

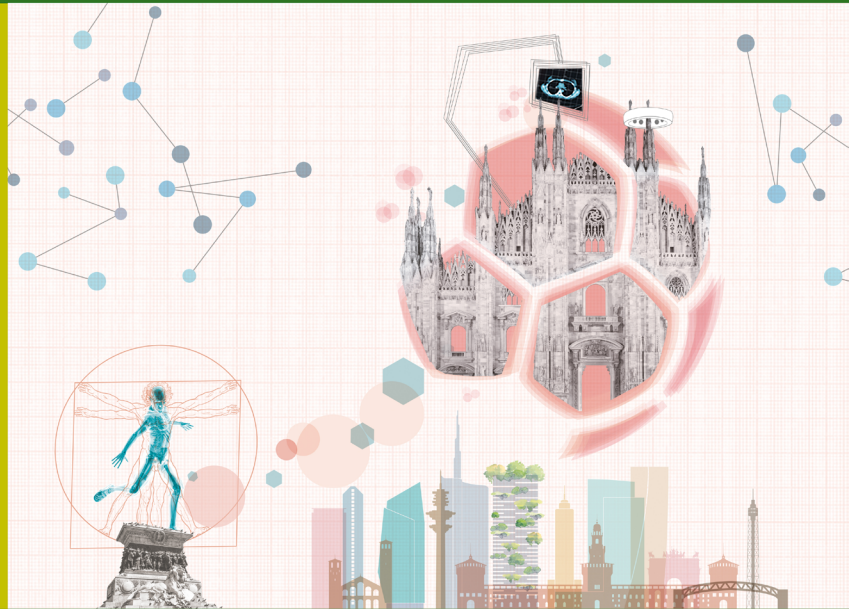
# Radiotherapy & Oncology

Journal of the European Society for  
Radiotherapy and Oncology

**ESTRO 38**

**Targeting optimal care, together**

26-30 April 2019  
Milan, Italy



# Radiotherapy & Oncology

Journal of the European Society for  
Radiotherapy and Oncology

**Volume 133 Supplement 1 (2019)**



Radiotherapy & Oncology is available online:  
For ESTRO members: <http://www.thegreenjournal.com>  
For institutional libraries: <http://www.sciencedirect.com>



ELSEVIER

Amsterdam • Boston • London • New York • Oxford • Paris • Philadelphia • San Diego • St. Louis

© 2019 Elsevier B.V. All rights reserved.

This journal and the individual contributions contained in it are protected under copyright by Elsevier B.V., and the following terms and conditions apply to their use:

**Photocopying**

Single photocopies of single articles may be made for personal use as allowed by national copyright laws. Permission of the Publisher and payment of a fee is required for all other photocopying, including multiple or systematic copying, copying for advertising or promotional purposes, resale, and all forms of document delivery. Special rates are available for educational institutions that wish to make photocopies for non-profit educational classroom use.

For information on how to seek permission visit [www.elsevier.com/permissions](http://www.elsevier.com/permissions) or call: (+44) 1865 843830 (UK)/(+1) 215 239 3804 (USA).

**Derivative Works**

Subscribers may reproduce tables of contents or prepare lists of articles including abstracts for internal circulation within their institutions. Permission of the Publisher is required for resale or distribution outside the institution.

Permission of the Publisher is required for all other derivative works, including compilations and translations (please consult [www.elsevier.com/permissions](http://www.elsevier.com/permissions)).

**Electronic Storage or Usage**

Permission of the Publisher is required to store or use electronically any material contained in this journal, including any article or part of an article (please consult [www.elsevier.com/permissions](http://www.elsevier.com/permissions)).

Except as outlined above, no part of this publication may be reproduced, stored in a retrieval system or transmitted in any form or by any means, electronic, mechanical, photocopying, recording or otherwise, without prior written permission of the Publisher.

**Notice**

No responsibility is assumed by the Publisher for any injury and/or damage to persons or property as a matter of products liability, negligence or otherwise, or from any use or operation of any methods, products, instructions or ideas contained in the material herein. Because of rapid advances in the medical sciences, in particular, independent verification of diagnoses and drug dosages should be made.

Although all advertising material is expected to conform to ethical (medical) standards, inclusion in this publication does not constitute a guarantee or endorsement of the quality or value of such product or of the claims made of it by its manufacturer.

---

**Orders, claims, and journal inquiries:** Please visit our Support Hub page <https://service.elsevier.com> for assistance.

**Funding Body Agreements and Policies**

Elsevier has established agreements and developed policies to allow authors whose articles appear in journals published by Elsevier, to comply with potential manuscript archiving requirements as specified as conditions of their grant awards. To learn more about existing agreements and policies please visit <http://www.elsevier.com/fundingbodies>



# ESTRO 38 CONTENT

27 APRIL 2019

## Teaching Lecture

Artificial Intelligence Applications in Radiation Oncology .....	Abs. 1
Using mice to model normal tissue responses to thoracic radiation .....	Abs. 2
State of the art in definitive treatment of locally advanced NSCLC .....	Abs. 3
New ILROG radiotherapy guidelines for haematological malignancies .....	Abs. 4
The role of postoperative radiotherapy in endometrial cancer: what have we learned of the PORTEC trials? .....	Abs. 5
Gating and breath-hold techniques in Radiation Therapy .....	Abs. 6
Technology for precision small animal radiotherapy research: Optimal use and challenges .....	Abs. 7
Ensuring Quality in an Image Guidance Era .....	Abs. 8

## Symposium

Artificial intelligence in Radiation Oncology .....	Abs. 9-12
Mouse models: Animal models the next step for RT .....	Abs. 13-16
Optimal management of patients with unresectable stage 3 NSCLC .....	Abs. 17-20
Combined modality treatment vs chemotherapy alone in lymphoma patients? .....	Abs. 21-24
Image guided adaptive brachytherapy IGABT for primary vaginal cancer in Europe and North America .....	Abs. 25-28

## Joint Symposium

ESTRO-AAPM: QA of on-line adaptive radiotherapy .....	Abs. 29-33
---	------------

## Symposium

Beyond Physical dose .....	Abs. 34-37
Quality in an IGRT .....	Abs. 38-40

## Poster Viewing

Poster viewing 1 : Breast and Skin .....	Abs. 41-49
--	------------

## Symposium

Challenging dose painting: Are we really painting what we aim to or the better outcome is only linked to higher dose spots within the CTV? .....	Abs. 50-53
--	------------

## Proffered Papers

RB 1: Pre-clinical models is the next step for radiotherapy .....	Abs. 54-58
CL 1: Proffered papers : Lung .....	Abs. 59-65
CL 2: Proffered papers Haematology, Sarcoma and oligometastases .....	Abs. 66-72
BT 1: Treatment verification .....	Abs. 73-79
PH 1: Adaptive radiotherapy: tools and technologies .....	Abs. 80-86
PH 2: Applications of dose modelling and calculation .....	Abs. 87-93
RTT 1: Motion management and adaptive strategies .....	Abs. 94-98

## Poster Viewing

Poster viewing 2: Advanced technologies .....	Abs. 99-107
---	-------------

## Award Lecture

Emmanuel van der Schueren Award Lecture .....	Abs. 108
Iridium Award Lecture .....	Abs. 109

## Symposium

MR-guided radiation therapy: hybrid machines and treatment adaptation .....	Abs. 110-113
How to exploit Immunogenic cell death Mechanism in Radiotherapy .....	Abs. 114-117
Oligo-metastatic prostate cancer – shedding light in a quickly emerging field .....	Abs. 118-121
New developments in gynaecological cancers .....	Abs. 122-124
Real time navigation technologies in brachytherapy .....	Abs. 125-127
Automatic / Knowledge based treatment planning:open issues .....	Abs. 128-131

## Joint Symposium

ESTRO-EFOMP: Multi-disciplinary working in Radiotherapy ..... Abs. 132-135

## Symposium

Younger people and radiotherapy ..... Abs. 136-138

## Poster Viewing

Poster viewing 3: Brachytherapy ..... Abs. 139-147

## Multidisciplinary Tumour Board

Soft tissue sarcomas

## Proffered Papers

RB 2: How to exploit immunogenic cell death mechanisms in radiotherapy ..... Abs. 151-157

CL 3: Proffered papers : Prostate and Bladder ..... Abs. 158-164

CL 4: proffered papers : CNS and Paediatrics ..... Abs. 165-171

BT 2: Cervix brachytherapy ..... Abs. 172-178

PH 3: Proffered paper: New developments in automated treatment planning ..... Abs. 179-185

PH 4: Proffered paper: New technologies ..... Abs. 186-192

RTT 2: A patient centered approach to follow up ..... Abs. 193-199

## Poster Viewing

Poster viewing 4: Head-Neck and Lung ..... Abs. 200-208

## Award Lecture

Honorary Members award lectures ..... Abs. 209-211

## 28 APRIL 2019

## Teaching Lecture

Re-irradiation for breast cancer ..... Abs. 212

Extracellular vesicles; are we there yet? ..... Abs. 213

Update on the management of SCLC ..... Abs. 214

How to combine checkpoint inhibitors with radiotherapy? ..... Abs. 215

How does brachytherapy fit in the modern management of penile cancer? ..... Abs. 216

Detector specific output correction factors: How to use them in practice ..... Abs. 217

Uncertainties in Radiomics ..... Abs. 218

New technology and modalities in Radiotherapy - What can the ESTRO School offer? ..... Abs. 219

Precision medicine and systems biology - transforming cancer research in the 21st century ..... Abs. 220

## Symposium

Balancing the risks and benefits of re-irradiation ..... Abs. 221-224

Circulating biomarkers for patient stratification and treatment monitoring ..... Abs. 225-228

## Debate

This house believes that Proton-beam be used routinely in the treatment of lung cancer

## Symposium

Radiation-drug combinations on the 2019 horizon ..... Abs. 229-232

Inverse planning in brachytherapy - A one click solution? ..... Abs. 233-235

Reference and non-reference dosimetry - CoPs and beyond ..... Abs. 236-239

New advances in image reconstruction in CBCT ..... Abs. 240-242

New technology and modalities ..... Abs. 243-245

Combining research and clinical/ professional training/ practice ..... Abs. 246-250

## Poster Viewing

Poster viewing 5: Health Services Research and Health-Related Quality of Life ..... Abs. 251-259

## Networking session

Speed Dating with Quiz

## Joint Symposium

ESTRO-JASTRO: Clinical trials for particle therapy: which ones to run and how? ..... Abs. 260-263

## Proffered Papers

RB 3: Tumour sensitization ..... Abs. 264-268

CL 5: Proffered papers : Randomised Clinical Trials ..... Abs. 269-274

CL 6: Proffered papers Radiation and Targeted Agents ..... Abs. 275-281

BT 3: Prostate HDR brachytherapy ..... Abs. 282-288

PH 5: Proffered paper: Innovations in dosimetry and dose measurements ..... Abs. 289-295

PH 6: Proffered paper: X-ray guided tumour tracking ..... Abs. 296-302

RTT 3: Impact of variations on treatment planning ..... Abs. 303-307

## Poster Viewing

Poster viewing 6 : Radiobiological modelling and quantitative imaging ..... Abs. 308-316

## Proffered Papers

BT 4: Breast and Skin brachytherapy ..... Abs. 317-323

## Presidential Symposium

Presidential symposium ..... Abs. 324

## Award Lecture

Claudius Regaud Award Lecture ..... Abs. 325

## Symposium

How to prevent burnout? ..... Abs. 326-330

The microbiome, inflammation and radiotherapy response ..... Abs. 332-334

Reducing the normal tissue effects of RT ..... Abs. 335-338

Radiotherapy in the era of the Silver Tsunami ..... Abs. 339-342

## Debate

This house believes that margin reduction is the key to improved outcome

Which is the best brachytherapy technique to deliver partial breast irradiation? Pitfalls, results and current recommendations ..... Abs. 343-346

## Symposium

Big data – big problems? ..... Abs. 347-349

From grid therapy to microbeam radiotherapy ..... Abs. 350-353

Focus on the lung ..... Abs. 354-356

Stronger together - news and projects in the young national societies ..... Abs. 357-360

## Poster Viewing

Poster viewing 7: CNS, Paediatrics, Haematology and Gynaecology ..... Abs. 361-369

## Multidisciplinary Tumour Board

Prostate cancer

## Networking session

Quiz and Young networking cocktail

## Joint Symposium

ESTRO-ASTRO: Translating discovery to cure ..... Abs. 370-373

## Proffered Papers

RB 4: Normal tissue effects of radiotherapy ..... Abs. 374-379

CL 7 :Proffered papers: GI ..... Abs. 380-386

CL 8: Proffered papers : Head and Neck ..... Abs. 387-393

BT 5: Optimising dose distribution ..... Abs. 394-400

PH 7: Proffered paper: Outcome modelling .....	Abs. 401-407
PH 8: Proffered paper: Handling intra-fraction motion in MR guided RT .....	Abs. 408-414
RTT 4: Reducing uncertainties in volume definition .....	Abs. 415-421

#### Poster Viewing

Poster viewing 8: TP Developments .....	Abs. 422-430
---	--------------

#### Proffered Papers

BT 6 : Innovative and uncommon indications .....	Abs. 431-437
--	--------------

#### Award Lecture

Jens Overgaard Legacy Award Lecture	
Honorary Physicist Award Lecture .....	Abs. 438

### 29 APRIL 2019

#### Teaching Lecture

Extreme hypofractionation in the treatment of localized prostate cancer .....	Abs. 439
Radio-immunotherapy: challenges and opportunities .....	Abs. 440
Tumor metabolism and radiation response .....	Abs. 441
Radiomic machine-learning to predict radiotherapy outcome .....	Abs. 442
Importance of volumetric staging and biological dose inhomogeneity in IMRT .....	Abs. 443
In-vivo dosimetry : Possibilities and Pitfalls .....	Abs. 444
The vital role of physicists in clinical trials: from design to data analysis .....	Abs. 445
New developments in the treatment of brain metastases: better prognostic tools, improved outcomes .....	Abs. 446

#### Symposium

Radiotherapy in bladder cancer: Standard of care and future perspectives .....	Abs. 447-450
--	--------------

#### Joint Symposium

ESTRO-EACR: Radio-immunotherapy: from concept to clinical practice .....	Abs. 451-454
--	--------------

#### Symposium

Tumor Metabolism and Radiotherapy .....	Abs. 455-458
---	--------------

#### Joint Symposium

ESTRO-ESR: Current status and future challenges in MR-integrated radiotherapy .....	Abs. 459-462
---	--------------

#### Symposium

Improved outcome by smarter use of radiotherapy .....	Abs. 463-465
Quantitative Imaging for Radiation Oncology .....	Abs. 466-468
Advanced methods to account for proton range uncertainties in treatment planning .....	Abs. 469-472
Care, communication and new technology in brain radiotherapy .....	Abs. 473-475

#### Poster Viewing

Poster viewing 9: Applied dosimetry .....	Abs. 476-484
---	--------------

#### Joint Symposium

ESTRO-IAEA: The role of hypofractionation in current radiotherapy and its impact in planning radiotherapy services .....	Abs. 485-488
--	--------------

#### Debate

Which is the best technique for the delivery of APBI? .....	Abs. 489-492
---	--------------

#### Proffered Papers

Biomarkers and bioimaging in radiotherapy .....	Abs. 493-499
CL 9: Proffered papers : Late breaking abstracts .....	Abs. 500-505
CL 10: Proffered papers : Pelvic Tumours .....	Abs. 506-512
PH 9: Proffered paper: Artificial intelligence and novel imaging approaches .....	Abs. 513-519
PH 10: Proffered paper: Treatment planning innovations .....	Abs. 520-526

RTT 5: Improving accuracy in patient positioning ..... Abs. 527-532

### Poster Viewing

Poster viewing 10: Radiobiology ..... Abs. 533-541

### Award Lecture

Klaus Breur Award Lecture ..... Abs. 542

Academic award: Jack Fowler University of Wisconsin Award ..... Abs. 543

Company Award Lectures ..... Abs. 544

### Symposium

Adaptive RT: reactive or proactive? ..... Abs. 545-548

Predictive models of toxicity and big data, big open issues ..... Abs. 549-552

Biological Imaging for Radiotherapy ..... Abs. 553-556

New developments for breast cancer irradiation ..... Abs. 557-560

### Joint Symposium

ESTRO-EORTC: Moving radiation oncology forward to improve patient outcomes ..... Abs. 561-563

### Debate

In 10 years physicists will need different training to include more ...

### Proffered Papers

PH 11: Proffered paper: Proton range and dose verification ..... Abs. 564-570

### Symposium

Education and Advance Practice ..... Abs. 571-573

### Poster Viewing

Poster viewing 11: Novel strategies in IGRT ..... Abs. 574-581

### Multidisciplinary Tumour Board

Bladder cancer

### Debate

Can early-regression-guided adaptive RT eRG-ART improve the pathological response in neo-adjuvant treatments?

### Symposium

Recent insights into adverse cardiac effects from multimodal radiation therapy ..... Abs. 582-585

### Proffered Papers

RB 6: Pre-clinical research in particle therapy ..... Abs. 586-590

CL 11: Proffered papers : Breast ..... Abs. 591-596

CL 12: Proffered papers : Health Economics and Health services research ..... Abs. 597-602

PH 12: Proffered paper: Multi centre analysis of quality ..... Abs. 603-609

PH 13: Proffered paper: Modelling toxicity ..... Abs. 610-616

RTT 6: Education and quality management for optimising patient care ..... Abs. 617-621

### Poster Viewing

Poster viewing 12: GI and Urological Cancers ..... Abs. 622-629

### Award Lecture

Donald Hollywood award lecture ..... Abs. 631

Highlights of proffered papers ..... Abs. 632-635

## 30 APRIL 2019

### Teaching Lecture

The DNA damage response to radiotherapy: mechanisms and therapeutic opportunities ..... Abs. 636

Are adolescents and young adults AYA a specific patients' population? .....	Abs. 637
Hypofractionation; Is there rationale from biology a/b ratio? .....	Abs. 638
Recent insights into radiotherapy tolerance from the REQUITE Consortium .....	Abs. 639
Integration of PET imaging in radiation treatment planning .....	Abs. 640
Implementation and practice of SRS and SBRT: Consensus guidelines and protocols .....	Abs. 641
How to select patients for radiotherapy with protons instead of photons .....	Abs. 642
MR-guided radiotherapy in the pelvic region .....	Abs. 643

### **Symposium**

Radiotherapy biomarkers: a confluence of imaging, genetics and pathology .....	Abs. 644-647
Palliation in RT - How much is enough? .....	Abs. 648-651
Mechanisms of treatment resistance in glioma .....	Abs. 652-655

### **Debate**

This house believes that there is still a role for radiotherapy in pancreatic cancer .....	Abs. 656-659
--	--------------

### **Symposium**

New developments in Head and Neck Cancer treatment .....	Abs. 660-662
New detector developments .....	Abs. 663-666

### **Proffered Papers**

PH 14: Proffered paper: Treatment planning of proton therapy .....	Abs. 667-673
--	--------------

### **Symposium**

Focus on the Pelvic Region .....	Abs. 674-676
----------------------------------	--------------

### **Joint Symposium**

ESTRO-RANZCR: Radiotherapeutical management of oligometastatic disease .....	Abs. 677-680
--	--------------

### **Symposium**

Plan of the day - present status and future aims .....	Abs. 681-684
--	--------------

### **Debate**

This house believes that immunotherapy is really changing radiation oncology .....	Abs. 685-688
This house believes that patients with squamous cell cancer of the esophagus no longer need surgery .....	Abs. 689-692

### **Symposium**

Controversies in the management of brain metastases .....	Abs. 693-696
Improving delineation in RT: not only for the doctor .....	Abs. 697-700
A new era for radiotherapy anthropomorphic phantoms .....	Abs. 701-704

### **Debate**

Workload/clinic logistics, and not technical uncertainties, are the main barrier to widespread implementation of adaptive RT practice .....	Abs. 705-706
---	--------------

### **Closing debate**

Data mining or data farming? .....	Abs. 707-708
------------------------------------	--------------

## **POSTER**

Clinical track: Head and Neck .....	Abs. 709-733
Clinical track: CNS .....	Abs. 734-757
Clinical track: Haematology .....	Abs. 758
Clinical track: Breast .....	Abs. 759-767
Clinical track: Lung .....	Abs. 768-785
Clinical track: Upper GI oesophagus, stomach, pancreas, liver .....	Abs. 786-813
Clinical track: Lower GI colon, rectum, anus .....	Abs. 814-821
Clinical track: Gynaecological endometrium, cervix, vagina, vulva .....	Abs. 822-833
Clinical track: Prostate .....	Abs. 834-862
Clinical track: Urology-non-prostate .....	Abs. 863-864

Clinical track: Skin cancer / malignant melanoma .....	Abs. 865-866
Clinical track: Sarcoma .....	Abs. 867-868
Clinical track: Paediatric tumours .....	Abs. 869-875
Clinical track: Palliation .....	Abs. 876-884
Clinical track: Elderly .....	Abs. 885
Clinical track: Other .....	Abs. 886-890
Physics track: Basic dosimetry and phantom and detector development .....	Abs. 891-898
Physics track: Dose measurement and dose calculation .....	Abs. 899-911
Physics track: Radiation protection, secondary tumour induction and low dose .....	Abs. 912-914
Physics track: Treatment plan optimisation: algorithms .....	Abs. 915-919
Physics track: Treatment planning: applications .....	Abs. 920-946
Physics track: Radiobiological and predictive modelling, and radiomics .....	Abs. 947-969
Physics track: Intra-fraction motion management .....	Abs. 970-979
Physics track: Adaptive radiotherapy and inter-fraction motion management .....	Abs. 980-998
Physics track: Quantitative functional and biological imaging .....	Abs. 999-1000
Physics track: Imaging acquisition and processing .....	Abs. 1001-1012
Physics track: Implementation of new technology, techniques, clinical protocols or trials including QA & audit .....	Abs. 1013-1039
Brachytherapy: Breast .....	Abs. 1040
Brachytherapy: Gynaecology .....	Abs. 1041-1043
Brachytherapy: Head and neck .....	Abs. 1044-1045
Brachytherapy: Physics .....	Abs. 1046-1052
Brachytherapy: Prostate .....	Abs. 1053-1059
Brachytherapy: Miscellaneous .....	Abs. 1060-1064
Radiobiology track: Radiobiology of normal tissues .....	Abs. 1065
Radiobiology track: Radiobiology of stem cells cancer and normal tissue .....	Abs. 1066-1067
Radiobiology track: Radiobiology of particles and heavy ions .....	Abs. 1068-1069
Radiobiology track: Radiation-induced signalling pathways .....	Abs. 1070-1071
Radiobiology track: Immuno-radiobiology .....	Abs. 1072-1074
Radiobiology track: Radiation and tumour metabolism .....	Abs. 1075-1079
Radiobiology track: DNA damage response .....	Abs. 1080-1085
Radiobiology track: Biological therapies e.g. viruses, vaccines .....	Abs. 1086
Radiobiology track: Radiation response biomarkers .....	Abs. 1087-1090
RTT track: Patient preparation, positioning and immobilisation .....	Abs. 1091-1095
RTT track: Imaging acquisition and registration, OAR and target definition .....	Abs. 1096-1105
RTT track: Treatment planning and dose calculation / QC and QA .....	Abs. 1106-1111
RTT track: Image guided radiotherapy and verification protocols .....	Abs. 1112-1116
RTT track: Motion management and adaptive strategies .....	Abs. 1117-1121
RTT track: Patient care, side effects and communication .....	Abs. 1122-1125
RTT track: Education and training/role development .....	Abs. 1126-1130
RTT track: Risk management/quality management .....	Abs. 1131-1132

## **ELECTRONIC POSTER**

Clinical track: Head and Neck .....	Abs. 1133-1205
Clinical track: CNS .....	Abs. 1206-1263
Clinical track: Haematology .....	Abs. 1264-1268
Clinical track: Breast .....	Abs. 1269-1333
Clinical track: Lung .....	Abs. 1334-1391
Clinical track: Upper GI oesophagus, stomach, pancreas, liver .....	Abs. 1392-1445
Clinical track: Lower GI colon, rectum, anus .....	Abs. 1446-1474
Clinical track: Gynaecological endometrium, cervix,vagina,vulva .....	Abs. 1475-1511
Clinical track: Prostate .....	Abs. 1512-1584
Clinical track: Urology-non-prostate .....	Abs. 1585-1592
Clinical track: Skin cancer / malignant melanoma .....	Abs. 1593-1600
Clinical track: Sarcoma .....	Abs. 1601-1608
Clinical track: Paediatric tumours .....	Abs. 1609-1614

Clinical track: Palliation .....	Abs. 1615-1635
Clinical track: Elderly .....	Abs. 1636-1652
Clinical track: Health services research / health economics .....	Abs. 1653-1660
Clinical track: Communication .....	Abs. 1661
Clinical track: Other .....	Abs. 1662-1681
Physics track: Radiation protection, secondary tumour induction and low dose incl. imaging .....	Abs. 1682-1691
Physics track: Basic dosimetry and phantom and detector development .....	Abs. 1692-1719
Physics track: Dose measurement and dose calculation .....	Abs. 1720-1807
Physics track: Treatment plan optimisation: algorithms .....	Abs. 1808-1823
Physics track: Treatment planning: applications .....	Abs. 1824-1891
Physics track: Radiobiological and predictive modelling, and radiomics .....	Abs. 1892-1942
Physics track: Intra-fraction motion management .....	Abs. 1943-1981
Physics track: Adaptive radiotherapy and inter-fraction motion management .....	Abs. 1982-2021
Physics track: Quantitative functional and biological imaging .....	Abs. 2022-2032
Physics track: Imaging acquisition and processing .....	Abs. 2033-2070
Physics track: Implementation of new technology, techniques, clinical protocols or trials including QA & audit .....	Abs. 2071-2117
Brachytherapy: Breast .....	Abs. 2118-2123
Brachytherapy: Gynaecology .....	Abs. 2124-2139
Brachytherapy: Head and neck .....	Abs. 2140
Brachytherapy: Physics .....	Abs. 2141-2147
Brachytherapy: Anorectal .....	Abs. 2148
Brachytherapy: Prostate .....	Abs. 2149-2155
Brachytherapy: Miscellaneous .....	Abs. 2156-2157
Radiobiology track: Radiobiology of particles and heavy ions .....	Abs. 2158-2159
Radiobiology track: Radiation-induced signalling pathways .....	Abs. 2160-2161
Radiobiology track: Tumour microenvironment .....	Abs. 2162
Radiobiology track: Immuno-radiobiology .....	Abs. 2163-2164
Radiobiology track: Radiation and tumour metabolism .....	Abs. 2165
Radiobiology track: DNA damage response .....	Abs. 2166-2168
RTT track: Patient preparation, positioning and immobilisation .....	Abs. 2169-2177
RTT track: Imaging acquisition and registration, OAR and target definition .....	Abs. 2178-2180
RTT track: Treatment planning and dose calculation / QC and QA .....	Abs. 2181-2189
RTT track: Image guided radiotherapy and verification protocols .....	Abs. 2190-2195
RTT track: Motion management and adaptive strategies .....	Abs. 2196-2197
RTT track: Patient care, side effects and communication .....	Abs. 2198-2208
RTT track: Education and training/role development .....	Abs. 2209-2213
RTT track: Risk management/quality management .....	Abs. 2214



# ABSTRACTS

ESTRO 38 Saturday 27 April

---

**Teaching Lecture: Artificial Intelligence Applications in Radiation Oncology**


---

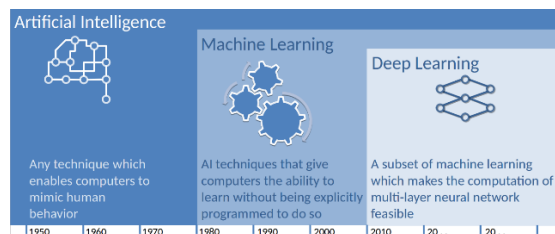
**SP-0001 Artificial Intelligence Applications in Radiation Oncology**

N. Dinapoli<sup>1</sup>, J. Lenkowicz<sup>2</sup>, C. Masciocchi<sup>2</sup>, A. Damiani<sup>2</sup>, I. Boldrini<sup>2</sup>, d. Cusumano<sup>3</sup>, v. Valentini<sup>1</sup>

<sup>1</sup>Fondazione Policlinico Universitario A. Gemelli IRCCS, UOC Radioterapia Oncologica- Dipartimento di Diagnostica per immagini- Radioterapia Oncologica ed Ematologia, Roma, Italy ; <sup>2</sup>Università Cattolica del Sacro Cuore, Dipartimento di Diagnostica per immagini- Radioterapia Oncologica ed Ematologia, Roma, Italy; <sup>3</sup>Fondazione Policlinico Universitario A. Gemelli IRCCS, UOC Fisica Sanitaria- Dipartimento di Diagnostica per immagini- Radioterapia Oncologica ed Ematologia, Roma, Italy

**Abstract text**

Artificial intelligence (AI) is a very generic concept defined as “the study of agents that receive percepts from the environment and perform actions” (S. Russell). It is being developed by using information technology, software and hardware, designed to create functions and procedures oriented to learn from, and process, data. First experiences of AI started from the beginning of computer age but thanks to the availability of high performance computing hardware (like GPUs or cloud computing) nowadays AI is booming in many fields of business, technology, e-commerce and, last but not least, health and medicine. What are the main tools available for creating AI based models in medicine? In a simplified slide published on Oracle® website (<https://blogs.oracle.com/bigdata/difference-ai-machine-learning-deep-learning>, Figure 1)



AI world includes applications as Machine Learning (ML), a part of which is constituted by so called Deep Learning (DL). In radiation oncology there are already many potential application of AI, ML and DL, being the number of the last ones increasing, step by step, in last years. For example, fields of application of AI can be the automatic target or organs at risk delineation process, the auto-planning procedures or different modeling processes of patients evaluation and prognosis. In literature there are several examples of AI applications, but a first summary of them needs to understand how AI algorithms can work and be applied to daily workflow, like DL and its use in imaging related applications. The complexity and extraordinary fast evolution of DL based applications seems to prelude the possibility of more and more self automated clinical workflows, starting from treatment prescription aids, going through volumes delineation and finally managing the whole treatment delivery process, both taking into account imaging (IGRT) based and clinical issue for toxicity management. Clinical and concurrent ethical issues will raise as soon as AI based applications will offer in medicine, and radiation oncology, a sufficient grade of automation, likewise the self-driving car are

provoking ethical discussions about how to proceed in case of accidents and damages to the human beings.

---

**Teaching Lecture: Using mice to model normal tissue responses to thoracic radiation**


---

**SP-0002 Using mice to model normal tissue responses to thoracic radiation**

Andy Ryan<sup>1</sup>

<sup>1</sup>Oxford University, Oncology, Oxford, United Kingdom

**Abstract text**

Thoracic radiotherapy is widely used for the treatment of cancer, with either curative or palliative intent depending on the stage of the disease. Radiation dose is limited by normal tissue effects where common side effects include oesophagitis, pneumonitis and pulmonary fibrosis. As new approaches to improving the effectiveness of radiation enter clinical trials, a key challenge to the field is to understand the potential impact of new agents on the therapeutic ratio in patients. Using PARP, ATR and ATM inhibitors as exemplars, the effects of radiation combination therapy will be described in established models of toxicity (C57BL/6 mice) and efficacy (subcutaneous xenografts grown in BALB/c nude mice). Recently, we have developed a new in vivo approach with the potential to evaluate both toxicity and efficacy in a single mouse model. A/J mice are treated with urethane which leads to the development of lung tumours over a period of 6-9 months. In this model, radiation treatment has significant anti-tumour effects, but also induces pneumonitis and fibrosis. Using this new model, we outline emerging data using PARP, ATR and ATM inhibitors in combination with localised radiation, and suggest this may be a better approach to determining the potential impact of new agents on the therapeutic index of radiation therapy.

---

**Teaching Lecture State of the art in definitive treatment of locally advanced NSCLC**


---

**SP-0003 State of the art in definitive treatment of locally advanced NSCLC**

C. Faivre-Finn<sup>1</sup>

<sup>1</sup>The Christie NHS Foundation Trust, Division of Cancer Sciences -Radiation Oncology, Manchester, United Kingdom

**Abstract text**

Approximately one third of patients with non-small cell lung cancer (NSCLC) present with stage III disease and the majority of these patients are inoperable. Treatment of inoperable stage III NSCLC requires both control of the local disease and the distant micrometastases. The international standard of care is concurrent chemoradiotherapy (CIRT) that is associated with a 5 year survival rate of 20-25% (Auperin, Ramnath, Eberhardt). The literature supports the use of concurrent CIRT, in selected patients with good performance status, without major co-morbidities and for whom the RT plan produces acceptable normal tissue doses. Data in the elderly population is limited. The addition of chemotherapy concurrently to RT increases the risk of severe oesophagitis but does not increase the risk of lung toxicity. To date there is no established standard concurrent CIRT regimen in Europe. Neither the addition of induction or consolidation CT to concurrent CIRT have led to improvements in survival in unresectable locally advanced NSCLC. There is no role for dose escalation in stage III NSCLC using conventional dose fractionation

(Bradley).

Major progress has been made in recent years in the field of radiotherapy planning/delivery (i.e. 4DCT, PETCT, IMRT and VMAT) and treatment verification (daily on-line cone beam CT).

For the majority of patients, concurrent CRT is not suitable due to performance status and co-morbidities. The alternative treatment options are chemotherapy followed by RT (sequential CRT), or RT alone. The latter is associated with a 5 year survival rate of less than 10 %, due to both locoregional and distant relapse. There is currently no established role for induction, consolidation chemotherapy or targeted agents in stage III NSCLC. The PACIFIC trial has recently established a new standard of care by showing a progression-free and overall survival advantage for consolidation immune check-point inhibitor (Antonia).

PCI in stage III NSCLC reduces the incidence of brain metastases but has not been demonstrated to reduce survival in the reported studies (Paumier). The role of post-operative RT in completely resected patients with N2 disease is controversial (Le Pécoux).

Aupérin A et al. Meta-analysis of concomitant versus sequential radiochemotherapy in locally advanced non-small-cell lung cancer. *J Clin Oncol.* 2010; 28(13):2181-90. Ramnath N, et al. Treatment of stage III non-small cell lung cancer: Diagnosis and management of lung cancer, 3rd ed: American College of Chest Physicians evidence-based clinical practice guidelines. *Chest.* 2013;143(5 Suppl):e314S-40S

Eberhardt WE et al. 2nd ESMO Consensus Conference in Lung Cancer: locally advanced stage III non-small-cell lung cancer. *Ann Oncol.* 2015 Aug;26(8):1573-88.

Bradley J, et al. Standard-dose versus high-dose conformal radiotherapy with concurrent and consolidation carboplatin plus paclitaxel with or without cetuximab for patients with stage IIIA or IIIB non-small-cell lung cancer (RTOG 0617): a randomised, two-by-two factorial phase 3 study. *Lancet Oncol.* 2015;16(2):187-99

Paumier A, et al. Prophylactic cranial irradiation in lung cancer. *Cancer Treat Rev.* 2011 Antonia SJ, et al. Durvalumab after Chemoradiotherapy in Stage III Non-Small-Cell Lung Cancer. *N Engl J Med* 2017 ;377(20):1919-1929.

Antonia SJ, et al. Overall Survival with Durvalumab after Chemoradiotherapy in Stage III NSCLC. *N Engl J Med.* 2018 Sep 25

Le Pécoux C. Role of postoperative radiotherapy in resected non-small cell lung cancer: a reassessment based on new data. *Oncologist.* 2011;16(5):672-81

---

### Teaching Lecture: New ILROG radiotherapy guidelines for haematological malignancies

---

#### SP-0004 New ILROG radiotherapy guidelines for haematological malignancies

L. Specht<sup>1</sup>

<sup>1</sup>The Finsen Center - Rigshospitalet, Oncology, Copenhagen, Denmark

#### Abstract text

The International Lymphoma Radiation Oncology Group (ILROG) is a worldwide organization of radiation oncologists interested in lymphomas and other haematological malignancies. Our goal is to improve outcome for patients by encouraging the appropriate integration of radiation therapy (RT) in the management of these diseases. One of the most important tasks has been to develop and teach the use of modern, image-guided and highly conformal RT for the many different disease entities and anatomic distributions. A very important task has been the development and publication of guidelines. In 2014-15 we published ILROG

guidelines on the treatment of Hodgkin lymphoma, pediatric Hodgkin lymphoma, nodal non-Hodgkin lymphoma, extranodal lymphomas, and primary cutaneous lymphomas. They proved very popular, being some of the most frequently downloaded publications in radiation oncology. In 2017 we gathered in Boston with the aim of defining other areas where guidelines were needed. We have subsequently published 9 new guidelines covering the following areas:

Relapsed or refractory Hodgkin lymphoma, where RT has long been demonstrated to be a powerful agent in the local control. It may even be effective when used alone in selected cases. Many patients undergo high-dose chemotherapy (HDCT) and stem cell transplant (SCT), but they frequently relapse in sites of prior disease, and this risk is reduced in patients treated with RT. The indications for RT in these patients are: 1) localized relapse, 2) disseminated relapse but with either bulky disease, persistent FDG-avid disease, or involvement of areas considered critical for local control. It is debated whether the RT should be given before or after the SCT. The doses and volumes depend on the response to chemotherapy and the extent of disease.

Relapsed/refractory diffuse large B-cell lymphoma, where RT may also provide effective local control. Young patients without comorbidities and with chemosensitive disease are often offered HDCT and SCT, and RT is used according to the same principles as for Hodgkin lymphoma. For patients who are not eligible for transplant, RT can offer effective palliation and for patients with locoregionally confined disease even cure. Doses vary according to the response to chemotherapy, and may in refractory disease go as high as 45-50 Gy. Volumes depend on disease location and extent.

Solitary plasmacytoma are potentially curable with RT. Doses vary from 35 Gy to small lesions to 40-50 Gy to large lesions. For patients with multiple myeloma RT is an effective palliative treatment at lower doses. Total body irradiation (TBI) continues to be an important part of conditioning regimens for allogeneic SCT. Many different techniques have been used, most often at extended source-to-skin distance (SSD). Increasingly, 3-dimensional planning and intensity modulated therapy are being used. This may allow reductions of the doses to risk organs. With some of these techniques the TBI is no longer delivered simultaneously to the entire body, possibly leading to some circulating leukemia cells receiving reduced doses. The TBI may be delivered at standard SSDs leading to higher dose rates, which has the potential to increase toxicity.

Extramedullary leukemia can pose therapeutic challenges for which RT can have an important role. RT should be considered for isolated choromas with inadequate response to chemotherapy, for isolated recurrences after SCT, and for palliation. Leukemia cutis may be treated with electron therapy, if large areas are involved total skin electron beam therapy may be used. A dose of 24 Gy results in excellent, rapid, and durable local control. Central nervous system leukemia may be an indication for RT, in particular in patients with recurrent or refractory CNS leukemia. Whole brain RT is usually given at doses of 24 Gy, but for selected patients treated with curative intent, cranio-spinal RT may be indicated. Lymphoblastic lymphoma with a large mediastinal mass often relapse in the mediastinum after treatment with intensive chemotherapy. Mediastinal RT can improve local control, but toxicity is a concern.

Proton therapy for mediastinal lymphoma may help to reduce the radiation dose to the normal structures thereby reducing long-term toxicity. There are many uncertainties in proton therapy, and these need to be considered. Imaging with FDG-PET plays a major role in the treatment planning of many lymphoma types. Accurate definition of sites of involvement before any systemic therapy is

important for RT planning. A baseline pre-treatment PET/CT is recommended. Smaller nodes that are not FDG-avid but seen on CT adjacent to FDG-avid nodes should be included. In masses seen on CT with partial FDG-uptake the entire mass should be included. Breathing control techniques are recommended for mediastinal treatment to reduce the doses to the critical structures.

---

**Teaching Lecture: The role of postoperative radiotherapy in endometrial cancer: what have we learned of the PORTEC trials?**

---

**SP-0005 The role of postoperative radiotherapy in endometrial cancer: what have we learned of the PORTEC trials?**

C. Creutzberg<sup>1</sup>

<sup>1</sup>Leiden University Medical Center LUMC, Department of Radiotherapy, Leiden, The Netherlands

**Abstract text**

In this presentation, the current evidence and recent developments in risk-based adjuvant treatment for endometrial cancer will be discussed, reviewing the data from the PORTEC-1 and PORTEC-2 trials which have been pivotal in determining the role of radiation therapy, especially vaginal brachytherapy, in (high)intermediate risk endometrial cancer.

The PORTEC-3 trial focused on the 15-20% of women with high-risk endometrial cancer (stage IB grade 3 and stage II-II endometrial cancers, and stage I-III non-endometrioid cancers), investigating the efficacy of combined adjuvant chemotherapy and radiation therapy, showing that radiation therapy alone is still standard treatment for stage I-II disease, while combined adjuvant treatment should be considered for women with stage III disease and those with serous cancers. Data on toxicity and quality of life from these trials are essential for shared decision making.

The PORTEC-4a trial builds on the recent knowledge on molecular characteristics of endometrial cancer and investigates the role of an integrated molecular profile to determine adjuvant treatment in high-intermediate risk disease, aiming to reduce overtreatment by sparing the expected 50% with a favourable profile adjuvant brachytherapy, while optimizing outcomes for the 5-10% with an unfavourable profile by using pelvic radiotherapy. Results of the pilot phase have shown the determination of the molecular factors within 2 weeks to be feasible in clinical practice.

The PORTEC-results will be put into perspective of results from other recent randomised trials, and future developments will be discussed.

---

**Teaching Lecture: Gating and breath-hold techniques in Radiation Therapy**

---

**SP-0006 Gating and breath-hold techniques in Radiation Therapy**

M. Aznar<sup>1</sup>

<sup>1</sup>The University of Manchester, Division of Cancer Sciences, Manchester, United Kingdom

**Abstract text**

This teaching lecture will summarise the upcoming ACROP guidelines on the practical implementation of breath hold techniques in different clinical sites (breast, lung, lymphoma, abdomen). The similarities and differences with gating approaches will be highlighted and special focus will be given to image guidance procedure (for planning purposes as well before treatment and during treatment).

---

**Teaching Lecture: Technology for precision small animal radiotherapy research: Optimal use and challenges**

---

**SP-0007 Technology for precision small animal radiotherapy research: Optimal use and challenges**

F. Verhaegen<sup>1</sup>, A. Vaniqui<sup>1</sup>, S. Van Hoof<sup>1</sup>, I.P. Almeida<sup>1</sup>, B. Van Der Heyden<sup>1</sup>, P. Granton<sup>2</sup>, J. Theys<sup>3</sup>, M. Vooijs<sup>3</sup>, L. Dubois<sup>3</sup>

<sup>1</sup>Maastricht Radiation Oncology Maastr, Clinical Physics Research, Maastricht, The Netherlands ; <sup>2</sup>Smart Scientific Solutions Bv, Maastricht, The Netherlands ; <sup>3</sup>Maastricht Radiation Oncology Maastr, Maastr Lab, Maastricht, The Netherlands

**Abstract text**

Two major recent developments have boosted radiobiology research in in vivo systems: (1) the development of high-precision image-guided photon irradiation platforms including treatment planning software, and (2) the development of ever more realistic disease models. These platforms have been developed mostly for cancer research, but can also be used for the study of other diseases e.g. in cardiology or neurology.

To guide the users towards optimal use of this new technology, recently ESTRO issued ACROP (Advisory Committee on Radiation Oncology Practice ) guidelines<sup>1</sup>. These guidelines identified several challenges including: (1) what are the key technologies required to downscale clinical treatments into small animal models, (2) how to deal with target motion, (3) which imaging modalities should be integrated into the radiation platforms, (4) what are the optimal irradiation margins, (5) what is the accuracy and precision of small field dosimetry, (6) which methods should be developed to verify the dose distribution, (7) which imaging modalities should be used for treatment planning, given the evolving clinical scenarios, (8) what is the difference between high and low-energy photon irradiation.

These novel platforms combine capabilities for precision irradiation with very small fields (e.g. in an arc), with various modalities of integrated onboard high resolution imaging. The platforms enable for the first time irradiation studies at the mouse/rat level, similar to the clinical standard of image-guided radiotherapy. These platforms include imaging modalities such as micro-cone beam CT, bioluminescent imaging (BLI), advanced targeting capabilities and a dedicated treatment planning system (e.g. SmART-ATP<sup>2</sup>). Further developments at the research stage include orthotopic tumor models, novel BLI targeting, novel CT contrast media, dual-energy CT imaging, spectral CT imaging, phase-contrast imaging, intravital microscopy, microbeam technology, motion-gated therapy, motion-dependent dose calculations, dose painting, margin recipes, autodelineation of anatomical structures, non-coplanar beams, dynamic field collimators, dose verification systems, advanced phantoms, and a preclinical data warehouse. Furthermore, the first studies on precision irradiation of rodent models with proton beams have been published<sup>3</sup>. From the overview to be given in this lecture it is clear the research platforms are reaching a level of maturity which will facilitate translational research. Many more developments are expected in the near future.

1. Verhaegen et al. *ESTRO ACROP: Technology for Precision Small Animal Radiotherapy Research: optimal use and challenges*. *Radiother Oncol*, 126/3, 471-78, 2018
2. van Hoof et al. *Development and Validation of a Treatment Planning System for Small Animal Radiotherapy: SmART-Plan*. *Radiother Oncol*, 109, 361-6, 2013
3. Almeida et al. *Exploring the feasibility of a clinical*

proton beam with an adaptive aperture for pre-clinical research. Br J Radiol 91: 20180446, 2018

---

### Teaching Lecture: Ensuring Quality in an Image Guidance Era

---

#### SP-0008 Ensuring Quality in an Image Guidance Era E. Miles<sup>1</sup>

<sup>1</sup>Mount Vernon Hospital, Academic Physics, Northwood Middlesex, United Kingdom

#### Abstract text

The radiotherapy process is a series of events during which discrepancies between the planned treatment and actual treatment delivered can occur. This necessitates a comprehensive quality assurance (QA) programme, including regular quality control (QC) checks and audits. As more advanced technology is introduced in the clinical setting, QA activities must continually evolve to provide a safe framework for implementation of technical radiotherapy.

With image guided and adaptive strategies being increasingly employed to ensure accurate delivery of treatment in scenarios such as dose escalation and hypofractionation; techniques must be implemented in a safe and effective manner.

QA in the clinical trial arena has played a leading role in striving for accuracy and consistency of radiotherapy treatment delivery through monitoring protocol compliance in a multi-centre setting. Clinical trials can also evaluate the feasibility and effectiveness of a new technology. A comprehensive trial QA programme not only accredits centres for recruitment to a trial but also benefits the general standard of radiotherapy delivered. This presentation will aim to demonstrate how we can extend the clinical trial QA experience to routine practice to ensure quality of image guidance through discussing examples of clinical trial benchmarking and credentialing processes and their perceived impacts on clinical practice.

---

### Symposium: Artificial intelligence in Radiation Oncology

---

#### SP-0009 Clinical applications of AI for Radiation Oncology

J. Bibault<sup>1</sup>

<sup>1</sup>Université Paris Descartes - Hôpital Européen Georges Pompidou, Paris, France

#### Abstract text

The application areas of Artificial Intelligence (AI) in radiation oncology include image segmentation and detection, image phenotyping and radiomic signature discovery, clinical outcome prediction, and treatment planning automation.

In this lecture, we will first explain the methods used in AI, such as K-Nearest Neighbor, Decision Trees, Support Vector Machines, and Artificial Neural Networks, with a focus on Deep Learning (DL).

In the second part of the lecture, we will describe studies using DL for image segmentation, outcome prediction (toxicity, treatment response and survival) or treatment planning.

Finally we will explain the limits of these methods and evaluate how they will transform radiation oncology.

#### SP-0010 Acceptance, commissioning, introduction, regulatory aspects and QA of AI

W. Verbakel<sup>1</sup>

<sup>1</sup>VU University Medical Center, Radiation Oncology Department, Amsterdam, The Netherlands

#### Abstract text

Artificial intelligence is increasingly being proposed for radiotherapy. It has the potential to support or even take over several factors in the radiotherapy chain. A few examples are automated delineation, prediction of dose calculation, guiding optimal plan optimization, QA of treatment plans, and verification on the linac. Generally, AI is based on historic information, and a mathematical model, or a deep learning convolutional neural network is built on the basis of a library of data which is used for training. The result is a product that can take over clinical tasks from clinicians, dosimetrists, physicists and technologists. Therefore, such product is considered as a medical device and it should obey the EU rules for medical devices. The data that is used for training is in general patient related data, and the hospital should follow the privacy rules / get patient consent / get permission from the medical ethics committee / use only anonymized data. Furthermore, the clinical data may not be as consistent as we hope. For contouring, it may contain wrongly assigned structure names, or quickly contoured structures that deviate from the standard, and for dose prediction, it may contain sub-optimal treatment plans where insufficient OAR sparing was achieved. This can influence the performance of the AI. The AI result will not necessarily be worse than the contour by the clinician, but it is advisable to always check the output of an AI system. Ideally, a prediction would include an uncertainty with which the prediction is made, which is an important field of work in deep learning. Finally, the output of an AI algorithm also needs to be accepted by the medical staff, which requires convincing testing.

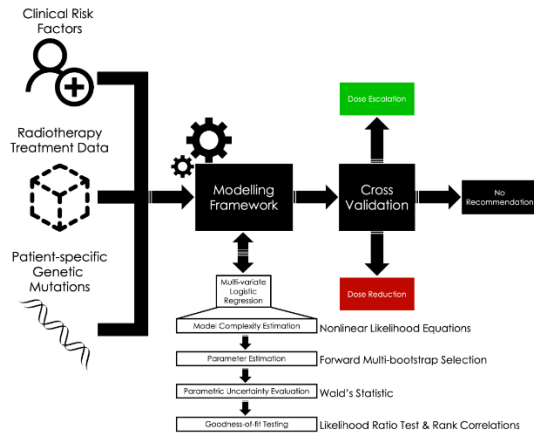
#### SP-0011 Unified Radiogenomic Prediction of Late Radiotherapy Toxicities

J. Coates<sup>1,2</sup>, A. Jeyaseelan<sup>2</sup>, N. Ybarra<sup>2</sup>, J. Tao<sup>2</sup>, M. David<sup>3</sup>, S. Faria<sup>3</sup>, L. Souhami<sup>3</sup>, F. Cury<sup>3</sup>, M. Duclos<sup>3</sup>, I. EL Naqa<sup>4</sup>

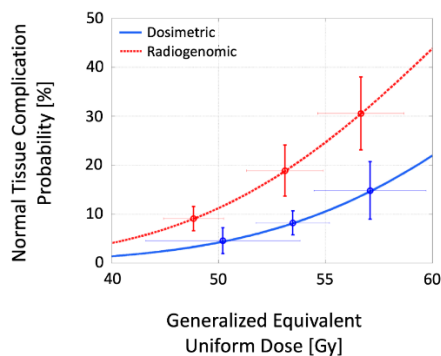
<sup>1</sup>Department of Oncology, University of Oxford, Oxford, United Kingdom ; <sup>2</sup>McGill University, Medical Physics Unit, Montreal, Canada ; <sup>3</sup>McGill University, Radiation Oncology Division, Montreal, CANADA; <sup>4</sup>University of Michigan, Department of Radiation Oncology, Ann Arbor, USA

#### Abstract text

Radiation-induced toxicities are the unavoidable result of damage to healthy tissues that surround solid tumours and directly limit the ability of clinicians to achieve local tumour control. Clinically, they present as acute events, becoming manifest and subsiding within days-to-weeks, or as late effects, in which case disease onset can take years. In this work, we integrate clinical risk factors, radiotherapy treatment plan parameters, and patient specific biological variables together to construct models that more accurately predict such side effects. We make use of a well-established data-driven modelling approach based on logistic regression and optimised specifically for radiotherapy-related data-mining.



We identified a cohort of 100 patients that underwent curative hypofractionated radiotherapy to the prostate (66 Gy in 22 fractions) and retrospectively genotyped for gene dosage (copy numbers) and nucleotide polymorphisms in six different genes reported previously to be involved in response to radiotherapy: XRCC1, XRCC3, ERCC2, SOD2, VEGFA and TGFB1. Predictive models of both late rectal bleeding and erectile dysfunction, two dose limiting side effects of prostate cancer radiotherapy, were identified and cross-validated. The best performing multi-metric models contained dosimetric and biological variables, reflecting the interlinked biophysical nature of late radiation-induced toxicities. Notably, the copy number of DNA repair gene XRCC1, acting via the base excision repair pathway, and TGFB1, a key player in modulating inflammation and matrix remodelling, were found to be valuable predictive markers.



Taken together, we demonstrate that the inclusion of patient-specific mutations in DNA repair genes coupled with dosimetric parameters derived from patient-specific radiotherapy treatment plans provides a significant improvement over non-biological models. We accomplished this using an automated data-mining framework able to deal with clinical, biological, and treatment-related radiotherapy data simultaneously. In

the future, similar frameworks are likely to be used by clinicians to dose-escalate patients at low-risk and reduce the dose for high-risk patient groups.

#### SP-0012 Impact of AI and automation on practice

L. Tagliaferri<sup>1</sup>

<sup>1</sup>Fondazione Policlinico Universitario Agostino Gemelli IRCCS, Radiation Oncology Department - Gemelli ART Advanced Radiation Therapy, Rome, Italy

#### Abstract text

Radiotherapy is involved in 45-55% of newly diagnosed cancer but also in the advanced stage disease thanks to the efficacy in the durable palliation and pain control. However, RT requires training and quality assurance[1] as it is a technologically complex advanced treatment[2]. To meet these needs, there will be an increased request of radiation therapy infrastructures and staffing but also the need to introduce Intelligence Artificial Guided Procedure (IAGP) and Automation in the clinical practice. The impact of this introduction will not be negligible, and it could improve overall health care quality thanks to the support of big data[3], deep learning[4], algorithmic innovation and powerful neural network models[5]. Automation using artificial intelligence is systematically involved in several fields of cancer care and, more specifically, in the radiation treatment workflow[6]. Many software aiming to improve and speed up the “contouring process” through autosegmentation[7] solutions have been released in the last years. Auto-segmentation also allows to perform the adaptive re-planning procedure during treatment[8]. Treatment planning step is also a very time-consuming task and the quality of its output is based on the physicist’s and physician’s knowledge and expertise. There is variability in this field, not only across centers, but even in the same center due to the presence of different planners. Inverse planning optimization and automated knowledge-based treatment planning approaches[9][10] improve the speed of the process and ensure that the quality of the results is optimal and not treatment planner dependent. Many AI applications have also been introduced in the radiation delivery process. Many technologies can indeed check the exact location of the target and the organs at risk improving the quality and speeding up the procedure of patient repositioning[11] and the radiation delivery[12]. Recently, Decision Support Systems (DSS) are spreading more and more: the implementation of large database and radiomics[13] provides physicians a huge amount of data that can improve clinical practice through the use of predictive models[14] and reduce the impact of knowledge gaps between domain-specific experts and non-experts[15] aiming to improve personalized cancer care. Aim of this talk is to present and discuss how the introduction of Intelligence Artificial Guided Procedure (IAGP) and Automation could impact the clinical practice and the radiotherapy workflow, especially in the fields of contouring and treatment planning, quality assurance, radiation delivery and clinical outcomes recording and prediction. It will be also analyzed how, thanks to the minimum human intervention and automatically error detection systems, automation could also provide a reduction in cure costs[16] and an escape from time-consuming repetitious tasks with significant advantages for the physicians and consequent of more time to dedicate to interaction with patients, increasing the level of humanity and patients care perception quality.

#### Bibliography

[1] Morganti AG et al. *Radiother Oncol.* 2008 [2] Valentini V et al. *Rays.* 2001 [3] Tagliaferri L et al. *J Contemp Brachytherapy.* 2016 [4] Damiani A et al. *Eur J Intern Med.* 2018 [5] Xing L et al. *J. Med Phys.* 2018 [6] Thompson RF et al. *Int J Radiat Oncol Biol Phys.* 2018 [7] Naceur MB et al. *Comput Methods Programs Biomed.* 2018 [8] Montanaro T et al. *Med Phys.* 2018 [9] Good D et al. *Int J Radiat Oncol*

Biol Phys. 2013 [10]Nwankwo O et al Radiat Oncol. 2015 [13]Arimura H et al. J Radiat Res. 2018.[14]Tagliaferri L et al. J ContempBrachytherapy. 2017 [16]Massaccesi M et al. Acta Oncol. 2015

---

**Symposium: Mouse models: Animal models the next step for RT**

---

**SP-0013 Linking radiation-induced damage to systemic effects: what can we learn from preclinical models of normal tissue complications**

V. Jendrossek<sup>1</sup>

<sup>1</sup>University Hospital Essen, Institute of Cell Biology Cancer Research- Department of Molecular Cell Biology, Essen, Germany

**Abstract text**

Radiotherapy (RT) is part of standard treatment for lung cancer patients but disease progression is common. Herein biological factors such as high intrinsic or microenvironment-mediated radiation resistance of the cancer cells and potentially tumour immune escape limit successful RT or combined radiochemotherapy (RCT). Moreover, adverse late effects in the highly radiosensitive normal lung preclude the use of curative doses leading to decreased quality of life or - as a consequence of treatment with suboptimal radiation doses - to fatal outcomes by local recurrence or metastatic disease. Historically, RT has been introduced as a highly efficient and spatially accurate local therapy. But under certain conditions RT can also elicit systemic effects that impact treatment outcome in normal and tumor tissues locally and occasionally at non-irradiated tumour sites outside the radiation field (abscopal effects). Elegant work in preclinical models in mice has demonstrated that the systemic effects of ionizing radiation are immune mediated. Further experimental work has helped to substantially advance our understanding of the contribution of radiation-induced immune changes in the pathogenesis of radiation-induced adverse late effects e.g. in the lung. The presentation will introduce the molecular and cellular processes that link radiation-induced DNA-damage to activation of cells from the innate and adaptive immune system, highlight the dual face of radiation-induced acute and chronic immune changes in normal and tumour tissues, and discuss the importance of dose and fractionation for RT-induced immune changes. Finally, the presentation will discuss the use of radiation-induced immunoregulatory mechanisms as therapeutic targets that may allow to limit RT-induced adverse late effects and to increase the therapeutic gain of RT. Such compounds may be of future clinical relevance in view of the increasing interest in combining RT with immune checkpoint blockade or other immune modulators to enhance the immune response against the tumour.

**SP-0014 New developments in small animal image guided radiotherapy: Bladder cancer**

A. Kiltie<sup>1</sup>

<sup>1</sup>CRUK/MRC Oxford Institute for Radiation Oncology, Dept. of Oncology, Oxford, United Kingdom

**Abstract text**

Muscle-invasive bladder cancer can be treated clinically by bladder removal (cystectomy) or bladder preservation, where the patient keeps their native bladder. Trimodality therapy, with complete transurethral resection of the tumour followed by concurrent chemoradiation, with or without neoadjuvant chemotherapy is the current standard of care, although many elderly patients receive only radiotherapy alone, due to the toxicity of current radiosensitising agents. There is therefore an urgent need

to find agents less toxic to the normal tissues. Preclinical studies are useful in this regard and use of image-guided radiotherapy in small animals allows the treatment to more closely mimic the radiotherapy delivered in human patients.

We have used our small animal radiation research platform (SARRP) to both treat orthotopic tumours in the bladder and to investigate normal tissue toxicity. As longer term *in vivo* studies of bladder cancer irradiation are hampered by the need to avoid small intestine, we have developed a method of irradiating bladder and large intestine/rectum only by treating the mice head down, which employs gravity to move the small intestine from the radiotherapy field. Image guidance allows us to verify that there is no small intestine in the proposed field.

We also use image guidance to treat mice for longer term toxicity studies, which include histological endpoints in the bladder and intestine evaluated by a veterinary pathologist and also functional assays including stool assessments.

Much of this work has only been made possible with the advent of small animal image-guided radiotherapy.

**SP-0015 RBE of protons: what can we learn from preclinical models?**

C.P. Karger<sup>1</sup>

<sup>1</sup>German Cancer Research Center DKFZ, Department of Medical Physics, Heidelberg, Germany

**Abstract text**

Proton therapy allows highly conformal tumor irradiation and thereby sparing of neighboring healthy tissues. Compared to photon treatments, proton irradiation exhibit a higher biological effectiveness, which is currently considered by a fixed RBE of 1.1. Recent *in-vitro* data, however, indicate that the RBE at the distal edge of the Bragg-peak may increase up to values of 2 [1] and beyond and models have been developed [2-5], which describe this increase as a function of LET, dose and cell-specific parameters. This increase could potentially increase the risk of side effects in normal tissue structure behind the distal edge of the spread-out Bragg-peak. While the clinical relevance and the need to introduce these models in patient treatments is controversially discussed [6, 7], strong supportive data from *in-vivo* experiments and patients are still lacking. This presentation gives an overview on existing data in animal models and discusses their impact and limitations on clinical conclusions. The needs for further research will be outlined.

**References**

1. Britten, R.A., et al., Radiat Res, 2013. 179(1): p. 21-8.
2. Jones, B., Acta Oncol, 2017. 56(11): p. 1374-1378.
3. Carabe, A., et al., Phys Med Biol, 2012. 57(5): p. 1159-72.
4. McNamara, A.L., et al. Phys Med Biol, 2015. 60(21): p. 8399-416.
5. Wedenberg, M., et al., Acta Oncol, 2013. 52(3): p. 5808.
6. Buchsbaum, J.C., Int. J. Radiat. Oncol. Biol. Phys, 2017. 97(5): p. 1085-1086.
7. Paganetti, H., Int J Radiat Oncol Biol Phys, 2015. 91(5): p. 892-4.

**SP-0016 Dynamics Changes in Immune Cells During Glioblastoma Response to Treatment: Macrophages at Play**

L. Akkari<sup>1</sup>

<sup>1</sup>Netherlands Cancer Institute, Tumor Biology and Immunology, Amsterdam, The Netherlands

**Abstract text**

New insights into the role of innate immune subsets in cancer requires a thorough investigation of the molecular mechanisms responsible of their evolution in the course of

malignancy and therapy response, in order to effectively harness their anti-cancer potential. This is particularly relevant to late-stage and recurrent disease which are refractory to standard of care treatment, do not respond to targeted or T cell immunotherapy and that are consequently fatal. Glioblastoma (GBM) is such a cancer type, and the most malignant form of primary brain tumor in the central nervous system. Despite aggressive standard of care treatment, the median survival of GBM patients does not exceed 15 months. Tumor-associated macrophages/microglia (TAMs) are the most abundant non-cancerous cell types in human and murine GBM. Using murine models of GBM in which we examined the relative contribution of TAM, we found that radiotherapy alters infiltrating bone marrow-derived macrophages (BMDM) and brain-resident microglia (MG) content and phenotype. These cells undergo profound proteomic and transcriptional changes in the treated GBM tumor immune microenvironment, and support radiotherapy resistance and relapse. We demonstrated that the convergence of MG and BMDM phenotype at recurrence relies on acquisition of neurodegenerating signals within the TIME, with activation of the Notch and TGF $\beta$  pathways at its core. Limiting the acquisition of this recurrent signature in both BMDM and MG led to enhanced radiotherapy response and delayed recurrence in multiple GBM murine models. We propose that dampening the dynamics of macrophage subpopulation phenotype in GBM post treatment may be a fundamental step to take in combinatorial therapy.

---

**Symposium: Optimal management of patients with unresectable stage 3 NSCLC**

---

**SP-0017 Standard of care in 2019**

F. McDonald<sup>1</sup>

<sup>1</sup>Royal Marsden NHS Foundation Trust/Institute of Cancer Research, Department of Radiotherapy, Sutton, United Kingdom

Abstract not received

**SP-0018 Optimal management of patients with unresectable stage III NSCLC: areas of controversy and ongoing research**

R. Dziadziszko<sup>1</sup>

<sup>1</sup>Medical University of Gdansk, Dept. of Oncology and Radiotherapy, Gdansk, Poland

**Abstract text**

Results of definitive treatment of patients with unresectable stage III NSCLC have changed favourably over the last decade. With more precise imaging, invasive staging, 4D-CT treatment planning, and image-guided treatment delivery, concurrent radiochemotherapy protocols lead to median survival of approximately 24 - 30 months and 5-year survival probability of approximately 30 - 35%. These indices are further improved with integration of consolidation immunotherapy as demonstrated in the PACIFIC trial with PDL1 inhibitor durvalumab. Further progress in this field is likely to result from improvements in both local and systemic therapies. Old dose/volume/fractionation research questions need still to be re-evaluated from the perspective of optimisation of local control versus toxicities. Most effective hypofractionation protocols and perhaps different radiotherapy doses to primary tumour and mediastinal lymph nodes are the key research questions. More research focus on late toxicity, particularly cardiac and pulmonary, is needed as our patients live longer and are more likely to experience this toxicity. Systemic research trials are designed to test the use of different immune checkpoint inhibitors as consolidation treatment with concurrent, sequential or even exclusive radiotherapy in properly selected patient subsets. Further

improvement is likely to occur with integration of novel immunotherapy agents, including multiple checkpoint inhibitors, personalised cancer vaccines, and other immune response modifiers. Tissue and blood-based biomarker data are needed to better understand how to personalise consolidation therapies most effectively.

**SP-0019 Active management of patient's comorbidities (including respiratory and cardiac comorbidities)**

V. Westeel<sup>1</sup>

<sup>1</sup>Hôpital Univ. Jean Minjot, Chest Disease Department, Besançon, France

**Abstract text**

The prevalence of comorbidity is high in lung cancer patients, up to 50 % in non-surgically treated patients. Pathologies, which share the same risk factor, smoking exposure, and diseases at increased risk after 70 years are particularly frequent in patients diagnosed with lung cancer. Chronic inflammation is also considered to contribute to lung cancer carcinogenesis in several comorbidities, such as COPD and cardiovascular diseases (CVDs). Because standard therapy includes chemotherapy, radiotherapy and immunotherapy in PD-L1 $\geq$ 1% NSCLC, many comorbidities can interfere with treatment decision.

**Pulmonary comorbidity**

Several lung diseases are associated with an increased risk of lung cancer. COPD is reported in approximately 50% of patients with NSCLC, including patients treated with chemo-radiotherapy. COPD is a risk factor for lung cancer, independent of smoking history, with COPD smokers five times more likely to develop lung cancer than smokers without COPD. Bronchiectasis has also been reported as an independent risk factor of lung cancer, because of recurrent microbial infections. Diagnosis of obstructive bronchial disease relies on spirometry to measure the FEV1 and the diffusing capacity for carbon monoxide. Therapeutic management can include smoking cessation, pharmacologic treatments, oxygen therapy and noninvasive ventilation, and early treatment and prevention of exacerbations (influenza and pneumococcal vaccination) and pulmonary rehabilitation ([www.goldcopd.org](http://www.goldcopd.org)).

Several studies suggest an association between interstitial lung diseases (ILDs), particularly pulmonary fibrosis, and lung cancer. Treatment-related mortality and the risk of radiation pneumonitis are high in patients with ILD. Therefore, the diagnosis should not be ignored and the benefit of radiotherapy carefully considered, taking into account this high risk of toxicity and patient prognosis.

**Cardiovascular diseases**

Cardiovascular diseases (CVDs) are observed in approximately 25% of patients and represent the first cause of non-cancer death, in locally advanced NSCLC. Heart failure and cardiac arrhythmia are predictive of cardiac complications after chemo-radiotherapy. Heart failure, myocardial infarction and cardiac arrhythmias are associated with decreased survival rates in patients treated with chemoradiation for stage III NSCLC, while hyperlipidaemia might have a protective effect. Beside diagnosis and optimal treatment of CVDs, treatment adaptations may be necessary. Cisplatin, which requires large hydration cannot be used in patients with pre-existing reduced LVEF.

**Other comorbidities**

Chronic renal disease is common in patients with lung cancer and impacts both systemic treatment and survival. The choice of the chemotherapy regimen and dose calculation should be adapted according to the glomerular filtration rate, using carboplatin rather than cisplatin, avoiding pemetrexed...(1)

Infections, especially hepatitis B and HIV infection need to be diagnosed before treatment for stage III NSCLC. Cytotoxic chemotherapy can be responsible for HBV

reactivation, which can be avoided with antiviral prophylaxis. People living with HIV are at high risk of cancer, and especially lung cancer. There are specific guidelines for the management of patients with HIV and cancer (2).

Diabetes mellitus is associated with higher mortality in patients with lung cancer, increasing the risk of cardiovascular and infectious events. Complications of diabetes, such as chronic renal insufficiency and peripheral neuropathy can interfere with the treatment of lung cancer. Frequent need for corticosteroids during chemotherapy requires closed monitoring of glycaemia. Adjuvant durvalumab after chemoradiotherapy has been shown to improve overall survival in stage III NSCLC. Autoimmune diseases or diseases requiring immunosuppressive therapy (including corticosteroids > 10 mg/day) and ILD can preclude their use.

The comorbidity burden of patients with stage III NSCLC is high, with a variety of diseases and a frequent association of several comorbidities. A thorough work-up of patients exploring these comorbidities is needed before treatment decision, which should be best taken after treatment optimization of all comorbidities within a multidisciplinary setting

#### References :

1. Lichtman SM, Wildiers H, Launay-Vacher V, Steer C, Chatelut E, Aapro M. International Society of Geriatric Oncology (SIOG) recommendations for the adjustment of dosing in elderly cancer patients with renal insufficiency. *Eur J Cancer*. janv 2007;43(1):14-34.
2. Reid E, Suneja G, Ambinder RF, Ard K, Baiocchi R, Barta SK, et al. Cancer in People Living With HIV, Version 1.2018, NCCN Clinical Practice Guidelines in Oncology. *J Natl Compr Canc Netw*. août 2018;16(8):986-1017.

#### SP-0020 Role of patient reported outcome in patients follow-up

L.Yolande<sup>1</sup>

<sup>1</sup>Ghent University Hospital and Ghent University, Department of Radiation Oncology, Ghent, Belgium

Abstract not received

---

#### Symposium: Combined modality treatment vs chemotherapy alone in lymphoma patients?

---

#### SP-0021 The role of radiotherapy in Hodgkin Lymphoma - results from the German Hodgkin Study Group (GHSg)

H.T. Eich<sup>1</sup>

<sup>1</sup>University of Münster, Department of Radiation Oncology, Münster, Germany

#### Abstract text

Thomas Hodgkin was the first who described the disease in 1832 in his publication entitled "On some morbid appearances of the absorbent gland and spleen". Nowadays Hodgkin's Lymphoma has rendered to one of the best curable malignancies. The treatment of patients in early favorable and early unfavorable consists of chemotherapy followed by Involved-Site Radiotherapy (RT). Patients in advanced stages are treated with intensified chemotherapy and PET-guided radiotherapy. Due to optimized chemotherapy regimen and modern RT Overall Survival (OS) is up to 96,8% for patients in early favorable stages, 94,5% in early unfavorable stages and 95,3% in advanced stages. The development of RT within the past decades is remarkable. Field designs and radiation techniques changed dramatically throughout the years. In early favorable stages RT-dose decreased to 20 Gy Involved-Site RT and in early unfavorable stages the dose is 30 Gy. The recently completed trials conducted by the EORTC and the GHSg tested whether RT can be

omitted in patients with a PET negative result after chemotherapy. The final results from these studies showed, that patients who received chemotherapy only due to a negative PET had a worse PFS. Therefore the combined modality approach remains the standard of care for patients in early stages.

#### SP-0022 State of the art for indolent lymphoma

J. Yahalom<sup>1</sup>

<sup>1</sup>Memorial Sloan Kettering Cancer Center, Department of Radiation Oncology, New York, USA

Abstract not received

#### SP-0023 Aggressive Lymphoma (DLBCL); when does addition of RT make a difference?

G. Mikhaeel<sup>1,2</sup>

<sup>1</sup>Guy's and St. Thomas' NHS Foundation Trust, Department of Clinical Oncology, London, United Kingdom; <sup>2</sup>King's College, Division of Cancer Studies, London, United Kingdom

Abstract not received

#### SP-0024 Aggressive Lymphoma (DLBCL) - when does addition of RT doesn't make a difference?

U.Vitolo<sup>1</sup>

<sup>1</sup>University of Turin, Department of Oncology and Hematology Turin, Italia

Abstract not received

---

#### Symposium: Image guided adaptive brachytherapy (IGABT) for primary vaginal cancer in Europe and North America

---

#### SP-0025 Evidence for image guided adaptive brachytherapy in primary vaginal cancer

H. Westerveld<sup>1</sup>

<sup>1</sup>Amsterdam UMC AMC, Radiation Oncology, Amsterdam, The Netherlands

#### Abstract text

Primary vaginal cancer (PVC) is a very rare disease. In most cases, definitive radiotherapy (external beam radiotherapy (EBRT) followed by a brachytherapy (BT) boost) combined with chemotherapy is the treatment of choice. PET (CT), ultrasound and MRI can all play a role in the diagnostic work-up, response assessment and planning of the EBRT and BT in PVC cases. However, due to its superiority of soft tissue contrast and the possibility of functional imaging, MRI is the best image modality in the diagnostic process and for delineation of the target at time of treatment. Due to its rarity, only limited data are available about the use of image guided adaptive brachytherapy (IGABT) in primary vaginal cancer. Most studies include small retrospective series of patients that have been included over a long period of time. The studies can be categorized in two groups with regard to the treatment technique. One group includes older studies where patients have been treated with 2D radiograph-based BT. The other group includes more recent monocenter studies where patients have been treated according to a 3D BT target concept adopted from GEC-ESTRO recommendations for cervical cancer. Although these 3D studies are very small, results are promising showing better local control without additional morbidity. Recently, a retrospective multicenter study was conducted to assess the outcome of patients treated for PVC with IGABT, defined by the use of MRI at time of brachytherapy. At a median follow-up of 29 months (range 3-167), the 3 years local control rate was 82%. Improved local control was found in patients with T2-4 tumor if >80

Gy was delivered to the CTV. In summary, more evidence is coming for the need of image guided adaptive brachytherapy, preferably with MRI, in primary vaginal cancer. A prospective multicenter study is warranted to gain more knowledge about this rare disease.

**SP-0026 GYN GEC-ESTRO Recommendations for IGABT target delineation in primary vaginal cancer**

M. Schmid<sup>1</sup>

<sup>1</sup>Medical University of Vienna, Department of Radiotherapy, Vienna, Austria

Abstract not received

**SP-0027 Brachytherapy for primary vaginal cancer - North American experiences**

M. Kamrava<sup>1</sup>

<sup>1</sup>Cedars-Sinai Medical Center, Radiation Oncology, Los Angeles, USA

**Abstract text**

While large prospective experiences with image guided adaptive brachytherapy (IGABT) are accumulating in definitive cervical cancer treatment there is more limited information on the impact of IGABT in the definitive management of vaginal cancers. There is no consensus regarding the ideal dose, definition of the high-risk clinical target volume, or definition of organs at risk (OAR) such as the vagina. The purpose of this talk is to review the literature from North America regarding IGABT for primary vaginal cancers with respect to dose, target/OAR definitions, and clinical outcomes. We will compare the North American experiences with those from Europe and finally review the North American experience with trying to find consensus regarding target definition.

**SP-0028 Dose planning for primary vaginal cancer - a multicentre comparison**

N. Nesvacil<sup>1</sup>

<sup>1</sup>Medical University of Vienna, General Hospital of Vienna- Vienna- Austria, Department of Radiation Oncology, Vienna, Austria

Abstract not received

---

**Joint Symposium: ESTRO-AAPM: QA of on-line adaptive radiotherapy**

---

**SP-0029 Setting the scene**

S. Mutic<sup>1</sup>

<sup>1</sup>Washington University School of Medicine, Radiation Oncology- Physics Division, Saint Louis, USA

Abstract not received

**SP-0030 QA of contour segmentation**

E.M. Vasquez Osorio<sup>1</sup>

<sup>1</sup>The University of Manchester, Division of Molecular & Clinical Cancer Studies- School of Medical Sciences- Faculty of Biology- Medicine and Health, Manchester, United Kingdom

**Abstract text**

Adaptive radiotherapy relies on fast identification of the structures (targets and organs at risk) on the daily image to adapt the treatment plan according to the patient's anatomy on the day of delivery. Two main alternatives for identifying these structures are 1) propagation of contours from the planning image (CT scan/MR scan) into the daily image and 2) generating contours from scratch on the daily image. Contour propagation is the most commonly used and it is implemented in clinical adaptive pathways. No matter how the contours are created, they are manually

edited, which is very time consuming. This delay could compromise the treatment efficacy due to intra-fractional anatomical changes happening while the patient is lying on the couch.

The question to be addressed in this talk is how we could perform quality checks on the daily contours to guarantee safe treatment delivery. To elaborate on that, metrics used to assess contour quality will be discussed, as well as the link between geometry and dosimetry to determine the areas where contours need to be more accurate. For contours propagation, strategies specifically defined for adaptive pathways will be discussed; and general issues with contour generation will be considered.

**SP-0031 QA of deformable image registration**

Marc Kessler<sup>1</sup>

<sup>1</sup>University of Michigan, Radiation Oncology, Ann Arbor, USA

**Abstract text**

Combined hardware and software systems are now available at the treatment unit to support daily dose assessment and enable on-line adaptive radiotherapy using image registration and data fusion to propagate contours and accumulate dose across image data acquired throughout patient treatment. The goal of these systems is to provide up-to-date estimates of anatomical changes and delivered dose. This information aids in the detection of changes that may demonstrate a clinical need to modify the original treatment plan or prescription.

As the output of the image registration process is always used as the input of another process for planning or delivery, it is important to understand and communicate the uncertainty associated with this process, both in general and for a specific registration. Unfortunately, there is no standard mathematical formalism to perform this analysis in actual clinical situations where overall uncertainty conflates image noise and distortion with underlying algorithm bias and complex anatomical variations. Validation of registration performance is also complicated by the lack of documentation available for commercial systems leading to use of these systems in a less-than-desirable 'black-box' fashion.

In view of this situation and the central role that image registration and data fusion play in various clinical workflows, the Therapy Physics Committee of the American Association of Physicists in Medicine commissioned Task Group 132. The resulting report reviews current approaches and solutions for image registration and provides recommendations for quality assurance and quality control of these clinical processes. These recommendations and examples of their use for on-line adaptive radiotherapy will be presented.

**SP-0032 QA of on-line adaptive radiotherapy: Experience of The Royal Marsden Hospital**

S. Nill<sup>1</sup>

<sup>1</sup>The Institute of Cancer Research and The Royal Marsden NHS Foundation Trust, Joint Department of Physics, London, United Kingdom

**Abstract text**

In room MR image guidance enables the online adaptation of treatment plans based on the current patient anatomy while the patient is on the treatment couch. Therefore conventional methods like pre-treatment plan QA using a phantom to validate the treatment plan are no longer applicable.

In 2016 The Royal Marsden NHS Foundation Trust and The Institute of Cancer Research installed the Elekta Unity system and the first patients were treated in September 2018. The Elekta Unity system consists of a 1.5T MR

scanner and a state of the art linear accelerator. During the commissioning and implementation phase of the MR Linac a series of programs and methods were developed to replace the traditional pre-treatment plan QA approach. This includes the commissioning of a non Monte Carlo dose engine within a second commercial planning system to perform the independent monitor unit check. A high degree of automation and integration is desirable to enable the operator to perform a comprehensive QA of the new treatment plan within the limited time available. While a strong focus of these checks will be on the dosimetric aspects other issues like contours and data transfer error must not be neglected. Within this presentation the methods developed at the RMH/ICR to tackle online plan QA will be presented.

**SP-0033 QA of on-line Adaptive Radiotherapy: Washington University Experience**

S. Mutic<sup>1</sup>

<sup>1</sup>Washington University School of Medicine, Department of Radiation Oncology, St. Louis, USA

**Abstract text**

Adaptive radiotherapy (ART) has been a concept for a long time but has become a practicality just in the past few years. This is especially the case for online ART. The online ART has been defined in many different ways and for the purposes of this presentation the online ART consists of 1) Daily volumetric patient imaging, 2) Creation of contours on the images of the day, 3) Creation of a new plan on contours of the day, including full IMRT optimization, 4) Review of the plan, 5) QA with the patient on the table, and 6) patient treatment with the new plan based on the daily anatomy and contours. It is worth noting that the desired time for this entire procedure should not add much time (minutes) to typical radiotherapy treatment appointments. While the main obstacle to practical online ART have been technological limitations, there are also operating paradigms that need to be evolved to enable practical online ART. One of the paradigms that needs to evolve is patient specific QA. While many will equate patient specific QA to IMRT QA, the QA for online ART has many more components. The online ART includes evaluation of daily imaging, contour accuracy, any image registrations or contour propagations, evaluation of clinical and technical integrity of the daily plan, evaluation of deliverability and safety of the daily plan, etc. While most, if not all, of these steps are performed with conventional radiotherapy and offline ART, the unique challenge of online ART is that all of these tests plus the treatment planning process have to be performed in minutes versus hours to days that are used in conventional and offline ART. In addition, during the entire time that planning and QA are performed the patient is on treatment table making any measurement based QA impractical. The needed speed for online ART QA and inability to follow conventional processes mandates reconsideration of conventional patient specific QA paradigms. This presentation is intended to provide systematic analysis of concepts for online ART QA, describe deployment of these concepts in a clinical setting, and description how lessons learned may affect future developments in this area. Learning Objectives: After this presentation, the audience should be able to 1) Describe systems based approach to design of online ART QA2) Describe practical considerations for online ART3) Understand direction in online ART QA as this procedure becomes more prevalent.

**SP-0034 Mathematical Modelling of radiation response in Proton Therapy**

K. Kirkby<sup>1</sup>, R.I. Mackay<sup>2</sup>, N.F. Kirkby<sup>1</sup>, J. Warmenhoven<sup>1</sup>, N. Henthorn<sup>1</sup>, A. Chadwick<sup>1</sup>, S. Ingram<sup>1</sup>, W. Rothwell<sup>1</sup>, E. Smith<sup>1</sup>, N.G. Burnet<sup>1</sup>, A. Aitkenhead<sup>2</sup>, M.J. Merchant<sup>1</sup>  
<sup>1</sup>The University of Manchester, Division of Cancer Sciences, Manchester, United Kingdom ; <sup>2</sup>The Christie NHS Foundation Trust, Christie Medical Physics and Engineering, Manchester, United Kingdom

**Abstract text**

Clinically, the Relative Biological Effectiveness (RBE) of protons compared to photons is 1.1. However, there is considerable variance between the experimental studies informing this value. It has been shown that RBE is not constant but instead depends on many factors, including dose, Linear Energy Transfer (LET) and cell type. Most studies on proton RBE have concentrated on phenomenological modelling based on linear energy transfer (LET) and parameters derived from the linear quadratic model fitted to cell survival. We have taken a different approach, centred on mechanistic mathematical models. Detailed models of the cell and its DNA are constructed in Geant4-DNA where the DNA volume energy depositions, resulting from radiation track-structure, are recorded. Mechanisms of direct and indirect DNA damage are incorporated by simulation and comparison to experimental data in the literature. Predictions of both the position and complexity in DNA damage are then passed to our model of DNA repair, named DaMaRiS, which incorporates both non-homologous end joining (NHEJ) and homologous recombination (HR). Here, predictions are made on the kinetics and fidelity of repair at various time points. We show preliminary results, which integrate mechanistic mathematical models of DNA damage and repair in the Eclipse™ Treatment Planning System (TPS). We score the dose and LET in each voxel and, using the previously established correlations, convert the scored parameters into biological predictions, specifically the yield of residual and misrepaired DSBs, which can be anatomically mapped. Predictably, residual DSBs across the LET and dose range dominate the biological outcome. The model shows a slight increase in complex damage with LET, i.e. with depth in the patient. We also predict that the increased LET produces more proximal Double Strand Breaks (DSBs), which increased misrepair events between DSBs. These maps can potentially provide valuable information to the clinician by allowing identification of regions of heightened biological effect (and are a step towards biologically augmented radiotherapy).

**SP-0035 Developing metrology support for biologically relevant dosimetry**

H. Rabus<sup>1</sup>

<sup>1</sup>Physikalisch-Technische Bundesanstalt PTB, Radiation Effects, Braunschweig, Germany

**Abstract text**

A number of radiation modalities require weighting factors applied to absorbed dose to account for the biological effectiveness of the particular radiation quality. Examples include proton and ion beams as well as kilovoltage X-rays [1-3]. Micro- and nanodosimetry have been developed to provide radiation quantities that capture the influence of the stochastic nature of radiation interactions and, hence, the properties of different radiation qualities responsible for their different relative biological effectiveness. The European Joint Research Project BioQuaRT (Biologically weighted quantities in radiation therapy) [4-6], funded within the European Metrology Research Programme [7], created a metrological basis for radiation quantities integrating properties of particle track structure and biological radiation effects (Fig. 1).

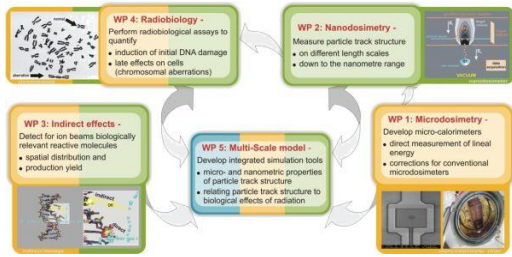


Fig. 1: The BioQuaRT multi-disciplinary approach.

Apart from findings like a simple correspondence between cellular biological endpoints and nanodosimetric parameters of track structure [8], BioQuaRT also came up with novel metrological approaches to radiobiological assays [9-13]. The increasing use of biological assays in radiology [14] and the long-term aim of biology-based treatment planning in radio-oncology require developing a metrological fundament for radiobiology. As the challenges involved require resources and skills beyond those presently available at Metrology Institutes, an initiative has been formed to establish a European Metrology Network (EMN) on Ionizing Radiation Effects within the European Association of National Metrology Institutes (EURAMET).

Such an EMN would link to existing networks in biological dosimetry [15] and would follow a strategic agenda for which four main topics have been identified in stakeholder consultations [16-17]: First, research towards identifying which microdosimetric or nanodosimetric radiation quantities best correlate with radiobiological effectiveness and the development of detectors for their primary realization as well as for practical measurements in clinical practice (Fig. 2). Second, measurements supporting uncertainty assessment and validation of numerical tools, e.g. Monte Carlo track structure codes, used in radio-oncology research. Third, metrology supporting the improvement of radiobiological assays in terms of reliability, reproducibility, solid measurement uncertainty assessment and model-based data interpretation. Fourth, cross-cutting the three aforementioned lines, standardization of procedures and development of tangible as well as written standards.

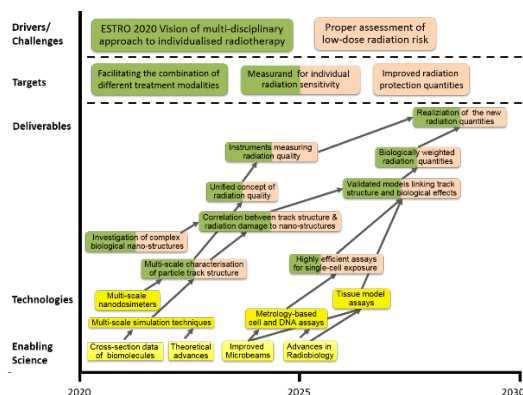


Fig. 2: Draft roadmap of the first EMN topic.

[1] IAEA, *Relative Biological Effectiveness in Ion Beam Therapy*, Technical Reports Series No. 461, International Atomic Energy Agency, Vienna 2008.  
 [2] Hill M. *The variation in biological effectiveness of x-rays and gamma rays with energy*, Radiat. Prot. Dosim. 112, 471-481 (2004).  
 [3] Nikjoo H. and Lindborg L. *RBE of low energy electrons and photons*, Phys. Med. Biol. 55, R65 (2010).

[4] <https://www.ptb.de/emrp/bioquart.html>  
 [5] Rabus H et al. *Biologically Weighted Quantities in Radiotherapy: an EMRP Joint Research Project*. EPJ Web of Conferences 77: 00021 (2014).  
 [6] Palmans H et al. *Future development of biologically relevant dosimetry*. Br. J. Radiol. 88: 20140392, (2015). [7] <http://www.emrponline.eu/>  
 [8] Conte V et al. *Track structure characterization and its link to radiobiology*, Radiat. Meas. 106, 506-511 (2017).  
 [9] Patrono C et al. "BioQuaRT" Project: design of a novel in situ protocol for the simultaneous visualization of chromosomal aberrations and micronuclei after irradiation at microbeam facilities, Radiat. Prot. Dosim. 166, 197-199 (2015).  
 [10] Villagrasa C et al., *Geant4-DNA simulation of DNA damage caused by direct and indirect effects and comparison with biological data*, EPJ Web of Conferences 153, 04019, 1-6 (2017).  
 [11] Testa A et al. *Analysis of radiation-induced chromosome aberrations on cell-by-cell basis after alpha-particle microbeam irradiation: experimental data and simulations*, Radiat. Res. 189, 597-604 (2018).  
 [12] Gonon G et al., *From Energy Deposition of Ionizing Radiation to Cell Damage Signaling: Benchmarking Simulations by Measured Yields of Initial DNA Damage after Ion Beam Irradiation*, under review at PloS Comp. Biol.  
 [13] Rabus H et al. *Investigation into the probability for miscounting in foci-based assays*, Proc. MICROS 2017, accepted for publication in Radiat. Prot. Dosim. (2018).  
 [14] IAEA, "Application of Biomarkers of Radiation Exposure in Radiological Clinical Practice" Human Health Series, International Atomic Energy Agency, Vienna, in preparation.  
 [15] <http://www.reneb.net/>  
 [16] Baek W Y et al. *Metrology for Biological Radiation Effects - Status and Metrological and Research Needs*, PTB Report Dos 60, ISBN 978-3-95606-419-7 (2018).  
 [17] Rabus H et al. *Proposal for a European Metrology Network on Biological Ionising Radiation Effects*, Proc. EPR BioDose 2018, to appear in Radiat. Prot. Dosim. (2019).

**SP-0036 Understanding biological response**

B.S. Sørensen<sup>1</sup>

<sup>1</sup>Aarhus University Hospital, Exp. Clin. Oncology, Aarhus C, Denmark

**Abstract text**

There are a number of biological characteristics that have been shown to influence differences in response to radiation for both the tumor and the surrounding normal tissue. These characteristic includes intrinsic radiosensitivity, hypoxia, HPV status, number of cancer stem cells (CSCs), and repopulation between radiotherapy fraction. In the last 20 years, significant progresses in the knowledge of the biological factors influencing radiation response and the causative molecular basis, such as the DNA-damage response and repair mechanisms, signaling pathways and tumor microenvironmental factors, have been made, which both has impact for therapeutic possibilities and has also generated a large number of potential biomarkers.

The issue of biological response becomes more complicated when considering particle radiation. Protons and high LET radiation have a higher relative biological effectiveness (RBE), but RBE is a complex quantity, depending on both biological and physical parameters. RBE is often established as measured by cell death, but emerging evidence also demonstrate an altered response in the surviving cells. This is both evident for high LET radiation and for proton radiation. This differential biological effect is not only relevant in the tumour, but also in the normal tissue. Current research in particle radiobiology is, in addition to the RBE, focusing on the

molecular tissue response, and on the signalling pathways. Studies indicate a differential DNA damage response (DDR) following high LET irradiation, with the double strand breaks DSB preferentially repaired by homologous recombination (HR), leading to an increased level of unrepaired damage, which is reflected in the RBE. This change in DDR may also lead to a differential response in cellular processes downstream of the DNA repair.

**SP-0037 Implementation of nanodosimetric based radiobiological models in treatment planning systems**  
F. Villegas<sup>1</sup>

<sup>1</sup>*Uppsala University, Immunology- Genetics and Pathology, Uppsala, Sweden*

**Abstract text**

Modelling for prediction of relative biological effectiveness (RBE) is a fast-growing research topic within hadron therapy. Carbon ion treatment centers have been at the forefront in the use of RBE models in treatment planning systems (TPS). However, the current exponential expansion of proton therapy seen in the last decades implies questioning of the convention of applying a constant RBE of 1.1 in clinical practice. Several planning studies have shown that proton treatments considering the expected biological outcome per tissue type and particle energy could reduce the side effect risk and increase the probability for tumour control. Unfortunately, the prediction accuracy of the radiobiological models used for optimization has been limited as correlations between simple macroscopic characteristics of the radiation (e.g. physical dose or linear energy transfer) and biological endpoints (e.g. cell survival) are not univocal. A key to strengthen the prediction power is to use nanoscopic properties of the radiation which characterize the textures of the radiation's energy deposition discrete events at the scale of biomolecules (e.g. DNA) directly causing the biological damage. Advancements in experimental and computational nanodosimetry have pushed forward the search for an operational and measurable nanodosimetric quantity capable of RBE prediction. The frequency of cluster size is a promising property upon which published phenomenological models have been based; although the cluster scoring is still a matter of debate whether it be inside a predefined volume [1] or be free from volume [2]. Multiscale energy deposition distributions have also been used for building mechanistic models such as the NanOx model [3] which elegantly incorporates the chemical stages of DNA damage. Regardless of the model, issues concerning benchmarking and uncertainty assessments of Monte Carlo simulations involved need to be addressed first. Validated computational tools can then simulate clinical beams to fully characterize them down to a nanometer level. Such dosimetric charts are the key to bypass the need for LET mapping used by existing TPS optimization engines. In parallel, another set of challenges need to be undertaken to produce a consistent and reproducible biological experimental database to aid the fine-tuning of both mechanistic and/or phenomenological models. Indeed, the fundamental parts towards an RBE optimized treatment planning are already in place thus the biggest challenge is to connect them through standardization processes which will not only make data transferable between facilities but also will help gain the trust of clinical community.

[1] Selva A, Conte V and Colautti P. A Monte Carlo tool for multi-target nanodosimetry. *Radiat Prot Dosim* 180, 182-6 (2018).

[2] Villegas F, Bäckström G, Tilly N and Ahnesjö A. Energy deposition clustering as a functional radiation quality descriptor for modelling relative biological effectiveness. *Med Phys* 43, 6322 (2016).

[3] Cunha M, Monini C, Testa E and Beuve M. NanOx, a new model to predict cell survival in the context of particle therapy. *Phys Med Biol* 62, 1248-68 (2017).

---

**Symposium: Quality in an IGRT**

---

**SP-0038 Continuous Quality Improvement Strategies to Support Volumetric IGRT**

W. Li<sup>1</sup>

<sup>1</sup>*Princess Margaret Cancer Center, Department of Radiation Oncology, Toronto, Canada*

**Abstract text**

Technological advances in the field of Radiation Therapy enables online image guidance of patient setup, increasing the precision and accuracy of treatment delivery. Maintaining sustained excellence in an IGRT environment require various continuous quality improvement strategies ranging from education and staff training to development of departmental protocols, procedures, and processes. This presentation will focus on supporting RTT education and training at a large urban cancer centre in Ontario, from initial training strategies and current annual refresher approach (team based and eLearning module approach), to development and implementation of RTT led IGRT rounds, where challenging clinical cases are shared and discussed.

**SP-0039 Audits in IGRT - Development of standardized image guidance registration documents and workflows**

H. De Boer

<sup>1</sup>*University Medical Center Utrecht, Department of Radiation Oncology, Utrecht, The Netherlands*

Abstract not received

**SP-0040 Exploiting IGRT to calculate delivered dose for normal tissue sparing**

L. Shelley<sup>1</sup>

<sup>1</sup>*University of Cambridge, Department of Engineering-JDG, Cambridge, United Kingdom*

**Abstract text**

Introduction

Image guided radiotherapy (IGRT) is essential in modern radiotherapy. The primary function of image guidance is to confirm tumour positioning to accurately deliver the planned dose to the PTV. Here we present evidence of the further usefulness of these routine images in the calculation of delivered dose to the organs at risk (OARs).

Due to daily organ deformation and anatomical changes, the delivered dose to OARs can be different to planned dose. However, provided that imaging protocol thresholds are met, this is generally not accounted for. Deviations from planned dose induce differences to the normal tissue complication probability (NTCP) since toxicity relates to dose actually delivered to the OAR. The hypothesis of the CRUK VoxTox research programme (UK CRN ID 13716) is that delivered dose can be a better predictor of toxicity than planned dose. Tracking motion-inclusive daily delivered dose allows us to build a more accurate picture of the total accumulated dose received by the OAR. By constructing NTCP models based on delivered dose, the ultimate aim is to identify patients on-treatment who are at increased risk of toxicity, for selectively targeted adaptive radiotherapy.

**Material and Methods**

Daily MVCT scans were acquired for patients undergoing TomoTherapy for prostate cancer (n = 528), head & neck (H&N) cancers (n = 319), and cancers of the CNS (n = 26). Here we focus on the former two cohorts. Automation was vital for large scale processing of over 26,000 MVCT scans, and multidisciplinary expertise spanned engineering,

mathematics, high energy, medical physics and radiation oncology, at the University of Cambridge and Cambridge University Hospitals.

Autosegmentation algorithms were applied for identifying the rectum in prostate radiotherapy (Chan-Vese), and the swallowing OARs (parotids and submandibular glands, pharyngeal constrictors, oral cavity and supraglottic larynx) in H&N radiotherapy (Elastix). CheckTomo, an independent dose calculation system for direct calculation on MVCT images, was integrated into the VoxTox automated processing system. Toxicity data were prospectively collected using electronic case report forms, and all coding to standard scoring systems was externally verified.

For accumulating delivered dose to the rectum, dose surface maps (DSMs) of the rectal wall were generated in order to conserve spatial dose features. Daily delivered DSMs were corrected for positional variations and differences in MVCT field of view, and accumulated. Final accumulated and planned DSMs were parametrised using equivalent uniform dose (EUD) and dose-widths (the lateral extent of an ellipse fitted to a given isodose). Associations with rectal bleeding (RB) at 2 years cumulative incidence were assessed.

For swallowing OARs, the difference between planned and accumulated dose were reported using mean dose. Univariate analyses were performed to assess correlations between baseline clinical factors, mean planned dose, and mean delivered dose, with three toxicity endpoints; xerostomia, salivary duct inflammation, and dysphagia.

#### Results

For a cohort of 109 prostate cancer patients, accumulated EUD to the rectal wall was systematically lower than planned EUD. Accumulated EUD was the strongest discriminator of RB (AUC 0.682). Spatial features of accumulated DSMs were more strongly associated with RB than those from planned DSMs for dose-widths up to 70 Gy. The accumulated DSM 65 Gy dose-width generated the strongest spatial correlation (AUC 0.664). The same trend was observed from a separate cohort of 140 patients in a subsequent analysis (accumulated EUD AUC = 0.651, 65 Gy dose-width AUC = 0.636). A multivariate NTCP model based on parameters of accumulated dose (incorporating baseline RB and previous pelvic or abdominal surgery) was more predictive of 1 year RB than planned dose (AUC 0.809 v 0.782). Model validation is underway.

Mean delivered dose was higher than mean planned dose for all OARs in a cohort of 141 H&N cancer patients. In addition to confirming previously reported relationships between concomitant systemic therapy and pre-treatment symptoms with toxicity 1 year post-treatment, results also suggest stronger associations with delivered dose than planned dose for all endpoints. For H&N patients receiving Proton Beam Therapy (PBT) this may be particularly important.

#### Conclusion

The unique VoxTox dataset exploits routine MVCT IGRT scans, already being acquired for the purposes of patient positioning, to calculate motion-inclusive delivered dose to OARs. Results suggest that associations between accumulated dose and toxicity are stronger than those from planned dose, and this has been verified in a separate cohort in the case of the rectum. Information on spatial dose features may reveal intra-organ radiosensitivities, which could be useful when identifying patients on treatment who would benefit from adaptive radiotherapy, and may also be relevant for patients receiving PBT.

#### PV-0041 Randomized therapeutic trial of combined pentoclo versus placebo in radiation-induced plexopathy

S. Delanian<sup>1</sup>, T. Maisonobe<sup>2</sup>, T. Lenglet<sup>2</sup>, D. Psimaras<sup>3</sup>, M. Resche-Rigon<sup>4</sup>, P. Pradat<sup>5</sup>

<sup>1</sup>Hopital Saint-Louis- APHP, Oncologie-Radiotherapie-Radiopathologie, Paris, France; <sup>2</sup>Hopital Pitié-Salpêtrière- APHP, Neurophysiologie, Paris, France;

<sup>3</sup>Hopital Pitié-Salpêtrière- APHP, Neurologie, Paris, France;

<sup>4</sup>Hopital Saint-Louis- APHP, Statistique, Paris, France; <sup>5</sup>Hopital Pitié-Salpêtrière- APHP, Neurologie, Paris, France

<sup>5</sup>Hopital Pitié-Salpêtrière- APHP, Neurologie, Paris, France

#### Purpose or Objective

Radiation-induced plexopathy (RIP) is a rare and severe peripheral nerve complication after RT for cancer, without any existing treatment that stabilize or slow down neurological progression. Preclinical and clinical studies showed that combined pentoxifylline-vitamin E treatment (PENTO) significantly reduced radiation-induced fibrosis, and that the combination with clodronate (PENTOCLO) allowed healing of progressive mandible osteoradionecrosis and a reduction of some neurological symptoms.

#### Material and Methods

We conducted a randomized, placebo-controlled, double-blind, monocentric trial in RIP patients. Subjects were screened among adults referred to Hôpital Saint-Louis, for limb RIP, after irradiation including axillar-subclavian (breast, lung) or lumbar-iliac lymph area (Hodgkin, seminoma, uterus), excluding recurrence with MRI and PETscan. Included patients were randomized for a daily oral 18 months treatment, in two arms, PENTOCLO (Pentoxifylline 800mg, Tocopherol 1000mg, Clodronate 1600 mg 5d/7) or triple PLACEBO.

Primary outcome measure at M<sub>18</sub> was the SOMA score quoting neurological symptoms divided in 3 domains: pain, paresthesia and motor disability. Secondary endpoints were sensitivity measures (pain - paresthesia VAS), motor function (ODSS, muscle testing), neurological examination, nine hole peg test/ timed 25-foot walk), quality of life (SF36, CGIC/PGIC); and electromyography.

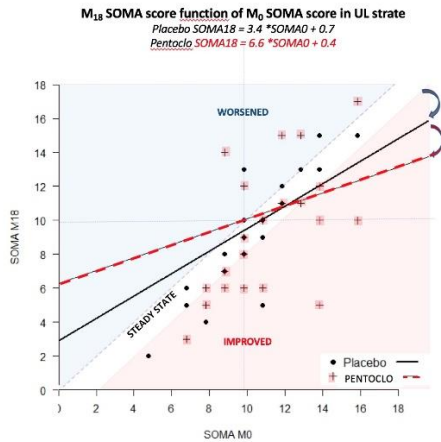
#### Results

Between 2011/03 and 2016/10, 59 patients were included (1 false inclusion developing neoplastic plexopathy): 29 in the placebo (P) group vs 29 in the active (A) group. 46 patients had upper limb RIP (mean 68y) and 12 lower limb RIP (59y), irradiated 26 ± 8y before, with neurological symptoms for 5 ± 5y. SOMA at M<sub>0</sub> was 9 (0-6-3 for each domain) in P vs 9 (1-6-3) in A, with severity bias in A group disfavor.

At M<sub>18</sub>, 51 patients (25 P vs 26 A) were analyzed (7 early discontinuations). No significant difference was observed at M<sub>18</sub> between P and A groups on the primary outcome: global SOMA 8.7 vs 8.8 (p 0.81) with a probable lack of sensitivity of our score. Secondary outcomes showed, in UL strata (figure), a trend for improvement of pain and paresthesia in A group, as assessed by the SOMA score subdomain for pain (1.22 in P vs 0.87 in A) and VAS paresthesia (4.4 in P vs 3.4 in A).

Adverse events were detected in 81% patients, but no difference was observed between the two groups. There was an unexpected excess of RI complications (30%) in both groups, while expected vascular and digestive complications were more frequent in A (+9%).

RIP natural history was lightened by an excess of vascular stenosis in UL stratum (60%), threatening in third, representing an unexpected neurological severity bias.



### Conclusion

This was the first randomized pharmacological drug trial in RIP. No significant therapeutic effect of PENTOCLO was detected. There is a need to develop more sensitive measures to detect the effect of investigational drugs in RIP.

### PV-0042 Radiation related lymphopenia as a predictor of locoregional recurrence in early breast cancer

O. Cho<sup>1</sup>, Y. Oh<sup>1</sup>, M. Chun<sup>1</sup>, O.K. Noh<sup>1</sup>, J. Heo<sup>1</sup>

<sup>1</sup>Ajou University Hospital, Radiation Oncology, Suwon City, Korea Republic of

### Purpose or Objective

Many studies reported that radiation related lymphopenia (RRL) was associated with treatment outcome in various cancers. However association between RRL and treatment outcome in early breast cancer (EBC) was rarely studied. This study aimed to investigate whether RRL could predict clinical outcome in EBC patients.

### Material and Methods

We analyzed 216 EBC patients (stage IA-IIB) treated with adjuvant radiotherapy (RT) after partial mastectomy from 2004 to 2012 in our institution using Kaplan-Meier plots and the Cox proportional hazards model. All patients did not receive chemotherapy. Peripheral absolute lymphocyte counts (ALCs) during two years after RT were collected from each patient. They were divided into pretreatment ALC (ALC0), ALC 3-5 months (ALC1), ALC 9-11 months (ALC2), ALC 15-17 months (ALC3), and ALC 21-23 months (ALC4) after RT.

### Results

ALCs after RT had a tendency of slow increase after rapid decline (median [range] ALC0 1847 cells/ $\mu$ L [623-4085], ALC1 1479 cells/ $\mu$ L [437-3500], ALC2 1626 cells/ $\mu$ L [775-3193], ALC3 1730 cells/ $\mu$ L [854-4408], and ALC4 1855 cells/ $\mu$ L [899-3793]). The 86 patients with ALC1 $\leq$ 1400 cells/ $\mu$ L had significantly lower 8 years locoregional control rate than 118 patients with ALC1>1400 cells/ $\mu$ L (80.5% vs. 98.3%,  $P=0.012$ ) while there was no difference in 8 years disease specific survival rate between two groups (98% vs. 97.1%,  $P=0.758$ ). Young age ( $\leq 40$  years), lymphopenia (ALC1 $\leq$ 1400 cells/ $\mu$ L), and high histologic grade were significant predictors of locoregional recurrence (LRR) in multivariate analysis (hazard ratio [97% confidence interval] 1.39 [1.18-13.7]  $P=0.026$ , 1.74 [1.21-26.8]  $P=0.028$ , and 2.3 [2.6-38.4]  $P<0.001$ ).

### Conclusion

Low ALCs 3-5 months after RT were associated with LRR in EBC patients. Therefore RRL could be a potential predictor for LRR of EBC.

### PV-0043 ESTRO guidelines for volume delineation for RT after immediate implant-based reconstruction

O. Kaidar-Person<sup>1</sup>, P. Poortmans<sup>2</sup>, B.V. Offeren<sup>3</sup>  
<sup>1</sup>Rambam Health Care Campus - Faculty of Medicine, Oncology Institute, Haifa, Israel; <sup>2</sup>Institut Curie, Radiation Oncology, Paris, France; <sup>3</sup>Aarhus University Hospital, Oncology, Aarhus, Denmark

### Purpose or Objective

on behalf of the ESTRO Working Group on Breast reconstruction and radiation therapy: a contouring project.

Immediate breast reconstruction is increasingly used after mastectomy, even if radiation therapy (RT) is indicated. Contouring guidelines in case of postmastectomy RT (PMRT) after implant-based immediate breast reconstruction are missing (IBR-i). We developed delineation guidelines based on a consensus between a global group of breast cancer experts.

### Material and Methods

After designing the project by the core group, an invitation letter was sent to an international multidisciplinary group of experts (including breast surgeons, radiation oncologists, and clinical oncologists) inviting them to participate in the consensus guidelines. The project included: a web-questionnaire, contouring exercise, group discussions, and literature review.

### Results

Based on mailings, the first contouring round, video conferences and a plenary discussion, guidelines are drafted to be validated in the prospective Danish DBCG RT Recon Trial randomising early breast cancer patients between immediate versus delayed breast reconstruction after mastectomy followed by loco-regional RT. Approximately 5-10% glandular tissue is retained after conventional total mastectomy, and more in cases of skin/nipple sparing mastectomy. Therefore, our recommendations include performing a careful evaluation of the patient using visualization/palpation, planning CT, and the extent of the contralateral breast (if intact), to determine the *cranio-caudal borders* of the CTV. The CTV includes the "residual breast tissue and the (subcutaneous) draining lymphatics", thereby excluding the implant. The location of the residual glandular tissue varies; in most cases it is found laterally in the breast, mainly in the "axillary-tail". We recommend consulting with the breast surgeon about the anatomical borders of the breast-skin. Moreover, in cases of a muscle flap/implant procedure, the transplanted flap including its overlaying skin is not part of the target volume, for which the scars should be marked for proper delineation.

The implant and the contralateral breast should be delineated on planning CT as well as all other organs at risk for treatment planning purposes.

Table 1: ESTRO delineation guidelines for the CTV in case of implant-based immediate breast reconstruction  
 Figure 1: Retro-pectoral implant. The CTV is delineated in pink.

### Conclusion

The use of target volume guidelines in the setting of IBR-i, based on recognised zones of tumour recurrence risk, aims to reduce inter- and intra-observer variation. They should be reserved for cases for which the disease staging (mainly T-stage) and surgical procedures used are well-defined. These guidelines are being validated in the DBCG reconstruction trial.

### PV-0044 Mastectomy or breast-conserving therapy for early breast cancer: outcome comparison of 7565 cases

S. Corradini<sup>1</sup>, M. Pazos<sup>1</sup>, D. Reitz<sup>1</sup>, S. Schönecker<sup>1</sup>, M. Niyazi<sup>1</sup>, U. Ganswindt<sup>1,2</sup>, F. Alongi<sup>3,4</sup>, M. Braun<sup>5</sup>, N. Harbeck<sup>6</sup>, C. Belka<sup>1</sup>

<sup>1</sup>LMU Munich, Department of Radiation Oncology, Munich, Germany ; <sup>2</sup>Medical University, Department of Radiation Oncology, Innsbruck, Austria ; <sup>3</sup>Hospital Sacro Cuore Don Calabria, Department of Radiation Oncology, Negrar, Italy ; <sup>4</sup>University of Brescia, Radiation Oncology, Brescia, Italy ; <sup>5</sup>Red Cross Hospital, Breast Centre, Munich, Germany ; <sup>6</sup>LMU Munich, Department of Obstetrics and Gynecology- Breast Centre, Munich, Germany

#### Purpose or Objective

Treatment of early stage breast cancer (BC) can be considered as a preference-sensitive care, where decision-making between treatment options can vary according to patient preferences. Typical factors that influence therapy choice in favour of mastectomy include: concerns about cancer recurrence or perceived consequences related to breast conserving surgery (BCT), including potential adverse effects of radiation therapy. Aim of the present study was to compare the oncologic outcome of mastectomy versus breast conserving therapy in patients treated in a modern clinical setting outside of clinical trials.

#### Material and Methods

Data were provided by the population-based Munich Cancer Registry. Between 1998 and 2014, all female patients diagnosed with early invasive BC (pT1pN0, pT2pN0, pT1pN1 and pT2pN1) and treated at two Breast Care Centres were included in this observational study. For comparison of the standard BCT and mastectomy approaches, we excluded patients with more than 3 positive lymph nodes (pN2) as postmastectomy RT (PMRT) would have been routinely recommended in these high-risk patients.

#### Results

The final study cohort consisted of 7565 women with a median follow-up of 95.2 months. After adjusting for age, tumour characteristics and therapies, Cox regression analysis for local recurrence-free survival identified BCS with RT as an independent predictor for improved local control (hazard ratio [HR], 1.476; 95% confidence interval [CI], 1.164-1.872, p<0.001) as compared to mastectomy without RT. Ten-year risk of local recurrences was 8.7% following BCS, compared to 14.8% in patients receiving mastectomy (p<0.001). Similarly, lymph node recurrences (10y LNR 2.4% vs 6.7%, p<0.001) and distant metastasis (10y DM 9.8% vs 15.2%, p<0.001) were more frequent in patients undergoing mastectomy only. This translated into an improved survival outcome among patients treated with BCS plus radiotherapy (10-year OS estimates 86.7% vs 77.6%, p<0.001), which was also significant on multivariate analysis (p=0.011).

#### Conclusion

In conclusion, the present study showed that patients treated with BCS followed by radiotherapy in clinical practice had an improved outcome regarding local control, distant control and overall survival as compared to mastectomy alone in a large cohort reflecting "real-life" clinical practice in this setting.

#### PV-0045 Is proton therapy a "pro" for breast cancer? A comparison of proton vs. non-proton RT using the NCDB

M. Chowdhary<sup>1</sup>, A. Lee<sup>2</sup>, S. Gao<sup>3</sup>, P. Barry<sup>1</sup>, R. Diaz<sup>4</sup>, N. Bagadiya<sup>5</sup>, H. Park<sup>3</sup>, J. Yu<sup>3</sup>, L. Wilson<sup>3</sup>, M. Moran<sup>3</sup>, S. Higgins<sup>3</sup>, C. Knowlton<sup>3</sup>, K. Patel<sup>3</sup>

<sup>1</sup>Rush University Medical Center, Radiation Oncology, Chicago, USA ; <sup>2</sup>SUNY Downstate Medical Center, Radiation Oncology, Brooklyn, USA ; <sup>3</sup>Yale School of Medicine, Therapeutic Radiology, New Haven, USA ; <sup>4</sup>Moffitt Cancer Center, Radiation Oncology, Tampa, USA ; <sup>5</sup>Emory University School of Medicine, Radiology, Atlanta, USA

#### Purpose or Objective

There is limited data demonstrating the clinical benefit of proton radiotherapy (PRT) in breast cancer. Here we investigate the impact of PRT on overall survival (OS) and evaluate predictors associated with PRT use for patients with breast cancer in the National Cancer Database (NCDB).

#### Material and Methods

Women with non-metastatic breast cancer treated with adjuvant radiotherapy from 2004-2014 were identified using the NCDB. Patients were stratified based on receipt of PRT or non-PRT (i.e. photons +/- electrons). A logistic regression model was used to determine predictors for PRT utilization. For OS, Multivariable analysis (MVA) was performed using Cox proportional hazard model. Subset analyses were performed for groups at risk for receiving higher heart dose.

#### Results

A total of 724,492 women were identified: 871 received PRT and 723,621 received non-PRT. 58.3% of the PRT patients were group stage 0-1. Median follow-up time was 62.2 months. On multivariate logistic analysis, the following factors were found to be significant for receipt of PRT (all p<0.05): academic facility (odds ratio [OR]=2.50), South (OR=2.01) and West location (OR=12.43), left-sided (OR=1.21), ER-positive (OR=1.59), and mastectomy (OR=1.47); pT2-T4 disease predicted for decrease PRT use (OR=0.79).

PRT was not associated with OS on MVA for all patients: Hazard Ratio: 0.85, p=0.168. PRT remained not significant on MVA after stratifying for subsets likely associated with higher heart radiation doses, including: left-sided (p=0.140), inner-quadrant (p=0.173), mastectomy (p=0.095), node positivity (p=0.680), N2-N3 disease (p=0.880), and lymph node irradiation (LNI) (p=0.767).

#### Conclusion

In this large national multicenter database, we found receipt of PRT to be associated with left-sided, ER+ tumors, mastectomy, South and West location, and academic facilities, but not higher group stages or LNI. PRT was not associated with OS, including in subsets likely at risk for higher heart doses.

In light of the high cost of proton RT, these data question the utilization of PRT, especially in early-stage patients with expected low heart doses, unless enrolled on a clinical trial.

#### PV-0046 Patient selection for proton therapy of early breast cancer - the DBCG phase II study strategy

L.B. Stic<sup>1</sup>, E.L. Lorenzen<sup>2</sup>, E.S. Yates<sup>3</sup>, C. Anandadas<sup>4</sup>, K. Andersen<sup>5</sup>, C. Ariste<sup>6</sup>, O. Byrne<sup>7</sup>, S. Hol<sup>8</sup>, I. Jensen<sup>9</sup>, A. Kirby<sup>10</sup>, Y.M. Kirova<sup>11</sup>, L. Marrazzo<sup>12</sup>, A. Matias-Pérez<sup>13</sup>, M.M.B. Nielsen<sup>14</sup>, H.D. Nissen<sup>15</sup>, S. Oliveros<sup>16</sup>, K. Verhoeven<sup>17</sup>, J. Vikström<sup>18</sup>, B.V. Offersten<sup>19</sup>

<sup>1</sup>Rigshospitalet, Department of Oncology, Copenhagen, Denmark ; <sup>2</sup>Odense University Hospital, Laboratory of Radiation Physics, Odense, Denmark ; <sup>3</sup>Aarhus University Hospital, Department of Medical Physics, Aarhus, Denmark ; <sup>4</sup>The Christie Hospital NHS Foundation Trust, Department of Clinical Oncology, Manchester, United Kingdom ; <sup>5</sup>Herlev & Gentofte Hospital, Department of Radiotherapy, Herlev, Denmark ; <sup>6</sup>University of Perugia & Perugia General Hospital, Department of Surgical and Biomedical Science, Perugia, Italy ; <sup>7</sup>Addenbrooke's Hospital - Cambridge University Hospitals NHS Foundation Trust, Department of Medical Physics, Cambridge, United Kingdom ; <sup>8</sup>Institute Verbeeten, Department of Radiation Oncology, Tilburg, The Netherlands ; <sup>9</sup>Aalborg University Hospital, Department of Medical Physics, Aalborg, Denmark ; <sup>10</sup>The Royal Marsden Hospital NHS Foundation Trust and Institute of Cancer Research, Department of Radiotherapy, London, United Kingdom ; <sup>11</sup>Institut Curie, Department of Radiation Oncology, Paris, France ; <sup>12</sup>Careggi University Hospital, Department of Medical Physics, Florence, Italy ;

<sup>13</sup>Institut Gustave Roussy, Département de Radiothérapie, Villejuif, France; <sup>14</sup>Zealand University Hospital, Department of Oncology, Næstved, Denmark; <sup>15</sup>Vejle Sygehus, Department of Oncology, Vejle, Denmark; <sup>16</sup>Oxford University Hospitals NHS Foundation Trust, Department of Oncology, Oxford, United Kingdom; <sup>17</sup>Maastriclinic - GROW School for Oncology and Developmental Biology - Maastricht University Medical Centre, Department of Radiation Oncology, Maastricht, The Netherlands; <sup>18</sup>Stavanger University Hospital, Department of Radiotherapy, Stavanger, Norway; <sup>19</sup>Aarhus University Hospital, Department of Experimental Clinical Oncology and Department of Oncology, Aarhus, Denmark

### Purpose or Objective

Recently, overall survival gain from radiation therapy (RT) of the internal mammary nodes (IMN) was documented. IMN RT inevitably leads to more radiation dose to heart and lungs, thus often target coverage is compromised to meet constraints for doses to organs at risk (OAR). Here, doses to heart and lung are estimated when target coverage is not compromised in consecutive high-risk breast cancer (BC) patients. The aim is to establish dose cut-off points for selection of patients for proton therapy (PT) in the Danish Breast Cancer Group (DBCG) single-arm phase II trial.

### Material and Methods

179 BC patients treated with adjuvant loco-regional RT including the IMN from 18 European departments were included in the study. Each department included 5 patients with left-sided and 5 patients with right-sided BC. The prescription dose ranged from 39.9 Gy to 51.52 Gy in 15 to 28 fractions. Planning techniques included both conformal and several inversely optimized techniques (see Table 1). If the clinically delivered treatment plan did not comply with defined target coverage requirements, the plan was modified retrospectively for this study until sufficient target coverage was reached by allowing OAR constraints to be exceeded. Sufficient target coverage was in this study defined as: V90%  $\geq$  95% of CTV<sub>IMN</sub>, V90%  $\geq$  95% of CTV<sub>n</sub> and V95%  $\geq$  95% of CTV<sub>breast</sub>/chest wall.

Table 1 Treatment characteristics	
	n (%)
Dose-fractionation scheme	
50 Gy in 25 fractions*	69 (39%)
40 Gy in 15 fractions**	101 (56%)
Other fractionation schemes	9 (5%)
Treatment technique	
3DCRT	90 (50%)
VMAT	26 (15%)
Hybrid	17 (9%)
Intensity modulated tomotherapy	35 (20%)
Step & shoot IMRT + static SCF	11 (6%)
Breath hold	
Yes	112 (63%)
No	67 (37%)
Modified plan	
Yes	71 (40%)
No	108 (60%)
Surgery	
Lumpectomy	65 (36%)
Mastectomy	95 (53%)
Reconstruction	19 (11%)
Simultaneous integrated boost	
Yes	12 (7%)
No	167 (93%)
No. of intercostal spaces in IMN target	
2	1 (<1%)
3	105 (59%)
4	71 (40%)
5	2 (1%)

Abbreviations: 3DCRT, 3D conformal radiotherapy; VMAT, volumetric modulated arc therapy; IMRT, intensity modulated radiotherapy; SCF, supraclavicular field; IMN, internal mammary nodes.  
\*Including patients receiving 51.52 Gy in 28 fractions (n=3). \*\*Including patients receiving 42.3 Gy in 18 fractions (n=2).

### Results

Forty percent of the treatment plans needed modification to fulfil the required dose for target coverage. Median mean heart dose (MHD) was 3.0 Gy (range, 1.1-8.2 Gy) for left-sided BC and 1.4 Gy (range, 0.4-11.5 Gy) for right-sided BC. For left-sided BC patients the median MHD was 2.8 Gy (range, 1.1-7.4 Gy) when breath hold (BH) was used (71%) and 5.2 Gy (range, 2.2-8.2 Gy) when no BH was used (29%). Median mean (ipsilateral) lung dose was 13.4 Gy (range, 5.1-24.9 Gy). Median V17Gy/V20Gy (hypofractionated/normofractionated plans) for lung was 31% (range, 0-57%). To guide selection criteria for referral to PT, we chose to set cut-off points for dose to OAR for departments that aimed for treating all patients with 3DCRT and in BH, which 9 departments did (98% 3DCRT and 93% BH). We chose MHD  $\geq$  4 Gy or lung V17Gy/V20Gy  $\geq$  37% as cut-off points for the PT study based on dose-response relationships for ischemic heart disease and radiation pneumonitis in combination with capacity limitations for PT. In the departments having 3DCRT and BH as standard, 22% of the patients had a MHD  $\geq$  4 Gy or lung V17Gy/V20Gy  $\geq$  37%. The remaining 9 departments mainly used inverse techniques (98%) where BH was used in 31% of the patients. Fifty-two percent of these patients had a MHD  $\geq$  4 Gy or lung V17Gy/V20Gy  $\geq$  37%.

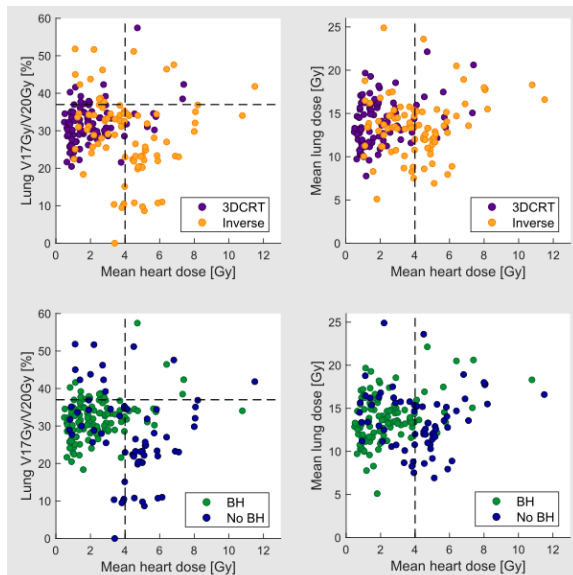


Figure 1: Upper panels show heart and lung dose metrics for 3DCRT (purple circles) and inverse treatment techniques (yellow circles). Lower panels show heart and lung dose metrics for breath hold (BH, green circles) and no breath hold (blue circles). The dashed lines represent the mean heart dose  $\geq 4$  Gy and lung V17Gy/V20Gy  $\geq 37\%$  thresholds.

### Conclusion

Using thresholds of MHD  $\geq 4$  Gy and lung V17Gy/V20Gy  $\geq 37\%$  in departments using 3DCRT and BH, we estimate that 22% of all the patients requiring loco-regional IMN RT will be eligible for the DBCG phase II PT study.

### PV-0047 IMRT versus VMAT for elderly patients with breast cancer: comparison of acute and late toxicities

F. Alongi<sup>1,2</sup>, F. Gregucci<sup>1</sup>, A. Fiorentino<sup>1</sup>, R. Mazzola<sup>1</sup>, V. Figlia<sup>1</sup>, F. Ricchetti<sup>1</sup>, G. Sicignano<sup>1</sup>, N. Gajj-Levra<sup>1</sup>, S. Naccarato<sup>1</sup>, A. Massocco<sup>1</sup>, S. Corradini<sup>3</sup>, R. Ruggieri<sup>1</sup>

<sup>1</sup>Hospital Sacro Cuore Don Calabria- Cancer Care Center, Radiation Oncology, Negrar, Italy; <sup>2</sup>University of Brescia, Radiation Oncology, Brescia, Italy; <sup>3</sup>LMU University Hospital, Radiation Oncology, Munich, Germany

### Purpose or Objective

To evaluate the differences between conventional fractionated intensity modulated radiotherapy (cIMRT) and hypofractionated (HypoRT) volumetric modulated arc therapy (VMAT) in elderly women affected by early stage Breast Cancer (BC) in terms of RT-related acute and late side effect.

### Material and Methods

Between October 2011 and July 2015, 80 consecutive elderly BC patients were treated with cIMRT for 5 weeks (40 patients) or HypoRT-VMAT for 3 weeks (40 patients). Inclusion criteria were: age  $\geq 70$  years, early stage BC (pT1-2 pN0-1), no prior neoadjuvant chemotherapy and non-metastatic disease. For patients receiving cIMRT or HypoRT-VMAT, a total dose of 50 Gy (25 fractions) or 40.5 Gy (15 fractions) were prescribed to the whole ipsilateral breast, respectively. All patients received a simultaneously integrated boost (SIB) up to a total dose of 60 Gy for cIMRT and 48 Gy for HypoRT-VMAT. Acute and late side effects were evaluated using the RTOG/EORTC radiation morbidity scoring system.

### Results

Median follow-up was 45 months. Compliance to treatment was 100% for each RT schedule, without any interruptions. The median age was 75 years (range 70-83). The median PTV breast was 929 cc (range 330-2527). In each group, 90% and 92% of patients received hormone-therapy, respectively. During RT delivery, only low grade acute skin toxicity was observed, with an advantage for

the HypoRT-VMAT group: grade 1 in 25 cases (62.5%) of the cIMRT group and 21 cases (52.5%) of the HypoRT-VMAT group (p=0.2); while grade 2 toxicity was reported in 10 cIMRT patients (25%) and 1 HypoRT-VMAT patient (2.5%) (p=0.001). No skin G3 or other side effects were observed at all. Regarding late adverse events, skin toxicity was overall mild without any grade 2 or higher toxicity, but resulted in significantly better outcome for patients treated with HypoRT-VMAT. Grade 1 side effects were reported in 13 cases (32.5%) of the cIMRT group as compared to 2 cases (5%) of the VMAT group (p=0.001). G1 fibrosis was registered in 4 cIMRT (10%) cases and 2 HypoRT-VMAT patients (5%) (p=0.4). No other late toxicities (e.g. pulmonary or arm edema) were observed. In patients treated with cIMRT, only the breast volume  $>700$  cc was statistically associated with acute G2 skin adverse events (p=0.04). In patients receiving Hypo-RT, factors like age or breast volume did not have any influence on the onset of acute or late skin toxicity. No differences in fatigue were observed for the two groups of treatment groups: 11 cIMRT patients vs 16 HypoRT-VMAT (p=0.1).

### Conclusion

The present study showed that whole breast cIMRT and HypoRT-VMAT are feasible and well tolerated in early stage BC elderly patients and that HypoRT-VMAT is affected by lower risk of acute and late RT-related side effects.

### PV-0048 The Radiosensitivity Index (RSI) predicts for outcomes in triple negative breast cancer

C. Liveringhouse<sup>1</sup>, N.B. Figura<sup>2</sup>, K.A. Ahmed<sup>2</sup>, G.D. Grass<sup>2</sup>, P. Blumencranz<sup>3</sup>, K. Allen<sup>3</sup>, C. Laronga<sup>4</sup>, M.C. Lee<sup>4</sup>, L.B. Harrison<sup>2</sup>, T.J. Robinson<sup>2</sup>, J.F. Torres-Roca<sup>2</sup>, R. Diaz<sup>2</sup>

<sup>1</sup>University of South Florida, Morsani College of Medicine, Tampa, USA; <sup>2</sup>Moffitt Cancer Center, Department of Radiation Oncology, Tampa, USA; <sup>3</sup>Baycare Morton Plant Hospital, Department of Breast Oncology Surgery, Clearwater, USA; <sup>4</sup>Moffitt Cancer Center, Department of Breast Oncology, Tampa, USA

### Purpose or Objective

While genomic biomarkers have been utilized to predict outcomes in ER+ breast cancer, further investigation is needed to develop similar predictors for triple negative breast cancer (TNBC). RSI is a previously validated multi-gene expression index that is thought to be radiotherapy (RT)-specific. Here, we evaluate whether RSI is an RT-specific predictive biomarker in TNBC.

### Material and Methods

Prospectively gathered breast tumor samples were identified from an IRB-approved tissue biorepository representing one academic and two community hospitals. Gene expression of tumor samples was assessed with Affymetrix microarray chips and the RSI 10-gene signature was calculated for each sample using the previously published rank-based algorithm. As in prior studies, radiophenotype was determined by dichotomizing at RSI=0.3745, where RSI $\geq$ 0.3745 is radioresistant (RR) and RSI<0.3745 is radiosensitive (RS). Clinical information was obtained by chart review. Endpoints were locoregional recurrence-free survival (LRF5), distant metastasis-free survival (DMFS), overall survival (OS), and progression-free survival (PFS). Outcomes were estimated with Kaplan Meier (KM) methods and compared with log-rank tests. Associations between characteristics and outcomes were explored with univariable (UVA) and multivariable (MVA) Cox regression.

### Results

97 TNBC tumors with available genomic profiling were identified for analysis. The median age was 55 years (range 25-82). 97.9% of tumors were pT1-T2, and 37.1% had positive lymph nodes. 80% of tumors were high grade. 40.2% were treated with mastectomy alone, 14.4% with

mastectomy + RT, and 42.3% with lumpectomy + RT. The median RT dose was 46.8 Gy. 85.6% received chemotherapy. There were no significant differences in characteristics between RS and RR patients ( $p>0.05$ ). Median follow-up was 7.6 years (range 0.21-17.2). There were 10 locoregional recurrences, 15 distant metastases, and 16 deaths. All results of KM analyses are included in the accompanying table. Among all patients, radiophenotype predicted for all outcomes as RS had superior LRF5, DMFS, OS and PFS. Radiophenotype remained predictive for outcomes among RT-treated patients, as RS patients had superior LRF5, DMFS, OS, and PFS compared to RR patients. In contrast, radiophenotype did not predict for outcomes in patients not treated with RT as there were no significant differences in LRF5, DMFS, OS, or PFS. In RT-treated patients, radiophenotype ( $p=0.034$ ) and surgery type ( $p=0.012$ ) were associated with PFS and both remained significant on MVA (RR vs RS, HR 4.6 95% CI 1.01-20.48,  $p=0.048$ ) (lumpectomy vs mastectomy, HR 0.29 95% CI 0.10-0.83,  $p=0.021$ ). In non-RT patients, no factors predicted for PFS on MVA.

	5-year LRF5	5-year DMFS	5-year OS	5-year PFS
<b>All patients (N=97)</b>				
Radiosensitive	100%	95%	98%	93%
Radioresistant	84%	77%	84%	71%
Log-rank P	0.033	0.020	0.035	0.035
<b>Treated with RT (n=55)</b>				
Radiosensitive	100%	100%	100%	96%
Radioresistant	75%	72%	81%	66%
Log-rank P	0.024	0.007	0.006	0.018
<b>Not treated with RT (n=42)</b>				
Radiosensitive	100%	89%	94%	89%
Radioresistant	96%	83%	88%	79%
Log-rank P	0.409	0.738	0.343	0.699

### Conclusion

In this cohort of consecutively treated patients, we show that RSI radiophenotype predicts for outcomes in TNBC and is specific to RT-treated patients. Patients with radioresistant TNBC have poor outcomes and may benefit from treatment intensification, warranting further prospective validation.

### PV-0049 Merkel cell polyoma viral load predicts overall survival in patients with Merkel cell carcinoma

J. Mueller-von der Gruen<sup>1</sup>, R. Winkelmann<sup>2</sup>, M. Meissner<sup>3</sup>, U. Wieland<sup>4</sup>, S. Silling<sup>4</sup>, D. Martin<sup>1</sup>, E. Fokas<sup>1</sup>, C. Rödel<sup>1</sup>, F. Rödel<sup>1</sup>, P. Balcermpas<sup>5</sup>

<sup>1</sup>University of Frankfurt, Department of Radiation Oncology, Frankfurt, Germany; <sup>2</sup>University of Frankfurt, Dr. Senckenberg Institute of Pathology, Frankfurt, Germany; <sup>3</sup>University of Frankfurt, Department of Dermatology, Frankfurt, Germany; <sup>4</sup>University of Cologne, Institute of Virology- National Reference Center for Papilloma- and Polyomaviruses, Cologne, Germany; <sup>5</sup>University Hospital of Zürich, Department of Radiation Oncology, Zürich, Switzerland

### Purpose or Objective

Merkel cell carcinoma (MCC) is a rare but aggressive neuroendocrine tumor of the skin and its tumorigenesis is linked to the presence of clonally integrated Merkel cell polyomavirus (MCPyV) in up to 80% of the cases. The aim of this study was to determine the prognostic value of quantitative MCPyV viral load and lymphocytic infiltration.

### Material and Methods

CD8+ tumor infiltrating lymphocytes (TILs) and PD-L1 status were assessed using immunohistochemistry in FFPE tissue obtained from 49 patients with MCC treated with

(n=22, 45%) or without postoperative radiotherapy. MCPyV DNA prevalence, DNA integration status and viral load were determined by virus-specific quantitative real-time PCR. Immune marker expression and MCPyV characteristics were correlated with clinicopathological factors and overall survival (OS).

### Results

Median age at diagnosis was 74 (range 42-100) and 51% of the patients were female. 1-, 3- and 5-years OS rates were 65%, 33% and 25%, respectively. Positive MCPyV status was recorded in 79% of the patients and was associated with female gender ( $p=0.033$ ). Further, tumor localization (head and arms vs. trunk) positively correlated with PD-L1 status as well as combined expression of CD8+/PD-L1 ( $p$ -values: 0.011 and 0.038). Stromal TILs correlated significantly with both PD-L1 expression ( $p=0.010$ ) and N-stage ( $p=0.037$ ). Also, N+ stage inversely correlated with TILs ( $p=0.048$ ). A high viral load was significantly associated with worse OS ( $p=0.026$ ) and high intratumoral CD8+ infiltration with improved OS for the entire cohort ( $p=0.045$ ).

### Conclusion

A High MCPy DNA viral load was associated with impaired OS and high intratumoral TILs with improved OS. Furthermore, stromal TILs positively correlated with PD-L1 status, possibly opening new future perspectives for combining treatment approaches such as RT and immune-checkpoint inhibitors.

### Symposium: Challenging dose painting: Are we really painting what we aim to or the better outcome is only linked to higher dose spots within the CTV?

### SP-0050 What is left from dose painting when adding all uncertainties

M. Alber<sup>1</sup>

<sup>1</sup>Heidelberg University Clinic, Radiation Oncology, Heidelberg, Germany

### Abstract text

Multiple levels of dose prescription to the target volume (simultaneous integrated boost, SIB) and highly conformal, yet inhomogeneous dose escalation to small targets (such as in stereotactic body radiotherapy) are becoming rather common in modern radiotherapy. Dose painting (DP) is in essence an image-guided SIB, so it is reasonable to assume that planning- and delivery-related uncertainties play no greater role in DP than in geometry-guided SIB. It is the element of biological guidance that adds the essential layers of uncertainty.

It is instructive to follow a thought experiment that starts with an indiscriminate, geometric SIB to the core target volume (usually the GTV) with the appropriate prescription (to be addressed later). Then, what image information is required to shape the SIB into DP by chipping away dose? The locations where dose can be reduced are tied to the true negative rate (absence of the biological feature) and thus to specificity, while the level of de-escalation is tied to the false negative rate (missing the biological feature) and thus to sensitivity. Thus, low specificity enlarges the boosted volume, low sensitivity forces the dose spread smaller to limit tumour control loss by underdosing. To arrive at the DP prescription, it is sufficient to demand optimum use of the image information content; no sophisticated biological modelling is required.

An imaging modality may appear to be very specific to a particular trait of a tumour, but this does not mean that it is specific to therapy resistance. For example, pre-treatment hypoxia image information may be invalidated by re-oxygenation during therapy, or further unknown tumour characteristics may play a large role in therapy resistance. Thus, any attempt to model tumour response

from imaging data has to cope with incomplete information and temporal changes, effectively degrading both image sensitivity and specificity. The combination of multiple imaging modalities (increase overall sensitivity) and multiple examinations to quantify therapy response (increase overall specificity) can remedy this, and seems to be the most promising route to DP. In practice, it could turn out very difficult to prove the non-inferiority of DP versus a SIB of equal dose. However, at the very least, any imaging modality that is shown to have predictive value stratifies patients into risk groups and can therefore be the basis of patient-specific dose prescriptions, be they applied as SIB or DP. Notwithstanding the difficulties with an evidence base for DP from the tumour control perspective, normal tissue sparing might be the strongest rationale.

**SP-0051 What are the limitations on dose escalation to sub-volumes in head and neck cancer: experience from dose painting**

F. Duprez<sup>1</sup>, J. Daisne<sup>2</sup>, W. de Gersem<sup>1</sup>, I. Goethals<sup>3</sup>, L. Olteanu<sup>1</sup>, T. Vercauteren<sup>1</sup>, W. de Neve<sup>1</sup>

<sup>1</sup>Universitair Ziekenhuis Gent, Radiotherapie-Oncologie, Gent, Belgium ; <sup>2</sup>UCL-CHU Namur, Radiotherapie, Namur, B Belgium; <sup>3</sup>Universitair Ziekenhuis Gent, Nuclear Medicine, Gent, Belgium

**Abstract text**

Dose escalation of radiotherapy above 70 Gy could potentially lead to higher locoregional control rates but is hampered by severe acute and late toxicities. Molecular imaging based dose-painting is an attractive concept for dose-escalation while keeping toxicity lower to equal. As per-treatment changes of anatomical as well as biological signal intensity often occurs, these techniques are mostly performed in an adaptive radiotherapy program, using re-imaging during the 7-weeks of radiotherapy. Many theoretical as well as planning studies have been performed employing the dose-painting concept, broadly investigating two molecular imaging dose-painting methods:

(1) dose painting by contours (DPBC): using discretely contoured subvolumes within the tumor based on molecular imaging.

(2) dose painting by number (DPBN): using molecular imaging voxel-intensities to directly optimize radiotherapy plans.

In contrast to the relatively high number of planning studies, few clinical trials have been performed. The research program for head and neck radiotherapy at Ghent University Hospital has been focusing on molecular based dose-painting since 2003. Consecutively, following prospective clinical trials have been performed, all of them based on <sup>18</sup>F-FDG-PET:

(1) 2003-2005: phase I, non-adaptive DPBC in fractions 1-10 of 32; n = 41. (2) 2007-2009: phase I, 2-phase adaptive DPBN in fractions 1-20 of 32; n = 21.

(3) 2010-2011: feasibility trial on 3-phase adaptive DPBN in fractions 1-30/30; n = 10.

(4) 2012-2014: feasibility trial on 3-phase adaptive DPBN in fractions 1-30/30 for reirradiation of recurrent head and neck cancer; n = 10.

(5) 2011-2018: phase II randomized trial comparing 3-phase adaptive DPBN in fractions 1-20/30 with standard non-dose painting, non-adaptive IMRT; n = 95.

Trials 2-3-4 demonstrated the feasibility of biological imaging based dose-painting in head and neck cancer. However, during the randomized phase II trial, the DPBN-dose prescription has been adapted twice due to an unanticipated high occurrence of late mucosal ulcers: at the last interim analysis available at time of abstract writing, 9/39 studied patients developed late grade 4 mucosal ulcers, that seemed to be strongly associated not only with the high-dose subvolumes, but also with continuation of smoking or alcohol drinking after DPBN.

Definitive results after closing of recruitment in this phase II randomized trial are awaited.

The presentation will focus on the findings related to the occurrence of acute toxicity and late mucosal ulcers, the latter being the identified dose-limiting factor for further dose-escalation.

**SP-0052 Heterogeneous dose adapted to treatment response during radiotherapy: clinical experience from cervix cancer IGABT**

I. Jürgenliemk-Schulz<sup>1</sup>

<sup>1</sup>UMC Utrecht, Radiation Oncology, Utrecht, The Netherlands

**Abstract text**

For many decades, technological developments in cervix cancer brachytherapy have been limited and treatment was based on 2D imaging and standard approaches as developed by the classical brachytherapy schools in the early 20th century. With ICRU38 a system for dose prescription and reporting became available; mainly based on X-ray determined applicator related dose points. In recent years, image guided adaptive brachytherapy (IGABT) has resulted in a major change of practice. The ICRU89/GEC-ESTRO recommendations support the introduction of IGABT. They are based on repetitive tumour assessment through clinical examination and imaging, preferably magnetic resonance imaging (MRI), with adaptation of dose according to the tumour extent at diagnosis, and the response to EBRT at the time of brachytherapy. Adaptive treatment planning takes into account the changes during treatment and prescribes specific doses to the various volumes of interest. For the primary tumour adaptive target volumes can in principle be defined after any treatment phase. The residual GTV reflects macroscopic tumour rest whereas the adaptive CTV takes into account the morphology and topography of the initial GTV and the morphology and/or functional response to treatment. For definitive cervical cancer radiotherapy, these volumes are boosted through brachytherapy to different dose levels according to estimated levels of remaining tumour cell burden and in order to achieve very high doses in defined small volumes. Several mono-institutional studies and the prospective multicentre international RetroEMBRACE and EMBRACE studies have demonstrated that a highly differential dose distribution with significant dose escalation is clinically feasible with IGABT in cervical cancer. This is because with IGABT, the "super-high" doses are only administered to small volumes. The response-adaptation of volume is the key factor to identify volumes which are small enough to tolerate such high doses. The excellent outcome of IGABT has been demonstrated in several mono-institutional reports as well as in the RetroEMBRACE study. The 3-year local and pelvic control rates reached 98-100% and 96%, respectively, for FIGO stage IB1 and IB2 disease, and 93-96% and 89-91%, respectively, for stage IIB disease. For stage III/IVA disease, the local and pelvic control rates between centres were more variable ranging from 73-86%. Comparing with data as published after (chemo)radiation and traditional brachytherapy for cervical cancer the estimated gain of IGABT in its early phase is about 10% for pelvic/local control and not to the cost of additional morbidity. Further fine tuning the therapeutic window of IGABT can be expected as our knowledge on dose levels needed for better control and less morbidity is constantly increasing. Evidence for clinical improvement in terms of local/pelvic control will be the main focus for this presentation but the way to achieve this will also be addressed.

**SP-0053 Exploiting low drug uptake volume for dose painting**

A. Yaromina<sup>1</sup>, L. Dubois<sup>1</sup>, P. Lambin<sup>1</sup>

<sup>1</sup>Maastricht university, Department of Precision Medicine- the m-lab- gUow - school for Oncology and Developmental biology, Maastricht, The Netherlands

#### Abstract text

Several clinical studies have shown the possibilities to give a higher dose to certain hypothetically more radioresistant tumour sub-volumes, typically with high accumulation of FDG or a hypoxia tracer. We have tested the therapeutic efficacy of dose-painting (DP) strategies, i.e. targeted dose escalation and dose redistribution, in a rat syngeneic rhabdomyosarcoma model based on FDG uptake [1]. Our data indicate that, while dose escalation to high FDG uptake sub-volume was not superior to the same dose increase in low FDG uptake areas, dose redistribution was even detrimental, consistent with the hypothesis that tumor response is dependent on the minimum intratumoral dose. Interestingly, in the same tumour model dose escalation to the hypoxic sub-volume, as determined by the highest uptake of HX4 hypoxia tracer, resulted in worse tumour response than the same dose increment to the non-hypoxic sub-volume [2]. This data suggests that dose to the tumour bulk should be sufficient to inactivate non-hypoxic cells.

It might be difficult to achieve clinically sufficient dose escalation to eradicate tumour cells in hypoxic tumor sub-volume. Therefore, we moved beyond the traditional DP approaches combining hypoxia-targeted drugs with inverse dose-painting of hypoxic sub-volume and thus offering, in our view, more efficient utilization of radiation, i.e. radiation boost to non-hypoxic tumour areas with simultaneous inactivation of hypoxic tumour cells by a HAP. Indeed, our results support targeted dose escalation to non-hypoxic sub-volume with no/low activity of HAPs. This strategy applies on average a lower radiation dose and is as effective as uniform dose escalation to the entire tumour.

Routine implementation particularly of hypoxia PET imaging in the clinic is problematic because it is expensive, labor intensive, not attractive for the patient, or even not accessible. Therefore, partial non-targeted tumour irradiation with high dose in combination with immunotherapy might be a new alternative approach to dose-painting, which is currently being tested in our laboratory. It is expected that partial tumour irradiation enables delivery of high doses to tumor sub-volumes reducing normal tissue injury, causes less total damage to intratumoral vasculature permitting immune cells infiltration and provides stronger induction of immunogenic cell death releasing antigens and stimulants to immune system, while immunotherapy boosts anti-tumour immune response with systemic therapeutic potential.

#### References:

1. Trani D, Yaromina A, Dubois L, Granzier M, Peeters SG, Biemans R, Nalbantov G, Lieuwes N, Reniers B, Troost EE, Verhaegen F, Lambin P. Preclinical Assessment of Efficacy of Radiation Dose Painting Based on Intratumoral FDG-PET Uptake. *Clin Cancer Res.* 2015;21(24):5511-8.
2. Yaromina A, Granzier M, Biemans R, Lieuwes N, van Elmpt W, Shakirin G, Dubois L, Lambin P. A novel concept for tumour targeting with radiation: Inverse dose-painting or targeting the "Low Drug Uptake Volume". *Radiother Oncol.* 2017;124(3):513-520.

---

Proffered Papers: RB 1: Pre-clinical models is the next step for radiotherapy

---

OC-0054 Tumor reoxygenation and image-guided SBRT for the treatment of murine colorectal liver metastases

M. Pruschy<sup>1</sup>

<sup>1</sup>University of Zurich, Applied Radiobiology, Zurich, Switzerland

#### Purpose or Objective

Reactive oxygen species are generated in response to ionizing radiation (IR) and produce amongst others irreversible DNA double-strand breaks. This IR-induced cytotoxic effect is less abundant under hypoxia and thus hypoxic cells are more resistant to IR. Hence, reoxygenation of the hypoxic tumor fraction by a combined treatment modality with a pharmaceutical agent is of high interest to reduce the required dose of IR and thereby to further minimize normal tissue toxicity. Here we investigated the combined treatment modality of the novel anti-hypoxia compound *myo*-inositol trispyrophosphate (ITPP) in combination with IR for the treatment of murine colorectal liver metastases (CLM).

#### Material and Methods

ITPP was developed as an effector of hemoglobin lowering the oxygen/hemoglobin affinity thereby resulting in an enhanced release of oxygen e.g. in hypoxic tumors. Murine colorectal cancer cells (MC38) were injected either subcutaneously or orthotopically in the right lateral liver lobe of female C57BL/6 mice. Mice were treated with a previously identified regimen of ITPP (2x 3g/kg, neoadjuvant) alone and in combination with single fractions of IR ranging from 2.5 to 30 Gy. Tumor detection and irradiation were performed by contrast-enhanced CT and a small-animal radiotherapy (X-Rad225Cx), respectively. Tumor volumes were probed either by caliper measurements (subcutaneous tumors) or by serial MRI. Liver functional parameters in the blood serum were assessed 7 weeks upon irradiation.

#### Results

Treatment with ITPP alone did not reduce the growth rate of subcutaneous tumors as compared to vehicle treatment. However, ITPP in combination with a single high dose fraction of IR (12 Gy) significantly delayed tumor growth in comparison to irradiation alone. Selective intraportal injection of colorectal cancer cells yields a high rate in colorectal liver metastasis formation. An initial IR-dose escalation study for the treatment of the right liver lobe in healthy mice demonstrated that single fractions of 20 Gy and higher resulted in substantial animal body weight loss and impairment of liver functional markers. Preliminary results in this murine CLM model revealed a partial radioprotective effect of ITPP in healthy liver. Targeted irradiation of the right liver lobe with single fractions of 10 and 15 Gy is effective in reducing the growth of metastatic lesions without causing radiation-induced toxicities.

#### Conclusion

Here we demonstrated that the combined treatment modality of ITPP and IR results in a supra-additive tumor growth delay, which is most probably linked to neoadjuvant tumor reoxygenation. Moreover, we demonstrate that the irradiation of murine CLMs is feasible, accurate and effective with a small-animal image-guided radiotherapy platform.

#### OC-0055 Zebrafish model to study the use of nanoparticles as a radiosensitizer in low Z target beams

M. Ha<sup>1</sup>, O. Piccolo<sup>2</sup>, N. Melong<sup>3</sup>, J. Lincoln<sup>4</sup>, D. Parsons<sup>5</sup>, A. Detappe<sup>6</sup>, O. Tillement<sup>7</sup>, R. Berbeco<sup>8</sup>, J. Berman<sup>9</sup>, J. Robar<sup>10</sup>

<sup>1</sup>Dalhousie University/Nova Scotia Health Authority, Radiation Oncology, Halifax, Canada; <sup>2</sup>Dalhousie University, Biology, Halifax, Canada; <sup>3</sup>IWK Health Centre/Dalhousie University, Pediatrics, Halifax, Canada; <sup>4</sup>Dalhousie University, Physics and Atmospheric Science, Halifax, Canada; <sup>5</sup>UT Southwestern Medical Centre, Radiation Oncology, Dallas, USA; <sup>6</sup>MIT, David H Koch Institute for Integrative Cancer Research, Cambridge, USA; <sup>7</sup>Universite de Lyon, Institut Lumiere

Matiere, Villeurbanne, France ; <sup>8</sup>Harvard Medical School, Radiation Oncology, Boston, USA; <sup>9</sup>IWK Health Centre/Dalhousie University, Pediatrics/Pathology/Microbiology and Immunology, Halifax, Canada; <sup>10</sup>Dalhousie University/Nova Scotia Health Authority, Radiation Oncology/Physics and Atmospheric Science/Medical Physics, Halifax, Canada

### Purpose or Objective

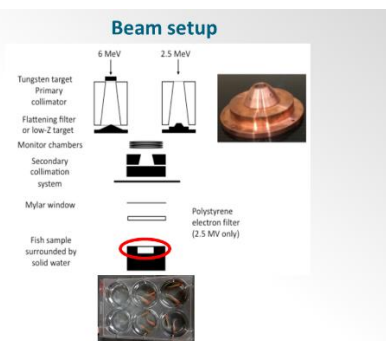
Nanoparticles made of high atomic number (Z) elements have been shown to sensitize cancer cells to radiation beams generated from linacs *in vitro* and *in vivo*. This effect occurs due to the emission of low energy photoelectrons and Auger electrons. Gold (GNP) and gadolinium (GdNP) based nanoparticles are biocompatible, and accumulate passively in tumours due to the enhanced permeability and retention effect, and there is growing evidence that localized radiation-induced tumour vascular damage can be used to clinical advantage. The introduction of low Z (sintered diamond) linac target instead of a standard Cu/W target results in a predicted 7.7 fold enhancement in the immediate proximity of the NP. The efficacy of combining the low Z target beam with NPs remains to be verified *in vivo*. To this end, we employed an established zebrafish xenotransplantation platform to quantify tumour cell proliferation. The zebrafish model offers the advantages of using a transparent fish to allow *in vivo* monitoring of grafts, as well as enabling large sample sizes.

### Material and Methods

**Beam setup:** The samples were irradiated using a standard 6 MV or a custom 2.5 MV/diamond target x-ray beam from a TrueBeam linac. The 2.5 MV/diamond beam was generated by 2.5 MeV electron beam incident upon a sintered diamond target in the carousel. (see figure)

**Cell line screen:** Panc1 (pancreas), FaDu (hypopharynx), A673 (Ewing), MDA-MB-231 (breast), LNCaP (prostate), A549 (lung) were labeled *in vitro* with NPs. They were irradiated with 8 Gy using the low Z or conventional target beam. Proliferation was assayed using Alamar Blue.

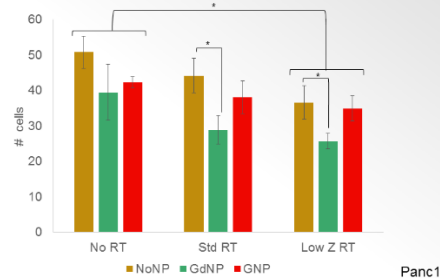
**Xenograft assay:** Cells were co-labeled *in vitro* with NPs and a lipophilic fluorescent dye. Labeled cells were injected into the yolk sac of dechorinated *casper* zebrafish embryos and irradiated 1 dpi (days post injection) with 8 Gy. Tumour viability was measured by a standard *ex vivo* proliferation assay at 3 dpi.



### Results

Cells showed differential responses to being irradiated with standard or low-Z target beam in the presence of GNP or GdNP. Among the cell lines tested, FaDu cells were the most sensitive to NP mediated irradiation. In Panc1 xenografts, there was a statistically significant decrease in the surviving cell numbers in samples treated with low Z target beams.

### Nanoparticle mediated response to low Z beam is seen in xenografted Panc1



### Conclusion

In a proof of principle experiment, we have shown enhanced radiologic cell kill in low-Z target irradiation in xenografted NP labeled cells. We are in the process of testing the model in additional cells with plans to examine tumour response in adult fish model.

### OC-0056 Multiple strategies for resolving radiation-induced neurocognitive dysfunction

C. Limoli<sup>1</sup>, M. Vozenin<sup>2</sup>, M. Acharya<sup>3</sup>

<sup>1</sup>University of California Medical Sciences I, Department of Radiation Oncology, Irvine, USA; <sup>2</sup>Radio-Oncology/CHUV, Department of Radiation Oncology, Lausanne, Switzerland; <sup>3</sup>University of California, Radiation Oncology, Irvine, USA

### Purpose or Objective

The progressive and debilitating side effects manifesting as cognitive dysfunction, mood disorders and a range of persistent pathologies have long hampered the radiotherapeutic management of CNS malignancies. For decades this problem has plagued therapeutic outcomes, and has not been restricted to brain cancer cases, as systemic chemotherapy elicits similar adverse outcomes, problems that remain an unmet medical need. Here we will highlight multiple strategies for resolving these long-standing clinical problems.

### Material and Methods

Work in our laboratories have focused on resolving many of these treatment-associated complications through a variety of stem cell based, genetic, pharmacologic and beam delivery strategies. Cranial transplantation of multiple stem cell types, systemic delivery of stem-cell derived exosomes, retrograde endocannabinoid blockade, microglial depletion, epigenetic modulation and ultra-high dose rate "FLASH" radiotherapy have all been used and characterized to provide significant relief from the normal tissue toxicities transpiring in the irradiated and/or chemotherapy treated brain.

### Results

Cranial grafting of 5 different pluripotent or multipotent human stem cell types, or stem cell-derived exosomes grafted intrahippocampally or systemically have been found to completely resolve radiation and chemotherapy-induced cognitive dysfunction from 1-8 months after treatment. Multiple spontaneous exploration tasks designed to interrogate learning and memory, and other tasks used to quantify anxiety, depression and fear extinction, demonstrate conclusively that our selected interventions improve behavioral performance in multiple preclinical rodent models over extended post-treatment times. This long term relief is associated with a significant preservation of host neuronal morphology, protection of the microvasculature and attenuation of neuroinflammation. Similar results have been obtained with the cannabinoid receptor 1 (CB1) antagonist AM251,

with the colony stimulating factor 1 receptor (CSF1R) antagonist PLX5662 and with inhibitors of adenosine kinase. Interestingly, more recent data implementing FLASH radiotherapy has achieved similar promising results in terms of sparing normal tissue complications in the irradiated brain without compromising tumor cure.

#### Conclusion

Progress in each of these research areas holds significant potential for translation to the clinic with the hope of improving the quality of life of millions of cancer survivors. These will be highlighted in further detail in our presentation.

#### OC-0057 Probing spatiotemporal fractionation on the preclinical level

I. Telarovic<sup>1</sup>, M. Pruschy<sup>1</sup>, I. Grgic<sup>1</sup>, J. Krayenbuehl<sup>1</sup>, M. Guckenberger<sup>1</sup>, J. Unkelbach<sup>1</sup>

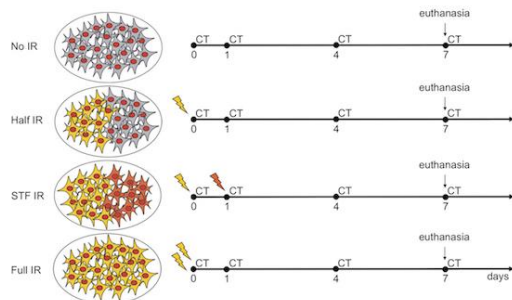
<sup>1</sup>Universitätsspital Zürich, Radiation Oncology, Zürich, Switzerland

#### Purpose or Objective

In contrast to conventional radiotherapy, spatiotemporally fractionated (STF) treatments deliver a distinct dose distribution in each fraction. The aim is to increase the therapeutic window by simultaneously achieving partial hypofractionation in the tumor along with near uniform fractionation in normal tissues. To that end, each fraction delivers high single fraction doses to alternating parts of the tumor while creating a similar dose bath in the surrounding normal tissue. This approach has been studied *in silico* (Unkelbach, 2015) based on the working hypothesis that different parts of the tumor can be treated in different fractions as long as each part receives the prescribed cumulative biological dose in the end. Here, we do an initial step towards verifying this assumption in an experimental animal model.

#### Material and Methods

We compare the tumor growth rate of conventionally treated xenografts derived from mouse colon cancer cells to a reductionistic preclinical model of STF. Upon reaching the tumor volume of  $300 \text{ mm}^3 \pm 10\%$ , animals are randomly assigned to 4 treatment groups (Fig. 1). No irradiation (IR) group is sham irradiated. Half IR group is irradiated with a partial 12 Gy IR covering the cranial half of the tumor. STF IR group receives two partial 12 Gy IRs given on day 0 and day 1, covering the cranial and caudal half of the tumor, respectively. Full IR group receives two partial 12 Gy IRs successively. All animals undergo CT imaging on days 0, 1, 4 and 7 post IR and are euthanized on day 7. To perform such fractionated IR of varying target volumes in small animals, we develop a pipeline that combines a dedicated small animal image-guided research platform (X-RAD 225Cx / SMART-Plan) with the clinical software MIM (MIM Software Inc.). Finally, we compare caliper-based (CALVM) growth rate curves with CT-volumetry (CTVM) in the context of tumor growth rate studies.

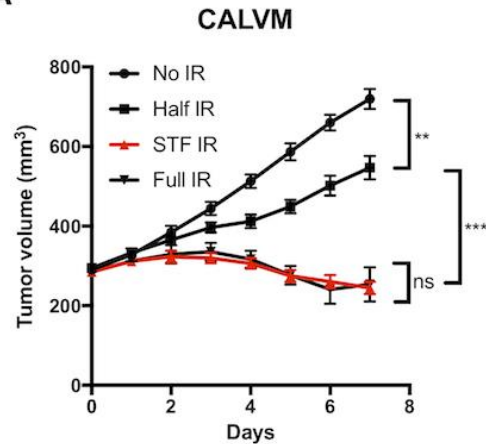


#### Results

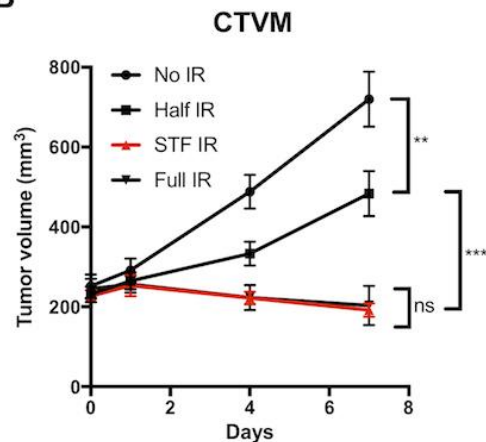
Tumors irradiated to the same dose, either immediately (Full IR) or with a 24 hour delay between two partial IRs (STF IR), exhibited no difference in growth rate (Fig. 2A,

area under tumor growth curve STF IR= $2060 \pm 204$  vs Full IR= $2095 \pm 343$ ,  $P=0.99$ ). Reduction in the irradiated volume resulted in a decreased response (Fig. 2A, Half IR). CTVM (Fig. 2B) measured overall significantly smaller starting volumes with an increased dispersion compared to CALVM ( $V_0$  CTVM= $238 \pm 53 \text{ mm}^3$  vs CALVM= $288 \pm 14 \text{ mm}^3$ ,  $P<0.001$ ), while the relative tumor growth curves (each point normalized to corresponding  $V_0$ ) did not differ between the two methods.

#### A



#### B



#### Conclusion

The assumption of spatiotemporal fractionation that the tumor response can be predicted by locally adding up biological doses from each fraction is confirmed in a reductionistic preclinical model whereby xenografts irradiated either immediately or with a 24 hour delay between two partial irradiations exhibit no difference in growth delay. The study suggests caliper- and CT-volumetry to be interchangeable when considering relative, but not absolute volumes in tumor growth studies.

#### OC-0058 Dose-volume effects in the central nervous system and sparing in microbeam/minibeam radiation

E. Bahn<sup>1,2</sup>, M. Alber<sup>1</sup>

<sup>1</sup>Heidelberg University Hospital, Radiation Oncology, Heidelberg, Germany; <sup>2</sup>Clinical Cooperation Unit Radiation Oncology, German Cancer Research Center DKFZ, Heidelberg, Germany

#### Purpose or Objective

Animal experiments with narrow proton beams in the mm-range and bath/shower dose distributions have produced evidence of an abnormally high volume effect in rat spinal cord more than a decade ago. Whether these results have

pertinence for the effects observed in microbeam radiation (whether a microbeam radiation is a kind of bath/shower dose) remains a fundamental question. We present a spinal cord dose response model that predicts relative frequency and localization of late radiation effects after irradiation with arbitrary dose distributions, over scales from few micrometers to the entire organ. The model can predict the posited sparing effect in micro-/minibeam radiation and thereby help to optimize microbeam patterns.

#### Material and Methods

The dynamic repair model (DRM) views a complication as a result of a failed repair/homeostasis process, caused by deletion of critical tissue information via radiation. From general thermodynamic principles, we derive a closed form that relies on only three parameters. In this framework, the volume effect emerges as a result of a finite communication distance in a network-like information storage system.

We tested the DRM on six well-known published datasets of volume effects and bath/shower effects in rat spinal cord, as well as one dataset of synchrotron-based microbeam radiation. Model parameters were obtained from regression to the volume-effect data. Model validation was subsequently performed on the bath/shower and microbeam data.

#### Results

The DRM provides a very good prediction of all small volume and bath/shower datasets. Fig. 1 shows 50 % response doses  $D_{50}$  as a function of irradiated length (or effective length in the case of inhomogeneous irradiation). For the rat spinal cord, we determine a critical information communication distance of  $(4.0 \pm 0.3)$  mm.

The microbeam experiment compares a 1.35 mm wide homogeneous field with an 11 mm wide comb of  $35 \mu\text{m}$  wide microbeams. The homogeneous field response is well predicted by the DRM. The microbeam  $D_{50}$  is underestimated (predicted:  $180 \pm 20$  Gy measured:  $370 \pm 90$  Gy).

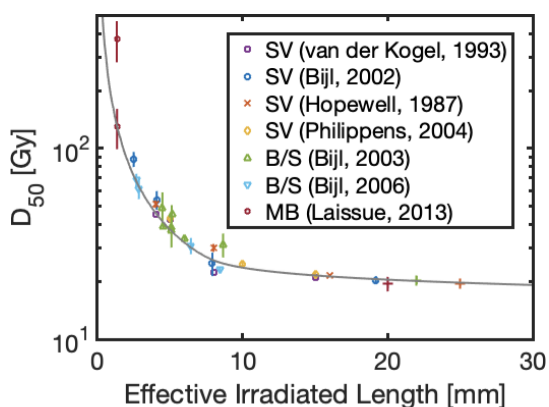


Fig. 1:  $D_{50}$  vs effective irradiated spinal cord length. Error bars denote 95% confidence intervals. SV: small volume; B/S bath/shower; MB: microbeam; Solid line: Model prediction.

#### Conclusion

In micro-/minibeam radiation, dose distributions are highly inhomogeneous on very small scales. The abnormally high volume effect on small scales might provide an explanation, but this requires a model that permits comparison of effects of inhomogeneous doses. The DRM allows a prediction of the dose response for arbitrary dose distributions and it particularly explains the effect of low dose baths adjacent to small high dose regions through a deleterious effect on information critical for repair. Microbeam experiments with peak doses in excess of 200 Gy may lie outside the valid range of the DRM because effects that arise from killing every cell in the high dose region are not modelled. Microbeam

dose response data are scarce and thus definitive conclusions are not justified, but comparison of model prediction with a published dataset indicates an additional dose tolerance beside the volume effect, possibly caused by overkill.

---

#### Proffered Papers: CL 1: Proffered papers : Lung

---

#### OC-0059 Stereotactic radiotherapy for oligoprogressive NSCLC: clinical scenarios affecting survival

S. Kroeze<sup>1</sup>, C. Fritz<sup>1</sup>, D. Kaul<sup>2</sup>, O. Blanck<sup>3</sup>, K.H. Kahl<sup>4</sup>, F. Roeder<sup>5</sup>, S. Siva<sup>6</sup>, J. Verhoeff<sup>7</sup>, A. Grosu<sup>8</sup>, M. Schymalla<sup>9</sup>, M. Glatzer<sup>10</sup>, M. Szücs<sup>11</sup>, M. Geier<sup>12</sup>, S. Mose<sup>13</sup>, I. Sackeler<sup>14</sup>, F. Lohaus<sup>15</sup>, F. Eckert<sup>16</sup>, M. Guckenberger<sup>1</sup>

<sup>1</sup>University Hospital Zürich, Radiation Oncology, Zurich, Switzerland; <sup>2</sup>Charité-University Hospital Berlin, Radiation Oncology, Berlin, Germany;

<sup>3</sup>Universitätsklinikum Schleswig-Holstein, Radiation Oncology, Kiel, Germany;

<sup>4</sup>Klinikum Augsburg, Radiation Oncology, Augsburg, Germany; <sup>5</sup>University Hospital Munich, Radiation Oncology, Munich, Germany;

<sup>6</sup>Peter MacCallum Cancer Center, Radiation Oncology, Melbourne, Australia; <sup>7</sup>University Medical Center

Utrecht, Radiation Oncology, Utrecht, The Netherlands; <sup>8</sup>University Medical Center Freiburg, Radiation Oncology, Freiburg, Germany;

<sup>9</sup>Universitätsklinikum Gießen und Marburg, Radiation Oncology, Marburg, Germany;

<sup>10</sup>Kantonsspital St. Gallen, Radiation Oncology, St. Gallen, Switzerland; <sup>11</sup>University Hospital Rostock, Radiation Oncology, Rostock, Germany;

<sup>12</sup>Ordensklinikum Linz- Barmherzige Schwestern, Radiation Oncology, Linz, Austria; <sup>13</sup>Schwarzwald-Baar Klinikum, Radiation Oncology, Villingen-Schwenningen, Germany;

<sup>14</sup>Strahlentherapie Freising und Dachau, Radiation Oncology, Freising, Germany; <sup>15</sup>University Hospital Dresden, Radiation Oncology, Dresden, Germany;

<sup>16</sup>University Hospital Tübingen, Radiation Oncology, Tübingen, Germany

#### Purpose or Objective

Developments of local and systemic therapies have improved the prognosis of metastatic NSCLC. Oligometastatic patients may especially benefit from a more aggressive treatment approach. However, the concept of "oligometastasis" is complex: e.g. limited progression or resistance of disease to systemic treatment. This study aimed to evaluate the outcome of stereotactic radiotherapy (SRT) to oligoprogressive or oligoresistant NSCLC in patients receiving concurrent immuno- or targeted therapy.

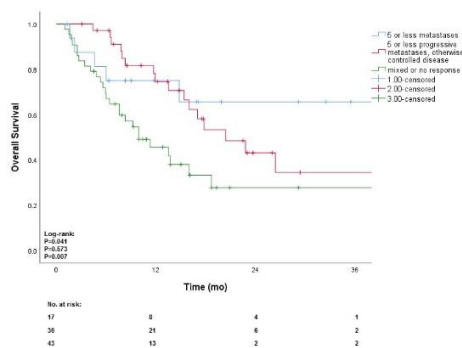
#### Material and Methods

The retrospective international multicenter register study (TOaSTT) collected data on metastatic NSCLC patients receiving SRT concurrent ( $\leq 30$ d) to immuno- or targeted therapy. Patients were grouped in: patients treated for  $\leq 5$  metastases without additional metastases (oligoprogression), treated for  $\leq 5$  progressive metastases with controlled disease of all other metastases (oligopersistent), and patients with mixed response/uncontrolled disease. SRT was performed to  $\leq 5$  extracranial or cranial lesions. Overall survival (OS) was analyzed using Kaplan-Meier survival curves and log rank testing. Secondary outcomes were progression free survival (PFS), local control (LC), time to switch of systemic therapy after SRT and toxicity as defined by the CTCAE v4 criteria.

#### Results

SRT of 192 lesions in 108 patients was performed between 7/2009 and 5/2018 in 16 clinics. Median age was 63y (range 33-80). 75% had synchronous metastatic disease, driver mutations were: EGFR 41%, ALK 14%, other 21%, unknown/no 24%. Median follow-up was 18.7 (range 1-102)

mo. The majority had metastases in 1-3 organs. 90% were ECOG 0-1. Median 1 (range 1-5) metastasis was treated with SRT; 69% cranial and 31% body SRT. Targeted therapies were started a median 5.8mo before SRT in 69%, during SRT in 8%, and a median 14d after SRT in 23% of patients. 60% received an ALK- or EGFR-TKI, 31% nivolumab or pembrolizumab, 8% bevacizumab. Oligoprogressive and oligopersistent patients showed improved OS compared to advanced metastatic disease ( $p=0.008$ ) (Fig.1). PFS was best in oligoprogressive patients; median 20.1 vs 7 and 4.4 mo., respectively ( $p=0.006$ ). LC was median 21.0, 12.0 und 9.0mo; no significant difference between groups. After 1y, 86%, 47% and 39% in the 3 groups continued the same immuno- or targeted therapy as before SRT. Grade 3 and 4 acute toxicity were observed in 6% and 1% ( $n=1$ , headache), late toxicity in 3% and 1% ( $n=1$ , hemiparesis), respectively.



## Conclusion

This study observed excellent survival with limited toxicity when definitive SRT to a limited number of metastases was combined with targeted- or immunotherapy in oligoprogressive and oligopersistent NSCLC patients. High-dose local radiotherapy of metastatic sites allowed continuation of targeted-, or immunotherapy for minimum 1 year in 39% to 86%, with best results observed in oligoprogressive patients. These observations need to be further evaluated within prospective trials.

## OC-0060 I-SABR induces local and abscopal responses in metastatic patients after failure to ICI treatment

R. Chicas Sett<sup>1</sup>, I. Morales-Orue<sup>1</sup>, J.F. Castilla-Martinez<sup>1</sup>, J. Blanco<sup>1</sup>, A. Kannemann<sup>1</sup>, J. Zafra<sup>1</sup>, M. Zajac<sup>1</sup>, M. Lloret<sup>1</sup>, P.C. Lara<sup>2</sup>

<sup>1</sup>Dr. Negrin University Hospital of Gran Canaria, Radiation Oncology, Las Palmas de Gran Canaria, Spain;

<sup>2</sup>San Roque University Hospital/Universiada Fernando Pessoa Canarias, Radiation Oncology, Las Palmas de Gran Canaria, Spain

## Purpose or Objective

The increased probability of abscopal responses that can be triggered by the combination of immune-checkpoint inhibitors (ICI) and stereotactic ablative radiotherapy (SABR) represents a promising therapeutic strategy for eradicating metastatic disease. The aim of the present study is to assess the role of I-SABR in patients with metastatic cancer in progression to ICI.

## Material and Methods

We conducted a prospective study based on metastatic patients (lung, melanoma, H&N, bladder and renal carcinoma) who had experienced disease progression while on ICI (anti-PD1/L1) treatment. SABR was performed by volumetric-modulated arc therapy and each fraction was delivered in a separate interval of 48 hours. Objective overall response (OR) including complete response (CR), partial response (PR) and stable disease (S), acute toxicity

(CTCAE v.4.3), and abscopal response (AR) were measured. One to three metastases were selected on each patient for SABR treatment. All patients had received at least 1 cycle of ICI prior to SABR. In order to evaluate the AR, 2 non-irradiated lesions were selected. AR was defined as 25% reduction in any non-irradiated predefined measurable lesions. These lesions were assessed according to RECIST (v1.1) by CT, MRI or PET at 8-week intervals.

## Results

From September 2017 to October 2018, 60 patients who had received anti-PD-1/L-1 immunotherapy [nivolumab ( $n=31$ ), pembrolizumab ( $n=22$ ) or atezolizumab ( $n=7$ )] were included. Twenty patients were excluded from analysis due to the lack of at least 8-weeks follow-up after SABR. All lesions received SABR doses  $> 6$  Gy/fraction, with a median dose of 35 Gy/5 fractions ( $BED_{10} = 59.5$  Gy). After a 7-month median follow-up (2-14 months), the acute ICI toxicity profile was similar before and after SABR. Median overall survival (OS) was 9 months (SD 0.5, IC95% 8.0-10.4). Local response was reported in 29 patients (73%). AR was observed in 13 patients (33%), 4 of whom had CR, 6 PR and 2 stable. Median time from SABR to AR was 2 months. All patients with AR are alive to date. Overall, 21 patients (53%) presented OR and 5 patients (13%) achieved a sustained systemic CR. OS sub-analysis was significantly higher in the AR group versus the Non-AR group (100% vs 60%,  $p=0.01$ ). OR rate was also higher in the AR group versus the Non-AR group (88% vs. 28%,  $p=0.002$ ). Patients continued to receive the same ICI for a mean of 6 months post-SABR (range: 2-14 months) before subsequent disease progression. Only 9 patients (23%) have required a new systemic treatment. Lastly, an analysis regarding SABR dose was performed. Patients were divided into two groups based on the biologically equivalent dose ( $BED_{10}$ ) received. Patients who received doses  $> 50$  Gy ( $BED_{10}$ ) achieved a superior median OS compared to  $< 50$  Gy ( $BED_{10}$ ) (9 vs 4 months,  $p=0.01$ ).

## Conclusion

Our results show that in patients unresponsive to ICI, I-SABR could rechallenge the immune system resulting in high local and abscopal effect improving survival with maintenance ICI treatment.

## OC-0061 EORTC 22113-8113 Lungtech trial on SBRT of central lung tumors

S. Adebahr<sup>1,2,3</sup>, Y. Liu<sup>4</sup>, S. Colette<sup>4</sup>, C. Faivre-Finn<sup>5</sup>, S. Ahmad<sup>6</sup>, M. Ahmed<sup>7</sup>, J. Belderbos<sup>8</sup>, N. Andratschke<sup>9</sup>, K. Franks<sup>10</sup>, X. Geets<sup>11</sup>, M. Guckenberger<sup>9</sup>, K. Konopa<sup>12</sup>, M. Lambrecht<sup>13</sup>, V. Lewitzki<sup>14</sup>, Y. Lievens<sup>15</sup>, N. Pourel<sup>16</sup>, D. De Ruysscher<sup>17,18,19</sup>, R. Dziadziuszko<sup>12</sup>, C. Fortpied<sup>4</sup>, F. McDonald<sup>7</sup>, H. Peulen<sup>8,20</sup>, A. Grosu<sup>1,2,3</sup>, C. Hurkmans<sup>20</sup>, C. Le Pechoux<sup>21</sup>, U. Nestle<sup>1,22</sup>

<sup>1</sup>Medical Center- Faculty of Medicine- University of Freiburg, Department of Radiation Oncology, Freiburg im Breisgau, Germany; <sup>2</sup>German Cancer Consortium DKTK, Partner Site Freiburg, Freiburg, Germany;

<sup>3</sup>German Cancer Research Center, dkfz, Heidelberg, Germany; <sup>4</sup>EORTC, Headquarters, Brussels, Belgium;

<sup>5</sup>Division of Cancer Sciences- University of Manchester, The Christie NHS Foundation Trust, Manchester, United Kingdom; <sup>6</sup>NHS Foundation Trust, Guy's & St Thomas', London, United Kingdom; <sup>7</sup>Royal Marsden NHS Foundation Trust/Institute of Cancer Research,

Department of Radiotherapy, Sutton, United Kingdom; <sup>8</sup>The Netherlands Cancer Institute, Department of Radiation Oncology, Amsterdam, The Netherlands;

<sup>9</sup>University of Zurich, Department of Radiation Oncology, Zurich, Switzerland; <sup>10</sup>St. James's University Hospital, Department of Clinical Oncology, Leeds, United Kingdom;

<sup>11</sup>Cliniques universitaires Saint-Luc- MIRO - IREC Lab, Department of Radiation Oncology, UCL-Bruxelles, Belgium; <sup>12</sup>Medical University of Gdansk, Department of Oncology and Radiotherapy, Gdansk, Poland;

<sup>13</sup>UZ Gasthuisberg Leuven and Department of

experimental Radiotherapy KU Leuven, Department of Radiotherapy-Oncology, Leuven, Belgium; <sup>14</sup>University Hospital Würzburg, Department of Radiation Oncology, Würzburg, Germany; <sup>15</sup>Ghent University Hospital and Ghent University, Department of Radiation Oncology, Ghent, Belgium; <sup>16</sup>Institut Sainte-Catherine- 250-chemin de Baigne-Pieds, Service de radiothérapie, Avignon, France; <sup>17</sup>KU Leuven-University of Leuven, Department of Oncology- Experimental Radiation Oncology, Leuven, Belgium; <sup>18</sup>GROW School for Developmental Biology and Oncology, Department of Radiation Oncology Maastricht, Maastricht, The Netherlands; <sup>19</sup>Maastricht University Medical, Center, Maastricht, The Netherlands; <sup>20</sup>Catharina Hospital, Department of Radiation Oncology, Eindhoven, The Netherlands; <sup>21</sup>Gustave Roussy- Paris Sud University, Department of Radiation Oncology, Villejuif, France; <sup>22</sup>Kliniken Maria Hilf GmbH Mönchengladbach, Department of Radiation Oncology, Mönchengladbach, Germany

### Purpose or Objective

The European Organization for Research and Treatment of Cancer (EORTC) phase II prospective multicentre Lungtech trial 22113-08113 assesses safety and efficacy of stereotactic body radiotherapy (SBRT) in inoperable patients with centrally located non-small cell lung cancer (NSCLC). The trial was closed early due to poor accrual. Here we report on two lethal complications.

### Material and Methods

Patients with centrally located (“tumor within 2 cm or touching the zone of the proximal bronchial tree (PBT) or tumor that is immediately adjacent to the mediastinal or pericardial pleura, with a planning target volume expected to touch or include the pleura”) non-metastatic NSCLC (T1-T3,  $\leq 7$ cm) were included. After prospective imaging review and radiation quality assurance (RTQA) patients were treated with SBRT (8x7.5Gy, ICRU 83). Follow-up is performed 6 weeks after treatment, then 3-monthly for 3 years, 6-monthly in year 4 and 5, including history, clinical examination, toxicity assessment and CT, FDG-PET and biopsy in case of suspected progression. The protocol included recruitment stop in case of potentially SBRT-related death triggering safety review.

### Results

Between 08/15 and 12/17, 39 patients from 13 sites and 6 European countries were included in the trial, 33 passed imaging and RTQA review (58% male, age 57-89 years, tumor size 1.4 - 5.5cm) and were treated per protocol. So far, 2 potentially treatment related deaths were observed.

An 88 year old patient died 3 months after SBRT and death was attributed to radiation pneumonitis. Safety review could not decide on the definite cause of death, also potentially related to pre-existing cardiac disease (CD) or amiodarone lung disease. As a consequence, patients with severe pre-existing CD, interstitial lung disease or concomitant amiodarone intake were excluded from recruitment and a formal policy to treat pneumonitis was added in the protocol. As this patient had a relatively high contralateral mean lung dose (CMLD), the amended recommendation restricted CMLD to  $< 3.6$ Gy.

An 83 year old patient with a tumor broadly abutting the right lower lobe bronchus died 15 months after SBRT, scored as SBRT-related hemoptysis. The PBT received 46.5Gy to 0.54cc, considered as acceptable protocol variation. Safety review revealed that in this patient taking anticoagulants, bronchoscopy, including a biopsy of a necrotic patch at the right lower lobe was performed 4 days before death. The event was categorized as expected toxicity and recommendations for a more careful management of procedures after SBRT were made available to investigators. Although it was not recommended to stop the study for safety reasons, the

repeated safety-related halt in recruitment contributed to the early closure of the trial.

### Conclusion

Safety of SBRT in centrally located lung tumors remains unclear. For the prospective investigation of radiotherapy related toxicities, alternative trial designs to those typically used to investigate medicinal products might be needed.

### OC-0062 Development & validation of prognostic and predictive models in limited-stage small-cell lung cancer

A. Salem<sup>1</sup>, H. Mistry<sup>2</sup>, S. Falk<sup>3</sup>, G. Price<sup>4</sup>, C. Faivre-Finn<sup>1</sup>  
<sup>1</sup>University of Manchester/ Christie NHS Foundation Trust, Division of Cancer Sciences/ Radiotherapy Related Research & Department of Clinical Oncology, Manchester, United Kingdom; <sup>2</sup>University of Manchester/ Christie NHS Foundation Trust, Division of Cancer Sciences & Division of Pharmacy/ Radiotherapy Related Research, Manchester, United Kingdom; <sup>3</sup>Christie NHS Foundation Trust, Radiotherapy Related Research, Manchester, United Kingdom; <sup>4</sup>University of Manchester/ Christie NHS Foundation Trust, Division of Cancer Sciences/ Radiotherapy Related Research, Manchester, United Kingdom

### Purpose or Objective

Assessment of prognosis & selection of limited-stage small-cell lung cancer (LS-SCLC) patients who benefit from chemoradiotherapy (CRT) could aid clinical decisions. We used the CONVERT trial & validation cohorts to investigate LS-SCLC prognostic & predictive covariates.

### Material and Methods

CONVERT is a phase III trial that randomised patients between twice-daily (45Gy in 30 fractions) & once-daily (66Gy in 33 fractions) CRT, followed by prophylactic cranial irradiation if indicated. The following covariates were investigated for prognostic & predictive significance (benefit from twice-daily radiotherapy & CRT completion) in CONVERT: clinical (age, performance score (PS), TNM stage, tumour laterality, smoking status, weight loss  $>10\%$  & lung function), laboratory (alkaline phosphatase, sodium & lactate dehydrogenase) & dosimetric (gross tumour volume (GTV), % heart dose & lung V20). Chemotherapy & radiotherapy completion were defined as delivery of all pre-planned cycles (4 or 6) & all radiotherapy fractions, respectively. Multivariate overall survival (OS) & chemotherapy completion regression analyses were conducted after correcting for multiple comparisons with a final model derived via a backward elimination approach using the likelihood ratio-test. The CONVERT OS model was validated in 2 independent LS-SCLC retrospective patient cohorts, treated in the routine setting at The Christie.

### Results

459 CONVERT participants & 2 Christie cohorts treated with CRT (cohort 1; n=108) and radiotherapy  $\pm$  chemotherapy (cohort 2; n=228) were included (table 1). In CONVERT, GTV was the strongest OS prognostic covariate (HR 1.3 (95% CI 1.14-1.48);  $p<0.001$ ). The addition of PS (ECOG 1/2 vs 0) & tumour laterality (bilateral/midline/unknown vs unilateral) modestly improved the models' concordance index (0.59 to 0.61). The HR for OS between high & low risk groups using this model, derived by splitting on the median risk score, was 1.96 (95% CI 1.54-2.49); median OS: 21 m (95% CI 18-25) vs 45 m (95% CI 34-NR), respectively (figure 1A). The models' prognostic significance was validated in the 2 independent Christie cohorts (cohort 1 concordance index=0.62, SE=0.04 & cohort 2 concordance index=0.59, SE=0.02); figure 1B-C. None of the covariates predicted benefit from twice-daily radiotherapy in CONVERT. In CONVERT, increasing patient age (continuous) alone or with hyponatremia & decrease in forced expiratory volume in 1sec (continuous) predicted non-completion of

6 or 4 pre-planned chemotherapy cycles ( $p < 0.05$ ), respectively. Due to high radiotherapy completion in CONVERT ( $\geq 80\%$  in both trial arms), a multivariate analysis to predict radiotherapy completion was not performed. Data on treatment completion were currently unavailable in the routinely treated cohorts.

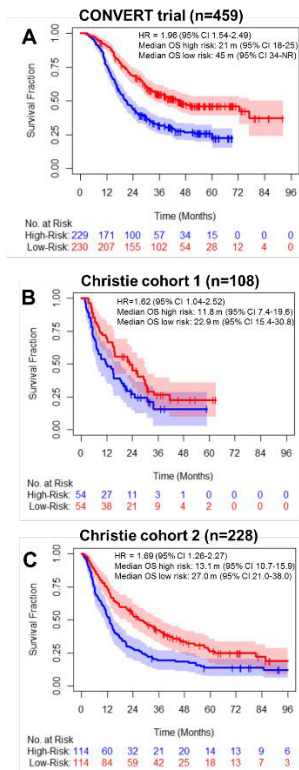
**Table 1:** Baseline characteristics of patients across all groups

	CONVERT (events=278; n=459)	Christie Cohort 1 (events=80; n=108)	Christie Cohort 2 (events=181; n=228)
<b>Age</b>	62 (29-81)	64 (41-84)	71 (36-93)
<b>Gender</b>			
Male	255 (56%)	36 (33%)	102 (45%)
Female	204 (44%)	72 (67%)	126 (55%)
<b>Therapy</b>			
Concurrent CRT	454 (99%)	48 (44%)	0 (0%)
Sequential CRT	2 (<1%)	60 (56%)	0 (0%)
No RT	3 (1%)	0 (0%)	0 (0%)
RT alone <sup>1</sup>	0 (0%)	0 (0%)	228 (100%)
<b>Smoking Status</b>			
Current	163 (36%)	46 (43%)	52 (23%)
Ex	291 (63%)	54 (50%)	39 (17%)
Never	5 (1%)	4 (4%)	1 (<1%)
Unknown	0 (0%)	4 (4%)	136 (60%)
<b>ECOG PS</b>			
0	215 (47%)	18 (17%)	23 (10%)
1	232 (51%)	59 (55%)	115 (50%)
2	12 (3%)	23 (21%)	67 (29%)
3	0 (0%)	8 (7%)	23 (10%)
<b>GTV (cubic cm)</b>			
median (range)	83.8 (0.5-593.0)	36.9 (0.5-535.0)	23.6 (0.1-375.3)
<b>Laterality</b>			
1	126 (27%)	23 (21%)	80 (35%)
2	323 (70%)	85 (79%)	148 (65%)
3	10 (2%)	0 (0%)	0 (0%)
<b>IMRT</b>			
Yes	79 (17%)	83 (77%)	69 (30%)
<b>Linear Predictor -Cox Model</b>			
Median (Range)	1.56 (0.14-2.28)	1.27 (-0.20 - 2.08)	1.05 (-0.74 - 1.97)

<sup>1</sup>: A small number of patients received chemotherapy, in addition to radiotherapy

ECOG PS – Eastern Cooperative Oncology Group Performance Score; GTV – Gross Tumour Volume; RT- Radiotherapy

**Figure 1:** Kaplan-Meier survival curves for CONVERT (A) and Christie cohorts 1 (B) and 2 (C) split into high & low risk groups using the median value derived from final Cox model (GTV, ECOG PS and tumour laterality)



## Conclusion

We report an independently validated LS-SCLC prognostic model from the CONVERT trial, providing information clinicians can relay to patients to aid clinical decisions. The addition of biological covariates could refine this model.

## OC-0063 CREO Project: exploratory radiomics for predicting adaptive radiotherapy in NSCLC

M. Fiore<sup>1</sup>, C. Greco<sup>1</sup>, E. Ippolito<sup>1</sup>, E. Molfese<sup>1</sup>, P. Trecca<sup>1</sup>, M. Miele<sup>1</sup>, E. Cordelli<sup>2</sup>, R. Sicilia<sup>2</sup>, P. Soda<sup>2</sup>, R.M. D'Angelillo<sup>1</sup>, L. Trodella<sup>1</sup>, S. Ramella<sup>1</sup>  
<sup>1</sup>Campus Biomedico University, Department of Radiation Oncology, Roma, Italy; <sup>2</sup>Campus Biomedico University, Research Center in Advanced Biomedicine and Bioengineering, Roma, Italy

## Purpose or Objective

The primary goal of precision medicine is to minimize side effects and optimize efficacy of treatments. Recent advances in medical imaging technology allow the use of more advanced image analysis methods beyond simple measurements of tumor size or radiotracer uptake metrics. The extraction of quantitative features from medical images to characterize tumor pathology or heterogeneity is an interesting process to investigate, in order to provide information that may be useful to guide the therapies and predict survival. The aim of this study was to investigate whether the radiomic features of initial imaging were able to predict tumor reduction during radio- chemotherapy (RCT) in patients with stage III non-small cell lung cancer (NSCLC).

## Material and Methods

We studied 91 patients with stage III NSCLC treated with concurrent RCT: 50 patients were treated at radical dose with adaptive approach (adaptive group), 41 patients underwent radical concurrent RCT in the same period, but who did not achieve target reduction (non-adaptive group). Clinical characteristics of these patients are listed in Table 1. The characteristics investigated were extracted from the initial simulation CT on which the Clinical Target Volume was manually delineated by expert radiation oncologists, providing a 3D ROI. Given each 3D ROI in the images, we computed the radiomic features using our in-house software tool coded in MATLAB (Mathworks Inc, MA, U.S.A.), taking into consideration 12 statistics features and 230 textural features extracted from the CT images. In our study, we used an ensemble learning method to classify patients' data into either the adaptive or non-adaptive group during RCT on the basis of the starting CT simulation. All the experiments were conducted according to a 10-fold cross validation, i.e., a model validation technique which provides a nearly unbiased estimate using only the original data.

	Adaptive group (%) (n=50)	Non-Adaptive group (%) (n=41)	Total (n=91)
Age:			
< 70 years	19 (38%)	18 (44%)	37 (41%)
≥ 70 years	31 (62%)	23 (56%)	54 (59%)
Sex:			
Male	39 (78%)	30 (73%)	69 (76%)
Female	11 (22%)	11 (27%)	22 (24%)
Histology:			
Adenocarcinoma	16 (32%)	23 (56%)	39 (43%)
Squamous	28 (56%)	15 (37%)	43 (47%)
NOS	3 (6%)	3 (7%)	6 (7%)
No histologic subtype available	3 (6%)	0 (0%)	3 (3%)
Stage:			
IIIA	29 (58%)	26 (63%)	55 (60%)
IIIB	21 (42%)	15 (37%)	36 (40%)
Chemo before RCT:			
Yes	23 (46%)	28 (68%)	51 (56%)
No	27 (54%)	13 (32%)	40 (44%)
Concurrent chemo:			
Duplets	19 (38%)	20 (49%)	39 (43%)
Mono	31 (62%)	21 (51%)	52 (57%)

Table 1: Patients' characteristics

## Results

Figure 1 shows the final performance, the area under the receiver operating characteristic curve (AUC). To the best of our knowledge, this is the first trial investigating radiomic strategy to predict tumor shrinkage during RCT and our data suggests that a specific signature can be identified (AUC 0.82).

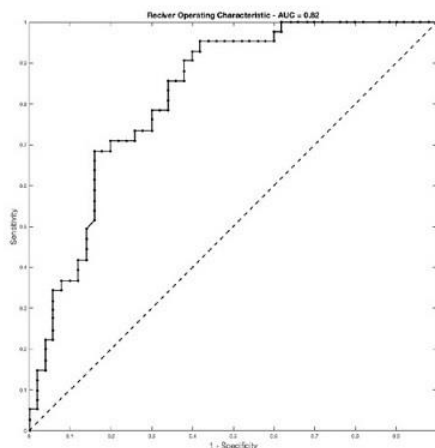


Figure 1: ROC curve of the proposed system

## Conclusion

The initial results of CREO Project obtained are an original and innovative topic that opens up new research in the field of personalized medicine in radiation therapy. The identification of the external validation dataset is actually ongoing.

### OC-0064 Reducing radiotherapy dose to involved lymph nodes in locally advanced NSCLC: efficacy and toxicity.

J. Van Diessen<sup>1</sup>, M. Kwint<sup>1</sup>, J. Sonke<sup>1</sup>, I. Walraven<sup>1</sup>, B. Stam<sup>1</sup>, J. De Langen<sup>2</sup>, J. Belderbos<sup>1</sup>  
<sup>1</sup>Netherlands Cancer Institute, Radiation Oncology, Amsterdam, The Netherlands; <sup>2</sup>Netherlands Cancer Institute, Thoracic Oncology, Amsterdam, The Netherlands

## Purpose or Objective

Radiotherapy for locally advanced non-small lung cancer (LA-NSCLC) causes oesophageal and pulmonary toxicity, which might be severe especially when concurrent chemotherapy is applied. A possible solution to decrease severe toxicities, is dose reduction to the involved lymph nodes, thereby reducing the dose to the mediastinal structures. The reported low incidence of regional (lymph node) failures compared to the primary tumour (6% versus 16%) supports this policy [1]. The goal of this study was to assess the safety and efficacy of a dose reduction to the involved lymph nodes in LA-NSCLC patients receiving (chemo)radiotherapy.

## Material and Methods

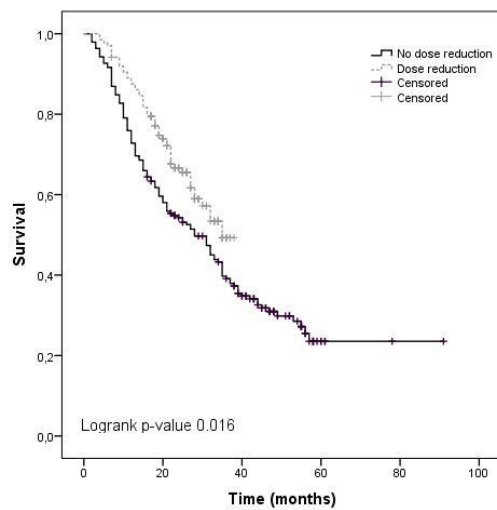
An observational study was performed with a sequential design cohort including 328 patients with LA-NSCLC. Both cohorts received hypofractionated radiotherapy of 24 x 2.75 Gy to the primary tumour. The standard cohort included 191 patients treated between June 2013 and June 2015 with a 24 x 2.75 Gy (EQD<sub>2</sub>=70Gy (α/β=10)) dose scheme to the involved lymph nodes. The dose-reduction cohort (treated from June 2015 until June 2017) consisted of 137 patients who received a reduced dose of 24 x 2.42 Gy (EQD<sub>2</sub>=60Gy (α/β=10)) to the involved lymph nodes. The effect of dose reduction on toxicity and OS was assessed using independent samples t-test, chi-square tests, Logrank and cox regression analyses. Additionally, we assessed whether patient, tumour and treatment characteristics significantly influenced the association between dose reduction and outcomes.

## Results

The median follow-up for the standard cohort and dose reduction cohort was 48 (2-85) and 29 (3-35) months, respectively. Patient and tumor characteristics were comparable between the 2 cohorts. Oes\_V<sub>50</sub> (the volume of the oesophagus receiving ≥50 Gy), mean lung dose (MLD) and mean heart dose were significantly lower in the dose-reduction cohort. The incidence of regional failures was non-significantly lower in the dose-reduction group, 12% versus 7%, respectively (P=0.430). Furthermore, a significantly improved OS was observed in the dose-reduction group, 28 versus 35 months respectively (P=0.016) (Fig 1). Acute toxicity grade ≥2, (dysphagia, pneumonitis, dyspnoea and cough, P=0.001) and late toxicity grade ≥2 (dysphagia, vertebrae fracture and cough, P=0.041) were significantly lower in the dose reduction cohort. MLD significantly influenced the association between dose reduction and OS. Nonetheless, after correction for MLD the independent association remained borderline significant (HR 0.733; 95% CI 0.526-1.021; P= 0.067).

## Figure 1.

Kaplan-Meijer curve for overall survival between the standard and dose reduction cohort.



### Conclusion

In conclusion, a dose reduction from 70 Gy to 60 Gy (EQD<sub>2</sub>) to the involved mediastinal lymph nodes in LA-NSCLC patients receiving (chemo)radiotherapy results in a lower incidence of severe toxicity and an increase OS and is therefore safe and promising. No increase in regional failures was observed.

### OC-0065 Cardiac dose and survival in lung cancer: which cardiac sub-structures matters most?

A. McWilliam<sup>1</sup>, J. Khalifa<sup>2</sup>, E. Vasquez Osorio<sup>1</sup>, A. Abravan<sup>1</sup>, A. Marianne<sup>1</sup>, C. Faivre-Finn<sup>1</sup>, M. Van Herk<sup>1</sup>

<sup>1</sup>University of Manchester, Division of Clinical Cancer Sciences, Manchester, United Kingdom; <sup>2</sup>Institut Universitaire du Cancer de Toulouse, Oncopole, Toulouse, France

### Purpose or Objective

There is increasing evidence that dose to the heart for non-small cell lung cancer (NSCLC) patients impacts overall survival. However, despite the growing body of evidence, cardiac sub-structures where excess dose has the greatest impact on overall survival have not been identified. In this work we implement two variable reduction techniques to identify these sub-structures and estimate radiotherapy dose-limits.

### Material and Methods

14 cardiac sub-structures were delineated on 5 template patients including: atria and ventricles, coronary arteries, valves and pulmonary arteries. 1,100 NSCLC patients were non-rigidly registered to the 5 template patients, mapping their planned radiotherapy dose to the template patient's anatomy. Mean and max dose to each cardiac sub-structure were extracted. Across the 5 template patients, a mean of the mean dose was calculated and the max of the max dose extracted for analysis. The cohort was split into training (2/3 patients) and test (1/3 patients) datasets.

Two variable reduction techniques were implemented: an elastic net LASSO model and a random forest survival model. Each model was optimised to extract the variables that contributed the most to overall survival. Models were tested on their ability to predict overall survival at 1 year in the test dataset, ROC analysis and area under the curve (AUC) calculated. The two most important variables, common to the two models, were selected for further analysis. Multivariate cox-proportional hazard models were created for each identified sub-structure. An optimal split on dose was performed for each variable with Kaplan Meier survival curves plotted for the test dataset to show significance.

### Results

978 patients remained in the analysis after visual inspection of the registration. The training and test datasets were well balanced for clinical parameters. The AUC for the elastic net model and the random forest model was 0.74 and 0.68, respectively. Both models identified the max dose to the right atrium (RA) and right coronary artery (RCA) as the most important factors associated with survival.

The individual multivariate models (table 1) showed both RA and RCA were significant with a hazard ratio (HR) of 1.02,  $p=0.02$ . In both model's (log) tumour volume was significant as well as N-stage. Interestingly, mean lung dose was not significant. The optimal cut point for the RA was 29.5Gy and for the RCA 15.5Gy. As these are neighbouring structures, the max dose was strongly correlated. The mean, 22.5Gy max dose, was applied to the test dataset and Kaplan Meier survival curves for the RA and RCA plotted, figure 1. The log rank for both curves was  $p<0.0001$ .

	Univariate		Multivariate		Multivariate	
	HR (95% CI)	p	HR (95% CI)	p	HR (95% CI)	p
Right coronary Max dose (continuous)	1.02 (1.01-1.02)	<0.001	1.02 (1.00-1.03)	0.02		
Right Atrium Max dose (continuous)	1.02 (1.01-1.03)	<0.001			1.01 (1.00-1.03)	0.02
Tumour size (log) (continuous)	1.34 (1.24-1.45)	<0.001	1.20 (1.02-1.40)	0.02	1.21 (1.03-1.41)	0.02
Age (continuous)	1.01 (1.00-1.01)	0.32	1.02 (1.00-1.04)	0.01	1.02 (1.00-1.04)	0.02
Mean lung dose (continuous)	1.06 (1.04-1.08)	<0.001	0.99 (0.94-1.05)	0.84	0.99 (0.93-1.05)	0.66
Gender (male vs. female)	1.14 (0.96-1.35)	0.13	1.05 (0.78-1.41)	0.76	1.07 (0.80-1.43)	0.64
Induction Chemotherapy (yes vs. no)	1.08 (0.89-1.31)	0.43	0.99 (0.67-1.45)	0.95	0.98 (0.67-1.45)	0.93
T-Stage (T1 ref)						
T2	1.32 (0.98-1.76)	0.06	0.69 (0.44-1.07)	0.10	0.74 (0.48-1.15)	0.19
T3	1.67 (1.23-2.27)	>0.01	0.70 (0.43-1.14)	0.15	0.72 (0.45-1.17)	0.19
T4	1.66 (1.19-2.32)	>0.01	0.69 (0.38-1.24)	0.21	0.62 (0.34-1.14)	0.12
N-stage (N0 ref)						
N1	0.99 (0.75-1.31)	0.95	1.27 (0.80-2.04)	0.32	1.28 (0.80-2.05)	0.29
N2	1.45 (1.18-1.79)	>0.01	1.68 (1.17-2.41)	0.01	1.57 (1.10-2.26)	0.01
N3	1.60 (1.15-2.24)	>0.01	1.24 (0.66-2.36)	0.50	1.30 (0.69-2.46)	0.42
Performance status (PS0 ref)						
1	1.30 (0.98-1.71)	0.06	0.93 (0.55-1.55)	0.78	0.98 (0.59-1.64)	0.94
2	1.55 (1.17-2.06)	>0.01	1.13 (0.67-1.92)	0.64	1.25 (0.74-2.12)	0.40
3	1.82 (1.21-2.73)	>0.01	1.51 (0.74-3.08)	0.26	1.46 (0.71-2.99)	0.30

Table 1. Uni-variate and multi-variate analysis including the two cardiac sub-structures identified using the variable reduction techniques. Log tumour volume and available clinical covariates are included in the analysis.

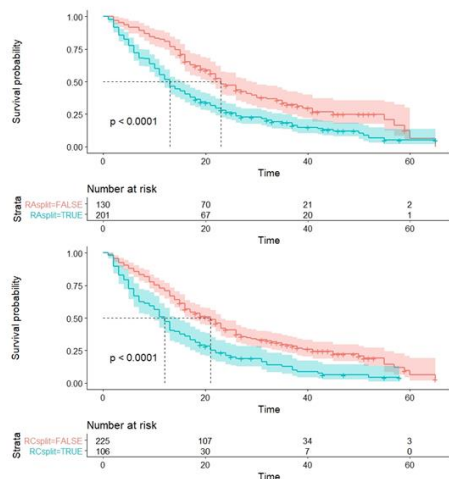


Figure 1. Kaplan Meier survival curves showing the survival difference split as patients receiving greater than or less than 22.5Gy, plotted for the test dataset. Patients receiving greater than 22.5Gy do significantly worse for overall survival.

## Conclusion

We have identified the max dose to the right atrium and right coronary artery as the cardiac sub-structures responsible for the greatest dose-related impact on patient survival. A max dose of 22.5Gy was identified and should be considered for these as avoidance structures in future planning studies.

Proffered Papers: CL 2: Proffered papers Haematology, Sarcoma and oligometastases

OC-0066 Effectiveness of radiotherapy for patients not in metabolic remission after chemotherapy for DLBCL

J. Brady<sup>1</sup>, N.G. Mikhaeel<sup>1,2</sup>

<sup>1</sup>Guy's and St. Thomas' NHS Foundation Trust, Department of Clinical Oncology, London, United Kingdom; <sup>2</sup>King's College, Division of Cancer Studies, London, United Kingdom

## Purpose or Objective

Persistent metabolic activity on 18-FDG PET-CT at completion of first-line chemotherapy in diffuse large B cell lymphoma (DLBCL) is associated with poor prognosis. Fit patients can be offered salvage high-dose therapy if refractory disease is confirmed, but there is no standard treatment for less fit patients.

Radiotherapy is as an effective treatment for DLBCL and commonly used as part of planned combined modality treatment for localised disease. Its value in patients with localised refractory disease remains to be defined. In this study we aim to evaluate to outcome for patients with incomplete metabolic response (Deauville score 4-5) following first-line chemotherapy who underwent RT to sites of persistent activity.

## Material and Methods

We performed a retrospective review of all patients with DLBCL who received RT at our institution having not achieved a complete metabolic response after first-line chemotherapy. This was defined as a Deauville Score (DS) of 4 or 5 on PET-CT. Eligible patients received RT to a radical dose ( $\geq 30$ Gy in 1.8-2Gy fractions). We collected data on patient, disease and treatment characteristics. Outcomes included relapse rate, site of relapse, time to progression and overall survival (OS). Post radiotherapy PET-CT response was also recorded.

## Results

41 patients who received RT between March 2011 and July 2018 were identified. Patient and disease characteristics are shown in the table below.

Table. Patient and treatment characteristics

Male	21 (51.2%)
Female	20 (48.8%)
Median Age /years (range)	64 (21-89)
Histopathology	
Germinal centre (GC)	17 (41.5%)
Non GC	8 (19.5%)
PMBCL	6 (14.6%)
NOS	10(24.4%)
Stage	
1	4 (9.8%)
2	19 (46.3%)
3	5 (12.2%)
4	13 (31.7%)
IPI	
0-1	16 (39%)
2	9 (22%)
3	8 (19.5%)
4-5	8 (19.5%)
Median no chemotherapy cycles (range)	6 (3-8)
Chemotherapy regimen	
R miniCHOP	8 (19.5%)
RCHOP	29 (70.7%)
RGCVP/RCVP	3 (7.3%)
LMB -B	1 (2.4%)
End of chemotherapy Deauville score	
4	32 (78%)
5	9 (22%)
Radiotherapy dose	
30Gy/30.6Gy	24 (58.5%)
36Gy	13 (31.7%)
40GY	4 (9.8%)

With median 24.3 months of follow up from completion of RT (range 1.7-78.5), 13/41 patients have relapsed/progressed (31.7%). 8 relapses were out of field, 3 both in and out of field and 2 progressed in field only. Median time from completion of RT to progression was 4.0 months (0.8-51).

Of patients with relapsed/progressive disease, 6 received salvage high-dose chemotherapy, and 3 are alive and in

remission. Median OS for all patients was 75 months (1.64-78.5). Median OS for patients with relapsed/progressive disease was 13 months (1.64-74.5).

Deauville score (DS) prior to RT was predictive of relapse risk. 5/9 patients (55.6%) with DS 5 post chemotherapy have relapsed/progressed compared to 8/32 (25%) of those with DS 4.

Response assessment PET-CT scans after RT were performed in 38/41 (92.6%) patients. 18 patients (47.4%) achieved a complete metabolic response (DS 2 or 3), 10 (26.3%) a partial metabolic response (DS 4) and 10 (26.3%) had DS 5. 9/10 (90%) patients with DS 5 post RT have clinically progressed. Only 1/10 (10%) patients with DS4 post RT has progressed.

### Conclusion

Our experience suggests that the majority of patients with an incomplete metabolic response, will not relapse following radiotherapy to the PET positive site. Relapses/progressions were more common in patients with Deauville Score 5 at end of chemotherapy, but a proportion can be successfully salvaged by RT.

### OC-0067 Continuous Positive Airway Pressure (CPAP): an innovative respiratory gating in lymphoma patients

M. Levis<sup>1</sup>, P. Solidoro<sup>2</sup>, S. Bartoncini<sup>1</sup>, E. Gallio<sup>3</sup>, F.R. Giglioli<sup>3</sup>, V. De Luca<sup>4</sup>, L. Focaraccio<sup>2</sup>, C. Cavallin<sup>4</sup>, G.C. Iorio<sup>4</sup>, R. Parise<sup>4</sup>, C. Palladino<sup>4</sup>, V. Di Martino<sup>4</sup>, G. Furfaro<sup>4</sup>, G. Rovere<sup>2</sup>, A. Mattei<sup>2</sup>, R. Ragona<sup>4</sup>, U. Ricardi<sup>4</sup>  
<sup>1</sup>A.O.U. Città della Salute e della Scienza, Radiation Oncology, Torino, Italy ; <sup>2</sup>A.O.U. Città della Salute e della Scienza, Pulmonology, Torino, Italy ; <sup>3</sup>A.O.U. Città della Salute e della Scienza, Medical Physics Unit, Torino, Italy; <sup>4</sup>University of Turin, Department of Oncology, Torino, Italy

### Purpose or Objective

Respiratory gating techniques, as deep inspiration breath holding (DIBH), are strongly encouraged for lymphoma patients with mediastinal involvement in reason of their ability in reducing the dose to normal tissues and to minimize the risk of long term complications. With this background, we aimed to investigate the potential role of Continuous Positive Airway Pressure (CPAP), as an alternative to DIBH, by comparing this innovative respiratory gating with free-breathing (FB) approach in Hodgkin lymphoma (HL) and primary mediastinal lymphoma (PMBCL) patients treated with an optimized volumetric arc therapy (VMAT) solution.

### Material and Methods

After institutional review board approval, 23 patients (9 males and 14 females; mean age 28 years, range 16-38) affected with mediastinal HL (18) or PMBCL (5) were included. All patients underwent computed tomographic simulation twice: with FB and with CPAP. The CPAP pressure used was 18 cm H<sub>2</sub>O for each patient. Median prescription dose to the PTV was 30 Gy in 2-Gy fractions (range 30-40 Gy). Lungs, female breasts, heart and cardiac structures (coronary arteries, valves, atria and ventricles) were all contoured as organs at risk and included in the optimization process of the same VMAT solution in FB or with CPAP for each patient. Maximum and mean dose were compared for all organs and CPAP was used during treatment if judged beneficial. Second breast and lung cancer risks were estimated by calculating the lifetime attributable risk (LAR). Coronary artery disease (CAD) and chronic heart failure (CHF) risks were estimated by calculating the relative risk (RR). CAD risk was derived from the mean dose received by the sum of coronary arteries, while CHF was derived from the mean dose received by the left ventricle, as recently published.

### Results

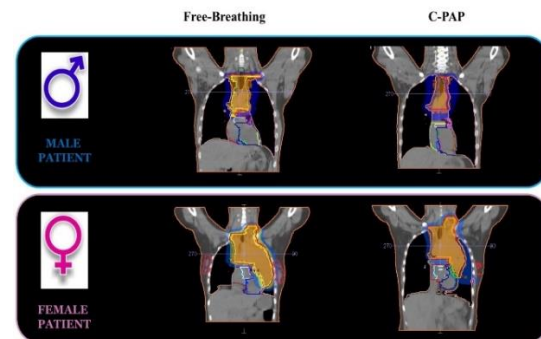
CPAP was well tolerated by all patients. Only one had no benefit from the addition of CPAP and received treatment in FB. CPAP increased mean lungs volume (4.21 vs 2.71 liters, p<0.01) and significantly reduced both lungs

V<sub>20Gy</sub> and V<sub>5Gy</sub> (p<0.01). Moreover, CPAP decreased the intersection between whole heart and PTV volumes (p<0.01) and resulted in lower dose to heart (p<0.01), whole coronary arteries (p<0.01), left ventricle (p<0.01) and aortic valve (p<0.01). Breast V<sub>4</sub> was similar for FB and CPAP (p=0.20). Dose parameters are reassumed in the table. Significant lower RR for CAD (p<0.01) and CHF (p<0.01) were observed for CPAP, with a mean 22% and 8% risk reduction, respectively. LAR for lung cancer was lower with CPAP (p<0.01), while LAR for second breast cancer was similar for CPAP and FB (p=0.81).

Table: Dose parameters comparison between Free-Breathing and C-PAP

Structure	Parameter	Free-Breathing	C-PAP	Wilcoxon test p-value	
PTV COVERAGE	V95	95.3%	95.2%	ns	
	Overall Volume (cc)	2.710	4.210	<0.01	
	V <sub>5Gy</sub>	12.9%	10.4%	<0.01	
LUNGS	V <sub>5Gy</sub>	40.6%	34.5%	<0.01	
	Life attributable risk (LAR)	240.9	207.7	<0.01	
	Intersection Heart/PTV	26.9	12.5	<0.01	
WHOLE HEART	Max dose	32.8 Gy	32.5 Gy	ns	
	Mean dose	5.3 Gy	3.9 Gy	<0.01	
CORONARY ARTERIES	1- Left main trunk	Max dose: 16.5 Gy Mean dose: 12.6 Gy	12.9 Gy 8.9 Gy	<0.01	
	2- Circumflex	Max dose: 15.5 Gy Mean dose: 7.4 Gy	11.2 Gy 4.9 Gy	<0.01	
	3- Left descending	Max dose: 22.4 Gy Mean dose: 10.1 Gy	17.6 Gy 7.2 Gy	<0.01	
	4- Right coronary	Max dose: 19.3 Gy Mean dose: 8.9 Gy	14.1 Gy 6.2 Gy	<0.01	
	5- Coronary SUM (overall)	Max dose: 22.6 Gy Mean dose: 3.2 Gy	19.0 Gy 2.1 Gy	<0.01	
	Relative Risk (for coronary events)	3.7	2.9	<0.01	
	LEFT VENTRICLE	Max dose	22.6 Gy	19.0 Gy	<0.01
		Mean dose	3.2 Gy	2.1 Gy	<0.01
		Relative Risk (for chronic failure)	1.29	1.19	<0.01
	AORTIC VALVE	Max dose	21.1 Gy	16.6 Gy	<0.01
Mean dose		10.5 Gy	6.9 Gy	<0.01	
BREASTS	Max dose	28.5 Gy	24.9 Gy	<0.01	
	Mean dose	4.25 Gy	3.71 Gy	ns	
BREASTS	V <sub>4Gy</sub>	28.9%	23.8%	ns	
	Life attributable risk (LAR)	83.2	82.1	0.81	

Figure: comparison between CPAP and free-breathing in a male and in a female patient



### Conclusion

In this pilot study, we first demonstrated the contribution of CPAP to a reduction in lungs and heart structures dose, with a significant impact on long term complications. CPAP was well tolerated, simple to implement, reproducible and does not require breath-holding. In our opinion, CPAP should be further implemented as a novel strategy for motion management and respiratory gating in lymphoma patients.

### OC-0068 MR-guided adaptive radiotherapy for intra-abdominal lymphoma

F. Spoelstra<sup>1</sup>, P. Cobussen<sup>1</sup>, M. Palacios<sup>1</sup>, A. Bruynzeel<sup>1</sup>, F. Lagerwaard<sup>1</sup>, B. Slotman<sup>1</sup>, S. Senan<sup>1</sup>  
<sup>1</sup>VU University Medical Center, Radiation Oncology, Amsterdam, The Netherlands

### Purpose or Objective

Radiotherapy for intra-abdominal lymphoma may be impaired by geographic misses arising from variations in gastric filling, bowel movement, or respiratory motion. Larger PTV margins are therefore used, resulting in

unnecessary doses to organs at risk. Despite use of larger PTV margins, verification of tumor position is essential. However, visualization of intra-abdominal tumor position is suboptimal using cone-beam CT scans. Daily MR-guidance can enable improved tumor verification, and adaptive radiotherapy may also allow for optimal target coverage. We report on our initial experience of MR-guided adaptive radiotherapy in intra-abdominal lymphoma patients.

#### Material and Methods

Five patients underwent both a planning CT and MRI scan (MRIdian; ViewRay Inc) during shallow inspiration breath hold after at least 3 hours of fasting. The gross tumor volume (GTV) was contoured on the planning MR, and a planning target volume (PTV) generated using a 10 mm margin. The liver, kidneys, spinal cord, and spleen were contoured as avoidance structures for initial treatment planning, but were not contoured daily due to low doses used. Daily breath-hold MR scans were performed before each fraction, and the GTV was manually adjusted when necessary. Re-optimized plans were routinely created and compared to the original plan that was recalculated on the anatomy of the day. Clinicians selected the most optimal of both plans. Treatment was delivered during video-assisted breath-hold based on tracking of the GTV, using the PTV as gating boundary. Inter-fractional changes in GTV were assessed, and the frequency of using re-optimized plans and the rationale for this were analyzed.

#### Results

Five patients, of whom three had a gastric lymphoma and two a mesenteric lymphoma, have been treated with MR-guided adaptive radiotherapy. A total of 67 MR-guided fractions were delivered, with total doses ranging from 24-36 Gy in 12-18 fractions. Daily adjustment of the GTV was performed in 4 patients (49 fractions), with mean GTVs ranging from 244cc to 296cc. Limited inter-fractional changes in GTV were seen in 3 patients, with relative GTV differences between the mean and 10<sup>th</sup>-90<sup>th</sup> percentiles of <11%. The relative difference was 38% in the fourth patient, because fasting instructions were not complied with. Re-optimized plans were superior to recalculated original plans in each fraction studied, with the reason being reduced PTV coverage in 4 patients (mean V95% of 85%, 10<sup>th</sup>-90<sup>th</sup> percentile: 74%-95%). In another patient, the recalculated original plan would have led to a V107% >5% in 12 fractions, whereas inadequate PTV coverage was the reason for using the re-optimized plans in the remaining 8 treatment fractions.

#### Conclusion

MRI guided treatment of intra-abdominal lymphoma allows for improved visualization of the GTV and permits daily plan re-optimization, which led to superior PTV coverage and reduction in plan inhomogeneity.

**OC-0069 5x5 Gy with chemotherapy in borderline resectable soft tissue sarcomas: early results of a trial**  
 M. Spalek<sup>1</sup>, H. Koseta-Paterczyk<sup>1</sup>, A. Borkowska<sup>1</sup>, M. Wągródzki<sup>2</sup>, A. Szumera-Ciećkiewicz<sup>2</sup>, A. Cieszanowski<sup>3</sup>, P. Castaneda-Wysocka<sup>3</sup>, T. Świtaj<sup>1</sup>, M. Dudzisz-Śledź<sup>1</sup>, A. Czarnecka<sup>1</sup>, E. Dąbrowska-Szewczyk<sup>4</sup>, P. Rutkowski<sup>1</sup>  
<sup>1</sup>Maria Skłodowska-Curie Institute - Oncology Center, Department of Soft Tissue/Bone Sarcoma and Melanoma, Warsaw, Poland; <sup>2</sup>Maria Skłodowska-Curie Institute - Oncology Center, Department of Pathology and Laboratory Diagnostics, Warsaw, Poland; <sup>3</sup>Maria Skłodowska-Curie Institute - Oncology Center, Department of Radiology I, Warsaw, Poland; <sup>4</sup>Maria Skłodowska-Curie Institute - Oncology Center, Department of Medical Physics, Warsaw, Poland

#### Purpose or Objective

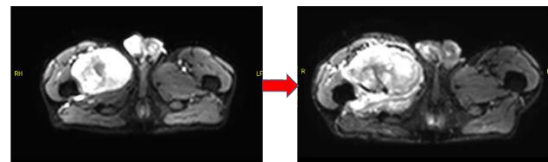
There is a lack of standard treatment of unresectable and marginally resectable sarcomas (STS). Results of commonly used approaches are unsatisfactory. The addition of neoadjuvant/induction chemotherapy before

the irradiation and in the prolonged gap between the end of hypofractionated 5x5 Gy radiotherapy and surgery may allow to obtain the R0 resection rate, high pathological response rate and/or a higher rate of limb-sparing/conservative surgery as well as to increase patients' survival.

#### Material and Methods

A single-arm prospective clinical trial was conducted (NCT03651375). Treatment consisted of one cycle of doxorubicin and ifosfamide (AI), then 5x5 Gy RT, and two cycles of AI in seven-eight weeks gap between the end of RT and surgery. STS response was assessed in DWI-MR imaging (Fig. 1) and pathologically by EORTC STBSG criteria. The primary endpoint is rate of limb-sparing surgeries and R0 resections.

**Figure 1.** UN-RESARC – MRI evaluation of STS response to the treatment

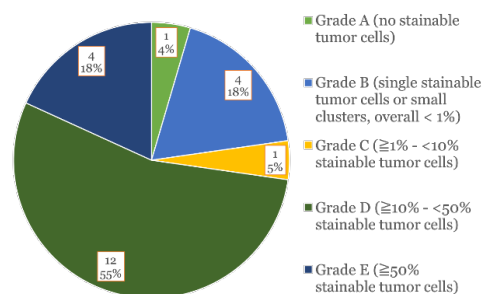


**Description of DWI-MRI after preoperative treatment:** The tumour located in the middle thigh compartment of the right thigh is slightly larger, but it contains slightly larger areas of necrosis and bleeding. Large oedema in the surrounding soft tissues - probably after treatment. The tumour shows smaller areas and less intensive diffusion restriction (the areas of increased signal in ADC) - which suggests a response to the treatment.

#### Results

30 patients(pts) met eligibility criteria, 23 received the whole planned protocol treatment, four are currently receiving the treatment, in three pts the treatment was prematurely stopped. 23 pts underwent limb-sparing or conservative surgery, 3 pts underwent extremity amputation, two after 1st AI cycle due to poor tolerance, one due to extensive tumour invasion without a possibility of vessels reconstruction. Among patients who underwent conservative treatment, in 15 of them resection margin was R0, in 7 pts R1. One toxic death occurred outside our centre related to severe bone marrow suppression with septic shock after the second AI cycle. Early tolerance of chemotherapy was acceptable. Grade 3+ CTCAE4.03 toxicity occurred in 11 pts. Early RT tolerance was good. EORTC grade 1 radiation dermatitis occurred in 14 and grade 2 in three pts. Postoperative wound complications occurred in 7 pts, in two were severe. Very good pathological response (<1% of stainable tumour cells; grade A/B) was found in 5 pts (Fig. 2). Good pathological response (<50% tumour cells; grade C/D) was found in 13 pts (Fig. 2).

**Figure 2.** Evaluation of response after preoperative treatment according to EORTC-STBSG recommendations for pathological examination



#### Conclusion

Preoperative AI combined with hypofractionated radiotherapy is a feasible method of the management of

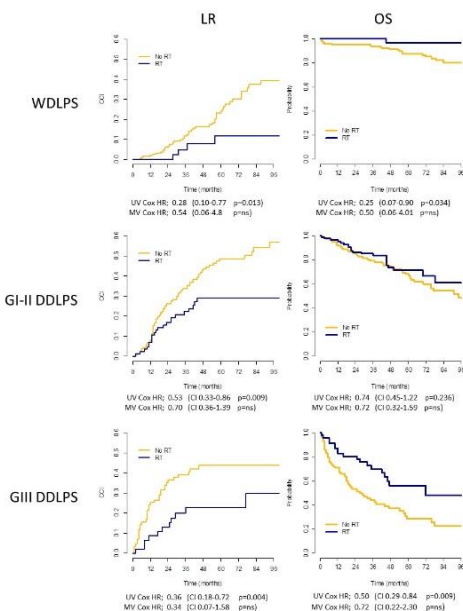
marginally resectable STS. It provides good pathological responses in advanced STS with acceptable treatment toxicity.

#### OC-0070 Radiation Therapy for Retroperitoneal Liposarcoma - A report from TARPSWG

R. Haas<sup>1</sup>, S. Bonvalot<sup>2</sup>, R. Miceli<sup>3</sup>, D. Strauss<sup>4</sup>, C. Swallow<sup>5</sup>, P. Hohenberger<sup>6</sup>, F. Van Coevorden<sup>7</sup>, P. Rutkowski<sup>8</sup>, D. Callegaro<sup>9</sup>, A. Hayes<sup>4</sup>, C. Honoré<sup>10</sup>, M. Fairweather<sup>11</sup>, R. Gladdy<sup>5</sup>, J. Jakob<sup>6</sup>, M. Szacht<sup>8</sup>, M. Fiore<sup>9</sup>, P. Chung<sup>12</sup>, W. Van Houdt<sup>7</sup>, C. Raut<sup>11</sup>, A. Gronchi<sup>9</sup>  
<sup>1</sup>Netherlands Cancer Institute, Radiotherapy, Amsterdam, The Netherlands; <sup>2</sup>Institute Curie, Department of Surgery, Paris, France; <sup>3</sup>Fondazione IRCCS Istituto Nazionale dei Tumori, Unit of Clinical Epidemiology and Trial Organization, Milan, Italy; <sup>4</sup>Royal Marsden Hospital NHS Foundation Trust, Department of Surgery, London, United Kingdom; <sup>5</sup>Mount Sinai Hospital and Princess Margaret Cancer Centre, Department of Surgical Oncology, Toronto, Canada; <sup>6</sup>University Medical Center Mannheim- University of Heidelberg, Division of Surgical Oncology & Thoracic Surgery, Heidelberg, Germany; <sup>7</sup>Netherlands Cancer Institute, Department of Surgical Oncology, Amsterdam, The Netherlands; <sup>8</sup>Maria Sklodowska-Curie Institute - Oncology Center, Department of Soft Tissue/Bone Sarcoma and Melanoma, Warsaw, Poland; <sup>9</sup>Fondazione IRCCS Istituto Nazionale dei Tumori, Department of Surgery, Milan, Italy; <sup>10</sup>Institute Gustave Roussy, Department of Surgery, Villejuif, France; <sup>11</sup>Brigham and Women's Hospital and Center for Sarcoma and Bone Oncology- Dana-Farber Cancer Institute- Harvard Medical School, Department of Surgery, Boston, USA; <sup>12</sup>Mount Sinai Hospital and Princess Margaret Cancer Centre, Radiation Medicine Program, Toronto, Canada

#### Purpose or Objective

This study investigates the role of radiotherapy (RT) in patients with primary non-metastatic retroperitoneal liposarcomas.



#### Material and Methods

607 patients with localized retroperitoneal WDLPS and DDLPS were resected with or without RT at 8 high-volume sarcoma centers: 234 WDLPS, 242 GI-II DDLPS and 131 GIII DDLPS. RT was applied in 19.7%, 34.7% and 35.1% of these cohorts respectively. Overall survival (OS) was estimated by Kaplan-Meier method, and the incidences of local recurrence (LR) and distant metastasis (DM) were

estimated in a competing-risk framework. To account for bias consistent with non-random RT-assignment, propensity scores were estimated. Cox univariable analyses of association between RT and oncological endpoints was performed by applying inverse-probability-of-treatment-weight (IPTW) using propensity scores.

#### Results

Age, tumor size, and chemotherapy administration were significantly imbalanced between irradiated and unirradiated patients in all cohorts. IPTW removed all imbalances in key prognostic variables. The 8-year LR incidence in surgery + RT versus surgery only was 11.8% and 39.2% (p=0.011; WDLPS), 29.0% and 56.7% (p=0.008; grade I-II DDLPS), and 29.8% and 43.7% (p=0.025; grade III DDLPS), respectively, however this significant benefit was lost after IPTW-analyses. There were no significant differences in DM and OS between irradiated and unirradiated patients across all three cohorts.

#### Conclusion

Perioperative RT was associated with better LC on univariable unadjusted analyses in all cohorts, but not after accounting for imbalances in prognostic variables. RT did not impact on DM or OS. Appropriate selection of RT in this disease remains challenging. Results of the EORTC-STBSG 62092/22092 study are awaited.

#### OC-0071 Stereotactic radiotherapy for nodal recurrences: an interim analysis from two phase I trials

F. Deodato<sup>1</sup>, S. Cilla<sup>2</sup>, A. Ianiro<sup>2</sup>, V. Picardi<sup>1</sup>, M. Ferro<sup>1</sup>, M. Boccardi<sup>1</sup>, G. Tolento<sup>3</sup>, R. Cardano<sup>3</sup>, S. Cammelli<sup>3</sup>, P. Assalone<sup>4</sup>, M. Buwenge<sup>3</sup>, G.C. Mattiucci<sup>5</sup>, V. Valentini<sup>5</sup>, A.G. Morganti<sup>3</sup>, G. Macchia<sup>1</sup>

<sup>1</sup>Fondazione di Ricerca e Cura "Giovanni Paolo II"- Università Cattolica S. Cuore, Radiotherapy Unit, Campobasso, Italy; <sup>2</sup>Fondazione di Ricerca e Cura "Giovanni Paolo II"- Università Cattolica S. Cuore, Medical Physics Unit, Campobasso, Italy; <sup>3</sup>Radiation Oncology Center, Dept. of Experimental- Diagnostic and Specialty Medicine - DIMES- University of Bologna-S. Orsola-Malpighi Hospital, Bologna, Italy; <sup>4</sup>Veneziale Hospital, Oncology Unit, Isernia, Italy; <sup>5</sup>Policlinico Universitario "A. Gemelli"- Università Cattolica del Sacro Cuore, Department of Radiotherapy, Roma, Italy

#### Purpose or Objective

Stereotactic body radiotherapy (SBRT) has been shown to achieve high local control rates in limited metastatic burden of disease. Few papers reported on the efficacy of SBRT in limited nodal metastases. The primary aim was to review institutional outcomes of patients with solitary or oligometastatic lymph nodes treated with SBRT.

#### Material and Methods

Data from DESTROY-1 phase I and SRS-DESTROY-2 phase I clinical trials were reviewed and analyzed. These trials were a 5 fractions SBRT trial and a single fraction radiosurgery study, respectively (Figure 1). End-points were the detection of toxicities, overall response rate (ORR), and local control (LC). Tumor response was assessed according to the RECIST and EORTC PET criteria. Patients with all metastatic sites, primary tumor types and histologies were included between December 2003 and January 2018.

**Dose Escalation STereotactic RadiOtherapy 1**

Level	Lung/extra-pulmonary tumors	Para-thoracic tumors or tumors near chest wall	Extra-thoracic tumors	Re-irradiation		ESRT boost	
				with prior radiotherapy > 60 Gy or re-irradiation of parotid or pelvic cancer	with prior radiotherapy > 60 Gy	after RT dose < 50 Gy	after RT dose > 50 Gy
1	25 Gy	25 Gy	25 Gy	20 Gy	25 Gy	25 Gy	20 Gy
2	37.5 Gy	30 Gy	30 Gy	25 Gy	30 Gy	30 Gy	25 Gy
3	45 Gy	35 Gy	35 Gy	30 Gy	35 Gy	35 Gy	30 Gy
4	50 Gy	40 Gy	40 Gy	35 Gy	40 Gy	40 Gy	35 Gy
5	45 Gy	45 Gy	45 Gy	40 Gy	45 Gy	45 Gy	40 Gy
6	50 Gy	50 Gy	50 Gy	45 Gy	50 Gy	50 Gy	45 Gy

**VMAT based Dose Escalated Stereotactic RadiOtherapy 2 (Radiosurgery)**

Level	Lung	Liver	Bone	Advanced	Vertebrae (after 25 Gy)
1	26 Gy/	26 Gy	12 Gy	16 Gy	8 Gy
2	28 Gy	28 Gy	14 Gy	18 Gy	10 Gy
3	30 Gy	30 Gy	16 Gy	20 Gy	12 Gy
4	32 Gy	32 Gy	18 Gy	22 Gy	
5	34 Gy		20 Gy	24 Gy	
6			22 Gy		
7			24 Gy		

**Results**

180 patients (M/F: 94/86); median age: 67, range 37-88) treated with SBRT for a total of 253 nodal recurrences were analyzed. Patients with different cancer types were included in the analysis, in particular the primary were: gynaecological (N°=49; 27.2%), prostatic (N°=38; 21.1%), gastrointestinal (N°=25; 13.9%), lung (N°=22;12.2%), breast (N°=16; 8.9%), genito-urinary (N°=12; 6.7%), head and neck (N°=11; 6.1%) and skin tumours (N°=7; 3.9%). The most common metastatic sites were the thorax (N°=92; 36.4%) and the pelvis (N°=88; 34.8%), followed by abdominal (N°=61; 24.1%) and neck regions (N°=12; 4.7%). The majority of lesions (79.8%) were treated with VMAT technique, while the former by 3DCRT or IMRT techniques. Dose prescription to the Planning Target Volume varied from 12 Gy/single fraction to 50 Gy/5 fractions. With a median follow-up of 21 months (2-124) no grade 3 acute or late toxicity was recorded. ORR based on CT/MRI/PET was 79.8 % (CI 95%: 73.3-85) with a complete response rate of 57.7% (CI 95%: 50.3-64.5). 24- and 48-months actuarial local control (freedom from progression in the irradiated site) was 81.3% and 69.6%, respectively.

**Conclusion**

These data on a large series of lymph node recurrences in oligometastatic patients demonstrate low risk of morbidity after SBRT and favourable long term local control

**OC-0072 Clinical outcomes of stereotactic MR-guided adaptive radiation therapy for adrenal oligo-metastases**

P. Cobussen<sup>1</sup>, M.A. Palacios<sup>1</sup>, F.O.B. Spoelstra<sup>1</sup>, I. Bahce<sup>2</sup>, A.M.E. Bruynzeel<sup>1</sup>, S.M.S. Hashemi<sup>2</sup>, A. Becker - Commissaris<sup>2</sup>, N.J. Haasbeek<sup>1</sup>, B.J. Slotman<sup>1</sup>, F.J. Lagerwaard<sup>1</sup>, S. Senan<sup>1</sup>

<sup>1</sup>VU University Medical Center, Radiation Oncology, Amsterdam, The Netherlands; <sup>2</sup>VU University Medical Center, Pulmonology, Amsterdam, The Netherlands

**Purpose or Objective**

Patients presenting with 1-5 distant metastases, so-called oligo-metastases, can have a survival benefit if all lesions are treated using stereotactic ablative radiotherapy (SABR). The delivery of SABR to adrenal metastases can be challenging due to respiration-induced organ motion and proximity of organs at risk (OAR). Consequently, lower radiation doses are often delivered to minimise the risk of toxicity, even though lower doses may be correlated with a worse local control. We implemented stereotactic magnetic resonance-guided adaptive radiation therapy (SMART) for abdominal tumors aiming for a BED 100 Gy<sub>10</sub>, and report on clinical outcomes in adrenal oligo-metastases.

**Material and Methods**

All patients treated for adrenal oligo-metastases on the MRIdian system (ViewRay Inc.) at our institution until June 2018 were included. The OAR and GTV's were contoured on a breath-hold planning MR, and a planning target volume (PTV) was created by adding a 3mm margin to the GTV, but excluding luminal OAR's (see figure). Relevant high dose OARs were stomach, bowel and ipsilateral kidney. A robust baseline plan was generated for daily adaptation. Our institutional protocol mandates accepting underdosage inside the PTV if deemed necessary to meet high dose OAR constraints (see figure). All patients underwent daily on-table MR-imaging before treatment, and to optimise delivery, a new on-table treatment plan was generated based on the anatomy-of-the-day. Gated SMART was delivered during repeated voluntary video-assisted breath-holds, with continuous tracking of the GTV and using the PTV as gating boundary. We analysed toxicity, local control (LC), disease free- and overall survival (DFS, OS).

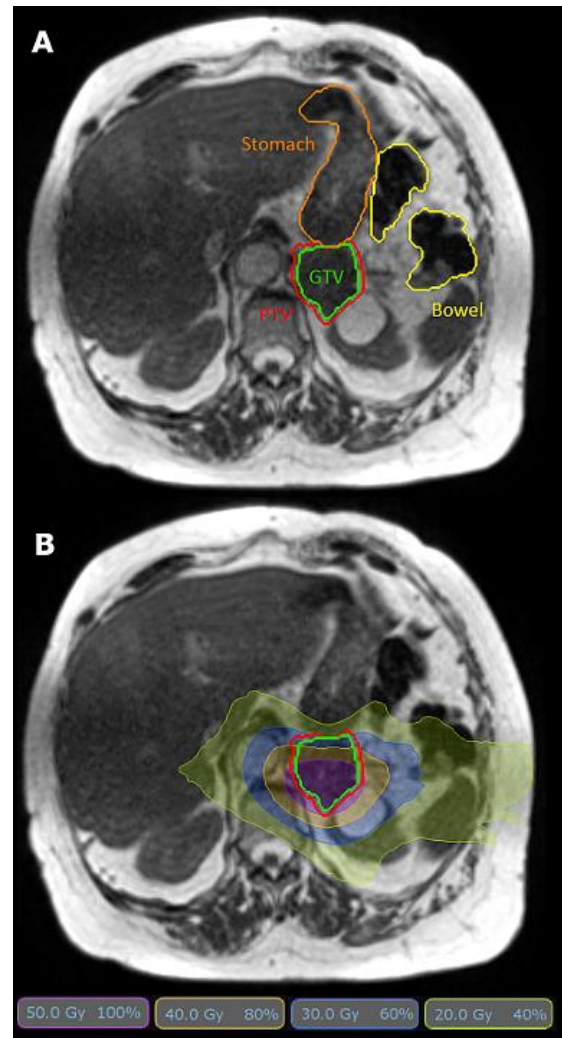


Figure. MR-scan of an adrenal gland metastasis patient showing relevant OARs (A). Dose distribution of a SMART treatment plan showing sparing of the stomach (B).

**Results**

Twenty-five patients underwent SMART for an adrenal oligo-metastasis (68% left-sided). Median patient age was 62 years, and the commonest primary tumor was lung cancer (72% NSCLC, 12% SCLC). The majority (64%) received a dose of 50 Gy in 5 fractions, with total doses

ranging from 24-60 Gy in 3-8 fractions. Thirty-two percent of patients received concurrent immunotherapy or targeted therapies. Median follow-up was 11.6 months. In 48% of patients, acute grade 1-2 toxicities (CTCAE v4) were reported, mostly fatigue and nausea. Acute grade 3 nausea and weight loss were observed in one patient. Another developed a lumbar insufficiency fracture six months post-SMART, a possible late grade 3 adverse event. Only one in-field tumor recurrence was observed eight months post-SMART, resulting in a 1-year LC of 93%. The 1-year DFS and OS rates were 47% and 76%, respectively.

#### Conclusion

Delivery of SMART to adrenal oligo-metastasis is associated with limited acute toxicity, even in a cohort where 32% of patients received concurrent immune and targeted therapies. Local control rates are promising, but long-term follow-up is awaited.

### Proffered Papers: BT 1: Treatment verification

#### OC-0073 BrachyView: A Real-time In-body HDR Source Tracking System with Simultaneous TRUS Image Fusion

S. Alnaghy<sup>1</sup>, D. Cutajar<sup>1</sup>, M. M. Safavi-Naeini<sup>1</sup>, G. Stuart<sup>1</sup>, H. Andrew<sup>2</sup>, A. Bece<sup>2</sup>, J. Jakubek<sup>3</sup>, S. Pospisil<sup>3</sup>, M. Lerch<sup>1</sup>, M. Petasecca<sup>1</sup>, A. Rosenfeld<sup>1</sup>

<sup>1</sup>University of Wollongong, Centre for Medical Radiation Physics, Wollongong, Australia; <sup>2</sup>St George Hospital, St George Cancer Care Centre, Kogarah, Australia; <sup>3</sup>Czech Technical University of Prague, Institute of Experimental and Applied Physics, Prague, Czech Republic

#### Purpose or Objective

HDR BrachyView is a real-time in-body gamma camera probe for 3D HDR prostate brachytherapy source tracking, providing real-time source position verification. This study constitutes the first experimental demonstration of the HDR BrachyView prototype, performed with a CIRS tissue-equivalent gel prostate phantom. The main objectives of this study are to evaluate the developed real-time acquisition software in terms of the accuracy of spatiotemporal source position estimation, and to evaluate the combination of BrachyView reconstructed positions and dwelling times and the 3D TRUS image data using a custom developed visualisation software.

#### Material and Methods

A prototype in-body gamma camera system with integrated TRUS and associated real-time image acquisition and analysis software was developed for intraoperative source tracking in HDR brachytherapy. The probe utilises a cylindrical 7-pinhole tungsten collimator and a 4x1 array of Timepix high-resolution pixelated silicon detectors. The developed real-time data acquisition and image fusion software is validated against CT measurements of source position during a full clinical treatment plan. The tracking accuracy and temporal resolution of the system was validated experimentally using a deformable tissue-equivalent prostate gel phantom and a full clinical HDR treatment plan. A global coordinate system was defined by CT scanning the phantom with the probe in situ. Fusion of the estimated source dwell positions and timing with the 3D prostate image was performed using an integrated 3D visualisation software.

#### Results

Figure 1 (a) shows the percentage of the reconstructed dwell positions distribution as a function of the discrepancy of the position in respect to the nominal location determined by the TPS and identified in the CT scan of the phantom using implanted CT markers in each catheter. The BrachyView system was able to measure 78% of the 200 source positions with an accuracy within 1 mm. A minimum acquisition time of 0.28 s/frame was required to achieve this accuracy, restricting dwell times to a

minimum of 0.3 s. Due to limitations in the temporal resolution of the system, dwell times of less than 0.3 s could not be resolved for reconstruction, resulting in 175/200 dwell positions being reconstructed. Figure (b) shows the reconstructed prostate volume taken from the TRUS, co-registered with the reconstructed dwell positions from the BrachyView system and CT determined dwell locations. Figure (c), shows the configuration of the experiment.

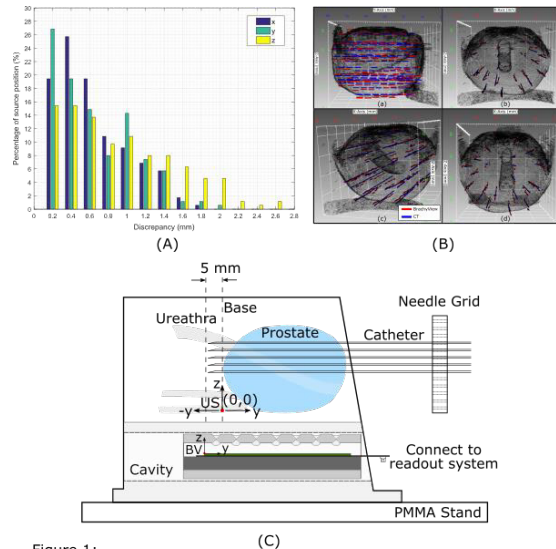


Figure 1:

#### Conclusion

HDR BrachyView is demonstrated to be a valuable tool for intraoperative source tracking in HDR brachytherapy. It can resolve source dwell locations in real-time and potentially in-vivo, with the advantage to visualise the source positions within the prostate anatomy when combined with TRUS. However, a faster readout system combined with a more efficient source localisation algorithm is required to be able to maximise the number of reconstructed dwell positions with short dwell times.

#### OC-0074 Accuracy of an integrated EMT/BT system for dwell-position detection in pelvic BT

L. Van Heerden<sup>1</sup>, J. Schiphof-Godart<sup>1</sup>, M. Christianen<sup>1</sup>, J. Mens<sup>1</sup>, M. Franckena<sup>1</sup>, M. Maenhout<sup>1</sup>, R. Rijnsdorp<sup>1</sup>, L. Luthart<sup>1</sup>, M. Hoogeman<sup>1</sup>, I. Kolkman-Deurloo<sup>1</sup>

<sup>1</sup>Erasmus Medical Center, Radiation Oncology, Rotterdam, The Netherlands

#### Purpose or Objective

Recently, a prototype High-Dose Rate Brachytherapy (HDR-BT) Flexitron afterloader with integrated Electromagnetic Tracking (EMT) has been developed by Elekta AB, enabling pre-treatment in-vivo verification of dwell positions. However, electromagnetic interference originating from surrounding equipment present during HDR-BT procedures could lead to dwell-position detection errors. As of yet, this has not been investigated for the integrated system in various clinical environments for pelvic brachytherapy. The goal of this study is to assess the impact of the interference on the accuracy of EMT-based dwell-position detection in prostate and cervix HDR-BT.

#### Material and Methods

Dedicated prostate and cervix phantoms were constructed holding an implant of 10 catheters and the Utrecht applicator with 6 needles, respectively. CT scans of the phantoms were acquired to reconstruct the implant geometry. Subsequently, BT plans were created with dwell positions at every 5mm. These BT plans were verified by EMT in an interference-free set-up and in

various clinical environments (delivery in the operating room (OR), CT scanner room (CT), and patient bed). To determine the accuracy of EMT-based dwell-position detection, the residual error, i.e. the distance between the EMT-measured and planned dwell positions, was averaged per catheter. In addition, we determined the minimum error that can be detected by EMT by calculating the detection limit, defined as the mean residual error in the x-, y- and z-direction + 2 standard deviations.

### Results

For the prostate phantom the residual error was on average over all catheters 0.6mm, 0.5mm and 0.3mm in the OR, CT room and the patient bed, respectively, compared to 0.3mm in the interference free set-up. For the catheters in the cervix applicator, the mean residual error was <0.4mm in the interference free set-up (Fig. 1). The minimum error that could be detected with EMT was <0.9mm in all cases (Table 1).

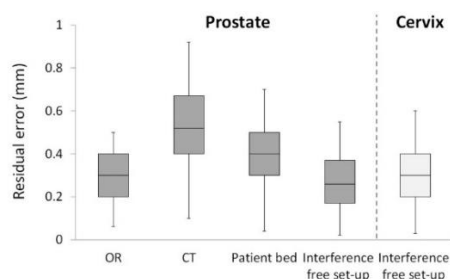


Fig. 1 Boxplot of the residual error between EMT-measured and planned dwell positions averaged over all catheters, in the prostate phantom (left) and the cervix phantom (right).

Minimum detection error (mm)	x-direction	y-direction	z-direction
	<b>Prostate</b>		
OR	0.7	0.4	0.3
CT	0.9	0.6	0.6
Patient bed	0.9	0.5	0.4
Interference free set-up	0.5	0.3	0.3
<b>Cervix</b>			
Interference free set-up	0.9	0.3	0.3

Table 1 The minimum error that can be detected by EMT, for the x- y- and z- direction.

### Conclusion

Using the integrated EMT/BT system, we quantified errors due to EM field interference in the BT clinical setting for pelvic tumours. We found a mean residual error <0.6mm, which is smaller than the dose calculation grid size (1mm). With our current method we are able to detect dwell position shifts >0.9mm. We therefore conclude that the effect of EM field interference due to medical equipment is limited and that EMT is sufficiently accurate for dwell position detection in prostate and cervical cancer.

### OC-0075 Error detection using an electromagnetic tracking system in multicatheter interstitial brachytherapy

S. Masitho<sup>1</sup>, K. Kallis<sup>1</sup>, V. Strnad<sup>1</sup>, R. Fietkau<sup>1</sup>, C. Bert<sup>1</sup>  
<sup>1</sup>Universitätsklinikum Erlangen, Radiation oncology, Erlangen, Germany

### Purpose or Objective

HDR interstitial brachytherapy (iBT) is a common treatment option for breast cancer patients. Despite its clinical success, errors which could occur during treatment planning or treatment delivery can have a dosimetric impact on the planned dose delivery. Currently, there is no extended quality assurance (QA) system available to detect these errors. The hybrid treatment delivery system (HTDS) is one of the possible QA methods for iBT. The system consists of an afterloader prototype system (Flexitron, Elekta, Veenendaal, The Netherlands) with an integrated electromagnetic tracking sensor, combined with an EMT system (Aurora, Northern Digital Inc., Canada). The HTDS allows the automatic measurement of the sensor's position in the implanted catheters. To test the feasibility of the system for error detection for breast cancer patients, possible planning and delivery errors in iBT were simulated using two phantoms.

### Material and Methods

A CT-based treatment plan for each phantom was used as the reference data. Planning errors such as: an incorrect offset value, an incorrect indexer length, tip/connector end swaps, partial swaps, and delivery error such as whole implant displacement were simulated by altering the treatment plan. Other delivery errors such as catheter shifts and catheter connection swaps were simulated using two different phantoms: a rigid phantom with 9 straight catheters and a breast equivalent phantom with 10 bent catheters. To simulate catheter shifts, 1.1 mm thick spacer discs were attached between the phantom's surface and the button at the catheter's tip end. Catheter connection swaps were simulated by connecting the catheters to the incorrect channels. Geometrical deviations between the dwell points of reference data and error-induced data were assessed using an in-house Matlab routine. The median deviation was used to confirm different errors, which were then differentiated visually. For catheter shifts, the median value corresponds to the detected magnitude of the shift.

### Results

The following errors were detected: Incorrect offset values (-10 mm and -15 mm), tip/connector end swaps, partial swaps between two catheters, and whole implant displacement (5 mm in lateral direction) in both phantoms. A total of 37 catheter connection swap measurements were conducted. Catheter connection swaps were detected 100% of the time. Shift measurements of one catheter were conducted 25 times for 1.1 to 5.07 mm shifts in each phantom. ROC analysis for shifts in the rigid phantom showed that 1.1 mm shifts in one catheter can be detected 98.36% of the time, while shifts larger than 2.21 mm can be detected 100% of the time. The measurement to determine the minimum detectable catheter shift in the breast equivalent phantom is still ongoing.

### Conclusion

Simulated treatment planning and delivery errors in iBT were detected. This study showed that it is feasible and beneficial to use the HTDS to detect planning and delivery errors prior irradiation in iBT for breast cancer patients.

### OC-0076 Real time treatment verification in HDR brachytherapy: an in-phantom proof of principle

M. Hanlon<sup>1</sup>, R. Smith<sup>2</sup>, V. Panettieri<sup>2</sup>, J. Millar<sup>2,3</sup>, R. Franich<sup>1,2</sup>  
<sup>1</sup>RMIT University, School of Science, Melbourne, Australia; <sup>2</sup>The Alfred, Alfred Health Radiation Oncology, Melbourne, Australia; <sup>3</sup>Monash University, Central Clinical School, Melbourne, Australia

### Purpose or Objective

HDR brachytherapy treatment verification can be achieved by tracking the source during treatment to confirm correct dwell delivery. Our system utilises a flat

panel detector (FPD) embedded in the treatment couch for source tracking and a ceiling mounted x-ray system for imaging and registration<sup>1</sup>. Here, we present the *real time* capabilities of the system, showing its ability to track the source, measure source position, and compare the measurement to the plan *during treatment*.

#### Material and Methods

An AP radiograph is captured of the phantom with implanted fiducial markers. The treatment plan, consisting of 81 dwell positions across 9 catheters, was registered to FPD coordinate space via the fiducial markers, allowing the tracked source positions to be directly compared to the plan. As the treatment was delivered, the FPD was run in cine mode at 15 fps, continuously capturing autoradiographs of the source radiation.

Each frame was analysed for 2D source position and compared to the planned dwell position. The process is completed in seconds: the analysis of each catheter is performed before the start of the next catheter treatment delivery. Any deviations, if present, are assessed against 'error signatures', shown in previous work<sup>2</sup> to correlate with common errors, enabling rapid identification of errors.

Plans were delivered both with and without deliberately introduced errors to validate the system in a phantom and to verify that treatment errors can be identified.

#### Results

To account for uncertainties and to minimise false positives, an error detection threshold of 5mm was set. When the plan was delivered without introduced errors, 0/81 dwells differed by more than the threshold, thereby, as all dwells were within uncertainty of expected positions, treatment was verified.

For one test of the system, the transfer tubes to two catheters were swapped. During delivery, the system correctly identified the error after the first incorrect catheter, allowing user notification before any additional incorrect catheters were delivered. The analysis was performed quickly: feedback was provided in time for the treatment to be interrupted before the start of the next catheter. Once adapted for clinical use, this will allow treatment to be paused and recover the prescribed plan. The success of the real time treatment verification system for other errors will be discussed.

#### Conclusion

Our *real time* HDR brachytherapy treatment verification system can identify gross errors *during delivery*, and confirm correct delivery with an error detection threshold of 5 mm. The process is performed *during treatment*, allowing for errors to be identified and corrected before completion of treatment. As more experience is gained with the system, it will be used routinely in real time as a treatment verification system with minimal impact on workflow and patient discomfort.

#### References

- Smith, R et al (2018) *Brachytherapy*, 17(1) 111-121
- Franich, R et al (2018) *APESM* 41(1) 307

#### OC-0077 Reconstruction of delivered dose based on in vivo dosimetry in prostate brachytherapy

E. Jørgensen<sup>1</sup>, S. Rylander<sup>1</sup>, S. Buus<sup>1</sup>, L. Bentzen<sup>1</sup>, S.B. Hokland<sup>1</sup>, A.K.M. With<sup>2</sup>, G. Kertzschner<sup>1</sup>, K. Tanderup<sup>1</sup>, J.G. Johansen<sup>1</sup>

<sup>1</sup>Aarhus University Hospital, Department of Oncology, Aarhus, Denmark; <sup>2</sup>Örebro University Hospital, Department of Medical Physics, Örebro, Sweden

#### Purpose or Objective

Novel in vivo dosimetry (IVD) systems for BT, have enabled source tracking (ST) with a sub-millimetre precision. We have used ST to reconstruct the delivered dose and dose volume histogram (DVH) parameters in HDR prostate treatments. Reconstructed DVH parameters are compared to the treatment plans to investigate, if current applicator

reconstruction uncertainties lead to clinically relevant deviations in dose.

#### Material and Methods

IVD was performed during 7 fractions of HDR prostate BT. Patients were treated with two HDR fractions of 8.5Gy delivered after 46Gy EBRT. The needles were implanted under trans-rectal ultrasound guidance. The needle reconstruction and organ delineation were done on MRIs. A dosimeter, based on a small luminescence crystal, was placed inside the prostate in a dedicated needle. Dose rates were recorded during the dose delivery at a read-out frequency of 20Hz and analysed post-treatment. The position of each needle relative to the dosimeter were determined with an optimisation process transforming dose rate patterns into positional shifts of the needles. The tracked needle positions were registered to the patient anatomy (relative to the dosimeter) on the planning MRI and used to reconstruct the delivered DVH parameters. Delivered and planned DVH parameters were compared to investigate the effect of positional uncertainties/changes.

#### Results

The ST analysis of all 117 needles (fig 1) showed longitudinal needle shifts (caudal-cranial direction) with a spread (1SD) of 1.5 mm and radial needle shifts (towards - away from the dosimeter) with a spread (1SD) of 0.5 mm. Any mean longitudinal shift on a fractional level was interpreted as an offset in the dosimeter position and corrected for before calculating the dose. The resulting changes in the dose distributions lead to a mean±1SD fractional change of  $-0.2\pm 0.1$ Gy in prostate  $D_{90}$ ,  $-0.1\pm 0.2$ Gy in urethra  $D_{2cm3}$ ,  $0.4\pm 2.1\%$  point in rectum  $D_{2cm3}$  and  $0.1\pm 4.5$ Gy in bladder  $D_{2cm3}$  (table 1). One needle was shifted 4 mm in the cranial direction into the bladder wall resulting in a bladder  $D_{0.1cm3}$  of 22.8 Gy.

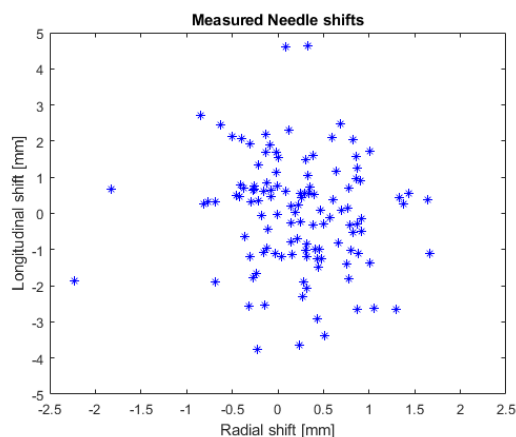


Figure 1: Measured needle shifts across all treatment fractions.

Volume	Planning Aim	Prescribed Dose	Delivered Dose
Prostate	$D_{90} \geq 8.5$ Gy	9.8 Gy (9.6 - 9.9)	9.5 Gy (9.3 - 9.6)
CTV	$D_{90} \geq 8.5$ Gy	9.1 Gy (8.7 - 9.3)	8.8 Gy (8.6 - 9.1)
	$V_{150\%} \leq 45\%$	34 % (32 - 36)	32 % (29 - 35)
	$V_{200\%} \leq 20\%$	12 % (10 - 15)	11 % (10 - 15)
Rectum	$D_{2cm3} \leq 75\%$	78 % (69 - 82)	77 % (71 - 84)
	$V_{100\%} = 0\%$	0 % (0 - 0)	0 % (0 - 0)
Urethra	$D_{0.1cm3} \leq 10$ Gy	9.9 Gy (9.8 - 10.1)	9.9 Gy (9.6 - 10.1)
	$D_{10} \leq 115\%$	114 % (113 - 116)	113 % (110 - 114)
	$D_{30} \leq 110\%$	112 % (110 - 114)	110 % (108 - 112)
Bladder	$D_{0.1cm3}$	11.1 Gy (9.7 - 13.0)	10.3 Gy (10.1 - 22.8)
	$D_{2cm3}$	8 Gy (7.1 - 8.5)	7.9 Gy (6.9 - 10.1)

Table 1: Median (range) of DVH parameters for delivered and planned dose.

## Conclusion

Novel IVD systems can be used to provide feedback on a reconstructed BT dose distribution. The observed needle shifts confirm a precise reconstruction of the needles on MR images and only limited discrepancies in the position of treatment needles ( $1SD < 2mm$ ). The dosimetric impact of the needle movements relative to the dosimeter was small except in one case where the source entered the bladder wall. Overall needle migration has previously been observed during prostate HDR-BT [1] and has a larger dosimetric impact than the needle shifts relative to the dosimeter when the bladder wall case is excluded. Needle migration cannot be observed with the ST method presented here as the dosimeter needle will typically migrate together with the entire needle implant.

[1] Buus S et al. Needle migration and dosimetric impact in high-dose-rate brachytherapy for prostate cancer evaluated by repeated MRI, Brachytherapy 17(2018).

## OC-0078 Error detection thresholds for routine real time in vivo dosimetry in HDR prostate brachytherapy

J. Mason<sup>1</sup>, A. Henry<sup>2</sup>, P. Bownes<sup>1</sup>  
<sup>1</sup>Leeds Cancer Centre, Medical Physics and Engineering, Leeds, United Kingdom; <sup>2</sup>Leeds Cancer Centre, Clinical Oncology, Leeds, United Kingdom

### Purpose or Objective

Real time in vivo dosimetry (IVD) for HDR prostate brachytherapy may provide independent verification of correct dose delivery and is part of our routine clinical workflow since 2014. This study evaluates the use of error detection thresholds in IVD.

### Material and Methods

IVD is implemented using a microMOSFET placed near the centre of the prostate in an additional needle. Error threshold calculation methodology was determined from the first 40 cases. IVD measurements were then performed for a further 72 patients treated with 15Gy or 19Gy single fraction treatments, applying the error thresholds to per-needle and per-plan measurements. Needle insertion and treatment planning use real-time trans-rectal ultrasound (TRUS).

Thresholds are determined individually for each patient using an uncertainty analysis; source-MOSFET distance uncertainty is the dominant component. A measurement is outside the error detection threshold if it is outside the ( $k=2$ ) uncertainty range. Additionally, per-needle measurements are only flagged as outside the threshold if absolute difference between measured and predicted reading is  $>20mV$  ( $-0.2Gy$ ). Plans/needles outside the thresholds were reviewed.

### Results

Table one summarises differences between measured and predicted reading per-plan and per-needle, and the uncertainty based thresholds. Figure 1 shows a measurement for one patient with two needles outside the threshold (highlighted).

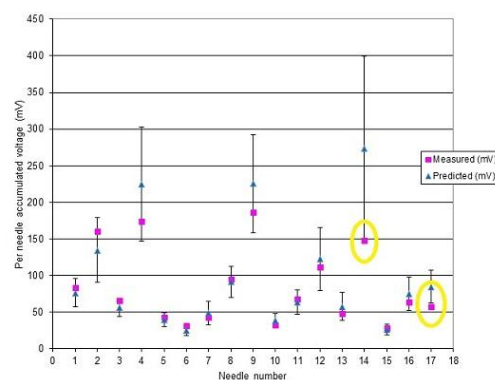
Of 3 plans outside the threshold, 1 was attributed to uncertainty in identifying the MOSFET position. 2 were due to uncertainty calculation limitation in the case where one needle is very heavily weighted so that the overall plan measurement fails even though each per-needle measurement passes. These false errors can be addressed by improvements in measurement technique and developing the method for aggregating per-needle uncertainties at the plan level.

Of 16 needles outside the error threshold, 2 were due to uncertainty in the reconstructed needle position of  $<2mm$ , 4 were due to uncertainty in identifying the MOSFET position. One needle reconstruction error when corrected caused the urethral D10 to increase by 3.5% which would have exceeded the dose constraint. For the remaining 10 needles no obvious error could be determined, however 8 of these were located posteriorly and previous work has

shown that the posterior prostate often drops between treatment planning and treatment.

Results	Number of measurements	Difference (measured - predicted)			K=2 error threshold		
		Median	Min	Max	Median	Min	Max
All plans	72	-5.2%	-15.8%	6.6%	$\pm 12.1\%$	$\pm 9.3\%$	$\pm 21.8\%$
Plans classed as error	3	-15.3%	-15.8%	-13.5%	$\pm 11.9\%$	$\pm 11.5\%$	$\pm 14.2\%$
All needles	1089	-5.4%	-8.6%	2.61%	$\pm 29.0\%$	$\pm 13.6\%$	$\pm 131\%$
Needles with dose difference $\geq 20 mV$	61	-13.4%	-6.9%	4.3%	$\pm 39.7\%$	$\pm 13.6\%$	$\pm 118\%$
Needles classed as error	16	-40.3%	-6.9%	3.9%	$\pm 32.5\%$	$\pm 14.5\%$	$\pm 49\%$

In-vivo Dosimetry - Measured v Predicted MOSFET Readings



## Conclusion

IVD in HDR prostate brachytherapy using a microMOSFET provides a high level of confidence that we are correctly delivering the planned dose to our patients, also allowing detailed analysis of dosimetric effects due to needle movement and reconstruction errors. In common with other IVD methods, it is difficult to completely avoid declaring false errors when defining error detection thresholds for real-time per needle IVD. The results of this analysis can be used to inform decisions on when to interrupt treatment if errors are detected during real-time IVD.

## OC-0079 Expanding Calibration Service for LDR Brachytherapy Seeds by Photon Fluence Determination

T. Schneider<sup>1</sup>  
<sup>1</sup>Physikalisch-Technische Bundesanstalt, Department 6.3 "Radiation Protection Dosimetry, Brunswick, Germany

### Purpose or Objective

The emitted radiation field and the dosimetric properties of LDR brachytherapy photon sources depends on the nuclide and the design of the seeds. BRAPHYQS and GEC-ESTRO encourage promotion of an efficient solution in Europe to monitor and assure seed design constancy, preferably like the CLA2004 - methodology controlled by AAPM.

In Europe, Aspects of the Quality Assurance (QA) in the production of seeds, including the constancy of the sources are not covered by the calibration of the seeds but by the process of CE-certification. Thereby the company's QA system must be outlined, and the effectiveness and permanent improvement must be demonstrated. Low energy photon spectrometry is a very sensitive tool to monitor the constancy of the radiation field of the seeds. However, establishing and maintaining a spectrometry unit requires considerable effort and such services are scarce within the brachytherapy community. The national metrology institute of Germany has decided to expand its calibration service for LDR seeds to include determination of photon fluence spectra at specific polar and azimuthal angles around the source from 2020 on. The inclusion of spectrometry into regular calibration service requires highly automated spectra measurement and data evaluation.

### Material and Methods

A commercially available detector system from Canberra (HPGe) is used controlled by the Genie 2000™ software

program.

To suppress stray radiation, the detector’s crystal is fully surrounded by a cylindrical steel cylinder. Collimators of 10 mm, 5 mm, 3 mm and 0.9 mm diameter are available. The detector’s efficiency was calibrated by means of radioactivity standards. The intensity of the discrete X-ray lines is analysed by a software package that follows the methodology of the “GUPIX” X-ray spectra-analysing software package.

The source holder is mounted to a computer-interfaced rotary stage, thus providing angular control while maintaining the proper orientation of the collimator axis to the source. In this way, spectra for a specific angle, as well as integral spectra, can be determined.

**Results**

In the figure below the step of automated peak detection is exemplify with a spectrum of an I-125 Bebig S17 seed. The upper panel shows the whole spectrum. The lower panel is an enlargement of the region marked red. The black frames represent the values for the detection limits calculated as the sum of three times the peak’s uncertainty plus the uncertainty of the fitted background at the peak’s position. As the peaks are of the Au-L-Lines at 9.7, 11.4 and 13.4 keV are below the frame they are not detected by the algorithm. This result is realistic, as the seed doesn’t feature any golden components. By contrast, the Ti-K-lines at 4.5 and 4.9 keV, arising from the capsule, are clearly detected, as well as the Mo-K-lines at 17.4 and 19.7 keV, arising from the marker.

**Conclusion**

An automated spectrometry set-up for LDR brachytherapy seeds will provide spectrometry as an integral part of the calibration service in the future.

ArcCheck (Sun Nuclear, Melbourne, FL) plus an ionization chamber (IC) and correlated with the independent dose calculation passing rates. An analysis of average changes in monitor units (MU) from one adapted plan to another was also performed.

**Results**

The average difference between the measured and TPS-predicted values for the end-to-end tests was 1.64% (maximum of 2.8%). The average gamma (2%/2mm) passing rate for the independently calculated dose vs the TPS-predicted dose was 98.5%. An example of the in-house software results for an adapted plan is shown in Figure 1. Table 1 shows the average IC, ArcCheck (3%/3mm) and independent QA (2%/2mm) rates for each patient. The average change in monitor units from fraction to fraction was 7.5%, with maximum observed of 20%.

ROI Name	Type	Volume (cc)	Gap	Density Override	Used in Optimization	# of Parts	Small Area Check
Skin	external	15000.5	No	No	Yes	4	Pass
WV_WREED_IC	others	0.6	Not Checked	No	No	-	Not Checked
DorsalHead	organ	301.5	No	No	Yes	1	Pass
Kidney_L	organ	169.7	No	No	Yes	1	Pass
Kidney_R	organ	152.0	No	No	Yes	1	Pass
LarynxHead	organ	276.4	No	No	Yes	1	Pass
Liver	organ	1239.9	No	No	Yes	1	Pass
SmallInt	organ	310.5	No	No	Yes	1	Pass
SpinalCord	organ	22.9	No	No	Yes	1	Pass
Stomach	organ	376.2	No	No	Yes	1	Pass
CTVtotal	target	21.8	No	No	Yes	1	Pass
CTVtotal	target	104.5	No	No	Yes	1	Pass
CTVtotal	target	104.5	No	No	Yes	1	Pass
PTV_Skin	skin	15041.1	No	No	Yes	1	Pass
PTV_Skin	others	11.2	Not Checked	No	Yes	-	Not Checked
GMRES	others	1303.9	Not Checked	No	No	-	Not Checked
GMRES	others	2317.2	Not Checked	No	No	-	Not Checked
GMRES	others	332.6	Not Checked	No	No	-	Not Checked
KIDNEY_L_COARDED	others	165.5	Not Checked	No	No	-	Not Checked
KIDNEY_L_COARDED	others	15000.7	Not Checked	No	No	-	Not Checked
COULON	others	300.4	Not Checked	Priority = 200.00	No	-	Not Checked
CT_Skin	others	15041.1	Not Checked	Priority = 210.00	No	-	Not Checked
SKIN_ARM	others	300.4	Not Checked	Priority = 210.00	No	-	Not Checked
SKIN_ARM	others	300.4	Not Checked	Priority = 210.00	No	-	Not Checked

Figure 1. An example of the in-house software check for contour integrity flagging the Kidney\_R structure as one for which the dose in the treatment plan is high enough to suggest being included in optimization objectives. The discontinuity of the Skin contour is also flagged as a potential issue.

**Proffered Papers: PH 1: Adaptive radiotherapy: tools and technologies**

**OC-0080 Comprehensive commissioning of MR-Linac online adaptive radiotherapy QA**

O. Green<sup>1</sup>, A. Price<sup>1</sup>, B. Cai<sup>1</sup>, J. Cammin<sup>1</sup>, V. Rodriguez<sup>1</sup>, J. Park<sup>1</sup>, S. Mutic<sup>1</sup>, D. Yang<sup>1</sup>

<sup>1</sup>Washington University School of Medicine, Radiation Oncology- Physics Division, Saint Louis, USA

**Purpose or Objective**

To establish the quality assurance process for online adaptive radiotherapy (ART) performed with a hybrid MR-linac system.

**Material and Methods**

The commissioning process consisted of three parts: independent validation of the vendor-provided Monte Carlo-based secondary dose calculation module; development of an in-house software package for plan integrity and deliverability checks; patient-specific phantom-based QA for each adapted fraction for the first five patients (a total of 42 fractions). The independent validation of the secondary dose calculation was performed via end-to-end tests with an MR-imageable phantom with inserts for ionization chambers (CIRS, Norfolk, VA). Five adaptive scenarios were simulated that included changes in target volume, changes in organ-at-risk positions, and changes in electron density (this was done by adding or subtracting water to the phantom). For each scenario, IC measurements were compared to predicted treatment planning system (TPS) dose values and correlated with independent dose calculation passing rates. The in-house software package was developed in MatLab (MathWorks, Natick, MA) to check contour integrity (gaps, islands, assigned density overrides, volumes, and whether it was used in optimization), flag undeliverable segments, and estimate plan delivery times. Patient-specific QA was performed after each adapted fraction for the first five patients using the MR-

Patient	Fractions adapted	IC % diff from TPS	Ind. Dose Calc.	
			AC 3%/3mm	2%/2mm
1	15	0.90%	96.90%	97.20%
2	15	1.20%	99.00%	91.90%
3	4	1.60%	97.84%	97.68%
4	4	2.30%	97.34%	96.97%
5	4	1.60%	99.08%	98.98%

Table 1 Phantom-based and independent dose calculation results for patient-specific adapted fractions using ionization chamber (IC) and ArcCheck (AC).

**Conclusion**

The complexity of online adaptation necessitates not only thorough commissioning but the establishment of on-going comprehensive quality assurance for each fraction that includes not only a phantom-less QA but also a method to ensure that all other components of the plan are accounted for and checked. In this work we have shown an example of such a comprehensive commissioning method for a hybrid MR-linac.

**OC-0081 Plan-library supported automated replanning for online-adaptive IMPT of cervical cancer**

T. Jagt<sup>1</sup>, S. Breedveld<sup>1</sup>, R. Van Haveren<sup>1</sup>, R. Nout<sup>2</sup>, E. Aresteinidou<sup>2</sup>, M. Staring<sup>3</sup>, B. Heijmen<sup>1</sup>, M. Hoogeman<sup>1</sup>  
<sup>1</sup>Erasmus MC University Medical Center Rotterdam, Department of Radiation Oncology, Rotterdam, The Netherlands; <sup>2</sup>Leiden University Medical Center, Department of Radiation Oncology, Leiden, The Netherlands; <sup>3</sup>Leiden University Medical Center, Division of Image Processing- Department of Radiology, Leiden, The Netherlands

**Purpose or Objective**

Intensity-modulated proton therapy (IMPT) is very sensitive to small daily density variations along the pencil beam paths and variations in target and OAR shapes. This makes IMPT for sites with large inter-fraction target

deformations extra challenging, such as in the treatment of cervical cancer. Online replanning is an option to achieve adequate target dose in each fraction. This study evaluates a novel approach employing a pre-treatment established plan-library as prior information in automated online replanning for IMPT of cervical cancer.

#### Material and Methods

CT data of 5 cervical cancer patients was available, comprising of a full and empty-bladder CT and 3-4 repeat CTs. Prescribed dose for the primary tumor and pelvic  $\pm$ para-aortic lymph nodes was 45 Gy. Pre-treatment plan-libraries were created to provide prior spot distributions for replanning on the repeat CTs. One consisted of two treatment plans based on the full and empty-bladder CT +8 mm margin and the other of one treatment plan encompassing all target deformation observed in the full and empty-bladder CT +10 mm margin, i.e. a large ITV. In case of the 2-plan-library the daily bladder volume was used to select the prior plan for replanning.

The reoptimization method starts with a spot-position (Bragg peak) restoration from the selected prior plan by adjusting the energy of each pencil beam to the water equivalent path length in the repeat CT. To further compensate for deformations, new spots are added. The reference point method (RPM) is then used to optimize the spot weights. The RPM has been automatically tuned on benchmark plans of 4 CTs (i.e. optimized from scratch without time constraints) and results in a reoptimized Pareto optimal plan for the new anatomy, with similar trade-offs as in the benchmark plan. Replanning was performed for each repeat CT using tight margins of 5/2 mm (primary tumor/nodes), only meant to account for intra-fraction motion. The prior and reoptimized plans were evaluated on the repeat CTs using the 5/2 mm-PTVs and compared to benchmark plans on the repeat CTs.

#### Results

Evaluating the prior plans on the repeat CTs without replanning resulted in  $V_{95\%} < 95\%$  in most CTs, with values down to 50% (see Fig 1). For both plan-library approaches, reoptimization increased the number of repeat CTs with adequate coverage ( $PTV V_{95\%} \geq 95\%$  and  $V_{107\%} \leq 2\%$ ) from 2/19 to 19/19 CTs. Fig 2 shows the differences between the reoptimized and benchmark plans on the repeat CTs using the ITV or 2-plan-library as prior. Median improvements are seen up to 4.5%-point for bladder  $V_{30Gy}$  when using the 2-plan-library instead of the ITV plan, with outliers up to 13.8%-point. Reoptimization took 3.6 min on average.

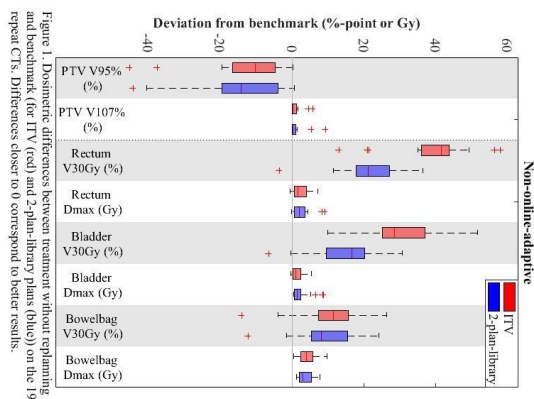


Figure 1. Dosimetric differences between treatment without replanning and benchmark (for ITV and 2-plan-library) on the 19 repeat CTs. Differences closer to 0 correspond to better results.

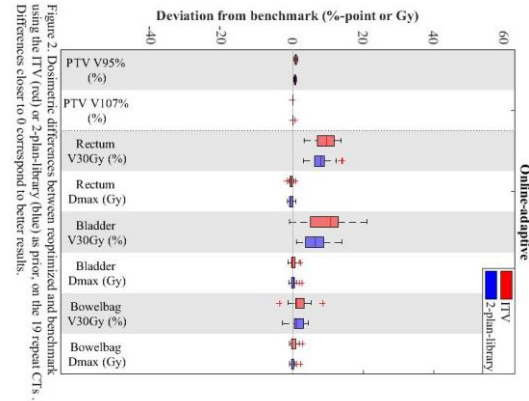


Figure 2. Dosimetric differences between reoptimized and benchmark using the ITV (red) or 2-plan-library (blue) as prior, on the 19 repeat CTs. Differences closer to 0 correspond to better results.

#### Conclusion

With fully automated replanning, adequate target coverage was restored for all CTs, as well as decreased OAR doses. The use of a 2-plan-library yielded lower OAR doses than a single ITV prior plan. With an average time of 3.6 minutes, this method is an important step towards online-adaptive IMPT in cervical cancer.

#### OC-0082 A biomechanical model to generate a library of cervix CTVs

C. Beekman<sup>1</sup>, S. Van Beek<sup>1</sup>, J. Stam<sup>1</sup>, J. Sonke<sup>1</sup>, P. Remeijer<sup>1</sup>  
<sup>1</sup>Netherlands Cancer Institute, radiation oncology, Amsterdam, The Netherlands

#### Purpose or Objective

Patients with cervical cancer treated with radiotherapy experience large daily CTV shape changes. To ensure good coverage while limiting the size of the PTV, a library of plans based on a series of CTVs has been implemented in various clinics. To obtain a series of cervix CTVs, a linear interpolation of a deformation vector field (DVF) between full and empty bladder anatomy is typically performed, leading to volume shrinkage of the intermediate structures. To overcome this shortcoming, we developed a biomechanical model that explicitly models the cervix deformation, which was used to generate a library of CTVs for intermediate bladder volumes.

#### Material and Methods

Twenty cervix cancer patients with empty and a full bladder CT-scans and associated delineations (bladder, cervix, uterus, rectum, bowel area, bones and external) were retrospectively selected. The delineations were converted to 3D surface meshes and imported into HyperWorks[1] for preprocessing and finite element analysis (FEA).

The bowel area was replaced by a constant pressure as they are highly deformable and hard to model explicitly. The empty bladder and rectum meshes were warped onto their corresponding full meshes, while motion of the bone mesh was fully constrained. These enforced displacements drove the deformation of the model. Elastic properties were taken from literature[2], except for the bowel pressure and the elasticity of the cervix CTV, which were subject of a parameter sweep.

A non-linear large-displacement analysis that allowed for continuous sliding between organs was performed. Residual errors between the simulated and target CTV mesh were corrected by an additional thin plate spline (TPS) deformation. Intermediate structural outputs of a linear superposition of the full biomechanical and residual deformation then constituted the library of CTVs for each patient. Optimal model parameters were identified as those that minimized the RMS distance of the residual deformation. Intermediate CTV volumes were compared with those from linearly interpolating the currently used anatomy mapping.

**Results**

Optimal model parameters are found for low bowel pressure and a cervix Young's modulus between 5 and 25 kPa (figure 1). Because the cervix is modeled as nearly incompressible, the FE method is less prone to intermediate volume shrinking effects than linear interpolation of a DVF, especially for large movers (figure 2).

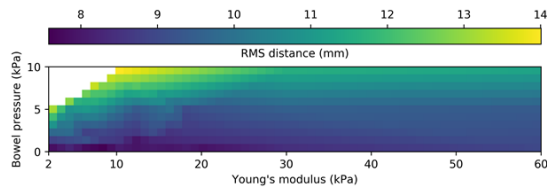


Figure 1. Elasticity of the cervix and bowel pressure against the RMS surface distance.

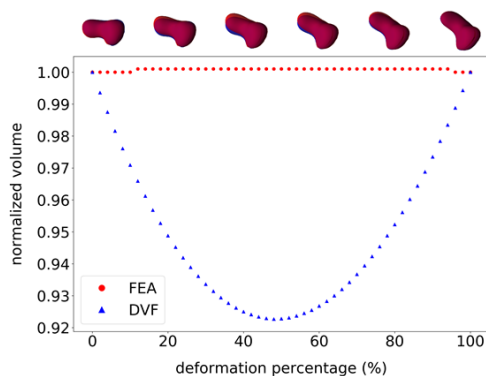


Figure 2. Volumetric comparison between FEA (red) and DVF (blue) CTV deformation. Volumes are normalized by the linear interpolation between the CTV volumes of empty and full bladder anatomy.

**Conclusion**

We developed a novel biomechanical library of plans method for the cervix CTV. By explicitly modeling CTV deformation due to variable bladder filling, volume shrinkage of intermediate library CTVs could be avoided. Moreover, finite element modeling has the potential to accurately describe anatomical deformations in 3D, allowing for improved dose accumulation in the future. However, validation on additional cervix anatomies or internal markers is necessary to further narrow down the optimal model parameter ranges.

[1] Altair Engineering Inc.

[2] Chai et al. Med. Phys. 38(1):142-50, 2011.

**OC-0083 MRI guided set-up corrections for esophageal cancer: what margin do we need?**

M. Boekhoff<sup>1</sup>, S. Mook<sup>1</sup>, A. Borggreve<sup>1</sup>, L. Goense<sup>1</sup>, P. Van Rossum<sup>1</sup>, N. Takahashi<sup>1</sup>, A. Van Lier<sup>1</sup>, A. Kotte<sup>1</sup>, J. Lagendijk<sup>1</sup>, G. Meijer<sup>1</sup>

<sup>1</sup>UMC Utrecht, Radiotherapy, Utrecht, The Netherlands

**Purpose or Objective**

MRI linacs allow for online target definition and online replanning for esophageal cancer irradiations, allowing high precision treatments. However, online planning requires online redefinition of target volumes and organs at risk and reoptimization of the plan, both of which can be time consuming. Alternatively, simple online setup corrections using rigid registration of the target volume can be done fast but on the downside do not correct for rotations and shape changes. The aim of this study is to quantify the proportion of treatment fractions at which a simple online setup correction can be safely applied at a given PTV margin in clinical practice.

**Material and Methods**

Thirty esophageal cancer patients underwent six T2-weighted MRI scans (1 prior to treatment and 5 during neo-

adjuvant chemoradiation (23x1.8 Gy) at weekly intervals. GTVs were delineated on each individual MRI. Follow-up scans were registered to the first (reference) scan. Registration consisted of a rigid translation of GTV masks with the Kappa-Statistic metric of the Elastix toolbox (Klein 2010) to ensure that the GTV in follow-up scans overlap with the reference GTV. Subsequently, artificial PTVs with varying margins from 1 to 12 mm around the reference GTV were created. Finally, the amount of voxels of the follow-up GTVs inside the PTV was analyzed for each margin.

**Results**

We found that when a PTV margin of 5 mm was applied the GTV was adequately covered by the PTV using an online correction strategy in 84% of the fractions (Figure 1/ Table 1). Conversely, when using a 5-mm PTV margin, 16% of the fractions would require an online replanning strategy as the shape changes of the target could not be absorbed by a 5-mm margin. At a patient level, replanning was needed for 43% of the patients at 1 or more treatment fractions using a 5-mm PTV margin, mostly for patients with distal tumors due to variable stomach filling (Figure 2). For the majority (57% of the patients) GTVs were properly covered in all instances, using a 5-mm PTV margin.

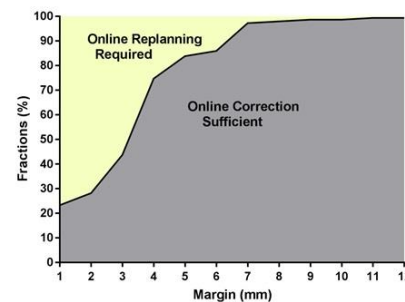


Figure 1) Percentage of fractions which require online replanning vs percentage of fractions where online correction is sufficient, for varying margins.

Margin (mm)	GTV correctly covered by PTV		GTV correctly covered by PTV for all fractions	
	Fractions (#)	Fractions (%)	Patients (#)	Patients (%)
1	33	23%	2	7%
2	40	28%	3	10%
3	62	44%	6	20%
4	106	75%	13	43%
5	119	84%	17	57%
6	122	86%	17	57%
7	138	97%	26	87%
8	139	98%	27	90%
9	140	99%	28	93%
10	140	99%	28	93%
11	141	99%	29	97%
12	141	99%	29	97%

Table 1) Covered fractions and patients for varying margins

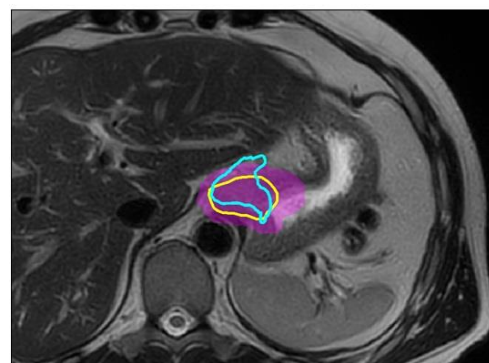


Figure 2) Example of a fraction where the GTV in a follow up scan (blue delineation) is not fully covered by the PTV with a margin of 5 mm (purple mask). This is caused by a change in tumor shape compared to the reference scan (yellow delineation)

## Conclusion

Tumor shape and position of esophageal cancer patients significantly vary on a daily basis. However, for the fast majority of fractions 5-mm PTV margins suffice when online MR guided setup correction are applied, enabling safe and efficient throughput MRI linac treatments for the majority of patients. Target coverage can be increased, but go along with an increased number of fractions that require online replanning. In both scenarios special attention should still be addressed to potential intrafraction tumor drifts.

## OC-0084 Baseline shifts towards the heart after IGRT are linked to overall survival in lung SABR patients

C. Johnson-Hart<sup>1</sup>, G. Price<sup>2</sup>, E. Vasquez Osorio<sup>1</sup>, C. Faivre-Finn<sup>2</sup>, M. Van Herk<sup>1</sup>

<sup>1</sup>University of Manchester, Radiotherapy Related Research, Manchester, United Kingdom; <sup>2</sup>The Christie NHS Foundation Trust, Radiotherapy Related Research, Manchester, United Kingdom

### Purpose or Objective

A recent study showed that in a cohort of NSCLC patients treated with standard fractionation, small residual set-up errors that move the high dose region towards the heart following image-guidance have a significant effect on overall survival. As SABR patients are setup daily matching to the tumour itself, baseline shifts of the tumour may influence the unintended irradiation of the heart and mediastinum. This study investigates the association of baseline shifts with survival in a SABR cohort.

### Material and Methods

136 NSCLC SABR patients treated with a daily soft tissue matching, 2mm action threshold, online CBCT IGRT protocol were studied. The mean shift of the high dose region in the direction of the heart due to baseline shifts was determined for each patient by performing a bony-anatomy match starting from the final soft tissue match position recorded during delivery for each fraction (taking bony anatomy as a surrogate for heart location), averaging this value over all fractions, and then projecting the resulting vector in the direction of the heart. This 'heart-baseline shift' was then used to categorise the patients into high and low risk groups based upon the median value. Correlations of this parameter with common clinical variables was tested. Kaplan-Meier survival curves were used to compare patients with baseline shifts towards/away from the heart, and the significance was determined through multivariable Cox regression, correcting for patient age, performance status, GTV volume and existing comorbidities.

### Results

The heart-baseline shifts had a median value of -0.5mm (range -9.0 - 8.6mm) and were independent of all tested clinical variables. Yet this parameter was significantly associated with survival, with patients with baseline shifts towards the heart having significantly worse prognosis as compared to cases with shifts away (Figure 1). Multivariable analysis found a hazard ratio of 1.261 per mm ( $p = 0.002$ ) for the baseline shift, when analysed as a continuous variable (Table 1).

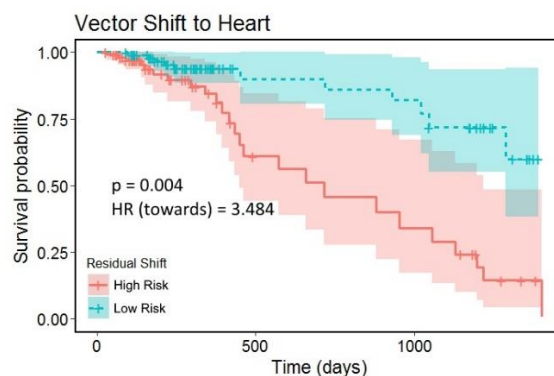


Figure 1: Multivariable Cox regression survival curves, stratified on the median baseline shift towards or away from the heart (-0.5mm) to ensure equal group sizes. High risk patients (those > -0.5mm, meaning that the majority of shifts will move the high dose region towards the heart) have worse overall survival ( $p=0.004$ ). The HR gives the hazard of death for high risk patients as compared to low risk patients.

Variable	p-value	Hazard ratio (95% CI)
Vector shift to the heart (per mm)	0.002	1.261 (1.086 – 1.466)
ECOG-PS	0.322	3.367 (0.305 – 37.207)
Age	0.130	1.035 (0.989 – 1.083)
ln(GTV)	<0.001	2.139 (1.376 – 3.324)
Comorbidity score	0.306	3.261 (0.339 – 31.364)

Table 1: Multivariate Cox regression results with shift to the heart as a continuous variable.

### Conclusion

Baseline shifts of the tumour towards the heart (thereby increasing the heart dose) during SABR significantly correlate with poorer overall survival in this cohort of early stage NSCLC patients. Such increase in dose to the heart appears to have an early effect on survival. These results provide evidence that stricter heart dose constraints are required when planning thoracic SABR. Furthermore, a PRV around the heart may be required to limit the effects of unavoidable baseline shifts.

## OC-0085 Correcting CBCT images for dose calculation using a U-shaped deep convolutional neural network

G. Landry<sup>1</sup>, D. Hansen<sup>2</sup>, F. Kamp<sup>3</sup>, M. Li<sup>3</sup>, B. Hoyle<sup>4</sup>, J. Weller<sup>4</sup>, K. Parodi<sup>1</sup>, C. Belka<sup>3</sup>, C. Kurz<sup>3</sup>

<sup>1</sup>Ludwig-Maximilians-Universität München, Department of Medical Physics, Garching, Germany; <sup>2</sup>Gradient Software, none, Aarhus, Denmark; <sup>3</sup>University Hospital-LMU Munich, Department of Radiation Oncology, Munich, Germany; <sup>4</sup>Ludwig-Maximilians-Universität München, Universitäts-Sternwarte- Fakultät für Physik, Munich, Germany

### Purpose or Objective

Radiotherapy (RT) dose calculations on daily cone beam computed tomography (CBCT) images may eventually allow online-adaptive workflows with current state of the art linac technology. Image correction is crucial when using CBCT for dose calculation; and for online-adaptive RT the corrections should be fast in addition to providing accurate dose calculation. This study evaluated three different deep learning based correction strategies using a U-shaped convolutional neural network architecture (Unet) in terms of their photon and proton dose calculation accuracy.

### Material and Methods

For training, CT to CBCT deformable image registration (DIR) was performed for 42 prostate cancer patients. This

yielded a virtual CT (vCT) which was used as prior for a previously validated projection-based correction method called CBCTcor (requiring >10 minutes of processing time). CBCTcor was used as reference throughout this study. A single Unet architecture was trained on three different datasets: (Unet1) raw and corrected CBCT projections, (Unet2) raw CBCT and vCT image slices and (Unet3) raw and CBCTcor image slices. Patients were distributed in training (27), validation (7) and testing (8) groups. Volumetric modulated arc therapy (VMAT) and proton pencil beam scanning (PBS) single field uniform dose (SFUD) plans with two opposed fields were optimized on the CBCTcor image and recalculated on the obtained Unet-corrected CBCT images. Figure 1 shows the Unet and the data used to train Unet1/2/3.

**Results**

The mean error (ME) and mean absolute error (MAE) over all patients for Unet1/2/3 were -1/2/3 Hounsfield units (HU) and 48/88/56 HU. The 1% dose difference pass rates were better than 98.4% for VMAT for 8 test patients not seen during training, with little difference between Unets. Gamma evaluation results were even better. For protons a gamma evaluation was employed to account for small range shifts, and 2%/2mm pass rates for Unet1/2/3 were better than 85%/89% and 91%. A 3 mm range difference threshold was established. Only for Unet3 the 5th and 95th percentiles of the range difference distributions over all fields, test patients and dose profiles were within this threshold. Example proton dose distributions are presented in Figure 2. The average time to correct an input projection for Unet1 was 12.5 ms, corresponding to 4.4 s for a 350 projections complete scan. For Unet2/3 the time to correct an image slice was 11 ms, with an entire image (264 slices) requiring 2.9 s.

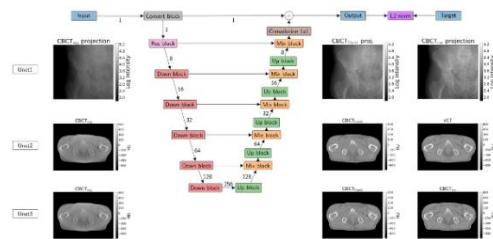


Figure 1. The Unet architecture and the data used for training Unet1, Unet2 and Unet3. The numbers next to the arrows indicate the number of channels.

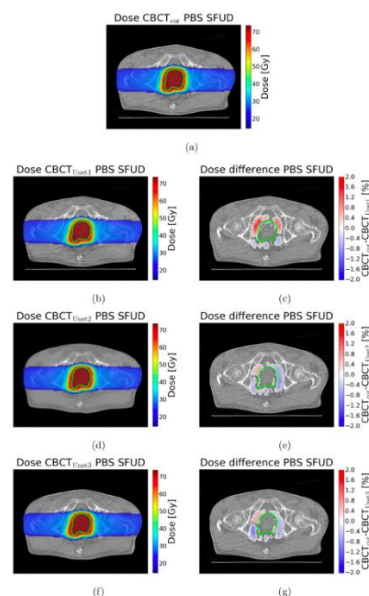


Figure 2. (a) Dose distribution from the PBS SFUD plan optimized on CBCTcor and recalculated on (b) CBCTUnet1, (d) CBCTUnet2 and (f) CBCTUnet3 and (c),(e),(g) the difference to the dose from CBCTcor, respectively

**Conclusion**

A single Unet architecture was successfully trained using both CBCT projections and CBCT image slices. Since the results of the other Unets were poorer than Unet3, we conclude that training directly on corrected CBCT image slices is optimal for PBS SFUD proton dose calculations, while for VMAT all Unets provided sufficient accuracy. Correction times were adequate for online adaptive RT workflows.

**Acknowledgements**

DFG-MAP, Deutsche Krebshilfe, NVIDIA

**OC-0086 Probabilistic Dose Accumulation Based Evaluation of Head and Neck Intensity Modulated Proton Therapy**

D. Wagenaar<sup>1</sup>, R.G.J. Kierkels<sup>1</sup>, A. Van der Schaaf<sup>1</sup>, M. Rodrigues Reis<sup>1</sup>, A. Meijers<sup>1</sup>, D. Scandurra<sup>1</sup>, M. Sijtsema<sup>1</sup>, E. Korevaar<sup>1</sup>, A. Knopf<sup>1</sup>, A. Van den Hoek<sup>1</sup>, J.A. Langendijk<sup>1</sup>, S. Both<sup>1</sup>

<sup>1</sup>UMCG University Medical Center Groningen, Department of Radiation Oncology, Groningen, The Netherlands

**Purpose or Objective**

Current robustness settings are based on systematic and random setup and range uncertainties. This study, incorporates treatment uncertainties in a probabilistic dose accumulation to investigate plan robustness requirements for clinical head and neck cancer (HNC) treatments.

**Material and Methods**

10 consecutive HNC patients treated with IMPT (IBA) were analyzed. Patients were treated with 70 Gy<sub>RBE</sub> to the primary CTV while immobilized using a 5-point mask (Orfit). Anatomy changes were monitored with daily CBCT and weekly offline verification CTs. For each fraction, 6D corrections were applied based on CBCT using a robotic table (Leoni). Plans were generated using worst-case MiniMax robust optimization with 3% range/ 5 mm setup uncertainties in the treatment planning system (RayStation v6.1). All plans were retrospectively re-optimized using 3%/3mm and 3%/2mm.

Treatment courses were robustly evaluated by sampling one systematic shift and 35 daily random shifts from their normal distributions. Fraction doses were calculated by computing dose on each verification CT 5 times for different shifts. The verification CT was considered representative of the patient anatomy for that week. A treatment course was evaluated 25 times for each plan, for each patient (26.250 fraction doses evaluated).

41 post-fraction CBCTs were acquired during patients' treatment course to assess intrafraction motion. Furthermore, we established the accuracy of the on-board imaging and robotic table from our machine QA results. An extra 0.5 mm was estimated to account for not considered residual systematic errors. From these data the distribution of the systematic and random error was determined. Range errors impact was studied for the patient with worst coverage by adding range uncertainties to the evaluation.

Treatment courses were analyzed in terms of target and organ at risk (OAR) DVH parameters and average tumor control probability (TCP) (Lühr et al.). A Wilcoxon signed rank test was performed ( $\alpha = 0.05$ ).

**Results**

The total random and systematic errors were found to be equal in each direction with  $\sigma = 0.7$  mm each. Treatment courses showed a significantly lower average OAR dose for the 3mm and 2mm plans compared to the 5mm plans for all OARs (Average  $\Delta D = 1.3$  and 2.3 Gy<sub>RBE</sub>). In terms of target coverage all simulations had a D99 > 95%. The average D99 slightly decreased from 69.0 to 68.7 and 68.4 Gy<sub>RBE</sub> for the 5mm, 3mm and 2 mm robust optimized plans, while remaining within the clinically acceptable level. Setup margin reduction resulted in virtually no change in

TCP (50.7% to 50.5% and 50.2%). No relevant change was observed when including range errors in the robust evaluation of the patient with the worst clinically acceptable coverage ( $< 0.1$  GyRBE).

### Conclusion

Reducing the robust optimization setting from 3%/5mm to 3%/2mm reduces OAR dose and can be safely implemented in our clinical practice for HNC IMPT treatment using a 5-point mask, a robotic couch and daily CBCT.

Figure 1: Average dose volume histogram of 25 robust evaluations of a single patient for a plan optimized with a 5mm, 3mm and 2mm robustness shift.

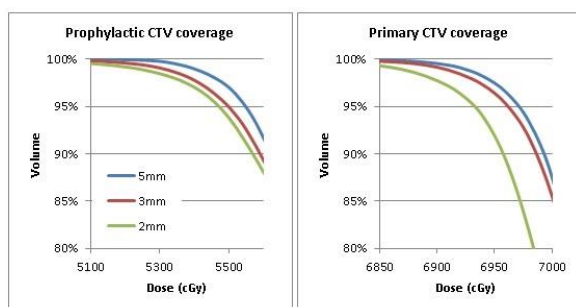


Table 1: Dose differences of 25 robust evaluations between a plan optimized with a 5mm robustness margin versus 3mm and 2mm. \*:  $p < 0.05$  in Wilcoxon signed rank test.

	5mm	3mm	$\Delta$	2mm	$\Delta$
<b>Organ at risk dose (Mean, Gy<sub>RBE</sub>)</b>					
Parotid ipsi	21.1	19.6	1.5*	18.5	2.6*
Parotid contra	10.2	9.0	1.2*	8.3	1.9*
Submand ipsi	40.8	40.2	0.5*	39.2	1.5*
Submand contra	25.4	24.5	0.9*	23.5	1.9*
Inferior PCM	19.1	17.7	1.4*	16.7	2.4*
Superior PCM	34.3	33.1	1.2*	31.9	2.4*
Cricopharyngeus M.	14.6	12.8	1.8*	11.8	2.8*
Supraglottic Larynx	23.6	21.7	1.9*	20.3	3.3*
Oral cavity	20.5	19.2	1.3*	18.4	2.1*
<b>Target coverage</b>					
D99 CTV7000 (Mean, Gy <sub>RBE</sub> )	69.0	68.7	0.3*	68.4	0.6*
D99 CTV5425 (Mean, Gy <sub>RBE</sub> )	54.7	54.0	0.7*	53.5	1.2*
D98 > 95% CTV7000 (%)	100.0	100.0	0	100.0	0
D98 > 95% CTV5425 (%)	100.0	100.0	0	100.0	0
TCP* (Mean, %)	50.7	50.5	0.2	50.2	0.5*

## Proffered Papers: PH 2: Applications of dose modelling and calculation

### OC-0087 A new method for modelling the tongue-and-groove in treatment planning systems

V. Hernandez<sup>1</sup>, J.A. Vera-Sánchez<sup>1</sup>, L. Vieilleveigne<sup>2</sup>, C. Khamphan<sup>3</sup>, J. Saez<sup>4</sup>

<sup>1</sup>Hospital Universitari Sant Joan de Reus, Medical Physics, Reus, Spain; <sup>2</sup>Institut Claudius Regaud - Institut Universitaire du Cancer de Toulouse & Centre de Recherche et de Cancerologie de Toulouse, Medical Physics, Toulouse, France; <sup>3</sup>Institut Sainte Catherine, Medical Physics, Avignon, France; <sup>4</sup>Hospital Clinic de Barcelona, Radiation Oncology, Barcelona, Spain

### Purpose or Objective

Accurate modeling of the MLC by TPSs is known to be a crucial aspect in IMRT dose calculations, the most important characteristics being MLC transmission, the leaf tip end and the tongue-and-groove (TG). However, TPSs typically model the TG by extending the projections of the leaf sides by a certain constant width and it has been found that this model may produce discrepancies of as much as 7-10% in the calculated average doses [1]. The purpose of this study is to introduce and validate a new method for modeling the TG that uses a non constant TG width.

### Material and Methods

We provide the theoretical background with analytical expressions and a detailed methodology to determine the optimal shape of the TG width from measurements of the aSG (asynchronous sweeping gap) tests with a Farmer ion

chamber [1]. For a difference between adjacent leaves equal to  $s$ , the total area of the TG profile to be subtracted from the fluence map,  $A(s)$ , can be obtained from measurements. The TG width  $w(s)$  can then be determined as the first derivative of  $A(s)$  and fitted to a function with two parameters  $a_1$  and  $a_2$ . Parameter  $a_1$  represents the TG width for large  $s$  values and  $a_2$  introduces a reduction in the TG width near the leaf tip end to account for the increased transmission through the tongue due to the rounded leaf design.

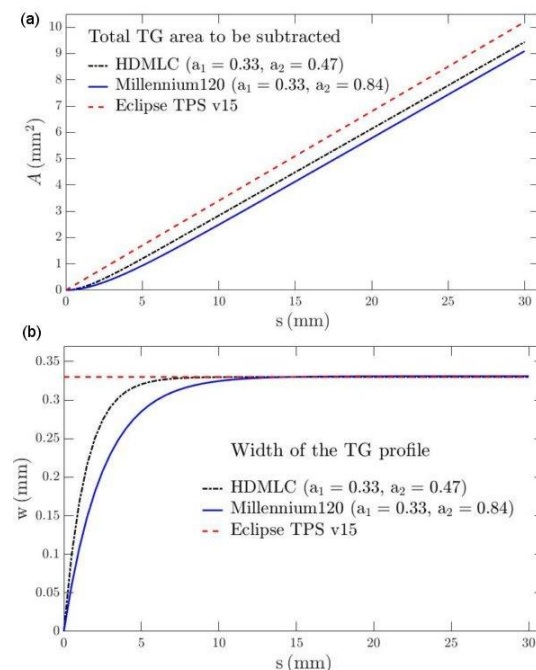
An MLC model similar to the one used by the Eclipse TPS was implemented in MATLAB. Calculated dose maps were obtained by convolution with a dose kernel [2] and were compared to Eclipse v15 calculations and to measurements from six Varian linacs from 4 different institutions: 3 linacs (2100CD, iX, TrueBeam) with the Millennium120 MLC and 3 (Trilogy and 2 TrueBeamSTx) with the HDMLC.

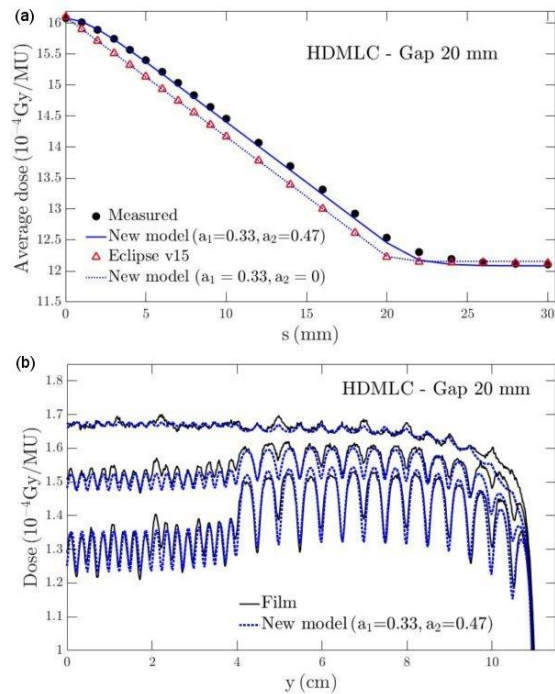
### Results

Parameters  $a_1$  and  $a_2$  were determined from the aSG tests. Parameter  $a_1$  was 0.33 mm for both MLC models, in agreement with the value used by Eclipse. Parameter  $a_2$  was 0.84 mm<sup>2</sup> and 0.47 mm<sup>2</sup> for the Millennium120 and the HDMLC, respectively (Fig 1).

Eclipse produced large discrepancies with respect to measurements, with differences in average doses as high as 4% and 6.5% for the Millennium120 and the HDMLC, respectively, and these calculations were accurately reproduced with the new model for  $a_2=0$ . On the other hand, with the experimentally determined parameters  $a_1$  and  $a_2$ , the new model produced calculations in close agreement with measurements, with all differences in average doses  $< 1\%$  (Fig 2a).

The new model was also in good agreement with radiochromic film results, recreating the fine spatial details associated to TG effects (Fig 2b). We also found that the parameters  $a_1$ ,  $a_2$  depend solely on the MLC design and are independent of the specific MLC device.





### Conclusion

A new method was presented that greatly improves the TG modeling. This method can be easily implemented in commercial TPSs and has the potential to further increase their accuracy, especially for MLCs with rounded leaf ends.

This method is currently in patent pending status.

[1] Phys Med Biol 62;2017:6688-6707

[2] Med Phys 9(37);2010:4634-4642

### OC-0088 A pilot study on the sensitivity of common beam modeling parameters in Eclipse

M. Glenn<sup>1</sup>, D. Followill<sup>1</sup>, R. Howell<sup>1</sup>, J. Pollard-Larkin<sup>1</sup>, S. Zhou<sup>2</sup>, S. Kry<sup>1</sup>

<sup>1</sup>The University of Texas MD Anderson Cancer Center, Radiation Physics, Houston, USA ; <sup>2</sup>The University of Texas MD Anderson Cancer Center, Biostatistics, Houston, USA

### Purpose or Objective

Recently, the accuracy of beam modeling parameter configuration has come into question, as IROC Houston has determined that considerable treatment planning system errors exist among institutions that fail its phantom credentialing test. The aim of this study was to determine the calculated dosimetric effects caused by the variations of several common beam modeling parameters in the Eclipse treatment planning system, based on realistic parameter values used by the radiotherapy community at large (as collected across the United States from over 500 institutions).

### Material and Methods

In this pilot study, a clinical 6 MV beam model for a Varian Clinac 2100iX was adapted in Eclipse (AAA 13.5.35) to match reference data collected from the IROC Houston site visit program, thus modeling an “average” performance linear accelerator. 23 output measurements, including PDD values, off-axis factors, and 12 square test fields ranging from 2x2 to 30x30 using both primary collimator- and multileaf collimator (MLC)-defined fields, were assessed in order to characterize the goodness of fit with respect to the reference output data. Once the model was verified, ten clinically acceptable head and neck phantom IMRT plans utilizing both dynamic MLC and VMAT techniques were recalculated following

modification of the dosimetric leaf gap (DLG), MLC transmission factor, and effective target spot size parameters. Parameter values chosen represented the 2.5<sup>th</sup>, 25<sup>th</sup>, 50<sup>th</sup>, 75<sup>th</sup>, and 97.5<sup>th</sup> percentiles of IROC survey responses in order to encompass the realistic extent of modeling variance in the radiotherapy community. Values examined for variations were the minimum dose, maximum dose, and mean dose to TLD structures, primary target volumes, and the organ at risk in the head and neck phantom.

### Results

The “average” performance 6 MV beam model represented the IROC reference data very well, having an average error of only 0.28%. Of the parameters tested herein, the dose calculations using the AAA algorithm were most sensitive to changes in the DLG, which ranged in value from 0.048 cm to 0.235 cm and produced changes from -6% to +3% of the calculated dose to identified structures. MLC transmission and effective target spot size contributed less significant changes, yielding up to  $\pm 1\%$  difference based on the most extreme values tested.

### Conclusion

Based on these initial findings, careful consideration should be made when commissioning clinical beam models, especially with respect to the measurement of the DLG. In this work the use of parameter values that are clinical but are still far from what is agreeable by the radiotherapy community are shown to potentially contribute to clinically significant changes in dose calculations.

### OC-0089 Mitigating inherent noise in Monte-Carlo dose distributions using UNet

U. Javaid<sup>1</sup>, J. Lee<sup>1</sup>, K. Souris<sup>1</sup>, S. Huang<sup>2</sup>, J. Madrigal<sup>1</sup>

<sup>1</sup>UCLouvain, IREC/MIRO, Brussels, Belgium ; <sup>2</sup>Memorial Sloan Kettering Cancer Center, Physics, New York, USA

### Purpose or Objective

Monte-Carlo (MC) algorithms offer accurate modeling of dose calculation by simulating the transport and interactions of many particles through the patient geometry. However, given their random nature, the resulting dose distributions from MC algorithms are affected by statistical uncertainty (*noise*), which renders it difficult to make accurate clinical decisions. This issue can be addressed to some extent using a huge number of simulated particles but it is computationally expensive. Therefore, there is a trade-off between the computation time and the noise level in MC dose distributions. Previous work on denoising the MC dose distributions is based on smoothing the distributions. In this work, we address the mitigation of noise inherent to MC dose distributions using UNet - an encoder-decoder styled fully convolutional neural network, which allows fast and fully automated denoising of whole-volume dose distributions.

### Material and Methods

We propose UNet that has three down-sampling layers for denoising whole-volume MC dose distributions. Mean-squared error (MSE) is used as loss function to train the model. MSE measures the pixel intensity difference between the denoised and reference image by summing all the squared differences. Lower the value of MSE, the similar the two images under observation therefore, we use it to evaluate the optimal weights for our model in its training phase. We train our model on proton therapy MC dose distributions of different tumor sites (*brain, head & neck, liver, lungs, prostate*) acquired from 31 patients. In training phase, we use three different noise realizations per patient to better model the noise inherent to MC dose distributions. We train the network in 3D manner with input MC dose distributions simulated using  $1e^6$  particles while keeping  $1e^9$  particles as reference.

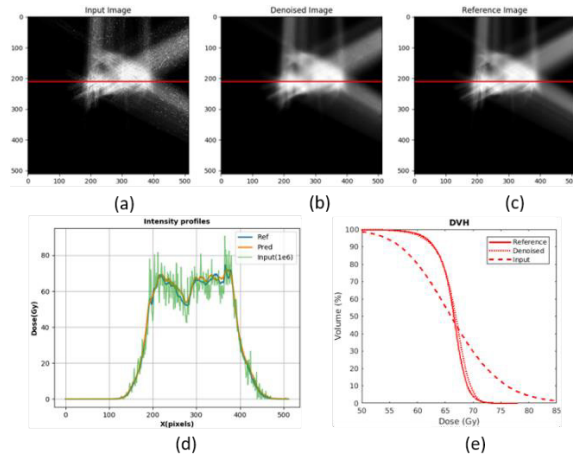
### Results

After training, our model successfully denoises new MC dose distributions. In the example test case (Figure 1), we

show that our model recovers  $D_{95}$  of 61.1 Gy from the noisy MC input of 54.3 Gy whereas the low noise MC (reference) offers 61.5 Gy. We observe higher *Peak signal-to-noise ratio* (PSNR) for reference vs denoised (39.70 dB) than reference vs input (28.12 dB) with an improvement factor of 11.58 dB. Moreover, the inference time of our model is only 7s for a dose distribution of an average dimension of 158x512x512.

### Conclusion

We propose an end-to-end, fast and fully automated UNet based framework for denoising the MC dose distributions. The proposed framework offers good generalization ability as it involves no pre-processing and can be trained on any tumor site. It provides comparable dose-volume histogram (DVH) to the MC simulation using  $1e^9$  particles and thus, identical  $D_{95}$ . We obtain a significant reduction in computational time: 7s vs 100 min (MC simulation using  $1e^9$  particles).



### OC-0090 Use of a realistic breathing lung phantom to verify 4D Monte Carlo dose calculations

S. Gholampourkashi<sup>1</sup>, J. Cygler<sup>1,2,3</sup>, B. Lavigne<sup>2</sup>, E. Heath<sup>1</sup>  
<sup>1</sup>Carleton University, Physics, Ottawa, Canada; <sup>2</sup>The Ottawa Hospital Cancer Center, Medical Physics, Ottawa, Canada; <sup>3</sup>University of Ottawa, Radiology, Ottawa, Canada

#### Purpose or Objective

To validate 4D Monte Carlo (MC) simulations of dose delivery to a programmable deformable lung phantom using realistic respiratory motion traces.

#### Material and Methods

A previously developed tissue-equivalent deformable lung phantom<sup>1</sup>, was modified to enable realistic breathing motion [Fig.1a]. A piston, attached to a programmable motor, provides variable peak-to-peak (P-P) amplitudes in the sup-inf direction.

Measurements were performed on an Elekta Agility linac with the phantom in stationary and breathing states [Fig.1b]. Dose within the tumor, located in the lung, was measured using the calibrated Gafchromic EBT3 film and the RADPOS 4D dosimetry system<sup>2</sup> [Fig.1c]. To measure the dose inside the lung, two RADPOS detectors were mounted on the top and bottom surfaces of the plug [Fig.1d]. RADPOS position tracker recorded the phantom motion with a temporal resolution of a 100 ms.

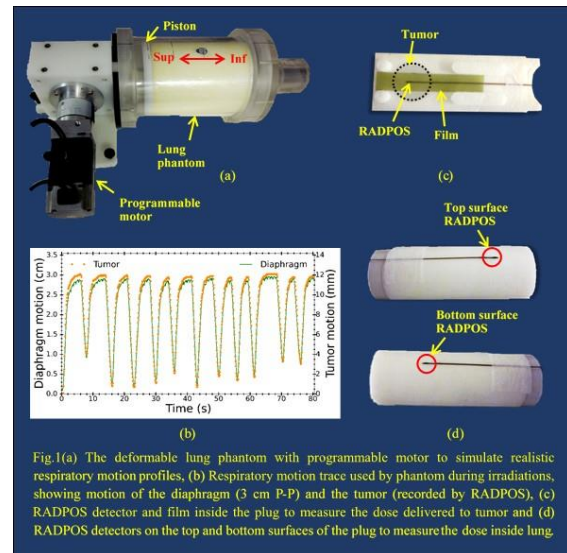


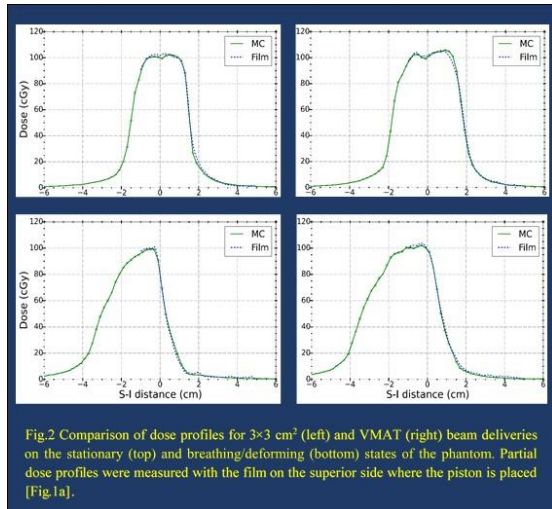
Fig.1(a) The deformable lung phantom with programmable motor to simulate realistic respiratory motion profiles, (b) Respiratory motion trace used by phantom during irradiations, showing motion of the diaphragm (3 cm P-P) and the tumor (recorded by RADPOS), (c) RADPOS detector and film inside the plug to measure the dose delivered to tumor and (d) RADPOS detectors on the top and bottom surfaces of the plug to measure the dose inside lung.

To capture full range of phantom motion, 3D CT scans of the phantom at end-of-inhale (0 cm) and end-of-exhale (3 cm) were acquired using a helical CT scanner. Static 3x3 cm<sup>2</sup> and VMAT plans were created on the end-of-inhale CT scans of the phantom in Monaco TPS V.5.11.01 to deliver 100 cGy to the center of the tumor.

A previously validated BEAMnrc model of our 6 MV Elekta Agility linac was used for all simulations<sup>3</sup>. DOSXYZnrc and 4DdefDOSXYZnrc<sup>3</sup> user codes were used, for stationary and moving anatomy dose simulations, respectively. We used  $8 \cdot 10^7$  histories to achieve a statistical uncertainty of 0.8% on a dose grid resolution of 2.0x2.0x2.0 mm<sup>3</sup>. Data from the linac delivery log files were extracted to generate input files for simulations. For 4D simulations, deformation vectors were obtained by deformably registering 4DCT scans of the end-of-exhale to end-of-inhale states using Velocity AI 3.2.0. Deformation vectors, along with the phantom motion trace measured with RADPOS, were used to model the phantom motion. The exact same motion as during irradiations was used in simulations by synchronizing the start of the phantom motion with the linac beam-on time.

#### Results

Dose values from MC simulations and measurements at the center of the tumor and bottom surface of the plug were found to be within 1s of experimental uncertainties (2.4%). Agreements on the top surface of the plug (high dose gradient region) were found to be better than 4.0%. On the stationary phantom all dose points from simulations passed a 2%/2 mm gamma analysis [Fig.2 top]. On the moving phantom, passing rates were better than 97.0% [Fig.2 bottom].



### Conclusion

Our 4DMC code accurately calculates dose delivered to a realistic breathing/deforming anatomy. This tool can be used for adaptive purposes to calculate the cumulative dose delivered to patients during treatments.

<sup>1</sup> Gholampourkashi S., *et al.* Phys. Medica 51, 2018;81-90

<sup>2</sup> Cherpak A., *et al.* Med. Phys. 36(5), 2009;1672-1679

<sup>3</sup> Gholampourkashi S., *et al.* Med. Phys. 44(1), 2017;299-310

### OC-0091 Patterns of failures among Imaging and Radiation Oncology Core lung and spine phantom irradiations

S. Edward<sup>1</sup>, H.A. Molineu<sup>2</sup>, P.E. Alvarez<sup>2</sup>, D. Followill<sup>1</sup>, S.F. Kry<sup>1</sup>

<sup>1</sup>The University of Texas MD Anderson Cancer Center, Radiation Physics, Houston, USA ; <sup>2</sup>The University of Texas MD Anderson Cancer Center, IROC Houston Quality Assurance Center, Houston, USA

### Purpose or Objective

To investigate and classify the reasons why institutions fail the Imaging and Radiation Oncology Core (IROC) SBRT spine and moving lung phantom (which are used to credential institutions for clinical trial participation).

### Material and Methods

A total of 189 IROC phantom irradiation results (61 spine and 128 lung) irradiated between 2012-present were randomly selected for investigation. Those that failed to meet established IROC criteria for a satisfactory irradiation were categorized as failures. The reports of the failing irradiations, including point dose disagreement, dose profiles, and gamma analyses, were qualitatively analyzed by IROC physicists. Classes of failure patterns were created and used to categorize each instance.

### Results

There were 34 phantom irradiation failures: 16 spine (26% of spine cases) and 18 lung (14% of lung cases). After individual analysis of each report, the phantom failures were classified as follows:

#### Spine

1. **Systematic dose:** uniform overdosing or underdosing of the PTV

2. **Dose fall-off region:** dose error in the steep dose-gradient between the PTV and spinal cord (Fig. 1D)

3. **OAR overdose:** overdose of the spinal cord structure

4. **Localization error:** dose distribution improperly aligned with target

#### Lung

5. **Systematic dose:** a uniform overdosing or underdosing of the PTV (all cases were underdosed)

6. **Local dose failure:** dose error in an isolated area of the plan

7. **ITV error:** dose error at end of motion range associated with using ITV technique (Fig. 1B)

8. **Localization error in the direction of motion (SI):** dose distribution improperly aligned with target in direction of motion

9. **Localization (SI) & ITV error:** a combination of 3 & 4 above

10. **Localization errors in multiple directions:** dose distribution improperly aligned with target in directions other than direction of motion

The number of failures in each category are listed in table 1, and dose profiles showing some of the phantom errors are illustrated in figure 1.

Spine Phantoms		Lung Phantoms	
Category	Number (%)	Category	Number (%)
Systematic:	8 (50)	Systematic dose	2 (11)
➤ Underdose	6 (38)	Local dose failure	2 (11)
➤ Overdose	2 (12)	ITV error	2 (11)
Dose fall-off region	2 (12)	Localization error in direction of motion (SI)	5 (28)
OAR overdose	3 (19)	Localization (SI) & ITV error	5 (28)
Localization error	3 (19)	Localization error in multiple directions	2 (11)

Table 1. Distribution of phantom failure categories

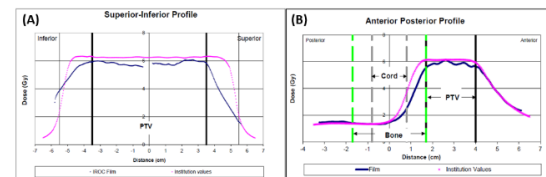


Fig. 1 Screenshots of lung and spine phantom dose profiles; pink represents the planned dose, blue is the measured dose. (A) shows an example of a lung phantom ITV error on the superior and inferior edges (direction of motion). (B) shows a spine phantom with an underdose in the dose fall off region.

### Conclusion

There are two distinct patterns of failure between phantoms. A majority (81%) of the spine phantoms failed due to a systematic dose error. Most (78%) of the moving lung phantom failures were due to localization of the moving target. Both of these errors are clinically relevant and will likely manifest as errors in patient cases. This information can help guide the community in improving the quality of radiation therapy.

### OC-0092 Portal dosimetry of small unflattened beams

A. Torres Valderrama<sup>1</sup>, I. Olaciregui-Ruiz<sup>1</sup>, P. González<sup>1</sup>, A. Mans<sup>1</sup>

<sup>1</sup>The Netherlands Cancer Institute, Radiation Oncology, Amsterdam, The Netherlands

### Purpose or Objective

Unflattened beams allow higher dose per pulse and faster delivery, but dosimetric difficulties arise with shrinking field size: (i) Electron range can exceed the field size yielding loss of equilibrium. (ii) Volume averaging effects smooth the penumbra and reduce the signal on the central axis (CAX). (iii) Accurate positioning of detectors becomes more critical than in large fields. Using traditional dosimetry under such circumstances has led to radiation accidents with over-dosage and harm to patients [1]. IAEA's code of practice TRS-483 [2] addresses these issues, providing output factors for several detector types, beam qualities and machine types. EPIDs have particular dosimetric characteristics requiring several corrections in order to match measurements of dose to water similar to those addressed in TRS-483. In this work we demonstrate that the back-projection algorithm in Ref. [3], after

modifications described below, can accurately convert portal images of small unflattened fields to dose distributions in patients and phantoms, both for static fields and VMAT arcs.

#### Material and Methods

The back-projection model in Ref. [3] was modified to render it applicable for small fields dosimetry as follows: (i) New reference measurements using the PTW microdiamond detector (type 60019) were used as input data for commissioning to reduce the volume effect.

(ii) The blurring EPID scatter kernel ([3] Eq. 5.11A), which mimics the ion chamber's volume effect, was removed for commissioning and dose reconstruction.

(iii) Square fields from  $10 \times 10 \text{ cm}^2$  down to  $1 \times 1 \text{ cm}^2$  were used to extract the primary signal, instead of the  $23 \times 23 \text{ cm}^2$  down to  $3 \times 3 \text{ cm}^2$  data in [3], better capturing the small fields regime.

(iv) Alignment errors between the portal images and the CAX microdiamond data arising from limitations in the accuracy of the EPID positioning system were corrected in the commissioning software.

#### Results

Fig. 1 compares TPS dose and portal dosimetry for small fields using the virtual reconstruction method [4], for a  $1 \times 1 \text{ cm}^2$  square field (a-b) and a VMAT plan (c-d). The standard reconstruction model (SRM) yields underdosage of about 8% compared to the TPS. Fig. (e) shows box plots of the dose difference at the isocenter for 15 VMAT plans expressed as a percentage. The small field model (SFM) reduces the discrepancy for all treatments to less than 3%, the tolerance value for clinical use. The mean dose error (not plotted) reduces from  $-2.9\%$  to  $-0.6\%$ .

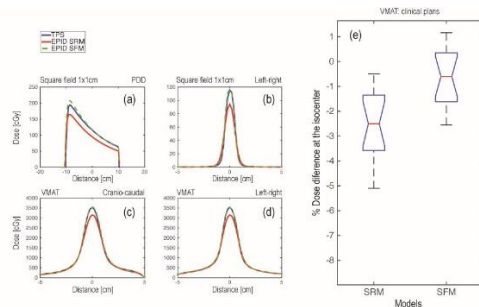


Figure 1: The left panel shows dose profiles obtained by the standard reconstruction model (SRM) and the small fields dosimetry model (SFM) for a  $1 \times 1 \text{ cm}^2$  square field on a polystyrene phantom aligned at the isocenter (a-b), and a VMAT plan reconstructed on the patient planning CT (c-d). (e) Shows box plots of the dose difference for 15 stereotactic VMAT brain plans, on each box the central mark is the median and the box edges are the 25th and 75th percentiles.

#### Conclusion

The EPID back-projection model in Ref. [3] was successfully extended to the small fields regime. With the modifications here described, portal dosimetry (in vivo as well as pre-treatment) can be used for accurate verification of both static fields and VMAT plans of small unflattened beams.

#### References

- [1] The New York Times, February 24.
- [2] IAEA (2017) Technical Reports Series No. 438. Vienna, Austria.
- [3] Medical Physics 33, 259-273 (2006).
- [4] Physica Medica 37, 49 - 57 (2017).

#### OC-0093 Microcavities in the lung affect the dose distribution in microbeam radiation therapy

G. Hombrink<sup>1,2,3</sup>, J.J. Wilkens<sup>1,2</sup>, S.E. Combs<sup>1,3</sup>, S. Bartzsch<sup>1,3</sup>

<sup>1</sup>Klinikum rechts der Isar, Department of Radiation Oncology, Munich, Germany; <sup>2</sup>Technical University of Munich, Physics Department, Munich, Germany; <sup>3</sup>Helmholtz Zentrum German Research Center for Environmental Health, Institute of Innovative Radiotherapy, Neuherberg, Germany

#### Purpose or Objective

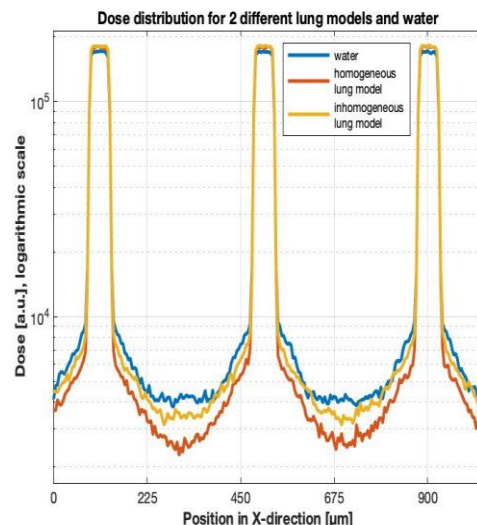
Microbeam radiation therapy (MRT) is a still preclinical technique in radiation oncology, which uses arrays of micro planar beams. High doses are delivered in the areas of the beams (peak dose, several 100 Gy) and a very low dose in between the beams (valley dose). This technique was suggested in the treatment of lung cancer as it promises less healthy tissue damage but equal tumor control when compared to conventional radiation therapy. However, as typical sizes of micro-cavities in the lung (alveoli, bronchioles, etc.) are in the same order of magnitude as microbeam widths and spacings the lung microstructure may have an effect on the dose distribution inside the lung tissue. The aim of this study is to quantify these differences in MRT dose distributions between the inhomogeneous lung tissue and the assumption of a homogeneous water-air mixture in Monte Carlo simulations.

#### Material and Methods

All simulations were performed with the Geant4 tool kit (vers. 10.0 patch 2). Two different lung models were developed, model 1 consisting of homogeneous tissue ( $\rho=0.26 \text{ g/cm}^3$ ) and model 2 of a water filled volume with small spherical air cavities ( $r=100 \text{ nm}$ ) in a cubic face centered packing to reach the same mean density as in model 1. Shape and size of the simulated volumes correspond to the geometry of an ongoing dosimetric validation using radiochromic films. Experimentally a slab of gel foam imitates the porous lung material. For reference the lung tissue and lung model in the phantom were replaced by pure water in a third simulation. A  $20 \times 20 \text{ mm}^2$  radiation field was used for all simulations comprising of 50 microbeams with a beam width of 50  $\mu\text{m}$  and a center to center distance of 400  $\mu\text{m}$ .

#### Results

Simulation results show that in the inhomogeneous lung model the valley dose is up to 41% higher than for the homogeneous model. There is also an up to 2% higher peak dose observed in the inhomogeneous lung model. Subsequently the peak to valley dose ratio (PVDR) is reduced in the inhomogeneous lung tissue (mean PVDR = 48.2) when compared to the homogeneous lung model (mean PVDR = 60.5).



#### Conclusion

The results show that the lung microstructure has a strong impact on the MRT dose distribution and cannot be neglected. At equal mean density the simple assumption of a homogeneous air-water mixture overestimates the PVDR by 25% on average in our simulations. The effect can be explained by secondary electrons that are produced in

the peak regions, traverse air cavities without substantial energy loss and deposit a higher dose distant to the peak in the valley regions. Our results show that the microstructure of the lung cannot be neglected for treatment planning of MRT in lung tissue. Currently, these findings are experimentally validated.

**Proffered Papers: RTT 1: Motion management and adaptive strategies**

**OC-0094 Retrospective evaluation of motion effects in robotic radiosurgery treatments of lung cancer**

S. Trivellato<sup>1,2</sup>, E. Rondi<sup>1</sup>, S. Vigorito<sup>1</sup>, E. Miglietta<sup>3</sup>, F. Castellini<sup>3</sup>, G. Piperno<sup>3</sup>, A. Ferrari<sup>3</sup>, B.A. Jercezek-Fossa<sup>3,4</sup>, F. Cattani<sup>1</sup>

<sup>1</sup>IEO- European Institute of Oncology IRCCS, Unit of Medical Physics, Milan, Italy; <sup>2</sup>University of Milan, Department of Physics, Milan, Italy; <sup>3</sup>IEO- European Institute of Oncology IRCCS, Division of Radiation Oncology, Milan, Italy; <sup>4</sup>University of Milan, Department of Oncology and Hemato-oncology, Milan, Italy

**Purpose or Objective**

Stereotactic body radiation therapy (SBRT) has emerged as a non-invasive standard treatment modality for early-stage lung cancer [1-3]. Respiratory management should be individually assessed to ensure SBRT dose conformity [4]. A treatment planning system for a robotic radiosurgery system is now offering the 4D treatment planning and optimization feature to consider organ motion recorded in a 4D computed tomography (4DCT) [5]. The aim of the study is to exploit this 4D module for a retrospective analysis of motion effects on target coverage and organs at risk (OARs) sparing during robotic radiosurgery in lung cancer treatment.

**Material and Methods**

Ten consecutive lung cancer treatments, 5 in upper and 5 in lower lobes, were retrospectively selected. The robotic system allows treating lesions that cannot be fully tracked. In this so-called 0-view modality, the internal target volume is defined as the envelope of the lesion volume in the full-exhale and full-inhale CT series. A set-up margin of 5 mm is added to get the planning target volume (PTV). The conventional 3D module optimizes and calculates dose distributions on the reference full-inhale phase. The 4D module uses b-splines deformable image registration to accumulate dose distributions calculated on each static 3D-CT image of the 4DCT dataset. For each patient, 3D optimization was performed and followed by both 3D and 4D calculations (3D<sub>opt+calc</sub> Plan and 3D<sub>opt</sub>4D<sub>calc</sub> Plan). A complete 4D optimization and calculation (4D<sub>opt+calc</sub> Plan) were performed when the 3D<sub>opt</sub>4D<sub>calc</sub> Plan resulted clinically suboptimal. All dose distributions were obtained using an 80% isodose prescription, the Ray Tracing algorithm, and 8 respiratory phases.

**Results**

The range of lesion displacement was 0-6 mm and 4-19 mm for upper and lower lobe, respectively. This difference resulted statistically significant at the Wilcoxon Mann Whitney test (*p*-value < 0.02). 3D<sub>opt+calc</sub> Plans showed a median volume covered by the 100% isodose (V<sub>100%</sub>) of 98.2% with a median minimum dose (D<sub>min</sub>) of 93.5%. 3D<sub>opt</sub>4D<sub>calc</sub> Plans resulted in a median V<sub>100%</sub> of 95.6% and a D<sub>min</sub> of 87.6%. Variations in V<sub>100%</sub> metric were in the range (-14.9%, 0%). Seven out of 10 patients were re-optimized with the 4D Module, all lower lesions and 2 upper lesions. 4D<sub>opt+calc</sub> Plans showed a median V<sub>100%</sub> of 97.3% with a median D<sub>min</sub> of 93.8%. Among OARs, most relevant variations were registered in the heart maximum dose. Details are reported in Table 1 and 2.

	SI [mm]	Plan	D <sub>min</sub> [%]	V <sub>100%</sub> [%]
Total (10 patients)	3.8 (0-17.5)	3D <sub>opt+calc</sub>	93.5 (85.1 - 96.7)	98.2 (95.2 - 98.8)
		3D <sub>opt</sub> 4D <sub>calc</sub>	87.6 (75.4 - 96.5)	95.6 (83.3 - 98.3)
		4D <sub>opt+calc</sub>	93.8 (85.6 - 95.5)	97.3 (96.0 - 98.7)
Lower lobe (5 patients)	11.3 (4.0 - 17.5)	3D <sub>opt+calc</sub>	94.2 (91.0 - 95.8)	98.2 (95.2 - 98.6)
		3D <sub>opt</sub> 4D <sub>calc</sub>	86.3 (75.4 - 93.9)	90.1 (83.3 - 96.8)
		4D <sub>opt+calc</sub>	93.8 (92.1 - 95.5)	97.3 (96.0 - 98.7)
Upper lobe (5 patients)	2.5 (0.0 - 3.8)	3D <sub>opt+calc</sub>	92.8 (85.1 - 96.7)	98.4 (97.0 - 98.3)
		3D <sub>opt</sub> 4D <sub>calc</sub>	88.9 (82.8 - 96.5)	97.0 (92.1 - 98.3)
		4D <sub>opt+calc</sub>	89.8 (85.6 - 93.9)	97.1 (96.8 - 97.4)

**Table 1** Dosimetric results for total population, upper and lower lobe lesions: comparison between 3D<sub>opt+calc</sub>, 3D<sub>opt</sub>4D<sub>calc</sub>, and 4D<sub>opt+calc</sub> Plans. Values are presented as median (min-max). 3D<sub>opt+calc</sub>: dose distribution of 3D optimized and calculated plans; 3D<sub>opt</sub>4D<sub>calc</sub>: dose distribution of 3D optimized and 4D calculated plans; 4D<sub>opt+calc</sub>: dose distribution of 4D optimized and calculated plans; D<sub>min</sub>: minimum target dose; V<sub>100%</sub>: percentage volume covered by the 100% isodose.

OARs. D <sub>max</sub>	Δ%
Spinal cord	0.1 (-3.4; 2.0)
Oesophagus	-0.1 (-4.8; 2.7)
Heart	-2.7 (-16.2; 2.5)
Trachea	0.4 (-1.6; 5.7)

**Table 2** Variation between 3D<sub>opt+calc</sub> and 3D<sub>opt</sub>4D<sub>calc</sub> dose distributions for main organs at risk (OARs). Values are presented as median (min-max). Δ%: percentage deviation of 3D<sub>opt</sub>4D<sub>calc</sub> maximum doses with respect to 3D<sub>opt+calc</sub> maximum doses.

**Conclusion**

Due to recorded variations, 70% of plans have been re-optimized. The 4D module is a powerful tool to manage organ motion when lesion tracking is not possible, especially for lesions in lower lobes or close to moving OARs. Further studies will increase the number of patients and a Monte Carlo calculation will permit dose prescription discussion. Results will be validated with film measurements in a 4D anthropomorphic phantom.

**OC-0095 Intrafraction motion management in VMAT breast radiotherapy with AlignRT system: comparison of ROIs**

V. Favre<sup>1</sup>, O. Ruiz Abrard<sup>1</sup>, F. Chabbert<sup>1</sup>, C. Garcia<sup>1</sup>, L. Gonzalez Casabianca<sup>1</sup>, H. Mailleux<sup>1</sup>

<sup>1</sup>Institut Paoli Calmettes, radiotherapy oncology, Marseille, France

**Purpose or Objective**

Intra-fraction motion represents a crucial issue in the era of precise radiotherapy in VMAT breast irradiation. Continuous surface imaging offers the capability to monitor patient movements in three-dimensional space without any additional radiation exposure. During the implementation phase of 3D surface imaging system (AlignRT, Vision RT™, London, UK) in our institution, we noticed that the video camera-based patient localization

system that captures and compares images of a patient's topography to a DICOM-formatted external contour could be broken by the gantry motion during the VMAT session. To increase the accuracy of intra-fraction motion management and to avoid this break, we intend to compare the use of two types of ROIs in VMAT radiotherapy for breast cancer treatment.

#### Material and Methods

From November 2017 to March 2018, sixty breast cancer patients who underwent whole breast radiotherapy (WBRT) with VMAT treatment were selected for this study. CBCT were performed at the 1<sup>st</sup>, 2<sup>nd</sup>, 3<sup>rd</sup> day of the treatment, and then weekly. Patients were divided into two groups of thirty. Group one (G1) was positioned with the aid of AlignRT using an isocentric region of interest (ROI) containing the treated breast and the upper part of the abdomen (limited ROI). In group two (G2), patients were also positioned with AlignRT with a ROI containing the treated breast and half part of the contralateral breast (extensive ROI). For both groups, extra-treatment sites' ROIs were the same: homolateral arm, neck and head position. All the fractions for each patient were consecutively analyzed.

#### Results

A break in the intra-fraction motion management with AlignRT was noticed in 283/721 (39%) sessions using limited ROIs (G1), versus 52/702 (7%) using extensive ROIs (G2). In G1, 3/30 patients could achieve their treatment without any break versus 18/30 in G2.

#### Conclusion

We demonstrated that intra-fraction motion management with AlignRT in VMAT for breast cancer is reproducible and accurate thanks to a modification of isocentric ROIs, and allows the use of 3D surface imaging system in deep-inspiration-breath hold with VMAT technique in our institution.

#### OC-0096 Implementation of DIBH for gated IMRT of left sided breast cancer using optical surface guidance

N. Gomes<sup>1,2</sup>, A.M. Furtado<sup>1</sup>, M.D.G. Coelho<sup>1,2</sup>, M. Possanzini<sup>3</sup>, J. Morales<sup>1</sup>, C. Greco<sup>1</sup>

<sup>1</sup>Fundação Champalimaud, Radiation Oncology, Lisboa, Portugal ; <sup>2</sup>Mercurius Health, Radiation Oncology, Lisboa, Portugal; <sup>3</sup>Azienda Ospedaliera G. Brotzu, Radiation Oncology, Cagliari, Italy

#### Purpose or Objective

To describe the implementation of a workflow for treating left breast cancer patients with hypofractionated IMRT in DIBH using SGRT (Surface Guided Radiotherapy). This is known to reduce heart dose and therefore cardiotoxicity risk.

#### Material and Methods

24 patients with left sided breast cancer confined to the breast were selected. First, they had a training session on the Linac. The procedure was explained and the breathing amplitude and reproducibility were verified using OSMS (Optical Surface Monitoring System). Patients had to maintain DIBH for a minimum of 25s (mean time for a treatment field delivery). Treatment isocenter was defined to allow spotlight CBCT acquisition in DIBH to confirm lung expansion. Suitable patients then had 2 planning CTs (Free Breathing (FB) and DIBH). As OSMS is not installed in the CT room, spotlight CBCT and DIBH planning CT were merged to confirm reproducibility. Treatment plans using IMRT (2.7Gy to whole breast and 3.2Gy to an integrated boost) in 15 fractions were planned for both CTs to validate DIBH's advantage. Patients selected to be treated with DIBH had their setup confirmed with CBCT in FB before each treatment. OSMS was used to automatically perform shifts to DIBH isocenter. Spotlight CBCT was performed to avoid centring the couch while allowing continuous monitoring, prevent collisions, confirm lung expansion and heart position. If shifts within departmental tolerances (<3mm), treatment

is delivered with a gated beam on threshold of 3mm (fig.1). A spotlight CBCT is acquired at the end of treatment to confirm patient positioning and OSMS accuracy (fig.2). CBCT shifts, DIBH times and overall treatment times were measured.



Fig. 1 – Treatment delivery: a) Patient setup and monitoring, b) Beam held with breathing outsider threshold, c) Beam enabled with DIBH within threshold

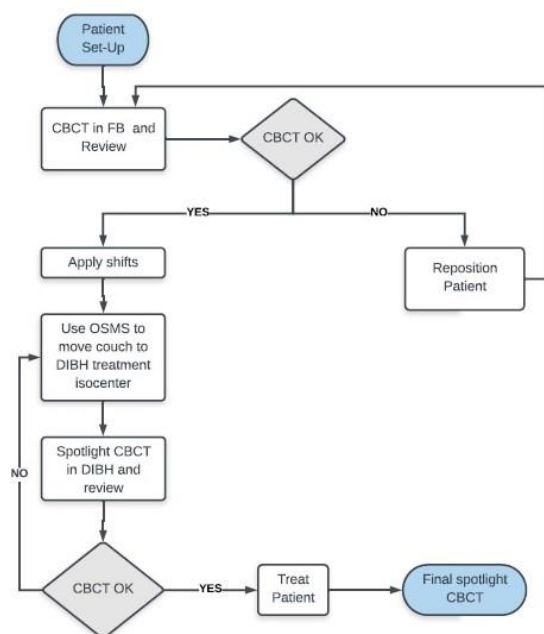


Fig. 2 - Workflow diagram.

## Results

5 patients were not suitable for DIBH. 2 did not meet training sessions criteria and 3 showed no dosimetric advantage when comparing both planning CT's. For the 19 suitable patients the mean DIBH time during training session was 31s, adding 6s to the minimum requisite. The mean overall treatment time was 26min about twice the departmental time slot of a standard FB treatment. For the first patient, adaptations of the planned workflow were made, due to inaccurate positioning of the OSMS cameras. During gantry rotation, cameras are blocked between 20° and 70°, interrupting the treatment repeatedly resulting in longer treatment time. This was solved by increasing the ROI and therefore the detected surface. In the 285 treatment sessions delivered, DIBH CBCT after OSMS positioning was within tolerances for 254 sessions. The remaining 31 sessions required repositioning and image reacquisition. With DIBH, the mean dose to the heart was reduced by 1.4Gy (5Gy in FB vs 3,6Gy in DIBH).

## Conclusion

DIBH using OSMS was successfully implemented in our department and is now a routine procedure. Careful selection of the patients is a key factor for a successful treatment delivery and the increased workflow has to be balanced out with its effective benefit. Our next aim is to implement SGRT in other thoracic treatment sites.

## OC-0097 Detection of GoldAnchor markers implanted in the liver during robotic radiosurgery in the CK system.

K. Szczepanik<sup>1</sup>, M. Stapo-Fudzinska<sup>2</sup>, B. Jochymek<sup>1</sup>, D. Bodusz<sup>1</sup>, L. Kleszyk<sup>1</sup>, E. Telka<sup>1</sup>, M. Kijonka<sup>3</sup>

<sup>1</sup>Maria Skłodowska-Curie Memorial Cancer Center and Institute of Oncology, Department of Radiotherapy, Gliwice, Poland ; <sup>2</sup>Maria Skłodowska-Curie Memorial Cancer Center and Institute of Oncology, Department of Planning Radiotherapy and Brachytherapy, Gliwice, Poland ; <sup>3</sup>Maria Skłodowska-Curie Memorial Cancer Center and Institute of Oncology, Department of Medical Physics, Gliwice, Poland

## Purpose or Objective

The study was to determine the migration values of applied GoldAnchor® intra-markers to the liver and to

assess their visibility in CT, MRI and the verification system.

## Material and Methods

The value of migration and change of the geometry of the system of implanted markers. The group of 66 patients was determined on the basis of a comparison of the distance between central points of all implanted markers during all treatment sessions. Measurement of the distance between the central points was carried out on the basis of images archived in the CyberKnife system.

The usefulness of tags is defined by determining the number of intra-markers used to locate the disc volume by the CyberKnife verification system. The analysis included a group of 66 patients who are treated in the Department of Radiotherapy, Oncology Center, the Branch Gliwice, from January 2010 to June 2017. In each patient, 2 to 5 markers were implanted percutaneously into the liver. In total, 198 gold markers were implanted. On the basis of CT scans, on which the contours of the tumor and critical organs were drawn, a treatment plan was prepared in the MultiPlan system. During each therapeutic session, the patient was positioned using a vacuum mattress, an infrared camera marker system and a Synchrony Vest. After making verification images in the CyberKnife system, the golden markers were located automatically. All detected markers were marked as active in the treatment panel. The number of detected markers by the system in individual treatment fractions was estimated based on a retrospective analysis of 352 archived images.

## Results

The average value of change in distance between markers along with the standard deviation was: 0.53 mm (SD = 0.86). The maximum value of change in distance between markers was 2.5 mm. In 57% of measurements, there was no change in the distance between individual markers during radiotherapy. In 39% of measurements, the measured change in distance was 1-2 mm, and in the case of 15% of measurements, the value was 3 mm. There was no case of tracer migration outside the liver area.

In 50% of patients, despite the implantation of at least 3 markers, the system detected only 2 during the entire treatment, and in the group of 16% of patients, the system detected only one marker. In all patients, where it was impossible to verify at least 3 markers, the implanted markers were developed or occurred in both forms. In the case of patients in whom all markers were folded up, the system correctly detected at least 3 markers.

In all cases, the markers were visible in CT and computed tomography images of nuclear magnetic resonance.

## Conclusion

1. The GoldAnchor® intra-tracer label applied in rolled form does not migrate in the liver parenchyma during the entire healing process,
2. The shape of the implanted tags determines the ability to detect them by the CyberKnife verification system; tags in the expanded form (line) are more often not recognized by the system than those that have a folded form,
3. The GoldAnchor® markers should be implanted in the liver only in rolled form (loops).

## OC-0098 Gated vs coached DIBH treatment in left sided breast cancer radiotherapy: a single centre study

K. Crowther<sup>1</sup>, S. Osman<sup>2</sup>, S. O'Hare<sup>1</sup>, S. Gray<sup>1</sup>, D.

Holland<sup>1</sup>, H. Vennard<sup>1</sup>, G. Hanna<sup>1,2</sup>

<sup>1</sup>Belfast Health and Social Care Trust, Cancer Centre-Radiotherapy, Belfast, United Kingdom ; <sup>2</sup>Queen's University, Centre for Cancer Research and Cell Biology, Belfast, United Kingdom

## Purpose or Objective

Deep inspiration breath hold (DIBH) reduces cardiac and pulmonary dose during tangential-field left breast radiotherapy (RT). We report preliminary results of an ongoing study, comparing voluntary moderate (vm) DIBH

and gated DIBH treatment for left sided breast cancer patients.

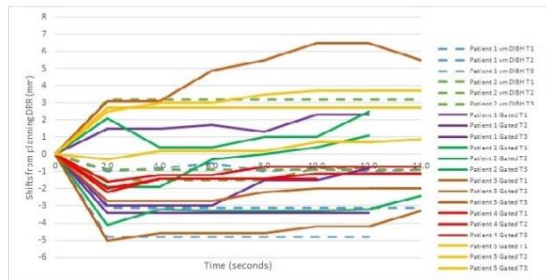
#### Material and Methods

Patients receiving adjuvant radiotherapy for breast cancer who had a maximum heart distance  $\geq 10$ mm from a standard free-breathing tangential field treatment plan underwent a second planning CT scan using a coached DIBH technique. All patients underwent whole-breast or chest wall DIBH RT. For 5 patients, Varian® Real-time Position Management (RPM™) system was used to monitor respiratory movement and to gate treatment delivery. In the other 5 patients, the vmDIBH technique was used to monitor the patient's breath-hold (BH) during treatment delivery by observing the marked isocentre in relation to the laser and treatment interrupted if there was concern that BH depth had changed. Daily cine electronic portal images were acquired, when possible, during delivery of the medial treatment field and treatment delivery times recorded. For every cine image acquired, the central lung distance (CLD), central flash distance, inferior central margin was measured at two-second intervals. Stability and reproducibility of BH was examined.

#### Results

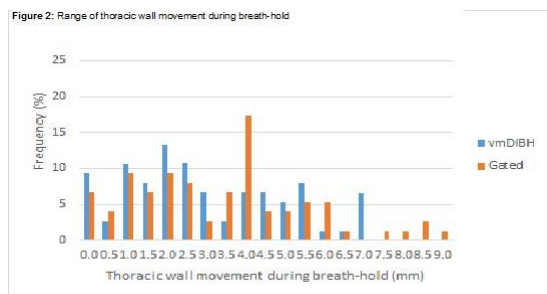
Ten patients were included in this analysis. Age ranged from 32 to 73 years (gated) and 40 to 55 years (vmDIBH). For all patients the treatment course was delivered as planned in DIBH (40Gy/15f) without interruption. Treatment delivery time per field was comparable between the gated (time= 162 seconds (s)) and vmDIBH groups (t=114s). For each patient, the stability of BH was determined from the difference in CLD relative to reference position in CT digitally reconstructive radiograph (DRR). (Figure 1). All images are within local breast imaging tolerance ( $\leq 6$ mm).

Figure 1: Thoracic wall movement during delivery of medial treatment field: first three fractions



The frequency of thoracic movements over a treatment course are presented in Figure 2 with the highest frequency observed thoracic movement for gated DIBH at 1.5mm and vmDIBH 2mm.

Figure 2: Range of thoracic wall movement during breath-hold



Reproducibility of BH was determined from the difference in thoracic movement on first frame of the cine image relative to the DRR. The population mean for vmDIBH was 1.7mm (SD 3.4mm) and the population mean for gated was 0.4mm (SD 3.7mm), indicating high reproducibility.

#### Conclusion

Two DIBH techniques have now been implemented into clinical practice with no significant difference observed between the treatment delivery times. Preliminary results indicate that both techniques ensure good reproducibility and stability of BH. This study will continue with the inclusion of additional patients. Future work will include the roll out of DIBH to enable IMC treatment but this will require a tightening of imaging tolerances and the evaluation of the dosimetric consequences to heart and left anterior descending artery.

#### Poster Viewing: Poster viewing 2: Advanced technologies

#### PV-099 MC simulations and dose measurements of a patient-specific 3D range-modulator for proton therapy

Y. Simeonov<sup>1</sup>, U. Weber<sup>2</sup>, C. Schuy<sup>2</sup>, K. Zink<sup>1</sup>  
<sup>1</sup>Technische Hochschule Mittelhessen - IMPS, Lse, Gießen, Germany; <sup>2</sup>GSI Helmholtzzentrum für Schwerionenforschung GmbH, Biophysics division, Darmstadt, Germany

#### Purpose or Objective

The purpose of this work was to develop and validate a novel 3D range-modulator for very fast treatment of moving targets. In contrast to the pencil beam scanning technique, where the multiple iso-energy layers are associated with relatively long irradiation times, the 3D modulator uses only one single energy to create a homogeneous and highly conformal 3D dose distribution, decreasing extremely the treatment time.

#### Material and Methods

Extending previous extensive research in this field, a 3D modulator was now developed from a real CT patient data, utilizing a ray-tracing algorithm to calculate the necessary information. A lung tumour with a complex 3D contour and irregular distal and proximal edges was deliberately chosen in order to simulate a worst-case scenario and investigate the limitations of the newly proposed technique.

The 3D modulator consists of many fine pyramid-shaped structures (pins) with  $\sim 4$  mm<sup>2</sup> base area (Fig.1). By using this pins an additional degree of freedom is introduced, i.e., the height and shape of each single pins can now be independently varied and optimised in such a way that the final 3D shape of the modulator corresponds to the 3D tumour form. When irradiated, the 3D range-modulator should create a quasi-static irradiation field, tightly shaped around the target.

The modulator was optimised for 151.77 MeV <sup>1</sup>H and was eventually triangulated and manufactured on a 3D-printer in high-quality rapid prototyping technique. The FLUKA Monte Carlo (MC) package was used to investigate the modulating properties of the range-modulator and calculate the resulting dose distribution. A sophisticated in-house user routine was additionally implemented into FLUKA to enable intensity modulated scanning and take into account the complex geometry contour of the modulator.

In order to validate the MC simulation results, dose measurements were conducted at the Marburg Ion-Beam Therapy Centre (MIT). The dose was measured with a 2D ionization chamber array (977 ICs) with 2.5 mm lateral resolution. The measurement depth was varied with a binary range shifter consisting of a set of retractable polyethylene plates.

#### Results

There is very good agreement between the measured and simulated dose. Fig 2. shows a homogeneous dose distribution conformed not only to the distal, but also to the proximal edge of the target.

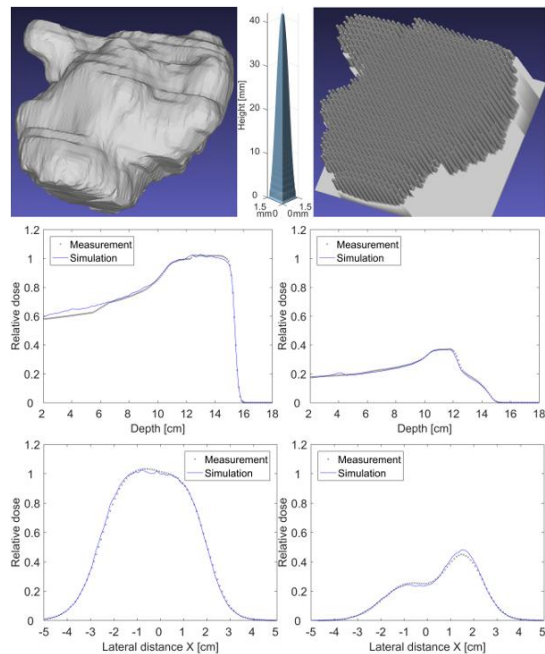


**Fig. 1** 3D tumour contour, a single pin and the corresponding 3D modulator (upper panel); Measured vs simulated dose distributions (middle/lower panel).

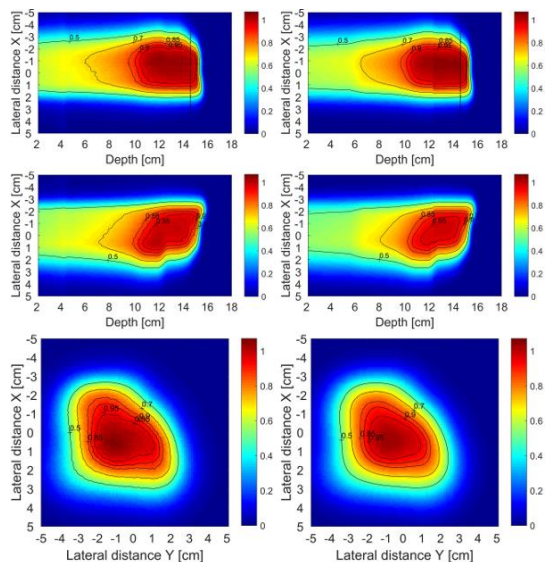


**Fig. 2** Measured vs. simulated X-Z (upper/middle panel) and X-Y (lower panel) dose distributions.

**Conclusion**

Utilizing state-of-the-art 3D printing technique to manufacture complex modulators is possible. Combining the advantages of very short treatment time, the 3D range-modulator could be an alternative to treat lung tumours with the same conformity as full raster-scanning treatment. Further measurements must be conducted to investigate the full potential of the 3D range-modulator.

**PV-100 Development of plan quality through EBRT dummy run in the EMBRACE-II study for cervical cancer**

Y. Seppenwoolde<sup>1</sup>, M. Sanggaard Assenholt<sup>2</sup>, D. Georg<sup>1</sup>, R. Nout<sup>3</sup>, L.T. Tan<sup>4</sup>, T. Rumpold<sup>1</sup>, A. De Leeuw<sup>5</sup>, I. Jürgenliemk-Schulz<sup>5</sup>, C. Kirisits<sup>1</sup>, R. Pötter<sup>1</sup>, J.C. Lindegaard<sup>2</sup>, K. Tanderup<sup>2</sup>, T.E. Collaborative Group<sup>1</sup>  
<sup>1</sup>Medical University of Vienna, Department of Radiotherapy, Wien, Austria; <sup>2</sup>Aarhus University

Hospital, Department of Oncology, Aarhus, Denmark ; <sup>3</sup>Leiden University Medical Centre, Department of Clinical Oncology, Leiden, The Netherlands; <sup>4</sup>Cambridge University Addenbrooke’s Hospital, Department of Radiotherapy, Cambridge, United Kingdom; <sup>5</sup>University Medical Center Utrecht, 6 Department of Radiotherapy, Utrecht, The Netherlands

**Purpose or Objective**

The international, multicentre EMBRACE II study combines Image-Guided Adaptive Brachytherapy for cervix cancer with an advanced protocol for external beam radiotherapy (EBRT) with specific target volume selection, contouring and treatment planning procedures. Well-defined EBRT is an integral part of the overall treatment strategy with the primary aim of improving nodal control and reducing morbidity. Before entering EMBRACE II, institutes had to go through accreditation regarding EBRT and brachytherapy. This study describes the development of EBRT plan quality through the accreditation dummy-run.

**Material and Methods**

The EMBRACE II EBRT planning concept is based on improved conformity[1] through eased coverage criteria for planning target volumes (PTV45Gy: V95%≥95% and Nodal PTV D90%≥98%) with the aim to reduce overall irradiated volume and spare OARs. Lymph nodes are irradiated by a simultaneous integrated boost and by coverage probability planning it is ensured that 98% of each nodal CTV is covered by 100% of the prescribed dose. As part of accreditation, a treatment planning dummy-run in combination with educational blocks and submission of an examination case was provided and evaluated by the study coordinators. Replanning and resubmission was required if hard constraints were violated or soft constraints were violated more than once or with a considerable amount. This study describes the plan quality of 113 submitted EBRT dose distributions from 67 centres.

**Results**

Twenty-four centres passed after first submission, and 23 and 10 centers needed one or more revisions, respectively. IMRT, VMAT and tomotherapy were used in 7%, 88% and 5% of the centers, and 6, 10 and 15 MV in 71%, 24% and 5% of centers, respectively. It was possible to produce acceptable plans with all techniques, energies, and treatment planning systems. The most common reasons for revisions were non-compliant conformity index, relatively high OAR doses or insufficient lymph node coverage. Only a few (6) first submissions were rejected because of (minor) hard constraint violations. Individual feedback improved plan quality considerably (Table 1 and Figure 1) with a significant improvement of conformity index from 1.12 to 1.03. A better cooling down of the PTV edges particularly resulted in a median V43Gy reduction of 133cm<sup>3</sup> from first plan submission to approved plan.

Parameter	constraint	Passed	SD (%)	Rejected	SD (%)	Paired analysis Difference after revision (rejected – passed)
Nr of plans		57		54		30
PTV45 (%) V95	95	97.0	1.4 1%	98.7	2.2 2%	-2.0
ITV45 (Gy) mindose	42.75	43.4	0.5 1%	43.5	1.1 3%	0.2
PTV LN1 CoP	90	92	2 2%	97	5 5%	-3
PTV LN2 CoP	90	92	2 2%	96	4 4%	-2
Conformality	115	1.03	0.04 4%	1.12	0.15 13%	-0.12
Bowel (cm3) V30Gy	450	428	58 14%	481	101 21%	-58
Bowel (cm3) V40Gy	222	164	20 13%	192	52 27%	-29
Sigmoid (%) V30Gy		88	8 9%	91	8 9%	-3
Sigmoid (%) V40Gy		69	6 8%	72	9 12%	-4
Bladder (%) V30Gy	80	72	8 11%	76	12 15%	-6
Bladder (%) V40Gy	55	42	4 10%	48	11 23%	-7
Rectum (%) V30Gy	90	72	5 7%	75	7 10%	-2
Rectum (%) V40Gy	75	51	6 12%	57	11 19%	-5
PIBS-2cm (Gy)	5	2.7	0.5 19%	2.8	1.1 38%	0
Body (cm3)* V43Gy		1725	71 4%	1869	246 13%	-133
Body (cm3)* V50Gy		38	10 25%	53	28 53%	-11

Table 1. Plan parameters and their median, SD values for all the passed plans, all rejected plans and the difference after revision (paired analysis).

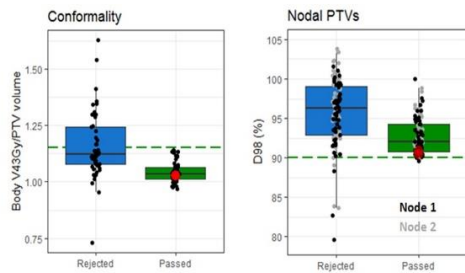


Figure 1. Average and 25%/75% percentile values for all rejected (blue) and passed (green) plans for conformity index and Nodal PTVs. Dotted line: constraint. Red dots: reference plan.

## Conclusion

A dummy-run accreditation as applied in EMBRACE II based on defined dose volume parameters for targets, OARs, conformity indices, V43Gy and including training and examination cases enables to test institutes' treatment planning capabilities and improves plan quality considerably whilst reducing inter-center variations.

[1] Defined as (V43Gy)/(PTV45Gy volume)

## PV-101 Clinical implementation of a dedicated brain treatment planning optimizer for stereotactic treatment

T. Gevaert<sup>1</sup>, A. Girardi<sup>1</sup>, B. Engels<sup>1</sup>, M. Boussaer<sup>1</sup>, C. El Aïsati<sup>1</sup>, M. De Ridder<sup>1</sup>

<sup>1</sup>Universitair Ziekenhuis Brussel, Radiotherapy, Brussels, Belgium

## Purpose or Objective

Clinical implementation of a novel dedicated and automated treatment-planning solution for cranial indications, Elements. Single lesions can be targeted with an inversely optimized VMAT approach using automated arc trajectory optimization (Cranial SRS Element, Brainlab, München, Germany) while up to fifteen metastatic brain tumors can be automatically targeted with a single isocenter and multiple inversely-optimized dynamic conformal arcs (Multiple Brain Mets SRS Element, Brainlab, München, Germany).

## Material and Methods

The very first 25 treated patients were analyzed, each representing a variable number of lesions (1-12). Depending on the number and location of the lesions a dedicated Element was selected and used in order to achieve the specific planning constraints. The plans were evaluated by means of Paddick conformity (CI) and gradient index (GI). Patient specific quality assurance (QA) was performed with gafchromic EBT3 film and portal imager.

## Results

The Elements software tools generated plans with CI of  $0.71 \pm 0.09$  and a gradient index of  $3.9 \pm 1.4$ . All plans achieved the organ at risk constraints. A gamma of 3%/3mm was used for the QA. A 98% and 98,2% passing rate was found for the EBT3 film and portal imager, respectively. This shows also the good concordance between film and EPID, suggesting that patient specific QA can be performed with the portal imager rather than the time-consuming films.

## Conclusion

The automated dose planning Elements revive dynamic conformal arcs as the paradigm for linac-based stereotactic radiosurgery of multiple brain metastases and at the same time implements an improved VMAT approach for single lesions with the use of automated arc trajectory optimization. This study shows the implementation of this technique in the routine clinical environment with an improved planning and treatment efficiency.

## PV-102 A prediction of intrinsic uncertainties in radiotherapy treatment planning systems

K. Kiers<sup>1</sup>, P. Van Horssen<sup>1</sup>, J.T. Trinks<sup>1</sup>, P.R. Pronk<sup>1</sup>, A. Mans<sup>1</sup>, C.J. Schneider<sup>1</sup>, E.M.F. Damen<sup>1</sup>, T.M. Janssen<sup>1</sup>

<sup>1</sup>The Netherlands Cancer Institute, Department of Radiation Oncology, Amsterdam, The Netherlands

## Purpose or Objective

In radiotherapy treatment planning, differences between the simulated and delivered dose can arise from intrinsic limitations of the treatment planning system (TPS) beam model. Among these limitations, we recognize two types: 1) approximating a continuous VMAT delivery with discrete control points and 2) uncertainties in the beam model. It is expected that increasing plan complexity leads to higher dosimetric uncertainty in both aspects.

The aim of this work is to predict for Pinnacle<sup>3</sup> v9.10 (Philips, Fitchburg, USA) the impact of these two intrinsic TPS problems which could lead independently to dosimetric errors, using complexity metrics (CMs) derived from the plan.

## Material and Methods

Regarding arc discretization, 80 clinical non-SBRT VMAT plans were selected. Each was computed with a control point gantry angle spacing of 4° and 2°. Plans which differed  $\geq 1\%$  in PTV-mean dose were classified as too complex. 9 CMs (Tab. 1) were calculated for all plans. A model to predict  $\Delta D_{\text{mean}} \geq 1\%$  (Prediction 1) was created using leave-one-out cross validated logistic regression and a combination of CMs, and validated on a stratified split train- and test set (80/20).

To test intrinsic beam model uncertainty, the dose distribution was recalculated for 77 non-SBRT VMAT plans comprising of three 'machines' (MLCi, 6 and 10MV; Agility, 10MV (Elekta, Stockholm, Sweden)), using two clinically commissioned beam models based on the same set of measurements. From the commissioning point of view both beam models per machine appear equivalent, only differing marginally in parameters like leaf offset correction, MLC transmission and penumbra blurring. Beam models of different machines were independent. Using CMs (Tab. 1), a linear regression model was trained to predict the  $\Delta D_{\text{mean}}$  between beam models for all MLCi 10MV plans (Prediction 2) and validated against the remaining plans. This model was then applied to 1412 independent plans and compared to their dosimetric outcome using the isocentre gamma value (3%/3mm) derived from in-vivo EPID dosimetry. Results were binned on Prediction 2 and per bin the 90<sup>th</sup> percentile of the isoc-gamma was used as a measure of dosimetric uncertainty.

## Results

Prediction 1: The  $\Delta D_{\text{mean}} \geq 1\%$  could be predicted with a specificity of 0.98 and a sensitivity of 1.0 by linear combination of three CMs (Tab. 1, Fig. 1).

Prediction 2: The predicting value was found using a linear regression of 7 CMs (Tab. 1, Fig. 1B1) with a fit of  $R^2=0.6$  ( $p<0.001$ ) for MLCi-10MV. The model was validated for Agility-10MV and MLCi-6MV with an  $R^2$  of 0.64 ( $p<0.001$ ) and 0.55 ( $p<0.001$ ) respectively. The predicting value has a strong linear correlation with the 90% CI isoc-gamma of the 1412 plans ( $R^2=0.6$ ,  $p<0.001$ , Fig. 1B2). The spread in the data in Figure 1B2 is due to the noisy nature of in vivo data.

Table 1. The complexity metrics. All metrics were calculated per control point and normalized to monitor units per beam and to control point.

	Complexity metrics	Explanation	Used in
Size and location	Field Aperture	Aperture size.	Pred. 2
	Wide Field Score	Sum of all distances from the center of the field aperture to the center of the MLC.	Pred. 2
Shape	Aperture Irregularity	Squared circumference of the aperture / $4\pi \cdot$ segment size.	Pred. 2
	Beam Modulation	$1 - (\text{Aperture size} / \text{union of all aperture sizes})$ .	Pred. 2
Dynamics (VMAT)	Leaf Travel	Average of the total travelled distance per leaf.	Pred. 2
	Modulation	Variation in segment area relative to the maximum aperture multiplied by the differences in position of the leaves relative to the maximum leaf differences.	Pred. 2
	Complexity Score		
	Dynamic Field Aperture	Absolute aperture difference between segments.	Pred. 1
	Traveled area	Traveled area between segments.	Pred. 1
	Segment Union	Union of the aperture area in two consecutive segments.	Pred. 1 and 2

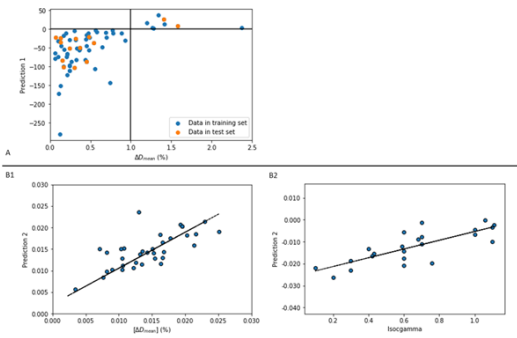


Figure 1 A: Prediction of the difference in dose calculation with a 2 and 4 degree gantry angle spacing ('Prediction 1') to the measured  $AD_{mean}$ . Orange data sets are the test data. B1: Prediction of the difference in dose calculation with different beam models ('Prediction 2') to the measured difference for MLG-10MV plans. B2: 90% CI of 'Prediction 2' of 1412 independent plans, packed in 35 bins, to their isocentre gamma value (3%/3mm).

### Conclusion

We demonstrated that CMs can be used effectively to predict intrinsic uncertainties in the TPS. These results can be used to indicate the probability of dosimetric errors for a given plan.

### PV-103 Linking ACROP guidelines to ICRU91: a multicentre study in lung SBRT on prescription and reporting

E. De Jong<sup>1</sup>, M. Guckenberger<sup>2</sup>, N. Andratschke<sup>2</sup>, K. Dieckmann<sup>3</sup>, M.S. Hoogeman<sup>4</sup>, M. Milder<sup>4</sup>, D. Sloth Moller<sup>5</sup>, T. Bisballe Nyeng<sup>5</sup>, S. Tanadini-Lang<sup>2</sup>, E. Lartigau<sup>6</sup>, T. Lacornerie<sup>6</sup>, A. Mendez Romero<sup>4</sup>, W. Verbakel<sup>7</sup>, D. Verellen<sup>8</sup>, G. De Kerf<sup>8</sup>, C.W. Hurkmans<sup>1</sup>  
<sup>1</sup>Catharina Ziekenhuis, Department of Radiation Oncology, Eindhoven, The Netherlands; <sup>2</sup>University Hospital Zurich, Department of Radiation Oncology, Zurich, Switzerland; <sup>3</sup>Medical University of Vienna, Department of Radiation Oncology, Vienna, Austria; <sup>4</sup>Erasmus MC Cancer Institute, Department of Radiation Oncology, Rotterdam, The Netherlands; <sup>5</sup>Aarhus University Hospital, Department of Medical Physics, Aarhus, Denmark; <sup>6</sup>Centre Oscar Lambret, Department of Radiation Oncology, Lille, France; <sup>7</sup>VU University Medical Center, Department of Radiation Oncology, Amsterdam, The Netherlands; <sup>8</sup>GZA St-Augustinus Iridium Cancer Network, Department of Radiation Oncology, Antwerp, Belgium

### Purpose or Objective

In 2017 the ESTRO Advisory Committee on Radiation Oncology Practice (ACROP) consensus guideline on implementation and practice of SBRT for peripherally located early stage NSCLC was published, recommending to prescribe  $3 \times 15$  Gy to the PTV as this results in a  $BED_{10Gy} > 100$  Gy. Later that year the ICRU published report 91 about prescribing, recording and reporting of stereotactic treatments with small photon beams advocating to also report the mean GTV dose. The purpose of this multicentre study is to establish the link between the ACROP and ICRU-91 recommendations.

### Material and Methods

From each of the eight participating centres, 15 consecutive clinical treatment plans of patients with peripherally located early stage NSCLC were selected. Treatment plans were generated following the institutional protocol, centres A and B prescribed  $3 \times 13.5$  Gy, centre C  $4 \times 12$  Gy, centres D and E  $3 \times 15$  Gy, centre F  $3 \times 17$  Gy and centres G and H  $3 \times 18$  Gy. Subsequently, dose parameters of the target volumes were reported as recommended by ICRU91 and also converted to  $BED_{10Gy}$ . The centres employed various techniques for motion management. Four centres used an ITV concept while two centres used the mid-ventilation concept, one centre a mix of the ITV and mid-ventilation concept and one centre

a mix of GTV tracking and the ITV concept. For the ITV planned patients no GTV volume was recorded.

### Results

Figure 1a shows that the minimum dose in the PTV ( $D_{98\%}$ ) is not for all centres higher than a  $BED_{10Gy}$  of 100 Gy (for a  $BED_{10Gy}$  of 100 Gy in 3 fractions, a total dose of 42 Gy is needed while for 4 fractions a total dose of 47.5 Gy is needed). Figure 1b shows that all centres had a GTV/ITV mean dose higher than a  $BED_{10Gy}$  of 100 Gy. The intra-centre variation in dose parameters was much smaller than the inter-centre variation.

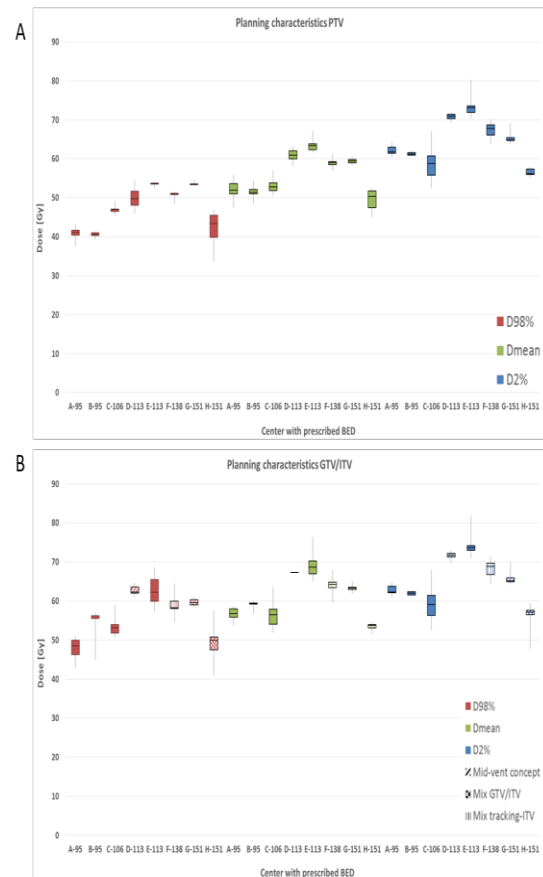


Figure 1: A) Boxplot of the minimum dose ( $D_{98\%}$ ; red),  $D_{mean}$  (green) and the maximum dose ( $D_{2\%}$ ; blue) of the PTV per centre; on the x-axis per centre the prescribed  $BED_{10Gy}$  is given; B) Boxplot of the minimum dose ( $D_{98\%}$ ; red),  $D_{mean}$  (green) and the maximum dose ( $D_{2\%}$ ; blue) of the GTV/ITV per centre; centres using the mid-ventilation concept are shown with a diagonal striped pattern, the centre using a mix of mid-vent and ITV is shown with a checkerboard pattern and the centre using a combination of tracking and ITV is shown with a vertical stripes pattern.

### Conclusion

Three out of 8 ACROP centres did not follow the ACROP guideline in having a  $BED_{10Gy} > 100$  Gy. This, together with the large variation in dose characteristics between centres raises the question whether or not further harmonization is warranted.

### PV-104 Out of field dose for three imaging modalities in case of image guided prostate cancer radiotherapy

C. Le Deroff<sup>1</sup>, R. Lefeuvre<sup>1</sup>, J. Bouvier<sup>1</sup>, R. De Crevoisier<sup>1,2</sup>, C. Lafond<sup>1,2</sup>

<sup>1</sup>Centre Eugène Marquis, Radiotherapy, Rennes, France; <sup>2</sup>Univ Rennes- CLCC Eugène Marquis- Inserm- LTSI-UMR 1099, Radiotherapy, Rennes, France

### Purpose or Objective

In prostate image guided radiotherapy (IGRT), a recent randomized trial reported an occurrence of other malignancies two times higher in case of a daily imaging

control compared to a weekly control (*de Crevoisier, IJROBP 2018*). The purpose of this study was to measure the additional out of field dose delivered by various imaging modalities.

#### Material and Methods

An anthropomorphic phantom was used to mimic a total dose of 78 Gy delivered in the prostate by IMRT/IGRT. We measured the dose related to three imaging techniques (a pair of orthogonal portal images (PI) (6 MV, 2 UM/image), a pair of orthogonal kV images (75 kV, 10 mAs and 105 kV, 80 mAs) and a standard full kV-CBCT (125 kV, 676 mAs)). The doses were measured for 21 points along the central axis of the phantom with thermoluminescent dosimeters (GR-200A). These doses were compared to the measured doses related to the treatment (IMRT, 5 beams, 6 MV, sliding window technique). Finally, the doses for various kV-CBCT parameters were computed: a low dose (260 mAs) and a high dose protocol (1300 mAs).

#### Results

Figure 1 shows the measured out of field dose for the three imaging modalities for one fraction/control. Orthogonal kV imaging (2D-kV) provides the minimum dose inside (1.12 mGy at 0 cm) and outside the field (0.11 mGy at 20 cm, corresponding to 10 cm from the imaging field edge). Standard kV-CBCT imaging provides less dose inside the field (18.6 mGy at 0 cm) than PI (28.8 mGy at 0 cm) but more dose outside the field (1.36 mGy at 20 cm) compared to PI (0.87 mGy at 20 cm). The high dose kV-CBCT protocol provides the maximum out of field dose (2.62 mGy at 20 cm), while using a low dose kV-CBCT protocol provides less dose (0.52 mGy at 20 cm) than PI. The out of field doses related to IMRT are superior to all the imaging control modalities (8.65 mGy at 20 cm).

Considering a weekly control by 2D-kV imaging (8 controls) and a daily control by a standard kV-CBCT imaging (39 controls), the doses at 20 cm were 0.90 mGy and 53.1 mGy, respectively. However, when considering a daily control by 2D-kV imaging and a weekly control by a low dose kV-CBCT imaging the doses are similar with 4.3 mGy at 20 cm.

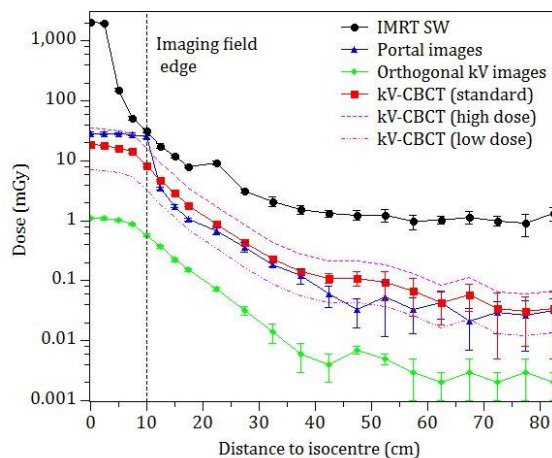


Figure 1: Measured dose profiles for one fraction of IMRT (SW: sliding window technique), one pair of orthogonal portal images (6 MV, 2 MU/image), one pair of orthogonal kV images (75 kV 10 mAs, 105 kV 80 mAs) and one full kV-CBCT (125 kV) with either 260 mAs (low dose), 676 mAs (standard) and 1300 mAs (high dose). The origin represents the treatment and imaging isocenters and is located at the prostate barycenter.

#### Conclusion

Both imaging modality and control frequency as well as treatment fields have an impact on the out of field dose. Regarding one imaging control session, the out of field

dose ranges from 0.1 to 2.6 mGy at 10 cm from the imaging field edge.

#### PV-105 <sup>68</sup>Ga-PSMA PET/CT for quantitative evaluation of radiotherapy-induced cell loss in salivary glands

V. Mohan<sup>1</sup>, N. Bruin<sup>2</sup>, J. Van de Kamer<sup>1</sup>, J. Sonke<sup>1</sup>, A. Al-Mamgani<sup>1</sup>, W. Vogel<sup>2</sup>

<sup>1</sup>The Netherlands Cancer Institute, Department of Radiation Oncology, Amsterdam, The Netherlands ; <sup>2</sup>The Netherlands Cancer Institute, Departments of Radiation Oncology and Nuclear Medicine, Amsterdam, The Netherlands

#### Purpose or Objective

Despite the precision of modern radiotherapy (RT) techniques that are applied to head and neck (H&N) cancer, xerostomia continues to be a complication that affects many patients. Current dose constraints for parotid glands (PGs) and submandibular glands (SMGs) are based on patient and physician-reported xerostomia that is subjective, multifactorial and difficult to quantify. Development of more accurate dose constraints requires quantitative dose-effect relationships. <sup>68</sup>Ga-PSMA is a highly specific and sensitive PET tracer designed for prostate cancer staging, but vital salivary gland cells also abundantly express the PSMA epitope. We aimed to explore the use of PSMA as a quantitative measure of radiation-induced cell loss in salivary glands.

#### Material and Methods

Five H&N cancer patients were included in an ongoing prospective study. They received treatment with 70 Gy in 35 fractions over 7 weeks. <sup>68</sup>Ga-PSMA PET/CT was acquired in treatment position at baseline and at 1-month post-treatment. The PET scans were rigidly registered to the planning CT and the associated dose distribution. The relative change in standard uptake values (SUV) between the two PET scans was compared with the absolute dose received, to establish the response per gland (SUV<sub>peak</sub>) and per voxel (8mm isotropic) within each gland. For the voxel-based evaluation the dose was binned per 5 Gy and the SUV change within each bin was averaged.

#### Results

Figure 1 shows the baseline and post-treatment PSMA PET images, and the RT dose distribution of patient 1. The relative SUV<sub>peak</sub> change for SMGs and PGs (20 glands in total) was highly correlated with the mean dose ( $r = -0.89$ ). At a mean dose of 70 Gy, the average reduction in SUV<sub>peak</sub> was 60% (without background subtraction). Figure 2 shows the relative SUV change in individual voxels, per gland type and averaged for symmetric glands within each patient. The PGs, being larger in volume, received a wider distribution of dose than the SMGs. The average response appears to reach a minimum at about 35 Gy for PGs and at about 45 Gy for SMGs.

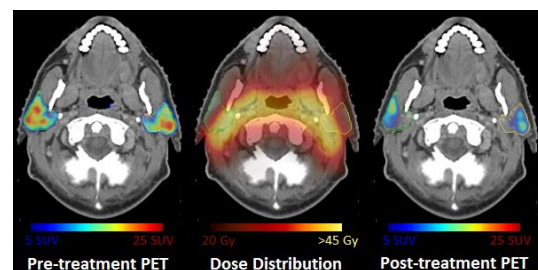
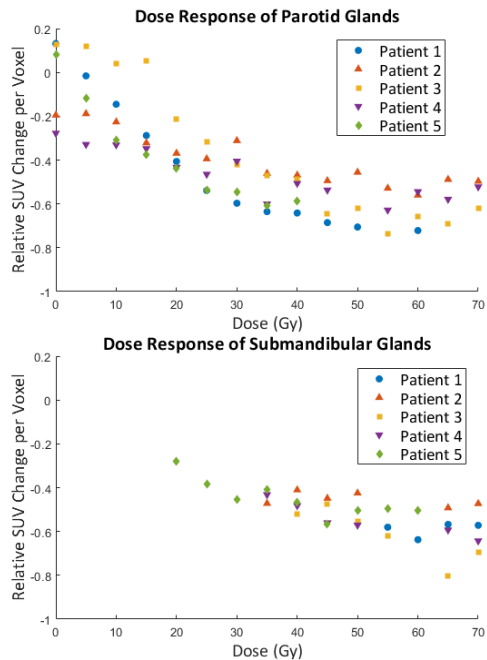


Figure 1. Anatomically registered pre/post-treatment PSMA PET scans and the dose distribution of patient 1, overlaid on the planning CT scan using colour maps. The loss of PET signal in the regions of high dose is evident on the post-treatment PET scan.



**Figure 2.** Dose response per voxel for parotid and submandibular glands of each patient. Dose is binned every 5 Gy and the relative change in SUV is averaged per bin.

### Conclusion

The PSMA PET response in salivary glands after radiotherapy demonstrates a significant dose-effect relationship on the glandular and voxel level, consistent with the hypothesized loss of glandular cells. The accuracy of this method appears to allow detection of differences in radiosensitivity between salivary gland types and between individual patients. If these dose-effect relations can be modelled and related to patient-reported outcomes, this could contribute to new dose constraints and potentially, a lower incidence of xerostomia in H&N RT patients.

### PV-106 An optimized compact microbeam source for preclinical studies

F. Treibel<sup>1,2,3</sup>, J.J. Wilkens<sup>1,2</sup>, S. Bartzsch<sup>2,3</sup>, S.E. Combs<sup>2,3</sup>

<sup>1</sup>Technical University of Munich, Physics Department, Garching, Germany; <sup>2</sup>Technical University of Munich, Department of Radiation Oncology, Munich, Germany; <sup>3</sup>Helmholtz Zentrum München, Institute of Innovative Radiotherapy, Neuherberg, Germany

<sup>1</sup>Technical University of Munich, Physics Department, Garching, Germany; <sup>2</sup>Technical University of Munich, Department of Radiation Oncology, Munich, Germany; <sup>3</sup>Helmholtz Zentrum München, Institute of Innovative Radiotherapy, Neuherberg, Germany

### Purpose or Objective

Microbeam Radiation Therapy (MRT) is based on spatial fractionation of the dose in arrays of highly collimated microbeams. In preclinical investigations MRT showed high normal tissue tolerance while preserving the degree of tumor control. Currently, MRT can only be delivered at large synchrotrons due to beam properties such as high dose rate and low beam divergence. To promote research on MRT, we developed a collimator for an alternative microbeam source using a small animal irradiator (SARRP by Xstrahl). In the design special attention was paid to an optimization of the peak-to-valley dose ratio (PVDR) and the achieved dose rate.

### Material and Methods

Considering the beam divergence of a conventional X-ray source, we developed a collimator with tilted slits. A movable middle plate framed by two fixed plates allows for variable slit widths between 0 and 100  $\mu\text{m}$  (Fig.1). Monte-Carlo simulations in Geant4 were performed to optimize the design of the setup with regard to variations in dose and improvement in PVDR in a water phantom. We

analyzed the impact of the slit widths and the collimator position relative to the X-ray tube. Modifications of the emission angle and respective reduction of the projected focal spot size were evaluated as an innovative approach increasing the PVDR. Apart from the PVDR, we considered a high peak dose rate, as well as small beam penumbra widths as figures of merit. Based on the simulations, the collimator setup was built and is now subject to experimental validation with radiochromic film dosimetry.

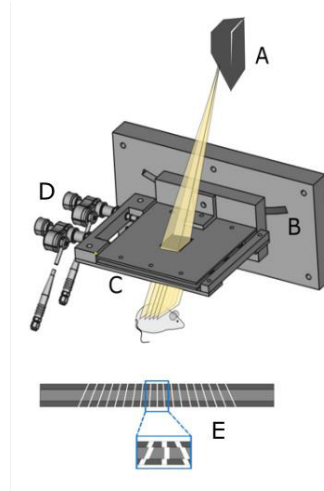


**Figure 1:** Setup of a microbeam source using a conventional X-ray tube (A). The three-layered collimator (C) is rotatorily mounted (B). The middle plate can be shifted by help of two piezo actuators (D). Tilted slits account for beam divergence (E).

### Results

Significant improvements were introduced compared to the previous design of Bartzsch, Cummings, Eismann and Oelfke in 2016 in *Medical Physics*. The source distance of the collimator was increased from 70 mm to 212 mm. We achieved a very high PVDR of up to 25 in 1 cm depth representing an enhancement of 62% versus the PVDR measured at 70 mm by Bartzsch et al. Simultaneously, the divergence of the microbeams is reduced. Larger treatment depths can be obtained, enabling *in vivo* studies in rodents.

Increased flexibility in beam width is achieved by the three-layered collimator design. The observed sensitivity of the dose to variations in slit width demands accuracies below 2  $\mu\text{m}$  which are obtained by use of piezo actuators. The projected focal spot width has a strong effect on the dose profile. At 2 cm depth in water, comparisons of 20° and 12° target angle revealed up to 22% deviation for the peak dose and 3% for the valley. In average, the PVDR was increased by 17% for the smaller projected focal spot size (Fig.2).

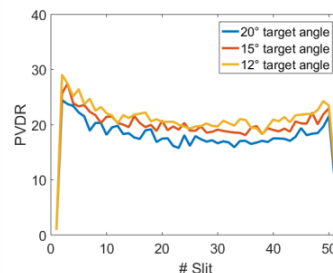


**Figure 2:** Impact of the target angle on the PVDR at 2 cm depth in a water phantom.

### Conclusion

Our investigations led to a new microbeam source. Precisely controlled positioning of the collimator and of the slit widths are crucial to provide reproducible dose profiles. Modification of the source distance and the



available. It needs prescription at the right time. It has to be given at the right form. The whole of these elements are covered by the process of 'Quality Assurance' which is the responsibility of all bodies involved". I met Emmanuel vander Schueren early in my career on a European Quality network in RT meeting, he made an impact on me. Since then I have had a special interest on Quality Management in RT and in particular in quality assessment. It is an honor and responsibility to receive this award and I commit myself to be an ambassador of his values.

---

#### Award Lecture: Iridium Award Lecture

---

#### SP-0109 The role of women in the brachytherapy field C. Haie-Meder<sup>1</sup>

<sup>1</sup>Institut Gustave Roussy, Radiation Oncology Department, Villejuif, France

##### Abstract text

Brachytherapy was initiated by a famous woman, Marie Sklodowska-Curie, after her radium discovery in 1898. She was awarded two Nobel prizes in 1903 and 1911, she was the first woman in Europe to get the degree of Doctor of Science, and she became the first female Professor at Sorbonne. She resigned patenting the radium isolation method, claiming that « Radium is a chemical element, a property of all humans ». The Radium Institute was founded in Paris in 1912 due to Marie Curie 's efforts. Thousands of patients were treated with radium for cancers. Her determination, her commitment, her humanity ideal were the basis for new generations of women researchers including medical physicists and radiation oncologists. Among them, at Gustave Roussy, Simone Laborde, head of the radiation department, was one of the first to write a book on brachytherapy technique. She fought against the concept that the heaviest treatments against cancer were the most efficient, after having seen severe complications among her cancer patients. In France, brachytherapy became very popular and women widely contributed to its development : The physicist Andrée Dutreix established the rules of the Paris system, still currently in use. Her pupil, Edith Briot, contributed to the spread of brachytherapy participating to the ESTRO courses and currently Isabelle Dumas who is in charge of brachytherapy physics at Gustave Roussy. Ginette Marinello, was the author of the famous « Practical Manual of Brachytherapy ». Monique Pernot, radiation oncologist in Nancy, accumulated a tremendous clinical experience, especially in head and neck cancer brachytherapy. Her numerous publications served as a basis for dose-rate values in low dose-rate brachytherapy. Outside France, a lot of physicists are dedicated to brachytherapy : Inger Lena Lamm, Taran Paulsen-Hellebust, Astrid de Leeuw, Nicole Nesvacil, Jamema Swamidas, Kari Tanderup, being now the Director of the ESTRO gynaecological course, and many others. Their commitments is the living proof of the continuous interest in brachytherapy. A lot of female doctors have contributed to the development of brachytherapy. Among them Ina Jürgenliemk-Schulz, who is the president elect of GEC-ESTRO, Li Tee Tan, Angela Rovirosa, Alina Sturdza, Henrike Westerveld, Claire Charra-Brunaud, Laurence Thomas, Hana Stankusova and many others. Outside Europe, important ladies, such as Judith Stitt, Beth Erickson , Akila Viswanathan and of course Patricia Eifel are among the most famous brachytherapists in the United States. Female doctors represent currently 60% of the medical community. Their contribution to the development of brachytherapy represents a tremendous step forward. Let's hope that their achievements will be more widely recognized in the future.

---

#### Symposium: MR-guided radiation therapy: hybrid machines and treatment adaptation

---

#### SP-0110 Magnetic resonance based small animal radiotherapy in neuro-oncology

C. Vanhove<sup>1</sup>, B. Descamps<sup>1</sup>, J. Bolcaen<sup>2</sup>, K. Deblaere<sup>3</sup>, M. Acou<sup>3</sup>, F. De Vos<sup>4</sup>, T. Boterberg<sup>5</sup>, C. De Wagter<sup>6</sup>, J. Kalala<sup>7</sup>, H. Giorgio<sup>7</sup>, C. Van Den Broecke<sup>8</sup>, L. Leybaert<sup>9</sup>, E. Decrock<sup>9</sup>, A. Vral<sup>9</sup>, S. Vandenberghe<sup>1</sup>, R. Van Hoken<sup>1</sup>, I. Goethals<sup>2</sup>

<sup>1</sup>Ghent University, Institute Biomedical Technology Ibitech, Gent, Belgium ; <sup>2</sup>Ghent University Hospital, Department Of Nuclear Medicine, Gent, Belgium ; <sup>3</sup>Ghent University Hospital, Department Of Radiology, Gent, Belgium; <sup>4</sup>Ghent University, Laboratory of Radiopharmacy, Gent, Belgium; <sup>5</sup>Ghent University Hospital, Department Of Radiation Oncology, Gent, Belgium; <sup>6</sup>Ghent University, Department of Radiation Oncology, Gent, Belgium; <sup>7</sup>Ghent University Hospital, Department Of Neurosurgery, Gent, Belgium; <sup>8</sup>Ghent University Hospital, Department of Pathology, Gent, Belgium ; <sup>9</sup>Ghent University, Department of Basic Medical Sciences, Gent, Belgium

##### Abstract text

Compared to computed tomography (CT), magnetic resonance imaging (MRI) provides vastly superior soft-tissue contrast. This makes it much easier to visualize lesion boundaries that will result in a much better delineation of the target volume, helping to better irradiate the lesion and avoid surrounding tissue. Therefore, combining MRI with CT data is increasingly used for radiotherapy planning in the clinic. This combined CT/MRI dataset contains both the information required for targeting and for dose calculations. During this presentation, three studies will be presented where MRI and small animal radiotherapy were combined in the field of neuro-oncology. In a first study, we used a combined CT/MRI dataset to guide the irradiation of brain tumours in a F98 glioblastoma rat model using a micro-irradiator. Contrast-enhanced MRI images were acquired to follow up tumour growth after orthotopic inoculation, to monitor treatment response, and to delineate the target volume during radiotherapy planning. Using multiple non-coplanar arcs the prescribed dose could be delivered to 90% of the target volume, while minimizing the dose to normal brain tissue. A challenging aspects of small animal CT imaging relates to the radiation dose received by the animals. This might become a very important issue when the therapeutic dose has to be delivered in multiple fractions spaced over time, where each individual irradiation requires a CT for accurate animal positioning. Therefore, in a second study we investigated the feasibility of a MRI-only based workflow for radiotherapy planning of the rat brain, that enables both accurate target delineation and accurate dose calculations using only MRI-based volumes. Multiple MRI sequences were used to generate synthetic CT images that could be used for dose calculations, because only one MRI volume was not sufficient to separate all major tissue types (air, soft tissue, bone) in the rat head. The synthetic CT images were sufficiently similar to the segmented CT images that are routinely used for radiotherapy planning on preclinical radiation research platforms. No significant differences were observed between CT and MRI based dose calculations when more complex beam configurations (multiple beams) were used in the dose plan. However, further research is required in the thoracic or abdominal region of small animals, where more tissue classes will be required to allow for accurate dose calculations compared to the rat head. Finally, discrimination between brain tumor recurrence (glioblastoma) and radiation necrosis (RN) remains a

diagnostic challenge because both entities have similar imaging characteristics on conventional MRI. Functional imaging techniques, such as dynamic contrast enhanced (DCE) MRI or positron emission tomography (PET), could overcome this diagnostic dilemma. A third study will be presented to investigate the potential of DCE-MRI and PET in discriminating high-grade glioma from RN in rats. Induction of RN was achieved by irradiating the right frontal region with 60 Gy using multiple arcs. Results suggested that functional imaging can be used to discriminate glioblastoma (recurrence) from RN.

#### SP-0111 On-line MRI-guidance for dose accumulation and plan adaptation

Bas Raaymakers<sup>1</sup>

<sup>1</sup>University Medical Center Utrecht, Radiotherapy, Utrecht, The Netherlands

#### Abstract text

There are two commercial, clinical hybrid MRI radiotherapy systems operational. The promise of these systems is to improve on the targeting accuracy by providing soft-tissue contrast images directly from the treatment table. These MRI data can be acquired both prior to- and during beam delivery. Such on-line visualization enables image guided Radiotherapy (IGRT) as we know it, but then based on soft-tissue contrast images. This presentation will mainly focus on the next steps of using on-line MRI data. The MR images can be used to reconstruct the delivered dose by combining the MRI with the linac output.

This can be done at various time scales. Daily MRI can be used for dose accumulation per day. Intra-fraction MRI, in combination with time-stamped linac output can yield time-resolved dose reconstruction at an intra-fraction level. The goal is to track the dose delivery in real-time, for this MRI, linac readings and dose calculations need to be optimized.

The accumulated dose can be used for treatment response assessment but clearly also as a metric for plan adaptation. Plan adaptation based on daily MRI from the treatment table is a next step for IGRT, the plan is adapted to the patient instead of trying to re-position the patient to the pre-determined plan. Similar to dose accumulation, the frequency of adaptation can be increased by also using intra-fraction MRI. The anatomical changes have to be interpreted live, various options are under investigation to allow real-time digestion of MRI, including faster MRI acquisitions and hybrid patient modelling-MRI techniques. Plan adaptations can be triggered by anatomical changes, but also by accumulated dose metrics. A loop to use the real-time dose accumulation as input for continuous (intra-fraction) plan adaptation will be presented.

In summary, this presentation aims to show that on-line MRI guidance as a next step for soft-tissue based IGRT is only the first step towards continuously adapted radiotherapy so moving targets can be treated as if they are static.

#### SP-0112 First clinical experience and future directions of MR-guided radiation therapy

D. Zips<sup>1</sup>

<sup>1</sup>University Hospital Tübingen, Radiation Oncology, Tübingen, Germany

#### Abstract text

Since September 2018 the 1.5 T MR-Linac system is in clinical use. I will discuss our first clinical experiences and reflect on expectations as well as on our long-term vision for MR-guided adaptive radiation oncology. In addition, I will discuss the potential of MRgRT to facilitate transformation of current radiation oncology into RO4.0.

#### OC-0113 MRI artifact simulation for clinically relevant MR sequences for guidance of HDR brachytherapy

E. Beld<sup>1</sup>, M.A. Moerland<sup>1</sup>, M.A. Viergever<sup>2</sup>, J.J.W. Legendijk<sup>1</sup>, P.R. Seevinck<sup>2</sup>

<sup>1</sup>UMC Utrecht, Department of Radiotherapy, Utrecht, The Netherlands; <sup>2</sup>UMC Utrecht, Image Sciences Institute, Utrecht, The Netherlands

#### Purpose or Objective

The purpose was to investigate the potential of several clinically relevant MR sequences for application during the HDR brachytherapy intervention to facilitate tracking/localization of brachytherapy devices (HDR source/titanium needle), which could simultaneously be used to visualize the anatomy. Simulations of the MR artifacts were implemented for a spoiled gradient echo sequence, a spin echo sequence, a balanced steady-state free precession (bSSFP) sequence and a bSSFP sequence with SPAIR fat suppression.

#### Material and Methods

##### Simulations

Simulation of the artifact for the spoiled gradient echo sequence was performed as described in [1]. To simulate the other sequences, the implemented MRI signal equation was adapted. For a spin echo sequence, no dephasing effect was included because of the 180° refocusing pulse. For bSSFP, the steady-state signal equation was included. For SPAIR, the spins at a frequency of the SPAIR pulse were set to 0.

##### MRI acquisition

The object, a non-active Ir Flexisource (Elekta)/a titanium needle (Ø1.9mm, Elekta), was positioned in the center of a doped water phantom. MR imaging was performed on a 1.5T MRI system (Ingenia, Philips). 4 types of 2D MR sequences were applied (2 intersecting 2D slices): spoiled gradient echo, spin echo, bSSFP and bSSFP-SPAIR (see Table1). Furthermore, the MR sequences of the clinical prostate HDR brachytherapy scan protocol were applied: a 3D bSSFP-SPAIR sequence, a T2-weighted and a T1-weighted spin echo sequence (both multi-slice 2D), see Table2. Angles of 0° and 20° between source/needle and B0 were applied.

##### Post-processing

The object position was determined by template matching between the MR images and the simulated artifacts, using a subpixel phase correlation algorithm [1]. A 2D phase correlation was performed for the 2D slices, and a 3D phase correlation for the 3D and multi-slice 2D acquired volumes. The average object position (of 7 obtained positions) and the mean deviation from this average were calculated.

**Table 1.** The scan parameters for the spoiled gradient echo sequence, the spin echo sequence, the bSSFP sequence and the bSSFP-SPAIR sequence that were applied (all 2D).

	Spoiled gradient echo	Spin echo	bSSFP	bSSFP-SPAIR
TE/TR (ms)	2.26/4.60	10.0/100.0	2.3/4.5	1.9/3.8
FOV (mm <sup>2</sup> )	256×256	256×256	256×256	256×256
Slice thickness (mm)	10.0	10.0	10.0	10.0
Acquisition matrix	256×256	256×256	256×256	256×256
Flip angle	30°	90°	20°	30°
Readout bandwidth (Hz/pixel)	434	158.8	434	775

**Table 2.** The scan parameters for the 3D bSSFP-SPAIR sequence, the multi-slice 2D T2-weighted (T2w) spin echo sequence and the multi-slice 2D T1-weighted (T1w) spin echo sequence that were applied (as provided in the current clinical scan protocol).

	bSSFP-SPAIR	T2w spin echo	T1w spin echo
TE/TR (ms)	1.76/3.52	110.0/7126.5	37.4/2000.0
FOV (mm <sup>3</sup> )	256×256×120	200×200×119	224×224×70
Reconstructed resolution (mm <sup>3</sup> )	1.0×1.0×1.0	0.5×0.5×3.0	1.0×1.0×2.0
Flip angle	30°	90°	90°
Readout bandwidth (Hz/pixel)	935.9	194.5	539.1

#### Results

Fig.1 shows the simulated and the MRI images for the 4 applied 2D MR sequences (with the object positions overlaid on the images). These results demonstrate that the simulations highly correspond to the acquired images

as well as that the obtained object positions within the artifacts correspond to the simulated object positions. The mean deviations of the object positions (from average) were 0.2-0.3mm, proving that all sequences were suitable for localization of the objects.

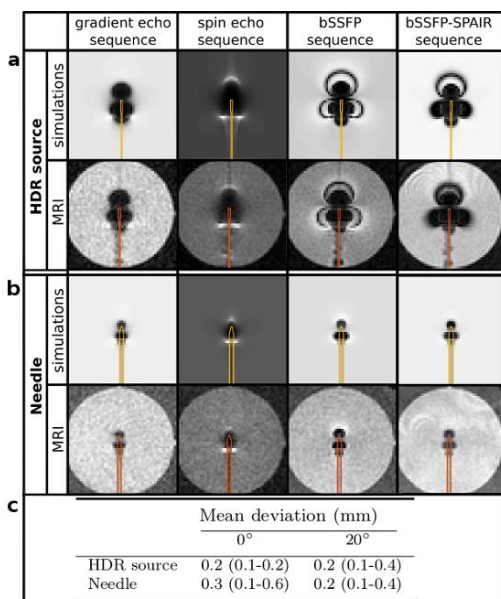


**Figure 1.** The simulated images (top rows) and the acquired MR images (bottom rows) for (a) the HDR brachytherapy source and (b) the titanium needle for an angle of 0°. The images represent the artifacts for the four 2D sequences applied (see the four columns). The contours of the simulated and the acquired object positions are overlaid in yellow and red respectively. (c) The mean deviation (and range) in mm from the average of all object positions obtained from the seven different MR sequences applied.

### Conclusion

This study demonstrated that the MR artifact induced by an HDR source or a titanium needle could be simulated for the 4 investigated types of MR sequences (spoiled gradient echo, spin echo, bSSFP and bSSFP-SPAIR), valuable for object localization in clinical practice. This could be applied for fast 2D acquisitions as well as for volumes acquired using the MR sequences currently provided in the clinical scan protocol, leading to flexibility in the choice of MR sequences for guidance of HDR brachytherapy. 1. Beld E et al 2018 PMB 63 085002

### Symposium: How to exploit Immunogenic cell death Mechanism in Radiotherapy

#### SP-0114 Immunogenic versus Non-Immunogenic Cell Death in Cancer

A. Garg<sup>1</sup>, L. Vandenberk<sup>2</sup>, S. Fang<sup>3</sup>, P. De Witte<sup>4</sup>, P. Salven<sup>3</sup>, P. Agostinis<sup>1</sup>

<sup>1</sup>Ku Leuven, Cell Death Research and Therapy Cdr Unit- Department Of Cellular And Molecular Medicine, Leuven, Belgium; <sup>2</sup>Ku Leuven, Department Of Microbiology And Immunology, Leuven, Belgium; <sup>3</sup>University Of Helsinki, Department Of Pathology, Helsinki, Finland; <sup>4</sup>Ku Leuven, Department Of Pharmaceutical Sciences, Leuven, Belgium

#### Abstract text

Innate immune detection of cells damaged lethally by sterile or pathogenic stimuli is orchestrated through several different immune-modulatory, inflammatory and/or danger signals. In pathogenic contexts, inflammatory chemokines guided (rapid) recruitment of specific innate immune cells from circulation, and their pathogen-associated molecular patterns (PAMPs)-triggered activation is a distinct feature of pathogen-

infected stressed or dying cells. Over the last two decades, it has been widely recognized that in some contexts, sterile dying cells can trigger a potent innate immune response by exposing specific endogenous molecules, analogous to PAMPs, termed damage-associated molecular patterns (DAMPs). This concept has been successfully applied to cancer cells wherein specific therapeutic stimuli have been found to induce immunogenic cell death owing to spatio-temporally defined exodus of immunogenic DAMPs. In some contexts, this immunogenic cancer cell death has been found to have potent anticancer vaccination effect - a feature that has driven its translational popularity. However, there are still a number of basic questions regarding this concept that remain unaddressed. For instance, the PAMPs::DAMPs analogy has frequently raised a challenging question that remains unanswered i.e. can sterile dying cancer cells stimulate innate immunity by moderately mimicking pathogen defense response-like signaling? We have found that sterile immunogenic dying cancer cells indeed trigger (a cell-autonomous) pathogen response-like chemokine (PARC)-signature, which is quite reminiscent of chemokine patterns orchestrated by mammalian cells infected with bacteria or viruses. In fact this PARC signature was specific to immunogenic apoptosis but not to accidental necrosis or non-immunogenic apoptosis. This PARC-signature was found to pave way for neutrophils based phagocytic-targeting of dead/dying cancer cells and subsequent cytotoxic-targeting of residual (live) cancer cells. These observations shed light on the possible evolutionary basis for sterile immunogenic signaling during cancer cell death that needs further systematic investigation in near future.

#### SP-0115 Immunogenic tumor cell death induced by chemoradiotherapy: a clinical point of view

K. Mimura<sup>1</sup>, K. Kono<sup>2</sup>

<sup>1</sup>Fukushima Medical University, Department Of Gastrointestinal Tract Surgery- Department Of Blood Transfusion and Transplantation Immunology- Department of Advanced Cancer Immunotherapy- Department of Progressive Dohad Research, Fukushima, Japan; <sup>2</sup>Fukushima Medical University, Department of Gastrointestinal Tract Surgery, Fukushima, Japan

#### Abstract text

Chemoradiotherapy is generally thought to be immunosuppressive, either by depleting T- and NK-cells or by rendering them functionally inactive, leading to infectious complications and growth of residual tumors. However, radiation oncologists realized a rare phenomenon called the 'abscopal effect' where local irradiation on the tumor causes regression of metastases at sites distant from the irradiated area, although the underlying mechanisms of this effect have not been completely elucidated. In immunogenic tumor cell death (ICD), dendritic cells (DC) were activated by danger signals such as high mobility group box 1 (HMGB1) and calreticulin released by dying cells. The activated DC could then efficiently phagocytize and present cancer antigens, resulting in the induction of tumor specific cytotoxic T lymphocytes. There is a possibility that the abscopal effect is induced by the ICD process. Although we reported that chemoradiotherapy can induce ICD, there was limited information to translate this theory directly in a clinical setting. However, it was recently reported cases of abscopal effect in melanoma patients treated with radiotherapy and immune checkpoint inhibitors (ICI). Further, many clinical trials with this combination approach (radiotherapy and ICI) are ongoing in several types of tumor including melanoma, NSCLC, RCC, Glioblastoma, and HNSCC etc. In this session, I present cellular mechanisms underlying ICD induced by chemoradiotherapy from a clinical point of view.

### SP-0116 Mechanisms of Radiotherapy Induced Inflammatory Signaling

S. Harding<sup>1</sup>

<sup>1</sup>University Health Network, Princess Margaret Cancer Centre, Toronto, Canada

#### Abstract text

Radiotherapy directly leads to clonogenic cell death which is accompanied by inflammatory cytokine signalling. These cytokines have the potential to influence the immune system and may contribute to success of radiotherapy alone and in combination with immune checkpoint blockade. We have recently identified viral response proteins, the pattern recognition receptors (PRRs), as key drivers of this response. In this seminar we will discuss mechanisms by which radiotherapy induces PRRs, drives inflammatory signalling and contributes to the abscopal response in murine models of radiotherapy-immune checkpoint blockade treatment. The goal of these studies is to determine how inflammatory signalling is activated, whether it can be used as a biomarker of treatment response, and if it represents a novel means for improving cancer therapy.

### SP-0117 Neoantigens in cancers

P. Kvistborg<sup>1</sup>

<sup>1</sup>The Netherlands Cancer Institute, Amsterdam, The Netherlands

Abstract not received

---

### Symposium: Oligo-metastatic prostate cancer - shedding light in a quickly emerging field

---

### SP-0118 What are realistic clinical goals in radical radiotherapy for oligometastatic prostate cancer?

T. Hölscher<sup>1</sup>

<sup>1</sup>Universitätsklinikum Carl Gustav Carus, Department Of Radiation Oncology / Oncoray, Dresden, Germany

#### Abstract text

Two decades ago, Hellmann and Weichselbaum postulated that for metastatic solid tumors a broad spectrum of transitional stages (spectrum hypothesis) exists, and that there may be an oligometastatic status potentially to be cured by ablative therapy. Next to the number of metastases (e.g. up to five?), the interval from treatment of the primary tumor and the pace of progression may define such an oligometastatic status.

In prostate cancer (PCa), prostate specific antigen (PSA) is an established tumor marker that is well ahead of clinically significant disease, thus allowing for screening for oligometastatic disease at an early time point. Median time from PSA recurrence to symptomatic disease is 8 years after primary curative treatment, and 2,5 years in patients with castration resistant PCa without detectable clinical metastases, only.

Beyond laboratory and pathology testing (Gleason score), modern anatomical and functional imaging (e.g. PSMA-PET-CT / -MR) has been shown to allow for an improved staging and thus a clinically sound patients selection. There may be different scenarios in prostate cancer, in which local ablative treatment of oligometastatic disease possibly plays a role:

- Identification of metastatic disease in high risk primary PCa
- Treatment failure after primary curative treatment in hormone-sensitive Pca
- Definition of an oligoprogressive status in castration resistant Pca.

Better clinical trials are urgently needed to establish the role of local ablative therapy in these cohorts of patients. These trials need to be competitive, i.e. randomized

against standard of care (comparator: systemic treatment), address proper endpoints (cure, reduction of secondary metastases, prolongation of life, maintenance of quality of life?) and incorporate translational research. In order to be accepted by the community, these trials have to contain optimal imaging and treatment methods and include sufficiently large numbers of patients (multicentre efforts).

During the presentation, I will highlight recent clinical studies in oligometastatic prostate cancer patients at different stages of disease and give a brief outlook on potential future studies the field of radiation oncology should embark on.

### SP-0119 What is the optimal staging for oligometastatic prostate cancer?

L. Miszczyk<sup>1</sup>, A. Napieralska<sup>1</sup>, M. Miszczyk<sup>2</sup>

<sup>1</sup>maria Skłodowska-Curie Memorial Cancer Center and Institute Of Oncology, Radiotherapy, Gliwice, Poland;

<sup>2</sup>Maria Skłodowska-Curie Memorial Cancer Center And Institute Of Oncology, 3rd Radiotherapy Ward, Gliwice, Poland

#### Abstract text

The TNM staging system does not reflect the needs of radiation therapy in terms of prognosis in prostate cancer (PC) patients in terms of oligometastatic disease, both - in the case of lymph nodes as well as bone metastases. It describes only their presence and in the case of lymph nodes metastases - location (in or outside the pelvis). It is known that tumor control probability (TCP) depends on the number of clonogenic cells (which, probably indirectly, is reflected by tumor volume) and delivered dose. TCP could also be dependent on lesion location, which is connected with treatment precision and dose delivery possibility (surrounding critical structures). The last factor influencing TCP is the kind of metastases - lymph nodes vs bones. An additional point which should be considered is imaging - how to find them and which examination ought to be a standard. Because aforementioned issues, we have discussed the usefulness of PC oligometastases volumetric staging relying on our own material. This material comprised 165 PC oligometastases (94 in lymph nodes, 71 in bone - 118 patients) treated locally between 2011 and 2017 with SABR. Up to three metastases were accepted as oligometastatic disease. The total dose (TD) varied from 8 to 60 Gy and was delivered in fraction doses 6-15 Gy. Tumor volume varied from 0.1 to 68.2 ccm (mean 4.8, median 1.6). The median of tumor volume was 1.1 for lymph nodes and 4.0 for bone metastases). Lymph node metastases were mainly located in the pelvis (57). During FU (up to 74.6 months; median 15.7), the tumor volume, local control (LC), biochemical control (BC) and overall survival (OS) were evaluated. For statistical assessment the ROC and Youden index, logrank test and scatterplots were used. On the basis of ROC we specified 2 ccm as a threshold volume. There was a significant difference (p=0.03) in 50 months LC for these two groups (98% vs 75%). We did not find a statistically significant difference for the thresholds 3 and 4 ccm, but there was a clear separation of KM LC curves. We also found significant impact of tumor volume for BC among bone metastases (p=0.006). None of the other analyzed factors had an impact on BC. The obtained results suggest that features of oligometastases have not a significant impact on BC (probably it is linked more to systemic treatment), so when thinking about oligometastatic disease staging we should consider features of these lesions and local result. The basic examination to find such lesions should be probably PSMA PET, which is connected with the issue of volume evaluation (the SUV threshold). Finally, the PC oligometastases staging system ought to take into account the volume of metastases, their number and location (lymph nodes vs bones) when considering the anatomy

(pelvis vs remote for lymph nodes; para-spinal vs rest for bones).

**SP-0120 What is the optimal target volume concept in radiotherapy for oligometastatic pelvic lymph nodes after radical prostatectomy?**

T. Zilli<sup>1</sup>

<sup>1</sup>*Hôpitaux Universitaires de Genève, Radiation Oncology, Geneva, Switzerland*

**Abstract text**

After radical prostatectomy, up to one third of the patients recur mainly with nodal lesions located in the pelvis. Radiation therapy (RT) has been demonstrated to be an effective salvage treatment for oligorecurrent ( $\leq 5$  metastases) prostate cancer, with promising results in terms of disease control and low treatment related toxicity. Both stereotactic body RT (SBRT) and elective nodal RT are been used in this setting and are considered valid, even if still investigational, treatment options. However, the best way to irradiate patients with an exclusive oligorecurrent nodal disease remains debated with many open questions on the performance of imaging techniques in reliably detect the recurrent disease. The aim of this talk is to discuss the rationale supporting the two different approaches (focal versus elective) for oligorecurrent nodal prostate cancer, and to present recent results and ongoing trials that will support the different treatment options.

**SP-0121 What is the optimal sequencing of local and systemic treatment in oligometastatic prostate cancer?**

G. De Meerleer<sup>1, 2</sup>

<sup>1</sup>*University Hospitals Leuven, Department of Radiation Oncology, Leuven, Belgium;* <sup>2</sup>*KU Leuven, Department of Oncology, Leuven, Belgium*

Abstract not received

---

**Symposium: New developments in gynaecological cancers**

---

**SP-0122 Integration of molecular prognostic factors in the management of endometrial cancer**

R. Nout<sup>1</sup>

<sup>1</sup>*Leiden University Medical Center LUMC, Department of Radiotherapy, Leiden, The Netherlands*

**Abstract text**

The majority of endometrial cancer (EC) patients present at an early stage (80% FIGO stage I) and have a good prognosis (overall survival stage I: 85%). Total hysterectomy and salpingo-oophorectomy is the mainstay of treatment. Clinicopathological risk factors (e.g. grade, depth of myometrial invasion, presence of LVSI) are currently used in clinical practice to help identify patients who may benefit from adjuvant (postoperative) therapy. More recently the TCGA group comprehensively assessed molecular alterations in endometrial cancer and found four groups with distinct prognosis: *POLE*-mutant ultramutated, MSI hypermutated, p53-mutant copy-number high (serous like), and a copy number low group without a specific mutation. The *POLE*-mutant group had a very low risk of recurrence despite their ultramutated phenotype and the p53 mutant group had an increased risk of disease progression. Subsequent studies have confirmed the distinct prognostic impact of these four groups, and have identified additional (targetable) prognostic molecular markers. In addition to these molecular features analysis of the impact of grading of LVSI pointed out that substantial LVSI in contrast to no or mild LVSI was a strong independent risk factor for regional and distant recurrence. Furthermore, risk groups based on combined

molecular and clinico-pathologic features were found to have a higher prognostic accuracy than either alone. This concept has been carried forward in the on-going randomised PORTEC-4a trial that investigates molecular profile-based versus standard recommendations for adjuvant therapy, with the overall aim is to further decrease both over- and undertreatment in early stage endometrial cancer.

**SP-0123 Improving outcomes in high-risk locally advanced cervical cancer: extended field RT, adjuvant chemotherapy or immunotherapy?**

C. Chargari<sup>1</sup>, C. Haie-Meder<sup>1</sup>, S. Gouy<sup>1</sup>, E. Deutsch<sup>1</sup>

<sup>1</sup>*Institut Gustave Roussy, Radiation Oncology, Villejuif, France*

**Abstract text**

The implementation of image guided adaptive brachytherapy has allowed achieving very high local control rates in locally advanced cervical cancer patients. However, a threshold seems to have been achieved in terms of survival, which remains alleviated by a high frequency of distant relapses, justifying the development of novel strategies aimed at further improving patients outcome. Conventional approaches are being tested, based on neoadjuvant or adjuvant combinatory chemotherapy. Another strategy relies on the better identification of patients warranting para-aortic irradiation, either through integration of primary para-aortic lymph node dissection or by inclusion of high-tech imaging modalities to better guided treatment fields. An adapted approach has also been proposed to tailor radiotherapy fields for each patient according to conventional risk factors, mainly based on the tumor stage. Finally, the increasing knowledge of tumor biology and the rapidly evolving field of anti-tumor immunity encourage pharmacological approaches in order to exploit the complex interplays between tumor and its microenvironment through radiotherapy.

**SP-0124 Chemo-radiation in Vulvar Cancer: recent developments in (neo)adjuvant and primary therapy**

S. Marnitz-Schulze<sup>1</sup>

<sup>1</sup>*University Clinic Cologne, Radiation Oncology, Cologne, Germany*

**Abstract text**

Chemoradiation in vulvar cancer patients is used postoperatively as adjuvant treatment for patients on high risk for recurrence, in a neoadjuvant setting with the aim to avoid mutilative surgery in patients with locally advanced disease and as a primary treatment to avoid surgery at all. In the recent years there has been a shift to more HPV-positive tumors, younger patients and those with unfavourable tumor localizations. Sentinel node technique has become a standard procedure for inguinal lymph node staging. The use of Sentinel technique lead to a dramatic decrease of morbidity like wound break down and lymph edema compared to full lymphadenectomy and also decreased the treatment related toxicity after radiation. Concerning the optimal diagnostic tool and treatment of pelvic and or para-aortic lymph node metastases, no internationally accepted standard has been established. In contrast to cervical cancer, no data are available with regard to the optimal radiation sensitizer. The talk discusses the data for pre-therapeutic lymph node staging with tailored chemoradiation concepts and the PROs and CONs of (neo-)adjuvant versus primary chemo-radiation, different drugs, dose and target concepts for contemporary treatment of vulvar cancer patients.

---

## Symposium: Real time navigation technologies in brachytherapy

---

### SP-0125 Multi-modal Image Fusion to support Minimally-invasive Therapy

D. Barratt<sup>1</sup>

<sup>1</sup>University College London Ucl, Department Of Medical Physics and Biomedical Engineering / Ucl Centre For Medical Image Computing / Wellcome Trust EPSRC Centre for Interventional and Surgical Science, London, United Kingdom

#### Abstract text

With the increasing availability of new treatment approaches for prostate cancer based on minimally-invasive surgical and radiation therapies, there is a growing need for computer-assisted therapy systems that enable high-accuracy, tumour-targeted therapy delivery within an easy-to-use and efficient clinical workflow. In this presentation, challenges to high-accuracy therapy delivery and clinical usability using computer-assisted planning and guidance systems will be discussed, with a focus on the impact and compensation of soft-tissue motion (including physical deformation). Approaches to automatic generation and application of computer-generated deformable organ models to compensate for organ motion within image fusion software will be described, drawing on the presenter's prior research in this area. Methodological aspects of validation and, in particular, accuracy evaluation, for such systems will then be discussed. Finally, the recent and potential future impact of contemporary machine learning techniques, such as convolutional neural networks, will be explored.

### SP-0126 Steering of needles and applicators

J. Dankelman<sup>1</sup>

<sup>1</sup>Delft University of Technology, Biomechanical Engineering, Delft, The Netherlands

#### Abstract text

It is challenging to steer needles accurately too difficult to reach places. In the first part of the presentation a short overview will be given of different principles to steer needles. Examples from hand held steerable needles and robotically steerable needles presented. Second part of the talk will focus on a novel way to steer needles during brachytherapy treatment of cervical cancer, in cases where the tumour is extending lateral to the pelvic wall or away from the vaginal surface. In these situations the use of an applicator is not sufficient to cover the target area, and free hand steering of needles is difficult and may result in incorrect placement or steering for a long distance through healthy tissue. To overcome this, a method will be presented based on personalised 3D-printed vaginal templates with curved channels. These curved channels are then used to steer needles. The shape of the template will be based on an MRI scans. In this study a template was printed having channels with different curvatures to examine the effect of curvature constraints on placement accuracy. The feasibility of needle steering using curved channels in a template was tested in an experimental set-up using gelatin phantoms.

### SP-0127 3D printed templates for steering of needles

J.C. Lindegaard<sup>1</sup>, P. Petric<sup>1</sup>, A. Traberg Hansen<sup>1</sup>, S. Kynde Nielsen<sup>1</sup>, B. Meisner<sup>1</sup>, K. Tanderup<sup>1</sup>, L.U. Fokdal<sup>1</sup>

<sup>1</sup>Aarhus University Hospital, Department Of Oncology, Aarhus C, Denmark

#### Abstract text

Standard templates for needles guidance have been used successfully for many years in brachytherapy. Brachytherapy has always been a field of innovative activity towards personalisation as exemplified

by the many customised devices designed and produced for implant optimisation over the years. In this context 3D printing is just a new tool for individualising the implant template in accordance with the distinctive patient anatomy and in close proximity to the clinical workflow, needs and possibilities within the individual departments. Several materials for 3D printing have the advantage of being MRI compatible, biocompatible, autoclavable and sufficiently cheap to allow for single use. However, in relation to safety and legal aspect it should be emphasized that the 3D printed product never should carry the radioactive source directly and only should serve as a platform for optimization of insertion and angulation of approved needles. Whereas commercially available templates can cover many clinical situations well with a standard implant configuration, 3D printed templates for steering of needles are in particular useful when individualised needles tracks are required. However, in such cases the local anatomical conditions should provide a reproducible and robust anchoring of the 3D printed template both with regard to rotation and angulation such that a meaningful pre-plan with virtual angulated needle tracks can be made. Ideally such a pre-plan should be based on MRI with a template in situ performed in a separate session not used for treatment. There is currently very limited data on the clinical use of 3D printed templates for steering of needles. This lecture will seek to review this experience using locally advanced cervical cancer as a practical example of the involved workflow, patient selection and possible outcome.

## Symposium: Automatic / Knowledge based treatment planning:open issues

---

### SP-0128 How can we get the best out of knowledge-based planning?

S. Currie<sup>1</sup>, E. Miguel-Chumacero<sup>1</sup>, N. Laverick<sup>1</sup>, G. Currie<sup>1</sup>  
<sup>1</sup>NHS Greater Glasgow And Clyde, Rt Physics, Glasgow, United Kingdom

#### Abstract text

Knowledge Based Planning (KBP) is now a recognised tool in the creation of high quality and consistent treatment plans. KBP was introduced as the standard planning approach for the majority of radical clinical sites at the Beatson West of Scotland Cancer Centre over three years ago based on the Varian RapidPlan solution. The presentation will describe the process of model implementation including the various barriers and pitfalls that were experienced. Additionally, the challenges faced in the continuing management of KBP models which now underpin over 50% of the daily clinical planning workload, across new software releases and updates, will be considered and how risks can be managed and addressed.

Following the implementation of KBP, a new development in treatment plan optimisation became available through Multi-Criteria Optimisation. This allowed a new strategy to be adopted in the creation of knowledge based planning models by combining Varian's Multi-Criteria Optimization-based Trade-Off Exploration to create base plans of the highest plan quality. These plans were optimised with emphasis in producing plans that offered reduced Organ at Risk (OAR) doses while always maintaining adequate and acceptable coverage of the planned tumour volume. These higher quality plans were then selected for the generation of new and updated knowledge based planning models. Results will be presented on the comparison of KBP plans generated with and without Trade-Offs, describing dose-volume parameters for both organs at risk and the PTVs, and target homogeneity, conformity, and plan complexity and deliverability. Finally, the opportunity afforded by knowledge based planning tools to aid in decision support will be

demonstrated, and specifically, the example of KBP models in the potential for spacing in moderately hypofractionated prostate treatments. KBP models were generated using twenty prostate patients, with and without a hydrogel spacer (SpaceOAR®, Augmenix Inc. Waltham, MA, USA). Four models were developed including plans generated for both pre and post gel implantation, and then a further two models, with these original plans re-optimised in combination with Multi-Criteria Optimisation, with focus in reducing the bladder and rectum doses, whilst ensuring adequate tumour coverage.

**SP-0129 Does automation jeopardise personalised treatment? Are we going back to prêt-à-porter instead of bespoke fashion?**

R.Moeckli

*UniversHospital CHUV Institut de Radiophysique(IRA)  
Lausanne, Switzerland*

Abstract not received

**SP-0130 The potential of automated treatment planning in clinical trials**

C. Hurkmans<sup>1</sup>

*<sup>1</sup>Catharina Ziekenhuis, Radiation Oncology, Eindhoven,  
The Netherlands*

**Abstract text**

Trial radiotherapy quality assurance (RTQA) is an important part of the good conduct of a clinical trial. Failure to perform the radiotherapy according to the trial protocol might lead to either a lower tumour control than expected or a higher morbidity. This in turn might lead to false positive or false negative trial results. The most important part of RTQA is a good protocol definition of what radiation treatment should be given in terms of fractionation, dose per fraction and dose to targets and organs at risk. This is assured by several RTQA steps: a facility questionnaire, standard beam output assessments (BOA) under reference conditions, benchmark planning exercises, Individual case reviews (ICRs) and complex dosimetric checks. Recently, it has been shown that BOA results have improved steadily over the last years and approximately only 0.5% of all BOA results are found to be out of the 5% tolerance level (Kerns 2018). This does however not guarantee that complex treatments can be administered with the same accuracy. Complex dosimetry checks have revealed that inaccurate beam modelling in a TPS can be an important reason why phantom dose measurements differ from the calculated dose (Kerns et al. IJROBP 2017). However, in general the current linear accelerators are very stable and individual plan quality assurance measurements show very good results. The most frequent failures to adhere to a trial protocol are found in the ICRs. Unacceptable trial protocol deviation rates between 11 and 48% have been reported and have shown to have a significant impact on the clinical outcome (Weber et al. RO 2012). Mostly, these ICRs were performed retrospectively and thus it seems clear ICRs should be conducted prospectively (Branquinho et al. RO 2018). Prospective feedback also potentially leads to a steeper learning curve on how to adhere to the trial guidelines. In the new EORTC 1735 ADHERE trial investigating the effect of an immune check-point inhibitor after chemoradiation in H&N patients, it will for the first time be prospectively investigated how much impact retrospective vs prospective ICRs will have on the proportion of acceptable patient plans. Until now, the ICR feedback given was usually limited to either per protocol, acceptable variation or unacceptable variation. Once prospective reviews are in place, unacceptable variations can be prevented. However, as protocol plan criteria are set such that most plans will be able to pass the criteria, the enormous potential further improvement in plan quality of

all the plans that pass these criteria is not exploited. With automated planning combined with rapid feedback to the institutions, this potential can be quantified on an individual patient level. The institutions can be presented with an alternative, improved plan which they might be able to use in their department. For example, for the RTOG 0933 whole brain with hippocampus sparing it was shown that automated planning could lead to better treatment plans than plans that were optimised just to adhere to the trial protocol (Krayenbuehl et al. RO 2017). Another example, comparing the plans actually used in the EORTC-1219 Dahanca H&N study plans, showed that the machine learning model was able to generate plans which could frequently improve OAR sparing (Tol et al. RO 2018). For another trial, comparing hypofractionated prostate treatment to conventional treatment, a higher grade 2 toxicity was found in the hypofractionated arm. Looking back at the treatment plans and generating new automated planning plans, it was shown that it was possible to reduce the NTCP of hypofractionated treatment to below the NTCP values of the clinically used standard fractionation schedule. This also indicates that potentially, automated planning could have led to a much lower late toxicity in the experimental arm and thus could have had a mayor influence on the trial outcome (Sharfo et al. RO 2018). In the Trendy trial of primary liver cancer, it was shown in a benchmark exercise that automated planning led to generally better plans with a lower liver NTCP (Habraken et al RO 2017). However, all these studies have been conducted retrospectively. There are still some challenges in order to fully use automated planning in clinical trials prospectively like easy to use software for up- and download of dicom-RT and CRFs including anonymization software which incorporates patient trial numbers and the use of standardized naming conventions for targets and OARs (AAPM TG report 263). Implementation of full prospective ICRs based on automated planning could lead to improved treatment of patients within the trial, a reduction of the number of patients needed in a trial and thus also a reduction of trial costs and more reliable trial outcomes leading to better treatment of future patients.

**SP-0131 Using automated planning for “bias-free” plan comparison**

L. Rossi<sup>1</sup>, A.W. Sharfo<sup>1</sup>, S. Breedveld<sup>1</sup>, B.J.M. Heijmen<sup>1</sup>

*<sup>1</sup>Erasmus Mc - Cancer Institute, Department Of Radiation Oncology, Rotterdam, The Netherlands*

**Abstract text**

Plan quality in current interactive trial-and-error treatment planning (designated ‘manual’ planning) is highly dependent on the planner’s skills and on allotted time. Many treatment planning studies may then suffer from considerable bias e.g. due to differences in planning experience for the investigated techniques, use of different treatment planning systems for the techniques, or a wish that one of the techniques will be superior. Due to the large manual planning workload numbers of plans may be small.

Automated planning can play a key role in substantially reducing bias in these planning studies. Erasmus-iCycle is a system for fully automated multi-criterial planning, based on a wish-list. Resulting plans are always Pareto-optimal and have clinically favourable trade-offs between objectives. Due to the involved prioritized optimization, plan generation is highly consistent among different patients. By using the same wish-list for all evaluated treatment techniques in the study, bias in the comparisons can be substantially reduced. Due to the automation excessive workload may be avoided and studies with large plan/patient numbers may be performed.

**Joint Symposium: ESTRO-EFOMP: Multi-disciplinary working in Radiotherapy**

**SP-0132 Working for radiotherapy applications: The perspective of a nuclear medicine physicist in the era of Hybrid Imaging Systems**

V. Bettinardi<sup>1</sup>, M.G. Cattaneo<sup>2</sup>

<sup>1</sup>IRCCS San Raffaele Hospital, Nuclear Medicine, Milano, Italy; <sup>2</sup>IRCCS San Raffaele Hospital, Medical Physics, Milano, Italy

**Abstract text**

Radiation therapy (RT) is a cornerstone of modern cancer therapy used in approximately 50% of all cancer patients during their clinical course of illness. A common feature of RT treatment with curative intent is to have very sharp dose gradients between the target and adjacent normal tissues. The introduction of more tailored RT planning/delivery techniques using intensity-modulated beams (IMRT), stereotactic radiotherapy (SBRT), tracking with gating or robotic radiosurgery, and precise image-guidance (IGRT) have largely contributed to improve the outcome both in terms of tumor control and in reducing toxicities. In this regard, multimodal imaging and in particular that of the latest generation of hybrid imaging systems (HIS) such as: PET/CT, SPECT/CT and more recently also PET/MRI, can play a crucial role to further exploit the potentialities of modern RT technology. Besides the great clinical value of HIS, technical aspects make these systems also particularly useful for RT applications. In fact, HIS allow the acquisition of anatomical and functional images with the patient being in the same position during the whole study session. This characteristic is further improved in fully integrated PET/MRI systems due to the possibility of truly simultaneous acquisition (spatial and temporal) of the two studies. This “hardware” alignment is very important for an accurate target volume delineation (TV) as errors introduced by image co-registration are minimized. Furthermore, the integration of anatomical, functional and molecular information allows the visualization of various pathophysiological aspects of the tumors which may be important for assessing individual parameters related to cancer cure procedure. In this highly technological scenario the perspective of a nuclear medicine (NM) physicist, who has access to HIS is to work on topics aiming to produce useful and accurate information (images and other type of data) for an optimal and personalized RT. A first of these topics is the set-up of a comprehensive quality control protocol, to guarantee stability/reproducibility of the systems' performance with particular reference to the need of RT applications. Definition and implementation of acquisition, reconstruction and post-processing protocols accounting for different tracers (e.g. 18F-FDG, 18F-FAZA, 11C-Methionine, etc.) and different targets (e.g. brain, lung, liver, etc.) are also important topics of a unique pipeline which aims at the most accurate TV. Delineation of the target volume, and in particular of the biological target volume, is still an open topic that needs to be improved. Several methods based on different image processing techniques (e.g. thresholding, probabilistic, clustering, etc.) have been proposed over the years but none of them have been accepted as standard for clinical use. This has left, to the human operator, the role of gold standard in the TV. However, new techniques based on a machine learning/deep learning, have shown to overtake human performance in computer vision, image recognition, and image interpretation challenges. Furthermore, the same techniques have shown very promising results also when applied to automatic segmentation for TV, in particular when a multimodal and/or a multiparametric imaging approach has been used. An accurate TV also allows a more accurate extraction of information that can be

useful for a more comprehensive characterization of image phenotypes of the tumor. Radiomics analysis has recently emerged as a promising tool for the definition of new imaging biomarkers by high-throughput extraction of quantitative image features. Several studies have shown that texture features extracted from PET, CT or MRI images may have a higher predictive and/or prognostic power than simpler, more “standard” metrics (SUV, tumor shape, tumor volume, etc.). Notwithstanding, such great promises, radiomics analysis presents several challenges that need to be carefully addressed. Standardization (features definition, features computation, features dependences etc ..) is one of the most important aspects which need to be defined to ensure robustness, reproducibility and dissemination of the obtained results among centers. In conclusion, all previously described topics find application when using HIS. HIS have an enormous potential in the generation of complementary information (images and other data type) that, once integrated in a unique model, may allow a more comprehensive understanding of the tumor pathology as well as a more accurate definition of the target for RT treatment. In this scenario the perspective of an NM physicist is to be active in this complex technological and methodological puzzle, working in strong collaboration with all the other people involved in the clinical and research work (physicists, engineers, physicians, technicians, etc.) having as a common objective the best treatment for each patient.

**SP-0133 Working in radiotherapy from the perspective of an MRI physicist**

L.E. Olsson<sup>1</sup>

<sup>1</sup>Lund University, Department of Medical Radiation Physics, Malmö, Sweden

**Abstract text**

There is a substantial increase of imaging in the recent development in radiotherapy. The on-going process of installing dedicated radiotherapy MR-scanners in the oncology/radiotherapy clinics is an obvious proof of this development. MRI is a much more complex modality and applications extend from diagnosis to specific imaging for target identification, treatment planning, treatment follow-up and adaptive regimes. An in-house MR-scanner also brings along many safety issues, both for personnel and patients. Altogether, there is an increasing need for MRI expertise in the radiotherapy department. The demand on accurate geometry and quantification of the data is considerably larger in therapy than diagnostic MRI applications. That means that what can easily be accepted as a well know harmless artefacts in the diagnostic setting can have detrimental negative effects if used for treatment guidance in radiotherapy. Therefore, the MRI-physicist needs specific training in how the image data will be used in the radiotherapy workflow. The MRI-expertise can be an in-house MRI-physicist working with radiotherapy or as a service provided by diagnostic radiology physicists. In any case, it is important that the MRI-physicist will be specifically trained and dedicated to radiotherapy. Not all MRI-physicists from radiology can have the knowledge needed in radiotherapy. Similarly, an MRI-physicist working in radiotherapy cannot be an expert on all MRI techniques. An ideal model is to have a dedicated MRI-physicist in-house in radiotherapy, which will act as a link to the other MRI-physicists in radiology, and thereby facilitate the discussion and knowledge transfer in both directions. The present question will be even more important to discuss when hybrid modalities, such as MR-linacs, will be implemented in the clinics. It is obvious that the MR-scanner is a part of the treatment machine. Therefore, the installation of MR-linacs should be combined with recruitment of in-house MRI-expertise. Traditionally, there have been different physicists

dedicated to radiotherapy, nuclear medicine, MRI and other radiology. The future hybrid modalities in both diagnostics (PET/MR, PET/CT) and therapy (MR/linac) will be the end of the era for "One Modality Physicist". This is a both a challenge as well as a source to opportunities to the physics profession.

#### SP-0134 Working with radiotherapy from the perspective of US physicist

E. Harris<sup>1</sup>

<sup>1</sup>The Institute of Cancer Research and The Royal Marsden NHS Foundation Trust, Joint Department of Physics, Sutton, United Kingdom

##### Abstract text

Ultrasound can be used to guide radiation therapy of the prostate and prostate bed, breast, gynaecological cancers, and some upper abdominal sites such as liver. The integration of ultrasound with the radiotherapy workflow presents a number of challenges for the ultrasound physicist. One key issue when using ultrasound to guide radiotherapy is the requirement of spatial registration of ultrasound data with the treatment coordinate system which is often not straight forward; ultrasound images are rarely obtained using rectilinear spatial sampling and proprietary information regarding the transducer geometry is not easily obtained. Furthermore, the transformation of ultrasound image data into Cartesian space reduces image quality but is necessary for image display and fusion with CT and CBCT. The pitfalls associated with geometrical registration of ultrasound with the RT treatment isocentre and the importance of working with radiotherapy colleagues to understand geometrical components of the radiotherapy workflow will be discussed.

QA has to be performed at a much greater frequency than is typical for the ultrasound physicist, which is commonly once per year. Traditional ultrasound imaging QA phantoms are typically not suitable to assess the use of ultrasound in radiotherapy (end-to-end testing) and for example, the development of X-ray and ultrasound compatible spatial registration phantoms and anthropomorphic test phantoms, even dynamic phantoms can be challenging. Multidisciplinary working is crucial to generate solutions to these problems. In the design of new systems, the ultrasound physicist has to appreciate there are several practical limitations associated with the radiotherapy setting which can reduce the ultrasound image quality obtainable, including: low (transducer) pressure scanning, high time-pressures, poor selection of imaging parameters, frequent rotation of skilled workforce. The need for greater automation and system redesign will be discussed, including a description of current methods to overcome these problems (used both in an RT setting and elsewhere in diagnostic ultrasound) and potential exciting new multidisciplinary research opportunities.

#### SP-0135 Working with radiotherapy from the perspective of data/computer scientist

D. Sarrut<sup>1</sup>, R. Simon<sup>1</sup>, A. Myriam<sup>2</sup>, C. Line<sup>2</sup>, B. Thomas<sup>1</sup>, B. Jean-Noel<sup>3</sup>, G. Anne-Laure<sup>3</sup>

<sup>1</sup>CNRS - Léon Bérard Cancer Center, Creatis, Lyon, France; <sup>2</sup>Léon Bérard Cancer Center, Radiation Therapy, Lyon, France ; <sup>3</sup>Léon Bérard Cancer Center, Nuclear Medicine, Lyon, France

##### Abstract text

I will present 3 short examples of collaborative experiences between computer scientist researchers and radiotherapy/nuclear medicine departments. The first one is the setup of radiotherapy NSCLC lung treatment using deformable image registration (DIR). The second example describes the development of motion

compensated Cone-Beam CT algorithms. The third example deals with image-based dosimetry in nuclear medicine therapy. All those examples illustrate the interest and the difficulty to access raw data, to provide new algorithms that may be difficult to insert into clinical routine.

---

#### Symposium: Younger people and radiotherapy

---

#### SP-0136 Considerations for Younger patients receiving RT: psychological, physical, and surveillance

C. Dickie<sup>1</sup>, N. Laperriere<sup>1</sup>

<sup>1</sup>Princess Margaret Cancer Centre- University of Toronto, Radiation Medicine Program, Toronto, Canada

##### Abstract text

Research has demonstrated that adolescents and young adults (AYAs) ages 15 to 39 have unique considerations for cancer care and survivorship. As they transition from pediatric to adult oncology, they also struggle with diverse life changes such as trying to establish independence and identity, a healthy separation from parents/family, employment decisions, higher education and having their own families. Studies show that this transitional period in life is more stressful than other stages with a diagnosis of cancer potentially exacerbating or adding to existing issues. This talk will provide an overview of some of the psychological, physical and surveillance issues that challenge this particular subset of patients with a focus on the supportive role a radiation therapist can play that may positively influence critical outcomes. Psychological distress is well documented in AYA survivors of childhood cancer and for AYAs undergoing therapy. In fact, there have been a series of unmet service needs identified for AYAs including issues involving emotional wellbeing, uncontrolled pain, fear, stress, anxiety, fertility preservation and sex drive / sexual health, fatigue, stressed social and romantic relationships, the inability to meet work demands, school and higher education concerns, and financial issues as they progress through their life during and after cancer therapy. Improvements in the effectiveness of cancer therapy have resulted in increased survival rates often accompanied by chronic toxicities associated with radiotherapy. Anatomical / physical issues include but are not limited to cardiopulmonary toxicity, neurocognitive dysfunction, musculoskeletal issues and secondary malignancy. Survivors also have difficulty with daily activities and physical function due to symptoms from medical interventions. Finally, surveillance considerations are important for the AYA population. A large proportion of adult survivors of childhood or adolescent cancer suffer from toxicities occurring very late and hence late effects screening is critical. In addition, the rate of secondary malignancies is higher than in the general age matched population. AYA patients should be made aware of this risk, have routine follow up, and should be informed to contact their health care team if new symptoms arise. Studies have demonstrated that AYAs frequently do not feel like they have received adequate information at discharge and are non-compliant with regular follow up. Radiation Therapists (RTTs) are in a unique position to improve the evaluation of AYAs unmet needs and management during radiotherapy. Although radiotherapy is often given at the end of the treatment trajectory, RTTs can facilitate access to services and information as the patient's daily point of contact. Research in AYA care shows underutilization of services with associated worse overall health related quality of life and outcomes. Increasing RTT awareness of these needs, how to identify an issue, and how to develop effective strategies to address concerns has the potential to contribute to the reduction of distress in the AYA

population. There may also be a role for an Advanced Practice RT in late effects clinics.

**SP-0137 Radiotherapy in children and adolescents. What do we know until now and what will the future bring?**

**T. Boterberg<sup>1</sup>**

<sup>1</sup>*Ghent University Hospital, Radiation Oncology, Gent, Belgium*

**Abstract text**

Cancer in children and adolescents is rare and at the same time characterized by a wide variety of tumour types, often different from the common adult cancers. Over the past decades, paediatric cancer treatment results have improved significantly: up to 80% of children and adolescents with cancer are currently cured of their disease, although survival figures for the individual cancers vary significantly. This is mainly the result of multi-modality treatment protocols including chemotherapy, surgery, and biological treatment, in addition to selective use of more sophisticated radiotherapy techniques. In addition to that, a better knowledge of molecular characteristics has led to an increasing personalisation of treatment based on risk stratification, which has allowed to further improve cure rates with a reduction in treatment-related morbidity. This is especially important for radiotherapy as treatment modality since almost every organ system is subject to some late effects caused by radiotherapy, in addition to the risk of developing secondary cancers. However, we should take into account that there is a significant variation in frequency of these long-term complications. They are more determined by the affected site, the irradiated volume, the age at time of treatment and the dose given than by the original tumour type treated. Obviously, interaction with chemotherapy may also play a role and should also be taken into consideration. The significant increase in paediatric cancer cure rate over the past years has also increased the number of cancer survivors at risk for developing late effects. While with the passing of time, the risks of cancer relapse recede, monitoring for late effects of treatment becomes more important as they can, as mentioned, affect any body system. The majority of patients will have some form of long-term sequelae, some minor, some major and some that can be ameliorated by timely intervention. Therefore it is strongly recommended that patients should be followed in a multidisciplinary clinic. A detailed treatment summary will help to predict the risk of complications and should guide this long-term follow-up. Finally, increasingly more sophisticated and well-targeted radiotherapy techniques should allow to further minimise the risk of late effects, but that too is still to be investigated and examined long after treatment has finished.

**SP-0138 (VAIRT) Video-Assisted Immobilisation during external beam RadioTherapy for Children**

**N. Ritt<sup>1</sup>**

<sup>1</sup>*Universitätsklinik für Strahlentherapie, Brachytherapie, Wien, Austria (VAIRT) Video-Assisted Immobilisation during external beam RadioTherapy for Children*  
Authors: N. Ritt, S. Hofstätter, A. Osztavics, B. Wisgrill, C. Chao, D. Berger, K. Dieckmann

**Purpose and Objective**

The aim of the pilot study at the Department of Radiotherapy at the Medical University of Vienna (General Hospital of Vienna) was to reduce the number of daily sedations, (which were necessary to keep the patient in treatment position during their radiotherapy fraction) including the presence of anaesthesiologist for children and young patient undergoing EBRT. Therefore, a short cartoon is shown on tablets, to the child lying on the

treatment couch. The impact of this method to reduce stress and anxiety by cognitive distraction, the acceptance by the patients and further the reduction of daily sedations shall be investigated in this work.

**Materials and Method**

In the pilot study between July 2017 and May 2018 the Video-Assisted Immobilisation during external beam RadioTherapy (VAIRT) was offered to all patients below the age of 18 years. The compliance of patients was identified during the preparation process for the radiotherapy treatment. If they were able keep calm during the head-immobilisation mask-preparation and/or CT simulation while watching the short video sequence, the radiation treatment at the LINAC can be performed without daily sedation. Involving the medical staff (Radiology Therapist- RTTs, Radiation Oncologists and Medical Physicists) during the briefing of assistant family member is necessary for the successful implementation of this method of immobilisation in young patients. Results Thirty-eight patients (24 male, 14 female) with a median age of 8 years [from 1 to 18 years] were treated during the pilot study period at the department of radiotherapy. Twenty out of 38 (52%) 7 [3-14] years were successfully cognitively distracted by movies during treatment so that no daily sedation and presence of an anaesthesiologist were needed. Of the remaining patients 13 (34%) at the age of 14 years [8-18] refused to watch any movie while five (13%) at 2 [1-7] year age had to be sedated during treatment. By the introduction of the VAIRT method in the radiotherapy department an increase of 50% of young patients who do not need a daily sedation was observed.

**Conclusion**  
The Video-Assist-Immobilisation method was successfully implemented in the clinical routine for patients below the age of 18 years. For the success of the VAIRT a professional briefing of the patient, relatives and all professional staff involved in the treatment is essential. Reducing sedation during radiation therapy, allows a meaningful handling of resources in saving time (30 min per fraction) and costs (2800€) per patient and treatment. The VAIRT can also be used in adult patients who are stressed and anxious during head-mask preparation and treatment.

---

**Poster Viewing: Poster viewing 3: Brachytherapy**

---

**PV-0139 Endorectal HDR brachytherapy boost with MRI guidance for non operative management of rectal cancer**

**R. Engineer<sup>1</sup>, A. Saklani<sup>2</sup>, A. D'Souza<sup>2</sup>, A. Baheti<sup>3</sup>, M. Patil<sup>1</sup>, S. Chopra<sup>1</sup>, P. Patil<sup>4</sup>**

<sup>1</sup>*Tata Memorial Hospital, Radiation Oncology, Mumbai, India;* <sup>2</sup>*Tata Memorial Hospital, Surgical Oncology, Mumbai, India;* <sup>3</sup>*Tata Memorial Hospital, Radlogy, Mumbai, India;* <sup>4</sup>*Tata Memorial Hospital, Gastrointestinal Oncology, Mumbai, India*

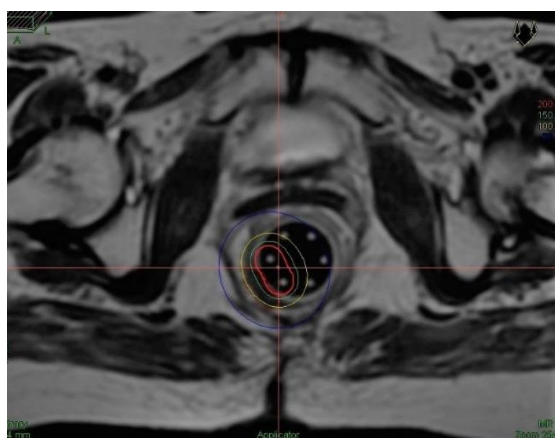
**Purpose or Objective**

In this study we evaluated the role of endorectal brachytherapy as a boost to escalate radiotherapy dose to achieve clinicoradiological complete response leading to organ preservation.

**Material and Methods**

This pilot study consisted of consecutive patients with T2-4 N0-2 M0 distal rectal cancer (within 6 cm from anal verge) treated with radical intent neoadjuvant chemotherapy (NACTRT) between October 2017 and May 2018. External beam radiotherapy consisted of 3D-CRT (4 field) or IMRT to a dose of 50Gy (1.8 to 2 Gy per fractions), to the primary and nodal regions along with daily capecitabine (825mg/msq). Response at conclusion was evaluated by digital per rectal examination (DRE) and those with a residual ulcerative disease and no greater than three-fourth circumferential involvement were

considered for further boost. A planning MRI scan with a multiple channel surface applicator in place was taken within 3 weeks of NACTRT completion. Residual tumour / fibrotic regions were contoured (CTV), dose prescribed at periphery of the residual tumor (7 - 10 mm) depending on depth of invasion and isodose distribution generated for 2-3 channels in closest proximity to the CTV. Plan evaluation consisted of ensuring that the CTV is completely covered by the 85% isodose cloud, while trying to limit the opposing rectal wall from being covered by the 50% isodose line (Fig. 1). High dose rate brachytherapy was delivered with iridium-192 source to a dose of 4 to 6 Gy in 2 fractions one week apart. Patients were assessed for tumor response at 6 weeks from radiation completion with DRE, rectal MRI scan and direct endoscopic visualization a 12 weeks. Patients with incomplete clinical response at 6 to 12 weeks were sent for immediate surgery. Patients with complete (CR) or near complete clinical response (NCR) were observed.



## Results

In all, 66 patients underwent NACTRT in the given period and 21 patients were found to be suitable for brachytherapy boost. 1 patient defaulted immediately after completion of brachytherapy. Four (20%) patients having partial response 3 underwent abdominoperineal resection and 1 had intersphincteric resection. Of these 1 patient had pathological complete response. Of the remaining 20 patients, 15 (75%) had CR to NCR at 12 weeks follow up and were enrolled for the wait and watch approach (Fig. 3). One with nCR underwent local excision.

At a median follow up of 27 weeks (range 16 - 44 weeks) only no patient has had a local regrowth and all 15 (75%) patients continue to be on observation. No rectal toxicity reported.

## Conclusion

Dose escalation with MRI guided endorectal brachytherapy for non operative management of rectal cancer is feasible and can lead to a larger number of patients to achieve complete clinicoradiological response leading to organ preservation.

Longer follow up and a larger sample size would be required to weigh the potential benefits of dose escalation with regard to local response, progression free interval, successful salvage and against risk of long term toxicity.

## PV-0140 Predictive factors and patients' selection for pulsed dose rate brachytherapy boost in anal cancer

T. Brahmi<sup>1</sup>, A.A. Serre<sup>1</sup>, F. Gassa<sup>1</sup>, F. Lafay<sup>1</sup>, M. Sandt<sup>1</sup>, P. Pommier<sup>1</sup>

<sup>1</sup>Centre Léon Bérard, Radiation Therapy, Lyon, France

## Purpose or Objective

The therapeutic standard of care for localized anal canal cancers is the association of pelvic radiation therapy,

possibly associated with concomitant chemotherapy, followed by a boost either by brachytherapy (BT) or external beam radiotherapy (EBRT). Pulsed Dose-Rate technique (PDR) has become a standard modality, with high local control rates, but questions are remaining regarding patient's selection and predictive factors for local control and toxicities.

## Material and Methods

Between 2005 and 2017, 179 consecutive patients with an anal canal cancer (all histological types), received PDR-BT as a boost after EBRT (+/- concomitant chemotherapy) in our institution. 159 were available for the analysis. Previously reported prognostic factors were analysed in univariate and multivariate analyses with a focus on the local extent of the tumour (T stage; circumference and anal margin and/or rectal mucosa involvement). Local control response was clinically assessed at the time of brachytherapy, then every 3 months for 2 years (MRI every 6 months), then every 6 months.

Late toxicities after BT were classified according to the CTCAE-v5.0.

## Results

The main characteristics of tumours and treatments are detailed in table 1.

With a mean follow-up of 44.5 months, the 5-years loco-regional control and Progression Free Survival (PFS) were respectively 89% (95%CI 86-92) and 82% (95%CI 78-86). Overall Survival (OS) rate was respectively 84% (±4) and 76% (±7) at 5 and 10 years.

Sixteen patients underwent abdominoperineal resection for local recurrence (14) or severe local toxicity (2). 14.5% experienced mucosal grade ≥2 late toxicity. In multivariate analysis, local control response at the time of BT (HR=4.46 for Partial Response rate); EBRT technique (HR = 3.25 for IMRT vs 3D conformal), histology and diabetes were significantly associated with PFS. In that series, gap between EBRT and BT was not significant, but was significantly greater in patients treated with 3D conformal EBRT (30.3 vs 17.6 days, p=0.002). Local extent of the tumour at the initial staging did not significantly influence the PFS in univariate and multivariate analyses. Only tumour recurrence was significantly associated with overall survival (OS).

No significant factors was identified for grade ≥2 late toxicity.

Variables	Number of patients	Percentages
<b>Histological classes</b>		
Squamous cells carcinoma	146	91.8%
Undifferentiated carcinoma	4	2.5%
Other	9	5.7%
<b>Circumference</b>		
<25	13	8.2%
[25 to <33]	37	23.3%
[33 to <50]	33	20.8%
≥50 to 66	76	47.8%
<b>Rectal mucosa involvement</b>		
None	50	31.4%
Present	89	56.0%
Missing data	20	12.6%
<b>Anal margin involvement</b>		
None	104	65.4%
Present	41	25.8%
Missing data	14	8.8%
<b>Staging cT</b>		
1	25	15.7%
2	100	62.9%
3	28	17.6%
4	4	2.5%
<b>Type of treatment</b>		
Exclusive EBRT	51	32.1%
Concurrent Radio-Chemotherapy	107	67.3%
<b>EBRT modalities</b>		
3D conformal	51	32.1%
IMRT	91	57.2%
Missing data	17	10.7%
<b>EBRT treatment time, in days</b>	Mean (SD)	
	38.8 (5.1)	
<b>Gap between EBRT and BT, in days</b>	Mean (SD)	
	23.0 (12.7)	

## Conclusion

PDR-BT is an effective boost modality after EBRT for anal carcinoma patients and may be also indicated in selected patients with a limited involvement of anal margin and rectal mucosa and/or a diameter > 50% (maximal 2/3) of the anal mucosa. The EBRT technique was significantly associated with PFS and IMRT should be applied in these

patients. Results from large multicentre prospective studies are awaited to confirm these observations.

#### PV-0141 Treatment outcomes of HDR brachytherapy for cervical cancer: a comparison of Ir-192 versus Co-60

T. Tantivatana<sup>1</sup>, R. Kanisa<sup>1</sup>

<sup>1</sup>Vajira Hospital, Radiation Oncology, Bangkok, Thailand

##### Purpose or Objective

To determine and compare treatment outcomes between cobalt-60 (Co-60) and iridium-192 (Ir-192) high dose rate (HDR) brachytherapy in stage IB2-IIIB cervical cancer patients at Department of Radiology, Faculty of Medicine Vajira Hospital, Navamindrahiraj University.

##### Material and Methods

A retrospective cohort study of patients diagnosed with cervical cancer and treated with radiotherapy at the Department of Radiation Oncology, Faculty of Medicine Vajira Hospital between 2004 and 2014. Survival rate was analyzed by Kaplan-Meier method and were compared between groups with log-rank test. Multivariate analysis was performed using Cox proportional hazards model.

##### Results

A total of 480 patients with cervical cancer and treated with radiotherapy were included, 274 patients for Ir-192 group and 206 patients for Co-60 group. The 2- and 5-year disease-free survival rate in Ir-192 group were 80.4% and 73.1% and in Co-60 group were 82.5% and 74.7%, respectively (p=0.365). Overall survival rates at 2 and 5 years were 89.4% and 77% of the Ir-192 group, and 91.6% and 81.9% in the Co-60 group, respectively (p=0.238). The complications were primarily grade 1 or 2. Grade 3 and 4 complications were found in 13 of 274 and 7 of 206 in Ir-192 and Co-60 groups, respectively (p=0.23). Grade and clinical stage of cancer significantly affected the survival outcome.

##### Conclusion

Cervical cancer patients who were treated with HDR Co-60 brachytherapy were comparable in survival and toxicity outcomes of those with HDR Ir-192 brachytherapy. Co-60 source has lots of economic advantages over Ir-192 and hence suitable for low resource radiotherapy setting.

#### PV-0142 HDR BRT treatment of non-melanoma skin cancer: outcome and feasibility in a retrospective analysis

D. Delishaj<sup>1</sup>, I.C. Fumagalli<sup>1</sup>, R. D'Amico<sup>1</sup>, G. Sangalli<sup>2</sup>, F. Declich<sup>2</sup>, C. Frigerio<sup>2</sup>, C.P. Soatti<sup>1</sup>

<sup>1</sup>Ospedale Manzoni di Lecco, Department of Radiotherapy, Lecco, Italy ; <sup>2</sup>Ospedale Manzoni di Lecco, Department of Medical Physics, Lecco, Italy

##### Purpose or Objective

Non-melanoma skin cancer (NMSC) is the most common malignancy in the white population, comprising about 2-3 million new diagnosis worldwide every year, with an increasing incidence observed in the last decades. High dose rate brachytherapy (HDR-BRT) is an advantageous treatment option both from dosimetric point of view and for patient convenience due to the small number of fractions.

The purpose of this study was to evaluate tumour control and toxicity in elderly patients treated with HDR-BRT.

##### Material and Methods

A total of 55 patients underwent skin HDR-BRT from October 2007 to July 2018 with Iridium-192 source. 34 lesions in 31 patients affected by NMSC were enrolled; lymphopietic, breast and benign histology (keloids) were excluded from the analysis. The median age at diagnosis was 79,6 years [48,5-102,4]. A surface flap was customized to the size of each target lesion and the catheters were embedded; every treatment was optimized with 3D planning using CT imaging. Different

prescribed doses and fractionation have been chosen: 24-31.5 Gy in 8-12 fractions for palliative treatment (5 cases, 15%), 34-52 Gy in 10-20 fractions for adjuvant treatment (20 cases, 59%) and 36,75-60 Gy in 7-30 fractions for radical treatment (9 cases, 26%); the average biological effective dose (BED) was 35.7, 51 and 60.9, respectively. The treatment was mostly delivered with daily fraction and some schedules were accelerated with 2 fractions a day. Acute and late toxicity has been recorded according to CTCAE 4.0.

##### CHARACTERISTICS

No of Patients 31 No of lesions 34

Age, years Median 79,6 Range 48,5-102,3

Sex Male 24 (70%) Female 10 (29%)

Histology Basal Cell Carcinoma 4 (12%) Squamous Cell Carcinoma 28 (82%) Kaposi Sarcoma 2 (6%)

Size, cm Median 3 Range 1-7

Localization Scalp 16 (47%) Ear 6 (18%) Face 7 (21%) Trunk 2 (6%) Extremity 3 (9%)

##### Results

At a median follow-up of 12 months (range 3-77,2 months), local control was 97%; in particular no patient treated with an adjuvant BRT HDR after radical surgery had local recurrence and 7 of the 9 lesions (78%) who received a radical dose showed a complete response. In only 4 lesions a partial response was observed, mostly in the palliative group, and just 1 case developed a progression. No severe acute toxicity was recorded; just 32% of the cases presented G2 acute toxicity, recovered within 2 months from the end of BRT. Late G1 toxicity was showed in almost a quarter of the lesions; no G2 or greater late toxicity was recorded. 62% lesions showed an excellent cosmetic impact and just 2 cases resulted in a fair cosmetic outcome.

##### Response tu BRT N %

radical 9

CR 7 78

PR 1 11

PD 1 11

adjuvant 20

Recurrence 0

palliative 5

CR 2 40

PR 3 60

##### Acute Toxicity

Grade

0 10 30

1 13 38

2 11 32

≥ 3 0

##### Late Toxicity

0 26 76

1 8 24

2 0

≥ 3 0

##### Cosmetic Result

Excellent	21 62
Good	11 32
Fair	2 6
Poor	0

### Conclusion

HDR-BRT represents an effective and safe solution for the treatment of NMSC, even in elderly population, with excellent clinical outcome and very low toxicity. More data with a longer follow-up are necessary.

### PV-0143 High-dose CT-guided interstitial brachytherapy of liver metastases in oligometastatic patients

F. Walter<sup>1</sup>, S. Gerum<sup>1</sup>, M. Rottler<sup>1</sup>, C. Maihöfer<sup>1</sup>, J. Well<sup>1</sup>, L. Nierer<sup>1</sup>, M. Seidensticker<sup>1</sup>, R. Seidensticker<sup>2</sup>, T. Streitparth<sup>2</sup>, F. Streitparth<sup>2</sup>, J. Ricke<sup>2</sup>, C. Belka<sup>1</sup>, S. Corradini<sup>1</sup>

<sup>1</sup>Radiation Oncology, Department of Radiation Oncology LMU, Munich, Germany; <sup>2</sup>Radiology, Department of Radiology LMU, Munich, Germany

### Purpose or Objective

Local treatment for liver oligometastases is a challenging issue. Aim of the present study is to report feasibility and outcome in this setting using high-dose CT-guided interstitial brachytherapy (BT).

### Material and Methods

36 patients (m:f 17:19) with a median age of 68 years (31-88) who received high-dose brachytherapy on liver metastases between 01/18 and 06/18 were retrospectively analysed. Primary tumours were as follows: rectosigmoid carcinoma in 16 patients (pts), breast cancer in 4 pts, NET in 5 pts, gastric cancer in 3 pts and others (sarcoma, GIST, pancreatic cancer, colon cancer, prostate cancer).

### Results

18 out of 36 pts presented with a single hepatic lesion, 12 pts had two lesions and 6 pts had 3 or more lesions. Between 1 to 9 catheters were utilized for the procedure (1=7pts, 2=14pts, 3=5pts, >3=10pts). The median metastases diameter was 2.1cm (range 0.8-13.6cm) with a median volume of 2.4ccm (0.1-550.8ccm). The total liver volume ranged from 891-2761ccm (median 1402ccm). A medium dose of 19.7Gy was achieved in D100 (8.7-26.1Gy), D98: 22.6Gy (9.6-33Gy), D95: 24.5Gy (10.1-39.6Gy), and D90: 26.6Gy (10.6-49.7Gy). Liver dose exposure parameters were V5: 290.3ccm (43.7-1792.2ccm), V10: 101.9ccm, and V15: 57.4ccm (8.4-689.5ccm). Follow-up was available in 32 out of 36 pts and was between 28-144 days (median 86 days). In 29 pts local control was achieved, while in 4pts a local recurrence occurred.

### Conclusion

CT-guided interstitial brachytherapy showed to be a safe and effective treatment approach for oligometastatic liver disease. Longer follow-up is needed to assess the role of this treatment modality in the oligometastatic setting as an alternative to other treatment approaches, including SBRT.

### PV-0144 Custom-made moulds plesiotherapy for non-melanoma skin cancer treatment

M.Á. González Ruiz<sup>1</sup>, J.L. Muñoz García<sup>2</sup>, J. Quirós Rivero<sup>2</sup>

<sup>1</sup>Punta de Europa Hospital, Radiation Oncology, Algeciras, Spain; <sup>2</sup>Badajoz University Hospital, Radiation Oncology, Badajoz, Spain

### Purpose or Objective

To evaluate our results in terms of local disease free survival (LDFS), cosmesis and toxicity in patients (pts) with non-melanoma skin cancer (NMSC) treated with high-dose-

rate brachytherapy (HDR-BT) treatment, plesiotherapy modality, with custom-made moulds.

### Material and Methods

87 pts out of 198 pts (44%) were treated with HDR-BT in our Department (110 NMSC lesions) from May 2015 to May 2017 with custom-made moulds. HDR-BT treatment (6 Gy/fraction; total dose 42 Gy) was used in 88.2% pts with an equivalent 2 Gy dose (EQD2) of 56 Gy. All the lesions were limited 3-4 mm depth. The median age was 79 years old (range 29-97), 60% of pts were males and 40% females. Basal-cell carcinoma (90%) was the most frequent histological type. 80.9% of the lesions were T1 stage (80.9%) and 100% were located on face and forehead. Treatment intention was radical in 83.6% of the pts and adjuvant in the 16.4%.

### Results

The median follow-up was 31 months (range 9-65). LDFS was 95.45%. There were no differences in terms of local control related to tumour stage (p 0.149). Pts had acute skin toxicity grade 1 (62.7%) and grade 2 (29.1%). Conjunctival toxicity appeared in 15.5 % (lesions near to the eyes). Cosmetic results were considered excellent and good in all of the patients.

### Conclusion

In base to our initial results, plesiotherapy with custom-made moulds is a safe, attractive and a good alternative of treatment in NMSC. This modality of treatment provides excellent results in terms of local control and cosmesis.

### PV-0145 The impact of modern imaging on low dose-rate prostate brachytherapy

D. Lamb<sup>1</sup>, L. Greig<sup>2</sup>, G. Russell<sup>3</sup>, J. Nacey<sup>4</sup>, L. Woods<sup>5</sup>

<sup>1</sup>Victoria University of Wellington, School of Biological Sciences, Wellington, New Zealand; <sup>2</sup>Capital and Coast District Health Board, Radiation Physics, Wellington, New Zealand; <sup>3</sup>Southern Cross Hospital, Prostate brachytherapy, Wellington, New Zealand; <sup>4</sup>University of Otago, Surgery, Wellington, New Zealand; <sup>5</sup>Victoria University, Statistics, Wellington, New Zealand

### Purpose or Objective

To determine if modern imaging has improved our understanding of why biochemical failure (BF) and urethral stricture develop in some men after low dose-rate prostate brachytherapy.

### Material and Methods

A prospectively maintained database containing information on 951 men with early stage prostate cancer treated with low dose-rate brachytherapy after transrectal ultrasound planning. In addition, 74 men implanted more recently after MRI planning.

### Results

Median follow up of the 951 men was 7.9 years, with a range 2.0 - 16.3 years. Ten-year prostate specific antigen control was 95% for 551 low-risk patients and 82% for 400 intermediate-risk patients. 73 men developed biochemical failure (BF) and 17 men urethral stricture.

Prostate specific membrane antigen PET-CT scanning performed on 34 men who underwent BF revealed that 27 (80%) had local recurrence, and of these, 25 (93%) had relapsed in the prostate base and/or seminal vesicles.

A low prostate Dose 90 ( $\leq 90\%$ ) did not increase the risk of BF (P=0.127), but a small prostate volume ( $\leq 35$  cc) increased both the risk of BF (P=0.02) and of urethral stricture (P=0.003). Men who developed urethral stricture were found to have twice as many seeds 10 mm below the prostate apex as men who did not, indicating that too low positioning of seed strands was usually responsible for this side effect. The increased risks associated with prostates  $\leq 35$  cc suggest that too low positioning occurs more often when the prostate is small.

Three-Tesla MRI planning of 74 more recently implanted men permitted accurate definition of the prostate capsule and the position of the membranous urethra. Prostates  $\leq 35$  cc were found to be nearly always 35 mm in length

rather than 40 mm as measured previously by trans-rectal ultrasound planning. In response to this finding, the plans of implants on 35 mm long prostates were altered to have less seeds placed in the 40 mm plane and more seeds in the 10 mm plane. Post implant, registered MR-CT images were used to measure the Dose 90 prostate base and Dose 0.1 cc membranous urethra, and these doses made it possible to identify men likely to be at higher risk of BF and urethral stricture.

#### Conclusion

Modern imaging has improved our understanding of factors influencing the risks of BF and urethral stricture after low dose-rate prostate brachytherapy, and has guided modifications to implant technique that could mitigate these risks.

#### PV-0146 RTOG versus CTCAE score: reporting toxicity of HDR brachytherapy Monotherapy for prostate cancer

M. Jolicoeur<sup>1</sup>, E. Hill<sup>1</sup>

<sup>1</sup>CICM Hôpital Charles Le Moyne, Radiation Oncology, Greenfield Park, Canada

#### Purpose or Objective

Compare the Radiation Therapy Oncology Group (RTOG) score and the Common Terminology Criteria for Adverse Events (CTCAE) score for reporting toxicities of HDR brachytherapy as monotherapy for prostate cancer.

#### Material and Methods

Mixed-method methodology was applied. The mixed-method consisted of direct comparison of the scores, a systematic literature review (25 selected articles), and the comparison of the acute toxicity scores classification in a sample of prostatic cancer patients treated by HDR brachytherapy. The patients included in this study were part of the protocol named: HDR Brachytherapy as Monotherapy for Low and Intermediate Risk Prostate Cancer (BRP2)

(<https://clinicaltrials.gov/ct2/show/NCT03424694>). 168 patients were followed up for 3 months after HDR brachytherapy for low and intermediate risk prostate cancer. Patients were evaluated at 1, 3, 6 weeks and 3 months after radiotherapy. Symptoms were classified according to RTOG and CTCAE scores. Descriptive statistics and Fisher Exact test were used to compare RTOG and CTCAE scores. Statistical significance was 0.05.

Toxicity grade	RTOG		CTCAE		
	n	%	n	%	
genitourinary	0	135	80.4	134	79.8
	1	15	8.9	27	16.1
	2	15	8.9	6	3.6
	3	0	0	1	0.6
	4	3	1.8	0	0
<b>Total</b>	<b>168</b>	<b>100</b>	<b>168</b>	<b>100</b>	
Fisher Exact Test p<0.01					
gastrointestinal	0	163	97	164	97.6
	1	3	1.8	4	2.4
	2	0	0	0	0
	3	2	1.2	0	0
	4	0	0	0	0
<b>Total</b>	<b>168</b>	<b>100</b>	<b>168</b>	<b>100</b>	
Fisher Exact Test p<0.01					

#### Results

RTOG score unifies several toxicity symptoms in each of the five grades, while CTCAE score classifies each symptom within five grades, according to their severity. RTOG score lacks reproducibility between acute and late toxicities. CTCAE proposes the same score for describing both late and acute toxicities. 64% of the systematic literature review selected studies were prospective. 76% of them used CTCAE, 20% used RTOG, 4% used neither to evaluate early toxicity. There was no standard for the toxicity reporting methodology. 24% of the articles did not report when the toxicity was evaluated. 48% did not inform how the toxicity was evaluated. Only 19% fully reported which symptoms were evaluated. 48% of the studies did not inform if the toxicity was reported per event or worse toxicity per patient. The early toxicity of

168 patients was compared between RTOG and CTCAE scores (Table 1). RTOG classified patients' genitourinary and gastrointestinal toxicities at higher grade than CTCAE. RTOG and CTCAE scores were associated in all scenarios (p<0.01), even with percentages of  $\geq$  grade 2 toxicities differing.

#### Conclusion

There is no significant statistical difference between the scores, even though RTOG score tends to increase the severity of the described symptoms. While, CTCAE appears to be more complex it is more reliable and reproducible in research, since each symptom is separately described with its corresponding grade. The use of the CTCAE score is preferable for reporting toxicities of HDR brachytherapy as monotherapy for prostate cancer. Detailed methodology and the use of guidelines can improve research quality, guarantee the report quality, and facilitate future research comparisons.

#### PV-0147 MRI-guided salvage HDR brachytherapy for locally recurrent prostate cancer

L. Joseph<sup>1</sup>, A. Sundaramurthy<sup>1</sup>, A. Berlin<sup>1</sup>, J. Helou<sup>1</sup>, C. Menard<sup>2</sup>, P. Warde<sup>1</sup>, C. Catton<sup>1</sup>, B. Lao<sup>1</sup>, A. Bayley<sup>1</sup>, A. Rink<sup>1</sup>, A. Beiki-Ardakani<sup>1</sup>, P. Chung<sup>1</sup>

<sup>1</sup>Princess Margaret Cancer Centre, Radiation Oncology, Toronto, Canada; <sup>2</sup>Centre Hospitalier de L'Université de Montreal, Radiation Oncology, Montreal, Canada

#### Purpose or Objective

Biochemical relapse (BCR) may occur in up to 40% of patients with localized prostate cancer treated with external beam radiotherapy (RT). A proportion of these, the disease recurrence is local alone. Radical salvage treatment options remain limited, and brachytherapy represents an attractive organ-preserving alternative. We report the results of a prospective study of MR-guided salvage brachytherapy.

#### Material and Methods

This was a phase II prospective cohort study. Eligibility were ECOG performance status 0-1, pathologically proven locally recurrent prostate cancer visible on multi-parametric MRI (mpMRI), > 18 months after primary RT, and PSA-doubling time > 6 months. All patients were treated with HDR brachytherapy under MR guidance alone. In cohort 1, patients were treated to a dose of 16Gy to the whole gland with an integrated 6Gy boost to the MR-visible tumor (GTV) in two fractions 7-14 days apart. Cohort 2 patients were treated to a dose of 26Gy to GTV alone in two fractions 1-2 weeks apart. The GTV was defined using mpMRI (T2-weighted, diffusion-weighted, dynamic contrast-enhanced). CTV margin expansion (5 mm in all directions) was restricted to adjacent organs at risk and 2 mm beyond the prostate boundary where applicable. PTV margins of 2 mm cranio-caudally and 1mm elsewhere were then applied. No patients were given neoadjuvant ADT. Patients were followed up with regular PSA, and mpMRI +/- prostate biopsy were performed after a minimum of 2 years. Toxicity was assessed using CTCAE version 4. BCR was determined using Phoenix definition (nadir+2).

#### Results

A total of 43 patients were enrolled, 14 in cohort 1, and 29 in cohort 2. Median age was 70 years (range 62-85). Median PSA pre-salvage was 4.54ng/mL (range 1.68-14). On pre-salvage biopsies, 7%, 72%, 12% and 7% had Gleason Score 6, 7, 8 and 9, respectively and 2% were ungraded. Overall median follow-up was 55 months (range 3-123), 100 in cohort 1, 38.5 in cohort 2. Crude rates of biochemical control at 2 years were 71% in cohort 1 and 82% in cohort 2. 3-year rates were 64% in cohort 1 and 68% in cohort 2. 5-year rates were 50% in cohort 1. Of those eligible and accepting of post-salvage MRI and/or biopsy, 42% (5/12) had localized recurrence confirmed in cohort 1 and 40% (6/15) in cohort 2 (4/15 recurrence within radiation field). Acute GI and GU toxicity was experienced in 13% (<grade 2) all patients, the majority of which

returned to baseline function. Late grade 4 GU toxicity (long-term urinary catheter) was observed in 1 patient.

#### Conclusion

MR-guided salvage brachytherapy appears to have a favourable therapeutic index in the post-RT local recurrence setting with minimal long-term toxicity. Focal brachytherapy alone may have comparable outcomes to whole gland treatment. Further study is needed to improve patient selection, and to determine optimal target volumes and dose schedules.

---

### Joint Symposium: ESTRO-CARO: Functional imaging in RT: from biology to guidance

---

#### SP-0148 Developments in techniques and processing tools for functional imaging in radiotherapy

Sara Leibfarth<sup>1</sup>, René M. Winter<sup>1</sup>, Simon Böke<sup>1,2,3</sup>, Daniela Thorwarth<sup>1,3</sup>

<sup>1</sup>University Hospital Tübingen, Section for Biomedical Physics, Tübingen, Germany

<sup>2</sup>University Hospital Tübingen,

Department of Radiation Oncology, Tübingen, Germany

<sup>3</sup>German Cancer Consortium Dtkk- Partner Site Tübingen, and German Research Center Dkfz- Heidelberg, Tübingen,

Germany

#### Abstract text

Functional imaging may be highly beneficial for radiotherapy (RT) planning, response monitoring, and follow-up. In magnetic resonance (MR) imaging, diffusion weighted MR (DW-MR) and dynamic contrast enhanced MR (DCE-MR), are promising functional imaging methods. PET tracers with potential benefit for RT are FDG and dedicated hypoxia tracers such as FMISO. Combined PET/MRI represents a technology allowing for simultaneous, intrinsically registered PET and MR data. In this talk, one focus will be on deriving quantitative parameter maps from functional imaging, discussing models for parameter extraction from DWI, DCE and dynamic FMISO acquisitions. In addition model-free, data-driven approaches such as principal component analysis will be discussed as an alternative approach for parameter map generation.

Another focus will be on approaches to combine single functional parameter maps into multiparametric models for specific tasks, such as the distinction between tumor and non-tumor tissue, the characterization of local tumor biology, and response evaluation. Such models might in the future allow for individually adapted treatment approaches based on multiparametric functional imaging.

#### SP-0149 Functional imaging in preclinical models for exploring new radiotherapy strategies

S. Stapleton<sup>1</sup>

<sup>1</sup>Massachusetts General Hospital, Massachusetts, USA

Abstract not received

#### SP-0150 Using functional imaging as a guidance and decision tool in radiotherapy

M. Milosevic<sup>1</sup>

<sup>1</sup>Princess Margaret Cancer Centre Department of Radiation Oncology

Abstract not received

---

### Proffered Papers: RB 2: How to exploit immunogenic cell death mechanisms in radiotherapy

---

#### OC-0151 Radiation and PI3K- $\alpha$ inhibitor enhanced anti-tumor effect of PD-1 blockade in syngeneic tumor model

I.A. Kim<sup>1,2,3</sup>, J.M. Park<sup>3</sup>, J.H. Lee<sup>1</sup>, D. Kim<sup>1</sup>, Y. Lim<sup>1</sup>

<sup>1</sup>Seoul National Univ. Bundang Hospital, Radiation Oncology and Medical Science Research Institute, Seongnam- Gyeonggi-Do, Korea Republic of; <sup>2</sup>Seoul National University College of Medicine, Radiation Oncology, Seoul, Korea Republic of; <sup>3</sup>Seoul National University Graduate School of Medicine, Tumor Biology and Cancer Research Institute, Seoul, Korea Republic of

#### Purpose or Objective

Breast cancer has been showing relatively poor response to immune checkpoint blockades potentially due to low immunogenicity of tumor and immunosuppressive tumor microenvironment. Radiation (RT) has been showing immune stimulatory effect and PI3K $\delta$  has immune suppressive effect via modulation of regulatory T cell (Treg). Therefore, we hypothesize that in situ tumor vaccination via RT and suppression of immune tolerance via PI3K $\delta$  inhibition could enhance the clinical efficacy of immune checkpoint blockade. As PI3KA controls a key oncogenic signaling pathway, we evaluated whether RT or novel PI3K $\alpha$  inhibitor or both could enhance the efficacy of antitumor effect of a PD-1 blockade in immune competent syngenic triple negative breast cancer (TNBC) model.

#### Material and Methods

4T1 murine breast cancer cells were grown subcutaneously in the hind limb of BALB/c mice. The mice were grouped as following seven groups: control, RT, PI3K $\alpha$  inhibitor, PI3K $\alpha$  inhibitor+ RT, PD-1 blockade, PD-1 blockade + RT, and triple combination group. Tumors were irradiated using 24 Gy/3 fractions. PD-1 blockade (10 mg/kg) and PI3K $\alpha$  inhibitor (4 mg/kg) were administered every other day for two weeks, respectively. Tumor size was measured periodically using a Vernier caliper and bioluminescence imaging to evaluate efficacy of each modality and combination therapy. Immune-modulatory function was evaluated using FACS, Elispot assay and immunohistochemical (IHC) staining.

#### Results

Triple combination of RT, PD-1 blockade, and PI3K $\alpha$  inhibitor significantly delayed tumor regrowth whereas PD-1 inhibitor alone showed only modest effect in 4T1 syngenic TNBC model. FACS and IHC study for immune repertoire using tumor samples showed that RT and PD-1 blockade modestly increased the proportion of cytotoxic CD8+ T cells and PI3K $\alpha$  inhibitor led to decrease the proportion of Treg. Triple combination showed remarkable increase of cytotoxic CD8+ T cells suggesting synergistic immune modulatory effect of RT, PD-1 blockade and PI3K $\alpha$  inhibitor. Triple combination led to significant upregulation of c-GAS/STING pathway in tumor and increased IFN-g level in blood compared to each modality alone.

#### Conclusion

Taken together, combination of RT and PI3K $\alpha$  inhibitors maximized immune stimulatory effect in immune competent syngenic TNBC model and enhanced the response of PD-1 inhibitor via non-redundant synergistic immune modulatory effect. This study provides a preclinical rationale for the combination of PI3K $\alpha$  inhibitor and RT with PD-1 blockade to overcome the immune tolerance of breast cancer. (Work supported by the grants from Korean Ministry of Science, Technology, Information & Communication, NRF#2017R1A2B4002710 & #2017M2A2A7A01018438 to In Ah Kim)

#### OC-0152 IDO inhibition strongly enhances effects of combined hRT and PD1/PD-L1 checkpoint blockade

T. Watanabe<sup>1,2</sup>, G. Niedermann<sup>1,3</sup>

<sup>1</sup>University of Freiburg, Department of Radiation Oncology- Faculty of Medicine, Freiburg, Germany;

<sup>2</sup>Kyoto University, Institute for Integrated Radiation and Nuclear Science, Osaka, Japan ; <sup>3</sup>German Cancer Research Center, German Cancer Consortium- Partner site Freiburg, Heidelberg, Germany

### Purpose or Objective

Indoleamine-2,3-dioxygenase (IDO) is an enzyme that degrades the essential amino acid tryptophan to the immunosuppressive metabolite kynurenine. IDO-expressing immune cells play critical roles in peripheral immune tolerance and energy. A recent phase 3 trial evaluating an IDO inhibitor/anti-PD1 antibody (aPD1) combination in metastatic melanoma patients missed its primary endpoint of improving progression-free survival compared to aPD1 monotherapy. However, IDO is induced by IFN-g, and hypofractionated radiotherapy (hRT) alone or in combination with immune checkpoint blockade can induce IFN-g-secreting, tumor-specific T cells. We therefore decided to study, in syngeneic mouse tumor models, whether the triple combination of hRT, aPD1, and an IDO inhibitor (IDOi) is superior to the respective double combinations.

### Material and Methods

We compared the triple treatment of hRT (12 Gy × 2) + aPD1 + IDOi with the double combinations of hRT + aPD1, hRT + IDOi, and aPD1 + IDOi, and with the respective monotherapies in mice bearing relatively large (300–500 mm<sup>3</sup>), aggressively growing B16 melanoma or 4T1 breast adenocarcinoma tumors. Tumor growth and survival of the mice were determined. The dependence of the therapeutic effects on CD8+ T cells and NK cells was studied by additional injection of depleting antibodies. Frequencies and functionality of tumor-specific CD8+ T cells in tumor and secondary lymphoid organs were determined flow cytometrically by using MHC tetramers and various types of antibodies.

### Results

In our models with relatively large tumors, the tumors did not regress following treatment with hRT + aPD1. The aPD1/IDOi double combination was not effective at all. In contrast, the triple treatment induced marked tumor regressions in both tumor models. The survival benefits were highly significant compared to hRT + aPD1 (B16 melanoma model  $p = 0.002$ ; 4T1 model  $p = 0.0001$ ). CD8+ T cell depletion strongly, and NK cell depletion partly, abrogated tumor control and survival benefits. Flow-cytometric analyses showed significant increases in tumor-specific CD8+ T cells for the triple combination group compared to the other groups. In addition, a significant increase in NK cell function was found.

### Conclusion

Our data in two aggressive tumor models show that the triple therapy with hRT, aPD1, and an IDOi can induce much stronger tumor regression than double combinations or monotherapy with the individual components. Our findings may serve as a rationale for the clinical evaluation of this triple combination therapy in patients with high-risk locally advanced tumors.

### OC-0153 Immune infiltrate modulation induced by preoperative radiotherapy in breast cancer patients

A. Matias Perez<sup>1</sup>, A. Bardet<sup>2</sup>, M. Lacroix-Triki<sup>3</sup>, F. Riet<sup>4</sup>, M.C. Mathieu<sup>3</sup>, E. Deutsch<sup>1</sup>, S. Michiels<sup>2</sup>, S. Rivera<sup>1</sup>  
<sup>1</sup>Institut Gustave Roussy, Département de Radiothérapie, Villejuif, France; <sup>2</sup>Institut Gustave Roussy, Service de Biostatistique et d'Epidémiologie, Villejuif, France; <sup>3</sup>Institut Gustave Roussy, Département de Biologie et Pathologie Médicales, Villejuif, France ; <sup>4</sup>Hôpital Pitié-Salpêtrière, Département de Radiothérapie, Paris, France

### Purpose or Objective

There is increasing evidence showing that tumor-infiltrating lymphocytes (TILs) are a marker for adaptive immune response. High level of TILs has been shown to

be associated with higher pathological complete response (pCR) after neoadjuvant anthracycline-based chemotherapy+ anti-HER2 agents, but very little is known regarding TILs and exclusive radiotherapy (RT) treatment in breast cancer (BC). Our series of exclusive preoperative RT is a unique opportunity to address such question. The objective of this study is to evaluate the impact of exclusive preoperative RT on immune infiltrate in BC.

### Material and Methods

TILs were estimated in a retrospective series of 187 BC patients with a median age of 49 years (43-60) with T2-T4 or N2 tumours treated between 1970 and 1984 with exclusive preoperative RT with a median follow-up of 32 years. Patients received a moderately hypofractionated RT (45-55 Gy in 18 fractions of 2.5 Gy over 34 days) to the whole breast and nodes, followed by a modified radical mastectomy plus axillary dissection. The percentage of stromal TILs was centrally evaluated for each patient on her diagnostic biopsy and her mastectomy specimen following the address International TILs working group recommendations.

### Results

Complete pathological response (pCR) was achieved in 18 (9.6%) of the 187 patients: six (8.4%) in Luminal A subtype, one (2.9%) in Luminal B, one (3.4%) in HER2 positive (3.4%) and eight (20%) in triple negative breast cancer (TNBC). The distribution of TILs in biopsies and mastectomy samples within subtypes is shown in figure 1. Overall, median TILs in biopsies was: <10% in 30.7%, between 10 - 40% in 64.5% and ≥50% in 4.8%. In the mastectomies TILs was <10% in 48.1%, between 10 - 40% in 50.3% and ≥50% in 1.6%. The subtypes with higher TILs levels were HER2 positive and TNBC (20% for both in biopsies and 15% and 20% for HER2 and TNBC in surgical samples) compared to Luminal A and B (10% in biopsies and 5% in surgical samples for both). Paired TILs measurements before and after radiotherapy were obtained in 122 (65.2%) patients. There was a slight decrease in TILs level with a mean change value of -3.0 ( $p=0.001$ ) in the whole population. The decrease was stronger in Luminal B subtype and HER2 positive, as shown in table 1.

Figure 1. Distribution of TILs in biopsies and surgical specimens (A= Luminal A; B= Luminal B; HER2 = HER2 positive; TN= Triple Negative; Miss.= missing data)

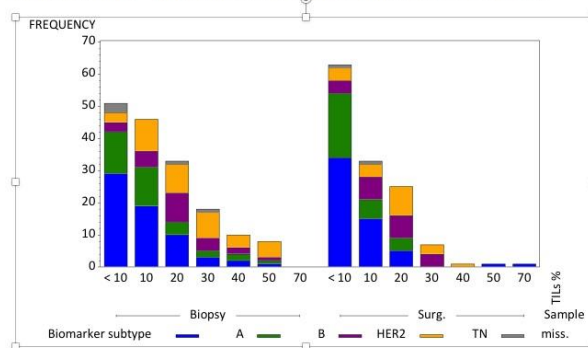


Table 1. TILs decrease within subgroups.

Molecular subtype	Number of analyzable patients	Mean change value (SD)	Median change value	p-value
All subtypes	122	-2.97 (12.01)	0	0.001
Luminal A	50	-1.02 (11.46)	0	0.14
Luminal B	29	-5.24 (12.21)	-4	0.02
HER2 positive	21	-4.29 (9.76)	0	0.05
TNBC	20	-3.00 (15.42)	-5	0.36

### Conclusion

Our preoperative RT series showed higher levels of TILs in HER2 positive and TNBC than in other subtypes before and after RT. In the paired samples, a slight decrease in TILs

was observed after preoperative RT. Specific assessment of lymphocytes in the scar area for patients in pCR and additional analyses of lymphocyte subtypes together with PD1 and FOXP3 Are planned and could be an innovative way to use lymphocytes dynamics after RT to guide the use of RT and immunotherapy combination in the future.

#### OC-0154 Radiation abrogates fibroblast-mediated immunosuppressive effects on dendritic cells

T. Hellevik<sup>1</sup>, R. Berzaghi<sup>2</sup>, M.A. Akhtar<sup>2</sup>, S. Tornaas<sup>2</sup>, I. Martinez-Zubiaurre<sup>2</sup>

<sup>1</sup>Univeristy Hospital of Northern Norway, Department of Radiation Oncology, Tromsø, Norway; <sup>2</sup>University of Tromsø, Clinical Medicine, Tromsø, Norway

#### Purpose or Objective

Recent reviews have highlighted the impact of cancer-associated fibroblasts (CAFs) in tumor development, dissemination and treatment resistance. Reactive CAFs - in contrast to normal fibroblasts - secrete a myriad of immunomodulatory soluble factors at high levels, which directly influence tumor immunity and inflammation, and promote an immunosuppressive tumor microenvironment. However, little is known about the mechanisms by which CAFs modulate immune responses after radiotherapy (RT). Previous studies by our group have uncovered the phenotypical and functional changes provoked by (high-dose) RT on human lung CAFs, characterized by induction of premature cellular senescence, as well as reduced proliferation, migration, and invasion rates. Changes have also been observed on the secretory profile by CAFs. The conditioned medium (CM) from irradiated-CAFs reduces the migratory capacity of endothelial cells, inhibits angiogenesis, and exerts a powerful immunosuppressive effect over activated T-cells. However, neither low-dose nor high-dose RT is affecting baseline CAF-mediated immunosuppressive effects. The present study focuses on effects of ionizing radiation, applied in different regimens, on CAF-mediated immunoregulation of macrophage polarization and dendritic cell phenotype and functions.

#### Material and Methods

CAFs were isolated by the outgrowth method from freshly resected NSCLC tumor specimens and characterized by the presence of lineage-specific markers. Highly pure CAF cultures (at passage 3) were irradiated with high-energy photons delivered as a single-high dose of 18 Gy or three consecutive daily doses of 6 Gy (3x6 Gy). CAF-CM were collected from (sham) irradiated cultures to examine CAF-induced paracrine effects on macrophage phenotype and dendritic cell differentiation, activation and function.

#### Results

We show that CAF-CM from non-irradiated cultures induces A) M2-polarization of monocyte derived-macrophages, promoting elevated surface expression of markers CD206 and CD163; and B) a tolerogenic phenotype of monocyte-derived DCs with decreased expression of differentiation surface markers (CD14, CD1a, CD209), decreased expression of maturation surface markers (CD80, CD86, CD40 and HLA-DR) and decreased functional capacities (migration, antigen-uptake, and T-CD4 cell priming). Interestingly, CM from CAFs irradiated with a single-high dose, or more prominently, with a fractionated medium-high dose (3x6 Gy) *reverts* the CAF-mediated tolerogenic induction on DCs. No significant differences in M2- or M1-macrophage polarization were observed between irradiated and non-irradiated CAFs.

#### Conclusion

Our results unveil advantageous effects elicited by defined radiotherapy regimens by reversing the baseline CAF-mediated immunosuppressive actions on DC phenotypes and functions.

#### OC-0155 Lxr Signaling Regulates Macrophage Survival and Phenotype Polarization Response To Ionizing Radiation

P.C. Lara Jimenez<sup>1</sup>, C. Tabraue<sup>2</sup>, M. Mirecki<sup>3</sup>, J.V. De La Rosa<sup>4</sup>, F. López-Blanco<sup>5</sup>, L. Bosca<sup>6</sup>, L. Fernandez<sup>5</sup>, A. Castrillo<sup>7</sup>

<sup>1</sup>Hospital Universitario San Roque/Universidad Fernando Pessoa Canarias, Oncology, Las Palmas de Gran Canaria-Ca, Spain; <sup>2</sup>Unidad Consejo Superior de Investigaciones Científicas, Grupo de investigación en Medio Ambiente y Salud, Las Palmas, Spain; <sup>3</sup>Universidad de Las Palmas de Gran Canaria, Ciencias Clínicas, Las Palmas de Gran Canaria, Spain; <sup>4</sup>Unidad del Consejo Superior de Investigaciones Científicas, Grupo de Estudio en Salud y Medio Ambiente, Las Palmas de Gran Canaria, Spain; <sup>5</sup>Universidad de Las Palmas de Gran Canaria, Ciencias Clínicas, Las Palmas de Gran Canaria, Spain; <sup>6</sup>Unidad de Consejo Superior de Investigaciones Científicas, Grupo de Investigación en Medio ambiente y salud, Las Palmas de Gran Canaria, Spain; <sup>7</sup>Unidad del Consejo Superior de Investigaciones Científicas, Grupo de Investigación en Medioambiente y Salud, Las Palmas de Gran Canaria, Spain

#### Purpose or Objective

Macrophages are a major cellular component of murine and human tumors, where they are commonly termed tumor-associated macrophages (TAMs). Recent studies indicate that ionizing radiation not only polarizes macrophages towards a M1-like phenotype leading an effective antitumor response, but also decreases macrophage survival through a pyroptosis mechanism.

The purpose of this study was to evaluate the role of LXR in the response of macrophages to irradiation, analyzing both cell viability and functional activity of the macrophage, as a possible strategy focused to deplete TAMs or re-program them towards a M1-like phenotype, in the context of cancer treatment with radiotherapy.

#### Material and Methods

Primary and immortalized murine bone marrow macrophages (BMDMs) from wild type or LXR double knock-out mice were exposed to X-ray irradiation. Subsequently, analysis of LXR signaling on cell proliferation and cytotoxicity induced by ionizing radiation was determined by time-lapse photomicroscopy. Genotoxic cell damage was evaluated by western blot of - H2AX and p53. Pyroptosis was analyzed through cell viability assay, lactate dehydrogenase (LDH) release assay and western-blot of caspase-1 active protein. We analyzed the expression of classic polarization markers, such as inducible nitric oxide synthase (iNOS) and interleukin-6 (IL-6) by real time RT-QPCR of messenger RNA levels of these M1 markers.

#### Results

Genetic and pharmacological inactivation of LXR induced radio sensitivity of macrophages.(figure 2) LXR deficiency decreased cell proliferation and enhanced cytotoxicity induced by ionizing radiation, in both immortalized and primary BMDMs. Protein levels of  $\gamma$ - H2AX and p53, both involved in response to cell damage, were exacerbated in LXR-deficient macrophages exposed to irradiation. Cell membrane damage augmented and cell viability decreased in LXR deficient macrophages compared to LXR-WT macrophages in response to irradiation. In addition, LXR deficiency enhanced both caspase-1 activation and LDH release in BMDM(figure 4) exposed inflammasome activators. Expression of pro-inflammatory markers IL-6 and iNOS was markedly higher in irradiated LXR-deficient macrophages than in LXR-WT macrophages(figure 4). This results show the role of LXR suppression favoring M1-polarization and therefore tumor control.

Fig.2

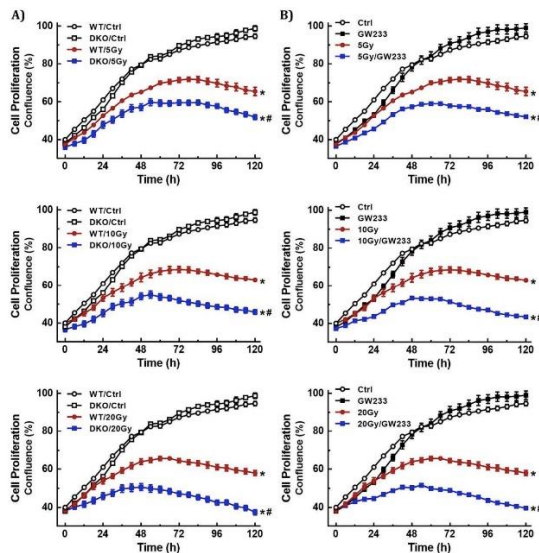
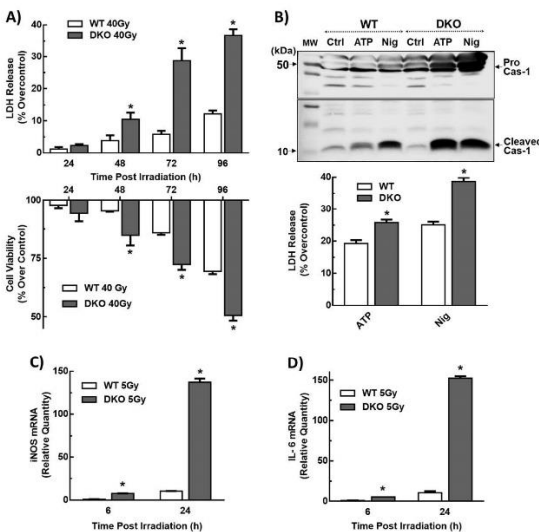


Fig.4



## Conclusion

The present work identifies LXR transcription factors as potential therapeutic targets to enhance the suppressive effects of radiotherapy on tumor growth, through induction of macrophage cell death and polarization towards a pro-inflammatory phenotype

### OC-0156 High-intensity focused ultrasound and radiotherapy: a promising combination?

G. Adema<sup>1</sup>, R. Van den Bijgaart<sup>1</sup>, T. Raaijmakers<sup>2</sup>, M. Den Brok<sup>1</sup>, M. Hoogenboom<sup>3</sup>, J. Fütterer<sup>4</sup>, J. Bussink<sup>1</sup>  
<sup>1</sup>UMC St Radboud Nijmegen, Radiation Oncology, Nijmegen, The Netherlands; <sup>2</sup>UMC St Radboud Nijmegen, Radiation Oncology and Anesthesiology- Pain Management and Palliative Care, Nijmegen, The Netherlands; <sup>3</sup>UMC St Radboud Nijmegen, Radiology and

Nuclear Medicine, Nijmegen, The Netherlands; <sup>4</sup>UMC St Radboud Nijmegen and University of Twente, Radiology and Nuclear Medicine and MIRA Institute for Biomedical Technology and Technical Medicine, Nijmegen, The Netherlands

## Purpose or Objective

In interventional oncology, a large variety of *in situ* tumor destruction techniques like cryo or thermal ablation, radiotherapy (RT) or high-intensity focused ultrasound (HIFU) are successfully applied. Although diverse in technology and the way of inducing cell death, ablative techniques share one key feature: they create *in situ* availability of ablated tumor material. During the efforts of the body to clear this dead material there is a time frame in which the immune system is actively controlling immune responses directed towards antigens from this antigen 'depot'<sup>1</sup>. The ability to stimulate the immune system upon scavenging antigens from dead tumor cells has led to the concept that *in situ* tumor destruction can be used to achieve systemic 'in vivo vaccination' against tumors, ultimately leading to the elusive 'abscopal effect'<sup>2,3</sup>. The aim of this study is to understand which (combination of) techniques results in the most effective release of tumor antigens, creates the most immunostimulatory environment from a molecular perspective, or combines most effectively with optimally timed immune stimulating therapies.

## Material and Methods

We have established multiple different ablation technologies in murine tumor models, including a MR-guided HIFU setup that can be used for thermal and mechanical destruction of murine tumors, including a melanoma (B16F10), a thymoma (EL4) and neuroblastoma (9464D) model<sup>4</sup>. Using these models we have explored the impact of multiple ablation treatments with immunotherapy, including the administration of different immune adjuvants. As read outs we have performed immune activation parameters (DC maturation, cytokine production), analysis of immune responses (T cell activation, proliferation and cytotoxicity) as well as tumor growth experiments.

## Results

Our data demonstrate that a tumor can serve as its own antigenic vaccine after different types of ablation, provided that additional immune activating signals are concomitantly given<sup>5-7</sup>. We have further established a HIFU based protocol to induce mechanical rather than thermal ablation of tumors. This mechanical HIFU based ablation of tissues induces complete subcellular fragmentation rather than tissue coagulative necrosis. RT is the main treatment modality for cancer, and around 50% of all cancer patients receive RT. Currently we are investigating the combination of HIFU and RT ablation with immunotherapy.

## Conclusion

Both HIFU and RT are non-invasive ablation techniques and can have immune modulatory effects<sup>8,9</sup>. Despite the obviously changing immunological parameters, their ablation-induced immunomodulation alone appears insufficient to generate consistent protective antitumor immunity. Combining HIFU with RT and immunotherapy may be more effective than either therapy alone, and is expected to be key to achieve systemic, long-lasting, antitumor immunity.

### OC-0157 Radiation and immunotherapy to fight cancer: a 'pushing the gas and releasing the brakes' approach.

V. Olivo Pimentel<sup>1</sup>, D. Marcus<sup>1</sup>, A. Van der Wiel<sup>1</sup>, R. Biemans<sup>1</sup>, N.G. Liewues<sup>1</sup>, D. Neri<sup>2</sup>, J. Theys<sup>1</sup>, A. Yaromina<sup>1</sup>, L.J. Dubois<sup>1</sup>, P. Lambin<sup>1</sup>

<sup>1</sup>Department of Precision Medicine- The M-Lab- GROW - School for Oncology and Developmental Biology, Maastricht Comprehensive Cancer Centre- Maastricht

University Medical Centre, Maastricht, The Netherlands; <sup>2</sup>Department of Chemistry and Applied Biosciences, Swiss Federal Institute of Technology, Zürich, Switzerland

### Purpose or Objective

Although immunotherapy is currently changing cancer treatment practice, primary resistance is still observed partly due to insufficient immunogenic priming. Radiotherapy (RT) induces the release of tumor antigens and thereby increases tumor immunogenicity. Therefore, combination of these therapies has high potential. Here, we investigated the therapeutic outcome of combining a single dose RT with the immunocytokine L19-IL2 and immune checkpoints inhibitors (ICIs) (aCTLA-4, aPD-L1 and aPD-1), aiming to further activate and prolong the RT-elicited anti-tumor immune response.

### Material and Methods

Balb/c or C57BL/6 mice were injected in the right flank with C51 and CT26 colon carcinoma or Lewis lung carcinoma (LLC) cells, respectively. Upon an average volume of 200mm<sup>3</sup>, animals were randomized in different treatment groups: RT + vehicle/L19-IL2 (1 mg/kg) + IgG or RT + vehicle/L19-IL2 + aPD-L1/aPD1/aCTLA-4 (all 10 mg/kg). Tumors were irradiated with 5Gy (C51 and CT26) or 10Gy (LLC), as the latter is less immunogenic. Vehicle/L19-IL2, aCTLA-4 and IgG were given i.v. on day 1, 3 and 5 after RT; aPD-1, aPD-L1 and IgG were given i.p. 1, 3, 5, 7 and 9 days after RT. Tumor response was quantified as time to reach 4 times starting tumor volume (T4xSV). For mechanistic studies, the same treatment schedule was used and mice were sacrificed at day 6 after RT.

### Results

In the CT26 model, RT + L19-IL2 ( $p < 0.001$ ), RT + aCTLA-4 ( $p < 0.01$ ) and RT + aPD-L1 ( $p < 0.05$ ) resulted in longer T4xSV compared to RT. In the C51 model solely RT + L19-IL2 ( $p < 0.001$ ) was better compared to RT. RT + L19-IL2 efficacy was significantly ( $p < 0.001$ ) better compared to RT + ICIs in the C51 model; a similar trend was observed for the CT26 model, albeit not significant. Adding ICIs to RT + L19-IL2 did not result in improved outcome in C51 and CT26 models. Conversely, in the LLC model the triple therapy of RT + L19-IL2 + aPD-L1 yielded a better outcome compared to RT + L19-IL2 ( $p < 0.05$ ) and RT + aPD-L1 ( $p < 0.001$ ). Mechanistically, in LLC tumors we found an increased infiltration of antigen-experienced (CD44+) CD8+ T cells and NK cells after triple therapy as compared to RT ( $p < 0.001$ ), RT + L19-IL2 ( $p < 0.01$ ) and RT + aPD-L1 ( $p < 0.01$ ). Percentage of regulatory T cells (Tregs) was surprisingly higher in tumors treated with RT + aPD-L1 vs RT + L19-IL2 ( $p < 0.05$ ), knowing that IL2 expands Tregs. Interestingly, other immunosuppressive proteins such as PD-1, Tim-3 and CD39 were upregulated on T cells upon PD-L1 blockade.

### Conclusion

Our results show that in the C51 and CT26 models, the therapeutic effect of RT + L19-IL2 is larger than RT + ICIs, while adding ICIs did not improved efficacy of RT + L19-IL2. In the LLC model, RT + L19-IL2 + aPD-L1 improved outcome compared to RT + L19-IL2 or aPD-L1 and was associated with increased infiltration of NK and CD44+ CD8+ T cells; functional co-culture assays are ongoing to prove their role on the anti-tumor response. PD-L1 blockade upregulated other immune-checkpoint proteins on T cells.

---

Proffered Papers: CL 3: Proffered papers : Prostate and Bladder

---

**OC-0158 Effect of EBRT underutilization in prostate cancer on overall survival and local control, NSW, Australia**

G. Gabriel<sup>1</sup>, M. Barton<sup>1</sup>, J. Shafiq<sup>1</sup>, G. Delaney<sup>1</sup>

<sup>1</sup>Ingham Institute for Applied Medical Research, Collaboration of Cancer Outcomes- Research and Evaluation CCORE and University Of New South Wales, Liverpool BC- NSW, Australia

### Purpose or Objective

Evidence-based modelling estimates show that 52% of all Australian prostate cancer patients would benefit from radiotherapy (RT) at diagnosis<sup>1-3</sup>. It was estimated that the 5-year overall survival (OS) shortfall for prostate cancer due to not receiving EBRT was 1.1% and the 5-year irreplaceable local control (LC) benefit for receiving EBRT was 12.4%<sup>4,5</sup>. Previous study indicated that radiotherapy utilization (RTU) rates decreased with increasing travel distance from patient residence to the nearest RT department (RTD)<sup>6</sup>. The objective of the study was to calculate actual RTU rate, to estimate the shortfall in OS and irreplaceable LC and to identify factors affecting RTU.

### Material and Methods

Data from NSW Central Cancer Registry for patients diagnosed with prostate cancer from 2009-2011 were linked to public and private radiotherapy, admitted patient, clinical cancer registry and death datasets. Patients located near the State border where their closest RT center was outside NSW (cross borders) were excluded from the analysis. To assess the irreplaceable benefit of EBRT, all treatment options where surgery or BT monotherapy were options over EBRT were set to 0% use of EBRT<sup>5</sup>. This method described a scenario where benefits of EBRT were counted only for cases where there was no guideline-recommended alternative treatment<sup>5</sup>. Analysis was performed using SAS, SPSS and ArcGIS software.

### Results

There were 19,816 patients diagnosed with prostate cancer during the study period. The median age was 67 years. Our study showed that 65% of prostate cancer patients had localized disease, 4% had distant disease and 30% had unknown or missing stage. Of patients with localized disease, 18% received EBRT, 37% had radical prostatectomy (RP) and 4% had both RP and EBRT. Twenty-eight percent of all prostate cancer patients had RP alone, 3% had RP & EBRT, 20% had EBRT alone and 49% had neither RP nor EBRT. Overall, 23% of all prostate cancer patients received RT within one year of diagnosis. Of the 5636 patients with complete TNM data available, 68% received RT compared to 6% of patients with no detailed TNM. The annual overall survival person-shortfall was estimated to be 41 and irreplaceable local control person-shortfall was 466. Univariate analysis showed that younger age, patients with loco-regional disease, living in more advantaged areas and outside major cities, and living >100 km of RTD were predictors for RT underutilization. On multivariate logistic regression model, all factors remained significant.

### Conclusion

Prostate cancer was the most diagnosed cancer in NSW and contributed to 18% of the total patients diagnosed with cancer during the study period. Actual RTU rate was half of the estimated optimal rate. Underutilization of RT increases the disease burden on health system due to local failure and overall survival shortfall. The study shows that giving EBRT according to evidence-based guidelines will probably prevent 41 immature death and 466 local failure annually.

**OC-0159 Long-Term Results of RTOG 0321: HDR Brachytherapy and External Beam Radiotherapy for Prostate Cancer**

I. Hsu<sup>1</sup>, J. Rodgers<sup>2</sup>, K. Shinohara<sup>3</sup>, J. Purdy<sup>4</sup>, J. Michalski<sup>5</sup>, G. Ibbott<sup>6</sup>, M. Roach<sup>7</sup>, E. Vigneault<sup>8</sup>, R. Ivker<sup>9</sup>, R. Pryzant<sup>6</sup>, M. Kuettel<sup>10</sup>, D. Tausky<sup>11</sup>, G. Gustafson<sup>12</sup>, A. Raben<sup>13</sup>, H. Sandler<sup>14</sup>

<sup>1</sup>University of California UCSF, Radiation Oncology, San Francisco CA, USA ; <sup>2</sup>NRG, Statistics, Philadelphia, USA ; <sup>3</sup>UCSF, Urology, San Francisco, USA; <sup>4</sup>University of

California Davis, Radiation Oncology, Sacramento, USA ;  
<sup>5</sup>Washington University, Radiation Oncology, St. Louis, USA ;  
<sup>6</sup>MD Anderson, Radiation Oncology, Houston, USA ;  
<sup>7</sup>UCSF, Radiation Oncology, San Francisco, USA; <sup>8</sup>Hotel-Dieu de Quebec, Radiation Oncology, Quebec, Canada;  
<sup>9</sup>Thomas Jefferson University, Radiation Oncology, Philadelphia, USA; <sup>10</sup>Roswell Park Cancer Institute, Radiation Oncology, Buffalo, USA ; <sup>11</sup>Centre Hospitalier de l'Université de Montreal-Notre Dame, Radiation Oncology, Montreal, Canada; <sup>12</sup>William Beaumont Hospital, Radiation Oncology, Royal Oak, USA; <sup>13</sup>Christiana Care Health Services, Radiation Oncology, Newark, USA; <sup>14</sup>Cedars-Sinai Medical Center, Radiation Oncology, Los Angeles, USA

### Purpose or Objective

This is a report of long-term patient outcome following treatment with external beam radiation therapy (EBRT) and prostate high dose rate (HDR) brachytherapy from a prospective phase II, multi-institutional collaborative trial conducted by RTOG.

### Material and Methods

Patients with clinically localized (T1c-T3b) prostate cancer without prior history of TURP or hip prosthesis were eligible for this study. All patients were treated with a combination of 45 Gy in 25 fractions from EBRT and one HDR implant delivering 19 Gy in 2 fractions. Adverse events (AE) were collected using CTCAE v3. Biochemical failure was assessed using the ASTRO definition and the Phoenix definition. Local failure was determined by clinical exam and distant failure required documentation of regional nodal recurrence or distant disease relapse. Disease-specific deaths included those due to prostate cancer, other causes with active malignancy, and complications of treatment. Cumulative incidence was used to estimate time to severe late GI/GU toxicity, biochemical failure, disease-specific mortality, local failure, and distant failure. Competing risks were death without an event. Overall survival was estimated using the Kaplan Meier method.

### Results

One hundred twenty-nine patients were enrolled from 7/04 to 5/06. One hundred and twenty-five patients were eligible and AE data was available for 115 patients. The pretreatment characteristics (NCCN intermediate to high risk) of the patients were as follows: median age was 68 (range: 48-80), T1c-T2c 91%, T3a-T3b 9%, PSA ≤ 10 70%, PSA >10-≤20 30%, GS 2-6 10%, GS 7 72%, and GS 8-10 18%. Forty-three percent of patients received adjuvant hormonal therapy.

There were 6 (5.2%) patients with grade 3 GI/GU AEs, and no late grade 4-5 GI/GU AEs. The single Grade 3 GI AE was proctitis. The grade 3 GU AEs were: cystitis (n=1), pollakiuria (n=1), renal/genitourinary, other (n=1), urethral stricture (n=1), urinary incontinence (n=1), and urinary retention (n=2). At 5 and 10 years, the rate of late grade 3-5 GI/GU AEs was 17.0% and 19.2%.

Five- and 10-years overall survival rates were 95.0% and 75.7%. The biochemical failure rates using the ASTRO definition: 5-year and 10-year rates of 9.8% and 14.7%; using Phoenix definition: 5- and 10-years rates of 14.0% and 22.6%. The 10-year rate of prostate specific mortality was 6.4%. At 5 and 10 years, the rates of distant failure were 4.2% and 7.7%. The rates of local failure at 5 and 10 years were 1.7% at both time points.

### Conclusion

This prospective trial demonstrates the feasibility to use HDR in a multi-institutional setting with excellent long-term outcomes and very modest toxicity.

This project was supported by grants U10CA180868 (NRG Oncology Operations), U10CA180822 (NRG Oncology SDMC) from the National Cancer Institute (NCI).

### OC-0160 When PI-RADS and ISUP meet each other: identification of candidates for pelvic lymph node dissection

C. Draulans<sup>1,2</sup>, W. Everaerts<sup>3,4</sup>, S. Isebaert<sup>1,2</sup>, T. Gevaert<sup>4</sup>, R. Oyen<sup>5,6</sup>, S. Joniau<sup>3,4</sup>, E. Lerut<sup>6,7</sup>, L. De Wever<sup>5</sup>, A. Laenen<sup>8</sup>, B. Weynand<sup>6,7</sup>, E. Vanhoutte<sup>5</sup>, G. De Meerleer<sup>1,2</sup>, K. Haustermans<sup>1,2</sup>

<sup>1</sup>University Hospitals Leuven, Department of Radiation Oncology, Leuven, Belgium ; <sup>2</sup>KU Leuven, Department of Oncology, Leuven, Belgium ; <sup>3</sup>University Hospitals Leuven, Department of Urology, Leuven, Belgium ; <sup>4</sup>KU Leuven, Department of Development and Regeneration, Leuven, Belgium; <sup>5</sup>University Hospitals Leuven, Department of Radiology, Leuven, Belgium ; <sup>6</sup>KU Leuven, Department of Imaging and Pathology, Leuven, Belgium; <sup>7</sup>University Hospitals Leuven, Department of Histopathology, Leuven, Belgium ; <sup>8</sup>KU Leuven, Leuven Biostatistics and Statistical Bioinformatics Center, Leuven, Belgium

### Purpose or Objective

The aim of this study is to update the current nomograms predicting lymph node invasion (LNI) in prostate cancer (PCa) patients with today's state-of-the-art available tumor information. This tumor information includes magnetic resonance imaging (MRI) based tumor staging and detailed biopsy information according to the International Society of Urological Pathology (ISUP).

### Material and Methods

Between 2008 and 2017, 420 clinical N0 staged PCa patients underwent a radical prostatectomy with pelvic lymph node dissection (PLND). The initial PSA value (iPSA), preoperative tumor stage by MRI (iT-stage), tumor multifocality on MRI, zonal tumor location on MRI, ISUP grade group on biopsy for each positive core, percentage of tumor involvement and exact tumor length in each core and percentage of positive biopsy cores were registered. Using this information, we developed a multivariable model predicting LNI to create a coefficient-based nomogram. A concordance index (C-index) was estimated to quantify the discriminative performance of the model.

### Results

On MRI, 180 (42.9 %) patients had iT1 or iT2 disease, 224 (53.3 %) iT3 and 16 (3.8 %) iT4 PCa based on features described in the literature, similar to the current PI-RADS v2 criteria. A median of 21 (IQR, 16 - 27) lymph nodes was removed per patient. Overall, 71 (16.9 %) patients were finally diagnosed with LNI. A multivariable model detected the iPSA value, MRI based iT-stage, maximum tumor length in one core (mm) and ISUP grade group corresponding to the maximum tumor involvement in one core as independent predictors of LNI (p < 0.05). After 5-fold internal cross validation, the predictive accuracy of our updated MRI and ISUP based nomogram for LNI (table 1) was 79.7 %.

Table 1 – Multivariable logistic regression analyses predicting the presence of LNI in 420 patients

	Odds Ratio (95 % CI)	p value	Parameter estimate
Intercept	-	-	-6.4605
MRI-based imaging T stage	1.467 (1.163; 1.850)	0.0012	0.3833
iPSA	1.023 (1.000; 1.046)	0.0457	0.0228
Maximum tumor length in one core (mm)	1.155 (1.061; 1.258)	0.0009	0.1443
ISUP grade group corresponding to maximum tumor length	1.863 (1.466; 2.367)	< 0.0001	0.6220

CI = confidence interval MRI = magnetic resonance imaging; iPSA = initial prostate specific antigen; ISUP = International Society of Urological Pathology

### Legend

Predicted probability =  $p(\text{LNI}) = \frac{e^{\mu}}{1+e^{\mu}}$

$\mu$ : model linear predictor, estimated by summation of the intercept term and all  $\beta$  values multiplied by that variable.

For example: Intercept +  $\beta$ var1 \* var1 +  $\beta$ var2 \* var2 + ...  $\beta$ varN \* varN

$\beta$  (variable name): parameter estimate associated with a variable

### Conclusion

We report an updated MRI and ISUP based nomogram predicting the presence of LNI in PCa patients. This nomogram will overcome stage migration and will prevent overtreatment, which is a potential risk when MRI

information is used in DRE based nomograms. Furthermore, by incorporating additional core-specific biopsy information instead of the percentage of positive cores as mentioned in the existing nomograms, this nomogram could handle with the paradigm shift from saturation biopsies towards targeted biopsies. This updated nomogram could be a useful tool that helps urologists and radiation oncologists to accurately predict the likelihood of LNI before treatment.

**OC-0161 Validation of clinical/dosimetric/genetic risk factor models for late RT-induced rectal bleeding**

T. Rancati<sup>1</sup>, P. Seibold<sup>2</sup>, A. Webb<sup>3</sup>, J. Chang-Claude<sup>4</sup>, A. Cicchetti<sup>1</sup>, D. Azria<sup>5</sup>, D. De Ruyscher<sup>6</sup>, R. Elliott<sup>7</sup>, S. Gutiérrez-Enríquez<sup>8</sup>, B.S. Rosenstein<sup>9</sup>, C.J. Talbot<sup>3</sup>, A. Vega<sup>10</sup>, L. Veldeman<sup>11</sup>, R. Valdagni<sup>12</sup>, C. West<sup>13</sup>  
<sup>1</sup>Fondazione IRCCS Istituto Nazionale dei Tumori, Prostate Cancer Program, Milan, Italy; <sup>2</sup>German Cancer Research Center, Division of Cancer Epidemiology- Unit of Genetic Epidemiology, Heidelberg, Germany; <sup>3</sup>University of Leicester, Department of Genetics, Leicester, United Kingdom; <sup>4</sup>German Cancer Research Center, Division of Cancer Epidemiology, Heidelberg, Germany; <sup>5</sup>University of Montpellier, Radiation Oncology, Montpellier, France; <sup>6</sup>Maastricht Clinic and Maastricht University Medical Centre, Department of Radiation Oncology / GROW - School for Oncology and Developmental Biology, Maastricht, The Netherlands; <sup>7</sup>University of Manchester, Institute of Cancer Sciences-Christie Hospital, Manchester, United Kingdom; <sup>8</sup>Vall d'Hebron Institute of Oncology, Oncogenetics Group, Barcelona, Spain; <sup>9</sup>Icahn School of Medicine at Mount Sinai, Genetics and Genomic Sciences, New York, USA; <sup>10</sup>Fundación Pública Galega Medicina Xenómica, Molecular Medicine, Santiago de Compostela, Spain; <sup>11</sup>Ghent University, Department of Radiotherapy and Experimental Cancer Research- Faculty of Medicine and Health Sciences, Ghent, Belgium; <sup>12</sup>University of Milan and Fondazione IRCCS Istituto Nazionale dei Tumori, Oncology and Hemato-oncology / Radiation Oncology 1 / Prostate Cancer Program, Milan, Italy; <sup>13</sup>University of Manchester, Division of Cancer Sciences, Manchester, United Kingdom

**Purpose or Objective**

REQUIRE is an international, prospective observational cohort study, which recruited patients (pts) in 8 countries (April2014-March2017). It is aimed at multinational validation of clinical/dosimetric/genetic risk factors for prediction of late toxicity following radiotherapy (RT). The purpose here was to present preliminary results on validation of such features for late rectal bleeding (LRB) after conventionally fractionated external beam RT (EBRT) for prostate cancer (PCa).

**Material and Methods**

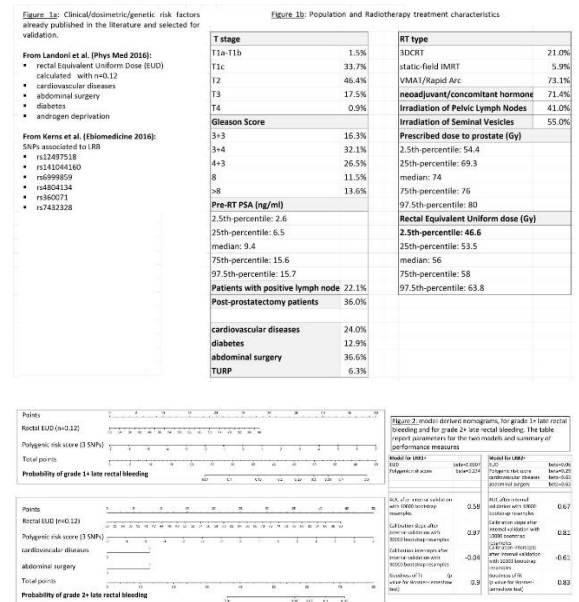
REQUIRE PCa pts treated with 2Gy/fr EBRT and complete 2-year follow-up were included. RT was prescribed according to local regimens, but centres used standardised data collection. Blood samples were collected for DNA extraction/genotyping. Grade≥1 LRB (LRB1+) and grade≥2 LRB (LRB2+) were considered as separate endpoints. Clinical/dosimetric/genetic risk factors already published in the literature were selected from Landoni (Phys Med 2016) and Kerns (Ebiomedicine 2016). Selected features are reported in Figure 1a. Association of selected features with LRB was investigated through logistic regression. A final logistic model including only validated predictors was fitted and a nomogram was developed. Confirmed SNPs were used to calculate a polygenic risk score which was included in modeling as a single genetic parameter.

**Results**

REQUIRE enrolled 1190 PCa pts with 2Gy/fr EBRT, 1178 had complete clinical/dosimetric data, 933/1178 had

complete 2-year follow-up and were included in this analysis. Description of the population is in Figure 1b. 147/933 (15.8%) LRB1+ and 29/933 (3.1%) LRB2+ were scored. Rectal EUD was confirmed as a predictor for both LRB1+ (OR=1.03 for 1Gy increase) and LRB2+ (OR=1.06 for 1Gy increase), with Odds Ratios similar to those reported in literature. Cardiovascular disease (OR=1.97) and abdominal surgery (OR=1.83) were confirmed for LRB2+, with slightly lower ORs with respect to those previously found.

Three SNPs were associated with LRB: rs6999859 (OR=1.37), rs4804134 (OR=0.97) and rs7432328 (OR=1.51) with ORs slightly lower than reported previously. The 3 SNPs were included in a polygenic risk score. Diabetes and androgen deprivation were not confirmed as risk factors, and not included in the final models. Figure 2 reports the two model-derived nomograms, model parameters and summary of performance measures.



**Conclusion**

REQUIRE highlighted the need to collect standardized data and the importance of model validation. The present analysis confirmed the predictive value for LRB of most clinical/dosimetric features previously published, together with validation of some SNPs. Resulting models including validated features well described clinical observation in the multi-center REQUIRE population, but discriminative power remained suboptimal. Use of 3-dimensional dose distributions might overcome the limitations of using dose-volume histogram parameters, which can be explored using the REQUIRE resource.

**OC-0162 PSMA PET/CT for intraprostatic tumor delineation and characterization based on radiomic features**

C. Zamboglou<sup>1</sup>, M. Carles<sup>2</sup>, S. Kiefer<sup>3</sup>, T. Fechter<sup>2</sup>, P. Bronsert<sup>3</sup>, K. Reichel<sup>4</sup>, A. Soerensen<sup>5</sup>, J. Ruf<sup>5</sup>, M. Fahrner<sup>3</sup>, H.C. Rischke<sup>1</sup>, O. Schilling<sup>3</sup>, C.A. Jilg<sup>4</sup>, D. Baltas<sup>4</sup>, M. Mix<sup>5</sup>, A.L. Grosu<sup>1</sup>

<sup>1</sup>Medical Center - University of Freiburg, Department of Radiation Oncology, Freiburg, Germany; <sup>2</sup>Medical Center - University of Freiburg, Division of Medical Physics - Department of Radiation Oncology, Freiburg, Germany; <sup>3</sup>Medical Center - University of Freiburg, Department of Pathology, Freiburg, Germany; <sup>4</sup>Medical Center - University of Freiburg, Department of Urology, Freiburg,

Germany; <sup>5</sup>Medical Center - University of Freiburg, Department of Nuclear Medicine, Freiburg, Germany

### Purpose or Objective

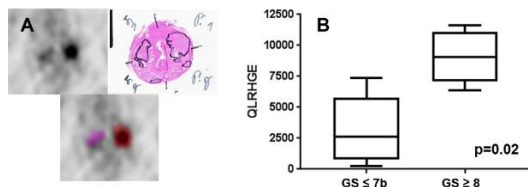
The usage of radionuclide-labelled inhibitors of prostate-specific membrane antigen for positron-emission tomography (PSMA PET) may enable accurate intraprostatic gross tumor volume (GTV) delineation and the characterization of its biological properties. To test these hypotheses we co-registered the PET images with whole-mount prostate sections after surgery in order to perform a correlation study between histology and PSMA PET information, including radiomic features.

### Material and Methods

20 patients with intermediate and high-risk PCa underwent <sup>68</sup>Ga-HBED-CC-PSMA PET/CT followed by radical prostatectomy. Histopathological information from resected prostates was processed and digitalized to obtain a 3D volume of PCa distribution. On each PET scan 5 contours were created: GTV-PET (expert contour of intraprostatic GTV based on PET information), GTV-histo (coregistered histopathology information, see figure 1A), GTV-histo-index (considering only lesions >5 mm in histology) and the subtraction volumes between the prostatic gland and GTV-histo and GTV-PET, respectively. To assess sensitivity and specificity in each CT slice the prostate was separated into 4 equal segments and the distribution of GTV-PET was compared with GTV-histo and GTV-histo-index, respectively. Furthermore, 133 radiomic features (including texture features) from PSMA PET were extracted from the respective volumes. False discovery rate-controlling procedures were implemented to account for multiple testing.

### Results

PSMA PET detected PCa in all patients. Mean sensitivity/specificity for GTV-PET were 81%/86% and 91%/88% considering GTV-histo and GTV-histo-index, respectively. In 83% of image features a strong correlation (Spearman  $\rho > 0.7$ ,  $p < 0.05$ ) between GTV-PET and GTV-histo was observed. Pairwise testing showed that 68% and 81% of image features had significant differences ( $p < 0.05$ ) between PCa and non PCa tissue considering GTV-histo and GTV-PET, respectively. 21% of image features derived from GTV-PET had a strong correlation (Spearman  $\rho > 0.7$ ,  $p < 0.05$ ) with the Gleason score (GS) and 70% of those image features had significant differences ( $p < 0.05$ ) between GS 7 and GS  $\geq 7$  PCa lesions (see exemplary figure 1B for feature: Long-Run High Gray-level Emphasis, QLRHGE).



### Conclusion

Based on histological validation a high sensitivity/specificity for PSMA PET-based GTV delineation was observed. In line with this observation we detected a strong correlation between image features extracted from GTV-PET and GTV-histo. The excellent diagnostic performance of PSMA PET enabled the usage of radiomic features for discrimination between PCa and non PCa tissue and for characterization of its biological aggressiveness.

**OC-0163 Risk classification for PSA relapse after PSMA-PET-guided RT for oligorecurrent prostate cancer**

M. Vogel<sup>1</sup>, S.G.C. Kroeze<sup>2</sup>, C. Henkenberens<sup>3</sup>, N.S. Schmidt-Hegemann<sup>4</sup>, S. Kirste<sup>5</sup>, J. Becker<sup>6</sup>, H. Christiansen<sup>3</sup>, C. Belka<sup>4</sup>, A.L. Grosu<sup>5</sup>, A.-C. Müller<sup>6</sup>, M. Guckenberger<sup>2</sup>, S.E. Combs<sup>1</sup>

<sup>1</sup>Klinikum rechts der Isar- Technical University of Munich TUM, Department of Radiation Oncology, Munich, Germany ; <sup>2</sup>University Hospital Zürich, Department of Radiation Oncology, Zürich, Switzerland ; <sup>3</sup>Medical School Hannover, Department of Radiotherapy and Special Oncology, Hannover, Germany; <sup>4</sup>University Hospital Munich LMU, Department of Radiation Oncology, Munich, Germany; <sup>5</sup>University of Freiburg, Department of Radiation Oncology, Freiburg, Germany; <sup>6</sup>University Hospital Tübingen, Department of Radiation Oncology, Tübingen, Germany

### Purpose or Objective

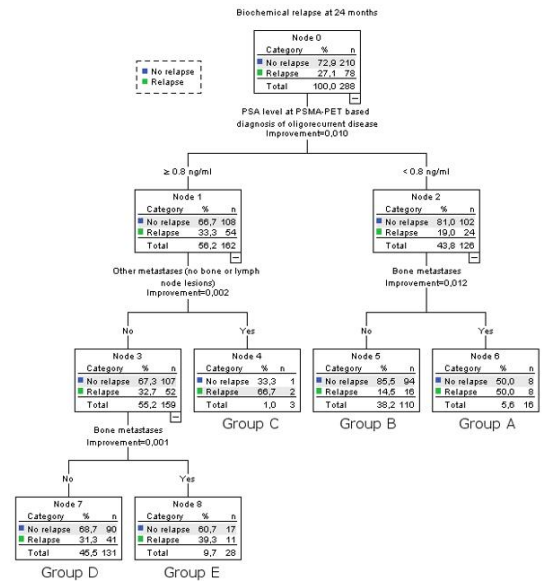
PSMA-PET-Imaging has changed the treatment for patients with few metastases, in particular in form of radical radiotherapy (RT) for oligorecurrent prostate cancer (PC) after prior definitive therapy. However, the majority of patients will develop progressive disease, despite accurate PSMA-PET-Staging and stereotactic RT; how to optimally select patients is unknown. In this analysis, we aimed to develop a risk classification predicting biochemical relapse free survival (BCRFS) after PSMA-PET-guided RT.

### Material and Methods

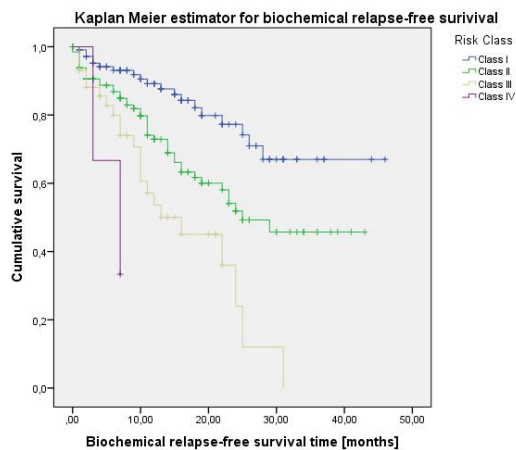
Data of 379 patients were collected at six radiation oncology departments. In this analysis we included 294 Patients with initial radical prostatectomy (RP) and subsequent diagnosis of oligorecurrent PC with positive findings in PSMA-PET-Imaging followed by radical RT. We used univariate and multiple Cox regression to determine significance for known risk factors. Significant factors were analyzed and grouped using recursive partitioning analysis (RPA) with classification and regression (CRT) method. Risk classes I to IV (low to very high risk) were generated using Kaplan-Meier estimator.

### Results

In univariate Cox regression initial nodal status (N0 vs. N1, HR: 0.59, 95%-CI: 0.38-0.90,  $p = 0.02$ ), PSA Persistence  $\geq 0.1$  ng/ml after RP (yes vs. no, HR: 1.61, 95%-CI: 1.05-2.47,  $p = 0.03$ ), PSA levels  $\geq 0.8$  ng/ml at PSMA-PET-based diagnosis of oligorecurrent disease (no vs. yes, HR: 0.51, 95%-CI: 0.33-0.81,  $p = 0.004$ ), presence of bone metastases (no vs. yes, HR: 0.38, 95%-CI: 0.23-0.62,  $p = 0.0001$ ), presence of other metastases than bone or lymph node lesions (no vs. yes, HR: 0.19, 95%-CI, 0.05-0.77,  $p = 0.02$ ), and total number of lesions (HR: 0.65, 95%-CI: 0.42-0.99,  $p = 0.04$ ) were significantly associated with relapse. PSA level at PSMA-PET-Imaging, bone metastases, and other metastases remained significant predictors in multiple regression. Figure 1 shows RPA for BCRFS at 24 months (mos) with a decision-making tree comprising end node groups A to E. 10-fold cross validation showed a risk for miscalculation of 0.295 (Standard error: 0.027), which results in 70.5% accuracy. Kaplan-Meier estimator showed a mean BCRFS of 15.6 mos (95%-CI: 11.2-30.0 mos) in group A, of 36.3 mos (95%-CI: 32.4-40.1 mos) in group B, of 5.7 mos (95%-CI: 2.6-8.7 mos) in group C, of 26.9 mos (95%-CI: 23.4-30.4 mos) in group D, and of 16.6 mos (95%-CI: 11.2-22.0 mos) in Group E. Subsequently, we built risk classes I (Group B), II (Group D), III (Group A and E), and IV (Group C). Kaplan-Meier curve and mean BCRFS stratified for risk classes ( $p < 0.0001$ ) is shown in figure 2 respectively.



Risk class	RPA group	Mean BCRF5 (95%-CI) in months	Predictive factors
Class I (low risk)	Group B	36.2 (32.4-40.1)	PSA level at PSMA-PET based diagnosis of oligorecurrent disease <0.8 ng/ml, no bone metastases
Class II (intermediate risk)	Group D	26.9 (23.4-30.4)	PSA level at PSMA-PET based diagnosis of oligorecurrent disease ≥0.8 ng/ml, bone metastases, no other metastases (no bone or lymph node lesions)
Class III (high risk)	Group A	16.0 (12.3-19.6)	PSA level at PSMA-PET based diagnosis of oligorecurrent disease <0.8 ng/ml, present bone metastases
	Group E		PSA level at PSMA-PET based diagnosis of oligorecurrent disease ≥0.8 ng/ml, no bone metastases, no other metastases (no bone or lymph node lesions)
Class IV (very high risk)	Group C	5.7 (2.6-8.7)	PSA level at PSMA-PET based diagnosis of oligorecurrent disease ≥0.8 ng/ml, present other metastases (no bone or lymph node lesions)



**Conclusion**

We developed a prognostic risk classification for patients with oligorecurrent PC treated with PSMA-PET-guided RT. Internal validation showed good accuracy. Patients with PSA levels at PSMA-PET-Imaging ≥0.8 ng/ml and the presence of other metastases (than bone or lymph node lesions) were at highest risk for biochemical relapse. External validation of the proposed RPA classification is planned as a next step.

**OC-0164 Hypoxia modification in bladder**

**preservation: relating long term outcomes to necrosis and hypoxia**

Y.P. Song<sup>1,2</sup>, H. Mistry<sup>2</sup>, L. Yang<sup>2</sup>, S. Chin<sup>1</sup>, C. West<sup>1,2</sup>, A. Choudhury<sup>1,2</sup>, P. Hoskin<sup>1,2,3</sup>

<sup>1</sup>The Christie NHS Foundation Trust, Radiotherapy Related Research, Manchester, United Kingdom ; <sup>2</sup>The University of Manchester, Division of Cancer Science,

Manchester, United Kingdom ; <sup>3</sup>Mount Vernon Cancer Centre, Clinical Oncology, Northwood, United Kingdom

**Purpose or Objective**

The BCON trial showed that the addition of carbogen and nicotinamide (CON) significantly improved recurrence free survival (RFS) and overall survival (OS) rates (Hoskin et al., 2010). Twelve years after the trial closed to recruitment, the long-term clinical outcomes and their relationship to hypoxia markers are reported.

**Material and Methods**

An updated analysis of patients with bladder cancer treated in the BCON trial was undertaken. Cox regression was carried out to relate clinical outcomes to previously published biomarkers: a 24 gene signature hypoxia score (Yang et al., 2017) and necrosis status (Eustace et al, 2013).

**Results**

333 patients were included in the original study. 12 patients were excluded from the analysis. Necrosis and hypoxia score were available for 148 of the remaining patients (73 RT+CON, 75 RT alone). There was a significant improvement in RFS at 5 years (41% vs 33%, p=0.040) which was maintained at 10 years (27% vs 20%). The 5 year OS was 49% vs 40% (p=0.068) with a continued effect seen at 10 years (32% vs 24%). The hypoxia score was prognostic in the RT alone group (p=0.041), but not in the RT+CON group (p=0.634). Necrosis status was a less strong prognostic indicator in the RT alone group (p=0.079) and had no effect in the RT+CON group. The prognostic value of both hypoxia score and necrosis remained following adjustment for other known prognostic factors. Hypoxia scores (p=0.013) (Figure 1) and presence of necrosis (p=0.05) were both independent predictors of benefit from hypoxia modification in the RT+CON group.

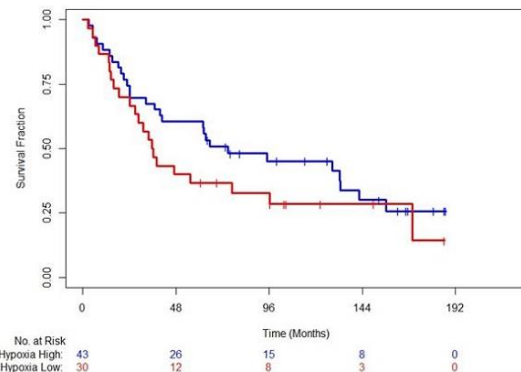


Figure 1. Survival of patients in RT+CON group with high and low hypoxia scores

**Conclusion**

With long-term follow up, there continues to be an advantage in RFS and OS with the addition of CON to radiotherapy, with a statistically significant improvement in 5 year RFS. These findings confirm the significant impact of hypoxia modification on long-term survival for bladder cancer patients undergoing organ preservation treatment. Similarly, the presence of necrosis and hypoxia predicts long-term benefit from hypoxia modification. A prospective biomarker driven clinical trial based on this data is now required to validate the use of hypoxia modification in patients most likely to benefit.

Proffered Papers: CL 4: proffered papers: CNS and Paediatrics

OC-0165 Patterns of treatment and outcomes for 1p19q co-deleted gliomas

D. Yebo<sup>1</sup>, J. Yu<sup>2</sup>, K.E. Liao<sup>3</sup>, J. Huse<sup>4</sup>, M. Penas-Prado<sup>5</sup>, B. Kann<sup>2</sup>, E. Sulman<sup>6</sup>, D. Grosshans<sup>1</sup>, J. Contessa<sup>2</sup>  
<sup>1</sup>MD Anderson Cancer Center, Radiation Oncology, Houston, USA; <sup>2</sup>Yale University School of Medicine, Department of Therapeutic Radiology, New Haven, USA ; <sup>3</sup>MD Anderson Cancer Center, Health Services Department, Houston, USA ; <sup>4</sup>MD Anderson Cancer Center, Department of Pathology, Houston, USA; <sup>5</sup>National Institute of Health, Neuro-Oncology Branch, Bethesda, USA; <sup>6</sup>New York University, Radiation Oncology Department, New York, USA

#### Purpose or Objective

Molecular markers are redefining classification of lower grade gliomas and ushering in a paradigm shift in their management. Our objective was to evaluate the impact of histologic grade on patterns of care and treatment outcomes for 1p19q co-deleted gliomas.

#### Material and Methods

We evaluated 1,618 patients in the National Cancer Database diagnosed with 1p19q co-deleted gliomas from 2010 through 2014 and treated with surgery followed by radiation therapy (RT), chemotherapy (CT), or combined-modality therapy. Kaplan-Meier analysis and log-rank tests were used to assess OS over time. Cox proportional hazards regression modeling was used to assess associations between the World Health Organization (WHO) glioma grade and the outcome of death when adjusting for significant clinical covariates, with a *p* value <0.05 defining significance. Additionally, propensity score matching was done in an attempt to further balance patients by known covariates.

#### Results

Most patients with grade II tumors received surgery alone (51.0%), whereas most patients with grade III tumors (86%) received surgery or biopsy followed by a form of post-operative therapy (*p*<0.001). In a propensity score matched cohort, the Cox multivariable proportional hazards model with frailty testing identified significant covariates were age, comorbidity, histology and grade. Patients ≥60 years had a higher likelihood of death as did those with at least one comorbidity. The hazard for death for grade III 1p19q co-deleted gliomas was about 3.6 times higher ([HR] 3.69, 95% confidence interval [CI] 2.03-6.68, *p*<0.001) than grade II 1p19q gliomas. Oligodendroglioma histology was associated with a lower likelihood of death (HR 0.40, 95% CI 0.23-0.70, *p*<0.001).

#### Conclusion

In conclusion, our study with one of the largest cohorts of specifically grade II versus grade III 1p19q co-deleted gliomas, provides relevant information on real-world outcomes in a national cohort. While we await the results of clinical trials such as CODEL and BN005, our study offers context regarding historical treatment patterns and outcomes in the community for 1p19q co-deleted gliomas.

#### OC-0166 Cumulative metastases volume, not number of brain metastases predicts survival in melanoma patients

J. Heitmann<sup>1</sup>, S.G.C. Kroeze<sup>1</sup>, O. Blanck<sup>2</sup>, S. Stera<sup>3</sup>, K.H. Kahl<sup>4</sup>, S. Gerum<sup>5</sup>, S.E. Combs<sup>6</sup>, A. Haap<sup>7</sup>, A. Claes<sup>8</sup>, M. Schymalla<sup>9</sup>, A. Grosu<sup>10</sup>, F. Eckert<sup>11</sup>, F. Lohaus<sup>12</sup>, N. Abbasi-Senger<sup>13</sup>, G. Henke<sup>14</sup>, M. Szuvecs<sup>15</sup>, M. Geier<sup>16</sup>, N. Sundahl<sup>17</sup>, D. Buerge<sup>18</sup>, M. Guckenberger<sup>1</sup>

<sup>1</sup>University Hospital Zürich, Radiation Oncology, Zurich, Switzerland ; <sup>2</sup>Saphir, Radiosurgery Center, Gustow, Germany ; <sup>3</sup>University Hospital Frankfurt, Radiation Oncology, Frankfurt, Germany ; <sup>4</sup>Klinikum Augsburg, Radiation Oncology, Augsburg, Germany ; <sup>5</sup>University Hospital Munich, Radiation Oncology, Munich, Germany ; <sup>6</sup>Technical University Munich, Radiation Oncology, Munich, Germany ; <sup>7</sup>Charité University Hospital, Radiation Oncology, Berlin, Germany ; <sup>8</sup>University Medical Center Utrecht, Radiation Oncology, Utrecht, The Netherlands ; <sup>9</sup>Philipps University Marburg,

Radiation Oncology, Marburg, Germany ; <sup>10</sup>University Medical Center Freiburg, Radiation Oncology, Freiburg, Germany; <sup>11</sup>University Hospital Tübingen, Radiation Oncology, Tübingen, Germany; <sup>12</sup>University Hospital Dresden, Radiation Oncology, Dresden, Germany ; <sup>13</sup>University Hospital Jena, Radiation Oncology, Jena, Germany ; <sup>14</sup>Kantonsspital St. Gallen, Radiation Oncology, St. Gallen, Switzerland; <sup>15</sup>University Hospital Rostock, Radiation Oncology, Rostock, Germany; <sup>16</sup>Ordensklinikum Linz, Radiation Oncology, Linz, Austria; <sup>17</sup>Ghent University Hospital, Radiation Oncology, Ghent, Belgium; <sup>18</sup>University Hospital Mannheim, Radiation Oncology, Mannheim, Germany

#### Purpose or Objective

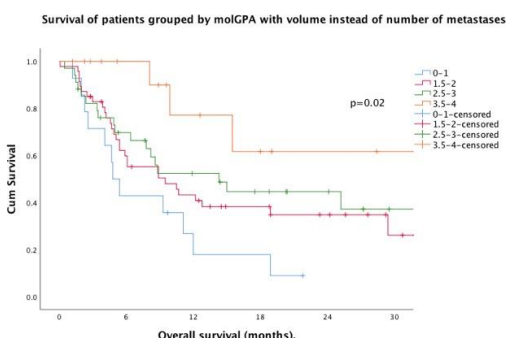
In 2017, Sperduto et al. proposed an updated Graded Prognostic Assessment for melanoma patients with brain metastases (molGPA score), which was validated by Nieder et al. in a cohort of 69 patients. However, both studies included many patients that received whole brain radiation therapy (WBRT). As melanoma patients are increasingly treated with stereotactic radiotherapy or radiosurgery (SRT) alone, we aimed to validate the score in a large cohort of 140 melanoma patients treated exclusively with SRT without WBRT, and concurrent targeted- or immunotherapy.

#### Material and Methods

We retrospectively analyzed data from the international database of efficacy and toxicity of combined SRT and immuno- or targeted therapy (TOaSTT). Patients that received a concurrent WBRT (n=5) with the SRT were excluded, as well as re-irradiations. The updated molGPA score was applied to our cohort to predict survival. The molGPA score included age (≥70 years or < 70 years), performance status, presence of extracranial metastases, BRAF mutational status and number of brain metastases. We used Kaplan-Meier curves to compare overall survival (OS) of groups defined by the score and compared by log rank test.

#### Results

18 centers treated 140 melanoma patients between 05/2011 and 02/2018 with concurrent targeted- or immunotherapy and SRT for 327 brain metastases with a median of 1 (1-6) fractions and a median of 20 Gy (12-30Gy). A median of 2 (1-30) metastases were treated per session with a median cumulative volume of 1.47cc (0.05-24.54cc). The molGPA score could not be validated in our patient cohort (*p* = 0.199). The four groups defined by the score did not show a significant difference in OS, as the number of metastases did not influence survival. However, in univariate analysis, the cumulative volume of irradiated metastases was significantly associated with OS: the group with an irradiated cumulative brain metastases volume smaller than the median volume (1.5cc) survived significantly longer than the group with a larger than or equal to 1.5cc cumulative brain metastases volume (*p* = 0.02). Therefore, the number of brain metastases in the molGPA score was substituted with cumulative brain metastases volume. Using this combination of factors, the four modified molGPA score prognostic groups showed significantly different OS (logrank *p* = 0.02).



**Conclusion**

For melanoma patients with brain metastases treated with concurrent targeted- or immunotherapy and SRT without concurrent WBRT, brain metastases volume impacts OS, but not the number of treated brain metastases. We propose adapting the molGPA score for melanoma patients treated with SRT and concurrent targeted- or immunotherapy.

**OC-0167 Identifying No Fly Zones to prevent long-term thinning of the cerebral cortex in glioma after RT**

S. Nagtegaal<sup>1</sup>, S. David<sup>2</sup>, H. Mesri<sup>2</sup>, M. Philippens<sup>1</sup>, A. Leemans<sup>2</sup>, J. Verhoeff<sup>1</sup>  
<sup>1</sup>UMC Utrecht, Radiation Oncology, Utrecht, The Netherlands ; <sup>2</sup>UMC Utrecht, Imaging Science Institute, Utrecht, The Netherlands

**Purpose or Objective**

Radiation induced brain injury consists of both anatomical and functional deficits in irradiated healthy brain tissue. Especially cognitive and executional impairments lead to a marked decrease in the patient’s quality of life after radiation therapy (RT), and have been linked to thinning of the healthy cerebral cortex. With the rise of more precise radiation techniques, like image-guided RT and proton RT, knowledge of the long-term effects of radiation on the cortex is important for optimal treatment planning. In this work, we present the results of structural morphometry of the cerebral cortex at different time points in glioma patients treated with RT, and compare the changes to the applied dose.

**Material and Methods**

We selected 31 patients with adequate follow-up scans who were treated with RT for glioma (grade II-IV) in our institution. Late follow-up was defined as >9 months after start of RT, and the cortical thickness was compared to baseline.

The CAT12 (Computational Anatomy Toolbox) was used for the automated preprocessing, segmentation and surface estimation of clinical 3T T1 scans. All scans were bias-field inhomogeneity and noise corrected, then segmented into grey matter, white matter and cerebrospinal fluid. Surface calculation was achieved via projection-based thickness estimation and reparametrized to the Freesurfer surface template, consisting of a 152k mesh per hemisphere. RT dose was 3D mapped to the surface. Change in cortical thickness was associated with locally applied dose via non-parametric permutations tests. Age and sex were included as covariates of no-interest, and correction for multiple comparisons with family wise error-rate adjustment was applied. The significance of a test was determined at  $p < 0.05$ . For each test the Cohen’s d was also calculated.

**Results**

Figure 1 shows the regions where a statistically significant dose-dependent decrease in cortical thickness was found. Data on the two regions are shown in Table 1. Figure 2

shows the change in cortical thickness per dose in the vertex with the greatest association between these two variables.

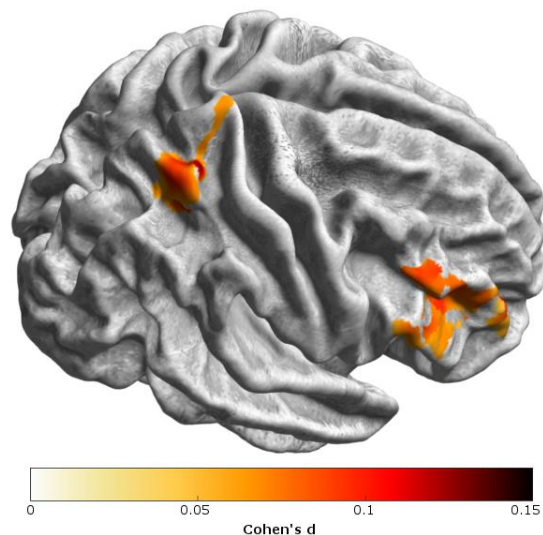


**Figure 1** Cortical areas with statistically significant ( $p < 0.05$ ) dose-dependent thinning between baseline and late follow-up

**Table 1** Data on the cortical areas in the right frontal (1) and parietal (2) lobes

Cluster	Number of vertices	Mean effect size (Cohen’s d)	p	Correspondence to brain atlas region*
1	2452	0.1	0.02	Middle frontal gyrus (45%)
				Inferior frontal sulcus (31%)
				Triangular part of the inferior frontal gyrus (17%)
				Middle frontal sulcus (3%)
				Opercular part of the inferior frontal gyrus (3%)
2	1841	0.1	0.02	Superior parietal lobule (55%)
				Intraparietal sulcus and transverse parietal sulci (28%)
				Postcentral sulcus (11%)
				Paracentral lobule and sulcus (6%)

\* According to Destrieux brain atlas

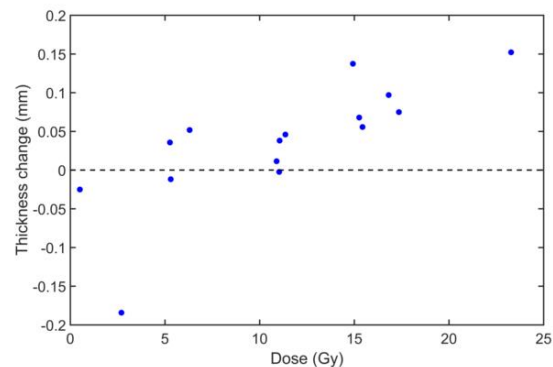


**Figure 2** Dose-dependant thickness change in a single vertex

**Conclusion**

This study shows that the cerebral cortex is susceptible to long-term radiation-induced cortical changes, and that the rate of change increases with the applied dose. This effect can be considered rapid aging of the healthy brain, which may accompany similar age-related cognitive impairments.

Despite this dose-dependent cortical thinning, changes in the cortex can already be seen at lower doses, suggesting

that sparing of healthy brain tissue should be a crucial aspect in the treatment of brain tumours. Luckily, new techniques are being developed that allow for very precise irradiation of the tumour area, which means cortical sparing is feasible. We here present 2 No Fly zones, to be avoided in cranial radiotherapy. In the future, cognitive symptoms after RT may be diminished further, vastly improving the quality of life of brain tumour patients.

#### OC-0168 Dose-dependent atrophy of the amygdala after radiotherapy

M. Huynh-Le<sup>1</sup>, R. Karunamuni<sup>1</sup>, V. Moiseenko<sup>1</sup>, N. Farid<sup>2</sup>, C. McDonald<sup>3</sup>, J. Hattangadi-Gluth<sup>1</sup>, T.M. Seibert<sup>1</sup>

<sup>1</sup>University of California San Diego, Radiation Medicine and Applied Sciences, San Diego, USA ; <sup>2</sup>University of California San Diego, Radiology, San Diego, USA;

<sup>3</sup>University of California San Diego, Psychiatry, San Diego, USA

#### Purpose or Objective

The amygdalae are deep brain nuclei critical to processing emotions such as fear, anger, and anxiety, as well as to the creation and storage of memory. The effects of brain radiotherapy (RT) on the amygdalae are currently unknown. We sought to quantify radiation dose-dependent change to the amygdalae in a retrospective cohort of patients with primary brain tumors.

#### Material and Methods

52 patients with primary brain tumors who received fractionated partial brain radiotherapy were identified. Study patients underwent high-resolution, volumetric magnetic resonance imaging before RT and 1 year afterward. Images were processed using software approved by the US Food and Drug Administration and Conformité Européenne for automated segmentation of amygdala volume. Results were inspected for accuracy. Tumor and surgical changes were manually censored. Mean dose to the amygdala was tested for correlation with amygdala volume change 1 year after RT via the Pearson correlation coefficient. A linear mixed-effects model was constructed to evaluate potential predictors of amygdala volume change, including patient (random effect), age, tumor hemisphere, sex, seizure history, and bevacizumab treatment during the study period. As 51 of 52 patients (98%) received chemotherapy during the study period, chemotherapy was not included as a predictive variable. A two-tailed *p*-value of <0.05 was considered to be statistically significant.

#### Results

The majority of patients were male (*n*=35, 67%), and the median age at the time of treatment was 54 years (range 19-77). Most patients had grade III-IV glioma (*n*=42, 81%). The most common tumor locations were frontal lobe (*n*=18, 35%) and temporal lobe (*n*=16, 31%). All patients were treated with intensity-modulated RT. Fifty patients (96%) received chemotherapy concurrent with RT; all of these patients received temozolomide. Fifteen patients (29%) had a major seizure during the study period and ten (19%) patients received bevacizumab. After censoring effects of tumor, surgery, or segmentation error, 40 right and 44 left amygdalae (total of 84 amygdalae) were included in the analyses. Mean dose to the amygdala (*r*=0.28, *p*=0.01) was significantly correlated with volume loss. On multivariable analysis, only radiation dose was a significant predictor of amygdala atrophy. The final linear mixed-effects model estimated amygdala volume loss of 0.17% for every 1 Gy increase in mean amygdala RT dose (*p*=0.008).

#### Conclusion

The amygdala demonstrates dose-dependent atrophy at one year after radiotherapy for brain tumors. The potential cognitive effects of radiotherapy to the amygdala warrant further exploration in prospective trials.

#### OC-0169 Spinal change after craniospinal irradiation for pediatric patients

Y. Oshiro<sup>1</sup>, M. Mizumoto<sup>2</sup>, H. Pan<sup>3</sup>, S. Kaste<sup>4</sup>, T.E. Merchant<sup>1</sup>

<sup>1</sup>St. Jude Children's Research Hospital-Memphis, Radiation Oncology, Memphis, USA; <sup>2</sup>University of Tsukuba, Radiation Oncology, Tsukuba, Japan; <sup>3</sup>St. Jude Children's Research Hospital- Memphis, Biostatistics, Memphis, USA; <sup>4</sup>St. Jude Children's Research Hospital-Memphis, Diagnostic Imaging, Memphis, USA

#### Purpose or Objective

To analyze spinal change after craniospinal irradiation (CSI).

#### Material and Methods

896 vertebral bodies in 220 pediatric patients who received CSI were analyzed. All met the following criteria: age at CSI ≤ 13 years, minimal follow up of 2 years with spinal MRI. CSI dose ranged from 15Gy to 43.2Gy. To analyze vertebral growth, vertebral body height were calculated. Signal change of vertebral body on MRI, scoliosis and kyphosis, degenerative change of vertebral bones and disc, and wedging or vertebral height loss were also analyzed on images. Then impact factors on these changes were investigated.

#### Results

Vertebral bone was significantly correlated radiation dose and growth hormone (GH) deficiency. The bone growth rate was 2.6%, 2.0%, 1.6%, 1.8%, 1.0%, and 0.8% for bones receiving < 20Gy, 23.4Gy, 36Gy, 39.6Gy, 40-50Gy, and >50Gy, respectively. Growth rate was significantly worse with the dose more than 38Gy. The growth rates were similar for vertebral bodies treated with growth hormone compared to those in whom growth hormone was not indicated (2.73% per year vs. 2.88% per year) whereas in those who refused or unable to receive growth hormone the rate of growth was significantly lower (1.38% per year) compared to those treated with growth hormone (*p*=0.0022). 83% of the patients showed fatty marrow change and 31% patients had disc degenerative change. Degenerative change of spinal bones and Wedging or spinal height loss was observed in 13% and 17% of the patients. Scoliosis was observed in 27% of the patients.

#### Conclusion

Vertebral bone growth was significantly disturbed with the dose >38Gy, and adequate GH replacement was very important for bone growth. Even with symmetrical irradiation, risk of scoliosis was high after CSI, and moreover, spinal demineralization and degenerative change frequently progressed after CSI, therefore, careful attention should be paid for future spinal symptoms as the patients grow old.

#### OC-0170 Proton beam radiation results in Pediatric Head and Neck Rhabdomyosarcoma

Abstract withdrawn

#### OC-0171 Hypofractionated SBRT in childhood cancer: preliminary results of a national prospective study

L. Claude Defez<sup>1</sup>, S. Bolle<sup>2</sup>, E. Blanc<sup>3</sup>, A. Laprie<sup>4</sup>, A. Huchet<sup>5</sup>, C. Vigneron<sup>6</sup>, A. Escande<sup>7</sup>, M. Morelle<sup>8</sup>, C. Carrie<sup>9</sup>, S. Supiot<sup>10</sup>

<sup>1</sup>Centre Leon Berard, Radiotherapy, Lyon, France;

<sup>2</sup>Gustave Roussy Cancer Campus, Radiation Oncology

Department, Villejuif, France; <sup>3</sup>Centre Léon Bérard,

Direction de la Recherche Clinique et de l'Innovation,

Lyon, France; <sup>4</sup>Institut Universitaire du Cancer de

Toulouse, Radiotherapy, Toulouse, France ; <sup>5</sup>University

Hospital of Bordeaux, Radiotherapy, Bordeaux, France;

<sup>6</sup>Centre Paul Strauss, Radiotherapy, Strasbourg, France;

<sup>7</sup>Oscar Lambret Comprehensive Cancer Center-,

Radiation Oncology, Lille, France ; <sup>8</sup>Centre Léon Bérard,

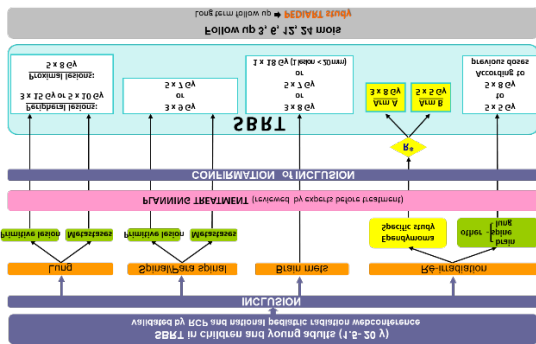
Direction de la Recherche Clinique et de l'Innovation-

**Purpose or Objective**

Hypofractionated Stereotactic Body Radiation Therapy (SBRT) is demonstrated as safe and efficient in many adult situations, including mainly primary/secondary tumors in brain, spine, and lung or in case of re-irradiation (re-RT). In pediatric situations, data are rare and needed to assess feasibility, efficiency and acute/long term toxicities in patients (pts) with radioresistant cancers (sarcomas, brain tumors such as ependymomas) or for re-RT. A multicentric national prospective study considering SBRT in young pts (1.5-20 y.) was opened in 12/2013, with multi-disciplinary staff confirmed indication of SBRT.

**Material and Methods**

The study was built as a prospective cohort study with several arms considering the site of lesion, summarized in Fig. 1. Only pts with ependymomas in relapse after radiotherapy (RT) could be included after complete surgery while the others had no surgery or incomplete macroscopic tumor resection. The main objective was to evaluate the 6-months local control (RECIST 1.1). Secondary objectives were to evaluate the feasibility of SBRT in childhood, 3-months, 1 and 2-years local control rates, acute, and middle-term toxicities (3-24 months) using NCI CTC v 4.0 criteria. Long-term toxicity will be evaluated using the national cohort study PEDIART.



**Results**

48 pts were included in 10 institutions. 4 pts did finally not receive SBRT (, 1 for early progression, 1 pt refusal, 2 pts due to medical decision after inclusion) and were excluded from the analysis. Among the population analysis (n=44), the median age was 12 y. (min 3 - max 20). 15 pts were irradiated in first intention: - 4 pts with brain lesions received a median dose of 32.5 Gy/5fr (isodose 80%).

- 5 pts with lung lesions received a median dose of 50 Gy/5 fr, (isodose 80%)

- 6 pts with spine lesions received a median dose of 50 Gy/5 fr, (isodose 80%)

29 pts were included for re-RT :

- 12 pts were treated by post-operative SBRT for locally relapsed ependymoma (median dose 25/5 fr., isodose 80%)

- 17 pts were treated for re-RT in other situations (brain, spine, lung...) without surgery (median dose 25 Gy/5 fr).

All the pts could receive SBRT. Median follow-up was 23 months (12-24). No pt required general anesthesia. Considering acute toxicity (< 3 months after SBRT), 1 pt reported epilepsy (grade 3). Grade 2 toxicity was observed in 3 pts (asthenia, transitory radiation pneumonitis, headache). Middle term RT toxicity (Grade > 2, 3-24 months after SBRT) was identified for 1 pt (pyloric spasm after spinal SBRT).

**Conclusion**

SBRT is feasible and safe in childhood, considering acute toxicity in brain, lung and spine treatment or in selected cases of re-RT. More follow-up is needed to better

**Proffered Papers: BT 2: Cervix brachytherapy**

**OC-0172 Performance of ring vs ovoids and intracavitary vs intracavitary-interstitial in the EMBRACE study**

M. Serban<sup>1</sup>, C. Kirisits<sup>2</sup>, A. De Leeuw<sup>3</sup>, R. Pötter<sup>2</sup>, I.M. Jürgenliemk-Schulz<sup>3</sup>, N. Nesvacil<sup>2</sup>, J. Swamidas<sup>4</sup>, R. Hudej<sup>5</sup>, G. Lowe<sup>6</sup>, T.P. Hellebust<sup>7</sup>, G. Menon<sup>8</sup>, A. Oinam<sup>9</sup>, P. Bownes<sup>10</sup>, B. Oosterveld<sup>11</sup>, M. De Brabandere<sup>12</sup>, K. Koedooder<sup>13</sup>, A.B.L. Marthinsen<sup>14</sup>, D. Whitney<sup>15</sup>, J. Lindegaard<sup>1</sup>, K. Tanderup<sup>1</sup>

<sup>1</sup>Aarhus University Hospital, Department of Oncology, Aarhus, Denmark; <sup>2</sup>Medical University of Vienna / General Hospital of Vienna- Vienna- Austria, Department of Radiation Oncology, Vienna, Austria ; <sup>3</sup>University Medical Centre Utrecht- The Netherlands, Department of Radiation Oncology, Utrecht, The Netherlands; <sup>4</sup>Tata Memorial Hospital- Mumbai- India, Department of Radiation Oncology, Mumbai, India; <sup>5</sup>Institute of Oncology Ljubljana- Slovenia, Department of Radiotherapy, Ljubljana, Slovenia; <sup>6</sup>Mount Vernon Hospital- London- UK, Cancer Centre, London, United Kingdom; <sup>7</sup>The Norwegian Radium Hospital- Oslo University Hospital- Oslo- Norway, Department of Oncology, Oslo, Norway; <sup>8</sup>Cross Cancer Institute- University of Alberta- Edmonton- Canada, Department of Oncology, Edmonton, Canada; <sup>9</sup>Postgraduate Institute of Medical Education and Research- Chandigarh- India, Department of Radiotherapy and Oncology, Chandigarh, India; <sup>10</sup>St James's University Hospital- Leeds- UK, Leeds Cancer Centre, Leeds, United Kingdom; <sup>11</sup>Arnhem-The Netherlands, Radiotherapiegroep, Arnhem, The Netherlands; <sup>12</sup>UZ Leuven- Belgium, Department of Radiation Oncology, Leuven, Belgium; <sup>13</sup>Academic Medical Center- University of Amsterdam- Amsterdam- The Netherlands, Department of Radiation Oncology, Amsterdam, The Netherlands ; <sup>14</sup>Cancer Clinic- St. Olavs Hospital- and Department of Physics- NTNU- Trondheim- Norway, Department of Radiotherapy, Trondheim, Norway; <sup>15</sup>Cambridge University Hospitals NHS Foundation Trust- Addenbrooke's Hospital- Cambridge- UK, Oncology Centre, Cambridge, United Kingdom

**Purpose or Objective**

To investigate the influence of brachytherapy (BT) technique and applicator type on target dose coverage, isodose surface volumes, and dose to organs at risk (OARs).

**Material and Methods**

949 patients treated with tandem/ovoids (T&O) and tandem/ring (T&R) BT applicators, from 18 centres in the EMBRACE study, were analysed. Patients received external beam radiotherapy with concomitant chemotherapy, followed by MRI guided adaptive brachytherapy with individualised dose prescription. Centres were divided into 4 groups, according to their applicator (T&O vs T&R) and intracavitary (IC) vs intracavitary/interstitial (IC/IS) usage: T&O and T&R IC centres treating mainly with the IC technique; T&O and T&R IC/IS centres treating routinely with the IC/IS technique (>20% of patients). V85Gy EQD2<sub>10</sub>, CTV<sub>HR</sub>D<sub>90%</sub> as well as bladder, rectum and vaginal (lateral point at 5mm with respect to the applicator) doses were evaluated. Data was analysed as independent samples based on Student's t-test or by multiple linear regression models.

**Results**

Patient characteristics, target and OAR doses for each center group are presented in Table 1. T&R IC compared to T&O IC centres had: mean CTV<sub>HR</sub>D<sub>90%</sub> higher by 4.9Gy EQD2<sub>10</sub> for a CTV<sub>HR</sub> volume of 30cm<sup>3</sup> and no statistically significant difference when > 45cm<sup>3</sup> (Fig.1a); mean V85Gy

EQD2<sub>10</sub> smaller by 19.2cm<sup>3</sup> at any given target volume (Fig.1b); mean Bladder ICRU and Rectovaginal Point doses (D2cm<sup>3</sup> is given in parenthesis) smaller by 9.1 (7.5) and 5.6 (3.3) Gy EQD2<sub>3</sub>, respectively; mean vaginal dose higher by 17.1GyEQD2<sub>3</sub>. IC/IS compared to IC centres had: significantly improved target coverage and smaller V85Gy EQD2 for intermediate and large CTV<sub>HR</sub> volumes (Fig. 1c-f); decreased OAR doses, mostly in T&O. T&R IC/IS compared to T&O IC/IS centres had: mean CTV<sub>HR</sub> D<sub>90%</sub> higher by 2.7Gy EQD2<sub>10</sub>; mean V85Gy EQD2<sub>10</sub> smaller by 8.3cm<sup>3</sup> at any given CTV<sub>HR</sub> volume; mean Bladder D2cm<sup>3</sup> and Rectovaginal Point doses smaller by 4.3Gy and 4.8Gy EQD2<sub>3</sub>, respectively; mean vaginal dose larger by 22.5Gy EQD2<sub>3</sub>. All above mentioned differences were statistically significant (p<0.01). For patients treated with IC/IS, needles were used for all fractions in 85% and 55% of cases in T&R IC/IS and T&O IC/IS centres, respectively. Average number of needles/patient was 4.9 (SD:2.5) and 3.5 (SD:1.8) in T&R IC/IS and T&O IC/IS centres, respectively.

Table 1. Patient characteristics, target and OAR doses for each centre group. Mean values and standard deviations (1 SD) are displayed.

	OVOIDS IC CENTRES	RING IC CENTRES	OVOIDS IC/IS CENTRES	RING IC/IS CENTRES
No. of Patients	119	161	180	489
Patient Age	52 (14)	51 (16)	49 (14)	51(13)
FIGO Stage (I / II / III+IV)	27%/55%/18%	30%/60%/10%	35%/54%/11%	9%/63%/28%
BT1 Tumour Width (cm)	4.3 (1.2)	3.9 (0.9)	4.1 (1.1)	4.5 (0.9)
CTV <sub>HR</sub> Vol. (cm <sup>3</sup> )	31.9 (16.5)	28.9 (18.0)	32.6 (15.9)	35.6 (18.9)
CTV <sub>HR</sub> D <sub>90%</sub> (Gy EQD2 <sub>10</sub> )	85.5 (7.4)	91.2 (10.0)	88.6 (5.9)	91.2 (5.1)
V85 Gy EQD2 <sub>10</sub> (cm <sup>3</sup> )	88.5 (23.6)	66.9 (18.7)	78.3 (22.0)	73.5 (23.8)
No. of patients with IC vs IC/IS (%)	89% / 11%	86% / 14%	38% / 62%	35% / 65%
Bladder ICRU Point (Gy EQD2 <sub>3</sub> )	74.5 (17.4)	65.4 (14.0)	69.5 (14.8)	67.5 (12.7)
Bladder D <sub>2cm<sup>3</sup></sub> (Gy EQD2 <sub>3</sub> )	82.9 (10.0)	75.4 (9.2)	79.4 (9.4)	75.1 (9.4)
Rectovaginal Ref. Point (Gy EQD2 <sub>3</sub> )	68.7 (7.1)	63.1 (7.6)	69.6 (10.1)	64.8 (7.0)
Rectum D <sub>2cm<sup>3</sup></sub> (Gy EQD2 <sub>3</sub> )	66.3 (7.2)	63.0 (6.6)	62.7 (7.4)	61.8 (6.3)
Vagina 5mm lateral (Gy EQD2 <sub>3</sub> )	87.5 (12.7)	104.6 (23.1)	87.0 (12.3)	109.5 (29.3)

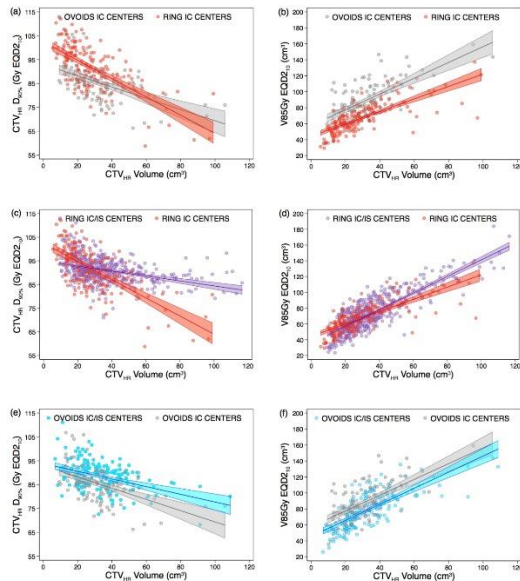


Figure 1. Scatter plots of CTV<sub>HR</sub> D<sub>90%</sub> and V85 Gy EQD2<sub>10</sub> for: (a,b) OVOIDS IC and RING IC centres; (c,d) RING IC and RING IC/IS centres; (e,f) OVOIDS IC and OVOIDS IC/IS centres. Each scatter plot displays the best fitting linear regression line (solid line) and the 95% CI (hatched band) for each center group.

**Conclusion**

The T&R IC applicator plans show better coverage and dose conformity than the T&O IC applicator plans for CTV<sub>HR</sub><45cm<sup>3</sup>. For large target volumes, both T&R and T&O IC plans fail to ensure adequate target coverage. Bladder and rectum are, in general, better spared with T&R IC, while the 5mm lateral vaginal dose is higher. Routine application of IC/IS improves target coverage and dose conformity, and better spares the OARs. With the addition of needles, the differences seen in target/OAR doses and in V85Gy EQD2 between the IC applicators become smaller. These differences are also related to both the number of needles and fractions with needles used.

**OC-0173 Dosimetric comparison of T-O brachytherapy with/without interstitial component in FIGO I-IIb tumors**

M. Federico<sup>1</sup>, A. Perez Fustero<sup>1</sup>, C. Catarina<sup>2</sup>, I. Fernandez<sup>3</sup>, J.L. Perez Molina<sup>3</sup>, I. Morales Orue<sup>1</sup>, M. Lloret<sup>1</sup>

<sup>1</sup>Hospital Universitario de Gran Canaria Dr. Negrin, Radiation Oncology, Las Palmas de Gran Canaria- Ca, Spain ; <sup>2</sup>ULPGC, Centro de Tecnologias de la Imagen CTIM, Las Palmas de Gran Canaria, Spain; <sup>3</sup>Hospital Universitario de Gran Canaria Dr. Negrin, Medical Physics, Las Palmas de Gran Canaria- Ca, Spain

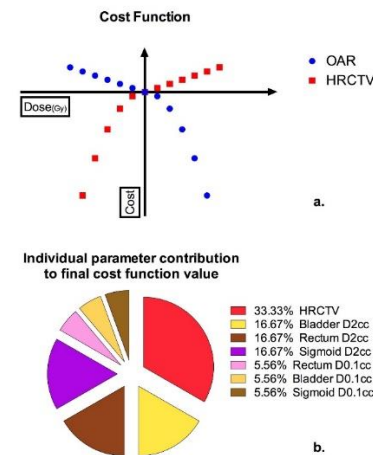
**Purpose or Objective**

Intracavitary/interstitial (IC/IS) brachytherapy (BT) improves HRCTV dose coverage in large locally advanced tumors resulting in improved local control and survival. In small tumors IC/IS brachytherapy may be useful in selected situations due to difficult OAR/tumor topography. A prospective trial was designed in order to evaluate in a series of consecutive patients with small cervical tumors potential gains of IC/IS vs. Intracavitary (IC) brachytherapy

**Material and Methods**

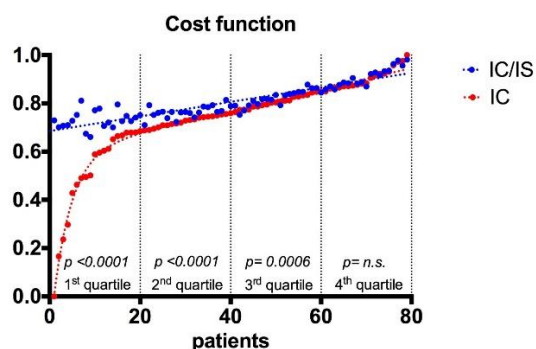
200 consecutive patients with histologically proven cervical cancers treated between 2013-18 with 45 Gy 3D CRT and MR-based IGABT (4 fraction of 7 Gy each in 2 different applications) were analyzed. Out of the original 200 patients the ones receiving TO application were selected (175 pts). To further select only the tumors potentially suited for IC BT application a standard IC 7 Gy point A plan was generated and patients with a HRCTV coverage <86 Gy<sub>EQD2</sub> were discarded (69 pts). Out of the 106 remaining patients 79 had IC/IS application in all 4 BT fractions and were selected for the present study. All pts had a FIGO stage I (20 pts) or II (59 pts).

At the time of their treatment all patients received IC/IS T-O application (Elekta Utrecht applicator) optimized upon the following constraints: HRCTV≥86Gy<sub>EQD2</sub>; Bladder≤90 Gy<sub>EQD2</sub>; Rectum≤70 Gy<sub>EQD2</sub>; Sigmoid ≤70 Gy<sub>EQD2</sub>. For the present study an IC plan was recalculated. To compare IC or IC/IS plans a cost function was generated Fig1a. To assign a specific cost to each individual planification a function was created with a linear and quadratic component. The zero of the function for each ROI was set to its specific constraint (86 Gy EQD2 for HRCTV, 90 Gy EQD2 for bladder, etc) or in case of D0.1 cc values to the median value of the delivered IC/IS planifications. The final cost of each plan was the sum of the individual ROI cost function normalized and weighted as follow (2/6 HRCTV cost, 1/6 for each OAR D2cc value and finally 1/6 for the D0.1cc values of the 3 OARs) (Fig 1b)



## Results

Average cumulative EQD2 doses (Gy) for IC/IS plan were the following: HRCTV D90 88.2±2.6; Bladder D2cc 72.1±7.9, D0.1cc 84.3±10.7; RectumD2cc 58±6.8, D0.1cc 66.7±11.3; Sigmoid D2cc 63±5.3, D0.1cc 73.9±8.6). Average cumulative EQD2 doses (Gy) for IC plan were the following: HRCTV D90 86.6±3.4; Bladder D2cc 74.4±9.9, D0.1cc 91±19.5; RectumD2cc 59.2±7.7, D0.1cc 69.5±13.7; Sigmoid D2cc 64.1±6.3, D0.1cc 76.4±10.4). Difference between IC/IS and IC plan was significant for all ROIs and dose points (wilcoxon test). Average cost function for IC/IS or IC plan was 0.8±0.1 and 0.7±0.2 respectively ( $p < 0.0001$ ). Quartile analysis of the cost function plot (Fig.2) shows that the difference between IC/IS and IC plans is not significant just in the 4th quartile.



## Conclusion

IC/IS plans achieved a significant dosimetric gain in a proportion of patients larger than expected. Given the comparable costs and complication rates between IC and IC/IS, a more extensive use of IS component in small tumors seems justified

## OC-0174 Advancement of brachytherapy for locally advanced cervical cancer in the era of image guidance

J.C. Lindegaard<sup>1</sup>, L.U. Fokdal<sup>1</sup>, P. Petric<sup>1</sup>, S.K. Nielsen<sup>1</sup>, K. Tanderup<sup>1</sup>  
<sup>1</sup>Aarhus University Hospital, Department of Oncology, Aarhus, Denmark

## Purpose or Objective

Two decades ago standard treatment for locally advanced cervical cancer (LACC) involved 4-field box external beam radiotherapy (EBRT) and 2D brachytherapy aiming for 80-85 Gy to point-A. In 2005 image guided adaptive brachytherapy (IGABT) was introduced in our department and we joined the newly formed international GEC ESTRO collaboration on IGABT in LACC. The aim of the present study was to evaluate the impact of this collaboration in terms of developments of BT techniques and dose-volume parameters over time.

## Material and Methods

400 consecutive pts treated 2005-2018 using EBRT ±concomitant cisplatin and IGABT were analysed. FIGO stage distribution was I-IIA 9%, IIB 61% and III-IV 30%. EBRT dose was 45-50 Gy delivered in 25-30 fx. A simultaneous integrated boost to 50 Gy (stage IIB) or 60 Gy (stage III-IV) for the primary tumour was used in the early years, but was gradually phased out and the EBRT dose reduced to 45 Gy/25 fx for all pts. IGABT was performed with PDR and was based on MRI with a gradual introduction of planning aims and DVH constraints from our collaborative GEC ESTRO experience as they became available. The Embrace II protocol (www.embracestudy.dk) was formally implemented in 2016.

Combined intracavitary/interstitial technique (IC/IS) was available from 2006, initially beside a tandem-ring

applicator, but from 2007 also with an intravaginal tandem-needle-template (TNT) with no ring. Time trends were visualized by sliding average calculation with 50 pts per frame (Figure 1). The planning aims and DVH hard and soft constraints were evaluated in relation to the Embrace II protocol (Table 1). Equivalent dose in 2 Gy fractions (EQD2) was calculated using  $\alpha/\beta=10$  for tumour and  $\alpha/\beta=3$  for organs at risk. Statistical analysis was done with t-test and Chi square.

## Results

The implant technique for IGABT changed significantly as the use of IC/IS went up from 32% to 68%, with 52% of the implants being performed with the TNT device in the last 50 pts (Table 1). The dose contribution of EBRT to D90 of CTV<sub>HR</sub> was reduced by 7 Gy while the contribution from IGABT enlarged by 11 Gy leading to an overall improvement in the D90 of CTV<sub>HR</sub> from 89 to 93 Gy. This improvement was realised with no increase in TRAK. For D2cm<sup>3</sup> of bladder, rectum and sigmoid the dose was significantly lowered by 3, 8 and 10 Gy, respectively. The dose to the ICRU recto-vaginal point was decreased by 8 Gy. Recording of D2cm<sup>3</sup> for bowel was initiated after the first 75 pts and stayed constant at about 60 Gy over the observation time. EMBRACE hard and soft constraints were fulfilled in 96% and 66% of the last 50 pts.

## Conclusion

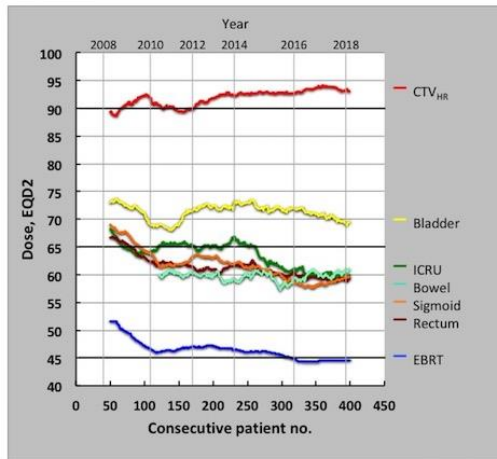
The constraints and planning aims obtained through the GEC ESTRO collaboration on IGABT in LACC has profoundly impacted our treatment practice with significant improvements in the dose-volume parameters. This improvement was primarily obtained by decreasing the dose contribution of EBRT and by use of advanced IC/IS implants for IGABT.

**Table 1**  
 Implant technique, DVH parameters and planning aim fulfillment in 400 consecutive patients treated with external beam radiotherapy +/- chemotherapy and MRI guided brachytherapy. Dose is equivalent dose in 2 Gy fractions, calculated using  $\alpha/\beta=10$  for tumour and  $\alpha/\beta=3$  for organs at risk.

Cohort, patient no.	1-400	1-50	351-400	p-value
<i>Applicator, no of pts (%)</i>				
Tandem-Ring	171 (43%)	34 (68%)	16 (32%)	
Tandem-Ring-Needle	131 (33%)	10 (20%)	8 (16%)	
Tandem-Needle-Template	98 (24%)	6 (12%)	26 (52%)	p<0.001
<i>Dose-volume-parameters (mean±SE)</i>				
TRAK, cGy/h	1.6±0.4	1.5±0.4	1.5±0.4	p=0.73
CTV <sub>HR</sub> D90 EBRT, Gy	47±3	52±4	45±2	p<0.001
CTV <sub>HR</sub> D90 BT, Gy	45±7	38±10	49±4	p<0.001
CTV <sub>HR</sub> D90, Gy	92±5	89±7	93±3	p<0.001
Bladder D2cm <sup>3</sup> , Gy	71±7	73±6	70±9	p<0.045
Rectum D2cm <sup>3</sup> , Gy	62±6	67±6	59±5	p<0.001
Sigmoid D2cm <sup>3</sup> , Gy	62±6	69±5	59±5	p<0.001
Bowel D2cm <sup>3</sup> *, Gy	60±8	n.a.	61±9	
ICRU RV point, Gy	64±7	68±7	60±5	p<0.001
<i>Hard constraints Aim Fulfilled in n (%)</i>				
CTV <sub>HR</sub> D90 >85 Gy	378 (95%)	40 (80%)	50 (100%)	
Bladder D2cm <sup>3</sup> <90 Gy	397 (99%)	50 (100%)	49 (98%)	
Rectum D2cm <sup>3</sup> <75 Gy	395 (99%)	48 (96%)	50 (100%)	
Sigmoid D2cm <sup>3</sup> <75 Gy	398 (99%)	48 (96%)	50 (100%)	
Bowel D2cm <sup>3</sup> * <75 Gy	323 (99%)	n.a.	50 (100%)	
ICRU recto-vaginal point <75 Gy	367 (92%)	41 (82%)	49 (98%)	
All hard	290 (73%)	33 (66%)	48 (96%)	p<0.001
<i>Soft constraints Aim Fulfilled in n (%)</i>				
CTV <sub>HR</sub> D90 >90 Gy	285 (71%)	23 (46%)	44 (88%)	
Bladder D2cm <sup>3</sup> <80 Gy	373 (93%)	47 (94%)	46 (92%)	
Rectum D2cm <sup>3</sup> <65 Gy	292 (73%)	20 (40%)	44 (88%)	
Sigmoid D2cm <sup>3</sup> <70 Gy	363 (91%)	26 (52%)	50 (100%)	
Bowel D2cm <sup>3</sup> * <70 Gy	297 (91%)	n.a.	44 (88%)	
ICRU recto-vaginal point <65 Gy	256 (65%)	21 (42%)	43 (86%)	
All soft	139 (35%)	4 (8%)	33 (66%)	p<0.001

\*D2cm<sup>3</sup> of bowel not recorded in the first 75 pts.

**Figure 1.** Sliding average (50 pts per frame) of dose to tumour (D90 CTV<sub>HR</sub>) and organs at risk (D2cm<sup>3</sup> bladder, bowel, sigmoid, rectum; dose ICRU recto-vaginal point) obtained in 400 consecutive pts treated 2005-2018 with external beam radiotherapy +/- chemotherapy and MRI guided brachytherapy. Dose contribution from external beam radiotherapy (EBRT) to D90 of CTV<sub>HR</sub> is also indicated.



### OC-0175 3D-printed tandem-needle-template for image guided adaptive brachytherapy in cervical cancer

P. Petric<sup>1</sup>, L.U. Fokdal<sup>1</sup>, A. Traberg Hansen<sup>1</sup>, S. Kynde Nielsen<sup>1</sup>, K. Tanderup<sup>1</sup>, J.C. Lindegaard<sup>1</sup>  
<sup>1</sup>Aarhus University Hospital, Department of Oncology, Aarhus C, Denmark

#### Purpose or Objective

Intracavitary/interstitial (IC/IS) image guided adaptive brachytherapy (IGABT) is being increasingly employed for locally advanced cervical cancer (LACC). However, narrow vagina and/or extensive local disease may compromise the use of tandem-ring or tandem-ovoid IC/IS applicators. We describe our experience with novel 3D printed vaginal tandem-needle templates (TNT) for insertion of needles in parallel (P) or parallel and oblique (P&O) direction.

#### Material and Methods

Fifty-nine consecutive patients treated with TNT from Jan 2015 - Jan 2018 were included. External beam radiotherapy (EBRT) consisted of 45 Gy/25 fx +/- nodal boost and concomitant cisplatin. Decision to use TNT and pre-planning of its optimal geometry were made after 4-5 weeks of EBRT, based on gynaecological examination and MRI with tandem-ring applicator in situ. Subsequently, TNT was 3D-printed in house, using biocompatible autoclavable material (Figure 1). TNT consisted of a 32- or 36-mm vaginal ring without a ring channel and with P and O holes for guidance of plastic needles. Standard (12 P needles or 8 P plus 7 O needles) or personalized TNT (individualized needle insertion points and angles) was printed. Following EBRT, 2 implants and 2 fractions of PDR IGABT were delivered about 1 week apart. TNT was fitted over commercially available uterine tandem. Plastic needles were placed through the guiding holes to pre-planned depths. The source was not in direct contact with the TNT. Dwell-positions in P needles were used to simulate the ring channel. Planning aims were based on the Embrace II protocol. TNT was discarded after single use.

#### Results

Patients selected for TNT were characterised by a median age of 69 years. Performance status (WHO) was > 0 in 49% and 56% of the patients had noteworthy co-morbidity. FIGO stage distribution was: IB 2%, IIB 48% and III-IV 50%. Median tumour width was 60 mm. Patients with P&O implants (n=32) had significantly larger tumours and more extensive parametrial involvement at diagnosis and BT when compared with P group (n=27). Bladder and rectum invasion also predicted for the use of P&O technique,

while vaginal and uterine involvement did not. Median number of implanted/active P and P&O needles at first implant was 8/7 and 12/10, respectively. Individualized 3D printing was used in 13 (57%) patients of the P&O group. Embrace II hard constraints were fulfilled in 95% (Table 1). With a median follow-up time of >18 months, local control was obtained in 56 (95%) and grade  $\geq 3$  radiation related complications observed in 3 pts (5%).

#### Conclusion

The use of 3D printed TNT for IGABT in LACC is promising. It allows for successful management of extensive local disease even in narrow vaginal conditions. 3D printing enables full and affordable control of the production process with the possibility for treatment individualisation and one-time use of the BT template.

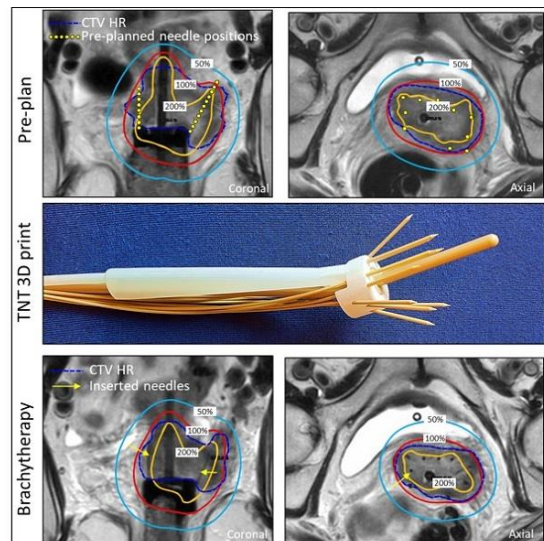


**Figure 1.** Concept of personalized applicator printing guided by MRI-based pre-planning. Isodoses are shown in % of planning aim for CTV HR D90.

DVH parameter	IMPLANT TYPE			p-value
	All	P	P&O	
TRAK [cGy/h]	1.59±0.46	1.45±0.38	1.71±0.50	p=0.027
HR-CTV [cm <sup>3</sup> ]	37±24	30±20	43±26	p=0.034
HR-CTV D90 [Gy]	94±3	95±3	93±3	p=0.01
Bladder D2cm <sup>3</sup> [Gy]	72±8	69±8	75±8	p=0.009
Rectum D2cm <sup>3</sup> [Gy]	60±5	58±4	62±6	p=0.005
Sigmoid D2cm <sup>3</sup> [Gy]	58±6	58±6	59±6	p=0.41
Bowel D2cm <sup>3</sup> [Gy]	60±9	61±9	60±9	p=0.60
ICRU RV <sup>2</sup> point [Gy]	60±5	58±6	61±5	p=0.028
	<b>Hard constraints</b>	<b>Constraint fulfilled [n (%)]</b>		
HR-CTV D90	>85 Gy	58 (98%)	27 (100%)	31 (97%)
Bladder D2cm <sup>3</sup>	<90 Gy	58 (98%)	27 (100%)	31 (97%)
Rectum D2cm <sup>3</sup>	<75 Gy	58 (98%)	27 (100%)	31 (97%)
Sigmoid D2cm <sup>3</sup>	<75 Gy	59 (100%)	27 (100%)	32 (100%)
Bowel D2cm <sup>3</sup>	<75 Gy	58 (98%)	27 (100%)	31 (97%)
ICRU RV point	<75 Gy	59 (100%)	27 (100%)	32 (100%)
All hard constraints		56 (95%)	27 (100%)	29 (91%)
	<b>Soft constraints</b>	<b>Constraint fulfilled [n (%)]</b>		
HR-CTV D90	>90 Gy	55 (93%)	27 (100%)	28 (88%)
Bladder D2cm <sup>3</sup>	<80 Gy	52 (88%)	26 (96%)	26 (81%)
Rectum D2cm <sup>3</sup>	<65 Gy	50 (85%)	27 (100%)	23 (72%)
Sigmoid D2cm <sup>3</sup>	<70 Gy	57 (97%)	26 (96%)	31 (97%)
Bowel D2cm <sup>3</sup>	<70 Gy	50 (85%)	22 (82%)	28 (88%)
ICRU RV point	<65 Gy	49 (83%)	24 (89%)	25 (78%)
All soft constraints		33 (56%)	20 (74%)	13 (41%)

**Table 1.** Dose-volume histogram parameters (EQD2) obtained in 59 patients with locally advanced cervical cancer treated with an intravaginal tandem-ring-template with needles implanted either in parallel (P) or parallel and oblique (P&O) to the tandem. <sup>2</sup>Fisher's exact test; <sup>3</sup>recto-vaginal

### OC-0176 A systematic analysis of delineation performance seen in EMBRACE-II brachytherapy quality assurance

S. Duke<sup>1</sup>, R. Pötter<sup>2</sup>, A. Sturdza<sup>2</sup>, M. Schmid<sup>2</sup>, T. Rumpold<sup>2</sup>, U. Mahantshetty<sup>3</sup>, N. Nesvacil<sup>2</sup>, A. De Leeuw<sup>4</sup>, C. Kirisits<sup>2</sup>, K. Tanderup<sup>5</sup>, R. Nout<sup>6</sup>, J. Lindegaard<sup>5</sup>, I. Jurgenliemk-Schulz<sup>4</sup>, L. Tan<sup>1</sup>

<sup>1</sup>Cambridge University Hospitals, Department of Oncology, Cambridge, United Kingdom; <sup>2</sup>Medical University of Vienna, Department of Radiotherapy, Vienna, Austria; <sup>3</sup>Tata Memorial Centre, Department of Radiation Oncology, Mumbai, India; <sup>4</sup>University Medical Center, Department of Radiation Oncology, Utrecht, The Netherlands; <sup>5</sup>Aarhus University Hospital, Department

of Radiation Oncology, Aarhus, Denmark ; <sup>6</sup>Leiden University Medical Center, Department of Radiation Oncology, Leiden, The Netherlands

### Purpose or Objective

EMBRACE-II is a prospective interventional multicentre study of IMRT and MRI-based image-guided adaptive brachytherapy (IGABT) in cervix cancer. The EMBRACE-II RTQA process for IGABT is mandatory for centres which did not participate in the first EMBRACE study.

The RTQA process comprised 1) a compliance questionnaire confirming that IGABT was established at the centre, 2) contouring on two benchmark cases by the principal investigator, and 3) submission of dosimetric data from 5 dummy run patients treated according to the study protocol. This abstract reports the results of the contouring assessments for the benchmark cases.

### Material and Methods

Delineation was performed using a bespoke online contouring tool.

Case 1 was a IIIB tumour with 40mm anterior vaginal extension at diagnosis. There was moderate response to chemoradiotherapy (CRT) with a small amount of residual anterior vaginal disease and palpable proximal parametrial disease at BT.

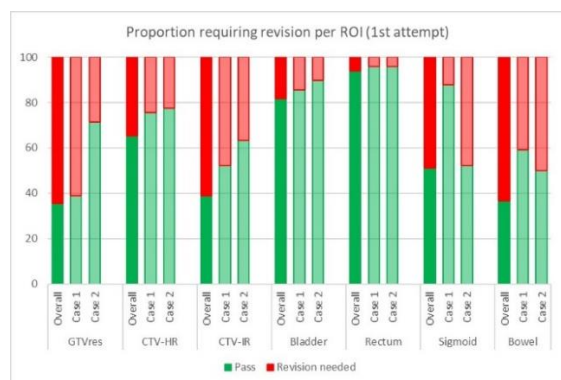
Case 2 was also a IIIB tumour but with no vaginal involvement at diagnosis. There was good response to CRT with no residual palpable or radiological parametrial disease.

The regions of interest (ROIs) assessed were the residual GTV (GTV<sub>res</sub>), high-risk CTV (CTV-HR), intermediate-risk CTV (CTV-IR), bladder, sigmoid, rectum and bowel. Each ROI was scored 0-10 by 2 assessors - a score of  $\geq 6$  was required to pass. Individualised feedback was also provided. A pass on every ROI for both cases was required for accreditation.

### Results

49 clinicians submitted contours for evaluation. 4 (8%) passed at the first attempt and 27 (62%) on resubmission after individualised feedback.

23% of submissions required revision of one ROI, 29% two ROIs, and 30% three or more ROIs. The most common ROIs requiring revision were the GTV<sub>res</sub> (65%), CTV-IR (61%), sigmoid (49%) and bowel (63%) [Figure 1].



A pair-wise comparison of individual performance for each ROI in the 2 cases was performed [Table 1]. The proportion of clinicians failing both cases ranged between 2-24% per ROI; a common conceptual difficulty was often identifiable from the qualitative feedback.

For the GTV<sub>res</sub>, CTV-IR and sigmoid, performance was worse in one case compared to the other which could be attributed to differences in case difficulty. For the CTV-HR, the causes for clinicians passing only one case were not obvious.

ROI	Pass both	Fail both	Fail only Case 1	Fail only Case 2	Common errors (frequency)	Consequence
GTV <sub>res</sub>	17 (35%)	12 (24%)	18 (37%)	2 (4%)	Normal cervix and/or grey zones included (47%) Tumour present on clinical examination missed - case 1 (32%)	Volume too large - unable to meet target dose constraint / objective Insufficient dose to residual tumour
CTV-HR	32 (65%)	6 (12%)	6 (12%)	5 (10%)	Too narrow axially (20%)	Insufficient dose to cervix / residual pathologic tissue
CTV-IR	19 (39%)	11 (22%)	12 (24%)	7 (14%)	Initial extent of disease not covered e.g. vagina - case 1 (33%) or parametrium (31%) Uninvolved tissue at diagnosis inappropriately included e.g. para-uterine tissues (33%)	Insufficient dose to areas of original macroscopic disease Increased dose to organs at risk near the uterine corpus (bowel, sigmoid)
Bladder	40 (82%)	3 (6%)	4 (8%)	2 (4%)	Inner wall contoured (14%)	Falsely low bladder D <sub>2cc</sub>
Rectum	46 (94%)	1 (2%)	1 (2%)	1 (2%)		
Sigmoid	25 (51%)	5 (10%)	1 (2%)	18 (37%)	Sigmoid mislabelled as bowel - case 2 (45%)	Bowel D <sub>2cc</sub> falsely high
Bowel	18 (37%)	12 (24%)	8 (16%)	11 (22%)	Individual bowel loops not contoured - case 1 (36%) Sigmoid mislabelled as bowel - case 2 (45%)	

### Conclusion

This is the first study to correlate the results of summative (pass/fail) assessments for benchmark cases in cervix cancer IGABT with a systematic analysis of qualitative feedback.

The first-time pass rate was low and most submissions required revision of more than one ROI. Qualitative analysis showed that while many errors were due to conceptual difficulties, there were also errors related to variation in case selection.

Individualised feedback improved contouring, but the time taken to manually assess and give relevant feedback was a significant burden.

Improved tools which will allow rapid contouring across a large number of cases with automated assessments are required.

### OC-0177 The value of kV-CBCT in adaptive HDR brachytherapy of cervical cancer patients

C. Constantinescu<sup>1</sup>, N. Jastaniyah<sup>2</sup>, S. Wadi-Ramahi<sup>1</sup>  
<sup>1</sup>King Faisal Specialist Hospital and Research Center, Biomedical Physics, Riyadh, Saudi Arabia; <sup>2</sup>King Faisal Specialist Hospital and Research Center, Radiation Oncology, Riyadh, Saudi Arabia

### Purpose or Objective

To assess the intra-fraction variation of dose delivered to organs-at-risk (OARs) using a kV-CBCT scanner and estimate the potential of this technology for adaptive HDR brachytherapy (BT) of cervical cancer.

### Material and Methods

Data of cervical cancer patients who underwent VMAT pelvic irradiation (45Gy/25fractions) followed by HDR BT (28Gy/4fractions) were retrospectively reviewed. Bladder-filling and rectum/bowel preparation protocols were performed.

A CT scan with 2 mm slice thickness was acquired and images imported to TPS for planning purposes. Contouring of the HR-CTV and the OARs (bladder, rectum and sigmoid) was performed on CT images, guided by MR images previously acquired. Planning objectives were according to (GYN) GEC-ESTRO recommendations. Immediately before treatment, a kV-CBCT scan was acquired with the patient in treatment position, using an in-built pelvis scanning protocol. CBCT images were manually registered with planning CT using the applicators as landmarks and the OARs were re-contoured.

Their D<sub>2cc</sub> and respective EQD2 were recalculated and compared to the planned ones using a Wilcoxon test. The dose variations were evaluated by the relative percentage difference between the doses calculated on planning CT and verification kV-CBCT images. Possible correlation between OARs dose and volume variation was investigated by a linear regression test.

### Results

Data of 19 patients and 57 BT fractions were analyzed. In each BT fraction, variations in OARs (as volume, shape

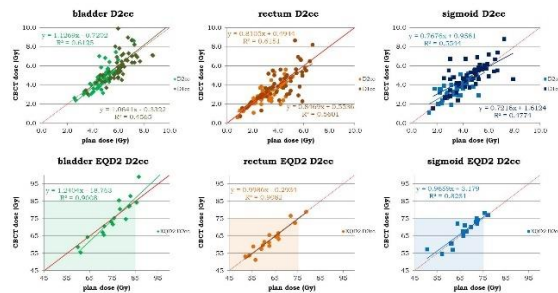
and/or position) always occurred between CT and kV-CBCT acquisition.

The mean relative percentage differences of  $D_{2cc}$  were:  $-2.7\% \pm 15.6\%$  for bladder,  $-1.2\% \pm 21.2\%$  for rectum and  $6.3\% \pm 24.1\%$  for sigmoid.

Table 1. Individual dosimetric variations for the bladder, rectum and sigmoid, expressed as EQD2.

		planning CT dose (Gy)			kV-CBCT dose (Gy)			diff. (%)		p
		mean	SD	range	mean	SD	range	mean	SD	
bladder	EQD2 <sub>2cc</sub>	77.2	9.9	60-102.1	77	12.9	55.3-107	-0.6	5.9	0.0001
	rectum	EQD2 <sub>2cc</sub>	63.3	7.6	53.6-78.7	62.9	7.9	53.7-78.8	-0.6	3.9
sigmoid	EQD2 <sub>2cc</sub>	66.7	6.9	50.5-77.2	67.6	7.3	54.6-78.2	1.4	5.1	0.0001

Figure 1. Correlation between the planning CT and kV-CBCT doses for OARs.



Variations higher than 10% of EQD2 were found in 1/19 (5%) patients for bladder and 2/19 (10%) for rectum and sigmoid, while the (GYN) GEC-ESTRO recommendations for OARs dose limits were met in 15/19 (79%) patients for bladder and 17/19 (89%) for rectum and sigmoid. A weak yet statistically significant correlation was found between volume and  $D_{2cc}$  variations for bladder ( $R^2=0.320$ ,  $p=0.0001$ ), but not for rectum and sigmoid. The time gap between CT and CBCT acquisitions was of  $125 \text{ min} \pm 48 \text{ min}$  (range: 47-204 min). No correlation was found between this time and OARs dose or volume variations.

#### Conclusion

OARs dose intra-fraction variations in HDR BT for cervical cancer are small on average, but large random variations were observed in individual patients. Differences are likely attributed to changes in volume for the bladder and to deformation and movement for the rectum and sigmoid.

A kV-CBCT scan acquired before dose delivery can detect unfavorable anatomical changes, warranting adaptive strategies.

Our data show that without adaptive planning, 21% of the patients will have a chance that at least one OAR will exceed the recommended limits, though a variation in EQD2 higher than 10% will occur in only 10% of them.

#### OC-0178 Indirect Excess Dose Volume Ratio (iRex): A Novel predictor of Late Toxicity in Cervical Cancer IGBT

T. Prasartseree<sup>1</sup>, P. Dankulchai<sup>1</sup>

<sup>1</sup>Faculty of Medicine- Siriraj Hospital- Mahidol University, Division of Radiation Oncology- Department of Radiology, Bangkok, Thailand

#### Purpose or Objective

Excess intermediate to high dose out of HR-CTV in IGBT associates with OAR toxicity.  $D_{2cc}$ ,  $D_{1cc}$ , and  $D_{0.1cc}$  demonstrate the dose-toxicity relationship with a limitation of identical locations of the most exposed volumes assumption. From observation, isodose surface volume (ISV) of intermediate dose usually covered the movable space of pelvic organs. To minimize effects of the organ motion in toxicity prediction, Excess Dose Volume (Vex) and its Excess Dose Volume Ratio (Rex), transformed from ISV, were proposed and probably be used as IGBT dose constraints. Indirect Excess Dose Volume Ratio (iRex), the more practical form derived

from Vex and Rex, was studied to demonstrate its correlation with late GI and/or GU toxicities in cervical cancer.

#### Material and Methods

149 cervical cancer patients treated with 44-52 Gy EBRT without central shielding, parametrial or pelvic nodal boost, or re-irradiation with/without chemotherapy with Gynaecologic GEC-ESTRO II directed HDR-IGBT in 2012-2015 were retrospectively reviewed. Late GI and/or GU toxicities were graded using CTCAE version 5.0. The iRex of each IGBT fraction was defined as  $ISV/V_{neg}$ . ISVs were transformed from isodose lines of fractional absorbed doses corresponded to EQD2 ( $\alpha/\beta=3$ ) of 60, 70, 80, 90 and 100 Gy.  $V_{neg}$  was the intercepted volume of ISV (60 Gy EQD2) and delineated toxicity-negligible regions including HR-CTV, uterus, and vagina. No further delineation of any OAR was performed. Numerical mean of iRex was established for each patient. The data of cumulative events of GI and/or GU toxicities was generated to determine the correlations between mean iRex and grade 2-4 late toxicities, using probit analysis.

#### Excess dose volume and its ratio: Vex, Rex, and iRex

**Isodose surface volume (ISV):** Transformed volume from isodose level of 60, 70, 80, 90, and 100 Gy EQD2 ( $\alpha/\beta=3$ )

**Toxicity-negligible volume (Vneg):**

$$V_{neg} = ISV(60 \text{ Gy EQD2}_3) \cap [HR-CTV \cup V_{uterus} \cup V_{vagina}]$$

**Excess dose volume (Vex):**

$$V_{ex} = ISV - V_{neg}$$

**Excess dose volume ratio (Rex):**

$$R_{ex} = V_{ex}/V_{neg} = ISV/V_{neg} - 1$$

**Indirect excess dose volume ratio (iRex):**

$$iR_{ex} = ISV/V_{neg}$$

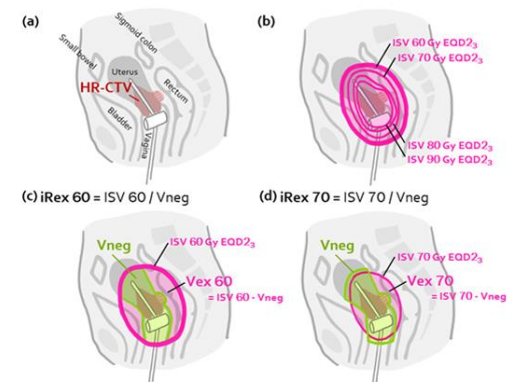


Diagram showing (a) Pelvic organs and HR-CTV, (b) ISV 60, 70, 80, 90 Gy EQD2, (c) ISV 60 Gy EQD2, Vneg, and Vex 60, (d) ISV 70 Gy EQD2, Vneg, and Vex 70

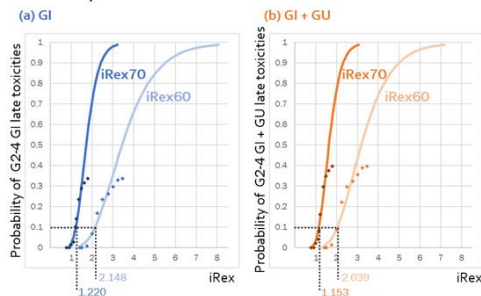
#### Results

50, 15, and 59 patients were affected from grade 2-4 late GI, GU, and combined GI and/or GU toxicities, respectively, with median follow-up time of 36 months. Mean iRex and toxicities correlations established the significant dose-response relationships for iRex60, iRex70 - late GI toxicities and iRex60, iRex70 - combined GI and/or GU toxicities. The effective ratio at 10 percent response values for iRex60 and iRex70 were 2.148 and 1.220 for grade 2-4 GI toxicities. For grade 2-4 combined GI and/or GU toxicities, the effective ratio at 10 percent response values for iRex60 and iRex70 were 2.039 and 1.153.

**Probability of G2-4 late toxicities according to iRex**

iRex	Probability of iRex for G2-4 late toxicities at the incidence rates shown (95% CI)			p value
	5%	10%	20%	
<b>Gastrointestinal toxicities (GI)</b>				
iRex60	1.880 (1.842-1.915)	2.148 (2.119-2.176)	2.525 (2.493-2.558)	0.000
iRex70	1.107 (1.093-1.119)	1.220 (1.210-1.230)	1.373 (1.362-1.385)	0.000
iRex80	0.79 (0.783-0.797)	0.865 (0.859-0.870)	0.965 (0.959-0.971)	0.286
iRex90	0.619 (0.613-0.624)	0.674 (0.670-0.678)	0.748 (0.744-0.753)	1.000
iRex100	0.510 (0.505-0.514)	0.557 (0.553-0.560)	0.619 (0.615-0.623)	0.934
<b>Genitourinary toxicities (GU)</b>				
iRex60	2.274 (2.237-2.311)	2.783 (2.726-2.849)	3.553 (3.422-3.715)	0.660
iRex70	1.199 (1.180-1.218)	1.439 (1.414-1.469)	1.796 (1.734-1.873)	0.516
iRex80	0.842 (0.829-0.850)	1.000 (0.984-1.018)	1.232 (1.193-1.260)	0.860
iRex90	0.665 (0.656-0.673)	0.775 (0.764-0.788)	0.934 (0.908-0.967)	0.991
iRex100	0.546 (0.539-0.553)	0.642 (0.633-0.653)	0.781 (0.758-0.809)	0.805
<b>Combined gastrointestinal and/or genitourinary toxicities (GI+GU)</b>				
iRex60	1.797 (1.755-1.834)	2.039 (2.007-2.069)	2.377 (2.349-2.406)	0.000
iRex70	1.045 (1.029-1.059)	1.153 (1.141-1.164)	1.300 (1.289-1.310)	0.000
iRex80	0.746 (0.738-0.753)	0.818 (0.813-0.824)	0.916 (0.911-0.921)	0.072
iRex90	0.589 (0.583-0.596)	0.643 (0.638-0.647)	0.714 (0.710-0.717)	0.997
iRex100	0.485 (0.480-0.489)	0.530 (0.526-0.533)	0.590 (0.587-0.593)	0.631

**Relationship between iRex and G2-4 late toxicities in**



**Conclusion**

iRex significantly established dose-response relationships with grade 2-4 late GI and/or GU toxicities in retrospective data, especially iRex60 and iRex70. Regarding of pelvic organ geometrical uncertainties, with further investigation, the proposed Vex, Rex, and iRex concept could probably be used as the novel IGBT dose constraints in addition to D2cc, D1cc, and D0.1cc.

**Proffered Papers: PH 3: Proffered paper: New developments in automated treatment planning**

**OC-0179 Clinical implementation of plan quality control for automated prostate planning**

M. Kusters<sup>1</sup>, F.J. Dankers<sup>1</sup>, P. Van Kollenburg<sup>1</sup>, R.J. Smeenk<sup>1</sup>, R. Monshouwer<sup>1</sup>

<sup>1</sup>Radboud University Medical Center, Academic Department of Radiation Oncology, Nijmegen, The Netherlands

**Purpose or Objective**

Currently most of our radiotherapy plans are automatically generated with a single treatment technique template in the Auto-Planning module in Pinnacle 16.0.2 (Philips Healthcare, Fitchburg, WI, USA). An inhouse-developed plan quality control tool (planQC) was built to check the quality of our automated prostate plans. This tool predicts a personalized dose-volume histogram (DVH) for each organ-at-risk (OAR) based on the anatomy of each individual patient. In this study the planQC tool was clinically implemented.

**Material and Methods**

Historical data of 129 automatically planned clinical prostate patient plans which all fulfill the clinical criteria were used to train and test a prediction model. In all these plans one single VMAT arc was used (95 to 265°), by which 70 Gy is given in 28 fraction of 2.5 Gy. The model was trained on 100 plans and validated on a separate test set of 29 plans based on a random split. The model was made by first calculating principal components (PCs) of the DVH and overlapping volume histogram (OVH), where the latter is a measure to capture individual patient anatomical information. Second, the calculated PCs were used to

train a support vector regression model that predicts DVH PCs from OVH PCs (see Figure 1). In our clinical workflow the planQC tool is initiated when the dicom data of a final clinical plan is exported from the treatment planning system to the planQC DICOM node, where the planQC tool application is executed. The application calculates the predicted and planned DVH curves and generates a personalized scorecard in a PDF report. The report is added to the departmental oncology information system (OIS) and reviewed by the planner. Threshold levels of 3 Gy for dose and 3% for dose and volume metrics at the OARs are set to detect if a plan is eligible for replanning. Plans are replanned by changing the treatment technique template for each of the OAR dose parameters that can be improved and starting the Auto-Planning again.

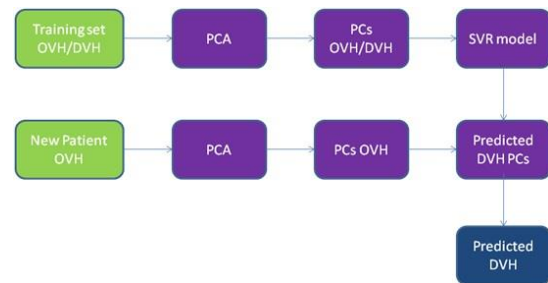


Figure 1

**Results**

The planQC tool was incorporated into the clinical workflow of automated prostate planning on March 1st 2018. Currently, 40 clinical prostate plans have been checked by planQC. For 8 of the 40 patients the plans did not pass the check and further optimization of the plan was done. In Figure 2 an example of a patient plan is shown where the planQC tool detected a suboptimal mean dose for the bladder (upper panel). After replanning the mean dose of the bladder was reduced by 5.3 Gy (lower panel), from 28.2 Gy to 22.9 Gy. In general, the mean improvement for the 8 plans was 3.6 Gy/% for the metrics of the OARs which were improved.

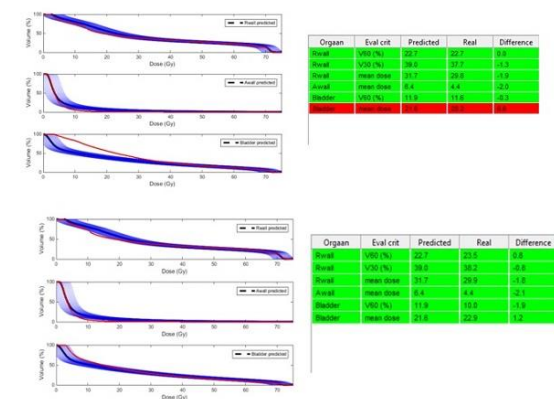


Figure 2: Result before (upper) and after replanning (lower panel)

**Conclusion**

A planQC tool was successfully introduced in the clinical workflow and monitor the quality of automated prostate plans. It can be used to detect plans that deviate from model development cohort and can therefore possibly be improved. For 8 of the 40 patients the plan was labelled suboptimal and could be improved.

### OC-0180 Towards a comprehensive automatic planning with deep neural networks: dose prediction for lung IMRT

A.M. Barragán Montero<sup>1,2</sup>, D. Nguyen<sup>2</sup>, W. Lu<sup>2</sup>, M. Lin<sup>3</sup>, X. Geets<sup>1</sup>, E. Sterpin<sup>1</sup>, S. Jiang<sup>2</sup>

<sup>1</sup>Université Catholique de Louvain- Institute of Experimental & Clinical Research, Molecular Imaging-Radiotherapy and Oncology MIRO, Brussels, Belgium ;

<sup>2</sup>UT Southwestern Medical Center, Medical Artificial Intelligence and Automation MAIA, Dallas, USA ; <sup>3</sup>UT Southwestern Medical Center, Radiation Oncology, Dallas, USA

#### Purpose or Objective

Most automatic planning strategies, such as knowledge-based planning, are based on the prediction of one-dimensional dose volume objectives that are insensitive to the spatial features of the dose distribution, hampering to achieve more individualized treatments. In addition, they rely on consistent beam and dosimetric characteristics among the training database, and often fail in cases where the beam configuration or the anatomy is significantly different. Our model uses neural networks to directly predict 3D dose distributions, combining both dosimetric and anatomical information in order to increase the robustness against heterogeneous patient populations.

#### Material and Methods

The model combines two recent deep learning architectures, UNet and DenseNet, to learn from previous clinical plans. The UNet is a type of convolutional neural network able to include local and global features from the input images. It was modified with the densely connected convolutional architecture used in DenseNet, to achieve a more efficient feature propagation. We used several input channels to include anatomical information from delineated contours (PTV and OARs, 9 channels) and per-beam dosimetric data (1 channel). A set of 129 lung cancer patients treated with IMRT, with heterogeneous beam configuration (4 to 9 beams) and orientation, was used for training/validation (100 patients) and testing (29 patients). Mean squared error was used as objective loss function.

The stability of the model was evaluated by using a 5-fold cross-validation approach, where the model was randomly initialized, trained with 80 patients, and validated with the remaining 20 patients, using a different training/validation combination for each fold. The accuracy of the model was evaluated by comparing the mean dose (Dmean) and other relevant metrics for clinical practice in the predicted and real doses.

#### Results

Figure 1 presents the average absolute error and its standard deviation (SD) on Dmean for the target and OARs for cross-validation (Figure 1.a, average prediction on the validation set for all 5 folds), and testing (Figure 1.b, average prediction on the test set for all 5 folds). The error on Dmean was below 2.5% of the dose prescription for all considered organs, in both cross-validation and testing. Figure 1.c and 1.d show the mostly overlapping DVHs for one of the test patients and the dose at the center of the target, respectively. Table 1 reports some relevant DVH metrics, most of them below 2%, except D2 for esophagus (> 4%) and spinal cord (> 5%). The training time was about 10h and the time employed to predict the 3D dose for a new patient was around 12 s.

Absolute mean error for DVH metrics			
		Cross-validation (mean ± SD)	Testing (mean ± SD)
PTV	D99 (% of D <sub>pre</sub> )	2.69±2.78	2.38±2.32
	D98 (% of D <sub>pre</sub> )	1.98±1.86	1.69±1.56
	D95 (% of D <sub>pre</sub> )	1.20±0.92	1.17±1.02
	D5 (% of D <sub>pre</sub> )	0.79±0.66	0.80±0.69
Esophagus	D2 (% of D <sub>pre</sub> )	4.13±4.59	4.85±5.41
	V40 (% of volume)	0.06±0.09	0.07±0.09
	V50 (% of volume)	0.07±0.09	0.07±0.08
Heart	V35 (% of volume)	0.09±0.14	0.10±0.16
Spinal cord	D2 (% of D <sub>pre</sub> )	6.95±5.57	5.83±4.36
	Dmean (% of D <sub>pre</sub> )	1.14±0.93	0.94±1.00
Lungs	V5 (% of volume)	0.02±0.04	0.02±0.05
	V20 (% of volume)	0.03±0.05	0.04±0.06

Table 1. Absolute error (mean±SD) for relevant metrics on the target and several organs. The values are expressed as percentage of the dose prescription (D<sub>pre</sub> = 60 Gy) for the metrics reporting the dose received by x% of volume (Dx), and as absolute difference for the metrics reporting the volume (in % receiving a dose of y Gy (Vy)).

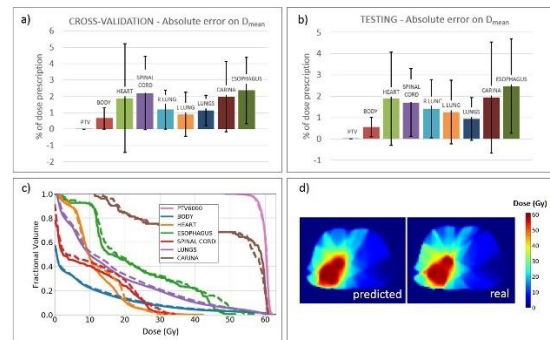


Figure 1. Absolute error on D<sub>mean</sub> for cross-validation (Figure 1.a) and testing (Figure 1.b), expressed as percentage of the dose prescription. The color bars represent the mean value, while the black solid lines represent the standard deviation. Figure 1.c contains the DVHs for one of the testing patients, solid lines correspond to the real dose and the dashed lines to the prediction. Figure 1.d shows the 3D dose (real and predicted) at the center of the target (axial view) for the same test patient.

#### Conclusion

The proposed architecture was able to learn from a very heterogeneous database in dosimetric terms, and generated accurate 3D dose distributions that can be later used as voxel-wise objective to create patient-specific treatment plans. This represents an important step towards an easier and more robust implementation of automatic planning techniques.

### OC-0181 Prostate auto-planning in clinical practice: evaluation of plan acceptance and manual adaptations

R. Van Der Bel<sup>1</sup>, D.A. Eekhout<sup>1</sup>, G.H. Wortel<sup>1</sup>, G. Van Der Veen<sup>1</sup>, R.H. Harmsen<sup>1</sup>, F.J. Pos<sup>1</sup>, T.M. Janssen<sup>1</sup>, E.M.F. Damen<sup>1</sup>

<sup>1</sup>The Netherlands Cancer Institute, Radiotherapy Oncology, Amsterdam, The Netherlands

#### Purpose or Objective

Implementation of auto-planning techniques may improve plan quality and consistency in plans and provide a possible time gain. In our clinic we have implemented auto-planning for prostate in 2016. In this retrospective study we aim to evaluate the effectiveness of prostate auto-planning. Therefore, we determined the acceptance rate of auto-plans and investigated the manual alterations made, their effect on the dose distribution and the clinical relevance of these interventions.

#### Material and Methods

Prostate auto-planning is performed using Pinnacle Auto-Planner (Pinnacle 9.10, Philips, Fitchburg, USA) in combination with an in-house post-script for fine tuning. A PTV coverage V<sub>95%</sub> of 99% was strived for. For 177 prostate cancer patients, irradiated at two dose levels with 35x2/2.2Gy between January 2017 and July 2018, DVH data of both the auto-plan (including post-script) as well as the clinically used plan were available for analysis.

DVH parameters and optimization objectives were extracted from archived DVH reports. Data were analysed in SPSS.

### Results

In 10.7% (n=19) of cases the auto-plan was directly accepted for treatment. In 46.9% (n=83) of cases, MUs were scaled before accepting the auto-plan. In 40.1% (n=71), the auto-plan was optimised further. In 2.3% (n=4) of all cases, the auto-plan was rejected entirely and a new plan was made manually. We could identify the following reasons for manual adaptations:

- **Bowel loop:** 14.7% of plans (n=26), a bowel loop was near the PTV. In 4 cases MU were scaled and 22 cases were optimised further.
- **Target coverage:** Upscaling of MUs (n=43) is done to improve target coverage. These auto-plans had a mean  $V_{95\%}$  of  $98.87 \pm 1.12\%$ , upscaling resulted in a mean  $V_{95\%}$  of  $99.41 \pm 0.25\%$  ( $p < 0.001$ ).
- **Hot or cold spots:** Downscaling of MUs (n=40) is mainly done to reduce the high dose volume. Before downscaling, auto-plans had a  $V_{103\%}$  of  $1.11 \pm 1.39\%$ , downscaling resulted in a  $V_{103\%}$  of  $0.48 \pm 0.62\%$  ( $p = 0.002$ ). In 22 cases additional objectives were required to counteract hot or cold spots in the plan.

Figure 1 shows PTV coverage of the auto-plan vs the clinical plan and denotes the reason for manual adaptation. These adaptations had no significant effect OAR mean dose (rectum, anal sphincter) ( $p > 0.141$ ). All manual plans were made due to the presence of a hip prosthesis or bowel loop.

### Conclusion

Although, clinical plans were based on the auto-plan in 97.7% of cases, the direct acceptance rate of auto-plans, including a post-script for fine tuning, was low at 10.2%. Rescaling of MU's was the most performed adaptation, which is easily automated by adding an auto-prescribe step. Overall, the effects of plan adaptations were small and might not have been clinically relevant. These data give rise to further discussion between physicists, physicians and RTTs to provide inside into what manual adaptations would be clinically relevant. Development of automated decisions tools to identify non-optimal treatment plans may be of great value for improvement of auto-planning practice.

### OC-0182 Automated (non-coplanar) beam selection for IMRT in young female lymphoma patients reduces OAR doses

P. Cambraia Lopes<sup>1</sup>, L. Rossi<sup>1</sup>, J. Leitão<sup>1</sup>, C. Janus<sup>1</sup>, M. Van de Pol<sup>1</sup>, J. Penninkhof<sup>1</sup>, B. Heijmen<sup>1</sup>  
<sup>1</sup>Erasmus MC Cancer Institute, Radiation Oncology, Rotterdam, The Netherlands

#### Purpose or Objective

There are as many variations in tumor location, shape and size in lymphoma patients, as in radiotherapy (RT) techniques clinically applied (Maraldo et al. Int J Radiat Oncol Biol Phys 2015, 92(1):151). This population might therefore benefit from patient-specific, computer selection of beam angles. We investigated the potential dosimetric advantages of automated beam angle selection (BAS), in both coplanar (CP) and non-coplanar (NCP) settings, for young mediastinal lymphoma females, with or without involvement of supraclavicular or axillar nodes, including bulky disease.

#### Material and Methods

A total of 23 patients were included with mediastinal lymphoma disease (PTV sizes: 97cc - 1308cc, median: 495cc; median age: 26 years). Erasmus-iCycle was used to automatically generate treatment plans with/without

BAS. The applied optimization protocol as defined by the 'wish-list' containing the planning hard constraints and prioritized objectives was tailored to RT of young females, where late toxicity to breasts, heart, and lungs are of great concern. The prescription dose was 30 Gy. Coplanar (BAS-CP) and fully non-coplanar (BAS-fNCP) plans were generated (min. beams=5, max.=15), for couch and gantry angles that are possible at the treatment unit. The optimal number of beams and the most common couch positions were investigated. For a subgroup of 16 patients, CP IMRT plans were generated with the clinically used beam angles, typically 5-7 beams manually selected from (and close to) anterior and posterior directions (CLIN-CP).

### Results

BAS-CP plans with the same number of beams as the CLIN-CP plans resulted in similar OAR doses for the same PTV coverage ( $V_{95\%}=98\%$ ), but lower integral patient dose ( $V_{15Gy}$ ,  $V_{20Gy}$ ). The addition of CP beams (10 vs 5) resulted in (1) improvements in heart and lung Dmean for all patients, on average -0.7 Gy (max. -2.4 Gy), and -0.8 Gy (max. -1.6 Gy) improvement respectively; (2) decrease in lung  $V_{5Gy}$  by more than 5% for 6 patients; and (3) a decrease in patients with breast Dmean over 2 Gy (5 vs 8). BAS-fNCP plans showed further reductions in OAR doses relative to BAS-CP: (1) the average lung and heart Dmean were lower by 0.5 Gy and 0.7 Gy, respectively; (2) a decrease in heart Dmean >1 Gy was found for 8 patients (max. 2.4 Gy); (3) a decrease in lung Dmean  $\geq 1$  Gy for 5 patients (max. 1.9 Gy), along with reductions in lung  $V_{5Gy}$  ranging from 6-20%, and (4) less patients with breast Dmean over 2 Gy (3 vs 5). BAS-fNCP with 15 beams resulted in the largest differences with CLIN-CP, with improvements (mean $\pm$ SD) of -1.3 $\pm$ 1.2 Gy (max. -3.6 Gy) and -1.2 $\pm$ 0.7 Gy (max. -3.0 Gy) for the heart and lung Dmean, respectively, and 5% lower lung  $V_{5Gy}$  on average (max. 20%), while the Dmean on both breasts was <2 Gy for 15/16 for BAS-fNCP, compared to 13/16 with CLIN-CP.

	N=16 patients			N=23 patients			N=23 patients		
	CLIN-CP Mean $\pm$ SD	BAS-fNCP <sub>15beams</sub> Mean $\pm$ SD	p	BAS-CP <sub>5beams</sub> Mean $\pm$ SD	BAS-CP <sub>10beams</sub> Mean $\pm$ SD	p	BAS-CP <sub>15beams</sub> Mean $\pm$ SD	BAS-fNCP <sub>15beams</sub> Mean $\pm$ SD	p
<b>Heart</b>									
Dmean [Gy]	4.4 $\pm$ 5.2	3.1 $\pm$ 4.2	<0.001	5.5 $\pm$ 5.6	4.8 $\pm$ 5.1	<0.001	4.6 $\pm$ 5.1	3.9 $\pm$ 4.7	<0.001
<b>Lungs</b>									
Dmean [Gy]	6.9 $\pm$ 3.2	5.7 $\pm$ 2.8	<0.001	7.6 $\pm$ 3.2	6.9 $\pm$ 2.9	<0.001	6.7 $\pm$ 2.8	6.2 $\pm$ 2.8	<0.001
$V_{5Gy}$ [%]	35 $\pm$ 15	29 $\pm$ 14	<0.001	41 $\pm$ 17	37 $\pm$ 16	0.001	37 $\pm$ 16	33 $\pm$ 15	0.001
<b>Right breast</b>									
Dmean [Gy]	0.9 $\pm$ 0.7	0.8 $\pm$ 0.5	NS	1.6 $\pm$ 1.3	1.3 $\pm$ 1.1	0.006	1.3 $\pm$ 1.1	1.1 $\pm$ 0.9	0.003
<b>Left breast</b>									
Dmean [Gy]	1.2 $\pm$ 0.9	1.0 $\pm$ 0.7	NS	1.4 $\pm$ 1.1	1.4 $\pm$ 1.1	NS	1.4 $\pm$ 1.1	1.2 $\pm$ 1.1	0.01

Table. Dose metrics.

All plans normalized to PTV  $V_{95\%}=98\%$ .

p values (Wilcoxon test) are given for the differences between the two plans on the left-hand side.

Statistically non-significant (NS):  $p > 0.05$ .

### Conclusion

We successfully implemented automated planning for young female lymphoma patients. Patient-specific computer optimization of (non-coplanar) beam angles can significantly reduce doses to breast, lung and heart.

### OC-0183 Multi-Institutional Evaluation of a Pareto Navigation Guided Automated Planning Solution

P. Wheeler<sup>1</sup>, N. West<sup>2</sup>, R. Powis<sup>3</sup>, R. Maggs<sup>1</sup>, M. Chu<sup>1</sup>, R.A. Pearson<sup>2</sup>, N. Willis<sup>2</sup>, B. Kurec<sup>3</sup>, M. Youings<sup>3</sup>, D.G. Lewis<sup>1</sup>, J. Staffurth<sup>4</sup>, E. Spezi<sup>5</sup>, A.E. Millin<sup>1</sup>

<sup>1</sup>Velindre Cancer Centre, Medical Physics, Cardiff, United Kingdom; <sup>2</sup>Northern Centre for Cancer Care, Cancer Services and Clinical Haematology, Newcastle upon Tyne, United Kingdom; <sup>3</sup>Worcestershire Acute Hospitals NHS Trust, Worcestershire Oncology Centre, Worcester, United Kingdom; <sup>4</sup>Cardiff University, School of Medicine, Cardiff, United Kingdom; <sup>5</sup>Cardiff University, School of Engineering, Cardiff, United Kingdom

#### Purpose or Objective

Automated treatment planning (AP) and multi-criteria optimization via Pareto navigation (MCO) are two important innovations within the field of radiotherapy

treatment planning, with AP promising step changes in planning efficiency, and MCO enabling a more intuitive exploration of competing trade-offs. Recently a novel fully automated solution (EdgeVcc), which incorporates MCO within the calibration process, has been developed in RayStation (RaySearch Laboratories, Stockholm, Sweden) using scripting and validated in a single institutional setting. This work presents results from a further study across two independent centers for prostate cancer and aims to evaluate the use of MCO in propagating automated solutions across institutions with differing planning techniques or aims.

### Material and Methods

For each institution ( $I_A$  and  $I_B$ ) 30 previously treated prostate cancer patients were randomly allocated into a calibration cohort ( $n=10$ ) and validation cohort ( $n=20$ ). A set of planning goals, comprising of constraints and trade-offs, were defined and the MCO guided calibration process performed on a single calibration patient. MCO enabled differing treatment options to be intuitively explored, with competing trade-offs balanced according to the institutional planning aims. The resultant automated solution was tested across all calibration patients, with planning goals or trade-off balancing (via MCO) refined as required. Following successful calibration, a single automated plan (VMAT<sub>Auto</sub>) was generated fully autonomously for each patient in the validation cohort. VMAT<sub>Auto</sub> plan quality was compared against the previously treated clinical plan (VMAT<sub>Clinical</sub>) quantitatively, using a range of DVH metrics, and qualitatively through blind review by an oncologist and dosimetrist pair based at the local institution.

### Results

A summary of the quantitative and qualitative results is provided in Table 1, with example dose distributions provided in Figure 1. For both institutions automation led to statistically significant improvements across the majority of rectal dose metrics, and D98% for the low and intermediate ( $I_A$  only) dose PTVs. VMAT<sub>Auto</sub> reduced bladder doses for  $I_B$  but for  $I_A$  they were increased. There were also small differences in the conformality indices and D2% between the two techniques, with VMAT<sub>Clinical</sub> performing slightly better, however this did not prevent both institutions from demonstrating a clear preference towards VMAT<sub>Auto</sub>. Across all study patients 92.5% and 95% of VMAT<sub>Auto</sub> plans were considered equivalent or better than VMAT<sub>Clinical</sub> by the reviewing oncologist and dosimetrist respectively.

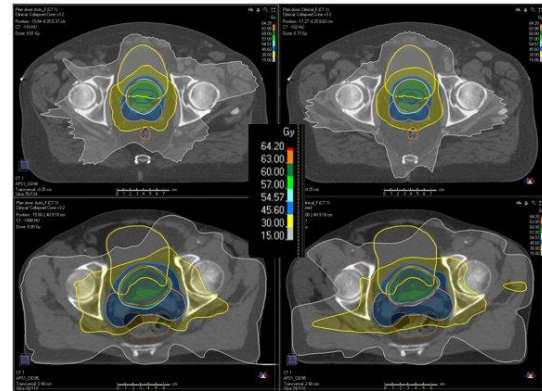


**Figure 1:** Example dose distributions for institution A (top) and institution B (bottom) with VMAT<sub>Auto</sub> to the left and VMAT<sub>Clinical</sub> to the right

### Conclusion

An MCO guided automated planning solution has been successfully validated against clinical practice in two independent institutions. The novel calibration process enabled intuitive adaptation of automated protocols to an institution's individual planning aims and yielded plans more congruent with the oncologist's clinical preference.

### OC-0184 Predicting patient specific treatment planning Pareto fronts based on anatomy only

E. Van der Bijl<sup>1</sup>, Y. Wang<sup>2</sup>, S.F. Petit<sup>2</sup>, T. Janssen<sup>1</sup>

<sup>1</sup>The Netherlands Cancer Institute, Department of Radiation Oncology, Amsterdam, The Netherlands;

<sup>2</sup>Erasmus MC Cancer Institute, Department of Radiation Oncology, Rotterdam, The Netherlands

### Purpose or Objective

Automated treatment planning is an effective solution to generate fast, consistent treatment plans on the Pareto front (PF). It leads to a single treatment plan that has a specific trade-off between conflicting objectives. Upfront knowledge of the PF will allow to direct automated planning to a plan with a non-standard trade-off tailored to the individual patient and helps with configuring new automated planning solutions. However, even with automatic planning systems a quick upfront estimate of the PF for every patient is clinically infeasible due to the large number of plans that needs to be generated. Since the PF in principle depends only on patient anatomy and delivery system, the purpose of this work is to demonstrate the feasibility of predicting the patient specific PF based only on patient anatomy since only the anatomy varies from patient to patient.

### Material and Methods

The inhouse TPS Erasmus-iCycle was used to generate 42 treatment plans for 115 prostate patients delivering 60Gy in 20 fractions (4830 treatment plans in total). Erasmus-iCycle uses a wish list of prioritized objectives and per definition generates plans on the PF. Here 42 different wish lists were used to create treatment plans on the PF spanned by rectum Dmean, the homogeneity (parameterized by PTV-Dmax) and the conformity, defined as the Dmax at 1cm distance to the PTV. All plans were normalized such that PTV D99% = 95%. First, for all patients the obtained PFs were parameterized using three parameters per patient that were estimated using least squares fitting. Then, patient specific features were selected to predict the parameters of the PF based on patient anatomy, using support vector regression with radial basis function kernels. The features were the proportion of the rectum and average area of the patient outline at the slices of the PTV, the volumes of PTV and rectum and the radii corresponding to 1,10, 50, 90 and 99% overlap of the PTV-rectum overlap volume histograms. The model was trained on 80% of the patients

**Table 1** Dosimetric comparison of VMAT<sub>Auto</sub> and VMAT<sub>Clinical</sub> for Institution A and B (mean  $\pm$  standard deviation). Results in bold indicate statistically significant differences ( $p < 0.05$ ). Dosimetrist plan rankings are provided in parenthesis where preference differs from the oncologist

Metric	Institution A		Institution B		
	VMAT <sub>Auto</sub>	VMAT <sub>Clinical</sub>	VMAT <sub>Auto</sub>	VMAT <sub>Clinical</sub>	
PTV60	D98% (Gy)	58.8 $\pm$ 0.1	59.0 $\pm$ 0.2	59.0 $\pm$ 0.1	58.7 $\pm$ 0.3
	D2% (Gy)	61.3 $\pm$ 0.1	60.8 $\pm$ 0.3	61.0 $\pm$ 0.1	60.9 $\pm$ 0.4
	CI	0.56 $\pm$ 0.03	0.57 $\pm$ 0.04	0.60 $\pm$ 0.03	0.64 $\pm$ 0.04
PTV57.5	D98% (Gy)	55.9 $\pm$ 0.1	55.5 $\pm$ 0.9	55.7 $\pm$ 0.2	54.7 $\pm$ 0.2
	D2% (Gy)	59.9 $\pm$ 0.1	60.2 $\pm$ 0.4	60.3 $\pm$ 0.13	60.1 $\pm$ 0.5
	CI	0.56 $\pm$ 0.06	0.59 $\pm$ 0.09	0.55 $\pm$ 0.07	0.55 $\pm$ 0.08
PTV48	D98% (Gy)	46.5 $\pm$ 0.3	45.8 $\pm$ 0.5	46.5 $\pm$ 0.2	45.5 $\pm$ 0.7
	D2% (Gy)	57.0 $\pm$ 0.4	57.3 $\pm$ 0.9	57.2 $\pm$ 0.3	56.5 $\pm$ 0.9
	CI	0.71 $\pm$ 0.02	0.75 $\pm$ 0.03	0.70 $\pm$ 0.02	0.68 $\pm$ 0.04
Rectum	V24.5Gy (%)	47.2 $\pm$ 13.0	62.3 $\pm$ 10.4	51.9 $\pm$ 11.6	60.3 $\pm$ 10.3
	V40.5Gy (%)	23.0 $\pm$ 9.1	26.5 $\pm$ 8.9	28.2 $\pm$ 8.8	29.7 $\pm$ 8.4
	V52.7Gy (%)	9.5 $\pm$ 2.8	10.4 $\pm$ 3.8	10.1 $\pm$ 3.0	10.4 $\pm$ 3.9
	V60.0Gy (%)	0.0 $\pm$ 0.0	0.3 $\pm$ 0.4	0.0 $\pm$ 0.1	0.3 $\pm$ 0.4
	DMean (Gy)	25.3 $\pm$ 4.7	29.0 $\pm$ 4.3	28.3 $\pm$ 4.1	30.1 $\pm$ 3.3
Bladder	V40.5Gy (%)	25.3 $\pm$ 14.7	24.0 $\pm$ 14.1	15.5 $\pm$ 7.4	16.4 $\pm$ 7.4
	V60.0Gy (%)	1.8 $\pm$ 1.6	2.3 $\pm$ 1.7	1.2 $\pm$ 0.9	1.1 $\pm$ 0.8
	DMean (Gy)	24.3 $\pm$ 9.3	23.8 $\pm$ 9.2	17.4 $\pm$ 5.3	18.7 $\pm$ 5.7
Beam MU	MU	636.5 $\pm$ 35.8	570.0 $\pm$ 36.7	739 $\pm$ 53	640 $\pm$ 118
Plan Ranking vs	Plans Superior (%)	90%		65%	
VMAT <sub>Clinical</sub>	Plans Equivalent (%)	0%		30% (35%)	
Plans Inferior (%)		10%		5% (0%)	

PTV suffix indicates prescribed dose in Gy.

CI: Paddick's Conformity Index for the specified PTV.

using a train-test split approach and validated on the remaining 20%. The performance of the predictions is scored using the rms difference of the actual versus the predicted rectum Dmean for given homogeneity and conformity.

**Results**

Observed rectum-Dmean values ranged 5-28 Gy over all plans and patients. Ranges for the homogeneity and conformity were 97-108%, 69-94% of the prescribed dose, indicating that we sampled a large part of the PF. The PFs could be described well using the 3 parameter parametrization (rms difference of 0.9 Gy in the rectum-Dmean direction), see Figure 1. The model led to an excellent prediction of the patient specific PF, the rms difference between the fit and the prediction was 0.5 Gy. The rms difference to the actual value was 1.1 Gy.

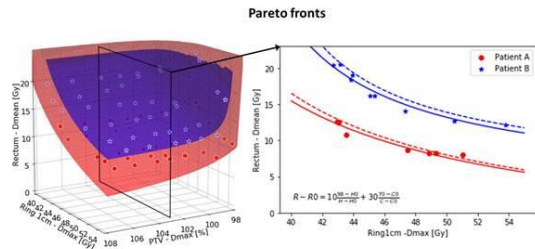


Figure 1: Pareto fronts for two patients in the validation set. The left panel shows the 3D distribution of plans and the surfaces. The right panel is the slice through the fronts at constant homogeneity (H = PTV-Dmax = 103%). The points corresponds to treatment plans with H in range 102%-104%. The Pareto fronts are parameterized by the equation with R0, H0 and C0 the patient-specific fit parameters and R and C the rectum Dmean and conformity respectively in percentage of the prescribed dose. Solid lines represent the fit to the data, the dashed lines is the predicted Pareto front based on the delineations only.

**Conclusion**

We successfully demonstrated that that patient specific PF could be predicted based on patient anatomy only, for a relatively simple site as the prostate.

**OC-0185 A multi-centre knowledge-based treatment planning model for radiotherapy of cervical cancer**

E. Adams<sup>1</sup>, M. Hussein<sup>2</sup>, S. Currie<sup>3</sup>, C. Thomas<sup>4</sup>, C. South<sup>1</sup>, A. Greener<sup>4</sup>, G. Currie<sup>3</sup>, A. Nisbet<sup>1</sup>

<sup>1</sup>Royal Surrey County Hospital NHS Foundation Trust, Radiotherapy Physics, Guildford, United Kingdom;

<sup>2</sup>National Physical Laboratory, Medical Radiation Physics, Teddington, United Kingdom ; <sup>3</sup>NHS Greater Glasgow and Clyde, Radiotherapy Physics, Glasgow, United Kingdom ;

<sup>4</sup>Guy's and St Thomas' NHS Foundation Trust, Radiotherapy Physics, London, United Kingdom

**Purpose or Objective**

There can be significant resource requirements in the initial setting up of Knowledge Based Treatment Planning (KBP) models for different treatment sites, particularly as the models depend on a sufficiently sized library of clinically acceptable plans. This can be a barrier for centres with a small number of patients and in rarer clinical sites. Sharing between cancer centres may overcome these issues. The purpose of this work was to address two key questions; whether a KBP model developed in one institution could be successfully used in another; and whether combining the expertise of the different institutions could lead to an improved model. These questions were addressed for the case of cervical cancer VMAT planning in the UK RapidPlan consortium (UKRC) of centres using Varian RapidPlan KBP.

**Material and Methods**

An RP model from one of the UKRC centres, C1, was selected for multi-centre testing. This model had been fully developed and benchmarked for planning cervical cancer cases using VMAT, including both post-hysterectomy and intact uterus cases, with prescribed doses of 45-50.4Gy in 1.8Gy/#. This model (Model<sub>C1</sub>) was shared with two other UKRC centres, C2 and C3, who used the model to generate plans for fourteen patients who had

previously been treated in their respective hospitals. The Model<sub>C1</sub> plans were compared to the clinical plans using the respective local plan acceptance; for C2, the clinical plans had been generated using their own validated in-house RP model; for C3 they were generated using template-based optimisation.

Based on the feedback and learning experience of the model comparisons, further refinements to the Model<sub>C1</sub> parameters were tested. Model<sub>C1</sub> and the refined models were evaluated for ten patients from C1 using a single optimisation without user interaction. The resultant plans were compared using a consensus set of plan acceptance criteria which incorporated the different metrics used in each of the three centres.

**Results**

Initial testing of Model<sub>C1</sub> compared to clinical plans from centres C2 & C3 showed improvements in OAR sparing at higher dose levels, but increased doses at lower dose levels, with higher mean doses for bladder and rectum in Model<sub>C1</sub> compared to clinical plans. Two different approaches (Model<sub>UKRC1</sub> and Model<sub>UKRC2</sub>) to addressing the potential areas for improvement were taken. Both gave statistically significant improvements in OAR sparing, but for Model<sub>UKRC1</sub>, this was at the expense of PTV coverage and homogeneity (see Table 1). However, Model<sub>UKRC2</sub> was able to achieve similar OAR dose reductions with only minimal impact on PTV doses (see Fig 1).

		Mean ± standard deviation			p-value		
		Model <sub>C1</sub>	Model <sub>UKRC1</sub>	Model <sub>UKRC2</sub>	UKRC1 vs C1	UKRC2 vs C1	UKRC2 vs UKRC1
PTV	D99% (%)	94.5 ± 0.4	91.8 ± 0.3	93.9 ± 0.4	0.01	0.01	0.01
	D95% (%)	96.1 ± 0.3	94.2 ± 0.4	95.8 ± 0.3	0.01	0.005	0.01
	D5% (%)	103.2 ± 0.4	105.0 ± 0.5	103.6 ± 0.4	0.01	0.01	0.01
	D2% (%)	104.1 ± 0.6	106.1 ± 0.6	104.4 ± 0.5	0.01	0.01	0.01
Bladder	D50% (Gy)	45.7 ± 3.1	45.2 ± 3.8	45.1 ± 3.9	-	0.01	-
	V50.4Gy (%)	0.6 ± 1.2	1.5 ± 2.1	0.8 ± 1.5	0.03	0.04	0.03
	V35Gy (%)	89.3 ± 11.3	82.4 ± 13.8	82.8 ± 13.9	0.01	0.01	-
	V40Gy (%)	76.2 ± 15.4	71.4 ± 16.1	72.0 ± 17.0	0.02	0.01	-
Rectum	V50Gy (%)	0.7 ± 1.1	1.6 ± 2.0	1.0 ± 1.6	0.01	0.04	0.04
	V30Gy (%)	61.6 ± 28.2	60.6 ± 27.4	60.8 ± 27.4	0.01	0.04	-
	V35Gy (%)	57.8 ± 24.8	56.3 ± 24.5	56.5 ± 24.2	0.01	0.04	-
	V45Gy (%)	42.3 ± 24.6	39.8 ± 23.7	41.2 ± 24.0	0.01	0.04	0.01
Bowel	D50% (Gy)	46.8 ± 2.1	45.4 ± 1.6	46.5 ± 2.3	-	0.05	-
	D60% (Gy)	45.4 ± 3.2	44.0 ± 2.9	44.9 ± 3.7	0.01	0.05	0.03
	D30% (Gy)	35.5 ± 10.9	33.3 ± 10.3	34.0 ± 10.7	0.01	0.01	0.07
	V15Gy (cm <sup>3</sup> )	683 ± 291	690 ± 290	689 ± 292	-	0.01	-
Right femoral head	V25Gy (cm <sup>3</sup> )	547 ± 262	513 ± 240	524 ± 249	0.02	0.06	0.09
	V45Gy (cm <sup>3</sup> )	159 ± 84	146 ± 68	152 ± 77	0.05	0.04	-
	V50.4Gy (cm <sup>3</sup> )	5.2 ± 8.5	9.6 ± 10.7	7.7 ± 12.0	0.01	0.01	0.09
	D15% (Gy)	32.1 ± 3.8	33.0 ± 3.1	32.4 ± 3.1	-	-	-
Left femoral head	D50% (Gy)	23.7 ± 2.9	26.0 ± 2.2	24.1 ± 1.7	0.01	-	0.02
	Dmax (Gy)	44.3 ± 3.5	44.7 ± 3.5	44.8 ± 3.4	-	-	-
	D15% (Gy)	35.2 ± 6.6	33.9 ± 3.8	32.7 ± 3.9	-	-	0.03
	D50% (Gy)	27.6 ± 8.3	26.5 ± 2.3	24.9 ± 2.1	0.09	-	0.01
Bone marrow	Dmax (Gy)	46.3 ± 3.9	45.7 ± 3.9	44.8 ± 4.0	-	-	-
	Dmean (Gy)	30.7 ± 2.2	29.7 ± 2.3	30.0 ± 2.1	0.01	0.005	0.07
	V10Gy (%)	91.9 ± 4.4	92.6 ± 4.5	92.4 ± 4.3	0.08	0.06	-
	V20Gy (%)	74.2 ± 5.3	75.8 ± 5.8	75.1 ± 5.0	0.01	0.03	-

Table 1: Summary of average dose-volume statistics for different models. p-values are based on the Wilcoxon signed-rank test

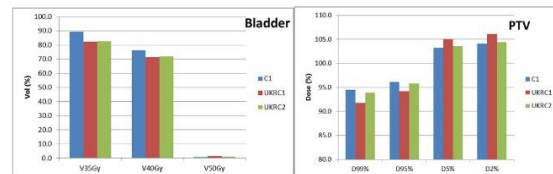


Fig. 1: Dose/volume statistics for bladder and PTV

**Conclusion**

Combining experience from multiple centres allowed the generation of a RapidPlan model for cervical cancer patients which gave improved results compared to single-institution models.

**Proffered Papers: PH 4: Proffered paper: New technologies**

**OC-0186 A system of materials capable of mimicking soft tissues and bone with both CT and MR imaging.**

K. Singhrao<sup>1</sup>, J. Fu<sup>1</sup>, Y. Gao<sup>2</sup>, P. Hu<sup>2</sup>, Y. Yang<sup>1</sup>, J.H. Lewis<sup>1</sup>  
<sup>1</sup>University of California Los Angeles, Radiation Oncology, Los Angeles, USA; <sup>2</sup>University of California Los Angeles, Radiology, Los Angeles, USA

### Purpose or Objective

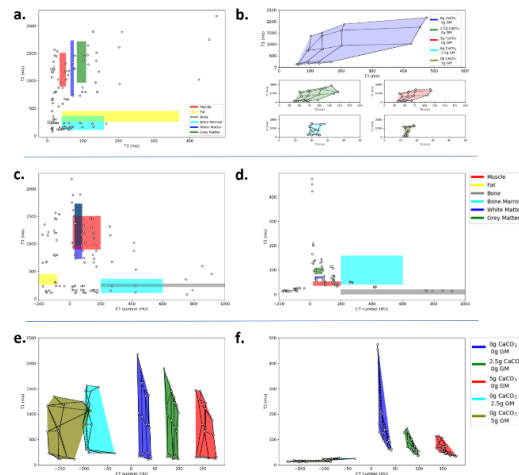
To develop a system of easily made and formed materials with adjustable T1 and T2 relaxation times, and x-ray attenuation properties for mimicking soft tissues and bone in both CT and MR imaging. The growing role of MR in radiotherapy has increased the demand for phantoms capable of cross-modality quality assurance or end-to-end testing. Most commercially available materials and phantoms do not mimic the T1 and T2 relaxation times, and CT numbers for different tissue types simultaneously on both modalities. Producing materials with the capability of producing tissue mimicking contrast on both modalities allows a ground truth to be established for validating a number of medical imaging and therapeutic applications such as MR-CT image registration and each component of MR-only radiotherapy workflows.

### Material and Methods

The effects on T1 and T2 relaxation times, and CT number were measured using a range of concentrations Gd contrast (0 - 250  $\mu\text{mol/g}$ ), agarose (0 - 4 g), glass microspheres (GMs) (0 - 5 g) and  $\text{CaCO}_3$  (0 - 25 g) in a common carrageenan-water gelatinizer. Samples were prepared with the additives, 1.5 g carrageenan and water to weigh a total of 50 g. Samples were imaged in a tissue validation phantom. Each tissue validation phantom contained 20 samples with fixed concentration of  $\text{CaCO}_3$  or GMs. MR images were acquired on a 3T Siemens Skyra and CT images were acquired on a Siemens Somatom. T1 and T2 relaxation time maps were generated using voxel-wise inversion recovery and spin echo signal fitting. A multivariate linear regression-based model (based on fitted coefficients) was generated to predict T1 and T2 relaxation times and CT number based on the concentrations of the 4 additives. Skeletal muscle, adipose tissue, white matter, gray matter, liver, prostate, bone marrow, glandular breast and trabecular bone tissues were mimicked to validate the fit model results and demonstrate the flexible range of values attainable with this system of materials.

### Results

Figure 1(a,c,d) demonstrates that the carrageenan-based system of materials can span a range of T1 values from 82 ms to 2180 ms, T2 values from 12 ms to 475 ms and CT numbers from -117 HU to 914 HU. Figure 1(b,e,f) demonstrates that the addition of 10%  $\text{CaCO}_3$  decreases the maximum T1 range by 36% and maximum T2 range by 83%. Addition of 10% glass microspheres decreases the maximum T1 range by 41% and maximum T2 range by 99%. Using the fit model, we were able to mimic the T1, T2 and CT numbers well compared to literature reported in vivo measurements (Table 1).



Tissue type	a. Tissue mimicking material composition				b. Phantom material measurements				c. Literature reported in vivo measurements		
	Gd (mmol/kg)	Agarose (w/w%)	$\text{CaCO}_3$ (w/w%)	GMs (w/w%)	T1 (ms)	T2 (ms)	CT number (HU)	T1 (ms)	T2 (ms)	CT number (HU)	
Muscle	0.0	1	0	0	1,160 ± 21	215 ± 8	20 ± 9	1,020 ± 18	180 ± 10	37 ± 1	
White Matter	0.0	1	0	0	1,020 ± 61	18 ± 20	21 ± 11	1,020 ± 80	21 ± 8	28	
Gray Matter	0.0	1	0	0	1,020 ± 7	87 ± 1	30 ± 3	1,080 ± 10	81 ± 8	31	
Liver	0.0	1	0	0	1,390 ± 10	161 ± 8	30 ± 10	1,390 ± 10	161 ± 8	30 ± 10	
Prostate	0.0	1	0	0	1,080 ± 10	215 ± 8	21 ± 8	1,020 ± 10	180 ± 10	30 ± 10	
Glandular breast	0	0.1	0	0	1,050 ± 10	21 ± 8	20 ± 8	1,080 ± 100	20 ± 8	181 ± 101	
Fat (noncontrast)	1.0	1	0	0	108 ± 10	11 ± 1	-111 ± 19	108 ± 10	68 ± 8	-16.70 ± 6.6	
Bone Marrow	0.0	0.1	1	0	400 ± 11	45 ± 8	22 ± 8	382 ± 10	11 ± 1 ± 2	70 ± 2 ± 3	
Trabecular Bone	0.0	0	0	0	1,027 ± 14	46 ± 2	102 ± 19	1,080 ± 22	11 ± 1 ± 2	100 ± 10	

### Conclusion

We have created a system of carrageenan-based materials capable of simultaneously producing tissue-like contrast for a wide range of human tissues in 3.0T MR and CT imaging. The materials can be cast and formed in the shapes of organs to create anthropomorphic phantoms.

### OC-0187 Comparison of proton range predictions between Single- and Dual-Energy CT using prompt gamma imaging

T. Boon-Keng<sup>2</sup>, Y. Xie<sup>1</sup>, F. O'Grady<sup>2</sup>, A. Lalonde<sup>3</sup>, J. Petzoldt<sup>4</sup>, J. Smeets<sup>4</sup>, G. Janssens<sup>4</sup>

<sup>1</sup>Massachusetts General Hospital, Department of Radiation Oncology, Boston, USA; <sup>2</sup>University of Pennsylvania, Department of Radiation Oncology, Philadelphia, USA; <sup>3</sup>University of Montreal, Department of Physics, Montreal, Canada; <sup>4</sup>Ion Beam Applications, Research, Louvain-la-Neuve, Belgium

### Purpose or Objective

Dual-energy CT (DECT) has been shown to be more accurate for predicting proton stopping power ratios (SPR) than traditional single-energy CT (SECT) calibrations in both surrogate and animal tissue phantoms. Prompt gamma imaging (PGI) is an in vivo imaging modality that has been used to demonstrate the feasibility of proton range verification. In this study, PGI was used to quantify the accuracy of SPR calibration from different CT modalities in a pelvic phantom.

### Material and Methods

Three sets of CT scans were obtained with the Rando phantom using a Siemens Definition Edge CT scanner: 1) 120 kVp SECT; 2) 80/140 kVp sequential DECT scan (SQCT); and 3) 120 kVp Twin-beam scan with Ti/Au dual filter (TBCT). The HU-to-SPR calibration curves were established using the stoichiometric method on SECT and the Eigen tissue decomposition method on DECT scans. Two pencil beam scanning proton plans were created: one with two iso-energy layers and one to cover an artificially drawn target mimicking a prostate treatment. Both plans

were first optimized on SECT then forward calculated on the DECT images. The 1D knife-edge prompt gamma camera system was used to measure the prompt gamma signal profile emitted during the proton beam delivery on a spot by spot basis in pencil beam scanning mode. The shifts in proton range were derived by comparing the recorded PGI profiles with simulations on the different CT images. Aggregation with nearby spots (4 and 8 mm radius) was applied to reduce statistical uncertainty of the retrieved shifts. The calculated range shift detected by the PGI camera was first calibrated on a rectangular water phantom to determine the systematic offset of the PGI system which was then applied to the Rando phantom studies.

**Results**

Figure 1 shows the retrieved proton range shifts with a two iso-energy layer proton plan. The median spot shifts for a 4mm spot aggregation were 6.8 mm/2.7 mm for SECT, 3.3 mm/1.6 mm for SQCT, and -3.3 mm/-4.9 mm for TBCT for 190 MeV (range= 23.8 cm water) and 205 MeV (range= 27.1 cm water) protons respectively.

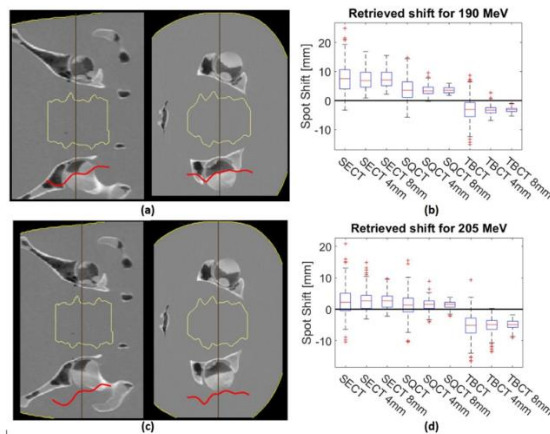


Figure 1: The proton range verification measurements on Rando phantom with two iso-energy layers. Top row figures are for the 190 MeV protons: (a) simulated Bragg peak location (red curve) on SECT (coronal and axial views) and (b) retrieved range shifts for the three CT calibrations (SECT, SQCT, and TBCT). Bottom row (c) and (d) are the corresponding plots for 205 MeV protons. Aggregation with nearby spots (4 and 8 mm radius) was applied to reduce statistical uncertainty of the retrieved shifts.

Figure 2 compared the retrieved shifts for a prostate plan obtained with simulations on three different CT calibrations. For all the layers within the camera’s field of view (FOV), SQCT calibration yielded the best agreement with measurements compared to SECT or TBCT.

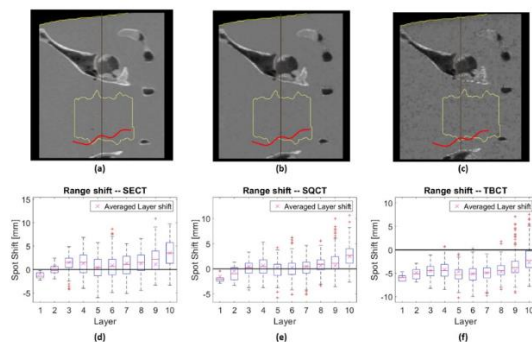


Figure 2: The range verification results comparison among three CT calibrations obtained with Rando phantom. The top row from left to right are the calculated Bragg peak position of one energy layer (red curve) on (a) SECT; (b) sequential DECT scan (SQCT); and (c) simultaneous DECT scan with Twin-beam (TBCT). The bottom row are the retrieved shifts in proton ranges for (d) SECT, (e) SQCT, and (f) TBCT. Only results of energy layers within the camera FOV are plotted.

**Conclusion**

Among the different CT calibrations, the sequential DECT

scan has the highest accuracy in proton range predictions, compared to the Twin-beam DECT method and traditional SECT calibration.

**OC-0188 Development and commissioning of a set-up optimization routine for ocular proton therapy**

G. Elisei<sup>1</sup>, R. Via<sup>2</sup>, A. Pella<sup>1</sup>, G. Calvi<sup>4</sup>, R. Ricotti<sup>1</sup>, B. Tagaste<sup>1</sup>, G. Fontana<sup>1</sup>, M.R. Fiore<sup>3</sup>, M. Ciocca<sup>6</sup>, F. Valvo<sup>5</sup>, G. Baroni<sup>1,2</sup>

<sup>1</sup>Centro Nazionale di Adroterapia Oncologica CNAO, Clinical Department- Bioengineering Unit, Pavia, Italy ;

<sup>2</sup>Center for Proton Therapy, Paul Scherrer Institut, Switzerland ;

<sup>4</sup>Centro Nazionale di Adroterapia Oncologica CNAO, Particle Accelerator Department, Pavia, Italy ;

<sup>5</sup>Centro Nazionale di Adroterapia Oncologica CNAO, Clinical Department, Pavia, Italy ;

<sup>6</sup>Centro Nazionale di Adroterapia Oncologica CNAO, Clinical Department- Medical Physics Unit, Pavia, Italy ;

<sup>7</sup>Politecnico di Milano, Department of Electronics Information and Bioengineering, Milano, Italy

**Purpose or Objective**

Proton therapy is an effective therapeutic option in the treatment of ocular melanomas. Treatment plan is optimized by defining two patients gazing angles (polar and azimuthal) and a brass collimator is used to shape the beam. The patient actively participates in the treatment by fixating a light source, prepositioned according to the treatment plan prescription. At our facility, the fixation light is embedded in an eye tracking (ETS) device which also features optical cameras for eye motion monitoring. The device is mounted on a dedicated robotic arm to guarantee the utmost precision and repeatability in ETS positioning. The system setup is depicted in Figure 1 (a). The close distance between the collimator and the treatment isocenter (7cm) makes for a complicated and sensible treatment setup, particularly considering that the patient wears eyelid retractors and an immobilization mask. Thus, an optimization of the ETS position is required to guarantee a fixation point consistent with the treatment plan while avoiding collisions with collimator and the patient and obstruction of the beam path. In this study we present the development and commissioning of a software application designed to optimize at a patient specific level the ETS position during treatment geometry planning.

**Material and Methods**

The ETS position optimizer is built on a three-dimensional rendering of the treatment setup including all elements: fixed (collimator holder), patient-specific (beam path and patient immobilization mask) and moving (ETS). For each gaze direction, the optimizer evaluates more than 600 ETS positions, consistent with the patient’s gazing angles, and select the one that maximizes distances and avoids collisions between all elements of the setup. To evaluate the capability of properly modelling the treatment scenario (Figure 1(b)), we have used the isocentric stereoscopic X-ray imaging system installed in the treatment room. The ETS and the thermoplastic mask were fitted with radiopaque beads and their 3D position, estimated with the optimizer, was compared to the one measured using radiographies. Errors in the optimizer model was quantified in terms of deviation from the planned gazing angles. The analysis was performed on 11 patients treated between Oct 2017 and Jul 2018, using their specific masks and treatment plans.

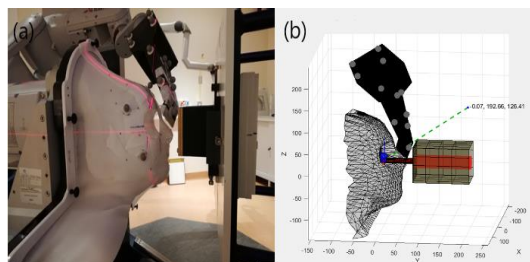


Figure 1: Treatment setup for ocular proton therapy (panel a); Modeling of treatment setup by software application (panel b).

## Results

Results are reported in Table 1. Three-dimensional errors were, on average,  $1.34 \pm 0.19$  mm and  $1.54 \pm 0.35$  mm for the ETS and the mask respectively. These uncertainties propagated into a maximum angular deviations of the fixation direction given to the patient by  $0.6^\circ$ , with an average of  $0.26^\circ$ .

Table 1: Three-dimensional discrepancies between measured and estimated ETS and mask positions. The corresponding deviations from the planned gazing angles are shown.

Patients	3D errors (mm)				Angular deviation ( $^\circ$ )	
	ETS		MASK		Polar	Azimuthal
	mean	std	mean	std		
Patient 1	1.49	0.31	1.63	0.34	0.54	0.19
Patient 2	1.14	0.20	1.34	0.24	0.46	0.60
Patient 3	1.48	0.27	2.17	0.34	0.26	0.03
Patient 4	1.08	0.19	1.02	0.22	0.06	0.10
Patient 5	1.37	0.18	1.34	0.27	0.05	0.26
Patient 6	1.45	0.12	1.74	0.49	0.11	0.14
Patient 7	1.17	0.14	2.14	0.77	0.35	0.50
Patient 8	1.44	0.12	1.45	0.28	0.13	0.43
Patient 9	1.40	0.17	1.03	0.21	0.18	0.36
Average	1.34	0.19	1.54	0.35	0.24	0.29

## Conclusion

The ETS position optimizer is capable of estimating the treatment setup on a geometrical level with errors lower than 1.5 mm. This translates into a deviation to the planned gazing angles below the threshold of clinical significance ( $1^\circ$ ). The proposed method automatically suggests the optimal treatment set-up geometry for a swifter treatment workflow and improved patient safety.

## OC-0189 Brain and Head-and-Neck MRI in immobilization masks: a novel and practical setup for radiotherapy

S. Mandija<sup>1</sup>, F. D'Agata<sup>1</sup>, R. Navest<sup>1</sup>, A. Sbrizzi<sup>1</sup>, C. Raaymakers<sup>1</sup>, R. Tijssen<sup>1</sup>, M. Philippens<sup>1</sup>, E. Seravalli<sup>1</sup>, J. Verhoeff<sup>1</sup>, J. Lagendijk<sup>1</sup>, C. Van den Berg<sup>1</sup>  
<sup>1</sup>UMC Utrecht, Radiotherapy, Utrecht, The Netherlands

### Purpose or Objective

In radiotherapy (RT), it is essential to perform the MRI and CT exams in treatment position. For this purpose and to minimize inter/intra-fraction movement, thermoplastic immobilization masks are used for brain/head and neck (HN) RT. However, standard immobilization masks are incompatible with diagnostic MR head/neck coils. As a compromise, flexible surface coils are adopted despite their technician dependent positioning and inferior signal-to-noise-ratio (SNR) compared to head/neck coils (2-channel vs. the 17-channel for head/neck receive coil). This leads to relatively poor image quality and reproducibility. Here, we explore the feasibility and performance of a new immobilization setup for brain/HN RT, redesigned to fit into the diagnostic head/neck MR coils thereby boosting MR image quality and reproducibility.

### Material and Methods

MR images were acquired on 2 volunteers using a 3T Ingenia MRI (Philips Healthcare, Best, The Netherlands).

The standard and the new RT setups are presented in Fig.1. Several comparative tests were performed.

- **Image quality test:** 3D T1w TFE, 3D T2w TSE FLAIR and 2D T2w TSE scans were acquired for brain, for neck 2D T1w TSE and 2D T2w TSE mDIXON scans were acquired.
- **SNR test:** SNR maps were computed from a T1w scan (2 dynamics, the second being a noise scan) as in (Kellman P., et al. *MRM* (2005)54:1439-47).
- **Motion restriction test:** the maximum motion in the feet-head/left-right directions was estimated from 2D cine-MR T1w bFFE acquisitions (300 dynamics) using Optical Flow (Zachiu C., et al. *Phys Med Biol* (2015)60:9003-29).
- **Inter-fraction repositioning test:** two high resolution 3D T1w sequences were acquired for each setup. Between acquisitions, the immobilization mask was removed and the subject was asked to move to mimic two different MRI sessions. The mean and the standard deviation of the subject movement between each pair of MR acquisitions were computed using Optical Flow as a proxy of the reproducibility of inter-fraction repositioning.

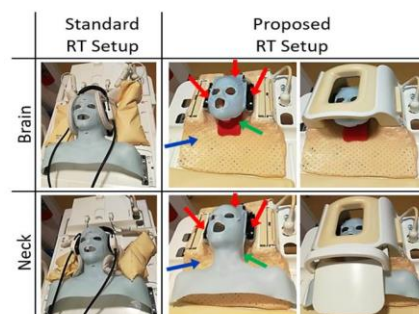


Fig. 1. **The standard RT setup:** individualized five-points head-and-shoulder mask fixated to the MRI flat table top and two MR flexible surface receive coils. **The new RT setup:** individualized three-points mask (for brain) or three-points head-and-shoulder mask (for neck) inside the head/neck coils. A new fixation thermoplastic base (blue arrow) hosting the anchor points (red arrows) for the immobilization masks was created to perfectly fit the head/neck MR coils. A neck support (same of the one used in the standard RT setup) is also integrated (green arrow), which can be made patient-specific. The new setup can be used for both 1.5T and 3T scanners given the same geometry for the base of the head/neck MR coils.

## Results

Brain images acquired with the standard RT coil setup had an inferior diagnostic quality compared to the new setup, especially for the FLAIR contrast (inferior sensitivity in detecting small lesions) (Fig. 2). For neck regions, the image quality was comparable between setups. The proposed setup allowed between 2 and 3 times higher SNR values for both brain/HN MRI (not shown - limited Fig. number).

Comparable motion restriction in the feet-head/left-right directions (maximum motion = 1 mm) and comparable repositioning accuracy (mean inter-fraction movement  $1 \text{ mm} \pm 0.5 \text{ mm}$ ) were observed for the standard and the new setup.

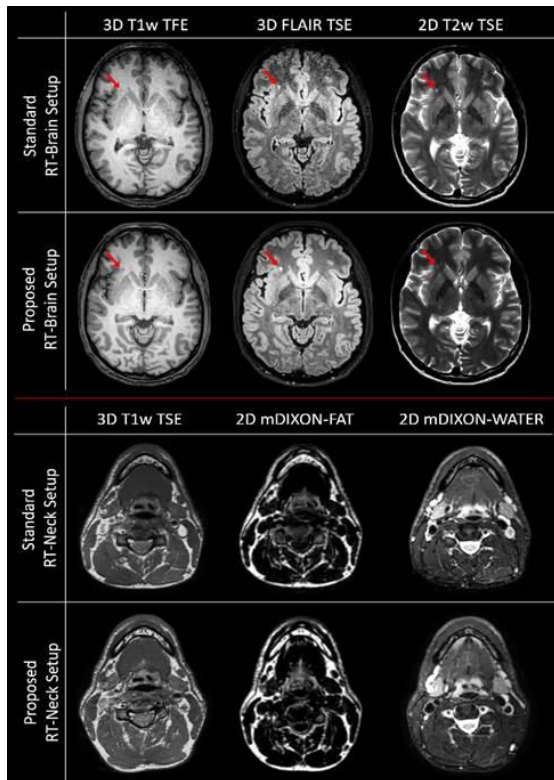


Fig. 2. Image quality comparison for the standard and the proposed RT brain/neck setups. The red arrow points to a white matter lesion.

### Conclusion

We integrated a fixation mask in the diagnostic head/neck MR coils. The proposed setup has several advantages: diagnostic image quality in RT treatment position, high SNR, homogenous signal, restricted motion (1 mm) and accurate inter-fraction repositioning. Translation of the new setup to the treatment table will be investigated.

### OC-0190 Development of Compton-scattered imaging technology for stereotactic radiotherapy of lung cancer

J. Chu<sup>1</sup>, K. Jones<sup>1</sup>, J. Strologas<sup>1</sup>, G. Redler<sup>2</sup>, G. Marwaha<sup>1</sup>, J. Turian<sup>1</sup>

<sup>1</sup>Rush University Medical Center, Department of Radiation Oncology, Chicago IL, USA; <sup>2</sup>University of Chicago, Department of Radiation Oncology, Chicago IL, USA

### Purpose or Objective

Compton scatter is a natural by-product of external beam radiation therapy. The scattered radiation contains information about the patient anatomy and the transient tumor location. Our previous geometrical phantom and computer simulation studies have demonstrated the potential of Compton-scattered imaging for monitoring lung tumor locations during stereotactic ablation radiation therapy (SABR). In preparation for an IRB-approved patient study, we now present experimental results from a new collimator with anthropomorphic and dynamic phantoms.

### Material and Methods

A pinhole collimator was constructed for the study. As seen in Fig 1, the collimator consists of 3 main components, with a wall thickness that can range from 7.6 to 34.7 mm lead equivalent when combinations of different components are used. Spherical tumors (2.1-2.9 cm diameter) embedded in an anthropomorphic LUNGMAN

phantom (Kyoto Kagaku Co.) and another spherical tumor of 3 cm diameter in a QUASAR respiratory motion phantom (Modus Medical Devices Inc.) were irradiated by 6 MV FFF beams from a Varian TrueBeam linear accelerator. The QUASAR phantom was programmed to move sinusoidally at 15 breaths per minute (0.25 Hz) over  $\pm(1.5-2)$  cm to simulate breathing motion. Experimental scatter images were acquired with a 550  $\mu\text{m}$  thick CsI scintillator detector and a pinhole collimator. Tumor centroid locations were measured from various scatter images and compared with the expected values. Contrast-to-noise ratio (CNR) of embedded tumors was calculated for test images to assess their potential for tracking tumor location during treatment.

### Results

The imaging system successfully acquired various phantom images over exposure of 2-1000 MU, or 0.1-50 second time scales. While the lung tumor was discernible for all anthropomorphic phantom images, the image quality improved with increasing collimator thickness. For example, the CNR increased by a factor of 3.6 at 10 MU over the range of collimator thickness studied. The measured tumor centroid locations agreed with the expected values for images from the QUASAR phantom. As shown in Fig 2, the root-mean-squared error (RMSE) for tumor tracking was 0.7-0.9 mm when the phantom was irradiated at 1200 MU/min with an image integration time of 300 ms/frame. As expected, RMSE improved with image integration time, reaching 0.6 mm with 600 ms/frame.

### Conclusion

This study on anthropomorphic and dynamic phantoms confirms the feasibility of using scatter imaging to track lung tumor movement during SABR treatments. The potential benefits may include real-time image guidance in 3D without additional radiation. With the IRB approval of patient studies, we are optimistic that this emerging technology will contribute to improved accuracy and workflow for this highly successful treatment modality.

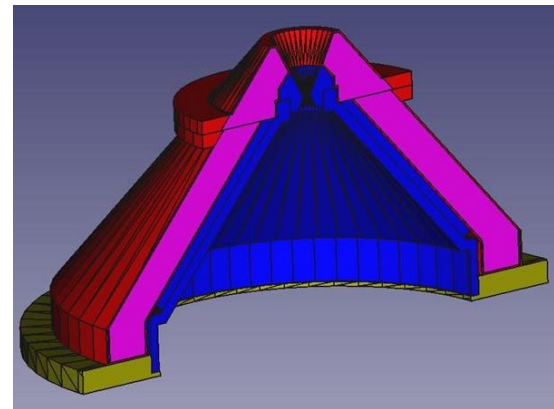


Fig. 1 Cross section of pinhole collimator. Selected shell components can be removed to allow effective wall thickness of 7.6 to 34.7 mm Pb equivalence.

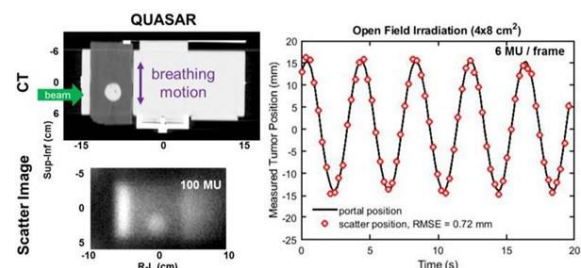


Fig. 2 (left, top): QUASAR phantom CT (coronal slice). (left, bottom) Static scatter image for 100 MU. (right): The scatter image measured position is compared to the true position measured by portal imaging. As shown above, a 3 cm diameter tumor was tracked with a root-mean-squared error (RMSE) of 0.7-0.9 mm for 300 ms (6 MU) frame integration.

**OC-0191 MLC-tracking latencies on Elekta Unity**

M. Glitzner<sup>1</sup>, P. Woodhead<sup>1</sup>, J. Lagendijk<sup>1</sup>, B. Raaymakers<sup>1</sup>

<sup>1</sup>UMC Utrecht, Department of Radiotherapy, Utrecht, The Netherlands

**Purpose or Objective**

Compared to previous guidance techniques, on-line MRI-guidance promises imaging during radiation and superior soft-tissue contrast. MR-images can be acquired in physiologically relevant frequencies and with clinically acceptable latencies [1]. In this work, we present the current status and latency figures of MRI-guided MLC-tracking on the Elekta Unity (Elekta AB, Sweden), which was previously discussed in [2].

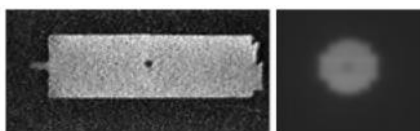
**Material and Methods**

Illustration 1: Phantom in MRI (left) and portal imager (right)

All experiments were performed on a clinical Elekta Unity with modified control software to enable MLC-tracking. The machine integrates a high-field (1.5T) MRI and a 7 MV linac. For the experiments, a circular beam was shaped using the on-board MLC (80 leaf pairs running in IEC1217-y direction). A cylindrical phantom was set in sinusoidal motion using a QUASAR MRI4D motion stage (Modus QA, Canada). The phantom was filled with agar to be detectable by MRI and a  $ZrO_2$  ball bearing for EPID-contrast (Illustration 1). To determine latency between real displacement and the MLC's reaction, EPID images (30Hz frame-rate) captured the position of the moving ball bearing and the projection position of the circular beam tracking the position of the phantom. Both positions were fit to a sinusoidal model which was used to extract the phase shift between the two curves. Real-time position variables for tracking were sourced from 1) the motion stage with real-time position feedback (<1ms latency, 25Hz, STAGE) and 2) MRI images sampled with 4Hz (MRI4Hz) and 8Hz (MRI8Hz), respectively. The MRI images were acquired using T<sub>1</sub>-weighted FFE -sequences (TR/TE=2.6/1.44ms,  $\alpha=6^\circ$ ) and streamed via a proprietary TCP-based interface. The current image position was extracted via detection of the edge of the phantom in the direction of motion.

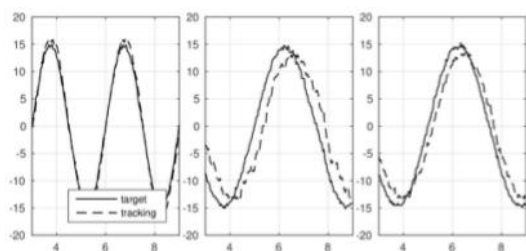
**Results**

Illustration 2: Tracking results for MLCONLY (left), MRI4Hz (center) and MRI8Hz (right)

Illustration 2 shows the tracking results. Naturally, because of the negligible position sensor latency, STAGE matches almost perfectly with the target position. The apparent latency was quantified at 20.67 ms. The tracked position overshoots. This is likely due to the control mode of the control system.

For the MRI-guided tracking, the impact of the longer latency for lower MRI-frequencies become apparent. MRI4Hz yields an apparent latency of 288 ms, while MRI8Hz has a lower latency of only 205 ms. Both MRI-guided

experiments show a loss of amplitude fidelity as the images cannot resolve the peaks of the excursion but can only interpolate between samples.

**Conclusion**

In this work we demonstrate stable tracking responses for the clinical MRI-linac system. Using the independent EPID imager, independent measurements of the tracking performance could be collected. Previously observed oscillatory behavior [2] could be stabilized using an improved version of the control system.

[1] Borman PTS et al. (2018) Characterization of imaging latency for real-time MRI-guided radiotherapy, Phys. Med. Biol. 63, 155023

[2] Glitzner M. et al. (2018) First MLC-tracking on the 1.5T MR-linac system, Radiotherapy and Oncology 127, S101 - S102

**OC-0192 Prerequisites for using "rapid learning" to optimise technical radiotherapy**

M. Aznar<sup>1</sup>, C. Johnson-Hart<sup>2</sup>, A. McWilliam<sup>2</sup>, M. Van Herk<sup>2</sup>, G. Price<sup>2</sup>

<sup>1</sup>The University of Manchester, Division of Cancer Sciences, Manchester, United Kingdom; <sup>2</sup>The University of Manchester c/o Christie Hospital- Dept 58- Floor 2A, Division of Cancer Sciences, Manchester, United Kingdom

**Purpose or Objective**

Technical improvements in radiotherapy such as image-guidance are often adopted with enthusiasm without trial or long-term evaluation due to their presumed benefit. "Rapid learning" describes a continuous improvement methodology to monitor the impact of changes and iteratively optimise clinical practice. We previously showed that the direction of residual set-up errors (i.e. shifting the high-dose region *towards* the heart) was *not* correlated with clinical parameters yet strongly correlated with poorer survival in lung cancer patients: this makes shift data vs survival an ideal model system for rapid learning. In this work, we demonstrate that the correlation between residual set-up errors and survival is removed after the application of a stricter IGRT protocol. Since rapid learning must be *rapid*, we also evaluate the minimal number of patients and minimal follow-up to detect this change.

**Material and Methods**

Locally advanced NSCLC patients treated with curative intent in our institution since 2008 were included in the analysis. Patients were treated with IGRT using bony anatomy registration on CBCT (Elekta XVI version 4.2 or 5.0).

Patients were divided into:

1. i) a "before" cohort (pre-November 2016, 780 patients), positioned using an extended non-action level protocol with a 5mm tolerance level,
2. ii) an "after" cohort (post-November 2016, 225 patients), positioned with daily CBCTs and a 2mm tolerance level.

We performed a sensitivity analysis using the "before" cohort to determine the minimal size of the subset of patients required to reliably observe the survival effect. Next, this number of patients was selected from both the "before" and "after" cohorts around the time of implementation of the change i.e. the last and first patients treated with both IGRT protocols, and the analysis repeated.

**Results**

Sensitivity analysis showed that 180 patients (~4 months accrual in our institution), followed up for 1 year, were sufficient to observe the survival effect in the "before" cohort with a power of 0.9 (Fig. 1). The survival discrepancy observed in the "before" cohort was not detected in "after" patients (Fig. 2) - i.e. changing IGRT

protocol significantly reduced the hazard of death to less than that in the “before” cohort.

This shows that a rapid learning approach can provide evidence of the impact of a change to clinical practice in a much shorter timeframe (<1.5 year) than that of a clinical trial.

#### Conclusion

This retrospective analysis demonstrates that continuous monitoring of patient outcomes, or rapid learning, can systematically provide evidence of the impact of even small changes in radiotherapy practice, and highlight where improvements can be made. Furthermore, as it necessarily takes place within a continuously monitored environment, it can make implementing such changes safer as adverse effects will be quickly detected. Rapid learning is complementary to clinical trials, provided that appropriate model system is used.

### Proffered Papers: RTT 2: A patient centered approach to follow up

#### OC-0193 Mobile application for daily patient scheduling during radiotherapy treatment course

J. Kauppinen<sup>1,2</sup>, M. Kokkonen<sup>2,3</sup>, M. Kaunisto<sup>4</sup>, J. Seppälä<sup>1</sup>  
<sup>1</sup>Kuopio University Hospital, Center of Oncology, Kuopio, Finland; <sup>2</sup>Healthcare Mobile Solutions, Medical department, Kuopio, Finland; <sup>3</sup>Kuopio University Hospital, Nuclear Medicine department, Kuopio, Finland ; <sup>4</sup>Kuopio University Hospital, Living Lab, Kuopio, Finland

#### Purpose or Objective

Currently most of the radiotherapy (RT) treatments are delivered with multiple treatment fractions in consecutive days. The RT patients are scheduled for a certain treatment machine and a daily pattern is given as a sequence of treatment days. Currently in most of radiotherapy departments in Finland the detailed timeslots are given to the patient once a week in advance on a paper. The purpose of this work was to determine whether a mobile phone application designed for patient scheduling can replace the previous workflow and simultaneously enhance the scheduling process overall and reduce the workload of the RT personnel.

#### Material and Methods

The testing of a mobile application (HMS, Healthcare Mobile Solutions) for patient scheduling was carried out at Kuopio University Hospital Radiotherapy department. During the three months testing phase (October 2017 - January 2018) 30 radiotherapy patients were involved in the test run. The initial and final patient daily scheduling was organized in Mosaiq (v2.62, Elekta AB, Stockholm, Sweden) patient verification system. The corresponding timeslots were given to the patients by the mobile application and also on the paper “time card”, since we wanted to investigate the patient reported difference between the two methods. In the final phase of the planned treatment (range of the total treatment fractions 5-30), the feedback was collected from the participating patients with five-point scale questionnaire (1 = strongly disagree, 2= disagree, 3 = neither agree or disagree, 4=agree, 5 = strongly agree).

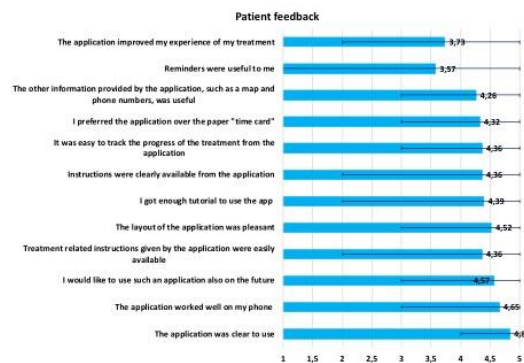
#### Results

The age distribution ranged between the participants in test run from 37-71 years. 75% of the patients were over 50 and 38% over 60 years old or older. 90,5% of the participants were using Android and 9,5% iPhone. The highest scores of the patient reported feedbacks were “the application was clear to use” (av 4.83, range 4-5), “the application worked well on my phone” (av 4.65, range 3-5) and “I would like to use such an application also on the future” (av 4.57, range 3-5). In addition, the overall feedback was that treatment related instructions given by the application were easily available (av 4.36, range 2-5)

and the patients would have chosen the application over the paper “time card” (av 4.32, range 3-5).

#### Conclusion

The mobile application was an effective tool for daily patient scheduling. The patient reported usability of the tested mobile application was high and none of the patients would have preferred the paper version of the time card, even though most of the patients were over 50 years old. In addition to the daily scheduling the application was used to give daily instructions and alerts for example for fasting and included treatment related instructions for the patients. This was the last step to convert our radiotherapy department into paper-less environment.



#### OC-0194 Continuous improvement by crossing patient satisfaction surveys, adverse events and complaints

S. Cucchiario<sup>1</sup>, M. Delgaudine<sup>2</sup>, F. Princen<sup>1</sup>, P. Coucke<sup>1</sup>  
<sup>1</sup>C.H.U. - Sart Tilman, Radiotherapy Department, Liège, Belgium ; <sup>2</sup>C.H.U. - Sart Tilman, STA Quality Department, Liège, Belgium

#### Purpose or Objective

Beyond the technological advances to improve Radiation Therapy (RT), the patient is a key player in security and improvement care processes. The patient's needs and expectations can be assessed through satisfaction surveys, adverse event declarations and records of complaints. However by crossing individual complaints, satisfaction surveys in combination with adverse events received we could get valuable information. The objective is to identify common elements of work between these different sources to improve care and to obtain additional views of caregivers and patients about an event to be more complete and accurate in choosing improvement actions.

#### Material and Methods

A retrospective analysis of patient's complaints, surveys and adverse events was carried out in order to highlight common improvement items between these 3 sources of information. Adverse events bring together caregiver statements and unexpected events completed by patients. Complaints are sent to us by the hospital Mediation. The complaints, adverse events and areas for improvement defined in the satisfaction surveys were examined. This analysis was conducted between June 2017 and June 2018, we have cross-pollated 249 improvement proposals from the surveys, with 7 complaints reporting and 13 patient completed adverse events.

#### Results

We first analyzed the 249 improvement proposals resulting from satisfaction surveys. We highlighted 5 criteria to improve: logistics and infrastructure (parking, waiting room), communication and information (brochure, information about treatment and on side effects), delays to treatment units (information delay, breakdowns), appointments (consultations) and the relationship with RT staff (doctors, nurses). We then compared them with complaints and patient related adverse events. Parking problem, treatment delays due to breakdowns as well as

poor communication about them were also reported through undesirable events. In the registered complaints, we found as concordance, a delay and a lack of communication about treatment and a problem of relationship with the Radiation Therapist staff. These common items have been chosen as events on which the RT department will implement improvement actions in priority (Figure1).

Monitoring decisions: Patient satisfaction surveys, complaints and adverse events				
Action	Decisions	Pilots	Status	Deadline
1	Revised brochures following patient feedback (with more information about treatment and on side effects)	SC FP	Work in progress	01/01/2019
2	Purchase of frames / decorations for waiting rooms	NR	Done	15/09/2018
3	Information given to the patient about the different parking options → Institutional brochure developed by the hospital with different parking possibilities	/	Done	/
4	Work on communication in the event of breakdowns, delays... → Creating a poster for occasional breakdowns or maintenance	FP SC	Work in progress	01/12/2018
5	Review the schedule sheet given to the patient	WS AP	Work in progress	01/10/2018

Figure 1

### Conclusion

By crossing these 3 information channels, we were able to highlight some areas on which we can reinforce improvement in order to increase patients' satisfaction as well as quality and safety of their care. This allows us to actively involve patient in quality processes of RT department so that he becomes a key actor in quality and safety of its own treatment. To continue this process of continuous improvement, a new crossover of these information will be organized at regular intervals.

Our final goal is to strengthen the quality and safety of treatments to create value for the patient and improve the patient experience.

And it's to adjust treatments to the life project of the patient and promote a participative approach focused on the patient's needs and expectations.

### OC-0195 Towards a Patient-Focused Organizational Model for Radiation Therapists

A. Shessel<sup>1</sup>, E. Moyo<sup>1</sup>, A. Koch<sup>1</sup>, J. Ringash<sup>1</sup>, J. Waldron<sup>1</sup>, F.F. Liu<sup>1</sup>, M. Velec<sup>1</sup>

<sup>1</sup>Princess Margaret Cancer Center, Radiation Medicine Program - Radiation Therapy, Toronto, Canada

#### Purpose or Objective

Patient experiences over their course of radiotherapy journey are fragmented by the many interactions from different Radiation Therapists (RTs), each focused on specific supportive care / technical activities (e.g. simulation, planning, delivery, etc.). The aim of this project was to determine the feasibility of reorganizing to provide continuity of care by identifying a primary RT partnering with each patient, throughout their entire radiotherapy trajectory.

#### Material and Methods

Two 4-month pilots were conducted in a single department (proof-of-concept phase in 2017, feasibility phase in 2018), with 16 RTs working in the new organizational model. Patients were triaged into the new model based on technique complexity or a perceived need for added psychosocial support (e.g. high anxiety, non-English speaking). Each patient was partnered with a 'primary' RT. This RT performed, all point-of-care activities identified as high priority (critical activities/time-points in the treatment course) for their patients as often as scheduling permitted. The high priority points-of-care were: all education and supportive care activities (including a new pre-treatment session and a new 2-week post treatment follow-up call), CT-simulation, dosimetry review, peer-review rounds and treatment delivery (at least 1st and last fractions). All 'primary' RT activities were documented to assess continuity of care. Patient satisfaction surveys were distributed at the final treatment and stakeholder surveys

were distributed to the multi-disciplinary clinical team following each phase.

#### Results

Over both phases, 312 patients (46% breast, 18% upper gastrointestinal, 36% head and neck) were treated in the new organizational model. On average, 75% of a patient's priority points-of-care were delivered by the primary RT in the new model, compared to 40% in the standard model. Overall, of the 173 patients surveyed, ≥95% of were satisfied with their experience. Compared to the fragmented standard model, 20% more patients in this model were satisfied with the patient education information they received and with staff consistency. Among the patients diagnosed with Breast cancer, 30% fewer reported accessing 'drop-in' nursing support clinics relative to the standard fragmented model. Multi-disciplinary stakeholders (n=83) saw improvements in patient support as a substantial benefit of the new model, with workflow challenges identified as a potential implementation barrier.

#### Conclusion

A patient-focused organizational model was developed to partner individual RTs with patients throughout their radiotherapy course. It was feasible to accrue substantial numbers of patients to this model. These early results suggest improved continuity of care, high quality supportive care and patient experience. Full-scale implementation of this organizational model is currently underway in our large comprehensive cancer centre.

### OC-0196 Predictors for radiation-induced oesophagitis in breast cancer patients

K. West<sup>1</sup>, M. Schneider<sup>2</sup>, C. Wright<sup>2</sup>, R. Beldham-Collins<sup>1,3</sup>, N. Coburn<sup>3</sup>, K. Tiver<sup>3</sup>, V. Gebiski<sup>4</sup>, K. Stuart<sup>1,5,6</sup>

<sup>1</sup>Crown Princess Mary Cancer Centre, Westmead Hospital, Wentworthville, Australia; <sup>2</sup>Monash University, Department of Medical Imaging and Radiation Sciences- Faculty of Medicine- Nursing and Health Sciences, Clayton, Australia; <sup>3</sup>Nepean Cancer Care Centre, Nepean Hospital, Penrith, Australia; <sup>4</sup>NHMRC Clinical Trials Centre, University of Sydney, Sydney, Australia; <sup>5</sup>Breast Cancer Institute, Westmead Hospital, Westmead, Australia; <sup>6</sup>Sydney Medical School, The University of Sydney, Sydney, Australia

#### Purpose or Objective

Radiation therapy (RT) for early breast cancer is increasingly more personalised. Treatment using intensity-modulated RT (IMRT) to the supraclavicular (SCF) nodes has shown potential for development of oesophagitis. This pilot study aims to identify predictors for the onset of radiation-induced oesophagitis.

#### Material and Methods

Patients prescribed RT to the breast or chest wall and SCF nodes (± other nodal groups) to a dose of ≥ 50 Gy in 25 fractions were considered eligible for the study. Patients were recruited consecutively at the time of simulation, and only excluded if they had previous treatment to the ipsilateral breast or chest wall or other contraindications to RT. A hybrid IMRT planning technique with a minimum of 95% of the prescribed dose to cover all PTVs was utilised for all patients. Grading was undertaken twice weekly using the RTOG system to determine the onset of moderate oesophagitis (grade 2). Mean and maximum doses to the oesophagus were recorded, as well as oesophageal length and length of pharynx included in the treatment area. Demographic data including age, treatment areas (SCF, internal mammary chain (IMC), axilla), laterality of disease site, chemotherapy and smoking history were recorded. Data were analysed using Fishers exact test and GraphPad Prism software with a 0.05 significance level.

#### Results

A total of 77 patients were enrolled from September 2012 until July 2015. Twenty-four patients reported a maximum

grade 2 oesophagitis. No patients reported grade 3 or higher oesophagitis. There was a significant difference in the number of patients receiving a mean oesophageal dose of  $\geq 31$  Gy with grade 2 toxicity compared to those receiving  $< 31$  Gy ( $p=0.025$ ). There was a significant difference in grade 2 toxicity in patients who had  $\geq 1$  cm of pharynx included in supraclavicular fields compared with those with  $< 1$  cm ( $p=0.0116$ ). A trend was observed in patients with left-sided SCF treatment, with more experiencing a grade 2 toxicity; this could be explained by the anatomical location of the oesophagus in this region. There was also an increased trend of grade 2 toxicity in patients who did not receive IMC RT; the reason for this may require further investigation. There were no overall significant differences in smoking history, oesophageal length and chemotherapy regimen.

#### Conclusion

This study has identified two potential predictors for moderate oesophageal toxicity in early breast cancer patients receiving RT to the breast or chest wall and supraclavicular nodes. By limiting the mean dose to the irradiated oesophagus to  $< 31$  Gy during the planning process, and if possible ensuring  $< 1$  cm of pharynx is included in the field, oesophageal toxicity could be reduced.

#### OC-0197 A survey of UK practice of radiotherapy skin care for breast patients

H. Nisbet<sup>1</sup>, S. Matthews<sup>1</sup>, R. Cooke<sup>1</sup>

<sup>1</sup>Oxford University Hospitals NHS Foundation Trust, Radiotherapy Department, Oxford, United Kingdom

#### Purpose or Objective

Radiation induced skin toxicity is one of the most common toxicities experienced with radiotherapy treatment and is characterised by erythema, heat, pain, swelling and pruritus. The management of skin toxicities has often been driven by established practices and local conventions rather than on research and evidence, resulting in non-standardised practice with little or no justification<sup>1, 2</sup>. In 2015 The Society and College of Radiographers (SCoR) published guidelines<sup>3</sup> to promote an evidence-based approach. However, a lack of evidence to support or refute the use of any particular product for topical application meant that only general guidance is given. In addition, it is advised that any moisturiser containing sodium lauryl sulphate (SLS) should be avoided as it causes skin irritation. The 2012 SCoR survey of UK practice showed that nearly 70% of radiotherapy departments advised the use of aqueous cream for prophylactic skin care<sup>2</sup>, a product that contains SLS. As a result, the new guidelines provided a review of the evidence base for skin care practice but simultaneously advised against the most common cream in use, creating uncertainty on what products can be recommended to patients. Therefore the objective was to survey current UK skin care practice for patients undergoing treatment to the breast following the implementation of the new guidelines and to evaluate if any one particular topical product had fewer associated skin toxicities.

#### Material and Methods

All UK departments were invited to participate via the SCoR Radiotherapy Information, Support and Review Special Interest Group online forum and provided with a skin assessment tool to record skin toxicity details. Extrinsic factors recorded were treatment technique and beam energy. Intrinsic factors included the co-morbidities of diabetes and cardiovascular disease, smoking, alcohol consumption, weight and patient demographics. The skin care products used during treatment were also documented. Participating departments had implemented the 2015 guidelines and for comparability only external beam radiotherapy to the breast and chest wall, excluding nodal treatment, were included. An assessment of the skin was recorded in week one using the

Radiation Therapy Oncology Group toxicity criteria<sup>7</sup> and for each subsequent week of treatment.

#### Results

594 total responses were received with 542 included in the survey after exclusions. The effect on skin toxicity of the skin care product used, as well as other patient and treatment factors were analysed. No significant differences were found in RTOG grades between any of the skin products used. Weight, cup size, diabetes, cardiovascular disease, mastectomy and beam energy were all found to have statistically significant higher RTOG grades.

#### Conclusion

This survey shows that intrinsic factors are more likely to determine skin toxicity and confirms the SCOR guidelines that any SLS free, topical product can be used for radiotherapy skin care.

#### OC-0198 Using PROs and PROMs in routine head and neck cancer care: what do RTs perceive as barriers?

H. Nguyen<sup>1</sup>, P. Butow<sup>2</sup>, H. Dhillon<sup>2</sup>, L. Morris<sup>1</sup>, A. Brown<sup>1</sup>, K. West<sup>1</sup>, P. Sundaresan<sup>1,3</sup>

<sup>1</sup>Radiation Oncology Network, Western Sydney Local Health District, Sydney, Australia; <sup>2</sup>Centre for Medical Psychology & Evidence-based Decision-making CeMPED, The University of Sydney, Sydney, Australia; <sup>3</sup>Sydney Medical School, The University of Sydney, Sydney, Australia

#### Purpose or Objective

Patient-reported outcomes (PROs) are direct reports from patients about the status of their health condition without amendment or interpretation by others. Patient-reported outcome measures (PROMs) are usually validated questionnaires that patients complete by self-assessing their health status. Domains assessed include the patient's physical, emotional, social and overall quality of life. The use of PROMs to measure PROs has been shown to improve patient overall survival and toxicity outcomes, patient-health professional (HP) communication and service-level quality. Yet, PROMs are not routinely used in many oncology institutions worldwide. The aim of this study was to examine HPs' perception of barriers to the routine use of PROs and PROMs in the care of head and neck cancer (HNC) patients. This report specifically focuses on perceptions of RTs caring for HNC patients.

#### Material and Methods

A custom survey was created to assess HNC HPs' perceptions of barriers to routine PRO use. To create the survey, existing literature was reviewed and potential barriers and enablers to routine PRO use were collated and categorised as patient-level, service-level or HP-level. Participants were asked to rate the degree to which they believe these items are barriers/enablers to PRO use by answering "not at all", "very little", "quite a bit" and "very much". The survey was pilot tested amongst selected HPs before being electronically disseminated to HPs involved in the care of HNC patients in Western Sydney Local Health District, Australia.

#### Results

There were 122 participants; 58% ( $n = 71$ ) of whom were RTs. The response rate amongst RTs was 94.7%. Most RTs (59.2%) had never heard of PROs whilst very few (2.9%) have used PROs to guide patient care. At the patient level, the perceived unavailability of PROMs in patients' preferred languages and patient difficulty understanding PROMs were rated as "quite a bit/very much" by 67.6% and 54.3% of RTs respectively. At the service-level, factors perceived as "quite a bit/very much" a barrier to PRO use included low workplace awareness of PROs (69.6%), low organisational support (69.6%) and insufficient staff resources (69.6%). At the HP-level, factors perceived as "quite a bit/very much" a barrier to PRO use included lack of knowledge regarding how to use PROs (66.7%), concern regarding need for additional time to interpret and action

PROs (56.5%) and lack of knowledge on how to integrate PROs into clinical practice (55.1%). Top enablers highlighted by RTs were staff education on how to use PROs (82.4%), clear definition of roles (80.9%) and designated time for staff to monitor and respond to PROs (80.9%).

#### Conclusion

This study has highlighted important barriers and enablers to the routine use of PROs in HNC care as perceived by RTs. Most barriers appear to lie at the service and HP levels. Findings from this study will guide future interventions to address these barriers such that successful and sustainable implementation of routine PRO collection may be achieved.

#### OC-0199 Patient-reported outcomes after stereotactic body radiotherapy in lung cancer: The Lung PLUS study

L. Van der Weijst<sup>1</sup>, R. Bultijnck<sup>1</sup>, A. Van Damme<sup>1</sup>, M. Van Eijkeren<sup>1</sup>, V. Surmont<sup>2</sup>, Y. Lievens<sup>1</sup>

<sup>1</sup>Ghent University Hospital, Radiation Oncology, Gent, Belgium; <sup>2</sup>Ghent University Hospital, Respiratory Medicine, Gent, Belgium

#### Purpose or Objective

Stereotactic body radiotherapy (SBRT) is the treatment of choice for early stage non-small cell lung cancer (ES-NSCLC) patients unwilling to undergo or ineligible for surgery. SBRT may bring along toxicities, adversely affecting health-related quality of life (HRQoL), with impact on the patients' physical, psychological and social wellbeing. Fatigue is a frequently reported side-effect in patients undergoing SBRT. We here report the initial results of patient-reported toxicity, HRQoL and fatigue in the Lung PLUS study.

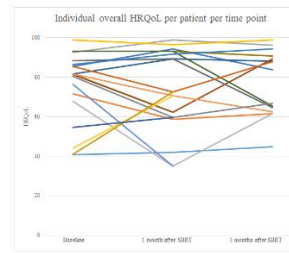
#### Material and Methods

Lung PLUS is a monocentric, prospective, longitudinal study, investigating the predictive value of Patient-Reported Outcomes (PROs), functional exercise capacity (6-minute walk test - 6MWT) and circulating cell-free DNA circulating DNA (cfDNA) on outcome in ES-NSCLC undergoing SBRT. PROs are collected at baseline, and at 1, 3, 6, 9 and 12 months after treatment. Outcome data (overall survival; local and loco-regional control; and metastatic relapse) are recorded during the entire course of follow-up. Socio-economic determinants are collected at baseline.

HRQoL is measured with a validated questionnaire (EORTC QLQ-C30). The patient-reported toxicities, collected with the patient-reported outcome measurement (PROM) version of the Common Terminology Criteria for Adverse Events (CTCAE) (PRO-CTCAE), are as follows: pain, fatigue, cough, anxiety and dyspnea. A meaningful clinically important difference (MCID) of HRQoL was defined as a 10-point difference on the total score of 100 of the EORTC QLQ-C30 between time points. The mixed model approach was applied to analyze the longitudinal data.

#### Results

Between June 2017 and October 2018, 25 patients (median age: 73) out of the 50 patients planned have been recruited. The majority was male (64%) and had stage I disease (96%). Total dose was 60Gy, delivered in 3 (26%), 5 (17%) or 8 fractions (57%). Data is available of 25, 19 and 17 patients at baseline, 1 and 3 months after SBRT respectively. So far, no significant differences in overall toxicity ( $p=0.681$ ), HRQoL ( $p=0.187$ ) and fatigue ( $p=0.221$ ) over time have been found. MCID in HRQoL was found in 50% (40% deterioration; 10% improvement) and 27% (all deteriorated) of patients respectively at 1 and 3 months after SBRT. Graph 1 provides an overview of individual overall HRQoL over time. Toxicity and HRQoL are significantly correlated ( $p<0.001$ ) over time.



Data based on 18 patients due to excessive missing data of one patient.

#### Conclusion

The initial results of the Lung PLUS study indicate that HRQoL, toxicity and fatigue levels remain stable after SBRT in ES-NSCLC. Updated results will be presented.

#### Poster Viewing : Poster viewing 4: Head-Neck and Lung

#### PV-0200 Accelerated- vs chemo-radiation as organ sparing strategies for laryngeal/hypopharyngeal carcinoma

A. M. Elamir<sup>1</sup>, S. Huang<sup>1</sup>, W. Xu<sup>2</sup>, M. Yu<sup>2</sup>, A. Spreafico<sup>3</sup>, A. Bayley<sup>1</sup>, S.V. Bratman<sup>1</sup>, J. Cho<sup>1</sup>, M. Giuliani<sup>1</sup>, A. Hope<sup>1</sup>, J. Kim<sup>1</sup>, B. O'Sullivan<sup>1</sup>, J. Ringash<sup>1</sup>, J.R. De Almeida<sup>4</sup>, D. Chepeha<sup>4</sup>, D. Goldstein<sup>4</sup>, J. Irish<sup>4</sup>, J. Waldron<sup>1</sup>, A. Hosni<sup>1</sup>

<sup>1</sup>Princess Margaret Cancer Centre / University of Toronto, Department of Radiation Oncology, Toronto-Ontario, Canada ; <sup>2</sup>Princess Margaret Cancer Centre / University of Toronto, Department of Biostatistics, Toronto- Ontario, Canada ; <sup>3</sup>Princess Margaret Cancer Centre / University of Toronto, Department of Medical Oncology, Toronto- Ontario, Canada ; <sup>4</sup>Princess Margaret Cancer Centre / University of Toronto, Department of Otolaryngology-Head and Neck Surgery/Surgical Oncology-, Toronto- Ontario, Canada

#### Purpose or Objective

To evaluate the outcomes of locoregionally advanced laryngeal/hypopharyngeal squamous cell carcinoma (SCC) following concurrent chemoradiation (CRT) and accelerated radiation therapy (ART).

#### Material and Methods

Retrospective review was conducted of stage III-IVB (AJCC/UICC-7th edition) laryngeal/hypopharyngeal SCC patients who were treated with curative-intent radiation therapy (RT) from 2000-2016. Patients were preferentially managed with CRT; those unfit or who declined chemotherapy received ART scheduled based on physician and patient preference: moderately accelerated, 70 Gy/35f/6w (A-Mod); hypofractionated, 60 Gy/25f/5w (A-Hypo); or accelerated hyperfractionation, 64 Gy/40f/4w (A-Hyper). Cases were matched 1:1 from our prospective quality assurance system based on: age, smoking and ECOG performance status (PS), T- and N-category, larynx vs hypopharynx, and IMRT vs 3D conformal RT. With propensity score matching, outcomes were compared following: 1) CRT vs the three ART regimens separately, 2) The three different AF-RT schedules. The primary endpoint was 5-yr local control (LC, evaluated by competing risk method) and secondary endpoints were 5-yr regional and distant control, cancer specific survival (analyzed by competing risk method), and overall survival (OS, measured by Kaplan-Meier method).

#### Results

Among 679 patients included, 195 received concurrent cisplatin (only 65 [33%] were able to receive 3 cycles of Q3-week cisplatin, 102 [52%] received 2 cycles, 14 [7%] tolerated only 1 cycle, while 14 patients [7%] received

weekly cisplatin). A total of 484 patients were managed with ART due to: age >70 years (n=216), comorbidity/poor PS (n=102), or declined chemotherapy (n=166). Patients and treatment characteristics are summarized in Table 1. The pattern of failure among the whole cohort is shown in Figure 1a. With a median follow up of 4.3 years, 5-yr LC following CRT, A-Mod (n=128), A-Hypo (n=141), and A-Hyper (n=215) were 81% (95%CI:74-85%), 70% (95%CI:60-78%), 68% (95%CI:59-75%) and 65% (95% CI:58-71%) respectively. Outcomes following propensity score matching are shown in Figure 2; the 5-yr LC following CRT was 80% (95%CI:72%-86%) vs 71% (95%CI:61%-78%) compared to A-mod (p=0.08), 82% (95%CI:72%-88%) vs 71% (95%CI:61%-79%) compared to A-Hypo (p=0.07), and 81% (95%CI:74%-86%) vs 66% (95%CI:58%-72%) compared to A-Hyper (p<0.001). There was no significant difference in 5-yr LC between different ART schedules (p>0.05, Figure 2b). Among patients who had locoregional recurrence (LRR) without synchronous distant metastases (n=202), 113 (56%) had salvage surgery (5-yr OS: 40% [95%CI:32%-51%]), while 89 were not surgical candidates (5-yr OS: 5% [95%CI:2-15%]). Late toxicities are summarized in Figure 1B.

Figure 1a. Distribution and pattern of failure among the whole cohort

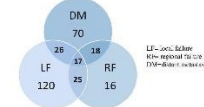


Figure 1b. Severe (grade ≥3) late toxicity

	Whole cohort (n=484)	Concurrent chemoradiation (n=197)	Moderately accelerated radiation (n=128)	A-Hypofractionation (n=141)	A-Hyperfractionation (n=215)
• Esophagus	• Esophageal obstruction: 17 (2.9%)	• Esophageal obstruction: 8 (4.1%)	• Esophageal obstruction: 2 (1.6%)	• Esophageal obstruction: 1 (0.7%)	• Esophageal obstruction: 2 (2.2%)
• Pharynx	• Dysphagia/odynophagia: 30 (44%)	• Dysphagia/odynophagia: 13 (6.7%)	• Dysphagia/odynophagia: 10 (7.8%)	• Dysphagia/odynophagia: 2 (1.4%)	• Dysphagia/odynophagia: 7 (3.3%)
• Trachea	• Tracheal stenosis: 20 (4.2%)	• Tracheal stenosis: 11 (5.6%)	• Tracheal stenosis: 4 (3.1%)	• Tracheal stenosis: 1 (0.7%)	• Tracheal stenosis: 1 (0.5%)
• Teeth	• Soft tissue necrosis: 20 (4.2%)	• Soft tissue necrosis: 7 (3.6%)	• Soft tissue necrosis: 4 (3.1%)	• Soft tissue necrosis: 5 (3.5%)	• Soft tissue necrosis: 1 (0.5%)
• Head	• Osteoradionecrosis: 4 (0.8%)	• Osteoradionecrosis: 2 (1.0%)	• Osteoradionecrosis: 1 (0.8%)	• Osteoradionecrosis: 1 (0.7%)	• Osteoradionecrosis: 1 (0.5%)
• Nerve	• Facial palsy: 1 (0.2%)	• Facial palsy: 1 (0.5%)	• Facial palsy: 1 (0.8%)	• Facial palsy: 1 (0.7%)	• Facial palsy: 1 (0.5%)
• Vascular	• Hypertension: 1 (0.2%)	• Hypertension: 1 (0.5%)	• Hypertension: 2 (1.6%)	• Hypertension: 1 (0.7%)	• Hypertension: 1 (0.5%)
• Overall	186 (38.4%)	43 (21.8%)	26 (20.3%)	10 (7.1%)	36 (16.7%)

Numbers were not available for a head-to-head comparison.

Figure 2a. Five year outcomes following propensity score match comparing chemoradiation versus accelerated radiation therapy schedules

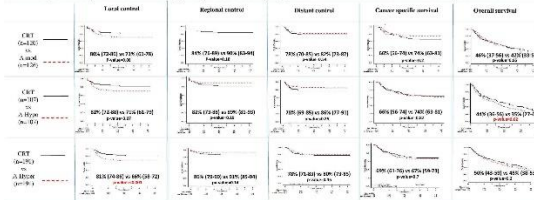
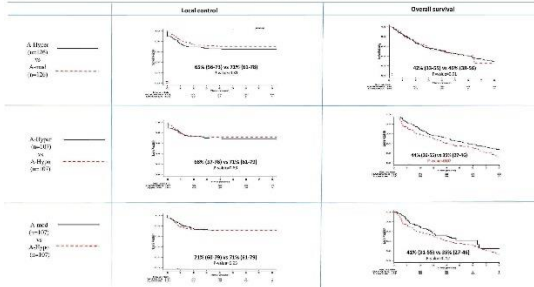


Figure 2b. Five year outcomes following propensity score match among accelerated radiation therapy schedules



	Concurrent chemoradiation (CRT) (n=197)	Accelerated fractionation radiation therapy (ART)				p-value
		Whole ART cohort (n=484)	Moderately accelerated radiation (n=128)	A-Hypofractionation (n=141)	A-Hyperfractionation (n=215)	
• Treatment description:						
- Total radiation dose (Gy)	70	70	60	64		
- Number of total fractions	35	35	25	40		
- Number of fractions/week	5	5	5	10 (two fractions/day)		
- Dose per fraction (Gy)	2	2	2.4	1.6		
- Overall treatment time (weeks)	7	6	5	4		
- Radiation BED10 (Gy10)	74.32	70.91	66.7	71.93		
- Concurrent chemotherapy	Cisplatin	No	No	No		
• Age (years; median (range))	59 (32-77)	68 (22-91)	72 (33-87)	71 (22-91)	65 (27-87)	<0.001
• Male gender	158 (81%)	400 (83%)	103 (80%)	117 (82%)	182 (85%)	0.66
• Smoking (pack-years; median (range))	20 (0-105)	40 (0-150)	49 (38-150)	40 (0-150)	40 (0-150)	<0.001
• Laryngeal primary tumor site	120 (61%)	358 (74%)	93 (73%)	99 (70%)	166 (77%)	<0.01
• cT3-4 category	140 (71%)	377 (78%)	104 (81%)	92 (66%)	181 (85%)	0.24
• cN3 category	141 (72%)	196 (40%)	55 (43%)	42 (30%)	79 (37%)	<0.001
• ECOG performance status:						
- ECOG 0	100 (51%)	211 (43%)	44 (35%)	58 (41%)	109 (51%)	0.34
- ECOG 1-2	92 (46%)	231 (47%)	82 (65%)	55 (39%)	94 (44%)	
- No reported	3	42	2	28	12	
• Radiation therapy technique:						
- Intensity modulated radiation therapy	159 (81%)	320 (66%)	128 (100%)	54 (38%)	138 (64%)	<0.001
- 3D conformal radiation therapy	36 (18%)	164 (34%)	0	87 (62%)	77 (36%)	

\* BED = D \* (1 + d/(α/β)) = 10.693 \* (1 + d/(2.5)) for tumor local control (BED)10; α/β = 10 Gy; ca = 0.3 Gy; β = 2.5 Gy; d = 2.5 Gy; n = 3.5.  
 - When BED = biologically effective dose (Gy), D = total dose (Gy), d = dose per fraction (Gy), n/F = linear (α) and quadratic (β) components of the linear-quadratic model (Gy<sup>2</sup>); T = overall treatment time (weeks), h = 168 h/F or coast of accelerated repopulation time (days), t = average doubling time during accelerated repopulation (days).  
 - BED for concurrent chemotherapy in the CRT group was considered as 8.8 Gy10

Conclusion

Approximately two thirds of stage III-IVB laryngeal/hypopharyngeal SCC patients who declined or were unfit for concurrent cisplatin achieved LC following ART. There was no significant difference in LC among the different ART regimens.

PV-0201 Development and validation of prediction models for salivary dysfunction in HN cancer patients L. Van den Bosch<sup>1</sup>, A. Van der Schaaf<sup>1</sup>, F.J.P. Hoebers<sup>2</sup>, H.P. Van der Laan<sup>3</sup>, E. Schuit<sup>3</sup>, E. Bakker<sup>1</sup>, O.B. Wijers<sup>4</sup>, A.M. Van der Wel<sup>4</sup>, R.J.H.M. Steenbakkers<sup>1</sup>, J.A. Langendijk<sup>1</sup>

<sup>1</sup>University of Groningen - University Medical Center Groningen, Radiation oncology, Groningen, The Netherlands ; <sup>2</sup>Maastro Clinics, Radiation Oncology, Maastricht, The Netherlands; <sup>3</sup>Utrecht University - University Medical Center Utrecht, Julius Center for Health Sciences and Primary Care, Utrecht, The Netherlands; <sup>4</sup>Radiotherapeutic Institute Friesland, Radiation Oncology, Leeuwarden, The Netherlands

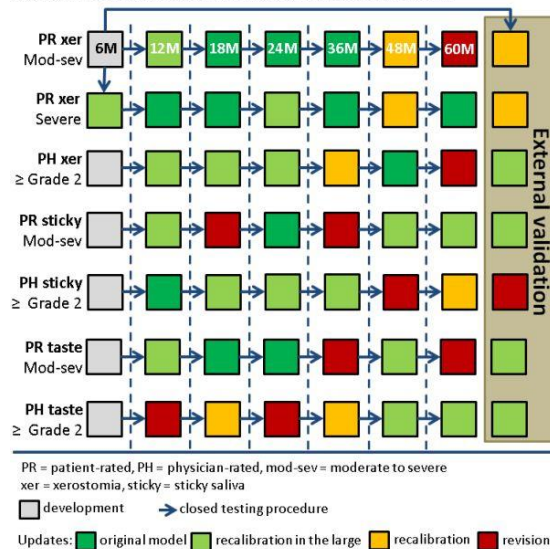
Purpose or Objective

NTCP-models for salivary dysfunction and other toxicities in head and neck cancer (HNC) patients can be used to optimize treatment plans and select the best RT technique. However, currently used NTCP-models have several shortcomings, such as retrospective assessments, being developed on limited data for only a single time point or grade without properly addressing missing data, non-linearity, and multicollinearity, no external validation and a limited number of organs at risk (OARs) investigated. Our aim was to address these shortcomings and to develop and externally validate an NTCP-profile based on a comprehensive set of NTCP-models for patient-rated (PR) and physician-rated (PhR) toxicities. Here we present the results for salivary dysfunction.

**Material and Methods**

This was a prospective cohort study including 750 HNC patients treated with definitive radiotherapy. All endpoints were scored prospectively and the compliance rate was > 80% for all endpoints. OARs were re-delineated according to international consensus guidelines. Multiple imputation was used to deal with missing data to avoid the potential bias of a complete case analysis. During model development we assessed non-linear dose-effect relations and dealt with multicollinearity. Models were developed for moderate-to-severe PR and grade 3 2 PhR (CTCAEv4.0) xerostomia, sticky saliva and changes in taste at 6 months after treatment. A closed testing procedure was used to validate and, if necessary, update the models at subsequent time points (up to 5 years) and higher toxicity grades (fig 1). The models at 6 months were externally validated on 260 HNC patients from 2 other RT-centers using the same closed testing procedure. The proposed model update was performed on the combined data to obtain a more generalized model.

Figure 1: Model development, validation and updating scheme



**Results**

Salivary dysfunction was best predicted by baseline complaints and mean dose to the parotid and submandibular glands and the oral cavity (table 1). For PR changes in taste, age was also a predictor. In most models, a square root or log transformation of the parotid glands or oral cavity dose improved model performance. All models performed well with an ROC-AUC ranging from 0.65 for PhR changes in taste to 0.77 for PhR xerostomia. When validated over time, none or minor model adjustments were necessary. The external validation showed good performance of the models and only minor updates sufficed to allow proper model performance,

thereby indicating good generalizability of the models.

Table 1: Model predictors and performance at 6 months

	PR xer	PH xer	PR sticky	PH sticky	PR taste	PH taste
Both parotid glands	sqrt	sqrt	sqrt		log	sqrt
Both submandibular glands						
Oral cavity					sqrt	
Baseline complaints						
Age						
AUC development	0.73	0.77	0.67	0.69	0.68	0.65
AUC external validation	0.65	0.74	0.73	0.64	0.71	0.67
Proposed update	Recal	RITL	RITL	Revis	RITL	RITL
AUC after update on combined data	0.72	0.78	0.69	0.64	0.69	0.65

variable in the model  
 sqrt = square root, log = natural logarithm  
 AUC = Area Under the Receiver Operation Characteristic (ROC) Curve  
 Recal = recalibration, RITL = recalibration in the large, Revis = revision

**Conclusion**

We developed and externally validated a comprehensive NTCP-profile for both PR and PhR salivary gland toxicities at different time points after head and neck radiotherapy, based on the newest OARs contouring guidelines. Such a profile can be used for treatment planning optimization and selection of patients for different RT techniques.

**PV-0202 3-D reconstruction of radiotherapy dose associated with advanced osteoradionecrosis after IMRT**

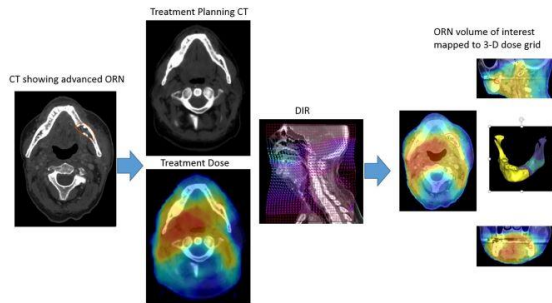
A.S.R. Mohamed<sup>1</sup>, K. Al Feghali<sup>1</sup>, S.P. Ng<sup>1</sup>, H. Elhalawani<sup>1</sup>, K. Hutcheson<sup>1</sup>, M. Chambers<sup>1</sup>, J. Phan<sup>1</sup>, J. Kraeima<sup>2</sup>, H. Glas<sup>2</sup>, M. Witjes<sup>2</sup>, G.B. Gunn<sup>1</sup>, A. Garden<sup>1</sup>, D. Rosenthal<sup>1</sup>, S. Frank<sup>1</sup>, W. Morrison<sup>1</sup>, C. Fuller<sup>1</sup>, S. Lai<sup>1</sup>  
<sup>1</sup>The University of Texas- MD Anderson Cancer Center, Radiation Oncology, Houston, USA; <sup>2</sup>University of Groningen- The Netherlands, Oral Surgery, Groningen, The Netherlands

**Purpose or Objective**

IMRT carries the ability to limit dose to organs-at-risk. However, recent findings by our group and others, reported no reduction in osteoradionecrosis (ORN) rates in oropharyngeal cancer (OPC) patients after IMRT in comparison to conventional radiotherapy techniques. We recently demonstrated that a wide range of two-dimensional dose-volume parameters in the intermediate and high dose beam-path are associated with the development of advanced ORN in patients with OPC treated with IMRT. To this end, we aim to further characterize the dosimetric correlated of advanced ORN by determining the three-dimensional (3-D) spatial dose distribution of the mandibular area of ORN.

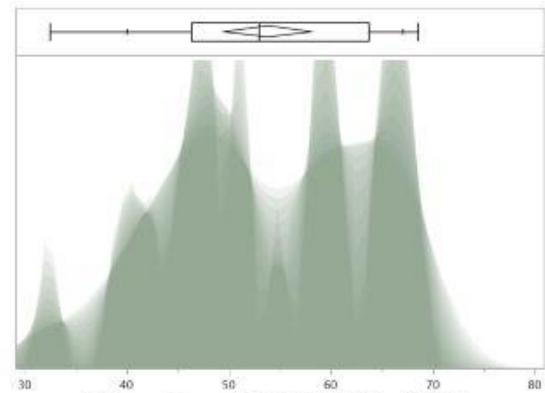
**Material and Methods**

After institutional review board (IRB) approval, we identified patients with grade IV ORN requiring major surgery among patients with OPC treated with IMRT between 2002 and 2013. The initial CT scans documenting the diagnosis of ORN were identified. The mandibular areas affected with ORN were manually segmented for all patients to create 3-D ORN volume of interest (ORN-VOI). Planning CTs and dose grids were subsequently retrieved. ORN-depicting CT scans were then co-registered to planning CT scans using a validated commercial image registration software (Velocity AI 3.0.1, Atlanta, GA). Finally, ORN-VOIs were mapped to planning CT scans, and dose grid then dosimetric parameters were extracted for each VOI (Figure 1).

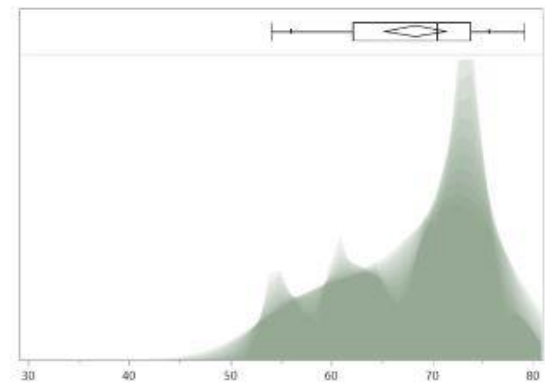


### Results

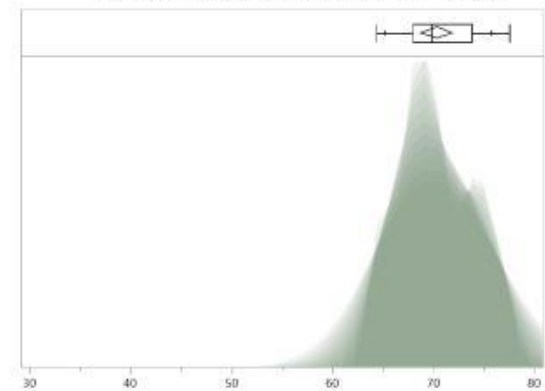
Twenty-five patients with grade IV ORN were identified. Median follow-up was 76 months (range 24-183) and median time to development of ORN was 22 months (range 5-132). Median age at diagnosis was 61 years (range 47-72), and 84% were men. The site of tumor origin was base of tongue, tonsil, and posterior pharyngeal wall in 12, 12, and 1 patient(s), respectively. Median radiation prescription dose was 70 Gy in 33 fractions. Only two patients developed ORN contralateral to the tumor site. The average of minimum dose to ORN-VOIs (i.e. the isodose line that covers 100% of the ORN volume) was 54.3 Gy. The first, second, third, and fourth quartile minimum dose distribution for ORN-VOI ranged from 32.4-46.7, 46.7-54.6, 54.6-64.6, and 64.6-68.5 Gy, respectively (Figure 2). The averages of mean and maximum doses to ORN VOIs were 66.3 Gy (range 54-75) and 72.5 Gy (range 64-78), respectively.



**Min. dose ORN VOIs (Gy)**



**Mean dose ORN VOIs (Gy)**



**Max dose ORN VOI (Gy)**

### Conclusion

The mandibular areas of origin of advanced ORN in OPC patients treated with IMRT received at least 55 Gy in approximately half of the examined cohort. However, lower doses, in the intermediate dose range (32-55 Gy), were also associated with mandibular ORN. Our findings suggest that the intermediate dose beam-path results in long-term bone toxicity for OPC survivors. Dose-volume constraints in both intermediate and high dose range of the mandibular organ at risk should be adopted in future IMRT plans.

### PV-0203 Adaptive proton therapy for patients with Head and Neck tumors involving skull base

S. Karaman<sup>1</sup>, R. Malyapa<sup>2</sup>, U. Langner<sup>2</sup>, T. Houser<sup>2</sup>, Z. Fellows<sup>2</sup>, J. Moreau<sup>2</sup>, Z. Vujaskovic<sup>2</sup>

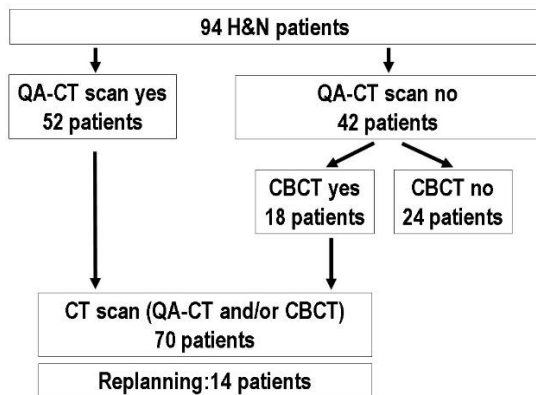
<sup>1</sup>Istanbul University Oncology Institute, Radiation Oncology, Istanbul, Turkey ; <sup>2</sup>Maryland Proton Treatment Center, Radiation Oncology, Baltimore, USA

### Purpose or Objective

To determine the impact of anatomical changes in target volume, sinus filling and weight on dose distribution in patients undergoing pencil beam scanning proton therapy (PBS-PT) for head and neck cancers (HNC) involving the skull base. This information was used in order to assess the need for adaptive replanning.

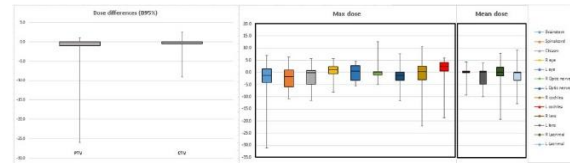
### Material and Methods

We analyzed 94 HNC patients treated with PBS-PT between 2016 and 2018 (Fig 1). The structures defined on initial planning CT were used as a reference to merge images on QA-CT scans to evaluate changes in anatomy and dose distribution during the course of treatment. For image registration we used a three-dimensional rigid registration algorithm. Patients' weekly QA-CT scans and/or daily cone beam CT (CBCT) was overlaid with the initial planning CT to evaluate target coverage and organs at risk (OAR) dose to assess the need for replanning as a result of anatomic changes. To evaluate target coverage, we looked at the dose difference for 95% of the volume (V95) for CTV and PTV, and for critical dose limiting OAR we looked at the absolute increase in maximum dose between initial planning CT and QA-CT scans.



### Results

Weekly QA-CT scans ± daily CBCT were performed for 70 patients. 24 patients did not have any CBCT since it became available only in late 2016. Daily CBCT alone was used to evaluate changes for 18 patients who had no gross disease or where disease site was not extending into sinus cavity and when the beams were not passing through sinus air cavity. Replanning was deemed necessary in 14 patients (20%) due to weight loss (40%), sinus filling (33%) and changes in tumor or in the post operative bed (27%). Replanning was necessary for the following tumor sites: Sinonasal undifferentiated carcinoma, skull base chordoma extending to cervical region, nasopharynx and maxillary sinus. Replanning was performed once in 13 patients and twice in one patient during the treatment course. Median differences for prescription dose coverage for 95% of the target volume between the initial planning CT and QA-CT scans were found to be -1 (range -26,+1) for CTV, and zero (range -9, +2.5) for PTV. Although we found median of maximum dose differences for all OARs to be <5%, we found our plans were robust to tolerate these changes. Only in two patients should we have continued to treat without replanning, the cumulative doses would have exceeded the tolerance dose (Fig 2).



### Conclusion

Despite the robustness of the initial treatment plan, replanning was necessary in 20% of patients due to anatomical changes during the treatment. While factors influencing plan robustness is important in HNC treatment, the importance of vigilance to anatomical changes and continuous monitoring during treatment is necessary for a safe and effective outcome.

### PV-0204 Mortality after radiotherapy or surgery in early stage NSCLC: a population based study

C. Ostheimer<sup>1</sup>, F. Palm<sup>1</sup>, E. Christoph<sup>1</sup>, M. Katharina<sup>1</sup>, M. Rafael<sup>2</sup>, D. Vordermark<sup>1</sup>, D. Medenwald<sup>1</sup>

<sup>1</sup>Martin Luther University Halle-Wittenberg,

<sup>1</sup>Department of Radiation Oncology, Halle/Saale,

Germany ; <sup>2</sup>Martin-Luther University Halle-Wittenberg,

Institute of Medical Epidemiology- Biostatistics and

Informatics, Halle Saale, Germany

### Purpose or Objective

Stereotactic body radiotherapy (SBRT) can achieve high tumour control with limited toxicity for inoperable early stage non-small-cell lung cancer (NSCLC) patients. The objective of this study is to evaluate the impact of the introduction of SBRT on survival of stage I lung cancer patients in the general population.

### Material and Methods

The German Epidemiologic Cancer Registries from the Robert Koch Institute were assessed in three time periods according to availability of SBRT: (1) 2000-2003 (pre-SBRT), (2) 2004-2007 (interim) and (3) 2007-2014 (broad availability of SBRT). To assess the association of cancer related parameters with mortality, hazard ratios (HR) from Cox proportional hazards models were computed. To evaluate the change of treatment related mortality, we performed interaction analyses and the relative excess risk due to interaction (RERI, additive scale) was computed. For the tumor-specific survival, subdistributional hazard ratios from Fine-Gray models were estimated.

### Results

A total of 16.292 patients with UICC stage I NSCLC diagnosed between 2000 and 2014 were analysed. Radiotherapy utilization increased from 5% in pre-SBRT era to 8.8% after 2007. Tumor-specific mortality was more favourable in all treatment groups in the years after 2007 compared to 2000-2003 (strongest for the radiotherapy group: HR=0.63, 95% CI: 0.5- 0.79). Comparing surgery and radiotherapy the interaction analysis revealed a stronger improvement for radiotherapy (multiplicative scale for 2000-2003 vs. >2007: 0.78, 95% CI: 0.62-0.98). On an additive scale, treatment\*period interaction revealed a RERI for 2000-2003 vs. >2007 of -1.18 (95% CI: -1.84, -0.52).

### Conclusion

Using population-based data, we observed a survival advantage in stage I lung cancer. With an increasing utilization of radiotherapy, a stronger improvement occurred in patients treated with radiotherapy when compared to surgery.

### PV-0205 Quantification of Changes in Lung Cancer during Radiotherapy: a comparison between CT and MRI

E. Huang<sup>1</sup>, S. Kumar<sup>1</sup>, D. Moses<sup>2</sup>, L. Holloway<sup>3</sup>, S. Vinod<sup>1</sup>

<sup>1</sup>Liverpool Hospital, Cancer Therapy Centre, Liverpool, Australia; <sup>2</sup>Prince of Wales Hospital, Department of Radiology, Randwick, Australia; <sup>3</sup>Liverpool Hospital, Ingham Institute of Applied Medical Research, Liverpool, Australia

### Purpose or Objective

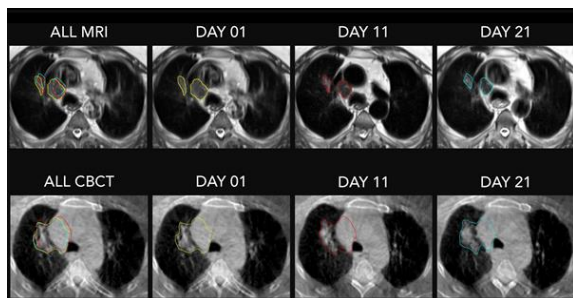
There has been growing interest in use of MRI in lung cancer radiotherapy. This study aims to evaluate the changes seen in lung cancer volume and position on MRI during a course of radiotherapy, and compare this with the current standard of practice, serial cone-beam CT (CBCT).

### Material and Methods

Patients with histologically or cytologically confirmed lung cancer receiving more than 12 fractions of radiotherapy, either alone or with concurrent chemotherapy, were enrolled in a prospective study of serial CBCT and MRI in during-treatment (Day 1, Day 11, & Day 21) scans. Time-matched CBCT and MRI primary gross tumour volumes (GTVp) were manually delineated by a single observer on MIM software. Derived parameters (volume, & centre of mass (COM)) were analysed descriptively and using Bland-Altman plots and linear regression.

### Results

20 patients with 23 GTVp were eligible for inclusion. 60 CBCT/MRI scan pairs were analysed. Mean ( $\pm$  standard deviation) CBCT vs MRI volume change compared to baseline (Day 1) were 81% ( $\pm$ 17) vs 80% ( $\pm$ 29), and 70% ( $\pm$ 31) vs 72% ( $\pm$ 46) for Day 11 and Day 21 respectively. CBCT contours were on average 23% larger than paired MRI contours. MRI vs CBCT demonstrated a systematic bias of -0.92 mL, with absolute volume of CBCT being greater than MRI. Bland-Altman analysis demonstrated CBCT and MRI were not equivalent imaging modalities. No significant regression was found in during-treatment CBCT or MRI ( $p=0.65$ ). No significant difference in slope of tumour regression was found between CBCT and MRI. A significant ( $> 0.5$  cm) COM shift was observed from Day 1 to Day 21, at 0.54 ( $\pm$ 0.42) vs 0.66 ( $\pm$ 0.41) cm for CBCT vs MRI respectively.



### Conclusion

Changes in lung cancer volume and position during radiotherapy are different on CBCT and MRI. Further investigation is warranted if MRI is to be used for adaptive radiotherapy in the future.

### PV-0206 Gross endobronchial disease: predictor of clinical outcomes for early stage NSCLC treated with SBRT

N. Aghdam<sup>1</sup>, S. Kataria<sup>1</sup>, M. Pernia<sup>2</sup>, C. Hall<sup>3</sup>, T. O'Connor<sup>3</sup>, L. Campbell<sup>1</sup>, S. Suy<sup>1</sup>, S.P. Collins<sup>1</sup>, R. Krochmal<sup>4</sup>, E. Anderson<sup>4</sup>, J. Lischalk<sup>1</sup>, B.T. Collins<sup>1</sup>  
<sup>1</sup>Georgetown University Hospital, Department of Radiation Medicine, Washington DC, USA ; <sup>2</sup>Metropolitan Hospital Center, Department of Internal Medicine, New York, USA ; <sup>3</sup>Cornell University, The college of arts and sciences, Ithaca, USA ; <sup>4</sup>Georgetown University Hospital, Division of Pulmonary and Critical Care Medicine, Washington DC, USA

### Purpose or Objective

SBRT with fiducial tracking is a safe and effective treatment for medically inoperable early stage non-small cell lung cancer (ES-NSCLC). Bronchoscopy affords an all-in-one evaluation of mediastinal lymph nodes, visualization of the central airway, biopsy of the primary tumor, and placement of fiducials for tracking. Tumor proximity to the central airway is a known risk factor for toxicity. In this report, we examine the clinical outcomes of a diverse cohort of patients with both central and peripheral tumors treated with 5 fraction SBRT using fiducial tracking. We identify endobronchial involvement as a predictor of poor clinical outcome and treatment-related death.

### Material and Methods

Medically inoperable patients were treated with frameless robotic SBRT per institutional protocol. Majority (41) underwent bronchoscopy with placement of 3 to 5 fiducials with the remainder placed under CT guidance. Clinical examination and PET/CT imaging were completed for staging and at 6 month follow up intervals. Follow-up was performed using a combination of clinical evaluation and PET/CT scans. Patients were stratified based on clinical stage, tumor location (central versus peripheral) and endobronchial involvement.

### Results

From December 2010 to December 2015, 50 patients with biopsy proven ES-NSCLC (stage I - 31; stage II - 19) deemed medically inoperable with median age of 75 were treated with fiducial-based SBRT to 50 Gy in 5 fractions. Twelve central and 38 peripheral tumors were treated with a median tumor diameter of 3.4 cm (range, 1.1 to 7.3 cm) and staged as T1 (n=18), T2 (n=22), and T3 (n=10) per the AJCC 7<sup>th</sup> edition. At median follow up of 36 months, overall survival (OS) was 52%. Survival did not differ between peripheral and central tumors (53% vs 50%;  $p=0.47$ ) nor between stage I and stage II disease (51% vs 52%;  $p=0.674$ ). Local control (LC), regional control (RC), distant metastasis free survival (DMFS), and disease free survival (DFS) were 88%, 89%, 83% and 73%, respectively. Of 41 patients who underwent bronchoscopy for fiducial placement, five tumors, all of which were centrally located, were found to have gross endobronchial involvement. LC and OS for this cohort was 66% and 20%. Cox regression analysis identified endobronchial involvement as a predictor of OS while controlling for age, location, and stage (OR: 4.096,  $p$ -value=0.046). Endobronchial involvement was also an independent predictor for grade 5 pulmonary toxicity (n=4,  $p=0.007$ ). Specifically, 3 patients with gross endobronchial disease went on to experience grade 5 bronchial stricture.

### Conclusion

Central location of ES-NSCLC is known to predict for SBRT-related toxicity. Here we report endobronchial involvement observed during staging bronchoscopy as a significant predictor of poor overall survival and Grade 5 pulmonary toxicity. The poor prognosis and high rates of treatment-related toxicity in patients with central ES-NSCLC may be due in part to gross tumor endobronchial involvement.

### PV-0207 Is V37Gy a Better Dose Predictor for Radiation Pneumonitis for Lung Proton Therapy?

W. Harris<sup>1</sup>, S. O'Reilly<sup>1</sup>, V. Jain<sup>1</sup>, B.K. Teo<sup>1</sup>, L. Dong<sup>1</sup>, S. Feigenberg<sup>1</sup>, A. Berman<sup>1</sup>, W. Zou<sup>1</sup>  
<sup>1</sup>University of Pennsylvania, Radiation Oncology, Philadelphia, USA

### Purpose or Objective

Radiation pneumonitis (RP) is one of the most common forms of toxicity that affect lung cancer patients. About 15-20% of locally-advanced non-small cell lung cancer (LA-NSCLC) patients treated with chemoradiotherapy (CRT) develop RP. The dosimetric parameters used clinically to reduce the likelihood of RP have traditionally been V20Gy

$\leq 30\%$  and mean lung dose  $\leq 20\text{-}23\text{Gy}$ ; however, these parameters are based on photon therapy. The purpose of this study is to evaluate if such dosimetric predictors for RP still hold for LA-NSCLC patients treated with proton therapy.

#### Material and Methods

A total of 129 (46 photon, 83 proton) LA-NSCLC patients treated with concurrent CRT between 2011-2016 were used in the study. In this selected cohort, with a higher rate than clinically observed, 46 (20 photon, 26 proton) were patients that exhibited RP (all grades using CTCAE v4.0) after photon or proton therapy. Dose volume histograms for the uninvolved lung were generated for each patient. The percent lung volume receiving above various dose levels (e.g. V35Gy) were obtained in addition to the traditional V20Gy and mean lung dose. These dosimetric parameters for RP and non-RP patients in photon and proton groups were evaluated with a two-tailed student's test and compared with the V20Gy and mean lung dose. Receiver Operating Characteristic (ROC) curves were generated for various dose levels. The volumetric constraint for the optimal dosimetric parameter was obtained through analyzing RP and non-RP sensitivity/specificity values.

#### Results

For proton patients, a greater separation between the RP and non-RP cohort was observed between V35Gy and V45Gy, when compared with the current clinical standard of V20Gy; however, the greatest difference between RP and non-RP photon patients remains around V20Gy. For proton patients, the maximum difference occurs at V37Gy, with  $24.65 \pm 4.62\%$  and  $18.96 \pm 6.38\%$  for RP and non-RP patients, respectively, while V20Gy was  $31.63 \pm 4.99\%$  and  $26.26 \pm 7.74\%$  for RP and non-RP patients, respectively. Mean lung dose values were consistent between proton and photon patients. A greater separation between RP and non-RP patients is observed when using V37Gy ( $p=0.0001$ ) as compared to V20Gy ( $p=0.002$ ) for proton patients. V20Gy ( $p=0.024$ ) is significant for photon patients, but V37Gy ( $p=0.053$ ) is not. V37Gy ROC curve had the highest Area Under the Curve (AUC) value compared with other dose levels for proton patients. Based on sensitivity/specificity, the optimal volume constraint of V37Gy is  $\leq 23\%$  for proton therapy and the constraint of V20Gy  $\leq 30\%$  is confirmed for photon patients.

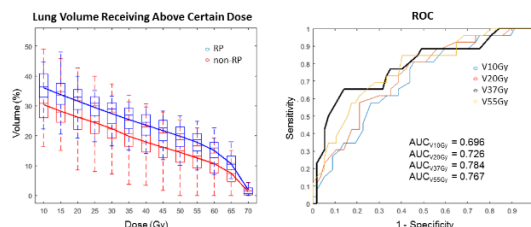


Figure 1: (Left) Box of lung volume receiving above a certain dose for proton therapy patients with radiation pneumonitis (RP - blue) and patients without RP (non-RP - red). (Right) ROC curves for V10Gy, V20Gy, V37Gy and V55Gy for proton patients. V37Gy resulted in the highest AUC value of 0.784 compared with the other dose levels.

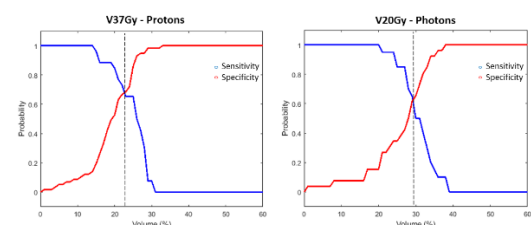


Figure 2: Sensitivity and specificity for V37Gy for proton patients (left) and V20Gy for photon patients (right). Blue line represents sensitivity and the red line represents specificity. The black vertical dotted line shows the point of intersect, which indicates at what volume level most likely predicts RP for V37Gy for protons and V20Gy for photons.

#### Conclusion

While V20Gy is a strong predictor for RP in photon therapy, the volume receiving a higher dose, such as V37Gy, may

be a better indicator for RP for LA-NSCLC patients treated with proton therapy. Further statistical analysis with this data needs to be performed. However, this new dosimetric criteria could potentially help with the RP control in LA-NSCLC treated with proton therapy.

#### PV-0208 Immune-related pneumonitis in NSCLC patients treated with ICI: impact of previous thoracic RT

A. Botticella<sup>1</sup>, T. Ibrahim<sup>2</sup>, L. Mezquita<sup>2</sup>, L. Hendriks<sup>2</sup>, J. Le Pavec<sup>3</sup>, R. Ferrara<sup>2</sup>, C. Caramella<sup>4</sup>, S. Champiat<sup>5</sup>, J. Michot<sup>5</sup>, P. Lavaud<sup>2</sup>, P. Gustin<sup>1</sup>, D. Planchard<sup>2</sup>, A. Gazzah<sup>2</sup>, A. Marabelle<sup>5</sup>, E. Deutsch<sup>1</sup>, B. Besse<sup>2</sup>, C. Le Pechoux<sup>1</sup>

<sup>1</sup>Institut Gustave Roussy, Radiation Oncology Department, Villejuif, France ; <sup>2</sup>Institut Gustave Roussy, Oncology Department, Villejuif, France ; <sup>3</sup>Centre Chirurgial Marie Lannelongue, Laboratoire de Chirurgie Expérimentale-UPRES EA-2705, Plessis Robinson, France ; <sup>4</sup>Institut Gustave Roussy, Radiology Department, Villejuif, France; <sup>5</sup>Institut Gustave Roussy, Département D'Innovation Thérapeutique et des Essais Précoces DITEP, Villejuif, France

#### Purpose or Objective

Pneumonitis is a potentially lethal side effect of immune checkpoint inhibitors (ICI), occurring in 1-5% of patients enrolled in clinical trials. Little is known about the interactions between ICI and previous thoracic radiotherapy (RT). This is the aim of the present study.

#### Material and Methods

Between December 2012 and November 2017, 318 consecutive non-small cell lung cancer (NSCLC) patients received ICI in our Institution and their charts were retrospectively analyzed. Primary endpoint was to determine whether previous radiotherapy had an effect on pulmonary toxicity. Pulmonary toxicity was retrospectively assessed by Common Terminology Criteria for Adverse Events version 4.0.

#### Results

Median follow-up was 32.8 months [95%CI: 5-190]. Median age at the start of ICI was 63 years. 205 patients (64,5%) were males, 103 (32,4%) smokers and 250 (78,6%) with PS  $\leq 1$ ; 206 (64,8%) had adenocarcinoma and 76 (23,9%) squamous; 79 (24,8%) were KRAS mutated, 18 (5,5%) EGFR mutated and 5 (1,6%) ALK positive. PDL1 was  $\geq 1\%$  by immunohistochemistry in 86 (27%), negative in 37 (11,6%) and unknown in 196 (61,3%) patients. ICI treatment was median 3<sup>rd</sup>line (range: 1-12), 89,4% monotherapy PD-(L)1 inhibition.

72 patients (22,6%) received a thoracic RT: 62 out of the 72 RT patients (87,5%) were irradiated with a curative intent. 53 patients (73,6% of the RT patients) received thoracic 3D-conformal RT or intensity modulated RT (normo- or mildly hypofractionated), whereas 9 received SBRT.

16,7% of the RT patients (12/72) showed a G1-4 immune-related pneumonitis (with a G $\geq 3$  of 11,1%), whereas for never-irradiated patients the G1-3 rate of immune-related pneumonitis was 2,4% (6/246), with only 1 G3 toxicity observed and no G $>4$  (t-test, p 0,001).

Median interval between the onset of the immune-related pneumonitis and the end of the RT was 22,4 months.

#### Conclusion

NSCLC patients treated with ICI may be at higher risk of developing immune-related pneumonitis if previously treated with curative-intent thoracic RT.

#### Award Lecture: Honorary Members award lectures

#### SP-0209 Multidisciplinary approaches as the keys to defeat lung cancer

G. Scagliotti<sup>1</sup>

<sup>1</sup>University of Turin, Department of Oncology, Turin, Italy

Abstract not received

**SP-0210 Are radiation specialists good global cancer citizens?**

J. Torode<sup>1</sup>

<sup>1</sup>Union for International Cancer Control (UICC), Geneva, Switzerland

Abstract not received

**SP-0211 Putting down the scalpel. The evolution of rectal cancer treatment**

A. Habr-Gama<sup>1</sup>

<sup>1</sup>Angelita and Joaquim Gama Institute, Colorectal Surgery, São Paulo, Brazil

**Abstract text**

The benefits of neoadjuvant chemoradiation were not restricted to long-term local disease control as confirmed by an update of the German Trial after 11 years of follow-up. Neoadjuvant treatment may lead to variable degrees of tumor regression, reflected by primary tumor reduction in size (downsizing), in depth of penetration and possible perirectal node sterilization (downstaging). In up to 42% of the cases, complete pathological tumor regression has been reported. Such findings challenged the role of standardized radical resection in all patients with rectal cancer irrespective of tumor response to neoadjuvant therapy. One could ask about the oncological benefit in a patient following radical rectal resection where not a single cancer cell is removed. But the solution is not straightforward, as it seems. Assuring complete tumor regression is not an easy task, unless radical resection is performed. However, exposing patients to considerable morbid procedure leading to urinary, sexual and fecal dysfunctions, the requirement for temporary or permanent stomas and the expected procedure-related mortality may not be considered the best alternative. In addition, the degree of tumor regression may be influenced by several different factors that should be taken into account. Studies have not definitively explained the reasons why after similar doses some tumors respond completely while others seem to be absolutely resistant to such therapy. Another factor that seems to influence tumor regression is the time elapsed between completion of treatment and response assessment. This was first suggested by data of patients with anal cancer. Similarly, in rectal cancer, retrospective studies also indicated that longer interval periods were associated with increased rates of complete tumor regression, suggesting that the more you wait, the more you get in terms of tumor regression. In this setting, patients with apparent complete clinical tumor regression would be ideal candidates for alternative treatment strategies including no immediate surgery and rigorous close observation. The main obstacle to this approach is the risk of leaving microscopic residual disease. Indeed, distinguishing transmural fibrosis from microscopic residual disease maybe quite difficult. Clinical assessment alone has been shown quite disappointing sensitivity and specificity rates in previous retrospective studies. However, some of these studies included tumor response assessment performed at 6 weeks from CRT completion, possibly too early and reflecting the detection of residual disease in the setting of ongoing necrosis. Also, studies have detected residual microscopic nodal disease in ypT0 patients. Again, these studies included patients managed by radical surgery after 6 weeks from CRT completion. This is suggested by the observation of absence of residual nodal disease in patients with ypT0 after periods of longer intervals than 6 weeks after CRT completion. It has been our strategy to assess tumor response at least after 8

weeks from CRT completion including clinical assessment with digital rectal examination, rigid proctoscopy and CEA levels in combination with radiological assessment, mainly performed to rule out residual extra-luminal disease. Only patients fulfilling these stringent criteria have been considered for this non-operative approach (Watch & Wait). Patients managed by this approach, did no worse than patients managed by radical surgery and pathological complete response in terms of survival. Late local relapses were all amenable to salvage resection, occurring in approximately 10% of these patients not immediately operated on and in a considerably longer interval when compared to systemic relapses. In a retrospective review, there was no survival compromise in patients with initial suspicion for complete clinical response who undergone delayed surgery for early tumor regrowth. Recently, other Institutions have observed similar results further supporting this treatment strategy in highly selected patients. Assessment of tumor response remains a challenging issue associated with a learning curve that has probably improved over time during our 25-year experience period. Even so, a subset of patients who were initially considered as complete responders presented with residual disease or early tumor regrowth/recurrence within 12 months of follow-up. It is worth mentioning that we have arbitrarily considered this period of 12 months as the minimum to consider a sustained complete clinical response in these patients. The share of patients with complete tumor regression may actually increase with modern CRT drugs and regimens and earlier baseline disease.<sup>20</sup> In fact the addition of chemotherapy cycles during the RT and the “resting” period between RT and surgery with a modest increase in RT dose (50.4Gy to 54Gy) has led to a significant increase in complete clinical response rates to over 50% of patients.

## Estro 38 Sunday 28 April

---

### Teaching Lecture: Re-irradiation for breast cancer

---

#### SP-0212 Re-irradiation for breast cancer

P. Poortmans<sup>1</sup>, O. Kaidar-Person<sup>2</sup>, S. Oldenburg<sup>3</sup>

<sup>1</sup>Institut Curie Ensemble Hospitalier, Department Of Radiation Oncology, Paris Cedex 05, France ; <sup>2</sup>Rambam Health Care Campus, Department Of Oncology- Radiation Oncology Unit, Haifa, Israel ; <sup>3</sup>Academic Medical Center, Departement of Radiation Oncology, Amsterdam, the Netherlands

#### Abstract text

Half of locoregional recurrences (LRR) after primary breast cancer treatment are isolated events. Re-staging should be done to rule out metastatic disease in order to select patients for potential curative salvage treatment. The treatment approach depends on the characteristics of the primary and recurrent cancer, previous locoregional and systemic treatments, site of recurrence, comorbidities and the patient's wishes. A multidisciplinary discussion should be associated to the shared decision-making process. As treatment has the potential to provide long-term disease-free survival, for radiation therapy (RT) meticulous target volume delineation and selection of the most appropriate techniques should be used to decrease the risk of toxicity, especially in patients who were previously treated with chemotherapy and/or RT. For patients who did not receive prior RT, resection followed by RT is the standard approach, including a boost to site of recurrent disease and with a higher radiation dose in case of residual macroscopic disease. Re-irradiation after previous RT should be considered also for all patients with isolated locoregional disease, preferably after surgical debulking. It can also be performed as primary treatment for gross disease, if surgery is not feasible or not accepted by the patient. The effective re-irradiation dose is generally limited to reduce adverse effects from the accumulated radiation dose. Combining lower re-irradiation doses combined with hyperthermia results in improved tumour control without additive toxicity. In selected patients, salvage breast-conserving surgery can be considered even in the case of earlier RT. Careful patient selection is needed and most experience is available with interstitial brachytherapy. Patients with LRR should also be considered for "adjuvant" systemic therapy as part of their treatment management, depending on the receptor status of the recurrent disease.

Reference: Kaidar-Person O, Oldenburg S, Poortmans P. Re-irradiation and Hyperthermia in Breast Cancer. Clin Oncol (R Coll Radiol). 2018 Feb;30(2):73-84.

---

### Teaching Lecture: Extracellular vesicles; are we there yet?

---

#### SP-0213 Extracellular vesicles and potential implications for radiation therapy

A. Dal Pra<sup>1,2</sup>

<sup>1</sup>University of Miami, Department of Radiation Oncology, Miami, USA; <sup>2</sup>University of Bern, Radiation Oncology, Bern, Switzerland

#### Abstract text

Extracellular vesicles are a heterogeneous group of cell-derived membranous structures comprising exosomes and microvesicles that reflect the genetic and non-genetic materials of parent cancer cells. They are present in biological fluids and are involved in multiple physiological and pathological processes. Extracellular vesicles are

currently deemed as an important mechanism to cell-cell communication, allowing cells to exchange proteins, lipids and genetic material. These vesicles carry molecules such as oncoproteins and oncopeptides, RNA species (e.g., microRNAs, mRNAs, and long non-coding RNAs), lipids, and DNA fragments from donor to recipient cells. These compounds are potential sources of prognostic and/or predictive biomarkers as well as markers of treatment response. We will review the current role of extracellular vesicles in radiation therapy, with a particular focus on the development of clinical assays for treatment personalization.

---

#### Teaching Lecture: Update on the management of SCLC

---

##### SP-0214 Update on the management of SCLC

C. Le Pechoux<sup>1</sup>, A. Botticella<sup>1</sup>, A. Levy<sup>1</sup>

<sup>1</sup>*Gustave Roussy Cancer Campus, Radiation Oncology, Villejuif Cedex, France*

##### Abstract text

Small cell lung cancer (SCLC) accounts for about 13% of lung cancers. With a decreasing incidence in the last twenty years, SCLC remains a cancer with a dismal prognosis due in particular to a short doubling time which explains the metastatic presentation in nearly two thirds of the cases at diagnosis. This disease has a particular propensity to recur locally and disseminate in the brain. Hence, there have been several randomized trials assessing the role of thoracic and brain radiotherapy. Two individual data-based meta-analyses showed that thoracic radiotherapy and prophylactic cranial irradiation (PCI) should be part of the therapeutic strategy. Although platinum based chemotherapy combined to etoposide remains the cornerstone of SCLC treatment, since the 1980s radiotherapy has taken a growing place in multidisciplinary care. The treatment of stages I to III, is based on concomitant chemoradiation in fit patients and prophylactic cranial irradiation at the dose of 25 Gy in 10 fractions. Recent studies have confirmed that concomitant hyperfractionated accelerated radiotherapy at the dose of 45 Gy in 30 twice daily fractions, in 3 weeks gives the best results. However for patients who cannot receive HFART, once daily radiotherapy at the dose of 66 Gy in 33 fractions, may be an alternative. Five-year survival in the latest randomized studies is around 30-35% in SCLC patients having received concomitant CRT and prophylactic cranial irradiation. Radiotherapy has also a place in metastatic SCLC. The pivotal treatment is of course systemic treatment with platinum based chemotherapy and Etoposide. There is however randomized evidence that consolidation thoracic radiotherapy at the dose of 30 Gy in 10 fractions, administered to responders may improve the outcome of patients with extensive disease. A randomized phase II trial has also tried to evaluate the role of consolidation radiotherapy, not only to intra-thoracic disease, but also to extracranial metastases in ED SCLC. The results were encouraging. Prophylactic cerebral irradiation (PCI) remains a standard of care in non metastatic disease in good responders but its place is more controversial in the metastatic setting. Most advances in SCLC management are based on a better integration of radiotherapy and chemotherapy, even in extensive disease.

---

#### Teaching Lecture: How to combine checkpoint inhibitors with radiotherapy?

---

##### SP-0215 How to combine checkpoint inhibitors with radiotherapy?

K. Harrington<sup>1</sup>

<sup>1</sup>*The Institute of Cancer Research and The Royal Marsden NHS Foundation Trust, Division of Radiotherapy and Imaging, Sutton, United Kingdom*

##### Abstract text

There is enormous excitement about the potential for combining radiotherapy with immune checkpoint inhibitors as a means of enhancing outcomes for patients with a variety of cancers. In recent years, we have begun to understand in great detail the biological effects of radiation on tumour (and normal) cells and this knowledge has informed our thinking on how we might best exploit radiation-induced immunogenic cell death for patient benefit. In particular, we have a much clearer perspective on the importance of molecular responses to DNA damage and their interactions with immune sensing mechanisms in the cell. In this presentation, the interplay between DNA damage and nucleic acid sensors will be reviewed, with specific focus on the cGAS/STING axis. However, other innate immune effectors such as toll-like receptors, RIG-I and mda5 will also be discussed. In addition, opportunities for combination therapies will be discussed in the context of neoadjuvant, concomitant and adjuvant use of immune checkpoint inhibitors, encompassing the PD-1/PD-L1 axis but also considering other more novel agents. The importance of the fractional and total dose of radiation will also be discussed with a view to interpreting existing clinical trial data and informing future trial design. Finally, the current and potential future roles for both predictive and prognostic biomarkers will be evaluated.

---

#### Teaching Lecture: How does brachytherapy fit in the modern management of penile cancer?

---

##### SP-0216 How does brachytherapy fit in the modern management of penile cancer?

J. Crook<sup>1</sup>

<sup>1</sup>*BC Cancer Agency - Southern Interior, Radiation Oncology, Kelowna, Canada*

##### Abstract text

Penile cancer is uncommon in western society, accounting for fewer than 1% of malignancies in men. When detected early, it is curable and penile conserving modalities should be considered first and foremost. If neglected and associated with spread to regional nodes, 5-year survival is reduced to 20-50% for inguinal node involvement and 10% when pelvic nodes are involved. The majority of penile cancers are of squamous cell (SCC) origin, and as such are both radiosensitive and radiocurable. About 50% are associated with HPV and as is the case for HPV-induced squamous cancer at other sites, may be more responsive to chemo-radiotherapy.

For SCC localized to the glans, brachytherapy is a convenient and effective means of delivering radiotherapy. There is abundant experience over several decades using low dose rate brachytherapy (LDR) employing temporary implantation of iridium-192 wire, or more recently using Pulse Dose Rate afterloading with a high intensity Ir-192 stepping source and hourly fractions that mimic LDR radiobiology. Penile preservation rates are about 85% at 5 years and 70% at 10 years. Ideal tumors are confined to the glans and < 4 cm in diameter. Higher grade is not a contraindication to brachytherapy but does determine nodal management. Surgical nodal staging is

recommended for all stage T2 or higher, grade 3, or T1b with LVI. The implant procedure is performed under either local (penile block) or general anesthesia and takes about 30-45 minutes. A minimum of a 2 plane implant is recommended, but up to 3 planes may be required. The median number of needles is 6 (4-12) and ideal spacing between adjacent needles and planes for LDR is 15 mm (range 12-18). Dosimetry can be calculated according to active length and spacing as per the rules of the Paris system for Iridium-192 wire manually after-loaded implants (dose prescribed at 85% of the dose rate minima in the central plane), or calculated from a planning CT scan performed with 1mm slice thickness through the region of interest. The patient is usually hospitalized during the treatment which takes about 5 days at an hourly dose rate of 50-60 cGy per hour. Needles can be removed at the bedside with suitable parenteral analgesia; bleeding is minimal.

With increasing availability and popularity of high dose rate brachytherapy, (HDR) and a growing general reluctance regarding manual after loading, HDR is taking a more prominent role in penile brachytherapy, with 4 recent series reporting on over 100 patients. Although the procedures are very similar, in contrast to an LDR implant, needle spacing should be closer in HDR, between 9 and 12 mm. Treatment is fractionated, twice daily with a minimum of 6 hours between. Fraction size is 3-3.5 Gy with a total prescribed dose of 42-51 Gy. Homogeneity parameters are important to minimize complications and it is recommended that the V125% be < 45% and the V150 < 20%. Penile preservation is reported at 93-100% at 2 years and 70% at 10 years.

Another HDR option involves an individualized or custom mold technique. This is suitable for Tis or minimally invasive T1a tumours. The prescribed dose is 40 Gy in 10 fraction given bid over 5 days. The dose can be prescribed at the required depth (3-5mm). Maximal skin dose should be limited to 120%, with central urethral sparing to receive < 90% of prescription. Two recent small series show promising results.

For both methods of brachytherapy, treatment is well tolerated with the acute reaction healing in 2-3 months. As the tumor resolves it will leave a crater which then must re-epithelialize. Cleanliness is maintained with saline soaks, and topical antibiotics, with the addition of Vitamin E as healing progresses. The most common long term complications are soft tissue ulceration in 5-25% (depending on implant volume, dose and tumour stage) which can usually be managed conservatively although hyperbaric oxygen will speed healing in more serious cases, and meatal stenosis requiring either urologic or self-dilatation in 9-45% (depending on proximity of the sources to the meatus).

With all the brachytherapy techniques for penile cancer, prolonged follow up is necessary. Although 80% of local failures are within the first 2 years, approximately 20% can occur late, after 5 years. Local recurrences can be managed surgically with no impact on cause specific survival but must be recognized and managed promptly. Patients must be aware of this limitation

---

#### Teaching Lecture: Detector specific output correction factors: How to use them in practice

---

#### SP-0217 Detector specific output correction factors: How to use them in practice

M. Aspradakis<sup>1</sup>

<sup>1</sup>Luzerner Kantonsspital Radio-Onkologie, Luzern Switzerland

Abstract not received

---

#### Teaching Lecture: Uncertainties in Radiomics

---

#### SP-0218 Uncertainties in Radiomics

M. Hatt<sup>1</sup>

<sup>1</sup>Inserm, Laboratory of Medical Information Processing Latim- Umr 1101, Brest, France

#### Abstract text

This lecture will highlight the major uncertainties and methodological pitfalls of radiomics studies. Building on previous experience as well as on a critical review of important published papers, the lecture will detail most important issues associated with image acquisition and pre-processing, object of interest (semi)automatic delineation, features definition, nomenclature and standardization, as well as statistical analysis and machine learning for models training and validation. For each pitfall and issue, the lecture will provide the most up-to-date and currently available methodological solutions, with a focus on options facilitating the transfer of radiomics to the clinical practice.

---

#### Teaching Lecture: New technology and modalities in Radiotherapy - What can the ESTRO School offer?

---

#### SP-0219 New technology and modalities in Radiotherapy - What can the ESTRO School offer?

J.G. Eriksen<sup>1</sup>

<sup>1</sup>Aarhus University Hospital, Dept. of Experimental Clinical Oncology, Aarhus, Denmark

#### Abstract text

Radiation Oncology is probably one of the most technology-driven medical specialties at all. This is very much reflected by the multidisciplinary nature needed for delivering the optimal treatment at the right time and in the right place. MD's, medical physicists and RTT's are some of the well-known key persons but also engineers, technicians and IT-professionals play an important role. The development of new technologies in radiotherapy are moving fast forward and it is both a privilege and an obligation of the ESTRO School to keep updated on the educational offers that reflect the technological development. The educational offer should be updated, being able to look into the future and be critical, objective and well balanced. The lecture will discuss why this obligation is so important, the current strategy of the School and give a glimpse of what we can expect in the near future.

---

#### Teaching Lecture: Precision medicine and systems biology - transforming cancer research in the 21st century

---

#### SP-0220 Precision medicine and systems biology - transforming cancer research in the 21st century

W. Kolch<sup>1</sup>

<sup>1</sup>University College Dublin- Ireland, Systems Biology Ireland and Conway Institute, Dublin, Ireland

#### Abstract text

Advances in technologies, especially genome sequencing and other omics methods, are enabling the precise molecular phenotyping of individual cancer patients. Major challenges are now unlocking the information contained in these data and integrating them with each other, but also with clinical data and imaging data. The aim is to obtain a clinically relevant and actionable view of an individual patient's cancer that allows finer diagnostic stratification, predictions of the course of

disease and response to therapies, ultimately enabling highly precise interventions with high efficacy and less side effects. Mathematical and computational modelling techniques developed by systems biology to analyse dynamic living systems play a key role in achieving these goals. I will discuss the role of such models for precise diagnostic stratification, the identification of efficacious drug combinations, and the personalisation of treatment.

---

**Symposium: Balancing the risks and benefits of re-irradiation**

---

**SP-0221 Indications for re-irradiation - changes in the era of effective systemic treatment options?**

M. Hoyer<sup>1</sup>

<sup>1</sup>Aarhus University Hospital, Danish Center For Particle Therapy, Aarhus, Denmark

**Abstract text**

The recent years have brought a number of drugs directed towards novel targets of the cancer cells. Many of these have given led to some improvement of the survival. This survival gain is moderate in most cancers, but it may a reason for reconsideration of strategies in treatment of radio-recurrent cancer? Reirradiation is always related to an increased risk of complication and selection of patients for reirradiation represents a delicate balance between disease control and survival gains on one hand and risk of severe complication on the other.

The presentation will give examples of considerations in selection of radio-recurrent patients for reirradiation. However, it will conclude that systemic therapies cannot replace radiation therapy in the attempt to achieve long lasting tumor control.

**SP-0222 Radiobiology of normal tissue repair - what are the implications for reirradiation?**

R. Coppes<sup>1</sup>

<sup>1</sup>University Medical Center Groningen, Radiation Oncology and Cell Biology, Groningen, The Netherlands

**Abstract text**

The response of normal tissues to irradiation is mainly determined by the survival and regenerative potential of the tissue stem cells, and modulated by inflammatory processes, vasculature damage and altered neuronal innervation and fibrosis. Interestingly, transplantation of tissue specific stem cells has been shown to restores tissue homeostasis and sparing stem cells may preserve tissue function and prevent late radiation effects. It is for long recognized that the number of surviving clonogens determines the time to recovery after irradiation and with that also the retreatment tolerance of many tissues. Since these clonogens are often stem cells or derived progenitor it seems eminent to spare these as much of possible to reduce normal tissue side effects and potentially allow reirradiation when needed. Recently much improvement has been made to described and characterized the tissues stem cells. This now allows localisation and studying of radiation responses in vitro and in vivo. In combination with accurate localised tissue proton irradiation this has yielded novel insight in the regenerative processes of several tissues. Dose volume effects, inhomogeneous irradiation field and uneven distribution of stem cells greatly influences the regenerative potential and with that the retreatment tolerance of normal tissue. Moreover, studies of post irradiation form in tissue isolated stem cells show regenerative potential in vitro being much higher than in situ, indicating that not only the radiation damaged stem cells themselves determine regenerative potential but also the affected environment. In this presentation the radiobiology of reirradiation will be discussed and examples of several tissue will be

provided to show insight in factors that influences stem cells functioning and how this may be used to enhance post-irradiation tissue regeneration and consequential retreatment tolerance.

**SP-0223 Protons, stereotactic radiotherapy and adaptive radiotherapy - what is their value for reirradiation?**

A. Richter<sup>1</sup>

<sup>1</sup>Universitätsklinikum Würzburg, Department of Radiation Oncology, Würzburg, Germany

**Abstract text**

For re-irradiation highly conformal treatment techniques are needed. Some technological developments such as proton therapy, stereotactic and adaptive radiation therapy have improved targeting accuracy and offer the possibility of highly conformal dose distributions. For proton therapy, the low exit dose is advantageous to achieve a high degree of dose conformity. The availability of proton therapy is limited to proton centers. The wider availability of in-room imaging and advanced treatment delivery systems means that more institutions are now offering stereotactic radiation therapy. The stereotactic approach uses an inhomogeneous dose distribution with a sharp fall-off dose and tight margins to achieve a high biological effective dose in the target and a dramatic sparing of normal tissue. For both techniques (proton and stereotactic radiotherapy), motion management strategies should be implemented to considered interfraction and intrafraction motion. Adaptive radiation therapy accounts for changes in patient's anatomy and/or physiology during the treatment course. The adaptive radiation therapy is based on repeated anatomical and/or functional imaging and the use of deformable image registration. Further elements of the adaptive workflow are the automatic recontouring, plan evaluation and reoptimization, dose calculation, and quality assurance. Adaptive radiation therapy can be performed in real-time, online or offline. The clinical realization of online adaptive radiotherapy is extremely challenging, mainly due to the inability for real-time treatment re-planning. The implementation of adaptive radiotherapy presents some challenges such as accuracy of deformable image registration and the higher workload for the staff. Despite some challenges, proton and stereotactic radiation therapy offer the possibility of highly conformal dose distributions. Adaptive radiation therapy holds significant promise in maximally compensating for intra and interfraction anatomical uncertainties.

**SP-0224 Brachytherapy in the reirradiation situation - what are benefits and limitations compared to modern EBRT?**

C. Gutiérrez Miguélez<sup>1</sup>

<sup>1</sup>Institut Català d'Oncologia, Brachytherapy Unit, L'Hospitalet de Llobregat, Spain

**Abstract text**

In this talk, I will do a revision of indications of Brachytherapy for reirradiation, a revision of the results in published in the literature and our results in different localizations. In the last years, due to the advances in imaging and dosimetry optimization, the interest and use of Brachytherapy (BT) for treating relapses is growing. The benefits of reirradiation with Brachytherapy versus External Radiotherapy (ERT) are: Smaller treated volume; Accuracy: no motion; Rapid dose fall-off; Accelerated treatment (therapeutic gain); Preferably intraoperative approach; If intra/peroperative implant, only 1 procedure. The limitations or disadvantages would be: Very small treated volumen; Operator dependent; Need of skills to insert applicator; Need of Operating Theatre; Help of other especialists (surgeons); Inhomogeneous dose distribution (Hot spots);

High complication rate. Currently there are some groups that are using BT for: Breast (second conservative approach). The GEC-ESTRO Breast group experience (JM Hannoun-Levy) published their experience with the same local control as the primary treatment and with good cosmetic results; Prostate (Salvage HDR or LDR BT): the rate of biochemical control, survival and complications by different groups are described. For Head&Neck, I will explain in detail Navarra's experience (R Martinez-Monge) and Erlangen's (V Strnad). I will also describe other indications, as Gynecology, Rectum, Chordoma, and other second primary cancers occurring in previously treated in-field. And finally I will describe our results in Breast (40 cases), Prostate: (96 analysed), Head&Neck: 13, Rectum: 14 and a miscellaneous.

---

**Symposium: Circulating biomarkers for patient stratification and treatment monitoring**

---

**SP-0225 Blood biomarkers to predict radiotherapy response**

G. Hanna<sup>1</sup>

<sup>1</sup>*Peter MacCallum Cancer Centre, Department of Radiation Oncology, Melbourne, Australia*

**Abstract text**

The use of predictive biomarkers in radiation oncology is a field still very much in its infancy. Very few validated biomarkers exist which are used to select or modify the treatment of a patient scheduled to receive radiotherapy and which are in routine use in clinical practice. Moving towards a precision medicine based approach in radiation oncology, it is hoped that predictive biomarkers may be used in a range of scenarios to inform clinical decision making. It is hypothesised that biomarkers could select patients for treatment versus no treatment, for selection of a specific radiation technique or dose and/or fractionation schedule and perhaps they may be used to select patients for a specific systemic therapy agent in combination with radiotherapy. It is hoped that circulating biomarkers could be used in combination with or in place of tissue samples. This presentation will review these considerations and will suggest potential blood based biomarkers which may be of potential clinical benefit in the future.

**SP-0226 ctDNA as a non-invasive liquid biopsy for patient stratification and treatment monitoring**

D. Gale<sup>1</sup>

<sup>1</sup>*University of Cambridge, Cancer Research UK Cambridge Institute- Li Ka Shing Centre, Cambridge, United Kingdom*

**Abstract text**

This talk will focus on the use of circulating tumour DNA (ctDNA) as a non-invasive liquid biopsy for treatment monitoring and patient stratification.

Different technologies will be discussed, including amplicon-based sequencing, exome sequencing, the use of patient-specific panels and digital PCR to monitor disease in advanced and early stage cancer in high-grade serous ovarian cancer, melanoma, breast and non-small cell lung cancer (NSCLC).

**SP-0227 Cancer detection using methylated cell-free DNA**

S. Bratman<sup>1</sup>

<sup>1</sup>*Princess Margaret Cancer Centre, Radiation Oncology, Toronto, Canada*

**Abstract text**

Circulating biomarkers play an important role in personalized cancer medicine and adaptive therapy. In

particular, liquid biopsies using circulating tumour DNA (ctDNA) are rapidly gaining acceptance in clinical settings. Current methods for the detection of ctDNA involve sequencing somatic mutations using cell-free DNA, but the sensitivity of these methods may be low among patients with localized cancer given the limited number of recurrent mutations. By contrast, large-scale epigenetic alterations—which are tissue- and cancer-type specific—are not similarly constrained and therefore potentially have greater ability to detect and monitor cancers in patients with localized disease. A prime example is DNA methylation, which differs between cancerous and normal tissues and between distinct cancer types. In this talk, I will describe current approaches to measuring methylated cell-free DNA. We have developed a new immunoprecipitation-based technique that addresses several limitations of previous assays. Our technique avoids chemical conversion of cell-free DNA (i.e., bisulfite treatment), therefore enabling genome-wide methylome analysis of small quantities of circulating cell-free DNA. We show that large-scale DNA methylation changes that are tumour-specific are enriched within cell-free DNA. Robust performance is seen in cancer detection and classification across an extensive collection of plasma samples from several tumour types. In a cohort of patients with head and neck squamous cell carcinoma, we demonstrate how methylated cell-free DNA analysis could be used for longitudinal monitoring and evaluating treatment response.

**SP-0228 Circulating biomarkers tumor immune response**

D. De Ruyscher<sup>1</sup>

<sup>1</sup>*Maastrro Clinic, Radiation Oncology, Maastricht, The Netherlands*

**Abstract text**

Immunotherapy (IO) is increasingly used to treat a variety of cancers, both in the curative and palliative setting. In contrast to TKIs, where biomarkers are in use for over a decade, leading to increased success and insights in resistance mechanisms and new targets, the landscape in IO is more sober. Although many IO targets are being identified in pre-clinical models and in human material, robust and highly predictive biomarkers are still lacking. The reasons may partly due to the complexity and dynamic nature of the immune system. Ideally, all parts of the immune system as well as the inflammatory status of the tumor at a certain moment in time should be known from a blood sample. The cancer immunogram was developed to describe the cancer-immune system interaction including a framework of seven parameters that are known to affect the anticancer immune response and that can be interrogated in individual cancer patients. These parameters are: tumor mutational burden; the general immune status of the patient; presence of T cell immune infiltrates; tumor PD-L1 expression; sensitivity of tumor cells to T-cell killing (including MHC expression, functional IFN-gamma receptor pathway); a myeloid cell-mediated inflammation (high C-reactive protein (CRP) and IL-6 levels); and high serum lactate dehydrogenase (LDH) (reflecting both tumor burden and anaerobic glycolysis). PD-L1 expression, with all its shortcomings, is the most commonly used biomarker for IO, but is not usable as a circulating biomarker.

In contrast, tumor mutational burden (MB), which is associated with response to IO, is experimentally detectable in the blood. The hypothesis is that the higher the number of mutations, the higher the probability of neo-antigen expression and thus the higher the likelihood that the tumor is being recognized as “foreign” by the immune system.

Patients with either germline or somatic mutations in mismatch repair genes have a very high number of non-synonymous mutations. This is reflected by unstable

microsatellite regions in the genome. Patients with mismatch repair deficient tumours (dMMR) have a high overall response rate to PD-1/PD-L1 blockade. TMB measurement is highly dependent on the method and a clear cut-off has not yet been defined. However, the likelihood that TMB will become a standard test is high. The diversity of the T-cell repertoire can be measured by DNA sequencing of the TCR V $\beta$  genes. The presence of a restricted or uneven TCR repertoire measured in the peripheral blood had a negative impact on survival in patients with melanoma or bladder cancer treated with IO. At present, this is still a highly experimental technique.

As the inflammatory status of the tumor micro-environment is also determining the response to IO, markers like lactate dehydrogenase (LDH), CRP, vascular endothelial growth factor (VEGF) and soluble CD25 are associated with response to anti-CTLA-4 and PD-1/PD-L1 blockade in advanced melanoma. However, more work is needed to validate these findings and to establish cut-off values that would make these clinically relevant. Baseline neutrophil-to-lymphocyte ratios and relative eosinophil count are associated with response to IO, but none of these have an accuracy which is high enough to be useful in the clinic.

Finally, circulating tumor DNA seems to be a very sensitive marker that allows to detect both tumor growth as well as response far before imaging does.

It is likely that the coming years circulating biomarkers will become available and more specific in order to change the landscape of IO to make it more efficient for more patients.

---

#### Symposium: Radiation-drug combinations on the 2019 horizon

---

##### SP-0229 Barriers and solutions to increase the number of clinical trials of new drug-radiotherapy combinations

R. Sharma<sup>1</sup>

<sup>1</sup>*UCL Cancer Institute, University College London, London, United Kingdom*

##### Abstract text

Radiotherapy is a fundamental component of treatment for the majority of patients with cancer. In recent decades, technological advances have enabled patients to receive more targeted doses of radiation to the tumour, with sparing of adjacent normal tissues. There is great potential for new drug-radiotherapy treatment strategies to improve clinical outcomes for patients. Novel combinations from the most relevant preclinical models of cancer biology and immune-oncology should be prioritised for rapid advancement to the clinic. Early and frequent communication between multiple stakeholders including industry, academia, regulatory agencies and patient advocates is essential to generate sufficient numbers of clinical trials and to increase the rate of progress. Intelligent trial designs are required to increase the number of studies which efficiently meet their primary outcomes. Endpoints including local control, organ preservation and patient-reported outcomes may demonstrate clinical benefit and are of specific relevance to clinical trials of new drug-radiotherapy combinations. In this talk, I will discuss barriers that have been identified to the development of new drug-radiotherapy combinations, and solutions to increase the number of clinical trials. Interested readers are recommended to read the review article published by the NCRI CTRad Academia-Pharma Joint Working Group: Sharma, R.A., et al., NCRI CTRad Academia-Pharma Joint Working Group. (2016). Clinical Development of New Drug-Radiotherapy

Combinations. *Nature Rev Clin Oncol*, 2016. doi: 10.1038/nrclinonc.2016.79.

##### SP-0230 Radiation and TKIs - what is the 2019 evidence?

C. Belka<sup>1</sup>

<sup>1</sup>*University Hospital- LMU Munich, Department of Radiation Oncology, Munich, Germany*

Abstract not received

##### SP-0231 Radiotherapy in combination with DNA damage response inhibitors in 2019: are we any closer to clinical benefit?

A. Chalmers<sup>1</sup>

<sup>1</sup>*Inst. of Cancer Sciences-Univ. Glasgow, Department of Clinical Oncology, Glasgow, United Kingdom*

##### Abstract text

Clinical evaluation of radiotherapy in combination with inhibitors of the DNA damage response has been underway for several years now and, while knowledge about effects on normal tissue toxicity is accruing, evidence of improved tumour control is still awaited. PARP inhibitors are the most advanced class of agents to be tested in the clinic, and this presentation will summarise the key observations made in the early phase trials that have been conducted to date. I will also consider how progress might have been accelerated if more efficient clinical trial designs had been adopted.

Inhibitors of additional DNA damage response proteins are also entering the clinic, both as single agents and in combination with radiotherapy, and pre-clinical data indicates that some of these may be more potent radiosensitizers than PARP inhibitors. After summarising the pre-clinical findings, I will review the key clinical trials and consider how we might select patients for particular radiation-DDRi combinations. Finally I will present some novel clinical trial designs that might enable us to make more rapid progress in this area.

##### SP-0232 Cost-estimate models for radiation-drug combinations

A.H. Ree<sup>1</sup>

<sup>1</sup>*Akershus University Hospital, Department of Oncology, Lørenskog, Norway*

##### Abstract text

Programs within precision cancer medicine are being conducted at an increasing number of cancer centers internationally, in line with recommendations from multiple governmental and independent initiatives. A common objective for such activities is the integration of existing resources and new investments in technologies and therapies that reside in the industrial, regulatory, academic, and clinical practice sectors. The presentation will discuss modeling of costs of the required infrastructure to conduct precision medicine studies with rational radiation-drug combinations in the public health services.

The model compares cost-per-patient figures for:

- Radiation alone (the benchmark)
- Radiation combined with biomarker-agnostic use of a given drug (combination A)
- Radiation combined with molecularly matched medication (combination B)

The estimations include costs for:

- The medication
- Outpatient clinic visits
- Admission from adverse events
- The biomarker-based diagnostic procedures

The input parameters comprise:

- A set of given diagnosis-related-group indicators
- Wholesale drug prices, including costs for required oncology nursing to administer intravenous drugs

- Personnel costs and factual investments within the biomarker-based procedures.
- The main cost drivers for radiation-drug combinations will probably be:
- The medication and management of adverse events for combination A
  - The diagnostic procedures for combination B

---

**Symposium: Inverse planning in brachytherapy - A one click solution?**

---

**SP-0233 Optimal use of inverse optimization in brachytherapy**

D. Baltas<sup>1</sup>

<sup>1</sup>Medical Center - University of Freiburg, Division of Medical Physics - Department of Radiation Oncology, Freiburg, Germany

Abstract not received

**SP-0234 Inverse treatment planning in clinical practice, one click and done?**

D. Todor<sup>1</sup>

<sup>1</sup>Virginia Commonwealth University, Radiation Oncology, Richmond- VA, USA

**Abstract text**

Treatment Plan Optimization is one of those subjects which strongly polarizes brachytherapy practitioners. Part of the problem is that we got where we are today by slowly building on decades of successful clinical experience, relying on clinical knowledge sublimated in collections of rules called 'systems': Stockholm, Paris, Manchester. These systems described, sometimes in great details, *how* things should be done; they represent practice not theory. This approach had a lot to do with reproducibility of treatments that seem clinically successful and little to do with understanding how things work, *why* a certain placement of radioisotopes actually works and explaining the mechanism behind.

Fast forward to the current era in which we learned how to compute radiation transport through the body very accurately and to describe our plans by employing dose volume histograms (DVH). Having now a set of DVH parameters that describes a dose distribution, one is in the position of optimizing that distribution by simultaneously maximizing those parameters to some structures (anatomical or disease related) while minimizing other parameters to structures related to normal anatomy, which typically one tries to spare.

Optimization is an interesting applied mathematical domain and attracts computer scientists, AI researchers, physicists and mathematicians.

The less than optimal reality (pun intended) is that optimization is seldom used in the clinic (at least in the brachytherapy practice) and when it is used, a physician or a physicist will typically 'adjust' a solution obtained straight out of the optimizer with the intent of further improving it.

My plan is to discuss the origins and the [i]rationale of this state of affairs as well as to describe possible avenues for increased utilization of true optimization. I will present three cases (cervical, prostate and breast cancer) as how-to examples of what optimization can deliver. I will devote a second part of my talk describing the obvious fact that plan optimization really is dose optimization and more precisely DVH-based optimization. I will do my best to question central concepts like prescription dose, targets, dose coverage, Ds and Vs, (all ingredients in the Optimization) and try to setup alternative constructs. An example based on cervical cancer data and/or prostate cancer will follow.

**SP-0235 Intuitive and Insightful Evolutionary Intelligent Treatment Planning**

P. Bosman<sup>1</sup>

<sup>1</sup>Centrum Wiskunde and Informatica CWI, Life Sciences and Health, Amsterdam, The Netherlands

**Abstract text**

Artificial Intelligence (AI) increasingly pervades the daily news, with self-driving cars, robots, and face recognition even on smart phones. The reason for this revolution is threefold: 1) several AI techniques have matured algorithmically, 2) there have been spectacular advances in computing hardware (e.g., GPUs), and 3) digitizing and storing large amounts of data has become common practice.

AI will increasingly be a key driver of automation, including in radiation oncology. In this talk, placed within the broader context of existing automation approaches to brachytherapy treatment planning in general, I will present the AI efforts undertaken so far by my research group to automate. These are mainly focused around a particular subfield of AI: that of Evolutionary Algorithms (EAs).

EAs are loosely based on the natural evolution principles and have the advantage of being relatively straightforward to apply to optimization and machine learning tasks. A disadvantage is that most textbook EAs are 'blind', as they randomly combine solutions. I will introduce the state-of-the-art Gene-pool Optimal Mixing Evolutionary Algorithm (GOMEA) family that automatically determines how to best combine solutions. I will illustrate the advantageous properties of GOMEAs over classical 'blind' EAs, showing how GOMEAs are capable of obtaining (near-)optimal results for problems with millions of variables in less than an hour on a normal desktop computer, where classic EAs can only do this for tens or a few hundred variables.

I will show how with GOMEA we are able to solve bi-objective problem formulations based directly on dose-volume indices for automated HDR brachytherapy treatment planning for the prostate, thereby finding not just one treatment plan, but trade-off curves consisting of many interesting potential treatment plans that trade-off target coverage with sparing organs at risk for large numbers of dose calculations points in mere minutes on a single modern GPU. Visualizing such a trade-off curve gives an insightful overview of what types of dose-volume indices are achievable for a particular patient.

Beyond this, I will briefly touch upon near-future avenues for further AI-based automation.

---

**Symposium: Reference and non-reference dosimetry - CoPs and beyond**

---

**SP-0236 MV reference dosimetry in TRS-398: State-of-the art and research supporting an updated code of practice**

F. Delaunay<sup>1</sup>, C. Andersen<sup>2</sup>, L. De Prez<sup>3</sup>, S. Duane<sup>4</sup>, M. Pimpinella<sup>5</sup>, P. Teles<sup>6</sup>, J. Tikkanen<sup>7</sup>, K. Zink<sup>8</sup>

<sup>1</sup>CEA- List, Laboratoire National Henri Becquerel Lne-Lnhb, F-91191 Gif-Sur-Yvette, France ; <sup>2</sup>DTU, Center For Nuclear Technologies, Kongens Lyngby, Denmark ; <sup>3</sup>VSL, Dutch Metrology Institute, Delft, The Netherlands ;

<sup>4</sup>National Physical Laboratory, Chemical- Medical and Environmental Science Department, Teddington, United Kingdom ; <sup>5</sup>ENEA, National Institute Of Ionizing Radiation Metrology Inmri, Rome, Italy; <sup>6</sup>University of Lisbon, GPSR- Centre of nuclear sciences and technology- IST, Lisbon, Portugal ; <sup>7</sup>Stuk, Radiation And Nuclear Safety Authority, Helsinki, Finland; <sup>8</sup>University Of Applied

*Sciences Giessen, Institute Of Medical Physics And Radiation Protection, Giessen, Germany*

#### Abstract text

The data in IAEA TRS-398 for MV beams was prepared in the mid-1990s, and since that date a number of new developments have taken place, such as the publication of ICRU 90 on key data for measurement standards in the dosimetry of ionizing radiation, free flattening filter beams, new detectors and dosimetry for small fields. IAEA decided to update its protocol and by the end of 2015 asked for volunteers to measure (based on primary standard dosimeters) and calculate (with Monte Carlo codes) updated  $k_{Q,Q_0}$  values for reference-class ionization chambers (IC).

Primary standard dosimeters for absorbed dose to water are water and graphite calorimeters. IAEA requested primary and secondary standard dosimetry laboratories to measure  $k_{Q,Q_0}$  values for at least 5 ICs of the same type, ideally from different manufactured batches and to include one chamber with well-known  $k_{Q,Q_0}$  values such as NE 2571. For calculations, the Monte Carlo codes have to pass the Fano test like EGSnrc and PENELOPE. One IC with well-known  $k_{Q,Q_0}$  values has to be simulated first to demonstrate appropriate skill for these calculations. The complete results are to be delivered by December 2018 and the data analysis is to begin in 2019. Following IAEA demand, EURAMET decided to launch the EMPIR project 16NRM03 RTNORM in mid-2017 to provide  $k_{Q,Q_0}$  factors to the IAEA. In the MV photon beams workgroup, DTU (Denmark), LNE-LNHB (France), NPL (United Kingdoms) and VSL (the Netherlands) were to measure  $k_{Q,Q_0}$  factors for 6 IC types and ENEA (Italy), IST-ID (Portugal), STUK (Finland) and THM (Germany) were to calculate  $k_{Q,Q_0}$  factors for 10 IC types. This presentation will give a description of the RTNORM measurements and calculations. The results will serve as examples to show which kind of data the IAEA received and how to evaluate them in order to select the ones that will be used for the TRS-398 update.

#### SP-0237 Clinical application of kQ factors for reference dosimetry in flattening filter free (FFF) photon beams

L. De Prez<sup>1</sup>, C. Andersen<sup>2</sup>, J. De Pooter<sup>1</sup>, H. Palmans<sup>3</sup>  
<sup>1</sup>VSL, *Ionizing Radiation Standards, Delft, The Netherlands*; <sup>2</sup>Center For Nuclear Technologies DTU Nutech, *Dosimetry, Roskilde, Denmark* ; <sup>3</sup>National Physical Laboratory, *Radiation Dosimetry, Teddington, United Kingdom*

#### Abstract text

Flattening filter free (FFF) photon beams were introduced several years ago and are now widespread for application in radiotherapy. There are several clinical advantages of FFF beams over conventional beams with flattening filter (WFF), however differences in beam spectra at the point of interest in a phantom potentially affect the ion chamber response. FFF beams are also non-uniform over the length of a typical reference ion chamber and recombination is usually larger because of the higher dose delivered per pulse. Several studies have described FFF beam characteristics and their effect on beam calibration using conventional reference dosimetry, including the use of  $k_Q$  factors. Some studies predicted significant discrepancies in  $k_Q$  factors (0.4% up to 1.0%) if TPR<sub>20,10</sub> based codes of practice (CoPs) were to be used. Recently the IAEA published a new code of practice for dosimetry of small and non-reference static fields, including a description on the application of reference dosimetry for FFF compared to conventional WFF beams. This presentation addresses the application of the new code of practice and how to perform reference dosimetry in FFF beams by applying  $k_Q$  factors in relation to  $k_Q$  values available literature and performed by the authors within

the EMPIR 16NRM03 RTNOM project. Examples of  $k_Q$  studies will be given and special attention will be paid on how to deal with, e.g., ion recombination and beam non-uniformity.

#### SP-0238 TRS 483: past, present and future

H. Palmans<sup>1,2</sup>

<sup>1</sup>EBG Medaustrom GmbH, *Medical Physics, Wiener Neustadt, Austria* ; <sup>2</sup>National Physical Laboratory, *Medical Radiation Science, Teddington, United Kingdom*

#### Abstract text

IAEA TRS-483 [1] is the first Code of Practice for the dosimetry of small high-energy photon fields published at either national or international level. The subsequent publication of a Summary paper in Medical Physics [2] marks the conclusion of a joint effort by the IAEA and the AAPM in publishing, for the first time, a Code of Practice for dosimetry together. In this presentation, the developments in the past decades that have shaped the small field recommendations in IAEA TRS-483 are presented, followed by an overview of the key steps in its application to the determination of small field output factors. A discussion will then be given on experience with the application of the Code of Practice and new developments and findings that have emerged from those. The aspects related to reference dosimetry for radiotherapy machines that cannot generate the conventional 10 cm × 10 cm reference field, and in particular those pertaining to the reference dosimetry of flattening-filter-free beams, are addressed in the previous presentation in this symposium.

The first part of this presentation discusses past developments that have been determining IAEA TRS-483 include the following. There has been the realization that for small fields the collimator setting and field size at FWHM are not congruent and an unambiguous definition of field size is needed. The definition of lateral charged particle equilibrium range has enabled a quantitative criterion to distinguish between fields for which small field conditions exist and broad beams. A paper by Alfonso et al [3] formally defined a small field output factor as a ratio of detector readings multiplied with a small field output correction factor which enabled the consistent determination of such factors using experiment or Monte Carlo simulations and the subsequent compilation of literature data for the Code of Practice. The work of Cranmer-Sargison et al [4] showed that for the representation of small field output factors and correction factors, the equivalent square field size of irregular small fields is better represented by a field with equal area than by a field with equal scatter conditions, as is the case for broad beams.

The second part of the presentation outlines the key steps in applying IAEA TRS-483 to the determination of field output factors. The first step is the selection of suitable measurement equipment. The second step consists of the characterisation of the small field profiles and the derivation of the equivalent square field size from those profiles. Then the alignment procedures for real-time and off-line detectors are considered followed by the selection and interpolation of output correction factors and the determination of their uncertainty. The last part of the presentation discusses the experience with applying the code of practice, new information that has become available in the literature and new detectors that have become commercially available.

[1] H. Palmans, P. Andreo, M. S. Huq, J. Seuntjens and K. Christaki, "Dosimetry of small static fields used in external beam radiotherapy: An IAEA-AAPM international Code of Practice for reference and relative dose determination," IAEA Technical Report Series No. 483, (Vienna, Austria: International Atomic Energy Agency), 2017.  
 [2] H. Palmans, P. Andreo, M. S. Huq, J. Seuntjens, K. E. Christaki and A. Meghziene, "Dosimetry of small static

fields used in external photon beam radiotherapy: Summary of TRS-483, the IAEA-AAPM international Code of Practice for reference and relative dose determination," *Med. Phys.* 2018; 45:e1123-e1145.

[3] R. Alfonso, P. Andreo, R. Capote, M. Saiful Huq, W. Kilby, P. Kjäll, T. R. Mackie, H. Palmans, K. Rosser, J. Seuntjens, W. Ullrich and S. Vatnitsky, "A new formalism for reference dosimetry of small and non-standard fields," *Med. Phys.* 2008; 35:5179-5186.

[4] G. Cranmer-Sargison, P. H. Charles, J. V. Trapp and D. I. Thwaites, "A methodological approach to reporting corrected small field relative outputs," *Radiother. Oncol.* 2013; 109: 350-355.

### SP-0239 Following TRS 483: reference and relative dosimetry in Tomotherapy

M.D.C. Lopes<sup>1</sup>, T. Santos<sup>1,2</sup>, T. Ventura<sup>1</sup>, M. Capela<sup>1</sup>  
<sup>1</sup>*Ipcfg- Epe, Medical Physics, Coimbra, Portugal* ; <sup>2</sup>*fc- University Of Coimbra, Physics, Coimbra, Portugal*

#### Abstract text

**Introduction and purpose:** The joint IAEA and AAPM international code of practice (CoP) for small static fields dosimetry - TRS 483- was issued on December 2017, after almost a decade from the publication, in 2008, of a formalism that outlined the extension of the dosimetry based on absorbed dose to water to small and composite fields and to non-reference conditions [1]. Both publications rely on universally adopted codes of practice like IAEA TRS 398 and AAPM TG 51, building on the established reference dosimetry for conventional reference 10 cm × 10 cm field and extending the dosimetry down to small and non-reference fields by introducing the concept of machine specific reference (*msr*) field. This concept applies to those treatment units where the conventional reference field is not permitted. Helical Tomotherapy (HT) is one of such machines. Exradin A1SL ionization chamber, from Standard Imaging, is the chamber included in the standard dosimetry package for HT but it is not included in the list of reference dosimeters in TRS 483. The motivation for the present work was to obtain the global correction factor for A1SL chamber that would account both for quality and geometry following the recommendations of TRS 483, in the context of performing reference dosimetry in Tomotherapy and exploring the different ways and concepts embodied in the document. Also relative dosimetry with A1SL has been explored through the determination of output factors using free-correction film results and other detectors suitable for small field dosimetry.

**Methods and materials:** According to TRS 483 the absorbed dose to water for the *msr* field ( $f_{msr}$ ), in the beam of quality  $Q_{msr}$ , at the reference depth in water is given by:

$$D_{w,Q_{msr}}^{f_{msr}} = M_{Q_{msr}}^{f_{msr}} N_{D,w,Q_0}^{f_{ref}} k_{Q_{msr},Q_0}^{f_{msr},f_{ref}}$$

where the chamber reading corrected for all charge collection influences ( $M$ ), multiplied by the chamber calibration factor from certificate ( $N$ ) has to be corrected both for beam quality and geometry by a correction factor

denoted by  $k_{Q_{msr},Q_0}^{f_{msr},f_{ref}}$ . This global correction factor for A1SL was obtained through different approaches following TRS 483 recommendations - cross calibration with reference chamber, radiochromic film independent dosimetry and using the hypothetical reference field concept. The results were compared with published values following other approaches like Monte Carlo calculations [1,2] or alanine dosimetry [3,4]. To underpinning small field relative dosimetry in HT, a set of small fields was configured through its pneumatically controlled binary multileaf collimator (MLC) for the three field slits - 1, 2, 5

and 5 cm. An intercomparison of output factors was done using different detectors like microdiamond, unshielded diode, micro chamber and also film dosimetry to set against A1SL chamber response. Once more the information conveyed in TRS 483 has been abundantly explored to reach a sustained way of performing relative dosimetry in HT.

#### Results

In agreement with values from literature, an average value of  $0.9962 \pm 0.0040$  has been obtained for the global correction factor of Exradin A1SL chamber to be applied in absolute dose determination for helical Tomotherapy. Concerning relative response, output factors obtained with different detectors were within agreement, given the level of uncertainty. Considering film output factors as free of corrections, the average value for A1SL output factors corrections was  $1.000 \pm 0.007$ .

#### Conclusions

The results of the present work justify Accuray practice of not correcting the A1SL chamber reading for quality and geometry in absolute dose determination in Tomotherapy as the derived factor is compatible with unity, within the associated uncertainty. Also in relative measurements, the ratio of A1SL chamber readings do not need further correction to be taken as output factors for the considered small clinical field sizes when normalized to the machine specific reference field in HT.

#### References:

- [1] Alfonso R, Andreo P, Capote R, Huq MS, Kilby W, Kjäll P, et al. A new formalism for reference dosimetry of small and nonstandard fields. *Med Phys* 2008; 35:5179-86.
- [2] Thomas SD, Mackenzie M, Rogers DWO, Fallone BG. A Monte Carlo derived TG-51 equivalent calibration for helical Tomotherapy. *Med Phys* 2005; 32:1346-53.
- [3] Sterpin E, Mackie TR, Vynckier S. Monte Carlo computed machine-specific correction factors for reference dosimetry of Tomotherapy static beam for several ion chambers. *Med Phys* 2012; 39:4066-72.
- [4] De Ost B, Schaecken B, Vynckier S, Sterpin E, Van den Weyngaert D. Reference dosimetry for helical tomotherapy: Practical implementation and a multicenter validation. *Med Phys* 2011; 38:6020-6.
- [5] Gago-Arias A, Rodriguez-Romero R, Sanchez-Rubio P, Gonzalez-Castano DM, Gomez F, Nunez L, et al. Correction factors for A1SL ionization chamber dosimetry in Tomotherapy: Machine-specific, plan-class, and clinical fields, *Med Phys* 2012; 39:1964-70.

---

### Symposium: New advances in image reconstruction in CBCT

---

#### SP-0240 Breathing motion in cone-beam CT

S. Rit<sup>1</sup>

<sup>1</sup>CREATIS CLB, Radiotherapy, Lyon, France

#### Abstract text

Breathing motion during cone-beam CT (CBCT) acquisition blurs moving structures and causes streaks along x-rays adjacent to these structures. Correcting for these artifacts is required to improve image-guided radiotherapy and for adapting the radiotherapy of lung and upper abdominal cancers. Current clinical solutions use respiration-correlated reconstruction: a large number of projection images is sorted in respiratory phases based on a breathing signal and a 3D CBCT image of the respiratory phase is reconstructed separately from each subset of projections to yield a 4D CBCT image. More advanced breathing motion correction techniques, which make use of less projection images, can be categorized in motion-compensated and iterative 4D CBCT. The former is essentially a 3D imaging technique in which the motion is first estimated and then compensated for during CBCT reconstruction. The latter compensates the lack of

projection images per respiratory phase with spatial and/or temporal regularization(s). This presentation will review these techniques, discuss the pros and cons of each and report on a recent attempt to evaluate them from the same dataset.

#### SP-0241 Deep image formation algorithms for CT and CBCT

M. Kachelriess<sup>1</sup>

<sup>1</sup>German Cancer Research Center DKFZ, Department of Medical Physics, Heidelberg, Germany

##### Abstract text

##### Purpose

To give an overview of the potential of deep learning in the field of x-ray CT and CBCT image formation.

##### Methods

With the introduction of deep learning in general, and with deep convolutional neural networks (CNNs) in particular, machine learning has spread into many medical areas with great success. In particular medical imaging may benefit from the new technology. Important applications such as image analysis, image segmentation and object recognition are well-known and start to become widely available.

The applications of machine learning to the field of image formation, which describes the process of data acquisition, preprocessing, image reconstruction and post processing, however, are less known, not as mature and not always available, yet. In CT and CBCT, which are the focus of this lecture, the use of machine learning can be mainly categorized into the categories 1) replacement of time-consuming computations (image reconstruction, scatter prediction, material decomposition, ...), 2) replacement of missing data (sparse view acquisition, limited angle tomography, ...), and 3) incorporation of a priori knowledge (non-contrast CT from contrast-enhanced CT, pseudo CT from MR, ...). This lecture discusses the underlying technology and application examples.

##### Results

Methods that promise to fill in missing data need to be taken with care because they are just another way of inter- or extrapolating data: Claims that a reduction of x-ray dose or of the number of x-ray projections, when combined with CNNs, yields the same image quality as high dose imaging are not proven and, if at all, demonstrated using simple phantoms or smooth CT images. In contrast, applications to replace time-consuming computations by real-time CNNs have the potential to provide accurate results even for a great input data variation because their output is typically a smooth but non-local function of the data input. Successful examples are networks that replace Monte Carlo calculations and compute deep scatter estimations (DSE) and deep dose estimations (DDE) in real time. Even more important are deep learning-based image reconstruction algorithms which also vendors have started to implement into their products. Such deep recons (DR) have the potential to outperform the conventional analytical reconstruction (AR) and iterative reconstruction (IR) algorithms, by far.

##### Conclusions

Deep learning has the potential to significantly improve CT and CBCT image formation. However, not all proposed methods may keep their promises. Care has to be taken in all cases because due to the large number of open parameters the behavior of neural networks is difficult to analyze or predict and it cannot be foreseen how they react to data that are not adequately represented by the training set.

#### SP-0242 Hounsfield corrected CBCT images - dose calculation and potential for bio-markers

C. Brink<sup>1</sup>

<sup>1</sup>Odense University Hospital, Laboratory of Radiation Physics, Odense, Denmark

##### Abstract text

CBCT scans are part of the daily clinic in many institutions. Quite often the 3D/4D CBCT information are reduced to three numbers indicating the patient translation needed in order to place the iso-center in the correct position. However, the CBCT images do contain much more information than just the positional uncertainty. An obvious use of the CBCT images is to validate that the overall patient anatomy is unchanged during a fractionated treatment schedule. Typically the RTT's will, as part of their online assessment of the images, notice whether anatomical changes are present. If there are anatomical changes the next question is whether these differences impact the planned dose distribution. Since grey levels in standard CBCT images are not representing the Hounsfield Units, the patient is often referred for a validation CT that can be used for dose calculation. If the CBCT images could be made to match Hounsfield Units it would be possible to use the CBCT images for dose validation directly. This would make it much faster to obtain information of the potential dose impact and also spare the patient for an additional visit to the CT scanner. Such a procedure is introduced as clinical practice for some of our local lung trial patients. During the talk different methods to obtain Hounsfield units from standard clinical CBCT images will be discussed. The potential of CBCT images are however even larger than just the ability to be used for dose calculation. CBCT and other medical images do have the potential to be used as early bio-markers that during RT could indicate the potential outcome of the patient. This could be used as a way to performed patient specific correction to the treatment plan based on the radiation sensitivity of the individual patient. However, the image noise is still a partly hindrance for obtaining valuable bio-markers. Some of the methods to reduce image noise will be discussed and some of the results related to bio-markers and CBCT images will be discussed during the talk.

---

#### Symposium: New technology and modalities

---

#### SP-0243 How to secure the right competencies when new modalities are implemented - a clinical aspect in proton therapy

H. Pennington<sup>1</sup>

<sup>1</sup>The Christie NHS Foundation Trust, Proton Therapy, Manchester, United Kingdom

##### Abstract text

In late autumn 2018 The Christie Foundation Trust in Manchester, United Kingdom, opened the first high energy proton therapy centre in England for National Health Service (NHS) patients.



In the opening of a new proton therapy service a new modality of radiation therapy was implemented with the intent of treating a wide range of complex and challenging cases. Key safeguards needed to, and have been, built into the service to ensure safe treatment of patients. One of these key safeguards was the training and education of the workforce. Such considerations started early in the project with a number of senior team members visiting operational proton therapy departments to gather as much information as possible to guide service development. We employed staff early and implemented extensive training packages. Clinical Oncologists, senior physicists and therapists have all undergone an extensive programme of training which included overseas education programmes and practical placements in established proton centres. This was complimented by bringing expertise to our site to discuss site specific treatment planning solutions, exercises in comparative planning, as well as discussion of the issues and challenges that are particular to proton therapy.



Overseas experience was backed up by on site applications training and a significant amount of time was incorporated into the commissioning schedule for end to end testing/patient treatment dry runs. During this time a comprehensive competency based in house training was developed and incorporated into an accredited quality system.

#### SP-0244 Personalized treatment planning and automation in modern radiotherapy

T. Piotrowski<sup>1</sup>

<sup>1</sup>Greater Poland Cancer Centre, Medical Physics, Poznan, Poland

##### Abstract text

Treatment planning for dynamic radiotherapy techniques (e.g. IMRT, VMAT, Tomotherapy), needs high knowledge of the planner to ensure high plan quality. Different level of knowledge and practical skills of planners can lead to variability in the quality of treatment plans and the time efficiency of productions of the plans.

The control of the realization is the additional aspect of the treatment plans and their potential modification during radiotherapy.

To standardize the planning process, the planning approaches with automation support were intensively developed in last years. There are also a lot of new technical solutions to control the accuracy of the dose delivery according to the prepared treatment plans.

This study critically reviews the body of publications up to the end of 2018.

The review is described for (i) automated planning - different types of automation algorithms and for (ii) the dose delivery - inaccuracies for the displayed doses caused from the actually implemented tools.

#### SP-0245 Advanced practice role in breast cancer radiation therapy

G. Lee<sup>1</sup>

<sup>1</sup>Princess Margaret Cancer Center, Radiation Medicine Program, Toronto, Canada

##### Abstract text

Implemented in 2007, the Clinical Specialist Radiation Therapist (CSRT) project is a model-of-care to develop advanced practice radiation therapy in Ontario, Canada. The breast-site CSRT is one of the first advanced practice roles piloted at the Princess Margaret Cancer Centre. The goal of this role is to enhance radiation therapy practice and patient-focused outcomes for patients requiring breast radiotherapy. The breast-site CSRT is an integral part of an inter-professional team and practices within the radiotherapy new patient clinic, follow-up clinic, and "on-treatment reviews" to provide clinical care and performs cavity target delineation for radiotherapy planning. As part of a multi-disciplinary team, the CSRT leads a rapid process for same-day breast radiotherapy. This session explores the breast-site CSRT role and evaluates the accumulated 10-year evidence in advanced practice role development.

---

#### Symposium: Combining research and (clinical/professional) training/ practice

---

#### SP-0246 Taking time off for full-time research - is it worth it?

A. Levy<sup>1</sup>

<sup>1</sup>Gustave Roussy, Radiation Oncology Department, Villejuif, France

##### Abstract text

For health practitioners, taking a break from clinics to undertake full-time research could be seen as an opportunity and/or a disadvantage. In this session, pros and cons of taking time off for full-time research will be discussed.

#### SP-0247 Why do we need to be trained in statistics? Need and pitfalls

A. Escande<sup>1</sup>, L. Lebellec<sup>2</sup>

<sup>1</sup>Oscar Lambret Comprehensive Cancer Center, Academic Department Of Radiation Oncology, Lille, France ; <sup>2</sup>Oscar Lambret Comprehensive Cancer Center, Biostatistics, Lille, France

##### Abstract text

Evidence based medicine is necessary for routine clinical practice. Understanding and taking into account large amount of data should permit to predict accurate outcome and tailoring the best individual treatment. However, clinicians need to understand statistical and data analysis in order to take the best decision and better criticize published studies. This need is also reinforce by the

increasing of treatment cost and the aim of treatment toxicity control. Some studies described misuse of statistical tests in medical studies but also difficulties to understand biostatistics for most of medical doctor. Thus, medical school should develop statistical tests and data analysis lessons. Moreover, we are now into artificial intelligence era partially based on advanced statistical analysis and medical doctor should be aware of multiple existing biases to not be victim of non-accurate conclusion but also better interact with biostatistical team. Here, we briefly explain how to use and pitfalls of most used tests such as Parametrical and non-parametrical tests, Kaplan Meier, Log Rank, Cox regression, Fine and Gray, Restricted Mean Survival and Classifier.

#### SP-0248 Research and training in medical physics

S. Petit<sup>1</sup>

<sup>1</sup>Erasmus Mc Cancer Institute, Department Of Radiation Oncology, Rotterdam, The Netherlands

##### Abstract text

In this session I will discuss how to acquire (and keep on having) a staff medical physicist position with dedicated and protected time for research. The first part of the talk is about the training to become a medical physicist. The training period is a period to decide in which direction you would like to develop yourself, gain relevant experience in different institutions, and making yourself seen among the medical physics community. The key for enhancing your visibility and increasing your attractiveness for institutes with combined medical physics and research positions, is research. I will present tips on how to achieve as much as possible with the limited time for research you may have during training. In the second part of the talk I will present the challenges and possible solutions of being a medical physicist with research time that sees his/her research time evaporate in the demanding and hectic environment called clinical practice.

#### SP-0249 Clinical vs lab research for clinicians Combining research and (clinical/professional) training practice

D. Milanovic<sup>1</sup>

<sup>1</sup>University Hospitals of Leicester NHS Trust, Department of Oncology, Leicester, United Kingdom

##### Abstract text

Radiation Oncologists are regularly confronted with a treatment of non-curative diseases. To improve their outcome the development of new treatment strategies will be necessary. Ideally more Radiation Oncologists should actively participate in relevant pre-clinical studies designing further clinical trials based on their findings. Realistically, this approach is challenging and difficult achievable due lack of ideas, facilities and financial support. In this presentation, possibilities to perform clinical and lab research during the training and afterwards in two large European Health Systems (German and British) will be elucidated. We can conclude that to retain motivated colleagues who want to actively participate in lab and clinical research projects, the appropriate length of time close to their routine clinical activities should be ensured.

#### SP-0250 Lessons learnt from a young head of department

R. Baumann<sup>1</sup>

<sup>1</sup>St. Marien Hospital Of Siegen, Radiation Oncology, Siegen, Germany

##### Abstract text

A head of department must be a true all-rounder in radiation oncology. In addition to the professional experience, the chief physician must show the economic competence, leadership, training and organizational skills

that are necessary for the development of his department and its integration into a scientific network. In Germany, a large part of the radiation therapy is performed at outpatient centers. Thus, university hospitals and maximum care hospitals have a particular responsibility to contribute to education and research. In addition to continuously securing high standards of care on a daily basis, it is also necessary to establish sufficient staff resources to be able to carry out high quality scientific projects.

Within the next two years, the Marien Hospital Siegen hospital together with three other regional hospitals will become a university hospital associated with a newly established medical school. Opportunities in the so called "Rethink Medicine" project include the economic cooperation of four hospitals within one city and the development of translational research projects in collaboration with international partners such as the Erasmus Medical Center Rotterdam (EMC) and the University of Oxford. One of the key challenges will be to establish basic and translational research programmes to complement the clinical research already taking place today.

In this lecture, the mentioned points are reflected from the perspective of a young head of a department (35 years old) for radiation oncology in Germany.

---

#### Poster Viewing: Poster viewing 5: Health Services Research and Health-Related Quality of Life

---

#### 1PV-0251 Inuit radiotherapy utilization: a multinational study of low-income regions in high-income countries

J. Chan<sup>1,2</sup>, T. Mee<sup>3,4</sup>, N.F. Kirkby<sup>3,4</sup>, R. Jena<sup>5</sup>, S. Waites<sup>6</sup>, J. Renaud<sup>7</sup>, K. Barker<sup>6</sup>, A. Polo<sup>8</sup>, D. Jones<sup>9</sup>, K.J. Kirkby<sup>3,4</sup>, R. Sullivan<sup>10</sup>, M. Brundage<sup>11</sup>, B. Slotman<sup>2</sup>, J. Bourque<sup>1,10</sup>

<sup>1</sup>University of Ottawa, Division of Radiation Oncology, Ottawa, Canada; <sup>2</sup>Vrije University Medical Center, Department of Radiation Oncology, Amsterdam, The Netherlands; <sup>3</sup>The University of Manchester, Division of Cancer Sciences, Manchester, United Kingdom; <sup>4</sup>Manchester Academic Health Science Centre, The Christie NHS Foundation Trust, Manchester, United Kingdom; <sup>5</sup>Cambridge University NHS Foundation Trust, Department of Oncology, Cambridge, United Kingdom; <sup>6</sup>Government of Nunavut, Department of Health, Iqaluit, Canada; <sup>7</sup>Radiation Medicine Program, the Ottawa Hospital, Ottawa, Canada; <sup>8</sup>International Atomic Energy Agency, Applied Radiation Biology and Radiotherapy Section, Vienna, Austria; <sup>9</sup>Canadian Partnership Against Cancer, First Nations- Inuit and Metis Program, Toronto, Canada; <sup>10</sup>Guy's Hospital Campus, Institute of Cancer Policy, London, United Kingdom; <sup>11</sup>Cancer Centre of Southeastern Ontario, Division of Radiation Oncology, Kingston, Canada

##### Purpose or Objective

The Inuit are one of three indigenous groups in Canada. Despite living in a high-income country (HIC), their unique sociodemographic characteristics mirrors those of low-and-middle income countries (LMIC) in terms of cancer care and outcomes. Geography is an important barrier. Inuit cancer patients from the northern Arctic territory of Nunavut must fly significant distances to access radiotherapy (RT) in southern Canada. RT utilization (RTU), the proportion of patients receiving RT, is an essential step to create policies for designing affordable and equitable RT service, which is a critical, and complex component of better cancer outcomes. However, RTU has never been specifically studied among the Inuit.

##### Material and Methods

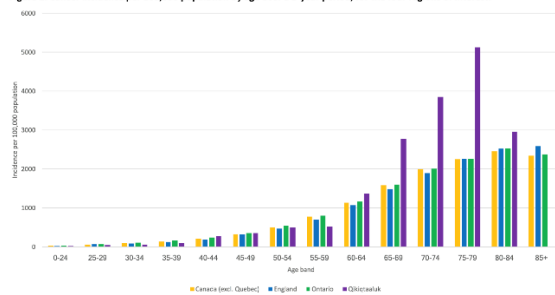
We conducted descriptive analyses comparing the cancer incidence among Nunavut's largest health region

(Qikiqtaaluk), to other regions in Canada and England. We calculated this region's RTU from 2011-2016, and compared it to the modelled optimal RTU (ORTU) using the evidence-based MALTHUS model, which contains 2,000 clinical decisions relating to RT. RTU for the Qikiqtaaluk region was obtained using incidence data from the Nunavut cancer registry and treatment data from the region's oncology referral centre, The Ottawa Hospital Cancer Centre (TOHCC).

### Results

The all-cancer incidence rate in the Qikiqtaaluk region was 265 per 100,000 over a 5-year period, compared to 524 in Canada, 546 in Ontario, and 536 in England. Figure 1 displays the incidence rate split by age range. This, in contrast to the lower overall cancer incidence rate, reveals a markedly higher incidence among older age ranges in the Qikiqtaaluk region compared to others. Of the cancer registry patients, 68% were seen at TOHCC. However, at least 20 cancer patients seen at TOHCC did not have a record in the cancer registry, suggesting under-reporting of Nunavut's cancer incidence. The majority of patients were diagnosed at stage IV (33%). The most common cancer type was lung (38%). The ORTU, based on the UK Malthus evidence-base, is 43% (excluding retreatments). Actual RTU for the Qikiqtaaluk region was 54%.

Figure 1. Cancer incidence per 100,000 population by age over a 5-year period, for the four regions of interest.



### Conclusion

This is the first study to describe RTU among any Inuit population worldwide. The Qikiqtaaluk region displays a lower overall cancer incidence, which may in part be due to under-reporting. Despite this, the 3-fold increased incidence among the region's older population is alarming. The higher calculated RTU among the Qikiqtaaluk region is also likely attributed to under-reporting of the cancer incidence. Solutions to increase RT uptake should include the development of robust systems for cancer reporting within the territory, in partnership with their oncology referral centres. Concurrently, novel models of RT delivery must not only address geographical barriers, but also the unique sociodemographic and cultural needs of this under-served population. Further in-depth analyses comparing incidence, stage and RTU for regions within HICs exhibiting LMIC traits is in progress.

### PV-0252 From theory to practice: assessing the use of radiotherapy in population based cancer registries

J.M. Borrás<sup>1</sup>, J. Corral<sup>1</sup>, J. Galceran<sup>2</sup>, R. Marcos-Gragera<sup>3</sup>, L. Vilardell<sup>3</sup>, J. Solà<sup>1</sup>, A. Ameijide<sup>2</sup>, M. Carulla<sup>2</sup>, X. Cardó<sup>2</sup>, À. Izquierdo<sup>3</sup>, J.A. Espinàs<sup>1</sup>

<sup>1</sup>IDIBELL, Catalan Cancer Plan, Hospitalet del Llobregat, Spain; <sup>2</sup>FUNCA, Registre de Càncer de Tarragona, Reus, Spain; <sup>3</sup>IDIBGI, Unitat d'Epidemiologia i Registre del Càncer de Girona, Girona, Spain

### Purpose or Objective

Planning for radiotherapy services requires evidence based information on the optimum and the actual use of this therapy in a population in order to assess the potential gaps in the utilization of external beam radiotherapy.

The objective of this study was to assess the actual utilization of external beam radiotherapy in two population based cancer registries in Girona and Tarragona, Catalonia, Spain. In addition, problems of access due to distance between patients residence to radiotherapy departments were analysed.

### Material and Methods

There are two cancer registries in Catalonia, Girona (750,000 inhabitants) and Tarragona (800,000 inhabitants), in both cases only one Radiation oncology department is available in each health region. All incident cancer patients (with the exception of non-melanoma skin cancers) of both regions diagnosed during the years 2009-2011 were linked to the reimbursement database of the Catalan Health Care Service. We calculated the proportion of patients receiving an external radiotherapy treatment during the first year after the diagnosis of the cancer, by type of tumour. Only the first radiotherapy treatment was included in this analysis, even if they subsequently received a retreatment.

### Results

The proportion of incident cases receiving radiotherapy treatment during the first year after diagnosis was 24.3%. The proportion of treatments decreased significantly at older ages (from 21.3% younger than 40 years old and 32% for 40-64 to 14.3% in patients older than 75 years). There were no differences in uptake of radiotherapy by distance from the residence of the patient to the Radiation oncology department.

The tumour sites (all stages at diagnosis) with highest proportion of radiotherapy use in the first year after diagnosis were breast (58%), head and neck (42%), Rectum (41%), Prostate (33%) and lung (30%).

### Conclusion

There is a significant gap between optimal use and actual use (although this study is focused on first year after diagnosis) and this is especially relevant in some tumour sites like bladder and haematological cancers. Population based data on actual use is an essential element for planning resources needed and it makes feasible to assess potential factors to explain the optimum-actual utilization gap and to reduce it when required to increase evidence based indications of radiation oncology.

### PV-0253 A critical quality appraisal of studies estimating the cost of radiotherapy

N. Defourny<sup>1</sup>, Y. Lievens<sup>2</sup>, C. Montens<sup>2</sup>, J. Monnet<sup>3</sup>, P.B. Dunscombe<sup>4</sup>, C. Grau<sup>5</sup>, L. Perrier<sup>6</sup>

<sup>1</sup>ESTRO A.I.S.B.L., HERO, Brussels, Belgium; <sup>2</sup>Ghent University Hospital, Department of Radiation Oncology, Ghent, Belgium; <sup>3</sup>Leon Berard Cancer Centre, Univ Lyon, Lyon, France; <sup>4</sup>University of Calgary, Department of Medical Physics, Calgary, Canada; <sup>5</sup>Aarhus University Hospital, Department of Oncology, Aarhus, Denmark; <sup>6</sup>Leon Berard Cancer Centre, Clinical research platform, Lyon, France

### Purpose or Objective

The rapid innovation in technique and technology of the radiotherapy increases the necessity of health economic evaluation (HEE). Indeed, given their increasing impact of HEE studies on policy, it is essential to appreciate their quality. We aim to assess the quality of selected HEE studies of radiotherapy against quality instruments, such as checklists. In addition, we want to evaluate differences between quality instruments and how well they perform in practice, with a dedicated focus on the costing side.

### Material and Methods

Building upon a previous systematic literature review of EBRT costing studies (Defourny et al., 2016) published from 2004-2015 in MEDLINE, Embase and the NHS EED databases, an assessment of the quality of the selected articles was performed by four independent reviewers. Based on 3 existing instruments - CHEC, CHEERS, and QHES - the selected articles were critically rated focusing on the

transparency of their reporting. Robustness of this analysis and instrument comparison were examined using the Kendall coefficient of concordance and Inter-Class-Correlation coefficients.

### Results

The systematic review lead to the selection of 15 records matching the search strategy: these were most frequently conducted in Canada (n=4) and France (n=3). Instruments' mean score were evaluated respectively at 59.4%, 69.7% and 73.6% for CHEC, CHEERS and QHES. The overall quality score was fairly good, even an in-depth analysis per criteria reveals that essential costing items - discount rate, time horizon, sensitivity analysis - were only partially completed.

Over time, instruments scores rise specifically for QHES. The statistical analysis confirms that raters have scored in a similar manner. In addition, as inter-rater reliability coefficients show that that the reviewers score converged more with CHEC (ICC=0.86\*\*\*) than for QHES (ICC=0.73\*\*\*) and CHEERS (ICC=0.64\*\*\*)).

Figure 1. Mean quality score of EBRT costing studies for each quality instrument.

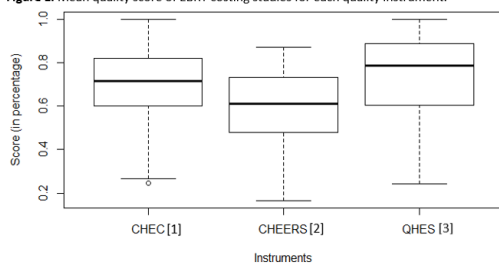
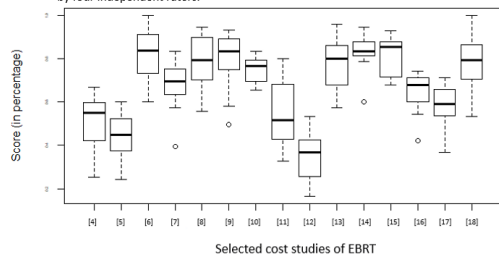


Figure 2. Mean quality score of each EBRT costing studies, reviewed against three instruments by four independent raters.



### Conclusion

The two-fold objectives of the present quality appraisal demonstrate a fairly good quality of reporting overall amongst EBRT costing studies published in the last decade. While we found no major difference in the instrument score, the CHEERS checklist has the most extensive consideration of cost components across all three instruments.

Yet essential improvement in reporting both acknowledged costing methodology and sufficient input information need to be put forward in order to continue improving the quality of future HEE study, supporting indirectly appropriate decision-making about the allocation of scarce healthcare resources.

### PV-0254 Mortality and Morbidity Review of serial radiotherapy accidents in Epinal, 1987-2006

J. Simon<sup>1</sup>, P. Maingon<sup>1</sup>, E. Francois<sup>2</sup>, E.H. Labib<sup>3</sup>, M. Vincent<sup>3</sup>, N. Alain<sup>3</sup>, L. Mihai<sup>3</sup>, M. Christian<sup>3</sup>, P. Didier<sup>3</sup>  
<sup>1</sup>Hôpital Pitié-Salpêtrière, Radiotherapy, Paris, France ;  
<sup>2</sup>Centre Antoine Bécélère, Centre Universitaire des Saints-Pères, Paris, France ;  
<sup>3</sup>Institut de cancérologie de Lorraine, Radiotherapy, Vandoeuvre-les-Nancy, France

### Purpose or Objective

Between 1987 and 2006, five serial accidents occurred in the radiotherapy department of the Jean Monnet Hospital in Epinal, France, resulting in over-irradiation of more

than 5,500 patients (pts) to varying degrees, from 3% to more than 50% of the prescribed dose. Five cohorts of pts were defined according to their specific cause of over-irradiation. We report the Mortality and Morbidity Review of those radiotherapy accidents.

### Material and Methods

Cohort 1: Between 2004 and 2005, 24 prostate cancer pts were over-irradiated more than 20%, because of the improper use of a treatment planning system. For prescribed doses between 69 Gy and 78 Gy, pts received doses between 81 Gy and 120 Gy.

Cohort 2: Between 2000 and 2006, 409 prostate cancer pts received 9-10% radiation overdose because of failure to consider doses delivered by daily portal imaging. For prescribed doses between 70 Gy and 78 Gy, pts received doses between 76.7 Gy and 85.5 Gy.

Cohort 3: Between 1987 and 2000, at least 5,000 pts were irradiated with 3% (1,100 pts), 5.5% (3,600 pts), or 7.1% (306 pts) more radiation than planned, depending on the photon energy used for their radiotherapy. The cause was an error in the homemade informatic program written to carry out calculations of monitor units (MU).

Cohort 4: in 1993, 8 breast cancer pts received a dose 20-68% higher than the prescribed dose because of an inappropriate correction factor used for the calculation of MU when filters for tangential beams were used.

Cohort 5: in 1999, 36 breast cancer pts had radiation overdose to the heart because of exclusive use of direct 6 MV photon beam to deliver 50 Gy to the internal mammary chain.

Moreover, one patient developed a radiation-induced myelitis after overlap of irradiation fields for breast cancer in 1998 and vertebral bone metastasis in 2003.

Adverse effects of radiotherapy were graded according to CTCAE v3.0 grading system. Accident severity was graded according to ASN/SFRO scale (classification of radiation protection events affecting patients).

### Results

Cohort 1: 10 pts died from radiation-induced injury of the gastrointestinal and/or genitourinary tract. This accident was rated level 7 (up to 7) on the ASN/SFRO scale.

Cohort 2: among 405 evaluable pts for toxicity, 372 (82.5%) developed late gastrointestinal toxicity (LGIT)  $\geq$  Grade 1, 155 pts (38%) had LGIT Grade  $\geq 2$ , 66 pts (16%) had LGIT Grade 3, and 2 pts died of radiation-induced rectovesical fistula (level 6 on the ASN/SFRO scale).

Cohort 3: 2 pts died of radiation-induced rectovesical fistula (level 6 on the ASN/SFRO scale).

Cohort 4: 1 patient developed a radiation-induced grade 3 skin complication (level 3 on the ASN/SFRO scale).

Cohort 5: 9 pts (24%) developed radiation-induced grade 4 cardiac adverse events (level 4 on the ASN/SFRO scale).

### Conclusion

Overall, 14 radiation-induced deaths occurred after these accidents. Since 2007, each French radiotherapy center is now inspected once a year by ASN. National measures have been taken to prevent recurrence of such accidents.

### PV-0255 Advocating for radiation oncology through the development of a massive open online course

M. Leech<sup>3</sup>, C. Poole<sup>1</sup>, S. Gallagher<sup>2</sup>, W. Fox<sup>2</sup>  
<sup>1</sup>Trinity College, Discipline of Radiation Therapy, Dublin, Ireland ;  
<sup>2</sup>Trinity College, Trinity Online Services, Dublin, Ireland ;  
<sup>3</sup>TCD Discipline of Radiation Therapy, Trinity College, Dublin, Ireland

### Purpose or Objective

Radiotherapy is an effective and cost effective treatment for most cancers however there is sub-optimal access worldwide and it is underutilised. Lack of information and awareness of radiation therapy is reported within the literature as a patient-related barrier to accessing radiation therapy. The aim of this project was to develop a massive open online course to inform cancer patients,

their families and health professionals about radiation oncology as a treatment for cancer.

#### Material and Methods

Online learning platform was designed with a focus on ensuring a rich learning environment by situating the course through the story of patients and allowing opportunity for reflection, questions and discussion. The platform consisted of 39 steps-15 videos, 15 articles, 2 discussion for a, 6 multiple choice quizzes and 1 final exercise. The Massive Open Online Course was launched in September 2018 and the steps were delivered over a 2 week period.

#### Results

1,489 people signed up to the MOOC from 111 countries. The majority were from the UK (24%), Ireland (20%), Australia (5%), India (4%), US (4%), Egypt (3%), Canada (2%), Spain (2%) and Mexico (2%). 50% of attendees were >56 years of age. A total of 958 comments were posted within the MOOC platform by 225 learners. In the post course evaluation survey, 97% stated that the course met or exceeded their expectations. 96% said the course provided them with new knowledge or skills. 65% have shared the knowledge they learned with other people and 51% have already applied what they learned.

#### Conclusion

Using online technology to explain radiation oncology is an engaging and effective methodology that has been very positively reviewed. This MOOC is available to an international audience and is one method that appears constructive in bridging the gap in knowledge of radiation oncology worldwide.

#### PV-0256 European survey on electronic patient-reported outcomes by the EORTC young Radiation Oncology Group

A.H. Thieme<sup>1</sup>, Y.G. Eller<sup>2</sup>, E. Rivin del Campo<sup>3</sup>, A. Abrunhosa-Branquinho<sup>4</sup>, S. Adebahr<sup>5</sup>, I. Desideri<sup>6</sup>, M. Fiore<sup>7</sup>, S. Hafeez<sup>8</sup>, B. Hoeben<sup>9</sup>, O. Kaidar-Person<sup>10</sup>, I. Kindts<sup>11</sup>, I. Meattini<sup>6</sup>, C. Mercier<sup>12</sup>, F. Mehrhof<sup>1</sup>, D. Nevens<sup>13</sup>, L. Ollivier<sup>14</sup>, M.H. Suppli<sup>15</sup>, L. Visani<sup>6</sup>, B.G. Baumert<sup>16</sup>, C. Ostheimer<sup>17</sup>

<sup>1</sup>Charité-Universitätsmedizin Berlin, Department of Radiation Oncology, Berlin, Germany; <sup>2</sup>University Hospital of Bern, Department of Radiation Oncology, Bern, Switzerland; <sup>3</sup>Tenon University Hospital - Sorbonne University, Department of Radiation Oncology, Paris, France; <sup>4</sup>Centro Hospitalar Lisboa Norte- E.P.E. - Hospital Santa Maria, Department of Radiation Oncology, Lisbon, Portugal; <sup>5</sup>University Medical Center Freiburg, Department of Radiation Oncology, Freiburg, Germany; <sup>6</sup>Azienda Ospedaliero Universitaria Careggi - University of Florence, Radiation Oncology Unit-Oncology Department, Florence, Italy; <sup>7</sup>Campus Bio-medico, Radiation Oncology, Rome, Italy; <sup>8</sup>Institute of Cancer Research - The Royal Marsden NHS Foundation Trust, Radiotherapy and Imaging, London, United Kingdom; <sup>9</sup>Radboud University Medical Center, Department of Radiation Oncology, Nijmegen, The Netherlands; <sup>10</sup>Rambam Medical Center, Oncology Institute- Radiation Oncology and Neuroncology Unit, Haifa, Israel; <sup>11</sup>University Hospitals Leuven, Lab of Experimental Radiation Oncology, Leuven, Belgium; <sup>12</sup>University of Antwerp, Molecular Imaging- Pathology- Radiotherapy & Oncology MIPRO, Antwerp, Belgium; <sup>13</sup>Iridium Cancer Network, Department of Radiation Oncology, Wilrijk- Antwerp, Belgium; <sup>14</sup>University Hospital CHRU Morvan, Radiation Oncology Department, Brest, France; <sup>15</sup>Rigshospitalet- Copenhagen University Hospital, Department of Oncology, Copenhagen, Denmark; <sup>16</sup>GROW - School for Oncology - Maastricht University Medical Centre, Dept. Radiation Oncology Maastricht, Maastricht, The Netherlands; <sup>17</sup>Universität Halle, Department of Radiation Oncology, Halle, Germany

#### Purpose or Objective

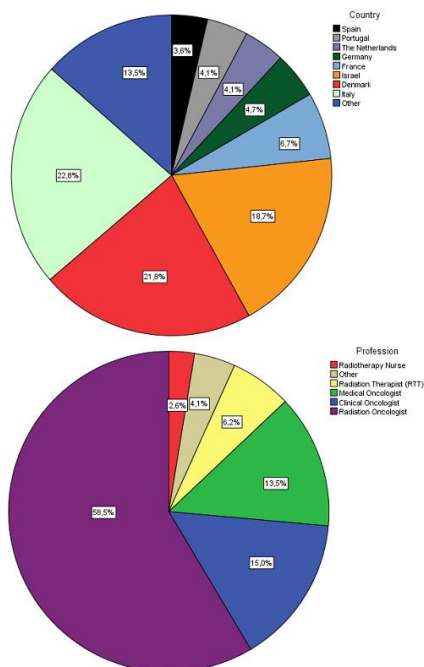
Complete and accurate examiner-independent documentation of meaningful patient orientated clinical outcomes is essential for both clinical trials and daily practice. Currently, adverse events (AEs) following radiotherapy (RT) are mostly investigator-reported, neglecting the essential perspective of the patient. Patient-reported outcomes (PROs) can be prognostic for clinical outcome and are becoming increasingly important. The young Radiation Oncology Group (yROG) of the European Organisation for Research and Treatment of Cancer (EORTC) is conducting a pan-European survey to capture utilization rates, importance and perceived benefits of PROs and to rank ideal features of an electronic tool for PRO assessment (ePRO) in regards to RT. The findings will be used to create an app for RT specific PRO assessment usable on handheld devices and PCs which will be freely available as a science tool for the radiation oncology community.

#### Material and Methods

The survey was addressed to physicians, radiation therapy technicians (RTTs) and nurses who regularly treat and manage patients undergoing radio(chemo)therapy. A publicly accessible online survey consisting of 40 questions and rating each ePRO-feature on a 5-point scale was created and promoted via newsletters. Members of the EORTC network and national radiation oncology societies from Belgium, Denmark, France, Germany, Israel, Italy, the Netherlands, Portugal, Spain, Switzerland and the United Kingdom participated in the survey. The survey is ongoing and will be closed as of 31st October 2018.

#### Results

The survey collected 199 replies up until 22nd October 2018. The distribution by profession and country is reflected in Figure 1. PROs were considered to be important for RT treatment, although assessments were implemented by less than half of the interviewees only (41.2%). Reasons for non-use of PROs were additional time consumption and absence or inaccessibility of ePRO. The majority of survey respondents confirmed the convenience of and demand for PROs. Almost unanimously (97.9%), respondents affirmed they would use ePRO in clinical routine if it were available at their institution. One of the features ranked most highly for ePRO was patient usability (on average 4.69 of 5 points). A first usable prototype of the app could be created and its further development will consider the rating of features (Figure 2).



Question 1 of 12

**In the last 7 days, what was the SEVERITY of your DRY MOUTH at its WORST?**

None  
 Mild  
 Moderate  
 Severe  
 Very severe

Next

© 2018 <http://www.toxicity.pro>

### Conclusion

A high demand for ePRO could be concluded from the survey. An app to assess PROs for RT-related AEs was successfully created and its design will be adapted to results of the survey.

### PV-0257 Radiotherapy impact on quality of life in localised prostate cancer: validation of EPIC-16 in Spain

A. Zapatero Laborda<sup>1</sup>, X. Maldonado Pijoan<sup>2</sup>, A. Gómez-Caamaño<sup>3</sup>, J. Pardo Masferrer<sup>4</sup>, V. Macías Hernández<sup>5</sup>, A. Hervás Morón<sup>6</sup>, J.L. Muñoz García<sup>7</sup>, A. Palacios Eito<sup>8</sup>, P. Anguita-Alonso<sup>9</sup>, C. González-Junco<sup>10</sup>, J. López Torrecilla<sup>11</sup>

<sup>1</sup>Hospital Universitario La Princesa, Department of Radiation Oncology, Madrid, Spain ; <sup>2</sup>Hospital Universitari Vall d'Hebron, Department of Radiation Oncology, Barcelona, Spain ; <sup>3</sup>Hospital Clínico Universitario de Santiago de Compostela, Department of

Radiation Oncology, A Coruña, Spain ; <sup>4</sup>Hospital Universitari Son Espases, Department of Radiation Oncology, Palma de Mallorca, Spain ; <sup>5</sup>Hospital Universitario de Salamanca, Department of Radiation Oncology, Salamanca, Spain ; <sup>6</sup>Hospital Ramon y Cajal, Department of Radiation Oncology, Madrid, Spain ; <sup>7</sup>El Hospital Infanta Cristina de Badajoz, Department of Radiation Oncology, Badajoz, Spain ; <sup>8</sup>Hospital Universitario Reina Sofía, Department of Radiation Oncology, Córdoba, Spain ; <sup>9</sup>Astellas Pharma Inc., Head of Medical Affairs Hospitals - Oncology, Madrid, Spain ; <sup>10</sup>Astellas Pharma Inc., Oncology, Madrid, Spain; <sup>11</sup>ERESA-Hospital General Universitario de València, Department of Radiation Oncology, València, Spain

### Purpose or Objective

Prostate cancer (PCa) is the third most prevalent type of cancer in Spain, with various treatment options, including radiotherapy (RT), depending on disease stage. Health-related quality of life (HRQoL) is greatly affected by functional alterations specific to PCa and its treatment. The Expanded Prostate Cancer Index Composite (EPIC-16), a shorter version of EPIC-50, was designed to be administered in routine clinical practice in patients (pts) with clinically localised prostate cancer, evaluating aspects of therapy that are most bothersome to pts. The objectives of this study were to measure the impact of RT on quality of life and to validate the Spanish version of EPIC-16 in routine clinical practice in Spain.

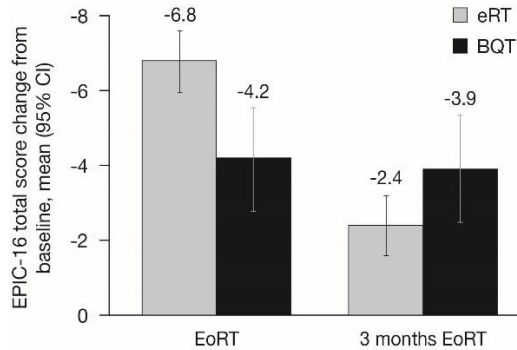
### Material and Methods

An observational, non-interventional, multicentre study was conducted in Spain with pts >40 years (yrs) of age with localised PCa, initiating treatment with external RT (eRT) or brachytherapy (BQT). Changes from baseline in EPIC-16 and UCLA Prostate Cancer Index (PCI) and patient-perceived state of health were measured at two follow-up visits. Psychometric evaluations of the Spanish version of EPIC-16 were conducted to assess its validity.

### Results

Of the 516 pts enrolled this study, 495 were included in the analysis (eRT, n=361; BQT, n=134). Mean (standard deviation [SD]) age was 71.7 (6.4) yrs [eRT] and 66.7 (7.5) yrs [BQT]. At baseline, 264 (73.1%) eRT and 21 (15.7%) BQT pts had a Gleason score  $\geq 7$ ; mean (SD) EPIC-16 global score (range 0-60, 60 being the worst) was 11.9 (7.5) in eRT pts and 10.3 (7.7) in BQT pts. For eRT pts, the total EPIC-16 score increased from baseline by a mean (SD) of 6.8 (7.6) for visit (V) 2 and 2.4 (7.4) at V3 (Figure). For BQT pts, total scores increased from baseline by a mean (SD) of 4.2 (7.6) and 3.9 (8.2) at end of treatment and 3 months after RT, respectively (Figure). Changes from baseline in individual domains (range 0-12, 12 being worse HRQoL) are shown in the table. Changes in the Spanish EPIC-16 domains correlated well with those of the UCLA-PCI for urinary, bowel and sexual domains. Patients perceived no change in their HRQoL status compared to baseline. EPIC-16 showed good internal consistency (Cronbach's  $\alpha=0.84$ ) and reliability, with a moderate intraclass correlation coefficient in all domains, with the exception of the bowel domain. Construct validity was shown with a 5-factor analysis indicating that EPIC-16 domains are conceptually distinct and merit an independent measure. Longitudinal validity was not evident in all HRQoL domains.

**Figure.** EPIC-16 total score mean (95% CI) change from baseline for eRT- and BQT-treated patients



BQT=brachytherapy; CI=confidence interval; EoRT=end of radiotherapy; EPIC-16=Expanded Prostate Cancer Index Composite; eRT=external radiotherapy

**Table.**

Change from baseline in EPIC-16 domains	Analysed patients (n=495)	
	eRT (n=361)	BQT (n=134)
Incontinence, V2/V3	n=322/n=320 -0.6 (1.7)/0 (1.7)	n=124/n=132 -0.3 (1.4)/-0.3 (1.8)
Irritation/obstruction, V2/V3	n=321/n=319 -2.2 (2.8)/-0.1 (2.6)	n=121/n=130 -2.5 (2.8)/-1.7 (3.2)
Bowel, V2/V3	n=322/n=320 -2.1 (3.1)/-0.7 (2.5)	n=123/n=130 -0.8 (2.8)/-0.6 (2.6)
Sexual, V2/V3	n=319/n=316 -1.5 (2.9)/-1.4 (3.1)	n=120/n=132 -1.0 (2.6)/-1.4 (3.1)
Vitality/hormonal, V2/V3	n=319/n=317 -0.5 (2.5)/-0.2 (2.5)	n=120/n=130 0.2 (2.3)/0.1 (2.8)

All data is mean (SD). BQT=brachytherapy; EPIC-16=Expanded Prostate Cancer Index Composite; eRT=external radiotherapy; RT=radiotherapy; SD=standard deviation; V2=visit 2, end of RT; V3=visit 3, 90 days after end of RT.

**Conclusion**

Overall, scores worsened after RT in different HRQoL domains, but pts did not perceive a global change in their HRQoL status. The Spanish version of the EPIC-16 questionnaire demonstrated sensitivity to detect PCa treatment-related effects and sensitivity for clinical improvement after RT. It also showed strong discriminative properties and reliability, demonstrating its validity for use in clinical practice and clinical trials to evaluate the effect of interventions.

**PV-0258 Patient reported outcome and survival analysis after stereotactic body RT (SBRT) of lung metastases**

R. Grosse<sup>1</sup>, K.A. Kessel<sup>1,2</sup>, D. Marciana-Nona<sup>2,3</sup>, M. Oechsner<sup>1</sup>, S.E. Combs<sup>1,2</sup>  
<sup>1</sup>Klinikum rechts der Isar- Technical University of Munich, Radiation Oncology, Munich, Germany; <sup>2</sup>Institute of Innovative Radiotherapy, Institute of Innovative Radiotherapy, Munich, Germany; <sup>3</sup>Klinikum rechts der Isar - Technical University of Munich, Radiation Oncology, Munich, Germany

**Purpose or Objective**

Stereotactic body radiation therapy (SBRT) is a high-precision method to irradiate extracranial targets. In this evaluation, we analyzed patients that underwent SBRT of pulmonary metastases. We focused on toxicity and the efficiency of SBRT in order to gain a long-term patient reported outcome (PRO).

**Material and Methods**

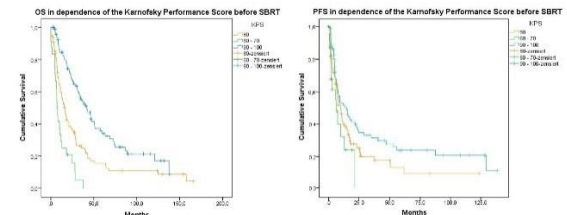
307 lung metastases in 209 patients were treated with SBRT between 2002 and 2017. All patients were enclosed into our retrospective study and documented in the research database of the department of radiation oncology.

We documented side effects according to the CTCAE criteria (v.4.03). Patients, that were still alive and had no follow-up visit for more than six months in our department, received an invitation to our patient survey via mail. The questionnaire contained 13 questions of PRO-CTCAE™ (developed by the NCI) and two self-created questions regarding their state of health and wellbeing. Patients were able to participate using our web-based survey system or if preferred paper-based.

**Results**

**Patients**

Median overall survival (OS) was 19 months (interquartile range (IQR) 7.8 to 41.3 months), median progression-free survival (PFS) was 6.4 months (IQR 2.2 to 16.9 months). The median local control (LC) was 11.6 months (IQR 4.6 to 27.6 months). The pulmonary lesions were treated with a median dose of 35 Gy to the 60% isodose. The Karnofsky Performance Score approved as a statistically significant impact on OS (p<0.001) and PFS (p=0.018).



**Toxicity**

The documented side-effects were mainly graded 1 or 2 (Table 1). Doctors only recorded severe side-effects (grade 3 or 4) in six participant's cases.

CTCAE grade	baseline RT n=209				6-12 months n=153				12-24 months n=114				patient reported n=47			
	1	2	3	4	1	2	3	4	1	2	3	4	1	2	3	4
fatigue	1.9%	3.4%			1.3%	3.3%			1.3%	3.5%			1.1%	3.2%		
nausea																
dermatitis																
hyperpigmentation																
edema																
neuropathy																
asthenia																
motor																
weightloss																
diarrhea																
anorexia																
alopecia																
hypocalcaemia																
cough																
hemoptysis																
apnoea																
stridor																

**PRO assessment**

Out of living 40 patients, 36 (90%) participated in our survey; four patients told us only the status of their actual disease which was stable. The median time between radiation therapy (RT) and PRO was 46.8 months (IQR 16.9 to 93.1).

Patients noted radiodermatitis grade 3 (n=1), sensory disorders grade 4 (n=1) and 3 (n=2), motor disorders grade 3 (n=2), dysphagia grade 3 (n=1), dyspnea grade 3 (n=2) and 4 (n=2) and cough grade 3 (n=1). All patients with severe dyspnea were diagnosed a COPD before SBRT. During PRO assessment, one patient noted four and another patient three grade 3 adverse effects. It appears that subjective personal sensitivity has a relevant influence on how patients filled out the questionnaire.

**Conclusion**

Our results showed low levels of acute, late, long and PRO toxicities. Hence, SBRT is a suitable treatment method for patients with lung metastases, who are unwilling to undergo surgery, or patients, who are functionally

inoperable or whose metastases are unresectable due to their location.

**PV-0259 Cosmetic outcome in irradiated breast cancer patients and association with patient reported outcomes**

M. Batenburg<sup>1</sup>, M. Gregorowitsch<sup>1</sup>, D. Van den Bongard<sup>1</sup>, W. Maarse<sup>2</sup>, H. Verkooijen<sup>3</sup>

<sup>1</sup>UMC Utrecht, Radiation Oncology, Utrecht, The Netherlands; <sup>2</sup>UMC Utrecht, Plastic Surgery, Utrecht, The Netherlands; <sup>3</sup>UMC Utrecht, Imaging Division, Utrecht, The Netherlands

**Purpose or Objective**

Locoregional treatment of breast cancer consists of surgery and, in the majority of cases, irradiation of the breast. These modalities affect cosmetic appearance of the breast. In this study, we evaluated the level of satisfaction with cosmetic outcome one to three years after the start of breast irradiation, determinants of low satisfaction, and its association with quality of life (QoL).

**Material and Methods**

This study was conducted within the UMBRELLA cohort, a prospective observational cohort including breast cancer patients referred for radiation treatment to the department of Radiation Oncology at the University Medical Centre Utrecht. In UMBRELLA, patients consent to collection of clinical and patient reported outcomes (PROs) for research purposes. All 821 patients treated with either lumpectomy or mastectomy followed by breast reconstruction between October 2013 and June 2018, with at least one year follow up were selected. Cosmetic satisfaction, QoL and depression were measured via self-reported questionnaires (resp. Sneeuw, EORTC QLQ-BR23 and C30, and HADS-NL). Patient reported cosmetic outcome was assessed in a 5 point scale: very satisfied, satisfied, neutral, dissatisfied and very dissatisfied with cosmetic outcome. For analysis, satisfied and very satisfied were considered "satisfied with cosmetic outcome" and dissatisfied and very dissatisfied were considered "dissatisfied with cosmetic outcome". Multivariate logistic regression analysis was used to assess the association between patient and tumor characteristics and poor cosmetic satisfaction.

**Results**

After respectively one, two and three years there were 64/821 (8%), 29/422 (7%), and 13/181 (7%) dissatisfied patients. BMI >25 and mastectomy followed by breast reconstruction were significantly associated with cosmetic dissatisfaction, (resp. adjusted OR 2.7 (95%CI 1.1-6.8) and 5.7 (95%CI 1.1-30.0)). High scores on the HADS depression subscale (>8) were significantly more common in dissatisfied patients than in satisfied/neutral patients after one and two years (Table 1). Patients who were dissatisfied with cosmetic outcome reported significantly lower scores for emotional functioning and body image than patients who were satisfied/neutral with their cosmetic outcome after one, two and three years (Figure 1).

**Conclusion**

Dissatisfaction with cosmetic outcome was present in 7-8% of the breast cancer patients one to three years after irradiation. BMI >25 and mastectomy followed by immediate reconstruction were associated with dissatisfaction with cosmetic outcome. Dissatisfied patients reported lower quality of life scores and higher depression scores. Late radiation complications like fibrosis, can occur years after radiation therapy. Therefore, to assess the impact of fibrosis on cosmetic outcome, long-term research has to be performed.

**Joint Symposium: ESTRO-JASTRO: Clinical trials for particle therapy: which ones to run and how?**

**SP-0260 International collaborations in proton therapy: networks, trials and data collection**  
C. Grau<sup>1</sup>

<sup>1</sup>Aarhus University Hospital, Danish Center for Particle Therapy, Aarhus N, Denmark

**Abstract text**

The key clinical research agenda for particle therapy (PT) is to establish the full range of indications for proton therapy. This will in most cases involve studies of PT applied to prevent radiation-induced side effects and/or induction of secondary tumours. In order to promote clinical research and integration of PT into radiation oncology, the European Particle Therapy Network (EPTN) will encourage and foster collaboration on trials and uniform prospective data registration. The vision and scope for clinical trials in the EPTN has been outlined in the special issue of *Radiother Oncol* July 2018:

- Emphasis should be on performing high quality clinical trials with properly selected patients and using relevant, validated clinical endpoints.
- A small number of pivotal RCTs are urgently needed. However, we need to develop, test and validate alternative evidence-based methodologies (e.g. "cohort multiple RCTs").
- Model-based selection (as predictive biomarker) is a useful concept for normal tissue complication probability (NTCP)-based clinical trials, and this concept should later be extended to incorporate Tumor Control Probability (TCP) as well.
- Trials involving state-of-the-art photon RT are welcome, as particle therapy should be an integral component of radiation oncology.
- European trials should be open to accredited centres with expertise and relative high numbers who wish to collaborate.
- Prospective collection of high-quality data for patients treated with proton therapy outside of clinical trials (using common ontology and data collection forms).
- Uniform guidelines for target and organ at risk delineation, as well as guidelines on dose constraints.
- There is a need to develop an IT-infrastructure and European QA platform, not only for particle therapy trials, but also for prospective data registries. The platform for data collection and clinical trials QA have been secured through the collaboration of ESTRO-EPTN with EORTC. With a network of many recently opened and upcoming PT centres in Europe, all with a high academic interest and a capacity to perform clinical trials, the prospects for new clinical trials in PT are encouraging.

**SP-0261 Trial quality assurance and audits for proton therapy**

C. Clark<sup>1</sup>

<sup>1</sup>National Physical Laboratory, Medical Radiation Physics, Teddington, United Kingdom

**Abstract text**

One of the roles of quality assurance (QA) in clinical trials is to enable high quality practice-changing techniques to be tested rigorously for the benefit of patients. This is undertaken by monitoring adherence to trial protocol and thus minimising variations between recruiting centres. Currently extensive proton trial investigations are relatively new in Europe (and world-wide) and hence the QA programmes are in early development across most groups. Particle therapy (PT) raises some different requirements for QA, however there is also much we can learn from the established photon therapy approaches. In an environment where individual countries have few

proton therapy centres there is a need for international cooperation and consensus in developing appropriate QA procedures. The Global Quality Assurance of Radiation Therapy Clinical Trials Harmonisation Group (GHG) is a multi-professional group with Clinicians, Physicists and RTTs collaborating to address this issue by learning from what has already been done for early trials and working together to find solutions to the unaddressed challenges. However, the centres also need confidence in their delivery from day one and other groups such as the European Particle Therapy Network (EPTN) are developing surveys and audits which can help to set the standards required for the implementation of practice-changing trials. Simultaneously, there is a need for calibration procedures which are specific to PT. Primary standards laboratories are working with clinical centres to develop calibration protocols and procedures which are straightforward to use whilst creating minimal uncertainty in the complete dosimetry chain. The aim will be to bring these endeavours together to determine which QA is important for PT clinical trials and how it impacts on clinical outcomes. Longer term this will create confidence that the trial outcomes reflect differences in randomisation schedules rather than variations in accuracy of treatment delivery across different centres. An additional benefit of comprehensive trials QA is the impact on the general standard of treatment delivered.

**SP-0262 Limitations of current RBE models and their implication for clinical trial design**

N. Matsufuji<sup>1</sup>

<sup>1</sup>National Institute of Radiological Sciences NIRS, Department for Accelerator and Medical Physics, Chiba, Japan

**Abstract text**

Unlike conventional X-ray, changing radiation quality within irradiation field and resultant enhancing relative biological effectiveness (RBE) toward its range end makes ion-beam therapy advantageous in realizing intense clinical effect on the deep-seated target while sparing surrounding normal tissues. On another front, this changing RBE of the ion beam makes it indispensable to use an appropriate RBE model that bridges between the radiation quality as input and biological effectiveness as output for safe and efficient ion-beam therapy. In Japan, the first RBE model dedicated for carbon-ion radiotherapy (CIRT) was established in a pragmatic manner, *i.e.*, dose distribution was at first designed from *in-vitro* cell survival response of a reference human salivary gland (HSG) cell as a verifiable biological endpoint, then it was scaled to meet clinical response for therapeutic purpose. Recently the model was updated by integrating the microdosimetric kinetic model (MKM) that realizes to estimate the biological effectiveness of any radiation accurately from its microdosimetric therefore measurable quantity while the indication of the RBE-weighted therapeutic dose has been inherited. At National Institute of Radiological Sciences (NIRS), clinical trials of CIRT have been conducted with the RBE model since 1994 for various solid tumors. More than 11,000 patients have been treated in the past 24 years, and the retrospective analysis of the derived clinical outcomes have revealed the appropriateness of the RBE model. At the same time, there is still certain room for future improvement in the ongoing RBE model especially for coming biologically adaptive therapy. Among possible biological factors, current model explicitly considers only the radiosensitivity of one HSG cells. The tumor-specific difference in response is treated just as the difference in optimum dose found in the dose-escalation clinical trials. In addition, heterogeneity of the tumor such as variation in O<sub>2</sub> pressure or the existence of radioresistant stem cells are not considered yet. The response of surrounding normal

tissues has been analyzed recently, however, further study is necessary to take them into consideration in the treatment planning. In the world, different approach has been adopted in European facilities. Local Effect Model (LEM), another biological model developed at GSI Helmholtzzentrum für Schwerionenforschung (GSI) in Germany, shows almost comparable performance with MKM as model itself, however, different biological endpoint and reference condition selected for therapeutic application results in different indication of the therapeutic RBE-weighted dose even though the same physical dose is delivered. The difference in RBE between the models needs careful translation of the therapeutic RBE-weighted dose from one to the other. For instance, in the international clinical trial for pancreatic cancer treatment CHIPHER (Trial of Carbon Ion Versus Photon Radiotherapy for Locally Advanced, Unresectable Pancreatic Cancer), 57.6 Gy (RBE) will be prescribed in total for those to be treated in Japanese CIRT facilities while 59.4 Gy (RBE) will be given for those placed to European facilities to deliver the identical absorbed dose. Translation of the tolerance dose of organs-at-risk (OARs) between the models is further complex therefore not yet achieved, however, add further weight in international clinical trials ahead.

**SP-0263 Clinical trials on carbon ion radiotherapy for locally advanced pancreatic cancer.**

T. Ohno<sup>1</sup>

<sup>1</sup>Gunma University, Gunma University Heavy Ion Medical Center, Maebashi, Japan

**Abstract text**

Carbon ion radiotherapy (C-ion RT) offers excellent dose distribution, enabling a concentrated administration of a sufficient dose within a target volume while minimizing the dose in the surrounding normal tissues. Additionally, C-ion RT provides biological advantages not seen in proton or photon therapy, owing to high linear energy transfer (LET); C-ion RT induces increased double-stranded DNA structures, causing irreversible cell damage independently of cell cycle phase or oxygenation, more so than lower LET irradiation such as proton and photon therapy. C-ion RT has been in use for more than 20 years in Japan and the efficacy and safety of this therapy, especially for photon-resistant tumors such as bone and soft tissue sarcoma, non-squamous cell carcinomas of the head and neck, pancreatic cancer, and rectal cancer is well accepted. For locally advanced unresectable pancreatic cancer, a phase I/II clinical study was conducted and recommended schedule of the combination of carbon ion radiotherapy (55.2 Gy (RBE) in 12 fractions for 3 weeks) and gemcitabine (1000 mg/m<sup>2</sup>/weekly) was determined. Subsequently operated C-ion RT centers have used the schedule. Recent multicenter retrospective clinical study demonstrated that the reproducible clinical efficacy was observed. The 2-year overall survival was 60% for patients treated with 55.2 Gy (RBE) in 12 fractions concurrent with chemotherapy. Based on these backgrounds, multicenter randomized clinical study on locally advanced pancreatic cancer comparing carbon ion radiotherapy with IMRT was conducted. In my talk, rationale, accumulated clinical outcomes, and future perspectives of C-ion RT for pancreatic cancer will be presented.

---

**Proffered Papers: RB 3: Tumour sensitization**

---

**OC-0264 CDK4/CDK6 inhibition radiosensitises HPV-neg HNSCC through inhibition of homologous recombination**  
E. Gottgens<sup>1</sup>, K. Leszczynska<sup>2</sup>, J. Bussink<sup>1</sup>, E. Hammond<sup>2</sup>, P. Span<sup>1</sup>

<sup>1</sup>UMC St Radboud Nijmegen, Department of Radiation Oncology, Nijmegen, The Netherlands; <sup>2</sup>CRUK-MRC

*Oxford Institute for Radiation Oncology, Department of Oncology, Oxford, United Kingdom*

#### **Purpose or Objective**

Radiotherapy is an important modality in the treatment of head and neck squamous cell carcinomas (HNSCC). Patients with human papillomavirus (HPV) negative carcinomas have a poorer treatment response and prognosis than patients with HPV+ HNSCC. Therefore, it is important to develop new treatment strategies to improve treatment for HPV- HNSCC patients. p16, a tumour suppressor and cyclin dependent kinase (CDK) 4/CDK6 inhibitor, is commonly overexpressed in HPV+ HNSCC and has been linked to the high radiosensitivity of HPV+ cells. We hypothesised that blocking CDK4/CDK6 using palbociclib in HPV- HNSCC would result in radiosensitisation.

#### **Material and Methods**

In this study, three HPV+ and ten HPV- HNSCC cell lines were exposed to clinically relevant levels of palbociclib, combined with ionising radiation (0-8 Gy). Cell survival was measured by colony forming assays. Levels of DNA damage and recruitment of DNA damage repair factors were assessed by 53BP1/RAD51/BRCA1 foci measurement and genome instability by metaphase spreading. Cell cycle analysis was performed by propidium iodide staining and flow cytometry. Mitotic catastrophe was measured by immunofluorescent staining for  $\alpha$ -tubulin and DAPI. Homologous recombination was measured using a GFP reporter-based system.

#### **Results**

A strong radiosensitising effect of palbociclib was observed in ten HPV- cell lines, whereas this did not occur in three HPV+ cell lines. This effect could also be observed in low oxygen tensions (1% O<sub>2</sub>) that are commonly known to cause radioresistance. Concurrent radiation with palbociclib resulted in elevated levels of residual 53BP1 foci in HPV- UT-SCC-24A cells (figure) and high levels of chromosomal aberrations. We discovered that palbociclib reduced the expression of RAD51 and BRCA1, leading to decreased protein expression, reduced localisation to DNA damage sites, and dysfunctional homologous recombination. In addition, we showed that this repression was cell cycle independent. As a consequence of this, we observed high amounts of mitotic aberrancies which suggests that combining radiation with palbociclib leads to cytotoxicity via mitotic catastrophe.

#### **Conclusion**

Palbociclib caused a strong radiosensitising effect in HPV-, but not HPV+ HNSCC cell lines. Taken together, we highlight a therapeutic strategy to improve the radiosensitivity of HPV-ve HNSCC, a patient group that has an unmet and urgent need for improved radiotherapy efficacy.

#### **OC-0265 MiR-205 enhances radiation sensitivity of prostate cancer cells through PKC $\epsilon$ and ZEB1 inhibition**

R. El Bezawy<sup>1</sup>, S. Tinelli<sup>1</sup>, A. Cicchetti<sup>2</sup>, R. Valdagni<sup>3</sup>, P. Gandellini<sup>1</sup>, N. Zaffaroni<sup>1</sup>

<sup>1</sup>Fondazione IRCCS Istituto Nazionale dei Tumori di Milano, Department of Applied Research and Technological Development, Milan, Italy ; <sup>2</sup>Fondazione IRCCS Istituto Nazionale dei Tumori di Milano, Department of Medical Physics, Milan, Italy ;

<sup>3</sup>Fondazione IRCCS Istituto Nazionale dei Tumori di Milano, Department of Radiation Oncology 1, Milan, Italy

#### **Purpose or Objective**

Radiotherapy is one of the main treatment options for non-metastatic prostate cancer (PCa). Although treatment technical optimization has greatly improved local tumor control, a considerable fraction of patients still experience relapse due to development of resistance. Radioresistance is a complex and still poorly understood phenomenon involving the deregulation of a variety of

signaling pathways as a consequence of several genetic and epigenetic abnormalities. In this context, cumulative evidence supports a functional role of microRNAs, endogenous small non-coding RNA molecules that negatively regulate gene expression, in affecting radioresistance, suggesting the modulation of their expression as a novel radiosensitizing approach. In this study, we investigated for the first time the ability of miR-205 to enhance the radiation response of prostate cancer cells.

#### **Material and Methods**

miR-205 reconstitution by a miRNA mimic in PCa cell lines (DU145 and PC-3) was used to elucidate miR-205 biological role. Radiation response in miRNA-reconstituted and control cells was assessed by clonogenic assay, immunofluorescence-based detection of nuclear  $\gamma$ -H2AX foci and comet assay. Target-protection experiments were performed by using a custom oligonucleotide designed to physically disrupt the pairing between the miRNA and its target PKC $\epsilon$ . For in vivo experiments, xenografts generated by implanting DU145 cells stably expressing miR-205 in SCID mice, were exposed to 5 Gy single dose irradiation using an image-guided animal micro-irradiator (225Cx, Precision X-ray).

#### **Results**

Experimental data showed that reconstitution of miR-205 is able to significantly enhance the radiation response of prostate cancer cell lines and xenografts. Specifically, miR-205 exerts its radiosensitizing effect through the impairment of radiation-induced DNA damage repair, as a consequence of PKC $\epsilon$  and ZEB1 inhibition. Indeed, phenocopy experiments based on knock-down of either PKC $\epsilon$  and ZEB1 were able to reproduce miR-205 radiosensitizing effect, hence confirming a functional role of both targets in the process. At the molecular level, miR-205-induced suppression of PKC $\epsilon$  counteracted radioresistance through the impairment of EGFR nuclear translocation and consequent DNA-PK activation. Consistently, disruption of miR-205-PKC $\epsilon$  3'UTR pairing almost completely abrogated the radiosensitizing effect, therefore further substantiating the role of PKC $\epsilon$  as a key effector of miRNA induced enhancement of radiation response.

#### **Conclusion**

Overall, our results uncovered the molecular and cellular mechanisms underlying the radiosensitizing effect of miR-205, suggesting this miRNA as a potential positive modulator of radiation response. These findings support the clinical interest in developing a novel therapeutic approach based on miR-205 reconstitution to increase Pca sensitivity to radiotherapy.

#### **OC-0266 Pancreatic ductal adenocarcinoma sensitization to radiotherapy by bioactive food components**

V. Vendrely<sup>1</sup>, S. Amintas<sup>2</sup>, C. Noël<sup>2</sup>, I. Moranvillier<sup>3</sup>, I. Lamrissi<sup>3</sup>, B. Rousseau<sup>2</sup>, S. Coulibaly<sup>4</sup>, A. Bedel<sup>2</sup>, F. Moreau-Gaudry<sup>2</sup>, E. Buscaïl<sup>5</sup>, L. Chiche<sup>5</sup>, G. Belleannée<sup>6</sup>, C. Dupin<sup>1</sup>, S. Dabernat<sup>2</sup>

<sup>1</sup>CHU de Bordeaux, Radiotherapy, Pessac, France ;

<sup>2</sup>Bordeaux University, Biotherapy, Bordeaux, France ;

<sup>3</sup>Inserm 1035, Biotherapy, Bordeaux, France ; <sup>4</sup>CHU

Bordeaux, radiotherapy, Bordeaux, France ; <sup>5</sup>CHU de

Bordeaux, Surgery, Pessac, France ; <sup>6</sup>CHU de Bordeaux,

Histopathology, Pessac, France

#### **Purpose or Objective**

Pancreatic ductal adenocarcinoma (PDAC) is of poor prognosis in part because of resistance to conventional treatments such as chemotherapy or radiotherapy. Some naturally occurring bioactive food components (BFCs), with pro-oxidant properties are able to potentiate the cytotoxic action of conventional drugs in the PDAC. In addition, these BFCs could increase the DNA breaks induced by ionizing radiation. Our objectives were to

evaluate the combined action of several BFCs in combination with chemotherapy and radiotherapy in PDAC models and to identify mechanisms involved in chemo / radiosensitization at the cellular and molecular levels

#### Material and Methods

Cell survival was evaluated *in vitro* in the presence of BFCs in combination on 4 pancreatic tumor cell lines. The production of reactive oxygen species (ROS) was measured by flow cytometry and fluorescence microscopy. Molecular mechanisms have been decrypted by western blot (signaling pathways) and flow cytometry (cell cycle and apoptosis). Finally, we evaluated the association of BFCs in gavage with intraperitoneal gemcitabine chemotherapy and with radiotherapy (2 Gy/fraction) *in vivo*, on subcutaneous CAPAN-2 cell xenografts.

#### Results

*In vitro*, resveratrol (R), capsaicin (C) and sulforaphane (S) were cytotoxic with significantly higher inhibitory effect in combination (R + C), (C + S) or (R + C + S), without effect on fibroblasts. In addition, the combinations potentiated the otherwise limited action of gemcitabine on cells tested *in vitro*. *In vivo*, the addition of R + C to treatment with gemcitabine at reduced dose allowed tumor inhibition equivalent to that obtained with gemcitabine at full dose. Furthermore, *in vitro*, the addition of BFCs alone and in combination with radiotherapy significantly increases cellular toxicity on the CAPAN-2 epithelial line, compared to radiotherapy alone and BFCs alone or combined. *In vivo*, the combination R + C associated with radiotherapy allowed a significant decrease in tumor volumes compared to radiotherapy alone. The study of signaling pathways showed an increase of pro-apoptotic proteins with the association R + C and radiotherapy, in relation with an increased induction of ROS, but also, surprisingly, an inhibition of the repair of the DNA by inhibition of ATM phosphorylation. These two combined effects precipitated the death of the tumor cells.

#### Conclusion

Combinations of R + C have a chemosensitizing and radiosensitizing effect in a preclinical model of PDAC, with identified molecular mechanisms relevant in the context of the therapies tested. By combining BFCs with radiochemotherapy with gemcitabine, we can hope for a double potentiation of radiotherapy and chemotherapy, by increasing the effectiveness of RT, and by reducing the dose of gemcitabine associated for similar efficiency and better tolerance treatment.

#### OC-0267 Imaging the effect of Atovaquone on the hypoxia-related marker CAIX in head and neck cancer models

F. Huizing<sup>1</sup>, B.A. Hoeben<sup>1</sup>, O.C. Boerman<sup>2</sup>, S. Heskamp<sup>2</sup>, J. Bussink<sup>1</sup>

<sup>1</sup>UMC St Radboud Nijmegen, Radiation oncology, Nijmegen, The Netherlands ; <sup>2</sup>UMC St Radboud Nijmegen, Nuclear Medicine, Nijmegen, The Netherlands

#### Purpose or Objective

Tumor hypoxia is an important cause of radio resistance and is associated with poor patient outcome. Therefore, methods to reduce hypoxia before or during radiotherapy are of great value. The drug Atovaquone shows great potential in this prospect. By reducing the oxygen consumption rate of cells it has been shown to reduce hypoxia both *in vitro* and *in vivo*.

Recently, the radioactive tracer <sup>111</sup>In-girentuximab-F(ab')<sub>2</sub> was developed for imaging of the hypoxia related marker Carbonic Anhydrase IX (CAIX). Successful imaging of the hypoxia reducing effect of Atovaquone could help predict the effectiveness of radiotherapy. Aim of this study is to assess the effect of Atovaquone on tumor hypoxia with the use of the SPECT tracer <sup>111</sup>In-girentuximab-F(ab')<sub>2</sub>.

#### Material and Methods

Athymic mice with subcutaneous FaDu or SCCNij202 head and neck carcinoma xenografts were treated with Atovaquone (50mg/kg) during 8 days or were held for 48 hours in a hypoxic chamber (8% O<sub>2</sub>). After treatment mice were injected with <sup>111</sup>In-girentuximab-F(ab')<sub>2</sub> and 24 hours after injection the mice were imaged using a microSPECT/CT. Tracer uptake was also measured by analyzing *ex vivo* radioactivity counting and autoradiography of the tumor sections. Immunohistochemical staining was used to determine CAIX expression and hypoxia.

#### Results

Atovaquone treatment decreased both CAIX expression and hypoxia staining by 54 ± 33% and 50 ± 21% in the FaDu tumor model, while in the SCCNij202 no difference was observed. Treatment with hypoxic breathing did not increase CAIX expression or hypoxia staining in both tumor models. <sup>111</sup>In-girentuximab-F(ab')<sub>2</sub> tumor uptake was generally in line with CAIX expression, however mice treated with hypoxic breathing showed an increased amount of necrosis and a decreased amount of tumor tracer uptake.

#### Conclusion

Atovaquone decreases tumor hypoxia in the FaDu tumor model, but not in the SCCNij202 model. <sup>111</sup>In-girentuximab-F(ab')<sub>2</sub> specifically targets to CAIX-expressing areas in head and neck cancer xenografts. The radiotracer has potential for therapy monitoring, but differences in tumor perfusion and necrosis can hamper accurate quantification.

#### OC-0268 Intrinsic radiosensitivity, genomic-adjusted radiation dose and patterns of failure of penile cancer

P. Johnstone<sup>1</sup>, G.D. Grass<sup>1</sup>, M. Azizi<sup>2</sup>, K. Ahmed<sup>1</sup>, G.S.J. Yoder<sup>3</sup>, E. Welsh<sup>4</sup>, W. Fulp<sup>4</sup>, J. Dhillon<sup>5</sup>, J. Torres-Roca<sup>1</sup>, A. Giuliano<sup>6</sup>, Z. Yuan<sup>1</sup>, P. Spiess<sup>2</sup>

<sup>1</sup>Moffitt Cancer Center, Radiation Oncology, Tampa, United States Minor Outlying Island ; <sup>2</sup>Moffitt Cancer Center, Urology, Tampa, United States Minor Outlying Island ; <sup>3</sup>Moffitt Cancer Center, Genomics Core, Tampa, United States Minor Outlying Island ; <sup>4</sup>Moffitt Cancer Center, Biostatistics and Bioinformatics, Tampa, United States Minor Outlying Island ; <sup>5</sup>Moffitt Cancer Center, Anatomic Pathology, Tampa, United States Minor Outlying Island ; <sup>6</sup>Moffitt Cancer Center, Cancer Epidemiology, Tampa, United States Minor Outlying Island

#### Purpose or Objective

Our group previously developed algorithms to characterize a genome-based radiosensitivity index (RSI) and a clinically actionable model to calculate genomic-adjusted radiation dose (GARD), which have been validated in various clinical cohorts. Herein, we characterized the RSI and GARD profiles in a cohort of patients with penile squamous cell carcinoma (PeSCC). We further assessed the potential correlation of GARD with the clinical outcomes in PeSCC patients treated with postoperative radiation therapy (PORT).

#### Material and Methods

A total of 25 PeSCC samples were identified from our institution's tissue bank to analyze RSI. Fresh frozen PeSCC tissue samples were analyzed using Affymetrix U133 2.0 microarray chips. RSI score (range 0-1.0) was derived for each sample using the previously published algorithm for a specific 10 genes signature. The comparison of RSI among PeSCC and various selected epithelial cancers were assessed. GARD values were calculated as described in our prior studies using a postoperative RT dose of 50 Gy. A cohort of 18 patients treated with PORT was reviewed for clinical correlation.

#### Results

The median RSI for the tissue cohort was 0.475 (range 0.215-0.682). The majority of the lesions (n=21; 84%) are radioresistant using a previously reported RSI cut-point of

0.375 (RSI >0.375 =radioresistant). In comparison to cohorts of other histologies including bladder transitional cell carcinoma, glioma, cervical SCC, esophageal adenocarcinoma, melanoma, non-melanoma skin cancer, non-opharynx and oropharynx head and neck SCC, PeSCC is one of the most intrinsically radioresistant cancers. Genomically, PeSCC is significantly more radioresistant while comparing with oropharynx head and neck SCC ( $p=0.01$ ) and cervical SCC ( $p=0.002$ ). The PeSCC GARD values ranged from 9.56 to 38.39 (median 18.25), suggesting various radiation therapeutic effects if treated with a uniform PORT dose of 50 Gy. GARD-modeled dose of 50 Gy controls only 52% of PeSCC lesions. Median follow-up from the completion of RT for the clinical cohort was 12.1 months. The majority of patients presented with pathological N2 or N3 disease ( $n=15$ ; 83%) and treated with adjuvant concurrent platinum-based chemoradiotherapy (CRT,  $n=16$ ; 89%). Nine out of the 18 patients had locoregional recurrence (LRR). Of whom, 6 patients presented with LRR within six months since completion of PORT.

### Conclusion

The majority of PeSCC are intrinsically radioresistant with low GARD-based radiation therapeutic effect. This finding is consistent with the observed high rate of LRR (50%) in the clinical cohort treated with PORT doses of 45-59.4 Gy. A GARD-based strategy may help personalize radiation therapy dose prescription to individual tumor biology and improve outcomes.

### Proffered Papers: CL 5: Proffered papers : Randomised Clinical Trials

#### OC-0269 A randomized phase III trial for alleviating radiation-induced xerostomia with chewing gum

J.K. Kaae<sup>1,2</sup>, L. Stenfeldt<sup>1</sup>, B. Hyrup<sup>3</sup>, C. Brink<sup>2,4</sup>, J.G. Eriksen<sup>5</sup>

<sup>1</sup>Odense University Hospital, Oncology, Odense, Denmark; <sup>2</sup>University of Southern Denmark, Clinical Research, Odense, Denmark; <sup>3</sup>Fertin Pharma A/S, Fertin Pharma, Vejle, Denmark; <sup>4</sup>Odense University Hospital, Laboratory of Radiation Physics, Odense, Denmark; <sup>5</sup>Aarhus University Hospital, Experimental Clinical Oncology, Aarhus, Denmark

### Purpose or Objective

Radiation-induced xerostomia is a serious problem affecting quality of life (QOL) after radiotherapy (RT) for head and neck cancer. The aim of this study was to assess the effect of tasteless chewing gum to improve salivary flow after radiation-induced xerostomia for Head and Neck Cancer Survivors (HNCS).

### Material and Methods

HNCS treated with curative intended primary RT and without loco-regional failure were recruited from the follow-up clinic. Inclusion criteria were subjective feeling of xerostomia as rated by the DAHANCA score, sufficient dental health, and minimum six months follow-up after end of RT. HNCS were randomized 2:1 to one month of daily chewing gum or best supportive care. Intervention was a customized experimental sugar-free chewing gum without flavors. Unstimulated and stimulated sialometry were performed to measure saliva flow. Saliva viscosity was tested with the Inclined Plane Test (IPT) by recording the saliva transit time on a 20 cm vertical plate with cutoff at 5 cm. The validated Groningen Radiotherapy-Induced Xerostomia (GRIX) questionnaire was completed to evaluate the subjective QOL in relation to xerostomia. The primary endpoint was the difference in salivary flow rate between unstimulated and stimulated sialometry after using chewing gum for one month.

### Results

From Aug 2016 to Aug 2018, 109 HNCS were enrolled. Ninety-one were eligible for analysis and randomized to intervention ( $n=55$ ) or control ( $n=36$ ) (Table 1). Median age was 61 years (range 34-80). Oropharynx was the predominant tumor location (95%). Prescribed treatment dose was 66-68 Gy. Sialometry showed an increase in mean salivary flow from unstimulated 0.15 ml/min to stimulated 0.57 ml/min ( $\Delta$ Saliva 0.42 ml/min) for the intervention group ( $p < 0.0001$ ) (Fig. 1). Viscosity on the IPT showed that the transit time of saliva at 5 cm was significantly faster for the stimulated saliva output (3 sec) compared to the unstimulated output (21 sec) for the intervention group ( $p = 0.02$ ) (Fig. 1). For the control group, mean salivary flow also increased with chewing gum stimulation ( $\Delta$ Saliva 0.56 ml/min,  $p < 0.001$ ) and saliva transit time for viscosity improved from 15 to 4 sec ( $p = 0.06$ ). No significant difference was seen between the unstimulated and stimulated mean salivary flow when comparing the two groups. The GRIX questionnaire showed improved QOL for the intervention group for items concerning xerostomia during the day (Q2,  $p = 0.001$ ), xerostomia when being outdoor (Q3,  $p = 0.001$ ) and while eating (Q4,  $p = 0.004$ ).

Table 1 Patient characteristics

	Randomized patients	Eligible patients Arm A	Eligible patients Arm B	P-value (2-sided)
Included patients	109	55	36	
Dropout	18	13	5	
Age (median)	61 [34-80]	61 [34-80]	60.5 [40-79]	0.5
Under 70 yr	95 (87%)	45 (82%)	33 (92%)	0.2
Above 70 yr	14 (13%)	10 (18%)	3 (8%)	
Gender (male)	72 (66%)	33 (60%)	27 (75%)	0.1
Weight, kg	76.9 [45-121]	76.9 [45-115]	78.4 [18-37]	0.4
BMI	25.4 [18-38]	25.5 [18-38]	25.6 [18-37]	0.6
Tumor site				
Oropharynx	103 (94%)	51 (93%)	35 (97%)	0.4
Oral Cavity	6 (6%)	4 (7%)	1 (3%)	
Concomitant chemotherapy	77 (71%)	39 (71%)	24 (67%)	0.7
Performance status				
PS 0	90 (73%)	46 (84%)	30 (83%)	1.0
PS 1	19 (17%)	9 (16%)	6 (17%)	
Time post RT				
Under 2 yrs (6-24 mths)	82 (75%)	39 (71%)	29 (81%)	0.3
Above 2 yrs (36-60 mths)	27 (25%)	16 (29%)	7 (19%)	
Smoking status				
Never smoker	39 (36%)	21 (38%)	15 (42%)	0.9
Former smoker	62 (57%)	30 (55%)	19 (53%)	
Active smoker	8 (7%)	4 (7%)	2 (5%)	
Comorbidity	72 (66%)	38 (69%)	21 (58%)	0.3
Daily aid with water	95 (87%)	48 (87%)	32 (89%)	0.8

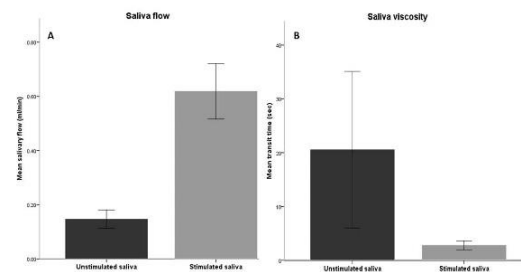


Fig 1 Saliva outputs before and after use of chewing gum at follow-up for the intervention group. (A) Mean salivary flow (ml/min) for unstimulated and stimulated saliva. (B) Mean transit time (sec.) for saliva viscosity at 5 cm on the inclined Plane Test (IPT) for unstimulated and stimulated saliva.

### Conclusion

Customized experimental chewing gum was able to increase salivary flow and decrease viscosity for Head and Neck Cancer Survivors experiencing radiation-induced xerostomia for both the intervention and control group. Xerostomia-related QOL only improved for the intervention group.

#### OC-0270 Antihormones with or without irradiation in breast cancer: 10-year results of the ABCSG 8A trial

G. Fastner<sup>1</sup>, F. Sedlmayer<sup>1</sup>, J. Widder<sup>2</sup>, M. Metz<sup>3</sup>, H. Geinitz<sup>4</sup>, K. Kapp<sup>5</sup>, L. Sölkner<sup>6</sup>, R. Greil<sup>7</sup>, R. Jakesz<sup>8</sup>, W.

Kwasny<sup>9</sup>, D. Heck<sup>10</sup>, V. Bjelic-Radicic<sup>11</sup>, M. Balic<sup>12</sup>, H. Stöger<sup>12</sup>, U. Wieder<sup>13</sup>, R. Zwrtek<sup>14</sup>, D. Semmler<sup>14</sup>, W. Horvath<sup>15</sup>, E. Melbinger-Zeinitzer<sup>16</sup>, M. Wiesholzer<sup>17</sup>, V. Wette<sup>18</sup>, M. Gnant<sup>19</sup>

<sup>1</sup>Paracelsus Medical University- University Hospital Salzburg- Landeskrankenhaus, Radiotherapy and Radio-Oncology, Salzburg, Austria ; <sup>2</sup>Medical University of Vienna, Radiation Oncology, Vienna, Austria ; <sup>3</sup>Wiener Neustadt Hospital, Radiooncology and Radiotherapy, Wiener Neustadt, Austria ; <sup>4</sup>Ordensklinikum Barmherzige Schwestern Linz, Radiation Oncology, Linz, Austria ; <sup>5</sup>Comprehensive Cancer Center CCC- Medical University of Graz, Therapeutic Radiology and Oncology, Graz, Austria ; <sup>6</sup>Austrian Breast and Colorectal Cancer Study Group, Biostatistics, Vienna, Austria; <sup>7</sup>Paracelsus Medical University- University Hospital Salzburg- Landeskrankenhaus, Medical Oncology, Salzburg, Austria ; <sup>8</sup>Austrian Breast and Colorectal Cancer Study Group, Vienna Study Centre, Vienna, Austria ; <sup>9</sup>Wiener Neustadt Hospital, Surgery, Wiener Neustadt, Austria; <sup>10</sup>Ordensklinikum Barmherzige Schwestern Linz, Surgery, Linz, Austria; <sup>11</sup>Medical University of Graz, Gynecology, Graz, Austria ; <sup>12</sup>Medical University of Graz, Internal Medicine- Division of Oncology, Graz, Austria ; <sup>13</sup>Hanusch Spital, Surgery, Vienna, Austria ; <sup>14</sup>Mistelbach Hospital, Surgery, Mistelbach, Austria; <sup>15</sup>Guessing Hospital, Surgery, Guessing, Austria; <sup>16</sup>Wolfsberg Hospital, Surgery, Wolfsberg, Austria ; <sup>17</sup>University Hospital St. Poelten- Karl Landsteiner University of Health Sciences, Internal Medicine I- Division of Nephrology and Hematology, St. Pölten, Austria ; <sup>18</sup>Krankenhaus der Barmherzigen Brüder St. Veit an der Glan, Surgery, St. Veit an der Glan, Austria; <sup>19</sup>Medical University of Vienna, Surgery and Comprehensive Cancer Center, Vienna, Austria

***This abstract is part of the media programme and will be released on the day of its presentation***

**OC-0271 First randomized study of Hafnium nanoparticles activated by radiotherapy in soft tissue sarcoma**

S. Bonvalot<sup>1</sup>, P. Rutkowski<sup>2</sup>, J. Thariat<sup>3</sup>, S. Carrere<sup>4</sup>, M. Sunyach<sup>5</sup>, E. Saada-Bouzi<sup>6</sup>, P. Agoston<sup>7</sup>, A. Hong<sup>8</sup>, A. Mervoyer<sup>9</sup>, M. Rastrelli<sup>10</sup>, C. Le Pechoux<sup>11</sup>, V. Moreno<sup>12</sup>, R. Li<sup>13</sup>, B. Tiangco<sup>14</sup>, A. Casado Herra<sup>15</sup>, A. Gronchi<sup>16</sup>, L. Mangel<sup>17</sup>, P. Hohenberger<sup>18</sup>, M. Delannes<sup>19</sup>, Z. Papp<sup>20</sup>  
<sup>1</sup>Institut Curie, Surgery, Paris, France ; <sup>2</sup>The Maria Skłodowska Curie Memorial Cancer Centre and Institute of Oncology MCMCC, Soft Tissue/Bone Sarcoma and Melanoma, Warsaw, Poland; <sup>3</sup>Cancer center Baclesse, Radiation Oncology, Caen, France ; <sup>4</sup>Centre Regional De Lutte Contre Le Cancer Paul Lamarque, Surgical Oncology, Montpellier, France; <sup>5</sup>Centre Leon Berard, Radiation Oncology, Lyon, France; <sup>6</sup>Centre Antoine Lacassagne, Medical Oncology, Nice, France; <sup>7</sup>Országos Onkológiai Intézet, Radiation Oncology Budapest, Hungary; <sup>8</sup>Chris O'Brien Lifeforce, Radiation Oncology, Sydney, Australia; <sup>9</sup>Centre Rene Gauducheau- CLCC Nantes Atlantique, Radiation Oncology, Saint Herblain, France ; <sup>10</sup>Institute of Oncology Veneto IOV, Surgical Oncology, Padova, Italy; <sup>11</sup>Institut Gustave Roussy, Radiation Oncology, Villejuif, France; <sup>12</sup>Hospital Fundación Jimenez Diaz, Medical Oncology, Madrid, Spain ; <sup>13</sup>St. Luke's Medical Center, Medical Oncology, Quezon City, Philippines; <sup>14</sup>The Medical City Cancer Center, Medical Oncology, Pasay City, Philippine; <sup>15</sup>Hospital Clinico Universitario San Carlos, Medical Oncology, Madrid, Spain; <sup>16</sup>Fondazione IRCCS - Istituto Nazionale dei Tumori, Surgery, Milan, Italy; <sup>17</sup>University of Pecs, Oncotherapy, Pécs, Hungary; <sup>18</sup>Universitätsklinikum Mannheim, Surgical Oncology and Thoracic Surgery, Mannheim, Germany; <sup>19</sup>Institut Claudius Regaud, Radiation Oncology, Toulouse, France; <sup>20</sup>Hungarian Defence Forces, Medical Centre, Budapest, Hungary

**Purpose or Objective**

Preoperative radiotherapy (RT) is an option for a subset of patients with locally advanced primary or relapsed tumors. Yet, its impact on efficacy in terms of pathological response is limited, highlighting the need for novel multimodal therapies aimed at local control with low toxicity.

NBTR3 is made of hafnium oxide nanoparticles which, injected intratumorally (IT) and activated by ionizing radiation, yield a tumor-localized high energy deposit and increase cell death compared to the same dose of RT alone.

We report here the results of a phase II/III randomized clinical trial of NBTR3 given as preoperative treatment to patients with locally advanced soft tissue sarcoma (STS) of the extremity and trunk wall [NCT02379845].

**Material and Methods**

Act.In.Sarc is an international, multicenter, open-label, active-controlled phase II/III trial in which patients (pts) with locally advanced STS of the extremity or trunk wall were randomized 1:1 to receive a single IT NBTR3 injection and RT (Arm A) or RT alone (Arm B), followed by surgical resection. RT consisted of Intensity Modulated RT or 3D-RT of 2Gy\*25 fractions (total 50 Gy) over 5 weeks.

The primary endpoint was pathological Complete Response Rate (pCRR), defined as the proportion of pts presenting <5% of residual viable cancer cells evaluated by a Central Review Board on anonymized tumor specimen. Key secondary endpoints included negative surgical margin (R0) and general safety.

#### Results

Among the 180 randomized pts, 176 were included in the intent-to-treat full analysis set (ITT-FAS). In the ITT-FAS population, pCRR was 16.1% in Arm A vs 7.9% in Arm B (p=0.0448). R0 margin was achieved in 77.0% of pts in Arm A vs 64.0% in Arm B (p=0.0424). The limb amputation rate, another secondary outcome, was decreased by 50% in Arm A as compared to Arm B. NBTXR3 showed very good local tolerance without any modification of RT alone safety profile. In all the treated pts in Arm A, who received any amount of NBTXR3 or at least one RT dose, the IT administration of NBTXR3 caused injection-site pain in 12 (13.5%) pts. NBTXR3 was also associated with grade 3-4 acute immune reactions in 7 (7.9%) pts, but these adverse events were of short duration, manageable, and, in some cases, resolved spontaneously. Long-term efficacy and safety results will be presented.

#### Conclusion

In this study both the primary and secondary endpoints (pCRR and R0 rate, respectively) were met with a safety profile of NBTXR3 activated by RT comparable to that of RT alone. As pCR is associated with improved progression-free and overall survival, NBTXR3 activated by RT represents a new preoperative treatment option for locally advanced STS. These data support ongoing studies investigating NBTXR3 in recurrent/metastatic HNSCC or metastatic non-small cell lung cancer [NCT03589339]; HNSCC [NCT01946867; NCT02901483]; prostate cancer [NCT02805894], liver cancer [NCT02721056] and rectal cancer [NCT02465593].

#### OC-0272 Hypofractionated vs conventional radiotherapy for prostate cancer: 7 yr results from the HYPROtrial

L. Incrocci<sup>1</sup>, K. De Vries<sup>1</sup>, R. Wortel<sup>1</sup>, E. Oomen<sup>1</sup>, W. Heemsbergen<sup>1</sup>, F. Pos<sup>2</sup>

<sup>1</sup>Erasmus Medical Center Rotterdam Daniel den Hoed Cancer Center, Department of Radiation Oncology, Rotterdam, The Netherlands ; <sup>2</sup>Netherlands Cancer Institute-Antoni van Leeuwenhoek Hospital, Department of Radiation Oncology, Amsterdam, The Netherlands

#### Purpose or Objective

In the phase 3, Hypofractionated irradiation for PROstate cancer (HYPRO) trial, hypofractionated radiotherapy was compared with conventionally fractionated radiotherapy. In previous reports, we could not demonstrate the postulated superiority of hypofractionation in terms of relapse-free survival (RFS) at 5-year follow-up. The use of long-term androgen deprivation therapy in more than 60% of the patients might have obscured potential benefits of hypofractionation at 5-year follow-up. In this analysis, we provide the 7-year outcomes on biochemical failure, clinical failure, local failure and overall survival (OS).

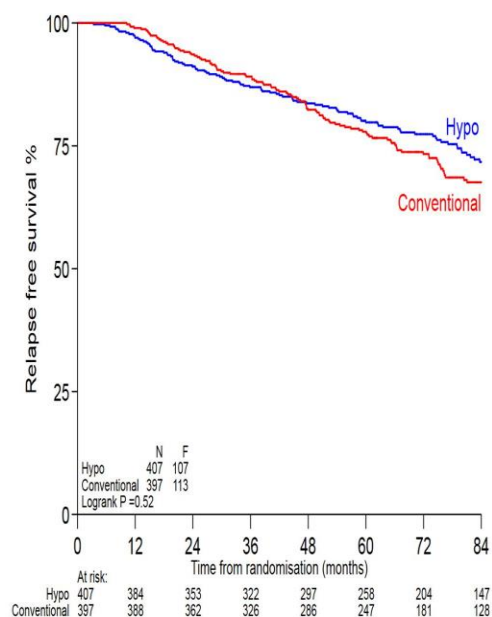
#### Material and Methods

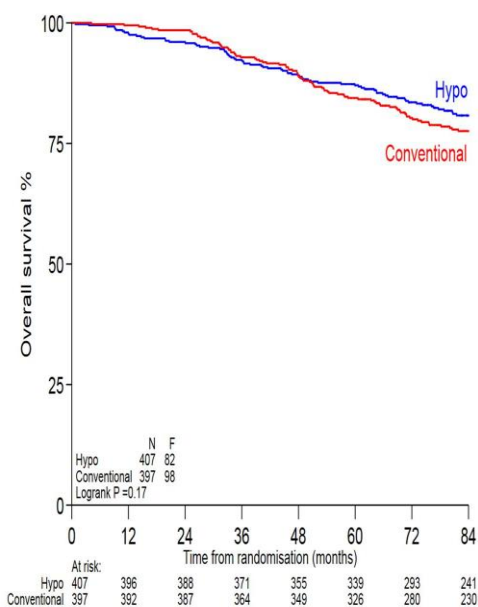
Patients with intermediate to high-risk localized prostate cancer (cT1-cT4NXOMX0), a PSA concentration  $\leq 60$   $\mu\text{g/L}$  and a WHO performance status of 0-2, were included in 7 Dutch radiotherapy centers. Patient were randomly assigned (1:1) to hypofractionated radiotherapy of 64.6 Gy (19 fractions of 3.4 Gy, three fractions per week) or conventionally fractionated radiotherapy of 78.0 Gy (39 fractions of 2.0 Gy, five fractions per week). Based on an estimated  $\alpha/\beta$  ratio for prostate cancer of 1.5 Gy, the equivalent total dose in fractions of 2.0 Gy (EQD2) was 90.4 Gy for hypofractionation versus 78.0 Gy for conventional fractionation. Primary outcomes have been previously published. This analysis will report on RFS en

OS survival at 7 year follow-up, and the effect of hypofractionation on local failure.

#### Results

Between 2007 and 2010, 820 patients were enrolled. A total of 804 were assessable for the current evaluation. Of these, 407 were assigned hypofractionated radiotherapy (HF) and 397 conventionally fractionated radiotherapy (CF). 537 (67%) of 804 patients received concomitant androgen deprivation therapy for a median duration of 32 months (IQR 10-44). Median follow-up was 89 months. Treatment failure at 7 years was reported in 183 (89 HF vs 94 CF) of 804 patients. 7-year relapse-free survival was 71.7 % (95% CI 66.4-76.4) for patients assigned hypofractionation and 67.6% (95% CI 62.0-72.5) for conventional fractionation (p=0.52). Overall survival was 80.8 % (95% CI 76.5-84.4) in the hypofractionated group versus 77.6 % (95 % CI 73.0-81.5) in the conventional fractionated group (p=0.17). Local failure as first site of recurrence was reported in 15 in the hypofractionated arm and 25 in the conventional arm (p=0.09). For Gleason  $\geq 8$ , a statistically significant difference in local failure free survival was found in favor of hypofractionation (p=0.003).





### Conclusion

The outcomes on 7-year relapse free survival and overall survival demonstrated no difference between hypofractionation versus conventional fractionation. A trend toward better local control was found after hypofractionation, whereas local control was statistically significant superior in patients with Gleason  $\geq 8$  tumors. These data on local control suggest that hypofractionation might be beneficial provided that high risk patients with subclinical metastasis at start of treatment are identified.

### OC-0273 Organ preservation after chemoradiotherapy for rectal cancer: 5-year results of the GRECCAR2 trial

V. Vendrely<sup>1</sup>, P. Rouanet<sup>2</sup>, J. Tuech<sup>3</sup>, A. Valverde<sup>4</sup>, B. Lelong<sup>5</sup>, M. Rivoire<sup>6</sup>, J. Faucheron<sup>7</sup>, J. Mehrdad<sup>8</sup>, G. Portier<sup>9</sup>, J. Asselineau<sup>10</sup>, E. Frison<sup>10</sup>, Q. Denost<sup>11</sup>, E. Rullier<sup>11</sup>

<sup>1</sup>CHU de Bordeaux, Radiotherapy, Pessac, France ; <sup>2</sup>ICM, Surgery, Montpellier, France; <sup>3</sup>CHU Rouen, Surgery, Rouen, France; <sup>4</sup>Hospital Diaconesses Croix saint Simon, Surgery, Paris, France ; <sup>5</sup>Institut Paoli Calmettes, Surgery, Marseille, France ; <sup>6</sup>Centre Léon Bérard, Surgery, Lyon, France; <sup>7</sup>CHU Grenoble, surgery, Grenoble, France; <sup>8</sup>Centre Oscar Lambret, Surgery, Lille, France; <sup>9</sup>CHU Toulouse, surgery, Toulouse, France ; <sup>10</sup>ISPED, Statistics, Bordeaux, France; <sup>11</sup>CHU Bordeaux, Surgery, Bordeaux, France

### Purpose or Objective

To evaluate the long term results at 5 years of the multicenter randomized trial comparing local excision (LE) vs. total mesorectal excision (TME) in good responders after chemoradiotherapy (CRT) for T2T3 low rectal cancer.

### Material and Methods

From March 2007 to September 2012, 148 patients clinically good responders after CRT for T2T3 rectal cancer, size  $\leq 4$  cm, were randomized in 74 LE vs. 74 TME, 3 were excluded and 145 analyzed. In the LE group, 26 had a completion TME for ypT2-3, which was part of the protocol. Kaplan-Meier and Cox regressions were used to estimate and compare local and metastatic recurrence and survival at 5 years.

### Results

Local recurrence (7% vs. 7%; hazard ratio (HR)=1.41, p=0.599), metastatic recurrence (18% vs. 19%; HR=0.86,

p=0.734), overall (84% vs. 82%; HR=0.92, p=0.845) and disease-free (70% vs. 72%; HR=0.87, p=0.682) survivals were not different between the LE and the TME groups at 5 years. No predictive factor of local recurrence was found, whereas ypT2-3 stage was independent factor of metastatic recurrence (HR=2.88, p=0.02).

### Conclusion

The 5-year results of this multicenter randomized trial suggest the oncologic safety of the strategy in selected patients with small T2T3 low rectal cancer.

### OC-0274 5x5 Gy and consolidation chemotherapy vs. chemoradiation for rectal cancer: a phase III study

K. Bujko<sup>1</sup>, X. On Behalf Of The Polish Colorectal Study Group<sup>2</sup>

<sup>1</sup>The Maria Skłodowska-Curie Memorial Cancer Center, Department Of Radiotherapy, Warsaw, Poland

### Purpose or Objective

This study evaluated whether preoperative short-course radiotherapy combined with consolidation chemotherapy (CCT) is superior to chemoradiation in terms of R0 resection rate. Previously we reported no differences in R0 resection, complete pathological response, postoperative complications, late complications, disease-free survival, incidence of local failure and distant metastases after 3 years of median follow-up (Ann Oncol 2016, 27:834-42). However, in the short-course/CCT group, we observed lower acute radiochemotherapy-induced toxicity (75% vs. 83%, p=0.006) and 8% benefit (p=0.046) in overall survival at 3 years. The main aim of the current analysis is to find out whether benefit in overall survival is sustained with longer observations.

### Material and Methods

Patients with fixed cT3 or cT4 rectal cancer were randomised either to 5x5 Gy and three cycles of FOLFOX4 given in tight sequence or to chemoradiation (50.4 Gy in 28 fractions combined with two 5-day cycles of bolus 5-Fu 325 mg/m<sup>2</sup>/day and leucovorin 20 mg/m<sup>2</sup>/day during the first and fifth week of irradiation along with five infusions of oxaliplatin 50 mg/m<sup>2</sup> once weekly). The protocol was amended during accrual to allow oxaliplatin to be omitted in both groups.

### Results

In total, 515 patients were eligible for analysis: 261 in the short-course/CCT group and 254 in the chemoradiation group. The median follow-up was 7.0 years (interquartile range 5.7-8.3 years). The benefit in overall survival at 3 years after short-course/CCT previously reported was also observed (71.6%, 95% confidence interval [CI] 66.1%-77.1% vs. 63.0%, 95% CI 57.1%-68.9%). However, this benefit disappeared later; at 8 years, overall survival was 48.8% in the short-course/CCT group vs. 48.6% in the chemoradiation group: hazard ratio (HR) 0.89 (95% CI 0.70-1.14), p=0.35. The corresponding values for disease-free survival were 42.6% vs. 41.0%, HR 0.94 (95% CI 0.75-1.19), p=0.64. The cumulative incidences of local failure and distant metastases did not differ between the short-course/CCT group and the chemoradiation group, and after 8 years were 35.0% vs. 31.9%, (relative risk [RR]=1.08, 95% CI 0.70 - 1.23), p=0.59 and 35.5% vs. 33.3%, (RR=1.11, 95% CI 0.67 - 1.21), p=0.49, respectively. The rate of late complications in the short-course/CCT group was 21.5% vs. 21.2% in the chemoradiation group, p=0.58.

### Conclusion

There was no difference in long-term overall survival between the short-course/CCT group and the chemoradiation group. Nevertheless, we suggest that benefits in short-term survival and acute toxicity favour short-course/CCT.

### OC-0275 Safety and efficacy of concurrent SRT and targeted- or immunotherapy for melanoma brain metastases

J. Heitmann<sup>1</sup>, S.G.C. Kroeze<sup>1</sup>, O. Blanck<sup>2</sup>, K.H. Kahl<sup>4</sup>, S. Gerum<sup>3</sup>, S.E. Combs<sup>6</sup>, D. Kaul<sup>7</sup>, A. Claes<sup>8</sup>, M. Schymalla<sup>9</sup>, A. Grosu<sup>10</sup>, F. Eckert<sup>11</sup>, F. Lohaus<sup>12</sup>, N. Abbasi-Senger<sup>13</sup>, G. Henke<sup>14</sup>, M. Szuëcs<sup>15</sup>, M. Geier<sup>16</sup>, N. Sundahl<sup>17</sup>, D. Buegy<sup>18</sup>, M. Guckenberger<sup>1</sup>

<sup>1</sup>University Hospital Zürich, Radiation Oncology, Zurich, Switzerland; <sup>2</sup>Saphir, Radiosurgery Center, Gustow, Germany; <sup>3</sup>University Hospital Frankfurt, Radiation Oncology, Frankfurt, Germany; <sup>4</sup>Klinikum Augsburg, Radiation Oncology, Augsburg, Germany; <sup>5</sup>University Hospital Munich, Radiation Oncology, Munich, Germany; <sup>6</sup>Technical University Munich, Radiation Oncology, Munich, Germany; <sup>7</sup>Charité University Hospital, Radiation Oncology, Berlin, Germany; <sup>8</sup>University Medical Center Utrecht, Radiation Oncology, Utrecht, The Netherlands; <sup>9</sup>Philipps University Marburg, Radiation Oncology, Marburg, Germany; <sup>10</sup>University Medical Center Freiburg, Radiation Oncology, Freiburg, Germany; <sup>11</sup>University Hospital Tübingen, Radiation Oncology, Tübingen, Germany; <sup>12</sup>University Hospital Dresden, Radiation Oncology, Dresden, Germany; <sup>13</sup>University Hospital Jena, Radiation Oncology, Jena, Germany; <sup>14</sup>Kantonsspital St. Gallen, Radiation Oncology, St. Gallen, Switzerland; <sup>15</sup>University Hospital Rostock, Radiation Oncology, Rostock, Germany; <sup>16</sup>Ordensklinikum Linz, Radiation Oncology, Linz, Austria; <sup>17</sup>Ghent University Hospital, Radiation Oncology, Ghent, Belgium; <sup>18</sup>University Hospital Mannheim, Radiation Oncology, Mannheim, Germany

#### Purpose or Objective

During their course of the disease, many melanoma patients develop brain metastases and receive stereotactic radiotherapy (SRT) concurrent to targeted- or immunotherapy. In this study, we investigated the safety and efficacy of this treatment combination and analyzed factors associated with toxicity and survival.

#### Material and Methods

This study is based on the international retrospective database on concurrent ( $\leq 30$  days) SRT and immunotherapy (TOASTT). Primary outcome of this study on malignant melanoma patients was overall survival (OS), secondary outcomes were progression free survival (PFS), local control (LC) and toxicity using CTCAE v4. Statistical analysis consisted of Kaplan Meier survival curves and log rank testing.

#### Results

Data of 145 melanoma patients from 18 international centers was analyzed. Patients were treated between 05/2011 and 02/2018. SRT was performed for 473 brain metastases in 180 sessions. At time of SRT, median patient age was 60 (25-92) years, patients were characterized by BRAF-mutation in 46.4%. Median number of treated brain metastases per patient was 2 (1-30), with a median of 1 fraction (1-6) and a total median dose of 20 (16-30) Gy, most commonly prescribed to the 80% isodose line. At 63.5% of treatments, immunotherapy was administered with SRT, in 28.7% SRT was combined with tyrosine kinase inhibitors (TKI; over 90% containing BRAF inhibitors) and 6.7% used a combination.

Median follow up was 10 (0-65) months from first concurrent treatment. Median PFS and OS was 4.1 (0.2-64.6) months and 9.5 (0-70) months, respectively. Median cumulative volume of brain metastases treated at one course of SRT was 1.5cc (0.04-24.54cc). For 42.7% of individual metastases imaging-based local metastases control was available: 176 metastases (85.8%) were controlled at last time of follow-up. Median time to local progression was 4.5 months. Infield toxicity of SRT was low: Acute grade 3 and 4 toxicities occurred in 5.5%, and 2.2%, respectively. One patient died of cerebral edema.

Late grade 3 toxicity occurred in only in 4.4%, no late grade 4 or 5 toxicities were reported. For the combination with systemic treatment, grade 3 and 4 toxicities were reported in 13.8% and 4.9%, respectively. 2 patients developed grade 5 toxicity and died of heart failure and a thromboembolic event, respectively. A longer OS was associated with controlled/non-existent other metastases vs. mixed response/uncontrolled other metastases ( $p=0.001$ ), and immunotherapy vs. TKI ( $p=0.01$ ). Need for steroids negatively impacted survival ( $p=0.01$ ), as did presence of body metastases ( $p=0.04$ ). BRAF status was not significant.

#### Conclusion

Concurrent targeted- or immunotherapy with SRT for melanoma brain metastases appears safe in this multicenter analysis. Longest OS was observed when SRT was combined with immune checkpoint inhibition; need for steroids was associated with worse OS.

### OC-0276 Stereotactic radiosurgery plus immunotherapy or targeted therapy for brain metastases from NSCLC

E. Olmetto<sup>1</sup>, C. Delli Paoli<sup>1</sup>, L.P. Ciccone<sup>1</sup>, M. Perna<sup>1</sup>, R. Grassi<sup>1</sup>, S. Erika<sup>1</sup>, S. Scoccianti<sup>1</sup>, D. Greto<sup>1</sup>, I. Desideri<sup>1</sup>, G. Simontacchi<sup>1</sup>, L. Marrazzo<sup>2</sup>, C. Arilli<sup>2</sup>, M. Casati<sup>2</sup>, A. Compagnucci<sup>2</sup>, G. Pecchioli<sup>3</sup>, S. Pallotta<sup>2</sup>, L. Livi<sup>1</sup>

<sup>1</sup>University of Florence, Azienda Ospedaliero Universitaria Careggi- Radiation Oncology Unit - Oncology Department, Florence, Italy; <sup>2</sup>University of Florence, Medical Physics Unit, Florence, Italy; <sup>3</sup>University of Florence, Azienda Ospedaliero Universitaria Careggi- Neurosurgery Unit, Florence, Italy

#### Purpose or Objective

Immunotherapy (IT) and Targeted Therapy (TT) have strongly changed the therapeutic management of Non-Small Cell Lung Cancer (NSCLC) patients. Radiosurgery (RS) is very effective in achieving local control of brain metastases (BM); moreover, it may have a symptomatic effect by reducing or preventing neurological deficits, in order to maintain a good quality of life longer. So far, data regarding the interactions between these novel drugs and RS in terms of efficacy and toxicity are not available. Aim of the present study is to evaluate outcome and safety of RS delivered in association to IT or TT for BM from NSCLC.

#### Material and Methods

We retrospectively analysed data from NSCLC patients with BM treated with RS plus IT or TT. We selected patients who received IT or TT within 4 weeks before or after RS. RS were performed with Gamma-Knife and Cyber Knife. Clinical toxicity was evaluated according to CTCAE v.4. During follow-up, all the patients underwent contrast-enhanced brain MRI every 3 months for the first year after RS, every 4 months thereafter. Local progression-free survival (L-PFS) was defined as the time from RS to radiological progression at the site of the treated lesion, while intracranial progression at a different site, defined as distant-PFS (D-PFS), was the time interval from RS to the appearance of new BM.

#### Results

We selected 30 patients treated at our centre from 2011 to 2018. There were 16 women (53%) and 14 men (47%) with a median age of 63 years (range 51-82). All patients were affected by adenocarcinoma; 13 (43%) were EGFR-mutated, 4 (13%) were ALK-rearranged and 4 (13%) were PD-L1 over-expressed. Twelve patients (40%) had metastatic disease when the lung tumor was newly diagnosed; among these, 10 patients (33%) had BM. At the time of RS, the majority of patients had a KPS of 90-100%, the median GPA-score was 2.6, while the median RPA-class was 2. The median number of treated lesions was 3 (range 1-11). Most of the patients ( $n=21$ , 70%) received a single-fraction of 24 Gy, whereas the others were treated with a dose of 18 or 21 Gy. IT and TT consisted of Pembrolizumab (4), Nivolumab (2), Erlotinib (11),

Gefitinib (4), Crizotinib (3), Ceritinib (1), Alectinib (1), Afatinib (1), Lorlatinib (1), Nintedanib (1), Rociletinib (1). IT or TT was started after the completion of RS in 18 patients; in the remaining cases (n=12), IT or TT was begun before RS (IT or TT was interrupted for a median period of seven days from RS in the majority of patients). Median follow-up was 12 months. One patient developed G1 radionecrosis after 18 months from RS. No G3 toxicity was observed. Median L-PFS and D-PFS were 10.6 and 7 months, respectively.

#### Conclusion

RS for BM may be safely associated with IT or TT in patients with NSCLC. Prospective studies are needed to confirm our results.

#### OC-0277 Interim safety analysis of RAPPOR trial - SABR with pembrolizumab in oligometastatic RCC

S. Siva<sup>1</sup>, M. Bressel<sup>2</sup>, S. Sandhu<sup>3</sup>, B. Tran<sup>3</sup>, J. Mooi<sup>3</sup>, J. Lewin<sup>3</sup>, S. Loi<sup>3</sup>, G. Toner<sup>3</sup>, D. Moon<sup>4</sup>, J. Goad<sup>4</sup>, M. Shaw<sup>1</sup>, S. Chander<sup>1</sup>, T. Eade<sup>5</sup>, A. Guminski<sup>5</sup>, D. Jayamanne<sup>5</sup>, D. Pryor<sup>6</sup>, K. Cuff<sup>6</sup>, S. Wood<sup>6</sup>, N. Lawrentschuk<sup>4</sup>, D. Murphy<sup>4</sup>  
<sup>1</sup>Peter MacCallum Cancer Centre, Department of Radiation Oncology, Melbourne, Australia; <sup>2</sup>Peter MacCallum Cancer Centre, Biostatistics and Clinical Trials, Melbourne, Australia; <sup>3</sup>Peter MacCallum Cancer Centre, Department of Medical Oncology, Melbourne, Australia; <sup>4</sup>Peter MacCallum Cancer Centre, Department of Surgical Oncology, Melbourne, Australia; <sup>5</sup>Northern Sydney Cancer Centre, Oncology, Sydney, Australia; <sup>6</sup>Princess Alexandra Hospital, Oncology, Brisbane, Australia

#### Purpose or Objective

SABR is a locally effective modality for metastatic renal cell carcinoma (RCC) (1, 2). Preclinical data in RCC has demonstrated improved disease control in both irradiated and unirradiated sites with single fraction SABR and anti-PD1 checkpoint blockade (3), although prospective clinical trials with this combination have not yet been reported.

#### Material and Methods

RAPPOR is a multi-institutional, single arm, phase 1b/II clinical trial (NCT02855203). Patients with 1-5 oligometastases from clear cell RCC were eligible. They received a single fraction SABR of 18-20Gy to all metastases (or 30Gy in 10 fractions of conventional radiotherapy if SABR was not feasible) followed by 8 x 3 weekly cycles of 200mg intravenous pembrolizumab. This is a preplanned interim safety analysis of the first 12 patients who completed SABR and 12 weeks of pembrolizumab. Adverse events were graded using CTCAE v4.0.

#### Results

At the date of reporting 25 patients with 76 metastases have been enrolled. The mean age is 62 years, with 18 males and 7 females enrolled. The commonest site of metastasis is lung (n=38, 50%). Most patients have ECOG performance status 0 (64%), with a minority ECOG 1 (36%). For the pre-specified interim safety analysis, 12 patients with a total 37 metastases were irradiated, with 32 (86%) receiving SABR and 5 (14%) receiving conventional radiotherapy. The number of lesions per patient was 1 in 3 patients (25%), 3 in 4 patients (33%), 4 in 3 patients (25%) and 5 in 2 patients (17%). The predominant site of metastases was the lung (n=24, 65%). No treatment courses were abandoned due to toxicity (radiotherapy + 8 cycles of pembrolizumab), although one patient ceased treatment early due to progressive disease. Grade 1 and graded 2 treatment related adverse events were recorded in 6 patients (50%, mixed events) and 1 patient (hypothyroidism, 8%), respectively. No grade 3 or greater treatment related adverse events were recorded.

#### Conclusion

The combination of SABR + pembrolizumab in a small cohort of patients to date is well tolerated. Based on this interim safety analysis the independent safety monitoring

committee have recommended continuation of planned recruitment (n=30).

**References** 1. Siva S, Kothari G, Muacevic A, Louie AV, Slotman BJ, Teh BS, et al. Radiotherapy for renal cell carcinoma: renaissance of an overlooked approach. *Nat Rev Urol.* 2017;14(9):549-63. 2. Kothari G, Foroudi F, Gill S, Corcoran NM, Siva S. Outcomes of stereotactic radiotherapy for cranial and extracranial metastatic renal cell carcinoma: a systematic review. *Acta oncologica.* 2015;54(2):148-57. 3. Park SS, Dong H, Liu X, Harrington SM, Krco CJ, Grams MP, et al. PD-1 Restrains Radiotherapy-Induced Abscopal Effect. *Cancer immunology research.* 2015;3(6):610-9.

#### OC-0278 Radiation-induced lymphopenia: Fractionation effect and association with infections and mortality.

C. Terrones Campos<sup>1</sup>, B. Ledergerber<sup>1</sup>, I. Vogelius<sup>2</sup>, M. Helleberg<sup>1</sup>, L. Specht<sup>2</sup>, J. Lundgren<sup>1</sup>  
<sup>1</sup>Rigshospitalet, Department of Infectious Diseases-Centre of Excellence for Health- Immunity and Infections CHIP, Copenhagen, Denmark; <sup>2</sup>Rigshospitalet, Department of Oncology- Radiation Oncology Section, Copenhagen, Denmark

#### Purpose or Objective

Radiotherapy may cause lymphocyte depletion in cancer patients. We designed this study to identify whether the radiation dose and duration of radiation exposure, among other factors, are associated with the end of radiotherapy (EoRT) lymphocyte count; and to determine the association of radiotherapy-induced lymphopenia with the risk of acquiring subsequent infections and mortality.

#### Material and Methods

Consecutive patients with a non-hematological cancer diagnosis were included in the study if they had received their first course of external beam radiotherapy (EBRT) with curative intent at Rigshospitalet, University of Copenhagen, from 01 January 2005 to 31 December 2016; and had a pre-treatment lymphocyte count collected within one year of radiotherapy start and an EoRT lymphocyte count collected within six months after radiotherapy ended. The EQD2 for every radiation scheme was calculated assuming an  $\alpha/\beta$  of 10. Factors associated with square-root transformed EoRT lymphocyte counts were identified using linear regression analysis, adjusting for cancer diagnosis and pre-treatment lymphocyte count, modelled as restricted cubic splines (tri-variable); and additionally, adjusting for age, gender and Charlson score (multivariable). Using negative binomial regression, the risk of acquiring a subsequent infection and mortality, according to the EoRT lymphocyte count, was determined after adjustment for age, gender, cancer diagnosis, and Charlson score.

#### Results

A total of 4,343 patients were studied. Compared to patients who received radiation schemes with EQD2 = 50-63 Gy delivered in 25-45 days, patients receiving a regimen with an EQD2 >63 Gy in <25 days (mostly NSCLC receiving stereotactic radiotherapy [77%]) had the highest predicted EoRT lymphocyte count (1,351 cells/ $\mu$ L 95% CI [1,210-1,492] vs. 804 cells/ $\mu$ L [774-834]; p<0.001), Figure 1. Radiation to multiple sites vs. single site (721 cells/ $\mu$ L [680-764] vs. 835 cells/ $\mu$ L [817-852]; p<0.001) and concomitant chemotherapy, particularly the use of platinum compounds vs. none (594 cells/ $\mu$ L [548-640] vs. 929 cells/ $\mu$ L [903-954]; p<0.001), also affected the EoRT lymphocyte count. An EoRT lymphocyte count <500 cells/ $\mu$ L was associated with both a higher risk for a new infection in the first year after EBRT (IRR=3.48 [2.54-4.77]; p<0.001) and death (IRR=1.31 [1.14-1.52]; p<0.001), compared to patients with an EoRT lymphocyte count >1,000 cells/ $\mu$ L, Figure 2.

#### Conclusion

Short duration (<25 days) treatment schedules with a higher radiation dose were associated with higher EoRT lymphocyte counts, an observation consistent with published models indicating less radiation dose of circulating blood by an approach of radiotherapy using fewer fractions. Radiation to multiple sites and concomitant chemotherapy conversely independently lowered EoRT lymphocyte count. Radiation-induced lymphopenia was associated with increased risk of acquiring a subsequent infection and mortality.

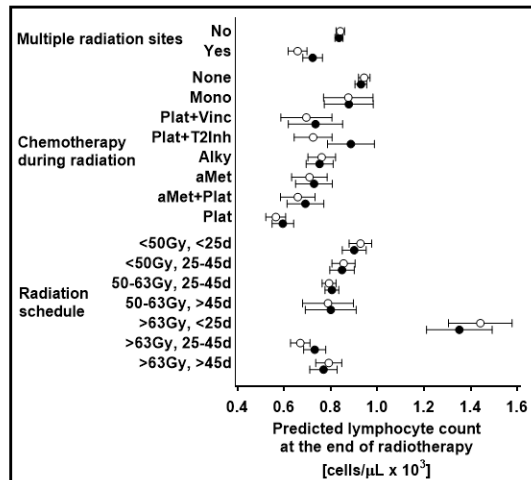


Figure 1. Factors associated with the lymphocyte count at the end of radiotherapy. Empty circles represent tri-variable and full circles multivariable analyses. Mono, monoclonal antibodies; Plat, platinum compounds; Vinc, vinca alkaloids; T2Inh, type II topoisomerase; Alky, alkylating agents; aMet, antimetabolite drugs.

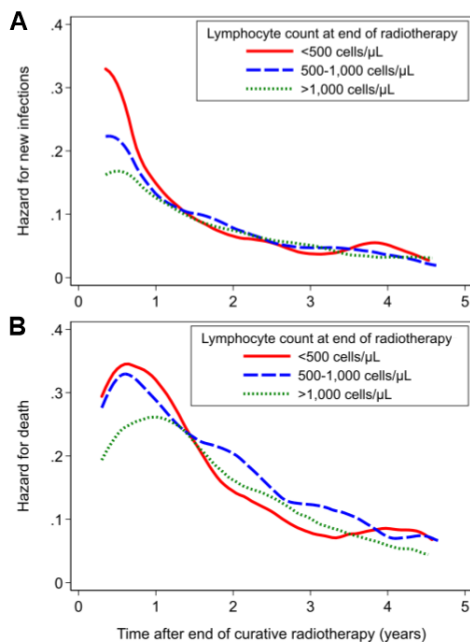


Figure 2. Risk of infections (A) and death (B).

**OC-0279** Concurrent and adjuvant effect of bevacizumab on hypofractionated tailor-made IMRT for glioblastomas

T. Iuchi<sup>1</sup>, R. Hara<sup>2</sup>, K. Hatano<sup>3</sup>, T. Sugiyama<sup>4</sup>, G. Togasaki<sup>2</sup>, T. Setoguchi<sup>1</sup>, Y. Hasegawa<sup>1</sup>, M. Itami<sup>4</sup>, T. Sakaida<sup>1</sup>

<sup>1</sup>Chiba Cancer Center, Neurological Surgery, Chiba, Japan; <sup>2</sup>Chiba Cancer Center, Radiation Oncology, Chiba,

Japan; <sup>3</sup>Tokyo Bay Advanced Imaging and Radiation Oncology Clinic Makuhari, Radiation Oncology, Chiba, Japan; <sup>4</sup>Chiba Cancer Center, Surgical Pathology, Chiba, Japan

**Purpose or Objective**

Hypofractionated high-dose IMRT had improved the local control of glioblastomas (GBMs), but still had higher risk of radiation injury even with tailor-made setting of radiation doses owing to the methylation status of *MGMT* gene promoter. We investigated the effect of bevacizumab (BEV) on control of the tumor and prevention of radiation injury after hypofractionated tailor-made IMRT.

**Material and Methods**

Newly diagnosed GBMs were enrolled. Residual enhanced lesions plus surgical cavity were defined as GTV, and 3-layered CTVs were contoured surrounding the GTV: CTV1=GTV+3mm, CTV2=GTV+18mm, and CTV3 was high-intensity volume on FLAIR images. PTV1, PTV2 and PTV3 were defined by expanding CTVs with 2mm margin. Prescribed doses for PTV2 and PTV3 were unified as 40Gy and 32Gy, but the dose for PTV1 was settled as 48Gy for *MGMT* methylated (Met) but 68Gy for unmethylated (UnMet) cases. IMRT was initiated 5 weeks after craniotomy, and the above doses were delivered with IMRT technique by 8 fractions. BEV was administered 3 weeks after craniotomy (2 weeks prior to IMRT), and continued bi-weekly for 6 cycles. Temozolomide (TMZ) was also initiated 3 weeks after craniotomy and administered for 42 days. Adjuvant BEV/TMZ was administered every 4 weeks for 12 cycles or until tumor progression. The primary endpoint was overall survival (OS), and secondary endpoints were progression-free survival (PFS), radiation necrosis-free survival (RNfS), and qualitative survival (QS) which was defined as the time to KPS<70%. The outcome of patients was compared with historical control of 76 patients with GBM treated by tailor-made IMRT without BEV.

**Results**

25 GBMs, 10 Met and 15 UnMet cases, were enrolled. The PFS of patients treated with BEV (median: 19.2m, 95%CI: 13.3m- not reached) was longer than that without BEV (9.7m, 7.8-16.3m), although this difference was not significant ( $P=0.140$ ). BEV improved the 6-months and 12-months RNfS rates from 83.0% to 98.8% and 58.5% to 72.6%. However, this difference disappeared after completion of the protocol treatment, and 18-months RNfS rates in BEV group (35.8m) was similar to that in historical group (40.9%). BEV significantly prolonged the median QS (13.8m vs. 19.0m,  $P=0.037$ ), but did not improve the OS of patients (not reached vs. 21.2m,  $P=0.657$ ).

**Conclusion**

BEV showed effect on prevention of radiation injury after hypofractionated IMRT, but this effect discontinued after withdrawal of this agent. Concurrent use of BEV had contributed to keep patients' performance status, but showed only limited efficacy on tumor control.

**OC-0280** ReRT with bevacizumab is related to lower rate of radionecrosis as reRT alone for recurrent glioma

D. Fleischmann<sup>1</sup>, J. Jenn<sup>1</sup>, S. Corradini<sup>1</sup>, V. Ruf<sup>2</sup>, R. Forbrig<sup>3</sup>, M. Unterrainer<sup>4</sup>, N. Thon<sup>5</sup>, F.W. Kreth<sup>5</sup>, C. Belka<sup>1</sup>, M. Niyazi<sup>1</sup>

<sup>1</sup>University Hospital- LMU Munich, Department of Radiation Oncology, Munich, Germany; <sup>2</sup>Faculty of Medicine- LMU Munich, Institute of Neuropathology, Munich, Germany; <sup>3</sup>University Hospital- LMU Munich, Institute of Neuroradiology, Munich, Germany; <sup>4</sup>University Hospital- LMU Munich, Department of Nuclear Medicine, Munich, Germany; <sup>5</sup>University Hospital- LMU Munich, Department of Neurosurgery, Munich, Germany

### Purpose or Objective

Reirradiation (reRT) was applied with concomitant bevacizumab (BEV) for glioma patients with tumour recurrence as in-house standard until 2016 in our department. After disapproval of BEV of the European Medical Agency for glioma treatment, BEV was no longer applied as concomitant therapy in the reRT setting. As treatment related side effects seemed to increase without concomitant BEV, we investigated the rate of radiation necrosis (RN) and RN related symptomatic edema in patients treated with reRT with and without concomitant BEV.

### Material and Methods

Glioma patients with tumour recurrence treated with reRT between April 2007 and December 2017 in our department were included into the cohort study. Study endpoints were the occurrence of RN and a compound endpoint of RN and/or symptomatic edema (RNSE). RN was diagnosed in contrast-enhanced MRI and verified in FET PET or histopathological examination after stereotactical biopsy, if available. Univariate and multivariate logistic regression analysis were performed to assess factors significantly related to the risk of RN and RNSE.

### Results

161 patients were included into the cohort study, of which 124 were treated with BEV and 37 without BEV concomitant to reRT. RN was detected in 6/124 patients treated with reRT with (4.8%) and in 5/37 patients treated with reRT without concomitant BEV (13.5%;  $p = 0.078$ ,  $p = 0.02$  on univariate and multivariate logistic regression analysis respectively). RN-free survival was significantly related to concomitant BEV treatment to reRT ( $p = 0.025$  on log-rank test;  $p = 0.036$ ,  $p = 0.013$  on univariate and multivariate cox-regression analysis respectively) and prescribed dose ( $p = 0.002$ ;  $p = 0.001$ ,  $p = 0.001$ ).

### Conclusion

reRT with concomitant BEV was significantly related to a lower rate of neurologic toxicity in our large monocentric cohort. Therefore, we strongly advise the use of concomitant BEV to reRT for glioma patients at tumour recurrence.

### OC-0281 Phase I/II trial of hafnium oxide nanoparticles activated by SBRT in the treatment of liver cancers

E. Chajon<sup>1</sup>, M. Pracht<sup>2</sup>, T. De Baere<sup>3</sup>, F. N'Guyen<sup>3</sup>, J. Bronowicki<sup>4</sup>, V. Vendrely<sup>5</sup>, A. Baumann<sup>6</sup>, V. Croisé-Laurent<sup>4</sup>, E. Rio<sup>7</sup>, Y. Rolland<sup>1</sup>, S. Le Sourd<sup>1</sup>, P. Gustin<sup>3</sup>, C. Perret<sup>7</sup>, F. Mornex<sup>8</sup>, D. Peiffert<sup>9</sup>, P. Merle<sup>8</sup>, E. Deutsch<sup>3</sup>  
<sup>1</sup>Centre Eugène Marquis, Radiotherapy, Rennes CEDEX, France; <sup>2</sup>Centre Eugène Marquis, Medical oncology, Rennes CEDEX, France; <sup>3</sup>Gustave Roussy, General surgery, Villejuif, France; <sup>4</sup>Hôpital de Brabois Adultes, Hepato-gastro-enterology, Nancy, France; <sup>5</sup>Groupe Hospitalier Sud - Hôpital Haut-Lévêque, Radiotherapy, Bordeaux, France; <sup>6</sup>Hôpital de Brabois Adultes, Radiotherapy, Nancy, France; <sup>7</sup>ICO - Site René Gauducheau, Radiotherapy, Saint Herblain Cedex, France; <sup>8</sup>Centre Hospitalier de la Croix Rousse, Hepato-gastro-enterology, Lyon, France; <sup>9</sup>Institut de Cancérologie de Lorraine, Radiotherapy, Nancy, France

### Purpose or Objective

Patients with hepatocellular carcinoma (HCC) and liver metastasis (mets) present with a wide range of underlying liver dysfunctions and concomitant malignancies. Stereotactic body radiation therapy (SBRT) is well-tolerated and a valuable alternative for patients who are not eligible for invasive procedures. Yet, like all radiation therapy (RT) techniques, the energy dose deposit to tumor cells is limited by the surrounding healthy tissues. NBTXR3, composed of hafnium oxide nanoparticles, was designed to effectively absorb ionizing radiation and augment the dose deposit within the tumor cells only

when activated by RT, thereby increasing tumor-specific physical killing through DNA damage/cell destruction and enhancing the immunogenic tumor cell death.

### Material and Methods

Patients suffering from primary HCC (with/without portal vein tumor thrombosis) or liver mets were included and treated with a single intralesional injection (IL) of NBTXR3 followed by SBRT (45 Gy/3 fractions/5 to 7 days).

The phase I part of the study was designed as a 3 + 3 escalation dose with tested dose levels at 10%, 15%, 22% and 33% of baseline tumor volume. Primary endpoints include the determination of the recommended dose and incidence of early dose limiting toxicities (DLTs). Secondary endpoints include assessment of global safety profile, characterization of the body kinetic profile, liver function evaluated by Child-Pugh score (CPS), AST to Platelet Ratio Index (APRI), and response rate (mRECIST/RECIST v1.1).

### Results

The enrollment is complete in the first 3 dose levels: 10% (6 pts), 15% (4 pts) and 22% (4 pts) and is ongoing at the last IL dose level at 33% with no early DLTs, no AE related to NBTXR3, and no serious AE related to RT or the injection. So far, four AEs related to the IL were observed (Malaise, grade 2; two Abdominal pain, grade 3 and Bilateral pleural effusion, grade 1) at dose level 10%, 15% and 22% respectively. NBTXR3 remained localized within the tumor, validating the relevance of the single IL. No relevant change in CPS or APRI was observed over time which is consistent with the low toxicity observed.

In 7 HCC pts evaluable for response, the mRECIST assessment by MRI on target lesions resulted in the following best observed response: 3 complete responses, 3 partial responses and 1 stable disease. In 5 evaluable liver mets pts, the RECIST v1.1 assessment by MRI on target lesions resulted in the following best observed response: 1 partial response, 3 stable disease and 1 local progressive disease.

### Conclusion

NBTXR3 was well tolerated and showed a promising safety profile. Recruitment at the highest dose level of 33% is ongoing for the IL part and, once completed, will be followed by the expansion phase.

NBTXR3 is also being evaluated in 6 other clinical trials, including a phase II/III trial in soft tissue sarcoma [NCT02379845] and phase I/II trials in prostate [NCT02805894], head and neck [NCT01946867] and rectum cancers [NCT02465593].

---

### Proffered Papers: BT 3: Prostate HDR brachytherapy

---

### OC-0282 HDR brachytherapy Monotherapy for prostate cancer: a one-day schedule phase II trial acute toxicity

M. Jolicoeur<sup>1</sup>, T.V. Nguyen<sup>1</sup>, T. Derashodian<sup>1</sup>, E. Hill<sup>1</sup>, M. Mondat<sup>1</sup>, M. Nachabe<sup>1</sup>, E. Antebi<sup>1</sup>, G. Wakil<sup>1</sup>, R. Héliou<sup>1</sup>  
<sup>1</sup>CICM Hôpital Charles Le Moyne, Radiation Oncology, Greenfield Park, Canada

### Purpose or Objective

To determine the early acute toxicity of a randomized phase II clinical trial of one 19.5 Gy fraction or two 14.5 Gy fractions of high-dose-rate (HDR) brachytherapy monotherapy delivered on a one day schedule.

### Material and Methods

205 patients with low or intermediate-risk prostate cancer were randomized between one fraction of 19.5Gy (Arm 1) or two fractions of 14.5Gy (Arm 2) on an HDR brachytherapy as monotherapy protocol (BRP2, NCT03424694), this the report of acute toxicities for the first 170 patients.

Treatments were delivered with a single implant on a one-day schedule. All patients had a post implant MRI based dosimetry with dominant intra prostatic lesion (DIL) boost

allowed. Patients on the 2 fractions arm had 2 dosimetries and fractions were delivered 6 hours apart. Toxicity was evaluated at 1, 3, 6 weeks and 3 months after treatment using Common Terminology Criteria for Adverse Events (CTCAE) score, IPSS and International Index of Erectile Function (IIEF-5), and compared to baseline. Descriptive statistics, t test, paired t test, Pearson Chi-Square and Fisher Exact test were used to describe and compare the groups. Statistical significance was 0.05

#### Results

Median Follow-up is 16 (3- 33) months. Pre-treatment median prostate-specific antigen for arm1 and arm 2 were 6.6±3and 6.7±2.7 respectively. T stages for arm 1 and arm2 were T1c = 55% and 57%, T2a = 31% and 31%, T2b = 9% and 12%, T2c 5% and 2 % respectively. Gleason score were mostly 7(3+4) 52% and 57%, 7(4+3) 28% and 30% respectively.

Evaluation of sexual function showed the following values: with a mean base line of 13±6.8 and 15.2±6.5 compared to 12.9±6.8 and 12.2±6.4 at 12 weeks for arm1 and arm 2 respectively.

IPSS categories at baseline were mild 6.3±4.4 and 6.7±4.4 for arm 1 and arm 2, respectively. At 1 week there was a small increase of the IPSS score 11.5±7.9 for arm 1 and 12.6±8.1 for arm 2. Patients start to recuperate at 3 weeks with IPSS being 8.4±5.7 vs 10±6.4 and returned to baseline at 3 months with 6.5±5.5 and 7.6±5.4 respectively. The most frequently symptoms at 3 weeks were urinary frequency and burning sensation. Most patients had Grade 0-1 acute urinary toxicity: 89.7 % or arm 1 and 90.4 % for arm 2. Urinary retention occurred in 6.7% of patients in arm 1 and 2.1% arm 2.

There was a small increase in Grade 2 acute gastrointestinal toxicity 1% for arm 1 and 4.8% for arm 2. However, acute toxicity did not differ between arms (GU p=0.62, GI p= 0.47).

#### Conclusion

Both arms of the protocol either a single fraction of 19.5Gy or 2 fractions of 14.5Gy delivered in a one-day schedule are well tolerated. Acute GI and GU toxicities are the same in both arms during the first 12 weeks, erectile dysfunction seems to follow the same pattern. Further report with longer follow-up on toxicity will follow.

#### OC-0283 Pattern of relapse and dosimetric analysis of a single dose 19Gy HDR-brachytherapy phase II trial

A. Gomez-Iturriaga<sup>1</sup>, D. Buchser<sup>2</sup>, P. Minguez<sup>3</sup>, J.M. Espinosa<sup>3</sup>, F. Perez<sup>3</sup>, J. Cacicedo<sup>2</sup>, F. Suarez<sup>2</sup>, A. Gonzalez<sup>2</sup>, P. Bilbao<sup>2</sup>, F. Casquero<sup>2</sup>

<sup>1</sup>Hospital Universitario Cruces- Biocruces Health Research Institute, Radiation Oncology, Barakaldo, Spain ; <sup>2</sup>Hospital Universitario Cruces- Biocruces Health Research Institute, Radiation Oncology, Barakaldo-Bizkaia, Spain ; <sup>3</sup>Hospital Universitario Cruces- Biocruces Health Research Institute, Radiation Physics, Barakaldo-Bizkaia, Spain

#### Purpose or Objective

To report the pattern of relapse within the prostate with reference to the initial site of disease in patients treated with single fraction 19-Gy and to determine the dose delivered to these areas of recurrence to inform potential strategies of focused dose escalation.

#### Material and Methods

A total of 44 patients with low and intermediate-risk prostate cancer were treated according to an institutional review board-approved prospective study of single-fraction HDR brachytherapy. Treatment was delivered using <sup>192</sup>Ir to a dose of 19 Gy prescribed to the prostate, no margins were applied.

Patients who experienced a biochemical failure underwent a re-staging multiparametric MRI(mpMRI) and MRI-TRUS fusion biopsy to rule-out local recurrence.

Forty-two patients (95%) had a pre-treatment mpMRI. In patients with visible Dominant intraprostatic lesions (DIL)

on pre-treatment mpMRI, the DIL was contoured with the use of 2 sequences (T2W and DWI). Contours were generated by consensus of two physicians. The site of local relapse was compared with the initial site of disease. The dose received by the site of recurrence was investigated.

#### Results

Forty-four percent of patients were low-risk and 56% intermediate-risk. The median prostate volume was 34cc (17-60). Median CTV and OAR doses were: V100: 96.5% (95-99.4), V150 20.5% (13.7-35.1), V200 5.3% (3.1-10.1), Urethral Dmax 106% (103-111) and rectum 2cc 53 % (45-48).

The median follow-up period was 37 months (range 23-50). The PSA nadir was reached at 24 months follow-up, with a median value of 1.07 ng/mL. To date, 14 patients (32%) have experienced biochemical failure (4 patients low-risk and 10 intermediate-risk; p=0.013). Re-staging mpMRI showed local relapse in 12 patients (27.2%) and 11/12 patients underwent MRI-TRUS fusion biopsy confirming local relapse in 10 patients.

The analysis of DVH of all 44 patients revealed that patients with biochemical failure had received significantly lower doses in terms of V100, V125 and D90 (p=0.032, p=0.018 and p=0.018 respectively).

Of the 25 patients with DILs on diagnostic mpMRI, the mean D90 and D98 on DIL were lower for patients with biochemical failure (21.8 Gy and 20.1 Gy vs 22.2 Gy and 20.8 Gy, respectively; p=n.s). And in patients with confirmed local failure, the doses received by the index lesion were median D90=21.8 Gy (range 19.9 Gy-24.7 Gy) and median D98=20 Gy (19.9 Gy-22.5 Gy)

#### Conclusion

This dosimetric analysis demonstrates a dose-response relationship in patients treated with single fraction 19Gy. Patients with intermediate-risk disease, with visible DIL on mpMRI and patients treated with cooler implants have higher incidence of biochemical and local failure. The recurrence pattern is predominantly local in patients with initial gross disease on mpMRI. Patients in this study failed after receiving doses as high as D90=24.7Gy providing some rationale for further dose escalation to dominant intraprostatic nodules.

#### OC-0284 Radiomic and dosimetric analysis of urethral strictures following prostate HDR monotherapy

Y.M. Tsang<sup>1</sup>, D. Vignarajah<sup>2</sup>, A. Mcwilliam<sup>3</sup>, H. Tharmalingam<sup>4</sup>, A. Choudhury<sup>3</sup>, P. Hoskin<sup>4,3</sup>

<sup>1</sup>Mount Vernon Cancer Centre, Radiotherapy, Northwood Middlesex, United Kingdom ; <sup>2</sup>Sunshine Coast University Hospital, Clinical Oncology, Queensland, Australia ; <sup>3</sup>University of Manchester, Division of Cancer Sciences-School of Medical Sciences- Faculty of Biology Medicine and Health- Manchester Academic Health Sciences Centre, Manchester, United Kingdom ; <sup>4</sup>Mount Vernon Cancer Centre, Clinical Oncology, Northwood Middlesex, United Kingdom

#### Purpose or Objective

High dose-rate (HDR) brachytherapy as monotherapy is accepted as a safe and effective local treatment for organ-confined prostate cancer. However, urethral stricture has been reported as one specific late effect with HDR monotherapy with conflicting results in and rethral dose. Radiomics is an emerging field in the era of precision medicine and there is great potential with mining MRI radiomics to capture the intra-tumour heterogeneity of prostate cancer. Against this background, we have analysed a cohort of HDR monotherapy patients to establish the frequency of non-malignant urethral stricture and explore the relation between stricture formation and (i) dose distribution along the length of the urethra and (ii) MRI radiomic features of the prostate gland.

**Material and Methods**

From Nov 2010 to July 2017, there were 178 patients treated with HDR monotherapy of 19Gy in a single fraction using the urethra dose constraints of D10% <22Gy, D30% <20.8Gy and maximum dose <28.5Gy. There were a total of five ≥grade2 strictures as defined by CTCAE v4.0 as being symptomatic, requiring dilatation or catheterization strictures (confirmed on cystoscopy). A matched pair analysis used one control for each stricture case matched for pre-treatment IPSS score, number of needles used and clinical target volume (CTV) size

For all data sets, pre-treatment T2-weighted MRI images were used to define regions-of-interests as urethra and the whole prostate gland. The urethra was divided into membranous urethra and inferior, mid and superior thirds of the prostatic urethra for the dosimetric analysis. MRI textural radiomic features associated with prostate cancer response in the literature of energy, contrast and homogeneity were selected. Pyradiomics was used to extract textural features on the whole prostate gland volumes.

Wilcoxon signed-rank test was performed to investigate significant differences in dosimetric parameters and MRI radiomic feature values between cases and controls.

**Results**

There were no statistically differences in pre-treatment IPSS score, number of needles used CTV and urethra volume size between the two groups of patients with and without strictures. As suggested in table 1, the urethral dosimetric parameters investigated were not statistically different between cases and controls (p>0,05). With regards to MRI radiomics feature analysis, significant differences were found in contrast and homogeneity between cases and controls (p<0.05). However, this did not apply to the energy feature.

		Patients with	Patient without	p value
		≥grade 2 stricture	≥grade 2 stricture	
		Median Value	Median Value	
Baseline Demographics	Pre-treatment IPSS	8.00	8.00	0.94
	Number of needles used	21.00	20.00	0.37
	CTV volume (cc)	40.90	41.10	0.39
	Whole urethra volume (cc)	2.20	2.10	0.31
Urethra D10% (Gy)	Whole	20.50	21.10	0.22
	Membranous	18.50	18.30	0.25
	Prostatic	20.60	21.20	0.22
	Inferior third prostatic	20.30	20.80	0.58
	Mid third prostatic	20.30	20.80	0.32
	Superior third prostatic	20.80	21.00	0.26
Urethra D30% (Gy)	Whole	19.90	20.60	0.17
	Membranous	17.10	16.90	0.20
	Prostatic	20.00	20.70	0.18
	Inferior third prostatic	19.80	20.00	0.77
	Mid third prostatic	19.80	20.20	0.46
	Superior third prostatic	20.40	20.60	0.18
Urethra Maximum Dose (Gy)	Whole	22.10	22.20	0.72
	Membranous	20.20	20.00	0.20
	Prostatic	22.10	22.10	0.72
	Inferior third prostatic	21.10	21.80	0.86
	Mid third prostatic	21.40	22.00	0.66
	Superior third prostatic	21.70	21.60	0.60
Urethra Mean Dose (Gy)	Whole	19.50	19.40	0.55
	Membranous	16.50	15.80	0.21
	Prostatic	20.10	20.40	0.63
	Inferior third prostatic	19.90	19.90	0.29
	Mid third prostatic	20.60	20.00	0.51
	Superior third prostatic	19.70	20.10	0.65
MRI Radiomic Feature	Energy	0.0036	0.0018	0.28
	Contrast	30.10	50.30	0.04
	Homogeneity	13.70	22.10	0.04

**Conclusion**

In this matched pair analysis, no association between post-treatment stricture and urethral dosimetry was identified. The MRI radiomic features of homogeneity and contrast of the prostate gland identified patients who develop strictures after HDR monotherapy. Although sample size is small, this warrants further investigation.

**OC-0285 Clinical outcomes of focal salvage high-dose-rate brachytherapy for radiorecurrent prostate cancer.**

M. Peters<sup>1</sup>, M.J. Van Son<sup>1</sup>, M.A. Moerland<sup>1</sup>, J.J.W. Lagendijk<sup>1</sup>, J.R.N. Van der Voort van Zyp<sup>1</sup>  
<sup>1</sup>UMC Utrecht, Radiation Oncology Department, Utrecht, The Netherlands

**Purpose or Objective**

Radiorecurrent prostate cancer is conventionally treated with palliative androgen deprivation therapy (ADT) or curative whole-gland salvage, both with a high risk of significant side-effects and a detrimental impact on quality of life (QoL). MRI-guidance has made focal salvage high-dose-rate (HDR) brachytherapy (BT) possible. Focal treatment could postpone or prevent ADT and substantially reduce side effects. Tumor control, toxicity and QoL of MRI-guided focal salvage HDR-BT are described here.

**Material and Methods**

From July 2013 to July 2018, 96 patients with locally recurrent, non-metastatic prostate cancer after primary radiotherapy were treated with MRI-guided focal salvage HDR-BT. Multiparametric-MRI and PSMA or Choline-PET/CT were used for intraprostatic disease assessment and exclusion of metastases. A single dose of 19Gy was prescribed. MRI compatible catheters allowed MRI-guided treatment planning after insertion. Biochemical failure was defined by the Phoenix-definition (nadir+2ng/ml). Prospective data collection included genitourinary (GU) toxicity, gastro-intestinal (GI) toxicity and erectile dysfunction (ED) with the Common Terminology Criteria for Adverse Events (CTCAE) 4.0. Urinary symptoms and erectile function were further assessed with IPSS and IIEF questionnaires. RAND-36, EORTC QLQ-C30 and EORTC QLQ-PR25 were used for QoL assessment.

**Results**

Median age pre-focal salvage was 72 years (interquartile range [IQR] 67-74). Median PSA was 5 (3-7), median PSADT 17 months (12-25). Tumor (rT)-stages were T2 (64%), T3 (34%), T4 (2%). Primary treatment was mostly EBRT (55%) and I-125 BT (42%). D95 was median 19Gy (18-20), urethral D10 16Gy (11-18), D1cc bladder 8Gy (5-11) and D1cc rectum 10Gy (8-12). Median follow-up was 11 months (5-23). Two patients had grade 3 urethral stricture, at 6 and 24 months (Figure 1). There was no grade 3 GI toxicity. IPSS scores increased until 12 months (8.3 to 11.1, p=0.001), after which they normalized (10.6 and 9.2 at 24 and 36 months [p=0.07, and p=0.26], respectively). IIEF decreased from 10.9 at baseline to 8.1 at 12 months (p<0.001) and 7.6 at 24 months (p=0.004). Corrected for multiple testing, QoL only deteriorated in the first month due to urinary complaints. At 2 years, biochemical disease-free survival was 77% (95% CI 65-91%), metastases-free survival 84% (95% CI 73-92%) (Figure 2) and overall survival 98% (95% CI 93-100%).

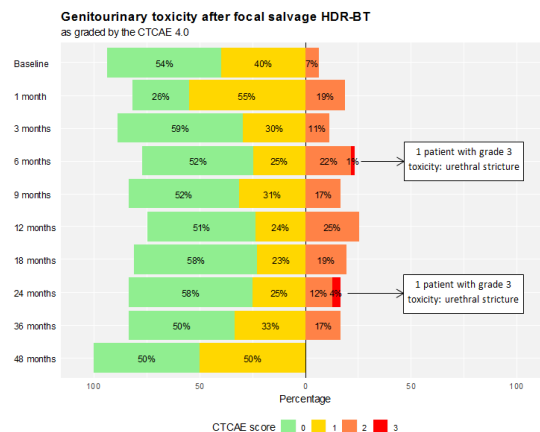


Figure 1: genitourinary toxicity as graded by the CTCAE 4.0.

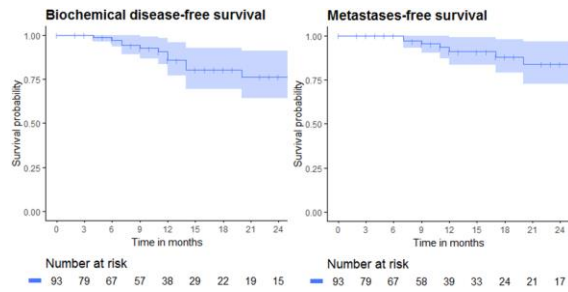


Figure 2: biochemical disease-free survival and metastases-free survival in the cohort with  $\geq 1$  month follow-up. 3/96 patients had not reached 1 month follow-up as of yet and are excluded from the calculations. 95% confidence intervals are presented here in blue.

## Conclusion

Focal salvage MRI-guided HDR-BT leads to high tumor control with low severe toxicity rates and short, self-limiting increases in urinary complaints.

**OC-0286 Focal high-dose-rate brachytherapy for localized prostate cancer: long-term clinical follow-up.**  
 M. Van Son<sup>1</sup>, M. Peters<sup>1</sup>, M.A. Moerland<sup>1</sup>, J.J.W. Lagendijk<sup>1</sup>, J.R.N. Van der Voort van Zyp<sup>1</sup>  
<sup>1</sup>UMC Utrecht, Radiotherapy, Utrecht, The Netherlands

## Purpose or Objective

Focal treatment of localized prostate cancer is an emerging paradigm in the search of optimal patient-tailored therapies with minimal toxicity. Though whole-gland treatments such as radiotherapy or prostatectomy reach excellent tumor control rates, they are associated with toxicity and quality of life (QoL) deterioration. Focal high-dose-rate brachytherapy (HDR-BT) may reduce toxicity and thereby preserve QoL in a selected patient group. Here we present long-term follow-up data.

## Material and Methods

Thirty patients with localized prostate cancer were treated with focal HDR-BT between May 2013-April 2016. Local disease status was evaluated by systematic biopsies and 3T MRI, using multiparametric MRI for the last 5 patients. After the brachytherapy implant procedure, 1.5T MRI's were made for organ contour adjustments and a final check of catheter positions. In a single dose, 19 Gy was delivered to the tumor area with a margin of 5 mm. Before treatment and during follow-up, genitourinary (GU) toxicity, gastro-intestinal (GI) toxicity and erectile dysfunction (ED) were graded according to the Common Toxicity Criteria for Adverse Events (CTCAE) 4.0. In addition, International Prostate Symptoms Score (IPSS) and International Index of Erectile Function score (IIEF-5) were obtained. QoL was measured with validated questionnaires (RAND-36, EORTC QLQ-C30 and EORTC QLQ-PR25). PSA was monitored, with biochemical recurrence defined as nadir+2 (Phoenix definition).

## Results

At baseline, median PSA was 7 ng/ml (range 1-10), median PSA doubling time was 4.5 years (range 0.5-38) and highest Gleason grade was 4+3=7 (2 patients). All tumors were stage T2. One patient received 1x45 mg Eligard 3 months before treatment. Median follow-up was 48 months (range 19-60). Improper removal of a brachytherapy catheter caused acute hemorrhage of the prostate in one patient. No grade >2 GU (Figure 1) or GI toxicity occurred and ED was relatively stable throughout follow-up. Mean IIEF-5 score decreased from 14 at baseline to 9.5 after 6 months, remaining stable around 10 afterwards (moderate ED,  $p < 0.01$ ). Mean IPSS increased in the first month from 6 to 9 (moderate symptoms,  $p = 0.02$ ), returning to baseline-level afterwards. There were no significant differences in QoL. Biochemical recurrence occurred in 10 patients, of which 9 had local recurrence on imaging (two in-field recurrences). Five patients were re-treated with curative salvage treatments. Two patients started ADT. After 4

years, biochemical disease-free survival was 70% (95% CI 52-93%) and metastases-free survival was 93% (95% CI 85-100%) (Figure 2).

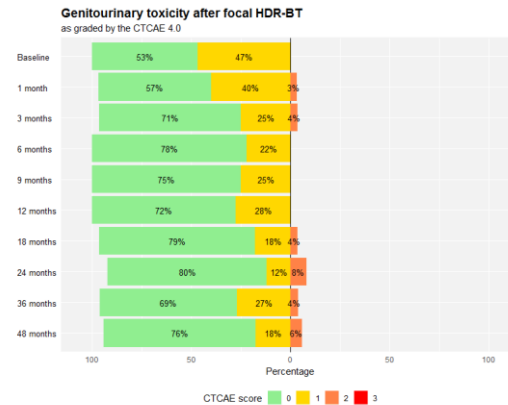


Figure 1: genitourinary toxicity as graded by the CTCAE 4.0.

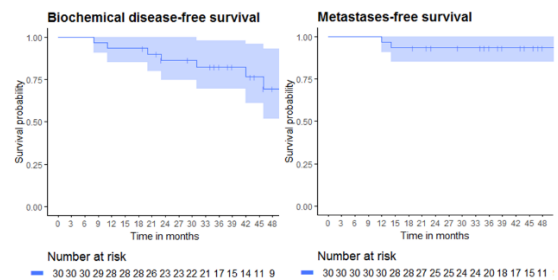


Figure 2: biochemical disease-free survival and metastases-free survival. 95% confidence intervals are presented here in blue.

## Conclusion

In terms of toxicity, focal HDR-BT is a safe treatment. Apart from one perioperative complication (3%), no grade >2 GU or GI toxicity occurred. Patient-reported QoL did not decrease over time. However, long-term biochemical control is inferior to whole-gland treatments. This might in part be attributed to inadequate patient selection.

## OC-0287 Dose to the dominant intraprostatic lesion using HDR vs. LDR monotherapy: Phase II Randomized trial

J. Crook<sup>1</sup>, D. Batchelar<sup>2</sup>, M. Hilts<sup>2</sup>, D. Anderson<sup>2</sup>, F. Bachand<sup>1</sup>, S. Tissaverasinghe<sup>1</sup>, B. Farnquist<sup>3</sup>, T. Bainbridge<sup>4</sup>, C. Araujo<sup>2</sup>  
<sup>1</sup>BC Cancer Agency - Southern Interior, Radiation Oncology, Kelowna, Canada; <sup>2</sup>BC Cancer Agency - Southern Interior, Radiation Physics, Kelowna, Canada; <sup>3</sup>Kelowna General Hospital, Radiology, Kelowna, Canada; <sup>4</sup>Kelowna General Hospital, Pathology, Kelowna, Canada

## Purpose or Objective

To present the dosimetric results of a Phase II randomized trial comparing dose escalation to the magnetic resonance imaging (MRI)-defined dominant intraprostatic lesion (DIL) using either low dose rate (LDR) or high dose rate (HDR) prostate brachytherapy.

## Material and Methods

Patients receiving prostate brachytherapy as monotherapy were randomized to LDR or HDR brachytherapy. Prostate and DILs were contoured on pre-operative multiparametric MRI. These images were registered with transrectal ultrasound (TRUS) for treatment planning. LDR brachytherapy was preplanned using I-125 seeds. Postplan dosimetry was performed at day 30 using MR-CT (computed tomography) fusion. HDR brachytherapy used intra-operative TRUS-based planning to deliver 27 Gy/2

fractions in separate implants. DIL location was classified as peripheral, central or anterior. Directed biopsies of DILs were performed at the time of brachytherapy for pathologic confirmation of mpMRI results. A student t-test compared DIL D90 between modalities and DIL locations.

#### Results

Of 60 patients, 31 underwent LDR and 29 HDR brachytherapy. Up to 3 DILs were identified per patient (100 total) with 74 peripheral, 6 central, and 20 anterior DILs. Mean DIL volume was 1.9cc (SD: 1.7cc) for LDR and 1.6 cc (SD 1.3cc) for HDR ( $p=0.279$ ). Mean DIL D90 was 151% (SD 30%) for LDR (217 Gy) and 132% (SD 13%) for HDR (17.8 Gy/fraction  $\times$  2). 88% of patients had biopsy confirmation of at least one DIL.

DIL D90 for peripheral lesions was higher than anterior and central ( $p<0.001$ ). The mean DIL D90 per location for LDR was 159% for peripheral lesions, but only 122% and 124% for central and anterior lesions, reflecting the planning algorithm which delivers 150% to the peripheral zone but limits the urethra to  $< 130\%$ . The mean D90 per location for HDR was 137% for peripheral lesions, and 123% and 118% for central and anterior DILs. DIL D90 coverage was further evaluated as a percentage of the desired peripheral zone dose coverage, which was 150% for LDR and 125% for HDR. For both central and anterior lesions, HDR DIL D90 values were significantly closer to the peripheral zone benchmark dose than for LDR ( $p=0.007$  and  $0.002$  respectively).

#### Conclusion

DIL location affects dose escalation, particularly because of urethral proximity, such as for anterior and central DILs. HDR brachytherapy may dose escalate better when target DIL is close to critical organs.

#### OC-0288 Long-term results of 15Gy HDRBT boost in intermediate risk-prostate cancer: Analysis of 500+ patients

L. Mendez<sup>1</sup>, K. Martell<sup>1</sup>, H. Chung<sup>1</sup>, C. Tseng<sup>1</sup>, Y. Alayed<sup>1</sup>, P. Cheung<sup>1</sup>, S. Liu<sup>1</sup>, D. Vesprini<sup>1</sup>, W. Chu<sup>1</sup>, E. Szumacher<sup>1</sup>, A. Ravi<sup>2</sup>, A. Loblaw<sup>1</sup>, G. Morton<sup>1</sup>

<sup>1</sup>Sunnybrook Odette Cancer Centre, Radiation oncology, Toronto, Canada; <sup>2</sup>Sunnybrook Odette Cancer Centre, Medical Physics, Toronto, Canada

#### Purpose or Objective

To report long-term biochemical control associated with single-fraction 15Gy high-dose-rate (HDR) brachytherapy boost followed by external beam radiation (EBRT) in intermediate-risk prostate cancer patients.

#### Material and Methods

All patients with intermediate-risk prostate adenocarcinoma that received treatment with 15Gy HDR brachytherapy (BT) boost followed by EBRT between 2009 and 2016 were retrospectively reviewed. Descriptive statistics were used to characterize the cohort. Biochemical failure was defined based on the Phoenix criteria. Kaplan-Meier method estimated biochemical relapse free survival (bRFS) at 5 and 7 years. Cumulative incidence of ADT use at 7 years was also calculated. R statistical software package v3.2.2 (www.r-project.org) was used for this analysis.

#### Results

545 patients met the inclusion criteria for this study. Median age at HDR BT was 67 years (IQR 61-72). Median baseline PSA was 7.4 ng/mL (IQR 5.4-9.9). 302 (55%) and 243 (45%) patients had cT1 and cT2 stage disease. 9 (2%), 346 (67%) and 164 (32%) had ISUP Gleason Grade Group 1, 2 and 3, respectively. A median of 5 (IQR 3-7) out of 12 (IQR 10-12) biopsied cores were positive. A total of 90 (18%) patients received neoadjuvant ADT for a median time of 6 months (IQR 3-6). The most frequent EBRT regimen was 37.5Gy in 15 fractions with 508 patients (93%) receiving this fractionation. All patients received 15Gy in a single HDR brachytherapy fraction. Median HDR prostate

V100, V150 and V200 were 97% (IQR 96-97), 36% (IQR 33-39) and 12% (IQR 10-14), respectively. After a median PSA follow-up time of 4.3 years (IQR 2.4-6.0), 44 (8%) patients experienced biochemical failure. After a median overall follow-up time of 4.9 years (IQR 2.6-6.4), 20 patients (4%) went on to receive ADT. Kaplan-Meier estimated bRFS rates were 91% (CI 88-94) and 82% (CI 77-87) at 5 and 7 years, respectively (Figure 1). The cumulative incidence of ADT use was 7% (CI 3-10) at 7 years (Figure 2). Figure 1- Kaplan-Meier estimate of biochemical relapse-free survival post 15Gy HDR-BT and EBRT

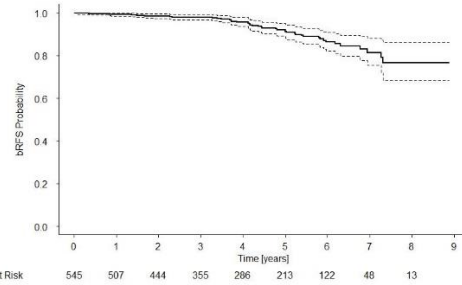
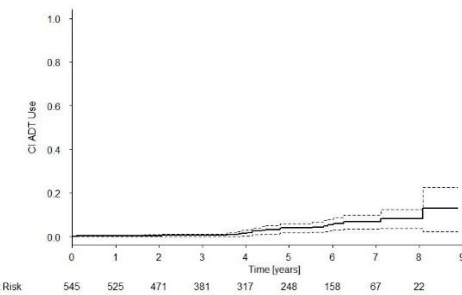


Figure 2- Cumulative incidence of ADT use post 15Gy HDR-BT and EBRT



#### Conclusion

In this large cohort of intermediate-risk prostate cancer patients, 15 Gy HDR BT boost plus EBRT results in durable long-term biochemical control and low rates of ADT salvage.

#### Proffered Papers: PH 5: Proffered paper: Innovations in dosimetry and dose measurements

#### OC-0289 A water calorimeter as a primary standard for absorbed dose in magnetic fields

L. De Prez<sup>1</sup>, J. De Pooter<sup>1</sup>, B. Jansen<sup>1</sup>, S. Woodings<sup>2</sup>, J. Wolthaus<sup>2</sup>, B. Van Asselen<sup>2</sup>, T. Van Soest<sup>2</sup>, J. Kok<sup>2</sup>, B. Raaymakers<sup>2</sup>

<sup>1</sup>VSL, Ionizing Radiation Standards, Delft, The Netherlands; <sup>2</sup>University Medical Center Utrecht, Department of Radiotherapy, Utrecht, The Netherlands

#### Purpose or Objective

MRI guided radiotherapy devices are currently in clinical use. Detector responses can be significantly affected by the magnetic field. Therefore, there is a need to characterize detectors in terms of absorbed dose to water,  $D_w$ , against primary standards that are operated under the magnetic field condition. The aim of this study was to commission a water calorimeter, accepted as the Dutch national standard for  $D_w$  and validate its claimed

standard uncertainty of 0.37 % in the 7 MV photon beam of an MRI linac in a 1.5 T magnetic field.

#### Material and Methods

Measurements were done with a magnetic field of 1.5 T and, after ramp-down, without magnetic field. Methods were developed for measurement of detector depth, distance and beam output. A thermodynamic description was used to demonstrate potential temperature effects due to the magneto-caloric effect (MCE). To evaluate the primary standard on a fundamental basis, realisation of  $D_w$  at 1.5 T was evaluated parameter by parameter.

#### Results

It was shown that the measurement of  $DT_w$ , are either independent of, or can be determined in, a magnetic field. The chemical heat defect,  $h$ , was considered zero within its stated uncertainty, as for 0 T. Evaluation of the MCE and measurements done during magnet ramp-down, indicated no changes in the specific heat capacity of water. However, variation of the applied transmission monitor in the bore was the limiting factor for output normalization.

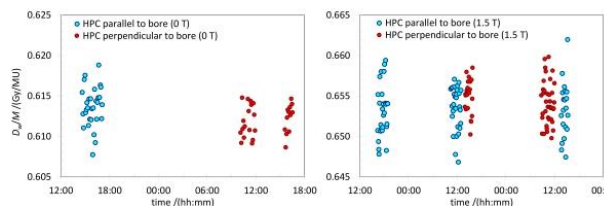
The table shows the calculated correction factors for heat conduction,  $k_c$  measured correction factors for perturbation of the calorimeter HPC both with and without magnetic field,  $k_{HPC}$  and the correction for beam non-uniformity  $k_{nu}$ . Hardly any significant effect of the magnetic field on the correction factors is observed.

The figure shows the corrected calorimetric  $D_w$  measurements in a 0 T magnetic field of an Elekta MRI-linac (left) and in the same machine with 1.5 T magnetic field (right). Both graphs show  $D_w$  measurements normalized to the monitor in the bore with the HPC perpendicular and in parallel direction to the bore. Note that values on the vertical axes cannot be compared due to the magnetic field dependence of the applied monitor.

#### Conclusion

This study confirmed that the uncertainty for measurement of  $D_w$  with a water calorimeter in a 1.5 T magnetic field is estimated to be the same as under conventional reference conditions at 0 T. The VSL water calorimeter can therefore be applied as a primary standard for  $D_w$  in magnetic fields and is currently the only primary standard operable in a magnetic field that provides direct access to the international traceability framework.

correction	$B = 0$ T	$B = 1.5$ T
$k_{c,\perp}$	0.9976 (18)	0.9979 (18)
$k_{c,\parallel}$	0.9970 (18)	0.9969 (18)
$k_{nu,\perp}$	1.0013 (5)	1.0015 (5)
$k_{nu,\parallel}$	1.0014 (5)	1.0016 (5)
$k_{HPC}$ (#06)	1.0033 (5)	1.0025 (5)
$k_{HPC}$ (#07)	1.0031 (5)	1.0028 (5)



#### OC-0290 Consistency of PTW30013 and FC65-G ion chamber magnetic field correction factors

S. Woodings<sup>1</sup>, B. Van Asselen<sup>1</sup>, T. Van Soest<sup>1</sup>, L. De Prez<sup>2</sup>, J. Lagendijk<sup>1</sup>, B. Raaymakers<sup>1</sup>, J. Wolthaus<sup>1</sup>

<sup>1</sup>UMC Utrecht, Radiotherapy, Utrecht, The Netherlands ;

<sup>2</sup>VSL, Dutch Metrology Institute, Delft, The Netherlands

#### Purpose or Objective

Reference dosimetry in a strong magnetic field is made more complex due to (i) the change in dose deposition and (ii) the change in sensitivity of the detector. Potentially it is also influenced by thin air layers, interfaces between media, orientations of field, chamber and radiation, and minor variations in ion chamber stem or electrode construction.

The PTW30013 and IBA FC65-G detectors are waterproof Farmer-type ion chambers that are suitable for reference dosimetry. The magnetic field correction factors have previously been determined for these chamber types.

The aim of this study was to assess the chamber-to-chamber variation and determine whether generic chamber type-specific magnetic field correction factors ( $k_{B,M,Q}$ ) can be applied for each of the PTW30013 and FC65-G -type ion chambers when they are oriented parallel (//) to, and perpendicular (|-) to, the magnetic field.

#### Material and Methods

The experiment was conducted with 12 PTW30013 and 13 FC65-G chambers. The  $k_{B,M,Q}$  were measured using the practical method of van Asselen et al. (2018, PMB, 63 p125008) that can be performed in the clinic. In this study each chamber was cross-calibrated against the local standard chamber twice; with and without magnetic field. Measurements with 1.5 T magnetic field were performed with the 7 MV FFF beam of the MRI-linac. Measurements without magnetic field (0 T) were performed with the 6 MV conventional beam of an Elekta Agility linac.

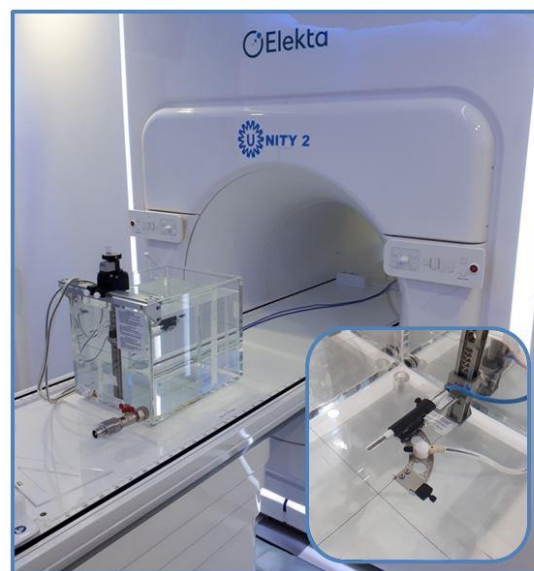


Figure 1: PTW prototype MR-compatible MP1 waterphantom at the MRI-linac with (picture insert) PTW prototype holder, with PTW30013 chamber and CC13 monitor chamber.

A prototype MR-compatible PTW MP1 phantom was used along with a prototype holder that facilitated measurements with the chamber aligned 90 degrees counter-clockwise (|-) and 180 degrees (//) to the direction of the magnetic field. A monitor chamber was also mounted on the holder and all measurements were normalized so that variations in the output of each linac were removed.

Measurements with the local standard chamber were repeated during the experiment to quantify the experimental uncertainty.

Recombination was measured in the 6 MV beam. Generic beam quality correction factors were applied. The differences in these factors between beams is constant within each chamber type (dependent on beam quality and dose-per-pulse).

By comparing the results for the two cross calibrations the  $k_{B,M,Q}$  can be determined for each chamber, and the variation within the chamber-type determined.

### Results

Table 1: Average results for each chamber type. The standard deviations of the results are shown in brackets.

Chamber-type	$N_{D,w,00}$ (cGy/nC)	$k_{B,M,Q}$ (parallel)	$k_{B,M,Q}$ (perpendicular)
PTW30013	5.384 (0.017)	0.995 (0.002)	0.966 (0.001)
FC65-G	4.817 (0.015)	1.005 (0.002)	0.961 (0.002)

The factors within both PTW30013 and FC65-G chamber-types were found to be very consistent, with observed standard deviations of  $k_{B,M,Q}$  for the PTW30013 of 0.19% (|-) and 0.13% (//), and for the FC65-G of 0.15% (|-) and 0.17% (//). These variations are comparable with the observed measurement uncertainties ( $1\sigma$ ) of 0.14% - 0.20%.

### Conclusion

The consistency of the results for the PTW30013 and FC65-G chambers implies that for these two chamber types it is not essential to measure the  $k_{B,M,Q}$  specifically for each individual chamber. Values for each chamber-type, magnetic field strength and relative chamber orientation can therefore be applied from the literature.

### OC-0291 Development of a deformable phantom for validation of adaptive irradiation methods in MRgRT

A. Elter<sup>1,2,3</sup>, S. Dorsch<sup>1,2,3</sup>, P. Mann<sup>1,2</sup>, A. Runz<sup>1,2</sup>, W.

Johnen<sup>1,2</sup>, S. Klüter<sup>2,4</sup>, C.P. Karger<sup>1,2</sup>

<sup>1</sup>German Cancer Research Center DKFZ, Medical Physics in Radiation Oncology, Heidelberg, Germany ;

<sup>2</sup>Heidelberg Institute for Radiation Oncology HIRO, National Center for Radiation Research in Oncology NCRO, Heidelberg, Germany; <sup>3</sup>University of Heidelberg, Faculty of Physics and Astronomy, Heidelberg, Germany;

<sup>4</sup>University Hospital Heidelberg, Department of Radiation Oncology, Heidelberg, Germany

### Purpose or Objective

One of the key features of MRgRT is the online adaption of treatment plans to account for daily anatomy changes. Due to the complex adaption process, specific end-to-end tests need to be performed that require the development of new phantoms. Such phantoms should include:

- flexible and reproducible geometric insert positioning
- various anthropomorphic MR and CT image contrasts
- dose measurement methods (1D-3D)

While (i) and (ii) are necessary to test the performance of the deformable imaging registration (DIR) method, (iii) allows verification of beam delivery. For this, a promising method is the use of 3D polymer gels (PG). However, due to the high reactivity with oxygen, its application is yet limited to few container materials and shapes.

The aim of this work was to evaluate different 3D printing materials for the use with PG and to develop a phantom that meets (i)-(iii), using arbitrarily-shaped structures filled with PG.

### Material and Methods

Using various 3D printing materials and techniques, PG containers were produced and filled with PAGAT [1] dosimetry gel. The containers were irradiated at a linear accelerator (Linac, Artiste, Siemens) with photons using either a homogenous large field or a small field (1x1cm<sup>2</sup>) to test the compatibility with the PG. The PG was evaluated by MRI and the results were compared with those obtained in already established BAREX<sup>TM</sup> containers [2]. Having found that the VeroClear printing material was compatible with the PG, the phantom was designed with variable components meeting requirements (i)-(iii). The phantom was used in a first experiment at a clinical MR-linac (MRidian, ViewRay) to test parts of the adaptive

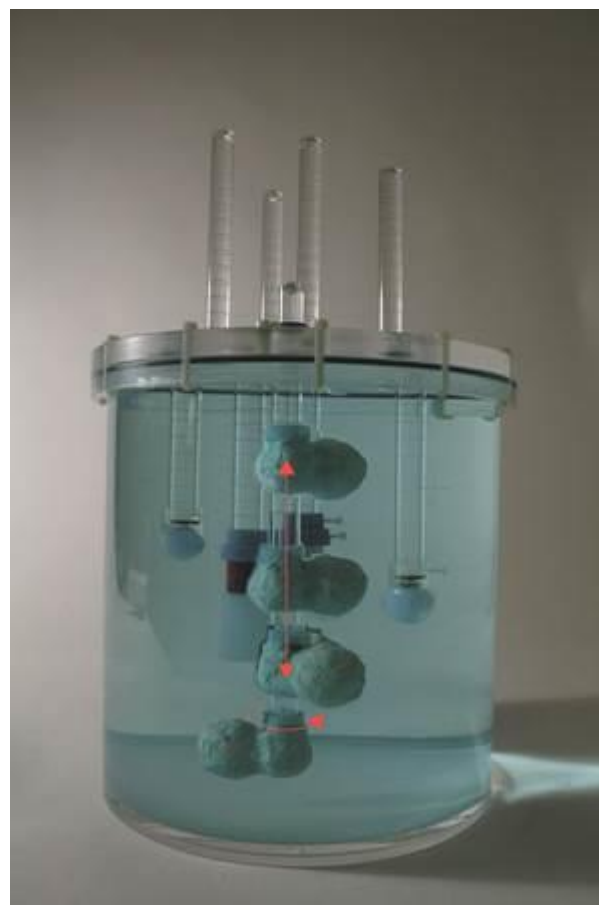
planning procedure in the presence of a target deformation.

[1]Baldock et al., doi:10.1088/0031-9155/55/5/R01

[2]Mann et al., doi:10.1088/1361-6560/aa51b1

### Results

The VeroClear material used in the Objet30 Pro printer (Stratasys) showed no significant interaction with the gel and provided a homogeneous dose response with differences of <3 % in the homogeneous irradiation. In addition, a high geometric accuracy when measuring the small field size was found (FWHM: 8.82 mm in VeroClear vs 8.96 mm in BAREX<sup>TM</sup>). Varying MR and CT imaging contrast can be realized by combining Agarose, Ni-DTPA and potassium chloride in various concentrations. First measurements showed a good performance of the DIR algorithms in case of linear component shifting but were not fully capable to detect rotations or changes in electron density like bone and air.



### Conclusion

We found a 3D printing material compatible with PG allowing to create arbitrary shaped and PG-filled inserts that can be used for 3D dose measurements. In a first experiment, the developed phantom could be used to test the performance of a DIR algorithm and to trigger a re-optimization process. Future experiments will focus on 3D-dosimetric validation of the adapted treatment plans and the development of a suitable end-to-end test for the validation of complete adaptive irradiation procedures in MRgRT.

### OC-0292 When we have to apply volume corrections in dosimetry?

K. Zink<sup>1</sup>, C. Andersen<sup>2</sup>, L. De Prez<sup>3</sup>, F. Delaunay<sup>4</sup>, S. Duane<sup>5</sup>, C. Gomà<sup>6</sup>, M. Pimpinella<sup>7</sup>, P. Teles<sup>8</sup>, J. Tikkanen<sup>9</sup>, M. Pinto<sup>7</sup>

<sup>1</sup>Universitätsklinikum Marburg- Klinik für

Strahlentherapie Partikeltherapie, Clinic for Radiotherapy and Radiation Oncology, Marburg, Germany; <sup>2</sup>DTU, Center for Nuclear Technologies, Kongens- Lyngby, Denmark; <sup>3</sup>VSL, Dutch Metrology Institute, Delft, The Netherlands; <sup>4</sup>CEA-Saclay, Laboratoire National Henry Bequerel- PtC 104, Gif-sur-Yvette-Cedex, France; <sup>5</sup>National Physical Laboratory, Chemical- Medical & Environmental Science Department, Teddington, United Kingdom; <sup>6</sup>KU Leuven, Department of Oncology, Leuven, Belgium; <sup>7</sup>ENEA, National Institute of Ionizing Radiation Metrology INMRI, Rome, Italy; <sup>8</sup>IST University of Lisbon, Centre of Nuclear Sciences and Technology, Lisbon, Portugal; <sup>9</sup>STUK, Stuk, Helsinki, Finland

### Purpose or Objective

In reference dosimetry we are interested in the absorbed dose,  $D_w$ , at a reference point in water. In small or non-reference fields it is common to apply a volume averaging correction,  $k_{vol}$ . The IAEA-AAPM report TRS-483 introduces  $k_{vol}$  for the non-uniformity of the lateral dose profiles in flattening-filter free beams (FFF). This approach is new compared to the treatment of conventional flattening-filter beams (cFF). In current codes of practice (e.g. IAEA TRS-398) volume averaging was not corrected for. In TRS-483, however,  $k_{vol}$  is applied as a contribution to the beam quality correction factor  $k_Q$ . Accordingly, TRS-483 gives independent tables of  $k_Q$  for cFF and FFF beams. When to apply or when not to apply  $k_{vol}$  might lead to confusion. Currently, the IAEA TRS-398 CoP is revised and new experimental and Monte Carlo based  $k_Q$  data are becoming available. Within the EMPIR 16NRM03 RTNORM project  $k_Q$  data were measured and calculated. As there are no clear recommendations on how to report or include the volume averaging, its impact for different ion chambers in cFF and FFF beams was determined.

### Material and Methods

$k_Q$  for beam quality  $Q$  is defined as a ratio of calibration coefficients  $N_{D,w,Q}/N_{D,w,Q_0}$  with  $N_{D,w,Q} = (D_w/M)_Q$  and reference beam quality  $Q_0$  (<sup>60</sup>Co).  $M$  is the corrected ion chamber reading. With Monte Carlo  $k_Q$  is calculated as  $(D_w/D_{det})_{Q,Q_0}$  with  $D_{det}$  the scored dose to the detector volume. However due to volume averaging, depending on the beam profile, measured and calculated  $k_Q$  values may differ:  $k_{vol}$  would be applied to the ion chamber corrections applied to  $M$  or removed in the MC calculated dose.

Calorimetric measurements were performed with a selection of ion chambers by different national standard labs in cFF and FFF beams. For all beams the dose profiles at the reference depth were measured with a small volume detector and the volume correction factor  $k_{vol}$  was determined. The  $k_Q$  factor for the different chambers was also calculated applying the Monte Carlo code EGSnrc. As in the experiments the dose profiles were determined for different source types (point source, phase space files, linac head) and  $k_{vol}$  was determined for the ion chambers and also for the water voxel used to determine  $D_w$ .

### Results

Table 1 shows measured  $k_{vol}$  data for three ion chambers in cFF and FFF beams of different accelerators. As can be seen, also in cFF beams  $k_{vol}$  may be in the range of several parts per mille. Similar results were obtained in the Monte Carlo simulations. Regarding the calculated dose to water  $D_w$  in Monte Carlo simulations, Fig. 1 shows, that the voxel size used to calculate  $D_w$  also has an impact of several parts per mille on the resulting  $k_Q$ .

**Figure 1:** Impact of the voxel radius  $r$  to determine the dose to water  $D_w$  in Monte Carlo simulations in beams of different accelerators. The voxel height is always 0.1 cm.

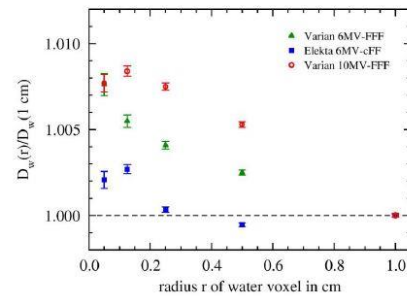


**Table 1:** Experimentally determined volume averaging corrections  $k_{vol}$  for three different ion chambers in cFF and FFF beams of a GE Saturne 43, an Elekta Versa HD, a Varian Truebeam accelerator and a cobalt-60 unit.

	<sup>60</sup> Co	GE Saturne 43			
		6 MV cFF	6 MV FFF	12 MV cFF	20 MV cFF
PTW 30013	1.0009	1.0009	0.9986	1.0039	
NE 2571	1.0010	1.0011	0.9985	1.0048	
Exradin A1SL	1.0002	0.9999	0.9997	1.0004	
Elekta Versa HD					
	6 MV cFF	6 MV FFF	10 MV cFF	10 MV FFF	
PTW 30013	0.9999	1.0033	0.9998	1.0054	
NE2571	0.9999	1.0036	0.9998	1.0059	
Varian TrueBeam					
	6 MV cFF	10 MV cFF	15 MV cFF	20 MV cFF	
PTW 30013	0.9991	0.9997	1.0004	1.0002	
NE 2571	0.9991	0.9997	1.0004	1.0003	
Exradin A1SL	0.9996	0.9999	0.9999	0.9996	

### Conclusion

The results show, that  $k_{vol}$  even for cFF beams may be not negligible and its contribution to  $k_Q$  should be indicated. Regarding Monte Carlo simulations especially the dose value  $D_w$  to calculate  $k_Q$  should be corrected for volume averaging to achieve a coherent  $k_Q$  data set in the revised TRS-398 protocol.

### OC-0293 Cerenkov emission-based dosimetry is a promising perturbation-free technique

Y. Zlateva<sup>1</sup>, B. Muir<sup>2</sup>, I. El Naqa<sup>3</sup>, J. Seuntjens<sup>1</sup>  
<sup>1</sup>McGill University, Medical Physics Unit, Montreal, Canada; <sup>2</sup>National Research Council of Canada, Measurement Science and Standards, Ottawa, Canada; <sup>3</sup>University of Michigan, Department of Radiation Oncology, Ann Arbor, USA

### Purpose or Objective

Cherenkov emission (CE)-based dosimetry is promising as a micrometer-resolution 3D perturbation-free in-water technique. Considering a potential formalism for broad-beam on-axis CE-based external radiotherapy dosimetry, we experimentally validate Monte Carlo (MC) calculation of the CE-to-dose conversion in a relative sense with a simple detector. We optimize detection configurations for electron beams and estimate achievable dosimetric uncertainties.

### Material and Methods

The EGSnrc code SPRRZnrc is modified to calculate the CE-to-dose conversion, kC, on beam axis in water. The code is validated through a relative experimental study with 6-20 MeV electron beams using a plano-convex lens pair/apertures and long optical fiber leading to a spectrometer outside (Fig. 1). The circular field-of-view is aligned at the water surface. Motivated by the experimental validation, kC is then calculated for 20 electron beam qualities (4 BEAMnrc models, 4-22 MeV). Detection geometry is considered, beam quality specification is addressed, and a preliminary dosimetric uncertainty is estimated.

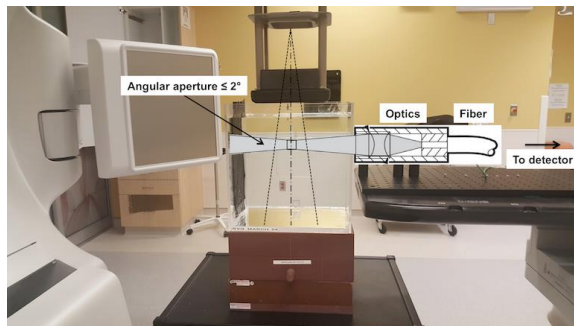


Fig. 1: Cherenkov detection setup. Not to scale.

## Results

MC and measured relative  $k_C$  factors agree to within 1% for percent-depth CE (PDC) > 50% (Fig. 2). At other depths, deviations are in accordance with approximations. Simulated electron beam quality specifier R50 is estimated from the depth of 50% CE C50 to within 0.1 mm and 0.4 mm (maximum) with large and small apertures respectively. The fit performance on measured R50 supports this finding. The  $k_C$  value is uniquely specified by R50 at a given depth with preliminary dosimetric uncertainty estimate of the order of 1% (Table 1). A PDC downstream shift by the R50-C50 difference is derived from theory and found to reduce the  $k_C$  depth dependence tenfold to 2.5%.

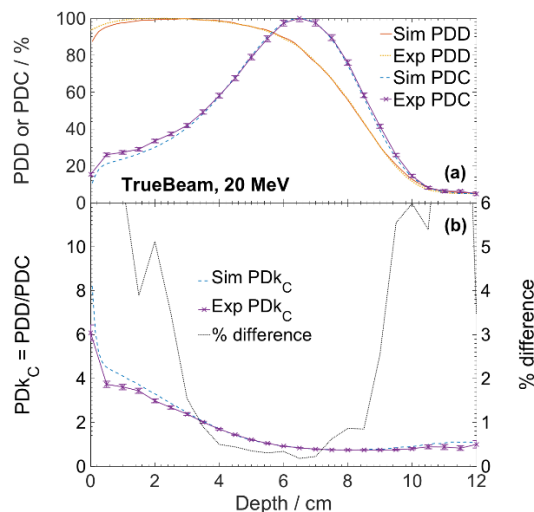


Fig. 2: (a) Simulated (Sim) and experimental (Exp) percent-depth dose, PDD, percent-depth Cherenkov emission (CE), PDC, at 90 degrees to beam, and (b) PDD/PDC (i.e., normalized CE-to-dose conversion,  $k_C$ ) in water from 20 MeV TrueBeam electrons. The error bars define an interval estimated to have 95% level of confidence.

Table 1: Preliminary best-case uncertainty budget of Cherenkov emission-based measurement of absorbed dose to water in electron beams at optimal depth  $d_{ref} = 0.6R50 - 0.1$  [cm] under reference conditions.

	4 $\pi$ detection	90°±5° detection
<b>Measurement</b>		
$M_{raw}$	0.3%	0.3%
SSD	0.10%	0.10%
Position	0.33%	0.33%
Field size	0.10%	0.10%
Temperature	0.06%	0.06%

## Calibration

Calibration factor	0.7%	0.7%
Calibration stability	0.1%	0.1%

## Conversion

$k_C$	0.50%	0.53%
$k_C$ assignment	0.40%	0.84%

## Influence quantities

Linac stability	0.05%	0.05%
<b>COMBINED (k=1)</b>	<b>1.1%</b>	<b>1.3%</b>

## Conclusion

The excellent agreement between MC and experiment motivate CE-based dosimeter design efforts. Based on these results, we recommend a large-aperture detector and downstream PDC shift for beam-axis CE-based electron beam dosimetry in water. This is an attractive alternative to current methods as it avoids perturbations, can be extended to 3D via tomography or optical sectioning, and is especially promising for small fields due to the high resolution achievable with optical methods.

## OC-0294 Separating initial and general recombination in reference dosimetry of proton pencil beam scanning

J.B. Christensen<sup>1</sup>, E. Almhagen<sup>2,3</sup>, L. Stolarczyk<sup>2,4</sup>, M. Liszka<sup>4</sup>, A. Vestergaard<sup>5</sup>

<sup>1</sup>Technical University of Denmark, Center for Nuclear Technologies, Roskilde, Denmark ; <sup>2</sup>The Skandion Clinic, The Skandion Clinic, Uppsala, Sweden ; <sup>3</sup>Uppsala University, Medical Radiation Sciences- Department of Immunology- Genetics and Pathology, Uppsala, Sweden ; <sup>4</sup>Institute of Nuclear Physics- Polish Academy of Sciences in Krakow, The Bronowice Cyclotron Centre, Krakow, Poland; <sup>5</sup>Aarhus University Hospital, Danish Centre for Particle Therapy, Aarhus, Denmark

## Purpose or Objective

Gas-filled ionization chambers are the detectors of choice for calibrating ion beams at proton therapy facilities. The charge liberated in the ionization chamber is collected via an applied voltage and related to the absorbed dose. However, ion pairs of opposite charge may recombine and lead to an underestimation of the dose. The recombination events cannot be corrected with Monte Carlo methods as the recombination cross sections contain too large uncertainties. As a result, recombination losses are traditionally corrected with methods dating anywhere from decades to a century back. The main objective is to obtain a more precise determination of the recombination correction by separation of initial and general recombination for use in reference dosimetry.

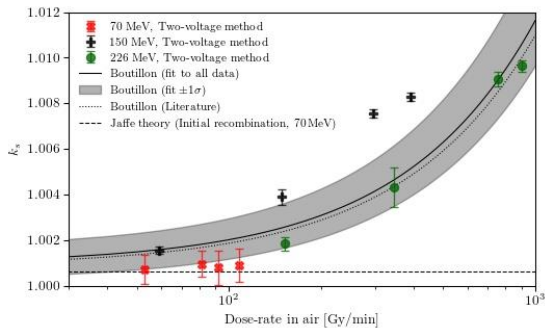
## Material and Methods

A Roos type parallel-plate ionization chamber was irradiated with a continuous scanned proton beam at 70, 150, and 226 MeV and 4 dose rates at in a water phantom. The liberated charge was for each configuration collected at 5 polarization voltages between 50 and 200 V. A detailed Monte Carlo model of the beam line enables an accurate calculation of both the particle spectrum and a conversion from delivered MU/minute to dose rate as the beam scans over the ionization chamber. The charge collection at several dose rates in turn permits a calculation of the recombination as a function of dose rate using the Boutillon theory [1]. The results are compared to the Jaffé theory [2] for initial recombination, the two-voltage-method (TVM) suggested in TRS-398 [3], and recombination corrections using extrapolation methods.

## Results

The experimentally determined recombination correction factors calculated with the TVM and extrapolation methods agree within 1.5%. The TVM data are in the figure plotted as a function of the calculated dose rate for a collecting voltage of 200 V. The dotted line represents the Boutillon theory for initial and general recombination

calculated with literature values from [1], whereas the Boutillon theory is fitted to all data points and shown with a solid line. The general recombination parameter  $m$  obtained from the fit is in 5% agreement with values in [1], and the initial recombination parameter  $A$  in the Boutillon theory is 11 % larger than that predicted by the Jaffe theory.



### Conclusion

The recombination for dose rates of proton pencil beams below 1 kGy/min in the Roos type ionization chamber is found to be below 1.1 %. The recombination for high energies and dose rates is completely dominated by general recombination where the recombination increases linearly with the dose rate. The recombination for low energies and dose rates below 0.1 kGy/min, on the other hand, is relatively constant. Such a behavior suggests a need to consider initial recombination for low dose-rates which also is indicated by the agreement with the Jaffe theory.

[1] Palmans H et al 2006 PMB 51 903-17

[2] Jaffe G 1913 Ann Phys 42 303-41

[3] TRS-398: IAEA, Vienna 2000.

### OC-0295 Comparison of PENH, FLUKA and Geant4/TOPAS for radiation transport calculations in proton beams

K. Baumann<sup>1</sup>, F. Horst<sup>2</sup>, K. Zink<sup>2</sup>, C. Gomà<sup>3</sup>

<sup>1</sup>University Medical Center Giessen-Marburg, Department of Radiotherapy and Radiooncology, Marburg, Germany ;

<sup>2</sup>University of Applied Sciences Giessen, Institute of Medical Physics and Radiation Protection, Giessen, Germany; <sup>3</sup>KU Leuven, Department of Oncology-Laboratory of Experimental Radiotherapy, Leuven, Belgium

### Purpose or Objective

At the time, the IAEA TRS-398 Code of Practice is being updated. Within this framework the RTNORM project is supporting the IAEA working group with experimental as well as Monte Carlo calculated beam quality correction factors for different ionization chambers and beam qualities such as photons and protons. Whereas the use of Monte Carlo codes like EGSnrc and PENELOPE for calculations in high energy photon beams is well established, data for protons are sparse. This work compares the performance of the Monte Carlo codes PENH, FLUKA and Geant4/TOPAS in the calculation of beam quality correction factors in therapeutic proton beams.

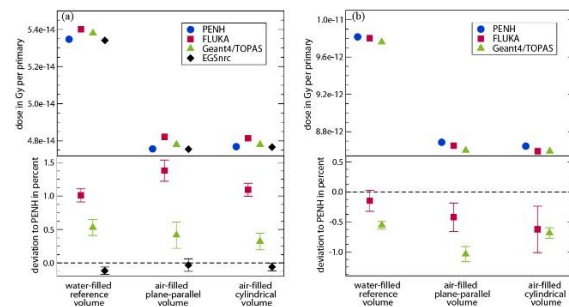
### Material and Methods

The absorbed dose to water ( $D_w$ ) in a reference volume in a water phantom was calculated with each of the Monte Carlo codes PENH, FLUKA and Geant4/TOPAS for the beam qualities  $Q_0$  (1.25 MeV mono-energetic photons) and  $Q$  (150 MeV protons). Additionally, the absorbed dose ( $D_{air}$ ) in two air cavities representing cylindrical and plane-parallel ionization chambers was calculated. EGS was also used to calculate  $D_w$  and  $D_{air}$  in the photon beams. From these absorbed dose values the ratios  $f_Q = (D_w/D_{air})$  (for

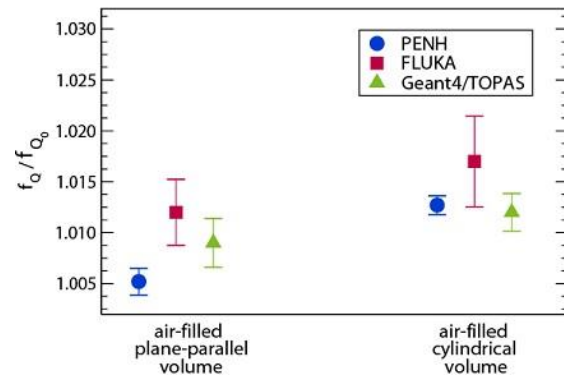
beam qualities  $Q$  and  $Q_0$ ) and the ratios  $f_Q/f_{Q_0}$  were calculated for both beam qualities and air cavities. This ratio  $f_Q/f_{Q_0}$  is the basis of beam quality correction factors. The particle transport settings and physics lists in each Monte Carlo code were adapted to simulate the radiation transport as accurately as possible.

### Results

In Figure 1 the dose values in the water reference volume and the air cavities for both beam qualities (panel (a) for photons, panel (b) for protons) are shown for the different Monte Carlo codes. In the bottom panel the deviations relative to PENH are shown. For the photon irradiation the results from EGSnrc and PENH agree within two standard deviations or better (largest deviation 0.1%). The dose values obtained with FLUKA and Geant4/TOPAS are up to 1.4% larger compared to PENH. For the proton irradiation the deviations of the three codes capable of transporting protons (PENH, FLUKA and Geant4/TOPAS) are 1% at maximum.



In Figure 2 the ratios  $f_Q/f_{Q_0}$  for the two air cavities and each Monte Carlo code are shown. The results agree within two standard deviations or better. The maximum deviation is 0.6%.



### Conclusion

It was shown that by using appropriate transport settings the results of the  $f_Q/f_{Q_0}$  - ratios agreed within 0.6%, although the dose values show deviations of up to 1.4%. However, these dose discrepancies tend to cancel out in the  $f_Q/f_{Q_0}$  -ratios. In other words, PENH, FLUKA and Geant4/TOPAS are suitable to calculate  $f_Q/f_{Q_0}$  - ratios in proton beams.

### Proffered Papers: PH 6: Proffered paper: X-ray guided tumour tracking

### OC-0296 Validation of motion-including dose reconstruction on a ground-truth time-resolved moving anatomy

J. Bertholet<sup>1</sup>, B. Eiben<sup>2</sup>, M.J. Menten<sup>1</sup>, E.H. Tran<sup>2</sup>, D.J. Hawkes<sup>2</sup>, S. Nill<sup>1</sup>, J.R. McClelland<sup>2</sup>, U. Oelfke<sup>1</sup>

<sup>1</sup>The Institute of Cancer Research and the Royal Marsden NHS Foundation Trust, Joint Department of Physics,

London, United Kingdom; <sup>2</sup>University College London, Centre for Medical Image Computing- Department of Medical Physics and Biomedical Engineering, London, United Kingdom

**Purpose or Objective**

Motion-including dose reconstruction (MIDR) aims at reconstructing the actually delivered dose to the moving anatomy during radiotherapy. However, the time-resolved patient anatomy during treatment is generally unknown and commonly estimated using 3D or 4D pre-treatment images. In this study, we reconstructed the delivered dose on a ground-truth, fully time-resolved anatomy (GT-MIDR) and used this to evaluate the accuracy of MIDR based on 3D and 4D CT images.

**Material and Methods**

The digital XCAT phantom was used to generate three regularly breathing thorax phantoms, each with a lung tumour moving according to its location (Fig 1). A 4DCT was generated and treatment plans were created for either a mid-ventilation approach (midVent) or treatment delivery with dynamic MLC tracking (tracking) (9-beam step-and-shoot IMRT, RTOG 1021). Treatment delivery under regular motion or regular motion and continuous drift was simulated in our in-house software.

For MIDR, the treatment fluence is discretized into sub-beams; each sub-beam is associated with the anatomy instance that it was delivered to and shifted to account for residual tumour position difference between the estimated anatomy and the actual target position if any. I.e. motion is modelled by a sub-beam isocenters shift, to emulate the actual relative target/beam position. The dose for each instance is then calculated in a research treatment planning system (TPS) and accumulated on the reference anatomy via deformable registration.

For GT-MIDR, ground-truth anatomy instances were generated from the XCAT. For 3D-MIDR, only one anatomy instance, the midVent 4DCT phase, was used and motion was accounted for by sub-beam isocenter shifts only. For 4D-MIDR, anatomy instances were chosen as the 4DCT phase where the tumour is closest to the actual tumour position and sub-beam isocenter shifts accounted for residual position differences.

**Results**

Differences between GT-MIDR and planning (Fig 2) show the effect of motion (midVent) or motion and mitigation (tracking) on dose delivery. Target underdosage was highest for tumour A. Tracking resulted in higher dose to the spinal cord and heart (tumour A, B) or aorta (tumour C).

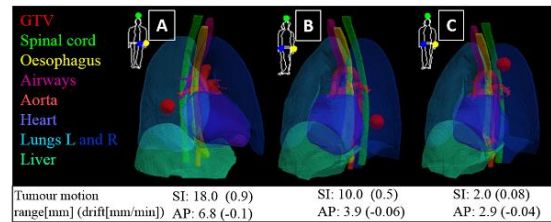


Fig 1. Anatomy, motion range and drift (if applicable) for tumours A, B and C. Tumour motion was determined by their location in the lungs.

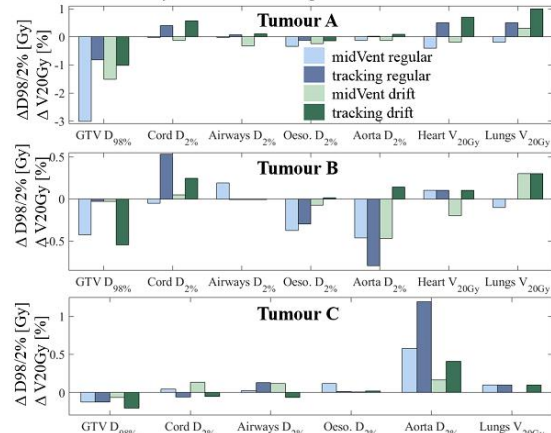


Fig 2. Ground truth reconstructed dose (GT-MIDR) minus plan dose to the target and the OAR for the tumour A (top), B (middle) and C (bottom).

Differences between 3D or 4D and GT-MIDR (Fig 3) show the accuracy of the respective methods. Reconstructed target dose errors above 1Gy were observed for 3D-MIDR. For tumour A, reconstructed dose to the organs-at-risks (OAR) were underestimated by 3D-MIDR. For tumour B, dose to the oesophagus and aorta was overestimated by 3D-MIDR. For tumour C, dose to the spinal cord and the oesophagus were overestimated by 4D-MIDR and dose to the aorta was underestimated by 3D and 4D-MIDR.

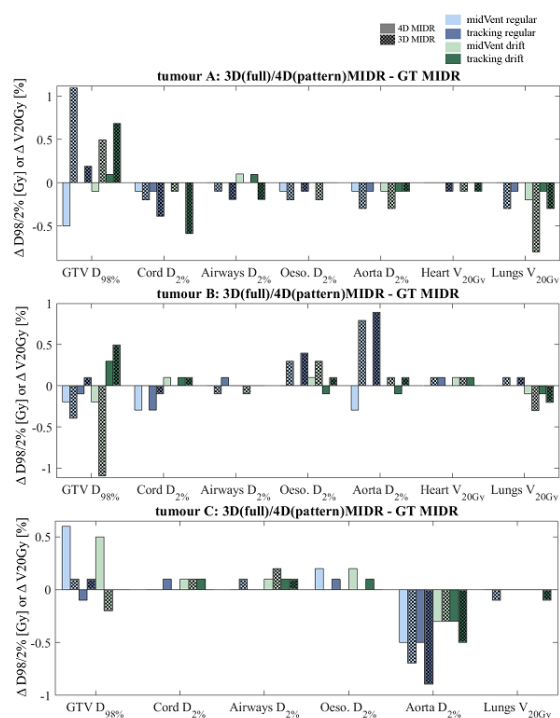


Fig 3. 3D(full) or 4D(pattern) MIDR minus Ground truth reconstructed dose (GT-MIDR) to the target and the OAR for the tumour A (top), B (middle) and C (bottom).

**Conclusion**

In the first demonstration of GT-MIDR, we calculated the delivered dose to target and OAR for a range of lung

tumour locations. We showed that MIDR based on planning data does not accurately resolve the delivered dose even in the case of regular motion. Our method may be used to validate MIDR for other motion models and treatment sites.

**OC-0297 Detailed PTV margin assessment for liver SBRT with CBCT-guidance or realtime monitoring and gating**

E. Worm<sup>1</sup>, R. Hansen<sup>1</sup>, M. Høyer<sup>2</sup>, J. Bertholet<sup>3</sup>, B. Weber<sup>2</sup>, A. Dolcet<sup>4</sup>, P.R. Poulsen<sup>1</sup>

<sup>1</sup>Aarhus University Hospital, Oncology, Aarhus C, Denmark; <sup>2</sup>Aarhus University Hospital, Danish Centre for Particle Therapy, Aarhus C, Denmark; <sup>3</sup>Institute of Cancer Research, Division of Radiotherapy and Imaging, London, United Kingdom; <sup>4</sup>University Hospital Virgen de las Nieves, Radiophysics, Granada, Spain

**Purpose or Objective**

Implanted markers are often used to guide liver SBRT treatments, but position errors remain due to marker localization uncertainties, liver deformations, and intrafraction motion. Knowledge of the full error budget is lacking thus hindering realistic margin estimations. Here, we analyze in detail all error contributions to determine appropriate PTV margins in marker-based liver SBRT in two treatment scenarios: (A) CBCT guided free breathing or (B) respiratory gating with realtime motion monitoring.

**Material and Methods**

The van Herk formalism of systematic ( $\Sigma$ ) and random ( $\sigma$ ) errors was used to quantify the geometric errors from (1) CBCT match uncertainties (only Scenario A), (2) intrafraction motion, (3) interfraction deformations and marker migration, and (4) intrafraction deformations. Here, (1) was obtained by re-analyzing data of 29 liver SBRT patients where online manual CBCT marker match (Fig.1C) was compared with the marker positions accurately obtained from marker segmentation in individual CBCT projections [Bertholet, Acta Oncol,56(2017)]. (2) was reported in a recent study [Worm, IJROBP,101(2018)] of 15 patients receiving 3-fraction Calypso-guided liver SBRT (3 implanted electromagnetic markers, continuous monitoring, Fig.1A). Treatment delivery was respiratory gated around the end-exhale phase. Non-gated treatment was also simulated. (3+4) were based on individual marker motion in the Calypso-data (Fig.1A) using one marker as surrogate-tumor (Fig.1B). (3) was derived from the mean difference between the marker-tumor vectors in the planning CT and the mean marker-tumor vectors during the first treatment field. Patients (n=1) with interfraction deformations >8mm were excluded since these receive re-planning in our daily clinical practice (based on marker-marker mismatch in CBCT). (4) was derived from the difference between the mean marker-tumor vectors during the first treatment field and the marker-tumor vectors during the rest of each treatment (Fig.1A+B).

**Results**

Table 1 shows the errors for scenarios A (CBCT guidance) and B (gating). For scenario A, errors were dominated by intrafraction motion and interfraction liver deformations. PTV margins of 4.6mm (LR), 9.6mm (CC), and 3.5mm (AP) were required for a 67% PTV dose prescription level (Nordic standard). Real-time monitoring and gating (scenario B) eliminated the need for the uncertain CBCT marker-match, reduced intrafraction motion, and slightly reduced the error of interfraction liver deformation. PTV margins of 2.9mm (LR), 3.9mm (CC) and 2.8mm (AP) were needed in (B).

**Conclusion**

Error analysis based on unprecedented detailed motion monitoring showed that intrafraction motion and interfraction deformations dominate the geometrical errors in liver SBRT. Gating based on realtime monitoring

largely reduces required PTV margins not only by decreasing motion, but also by reducing deformations and avoiding error-prone marker localization in CBCT's. Target delineation errors were not considered in this study.

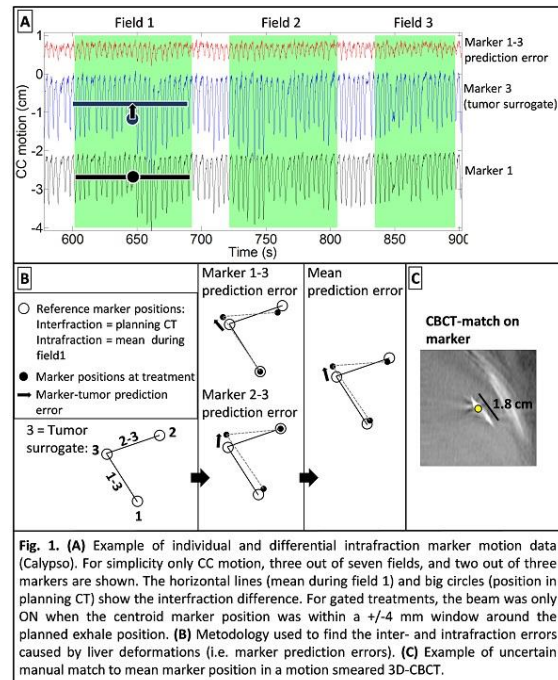


Fig. 1. (A) Example of individual and differential intrafraction marker motion data (Calypso). For simplicity only CC motion, three out of seven fields, and two out of three markers are shown. The horizontal lines (mean during field 1) and big circles (position in planning CT) show the interfraction difference. For gated treatments, the beam was only ON when the centroid marker position was within a +/-4 mm window around the planned exhale position. (B) Methodology used to find the inter- and intrafraction errors caused by liver deformations (i.e. marker prediction errors). (C) Example of uncertain manual match to mean marker position in a motion smeared 3D-CBCT.

**Table 1.** Required PTV margins calculated from the observed systematic ( $\Sigma$ ) and random errors ( $\sigma$ ) in non-gated and respiratory gated liver SBRT

	(A) Non-gated based on CBCT setup						(B) Respiratory gated based on real-time motion monitoring					
	LR (mm)		CC (mm)		AP (mm)		LR (mm)		CC (mm)		AP (mm)	
	$\Sigma$	$\sigma$	$\Sigma$	$\sigma$	$\Sigma$	$\sigma$	$\Sigma$	$\sigma$	$\Sigma$	$\sigma$	$\Sigma$	$\sigma$
CBCT match on markers (1)	0.6	0.7	1.1	1.0	0.5	0.7	-	-	-	-	-	-
Intrafraction motion (2)	1.1	1.2	2.4	4.8	0.9	2.2	0.4	0.6	0.3	1.8	0.2	1.1
Interfraction deformations (3)	1.2	0.8	2.1	0.5	0.7	0.8	1.0	0.8	1.4	0.6	1.0	0.9
Intrafraction deformations (4)	0.3	0.9	0.2	0.9	0.2	0.7	0.3	0.7	0.3	0.7	0.2	0.7
PTV margin (67% prescrip.)	4.6		9.6		3.5		2.9		3.9		2.8	
PTV margin (95% prescrip.)	5.2		12.9		4.6		3.2		4.6		3.2	

$PTV = 2.5 \Sigma_{tot} + \beta(\sigma_{tot}^2 + \sigma_p^2)^{1/2} - \beta \sigma_p$   
 $\Sigma_{tot}$  and  $\sigma_{tot}$  = quadratic sum of  $\Sigma$ 's and  $\sigma$ 's.  $\sigma_p = 3.2$  mm,  $\beta = 0.44$  (67%) or 1.64 (95% PTV prescription level) [van Herk, Semin Radiat Oncol, 14 (2004)].

**OC-0298 MLC tracking for lung cancer SABR is clinically feasible: results of first-in-human clinical trial**

J. Booth<sup>1</sup>, V. Caillet<sup>1</sup>, A. Briggs<sup>1</sup>, N. Hardcastle<sup>2</sup>, D. Jayamanne<sup>1</sup>, K. Szymura<sup>1</sup>, O. Ricky<sup>3</sup>, T. Eade<sup>1</sup>, P. Keall<sup>3</sup>  
<sup>1</sup>Royal North Shore Hospital, Northern Sydney Cancer Centre, St Leonards, Australia ; <sup>2</sup>PeterMacCallum Cancer Centre, Radiation Oncology, Melbourne, Australia ; <sup>3</sup>ACRF Image X Institute, University of Sydney, Sydney, Australia

**Purpose or Objective**

MLC tracking is an emerging technology to improve tumor targeting and reduce normal tissue irradiation during radiotherapy. The purpose of this work was to determine if MLC tracking for lung cancer SABR is clinically feasible, measure the target and normal tissue doses with comparison of these to SABR treatment.

**Material and Methods**

Seventeen patients with stage 1 lung cancer or lung metastases were recruited into the ethics-approved MLC

tracking clinical trial (NCT02514512). Each patient had three electromagnetic beacons (Calypso) inserted into the lung surrounding the tumor. An MLC tracking SABR plan was generated with the planning target volume (PTV) expanded 5mm from the end-exhale gross tumor volume (GTV). For comparison a conventional motion-encompassing SABR plan was generated with PTV expanded 5mm from a 4DCT-derived internal target volume (ITV). Treatment was delivered using a standard linear accelerator using in-house developed software to continuously adapt the MLC motion based on the Calypso beacons' movement. The rate of successful treatment fractions with MLC tracking, tumor motion, treated volume and reconstructed delivered dose were compared between MLC tracking and conventional ITV treatment planning.

#### Results

All seventeen patients were treated successfully with MLC tracking (70 successful fractions), completing the primary endpoint of this study. Tumor motion range varied during treatment, between fractions and from the planning 4DCT; significantly, larger motion was observed during treatment that exceeded standard PTV boundaries. The MLC tracking PTVs for all patients was smaller than with ITV based planning (mean 29%, range 2%-47% reduction, or 2-18 cm<sup>3</sup> with MLC tracking). Subsequent reductions in normal lung dose were observed. Reconstruction of delivered treatments confirmed accurate delivery of MLC tracking, with 100% of the prescribed dose delivered to the GTV for all 70 fractions.

#### Conclusion

Real-time adaptation via MLC tracking on a standard linac has been successfully performed in seventeen lung cancer patients. Reductions in treated volumes up to 47% were observed, which translated to reductions in lung dose.

#### OC-0299 Fully automatic detection of heart irradiation in cine MV images during breast cancer radiotherapy

P.R. Poulsen<sup>1</sup>, M.S. Thomsen<sup>2</sup>, R. Hansen<sup>2</sup>, E. Worm<sup>2</sup>, E. Yates<sup>2</sup>, H. Spejlborg<sup>2</sup>, B. Offersen<sup>1</sup>

<sup>1</sup>Aarhus University Hospital, Department of Oncology, Aarhus, Denmark; <sup>2</sup>Aarhus University Hospital, Department of Medical Physics, Aarhus, Denmark

#### Purpose or Objective

Heart irradiation during radiotherapy of breast cancer can lead to late cardiac morbidity and increased mortality for long-time survivors. Left-sided breast cancer patients are therefore often treated in deep-inspiration breath-hold (DIBH) to better separate the breast and the heart. However, daily variations in the heart position can give heart exposures that are much larger than planned. For tangential treatments, continuous portal images (cine MV images) may be used to monitor the heart exposure at each treatment fraction with no additional dose to the patient. Challenges include low image contrast and the location of the heart edge in or near the field penumbra. In this study, we develop and test automated heart detection in cine MV images.

#### Material and Methods

Cine MV portal images (Figure 1A) of 302 tangential field deliveries were recorded at 7.7 Hz for ten left-sided breast cancer patients who received DIBH radiotherapy in 15-18 fractions. An algorithm for fully automatic detection of the heart edge in cine MV images was developed and tested for all available images. The algorithm exploits that the intensity of pixels at the edge of the heart will change cyclically with frequencies of 1-3 Hz due to heartbeat and that the intensity changes of all pixels at the heart edge will be highly correlated with each other because they have the same physical origin (heartbeat). The algorithm first identifies a candidate pixel on the heart edge as the pixel in the image with highest value of (1) intensity variations in the 1-3 Hz frequency range multiplied by (2)

intensity variation correlation with a set of neighboring pixels. Next, an enhanced heart edge image is generated by multiplying the 1-3 Hz intensity variation of each pixel with the correlation of intensity variations between the pixel and the heart edge candidate pixel (Figure 1B). Finally, the heart edge is segmented in the enhanced heart edge image and the exposed heart area is calculated as the area between the heart edge and the medial field edge (Figure 1C).

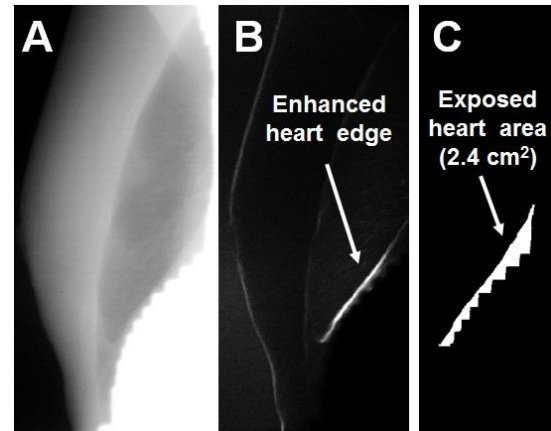


**Figure 1.** Cine MV image of a tangential breast treatment field (A) before processing and (B) after enhancement of the heart edge by the proposed algorithm. (C) Automatically extracted heart exposure area.

#### Results

Part of the heart was exposed at 169 out of 302 field deliveries. Using all cine MV images, the heart edge was correctly identified in all cine MV series except for 11 cases with heart drift motion during field delivery. For these cases, analysis of a shorter time series with less drift motion (30-50% of the MV images) correctly identified the heart edge. Figure 2 shows an example of the exposed heart area for a patient. While large interfraction variations occurred the intrafraction variations were smaller with high correlation between the heart exposure at field 1 and field 2 at a fraction ( $r = 0.85$ ,  $p < 0.001$ ).

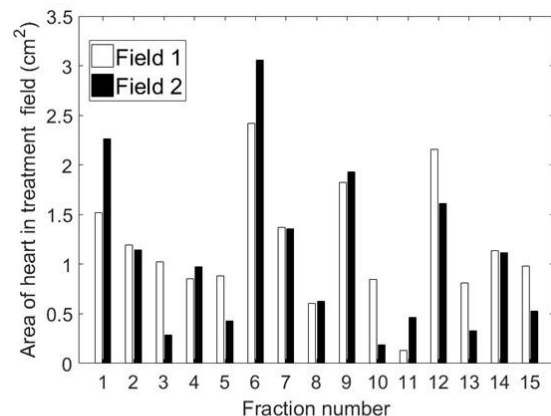


**Figure 2.** Example of exposed heart area at all fractions for a patient as extracted automatically in cine MV images as illustrated in Figure 1.

#### Conclusion

An algorithm for automatic identification of pixels at the heart edge in cine MV images was proposed, developed and shown to be highly efficient for heart exposure detection in tangential breast fields. The algorithm can be

used in a surveillance program with automated heart exposure monitoring of all breast cancer treatments in a clinic.

### OC-0300 Experimental validation of an MLC tracking treatment simulator with dose reconstruction

A. Hagner<sup>1</sup>, T. Ravkilde<sup>2</sup>, S. Skouboe<sup>3</sup>, C.G. Muurholm<sup>3</sup>, R. Hansen<sup>2</sup>, E.S. Worm<sup>2</sup>, P.R. Poulsen<sup>4</sup>

<sup>1</sup>Aarhus University, Department of Physics and Astronomy, Aarhus, Denmark; <sup>2</sup>Aarhus University Hospital, Department of Medical Physics, Aarhus, Denmark; <sup>3</sup>Aarhus University Hospital, Department of Oncology, Aarhus, Denmark; <sup>4</sup>Aarhus University, Department of Clinical Medicine, Aarhus University, Denmark

#### Purpose or Objective

Tumour motion may cause substantial deterioration of planned dose distributions. However, the dosimetric impact of tumour motion can be mitigated by MLC tracking. Current QA for MLC tracking involves pre-treatment delivery of the treatment plan to a moving dosimeter to determine its suitability for MLC tracking. This is a time-consuming process that may be replaced by dose delivery simulations for easier assessment of the suitability of MLC tracking for a given plan. In this study, we simulate delivered doses to a moving dosimeter with and without MLC tracking and validate the simulations by comparison with measurements.

#### Material and Methods

MLC tracking experiments were performed on a TrueBeam linear accelerator using iTools Tracking (Varian, CA) guided by an optical marker block. Delivered doses were measured at 72 Hz using a Delta4 dosimeter mounted in a HexaMotion motion stage (Scandidos, Sweden). The motion stage reproduced motion from four liver SBRT patients previously treated using VMAT plans with tumor motion monitoring by kilovoltage intrafraction monitoring. Three VMAT fields per patient were delivered to the dosimeter both with and without MLC tracking. The time-resolved motion-induced 3%/3mm gamma failure rate was determined for each VMAT field delivery faced with motion by comparing measured cumulative dose distributions with a measured static reference. In order to simulate the experiments, two in-house developed programs for 1) treatment delivery simulation and 2) dose reconstruction (DoseTracker) were combined. The treatment simulator took as input the DICOM treatment plans and motion stage trajectories used at the experiments and generated a log file with synchronized target positions and simulated linac parameters (gantry, MLC positions, MU, etc.) with 21Hz resolution. The log file was used by DoseTracker to reconstruct time-resolved delivered doses to all 1069 diodes in the dosimeter and calculate gamma failure rates comparing simulated and planned cumulative doses.

Finally, the time-resolved gamma failure rates of simulations and experiments were compared and the root-mean-square deviation (RMSD) calculated.

#### Results

The simulated gamma failure rates agreed well with the measurements throughout beam delivery for both MLC tracking and standard non-tracking treatments (Fig 1-2) with a root-mean-square deviation of 2.0 %-points.

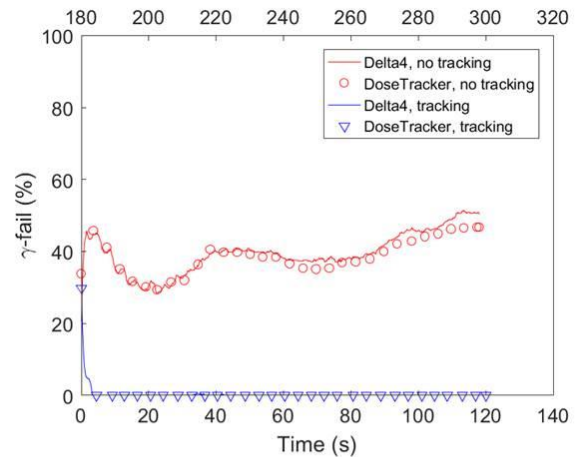


Figure 1: Example of measured (lines) and simulated (circles/triangles) motion-induced 3%/3mm gamma failure rates during delivery of the third field for patient 4 with MLC tracking and without.

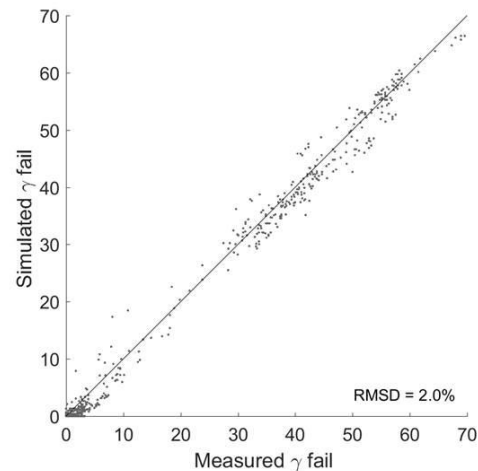


Figure 2: Scatter plot of all simulated vs. measured motion-induced 3%/3mm gamma failure rates. The unity line represents perfect simulation of motion-induced gamma failure rates.

#### Conclusion

End-to-end simulations of advanced radiotherapy delivery, from treatment plan to delivered dose distributions, were demonstrated and experimentally validated. The simulator accurately predicted motion-induced dose errors for VMAT liver SBRT to a moving target throughout both MLC tracking and standard non-tracking deliveries.

An accurate tracking simulator can eliminate the need for time-consuming experiments and QA measurements for MLC tracking. It allows easy evaluation of the motion robustness of treatment plans and their suitability to MLC tracking for a wider range of motion than practically possible with experiments.

### OC-0301 Real-time kV image guidance in the treatment of pancreatic SBRT: quantifying the purpose and impact

B. Jones<sup>1</sup>, Y. Vinogradskiy<sup>1</sup>, W. Campbell<sup>1</sup>, Y. Ding<sup>1</sup>, T. Schefter<sup>1</sup>, K. Goodman<sup>1</sup>, M. Miften<sup>1</sup>

<sup>1</sup>University of Colorado School of Medicine, Radiation Oncology, Aurora, USA

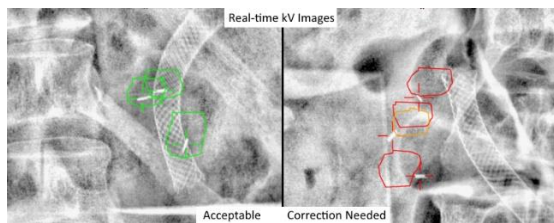
#### Purpose or Objective

Ablative radiotherapy of the pancreas requires extremely precise delivery in order to achieve local control while minimizing toxicity to the duodenum and

stomach. However, the pancreas undergoes erratic and unstable respiratory-induced motion, which makes it challenging to deliver dose accurately. Recent studies have demonstrated that traditional motion-mitigation techniques are often insufficient in guiding SBRT to the pancreas. The purpose of this study was to evaluate real-time imaging and tracking as a tool for pancreatic SBRT and quantify the ability of real-time imaging to correct for unpredictable tumor motion.

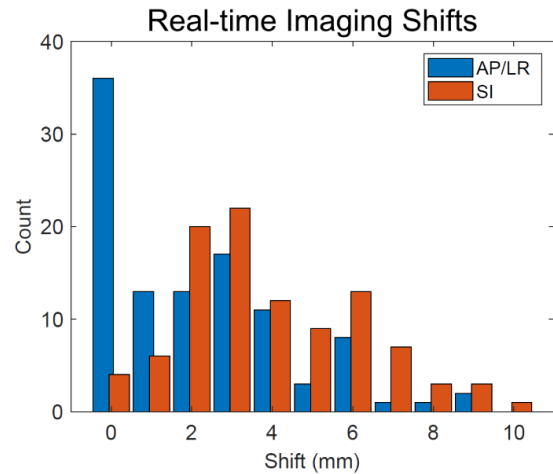
#### Material and Methods

To understand the effects of tumor motion on treatment, we apply a computational technique that uses the location of implanted fiducial markers in CBCT projection data to reconstruct the motion of these tumors. These data were used to determine the accuracy of 4DCT, and to analyze the impact of respiratory gating, abdominal compression, and real-time imaging on treatment accuracy. Following this, 68 patients were treated with pancreatic SBRT under real-time kV image guidance. Corrections were made to the position if the markers were observed >3 mm from the expected reference position. To understand impact of this imaging on treatment accuracy and clinical workflow, we retrospectively analyzed all treatment interruptions and corrections made based on this imaging. Throughout, we analyzed the effects of tumor motion by developing an artificial neural network-based dosimetric framework to model the dose distribution in the area immediately adjacent to the tumor.



#### Results

On average, 4DCT underestimated the 3D range of pancreatic tumor motion by 5.1 mm. These differences were driven by erratic components of respiratory and digestive motion. In retrospective analysis, respiratory gating outperformed abdominal compression, with an average superior-inferior range of motion of 5.5 mm vs 8.5 mm. In the dosimetric model, mean dose errors were less than 5% at all distances from the PTV, and mean absolute dose errors were 5-10%. Real-time imaging resulted in 0.81 pauses per fraction of treatment, with 40% of these resulting in re-localization of the target. The median 3D shift for patient re-alignment was 5.2 mm. 45% of shifts resulted in dosimetric differences to the tumor; of these, the median point dose difference was  $23\% \pm 22\%$  of prescription dose.



#### Conclusion

The pancreas undergoes unpredictable motion, which decreases the accuracy of 4DCT. Traditional methods of motion mitigation (compression and gating) were unable to decrease the average range of motion below 5 mm. We successfully treated 68 patients using a real-time imaging protocol that corrected positional variations >3 mm, resulting in significant dosimetric benefit to target coverage. In this way, real-time kV imaging allows for the correction of erratic and unpredictable pancreatic motion, and may allow for the safe delivery of future dose-escalated therapies.

#### OC-0302 Dose-guided motion management during liver SBRT delivery using real-time reconstructed tumor DVHs

C.G. Muurholm<sup>1</sup>, T. Ravkilde<sup>2</sup>, S. Skouboe<sup>1</sup>, E. Worm<sup>2</sup>, R. Hansen<sup>2</sup>, M. Høyer<sup>3</sup>, P.J. Keall<sup>4</sup>, P.R. Poulsen<sup>1</sup>

<sup>1</sup>Aarhus University Hospital, Department of Oncology, Aarhus, Denmark; <sup>2</sup>Aarhus University Hospital, Department of Medical Physics, Aarhus, Denmark;

<sup>3</sup>Aarhus University Hospital, Danish Center for Particle Therapy, Aarhus, Denmark; <sup>4</sup>Sydney Medical School -

The University Of Sydney, Radiation Physics Laboratory, Sydney, Australia

#### Purpose or Objective

Abdominal SBRT is susceptible to tumor motion due to high fraction doses and steep dose gradients. As a QA tool, we have developed a computer program, DoseTracker, that uses streamed tumor positions and linac parameters to reconstruct the dose to a moving tumor in real time during treatment delivery. While the tumor DVH provides intuitive and clinically relevant information on the fully delivered fraction dose it is often not meaningful for a partially delivered fraction. Here, we propose a time-resolved DVH that is useful for partial treatments and demonstrate its use for dose evaluation and dose-guided treatment adaptation in simulated liver SBRT treatments with real-time dose reconstruction.

#### Material and Methods

The proposed time-resolved DVH(t) describes the current deviations between the actual delivery with motion and the planned static delivery. Before treatment start DoseTracker calculates the planned static DVH (plan-DVH) of the full treatment. During treatment DoseTracker continuously calculates the cumulative actual dose with motion and planned static dose in all calculation points. The DVH(t) is then obtained by multiplying each calculation point used in the plan-DVH with the ratio of actual and planned dose. Hereby, the full treatment DVH is adjusted based on the current dosimetric state, which results in a real-time calculated DVH that meaningfully describes the current cumulative dose delivery and

converges towards the final motion-including DVH. The accuracy of DoseTracker's real-time calculated DVHs was first investigated by simulating 39 fractions from 13 liver SBRT patients with Calypso-measured motion. The motion-induced reduction in the CTV D95% ( $\Delta D95\%$ ) after each fraction was compared between DoseTracker and our treatment planning system (TPS; Eclipse). Next, the real-time DVH concept was used in two simulated dose-guided treatment scenarios where inter-field couch corrections were performed to correct mean position errors if  $\Delta D95\%$  exceeded either 5% or 10%.

### Results

Fig 1A compares the motion-including DVH(t) with the planned static DVH at different time points during a treatment. DoseTracker's final real-time estimated  $\Delta D95\%$  was in general in good agreement with the TPS with a root-mean-square error of 2.3 %-points and with the largest errors for small tumors (Fig 1B).

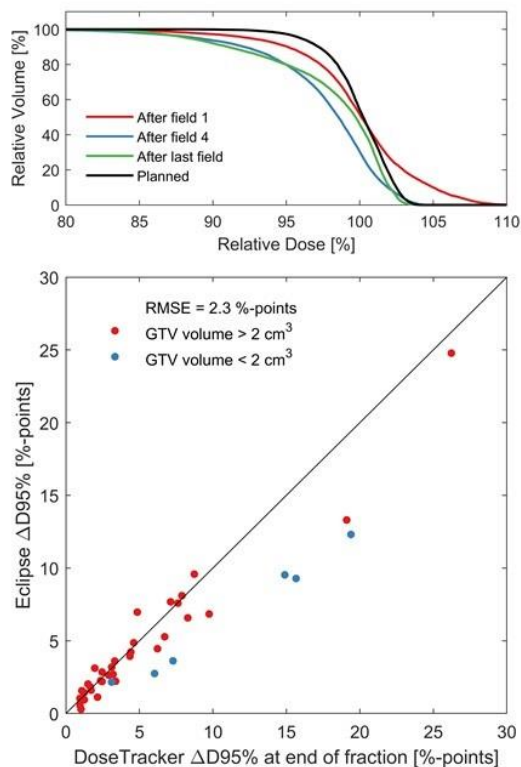


Figure 1. A: Examples of liver tumor DVHs without motion (black) and with motion calculated at different time points during a treatment. B: Motion-induced reduction in D95% after each fraction calculated with DoseTracker versus the treatment planning system (Eclipse).

Fig 2 shows the evaluation of  $\Delta D95\%$  during simulated treatments with and without dose-guided couch corrections. The mean (range) of the final  $\Delta D95\%$  was 5.9 %-point (1.0-26.2 %-point) without inter-field couch corrections and 3.8 %-point (1.0-10.0 %-point), and 3.1 %-point (0.6-9.5 %-point) with dose-guided couch corrections using 10% and 5%  $\Delta D95\%$  thresholds, respectively. The mean number of dose-guided couch shifts per fraction was 0.4 (10% threshold) and 1.1 (5%).

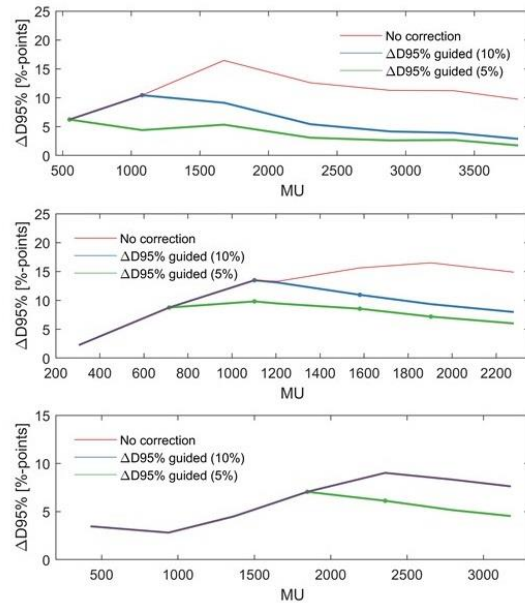


Figure 2.  $\Delta D95\%$  using the time-resolved DVH method as a function of MU delivered for 3 of the 39 simulated fractions.

### Conclusion

A new method for real-time motion-including dose evaluation that relates to a traditional DVH was presented and used for simulated dose-guided couch corrections based on reconstructed tumor dose deficits.

### Proffered Papers: RTT 3: Impact of variations on treatment planning

#### OC-0303 Dosimetric benefit of a clinically applied adaptive plan selection strategy for rectal cancer

R. De Jong<sup>1</sup>, J. Visser<sup>1</sup>, N. Van Wieringen<sup>1</sup>, K. Crama<sup>1</sup>, J. Wiersma<sup>1</sup>, D. Geijsen<sup>1</sup>, A. Bel<sup>1</sup>  
<sup>1</sup>Amsterdam UMC, Radiation Oncology, Amsterdam, The Netherlands

#### Purpose or Objective

For rectal cancer radiotherapy, an adaptive strategy by means of plan selection was clinically implemented in May 2016. We evaluated target coverage and dose to the organs at risk for the clinically used adaptive plan selection strategy compared to a non-adaptive approach for both short (5x5Gy) and long (25x2Gy) treatment schedules for rectal cancer patients.

#### Material and Methods

For this study the first 20 consecutive patients treated between May and September 2016 were included, if the length of the upper part of the mesorectum, as measured from the base of the bladder, was over 4.5 cm. For each patient 3 plans were created with different ventral PTV margins to the upper mesorectum (fig 1), i.e. the most mobile part of the target volume. The chosen margins depended on status of rectal filling on the CT scan: 25/15/0 mm for empty rectum versus 15/0/-15 mm for full rectum. All patients were planned with VMAT. Based on daily Conebeam CT (CBCT) scans RTTs selected the plan with the smallest PTV that encompassed the complete target volume for treatment. These plans were compared to a non-adaptive strategy with a single plan and a ventral PTV margin of 20 mm. For each fraction bowel cavity, bladder and target volume (mesorectum) were delineated on the CBCT scan by a single observer. The dose

distribution of each selected plan and the non-adaptive plan were used to calculate daily DVHs. To evaluate the dose levels as suggested in the QUANTEC papers (V15Gy, V30Gy, V40Gy, V45Gy), the corresponding dose levels per fraction were tested for significance: V0.6Gy, V1.2Gy, V1.6Gy, V1.8Gy and V95% for long, and V3.0Gy, V95% for short treatment schedules, respectively. Significance was tested using Wilcoxon signed ranks test for related samples. Coverage of the total CTV, as expressed by V95%, was also tested.

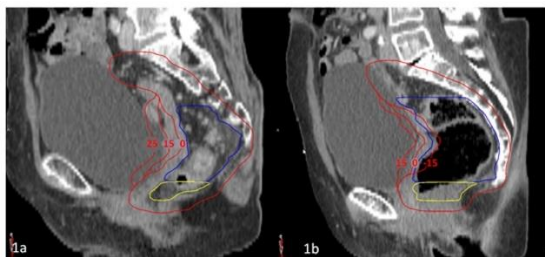


Fig. 1. Margin sets based on anatomy as captured on planning CT. (1a) shows empty rectum with a set of 25 mm, 15 mm, and 0 mm anterior margins (red) for upper mesorectum (blue). (1b) shows full rectum with a set of 15 mm, 0 mm, and -15 mm anterior margins (red) for upper mesorectum (blue)

## Results

In total, 10 short and 10 long treatment schedules were included, resulting in 300 plan selections. The margin set of 25/15/0 mm margins was used for 13 patients, the margin set of 15/0/-15 for 7 patients. Overall the -15mm, 0 mm, 15, and 25 mm plans were selected in 2%, 41%, 40%, 17% of fractions, respectively. For bowel cavity, limited but significant reductions were found in favor of the adaptive strategy for the long treatment schedule for V0.6Gy, V1.6Gy, V1.8Gy, and V95% ( $p < 0.05$ ). For the short treatment schedule the tested dose parameters (V3.0Gy and V95%) were not significantly different. For bladder limited but significant reductions were found in all dose parameters and both schedules (Table 1). Target volume V95% increased from 98% to 99%, but this increase was not significant.

Table 1. Dose to the organs at risk for all patients all fractions.

	Dose level per fraction	Median values (range)		p-value
		ART	non ART	
long schedule (25x2 Gy)				
Bladder	V0.6Gy (%)	99.8 (87.6-100.0)	100.0 (85.6-100.0)	.000
	V1.2Gy (%)	43.0 (12.6-99.3)	49.6 (19.1-96.8)	.000
	V1.6Gy (%)	22.8 (1.8-91.1)	29.0 (4.2-85.3)	.000
	V1.8Gy (%)	15.0 (0.2-87.0)	21.8 (0.4-77.6)	.000
	V95% (%)	10.8 (0.0-82.2)	17.8 (0.0-72.4)	.000
	Dmean (Gy)	1.23 (0.89-1.95)	1.30 (0.98-1.88)	.000
Bowel cavity	V0.6Gy (cm3)	847 (332-1447)	853 (294-1363)	.001
	V1.2Gy (cm3)	309 (119-554)	309 (120-557)	.542
	V1.6Gy (cm3)	205 (99-431)	214 (99-434)	.000
	V1.8Gy (cm3)	179 (93-381)	187 (90-390)	.000
	V95% (cm3)	160 (83-358)	170 (82-366)	.000
short schedule (5x5 Gy)				
Bladder	V3.0Gy (%)	29.7 (5.7-58.6)	33.8 (9.9-60.5)	.001
	V95% (%)	4.4 (0.0-16.4)	7.1 (0.0-27.7)	.013
	Dmean (Gy)	2.7 (2.1-3.5)	2.8 (2.3-3.6)	.001
Bowel cavity	V3.0Gy (cm3)	329 (139-456)	317 (137-477)	.237
	V95% (cm3)	176 (87-274)	191 (93-275)	.135

Dose levels per fraction V0.6Gy, V1.2Gy, V1.6Gy, V1.8Gy for long schedule corresponding to total dose V15Gy, V30Gy, V40Gy, V45Gy respectively and V3.0Gy for short treatment schedule corresponding to V15Gy total dose.

## Conclusion

The adaptive strategy with plan selection improved target coverage and lowered the dose to the organs at risk. Over all patients the clinical benefit seems limited.

### OC-0304 Dosimetric impacts of VMAT FFF large-field on standard dose fractionation

D. Julian<sup>1</sup>, S. Muraro<sup>1</sup>, O. Lauche<sup>1</sup>, A. Moustamia<sup>1</sup>, K. Serre<sup>1</sup>

<sup>1</sup>Clinique Clementville, CCGM Unité de Physique, Montpellier, France

## Purpose or Objective

Volumetric modulated arc therapy (VMAT) combined with flattening filter free beams (FFF) is generally used for stereotactic body radiation therapy (SBRT). Compared to flattened beams (FF), FFF provides advantages clearly identified in the literature to treat small lesions. In this study, an analysis of the dosimetric impacts of large X6<sub>FFF</sub> beams used in VMAT plans is developed for three major cancer locations.

## Material and Methods

A retrospective cohort of 90 patients treated between 2016 and 2017 includes 30 lung, 30 brain and 30 head & neck (H&N) cancers. The prescribed doses are respectively ranging from 50 to 66 Gy, 30 to 50 Gy and 60 to 70 Gy, 2 Gy per fraction. Planned target volumes (PTV) range from 35.0 to 482.0 cm<sup>3</sup>. Patients treated with VMAT X6<sub>FFF</sub> plans with 2 opposed coplanar arcs at 600 UM.min<sup>-1</sup> maximum dose rate on Varian Clinac® system. Plans are optimized on Varian Eclipse® TPS (AAA, PRO, V13.6). For each case, a new VMAT objective function and dose distribution are determined using X6<sub>FFF</sub> beams at 1400 UM.min<sup>-1</sup>. Both results are normalized so as 95% of the dose covers 98% of the PTV. VMAT X6<sub>FFF</sub> and X6<sub>FF</sub> plan comparisons included doses at the PTV and at 2 cm, specific organ-at-risk (OAR), 50% isodose prescription volumes (V50%), number of monitor units (MU) and treatment time. 3D  $\gamma$ -indexes (3%, 3mm, local dose) on Varian Portal Dosimetry® software is used to validate the plans.

## Results

PTV coverage do not differ significantly between the X6<sub>FF</sub> and X6<sub>FFF</sub> energies (<0.2%,  $p=0.5$ ) for any given location. At 2 cm around PTV, an average dose reduction of  $-4.0\% \pm 0.1\%$  ( $p < 0.001$ ) stands out for lung location,  $-2.75\% \pm 2.4\%$  ( $p < 0.001$ ) for brain and  $-0.8\% \pm 1.7\%$ ; ( $p=0.004$ ) for H&N targets. The V50% average dose decreases by  $3.9\% \pm 2.1\%$  ( $p=0.001$ ) for lung but no significant difference for brain and H&N is found. For all lung plans, doses at OAR decrease between  $-2.9\%$  and  $-6.5\%$  for normal lung, heart, spinal cord and esophagus; the overall decrease is due to the lower energy spectrum and scattered radiation. However, lower doses to the OAR are found for only 24 plans in brain and 20 plans in H&N with X6<sub>FFF</sub> beams. VMAT X6<sub>FFF</sub> plans requires a global greater MUs, with  $+10.7\% \pm 4.9\%$  than in X6<sub>FF</sub> for the lung,  $+8.7\% \pm 10.9\%$  for the brain,  $+28.3 \pm 16.1\%$  in H&N. X6<sub>FF</sub> and X6<sub>FFF</sub>  $\gamma$ -indexes do not show significant differences except for H&N: pass rate is less than 95% score for 70% of plans. Treatment time reductions using X6<sub>FFF</sub> high dose rate is limited by the gantry rotation speed. To ensure dosimetric objectives, X6<sub>FFF</sub> large field fluence is compensated by the segmentation algorithm. Except for lung location, X6<sub>FFF</sub> does not improve outcomes systematically.

## Conclusion

For lung localizations, the use of large X6<sub>FFF</sub> VMAT plans improves dose conformity to the target volume and generate high dose gradients which spare surrounding normal tissues and organs at risk. However, large X6<sub>FFF</sub> fields do not seem suitable for systematic brain and H&N plan management.

### OC-0305 Organ sparing potential and inter-fraction robustness of IMPT for cervical cancer

E.M. Gort<sup>1</sup>, J.C. Beukema<sup>1</sup>, M.J. Spijkerman-Bergsma<sup>1</sup>, S. Both<sup>1</sup>, J.A. Langendijk<sup>1</sup>, W.P. Matysiak<sup>1</sup>, C.L. Brouwer<sup>1</sup>  
<sup>1</sup>University Medical Center Groningen, Department of Radiation Oncology, Groningen, The Netherlands

## Purpose or Objective

Current chemoradiation (CHRT) for cervical cancer results in severe chronic bowel toxicity in one out of eight patients. Moreover, severe hematologic toxicity is a frequent cause of discontinuation of CHRT which may have an impact on treatment outcome. Our pencil beam scanning proton facility allows highly conformal intensity modulated proton therapy (IMPT), however inter-fraction

motion and increased sensitivity to range uncertainties may affect target dose coverage and dose to OAR. This in silico planning study was performed to evaluate robustness and the potential of IMPT to reduce dose to OAR in locally advanced cervical cancer, compared to the current photon treatment (VMAT).

#### Material and Methods

Five weekly repeated CT scans from 5 cervical cancer patients treated with CHRT were available for this study. The target volumes, with the para-aortic region included, were delineated according to the EMBRACE II intermediate IGRT protocol and three different primary treatment plans were created for 25 fractions of 1.8 Gy<sub>RBE</sub> using RayStation 6.99: a two-field IMPT (2F), a four-field IMPT (4F) and a two-arc VMAT plan. Robustness evaluation using a 5-mm setup and 3% range uncertainty margin was performed. Each repeated CT scan was contoured and registered to the plan CT scan and subsequently the primary treatment plan was recomputed on each repeated CT scan. The voxelwise minimum dose (worst case dose) delivered to 98% of the GTV (D<sub>98%</sub>GTV) and lymph nodes (D<sub>98%</sub> nodes) as well as the nominal OAR doses were evaluated on each of the CT scans. The selected clinical relevant OAR dose parameters were bone marrow V<sub>10Gy</sub> and V<sub>20Gy</sub> [1], femoral head D<sub>mean</sub> [2], sacrum D<sub>mean</sub> [2] and D<sub>50%</sub> [3] and whole bowel V<sub>15Gy</sub> [4]. In addition, entire DVHs for the whole bowel were compared.

#### Results

IMPT (2F and 4F) and VMAT showed similar plan robustness with regard to target coverage (GTV and nodes), with a mean dose deviation from the planCT of  $-0.11 \pm 0.43$  Gy<sub>RBE</sub> (IMPT 2F),  $-0.40 \pm 0.58$  Gy<sub>RBE</sub> (IMPT 4F) and  $0.04 \pm 0.90$  Gy<sub>RBE</sub> (VMAT) (Figure 1A). The DVHs of the whole bowel showed a lower mean dose in the range of 0 - 40 Gy<sub>RBE</sub> for the IMPT plans compared to VMAT (Figure 1B). Bone marrow V<sub>10Gy</sub> and whole bowel V<sub>15Gy</sub> were significantly lower for IMPT 2F and 4F compared to VMAT (Figure 1C and 1D). For both dose parameters the dose on the planCT was predictive for the resulting dose on the repeated CT. Mean bone marrow V<sub>10Gy</sub> and V<sub>20Gy</sub>, femoral heads D<sub>mean</sub>, sacrum D<sub>mean</sub> and D<sub>50%</sub> and whole bowel V<sub>15Gy</sub> were markedly lower in both types of IMPT plans compared to VMAT treatment plans (Table 1). IMPT 4F resulted in significantly lower bone marrow V<sub>20Gy</sub> in comparison to IMPT 2F.

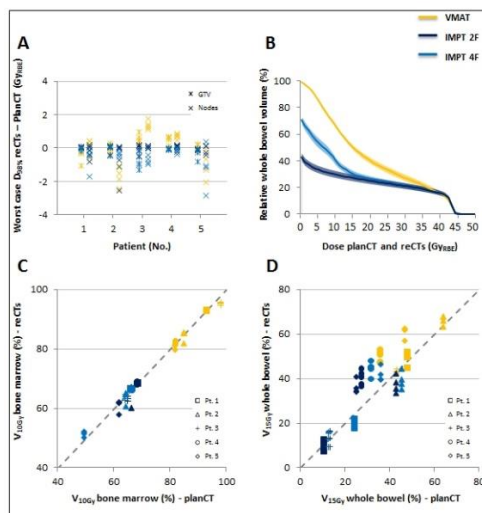


**Figure 1.** Comparison of IMPT two-field (2F), four-field (4F) and VMAT plans for five patients with ITV prescription dose 45 Gy<sub>RBE</sub>. A: Worst case D<sub>98%</sub>GTV and D<sub>98%</sub> nodes (Gy<sub>RBE</sub>) difference between each repeated CT and its corresponding planCT for each patient. B: relative volume (%) vs received dose (Gy<sub>RBE</sub>) for the whole bowel for the plan CT and repeated CTs, the error bands display the standard error. C: V<sub>10Gy</sub> bone marrow (%) repeated CTs vs corresponding planCT. D: V<sub>15Gy</sub> whole bowel (%) repeated CTs vs corresponding planCT. The symbols in Figure 1.C and 1.D represent the different patients.

**Table 1.** Average  $\pm$  SD OAR dose for VMAT, IMPT two-field (2F) and IMPT four-field (4F) evaluations on all 5 planCTs and 25 repeated CTs. For each OAR dose parameter, the results for all 5 patients are combined.

OAR parameter	OAR doses for 5 patients		
	VMAT	IMPT 2F	IMPT 4F
V <sub>10Gy</sub> bone marrow (%)	87.6 $\pm$ 6.0	65.6 $\pm$ 3.2	62.7 $\pm$ 5.7
V <sub>20Gy</sub> bone marrow (%)	66.4 $\pm$ 3.8	54.7 $\pm$ 2.5	40.9 $\pm$ 3.6
D <sub>mean</sub> femoral heads (Gy <sub>RBE</sub> )	20.4 $\pm$ 3.4	6.2 $\pm$ 1.9	8.1 $\pm$ 2.5
D <sub>mean</sub> sacrum (Gy <sub>RBE</sub> )	36.4 $\pm$ 1.7	35.6 $\pm$ 1.0	33.5 $\pm$ 2.1
D <sub>50%</sub> sacrum (Gy <sub>RBE</sub> )	35.9 $\pm$ 1.9	35.8 $\pm$ 1.1	34.1 $\pm$ 3.1
V <sub>15Gy</sub> whole bowel (%)	52.6 $\pm$ 9.7	27.4 $\pm$ 13.7	31.7 $\pm$ 13.3

1. L. K. Meil et al., "Dosimetric predictors of acute hematologic toxicity in cervical cancer patients treated with concurrent cisplatin and intensity-modulated pelvic radiotherapy," *Int. J. Radiat. Oncol.*, vol. 66, no. 5, pp. 1356–1365, Dec. 2006.
2. A.-C. Waldenström et al., "Relative Importance of Hip and Sacral Pain Among Long-Term Gynecological Cancer Survivors Treated With Pelvic Radiotherapy and Their Relationships to Mean Absorbed Doses," *Int. J. Radiat. Oncol.*, vol. 84, no. 2, pp. 428–436, Oct. 2012.
3. A. Ramlov et al., "Risk Factors for Pelvic Insufficiency Fractures in Locally Advanced Cervical Cancer Following Intensity Modulated Radiation Therapy," *Int. J. Radiat. Oncol.*, vol. 97, no. 5, pp. 1032–1039, Apr. 2017.
4. S. Chopra et al., "Predictors of Grade 3 or Higher Late Bowel Toxicity in Patients Undergoing Pelvic Radiation for Cervical Cancer: Results From a Prospective Study," *Int. J. Radiat. Oncol.*, vol. 88, no. 3, pp. 630–635, Mar. 2014.

#### Conclusion

Robustly optimized IMPT treatment plans for cervical cancer patients show equivalent target coverage robustness when compared to VMAT treatment plans, but offer significantly better OAR sparing. Potentially, this could reduce bowel and hematologic toxicity for this young patient population.

#### OC-0306 Using CBCT and VelocityTM Software for delivered dose verification during head and neck radiotherapy

L. Hay<sup>1</sup>, A. Duffton<sup>1</sup>, P. McLoone<sup>2</sup>, E. Miguel<sup>1</sup>, S. Currie<sup>1</sup>, C. Paterson<sup>1</sup>

<sup>1</sup>NHS Greater Glasgow and Clyde, The Beatson West of Scotland Cancer Centre, Glasgow, United Kingdom; <sup>2</sup>The Institute of Health & Wellbeing, University of Glasgow, Glasgow, United Kingdom

#### Purpose or Objective

Anatomical changes during head and neck radiotherapy (RT) can increase dose to OAR and under dose target volumes. On-treatment dose verification with Image Guided RT can aid the reduction of set-up uncertainties, ensuring planned dose is delivered to the correct structures. Currently a mid-treatment (#16) CT2 scan is compared with the initial planning CT (pCT1) to verify dose distribution. IGRT using cbCT and deformable image registration (IR) may allow the development of a process to reduce the number of patients receiving #16CT2 scans during RT. The study aimed to determine the suitability of Velocity<sup>TM</sup> Software in creating synthetic CT (sCT) images for mid-treatment dose verification, in patients receiving RT for locally advanced SCC of the oropharynx.

#### Material and Methods

20 patients treated with VMAT, 65Gy in 30#s, underwent weekly cbCT scans #s 1, 6, 11, 16, 21 and 26, post-treatment. Image registration between the pCT1 and cbCTs was undertaken and the structure set duplicated to the cbCTs. Within Velocity<sup>TM</sup> the pCT1 was deformed with the weekly cbCT volumes, and re-sampled to create a new primary sCT volume, which had the unit values of the pCT1 volume. IR between the cbCT and sCT1 was performed and the structures applied to the sCT volumes. VMAT #16sCT1 plans were re-calculated in Eclipse<sup>TM</sup> applying the pre-set values of the original plan optimisation. #16sCT2 verification plans were generated by the #16cbCT being deformed with the mid-point #16CT2, to compare plan

differences at the same point in the treatment course. The #16sCT1 plans were also compared with #16CT2 plans. pCT and sCT plans were compared for equivalent dose and fractions.

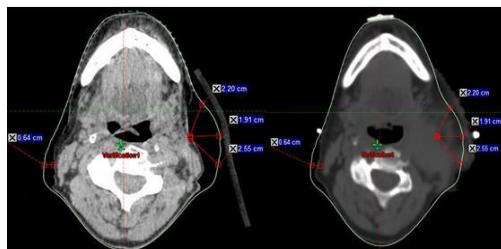
**Results**

D95% to PTV1 was visually comparable between CT and sCT plans. There were no statistically significant differences in the mean cumulative dose difference between sCT and pCT plans for any of the OAR, at the weekly intervals (p<0.05). The #16sCT2 verification plans were comparable with the CT2 verification plans, with no statistically or clinically significant differences in the mean doses between the planning structures (Table 1). There were no statistically or clinically significant differences in the maximum dose to brainstem (p=0.19) or spinal cord (p=0.51) detected between the #16sCT1 and CT2 plans. Mean dose difference between the #16sCT1 and #16CT2 plans for brainstem was 4cGy (SD5.0) and spinal cord 0cGy (SD3.6). Where large contour changes arose through weight loss and mass reduction, visible air gaps between the body structure and skin surface were illustrated on cbCT and Velocity™ overestimated the soft tissue distortion (Figure 1). This occurred where gaps >1-1.5cm were visible.

Table 1: Mean dose (cGy) differences between #16sCT2 and CT2 at fraction 16

PRV Brainstem:	Mean (cGy)	95% Conf. Interval	
Dose sCT	133.0	120.8	149.3
Dose pCT	135.3	120.8	149.8
Difference	-0.2	-4.1	3.7
			p=0.990
PRV Spinal Cord:	Mean	95% Conf. Interval	
Dose sCT	186.4	184.5	188.3
Dose pCT	185.1	184.0	186.2
Difference	1.3	-0.2	2.8
			p=0.409
Contralateral PG:	Mean	95% Conf. Interval	
Dose sCT	88.4	74.9	101.9
Dose pCT	88.9	75.0	102.9
Difference	-0.5	-3.2	2.2
			p=0.70
Ipsi-lateral PG:	Mean	95% Conf. Interval	
Dose sCT	49.3	40.0	58.9
Dose pCT	47.8	39.3	56.3
Difference	1.6	-0.6	3.9
			p=0.1441
PTV1	Mean	95% Conf. Interval	
Dose sCT	217.9	216.7	219.1
Dose pCT	217.9	216.2	219.6
Difference	-0.0	-1.1	1.0
			p=0.9830

Figure 1: Overestimation of tissue by Velocity™



**Conclusion**

It appears feasible for sCTs to be used for dose calculation within Eclipse™ for select patients. Where weekly cbCT indicates large contour changes, a mid-point #16CT2 scan would be recommended. The process may reduce the number of repeat #16CT2 scans required during RT.

**OC-0307 Feasibility of cardiac sparing in isotoxic dose escalated radiotherapy for NSCLC**

L. Turtle<sup>1</sup>, A. Willett<sup>2</sup>, J. Leadbetter<sup>1</sup>, M. Brada<sup>3</sup>, J. Fenwick<sup>3</sup>

<sup>1</sup>Clatterbridge Cancer Centre NHS Foundation Trust, Radiotherapy, Wirral, United Kingdom; <sup>2</sup>Clatterbridge Cancer Centre NHS Foundation Trust, Physics, Wirral, United Kingdom; <sup>3</sup>University of Liverpool, Institute of Translational Medicine, Liverpool, United Kingdom

**Purpose or Objective**

Heart dose-volume constraints used in the planning of NSCLC radiotherapy have not changed greatly in the past two decades, despite increasing evidence that there may

be an association between heart irradiation and decreased survival following treatment. Consequently heart constraints have easily been met in recent trials of dose escalated concurrent CRT for NSCLC, such as the phase I/II isotoxic IDEAL-CRT study in which prescribed doses were the highest possible between 63 and 73Gy while meeting several normal tissue dose constraints. We have therefore carried out a planning study to determine the extent to which heart doses can be reduced without diminishing plan quality, in particular target coverage. Specifically, we investigated the feasibility of reducing mean heart doses, and the volume of left atrial wall receiving doses in excess of 63Gy, both of which have been associated with survival.

**Material and Methods**

20 NSCLC patients planned using 4D-CT were selected for this study (IIIA (n=12) and IIIB (n=8), with an even number of left and right sided tumours), and re-planned following the IDEAL-CRT protocol using a VMAT technique. We identified new target levels for mean heart dose (MHD) and the volume of left atrial wall (LAW) receiving ≥ 63Gy (V<sub>LAW63</sub>). These levels are listed in Table 1 as ambitious, moderate and basic, and were identified from the 20<sup>th</sup>, 50<sup>th</sup> and 80<sup>th</sup> percentiles of treated values reported in related trials. Patients were then re-planned, more highly prioritising heart and LAW dose constraints, and determining the extent to which heart and LAW irradiation could be reduced while still meeting the IDEAL-CRT protocol target dose coverage levels (PTV V98 > 90%; CTV V99 > 95%) and dose constraints on other normal tissues.

**Results**

Table 1 shows numbers of patients (n) achieving the ambitious, moderate and basic levels of the (a) V<sub>LAW63</sub> and (b) MHD constraints, following baseline IDEAL-CRT planning and again after tightening of the V<sub>LAW63</sub> and MHD constraints while continuing to meet all other IDEAL-CRT dose-constraints. After routine IDEAL-CRT planning, 8 patients met the ambitious level for V<sub>LAW63</sub>; however after prioritising constraints on LA Wall irradiation the ambitious level could be achieved for 19/20 patients. Similarly after routine IDEAL-CRT planning the ambitious level for MHD was met for only 3 patients, and 5 failed to meet the basic level; but after prioritising reductions in MHD, the ambitious level was achieved in 8 patients and none failed to meet the basic level.

Table 1a

	V <sub>LAW63</sub> Constraint				
	Constraint Level	Ambitious	Moderate	Basic	Failed
		0%	≤2.2%	≤20%	>20%
	Prescribed Dose (Gy)				
	Median [range]				
IDEAL Baseline	68.8 [63, 73]	n=8	n=8	n=4	n=0
Tighter V <sub>LAW63</sub> planning	68.8 [63, 73]	n=19	n=1	n=0	n=0

Table 1b

	Mean Heart Dose Constraint				
	Constraint Level	Ambitious	Moderate	Basic	Failed
		≤5Gy	≤11Gy	≤20Gy	>20Gy
	Prescribed Dose (Gy)				
	Median [range]				
IDEAL Baseline	68.8 [63, 73]	n=3	n=9	n=3	n=5
Tighter MHD planning	68.8 [63, 73]	n=8	n=8	n=4	n=0

**Conclusion**

By setting more demanding and more highly prioritised heart dose constraints, MHD and LAW doses can be substantially reduced while continuing to meet the target coverage and normal tissue constraints of the IDEAL-CRT protocol, potentially improving survival.

Poster Viewing: Poster viewing 6: Radiobiological modelling and quantitative imaging

**PV-0308 MRI based radiomics improves prognostic assessment in soft tissue sarcoma patients**

J. Peeken<sup>1</sup>, A. Ott<sup>2</sup>, M.B. Spraker<sup>3</sup>, D. Münzel<sup>4</sup>, M. Devecka<sup>1</sup>, A. Thamer<sup>1</sup>, M.A. Shouman<sup>1</sup>, F. Nüsslin<sup>1</sup>, N.A. Mayr<sup>3</sup>, M.J. Nyflot<sup>3</sup>, S.E. Combs<sup>1</sup>

<sup>1</sup>Klinikum rechts der Isar- Technical University of Munich, Department of Radiation Oncology, Munich, Germany; <sup>2</sup>Technical University of Munich, Institut für Medizinische Statistik und Epidemiologie, Munich, Germany; <sup>3</sup>University of Washington, Department of Radiation Oncology, Seattle, USA; <sup>4</sup>Klinikum rechts der Isar- Technical University of Munich, Department of Radiology, Munich, Germany

**Purpose or Objective**

Multimodal therapy involving surgical resection and radiotherapy (RT) is regularly performed in patients with high-grade soft tissue sarcomas (STS) of the extremities and other anatomic sites. While local progression-free survival (LPFS) is high, distant progression-free survival (DPFS) and overall survival (OS) remain comparably low. In this work, we sought to determine whether radiomic analysis of multiparametric MRI carries a prognostic benefit for pre-therapeutic individual risk assessment.

**Material and Methods**

Fat-saturated T2-weighted sequences (T2FS) and contrast-enhanced T1-weighted fat-saturated (T1wFSGd) sequences were collected from two independent retrospective patients cohorts from the Technical University of Munich (TUM: 73 patients) and the University of Washington (UW: 136 patients). Patient records were assessed for demographics, staging and therapy information. After preprocessing, 2052 radiomic features were extracted. Features with a low correlation between a set of independent segmentations were excluded. For feature reduction and model building to predict OS, DPFS and LPFS the least absolute shrinkage and selection operator (LASSO) method was applied to the TUM cohort. External validation was performed on the UW cohort.

**Results**

The LASSO algorithm selected 10, 2, and, 5 features to predict OS, DPFS and LPFS using T1wFSGd-derived radiomic features. Prediction of OS and LPFS achieved better performances (OS: C-index: 0.80 (95% confidence interval: 0.68-0.92), LPFS: C-index: 0.81 (0.66-0.95)) than of DPFS (C-index: 0.65 (0.55-0.75)). All three models showed lower but significant performance in the validation set (OS: C-index: 0.66 (0.56-0.75), LPFS: C-index: 0.65 (0.54-0.77), DPFS: C-index 0.58 (0.50-0.67)). A clinical model performed better for OS (C-index: 0.74 (0.65-0.83)) and DPFS (C-index: 0.70 (0.62-0.79)) but similar for LPFS (C-index: 0.65 (0.53-0.77)) in the validation set. In multivariate cox-regression models accounting for age, grading and TNM staging, the radiomic scores of OS (HR=2.3, p=0.003) and LPFS (HR=3.7, p=0.007) were significantly associated and improved total model performance up to C-indices of 0.78 (0.68-0.87) and 0.69 (0.57-0.80), respectively. A model combining age and AJCC TNM staging groups with the radiomics scores showed a similar performance. T2FS-based radiomic phenotypes showed overall lower prognostic capabilities (validation set: OS: C-index: 0.61 (0.50-0.72), LPFS: C-index: 0.58 (0.45-0.72), DPFS: C-index: 0.57 (0.44-0.66)). Combining both MRI sequences did not effect an incremental benefit.

**Conclusion**

We first show that a T1-based radiomic phenotype is able to improve prognostic assessment above clinical staging and independent of the T2-based radiomic phenotype for OS and LPFS. As consequence, the radiomics analysis can be simplified by focusing on the T1wFSGd sequence. Such a radiomic phenotype may help to personalize sarcoma therapy above the current clinical staging system.

**PV-0309 Pretreatment ADC does not predict local recurrences in head and neck squamous cell carcinoma**

B. Peltenburg<sup>1</sup>, J. Driessen<sup>2</sup>, J. Vasmel<sup>1</sup>, R. De Bree<sup>3</sup>, C. Terhaard<sup>1</sup>, M. Philippens<sup>1</sup>

<sup>1</sup>UMC Utrecht, Radiotherapy, Utrecht, The Netherlands; <sup>2</sup>UMC Utrecht, Otorhinolaryngology, Utrecht, The Netherlands; <sup>3</sup>UMC Utrecht, Head and Neck Surgical Oncology, Utrecht, The Netherlands

**Purpose or Objective**

In head and neck squamous cell carcinoma, pretreatment identification of radio-insensitive tumors would affect treatment planning. ADC has been reported to be a predictor of local recurrence. However, correction for known clinical parameters such as tumor volume has rarely been performed. The aim of this study is to find the added value of ADC to tumor volume in predicting local recurrence.

**Material and Methods**

This retrospective cohort study included 217 patients with T2-T4 oral cavity, oropharyngeal, laryngeal or hypopharyngeal squamous cell carcinoma. All patients were treated with (chemo)radiotherapy, prior to treatment an MRI examination was performed. The tumor delineation procedure was semi-automatic. First, a seed point was placed in the tumor on the axial DW-MRI with the highest available b value (800 or b1000 s/mm<sup>2</sup>) and with a maximum intensity threshold of 50% the tumor was segmented. The delineation was transferred to the ADC map and high intensity areas at the edges of the segmentation were manually removed. The variables obtained from this segmentation were median ADC and total volume. The predictive effect of the variables on local recurrence was analyzed in univariable and multivariable regression.

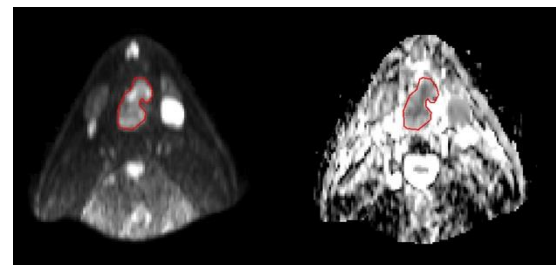
**Results**

Univariable analysis showed no significant correlation between tumor ADC and local control within three years after (chemo)radiotherapy. However, tumor volume was predictive for local recurrence. Multivariable cox regression including ADC and volume showed that tumor volume was an independent predictor of local recurrence with a hazard ratio of 1.032 (CI95% 1.020 - 1.044). ADC was not an independent predictor of local recurrence.

**Conclusion**

ADC has no added value in predicting local control in patients with HNSCC. Tumor volume, however, is predictive of recurrence.

Figure 1: Example of the delineation of a T3N2cM0 oropharyngeal carcinoma. Left: Diffusion weighted image (b800 s/mm<sup>2</sup>). Right: Corresponding ADC map.



**PV-0310 A field strength independent MR radiomics model for pathological complete response in rectal cancer**

D. Cusumano<sup>1</sup>, G. Meijer<sup>2</sup>, J. Lenkowicz<sup>3</sup>, G. Chiloiro<sup>3</sup>, L. Boldrini<sup>3</sup>, C. Masciocchi<sup>3</sup>, N. Dinapoli<sup>4</sup>, R. Gatta<sup>3</sup>, C. Casà<sup>3</sup>, A. Damiani<sup>3</sup>, B. Barbaro<sup>3</sup>, G. Maria Antonietta<sup>4</sup>, L. Azario<sup>1</sup>, M. De Spirito<sup>4</sup>, M. Intven<sup>2</sup>, V. Vincenzo<sup>3</sup>

<sup>1</sup>Fondazione Policlinico Universitario A.Gemelli IRCCS, U.O.C. Fisica Sanitaria- Dipartimento di Diagnostica per immagini- Radioterapia Oncologica ed Ematologia, Roma, Italy; <sup>2</sup>University Medical Center Utrecht,

Department of Radiotherapy, Utrecht, The Netherlands ;  
<sup>3</sup>Università Cattolica del Sacro Cuore, Istituto di Radiologia, Roma, Italy ;  
<sup>4</sup>Fondazione Policlinico Universitario A.Gemelli IRCCS, U.O.C. Radioterapia Oncologica- Dipartimento di Diagnostica per immagini- Radioterapia Oncologica ed Ematologia, Roma, Italy

### Purpose or Objective

Magnetic Resonance Imaging (MRI) is a complex and extreme versatile imaging technique. This may potentially jeopardize the generalizability of radiomics of images acquired with different field strengths and scan protocols. Aim of this study was to develop a generalized radiomics model for predicting pathological complete response (pCR) after neoadjuvant chemo-radiotherapy (CRT) in locally advanced rectal cancer (LARC) patients (pts) using pre-CRT T2-weighted (T2-w) images acquired at a 1.5 T and a 3 T scanner.

### Material and Methods

In two institutions 195 patients were scanned with a T2-weighted imaging protocol. In institution A 142 patients were scanned on a 1.5 T MR scanner (GE Signa Exite, Little Chalfont, United Kingdom) whereas in institution B 59 pts were scanned on a 3-T MR-scanner (Philips Medical System, Eindhoven, The Netherlands).

The heterogeneity between the two cohorts of pts was evaluated in terms of Wilcoxon Mann Whitney (WMW) and Pearson's  $\chi^2$  test.

Gross Tumor Volumes (GTV) were delineated on the MR images and all the images were resampled to a fixed spatial planar resolution of 0.7x0.7 mm<sup>2</sup> before to perform features extraction.

A total of 225 radiomic features belonging to four families (fractal, statistical, textural and morphological features) were extracted, applying two image filters (Laplacian of Gaussian (LOG) and Intensity Based (IB)). Features were standardized with Z-score normalization and an initial feature selection was carried out using WMW test: the most significant features at 1.5 T and 3 T were selected as main features.

Several logistic regression models combining the main features with a third one selected by those resulting significant in both datasets were elaborated and evaluated in terms of Area Under Curve (AUC) of the Receiver Operative Curve (ROC).

Features that combined together maximised the AUC value and minimised the Aikake Information Criteria (AIC) were selected. A 10-fold cross validation was repeated 300 times to evaluate the model robustness.

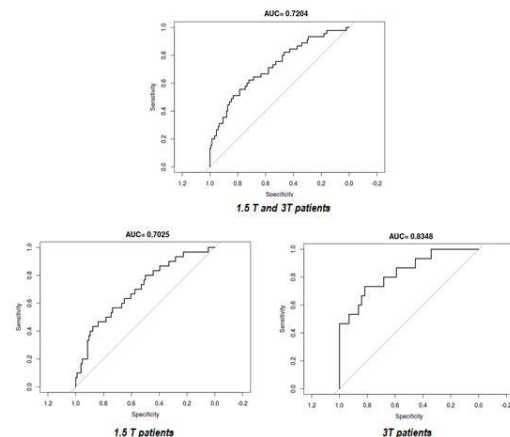
### Results

Table 1 reports the clinical characteristics: no statistical difference was observed between the two cohorts of patients demonstrating matched populations.

Table 1. Patients (pts) characteristics and descriptive statistics of variables in the cohort of 1.5 T and 3T patients. For statistical test were used the Pearson's  $\chi^2$  test ( $\chi^2$  test) for categorical variables and the Mann-Whitney Test (MW test) for continuous ones.

Patient Characteristics		1.5 T pts		3 T pts		p-values of differences		
		Mean	Range	Mean	Range	$\chi^2$ test	MW test	
Age	M	64	28-84	63	40-79	-	0.57	
	F	61.9	43-80	64	49-76	-	0.69	
Age (overall)		63.0	28-84	63	40-79	-	0.87	
Clinical Characteristics		N	%	N	%	$\chi^2$ test	MW test	
Response	pCR	30	22	15	25	0.74	-	
	not pCR	106	78	44	75			
Stage	cT	3	89	65	49	83	0.13	-
		4	47	35	10	17		
	cN	0	6	4	2	3	0.44	-
		1	43	32	5	8		
	2	87	64	52	88			

Three features were selected based on their performance: maximum fractal dimension with IB=0-50, energy and grey level non uniformity calculated on the run length matrix with IB=0-50. Figure 1 reports the ROC curves of the model: the AUC of the model tested on the whole dataset after cross-validation was 0.72, while 0.70 and 0.83 were obtained when only 1.5T and 3T patients were respectively considered.



### Conclusion

A MR radiomics prediction model for pCR after neoadjuvant therapy in locally advanced rectal cancer was developed. The model showed good performance, even when data from patients scanned on 1.5T and 3.0T were merged. This shows that magnetic field intensity variability can be overcome by means of selecting appropriate images features.

### PV-0311 MRI-based tumour control probability model in particle therapy

G. Buizza<sup>1</sup>, S. Molinelli<sup>2</sup>, E. D'ippolito<sup>3</sup>, G. Fontana<sup>4</sup>, L. Anemoni<sup>5</sup>, L. Preda<sup>6</sup>, G. Baroni<sup>1</sup>, F. Valvo<sup>3</sup>, C. Paganelli<sup>1</sup>  
<sup>1</sup>Politecnico di Milano, DEIB - Department of Electronics Information and Bioengineering, Milano, Italy ;  
<sup>2</sup>National Centre of Oncological Hadrontherapy CNAO, Medical Physics Unit, Pavia, Italy ;  
<sup>3</sup>National Centre of Oncological Hadrontherapy CNAO, Radiation Oncology Unit, Pavia, Italy ;  
<sup>4</sup>National Centre of Oncological Hadrontherapy CNAO, Clinical Bioengineering Unit, Pavia, Italy ;  
<sup>5</sup>National Centre of Oncological Hadrontherapy CNAO, Medical Radiology Technicians

Unit, Pavia, Italy; <sup>6</sup>National Centre of Oncological Hadrontherapy CNAO, Diagnostic Imaging Unit, Pavia, Italy

### Purpose or Objective

To estimate a tumour control probability (TCP) model from a group of patients affected by skull-base chordoma and treated with C-ions radiotherapy (CIRT), integrating information from diffusion-weighted (DW-) MRI.

### Material and Methods

From 2013 to 2016, 59 patients were enrolled for CIRT (70.4 GyE total prescribed dose) and 20 of them underwent a pre-treatment harmonized imaging protocol, including DW-MRI scan (b-value=50,400,1000 s/mm<sup>2</sup>). Local control (LC) was clinically assessed at a median follow-up time of 45.8 months as a binary variable, which was found to relate to D<sub>98</sub> (the maximum dose received by at least 98% of the volume) in the target. Survival fraction was defined by the linear-quadratic (LQ) formalism and the probability of killing was assumed to be Poissonian, thus following a classical analytical formulation of the TCP. The linear LQ parameter,  $\alpha$ , was obtained by setting the population TCP to 79%, which corresponds to the LC for all the chordoma patients treated at the facility, and by fitting an average TCP based on D<sub>98</sub>;  $\beta$  was set to 0 to account for the in-vitro experiments. Apparent diffusion coefficient (ADC) maps were computed from DW-MRI and converted into cellular density (cells/cm<sup>3</sup>) by using a relationship found in a histology-based study [1]. Therefore, two types of TCP, one based on ADC (TCP<sub>ADC</sub>) and one based on parameters from the literature (TCP<sub>LIT</sub>), were computed for each patient and their diagnostic performance with respect to LC was evaluated through a ROC curve analysis.

### Results

TCP<sub>ADC</sub> and TCP<sub>LIT</sub> were found to agree with the relation between LC and D<sub>98</sub>, showing a good fitting performance (R<sup>2</sup>=0.981 and R<sup>2</sup>=0.976), and the first being more conservative in estimating patients' TCP values (Fig.1). ROC curves (Fig.2) identified the same sensitivity (0.867) and specificity (0.600) and the same optimal threshold, at which the pointwise confidence bounds at 95% confidence were CI<sub>95%</sub>=[0.539 1] and CI<sub>95%</sub>=[0.625 1] for TCP<sub>ADC</sub> and TCP<sub>LIT</sub>, respectively. This allows to state the significant difference from the random performance but not between the two models.

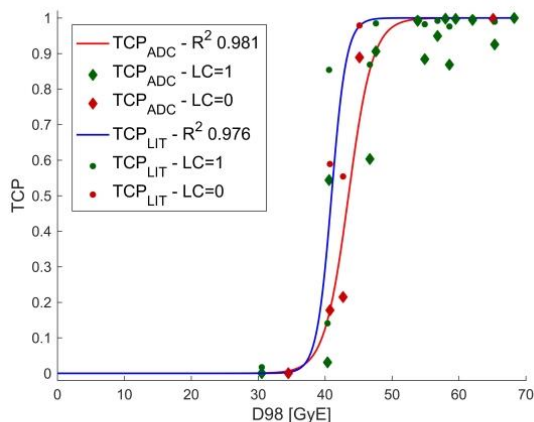


Figure 1 – TCP<sub>ADC</sub> (red) and TCP<sub>LIT</sub> (blue) curves with the respective datapoints (diamonds and dots), for patients with positive (green) and negative (red) LC, with respect to D<sub>98</sub> expressed in [GyE].

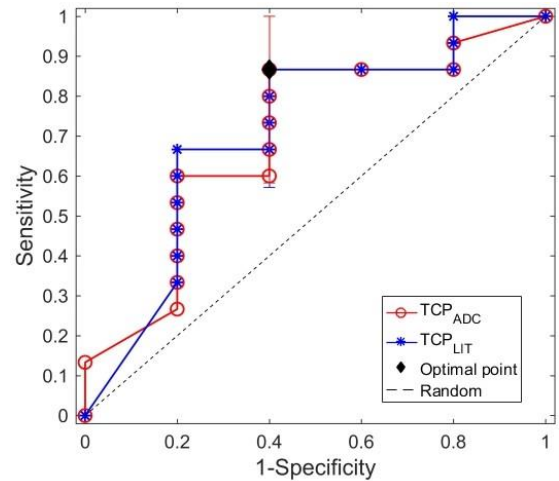


Figure 2 – ROC curves for TCP<sub>ADC</sub> (red) and TCP<sub>LIT</sub> (blue) models, with pointwise confidence intervals reported at the point (black diamond) with the best trade-off between specificity and sensitivity. The line describing random performance is shown as well.

### Conclusion

Two TCP models were obtained for a homogeneous group of patients, as for dose prescription, and they were both found to agree with clinically assessed LC. In particular, DW-MRI has confirmed to be a promising tool to predict the outcome in particle therapy, when coupled to dose information. Nevertheless, a more robust relationship between ADC and tissue microstructure is needed before DW-MRI usefulness can be established.

### Bibliography:

[1] D.T. Ginat, R. Mangla, G. Yeane, M. Johnson, and S. Ekholm, "Diffusion-weighted imaging for differentiating benign from malignant skull lesions and correlation with cell density," *Am. J. Roentgenol.*, vol. 198, no. 6, pp. 597-601, 2012.

### PV-0312 Distributed learning in radiomics to predict overall survival in head and neck cancer

M. Bogowicz<sup>1,2</sup>, A. Jochems<sup>2</sup>, S.H. Huang<sup>3</sup>, B. Chan<sup>3</sup>, J.N. Waldron<sup>3</sup>, B. O'Sullivan<sup>3</sup>, S. Tanadini-Lang<sup>1</sup>, O. Riesterer<sup>1,4</sup>, G. Studer<sup>1,5</sup>, J. Unkelbach<sup>1</sup>, R.H. Brakenhoff<sup>6</sup>, I. Nauta<sup>6</sup>, S.E. Gazzani<sup>7</sup>, G. Calareso<sup>8</sup>, K. Scheckenbach<sup>9</sup>, F. Hoebbers<sup>10</sup>, S. Barakat<sup>2</sup>, S. Keek<sup>2</sup>, S. Sanduleanu<sup>2</sup>, M. Vergeer<sup>11</sup>, R.C. Leemans<sup>6</sup>, C.H. Terhaar<sup>12</sup>, M.W. Van den Brekel<sup>13</sup>, M. Guckenberger<sup>1</sup>, P. Lambin<sup>2</sup>

<sup>1</sup>University Hospital Zurich and University of Zurich, Radiation Oncology, Zurich, Switzerland ; <sup>2</sup>GROW - School for Oncology and Developmental Biology- Maastricht University Medical Centre-, The D Lab: Decision Support for Precision Medicine-, Maastricht, The Netherlands ; <sup>3</sup>Princess Margaret Cancer Center- University of Toronto, Department of Radiation Oncology, Toronto- Ontario, Canada ; <sup>4</sup>Kantonsspital Aarau, Center for Radiation Oncology- KSA-KSB-, Aarau, Switzerland ; <sup>5</sup>Cantonal Hospital Lucerne, Institute for Radiation Oncology, Lucerne, Switzerland ; <sup>6</sup>VU University Medical Center, Department of Otolaryngology/Head and Neck Surgery, Amsterdam, The Netherlands ; <sup>7</sup>Parma University Hospital, Radiology department, Parma, Italy ; <sup>8</sup>IRCCS Fondazione Istituto Nazionale dei Tumori, Radiology Department, Milan, Italy ; <sup>9</sup>University Hospital Duesseldorf- Heinrich Heine University, Department of Otorhinolaryngology & Head/Neck Surgery, Duesseldorf, Germany ; <sup>10</sup>GROW- School for Oncology and Developmental Biology- Maastricht University Medical Centre, Department of Radiation Oncology, Maastricht, The Netherlands ; <sup>11</sup>VU University Medical Center, Department of Radiation

Oncology, Amsterdam, The Netherlands ; <sup>12</sup>University Medical Center Utrecht, Department of Radiotherapy, Utrecht, The Netherlands ; <sup>13</sup>The Netherlands Cancer Institute, Department of Head and Neck Oncology and Surgery, Amsterdam, The Netherlands

### Purpose or Objective

Radiomics has been shown a promising prognostic biomarker for different tumor types. However, one of the major challenges in radiomics is collection of data from large, preferably multicenter cohorts, which is important for reliable model training. Sharing data between the hospitals is restricted by legal and ethical regulations. Distributed learning is a technique to train models on multicenter data without data leaving the hospitals. In this study we tested the feasibility of distributed learning with radiomics data in the context of overall survival prediction in head and neck cancer patients.

### Material and Methods

Pretreatment, contrast-enhanced CT images were collected from 1005 head and neck cancer patients in 5 different centers Tab. 1. All patients underwent definitive radiochemotherapy. 981 radiomic features were extracted from the tumor region using Z-Rad software implementation. Two years overall survival was chosen as endpoint. For comparison, both feature selection and final classification was performed in a centralized and distributed manner. Five different models were trained, four datasets were always used for training while one of the datasets was left out for validation. The maximum relevance minimum redundancy (MRMR) method was used in the feature selection step. The MRMR was performed over 100 bootstrap samples, but in the distributed setting the selection rate was averaged over the different datasets. The final models for 2y-OS was trained with logistic regression. For the distributed solution the grid binary logistic regression was implemented. In the validation dataset, the receiver operating characteristics were compared between the models trained in the centralized and distributed manner using DeLong test ( $p < 0.05$ ). Additionally, patients were split into two risk groups based on median prediction from the training cohort and the misclassification error rate between the centralized and distributed models was calculated.

	center	A	B	C	D	E
	number of patients	176	441	100	147	141
HPV	positive	58	274	23	8	0
	negative	82	116	77	28	141
	unknown	36	51	0	111	0
subtype	oropharynx	113	441	100	81	63
	hypopharynx	37	0	0	10	47
	larynx	16	0	0	12	31
	oral cavity	10	0	0	44	0

Table 1. Patient characteristic

### Results

In the centralized training, 16-18 features were selected in the MRMR step. 7-11 features were selected in distributed setting, but 78-100% of those features overlapped with features selected centrally. Fig. 1 shows the area under the curve (AUC) for models trained in the centralized and distributed manner. No difference was observed between AUC for models with features selected with two methods, indicating no loss of prognostic power with smaller feature set. Also, final logistic regression coefficients resulted in similar predictions for both methods. No significant difference in AUC was observed. The misclassification rate was 5-12% and considered only patients close to splitting threshold. For the center E model validated poorly, however these was a subgroup of solely HPV negative patients.

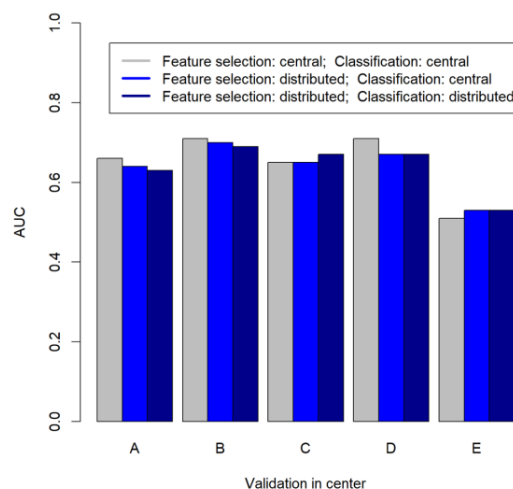


Fig 1. Area under receiver operating characteristic (AUC) for a logistic regression models in the validation cohort. No significant difference was observed between models trained in central and distributed manner.

### Conclusion

We have shown that both feature selection and classification are feasible in distributed manner for radiomics data. This opens new possibility for training more reliable radiomics models by gaining access to larger multi-institutional data.

**PV-0313 Ventilation functional lung volumes obtained from SPECT and 4D-CT do not identify the same voxels.**  
T. Nyeng<sup>1</sup>, L. Hoffmann<sup>1</sup>, K.P. Farr<sup>2</sup>, A.A. Khalil<sup>2</sup>, C. Grau<sup>2</sup>, D.S. Møller<sup>1</sup>

<sup>1</sup>Aarhus University Hospital, Medical Physics Department of Oncology, Aarhus C, Denmark; <sup>2</sup>Aarhus University Hospital, Department of Oncology, Aarhus C, Denmark

### Purpose or Objective

Several imaging modalities are available to obtain functional lung (FL) information. The overall lung toxicity may be decreased by reducing dose to the highly functional lung tissue during radiotherapy (RT), at the expense of added dose to the less functional lung regions. Recently, methods using 4D-CT and deformable registration have been shown to produce a map of ventilated lung regions. We have compared 4D-CT derived ventilation volumes with SPECT derived ventilation volumes, generally considered the gold standard for lung ventilation imaging.

### Material and Methods

Seventeen non-small cell lung cancer patients had a 4D-CT scan (10 bins phase sorted), and a ventilation SPECT-CT (V-SPECT) scan prior to RT treatment. For each patient, the total lung volume ( $V_{LUNG}$ ) was delineated on the exhale phase of the 4D-CT (4D-ex) and on the CT-part of the V-SPECT. The inhale and exhale phases of the 4D-CT were deformably registered using a free form intensity based deformable registration algorithm (DRA) (MIMv6.7) and the Jacobian determinant of the deformation matrix was used to segment expanding regions within the  $V_{LUNG}$ . The best ventilated third of the lungs ( $V_{FL-4D}$ ) was segmented and transferred to the 4D-ex. The best ventilated third of the lungs as defined using the V-SPECT ( $V_{FL-SPECT}$ ) was also segmented. The V-SPECT was then deformably registered to the 4D-ex, using the same DRA.  $V_{FL-SPECT}$  was propagated to the 4D-ex and the two FL volumes were compared in terms of overlap fraction (OF) with respect to  $V_{FL-SPECT}$ ,  $(V_{FL-SPECT} \cap V_{FL-4D}) / V_{FL-SPECT}$ . The fraction of the total lung volume indicated as inferiorly functional by both methods,  $V_{non-FL-SPECT}$  and  $V_{non-FL-4D}$ , was calculated as  $(V_{non-FL-SPECT} \cap V_{non-FL-4D}) / V_{LUNG}$ .

**Results**

The employed 4D-CT phases were of an acceptable quality. A few patients had breathing motion artefacts close to the diaphragm. The DRA performed well in regions of reasonable image contrast. Some patients with very low contrast lung regions showed several deformation artefacts influencing the FL segmentation especially near the diaphragm. The V-SPECT segmentations also often indicated regions near the diaphragm. The  $V_{LUNG}$  varied widely, with a median volume [range] on the 4D-ex of  $3159\text{cm}^3$ [2093-5446] (see Table1). The two segmented FL volumes for each patient were comparable in size, with a median difference between the two volumes ( $V_{FL-SPECT}-V_{FL-4D}$ ) of  $33\text{cm}^3$ [-80-142] (see Figure 1a). The median OF of the two volumes was 38%[27%-69%]. The volume of lung indicated as inferiorly functional by both methods, corresponded to a median 47%[42-58] of  $V_{LUNG}$  (see Figure1b).

**Conclusion**

The ventilation FL segmentations obtained using 4D-CT and V-SPECT did not identify the same lung voxels. However, though the overlap of the two FL volumes was low, the two methods indicated the same general areas as inferiorly functional. It is possible that the 4D-CT ventilation FL segmentations may highly depend on the quality of the 4D-CT scans and the quality of the deformation in low contrast areas.

Patient	Total lung volume [cm <sup>3</sup> ]	$V_{FL-SPECT}$ [cm <sup>3</sup> ]	$V_{FL-4D}$ [cm <sup>3</sup> ]	Volume difference [cm <sup>3</sup> ]	FL overlap [cm <sup>3</sup> ]	FL union [cm <sup>3</sup> ]	NonFL relative to total lung [%]	OF
1	5338	1630	1771	142	699	2701	49	0.43
2	3159	995	1055	60	431	1618	49	0.43
3	3358	1141	1117	-24	560	1697	49	0.49
4	3437	1100	1146	46	387	1860	46	0.35
5	5446	1844	1814	-30	790	2868	47	0.43
6	2785	908	930	22	327	1511	46	0.36
7	2207	704	737	33	311	1129	49	0.44
8	2093	710	698	-13	232	1177	44	0.33
9	2554	929	849	-80	308	1470	42	0.33
10	2497	866	835	-31	396	1305	48	0.46
11	4050	1319	1355	36	400	2275	44	0.30
12	4355	1365	1452	88	370	2447	44	0.27
13	3832	1177	1277	100	414	2039	47	0.35
14	2746	891	911	21	377	1425	48	0.42
15	2490	844	829	-15	317	1356	46	0.38
16	5146	1676	1710	34	642	2745	47	0.38
17	2508	721	833	112	499	1055	58	0.69
<b>Median</b>	<b>3159</b>	<b>995</b>	<b>1055</b>	<b>33</b>	<b>396</b>	<b>1618</b>	<b>47</b>	<b>0.38</b>

**Table 1:** Functional lung (FL) volume statistics for all 17 patients. All volumes are measured on the 4D-CT exhale phase. The FL volume difference is calculated relative to the V-SPECT FL volume. The overlap and union of the FL volumes are denoted FL overlap and FL union respectively. The inferiorly functional lung volume (nonFL) is the total lung volume minus FL union, relative to the total lung volume. The overlap fraction is  $(V_{FL-SPECT} \cap V_{FL-4D}) / V_{FL-SPECT}$ .

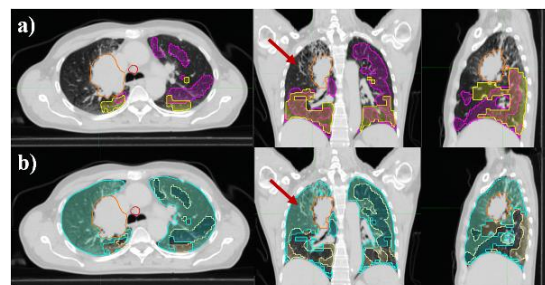


**Figure 1.** Orange = GTV tumour; Red = GTV lymph node; a) Yellow = FL as defined by ventilation SPECT-CT; Magenta = FL as defined by 4D-CT. The two methods do not define the same voxels and the OF is 0.43 for this patient. b) Cyan = Lung volume minus SPECT-CT FL; Sand = Lung volume minus 4D-CT FL. The large contiguous area in the top right lung (red arrow) is indicated by both methods as inferiorly-functional. The total volume indicated as non-functional by both methods, corresponds to 49% of the total lung volume for this patient.

**PV-0314 Machine learning helps identifying relations and confounding factors in radiomics-based models**  
 A. Traverso<sup>1,2</sup>, M. Kazmierski<sup>1</sup>, L. Wee<sup>1</sup>, A. Dekker<sup>1</sup>, M. Welch<sup>2</sup>, A. Hosni<sup>3</sup>, D. Jaffray<sup>2</sup>, A. Hope<sup>3</sup>

<sup>1</sup>Maastricht Radiation Oncology Maastricht Clinic, Radiotherapy, Maastricht, The Netherlands; <sup>2</sup>Princess Margaret Cancer Centre, Radiation Physics, Toronto, Canada ; <sup>3</sup>Princess Margaret Cancer Centre, Radiation Oncology, Toronto, Canada

**Purpose or Objective**

Imaging biomarkers derived from computed tomography (CT) scans (“radiomics”) have been used to generate predictive models for clinical outcomes such as overall survival (OS) following radiation therapy. Models based on imaging features have been shown to achieve similar performance to traditional models based on semantic features (e.g. tumor volume and staging). However, several challenges remain including: generalizability and reproducibility of radiomics-based models, risk of overfitting due to high number of model covariates, and strong correlations between features and clinical variables. These issues limit usage of radiomics-based prediction models in decision support systems. In our study, we applied unsupervised and supervised learning techniques to investigate the relationships between radiomics features, clinical features, and clinical outcomes with a special focus on the relationship between radiomics features and tumor volume.

**Material and Methods**

We used two publicly available datasets: 420 Non Small Cell Lung Cancer patients and 130 Squamous Cell Carcinoma oropharynx patients. CT scans, manually delineated GTV (Gross Tumor Volumes), clinical variables were available. Radiomics features were extracted from GTVs using the open source Pyradiomics library. Hierarchical clustering was used to discover groups of patients with similar radiomic signatures. Dependencies between radiomics features and tumor volume were evaluated with the Spearman concordance correlation coefficient ( $\rho$ ). Overall survival was compared between clusters using Kaplan-Meier analysis. Tumor volume distributions were also compared. Bootstrap-based methods were used to evaluate the stability and importance of radiomic features in predicting 2-year OS.

**Results**

As shown in Figure1A, it is possible to identify two groups of patients with different OS by using all radiomics features. However, when only using volume-independent features ( $\rho < 0.2$ ) the groups cannot be distinguished (1B). PCA (1C) revealed that tumour volume is highly correlated with the first and second dimensional PCA, which explains the higher variability in the data. Semantic features and volume explained most of OS variability in both datasets (1D).

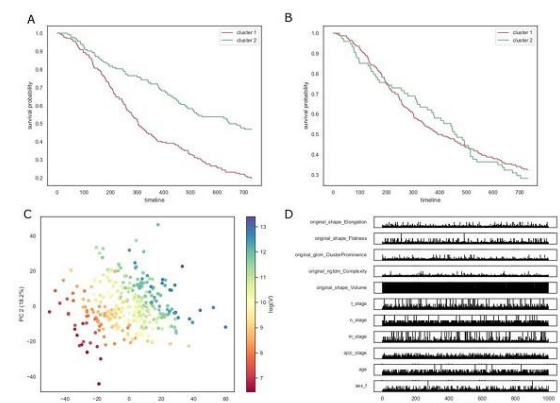


**Figure 1.** 2-year OS in patients clustered by A) full set of radiomic features B) volume-independent features ( $\rho < 0.2$ ). C) shows the patient radiomic signatures projected on first 2 principal components and colored by volume. D) shows the relative importance of covariates in a logistic regression model of 2-year OS across bootstrap resamples (higher bar indicates greater importance in a particular resample).

**Conclusion**

We demonstrated a significant dependence of radiomic features on tumor volume in lung and head & neck CT images. Volume could be reconstructed as a linear combination of even moderately correlated features. Volume-independent features did not show substantial discriminating power. We highlight the importance of accounting for the volume effect when evaluating the predictive performance of imaging biomarkers. Unsupervised and supervised machine learning techniques provide powerful tools to investigate the robustness of radiomics models and relations / redundancies with clinical features.

**PV-0315 A risk assessment method including credible intervals for lymphatic metastatic spread for HNSCC**

B. Pouymayou<sup>1</sup>, O. Riesterer<sup>1</sup>, M. Guckenberger<sup>1</sup>, J. Unkelbach<sup>1</sup>  
<sup>1</sup>Universitätsspital Zürich, Radiation Oncology, Zürich, Switzerland

**Purpose or Objective**

When treating head and neck squamous cell carcinoma (HNSCC) with radiotherapy, a large portion of the CTV aims at a prophylactic irradiation of the lymph node levels (LNL) at risk of harboring microscopic tumor despite the absence of visible metastases on imaging. We present a statistical model to estimate a probability range of ipsilateral microscopic involvement of LNL based on the patient's observed state of tumor progression, i.e. the location of metastases detected in imaging.

**Material and Methods**

We apply Bayesian Networks (BN) to model tumor progression. Each LNL is associated with 2 binary random variables (nodes on Fig. 1), the first corresponding to the hidden microscopic state of involvement and the second to the observable macroscopic state, i.e. whether metastases are detected on imaging for a LNL. The relationship between these two states is given by the sensitivity and specificity of the imaging modality.

The model assumes that tumor cells can spread directly from the primary tumor (PT) to a LNL or from one LNL to the next. The possible spreading paths are given by the graph of the BN and are depicted by arrows on Fig. 1. In this work, we investigate ipsilateral lymphatic spread (levels Ib to IV) for oropharyngeal (T1-T2) tumors. For learning the BN network parameters, we reconstructed a training data set of 103 cases from a published neck dissection series [1]. To assess parameter accuracy, we apply multinomial parameter learning (MPL) [2] to estimate the posterior distribution of parameters. An inference algorithm retrieves the probabilities of microscopic involvement of LNL, given the observed macroscopic involvement.

**Results**

Fig. 1 shows the BN model together with the posterior distribution over the parameters describing lymphatic spread. For example, p02 is the probability of the primary tumor to spread to LNL II, and p23 is the probability to spread from II to III. As a result, we can define credible intervals (CI) similar to confidence intervals. We construct 3 models describing the microscopic spread: one where all the parameters are set to the CI lower bounds, one where they are set to the expectation of the distribution and one where they are set to the upper CI bound. Fig. 2 summarizes the ranges of microscopic risk of involvement for each LNL and different scenarios. For example, even for the most pessimistic model, the probability of microscopic involvement of level IV despite negative finding on imaging does not exceed 10% as long as level III is not harboring macroscopic metastases.

**Conclusion**

Bayesian networks provide a framework for combining patient characteristics with population based patterns of lymphatic progression and thereby guide an individualized

CTV definition. We present a model that addresses the limitations of small size datasets by providing a range of risks of microscopic involvement.

**References:**

- [1] G. Sanguineti et al, IJROBP, V. 74(5), p.1356-64, 2009
- [2] Y. Zhou et al, Int. J. of Approximate Reasoning, V. 55(5), p. 1252-1268, 2014

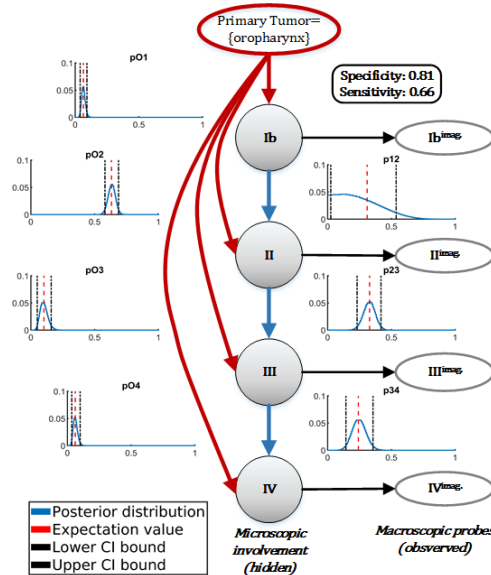


**Figure 1:** Bayesian Network modeling the microscopic ipsilateral spread (level Ib to IV) of an oropharyngeal primary tumor. The posterior distribution of the microscopic spread parameters are reported in blue, the expectation value in red and the boundaries of the credible interval (CI) containing 95% of the probability density in black. The sensitivity and the specificity of the macroscopic (e.g. imaging) are fixed.

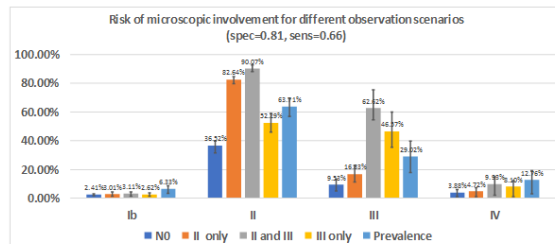


**Figure 2:** Probability of microscopic involvement at level II, III and IV given different combinations of macroscopically involved LN levels, assuming a primary tumor in the oropharyngeal region. Percentages are reported for the model built with the parameter expectation values. The lower and upper error bars report the predictions of the models built with the parameter lower and upper CI bounds, respectively. Prevalence refers to the probability of microscopic involvement without any macroscopic observation except for the primary tumor.

**PV-0316 Deep Learning Based Automatic Grading of Colon Cancer in Digitized Histopathology Images**

S. Chen<sup>1</sup>, J. Wang<sup>1</sup>, W. Hu<sup>1</sup>, Z. Zhang<sup>1</sup>, M. Zhang<sup>2</sup>, M. Xu<sup>2</sup>, D. Huang<sup>2</sup>, W. Sheng<sup>2</sup>  
<sup>1</sup>Fudan University Shanghai Cancer center, Radiation Oncology, Shanghai, China ; <sup>2</sup>Fudan University Shanghai Cancer center, Pathology, Shanghai, China

**Purpose or Objective**

The status of tumor differentiation is a crucial reference for cancer diagnosis and prognostication. However, the tumor differentiation grading can be difficult and time-consuming for pathologists. In this study we manage to use deep learning algorithm to automatic grading colon cancer.

**Material and Methods**

The workflow was presented in figure 1. 169 whole slide images (WSI) were enrolled into this study. These data were come from The Cancer Genome Atlas (TCGA). Two-

thousand-three-hundred-ninety rectangle regions were selected and annotated by pathologist with four categories including normal tissue, low, middle and high differentiation tumor. A convolutional neural networks (CNN) model which is similar to Xception model structure was used to training. Briefly, 256 \* 256 pixels' small patches with 40x magnification were extracted from WSI and assigned to their category. In model training, 152(90%) WSI images were used for training and 17 (10%) WSI images were used for validation. The initial learning rate is 1e-4 and the optimization algorithm is Adam. Each epoch has 1000 batches; each batch have 32 patches. The learning rate will decrease 10 times after every 150 epochs. An additional test WSI, which was not enrolled in model training and validation, was selected for demonstration our model's results.

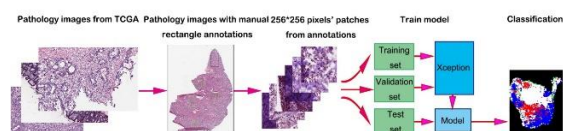


Fig1. Workflow of our current works.

## Results

The results were presented in table 1. The category accuracy of predicting small patch was 81.6% for training set and 79.6% for validation set. The model has consumed 8 days to research this accuracy. Figure 2 demonstrated a results of test WSI.

Table.1 Performance (accuracy) of model for series classes.

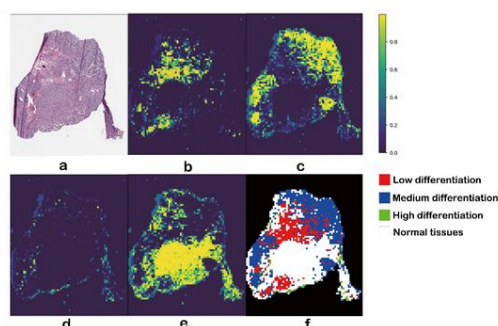


Figure 2. The pathology images and category heatmaps. a. Origin pathology image; b. Low differentiation; c. Medium differentiation; d. High differentiation; e. Normal tissue. f. Result of classification

## Conclusion

Our model can precisely distinguish tumor and normal tissue on small patches. The accuracy for single WSI may further improve by combining these patches results. And deep-learning model can assist pathologists in the detection cancer differentiation. Meanwhile it can be used for prognosis prediction and assist decision making in the future study.

Proffered Papers: BT 4: Breast and Skin brachytherapy

## OC-0317 2nd Conservative Treatment for 2nd Breast Tumor Event: GEC-ESTRO Breast Cancer WG updated results

J. Hannoun-Levi<sup>1</sup>, K. Daniele<sup>2</sup>, G. Benjamin<sup>3</sup>, G. Jocelyn<sup>4</sup>, S. Renaud<sup>4</sup>, P. Csaba<sup>5</sup>, G. Cristina<sup>6</sup>, N. Pieter<sup>7</sup>, G. Ravzan<sup>8</sup>, L. Kristina<sup>9</sup>, P. Bulent<sup>10</sup>, K. Georgy<sup>11</sup>, V.L. Erick<sup>12</sup>, S. Vratislav<sup>13</sup>

<sup>1</sup>Centre Antoine Lacassagne, Radiation Therapy, Nice, France ; <sup>2</sup>Medical University of Vienna, Department of

Radiation Oncology, Vienna, Austria ; <sup>3</sup>Institute Medic Onco Radioterapia, Department of Radiation Oncology, Barcelona, Spain ; <sup>4</sup>Antoine Lacassagne Cancer Center & University of Cote d'Azur, Biostatistics' Unite, Nice, France ; <sup>5</sup>National Institute of Oncology, Department of Radiation Oncology, Budapest, Hungary ; <sup>6</sup>Catalan Institute of Oncology, Department of Radiation Oncology, Barcelona, Spain ; <sup>7</sup>Offenbach University Hospital, Department of Radiation Oncology, Offenbach, Germany ; <sup>8</sup>University of Kiel- Kiel, Department of Radiation Oncology, Kiel, Germany ; <sup>9</sup>University Hospital Berne- Berne- Switzerland, Department of Radiation Oncology, Berne, Switzerland; <sup>10</sup>University of Wurzburg, Department of Radiation Oncology, Wurzburg, Germany ; <sup>11</sup>University of Lubeck, Department of Radiation Oncology, Lubeck, Germany; <sup>12</sup>Experimental Radiotherapy Laboratory, Department of Radiation Oncology, Leuven, Belgium ; <sup>13</sup>University Erlangen-Nuremberg, Department of Radiation Oncology, Erlangen, Germany

## Purpose or Objective

In case of second ipsilateral breast tumor event (2<sup>nd</sup>IBTE) occurring after primary breast conserving surgery, salvage mastectomy or 2<sup>nd</sup>conservative treatment (2<sup>nd</sup>CT) including breast conserving salvage-surgery and salvage accelerated partial breast re-irradiation (APBrI) with brachytherapy can be performed. We report update results of 2<sup>nd</sup>CT from the database of the GEC-ESTRO Breast Cancer Working Group.

## Material and Methods

Between 2000 and 2014, 331 patients (pts) underwent a 2<sup>nd</sup>CT in 12 hospital/cancer centers from 7 European countries. After salvage-lumpectomy, APBrI was performed using either low (30 - 55 Gy reference isodose) or high dose-rate brachytherapy (28 - 34 Gy). Oncological outcome including 3<sup>rd</sup>IBTE, regional (RFS) or metastasis-free survival (MFS), specific (SS) and overall survival (OS) was analyzed. The belonging to a specific group of the GEC-ESTRO APBI classification (GAC) was also investigated. Simultaneously late side effects and prognostic factors for 3<sup>rd</sup>IBTE were analyzed.

## Results

With a median follow-up of 72 months (range: 67 - 80 months), 143 pts (43%), 140 pts (42 %) and 48 pts (15%) were classified as low (LR), intermediate (IR) and high-risk (HR) respectively. For the whole cohort, 6-year 3<sup>rd</sup>IBTE free survival, RFS, MFS, SS and OS rates were 92.9%, 96.4%, 87.4%, 90.1% and 85.8% respectively. 6-year 3<sup>rd</sup>IBTE free-survival rates for LR, IR and HI were 99.3%, 90.4% and 92% respectively (p = 0,009). 6-year RFS, MFS, SS and OS rates according to GAC are reported in Table 1. In UVA, SBR (1,2 vs 3 - p = 0.008), age (< 50 y vs. <sup>35</sup>50 y - p = 0.002) and GAC (p = 0.009) were considered as significant prognostic factors for 3<sup>rd</sup>IBTE, while, in MVA, SBR (p = 0.046) and GAC (p = 0.01) were the two remaining prognostic factors. In terms of late toxicity, 194 pts (87%) presented G1,2 complications while G<sup>3</sup>3 complication rate was 13%.

6 years	3 <sup>rd</sup> IBTE-FS	RFS	MFS	SS	OS
Whole cohort	92.9	96.4	87.4	90.1	85.8
APBI LR	99.3	94.4	87.2	92.0	87.8
APBI IR	90.4	92.7	89.6	91.8	86.7
APBI HR	92.0	88.9	81.0	80.4	77.8

Table 1: Oncological outcomes for the whole cohort and according to the GEC-ESTRO APBI classification

## Conclusion

In case of 2<sup>nd</sup>IBTE, 2<sup>nd</sup>CT combining re-lumpectomy + APBrI represent a valid therapeutic option in terms of oncological outcome as well as toxicity profile. Patient and tumor characteristics have to be carefully evaluated

while patient information remains crucial for the discussion of treatment choice.

#### OC-0318 10-year clinical and cosmetic outcomes of high-dose-rate brachytherapy for early breast cancer

F. Arcidiacono<sup>1</sup>, F. Trippa<sup>1</sup>, P. Anselmo<sup>1</sup>, M. Italiani<sup>1</sup>, M. Casale<sup>1</sup>, L. Draghini<sup>1</sup>, S. Fabiani<sup>1</sup>, A. Di Marzo<sup>1</sup>, S. Terenzi<sup>1</sup>, E. Maranzano<sup>1</sup>

<sup>1</sup>Radiotherapy Oncology Centre, "S.Maria" Hospital, Terni, Italy

##### Purpose or Objective

In GEC-ESTRO randomised trial accelerated partial breast irradiation (PBI) with high-dose-rate brachytherapy (HDR-BRT) was not inferior to adjuvant whole breast irradiation at 5-year follow-up. The long-term results are lacking in literature. We report 10-year clinical and cosmetic outcomes of PBI with <sup>192</sup>Ir HDR-BRT in early breast cancer patients (pts).

##### Material and Methods

From May 2005 to July 2013, 129 early breast cancer pts were recruited in a phase II trial of exclusive <sup>192</sup>Ir HDR-BRT. Inclusion criteria were: age >40, PS 0-2, unifocal invasive ductal cancer, intraductal cancer component <25%, negative axillary nodes and tumor size ≤2.5 cm. Treatment schedule was 4 Gy twice a day for 4-5 days, up to a total dose of 32 Gy in 8 fractions with a minimum interval between daily fractions of at least 6 hours. Late toxicity was graded according to RTOG/EORTC scoring criteria and cosmetic outcomes according to Harvard criteria (i.e., excellent, good, fair and poor).

##### Results

Median age was 67 years (range, 42-85). There were 11 (8.5%) pT1a, 44 (34%) pT1b, 68 (53%) pT1c and 6 (4.5%) pT2. Estrogenic and/or progestinic receptors were positive in 118 (91.5%) pts. 116 (90%) and 20 (15.5%) patients received adjuvant hormonal therapy and chemotherapy, respectively. Median follow-up was 108 months (range, 8-162). 3(2%) isolated in-field breast relapse occurred 92, 123 and 129 months after HDR-BRT; 1(0.7%) isolated out-field breast relapse occurred 107 months after HDR-BRT. 4(3%) patients developed contralateral breast cancer, another one (0.7%) isolated regional relapse in axillary node and 4(3%) distant progression of disease. 16(12.5%) patients reported a second primary cancer. 5- and 10-year overall survival and cancer specific survival were 95% and 86%, 100% and 100%, respectively. At last follow-up, 105(81%) patients were alive without disease and 4(3%) with systemic disease. 20 (16%) patients died: 10 (8%) for other cancers and 10 (8%) for other causes. Cosmetic outcomes were excellent in 106 (82.5%), good in 12 (9.5%), fair in 8 (6%) and unknown in 3 (2%) pts. Late skin toxicity was registered in 29 (23.4%) pts, grade 1-2 in 28 (22.5%), grade 3 in 1 (0.8%). Late toxicity was significantly related to the skin administered doses (≤ 55% vs. > 55%, P < 0.05).

##### Conclusion

PBI delivered with <sup>192</sup>Ir HDR-BRT in selected breast cancer patients was associated to high local control and survival with excellent cosmetic outcomes overall when skin dose was ≤ 55%.

#### OC-0319 Twelve-year clinical outcomes with APBI with interstitial multicatheter brachytherapy after BCS

S. Kellas-Sleczyka<sup>1</sup>, B. Bialas<sup>1</sup>, P. Wojcieszek<sup>1</sup>, A. Cholewka<sup>2</sup>, M. Szlag<sup>2</sup>, M. Fijalkowski<sup>1</sup>, T. Krzysztofkiak<sup>1</sup>, K. Trzaska<sup>2</sup>, A. Pruefer<sup>2</sup>, L. Piotr<sup>1</sup>, M. Wesolowski<sup>3</sup>, B. Lange<sup>4</sup>

<sup>1</sup>Maria Sklodowska-Curie Memorial Cancer Center and Institute of Oncology, Brachytherapy Department, Gliwice, Poland; <sup>2</sup>Maria Sklodowska-Curie Memorial Cancer Center and Institute of Oncology, Radiotherapy Planning Department, Gliwice, Poland; <sup>3</sup>Maria Sklodowska-Curie Memorial Cancer Center and Institute

of Oncology, Tumor Pathology Department, Gliwice, Poland; <sup>4</sup>Maria Sklodowska-Curie Memorial Cancer Center and Institute of Oncology, III Department of Radiotherapy and Chemotherapy, Gliwice, Poland

##### Purpose or Objective

To report the long-term results, toxicity, and pattern of failure of 481 patients treated with APBI using interstitial multicatheter high-dose-rate brachytherapy (HDR-BT) after breast-conserving surgery in a single institution.

##### Material and Methods

Between July 2006 and September 2018, a total of 481 women with low-risk invasive and in-situ carcinoma after breast-conserving surgery (BCS) were treated with APBI using interstitial multicatheter HDR-BT at our department. The inclusion criteria were: ZUBROD 0 or 1, age ≥50 years, T1-2aN0M0, T≤3 cm, unifocally, invasive carcinoma without neuroinvasion, angioinvasion, a minimal surgical margin of 2 mm or DCIS with a minimal margin of 5 mm, without extensive intraductal component (EIC), positive estrogen receptors.

The total dose was 32 Gy in 8 fractions delivered twice daily with a minimum 6-hour break. The primary endpoint was local recurrence.

##### Results

The median age was 61 years (range 47-86 years). The median follow-up was 55 months (range 1-146 months). In the analyzed group, 262 patients were followed up for 5 years or longer. The mean volume of the PTV was 71.5 cm<sup>3</sup>, with the mean value of its coverage with the prescribed dose (PTV ref) amounting to 94.6%. The PTV mean value was 67.6%, and D90 was 105%. The mean values of key indices were acceptable, with a mean conformity index (COIN) of 0.69 and a mean dose homogeneity index (DHI) of 0.68.

The mean value of the maximum skin dose was 41% of the prescribed dose. The mean value of the ipsilateral lung dose to 2 cm<sup>3</sup> volume was 40.3% of the prescribed dose, and the mean value to 10 cm<sup>3</sup> volume was 30.1%; the maximum dose for ipsilateral lung was 50% on average. The mean maximum dose for the closest rib was 77.8% of prescribed dose.

There was no acute severe toxicity. The treatment was well tolerated. In 19.7% a hematoma following catheter insertion was noted. In 2.1% local inflammation requiring oral antibiotic therapy was noted, but in 22.2% of cases prophylactic antibiotic therapy was given. There was no late severe toxicity, and cosmetic outcome was good. In the whole group of patients, 11 failures (2.3%) were noted: seven local recurrences (1.5%) treated with amputations and four cases (0.8%) of distant metastases. All patients with local recurrence are alive without any symptoms of disease; two patients with distant metastases have died; two are still undergoing therapy.

The 5- and 10-year OS was 94.4% and 83.5% respectively. The 5- and 10-year DFS was 92.3% and 78.6% respectively.

##### Conclusion

APBI with Interstitial Multicatheter High-Dose-Rate Brachytherapy is an effective treatment modality, associated with very low toxicity and a low relapse rate. In our opinion, patient selection criteria should be revised and could likely be extended. Further studies are needed to validate this approach.

#### OC-0320 Comparing toxicities between Multicatheter Brachytherapy and Whole Breast External Beam Radiotherapy

T. Chan<sup>1</sup>, P.W. Tan<sup>1</sup>, J.I.H. Tang<sup>1</sup>

<sup>1</sup>The National University Cancer Institute- Singapore NCIS, Radiation Oncology, Singapore, Singapore

***This abstract is part of the media programme and will be released on the day of its presentation***

**OC-0321 Phase I-II multicenter trial Very Accelerated Partial Breast Irradiation (VAPBI): early effects**

J. Guinot<sup>1</sup>, V. Gonzalez-Perez<sup>2</sup>, N. Meszaros<sup>3</sup>, C. Polgar<sup>3</sup>, T. Major<sup>3</sup>, M.A. Santos<sup>1</sup>, D. Najjari<sup>4</sup>, C. Gutierrez<sup>4</sup>

<sup>1</sup>Fundación Instituto Valenciano de Oncología, Department of Radiation Oncology, Valencia, Spain ;

<sup>2</sup>Fundación Instituto Valenciano de Oncología, Department of Radiation Physics, Valencia, Spain ;

<sup>3</sup>National Cancer Institute., Department of Radiation Oncology, Budapest, Hungary ; <sup>4</sup>Catalan Institute of Oncology, Department of Radiation Oncology, Barcelona, Spain

**Purpose or Objective**

Accelerated partial breast irradiation (APBI) is a standard treatment for early breast carcinoma after conserving surgery. High dose rate (HDR) with multi-catheter interstitial brachytherapy (MIBT) is used twice a day (3.4Gy x 10, 4Gy x 8 or 4.3Gy x 7 fractions), to a total irradiation time of 4-5 days. We present the preliminary results of the first part of a Phase I-II trial endorsed by the GEC-ESTRO Breast Working Group, using a very accelerated scheme (VAPBI) with HDR-MIBT in 4 fractions, to decrease the total time of treatment to 2-3 days.

**Material and Methods**

The criteria to include patients were the same as the APBI GEC-ESTRO Phase III trial, only invasive carcinomas were included. Between August 2017 and July 2018, 31 patients from three centers, with low risk early invasive breast carcinoma have been treated with 4 fractions of 6.25Gy. The total dose was 25Gy prescribed to the CTV. Ten patients have been implanted perioperatively (32%), during the surgical procedure, and 22 postoperatively using CT or US-guided implantation of plastic tubes. 22 cases (71%) have been treated in two days. Mean age was 64 (51-87). Pathology showed invasive ductal carcinoma in 27 cases, invasive lobular carcinoma 2, tubular carcinoma 1 and colloid carcinoma in 1 case. All were with negative sentinel node, free margins 2mm or greater. Luminal A: 23

cases, Luminal B: 8. Grade 1: 20, G 2:10, G3: 1 case. Mean time between surgery and MIBT was 67 days (39-104) in postoperative cases. Median number of plastic tubes was 13 (range 7-24) implanted in a median of 3 planes (2-5). Regarding the dosimetry, mean V100 was 86cc (19.5-171cc) mean V150 was 24.2cc (6-41cc); mean D90: 105.4% (96-112.4%); mean DNR: 0.29 (0.23-0.41).

**Results**

The technique is the same as used for the GEC-ESTRO Phase III trial, and no differences have been recorded during the implantation and removal. Temporary hematoma developed in 7 cases (5 after perioperative implantations). Pain was referred in one third of cases, well managed with painkillers, and the tolerance was good. No case of infection. With a median follow-up of 7 months, and minimum of three months, slight pigmentation changes (G1) in the entrance of tubes were described in 26%, but with progressive attenuation with longer follow-up. Slight induration or fibrosis (G1) in 16%.

**Conclusion**

VAPBI with MIBT using four fractions of 6.25Gy in two or three days is feasible. No differences have been observed after a median follow-up of six months (minimum three months), compared with the previous experience of the APBI Phase III trial. Acute effects are similar. A longer follow up is needed to evaluate chronic effects. The shorter total time is beneficial for the patients and reduces the workload of the Brachytherapy unit.

**OC-0322 HDR Skin applicator fabrication for clinical cases: handmade vs digitally designed and 3D printed**

S. Nic A Bhaïrd<sup>1</sup>, R. Caines<sup>1</sup>, C. Lee<sup>1</sup>

<sup>1</sup>Clatterbridge Cancer Centre, Department of Physics, Liverpool, United Kingdom

**Purpose or Objective**

Several studies have demonstrated feasibility of digitally designed 3D-printed HDR skin applicators [1-2], but none have systematically compared this process against traditional hand-formed methods. This study compared five clinical hand-formed applicators previously used for treatment to digitally designed 3D-printed applicators retrospectively created for the same cases. Geometric and dosimetric measurements were performed.

**Material and Methods**

The traditional applicators comprised of a thermoplastic shell, hand-formed wax stand-off and catheters for source transfer. These applicators were constructed to meet specifications for skin-catheter distances and catheter-catheter distances. A process was developed to design these applicators digitally in the contouring module of an EBRT treatment planning system (TPS) (Eclipse v13.6, Varian Medical Systems, CA). The thermoplastic shell of the original applicators was used as a base for the 3D printed applicators. Applicator designs were exported and printed locally with the Axium 20 3D printer (Airwolf3D, CA).

All applicators were CT scanned at high resolution and over 3,800 geometric measurements made in the TPS. Skin-catheter and catheter-catheter distances were inspected and for each applicator type the proportion of measurements within a 1 mm tolerance determined.

Treatment planning and delivery was performed for both applicator types according to local protocol. Dosimetry at the centre of each treatment area was verified by TLD.

**Results**

**Skin-catheter distances:** The proportion of geometrical measurements within 1 mm of specification was 0.56 [95% CI: 0.53-0.59] for the hand-formed applicators compared with 0.69 [95% CI: 0.67-0.72] for the 3D-prints (p<0.01, Fig. 1)

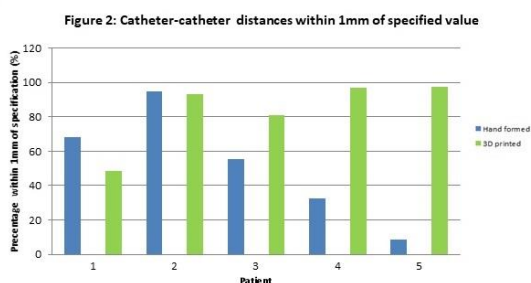
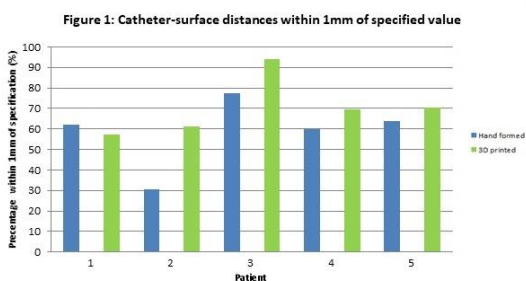
**Catheter-catheter distances:** The proportion of geometrical measurements within 1 mm of specification was 0.58 [95% CI: 0.55-0.61] for the hand-formed

applicators and 0.82 [95% CI: 0.80-0.85] for the 3D-prints ( $p < 0.01$ , Fig. 2)

Dosimetry: TLD measurements for both types of applicators agreed with the expected doses predicted by the TPS within a local tolerance of  $\pm 5\%$ .

#### Conclusion

The applicators made using the digitally designed 3D printing process were more geometrically accurate compared with the applicators made using the current traditional fabrication process. Both types of applicators gave satisfactory dosimetric performance. The 3D-printing process is faster and less labour intensive. The resulting applicators are durable, lightweight, low cost and visually appealing. They can be easily reprinted for teaching or further studies. As a result of this study digitally designed 3D-printed HDR skin applicators will be incorporated into our routine clinical practice.



[1] Ricotti, R et al. 2016. 3D-printed applicators for high dose rate brachytherapy: Dosimetric assessment at different infill percentage. *Physica Medica*, 32(12), p.1698-1706

[2] Jones, EL et al. 2017. Introduction of novel 3D-printed superficial applicators for high-dose-rate skin brachytherapy. *Brachytherapy*, 6(2), p.409-414

#### OC-0323 Perioperative interstitial high dose rate brachytherapy for keloids scars

V. Vera Barragam<sup>1</sup>, M. De Juan Marín<sup>2</sup>, S. Blanco Parajón<sup>1</sup>, J. Fernández García<sup>3</sup>, G. Juan Rijo<sup>1</sup>, A.I. Alonso García<sup>1</sup>

<sup>1</sup>Hospital Universitario Central de Asturias, Radiotherapy oncology, Oviedo, Spain ; <sup>2</sup>Hospital Universitario Central de Asturias, Plastic Surgery, Oviedo, Spain; <sup>3</sup>Hospital Universitario Central de Asturias, Physics, Oviedo, Spain

#### Purpose or Objective

The treatment of keloid scars is still a clinical challenge due to their high recurrence rate, which can happen in up to 30% of the cases. The use of radiation therapy combined with surgical excision is considered as one of the most effective treatments. However, there is little consensus among the medical community about the most optimal treatment in terms of dose, fractionation, and type of treatment: external or internal, i.e. brachytherapy. This study evaluates the treatment outcome in terms of local control, as well as from a cosmetic point of view, of keloid

scars treated with perioperative interstitial high dose rate (HDR) brachytherapy.

#### Material and Methods

The patient cohort under study comprised 61 keloids in 51 patients. All keloid lesions were treated with 12Gy in 4 fractions, during 48h, i.e., one fraction every 12h. The treating physician inserted a catheter along the scar during the surgical procedure, which served for the delivery of the subsequent brachytherapy fractions. The lapse of time between surgery and brachytherapy was less than 90 minutes.

Local failure was defined as recurrence of the apparent keloid as well as symptoms at the same location. The median age of the patients was 46 years (20-89 years). Keloids had an average size of 6.3cm and were located on the chest (41%), ear lobe (21%), back (1.6%), and extremities (11.5%). The IBM SPSS v.24 software was used for statistical analysis of quantitative variables (Analysis of Variance, ANOVA test) and qualitative variables (Chi-square test), such as the scar size or patient's race. P-value  $\leq 0.05$  was taken as significant.

#### Results

The recurrence rate, with a median follow-up of 48 months (range 1-96 months), was only of 4.9%, all of them located on the chest. In addition, most patients with successful treatment presented an excellent cosmetic result at the scar location, except some patients (below 20%) for which a small part of the scar remained but no pain, stinging or tissue thickening was reported.

The ANOVA and Chi-square tests showed no significant statistical relationship between the recurrence rate and the race ( $p=0.312$ ), or the size of the scar ( $p=0.525$ ).

Figure 1 illustrates the cosmetic outcome in one of the patients with a keloid scar located in the ear lobe, before (Figure 1.a) and after treatment (Figure 1.b).



#### Conclusion

Perioperative interstitial HDR brachytherapy appears to be a high effective treatment against keloid scars, with a decreased recurrence rate below 5%. All failed treatments happened in the chest, which suggests the investigation of higher dose for this site. The treatment was well tolerated by all patients and did not present significant side effects. The cosmetic results were also excellent and the patients reported great satisfaction after treatment.

#### Presidential Symposium: Presidential symposium

#### SP-0324

Umberto Ricardi<sup>1</sup>

<sup>1</sup>University of Turin, Turin, Italy

Abstract not received

#### Award Lecture: Claudius Regaud Award Lecture

#### SP-0325 Is fractionation history?

D. De Ruyscher<sup>1</sup>

*<sup>1</sup>Maastricht Clinic, Radiation Oncology, Maastricht, The Netherlands*

#### Abstract text

Claudius Regaud will mostly be remembered as the father of fractionation and therefore the possibility to spare better normal tissues than tumors. Already in 1906, he hypothesized that X-rays could be used against rapidly growing cells other than gametes, such as cancer. Historical experiments in rams indeed established the concept of fractionation. Regaud was a pathologist who tried to understand the biology of radiation in a real multidisciplinary way.

While even in the earlier days of radiotherapy attempts were made to test hypotheses in pre-clinical models and to understand the underlying biology, increasingly hypotheses were directly applied in patients. Large numbers of patients were exposed to potentially toxic treatments and as there was nor is a comprehensive database, nobody could evaluate the outcome. The standard fractionation scheme for stage III NSCLC, 60 Gy in 2 Gy QD fractions was established in the 1980's, but was already in use for many decades and has largely remained the same, while there have been countless patients who received other doses, fractions sizes and overall treatment times (OTT). Nobody knows what the results are. Accelerated radiotherapy was used since the 1920s, but before an influence on survival was demonstrated, we had to wait for the CHART trials in the 1990s and for level I evidence until 2012. At that time, concurrent chemoradiotherapy had become standard and we and others, without understanding the biology, used the same strategy of acceleration for the latter patients, unfortunately without benefit. Fortunately, improved techniques and integration of molecular imaging lead to less side effects than ever.

Stereotactic radiotherapy (SBRT) truly revolutionized our field, but at some moment, it was used at anatomical sites where it was predicted to be very toxic. Implementation without proper understanding of the underlying biology and prospective studies led to a high incidence of side effects and here again, the absence of a prospective database and the lack of formal testing precludes us to get more insights in the relation between toxicity and treatment and patients parameters.

The technological evolution has overwhelmed the complex biology and its benefit is not assessed properly. Assumptions about gains are in general not supported by reproducible data with dose-escalation and adaptive radiotherapy as a good examples.

Immune treatment is now changing oncology profoundly and we should embrace this evolution. It gives us the platform to investigate the biology thoroughly, not only of photons, but also of protons and to revise fractionation and volumes. This will only work when we work with many other disciplines, perform pre-clinical and clinical trials and establish usable prospective databases. AI will be needed to learn from these networks with countless nodes and to implement the results. AI will also enable to take into account the (forgotten) knowledge of the past, to avoid making the same mistakes.

Fractionation will however remain relevant.

---

#### Symposium: How to prevent burnout?

---

#### SP-0326 Perspectives on burnout in the medical professions

P. Franco<sup>1</sup>

*<sup>1</sup>University of Turin, Department of Oncology- Radiation Oncology, Turin, Italy*

#### Abstract text

Human beings are able to survive within a given environment as far as they are able to maintain an individual balance (homeostasis), which is constantly challenged by intrinsic and extrinsic causes, also known as stress factors (1). Stress can be seen as a physiological response in the shape of a 'general adaptation syndrome' and can be subdivided into 3 different phases: a) alarm, b) resistance c) exhaust (1). Individual can implement coping strategies in response to stress. They have 2 main goals: changing the situation causing stress and controlling the emotional response to the stressful agent. Certain coping strategies (emotional response) may lead to exhaustion, a final step in which the individual cannot accomplish to re-establish the inner balance. This may lead to the so-called 'Burn-out Syndrome' (BOS), which has been described by Maslach et al in the '90s (2). The terms forwards to a significance implying to burn something to exhaustion, until it is consumed (3). It is considered one of the mostly impacting factor for physical and mental well-being within the working environment. It particularly affects healthcare professionals (4). The three classic presentation clusters are loss of enthusiasm for work (emotional exhaustion), reduced empathy and increased cynism (depersonalisation) and a decreased perception of the meaningfulness of someone's work, finally leading to inefficacy (personal accomplishment) (2,4). Symptoms can be classified into physical (insomnia, lack of energy, back pain, loss of appetite, ulcer, migraine, nausea) and psychological (cynism, irritability, denial of failures, loss of sense of humor, indifference, insecurity, disinterest, indecision, reduction of self-esteem and loss of memory) cluster. BOS is a stress-related syndrome and it is particularly frequent within Oncology professionals and staff (5). The incidence has been shown to be as high as 50-70% (5-7). In team environments, such as in radiation oncology, situations of increased job stress and burn-out can lead to impaired cognitive functioning, increasing the potential for patient harm. BOS for hospital staff include illness, absenteeism, staff conflict, distrust of management, poor coping and substance abuse. Clinical consequences may include medical errors and adverse events, poor prescribing habits, low patients satisfaction and low adherence to physician recommendations (4). Different inherent factors may be related to BOS development. One of the most important is each individual's coping style. Poor coping may lead to impairment in job performance and ineffective coping strategies may lead to a higher likelihood to develop BOS. In general, emotion-oriented coping styles are associated to higher levels of BOS (9). Personality traits may also predispose individuals to develop BOS. Alexithymia and empathy are personality traits. Alexithymia is a psychological construct broadly describing individuals with deficits in emotion processing and awareness (10). Those who score high on measure of alexithymia show difficulty distinguishing emotions from bodily sensations, discriminating between cognition and emotions and describing and communicating emotions to others (11). Empathy is the ability to share and understand another's 'state of mind' or emotion. It is often characterized as the capacity to 'put oneself into another's shoes'. In the healthcare environment, effective emphatic communication enhances the therapeutic effectiveness of the clinician-patient relationship. The Young ESTRO Committee developed the PRO BONO study (PROject on Burn-Out in Radiation Oncology) to explore BOS in the field of radiation oncology and to investigate whether alexithymia and empathy may potentially affect the likelihood for BOS development. The project is also endorsed by the Young Radiation Oncology Group (yROG) of EORTC. The survey was aimed at all radiation oncology professionals and was completely anonymous. This project will provide useful information. Being aware of potential risk factors may help in implementing

protection strategies for radiation oncology professionals more prone to undergo BOS. Participants were asked to provide some general information and fill-in 3 different validated questionnaires (TAS-20, IRI, ProQoL) to investigate alexithymia trait, empathy and to quantify eventual BOS. The PRO-BONO initiative, is a valuable way to address an important issue, to analyze it and to define management strategies for individuals at risk of developing BOS.

#### OC-0327 The PRO BONO survey (PROject on Burn-Out in RadiatioN Oncology)

P. Franco<sup>1</sup>, V. Tesio<sup>2</sup>, J. Bertholet<sup>3</sup>, A. Gasnier<sup>4</sup>, E. Gonzalez del Portillo<sup>5</sup>, M. Spalek<sup>6</sup>, J. Bibault<sup>7</sup>, G. Borst<sup>8</sup>, W. Van Elmpt<sup>9</sup>, D. Thorwhart<sup>10</sup>, L. Mullaney<sup>11</sup>, K. Roe Redalen<sup>12</sup>, L. Dubois<sup>9</sup>, M. Bittner<sup>13</sup>, C. Chargari<sup>14</sup>, M. Lybeer<sup>15</sup>, L. Castelli<sup>2</sup>

<sup>1</sup>University of Turin, Department of Oncology- Radiation Oncology, Turin, Italy; <sup>2</sup>University of Turin, Department of Psychology, Turin, Italy; <sup>3</sup>The Institute of Cancer Research, Department of Medical Physics, London, United Kingdom; <sup>4</sup>Hopital Europeen Georges Pompidou- Universite Paris Descartes, Medical Physics Department, Paris, France; <sup>5</sup>University of Salamanca, Department of Radiation Oncology, Salamanca, Spain; <sup>6</sup>Maria Sklodowska Curie Institute, Department of Radiotherapy, Warsaw, Poland; <sup>7</sup>Hopital Europeen Georges Pompidou- Universite Paris Descartes, Radiation Oncology Department, Paris, France; <sup>8</sup>The Netherlands Cancer Institute- Antoni van Leeuwenhoek Hospital, Department of Oncology- Radiation Oncology Department, Amsterdam, The Netherlands; <sup>9</sup>Maastricht University Medical Center, Department of Radiation Oncology- GROW - School for Oncology and Developmental Biology, Maastricht, The Netherlands; <sup>10</sup>University Hospital for Radiation Oncology Tubingen, Section for Biomedical Physics, Tubingen, Germany; <sup>11</sup>School of Medicine- Trinity College Dublin, Applied Radiation Therapy Trinity Research Group- Discipline of Radiation Therapy, Dublin, Ireland; <sup>12</sup>Institute of Clinical Medicine, University of Oslo, Oslo, Norway; <sup>13</sup>Trinity College, Department of Radiation Oncology, Oxford, United Kingdom; <sup>14</sup>Institute Gustave Roussy, Department of Radiation Oncology, Villejuif, France; <sup>15</sup>ESTRO Office, Young ESTRO Committee, Brussels, Belgium

#### Purpose or Objective

Burn-out syndrome (BOS) is a stress-related syndrome, particularly frequent within Oncology professionals and staff. It may affect performance within the working environment and impact on individual physical and mental well-being. Personality traits may predispose to develop BOS. Alexithymia is a psychological construct describing deficits in emotion processing and awareness. Empathy is the ability to share and understand another's 'state of mind' or emotion. The PROject on Burn-Out in RadiatioN Oncology (PRO BONO study) was developed to explore BOS in the field of radiation oncology and to investigate whether personality traits such as alexithymia and empathy may potentially affect the likelihood to develop BOS.

#### Material and Methods

An anonymous survey was conducted online using the web-based platform Survey Monkey (www.surveymonkey.com), addressed to ESTRO members, reached out via e-mail, social media or through the collaboration of National Societies. All professionals within ESTRO were involved (radiation oncologists, medical physicists, radiation therapists, radiobiologists). Participants were asked to provide specific individual and professional information and fill-in 3 different validated questionnaires to investigate alexithymia trait, empathy and to quantify BOS, namely the Toronto Alexithymia Scale (TAS-20), the Interpersonal Reactivity Index (IRI) and the Professional

Quality of Life Scale (ProQoL). Answers were collected and results analysed by the Young ESTRO Committee.

#### Results

The survey is still open for response. So far, a total of 1958 ESTRO members took part, from 94 different countries and 5 continents. Male were 56%, female 44%. Most of respondents were radiation oncologists (53%), while radiation technologists were 26%, medical physicists 20% and radiobiologists 1%. As for educational level of respondents, most of them were MD (44%), MSc (18%) or BSc (13%), being in the field of radiation oncology for < 5 year (28%) or between 11 and 20 years (27%). Up to 49% of them had on-call duties. Most of them (84%) pointed out that medical practice affected their private life. They felt valued by their patients in 88% of cases (not enough:12%) and by their supervisor in 72% (not enough:28%). Up to 32% had a 1-year leave from work. Preliminary results using Person correlation coefficient (PCC) showed a significant correlation (PCC=0.82) between a higher score (>61) on TAS-20 and a higher score (>57) on the burn-out subscale of the ProQoL questionnaire. A higher score for Empathy Concern within the IRI questionnaire was also significantly correlated (PCC =0.79) to higher burn-out on ProQoL.

#### Conclusion

The PRO BONO study provided an overview on BOS, alexithymia and empathy in radiation oncology professionals worldwide. Personality traits such as alexithymia and empathy seem to be correlated to the likelihood to develop BOS. After the upcoming end of the study, detailed analysis on subset population and individual domains within administered questionnaires will better clarify the scenario.

#### SP-0328 Report back from ESTRO mobility grants clinical: SRS and SBRT in the management of oligometastatic disease

I. Zumbadze<sup>1</sup>

<sup>1</sup>Research Institute of Clinical Medicine, Department of Radiation Oncology, Tbilisi, Georgia

#### Abstract text

Concept of oligometastatic state, proposed by Hellman and Weichselbaum, implies that "there exists a subset of patients with limited volume metastases in whom treatment of oligometastatic sites impacts survival". Randomized studies have demonstrated that surgical treatment of oligometastatic lesions can improve survival. Stereotactic body radiotherapy (SBRT) and Stereotactic Radiosurgery (SRS) has emerged as an attractive alternative or as an adjuvant to surgical resection. In this report we would like to review: the results of ablative radiotherapy for the intracranial and extracranial (lung, liver, spine) oligometastases; recent attempts to identify the patients with limited number of metastases who mostly benefit from aggressive local treatment; data addressing fractionation regimens in regard to feasibility and safety of ablative radiotherapy for various localization, volume and size of metastases and short summary of my experience at the University Hospital Turin. Aiming to develop the concept of stereotactic body radiotherapy and radiosurgery and introduce it in the clinical practice, we have set up collaborations and engaged discussion with Georgian colleagues. This process was enhanced by my visit to the department of Prof. Umberto Ricardi thanks to the mobility grant. Sharing the expertise of this department and inspiring our self from the irradiation protocols developed by Prof. Umberto Ricardi and his group, now we are treating this group of patients with oligometastatic disease and keeping institutional registry. The accumulating clinical data could be used in future to draw conclusions for safe and beneficial implementation of the existing guidelines.

#### SP-0329 Modelling Head and Neck Radiotherapy outcomes using radiomics biomarkers

P. Kalendralis<sup>1</sup>, Z. Shi<sup>1</sup>, J. Van Soest<sup>1</sup>, A. Ryczkowski<sup>2</sup>, J. Kazmierska<sup>2</sup>, J. Malicki<sup>2</sup>, A. Dekker<sup>1</sup>, L. Wee<sup>1</sup>  
<sup>1</sup>Maastricht University, Department Of Radiation Oncology  
 Maastricht- Grow School For Oncology And Developmental  
 Biology- Maastricht University Medical Centre+- Dr  
 Tanslaan 12- 6229et- Maastricht- The Netherlands,  
 Maastricht, The Netherlands ; <sup>2</sup>Radiotherapy Department  
 li- Greater Poland Cancer Center- Poznan- Poland,  
 Radiotherapy Department, Poznan, Poland

#### Abstract text

**Introduction:** Predictive models of radiotherapy (RT) treatment outcomes for head and neck cancer (HNC) patients have clinical value in personalized treatment. Presently, few externally validated models for HNC tumour control and treatment-related toxicity exploit the potential of quantitative image-derived biomarkers (i.e. radiomics) to individually characterize the tumor phenotype. Our primary hypothesis is that adding radiomic features from Planning CT scans improves predictive performance of models for Overall Survival, Xerostomia and Dysphagia, which can be tested by independent external validation between two RT centres. **Materials and methods:** A “personal health train” architecture

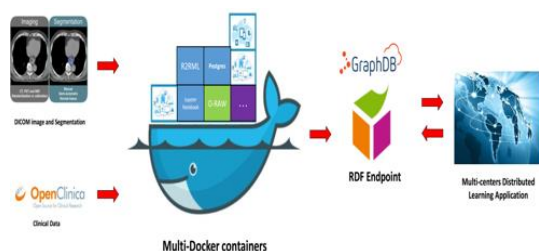
(<https://www.youtube.com/watch?v=mktAtHmy-FM> ) is implemented to connect Maastricht Clinic (Maastricht, Netherlands) and the Greater Poland Cancer Centre (GPCC-Poznan, Poland). The workflow of PHT is shown in Figure-1. These centres will independently develop and validate multi-variate prediction models on each other’s patient data without transferring any subject-level information. This methodology could maximally preserve medical data privacy because no individually-identifiable records are shared among centres. Instead, distributed machine learning algorithms shuttle between data sites to fit statistical models of outcome. The data from the two participated centres consist of retrospective clinical observation records and RT Computed Tomography (CT) planning scans approved for research from the Institutional Review Boards (IRBs) of each centre.

#### Results

We do not have preliminary results from our study as the workflow will be in progress during the visit to the GPCC. We aim to have local processing of retrospectively collected clinical and imaging data of H&N patients in combination with the development of a clinical prediction model in Poznan’s data performing distributed validation in MAASTRO’s dataset. Furthermore, as an extension of our results we are planning to distribute the final fitted models to a third RT centre for fully independent external validation of the models.

#### Conclusion

The collaboration between Maastricht and GPCC will potentially increase the sample size for model development, and provide essential alternative cohorts for fully independent external validation of prediction models. In addition, Maastricht’s technical infrastructure expertise establishes in return a long-term collaboration in Poland aiming to establish an innovative clinical research into the future.



#### SP-0330 Science slam: To breathe or not to breathe. ESTRO Mobility Grant report

S. Pracic<sup>1</sup>

<sup>1</sup>University Medical Centre Maribor, Department of Oncology, Maribor, Slovenia

#### Purpose

To learn about Voluntary Deep Inspiration Breath Hold radiotherapy technique.

#### Abstract text

Royal Marsden Hospital is one of the first hospitals which has implemented voluntary Deep Inspiration Breath Hold Technique (vDIBH) in a daily clinical practice. Their approach to this technique is unique, very simple and with no additional costs or investments in additional equipment, and therefore it is possible to copy their work onto our Department.

My primary goal was to learn how to train patients to breathe during the CT simulation and to learn the procedure of treatment delivery and treatment verification. It was also important to see the whole procedure and do some practical work for better understanding.

At the Pre-treatment Unit, I worked together with their radiographers during the CT simulation. Training the breathing technique with patient was of great benefit to further understand the principle of vDIBH. At the Treatment Unit, I was able to see what treatment delivery looks like in clinical practice. Working together with experienced radiographers and with patients, I was able to strengthen and further develop my knowledge gained through CT simulations, and better understand patient setup, treatment delivery and verification. I was also able to discuss outcomes of this technique, patient experience and satisfaction.

In a two week period, it was possible to see enough clinical cases and to overcome the challenges of such a technique.

---

#### Symposium: The microbiome, inflammation and radiotherapy response

---

#### SP-0331 Gut microbiota SCFAs modulate dendritic cell antigen presentation and impact radiotherapy

Andrea Facciabene<sup>1</sup>, S Rafail<sup>2</sup>, M Uribe-Herranz<sup>3</sup>, C Koumenis<sup>2</sup>

<sup>1</sup>University Of Pennsylvania,

Department Of Radiation Oncology-

Rand The Ovarian Canc. Res. Center\R, Philadelphia, Usa

<sup>2</sup>Upenn, Radiation Oncology, Philadelphia, Usa

<sup>3</sup>Upenn, Radiaiton Oncology, Philadelphia, Usa

#### Abstract text

Alterations in gut microbiota impact the pathophysiology of several diseases, including cancer. Radiotherapy (RT), an established curative and palliative cancer treatment, exerts potent immune modulatory effects, inducing tumor-associated antigen (TAA) cross-priming with anti-tumor CD8+ T cell elicitation and abscopal effects. Herein, we tested whether the gut microbiota modulates anti-tumor immune response following RT distal to the gut. Vancomycin, an antibiotic that acts mainly on gram-positive bacteria and is restricted to the gut, potentiated the RT-induced anti-tumor immune response and tumor growth inhibition. This synergy was dependent on TAA cross presentation to cytolytic CD8+ T cells and on IFN-g. Notably, butyrate, a metabolite produced by the vancomycin-depleted gut bacteria, abrogated the vancomycin effect. In conclusion, depletion of vancomycin sensitive bacteria enhances the anti-tumor activity of RT, which has important clinical ramifications.

**SP-0332 The Microbiome & Cancer Therapies**V. Paziienza<sup>1</sup><sup>1</sup>Fondazione IRCCS "Casa Sollievo della Sofferenza"  
Hospital, Gastroenterology, San Giovanni Rotondo, Italy**Abstract text**

Despite continuous advances in cancer related therapies, resistance to standard drugs and adverse effects still represent an important cause of therapeutic failure. Cancer is a major health burden worldwide being among the top two killing disease in the frame of non communicable diseases that are responsible of the 70% of deaths worldwide. There is a growing evidence that gut bacteria can affect the response to chemo, immuno and radiotherapeutic drugs by modulating either efficacy or toxicity. Moreover, intratumor bacteria have been shown to modulate chemotherapy response. At the same time, anticancer treatments themselves significantly affect the microbiota composition, thus disrupting homeostasis and exacerbating discomfort to the patient. In this lecture is presented the existing knowledge concerning the role of the microbiota in mediating chemo, immuno and radiotherapy efficacy and toxicity and the ability of these therapeutic options to trigger dysbiotic condition contributing to the severity of side effects. In addition, we discuss the use of probiotics, prebiotics, synbiotics, postbiotics, and antibiotics as emerging strategies for manipulating the microbiota in order to improve therapeutic outcome or at least ensure patients a better quality of life all along of anticancer treatments.

**SP-0333 Immune effects of the microbiome on cancer treatment**M. Nuti<sup>1</sup><sup>1</sup>Sapienza University of Rome, Division of Medical Oncology B- Department of Radiological- Oncological and Pathological Sciences- Policlinico Umberto I, Rome, Italy**Abstract text**

The microbiome is associated with immunity and the development of a healthy immune system. Several factors are known to influence the variable part of the microbiome such as host lifestyle, environment, diet, genotype, pathobiology, inflammation etc.. Parameters associated with a healthy and fit microbioma are essentially the high diversity and a resilient feature i.e the capacity to cope with a physiological stress. An unbalanced scenario together with a concomitant factors such as an inflammation process and/or presence of pathogens can cause complex diseases. It was not surprising the finding that outcome of immunotherapeutic strategies in cancer patients can be dependent on the gut microbiome. Treatment of cancer with check point inhibitors capable to unleash T cells to expand exponentially and kill transformed cells, is the newest and best treatment strategy being developed in the last decade. A true revolution in oncology is ongoing and we are seeing dramatic responses and long term overall survival in critical deadly tumors like advanced melanoma, non-small cell lung cancers, renal cell carcinomas. Not all patients respond and some of them show severe autoimmune toxicities. Data are now emerging suggesting that response to ICI therapy, particularly anti-CTLA4, is associated to microbioma composition and that restored immunity and antitumor activity of ICI could be achieved only with transplantation of stool samples from responder patients. Immunological mechanisms underlying these findings are still in the process of being fully elucidated. Significance of these findings is quite relevant for future strategies in oncology. We are today facing the possibility that modulation of microbioma with probiotics or fecal transplants can

increase the prevalence of bacteria linked to anticancer immunosurveillance and adapt bacteria ecosystem accordingly.

**SP-0334 The Microbiome and treatment side-effects**Y. Touchefeu<sup>1</sup><sup>1</sup>Institut des Maladies de l'Appareil Digestif- University Hospital- Nantes- France, Hepato-Gastroenterology, Nantes, France**Abstract text**

Radiation therapy and chemotherapy induce major changes in the composition of the gut microbiota. Basic and clinical data suggest that the intestinal microbiota may play an important role in the pathogenesis of chemo- or radiation-induced mucositis. Further metagenomic studies, investigating microbiota gene functions, are required to better understand the impact of microbiota disruption during cancer treatments. Strategies can be developed to prevent or treat potentially life threatening treatment complications, using manipulations of the intestinal microbiota. Probiotics may be beneficial to prevent chemo or radiation-induced diarrhoea. Gut microbiota identification could also be used as a predictive marker for radiation and chemotherapy adverse effects such as mucositis, diarrhoea, fatigue, pain and bacteremia, and could guide preventive strategies.

---

**Symposium: Reducing the normal tissue effects of RT**

---

**SP-0335 Stem cell replacement to overcome RT induced xerostomia**C. Von Buchwald<sup>1</sup>, C. Groenhoej<sup>1</sup>, C.D. Lynggaard<sup>1</sup><sup>1</sup>Rigshospitalet- Copenhagen- Denmark, Department of Orl- H and N Surgery And Audology, Copenhagen, Denmark**Abstract text**

**Background:** Salivary gland hypofunction and xerostomia are major complications to head and neck radiotherapy. We have conducted a trial assessing the safety and efficacy of adipose tissue-derived mesenchymal stem cell (ASC) therapy for radiation-induced xerostomia. **Patient and Methods:** A randomized, placebo-controlled phase I/II trial included 30 patients, randomized in a 1:1 ratio to receive ultrasound-guided transplantation of ASCs or placebo to the submandibular glands. Patients had previously received radiotherapy for a T1-2, N0-2A, human papillomavirus-positive, oropharyngeal squamous cell carcinoma. The primary outcome was the change in unstimulated whole salivary flow rate, measured before and four months after the intervention. **Results:** No severe adverse events were detected. Unstimulated whole salivary flow rates significantly increased in the ASC-arm at one (33%; p=0.048) and four months (50%; p=0.003), but not in the placebo-arm (p=0.6 and p=0.8), compared to baseline. The ASC-arm symptom scores significantly decreased on the xerostomia and VAS questionnaires, in the domains of thirst (-22%, p=0.035) and difficulties in eating solid foods (-2%, p=0.008) after four months compared to baseline. The ASC-arm showed significantly improved salivary gland functions of inorganic element secretion and absorption, at baseline and four months, compared to the placebo-arm. Core-needle biopsies showed increases in serous gland tissue and decreases in adipose and connective tissues in the ASC-arm compared to the placebo-arm (p=0.04 and p=0.02, respectively). MRIs showed no significant differences between groups in gland size or intensity (p < 0.05). In addition, outcome from one-year follow-up study along with next the stem cell studies in the pipeline will be presented. **Conclusions:** We have conducted the first-in-man transplantation of

ASCs for radiation-induced salivary hypofunction and xerostomia and found it safe and significantly improved salivary gland functions and patient-reported outcomes.

**SP-0336 Reducing normal tissue damage by sparing of stem cells using protons**

P. Van Luijk<sup>1</sup>

<sup>1</sup>*University of Groningen- University Medical Center Groningen, Radiation Oncology, Groningen, The Netherlands*

**Abstract text**

Radiotherapy plays an important role in the treatment of many forms of cancer. However, dose to normal tissue frequently leads to damage, toxicity and reduction of quality of life of the patient.

Xerostomia is a frequently-observed side-effect of the treatment of head-and-neck tumors, associated with irradiation of the parotid gland. Recently it has been shown that the response of the parotid gland critically depends on dose to its major ducts, containing most of its stem cells. The observation that sparing of a relatively small substructure of an organ is important to preserve its function after radiotherapy opened new opportunities for reducing toxicity. In addition, recent pre-clinical work suggests that tissue-specific stem cells are particularly sensitive to low doses of radiation.

Interestingly, these findings coincides with an increasing availability of proton therapy world-wide. The precision of protons provides unique opportunities to specifically spare such substructures. In addition they offer more opportunities to limit the large volumes receiving low doses, as typically observed in Intensity Modulated Radiotherapy.

In conclusion, based on the unique properties of protons and available information from radiobiology, proton therapy may offer unique opportunities to reduce toxicity of radiotherapy.

**SP-0337 Mechanisms of radiotherapy-induced neurocognitive decline**

L. Barazzuol<sup>1,2</sup>

<sup>1</sup>*UMCG, Department Of Radiation Oncology, Groningen, The Netherlands;* <sup>2</sup>*umcg, Department Of Biomedical Sciences Of Cells And Systems, Groningen, The Netherlands*

**Abstract text**

Radiotherapy is an essential part of the treatment of paediatric and adult primary brain tumours. Although long-term survival rates are increasing, 50 to 90% of the surviving patients develop neurological dysfunction leading to a reduced quality of life. Symptoms include a progressive impairment in memory, executive function and processing speed. In particular, children and young adults suffer from significant loss of intelligence quotient, with an average IQ decline of over 2 points per year. The pathogenesis of radiation-induced neurocognitive dysfunction is not well understood and consequently no effective treatment or prevention strategy exist. My laboratory, by using a combination of methodologies, including cerebral organoids and *in vivo* models, aims to reduce radiotherapy-induced neurocognitive dysfunction. Radiotherapy mainly works by damaging the DNA. To date, the link between DNA damage and neuropathology is not fully understood. Yet it is widely accepted that diminished protein homeostasis can cause neurodegeneration in aging and protein-misfolding diseases (such as Alzheimer's and Parkinson's disease).

Our recent data provide the first evidence that radiation-induced DNA damage leads to loss of protein homeostasis. Using different model systems, from primary neuronal and glial cells, human ES/iPS-derived cortical organoids to mouse and rat models, we have shown elevated protein

aggregation levels after DNA damage caused either directly by radiation or indirectly by impairment of the DNA damage response. This imbalance in protein homeostasis can be reduced by modulating the protein quality control capacity. In this presentation, new molecular targets for the future development of interventions will be presented.

**SP-0338 Neurocognition and brain irradiation**

S. Deprez<sup>1</sup>

<sup>1</sup>*KULeuven, Imaging and Pathology, Leuven, Belgium*

**Abstract text**

Whole brain irradiation (WBRT) is an important treatment modality in the management of brain metastases. Additionally, WBRT in the form of prophylactic cranial irradiation (PCI) is often used to reduce the incidence of brain metastases in for example small-cell lung cancer. Although effective in cancer control, WBRT has important neurotoxic side effects. Fifty percent or more of patients who survive 6 months or longer after WBRT report cognitive dysfunction. Functional deficits including impairments in memory, attention and executive functioning can have a serious impact on quality of life. Mechanisms of radiation-induced cognitive impairment are still poorly understood. The pathophysiology of brain injury after RT is multifactorial and complex. Possible mechanisms include CNS-irradiation triggered neuroinflammation, decreased hippocampal neurogenesis and vascular injury. Both early stage (< 6m after RT) and late delayed (>6m) brain injury can contribute to the observed cognitive dysfunction. Various pharmacologic and non-pharmacologic strategies to prevent or alleviate these toxicities are being investigated. In this talk an overview will be given of current knowledge in the field of neurocognition and brain irradiation, possible mechanisms of radiation-induced cognitive impairment and strategies for preservation being investigated.

---

**Symposium: Radiotherapy in the era of the Silver Tsunami**

---

**SP-0339 Cancer epidemiology in Europe with focus on indications for RT**

J. Overgaard<sup>1</sup>

<sup>1</sup>*Aarhus University Hospital, Dept. of Clinical Experimental Oncology, Aarhus, Denmark*

Abstract not received

**SP-0340 Does normal tissue in elderly patients have different sensitivity and tolerance and do tumors require different treatment?**

C. Herskind<sup>1</sup>,

<sup>1</sup>*Universitätsmedizin Mannheim- Medical Faculty Mannheim- Heidelberg University, Department of Radiation Oncology, Mannheim, Germany*

**Abstract text**

In clinical practice patients are often considered elderly from the age of 65-70 years. However, in the developed world with high life expectancy, healthy persons of this age have an expected remaining life span of 15-20 years, and even persons with an attained age of 75-80 years are expected to live for another 8-12 years or longer. Therefore, long-term survival and quality of life is as important for cancer patients in this age group as in younger patients. It is a commonly made assumption that elderly patient show poorer tolerance and may not be eligible for radiotherapy protocols used in curative treatment of patients below this age. However, there is little high-level evidence to support this view. The

presentation will summarize the biological changes associated with increasing age and will emphasize the large individual variation observed. Clinical studies of the sensitivity and tolerance of normal tissue in elderly patients will be reviewed and the role of co-morbidities will be discussed. Furthermore, the available data on survival outcome of standard treatment protocols for different tumour entities will be considered. The bulk of the current evidence seriously questions the common practice of excluding cancer patients from study protocols solely on the basis of their chronological age

**SP-0341 Influence of age and comorbidity on outcome and compliance to RT**

C.R. Boeje<sup>1</sup>, J. Overgaard<sup>2</sup>

<sup>1</sup>Aalborg University Hospital, Dept of Oncology, Aalborg, Denmark; <sup>2</sup>Aarhus University Hospital, Dept. of Clinical Experimental Oncology, Aarhus, Denmark

**Abstract text**

Head and neck cancer (HNC) patients are often long term users of tobacco and/or alcohol. Besides the carcinogenic effect of these substances they also lead to other chronic diseases and thus contributes to a high prevalence of comorbidities among HNC patients. Due to demographic changes the general population becomes older and consequently more HNC patients may suffer from comorbidity. Severe comorbidity may impact on prognosis for HNC patients and may impact treatment decision, compliance and subsequent outcome. This talk will focus on comorbidity and age in HNC patients and the impact on survival. Data will be presented from different studies including large population based study from the DAHANCA group. These studies show that comorbidity is common among HNC patients and is a negative prognostic factor for overall survival. Comorbidity also have a negative impact on cancer specific survival, while age does not. Therefore, critical assessment of comorbidity can significantly improve the decision-making proces for clinicians and may influence and improve patient outcome.

**SP-0342 From geriatric assessment in radiation oncology to interventions: experience from the PIVOG trial**

D. Vordermark<sup>1</sup>

<sup>1</sup>Martin Luther University Halle-Wittenberg, Dept. of Radiation Oncology, Halle/Saale, Germany

**Abstract text**

The demographic development in Europe e. g. in Germany leads to increasing need of adapted care concepts for elderly cancer patients. General principles (e. g. "go-go, slow-go, no-go" for very fit, quite fit and unfit elderly patients, respectively) are difficult to translate into clinical treatment recommendations for individual patients. Maintaining quality of life is highly important for elderly cancer patients. Its measurement, however, has only become possible recently with established of normal reference values for elderly age groups (e. g. for the EORTC QLQ-C30 questionnaire) and the validation of an elderly-specific instrument (QLQ-ELD 14; Wheelwright et al., Br J Cancer 2013).

Using these tools, we could show in an observational study of n=50 very elderly (>80 years old) cancer patients undergoing radiotherapy, that general and elderly-specific quality of life remained stable from beginning to end of radiotherapy, but deteriorated in several domains, including physical function, role function and family support by 6 months after treatment (Kaufmann et al., Support Care Cancer 2015). A possible explanation was the good access to supportive treatment during radiotherapy, but lack thereof after treatment.

We interpreted this as a need to develop an intervention to stabilize quality of life of elderly cancer patients after

the end of treatment and developed a complex intervention containing (a) a clinically feasible comprehensive geriatric assesmentn (CGA) before the start of cancer treatment and (b) regular telephone contact with an oncology nurse during the first six months after treatment to counsel patients on the management of symptoms and provide additional ressources of care. This intervention was pilot tested in n=100 elderly patients over 70 years with at least one comorbidity and / or one functional impairment in the PIVOG trial (Patient-centered Interdisciplinary Care Concept for Geriatric Oncology Patients; Schmidt et al., J Geriat Oncol 2017). The geriatric assessment was feasible and took on average one hour. The nurse-led telephone contact was well accepted (used by 79% of patients, mean 7.8 calls per patient, mean duration 14 minutes). In the primary endpoint, global quality of life at 6-month follow-up, mean scores were stabilized compared to baseline. Clinically relevant improvement and deterioration were seen in 35% and 28% of patients, respectively, no change in 37%. Details on the experience with specific elements of the geriatric assessment and development in subscales of quality of life will be presented. Ongoing work is focussed on developing the complex intervention for evaluation in a randomized trial, on physical exercise to improve or stabilize physical function in elderly cancer patients and on the implementation of electronic patient-reported outcome measurement in geriatric oncology using the CHES platform.

---

**Debate: Which is the best brachytherapy technique to deliver partial breast irradiation? Pitfalls, results and current recommendations**

---

**SP-0343 Postoperative multicatheter brachytherapy**

J. Hannoun-Levi<sup>1</sup>

<sup>1</sup>Centre Antoine Lacassagne, Radiation Therapy, Nice, France

**Abstract text**

Whatever the breast brachytherapy indication (boost, APBI for primary or APBrI for salvage irradiation), breast brachytherapy can be performed intra or post-operatively. We listed the different point which can be positively or negatively impacted if the implant is performed intra or postoperatively. Regarding breast brachytherapy applicators, in case of intra-operative implant, both multicatheter and balloon devices (single or multilumen) can be used, while in case of postoperative implant multicatheter brachy is the only one possible technique. For patient comfort regarding to anesthesia, in case of intra-op implant, the patient is under general anesthesia which is more comfortable compare to a local one in a postoperative implant. Regarding to "Vectors in place" duration, in case of intra-operative implant, before starting the irradiation, it is warranted to obtain the full postoperative pathological report which takes between 5 to 8 days plus 4 to 5 more days for the treatment itself for a total duration ranged between 10 to 15 days (patient discomfort, risk of local infection and/or pain). However, in case of post-operative implant, the "Vectors in place" duration is reduced to the treatment duration itself plus/minus the delay between the implant and the first day of irradiation. For brachytherapist comfort regarding to anesthesia in case of intra-op implant, surgeon and brachytherapist can work together, with a full visibility of the tumor bed and the clip position. No pressure due to potential patient pain. In case of post-operative implant, it is sometimes difficult to perform the implant when the patient is not totally relaxed, obliging the brachytherapist to do the implant in a shorter time (potential stress). In terms of organization, in case of intra-operative implant, the brachytherapist must be available at the time of the

surgical procedure (which is often delayed for some reasons). However, in case of post-operative implant, the implant can be scheduled according to the brachytherapist activity/program. For vector implantation, in case of intra-operative implant, whatever the location of the tumor bed, it is always possible to place the vectors even if (in some cases) it is necessary to insert the needles in two times (for large breast, deep tumor bed, complex angulation ...). But in case of post-operative implant, it is sometimes possible to switch from brachy to external beam APBI in the clinical situations listed above (impossibility to properly place the vectors). For CTV delineation, in case of intra-operative implant, it is sometimes possible to (post-operatively) add some extra-needles in order to more accurately cover the target volume in regards to the clips and considering the delineation rules (SM = 2 cm = Surgical margin + brachy margin). In case of post-operative implant, it is possible to use all the imaging supports and mainly a pre-implant CT-scan allowing a pre-planning calculation considering all the delineation parameters. For treatment modification after post-op histology, according to the post-operative final pathological report, APBI is sometimes not possible in regards to the GEC-ESTRO APBI criteria. In this situation and after intra-operative implant, it is possible to remove applicator/vectors and continue the treatment either with WBI or systemic therapy. It is also possible to propose an anticipated boost which is acceptable only if there is no indication of chemotherapy. But in case of post-operative implant intent, if the final pathological data do not match with APBI criteria, no implant will be performed. The export of breast brachytherapy technique ( $\neq$  centers: surgery & brachy) is a very important point. In case of intra-operative implant, and if the surgeon works in a different place, the later must perform the lumpectomy in the brachytherapist hospital or, the brachytherapist must go to the surgeon hospital. Leading to consider that breast brachytherapy will be difficult to export because the surgeon, in the large majority of the cases, will not accept to refer his patient to another surgeon who works in the brachytherapist hospital. However, in case of post-operative implant, each doctor (surgeon and brachytherapist) will perform his procedure in his own hospital.

#### SP-0344 Intraoperative multicatheter brachytherapy

K. Lössl<sup>1</sup>

<sup>1</sup>University of Bern, Inselspital Bern University Hospital, Bern, Switzerland

Abstract not received

#### SP-0345 Single catheter balloon brachytherapy (MammoSite, Contura)

P. Niehoff<sup>1</sup>

<sup>1</sup>Klinikum Offenbach GmbH, Dep. of Radiotherapy, Offenbach am Main, Germany

##### Abstract text

APBI is elegant method for treating low risk breast cancer patients. Single balloon catheter (MammoSite/ Contura) is the easiest way to treat pts. with APBI. If a open cavity method surgery has been used a geographic miss is extreme rare. Target definition is related to the applicator. The disadvantages are limited options for dose painting and covering the target volume. Another problem is the necessary for a minimum skin distance of 1.5 cm. Compared to other technique single lumen catheter have there limitation for breast size. The toxicity might be higher and the dose distribution worse compared to other techniques. But for deep sited small tumors and a large breast single lumen catheter are suitable.

#### SP-0346 Single catheter brachytherapy (SAVI) - Pitfalls, results and current recommendations.

A. Chichel<sup>1</sup>

<sup>1</sup>Greater Poland Cancer Centre, Department of Brachytherapy, Poznan, Poland

##### Abstract text

##### Introduction

Strut Adjusted Volume Implant (SAVI) serves as a single-entry Accelerated Partial Breast Irradiation (APBI) device that mimics, fastens and simplifies multicatheter interstitial brachytherapy (BT). In breast conserving therapy (BCT) radiation is mandatory, substantially reduces local recurrence rate and also improves overall survival. In low risk breast cancer patients APBI is proven safe alternative for whole breast irradiation. Amongst a number of possible techniques there is SAVI, which conforms with open cavity approach and fits the cavities easily with a set of applicator sizes. Single-entry device minimizes the risk of infection and improves patients' comfort.

##### Aim

The study is to report the long-term results in regard to loco-regional control and single institution experience in high-dose rate (HDR) BT APBI with the usage of single-entry applicator (SAVI) for early breast cancer patients treated with breast conserving approach.

##### Material and methods

Between Jan 2012 and Dec 2012, 11 stage I-IIA breast cancer patients (pT<sub>is</sub> - 1, pT<sub>1</sub> - 9, pT<sub>2</sub> - 1) were treated with BCT + adjuvant hormonal therapy and APBI HDR BT. All were implanted with SAVI in about 6 weeks after surgery and after receiving full pathological report. Each patient had a CT scan and treatment plan prepared on the day of implantation and started the treatment consisted of 10 daily fraction of 3,4 Gy. In this study overall survival (OS), disease-free survival (DFS), loco-regional control (LRC), cosmetic outcome (CO) and the tumor bed (TB) appearance were noted.

##### Results

Median follow-up was 58,5 months (range 19-78). One patient was lost from observation. Treatment plan parameters were as listed: PTV\_EVAL\_95 mean 96,89% (range 86,71 - 101,19%), PTV\_EVAL\_90 mean 101,74% (range 93,29 - 106,01%), skin 0,1 cc mean 60,9% (range 17,81 - 101,16%), chestwall 0,1 cc mean 72,1% (range 19,05 - 111,55%), lung 0,1 cc mean 51,99% (range 17,39 - 78,8%). In all cases treatment was completed without procedural complications and on time. OS was 10/10, DFS was 9/10 (1 case of multiple bone metastases), LRC was 100%. CO was excellent in 6/10 and good in 4/10. There were no outcomes assessed as satisfactory or poor. 5/10 patients resulted with soft breast and 5/10 had palpable painless TB (slight induration). No fat necrosis was identified on control mammograms. No superficial skin changes were observed.

##### Conclusions

APBI with HDR brachytherapy based on SAVI was feasible and well tolerated. As other APBI techniques SAVI results with perfect local control and itself saves very good breast appearance after proper surgery. SAVI application is fast and easy in experienced hands, needs only adequately prepared tumor bed, palpation and ultrasound. May be considered as intraoperative technique. SAVI offers better optimization abilities in comparison with single or multilumen balloon applicators, mimics and simplifies multicatheter interstitial BT. SAVI with its single entry minimizes the risk of infection and improves patients' comfort. Other advantages as well as important pitfalls, current recommendations and sights for future for SAVI will be discussed during the debate.

**Keywords:** SAVI, brachytherapy, APBI, breast cancer.

**SP-0347****The need and potential for use of big data for research and development of radiotherapy**

Leonard Wee<sup>1</sup>, J Van Soest<sup>2</sup>, I Bermejo<sup>3</sup>, R Fijten<sup>1</sup>, A Dekker<sup>2</sup>

<sup>1</sup>*School For Oncology and Developmental Biology-, Maastric Clinic, Maastricht, The Netherlands*

<sup>2</sup>*Institute Of Data Science, Maastricht University, Maastricht, The Netherlands*

<sup>3</sup>*School Of Oncology And Developmental Biology, Maastric Clinic, Maastricht, The Netherlands*

**Abstract text**

Radiation oncology is an area of medicine that stands to benefit enormously from clinical knowledge extracted from “big data”. Radiotherapy departments worldwide generate a vast quantity and variety of data daily, due to the extensive use of medical imaging and a relative high degree of process automation already in place. It is important to understand the scope, type, quality and distribution of variegated oncology data if we wish to extract knowledge using machine learning and artificial intelligence. The potential benefits that can be addressed through utilization of big data approaches in healthcare generally fall into two domains - operational improvements and direct patient benefit. Among the major clinical needs in radiation oncology are : appropriate patient stratification, optimal treatment selection and reducing unjustified variation in procedures. Operational excellence, such as automating routine steps in clinical workflow, are more easily introduced into clinical practice but tend to have limited or indirect patient impact. Prediction of prognosis and treatment outcome (hence exerting direct influence on clinicians’ decision making) is much more cautiously being introduced into the clinic, but has immense future potential for substantial patient benefit. There are still major challenges impeding research and clinical utilization, chiefly focussed around issues of consent, privacy, generalizability and quality assurance.

**SP-0348 Challenges of collection, sharing and analysis of data at scale**

M. Modat<sup>1</sup>

<sup>1</sup>*Kings College London, London, United Kingdom*

Abstract not received

**SP-0349 Practicalities and issues of setting up the infrastructure to collect big data in a hospital environment**

G. Price<sup>1</sup>

<sup>1</sup>*The University Of Manchester, The Christie Nhs Foundation Trust, Manchester, United Kingdom*

**Abstract text**

Recent years have seen increased interest in the clinical value of routinely collected patient data. The migration to electronic patient record systems coupled with the increased ease with which powerful machine learning techniques can be employed has led to huge growth in the volume of retrospective observational studies reported in the radiation oncology literature. High quality studies can provide valuable insight where gold standard randomized trial evidence is lacking or where traditional methodologies are not appropriate.

The Christie NHS Foundation Trust in partnership with the Manchester Cancer Research Centre has invested significant effort in establishing an informatics infrastructure to enable such studies. Use of the system has underpinned a rapid expansion in the volume of related research within the institutes and streamlined

collaboration with international partners. In this talk we describe the practicalities of implementing this system, focusing on the organizational, resource and governance aspects as well as the technical detail. We explore both the barriers overcome and the remaining challenges, and consider, with examples and case studies, how the system fits into both the academic and clinical aspirations of the host institutions.

**Symposium: From grid therapy to microbeam radiotherapy****SP-0350 Introduction to microbeam radiation therapy: radiosurgical grid therapy at the microscopic scale**

E. Schültke<sup>1</sup>

<sup>1</sup>*Rostock University Medical Center, Radiooncology, Rostock, Germany*

**Abstract text**

Microbeam radiation therapy (MRT) is a still experimental concept of spatially fractionated radiotherapy. Clinically, it compares closets to radiosurgery and grid radiotherapy. In MRT, the irradiation target is covered by an array of quasi parallel microbeams. Microbeams are typically between 25 and 100 µm wide and spaced at center-to-center distances of several hundred micrometers. Thus, an inhomogeneous dose distribution with characteristic peak dose (high dose) and valley dose (low dose) zones is generated. The X-ray doses deposited in the peak dose zones are typically in the order of several hundred Gy. It has been shown in small animal models of malignant brain tumour that MRT allows a superior tumour control compared to current clinical radiotherapy concepts. The original concept of MRT has been developed in the 1980s by a group of researchers at the NSLS (synchrotron radiation source at Brookhaven, USA) with the experiences of classic clinical grid radiotherapy in mind. Since then, an increasing number of research groups has expanded the field to understand the therapeutic potential of MRT. Different irradiation schedules were tested, with MRT as single fraction treatment similar to clinical radiosurgery or with MRT integrated in a conventional radiotherapy schedule. Studies were designed to assess the tolerance of normal tissue and the potential adverse effects of MRT. During the first decade, MRT research focused mainly on brain tumours as target indications. More recently, there have been interesting developments within the MRT research community to include other tumour entities as possible targets, such as malignant melanoma and carcinoma of the lung.

This presentation will highlight key achievements of MRT research in preparation of its transition from bench to bedside.

**SP-0351 Spatial fractionation of the dose: from photons to charged particles**

Y. Prezado<sup>1</sup>

<sup>1</sup>*Imagerie et Modélisation en Neurobiologie et Cancérologie, New Approaches in Radiotherapy, Orsay, France*

**Abstract text**

The therapeutic use of ionizing radiation has been largely guided by the goal of directly eliminating all cancer cells while minimizing the toxicity to adjacent tissues. Nowadays, technological advances in radiation delivery, including image guidance and particle therapy (i.e. proton therapy), have notably improved tumor dose conformation, thus reducing the dose to the organs-at-risk. Despite remarkable advancements, the dose tolerances of normal tissues continue to be the main limitation in RT and still compromise the treatment of some radioresistant tumors, tumors close to a sensitive

structure (e.g. central nervous system (CNS)) and paediatric cancer. One possible way to overcome this limitation is to employ new modes of radiation dose deposition that activate biological processes different from those acting in standard radiotherapy. An example is the spatial fractionation of the dose. This lecture will give a general overview about this strategy. A particular focus will be put on minibeam radiation therapy (MBRT) and its advantages. MBRT, originated at synchrotrons, can now be explored outside large facilities thanks to its successful transfer into cost-effective equipment [1]. This allows a widespread implementation, the realisation of comprehensive and systematic biological studies and an easy transfer to potential clinical trials. In the recent years, the exploration of the possible synergies between the advantages of MBRT and the benefits of charged particles for therapy has started, with techniques like proton and heavy ions MBRT [2-7]. In particular, proton MBRT [2] has been implemented at a clinical center (Orsay proton therapy center) and it has already shown an effectiveness of tumor control equivalent or superior than that of standard PT without the important side effects observed in the latter, thus opening the possibility for more aggressive irradiation schemes [3-5]. Concerning heavy ions MBRT, the dosimetric data obtained supports the exploration of this radiotherapy approach [6,7]. Among the different ions species evaluated, Ne stands as the one leading to the best balance between high peak-to-valley dose ratio and peak-to-valley-LET ratio in normal tissues and high LET values in the target region [6]. The biological mechanisms in MBRT, which are not completely known, seem to contradict the classic RT paradigms. Its exploration offers a whole new horizon of both scientific research and potential future clinical practice. The spatial fractionation of the dose could especially benefit paediatric oncology (central nervous system), whose treatments are limited to the high risk of complications in the development of the infants.

[1] Y. Prezado et al, *Sci. Reports* 7, article number 17295 (2017).

[2] Y. Prezado and G. Fois, *Med. Phys.* 40, 031712, 1-8 (2013).

[3] Y. Prezado et al., *Scie. Reports* 7, article number 14403 (2017).

[4] Y. Prezado et al. *Scientific Reports* 8, article number 16479 (2018).

[5] Y. Prezado et al, *IJROBP* (2018).

[6] W. Gonzalez and Y. Prezado, *Medical Physics* 45, 2620-2627 (2018).

[7] I. Martinez-Rovira et al. *Med. Phys.* 44, 4223-4229 (2017).

#### SP-0352 Dosimetry measurement in microbeam therapy

J. Lye<sup>1</sup>, P. Harty<sup>2</sup>, D. Butler<sup>2</sup>

<sup>1</sup>Australian Radiation Protection And Nuclear Safety Agency, Australian Clinical Dosimetry Service, Melbourne- Victoria, Australia; <sup>2</sup>Australian Radiation Protection And Nuclear Safety Agency, Psdl, Melbourne-Victoria, Australia

##### Abstract text

Microbeam radiation therapy (MRT) with Synchrotron beams continues to evolve from promising research towards clinical or veterinary radiotherapy. The change from research to clinical applications requires many developments including dedicated treatment planning, image guidance, patient quality systems and high quality dosimetry. The focus of this presentation is on the challenge of absolute and relative dosimetry as performed at the Australian Synchrotron. The Synchrotron dosimetry chain consists firstly of absolute dosimetry in a "broadbeam"- in this context field sizes of a few centimetres. The next stage is relative dosimetry in the microbeams approximately 10-100 microns in

width. Secondary standard dosimeters such as ionization chambers require calibration in conventional x-ray sources with substantially different field sizes, dose-rates, polarizations and spectra to synchrotron beams. These differences add significant uncertainties to measurements of the dose in the synchrotron beam. Calorimeters and free air chambers can determine dosimetric quantities from first principles. Calorimetry has been successfully performed directly on Synchrotron beams as the high dose rates offers the advantage of increased temperature rise compared to conventional clinical linac calorimetry. Free air chambers (FAC) can also be used for absolute dosimetry, however they suffer from strong recombination and electron loss effects in Synchrotron beams. FAC are also useful tools for continuously monitoring in Synchrotron beams. The determination of the peak and valley dose of the microbeams is challenging. Understanding the valley dose is particularly important as this is a key parameter to spare the normal tissue, limiting the clinical dose delivered. Film and microdiamond detectors are commercially available and with careful use and analysis have had success in microbeam dosimetry. Other promising detectors are high spatial resolution fibre optic dosimeters (FOD) and silicon detector arrays.

#### SP-0353 Compact microbeam sources and microbeam treatment planning

S. Bartzsch<sup>1,2</sup>

<sup>1</sup>Klinikum Rechts Der Isar- Technical University Munich, Department of Radiation Oncology, Munich, Germany; <sup>2</sup>Helmholtz-Zentrum Munich, Institute Of Innovative Radiotherapy, Munich, Germany

##### Abstract text

Microbeam radiation therapy (MRT) is an approach in radiation oncology that modulates radiation doses on a micrometre scale. Homogeneous radiation fields are collimated into 25-100 micrometre wide beamlets with a few hundred micrometre spacing between each other. Abundant preclinical research demonstrated that MRT has the potential to change radiotherapy treatment paradigms for certain tumour types. However, the technical demands of MRT on dosimetry, dose calculation, treatment planning and on the radiation source are high.

So far dose calculations in MRT have largely been based on Monte Carlo simulations. However, the small dimensions of the treatment fields, subsequent small voxel sizes and substantial dose differences between high and low dose regions entail long simulation times and often poor statistics. An alternative to Monte Carlo simulations are kernel based dose calculation approaches. Although these approaches are much faster they often lack accuracy at material boundaries due to the utilization of low energy photons in MRT. Hybrid dose calculation approaches use elements of both approaches and provide a very accurate and efficient way to calculate peak doses, valley doses and dose profiles. Even complicated cross-firing geometries can easily be calculated. Currently we implement a hybrid dose calculation engine in the popular treatment planning system Eclipse® (Varian), enabling treatment planning for first clinical trials in MRT.

The meaning of peak and valley doses in MRT on tissue reactions remains controversial. In order to plan and carry out first clinical trials in MRT, estimates on the biological effectiveness of microbeams based on the physical dose distribution are required. Recently, it has been suggested to use the concept of equivalent uniform dose (EUD). This concept can be calculated for arbitrary and complex beam geometries and our own in-vitro data demonstrates its applicability.

The major obstacle for a clinical application of MRT is the availability of adequate radiation sources. MRT requires high dose rates of more than 100 Gy/s, small beam divergence and photon energies of around 100 to 300

keV. Currently only a few large third generation synchrotrons around the world, such as the European Synchrotron in Grenoble (France) provide such beam properties. Various alternative approaches have been discussed in the past, including inverse Compton scattering sources and carbon nanotube x-ray tubes. Another strategy is the Line-Focus x-ray tube (LFxT), a source based on classical x-ray tubes, where the electron beam is focused to an extremely eccentric focal spot on a rapidly rotating tungsten target. The rapid relative movement between target and focal spot leads to a change in the energy transport within the target. Our simulations show that such a source can provide up to 200 Gy/s MRT peak entrance dose rate in a clinical setting.

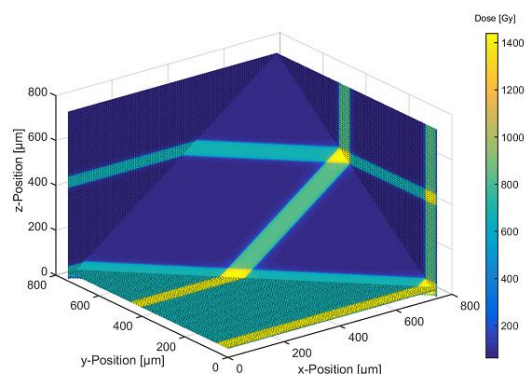


Figure 1: Hybrid dose calculation approaches can calculate complex MRT treatment geometries within a few minutes. The resulting dose distributions can be used to calculate the equivalent uniform dose a promising predictor for normal tissue reactions.

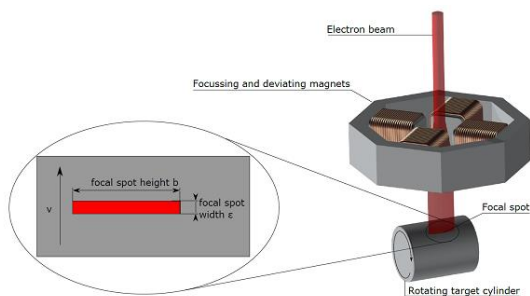


Figure 2: The concept of the line focus x-ray tube is based on conventional x-ray tube technology. An eccentric focal spot hits a fast rotating target cylinder.

## Symposium: Focus on the lung

### SP-0354 Image-guided adaptive radiotherapy in the treatment of lung cancer patients

M. Tvilum<sup>1</sup>, M. Marquard Knap<sup>1</sup>, L. Hoffmann<sup>2</sup>, A. Ahmed Khalil<sup>1</sup>, C.M. Lutz<sup>2</sup>, D. Sloth Møller<sup>2</sup>

<sup>1</sup>Aarhus University Hospital, Department Of Oncology, Aarhus C, Denmark; <sup>2</sup>Aarhus University Hospital, Department Of Medical Physics, Aarhus C, Denmark

#### Abstract text

Anatomical changes often occur during treatment of lung cancer patients with curative intended radiotherapy. These changes affect both the dose delivered to the tumour and to the normal tissue. By using the concepts of adaptive radiotherapy, the planned dose distribution can

be restored. Daily cone-beam CT scans based on soft tissue match are used for patient setup at Aarhus University Hospital. The combination of soft tissue match and an adaptive strategy allows for reduction in treatment margins, reduction in dose to normal tissue and enables dose escalation. This lecture focusses on the clinical implementation of image-guided adaptive radiotherapy in the treatment of lung cancer patients. It presents both the dosimetric and clinical outcome of the first patients treated with the strategy at Aarhus University Hospital.

### SP-0355 Selection of lung cancer patients for adaptive radiotherapy using cone-beam CT imaging

D. Hattu<sup>1</sup>

<sup>1</sup>Maastricht Radiation Oncology Maastricht Clinic, Radiotherapy, Maastricht, The Netherlands

#### Abstract text

Image-guided radiotherapy using cone-beam CT (CBCT) allows for precise patient set-up procedures and accurate treatment delivery. Besides image-guided patient set-up, CBCT can detect anatomical changes previously not visible on lateral port films. This additional information leads to an increased workload and decision criteria when to adapt need to be in place. Therefore in our department a traffic light protocol is part of the online matching protocol for lung cancer patients and is used for the evaluation of the correct positioning of the patient. It also serves as a decision support tool to guide Radiation Therapy Technologists (RTT) with potential follow-up investigations to be undertaken for e.g. changes in lung density, changes in tumor volume or tumor shifts. Requests for follow-up investigations are collected and reviewed offline by a dedicated RTT and a radiation oncologist specialized in lung cancer treatment to determine if further action is necessary (e.g. dose (re)calculation, new CT or even an adapted treatment plan). In this presentation an overview of the current protocol is given but also practical examples will be shown.

### SP-0356 Image-guided radiotherapy and motion management in lung cancer

V. Gram<sup>1</sup>

<sup>1</sup>University Hospital of Copenhagen- Rigshospitalet, section of Radiotherapy- Clinic of Oncology, Copenhagen, Denmark

#### Abstract text

Modern radiotherapy techniques as IMRT and VMAT have already contributed to a reduction of the radiation dose to the lungs and heart for patients with lung cancer, and there are still modern techniques that are being explored for this patient group today. Image guidance and motion management offer great advantages for lung cancer patients, including the ability of monitoring tumour size and motion. Motion management techniques, such as DIBH offer advantages including a reduced dose to the healthy part of the lung and the heart, improved image quality and intra-fractional motion management of the tumour and have been used for breast cancer patients for over a decade with good results, as this technique expands the lungs and pushes the heart down with the diaphragm. The use of breath hold techniques is however not a standard approach in lung cancer, despite its advantages. There are a number of considerations to be evaluated in the implementation of breath-hold techniques; both technical, practical and patient-related. This presentation will include clinical experience in implementing DIBH for lung cancer patients from the perspective of an RTT and include ethical aspects, choice of technique, patient selection, patient and staff training, patient compliance and extra time required for adding this technique.

**Symposium: Stronger together - news and projects in the young national societies**

**SP-0357 Perspective of an established young society: the Spanish Young Society**

V. Morillo<sup>1</sup>, R. Hernanz<sup>2</sup>

<sup>1</sup>*Consorcio Hospitalario Provincial De Castellon, Radiation Oncology, Castellon, Spain* ; <sup>2</sup>*ramon And Cajal Hospital, Radiation Oncology, Madrid, Spain*

**Abstract text**

The SYROG was formed about a decade ago, with the intention of fostering collaboration (research) and training (education) among young members of society as well as with other societies, both nationally and internationally. An executive committee was set up to oversee the objectives and functions of the group, made up of young specialists who wished to promote their spirit to the other doctors in training. We encountered many difficulties during our journey, but the ones that had the greatest impact were the lack of funding and recognition, slowing down our progress. In spite of this, numerous training courses have been carried out focused on the achievement of our objectives, the elaboration of articles with clinical impact, as well as the collaboration with fully constituted international societies. We promote the use of social networks as a means of disseminating evidence-based clinical guidelines, fundamental publications in healthcare practice, and reporting on scientific congresses and conferences. As far as future perspectives are concerned, it is necessary to be actively involved in young European society in order to be able to grow in opportunities, research and healthcare.

**SP-0358 An emerging young society: Young Romanian Radiotherapists and Oncologists Group (YRROG)**

M. Zerbea<sup>1</sup>

<sup>1</sup>*Institute of Oncology Prof. Dr. I. Chiricuta, Radiation Oncology, Cluj Napoca, Romania*

**Abstract text**

**Introduction**

The aim of a young society is to gain gratitude among the well known national and international societies. The Romanian residents in the oncology formed a society that is gaining members and visibility year by year. Projects Our society collaborates with the Romanian Surgery and Oncologic Gynecology Society in organizing the Multimodal Approach in Oncology, a conference held in Cluj Napoca once every month. It includes presentations on surgery, oncology, imaging, pathology, nuclear medicine for a better communication between all professionals in oncology. We also organize every week article presentations among residents. The goal is continuous medical education and improving qualities such as public speaking and presentation skills.

**Administration**

Our society is a non-profit organization managed by a representative, vice - representative and a secretary. It is holding over 500 members from diverse romanian medical fields. We promote our group through social media, national events such as the Romanian National Congress and international meetings such as ESTRO and ESMO Congress. The best papers presented by the residents are published in the society journal.

**Visión**

Our collaboration at ESTRO 38 with the other national societies is a step forward in organizing European projects, gaining better visibility in ESTRO and improving the medical education among the young residents.

**SP-0359 Creating a new young radiation oncology society - the case of Poland**

M. Spalek<sup>1</sup>

<sup>1</sup>*Maria Skłodowska-Curie Institute-Cancer Center, Department Of Soft Tissue/Bone Sarcoma And Melanoma, Warsaw, Poland*

**Abstract text**

Some young radiation oncology national societies (yNS) exist within Europe. However, the creation of a new yNS is a demanding task. Is it really important and worth this effort? The first step is to gather a group of enthusiastic people who will break the walls and face many legal issues. The presentation covers the process of creation of a new yNS in Poland, and also discusses ideas for first projects and possibilities of collaboration with the Young ESTRO Committee.

**SP-0360 Working together across borders: Young Academics in Radiation Oncology**

C. Ostheimer<sup>1</sup>

<sup>1</sup>*Universitaetsklinikum HalleSaale, Radiation Oncology, Halle, Germany*

**Abstract text**

Radiation Oncology is a crucial therapeutic pillar in modern Oncology, offering up-to-date and efficient treatment concepts for cancer patients. In cancer research, Radiation Oncology contributes with innovative research projects and approaches in clinical radiotherapy, radiation biology and physics.

In order to keep this status for the future, Radiation Oncology needs to stay attractive for young medical professionals and academics. As the "Motor of Innovation" in Radiation Oncology, research needs to motivate and support young academics to pursue own research activities - not only on the national level. In a world of globalization and internationalization, research needs to adapt to this trend and offer young academics and researchers structures, resources and platforms to collaborate on a multinational level. Only by establishing strong international research collaborations and networks already on the level of young academics can ensure and secure a lasting and significant impact of Radiation Oncology in cancer research.

This presentation gives an overview of the activities of the "Young Radiation Oncology Group" (YROG) of the EORTC ROG.

**Poster Viewing : Poster viewing 7: CNS, Paediatrics, Haematology and Gynaecology**

**PV-0361 Minor changes in neurocognition and quality of life after proton therapy for brain tumour patients**

A. Dutz<sup>1,2</sup>, L. Agolli<sup>1,3</sup>, C. Valentini<sup>1,3</sup>, R. Bütof<sup>1,3,4</sup>, E.G.C. Troost<sup>1,2,3,4,5</sup>, M. Baumann<sup>1,2,3,4,5,6</sup>, A. Lühr<sup>1,2,5</sup>, M. Krause<sup>1,2,3,4,5</sup>, S. Löck<sup>1,3,5</sup>

<sup>1</sup>*OncoRay - Center for Radiation Research in Oncology, Faculty of Medicine and University Hospital Carl Gustav Carus- Technische Universität Dresden, Dresden, Germany*; <sup>2</sup>*Helmholtz-Zentrum Dresden - Rossendorf, Institute of Radiooncology - OncoRay, Dresden, Germany* ; <sup>3</sup>*Department of Radiotherapy and Radiation Oncology, Faculty of Medicine and University Hospital Carl Gustav Carus- Technische Universität Dresden, Dresden, Germany*; <sup>4</sup>*National Center for Tumor Diseases NCT- Partner Site Dresden- Germany*; *German Cancer Research Center DKFZ- Heidelberg- Germany- Faculty of Medicine and University Hospital Carl Gustav Carus- Technische Universität Dresden- Dresden- Germany- and Helmholtz* ; <sup>5</sup>*German Cancer Consortium DKTK- partner site Dresden, and German Cancer Research Center DKFZ, Heidelberg, Germany* ; <sup>6</sup>*German Cancer Research Center, Deutsches Krebsforschungszentrum DKFZ, Heidelberg, Germany*

### Purpose or Objective

To investigate changes in neurocognitive function and quality of life (QoL) and their association with dosimetric parameters of various brain structures as well as clinical cofactors in adult brain tumour patients following proton beam therapy (PBT).

### Material and Methods

Sixty-nine adult patients with primary brain tumours who received conventionally fractionated PBT were included in this study. Neurocognitive function according to the Montreal Cognitive Assessment (MoCA) test and QoL according to general EORTC-QLQ-C30 and brain tumour specific QLQ-BN20 questionnaires were scored prospectively at baseline and within 3-month-intervals up to one year after PBT. Dose-volume parameters of the retrospectively contoured structures hippocampus, thalamus, frontal and temporal lobes, amygdala, entire cerebellum, anterior cerebellum, and posterior cerebellum were extracted. Clinical parameters comprised age, sex, diagnosis and WHO grading, tumour volume, prescribed dose, concomitant chemotherapy, tumour resection and administration of corticosteroids. MoCA scores and differences to baseline values at different time points were correlated with self-reported QoL items (Spearman correlation  $r_s$ ), clinical and dosimetric parameters (Mann-Whitney  $U$  test, logistic regression). A change of  $\geq 3$  points of the MoCA total score compared to baseline was considered clinically relevant. Unless otherwise stated, differences at 3 months after PBT compared to baseline are given.

### Results

The MoCA total score remained stable over time for the majority of patients: Less than 10% of the patients had clinically relevant changes at respective time points. The QLQ-C30 items did not change over time. On the QLQ-BN20 symptom scale, significant increases were observed for the items hair loss ( $p=0.002$ ) and seizure ( $p<0.042$ , up to 9 months after PBT). However, future uncertainty decreased significantly ( $p<0.042$ ). MoCA scores were significantly correlated with self-reported QoL scores. At all time-points, MoCA total score correlated with QLQ-C30 cognitive function ( $r_s$ : 0.31-0.57) and MoCA language scores with QLQ-BN20 communication deficit ( $r_s$ : 0.36-0.59). Clinically relevant differences in the MoCA total score were significantly associated with high dose parameters in the anterior, posterior and entire cerebellum (V55Gy,  $p<0.05$ ), but not with clinical parameters.

### Conclusion

Neurocognitive function and QoL remained stable in the majority of brain tumour patients following PBT. Self-reported QoL was in accordance with the results of the objective MoCA test. Significant associations between dose-volume parameters and clinically relevant neurocognitive changes suggest that further sparing of organs at risk in treatment planning may lead to increased neurocognitive function and QoL for brain tumour patients. New planning constraints for further potential organs at risk, such as the cerebellum [1], should be discussed.

[1] Eekers DBP et al. (2017) Clin Transl Radiat Oncol 8, 22-26.

### PV-0362 Long term outcomes of high-dose single-fraction radiosurgery for chordomas of the spine and sacrum

C.J. Jin<sup>1</sup>, J. Berry-Candelario<sup>2</sup>, A. Reiner<sup>3</sup>, E. Lis<sup>4</sup>, M. Bilsky<sup>2</sup>, I. Laufer<sup>2</sup>, A. Schmitt<sup>1</sup>, D. Higgison<sup>1</sup>, Y. Yamada<sup>1</sup>  
<sup>1</sup>Memorial Sloan Kettering Cancer Center, Radiation Oncology, New York, USA; <sup>2</sup>Memorial Sloan Kettering Cancer Center, Neurosurgery, New York, USA; <sup>3</sup>Memorial Sloan Kettering Cancer Center, Biostatistics, New York, USA; <sup>4</sup>Memorial Sloan Kettering Cancer Center, Neuroradiology, New York, USA

### Purpose or Objective

To evaluate outcomes of patients with primary chordomas treated with spine stereotactic radiosurgery (SRS) alone or in combination with surgery, drawing from a single-institution database to elucidate treatment options associated with durable control of these conventionally radioresistant tumors.

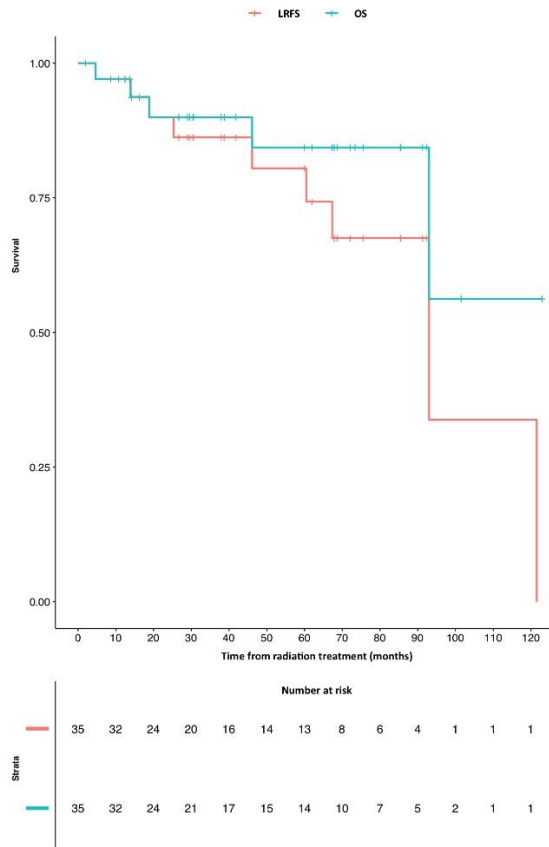
### Material and Methods

Clinical records were reviewed for outcomes of patients with primary chordoma of the mobile spine and sacrum who underwent single-fraction SRS between 2006 and 2017. Patients were followed with spine MRI to determine local recurrence-free survival (LRFS). LRFS and overall survival (OS) were analyzed using the Kaplan-Meier method. Tumor location and extent of surgery were analyzed for significance in relation to LRFS and OS using univariate Cox regression. CTCAE v. 5.0 toxicity in relation to extent of surgery was analyzed using Fisher's Exact Test.

### Results

In total, 35 patients with de novo chordoma of the mobile spine (46%) and sacrum (54%) received SRS, with a median post-SRS follow-up of 40.3 months (range 2.0-122.9). The median PTV volume was 155.6 cm<sup>3</sup> (29.2-903.8 cm<sup>3</sup>). The median PTV dose was 24 Gy (18-24 Gy), with a median V95 = 99.5% and D95 = 2395 cGy. Among 23 patients also undergoing surgery (66%), 39% underwent epidural decompression and instrumentation prior to SRS, while 61% underwent extensive resection including corpectomy or partial sacrectomy. One-third received SRS alone, including 4 patients who did not proceed to planned surgery based on lack of progression and patient preference. The 3- and 5-year LRFS rates were 86.2% and 80.5% respectively. Among 32 patients receiving 24 Gy (91%), the 3- and 5-year LRFS were 96.3% and 90.0%. Four developed metastatic disease (11%) at a median of 5.1 years (range 1.0-10.2). The 3- and 5-year OS rates were 90.0% and 84.3%. Spinal location (mobile spine, sacrum) and extent of surgery (none, epidural decompression, extensive resection) were not associated with LRFS or OS ( $p>.05$ ). Patients undergoing partial sacrectomy or corpectomy developed higher surgical toxicity rates compared to patients undergoing decompression surgery (85%  $\geq$ Grade 2; 54% Grade 3 vs. 22%  $\geq$ Grade 2; 0% Grade 3) ( $p=0.001$ ). The long-term  $\geq$ Grade 2 SRS toxicity rate was 31%, including 14% Grade 3 tissue necrosis, recurrent laryngeal nerve palsy, fracture, and secondary malignancy. Among 30 patients presenting with pain (100%), radiculopathy (23%), or neuropathy (34%), two-thirds reported symptom response to treatment, with rates of 40% complete response (CR), 23% partial response (PR), and 7% CR for pain with PR for neuropathy.

FIGURE: Kaplan-Meier estimate of local recurrence-free survival and overall survival.



### Conclusion

High-dose spine SRS can offer patients with chordoma the chance of durable radiographic control and effective symptom relief, with acceptable toxicity. SRS should be considered as definitive therapy for unresectable tumor due to surgical morbidity, neoadjuvant prior to resection, and adjuvant post-subtotal resection or for positive margins.

### PV-0363 Cognitive Outcomes after Conformal Radiotherapy in Pediatric Patients with Supratentorial Ependymoma

M. Mizumoto<sup>1</sup>, Y. Oshiro<sup>2</sup>, S. Wu<sup>3</sup>, T.E. Merchant<sup>1</sup>  
<sup>1</sup>St Jude Children's Research Hospital, Radiation Oncology, Memphis, USA; <sup>2</sup>Tsukuba Medical Center Hospital, Radiation Oncology, Tsukuba, Japan; <sup>3</sup>St Jude Children's Research Hospital, Biostatistics, Memphis, USA

### Purpose or Objective

This study investigated cognitive function after conformal radiotherapy (CRT) for pediatric supratentorial ependymoma.

### Material and Methods

From 1997 to 2009, 30 pediatric patients diagnosed with supratentorial ependymoma received photon-based CRT (54.0 or 59.4Gy) using a 0.5-1.0cm clinical target volume margin and were evaluated for change in cognitive function. The median age was 6 years (range 1 - 19 years). The tumor location was frontal (n=8), parietal (n=5), occipital (n=4), fronto-parietal (n=4), IIIrd ventricle (n=3) and other (n=6). The median follow-up period was 12.8 years (range, 2.2-19.0 years). 877 evaluations were performed including estimated IQ (n=209), WIAT Reading (n=174), WIAT Math (n=174), WIAT Spelling (n=173), and VAL (n=147).

### Results

Baseline mean neurocognitive scores were IQ (99.7±22.5), WIAT Reading (97.4±10.3), WIAT Math (98.2±12.2), WIAT Spelling (94.5±10.3), and VAL (97.3±22.2). Linear mixed models with random coefficients revealed no significant change over time and a slightly decline in WIAT reading scores during follow-up (WIAT Reading slope estimate -0.7444±0.3818 points/year; P=0.0631). Gender, age at time of radiotherapy, radiation dose to the supratentorial brain, temporal lobes and entire brain, the use of pre-CRT chemotherapy and number of surgeries was not significantly associate with cognitive function. Only tumor location (frontal vs. other) was significantly associated with WIAT Spelling (p=0.0223).

### Conclusion

In a cohort of children with supratentorial ependymoma and extended follow-up, CRT using photons spared cognitive function. These results challenge the premise that newer methods of radiation therapy will improve outcomes in these patients.

### PV-0364 Pulmonary function after high dose chemotherapy + total lung irradiation for pediatric Ewing sarcoma

B. Diletto<sup>1</sup>, E. Pecori<sup>1</sup>, N. Puma<sup>2</sup>, O. Alessandro<sup>3</sup>, S. Meroni<sup>4</sup>, M. Podda<sup>2</sup>, A. Busia<sup>5</sup>, F. Allegri<sup>5</sup>, A.C. Ogliari<sup>5</sup>, C. Materazzo<sup>6</sup>, R. Boffi<sup>5</sup>, E. Pignoli<sup>4</sup>, R. Luksch<sup>2</sup>, L. Gandola<sup>1</sup>  
<sup>1</sup>Fondazione IRCCS Istituto Nazionale dei Tumori, Radiation Oncology 1, Milan, Italy; <sup>2</sup>Fondazione IRCCS Istituto Nazionale dei Tumori, Pediatric Oncology, Milan, Italy; <sup>3</sup>Università degli Studi di Milano, Residency Program in Radiation Oncology, Milan, Italy; <sup>4</sup>Fondazione IRCCS Istituto Nazionale dei Tumori, Medical Physics, Milan, Italy; <sup>5</sup>Fondazione IRCCS Istituto Nazionale dei Tumori, Pulmonary Unit, Milan, Italy; <sup>6</sup>Fondazione IRCCS Istituto Nazionale dei Tumori, Cardiology Unit, Milan, Italy

### Purpose or Objective

Total lung irradiation (TLI) following high dose chemotherapy with busulfan and melphalan (BuMel) and autologous stem cell transplantation (ASCT) is an intensive strategy improving outcomes of pediatric Ewing sarcoma (ES) pts with lung metastases. A critical issue regarding the combination of BuMel-ASCT and TLI is the supposed additional lung toxicity. Results of pulmonary function of a subgroup of metastatic ES children treated with this approach in a single Institution within a multicentric prospective study are reported.

### Material and Methods

Clinical records of lung metastatic ES children treated in our Institution were collected. Pts were treated according to 3 international and national protocols: ISG/SSG (Italian Sarcoma Group/Scandinavian Sarcoma Group) IV, ISG-AIEOP (Associazione Italiana Ematologia Oncologia Pediatrica) EW-2, ISG/AIEOP-Rel. TLI was administered at least 8 weeks after BuMel-ASCT, and the prescribed total dose was 15 Gy in 10 daily fractions. Lung and cardiac functions were assessed by pulmonary function tests (PFTs) (including spirometry, lung volume measurements and single-breath carbon monoxide-diffusion capacity - DLCO-) and echocardiogram before BuMel-ASCT, between BuMel-ASCT and TLI, after TLI and regularly during the F-UP. Ejection fraction (EF), forced vital capacity (FVC), forced expiratory volume in 1 second (FEV1), total lung capacity (TLC), and DLCO were recorded.

### Results

Data from 17 pts (ISG/SSG IV: 6, ISG-AIEOP EW2: 10, ISG/AIEOP-Rel: 1) were collected (10 F, 7 M, median age 15.3 y, range 3.9-20). All pts performed PFTs and echocardiogram regularly. Median time from BuMel-ASCT to TLI was 95 days (73-335). After BuMel-ASCT a mild restrictive syndrome was observed in 7 pts (41%) and a mild obstructive syndrome in 1 pts (6%). After TLI 9 (53%) patients presented a mild and 1 pts (6%) a moderate restrictive syndrome, 1 pts showed a mild obstructive

syndrome (6%). At last F-UP (median 70.8 mo, 14.3-207.9) 5 mild (30%), 1 moderate restrictive (6%) and 1 mild obstructive syndrome (6%) were recorded. No EF pathological reduction were observed. Mean trend of most significant PFTs (FVC, FEV1, DLCO) showed a rapid decline after BuMel-ASCT, reaching the lowest values (< 80% of basal value) after TLI, and they recovered gradually up to 90% of basal value over time. Only 1 reversible G2 interstitial pneumopathy was detected after BuMel-ASCT.

#### Conclusion

The combined strategy of BuMel-ASCT and TLI for treatment of lung and metastatic ES children seems to not compromise pulmonary and cardiac functions, demonstrating an acceptable toxicity profile. Nevertheless, it is mandatory to strictly and regularly assess pulmonary function before and after BuMel-ASCT to identify pts possibly ineligible for TLI, and during the F-UP.

#### PV-0365 Adoption of expansion margins to reduce the dose received by coronary arteries in lymphoma patients

V. De Luca<sup>1</sup>, S. Bartoncini<sup>2</sup>, M. Levis<sup>1</sup>, E. Gallio<sup>3</sup>, C. Cavallin<sup>1</sup>, G.C. Iorio<sup>1</sup>, R. Parise<sup>1</sup>, C. Palladino<sup>1</sup>, F.R. Giglioli<sup>3</sup>, C. Fiandra<sup>3</sup>, U. Ricardi<sup>1</sup>

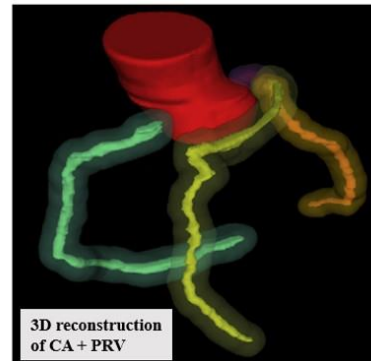
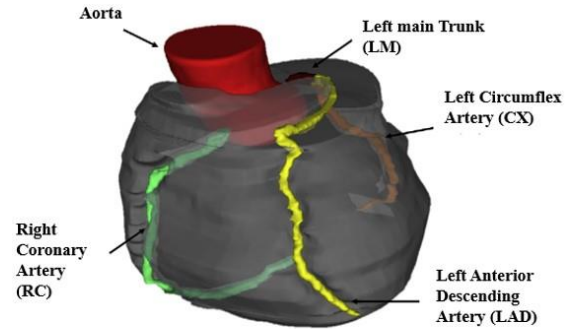
<sup>1</sup>University Of Turin, Department Of Oncology- Radiation Oncology, Turin, Italy ; <sup>2</sup>A.O.U. Citta' Della Salute E Della Scienza Di Torino, Department Of Oncology- Radiation Oncology, Turin, Italy ; <sup>3</sup>a.O.U. Citta' Della Salute E Della Scienza Di Torino, Medical Physics Unit, Turin, Italy

#### Purpose or Objective

Many studies have demonstrated a linear correlation between the heart dose and the risk of coronary artery disease in lymphoma patients receiving mediastinal radiotherapy (RT). In order to reduce long term ischemic events, a detailed contouring of cardiac structures - particularly of coronary arteries (CA) - is needed. Anyway, heart motion impacts on the precise estimation of the dose received by small volumes as CA. An isotropic margin (PRV) for CA may compensate the uncertainties due to their displacement during the heart cycle. In this study, we aimed to evaluate the potential dosimetric benefit obtained by the coronary tree with the optimization of the treatment plan on each PRV volume rather than just on CA volumes.

#### Material and Methods

We enrolled fifteen patients (mean age 30, range 16-54) affected with Hodgkin lymphoma or primary mediastinal B cell lymphoma (4 males and 11 females) with high prevalence of bulky presentation at baseline (13/15 patients: 87%). Median prescription dose to the PTV was 31 Gy (range 24-40). The following CA were contoured as organs at risk (OARs): left main trunk (LM), left anterior descending artery (LAD), left circumflex artery (CX) and right coronary artery (RC). We designed a dedicated PRV for each CA by applying an isotropic margin of 3 mm to LM, 4 mm to CX and 5 mm to LAD and RC, as suggested by a recent publication (Fig. 1).

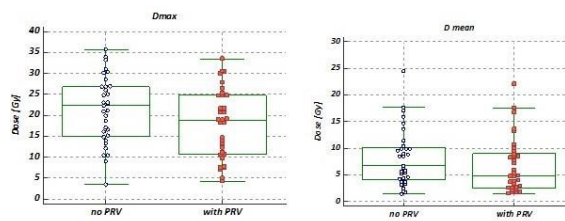


We then compared two care plans, either optimized on the original OARs (CA) or on their dedicated PRV in order to test potential dosimetric benefit conferred by the integration of PRV in the optimization process. Similar PTV coverage was deemed mandatory to proceed with the planning workflow. We included only those CA that were located in the close proximity of the target of treatment; we thus evaluated 33 CA and their relative PRVs. Seven patients (47%) had 3 CA, 4 (27%) had 2 CA and the remaining 4 (27%) had only 1 CA close to the PTV. Maximum and mean doses (Dmax and Dmean) were estimated for all the structures and were then compared with t-Student Test.

#### Results

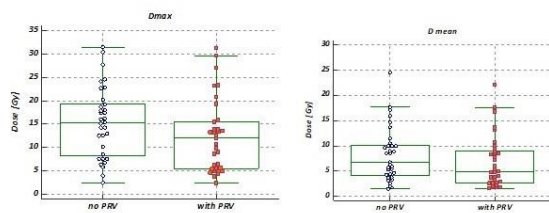
The plan optimization on PRVs shows a significant dosimetric benefit, both in terms of Dmax and Dmean, for the CA volumes, with a mean dose reduction of 20% for Dmax (12.3 vs 15.4 Gy,  $p < 0.05$ ) and of 16% for Dmean (6.8 vs 8.1 Gy,  $p < 0.05$ ). Moreover, we obtained a significant dosimetric gain also for the PRV volumes: in fact, we observed a mean dose reduction of 15,5% for Dmax (18.0 vs 21.3 Gy,  $p < 0.05$ ) and of 15,3% for Dmean (7.2 vs 8.5 Gy,  $p < 0.05$ ), respectively (Fig. 2).

## Plan optimized on PRVs



p - value	OAR PRV Dmax [Gy] [mean ± s.d.]		OAR PRV D mean [Gy] [mean ± s.d.]	
	NO	YES	NO	YES
	21.3 ± 8.0	18.0 ± 8.3	8.5 ± 8.5	7.2 ± 5.4
	< 0.05		< 0.05	

## Plan optimized on CAs



p - value	OAR PRV Dmax [Gy] [mean ± s.d.]		OAR PRV D mean [Gy] [mean ± s.d.]	
	NO	YES	NO	YES
	15.4 ± 7.5	12.3 ± 7.8	8.1 ± 5.4	6.8 ± 5.2
	< 0.05		< 0.05	

Notes: NO = OAR corresponds to Coronary Artery; YES = OAR corresponds to Coronary Artery's PRV.

## Conclusion

Our study shows that the optimization of the treatment plan to the PRV volumes of CA located in the proximity of the target volumes ensures a significant reduction (ranging from 15 to 20%) of the mean and maximal dose received by the coronary tree. We thus recommend to integrate PRVs in the optimization process of mediastinal RT for lymphoma patients because they decrease the dose received by CA and may potentially limit the risk of long term ischemic complications.

**PV-0366 Helical Total Lymphoid Irradiation: radiotherapy still works in lymphoma transplantation**  
S. Vagge<sup>1</sup>, F. Guolo<sup>2</sup>, A. Dominietto<sup>3</sup>, S. Agostinelli<sup>4</sup>, M. Gusinu<sup>4</sup>, A. Ibaticci<sup>3</sup>, F. Ballerini<sup>2</sup>, R.M. Lemoli<sup>2</sup>, E. Angelucci<sup>3</sup>, M. Gobbi<sup>2</sup>, R. Corvò<sup>5</sup>

<sup>1</sup>IRCCS Ospedale Policlinico San Martino- academic hospital, Radiation Oncology, Genova, Italy; <sup>2</sup>IRCCS Ospedale Policlinico San Martino, Clinica Ematologica, Genova, Italy; <sup>3</sup>IRCCS Ospedale Policlinico San Martino, Ematologia, Genova, Italy; <sup>4</sup>IRCCS Ospedale Policlinico San Martino, Medical Physics, Genova, Italy; <sup>5</sup>IRCCS Ospedale Policlinico San Martino, Radiation Oncology, Genova, Italy

## Purpose or Objective

Assessing feasibility and preliminary outcomes of a conditioning strategy based on high dose chemotherapy (HDC) and Helical Total Lymphoid Irradiation (HT-TLI) as preparation for autologous stem cell transplantation (ASCT) in patients affected by relapsed/refractory (R/R) Hodgkin's Lymphoma (HL) and non-Hodgkin lymphoma (NHL). Salvage chemotherapy followed by ASCT is the standard of care for patients with R/R. However conventional conditioning regimens have low efficacy in R/R patient and only a minority of them is cured by this approach. Promising results with a technical "old suite" total lymphoid irradiation (TLI) and with hyperfractionated schedules, followed by high-dose chemotherapy and ASCT have been reported in advanced HL patients, despite relevant toxicity due to radiation-induced damage of healthy tissues.

## Material and Methods

From February 2011 to December 2017, 15 patients with R/R HL (n=7), diffuse Large B Cell NHL (n=6) and T-cell NHL (n=2) were treated. Median age was 42 years (range 20-68) and median number of previous lines of therapy was 3 (range 2-4). Of note, 4 patients had already received prior ASCT. Salvage chemotherapy was decided case by case and clinical response was determined by functional imaging prior to ASCT. HT-TLI delivered 12 Gy in 3 daily fractions, by a dedicated setup, to all the body nodal chain with regards to the tumor burden area. HDC consisted of high-dose Bendamustine (400 mg/sqm) and Melphalan 140 (mg/sqm) for patients older than 40 years (n=10) and conventional FEAM (Fotemustine, Ethoposide, Cytarabine and Melphalan) for younger patients.

## Results

Salvage chemotherapy induced complete response (CR) in 7 patients (5 HL, 2 NHL), partial response (PR) in 5 (2 HL, 3 NHL), less than partial response (LPR) 3. Conditioning strategy was well tolerated. Six patients (40 %) experienced fever of unknown origin and 5 patients (33%) developed grade 3/4 mucositis. None experienced grade 3/4 extra-hematological toxicity. All patients showed complete engraftment and median time to neutrophil and platelet recovery was 11 (range 9-21) and 12 days (range 9-21) respectively. Median follow-up was 38 months (CI 95%: 1.3-66.1 months). All patients in PR or less before transplant achieved CR. There were no cases of treatment-related death. The 3-year overall PFS and OS were 78% and 93% (Fig. 1) respectively. Post-ASCT relapse occurred in 3 patients (HL=2 and NHL=1) at a median time of 8 months and 1 NHL patient subsequently died of progressive disease 7 months after ASCT.

## Conclusion

Our preliminary results show that HT-TLI can be safely used in advanced lymphomas with sequential high dose chemotherapy as combined conditioning. With the limit deriving from the small size of this series, we observe that all patients achieved CR after the procedure, even if heavily pretreated, and that relapse rate was low. Overall these results encourage the implementation of HT-TLI in the standard conditioning for R/R lymphomas.

**PV-0367 TMLI-based low-toxic myeloablative conditioning regimen in haploidentical HSCT for AML**  
C. Aristei<sup>1</sup>, V. Lancellotta<sup>1</sup>, A. Carotti<sup>2</sup>, C. Zucchetti<sup>3</sup>, S. Saldi<sup>4</sup>, A. Pierini<sup>2</sup>, L. Ruggeri<sup>2</sup>, S. Piccinini<sup>2</sup>, L. Amico<sup>2</sup>, M. Iacco<sup>3</sup>, A. Velardi<sup>2</sup>, M.F. Martelli<sup>2</sup>

<sup>1</sup>Radiation Oncology Section- University of Perugia and Perugia General Hospital, Surgery and Biomedical Sciences, Perugia, Italy; <sup>2</sup>Division of Hematology and Clinical Immunology and Bone Marrow Transplant Program- University of Perugia and Perugia General Hospital, Medicine, Perugia, Italy; <sup>3</sup>Medical Physics Unit- Perugia General Hospital, Medical Physics, Perugia, Italy; <sup>4</sup>Radiation Oncology Section- Perugia General Hospital, Surgery and Biomedical Sciences, Perugia, Italy

## Purpose or Objective

Hematopoietic stem cell transplantation (HSCT) is elective post-remission treatment for patients with intermediate-high risk acute myeloid leukemia (AML). The best donor is the matched sibling which is available for 25% of cases. The 1-haplotype mismatched relative (haploidentical) is a valid alternative as it is immediately available for 95% patients. In haploidentical HSCT total body irradiation is an essential component of the myeloablative conditioning regimen which, in elderly or young unfit patients, is associated with high toxicity and non-relapse mortality rates. In order to reduce the treatment-related toxicity we designed a conditioning regimen with total marrow/lymphoid irradiation (TMLI) and low chemotherapy doses. Furthermore, to induce a Graft versus Leukemia (GvL) effect with a low incidence of Graft versus Host Disease (GvHD) the graft contained, as

adoptive immunotherapy, a ratio of conventional T cells (Tcons) and T regulatory cells (Tregs).

#### Material and Methods

From July 2015 to July 2018 26 AML patients (14 in first and 10 in second complete remission, 2 in partial remission) and 2 patients with myelodysplasia underwent haploidentical HSCT. There were 15 male and 13 female; median age was 60 years (range 42-70). Composite comorbidity/age scores were 1/2 in 10 patients and  $\geq 3$  in 18. TMLI target volumes were skeletal bones, major lymph node chains and spleen. TMLI was delivered by helical tomotherapy in 4 and half days (from day -15 to day -11) in 2 daily fractions of 1.5 Gy (TMI) and 1.3 Gy (TLI) (total doses 13.5Gy and 11.7Gy respectively). Chemotherapy schedule included tiothepa 2.5 mg/kg on days -10 and -9; fludarabine 30 mg/m<sup>2</sup> from days -10 to -6; cyclophosphamide 15 mg/kg on days -8 and -7. Haploidentical grafts consisted of 10x10<sup>6</sup>/kg purified CD34+cells, 1x10<sup>6</sup>/kg Tcons, 2 x10<sup>6</sup>/kg Tregs. No post-transplant immunosuppression was given.

#### Results

TMLI-related acute toxicity was G1-G2 in 23 patients, G3 in 4 and G4 in 1. All patients sustained primary full-donor type engraftment. Grade II-IV acute GvHD developed in 8 patients (29%) and chronic GvHD in none. Transplant-related causes of death in 6 patients were veno-occlusive disease (1), hemorrhage (1) sepsis (2) and acute GvHD (3). Immune reconstitution was good, with peripheral blood T cells rapidly increasing. Relapse did not occur in any patients. Twenty two (79%) patients are alive and relapse-free at a median follow up of 19 months (3-40 months).

#### Conclusion

This transplant strategy (TMLI, low doses of tiothepa, fludarabine, cyclophosphamide and adoptive immunotherapy with Tregs-Tcons) was successful in haploidentical transplantation for elderly and young unfit AML patients. TMI provides strong myeloablation and TLI provides efficient immunosuppression. The conditioning regimen was associated with low toxicity and mortality. The appropriate Tcon/Treg ratio was confirmed to exert a powerful T-cell dependent GvL effect with a low incidence of GvHD.

#### PV-0368 Persistence of late substantial patient reported symptoms (LAPERS): A report from the EMBRACE study

A.S. Vittrup<sup>1</sup>, L.U. Fokdal<sup>1</sup>, R. Pötter<sup>2</sup>, S.M. Bentzen<sup>3</sup>, J.C. Lindegaard<sup>1</sup>, A. Sturdza<sup>2</sup>, B. Segedin<sup>4</sup>, K. Bruheim<sup>5</sup>, I.M. Jürgenliemk-Schulz<sup>6</sup>, U. Mahantshetty<sup>7</sup>, B. Rai<sup>8</sup>, C. Haie-Meder<sup>9</sup>, R. Cooper<sup>10</sup>, S. Marit<sup>11</sup>, F. Huang<sup>12</sup>, E. Van der Steen-Banasik<sup>13</sup>, E. Villafranca<sup>14</sup>, R.A. Nout<sup>15</sup>, K. Tanderup<sup>1</sup>, K. Kirchheiner<sup>2</sup>

<sup>1</sup>Aarhus University Hospital, Department of Oncology, Aarhus, Denmark ; <sup>2</sup>Medical University of Vienna/General Hospital of Vienna, Department of Radiation Oncology- Comprehensive Cancer Center, Vienna, Austria; <sup>3</sup>University of Maryland School of Medicine, Department of Epidemiology and Public Health, Baltimore, USA ; <sup>4</sup>Institute of Oncology Ljubljana, Department of Radiotherapy, Ljubljana, Slovenia; <sup>5</sup>The Norwegian Radium Hospital- Oslo University Hospital, Department of Oncology, Oslo, Norway ; <sup>6</sup>University Medical Centre Utrecht, Department of Radiation Oncology, Utrecht, The Netherlands ; <sup>7</sup>Tata Memorial Hospital, Department of Radiation Oncology, Mumbai, India ; <sup>8</sup>Postgraduate Institute of Medical Education and Research, Department of Radiotherapy and Oncology, Chandigarh, India ; <sup>9</sup>Gustave-Roussy, Department of Radiotherapy, Villejuif, France; <sup>10</sup>St James's University Hospital, Leeds Cancer Centre, Leeds, United Kingdom ; <sup>11</sup>St. Olavs Hospital, Clinic of Oncology and Women's Clinic, Trondheim, Norway; <sup>12</sup>Cross Cancer Institute and University of Alberta, Department of Oncology, Edmonton, Canada ; <sup>13</sup>Radiotherapiegroep Arnhem, Department of

Radiotherapy, Arnhem, The Netherlands ; <sup>14</sup>Hospital of Navarra, Department of Radiation Oncology, Pamplona, Spain ; <sup>15</sup>Leiden University Medical Center, Department of Radiation Oncology, Leiden, The Netherlands

#### Purpose or Objective

Incidence methods and prevalence rates are commonly used statistical approaches for summarizing late side effects after radiotherapy. Incidence methods capture the first occurrence of an event; but are unable to distinguish transient from persistent symptoms. Prevalence rates contain information on persistence of symptoms in the cohort; but not on an individual patient level. A novel method to identify patients with LAte, PERsistent, Substantial and likely treatment related symptoms (LAPERS) is applied on patient reported outcomes (PRO) from the prospective, observational, and longitudinal study on MRI image-guided, adaptive brachytherapy in locally advanced cervical cancer (EMBRACE study).

#### Material and Methods

PRO (EORTC QLQ-C30 + CX24) were analyzed in 657 out of 1416 patients within the EMBRACE study who had a valid baseline, 3 months' assessment and at least 3 late follow ups (6 months and ongoing). A LAPERS event for an individual patient was defined when the median scoring over late follow-ups was "quite a bit" or "very much" (substantial symptoms). For organ-related symptoms (e.g. urinary frequency) baseline morbidity was taken into account by requiring the median to be worse than the minimum of baseline and 3 months scoring (treatment-related); whereas for more unspecific symptoms (e.g. tiredness) baseline correction was not applied. Crude incidences and median prevalence rates of substantial symptoms from 6 to 60 months were calculated in the same cohort and put into perspective with LAPERS via ratio calculations.

#### Results

Median follow-up was 42 months (IQR 30-59). Table 1 presents the outcome of the different methods for reporting. LAPERS was  $\geq 10\%$  in 10 out of 31 symptoms; amongst them swelling in one or both legs, tiredness, urinary frequency and trouble sleeping. LAPERS was below 2% in 8 symptoms for example pain/burning feeling passing urine and blood in stools. LAPERS/crude incidence ratios lower than 0.1 was seen in vaginal symptoms, pain/burning feeling passing urine, blood in stools, nausea and vomiting; indicating that less than 10% of patients experiencing substantial symptoms did so persistently. LAPERS/median prevalence ratios lower than 0.4 was seen in the same symptoms; indicating that the patients experiencing substantial symptoms do not consist of the same individuals over time. LAPERS/median prevalence ratios close to 1 (e.g. swelling in one or both legs) indicate that patients experiencing substantial symptoms over time

are the same.

	Symptom	Baseline	LAPERS	Crude incidence	LAPERS/ crude incidence ratio	Median prevalence 6-60 months	LAPERS/ median prevalence ratio
Gastro-intestinal symptoms	Nausea	6.0%	<u>1.2%</u>	17.4%	0.07	3.80%	0.32
	Vomiting	2.6%	<u>0.3%</u>	7.3%	0.04	1.40%	0.21
	Constipation	10.6%	<u>2.0%</u>	16.4%	0.12	5.00%	0.40
	Diarrhea	5.2%	<u>6.5%</u>	31.5%	0.21	9.60%	0.68
	Difficulty controlling bowel	1.2%	<u>4.6%</u>	22.3%	0.21	6.50%	0.71
	Blood in stools	1.7%	<u>0.5%</u>	10.8%	0.05	2.00%	0.25
Urinary symptoms	Abdominal cramps	11.2%	<u>3.1%</u>	27.8%	0.11	7.70%	0.40
	Urinary frequency	21.7%	<u>10.0%</u>	44.9%	0.22	16.00%	0.63
	Pain/burning feeling passing urine	4.5%	<u>0.8%</u>	16.3%	0.05	3.40%	0.24
Vaginal symptoms	Leaking of urine	4.1%	<u>5.1%</u>	20.0%	0.26	6.70%	0.76
	Difficulty emptying bladder	3.4%	<u>1.7%</u>	15.0%	0.11	4.20%	0.40
	Irritation/soresness in vagina/vulva	5.2%	<u>1.5%</u>	18.5%	0.08	3.80%	0.39
Symptoms from other organs	Vaginal discharge	30.5%	<u>0.8%</u>	18.3%	0.03	2.80%	0.18
	Abnormal vaginal bleeding	21.7%	<u>0.0%</u>	7.4%	0.00	1.10%	0.00
	Shortness of breath	5.5%	<u>3.8%</u>	19.4%	0.20	6.00%	0.63
General symptoms	Tingling/numbness in hands/feet	6.3%	<u>10.6%</u>	38.5%	0.28	14.70%	0.72
	Swelling in one or both legs	4.0%	<u>10.6%</u>	29.4%	0.36	11.40%	0.93
	Pain in lower back	23.4%	<u>9.5%</u>	41.8%	0.23	15.60%	0.61
	Pain	22.9%	<u>8.3%</u>	41.6%	0.20	14.00%	0.59
	Lack of appetite	13.9%	<u>2.6%</u>	21.1%	0.12	5.30%	0.49
	Hot flashes/sweats	9.8%	<u>16.7%</u>	47.3%	0.35	21.00%	0.80
	Trouble sleeping	23.0%	<u>16.6%</u>	47.9%	0.35	19.10%	0.87
	Tiredness	22.8%	<u>20.0%</u>	51.0%	0.39	19.90%	1.01
	Need to rest	25.3%	<u>19.3%</u>	48.2%	0.40	19.10%	1.01
	Felt weak	18.7%	<u>12.2%</u>	41.7%	0.29	13.40%	0.91
Emotional symptoms	Difficulty concentrating	10.6%	<u>5.8%</u>	25.8%	0.22	8.30%	0.70
	Difficulty remembering	8.8%	<u>10.0%</u>	28.5%	0.35	11.20%	0.89
	Felt tense	23.9%	<u>8.6%</u>	36.4%	0.24	12.30%	0.70
	Worry	37.3%	<u>13.1%</u>	40.9%	0.32	13.50%	0.97
	Felt irritable	15.1%	<u>8.0%</u>	31.6%	0.25	10.40%	0.77
	Felt depressed	15.7%	<u>7.4%</u>	29.0%	0.26	9.20%	0.80

Table 1. Overview of LAPERS, crude incidence, prevalence rates of substantial symptoms (summarizing "Quite a bit" and "Very much") of the EORTC QLC30 and CX24. LAPERS calculation with baseline corrections applied are underlined. LAPERS ≥ 10% are marked with grey.

**Conclusion**

Incidence methods capture the first occurrence of an event; LAPERS in contrast excludes transient symptoms and identifies patients with persisting symptoms. When analyzing longitudinal morbidity data, a complementary approach combining the information of both methods improves the understanding of the morbidity profile of a treatment. LAPERS can be utilized to improve tools for informing patients about the burden and duration of toxicity (e.g. figure 1); thus improving the basis for shared

decision making.

**Difficulty controlling bowel**

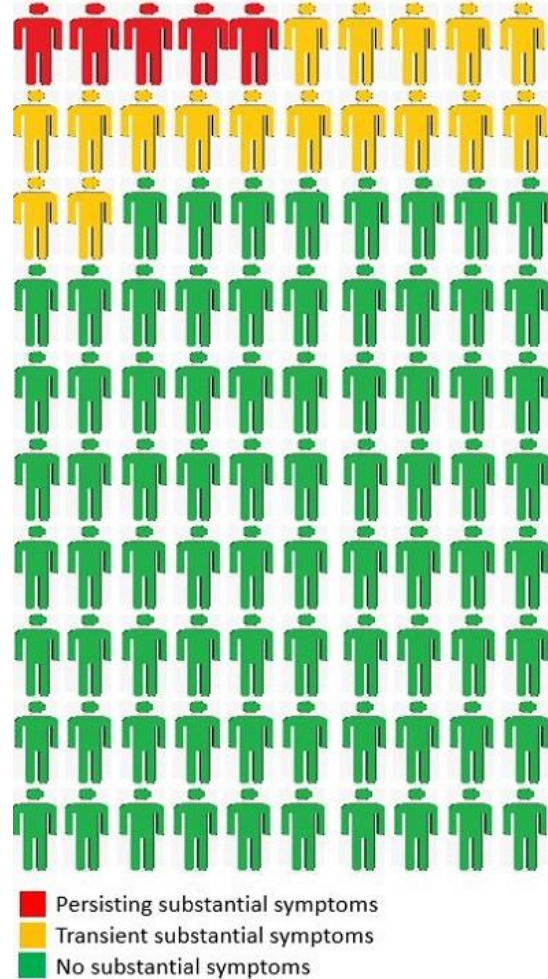


Figure 1. LAPERS events are the red persons, while crude incidence is the total of red and yellow persons.

**PV-0369 Radiomics in Magnetic Resonance Imaging for prediction of radiotherapy outcomes in cervical cancer**

N. Thanamitsomboon<sup>1</sup>, N. Kosaisawe<sup>2</sup>, K. Thephamongkhon<sup>1</sup>, P. Dankulchai<sup>1</sup>  
<sup>1</sup>Siriraj hospital, Division of Radiation Oncology- Department of Radiology, Bangkok, Thailand ;  
<sup>2</sup>University of California- Davis, Department of Molecular and Cellular Biology, Davis, USA

**Purpose or Objective**

The aim of this study is to investigate the predictive value of radiomics features from pre-treatment T2-weighted MR images for clinical outcome of radiotherapy with or without concurrent chemotherapy in cervical cancer patients. The primary and secondary clinical outcomes in this study were loco-regional recurrence (LRR) and overall survival respectively

**Material and Methods**

90 cervical cancer patients with stage IB-IVA between January 2015 to June 2016 were retrospectively enrolled in this study. All patients received definitive radiotherapy with or without concurrent chemotherapy as a primary treatment after underwent T2-weighted MRI simulation before the first fraction of external beam radiotherapy. Gross tumor volume (GTV) was delineated by a radiation oncologist who was an expertise in the gynecological field. Radiomics features [First orders, Gray level co-occurrence matrix (GLCM), and Gray level run length matrix (GLRLM)]

were extracted from GTV on pre-treatment T2-weighted MRI as a 3D contouring volume with MATLAB program. The association between radiomics features and loco-regional recurrence (LRR) were analyzed by T-Test and controlled by false discovery rate to reduce type I error from multiple testing. Then, the multivariable analysis was performed with significant radiomics features and known clinical prognostic factors using Cox-proportional hazard model.

### Results

The median follow-up time was 29.2 months in this study. 12 of 90 patients (13.3%) had LRR. 80 radiomics features were collected. The statistically significant association between each radiomics features with LRR showed as table below.

Table : P-value of T-test and Cox regression model with clinical factors

	P-value(t-test)	P-value(Cox)	Hazard Ratio	Lower CI	Upper CI
Max	0.00023	0.03818	1.002	1.0001	1.0039
Correlation135	0.00145	0.01305	1075.904	4.3454	266387.4092
Correlation90	0.00155	0.01522	1943.678	4.2945	879705.5522
Correlation45	0.00346	0.02480	915.340	2.3733	353027.4518
Correlation0	0.01062	0.05700	1345.319	0.8069	2242956.5340
HGRE0	0.01699	0.12562	1.100	0.9737	1.2424
Range	0.01791	0.04131	1.002	1.0001	1.0038
HGRE45	0.01888	0.13508	1.259	0.9307	1.7041
Entropy	0.02117	0.08858	7748.187	0.2588	232011519.3464
Contrast135	0.02129	0.04449	0.582	0.7810	0.9969

P-value(t-test) = P-value with t-test

P-value(Cox) = P-value of cox regression of radiomics feature and 6 clinical prognostic factors

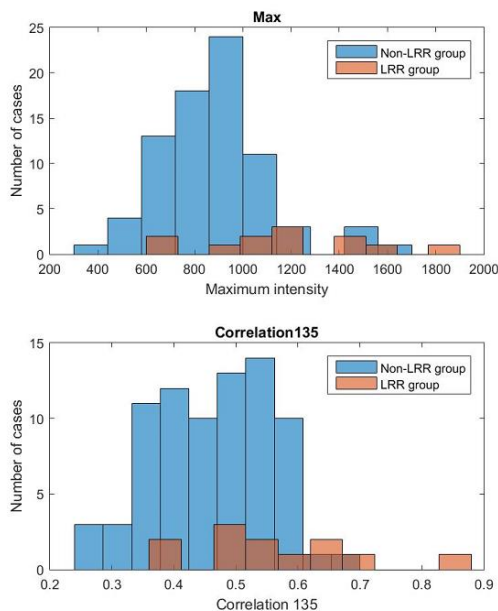
Max = Maximum intensity, Correlation135 = Correlation of gray-level co-occurrence matrix(GLCM) in 135 degree

Correlation90, Correlation45 and Correlation0 = Correlation of GLCM in 90, 45 and 0 degree,

HGRE0 and HGRE45 = High Gray-Level Run Emphasis in 0 and 45 degree, Range = Range of intensity,

Entropy = entropy of intensity, Contrast135 = Contrast of GLCM in 135 degree

The maximum intensity feature ( $p = 0.00023$ ) and correlation135 GLCM feature ( $p = 0.0015$ ) were the lowest p values.



Cox-regression analysis of radiomics features controlled for known clinical prognostic factors also confirmed significant hazard ratio for maximum intensity ( $p = 0.038$ ) and correlation135 GLCM ( $p = 0.013$ ) features. For overall survival outcome, there was no statistically significant association in any radiomics features

### Conclusion

The pre-treatment T2-weighted MR images in cervical cancer patients could provide additional information in predictive value of radiomics features with radiotherapy outcomes. Maximum intensity and correlation135 GLCM

features in our study were the most significant predictive values. To the best of our knowledge, this is the first work that shows predictive value of radiomics features in T2-weighted MRI for cervical cancer patients. These features need to be validated in subsequent more patients. Thus, the further investigation as comprehensive prediction model of LRR in cervical cancer patients would provide more statistical power and confirmation of these valuable features.

### Joint Symposium: ESTRO-ASTRO: Translating discovery to cure

#### SP-0370 Integrating Immunotherapy with Radiation

J. Schoenfeld<sup>1</sup>

<sup>1</sup>Dana Faber Cancer Institute, Radiation Oncology, Boston, USA

#### Abstract text

Immunotherapy has revolutionized the field of oncology. However, only a minority of patients with solid tumors respond to current immunotherapy treatments. Here, we will review the mechanism of action of immune checkpoint blockade and outcomes in recent seminal immunotherapy trials. Preclinical and an increasing amount of clinical data suggest that radiation can augment the clinical effectiveness of immune checkpoint blockade - we will review these data and discuss ongoing clinical trials.

#### SP-0371 A retrospective overview and future perspectives of developments in MRgRT

J. Lagendijk<sup>1</sup>

<sup>1</sup>UMC Utrecht, Department of Radiation Oncology, Utrecht, The Netherlands

#### Abstract text

Currently, MR linacs systems are entering the clinic. Those systems move radiotherapy in the direction of real-time MRI guided treatment optimization, greatly reducing the targeting uncertainty in radiotherapy. This development puts great importance on all forms of high quality imaging needed for tumour localization and characterization; the step from relative large PTV volumes to stereotactic body irradiation requires better target definition. The reduction of the PTV both facilitates dose optimization and the further development of hypofractionation for the majority of tumours. This process transforms radiotherapy towards interventional radiology, re-inventing radiotherapy and finally allowing dose painting as pointed out by every TCP model. The impact on the organization of radiotherapy will also be discussed. The new focus on complex, large imaging departments with interventional treatments will steer away from the old model with small radiotherapy satellites with a focus on closeness to the patient.

#### SP-0372 Real Time Adaptive Radiation, Lessons from Clinical Practice Teams

M. Bassetti<sup>1</sup>

<sup>1</sup>University of Wisconsin School of Medicine and Public Health, Human Oncology, Madison, USA

#### Abstract text

Radiation treatment plans are traditionally created pre-treatment and are unchanged during the course of delivery. Recent advances in radiation treatment delivery systems, including integration of MRI and rapid treatment planning software, enable oncologists to adapt radiation treatment plans in real time. This capability to adjust treatment to account for daily anatomical position changes allows the potential to increase dose to tumors and minimize dose to normal organs. While opening

avenues for potentially safe dose escalation in difficult to treat anatomical locations such as pancreatic cancers, it also creates increased demand and time pressures on clinical care teams. Here we discuss examples from clinical practice highlighting the benefits, challenges, and practical solutions for clinical use of real time MR-guided adaptive radiation.

#### SP-0373 Fractionation and breast cancer: towards more efficient schedules

J.R. Yarnold<sup>1</sup>

<sup>1</sup>The Institute of Cancer Research and The Royal Marsden NHS Foundation Trust, Radiotherapy & Imaging Department, Sutton, United Kingdom

#### Abstract text

In 1952, Lionel Cohen, reported a retrospective analysis of fractionation parameters associated with local control in women treated in Johannesburg for locally advanced/recurrent breast cancer. He found that breast cancer is sensitive to fraction size, an interpretation confirmed in 1984 when Bruce Douglas re-analysed Cohen's data using the new L-Q model. This historical observation simulated a series of UK randomised trials that have generated direct estimates of alpha/beta (a/b) for breast cancer and late reacting normal tissues in patients irradiated after primary surgery. An a/b value of around 3 Gy has been generated for both endpoints. So, conventional 2 Gy fractions are equally sparing of cancer and the late reacting normal tissue and have no clinical advantages. 40 Gy in 15 fractions of 2.7 Gy in 3 weeks has become an international standard, but it may not represent the safe and effective limit of hypofractionation. The FAST randomised trial controlled for time by testing 5 fractions delivered once-weekly for 5 weeks against 50 Gy in 25 fractions in 5 weeks. The results informed the FAST forward randomised trial testing two dose levels of a 5-fraction regimen delivered in 1 week against 40 Gy in 15 fractions in 3 weeks and 3-yr late normal tissue responses have been presented. The UK trial designs, incorporating 2 test dose levels, enable interpolation, where needed, to identify test schedules iso-effective with the Control regimen for tumour and normal tissues without distinguishing fraction size and time-related effects.

---

#### Proffered Papers: RB 4: Normal tissue effects of radiotherapy

---

#### OC-0374 GWAS identifies new susceptibility loci for late toxicity following prostate cancer radiotherapy

C. West<sup>1</sup>, S. Kerns<sup>2</sup>, L. Dorling<sup>3</sup>, G. Barnett<sup>4</sup>, D. Dearnaley<sup>5</sup>, L. Fachal<sup>6</sup>, L. Veldeman<sup>7</sup>, M. Parliament<sup>8</sup>, A. Vega<sup>9</sup>, A. Dunning<sup>10</sup>, B. Rosenstein<sup>11</sup>

<sup>1</sup>The University of Manchester, Translational Radiobiology, Manchester, United Kingdom ; <sup>2</sup>University of Rochester Medical Center, Department of Radiation Oncology, Rochester, USA; <sup>3</sup>University of Cambridge, Department of Public Health & Primary Care, Cambridge, United Kingdom ; <sup>4</sup>Addenbrookes Hospital, Department of Oncology, Cambridge, United Kingdom; <sup>5</sup>Institute of Cancer Research, Academic Unit of Radiotherapy, Sutton, United Kingdom ; <sup>6</sup>University of Cambridge, Department of Public Health and Primary Care, Cambridge, United Kingdom ; <sup>7</sup>Universiteit Gent, Department of Radiation Oncology & Experimental Cancer Research, Gent, United Kingdom; <sup>8</sup>University of Alberta, Department of Oncology, Alberta, Canada ; <sup>9</sup>Fundación Pública Galega Medicina Xenómica, Complejo Hospitalario Universitario de Santiago, Santiago de Compostela, Spain ; <sup>10</sup>University of Cambridge, Centre for Cancer Genetic Epidemiology, Cambridge, United

Kingdom ; <sup>11</sup>Mount Sinai, Icahn School of Medicine, New York, USA

#### Purpose or Objective

There is a risk of long-term side-effects following radiotherapy for cancer. Identification of common genetic variants can provide information on susceptibility, and may lead to improve risk prediction and inform functional work to better understand biological mechanisms. The purpose of this Radiogenomics Consortium study was to expand our previous meta-analysis from ~1,600 patients to 4,000 patients in an attempt to identify new loci associated with risk of late toxicity following radiotherapy.

#### Material and Methods

An individual patient data meta-analysis was carried out in six European-ancestry genome-wide association studies (n=3,871) of radiotherapy-treated prostate cancer survivors. Radiotherapy side-effects were graded prospectively in all studies. Cox proportional hazards regression tested associations of ~6 million genotyped or imputed variants with urinary and rectal toxicity endpoints (time to first ≥grade 2 event).

#### Results

Individual patient data meta-analysis of the European ancestry cohorts identified three signals with genome-wide significance and low Bayesian false discovery probability (<2%): rs17055178 (p=6.2x10<sup>-10</sup>), rs10969913 (2.9x10<sup>-10</sup>), rs11122573 (p=1.8x10<sup>-8</sup>), associated with rectal bleeding, decreased urinary stream, and haematuria radiation induced risk, respectively. Fine mapping the regions containing these signals identified an additional independent signal associated with haematuria. Credible causal variants at the four signals lie in gene-regulatory regions and some modulate expression of nearby genes. All variants retained significance in multivariable models including clinical and dosimetric risk factors. Previously identified variants showed a consistent association effect in the new cohorts (*KDM3B*, *DHAH5*, *ATM*). Two new and two previously identified signals showed a similar effect in two Japanese ancestry cohorts.

#### Conclusion

Our study highlights the importance of common genetic variants as a determinant of long-term side-effects following radiotherapy, increases understanding of the architecture of common genetic variants affecting risk of late radiotherapy side-effects, and shows further multinational studies in larger cohorts are worthwhile.

#### OC-0375 Improving lung cancer outcome by reducing normal lung tissue toxicity

L. Giuranno<sup>1</sup>, E. Roig Moreno<sup>1</sup>, R. Iannone<sup>1</sup>, M. Vooijs<sup>1</sup>  
<sup>1</sup>Maastricht Radiation Oncology Maastricht, Radiotherapy, Maastricht, The Netherlands

#### Purpose or Objective

Lung cancer is the leading cause of cancer death in western countries. The current standard of care includes surgery, chemotherapy and radiotherapy. While significant progress has been made in terms of treatment modality radiotherapy is limited by dose-limiting side-effects which negatively affect tumour control and patient's quality of life. Reducing side-effects may improve tumor control by dose-escalation and treatment-time. The Notch signaling pathway plays an important role in lung cell differentiation and regeneration of the airway epithelium and its deregulation is associated with several cancers including lung cancer. Notch signaling pathway alteration leads to poor outcome and treatment resistance in patients and in preclinical models suggesting Notch signaling as a novel therapeutic target. However, the mechanism through which Notch inhibition integrates with airway repair and cellular differentiation is not fully understood. What is currently lacking are primary human lung tissue models that enable robust evaluation of normal

tissue effects prior to clinical studies. We hypothesize that Notch inhibition has a protective effect in cells exposed to radiotherapy and may represent a potential target for intervention to modulate normal tissue toxicity.

#### Material and Methods

We established and characterized primary lung organoids and air liquid interface system (ALI), pseudo-stratified cultures derived from primary human bronchial epithelial cells (PBEcs) from 6 different donors. In these cultures, basal cells proliferate and differentiate into ciliated and mucous/secretory cell types resembling the human bronchus. We irradiated lung epithelium with 2 and 4 Gy and early and late response to radiotherapy were evaluated. We investigated the consequences of blocking Notch signaling pathway using the pan-notch  $\gamma$ -secretase inhibitor DBZ (1 $\mu$ M) alone and when combined with irradiation (2, 4 Gy).

#### Results

Using immunofluorescence, western blot and q PCR we found that basal cells (p63<sup>+</sup>, CK5<sup>+</sup>) cease proliferation (Ki67, EdU) at day 21 and mucous cell differentiation (Muc1/5ac<sup>+</sup>) precedes ciliary differentiation (Ac-Tub<sup>+</sup>) and both complete at day 28. Proliferation decreases overtime but inhibiting Notch in undifferentiated progenitors and in differentiated cells at day 21 increases p63 proliferation alone and even more in combination with radiotherapy. In all the 6 donors and in murine cultures Notch inhibition increases p63+basal progenitors and ciliated cells and decreases mucous cells alone and in combination with radiation. In irradiated cultures we observed increased pATM and pCHK2 12h and 24h post-irradiation when Notch signaling was inhibited. 53BP1 staining shows reduced DNA breaks 24h and 3 days post-irradiation when Notch was inhibited.

#### Conclusion

These data support the use of normal patient tissue for predictive toxicity, screening of combination treatments and disclose important novel interactions between Notch inhibition and radiotherapy.

#### OC-0376 Radio-selective effects of natural occurring muscle-derived dipeptide in A549 and normal cell lines

N. Ybarra<sup>1</sup>, J. Seuntjens<sup>1</sup>

<sup>1</sup>McGill University, Oncology Department, Montreal, Canada

#### Purpose or Objective

Radiotherapy (RT) causes morbidity and long-term side effects. A challenge in RT is to maximize cancer cell killing while minimizing damage to normal tissue. The ideal radio-protector selectively improves survival and limits damage to normal tissues while reducing survival or proliferation of cancer cells. Muscle-derived dipeptide, L-carnosine (CAR) has been described as a potent antioxidant, with radio-protective, but also anticancer properties, affecting the cell cycle of cancer cells. We aimed to test CAR effects in 3 cell types affected by RT: cancer cells, differentiated and undifferentiated normal cells. We hypothesized that 1) CAR antioxidant properties will confer protection to normal cells against RT while preventing cancer cell proliferation, and 2) CAR may act as a radiosensitizer of cancer cells due to its effect on their cell-cycle progression.

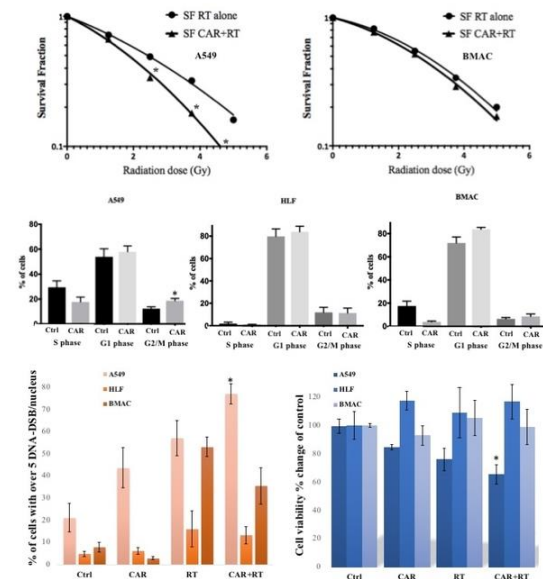
#### Material and Methods

The radio-selective effects of CAR were tested in cell lines: a) differentiated normal cells (human lung fibroblasts, HLF), b) normal undifferentiated cells (bone marrow adherent cells, BMAC), and c) lung cancer cell line (A549 cells). Treatment consisted of adding CAR to the media of growing cells. Cell cycle progression and short-term effects in proliferation were tested in control and CAR treated cells. Clonogenic assay, also performed in control and CAR-treated, was used to test CAR long-term effects in cells exposed to different radiation doses. In addition, the 3 cell lines were randomized in four groups:

control, CAR, RT, RT+CAR. Effects on cell viability were measured using XTT assay. DNA-DSB was done by quantifying foci of positive  $\gamma$ -H2AX staining. Cell bioenergetics were measured using Cell mitostress test (Seahorse Bioscience), and ROS production detected with the probe CM-H<sub>2</sub>DCFDA.

#### Results

Clonogenic assay: CAR reduced the number of colonies in non-irradiated cells, and decreased SF of A549 cells at increasing RT doses, not observed in BMACs. At short term, CAR reduced proliferation of the three cell lines and affected their cell cycle, but it only increased the percentage of A549 in the G2/M radiosensitive phase. In A549 cells CAR reduced cell viability, increased frequency of DNA-DSB, and production of ROS. These effects were exacerbated in RT+CAR; opposite effects were observed in normal cells. In terms of A549 cells bioenergetics, CAR reduced their metabolic potential (ability to meet energy demands via respiration/glycolysis), CAR did not induce negative effects on normal cells metabolic potential.



#### Conclusion

CAR increased radio-sensitivity of A549 cancer cells by selectively increasing ROS production and negatively affecting A549 cell bioenergetics, therefore reducing cells viability and DNA-DSB repair capacity. CAR had either no effect or reduced RT-induced damage in normal cells, depending on the cell type. CAR is a versatile naturally occurring compound, that could improve RT-induced cancer cell killing, while reducing the damage to normal differentiated and undifferentiated cells.

#### OC-0377 Individual radiation toxicity prediction, how does mtDNA influence normal tissue response?

M. Van Gisbergen<sup>1</sup>, S. Masroor<sup>2</sup>, E.E.J.M. Smeets<sup>1</sup>, M.J. Verhesen<sup>1</sup>, A.P.M. Stassen<sup>3</sup>, L. Dubois<sup>1</sup>, C. Oberije<sup>2</sup>, H.J.M. Smeets<sup>3</sup>, P. Lambin<sup>1,2</sup>

<sup>1</sup>GROW - School for Oncology and Developmental Biology- Maastricht Comprehensive Cancer Centre- Maastricht University Medical Centre, Department of Precision Medicine- The M-Lab, Maastricht, The Netherlands;

<sup>2</sup>GROW - School for Oncology and Developmental Biology- Maastricht Comprehensive Cancer Centre- Maastricht University Medical Centre, Department of Precision Medicine- The D-Lab, Maastricht, The Netherlands ;

<sup>3</sup>GROW - School for Oncology and Developmental Biology- Maastricht University Medical Centre, Department of Genetics and Cell Biology, Maastricht, The Netherlands

### Purpose or Objective

Mitochondria are structures within eukaryotic cells having their own genome. The mtDNA encodes for structural subunits of the OXPHOS chain, rRNAs and tRNAs. Although, variations in the mtDNA are very common (every individual carries variations), mtDNA variations can potentially lead to a stress-induced decrease in mitochondrial function. The main functions of mitochondria are ATP and ROS production, molecular properties important for radiotherapy (RT), suggesting that there is a role for mtDNA variations in RT response. We hypothesize that mtDNA variants are associated with RT response, and influence the DNA damage/repair capacity and/or induced ROS damage.

### Material and Methods

**Patient study:** Random forest modeling has been shown to perform well in situations where there are large numbers of predictor variables with complex interactions. We used this method to study the association between mtDNA variations of lung cancer patients and their dyspnea score as an outcome of radiation-induced lung toxicity (RILT). In our analysis, 137 patients with 3-month dyspnea score of 0 were marked to be not sensitive to RT and 41 patients with a change of at least 2 in the dyspnea score (3-month vs baseline) were marked as radiosensitive.

**In vitro study:** Primary fibroblasts were obtained from either healthy controls or mitochondrial patients, with a m.11778G>A mutation causative for a mild phenotype mitochondrial disease. Assays were performed using galactose containing medium in order to exhibit the mitochondrial phenotype of the cell lines.

### Results

Here, we performed a number of modeling efforts where each time we restricted the features to only a chosen subset of all mtDNA variants. We used a three-fold cross-validation (CV) on our data set and repeated the CV 100 times with random shuffling. We found predictive value when we restricted the features to all tRNA and rRNA variants together with the non-synonymous variants that:

1. are on genes COI, COII, COIII, and CYBT (AUC = 0.61±0.04)
2. are at positions that are at least 50% conserved (AUC = 0.59±0.04)

In our proof-of-concept study, trends in mitochondrial metabolism show that less mitochondrial spare capacity was present for the m.11778 G>A cells compared to the controls. Additionally, preliminary results show an upregulation of RT stress-induced genes (*NFKB*, *NRF2*). DNA damage (γH2AX foci) and apoptosis (cleaved PARP) were increased, although this needs to be further validated; also other stress response pathways are currently explored.

### Conclusion

Our data showed that mtDNA variation could be a valuable biomarker for RILT. Furthermore, we have preliminary data indicating that RT-induced stress response pathways are differently expressed in cells with a mild mtDNA phenotype.

### OC-0378 Regeneration after radiation and T cell-induced tissue injury is not enhanced by type III interferon

J. Fischer<sup>1</sup>, C. Lin<sup>2</sup>, S. Heidegger<sup>2</sup>, A. Wintges<sup>2</sup>, M. Schlapschy<sup>3</sup>, M. Beudert<sup>3</sup>, S.E. Combs<sup>1</sup>, F. Bassermann<sup>2</sup>, A. Skerra<sup>3</sup>, T. Haas<sup>2</sup>, H. Poock<sup>2</sup>

<sup>1</sup>Klinikum rechts der Isar- Technische Universität München, Department of Radiation Oncology, Munich, Germany; <sup>2</sup>Klinikum rechts der Isar- Technische Universität München, Klinik und Poliklinik für Innere Medizin III, Munich, Germany; <sup>3</sup>Technische Universität München, Munich Center for Integrated Protein Science CIPS-M and Lehrstuhl für Biologische Chemie, Freising, Germany

### Purpose or Objective

Type I interferon (IFN-I) and IL-22 modulate regeneration of the thymus and intestinal epithelial cells (IECs) after cytotoxic stress like irradiation. Radiation-induced damage to thymic tissues and IECs is a crucial aspect during the pathogenesis of inadequate immune reconstitution and acute graft-versus-host disease (GVHD) after allogeneic hematopoietic stem cell transplantation (allo-HSCT) with myeloablative total body irradiation (TBI), respectively. IL-22 and IFN-I reduce severity of acute GVHD after allo-HSCT with myeloablative TBI. However, the role of biologically related type III interferon (IFN-III), also known as interferon lambda (IFN-λ) or IL-28, in this context is unclear. We therefore studied the role of the IFN-III pathway in thymic regeneration and GVHD after TBI and allo-HSCT.

### Material and Methods

Co-housed wild-type (WT) and IFN-III receptor-deficient (IL-28 receptor-alpha-deficient/IL-28Ra<sup>-/-</sup>) mice were analyzed in models of TBI-induced thymus damage and a model of GVHD after allo-HSCT with myeloablative TBI. PASylated IFN-III (PASylated IL-28A) was generated to prolong plasma half-life of IFN-III. Pharmacological activity and effects of PASylated IL-28A on radiation-induced thymus damage and the course of GVHD after allo-HSCT with myeloablative TBI were tested.

### Results

Course and severity of GVHD after myeloablative TBI and allo-HSCT in IL-28 receptor-alpha-deficient mice were comparable and not significantly different compared to WT mice. Also, activation of the IFN-III pathway with PASylated IL-28A did not significantly modulate GVHD after allo-HSCT with TBI. Furthermore, IL28Ra<sup>-/-</sup> mice and WT mice showed similar thymus regeneration after radiation, which could also not be significantly modulated by IFN-III receptor activation using PASylated IL-28A.

### Conclusion

We have analyzed the role of IFN-III signaling during radiation-mediated acute tissue injury. We found that despite molecular and biological homologies with IFN-I and IL-22, IFN-III signaling did not regulate thymus regeneration after irradiation or the course of GVHD after myeloablative TBI and allo-HSCT.

### OC-0379 Radiation response mechanisms of mesenchymal stem cells in dependence on their tissue of origin

N. Nicolay<sup>1,2</sup>, A. Rühle<sup>2</sup>, R. Lopez Perez<sup>2</sup>, R. Saffrich<sup>3</sup>, S. Sisombath<sup>2</sup>, T. Trinh<sup>4,5</sup>, J. Debus<sup>4,5</sup>, P.E. Huber<sup>2,4</sup>

<sup>1</sup>University of Freiburg Medical Center, Radiation Oncology, Freiburg, Germany; <sup>2</sup>German Cancer Research Center, Molecular Radiation Oncology, Heidelberg, Germany; <sup>3</sup>German Red Cross Blood Donor Service, Transfusion Medicine and Immunology, Mannheim, Germany; <sup>4</sup>Heidelberg University Hospital, Radiation Oncology, Heidelberg, Germany; <sup>5</sup>German Cancer Research Center, Clinical Cooperation Unit Radiation Oncology, Heidelberg, Germany

### Purpose or Objective

Human mesenchymal stem cells (MSCs) aid the regeneration of tissue damage caused by ionizing radiation (IR), and early clinical results indicate a potential of MSC-based therapies for the treatment of IR-induced toxicities. While MSCs can be harvested from different tissues, the influence of the tissue source on the radiation response of MSCs remains largely unknown.

### Material and Methods

Human MSCs were harvested from adipose tissue (adMSCs), bone marrow (bmMSCs) and umbilical cord Wharton's jelly (wjMSCs) from 9 voluntary donors and characterized according to the established defining criteria: Cellular adhesion was measured, and multi-lineage differentiation was assessed after IR. Proliferation and survival of MSCs were examined after IR, and IR-

induced cell cycle distribution was quantified by flow cytometry. Apoptosis and senescence levels were determined using caspase-3, annexin-V and  $\beta$ -galactosidase stainings. Immunofluorescence analyses of  $\gamma$ H2AX foci were performed to assess DNA double strand break (DSB) repair, and the expression and activation of various proteins involved in human damage signaling and DSB repair were elucidated by Western blot in MSCs from different tissues of origin.

### Results

All MSCs exhibited a relative radioresistance independent of their tissue source and comparable to adult fibroblasts. The defining stem cell characteristics and multi-lineage differentiation potential remained largely unaffected by IR independent of the MSCs' tissue source. While adMSCs and bmMSCs showed a strong IR-induced accumulation in the G2/M phase, wjMSCs exhibited virtually no G2/M phase arrest. Very low apoptosis levels were found in adMSCs and bmMSCs after IR, whereas IR induced apoptosis in up to 20% of wjMSCs as measured by caspase-3 activation. In adMSCs and bmMSCs,  $\gamma$ H2AX foci numbers induced by up to 8 Gy returned to baseline levels within 24 hours after treatment. In contrast, 8 Gy led to significant residual  $\gamma$ H2AX foci and hence unrepaired DSBs in wjMSC1. Expression of  $\beta$ -galactosidase cells was found to be unaffected in wjMSCs, while irradiated adMSCs and bmMSCs demonstrated an increase of  $\beta$ -galactosidase-positive cells. Levels of phospho-ATM and phospho-Chk2 observed after IR were found strongly decreased in all MSCs at 24 hours after IR. Contrary to adMSCs and bmMSCs, wjMSCs exhibited increased phospho-BRCA1 expression still at 24 hours after IR.

### Conclusion

Despite a comparable radiation resistance of MSCs derived from different human tissues, MSCs exhibited differential responses to IR regarding apoptosis, senescence and cell cycle distribution that depended on their tissue source. As the radiation resistance of human MSCs was found independent of their tissue of origin, MSCs from various tissues may aid the regeneration of radiation-induced tissue damages. However, the observed tissue-specific differences of MSCs may need to be taken into account in order to find the optimal tissue source when devising MSC-based clinical therapies for IR-induced tissue damage.

## Proffered Papers: CL 7 :Proffered papers: GI

### OC-0380 Dose response relation in esophageal cancer after neoadjuvant therapy: multi-institutional analysis

M. Thomas<sup>1,2</sup>, A.S. Borggreve<sup>3,4</sup>, P.S. Van Rossum<sup>4</sup>, C. Perneel<sup>5</sup>, J. Moons<sup>6</sup>, E. Van Daele<sup>7</sup>, R. Van Hillegersberg<sup>3</sup>, W. Deng<sup>8</sup>, P. Pattyn<sup>7</sup>, S. Mook<sup>4</sup>, T. Boterberg<sup>9</sup>, J.P. Ruurda<sup>3</sup>, P. Nafteux<sup>6</sup>, S.H. Lin<sup>8</sup>, K. Haustermans<sup>1,2</sup>  
<sup>1</sup>KU Leuven - University of Leuven, Department of Oncology - Laboratory Experimental Radiotherapy, B-3000 Leuven, Belgium; <sup>2</sup>UZ Leuven - University Hospitals Leuven, Department of Radiation Oncology, B-3000 Leuven, Belgium; <sup>3</sup>University Medical Center Utrecht, Department of Surgery, 3584CX Utrecht, The Netherlands; <sup>4</sup>University Medical Center Utrecht, Department of Radiation Oncology, 3584CX Utrecht, The Netherlands; <sup>5</sup>Royal Military Academy, Department of Applied Mathematics, B-1000 Brussels, Belgium; <sup>6</sup>UZ Leuven - University Hospitals Leuven, Department of Thoracic Surgery, B-3000 Leuven, Belgium; <sup>7</sup>UZ Gent - Ghent University Hospital, Department of Pediatric and Gastrointestinal Surgery, B-9000 Ghent, Belgium; <sup>8</sup>The University of Texas MD Anderson Cancer Center, Department of Radiation Oncology, Houston - Texas, USA; <sup>9</sup>UZ Gent - Ghent University Hospital, Department of Radiation Oncology, B-9000 Ghent, Belgium

### Purpose or Objective

Curative treatment for locally advanced esophageal cancer (EC) consists of neoadjuvant chemoradiotherapy (nCRT) followed by surgery. Various chemotherapy and radiotherapy regimens are currently used worldwide. The aim of this study was to explore whether a higher total radiation dose leads to a higher probability to obtain a pathological major response (pMR).

### Material and Methods

All consecutive patients who underwent nCRT followed by surgery for locally advanced squamous cell carcinoma (SCC) or adenocarcinoma (AC) of the esophagus between 2000 and 2017 at four major university medical centres were included and stratified according to a prescribed dose of 36Gy, 40Gy, 41.4Gy, 45Gy or 50.4Gy in fractions of 1.8Gy or 2Gy. Clinical and treatment-related characteristics were collected from the prospectively obtained databases: age at diagnosis, sex, clinical tumor and nodal stage, histology, chemotherapy regimen, use of induction chemotherapy and the time interval from nCRT to surgery. The primary endpoint for the analysis was a pMR, defined as Mandard 1 (no residual tumor cells) or Mandard 2 (fibrosis with scattered tumor cells). A multivariable logistic regression analysis was used to analyse the relation between neoadjuvant radiation dose and pMR. Subgroup analysis was performed according to histology.

### Results

A total of 1102 patients were eligible for analysis, who received either 36Gy (162; 14.7%), 40Gy (79; 7.2%), 41.4Gy (211; 19.1%), 45Gy (271; 24.6%) or 50.4Gy (379; 34.4%). A pMR was achieved in 604 patients (54.8%). In multivariable analysis, the total radiation dose was the only factor increasing the probability of reaching a pMR (odds ratio (OR) 1.031), Table 1. Factors reducing this probability were a higher cT stage (cT1: reference; cT2: OR 1.030; cT3: OR 0.556; cT4: OR 0.448), the presence of an AC (OR 0.362) and the use of non-platinum versus platinum based chemotherapy (OR 0.294). The interaction between tumor type and chemotherapy regimen indicated that using non-platinum based chemotherapy for AC patients increases the likelihood of achieving a pMR (OR 4.336). The interaction between tumor type and the use of induction chemotherapy showed that the use of induction chemotherapy is beneficial to reach a pMR in AC patients (OR 1.731).

For AC, 417 of 819 patients (50.9%) achieved a pMR. Factors increasing the probability to achieve a pMR were total radiation dose (OR 1.027) and the use of induction chemotherapy (OR 1.702), Table 1. Tumor stage was the only factor reducing this probability (cT1: reference; cT2: OR 0.423, cT3: OR 0.260; cT4: OR 0.241).

For SCC, 187 of 283 patients (66.1%) achieved a pMR. No subgroup analysis with reliable adjustment of covariables was possible for the cohort of SCC patients.

Table 1: Explanatory model for pathological major response in the entire cohort and in patients with an adenocarcinoma.  
 n = number; OR = odds ratio; 95% CI = 95% confidence interval; SCC = squamous cell carcinoma; AC = adenocarcinoma; df = degrees of freedom.

\*51 and \*43 patients with a missing endpoint or variable were excluded for model building

	Entire patient cohort: n=1051*		Patients with AC: n=776*	
	OR (95% CI)	p-value	OR (95% CI)	p-value
Total dose	1.031 (1.007-1.056)	0.012	1.027 (1.001-1.053)	0.044
Histology (0=SCC; 1=AC)	0.362 (0.257-0.508)	<0.001	/	/
Tumour stage (cT1=reference)		0.011		0.025
cT2	1.030 (0.352-3.016)	0.957	0.423 (0.125-1.432)	0.167
cT3	0.556 (0.202-1.531)	0.256	0.260 (0.081-0.831)	0.023
cT4	0.448 (0.150-1.345)	0.152	0.241 (0.062-0.926)	0.039
Type of chemotherapy (0=platinum based; 1=non-platinum based)	0.294 (0.096-0.985)	0.031	/	/
Induction chemotherapy (0=no induction; 1= induction)	/	/	1.702 (1.261-2.296)	0.001
Interaction histology and induction chemotherapy	1.731 (1.281-2.340)	<0.001	/	/
Interaction histology and chemotherapy	4.336 (1.373-13.692)	0.012	/	/
	Hosmer-Lemeshow goodness: p=0.071 (df=7)		Hosmer-Lemeshow goodness: p=0.499 (df=7)	

### Conclusion

In this cohort of 1102 patients with EC who were treated with nCRT followed by surgery at four high volume institutes, it was demonstrated that the total radiation dose has a major impact on pathological response, especially in AC patients.

**OC-0381 Benchmark case in the ongoing PRODIGE 26 trial : quality assurance of dose escalated radiotherapy**

J. Boustani<sup>1</sup>, R. Rivin Del Campo<sup>2</sup>, J. Blanc<sup>3</sup>, D. Peiffert<sup>4</sup>, K. Benezery<sup>5</sup>, R. Pereira<sup>6</sup>, E. Rio<sup>7</sup>, E. Le Prisé<sup>8</sup>, G. Créhange<sup>1</sup>, F. Huguet<sup>2</sup>

<sup>1</sup>Centre Georges François Leclerc, Radiation Oncologist, Dijon, France ; <sup>2</sup>Tenon Hospital, Radiation oncology, Paris, France ; <sup>3</sup>Centre Georges François Leclerc, Biostatistics, Dijon, France ; <sup>4</sup>Institut de Cancérologie de Lorraine, Radiation Oncology, Vandoeuvre-Lès-Nancy, France ; <sup>5</sup>Centre Antoine Lacassagne, Radiation oncology, Nice, France ; <sup>6</sup>Centre Guillaume Le Conquérant, Radiation Oncology, Le Havre, France ; <sup>7</sup>Institut de Cancérologie de l'Ouest, Radiation Oncology, Saint Herblain, France ; <sup>8</sup>Centre Eugène Marquis, Radiation Oncology, Rennes, France

**Purpose or Objective**

The ongoing phase II/III PRODIGE 26 trial compares chemoradiotherapy with or without dose escalation in patients with locally advanced or unresectable oesophageal cancer. The results of a benchmark case procedure are reported here to evaluate the protocol compliance of participating centers as part of the radiation therapy quality assurance (RTQA) program.

**Material and Methods**

Volume delineation, target coverage, and dose constraints to the OARs were assessed on treatment plans performed by each participating center and compared to parameters defined in the protocol (Table 1). Centers were classified in three categories: per protocol (PP), minor acceptable deviation (MiD), or major unacceptable deviation (MaD). A plan was rejected if  $\geq 4$  MiD or one MaD were found.

**Results**

Thirty-seven centers submitted 52 plans. Among them, 17 (32.7%) were PP, 30 (57.7%) presented MiD, and 11 (21.1%) had MaD. Overall, 12 (23%) plans were rejected. One plan was rejected because the GTV was not correctly delineated. There were 8 (15.4%) MiD for CTV1 margins and 11 (21.2%) for CTV2 margins, due mostly to insufficient margins. The OARs delineation and the PTVs margins were respected in all cases. As for the target volume coverage, 10 plans had under-dosage among which 3 (5.8%) were major. Six plans had over-dosage among which 1 (1.9%) was major. When considering the maximal dose (Dmax) to the spinal cord, there were 2 (3.8%) plans with MiD and 1 (1.9%) plan with MaD. Regarding the lungs V20 and V30, 1 (1.9%) and 3 (5.8%) plans presented MiD and MaD, respectively. As for the heart V40, only 35 (67.3%) plans were PP, 13 (25%) had MiD and 4 (7.7%) had MaD. The liver V30 and the kidneys V20 were respected in all plans. Overall, 52% (n=27) of all treatments were planned with IMRT, while 48% (n=25) were planned with 3D-CRT. Deviations for target volume and OARs between 3D-CRT and IMRT plans are illustrated in Figure 1. The median PTV2 D2% was significantly lower in the IMRT group (p=0.01). The spinal cord Dmax was significantly lower in the IMRT group (median: 37.0 Gy (15.0-48.0), vs. 41.0 Gy (33.0- 46.0), respectively; p=0.003). The lungs V20 did not differ between groups (p=0.31), whereas the median V30 was significantly lower in the IMRT group, 9.0% (6.0-18.0) vs. 13.0% (7.0-28.0), respectively (p=0.003). The median heart V40 was significantly lower in the IMRT group (25.0% (14.0-36.0) vs. 30.0% (17.0-58.0), respectively; p=0.02). The liver V30 and the kidneys V20 did not differ significantly between groups. Overall, there were 13 (48.1%) and 4 (16%) PP plans in the IMRT and 3D-CRT groups (p=0.01), respectively. Significantly more plans in

the IMRT group were accepted (24 (88.9%) vs 16 (64%), respectively; p=0.03).

**Conclusion**

The high frequency of protocol deviations underlines the importance of a QA program in clinical trials. Further work should assess the impact of deviations on patient outcomes. IMRT might allow dose escalation without increasing normal tissue complications.

**OC-0382 Patterns of local failure after SBRT for pancreatic cancer: implications of target volume design**

X. Zhu<sup>1</sup>, C. Yangsen<sup>1</sup>, Z. Xianzhi<sup>1</sup>, S. Yuxin<sup>1</sup>, J. Xiaoping<sup>1</sup>, Q. Shuiwang<sup>1</sup>, C. Fei<sup>1</sup>, J. Zhen<sup>1</sup>, F. Fang<sup>1</sup>, G. Lei<sup>1</sup>, Z. Huojun<sup>1</sup>

<sup>1</sup>Changhai Hospital, Radiation Oncology, Shanghai, China

**Purpose or Objective**

To identify prognostic factors and patterns of local failure in patients with pancreatic cancer receiving stereotactic body radiation therapy (SBRT) plus chemotherapy as initial treatment, for the optimal design of target volumes encompassing a majority of local recurrences.

**Material and Methods**

Consecutive patients with resectable or borderline resectable but medically inoperable due to comorbidities and locally advanced pancreatic cancer undergoing SBRT and chemotherapy in our center were reviewed. Local recurrences were plotted with respect to the celiac trunk (CT), superior mesenteric artery (SMA) and splenic artery (SA) on 1 CT scan of a template patient.

**Results**

Five hundred and ten patients were included. Median follow-up of the entire group was 21.8 months (range: 3.1- 54.9 months). Two hundred and seventeen patients had locoregional recurrences while local and distant progressions were found in 293 patients. One hundred and sixty-nine (33.2%) and 144 (28.2%) patients had recurrences closer to the CT and SMA, respectively, while both invasions of the CT and SMA were found in 115 patients (22.5%). Additionally, 33 patients (6.5%) and 49 patients (9.6%) had recurrences at the hepatic hilum and invasions of the SA, respectively. Besides these patterns of failure, 138 patients (27.1%) also experienced retroperitoneal progressions. The mean distance to the CT, SMA and retroperitoneal recurrence was 9.0mm, 8.3mm and 11.7mm, respectively. Multivariable analysis demonstrated that advanced pancreatic cancer, recurrences at both the CT and SMA and the hepatic hilum, CA19-9 non-responders and BED<sub>10</sub> <60Gy were predictive of worse survival. Moreover, failures stratified by volumes of recurrences in the radiation field were also analyzed. In-field and outside-the-field recurrences alone were found in 127 (24.9%) 111 patients (21.8%), respectively, while 51 (10.0%) and 67 patients (13.1%) had in-field plus outside-the-field recurrences and marginal plus outside-the-field recurrences, respectively. Compared with patients with BED<sub>10</sub> <60Gy, fewer patients with BED<sub>10</sub>  $\geq$ 60Gy had in-field recurrence alone (68 patients vs. 59 patients, P=0.003) and in-field plus outside-the-field recurrences (29 patients vs. 22 patients, P=0.027). No differences were found in the incidences of margin recurrence alone (57 patients vs. 97 patients, P=0.108), outside-the-field recurrence alone (40 patients vs. 71 patients, P=0.128) and marginal plus outside-the-field recurrences (22 patients vs. 45 patients, P=0.091) between patients receiving BED<sub>10</sub> <60Gy and BED<sub>10</sub>  $\geq$ 60Gy, respectively.

**Conclusion**

Areas closer to the CT, SMA and retroperitoneal space were at a high risk of local recurrences. Non-uniform and enough expansions from gross tumor volumes may be necessary and the splenic vessels abutting to the tumor might also be included in the target volume without compromise of dose constraints of organs at risk.

### OC-0383 Randomised controlled trial for dose-escalated radiotherapy in locally advanced rectal cancer

A. Couwenberg<sup>1</sup>, H.M. Verkoijen<sup>2</sup>, M. Berbee<sup>3</sup>, J.P.M. Burbach<sup>4</sup>, S. Hoendervangers<sup>1</sup>, O. Reerink<sup>5</sup>, M.E.P. Philippens<sup>1</sup>, E.C.J. Consten<sup>6</sup>, A.B. Smits<sup>7</sup>, J. Heikens<sup>8</sup>, N. Wijffels<sup>7</sup>, A. Schiphorst<sup>9</sup>, M.M. Lacle<sup>10</sup>, F.J. Wessels<sup>11</sup>, M. Koopman<sup>12</sup>, W.M.U. Van Grevenstein<sup>13</sup>, M.P.W. Intven<sup>1</sup>

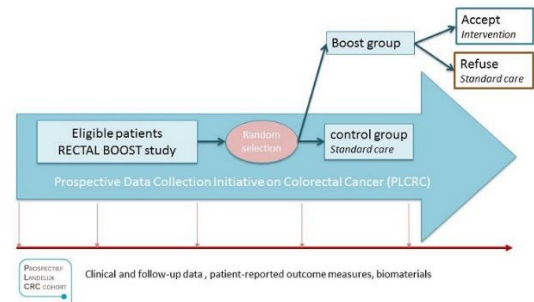
<sup>1</sup>UMC Utrecht, Radiotherapy, Utrecht, The Netherlands ; <sup>2</sup>UMC Utrecht, Imaging Division, Utrecht, The Netherlands; <sup>3</sup>Maastric Clinic, Radiotherapy, Maastricht, The Netherlands; <sup>4</sup>Medisch Centrum Leeuwarden, Surgery, Leeuwarden, The Netherlands ; <sup>5</sup>Isala clinic, Radiotherapy, Zwolle, The Netherlands ; <sup>6</sup>Meander Medical Center, Surgery, Amersfoort, The Netherlands; <sup>7</sup>St. Antonius Hospital, Surgery, Nieuwegein, The Netherlands ; <sup>8</sup>Ziekenhuis Rivierenland, Surgery, Tiel, The Netherlands; <sup>9</sup>Diakonessenhuis, Surgery, Utrecht, The Netherlands; <sup>10</sup>UMC Utrecht, Pathology, Utrecht, The Netherlands; <sup>11</sup>UMC Utrecht, Radiology, Utrecht, The Netherlands; <sup>12</sup>UMC Utrecht, Oncology, Utrecht, The Netherlands; <sup>13</sup>UMC Utrecht, Surgery, Utrecht, The Netherlands

#### Purpose or Objective

Patients with locally advanced rectal cancer (LARC) who achieve a good response following neoadjuvant chemoradiation (CRT) are potential candidates for organ-sparing treatment instead of surgery. As the response to radiotherapy is dose dependent, dose-escalated radiotherapy for LARC may render more patients eligible for organ preservation. In this trial, the RECTAL BOOST study, we have investigated the effect of a radiation boost to the primary tumour prior to standard CRT on complete tumour response in LARC patients.

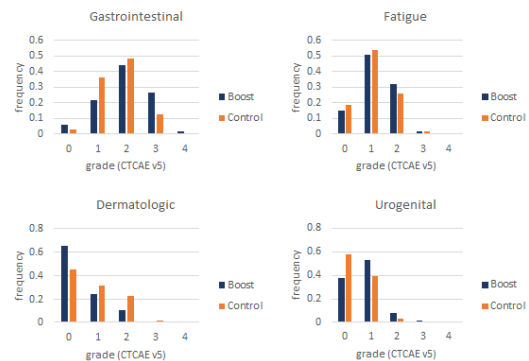
#### Material and Methods

This is a multicentre randomised controlled trial (RCT) nested within a cohort according to the cohort multiple RCT design (Figure 1). Patients with LARC participating in a prospective cohort, referred for CRT and with a tumour <10cm from the anorectal angle were randomised. The control arm received standard CRT (25x2Gy with capecitabine 825mg/m<sup>2</sup> bid). The intervention arm was offered a stereotactic, sequential radiation boost of 5x3Gy to the GTV prior to standard CRT. Dose planning for boost treatment involved equal dose constraints for organs at risk as in standard CRT. The primary endpoint was complete tumour response defined as pathological complete response (pCR), or, in patients who opted for a wait-and-see (WS) approach, 2-years local recurrence-free survival (2-yLRFS). We also assessed organ-sparing potential after CRT defined as (near-)pCR, ypT0-1N0, or wait-and-see with the hypothesis that ypT1N0 patients could have received local excision or could have waited longer. Acute toxicity was measured using CTCAE scores v5.0. Patients were included between Sept 2014 and July 2018. Because this abstract includes preliminary results, differences in outcomes were not tested for significance.



#### Results

Of the 64 patients who were offered boost CRT, 52 (81%) accepted and 51 (80%) received boost treatment. At abstract submission, 52 patients in the intervention group and 55 in the control group had complete follow up. In the boost group, 20/52 (38%) patients had a complete response (15 pCR and 5 2-yLRFS after WS) versus 20/55 (36%) patients in the control group (18 pCR and 2 2-yLRFS after WS). Organ-sparing potential was 50% in the boost arm (20 complete responses, 5 ypT1N0 and 1 ypTisN0) versus 36% in the control arm (20 complete responses, no ypT1N0). Grade 3/4 acute toxicity rate was 20/64 (31%) in the boost arm and 10/64 (16%) in the control arm, primarily due to gastrointestinal toxicity (Figure 2). No grade 5 toxicity was observed. Of all patients who underwent surgery, postoperative complications occurred in 21/46 (46%) in the boost arm versus 32/52 (62%) in the control arm.



#### Conclusion

Results suggest that the rate of complete tumour response is comparable between dose-escalated CRT and standard CRT. However, organ-sparing potential after dose-escalated CRT seems higher. Unfortunately, at the expense of an increase in grade 3-4 acute toxicity. Updated results on this RCT will be presented at the meeting.

### OC-0384 QoL after multimodal treatment of rectal cancer with/without oxaliplatin (phase 3, CAO/ARO/AIO-04)

R. Kosmala<sup>1</sup>, E. Fokas<sup>2</sup>, M. Flentje<sup>1</sup>, R. Sauer<sup>3</sup>, T. Liersch<sup>4</sup>, U. Graeven<sup>5</sup>, R. Fietkau<sup>3</sup>, W. Hohenberger<sup>6</sup>, D. Arnold<sup>7</sup>, R. Hofheinz<sup>8</sup>, M. Ghadimi<sup>4</sup>, H. Raab<sup>9</sup>, P. Ströbel<sup>10</sup>, L. Staib<sup>11</sup>, G.G. Grabenbauer<sup>12</sup>, G. Folprecht<sup>13</sup>, W. Uter<sup>14</sup>, C. Gall<sup>14</sup>, C. Rödel<sup>2</sup>, B. Polat<sup>1</sup>

<sup>1</sup>University Hospital Würzburg, Department of Radiation

Oncology, Würzburg, Germany ; <sup>2</sup>University of Frankfurt and German Cancer Consortium DKTK partner site, Department of Radiotherapy and Oncology, Frankfurt, Germany ; <sup>3</sup>University Hospital Erlangen, Department of Radiation Oncology, Erlangen, Germany; <sup>4</sup>University Medical Centre Göttingen, Department of General-Visceral and Paediatric Surgery, Göttingen, Germany; <sup>5</sup>Kliniken Maria Hilf GmbH Mönchengladbach, Department of Haematology/Oncology and Gastroenterology, Mönchengladbach, Germany; <sup>6</sup>University Hospital Erlangen, Department of Surgery, Erlangen, Germany; <sup>7</sup>Tumour Biology Centre Freiburg, Tumour Biology Centre Freiburg, Freiburg, Germany ; <sup>8</sup>University Hospital Mannheim- University of Heidelberg, Interdisciplinary Tumour Centre, Heidelberg, Germany ; <sup>9</sup>University of Oldenburg, Department of General and Visceral Surgery, Oldenburg, Germany ; <sup>10</sup>University Medical Centre Göttingen, Institute of Pathology, Göttingen, Germany; <sup>11</sup>Klinikum Esslingen, Department of Surgery, Esslingen, Germany ; <sup>12</sup>DiaCura & Klinikum Coburg, Department of Radiation Oncology and Radiotherapy, Coburg, Germany ; <sup>13</sup>University Hospital Carl Gustav Carus, Medical Department I- University Cancer Centre, Dresden, Germany ; <sup>14</sup>University Erlangen-Nürnberg, Department of Medical Informatics-Biometry and Epidemiology, Erlangen, Germany

#### Purpose or Objective

In a phase 3, open label randomised multicentre trial we previously confirmed that the inclusion of oxaliplatin (OX) into standard fluorouracil-based (5-FU) combined modality treatment for locally advanced rectal cancer (UICC II/III) was well tolerated and led to an improved disease-free survival (DFS) at 3 years. Here, we present 5-year results of patient reported quality of life (QoL).

#### Material and Methods

Between July, 2006, and February, 2010, 1236 patients aged 18 years or older with rectal carcinoma (clinically staged T3-4 or any node-positive) were randomly assigned to two groups at 88 participating German centres. Treatment was either standard 5-FU-based chemoradiotherapy (CRT) followed by total mesorectal excision (TME-surgery) and postoperative chemotherapy (CTx) with 5-FU, or preoperative CRT with 5-FU and OX, followed by TME-surgery and postoperative CTx with OX, leucovorin and 5-FU. 613 patients were randomised to the investigational group and 623 patients to the control group. The primary endpoint was DFS. QoL questionnaires (EORTC QLQ-C30, colorectal module CR38) were completed pretherapeutically, at the end of postoperative Ctx and during follow-up (1-, 3-, and 5-year visit). QoL assessment did not comprise specific questions on neurotoxicity. Analysis was done according to intention-to-treat. Recruitment and long-term follow-up are completed. ClinicalTrials.gov identifier: NCT00349076.

#### Results

Available questionnaires at baseline were 84,0% (n=515) in the investigational group and 82,5% (514) in the control group, 39,0% (239) vs. 36,8% (229) at 3 years, and 15,2% (93) vs. 16,4% (102) at 5 years (for all patients). General health status (GHS) for disease-free patients was stable in both groups (range 0 to 100): baseline: OX arm mean 63,2 (SD +/- 22; n=503) vs. standard arm 62,0 (+/- 21,6; n=491), 95% CI [-1,5;3,9]; at 5 years: OX arm 65,5 (+/- 22,4; n=83) vs. standard arm 64,9 (+/- 21,1; n=85), 95% CI [-6;7,2]. At the end of treatment and during follow-up, no moderate or large clinically relevant and statistically significant differences (differences of more than 10 points) between groups were found in QoL domains, including scales for diarrhea, gastrointestinal symptoms, chemotherapy side-effects or fatigue. Adjusting for age and gender, as well as including non-disease-free patients did not induce considerable changes. Regardless of the treatment arm, disease-free patients experiencing neurotoxic side-effects (grade 1-4) showed worse GHS at

3-year visit than patients without neurotoxicity (n=65 vs. n=296; mean 59,0 vs. 69,3; difference of means -10,4; 95% CI [-16,1;-4,6]).

#### Conclusion

The addition of oxaliplatin to a 5-FU-based preoperative CRT and postoperative CTx is not associated with worse overall QoL during follow-up. Given the benefit of improved DFS, our findings support the addition of oxaliplatin as a potential treatment option for patients with locally advanced rectal adenocarcinomas.

#### OC-0385 Gender associated differences in outcome after neoadjuvant chemoradiotherapy for rectal cancer

S. Meltzer<sup>1</sup>, K.M. Bakke<sup>1</sup>, K.L. Rød<sup>2</sup>, S. Dueland<sup>3</sup>, K. Flatmark<sup>4</sup>, A.T. Kristensen<sup>4</sup>, F.O. Larsen<sup>5</sup>, J.V. Schou<sup>5</sup>, A.J. Fuglestad<sup>6</sup>, C. Kersten<sup>6</sup>, K.R. Redalen<sup>2</sup>, A.H. Ree<sup>7</sup>  
<sup>1</sup>Akershus University Hospital, Department of Oncology, Lørenskog, Norway ; <sup>2</sup>Norwegian University of Science and Technology, Department of Physics, Trondheim, Norway ; <sup>3</sup>Oslo University Hospital, Department of Oncology, Oslo, Norway ; <sup>4</sup>Oslo University Hospital - Norwegian Radium Hospital, Department of Tumor Biology, Oslo, Norway ; <sup>5</sup>Herlev and Gentofte Hospital, Department of Oncology, Herlev, Denmark ; <sup>6</sup>Sørlandet Hospital, Center for Cancer Treatment, Kristiansand, Norway; <sup>7</sup>Institute of Clinical Medicine, University of Oslo, Oslo, Norway

#### Purpose or Objective

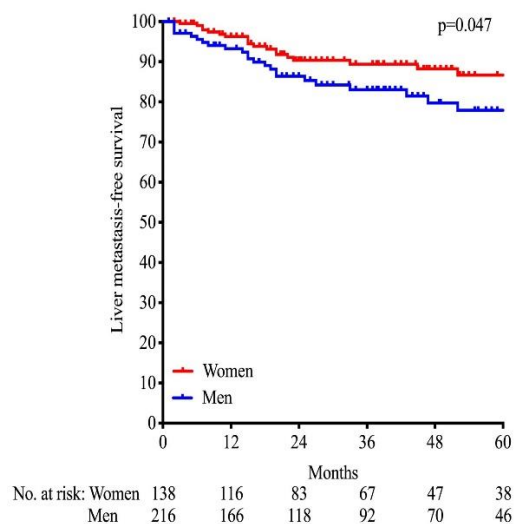
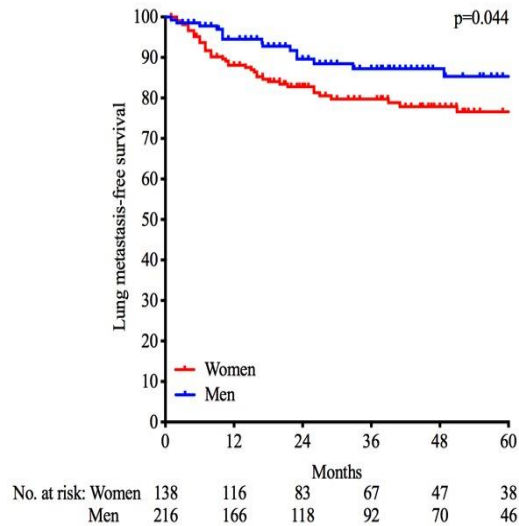
As combined-modality treatment of rectal cancer has resulted in high local control rates, dissemination to distant organs remains the foremost reason of treatment failure, disease-related morbidity, and impaired survival. While colon cancer primarily metastasizes to the liver, probably due to mesenteric venous drainage into the portal vein, rectal cancer is more prone to primarily spread to the lungs. We hypothesized that this may relate to anatomic and hemodynamic factors in the pelvic cavity.

#### Material and Methods

From 705 rectal cancer patients prospectively enrolled onto six clinical studies at four centers in Norway and Denmark between October 2005 and December 2017, 354 patients (216 men, 138 women) with locally advanced rectal cancer (LARC) were included for analysis of gender disparities in metastasis outcome. The selected patients had disease confined to the pelvic cavity at diagnosis and underwent study cohort-specific schedules of neoadjuvant chemoradiotherapy with curative intent. Progression-free survival was recorded as time from study enrolment until the first metastatic event or up to five years after surgery in the case of no event. In one of the study cohorts, dynamic susceptibility contrast-based magnetic resonance and computed tomography imaging at diagnosis enabled measurements of tumor blood perfusion (n=94) and the diameter of the inferior mesenteric vein (IMV; n=137), from patients who either proceeded directly to primary surgery or to standard neoadjuvant chemoradiotherapy. The IMV diameter was measured following the left colic, superior rectal and sigmoid veins to their confluence and then measuring the widest diameter of the IMV just after.

#### Results

Significantly more women than men developed lung metastasis (Figure 1), while the opposite was the case for liver metastasis (Figure 2). Women had both higher tumor blood perfusion than men (mean of 122.1 versus 99.83 ml/min/100g, p=0.004 by Student's t-test, parameters were normally distributed) and smaller IMV diameter (mean of 4.69 versus 5.48 mm, p<0.001 by Student's t-test). Finally, IMV diameter ≥5 mm was associated with progression to liver metastasis (p=0.016 by log-rank test, cutoff selected by receiver operating characteristics curve).



### Conclusion

Following neoadjuvant chemoradiotherapy for LARC, women had higher risk of developing lung metastasis, while men were more prone to develop liver metastasis. In a cohort consisting of rectal cancer patients that either proceeded directly to surgery or to standard neoadjuvant chemoradiotherapy, men's tumors had lower blood perfusion and wider IMV diameter. The latter was strongly associated with development of liver metastasis. Even though the LARC patients received study cohort-specific neoadjuvant treatments, the results indicate that women and men with rectal cancer have different outcomes of tumor-directed therapies, which may be related to hemodynamic factors in both the tumor and the pelvic cavity.

**OC-0386 A PET-based patterns of failure analysis in the context of contouring guidelines in anal cancer**  
 H. Dapper<sup>1</sup>, K. Schiller<sup>1</sup>, S. Münch<sup>1</sup>, J. Peeken<sup>1</sup>, K. Borm<sup>1</sup>, W. Weber<sup>2</sup>, S.E. Combs<sup>1,3,4</sup>

<sup>1</sup>Klinikum rechts der Isar- TU München, Department of Radiation Oncology, München, Germany ; <sup>2</sup>Klinikum rechts der Isar- TU München, Department of Nuclear Medicine, München, Germany; <sup>3</sup>Deutsches Konsortium für Translationale Krebsforschung DKTK, Partner Site Munich, München, Germany; <sup>4</sup>Helmholtz Zentrum München, Institute for innovative Radiotherapie iRT, München, Germany

### Purpose or Objective

Definitive radiotherapy combined with chemotherapy (CRT) is the standard treatment for patients with loco-regional squamous-cell carcinoma of the anal canal. There are different contouring guidelines for anal cancer, which still vary concerning recommendations for radiation margins in different anatomical regions, especially on inguinal site. PET-imaging has become more important in primary staging of anal cancer, as it is a very sensitive method to detect lymph node (LN) metastases. Using PET-imaging, we evaluated patterns of LN spread, and examined the differences of the respective contouring guidelines on the basis of our results.

### Material and Methods

We carried out a retrospective study of 37 anal cancer patients treated with RCHT who underwent FDG-PET imaging for primary staging in our department between 2011 and 2018. Patients showing PET-positive LNs were included in this analysis. LN metastases of all patients were delineated in one patient's dataset. Using a color-code, LNs were divided indicating whether its location was in- or out-field of the standard clinical target volume as recommended by Radiation Therapy Oncology Group (RTOG), Australasian Gastrointestinal Trials Group (AGITG) or British National Guidance (BNG). Furthermore, a detailed analysis of the location of LNs of the inguinal region was performed.

### Results

Twenty-two out of 37 AC patients with pre-treatment PET-imaging had PET-positive LN metastases, accumulating to a total of 154 LNs. The most commonly affected anatomical region was inguinal (49 LNs, 32%). All para-rectal, external & internal iliac and pre-sacral LNs were covered by the recommended CTVs of the three different guidelines. Twenty-six out of the 154 positive LNs (17%) were above all three CTVs (13 para-iliac, 13 para-aortic). Of 49 involved inguinal LNs, 14 (29%), 7 (14%) and 5 (10%) inguinal LNs were outside the recommended CTVs by RTOG, AGITG and BNG. Inguinal LNs could be located up to 5.7cm inferiorly to the femoral saphenous junction and 2.8cm medial or laterally to the big femoral vessels.

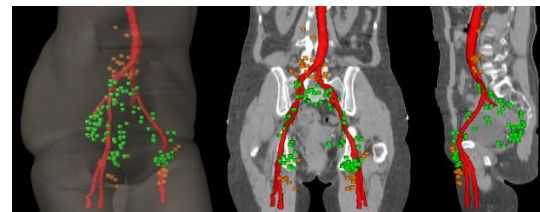


**Table 2** PET-positive lymph nodes in anal cancer patients with number of misses using different contouring guidelines<sup>1</sup>

Location/ Patient	1	2	3	4	5	6	7	8	9	10	11	12	13	14	15	16	17	18	19	20	21	22	Σ	
<b>Para-aortic</b>	6	6														1								13
RTOG	6	6														1								13
AGITG	6	6														1								13
BNG	6	6														1								13
<b>Common iliac</b>	13	1									1						1		1					17
RTOG	12	0								0							1	0						13
AGITG	12	0								0							1	0						13
BNG	12	0								0							1	0						13
<b>External iliac</b>	2	11		1		2					1		2	1	3	3								26
RTOG	0	0	0	0	0	0				0	0	0	0	0	0	0								0
AGITG	0	0	0	0	0	0				0	0	0	0	0	0	0								0
BNG	0	0	0	0	0	0				0	0	0	0	0	0	0								0
<b>Internal iliac</b>	1	5	1	1	1						1		1	1	4									16
RTOG	0	0	0	0	0					0			0	0	0									0
AGITG	0	0	0	0	0					0			0	0	0									0
BNG	0	0	0	0	0					0			0	0	0									0
<b>Pre-sacral</b>	3	1	1	1	2						1		2						2	1				14
RTOG	0	0	0	0	0					0			0	0	0				0	0	0			0
AGITG	0	0	0	0	0					0			0	0	0				0	0	0			0
BNG	0	0	0	0	0					0			0	0	0				0	0	0			0
<b>Peri-sacral</b>	1	2		1	2	1	1	1	2				2						2	1	2			19
RTOG	0	0		0	0	0	0	0	0				0	0	0				0	0	0			0
AGITG	0	0		0	0	0	0	0	0				0	0	0				0	0	0			0
BNG	0	0		0	0	0	0	0	0				0	0	0				0	0	0			0
<b>Inguinal</b>	2	5	1	14				1	1		1	6		2	16									49
RTOG	0	3	0	6				0	0		1	0	0	4										14
AGITG	0	1	0	3				0	0		1	0	0	2										7
BNG	0	0	0	3				0	0		1	0	0	1										5
<b>Total LNs</b>	3	32	1	38	1	2	2	3	4	5	3	3	1	10	3	13	19	1	2	4	3			154

## Conclusion

In this study, we demonstrated patterns of LN involvement based on PET-imaging. In the pelvis, various recommendations are largely consistent and all LNs were covered by the recommended CTVs. LN "misses" appear generally cranially (common iliac or para-aortic) or caudally (inguinal) to the recommended CTVs. The established guidelines differ significantly, particular regarding the inguinal region. Based on our results, we finally presented our recommendation for contouring of the elective CTV of the inguinal region. Lymph node involvement of a larger number of patients should be investigated to enable final recommendations.

## Proffered Papers: CL 8: Proffered papers : Head and Neck

### OC-0387 radiotherapy with paclitaxel/cisplatin vs. fluorouracil/cisplatin for head and neck cancer

R. Fietkau<sup>1</sup>, M. Hecht<sup>1</sup>, B. Hofner<sup>2</sup>, H. Iro<sup>3</sup>, O. Gefeller<sup>2</sup>, C. Rödel<sup>4</sup>, M. Hautmann<sup>5</sup>, O. Kölbl<sup>5</sup>, A. Salay<sup>6</sup>, C. Rube<sup>7</sup>, P. Breinl<sup>8</sup>, W. Krings<sup>9</sup>, S. Gripp<sup>10</sup>, B. Wollenberg<sup>11</sup>, R. Keerl<sup>12</sup>, U. Schreck<sup>13</sup>, B. Siemeyer<sup>14</sup>, G.G. Grabenbauer<sup>15</sup>, P. Balermipas<sup>16</sup>

<sup>1</sup>University Hospital of Erlangen- Erlangen- Germany, Department of Radiation Oncology, Erlangen, Germany ;

<sup>2</sup>FAU Erlangen-Nürnberg, Institut Medizininformatik-Biometrie und Epidemiologie IMBE, Erlangen, Germany ;

<sup>3</sup>University Hospital of Erlangen- Erlangen- Germany, Department of Otorhinolaryngology-Head and Neck Surgery, Erlangen, Germany ;

<sup>4</sup>J.W. Goethe University Hospital Frankfurt, Department of Radiotherapy and Oncology, Frankfurt, Germany ;

<sup>5</sup>University Hospital of Regensburg, Department of Radiotherapy, Regensburg, Germany ;

<sup>6</sup>Brüderkrankenhaus St. Josef, Department of Radiotherapy, Paderborn, Germany ;

<sup>7</sup>Saarland University Medical Centre, Department of Radiotherapy and Radiation Oncology, Homburg, Germany ;

<sup>8</sup>Kliniken Pasing und Perlach, Department of Otorhinolaryngology-Head and Neck Surgery, Munich, Germany ;

<sup>9</sup>Kliniken Maria Hilf- Mönchengladbach, Department of Radiotherapy, Mönchengladbach, Germany ;

<sup>10</sup>University Hospital of Düsseldorf, Department of Radiation Oncology, Düsseldorf, Germany ;

<sup>11</sup>University of Schleswig-Holstein- Lübeck, Department of Otorhinolaryngology, Lübeck, Germany ;

<sup>12</sup>Klinikum St. Elisabeth- Straubing, Department of

Otorhinolaryngology, Straubing, Germany ; <sup>13</sup>Klinik am Eichert- Göppingen, Department of Radiotherapy, Göppingen, Germany ; <sup>14</sup>MVZ Mutterhaus der Borromäerinnen- Trier, Department of Radiotherapy, Trier, Germany ; <sup>15</sup>Coburg Cancer Center, Department of Radiation Oncology, Coburg, Germany ; <sup>16</sup>University Hospital Zurich, Department of Radiation Oncology, Zurich, Switzerland

## Purpose or Objective

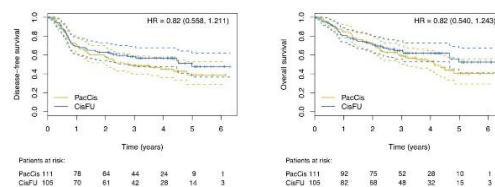
The utilization of taxanes has demonstrated promising results in squamous cell carcinoma of the head and neck (SCCHN) as induction chemotherapy prior to definitive chemoradiotherapy (CRT). The purpose of this multicenter, phase 3 trial was to investigate whether the incorporation of concurrent paclitaxel and cisplatin together with a slightly reduced total dose of radiotherapy (RT) is superior compared with standard fluorouracil-cisplatin based CRT.

## Material and Methods

Previously untreated patients with non-metastatic SCCHN, stage III-IVB, were randomized to receive paclitaxel/cisplatin(PacCis)-CRT (arm A; paclitaxel 20 mg/m<sup>2</sup> on days 2, 5, 8, 11 and 25, 30, 33, 36; cisplatin 20 mg/m<sup>2</sup>, days 1-4 and 29-32; RT to a total dose of 63.6 Gy) or fluorouracil/cisplatin(CisFU) -CRT (arm B; fluorouracil 600 mg/m<sup>2</sup>; cisplatin 20 mg/m<sup>2</sup>, days 1-5 and 29-33; RT: 70.6 Gy). Primary endpoint was 3-year-disease free survival (3y-DFS). Secondary endpoints included overall survival (OS), locoregional failure rate (LFR), distant failure rate (DFR), and toxicity.

## Results

A total of 221 patients have been enrolled in 14 sites between 2010 and 2015. With a median follow-up of 3.7 years, 3y-DFS in the CisFU arm and PacCis arm was 58.2% and 48.4%, respectively (HR 0.82, 95% CI 0.56-1.21, p=0.52). The 3y-OS amounted to 64.6% in the CisFU arm, and to 59.2% in the PacCis arm (HR 0.82, 95% CI 0.54-1.24, p=0.43). There were no significant differences for LFR and DFR. In the subgroup of p16-positive oropharyngeal carcinomas, 3y-DFS and 3y-OS was 84.6% vs 83.9% (p=0.653), and 92.3% vs. 83.5% (p=0.76) in arm A and B, respectively. Hematological toxicities grade 3-4 were significantly reduced in arm A (anemia, p=0.01; leukocytopenia, p=0.003).



## Conclusion

Paclitaxel/cisplatin-CRT with a slightly reduced total RT-dose is not superior to standard fluorouracil/cisplatin-CRT. Subgroup analyses indicate that a reduced radiation dose seems to be sufficient for p16+ oropharyngeal cancer and/ or in non-smokers.

### OC-0388 A prospective multicenter DAHANCA study of hyperfractionated accelerated RT for head and neck cancer

M. Saksø<sup>1</sup>, E. Andersen<sup>2</sup>, J. Bentzen<sup>2</sup>, M. Andersen<sup>3</sup>, J. Johansen<sup>4</sup>, J. Overgaard<sup>1</sup>, J.G. Eriksen<sup>1</sup>

<sup>1</sup>Aarhus University Hospital, Dept. of Experimental Clinical Oncology, Aarhus, Denmark ;

<sup>2</sup>Herlev Hospital, Dept. of Oncology, Herlev, Denmark ;

<sup>3</sup>Aalborg University Hospital, Dept. of Oncology, Aalborg, Denmark ;

<sup>4</sup>Odense University Hospital, Dept. of Oncology, Odense, Denmark

## Purpose or Objective

The DAHANCA9 hyperfractionation study and the MARCH meta-analysis (Bourhis et al, Lancet 2006) on altered fractionation showed that Hyperfractionated Accelerated Radiotherapy (HART) is superior in terms of loco-regional control (LRC) and overall survival (OS) compared to conventional or moderately accelerated radiotherapy for Head and Neck Squamous Cell Carcinomas (HNSCC). Since 2007, HART has been included as a treatment option in the Danish DAHANCA radiotherapy guidelines. The aim of the present study was to evaluate this treatment strategy using LRC, OS and late morbidity as endpoints.

## Material and Methods

Prospectively registered patients (pts) with HNSCC treated with HART according to national guidelines prescribed as 76Gy/56fx, 10 fx/week, as primary treatment were identified in the DAHANCA database and updated. The study was evaluated as intention to treat and elective neck-dissection was not an option.

## Results

From July 2007 to December 2017, 271 pts with HNSCC treated with HART were identified in four national cancer centers that on a regular basis offers HART according to treatment guidelines. The median age was 64 years (32-81 years) and 74% were males. The majority of pts were WHO PS 0-1 (94%) and only 6% were WHO PS  $\geq 2$ . Most (84%) were current or previous smokers with a smoking history of median 42 pack-years (1-140 pack-years). The primary site was larynx in 65 cases (24%); 176 cases were in the pharynx (65%) and 30 pts had oral cavity cancer (11%). In total, 62% of the cases were stage III-IV (UICC7). In the pharynx, 138 cases (78%) were of oropharyngeal origin and of those, 48% were HPV/p16+. The proportion of pts receiving HART as planned was 96%. No patients received adjuvant or concomitant chemotherapy. As per September 1<sup>st</sup> 2018, 50 loco-regional failures (19% of the pts) were detected with a median follow-up time of 29 months: 47 occurred in T-site and 15 in N-site. Among those, 12 pts had both T- and N-site failure. Three-year actuarial LRC was 81% and OS was 68%. LRC at three years was significantly different for stage I-II and stage III-IV HNSCC (90% vs. 74%, HR 0.44 (range 0.23-0.81)) but not significantly better for HPV/p16+ oropharyngeal carcinomas compared to the HPV/p16- oropharynx pts (94% vs 89%). The proportion of pts reporting severe late dysphagia was 16%, and 9% reported late, severe dryness of the mouth; 8% were observed with late tardive edema of the larynx, 10% with severe mucosal atrophy and 5% with severe fibrosis of the subcutaneous tissue in the neck region.

## Conclusion

Hyperfractionated accelerated radiotherapy is an attractive treatment approach in patients with HNSCC. Three-year loco-regional control as observed in this study is more than 80% and that is reflected in an acceptable overall survival. In this study, HART produced equally good results for HPV/p16+ and HPV/p16- oropharyngeal cancer patients. Severe late morbidity is reasonably low and comparable to treatment with chemo-radiotherapy.

## OC-0389 Individualized prophylactic irradiation based on sentinel lymph node(s) identification in cN0 HNSCC

E. Longton<sup>1</sup>, G. Lawson<sup>2</sup>, S. Deheneffe<sup>1</sup>, B. Bihin<sup>3</sup>, I.

Mathieu<sup>4</sup>, F. Hanin<sup>4</sup>, T. Vander Borgh<sup>5</sup>, J. Daisne<sup>1</sup>

<sup>1</sup>CHU UCL Namur- site Sainte-Elisabeth, Radiation oncology, Namur, Belgium; <sup>2</sup>CHU UCL Namur- site Godinne, Head and Neck Surgery, Yvoir, Belgium ;

<sup>3</sup>Namur Research Institute for Life Sciences Narilis, Unit of Biostatistics, Namur, Belgium ; <sup>4</sup>CHU UCL Namur- site Sainte-Elisabeth, Nuclear Medicine, Namur, Belgium ;

<sup>5</sup>CHU UCL Namur- site Godinne, Nuclear Medicine, Yvoir, Belgium

## Purpose or Objective

Due to a risk of occult nodal metastases in clinically node-negative (cN0) head and neck squamous cell carcinoma

(HNSCC) patients, prophylactic and often bilateral neck irradiation is mandatory. However, it leads to a large irradiation of healthy tissues and could miss unexpected nodal basins drained by the tumor. This prospective, non-randomized, interventional phase II study investigated how sentinel lymph node (SLN) mapping by SPECT/CT may help to individualize prophylactic neck irradiation and its potential impact on radiation-related toxicities and tumor control. The final results are presented.

## Material and Methods

Forty-four patients with newly diagnosed cN0 squamous cell carcinoma of the oral cavity, oropharynx, larynx or hypopharynx were included and treated with upfront (chemo)radiotherapy with a curative intent. After simulation, all patients were imaged in treatment position with SPECT/CT after <sup>99m</sup>Tc nanocolloid injection around the tumor. The neck levels containing up to four hottest SLN were selected for prophylactic irradiation (CTVn-LS). A comparative virtual planning was performed by including the levels selected on the basis of the current international guidelines (CTVn-IG). Dosimetric data to the different organs-at-risk (OAR) were compared between both plans. Normal tissue complication probability (NTCP) models for xerostomia and dysphagia as well as quality of life assessments (EORTC C30 and H&N35 scales) are being investigated to predict the clinical benefit of this technique.

## Results

Lymphatic migration was observed in all of the 44 patients. Four patients (9%) presented an unpredicted lymphatic drainage and 21 patients (48%) had only an unilateral drainage. The volumes of CTVn-LS and PTVn-LS (median volumes of 91.8 cc and 219.1 cc, respectively) were systematically smaller than CTVn-IG and PTVn-IG (median volumes of 188.3 cc and 405.3 cc, respectively). This led to a significant dose decrease in identified OAR, particularly to the contralateral parotid gland, contralateral submandibular gland, inferior constrictor muscle for oral/oropharynx tumors and superior constrictor muscle for larynx/hypopharynx tumors (Table 1). NTCP values and QoL data processing is still work in progress and will be presented during the congress. At a median follow-up of 42 months, 3 patients experienced a regional relapse: 2 in an irradiated area (4.5%) and 1 in a non-irradiated area (2.3%). Currently, 4 patients had a local recurrence and 6 patients died (2 patients from geriatric degradation and 4 patients experienced fatal local relapse).

Comparative dosimetry of clinically significant organs-at-risk

OARs	IG plan Median Dmean (Gy)	LS plan Median Dmean (Gy)	p-Value*	Median ΔDmean (Gy)
<b>Unilateral lymph drainage on SPECT/CT (n = 21)</b>				
Oral cavity and oropharynx carcinoma				
Parotid gland (ipsilateral)	28.5	29.7	0.69	-0.1
Parotid gland (contralateral)	25.3	18.6	0.03	10.4
Submandibular gland (ipsilateral)	45.0	47.1	0.87	0.4
Submandibular gland (contralateral)	49.8	20.9	<0.01	28.0
Superior PCM	57.3	55.2	0.09	1.0
Middle PCM	38.2	32.2	0.14	7.1
Inferior PCM	33.8	13.4	0.01	22.5
Hypopharynx and larynx carcinoma				
Parotid gland (ipsilateral)	18.9	18.0	0.03	1.9
Parotid gland (contralateral)	19.5	4.0	<0.01	15.2
Submandibular gland (ipsilateral)	39.2	36.3	0.08	3.1
Submandibular gland (contralateral)	41.6	11.0	<0.01	29.1
Superior PCM	56.0	20.9	<0.01	34.4
Middle PCM	49.1	42.2	0.22	6.2
Inferior PCM	58.6	57.3	0.66	2.2
<b>Bilateral lymph drainage on SPECT/CT (n = 22)</b>				
Oral cavity and oropharynx carcinoma				
Parotid gland (ipsilateral)	27.15	25.75	0.43	1.5
Parotid gland (contralateral)	25.05	23.67	0.45	1.7
Submandibular gland (ipsilateral)	50.15	46.3	0.55	0.4
Submandibular gland (contralateral)	42.1	38.4	0.31	1.5
Superior PCM	64.25	62.5	0.66	0.0
Middle PCM	47.6	44.2	0.70	0.8
Inferior PCM	46.7	19.05	<0.01	24.9
Hypopharynx and larynx carcinoma				
Parotid gland (ipsilateral)	20.7	18.9	0.02	0.3
Parotid gland (contralateral)	20.2	18.7	0.02	0.6
Submandibular gland (ipsilateral)	39.5	26.95	0.06	1.8
Submandibular gland (contralateral)	37.25	33.55	0.04	2.8
Superior PCM	36.95	30.55	0.05	6.0
Middle PCM	56.3	56.15	0.44	0.4
Inferior PCM	60.05	58.3	0.74	0.3

Abbreviations: IG: International guidelines; LS: Lymphoscintigraphy; PCM: pharyngeal constrictor muscle

\* Mann-Whitney-U test, two-sided test.

## Conclusion

SLN mapping using SPECT/CT allowed to significantly reduce the prophylactically irradiated neck volumes in cN0 HNSCC patients. This resulted in a significant dose decrease in OAR, especially in patients presenting an unilateral lymphatic drainage, while uncompromising the

oncological outcome. The final analysis of the clinical impact of dose reduction to OAR will be presented.

**OC-0390 TCGA molecular subclassification is prognostic for LRC of HNSCC after postoperative RCTx**  
 A. Linje<sup>1,2,3,4</sup>, B. Tawik<sup>5,6,7</sup>, S. Löck<sup>1,2,3,4</sup>, M. Großer<sup>8</sup>, F. Lohaus<sup>1,2,3,4</sup>, V. Gudziol<sup>4,9</sup>, A. Nowak<sup>4,10</sup>, I. Tinhofer<sup>11,12</sup>, V. Budach<sup>11,12</sup>, M. Stuschke<sup>13,14</sup>, P. Balermipas<sup>15,16</sup>, C. Rödel<sup>15,16</sup>, H. Schäfer<sup>17,18</sup>, A. Grosu<sup>17,18</sup>, J. Debus<sup>5,7,19,20,21</sup>, U. Ganswindt<sup>22,23,24</sup>, C. Belka<sup>22,23,24</sup>, S. Pigorsch<sup>23,25</sup>, S.E. Combs<sup>23,25,26</sup>, D. Mönnich<sup>27,28</sup>, D. Zips<sup>27,28</sup>, G.B. Baretton<sup>3,4,8,29</sup>, A. Abdollahi<sup>5,6,7,20,21</sup>, M. Krause<sup>1,2,3,4,30</sup>, M. Baumann<sup>1,2,3,31</sup>

<sup>1</sup>Department of Radiation Oncology, Faculty of Medicine and University Hospital Carl Gustav Carus, Technische Universität Dresden, Germany ; <sup>2</sup>OncoRay - National Center for Radiation Research in Oncology, Faculty of Medicine and University Hospital Carl Gustav Carus Dresden, Technische Universität Dresden, Germany ; <sup>3</sup>German Cancer Research Center, Heidelberg and German Cancer Consortium, partner site Dresden, Germany ; <sup>4</sup>National Center for Tumor Diseases, partner site Dresden and Faculty of Medicine and University Hospital Carl Gustav Carus, Technische Universität Dresden, Germany ; <sup>5</sup>Heidelberg Institute of Radiation Oncology and National Center for Radiation Research in Oncology, University of Heidelberg Medical School and German Cancer Research Center, Heidelberg, Germany ; <sup>6</sup>Translational Radiation Oncology, University of Heidelberg Medical School and German Cancer Research Center, Heidelberg, Germany ; <sup>7</sup>German Cancer Research Center, Heidelberg and German Cancer Consortium, partner site Heidelberg, Germany ; <sup>8</sup>Institute of Pathology, Faculty of Medicine and University Hospital Carl Gustav Carus, Technische Universität Dresden, Germany ; <sup>9</sup>Department of Otorhinolaryngology, Faculty of Medicine and University Hospital Carl Gustav Carus, Technische Universität Dresden, Germany ; <sup>10</sup>Department of Oral and Maxillofacial Surgery, Faculty of Medicine and University Hospital Carl Gustav Carus, Technische Universität Dresden, Germany ; <sup>11</sup>Department of Radiooncology and Radiotherapy, Charité University Hospital, Berlin, Germany ; <sup>12</sup>German Cancer Research Center, Heidelberg and German Cancer Consortium, partner site Berlin, Germany ; <sup>13</sup>Department of Radiotherapy, Medical Faculty, University of Duisburg-Essen, Germany ; <sup>14</sup>German Cancer Research Center, Heidelberg and German Cancer Consortium, partner site Essen, Germany ; <sup>15</sup>Department of Radiotherapy and Oncology, Goethe-University Frankfurt, Frankfurt, Germany ; <sup>16</sup>German Cancer Research Center, Heidelberg and German Cancer Consortium, partner site Frankfurt, Germany ; <sup>17</sup>Department of Radiation Oncology, Medical Faculty, University of Freiburg, Germany ; <sup>18</sup>German Cancer Research Center, Heidelberg and German Cancer Consortium, partner site Freiburg, Germany ; <sup>19</sup>Clinical Cooperation Unit Radiation Oncology, University of Heidelberg Medical School and German Cancer Research Center, Heidelberg, Germany ; <sup>20</sup>National Center for Tumor Diseases, University of Heidelberg Medical School and German Cancer Research Center, Heidelberg, Germany ; <sup>21</sup>Heidelberg Ion Therapy Center, Department of Radiation Oncology, University of Heidelberg Medical School, Germany ; <sup>22</sup>Department of Radiotherapy and Radiation Oncology, University Hospital, Ludwig-Maximilians-Universität Munich, Germany ; <sup>23</sup>German Cancer Research Center, Heidelberg and German Cancer Consortium, partner site Munich, Germany ; <sup>24</sup>Clinical Cooperation Group Personalized Radiotherapy in Head and Neck Cancer, Helmholtz Zentrum Munich, Neuherberg, Germany ; <sup>25</sup>Department of Radiation Oncology, Technische Universität München, Munich, Germany ; <sup>26</sup>Institute of Innovative Radiotherapy, Helmholtz Zentrum München, Oberschleißheim, Germany ; <sup>27</sup>Department of Radiation Oncology, Faculty of

Medicine and University Hospital Tübingen, Eberhard Karls Universität Tübingen, Germany ; <sup>28</sup>German Cancer Research Center, Heidelberg and German Cancer Consortium, partner site Tübingen, Germany ; <sup>29</sup>Tumour and Normal Tissue Bank- University Cancer Centre, University Hospital Carl Gustav Carus, Technische Universität Dresden, Germany ; <sup>30</sup>Helmholtz-Zentrum Dresden - Rossendorf, Institute of Radiooncology, Dresden, Germany ; <sup>31</sup>German Cancer Research Center, Heidelberg, Heidelberg, Germany

#### Purpose or Objective

The Cancer Genome Atlas (TCGA) recently provided a molecular subclassification of head and neck squamous cell carcinomas (HNSCC) including an atypical, classical, basal and mesenchymal subtype. The aims of the present study are to investigate (I) the impact of this subclassification on loco-regional control (LRC) in patients with locally advanced HNSCC who received postoperative radiochemotherapy (RCTx); and (II) the enrichment of those subtypes in radiobiologically relevant aspects such as hypoxia, epithelial-mesenchymal transition (EMT) and cancer stem cells (CSCs).

#### Material and Methods

In this retrospective multicentre study, 195 patients with locally advanced squamous cell carcinoma of the oral cavity, oropharynx and hypopharynx were included. All patients received surgery followed by postoperative RCTx between 2005 and 2011. Their median follow-up was about 26 months. Whole transcriptome analysis was performed using the HTA 2.0 Array (Affymetrix). Tumours were classified into the four subtypes atypical, classical, basal or mesenchymal, based on four cluster centres of the expressions of 838 genes that were previously reported. A clear classification was possible for 141 out of 195 patients. Hypoxia was assessed using an established hypoxia-associated 15-gene signature. For EMT, a previously developed 31-gene signature was applied and for the analysis of CSC markers, previously reported putative CSC markers *CD44*, *SLC3A2* and *MET* were used since no CSC signature is available to date. Primary endpoint was loco-regional control (LRC).

#### Results

Tumours were classified into all four subtypes (43% atypical, 19% classical, 15% basal and 23% mesenchymal). The atypical subtype represented the subgroup with the highest LRC, while the mesenchymal subtype showed the lowest LRC (p=0.002, log-rank test). The basal and classical subtypes represented intermediate subgroups. Interestingly, the atypical subtype showed low expressions of the EMT signature, the hypoxia signature as well as low expressions of CSC markers. In contrast, the mesenchymal subtype was associated with increased expression of the EMT signature as well as hypoxia-associated genes and CSC markers.

#### Conclusion

We have shown for the first time, that the molecular subclassification reported for the TCGA HNSCC cohort allows for stratification of patients who were treated with postoperative RCTx regarding their loco-regional control. This was further supported by the enrichment of radiobiologically relevant aspects within those subtypes.

#### OC-0391 Treatment outcome of 265 patients with sinonasal adenoid cystic carcinoma (ACC)

S. Akbaba<sup>1</sup>, D. Ahmed<sup>1</sup>, A. Mock<sup>2</sup>, K. Lang<sup>1</sup>, T. Held<sup>1</sup>, K. Herfarth<sup>1</sup>, S. Rieken<sup>1</sup>, P. Plinkert<sup>3</sup>, J. Debus<sup>1</sup>, S. Adebeg<sup>1</sup>  
<sup>1</sup>University Hospital Heidelberg, Radiation Oncology, Heidelberg, Germany ; <sup>2</sup>University Hospital Heidelberg, Oncology, Heidelberg, Germany ; <sup>3</sup>University Hospital Heidelberg, Otorhinolaryngology- Head and Neck Surgery, Heidelberg, Germany

### Purpose or Objective

The authors aimed to evaluate treatment outcome of primary and postoperative radiotherapy (RT) for 265 sinonasal adenoid cystic carcinomas, the currently available largest single-center patient collective for this cohort.

### Material and Methods

265 patients who received either an intensity modulated radiotherapy (IMRT) alone or a dose-escalated bimodal treatment with IMRT and carbon ion boost for sinonasal adenoid cystic carcinoma at the Department of Radiation Oncology, University Hospital Heidelberg and at the Heidelberg Ion-Beam Therapy Center (HIT) between 2003 and 2018 were analyzed retrospectively for local control (LC), distant progression-free survival (DPFS) and overall survival (OS) using Kaplan-Meier estimates. The majority of patients had tumors in advanced stages (T4 stage, n=208, 78.5%) or were irradiated for a macroscopic tumor disease (n=200, 76%). Overall, 35% of the patients received primary (n=93) and 65% postoperative RT (n=172). Additionally, toxicity was assessed according to the Common Toxicity Terminology Criteria for Adverse Events (CTCAE) v5.

### Results

Median follow-up was 49 months. At last follow up, 61% of the patients were still alive (n=90/231) while local recurrence occurred in 38% (n=84/231) and distant relapse in 39% (n=87/231), respectively. In univariate and multivariate analysis, we could identify three prognostic subgroups (postoperative bimodal RT vs. postoperative IMRT vs. definite bimodal RT) resulting in significantly different LC ( $p=0.003$ ), DPFS ( $p=0.005$ ) and OS rates ( $p<0.0001$ ). Best survival outcome could be achieved for the postoperative bimodal RT subgroup with a 5-year OS and DPFS of 78% and 72% vs. 69% and 70% for postoperative IMRT vs. 60% and 50% for definite bimodal RT, respectively. Bimodal RT resulted in a significantly increased LC compared to IMRT alone with a 5-year LC rate of 82% for postoperative bimodal RT vs. 76% for definite bimodal RT vs. 58% for postoperative IMRT alone. The majority of recurrences occurred in-field (n=37/84, 44%) and at critical structures where dose was spared (n=34/84, 40%). Toxicity was moderate with 29% acute and 16% late grade 3 toxicity.

### Conclusion

The authors conclude that bimodal RT in a primary or postoperative setting results in superior LC rates with moderate toxicity. Nevertheless, regarding overall survival outcome including OS, LC and DPFS, patients may profit the most from postoperative dose-escalated bimodal RT.

### OC-0392 Risk of ischemic cerebrovascular events is associated with carotid artery radiation dose

E. Van Aken<sup>1</sup>, H. Bijl<sup>1</sup>, H.P. Van der Laan<sup>1</sup>, L. Van den Bosch<sup>1</sup>, A. Van den Hoek<sup>1</sup>, M. Dieters<sup>1</sup>, R. Steenbakkers<sup>1</sup>, H. Langendijk<sup>1</sup>

<sup>1</sup>University Medical Center Groningen, Radiation Oncology, Groningen, The Netherlands

### Purpose or Objective

Radiotherapy in the head and neck area may cause vascular damage to the carotid arteries, increasing the risk of ischemic cerebrovascular events (ICVEs). However, limited data exists on the relationship between radiation dose and the risk of ICVE. This information is crucial to identify patients at risk and to optimize radiotherapy treatment plans. Therefore, the purpose of this study was to determine the relationship between radiation dose to the carotid arteries and anterior circulation ICVE risk and to identify the most relevant dose-volume parameters.

### Material and Methods

A retrospective analysis was performed using data of a prospective cohort study of 750 patients treated with definitive radiotherapy (either or not combined with

systemic treatment) for head and neck squamous cell carcinomas. Based on treatment planning CT scans, carotid arteries were delineated and dose-volume parameters were calculated bilaterally for the entire carotid arteries (external carotid arteries were excluded) and for the common carotid artery (CCA), bifurcation and internal carotid artery (ICA). ICVEs were scored prospectively and additional information was added by reviewing patient records. Cox proportional hazards analysis was performed to analyse the relationship between radiation dose and the risk of ICVE.

### Results

In the univariate analysis, anterior circulation ICVE risk was significantly associated with dose variables to the entire carotid arteries, particularly to the CCA and the bifurcation. Multivariable analysis showed that the absolute volume (cc) of the entire carotid arteries that receives at least a radiation dose of 10 Gy was the most important prognostic factor for ICVE (Figure 1), with a HR of 1.14 per cc (95% CI 1.064-1.222;  $p<0.001$ ). No relevant confounding patient and treatment characteristics were found, meaning that the absolute V10 to the entire carotid arteries can be considered as an independent prognostic factor for the cumulative incidence of ICVE.

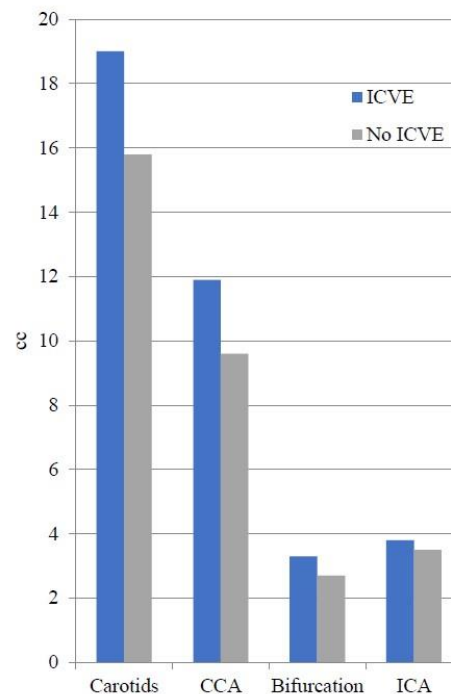


**Figure 1.** Absolute V10 of the carotid arteries and the individual bilateral portions.

### Conclusion

This is the first prospective cohort study that demonstrates an independent dose-effect relationship between radiation dose to the carotid arteries and the risk of ICVE. These findings may lead to more adequate ICVE risk prediction and prevention in these patients. ICVE prevention can be achieved by radiotherapy treatment optimization, regular screening or pharmacological treatment.

### OC-0393 Impact of sarcopenia on survival and late toxicity in head and neck cancer patients treated with RT

I. Van Rijn - Dekker<sup>1</sup>, L. Van den Bosch<sup>1</sup>, A. Van den Hoek<sup>1</sup>, H. Bijl<sup>1</sup>, M. Dieters<sup>1</sup>, E. Van Aken<sup>1</sup>, H.P. Van der Laan<sup>1</sup>, H. Langendijk<sup>1</sup>, R. Steenbakkers<sup>1</sup>

<sup>1</sup>University Medical Centre Groningen UMCG, Radiotherapy, Groningen, The Netherlands

### Purpose or Objective

Sarcopenia, defined as the loss of skeletal muscle mass and strength, is emerging as an adverse prognostic factor for both survival and complication risk in cancer patients. The aim of this study was to determine the impact of sarcopenia on several survival parameters and late toxicity in a large cohort of patients with head and neck squamous cell carcinoma (HNSCC) treated with primary radiotherapy (RT).

### Material and Methods

Patients with HNSCC who were treated with definitive RT with or without systemic treatment from January 2007 to June 2016 were included. Prospectively collected variables were retrospectively analysed. The planning CT-scan was used to measure the cross-sectional area (CSA) of skeletal muscles at the level of the third cervical vertebra (C3). The prediction rule by Swartz et al. was used to estimate CSA at the third lumbar vertebra (L3). L3 skeletal muscle index (SMI) was calculated.

The impact of sarcopenia on overall survival (OS) and disease-free survival (DFS) was investigated using univariate (Kaplan Meier) and multivariate (Cox proportional hazards regression) analysis. To analyse the association of sarcopenia with physician-rated grade  $\geq 2$  toxicity (i.e. xerostomia and dysphagia) and with moderate-to-severe patient-rated xerostomia, multivariable logistic regression analyses were performed to create association models.

### Results

The study population was composed of 750 patients with HNSCC. The cut-off value of sarcopenia was set at SMI  $<42.4 \text{ cm}^2/\text{m}^2$  (men) and  $<30.6 \text{ cm}^2/\text{m}^2$  (women) corresponding with the lowest gender specific quartile. Patients with sarcopenia had significantly poorer survival rates than others. The 3-year OS in sarcopenic patients was 53% compared to 73% in non-sarcopenic patients ( $p < 0.001$ ) and the 3-year DFS was resp. 59% and 76% ( $p < 0.001$ ). However, sarcopenia was only significantly associated with OS and DFS in patients with WHO performance score (WHO-score)  $> 0$  (resp.  $p < 0.001$  and  $p = 0.003$ ) and in those with locally advanced disease (stage III-IV) (both  $p < 0.001$ ) (Figure 1 OS stratified by stage of disease). The multivariate analysis showed that sarcopenia was an independent adverse prognostic factor for OS ( $p = 0.004$ ), next to age, WHO-score, tumour stage and primary tumour site and for DFS ( $p = 0.013$ ), next to age, WHO-score and tumour stage (Table 1).

In the univariate analysis, sarcopenia was associated with more radiation-induced xerostomia and dysphagia at six and twelve months after treatment, but no such association was found in multivariate analysis after correcting for confounders.

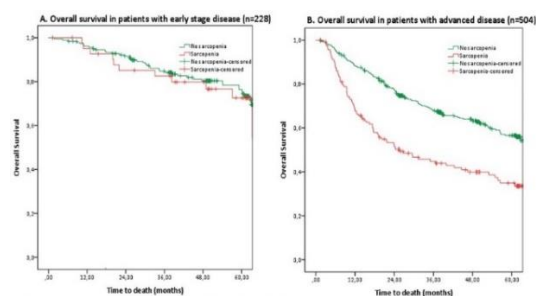


Figure 1 Kaplan Meier curves of overall survival in HNSCC patients treated with radiotherapy. A. OS of patients with early stage disease (I-II) ( $p = 0.596$ ) B. OS of patients with locally advanced disease (III-IV) ( $p < 0.001$ ) HNSCC = head neck squamous cell carcinoma, OS = overall survival

Table 1 Cox regression analysis of overall survival and disease-free survival in HNSCC patients treated with radiotherapy

Variable	Overall survival (n=729)		Disease-free survival (n=641)	
	HR (95% CI)	p-value	HR (95% CI)	p-value
<i>Univariate analysis</i>				
Gender (male vs. female)	1.103 (0.853 - 1.425)	0.456	1.058 (0.794 - 1.409)	0.700
Age	1.014 (1.003 - 1.025)	0.011	1.024 (1.012 - 1.037)	$< 0.001$
WHO-score (0 vs. 1-3)	0.374 (0.299 - 0.467)	$< 0.001$	0.426 (0.333 - 0.546)	$< 0.001$
Sarcopenia (no vs. yes)	0.533 (0.421 - 0.675)	$< 0.001$	0.566 (0.433 - 0.740)	$< 0.001$
Smoking history (never vs. ever)	0.758 (0.520 - 1.105)	0.150	0.950 (0.644 - 1.402)	0.797
Tumour stage (I-II vs. III-IVb)	0.472 (0.360 - 0.617)	$< 0.001$	0.629 (0.479 - 0.827)	0.001
Primary tumour site (larynx vs. other)	0.521 (0.412 - 0.659)	$< 0.001$	0.662 (0.515 - 0.851)	0.001
Treatment modality (RT alone vs. RT with systemic treatment)	0.663 (0.531 - 0.828)	$< 0.001$	0.852 (0.662 - 1.096)	0.214
Technique (conventional vs. IMRT)	0.593 (0.417 - 0.843)	0.004	0.695 (0.484 - 0.997)	0.048
<i>Multivariate analysis</i>				
Age	1.020 (1.009 - 1.032)	0.001	1.024 (1.011 - 1.038)	$< 0.001$
WHO-score (0 vs. 1-3)	0.442 (0.352 - 0.556)	$< 0.001$	0.501 (0.387 - 0.647)	$< 0.001$
Sarcopenia (no vs. yes)	0.697 (0.545 - 0.892)	0.004	0.705 (0.535 - 0.930)	0.013
Tumour stage (I-II vs. III-IVb)	0.601 (0.440 - 0.821)	0.001	0.624 (0.467 - 0.835)	0.001
Primary tumour site (larynx vs. other)	0.674 (0.515 - 0.883)	0.004		

HNSCC = head neck squamous cell carcinoma; HR = hazard ratio; 95% CI = 95% confidence interval; WHO-score = WHO performance score; RT = radiotherapy; IMRT = intensity modulated radiotherapy

### Conclusion

In this prospective cohort study, sarcopenia was significantly associated with poorer OS and DFS, for patients with lower performance (WHO-score  $> 0$ ) and locally advanced disease (stage III-IV), with similar prognostic value as WHO-score, tumour stage and primary tumour site. Given that the SMI can be easily assessed on planning-CT scan, clinical introduction is easy and adds important and clinically relevant information to assess patient outcome.

### Proffered Papers: BT 5: Optimising dose distribution

#### OC-0394 Brachytherapy quality assurance in the PORTEC-4a trial for high-intermediate risk endometrial cancer

B. Wortman<sup>1</sup>, E. Astreimidou<sup>1</sup>, M. Laman<sup>1</sup>, L. Lutgens<sup>2</sup>, E. Van der Steen-Banasik<sup>3</sup>, A. Slot<sup>4</sup>, H. Westerveld<sup>5</sup>, K. De Winter<sup>6</sup>, H. Van den Berg<sup>7</sup>, M. Bloemers<sup>8</sup>, T. Stam<sup>9</sup>, J. Mens<sup>10</sup>, L. Zwanenburg<sup>11</sup>, S. Bijmolt<sup>12</sup>, I. Jürgenliemk-Schulz<sup>13</sup>, A. Snyers<sup>14</sup>, C. Creutzberg<sup>1</sup>, R. Nout<sup>1</sup>  
<sup>1</sup>Leiden University Medical Center LUMC, Radiation Oncology, Leiden, The Netherlands; <sup>2</sup>Maastricht Radiation Oncology Clinic, Radiation Oncology, Maastricht, The Netherlands; <sup>3</sup>Radiotherapiegroep, Radiation Oncology, Arnhem, The Netherlands; <sup>4</sup>Radiotherapy Institute Friesland, Radiation Oncology, Leeuwarden, The Netherlands; <sup>5</sup>Amsterdam University Medical Center, Radiation Oncology, Amsterdam, The Netherlands; <sup>6</sup>Institute Verbeeten, Radiation Oncology, Tilburg, The Netherlands; <sup>7</sup>Catharina Hospital Eindhoven, Radiation Oncology, Eindhoven, The Netherlands; <sup>8</sup>Netherlands Cancer Institute, Radiation Oncology, Amsterdam, The Netherlands; <sup>9</sup>Haaglanden Medical Center, Radiation Oncology, Leidschendam, The Netherlands; <sup>10</sup>Erasmus MC-Cancer Institute, Radiation Oncology, Rotterdam, The Netherlands; <sup>11</sup>Isala, Radiation Oncology, Zwolle, The Netherlands; <sup>12</sup>University Medical Center Groningen, Radiation Oncology, Groningen, The Netherlands; <sup>13</sup>University Medical Center Utrecht, Radiation Oncology, Utrecht, The Netherlands; <sup>14</sup>Radboud University Medical Center, Radiation Oncology, Nijmegen, The Netherlands

### Purpose or Objective

The international multicenter PORTEC-4a trial investigates molecular-integrated risk profile guided adjuvant treatment for women with high-intermediate risk (HIR) endometrial cancer (EC). As part of the quality assurance (QA) program, all participating centers had to pass a mandatory vaginal brachytherapy (VBT) dummy run procedure before site activation. Subsequently, QA review of one VBT treatment plan is done annually for each site to verify protocol adherence. Aims of the current study

were to evaluate VBT planning quality and protocol adherence.

#### Material and Methods

Each participating center was asked to provide anonymised CT or MRI scan data used for a VBT plan for a randomly selected case. Quality review included the delineation of organs at risk (OAR) and clinical target volume (CTV), applicator reconstruction, dose plan, DVH parameters and printouts of the dose plan including the dose to the reference points (see Figure 1). In an additional questionnaire, changes in type of afterloader, applicator set and software used were recorded. Data was imported into Oncentra Brachytherapy at Leiden University Medical Center. A local expert panel reviewed all information and scored the compliance of plans according to a QA item checklist. After the review, feedback was sent to the study PI and physicist of each participating site.

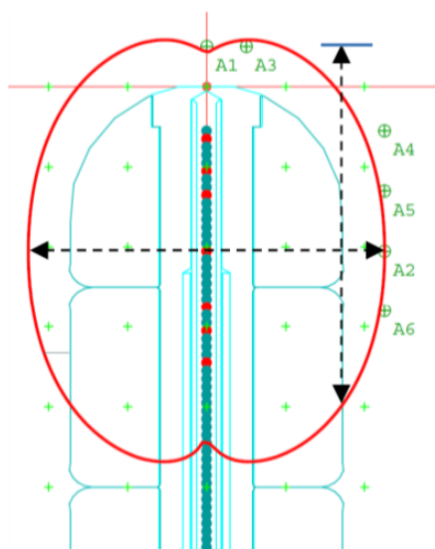


Figure 1. Dose distribution for a vaginal cylinder diameter 3.5cm. 100% isodose line (red). Dose is specified to point A2; average dose of A1+A3 should be approximately 100%; dose to A1 >90% and A3 <110%; A4-6 aim for dose reporting with the aiming to reach 100%. Reference length/width (dotted arrows), reference length should aim for 4.5 cm.

#### Results

Currently a total of 152 patients have been included in the PORTEC-4a trial and 14 sites are actively recruiting. In total, 21 cases were requested for the annual QA review, five in the first and eight in the second round were evaluated; eight data requests are pending. 12 centers used CT planning, two used MRI planning. Three different treatment planning systems and HDR afterloaders were used. During the trial, two centers changed to a different cylinder applicator and two centers changed their planning software. Compliance results of the QA checklist are shown in Table 1. Seven out of thirteen evaluable plans were fully compliant. Most common reasons for feedback were related to target (CTV was not a ring structure or too long) and OAR delineation, and applicator positioning (applicator not horizontal or in optimal contact). Feedback concerning the symmetry of the loading pattern and the reference length (when > 5cm) was provided for six plans (mean reference length 5.0cm, range 4.3 - 5.6; Figure 1). The mean % dose (7Gy = 100%) in A2 was 100.7% (SD 2.4, range 99.3-108.7); in A1: 90.4% (SD 7.1, 67.8-95.7); and in A3: 105.3% (SD 7.7, 81.7-110.0).

Table 1. Checklist QA

Items	Fully compliant	Partly compliant
<b>Applicator positioning</b>		
Position and angle of cylinder	8	5
Contact of cylinder to vaginal mucosa	10	3
<b>Delineation</b>		
CTV delineation	6	7
OAR delineation	9	4
<b>Treatment planning</b>		
Reconstruction	10	3
Position of A points	9	4
Prescribed dose in point A2	12	1
Symmetry of loading pattern	7	6
<b>Evaluation of dose distribution</b>		
Average dose in A1+A3 = 100%	8	5
Dose in point A1 >90% and A3 <110%	10	3
Reference length/width	7	6
CTV D90/D98	11	2
OAR D2cm <sup>3</sup>	13	0

#### Conclusion

Most feedback during the continuous QA of VBT planning in the PORTEC-4a trial was related to target and OAR delineation, applicator positioning, symmetry of the loading pattern and reference length. Changes in type of afterloader, applicator and planning software were recorded and can affect VBT protocol compliance. Annual QA contributes to protocol compliance, to ensure uniform high quality VBT in all participating centers.

#### OC-0395 Bi-objective optimization of dosimetric indices for HDR prostate brachytherapy within 30 seconds

A. Bouter<sup>1</sup>, T. Alderliesten<sup>2</sup>, B.R. Pieters<sup>2</sup>, A. Bel<sup>2</sup>, Y. Niatsetski<sup>3</sup>, P.A.N. Bosman<sup>1</sup>

<sup>1</sup>Centrum Wiskunde & Informatica, Life Sciences and Health, Amsterdam, the Netherlands; <sup>2</sup>Amsterdam UMC-University of Amsterdam, Radiation Oncology, Amsterdam, The Netherlands; <sup>3</sup>Elekta, Physics and Advanced Development, Veenendaal, the Netherlands

#### Purpose or Objective

In clinical practice, plan quality is judged based on dosimetric indices. However, for the purpose of efficiency, typical automated planning methods do not directly optimize dosimetric indices. This creates a mismatch between what is optimized and what is evaluated. A bi-objective optimization approach was recently proposed that directly optimizes dosimetric indices, finding many high-quality plans with different trade-offs between target coverage and organ sparing. This allows for insightful comparison of high-quality plans and patient-specific plan selection. We now aim to accelerate this approach to the extent that it can be used in clinical practice by applying parallelization on a Graphics Processing Unit (GPU).

#### Material and Methods

The two objectives of our bi-objective optimization are the dosimetric indices having the largest deviations from the clinical protocol (see Table 1) in terms of aspired target coverage and organ sparing, the Least Coverage Index (LCI) and Least Sparing Index (LSI), respectively. Optimization is done using the Gene-pool Optimal Mixing Evolutionary Algorithm (GOMEA). The main acceleration is obtained by calculating dosimetric indices on an NVIDIA Titan Xp GPU, programmed in CUDA.

We perform bi-objective planning for 18 HDR prostate brachytherapy cases. Prior to acceleration, results for these cases after 1 hour of optimization were found to be clinically superior to manually optimized plans. We optimize on 20,000 dose calculation (DC) points, whereas typical planning methods (e.g., IPSA, HIPO) use in the order of 5,000 DC points for the purpose of efficiency. All

final reported dosimetric indices are computed on 500,000 DC points, the standard setting in Oncentra Brachy. Bi-objectively optimized plans are compared to clinical plans obtained by experienced planners using IPSA/HIPO, followed by graphical optimization, in 30 to 60 minutes.

**Results**

For all cases, a trade-off curve of plans similar to or better than the clinical plan was found. The clinical plans satisfied all clinical criteria for only 4 cases. Our optimization found plans satisfying all clinical criteria for 15 cases, including these 4. Optimizing for more than 30 seconds did not substantially improve results.

Figure 1 shows plans generated in 30 seconds by the bi-objective planning for 3 patients.

In Table 1, we highlight selected plans for the same patients. Plans with maximum coverage while satisfying all sparing constraints were selected. To satisfy the clinical constraint on the urethra for patient 2, dose to rectum and bladder are increased compared to the clinical plan. For patient 3, all dosimetric indices of the optimized plans are better than the clinical plan.

**Conclusion**

Bi-objective planning allows for insightful plan selection from a large set of high-quality plans, each with a different trade-off between target coverage and organ sparing. We can now generate such sets computer-aided in as little as 30 seconds by applying GPU acceleration, which permits use in clinical practice.

M.C. Van der Meer<sup>1</sup>, P.A.N. Bosman<sup>2,3</sup>, B.R. Pieters<sup>1</sup>, Y. Niatsetski<sup>4</sup>, T. Alderliesten<sup>1</sup>, A. Bel<sup>1</sup>  
<sup>1</sup>Amsterdam UMC- University of Amsterdam, Radiation Oncology, Amsterdam, The Netherlands; <sup>2</sup>Centrum Wiskunde and Informatica, Life Sciences and Health, Amsterdam, The Netherlands; <sup>3</sup>Delft University of Technology, Software Technology, Delft, The Netherlands; <sup>4</sup>Elekta, Physics and Advanced Development, Veenendaal, The Netherlands

**Purpose or Objective**

Recently, a bi-objective optimization model has been introduced, to automatically create a set of clinically good HDR prostate brachytherapy (BT) plans. The model uses separate objectives for target coverage and organ sparing, based solely on dose-volume indices (DVIs). To calculate DVIs, a reconstruction algorithm is used to determine the 3D organ shape from 2D contours, containing settings that influence the result. In this work, we augment the automatic planning model to find plans that are robust to differences in 3D reconstruction. We investigated the impact on the resulting plans.

**Material and Methods**

The original model is based on the clinical protocol (Table). DVIs of the protocol are combined into two objectives: Least Coverage Index (LCI) and Least Sparing Index (LSI), and a hard optimization constraint value C. Studied reconstruction settings were:

1. The urethra is considered as part of the prostate, or not.
2. Contours fill the volume spanned by their slice, or interpolation is used.

3. Top/bottom contours span the half-slice-thickness towards the other contours, or the full-slice-thickness.

Combinations of these settings yield 8 possible 3D organ reconstructions per patient, hence 8 combinations of (LCI<sub>i</sub>, LSI<sub>i</sub>, C<sub>i</sub>) per plan. We define the robust model as  $LCI = \min_{i=1, \dots, 8} \{LCI_i\}$ ,  $LSI = \min_{i=1, \dots, 8} \{LSI_i\}$ ,  $C = \min_{i=1, \dots, 8} \{C_i\}$ .

Both models were tested on data of 5 prostate cancer patients consecutively treated with HDR BT, with contours delineated on axial MRI scans (slice thickness: 3.3mm). For the original model, settings were based on the standard of our TPS (Oncentra Brachy version 4.5: urethra as part of the prostate, interpolation, half-slice-thickness). Plans were optimized using the evolutionary algorithm GOMEA, which previously obtained excellent results for the original model. Optimization was performed on 20,000 dose-calculation points, and re-evaluation on 500,000 points. To compare the two models, all optimized plans were re-evaluated both in the original, and in the robust model.

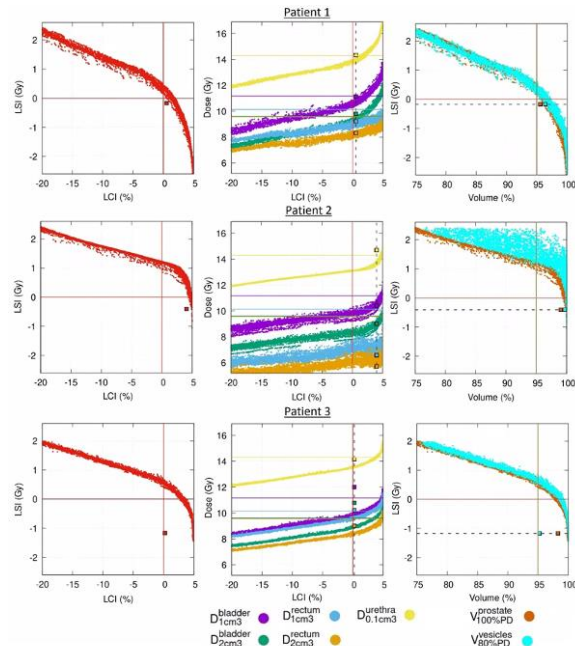


**Figure 1:** All optimized plans of 30 runs (to show variation) of bi-objective planning for 30 seconds. Leftmost figures show the LCI and LSI for all plans. Plans with positive LCI and LSI satisfy all clinical coverage and sparing constraints, respectively. Middle figures show each plan in 5 different colors, aligned parallel to the dashed line, to indicate the 5 different dose indices for a plan with a given LCI. Rightmost figures show each plan in 2 colors, and corresponding volume indices for a given LSI. Clinical constraints are shown as solid lines in corresponding colors. The clinical plan is shown as a square in all plots, colored corresponding to the displayed dosimetric index.

	Planning-aim Dose (PD) = 13.00 Gy						
	$V_{100\%}^{prostate}$	$V_{95\%}^{prostate}$	$D_{100\%}^{bladder}$	$D_{95\%}^{bladder}$	$D_{100\%}^{rectum}$	$D_{95\%}^{rectum}$	$D_{100\%}^{urethra}$
Protocol	> 95%	> 95%	< 11.18 Gy	< 9.62 Gy	< 10.14 Gy	< 9.62 Gy	< 14.30 Gy
P1 Clin.	95.5	96.4	11.15	9.79	9.22	8.33	14.35
P1 Bi-obj.	96.5±0.3	97.3±0.6	10.80±0.10	9.55±0.06	9.12±0.17	8.30±0.17	14.20±0.11
P2 Clin.	99.0	99.7	10.42	9.01	6.58	5.70	14.70
P2 Bi-obj.	99.8±0.1	100±0.0	11.03±0.14	9.42±0.11	7.26±0.44	6.29±0.36	14.13±0.17
P3 Clin.	98.3	95.2	12.02	10.79	10.22	9.01	14.16
P3 Bi-obj.	98.3±0.6	98.6±0.9	10.56±0.11	9.55±0.08	10.08±0.05	8.84±0.06	14.07±0.11

**Table 1:** Dosimetric indices of selected, bi-objectively optimized plans (Bi-obj.) for 3 patients (P1-3), compared to the clinical (Clin.) plans. The clinical protocol for HDR prostate BT at our medical center is listed, and dosimetric indices violating the protocol are marked in red. Means and standard deviations of 30 runs are displayed.

Target coverage		Organ sparing		
Prostate	Vesicles	Bladder	Rectum	Urethra
$V_{100\%} > 95\%$	$V_{80\%} > 95\%$	$D_{1cm3} < 86\%$	$D_{1cm3} < 78\%$	$D_{0.1cm3} < 110\%$
$D_{90\%} > 100\%$		$D_{2cm3} < 74\%$	$D_{2cm3} < 74\%$	
$V_{150\%} < 50\%$				
$V_{200\%} < 20\%$				

$$LCI = \min\{V_{100\%}^{prostate} - 95, V_{80\%}^{vesicles} - 95\}$$

$$LSI = \min\{86 - D_{1cm3}^{bladder}, 74 - D_{2cm3}^{bladder}, 78 - D_{1cm3}^{rectum}, 74 - D_{2cm3}^{rectum}, 110 - D_{0.1cm3}^{urethra}\}$$

$$C = \min\{50 - V_{150\%}^{prostate}, 20 - V_{200\%}^{prostate}\}$$

**Table:** The DVIs and the clinical protocol for HDR prostate BT used at our center, and the original bi-objective optimization model used. The unit of each DVI is either percentage of total organ volume for volume indices V, or percentage of planning-aim dose (13Gy) for dose indices D. During optimization, only plans with a positive constraint violation index (C) are considered feasible. For feasible plans, the clinical protocol is satisfied if the two objectives Least Coverage Index (LCI) and Least Sparing Index (LSI) are positive.

**Results**

Re-evaluated in the original model, differences were negligible for all patients between plans optimized using the original model (fig. (a)), and plans optimized using the robust model (fig. (b)), hence the cost for robust optimization as observed in the original model was negligible. Re-evaluated in the robust model, the difference between the original model (fig. (c)) and the

robust model (fig.(d)) was large for 2 of the 5 patients (2,5), hence the benefit of robust optimization could be large. For patient 2, plans that appeared good when optimized in the original model, often violated the clinical protocol when considering different settings. This was not the case for robustly optimized plans.

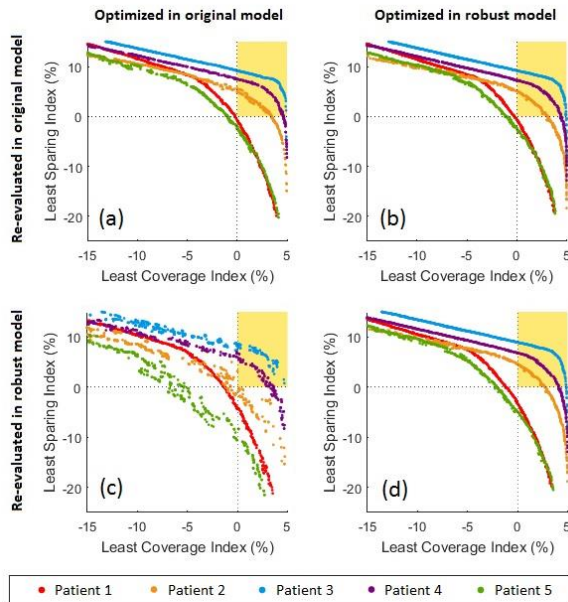


**Figure:** Original and (new) robust bi-objective HDR prostate BT planning results for 5 patient cases. All plans, optimized with either the original (a, c) or robust (b, d) bi-objective model, are re-evaluated in the original (a, b) or the robust (c, d) bi-objective model. Plans in the yellow rectangle where the LCI and LSI are both larger than zero satisfy the clinical protocol.

## Conclusion

Different settings for organ reconstruction can have a non-negligible impact on automatically optimized plans. Robust optimization generated plans of high quality, irrespective of organ reconstructions, and therefore offers a solution to accounting for dosimetric uncertainties.

## OC-0397 Intensity modulated brachytherapy for prostate cancer: plan quality, robustness and delivery time

G. Famulari<sup>1</sup>, S.A. Enger<sup>1,2,3</sup>

<sup>1</sup>McGill University, Medical Physics Unit, Montreal, Canada; <sup>2</sup>McGill University, Department of Oncology, Montreal, Canada; <sup>3</sup>McGill University Health Centre, Research Institute, Montreal, Canada

### Purpose or Objective

Intensity modulated brachytherapy (IMBT) is a novel high dose rate brachytherapy (HDR-BT) technique which incorporates rotating metallic shields inside brachytherapy catheters to dynamically direct the radiation towards the tumor and away from healthy tissues. A delivery system that can enable IMBT for prostate cancer was proposed in a previous study. The purpose of this study is to evaluate the plan quality, robustness and delivery time for IMBT.

### Material and Methods

The IMBT delivery system dynamically controls the rotation of platinum shields placed inside interstitial catheters (Fig. 1). The platinum shield partially collimates the radiation emitted from an <sup>169</sup>Yb source to produce a highly anisotropic dose distribution. The shield contains an emission window of 180° and a groove which guides the translation of the source through the catheter. The device can be connected to the standard 6F transfer tubes for interstitial brachytherapy. Conventional <sup>192</sup>Ir-based HDR-BT and <sup>169</sup>Yb-based IMBT plans were generated for 12

prostate cases using an in-house column generation-based optimizer coupled to a Geant4-based dose calculation engine, RapidBrachyMC. The optimized treatment plans were normalized to match the same PTV D<sub>90</sub> coverage as the original clinical plans. A sensitivity analysis was performed to evaluate the impact of longitudinal source positioning errors ( $\pm 1$  mm,  $\pm 2$  mm and  $\pm 3$  mm) and rotational errors ( $\pm 5^\circ$ ,  $\pm 10^\circ$  and  $\pm 15^\circ$ ) on plan quality indices (PTV D<sub>90</sub> and urethra D<sub>10</sub>).

## Results

The platinum shield reduced the dose on the shielded side at 1 cm off-axis to 18.1% of the dose on the unshielded side (Fig. 2a). For equal PTV D<sub>90</sub> coverage, the urethral D<sub>10</sub> was reduced by 12.9% $\pm$ 4.6%, without change to other plan quality indices (Fig. 2b). The maximum decrease for a single case was 21.3%. Delivery times for IMBT using a 3.1 Ci <sup>169</sup>Yb source, which has the same dose rate at 1 cm off-axis as a 10 Ci <sup>192</sup>Ir source, were, on average, 35% higher compared to conventional HDR-BT. Systematic translational and rotational shifts led to a decrease (increase) in PTV coverage (urethral dose). In general, the PTV D<sub>90</sub> was more sensitive to source positioning errors, while the urethral D<sub>10</sub> was more sensitive to rotational errors (Fig. 2cd). For a typical range of delivery errors ( $\pm 1$  mm,  $\pm 5^\circ$ ), the plan quality indices varied by <2%.

## Conclusion

A system was developed to deliver IMBT for prostate cancer. IMBT has the potential to create a low dose tunnel within the urethra. Delivery times for IMBT with a 4 Ci <sup>169</sup>Yb source are comparable to that of conventional HDR-BT with a 10 Ci <sup>192</sup>Ir source. Treatment plans are robust with respect to delivery errors.

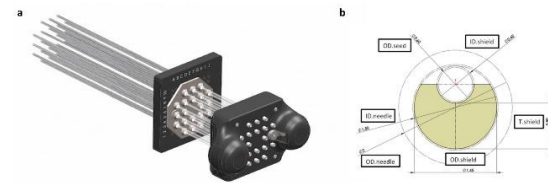


**Figure 1:** (a) IMBT system. (b) Transverse cross section of the shielded needle with dimensions.

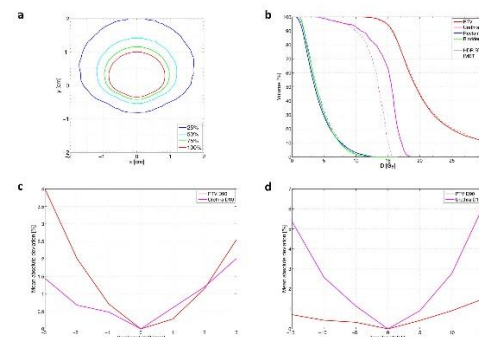


**Figure 2:** (a) Relative dose distribution in the transverse plane of a shielded <sup>169</sup>Yb source. (b) Average DVH for prostate cancer treated with conventional HDR-BT and IMBT. Impact of (c) source position errors and (d) rotational shield errors on plan quality indices.

## OC-0398 Clinical introduction of 3D printed applicators for endocavitary and interstitial brachytherapy.

W. Bazen<sup>1</sup>, P. Kroon<sup>1</sup>, R. Moerland<sup>1</sup>, S. Van de Vegt<sup>1</sup>, P. Mulder<sup>1</sup>, R. Schokker<sup>1</sup>, K. Van Vliet - van den Ende<sup>1</sup>, S. Kloosterman<sup>1</sup>, H. Dehnad<sup>1</sup>

<sup>1</sup>UMC Utrecht, Radiotherapy, Utrecht, The Netherlands

### Purpose or Objective

In our institute, we used handmade applicators and needle templates for brachytherapy of head and neck tumors. The needle entry points were defined on the template according to a clinical drawing of anatomy and clinical target volume (CTV). The drawback of this method is the difficulty of finding the optimal needle configuration. The introduction of 3D printing based on CT and/or MR imaging gives the opportunity to create more conformal applicators and templates.

The aim of this work is:

- to compare simulated dose distributions based on 3D printed applicators with clinically achieved dose distributions
- to demonstrate the clinical workflow and to share our first clinical experiences with 3D printed applicators.

### Material and Methods

Before introduction of 3D printed applicators and templates, an in-silico treatment plan study was performed using the Oncentra Brachy (OCB) treatment planning system (Elekta).

In 4 patients treated for cancer of the vestibulum nasi, a plan based on a 3D printed template was compared to the clinical plan (Figure 1).

Subsequently, a clinical workflow for the use of 3D printed applicators and templates was developed, which consists of the following steps (Figure 2):

- 1) A CT and/or MRI is made for defining the CTV and the body contours;
- 2) The virtual placement of catheters is simulated in the TPS and optimized until an adequate dose distribution is achievable;
- 3) In a 3D design program (Autodesk, Fusion 360) the preplanned catheters and the lock inserts (Elekta) to fix the needles are subtracted from the applicator;
- 4) The applicator is fitted on the patient and a CT scan is made for reconstruction and dose planning;
- 5) The applicator is sterilized and used for treatment;
- 6) The treatment plan is made;
- 7) The treatment plan is executed;
- 8) During treatment a position verification CT is made;
- 9) The applicator is removed.

Between November 2017 and September 2018 17 patients (10 lip, 4 vestibulum nasi, 3 other) have been treated using 3D printed applicators).

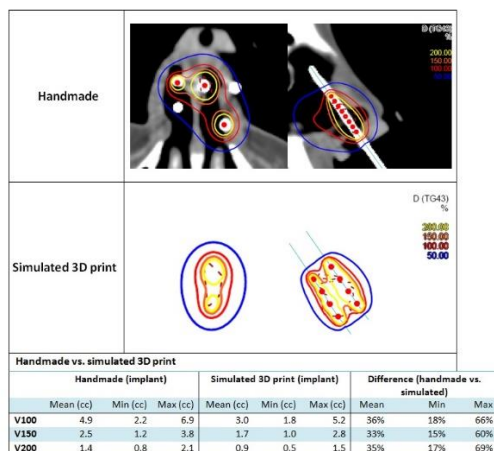


Figure 1: In-silico comparison handmade applicator vs. 3D printed applicator

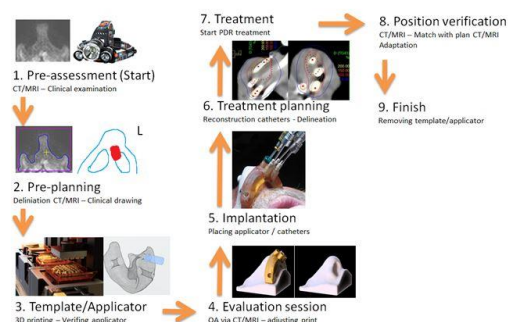


Figure 2: Workflow of creating individual templates and applicators (example vestibulum nasi)

### Results

The in-silico study showed a reduction of the dose volumes V100, V150 and V200 when using 3D printed applicators without compromising CTV coverage (Figure 1). 17 patients were treated according to the new workflow (Figure 2). The applicators fitted well in and on the patients and the needles were placed according to the preplanned positions resulting in adequate CTV dose coverage. On average it took about 3 hours to create a 3D model for printing, whereas handcrafting a template may take up to 6 hours.

### Conclusion

The possibility to optimize needle positions based on CT and/or MR imaging in a single implant gives the advantage to adapt to a wide range of tumor shapes and anatomy constraints. This translates into a reduction of dose volumes when using 3D printed applicators without compromising CTV coverage. The clinical workflow using 3D printed applicators for brachytherapy was successfully implemented and resulted in a reduction of production and processing time.

### OC-0399 Comparison of high-dose interstitial brachytherapy vs. stereotactic treatment in patients with HCC

F. Walter<sup>1</sup>, S. Gerum<sup>1</sup>, J. Well<sup>1</sup>, R. Shpani<sup>1</sup>, N. Lukas<sup>1</sup>, M. Cornelius<sup>1</sup>, F. Streitparth<sup>2</sup>, J. Ricke<sup>2</sup>, C. Belka<sup>1</sup>, S. Corradini<sup>1</sup>

<sup>1</sup>Radiation Oncology, Department of Radiation Oncology LMU, Munich, Germany; <sup>2</sup>Radiology, Department of Radiology, Munich, Germany

### Purpose or Objective

The role of brachytherapy (BT) in hepatocellular carcinoma is under investigation. Objective of the study was to evaluate and compare normal liver tissue exposure of CT-guided high-dose interstitial BT to SBRT.

### Material and Methods

The treatment plans of 11 patients (m:f 9:2) with a median age of 65 years (47-82) who received high-dose BT for hepatocellular carcinoma between 07/17 and 06/18 were retrospectively analysed. Lesions with a maximal diameter of <6cm were included. In all cases a prescription dose of 15Gy in single fraction was aimed. SBRT plans prescribing 37.5Gy in 3 fractions to the 65%-Isodoseline were retrospectively planned using the BT planning CT images. Regarding liver exposure, the V5 and V10 Gy of the single BT treatment was compared to the V15, V15.9 and V20Gy of SBRT in 3 fractions (EQD2;  $\alpha/\beta = 3\text{Gy}$ ).

### Results

A total of 13 lesions were treated with high-dose CT-guided interstitial BT using 1 catheter in 7 patients (pts), two in 5pts and three in one case. GTV had a median diameter of 2.73cm (1.17-6.53cm), and a median volume of 5.03ccm (1.39-66.43ccm). The total liver volume ranged from 832.55-2194.46ccm (median 1461.88ccm). A medium dose of 15.1Gy was achieved in D100 (11.4-

15.5Gy), D98=18Gy (14.2-19.1Gy), D95=19.5Gy (15.8-21.5Gy), and D90=21.5Gy (17.8-24.2Gy). In BT 5Gy was administered to 87.7ccm (19.28-570.75ccm) of the liver, 10Gy (EQD2 26Gy,  $\alpha/\beta$ 3) to 35.92ccm (8.38-254.42ccm). Correspondingly in SBRT normal liver tissue received 15Gy median 135.53 (56.88-827.2ccm), 15.9Gy (EQD2 26.4Gy,  $\alpha/\beta$ 3) 120.93 ccm (51.18-734.91ccm), and 20Gy to 73.11ccm (16.59-390.73ccm) of normal liver tissue.

Figure: plan comparison

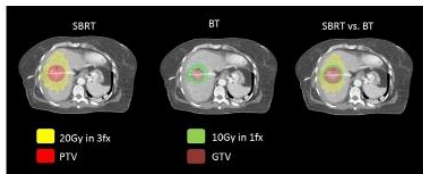


Table: Comparison of delivered doses to normal liver tissue:

Pts	Brachytherapy		SBRT		
	5Gy	10Gy	15Gy	15.9Gy	20Gy
1	39.66	18.17	34.23	30.98	21.58
2	31.14	136.62	335.25	363.35	215.8
3	88.52	31.38	136.37	120.51	75.11
4	87.7	85.92	58.89	49.49	34.88
5	217.64	135.88	387.38	287.13	218.47
6	45.48	20.01	115.15	101.88	50.5
7	970.79	124.42	610.29	382.88	200.19
8	81.85	33.57	49.19	44.86	32.82
9	147.78	47.04	140.5	181.55	145.75
10	27.38	8.88	29.22	24.09	28.59
11	120.02	108.49	91.71	284.81	179.78
12	18.38	8.81	54.94	49.05	32.45
13	272.28	114.27	395.46	322.87	299.99

### Conclusion

Compared with SBRT, high-dose interstitial brachytherapy in patients with hepatocellular carcinoma allows for a good dose coverage while sparing normal liver tissue.

### OC-0400 Are prostate contours affected by the RO's clinical experience in prostate HDR brachytherapy?

H. Lavoie<sup>1</sup>, E. Poulin<sup>1</sup>, A. Martin<sup>1</sup>, L. Pilote<sup>1</sup>, E. Vigneault<sup>1</sup>, W. Foster<sup>1</sup>, L. Archambault<sup>1</sup>, F. Lacroix<sup>1</sup>

<sup>1</sup>CHU de Quebec, Radiation Oncology, Quebec, Canada

### Purpose or Objective

The aim of this study was to compare the prostate contours for two imaging modalities, computed tomography (CT) and trans-rectal ultrasound (TRUS), used in HDR brachytherapy. The authors hypothesized that the contour variability was affected by the radiation oncologists (ROs) clinical experience.

### Material and Methods

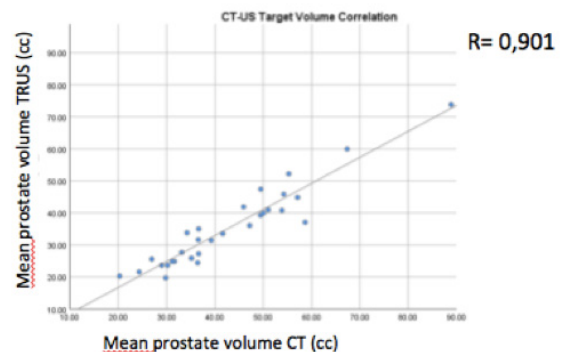
CHU de Québec is a high volume prostate brachytherapy center (>250 patients/year) employing multiple ROs that have performed CT-based HDR brachytherapy since 1999. A TRUS-based HDR procedure was introduced in 2016. The first thirty patients to undergo the TRUS procedure were given a 15 Gy HDR boost. While still under general anesthesia, a CT on rails located in the brachytherapy suite was used to image the pelvis after the treatment. The treating RO (RO1, 2 or 3 in 2016) then contoured the prostate on both modalities. Two years later, four ROs (RO4 started in 2017) re-contoured the prostate on the CT and TRUS images for each patient. The RO's CT clinical experience was as follow: RO1=13, RO2= 18 RO3=7 and

RO4= 1 (years). In 2018, all 4 ROs had 2 years of experience in TRUS. A volume comparison between both modalities and between ROs was performed. A rigid registration between CT and TRUS images was completed for 16 patients using gold fiducial markers. The Jaccard Index (JI) was computed to evaluate the inter-observer variability. In addition, the intra-observer variability was evaluated by comparing the volumes contoured in 2016 and 2018. Paired t-tests were used to evaluate the volume and JI differences.

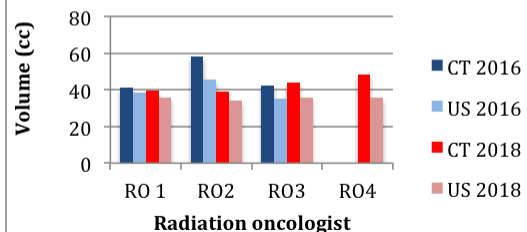
### Results

The mean CT and TRUS volumes showed a significant correlation for the prostate of 0.95 ( $p<0.001$ ). The volume ratio of TRUS/CT was 0.82 (95% interval 0.79-0.87), meaning the volume was 18% bigger on CT. The mean JI was 87% for CT and 92% for TRUS when comparing all 4 ROs; CT and TRUS JIs were significantly different ( $p<0.001$ ). The mean JI for the prostate on CT was significantly better ( $p<0.05$ ) when comparing RO1, 2 and 3 together (RO1-2, RO1-3, RO2-3, mean=89%) than when comparing RO4 to the others (RO1-4, RO2-4, RO3-4, mean=85%). For TRUS planning, the mean JI was not significantly different ( $p>0.05$ ) when comparing all ROs (91-93%). The intra-observer volume variability between 2016 and 2018 for CT and TRUS was evaluated and revealed a bigger mean difference for CT than for TRUS, 6.9 cc vs 4.5 cc respectively ( $p<0.001$ ). The average ROs intra-observer variability was not significant in TRUS ( $p>0.05$ ).

### Correlation between CT and TRUS mean prostate volume (2018)



### Mean prostate volume by RO and imaging modality



### Conclusion

Contoured prostate volumes were 18% bigger on CT compared to TRUS. In CT, the inter-observer variability is significant even for ROs with more than 7 years' experience. Interestingly, the inter-observer and intra-observer variability were significantly smaller in TRUS

compared to CT-based planning, despite different clinical experiences. Finally, the superior soft tissue contrast offered by TRUS seems to insure a RO independent prostate planning, which might lead to more homogeneous clinical outcomes.

### Proffered Papers: PH 7: Proffered paper: Outcome modelling

#### OC-0401 Pre-treatment radiomic features predict individual nodal failure in head and neck cancer

T. Zhai<sup>1,2</sup>, R.J.H.M. Steenbakkers<sup>1</sup>, L.V. Van Dijk<sup>1</sup>, J.G.M. Vemer-van den Hoek<sup>1</sup>, H.P. Bijl<sup>1</sup>, M. Dieters<sup>1</sup>, W. Noordzij<sup>3</sup>, A. Van der Schaaf<sup>1</sup>, N.M. Sijtsema<sup>1</sup>, J.A. Langendijk<sup>1</sup>

<sup>1</sup>University Medical Center Groningen, Department of Radiation Oncology, Groningen, The Netherlands ;

<sup>2</sup>Cancer Hospital of Shantou University Medical College, Department of Radiation Oncology, Shantou, China ;

<sup>3</sup>University Medical Center Groningen, Department of Nuclear Medicine and Molecular Imaging, Groningen, The Netherlands

#### Purpose or Objective

Optimal management of neck nodes after definitive radiotherapy for head and neck cancer patients is still under debate. The main concerns are how to identify patients that need neck dissection and lymph nodes that need super-selected neck node resection after treatment. The main objective of this study was to test whether the addition of pre-treatment radiomic features of pathological lymph nodes to clinical prediction models improves the prediction of nodal failure for individual lymph nodes.

#### Material and Methods

This was a retrospective analysis in a prospective cohort study, which was composed of 277 node-positive head and neck squamous cell carcinoma patients with 1025 pathological neck nodes treated with definitive radiotherapy with or without systemic treatment. A total of 165 patients with 558 pathological lymph nodes treated before January 2013 were enrolled in the training cohort and 112 patients with 467 pathological lymph nodes treated between January 2013 and June 2016 were enrolled in the validation cohort. Overall 82 pre-treatment CT radiomic features and 8 clinical features from each positive lymph node were analyzed. The endpoint was the cumulative incidence of nodal failure. Clinical, radiomic and combined models were created from the multivariable Cox proportional hazard analysis based on clinical features, radiomic features, and both clinical and radiomic features, respectively. The performances of the models were assessed in the validation cohort. A nomogram was constructed for individualized nodal failure estimation.

#### Results

There were 71 and 28 lymph node failures in the training and validation cohorts with 31.1 and 29.0 months median follow up, respectively. Multivariable analysis revealed two radiomic features (Least axis length (LALLN,  $p < 0.001$ ) and Correlation of Grey level co-occurrence matrix (Corre-GLCM,  $p = 0.039$ ) and three clinical risk factors (WHO performance score (PS,  $p < 0.001$ ), T stage ( $p = 0.009$ ) and gender ( $p = 0.005$ )). LALLN means the shortest diameter and Corre-GLCM represents the heterogeneity of the lymph node. The combined model showed good discrimination with a c-index of 0.87 (95% CI: 0.80 to 0.95) in the training cohort and 0.79 (95% CI: 0.78 to 0.80) in the validation cohort and was significantly better than models based on clinical features ( $p < 0.001$ ) or radiomics ( $p = 0.002$ ) only (Fig.1). The relation between the risk of nodal failure for male patients with WHO PS > 0 and the radiomic features is shown in Fig.2. Lymph nodes with a

high risk to persist or recur could be identified before treatment by using the nomogram constructed for this model to guide decisions on the preferred treatment strategies such as neck dissection or treatment intensification.

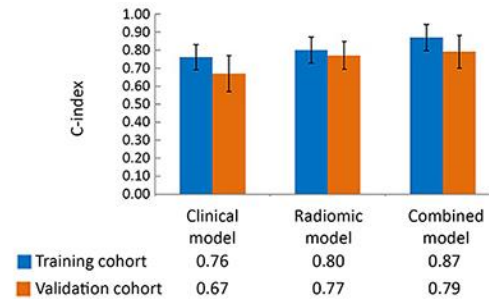


Fig.1. The performance of clinical, radiomic and combined models.

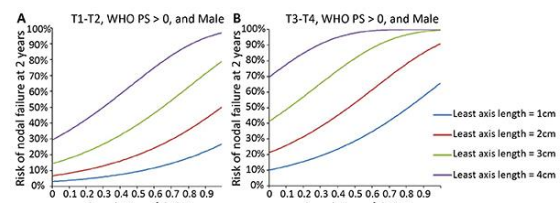


Fig.2. The risk of nodal failure for male patients with worse WHO PS at 2 years as a function of the radiomic features (Correlation of GLCM and Least axis length) for different tumor stages: (A) T1 and T2 and (B) T3 and T4. Abbreviations: WHO PS = WHO performance score; GLCM = Grey level co-occurrence matrix.

#### Conclusion

A pre-treatment prediction model was developed to predict the risk of individual lymph node failure based on non-invasive radiomic and clinical features. This model may support personalized lymph node treatment adaptations in clinical practice after further multi-center validation.

#### OC-0402 Tumour blood perfusion from baseline contrast-based MRI predicts radiation outcome in rectal cancer

K. Bakke<sup>1,2</sup>, S. Meltzer<sup>1</sup>, E. Grøvik<sup>3,4</sup>, A. Negård<sup>5,6</sup>, H. Stein Harald<sup>5</sup>, A. Hansen Ree<sup>1,6</sup>, K. Gjesdal<sup>1</sup>, K. Røe Redalen<sup>1,7</sup>

<sup>1</sup>Akershus University Hospital, Department of Oncology, Lørenskog, Norway; <sup>2</sup>University of Oslo, Department of Physics, Oslo, Norway; <sup>3</sup>Oslo University Hospital, Department of Diagnostic Physics- Division of Radiology and Nuclear Medicine, Oslo, Norway; <sup>4</sup>University of South-Eastern Norway, Department of Optometry-Radiography and Lighting Design, Drammen, Norway; <sup>5</sup>Akershus University Hospital, Department of Radiology, Lørenskog, Norway; <sup>6</sup>University of Oslo, Institute of Clinical Medicine, Oslo, Norway; <sup>7</sup>Norwegian University of Science and Technology, Department of Physics, Trondheim, Norway

#### Purpose or Objective

To evaluate the prognostic and predictive potential of parameters obtained from baseline intravoxel incoherent motion (IVIM) diffusion-weighted MRI and multi-echo contrast-based dynamic MRI in locally advanced rectal cancer.

#### Material and Methods

192 patients with suspected rectal cancer were enrolled onto a prospective biomarker study. 45 of these patients scheduled for neoadjuvant radiation consisting of either short-course radiotherapy (5 Gy x 5) (n = 10) or long-course chemoradiotherapy (2 Gy x 25 with concomitant capecitabine) (n = 35) were selected for analysis. At baseline, patients underwent routine MRI followed by an extended diffusion weighted sequence for IVIM analysis and a multi-echo contrast-based dynamic sequence with

gadolinium injection (Dotarem® 279.3 mg/ml, Guerbet Roissy, France). From the multi-echo data both the  $T_1$ -weighted dynamic curve and the  $R_2^*$ -weighted curve were extracted for dynamic contrast enhanced (DCE) and dynamic susceptibility contrast (DSC) analysis, respectively. The extended Tofts model was applied for DCE analysis, estimating transfer constants ( $K^{trans}$ ,  $k_{ep}$ ) and plasma- and interstitial volumes ( $V_p$ ,  $V_e$ ). The model-free deconvolution approach was used for DSC analysis, calculating tumour blood flow (BF). For both DCE and DSC analysis, individual arterial input functions were used. A bi-exponential model was used for IVIM analysis, estimating perfusion fraction ( $f$ ), pseudo-diffusion ( $D^*$ ) and diffusion ( $D$ ). Tumours were delineated by two radiologists on  $T_2$ -weighted images and co-registered to parametric images before median tumour values were extracted. Pearson correlation coefficients were estimated to evaluate correlations between parameters, Student's  $t$ -test to assess differences between patients with good and poor tumour response to the neoadjuvant radiation and Cox-regression for survival analysis. The median follow-up for the selected patients was 21 months (range 3 - 51 months).

### Results

BF was significantly higher in tumours with good response to the treatment (ypT0-1,  $n = 9$ ; BF = 120 ml/min/100 g) compared to those with poor response (ypT2-4,  $n = 34$ ; 96 ml/min/100 g) ( $p = 0.014$ ). High BF was also significantly associated with overall survival (hazard ratio = 0.97,  $p = 0.017$ ), Figure 1. Further, BF was correlated to both  $D^*$  ( $r = 0.46$ ,  $p = 0.001$ ) from IVIM and  $v_p$  ( $r = 0.57$ ,  $p < 0.001$ ) from the DCE analysis.

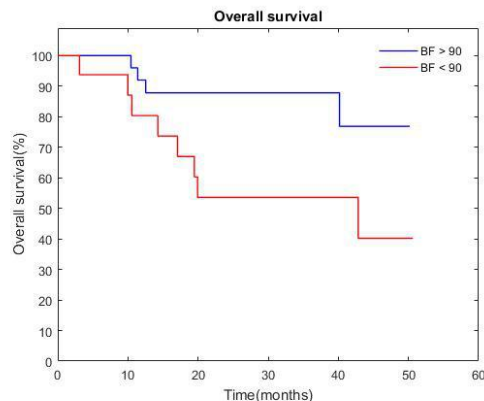


Figure 1: Kaplan-Meier plot showing overall survival for patients with low (< 90 ml/min/100 g) versus high (> 90 ml/min/100 g) tumour blood flow (BF) at baseline.

### Conclusion

In this cohort of rectal cancer patients, BF from DSC acquired at baseline, reflecting tumour perfusion, predicted both local tumour response to neoadjuvant radiation as well as overall survival.

### OC-0403 Type 4 TRIPOD external validation of a larynx survival model

C. Rønn Hansen<sup>1,2,3,4</sup>, N. Sarup<sup>1</sup>, R. Zukauskaitė<sup>4,5</sup>, J. Johansen<sup>3</sup>, J.G. Eriksen<sup>5,6</sup>, S.L. Krogh<sup>1</sup>, A. Bertelsen<sup>1</sup>, D.I. Thwaites<sup>2</sup>, U. Bernchou<sup>1,4</sup>, C. Brink<sup>1,4</sup>

<sup>1</sup>Odense University Hospital, Laboratory of Radiation Physics, Odense, Denmark; <sup>2</sup>The University of Sydney, Institute of Medical Physics- School of Physics, Sydney, Australia; <sup>3</sup>Aarhus University Hospital, Danish Centre for Particle Therapy, Aarhus, Denmark; <sup>4</sup>University of Southern Denmark, Department of Clinical Research, Odense, Denmark; <sup>5</sup>Odense University Hospital, Department of Oncology, Odense, Denmark; <sup>6</sup>Aarhus University Hospital, Department of Experimental Clinical Oncology, Aarhus, Denmark

### Purpose or Objective

Prediction of overall survival is important to select appropriate treatment for the individual patient. In order to use prediction models clinically, they require independent validation to check their robustness between different institutions (Type 4 TRIPOD external validation). The aim of this study was to validate the larynx survival model published by Egelmeier et al 2011 in an external cohort from one institution.

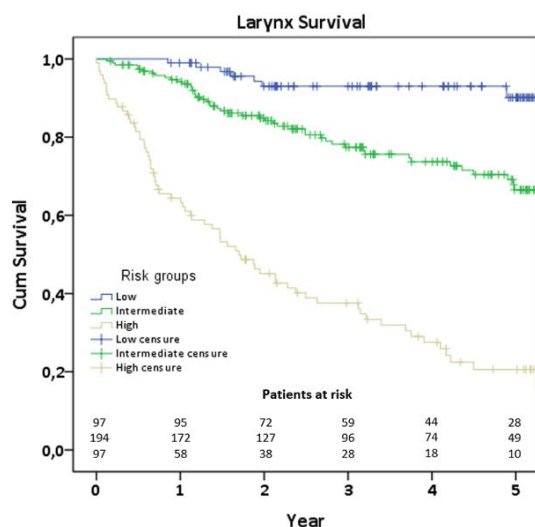
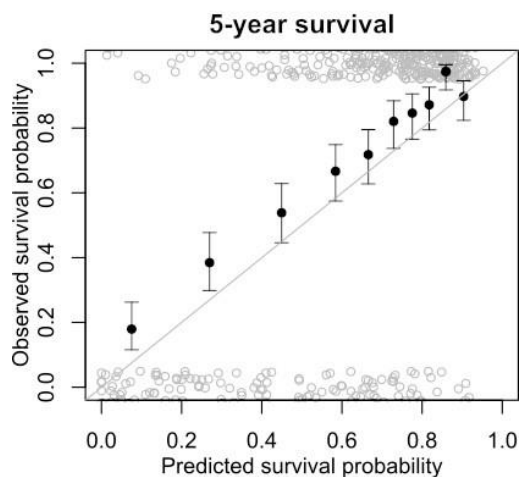
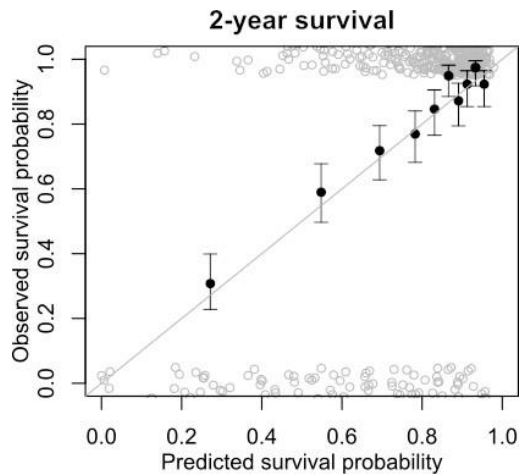
### Material and Methods

Using the Computer Assisted Theragnostics (CAT) approach all ( $n=615$ ) patients treated for larynx cancer were retrieved from the Danish DAHANCA database from 2005-2015 and using the CAT system combined with data from our local Record and Verify system (Mosaik). Patients that received surgery alone ( $n=58$ ) or those with missing data ( $n=169$  - predominantly hemoglobin at start of RT) were excluded. In total, 388 patients were used for the validation. All patients were treated according to the DAHANCA guidelines and followed up yearly until year 5. The median follow-up of the 388 patients was 2.6 years. The parameters used in the model were: age, hemoglobin and equivalent dose (EQD2T) as continuous variables, and T-classification (1-4), N- classification (-/+), sex (F/M) and tumor site (glottis/other) as categorical variables.

The 2-year and 5-year model performance was validated using calibration plots with the patients grouped in 10 equal sized groups. The plots contain raw data as open circles (1 = alive) and group averages as filled circles. The error bars represent one standard deviation. The validation cohort was split into three groups (two outer quartiles and the inner quartiles as one group) according to the risk assessment of the published model in a Kaplan-Meier plot. The Harrell C-index, the equivalent of AUC for a survival model, was calculated. Bootstrap was used to calculate a 95% confidence interval.

### Results

The external model validation shows a very good calibration for the 2 year survival, while the 5-year survival model underestimates the survival (offset), however with a good calibration slope (fig. 1). The three risk groups showed highly significant ( $p < 0.001$ ) different survival rates in the Kaplan-Meier plot (fig. 2), validating that the model discriminates this larynx patient cohort well. The 2- and 5-year survival rates for the three risk groups were: low risk  $93.0 \pm 2.8\%$  and  $90.1 \pm 3.9\%$ , intermediate risk  $84.9 \pm 2.7\%$  and  $66.5 \pm 4.3\%$ , and high risk  $45.1 \pm 5.2\%$  and  $20.6 \pm 4.8\%$  (std error). The model has a high Harrell C-index of 0.78 [0.74-0.82] compared to 0.73 [0.70-0.77] from the original article.



### Conclusion

The data collection and merging in the CAT-system work smoothly and show good potential. The models perform very well on this external patient cohort and could provide doctors and patients with valuable information on patient-specific survival. The model does not include smoking status of the patients, which has been shown to have a major impact on tumor control and survival and therefore could potentially improve the model predictions further.

### OC-0404 Dose to vascular calcifications is predictive for overall survival in lung cancer patients

E.M. Vasquez Osorio<sup>1</sup>, F. Brewster<sup>2</sup>, A. McWilliam<sup>1</sup>, A. Scaife<sup>3</sup>, K. Banfill<sup>1</sup>, A. Abravan<sup>1</sup>, D. Cobben<sup>1</sup>, C. Faivre-Finn<sup>1</sup>, M. Van Herk<sup>1</sup>

<sup>1</sup>The University of Manchester, Division of Cancer Studies- School of Medical Sciences- Faculty of Biology-Medicine and Health, Manchester, United Kingdom ; <sup>2</sup>The Christie NHS Foundation Trust, Christie Medical Physics & Engineering, Manchester, United Kingdom; <sup>3</sup>The University of Manchester, Jodrell Bank Centre for Astrophysics - School of Physics and Astronomy - Faculty of Science and Engineering, Manchester, United Kingdom

### Purpose or Objective

Recent studies suggest that incidental dose to the heart can have an early detrimental effect on overall survival for lung cancer patients receiving radiotherapy. We investigated whether irradiation of vascular calcifications, identified on the radiotherapy planning CT, also affects overall survival.

### Material and Methods

Data from 1002 unselected non-small cell lung cancer patients, all treated with 55Gy in 20 fractions, were used. Calcifications within the thoracic cavity were automatically segmented in the planning CT scans using standard image processing algorithms, including morphological operations, connected pixel analysis and shape analysis. Calcifications for 10 CT scans were manually segmented to evaluate the quality of the automatic segmentation. To explore the interaction of the identified calcifications and the radiation dose on overall survival prediction, the volume of calcifications receiving  $\geq 0$ , 10, 20, 30, 40 and 50 Gy was determined. We subsequently refer to them as Cx. These variables were included in a Cox-regression analysis alongside log tumour volume, age, mean dose to the lungs, and gender. Heart structures were created for all patients using atlas-based segmentation in ADMIRE v2.0 (Elekta AB, Stockholm, Sweden). The analysis was repeated for calcifications within the heart only.

### Results

The average calcification volume found was 2.6 cm<sup>3</sup> (SD 2.8 cm<sup>3</sup>), of which 1.3 cm<sup>3</sup> (SD 2.0 cm<sup>3</sup>) was within the heart. The success rate of the algorithm for identifying calcifications was 81.8%, with an error rate of 8.8%. Figure 1 shows the hazard ratios and significance levels for univariate and multivariate Cox-regressions. Univariate analysis of C10, C20, C30, C40 and C50 were significant for all calcifications, but only C10, C20 and C30 for calcifications within the heart. Tumour volume, age, mean dose to the lungs, and gender were significant in all models. In the multivariate analysis, C20 remained significant when using all calcifications (HR=1.27, CI=1.01, 1.59, p=0.04) but only borderline significant for calcifications within the heart.

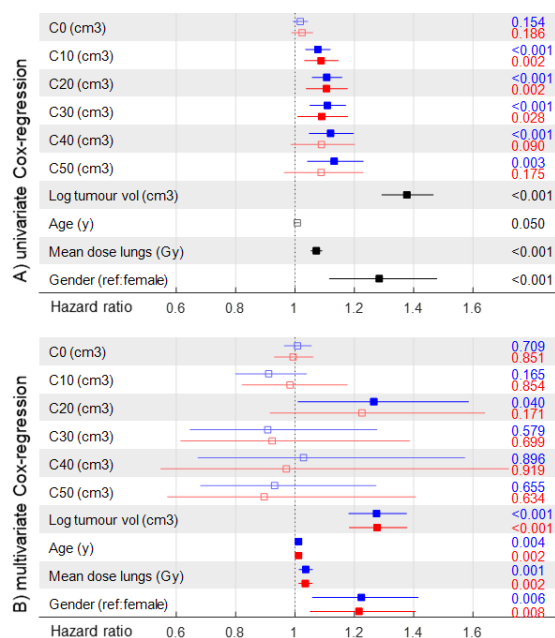


**Fig 1:** Forest plots of the hazard ratios for A) univariate and B) multivariate survival analysis. Blue indicates all calcifications, red only in the heart and black other variables. Filled markers represent significance at 0.05 threshold. n=1002,803 events for all variables.

Using median C20 to stratify the patient data resulted in two significantly different survival distributions when all calcifications were used ( $p=0.003$ , log-rank test) but border-line for calcifications only in the heart. Figure 2 shows the corresponding Kaplan-Meier survival estimates.

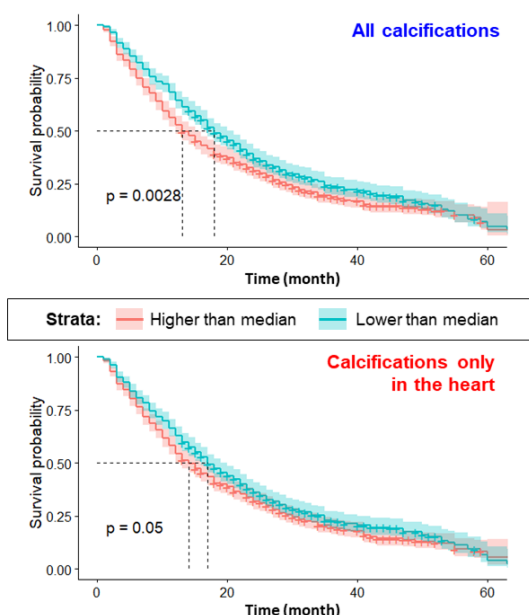


**Fig 2:** Kaplan-Meier survival estimators for the univariate models for calcification volume receiving  $\geq 20$  Gy. Median survival times across groups are significant different when stratifying based on all calcifications but border-line for calcifications only in the heart.

## Conclusion

Our results suggest that the risk of death increases by 27% for every extra  $\text{cm}^3$  of calcifications receiving at least 20 Gy. Moreover, the loss of significance when analysing data to only the calcifications within the heart suggest an important dose/effect relation for calcifications outside the heart and these should not be ignored. We are planning to validate of our findings in an external cohort.

## OC-0405 Registry-based modelling of early mortality following radiotherapy of lung cancer

L. Stervik<sup>1</sup>, N. Pettersson<sup>2</sup>, J. Scherman<sup>3</sup>, C.F. Behrens<sup>4</sup>, C. Ceberg<sup>5</sup>, S. Engelholm<sup>6</sup>, G.F. Persson<sup>7</sup>, M. Pohl<sup>8</sup>, A. Hallqvist<sup>9</sup>, J. Nyman<sup>9</sup>, I.R. Vogelius<sup>10</sup>, A. Bäck<sup>2</sup>

<sup>1</sup>University of Gothenburg, Department of Radiation Physics, Gothenburg, Sweden ; <sup>2</sup>Sahlgrenska University Hospital- University of Gothenburg, Department of Therapeutic Radiation Physics- Department of Radiation Physics, Gothenburg, Sweden ; <sup>3</sup>Skåne University Hospital, Department of Radiation Physics, Lund, Sweden ; <sup>4</sup>Herlev and Gentofte Hospital- University of Copenhagen, Department of Oncology, Copenhagen, Denmark ; <sup>5</sup>Lund University, Department of Medical Radiation Physics, Lund, Sweden ; <sup>6</sup>Skåne University Hospital, Department of Oncology, Lund, Sweden ; <sup>7</sup>Herlev and Gentofte Hospital- University of Copenhagen, Department of Oncology- Department of Clinical Medicine, Copenhagen, Denmark ; <sup>8</sup>Rigshospitalet- University of Copenhagen, Department of Oncology, Copenhagen, Denmark ; <sup>9</sup>Sahlgrenska University Hospital, Department of Oncology, Gothenburg, Sweden ; <sup>10</sup>Rigshospitalet- University of Copenhagen, Department of Oncology- Department of Clinical Medicine, Copenhagen, Denmark

## Purpose or Objective

To demonstrate registry based outcome modeling using multivariable models of 90- and 180-day mortality rates following conventionally fractionated, curative radiotherapy treatments (RTs) for non-small cell lung cancer (NSCLC) as exemplar.

## Material and Methods

The scripting capabilities of a modern oncology information system was used to automatically identify patients and extract dose volume information. We considered all patients available in the oncology information systems diagnosed with NSCLC treated with conventionally fractionated, curative RT between 2002 and 2017 at two Danish and two Swedish hospitals. Date of death was available through national registries or hospital records. Exclusion criteria were previous dose exposure in the thoracic region, another RT concurrently or during the observation period for early mortality (90- or 180-days), and/or dose or treatment time outside of normal range (see Figure 1).

Maximum likelihood estimation and univariable logistic regressions (LRs) for the binary endpoints death within 90- and 180-days from the treatment start were used. Predictor variables with a p-value for the regression coefficient less than 0.1 in likelihood ratio tests were considered eligible for multivariable LR to model the same endpoints. The statistical significance of each multivariable model as a whole was evaluated with likelihood ratio tests.

## Results

Data were automatically extracted for 2018 patients. Applying exclusion criteria, 1721 patients and 1621 patients remained for modelling of the 90- and 180-day mortality rate, respectively. Figure 1 shows a CONSORT diagram of the patient cohort. The 90- and 180-day mortality rates were 2.9% (50/1721) and 10% (170/1621), respectively. MLD and patient age were significantly associated with mortality after both 90 and 180 days (all  $p<0.01$ ). Predicted 90-day mortality rate (Figure 2, upper panel) of 5% for patients aged 50, 60, 70 and 80 years were reached at MLD of 34, 28, 22 and 16 Gy, respectively. Calibration plots showed a good agreement between observed and modelled 90- (Figure 2, lower panel) and 180-day mortality rates.

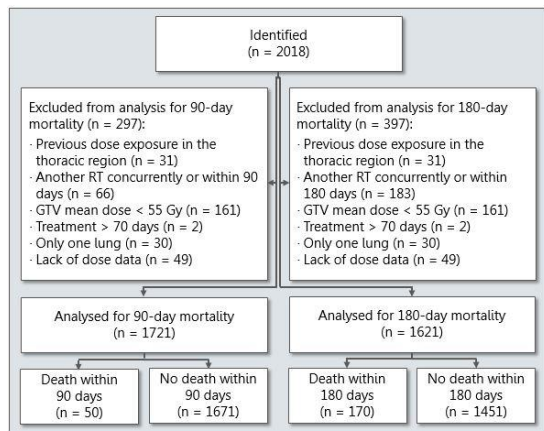


Figure 1. CONSORT diagram of the patient cohort.

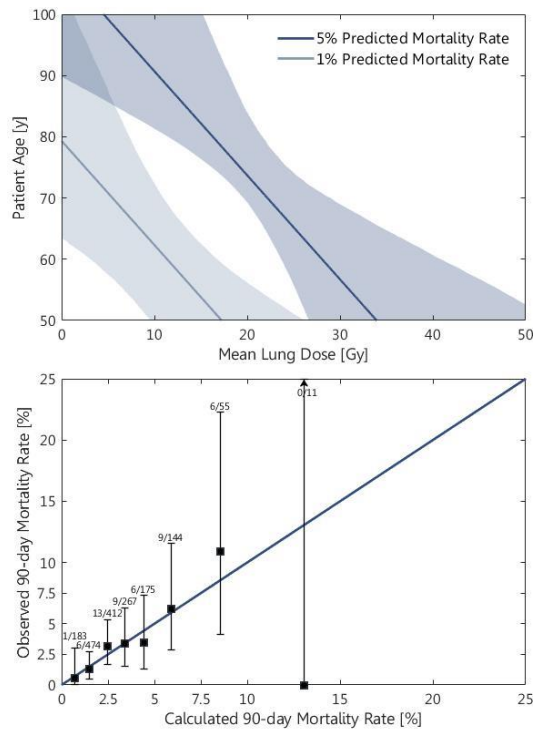


Figure 2. Upper panel: Isocurves of the predicted 90-day mortality rates 1% and 5% as a function of the mean lung dose and patient age. The shaded areas corresponds to the 95% confidence intervals. Lower panel: Calibration plot comparing observed and modelled 90-day mortality rates. The vertical error bars are the 95% binomial confidence interval and the numbers above are the observed data in each bin.

#### Conclusion

We demonstrated registry based outcome modeling as a means to predict the infrequent endpoint of early mortality following curative intended radiotherapy for NSCLC. Age and MLD were found to be associated with a higher risk of early mortality.

#### OC-0406 Early survival prediction in non-small cell lung cancer with PET/CT size aware longitudinal pattern

M. Astaraki<sup>1,2</sup>, C. Wang<sup>1</sup>, G. Buizza<sup>3</sup>, I. Toma-Dasu<sup>2,4</sup>, M. Lazzeroni<sup>2,4</sup>, Ö. Smedby<sup>1</sup>

<sup>1</sup>KTH Royal Institute of Technology, Department of Biomedical Engineering and Health Systems, Stockholm, Sweden ; <sup>2</sup>Karolinska Institutet, Department of

Oncology-Pathology, Stockholm, Sweden ; <sup>3</sup>Politecnico di Milano, - Department of Electronics- Information and Bioengineering, Milan, Italy; <sup>4</sup>Stockholm University, Department of Physics, Stockholm, Sweden

#### Purpose or Objective

Recently, numerous studies have developed advanced imaging biomarkers in order to capture cancer imaging phenotypes. By extracting large numbers of quantitative features, radiomics offers new opportunities in cancer outcome modeling. However, radiomic features are quite sensitive to different factors, and it is often difficult to interpret their physiological meanings. The objective of this study was to develop a novel physiologically interpretable feature set describing intra-tumor heterogeneity in patients with lung cancer and test it as an imaging biomarker for survival prediction.

#### Material and Methods

Longitudinal PET-CT images from 30 patients diagnosed with non-small cell lung cancer were analyzed. After preprocessing the images, gross target volumes (GTV) were segmented semi-automatically. Inspired by the assumption that partial tumor response to the therapy would be explained by the existence of sub-regions within the GTV, we introduced the size-aware longitudinal pattern (SALoP), which aims at quantifying variations in the structure and function of the tumor. To compute SALoP, we partitioned the GTVs into separate subregions based on the distance of each voxel inside the GTV from the tumor border, i.e. for every 0.5cm of distance from the tumor border, one region was added. Then, the change in average intensity of each subregion between the two scans was calculated. For comparison, radiomic analysis was performed by extracting 451 features. Reproducibility of SALoP and radiomic features were investigated on an external test-retest dataset. Dimensionality reduction was performed by applying a forward feature selection (FFS) algorithm, and a support vector machine (SVM) was employed as the prediction model.

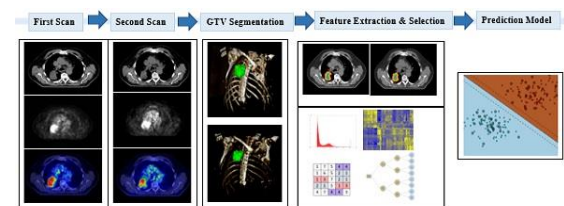


Figure 3. Schematic illustration of the study pipeline.

#### Results

Reproducibility of the SALoP set was substantiated by achieving a high agreement when it was applied on test-retest dataset. Without FFS, SALoP features outperformed radiomics significantly. Feeding the prediction model with only selected features, the combination of SALoP and radiomics resulted in the highest predictive values. For SALoP, a combination of PET and CT features led to higher predictive values than CT and PET features separately either with or without FFS. Applying FFS contributed an improvement of 15 percent (0.71 to 0.86) in predictive power of radiomics and 5 percent (0.90 to 0.95) for the SALoP. This implies that large numbers of radiomic features were either redundant or lacking informative value, whereas the SALoP features were more consistent

with each other.

Table1. Predictive values of SALoP feature set, radiomics and their combination with and without Forward Feature Selection (FFS), in terms of area under the receiver operating characteristic curve (AUROC) calculated on leave one out cross validation. For each case, the highest values are marked in bold. AUROC values significantly different from randomness (0.5) are indicated with \*

Modality	Therapy	AUROC					
		Without FFS			With FFS		
		SALoP	Radiomics	SALoP+ Radiomics	SALoP	Radiomics	SALoP+ Radiomics
CT	Sequential	0.87*	0.80	<b>0.92*</b>	0.92*	0.76	<b>0.95*</b>
	Concurrent	<b>0.70</b>	0.49	0.50	0.53	0.50	<b>0.70</b>
	All	0.66	0.56	<b>0.69</b>	0.71*	0.87*	<b>0.89*</b>
PET	Sequential	<b>0.85*</b>	0.73	0.73	0.91*	0.97	<b>0.99</b>
	Concurrent	<b>0.80*</b>	0.63	0.65	0.90*	<b>1*</b>	<b>1*</b>
	All	<b>0.86*</b>	0.61	0.63	0.89*	0.87*	<b>0.96*</b>
PET-CT	Sequential	<b>0.94*</b>	0.78	0.76	0.95*	0.96*	<b>0.98</b>
	Concurrent	<b>0.83*</b>	0.65	0.69	0.91*	<b>1</b>	<b>1*</b>
	All	<b>0.90*</b>	0.71	0.66	<b>0.95*</b>	0.86*	<b>0.95*</b>

### Conclusion

Assuming that the sensitivity of tumor cells to treatment may vary as a function of distance from the tumor border, dividing the tumor volume into subregions can characterize tumor cells and identify them from more homogeneous regions. The proposed novel feature set was capable of describing intra-tumor heterogeneity with only 20 features and outperformed conventional radiomics.

### OC-0407 CT-based Radiomics for Risk Stratification in Prostate Cancer

S. Osman<sup>1,2</sup>, R.T.H. Leijenaar<sup>3</sup>, A.J. Cole<sup>1,4</sup>, A.R. Hounsfield<sup>2</sup>, K.M. Prise<sup>1</sup>, J.M. O'Sullivan<sup>1,4</sup>, P. Lambin<sup>3</sup>, C.K. McGarry<sup>1,2</sup>, S. Jain<sup>1,4</sup>

<sup>1</sup>Queen's University Belfast, Centre for Cancer Research & Cell Biology, Belfast, United Kingdom; <sup>2</sup>Northern Ireland Cancer Centre, Medical Physics, Belfast, United Kingdom; <sup>3</sup>The D-Lab: Decision Support for Precision Medicine- GROW- Maastricht University Medical Centre- The Netherlands, School for Oncology and Developmental Biology, Maastricht, The Netherlands; <sup>4</sup>Northern Ireland Cancer Centre, Department of Clinical Oncology, Belfast, United Kingdom

### Purpose or Objective

The prognostic and predictive value of MRI- based radiomics imaging features for prostate cancer (PCa) has been demonstrated in a number of publications. However, there is no clear consensus on the most important imaging biomarkers for prostate or their clinical applicability. This could be due to the lack of interoperability (i.e. variable imaging protocols, scanners, software or uncertainties in the manual definition of tumours). Planning CT scan protocols for PCa are typically standardised for all patients treated with external beam radiation therapy (EBRT). This study explored the role of CT-based radiomics features in PCa Gleason score (GS) and risk group classification.

### Material and Methods

The study population consisted of 506 PCa patients from a clinically annotated database all treated in a single centre using EBRT. After applying exclusion criteria (available CT scans with 2.5mm slice thickness and no artefact), 342 patients were included in the final analysis. CT-based radiomics features were extracted for prostate gland only (PO) structure. CT scans were re-sampled to 2.5mm isotropic voxels and the range of Hounsfield Units (HU) discretised to 10 HU bins prior to feature extraction. For 20 patients with scan and re-scan data the interclass correlation coefficient ICC was used to identify a set of robust features to use for our analysis. Features with ICC > 0.8 were considered reproducible. Pairwise correlation testing was also employed to remove redundant features. Penalized regression analysis using LASSO generalized linear model was used. Optimal lambda was estimated using 10-fold cross validation (CV) repeated 100 times, the lambda value one standard error away was used. Models were evaluated through 10-fold CV repeated 100 times.

Models' discriminatory performance was assessed using receiver operating characteristic (ROC) area under the curve (AUC) analysis, accuracy, and Youden index (YI = specificity + sensitivity - 1).

Table 1(a): Patient grouping based on Gleason Score (GS)

Gleason Score	Number of patients
6(3+3)	100
7(3+4)	87
7(4+3)	49
>7	106

Table 1(b): Patient grouping based on Risk Group (RG)

Risk Group	Criteria	n
Low risk	T1 or T2a and Gleason score 6 and PSA <10 ng/ml	33
Intermediate risk	T2b or T2c or Gleason score 7 or PSA 10-20ng/ml	76
High Risk	>T2c Gleason score 8-10 or PSA > 20ng/ml	233

### Results

Classifiers employing CT-based radiomics features distinguished between GS ≤ 6 vs. GS ≥ 7 with (AUC = 0.83, YI = 0.16) and GS=7(3+4) vs. GS=7(4+3) with (AUC = 0.98, YI = 0.80). Excellent performance was observed for radiomics-based classification of PCa risk groups for low vs. high risk group (AUC = 1.00, YI = 0.81), low vs. intermediate risk (AUC = 0.97, YI = 0.58). Models showed poor performance in distinguishing between GS 7 vs. GS > 7 (AUC = 0.65, YI = 0.02) as well as intermediate vs. high risk patients (AUC = 0.66, YI = 0.00). Applying augmentation methods to balance the data improved classifiers' performance in all cases.

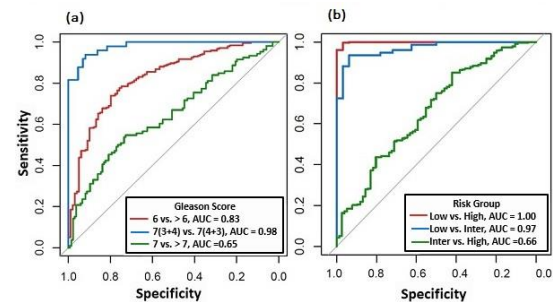


Figure 1: ROC curves for (a) Gleason score and (b) risk group classification.

### Conclusion

Results show that radiomics features from routinely acquired planning CT scans may provide insights into prostate cancer aggressiveness (i.e. Gleason score and risk-group) in a non-invasive manner. Our classifiers were especially accurate in identifying high-risk patients. External validation, and prospective studies are warranted to verify the presented findings.

Proffered Papers: PH 8: Proffered paper: Handling intra-fraction motion in MR guided RT

OC-0408 Impact of bladder filling on the magnitude of prostate intra-fraction motion assessed in 3D Cine-MR  
H. De Boer<sup>1</sup>, D.M. De Muinck Keizer<sup>1</sup>, J.R.N. Voort van Zyp<sup>1</sup>, N.A.T. Van den Berg<sup>1</sup>, F.J. Pos<sup>2</sup>, U.A. Van der Heide<sup>2</sup>, B.W. Raaymakers<sup>1</sup>, J.J.W. Lagendijk<sup>1</sup>, L.G.W. Kerkmeijer<sup>1</sup>

<sup>1</sup>University Medical Center Utrecht, Department of Radiation Oncology, Utrecht, The Netherlands ;  
<sup>2</sup>Netherlands Cancer Institute, Department of Radiation Oncology, Amsterdam, The Netherlands

### Purpose or Objective

We have collected and analyzed an extensive 3D cine-MR dataset to study the visualization of intrafraction motion of the prostate and surrounding organs in MR-guided RT. Here we report on a remarkable relationship of prostate intrafraction motion with initial bladder volume.

### Material and Methods

Fifty-nine patients had repeated weekly cine-MR imaging sessions over five weeks in a multicenter Medical Ethics Review Board approved study. Each session was scheduled shortly after a radiotherapy fraction. 30 patients were instructed to drink 400 mL prior to irradiation as well as scanning, while 29 patients were instructed to drink 200 mL only prior to irradiation. A cine-MR session consisted of 55 sequentially obtained 3D datasets ('dynamics'), using a balanced 3D gradient echo sequence. Each dynamic was acquired over a 11 second period, with the complete cine-MR session covering a ten minute period, similar to the duration of RT fraction delivery. The bladder volume (BV) in each dynamic was obtained with an in-house developed bladder segmentation algorithm. In total, 238 sessions were available for analysis. Prostate intrafraction motion results were obtained with an in-house developed automatic soft-tissue tracking algorithm that was validated with an independent marker tracking algorithm (success rate > 98%, ESTRO 37). We assigned cine-MR sessions to either a group with a BV in the first dynamic below the overall mean BV (Group 1) or to a group with a BV above the group mean (Group 2). We analyzed differences in prostate intrafraction behavior between these two groups.

### Results

Deviations between the automatic segmentation of the bladder and manual delineations were typically < 10 mL. The mean bladder volume  $\pm$  SD was  $0.17 \pm 0.07$  L,  $0.12 \pm 0.03$  L and  $0.24 \pm 0.05$  L in respectively all sessions, group 1 (135 sessions) and group 2 (103 sessions). BV increase during the ten minute sessions was small ( $0.014 \pm 0.013$  L). The distributions of intrafraction translations in AP as well as CC directions were significantly different between groups 1 and 2 for all time points > 2 minutes ( $p < 0.05$ , Kolmogorov-Smirnov test). Particularly the magnitude of motions in the AP direction was markedly larger in group 2 (Fig. 1). The distributions of 3D displacements were equally different between the two groups, as illustrated by Fig. 2. The frequency of displacements > 5 mm almost doubled in group 2 relative to group 1 near the end of the sessions.

### Conclusion

We have found a significant and clinically meaningful increase of prostate intrafraction motion in patients with an initial high bladder volume. Our working hypothesis is that this is due to increased discomfort for larger BV. The presented results suggest that caution should be applied with too strict drinking instructions for prostate cancer patients as full bladder conditions may deteriorate targeting accuracy even after daily on-line corrections.

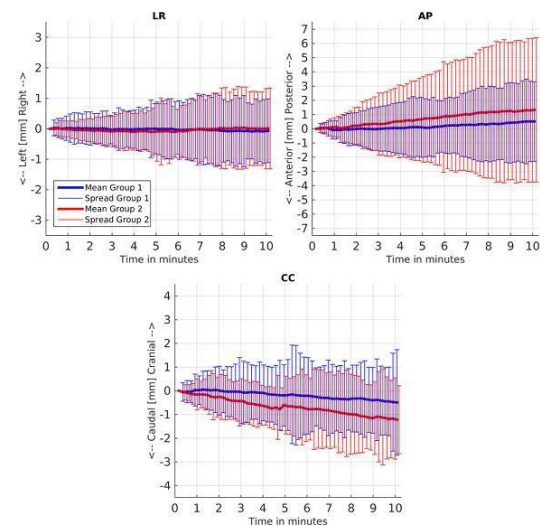


Figure 1: The time evolution of group mean translations (bold) and spread (95 percentile error bars) for both groups.

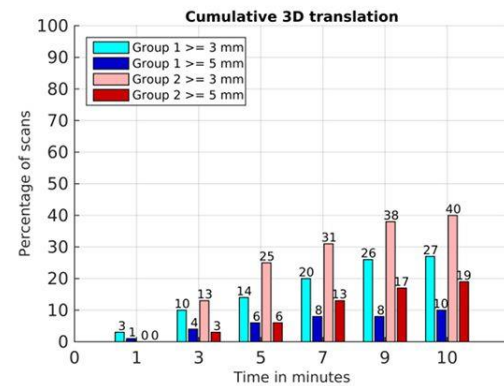


Figure 2: Cumulative distribution of 3D intrafraction translations of group 1 and 2, for various time points.

### OC-0409 Comparison of different strategies to derive time-resolved volumetric MRI in MRI-guided radiotherapy

C. Paganelli<sup>1</sup>, S. Portoso<sup>1</sup>, N. Garau<sup>1</sup>, G. Meschini<sup>1</sup>, R. Via<sup>2</sup>, P. Keall<sup>3</sup>, M. Riboldi<sup>4</sup>, G. Baroni<sup>1</sup>

<sup>1</sup>Politecnico di Milano, Dipartimento di Elettronica- Informazione e Bioingegneria, Milano, Italy; <sup>2</sup>Paul Scherrer Institute, Center for Proton Therapy, Villigen, Switzerland; <sup>3</sup>University of Sydney, ACRF Image X Institute- Sydney Medical School, Sydney, Australia ; <sup>4</sup>Ludwig-Maximilians-Universität München, Department of Medical Physics, Munich, Germany

### Purpose or Objective

MRI-Linacs enable 2D cine-MRI centred in the tumour for motion detection in radiotherapy. However, they lack 3D information due to temporal-spatial limits. To derive time-resolved 3D information, different approaches have been proposed in the literature, but a rigorous comparison between these strategies has not yet been performed. The goal of this study is to quantitatively investigate published strategies to derive time-resolved volumetric MRI in MRI-guided radiotherapy.

### Material and Methods

Five published strategies to derive time-resolved 3DMRI were selected: propagation (PROP)<sup>1</sup>, out-of-plane motion

compensation (OOPM)<sup>2</sup>, Fayad model (FAY)<sup>3</sup>, ROI-based model (ROI)<sup>4</sup> and Stemkens model (STEM)<sup>5</sup>. Comparison among these methods was performed by means of a digital phantom. 3D Digital XCAT-based MRI phantoms were generated from six patient-measured tumour shapes, positions and motion signals: 4DMRI (mean cycle) was generated prior to treatment, with sagittal/coronal 2D cine-MRI acquired during treatment (1x1x3mm<sup>3</sup> resolution, 300ms acquisition). Quantitative analysis was performed by comparing the estimated 3D volume to the ground truth available for each 2D cine-MRI using the centre of mass distances (CD) and dice coefficient (DSC) for the tumour and the apex distance for the diaphragm (Dd).

### Results

Figure A shows the boxplot for each method over the six cases (Friedman test for statistical analysis). For the tumour region (patient motion of 0.4-6.3mm) better results were achieved by PROP and ROI with an overall median CD of 1.14mm and 1.44mm, respectively. Higher errors and variabilities were instead quantified for OOPM, FAY and STEM, with CD>2mm (DSC<0.90) for patients with irregular breathing patterns (CD<1.8mm and DSC>0.92 for PROP and ROI). All methods presented median errors on Dd below 2.5mm (patient motion of 2.2-9.3mm), with PROP and ROI being the most accurate (Dd<3.1mm for irregular patients). Figure B shows a qualitative result for a regular and irregular patient.

### Conclusion

A comparison between different strategies to derive time-resolved 3DMRI is proposed, with PROP and ROI outperforming other methods due to the capability to directly compensate for in-room variations and to account for regional changes, respectively. Future analysis will evaluate the performance of each method according to relevant patient-specific characteristics.

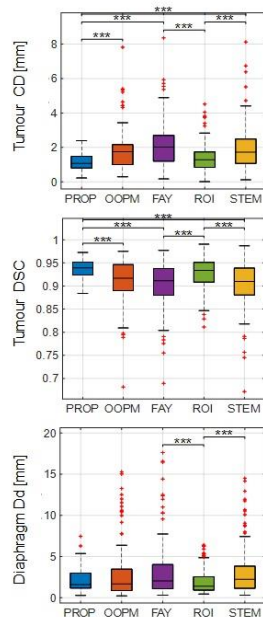


Figure A. Error distributions for tumour (CD and DSC) and diaphragm (Dd) in case of Propagation, OOPM compensation, Fayad model, ROI-based model and Stemkens model. \*\*\* for significant difference ( $p < 0.001$ ).

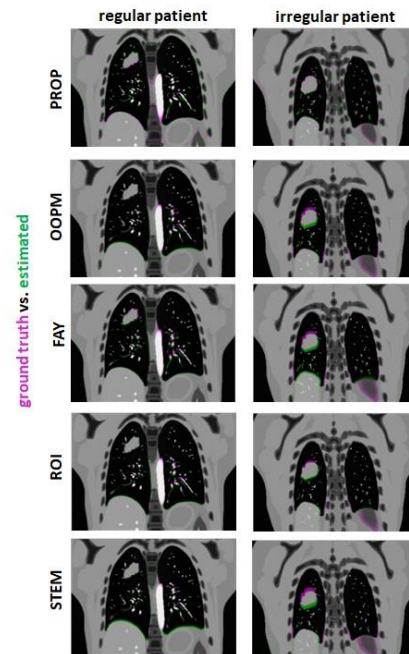


Figure B. Performance of the considered methods on a regular and irregular case: overlap between the estimated volume and the ground truth. Patient-specific signals and tumours animate the phantom.

<sup>1</sup>Paganelli et al. 2018. Feasibility study on 3D image reconstruction from 2D orthogonal cine-MRI for MRI-guided radiotherapy. JMIRO

<sup>2</sup>Seregni et al. 2017. Out-of-plane motion correction in orthogonal cine-MRI registration. Radiother Oncol

<sup>3</sup>Fayad et al. 2012. A generic respiratory motion model based on 4D MRI imaging and 2D image navigators. IEEE

<sup>4</sup>Garau et al. 2018. A ROI-based global motion model for MRI-guidance in radiation therapy: a phantom study. Radiother Oncol

<sup>5</sup>Stemkens et al. 2016. Image-driven, model-based 3D abdominal motion estimation for MR-guided radiotherapy. PMB

### OC-0410 Soft-tissue based on-line prostate motion assessment in 4D Cine-MR for MR-Linac treatments

D. De Muinck Keizer<sup>1</sup>, L.G.W. Kerkmeijer<sup>1</sup>, M. Maspero<sup>1</sup>, J.R.N. Van der Voort van Zyp<sup>1</sup>, C.A.T. Van den Berg<sup>1</sup>, B.W. Raaymakers<sup>1</sup>, J.J.W. Lagendijk<sup>1</sup>, H.C.J. De Boer<sup>1</sup>

<sup>1</sup>UMC Utrecht, Radiotherapy, Utrecht, The Netherlands

#### Purpose or Objective

We develop real-time MR-guided extremely hypofractionated (HF) prostate radiotherapy (RT) with active correction for prostate intrafraction motion. We have collected an extensive 4D cine-MR dataset to study the intrafraction motion of the prostate during the period of a RT fraction. Previously, we have presented a method for accurate automatic prostate tracking based on fiducial gold markers (ESTRO 37). Now we present a method for soft-tissue contrast based tracking that obviates the need for fiducial markers on an MR-Linac.

#### Material and Methods

Thirty patients undergoing HF prostate RT had repeated cine-MR imaging sessions after each of five weekly fractions in a multicenter Medical Ethics board approved study. Each cine-MR session consisted of 55 sequentially obtained 3D datasets ('dynamics'), acquired with a balanced 3D gradient echo sequence and a voxel spacing of 0.96x0.96x2mm<sup>3</sup>. Each dynamic was acquired over an 11 second period, with the cine-MR session covering a 10 minute period, similar to the duration of a RT fraction. A clinician delineated the prostate on the first dynamic from

which in-house developed Python code performed soft-tissue (ST) tracking of the prostate in subsequent dynamics using a mutual information metric and rigid transformations. We validated the performance of the ST algorithm with previously obtained, ground truth marker tracking (MT) data of the same dataset.

**Results**

The algorithm was applied to 7645 dynamics from 139 sessions with a mean processing time of  $5.47 \pm 0.77$  sec (mean $\pm$ stdev) per dynamic. The success rate (difference between MT and ST result < 1 mm) was 98.93%. We found group translations after 10 minutes of  $0.05 \pm 0.81$ mm for X (LR),  $0.83 \pm 1.90$ mm for Y (AP),  $-0.90 \pm 1.85$ mm for Z (CC) and corresponding rotations of  $-0.49 \pm 2.13^\circ$  about X,  $0.09 \pm 0.58^\circ$  Y and  $0.09 \pm 0.73^\circ$  for Z. After 10 min, 12% of all sessions had demonstrated a 3D displacement > 5 mm. Linear regression and Pearson correlation analysis indicated a good correlation and non-significant difference with all p-values <  $1e^{-5}$  between the ST and MT algorithm in the X (R=0.934), Y (R=0.966) and Z (R=0.953) directions as shown in Fig. 1. An overview of the ST intrafraction visualization tool is provided in Fig. 2, showing the rotation, translation and full 3D segmentation of the prostate at a specific time point.

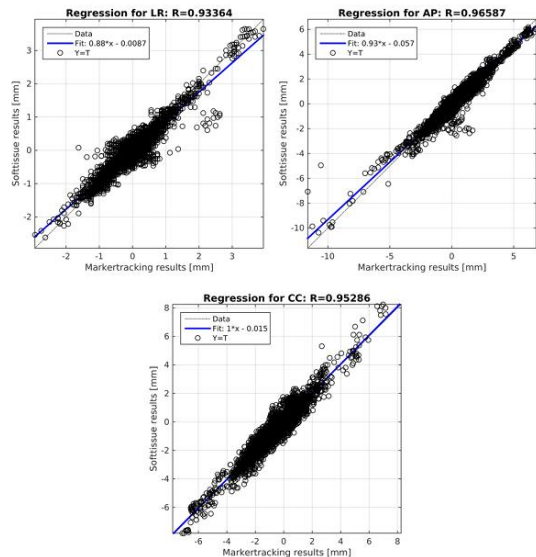


**Figure 1:** Overview of the linear regression analysis between the ST and MT algorithm results in the three translation directions.

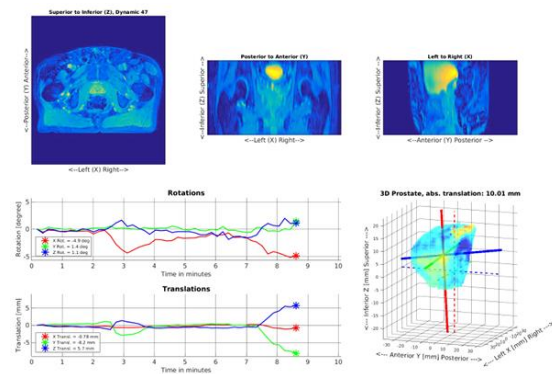


**Figure 2:** Overview of the prostate intrafraction visualization tool, showing the different slices of the prostate, the found rotations and translations and the current 3D segmentation of the prostate.

**Conclusion**

We have developed a fast, robust and accurate ST tracking algorithm in cine-MR data which was validated against marker tracking. The presented method for soft-tissue contrast based tracking obviates the need for surgically implanted fiducial markers during MR-guided prostate RT on an MR-Linac.

**OC-0411 Geometric efficacy of breath-hold gated MR-guided SABR for adrenal metastases**

J. Van Sornsen de Koste<sup>1</sup>, M. Palacios<sup>1</sup>, A. Bruynzeel<sup>1</sup>, F. Spoelstra<sup>1</sup>, B. Slotman<sup>1</sup>, F. Lagerwaard<sup>1</sup>, S. Senan<sup>1</sup>  
<sup>1</sup>Amsterdam UMC- Vrije Universiteit Amsterdam- VU Medical Center, Department of Radiation Oncology, Amsterdam, The Netherlands

**Purpose or Objective**

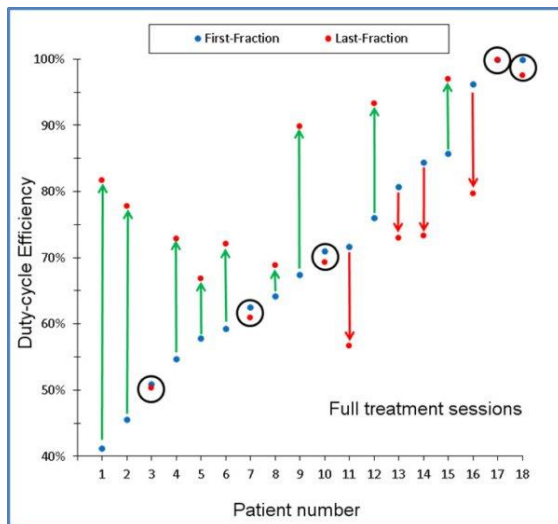
Magnetic Resonance (MR) guided stereotactic ablative radiotherapy (SABR) improves target coverage and reduces organ-at-risk doses. We studied target coverage and breath-hold performance in patients undergoing MR-guided adrenal SABR.

**Material and Methods**

Breath-hold SABR data from 18 patients treated on a MRIdian unit (ViewRay Inc) was analyzed. Real-time tumor tracking during SABR was performed using repeated fast planar MR imaging in a single sagittal plane, at 4 frames-per-second with 3.5mm x 3.5mm in-plane resolution via deformable image registration. An in-room MR-compatible monitor projects sagittal images to allow patient visualization of tracked GTV (GTV<sub>t</sub>) and PTV (GTV+3mm) contours. Simulation MR-imaging is performed in quiet inspiration. A delivery threshold-ROI% determines the maximum permitted percentage of GTV<sub>t</sub>-area that can be outside the PTV-area, before a beam-hold is triggered. Breath-hold related tumor coverage during SABR was analyzed for 82 fractions (40 hours of MR-cine series). For each fraction, we analyzed: [1] geometric coverage of GTV<sub>t</sub> within PTV; [2] duty-cycle efficiency; [3] stability of breath-holds during each session [4] beam-off latency effects on target coverage using a 500msec system-latency time as a worst case scenario.

**Results**

Different threshold-ROI% settings were used (range 7-20%), but 75% of fractions used a 15% threshold-ROI. Mean geometric GTV<sub>t</sub> coverage was 94.2% (5<sup>th</sup>-95<sup>th</sup> Percentile range: 90.6%-96.7%); corresponding mean duty-cycle efficiency was 71.7% (range: 45.5%-99.5%). Average duty-cycle efficiency increased from 70.5% during the first fraction, to 76.7% during the last fraction (Figure), and treatment delivery times decreased from 32.4 to 28.6 minutes, respectively (p<0.04). Gating efficacy in patients during the initial 10 minutes of SABR delivery correlated with efficacy during the full SABR session (~ 31 minutes). On average, beam latency effects had marginal impact on GTV<sub>t</sub> coverage during repeated inspiration breath-holds, leading to a reduction in mean GTV<sub>t</sub> coverage by only -0.9%. Increased latency effects were seen when (i) relatively short breath-hold gates occurred in combination with mean large tumor motion (>15mm, Peak-to-Peak), (ii) both very short and high frequent gates occurred, and (iii) different breathing phases were used during gating (e.g. mid-ventilation), leading to system-latency effects causing up to -3.0% in mean GTV<sub>t</sub> coverage. Analysis of the first, middle and last fractions revealed that some patients used different breathing phases than light inspiration in 10/54 fractions; in those patients latency effects increased for tumors showing an initial mean motion >12mm.



Comparison of first and last SABR fractions: Duty-cycle efficiency increased in nine patients (green arrows), decreased in four patients due to an increase tumor motion amplitude (red arrows), and remained stable in five other patients in both low and high efficiency ranges (black circles). Small tumor motion amplitude generally results high duty cycle efficiency.

### Conclusion

In breath-hold adrenal SABR, use of visual MR feedback achieved high geometric tumor coverage, but beam latency effects increased in patients who performed subsequent breath-holds in other phases of respiration.

**OC-0412 Dosimetric impact of marker-based intrafraction motion from cine-MRI in prostate SBRT**  
 C. Kontaxis<sup>1</sup>, D. De Muinck Keizer<sup>1</sup>, L. Kerkmeijer<sup>1</sup>, H. De Boer<sup>1</sup>, B. Raaymakers<sup>1</sup>  
<sup>1</sup>UMC Utrecht, Radiotherapy department, Utrecht, The Netherlands

### Purpose or Objective

To investigate the effect of intrafraction translation and rotation motion, as extracted from 3D cine-MRI based on fiducial marker tracking, on the dose distributions of extremely hypofractionated (SBRT) prostate patients.

### Material and Methods

Twenty prostate patients treated with extremely hypofractionated radiotherapy (4 mm CTV to PTV margin,  $5 \times 7$  Gy, with focal boosts up to  $5 \times 10$  Gy) underwent weekly cine-MRI within an Ethical Review Board approved study. Fiducial marker-based online corrections were applied during treatment. Each cine-MRI session consisted of a balanced 3D gradient echo sequence, acquiring one volume every 11 sec over 10 min. A marker tracking algorithm was used to obtain the prostate marker-based intrafraction motion in subsequent dynamics for each session (ESTRO 37). The fiducial positions from the first cine-MR dynamics were registered to the planning CT, thus transferring the local cine-MRI motion to the CT coordinate system. Then for each patient fraction, the treatment plan delivery consisting of two VMAT arcs was played back, by proportionally splitting the MUs into 11 sec intervals leading to 33 partial plans during a 6 min delivery. For each partial plan, the corresponding volume was generated by applying the cine-MRI rigid transformation to the CT, the partial dose was calculated using our research treatment planning system and was then warped back to the reference volume by using the inverse transformation. The mean $\pm$ SD translations (mm) were  $0.04 \pm 0.79$  (LR),  $0.4 \pm 1.9$  (AP),  $-0.5 \pm 1.73$  (CC) and rotations (degrees) were  $-0.84 \pm 2.91$  (LR),  $0.13 \pm 1.15$  (AP),  $0.25 \pm 1.84$  (CC) among all patients and timepoints. For each fraction the 33 partial doses were summed leading to the accumulated fraction and total treatment dose

(INTRA) which was compared to the original reference (REF) dose.

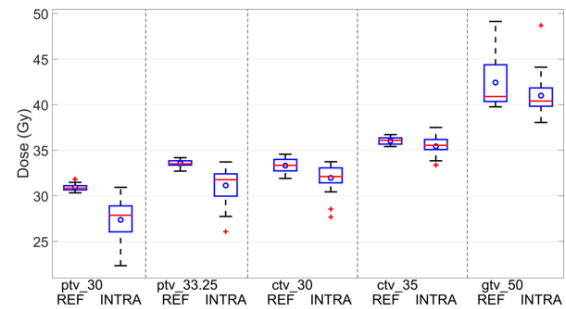


Figure 1: Boxplots including the D99% DVH point of the different target structures: CTV\_35 corresponds to the prostate, CTV\_30 to the seminal vesicles along with their corresponding PTV expansions and integrated GTV\_50

### Results

Figure 1 shows the D99% point of the target structures between REF and INTRA dose for these 20 patients. The PTVs (average decrease of  $9.4 \pm 6.8\%$ ) ensured the full CTV/GTV coverage for 80% patients. The average drop in D99% coverage for CTV\_35 (prostate) and CTV\_30 (seminal vesicles) was  $1.7 \pm 2.8\%$  and  $4.1 \pm 4.7\%$  respectively while the GTV dropped by  $3.2 \pm 3.6\%$  with a mean dose reduction of  $2.8 \pm 2.4\%$ . Figure 2 shows boxplots of the Dmax for rectum and urethra respectively. Rectum Dmax (40 Gy) was exceeded in 4 cases while V35Gy was stable ( $0.1 \pm 1.1\%$ ).

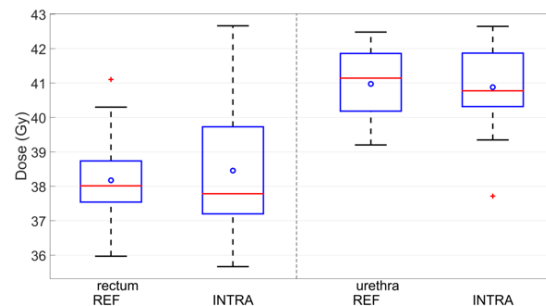


Figure 2: Boxplots including the Dmax DVH point of Rectum and Urethra OARs

### Conclusion

We have simulated the dosimetric impact due to prostate intrafraction motion as extracted by marker-based tracking on cine-MRI for extremely hypofractionated treatments. Evaluating the impact of intrafraction motion with such high spatial and temporal resolution has now become possible with MRI-linacs. The analysis presented is essential to establish the optimal inter/intrafraction adaptation strategies for MRI-guided radiotherapy, which will ensure continuous online target coverage while safely decreasing margins. We are now working towards a full dosimetric analysis of both targets and OARs for more patients.

**OC-0413 MR-derived signals for respiratory motion models evaluated using sagittal and coronal datasets**  
 E.H. Tran<sup>1</sup>, B. Eiben<sup>1</sup>, A. Wetscherek<sup>2</sup>, U. Oelfke<sup>2</sup>, G. Meedt<sup>3</sup>, D.J. Hawkes<sup>1</sup>, J.R. McClelland<sup>1</sup>

<sup>1</sup>University College London, Medical Physics and Biomedical Engineering, London, United Kingdom ; <sup>2</sup>The Institute of Cancer Research and the Royal Marsden NHS Foundation Trust, Joint Department of Physics, London, United Kingdom; <sup>3</sup>Elekta, Medical Intelligence Medizintechnik GmbH, Schwabmünchen, Germany

### Purpose or Objective

MR-Linac systems can provide 2D cine-MR images to monitor the motion of a tumour during beam delivery, enabling gated or tracked radiotherapy treatments.

Respiratory motion models can potentially estimate the motion of the full 3D anatomy using internal surrogate signals extracted from the real-time 2D images. In this study, we used 2D motion models to quantitatively evaluate potential surrogate signals with data from lung cancer patients.

#### Material and Methods

Surrogate cine-MR images from a fixed location and with sagittal orientation were used to generate surrogate signals by tracking the diaphragm motion, and performing principal component analysis (PCA) on image intensities, or PCA on deformation fields (DFs) resulting from deformable registration of the images. The surrogate images were interleaved in time with motion images from another fixed location. The motion images had sagittal orientation for 8 datasets and coronal orientation for 4 datasets. Deformable image registration was used to measure the motion in the motion images relative to an end-exhale reference image. The registration algorithm can account for sliding motion by taking a sliding interface (manually defined for each dataset) as input. The motion images were divided into a training set and a test set. Linear correspondence models were fit to the motion measurements using a variable number of training images and the corresponding interpolated surrogate signals. The models driven by the surrogate signals were used to estimate the motion for the test images. The different surrogate signals were evaluated by calculating the deformation field error (DFE) which is the difference between the DFs estimated by the model and the DFs from the sliding registration.

#### Results

The motion models are able to model the sliding motion. Figure 1 shows an example of the estimated DFs for a sagittal and a coronal dataset respectively. Figure 2 reports the mean of the L2 norm of the DFE against the number of training images for the different surrogate signals. For each dataset the mean DFE was computed over all pixels of all test images within the sliding interface (excluding the gastrointestinal organs) and averaged over all datasets for each slice orientation. The mean DFE when not using a motion model was equal to 3.41 mm for the sagittal datasets and 4.54 mm for the coronal datasets. The models for the different surrogate signals all give good results when using 8 or more training images, with mean DFEs below the in-plane pixel size (1.98 mm).

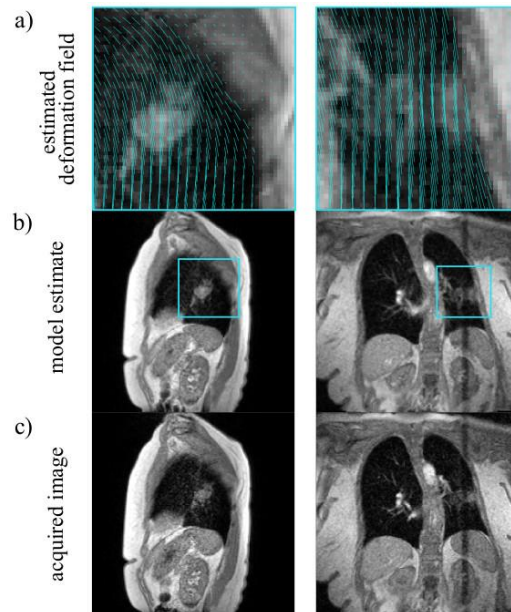


Figure 1. Model estimates using PC1 and PC2 on DFs as surrogate signals for a sagittal (left) and a coronal (right) dataset. a) DF estimated by the model in a region containing the tumour, showing the sliding motion of the lung. b) Motion image estimated by the model and obtained by warping the reference image with the estimated DF. c) Corresponding acquired motion image.

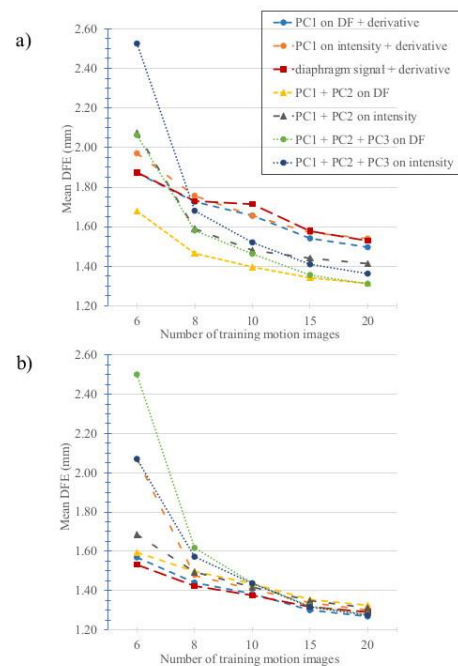


Figure 2. Mean of the L2 norm of the DFE for different numbers of training motion images with sagittal (a) and coronal (b) orientation. The different combinations of signals used to build and drive the motion models are indicated with different lines and colors.

#### Conclusion

The investigated surrogate signals are suitable to model the 2D motion, including sliding, in both sagittal and coronal planes, using few training images. Future work will extend the study to 3D motion models from multi-slice MR images. The 3D models can potentially estimate the motion of the tumour as well as the organs-at-risk during treatment on an MR-Linac from 2D cine surrogate images, and facilitate accurate dose calculations.

**OC-0414 Intrafraction displacement of breast tumor (bed) and individual axillary lymph nodes on cine MRI**  
 M. Groot Koerkamp<sup>1</sup>, H.J.G.D. Van den Bongard<sup>1</sup>, M.E.P. Philippens<sup>1</sup>, J.J.W. Lagendijk<sup>1</sup>, A.C. Houweling<sup>1</sup>  
<sup>1</sup>UMC Utrecht, Radiotherapy, Utrecht, The Netherlands

### Purpose or Objective

The purpose of this study was to evaluate intrafraction displacement of breast tumor (bed) and individual axillary lymph nodes (LN) on cinematic MRI (cine) scans. Evaluation of displacement in local and regional target regions will help us to assess the potential impact of these displacements on future MRI-guided (stereotactic) RT for breast cancer patients.

### Material and Methods

2D cine scans (0.3-0.6s/slice) of 25 breast cancer patients participating in an MR imaging study were acquired on a 1.5T MRI scanner. Transverse-sagittal interleaved imaging of the breast was performed in both prone and supine position. Coronal-sagittal interleaved imaging of regional LNs was performed in supine position only. Additionally, sagittal cine scans (0.3s/slice) of LNs of 7 healthy volunteers were assessed. All cine scans were acquired during 1-3 minutes of free breathing.

Intrafraction displacement in the cine scans was investigated with an optical-flow algorithm. With this method we applied a deformable registration of the cine scan frames to a reference frame of the same cine series. The mean displacement of pixels within a region of interest was calculated to determine tumor (bed) or LN displacement with respect to the reference frame. In preoperative patients the visible tumor or biopsy marker was chosen as the region of interest; in postoperative patients the best visible surgical clip was used. The maximum peak-to-peak difference (Figure 1) was determined in left-right (LR), superior-inferior (SI), and anterior-posterior (AP) direction.

### Results

In total 40 cine scans of LNs (17 patients, 7 volunteers), and 21 cine scans of the breast (6 pre- and 4 postoperative patients) in prone (12) and supine (9) position were analyzed (Figure 1). The median maximum displacement for LNs was around 2mm in all directions (Table 1). Tumor or surgical clip position in prone position was very stable (median maximum displacements around 1mm in all directions). In supine position median maximum displacements were 1.5mm in LR, 2.6mm in SI, and 3.7mm in AP direction.

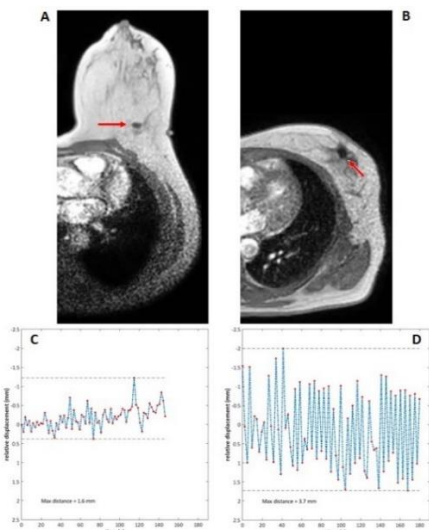


Figure 1. Prone (A) and supine (B) cine scans for intrafraction tumor displacement analysis with AP displacements (C and D) in two different breast cancer patients. This example illustrates that on average the maximum displacement in AP direction was larger in supine position than in prone position.

Table 1. Median maximum [range] intrafraction displacements [mm] in individual axillary lymph nodes and breast tumor (bed).

	Lymph nodes		Tumor (bed)*			
	Median (range)	# cine scans	Prone median (range)	# cine scans	Supine median (range)	# cine scans
Left-Right	1.9mm (1.2 – 4.1mm)	33	1.0mm (0.2 – 1.9mm)	12	1.5mm (0.8 – 3.4mm)	7
Superior-Inferior	2.1mm (0.9 – 3.9mm)	34	0.9mm (0.1 – 1.4mm)	11	2.6mm (1.1 – 3.1mm)	9
Anterior-Posterior	1.9mm (0.7 – 3.8mm)	34	1.2mm (0.7 – 1.9mm)	12	3.7mm (2.6 – 6.5mm)	7

\* In preoperative patients: tumor or biopsy marker depending on visibility;  
 In postoperative patients: best visible surgical clip

### Conclusion

Intrafraction displacement of both the tumor (bed) and axillary lymph nodes was small. With the current PTV margins (5-8mm) these displacements are not clinically relevant. However, the displacements should be considered for future MRI-guided stereotactic (single fraction) breast RT with smaller PTV margins, e.g. for tumor-positive LNs or partial breast irradiation. For local stereotactic breast RT, prone positioning might be beneficial, since the displacements in the breast were smaller in prone than in supine position, especially in AP direction.

### Proffered Papers: RTT 4: Reducing uncertainties in volume definition

#### OC-0415 MERINO study: Defining a standardised delineation method for repeated GTV assessment using DW MRI

A. Duffton<sup>1</sup>, I. McCrea<sup>2</sup>, S. Allwood-Spiers<sup>3</sup>, L. Hay<sup>4</sup>, L. Devlin<sup>4</sup>, M. Sankaralingam<sup>3</sup>, M. Thomson<sup>4</sup>, P. McLoone<sup>5</sup>, M. McJury<sup>3</sup>, J. Foster<sup>3</sup>, C. Paterson<sup>6</sup>

<sup>1</sup>Inst. of Cancer Sciences-Univ. Glasgow, Research & Development Radiographer, Glasgow, United Kingdom ;

<sup>2</sup>Queen Elizabeth University Hospital, Department of Radiology, Glasgow, United Kingdom ; <sup>3</sup>Beatson West of Scotland Cancer Centre, Department of Clinical Physics and Bioengineering, Glasgow, United Kingdom ; <sup>4</sup>Beatson West of Scotland Cancer Centre, Radiotherapy, Glasgow, United Kingdom ; <sup>5</sup>University of Glasgow, West of Scotland cancer surveillance unit, Glasgow, United Kingdom ; <sup>6</sup>Beatson West of Scotland Cancer Centre, Clinical Oncology, Glasgow, United Kingdom

### Purpose or Objective

Diffusion-weighted MRI (DW MRI) enhances anatomical imaging obtained from MR, by providing information on the cellularity of tumours by measuring Brownian motion. Studies show promising results in defining a threshold change in ADC that predicts non-responders to treatment. However, these studies have; low patient numbers, include a number of sub-sites, and often don't describe the delineation method. The overall aim of the MERINO study is to determine threshold change in ADC that determines responders from non-responders, which may allow intensification of RT treatment for those who require it [1].

The aim of this work is to:

- Quantify primary gross target volume (GTV) change between; baseline MR (GTV\_T1\_Base) to repeat MR (GTV\_T1\_Rpt) as defined on T1 post contrast fat sat (T1PCFS) anatomical imaging, and baseline MR (GTV\_b0\_Base) to repeat MR (GTV\_b0\_Rpt) on DW MRI.
- Describe a standardised method of defining a region of interest (ROI) to allow repeated measurements within clinical studies

### Material and Methods

This is a prospective observational imaging study (REC approval (15/WS/0159). Patients with intermediate and high risk, locally advanced SCC oropharynx (OPSCC)

receiving radical RT or chemo-RT(65Gy in 30 fractions) were eligible for the study.

DW- MRI images were acquired immediately prior to fraction 1, and repeated immediately before 11. MRI scans were acquired on a GE Signa 1.5T HDxT scanner including T1PCFS image with slice thickness of 3mm. Diffusion weighted images were acquired using a single shot EPI sequence with five b-values between 0 and 1000 s/mm<sup>2</sup>. Parallel imaging was utilised to reduce distortion in the images. Apparent diffusion coefficient (ADC) maps were calculated using a monoexponential fit.

A clinical oncologist, radiologist and RTT delineated GTV on axial slices on MR baseline and repeat MR to evaluate volume change. For ADC measurements, a ROI was defined on T1PCFS, copied to DW b=0 image, slightly adjusted for artefacts and patient motion. This volume was then copied to the ADC map. To ensure ROI include only disease, an inner margin of 1mm was created. ADC was recorded for each ROI, and % ADC change was calculated.

**Results**

20 patients with intermediate-high risk, locally advanced OPSCC were included in the analysis. Primary GTV volumes were successfully delineated in 18/20 patients using the described method Figure 1. Mean (SD,range) GTV\_T1\_Base was 15.1cm<sup>3</sup> (8.5, 3.3-34.2) with GTV\_T1\_Rpt volume reducing to 8.3cm<sup>3</sup> (6.3, 0.1-18.1). On b value 0 images, GTV\_b0\_Base volume was 12.4cm<sup>3</sup> (8.1, 2.1-26.1), reducing to 6.9cm<sup>3</sup> (5.6, 0.1-17.0) on GTV\_b0\_Rpt.

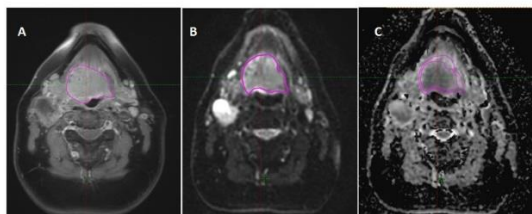


Figure 1. Images showing method of delineation used to define ROI. Primary GTV on: A - T1PCFS image, B – b=0 image, C – ADC map. Primary GTV with inner margin of 1mm shown on C.

**Conclusion**

There are many challenges in quantifying ADC as a predictor of outcome. We imported MR scans into the treatment planning system, allowing 3D ROI to be created. Here we described a standardised method of creating a ROI for repeated assessment of volume change and ADC within a large clinical study. MERINO study will use these analytical method for all patients.

1.Paterson, C et al.The MeRInO study.Clinical and Translational Radiation Oncology , Volume 2 , 13 - 18

**OC-0416 Assessing the quality of oesophageal cancer target volume delineation in the SCOPE1 trial**

S. Cox<sup>1</sup>, S. Gwynne<sup>1</sup>, J. Staffurth<sup>2</sup>, T. Crosby<sup>2</sup>  
<sup>1</sup>South West Wales Cancer Centre, Oncology Department, Swansea, United Kingdom; <sup>2</sup>Velindre Cancer Centre, Oncology Department, Cardiff, United Kingdom

**Purpose or Objective**

The SCOPE1 trial, which standardised RT planning within the UK, demonstrated survival rates for oesophageal cancer patients treated with definitive chemoradiotherapy (dCRT) comparable with the best published results worldwide. We present the planned retrospective analysis of adherence to the trial protocol for target volume delineation (TVD).

**Material and Methods**

A single RT plan was selected at random from each of the 32 centres. Using the Global Harmonisation Group’s (GHG) system for classifying RT protocol adherence, each step (protocol item) of TVD was retrospectively assessed. RT

plans without deviations were graded as ‘acceptable-per protocol’. Variations in TVD which were unlikely to affect the trial outcome were graded as ‘acceptable’, whilst those with a potential impact graded as ‘unacceptable’. Unacceptable deviations were further categorised according to their potential impact on tumour control probability (TCP) and toxicity. An initial review was conducted by an experienced RTQA reviewer; plans with deviations underwent a secondary review by the RTQA lead for the SCOPE2 trial. Reviewers were blinded to the trial treatment arm & recruiting centre.

**Results**

32 RT plans were reviewed (19 upper/mid and 13 lower third oesophageal tumours) with 463 protocol items in total (figure 1). Overall, 15 (47%) plans were deemed to have either acceptable or no deviations, the majority of which had upper/mid oesophageal tumours; 9 (28%) such plans did not have any deviations at all. 17 (53%) plans had at least one unacceptable deviation, the majority being lower third oesophageal tumours. The pre-trial benchmark test case was for a mid-oesophageal tumour; lower third TVD and elective lymph node irradiation (ELNI) is more complex and was not assessed with a benchmark case which may explain the higher number of unacceptable deviations for this sub site. When the total number of protocol items was assessed, 413 (89.2%) were acceptable-per protocol; 18 (3.9%) were graded as acceptable deviations. 28 (6.0%) protocol items were graded as unacceptable, 8 (1.7%) of which were deemed unlikely to affect tumour control probability (TCP) or treatment-related toxicity rates (table 1).

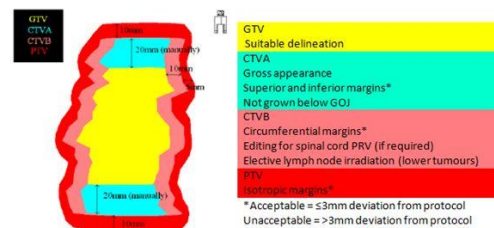


Figure 1: TVD protocol for SCOPE1 and assessment criteria for deviations  
 Abbreviations: GTV – gross tumour volume; CTV – clinical target volume; GOJ – gastro-oesophageal junction; PRV – planning risk volume; TV – planning target volume

	Potential to increase treatment-related toxicity n (%)	Unlikely to affect treatment-related toxicity n (%)	Total n (%)
Potential impact on TCP n (%)	2/463 (0.4%) <i>Most commonly relating to inadequate ELNI</i>	11/463 (2.4%) <i>Most commonly relating to inadequate ELNI</i>	13 (2.8%)
Unlikely to affect TCP n (%)	7/463 (1.5%) <i>Most commonly relating to CTVa stopping at GOJ</i>	8/463(1.7%) <i>Most commonly relating to CTVa inferior margin</i>	15 (3.2%)
Total n (%)	9/463 (1.9%)	19/463 (4.1%)	28 (6.0%)

Table 1: Frequency of unacceptable deviations according to potential impact on clinical outcomes  
 Abbreviations: CTV – clinical target volume, ELNI – elective lymph node irradiation; GOJ – gastro-oesophageal junction; TCP – tumour control probability

**Conclusion**

Adherence to the TVD protocol in this sample from SCOPE1 was high with only 4.3% of protocol items graded as unacceptable deviations with potential clinical impact. Our results show that even with a detailed TVD protocol and benchmark case, clinically significant errors still occur. As RTQA programmes are being streamlined appropriate benchmark cases need to be carefully considered, especially for trials that may introduce a new standard of care.

### OC-0417 Impact of CT myelogram vs. MR imaging on spinal cord delineation in spine stereotactic radiosurgery

C.J. Jin<sup>1</sup>, N. Tyagi<sup>2</sup>, E. Lis<sup>3</sup>, M. Patel<sup>1</sup>, J. Haseltine<sup>1</sup>, P. McLaughlin<sup>4</sup>, X. Cai<sup>1</sup>, X. Huang<sup>1</sup>, Y. Yamada<sup>1</sup>

<sup>1</sup>Memorial Sloan Kettering Cancer Center, Radiation Oncology, New York, USA; <sup>2</sup>Memorial Sloan Kettering Cancer Center, Medical Physics, New York, USA;

<sup>3</sup>Memorial Sloan Kettering Cancer Center, Neuroradiology, New York, USA ; <sup>4</sup>Dana-Farber Cancer Institute- Harvard Medical School, Radiation Oncology, Boston, USA

#### Purpose or Objective

Accurate identification of spinal cord and cauda equina is paramount for spine stereotactic radiosurgery (SRS). This study investigates the inter-observer variability in contouring spinal cord (SC), cauda equina (CE) and thecal sac (TS) using CT myelogram vs. MRI T2 sequences.

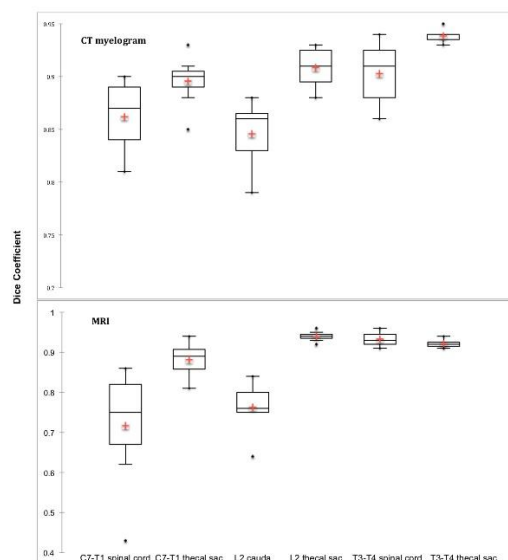
#### Material and Methods

7 radiation oncology (RO) observers (3 ROs and 4 RO residents) and 1 diagnostic neuroradiologist (DR) delineated SC, CE, and TS in the regions of interest for 6 spine SRS cases. Cases included 3 with CT myelogram pre-simulation and 3 with diagnostic MR spine fusion. Cases were evenly distributed between the junctional (C7-T1), mobile (L2), and semirigid (T3-T4) spine. Inter-observer variability was quantified using volumetric coefficient of variation (VCV), mean Hausdorff distance (HD), and the Dice coefficient (DSC). Segmentation variability in relation to imaging modality and spinal region was analyzed using the Wilcoxon rank sum test.

#### Results

In total, 96 contours were analyzed within the CT myelogram and MRI datasets. Across the 6 cases, no significant difference was found in mean VCV for CT myelogram vs MRI (10.7% vs 12.3%  $P = .675$ ). The mean HD between RO and DR contours was significantly lower for CT vs MRI (0.32 vs 0.46 mm  $P = .008$ ). The mean DSC agreement between RO and DR contours was  $0.89 \pm 0.04$  for CT and  $0.89 \pm 0.11$  for MRI ( $P = .063$ ). Substantial differences in contour variability were seen in different spine locations. The mean VCV for SC/CE contours based on MRI varied across the junctional (21.1%), mobile (25.5%), and semirigid (10.1%) spine, while there was less variability based on CT myelogram (14.0%, 13.4%, and 16.3% respectively). TS volumes were less variable across all spine locations (mean VCV 6.3% TS vs 16.7% SC/CE,  $P = .036$ ). Mean HD between RO and DR contours was significantly greater in the junctional vs semirigid spine for both SC (0.57 vs 0.19 mm,  $P = .002$ ) and TS (0.49 vs 0.26 mm,  $P = .005$ ), and this difference persisted across imaging modalities (CT: 0.37 vs 0.21 mm,  $P = .002$ ; MR: 0.68 vs 0.24 mm,  $P = .003$ ). Similarly, the DSC agreement was significantly lower in the junctional vs semirigid spine for SC (0.78 vs 0.92,  $P = .003$ ) and TS (0.89 vs 0.93,  $P = .001$ ), for both imaging modalities (CT: 0.88 vs 0.92,  $P = .001$ ; MR: 0.79 vs 0.93,  $P = .003$ ). Compared to RO volumes, DR volumes were larger for SC/CE ( $P = .036$ ) and TS ( $P = .036$ ), particularly for the MRI dataset ( $P = .036$ ), with a similar trend for the CT myelogram dataset ( $P = .059$ ).

Figure: DSC agreement between RO and DR contours based on CT myelogram and MRI.



#### Conclusion

Inter-observer variability differences in contouring SC, CE, and TS between CT myelogram and MRI were minor. CT myelogram produces slightly better agreement between RO and DR contours, but similar segmentation can be achieved from either imaging modality when there is no registration error. Contouring uncertainties that need to be considered include the greater inter-observer variability in the junctional spine, and the comparatively larger DR volumes.

### OC-0418 Residual misalignment of supraclavicular lymph nodes for NSCLC patients, to determine GTV-PTV margin

J. Stam<sup>1</sup>, S. Gerrets<sup>1</sup>, R. De Haan<sup>1</sup>, J. Belderbos<sup>1</sup>, E. Damen<sup>1</sup>, P. Remeijer<sup>1</sup>

<sup>1</sup>Netherlands Cancer Institute, Department of Radiation Oncology, Amsterdam, The Netherlands

#### Purpose or Objective

For locally advanced non-small cell lung cancer (NSCLC) patients besides the primary tumor, the mediastinal lymph nodes and supraclavicular lymph nodes (SLN) are often involved. In case of SLN involvement a thermoplastic mask is used for immobilization. For the SLN a GTV-PTV margin of 1-1.2 cm in all directions is used in our institute. In this analysis the positioning-errors of the SLN were evaluated to determine the optimal GTV-PTV margin to cover involved SLN adequately.

#### Material and Methods

A total 720 CBCT's of 30 patients with a fractionated treatment dose > 44Gy were analyzed. All patients were positioned on a thorax support and immobilized with a thermoplastic mask. The IMRT treatment plan included the primary tumor, mediastinal lymph nodes and SLN in one isocenter. For each fraction online CBCT registrations were performed using a 3D rectangular shaped region-of-interest (ROI) around the vertebrae (Clipbox 1) and a ROI around the carina (Clipbox 2) followed by an online table shift to correct for the carina misalignment. When the spinal cord dose was critical, the table shift was performed based on the vertebrae registration instead. To measure the residual set up error of the SLN, a grey value registration was performed using an additional ROI around the SLN (Clipbox 3), see figure 1. After the automatic grey

value registration of Clipbox 3, the position of the SLN was visually checked. If necessary, the registration was manually adapted to make sure the position of the SLN was correct.

Next, the residual errors of the SLN lymph nodes relative to the carina and vertebrae registration were analyzed. For both residuals the grand mean ( $M$ ), systematic errors ( $\Sigma$ ) and random errors ( $\sigma$ ) were calculated. From these results the required GTV to PTV margins were derived using the margin recipe from van Herk et. al., taking delineation uncertainty and intra-fraction motion [1] in account as well.

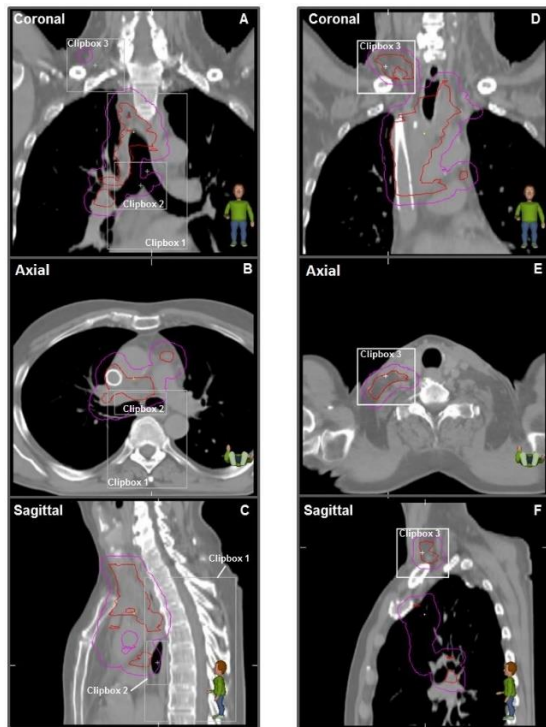


Figure 1. Example of the three clipboxes used for the CBCT registrations. Clipbox 1 (vertebrae) and Clipbox 2 (carina) are shown in a coronal, axial and sagittal view in respectively picture A, B and C. Clipbox 3 (SLN) is shown in a coronal, axial and sagittal view in respectively picture D, E and F.

**References** 1. A. Licup, Data mining in RT: Intrafraction motion and treatment time analysis for SBRT lung cancer patients (ESTRO37 2018)

**Results**

For all CBCT's a successful SLN registration was performed, automatically or either after manual adaptation. The mean, systematic and random error (translations and rotations) for the SLN in relation to the correction based on the vertebrae or carina are summarized respectively in table 1. A and B.

Table 1: Grand mean, systematic ( $\Sigma$ ) and random error ( $\sigma$ ) for the SLN relative to the Vertebrae (A) and the Carina (B) position. LR: left-right, CC: cranial-caudal, AP: anterior-posterior							
		LR (mm)	CC (mm)	AP (mm)	Roll (deg)	Pitch (deg)	Yaw (deg)
A Vertebrae	Mean	0.28	0.65	0.29	0.39	-0.18	0.05
	$\Sigma$	0.87	1.70	1.67	0.85	1.01	0.77
	$\sigma$	1.30	1.45	1.45	1.03	1.14	1.07
	Margin	7	9	9			
B Carina	Mean	-0.11	0.85	0.68	-0.09	0.29	-0.22
	$\Sigma$	1.39	3.27	1.92	0.90	0.97	0.63
	$\sigma$	1.45	1.73	1.57	0.98	1.04	0.97
	Margin	8	12	9			

**Conclusion**

Positioning errors of the SLN lymph nodes were analyzed for locally advanced NSCLC patients using a thermoplastic mask. Based on the found results the initial GTV-PTV margin of 1-1.2 cm in our institute could be reduced as following: in case the table correction was based on the vertebrae registration, the required GTV-PTV margin for

the SLN was LR: 7 mm, CC: 9 mm and AP: 9 mm. When the table correction was based on the carina registration, the required GTV-PTV margin for the SLN was LR: 8 mm, CC: 12 mm and AP: 9 mm.

**OC-0419 Evaluation of Metabrain: a semi-automated delineation tool for edema surrounding brain metastasis**

Y. Pin<sup>1</sup>, D. Antoni<sup>1</sup>, A. Keller<sup>1</sup>, P. Truntzer<sup>1</sup>, J. Clavier<sup>1</sup>, O. Schaeffer<sup>1</sup>, M. Schmitt<sup>1</sup>, W. Waissi<sup>1</sup>, G. Noël<sup>1</sup>  
<sup>1</sup>Centre de Lutte Contre le Cancer Paul Strauss, Radiation Oncology, Strasbourg, France

**Purpose or Objective**

The edema surrounding brain metastasis (BM) was the subject of several studies but the measurement methods remain controversial. The edema volume is an objective and relatively reproducible feature but its determination by contouring is time consuming which can limit its use. In this study, we propose and test a semi-automated tool to segment brain edema and measure its volume in patients with BM.

**Material and Methods**

We developed Metabrain, a threshold based automated segmentation tool to extract edema surrounding BMs on FLAIR sequence MRI. Developed in Python, the software imports image datasets and BMs GTV contours. Each edema, corresponding to a BM, is segmented and its volume measured based on a windowing (level and width) manually defined by the user. A contouring study was performed to assess the reliability and similarity of Metabrain contours. Ten BM edemas were contoured two times by 9 radiation oncologists: manually (MC) and with Metabrain (AC). A Dice index (DI) was calculated in the MC and AC groups, compared to the intersection of all contours in each group. The DI was also calculated between each manual and automated contour of each edema for each radiation oncologist. The volume of each edema and the total time for manual and automated contouring were recorded. DI, volumes and contouring time were compared using a paired Wilcoxon signed rank test. Contouring time and DI were compared between experimented physicians and residents.

**Results**

Ninety manual and semi-automated edemas were delineated. One edema on ten was removed because it was in contact with the skull and lead to an aberrant segmentation. In the AC group, the DI was significantly better than in the MC group (median DI of 0.95 vs 0.81,  $p < .001$ ) and the contouring time significantly shorter (18 vs 40 minutes,  $p = 0.01$ ). The median volume was significantly lower in the AC group than in the MC group (respectively a median volume of 1.89 and 2.16 mL,  $p < .001$ ). The median DI between manual and Metabrain contours from a same radiation-oncologist was 0.80. No significant difference was found in DI and contouring time between experimented physicians and residents.

**Conclusion**

Metabrain is an efficient tool to measure the volume of edema surrounding brain metastasis. It performs contours more similar, accurate and time saving than manual contouring. Its use would make it easier to include the volume of cerebral edema in BM studies.

**OC-0420 How accurate is automatic determination of the Mid-Ventilation position and tumour motion?**

A. Van Nunen<sup>1</sup>, D. Schuring<sup>1</sup>  
<sup>1</sup>Catharina hospital, Radiotherapy, Eindhoven, The Netherlands

**Purpose or Objective**

Different approaches can be applied to determine target position and PTV margins for lung cancer patients. In our hospital the Mid-Ventilation (MidV) approach is used. For quantifying the MidV position (MidV-P) and tumour motion,

several manual actions have to be performed which are time consuming, and interobserver variation can occur. An automatic procedure can reduce the workload and variability. Aim of this study was to compare the results of the manual approach with the automatic approach using the Deformable Image Registration (DIR) module in RayStation.

#### Material and Methods

For 23 patients, the automatic procedure was applied and compared to the manually determined MidV. The tumour was delineated at one of the 10 reconstructed phases of the 4D CT-scan. This delineation is then copied to the other phases and translated manually to the correct position. For the automatic approach, all phases were registered deformably to the 0% phase scan using the Anaconda algorithm. To improve the DIR in the close proximity of the tumour, a 2 cm expansion was used as focus region. After visually inspecting the DIRs (figure 1), the delineated tumour was propagated automatically to the other phases. The center of mass position of the translated or propagated contour was used for calculating the MidV-P and tumour motion.

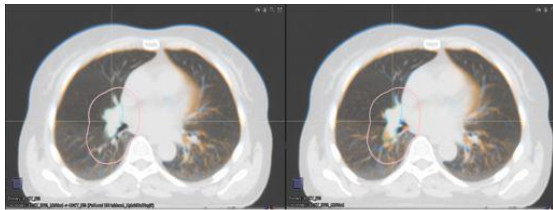


Figure 1: Transversal CT slice with the results of a DIR (left) compared to the rigid registration (right). (pink = focus region and lightblue = tumour)

#### Results

For all patients, the DIRs were considered acceptable for calculating the MidV-P and tumour motion. The difference in MidV-P was  $0.0 \pm 0.5$  mm in LR direction,  $0.4 \pm 1.0$  mm in CC direction and  $0.1 \pm 0.6$  mm in AP direction (mean  $\pm$ SD). For 22/23 patients the maximum difference in position was 2 mm and a high correlation was found in all directions. For 4/23 patients a difference in tumour motion larger than 2 mm was observed (figure 2). The mean difference in tumour motion was  $0.6 \pm 0.8$  mm in LR direction,  $0.1 \pm 1.4$  mm in CC direction and  $0.2 \pm 0.9$  mm in AP direction (mean  $\pm$ SD). These variations are similar to the interobserver variation for the manual procedure. For one patient, manual determination of the MidV-P and tumour motion was difficult due to poor soft tissue contrast between tumour and surrounding tissue. This resulted in a difference in MidV-P in the CC direction of 3.6 mm and a difference in tumour motion in LR and CC direction of 2.4 and 4.4 mm respectively. By using the automatic approach with the enlarged focus region, the surrounding vessels are included in this region to obtain more consistent results compared to the manual approach.

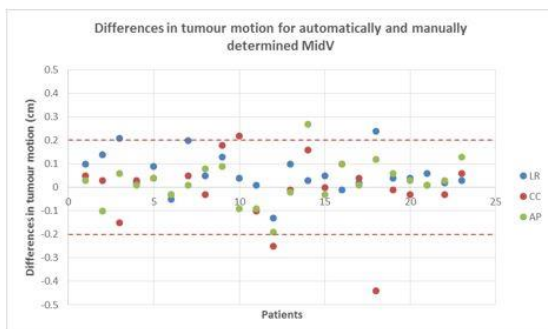


Figure 2: difference in tumour motion for automatically and manually determined MidV for all directions.

#### Conclusion

MidV determination based on DIR is accurate. A high correlation was found in MidV-P for the evaluated methods and the differences in tumour motion were small. Different results were found for patients with poor soft tissue contrast between tumour and surrounding tissue. For these patients, the automatic approach can reduce the interobserver variation and can obtain more consistent results by using an enlarged focus region. The automated method is now clinically used to determine tumour motion and MidV-P.

#### OC-0421 Stage migration in planning PET/CT scans in lung cancer patients referred to radiochemotherapy

S. Kivistik<sup>1</sup>, L. Randle<sup>1</sup>, M. Vardja<sup>1</sup>, A. Aasa<sup>1</sup>, J. Jaal<sup>1</sup>  
<sup>1</sup>Tartu University Hospital, Dept of Radiotherapy and Oncological Therapy, Tartu, Estonia

#### Purpose or Objective

With recent advances in immune-oncology and the introduction of checkpoint inhibitors into clinical practice, the treatment landscape of lung cancer has changed dramatically. Immune checkpoint inhibitors can be used as adjuvant therapy after completion of radiochemotherapy in stage III non-small cell lung cancer (nsclc) and as systemic treatments in stage IV nsclc as well as small-cell lung cancer (sclc). Cancer treatment costs are rising, therefore, it is extremely important to assure that patients receive most effective treatment at the right time based on the exact stage of the disease. In our institution, 18-fluoro-deoxyglucose positron emission tomography (FDG-PET) is mostly used for patients that are considered to have stage III disease based on previous computed tomography (CT) findings and are consequently referred to receive radiochemotherapy. The aim of this study was to assess the impact of radiotherapy planning PET-CT on stage migration in these patients.

#### Material and Methods

The stage migration after PET-CT was evaluated in 82 patients referred to our department to receive radiochemotherapy. All patients were previously assessed in multidisciplinary team meetings (including radiologist) and had stage III disease based on available CT scans.

#### Results

Out of 82 patients, 65 had nsclc (79%) and 17 sclc (21%). After planning PET-CT, metastatic stage IV disease was detected in 31 lung cancer patients (38%). The stage migration was seen in 22 patients (34%) with nsclc and in 9 patients (53%) with sclc. In nsclc, metastases were most frequently found in bones (55%), lymph nodes (55%), lungs (32%), pleura (23%), adrenal glands (18%) and liver (9%). In sclc, metastases were most frequently detected in lymph nodes (67%), bones (22%), lungs (11%), pleura (11%) and liver (11%). Radiochemotherapy was given to 45 patients (88%) with locoregional disease. Some patients did not receive radiochemotherapy due to refusal (n=1), treatment in another hospital (n=1), or not acceptable mean lung dose (n=4).

#### Conclusion

In the situation, where PET-CT is not routinely used for staging of all lung cancer patients and it is mainly utilized for radiotherapy planning, significant stage migration can be detected. Big proportion (38%) of lung cancer patients that were previously considered to have stage III disease showed metastatic lesions after planning PET-CT. This study confirms that proper selection of patients with PET-CT is mandatory to guarantee optimal use of cancer care resources.

Poster Viewing : Poster viewing 8: TP Developments

PV-0422 Consequences of respiratory motion variability in lung 4DMRI datasets

M. Krieger<sup>1,2</sup>, A. Giger<sup>3</sup>, D.C. Weber<sup>1,4</sup>, A.J. Lomax<sup>1,2</sup>, Y. Zhang<sup>1</sup>

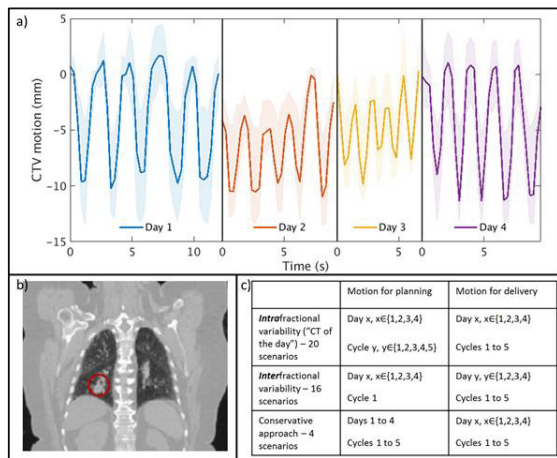
<sup>1</sup>Paul Scherrer Institute, Centre for Proton Therapy, Villigen PSI, Switzerland ; <sup>2</sup>ETH Zurich, Department of Physics, Zurich, Switzerland ; <sup>3</sup>University of Basel, Center for medical Image Analysis and Navigation CIAN-Department of Biomedical Engineering, Basel, Switzerland ; <sup>4</sup>University Hospital Zurich, Department of Radiation Oncology, Zurich, Switzerland

### Purpose or Objective

To investigate the consequences of respiratory motion pattern variability on ITV definition for treatment planning and 4D dosimetric evaluation.

### Material and Methods

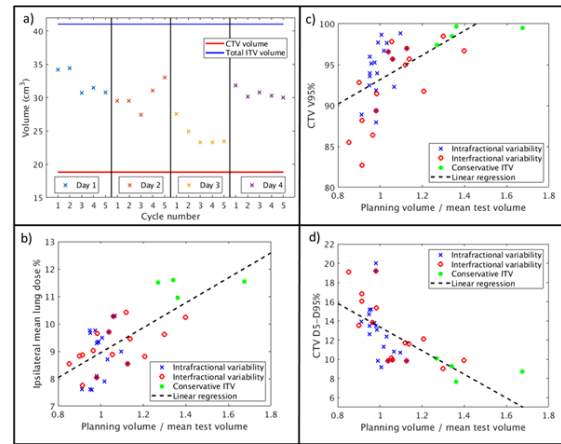
Synthetic 4DCT (4DCT(MRI)) data sets (Fig. 1b) have been generated by warping a single phase 3DCT using multiple motions extracted from 4DMRI datasets of a single subject (Boye et al 2013, Med.Phys. 40(6)). 20 such 4DCT(MRI) data sets have been generated from 20 respiratory cycles (128 phases) with large amplitude/period variations (Fig. 1a), which were then sorted as 4 sub-datasets (each of 5 cycles), each of which simulates motions that might occur on four different fractions. To evaluate the influence of *intra*- and *inter*-fractional motion variabilities from this data, two field PBS proton treatment plans were optimised on different geometric ITVs by considering several definitions (see Fig. 1c for details of each scenario). 4D dose calculations were applied to quantify the dosimetric effects by assuming different motion scenarios during dose delivery, using 9 volumetric rescans in order to minimise the influence of the interplay effect. Additionally, a ‘conservative’ ITV was calculated as a reference by considering all cycles together. Planning was performed on phase-averaged 4DCT(MRI) data sets, but using maximum intensity projections within the ITV. The resulting 4D dose distributions were analysed in terms of CTV coverage and homogeneity (V95%, D5-D95%) as well as mean lung dose. Linear regression was used to extract trends between relative ITV volumes and the aforementioned dose parameters.



### Results

Based on 4DMRI extracted motions, mean ITV size (29.4cc) was 156% of the static CTV (18.8cc), with large variations of ITV size of up to ±20% (range: 23.3-34.4cc) observed depending on the considered motion cycle during treatment planning (see Fig. 2a). Coverage (range: 82.7%-99.7%) and homogeneity (range: 7.7%-20.0%) for all 4D plan scenarios (Fig. 2c-d) show a clear trend of improved coverage and homogeneity for plans optimised on the larger ITVs and encountering smaller motions during delivery ( $R^2=0.39$  for D5-D95%, 0.28 for V95%). Moreover, considering the conservative ITV, the volume is between 16% and 43% larger than any individual ITV and induced a

significantly ( $R^2=0.46$ ) increased mean lung dose of up to 57% (range: 7.6%-11.6%, Fig. 2b). Generally, dosimetric impacts due to the variation of ITV volume definition are larger for *inter*-fractional than *intra*-fractional variability.



### Conclusion

The ITV defined at treatment planning phase can vary up to ±20% depending on the motion cycle considered by a 4DCT and could become invalid when motions are considerably different during dose delivery, thus substantially compromising the quality of the dose delivered in a fraction. Thus, careful consideration of motion variability is required for 4D treatments at both planning and delivery phase.

### Acknowledgement

This study was funded by Swiss National Science Foundation grant No 320030\_163330/1.

### PV-0423 Fast automated IMRT sequencing using deep-learned dose from generative adversarial networks

C. Kontaxis<sup>1</sup>, G. Bol<sup>1</sup>, J. Lagendijk<sup>1</sup>, B. Raaymakers<sup>1</sup>

<sup>1</sup>UMC Utrecht, Radiotherapy Department, Utrecht, The Netherlands

### Purpose or Objective

In this work we utilize generative adversarial networks (GANs) to perform fast dose prediction along with a two-step IMRT optimization pipeline capable of fast automated plan optimization for prostate radiotherapy.

### Material and Methods

A conditional GAN network was trained to predict the 3D clinical dose distributions from data of previously treated patients in our clinic. For 291 prostate patients the masks of the relevant optimization volumes, including bladder, rectum, femur heads, PTV and EBV were calculated. Then, for each 3 mm transversal PTV slice, a 256x256 image of the combined masks and background Hounsfield Units was extracted along with its corresponding slice from the clinical dose distribution of that patient (Figure 1). For each input mask slice  $i$ , a three-channel image was formed by placing slice  $i-1$  into red, slice  $i$  into green and slice  $i+1$  into blue channel respectively; in a caudal-to-cranial direction encoding the local 3D anatomical information into the 2D image. Then, the pix2pix framework was used to train the network with the data of 215 patients, totalling 5907 images. The resulting network was used to predict the dose distribution for the remaining independent 76 patients per slice. The 2D slices are then concatenated into the final predicted 3D dose distribution and fed into our previously developed Adaptive Sequencer (ASEQ) to perform IMRT optimization generating deliverable plans targeting that input dose. ASEQ is an IMRT optimizer which uses a per-voxel dose prescription along with minimum/maximum weights to penalize under- and overdosage. For automated planning a generic weights set is selected following the clinical structure priority:

bladder (low), rectum, PTV, EBV (high).

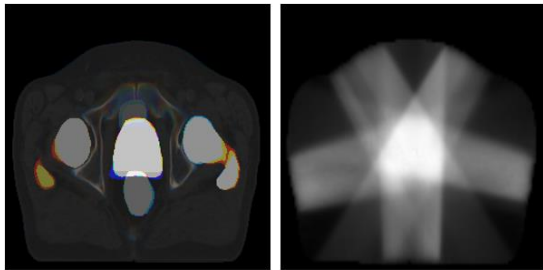


Figure 1: Input (left) / target (right) pair for one 2D transversal slice

## Results

The GAN network was trained over 75 epochs. The average difference between the 3D predicted and clinical dose distributions was  $0.1\% \pm 2.6\%$  and  $0.9\% \pm 1.9\%$  for PTV and EBV among 76 patients. For 5 patients, ASEQ was used to generate automated IMRT plans targeting the predicted dose (Figure 2). The average difference between the clinical and ASEQ dose was  $-1.1\% \pm 3.1\%$  and  $-0.3\% \pm 2.4\%$  for PTV and EBV while bladder and rectum were more spared ( $10.7\%$  and  $3.6\%$  on average). Total time per patient for dose prediction and plan optimization was 47 and 109 sec respectively.

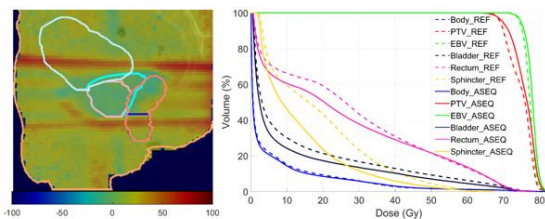


Figure 2: Central sagittal slice of the relative dose difference (%) between the clinical (REF) and ASEQ dose distribution (positive value means REF is higher) (left) and DVH plot of the relevant structures (right) for one case

## Conclusion

We demonstrate that conditional GAN networks can be used to accurately predict the 3D dose distribution of prostate patients. Moreover, the GAN output can be directly used into our fast automated optimization as a voxel-by-voxel prescription to generate deliverable plans closely matching the clinical plans. Application of this pipeline can be twofold: the initial dose prediction could assist the radiation therapist during the offline plan generation, while in an MRI-linac setting the ASEQ pipeline can be used for fast plan generation on an online inter/intrafraction basis. We are now evaluating automated plan generation for all test patients and further exploring both the network and ASEQ-specific parameters.

### PV-0424 Deliverable multi-criteria navigation for VMAT in RayStation

R. Bokrantz<sup>1</sup>

<sup>1</sup>RaySearch Laboratories, Research, Stockholm, Sweden

#### Purpose or Objective

To develop and evaluate a method for deliverable multi-criteria VMAT navigation: a form of real-time planning based on exploration of a Pareto surface represented by a set of plans and their linear combinations. Navigation has conventionally relied on Pareto surface representations composed of plans generated by fluence map optimization. Such a representation necessitates a post-processing step where the navigated dose is converted to control points, which can degrade the dose. Deliverable navigation, in contrast, uses plans that are segmented into control points in combination with a control point interpolation technique that after the navigation is used

to collapse the Pareto surface plans into a single deliverable plan. The goal is to make the navigated dose as realistic as possible representation an achievable dose distribution.

#### Material and Methods

The multi-criteria optimization (MCO) module of RayStation (RaySearch Laboratories) was augmented with the capability to generate Pareto surfaces composed of VMAT plans represented by control points. All plans were made to satisfy a movement pattern where the MLC leaves sweep back and forth across the target volume as the gantry rotates, defined such that the leaf motion was unidirectional within sub-sectors of an arc. A deliverable plan was, following navigation, constructed by interpolation of the leaf trajectories of the Pareto surface plans. The interpolated trajectories were sampled into control points at equispaced gantry angles and the control points optimized towards minimization of any dose error relative to the navigated dose.

#### Results

The new form of MCO was evaluated for three patients (head and neck, lung, and brain with multiple metastases). All patients were planned for treatment with a 360-degree arc. For each patient, a Pareto surface was generated using a fast optimization dose algorithm. A navigated dose satisfying the patient's clinical goals was then identified and this dose converted to a deliverable plan. Final dose for the deliverable plan was calculated using an accurate dose algorithm and the accuracy between this dose and the navigated dose then assessed. The resulting differences are quantified in Table 1 and summarized qualitatively as DVHs in Figure 1.

Table 1. Voxelwise dose differences between the navigated dose and the deliverable plan, with differences corresponding to an improved dose (a dose closer to the prescription level for targets and closer to zero otherwise) truncated to zero.

	Average (cGy)	90 <sup>th</sup> percentile (cGy)	98 <sup>th</sup> percentile (cGy)
<b>Head and neck</b>			
PTV 69	16	52	91
PTV 50	24	76	129
Healthy tissues $\geq 20$ Gy	31	101	366
<b>Lung</b>			
PTV 70	12	37	65
Healthy tissues $\geq 20$ Gy	15	17	247
<b>Brain</b>			
PTV 54	11	30	43
PTV 48	9	20	30
PTV 42	4	13	35
Healthy tissues $\geq 20$ Gy	13	24	202

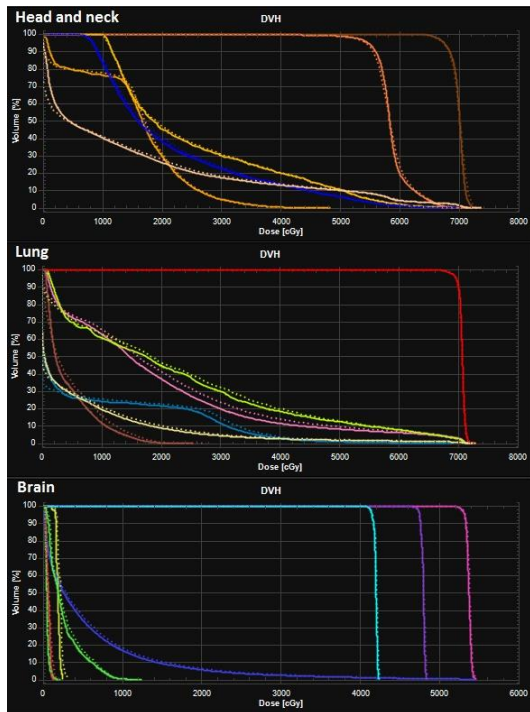


Figure 1. DVH comparison between the deliverable plan (solid lines) and the navigated dose (dotted lines).

**Conclusion**

A form of multi-criteria navigation for VMAT that gives only minor or negligible errors between the deliverable plan and the navigated dose has been demonstrated. A highly realistic navigated dose has the potential to simplify clinical decision making and improve planning efficiency thanks to a decreased or eliminated need for manual tuning after the conversion of the navigated dose into a deliverable plan.

**PV-0425 Automated configuration of an algorithm for fully automated Pareto-optimal treatment planning**  
 R. Van Haveren<sup>1</sup>, B. Heijmen<sup>1</sup>, S. Breedveld<sup>1</sup>  
<sup>1</sup>Erasmus Medical Center Rotterdam Daniel den Hoed Cancer Center, Radiation Oncology, Rotterdam, The Netherlands

**Purpose or Objective**

The Lexicographic Reference Point Method (LRPM) is a novel algorithm for automated, fast and consistent generation of clinically favourable Pareto-optimal treatment plans. Current configuration of the LRPM requires manual tweaking of the algorithm’s parameters. This is a labour-intensive and time-consuming trial-and-error procedure. We propose a novel configuration method to automatically tune the algorithm’s parameters based on historical treatment plans. We demonstrate the method for prostate, and head and neck (HN) cancer.

**Material and Methods**

The LRPM for fast automated multi-criterial treatment planning has previously been introduced for generating Pareto-optimal plans with clinically favourable trade-offs between all plan criteria. The proposed novel configuration method generates a single LRPM configuration per treatment site. Validation was performed with patient/plan databases for prostate cancer (287 plans) and HN cancer (105 plans). All database plans were generated with an in-house developed clinically applied algorithm for automated multi-criterial planning (other than LRPM).

Configuration of the LRPM was based on 90 training plans for prostate cancer and 30 plans for HN cancer. For each criterion, differences between the training plans and

LRPM generated plans were compared. To steer towards relevant trade-offs between all criteria for all training patients, the user specifies preferences for each criterion. E.g., for prostate cancer, the preferences encourage reducing high rectum dose and mean bladder dose, while retaining similar PTV coverage and allowing slight degradation in mean anus dose. The quality of the automatic LRPM configurations was tested by comparing database plans with LRPM generated plans for 197 prostate cancer evaluation patients (not used for training) and 75 HN evaluation patients.

**Results**

With the automatically generated LRPM configurations, all automatically LRPM generated plans had sufficient PTV coverage ( $V_{95\%} \geq 99\%$  for prostate,  $V_{95\%} \geq 98\%$  for HN). For the evaluation patients, differences in OAR doses between database plans and LRPM generated plans (both Pareto-optimal) are shown in fig. 1 (prostate) and fig. 2 (HN) using boxplots. Medians of criteria differences marked with \* were statistically significantly different from zero (paired two-sided Wilcoxon signed-rank test,  $p < 0.05$ ). For prostate cancer, the LRPM generated plans had on average a decreased high rectum dose at the cost of slight increases in mean anus dose and maximum dose to the femoral heads (while still within constraints). For HN, we found more variation: generally, the LRPM generated plans had large improvements for some criteria at the cost of slight degradations for other criteria.

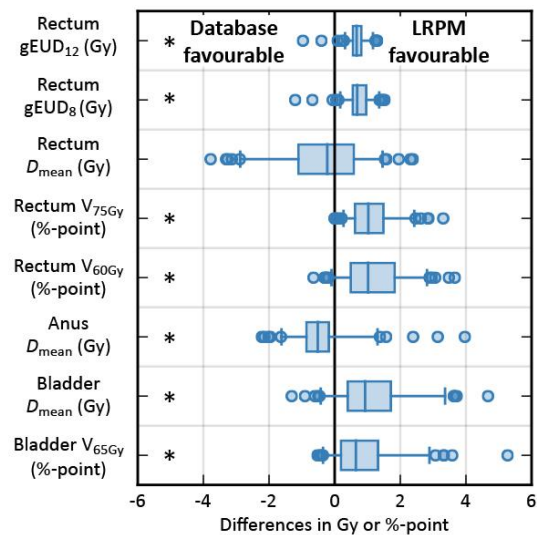
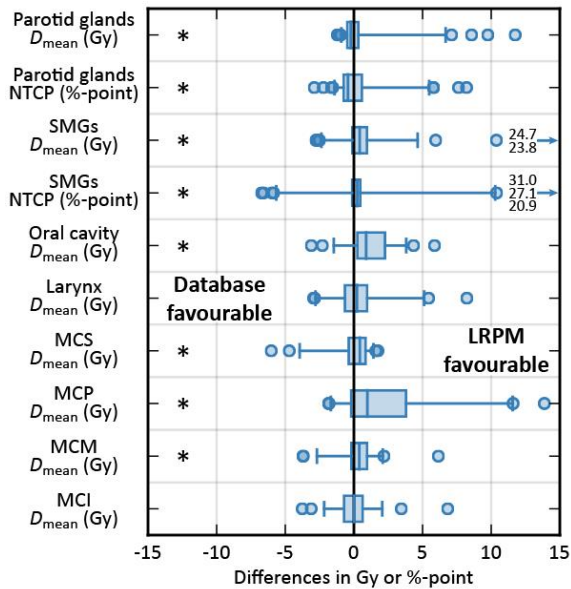


Figure 1. Plan parameter differences between database plans and LRPM generated plans for the 197 prostate evaluation patients. Vertical lines in boxes are medians, boxes are within 1<sup>st</sup> and 3<sup>rd</sup> quartile, whiskers are between the 2.5<sup>th</sup> and 97.5<sup>th</sup> percentile, and circles are outliers.



**Figure 2.** Plan parameter differences between database plans and LRPM generated plans for the 75 HN evaluation patients. Vertical lines in boxes are medians, boxes are within 1<sup>st</sup> and 3<sup>rd</sup> quartile, whiskers are between the 2.5<sup>th</sup> and 97.5<sup>th</sup> percentile, and circles are outliers. Arrows display values of large outliers outside of the specified range.

### Conclusion

The novel method for automatic configuration of the LRPM resulted in clinically favourable Pareto-optimal treatment plans. Due to the vast reduction in configuration workload, a major obstacle for introducing large-scale automated multi-criterial planning with the LRPM has been overcome.

### PV-0426 First system for fully automated multi-criterial planning for an MR-Linac applied to rectal cancer

R. Bijman<sup>1</sup>, L. Rossi<sup>1</sup>, T. Janssen<sup>2</sup>, P. De Ruijter<sup>2</sup>, C. Carbaat<sup>2</sup>, B. Van Triest<sup>2</sup>, S. Breedveld<sup>1</sup>, J.J. Sonke<sup>2</sup>, B. Heijmen<sup>1</sup>

<sup>1</sup>Erasmus MC Cancer Center, Radiation Oncology, Rotterdam, the Netherlands ; <sup>2</sup>The Netherlands Cancer Institute, Radiation Oncology, Amsterdam, The Netherlands

### Purpose or Objective

High-quality Pareto-optimal treatment plans are mandatory for MR-Linac (MRL) treatment units to maximally benefit from the offered high geometrical accuracy. In this study we have adapted our system for fully automated multi-criterial planning on regular linacs for plan generation on a 1.5T MRL. We evaluated automated MRL planning for rectal cancer by comparing automatically and manually generated plans regarding planning workload and plan quality.

### Material and Methods

A fully automated planning workflow for generation of clinically deliverable Pareto-optimal plans was implemented by coupling the in-house Erasmus-iCycle optimizer to a dedicated version of the Monaco TPS (Elekta AB, Sweden). The integrated system can handle the dosimetric impact of the magnetic field, enlarged source-isoc. distance, etc. 15 rectal cancer patients were manually planned for a 9-beam Step and Shoot IMRT treatment, delivering 50 Gy in 25 fractions. The 9 fixed beam directions were selected to avoid irradiation through the MRL cryostat pipe and the high attenuation regions of the MRL treatment couch. Automated plans were generated with the same beam directions as used for

the manual plans. The clinical protocol was leading in both manual and automated plan generation and evaluation. For the healthy tissues the goal was to maximally reduce the mean dose in a composite OAR consisting of small-bowel-bag + bladder excluding overlaps with the PTV. For consistent plan comparisons based on the OAR sparing, all plans were rescaled such that 95% of the PTV received 99% of the prescribed dose, as required by the clinical protocol. The two-sided paired Wilcoxon signed rank test was applied for statistical analyses.

### Results

Differences in plan quality are presented in Table 1. With equal PTV coverage and PTV D<sub>99%</sub>, automated plans had favourable V<sub>107%</sub> and homogeneity index (HI). Compared to the manual plans, the OAR D<sub>mean</sub> was reduced in the automated plans by 1.2 Gy (6.4%) on average and a maximum reduction of 4.2 Gy (21.3%). A large reduction in planning time was obtained, going from ~4-6 hours per patient for manual plans (mainly hands-on time) to ~1-2 hours per patient (mainly computational time).

**Table 1** Comparison of dosimetric parameters for manual plans and automated plans for 15 rectal cancer patients.

PTV	Parameter	Manual		Manual – Automated			
		Mean	SE	Mean	Range	SE	P (Wilcox)
PTV	V <sub>99%</sub> [%]	99*	-	0*	-	-	-
	D <sub>99%</sub> [Gy]	95*	-	0*	-	-	-
	V <sub>107%</sub> [%]	0.3	0.04	0.2	[-0.4 – 0.5]	0.06	0.02
	D <sub>mean</sub> [Gy]	50.2	0.03	-0.1	[-0.8 – 0.8]	0.1	0.3
	CI	0.5	0.01	-0.05	[-0.3 – 0.3]	0.04	0.2
	HI [%]	9.5	0.08	0.8	[-0.7 – 2.5]	0.2	0.003
Composite OAR	D <sub>mean</sub> [Gy]	19.1	0.5	1.2	[-1.0 – 4.2]	0.8	0.004

\* all plans normalized to 99%, \* related to plan normalization, SE = standard error, PTV = planning target volume, OAR = organ at risk, CI = conformity index, HI = homogeneity index

### Conclusion

A system for fully automated multi-criterial planning for a high magnetic field MR-Linac has been developed and tested for rectal cancer patients. Plan quality of automated plans was better with an improvement in OAR dose. Automated planning resulted in a major reduction in manual planning workload.

### PV-0427 Improving cumulative dose evaluation for re-irradiation: first results from the STRIDeR project

L. Murray<sup>1,2</sup>, S. Gregory<sup>3</sup>, M. Nix<sup>3</sup>, M. Aldred<sup>3</sup>, L. Aspin<sup>3</sup>, J. Uzan<sup>4</sup>, J. Lilley<sup>3</sup>, B. Al-Qaisieh<sup>3</sup>, A. Appelt<sup>1,3</sup>

<sup>1</sup>University of Leeds, Leeds Institute of Cancer and Pathology, Leeds, United Kingdom ; <sup>2</sup>Leeds Cancer Centre, Department of Clinical Oncology, Leeds, United Kingdom ; <sup>3</sup>Leeds Cancer Centre, Department of Medical Physics, Leeds, United Kingdom ; <sup>4</sup>Raysearch Laboratories, Service Department, Stockholm, Sweden

### Purpose or Objective

Accurately evaluating cumulative doses in the re-irradiation (reRT) setting is challenging due to anatomical and positional changes between radiotherapy courses. Furthermore, treatment planning systems (TPS) do not routinely incorporate radiobiology (e.g. fraction size correction) into dose summation. The STRIDeR (Support Tool for Re-Irradiation Decisions guided by Radiobiology) project aims to develop a software tool for use in a commercially available TPS to address these issues and so facilitate more informed reRT. We evaluated three approaches to dose summation, incorporating anatomical change and radiobiology to differing extents.

### Material and Methods

Ten patients who received pelvic reRT were included. All originally had conventionally fractionated radiotherapy. ReRT was Stereotactic Ablative Radiotherapy (SABR, 30Gy/5 fractions) to oligometastatic nodal disease in the previously irradiated pelvis. For clinical reRT planning, permitted doses to organs at risk (OAR) were at the

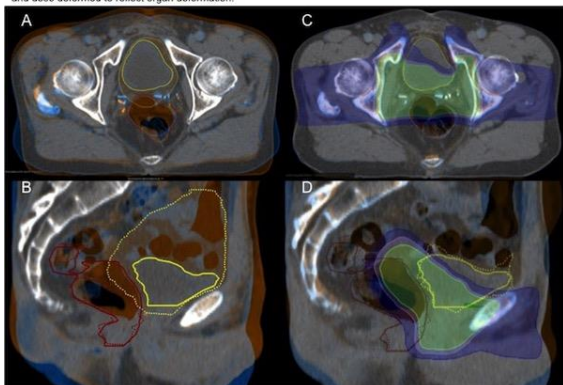
clinicians' discretion, after review of the former treatment plan.

Using RayStation (RaySearch Laboratories, Stockholm, Sweden), cumulative doses were calculated in 3 ways:

1. Rigid image registration (RIR) of former and reRT plans with physical dose summation (current clinical standard)
2. RIR with full radiobiological dose
3. e summation (i.e. each dose distribution converted to equivalent dose in 2Gy fractions (EQD2), then summated, using  $\alpha/\beta=3\text{Gy}$  for all tissues, except nerves, where  $\alpha/\beta=2\text{Gy}$ )
4. Deformable image registration (DIR) with dose mapping and radiobiological dose summation as per 2. above (Fig. 1).

Registrations were assessed by two clinicians who considered all DIR images of greater clinical relevance than RIR images.

Figure 1. Example case. A and B: rigid registration: solid line represents reRT contours and dotted line represents former radiotherapy contours. Substantial difference in bladder volume between courses apparent. C and D: deformable registration with dose mapping and radiobiologically summed dose distribution: solid line represents reRT contours and dotted line represents deformed former radiotherapy contours. Bladder volumes now more similar and dose deformed to reflect organ deformation.



## Results

Table 1 shows cumulative OAR doses based on each strategy. Summated physical doses (Strategy 1) should not be evaluated against constraints given the different dose per fraction from each treatment course, potentially masking OAR overdose. For example, incorporating radiobiology (Strategy 2) revealed that one patient received cumulative maximum EQD2 of 94.8/106.9/119.5Gy to colon/small bowel/sacral plexus, not appreciated at the time of clinical plan prescription, or identified by physical dose summation. By incorporating DIR and radiobiology (Strategy 3), for 11/114 threshold/maximum doses, there was  $\geq 20\%$  difference in cumulative EQD2 (range -33 to +43%) compared to RIR with radiobiology, affecting at least one OAR in 7/10 cases: cumulative doses were lower based on DIR in 5/7.

Table 1. Cumulative doses

	Threshold volume (used in addition to maximum dose constraints for selected OAR)	Strategy 1: Rigid registration with physical dose summation		Strategy 2: Rigid registration with dose summation in EQD2		Strategy 3: Deformable registration with dose summation in EQD2	
		Median of Dose to threshold volume (range)	Median of Maximum doses to 0.5cm <sup>3</sup> * (range)	Median of Dose to threshold volume (range)	Median of Maximum doses to 0.5cm <sup>3</sup> ** (range)	Median of Dose to threshold volume (range)	Median of Maximum doses to 0.5cm <sup>3</sup> ** (range)
Small bowel	5cm <sup>3</sup>	19.4 (4.6-63.4)	26.2 (6.1-77.8)	21.0 (3.2-73.8)	33.1 (4.4-106.9)	15.3 (2.9-58.6)	31.4 (4.2-90.1)
Colon	-	-	52.6 (17.5-73.5)	-	55.9 (18.9-94.8)	-	53.3 (18.4-70.0)
Rectum	-	-	53.1 (36.4-73.8)	-	59.7 (42.1-73.5)	-	59.2 (41.9-72.1)
Vessels	-	-	35.1 (27.7-79.3)	-	61.8 (36.5-116.6)	-	61.6 (37.1-86.9)
Sacral plexus*	5cm <sup>3</sup>	24.0 (13.6-62.3)	35.6 (23.7-79.2)	21.6 (10.2-82.5)	53.2 (23.5-119.5)	20.6 (9.4-78.2)	53.8 (25.2-95.6)
Cauda equina*	5cm <sup>3</sup>	9.7 (2.4-14.6)	9.0 (3.2-34.1)	9.1 (1.3-14.3)	8.1 (1.6-40.5)	9.0 (1.2-14.4)	8.1 (1.6-34.6)
Bladder	15cm <sup>3</sup>	53.1 (35.0-65.6)	54.0 (35.8-83.0)	59.8 (39.8-66.6)	61.3 (41.2-110.1)	54.6 (36.4-67.1)	61.1 (41.3-110.7)
Left femoral head**	10cm <sup>3</sup>	38.7 (19.3-48.1)	-	35.8 (16.9-44.9)	-	35.5 (16.7-42.1)	-
Right femoral head**	10cm <sup>3</sup>	40.2 (7.7-50.2)	-	38.8 (5.5-46.0)	-	38.9 (5.6-45.5)	-

\*Dose to 0.1cm<sup>3</sup> presented for neural structures; \*\*Maximum doses to femoral heads not used clinically so not reported

## Conclusion

Evaluation of cumulative doses in the reRT setting has traditionally been crude. Physical dose summation is radiobiologically meaningless, thus clinically unhelpful. An approach that incorporates radiobiology has revealed cases where OARs received higher doses than intended. DIR substantially influenced dosimetry in 70% of cases. We have developed a clinically implementable solution for radiobiological dose summation. This can be applied in many situations, including reRT and adaptive radiotherapy.

## PV-0428 A multi-centre study for implementation of MRI-only prostate planning

P. Greer<sup>1,2</sup>, P. Pichler<sup>1</sup>, T. Young<sup>3</sup>, J. Martin<sup>1,4</sup>, P. Hunter<sup>1</sup>, C. Wratten<sup>1,4</sup>, J. Denham<sup>1,4</sup>, L. Holloway<sup>3,5</sup>, M. Sidhom<sup>3,5</sup>, J. Dowling<sup>6</sup>

<sup>1</sup>Calvary Mater Newcastle Hospital, Department of Radiation Oncology, Newcastle, Australia; <sup>2</sup>University of Newcastle, School of Mathematical and Physical Sciences, Newcastle, Australia; <sup>3</sup>Liverpool Hospital, South Western Sydney Radiation Oncology, Sydney, Australia; <sup>4</sup>University of Newcastle, School of Medicine and Public Health, Newcastle, Australia; <sup>5</sup>University of New South Wales, South Western Sydney Clinical School, Sydney, Australia; <sup>6</sup>CSIRO, E-Health Research Centre, Brisbane, Australia

## Purpose or Objective

MRI-only planning is a departure from conventional CT based planning practice where dose calculations are performed on artificially created pseudo-CT (pCT) scans. It is paramount that procedures and processes are developed to ensure the safe implementation of this new technology. This project aims to investigate whether MRI-only prostate planning can be implemented effectively and safely in a prospective multi-centre study.

## Material and Methods

The protocol was a 2 phase design, where for phase 1 centres that had not previously validated MRI-only plans recruited 5 patients for retrospective analysis. Following successful completion of this phase centres then recruited to the prospective MRI-only treatment phase. To date 22 patients have been recruited and analysed across two treatment centres with 17 prospective. Whole-pelvic MRI scans were converted to pCT using an established atlas-based method. Dose plans were generated using MRI-based anatomy and pCT dose calculations. A conventional QA CT scan was acquired subsequent to MRI-only plan

development. Comprehensive QA procedures and tolerances were developed to evaluate pCT dose calculation accuracy and gold fiducial marker positions for image guidance prior to treatment. 3D Gamma evaluation was performed between pCT calculated plan dose and recalculation on QA CT following image registration. Distances of each of three gold fiducial markers to the centroid and isocentre were compared between pCT and QA CT scan.

### Results

Isocentre dose differences between pCT and QA CT were (mean=-0.1%, SD=1.1%). The 3D Gamma dose comparison pass-rates were (mean=99.3%, SD=0.7%) with mean gamma (mean=0.239, SD=0.074) for 2%, 2 mm criteria with 20% low dose threshold and QA CT as reference dose distribution. Results were similar for the two centres using two different scanners. All gamma comparisons exceeded the 90% pass-rate tolerance with a minimum gamma pass-rate of 97.6%. In all cases the gold fiducial markers were correctly identified on MRI and the distances of all seeds to centroid were within the tolerance of 1.0 mm of the distances on QA CT (mean=0.1 mm, SD = 0.5 mm). Differences in distances to isocentre were larger (mean=1.8 mm, SD=5.4 mm). This reflects displacements due to the image registration of QA CT to the pCT scan to copy the plan to the QA CT. All MRI-only treatment plans passed the QA criteria. All 17 prospective MRI-only plans were approved by the radiation oncologist and used for patient treatment.

### Conclusion

To our knowledge this is the first multi-centre study examining prospectively the implementation of MRI-only radiotherapy planning. The results to date support the hypothesis that MRI-only prostate planning can be implemented safely and accurately. Alternatives to comparison to QA CT scans for quality assurance of MRI-only planning are currently under development.

### PV-0429 A machine learning method to improve duodenum dose prediction for pancreatic cancer radiotherapy

Z. Feng<sup>1</sup>, K. Ding<sup>1</sup>

<sup>1</sup>John Hopkins School of Medicine, Department of Radiation Oncology and Molecular Radiation Sciences, Baltimore, USA

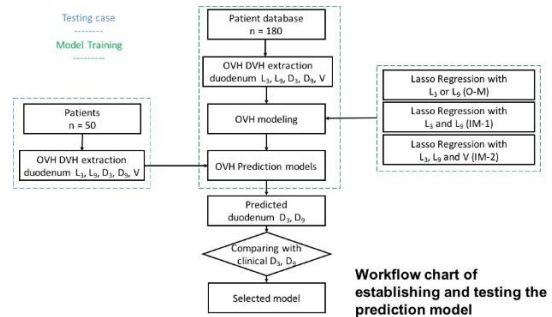
### Purpose or Objective

Our goal is to use machine learning based method to improve the accuracy of overlap-volume-histogram (OVH) based duodenum dose prediction for pancreatic cancer radiotherapy. We have previously proposed a method to reduce duodenum dose using biodegradable pancreas-duodenum spacer and accurate dose prediction is an important step to understand if a patient needs spacer.

### Material and Methods

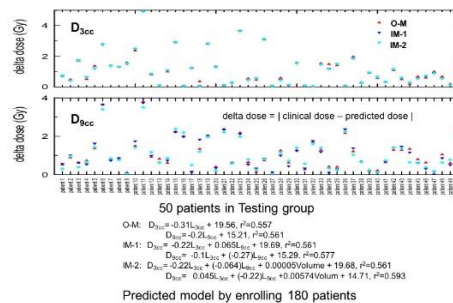
A database of OVH and dose-volume-histogram (DVH) metrics, was collected from the stereotactic body radiation therapy (SBRT) plans of 230 previous patients with unresectable pancreatic cancer (33Gy in 5 fractions). OVH metrics L9cc and L3cc were defined as the tumor volume expansion distance at which 9cc and 3cc volume of the duodenum overlap with tumor. DVH metrics D9cc and D3cc of the duodenum were defined as the dose to 9cc and 3cc of the duodenum. We randomly selected 180 patients in the database as the training group and the rest of the 50 patients as testing and validation group. Our previously published prediction model, a linear regression model (O-M) between Lx and Dx, where x=3cc and 9cc, served as the baseline for comparison. For machine learning based method, we used multivariate regression model with Least Absolute Shrinkage and Selection Operator (LASSO). We included OVH data (L9cc, L3cc, duodenum volume) as explanatory variables to predict Dx of duodenum: I-Model-1 was a linear equation in two variables which is to model the relationship between L3cc,

L9cc and Dx. I-Model-2 included L3cc, L9cc and volume of duodenum as explanatory variables to establish a linear equation in three variables to predict the response variable, Dx. For validation, the difference between the predicted dose (D3cc, D9cc) from these three models and the achieved dose of clinical plans, was defined as delta dose (Gy) to evaluate the prediction accuracy.



### Results

For the training group, the ANOVA results of these models showed that the predicted accuracy of D9cc was significantly improved by including one or two parameters data in the IM-1 (p=0.048) and IM-2 (p=0.014) compared with O-M. Furthermore, by comparing between IM-1 and IM-2, adding volume of duodenum could lead to a significantly improved fit over the I-Model-1 (p= 0.0087). For the testing group, the goodness of fitting between predicted dose and clinical dose was higher in IM-1 (r<sup>2</sup>=0.366 and 0.289 for D3cc and D9cc, respectively) and IM-2 (r<sup>2</sup>=0.366 and 0.324 for D3cc and D9cc, respectively), compared to the O-M (r<sup>2</sup>=0.358 and 0.282 for D3cc and D9cc, respectively). All the predicted doses of D3cc and D9cc were in corresponding predicted ranges of three types predicted models. The root mean square error (RMSE) of D3 is lower in IM-1(1.50) and IM-2(1.50) compared to the O-M(1.51). IM-2 produces the lowest RMSE value of D9(1.31) than O-M(1.35) and IM-1(1.35).



### Conclusion

By utilizing machine learning method, the multivariate regression models can more accurately predict achievable duodenum planning dose.

### PV-0430 automated IMRT planning integrating knowledge-based model with Auto-Planning for cervical cancer

C. Tao<sup>1</sup>, B. Liu<sup>1</sup>, C. Li<sup>1</sup>, J. Zhu<sup>1</sup>, J. Lu<sup>1</sup>, Y. Yin<sup>1</sup>

<sup>1</sup>Shandong Cancer Hospital Affiliated to Shandong University, Department of Radiation Oncology, Jinan, China

### Purpose or Objective

In this study, a fully automated hybrid IMRT planning platform, integrating knowledge-based model and Auto-Planning engine, were established by Pinnacle scripts and Python codes for cervical cancer. And the advantages of this hybrid planning platform were investigated.

## Material and Methods

60 patients with clinical approved IMRT plans for cervical cancer were selected into establishing a knowledge-based model by linear fitting the equivalent uniform dose (EUD,  $a=1$ ) and equivalent uniform distance (EUL,  $a=1$ ), developed from the overlap volume histograms (OVH) method. Another 20 patients were used as the test group. By integrating the EUD-EUL model with Auto-Planning module, a fully automated hybrid IMRT planning platform was developed based on Pinnacle scripts and python codes. IMRThy plans, generated this hybrid planning platform, were compared with corresponding IMRTap plans, generated by Auto-Planning module with default pre-setting objectives from a template. The quality and consistency of IMRThy plans produced by this hybrid planning platform were evaluated by dose/volume indices and EUD-EUL metrics.

## Results

The linear regression between EUD and EUL for bladder and rectum of 60 previous clinical approved plans were shown in figure 1. Therefore, correlation functions between EUD and EUL for bladder and rectum were obtained:

$$\text{EUD}_{\text{bla}} = 45.37 - 5.78 \cdot \text{EUL}_{\text{bla}} \text{ with } R^2 = 0.79$$

$$\text{EUD}_{\text{rec}} = 44.23 - 5.38 \cdot \text{EUL}_{\text{rec}} \text{ with } R^2 = 0.69$$

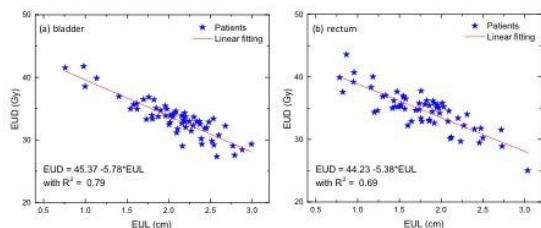


Figure 1: Linear regression between EUD and EUL for bladder and rectum of 60 previous clinical approved plans.

The dose/volume indices of IMRThy plans and IMRTap plans were listed in table 1. For PTV, V95 of IMRThy plans were a little worse than that of IMRTap plans with significant differences (IMRThy:  $95.38 \pm 0.92\%$ , IMRTap:  $96.04 \pm 0.73\%$  with  $p=0.02$ ). While HI and CI of IMRThy and IMRTap plans were very similar without significant differences. Considering bladder and rectum, the organs predicted by the EUD-EUL model, dose/volume indices including V20, V30, V40 and Dmean of IMRThy plans were dramatically reduced than IMRTap plans with significant differences. While V50 and V60 of IMRThy plans were lower than that of IMRTap plans without significant differences. For femoral heads, which were not considered in the predicting model, all dose/volume indices were comparable between these two type plans.

Table 1: Evaluation of dose/volume indices of IMRThy plans and IMRTap plans.

Structures	Parameters	IMRThy plans	IMRTap plans	p value
PTV	V95	95.38±0.92	96.04±0.73	0.02
	HI	0.11±0.01	0.11±0.01	0.06
	CI	0.74±0.04	0.74±0.04	0.94
Bladder	V20	72.55±6.58	77.94±8.14	0.03
	V30	50.55±6.33	57.87±6.43	<0.01
	V40	30.00±5.76	35.10±6.55	0.02
	V50	14.36±4.00	16.69±4.51	0.11
	V60	3.45±1.90	3.96±2.02	0.43
	Dmean	31.48±1.97	33.65±2.27	<0.01
Rectum	V20	81.77±9.24	88.40±8.68	0.04
	V30	50.43±9.44	58.70±7.62	<0.01
	V40	28.31±6.91	33.85±6.06	<0.01
	V50	10.94±4.69	13.77±5.01	0.08
	V60	1.08±0.98	1.54±1.46	0.27
	Dmean	32.11±2.21	34.46±1.68	<0.01
Femoral head-L	V20	43.49±4.52	43.92±4.42	0.75
	V30	15.23±4.25	14.37±3.86	0.47
	V40	2.28±1.40	2.19±1.71	0.84
	V50	0.10±0.15	0.11±0.21	0.85
	V60	0.00±0.00	0.00±0.00	-
	Dmean	20.12±0.64	20.16±0.69	0.86
Femoral head-R	V20	41.49±9.81	41.75±9.79	0.94
	V30	14.00±6.12	14.01±6.38	0.99
	V40	2.42±2.11	2.61±2.41	0.81
	V50	0.16±0.37	0.14±0.35	0.91
	V60	0.00±0.00	0.00±0.00	-
	Dmean	19.81±1.84	19.96±1.58	0.78

## Conclusion

The fully automated hybrid IMRT planning platform, combining knowledge-based model and Auto-Planning module, could generate clinical accepted plans and significantly improve the quality and consistency of IMRT plans.

## Proffered Papers: BT 6 : Innovative and uncommon indications

### OC-0431 Esophageal brachytherapy: Institut Gustave Roussy's experience

M. Kissel<sup>1</sup>, E. Chirat<sup>1</sup>, P. Annede<sup>1</sup>, P. Burtin<sup>2</sup>, I. Fumagalli<sup>1</sup>, E. Bronsart<sup>1</sup>, F. Mignot<sup>1</sup>, A. Schernberg<sup>1</sup>, I. Dumas<sup>1</sup>, C. Haie-Meder<sup>1</sup>, C. Chargari<sup>1</sup>

<sup>1</sup>Institut Gustave Roussy, Radiotherapy, Villejuif, France;

<sup>2</sup>Institut Gustave Roussy, Gastroenterology, Villejuif, France

### Purpose or Objective

Esophageal cancer is characterized by its propensity to local evolution, which conditions prognosis but also quality of life. Brachytherapy may be a therapeutic option for all stages of esophageal cancer, especially for inoperable patients.

### Material and Methods

This retrospective unicentric study included all consecutive patients treated for an esophageal high dose rate brachytherapy in our institution from 1992 to 2018.

### Results

90 patients were included. They were treated in four distinct indications : exclusive (7 patients), boost after external beam radiotherapy (41), reirradiation (36) or palliative aim (6). Most frequently prescribed schemes were 3x5Gy (boost) or 6x5Gy (exclusive treatment and reirradiation). At the end of follow-up, 50% of patients had presented with local recurrence : 46% in the boost setting, 71% for exclusive brachytherapy, 47% for reirradiation and 100% for palliative treatment. 17% of patients had a metastatic relapse. Median overall survival (OS) was 15 months in the whole cohort : 22 months in the boost setting, 25 months for exclusive brachytherapy, 15 months for reirradiation and only 2 months for palliative treatment. Tumor length at brachytherapy, brachytherapy dose and interfraction response were significantly associated to OS. 40% of patients presented with grade 2+ toxicity, mostly esophagitis, including 3 toxic deaths.

### Conclusion

Phase III trial RTOG9405, showing the absence of dose-effect on esophageal cancer, has led teams to progressively give up the technique in the boost setting. Although local control outcomes are still poor, one must remember that patients are unfit for any curative therapeutic option and that palliative chemotherapy offers mediocre results. The most promising setting probably is reirradiation since brachytherapy offers a remarkable dose gradient allowing best OAR sparing. Esophageal brachytherapy deserves to be further investigated since some patients, even unfit, may benefit from it in some indications, with acceptable toxicity. Prospective studies are warranted.

### OC-0432 Endoluminal brachytherapy with induction chemotherapy and definitive chemoradiation in Ca. Esophagus

S. Raghunath<sup>1</sup>, R. Tiwari<sup>1</sup>, G. Narayanan<sup>1</sup>, B. Vishwanathan<sup>1</sup>, R. Sultana<sup>1</sup>

<sup>1</sup>Vydehi Institute of Medical Sciences and Research Center, Radiation Oncology, Bangalore, India

### Purpose or Objective Need for the Study:

Over 75% of people with cancer worldwide have no access to safe surgery. Access is worse in low income countries where 95% of people with cancer do not receive basic cancer surgery.

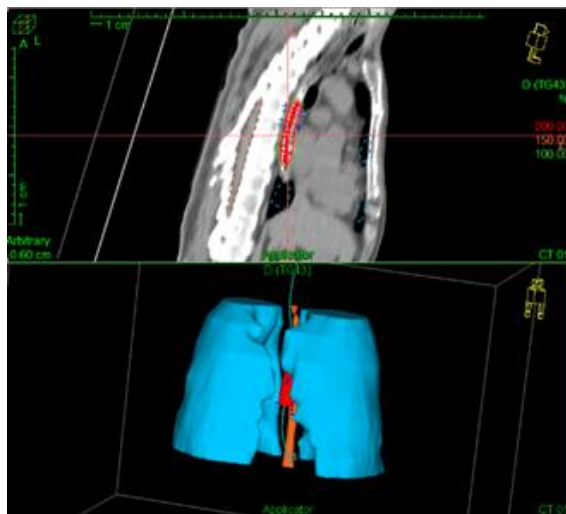
Patients in remote areas in Rural India, South Asia, Africa and Poorer EU Member States do not have access to surgical infrastructure or qualified personnel to deliver high quality surgery in locally advanced esophageal carcinoma. Further, Esophageal Cancer has an abysmal response despite multimodality treatment. Endoluminal Brachytherapy is an under-utilized modality in the curative setting and an elegant tool to escalate the dose to improve the clinical response and clinical symptoms.

This study examines if Dose Escalation with Endoluminal Brachytherapy after Induction Chemotherapy and Definitive Chemoradiation is feasible in the background of the above scenarios in underserved populations.

### Objective:

To evaluate Dysphagia Free Interval (DFI), Disease Free Survival (DFS), Overall Survival (OS) and Toxicity Profile in Endoluminal Brachytherapy in Ca. Esophagus with Induction Chemotherapy and Definitive Chemoradiation.

### Material and Methods



31 patients with biopsy proven Esophageal Carcinoma Stage IIA-IVA with Node (-) Status were enrolled at our Institute from June 2007 to July 2018. ILRT 10Gy/2# was delivered following Definitive CRTT 50.4Gy/28# with 3-weekly CDDP/5-FU after 6-10 cycles of Pacli/Carbo.

Proximal and Distal borders were marked from the Prechemotherapy tumor volume on OGD. Patients were simulated in a GE Multislice CT scanner to confirm accurate coverage of the pre-chemotherapy disease.

Positions were marked and secured to prevent any shift in placement before and during treatment. ILRT Dose was prescribed to 1 cm from the center of the source.

Swallowing Status was established on follow up. OS and DFS was censored at death or last follow up. Statistical Analysis was performed using SPSS.

### Results

Patient Characteristics	
Total No. of Patients	31
Median Age of Recruitment	62.5 years
Distribution by Sex	
Male	20
Female	11
Distribution by Stage	
T2N0M0	3.22%
T3N0M0	87.09%
T4N0M0	9.6%
Histology	
Squamous Cell Carcinoma	87.09%
Adenocarcinoma	12.91%

- Median Age of Recruitment was 62.5 years. All 31 Patients completed treatment and were clinically stable at discharge. 83.97% Completed Chemotherapy, 96.77% completed Radiation Therapy according to protocol. 35.48% patients were alive on last follow up.
- Median OS was 21 months. OS at 2 years was 53.6% . Median DFI was 10.7 months. Those with a Cumulative EQD2 >60 Gy had a significant 5 year OS of 59.1% vs. 33.3% for those who received EQD2 <60 Gy (p=0.061, CI=76.3-91.4). 5 year DFS for EQD2 >60 Gy was 56.1% vs. 16.7% for those who received Cumulative EQD2 <60Gy (p=0.079, CI=74.2-93.8).
- There were no Grade III/IV acute toxicities. There were no Fistulas on follow up. 2 patients required stenting within 1 year of treatment and died within 2 months thereafter. 2 Patients developed CHF at 4 years.1 Patient Developed Left Breast Fibrosis at 4.5 years.

### Conclusion

Endoluminal Brachytherapy with Induction Chemotherapy and Definitive Chemoradiation is a feasible option in the absence of conventional alternatives.

### OC-0433 Feasibility and early clinical response of interstitial BT for hepatocellular carcinoma

S. Corradini<sup>1</sup>, F. Walter<sup>1</sup>, C. Maihöfer<sup>1</sup>, M. Rottler<sup>1</sup>, J. Well<sup>1</sup>, L. Nierer<sup>1</sup>, M. Seidensticker<sup>2</sup>, R. Seidensticker<sup>2</sup>, T. Streitparth<sup>2</sup>, F. Streitparth<sup>2</sup>, J. Ricke<sup>2</sup>, C. Belka<sup>1</sup>  
<sup>1</sup>Radiation Oncology, Department of Radiation Oncology LMU, Munich, Germany; <sup>2</sup>Radiology, Department of Radiology LMU, Munich, Germany

### Purpose or Objective

Several local approaches for hepatocellular carcinoma have been evaluated in clinical practice. Interstitial CT-guided brachytherapy (BT) has been shown to be a safe and effective treatment option in various sites, but remains under investigation in the setting of hepatocellular carcinoma.

### Material and Methods

Between 07/2017-07/2018 patients treated with CT-guided high-dose interstitial brachytherapy for hepatocellular carcinoma were evaluated. All patients with a minimum follow-up of 2 months were included in the present Analysis.

### Results

Between 07/2017-07/2018 patients treated with CT-guided high-dose interstitial brachytherapy for hepatocellular carcinoma were evaluated. All patients with a minimum follow-up of 2 months were included in the present analysis.

### Results

Overall, 82 hepatocellular carcinoma lesions were treated with BT in 36 patients. Median age was 66 years (range 46-85 years). 29 patients presented with a liver cirrhosis Child-Pugh A and 11 patients with Child-Pugh B cirrhosis at the time of brachytherapy. Prior treatments were: transarterial chemotherapy embolization (TACE), radiofrequency ablation (RFA), surgical resection, selective internal radiotherapy (SIRT), SBRT. In 22 patients more than one lesion was treated per fraction (mean 1.6, range 1-5 per fraction). Mean liver volume was 1654cc (range 800-2488cc). Brachytherapy was performed in a single fraction with an aimed prescription dose of 15Gy, taking into account constraints of organs at risk. A mean dose of D100: 14.4 Gy was reached, D95: 18.9 Gy, D90: 21.0 Gy. Mean CTV volume of single lesions was 14cc (range 0.2-103cc) and cumulative CTV volume per fraction of 36cc (range 1.4-282cc). Mean liver volume receiving > 5Gy was 326cc (range 21-1330cc).

After a mean follow-up of 6 months (2-12months), 3 patients who received brachytherapy as a bridging treatment, had undergone liver transplantation after 2-5month. Regarding overall local control of treated lesions, 26 complete responses, 24 partial responses and 1 progression were recorded. 15 patients developed new HCC lesions within the liver and 5 patients developed distant metastases. 4 patients died during the follow-up period, resulting in a 6- and 12-months overall survival of 96% and 74%, respectively.

### Conclusion

Interstitial CT-guided BT showed to be an effective treatment option due to its good rate of local control. However, longer follow-up is needed to definitively assess its role in this Setting.

### OC-0434 Sphincter function after EBRT and Pulsed Dose Rate Brachytherapy (PDR-BT) in anal cancer patients

T. Brahmi<sup>1</sup>, A.A. Serre<sup>1</sup>, F. Gassa<sup>1</sup>, M. Sandt<sup>1</sup>, F. Lafay<sup>1</sup>, P. Pommier<sup>1</sup>

<sup>1</sup>Centre Léon Bérard, Radiation Therapy, Lyon, France

### Purpose or Objective

One of the objectives of the anal canal cancer treatment is the preservation of the pelvic sphincter system to avoid a definitive stoma. However, the sphincter function is poorly evaluated, especially regarding patients' perspective.

### Material and Methods

Between 2005 and 2017, 179 consecutive patients with anal canal cancer (all histological types) received PDR-BT as a boost after EBRT (+/- concomitant chemotherapy) in our institution. 79 out of 131 of them eligible for the study (alive with a minimum 7 months follow-up; no recurrence) were included.

Sphincter function was self-evaluated by the Wexner questionnaire, that assess different types of incontinence (solids, liquids, gases) and their impact on the quality of life, leading to a score from 0 to 20. Interpretation of Wexner's score was defined as follows: None (0), Minimal (1 to 4), Moderate (5 to 9), Important (10 to 16) and Severe (17 to 20). Threshold of 9 has also been used, associated in the literature to a poorer quality of life. Additional items issued from the questionnaire developed by Vaizey (impact on sexuality, faecal urgency and self-medication) were also assessed.

### Results

Patients who responded to the questionnaire had similar characteristics to those of the whole cohort, except for average follow-up (43 vs 23 months, p<0.001). Average Wexner score was 4.1 (25%IQ: 0 - 75%IQ: 7). 19% had a score > 9. 41.8% of this cohort did not report any symptoms (score 0). Only 2.5% had severe symptoms. Regarding sexual symptoms, 56.5% of our patients have expressed no discomfort. Faecal urgency was present in 45.6% of our cohort. Only 11.4% of patients have used drugs for a constipation purpose.

No pre-therapeutic or therapeutic factors have been identified as associated with the occurrence of anal incontinence. The occurrence of a late gastrointestinal or cutaneous toxicity (> grade 2) does not have a significant influence on the occurrence of these symptoms (HR: 1.693 [95%CI: 0.573 - 5.008], p=0.357).

We observed a non-significant (p=0.185) decrease of the average score with the delay between the BT and the evaluation: 6.3, 3.8 and 3.5 respectively when the questionnaire was applied less than 2; 2 to 5; or more than 5 years after BT. Incontinence for solid stools was statistically reducing with time (average score: 1.3, 0.4 and 0.3 respectively, p=0.011) as well as the proportion of patients without symptoms (13.3%, 40% and 55.9% respectively, p=0.019).

### Conclusion

Anal incontinence after conservative treatment of the sphincter system remains a poorly explored pathology, with multiple scores available in the literature. Our homogeneous retrospective cohort reports a low incidence of incontinence, but faecal urgency remains important with a definite impact on the quality of life of these patients. With reservation of confounding factors (modifications of the indications and treatments' modalities during the period of observation), the function of the sphincter may improve over time.

### OC-0435 Contact X-Ray Brachytherapy (CXB) after local excision (LE) for early rectal adenocarcinoma.

J. Gérard<sup>1</sup>, S.M. Arthur<sup>2</sup>, F. Antoine<sup>3</sup>, D. Amandeep<sup>4</sup>  
<sup>1</sup>Centre Antoine Lacassagne, Radiotherapy - University Côte d'Azur, Nice, France ; <sup>2</sup>Clatterbridge Cancer Centre, Radiotherapy Papillon Suite, Liverpool - Clatterbridge, United Kingdom; <sup>3</sup>Centre Antoine Lacassagne, Biostatistiques - University Côte d'Azur, Nice, France ; <sup>4</sup>East Yorkshire Hospitals, Radiotherapy Oncology, Hull, United Kingdom

### Purpose or Objective

Early rectal cancers, increasingly diagnosed through screening programmes, are often treated using local excision (LE). In case of pathological pejorative features a radical surgery (TME) is the standard recommendation. The risks and sequelae of TME have stimulated alternative option using radiotherapy to preserve the rectum. We present the results of adjuvant CXB with or without external beam radiotherapy (EBRT) after LE in a multicenter cohort.

### Material and Methods

Between 2009-2017 CXB was given after LE in three centers to 197 patients (Clatterbridge :120, Hull: 35, Nice:34). All patients were M0. Negative pathological features were: lymphovascular invasion (LVI), sm2-3

kikuchi level, budding, pT2, R1. CXB was performed with the Papillon50™ machine and dose was 40 to 60 Gy in 2 or 3 fractions (depending on association with EBRT) over 2 to 4 weeks. Kaplan Meier estimates was used for outcomes measures.

**Results**

Median age was: 70 years. Male:127, Female :70. cN0: 189, cN1: 8 (4%). pT staging was : pT1: 146, pT2: 46, pT3: 5 . CXB alone was given in 27 pts and combined with EBRT in 170 (EBRT alone(45 -50 Gy/ 5 weeks):35, chemoRT :107, EBRT “short course”: 28 pts. Median follow-up time was 41 months. Local relapse rate at 5 years was 8% and distant metastases 11%. Organ preservation was achieved in 95% with good bowel function in nearly all patients. Main toxicity was rectal bleeding due to radiation mucosal telangiectasia. Due to small number of events only few prognostic parameters were observed: LVI for local relapse (4% vs 19% out of 63 pts with LVI reported ) and sm3 vs sm1-2 for distant metastases (DM). A local relapse was associated with a higher risk of DM (5% vs 44%, p< 0.0001)

**Conclusion**

This appears to be the largest ever presented multicenter cohort study using adjuvant CXB for early rectal cancer with pejorative features after local excision. This strategy brings high rate of local control and rectal preservation with good bowel function. It appears to be a good option for well-informed patients to avoid safely the risks of a radical TME after LE.

**OC-0436 13 SCC penis treated with HDR brachytherapy, results and dosimetric analysis**

M. Marban Orejas<sup>1</sup>, J. Crook<sup>1</sup>, M. Keyes<sup>2</sup>, D. Batchelar<sup>1</sup>, R. Dubash<sup>2</sup>, F. Bachand<sup>1</sup>  
<sup>1</sup>BCCA, Radiation Oncology, Kelowna BC, Canada ; <sup>2</sup>BCCA, Radiation Oncology, Vancouver BC, Canada

**Purpose or Objective**

We report a retrospective analysis of treatment features and results for 13 localized penile SCC treated with HDR brachytherapy (BT)

**Material and Methods**

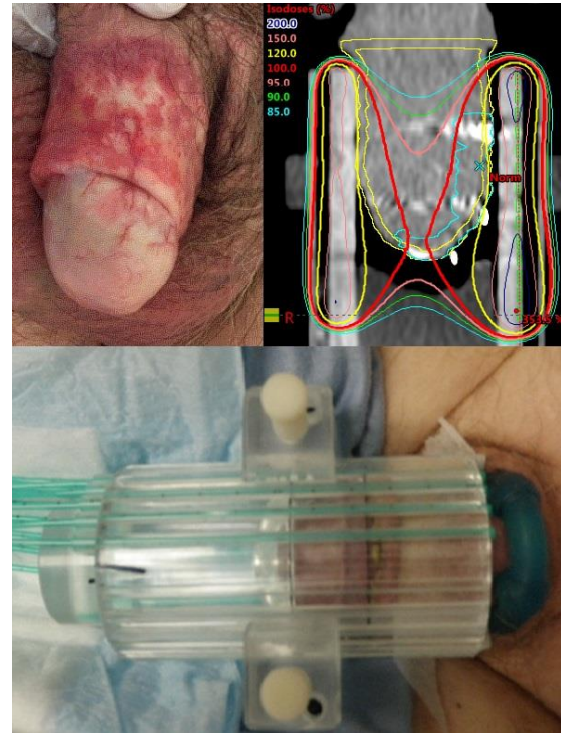
6 patients (T1a-b) received plesiotherapy and 7 (T1-2) interstitial BT. CTV was defined as GTV+5mm, or 3mm below the skin after excisional biopsy (n=2). Skin refers to a 2mm rind on the penis within the applicator and urethra is a central 1cm circle or the catheter contoured on CT. We performed a descriptive analysis to correlate dosimetry with clinical outcomes

**Results**

HDR mold BT was used for 5 T1a tumors and 1 T1b(G3 pN0) between 11/15-02/17. Median age was 68(51-78) 40Gy/10 was prescribed BID 6hours apart. Median CTV was 4.4cc(2.6-11.8)

Median dosimetric parameters were CTV V100 80.3%, V125 0.2%; skinD5 118%(125-107); urethral Dmax 102%(118-75), D5 95% and D30 89%.

Median follow up is 29.3months(20-35). All patients are alive and free of disease(NED). 1 patient had a local failure at 17months presenting as a non-healing ulcer and urethral stricture. He had a partial penectomy for pT3 recurrence, and remains NED 15months later. No other urethral or soft tissue toxicity occurred. First 2patients treated have G2 telangiectasias on the shaft(image1), proximal to treated site, attributed to redundant penile skin sliding into treatment volume. Subsequently, a Lucite applicator allowed visual position check and a constriction ring at the penile base immobilized the skin(image3). All sexually active patients remain potent.



HDR interstitial BT was used for 7patients between11/09-05/18. Median age was 51.7(33-77). 2patients had T1 and 5 had T2 disease. 2 underwent inguinal LND, one for G3(pN0) and one cN1(pN2) Dose prescribed was 42Gy/12 in 3patients while the other 4 received 42/14, 45/12, 53/17 and 38.4/12, BID 6h apart.

Interstitial HDR dosimetric parameters															
cGy	PTV α/β 10.5			vol (cc)	V100 (% V125 (% V150 (% V200 (%			Urethra α/β 3			Skin α/β 8				
	D5 (%)	D30 (%)	Dmax (%)		D5 (%)	D30 (%)	V125 (cc)								
4200/12	5600	6040	910	35	99.7	75.7	26.8	9.3	145.7	132.6	208	149.42	74.15	1.31	
4200/12	5600	6040	910	57.3	99.9	88.2	88.7	27.3	194.5	178.5	218.5	258.2	180.81	7.6	
4500/12	6110	6610	1012	15.6	100	75.4	15.4	3.7	128	118.7	146	187.37	117	2.79	
4200/12	5600	6040	910	26.5	98.6	90.5	71	32	108.9	98.5	115.7	134.85	77.53	0.96	
5300/17	6880	7370	1082	14.3	84.4	72.7	56.3	24.2	184.7	88.7	207.9	70.72	29.71	0.15	
				14.3	84.6	39	21	8	114.5	80.46	207.9	70.72	29.71	0.15	
3840/12	5010	5380	794	3.9	88.1	40.4	19	4.7	85.7	74.8	99.9	117.2	28.21	0.48	
4200/14	5400	5780	840	17.9	92	49	18.6	5.29	148.4	130.14	162.4	146.12	80	0.78	
				median	21.05	98.60	75.40	26.80	9.30	128.00	98.50	207.90	134.85	74.15	0.96

Table1 summarizes dosimetric parameters

Median follow up is 98 months(5-106). All patients are alive and NED at last follow up, 5 with intact penis, and 3 remain potent 1patient failed locally at 21months with a non-healing ulcer unresponsive to hyperbaric oxygen. 6 years after partial penectomy and pelvic/groin dissection(pN1), he is alive and NED. The first 4 patients had G2necrosis, 3 received hyperbaric oxygen. The implant had catheter spacing >12mm(14-17mm) and unacceptable inhomogeneity (V150mean 47%, V125mean 85%). For the final 2patients, catheter spacing 9-12mm was used and V150 limited to<20%,V125 to-45% 1 patient presented with G1 meatal stenosis, 1 with urethral stenosis requiring dilatations(G2) and 1 perineal urethrostomy(G3). There was no correlation between toxicity and implant geometry in those cases, but BED, considering urethral α/β=3, was higher(101.2 and 108.2Gy), and they had diabetes.

**Conclusion**

HDR brachytherapy is effective treatment for SCC penis either as a surface mold or interstitial. Homogeneity parameters should be followed. There may be a correlation between urethral BED and complications. A constriction ring is advisable in mold treatment to avoid skin toxicity More prospective analyses are warranted

**OC-0437 Update of moderate dose-escalation with perioperative HDR brachytherapy in soft tissue sarcomas**

X. Chen<sup>1</sup>, A. Montero<sup>1</sup>, J. De las Heras<sup>2</sup>, E. Sanchez<sup>1</sup>, O. Hernando<sup>1</sup>, M. Lopez<sup>1</sup>, J. Garcia<sup>3</sup>, M.A. De la Casa<sup>3</sup>, D. Zucca<sup>3</sup>, R. Ciervide<sup>1</sup>, M. Garcia-Aranda<sup>1</sup>, J. Valero<sup>1</sup>, R. Alonso<sup>1</sup>, J. Marti<sup>3</sup>, L. Alonso<sup>3</sup>, P. Garcia de Acilu<sup>3</sup>, P. Fernandez-Leton<sup>3</sup>, C. Rubio<sup>1</sup>

<sup>1</sup>University Hospitals HM Sanchinarro - Puerta del Sur, Radiation Oncology, Madrid, Spain; <sup>2</sup>University Hospitals HM Sanchinarro, Orthopaedic Surgery, Madrid, Spain; <sup>3</sup>University Hospitals HM Sanchinarro - Puerta del Sur, Medical Physics, Madrid, Spain

**Purpose or Objective**

Conservative surgery in combination with local radiation therapy is considered a standard approach for soft tissue sarcomas (STS). A close relationship exists between total radiation dose and local control. We report our experience about the feasibility of perioperative brachytherapy (PoBT) with a moderate dose-escalation in the multidisciplinary management of soft tissue sarcoma.

**Material and Methods**

From May 2015 to October 2018, 22 patients (p), 13 men and 9 women, with a median age of 61.5 years (range 7 - 77 years) underwent perioperative brachytherapy (PoBT). Histology: 7 p (32%) liposarcoma, 5 p (23%) fusocellular sarcoma, 3 p (14%) desmoids tumor, 5 p (23%) fibroblastic sarcoma, 1 p (4%) pleomorphic sarcoma and 1 p (4%) malignant glomus tumour. Tumor location: thigh 14 p (63%), trunk 4 p (18%), arm 3 p (14%), neck 1p (4%). Tumor staging according to the AJCC 8th ed (2016): 5 p IA, 9 p IB, 5 p II, 2 p IIIA and 1 p IIIB. PoBT procedure was performed by using 6F plastic catheters placed on the surgical bed at the time of tumor excision. Sixteen (73%) patients obtained R0 resection and 5 p (23%) R1 resection. Plastic catheters were placed either parallel or perpendicular to the surgical incision at 1.5- 2 cm intervals to ensure adequate dosimetry. CT simulation with 1.5 mm slice thickness was done in the fourth or fifth day after surgery once the sewer system was retired. A total 16.5 Gy was delivered to the PTV in 3 fractions of 550 cGy in 20 p; 1 p received 4 fractions of 400 cGy and 1p received 3 fractions of 500 cGy. Fractions were separated at least 6 hours. Catheters were retired after the last fraction.

**Results**

All p received external beam radiotherapy (EBRT) before or after brachytherapy at a mean dose of 50 Gy in 25 fractions. Conformal 3D radiotherapy planning was used in 7 p (32%), intensity modulated radiotherapy (IMRT) in 10 p (45%) and volumetric modulated arc therapy (VMAT) in 4 p (18%). Six p (27%) underwent pre-operative radiotherapy whereas 16 p (73%) post-operative radiotherapy. One of the biological characteristics of sarcoma is their relatively low  $\alpha$ -B ratio. Assuming an  $\alpha$ /beta ratio of sarcoma cells as 4 our calculation of tumor BED is as following: (2Gy x 25fx) + (5.5Gy x 3fx) = 114.19Gy which corresponds to an accumulated EQD2Gy for tumor of 76.12Gy. With a median follow-up of 16 months (range 0.2 - 37.5 months), 1 p had developed marginal local relapse at 7.6 months of follow-up. In-field local control, distant-metastases free survival and overall survival are of 100%. No grade 3 or higher toxicity was observed.

**Conclusion**

Peri-operative brachytherapy is feasible and well tolerated and allows a moderate dose-escalation in patients with soft-tissue sarcomas.

<sup>1</sup>University Hospital Zürich, Department of Radiation Oncology, Zurich, Switzerland

**Abstract text**

Radiation Oncology is unique as a field, where excellence in care and advances in research are only possible by closest collaboration of multiple professions: medical physics, nursing, radiation oncology, radiation technologists and radiobiology. The progress in our field is documented by significantly and clinically relevant improved outcome over time and this has been achieved in all frequent cancer sites of lung cancer, prostate cancer, breast cancer, rectal cancer and many small cancer sites. Medical physics has been a key driver of these advances and has strongly contributed to reshape the way radiation oncology is practiced and perceived today: clinically effective, well tolerated and cost-effective. Both innovation AND translation are responsible for these success stories. Intensity-modulated radiotherapy, image-guidance and stereotactic-body radiotherapy are just some exemplary innovations which all improve outcome of our today's cancer patients: these advances have been (co-)developed by Medical Physics, jointly implemented by all professions, successfully evaluated in clinical trials, incorporated into international and multidisciplinary guidelines and are today standards of care in our societies. All innovations can be summarized under the umbrella of precision medicine: to adapt radiation oncology to the patient-individual disease aiming to deliver the right treatment to the right patient and the right time. Consequently, radiation oncology has practiced precision medicine long before this "buzz-word" was adopted in medicine and oncology. This is a huge opportunity for radiation oncology in general and medical physics in particular: to be at the forefront of current research and clinical advances in oncology and medicine. Precision medicine is fundamentally based on individual patient and disease characterization: digitalization, standardization, collection, analysis and interpretation of various patient and disease characteristics within multi-level prognostic and predictive models has already been established in radiation oncology. More comprehensive patient and disease characterization beyond currently available biomarkers has been pioneered by Medical Physics using e.g. quantitative image analysis - Radiomics. Artificial intelligence and machine learning will be mandatory for handling and interpretation of these massive data and are already today routine in radiation oncology. Medical physics has therefore a lot to offer to the progress of precision medicine in general, not only in the field of radiation oncology and also not restricted to oncology. It will be critical to distribute and balance the limited resources between these different fields of research, between "traditional" radiation oncology medical physics and "beyond borders" radiation oncology. This will strengthen Medical Physics. However, if Radiation Oncology overall is open for these developments, our discipline and finally our cancer patients will benefit from continuing our multi-professional nature.

**Award Lecture: Honorary Physicist Award Lecture**

**SP-0438 Precision medicine - an opportunity for medical physics and radiation oncology**

M. Guckenberger<sup>1</sup>

## ESTRO 38 Monday 29 April

---

### Teaching Lecture: Extreme hypofractionation in the treatment of localized prostate cancer

---

#### SP-0439 Extreme hypofractionation in the treatment of localized prostate cancer

R. Valdagni<sup>1</sup>

<sup>1</sup>Fondazione IRCCS Istituto Nazionale dei Tumori, Radiation Oncology 1, Milan, Italy

#### Abstract text

Over the past two decades, the radiation oncology community is being experiencing a major technical evolution in the radical irradiation (RT) of localized prostate cancer. Most significant improvements consist of the routine utilization of IMRT, of IGRT, also including active (e.g. electromagnetic transponders) or passive (e.g. gold fiducials markers) localization systems, of devices aimed to improve dosimetry in the perirectal space (e.g. rectal spacer and endorectal balloons) as well advances in prostate imaging.

Such technical sophistication facilitates the definition, localization and monitoring of the tumor position, size and shape before and during treatment, together with the possibility of higher, targeted radiation doses to improve tumor control and decreased radiation exposure to normal tissues surrounding the tumor. Highly precise treatment delivery is leading to safely administer very conformal treatment at increased total doses in small volumes. This allows to overcome conventional fractionation (CF) and to routinely utilize moderate hypofractionation (M-HF) as well as to explore feasibility and safety of extreme hypofractionated (E-HF). The recently published guidelines on localized prostate cancer by ASTRO, ASCO, and AUA define M-HF as the daily fraction of 2.40-3.4 Gy and of  $\geq 5$  Gy for E-HF; this guideline underlines that, being HF a "spectrum" of fraction sizes and lacking a "universally accepted definition", the above mentioned subdivision between M-HF and U-HF is "necessarily arbitrary" and pragmatically reflects most of the available clinically experience with M-HF and E-HF. The almost acquired evidence that the  $\alpha/\beta$  ratio of prostate cancer is in the range of 1.5-2 Gy and that surrounding critical organs (rectum and bladder) tend to exhibit lower fractionation radiosensitivity (i.e.  $\alpha/\beta$  range: 3-5 Gy), suggest the use of hypofractionated schemes to improve the therapeutic gain, exploiting high doses per fraction to achieve better tumor control probability.

E-HF, particularly at single doses  $\geq 8$ Gy, shows further radiobiological advantages with respect to C-F and M-HF, tumor microvasculature induced disruption appearing to be a significant ablative determinant which concurs in considerably increasing tumor cell death. Beside radiobiological and clinical considerations, E-HF implies additional advantages in terms of economical cost reduction and patients' convenience (mainly but not only related to the possibility of gaining time), over CF- and M-HF, brachytherapy, proton irradiation and, because of non-invasiveness and of the evidence that radio-induced toxicities do not depend on patient's age, over radical prostatectomy. To date, E-HF in localized prostate cancer has been used in low, intermediate and high risk tumors and appears very attractive for intermediate risk and potentially for high risk patients (the non malignant nature of GG I/GPS 3+3 strongly suggests to avoid overtreatment in low risk patients), showing good biochemical control and, with few exceptions, limited toxicities in the early-mid term follow up. However, the long survival of prostate cancer patients with localized disease and the present

lack of published randomized trials comparing E-HF with C-F and/or M-HF, suggest that E-HF should remain an area of investigation.

The aim of this teaching lecture is to review the present clinical experience of extreme hypofractionation in localized prostate cancer, discussing patient and disease selection, different fractionation schemes, major technical features of available treatments, the present evidence re toxicities and oncologic outcomes, and future developments in the use of E-HF.

---

#### Teaching Lecture: Radio-immunotherapy: challenges and opportunities

---

#### SP-0440 Immunotherapy and Radiotherapy: challenges and opportunities

S. Formenti<sup>1</sup>

<sup>1</sup>Weill Cornell Medical Center of Cornell University, Radiation Oncology, New York- NY, USA

##### Abstract text

Radiotherapy has revealed an ideal adjuvant to cancer immunotherapy, because of its ability to convert the irradiated tumor into an individualized, in situ vaccine. When successful at immunizing, radiotherapy evokes T cell memory, and induces effects outside the treated field, defined as abscopal effects (responses at a distant, synchronous, un-irradiated established tumor or metastasis). In the setting of clinical cancer, however, abscopal effects are extremely rare, because of immune-suppressive characteristic of established solid tumors (Curr Probl Cancer 40:25-37, 2016). Thus, strategies to exploit the pro-immunogenic effects of radiotherapy require combination with immunotherapy: experiments in several syngeneic mouse models that mimic the setting of advanced cancer have demonstrated promise of combining radiation with immune checkpoint blockade (Clin Cancer Res. 2005;11:728-734). Radiation can compensate tumors with a low mutational load, by inducing de novo T cell priming to multiple tumor antigens and therefore, achieve responses in the absence of pre-existing neoantigens with anecdotal clinical examples confirming the preclinical data (Trends Cancer 2016;2,6:286-294). Currently, multiple clinical trials are exploring optimal regimes of radiotherapy and immunotherapy, with some initial success. The issue of dose and fractionation seems to be particularly relevant to abscopal responses. A mechanism underlying the dose dependence of abscopal response was recently elucidated (Nature Communications 2017; Jun 9;8:15618 ). In mice bearing bilateral TSA murine breast carcinoma when combined with ICB a single dose of 20 or 30Gy achieved comparable in field control to that of a regimen of 8GyX3 fractions, but only the fractionated regimen induced abscopal responses. Radiation-generated double strands (ds) DNA fragments reach the cytoplasm of irradiated cells where they are "sensed" by the cGAS/STING pathway (cGAS=cyclic GMP-AMP synthase and its adaptor protein STING= stimulator of interferon genes, aka transmembrane protein 173 - TMEM173). cGAS binds cytosolic dsDNA to initiate interferon (IFN-I) responses upon STING stimulation, resulting in dendritic cell recruitment and cross-priming of effector T-cells, the key steps to convert the tumor into an in situ vaccine. When tested in multiple carcinoma murine and human carcinoma cells as the radiation dose per fraction increases, cytosolic dsDNA was found to accumulate to a threshold above which induction of three prime repair exonuclease 1 (Trex1) occurred, an enzyme that degrades cytoplasmic DNA. Single doses in excess of 10-12Gy induced Trex1 to rapidly degrade cytosolic dsDNA, the substrate for cGAS/STING. As a result, signaling to induce IFN was abrogated, impairing RT-induced abscopal effects. Consideration to these findings suggest that a

hypo-fractionated regimen, ideally with 3-5 doses of less than 10-12 Gy each, should be used when radiotherapy is combined with immunotherapy. Recent clinical data confirms the use of this dose and fractionation regimens, demonstrating efficacy in human cancers (Nature Medicine 2018:24, 1845-51).

---

#### Teaching Lecture: Tumor metabolism and radiation response

---

#### SP-0441 Inhibiting mitochondrial TCA cycle unravels tumor growth inhibitory and radiosensitizing effects

O. Feron<sup>1</sup>

<sup>1</sup>UCLouvain, Institut De Recherche Expérimentale Et Clinique Irec, Brussels, Belgium

##### Abstract text

Lactate exchange between glycolytic and oxidative cancer cells optimizes tumor growth. Blocking lactate uptake through monocarboxylate transporter 1 (MCT1) thus represents an attractive therapeutic strategy but may in turn stimulate glucose consumption by oxidative cancer cells. Here, we found that inhibition of mitochondrial pyruvate carrier (MPC) activity could fulfill the tasks of blocking lactate use while preventing glucose oxidative metabolism. Using *in vitro* <sup>13</sup>C-glucose and *in vivo* hyperpolarized <sup>13</sup>C-pyruvate, we identified TACC2 as a potent inhibitor of mitochondrial pyruvate transport which consecutively blocks extracellular lactate uptake by promoting intracellular pyruvate accumulation. Also while in spheroids MCT1 inhibition leads to cytostatic effects, pharmacological inhibition of MPC activity induces profound cytotoxic effects together with glycolysis stimulation and uncompensated inhibition of mitochondrial respiration. Hypoxia reduction obtained with TACC2 was further shown to sensitize tumor xenografts to radiotherapy. Hence, this study positions MPC as a control point not only for pyruvate but also lactate metabolism and expands on the radiosensitizing potential of MPC inhibition.

---

#### Teaching Lecture: Radiomic machine-learning to predict radiotherapy outcome

---

#### SP-0442 Machine learning in radiomic analyses to predict radiotherapy outcome

S. Löck<sup>1</sup>

<sup>1</sup>OncoRay - National Center for Radiation Research in Oncology, Faculty of Medicine and University Hospital Carl Gustav Carus- Technische Universität Dresden-Helmholtz-Zentrum Dresden-Rossendorf, Dresden, Germany

##### Abstract text

This lecture will focus on specific methods for the development and validation of prognostic or predictive models based on features extracted from medical imaging. The radiomic workflow, starting from available medical images to finally validated models, will be presented. Different machine-learning algorithms for the tasks of feature selection and model development will be explained in detail. Furthermore, the steps of hyperparameter tuning and model validation will be discussed. The results of systematic comparisons between machine-learning algorithms for the tasks of feature selection, patient classification or survival analysis allow for selecting suitable methods, which is an important step to increase the robustness of radiomic studies. After this lecture the participants may have a general impression on the radiomic workflow and on specific machine-learning algorithms applied for radiomic analyses.

---

**Teaching Lecture: Importance of volumetric staging and biological dose inhomogeneity in IMRT**


---

**SP-0443 Importance of volumetric staging and biological dose inhomogeneity in IMRT**

B. Maciejewski<sup>1</sup>

<sup>1</sup>*Maria Skłodowska-Curie Memorial Cancer Center and Institute of Oncology, Dept. Radiotherapy, Gliwice, Poland*

**Abstract text**

Basic biological aim of radiotherapy is to kill tumour cells (stem and clonogenic cells) and kill them all to achieve the highest TCP. Therefore, dose fractionation should be tailored to the initial number of tumour cells, which strictly corresponds with tumour volume. However, fractionation schedule is still individually designed based on quasi-quantitative rank - TNM system, which radiobiologically sounds illogical. Within a given T stage, i.e. T<sub>2</sub>N<sub>0</sub>M<sub>0</sub>, there is at least one decade difference in tumour cell number between the smallest and the largest tumours within this T category but practically, prescribed total dose is usually the same. This problem is discussed in details and illustrated with own data and the published results. Simple methods, how to convert tumour volume into the number of tumour cells and to tailor dose-fractionation for the highest TCP as possible, using single parameter D<sub>10</sub> is presented. The use of Volumetric Staging instead of the TNM to plan optimal radiotherapy is documented by practical examples. In the era of the 3D, 4D-IMRT, IGRT, SHRS, Fowler strongly recommended to plan D<sub>100</sub> instead of D<sub>95</sub> for the GTV. Results of the own pilot study clearly show, that even small “cold spots” within GTV subvolume can ruin the TCP initially predicted. The study shows how important is to convert physical DVHs into Biologically Normalized Histograms (BNDVHs) and the way how to replan dose distribution within GTV to eliminate biological “cold spots” in order to estimate real TCP to be close or even equal to that initially prescribed. Main goal of the lecture is to convince the audience that clinical radiobiologic principles are undoubtedly a basic requirement of all 3D conformal radiotherapy strategies. Key words: 3D-IMRT, Volumetric Staging, biological dose fractionation planning, D<sub>100</sub> instead of D<sub>95</sub>, BNDVHs

---

**Teaching Lecture: In-vivo dosimetry : Possibilities and Pitfalls**


---

**SP-0444 In-vivo dosimetry: Possibilities and Pitfalls**

V.N. Hansen<sup>1</sup>

<sup>1</sup>*Odense University Hospital, Laboratory of Radiation Physics, Odense C, Denmark*

**Abstract text**

In-vivo dosimetry (IVD) is the final verification of correct radiotherapy delivery. IVD is verifying that the radiotherapy plan, as designed within the treatment planning system (TPS), is delivered correctly to the individual patient, at the time of treatment. Historically IVD has focused on correct output of the linear accelerator and the focus has been point dose measurements. This is often measured as entrance dose verification, which does give assurance that at the specific point the output of the linac is correctly calibrated. This worked well in an era of simple open beams. However, the focus has changed from the “simple” output of the linac due to the fact that most TPS plans are IMRT or VMAT. Hence a point dose is no longer representative of the treatment. In addition the focus is not only on the capability of the linac delivery, but it is increasingly the patient anatomy and the possible

changes of the individual’s anatomy. The lecture will review options for IVD based on 2D detectors either place at the head of the linac for forward projected 3D IVD, or EPID detectors for back-projected 2D or 3D IVD. Clinical examples and challenges of IVD will be discussed.

---

**Teaching Lecture: The vital role of physicists in clinical trials: from design to data analysis**


---

**SP-0445 The vital role of physicists in clinical trials: from design to data analysis**

A.L. Appelt<sup>1</sup>

<sup>1</sup>*University of Leeds & St James’s University Hospital, Leeds Institute of Medical Research and Leeds Cancer Centre, Leeds, United Kingdom*

**Abstract text**

Medical physicists are vital players in the conducting of radiotherapy trials. Evidence clearly points to the importance of treatment quality assurance in clinical trials [1,2], where protocol violations and sub-optimal radiotherapy results in worse patient outcomes [3]. Consequently, the need for medical physics expertise for trial QA is well-recognised, and major organisations directly employ physicists to conduct multi-centre QA, e.g. in EORTC, IAEA, RTOG, TROG, and the UK RTTQA [4].

This lecture will argue, however, that the role to be played by physicists is considerably more extensive and more impactful than “just” thorough trial QA. Through specific trial examples, the impact of physicists on hypothesis generation, trial design, protocol development, and imaging / treatment delivery sub-studies will be demonstrated - and a case will be made for physics leadership on trials. Trials discussed will include an early phase dose finding trial [5] in head & neck cancer and a large multi-centre phase III trial in NSCLC [6]. Furthermore, the added scientific depth offered by radiotherapy physicists from exploratory secondary analysis of trial data will be touched upon (see e.g. [7]). Finally, we will go through some practical tips and tricks on how to get involved in clinical trials work - all directly sourced from physicists actively working on clinical trials.

1. Ohri N, Shen X, Dicker AP, et al. Radiotherapy protocol deviations and clinical outcomes: A meta-analysis of cooperative group clinical trials. *J Natl Cancer Inst* 2013;105:387-393.
2. Weber DC, Tomsej M, Melidis C, Hurkmans CW. QA makes a clinical trial stronger: evidence-based medicine in radiation therapy. *Radiother Oncol.* 2012;105:4-8.
3. Peters LJ, O’Sullivan B, Giral J, et al. Critical impact of radiotherapy protocol compliance and quality in the treatment of advanced head and neck cancer: results from TROG 02.02. *J Clin Oncol.* 2010;28:2996-3001.
4. Melidis C, Bosch WR, Izewska J, et al. Radiation therapy quality assurance in clinical trials - Global Harmonisation Group. *Radiother Oncol.* 2014;111:327-9.
5. Rasmussen JH, Håkansson K, Vogelius IR, et al. Phase I trial of 18F-Fluorodeoxyglucose based radiation dose painting with concomitant cisplatin in head and neck cancer. *Radiother Oncol.* 2016;120:76-80.
6. Møller DS, Nielsen TB, Brink C, et al. Heterogeneous FDG-guided dose-escalation for locally advanced NSCLC (the NARLAL2 trial): Design and early dosimetric results of a randomized, multi-centre phase-III study. *Radiother Oncol.* 2017;124:311-317.
7. Yahya N, Ebert MA, House MJ, et al. Modeling Urinary Dysfunction After External Beam Radiation Therapy of the Prostate Using Bladder Dose-Surface Maps: Evidence of Spatially Variable Response of the Bladder Surface. *Int J Radiat Oncol Biol Phys.* 2017;97:420-426.

---

**Teaching Lecture: New developments in the treatment of brain metastases: better prognostic tools, improved outcomes**

---

**SP-0446 New developments in the treatment of brain metastases: better prognostic tools, improved outcomes**

C. Nieder<sup>1</sup>

<sup>1</sup>Nordlandssykehuset HF, Dept. of Oncology and Palliative Medicine, Bodoe, Norway

**Abstract text**

Compared to previous decades where treatment options for brain metastases were limited to surgical resection and whole-brain radiotherapy, with stereotactic radiosurgery as an emerging modality, the current era is characterized by highly individualized treatment concepts, often combining different modalities and also integrating systemic drug therapy. Unprecedented CNS activity has been reported for different drugs, e.g., in subsets of patients with non-small cell lung cancer and malignant melanoma. It also appears possible to extend the survival of patients with oligometastatic disease by adding consolidative, ablative radiotherapy to extracranial metastatic sites after standard of care systemic treatment. On the other hand, many patients still present with widespread metastases and sometimes additional adverse prognostic features. These patients are at risk of early death and may be managed with optimal supportive care. Therefore, the invited lecture will focus on recent clinical studies and refined prognostic models, e.g., for non-small cell lung cancer, malignant melanoma and renal cell cancer.

---

**Symposium: Radiotherapy in bladder cancer: Standard of care and future perspectives**

---

**SP-0447 Do we have the evidence for radiation therapy as standard of care in bladder cancer?**

V. Fonteyne<sup>1</sup>

<sup>1</sup>Fonteyne Valerie, Radiotherapy-Oncology- Ghent University Hospital, Lovendegem, Belgium

**Abstract text**

Nowadays a radical cystectomy is still the golden standard for patients with muscle invasive bladder cancer although there is growing interest in bladder sparing approaches as an alternative for radical cystectomy. Level 1 evidence has clearly demonstrated the superior effect in outcome by combining chemotherapy and radiotherapy in a trimodality approach compared to radiotherapy alone. Similarly adding the tumour radiosensitizers carbogen and nicotinamide to radiotherapy results in increased permanent control of bladder disease. In the meanwhile several publications have proven the efficacy and safety of these trimodality therapies. Randomised trials comparing the outcome after radical cystectomy and trimodality therapy are lacking and one attempt to randomise patients between both treatment options failed due to poor accrual. Several retrospective analyses have tried to resolve the issue whether or not trimodality therapy is a valuable alternative for radical cystectomy. Conflicting results have been published. However it is of importance to point out that these analyses are not free from limitations. Misclassification and selection bias impair the interpretation of these data leading to overstated results and misleading conclusions. Rather than seeing both modalities as competing strategies one should regard them as complementary approaches in a very heterogenous population and one must absolutely avoid to deny a curable treatment with a bladder sparing

approach to patients who are unfit for surgery. This is of specific interest in an increasing elderly population.

**SP-0448 Bladder brachytherapy: an undoubtable importance of close multidisciplinary collaboration**

E. Van Der Steen-Banasik<sup>1</sup>, B. Oosterveld<sup>1</sup>, M.A.D.

Haverkort<sup>1</sup>, C. Wijburg<sup>2</sup>, G. Smits<sup>2</sup>

<sup>1</sup>Radiotherapy Group, Radiotherapy, Arnhem, The Netherlands ; <sup>2</sup>Rijnstate Hospital, Urology, Arnhem, The Netherlands

**Abstract text**

The first report of brachytherapy (BT) as part of a bladder-sparing treatment in MIBC appeared in 1915, followed by hundreds of treatments in the US and since the 50s in Europe with the majority of patients treated in the Netherlands. The biggest population was published by Koning et al in 2012, reporting a cohort of 1040 patients with a 5-years local control of 75 %. Two other bladder sparing modalities: partial cystectomy (PC) and chemoradiation report resp. 5-years DFS of 39%-67% and 60-73%. In a match-controlled study, comparing open radical cystectomy with BT in solitary MIBC, we have shown superior recovery, less complications and at least equal oncological outcome in the BT group. BT catheter placement was then performed by open surgery. Since 2009, we uniquely transformed the open technique in minimal invasive laparoscopy, in 2010 modified to a robot assisted approach. Here we show data of 130 consecutive, minimal invasively treated and prospectively monitored patients.

**Methods**

The indication is <5cm unifocal MIBC, no CIS, staged  $\leq$ T3a (CT and MRI.)

Ca 8 wks after TURB external beam irradiation EBRT starts, 40 Gy, 20 fractions in 4 weeks, including bladder and regional lymph nodes.

10 days afterwards the surgery consists of BT catheter implantation and (PC) if thicker than 1 cm residual tumor, localization in urachus, diverticulum or tumor nearby distal ureter/ostium.

The HDR (Ir-192) scheme is 25 Gy in 10 fractions, 3 fractions/day, starting 3hrs after surgery. In 2016 the decision was made to de-escalate the brachytherapy dose to 17.5 Gy in 7 fractions if PC was performed.

**Results**

130 consecutive patients (2% recurrent pT1, 98% MIBC) were treated. 5 patients were excluded from final analysis. PC was performed in 42 patients, with the last 16 receiving a reduced BT dose. Selective Lymph node dissection was performed in 42 patients, we found 7 positive of 252 resected nodes. Median hospitalization was 5.0 days, significantly reduced compared to the previous published open procedure (13.5 days). The average FU was 2.9 year (1 month - 9 year). 16 patients developed toxicity (CTCAEv4): acute G3-4: delirium(3), ileus(1), pulmonary embolism(1), late G2-3: hematuria(3), urinary urgency(3), lymphedema(2), bladder necrosis(1), recurrent cystitis(1), hydronephrosis(1). No changes in sexual functions nor late deterioration of bladder functions were

observed. Survival analysis: Kaplan-Meier method; 2y local control is 82%, 2y disease specific survival is 89%. No in-field local recurrences are observed in the PC group. This subgroup consists of 49% pT0, 11% pT1, 40% pT2 or more and showed 97% cancer specific survival, 97% loco-regional control and 94% NED (median follow-up of 2,5y). Fortunately this method is adopted: the group from Amsterdam recently reported 3 in-field recurrences in a cohort of 26 patients, treated between 2011 - 2016 and in the group from Lisbon reported on feasibility and reproducibility of the treatment.

**Conclusions:**

In these selected MIBC patients this minimally invasive multi-modality treatment results in excellent oncological

and functional outcomes. We consider this bladder sparing treatment as the gold standard in bladder preserving therapies. A multidisciplinary collaboration is indispensable.

**SP-0449 Stepwise Development of Personalized Radiation Therapy for Bladder Cancer**

V. Kong<sup>1,2</sup>, P. Chung<sup>1,2</sup>, S. Chen<sup>1</sup>, T. Craig<sup>1,2</sup>, T. Rosewall<sup>1,2</sup>

<sup>1</sup>Princess Margaret Cancer Centre, Radiation Medicine Program, Toronto, Canada ; <sup>2</sup>University of Toronto, Department of Radiation Oncology, Toronto, Canada

**Abstract text**

The introduction of new technology has revolutionized the way radiotherapy is delivered for bladder cancer: developing from the use of basic conventional techniques to a high precision, personalized approach. In order to demonstrate that the new technology is beneficial to the patient and to ensure its safe implementation, there is a need to integrate clinical expertise, patient values and research evidence into the development of evidence-based best practices (EBP). Since 2005, a series of prospective and retrospective studies were conducted to investigate different aspects of bladder radiotherapy, such as the accurate definition of treatment volumes, quantification of inter- and intrafractional bladder volumes changes and surface displacements, conformity and normal organ avoidance for dose distributions, mode and frequency of image-guidance interventions, reliability of image guidance surrogates and the cost/benefit of adaptive strategies. At each stage, the impact on geometric and dosimetric precision was quantified as evidence to substantiate the use of EBPs. Currently all bladder patients at our institution are treated with daily image guidance using CBCT with soft tissue alignment, with dose delivered to an individualized clinical target volume and planning target volume using IMRT.

**SP-0450 Radiosensitization strategies for the treatment of bladder cancer**

A. Choudhury<sup>1</sup>

<sup>1</sup>The Christie NHS Foundation Trust, Clinical Oncology, Manchester, United Kingdom

**Abstract text**

Bladder preservation is increasingly being accepted as an important alternative to radical cystectomy for muscle-invasive urothelial cancers. This talk will cover the evidence for bladder preservation using radiotherapy with radiosensitisation, dose, fractionation and radiotherapy technique. There are no robust ways to stratify patients for treatment, but there are a number of promising candidates. An overview of novel biomarkers for stratification will be presented.

---

**Joint Symposium: ESTRO-EACR: Radio-immunotherapy: from concept to clinical practice**

---

**SP-0451 Radiation-induced microenvironmental changes in cancer**

A. Gros<sup>1</sup>

<sup>1</sup>Valle de Hebrón Instituto de Oncología (VHIO), Tumor Immunology and Immunotherapy Group, Barcelona, Spain

Abstract not received

**SP-0452 Radiotherapy and cisplatin increase immunotherapy efficacy by enabling local and systemic intratumoral T-cell activity**

P. Kroon<sup>1</sup>, E. Frijlink<sup>1</sup>, V. Iglesias-Guimaraes<sup>1</sup>, A. Volkov<sup>1</sup>, M. Van Buuren<sup>2</sup>, T. Schumacher<sup>2</sup>, M. Verheij<sup>3</sup>, J. Borst<sup>1</sup>, L. Verbrugge<sup>1</sup>

<sup>1</sup>The Netherlands Cancer Institute, Division Of Tumor Biology And Immunology, Amsterdam, The Netherlands; <sup>2</sup>The Netherlands Cancer Institute, Division Of Molecular Oncology And Immunology, Amsterdam, The Netherlands; <sup>3</sup>The Netherlands Cancer Institute, Department Of Radiation Oncology, Amsterdam, The Netherlands

**Abstract text**

To increase cancer immunotherapy success, PD-1 blockade must be combined with rationally selected treatments. Here, we examined in a poorly immunogenic mouse breast cancer model the potential of antibody-based immunomodulation and conventional anti-cancer treatments to collaborate with anti-PD-1 treatment. One important requirement to improve anti-PD-1-mediated tumor control was to promote tumor-specific cytotoxic T cell (CTL) priming, which was achieved by stimulating the CD137 costimulatory receptor. A second requirement was to overrule PD-1-unrelated mechanisms of CTL suppression in the tumor micro-environment (TME). This was achieved by radiotherapy and cisplatin treatment. In the context of CD137/PD-1-targeting immunotherapy, radiotherapy allowed for tumor elimination by altering the TME, rather than intrinsic CTL functionality. Combining this radioimmunotherapy regimen with low-dose cisplatin improved CTL-dependent regression of a contralateral tumor outside the radiation field. Thus, systemic tumor control may be achieved by combining immunotherapy protocols that promote T cell priming with (chemo)radiation protocols that permit CTL activity in both the irradiated tumor and (occult) metastases.

**SP-0453 Targeting DNA repair to improve immune-surveillance and restrict cancer growth**

G. Germano<sup>1</sup>, S. Lamba<sup>2</sup>, G. Rospo<sup>2</sup>, L. Barault<sup>2</sup>, A. Magri<sup>3</sup>, F. Maione<sup>2</sup>, M. Russo<sup>2</sup>, F. De Braud<sup>4</sup>, S. Marsoni<sup>5</sup>, M. D'incalci<sup>6</sup>, A. Sartore-Bianchi<sup>7</sup>, S. Siena<sup>7</sup>, F. Pietrantonio<sup>4</sup>, F. Di Nicolantonio<sup>1</sup>, A. Bardelli<sup>1</sup>

<sup>1</sup>Candiolo Cancer Institute, Department Of Oncology-University Of Torino, Torino, Italy; <sup>2</sup>Candiolo Cancer Institute, Fpo- Irccs, Candiolo To, Italy ; <sup>3</sup>Candiolo Cancer Institute, Fpo-Irccs, Candiolo To, Italy ; <sup>4</sup>Fondazione Irccs Istituto Nazionale Dei Tumori, Medical Oncology Department, Milano, Italy; <sup>5</sup>IOM - The Firc Institute Of Molecular Oncology, Precision Oncology, Milano, Italy; <sup>6</sup>irccs-Istituto Di Ricerche Farmacologiche Mario Negri, Department Of Oncology, Milano, Italy ; <sup>7</sup>Niguarda Cancer Center- Grande Ospedale Metropolitano Niguarda, Department Of Oncology, Milano, Italy

**Abstract text**

Colorectal, ovarian, endometrial and other tumors carrying defects in DNA mismatch repair often show favorable prognosis and indolent progression. The genomes of these tumors bear hundreds of thousands of somatic mutations, a feature which fosters cancer progression and might lead to rapid evolution of resistance to targeted therapies. Recent evidences that a subset of MSI (microsatellite instable) tumors respond prominently to immune checkpoint blockade led to the hypothesis that the presence of high number of somatic mutations may be responsible for effective immune-surveillance. However, several reports indicate that a relevant fraction of hyper-mutated tumors have unfavorable prognosis and do not respond to immune-modulators. To understand the molecular and functional bases of response to immune checkpoint inhibitors, we genetically inactivated MutL homolog 1 (MLH1) in colorectal, breast and pancreatic mouse cancer cells. The growth of MMR deficient cells was comparable to their proficient counterparts in vitro and upon transplantation in immune-compromised mice. However, isogenic MMR deficient cancer cells, acquiring alterations over time, were unable to form tumors when

injected subcutaneously or orthotopically in syngeneic mouse models according to cell-passage number. Moreover, we found that MMR-driven dynamic generation of neoantigens, when restricted to a clonal population, further increases immune detection. Mechanistically, MLH1 inactivation increased the mutational burden and led to dynamic mutational profiles, resulting in persistent renewal of neoantigens *in vitro* and *in vivo*, while control cells exhibited stable mutational loads and neoantigen profiles over time. These results led us to hypothesize that enforced increase of the number of mutations in cancer cells could restrict cancer growth and might be beneficial for therapeutic purposes. We therefore performed a pharmacological screen to identify agents capable of permanent inactivation of MMR in colorectal, breast and PDAC cancer cells. We found that temozolomide triggers MLH1 inactivation in cancer cells that -as a result- are unable to form tumors in syngeneic animals. Genomic analysis of temozolomide resistant cells revealed that fluctuating levels of neoantigens, rather than the absolute number of mutations, might be critical to provoke immune surveillance. Overall, these results provide the rationale for developing innovative anticancer therapies based on inhibition of DNA repair mechanisms.

**SP-0454 Trial design: early clinical studies and learning from the laboratory**

T. Illidge<sup>1</sup>

<sup>1</sup>The University of Manchester, Manchester Cancer Research Centre- Christie NHS Foundation Trust, Manchester, United Kingdom

**Abstract text**

Radiotherapy (RT) is a highly effective cancer treatment and research for much of the last century focused on understanding the mechanisms underlying its tumoricidal properties. Only relatively recently have the local and systemic immunomodulatory properties of RT been investigated. RT is now known to stimulate an immune response by inducing a variety of immunogenic and phenotypic changes in malignant cells that can recalibrate the immune contexture of the tumour microenvironment. If the immunoregulatory effects could be harnessed this could significantly increase the anti-cancer effect of RT. The recent major breakthrough of the immune checkpoint inhibitors (ICI) anti-CTLA-4 (cytotoxic T-Lymphocyte-associated protein 4) and anti-PD1/PD-L1 (programmed death-ligand 1) has led to durable remissions and improved survival in a number of incurable cancers including metastatic malignant melanoma, Non Small Cell lung cancer, renal cell cancer and other cancers. This remarkable clinical efficacy has established immunotherapy as another effective form of cancer therapy and stimulated the “immunotherapy revolution” leading to the large scale development of a new class of therapeutics termed immuno-oncology (IO) agents. Given that both RT and IO agents are potentially immunomodulatory combining RT with IO agents provides a unique opportunity to increase systemic anti-tumour immunity and transform cancer therapy. This goal would be achieved with RT and IO agents combinations by improving the outcomes for those patients who present with localised disease and who currently fail with localised recurrence or the development of metastatic disease as well as tackling those with oligometastatic disease who are currently incurable and thus converting RT into an effective part of systemic therapy. Proof of principle preclinical studies using RT in combination with Immune check point inhibition (ICI) using anti-CTLA-4 and PD-1/PD-L1 blockade have demonstrated “abscopal” systemic anti-tumour immune responses in tumours outside of the RT field leading to long term clearance. These systemic immune responses have also been reported in a number of clinical case reports. This preclinical evidence and these interesting clinical reports led to hundreds of clinical trials

being launched with the aim of testing the efficacy of radiotherapy in combination with immunotherapy to improve outcomes. However converting clinical responses seen with in a minority of patients in solid tumours with ICI using a single site of RT for “abscopal” responses and expecting the majority of patients to respond to ICI in combination with RT is unlikely to happen. In order to see more durable responses to RT and IO agent combinations we need firstly to further understand how RT influences the tumour cells, tumour microenvironment and surrounding immune effector cells. We also need to explore irradiation of multiple lesions in order to enhance the likelihood of obtaining meaningful clinical outcomes in some clinical situations. Secondly we need to partner RT with the optimal immunomodulatory IO agent to generate the most effective systemic anti-tumour immune responses. For tumours rich in T cell infiltrates, RT and anti-PD1 might be effective combinations overcoming T cell exhaustion and increasing systemic T cell anti-tumour immunity. For those with more immunosuppressive microenvironments that might be devoid of T cell and / or rich in myeloid cells other types of immunostimulatory agents are likely to be required. In this presentation the current challenges in translating recent findings with RT and IO agents in the laboratory into the clinic and a review of the progress made to date in clinical trials will be discussed.

---

**Symposium: Tumor Metabolism and Radiotherapy**

---

**SP-0455 Inhibition of glycolysis and redox metabolic pathways in cervical cancer**

J. Schwarz<sup>1</sup>

<sup>1</sup>Washington University School of Medicine, Department of Radiation Oncology, St. Louis, USA

**Abstract text**

One third of locally advanced cervical cancers treated with standard of care chemoradiation (pelvic irradiation plus concurrent cisplatin chemotherapy) fail this treatment, and there is currently no cure for recurrent or metastatic disease. Our previous work has shown that the results of <sup>18</sup>F-fluoro-deoxy-glucose positron-emission-tomography (FDG-PET) can be used to identify treatment-resistant cervical cancers. Cervical tumors that take up large quantities of FDG, a glucose analog, prior to treatment are resistant to radiation, and tumors that maintain high levels of FDG uptake after radiation is complete are likely to recur. Given these clinical observations, a reasonable hypothesis is that inhibiting cervical tumor glucose metabolism may improve radiation sensitivity. The hexokinase inhibitor, 2-deoxyglucose (2-DG), has been evaluated in *in vitro* and *in vivo* as a radiosensitizer in a number of cancer models, and 2-DG has been administered to patients in the context of clinical trials. The results of these studies show that while inhibition of glucose metabolism with 2-DG can transiently increase radiation sensitivity, long term therapeutic gains are limited by the normal tissue toxicity that occurs at the doses required to maintain effective inhibition of glycolysis in tumors. In addition, new concerns have arisen over the capacity of tumor cells to rewire their metabolism in response to metabolic therapy (metabolic plasticity). Glycolytic tumor cells exist in a relative state of oxidative stress due to increased levels of reactive oxygen species (ROS) and compensate for this by upregulating redox metabolic pathways. Indirect effects of irradiation also result in transient increases in ROS that are metabolized by tumor cells. We hypothesized that simultaneous inhibition of glycolysis and the redox metabolic pathways would be more effective as a radiation sensitizer than inhibition of glycolysis alone. Using a panel of cervical cancer cell lines, we

demonstrate that sensitivity to 2-DG monotherapy is increased in tumor lines that are highly glycolytic, and that 2-DG enhances the efficacy of cisplatin chemotherapy and radiation in glycolytic tumor cells. When 2-DG is combined with L-buthionine sulfoximine (BSO), an inhibitor of glutathione biosynthesis, and auranofin (AUR), a thioredoxin reductase inhibitor, glycolytic cervical cancer cells are unable to proliferate. Detailed analysis of intracellular redox parameters indicates that these effects are mediated primarily by increases in intracellular reactive oxygen species, which can promote autophagic and non-autophagic forms of cell death depending on the oncogenic context. In cervical tumor models in the mouse, this drug strategy can be used to limit tumor growth for highly glycolytic cancers and to radio-sensitize cancers that display intermediate levels of Warburg-related glucose metabolism. Consistent with our hypothesis, combined treatment with 2-DG, BSO and AUR is more effective as a radio-sensitizer in vivo than 2-DG alone. Most recently, we have found that glutamine deprivation or treatment with glutaminase inhibitors can also be used to promote increases in intracellular oxidative stress that facilitate radiation therapy efficacy.

**SP-0456 Sex differences in cancer metabolism: implications for therapy**

J. Ippolito<sup>1</sup>

<sup>1</sup>Washington University School of Medicine, Radiology, Saint Louis, USA

**Abstract text**

There is a sex disparity in many cancers throughout the body where males have a higher incidence and mortality compared to females. Moreover, these effects are independent of age suggesting that cell-intrinsic phenomena, rather than the effects of sex hormones, may play a key role in this clinical phenotype. Metabolism is one potential factor underlying this disparity where nutrient uptake and metabolism are enhanced in males relative to females beginning at the earliest stages of embryogenesis and are carried into adulthood. Because of the established inverse correlation between enhanced glucose metabolism and patient survival in many cancers, we hypothesized that sex differences in central carbon metabolism underlie sex differences in cancer patient survival. We developed a data mining algorithm using The Cancer Genome Atlas (TCGA) to identify metabolic gene expression patterns that correlated with poor sex-specific outcomes. We applied this algorithm to the lower grade glioma (LGG) transcriptome and identified numerous enzymes involved in glycolysis, glutamine-fueled tricarboxylic acid (TCA) cycle metabolism, and oxidative phosphorylation that uniquely identified men, but not women, with poor outcomes. We validated these findings using an established mouse model for sex differences in gliomas, the *Nf1*<sup>-/-</sup>*DNp53* model, where transformed mouse astrocytes are deficient for neurofibromin 1 (*Nf1*) and express dominant negative p53 (*DNp53*) protein. We identified that a critical metabolic sex difference was glutamine-fueled TCA cycle metabolism that was significantly higher in transformed male astrocytes. We also identified that transformed male astrocytes were more susceptible to inhibition of glutamine metabolism with glutaminase inhibitors compared to females. Together, these findings highlight sex-specific dependencies of specific nutrients and metabolic pathways on tumor growth that may potentially be exploited for therapy. Moreover, clinically-relevant metabolic imaging modalities such as fluorodeoxyglucose-PET, fluoroglutamine-PET, or hyperpolarized carbon-13 MRI may identify prognostic sex differences in patients.

**SP-0457 Hypoxia-induced Replication Stress**

TBC

**SP-0458**

**Targeting metabolism to sensitize hypoxic tumor cells**

M. Koritzinsky<sup>1</sup>

<sup>1</sup>University Health Network, Princess Margaret Cancer Centre, Toronto, Canada

**Abstract text**

Tumor hypoxia has long been recognized as a limiting factor for radiotherapy response due to the strong radiosensitizing effect of oxygen. Although randomized clinical trials have demonstrated some benefit of increasing the oxygen supply or replacing oxygen with radiosensitizers during radiotherapy, these strategies have not resulted in widespread clinical adoption. Over the last few years, a common theme has emerged from experimental studies, highlighting the potential for various clinically approved drugs to enhance tumor oxygenation through inhibition of the oxygen consumption of tumor cells close to blood vessels. These studies have hence led to several ongoing randomized clinical trials in which these drugs are repurposed to enhance tumor oxygenation during radiotherapy. A complimentary approach to sensitize hypoxic tumors is to target hypoxia adaptation mechanisms that render cancer cells vulnerable to the lack of oxygen. Many aspects of metabolism are altered or specifically required under hypoxic conditions, including the cellular metabolism of reactive oxygen species (ROS). Cancer cells frequently have high ROS production due to deregulated proliferation and metabolism. Hypoxia further increases overall cellular levels of ROS, and reoxygenation triggers substantial ROS bursts. Together, this renders tumor cells vulnerable to targeting anti-oxidant defense systems. Here we will present data demonstrating that the protein peroxiredoxin 4 (PRDX4) is essential in both normoxia and fluctuating oxygen conditions in vitro and in experimental tumor models. Loss of PRDX4 leads to increase ROS and DNA damage, resulting in cell toxicity and radiosensitization. These data support the potential for combining disruption of redox homeostasis with radiotherapy for improved therapeutic ratio.

---

**Joint Symposium: ESTRO-ESR: Current status and future challenges in MR-integrated radiotherapy**

---

**SP-0459 Clinical status of MR-integrated photon therapy**

L. Boldrini<sup>1</sup>

<sup>1</sup>Fondazione Policlinico Universitario "A. Gemelli" Ircs, Radiation Oncology, Rome, Italy

**Abstract text**

The introduction of MR integrated delivery units represents one of the most significant and promising innovations of the last years in radiotherapy delivery technology. The advantages assured by the better visualization of the therapy volumes allowed by on board MR imaging and the possibility to use active gating and motion management solutions embedded in this novel workflow need to be further explored and quantified both from a technical and a clinical perspective. Aim of this talk is to describe the current clinical status of the MR-integrated photon radiotherapy and to present the clinical evidence to date available. Its most common applications will be reported, ranging from the patient selection methods to the choice of the most appropriate therapy delivery protocol. Furthermore, the possibility to implement innovative hypothesis generating approaches (movement management, radiomics, new delivery techniques) in clinical MR-integrated radiotherapy will be presented.

**SP-0460 Integration of MR and particle therapy - how far are we?****A. Hoffmann<sup>1</sup>**<sup>1</sup>*OncoRay - Center for Radiation Research in Oncology, Medical Radiation Physics, Dresden, Germany***Abstract text**

Precise targeting in proton therapy (PT) is even more important than in conventional photon-based radiation therapy (XT), because the usage of fewer radiation fields make PT dose distributions more sensitive to anatomical variations (e.g., organ motion and deformation) and patient set-up inaccuracies than XT. This is due to the steep dose fall-off behind the Bragg peak and to the fact that the range of the proton beam strongly depends on the material composition in the beam path. Especially for moving tumours, these uncertainties translate into relatively large safety margins, thus compromising the dosimetric benefit of PT. This urges the need for real-time image guidance during PT dose delivery. Magnetic resonance imaging (MRI) offers real-time image guidance with unparalleled soft-tissue contrast and absence of radiation dose. PT is therefore expected to benefit even more from the integration with real-time MRI than XT. Hence, in recent years there has been a growing interest to investigate the potential of MR-integrated PT (MRiPT), but so far no hybrid system has been realized due to a number of hitherto open technological problems. To study the technological feasibility of MRiPT, mutual interactions between the PT and MRI system have to be taken into account, some of which have already been addressed or are subject of ongoing research. Lorenz-force induced dose distortions (i.e. beam deflection and electron return effect for transverse magnetic fields and beam focussing effect for longitudinal magnetic fields) need to be quantified and taken into account during treatment planning and dose delivery. The magnetic interaction with dosimetry detectors may compromise the results of such measurements. Methods and procedures for proton beam dosimetry in the presence of magnetic fields have to be established. The mutual electromagnetic interaction between the MRI scanner and the PT system needs to be assessed and understood as this can compromise both the beam and image quality. For simultaneous operation of both systems, magnetic shielding may be required in addition to RF shielding. For on-line adaptive treatment planning, the proton dose distribution needs to be calculated directly from MR images. Fast and accurate methods that translate MR image information into electronic stopping power need to be developed.

Recent research efforts have realized a proof-of-concept system where first MR images of tissue-mimicking phantoms have been successfully acquired with a clinical in-beam MR scanner during proton beam irradiation. This offers the prospect that the development of a clinical prototype MRiPT system within the next 5 years should not be considered beyond the realms of possibility.

The contribution provides an overview of the current status of MRiPT research achievements and discusses technology issues that need further investigation. Implications for future developments and clinical treatment workflow are also addressed.

**SP-0461 MR-based functional imaging****R. Beets-Tan<sup>1</sup>**<sup>1</sup>*Maastricht Radiation Oncology (Maastricht), Maastricht, The Netherlands*

Abstract not received

**SP-0462 Adaptive workflow - current status and challenges****S. Kharuzhyk<sup>1</sup>**<sup>1</sup>*N.N. Alexandrov National Cancer Center, Department of Radiology, Minsk, Belarus***Abstract text**

MRI is used at different stages of oncological patient management including tumor staging, treatment (surgery, radiation therapy) planning and tumor response assessment. Traditional radiation therapy planning workflow integrates high contrast resolution and anatomical details provided by MRI with electron density values obtained from CT. More recently MRI-only radiotherapy planning workflow has been implemented with synthetic CT images generated from MRI data. On-treatment MRI-guidance is a new paradigm of precision radiotherapy that enables a scan-plan-treat approach or adaptive radiotherapy. MRI linac machines integrating clinical MRI scanner with linear accelerator are current reality in some cancer centers around the globe.

**Symposium: Improved outcome by smarter use of radiotherapy****SP-0463 Towards less radiotherapy in breast cancer treatment****I. Meattini<sup>1</sup>**<sup>1</sup>*University of Florence - Azienda Ospedaliero Universitaria Careggi, Radiation Oncology Unit - Oncology Department, Florence, Italy***Abstract text**

Overdiagnosis and overtreatment represent great challenges in modern treatment for breast cancer. During the last decades several trials aiming less radiotherapy have been performed: reduction of overall treatment course (hypofractionation), reduction of overall treatment courses and breast target volumes (partial breast irradiation), omission of radiotherapy (whole breast and/or tumour bed boost). Hypofractionated whole breast irradiation, based on precedent studies over the past two decades, offers an opportunity for improved patient convenience, lower healthcare costs, and greater access to care without sacrificing treatment outcomes. Four randomized trials fully supported the use of hypofractionated whole breast irradiation as standard of treatment: the RMH/GOC trial, the UK START trial A and B, and the Canadian trial [1-6]. Partial breast irradiation has been introduced as an alternative treatment method for selected patients with early stage breast cancer. Potential advantages include shorter treatment time (accelerated), improved cosmesis secondary to a reduction in volume of breast tissue treated, and cost reduction compared with standard fractionation. Initial trials investigating partial breast irradiation showed conflicting results. The recent new high-level evidence provided by the results of the IMPORT-LOW trial clearly showed that adequate patients' selection led to low LRR. Tumour biology seems to play a crucial role on treatment outcome, thus it should always be considered together with disease stage, comorbidities, and patient's quality of life. Breast cancer should be always considered as a heterogeneous disease, for which a one treatment fit all strategy rarely represented the best option e giving the patients the final word in the shared decision-making process [7-10]. Whether radiotherapy is beneficial in elderly patients undergoing conservative surgery for early breast cancer has long been controversial. In the PRIME II trial, patients  $\geq 65$  years with tumours  $< 3$  cm in size with primarily grade I/II disease, all oestrogen receptor-positive and pathologically node-negative, were randomly assigned to whole-breast radiation therapy plus hormone therapy vs hormone therapy alone. The findings parallel those of CALGB 9343, which included an even lower-risk cohort of

patients ( $\geq 70$  years with tumours  $\leq 2$  cm, clinically node-negative, oestrogen-positive). Both studies showed significantly higher rates of local relapse in the endocrine therapy alone arms; though these differences, the addition of whole-breast radiation therapy did not result in differences in breast cancer-specific survival. The BASO II trial confirmed that patients treated with either exclusive adjuvant radiotherapy or endocrine therapy with tamoxifen had an equivalent local relapse rate per annum of 0.8%. These data suggest that radiation or endocrine therapy alone resulted in excellent disease control in older women with early breast cancer, and that the combination of treatments may have less benefit than expected. A direct comparison between radiation or endocrine therapy omission as adjuvant treatment is lacking in the existing literature [11-13]. The use and dose of a boost on the tumour bed has been largely investigated. In a phase 3 randomised controlled trial, the effect of a radiation boost of 16 Gy on overall survival, local control, and fibrosis for patients with stage I and II breast cancer compared with patients who received no boost has been evaluated. At a 20-year follow-up time, a radiation boost has no effect on long-term overall survival, but can improve local control, with the largest absolute benefit in young patients, although it increases the risk of moderate to severe fibrosis. Conversely, boost can be avoided in most patients older than age 60 [14,15].

#### References

- [1]. Yarnold J, Ashton A, Bliss J, et al. *Radiother Oncol*. 2005;75:9-17.
- [2]. Owen JR, Ashton A, Bliss JM, et al. *Lancet Oncol*. 2006;7:467-71.
- [3]. START Trialists' Group. Bentzen SM, Agrawal RK, et al. *Lancet Oncol*. 2008;9:331-41.
- [4]. START Trialists' Group. Bentzen SM, Agrawal RK, et al. *Lancet*. 2008;371:1098-107.
- [5]. Haviland JS, Owen JR, Dewar JA, et al. *Lancet Oncol*. 2013;14:1086-94.
- [6]. Whelan TJ, Pignol JP, Levine MN, et al. *N Engl J Med*. 2010;362:513-20.
- [7]. Coles CE, Griffin CL, Kirby AM, et al. *Lancet*. 2017;390(10099):1048-1060.
- [8]. Meattini I, Livi L, Pallotta S, Marrazzo L. *Breast*. 2018;38:98-100.
- [9]. Polgar C, Van Limbergen E, Potter R et al. *Radiother Oncol* 2010;94:264-73.
- [10]. Correa C, Harris EE, Leonardi MC et al. *Pract Radiat Oncol* 2017;7:73-9.
- [11]. Kunkler IH, Williams LJ, Jack WJL, et al. *Lancet Oncol*. 2015;16:266-273.
- [12]. Hughes KS, Schnaper LA, Bellon JR, et al. *J Clin Oncol*. 2013;31:2382-2387.
- [13]. Blamey RW, Bates T, Chetty U, et al. *Eur J Cancer*. 2013;49:2294-2302.
- [14]. Vrieling C, van Werkhoven E, Maingon P, et al. *JAMA Oncol*. 2017;3:42-48.
- [15]. Bartelink H, Maingon P, Poortmans P, et al. *Lancet Oncol*. 2015;16:47-56.

#### SP-0464 Image-guided elective neck irradiation in head and neck cancer

A. Al-Mamgani<sup>1</sup>

<sup>1</sup>Netherlands Cancer Institute, Department of Radiation Oncology, Amsterdam, The Netherlands

#### Abstract text

Because of the rich lymphatic supply of the head and neck region, head and neck squamous cell carcinoma (HNSCC) has the tendency to metastasize to the regional lymph nodes, also to the contralateral side. The concept of elective nodal irradiation (ENI) was introduced in the sixties by Fletcher and supported later on by others. Since then, there is a long-standing empirical convention to irradiate the vast majority of HNSCC electively to both

sides of the neck (with the exception of T1 laryngeal and small lateralized tonsillar fossa cancer), in order to reduce the risk of contralateral RF (cRF). Meanwhile, there is slowly growing evidence that the incidence of cRF in well-selected HNSCC is very low (<5%). Furthermore, unilateral ENI will result in significant decrease in the incidence and severity of acute and late toxicity and improve QoL. In different studies, large treated volumes, chemoradiation and bilateral neck irradiation were the most important predictors for radiation-related toxicity. Therefore, there is increasing need for selection tools to expand the indication for unilateral ENI to reduce toxicity and improve QoL. As a consequence of the improved prognosis and increased incidence of HPV-positive oropharyngeal cancer among young people, these issues are becoming increasingly important since these young patients will live longer with the burden of troublesome late toxicities. At the Dutch Cancer Institute, we initiated a proof-of-concept study, the SUSPECT study (mapping of sentinel lymph node drainage using SPECT to tailor ENI in node-negative neck of patients with head and neck cancer) (ClinicalTrials.gov Identifier NCT02572661). The aim of this study was to investigate the role of SPECT/CT for the lymph drainage mapping (LDM) and to explore the incidence of cRF in patients electively treated to one side of the neck, based on SPECT/CT-guided LDM. In this study, 50 patients with primary HNSCC, T1-3N0-2bM0 located in the oral cavity, oropharynx, larynx (except T1 glottic), and hypopharynx, not crossing the midline and planned for treatment with (chemo)radiotherapy in curative setting, were included. LDM was performed using SPECT/CT scan 2-4 hours after injection of the primary tumor with radioactive Tc-Albumin (80MBq). Patients without any contralateral drainage, only the ipsilateral neck was electively irradiated. In case a contralateral tracer accumulation was identified, the elective treatment included the ipsilateral neck and only the level containing tracer accumulation, instead of the whole contralateral neck. The preliminary results are very promising. The dosimetric analysis showed highly significant reduction of dose to the salivary glands, swallowing muscles, speech structures, larynx, supraglottic region and thyroid glands. These dosimetric advantages was translated in significant reduction of the frequency, severity, and duration of acute and late toxicities such as grade 3 dysphagia (tube-feeding) and dry mouth, compared to a historical cohort of 50 consecutive patients treated bilaterally, outside the framework of the study. The first 40 patients included have meanwhile a follow-up time of at least 1 year. Only one patient with cRF was seen (2.5%). This patient was successfully salvaged by ND and is still alive with NED, 1.5 years after treatment.

#### SP-0465 Adapting RT in soft tissue sarcoma: the influence of anatomy, biology and response

B. O'Sullivan<sup>1</sup>

<sup>1</sup>Princess Margaret Cancer Centre, Radiation Oncology, Toronto, Canada

#### Abstract text

Traditional combined modality approaches to the local management of soft tissue sarcoma have used post-operative radiotherapy (RT) in a "shrinking field" concept to deliver an elective dose (e.g. 50 Gy) to a clinical target volume (CTV2) encompassing potential microscopic involvement beyond the original location of the gross tumour volume (GTV) and a higher dose to the originally site of the GTV (CTV1). These CTVs can be treated simultaneously or sequentially and generally are facilitated by the use of IMRT to deliver a dose of 60-66 Gy to the combined volume. Alternatively, pre-operative RT to CTV2 alone is often favored with RT reserved for CTV1 as a "boost" if involved resection margins occur at the resection. However, adequate and safe RT administration may not be feasible in some sites such as

skull base or retroperitoneum occupied by vulnerable anatomy. Therefore, modifications have been introduced by some groups in the interest of dose reduction to spare late morbidity. For example, a post-operative “boost” of 10-16 Gy to CTV1 to complete the 66 Gy total dose prescription was traditional in pre-operative radiotherapy but has generally been omitted in recent years when resection margins are not involved. Moreover some centres now also omit this “boost” when the margins are involved if this was a “planned positive” margin in a very small region juxtaposed to a vulnerable structure. Some colleagues, e.g. in Scandinavia and France, have also restricted post-operative radiotherapy courses to approximately 50 Gy in 25 fractions or equivalent rather than delivering an additional boost to CTV1 for a total of 66 Gy if the resection margins are uninvolved. The concept of restricting the dose to 50 Gy pre-operatively and post-operatively is currently being tested in the Canadian 50/50 randomized trial (NCT02565498). Differences in RT response of different sarcoma histological subtypes exists and has been shown to convert to improved local control in myxoid liposarcoma, with further potential for treatment with lower pre-op RT doses (36 Gy) in this pathological subtype currently under evaluation in the Doremy study (NCT02106312). There is also evidence that RT volume adaptation may be facilitated based on on-treatment response during pre-operative RT evident in patients treated in the first clinical trial of IMRT in extremity (STS NCT00188175). With daily CBCTs online, we have seen incremental changes in volume, and a 1 cm change affects dosimetry and coverage. This may be facilitated by implementation of MRgRT systems, with eventual potential generation of new IMRT plans for patients while still on treatment. Additional possibilities for RT dose reduction with shorter overall treatment time seem possible using RT regimens combined with chemotherapy or targeted agents. Finally, RT doses may be reduced through volume restriction by modification of RT delivery including use of particle beam, intra-operative RT, or pathological response following intratumoral injection of hafnium oxide nanoparticles with RT.

---

**Symposium: Quantitative Imaging for Radiation Oncology**

---

**SP-0466 A Critical Look of Quantitative Dynamic Contrast Enhanced MRI: From QIBA guidelines to Clinical Implementation**

**C. Chung<sup>1</sup>**

<sup>1</sup>MD Anderson Cancer Center, Radiation Oncology, Houston, USA

**Abstract text**

The promise of dynamic contrast-enhanced MRI (DCE-MRI) as a prognostic and predictive biomarker in solid malignancies is not a new concept. There have been efforts over several decades to investigate the methods and clinical value of DCE-MRI in oncological assessment. Many studies from individual institutions have suggested that DCE-MRI can characterize tumor angiogenesis and serial measurements may reflect changes in tumor vascular physiology in response to treatment or with further tumor progression. In Radiation Oncology, DCE-MRI has frequently been investigated in conjunction with tumor hypoxia, which has been associated with greater tumor aggressiveness and metastatic potential. In Medical Oncology, DCE-MRI was of particular interest when anti-angiogenic and anti-vascular therapies were discovered, but remain of interest in the context of drug delivery and early biomarkers of response.

Despite strong interest and promising single site studies, there have been great challenges in using DCE-MRI as a

quantitative imaging measure, particularly in multisite trials. This motivated the Quantitative Imaging Biomarker Alliance (QIBA), which initially formed in 2007, to write one of their earliest profiles on DCE-MRI. The DCE-MRI Quantification QIBA Profile places requirements on the acquisition device, the actors (technologists, radiologists, physicists), reconstruction software and image analysis tools involved in image acquisition, image data reconstruction, and image analysis. As QIBA recognized that the clinical and research environment for these quantitative imaging tools is ever evolving, the Profile sits online as a living document and there are current ongoing revisions to address the increasing use of 3.0T magnets and parallel imaging. The Profile requirements are determined based on published literature on repeatability and reproducibility. Despite a long history of interest by the oncology community in using DCE-MRI as a quantitative imaging biomarker, the recent systemic review of clinical literature by the DCE-MRI Committee within QIBA discovered a very limited number of publications on repeatability and reproducibility data.

In the era of precision medicine, the community-at-large is starting to understand that variability in measurement limits our ability to quantitatively characterize tumors or evaluate treatment response. Only through standardized processes of image acquisition, quality assessment, processing and analysis will there be the potential for collaborative, quantitative investigation. As part of this standardization process, the community will need to come together to determine shared nomenclature and define reporting standards that ensure enough transparency to enable cross-validation as well as supportive data collection, including repeatability and reproducibility data.

**SP-0467 Quality assurance for quantitative MRI in a multicenter trial**

**P. Van Houdt<sup>1</sup>**

<sup>1</sup>The Netherlands Cancer Institute, Radiation Oncology, Amsterdam, The Netherlands

**Abstract text**

Quantitative MRI (qMRI) is promising as a biomarker for prediction of treatment outcome and for treatment response monitoring. However, current evidence is mainly built on small patient cohorts. Large, multi-center studies are necessary to investigate the clinical application of qMRI. However, these studies typically involve a wide variety in MRI systems, with different vendors, field strengths, and generations. As a result novel sequences may be available in one institute, but not in another. One approach to reach consistency would be to use standardized MRI protocols in all centers. The drawback is, however, that this will force us to design the sequences for the oldest system. Therefore, we have built a framework where we deal with this variety by optimizing the trial sequences on each system individually. In this way all institutes are free to choose the sequence to their preference and system possibilities. We have set up a quality assurance (QA) procedure using calibration phantoms to assess consistency of the trial sequences between institutes. This includes the measurement of benchmark sequences to investigate whether deviations between institutes result from protocol differences in the trial sequences or from system variations. These benchmark sequences are well known reference standards that are available on all systems using identical parameter settings.

In this talk, we will illustrate how we applied this framework in the IQ-EMBRACE trial and for treatment response monitoring studies using MR-linac systems. IQ-EMBRACE (sub-study of the EMBRACE-II trial) is a large, multi-center trial in which patients with cervical cancer will undergo an MRI exam prior to radio(chemo)therapy to investigate qMRI as a potential biomarker for treatment

outcome. So far, measurements have been performed in ten institutes. With the QA procedure we were able to identify inaccurate results and optimize the sequences such that consistent results were obtained. Similar results were obtained with measurements on MR-linac Unity systems, where we compared the repeatability and reproducibility in comparison to standard diagnostic systems.

**SP-0468 Quality assurance and validation for Quantitative PET in Multicenter Trials**

M. Lubberink<sup>1</sup>

<sup>1</sup>*Uppsala University, Department Of Surgical Sciences-Radiology, Uppsala, Sweden*

**Abstract text**

In recent years, a lot of effort has been put into harmonization of clinical PET procedures with <sup>18</sup>F-fluorodeoxyglucose (FDG) in oncology. For example, the European Association of Nuclear Medicine's EARL accreditation program aims to ensure comparable quantitative results among patients and sites, and as such provide quality assurance for multi-center trials. This lecture will cover the use quantitative imaging with PET-CT and PET-MR, especially related to the use of PET in multi-center trials concerning dose planning and treatment response monitoring.

First, the concept of quantitative PET will be discussed. PET is unique amongst medical imaging techniques in its ability to absolutely measure a wide range of molecular and physiological biomarkers. These quantitative measurements are based on time-varying measurements of radioactivity concentrations and the tracer kinetic models that describe the in-vivo behaviour of PET tracers. This will be illustrated using its most common application, measurement of glucose metabolism using FDG. The simplifications necessary to use these methods clinically in radiation oncology will be addressed, such as standardized uptake values (SUV), and the challenges associated with them both in terms of biology and instrumentation. Then, the harmonization efforts to ensure comparable SUV measurements between different scanners and hospitals will be discussed. PET-MR provides additional challenges in quantification associated with the limitations of MR-based attenuation correction. Improvements in quantification using recent developments in instrumentation, such as digital PET detectors and time-of-flight, and novel image reconstruction methods, will be reviewed in the context of multi-center studies in oncology.

Finally other tracers than FDG and their possible quantitative applications in radiation oncology will be presented, such as those measuring hypoxia, proliferation, blood flow and oxygen consumption.

---

**Symposium: Advanced methods to account for proton range uncertainties in treatment planning**

---

**SP-0469 Mitigation of range uncertainties with probabilistic IMPT optimization**

M. Bangert<sup>1,2</sup>, N. Wahl<sup>1,2</sup>, H. Wieser<sup>2,3,4</sup>

<sup>1</sup>*German Cancer Research Center Dkz, Medical Physics In Radiation Oncology, Heidelberg, Germany* ; <sup>2</sup>*Heidelberg Institute Of Radiation Oncology Hiro, Heidelberg, Germany*; <sup>3</sup>*German Cancer Research Center, Medical Physics in Radiation Oncology, Heidelberg, Germany*; <sup>4</sup>*Heidelberg University, Faculty For Medicine, Heidelberg, Germany*

**Abstract text**

At the time of planning it is impossible to estimate the range of charged particles within a patient with absolute certainty. Due to, among others, inevitable limitations in

computed tomography imaging and patient motion, particles stop at different geometric locations during treatment than predicted during dose calculation. This may heavily compromise the quality of the computed treatment plan.

Conventional radiation therapy planning does not explicitly model this range uncertainty, usually relying only on a single "best-guess" scenario for dose optimization. Probabilistic optimization, in contrast, may incorporate explicit assumptions about the probability distribution over range uncertainty. Thereby it is possible to reduce a potentially deteriorating impact of uncertainties within a structured probabilistic optimization process.

The first part of the presentation will give a thorough introduction to the fundamentals of probabilistic optimization in radiation therapy planning. This includes (1) intuitive visualizations on how uncertainty in particle ranges translate into uncertainty in the dose, depending on different correlation and fractionation assumptions, and (2) a brief overview of facilitated objective functions for probabilistic optimization.

Within the second part of the presentation we will discuss advantages and disadvantages associated with probabilistic optimization in radiation therapy as compared to conventional optimization and robust ("worst case") optimization. In particular, this includes an illustration of the challenges associated with probabilistic and robust optimization regarding the exact control of the robustness level of the optimized treatment plans. In the third part of the presentation we will elaborate on prerequisites for exact uncertainty control within probabilistic radiation therapy optimization with regard to (1) the underlying uncertainty models, (2) the facilitated uncertainty quantification pipeline, and (3) the mathematical formulation of the uncertainty minimization algorithms. We will show how this issue is currently addressed within the academic community using e.g. Gaussian Processes, Polynomial Chaos Expansion, and Analytical Probabilistic Modeling.

**SP-0470 Multi-energy CT for improved SPR determination: Proposed methods and their experimental validation**

V. Taasti<sup>1</sup>, G.J. Michalak<sup>2</sup>, A.J. Deisher<sup>3</sup>, J.J. Kruse<sup>3</sup>, C.H. McCollough<sup>2</sup>, L.P. Muren<sup>4</sup>, J.B.B. Petersen<sup>4</sup>, D.C. Hansen<sup>4</sup>  
<sup>1</sup>*Memorial Sloan Kettering Cancer Center, Medical Physics, New York, Usa*; <sup>2</sup>*Mayo Clinic, Radiology, Rochester, Usa* ; <sup>3</sup>*Mayo Clinic, Medical Physics, Rochester, Usa*; <sup>4</sup>*Aarhus University Hospital, Medical Physics, Aarhus, Denmark*

**Abstract text**

*Introduction*

Dual energy CT (DECT), Multi energy CT (MECT) and Photon Counting Detector CT (PCD-CT) have been investigated for their ability to improve the accuracy of the stopping power ratio (SPR) estimation, which is used in the treatment planning process for proton therapy. Especially DECT has been intensively investigated. Most DECT based methods have been shown to provide better results for the SPR estimation than the conventional method based on single energy CT (SECT). The CT number and the SPR are both proportional to the electron density of the tissue whereby they are also proportional to each other. This is exploited in the standard SECT based SPR estimation. However, the proportionality factor is not constant. This has been considered by making a piecewise linear fit between the single energy CT number and the SPR, approximating the proportionality factor with a local constant. Using DECT or even MECT and PCD-CT this approximation is not needed, directly, but approximations are still exploited. Some of these SPR methods are more empirical than others, but often their parameter fitting is

less ambiguous than the empirical SECT based stoichiometric method.

#### Methods and Materials

To investigate the accuracy of SPR estimation methods, experimental validation was performed on organic tissues. Measurements of the proton range were made with pristine pencil beams, and CT scans were acquired in SECT and DECT mode, as well as PCD-CT mode. Firstly, the SECT scans were evaluated with a clinical stoichiometric conversion curve, and the DECT scans were evaluated with commercial DECT software. The SECT and DECT scans were later re-evaluated with our own implementation of (other) SPR methods. No software is available for evaluation of SPR estimation based on PCD-CT scans and these were therefore evaluated with our own implementation of different SPR estimation methods. The accuracy of the methods was evaluated based on the root-mean-square error (RMSE) and the mean error, with main focus on the RMSE as too few tissues were examined to assume Gaussian distributed errors.

#### Results

It was found that DECT was superior to SECT, following the trend of other recent investigations. However, re-evaluation using another implementation of the stoichiometric curve, it was found that the SECT based SPR estimation error could be significantly reduced (Table 1). The mean errors stayed lower for the DECT based methods. The same tissues (a subset) were scanned with a PCD-CT scanner, acquired in four, two and one energy bin mode. For the one-bin images the stoichiometric method was applied, here the result was consistent with the second implementation for SECT (compare Table 1 and 2). Two different SPR methods developed for MECT and a DECT method were tested. The results for all the methods were comparable (Table 2).

#### Discussion

In the comparison of SECT and DECT (Table 1), the fitting of the second stoichiometric curve was not guided by the measurements of the organic tissues. This shows that when comparing any DECT or MECT based SPR method to the SECT based stoichiometric method an effort should be made to improve the stoichiometric curve to have a fair comparison. More importantly, it shows that SECT based SPR estimation as applied in most proton centers today can provide fairly good results, but the curve fit should be carefully considered. At best, it should be experimentally validated to ensure the connection points between the individual line sections are placed appropriately; generally, more than two line sections are needed. Moreover, it was found that the stoichiometric curve could also be improved by implementing different methods for estimating the CT numbers of the literature data for the reference human tissues (first step of the stoichiometric method). The standard stoichiometric method was based on an empirical parametrization of the linear photon attenuation coefficient, which is less accurate for high density tissues. The second method applied a CT number estimation was based on effective energies for the x-ray energy spectrum, which improved the accuracy (Table 3). DECT and PCD-CT provided low errors for the SPR estimation of the organic tissues, but it was found that two-bin PCD-CT images were sufficient, and a further increase of the number of energy bins was not needed. It has previously been shown that three or four CT numbers improved the accuracy above the results for DECT. However, for our experimental results this was not the case, which most likely can be explained by the favorable energy separation which can be obtained using two-bin PCD-CT scans. In conclusion, DECT, MECT and PCD-CT can improve the SPR accuracy compared to SECT. But until these CT techniques can be used in commercial treatment planning software, improvements of the SPR estimation can be obtained by carefully fitting the stoichiometric method, and optimization of the CT scanning protocols.

**Table 1:** SPR accuracy in experimental evaluation based on fourteen organic tissues for comparison of SECT vs DECT. The results are stated as root-mean-square errors (RMSE) and mean errors.

SPR methods – SECT vs DECT	RMSE (%)	Mean (%)
SECT version 1	2.8	-0.6
DECT method 1	1.3	-0.3
SECT version 2	0.8	-0.6
DECT method 2	0.9	0.2

**Table 2:** Results for SPR estimation based on PCD-CT compared to measured SPR for nine organic tissues.

SPR methods – PCD-CT	RMSE (%)	Mean (%)
4 energy bins, PCD method 1	1.0	0.3
4 energy bins, PCD method 2	0.8	-0.7
2 energy bins, PCD method 1	0.8	0.1
2 energy bins, DECT method	1.3	0.1
1 energy bin, SECT method	0.8	-0.1

**Table 3:** CT estimation accuracy. Results presented in the upper part of the table is based on the accuracy of the CT number estimation for tissue equivalent phantom materials. The lower part of the table present SPR accuracy for the stoichiometric method applying the two different CT number estimation methods, evaluated on the fourteen organic tissues.

CT number estimation	RMSE (%)	Mean (%)
X-ray attenuation parametrization	3.1	-1.2
Effective energies	0.2	0.0
SPR estimation	RMSE (%)	Mean (%)
X-ray attenuation parametrization	0.7	-0.2
Effective energies	0.5	-0.1

#### SP-0471 Treatment Planning and Verification with Proton CT and Proton Radiography to Reduce Range Uncertainties in Proton Therapy

R. Schulte<sup>1</sup>

<sup>1</sup>Loma Linda University, Division of Biomedical Engineering Science- Department of Basic Sciences, Loma Linda, USA

#### Abstract text

Proton CT was originally proposed as a low-dose imaging modality by physicist Allan M. Cormack, winner of the 1979 Nobel Prize in Physiology or Medicine. Cormack had in mind to use protons for diagnostic imaging instead of x-rays but was discouraged by the need for large accelerators, rotating gantries, and other expensive equipment, besides the difficulties imposed by multiple Coulomb scattering. The real value of pCT became apparent with the expansion of proton therapy; currently, there are 27 proton treatment centers operational in the United States. Proton CT (pCT) provides artifact-free images of the true relative stopping power values of the patient tissues (not converted from x-ray CT HU), thus avoiding the uncertainties in HU-to-RSP conversions. The use of pCT in treatment planning would reduce distal margins added to clinical proton beams and allow the use of beam directions where the beam stops near critical organs at risk like brain stem and optic chiasm. In this presentation, the possible technological realizations of proton CT scanners, all still at the preclinical stage and ranging from single-particle tracking systems operating in list-mode data acquisition to simpler technology using equipment already in use in the clinic. Proton radiography can be used as a pre-treatment verification of water-equivalent range-checking tool for each treatment field. In addition, proton CT may be used for pretreatment volumetric imaging and treatment adaptation, thus closing the gap in image guidance with respect to photon therapy.

#### SP-0472 Accounting for organ motion in proton therapy at the planning stage

T. Lomax<sup>1</sup>

<sup>1</sup>Paul Scherrer Institute (PSI) Centre for Proton Therapy, Villigen PSI, Switzerland

Abstract not received

---

**Symposium: Care, communication and new technology in brain radiotherapy**

---

**SP-0473 Stereotactic radiosurgery for brain metastases: treating multiple lesions**

A. Williamson<sup>1</sup>

<sup>1</sup>Beatson West Of Scotland Cancer Centre, Radiotherapy, Glasgow, United Kingdom

**Abstract text**

Stereotactic radiosurgery (SRS) has become an increasingly utilised treatment option in the initial management of patients with brain metastases. Its efficacy has been well demonstrated with a local control rate of >75% at 1 year with minimal treatment related toxicity. Novel plan optimisation and treatment delivery platforms for linear accelerator-based SRS techniques have shown that single isocentre SRS for multiple targets can be efficiently delivered without increasing the dose to organs at risk. Evolving radiation therapy and imaging technology has increased interest in SRS for hypofractionated stereotactic radiotherapy (HFSRT) for large metastases and for lesions close to organs at risk (e.g. the brainstem).

The aim of this presentation is to review and discuss results of selected SRS studies in light of technological advances and the emerging clinical needs. The session will include discussion on the optimal technique for delivery, including; different treatment platforms and technologies, treatment planning methods, methods of dose prescribing and calculation of appropriate margins. New and emerging evidence will be presented with an overview of future areas of interest.

**SP-0474 Linac isocentric accuracy and its influence on treatment margins**

E. Kouwenhoven<sup>1</sup>, J. Van Egmond<sup>2</sup>, J. Van Santvoort<sup>2</sup>

<sup>1</sup>Haaglanden Medical Centre Location Westeinde Hospi, Medical Physics, Den Haag, The Netherlands ;

<sup>2</sup>Haaglanden Medical Centre, Medical Physics, Den Haag, The Netherlands

**Abstract text**

The majority of linear accelerators used for radiotherapy is isocentric. Their design is such that the three major rotation axes, for rotation of collimator, gantry and table, pass through one point, the isocenter. Several factors hinder the ideal situation of an isocenter having a fixed position in space. As a result the location of the tumor with respect to the beam's central axis is displaced due to gantry, table or collimator rotation. The isocentric accuracy is an important parameter in stereotactic treatment, as it is a major determinant of the treatment accuracy.

Measurement of isocentric accuracy is part of the quality assurance program. Ideally, it should be carried out quickly, and, considering the requirements on accuracy, have high spatial resolution.

We developed a procedure to measure isocentric accuracy, based on the Winston-Lutz test. To quantify isocentric accuracy due to gantry rotation (no table rotation) a ball bearing was imaged at various gantry and collimator angles. The accuracy of the procedure was established and found to be better than 10 µm. Several system quality parameters could be derived from these measurements, such as:

-Lateral vs. longitudinal excursion of isocenter due to gantry rotation

- EPID tilt
- Field size
- Position of beam focus, and the influence of beam steering
- MLC symmetry

The influence of inaccuracies of table rotation are mainly due to differences in location of collimator rotation axis vs. table rotation axis, as a function of table rotation angle. A simple procedure to measure this distance is discussed. The consequences of such an inaccuracy are variations in coincidence of the beam central axis and the target position in the patient. These should be accounted for by including its effect in the treatment margins that are applied. A procedure to calculate the contribution to treatment margins is given and discussed using results of our linacs.

**SP-0475 Communication care and side effect - brain radiotherapy - What's the role of the RTT?**

H. Simonsen<sup>1</sup>

<sup>1</sup>Nurse, Radioterapi, Aarhus, Denmark

**Abstract text**

Abstract Estro April 2019 Presenter: Hanne Simonsen, Department of Oncology, Aarhus University Hospital, Denmark. Topic category: Cancer care. Key words: Patient care, side effects and communication. Presentation preference: Oral, I am an invited speaker. Title: Individual network meetings in cancer care -From young people with cancer to adults with brain tumours Purpose/objective: The aim of the network meetings is to facilitate the involvement of a supportive social network around the patient and relatives. A malignant brain tumour often includes cognitive impairment. This affects both patients and families. Compared to other cancer patients, studies show that they are significantly in more need of social support and help for everyday activities. A network focused approach offering individual network meetings with and for young people with cancer has shown to facilitate the involvement of a social network around the patient and the family, with can assist them in keeping their world together. Methods: A participatory action research design was employed to develop and implement a researched based service that would promote and encourage a supportive social network for patients with primary brain tumours and their families. Patients and close relatives preferences and attitudes towards an offer of a network meeting were explored. The study involved parallel processes of interviews with patients and usually their spouses, education and interaction between the researcher and a group of ten clinical nurses. Results: Based on the findings the individual network meeting for patients with brain tumours has been shaped to fit their needs and wishes and are now fully implemented in the clinic. A group of nurses has been trained in planning and leading network meetings and acts as implementation agents. Early presentation of individualised network meetings is welcomed as an opportunity and accepted by about 40 % of the patients and relatives. Conclusion: Network meetings are feasible in clinical practice. They are highly valued by patients, who has participated and their social network. The interactive approach in action research has supported the implementation of the complex service - a service which has potential in other nursing areas. The presentation will focus on preparing and conducting network meetings.

---

**Poster Viewing : Poster viewing 9: Applied dosimetry**

---

**PV-0476 Effect of updated ICRU90 data on Monte Carlo kQ calculations: results from the Australian PSDL**  
M. Hanlon<sup>1</sup>, C. Oliver<sup>1</sup>, T. Bailey<sup>1</sup>, J. Lye<sup>2</sup>, D. Butler<sup>1</sup>

<sup>1</sup>Australian Radiation Protection and Nuclear Safety Laboratory, Primary Standards Dosimetry Laboratory, Melbourne, Australia ; <sup>2</sup>Australian Radiation Protection and Nuclear Safety Laboratory, Australian Clinical Dosimetry Service, Melbourne, Australia

### Purpose or Objective

The publication of the updated key data for ionizing-radiation dosimetry in ICRU90<sup>1</sup> includes changes to the mean excitation energy (I-value) of graphite and water, and the renormalised photoelectric cross sections. Both of these changes will affect the Monte Carlo calculated beam quality correction factor  $k_Q$ , which is being considered with the update to TRS-398. Here, we have modelled the change that the ICRU90 data has on  $k_Q$  for several common ionisation chambers.

### Material and Methods

All modelling was done in the EGSnrc c++ user code egs\_chamber. Various ionisation chambers commonly calibrated by the Primary Standards Dosimetry Laboratory (PSDL) at ARPANSA were modelled (Including the NE 2571, PTW 30013, IBA FC65-5, ICA CC-13, and the Exradin A12) according to detector specifications from obtained from the manufacturers, including accurate modelling of the stem. Two source inputs have been used; a commissioned full linac head model (6, 10, 18 MV) and tabulated photon source spectra from both published results (4-25 MV) and results from the ARPANSA modelled linac. The dose to the air cavity in the chamber and the dose to water were scored at 5 cm depth in <sup>60</sup>Co beams and at 10 cm depth in MV photon beams, as per the IAEA TRS-398 protocol, and the ratio used to calculate  $k_Q$ . The simulations were repeated with the previous (ICRU37) and updated (ICRU90) key datasets.

### Results

All simulations were run until a combined uncertainty from all four measurements was <0.1%. All simulations compare well to TRS-398, agreeing within similar ranges to other published studies. When using the ICRU37 data, results agreed with published values<sup>2</sup> to within 0.4%. When comparing the same inputs with the updated ICRU90 data, the values for  $k_Q$  were on average 0.2% higher/lower, indicating that the impact of the updated data from ICRU90 has a small effect on  $k_Q$ , which agrees with other published works. Figure 1 shows the calculated values for the NE-2571 ionisation chamber, including the difference. The difference of 0.2% is small, and within the 1% uncertainty quoted in TRS-398.

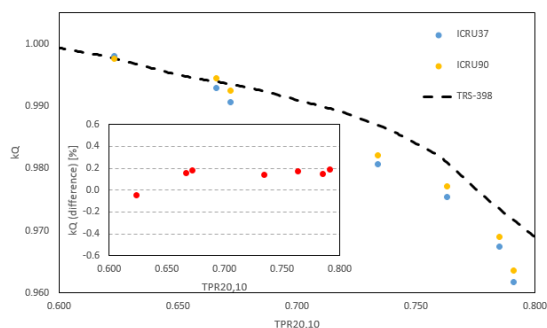


Figure 1: Calculated  $k_Q$  values for the NE-2571 ionisation chamber using ICRU37 and ICRU90 data, with the differences (positive shows ICRU 90 is higher than ICRU37) between the two datasets.

### Conclusion

Several ionisation chambers have been successfully modelled, allowing for the beam quality correction  $k_Q$  to be calculated. We have shown good agreement with published protocols and published Monte Carlo studies.

The updated ICRU90 data has a small effect on  $k_Q$ , in the order of 0.2%, but this is well within the quoted uncertainty associated with  $k_Q$  in TRS-398 of 1%.

### References:

1. Seltzer, S. et al (2016). ICRU Report 90.
2. Muir, B. R., & Rogers, D. W. O. (2010). *Medical physics*, 37(11), 5939-5950.

### PV-0477 A Monte Carlo study of collimator angle dependence of extra focal dose during VMAT

F. Ghareeb<sup>1</sup>, J. Lencart<sup>2</sup>, J. Oliveira<sup>1</sup>, J. A. M. Santos<sup>1,2,3</sup>  
<sup>1</sup>Instituto Português de Oncologia do Porto Francisco Gentil- EPE, Medical Physics- Radiobiology and Radiation Protection Group- IPO Porto Research Center CI-IPOP, Porto, Portugal; <sup>2</sup>Instituto Português de Oncologia do Porto Francisco Gentil- EPE, Medical Physics, Porto, Portugal; <sup>3</sup>University of Porto, Instituto de Ciências Biomédicas Abel Salazar ICBAS, Porto, Portugal

### Purpose or Objective

Patients undergoing 3DCRT radiotherapy using linac head equipped with HD120MLC are subjected to out-of-field transmitted localized extra-focal dose (LEFD) in a very specific region in the direction perpendicular to the MLC leaves motion direction [1]. The goal of this work is to study the effect of collimator rotation angle on the location and the magnitude of the extra-focal dose regions in case of VMAT using Monte Carlo (MC) technique.

### Material and Methods

Several VMAT treatment plans were created using Varian Eclipse TPS for the same hypothetical abdominal lesion. The plans were based on a whole-body CT dataset of a pediatric anthropomorphic phantom (CIRS, ATOM model 705-C, Norfolk, VA). Each plan consisted of two 6 MV full arcs and they were optimized to achieve the same PTV and OAR objectives with different collimator rotations ranged from 0°(360°) to 50°(310°). The treatment plans were then simulated with Monte Carlo (MC) technique using PRIMO software. The dose out of the treatment field was evaluated using 10 spherical structures (1 cm<sup>3</sup>) located along the central axis at several distances from the isocenter (5 spheres) and along the lateral axis (5 spheres) located 7.5 cm to the right of the isocenter (Figure 1a). For each collimator angle all the mean dose values inside each spherical structure were normalized to the corresponding mean dose value inside an identical spherical structure located at the isocenter.

### Results

The localized extra focal dose distribution is located after 11 cm from the isocenter in the direction perpendicular to the leaves motion direction. At 0° of collimator rotation a cylindrical dose distribution with a diameter equal to the Y-jaws aperture is noticed (as shown in Figure 1b). The dose inside the cylinder is up to 3 folds of the background dose. As the collimator angle increases, the dose distribution start to decrease along the central axis and to increase at the peripheral regions (as shown in Figure 1c for a collimator rotation of 30°) until the extra focal dose disappears from all the evaluated structure at a collimator rotation > 40°. The collimator angle dependence of dose in points 1, 9 and 10 are shown in Figure 2.

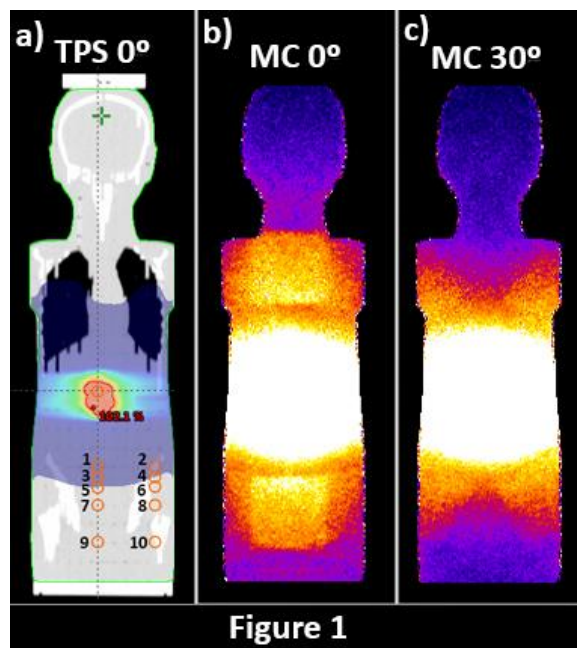


Figure 1

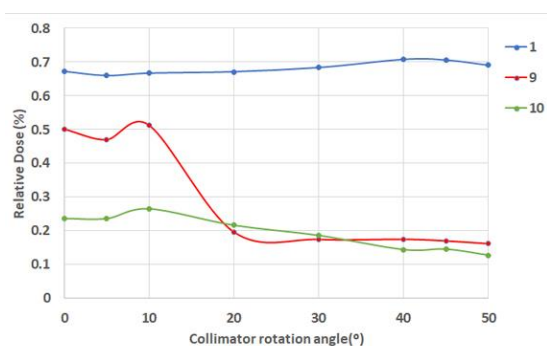


Figure 2

### Conclusion

From the above results, one notices that highly inhomogeneous out-of-field distributions in the patient can easily be achieved for different collimator rotations during VMAT irradiations. Extra precautions can be taken into consideration when treating patients with HD120MLC or other devices presenting the same behavior. To avoid directing the extra-focal radiation into a radiosensitive organ during VMAT treatment, the collimator angle can be optimized as described to avoid sensitive organs at risk. This issue is of major importance in pediatric patients.

[1] Ghareeb, F., et al., *Physica Medica*, 2018. 52: p. 57-58

### PV-0478 A new tool to test tracking systems based on tumour detection

S. Pallotta<sup>1</sup>, S. Calusi<sup>2</sup>, L. Masi<sup>2</sup>, L. Marrazzo<sup>3</sup>, C. Talamonti<sup>1</sup>, L. Livi<sup>4</sup>, G. Simontacchi<sup>4</sup>, L. Foggi<sup>5</sup>, R. Lisci<sup>6</sup>  
<sup>1</sup>University of Florence- Azienda Ospedaliero Universitaria Careggi, Department of Biomedical Experimental and Clinical Sciences "Mario Serio"- Medical Physics Unit, Florence, Italy ; <sup>2</sup>IFCA, Medical Physics and Radiation Oncology, Florence, Italy ; <sup>3</sup>Azienda Ospedaliero Universitaria Careggi, Medical Physics Unit, Florence, Italy ; <sup>4</sup>University of Florence- Azienda Ospedaliero Universitaria Careggi, Department of Biomedical Experimental and Clinical Sciences "Mario Serio"- Radiotherapy Unit, Florence, Italy ; <sup>5</sup>University of Florence, Department of Biomedical Experimental and Clinical Sciences "Mario Serio", Florence, Italy ; <sup>6</sup>University of Florence, of Agricultural- Food and Forestry System, Florence, Italy

### Purpose or Objective

To report on an upgrade of the Anthropomorphic Dynamic breAthing Model (ADAM) phantom for QA of real time respiratory tracking systems.

### Material and Methods

ADAM is a 3D printed human torso with realistic embedded ribs and spinal cord, a moving upper chest wall and simulated lungs. An Arduino programmable board, integrated in the phantom body, drives movements of lung along linear or elliptical paths and of upper chest wall up and down. Linear paths dephasing thorax motion and signals based on real patient breathing traces are implemented.

In the current version a new Tracking Tool (TT) (fig 1A) has been realized to enable accuracy tests of tracking systems based on fiducial-less tumor detection. The TT consists in four blocks, each hosting a quarter of sphere, simulating a lung-tumor structure, built using a 3D printer and different filling percentage. This results in X rays images with realistic contrast between the target and the surrounding material. The TT can host two small films and can be inserted in any position inside the phantom thorax enabling to simulate different tumor detection uncertainties, as observed in real patient cases (fig 1 B). The TT is moved by the same system used to move lungs.

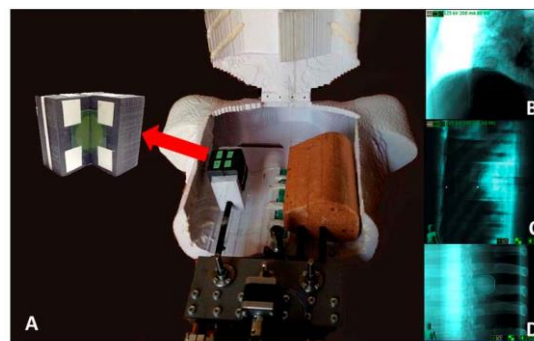


Figure 1. ADAM and a zoomed view of the Tracking Tool containing radio-chromic films. A. X-rays projections acquired with the Cyber-Knife imaging system showing detected structures in patient B, in ADAM C, and in a commercial phantom D.

ADAM and the new TT were used to perform end-to-end tests of a CyberKnife® System (Accuray, USA). An isocentric plan was created targeting the beams on the TT. Two orthogonal EBT3 films were inserted in the sphere and the plan was delivered while moving the sphere and the thorax according to: Linear, Elliptical, Linear no sync (thorax and TT motion not always synchronized), Linear patient (based on a real patient breathing) and Linear patient no tracking (with the tracking system deactivated) respiratory traces. The same plan was delivered also in static condition.

Films were analyzed using an E2E dedicated software (Accuray, USA), which provides the distance between the centroid of planned and delivered dose distributions as global tracking error. Films irradiated in static and moving conditions were compared with FilmQA™ Pro (Ashland Inc., USA).

### Results

The TT was detected by the tracking algorithm with an uncertainty (range 10%-20%) close to what observed in real patient treatments (mean 15.5%; range 5%-32). In one of the two projections, uncertainty was higher (15%-20%) due to the superimposition of a radiopaque heart-like structure (fig 1C). Tracking errors derived by the E2E software were all below 0.95 mm (range 0.6-0.9 mm). The maximum difference in tracking error between two repeated tests was 0.4 mm. In table 1 gamma passing rates obtained by comparing films acquired in dynamic and static conditions are reported. In particular  $GI_{3\%/1mm}$  (local criteria) pass-rates scored above 90% for all respiratory

traces using tracking, while dropping below 50% when the tracking system was deactivated.

Table 1. Gamma passing rates of films (lying on the sagittal plane) acquired in different dynamic conditions using films irradiated in stationary conditions as reference.

path	TT amplitude in CC [mm]	Chest wall amplitude in UD [mm]	Breathing frequency [bpm]	GI <sub>25%/2mm</sub>	GI <sub>50%/2mm</sub>
Linear	10	10	11.2	96%	97%
Linear no sync	10	10	11.2	90%	97%
Elliptical	10 (5 AP)	10	10.4	96%	99%
Linear patient	10 (max)	10 (max)	11 (max)	94%	97%
Linear patient no tracking	10 (max)	10 (max)	11 (max)	30%	45%

TT tracking tool, CC craniocaudal, AP anterior-posterior, UD up and down

## Conclusion

The new ADAM's tool demonstrates suitable performances to test, in realistic patient-like conditions, tracking systems based on soft tissue detection.

## PV-0479 Development of an anthropomorphic multimodality pelvis phantom for PET/MRI- and CT-based RT planning

N. Homolka<sup>1,2,3</sup>, A. Pfaffenberger<sup>1,3</sup>, B. Beuthien-Baumann<sup>3,4,5</sup>, P. Mann<sup>1,3</sup>, V. Schneider<sup>3,4</sup>, W. Johnen<sup>1,3</sup>, A. Runz<sup>1,3</sup>, G. Echner<sup>1,3</sup>, A.L. Hoffmann<sup>6,7,8</sup>, E. Troost<sup>6,7,8,9,10</sup>, S.A. Koerber<sup>3,5,11</sup>, J. Seco<sup>2,12</sup>, C. Gillmann<sup>1,3</sup>

<sup>1</sup>German Cancer Research Center DKFZ, Medical Physics in Radiation Oncology, Heidelberg, Germany ; <sup>2</sup>University of Heidelberg, Faculty for Physics and Astronomy, Heidelberg, Germany ; <sup>3</sup>Heidelberg Institute for Radiation Oncology HIRO, National Center for Radiation Research in Oncology NCRO, Heidelberg, Germany ; <sup>4</sup>German Cancer Research Center DKFZ, Radiology, Heidelberg, Germany ; <sup>5</sup>National Center for Tumor Diseases NCT, Partner Site Heidelberg, Heidelberg, Germany ; <sup>6</sup>Helmholtz-Zentrum Dresden-Rossendorf, Institute of Radiooncology - OncoRay, Dresden, Germany ; <sup>7</sup>Technische Universität Dresden- Faculty of Medicine and University Hospital Carl Gustav Carus, Department for Radiotherapy and Radiation Oncology, Dresden, Germany ; <sup>8</sup>OncoRay - National Center for Radiation Research in Oncology, Dresden, Germany ; <sup>9</sup>German Cancer Consortium DKTK, Partner Site Dresden, Dresden, Germany ; <sup>10</sup>National Center for Tumor Diseases NCT, Partner Site Dresden, Dresden, Germany ; <sup>11</sup>University Hospital Heidelberg, Radiation Oncology, Heidelberg, Germany ; <sup>12</sup>German Cancer Research Center DKFZ, BioMedical Physics in Radiation Oncology, Heidelberg, Germany

## Purpose or Objective

The aim of the study is the further development of an anthropomorphic multimodality pelvis phantom (ADAM, [1]) for the integration of PSMA-PET/MRI-based treatment planning of prostate cancer patients.

## Material and Methods

CT and 3T-MRI characteristics of different tissue types are mimicked using agarose gels (Agarose NEO Ultra-Qualität Carl Roth GmbH + Co. KG, Germany) mixed with different concentrations of Gadolinium (Gd, MultiHance® 0.5 M, Bracco Imaging Deutschland GmbH) and sodium fluoride (NaF, Carl Roth GmbH + Co. KG). Gels were scanned using a 3T PET/MRI (Biograph mMR, Siemens Healthineers, Erlangen, Germany) using a saturation recovery sequence with multiple inversion times and a spin-echo sequence with multiple echo times. Based on the resulting images, T1- and T2-relaxation times were determined using in-house written software. CT scans of the agarose mixtures were performed on a stand-alone CT scanner (Somatom Definition Flash, Siemens Healthineers) at 120 kV and 390 mAs.

Agarose mixtures that agreed best with reference values derived from literature data [2-4] were subsequently doped with patient-specific activity concentrations of <sup>18</sup>F and <sup>68</sup>Ga (e.g. 3 kBq/ml <sup>68</sup>Ga and 11 kBq/ml <sup>18</sup>F for the primary tumor). Organ shells (prostate with two

intraprostatic lesions, lymph nodes and bone metastases) were printed using a 3D printer (Stratasys Objet 300 Connex 3, print material: VeroClear). The doped, liquid agarose gels were filled into the organ shells where they solidified within seconds. Organ shells were scanned at the 3T PET/MRI scanner (PET acquisition time: 10 min, MRI: T2-weighted morphological sequence).

## Results

The final compositions of agarose gels are the following (given as mass fractions of agarose/NaF/Gd): Prostate (1.35%/3.2%/0.011%), lesions (2.25%/3.2%/0.0085%) and lymph nodes (3.2%/1.4%/0.025%).

T1- and T2-relaxation times and CT numbers of the developed agarose gels fit well to reference values (Figure 1). Exemplary PET- and MR-images of a prostate with two intraprostatic lesions doped with 11 kBq/mL <sup>18</sup>F are shown in Figure 2. The PET signal can be detected and the tumors appear hypointense on T2-weighted MRI.

## Conclusion

Agarose gel mixtures with organ-specific MR-relaxation times at 3T and CT numbers have been developed and doped with radioactive tracers. The gels will be used in the pelvis phantom which will be central to simulate and optimize the technical workflow for the integration of PSMA-PET/MRI-based RT planning of prostate cancer patients.

## References

- [1] Niebuhr et al, DOI: 10.1118/1.4939874
- [2] de Bazelaire CM et al, DOI: 10.1148/radiol.2303021331
- [3] C. Wagner-Manslau et al, DOI: 10.1007/BF00599063
- [4] W. Schneider et al, DOI: 10.1088/0031-9155/45/2/314

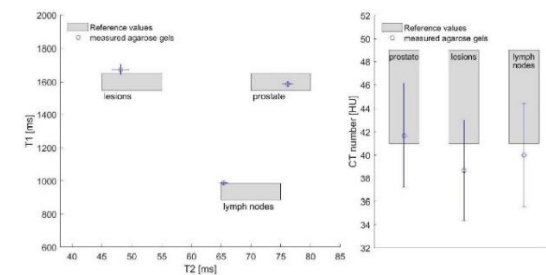
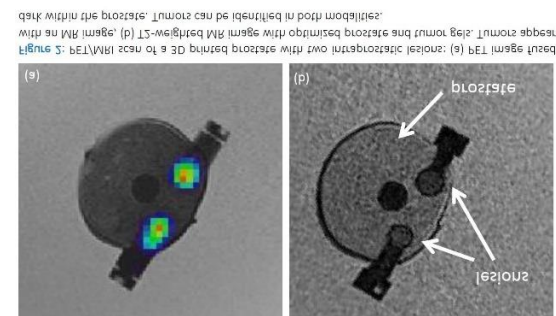


Figure 1: Comparison of T1- and T2-relaxation times (left) and CT numbers (right) of optimized agarose gels with reference values. Reference values were derived based on literature data [1-3].



## PV-0480 Plastic-scintillator based PET detector for proton beam therapy range monitoring: preliminary study

A. Rucinski<sup>1</sup>, J. Baran<sup>1</sup>, M. Garbacz<sup>1</sup>, M. Pawlik-Niedzwiecka<sup>1</sup>, P. Moskal<sup>2</sup>

<sup>1</sup>Institute of Nuclear Physics PAN, Proton Radiotherapy Group, Krakow, Poland ; <sup>2</sup>Jagiellonian University, Faculty of Physics- Astronomy and Applied Computer Science, Krakow, Poland

## Purpose or Objective

Proton beam therapy (PBT) range monitoring is required to fully exploit the advantages of a proton beam in the clinic. In PBT the distribution of beta+ emitters induced

by a proton beam in a patient can be detected by PET scanners, the emission distribution can be reconstructed and used for monitoring of the beam range. A prototype of a diagnostic strip-based whole-body PET scanner (J-PET) has been developed and tested at the Jagiellonian University in Krakow (Moskal et al. Phys. Med. Biol. 61 (2016) 2025-2047). The advantages of the system over commercial PET scanners is that it increases the geometrical acceptance and facilitates integration in the treatment room, off-line or in the treatment position. The aim of this work is to study a feasibility of the J-PET technology for range verification in PBT.

#### Material and Methods

A single detection module of the strip-PET scanner is constructed out of thirteen 50-cm long organic scintillator strips. The light pulses produced in a strip by gamma quanta are propagated to its edges and converted into electrical signals by silicon photomultipliers (see Fig. 1). They are read-out by fast on-board front-end electronics allowing excellent overall coincidence resolving time (CRT) of about 300 ps, which shows a significant improvement compared to the standard LSO-based PET scanners. Three different configurations of the modular system were investigated: (i) a single layer consisting of 24 modules, (ii) a two-layer consisting of 20 and 24 modules, and (iii) three-layer consisting of 20, 24 and 28 modules. GATE Monte Carlo (MC) toolkit has been used to investigate the modular JPET system efficiency for detection of beta+ annihilation back to back photons induced in PMMA target by a proton beam (see Fig. 2). A MC based comparison of a J-PET based dual head system consisting of 2x5 modules configured as two opposing heads with the clinically operated inter-spill dual-head PET system installed at CNAO (V. Ferrero et al. Sci. Rep. 8:4100 2018) has been performed.

Fig. 1.

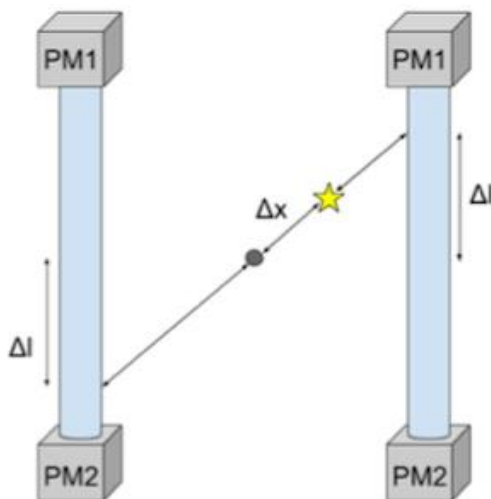
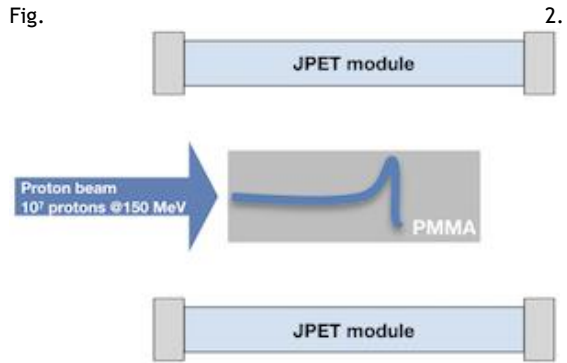


Fig.



#### Results

The efficiency of the system in the proton beam simulation increases quadratically with the number of detector layers. It ranges from 0.12% for single layer setup to 0.75% for three-layer setup. Detected coincidences per primary proton for the single layer, two and three layer modular JPET configurations is  $4.0 \cdot 10^{-5}$ ,  $1.3 \cdot 10^{-4}$  and  $2.5 \cdot 10^{-4}$ , respectively. The comparison of the dual head JPET and PET system installed at CNAO reveals comparable results.

#### Conclusion

Performed simulations suggest the signal obtained with the J-PET detector technology during proton beam therapy is sufficient for range monitoring. The results revealed that inter-spill beam range monitoring is achievable with both, dual-head and multi-layer JPET configurations. Experimental verification of the performed simulations is planned.

**PV-0481 IMRT/VMAT QA in heterogeneous media: first experience with a 2D solid-state detector prototype**  
G. Biasi<sup>1</sup>, N. Stansook<sup>1,2</sup>, M. Petasecca<sup>1</sup>, M. Carolan<sup>3</sup>, V.L. Perevertaylo<sup>4</sup>, P. Metcalfe<sup>1</sup>, M.L.F. Lerch<sup>1</sup>, T. Kron<sup>5,6</sup>, A.B. Rosenfeld<sup>1</sup>

<sup>1</sup>University of Wollongong, Centre for Medical Radiation Physics, Wollongong, Australia; <sup>2</sup>Mahidol University, Department of Radiology, Bangkok, Thailand;

<sup>3</sup>Wollongong Hospital, Illawarra Cancer Care Centre, Wollongong, Australia; <sup>4</sup>SPA-BIT, n/a, Kiev, Ukraine;

<sup>5</sup>Peter MacCallum Cancer Centre, Department of Physical Sciences, Melbourne, Australia; <sup>6</sup>University of Melbourne, Sir Peter MacCallum Cancer Institute, Melbourne, Australia

#### Purpose or Objective

Under-sampling dose distributions in IMRT/VMAT QA may potentially lead to incorrect gamma index analysis. At the present time, the spatial resolution of commercially available phantom-based array detectors is generally larger than 3 mm.

These devices are also not designed for measurements in heterogeneous media.

In this context, the present study aimed at introducing the use of a high-resolution (2 mm) 2D solid-state detector prototype 'MP512' embedded into a customized (in terms of density, dimensions, shape and location of inhomogeneities with respect to the active area of the detector) heterogeneous phantom.

#### Material and Methods

The MP512 has diode-sensitive volumes with a square area of 0.5 m side each.

They are uniformly distributed with a pitch of 2mm over a square area of 52 mm side.

The MP512 and Gafchromic™ EBT3 films were lodged into a phantom (cedar wood,  $\rho=0.38 \text{ g/cm}^3$ , to simulate lung tissue) of total thickness 5 cm with a small solid water insertion (0.5 cm radius,  $\rho=1 \text{ g/cm}^3$ , to simulate the tumour target).

We considered a lung treatment plan delivered with step-and-shoot IMRT, and a lung treatment plan delivered with VMAT.

We used the Pinnacle<sup>3</sup> treatment planning system (TPS), version 14 (Philips Medical Systems, Eindhoven, The Netherlands) and dose calculations were performed with Pinnacle's adaptive convolution-superposition (CS) algorithm with a 2 mm grid.

In all cases, fields were produced by a 6 MV flattened photon beam delivered by a Varian Clinac® iX linear accelerator equipped with a Millennium 120-multi-leaf collimator (MLC).

To assess the performance of the MP512, we used a gamma index analysis (acceptance criteria: 3%/3 mm and 2%/1 mm) considering absolute dose map measurements with the detector, with films and calculations with the TPS.

### Results

3%/3 mm: gamma passing rates (%GP) were >99% for all plans when comparing the MP512 and films, and =100% when comparing the MP512 and TPS.

2%/1 mm: %GP were >95% for all plans when comparing the MP512 and films, and >96% when comparing the MP512 and TPS.

For %GP, we found a better agreement between the MP512 and TPS than with films and TPS.

This may be explained by noise artefacts created by scanning procedures and/or film handling, heterogeneities affecting film response, or the higher spatial resolution of films.

Selected dose profiles measured with the MP512 and with films are in Figure 1.

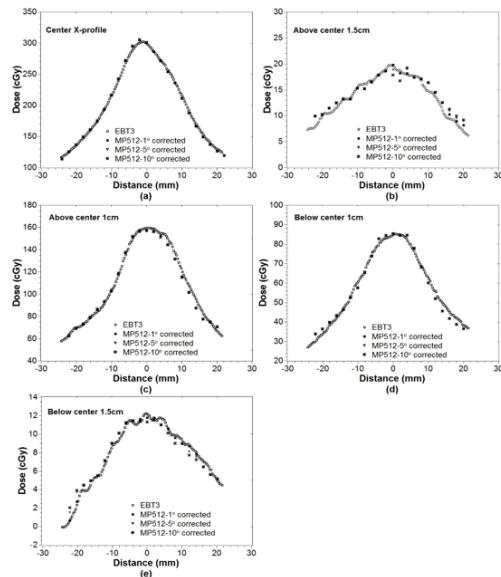


Figure 1. VMAT plan, lung: superior-inferior dose profiles measured with the MP512 and with films. Profiles are shown at the centre (a) and for different distances from the latter: 1.5 cm above (b), 1 cm above (c), 1 cm below (d), 1.5 cm below (e). The response of the MP512 was corrected for its angular dependence by applying correction factors calculated at either 10°, 5° or 1° intervals. However, results were not significantly different.

### Conclusion

Results suggest that the MP512 system has the required characteristics for high-resolution (2 mm) absolute dose maps measurements in fully-customizable heterogeneous phantoms in the context of IMRT/VMAT QA. The MP512 could potentially be used to verify dose calculations with a TPS in heterogeneous media.

### PV-0482 Dosimetric verification of Elekta MR-linac adaption workflow using 3D dosimeters

F. Costa<sup>1</sup>, I. Hanson<sup>1</sup>, S. Doran<sup>2</sup>, J. Adamovics<sup>3</sup>, S. Nill<sup>1</sup>, U. Oelfke<sup>1</sup>

<sup>1</sup>The Institute of Cancer Research and The Royal Marsden NHS Foundation Trust, Joint Department of Physics,

London, United Kingdom ; <sup>2</sup>Institute of Cancer Research, CRUK and EPSRC Cancer Imaging Centre, London, United Kingdom ; <sup>3</sup>Rider University, Department of Chemistry and Biology, Lawrenceville, USA

### Purpose or Objective

The Elekta MR-linac (Elekta Unity, AB, Stockholm, Sweden) system comprises a 1.5T Phillips magnet, a 7 MV Linac and a treatment table which cannot be used to correct for target miss-positioning. An MRI scan of the patient position and anatomy is used to localize the target and adapt the treatment plan. In this work, PRESAGE® 3D dosimeters are used together with a lung phantom as an end-to-end test to verify the dose distributions obtained by following this daily adaptation workflow.

### Material and Methods

A CT scan of a dummy PRESAGE® sample (3.5 cm diameter and 5.7 cm length) placed in the central cylinder of the QUASAR™ MRI4D motion phantom was performed. The scan was transferred to Monaco (version 5.4, Elekta AB, Stockholm, Sweden) and an IMRT plan with 5 beams was calculated with a maximum dose to the target of 9.4Gy. Three irradiations were performed using different PRESAGE® samples. One sample (sample 1) was placed at the linac isocenter, verified via EPID images acquired at gantry 0° and 90°, and irradiated as per the plan. The two other samples were irradiated with the phantom away from the isocenter to test the “adapt segments” option of the MR-linac, in which the isocenter shift is accounted for by repositioning the MLC leaves to match the original plan aperture shapes. Prior to the adaptation an MRI scan of the phantom on the table was taken and registered with the planning CT. Sample 2 was irradiated with the phantom placed 3 cm away from the isocenter in the sup-inf direction, while for sample 3 the phantom was moved an additional 3 cm in the left-right direction (Figure 1).

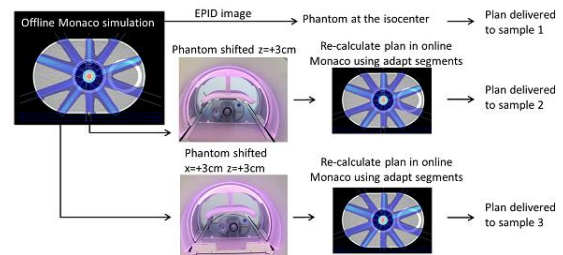


Figure 1. Scheme of the study workflow

Samples were imaged before and after irradiation with an in-house telecentric optical-CT scanner with a voxel size of  $-0.2 \text{ mm}^3$ . PRESAGE® samples have shown a higher sensitivity to radiation at the axial edges, so a correction image, which was obtained previously by uniformly irradiating samples from the same batch, was applied here.

### Results

PRESAGE® measured and Monaco simulated dose distributions agreed well with adapted plans (Figure 2). For a local gamma criterion of 2%, 2mm and 10% threshold, the gamma passing rate was 98.5% for sample 1, 99.7% for sample 2 and 98.4% for sample 3.

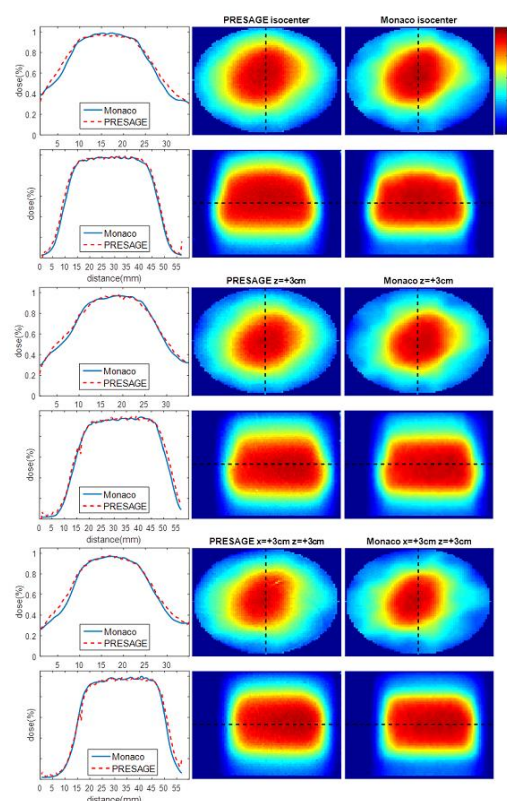


Figure 2. Axial and sagittal slices showing normalized 2D colour coded measured (PRESAGE) and simulated (Monaco) dose distribution and respective profiles given by the black dashed lined.

## Conclusion

The dosimetric accuracy of the MR-linac online adaption workflow was tested for the first time using PRESAGE® dosimeters and a phantom mimicking a tumour in the lungs. The dose distributions were accurately delivered to the target by positioning the phantom at the isocenter and by shifting it and applying the adaptive planning workflow. Complex IMRT plans will be evaluated in the future using larger samples of PRESAGE®.

## PV-0483 Pre-treatment portal dosimetry for the MR-Linac

I. Torres Xirau<sup>1</sup>, I. Olaciregui-Ruiz<sup>1</sup>, A. Mans<sup>1</sup>, U. A. van der Heide<sup>1</sup>

<sup>1</sup>Netherlands Cancer Institute, Radiation Oncology, Amsterdam, The Netherlands

## Purpose or Objective

The implementation of MRI-guided radiotherapy systems has become a reality in our clinic with the first patients being treated in the Elekta's Unity MR-Linac (Elekta AB, Stockholm, Sweden). The system introduces the possibility of real-time adaptation of the plan based on the actual anatomy of the patient during treatment. Given the complexity of the system, in combination with novel techniques for daily re-planning, the verification of the dose delivered to the patient is very important. For this purpose, the use of an Electronic Portal Imaging Device (EPID) for independent *in vivo* dose verification in the MR-Linac is being developed and the first phantom validation results are presented.

## Material and Methods

An existing back-projection algorithm used with conventional linacs was adapted for the Unity system, accounting for the increased amount of scatter received by the panel and the extra attenuation by the MR elements in the beam. The algorithm parameters were determined

by performing square field measurements under a variety of different phantom setups (varying SSD, phantom thickness and field size), which were semi-empirically fitted to EPID images of the corresponding fields. The algorithm was commissioned for three gantry angles (0, 90 and 180 degrees) and a solution to adapt the back-projection to arbitrary intermediate gantry angles was introduced and validated with phantom experiments. Phantom verification was performed for 75 IMRT fields irradiated to a solid water slab phantom at gantries 0, 90 and 180 degrees. The EPID images were back-projected to the isocenter at 10 cm depth using the model commissioned at its corresponding gantry angle. The reconstructed dose distributions were compared to 2-D measurements acquired at 10 cm depth with an ionization chamber (IC) array (OCTAVIUS 1500 PTW array).

The same IMRT fields were back-projected using a model commissioned at a different gantry angle and incorporating the gantry angle adaptation in the algorithm, and compared to 2-D measurements.

## Results

In the phantom study, the gamma results (global, 3%, 2mm, within the 10% isodose) averaged over 75 IMRT fields were  $\gamma_{\text{mean}} = 0.37 \pm 0.07$  and  $\gamma_{\text{passrate}} = 98.1 \pm 2.4$ , with an average dose difference in reference point of  $\Delta\text{DRP} = -0.5\% \pm 1.8\%$ . Gamma results for the fields reconstructed from a different commissioned gantry angle were  $\gamma_{\text{mean}} = 0.39 \pm 0.08$  and  $\gamma_{\text{passrate}} = 97.6 \pm 3.3$ , with an average  $\Delta\text{DRP} = -0.1\% \pm 1.8\%$ .

## Conclusion

We have successfully demonstrated the feasibility of back-projection portal dosimetry for the MR-Linac. Verification of IMRT fields irradiated to a phantom shows good agreement between EPID reconstructed and IC array dose distributions. The first MR-Linac prostate and rectum patients are being treated in our clinic and EPID images acquired during treatment for validation of the described method.

This research was partly sponsored by Elekta AB, Stockholm, Sweden.

## PV-0484 In vivo dosimetry using CBCT and EPID device: analysis of sources of errors in VMAT treatments

S. Bresciani<sup>1</sup>, L. Botez<sup>1</sup>, A. Miranti<sup>1</sup>, M. Stasi<sup>1</sup>

<sup>1</sup>Candiolo Cancer Institute - FPO- IRCCS, Medical Physics, Candiolo TO, Italy

## Purpose or Objective

*In vivo* dosimetry (IVD) using an electronic portal imaging device (EPID) combined with CBCT imaging may provide an effective means for quantify dose discrepancies and preventing errors in radiotherapy. The aim of this work is to evaluate the daily dose delivery discrepancies catching sources of errors in VMAT treatments with a 3D EPID-based IVD system

## Material and Methods

The IVD software PerFRACTION (Sun Nuclear Corporation) was used.

PerFRACTION is based on the information concerning MLC and collimator positions obtained by EPID images and on the information of log files, such as the MUs and the gantry angles. From these informations, a collapsed-cone/superposition algorithm (SDC) is used to calculate the dose distribution on daily CBCT images. It also uses the SDC to produce an entire dose volume to check against that from the TPS. First of all we calculated the dose discrepancies (DD%) at the isocenter (ID) and the 3D 2%/2mm gamma passing rate (% GP) between our reference (AAA) and SDC algorithm for 180 plans. About IVD, 3D dose distributions were reconstructed for 961 fractions of 133 patients, including prostates (17%), lungs (15%), Head & Neck (6%), PBI (17%), and palliatives (28%). We evaluated DD% between reference and daily

dose distribution in terms of dose to 95% of the volume ( $D_{95\%}$ ), dose to 2% of the volume ( $D_{2\%}$ ) and average dose to the target.

#### Results

We obtained for ID an average DD% equal to  $(1.8 \pm 0.9)\%$  and an average %GP equal to  $(98 \pm 2)\%$ . For IVD, the mean DD% was equal to  $(-1.6 \pm 5.4)\%$  for  $D_{95\%}$ ,  $(1.0 \pm 1.7)\%$  for  $D_{2\%}$ , and  $(0.3 \pm 1.8)\%$  for average dose. 74% of fractions showed DD% inferior to 2%. For 16% and 5% of the analyzed dose points, DD% was greater than 3% and 5%, respectively. Dose failures occur mainly in air-tissue interfaces and in superficial regions, in fact the deviations greater than 5% were observed in lung patients (30%), partial breast irradiation plans (27%) and palliative treatments (20%). For the 57% of fractions the delivered dose is higher than calculated one. For the fractions that exceed 3%, the errors are due to setup (29%), patient anatomy (40%), setup + anatomy (27%) and bolus positioning (4%). Among set-up errors, 48% is due to SSD variations, 5% are rotational errors, 12% are errors due to difficult art and shoulder positioning, and 35% is due to weight variation. No machine-based errors were observed for these patients.

#### Conclusion

EPID-based IVD is a powerful method to catch and quantify delivery discrepancies during radiotherapy process.

---

### Joint Symposium: ESTRO-IAEA: The role of hypofractionation in current radiotherapy and its impact in planning radiotherapy services

---

#### SP-0485 Hypofractionation from a radiobiological perspective

M.R. Horsman<sup>1</sup>

<sup>1</sup>Aarhus University Hospital, Dept. Experimental Clinical Oncology, Aarhus C, Denmark

#### Abstract text

Hypofractionation is the application of dose fractions larger than the conventional 2 Gy per fraction. It includes moderate doses per fraction of approximately 3.5 Gy routinely used with curative intent, as well as stereotactic treatments with a few large fractions that has been widely applied in palliative radiotherapy, but now suggested to have a curative application, especially for oligometastases. Radiobiologically, when compared to conventional fractionation, hypofractionation would be expected to lower the therapeutic ratio between tumors and late-responding normal tissues. However, technological advances in image guidance and treatment delivery can reduce the dose delivered to normal tissues, allowing tumors to receive higher doses per fraction. There are reports that in addition to direct cell killing seen with high doses per fraction, one also finds dose-dependent secondary cell death that occurs following the induction of vascular damage. However, this is controversial, because changes to the tumour microenvironment (i.e., increased hypoxia) seen following vascular damage are not always apparent after stereotactic irradiation. In fact, hypoxia in tumours, a known factor for resistance to conventional radiotherapy, may play a more significant role with stereotactic radiation. These vascular and microenvironmental effects may depend on the dose per fraction. Recent studies suggest that high-doses per fraction has the potential to induce an immune response that not only improves response of the primary tumor, it also has the potential to cause an abscopal effect. However, the radiation dose and number of fractions necessary to induce this effect is unclear. In this presentation, we will review some of these radiobiological issues associated with hypofractionation and discuss how they can play a role in future radiation therapy.

*Supported by funding from the Danish Cancer Society and the Danish Council for Independent Research: Medical Sciences.*

#### SP-0486 Clinical outcome and effectiveness of extreme hypofractionation together with the different scenarios in terms of resources and costs

J.A. Polo Rubio

*Hospital Ramon y Cajal, Madrid Spain*

Abstract not received

#### SP-0487 How we deliver extreme-hypofractionated radiotherapy with current technology - a physicist perspective

J. Cuijpers<sup>1</sup>

<sup>1</sup>Amsterdam University Medical Centers, Radiation Oncology Department, Amsterdam, The Netherlands

#### Abstract text

The successful clinical implementation of hypofractionated radiotherapy is strongly connected to current advances in treatment technology that enable the safe and precise delivery of high fraction doses to the target with optimal sparing of the adjacent healthy tissue. This starts with a reliable definition of the target volumes and organs at risk using multimodality pretreatment imaging incorporating breathing motion for tumors in the lung or abdomen. Advanced dose delivery techniques, like multiple field IMRT or VMAT, using complex shaped beam portals are applied to achieve steep dose gradients outside the target. This sets high demands on dose planning, especially for small targets in low density lung tissue, and machine performance. Due to the multi-directional or rotational beam setup high beam energies are becoming of less importance, but instead the use of flattening filter free modalities will be important for reduction of treatment times for the delivery of high fraction doses. Of utmost importance is a reliable positioning of the tumor before but also during treatment using on-line image guidance, setting high standards in accuracy and precision for IGRT equipment. This is even more important in the case of hypo-fractionation since the dose averaging effect of geometric random errors does not occur if only a few fractions are administered. Ultimately, if the superior soft tissue contrast of MRI is required, an integrated MR-treatment unit will allow to meet these requirements. Also, demands for quality assurance programs and the necessary equipment will be affected by the requirements for high-precision hypo-fractionated treatments. The consequences on how this affects the program of requirements for radiotherapy equipment will be discussed in this presentation.

#### SP-0488 What's the impact of extreme-hypofractionated radiotherapy in operating a radiotherapy department - an RTT perspective

Y.M. Tsang<sup>1</sup>

<sup>1</sup>Mount Vernon Cancer Centre, Radiotherapy, Northwood Middlesex, United Kingdom

#### Abstract text

Radiotherapy plays a key role in cancer management. The conventional radiotherapy treatment course is divided into a number of small doses called fractions, which are usually given once a day, Monday to Friday, over a number of weeks. Currently, there is a wide range of radiotherapy fractionation schemes available clinically based on treatment intents and disease sites. Hypofractionation, the delivery of a course of radiotherapy using a smaller number of fractions with a higher dose of radiation within each fraction than what is given conventionally as 1.8 - 2Gy, is increasingly studied and adopted for clinical use. In the last decade, there have been rapid changes and progressive developments in the technology used for

planning and delivery of radiotherapy. Intensity modulated radiotherapy and volumetric modulated arc therapy are now commonly implemented for clinical use. Combining the concept of hypofractionated radiotherapy and the use of image guided radiotherapy, these advanced highly precise treatment techniques can be utilised to deliver ablative doses of radiation to tumours while sparing the surrounding normal tissues as commonly known as stereotactic radiotherapy.

Hypofractionated high dose per fraction requires greater clinical, dosimetric and geometric accuracy. Interval between fractions and gaps in radiotherapy schedules can be critical in maintaining the overall treatment outcome. With the introduction of advanced radiotherapy technology, this has increased the complexity of the treatment process resulting in a shift in types and levels of responsibility taken between clinicians, physicists and radiation therapists (RTTs). It provides an opportunity for RTTs to extend their roles and scopes of practice. RTTs should understand the scientific basis and clinical rationale of extreme-hypofractionated radiotherapy and the importance of accurate delivery to tackle both systematic and random errors in this setting. Development of a comprehensive training and competency assessments is an essential aspect of introducing a culture of accuracy in the advanced hypofractionated radiotherapy delivery, irrespective of resource constraints. Before implementing advanced hypofractionated radiotherapy, an institution should review its resources and working practices to define the level of accuracy that is realistically achievable. The number of patients who can be treated accurately within a given time frame and the level of complexity that can be safely implemented into daily practice should be considered. All of these will be discussed in this presentation with the aim to explore the perceived impact of extreme-hypofractionated radiotherapy in operating a radiotherapy department with a RTT's perspective.

---

**Debate: Which is the best technique for the delivery of APBI?**

---

**SP-0489 This house believes that the EBRT is the best technique**

C. Coles<sup>1</sup>

<sup>1</sup>University of Cambridge, Oncology, Cambridge, United Kingdom

**Abstract text**

External beam partial breast radiotherapy: Is non-inferior to whole breast radiotherapy with excellent local control rates, DFS and OS and is the only technique whereby patients have reported better breast appearance and less late side effects<sup>1</sup>.

Can be given in just 5 daily outpatient treatments as illustrated by the UK FAST Forward trial 3-year toxicity results and is non-invasive.

Does not require specialist training and is therefore far more accessible for patients.

Uses existing standard equipment and this simple technique can be implemented in all radiotherapy centres worldwide with no/minimal additional resources.

1. Coles CE, Griffin CL, Kirby AM, Titley J, Agrawal RK, Alhasso A, Bhattacharya IS, Brunt AM, Ciurlionis L, Chan C, Donovan EM, Emson MA, Harnett AN, Haviland JS, Hopwood P, Jefford ML, Kaggwa R, Sawyer EJ, Syndikus I, Tsang YM, Wheatley DA, Wilcox M, Yarnold JR, Bliss JM; IMPORT Trialists. Partial-breast radiotherapy after breast conservation surgery for patients with early breast cancer (UK IMPORT LOW trial): 5-year results from a multicentre, randomised, controlled, phase 2, non-inferiority trial. *Lancet* 2017 Sep 9;390(10099):1048-1060.

**SP-0490 This house believes that the multicatheter brachytherapy is the best technique**

V. Strnad<sup>1</sup>

<sup>1</sup>University Hospital Erlangen, Dept. Radiation Oncology, Erlangen, Germany

**Abstract text**

**Purpose:** To analyze the facts about adjuvant interstitial brachytherapy-based Accelerated Partial Breast Irradiation (APBI) after breast conserving surgery in terms of clinical experience, quality assurance and clinical results. **Methods and Materials:** The multicatheter brachytherapy is unique among the different techniques of APBI for a lot of reasons. The author analyses in a matter-of-fact and detailed fashion the facts in this context: 1. *High Quality assurance and reproducibility*; 2. *Technique with the longest experience among all APBI techniques*; 3. *Level 1 evidence - excellent efficacy - the same whole breast irradiation (WBI)*; 4. *Level 1 evidence - lower incidence of late side effects in comparison to WBI*; 5. *Level 1 evidence - better Quality of Life (QoL) in comparison to WBI*; 6. *In comparison to APBI using different external beam therapy techniques the multicatheter brachytherapy reduces in majority of anatomic scenarios significant doses to all relevant organs at risk.*

**Results**

The published data imposingly demonstrate the very long experience of brachytherapy as a technique for APBI. The first Phase II APBI-trials were started more than 20 years ago and over the same time the basic rules of image-guided multicatheter brachytherapy techniques have been developed and guidelines published. Long-term follow-up outcomes in two Phase 3 trials show that APBI using multicatheter brachytherapy yields equivalent local control, disease-free survival, and overall survival after breast-conserving treatment compared with conventional whole-breast irradiation. In large multicentre GEC-ESTRO trial after median follow-up of 6.6 years exceptionally low overall recurrence about 1% at 5 years in both treatment arms has been reported (p=0.4). Analogous also 5-year disease-free survival was 94,5% with whole-breast irradiation and 95% with APBI (p=0.8) and breast cancer-related mortality did, hitherto, not differ between groups (four events vs four events; p=0.8). Furthermore 5-year toxicity profiles and cosmetic results were similar in patients treated with breast-conserving surgery followed by either APBI with interstitial brachytherapy or conventional whole-breast irradiation, with significantly fewer grade 2-3 late skin side-effects after APBI with interstitial brachytherapy. APBI with multicatheter brachytherapy is also associated in general with equal quality of life (QoL) compared with whole-breast irradiation, but in details moderate, statistically and clinical significant difference of QoL between the groups was found in the breast symptoms scale in favour for brachytherapy based APBI. In addition to it the published dosimetric comparisons of different APBI techniques described, that the multicatheter brachytherapy in comparison to external beam based APBI-techniques reduces in majority of anatomic scenarios significant the mean doses to all relevant organs at risk and in consequence the multicatheter-based APBI is able to reduce significant as well deterministic as the stochastic late side effects in all surrounding organ at risk as heart and lung.

**Conclusions**

Summarizing the facts available to date it is obvious that APBI using brachytherapy techniques works excellently. No other technique of APBI is supported by such robust, broad positioned and encouraging data. In addition to it comparing the dose distributions of different APBI techniques, and given the long-term experience and excellent clinical results the high adaptability, versatility, precision, quality and reproducibility of brachytherapy

based APBI is also proven. All these facts should be a stimulus for radiation oncologists to make available brachytherapy based APBI worldwide for each suitable patient with early breast cancer.

**SP-0491 For which patient which technique is the best from view of the physicist?**

T. Major<sup>1</sup>

<sup>1</sup>National Institute of Oncology, Radiotherapy, Budapest, Hungary

**Abstract text**

Accelerated partial breast irradiation (APBI) can be performed with various techniques including both brachytherapy (BT) and external beam radiotherapy (EBRT) having different dosimetric characteristics. All methods are clinically feasible and there is no „one size fits all” technique. The best technique depends on patient anatomy and tumour location. However, the choice for treatment in the institutions mostly depends on the physician's preference and the technical availability.

Among all techniques multicatheter interstitial BT (MIBT) has the longest experience. MIBT can provide highly conformal dose distribution, large dose gradient at target edge, low doses to organs at risk (OARs), but a possible geometric miss can result in significant under dosage of the target.

Technically, the use of single-entry intracavitary applicators is easier. With balloon-type applicators no geometric miss can occur, but proper tissue conformance is not always guaranteed. With multi-lumen balloons sphere-like target volume with limited asymmetric margins can be irradiated, and the dose modulation potential is modest. In some anatomical situation the balloon can be asymmetric resulting in asymmetric target coverage. The intracavitary hybrid applicators are more flexible regarding shaping the dose distribution and reducing dose to OARs without compromising the target volume coverage.

During intraoperative radiotherapy (IORT) large dose is given in one fraction without imaging and 3D treatment planning. In intraoperative electronic BT using spherical applicator the dose distribution is also spherical and a large dose inhomogeneity develops due to the sharp dose fall-off of the low energy X-ray beam. The margin is always symmetric, but the geometric accuracy is always ensured.

At IORT with electron beam dose modulation possibility to shape the dose distribution is very limited. Standard dose distributions are used, the thoracic wall is protected with a physical device and the skin with retraction.

Linear accelerator based EBRT techniques expose relatively large volumes of non-target breast to high dose mainly due to the extended target volume created from CTV. In three-dimensional conformal radiotherapy (3D-CRT) dose to contralateral breast, lung or heart can be reduced with proper selection of beam orientations. With intensity modulated radiotherapy (IMRT) highly conformal dose distribution can be achieved, but volumes irradiated by low doses can be larger than with 3D-CRT. Regarding the dose to OARs, with MIBT the critical structures can be better spared than with 3D-CRT/IMRT except for the heart. The dose to heart in BT is strongly dependent on the location of the PTV. With image guidance in EBRT the dose to OARs can be significantly reduced due to smaller target volume. At left sided lesion the dose to heart can be considerably decreased with deep inspiration breath-hold technique.

With special EBRT devices such as Cyberknife or Tomotherapy which are equipped with image guidance smaller CTV-PTV margin can be applied which reduces the dose to OARs while maintaining proper target coverage. Real-time tracking with Cyberknife can provide good target volume coverage and spares nearby critical organs, but the treatment time is too long.

Proton beam irradiation, due to the more favourable dose characteristics of proton beam, can provide the least dose to organs at risk, but the accessibility of the technique is limited and the available data are scarce.

**SP-0492 Radiobiology of APBI: aspects and limitations**

J. Guinot<sup>1</sup>, V. Gonzalez-Perez<sup>2</sup>

<sup>1</sup>Fundación Instituto Valenciano De Oncología,

Department Of Radiation Oncology, Valencia, Spain;

<sup>2</sup>Fundación Instituto Valenciano De Oncología,

Department Of Radiation Physics, Valencia, Spain

**Abstract text**

Accelerated partial breast irradiation (APBI) has become a standard in early low-risk breast carcinomas. Alfa/beta around 4 is accepted for breast, what means that higher doses per fraction are recommended, and are favourable for patients due to a shorter total time of treatment in five days or less. Several techniques are being used, but with different dosimetries and different biological effects. Intracavitary procedures limit the irradiation to a certain margin from the cavity edge, but with a high gradient of dose on the surface. The volume of treatment is several times larger with external beam radiotherapy (EBRT) compared with multicatheter interstitial brachytherapy (MIBT) because a PTV must be added due to positional uncertainties. The skin and ribs cannot be easily preserved with EBRT. The accelerated schemes of EBRT with 38.5Gy in ten fractions or 30 Gy in 5 five fractions, correspond to a higher EQD2 dose than MIBT for alfa/beta 4, but the difference is greater for alfa/beta 2, chosen for late effects. We do not know if it has some impact on long term results and complications, as it happens with intracavitary devices, where rib fractures and skin necrosis are described in a small amount. On the other hand, the prescription dose with EBRT is quite homogeneous. With MIBT it corresponds with the peripheral dose, and the gradient of dose around every catheter supposes a higher biological effect inside the treated volume, but a higher risk of fibrosis. Five-year results are only the first step to know the efficacy of APBI, and longer follow-up is needed to be sure that the low total EQD2 doses are similar for EBRT and MIBT. Shorter number of fractions are under investigation, and will probably be implemented in the next future, to increase the comfort and compliance of APBI. The extremely low percentage of recurrences, under 2-3% at five years, indicates that low total doses are enough to control the remaining tumour cells after conserving surgery. Very accelerated partial breast irradiation (VAPBI) in a few or even a single fraction are promising. But the radiobiological effect is not well known and we must wait for the clinical trials to find the best option. Probably, several approaches will be useful and must be offered to each patient according to the availability, experience and preferences.

---

**Proffered Papers: Biomarkers and bioimaging in radiotherapy**

---

**OC-0493 CTCs in patients with brain metastases under radiotherapy: do they indicate treatment response?**

C. Petersen<sup>1</sup>, Y. Goy<sup>1</sup>, A. Krüll<sup>1</sup>, K. Pantel<sup>2</sup>, H. Wikman<sup>2</sup>, K. Borgmann<sup>3</sup>

<sup>1</sup>University Medical Center Hamburg - Eppendorf UKE, Department of Radiation Oncology, Hamburg, Germany ;

<sup>2</sup>Institut of Tumor Biology, Center of Oncology, Hamburg, Germany; <sup>3</sup>Laboratory of Radiobiology & Experimental Radio-Oncology, Department of Radiotherapy, Hamburg, Germany

### Purpose or Objective

Circulating tumor cells (CTCs) are detectable in many cancers, including breast and lung cancer, where they can have prognostic significance. However, because of the lack of a suitable detection method, there are no useful data on CTCs in patients undergoing radiotherapy. The only US Food and Drug Administration-approved methodology, the CellSearch platform, uses epithelial cellular adhesion molecule EpCAM, exploiting the positivity of carcinomas to common epithelial markers. The monitoring of CTCs under chemotherapy showed a correlation of persistent CTCs and shorter survival in breast cancer. This indicates stronger defense mechanisms in the remaining CTCs. More efficient DNA repair capacity could contribute to such stronger resistance. The aim of this study is to identify relevant DNA damage response pathways in CTCs and peripheral blood lymphocytes under radiotherapy and their possible implications for the adjustment of future therapies.

### Material and Methods

Up to now 47 patients with brain metastases of breast and lung cancer (n=21/26) receiving radiotherapy were included in the study. Blood samples were collected before, at the end of radiotherapy and at the first follow-up (87 blood samples so far). The number of CTCs at the first follow-up was compared with clinical treatment response (e.g. MRI/CT and performance status). Enumeration and characterization of CTCs were done using the CellSearch® system. Apoptosis was measured in CTCs (*in vivo* irradiation) with the help of the M30 antibody in the CellSearch® system and DNA damage repair analyzed by γH2AX and 53BP1 foci detection was analyzed in primary lymphocytes (*ex vivo* irradiation).

### Results

CTCs were detectable in 19% of lung cancer and 38% of breast cancer patients with brain metastases before start of radiotherapy. Quantitative changes in the number of CTCs under local radiotherapy were measurable in all patients. In the lung cancer group, 40% of patients showed an increase of CTCs after irradiation. This percentage was much higher in the breast cancer group with 75%. To specify whether the observed increase in number was due to vital or lethal CTCs an apoptotic marker (M30) was stained in addition in the same samples. In 82% the increase in CTC number was accompanied by apoptosis. After correction for this the number of vital CTCs decreased, indicating treatment response. This is mirrored by the clinical follow up via MRI/CT (evaluation under way) after different radiation schedules (whole brain vs. stereotactic treatment). The same treatment response was detectable in the DNA-damage response assessment parameters.

### Conclusion

The results indicate that monitoring DNA repair in CTCs and primary lymphocytes is already showing promising potential for judging treatment response after radiotherapy in the metastatic state of disease. The increase in apoptotic cells under radiotherapy suggests ineffective DNA repair and thus a local response to therapy. On the other hand, if persistent CTCs are present, this indicates efficient DNA repair and a poor prognosis.

### OC-0494 Genetic variants associated with radiation-induced xerostomia in head and neck cancer: a GWA study

E. Naderi<sup>1,2</sup>, A.P. Crijns<sup>1</sup>, R.J. Steenbakkers<sup>1</sup>, H.P. Bijl<sup>1</sup>, J.F. Van den Hoek<sup>1</sup>, M. Dieters<sup>1</sup>, M.H. Boezen<sup>2</sup>, B.Z. Alizadeh<sup>2</sup>, J.A. Langendijk<sup>\*1</sup>

<sup>1</sup>The University of Medical Center Groningen, Radiation Oncology, Groningen, The Netherlands ; <sup>2</sup>The University of Medical Center Groningen, Epidemiology, Groningen, The Netherlands

### Purpose or Objective

We aimed to find genetic variants associated with radiation-induced late Xerostomia in head and neck cancer (HNC) patients population treated with definitive or postoperative radiotherapy (RT).

### Material and Methods

We included 1,061 HNC patients treated with definitive or postoperative RT with or without chemotherapy from a prospective cohort study. All baseline patient- tumor- and treatment characteristics and acute and late toxicity was prospectively scored. Patients were followed up to 5 years after treatment. Patient phenotype data were imputed to correct for missingness of samples. Patients were genotyped on Illumina human hap 550k v.3.0 (n=607) or Illumina global screening array (n=464). Genotypes were imputed on Haplotype Reference Consortium reference panel version R1.1. Principal component analysis (PCA) was performed to identify population substructures among samples. Eventually, 957 patients and 6,334,277 SNPs passed quality controls which were included in the final analysis. Xerostomia was defined as moderate to severe xerostomia at 6 months (XER6M). We fitted first a phenotype model (model I) to identify the significant non-genetic clinical and baseline factors associated with XER6M by using imputed samples. Next logistic regression was used to estimate the association of the additive effect of genetic variants with XER6M while adjusting for other predictors from the model I and the top four eigenvectors obtained from PCA analysis. A p-value<0.05 for clinical co-variable, and a genome-wide p-value<5.0x10<sup>-8</sup> for genetic variants was considered statistically significant.

### Results

Full data were available in 763 patients, of whom 280 (36.7%) had XER6M. These cases were compared to 483 patients without XER6M. Clinical factors including N stage (OR=0.29; 95%CI 0.12 to 0.68; p=0.004), volume surrogate (5.97; 3.11 to 11.46; p=7.16x10<sup>-8</sup>), definitive radiotherapy (0.22; 0.15 to 0.32; p=1.61x10<sup>-15</sup>) and baseline xerostomia (2.60; 2.00 to 33.36; p=5.48x10<sup>-13</sup>) were significantly associated with XER6M. In total, 26 variants across eight genomic regions showed a suggestive association at (5.0x10<sup>-8</sup><p<5.0x10<sup>-6</sup>) to XER6M, including one variant on chr1.q41 at p=7.8x10<sup>-7</sup> with an OR of 2.5 (95%CI 1.74 to 3.61).

### Conclusion

We found suggestive genetic variants associated to in XER6M, independent of clinical predictors of XER6M. Further replication is required in independent cohorts while also adjusting for dose distributions in related organs at risk. Identification of genetic variants associated with radiation-induced XER6M may eventually improve predictive models for radio-toxicity in HNC patients.

### OC-0495 Use of radiomics in the recurrence patterns after IMRT for head and neck cancer: a preliminary study

S. Li<sup>1</sup>, K. Wang<sup>1</sup>, Z. Hou<sup>1</sup>, J. Yang<sup>1</sup>, W. Ren<sup>1</sup>, S. Gao<sup>1</sup>, F. Meng<sup>1</sup>, P. Wu<sup>1</sup>, B. Liu<sup>1</sup>, J. Liu<sup>1</sup>, J. Yan<sup>1</sup>

<sup>1</sup>The Comprehensive Cancer Centre of Drum Tower Hospital- Medical School of Nanjing University & Clinical Cancer Institute of Nanjing University, The Comprehensive Cancer Centre of Drum Tower Hospital, Nanjing, China

### Purpose or Objective

To analyze the recurrence patterns and reasons in patients with head and neck cancer (HNC) treated with intensity-modulated radiotherapy (IMRT) and to investigate the feasibility of radiomics for analysis of nasopharyngeal carcinoma (NPC) radioresistance.

### Material and Methods

We analyzed 504 HNC patients treated with IMRT from Jul-2009 to Aug-2016, 26 of whom developed with recurrence. For the HNCs with recurrence, CT, MR or PET/CT images of recurrent disease were registered with the primary

planning CT for dosimetry analysis. The recurrences were defined as in-field, marginal or out-of-field, according to dose-volume histogram (DVH) of the recurrence volume. To explore the predictive power of radiomics for NPCs with in-field recurrences (NPC-IFR), 16 NPCs with non-progression disease (NPC-NPD) were used for comparison. For these NPC-IFRs and NPC-NPDs, 1117 radiomic features were quantified from the tumor region using pre-treatment spectral attenuated inversion-recovery T2-weighted (SPAIR T2W) magnetic resonance imaging (MRI). Intraclass correlation coefficients (ICC) and Pearson correlation coefficient (PCC) was calculated to identify influential feature subset. Kruskal-Wallis test and receiver operating characteristic (ROC) analysis were employed to assess the capability of each feature on NPC-IFR prediction. Principal component analysis (PCA) was performed for feature reduction. Artificial neural network (ANN), k-nearest neighbor (KNN) and support vector machine (SVM) models were trained and validated by using stratified 10-fold cross validation.

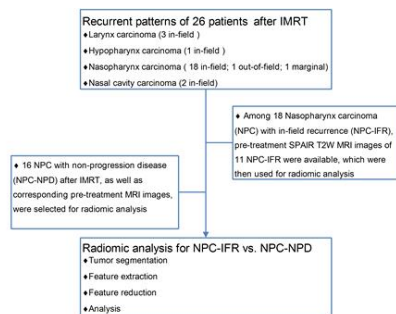


Figure 1. Flowchart of using radiomic analysis in recurrent pattern.

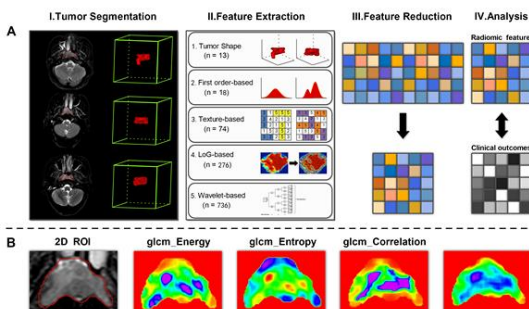


Figure 2. (A) Workflow of radiomic analysis for nasopharyngeal carcinoma (NPC) with in-field recurrence (IFR). (B) Examples of feature maps computed from the tumor region by using GLCM method (e.g. Energy, Entropy, Correlation, InverseDifferenceMoment [IDM]).

## Results

The median follow up was 26 (range 3-65) months. 13/26 (50%) occurred in the primary tumor, 8/26 (31%) occurred in regional lymph nodes, and 5/26 (19%) patients developed a primary and regional failure. Dosimetric and target volume analysis of the recurrence indicated that there were 24 in-field, and 1 marginal as well as 1 out-of-field recurrence. Among the HNCs with recurrence, 20 NPCs developed in-field failure (NPC-IFR). With pre-therapeutic SPAIR T2W MRI images available, 11 NPC-IFRs (11 of 20 NPC-IFRs who had available pre-therapeutic MRI) and 16 NPC-NPDs were subsequently employed for radiomic analysis. Results showed that NPC-IFRs versus NPC-NPDs could be differentiated by 8 features (AUCs: 0.727-0.835). The classification models showed potential in prediction of NPC-IFR with higher accuracies (ANN: 0.812, KNN: 0.775, SVM: 0.732).

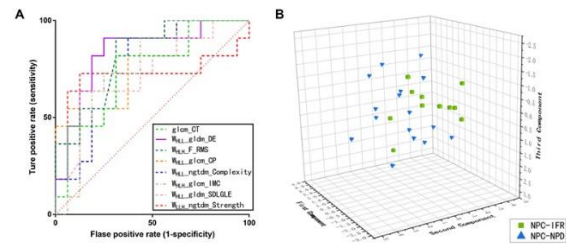


Figure 3. (A) Receiver operating characteristics (ROC) curves on the basis of the significant features. (B) Three-dimensional scatter plot of the NPC-IFR and NPC-NPD by using three principal components derived from the above eight significant features.

## Conclusion

In-field and high-dose region relapse were the main recurrence patterns which may be due to the radioresistance. After integration in the clinical workflow, radiomic analysis can be served as imaging biomarkers to facilitate early salvage for NPC patients who are at risk of in-field recurrence.

## OC-0496 Deep-learning based estimation of loco-regional control for patients with locally advanced HNSCC

S. Starke<sup>1,2,3</sup>, S. Leger<sup>1,3,4</sup>, A. Zwanenburg<sup>1,3,4,5</sup>, K. Piltz<sup>1,3,4,5</sup>, F. Lohaus<sup>1,3,4,5</sup>, A. Linge<sup>1,3,4,5</sup>, K. Zöpfel<sup>6,7</sup>, J. Kotzerke<sup>6,7</sup>, A. Schreiber<sup>8</sup>, I. Tinhofer<sup>9,10</sup>, V. Budach<sup>9,10</sup>, M. Stuschke<sup>11,12</sup>, P. Balermipas<sup>13,14</sup>, C. Rödel<sup>13,14</sup>, U. Ganswindt<sup>15,16,17</sup>, C. Belka<sup>15,16,17</sup>, S. Pigorsch<sup>15,18</sup>, S.E. Combs<sup>15,18,19</sup>, D. Mönlich<sup>20,21</sup>, D. Zips<sup>20,21</sup>, M. Krause<sup>1,3,4,5,22</sup>, M. Baumann<sup>1,3,4,5,22,23</sup>, C. Richter<sup>1,3,5,22</sup>, E.G.C. Troost<sup>1,3,4,5,22</sup>, S. Löck<sup>1,3,5</sup>

<sup>1</sup>OncoRay - National Center for Radiation Research in Oncology, Faculty of Medicine and University Hospital Carl Gustav Carus- Technische Universität Dresden-Helmholtz-Zentrum Dresden - Rossendorf, Dresden, Germany; <sup>2</sup>Helmholtz-Zentrum Dresden - Rossendorf, Department of Information Services and Computing, Dresden, Germany; <sup>3</sup>German Cancer Research Center DKFZ, Heidelberg and German Cancer Consortium DKTK partner site, Dresden, Germany; <sup>4</sup>National Center for Tumor Diseases NCT, Partner Site Dresden: German Cancer Research Center DKFZ Heidelberg- Faculty of Medicine and University Hospital Carl Gustav Carus- Technische Universität Dresden and Helmholtz Association / Helmholtz-Zentrum Dre; <sup>5</sup>Faculty of Medicine and University Hospital Carl Gustav Carus- Technische Universität Dresden, Department of Radiotherapy and Radiation Oncology, Dresden, Germany; <sup>6</sup>Faculty of Medicine and University Hospital Carl Gustav Carus- Technische Universität Dresden, Department of Nuclear Medicine, Dresden, Germany; <sup>7</sup>Helmholtz-Zentrum Dresden - Rossendorf, PET Center-Institute of Radiopharmaceutical Cancer Research, Dresden, Germany; <sup>8</sup>Hospital Dresden-Friedrichstadt, Department of Radiotherapy, Dresden, Germany; <sup>9</sup>German Cancer Research Center DKFZ, Heidelberg and German Cancer Consortium DKTK partner site, Berlin, Germany; <sup>10</sup>Charité University Hospital, Department of Radiooncology and Radiotherapy, Berlin, Germany; <sup>11</sup>German Cancer Research Center DKFZ, Heidelberg and German Cancer Consortium DKTK partner site, Essen, Germany; <sup>12</sup>Medical Faculty- University of Duisburg-Essen, Department of Radiotherapy, Essen, Germany; <sup>13</sup>German Cancer Research Center DKFZ, Heidelberg and German Cancer Consortium DKTK partner site, Frankfurt, Germany; <sup>14</sup>Goethe-University Frankfurt, Department of Radiotherapy and Oncology, Frankfurt, Germany; <sup>15</sup>German Cancer Research Center DKFZ, Heidelberg and German Cancer Consortium DKTK partner site, Munich, Germany; <sup>16</sup>Helmholtz Zentrum München, Clinical Cooperation Group- Personalized Radiotherapy

in Head and Neck Cancer, Munich, Germany ; <sup>17</sup>Ludwig-Maximilians-Universität, Department of Radiation Oncology, Munich, Germany ; <sup>18</sup>Technische Universität München, Department of Radiation Oncology, Munich, Germany ; <sup>19</sup>Helmholtz Zentrum München, Institute of Innovative Radiotherapy iRT, Oberschleißheim, Germany ; <sup>20</sup>German Cancer Research Center DKFZ, Heidelberg and German Cancer Consortium DTK partner site, Tübingen, Germany ; <sup>21</sup>Faculty of Medicine and University Hospital Tübingen- Eberhard Karls Universität Tübingen, Department of Radiation Oncology, Tübingen, Germany ; <sup>22</sup>Helmholtz-Zentrum Dresden - Rossendorf, Institute of Radiooncology - OncoRay, Dresden, Germany ; <sup>23</sup>German Cancer Research Center DKFZ, Scientific Director, Heidelberg, Germany

### Purpose or Objective

In order to improve radiotherapy outcomes, further treatment personalisation is considered beneficial. Radiomics analyses aim to predict treatment outcomes based on medical imaging data. Commonly, hand-crafted imaging features are used that require domain knowledge and further feature selection steps. This may cause relevant information to be lost. Deep convolutional neural networks (CNNs) on the other hand can act as automatic feature detectors and are able to learn highly nonlinear relationships directly from imaging data, thus addressing the drawbacks of conventional radiomics approaches and enabling end-to-end learning. We investigated whether CNNs are capable of quantifying loco-regional tumour control (LRC) based on CT imaging of patients with locally advanced head and neck squamous cell carcinoma (HNSCC).

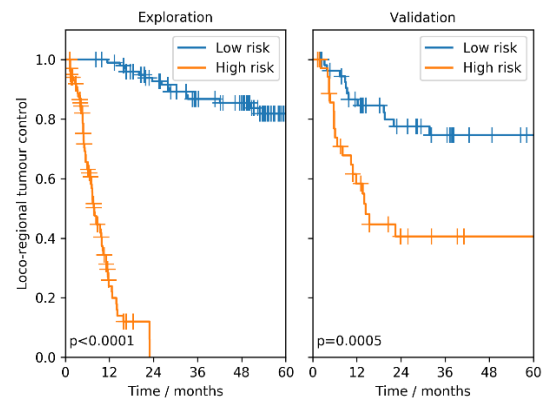
### Material and Methods

A multicentre cohort consisting of 302 patients with locally advanced HNSCC was collected and divided into an exploratory and a validation cohort (207 and 95 patients, respectively). All patients received a CT scan for treatment-planning and were treated by primary radio(chemo)therapy. 9725 transverse CT slices from the exploratory cohort were used to train a CNN with eight convolutional layers. For every patient (with one exception) we used 23 CT slices cranial and caudal of the slice with the largest tumour area, resulting in 47 slices per patient. Discriminative performance was evaluated using 4465 slices of the validation data set. The hazard of loco-regional recurrence was estimated by the CNN maximising the likelihood of the Cox proportional hazards model, which allows for incorporation of nonlinear relationships between the imaging features and the hazard prediction. The final hazard for every patient was obtained by averaging the results of the individual slices. The prognostic value of the model was evaluated by the concordance index (C-Index). Patients were stratified into groups of low and high risk of recurrence using the median hazard in the exploratory cohort.

### Results

The validation of our CNN model revealed a C-Index of 0.68 (95% confidence interval: 0.57-0.79) for the prognosis of LRC. The estimated hazards were used to stratify patients into two risk groups. LRC significantly differed between these groups, both in the exploratory and the validation cohort (log-rank  $p < 0.0001$  and  $p = 0.0005$ , respectively). Compared to previously published results with an average validation C-Index of 0.62 based on conventional radiomics [1], prognostic performance was slightly improved.

[1] Leger et al. Sci Rep 7: 13206 (2017).



### Conclusion

We showed that CNNs are capable of automatically stratifying patients with locally advanced HNSCC into high and low-risk groups for loco-regional tumour recurrence. The obtained results suggest that deep-learning based approaches can become useful for non-invasively evaluating individual recurrence risks encouraging future research in this area.

### OC-0497 Predictive modelling of risk of breast fibrosis at >10 years after radiotherapy using the RILA assay

C. Herskind<sup>1</sup>, P. Seibold<sup>2</sup>, I. Helmbold<sup>2</sup>, E. Sperk<sup>1</sup>, F.A. Giordano<sup>1</sup>, S. Behrens<sup>2</sup>, F. Wenz<sup>1</sup>, J. Chang-Claude<sup>2</sup>, M.R. Veldwijk<sup>1</sup>

<sup>1</sup>Universitätsmedizin Mannheim- Medical Faculty Mannheim- Heidelberg University, Department of Radiation Oncology, Mannheim, Germany ; <sup>2</sup>German Cancer Research Center, Division of Cancer Epidemiology, Heidelberg, Germany

### Purpose or Objective

The radiation-induced lymphocyte apoptosis (RILA) assay has shown associations with the risk of late adverse reaction in cohorts of radiotherapy patients with mixed and single-entity tumors. However, most published studies have scored late reactions up to three years only. The purpose of the present study was to test the assay in breast cancer patients who had undergone radiotherapy after breast-conserving surgery (BCS) more than 10 years earlier. A particular aim was to compare the predictive value of RILA for fibrosis within and outside the surgical area, as well as for telangiectasia, and to assess the influence of other clinical risk factors.

### Material and Methods

Patients from the German ISE cohort (BCS and adjuvant radiotherapy without chemotherapy) with median 11.6 years of follow-up were included in the analysis. RILA for CD4<sup>+</sup> and CD8<sup>+</sup> T cells was determined by flow cytometry of peripheral blood cells 48h after irradiation with a dose of 8 Gy (6 MV X-rays). Late reactions scored by LENT-SOMA were dichotomized as moderate-severe (grade 2-3) vs non-mild (grade 0-1). Fibrosis was scored outside and within the surgical area. Multivariate logistic regression model included: Age at surgery, BMI, hypertension, smoking status, total dose (EQD2), and hormonal treatment. Multivariate predictive modelling was performed by bootstrapping using c statistics to evaluate discrimination of risk.

### Results

High CD4<sup>+</sup> RILA values were inversely correlated with the risk of fibrosis ( $p = 0.011$ ) and telangiectasia ( $p < 0.001$ ) while CD8<sup>+</sup> RILA showed a trend ( $p = 0.06$ ) for telangiectasia only. Univariate ROC analysis and multivariate analysis showed higher AUC and c-stat values outside than within the surgical area. Notably, the improvement by including CD4<sup>+</sup> RILA in the multivariate analysis relative to including

only the clinical factors was larger outside than inside the surgical area. The data showed better discrimination for predicting resistance than sensitivity to developing late reaction. In univariate analysis of the upper RILA tertile versus the lower and middle tertiles, the positive predictive value (PPV) for resistance to fibrosis was 95.1% outside and 73.2% within the surgical area whereas the negative predictive values (NPV) were 21.0% and 16.0%, respectively. For resistance to telangiectasia, PPV was 97.5% and NPV was 12.7%.

#### Conclusion

CD4<sup>+</sup> RILA predicted fibrosis and telangiectasia although it seemed better at predicting resistance. The higher PPV for resistance to fibrosis outside the surgical area supports that CD4<sup>+</sup> RILA is indeed associated with risk of radiation-induced fibrosis whereas fibrosis within the surgical area could be partly explained by clinical factors. Although the patients in this study were recruited prospectively and had a long follow-up (>10y), the predictive modeling is limited by blood samples being taken at the time of follow-up rather than prospectively. Future prospective studies are needed to validate the present findings.

#### OC-0498 Results of the prospective trial evaluating radiation-induced lymphocyte apoptosis and prostate RT

D. Azria<sup>1</sup>, G. Crehange<sup>2</sup>, F. Castan<sup>3</sup>, E. Schwartz<sup>4</sup>, Y. Belkacemi<sup>5</sup>, J. Lagrange<sup>6</sup>, T. NGuyen<sup>7</sup>, O. Chapet<sup>8</sup>, F. Mornex<sup>9</sup>, G. Noel<sup>10</sup>, E. Lartigau<sup>11</sup>, D. Pasquier<sup>11</sup>, S. Clippe<sup>12</sup>, C. Hennequin<sup>13</sup>, S. Gourgu<sup>14</sup>, M. Brengues<sup>15</sup>, P. Fenoglio<sup>4</sup>, M. Farcy-Jacquet<sup>16</sup>, E. Ozsahin<sup>17</sup>  
<sup>1</sup>ICM-Val d'Aurelle, Radiation Oncology and Radiobiology Unit, Montpellier, France ; <sup>2</sup>Centre GF Leclerc, Radiation Oncology, Dijon, France ; <sup>3</sup>ICM Val d'Aurelle, Biometry Unit, Montpellier, France ; <sup>4</sup>ICM-Val d'Aurelle, Radiation Oncology, Montpellier, France ; <sup>5</sup>AP-HP Henri Mondor, Radiation Oncology, Creteil, France ; <sup>6</sup>AP-HP Henri Mondor, Radiation Oncology, Créteil, France ; <sup>7</sup>Institut Jean Godinot, Radiation Oncology, Reims, France ; <sup>8</sup>Centre Hospitalier Lyon Sud, Radiation Oncology, Pierre Bénite, France ; <sup>9</sup>Centre Hospitalier Lyon Sud, Radiation Oncology, Pierre Benite, France ; <sup>10</sup>Centre Paul Strauss, Radiation Oncology, Strasbourg, France ; <sup>11</sup>Centre Oscar Lambret, Radiation Oncology, Lille, France ; <sup>12</sup>Centre Marie Curie, Radiation Oncology, Valence, France ; <sup>13</sup>AP-HP Saint Louis, Radiation Oncology, Paris, France ; <sup>14</sup>ICM-Val d'Aurelle, Biometry Unit, Montpellier, France ; <sup>15</sup>IRCM ICM-Val d'Aurelle, Radiobiology unit, Montpellier, France ; <sup>16</sup>CHU Nimes, Radiation Oncology, Nimes, France ; <sup>17</sup>CHUV, Radiation Oncology, Lausanne, Switzerland

#### Purpose or Objective

Monocentric cohorts suggested that radiation-induced CD8 T-lymphocyte apoptosis (RILA) can predict late toxicity after curative intent radiotherapy (RT). We assessed the role of RILA as a predictor of pelvic toxicities (pt+) after localized prostate RT in a prospective multicentre trial.

#### Material and Methods

A total of 383 prostate-cancer patients (pts) treated by RT were recruited at eight centres. Before the amendment (2014), only favourable stage prostate cancers were included (n=205). The amendment allowed inclusions of prostate cancers treated with pelvic irradiation for higher risk disease or postoperative RT (n=179). RILA was assessed before RT by flow cytometry. Impact of RILA on pt+ (primary endpoint) or relapse was assessed using a competing risks method. Receiver-operator characteristic (ROC) curve analyses were also performed in intention to treat. This study is registered with ClinicalTrials.gov, number NCT00893035 and analyses of the 205 localized prostate-cancer pts are presented here.

#### Results

All pts received 80 Gy to the planning target volume defined as the prostate only plus a margin of 10 mm except in regard to the rectum (5 mm). Concomitant

hormonotherapy was administered to 91 pts (44.4%). With a median follow-up of 38 months (179 pts presented a minimum follow-up of 36 months), acute and late grade  $\geq 2$  pt+ was observed in 95 pts (46.3%) and 60 pts (29.3%), respectively. No correlation was observed between values of RILA and acute pt+. A decreased incidence of late grade  $\geq 2$  pt+ was observed for increasing values of RILA (p = 0.04). The area under the ROC curve was 0.60. For cut-off values of RILA  $\geq 24\%$  and  $< 14\%$ , sensitivity and specificity were 75% and 37%, 45% and 74%, respectively. Negative predictive value for grade  $\geq 2$  pt+ was equal to 76% for RILA  $\geq 24\%$  and positive predictive value was equal to 45% for RILA  $< 14\%$  where the overall prevalence of grade  $\geq 2$  pt+ was estimated at 29%. A significant increase in the risk of grade  $\geq 2$  pt+ was found if patients had pre-treatment urinary symptoms (sHR = 1.90, p = 0.016) and decreased if pts presented a RILA  $\geq 14\%$  (sHR = 0.58, p = 0.04).

#### Conclusion

RILA significantly predicts the risk of pt+ in case of prostate radiotherapy associated with pre-treatment clinical symptoms. This study validates the use of RILA in a predictive multiparametric nomogram as a rapid screening test before RT delivery and may guide physicians in personalizing radiation therapy scheme.

#### OC-0499 Neutrophilia as prognostic factor for outcome in the CAO/ARO/AIO-04 phase 3 rectal cancer trial

M. Diefenhardt<sup>1</sup>, R. Hofheinz<sup>2</sup>, T. Beissbarth<sup>3</sup>, D. Arnold<sup>4</sup>, J. Müller von den Grün<sup>1</sup>, T. Liersch<sup>5</sup>, P. Ströbel<sup>6</sup>, G. Grabenbauer<sup>7</sup>, R. Fietkau<sup>8</sup>, J. Weitz<sup>9</sup>, M. Ghadimi<sup>5</sup>, C. Rödel<sup>1</sup>, E. Fokas<sup>1</sup>  
<sup>1</sup>Klinikum der Johann Wolfgang Goethe Univ, Department of Radiotherapy and Oncology, Frankfurt, Germany ; <sup>2</sup>University Hospital Mannheim, Department of Medical Oncology, Mannheim, Germany ; <sup>3</sup>University Medical Center Göttingen, Department of Statistics-, Göttingen, Germany ; <sup>4</sup>Helios Klinikum Hamburg, Department of Medical Oncology, Hamburg, Germany ; <sup>5</sup>University Medical Center Göttingen, Department of General-Visceral and Pediatric Surgery, Göttingen, Germany ; <sup>6</sup>University Medical Center Göttingen, Institute of Pathology, Göttingen, Germany ; <sup>7</sup>DiaCura & Klinikum Coburg, Department of Radiation Oncology and Radiotherapy, Coburg, Germany ; <sup>8</sup>University of Erlangen-Nürnberg, Department of Radiation Therapy, Erlangen, Germany ; <sup>9</sup>University of Dresden, Department of General and Visceral and Pediatric Surgery, Dresden, Germany

#### Purpose or Objective

Peripheral blood leukocytosis and neutrophilia reflect cancer inflammation and have been proposed as prognostic immunological biomarkers in various malignancies. However, previous studies were limited by their retrospective nature and small patient numbers.

#### Material and Methods

The CAO/ARO/AIO-04 randomized phase 3 trial accrued 1236 patients with locally-advanced rectal adenocarcinoma. Patients were randomized to receive either fluorouracil-based preoperative chemoradiotherapy alone (5-FU CRT) or with oxaliplatin (5-FU/Oxaliplatin CRT) followed by surgery and adjuvant chemotherapy. The baseline level of peripheral blood leukocytes, neutrophils, hemoglobin, platelets, lactate dehydrogenase (LDH) and carcinoembryonic antigen (CEA) was correlated with clinicopathologic characteristics and clinical outcome. Multivariable analyses adjusted for treatment arm, pathologic stage, resection status and blood biomarkers were performed using Cox regression models.

#### Results

After a median follow-up of 50 months, neutrophilia remained an independent adverse prognostic factor for disease-free survival (DFS; HR 1.528; 95% CI 1.181-1.977;

P=0.001), the cumulative incidence of distant metastasis (HR 1.957; 95% CI 1.388-2.761; P<0.001) and overall survival (OS; HR 2.161; 95% CI 1.507-3.10; P<0.001) in multivariable analysis. Similar significant findings were observed for leukocytosis and high CEA levels, whereas thrombocytosis was an independent prognostic factor for local recurrence (HR 2.731; 95% CI 1.308-5.701; P=0.007) in multivariable analysis. Conversely, treatment-induced leukopenia correlated with significantly better DFS (P=0.037). Addition of oxaliplatin to 5-FU CRT resulted in a significant DFS improvement only in patients with neutrophilia and leucocytosis (both P=0.005).

#### Conclusion

We here demonstrate that peripheral blood leukocytosis and neutrophilia were associated with adverse clinical outcome in patients with rectal cancer treated within the CAO/ARO/AIO-04 phase 3 trial. Our findings have important implications for the daily clinical practice and provide high-level evidence on the prognostic role of leukocytes and neutrophils. These data could help guide patient stratification to escalation or de-escalation strategies, also as part of the increasingly explored concept of non-operative management, and provide a rationale for neutrophil inhibition with CRT and chemotherapy in future trials in rectal cancer.

---

#### Proffered Papers: CL 9: Proffered papers : Late breaking abstracts

---

#### OC-0500 Radical Hemi-thoracic Radiotherapy vs. Palliative Radiotherapy for Malignant Pleural Mesothelioma.

E. Minatel<sup>1</sup>, M. Trovo<sup>2</sup>, J. Polesel<sup>1</sup>, C. Furlan<sup>1</sup>, A. Revelant<sup>1</sup>, A. Drigo<sup>1</sup>, L. Barresi<sup>1</sup>, A. Bearz<sup>1</sup>, A. Del Conte<sup>1</sup>, A. Follador<sup>3</sup>, U. Zuccon<sup>4</sup>, A. Dicorato<sup>5</sup>, P. Fontana<sup>6</sup>, G. Franchin<sup>1</sup>

<sup>1</sup>Centro Di Riferimento Oncologico, Radiation Oncology, Aviano, Italy ; <sup>2</sup>azienda Sanitaria Universitaria Integrata Udine, Radiation Oncology, Udine, Italy; <sup>3</sup>Azienda Sanitaria Universitaria Integrata Udine, Medical Oncology, Udine, Italy; <sup>4</sup>Pordenone General Hospital, Pneumology, Pordenone, Italy; <sup>5</sup>Azienda Sanitaria Universitaria Integrata Trieste, Medical Oncology, Trieste, Italy; <sup>6</sup>Mestre General Hospital, Thoracic Surgery, Mestre, Italy

***This abstract is part of the media programme and will be released on the day of its presentation***

#### OC-0501 Chemo-RT plus induction or consolidation chemotherapy for rectal cancer: a randomised phase 2 trial

E. Fokas<sup>1</sup>, M. Allgäuer<sup>2</sup>, B. Polat<sup>3</sup>, G. Klautke<sup>4</sup>, G. Grabenbauer<sup>5</sup>, R. Fietkau<sup>6</sup>, T. Kuhnt<sup>7</sup>, L. Staib<sup>8</sup>, T. Brunner<sup>9</sup>, A.L. Grosu<sup>10</sup>, W. Schmiegel<sup>11</sup>, L. Jacobasch<sup>12</sup>, J. Weitz<sup>13</sup>, G. Folprecht<sup>14</sup>, A. Schleska-Lange<sup>15</sup>, R. Grützmann<sup>16</sup>, M. Schwarzbach<sup>17</sup>, V. Paolucci<sup>18</sup>, W.O. Bechstein<sup>19</sup>, T. Friede<sup>20</sup>, M. Ghadimi<sup>21</sup>, R.D. Hofheinz<sup>22</sup>, C. Rödel<sup>1</sup>

<sup>1</sup>University Of Frankfurt, Department Of Radiotherapy And Oncology, Frankfurt, Germany ; <sup>2</sup>Barmherzige Brüder Hospital Regensburg, Department Of Radiotherapy, Regensburg, Germany ; <sup>3</sup>University Of Würzburg, Department Of Radiation Therapy, Würzburg, Germany ; <sup>4</sup>poliklinik Chemnitz Gmbh, Department Of Radiation Therapy, Chemnitz, Germany ; <sup>5</sup>Diacura and Klinikum Coburg, Department of Radiation Oncology And Radiotherapy, Coburg, Germany ; <sup>6</sup>University Of Erlangen-Nürnberg, Department of Radiation Therapy, Erlangen, Germany ; <sup>7</sup>university Of Leipzig, Department Of Radiation Therapy, Leipzig, Germany ; <sup>8</sup>klinikum Esslingen, Department Of General And Visceral Surgery, Esslingen, Germany ; <sup>9</sup>University Of Freiburg, Department of Radiation Therapy, Freiburg, Germany ; <sup>10</sup>Department of Radiation Therapy, University of Freiburg, Freiburg, Germany ; <sup>11</sup>Ruhr-University Bochum, Department Of Haematology and Oncology, Bochum, Germany ; <sup>12</sup>Clinic Of Haematology and Oncology, Dresden, Department of Haematology and Oncology, Dresden, German ; <sup>13</sup>University of Dresden, Department of General and Visceral Surgery, Dresden, Germany ; <sup>14</sup>University Of Dresden, Department of Haematology and Oncology, Dresden, Germany ; <sup>15</sup>Barmherzige Brüder Hospital Regensburg, Department of Haematology and Oncology, Regensburg, Germany ; <sup>16</sup>university Of Erlangen-Nürnberg, Department of General And Visceral Surgery, Erlangen, Germany ; <sup>17</sup>klinikum Frankfurt Höchst, Department Of General and Visceral Surgery, Frankfurt, Germany ; <sup>18</sup>ketteler Krankenhaus Offenbach, Department of General and Visceral Surgery, Offenbach, Germany ; <sup>19</sup>University of Frankfurt, Department Of General And Visceral Surgery, Frankfurt, Germany ; <sup>20</sup>University Medical Center Göttingen, Department of Medical Statistics, Göttingen, Germany ; <sup>21</sup>University Medical Center Göttingen, Department of General and Visceral Surgery, Göttingen, Germany ; <sup>22</sup>University Hospital Mannheim, Department of Medical Oncology, Mannheim, Germany

#### Purpose or Objective

Total neoadjuvant therapy (TNT) is a new paradigm for locally-advanced rectal cancer treatment. Two TNT

sequences have emerged: induction chemotherapy (CT) followed by chemoradiotherapy (CRT), and CRT followed by consolidation CT. Despite the increasing interest in the concept of TNT, optimal scheduling of preoperative CRT and CT remains to be established.

#### Material and Methods

We conducted the CAO/ARO/AIO-12 multicentre, randomised, phase 2 trial using a “pick the winner” design to select the better TNT sequence. Patients with stage II-III rectal cancer were randomly assigned to group A for induction CT prior to CRT, or to group B for consolidation CT following CRT. CRT consisted of 50.4 Gy in 28 fractions plus infusional fluorouracil (250 mg/m<sup>2</sup> days 1-14 and 22-35) and oxaliplatin (50 mg/m<sup>2</sup> days 1, 8, 22, and 29). Induction-/consolidation CT consisted of oxaliplatin (100 mg/m<sup>2</sup> day 1), leucovorin (400 mg/m<sup>2</sup> day 1), and infusional fluorouracil (2400 mg/m<sup>2</sup> days 1-2) repeated every 15 days for a total of 3 cycles. Total mesorectal excision surgery was scheduled on day 123 after start of TNT. Randomisation was done with computer-generated block randomisation codes stratified by centre and clinical N category (cN0 vs cN1-2) without masking. The primary endpoint was pathological complete response (pCR). Secondary endpoints included toxicity, compliance and surgical complications (ClinicalTrials.gov, registration number NCT02363374).

#### Results

Of the 311 patients enrolled, 306 patients were evaluable (156 in group A and 150 in group B). CRT-related grade 3-4 toxicity was lower (37% vs 27%) and compliance to CRT higher in group B (91%, 78%, and 76% vs 97%, 87%, and 93% received full dose radiotherapy, fluorouracil, oxaliplatin in group A and B, respectively); 92% vs 85% completed all CT cycles. The longer interval between completion of CRT and surgery in group B (median 90 vs 45 days in group A) did not increase surgical morbidity. A pCR in the intention-to-treat population was achieved in 17% (95% CI [12%; 24%]) in group A and in 25% (95% CI [18%; 32%]) in group B. Thus, only group B (p=0.0002) but not group A (p=0.210) fulfilled the predefined statistical hypothesis of significantly increased pCR versus 15% expected after standard CRT. In an exploratory analysis, comparison between groups yielded an odds ratio for pCR of 1.69 in favour of group B (95% CI [0.96; 2.99], p=0.0705).

#### Conclusion

In summary, this is, to our knowledge, the first randomised trial to report safety and efficacy of TNT sequences. CRT followed by consolidation CT was feasible and led to more patients achieving a pathological complete response. This TNT sequence fulfilled the predefined trial hypothesis of an increased pCR rate of 25% based on the “pick the winner” design, and has been selected for further phase 3 comparison with standard preoperative CRT in the CAO/ARO/AIO-18 trial.

#### OC-0502 Role of consolidation RT to bulky lesions of advanced Hodgkin lymphoma: results of FIL HD0801 trial

U. Ricardi<sup>1</sup>, M. Levis<sup>1</sup>, A. Evangelista<sup>2</sup>, D.M. Gioia<sup>3</sup>, L. Rigacci<sup>4</sup>, B. Botto<sup>5</sup>, G. Simonacchi<sup>6</sup>, P. Franzoni<sup>7</sup>, G. Rossi<sup>8</sup>, M. Buglione<sup>9</sup>, V. Pavone<sup>10</sup>, M. Bonfichi<sup>11</sup>, C. Rusconi<sup>12</sup>, R. Freilone<sup>13</sup>, A. Pulsoni<sup>14</sup>, V. De Sanctis<sup>15</sup>, G. Gaidano<sup>16</sup>, C. Stelitano<sup>17</sup>, M. Tani<sup>18</sup>, A. Castagnoli<sup>19</sup>, G. Ciccone<sup>2</sup>, F. Zaja<sup>20</sup>, A. Santoro<sup>21</sup>, P.L. Zinzani<sup>22</sup>

<sup>1</sup>University of Torino, Department Of Oncology, Torino, Italy ; <sup>2</sup>A.O.U. Città Della Salute E Della Scienza, Unit of Cancer Epidemiology, Torino, Italy ; <sup>3</sup>Fondazione Italiana Linfomi, Trial Office, Alessandria, Italy; <sup>4</sup>San Camillo Forlanini Hospital, Hematology Unit, Roma, Italy ; <sup>5</sup>A.O.U. Città della Salute e della Scienza, Hematology Unit, Torino, Italy; <sup>6</sup>University Of Firenze, Department of Radiation Oncology, Firenze, Italy ; <sup>7</sup>S. S. Antonio E Biagio Hospital, Department of Radiation Oncology, Alessandria, Italy ; <sup>8</sup>Spedali Civili, Department of Hematology, Brescia, Italy ; <sup>9</sup>Spedali Civili, Department

Of Radiation Oncology, Brescia, Italy ; <sup>10</sup>Azienda Ospedaliera Cardinal Panico, Hematology Unit, Tricase, Italy ; <sup>11</sup>Policlinico San Matteo, Department of Hematology, Pavia, Italy; <sup>12</sup>Azienda Ospedaliera Niguarda Ca' Granda, Department of Hematology, Milano, Italy; <sup>13</sup>Stabilimento Ospitaliero Ivrea, Hematology Unit, Ivrea, Italy; <sup>14</sup>Sapienza University, Department of Hematology, Roma, Italy; <sup>15</sup>Sapienza University- Sant'andrea Hospital, Department of Radiation Oncology, Roma, Italy ; <sup>16</sup>Amedeo Avogadro University, Department Of Hematology, Novara, Italy; <sup>17</sup>Azienda Ospedaliera Bianchi Melacrino Morelli, Department of Hematology, Reggio Calabria, Italy; <sup>18</sup>Santa Maria Delle Croci Hospital, Department of Hematology, Ravenna, Italy; <sup>19</sup>Ospedale Santo Stefano, Nuclear Medicine Unit, Prato, Italy; <sup>20</sup>Azienda Sanitaria Universitaria Integrata, Department of Hematology, Trieste, Italy; <sup>21</sup>Istituto Clinico Humanitas, Department of Oncology and Hematology, Rozzano Milanese, Italy; <sup>22</sup>Sant'orsola Malpighi University Hospital, Institute of Hematology "L. E. A. Seragnoli", Bologna, Italy

*This abstract is part of the media programme and will be released on the day of its presentation*

**OC-0503 Phase III trial of Prophylactic Cranial Irradiation with or without Hippocampus Avoidance in SCLC**

J. Belderbos, Md PhD<sup>1</sup>, D. De Ruyscher<sup>2</sup>, K. De Jaeger<sup>3</sup>, F. Koppe<sup>4</sup>, M. Lambrecht<sup>5</sup>, Y. Lievens<sup>6</sup>, E. Dieleman<sup>7</sup>, J. Jaspers<sup>8</sup>, J. Van Meerbeeck<sup>9</sup>, J. Ubbels<sup>10</sup>, M. Kwint<sup>1</sup>, M. Kuenen<sup>11</sup>, S. Deprez<sup>12</sup>, M. De Ruiter<sup>11</sup>, K. Sikorska<sup>13</sup>, H. Van Tinteren<sup>13</sup>, S. Schagen<sup>11</sup>

<sup>1</sup>The Netherlands Cancer Institute, Radiation Oncology, Amsterdam, The Netherlands; <sup>2</sup>Maastricht University Medical Center- School For Oncology and Developmental Biology Grow, Radiation Oncology, Maastricht, The Netherlands; <sup>3</sup>Catharina Hospital, Radiation Oncology, Eindhoven, The Netherlands; <sup>4</sup>Institute Verbeeten, Radiation Oncology, Tilburg, The Netherlands; <sup>5</sup>Uz Gasthuisberg, Radiation Oncology, Leuven, Belgium; <sup>6</sup>Ghent University Hospital And Ghent University, Radiation Oncology, Gent, Belgium; <sup>7</sup>Amsterdam Umc- Location Amc, Radiation Oncology, Amsterdam, The Netherlands; <sup>8</sup>Erasmus Mc Cancer Institute- Erasmus Mc University Medical Center, Radiation Oncology, Rotterdam, The Netherlands; <sup>9</sup>Antwerp University Hospital, Department Of Pulmonology and Thoracic Oncology, Antwerp, Belgium; <sup>10</sup>University of Groningen- University Medical Center Groningen, Radiation Oncology, Groningen, The Netherlands; <sup>11</sup>The Netherlands Cancer Institute, Division of Psychosocial Research and Epidemiology, Amsterdam, The Netherlands; <sup>12</sup>University Hospitals Leuven- Kul, Imaging and Pathology, Leuven, Belgium; <sup>13</sup>The Netherlands Cancer Institute, Department of Biometrics, Amsterdam, The Netherlands

**Purpose or Objective**

Neurocognitive decline after Prophylactic Cranial Irradiation (PCI) may be related to the dose in the hippocampus. This multicenter randomized phase III trial (NCT01780675) investigated hippocampus dependent memory functioning and safety after PCI with or without hippocampus sparing in Small Cell Lung Cancer (SCLC) using the Hopkins Verbal Learning Test-Revised (HVLTR).

**Material and Methods**

Patients with limited or extensive stage SCLC who received PCI (25 Gy in 10 fractions) were randomized to standard PCI or hippocampus avoidance PCI (HA-PCI), using IMRT or VMAT. In the HA-PCI group the objective was to get the mean dose in the right and left hippocampus  $\leq$  8.5 Gy (biological dose  $\leq$  6.1 Gy for  $\alpha/\beta=2\text{Gy}$ ) and  $D_{1\%}$

hippocampus  $\leq$  10 Gy,  $D_{\text{max}}$  PTV  $<$  28.75 Gy (115%) and  $V_{115\%}$  PTV  $\leq$  1%. Neurocognitive functioning was assessed by a neuropsychological test battery at baseline, 4, 8, 12, 18 and 24 months after the irradiation. The primary endpoint was a decline in the HVLTR total recall at 4 months, where a decline of 5 or more out of a possible 36 points was considered a failure. Secondary objectives were other cognitive outcomes/quality of life, radiological brain abnormalities on MRI (baseline, 4 and 12 months) and evaluation of the incidence and location of brain metastases following HA-PCI compared with standard PCI and overall survival (OS) using the Kaplan-Meier method.

**Results**

From April 2013 until March 2018 a total of 168 patients were randomized in 10 centers in the Netherlands and Belgium. The median follow-up time was 24.6 months. Median age was 64 years, 51% was female, and performance score at baseline was WHO 0-1 in 93%. The stage distribution was comparable in both arms (70% limited- and 30% extensive stage). All patients were treated using 25 Gy in 10 fractions. A total of 75% of all patients alive and treated had neurocognitive tests at 4 and this was 66% at 8 months. The HVLTR total recall score was  $\geq$  5 points lower compared to baseline in 28% PCI and 29% HA-PCI at 4 months ( $P=0.99$ ) and 34% PCI and 26% HA-PCI at 8 months ( $P=0.46$ ). Compared to baseline, the average HVLTR total recall score dropped 2 points for both arms at 4 months and 3 points in the PCI arm and 1 point in the HA-PCI arm at 8 months. Nineteen patients developed brain metastases of which 50% were multiple. No patient developed an isolated brain metastasis in the HA zone. The OS at 18 months was 54% in the PCI arm and 53% in the HA-PCI arm.

**Conclusion**

This randomized phase III trial investigating the neurocognitive decline at 4 and 8 months after treatment of HA-PCI compared to conventional PCI revealed a decline by  $\geq$  5 points at HVLTR total recall score in 28% of the total group. However, no significant difference between the two arms was seen. The incidence of brain recurrences was not increased in the avoidance region.

**OC-0504 Randomized phase 2 trial of adaptive dose painting vs. standard IMRT for head and neck cancer.**

F. Duprez<sup>1</sup>, J. Daisne<sup>2</sup>, D. Berwouts<sup>3</sup>, W. De Gerssem<sup>1</sup>, I. Goethals<sup>3</sup>, L. Olteanu<sup>1</sup>, T. Vercauteren<sup>1</sup>, W. De Neve<sup>1</sup>  
<sup>1</sup>Universitair Ziekenhuis Gent, Radiotherapie-Oncologie, Gent, Belgium; <sup>2</sup>CHU-UCL Namur, Radiotherapie, Namur, Belgium; <sup>3</sup>Universitair Ziekenhuis Gent, Nuclear Medicine, Gent, Belgium

**Purpose or Objective**

We report final results of a randomized phase 2 trial comparing adaptive dose painting by numbers (A-DPBN) using <sup>18</sup>F-FDG-PET with standard IMRT (S-IMRT) in 2 centres.

**Material and Methods**

Patients were stratified per centre before randomisation. Ninety-five patients were randomized: 47 in A-DPBN and 48 in S-IMRT. Patient characteristics can be found in Table 1.

The dose prescription protocols for both arms are given in Figure 1. As we unexpectedly observed late grade 3 and 4 mucosal ulcers in 1/7 and 3/7 A-DPBN-patients, respectively, in the first dose prescription protocol for A-DPBN, the levels of dose-escalation in A-DPBN have been adapted in 2 steps during the trial.

Kaplan-Meier statistics were used to estimate local (LC), regional control (RC) and overall survival (OS).

Acute toxicity was assessed during radiotherapy in all patients. Late toxicity could be assessed in 83 patients (DPBN-arm 42 and S-IMRT 41) from 3 months after radiotherapy.

	3-phase adaptive DPBN (n = 47)	Standard IMRT (n = 48)	p-value
Median age (range) (in years)	60 (40-74)	58 (43-81)	
Male / female	40/7	40/8	1
Site:			0,012
Oropharynx	34	19	
HPV related	7	4	
Not HPV related	17	10	
HPV status unknown	10	5	
Hypopharynx	8	18	
Larynx	4	8	
Oral cavity	1	3	
Stage grouping (TNM 7)			0,15
- I	1	1	
- II	3	3	
- III	12	9	
- IVA	29	27	
- IVB	2	8	
T-staging (TNM 7)			0,17
- T1	6	8	
- T2	17	15	
- T3	15	8	
- T4a	7	9	
- T4b	2	8	
N-staging (TNM 7)			0,51
- N0	8	6	
- N1	8	11	
- N2a	3	3	
- N2b	11	11	
- N2c	17	17	
Pre-IMRT neck dissection	7/47	2/48	0,09
Concomitant systemic therapy	16/47	20/48	0,52
Treating centre			1
- 1	39	8	
- 2	39	9	

local recurrence); spontaneous healing was seen in 3/3 patients of S-IMRT and in 9/14 of A-DPBN. Post-hoc analysis revealed more grade ≥3 late mucosal toxicity in active smokers (29% vs. 3%, p=0.005) and alcohol drinkers (33% vs. 13%, p=0.024) at diagnosis. For grade ≥4 late mucosal toxicity, comparable results were observed in active smokers at diagnosis (19% vs. 0%, p=0.013) but not in active alcohol drinkers at diagnosis.

There was no patient with grade 3 late dysphagia or xerostomia, but 1 patient presented with grade 4 dysphagia in S-IMRT due to esophageal stenosis (primary hypopharyngeal carcinoma).

**Conclusion**

Superior local control was achieved with A-DPBN compared to standard-IMRT, at the cost of more late grade ≥3 mucosal toxicity in active smokers/drinkers at diagnosis. An appropriately powered multicenter phase-3 trial comparing A-DPBN with S-IMRT in non-smokers could lead to better OS or disease-free survival without high rates of mucosal ulcers.

**OC-0505 Evidence-based practice in the global setting: an international survey of hypofractionation**

**D. Rodin**<sup>1</sup>, M. Osama<sup>2</sup>, B. Tawk<sup>3</sup>, S. Grover<sup>4</sup>, F. Moraes<sup>5</sup>, M.L. Yap<sup>6</sup>, E. Zubizarreta<sup>7</sup>, Y. Lievens<sup>8</sup>  
<sup>1</sup>Princess Margaret Cancer Centre, Department of Radiation Oncology, Toronto, Canada; <sup>2</sup>University of Texas Southwestern Medical Center, Department of Radiation Oncology, Dallas, Usa ; <sup>3</sup>Heidelberg and German Cancer Consortium, German Cancer Research Center, Heidelberg, Germany; <sup>4</sup>University of Pennsylvania, Department of Radiation Oncology, Philadelphia, USA ; <sup>5</sup>Kingston General Hospital, Department Of Oncology, Kingston, Canada ; <sup>6</sup>Ingham Health And Medical Research Institute, Liverpool Cancer Therapy Centre- Macarthur Cancer Therapy Centre, Liverpool, Australia; <sup>7</sup>International Atomic Energy Agency, Section of Applied Radiation Biology And Radiotherapy, Vienna, Austria ; <sup>8</sup>Ghent University Hospital, Department of Radiation Oncology, Ghent, Belgium

**Purpose or Objective**

Multiple large clinical trials have established the equivalence or non-inferiority of hypofractionated radiotherapy compared to conventionally fractionated treatment. The objective of this study is to determine real-world variations in the adoption of hypofractionation across different geographic regions and practice settings for cancers of the breast, prostate, and cervix, and for bone metastases, and barriers and facilitators to such adoption.

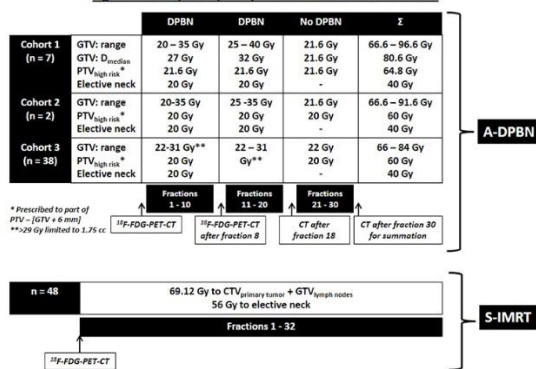
**Material and Methods**

An anonymous, electronic survey was distributed internationally from January to December 2018 in English, Spanish, and Mandarin to radiation oncology consultants through the ESTRO Global Impact of Radiotherapy in Oncology initiative. There were 2,259 respondents from Europe (56%), Asia Pacific (19%), Middle East (5%), 12% Latin America, (12%), North America (6%), and Africa (2%). This survey assessed preference for hypofractionation and specific fractionation regimens across 4 disease sites (breast, prostate, and cervical cancer, and bone metastases) in curative and palliative scenarios. Perceived barriers and facilitators to adoption were evaluated. In regression analyses, hypofractionation preference was defined as the use of hypofractionation for >75% of patients within each disease site and in >50% of clinical scenarios overall.

**Results**

Hypofractionation preference was more common in node-negative than in node-positive breast cancer (83% vs 46%, respectively; p<0.001), in low- and intermediate- vs. high-risk prostate cancer or that requiring pelvic irradiation (56% vs. 32%, respectively; p=0.00001); hypofractionation

Figure 1. Dose prescription protocols in A-DPBN and S-IMRT



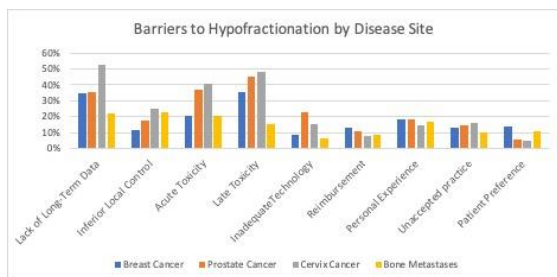
**Results**

Table 1 shows an imbalance in site distribution. Median follow-up was 25 months. Better local control was achieved in A-DPBN: 1- and 2-year local control were 91% and 88% vs. 78% and 75% in A-DPBN vs. S-IMRT (p=0.033). One- and 2 year regional control were equal in A-DPBN vs. S-IMRT: 86% and 84% vs. 84% and 82%, respectively (p=0.8). One- and 2 year OS were equal in A-DPBN vs S-IMRT: 85% and 80% vs. 90% and 70%, respectively (p=0.2). There was no difference in grade ≥3 acute dermatitis, dysphagia or mucositis between both arms. More grade 3 acute dysphagia was observed in patients with concomitant chemotherapy (13/42; 49% vs. 3/41; 22%, p=0.016) and depended from site (oral cavity 100%, oropharynx 42%, larynx 25% and hypopharynx 28%, p=0.036). We observed more grade ≥3 late mucosal toxicity (33% vs. 7%, p=0.003) and grade ≥4 late mucosal toxicity (19% vs. 5%, p=0.047) in A-DPBN than S-IMRT. One grade 5 toxicity was observed in A-DPBN (mucosal blow-out in absence of

was more common in North America and Europe than in other regions. In cervix cancer, hypofractionation was preferred in 30% of locally advanced cervical cancer cases in Africa, but in <10% of cases in other regions. For palliative symptom control, hypofractionation was preferred by 93%, 91%, and 84% of respondents for breast cancer, prostate cancer, and cervix cancer respectively, and in 95% for bone metastases ( $p < 0.001$ ) across geographic regions. Lack of long-term data, inferior local control, toxicity, and inadequate technology were the most commonly cited barriers. In adjusted analyses, hypofractionation preference was associated with age <55 (odds ratio [OR] = 1.46, 95% CI 1.23 to 1.88), practice in a high-income country (OR=2.72, 95% CI 2.12 to 3.49), in a university setting (OR=1.30, 95% CI 1.04 to 1.67), in a centre with a catchment area with >1,000,000 population (OR=1.57, 95% CI 1. to 2.0), and with intensity modulated radiotherapy (OR=1.70, 95% CI 1.22 to 2.34).

Table 1. Preference for hypofractionation by indication and by region

	Africa (N=64)	North America (N=117)	Asia-Pacific (N=433)	Europe (N=1254)	Latin America (N=269)	Middle-East (N=122)
<b>Breast Cancer</b>						
Lumpectomy, node negative	40%	100%	73%	89%	77%	79%
Lumpectomy, node positive	37%	48%	43%	48%	36%	61%
Mastectomy, node negative	49%	62%	33%	49%	38%	70%
Mastectomy, node positive	49%	40%	23%	34%	25%	51%
Palliative symptom control	80%	98%	90%	95%	91%	96%
<b>Prostate Cancer</b>						
Low-Risk	18%	92%	42%	66%	45%	32%
Intermediate-Risk	21%	92%	41%	64%	37%	32%
High-Risk	30%	65%	35%	49%	25%	23%
Pelvic Irradiation	27%	31%	16%	28%	15%	11%
Palliative symptom control	85%	100%	91%	93%	83%	81%
<b>Cervix Cancer</b>						
Locally advanced	30%	0%	5%	9%	10%	6%
Palliative symptom control	79%	100%	79%	85%	82%	81%
<b>Bone Metastases</b>						
Bone Metastasis, Uncomplicated	100%	100%	96%	98%	90%	96%
With Fracture	93%	98%	96%	95%	92%	98%
With Cord Compression	97%	97%	98%	95%	92%	91%
With Soft Tissue Component	93%	96%	91%	94%	85%	89%



### Conclusion

Significant variation was observed in preference for hypofractionation across indications and between geographic regions, with greater concordance in preference for palliative indications. Improving the cost-effectiveness of radiotherapy and the quality of care delivered requires greater international attention to continuing medical education and policy reform that aligns evidence-based practice with physician incentives.

### Proffered Papers: CL 10: Proffered papers : Pelvic Tumours

#### OC-0506 Patient-reported sexual outcomes after definitive RCHT+IGABT for cervical cancer (EMBRACE study)

K. Kirchheiner<sup>1</sup>, I.M. Jürgelemk-Schulz<sup>2</sup>, C. Haie-Meder<sup>3</sup>, J.C. Lindegaard<sup>4</sup>, A. Sturdza<sup>1</sup>, U. Mahantshetty<sup>5</sup>, B. Segegin<sup>6</sup>, K. Bruheim<sup>7</sup>, B. Rai<sup>8</sup>, R. Cooper<sup>9</sup>, E. Van der Steen-Banasik<sup>10</sup>, E. Wiebe<sup>11</sup>, M. Sundset<sup>12</sup>, E. Van Limbergen<sup>13</sup>, E. Villafranca<sup>14</sup>, H. Westerveld<sup>15</sup>, L.T. Tan<sup>16</sup>,

K. Tanderup<sup>4</sup>, R. Pötter<sup>1</sup>, R.A. Nout<sup>17</sup>

<sup>1</sup>Medical University of Vienna / General Hospital of Vienna, Department of Radiation Oncology-Comprehensive Cancer Center, Vienna, Austria ;

<sup>2</sup>University Medical Centre Utrecht, Department of Radiation Oncology, Utrecht, The Netherlands ;

<sup>3</sup>Gustave-Roussy, Department of Radiotherapy, Villejuif, France ; <sup>4</sup>Aarhus University Hospital, Department of Oncology, Aarhus, Denmark ;

<sup>5</sup>Tata Memorial Hospital, Department of Radiation Oncology, Mumbai, India ;

<sup>6</sup>Institute of Oncology Ljubljana, Department of Radiotherapy, Ljubljana, Slovenia ;

<sup>7</sup>The Norwegian Radium Hospital- Oslo University Hospital, Department of Oncology, Oslo, Norway ;

<sup>8</sup>Postgraduate Institute of Medical Education and Research, Department of Radiotherapy and Oncology, Chandigarh, India ;

<sup>9</sup>St James's University Hospital, Leeds Cancer Centre, Leeds, United Kingdom ;

<sup>10</sup>Arnhem, Department of Radiotherapy, Arnhem, The Netherlands ;

<sup>11</sup>Cross Cancer Institute and University of Alberta, Department of Oncology, Edmonton, Canada ;

<sup>12</sup>St. Olavs Hospital, Clinic of Oncology and Women's Clinic, Trondheim, Norway ;

<sup>13</sup>UZ Leuven, Department of Radiation Oncology, Leuven, Belgium ;

<sup>14</sup>Hospital of Navarra, Department of Radiation Oncology, Pamplona, Spain ;

<sup>15</sup>Amsterdam UMC- Location Academic Medical Center, Department of Radiation Oncology, Amsterdam, The Netherlands ;

<sup>16</sup>Cambridge University Hospitals NHS Foundation Trust-Addenbrooke's Hospital, Oncology Centre, Cambridge, United Kingdom ;

<sup>17</sup>Leiden University Medical Center, Department of Radiation Oncology, Leiden, The Netherlands

### Purpose or Objective

To evaluate the pattern of sexual activity and its associations to sexual/vaginal functioning within the prospective, observational, multi-center EMBRACE study (An international study on MRI-guided brachytherapy in locally advanced cervical cancer).

### Material and Methods

From 2008-2015, 1416 patients from 22 centers were included and treated with combined EBRT±chemotherapy and image-guided adaptive brachytherapy (IGABT) following the GEC-ESTRO guidelines.

Sexual outcomes were prospectively assessed according to EORTC-QLQ-CX24 questionnaires at baseline and follow-ups (FUP) every 3 months (1<sup>st</sup> year), every 6 months (2<sup>nd</sup>, 3<sup>rd</sup> year) and yearly thereafter. Prevalence rates over time were displayed. Associations between pain during intercourse (dyspareunia) and vaginal functioning were evaluated with Spearman's rank correlations, pooling observations over all FUP (N=2670).

Longitudinal analyses of individual patterns for sexual activity and dyspareunia were performed in patients with at least 3 FUP (N=850). Frequent dyspareunia was defined, if ≥50% of all sexual encounters were "quite a bit" or "very much" painful; occasional dyspareunia if less than half of all encounters were experienced painful.

### Results

Information on baseline sexual activity was available in 1027, in FUP in 1044 patients, with a median FUP time of 36 months. Sexual functioning was assessed in sexually active patients (incidence in FUP: 611 patients, 58.5%). Prevalence rates (figure 1A-F) revealed a slow increase of sexual activity during the 1<sup>st</sup> year of FUP, reaching a plateau up to 5 years. Vaginal functioning problems such as dryness, shortening, tightening and dyspareunia showed a substantial increase after treatment and remained either elevated or showed signs of slight improvement during the observation period. Sexual enjoyment was impaired over all time points, with a range of 37-48% of patients reporting to have "not at all" or "a little" sexual enjoyment.

The vaginal functioning problems dryness, shortening and tightening were significantly correlated with dyspareunia to  $r=0.407$ ,  $0.539$ ,  $0.552$ , respectively (figure 2A-C). The analysis of individual longitudinal pattern revealed 179 patients reporting dyspareunia at least once during FUP (incidence). Of those, the symptom was experienced frequently by 89 (49.7%), but only occasionally by 90 (50.3%) patients, with significant impact on the sexual frequency. 28.1% of patients with frequent dyspareunia showed lower sexual activity (to less than 50% of FUPs). In contrary, only 6.7% of patients with occasional dyspareunia reported a low sexual frequency to the same degree.

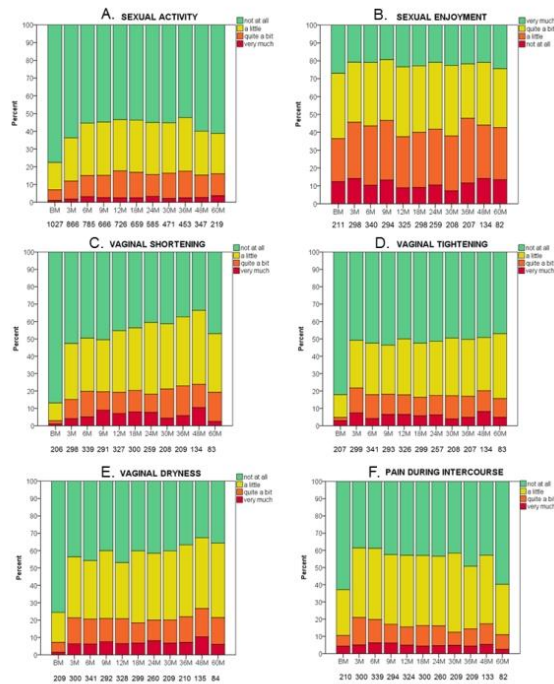


Figure 1: Prevalence rates of A. sexual activity, B. sexual enjoyment, C. vaginal shortening, D. vaginal tightening, E. vaginal dryness and F. pain during intercourse. BM = baseline, M = months in follow-up

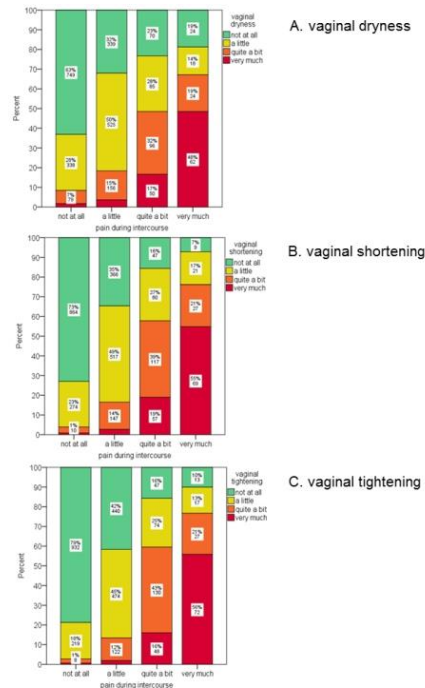


Figure 2: Association between pain during intercourse and A. vaginal dryness, B. vaginal shortening and C. vaginal tightening. Observations pooled over all follow-ups.

**Conclusion**

More than half of locally advanced cervical cancer patients are sexually active after definitive radiochemotherapy plus IGABT. Treatment-induced vaginal changes, such as patient-reported vaginal dryness, shortening and tightening can be associated with pain during intercourse and can impact sexual functioning and frequency.

**OC-0507 Risk factors for bladder fistula, bleeding and cystitis in cervix cancer: an EMBRACE analysis**

S. Spampinato<sup>1</sup>, L.U. Fokdal<sup>1</sup>, R. Pötter<sup>2</sup>, C. Haie-Meder<sup>3</sup>, J.C. Lindegaard<sup>1</sup>, M. Schmid<sup>2</sup>, I. Jürgenliemk-Schulz<sup>4</sup>, U. Mahantshetty<sup>5</sup>, B. Segedin<sup>6</sup>, K. Bruheim<sup>7</sup>, P. Hoskin<sup>8</sup>, B. Rai<sup>9</sup>, F. Huang<sup>10</sup>, R. Cooper<sup>11</sup>, E. Van der Steen-Banasik<sup>12</sup>, E. Van Limbergen<sup>13</sup>, K. Kirchner<sup>2</sup>, C. Kirisits<sup>2</sup>, K. Tanderup<sup>1</sup>

<sup>1</sup>Aarhus University Hospital, Department of Oncology, Aarhus, Denmark ; <sup>2</sup>Medical University/General Hospital of Vienna, Department of Radiation Oncology-Comprehensive Cancer Center, Vienna, Austria ; <sup>3</sup>Gustave-Roussy, Department of Radiotherapy, Villejuif, France ; <sup>4</sup>University Medical Centre Utrecht, Department of Radiation Oncology, Utrecht, The Netherlands ; <sup>5</sup>Tata Memorial Hospital, Department of Radiation Oncology, Mumbai, India; <sup>6</sup>Institute of Oncology Ljubljana, Department of Radiotherapy, Ljubljana, Slovenia ; <sup>7</sup>The Norwegian Radium Hospital- Oslo University Hospital, Department of Oncology, Oslo, Norway ; <sup>8</sup>Mount Vernon Hospital, Mount Vernon Cancer Centre, Northwood, United Kingdom ; <sup>9</sup>Postgraduate Institute of Medical Education and Research, Department of Radiotherapy and Oncology, Chandigarh, India ; <sup>10</sup>Cross Cancer Institute and University of Alberta, Department of Oncology, Edmonton, Canada; <sup>11</sup>St James's University Hospital, Leeds Cancer Centre, Leeds, United Kingdom; <sup>12</sup>Radiotherapiegroep Arnhem, Department of Radiotherapy, Arnhem, The Netherlands ; <sup>13</sup>UZ Leuven, Department of Radiation Oncology, Leuven, Belgium

### Purpose or Objective

To identify risk factors for bladder fistula, bleeding and cystitis within the prospective, multi-institutional, observational EMBRACE I study (An international study on MRI-guided brachytherapy in locally advanced cervical cancer) that enrolled 1416 patients treated from 2008 to 2015.

### Material and Methods

Bladder fistula, bleeding and cystitis (CTCAEv.3) were analysed in Locally Advanced Cervical Cancer (LACC) patients treated with radiochemotherapy and Image-Guided Adaptive Brachytherapy (IGABT). Adverse events arising at any time in the course of follow-up were considered. Patient, disease and treatment characteristics were tested as risk factors for moderate grade (G)  $\geq 2$  with univariate (UVA) and multivariable (MVA) analyses (Cox proportional hazards model) in patients without bladder involvement. UVA and MVA were also performed for severe G $\geq 3$  incidence pooled over the three endpoints. The cumulative (EBRT+IGABT) minimal dose to the most exposed 2cm<sup>3</sup> of the bladder (D2cm<sup>3</sup>) and ICRU Bladder Point dose (EQD2) were considered as continuous variables in UVA and MVA. Urinary frequency and incontinence were not included in the analysis.

### Results

In 1146 patients without bladder involvement, the crude incidences for G $\geq 2$  fistula, bleeding and cystitis were 0,7% (n=8), 2,0% (n=23) and 7,4% (n=84), respectively. The pooled incidences for G $\geq 2$  and G $\geq 3$  were 8,5% (n=97) and 1,4% (n=16), respectively, with 15% of symptomatic patients experiencing more than one endpoint. In 67 patients with bladder involvement, the incidences for G $\geq 2$  fistula, bleeding and cystitis were 2,5% (n=8), 12% (n=2) and 17% (n=11), respectively, and G $\geq 3$  in 15% (n=10) (pooled incidence). Mean (SD) bladder D2cm<sup>3</sup> was 75,8 $\pm$ 9,7Gy and 83 $\pm$ 11,5Gy in patients without and with bladder involvement, respectively. Median follow-up was 35 (range:1-97) months, median age was 49 (range:22-91) years, and 31% were smokers. Table 1 shows the covariates tested in UVA and MVA for G $\geq 2$  fistula, bleeding and cystitis, and G $\geq 3$  for pooled symptoms in patients without bladder involvement. The Hazard Ratios (HR) are shown for significant variables in UVA (p $\leq$ 0.10) and MVA (p $\leq$ 0.05). Bladder D2cm<sup>3</sup> was significant on MVA for all individual and pooled endpoints. ICRU Bladder Point dose was significant in UVA for fistula and pooled incidence, but was not included in the MVA because of correlation with bladder D2cm<sup>3</sup> and a lower HR. Smoking status was predictive for bleeding, cystitis and pooled incidence, with smokers at higher risk. Younger patients had a higher risk for cystitis compared to older patients.

**Table 1:** Covariates tested in UVA and MVA for G $\geq 2$  fistula, bleeding and cystitis and for G $\geq 3$  pooled incidence. HRs are shown for variables significant in UVA. Significant HRs in MVA are highlighted in bold.

Variables	Fistula (G2) (n=8)	Bleeding (G2) (n=23)	Cystitis (G2) (n=84)	Pooled (G3) (n=16)
	HR (95%CI)	HR (95%CI)	HR (95%CI)	HR (95%CI)
Age (C)	ns	ns	0.978(0.961-0.996)*	ns
BMI (C)	ns	1.067(1.003-1.134)*	1.033(0.997-1.07)*	ns
Smoke "Yes" vs. "No(R)"	6.973(1.407-3.4E1)*	2.311(1.002-5.332)*	1.628(1.051-2.522)*	2.317(0.869-6.173)*
Anterior vaginal wall involvement "Yes" vs. "No(R)"	ns	<b>2.948(1.264-6.876)**</b>	<b>1.854(1.165-2.95)**</b>	<b>3.334(1.031-11.1E1)**</b>
Chemotherapy "<4" vs. "4-8(R)" cycles	ns	ns	ns	ns
EBRT technique "IMRT" vs. "3DCRT(R)"	ns	ns	ns	ns
EBRT prescription dose (C)	ns	ns	ns	ns
IGABT technique (C, % of ICIS fractions)	ns	ns	ns	ns
Bladder D2cm <sup>3</sup> (C)	1.102(1.007-1.206)*	1.071(1.028-1.116)*	1.026(1.004-1.049)*	1.083(1.024-1.145)*
ICRU BP dose (C)	<b>1.123(1.024-1.231)**</b>	<b>1.076(1.029-1.125)**</b>	<b>1.034(1.01-1.058)**</b>	<b>1.104(1.04-1.173)**</b>
ICRU BP dose (C)	1.044(1-1.091)*	ns	ns	1.041(1.012-1.07)*

Abbreviations: n=number of events. ns=not significant. C=continuous variable. (R)=reference value. HR=Hazard Ratio. 95%CI= 95% Confidence Interval. BMI=Body Mass Index. IMRT= Intensity Modulated RadioTherapy. 3DCRT= 3D Conformal RadioTherapy. % of ICIS fractions= percentage of brachytherapy fractions with needles. ICRU BP=ICRU Bladder Point.  
\*univariate analysis. \*\*multivariable analysis. Bold: MVA significance.

### Conclusion

In the present study, bladder D2cm<sup>3</sup> was a dominant risk factor for developing bladder fistula, bleeding or cystitis

after IGABT in LACC patients. The risk of bleeding and cystitis was considerably higher in smokers. Finally, age was a predictor for cystitis, with younger patients at higher risk.

### OC-0508 MRI guided chemoradiation and brachytherapy for postsurgical vaginal recurrences: A phase II study

S. Chopra<sup>1</sup>, R. Engineer<sup>2</sup>, U. Mahantshetty<sup>2</sup>, S. Mechanery<sup>3</sup>, T. Dora<sup>3</sup>, R. Shukla<sup>4</sup>, P. Popat<sup>5</sup>, J. Swamidas<sup>3</sup>, J. Ghosh<sup>3</sup>, S. Gupta<sup>3</sup>, S. Shrivastava<sup>2</sup>  
<sup>1</sup>Advanced Centre for Treatment- Research and Education in Cancer- Mumbai, Radiation Oncology, Mumbai, India ; <sup>2</sup>Tata Memorial Hospital, Radiation Oncology, Mumbai, India ; <sup>3</sup>Advanced Centre for Treatment Research and Education in Cancer, Radiation Oncology, Navi Mumbai, India ; <sup>4</sup>Advanced Centre for Treatment- Research and Education in Cancer, Radiation Oncology, Mumbai, India ; <sup>5</sup>Tata Memorial Hospital, Radiodiagnosis, Mumbai, India

### Purpose or Objective

To report outcomes of prospective phase II study that integrated MRI for planning external radiation and brachytherapy for postsurgical recurrences of cervical cancer.

### Material and Methods

The prospective phase II study (NCT 01391065) recruited patients from January, 2011 until December, 2016. Patients with local residual or recurrent tumour after hysterectomy without any evidence of distant metastasis were included. All patients underwent baseline T2 MR imaging to define the extent and volume of disease and were planned for external radiation (50 Gy/25#/5weeks (IMRT or 3DCRT)) with concurrent weekly cisplatin (40mg/m<sup>2</sup>). Response assessment MRI was performed in all patients at completion of brachytherapy. While patients with baseline parametrial disease received interstitial high dose rate brachytherapy including vagina and parametrium (16-20Gy/4-5#) those with only central disease at presentation received only central vaginal brachytherapy (12-14 Gy/2-4#). Information from MR was utilized to delineate clinical target volume on CT obtained for planning interstitial or intracavitary brachytherapy. MRI was done at first follow up followed by clinical examination with additional imaging as and when indicated. Kaplan Meier Analysis was performed to evaluate Locoregional Relapse, Disease Free and Overall Survival. Univariate and multivariate analysis was performed to evaluate impact of known prognostic factors.

### Results

A total of 60 patients were included of which 51 were identified to have nonmetastatic disease. The median age of the cohort was 48 years (35-65 yrs). The median and mean tumour volume on T2W MRI was 25 cc (IQR 8.4-145 cc) and 118 cc ( IQR8.4-145) cc[A1] ). A vast majority of patients had squamous carcinoma (82.4%). Overall 16/50 (31.4%) patients had radiologically positive lymph nodes prior to treatment initiation. Overall 40 patients (78%) had complete response after external radiation, 8 had partial response and 3 patients had progressive disease. Planned treatment was completed in 47/50 patients. The median EQD2 was 70.8Gy (50-73 Gy). The median D 2cc for rectum, bladder and sigmoid was 65.8 Gy, 68 Gy and 62 Gy respectively. At a median follow up of 60 months (5-93) local control was 88%. Of the 6 patients (12%) with local relapse 4 were local only and another 2 also had distant metastasis. Five patients (10%) had distant relapse in the absence of local relapse leading to 5 and 7 year disease free and overall survival of 72% and 69% and 88% and 77% respectively. Grade III proctitis and cystitis was observed in 4% and 2% patients respectively. Of the known prognostic, predictive and treatment related factors only baseline tumour volume >20 cc adversely impacted 7 year

DFS (91% vs 65%,  $p=0.03$ ) and overall survival (96% vs 77%,  $p=0.06$ ).

**Conclusion**

MRI assisted external radiation and brachytherapy results in excellent 7-year disease free and overall survivals in patients with post surgical vaginal recurrences

**OC-0509 MRI radiomics analysis for predicting prognosis of cervical cancer after definitive radiotherapy**

A. Takada<sup>1</sup>, H. Yokota<sup>1</sup>, M. Watanabe<sup>1</sup>, T. Horikoshi<sup>1</sup>, T. Uno<sup>1</sup>  
<sup>1</sup>Chiba University, Department of Radiology, Chiba, Japan

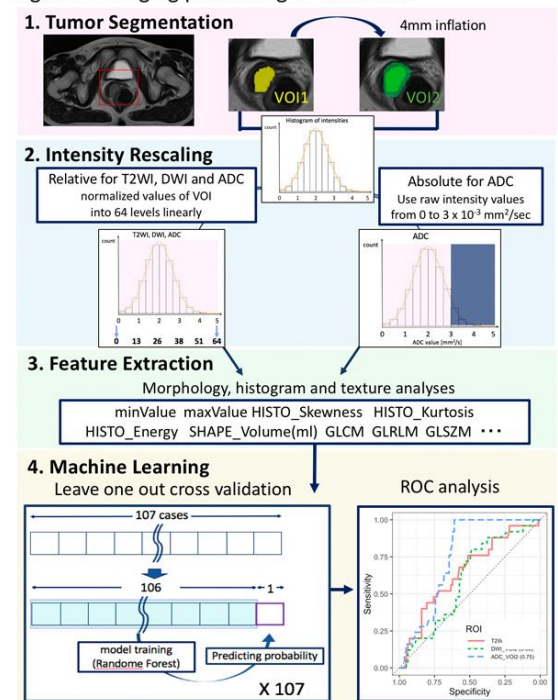
**Purpose or Objective**

Although many clinical prognostic factors for uterine cervical cancer have been reported, prediction accuracy is still insufficient. Radiomics is a method to construct predictive machine learning models for treatment prognosis or benign/malignant using many image features, which are extracted from a lesion site on medical images such as MRI, CT, and PET. However, machine learning is theoretically weak for differences in imaging acquisition conditions. The purpose of this study was to investigate whether radiomics analysis with MRI images of different scanners can predict the prognosis in cervical cancer after definitive radiotherapy.

**Material and Methods**

Totally 107 patients ( $58.8 \pm 13.5$  years) were included. All underwent MRI of 16 multi-center scanners and definitive radiotherapy for cervical cancer between April 2012 and March 2016. Spatial resolution of MRI was converted into  $0.5 \times 0.5 \times 5.0$  mm for T2-weighted image (T2WI), and  $1.0 \times 1.0 \times 5.0$  mm for diffusion-weighted image (DWI) and apparent diffusion coefficient map (ADC). A radiologist delineated the volume of interest (VOI) within each tumor region on axial T2WI, DWI and ADC map (VOI1). In addition, VOI2 was created by expanding the entire circumference by 4 mm. Using open-source software (LIFEx: <https://www.lifexsoft.org>), two intensity rescaling methods were applied; i.e. relative rescaling for T2WI and DWI, and relative and absolute rescaling for ADC. The Relative method can be applied for any imaging modalities, whereas the absolute method is robust for outliers although it is available for images with absolute values such as ADC. From T2WI, DWI and ADC each, 45 imaging features of morphology, histogram and texture analyses in the VOIs were extracted. The prognosis was defined based on whether recurrence within the irradiation field within two years after treatment. We constructed prediction models for locoregional recurrence with leave-one-out cross-validation using random forest algorithm, and receiver operating characteristic (ROC) analysis to evaluate diagnostic performance.

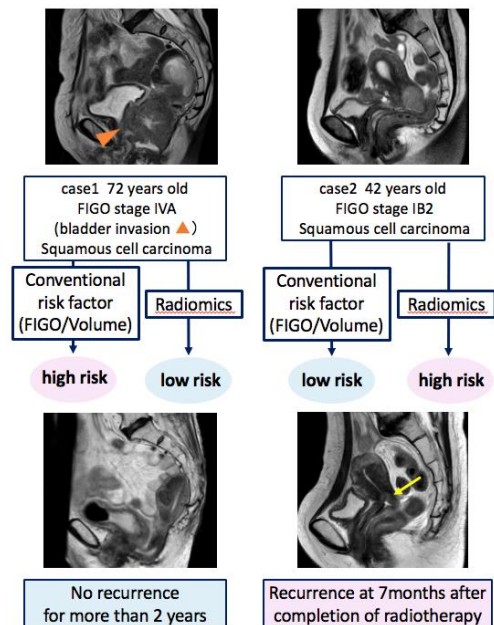
Figure 1. Imaging processing of radiomics



**Results**

Cervical cancer relapsed in 25 of 107 patients within the irradiation field. The area under the curve (AUC [95% confidence interval]) calculated by ROC analysis was summarized in Table. Absolute rescaling improved AUC of ADC into 0.79 (sensitivity 69.5% and specificity 88.0% at the closest top-left point of ROC curve) on VOI2. AUCs of conventional risk factors such as volume (AUC=0.52) was significantly lower than that of ADC with radiomics ( $p=0.001$ , Delong test).

Figure2. An example with discrepancy between conventional risk factor and Radiomics



**Conclusion**

Radiomics machine learning approach for ADC with absolute rescaling and VOI delineation including tumor surroundings was useful for predicting locoregional recurrence of cervical cancer after definitive radiotherapy even using multi-center MRI data.

Intensive Rescaling	VOI	T2WI	DWI	ADC
Relative	VOI1	0.52 [0.390-0.65]	0.70 [0.59-0.80]	0.68 [0.57-0.79]
Relative	VOI2	0.66 [0.53-0.79]	0.73 [0.63-0.84]	0.5 [0.43-0.70]
Absolute	VOI1	N/A	N/A	0.67 [0.56-0.79]
Absolute	VOI2	N/A	N/A	0.79 [0.70-0.87]

### OC-0510 MRI radiomics to predict tumour response in patients with locally advanced rectal cancer

P. Bulens<sup>1</sup>, A. Couwenberg<sup>2</sup>, M. Intven<sup>2</sup>, A. Debucquoy<sup>1</sup>, V. Vandecaveye<sup>3</sup>, M. Philippens<sup>2</sup>, P. Mukherjee<sup>4</sup>, O. Gevaert<sup>4</sup>, K. Haustermans<sup>1</sup>

<sup>1</sup>University Hospital Gasthuisberg, Radiation Oncology, Leuven, Belgium ; <sup>2</sup>University Medical Center Utrecht, Radiation Oncology, Utrecht, The Netherlands;

<sup>3</sup>University Hospital Gasthuisberg, Radiology, Leuven, Belgium; <sup>4</sup>Stanford University, Center for Biomedical Informatics Research, Stanford, USA

#### Purpose or Objective

To implement organ-sparing strategies into the multimodality treatment of patients with locally advanced rectal cancer (LARC), response prediction to select eligible patients is needed. In this research, we investigate the use of different multiparametric MRI-based radiomics models that predict (near-)complete response to chemoradiotherapy (CRT) in patients with LARC and compare their performances with the performance our previously developed and validated semantic model based on two volumetric and two ADC parameters.

#### Material and Methods

Radiomics models were developed in a cohort of 70 patients with LARC, prospectively recruited between 2012 and 2015. The external validation cohort consisted of 55 patients, recruited between 2008 and 2011. All patients were treated with CRT followed by surgery and underwent T2-weighted and diffusion-weighted imaging (DWI) before CRT and before surgery. The outcome measure for this study was (near-)complete pathological tumour response (ypT0-1N0).

The tumour was segmented on T2-images and the ROI was transferred to DWI b800 images and ADC maps, after which radiomics features were extracted. Also, the two volumetric and two ADC parameters of the semantic model were calculated. Principal component analysis was used to linearly combine the radiomics and semantic features and regression analysis with LASSO was applied to develop the models. The best three models based on performance using receiver operating characteristic (ROC) and precision were selected for external validation and for comparison with the four-feature semantic model.

#### Results

21/70 patients (30%) achieved ypT0-1N0 in the development cohort versus 13/55 patients (24%) in the validation cohort. The four-feature semantic model had a predicting performance of AUC 0.86 (95% confidence interval (CI) 0.76-0.95) on the development cohort and

AUC 0.87 (95% CI 0.76-0.97) on the validation cohort. The best three models using radiomics with or without semantic features (semantic\_dwi\_post, semantic\_dwi\_adc\_pre, t2\_dwi\_pre\_post) were identified with performances on the development cohort with an AUC of 0.84 (95% CI 0.75-0.94), 0.85 (95% CI 0.75-0.98) and 0.83 (95% CI 0.70-0.95) respectively. Two models (semantic\_dwi\_post, t2\_dwi\_pre\_post) validated well in the external patient cohort with an AUC of 0.86 (95% confidence interval 0.76 - 0.97) and 0.83 (95% confidence interval 0.70 - 0.95) respectively.

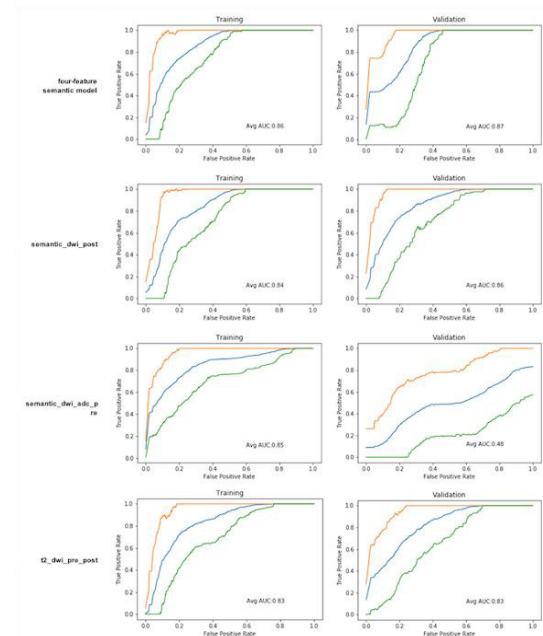


Figure 1. Receiver operating characteristic curves for the four-feature semantic model and the three radiomics models on both the training and the validation cohort. Orange and green curves represent the 95% confidence interval.

	Development Cohort	Validation Cohort
semantic	AUC	0.857 (0.765 – 0.950)
	PPV	77%
	Sensitivity	53%
	Specificity	94%
semantic_dwi_post	AUC	0.842 (0.747 – 0.936)
	PPV	67%
	Sensitivity	63%
	Specificity	88%
semantic_dwi_adc_pre	AUC	0.864 (0.749 – 0.979)
	PPV	92%
	Sensitivity	52%
	Specificity	98%
t2_dwi_pre_post	AUC	0.828 (0.728 – 0.929)
	PPV	67%
	Sensitivity	50%
	Specificity	90%

Table 1. Performance and operating points of the selected models that predict response to chemoradiation for patients with rectal cancer, for both the development and the validation cohort. Data between brackets represents the 95% confidence interval. Abbreviations: AUC = Area Under the Curve; PPV = Positive Predictive Value.

### Conclusion

Prediction models based on T2- and DW-MRI radiomics can be used for adequate non-invasive detection of patients with rectal cancer that will achieve a (near-)complete response after CRT. These radiomics models, however, do not outperform a previously reported prediction model based on two volumetric and two ADC parameters.

### OC-0511 Organ Preservation with Image Guided and Adaptive Brachytherapy for Patients with Rectal Cancer

A. Garant<sup>1</sup>, S. Magnan<sup>2</sup>, S. Devic<sup>3</sup>, A. Martin<sup>2</sup>, M. Boutros<sup>4</sup>, C. Vasilevsky<sup>4</sup>, S. Ferland<sup>5</sup>, A. Bujold<sup>6</sup>, S. Desgroseilliers<sup>7</sup>, H. Sebahang<sup>8</sup>, C. Richard<sup>9</sup>, T. Vuong<sup>10</sup>

<sup>1</sup>UT Southwestern Medical Center, Radiation Oncology, Dallas, USA ; <sup>2</sup>Laval University, Radiation Oncology, Quebec City, Canada ; <sup>3</sup>McGill University, Medical Physics, Montreal, Canada ; <sup>4</sup>Jewish General Hospital, Colorectal Surgery, Montreal, Canada ; <sup>5</sup>Gatineau Hospital, Radiation Oncology, Gatineau, Canada ; <sup>6</sup>Maisonneuve-Rosemont Hospital, Radiation Oncology, Montreal, Canada ; <sup>7</sup>Pierre-Boucher Hospital, Surgery, Longueuil, Canada ; <sup>8</sup>University of Montreal Hospital Center, Surgery, Montreal, Canada ; <sup>9</sup>University of Montreal Hospital Center, Colorectal Surgery, Montreal, Canada ; <sup>10</sup>Jewish General Hospital, Radiation Oncology, Montreal, Canada

### Purpose or Objective

Organ preservation or non-operative management (NOM) of rectal cancer is of growing interest among colorectal experts. Image guided and adaptive endorectal brachytherapy (IG-AEBT) is a radiation dose escalation modality: we explored its role as a tumor-response adaptive therapy in elderly patients unfit for surgery and patients refusing surgery.

### Material and Methods

In this prospective registry study, patients with rectal cancer who were ineligible for surgery began treatment with pelvic external beam radiotherapy (EBRT) to a dose of 40 Gy in 16 fractions; in patients refusing surgery, EBRT was prescribed at a dose of 45- 50 Gy in 25 fractions with concurrent 5-FU. This was followed by three weekly IG-AEBT boosts of 10 Gy to the residual clinical target volume, for a total of 30 Gy in 3 weekly fractions. Complete clinical response (cCR) was the primary endpoint.

### Results

A total of 118 patients were included; the median age was 81 years. With a median follow-up of 2.5 years for living patients, the proportion of cCR was 86.4%, the tumor regrowth proportion was 12.8%, and the cumulative incidence of local relapse was 4.3% at 1 year and 16.4% at 2 years. When considering responders and non-responders, the 2-year local control was 72.8%. The overall survival at 2 years was 66.1%. Acute rectal grade 1-2 toxicity included all patients: 25.5% of patients had late rectal bleeding requiring iron replacement, or blood transfusions and/or argon plasma therapy.

### Conclusion

The results of our registry study exploring IG-AEBT as a boost modality for an elderly medically unfit patient population with unselected tumors reveal that a high proportion of patients achieved cCR with a reasonable toxicity profile. Consequently, it is our belief that this technology will contribute to the challenging NOM paradigm of rectal cancer.

### OC-0512 Radiochemotherapy and hyperthermia in locally advanced rectal cancer - A prospective phase II trial

C. Gani<sup>1</sup>, U. Lamprecht<sup>1</sup>, M. Bitzer<sup>2</sup>, J. Gellermann<sup>3</sup>, O. Voigt<sup>1</sup>, A. Ziegler<sup>4</sup>, M. Moll<sup>1</sup>, A. Königsrainer<sup>5</sup>, D. Zips<sup>1</sup>  
<sup>1</sup>University Hospital Tübingen, Radiation Oncology, Tübingen, Germany ; <sup>2</sup>University Hospital Tübingen,

Gastroenterology, Tübingen, Germany; <sup>3</sup>Zentrum für Strahlentherapie und Radioonkologie, Radiation Oncology, Berlin, Germany ; <sup>4</sup>Städtische Kliniken Esslingen am Neckar, Oncology, Esslingen am Neckar, Germany ; <sup>5</sup>University Hospital Tübingen, Surgery, Tübingen, Germany

### Purpose or Objective

Despite excellent local control rates after preoperative radiochemotherapy and total mesorectal excision there is growing interest in local treatment escalation strategies which could increase pathological complete response rates and therefore qualify more patients for non-operative management. Therefore, the goal of the present study was to evaluate tumor regression after preoperative radiochemotherapy combined with deep regional hyperthermia in locally advanced rectal cancer.

### Material and Methods

A total of 78 patients with locally advanced rectal cancer, UICC stage II or III, were enrolled in this prospective phase 2 study. Radiotherapy consisted of 50.4 Gy and concomitant chemotherapy with 5-Fluorouracil (1000mg/m<sup>2</sup> CVI) during the first and fifth week of treatment. Deep regional hyperthermia was applied biweekly with a target of at least eight treatments. Tumor regression was graded according to the Dworak classification with "Dworak 4" corresponding to a pathological complete response. The primary endpoint was the pathological complete response rate, a good response (GR) was defined as Dworak grades three and four.

### Results

All patients completed radiotherapy as prescribed. Sixty of 78 patients (77%) completed eight or more hyperthermia treatments, all patients underwent surgery. Five patients experienced grade three or higher hyperthermia related toxicity (Three with claustrophobia, two with bolus pressure). Dworak grades 1/2/3 and 4 were 11.5% / 38.5% / 34.6% and 15.4%. A GR to treatment was achieved by 50% of all patients. Patients with a GR had significantly higher cumulative equivalent minutes at 43 degrees (CEM43) compared with patients with Dworak grades 1 and 2 (7.22 vs 4.47, p=0.012).

### Conclusion

Our study showed a very favorable toxicity profile of deep regional hyperthermia and a promising proportion of patients with a high degree of tumor regression. The higher CEM43 in good responders suggests a causal relationship between temperature and tumor regression. We will further investigate the potential of hyperthermia to maximize pathological complete response rates in the ongoing multicentric CAO/ARO/AIO-16 organ preservation trial.

(Parts of the study results were presented at the "European Society of Hyperthermia in Oncology" Meeting in 2018)

---

### Proffered Papers: PH 9: Proffered paper: Artificial intelligence and novel imaging approaches

---

### OC-0513 Cone-beam CT intensity correction using a generative adversarial network and unpaired training

C. Kurz<sup>1,2,3</sup>, M. Maspero<sup>3</sup>, M.H.F. Savenije<sup>3</sup>, G. Landry<sup>2</sup>, F. Kamp<sup>1</sup>, M. Li<sup>1</sup>, K. Parodi<sup>2</sup>, C. Belka<sup>1,4</sup>, C.A.T. Van den Berg<sup>3</sup>

<sup>1</sup>University Hospital- LMU Munich, Department of Radiation Oncology, Munich, Germany ; <sup>2</sup>Faculty of Physics- Ludwig-Maximilians-Universität München, Department of Medical Physics, Munich, Germany ; <sup>3</sup>Universitair Medisch Centrum Utrecht, Center for Image Sciences, Utrecht, The Netherlands; <sup>4</sup>DTK, German Cancer Consortium, Munich, Germany

### Purpose or Objective

In adaptive photon and proton radiotherapy (RT and PT) it is desirable to utilize pre-treatment CBCT images for online dose calculation and adaptation. Due to various imaging artifacts CBCTs are, however, not suitable for accurate dose determination and current correction methods lack speed for online application. This work aimed at investigating the feasibility of using a cycle-consistent generative adversarial network (cycleGAN) for CBCT intensity correction to enable fast and accurate RT and PT dose calculation. The dedicated loss-function of the network allowed for using unpaired (not registered) training data despite inter-scan anatomical deviations.

### Material and Methods

Planning CT (pCT) and daily CBCT imaging data of 25 prostate cancer patients were used for training in this study. A cycleGAN was trained using 18/25 patients and 4-fold cross-validation, aiming at translating the uncorrected CBCT images ( $CBCT_{org}$ ) to a pCT-like image ( $CBCT_{cycleGAN}$ ) in 2D (slice-by-slice). No initial matching of the data was performed (unpaired). A previously validated CBCT correction method ( $CBCT_{cor}$ ) applying corrections in projection space on the basis of a prior virtual CT, obtained from pCT to CBCT deformable image registration (DIR), served as reference.  $CBCT_{cycleGAN}$  was compared to  $CBCT_{cor}$  in terms of mean Hounsfield Unit (HU) error within the body outline. Dose calculation accuracy was evaluated using volumetric modulated arc therapy (VMAT) photon and opposing single field uniform dose (OSFUD,  $90^\circ/270^\circ$  gantry angle) proton plans generated on  $CBCT_{cor}$  and recalculated on  $CBCT_{cycleGAN}$ . Single-sided SFUDs were utilized to compare the proton range in beam's eye view (BEV).

### Results

The average (over all patients) HU error comparing  $CBCT_{cor}$  and  $CBCT_{cycleGAN}$  was -0.5 HU. In comparison,  $CBCT_{org}$  showed an average deviation of 33HU with respect to  $CBCT_{cor}$  (Fig. 1). For VMAT the average pass-rates for a 2%/1% dose-difference criterion were 100%/94%. For the OSFUD plans the 2% pass-rate was lower, at 77% (Fig. 2). Using a 2%/2mm gamma criterion the pass-rate increased to 94%. In terms of the proton range 87% of all analyzed BEV profiles agreed better than 3mm on  $CBCT_{cor}$  and  $CBCT_{cycleGAN}$ . The average range difference was 0.4mm. Application of the cycle consistent GAN allowed for a considerable increase in speed: time to correct a 3D CBCT was reduced from 8-10 min ( $CBCT_{cor}$ ) to about 3 s ( $CBCT_{cycleGAN}$ ).

### Conclusion

Our study demonstrated for the first time the feasibility of using a cycleGAN and unpaired training for CBCT intensity correction. Results suggest high RT dose calculation accuracy. In PT, agreement to the reference  $CBCT_{cor}$  was reduced due to the sensitivity of the proton range on HU values. The substantial speed-up with respect to the reference method renders  $CBCT_{cycleGAN}$  particularly interesting in the scope of online adaptive therapy approaches. Due to unpaired training the method is independent from anatomical inconsistencies in the training data.

**Acknowledgements:** German Cancer Aid, DFG-MAP, IMDI

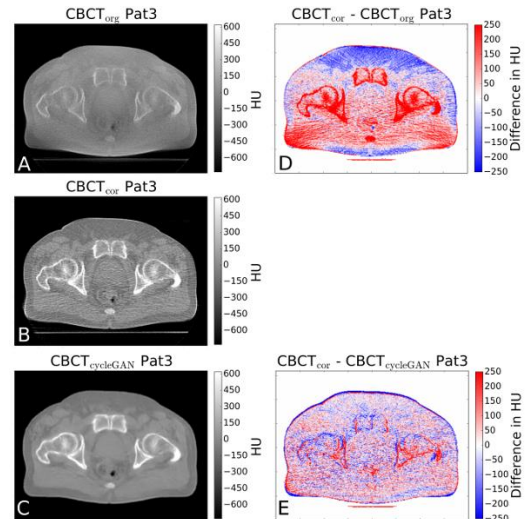


**Figure 1.** CBCT images used in this study: Original CBCT ( $CBCT_{org}$ , A), reference corrected CBCT ( $CBCT_{cor}$ , B) and CBCT corrected using the cycle-consistent GAN ( $CBCT_{cycleGAN}$ , C). Panels D and E illustrate the difference between  $CBCT_{cor}$  and  $CBCT_{org}$  (D), as well as  $CBCT_{cycleGAN}$  (E).

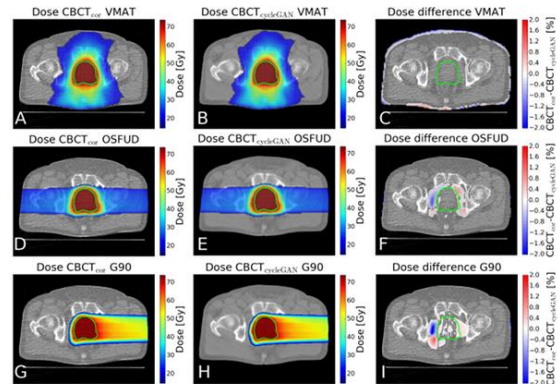


**Figure 2.** Dose distribution optimized on  $CBCT_{cor}$  (A, D, G) and recalculated on  $CBCT_{cycleGAN}$  (B, E, H) for the VMAT (A, B) the OSFUD (D, E) and the single-sided SFUD plan at  $90^\circ$  gantry angle (G, H). Deviations between  $CBCT_{cor}$  and  $CBCT_{cycleGAN}$  based dose calculations are depicted in panels C, F and I.

### OC-0514 Unsupervised deep learning for fast and accurate CBCT to CT deformable image registration

S.R. Van Kranen<sup>1</sup>, T. Kanehira<sup>1</sup>, R. Rozendaal<sup>1</sup>, J. Sonke<sup>1</sup>

<sup>1</sup>Netherlands Cancer Institute, Radiation Oncology, Amsterdam, The Netherlands

### Purpose or Objective

CBCT based online adaptive radiotherapy requires fast deformable image registration (DIR) to facilitate plan adaptation within a reasonable timeslot. Deep learning convolutional neural networks (CNNs) have demonstrated fast and accurate alignment of MR datasets of brain images[1]. The goal of this study is to train such networks for head & neck CBCT-to-CT DIR and to compare the accuracy with our clinically implemented bSpline method.

### Material and Methods

VoxelMorph [1], a U-net based CNN with a spatial transformation block for image registration, was modified to capture deformations up to 3 cm. Networks were trained unsupervised on 7899 CBCT-CT scan pairs of 232 patients. The loss function consisted of local cross correlation regularized on the bending energy to enforce smooth deformations. Several trainings were performed to determine the optimal weighting ( $\lambda=0.1-10$ ). An independent set of 10 CBCT-CT pairs was regularly evaluated during training to determine convergence (no improvement during 200 iterations). Training typically took 1.5 days on a single GTX 1080 GPU.

The accuracy of both methods was determined with a modified distance discordance metric[2] (DDM): a deformation vector field (DVF) between a planning CT (pCT) and a repeat CT (rCT) was constructed by concatenating DVFs between the pCT and a CBCT and the CBCT and the rCT. With 35 CBCTs per patient, the distribution of the DVF end points was determined (per pCT voxel as the vector length of the standard deviation per direction). Finally the accuracy for relevant structures was quantified. The DDM was collected over a held-out test set of 5 patients.

### Results

Training typically converged within three epochs. Regularization weights in the range 0.5-2 showed a shallow optimum and resulted in an absence of folding effects and unrealistic micro deformations. Applying trained models to scan-pairs took ~10 sec, vs minutes with our bSpline method. Figure 1 shows an example DDM color overlay. VoxelMorph generally showed accurate mapping, but failed at occasional large deformations (weight loss, shoulders) and areas with sliding tissue (uvula, epiglottis) or (dis)appearing air gaps (nose, oral cavity). Figure 2 shows the distribution of DDM vector lengths of target areas and various organs. Both deformation methods showed excellent mapping-accuracy: 50% of voxels within the patient-external lay within 0.5mm, 90% within 1.5mm. Outliers within the external were found to correspond with above mentioned failures. Specified per structure, bSplines DIR was more accurate than VoxelMorph.

[1] Balakrishnan G, CVPR, 2018

[2] Saleh ZH, PMB, 2014

### Conclusion

CNN based DIR resulted in fast and accurate head & neck CBCT-to-CT mappings, creating opportunities for on the fly DIR for online plan adaptation. Accuracy was acceptable but less than our clinically applied bSpline DIR and failed at occasional large deformations. Diversifying the training with large deformations and other tumor sites may improve accuracy and robustness, and prevent failures.

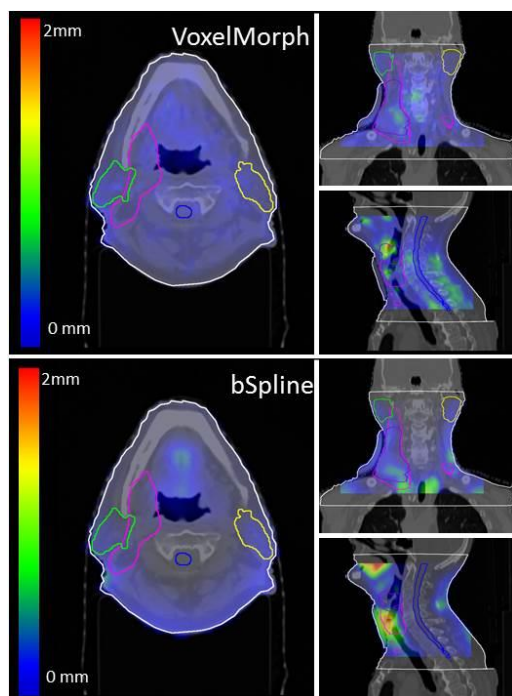


Figure 1. DDM color overlay for an example patient. Tumor regression, sliding tissue and (dis)appearing airgaps are challenges to both VoxelMorph and bSpline DIR.

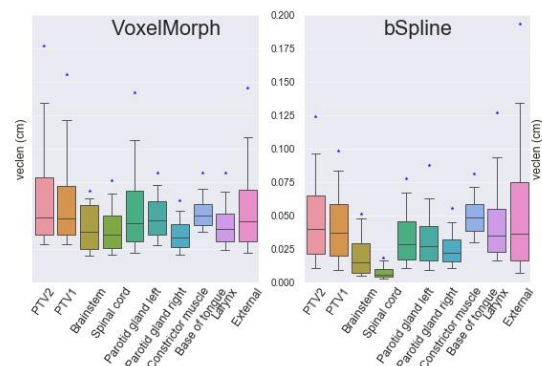


Figure 2. DDM comparison of the DIR accuracy of VoxelMorph vs. bSpline. The boxes represent the median and interquartile ranges, the whiskers the 10/90-percentile, the stars the 95-percentile.

### OC-0515 Synthetic CT generation for Head and Neck radiotherapy by a 3D convolutional neural network

A. Dinkla<sup>1</sup>, M. Florkow<sup>2</sup>, M. Maspero<sup>1</sup>, M. Savenije<sup>1</sup>, F. Zijlstra<sup>2</sup>, P. Doornaert<sup>1</sup>, M. Van Stralen<sup>2</sup>, M. Philipppens<sup>1</sup>, P. Seevinck<sup>2</sup>, N. Van den Berg<sup>1</sup>

<sup>1</sup>UMC Utrecht, Department of Radiation Oncology, Utrecht, The Netherlands; <sup>2</sup>UMC Utrecht, Centre for Image Sciences, Utrecht, The Netherlands

### Purpose or Objective

Synthetic CT generation is required for MR-only simulation workflow where CT-MRI registration can be avoided. More recently, also sCTs are becoming desirable for MRI-guided Radiotherapy where planning is performed based on daily MR images.

In the Head and Neck region (H&N), atlas-based methods have been adopted. However, their robustness is limited as in H&N abnormal patient anatomies can occur due to large tumors or surgical excision. Therefore, here a patch-based deep learning method was chosen to improve robustness. In particular, we used a 3D patch-based convolutional neural network (CNN) to generate sCTs based on T2-weighted Turbo Spin echo (TSE) images and evaluated its image and dosimetric performance.

### Material and Methods

We conducted a retrospective study on 34 patients with Head and Neck cancer who underwent CT (Philips Brilliance Big Bore) and MR imaging (3T Philips Ingenia) for radiotherapy simulation. To generate the sCTs, a large field-of-view (FOV) transverse T2-w TSE mDixon MRI, originally used for tumor/OAR contouring, was selected from the clinical protocol. 83 transverse slices with 3 mm thickness were acquired with a FOV of 45x45 cm<sup>2</sup> and 0.94x0.94 mm<sup>2</sup> resolution in 5min24s and readout bandwidth of 876 Hz/px. Cases with severe image artefacts from dental implants (CT) or motion (MRI) were excluded from the training. To align images for training and evaluation, CT scans were non-rigidly registered (CTreg) to the in-phase MR images (Elastix 4.7) and all images were resampled to 1x1x1 mm<sup>3</sup> isotropic resolution. The CNN was based on a U-net architecture and consisted of 14 layers with 3x3x3 filters. Patches of 48x48x48 were randomly extracted and fed into the training. sCTs were created for all patients using three-fold cross validation. The CT-based treatment plan was recalculated on sCT using Monaco TPS (Elekta).

### Results

sCT generation took 4 min. on a single GPU. The patch-based approach allowed proper sCT generation for non-standard anatomies (fig. 1). Mean absolute error (MAE) over the patient population of the sCT within the intersection of body contours was 75±9 HU, and the mean error (ME) was 9±11 HU. Dice scores of the air (<200HU) and bone (>250HU) masks (CTreg vs sCT) were 0.79±0.08 and 0.70±0.07 respectively. Dosimetric analysis showed mean differences of -0.03±0.05% for dose within the body

contours and  $-0.07 \pm 0.22\%$  inside the high dose region (dose  $>90\%$ ). Dental artefacts obscuring the CT, could be circumvented in the sCT by the CNN-based approach in combination with TSE MRI sequence that typically is less prone to susceptibility artefacts (fig. 2).

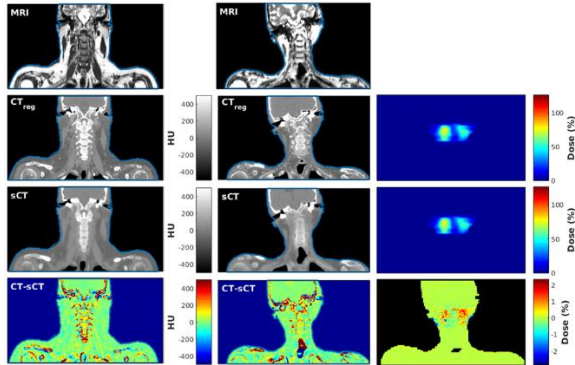


Figure 1: Coronal slice through the MRI, CT<sub>reg</sub>, sCT and HU difference map of a regular case (left) and for a postoperative case with non-standard anatomy (centre). For the latter, the dose maps calculated on the CT<sub>reg</sub>, sCT and dose difference map are shown (right).

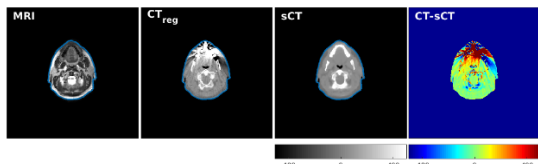


Figure 2: Example of a patient with streaking artefacts on the CT from dental implants. Since no artefacts are present on the MRI, the sCT can be reconstructed without artefacts.

## Conclusion

The 3D patch-based CNN generated sCTs of the H&N region that were dosimetrically accurate. The sCT were generated based on T2W TSE images already used for tumor/OAR contouring and thus no extra scan time was added. Moreover, for H&N cancers, the use of TSE as input for sCT generation has as particular advantage that it is less affected by dental artefacts compared to commonly used gradient echo sequences.

## OC-0516 Whole-frame 2D cineMR prediction using deep neural networks

P. Borman<sup>1</sup>, L. Kerkmeijer<sup>1</sup>, B. Raaymakers<sup>1</sup>, M. Glitzner<sup>1</sup>  
<sup>1</sup>UMC Utrecht, Radiotherapy, Utrecht, The Netherlands

### Purpose or Objective

Accurate target localization during radiotherapy treatments is becoming increasingly feasible with the recent clinical introduction of MR-guided radiotherapy systems such as the Elekta Unity and ViewRay MRIdian. These systems will facilitate real-time treatment adaptation based on continuous MR imaging, to correct for e.g. respiratory motion. It is important to minimize the latency of this control loop, which is largely determined by the MR imaging due to its relatively long acquisition time [1]. The control loop latency may be reduced by predicting the next state based on previous states, a concept that has been previously applied to 1D respiratory signals [2]. In this work we present full frame, image-based, prediction results using the readily available deep learning library pix2pix [3].

### Material and Methods

MR images were acquired on a 1.5T Philips Ingenia system in five renal cell carcinoma patients, with IRB approval. A 2D balanced gradient echo sequence was used consisting of 300 sagittal frames, with a frame rate of 2 Hz. A TensorFlow implementation of pix2pix was used to train a model that predicts a frame based on three previous frames. For each frame (n), the input images consisted of frames (n-2), (n-1), and (n), while the target image was set to frame (n+1). The model was trained and tested on

a per patient basis, where the first 200 frames were used for training and the last 100 frames for testing. The training time was 45 minutes using a nVidia Titan Xp GPU. For evaluation, motion fields of 1) the predicted frames (n+1)' and 2) the most current frames (n) were calculated with respect to the ground truth frames (n+1). The motion fields were then used to calculate per-voxel displacement curves and RMSE maps, with and without prediction.

## Results

The RMSE maps show that the error with prediction is substantially lower than without prediction in almost all areas of the image (figure 1). Displacement curves at points around the tumor (figure 2) show that phase and baseline of the predicted signal correspond with the ground truth, reducing the RMSE from 2.4 mm with no prediction to 1.1 mm with prediction, in this patient. Averaged over all patients, the RMSE was reduced from 1.47 mm to 0.74 mm, an average reduction factor of 2.0.

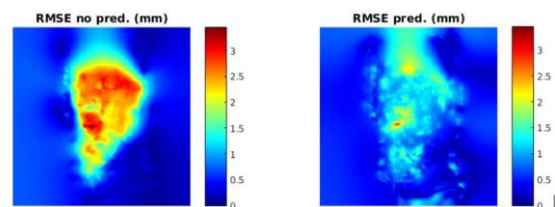


Figure 1: Root mean squared error maps without prediction (left) and with prediction (right).

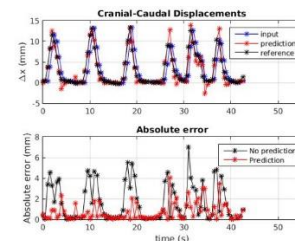


Figure 2: Displacement curves of the tumor for the input, prediction, and ground truth reference (top). The absolute error with and without prediction is shown in the bottom graph.

## Conclusion

A deep learning based prediction model is indeed able to learn a patients breathing pattern and predict a full frame 500 ms ahead. This may help to reduce the influence of imaging latency, which is important for real-time MR-guided treatment applications.

[1] Borman et al. PMB 63(15)

[2] Sun et al. PMB 62(17)

[3] Isola et al. arXiv:1611.07004

## OC-0517 Automatic tumor delineation in rectal cancer using functional MRI and machine learning

F. Knuth<sup>1</sup>, A. Rosvoll Grøndahl<sup>2</sup>, T. Torheim<sup>3,4</sup>, A. Negård<sup>5,6</sup>, S.H. Holmedal<sup>5</sup>, K.M. Bakke<sup>7,8</sup>, S. Meltzer<sup>7</sup>, C. Futsaether<sup>2</sup>, K.R. Redalen<sup>1,7</sup>

<sup>1</sup>Norwegian University of Science and Technology, Department of Physics, Trondheim, Norway; <sup>2</sup>Norwegian University of Life Sciences, Faculty of Science and Technology, Ås, Norway; <sup>3</sup>University of Oslo, Department of Informatics, Oslo, Norway; <sup>4</sup>Oslo University Hospital, Institute for Cancer Genetics and Informatics, Oslo, Norway; <sup>5</sup>Akershus University Hospital, Department of Radiology, Lørenskog, Norway; <sup>6</sup>University of Oslo, Institute of Clinical Medicine, Oslo, Norway; <sup>7</sup>Akershus University Hospital, Department of Oncology, Lørenskog, Norway; <sup>8</sup>University of Oslo, Department of Physics, Oslo, Norway

### Purpose or Objective

Tumor delineation is a time- and labor-intensive procedure both for radiotherapy planning and for quantitative imaging biomarker purposes. In addition, it is

prone to inter- and intra-observer variations. The movement towards a plan-of-the-day approach further intensifies this issue and increases a need for fast and automatic tumor delineation methods. The objective of our study was to use functional magnetic resonance imaging (MRI) to develop and evaluate a voxelwise tumor classification method in rectal cancer utilizing a machine learning approach.

#### Material and Methods

Eighty-nine patients with rectal cancer were subjected to MRI scans at baseline. Routine T2-weighted (T2w) MRI was performed before an extended diffusion-weighted (DW) sequence with b-values of 0, 25, 50, 100, 500, 1000 and 1300 s/mm<sup>2</sup>. In addition, static R2\* (1/T2\*) MR data was acquired using a sequence with five different echo times. Intensity and spatial information extracted from the different image series served as input to an image voxel classification based on Fisher's linear discriminant analysis (LDA) model. The model was trained and assessed using tumor delineations from two radiologists as reference. Their tumor delineations were defined on T2w-images but guided by T2w and DW images.

The ability to distinguish tumor from healthy tissue was assessed by using the Dice similarity coefficient (DICE), kappa statistics (K) as well as sensitivity (Sens) and specificity (Spec) as performance measures. In addition, the receiver operating characteristic (ROC) curve was inspected for each model adjustment by use of the area under the curve (AUC). The effect of combining the different image series was investigated as well as the effect of different pre- and postprocessing options.

#### Results

LDA models based on T2w images alone resulted in an AUC of 0.72 (DICE: 0.24; K: 0.19; Sens: 0.82; Spec: 0.67). R2\* images alone resulted in similar performance measures (AUC: 0.76; DICE: 0.23; K: 0.18; Sens: 0.78; Spec: 0.66). Models based on DW images or a combination of DW and T2w and/or R2\* images improved the performance measures (AUC: 0.86-0.88; DICE: 0.42-0.43; K: 0.39-0.40; Sens: 0.75-0.78; Spec: 0.88-0.89). Inclusion of spatial information in the form of intensity information of neighboring voxels improved the performance as well as preprocessing by calculating the standardized z-scores. A further improvement was achieved by postprocessing the binary tumor mask utilizing morphological closing and opening.

#### Conclusion

We demonstrate an automatic method for MR-based classification of tumor voxels in rectal cancer using a machine-learning approach. The classification results improved significantly when functional MRI sequences were added to the anatomical sequences.

#### OC-0518 Feasibility of MRI-guided VMAT: investigating image quality during gantry rotation on an MR-linac

S. Jackson<sup>1</sup>, M. Glitzner<sup>2</sup>, R.H.N. Tijssen<sup>2</sup>, B.W. Raaymakers<sup>2</sup>

<sup>1</sup>The Christie NHS Foundation Trust, Christie Medical Physics and Engineering, Manchester, United Kingdom ;

<sup>2</sup>University Medical Hospital, Department of Radiotherapy, Utrecht, The Netherlands

#### Purpose or Objective

During a step and shoot or VMAT radiotherapy treatment the linac gantry is repositioned many times. On the Elekta Unity MR-Linac if the patient is continuously MR imaged then the active shimming of the magnet will no longer be correct as soon as the gantry moves away from its original position. Incorrect shimming can result in inhomogeneity of the principal (B0) magnetic field, leading to geometric distortion that could affect real-time treatment plan adaptation.

For a static linac gantry it has been shown that the inhomogeneity difference is negligible between a shimmed and unshimmed magnet, using a clinical pulse

sequence at several gantry angles. Our objective was to measure B0 inhomogeneity changes during linac gantry rotation and to measure geometric distortion in MR images during linac gantry rotation using a clinical balanced steady state (bFFE) sequence and a single shot spin echo EPI (SS-SE-EPI) sequence.

The clinical bFFE sequence has high receive bandwidth to minimise geometric distortion caused by B0 inhomogeneity. The EPI sequence was chosen to demonstrate the sensitivity of the method due to its susceptibility to geometric distortion and because it is often used in diffusion weighted imaging (DWI).

#### Material and Methods

**Continuous rotation:** Sequential single slice acquisitions were obtained while the gantry completed one rotation around the magnet. The centre point of a 10cm diameter spherical phantom was estimated for both the bFFE and SS-SE-EPI pulse sequences, with a temporal resolution of <1s/frame. These were compared to the static gantry cases.

**Inhomogeneity:** Analysis of the root-mean-squared deviation from perfect magnetic homogeneity was obtained for sequential, single slice B0 maps obtained coronally using a dual echo FFE sequence with a temporal resolution of 1.5s/frame during continuous gantry rotation for a 35cm diameter ROI in a flood phantom. This was compared to the static gantry case.

**Step-and-shoot:** the average of fifty coronal, dynamic, single-sliced SS-SE-EPI MR images was calculated with the gantry static at 12 gantry angles spaced 30° apart, with the magnet shimmed for the first gantry position only. The centre point of a 10cm diameter spherical phantom on the resulting images was estimated and plotted against gantry angle.

#### Results

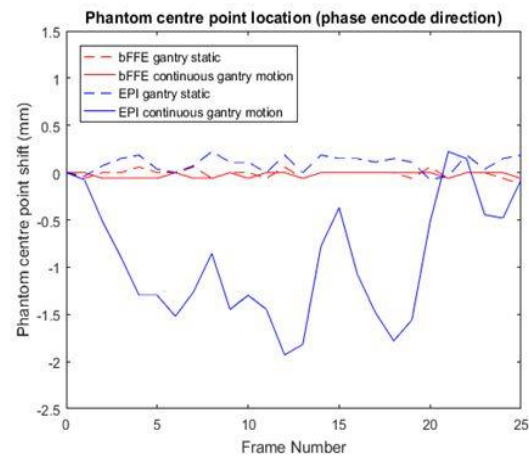


Figure 1 Measured phantom centre point position during static and continuous gantry motion for the clinical bFFE and EPI sequences

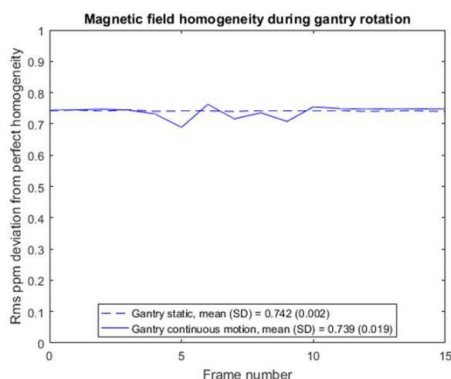


Figure 2 Rms ppm deviation from perfect homogeneity during static and continuous gantry motion using the B0 map.

The 10cm diameter spherical phantom deviated by less than 1mm in the phase encode direction between different gantry angle positions during the step and shoot SS-SE-EPI test.

#### Conclusion

We conclude that VMAT with real-time MR monitoring is feasible, SS EPI-based DWI is permitted as the geometric shifts measured are sub-pixel sized for this sequence and re-shimming the magnet is not required during continuous monitoring of step and shoot treatments.

#### OC-0519 Registration and image quality of T2w 3D TSE scans of the Unity MR-linac

V. Van Pelt<sup>1</sup>, T. Janssen<sup>1</sup>, I. Walraven<sup>1</sup>, C. Liskamp<sup>1</sup>, D. Lambregts<sup>2</sup>, U. Van der Heide<sup>1</sup>, M. Nowee<sup>1</sup>  
<sup>1</sup>Netherlands Cancer Institute, Radiation Oncology, Amsterdam, The Netherlands; <sup>2</sup>Netherlands Cancer Institute, Radiology, Amsterdam, The Netherlands

#### Purpose or Objective

With the Unity MR-linac (Elekta AB, Stockholm, Sweden) a new paradigm in radiation oncology has emerged allowing daily adaptive radiotherapy. Currently, a 3D TSE sequence with an acquisition time of over 6 minutes is used clinically as pre-beam MR. The aim of this study was to investigate the impact of the acquisition time and scan quality on the accuracy in registration of the pre-beam MR for plan adaptation.

#### Material and Methods

After informed consent, 8 patients with prostate cancer were scanned on the Unity MR-linac. Four T2w 3D TSE sequences were acquired with different acquisition times and resolutions (Table 1). Seven experienced observers independently registered the MR sequences on the planning CT using Monaco 5.4 (Elekta AB). Automatic prostate matching was performed and manually adjusted when necessary. Sequences were compared on 3 measures. 1) Registration accuracy for each sequence was quantified by the standard deviation of the registrations per patient. 2) Differences between the sequences was quantified by the mean deviation from the mean registration. 3) A dedicated radiation oncologist and radiologist assessed the overall image quality using a 5 point scale (1: poor; 2: moderate; 3: satisfactory; 4: good; 5: excellent).

#### Results

Acquisition times ranged between 6.25 and 1.27 minutes (Table 1) and an example of corresponding image quality is presented in Figure 1.

Mean deviation from the mean registration per sequence was maximally 0.3mm (sequence A) and the root mean square of the standard deviations of each registration per sequence was <0.7mm. Comparing the different sequences, only small differences were seen, where

deviations in registration of sequence A seem to be slightly larger compared to the other sequences (Table 1).

The qualitative assessment by radiologist and radiation oncologist is listed in Table 1. Median scores per patients ranged from 1.5 - 4.0.

	Voxel size	Acquisition time	Mean deviation of the mean (mm)			RMS of standard deviation (mm)			Median qualitative assessment (range)	
			LR	AP	CC	LR	AP	CC	Rad. Onc.	Radiologist
A	1.2x1.2x1.2 mm	6.25 min	+0.3	+0.3	+0.2	0.50	0.41	0.66	3 (1-3)	3 (3-4)
B	1.2x1.2x2.4 mm	3.12 min	-0.2	0.0	0.0	0.35	0.28	0.69	3 (1-3)	3 (1-4)
C	1.7x1.7x1.7 mm	3.15 min	0.0	-0.2	-0.2	0.45	0.25	0.56	3 (2-3)	3 (2-4)
D	1.8x1.8x1.8 mm	1.27 min	-0.1	-0.1	0.0	0.45	0.30	0.63	2 (2-3)	2 (1-3)

Table 1. voxel size and acquisition time of the T2w 3D TSE sequences. LR: left-right, AP: anterior-posterior, CC: cranial-caudal.

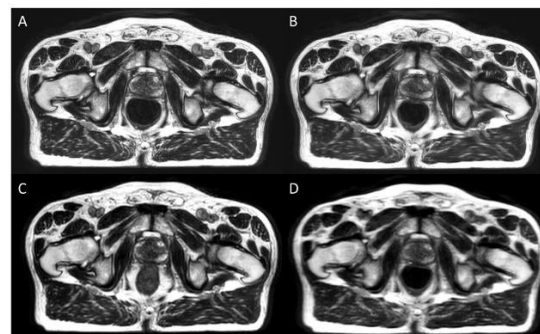


Figure 1. Example of a prostate cancer patient scanned with different acquisition times (A: 6.25 min; B: 3.12 min; C: 3.15 min; D: 1.27 min)

#### Conclusion

We studied scan quality and registration accuracy comparing a 6.25 minute T2w 3D TSE scan with shorter sequences of up to 1.27 minutes. We found registration accuracy was on average high (sub-millimetre) and changed only mildly for the different sequences. A qualitative assessment shows only a lower judgement for the shortest (1.27 minute) sequence and variation of image quality between patients is larger than between the different acquisition times. These results can be used to effectively improve overall fraction time for adaptive treatment on the MR-linac, by optimising the imaging sequence used for registration.

#### Proffered Papers: PH 10: Proffered paper: Treatment planning innovations

#### OC-0520 Inter-observer variations in plan evaluation

L.P. Kaplan<sup>1</sup>, A.I.S. Holm<sup>1</sup>, U.V. Elstrøm<sup>1</sup>, J.G. Eriksen<sup>2</sup>, K. Jensen<sup>3</sup>, H. Primdahl<sup>3</sup>, C.N. Andreassen<sup>2</sup>, S.S. Korreman<sup>1</sup>

<sup>1</sup>Aarhus University Hospital, Dept. of Medical Physics, Aarhus C, Denmark ; <sup>2</sup>Aarhus University Hospital, Dept. of Experimental Clinical Oncology, Aarhus C, Denmark ; <sup>3</sup>Aarhus University Hospital, Dept. of Oncology, Aarhus C, Denmark

#### Purpose or Objective

Use of dose-volume parameters is the standard way of quantifying plan quality. Secondary plan characteristics can be quantified using metrics such as dose gradient or dose homogeneity but are in practice often evaluated qualitatively. Subjective qualitative evaluation and comparison of RT treatment plans can be arbitrary and hence suffer from inter-observer variations. The aim of this study was to compare subjective vs. quantitative evaluations and determine how much consistency there is between the two.

**Material and Methods**

Twenty head-and-neck cancer pts were included. Two planning strategies were used for all pts: one with and one without using the knowledge-based planning (KBP) software RapidPlan included in the Eclipse TPS (v13.7 Varian Medical Systems). All plans were three-arc VMAT plans, made to be clinically acceptable according to current national guidelines. Four radiation oncologists performed a blinded clinical evaluation of the plans. Each chose which plan they preferred for each patient, giving scores for target coverage and OAR doses, respectively, from six (good) to one (bad). In addition, they gave scores for importance in choosing between two plans, from six (important) to one (not important), for five different secondary plan characteristics. Corresponding quantitative metrics from the literature were calculated. Subjective scores and quantitative metrics are shown in table 1. Consistency between the score-metric pairs was evaluated and the calculated metrics were compared for KBP vs. non-KBP plans.

Subjective scores	Metrics	Definitions	Significant difference KBP/non-KBP?
Target score	Target coverage index	$TCl = TV_{PD} / TV \times 100$	No
	Cold volume	$CV = TV < 95\% PD$	No
OAR score	OAR mean dose		Yes, KBP lower for: PCM <sub>sp</sub> $p = 0.025$ PCM <sub>int</sub> $p < 0.001$ PCM <sub>low</sub> $p < 0.001$ Thyroid $p = 0.036$ GI larynx $p = 0.003$
Dose homogeneity in target	Homogeneity index	$HI = (D_{2\%} - D_{98\%}) / D_{95\%}$	Yes, KBP dose less homogenous in low-risk target $p < 0.001$
Steep dose fall-off	Gradient index	$GI = R_{eff,50\%PD} - R_{eff,PD}$	Yes, steeper gradient for KBP $p = 0.004$
	Conformity index	$CI = TV_{90\%} / (TV \times PDV)$	Yes, KBP plans less conformal to high-risk target $p < 0.001$
Hot spots outside target	Hot volume	$HV = HT > 95\%PD$	Yes, larger for KBP for High-risk target: $p < 0.001$ Low-risk target: $p = 0.033$ Elective target: $p = 0.019$
Low-dose bath	$V_{X\%}, X = 1, 5, 10, 15$	Volume given a minimum dose of X Gy	Yes, smaller for KBP for 10 Gy $p = 0.030$ 15 Gy $p = 0.002$
Integral dose	Body mean dose times body volume		Yes, lower for KBP $p = 0.019$

Table 1: List of the plan characteristics which were scored subjectively. Each has one or more quantitative metrics associated with it. If the quantitative metrics differ significantly from KBP to non-KBP plans this is noted in the rightmost column.  $D_{X\%}$ : minimum dose given to the hottest X% of a volume, HT: healthy tissue volume, PD: prescription dose, PCM: pharyngeal constrictor muscle,  $R_{eff,50\%PD}$ : effective radius of the 50% prescription isodose volume,  $R_{eff,PD}$ : effective radius of the prescription isodose volume, TV: target volume,  $TV_{PD}$ : target volume given at least 95% of the prescription dose.

**Results**

All plans complied with critical OAR (spinal cord, brainstem) and target coverage constraints. KBP plans were preferred in 65% of all evaluations. In only six cases did all physicians prefer the same plan. Mean[SD] scores given for target coverage were 5.28[0.70] (KBP) and 5.40[0.54] (non-KBP). For OAR dose they were 5.16[0.66] (KBP) and 4.71[0.67] (non-KBP). For all scores except OAR for non-KBP plans a Friedman's ANOVA test showed significant ( $p < 0.05$ ) variations between observers. Table 1 shows for which quantitative metrics KBP and non-KBP plans differed significantly (Wilcoxon signed rank test,  $p < 0.05$ ). Subjective scores and corresponding metrics are shown in fig. 1 for dose gradient and conformity. The figure shows little consistency between the subjective scores and the quantitative metrics. The same was found for all score-metric pairs investigated. Spearman's  $\rho$  for correlations in each score-metric pair (including scores from all physicians) ranged from -0.34 to 0.20 (median -

0.07).

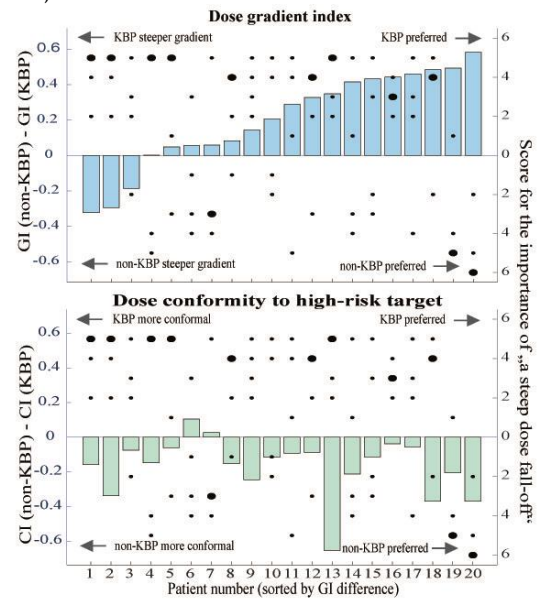


Figure 1: The bars (left y-axes) show the gradient (upper) and conformity (lower) index for non-KBP plans minus the same index for KBP plans for each patient. The black dots (right y-axes) show subjective scores given for the importance of a steep dose fall-off outside the target in the choice between two plans for a patient. A dot in the upper half of the figure indicates the corresponding physician preferred the KBP plan for this patient, a dot in the lower half that the non-KBP plan was preferred. Large dots mark where two physicians gave the same score.

**Conclusion**

There were substantial inter-observer variations in subjective scores. Little to no consistency was seen between qualitative scores and corresponding quantitative metrics. Often physicians gave a high importance score to a plan characteristic but chose the plan which scored worse on the quantitative metric. Consistent use of quantitative metrics in addition to subjective plan evaluation should be investigated as a way of mitigating such inconsistencies and variations.

**OC-0521 SRS plan quality with variation in modality: Results of an international planning competition**

N. Hardcastle<sup>1</sup>, B. Nelms<sup>2</sup>, L. O'Connor<sup>3</sup>, J. Shakeshaft<sup>4</sup>, A. Haworth<sup>5</sup>, O. Cook<sup>6</sup>, M. Harris<sup>6</sup>, C. Phillips<sup>7</sup>  
<sup>1</sup>Peter MacCallum Cancer Centre, Physical Sciences, Melbourne, Australia ; <sup>2</sup>ProKnow Systems, Development, Madison, USA ; <sup>3</sup>Calvary Mater Hospital, Radiation Therapy, Newcastle, Australia ; <sup>4</sup>Radiation Oncology Centres, Medical Physics, Brisbane, Australia ; <sup>5</sup>University of Sydney, School of Medical Physics, Sydney, Australia ; <sup>6</sup>Trans-Tasman Radiation Oncology Group, Quality Assurance, Newcastle, Australia; <sup>7</sup>Peter MacCallum Cancer Centre, Radiation Oncology, Melbourne, Australia

**Purpose or Objective**

Stereotactic radiosurgery (SRS) delivers highly conformal doses cranial targets. There is large variation in treatment planning and delivery technology, with recent linac developments enabling treatment of complex and multiple targets. In this study, we evaluate the treatment plan quality for plans submitted to an international competition for a case of SRS to multiple brain metastases.

**Material and Methods**

A single SRS patient was used, with five brain metastases of volumes 0.07-2.82 cm<sup>3</sup> located throughout the brain including adjacent to the brainstem. A planning CT scan with tumour and OAR contours was provided via the ProKnow system. Targets were provided as PTVs, without margin adjustment for SRS delivery technology. A dosimetry scoring matrix based on the TROG 16.02 Local-

HERO trial protocol was created in which approximately equal points were allocated to target dosimetry including conformity index (CI), and to OAR dosimetry. Where applicable, progressive scoring was used; for example, participants received a minimum score for meeting trial protocol and increasing points when OAR dose was reduced further below protocol. In addition to dosimetry metrics, delivery parameters including treatment plan geometry, delivery time and monitor units were analysed for the top 50 plans.

### Results

A total of 160 plans were submitted from 28 countries. Treatment devices included linacs, CyberKnife (CK), GammaKnife (GK), TomoTherapy and particle therapy. The majority of plans were VMAT (101), followed by GK (20), CK (16) and IMRT (7) (Figure 1). The median score was 124.8 (out of 150) and maximum was 146.2, achieved with CK. The top 50 plans scored 134.5-146.2. Of these, VMAT/IMRT plans had superior CI100% compared with CK and GK, however VMAT was inferior to IMRT, CK and GK for CI50%. IMRT achieved lower normal brain receiving 12 Gy compared with VMAT, CK and GK (Figure 2). It should be noted that GK PTV margin in practice may be lower than for linac plans. For all techniques, all top 50 plans had at least 125% target maximum dose. Top 50 linac plan score was independent of monitor units, but all had at least three couch angles. Median VMAT delivery time was 14 minutes, compared with 25, 120 and 169 minutes for IMRT, CK and GK respectively (Figure 2).

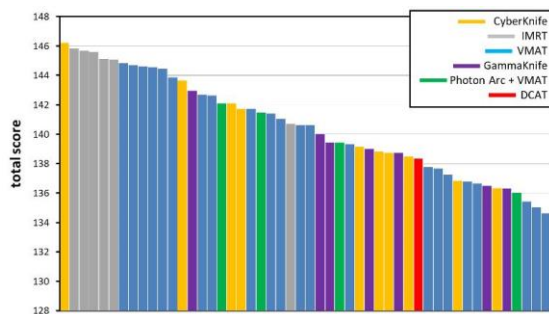


Figure 1: Waterfall plot of plan scores for the top 50 plans with delivery or planning technique denoted by colour

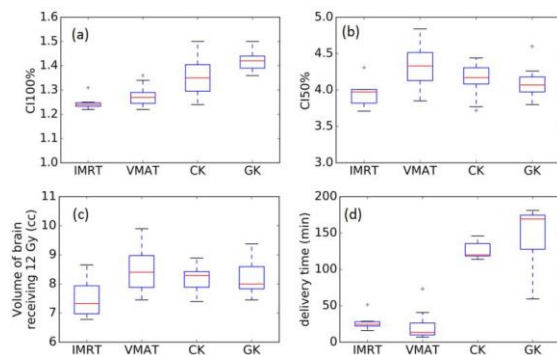


Figure 2: (a) 100% CI (b) 50% CI (c) volume of normal brain receiving 12 Gy and (d) delivery time for IMRT, VMAT, GammaKnife and Cyberknife in the top 50 scoring plans

### Conclusion

In this international multi-metastases SRS planning competition, similar plan quality was achieved with across various SRS delivery systems. There was a vast range in delivery time required between different SRS delivery systems. This study did not however collect planning and QA time, or QA results, for which large variations between systems may be present.

### OC-0522 Characterising dose changes due to unplanned gas cavities in Magnetic Resonance guided Radiotherapy

J. Shortall<sup>1</sup>, E. Vasquez Osorio<sup>1</sup>, A. Green<sup>1</sup>, R. Chuter<sup>2</sup>, A. McWilliam<sup>1</sup>, K. Kirkby<sup>1</sup>, R. Mackay<sup>2</sup>, M. Van Herk<sup>1</sup>

<sup>1</sup>The University of Manchester, Division of Cancer Sciences, Manchester, United Kingdom ; <sup>2</sup>The Christie NHS Foundation Trust, Medical Physics and Engineering, Manchester, United Kingdom

### Purpose or Objective

Due to Lorentz Forces, electron dose deposition within patients is altered during Magnetic Resonance guided Radiotherapy (MRgRT). Effects of the magnetic field are of particular interest at air-tissue boundaries, named the Electron Return Effect (ERE). Little work has been done on characterising the dosimetric effects of unplanned gas cavities in MRgRT on Organs At Risk (OAR), which could affect their dose constraints, depending on beam directions and the frequency of gas cavity presence. Here we characterise superficial dose changes around unplanned spherical air cavities during MRgRT in a single beam, as part of development a simulation platform for the dosimetric accuracy of MRgRT.

### Material and Methods

Three cuboid water phantoms containing varying spherical air cavities (0.5, 3.5, 7.5cm diameter) and a reference phantom without an air cavity were created. Monte Carlo dose calculations of a single 7MV photon beam under the influence of a 1.5T transverse magnetic field were produced using research Monaco 5.19.02 treatment planning system (Elekta AB, Stockholm, Sweden). Calculated dose distributions of phantoms with and without air cavities were compared using a spherical coordinate system originating in the centre of the cavity. Dose changes over the surface of the cavities,  $\Delta D\%(\theta, \Phi)$ , were fit to a modulated sinusoidal function of the form:  $\Delta D\%(\theta, \Phi) = A \sin(k_1 \theta + \psi_1) \sin(k_2 \Phi + \psi_2) + E$ .

Absolute residual errors, defined as simulated-fitted delta dose, for the fit were quantified and reported.

### Results

Figure 1 shows  $\Delta D\%(\theta, \Phi)$  for all tested cavities. Hot and cold spots of up to +/- 70% are observed for larger cavities, with the largest effects observed about 12° off-axis.

The fitted  $\Delta D\%(\theta, \Phi)$ , fitting parameters and absolute residual error of the fit for the cavities are presented in Figure 2. All fits have a mean error <3% of the dose at the air cavity (<0.3% for the two larger cavities), and standard deviation of <6%, i.e., the sinusoidal function characterises the effect well. However, for all cavities the fit deteriorates at the sides of the cavities (indicated by the blue areas in figure 2(panels D-F)), mainly due to lack of attenuation by the cavity. Calculating the dosimetric effect for multiple beams is done by applying the equation per beam, while rotating the coordinate system according

to the beam direction.

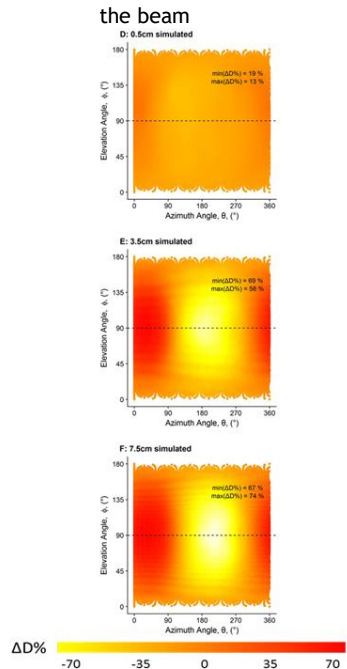


Figure 1: The dose changes,  $\Delta D\%(\theta, \phi)$ , occurring due to unplanned spherical air cavities (diameter 0.5, 3.5, 7.5 cm respectively) forming in the path of a single beam during MRgRT using a 1.5 T transverse magnetic field. Clear areas of dose increase (red) and decrease (yellow) are observed around the cavities. Minimum and maximum dose changes become larger for larger air cavities, increasing from the region of 15% in small cavities to 70% in the largest cavity for cavities.

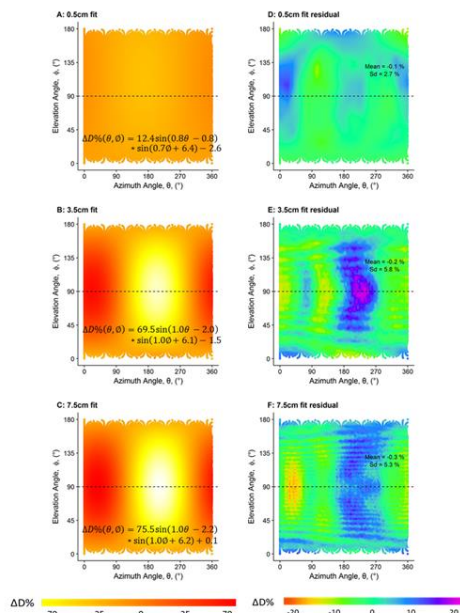


Figure 2: A-C: The fitted dose change maps for the surface of the cavities, produced using reduced-squared optimization to fit simulated data (figure 1) to a modulated sinusoidal function. The fitting parameters for each cavity are shown. D-F: The residual error of the fit for each cavity. The sinusoidal function fits the simulated data well overall, with all mean errors  $<3\%$  and the standard deviation  $<6\%$ . The fit deteriorates in the same location around the larger cavities however, indicated by the blue area. This could be due to the lack of attenuation through the cavity, which does not appear to follow a sinusoidal pattern as effects due to ERE do.

## Conclusion

We quantified dosimetric changes due to unplanned gas cavities in MRgRT using Monte Carlo dose calculations. Dose changes around the surface of unplanned spherical air cavities can be well characterised as a modulated sinusoidal function. The fit does deteriorate slightly in a consistent place around each cavity. Work is currently being done to extend the model beyond the cavity surface, create a generalised form for the relevant cavity diameters, and to implement the fit function into a

simulation platform that takes multiple beam directions into account.

## OC-0523 $^3\text{He}$ MRI for functional lung avoidance VMAT treatment planning in lung cancer

K. Hart<sup>1,2</sup>, H. Marshall<sup>3</sup>, J. Swinscoe<sup>2</sup>, S. Robinson<sup>2,3</sup>, T. Matthew<sup>4</sup>, S. Tozer-Loft<sup>1,2</sup>, M. Hatton<sup>2,4</sup>, J. Wild<sup>3</sup>, R. Ireland<sup>2,3</sup>, B. Tahir<sup>2,3</sup>

<sup>1</sup>Weston Park Hospital, Radiotherapy Physics, Sheffield, United Kingdom ; <sup>2</sup>University of Sheffield, Academic Unit of Clinical Oncology, Sheffield, United Kingdom; <sup>3</sup>University of Sheffield, Academic Radiology, Sheffield, United Kingdom; <sup>4</sup>Weston Park Hospital, Oncology, Sheffield, United Kingdom

## Purpose or Objective

Radiation-induced lung toxicity (RILT) is a dose limiting complication of thoracic radiotherapy that impacts on the clinical benefits of dose escalation strategies in lung cancer. Lung dose volume parameters have a limited ability to identify patients at risk of RILT and recent studies suggest functional dosimetric parameters provide stronger predictive values than conventional anatomical parameters. The incorporation of regional ventilation information obtained via hyperpolarised gas MRI has been shown to reduce functional lung dose in conformal (3D-CRT) and fixed-field intensity-modulated radiotherapy (ff-IMRT) planning. Here we report the effects of hyperpolarised  $^3\text{He}$  MRI for volumetric modulated arc therapy (VMAT) in a cohort of lung cancer patients.

## Material and Methods

Ten non-small cell lung cancer (NSCLC) patients being planned for radical radiotherapy underwent inspiratory breath-hold CT and same-breath anatomical  $^1\text{H}$  MRI and hyperpolarized  $^3\text{He}$  MRI ventilation at the same inflation state as CT. The ventilated lung was segmented using a fuzzy c-means clustering algorithm. Binary ventilation maps were registered to breath-hold CT via its same-breath anatomical  $^1\text{H}$  MRI. VMAT plans with two partial arcs that minimised dose to the anatomical lung volume were compared with plans that minimised dose to the  $^3\text{He}$  defined functional lung volume. For each pair of plans, the volume of functional lung receiving  $\geq 10\text{Gy}$  ( $fV_{10}$ ) and  $\geq 20\text{Gy}$  ( $fV_{20}$ ), mean functional lung dose ( $fMLD$ ) and percentage of planning target volume (PTV) receiving 95% of the prescription dose ( $PTV_{95}$ ) were compared.

## Results

Incorporation of  $^3\text{He}$  MRI ventilation information led to statistically significant median reductions in  $fV_{10}$  of 1.3% (range: -0.1-2.4%;  $p=0.016$ ) and  $fV_{20}$  of 0.8% (range: -0.2-1.1%;  $p=0.007$ ). A small but significant reduction in  $fMLD$  of 0.3Gy (range: 0.1-0.4 Gy;  $p=0.005$ ) was also observed. There was no difference in target coverage: median difference in  $PTV_{95}$  of 0.0% (range: -0.2-0.1%;  $p=0.447$ ). Patients with the largest individual reductions in  $fV_{10}$  and  $fV_{20}$  demonstrated large functional defects either in close proximity to the target volume or at the periphery of the ipsilateral lung. Significant negative correlation between the percentage of ventilated ipsilateral lung and both  $fV_{10}$  and  $fV_{20}$  was also observed ( $R_s = -0.707$ ,  $p = 0.022$  and  $R_s = -0.665$ ,  $p = 0.036$  respectively).

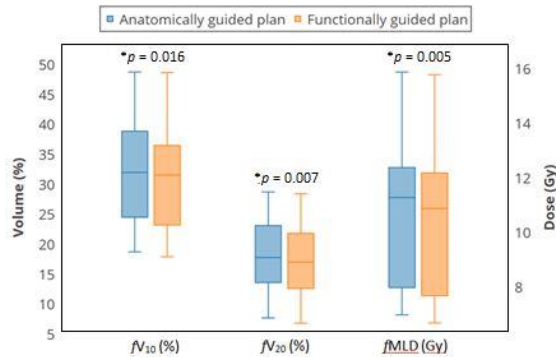


Fig1: Boxplot of functional dosimetric parameters for anatomically and functionally guided VMAT plans.

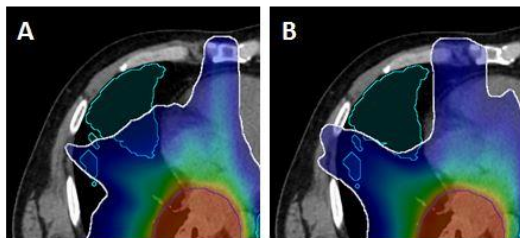


Fig2: Transverse views of anatomically guided (A) and functionally guided (B) VMAT plans for a representative patient. Cyan contour indicates the ventilated volume within the lung as defined via  $^3\text{He}$  MRI. White contour shows the 20Gy isodose, which can be seen to preferentially avoid the ventilated volume in the functionally guided plan.

## Conclusion

Functionally-guided VMAT plans incorporating regional ventilation information from hyperpolarised  $^3\text{He}$  MRI can permit dosimetric reduction to the ventilated lung volume without compromising PTV coverage. The degree of reduction is however less than that previously reported for 3D-CRT and ff-IMRT planning, which may be attributable to increased dose conformity with VMAT. The location of ventilation defect in relation to target volume is an important factor in reducing function lung dose, with the greatest reduction possible in patients with significant ventilation defects located in the ipsilateral lung.

## OC-0524 A two-beam non-coplanar class solution to supplement VMAT in prostate SBRT

A.W. Sharfo<sup>1</sup>, L. Rossi<sup>1</sup>, M. Dirckx<sup>1</sup>, S. Aluwini<sup>2</sup>, S. Breedveld<sup>1</sup>, B. Heijmen<sup>1</sup>

<sup>1</sup>Erasmus MC Cancer Institute, Radiation Oncology, Rotterdam, The Netherlands ; <sup>2</sup>University Medical Center Groningen, Department of Radiation Oncology, Groningen, The Netherlands

## Purpose or Objective

An advantage of coplanar VMAT in SBRT is short delivery time. It also avoids long planning times related to optimization of non-coplanar beam arrangements, and most commercial TPSs lack advanced options for beam angle optimization (BAO). On the other hand, optimized non-coplanar setups can often significantly improve SBRT dose distributions. In this study we used automated planning with integrated BAO to explore advantages of VMAT supplemented with  $\leq 5$  noncoplanar IMRT beams, aiming at plan quality improvement relative to VMAT while limiting the increase in treatment time. The analyses resulted in a proposal for a two-beam noncoplanar class solution to supplement VMAT.

## Material and Methods

For 20 prostate SBRT patients with a prescribed dose of 38 Gy in 4 fractions, our platform for fully automated multi-criterial treatment planning was first used to generate dual-arc VMAT plans supplemented with five non-coplanar

IMRT beams with optimized patient-specific beam orientations (VMAT+5). Next, based on the selected non-coplanar beam directions in the patient group (20x5 beams in total), two preferred non-coplanar beam directions were selected as class solution (CS), and for each of the 20 patients a VMAT+CS plan was automatically generated. The VMAT+CS plans were benchmarked against a) dual-arc coplanar VMAT plans, b) the VMAT+5 plans, and c) IMRT plans with 30 computer-optimized non-coplanar beams (30NCP). For comparison, all plans were normalized to have identical PTV coverage. Deliverability of generated plans was verified with QA measurements by executing plans at the linac, where treatment delivery times were also measured.

## Results

Fig. 1 shows treatment plan parameters for the four treatment approaches normalized to the values of VMAT. Overall the quality of VMAT+CS plans is similar to VMAT+5, while optimization times were reduced by a factor of 25 due to the omission of BAO. Compared to VMAT, VMAT+CS significantly reduced doses to rectum and bladder and dose bath, showing median percentage differences from 1-24% for rectum  $D_{1cc}$ ,  $D_{mean}$ ,  $V_{40GyEq}$ , and  $V_{60GyEq}$ , bladder  $D_{mean}$ , and patient  $V_{xGy}$  (all  $p < 0.001$ , Fig. 1). All VMAT and VMAT+CS plans passed the dosimetric QA tests (3%/1 mm criteria) with average Gamma passing rates of  $98.3 \pm 1.0\%$  and  $98.3 \pm 0.7\%$ , respectively. Compared to VMAT, VMAT+CS plans required 3% less MU on average and only  $1.9 \pm 0.7$  min longer total delivery time. Compared to 30NCP, VMAT+CS plans were considered clinically equivalent with respect to high doses in the rectum and bladder (Fig. 1A) and much faster to deliver, while 30NCP had more favorable low dose bath (Fig. 1B).

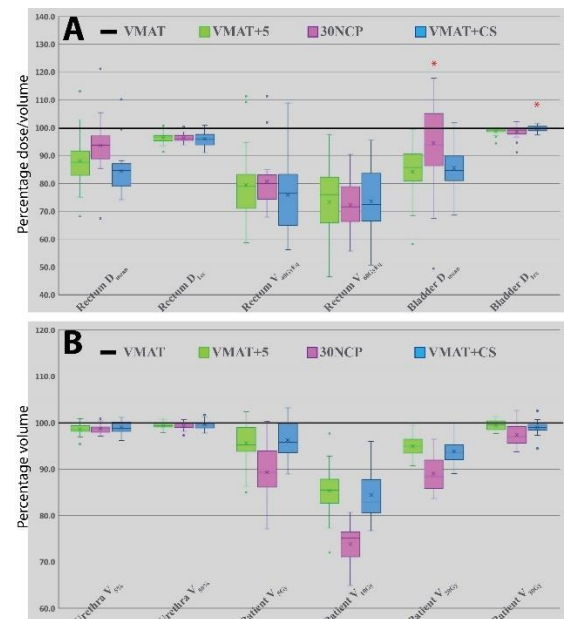


Fig 1. Percentage dose/volume values for healthy tissues across the 20 study patients, relative to VMAT. The central line of each box represents the median value, and its upper and lower edge the 25<sup>th</sup> and 75<sup>th</sup> percentiles, respectively. The x mark inside each box represents the mean value. The whiskers extend to the minimum and maximum values, or to 1.5 times the inter-quartile range from the top/bottom of the box. Values outside this range are plotted individually as outliers.

\* indicates no statistically significant difference compared to VMAT.

## Conclusion

Using an algorithm for fully automated multi-criterial beam profile and beam angle optimization (BAO), we derived a two-beam non-coplanar class solution (CS) to supplement VMAT for prostate SBRT. Adding the CS beams to a coplanar VMAT plan resulted in substantial improvements in treatment plan quality with a minimal increase in treatment time. The fixed CS avoids the need for patient-specific BAO.

### OC-0525 4D Monte Carlo dose calculations on different CT image sets for SBRT using patient breathing data

P. Freislederer<sup>1</sup>, A. Von Münchow<sup>1</sup>, F. Kamp<sup>1</sup>, C. Heinz<sup>1</sup>, S. Gerum<sup>1</sup>, F. Roeder<sup>1,2</sup>, S. Corradini<sup>1</sup>, R. Floca<sup>3,4</sup>, M. Alber<sup>3,5</sup>, M. Söhn<sup>1</sup>, M. Reiner<sup>1</sup>, C. Belka<sup>1,6,7</sup>, K. Parodi<sup>8</sup>  
<sup>1</sup>University Hospital LMU Munich, Department of Radiation Oncology, Munich, Germany; <sup>2</sup>German Cancer Research Center DKFZ, CCC Molecular Radiation Oncology, Heidelberg, Germany; <sup>3</sup>National Center for Radiation Research in Oncology NCRO, Heidelberg Institute of Radiation Oncology HIRO, Heidelberg, Germany; <sup>4</sup>German Cancer Research Center DKFZ, Division of Medical Image Computing, Heidelberg, Germany; <sup>5</sup>Heidelberg University Hospital, Department of Radiation Oncology, Heidelberg, Germany; <sup>6</sup>Comprehensive Pneumology Center Munich CPC-M, Member of the German Center for Lung Research DZL, Munich, Germany; <sup>7</sup>DKTK, German Cancer Consortium, Munich, Germany; <sup>8</sup>LMU Munich, Department of Experimental Physics - Medical Physics, Munich, Germany

#### Purpose or Objective

The need for four-dimensional treatment planning becomes indispensable for radiation therapy of tumors with breathing-induced motion. In this study, we combined the actual patient breathing trace with the Linac's log file and a Monte Carlo (MC) dose engine to recalculate a 4D dose distribution for 3D-conformal radiation therapy (3D-CRT) and volumetric modulated arc therapy (VMAT) for lung SBRT and compared the 4D dose to MC dose calculations based on different CT image datasets.

#### Material and Methods

For 5 lung patients, 3D-CRT and VMAT treatment plans were calculated on four different 3DCT image datasets: a three-dimensional CT (3DCT), an average intensity projection (AIP) and a maximum intensity projection (MIP) CT both generated from a 4DCT, and a 3DCT with density overrides (DO) in the internal target volume (ITV) and planning target volume (PTV) based on the 3DCT. The MC 4D dose has been calculated on each 4DCT phase using the Linac's log file and the patient's breathing trace (acquired during clinical treatment). Dose calculation on 10 4DCT breathing phases was performed using MCverify, a scriptable sub-module XVMC dose engine of Hyperion V2.4.5 (University Tübingen, Germany; research version of Elekta MONACO 3.2). Dose was accumulated to the gross tumor volume (GTV) at the 50% breathing phase (end of exhale) using deformable image registration with AVID (Analysis of Variations in Interfractional Radiotherapy, DKFZ, Germany). Dose-volume-histograms (DVHs) were created and  $\Delta D98\%$  and  $\Delta D2\%$  were calculated as the difference between 4D recalculated and planned dose.

#### Results

For 3DCT-based planning,  $\Delta D98\%$  is higher in mean over all patients for all treatment plans while  $D2\%$  is lower for 3D-CRT. AIP-based planning increases the low dose areas in the GTV in 3D-CRT and slightly less using VMAT, while  $D2\%$  stays within the same range for both treatment planning methods. Absorbed dose in high dose areas is in good agreement for MIP-based planning over the patient cohort, although less dose was calculated and both treatment techniques. DO-based planning leads to a lower  $D2\%$  in the GTV due to the higher density in ITV and PTV but also to fewer cold spots for low dose areas ( $D98\%$ ) in the GTV.

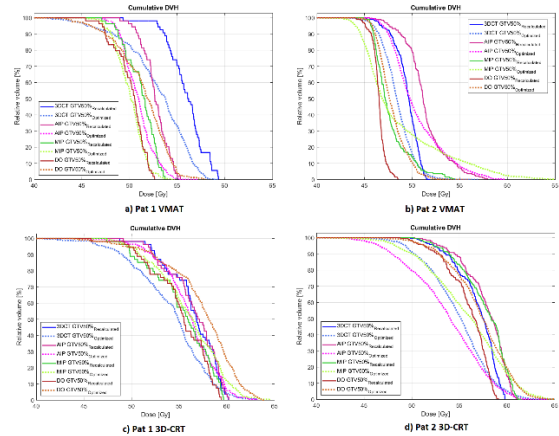


Fig. 1: GTV<sub>50%</sub> DVHs of 4D MC recalculated (solid) and optimized dose (dashed) for 2 patients: 3DCT (blue), AIP (magenta), MIP (green), DO (brown)

#### Conclusion

AIP and MIP served as the most stable base for treatment planning and both tend to be superior to DO, but the results indicate a dependency on breathing variability, tumor motion, and size. Both methods can be recommended for SBRT treatment planning but DO could perform better in individual cases due to the highly patient-specific character of breathing motion. An interplay effect could not be observed in the small patient cohort. Our workflow, after adaptation for clinical use, could help to provide a 4D dose calculation tool in modern treatment planning systems, where evaluation tools for the effects of tumor motion have not been incorporated adequately.

### OC-0526 Dependency of the interplay effect on the fractionation for proton therapy of pancreatic cancer

K. Dolde<sup>1,2,3</sup>, Y. Zhang<sup>4</sup>, N. Chaudhri<sup>3,5</sup>, C. Dávid<sup>2,6</sup>, M. Kachelriess<sup>6</sup>, A.J. Lomax<sup>4,7</sup>, P. Naumann<sup>8</sup>, N. Saito<sup>8</sup>, D.C. Weber<sup>4</sup>, A. Pfaffenberger<sup>1,3</sup>

<sup>1</sup>German Cancer Research Center DKFZ, Medical Physics in Radiation Oncology, Heidelberg, Germany; <sup>2</sup>University of Heidelberg, Department of Physics and Astronomy, Heidelberg, Germany; <sup>3</sup>National Center for Radiation Research in Oncology, Heidelberg Institute for Radiooncology, Heidelberg, Germany; <sup>4</sup>Paul Scherrer Institute, Center of Proton Therapy, Villigen, Switzerland; <sup>5</sup>Heidelberg Ion-Beam Therapy Center HIT, Heidelberg Ion-Beam Therapy Center HIT, Heidelberg, Germany; <sup>6</sup>German Cancer Research Center DKFZ, Division of X-Ray Imaging and Computed Tomography, Heidelberg, Germany; <sup>7</sup>ETH Zurich, Department of Physics, Villigen, Switzerland; <sup>8</sup>University Clinic Heidelberg, Department of Radiation Oncology, Heidelberg, Germany

#### Purpose or Objective

In particle therapy treatments of pancreatic cancer, interplay effects between the scanning pencil beam and intrafractional abdominal organ motion may lead to pronounced hot and cold spots in the resulting dose distributions. These effects can be assessed and quantified by means of 4D dose calculations. To furthermore account for interfractional motion variability, repeated 4D image acquisitions are required. In this study, we performed 4D dose calculations based on repeated time-resolved volumetric MR images (4D-MRI) to investigate both the magnitude and the mitigation effectiveness of the interplay effect by means of fractionation for pancreatic cancer patients.

#### Material and Methods

For a cohort of 9 pancreatic cancer patients (P1-P9), up to six repeated 4D-MRI were acquired, which were

reconstructed by an iterative algorithm which provides 20 breathing phases per measurement. The deformation vector fields between the breathing phases were used to warp a 3D planning CT of the corresponding patient to obtain multiple synthetic 4DCTs per patient. These synthetic 4DCTs were used to perform single field uniform dose 4D dose calculations with 1.8 Gy (RBE) per fraction and two oblique proton beams. The interplay effect was quantified by means of the homogeneity index  $d5/d95$  and CTV coverage  $v95$  for gradually increasing numbers of treatment fractions. This was realized by randomly accumulating single fraction dose distributions with both variable initial breathing phases and underlying synthetic 4DCTs. Moreover, correlations between the interplay effect and pancreatic motion amplitudes were analyzed.

### Results

Variable initial breathing phases and day-to-day organ motion variations lead to an incremental mitigation of the interplay effect. For single fractions, pronounced underdosage down to  $v95=70\%$  with heterogeneous dose distributions were observed. On average, after 7 fractions, sufficient CTV coverage of 95%-107% was obtained for the patients. However, for patients with large underlying motion amplitudes, more fractions were needed to mitigate the interplay effect sufficiently. Despite of the pronounced interplay impact on the CTV, no significant differences were found for the organs at risk, comparing static and 4D dose distributions. Significant correlations were found between the CTV motion amplitudes and the resulting interplay effect.

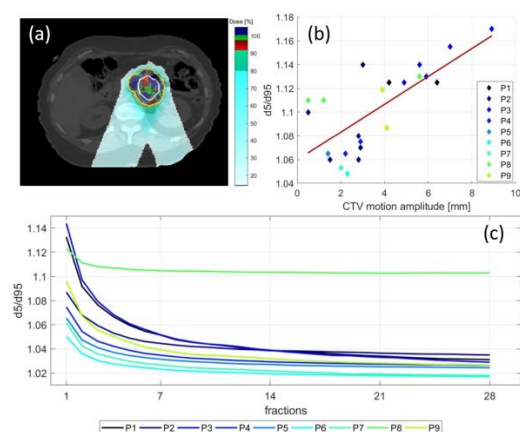


Figure 1: (a) 4D dose distribution of a single fraction. (b) The interplay effect, quantified by  $d5/d95$  is correlated with the CTV motion amplitudes. (c) By means of fractionation, the interplay effect is mitigated patient-specifically.

### Conclusion

4D dose evaluations, based on repeated 4D-MRI images, are a promising tool to investigate interplay effects and their dependency on the number of fractions. Without exposing the patients to additionally ionizing radiation, repeated 4D-MRI are useful to include motion variability into 4D dose analyses. Generally, for hypofractionated treatments, the interplay effect showed to be more pronounced than for standard fractionation schemes for pancreatic cancer treatments.

### Proffered Papers: RTT 5: Improving accuracy in patient positioning

**OC-0527 Evaluation of AlignRT for deep inspiration breath hold positioning and intrafraction monitoring**  
 V. Hamming<sup>1</sup>, C. Visser<sup>1</sup>, D. Busz<sup>1</sup>, E. Batin<sup>1</sup>, J.A. Langendijk<sup>1</sup>, S. Both<sup>1</sup>, N.M. Sijtsema<sup>1</sup>  
<sup>1</sup>UMCG University Medical Center Groningen, Radiation Oncology, Groningen, The Netherlands

### Purpose or Objective

To determine the accuracy of a surface imaging system (AlignRT) for positioning of breast cancer patients in breath hold (BH) by comparison with conebeam computed tomography (CBCT) data. Second, to evaluate with AlignRT the intrafraction variability and stability of the breast surface position during BHs guided with the active breathing coordinator (ABC) system.

### Material and Methods

eighteen consecutive left-sided breast cancer patients treated with deep inspiration breath hold radiotherapy (DIBH-RT) were included. During CBCT acquisition and treatment, AlignRT monitored the breast surface. CBCT registrations were performed both on the target volume and on the patient's surface. The setup error differences between the CBCT and AlignRT were analyzed in terms of the group mean ( $M$ ), the systematic error ( $\Sigma$ ), the random error ( $\sigma$ ) and the 95% limits of agreement (LOA). A linear regression analysis was performed to determine the correlation. Furthermore, the intrafraction variability and stability of the ABC guided BHs were evaluated with AlignRT. The variability was determined as the average over the maximum differences between different BH levels within a treatment fraction for a patient. The stability was determined as the difference between the start and end position of a BH.

### Results

In total 143 treatment fractions were included with an average of  $7.9 \pm 3.6$  CBCTs per patient. Figure 1 shows the Bland-Altman plots for the setup errors of AlignRT and the CBCT registrations. The LOA values are on average tighter when the CBCT is registered to the patient's surface. The LOA values (mean  $\pm$  2SD) were  $0.1 \pm 3.0$ ,  $0.6 \pm 4.1$  and  $0.4 \pm 3.4$  mm in left-right, craniocaudal and anterior-posterior directions respectively for the CBCTs registered to the patient's surface. Systematic and random errors of the setup error differences were  $\leq 2$  mm in all directions. AlignRT data showed higher correlations with CBCT data for the patient's surface than for the target volume (0.61 vs 0.44 respectively). This was as expected as AlignRT monitors the same surface as was registered during the CBCT surface registration. For the variability and stability a total of 1705 BHs were analyzed. The results are presented in Table 1. The average intrafraction variability between BHs was 2.2, 2.8 and 2.3 mm whereas the average stability was -1.0, 2.1 and 1.5 mm in left-right, craniocaudal and anterior-posterior directions respectively. The largest error in intrafraction variability was 12.4 mm (craniocaudal direction) and in stability it was 11.7 mm (anterior-posterior direction).

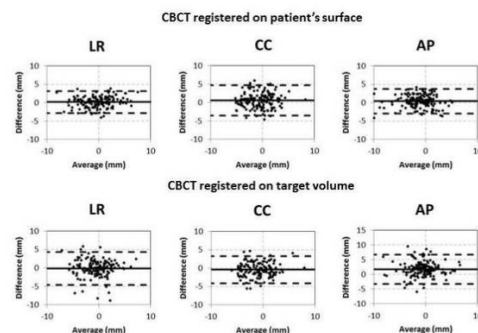


Figure 1: Bland-Altman plots for the setup errors of AlignRT and the CBCT registrations. The top and bottom dashed lines represent the 95% limits of agreement. The central solid line represents the mean of the differences between the AlignRT and CBCT setup errors. LR: left-right, CC: craniocaudal, AP: anterior-posterior.

Table 1. Intrafraction BH variability and stability evaluation

	LR (mm)	CC (mm)	AP (mm)
<u>Average (<math>\pm</math> 1SD)</u>			
BH deviation with planning CT	0.2 ( $\pm$ 3.1)	-1.0 ( $\pm$ 2.6)	-1.2 ( $\pm$ 2.9)
Variability	2.2 ( $\pm$ 1.4)	2.8 ( $\pm$ 1.5)	2.3 ( $\pm$ 1.3)
Stability	-1.0 ( $\pm$ 1.3)	2.1 ( $\pm$ 2.5)	1.5 ( $\pm$ 2.8)
<u>Maximum</u>			
Variability	7.5	12.4	6.4
Stability	-5.8	9.6	11.7

### Conclusion

With AlignRT, left-sided breast cancer patients can be positioned accurately (on average  $0.4 \pm 1.3$  (1SD) mm) based on comparison with CBCT data. Low intrafraction variability and good stability were observed for the active breathing coordinator guided breath holds.

### OC-0528 A clinical evaluation of the stability, patient comfort and ease in use of the new Nanor mask

L. Mesch<sup>1</sup>, M. Essers<sup>2</sup>, T. Rozema<sup>1</sup>

<sup>1</sup>Dr. Bernard Verbeeten Instituut, Department of Radiation Oncology, Tilburg, The Netherlands; <sup>2</sup>Dr. Bernard Verbeeten Instituut, Department of Medical Physics and Engineering, Tilburg, The Netherlands

### Purpose or Objective

The Nanor mask (Orfit Industries) is a mask with a “thin thermoplastic material that makes use of nanotechnology to improve the mechanical properties of the thermoplastic material”. The goals of this study were to compare the stability and patient comfort of the Nanor Mask with two Efficast mask materials, as well as the ease in use for the RTT.

### Material and Methods

From January 2017 until December 2017, 48 patients referred for radiotherapy of the brain for at least 10 fractions were randomized to 3 categories:

1. Orfit Efficast mask 2 mm maxi perforation (16, 1 stopped)
2. Orfit Efficast mask 1,6 mm micro perforation (16, 2 stopped)
3. Orfit Nanor mask 1,6 mm micro perforation (16, 2 stopped)

Each patient was immobilized with a mask in combination with Raycast® Head supports regular density with lateral neck flaps (Orfit Industries).

### Stability

Two orthogonal kV images were acquired for daily image-guided patient setup (Varian Medical Systems). After the online correction, CBCT1 was acquired. After delivery of the treatment fields, CBCT2 was acquired to determine the intra fraction error. Proper PTV margins were determined taking these intrafraction errors into account<sup>1</sup>.

### Patient comfort

After the treatment, the RTT marked the straining zones on a picture of the head and asked the patient where they felt any discomfort or pressure, which was also marked on another picture of the head. Figure 1 shows the colour scale (0-100%): 0% means there was no straining on any day and 100% means patient felt straining zones on each treatment day.

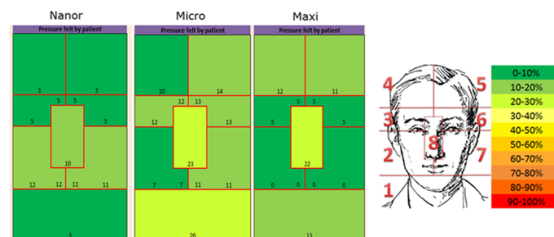


Figure 1: patient comfort

### Questionnaire

A questionnaire about ease in moulding, positioning and removing the mask was answered by:

- 4 Mouldroom RTTs
- 5 CT RTTs
- 38 Treatment room RTTs

1. van Herk M, Remeijer P, Rasch C, et al: The probability of correct target dosage: Dose-population histograms for deriving treatment margins in radiotherapy. Int J Radiat Oncol Biol Phys 47:1121-1135, 2000

### Results

#### Stability

The stability of the Nanor mask is slightly better than the Efficast Maxi and Micro mask. A reduction in intrafraction margin of 5mm is possible (Table 1).

Table 1: Intrafraction motion margin

	Margin			
	Vrt (mm)	Lng (mm)	Lat (mm)	Proper PTV Margin (mm)
Nanor mask	1,5	1,5	1,7	1,5
Efficast mask Micro	2,2	1,7	1,8	2,0
Efficast mask Maxi	1,8	2,2	1,7	2,0

### Patient comfort

Patient comfort of all masks is good. The pressure felt by the patient is comparable for the Efficast Maxi and Nanor masks and slightly less for Efficast Micro mask. Similar results were found for compression seen by the RTT. Patient comfort is slightly better for the Nanor mask for fractions where patients use dexamethasone (figure 1).

### Questionnaire

User friendliness is comparable for all masks. There is a slight preference for Nanor mask, especially for positioning the patient in the mask at the CT and the treatment unit.

### Conclusion

The stability and patient comfort for the Nanor, Efficast micro and Efficast maxi mask are good. Although the Nanor mask feels more comfortable and softer than the Efficast micro mask, in fact the stability is slightly improved.

### OC-0529 Evaluation of the potential treatment delivery benefits of Varian HyperArc for brain metastases

A. Williamson<sup>1</sup>, A. James<sup>1</sup>, A. Chalmers<sup>2</sup>, R. Carruthers<sup>2</sup>, S. Nowicki<sup>1</sup>, P. McLoone<sup>3</sup>

<sup>1</sup>Beatson West of Scotland Cancer Centre, Radiotherapy, Glasgow, United Kingdom; <sup>2</sup>Institute of Cancer Sciences-University of Glasgow, Radiotherapy, Glasgow, United Kingdom; <sup>3</sup>University of Glasgow, Statistics, Glasgow, United Kingdom

### Purpose or Objective

Varian HyperArc is a stereotactic radiosurgery solution, designed to automate and simplify sophisticated treatments which became clinically available in October 2017. HyperArc uses the Encompass immobilisation device and 6DOF couch, with a single button delivery and automated couch movement eliminating the need to re-

enter the room during treatment. Before the implementation of HyperArc, patients were immobilised with BrainLab mask system and planned using 10X FFF VMAT.

#### Objective

- Compare the positioning accuracy of Encompass and the BrainLab frameless mask system
- Determine the potential treatment delivery advantages of HyperArc
- Investigate the intrafraction motion for the Encompass device

#### Material and Methods

50 patients with brain metastases were treated with SRS. Lesions were <3cm and treated with a dose between 18-24Gy.

25 patients, set up with Brainlab, were planned using mono-isocentre 10XFFF VMAT with co-planar arcs. These were compared to 25 subsequent patients, set up with Encompass, and planned with Hyperarc using a mono-isocenter technique with multiple non-coplanar arcs. CBCT imaging was acquired immediately before treatment and registered to the reference CT using a 6DOF automatching procedure. All corrections were applied before delivery. Beam on time (BOT) (min:sec) is defined as the aggregate time for delivery of total MU for all arcs in a given plan. Time In Room (TIR) (min:sec) is measured from the first alignment image to last beam off, inclusive of all pre-treatment imaging and/or shifts to correct patient position. Post treatment CBCT scans were acquired for Encompass to assess intrafraction motion. Two sample t-tests (two-tailed with a significance level of < 0.05) were used to test for differences between the techniques.

#### Results

Brainlab patients were treated with 2 coplanar arcs. Encompass patients were treated with 4 arcs delivered at floor rotation angles of 0, 45, 315 and 270. Mean setup shifts for Encompass and Brainlab were 1mm or less (Table 1). There was no statistically significant difference in mean set-up shifts comparing Encompass with BrainLab patients, although the mean values for Brainlab patients were slightly smaller and sub 1 mm.

Mean BOT for HyperArc was on average 0.6 minutes less than 10XFFF VMAT ( $p=0.0005$ ) - a 20% reduction (Table 2). Mean TIR for HyperArc was on average 7.1 minutes shorter ( $p<0.0001$ ) - a 41% reduction.

Intrafraction motion for Encompass is shown in Table 3.

	Vrt mm Mean (SD)	Lng mm Mean (SD)	Lat mm Mean (SD)	Pitch° Mean (SD)	Roll° Mean (SD)	Rot° Mean (SD)
Encompass	1.18 (0.76)	1.04 (0.74)	0.87 (0.60)	0.43 (0.50)	0.55 (0.48)	0.74 (0.62)
BrainLab	0.78 (0.68)	0.79 (0.72)	0.78 (0.62)	0.61 (0.52)	0.34 (0.31)	0.44 (0.34)
P value	0.06	0.23	0.58	0.22	0.08	0.06

	Mean BOT (SD) (mins)	Mean TIR (SD) (mins)
HyperArc	2.5 (0.3)	10.1 (1.1)
10X FFF VMAT	3.1 (0.6)	17.2 (5.0)

	Vrt mm	Lng mm	Lat mm	Pitch°	Roll°	Rot°
Mean	0.18	0.23	0.12	0.13	0.11	0.15
SD	0.12	0.26	0.12	0.10	0.05	0.17

#### Conclusion

To our knowledge this is the first study to evaluate the benefits of Varian Hyperarc for treatment delivery. The setup accuracy of Encompass is comparable to BrainLab, and treatment position with Encompass is maintained during the delivery of non-coplanar beams. HyperArc delivers linac based SRS efficiently, with a faster treatment time than 10XFFF VMAT and a statistically significant improvement in TIR. This significant reduction in delivery time (TIR) could result in a clinically

meaningful reduction in risk of intrafraction motion than previous technique.

#### OC-0530 Improving OAR volumes during prostate RT using daily patient feedback and standardized protocols

I. Gagne<sup>1</sup>, K. Earnshaw<sup>2</sup>, S. Cowan<sup>2</sup>, J. Goulart<sup>3</sup>, A. Alexander<sup>3</sup>

<sup>1</sup>BC Cancer - Victoria, Medical Physics, Victoria, Canada ;

<sup>2</sup>BC Cancer - Victoria, Radiation Therapy, Victoria, Canada; <sup>3</sup>BC Cancer - Victoria, Radiation Oncology,

Victoria, Canada

#### Purpose or Objective

Prostate radiotherapy accuracy is impacted by inter- and intra-fraction volume variations associated with proximal organs at risk (OARs) such as bladder and rectum. Patients are therefore often advised to have a comfortably full bladder and empty rectum at the time of CTsim and treatment. The optimal hydration and bowel preparation is a topic of many studies and there exists to date no consensus. The goal of this study was to evaluate the impact of a standardized hydration and bowel preparation protocol (SHBPP) in conjunction with daily patient engagement on bladder and rectum volumes.

#### Material and Methods

In 2018, 32 patients with prostate cancer were sent a SHBPP advising them to administer a micro-enema 2-3 hours before CTsim and the first 10 treatments and to empty their bladder 1hour before CTsim and treatment and consume within 15 minutes, 750 ml of water. At the time of CTsim and treatment, radiation therapists (RTs) recorded the details of the preparation in the patient's technical notes. Daily CBCT was performed and the consistency of bladder and rectal volumes in comparison to CTsim was assessed and recorded using a locally developed bladder and rectum scoring system. Scores and CTsim volumes obtained for this cohort were compared to 20 patients treated in 2013 who had CBCT on days 1,2,3 and weekly, and no SHBPP and daily feedback. In this non-SHBPP cohort, therapists were instructed to ensure bladder filling at time of CTsim placed the bladder dome at least 2 cm above the femoral head.

#### Results

To date, 19 patients on SHBPP have completed treatment, leading to 19 CTsim volumes and 533 CBCT scores for analysis. Using the Mann-Whitney test, the median bladder (279cc vs 387cc) and rectal (57cc vs 79cc) volumes were found to be statistically different at the  $P=0.05$  level, with CTsim bladder and rectal volumes being on average, 15% and 30% smaller, respectively with SHBPP. While rectal volumes were found to have less variability (SD: 20cc vs 37cc), bladder volumes had slightly larger variability (SD: 200cc vs 180cc). The smaller variability in the non-SHBPP cohort could be due to the bladder filling requirement at CTsim. On treatment, the fraction of treatments with rectal volumes within "rectum+5mm" where the same (75%) while the fraction of treatments with anterior rectal distensions >10mm decreased by 3% (8% vs 11%) for the SHBPP group. The fraction of treatments with bladder volumes <2/3 decreased by 28% (13% vs 41%). On average, the difference in bladder filling scored by measuring the dome location difference between CBCT and CTsim was  $-0.3\text{cm}\pm 0.9\text{cm}$  for the SHBPP group vs  $-2.0\pm 2.5\text{cm}$  for the non-SHBPP group.

#### Conclusion

The implementation of SHBPP resulted in significantly smaller and less variable rectal volumes and slightly smaller bladder volumes at CTsim. The use of daily feedback significantly reduced the variability of bladder volumes at treatment and also reduced the fraction of treatments with rectal distensions >10mm by 3%.

### OC-0531 Can SGRT be used with open masks to set-up HNC patients and reduce intrafractional motion?

A. Moreira<sup>1</sup>, N. Weitkamp<sup>1</sup>, M. Zamburlini<sup>1</sup>, H.I. Garcia Schüler<sup>1</sup>, M. Guckenberger<sup>1</sup>

<sup>1</sup>University hospital Zurich, Radiation Oncology, Zurich, Switzerland

#### Purpose or Objective

To evaluate the set up and treatment of head and neck cancer patients in an open mask with the aid of surface guided radiotherapy (SGRT). We investigated the initial setup accuracy of an open mask (OM) with SGRT vs. traditional closed mask (CM) system. Additionally, data from the SGRT system was used to evaluate intrafractional motion.

#### Material and Methods

14 Patients being treated for T1 or T2 larynx carcinomas were evaluated in this study. Patient setup at planning CT was performed using a CIVCO Posifix® thermoplastic mask. For 7 patients the mask was cut out around the face (from 2-5cm above the eyebrow, until 1cm above the lips and on the sides until their ears) as well as over the neck (Fig 1.). Patients' reference surface was imported from the CT scan and regions of interest for both the face and the neck were selected. The patients were positioned until all pre-shift deltas displayed on the SGRT system were as close to zero as possible. After positioning, CBCT imaging was performed to verify the patient's position. The residual set up error as defined by shifts seen on the CBCT image were compared to a control group of 7 patients who were treated using the standard closed mask to evaluate any loss in stability as well as set up accuracy. For the 7 patients treated with an open mask, the intra-fractional motion caused by swallowing was also evaluated using SGRT to monitor the neck area. Gating margins on the SGRT system were set at  $\pm 2\text{mm}/2^\circ$  in each direction and log files were retrospectively analyzed to determine how often the patients swallowed during treatment and how large this motion was.

#### Results

In total, 153 CBCTs were analyzed: 80 from the OM group and 73 from the CM group. Mean post-match shifts based on CBCT PTV match was  $-0.1 \pm 0.2\text{cm}$ ,  $0.2 \pm 0.4\text{cm}$ ,  $-0.04 \pm 0.13\text{cm}$ ,  $0.4 \pm 1.8^\circ$ ,  $0.7 \pm 2.7^\circ$ ,  $0.6 \pm 2.5^\circ$  in the OM plus SGRT group and  $0.0 \pm 0.3\text{cm}$ ,  $-0.1 \pm 0.5\text{cm}$ ,  $-0.1 \pm 0.4\text{cm}$ ,  $0.2 \pm 1.4^\circ$ ,  $0.6 \pm 1.4^\circ$ ,  $0.7 \pm 1.2^\circ$  in the CM group, in the VRT, LNG, LAT, Rotation, Roll and Pitch directions respectively. In 27% out of the 211 fractions monitored using SGRT, the radiotherapy delivery was interrupted at least once during treatment due to motion caused by swallowing. During this time, the mean absolute shifts were  $1.5 \pm 2.6\text{ mm}$ ,  $3 \pm 7\text{ mm}$ ,  $1.7 \pm 1.9\text{ mm}$  in VRT, LONG, LAT directions. This proves that treatment disruption is due to longitudinal motion. Mean absolute motion observed during beam delivery were  $0.27 \pm 0.23\text{ mm}$ ,  $0.3 \pm 0.3\text{ mm}$ ,  $0.3 \pm 0.4\text{ mm}$  in the VRT, LNG, LAT directions.

#### Conclusion

Our study shows that SGRT allows for HNC treatment in an open mask with clinically acceptable setup accuracy of less than 2mm in each direction. An open mask creates a better treatment experience for patients with claustrophobia and any potential benefit of increased patient comfort will be investigated in future studies. Additionally, OM allows monitoring and if necessary gating of radiotherapy delivery for swallowing motion, which could influence future PTV definition.

### OC-0532 Virtual reality animations, a new strategy to reduce patients' anxiety induced by radiotherapy

G. Van Ooteghem<sup>1,2</sup>, X. Geets<sup>1,2</sup>

<sup>1</sup>Institut de Recherche Expérimentale et Clinique, Molecular Imaging- Radiotherapy and Oncology - MIRO, Brussels, Belgium; <sup>2</sup>Cliniques Universitaires Saint Luc, Radiation Oncology, Brussels, Belgium

#### Purpose or Objective

Patients facing medical and technological interventions such as radiotherapy, mechanically-assisted and non-invasive ventilation (MANIV), or MRI can experience a high level of anxiety and discomfort in addition of the stressful background linked to cancer. This can lead to negative impacts on their mental status but also have deleterious consequences during radiation treatments (difficulties in positioning, movements during irradiation, impaired breathing) and thus also impact the treatment efficacy. Virtual reality and hypnosis are stress management strategies that showed encouraging results in different medical fields. The efficacy on anxiety of a dedicated hypnotising Virtual Reality Animation (VRA) commercialised by Oncomfort® was evaluated in patients included in a trial assessing MANIV. This trial aimed to demonstrate the safety and the efficacy of MANIV to stabilize and modulate the breathing pattern without any sedation. Patients were therefore connected to a mechanical ventilator and asked to give up control on their breathing. They could thus experience anxiety.

#### Material and Methods

VRA lasted for 10 to 20 minutes and was proposed before each MANIV session (one coaching session, one simulation session and 2 MRI sessions) (Figure 1).

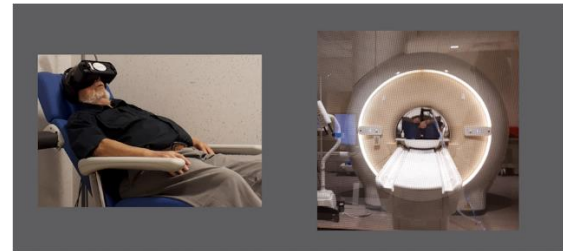


Figure 1: The Oncomfort® device was used for a hypnotising Virtual Reality Animation (VRA) with the aim to decrease the patient anxiety level before that he underwent a MRI acquisition session with Mechanically-assisted and non-invasive ventilation (MANIV).

VRA assessment was done with questionnaires fulfilled at each session. Patients answered first to multiple choice questions (MCQ), then to the same questions but with a Visual Analogic Scale (VAS) ranging from 0 to 100. On VAS, an effect on anxiety was considered when a difference greater than 10 was observed between two scores.

#### Results

Twenty-one patients (49-83 years old) participated to the trial. Comfort level obtained during the coaching and simulation sessions and rated before the VRA, after the VRA and during MANIV were 54, 67 and 66 respectively. During the 2 MRI sessions, the comfort level before the VRA, after the VRA were similar (57.5 and 66.5 respectively) but was clearly decreased during the MRI acquisitions (50), raising a probable MRI-driven loss of comfort.

Based on the MCQ, 17 patients (81%) appreciated the VRA experience. Nine patients (43%) felt an improvement of their comfort while 9 patients (43%) did not and 3 (14%) experienced a comfort degradation. VAS scores led to identical conclusions, with only one patient having discrepancies in his answers. Patients with the lowest VAS scores in comfort before the trial were those with the greatest improvement after the VRA. Eight patients (38%) stopped the trial at their request for convenience reasons or due to the degradation of comfort.

#### Conclusion

The hypnotising Virtual Reality Animation proposed by Oncomfort® can be a good support, especially in very anxious patients. However, some patients may not benefit of this strategy, highlighting the need to adapt to each patient and to further enlarge our stress management strategies.

---

 Poster Viewing : Poster viewing 10: Radiobiology
 

---

**PV-0533 HPV16 viral load may explain gender differences in treatment outcome of anal squamous cell carcinoma**

D. Martin<sup>1</sup>, P. Balermphas<sup>1</sup>, R. Winkelmann<sup>2</sup>, U. Wieland<sup>3</sup>, M. Rave-Fränk<sup>4</sup>, J. Kitz<sup>5</sup>, C. Rödel<sup>1</sup>, E. Fokas<sup>1</sup>, F. Rödel<sup>1</sup>  
<sup>1</sup>Klinikum der Johann Wolfgang Goethe Univ, Department of Radiotherapy and Oncology, Frankfurt, Germany ;  
<sup>2</sup>Klinikum der Johann Wolfgang Goethe Univ, Senckenberg Institute for Pathology, Frankfurt, Germany ;  
<sup>3</sup>University of Cologne, Institute of Virology- National Reference Centre for Papilloma- and Polyomaviruses, Cologne, Germany ;  
<sup>4</sup>University Medical Center Göttingen, Department of Radiotherapy and Radiation Oncology, Göttingen, Germany ;  
<sup>5</sup>University Medical Center Göttingen, Department of Pathology, Göttingen, Germany

**Purpose or Objective**

Female gender is a well-established favorable prognostic factor after definitive chemoradiotherapy (CRT) for patients with anal squamous cell carcinoma (ASCC), however, no clear explanation for this gender difference has been elucidated so far. ASCC is associated with high-risk strains of human papilloma virus (HPV) infection and HPV-positive patients have improved treatment outcomes. We hypothesized that the differences in outcome according to gender are due to differences in HPV infection parameters.

**Material and Methods**

We examined pretreatment tumor samples of 141 patients (64 male/77 female) with ASCC treated with standard chemoradiotherapy. Expression of p16<sup>INK4a</sup> was measured semiquantitatively by a immunohistochemical score. The HPV16 viral load was assessed via a quantitative PCR approach. Clinical outcomes of these patients were correlated with clinicopathological factors and p16 expression/HPV16 viral load.

**Results**

After a median follow-up of 46 months, the 5-year locoregional control rate (LRC) and disease-free survival (DFS) was 80.4% and 75.3%, respectively. There were no significant differences in age, cT/N-categories, pretreatment white blood cell and platelet count according to gender, but female patients had significantly lower hemoglobin levels at baseline. A high HPV16 viral load (using maximally selected rank statistics) was associated with a favorable LCR ( $p < 0.01$ ), DFS ( $p < 0.01$ ), and overall survival ( $p < 0.01$ ). A high expression of p16<sup>INK4a</sup> (score >6) was associated with a favorable LRC ( $p < 0.01$ ) and DFS ( $p < 0.05$ ). Female patients showed a significantly higher HPV16 viral load ( $p = 0.012$ ) at baseline. In a multivariate cox regression model, including gender and HPV16 viral load, only the viral load was significantly associated with LRC (HR 0.3,  $p < 0.01$ ) and DFS (HR 0.39,  $p < 0.05$ ).

**Conclusion**

A high HPV16 viral load in pretreatment tissue was associated with better treatment outcome and significantly higher in female patients. Multivariate analyses revealed that HPV16 viral load remained as a significant predictor of treatment outcome when combined with gender. These data suggest a possible biological background for gender differences after CRT in ASCC.

**PV-0534 Carbon ions and microRNAs: new insights into hadrontherapy biology in prostate cancer**

I. Salido<sup>1</sup>, R. El Bezawy<sup>1</sup>, M. Ciocca<sup>2</sup>, F. Valvo<sup>2</sup>, A. Facchetti<sup>2</sup>, P. Gandellini<sup>1</sup>, R. Valdagni<sup>3</sup>, N. Zaffaroni<sup>1</sup>  
<sup>1</sup>Fondazione IRCCS Istituto Nazionale dei Tumori di Milano, Applied Research and Technological

Development, Milan, Italy; <sup>2</sup>Fondazione CNAO- Centro Nazionale di Adroterapia Oncologica, Clinical Department, Pavia, Italy; <sup>3</sup>Fondazione IRCCS Istituto Nazionale dei Tumori di Milano, Department of Radiation Oncology 1, Milan, Italy

**Purpose or Objective**

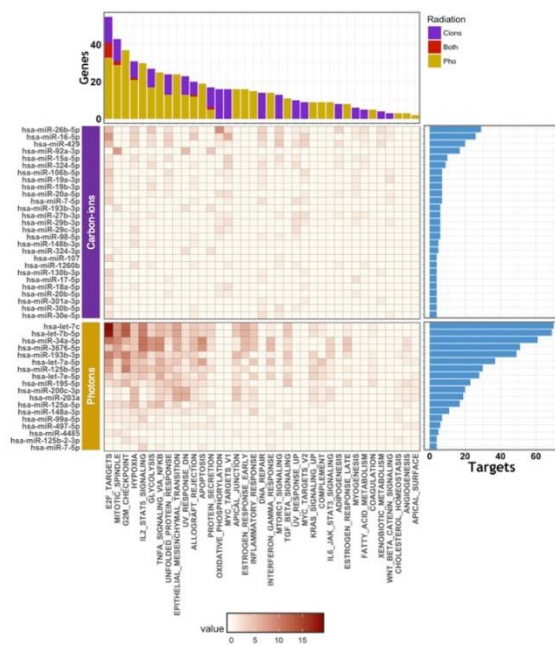
Considering the relative radioresistance of prostate cancer (PCa) to conventional photon therapy, a novel form of external radiation therapy, hadrontherapy, has been recently proposed. Hadrontherapy uses high-linear energy transfer (LET) particle beams, such as carbon ions, and exhibits favorable results for several malignancies that poorly respond to conventional radiotherapy, including PCa. However, from a radiobiological perspective, the molecular basis underlying carbon ions is not yet fully understood. In this regard, among the various molecular determinants of response to radiotherapy are microRNAs (miRNAs).

**Material and Methods**

We explored changes in the miRNome and gene expression profile of PCa cell lines (LNCaP and DU145) upon carbon ion beam and photon irradiation -a study never pursued in the available literature- to search for commonalities and differences between the two irradiation sources. Considering the higher relative biological effectiveness (RBE) of carbon ions, PCa cells were exposed to different doses of photons (10 Gy) and high-LET carbon ion beams (5 Gy) delivered by a <sup>137</sup>Cs irradiator and a synchrotron (at CNAO, Pavia), respectively. miRNA and gene differential expression following irradiation was assessed by microarray analyses at different time points and then validated by qRT-PCR.

**Results**

We found that, among the 102 miRNAs modulated by photons and the 186 miRNAs affected by carbon ions, only 6 (2%) were shared by the two irradiation sources in both LNCaP and DU145 cell lines. Accordingly, the analysis of miRNA targets, selected from the intersection of targets predicted by in silico tools and genes found anticorrelated among those modulated upon irradiation, revealed that there was only a partial overlap (4%) between photons and carbon ions. These findings suggest that, unexpectedly, the two irradiation sources act by affecting different miRNAs and genes, still producing the same biological effect. Paradoxically, GSEA analyses revealed that genes significantly modulated by photons and/or carbon ions were prevalently enriched for common biological processes, including mitotic spindle and UV response, known to be strictly related to radiation response. This provides the first evidence that photons and carbon ion beams modulate different factors still converging on common cell processes, thus determining a comparable final biological effect.



### Conclusion

Overall, our findings show that photons and carbon ions may modulate the expression of different miRNAs still affecting the same biological processes. While photon radiobiology has been extensively characterized, a deeper understanding of the biological dynamic underlying the modus operandi of carbon ions might contribute to the design of more precise and honed hadrontherapy treatment schedules on the basis of patient miRNA expression patterns. In addition, miRNAs may be envisaged as a novel class of predictive biomarkers also for this promising frontier in radiotherapy.

### PV-0535 Pilot study on immunomodulation role of radiotherapy in oropharyngeal cancer: preliminary results

L. Belgioia<sup>1</sup>, A. Bacigalupo<sup>2</sup>, F. Missale<sup>3</sup>, S. Negrini<sup>4</sup>, G. Filaci<sup>4</sup>, D. Fenoglio<sup>4</sup>, F. Incandela<sup>3</sup>, S. Vecchio<sup>5</sup>, G. Peretti<sup>3</sup>, R. Corvò<sup>1</sup>

<sup>1</sup>University of Genoa and IRCCS Ospedale Policlinico San Martino, Department of Health Science DISSAL and Radiation Oncology, Genoa, Italy; <sup>2</sup>IRCCS Ospedale Policlinico San Martino, Department of Radiation Oncology, Genoa, Italy; <sup>3</sup>University of Genoa, Department of Otorinolaringology- Head and Neck Surgery, Genoa, Italy; <sup>4</sup>University of Genoa and IRCCS Ospedale Policlinico San Martino, U.O. Immunologia Clinica and Centro di Eccellenza per le Ricerche Biomediche CEBR, Genoa, Italy; <sup>5</sup>IRCCS Ospedale Policlinico San Martino, Department of Medical Oncology, Genoa, Italy

### Purpose or Objective

The discovery of the key role of the immune system in the pathogenesis of tumors prompted studies aimed at identifying immunological prognostic biomarkers. The encouraging results of immunotherapy in recurrent non-resectable head and neck cancer may indicate its potential efficacy, combined to conventional therapies, also as primary treatment. The aim of our prospective study is to perform a comprehensive analysis of the circulating and intratumoral T cell compartments in patients affected by Oropharyngeal Squamous Cell Carcinoma (OSCC) to search for new prognosticators and

to get insights on new possible immunotherapeutic strategies.

### Material and Methods

From May to November 2017 20 untreated patients affected by moderately to advanced stage OSCC and treated by radiotherapy or chemo/bio-radiotherapy have been enrolled in the study. Peripheral blood and tumor biopsies were collected and evaluated by multiparametric flow cytometry panels to delineate: CD4+ and CD8+ T cell maturation stages, frequency of CD4+ and CD8+ T regulatory cells (Treg), expression of exhaustion/immune checkpoints (CD39, PD-1, CTLA-4, TIM3).

### Results

The results showed: a) CD4+ and CD8+ effector memory cells were the most represented population among tumor infiltrating lymphocytes (TIL) but not among peripheral blood lymphocytes; b) CD4+ and CD8+ TIL showed decreased expression of co-activatory receptors, as CD28 molecule, and increased expression of inhibitory receptors, as PD-1, TIM-3, CTLA-4, than circulating CD4+ and CD8+ T cells; c) intratumoral CD4+ and CD8+Treg frequencies resulted statistically increased in cancer specimens with respect to blood; d) Treg exhibited an active functional phenotype, as demonstrated by their elevated FoxP3, CTLA-4 and CD39 expression and high expression of immune checkpoints (PD1, CTLA-4 and TIM3).

### Conclusion

Collectively, the results highlight expansion in the tumor of T cells in advanced stage of maturation, characterized by high expression of immune checkpoints and enrichment of Treg, suggesting a pressure by tumor toward regulatory function induction. Interestingly, immune checkpoint expression only partially overlapped in the different intratumoral T cell subsets indicating that immunotherapy by immune checkpoint inhibitors might develop new combinatorial protocols associating at least 3 different agents targeting CTLA-4, PD1-PDL1 and TIM3-Galectin-9 axes in order to be effective in HNSCC patients.

### PV-0536 On the impact of HPV status and radiation dose on survival in a large cohort of anal cancer patients

R. Kabarriti<sup>1</sup>, P. Brodin<sup>2</sup>, R. Narang<sup>3</sup>, R. Huang<sup>3</sup>, J. Chuy<sup>3</sup>, L. Rajdev<sup>3</sup>, S. Kalnicki<sup>2</sup>, C. Guha<sup>2</sup>, M. Garg<sup>2</sup>  
<sup>1</sup>Montefiore Medical Center- Albert Einstein College, Radiation Oncology, New York, USA ; <sup>2</sup>Montefiore Medical Center, Radiation Oncology, Bronx, USA; <sup>3</sup>Montefiore Medical Center, Oncology, Bronx, USA

### Purpose or Objective

To determine whether patients with anal cancer with human papilloma virus (HPV) infections have different overall survival compared to those without HPV infections, and to elucidate the radiation dose-response relationship in a large retrospective cohort of anal cancer patients.

### Material and Methods

We utilized the National Cancer Database (NCDB) registry to identify a cohort of non-metastatic anal cancer patients treated with curative intent between 2008 - 2015 with available treatment data and follow-up for vital status. HPV status was dichotomized into positive vs. negative for those with available HPV markers from diagnostic work-up. For patients receiving definitive radiation therapy (RT), the total dose delivered to the tumor was used for analysis. Multivariable Cox proportional hazards regression models were used to determine the association between HPV status and overall survival (OS), as well as varying levels of total RT dose delivered. Kaplan-Meier survival analysis with log-rank test was used to illustrate and compare actuarial survival estimates between groups.

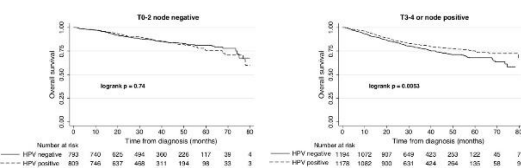
### Results

We identified 33,537 patients for this analysis, of which 5,961 patients had information on HPV infection. Of those, 3,550 (59.6%) were HPV positive and 2,411 (40.4%) were

HPV negative. In a propensity-matched analysis adjusted for age, sex, Charlson-Deyo score, systemic therapy use, treatment facility, income, ethnicity and race; HPV positive patients had significantly better OS, but only in patients with locally advanced disease (T3-4 or node positive; HR = 0.77 (95% CI: 0.64-0.93),  $p=0.005$ ), whereas for patients with early stage disease (T1-2 and node negative) there was no association with OS (HR = 1.08 (95% CI: 0.83-1.42),  $p=0.56$ ). Similar results were found in unmatched multivariable analysis (Locally advanced disease: HR: 0.79;  $p=0.005$  and early-stage disease HR: 1.12;  $p=0.34$ ). The table shows the results from the propensity-matched multivariable analysis and the figure the propensity-matched unadjusted Kaplan-Meier curves, illustrating HPV infection as a prognostic marker in locally advanced disease. The multivariable model for radiation dose showed a clear dose-response for all patients with decreasing HRs for increasing total RT dose up to 55 Gy (compared to total RT doses less than 40 Gy, 40-45 Gy- HR: 0.71;  $p<0.001$ ; >45-50 Gy- HR: 0.74;  $p<0.001$ ; >50-55 Gy- HR: 0.60,  $p<0.001$ ; >55-60 Gy- HR: 0.69;  $p<0.001$ ; >60-65 Gy- HR: 0.78;  $p=0.003$ ; >65 Gy- HR: 0.84;  $p=0.11$ ). A stronger dose-response was seen for locally advanced patients who were HPV negative (HR: 0.43 for >50-55 Gy), compared to those that were HPV positive (HR: 0.72 for >50-55 Gy).

Patients with T3-4 or node positive disease	Hazard ratio (95% CIs)	p-value
HPV status (Positive vs. Negative)	0.77 (0.64, 0.93)	0.005
Systemic therapy		
No systemic therapy	Ref	
Single agent chemotherapy	1.93 (1.41, 2.65)	<0.001
Multi agent chemotherapy	1.78 (1.42, 2.24)	<0.001
Age ( $\geq 65$ y vs. <65y)	1.85 (1.53, 2.25)	<0.001
Sex (Female vs. Male)	0.65 (0.55, 0.77)	<0.001
Charlson-Deyo score		
0	Ref	
1	1.40 (1.07, 1.83)	0.013
2	2.66 (1.74, 4.05)	<0.001
3	2.53 (1.68, 3.82)	<0.001
Facility type		
Community cancer program	Ref	
Comprehensive community cancer program	0.71 (0.52, 0.97)	0.032
Academic/Research Program	0.81 (0.59, 1.11)	0.19
Integrated Network Cancer Program	0.56 (0.37, 0.86)	0.008

\*also adjusted for income, ethnicity and race



## Conclusion

We found that HPV infection is a positive prognostic marker for patients with locally advanced anal cancer, but not for those with early stage disease. We further found that higher radiation dose up to 55 Gy was associated with better survival, especially for locally advanced disease in HPV negative patients, and less so in those with HPV positive disease.

## PV-0537 Optimized fractionated radiotherapy with anti-PD-L1 and anti-TIGIT: a promising combination

M. Grapin<sup>1</sup>, E. Limagne<sup>2</sup>, C. Richard<sup>2</sup>, R. Boidot<sup>2</sup>, M. Thibaudin<sup>2</sup>, V. Morgand<sup>1</sup>, G. Créhanche<sup>1</sup>, F. Ghiringhelli<sup>2</sup>, C. Mirjoret<sup>1</sup>

<sup>1</sup>Centre Georges-François Leclerc, Radiation Oncology, Dijon, France ; <sup>2</sup>Centre Georges-François Leclerc, Platform of Transfer in Biological Oncology, Dijon, France

## Purpose or Objective

Radiotherapy (RT) is able to induce an immunogenic antitumor response, but also to increase some

immunosuppressive barriers. It is still unclear how each fractionation protocol can modulate the immune microenvironment. Nevertheless, it is essential to determine the best RT fractionation protocol to associate with checkpoint inhibitors (CPI). Currently, in the setting of localized rectum cancer, RT can be delivered before surgery according to two validated schemes with a different dose per fraction. Clinical studies are ongoing to evaluate CPI (such as anti-PD-L1) in association with RT. However, only few trials aim to optimize the RT fractionation to improve efficacy of these associations. Here we wanted to characterize different fractionation protocols effect on immune response and associate them with CPI.

## Material and Methods

Mice bearing subcutaneous CT26 colon tumors were irradiated using SARRP device according to different radiation schemes (1, 3 or 18 fractions) with a same biologically effective dose. The mice were monitored for tumor growth. The radiation immune response (lymphoid, myeloid cells, lymphoid cytokines and immune checkpoints) was monitored by flow cytometry at different time points after treatment. The same fractionation protocols were performed with or without CPI against immune checkpoints modulated by RT.

## Results

In absence of CPI, we showed that 18x2Gy and 3x8Gy induced the longest tumor growth delay compared to 1x16.4Gy. While 3x8Gy and 1x16.4Gy induced a lymphoid response (CD8<sup>+</sup>T cells, Regulators T cells (Treg) and natural killer cells); 18x2Gy induced a myeloid response (MDSC, neutrophils, tumor-associated macrophages 2). The secretion of granzyme B by CD8<sup>+</sup>T cells and interferon  $\gamma$  by CD4<sup>+</sup>T cells was more importantly increased with 3x8Gy. The expression of PD-L1 by tumor cells was moderately increased by RT but the most durably with 18x2Gy. While TIGIT expression by CD4<sup>+</sup>, CD8<sup>+</sup>T and NK cells was increased or maintained by 3x8Gy compared to control group, it was decreased or maintained by 18x2Gy and 1x16.4Gy. There was a synergistic effect of any CPI with RT whatever the dose per fraction compared to RT and IgG. The 18x2Gy protocol did not seem to benefit from anti-TIGIT when associated with anti-PD-L1. RT was dramatically more effective with 3x8Gy compared to all the other treatments schemes when associated with anti-TIGIT and anti-PD-L1 with more than 90% of the tumor in complete response.

## Conclusion

Each fractionation scheme induced different lymphoid and myeloid responses as well as various modulation of PD-L1 and TIGIT expression. Furthermore, 3x8Gy was the most effective protocol when associated with anti-PD-L1 and anti-TIGIT. This is the first study combining RT and anti-TIGIT with promising results; further studies are warranted.

In order to describe mechanisms, which may explain differential effects of the different fractionation protocols on immune response, RNA sequence-analysis is still ongoing.

## PV-0538 Prostaglandin related distinct regenerative activities in hair follicles following radiation injury

S. Lai<sup>1,2</sup>, W. Huang<sup>3</sup>, S. Chen<sup>1</sup>, S. Lin<sup>1,4,5</sup>

<sup>1</sup>National Taiwan University, Institute of Biomedical Engineering- College of Medicine and College of Engineering, Taipei, Taiwan ; <sup>2</sup>National Taiwan University Hospital and College of Medicine, Division of Radiation oncology- Department of Oncology, Taipei, Taiwan ; <sup>3</sup>National Taiwan University, Institute of Biomedical Engineering- College of Medicine and College of Engineering-, Taipei, Taiwan ; <sup>4</sup>National Taiwan University, Research Center for Developmental Biology and Regenerative Medicine, Taipei, Taiwan ; <sup>5</sup>National Taiwan University Hospital and College of Medicine, Department of Dermatology, Taipei, Taiwan

### Purpose or Objective

The highly proliferative hair follicles are sensitive to radiation and hair loss (alopecia) often develops. We found, local prostaglandin E<sub>2</sub> (PGE<sub>2</sub>) pretreatment could reduce hair loss from radiation injury by preventing entry into catagen (regression phase) and telogen (resting phase) (Figure 1a). Whether and how anagen hair follicles attempt to repair themselves in response to ionizing radiation (IR) under PGE<sub>2</sub> local treatment has not been characterized. In this work, we try to investigate the proceeding regenerative process in hair follicle cells following radiation injury under prostaglandin treatment.

### Material and Methods

The dorsal hair of female C57BL/6 mice on postnatal day 32 when hair follicles were in the early full anagen (growth phase) was carefully shaved. Single dose of 8.5Gy was given from dorsal side 2 hours after dmPGE<sub>2</sub> (A stabilized derivative of prostaglandin E<sub>2</sub>, 16,16-dimethyl-PGE<sub>2</sub>) locally injected. Skin specimen was harvested at multiple time points after radiation exposure. H&E staining, Immunohistochemical analysis and double staining with hair follicle cell markers were used to monitor the dynamics of cell differentiation at different time points. The fluorescence ubiquitination cell cycle indicator (FUCCI) system, which can easily determine G1 and/or S/G2/M phases of the cell cycle through analyzes living cells in a spatio-temporal manner using a dual color scheme of orange and green, is used for evaluating cell cycle condition.

### Results

Severe dystrophic change of anagen hair follicles were observed after 8.5Gy radiation injury. We found anagen hair follicles were able to initiate spatially and temporally repair activities to restore their structure under PGE<sub>2</sub> pretreatment after radiation injury. The hair follicle bulge stem cells were not activated during the repair process. (Figure 1b) Continuous BrdU pulse labeling after PGE<sub>2</sub> local pretreatment revealed that the proliferation of hair follicle bulb matrix cells (hair follicle transit amplifying cells (TACs) ) was transiently halted (Figure 2a). Immunostaining of cell cycle marker of cyclin D showed decrease level after PGE<sub>2</sub> pretreatment. (Figure 2b). These suggested PGE<sub>2</sub> might reduce the radiosensitivity of TACs through cell cycle G1 phase arrest. We further took advantage of the fluorescence ubiquitination cell cycle indicator (FUCCI) system and confirmed the process.

Figure. 1

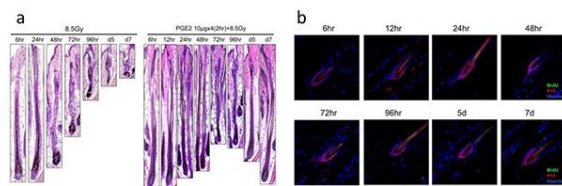
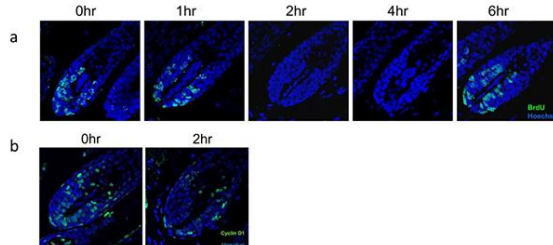


Figure. 2



### Conclusion

Under radiation injury, anagen hair follicles were able to initiate distinct repair activities to restore their structure after PGE<sub>2</sub> pretreatment through cell cycle modification.

Radiation-induced alopecia might be prevented by modulating cell cycle associated signaling to enhance spontaneous repair.

### PV-0539 Antidiabetic biguanides radiosensitize hypoxic cancer cells through a decrease in oxygen consumption

S. De Mey<sup>1</sup>, H. Jiang<sup>1</sup>, C. Corbet<sup>2</sup>, H. Wang<sup>1</sup>, I. Dufait<sup>1</sup>, K.L. Law<sup>1</sup>, T. Gevaert<sup>1</sup>, O. Feron<sup>2</sup>, M. De Ridder<sup>1</sup>  
<sup>1</sup>University Hospital Brussels, Radiotherapy, Jette, Belgium; <sup>2</sup>Université catholique de Louvain, Pole of Pharmacology and therapeutics, Brussels, Belgium

### Purpose or Objective

The anti-diabetic biguanide drugs metformin and phenformin exhibit antitumor activity in various models. However, their radiomodulatory effect under hypoxic conditions, particularly for phenformin, is largely unknown. This study therefore examines whether metformin and phenformin as mitochondrial complex I blockades could overcome hypoxic radioresistance through inhibition of oxygen consumption.

### Material and Methods

A panel of colorectal cancer cells (HCT116, DLD-1, HT29, SW480, and CT26) was exposed to metformin or phenformin for 16 h at indicated concentrations. Afterward, cell viability was measured by MTT and colony formation assays. Apoptosis and reactive oxygen species (ROS) were detected by flow cytometry. Phosphorylation of AMP-activated protein kinase (AMPK) was examined by western blot. Mitochondria complexes activity and oxygen consumption rate (OCR) were measured by seahorse analyzer. The radiosensitivity of tumor cells was assessed by colony formation assay under aerobic and hypoxic conditions. The *in vitro* findings were further validated in colorectal CT26 tumor model.

### Results

Metformin and phenformin inhibited mitochondrial complex I activity and subsequently reduced OCR in a dose-dependent manner starting at 3 mM and 30  $\mu$ M, respectively. As a result, the hypoxic radioresistance of tumor cells was counteracted by metformin and phenformin with an enhancement ratio about 2 at 9 mM and 100  $\mu$ M, respectively. Regarding intrinsic radioresistance, both of them did not exhibit any effect although there was an increase of phosphorylation of AMPK and ROS production. In tumor-bearing mice, metformin or phenformin alone did not show any anti-tumor effect. While in combination with radiation, both of them substantially delayed tumor growth and enhanced radioresponse, respectively, by 1.3 and 1.5-fold.

### Conclusion

Our results demonstrate that metformin and phenformin overcome hypoxic radioresistance through inhibition of mitochondrial respiration, and provide a rationale to explore metformin and phenformin as hypoxic radiosensitizers.

### PV-0540 Tumor modifications recorded with IVIM and DCE-MRI after Neoadjuvant radiotherapy

F. Lallemand<sup>1,2,3</sup>, N. Leroi<sup>3</sup>, M. Bahri<sup>2</sup>, E. Balteau<sup>2</sup>, A. Noël<sup>3</sup>, P. Coucke<sup>1</sup>, A. Plenevaux<sup>2</sup>, P. Martinive<sup>1,3,4</sup>  
<sup>1</sup>C.H.U. - Sart Tilman, Department of Radiotherapy-Oncology, Liège, Belgium; <sup>2</sup>University of Liège, Cyclotron Research Centre, Liège, Belgium; <sup>3</sup>University of Liège, Laboratory of Tumor and Development Biology, Liège, Belgium; <sup>4</sup>Institut Jules Bordet, Department of Radiotherapy-Oncology, Brussels, Belgium

### Purpose or Objective

Neoadjuvant radiotherapy (NeoRT) improves tumor local control and facilitates tumor resection in many cancers. We hypothesized anti-cancer treatments (i.e. radiotherapy) modify tumor microenvironment and could potentially impact distant metastases occurrence.

Previously, we developed a pre-clinical model demonstrating an impact of NeoRT schedule and the timing of surgery on metastatic spreading (Leroi et al. *Oncotarget* 2015). Here, we aim to identify by fMRI non-invasive markers reflecting NeoRT related tumor microenvironment modifications that could predict the best timing for performing surgery and avoiding tumor spreading.

#### Material and Methods

To briefly delineate the NeoRT model, MDA-MB 231 tumor cells implanted in the flank of SCID mice were locally irradiated with 2x5Gy when tumor reached 100mm<sup>3</sup> and then surgically removed at different time points. We performed fMRI, Diffusion Weighted (DW) and Dynamic Contrast enhancement (DCE) - MRI, before RT and every 2 days between RT and surgery. We acquired 8 slices of 1 mm thickness and 0.5 mm gap with an "in plane voxel resolution" of 0.5 mm. For DW-MRI, we performed FSEMS (Fast Spin Echo MultiSlice) sequences, with 9 different B-value (from 40 to 1000) and B0. We performed IVIM (IntraVoxel Incoherent Motion) analysis to obtain information on intravascular diffusion, related to perfusion ( $F$ : perfusion factor) and subsequently tumor vessels perfusion. For DCE-MRI, we performed a T1 mapping with multiple TR and DCE acquisition with 200 repetitions of 3 sec each and gadolinium IV injection after 10 repetitions. We performed semi-quantitative analysis. We validated tumor perfusion by immunohistochemistry with injection of FITC-dextran IV 3 min before surgery and CD31 labelling. Human Ki67 was used for lung metastases labelling and quantification.

#### Results

After the tumor irradiation, we observed a significant and transient increase at day 6 (60% of the basal value ( $n=6$ ,  $p<0,05$ )) of  $F$  and  $D^*$  parameters related to perfusion. The other parameters of the DW-MRI, ADC and  $D$  presented no modifications. The sham irradiated tumors used as control showed no modifications of all fMRI parameters. At the same timing, 6 days post-radiotherapy, DCE-MRI significantly demonstrated a WashinSlope ( $n=13$ ,  $p<0,05$ ) increase. Immunohistochemistry confirmed the increase of tumor perfusion when surgery is performed at day 6. The sham irradiated tumors never demonstrated such changes. Finally, when surgery is performed on tumor increased perfusion measured by fMRI, it demonstrated a burst of lung metastasis compared to the other timings.

#### Conclusion

We showed a significant difference in perfusion-related parameters with fMRI and immunohistochemistry at a specific time point after NeoRT. These modifications are correlated with an increase of metastasis spreading related to surgery procedure. These results open new perspectives in the personalized medicine and MRI guided surgery timing after NeoRT.

#### PV-0541 Immune modulation by brachytherapy in peripheral blood

M.A. Berenguer Francés<sup>1</sup>, I. Linares Galiana<sup>1</sup>, R. Cañas<sup>2</sup>, C. Gutierrez<sup>1</sup>, D. Najjari<sup>1</sup>, A. Slocker<sup>1</sup>, S. Marin i Borrás<sup>1</sup>, C. Bellobi<sup>1</sup>, F. Guedea<sup>1</sup>

<sup>1</sup>Instituto Catalan De Oncologia, Radiation Oncology, Hospitalet De Llobregat, Spain; <sup>2</sup>Idibell-Oncobell, Radiobiology and cancer, Hospitalet De Llobregat, Spain

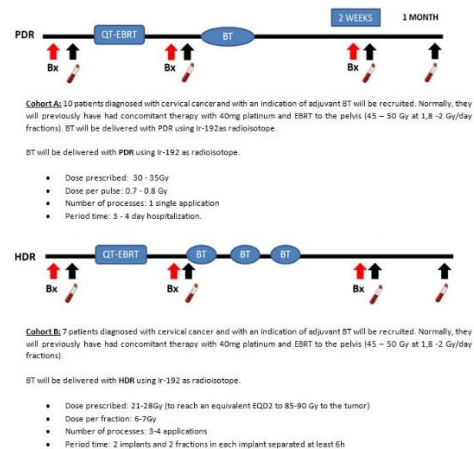
#### Purpose or Objective

Treatment with brachytherapy, either High Dose Rate (HDR) or Pulsed Dose Rate (LDR), is an effective treatment with consolidated results in cervical cancer, but its effect on the immune system is unknown. The effect of HDR-BQT as well as SBRT or IORT, can generate an individual immunity that can lead to lasting systemic responses, causing superior tumor control in these patients. These changes should be greater in HDR than in LDR. Our objective was to compare the effect on the immune system of both treatment in cervical cancer with the idea

of being able to find predictive and prognostic factors for diagnosis in these patients.

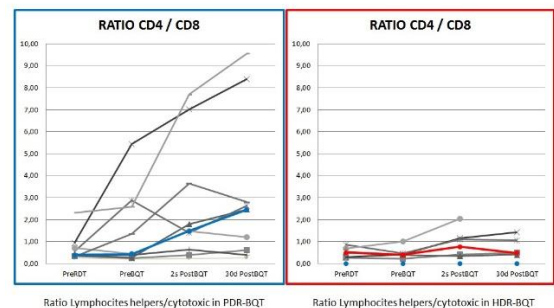
#### Material and Methods

We studied immunological factors in peripheral blood of 17 patients diagnosed with cervical cancer, 10 were treated with LDR-BQT and 7 with HDR-BQT. Four blood samples were obtained at different times of chemotherapy + radiotherapy and LDR / HDR-BQT. A blood sample was obtained prior to the start of treatment with RT, second sample before the start of the BQT, another sample at 2 weeks after the end of the BQT and a fourth sample one month after the end of the treatment. These samples were studied by flow cytometry in 3 panels. In the first panel the lymphocyte phenotype is studied; B lymphocytes, T lymphocytes, NK cells and monocytes. In another panel the regulatory T cells (Treg) were studied and in the third panel the suppressor cells derived from myeloid cells (MDSC). Subsequently, the effect on the tumor microenvironment will be analyzed with biopsies taken at different times of treatment.



#### Results

In the phenotyping panel there was an increase in TCD8 cell values and a decrease in TCD4 cells in BQT-HDR with a CD4 / CD8 ratio favorable to the BQT-HDR arm. An increase of NK cells in HDR-BQT was observed. At the Treg cell level there was a decrease in the HDR-BQT arm. In the MDSC panel an increase of the CD4 + CD45Ra-CD25 + and FOXP3 + cells in the HDR-BQT arm was evidenced.



#### Conclusion

Radiation doses delivered with HDR-BT in cervix cancer patients could trigger immune stimulation by modulating immune cells in plasma and tumor microenvironment. Deciphering immune-responses to treatment in cervix cancer patients could introduce new biomarkers helpful for treatment choice in the future.

**SP-0542 A stroll in Rome, together**V. Valentini<sup>1</sup><sup>1</sup>Fondazione Policlinico Universitario A.Gemelli IRCCS, Diagnostica Immagini- Radiation Oncology And Hematology, Roma, Italy**Abstract text**

In Rome every period of history has written pages of great artistic beauty.

These testimonies are randomly distributed throughout the city, sometimes one inside the other. What makes it unique to walk through the streets of Rome is that you never lose the sense of unity that there is, however, among all these beauties.

Radiation oncology is like Rome: it has pages of great beauty that combine together in great unity. The interweaving of basic sciences with clinical activity, of the relationship with the patient and technological innovation, of the molecular world with value-based medicine make this profession as unique and fascinating as Rome.

Being able to reread one's professional career in the light of this unified perspective helps me and perhaps the youngest to predict the future of our discipline.

---

**Award Lecture: Academic award: Jack Fowler University of Wisconsin Award**

---

**OC-0543 First clinical real-time motion-including tumor dose reconstruction during radiotherapy delivery**S. Skouboe<sup>1</sup>, T. Ravkilde<sup>2</sup>, J. Bertholet<sup>3</sup>, R. Hansen<sup>2</sup>, E. Worm<sup>2</sup>, C.G. Muurholm<sup>1</sup>, B. Weber<sup>1</sup>, M. Høyer<sup>4</sup>, P.R. Poulsen<sup>1</sup>

<sup>1</sup>Aarhus University Hospital, Department of Oncology, Aarhus, Denmark; <sup>2</sup>Aarhus University Hospital, Department of Medical Physics, Aarhus, Denmark; <sup>3</sup>The Institute of Cancer Research and the Royal Marsden Hospital, Joint Department of Physics, London, United Kingdom; <sup>4</sup>Aarhus University Hospital, Danish Center for Particle Therapy, Aarhus, Denmark

**Purpose or Objective**

Organ and tumor motion during radiotherapy delivery can deteriorate the planned dose. Real-time reconstruction of the delivered dose to a moving tumor may be used for quality assurance (QA) or dose-guided decision-making during treatment. This study presents the first clinical real-time motion-including tumor dose reconstruction performed during radiotherapy delivery.

**Material and Methods**

Seven liver SBRT patients with 2-3 implanted gold markers were treated using 3-arc VMAT.

The 3D tumor motion was monitored in real time during one fraction per patient by our in-house developed software that used continuous monitoring of an external marker block combined with x-ray images acquired every 3 seconds by a gantry-mounted imager. The monitoring relied on a correlation model between external block motion and internal marker motion that was established just before treatment from setup cone-beam CT projections and updated during treatment by the x-ray images. The tumor position and all accelerator parameters were streamed at 9.5Hz to another in-house program, DoseTracker, that reconstructed the actual motion-including dose and the planned static dose to the same calculation points as used by the treatment planning system (TPS) within the PTV. A modified pencil beam algorithm that assumes water density inside the patient contour was used.

Post-treatment, the real-time tumor localization accuracy was estimated by comparing the real-time 3D marker positions at the time of x-ray imaging with ground truth

3D positions obtained from accurate post-treatment marker segmentations in all intra-treatment x-ray images. The real-time DoseTracker doses were compared with ground truth doses obtained with post-treatment TPS calculations that emulated tumor motion as multiple isocenter shifts.

**Results**

The mean 3D root-mean-square error (RMSE) of the real-time tumor localization was 1.90mm as estimated from a mean of 174 intra-treatment x-ray images per fraction. DoseTracker reconstructed pairs of actual and planned doses at a mean frequency of 9.5Hz with a mean of 3194 calculation points per patient. The time-resolved dose in single points and the reconstructed dose distributions generally agreed well with the ground truth TPS doses (see examples in Fig 1). The actual transient point dose deviated substantially from the planned dose as the point moved in and out of the beam (Fig 1A). The motion-induced reduction in CTV D95 (minimum dose to 95% of the CTV) as reconstructed by DoseTracker was in most cases in very good agreement with that of the TPS (Fig 2A) with a RMSE over all patients of 2.0%-points (Fig 2B). Outliers were mainly caused by approximations such as water density in the current version of DoseTracker.

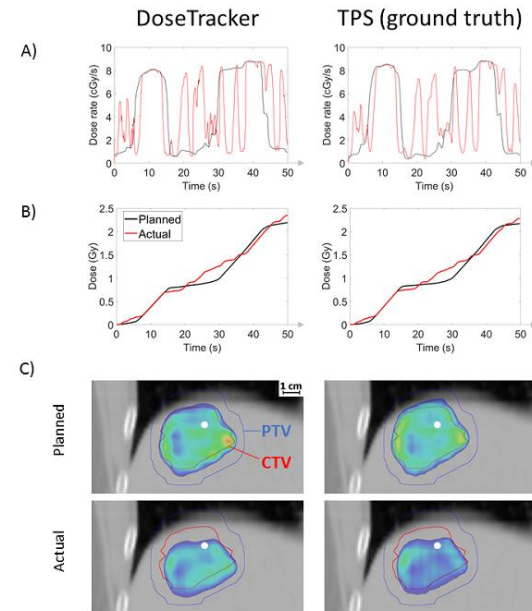


**Figure 1:** Example of planned (black) and actually delivered (red) transient (A) and cumulative (B) dose to one out of 4200 calculation points as determined in real time during treatment by DoseTracker (left) and after treatment by the treatment planning system (right). The doses are only shown for the first 50s of treatment. (C) Planned and actually delivered dose distribution in the coronal plane through the isocenter after delivery of the whole plan (dose range of 95%-107% is shown, 67% was prescribed to the PTV). The white dot indicates the calculation point presented in (A) and (B).

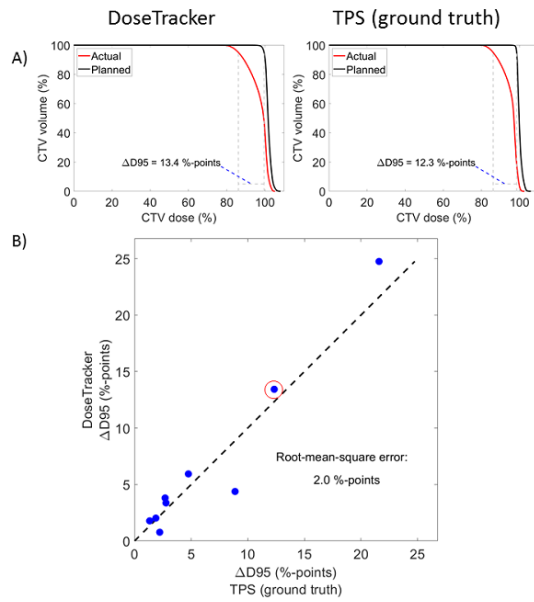


**Figure 2:** (A) DVH for the planned (black) and actually delivered (red) CTV dose for the same case as in Fig 1 determined in real time during treatment by DoseTracker (left) and after treatment by the treatment planning system (right). The specified  $\Delta D95$  is the reduction in CTV D95 caused by motion. (B)  $\Delta D95$  from DoseTracker plotted against the ground truth from the TPS for all nine tumors (two of the seven patients had two tumors). The red circle indicates the patient in Fig 1 and Fig 2A. The black, dotted unity line indicates perfect agreement of dose error reconstruction.

## Conclusion

The world's first clinical real-time motion-including tumor dose reconstruction during radiotherapy was demonstrated. This milestone marks a significant step towards real-time monitored radiotherapy with important potential applications for real-time QA and dose-guided treatment adaptation.

## Award Lecture: Company Award Lectures

### OC-0544 Distributed learning on 20 000+ lung cancer patients

T. Deist<sup>1</sup>, F.J.W.M. Dankers<sup>2</sup>, P. Ojha<sup>3</sup>, S. Marshall<sup>3</sup>, T. Janssen<sup>3</sup>, C. Faivre-Finn<sup>4</sup>, C. Masciocchi<sup>5</sup>, V. Valentini<sup>5</sup>, J. Wang<sup>6</sup>, J. Chen<sup>6</sup>, Z. Zhang<sup>6</sup>, E. Spezi<sup>7</sup>, M. Button<sup>8</sup>, J.J. Nuytens<sup>9</sup>, R. Vernhout<sup>9</sup>, J. Van Soest<sup>10</sup>, A. Jochems<sup>1</sup>, R. Monshouwer<sup>2</sup>, J. Bussink<sup>2</sup>, G. Price<sup>4</sup>, P. Lambin<sup>1</sup>, A. Dekker<sup>10</sup>

<sup>1</sup>Maastricht University Medical Centre+, The D-Lab: Decision Support for Precision Medicine- GROW - School for Oncology and Developmental Biology, Maastricht, The Netherlands; <sup>2</sup>Radboud University Medical Center, Department of Radiation Oncology, Nijmegen, The Netherlands; <sup>3</sup>The Netherlands Cancer Institute - Antoni van Leeuwenhoek, Department of Radiation Oncology, Amsterdam, The Netherlands; <sup>4</sup>The University of Manchester, Manchester Academic Health Science Centre- The Christie NHS Foundation Trust, Manchester, United Kingdom; <sup>5</sup>Università Cattolica del Sacro Cuore, Radiotherapy Department, Rome, Italy; <sup>6</sup>Fudan University, Department of Radiation Oncology- Fudan University Shanghai Cancer Center- Department of Oncology- Shanghai Medical College, Shanghai, China; <sup>7</sup>Cardiff University, School of Engineering, Cardiff, United Kingdom; <sup>8</sup>Velindre Cancer Centre, Clinical Oncology, Cardiff, United Kingdom; <sup>9</sup>Erasmus MC Cancer Institute, Department of Radiation Oncology, Rotterdam, The Netherlands; <sup>10</sup>Maastricht University, Department of Radiotherapy, Maastricht, The Netherlands

## Purpose or Objective

Access to healthcare data is crucial for scientific progress and technological innovation. Sharing healthcare data is time-consuming and notoriously difficult due to privacy and regulatory concerns (e.g., GDPR). Leaving health data at its source and bringing research questions to the data overcomes these privacy issues. Our infrastructure connects FAIR (Findable, Accessible, Interoperable, Reusable) data sources and allows distributed data analysis and machine learning. The infrastructure facilitates assembling study consortia and executing analyses in a short time frame, therefore paving the way for the era of *rapid learning healthcare*. We present results of the infrastructure's application across 8 healthcare institutes in 5 countries on 20 000+ patients: a registered study to predict 2-year survival in non-small cell lung cancer (NSCLC) patients executed and analyzed in 4 months.

## Material and Methods

NSCLC-specific databases (tumor staging and post-treatment survival information) of oncology departments were translated according to FAIR principles. Distributed learning software was installed on-site to receive machine learning algorithms. An iterative alternating direction method of multipliers-based logistic regression (LR) algorithm and data analysis procedures were implemented in MATLAB. These algorithms are privacy-preserving by design as only summary statistics and LR coefficients are exchanged between healthcare institutes and the central server. The LR algorithm was trained to predict post-treatment 2-year survival on 2/3 of the eligible patient data. The LR model performance was evaluated on the remaining 1/3 by receiver operating characteristic curves (ROC) per site and their area under the curve (AUC), and root mean square error (RMSE).

## Results

Eight healthcare institutes in Europe and Asia supplied data of 37 090 patients on which descriptive statistics were computed. Strong variation in patient cohorts across sites was observed. Inclusion criteria for prediction modelling of 2-year survival were met for 23 203 patients (Fig. 1). An LR model was distributively trained on 14 810 patients diagnosed between 1978-2011. The LR training algorithm converged after 81 iterations (25 minutes). When applying the final LR model on the validation cohort of 8 393 patients diagnosed between 2012-2015, the total RMSE was 0.43 and the AUCs ranged between 0.58-0.85 across sites (Fig. 2).

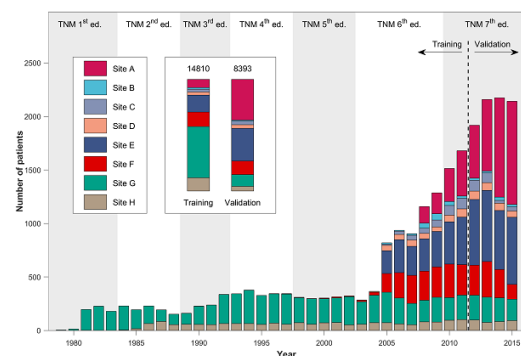


**Figure 1:** The number of patients available for training or validation per year per site.

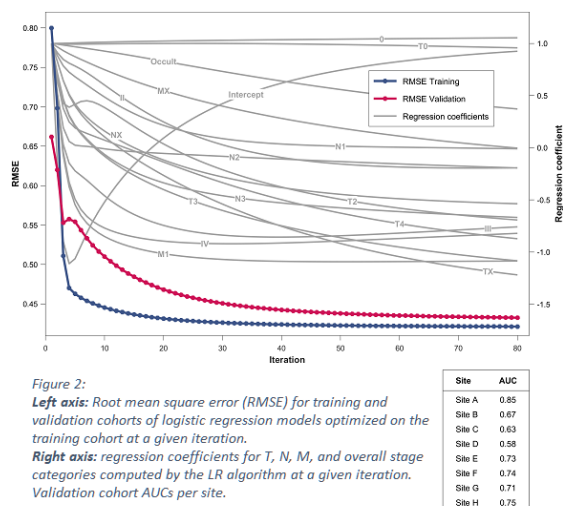


Figure 2:

Left axis: Root mean square error (RMSE) for training and validation cohorts of logistic regression models optimized on the training cohort at a given iteration.

Right axis: regression coefficients for T, N, M, and overall stage categories computed by the LR algorithm at a given iteration.

Validation cohort AUCs per site.

## Conclusion

Our infrastructure was deployed across 8 healthcare institutes in 5 countries in 4 months. A 2-year survival prediction model was trained and validated in more than 20 000 NSCLC patients. This infrastructure demonstrably overcomes patient-privacy barriers to healthcare data sharing and allows training population-based predictive models. Scaling up and combining future imaging and genomic data analyses via the infrastructure will bring us closer to the ultimate goal of model-based treatment individualization.

## Symposium: Adaptive RT: reactive or proactive?

### SP-0545 Clinical perspective and evidence on RT adaptation, has it improved outcome?

M. Guckenberger<sup>1</sup>

<sup>1</sup>University Hospital Zürich, Department of Radiation Oncology, Zurich, Switzerland

#### Abstract text

Already in 1997, Di Yan et al. described the aims and process of adaptive radiotherapy “Adaptive radiation therapy is a closed-loop radiation treatment process where the treatment plan can be modified using a systematic feedback of measurements. Adaptive radiation therapy (ART) intends to improve radiation treatment by systematically monitoring treatment variations and incorporating them to re-optimize the treatment plan early on during the course of treatment”. More than 20 years later, we have predominantly been working on solving the methodological challenges of ART, in particular improving in-room image quality, fast and automatic image segmentation, re-define adaptive planning objectives, fast and robust treatment plan optimization and quality assurance. Many in-silico planning studies have been conducted, focusing in particular on conventionally fractionated radiotherapy of lung cancer and head and neck cancer; whereas most studies reported a clinically relevant benefit of ART - organs-at-risk sparing or iso-toxic dose escalation - the magnitude of benefit varies substantially, most likely because of variation in ART methodology and endpoints. Clinical results of ART are still very rare, because its clinical implementation has only recently accelerated due to the commercial availability of the MRI-Linac technology and advances in software for image processing and treatment planning. On 12/2018, a total of 15 clinical trials are listed in clinicaltrials.gov with ART as the intervention: head and neck cancer is the most frequent indication (4/15 trials).

Results of these trials are eagerly awaited to evaluate the true clinical benefit of ART.

### SP-0546 Physics perspective on RT adaptation including role of predictive modelling in RT adaptation

J. Sonke<sup>1</sup>

<sup>1</sup>Netherlands Cancer Institute, Department of Radiation Oncology, Amsterdam, The Netherlands

#### Abstract text

Adaptive radiotherapy (ART) utilizes an imaging feedback loop and replanning to 1) improve target coverage, 2) reduce toxicity and/or 3) improve tumor control after radiation therapy. Firstly, when adequate PTV margins are used to account for geometrical uncertainties, ART is only required for a limited number of patients with large variability to restore target coverage. On the other hand, more extensive use of ART allows for margin reduction with constant target coverage and reduced organ at risk exposure. Secondly, ART can be utilized to modify the treatment plan for patients where the delivered dose deviates from the planned dose. Effective use of such strategies requires normal tissue complication probability (NTCP) models to discriminate clinically relevant from irrelevant changes. Most NTCP models available, however, are based on the planned dose instead of the delivered dose. These models need to be updated using delivered dose to effectively use such adaptive strategies. Similarly, in the context of daily adaptive replanning, dose objectives and constraints should be reevaluated. Thirdly, adaptive strategies utilizing repetitive biological imaging aim to characterize treatment response and modify the treatment plan accordingly. Such strategies also require predictive models to translate (heterogeneous) treatment response to modified dose prescription between patients or even within the target itself.

### SP-0547 Role of the RTT in the clinical implementation of adaptive radiotherapy

A. Baker<sup>1</sup>, H. Mcnair<sup>2</sup>

<sup>1</sup>Oxford University Hospitals NHS Foundation Trust, Radiotherapy, Oxford, United Kingdom; <sup>2</sup>The Royal Marsden NHS Foundation Trust, Radiotherapy, London, United Kingdom

#### Abstract text

In the UK we are aiming for adaptive radiotherapy (ART) to be the standard of care<sup>1</sup> with IGRT as a core, essential component. These national recommendations define a roadmap to modern 4D-ART within a multi-professional team (MPT) environment with each profession bringing different perspectives to the development and implementation process. ART can be reactive, proactive, scheduled and real-time. Each have workflow considerations which should be carefully considered including roles and responsibilities of the MPT. Standardisation of clinical practice is essential for the delivery of safe, accurate radiotherapy treatments. New protocols and processes for ART should be developed which can be at both local and national levels. These can be established using existing evidence, through clinical trial participation and driven by technology. Examples of these approaches, from a radiation therapist (RTT) perspective, will be discussed.

Clinical trials enable new technologies to be evaluated with regard to outcome, in a controlled environment. There have been a number of ART clinical trials in the UK which use a proactive plan of the day technique for bladder treatments. This assisted the centres involved to develop ART standards within their departments within a quality assured clinical trial. One such standard was the competency of RTT's to select the plan of the day. Clearly defined guidelines within the protocol and the advice and support of the QA team enabled successful implementation throughout the UK.

It is important to consider the role of QA together with audit programmes both during the implementation phase and also on a routine basis following the implementation of the new evidence based standards. This should include process mapping and resource assessments for each step in the ART process. RTTs are a key component of this process within the MPT.

The advent of real-time ART techniques, particularly utilising the MR-linac technology, presents an opportunity to improve outcomes for a number of disease sites and for RTTs to further extend their role within the patient pathway. However, this also presents challenges from a training perspective for RTTs to ensure correct interpretation of on-line image guidance, now with both CBCT and MR modalities.

#### Conclusion

Utilisation of national recommendations or clinical trial processes ensure that ART can be developed and implemented safely and accurately within a multi-professional team environment. Advanced ART techniques provide an opportunity for RTTs to extend their roles and scope of practice. This can be achieved by developing an educational framework which includes ART.

References <sup>1</sup>National Radiotherapy Implementation Group Report. Image Guided Radiotherapy. Guidelines for Implementation and use.

#### SP-0548 Adaptive and Real-time Approaches in Brachytherapy

T.P. Hellebust<sup>1</sup>

<sup>1</sup>Oslo University Hospital/University of Oslo, Department of Medical Physics/Physics Department, Oslo, Norway

#### Abstract text

For the last 25 years radiotherapy treatment planning has evolved from a 2-dimensional (2D)-approach using radiographic films to an approach where the planning is based on 3D imaging showing the target volumes and the normal tissue. This enables conformation of the dose distribution to the target volume(s) and avoidance of high dose to organs at risk (OARs). Broad implementation of 3D planning in external beam radiotherapy (EBRT) already took place around the end of the 90ties and was considered as state of the art rather soon. In brachytherapy (BT), however, the transition from 2D to 3D based planning started much later and is not until recently considered as the state of the art, especially for GYN, prostate and breast BT. The 3D imaging approach for treatment planning is rather different for EBRT and BT. In EBRT the treatment is traditionally based on pre-treatment imaging acquired typically a few days or up to a week before treatment start. Due to development of on board anatomical imaging, using cone beam CT and lately MR imaging, many groups have for the last years worked on procedures for treatment plan adaptation during the EBRT treatment schedule. In BT, on the other hand, many centres developed procedures with a dedicated imaging procedure for each fraction already from the beginning of the 3D area. Such procedure facilitates the opportunity to prepare a new fraction specific treatment plan taking into account the dose distribution in previous fractions, in fact the core principle of adaptive radiotherapy. Additionally, the limited requirement of tissue density to have accurate dose calculation, means that MR and/or ultrasound (US) based treatment planning has played an important role since 3D planning was introduced in brachytherapy more than a decade ago.

Image guidance in BT is used for navigation of the implant and individual dose adaptation. In fact, when image guided brachytherapy is given as boost at the last part an EBRT schedule, an adaptive target volume is identified. This means that the dose is delivered to the residual limited sized target volume and not to the initial target volume which may be significantly larger. Such approach has successfully been applied in definitive treatment of

cervical cancer the last decade [Sturdza et al 2016]. Several studies have addressed the added value of fraction specific imaging and re-planning, e.g. for breast [Altman et al 2018], bladder [Bus et al 2018], cervix [Nesvacil et al 2013 and Skliarenko et al 2018] and prostate [Simnor et al 2009]. Skliarenko et al suggested for example that the first implant, used for delivering two fractions, could be performed only with intracavitary applicators and that the addition of needles in the second implant could be performed if the dosimetry of the first implant was suboptimal.

Another important principle of adaptive radiotherapy is to record the actual dose distribution that is delivered to the patient. In EBRT the CBCT is performed in room with the patient on the treatment couch. Except for US-guided brachytherapy, such in room imaging systems is usually not used in brachytherapy centers, even though some centers has developed in room MR and CT facilities. This means that the patient is moved from the brachytherapy suite to the imaging device and then to the treatment room with inherent risk of altering the position of the applicator. Therefore, the need of treatment monitoring and verification has emerged. Some very interesting technology has been developed and implemented recently. One of them is electromagnetic (EM) tracking where the position and orientation of one or several small coils (sensors) are detected within a known electromagnetic field. Additional, new developments in real-time in vivo dosimetry are also promising and it has been demonstrated that it can be used for source tracking during treatment delivery. However, the limitation of source tracking is of course that it tracks the source in relation to the detector, and not in relation to the anatomy. The ultimate goal would be to combine the source tracking with imaging, which some groups are working on. Moreover, at the end of the day the ability to perform true adaptive BT treatment requires fast recalculation algorithms/procedure, which is rather similar to challenges seen in EBRT.

---

#### Symposium: Predictive models of toxicity and big data, big open issues

---

#### SP-0549 How to organise your department to have a structured way of collecting toxicity data

J. Widder<sup>1</sup>

<sup>1</sup>Medical University Vienna, Radiation Oncology, Vienna, Austria

#### Abstract text

Reducing toxicity is a central paradigm for all local treatment modalities in oncology. Minimally invasive and robot assisted surgery, local ablation options, increasing conformality and beam modulation in radiotherapy as well as the implementation of protons all intend to reduce toxicity. RT has highly quantitative, modellable, and actionable causal data of toxicity, more than any other discipline: this renders RT a paradigm discipline of precision medicine striving towards improving the fit between oncological condition of a patient and tailored treatment. Why then are actionable RT toxicity data still relatively scarce? How to assess toxicities is navigating between specificity (is this toxicity radiation-induced?) and relevance-for-patients (does this toxicity actually bother patients?). Quality-of-life, functioning, symptoms, toxicity scores: which outcomes matter most, and which are actually used in treatment decisions. Clinical relevance is crucial, and any threshold-level of clinical relevance will require consensus. In order to be effective, collecting toxicity data at a department need to be part of a larger endeavour of collecting patient-data, data about the disease and comorbidity, surgery and systemic treatments and detailed

radiotherapy data: dose-matrix, dose administered, and time. Survival and patterns of recurrence are essential to render toxicity data interpretable. This requires a department policy commitment as it will change workflows and even clinical routine (e.g., organisation of patient follow-up). Using common terminology for regions-of-interest is a prerequisite, just like adequate software and IT-support, which is crucial as data incompleteness and inconsistencies are an issue.

**SP-0550 Dreams and reality of toxicity data-sharing/farming: quality vs quantity?**

A. Dekker<sup>1</sup>

<sup>1</sup>*Department Of Radiation Oncology Maastrro- Grow School For Oncology And Developmental Biology- Maastricht University Medical Centre+, Maastrro, Maastricht, The Netherlands*

**Abstract text**

Big, real world data has opened a new paradigm of modeling. The large quantity and diversity of data becoming available, may enable new predictive models of toxicity after radiation therapy which are better in terms of performance and more holistic (i.e. taking into account data elements from a wide variety of domains such as biological, clinical, imaging and treatment factors). But big, real world data is usually of much lower quality compared to clinical trial data that was until now used to derive toxicity prediction models. The hypothesis is that knowing and planning for data quality problems, using data quantity to our advantage and ensuring proper validation strategies will enable big real world data to start playing a larger role in toxicity prediction models.

Typical big, real world data quality problems include unstructured data, incomprehensible data, missing data, incorrect/implausible data, contradicting data, biased data and biased-missing data. Being aware of and identifying these data quality problems is a first step towards addressing them.

There are a number of ways to improve and mitigate quality once the problems are known. E.g. tools are becoming available to convert unstructured and incomprehensible data into FAIR (Findable Accessible Interoperable Reusable) data; missing data can be imputed; incorrect data removed; contradictions solved by a trust hierarchy of sources; biased data can be transformed to a common, unbiased data domain. Besides improving the data quality, careful selection of the modeling approach taking into account the approach's sensitivity to data quality problems is also important. In almost all the above data quality improvement approaches, a high data quantity is an important enabler. Finally, even if the toxicity prediction model is based on low quality data, it does not necessarily mean the model is bad nor vice versa (a model on good data may be bad). It is therefore important to validate the model on locally recorded data so that confidence and trust in the model is increased. Such acceptance and commissioning of models requires effort on the implementing site to capture their toxicity data and other data elements required for model validation. This effort leads to more and high quality data to become available which can then be fed back for the development of a new iteration of the prediction model. Such a learning system, which implements the model development - validation - development cycle, is expected to lead to both improved data quality and data quantity and finally better toxicity prediction models.

**SP-0551 Exploiting large data base to build robust predictive models: validation issues**

T. Rancati<sup>1</sup>

<sup>1</sup>*Fondazione IRCCS Istituto Nazionale dei Tumori, Prostate Cancer Program, Milan, Italy*

**Abstract text**

The final purpose of any predictive model in the oncological domain is to provide valid outcome predictions for new patients. Essentially, the data set used to develop a model is not of interest other than to learn for the future.

Validation hence is a crucial aspect in the process of predictive modelling. Validation is the process of determining the degree to which a model is an accurate representation of the real world from the perspective of the intended uses of the model. It is a process that accumulates evidence of a model correctness or accuracy for specific scenarios, with external validation providing a measure of "generalizability" and "transportability" of the prediction model to populations that are "plausibly related".

"Plausibly related" populations can be defined as cohorts that could be slightly different from the one used for model development, e.g. treated at different hospitals, at different dose levels, with different RT techniques, in different countries or in different time frames. Generalizability and transportability are desired properties from both a scientific and practical perspective.

Quantifying the confidence and predictive accuracy of model calculations provides the decision-maker with the information necessary for making high-consequence decisions.

The more often a model is externally validated and the more diverse these settings are, the more confidence we can gain in use of the model for prospective decision-making and its possible use in interventional trials. Within this frame, the following specific issues will be considered:

1. Detecting signal from noise: the importance of model validation
2. Internal vs external validation
3. External validation: homogeneity vs heterogeneity issues, harmonization issues
4. Using large distributed datasets vs large benchmark datasets
5. Extrapolation of models: defining model applicability domain
6. Using models: continuous refinement opportunity

**SP-0552 Radiogenomics: big data to understand genetic risk factors of toxicity**

C.N. Andreassen<sup>1</sup>

<sup>1</sup>*Aarhus University Hospital, Department of Experimental Clinical Oncology, Aarhus C, Denmark*

**Abstract text**

The ability to predict normal tissue radiosensitivity has been a long sought goal in radiobiology. During the last 15 years, efforts were made to identify genetic germline alterations that affect the risk of toxicity after radiotherapy. This research is to an increasing extent undertaken by international cooperative research groups. Certain challenges relate research in radiogenomics: Large cohorts are needed to identify genotype-phenotype associations. Furthermore, normal tissue radiosensitivity is a relatively complex phenotype in several respects. It is made up by a number of sub-phenotypes that are not necessarily strongly associated. In addition the risk of normal tissue toxicity is dependent on complicated and not entirely understood dose-volume relationships. Some sequence alterations are likely to be specifically associated with certain types of normal tissue toxicity whereas others are likely to have a general impact on normal tissue toxicity.

In order to meet these challenges, 'big data approaches' will be needed. These include development of detailed NTCP-models, machine learning algorithms to analyze

complex genotype data and approaches that combine biological knowledge with genotype data.

---

### Symposium: Biological Imaging for Radiotherapy

---

#### SP-0553 Imaging of tumor infiltrating lymphocytes with [<sup>18</sup>F]FB-IL2 PET

E. De Vries<sup>1</sup>, S. Hartimath<sup>1</sup>, O. Draghiciu<sup>2</sup>, V. Manuelli<sup>1</sup>, A. Van Waarde<sup>1</sup>, R. Dierckx<sup>1</sup>, T. Daemen<sup>2</sup>, H. Nijman<sup>3</sup>  
<sup>1</sup>University of Groningen- University Medical Center Groningen, Nuclear Medicine and Molecular Imaging, Groningen, The Netherlands; <sup>2</sup>University of Groningen- University Medical Center Groningen, Medical Microbiology- Tumor Virology and Cancer Immunotherapy, Groningen, The Netherlands ; <sup>3</sup>University of Groningen- University Medical Center Groningen, Gynecological Oncology, Groningen, The Netherlands

#### Abstract text

Cytotoxic T-cells play an important role in the response to cancer treatment. T-cells can be (re)activated by e.g. immunotherapy, chemotherapy or radiotherapy and subsequently contribute to the destruction of the tumor. Insight in the immune response in the tumor can facilitate optimal treatment with minimal side effects. Non-invasive imaging of infiltrating activated T-cells would be very useful for monitoring the immune response within the tumor. Positron Emission Tomography (PET) could be such a tool, provided that a suitable tracer is available. Therefore, we have developed the PET tracer, [<sup>18</sup>F]FB-IL2, that binds specifically to interleukin-2 (IL2) receptors, that are predominantly expressed by activated T-cells. Since chemokine receptors direct the migration of T-cells to the tumor, we have also developed the PET tracer N-[<sup>11</sup>C]methyl-AMD3465 for imaging of CXCR4 receptors on T cells. The imaging properties of both tracers were successfully evaluated in several rodent models. To demonstrate the feasibility of the imaging methods to monitor the immune response to treatment, PET imaging with [<sup>18</sup>F]FB-IL2 and N-[<sup>11</sup>C]methyl-AMD3465 was performed in TC-1 tumor-bearing mice. Mice were treated with sham-irradiation (control), with a single 14Gy dose of tumor irradiation alone, or with tumor irradiation in combination with vaccination against human papilloma virus antigens that are expressed by the tumor cells. To investigate whether infiltration of lymphocytes is mediated by the CXCR4 receptor signaling pathway, a group of animals were treated with radiotherapy in combination with the CXCR4 antagonist Plerixafor (AMD3100).

PET imaging of IL2 receptors on activated T-cells 4 days after (sham-)irradiation showed a 10-fold increase in [<sup>18</sup>F]FB-IL2 uptake in the tumor of mice treated with radiotherapy alone, when compared to controls. When radiotherapy was combined with vaccination, the tumor uptake of [<sup>18</sup>F]FB-IL2 was even further increased by another 2.7-fold. These results were in line with flow cytometry data of CD8+ T-cells in the tumor. Interestingly, the combination of radiotherapy and vaccination - but not tumor irradiation alone - significantly increased the [<sup>18</sup>F]FB-IL2 uptake in various organs, indicating that the immune response to tumor irradiation is restricted to the tumor, whereas the addition of vaccination induced a more widely spread immune response. PET imaging of CXCR4 receptor expression showed similar results as [<sup>18</sup>F]FB-IL2 PET, with N-[<sup>11</sup>C]methyl-AMD3465 uptake being increased 2.5- and 4-fold in mice treated with radiotherapy alone, or radiotherapy in combination with vaccination, respectively. Moreover, [<sup>18</sup>F]FB-IL2 PET showed that blocking of the CXCR4-mediated signaling pathway with the antagonist Plerixafor, resulted in a 2.8-fold reduction tracer uptake in the irradiated tumor,

indicative of a reduction in T-cell infiltration. These results suggest that tumor irradiation and vaccination increase the influx of activated T-cells and that CXCR4 receptor-mediated signaling is involved in the migration and infiltration of these T-cells. Taken together, this study demonstrates the potential of PET imaging for non-invasively monitoring of the immune response to anti-cancer treatments, like immunotherapy and radiotherapy. Currently, the first clinical studies evaluating the feasibility of [<sup>18</sup>F]FB-IL2 PET to detect the immune response in tumor lesions during immunotherapy and chemo-radiotherapy are in progress.

#### SP-0554 Imaging DNA damage response

B. Cornelissen<sup>1</sup>

<sup>1</sup>Oxford Cancer Center - Churchill Hospital Oxford inst for RO, Radiopharmaceuticals and Molecular Imaging Group, Oxford, United Kingdom

#### Abstract text

DNA integrity is continuously challenged by endogenous and exogenous factors that can damage or alter the DNA sequence, leading to mutagenesis, aberrant transcriptional activity, and cytotoxicity. Left unrepaired, damaged DNA can ultimately lead to the development of cancer. To overcome this threat, a series of complex mechanisms collectively known as the DNA damage response (DDR) are able to detect the various types of DNA damage that can occur and stimulate the appropriate repair process. Each DNA damage repair pathway leads to the recruitment, upregulation, or activation of specific proteins within the nucleus, which, in some cases, represent attractive targets for molecular imaging. Given the dominant involvement of DNA damage and its repair during radiotherapy, the ability to monitor these repair processes non-invasively using nuclear imaging techniques may facilitate monitoring response to DNA damaging treatments. The aim of this talk is to provide an overview of recent efforts to develop PET and SPECT radiotracers for imaging of DNA damage repair proteins.

#### SP-0555 MRI-CEST Imaging of tumor acidosis

D. Longo<sup>1</sup>

<sup>1</sup>Italian National Research Council (CNR) Institute of Biostructures and Bioimaging (IBB)

#### Abstract text

Up-regulated glucose metabolism, upon hypoxia-induced shift toward glycolysis, leads to enhanced acidification of the extracellular pH (pHe) to values in the range 6.5-7.0, which is a salient feature of the tumor microenvironment. Consequently, tumor cells have evolved several sophisticated mechanisms to regulate pH homeostasis: they eliminate acidic catabolites by ion transporters and pumps to preserve a slightly alkaline intracellular pH (pHi), which is optimal for cell proliferation and tumor survival. Imaging based methods are already been established, at a clinical level, to assess glucose metabolism (by positron emission tomography - PET imaging of 18F-fluorodeoxyglucose FDG tumor uptake) providing a formidable tool for evaluating treatment response.

Conversely, despite the excellent studies regarding tumor acidosis, we still do not have an effective imaging protocol that allow to quantify extracellular tumor pH and to assess pHe related changes following therapeutic treatment. Furthermore, new anticancer drugs that, upon inhibiting one or more of these pH regulators causing both the pHi and the pHe values to return to normal, with the consequent impairment of tumour growth, cannot be in vivo evaluated both at preclinical and clinical level. We have developed innovative MRI-based approaches for assessing in vivo tumor acidosis by exploiting already clinically-used x-ray contrast agents that are translatable to the clinical scenario. We have exploited tumor pH

imaging for assessing its relationship with cancer metabolism and metastatic potential as well as for assessing treatment response to novel anticancer therapies.

We will discuss different MRI-based approaches developed for imaging tumor acidosis, using examples from our own research and from recent literature. Based on these data, tumor pH imaging may be a potential innovative diagnostic tool for characterizing tumor metabolism and to evaluate treatment response.

#### SP-0556 Tracing Tumor Hypoxia

M. Vooijs<sup>1</sup>, J. Ient<sup>1</sup>, A.J. Groot<sup>1</sup>, J.A.F. Vermeer<sup>2</sup>, R. Muschel<sup>2</sup>, J. Van Rheenen<sup>3</sup>, D. Postrach<sup>3</sup>, B. Markelc<sup>2</sup>  
<sup>1</sup>Maastricht University Medical Center MUMC+, Radiotherapy, Maastricht, The Netherlands ; <sup>2</sup>Cruk/Mrc Oxford Institute For Radiation Oncology, Radiation Oncology, Oxford, United Kingdom ; <sup>3</sup>Netherlands Cancer Institute / Oncoade, Molecular Pathology, Amsterdam, The Netherlands

##### Abstract text

Hypoxia is known to play a role in many types of cancer and is linked to metastasis, genetic instability, resistance to therapy and poor prognosis. Despite the overwhelming prognostic and predictive significance of tumor hypoxia, hypoxia modification strategies have been mostly unsuccessful in patients. There is a knowledge gap in the characterization and behavior of hypoxic tumor cells during tumorigenesis and treatment. We have optimized a system that allows hypoxic cells to be lineage traced using genetically encoded fluorescent sensors and cytotoxins to investigate their dissemination within the primary tumor and in distant metastasis. I will present data showing the application of these systems to the intravital imaging of hypoxic tumor cells.

---

#### Symposium: New developments for breast cancer irradiation

---

#### SP-0557 Neoadjuvant radiotherapy in breast cancer

Y. Kirova<sup>1</sup>  
<sup>1</sup>Institut Curie Ensemble Hospitalier, Department of Radiation Oncology, Paris cedex 05, France

##### Abstract text

Previous experience with preoperative RT with or without systemic treatment was reported with long term results. The studies have shown the excellent response rate, increasing the breast conserving surgery. These studies helped to numerous patients to preserve their breasts. Conventional scheduling in breast cancer treatment has been challenged in recent years with primary systemic therapy now widely used. The potential advantages of delivering RT before surgery are now under investigation, with current and upcoming trials. These new studies are asking new questions: how to optimize timing with mastectomy and reconstruction when the breast conserving surgery is not feasible, as well as the interest of combination with novel drugs to improve the response rates in chemo resistant tumours. The associations between radiotherapy and systemic treatments are also useful in patients who did not responded to primary systemic therapy as salvage treatment. Technically the neoadjuvant radiotherapy is interesting option because the radiation oncologist can visualize and directly delineate the tumour. Other advantage of the preoperative radiotherapy is that it can avoid the challenging techniques after oncoplastic and reconstruction surgical techniques in terms of volumes definition, as well as the sparing of organs at risk (OAR). With the hypofractionation regiments, the toxicity is

lower and the postoperative complications can be decreased. There is also currently increased interest of association between neoadjuvant irradiation and new targeted molecules as PARP inhibitors, immunotherapy agents with the aim to improve the treatment results. These associations realized in clinical trials open the door for the translational research with understanding the mechanisms of tumour resistance, as well as the discovery of new biomarkers to permit individualized optimal treatment.

#### SP-0558 Response to preoperative therapy - prediction, assessment and indications for adjuvant radiotherapy

M. Jarzab<sup>1</sup>  
<sup>1</sup>Maria Sklodowska-Curie Memorial Cancer Center and Institute of Oncology, Gliwice, Poland

Abstract not received

#### SP-0559 Nodal irradiation with or instead axillary lymph node dissection

M. Molla<sup>1</sup>  
<sup>1</sup>Hospital Clinic Barcelona, Radiation Oncology, Barcelona, Spain

##### Abstract text

The management of the node positive axilla in breast cancer remains a controversial topic.

A negative finding on examination of the axilla identifies patients who are candidates for axillary staging with SLNB. The absence of cancer cells in the SLNB confirms that no further surgical management of the axilla or nodal RT is warranted.

Clinical trials (EBCTCG metaanalysis /EORTC 22922/10925 and NCIC MA209) support the use of regional nodal irradiation (RNI) in breast cancer patients with 1-3 axillary nodal metastases following ALND. However, the controversy lies in regarding the need for ALND and/ or RNI in T1-2 clinically node negative breast cancer undergoing conservative breast surgery and systemic therapy and have metastases in 1 or 2 sentinel nodes. Ten year results of ACOSOG Z0011 (ALND or no further axillary treatment) and 5 year results of AMAROS (ALND or axillary radiotherapy) confirm no differences in nodal recurrence, disease-free survival or overall survival. The presence of risk factors such as: younger patient age, large tumor size, extent of nodal involved, lymphovascular invasion, and high tumor grade strongly support the use of RNI in this group of patients. Future work is ongoing to examine whether genes that are frequently associated with risk of recurrence can be used to assign patients to the most appropriate loco-regional treatment.

In those patients with T1-2 and sentinel node metastases undergoing mastectomy, there is little evidence to support omitting ALND and/or RNI. There are some scenarios in which axillary treatment could be omitted, such as: sentinel node micrometastases (AATRM 048/13/2000 and IBCSG 23-01) and the use of neoadjuvant chemotherapy (NAC).

The increasing use of NAC has significantly affected local-regional decision-making. Higher rates of loco-regional recurrence was seen in patients with extensive disease at presentation or nodal positive after NAC, which could decrease with RNI. However, there are some clinical data suggesting that in women who experience a complete response with NAC, ALND and/ or RNI could be omitted. Achieving a pathological response following NAC has been associated with improved survival. The NSABP B-18 and B-27 trials and data from retrospective studies found that the incidence of locoregional recurrence failure is less than 10% in patients with stage II and non residual lymph node disease. However, there are other factors that have to be taken into consideration, such as: presence of residual disease in the breast, young age and

the presence of lymphovascular invasion. In patients with these risks factors RNI would be recommended. Currently, there are two prospective trials (Alliance A11202 and RTOG 1304) that will potentially allow us to optimize nodal treatment.

**SP-0560 Radiotherapy after breast reconstruction**  
B. Offersen<sup>1</sup>

<sup>1</sup>Aarhus University Hospital, Department Of  
Experimental Clinical Oncology, Aarhus, Denmark

**Abstract text**

Immediate breast reconstruction (IBR) rates are increasing in high risk breast cancer patients having postmastectomy radiation therapy (PMRT). PMRT combined with reconstruction increases the rate of complications regardless of the type (implant or autologous) and the timing of reconstruction. Fewer complications and better long-term cosmetic outcome are seen with autologous flap-based reconstruction compared to implant-based reconstruction, however, implant-based reconstruction is increasing in combination with PMRT. Despite thousands of women are treated, contouring guidelines for target volumes in the setting of IBR are lacking. Therefore, many patients who have IBR receive PMRT to target volumes similar to CT-simulator based conventional breast irradiation. The aim of this presentation is to present a delineation guideline for PMRT after IBR with implant endorsed by a consensus among a global multidisciplinary group of breast cancer experts. If a consensus for patients having autologous IBR is reached before the ESTRO38 conference, this will also be presented.

---

**Joint Symposium: ESTRO-EORTC: Moving radiation oncology forward to improve patient outcomes**

---

**SP-0561 EORTC State of Science in Radiation Oncology: Overcoming barriers to practice change by collaboration; why now, and how....**

R. Bristow<sup>1</sup>

<sup>1</sup>Manchester Cancer Research Centre University of Manchester, Division of Cancer Sciences, Manchester, United Kingdom

**Abstract text**

The EORTC conducted a State of Science in Radiotherapy Workshop in September 2018 to explore collaborative research in radiobiology as applied to radiation oncology. The workshop was attended by clinicians, medical physicists and basic scientists in order to delineate areas of innovative research potential in the biological sciences that could augment technologic approaches within the speciality of radiation oncology. This was particularly of interest in an era where the cost-effectiveness of new technologies, including particle therapies, are being evaluated for their ability to step-change clinical practice in relation to biological approaches. The latter approaches include stratified medicine approaches using big data and genomics, immuno-modulation of treatment response using radiotherapy, molecular predictive assays married to molecular drug treatments in combination with precision radiotherapy for localised and (oligo)metastatic disease. Using an interactive group discussion approach, a number of new areas for clinical trials were explored that marry technology with best biology in a multidisciplinary manner: these will be discussed in the session. Other important elements were the interactive team science approaches to novel ideas generation and implementation across disparate health care jurisdictions and competing health resources within the EORTC. Exciting areas for collaboration can come from discrete team science approaches which focus on specific clinical impact and

routes that afford rapid translation from the basic through discovery to clinical trials sciences.

**SP-0562 Cohorts studies versus randomised controlled trials: can we combine the best of both worlds?**

L. Verkooijen<sup>1</sup>

<sup>1</sup>UMC Utrecht, Imaging Division University Medical Center Utrecht, Utrecht, The Netherlands

**Abstract text**

Randomised controlled trials (RCTs) provide the best evidence for effectiveness of new interventions. RCTs are often hampered by slow and time-consuming recruitment, and complicated informed consent procedures. RCTs may also suffer from limited generalisability, due to strict in- and exclusion criteria, and enrolment of healthier and more educated individuals. In cohort studies, recruitment of large groups of representative patients is more straightforward. However, the cohort study design is less suitable for evaluation of treatment effectiveness, due to the 'selection by indication' phenomenon. The 'Trials within Cohorts' (TwiCs) design, also known as the cohort multiple RCT (cmRCT) design, aims to combine the advantages of RCTs and cohorts and is increasingly being applied as an alternative for classic RCTs. The basis of TwiCs is a prospective cohort of people with a condition of interest, in which trials can be embedded. According to the classic cohort study design, characteristics and outcomes of participants (eg. demographics, clinical data, laboratory findings, patient-reported outcomes etc.) are collected at baseline and at fixed time intervals during follow-up. In addition, at cohort entry, participants provide broad consent to be either randomly selected to be approached for experimental interventions, or to serve as control without further notice. In a second stage, at the start of an RCT, cohort participants eligible for an experimental intervention are identified within the cohort and randomized to the intervention or control arm. Only those randomized to the intervention arm are informed about the trial, and offered the intervention, which they can accept or refuse. Participants randomized to the control arm are not informed about the trial and receive treatment as usual. Relevant outcomes of participants who have been offered the the intervention are compared with those of participants who were not offered the intervention and who received standard care. Starting in 2013, several radiotherapy TwiCs cohorts have been set up including patients with breast cancer (2400+), bone metastases (1400+), oligo lymph nodes (n=20), brain metastases (starting), and rectal cancer (700+). Of those patients, 80-85% provided broad consent for future randomization. Response rates of patient-reported outcome questionnaires varied from >85% at baseline to 60-70% at 3 years follow-up. Three RCTs have now been completed: RECTAL BOOST (n=128), VERTICAL (SBRT for vertebral metastases, n=110) and FIT (exercise trial, n=260).

Advantages of the TwiCs design included easier and more representative recruitment (>60% of all eligible patients were enrolled), and prevention of contamination and cross-over in the control arm. One of the main challenges of TwiCs was the selective drop-out in the intervention arm (i.e. patients refusing to undergo the experimental intervention), which was substantial in some of the trials. This presentation will address the above challenges, as well as other practical, ethical, and statistical issues associated with the TwiCs design.

**OC-0563 First experience with the model-based selection of head and neck cancer patients for proton therapy**

M. Tambas<sup>1</sup>, H.P. Van der Laan<sup>1</sup>, J.G.M. Van den Hoek<sup>1</sup>, H.P. Bijl<sup>1</sup>, M. Dieters<sup>1</sup>, R.G.J. Kierkels<sup>1</sup>, D. Scandurra<sup>1</sup>, S. Both<sup>1</sup>, R.J.H.M. Steenbakkers<sup>1</sup>, J.A. Langendijk<sup>1</sup>

<sup>1</sup>Department of Radiation Oncology- University of Groningen- University Medical Center Groningen, Radiation Oncology, Groningen, The Netherlands

### Purpose or Objective

In the Netherlands, head and neck cancer (HNC) patients are selected for intensity modulated proton therapy (IMPT) according to so-called 'model-based selection' approach (MBS). In this approach, a VMAT-plan and IMPT-plan is generated per patient, to determine the differences in dose to the OARs ( $\Delta$ Dose), and to translate  $\Delta$ Dose into the differences in normal tissue complication probabilities ( $\Delta$ NTCP-profile), which can be considered as a biomarker for the expected reduction in toxicity. The aim of this study was to evaluate the first experience in MBS of HNC patients.

### Material and Methods

According to the Dutch National Indication Protocol, three NTCP-models are used for the selection for IMPT, including NTCP models for tube feeding dependence, grade 2 xerostomia and dysphagia. These models include the following predictors:  $D_{\text{mean}}$  contralateral parotid gland, superior and inferior pharyngeal constrictor muscles, cricopharyngeal muscle and oral cavity, T stage, treatment modality, baseline weight loss, xerostomia and dysphagia status. The  $\Delta$ NTCP-thresholds to be selected for IMPT were defined as  $\geq 10\%$  and  $\geq 5\%$ , for grade  $\geq 2$  and grade  $\geq 3$ , respectively; or  $\geq 15\%$  for the summed risk reduction ( $\Sigma$ ANTCP) for grade 2 side effects.

63 consecutive patients with HNC who were treated with definitive RT alone (conventional or accelerated RT) with or without systemic treatment at our center since January 2018 and were subject to the MBS were evaluated. Most patients had either oropharyngeal (42%) or laryngeal (42%) carcinoma.

First, a VMAT plan was created for each patient with optimal sparing of OARs relevant for the  $\Delta$ NTCP-profile (model-based optimization). Then the subsequent NTCP-profile was calculated. An IMPT-plan with robustness evaluation was only created if the NTCP-values were beyond the thresholds. The  $\Delta$ NTCP-profile was derived from the VMAT and IMPT plans. If the  $\Delta$ NTCP-profile met the decision criteria, the patient was selected for IMPT (Fig. 1).

### Results

10 patients were excluded from the MBS plan comparison since they were not eligible for IMPT for various reasons and 5 patients because NTCP values in the VMAT plan were already below the thresholds (Fig. 1).

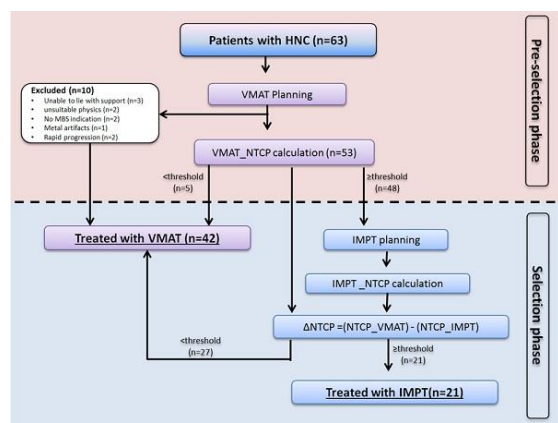


Figure 1. Selection of patients with model-based approach for proton therapy.

A planning comparison was performed for 48 patients, of which 27 were not selected since their  $\Delta$ NTCP-profile did not meet the MBS criteria (Fig. 1). Among the 21 patients who were selected for IMPT, 3 patients qualified based on  $\Delta$ NTCP xerostomia, 11 based on  $\Delta$ NTCP dysphagia, 6 based

on  $\Delta$ NTCP tube feeding dependence and 14 based on  $\Sigma$ ANTCP of  $\geq 15\%$ . Three patients were selected for IMPT based on only  $\Sigma$ ANTCP value. The NTCP values of patients with a plan comparison are summarized in Fig.2.

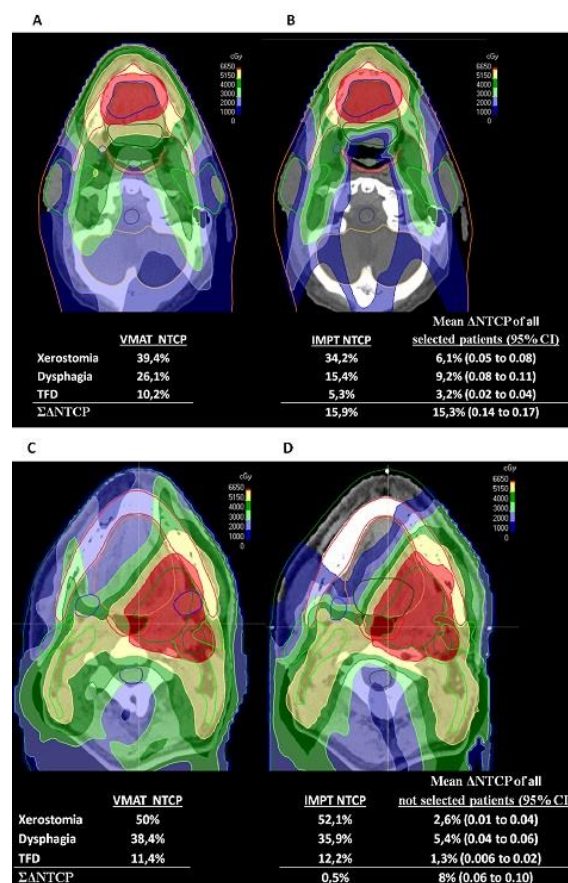


Fig. 2. The dose distributions of two patients who were selected for proton therapy (VMAT=A, IMPT=B) and photon therapy (VMAT=C, IMPT=D). The  $\Delta$ NTCP and  $\Sigma$ ANTCP values of all the patients for whom a plan comparison was performed were also shown.

### Conclusion

Our first experience is that MBS is logistically time consuming but feasible. Of the 63 patients included in this procedure, 21 were selected for IMPT. Using MBS for IMPT, only patients who most likely benefit from IMPT are selected. Our next step is to develop highly efficient pre-selection tools and new (updated) NTCP models.

### Proffered Papers: PH 11: Proffered paper: Proton range and dose verification

#### OC-0564 A novel range probing-based optimization of CT calibration curve for Proton Therapy

A. Meijers<sup>1</sup>, J. Free<sup>1</sup>, D. Wagenaar<sup>1</sup>, S. Deffet<sup>2</sup>, A.C. Knopf<sup>1</sup>, J.A. Langendijk<sup>1</sup>, S. Both<sup>1</sup>

<sup>1</sup>University of Groningen - University Medical Centre Groningen, Department of Radiation Oncology, Groningen, The Netherlands ; <sup>2</sup>Université catholique de Louvain, Icteam, Louvain-la-Neuve, Belgium

### Purpose or Objective

Proton therapy is affected by range uncertainty. CT calibration curves (CC) are institution specific and may be a source of systematic errors for proton treatment planning. Therefore, a novel range probing method to optimize and validate a CT CC for proton treatment planning using an end-to-end approach is proposed.

### Material and Methods

An initial CT CC was determined according to the stoichiometric approach. The CC consists of 5 segments: 3 lines that each describe organ-like, fat-like and bone-like tissues respectively and 2 lines as transitions between the primary segments. Unlike in routine practice, 3 types of vacuumed “fresh” animal tissue phantoms were made, consisting of (1) a pig’s head, (2) “thorax”, consisting of ribs, fat, liver and muscle, and (3) femoral bone. These phantoms were scanned on the CT (Somatom, Siemens) and transferred to the treatment planning system (RayStation, RaySearch) to calculate individual pencil beams directed through each phantom. On the CT scans a water slab was added behind the tissue samples to simulate the detector that was used for integral depth dose curve measurements. Tissue phantoms were positioned in the planned position at the proton therapy system (ProteusPlus, IBA) isocenter using the on-board x-ray imaging. A set of shot-through pencil beams of a 210 MeV energy was delivered, and depth dose profiles were measured using a multi-layer ionization chamber (Giraffe, IBA). Measured depth dose curves were compared to TPS calculated ones and the residual range error per spot was defined. Additionally, based on the WEPL of every spot through the tissue, the range error margin according to the published uncertainty recipe of 2.4% + 1 mm was defined. Ratios between measurement based and theoretical range error margins per spot were calculated (fig 1). The CT CC optimization was performed by identifying systematic shifts of the mean range error value per phantom type and minimizing the spread of ratios between residual range errors and range uncertainty margins.

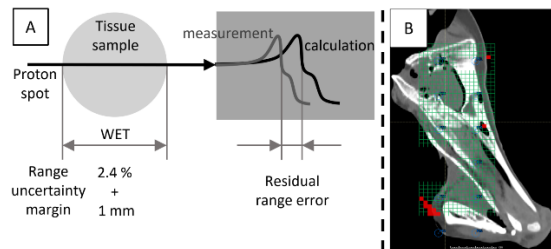


Fig 1. A illustrates the principle of the experiment, where proton beam is shot through a tissue sample and depth profile is measured behind the sample by the detector. Afterwards residual range error is defined as discrepancy between measurement and TPS calculation. The WEPL through tissue is defined for every spot and range uncertainty margin is calculated. A ratio between range error and uncertainty margin is defined. B Shows an overlay between pig’s head and measured spots, where every green square is a measurement; red squares indicates spots for which range error exceeds uncertainty margin.

## Results

When performing the analysis using the initial CT CC, increased range errors were observed for the femoral bone measurement set. Therefore, the slope of the CT CC line segment representing bone-like tissues was adjusted to ensure better agreement between measurements and calculations. Afterwards an independent measurement set for another femoral bone was included in the analysis and all data sets were recalculated using the optimized CT CC. For a full data set (about 1600 spots over all phantoms) the ratio of the actual range error and the uncertainty margin for 1.5 $\sigma$  did not exceed 0.75, indicating that the theoretical uncertainty recipe overestimates the actual range errors (fig 2).

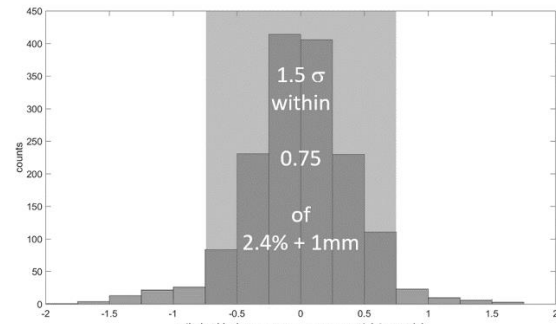


Fig 2. Histogram of ratios between measured residual range errors and range uncertainty margin as defined per individual spot. 1.5 $\sigma$  of ratios are within 0.75, which indicates that theoretical uncertainty margin is an overestimation.

## Conclusion

The feasibility of using range probing to assess the residual range errors was demonstrated in an institution specific setup. As a result, the published uncertainty margins may be reduced by ~25%, allowing for potentially more conformal proton plans in the future.

## OC-0565 The optimization of prompt gamma based range estimation in proton therapy using Cramér-Rao theory

E. Lens<sup>1</sup>, E. Tolboom<sup>1</sup>, D. Schaart<sup>1</sup>

<sup>1</sup>Delft University of Technology, Radiation Science and Technology, Delft, The Netherlands

## Purpose or Objective

Various methods for *in vivo* range estimation during proton therapy based on the measurement of prompt gamma (PG) photons have been proposed. However, optimizing the method of detection by trial-and-error is a tedious endeavor. Here, we demonstrate the use of the Cramér-Rao lower bound (CRLB) to more quickly, and more objectively, arrive at an optimal detector design.

## Material and Methods

The CRLB is based on the Cramér-Rao inequality and can be used to find the lower bound on the variance of any unbiased estimator of a parameter, given a statistical model of the observables. In this study the CRLB was used to derive the smallest possible variance on the proton range obtained from the detected PG photons, making use of the fact that the PG emission process is covered by Poisson statistics. The observables considered are the position, energy, and time of detection of the detected PG photons.

We used the TOPAS (Geant4 based) Monte Carlo code to simulate a clinical proton pencil beam with  $4 \cdot 10^9$  protons targeting a cylindrical, soft-tissue equivalent phantom. PG photons were scored on a cylindrical surface (i.e. detector;  $\varnothing=40$  cm) coaxially surrounding the phantom. Spatially-, temporally-, and spectrally-resolved PG emission profiles corresponding to different proton ranges were generated by changing the initial proton energy. The detected photons were selected and tallied based on the location, energy, time, and angle of incidence on the simulated ideal detector. From the resulting signals, we calculated the CRLB as a function of several detector setup parameters such as detector size and location, bin size, energy resolution, and photon acceptance angle.

## Results

We obtained relations between the CRLB and different detector setup parameters that allowed us to determine the optimal values for these detector properties. For most detector parameters there is a clear optimal value while the energy resolution and proton bunch width were preferably kept as small as possible.

We found comparable CRLB values for proton range estimation based on either spatial, spectral, or temporal information, of 0.26 mm, 0.24 mm and 0.25 mm, respectively, if the detection parameters were optimized

for each case (Table). The figure illustrates this optimization when using the PG photon energy. The table lists the optimal detection parameters for all (combinations of) observables. Combined detection of spatial and energy information yielded the lowest CRLB values.

**Conclusion**

We conclude that the CRLB is a promising tool for the optimization of the detector setup for PG based range estimation in particle therapy. With the current, idealized detector setup, similar accuracy could be achieved when using either the position, energy, or time of detection of the detected PG photons. Moreover, simultaneous measurement of the spatial information and energy of the PG photons yielded the highest accuracy when determining the proton range.

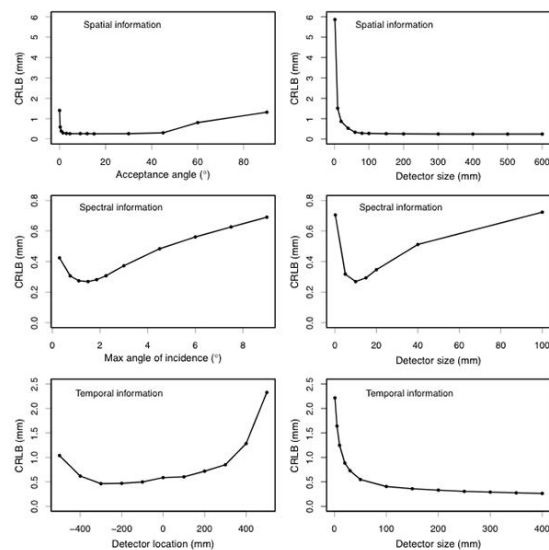


Figure: CRLB values as a function of different detection parameters when using the spatial, spectral or temporal information of incoming prompt gamma photons.

Table: Optimized CRLB values and detection parameters for the different observables

	Spatial	Energy	Timing	Spatial + energy	Spatial + timing
Max. angle of incidence <sup>1</sup> (°)	9.0	1.5	90.0	3.0	3.0
Detector size (cm)	60.0	1.0	60.0	40.0	40.0
Detector location <sup>2</sup> (cm)	0.0	0.2	-30.0	0.0	0.0
Pixel size (cm)	1.25	1.25	1.25	0.5	0.5
Energy resolution <sup>3</sup> (%)	5.0	5.0	5.0	5.0	5.0
Proton bunch width <sup>4</sup> (ns)	1.0	1.0	1.0	1.0	1.0
<b>CRLB (mm)</b>	<b>0.26</b>	<b>0.24</b>	<b>0.26</b>	<b>0.18</b>	<b>0.26</b>

<sup>1</sup> Particles with larger angles of incidence were rejected

<sup>2</sup> A location of 0 cm indicates a detector centered around the proton range

<sup>3</sup> At a particle energy of 1 MeV

<sup>4</sup> Based on a pulsed proton beam delivery

**OC-0566 Range verification in proton therapy: Can prompt-gamma imaging identify the source of deviation?**

C. Khamfongkhrua<sup>1</sup>, G. Janssens<sup>2</sup>, J. Petzoldt<sup>2</sup>, J. Smeets<sup>2</sup>, G. Pausch<sup>1,3,4,5</sup>, C. Richter<sup>1,3,4,5</sup>

<sup>1</sup>OncoRay - National Center for Radiation Research in Oncology, Faculty of Medicine and University Hospital Carl Gustav Carus- Technische Universität Dresden-Helmholtz-Zentrum Dresden - Rossendorf, Dresden, Germany ; <sup>2</sup>Ion Beam Applications SA, Research, Louvain-la-Neuve, Belgium; <sup>3</sup>Helmholtz-Zentrum Dresden - Rossendorf, Institute of Radiooncology - OncoRay, Dresden, Germany ; <sup>4</sup>German Cancer Consortium DKTK-partner site Dresden, German Cancer Research Center DKFZ- Heidelberg, Dresden, Germany; <sup>5</sup>Faculty of Medicine and University Hospital Carl Gustav Carus- Technische Universität Dresden, Department of Radiotherapy and Radiation Oncology, Dresden, Germany

**Purpose or Objective**

In-vivo prompt-gamma imaging (PGI) is a promising method for directly assessing deviations in the proton

range during proton therapy. However, several effects that can cause range shifts in patients need to be distinguished, e.g. global range errors in CT conversion to stopping power ratio (SPR), variations in patient setup, and changes in the patient anatomy. Here, we evaluate if the source of range deviation in proton pencil-beam scanning (PBS) can be distinguished based on PGI information using a slit camera [1].

**Material and Methods**

For a virtual head-and-neck tumor in an anthropomorphic head phantom, a PBS treatment plan with simultaneous integrated boost (3 beams, 70Gy and 57Gy in 33 fractions) was generated. For all PBS spots in the investigated beam, PGI profiles were simulated using a verified analytical model of the slit camera [2, 3] for the reference scenario as well as for different error scenarios: SPR change of ±1.0, ±2.0 and ±3.5%, setup error in beam direction of ±1mm and ±3mm, and 10 scenarios of realistic anatomical changes (Fig. 1). A decision-tree approach was proposed to classify different groups of error sources. This included preceding filtering of PBS spots containing reliable PGI information for range verification. For simplification and better hypothesis generation, the head phantom was first overridden with water density. Afterwards, the real phantom anatomy including all heterogeneities was analyzed. It was evaluated whether the different error scenarios could be classified correctly.

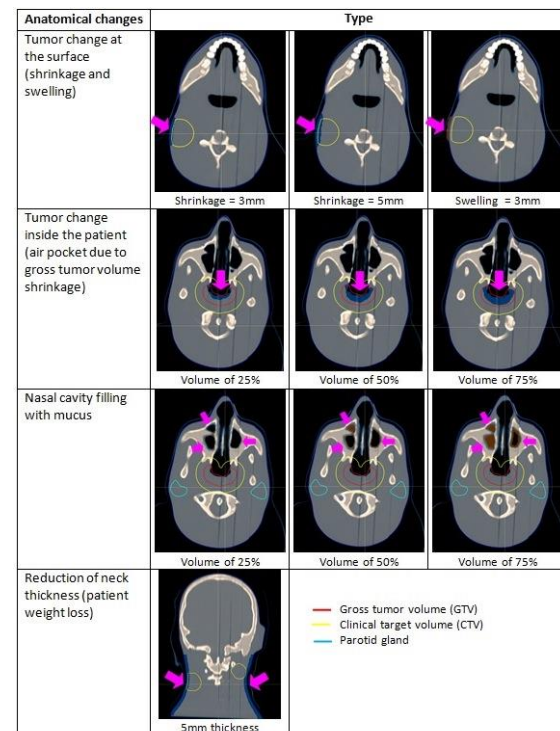


Figure 1: Simulated anatomical changes based on modified CT images of an anthropomorphic head phantom.

**Results**

An automated filter to identify reliable PBS spots was developed, e.g. assuring that the spot position is within the effective field of view (FOV) of the camera and that the fall-off of the PGI profile is completely included in the FOV - even in case of range shifts. For subsequent decision-tree-based error source classification (Fig. 2), the following parameters were selected: The coefficient of determination (R<sup>2</sup>), the slope and intercept of the linear regression between range shift and penetration depth as well as the 2D range shift map. With this approach, 27 of 30 error scenarios could be identified correctly. However, the three error scenarios with anatomical changes in the nasal cavity could not be identified because the

automated filtering approach had removed most relevant spots in this region.

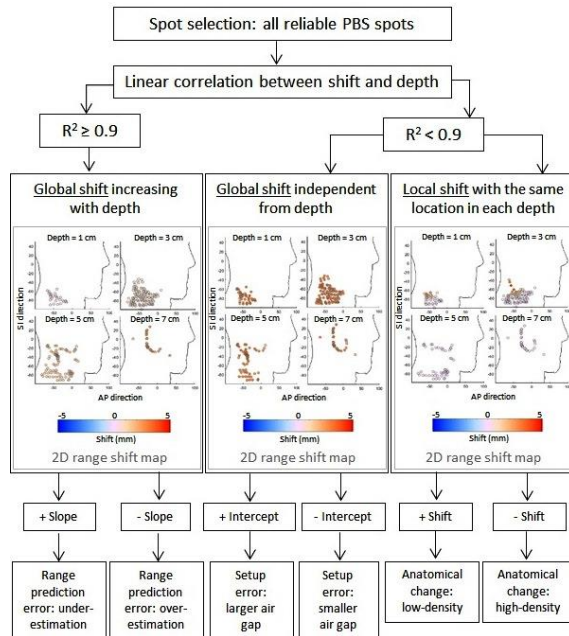


Figure 2: Decision tree to identify the source of range deviation based on PGI information.

## Conclusion

An automated classification approach was introduced to identify the source for range deviation solely from prompt-gamma information. Based on phantom data, including simulation of realistic anatomical variation, the results are promising. Further refinement of this initial approach might be beneficial. An extension of the validation with patient CT data is in preparation. In the future, an application of the approach on clinically measured PGI data is planned. Also other classification methods could be evaluated.

[1] Smeets et al., PMB, 2012

[2] Sterpin et al., PMB, 2015

[3] Nenoff et al., Radiother Oncol, 2017

## OC-0567 Reconstructing the 3-D proton dose distribution from the modelled iono-acoustic wave field

E. Lens<sup>1</sup>, A. De Blécourt<sup>2</sup>, D. Schaart<sup>1</sup>, F. Vos<sup>2</sup>, K. Van Dongen<sup>2</sup>

<sup>1</sup>Delft University of Technology, Radiation Science and Technology, Delft, The Netherlands ; <sup>2</sup>Delft University of Technology, Imaging physics, Delft, The Netherlands

### Purpose or Objective

Real-time range verification during proton therapy is paramount to ensure patient safety as well as treatment effectiveness, but remains a major challenge. Here, we investigate if the iono-acoustic wave field generated by the protons can be used to reconstruct the 3-D dose distribution during treatment.

### Material and Methods

We developed a new numerical method to model the pressure field generated by a clinical proton pencil beam. To compute the field, we convolved a 3-D Green's function, representing the impulse response of the medium, with a volume density of injection rate source. This source describes the expansion of the medium due to a local temperature increase caused by the energy deposited by the protons. An analytical model is used to describe the spatial and temporal shape of the proton dose distribution. Next, we used this method to compute the

pressure field as would be measured by a 2-D transducer array consisting of 900 point-receivers. During a measurement the pressure field resulting from a number of proton spills is detected, this set of proton spills is defined as a proton pulse (Table).

For the model-based reconstruction of the proton dose distribution, we assumed prior knowledge of the temporal behaviour of the proton beam. To solve the resulting linear inverse problem, we used a conjugate gradient minimization scheme.

### Results

To validate our method, we modelled the acoustic wave field generated by a 100 MeV clinical proton therapy beam in water. All selected beam parameters such as beam width, beam current and proton pulse duration were selected such as to reflect clinical values based on an isochronous cyclotron (Table). A cross section of the original proton dose distribution used to model the pressure field is shown in the figure (top row). Next, the figure illustrates a snapshot of the resulting pressure field (middle row). The bottom row shows the reconstructed dose distribution using the proposed method.

The simulated measured wave-field had a centre frequency around 30 kHz and an amplitude of approximately 55 mPa. It also showed all the characteristics typical for the iono-acoustic wave field with a clear pulsed behaviour, corresponding to the field generated by the protons at the Bragg-peak location. The resulting reconstructed dose is similar to the original dose distribution and the error in the location of the Bragg peak is 3.9 mm.

### Conclusion

The iono-acoustic wave field resulting from a proton beam with clinically relevant parameters has been modelled using Green's functions. Imaging the proton dose distribution is feasible by solving the linear inverse problem, while taking the temporal profile of the proton dose distribution as prior knowledge. It is expected that the error can be reduced significantly, e.g. by optimizing the positions of the receivers or by taking more prior knowledge about the beam properties into account.

Table: Parameters used for the simulation

Parameter	Value	Parameter	Value
$\sigma_t$	1 ns	$R$	63 mm
$\tau$	13 ns	$\sigma_r$	4.5 mm
$\tau_{pulse}$	6.4 $\mu$ s	$c_0$	1520 m/s
$N_{spill}$	492	$\rho_0$	996 kg/m <sup>3</sup>
$N_{proton}$	$1.2 \times 10^6$	$\Gamma_0$	0.8
$I_{proton}$	30 nA		

$\sigma_t$  = Gaussian temporal width of a proton spill

$\tau$  = Temporal spacing between proton pulses

$\tau_{pulse}$  = Duration of a proton pulse

$N_{spill}$  = Number of proton spills in a proton pulse

$N_{proton}$  = Total number of protons

$I_{proton}$  = Proton beam current

$R$  = Proton range

$\sigma_r$  = Initial proton beam Gaussian spatial width

$c_0$  = Speed of sound in the medium

$\rho_0$  = Mass density of the medium

$\Gamma_0$  = Grüneiser parameter of the medium

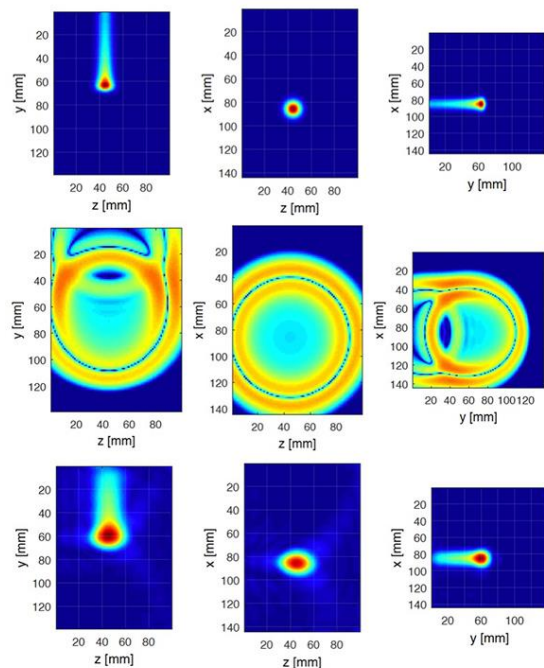


**Figure:** original proton pencil beam dose distribution (top row), Snap shot of the iono-acoustic pressure field at  $t = 0.35 \mu\text{s}$  (middle row) and reconstructed dose distribution (bottom row).

#### OC-0568 Experimental dosimetric characterization of a proton beam in the presence of a magnetic field

F. Padilla Cabal<sup>1</sup>, L. Fetty<sup>1</sup>, P. Kuess<sup>1</sup>, D. Georg<sup>1</sup>, H. Fuchs<sup>1</sup>

<sup>1</sup>Medizinische Universität Wien, Department of Radiotherapy, Vienna, Austria

#### Purpose or Objective

Advancements in Magnetic Resonance Image guided photon therapy have recently stimulated research towards MR guided proton therapy. From a physics point of view, magnetic fields induce dose distortions due to proton beam deflections and thus challenge dose measurements and dose calculations. This work aims to study the response of conventional detectors used for absolute dose verification in proton therapy in the presence of external magnetic fields up to 1T.

#### Material and Methods

Measurements were performed using a proton research beam line in the clinical energy range of 62.4 - 252.7 MeV. A resistive dipole magnet was positioned in the isocenter, thus allowing to apply magnetic fields between 0 - 1T perpendicular to the beam incidence plane. An in-house built PMMA phantom ( $200 \times 120 \times 300 \text{ mm}^3$ ) was carefully placed in the center of the magnet, assuring homogeneous irradiations within the entire phantom volume.

To evaluate the effect of the magnetic fields on different dosimetric methods, calibration curves were determined for EBT3 films and measurements using a Roos chamber were performed. Film calibration was conducted using 148.2 MeV protons at 20 mm depth in PMMA, for dose levels between 0.2-10 Gy, see Fig. 1. Afterwards, dose verification measurements were performed for different targets sizes using the same batch of calibrated films and the Roos chamber. Detectors were placed transverse to the beam, at depths between 20-150 mm covering the plateau and Bragg peak region. Results were compared for B=0T and B=1T. Monte Carlo simulations using the GATE/Geant4 toolkit were used to predict the effect of magnetic fields on dose distributions.

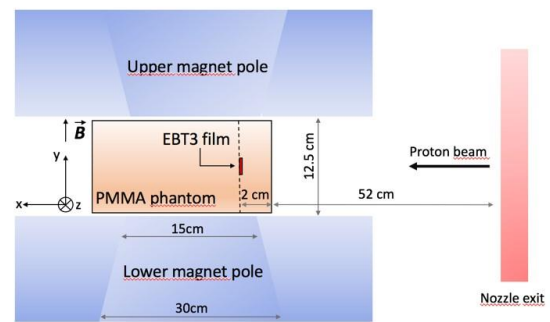


**Fig. 1** Sketch view of the experimental setup used for the EBT3 films calibration.

#### Results

Net optical density calibration curves for EBT3 films up to 10 Gy showed no significant differences ( $p\text{-value}=0.05$ ) between the different applied magnetic fields ( $B = 0, 0.5, 1\text{T}$ ). Relative differences in the Roos ionization chamber response at 20 mm depth in PMMA with/without magnetic fields were below 0.3%. Figure 2 summarizes measured and calculated proton depth dose distributions reaching a box target placed in the center of the magnet, for field strengths of  $B=0\text{T}$ ,  $B=1\text{T}$ . Absolute dose measurements with films showed an under-response up to -8% in the Bragg peak region, exhibiting a similar quenching effect as already observed without magnetic field.

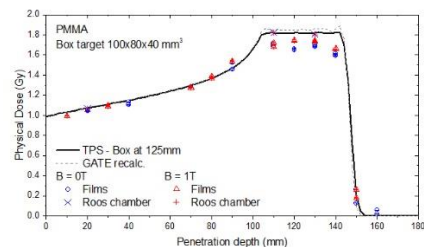


**Fig. 2** Spread out Bragg peak measured without/within a magnetic field region. The continue and dash lines correspond to the planned and MC-recalculated dose distributions respectively.

#### Conclusion

For the first time the effect of magnetic fields on the dose response function was investigated for different detectors in the context of protons dosimetry. The proposed calibration and experimental method offer a viable solution for dose measurements within magnetic fields, considering the neglectable field influence observed. Further investigations using different detectors and irradiation geometries are foreseen.

#### OC-0569 A framework for variance-based sensitivity analysis of uncertainties in proton therapy

J. Hofmaier<sup>1</sup>, G. Dedes<sup>2</sup>, D.J. Carlson<sup>3</sup>, K. Parodi<sup>2</sup>, C. Belka<sup>1,4</sup>, F. Kamp<sup>1</sup>

<sup>1</sup>University Hospital LMU Munich, Department of Radiation Oncology, Munich, Germany; <sup>2</sup>Faculty of Physics LMU Munich, Department of Medical Physics, Munich, Germany; <sup>3</sup>Yale University School of Medicine, Department of Therapeutic Radiology, New Haven, USA; <sup>4</sup>German Cancer Consortium DKTK, partner site Munich, Munich, Germany

#### Purpose or Objective

Due to the physical properties of proton beams, treatment outcomes in particle therapy are more sensitive to uncertainties than conventional X-ray therapy. Sources of

uncertainty include motion, range and prediction of relative biological effectiveness (RBE). We present a platform to assess the combined impact of these uncertainties on dose distributions and DVHs in a variance-based sensitivity analysis (SA).

#### Material and Methods

Since the statistical approach of the variance-based SA requires a large number of RBE-weighted dose (RWD) calculations ( $10^5$ - $10^6$ ), a fast, GPU-accelerated modeling of patient and range shifts was implemented, based on the pencil beam algorithm in an ion therapy extension of the research treatment planning system CERR. It was combined with the repair-misrepair-fixation (RMF) model for fast RBE calculation. In each calculation the input parameters (motion, range shifts, the biological reference parameter  $\alpha/\beta$  for X-rays and RMF model parameters) are sampled independently within their assumed normal distributions (range: 3%+1mm, biological parameters: 10%, motion: 1mm in all 3 dimensions). The parameters are ranked by statistical formalisms according to their impact on the uncertainty of the RWD in every voxel, resulting in relative, normalized sensitivity indices ("S=0: no impact, S=1: only influential input"). Results are visualized in sensitivity maps and DVHs.

#### Results

The complete SA calculation including  $5 \cdot 10^5$  RWD calculations was performed in <2 hours for a meningioma proton plan (dose/fx: 1.8 Gy (RBE)). The largest local uncertainty (0.6 Gy (RBE)) was discovered towards and after the distal fall-off of the spread out Bragg peak (SOBP) (fig. 1), where it is dominated by range uncertainties. In the lateral direction the overall uncertainty is governed by motion, while biological modeling is the most relevant contribution to the smaller uncertainty (0.15 Gy (RBE)) in the center of the SOBP. Consequently, OARs downstream of the target are affected primarily by range uncertainties and OARs lateral to the beam are affected more by motion. The uncertainty of the CTV D95% is affected by mostly by range and biology (fig. 2).

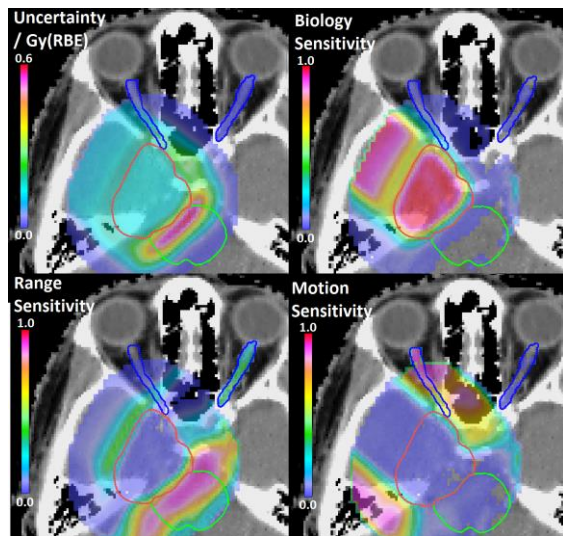


Fig.1: Impact of uncertainties in motion, biological modeling and range on the overall uncertainty (local empirical standard deviation) on a meningioma treatment plan consisting of one IMPT field. The structures shown are the CTV (red), brain stem (green) and optic nerves (blue).

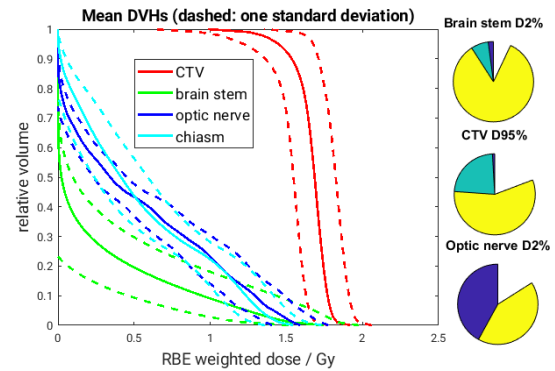


Fig.2: DVHs and sensitivities of selected quantiles. In the pie charts, the sensitivities of the input parameters are combined to three groups: motion (blue), range (yellow) and biology (turquoise).

#### Conclusion

A comprehensive sensitivity analysis framework for uncertainties in particle therapy was implemented. It is a powerful and flexible tool to assess the combined impact and interplay of motion, range and biological uncertainties, with possible implications for PTV definition and robust planning.

Acknowledgment DFG-KA4346/1-1

#### OC-0570 Dosimetric study to guide preclinical trials in proton minibeam radiotherapy

G. Consuelo<sup>1</sup>, L. De Marzi<sup>2</sup>, Y. Prezado<sup>3</sup>

<sup>1</sup>Centre national de la recherche scientifique, Imagerie et Modélisation en Neurobiologie et Cancérologie, Orsay Ville, France; <sup>2</sup>Institut Curie, Centre de Protonthérapie d'Orsay, Orsay Ville, France; <sup>3</sup>Imagerie et Modélisation en Neurobiologie et Cancérologie, Imagerie et Modélisation en Neurobiologie et Cancérologie, Orsay Ville, France

#### Purpose or Objective

Proton minibeam radiation therapy (pMBRT) is a novel concept that combines the benefits of protons for therapy with the remarkable normal tissue preservation observed when irradiated with submillimetric spatially fractionated beams [1]. Thanks to multiple Coulomb scattering, the tumor may receive a homogeneous dose distribution, while normal tissues in the beam path benefit from the spatial fractionation of the dose. This promising technique [2] has already been implemented at a clinical center (Institut Curie-Proton therapy center of Orsay, ICPO) by means of a first prototype of a multislit collimator [3]. The goal of this work was to develop a set of dosimetric tools to be able to guide reliably preclinical studies.

#### Material and Methods

The complete ICPO beamline and pMBRT irradiations setup were modelled using GATEv7.0 simulations. A clinically relevant energy (100 MeV) was used. For minibeam generation the brass multi-slits collimator used in the experiments was modelled [3]. Dose distributions were recorded in a water phantom and voxelized rat CT images (7 week male Fischer rats), whose whole brains were irradiated at ICPO. One part of the animals was implanted RG2 glioma tumors intracranially. This study includes a control group (tumor-bearing rats, non-irradiated) and a group of tumor-bearing rats that received pMBRT (70 Gy peak dose in one fraction) with very heterogeneous dose distributions.

#### Results

The agreement between the MC and experimental data provided us with a benchmark. We generate a virtual source in the nozzle exit in good agreement with the measurements. Starting from our modelling, we are able to perform preclinical simulations with a significant reduction of the computational time. Hence, we have

performed simulations with voxelized rat CT images of those animals used in experimental trials. Fig.1 shows representative dosimetry maps in three irradiation scenarios. Simulated results provide us a powerful quantitative understanding of the dose distributions within the animal brain. pMBRT leads to a significant increase of glioma tumor control, with 22 % of tumor sterilization. No substantial brain damage was observed neither in the long-term survival tumor-bearing rats nor in the irradiated normal rats, which confirms the widening of the therapeutic window for gliomas offered by pMBRT.

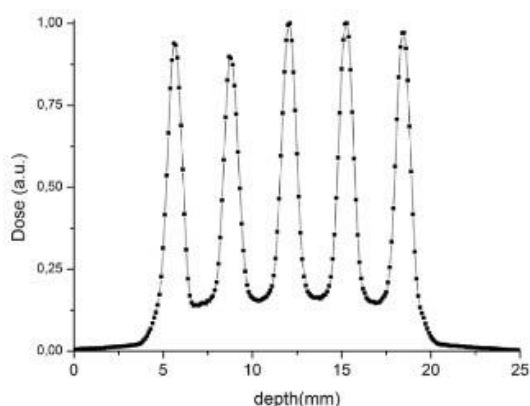
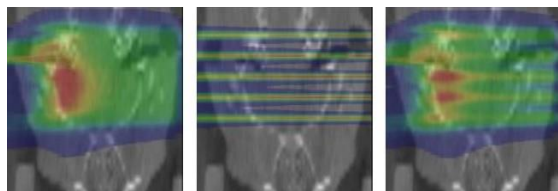


Figure 1: Left: Dose distribution inside the CT rat head in three main irradiation scenarios: broad beam (left), pMBRT (center), and pMBRT (plus solid-water) targeting the tumor position. Right: Corresponding lateral dose profile for the pMBRT case at the tumor position (ML: 5 mm, AP: -3 mm, DV: 5.5 mm).

#### Conclusion

A dose calculation engine for pMBRT has been developed. This tool allows us to reliable guide and interpret the results of our biological experiments.

[1] Prezado Y, Fois G. *Med Phys.* 2013; 40:031712

[2] Prezado et al., *Scientific Reports* 7, Article number: 14403 (2017)

[3] Peucelle C, Nauraye C, Patriarca A, et al. *Med Phys.* 2015; 42:7108-7113

---

### Symposium: Education and Advance Practice

---

#### SP-0571 Defining advanced practice roles specifically in radiotherapy

A. Duffton<sup>1</sup>

<sup>1</sup>*Inst. of Cancer Sciences-Univ. Glasgow, Research and Development Radiographer, Glasgow, United Kingdom*

#### Abstract text

The demand for radiotherapy services in the management of cancer has continued to increase over recent years. This has been due to a number of factors including: an ageing population, the ability to treat previously untreated cancers and the curative benefit of RT being realised within clinical trials. As more patients require RT to be delivered as part of their curative or palliative disease management, it has been necessary for service delivery and the workforce to evolve and meet these demands. To deliver good outcomes, professionals must ensure these

treatments are delivered with a timely and high quality approach. An established change in the oncology team workforce has been the diversifying role of the radiation therapist (RTT). This is evident in advanced practice (AP) roles detailed in the evidence base. The aim of this presentation is to describe the background of AP role development throughout Europe for RTTs, and give an overview of the literature supporting benefits of their implementation. Examples of AP roles within the RTT profession will be given, illustrating how their development has been in response to service/departmental needs. The evaluation of AP roles will be discussed, giving consideration to the benefit and impact they have on patient care. Finally, new roles bring about many opportunities for career development and progression to expert practice. This is advantageous to the RTT profession and the multi-disciplinary team.

#### SP-0572 Education and Advance Practice - Defining level EQF 7 and 8 competencies

M. Coffey<sup>1</sup>

<sup>1</sup>*Trinity College Dublin, Discipline of Radiation Therapy, Dublin, Ireland*

#### Abstract text

From an RTT perspective radiotherapy is the use of rapidly evolving technology in the preparation and treatment of cancer patients. This incorporates consideration of the technology and techniques used, the psychosocial management of a diverse patient population, the organisational structure and departmental relationships and current working practices. As a member of the radiotherapy team the RTT must be in a position to positively influence practice and to support effective and efficient service delivery. Evidence from many countries has shown how the development of diverse roles and responsibilities of RTTs has succeeded in achieving this. Unfortunately, in most instances, these developments are not linked to specialist education, professional development, career progression or associated salary increase. The failure to link these elements together results in lack of professional recognition in the wider context leading ultimately to role erosion and restriction of the potential of RTTs going forward. It is important for the recognition of the profession that education underpins defined advanced practice roles to enable a career structure to be put in place at a national and international level. While non-specific education is directly beneficial to the individual and is therefore worthwhile, it does not progress the overall profession in the same way. In this context we decided to define specific roles and responsibilities in the EQF 7 & 8 although the context and content is sufficiently broad to also enable individual development in other areas as they evolve. The roles associated with each area are sub-divided into level 7 or 8 depending on the level of responsibility expected and the education level achieved. This underpins the development of a career structure which supports professional advancement of RTTs and the provision of more efficient and effective service delivery. The roles defined in the ESTRO EQF level 7 & 8 benchmarking document include: advanced contouring and volume determination, treatment planning, advanced imaging: IGRT and ART, management, patient care and support, brachytherapy, research and education.

#### SP-0573 Incorporation radiation therapist RTT into radiation oncologist RO team

B. Bak<sup>1</sup>, J. Michalewska<sup>1</sup>, A. Machtyl<sup>1</sup>, P. Martenka<sup>2</sup>

<sup>1</sup>*Greater Poland Cancer Centre, Department Of Radiotherapy, Poznan, Poland* ; <sup>2</sup>*Greater Poland Cancer Centre, Radiotherapy Ward 1, Poznan, Poland*

## Abstract text

### Purpose

The study assessed the impact of incorporation radiation therapist (RTT) into radiation oncologist RO team in Radiotherapy Wards. We intended to estimate the efficiency of workflow improvement and to investigate whether this would reduce the time gap between the preparation and the start of treatment.

### Material and Methods

For one year RTT worked as a member of interdisciplinary team in two independent Wards. During the first six months selected RTT had worked strictly with RO at Radiotherapy Ward 1 (WR1) and focused on coordination and treatment preparation of patients with oesophagus, stomach, prostate and H&N cancer. In the second half of the year RTT managed patients with H&N and prostate cancer in the Radiotherapy Ward 2 (WR2). The main responsibilities were as follows: 1. participation in the morning report, 2. making an appointment and educating the patient, 3. coordinating the different phases of preparation for radiotherapy (RT) including: initial simulation, initial computed tomography (iCT) and virtual simulation, contouring of organs at risk (OAR), initial verification of treatment plans.

### Results

Mean reduce of time from iCT to intent order was 1 day comparing to period without RTT. Mean time from intent order to initial simulation was > 4 days and from intent order to beginning of the treatment > 5 days. There was no statistically significant time reduction at that point. Average contouring time of OAR's for RTT was 92 min for stomach 115 min for oesophagus case and 81min for prostate and 129 min for H&N cases. In the period when RTT coordinated and managed the radiotherapy pathway the number of treated patients increased by 23% and 11% in WR1 and WR2, respectively.

### Conclusions

Cooperation with RTT results in reduced time of patient's preparation for radiotherapy and increased number of treated patients.

## Poster Viewing: Poster viewing 11: Novel strategies in IGRT

### PV-0574 Evaluation of a clinical decision support protocol during radiotherapy for H&N cancer patients

F. Rodrigues Sousa<sup>1</sup>, Y. Jourani<sup>2</sup>, M. Somoano<sup>1</sup>, T. Dragan<sup>1</sup>, S. Beauvois<sup>1</sup>, D. Van Gestel<sup>1</sup>

<sup>1</sup>Institut Jules Bordet - Université Libre de Bruxelles, Radiotherapy, Brussels, Belgium ; <sup>2</sup>Institut Jules Bordet - Université Libre de Bruxelles, Medical Physics, Brussels, Belgium

### Purpose or Objective

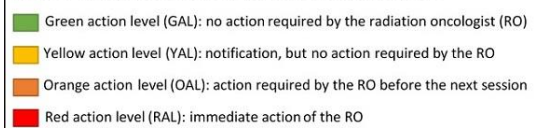
During radiotherapy (RT) treatment, variations such as patient weight loss, tumor regression and diminution of the volume of organs at risk (OARs) are likely to occur. These variations may result in changes in the dose distribution with a risk of overdose to the OARs which cannot be compensated for by a simple rigid repositioning. In order to more easily prioritize these variations according to their potential impact, an action level protocol (ALP) has been put into practice as a clinical decision support system (CDSS). In this study we analyze whether the used ALP criteria are adequate and clinically useful for adaptive planning and whether further optimization of the protocol can reduce the workload.

### Material and Methods

An ALP (Figure 1) based on online provided papers was designed in an in-house developed informatics tool through collaboration between physicians, physicists and RTTs. All CBCT review orders from head and neck patients

treated with VMAT between February and July 2018 were analyzed. These orders were categorized based on the following criteria: change of body contour, gap between skin and bolus (when used), tumor progression or inflammation of healthy tissue, tumor regression, shift of the target, tracheotomy performed after the reference computed tomography (CTref) images, teeth extraction after the CTref, second opinion on matching or other. For these criteria, frequency and follow-up action (i.e. no action required, new CT and plan adaptation) were scored.

Figure 1 - Action levels of the clinical decision support system

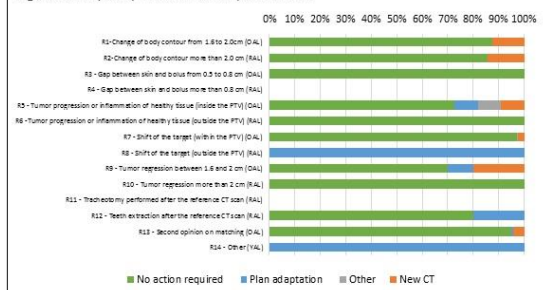


### Results

In the 50 patients, our protocol resulted in 397 review orders: the majority (372; 94%) did not require any further action after investigation; in 17 cases (4%), a new CT scan was made; and in 7 cases (2%), a plan adaptation was done. The latter was seen in categories R5, R8, R9, R12, R13 and R14 (Figure 2). Clinically relevant indicators of potential adaptation were mostly found in time, i.e. in the OAL rather than in the RAL.

CBCT review orders regarding shift of the target (within the PTV; R7) were most often reported, but required hardly any further action. Therefore we could safely decrease the action level of this criterion from an orange action level (OAL) to a yellow action level (YAL; Figure 1), reducing the radiation oncologists (ROs) workload by 57%.

Figure 2: Frequency of action taken per criterion



### Conclusion

Our action level protocol has been proven adequate for identifying patients in need of adaptive re-planning, but it also led to many false alerts. The revised and optimized protocol leads to a reduction of 57% in the workload.

### PV-0575 Is diaphragm dome or bone fusion adequate to IGRT in liver-SBRT compare to fiducial markers?

C. De la Pinta Alonso<sup>1</sup>, D. Sevillano<sup>2</sup>, R. Colmenares<sup>2</sup>, M. Martín<sup>1</sup>, C. Vallejo<sup>1</sup>, E. Fernández-Lizarbe<sup>1</sup>, S. Barrio<sup>3</sup>, V. Pino<sup>3</sup>, J.A. Rojo<sup>3</sup>, S. Sancho<sup>1</sup>

<sup>1</sup>Hospital Ramon y Cajal, Radiation Oncology, Madrid, Spain; <sup>2</sup>Hospital Ramon y Cajal, Medical Physics, Madrid, Spain; <sup>3</sup>Hospital Ramon y Cajal, Radiotherapist, Madrid, Spain

### Purpose or Objective

Stereotactic body radiotherapy (SBRT) in liver tumours is increasingly being used to treat primary and metastatic tumours. The purpose of this study was to compare the liver motion variability between using implanted fiducial markers as surrogates and alternatives methods with diaphragm dome or bone registration. We analyzed in this abstract our preliminary results.

### Material and Methods

Eight patients undergoing SBRT with abdominal compression for primary or metastatic liver cancer were analyzed. We determined the day-to-day correlation between metallic markers compare to diaphragm dome and bone tumour positions in conebeam-CT (CBCT) acquired before each treatment session. A total of 38 CBCT were analyzed. The liver variability observed in metallic markers and bone or diaphragm dome fusion and agreement was assessed using kappa statistic was analyzed. Agreement interpretation was evaluated using Landis and Koch's interpretation of strength of agreement.

#### Results

Fiducial marker-guidance was our gold standard to guiding treatment in this study. Median displacement in anterior-posterior (AP) direction of fiducial, diaphragm dome and bone was 0.06, 0.12, and 0.13cm respectively. Median displacement in lateral direction of fiducial, diaphragm dome and bone was 0.02, 0.05, and 0.06cm respectively. Median displacement in superior-inferior (SI) direction of fiducial, diaphragm dome and bone was 0.05, 0.05, and 0.18cm respectively. In the AP direction displacements of fiducial and diaphragm dome showed substantial agreement ( $\kappa=0,65$ ); and fiducial and bone light agreement ( $\kappa=0,1$ ). In the lateral direction displacements of fiducial and diaphragm dome showed substantial agreement ( $\kappa=0,64$ ); and fiducial and bone light agreement ( $\kappa=0,07$ ). In the SI direction displacements of fiducial and diaphragm dome showed just agreement ( $\kappa=0,36$ ); and fiducial and bone showed light agreement ( $\kappa=0,06$ ). In all group, the largest deviations were observed in the SI direction (variance 0,29).

#### Conclusion

These are preliminary results of our study but we consider image-guided radiotherapy (IGRT) with soft tissue match (diaphragm dome) provides a non-invasive option for daily localization and is accurate within treatment uncertainly for the majority of cases. In this moment we continuing use metallic markers until finish the study.

#### PV-0576 Simulation of EHRT for prostate cancer without monitoring intra-fractional prostate motion

Y. Oguma<sup>1</sup>, H. Shiomi<sup>2</sup>, K. Nagata<sup>3</sup>, K. Okajima<sup>1</sup>, H. Morikawa<sup>3</sup>, Y. Watanabe<sup>3</sup>, K. Mizuno<sup>3</sup>, K. Komatsubara<sup>3</sup>, K. Hata<sup>3</sup>

<sup>1</sup>Nara hospital Kindai University, Radiology, Ikoma, Japan; <sup>2</sup>Miyakojima IGRT clinic, Radiation oncology, Osaka, Japan; <sup>3</sup>Ishikiri Seiki Hospital, Radiation oncology, Higashi Osaka, Japan

#### Purpose or Objective

To examine the effectiveness of extreme hypofractionated radiation therapy (EHRT) for prostate cancer without the monitoring of the intra-fractional prostate motion.

#### Material and Methods

Between January 2015 and December 2016, data from 631 fractions obtained from 43 patients with prostate cancer who underwent more than 10 sessions of intensity-modulated radiation therapy (IMRT) (74 Gy/37 Fr, D50) with image guided radiation therapy (IGRT) before and after irradiation were analyzed. Three-dimensional prostate motions were detected using computed tomography, and the probability distributions (mean and standard deviation for each direction) were calculated. Assuming EHRT (35 Gy/5 Fr), dose distribution changes were simulated 1000 times using the dose shift method with the assumption of the worst outcome, i.e. that the prostate had shifted to the end position immediately. The all-fraction dose distributions were integrated, the equivalent dose was converted into 2 Gy fractions (EqD2) using the Liner-Quadratic model, the equivalent uniform dose (EUD) ( $\alpha = -13$ ) was obtained, and then the TCP ( $\gamma50 = 2.2$ ,  $TD50 = 67.5$ ,  $\alpha/\beta = 1.5$ ) was calculated. Finally, the

decrease in TCP caused by prostate motion was calculated.

#### Results

The maximum prostate motions were  $0.4 \pm 0.9$  mm (L-R),  $1.5 \pm 4.7$  mm (A-P), and  $0.2 \pm 4.5$  mm (S-I). The TCP was estimated to be 71% for conventional IMRT (74 Gy/37 Fr), and 89% for EHRT (35 Gy/5 Fr) without prostate motions. In the worst-case scenario, prostate motion induced the TCP to decrease to 68-70% (90% confidence interval, 74 Gy/37 Fr) and 86-89% (90% confidence interval, 35 Gy/5 Fr).

#### Conclusion

EHRT for the treatment of prostate cancer was observed to be efficient, even when the intra-fractional prostate motion was not monitored and it was divided into 5 or more fractions.

#### PV-0577 Single-institution report of whole breast VMAT radiotherapy implemented with 3D surface imaging

V. Favrel<sup>1</sup>, O. Ruiz Achard<sup>1</sup>, L. Gonzague Casabianca<sup>1</sup>, F. Chabbert<sup>1</sup>, A. Louis<sup>1</sup>, J. Paumont<sup>1</sup>, H. Maillieux<sup>1</sup>, P. Eustache<sup>1</sup>, A. Tallet<sup>1</sup>

<sup>1</sup>Institut Paoli Calmettes, Radiotherapy Oncology, Marseille, France

#### Purpose or Objective

Inter and Intra-fraction motion is a key issue for VMAT breast irradiation. 3D surface imaging allows us to monitor patient movements for all breast VMAT treatment with AlignRT (VisionRT, London, UK). However, we continue to apply CBCT for day 1, 2, 3 and then weekly. We analyzed the rate and causes of definitive stops of AlignRT use during the treatment for all patients (pts), with the aim to elaborate a decision tree to help the team to take the adequate decision for complex cases of discrepancies between CBCT and AlignRT.

#### Material and Methods

From February 2017 to August 2018, 506 patients (pts) were consecutively treated with breast VMAT radiotherapy and AlignRT system. We retrospectively collected data from 11375 sessions to assess the rate and the time of definitive stops of use AlignRT treatment monitoring, with intent to identify causes of the stops.

#### Results

We have identified two groups: G1 (413 pts; 89%) in which all the pts were treated without any stop, and G2 where AlignRT was definitively stopped during the treatment (56 pts; 11%). A subgroup of G1 (G1bis; 37 pts; 7%) represents pts who had to perform a new CT scan +/- new plan during treatment but could continue to be managed with AlignRT.

Data are summarized in the table 1

Sites treated with VMAT	Use of AlignRT during the whole treatment group 1 (G1)			Definitive stop AlignRT group 2 (G2)			
	Without new CT scan	With new CT scan group 1bis (G1bis)		Without new CT scan	With new CT scan		
Breast +/- LN +/- tumor bed	403 (79.64%)	No new planning <sup>2</sup>	New planning	31	No new planning <sup>2</sup>	20	5
496 (98.03%)		14	23				
Tumor bed only	10	0		0			
10 (1.97%)							
Total: 506 patients	413 (82%)	37 (7%)		56			
	450 (89%)			56 (11%)			

Table 1: <sup>1</sup> lymph nodes; <sup>2</sup> after reviewing, the initial plan remained relevant

The median stop occurred at the 9<sup>th</sup> session in G2 vs the 6<sup>th</sup> in G1bis (for G1bis: stop and go with AlignRT). There was no difference due to learning curve between treatments done in 2017 vs 2018 in both groups. The main reasons to perform a new CT scan during the treatment are anatomy changes, patient motion due to pain, and

AlignRT out of tolerances data compared to CBCT. In part because of the lack of homogeneous procedures for complex cases in the Department before July 18, 25/506 pts in G2 couldn't be further managed with AlignRT despite a new scan +/- new plan vs 37/506 in G1; 31/506 pts in G2 did not perform a new CT scan despite persistent discrepancies between AlignRT and CBCT.

#### Conclusion

In our series, AlignRT motion management is robust and efficient for 89% of breast cancer VMAT treatments. For the remaining 11%, AlignRT has been definitely stopped during the treatment for several reasons i.e. anatomy changes, pain, and out-of-tolerance-data compared to CBCT. An inhomogeneous decision-making among the team could be involved in some of these stops. We thus implemented a decision tree since July 18 with the aim to increase the rate of treatments without any stop. We now prospectively collect data to evaluate this implementation

#### PV-0578 Image quality of cone beam CT used as image-guidance for pelvic Stereotactic Ablative Radiotherapy

F. Slevin<sup>1</sup>, M. Beasley<sup>2</sup>, A. Needham<sup>2</sup>, J. Lilley<sup>3</sup>, R. Speight<sup>3</sup>, L.J. Murray<sup>1</sup>, A.M. Henry<sup>1</sup>

<sup>1</sup>Leeds Cancer Centre, Clinical Oncology, Leeds, United Kingdom; <sup>2</sup>Leeds Cancer Centre, Therapeutic radiography, Leeds, United Kingdom; <sup>3</sup>Leeds Cancer Centre, Medical Physics, Leeds, United Kingdom

#### Purpose or Objective

Abdomino-pelvic Stereotactic Ablative Radiotherapy (AP-SABR) is increasingly used to treat oligo-metastatic pelvic nodal disease. Cone beam CT (CBCT) is used for image-guided radiotherapy (IGRT), but image quality is limited by scattered radiation, use of low-dose protocols and streak artefacts from moving bowel gas. These factors could make the process of AP-SABR target-matching more difficult. This retrospective single centre study investigated the extent to which CBCT image quality influenced the ease of AP-SABR target-matching and determined the proportions of images affected by factors limiting image quality.

#### Material and Methods

11 consecutive patients treated with AP-SABR were investigated. Two experienced therapy radiographers retrospectively independently reviewed 139 CBCTs acquired before and after each SABR fraction from these patients in the XVI (Elekta) IGRT system. Target-matching was performed between the planning CT and each CBCT image. Image quality was assessed using a four-point Likert scale (image quality for target-matching excellent, satisfactory, poor or impossible to use). Factors used to determine chosen score were presence of streak artefacts close to the target, lack of soft tissue contrast, small size of target and lack of surrogate structure to aid target matching. Descriptive statistics are presented.

#### Results

CBCT image quality scores were judged by assessors 1 and 2 as excellent in 6 (4.3%) and 8 (5.8%) of 139 images respectively; satisfactory in 63 (45.3%) and 89 (64%) respectively; poor in 66 (47.5%) and 40 (28.8%) respectively; and impossible to match in 4 (2.9%) and 2 (1.4%) images respectively (Figure 1). Streak artefact close to the target was observed in 89 (64%) and 62 (44.6%) images respectively. Source of artefacts was small bowel or combination of small and large bowel in a quarter and three-quarters of images respectively. Lack of soft tissue contrast was observed in 86 (61.9%) and 70 (50.4%) images respectively. Small size of target was found in 70 (50.4%) and 10 (7.2%) images respectively. Lack of surrogate was observed in 13 (9.4%) and 0 images respectively (Figure 2). Agreement between assessors for Likert scores, presence of streak artefacts, lack of soft tissue contrast, small target size and lack of surrogate was seen in 54 (38.8%),

56 (40.3%), 83 (59.7%), 73 (52.5%) and 126 (90.6%) of images respectively.

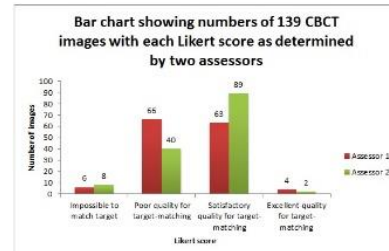


Figure 1 Bar chart showing numbers of CBCT images with each Likert score as determined by two assessors. Large proportion of images judged poor quality for target-matching.

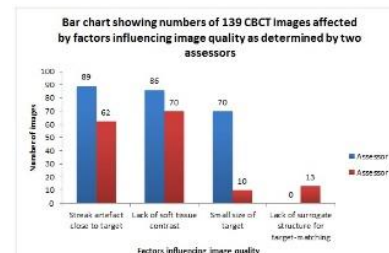


Figure 2 Bar chart showing numbers of CBCT images affected by factors influencing image quality as determined by two assessors. Note large proportion of images affected by streak artefact close to target and lack of soft tissue contrast.

#### Conclusion

Streak artefacts from moving bowel gas close to the target, especially from small bowel or combination of small and large bowel, affected over half of CBCT images. Images were also affected by lack of soft tissue contrast in over half of images. In over a third of cases image quality was felt to be poor or impossible to use because of factors negatively affecting image quality. Use of anti-peristaltic agents to reduce streak artefacts and modification of CBCT dose to improve soft tissue contrast should be investigated. Considerable variation between assessor scores reflects the subjectivity of this assessment process.

#### PV-0579 The impact of intra-thoracic anatomical changes on the delivery of lung SABR

M. Beasley<sup>1</sup>, S. Brown<sup>2</sup>, R. Chuter<sup>2</sup>, C. Favier-Finn<sup>3</sup>, K. Franks<sup>1</sup>, L. Murray<sup>4</sup>, M. Van-Herk<sup>2</sup>, A. Henry<sup>4</sup>

<sup>1</sup>Leeds Cancer Centre- Leeds Teaching Hospitals NHS Trust, Radiotherapy Research Group, Leeds, United Kingdom; <sup>2</sup>The Christie NHS Foundation Trust, Radiotherapy Related Research, Manchester, United Kingdom; <sup>3</sup>University of Manchester and The Christie NHS Foundation Trust, Radiotherapy Related Research, Manchester, United Kingdom; <sup>4</sup>University of Leeds- Leeds Institute of Cancer and Pathology and Leeds Cancer Centre- Leeds Teaching Hospitals NHS Trust, Radiotherapy Research Group, Leeds, United Kingdom

#### Purpose or Objective

Although evidence is limited, it has been suggested that approximately 70% of locally advanced non-small cell lung cancer (NSCLC) patients undergoing curative radiotherapy develop intra-thoracic anatomical changes (ITACs), with fewer than 10% requiring a completely new treatment plan.<sup>1</sup> The impact of ITACs on patients receiving SABR for early stage NSCLC, however, is unknown.

The aim of this study is to describe the occurrence of ITACs on CBCT imaging and the impact in lung cancer patients treated with SABR. This study was conducted on behalf of the UK Advanced Radiotherapy Technologies Network (ART-NET).

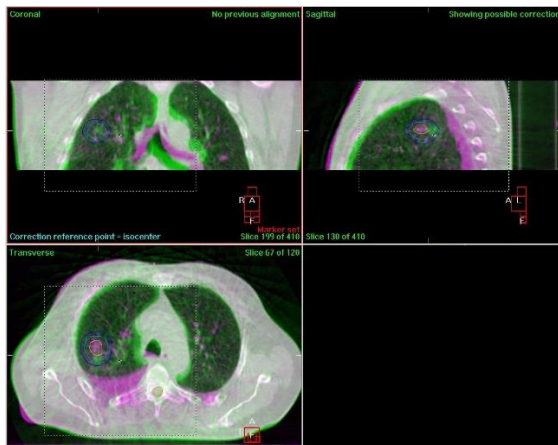
### Material and Methods

100 patients treated with SABR for early non-small cell lung cancer at two large UK NHS radiotherapy centres were identified. CBCTs acquired from 546 treatment fractions were reviewed for the presence of the following ITACs: atelectasis, infiltrative change, pleural effusion, baseline shift, gross tumour volume (GTV) increase and GTV decrease. These were graded using a traffic light protocol, similar to Kwint *et al.*, 2014<sup>1</sup>, in order to assess potential target under-coverage. The frequency of requests for physicists or clinicians to review the impact of ITACs was also recorded.

### Results

ITACs were observed in 23% of patients undergoing SABR for lung cancer at two UK radiotherapy centres. An example of a 'red' ITAC is depicted in Figure 1. The majority of CBCTs demonstrated no ITACs (85%, in 77% of patients). However, 18% of ITACs were graded as 'red', indicating a potential risk of target under-coverage. The highest proportion of ITACs observed (49%) were graded as 'yellow', indicating minimal impact upon PTV coverage. Physicist or clinician review was required for 9% of treatment fractions. Three patients needed to have their treatment re-planned.

**Figure 1:** From clockwise: coronal, sagittal and axial slices of the CBCT acquired at a 1<sup>st</sup> fraction of SABR. This shows the resolution of pleural effusion and a consequential tumour baseline shift. This was scored as red. The GTV, ITV and PTV are represented by the pink, light blue and dark blue isodose lines, respectively.



### Conclusion

The majority of ITACs were minor; however, they are associated with unplanned physicist or clinician review representing a potentially significant resource burden. There is a need to incorporate detailed guidance on the management of ITACs into IGRT workflows. This would provide an evidence-based approach to support Therapeutic Radiographer decision making when treating lung SABR, potentially reducing the impact of ITACs on workflow and the wider radiotherapy service.

### References:

Kwint M, Conijn S, Schaake E, et al. Intra thoracic anatomical changes in lung cancer patients during the course of radiotherapy. *Radiother Oncol.* 2014;113(3):392-397.

### PV-0580 CBCT-based analysis of target coverage-volume changes after prostate SABR with triggered kV-imaging

K. Kisiván<sup>1</sup>, A. Farkas<sup>1</sup>, D. Gugyerás<sup>1</sup>, C. Glavák<sup>1</sup>, Z. László<sup>1</sup>, M. Petóné Csima<sup>2</sup>, Z. Cselik<sup>3</sup>, J. Hadjiev<sup>1</sup>, A. Gulyban<sup>4</sup>, F. Lakosi<sup>1</sup>

<sup>1</sup>Somogy County Kaposi Mor Hospital- Dr. Baka József Diagnostic- Radiation Oncology- Research and Teaching Center, Radiation Oncology, Kaposvar, Hungary;

<sup>2</sup>Kaposvar University, Faculty of Pedagogy, Kaposvar, Hungary; <sup>3</sup>Cholnoky Ferenc Hospital, Department of Radiation Oncology, Veszprem, Hungary; <sup>4</sup>Europe Hospitals, Department of Radiation Oncology, Brussels, Belgium

### Purpose or Objective

To evaluate target coverage and normal volume changes after gold marker-based prostate stereotactic ablative radiotherapy (SABR) with triggered kV imaging using multiple CBCTs.

### Material and Methods

A total of 11 patients (8 monotherapy: 5x7.25 Gy, 3 boost:50.4+3x6.5 Gy) were treated with VMAT based SABR. All patients were prepared according to an institutional bladder and rectal filling protocol. Treatment verification consisted of pre-and post RT CBCTs, while during treatment online triggered kV imaging at an interval of 3 seconds was acquired. In case of  $\geq 3$ mm (deviation limit, DL) displacement, treatment was interrupted and corrected with additional imaging (2D/3D match, kV pair and/or CBCT). Beam interruptions, intrafractional shifts, treatment time were also recorded. Prostate, rectum, bladder were delineated on each CBCT. Target coverage was evaluated by comparing the individual prostate delineations with 95% isodose contour volumes using Supplementary Volume Contoured (% of the evaluated volumes exceeding the reference, SVC) metrics. Furthermore, volumetric changes of the delineated organs were assessed to evaluate bladder and rectal filling compared to baseline, and their intrafractional variations using paired t-test at  $p < 0.05$  significance level.

### Results

The average ( $\pm$  SD) treatment time was: 16 $\pm$ 12 min. On average, beams had to be interrupted twice (range: 0-10) per treatment sessions with a mean of 2.5 mm 3D shifts exceeding the DL in 30% (15/51) of the fractions. Patients were re-positioned 15 times due to inadequate rectal (14) or bladder (1) filling status. Only 4/98 evaluation (2 pre-, 2 post-CBCT) showed deviation from the ideal SVC (=0%) of the target (vs. 95% isodose line) with a maximum of 3%. In contrast, in the 15 re-positioned sessions the SVC analysis showed relevant (>5%) deviation in one third of the cases with up to 34%. The bladder volume on pre-CBCT was significantly larger compared to baseline (271 $\pm$ 161 cm<sup>3</sup> vs. 321 $\pm$ 199 cm<sup>3</sup>,  $p=0.02$ ), and further increased during treatment by an average of 17% ( $p < 0.001$ ). There were no significant inter- and intrafractional changes of the rectal volume.

### Conclusion

Gold marker-based prostate SABR with triggered kV imaging and pre/post-treatment CBCT was successfully implemented in our clinic. The 3D evaluation confirmed sufficient target coverage beside significant bladder volume changes.

### PV-0581 Image Gently for pediatric IGRT on Varian Halcyon and Edge systems: dose and positioning accuracy

Y. Zhang<sup>1</sup>, M. Wang<sup>1</sup>, Y. Huang<sup>1</sup>, H. Wu<sup>1</sup>, W. Wang<sup>1</sup>

<sup>1</sup>Key Laboratory of Carcinogenesis and Translational Research Ministry of Education/Beijing- Department of Radiation Oncology- Peking University Cancer Hospital and Institute, Department of Radiotherapy, Beijing, China

### Purpose or Objective

Reduced-dose protocols have been made available on Varian Edge kV cone beam CT (CBCT) and Halcyon MV CBCT. To assist clinicians in choosing optimal imaging modality for specific patient anatomy, this work compared the imaging dose and positioning accuracy of kV and MV CBCT using various scanning protocols and phantoms.

## Material and Methods

The settings of standard and image gently protocols of kV CBCT was listed in table 1 (OBI V.2.5). The kV imaging dose to the CT dose index (CTDI) phantom was measured using a calibrated PTW CT chamber. After measurement-based validation, the Halcyon MV CBCT imaging dose (V.1.0) to the corresponding volumes were calculated on Eclipse Treatment Planning System (V.15.1), since Halcyon uses identical 6 MV flattening-filter-free photons for both imaging and treatment, enabling the automated incorporation of the two doses. The 'High Quality' and 'Low Dose' modes uses dose rates of 45 MU/min and 27 MU/min, delivering 10 MU and 5 MU per scan respectively. The weighted CTDI (CTDI<sub>w</sub>) were computed for both systems. Using various modalities and protocols, the accuracy of correcting a known couch shift (5 mm on three directions) for the head, thorax and pelvis regions of CIRS 1-year, 5-year and RANDO adult anthropomorphic phantoms were compared.

**Table 1** Comparisons between the Image Gently parameters and the standard scanning protocols

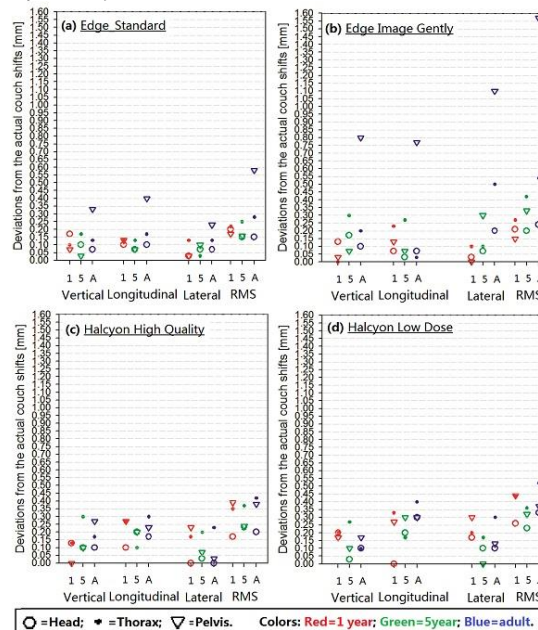
	Image Gently	Head	Thorax	Pelvis
<b>Fan*</b>	Full	Full	Half	Half
<b>Trajectory</b>	200°	200°	360°	360°
<b>kVp</b>	80	100	125	125
<b>mAs</b>	100	150	270	1080

\*The Full Fan and Half Fan modes utilize full and half bow-tie filters, providing maximum field-of-view (FOV) diameters of 26.2 cm and 46.5 cm respectively.

## Results

The CTDI<sub>w</sub> for the standard 'Head', 'Thorax', 'Pelvis' and 'Image Gently' (measured on both CTDI head and CTDI body phantoms respectively) protocols of kV CBCT were 0.45 cGy, 0.54 cGy, 1.93 cGy, 0.11 cGy, and 0.05 cGy respectively. The computed CTDI<sub>w</sub> for MV CBCT in the CTDI head and body phantoms were 8.45 cGy and 6.38 cGy (imaging length=28 cm, the maximum field of Halcyon), 6.88 cGy and 5.55 cGy (imaging length=16 cm, equivalent to that of Edge kV CBCT) respectively, using the 'High Quality' protocol. The exposure of 'Low Dose' MV CBCT was approximately halved. Figure 1 displays the deviations of image registrations from the actual couch shifts [mm] on the vertical, longitudinal, lateral directions and the root-mean-square (RMS), as guided by Edge kV CBCT and Halcyon MV CBCT. Only the positioning error of adult pelvis guided by 'Image Gently' kV CBCT (1.57 mm) exceeded our clinical tolerance of 1.00 mm. All other registrations were satisfactory: the maximum deviations for the 1-year, 5-year and adult phantoms were 0.22 mm, 0.25 mm, 0.58 mm (standard kVCBCT); 0.27 mm, 0.42 mm, 0.54 mm ('Image Gently' kV CBCT excluding adult pelvis); 0.39 mm, 0.37 mm, 0.42 mm ('High Quality' MV CBCT); and 0.44 mm, 0.36 mm, 0.52 mm ('Low Dose' MV CBCT)

respectively.



## Conclusion

'Image Gently' kV CBCT is inadequate for adult pelvis, but is applicable to other anatomies achieving comparable positioning accuracy as standard kV CBCT. Similar registration results were achievable using MV CBCT, but the 'Low Dose' mode is most cost-effective for all phantoms than the 'High Quality' protocol.

## Symposium: Recent insights into adverse cardiac effects from multimodal radiation therapy

### SP-0582 Prediction models for adverse cardiac effects to target optimal cardiac radiation dose distributions in breast cancer patients

A. Crijs<sup>1</sup>

<sup>1</sup>UMC Groningen, Radiotherapy, Groningen, The Netherlands

#### Abstract text

Incidental cardiac radiation in breast cancer radiotherapy results in an increased risk of major cardiac events. Darby et al. found that the lifetime excess risk of an acute coronary event [ACE] increases linearly by 7.4% per Gray of the mean heart dose. However, we have validated that the first 9 years following radiotherapy the excess risk of an ACE even increases by 16% per Gray of the MHD. In the Netherlands, the model-based approach is applied to select breast cancer patients for proton therapy. To qualify for proton therapy, breast cancer patients should have a  $\geq 2\%$  decrease in the absolute lifetime risk of an ACE after planning comparison between photon and proton therapy. To calculate the absolute lifetime risk of an ACE, the validated Darby model is used, with the difference that the observed baseline risk of an ACE is based on the numbers of ACEs in females and males in the Dutch population. However, for optimization of cardiac photon dose distributions and better selection of patients for proton therapy validated prediction models are essential, describing the relationship between radiation dose to cardiac substructures and MCEs. Furthermore, knowledge about early subclinical cardiovascular effects (ESCEs) induced by radiotherapy that eventually develop into MCEs is also needed for development of primary and secondary preventive strategies. Currently these issues are addressed in the European MEDIRAD-BRACE and -EARLY

HEART Projects. An overview of these studies will be presented.

**SP-0583 Practical aspects of estimating and measuring of CIED dose in radiotherapy procedures**

E. Konstanty<sup>1</sup>, B. Bak<sup>2</sup>, W. Szyszka<sup>2</sup>

<sup>1</sup>Greater Poland Cancer Centre, Department Of Medical Physics, Poznan, Poland ; <sup>2</sup>Greater Poland Cancer Centre, Radiotherapy Department II, Poznan, Poland

**Abstract text**

According to AAPM Report No. 45 “Management of radiation oncology patients with implanted cardiac pacemakers” cardiac pacemakers can fail from radiation damage and can exhibit functional changes. Total dose to each type of cardiovascular implantable electronic device (CIED) should be estimated for each patient who undergoes radiotherapy. One of the recommendations of the task group is to estimate the absorbed dose to be received by the device before treatment. Another important document that contains practical recommendations for specialists treating patients with CIEDs with radiation therapy is a clinical guideline of the Heart Rhythm Society: “2017 HRS expert consensus statement on magnetic resonance imaging and radiation exposure in patients with cardiovascular implantable electronic devices”. Maximum expected cumulative incident dose  $\int_{SEP} dD$  should be estimated and minimize (threshold of 5 Gy).

In some cases national guidelines introduce the obligation to perform not only the estimation but also the measurement of CIED dose during radiotherapy session. In this presentation possible methods and technical difficulties of the CIED dose estimation and in-vivo dosimetry will be discussed. Finally, the results of in-vivo dosimetry of CIEDs treated in Greater Poland Cancer Centre will be presented.

**SP-0584 From biological basis of RI cardiac toxicity to the new application of SBRT in the cardiovascular field**  
M. Vozenin<sup>1</sup>

<sup>1</sup>Centre Hospitalier Universitaire Vaudois, Department of Radiation Oncology, Lausanne Vaud, Switzerland

**Abstract text**

Cardiac toxicity induced by anti-cancer treatments including radiotherapy is today an issue for long-term cancer survivors<sup>1, 2</sup> without therapeutic management. The first part of this talk will be dedicated to summarize biology-driven efforts made to develop translatable therapeutic approaches to prevent, mitigate or reverse radiation injury to the heart. Then, recent results will be shown including a yet never described gender difference in both radiation-induced sensitivity and sensitivity to combined treatment based upon RT, paclitaxel and herceptine. Female mice are protected from cardiac defect and this protection is mediated by small GTPase RhoB via its interaction with ERa. In the second part, possible new application SBRT (Stereotactic body radiotherapy) in cardiology will be discussed such as the non-invasive management of ventricular tachycardia (VT) refractory to standard treatments<sup>3,4</sup>. In addition, the first preclinical data will be shown that investigates the physiopathological impact of such large but localized dose of irradiation on the heart using experimental mouse model and Image guided radiotherapy device (XRad225CX-PXi) that enable to mimic clinical SBRT configuration.

1. Andratschke N, Maurer J, Molls M, Trott KR. Late radiation-induced heart disease after radiotherapy. Clinical importance, radiobiological mechanisms and strategies of prevention. *Radiother Oncol.* 2011;100(2):160-6.

2. Darby SC, McGale P, Taylor CW, Peto R. Long-term

mortality from heart disease and lung cancer after radiotherapy for early breast cancer: prospective cohort study of about 300,000 women in US SEER cancer registries. *Lancet Oncol.* 2005;6(8):557-65.

3. Cuculich PS, Robinson CG. Noninvasive Ablation of Ventricular Tachycardia. *N Engl J Med.* 2018;378(17):1651-2

4. Jumeau R, Ozsahin M, Schwitter J, Vallet V, Duclos F, Zeverino M, et al. Rescue procedure for an electrical storm using robotic non-invasive cardiac radio-ablation. *Radiother Oncol.* 2018;128(2):189-91.

**SP-0585 Managing cardiotoxicity in oncology follow up and primary care services**

S. Faithfull<sup>1</sup>

<sup>1</sup>University of Surrey, Faculty of Health and Medical Sciences, Guildford, United Kingdom

**Abstract text**

The purpose of this paper is to explore how primary care and oncology can work together to identify those at risk of cancer related cardiovascular disease (CVD) to provide primary and secondary prevention. Cancer therapeutic agents impact directly on the coronary endothelium, myocardium, heart valves and other structures and the increase in multi-modality treatment with radiotherapy means more patients are likely to be affected in the future. Many of the factors associated with increased prevalence of cancer are also associated with cardiovascular disease for example, ageing, low physical activity, smoking and obesity. Cancer treatment cardiac damage is more responsive to therapy if treated early, so this paper focuses on how as clinical oncologists, nurses and therapy radiographers we can work more closely with primary care to promote earlier diagnosis of cardiac toxicity and instigate protocols for monitoring heart health in those at higher risk during radiotherapy follow-up. Improving cardio-toxicity management requires primary prevention before treatment starts, to reduce the likelihood of a cardiac events after cancer treatment, by active risk reduction [1]. Evaluation of coronary risk primarily by means of screening for elevated cholesterol, diabetes, hypertension, diabetes, smoking and family history can identify patient’s CVD risk profiles. CVD risk reduction should be considered prior to cancer therapy, promoting lifestyle advice and cardio protective measures. Secondary prevention is also important in treating cardiac dysfunction especially in patients at higher risk. Heart failure treatment within 3 months of symptom development is reversible >90% over 2 years whilst after 6 months’ post symptom development management is less effective [2]. Furthermore, in cancer surveillance and follow up, unexpected changes in patients existing CVD should be investigated and that these symptoms may be early signs of cardio toxicity. Primary care services are involved in managing the long-term health of people with cancer as well as holistically their long-term conditions (LTC). More than 40% of cancer patients have one and 15% two LTC. However primary care physicians have limited knowledge of cancer therapies and how these may destabilise previously well controlled cardiovascular disease and diabetes [3]. In recent surveys, primary care physicians, oncology nurses and allied health professionals undertaking follow up of cancer patients were unaware of cardiac toxicity or how best to identify or manage symptoms [4]. Clear reporting and assessment communication between cancer centres and primary care services with potential side-effects listed, risk of occurrence, cumulative dose and referral guidance if symptoms occur should be provided.

1. Zamorano L, Lancellotti P et al, ESC Scientific Document Group; 2016 ESC Position Paper on cancer treatments and cardiovascular toxicity developed under the auspices of the ESC Committee for Practice Guidelines: The Task

Force for cancer treatments and cardiovascular toxicity of the European Society of Cardiology (ESC), *European Heart Journal*, Volume 37, Issue 36, 21 September 2016, Pages 2768

2801, <https://doi.org/10.1093/eurheartj/ehw211>

2. Hamo CE, Bloom MW et al, Cancer-therapy-related cardiac dysfunction and heart failure. Part 2 Prevention, treatment, guidelines and future directions, *Circ Heart Fail*, 2016 Volume 9, issue 2

<https://doi.org/10.1161/Circheartfailure.115.002843>

3. Kapoor, A et al Monitoring risk factors of cardiovascular disease in cancer survivors, *Clinical Medicine*, 2017 Volume 17, no4 293

4. Faithfull, Kirby M et al. Mitigating risk of Cardiovascular disease *Cancer Nursing Practice*. 16, 1, 18-23. <https://doi.org/10.7748/cnp.2017.e1352>

### Proffered Papers: RB 6: Pre-clinical research in particle therapy

#### OC-0586 Immunological contexture basis of a prognostic radiomics signature in head and neck cancers

D. Ou<sup>1,2,3,4</sup>, J. Adam<sup>5</sup>, I. Garberis<sup>5,6</sup>, P. Blanchard<sup>2</sup>, F. Nguyen<sup>2</sup>, A. Levy<sup>2,3,4</sup>, O. Casiraghi<sup>5</sup>, R.T.H. Leijenaar<sup>7</sup>, P. Gorphe<sup>8</sup>, I. Breuskin<sup>8</sup>, F. Janot<sup>8</sup>, C. Robert<sup>2,3,4</sup>, P. Lambin<sup>7</sup>, S. Temam<sup>8</sup>, J. Scoazec<sup>3,5,6</sup>, E. Deutsch<sup>2,3,4</sup>, Y. Tao<sup>2,3,4</sup>

<sup>1</sup>Fudan University Shanghai Cancer Center, Department of Radiation Oncology, Shanghai, China ; <sup>2</sup>Gustave Roussy Cancer Campus, Department of Radiation Oncology, Villejuif, France ; <sup>3</sup>Université Paris Sud, Université Paris Sud, Paris, France ; <sup>4</sup>INSERM, INSERM1030 molecular radiotherapy, Villejuif, France ; <sup>5</sup>Gustave Roussy Cancer Campus, Department of Pathology, Villejuif, France ; <sup>6</sup>INSERM, INSERM US23/CNRS UMS3655- Molecular analysis- modelling and imaging of cancer disease- Experimental and Translational Pathology, Villejuif, France ; <sup>7</sup>Maastricht University Medical Centre+, The D-Lab: Decision Support for Precision Medicine- GROW - School for Oncology and Developmental Biology, Maastricht, The Netherlands ; <sup>8</sup>Gustave Roussy Cancer Campus, Department of Head and Neck Surgical and Medical Oncology, Villejuif, France

#### Purpose or Objective

While in recent years radiomics has been increasingly studied and often associated with clinical endpoints, the relationships of radiomics and tumor biology are largely unknown. In this study, we sought to explore the immunological contexture basis of a previously developed prognostic radiomic signature in head and neck cancers.

#### Material and Methods

Ninety-five patients were included in the analysis. Evaluation for density of CD8+ T cells, FoxP3+ T cells, CD68+ cells, PD-L1 expression and p16 expression was performed on pretreatment biopsy tissue samples with immunohistochemistry methods. A total of 544 radiomics features of the primary tumor were extracted from radiotherapy planning computed tomography scans. We categorized patients into four phenotypes based on p16 expression and a previously developed 24-feature based prognostic radiomic signature [1]: p16+/radio<sup>low</sup>(PL), p16+/radio<sup>high</sup>(PH), p16-/radio<sup>low</sup>(NL), p16-/radio<sup>high</sup>(NH). The correlations between the four phenotypes and biomarker expressions in the tumor micro-environment were analyzed using Spearman's rank correlation test. Survival rates were calculated with the Kaplan-Meier method and compared using the log-rank test.

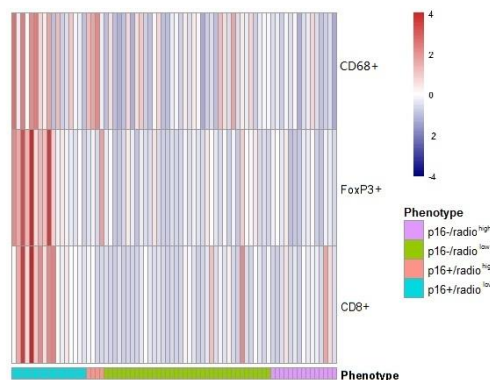
#### Results

The median follow-up was 50 months (range: 4-104). IHC results of CD68 were evaluable for all the 95 patients, CD8 and FoxP3 were evaluable for 74 patients, and PD-L1 was

evaluable for 31 patients. Overall survival (OS) and progression-free survival (PFS) of the four phenotypes were significantly different (5-year OS: PL 95.2%, PH 80%, NL 53.7%, NH 20.8%,  $p < 0.001$ ; 5-year PFS: PL 79.6%, PH 50%, NL 48.7%, NH 7.4%,  $p < 0.001$ ). We found a significant correlation of the p16-radiomic phenotype with density of CD8+ T cells ( $r = 0.39$ ,  $p = 0.001$ ), FoxP3+ T cells ( $r = 0.45$ ,  $p < 0.001$ ) and CD68+ cells ( $r = 0.40$ ,  $p < 0.001$ ), but not with PD-L1 expression. Specifically, all patients with high density of CD8+ T cell, high FoxP3 and high CD68+ macrophages simultaneously, which suggests a favorable immune activated state, exhibit as p16+/radio<sup>low</sup> phenotype (Figure 1).

#### Legend:

Figure 1. Heatmap of distribution of density of CD8+ T cells, FoxP3+ T cells and CD68+ cells according to the four p16-radiomic phenotype (N=74). The columns represent patients and the rows indicate the 3 immune biomarkers. In the bottom color bars each color represents a p16-radiomic phenotype.



#### Conclusion

We demonstrate that radiomic approaches permit noninvasive assessment of immunological characteristic of tumors in head and neck cancers. Further validation in external cohort is required.

#### OC-0587 Preclinical studies of MRI guided BNCT at Torino and Pavia Universities

N. Protti<sup>1</sup>, D. Alberti<sup>2</sup>, A. Toppino<sup>3</sup>, S. Bortolussi<sup>4</sup>, S. Altieri<sup>4</sup>, A. Deagostino<sup>3</sup>, S. Aime<sup>5</sup>, S. Geninatti-Crich<sup>2</sup>  
<sup>1</sup>National Institute of Nuclear Physics INFN, Pavia Unit, Pavia, Italy ; <sup>2</sup>University of Torino, Department of Molecular Biotechnology and Health Sciences, Torino, Italy ; <sup>3</sup>University of Torino, Department of Chemistry, Torino, Italy ; <sup>4</sup>National Institute of Nuclear Physics INFN / University of Pavia, Pavia Unit / Department of Physics, Pavia, Italy ; <sup>5</sup>University of Torino / IBB-CNR, Department of Molecular Biotechnology and Health Sciences / MBC, Torino, Italy

#### Purpose or Objective

Boron Neutron Capture Therapy (BNCT) is a binary hadrontherapy performed on head and neck recurrent and primary cancers, skin melanomas and highly malignant brain tumours. BNCT is based on the capture reaction induced by low energy neutrons on <sup>10</sup>B selectively delivered by tumour-targeting drugs. A couple of high LET hadrons triggers cell death through the local energy deposition along densely ionizing tracks with ranges of 5-9  $\mu$ m, which destroy tumour cells without affecting adjacent healthy tissues. This makes BNCT a promising treatment for disseminated and infiltrating tumours that cannot be handled by surgery, conventional radiotherapy or heavy ion therapy, which require a precise localisation of the pathology.

The real time knowledge of  $^{10}\text{B}$  concentration in tumour is crucial to exploit BNCT selectivity. Aim of the present work is the efficiency evaluation of a theranostic agent for MRI guided BNCT.

#### Material and Methods

The theranostic agent, developed at Torino University, consists of a carborane cage (10 atoms of boron) bound on one side to a Low Density Lipoprotein (LDL) used to target tumour cells, and a  $\text{Gd}^{3+}$  complex on the other for the detection of the agent through Magnetic Resonance Imaging (MRI). The expression of LDLs transporters is upregulated in many tumours and here is exploited to reach the  $^{10}\text{B}$  selective uptake.

The theranostic agent was tested in different murine tumour models including: B16 skin melanoma, Her2+ breast tumour, ZL34 and AE17 malignant pleural mesothelioma. EML4-ALK transgenic mouse model was used as primary lung tumour.

The *in vitro* and *in vivo* studies of selective accumulation and  $^{10}\text{B}$  quantification were carried out at Torino University, while the thermal neutron irradiation was designed and performed at the TRIGA Mark II research nuclear reactor of Pavia University.

#### Results

The *in vitro* studies showed the tumour selective uptake of the theranostic agent and led to the identification of the optimum post injection time to realise BNCT. Three groups of animals for each models were considered: the cold control group, the neutron irradiated group (without  $^{10}\text{B}$  administration) and the BNCT treated group. The animals were followed up for 20 up to 40 days after irradiation and in all the experiments the BNCT treated groups showed a significant reduction in tumour growth with respect to the control groups.

#### Conclusion

A theranostic agent for MRI guided BNCT was developed and positively applied in preclinical treatment of small animal tumour models. The possible use of this kind of boronated agents in clinical BNCT will improve BNCT outcomes making possible the personalisation of the treatment on the  $^{10}\text{B}$  accumulation response of each single patient.

#### OC-0588 Combing hyperthermia and/or OXi4503 with low LET radiation is equivalent to high LET radiation alone

P.B. Elming<sup>1</sup>, B.S. Sørensen<sup>1</sup>, H. Spejlborg<sup>2</sup>, J. Overgaard<sup>1</sup>, M.R. Horsman<sup>1</sup>

<sup>1</sup>Aarhus University Hospital, Dept. of Experimental Clinical Oncology, Aarhus, Denmark ; <sup>2</sup>Aarhus University Hospital, Dept. Oncology, Aarhus, Denmark

#### Purpose or Objective

Tumor hypoxia is a major factor causing resistance to low linear energy transfer (LET) radiation (i.e., photons). One solution to this problem is to use high LET radiation (i.e., carbon ions), but such an approach is not so readily accessible. However, additional therapies increase the efficacy of low LET radiation and may make tumor response equivalent to that seen with high LET radiation. We investigated this by combining low LET radiation with hyperthermia and/or the vascular disrupting agent (VDA) OXi4503.

#### Material and Methods

A C3H mammary carcinoma, implanted in the right rear foot of CDF1 mice, was used for all experiments when at 200 mm<sup>3</sup> in size. Treatments were performed on restrained, non-anaesthetised, animals with the tumor bearing leg exposed and immersed in a water bath maintained at 25°C for radiation (240 kV X-rays) alone or with heating at 41-43°C for 60 minutes. Radiation was applied either in the middle of the heating period (simultaneous treatment), or 1-hour (early sequential treatment) or 4-hours (late sequential treatment) prior to heating. OXi4503 (50 mg/kg) was intraperitoneally

injected 1.5 hours prior to irradiating. Tumor response was the percentage of mice showing local tumor control 90 days after treatment with graded radiation doses, and following logit analysis of the radiation dose-response curve, the TCD50 value (radiation dose causing tumor control in 50% of mice) was estimated.

#### Results

The TCD50 value for low LET photon irradiation alone was 54 Gy. Our previous studies with carbon ions in the same tumor model reported a TCD50 value that was 1.5 times lower than that seen with photons (Sørensen et al., Acta Oncol., 2015;54:1623-30). A similar enhancement ratio (ER; ratio of TCD50 values for radiation alone and radiation + modifier) of 1.5 was obtained with a temperature of 41.5°C when administered simultaneously with the low LET radiation. For a late sequential radiation and heat treatment, temperatures of 42.5°C and above were necessary, although an ER of 1.5 was observed at 41.5°C if this sequential treatment was combined with OXi4503; the VDA alone gave an ER of around 1.3. The effect of using an early sequential approach is under investigation.

#### Conclusion

The local tumor control obtained with high LET carbon ions is also possible with low LET photons if combined with hyperthermia. However, the temperature at which this equivalent response is observed is dependent on the radiation and heat sequence, and whether a VDA is included in the treatment schedule.

#### OC-0589 RBE-weighted dose in carbon ion therapy: impact of the RBE model translation on clinical outcomes

S. Molinelli<sup>1</sup>, M. Bonora<sup>2</sup>, B. Vischioni<sup>2</sup>, J.E. Dale<sup>3</sup>, S. Russo<sup>1</sup>, S. Casale<sup>4</sup>, M.R. Fiore<sup>2</sup>, I. Fumagalli<sup>5</sup>, A. Hasegawa<sup>6</sup>, L. Preda<sup>7</sup>, P. Fossati<sup>8</sup>, F. Valvo<sup>2</sup>, M. Ciocca<sup>1</sup>  
<sup>1</sup>National Center for Oncological Hadrontherapy, Medical Physics, Pavia, Italy; <sup>2</sup>National Center for Oncological Hadrontherapy, Clinical Department, Pavia, Italy; <sup>3</sup>Haukeland University Hospital, Department of Oncology and Medical Physics, Bergen, Norway; <sup>4</sup>Institute of Radiology IRCCS San Matteo University Hospital, Department of Diagnostic Medicine, Pavia, Italy; <sup>5</sup>University of Milano Bicocca, Faculty of Medicine, Milano, Italy; <sup>6</sup>Osaka Heavy Ion Therapy Center, Clinical Department, Osaka, Japan; <sup>7</sup>National Center for Oncological Hadrontherapy, Radiology Department, Pavia, Italy; <sup>8</sup>MedAustron, Clinical Department, Wiener Neustadt, Austria

#### Purpose or Objective

With the aim of taking advantage of the long term experience in carbon ion radiotherapy (CIRT) of the National Institute of Radiological Sciences (NIRS), we implemented at the National Center for Oncological Hadrontherapy (CNAO) a conversion scheme for relative biological effectiveness (RBE)-weighted prescription doses ( $D_{\text{RBE}}$ ) to account for the use of a different carbon ion RBE model (1). No correction was applied for NIRS defined constraints to optic pathways, brainstem and rectum, thus following a conservative approach. The purpose of this study is to assess the clinical implications of the described method on tumor control.

#### Material and Methods

Plans of 60 Adenoid Cystic Carcinoma (ACC) and 25 sacral chordoma (SC) patients, previously treated at CNAO with a Local Effect Model I (LEM1)- $D_{\text{RBE}}$  optimization, were exported for recalculation with a Microdosimetric Kinetic Model (MKM)- $D_{\text{RBE}}$  calculation system. The latter model is currently in use at NIRS. In addition, 10 patients treated at NIRS for a pancreatic lesion were used for RBE evaluation in this tumor site. LEM1 prescription doses were 68.8 Gy(RBE) and 70.4 Gy(RBE) in 16 fractions and 57.6 Gy(RBE) in 12 fractions for the ACC, SC and pancreas cases, respectively.  $D_{\text{RBE}}$  to 95%, 50% and 2% of the clinical

target volume (CTV), for LEMI- and MKM-RBE computations, were criteria to assess target dose. Selected ACC and SC included patients presenting a tumor relapse at follow-up. Recurrences were retrospectively contoured on the follow-up MR scan corresponding to first diagnosis. The relapse location, with respect to CTV and spared OARs, and relative dose distributions in the two RBE systems were analyzed.

### Results

The MKM- $D_{RBE}$  analysis showed that prescription dose conversion factors correctly acted on median CTV  $D_{RBE}$ , but allowed the generation of low and high MKM- $D_{RBE}$  regions (figure 1a-b) linked to the steeper MKM-RBE variation along the beam path. Location of inhomogeneities was related to tumor volume, beam number and configuration. The average MKM- $D_{RBE}$  reduction at 95% of CTV ranged from 8% to 2% of the expected value, for the lower and higher fraction doses, respectively. ACC and SC relapses were mainly (38% ACC and 25% SC) related to poor CTV coverage due to OARs sparing to a MKM- $D_{RBE}$  significantly lower than expected (figure 1c). No clear evidence was found of a cause-effect relation between low MKM- $D_{RBE}$  to 95% of CTV and loss of tumor control.

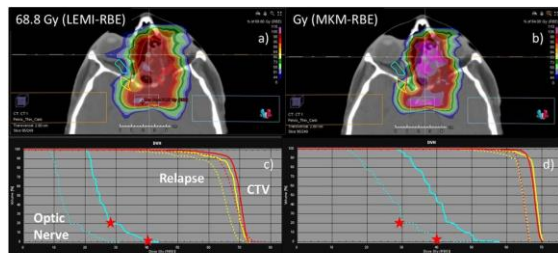


Figure 1: a) Transversal  $D_{RBE}$  distribution of a LEMI-optimized ACC plan to 68.8 Gy (RBE). The CTV contour is plotted in red, the optic nerve in light blue and the relapse in yellow. b) Transversal  $D_{RBE}$  distribution of the corresponding MKM-re-calculated plan, showing the appearance of CTV hot and cold spots. c) DVHs corresponding to LEMI (solid lines) and MKM (dotted lines) computations. The red stars point to the MKM-defined NIRS constraint to the optic nerve. d) DVHs corresponding to a MKM-optimized plan to 64 Gy (RBE) (dotted lines) and corresponding LEMI-re-calculated plan (solid lines).

### Conclusion

The use of a MKM system, as a starting point for LEMI optimization, could reduce CTV dose inhomogeneities and their potential impact on tumor local control and patient toxicity (figure 1d).  $D_{RBE}$  deviations between LEMI and MKM plans were significantly higher in regions where steep dose gradients were applied to spare OARs, than in the target region. New constraints are currently being defined for optic pathways, brainstem and rectum at CNAO to improve target coverage with no expected increase in tissue complications.

(1) Molinelli S. et al. Radiotherapy and Oncology 120 (2016).

### OC-0590 Avoidance of DNA replication stress by functional HR leads to radioresistance in stem cell-like TNBC

K. Borgmann<sup>1</sup>, M. Felix<sup>1</sup>, E. Anna Maria<sup>1</sup>, B. Saskia<sup>1</sup>, H. Linda<sup>2</sup>, P. Claudia<sup>2</sup>, D. Anna<sup>2</sup>, W. Sabine<sup>3</sup>, W. Harriet<sup>4</sup>, R. Kai<sup>1</sup>, P. Cordula<sup>5</sup>

<sup>1</sup>Laboratory of Radiobiology & Experimental Radiooncology, Department of Radiotherapy- Center of Oncology- University Medical Center Hamburg - Eppendorf UKE, Hamburg, Germany ; <sup>2</sup>Institute of Radiooncology- OncoRay- National Center for Radiation Research in Oncology-, Faculty of Medicine and University Hospital Carl Gustav Carus- Technische Universität Dresden- Helmholtz-Zentrum Dresden - Rossendorf, Dresden, Germany ; <sup>3</sup>Institute of Biochemistry, University Medical Center Hamburg-Eppendorf UKE, Hamburg, Germany; <sup>4</sup>Department of Tumor Biology, University Medical Center Hamburg-Eppendorf UKE, Hamburg, Germany; <sup>5</sup>Department of

Radiotherapy, Center of Oncology- University Medical Center Hamburg-Eppendorf UKE, Hamburg, Germany

### Purpose or Objective

Breast cancer comprises a heterogeneous group of tumors of whom 20% are categorized as triple-negative (TNBC). A specific tumor therapy for this subgroup is still lacking. Important biological characteristics and potential therapeutic targets of TNBC include a basal-like and mesenchymal so called stem-cell phenotype and a defect in the DNA repair pathway Homologous Recombination (HR), which feeds the observed elevated chromosomal instability (CIN) in these tumors. This project aims to develop treatment intensification strategies based on the simultaneous exploitation of the HR-deficiency and the stem-like phenotype, using specific inhibitors such as ATR, CHK1, RAD51, and PARP1 in combination with irradiation.

### Material and Methods

The investigations were performed in three TNBC cell lines MDA-MB-231 which metastasize systemically (WT), into the brain (BR) or into the bone marrow (SA) and their respective radiation resistant subclones selected by repeated irradiation (10x4Gy). Luminal MCF7 cells served as controls. Expression of HR-related and stem-like factors was determined and DNA repair in general (53BP1) as well as HR functionality (RAD51 foci formation, MMC-sensitivity and plasmid reporter assay) was analyzed. Replication processes were examined by using the DNA fiber assay and migration assays were also performed. Radiosensitizing effect of several HR and S-phase specific inhibitors were analyzed by colony assay and correlated with expression profiles of stem cell markers and DNA repair proteins in the METABRIC database.

### Results

A significantly increased expression of the stem cell markers ALDH1, ZEB1 and Vimentin was observed in all four radioresistant sublines, both on single cell basis and in Western blots. This led to an increased activation of ALDH1 in the Aldefluor assay in all investigated clonal subpopulations. After irradiation, survival in the clonal subpopulation was significantly increased compared to the original cell line. In accordance with this, the radioresistant subclones showed a lower number of 53-BP1 foci, indicating improved DNA repair. Also HR capacity seem to be improved. This is confirmed by a significantly stronger activation of the Intra-S phase control point, with an increased activation of CHK1. This results in a distinct radiosensitization after CHK1i; the most radioresistant cell line was most strongly sensitized (EF=3) and also showed up in DNA replication processes: the higher the EF the stronger the inhibitory effect on DNA replication. The effect of other inhibitors on radiosensitivity is currently being investigated. A second promising target is RAD51, because a METABRIC analysis (952 TNBCs) showed that both, RAD51 and CHK1 are differentially expressed according to their degree of chromosomal instability.

### Conclusion

In conclusion the results presented here show that DNA repair and a stem-like phenotype are closely intertwined in determining resistance to tumor therapy of TNBCs with high CIN.

Proffered Papers: CL 11: Proffered papers : Breast

### OC-0591 Response after MR-guided single dose ablative preoperative partial breast irradiation

J. Vasmel<sup>1</sup>, R. Charaghvandi<sup>1</sup>, A. Houweling<sup>1</sup>, M. Philippens<sup>1</sup>, C. Vreuls<sup>2</sup>, P. Van Diest<sup>2</sup>, G. Van Leeuwen<sup>3</sup>, J. Van Gorp<sup>4</sup>, A. Witkamp<sup>5</sup>, C. Van der Pol<sup>5</sup>, R. Koelemij<sup>6</sup>, A. Doeksen<sup>6</sup>, M. Sier<sup>7</sup>, T. Van Dalen<sup>8</sup>, E. Van der Wall<sup>9</sup>, W. Veldhuis<sup>10</sup>, M. Hobbelink<sup>11</sup>, A. Kirby<sup>12</sup>, H. Verkoijen<sup>13</sup>, D. Van den Bongard<sup>1</sup>

<sup>1</sup>UMC Utrecht, Radiotherapy, Utrecht, The Netherlands ; <sup>2</sup>UMC Utrecht, Pathology, Utrecht, The Netherlands ; <sup>3</sup>St Antonius Hospital, Pathology, Nieuwegein, The Netherlands ; <sup>4</sup>Diakonessenhuis, Pathology, Utrecht, The Netherlands ; <sup>5</sup>UMC Utrecht, Surgery, Utrecht, The Netherlands ; <sup>6</sup>St Antonius Hospital, Surgery, Nieuwegein, The Netherlands ; <sup>7</sup>Rivierenland Hospital, Surgery, Tiel, The Netherlands; <sup>8</sup>Diakonessenhuis, Surgery, Utrecht, The Netherlands; <sup>9</sup>UMC Utrecht, Medical Oncology, Utrecht, The Netherlands ; <sup>10</sup>UMC Utrecht, Radiology, Utrecht, The Netherlands; <sup>11</sup>UMC Utrecht, Nuclear Medicine, Utrecht, The Netherlands ; <sup>12</sup>The Royal Marsden NHS Foundation Trust, Radiotherapy, Sutton, United Kingdom; <sup>13</sup>UMC Utrecht, Imaging, Utrecht, The Netherlands

### Purpose or Objective

This single arm interventional multi-center cohort study was designed to evaluate the pathologic and radiologic response after MR-guided single dose ablative preoperative partial breast irradiation (PBI) in early-stage breast cancer patients with low risk on local recurrence.

### Material and Methods

In the ABLATIVE study (ClinicalTrials.gov: NCT02316561), we included women with unifocal, estrogen-receptor positive and HER2-negative tumors with a maximum diameter of 20mm (age 50-70 years), or 30mm (age  $\geq$ 70 years) as assessed on MRI. Furthermore, patients were required to have a tumornegative sentinel lymph node biopsy, no history of breast cancer and no indication for chemotherapy. Patients were treated with MR-guided single dose ablative preoperative PBI: 20Gy to the gross tumor volume (GTV) and 15Gy to the clinical target volume (CTV=GTV+2cm margin). GTV and CTV were expanded by 3mm to create the planning target volume. Breast-conserving surgery (BCS) was originally performed 6 months after PBI. After the first 15 patients this interval was prolonged to 8 months to evaluate whether this would increase the rate of pathologic complete response (pCR). Primary outcome was the rate of pCR, which was defined as no residual tumor cells. Secondary outcomes were radiologic response and treatment-induced toxicity. Radiologic response was evaluated by dedicated breast radiologists on tumor morphology, diffusion restriction and contrast enhancement kinetics using DCE- and DW-MRI every 2 months until BCS was performed. Toxicity was assessed according to CTCAE v4.03.

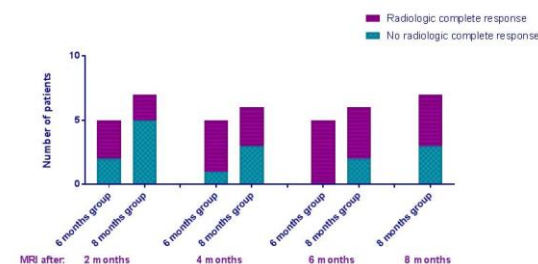
### Results

From May 2015 until November 2017, 32 patients were recruited. Median follow-up was 18 months (range 9-36). The median tumor size was 13mm (range 5-20) and median age 64 years (range 51-78). pCR was reported in 5 and 7 patients (33% and 41%), and near pCR in 5 and 6 patients (33% and 35%), after 6 and 8 months respectively (table 1). Radiologic response assessment showed an increase in complete response during follow-up. Radiologic complete response was only observed in patients with pCR or near pCR, however, 11 of the 23 patients with pCR or near pCR did not show a radiologic complete response (figure 1). Five patients received preoperative endocrine treatment which was initiated after PBI; 2 of these patients had pCR. Only mild treatment-induced toxicity (i.e. grade 1-2) was observed and all grade 2 toxicity was transient. Observed toxicity was grade 1 fibrosis (91%), grade 1 breast pain (59%) and transient grade 2 breast pain (3%).

Table 1: Pathologic response according to interval between single dose ablative preoperative PBI and BCS.

	6 month interval (N=15)	8 month interval (N=17)
pCR (no residual tumor cells)	5 (33%)	7 (41%)
Near pCR ( $<$ 10% residual tumor cells)	5 (33%)	6 (35%)
Partial response (10-50% residual tumor cells)	4 (27%)	2 (12%)
Stable disease ( $>$ 50% residual tumor cells)	1 (7%)	2 (12%)

Figure 1. Radiologic response in patients with pCR at 6 and 8 months following PBI.



### Conclusion

MR-guided single dose ablative preoperative PBI resulted in pCR in one third of the patients. Radiologic complete response on MRI was not recognized in all patients with pCR. Further assessment of MRI and other response monitoring techniques should be considered in single-dose ablative preoperative PBI.

### OC-0592 5 year results of the Preoperative Accelerated Partial Breast Irradiation (PAPBI) trial

S. Bosma<sup>1</sup>, F. Leij van der<sup>1</sup>, S. Vreeswijk<sup>1</sup>, M. Vijver van der<sup>2</sup>, S. Rivera<sup>3</sup>, T. Foukakis<sup>4</sup>, D. Bongard van den<sup>5</sup>, E. Rutgers<sup>6</sup>, A. Scholten<sup>1</sup>, H. Bartelink<sup>1</sup>, P. Elkhuisen<sup>1</sup>  
<sup>1</sup>The Netherlands Cancer Institute, Radiation oncology, Amsterdam, The Netherlands; <sup>2</sup>Amsterdam UMC, Pathology, Amsterdam, The Netherlands; <sup>3</sup>Institute Gustave Roussy, Radiation Oncology, Paris, France; <sup>4</sup>Karolinska institutet, Radiation Oncology, Stockholm, Sweden ; <sup>5</sup>UMCU, Radiation Oncology, Utrecht, The Netherlands ; <sup>6</sup>The Netherlands Cancer Institute, Surgery, Amsterdam, The Netherlands

### Purpose or Objective

Accelerated Partial Breast Irradiation (APBI) is a treatment option for low-risk early stage breast cancer. Preoperative APBI (PAPBI) provides several advantages compared to conventional postoperative radiotherapy (RT), including improved target localization, accurate tumor delineation, the possibility for response evaluation and excision of the high dose irradiated volume. Here, we present the 5-year results of the PAPBI trial providing novel data from a large set of preoperatively irradiated patients.

### Material and Methods

In the multicentre PAPBI trial, 138 patients were included between 2010-2017. Women aged  $\geq$  60 years with an invasive, unifocal  $\leq$  3 cm on MRI, (non-lobular) adenocarcinoma of the breast and a negative SN received PAPBI (40 Gy in 10 fractions in 2 weeks or 30 Gy in 5 fractions in 1 week). 6 weeks after RT a wide local excision was performed. The primary endpoints were breast fibrosis and cosmetic outcome. Local recurrences (LR) should not exceed 4% at 5 years. Toxicity was scored 3-monthly in the first year, then every 6 months for the first 5 years and yearly thereafter. Cosmetic outcome was evaluated by the treating physician and the (Dutch) patients before start of treatment, 6 months after treatment and then yearly.

### Results

133 patients were analyzed with a median follow-up of 4.6 yrs (0.9-8.3 yrs). Baseline characteristics are displayed in table 1. 78 (59%) patients were treated with 10x4 Gy and 55 (41%) with 5x6 Gy. A postoperative complication occurred in 14% of patients, of which 4 patients required re-surgery. 11% had a postoperative infection requiring treatment. Acute skin toxicity was absent in 65% of patients and 34% of patients had grade 1 skin toxicity. At 1 year of follow-up, induration/fibrosis at the tumor area was absent in 30(26%) and mild in 69(60%) of 115 patients. At 3 (n=94) and 5 years (n=55) of follow-up, respectively

37% and 65% of patients had no fibrosis and 50% and 29% mild fibrosis at the tumor area. The global cosmetic outcome was good-excellent in 70% after 6 months, 88% after 2 years and 93% after 5 years (figure 1). Patients were very satisfied/satisfied with the cosmetic outcome in 78% after 6 months, 84% after 2 years and 93% after 5 years. An LR was detected in 4 patients: 3 were located along the biopsy trajectory. Subsequently, we adjusted the protocol by surgical removal of the biopsy route.

#### Characteristics

Median age (yrs) 68 (60-87)

Tumour size (mm) 12 (5-27)

#### Grade

1 35 (27%)

2 89 (68%)

3 7 (5%)

#### Subtype

ER+/PR+/HER2- 86 (65%)

ER+/PR-/HER2- 36 (27%)

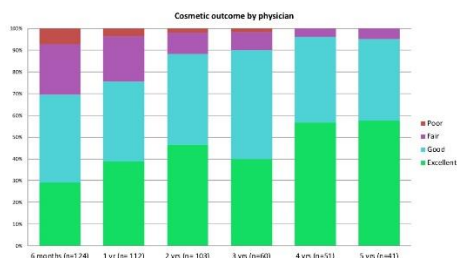
ER-/PR-/HER2- 8 (6%)

HER2+ 2 (2%)

#### Systemic therapy

Hormonal 89/129 (64%)

Chemotherapy 5/129 (4%)



#### Conclusion

PAPBI is a feasible and promising treatment for low-risk breast cancer patients resulting in excellent cosmetic outcome and limited fibrosis, presumably due to removal of the high dose area. Postoperative complications are comparable to surgical complications before PBI. Cosmetic outcome improved over time. A few recurrences in the biopsy tract occurred before adjustment of the protocol.

#### OC-0593 Prone breast radiotherapy reduces acute skin toxicity - results from a multicentre single blind RCT

D. Vesprini<sup>1</sup>, M. Davidson<sup>2</sup>, S. Bosnic<sup>3</sup>, L. Fenkell<sup>4</sup>, D. Comsa<sup>4</sup>, P. Truong<sup>5</sup>, E. Wai<sup>5</sup>, M. El-Mallah<sup>6</sup>, L. Garcia<sup>6</sup>, C. Stevens<sup>7</sup>, M. Follwell<sup>7</sup>, H. Gotthardt<sup>3</sup>, S. Zhu<sup>3</sup>, A. Kiss<sup>8</sup>, E. Rakovitch<sup>1</sup>, J. Pignol<sup>9</sup>

<sup>1</sup>Sunnybrook Odette Cancer Centre- University of Toronto, Radiation Oncology, Toronto, Canada ;

<sup>2</sup>Sunnybrook Odette Cancer Centre- University of Toronto, Medical Physics, Toronto, Canada ;

<sup>3</sup>Sunnybrook Odette Cancer Centre, Radiation Oncology, Toronto, Canada ;

<sup>4</sup>Southlake Regional Health Centre- University of Toronto, Radiation Medicine Program, Newmarket, Canada ;

<sup>5</sup>Victoria and University of British Columbia, Radiation Oncology, Victoria, Canada ;

<sup>6</sup>Durham Regional Cancer Centre, Radiation Oncology, Oshawa, Canada ;

<sup>7</sup>Simcoe Muskoka Regional Cancer Centre- University of Toronto, Radiation Oncology, Barrie, Canada ;

<sup>8</sup>University of Toronto, Institute of Health Policy- Management and Evaluation, Toronto, Canada ;

<sup>9</sup>Dalhouse University, Radiation Oncology, Halifax, Canada

#### Purpose or Objective

To determine if treating large breasted women with adjuvant breast radiotherapy (RT) in the prone position reduces acute skin toxicity when compared to the supine position.

#### Material and Methods

From 2013 to 2018 a total of 357 large breasted women (bra size 40in and/or D cup or greater) from 5 centres in Canada receiving adjuvant RT to the breast alone were randomized to the supine or prone position. Patients were initially treated to 50Gy/25 fractions (conventional fractionation), though the protocol was amended at 3 years to allow 42.5Gy/16 fractions (hypofractionation) which was almost exclusively used from that time onwards. Randomization was blocked on postoperative RT boost. Acute toxicity including moist desquamation (MD), erythema, and pain as per CTCAE 4.03, was assessed by an observer blinded to treatment position at baseline, weekly during RT and up to 6 wks post treatment. Comparison of the frequency of grade 2-3 MD between treatment arms was performed using a two sample two-sided test of proportions providing an OR and its associated 95% CI. Multivariable logistic regression analysis evaluated the relative risk of acute skin toxicity as the dependent variable. The various independent variables tested included the treatment position, boost delivery, fractionation, breast size, and chemotherapy.

#### Results

A total of 357 patients were accrued, 182 treated supine and 175 prone. 180 received conventional fractionation (92 supine, 88 prone) and 177 treated with hypofractionation (90 supine, 87 prone). On bivariate analysis there was significantly more acute MD in patients treated supine compared to prone (39.6% vs 26.9%; OR 1.8, CI 1.1-2.8, P=0.01). This association was confirmed on multivariate analysis with increased MD in the supine position (OR 1.9, CI 1.2-3.1, P<0.01). Additional factors independently associated with MD included use of RT boost (OR 2.8, CI 1.6-4.7, P<0.01), conventional fractionation (OR 3.0, CI 1.8-4.9, P<0.01) and larger bra size (OR 2.4, CI 1.4-3.9, P<0.01). There was no association between MD and chemotherapy. Similar analyses showed only boost and conventional fractionation were associated with erythema and pain. In an unplanned subset analysis, there was significantly more acute MD in patients treated with conventional fractionation compared to those treated with hypofractionation (OR 2.5, CI 1.6 - 4.0, P < 0.0001) and this was true for both the supine (OR 2.7, CI 1.5-5.0, P<0.0001) and prone (OR 2.4, CI 1.2-4.8, P<0.0001) positions.

#### Conclusion

This multicentre single blinded RCT confirms that treatment in the prone position leads to significantly less acute MD compared to the supine position in large breasted women receiving adjuvant radiotherapy. It also shows increased toxicity using an RT boost and conventional fractionation.

#### OC-0594 Acute toxicity results after breast-conserving therapy in "boost vs no boost (BONBIS)" DCIS trial

C. Bourcier<sup>1</sup>, D. Cowen<sup>2</sup>, C. Lemanski<sup>1</sup>, F. Castan<sup>3</sup>, S. Rivera<sup>4</sup>, B. De La Lande<sup>5</sup>, K. Peignaux<sup>6</sup>, M. Le Blanc-Onfroy<sup>7</sup>, A. Benyoucef<sup>8</sup>, A. Mege<sup>9</sup>, Z. Douadi-Gaci<sup>10</sup>, S. Racadot<sup>11</sup>, I. Latorzeff<sup>12</sup>, U. Schick<sup>13</sup>, S. Jacquot<sup>14</sup>, C. Massabeau<sup>15</sup>, P. Guilbert<sup>16</sup>, J. Geffrelot<sup>17</sup>, S. Ellis<sup>18</sup>, I. Lecouillard<sup>19</sup>, C. Breton-Callu<sup>20</sup>, A. Richard-Tallet<sup>21</sup>, P. Bontemps<sup>22</sup>, P. Fenoglio<sup>1</sup>, D. Azria<sup>1</sup>

<sup>1</sup>ICM-Val d'Aurelle, Radiation Oncology, Montpellier, France;

<sup>2</sup>CHU La Timone, Radiation Oncology, Marseille, France;

<sup>3</sup>ICM-Val d'Aurelle, Biostatistic Department, Montpellier, France;

<sup>4</sup>Gustave Roussy, Radiation Oncology, Villejuif, France ;

<sup>5</sup>Curie Saint Cloud, Radiation Oncology, Saint Cloud, France ;

<sup>6</sup>Centre Georges François Leclerc, Radiation Oncology, Dijon, France ;

<sup>7</sup>Centre René Gauducheau, Radiation Oncology, Saint Herbain, France ;

<sup>8</sup>Centre Henri Becquerel,

Radiation Oncology, Rouen, France ; <sup>9</sup>Institut Sainte Catherine, Radiation Oncology, Avignon, France ; <sup>10</sup>Centre Catherine de Sienne, Radiation Oncology, Nantes, France; <sup>11</sup>Centre Léon Bérard, Radiation Oncology, Lyon, France; <sup>12</sup>Groupe ONCORAD GARONNE, Radiation Oncology, Toulouse, France ; <sup>13</sup>CHU Brest, Radiation Oncology, Brest, France ; <sup>14</sup>Centre de Cancérologie de Grand Montpellier, Radiation Oncology, Montpellier, France; <sup>15</sup>Institut Claudius Regaud, Radiation Oncology, Toulouse, France ; <sup>16</sup>Institut Jean Godinot, Radiation Oncology, Reims, France ; <sup>17</sup>Centre François Baclesse, Radiation Oncology, Caen, France ; <sup>18</sup>Centre Catalan d'Oncologie, Radiation Oncology, Perpignan, France ; <sup>19</sup>Centre Eugène Marquis, Radiation Oncology, Rennes, France ; <sup>20</sup>Institut Bergonié, Radiation Oncology, Bordeaux, France ; <sup>21</sup>Institut Paoli Calmette, Radiation Oncology, Marseille, France ; <sup>22</sup>CHU Jean Minoz, Radiation Oncology, Besançon, France

### Purpose or Objective

To analyze the tolerance in the French randomized phase 3 trial (BONBIS) that investigated the role of the boost to the tumor bed after breast-conserving surgery for ductal carcinoma in situ (DCIS).

### Material and Methods

From November 2008 to July 2014, 2004 DCIS patients were treated by tumorectomy followed by whole-breast irradiation (WBI) to a dose of 50 Gy in 25 fractions for 5 weeks. Patients were randomized after surgery and before WBI between an additional boost to the primary tumor bed (16 Gy in 8 fractions of 2 Gy, n=1002) and no further treatment (n=1002). Stratification factors were centre, age (below or above 40), hormone therapy (yes or no), histological grade (low or intermediate or high), diagnosis mode (clinically or by mammography), surgical margins (1-2 mm vs 3 mm). Acute toxicities were prospectively recorded from baseline to 3 months after radiotherapy completion.

### Results

A total of 1928 DCIS patients were evaluable for acute tolerance. Median age was 57 years. Re-excision was needed in 20% of patients in each treatment arm, mainly due to involved margins or postoperative complications. Median time for radiotherapy initiation was 54 days from surgery [min; max=5; 146]. Mean volumes of breast (CTV1) and of boost (CTV2) were 545 cc [min; max= 6; 2818] and 25 cc [min; max= 0; 754], respectively. A significant higher rate of radiotherapy disruption was observed in boost arm (3.9% vs 1.5%; p=0.015) due to acute toxicities occurrence with a mean time of disruption of 3 days. A significantly higher rate of grade ≥2 overall toxicities (including skin, edema, pain) was observed in the boost arm (54.6% vs 36.4%; p<0.001). Similarly, grade 3 erythema was significantly increased in the boost arm (5.4% vs 2.1%; p<0.001).

### Conclusion

In the boost arm, a higher rate of grade ≥2 acute toxicities was observed compared to the control arm. However, grade 3 erythema was quite low even though its occurrence was significantly higher in the boost arm. A multivariate analysis of acute toxicities will be presented at the congress.

### OC-0595 Does seroma predict patient-reported adverse effects following breast radiotherapy in IMPORT HIGH?

I.S. Bhattacharya<sup>1</sup>, J.S. Haviland<sup>1</sup>, C. Perotti<sup>2</sup>, D. Eaton<sup>3</sup>, S. Gulliford<sup>4</sup>, E. Harris<sup>4</sup>, C.E. Coles<sup>5</sup>, C.C. Kirwan<sup>6</sup>, J.M. Bliss<sup>1</sup>, A.M. Kirby<sup>7</sup>

<sup>1</sup>Institute of Cancer Research, Clinical Trials and Statistics Unit, London, United Kingdom ; <sup>2</sup>Royal Marsden NHS Foundation Trust, Radiotherapy and Imaging, London, United Kingdom ; <sup>3</sup>Mount Vernon Hospital, National Radiotherapy Trials QA Group, London, United Kingdom ; <sup>4</sup>Institute of Cancer Research, Radiotherapy

and Imaging, London, United Kingdom ; <sup>5</sup>Cambridge University, Department of Oncology, Cambridge, United Kingdom ; <sup>6</sup>University of Manchester, Division of Cancer Sciences, Manchester, United Kingdom ; <sup>7</sup>Royal Marsden NHS Foundation Trust and Institute of Cancer Research, Radiotherapy and Imaging, London, United Kingdom

### Purpose or Objective

Seroma describes collection of serous fluid within a cavity and can occur following breast surgery. A seroma prevalence of 37-57% has been reported. Seroma is associated with adverse effects (AE) following breast radiotherapy. These AE have been predominantly assessed by clinicians and photographs, and not by patients. This study investigates if seroma is associated with patient-reported AE in IMPORT HIGH (CRUK/06/003).

### Material and Methods

IMPORT HIGH (ISRCTN47437448) is a randomised, multi-centre phase III trial testing dose-escalated simultaneous integrated boost against sequential boost each delivered by intensity modulated radiotherapy (RT) in women with breast cancer. AE assessment included patient-reported outcome measures (PROMs) in a planned sub-set of patients. A case-control methodology was used to investigate the association of seroma with patient-reported AEs at 3 years. Cases were patients who reported moderate/marked breast appearance change and controls were those who reported none/mild changes. One control was selected at random for each case (unmatched). Seromas were identified on RT CT planning scans and graded as not visible/subtle or visible/highly visible. Logistic regression models were used to test associations between seroma and moderate/marked breast appearance change at 3 years, adjusting for patient and tumour/treatment factors. Tumour and treatment factors were reported by clinicians.

### Results

2621 patients were recruited to IMPORT HIGH. 1078/1149 patients at centres participating in the PROMs sub-study consented to PROMs. 836 patients responded to whether they had breast appearance change at 3 years, of whom 231 (28%) patients reported moderate/marked changes (cases); 231 controls were identified. RT CT planning data were available for 202 cases and 205 controls. 156/231 (68%) cases and 148/231 (64%) controls received chemotherapy respectively. Seroma prevalence was 41/202 (20%) in cases and 32/205 (16%) in controls. No significant association was found between visible seroma and moderate/marked breast appearance change [odds ratio 1.38 (95% confidence interval 0.83-2.29), p=0.22] regardless of chemotherapy use. Larger seroma volume was significantly associated with worse breast appearance change on univariate analysis only [1.21 (1.02-1.44), p=0.03]. Treatment group was not significant on univariate analysis. On multivariable analysis, independent risk factors for worse breast appearance change were larger tumour size [1.43 (1.13-1.82), p=0.003], haematoma [5.96 (2.20-16.11), p<0.001], current smoking [2.25 (1.06-4.74), p=0.03] and body image concerns at baseline [1.04 (1.00-1.09), p=0.04].

### Conclusion

Seroma prevalence in this study was lower than previously reported, perhaps reflecting the proportion of patients receiving chemotherapy in whom seroma resolves. Seroma was not associated with patient-reported breast appearance change but haematoma was a significant risk factor. Smoking cessation pre-radiotherapy should be encouraged to reduce AE.

### OC-0596 Importance of dose to the atherosclerotic plaque in the LAD for cardiac toxicity in breast cancer

V. Van den Bogaard<sup>1</sup>, D. Spoor<sup>1</sup>, A. Van der Schaaf<sup>1</sup>, L. Van Dijk<sup>1</sup>, J. Langendijk<sup>1</sup>, J. Maduro<sup>1</sup>, A. Crijns<sup>1</sup>

<sup>1</sup>University Medical Center Groningen, Radiation Oncology, Groningen, The Netherlands

### Purpose or Objective

Recent studies have demonstrated a dose-effect relationship between radiation dose to the heart and the risk of an acute coronary event (ACE). However, knowledge on the exact underlying mechanisms behind this radiation-induced cardiac toxicity is lacking. Such information is crucial for the development of new strategies to optimize radiotherapy (RT) treatment planning.

We hypothesized that radiation dose to atherosclerotic plaques leads to subsequent inflammatory reactions and increased risk of ACEs. Thus, dose to the plaques may be a stronger predictor of an ACE after RT than the dose to the left anterior descending coronary artery (LAD). Therefore, the aim of this study was to investigate the association between radiation dose to the LAD and the LAD-plaques and the risk of an ACE in breast cancer (BC) patients treated with 3D conformal radiation therapy.

### Material and Methods

The study cohort consisted of 952 BC patients treated with postoperative RT after breast conserving surgery. The LAD was delineated using an auto-segmentation tool. After calculation of the coronary artery calcium score, LAD-plaques with Hounsfield units  $\geq 130$  were manually delineated. The primary endpoint was the cumulative incidence of an ACE (defined according to Darby *et al.*) 9 years after treatment. For each individual patient, the mean heart dose (MHD), mean dose to the LAD and the mean dose to the LAD-plaques were collected from planning CT scans.

First, the relation between the dose to the LAD and the LAD-plaques and ACEs was analyzed with an univariable Cox-regression analysis. Then, an association analysis using a Cox-regression model was performed, only including patients who had a LAD-plaque. Furthermore, we used a multivariable Cox-regression analysis to calculate the excess risk of an ACE per patient including age, cardiac risk factors (0 or  $\geq 1$ ) and mean dose to the heart and LAD-plaques.

### Results

The median follow-up time was 7.5 years (range: 0.1-10.1 years). In total, 31 patients developed an ACE during follow-up. 167 patients (17.5%) had a LAD-plaque. Univariable Cox-regression analysis showed that the impact of the dose to the LAD-plaque was much stronger than the impact of the MHD and the mean dose to the LAD (Figure 1). A significant but modest association between radiation dose to the LAD and ACEs was found (regression coefficient 0.053 (95% CI 1.014-1.096),  $P=0.008$ ). However, a much stronger and significant association was found between the mean dose to the LAD-plaques and ACEs (regression coefficient 0.323 (95% CI 1.129-1.689),  $P=0.002$ ). In figure 2, the NTCP-curves are shown for a 50-year old patient in the presence of a cardiac risk factor for ACE.

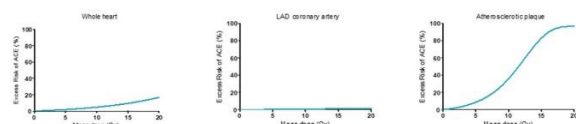


Fig. 1: Univariable Cox-regression analysis for the cumulative incidence of ACEs within the first 9 years after RT

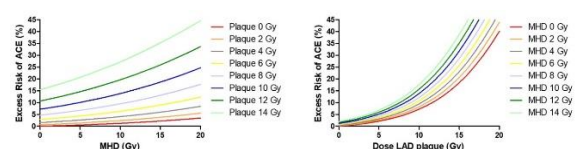


Fig. 2: NTCP-models for the cumulative incidence of ACEs within the first 9 years after RT in a 50-year old patient in the presence of a cardiac risk factor for ACE.

### Conclusion

The results of this study suggest that mean dose to the atherosclerotic plaque in the LAD is more important for the development of an ACE in BC patients than the MHD, possibly due to radiation-induced inflammatory reactions in pre-existent plaques. This will be further investigated.

### Proffered Papers: CL 12: Proffered papers : Health Economics and Health services research

#### OC-0597 Implementing a quality indicator project on a national basis: a feasibility study

A. Vaandering<sup>1</sup>, Y. Lievens<sup>2</sup>, N. Jansen<sup>3</sup>, C. Weltens<sup>4</sup>, L. Moretti<sup>5</sup>, K. Stellamans<sup>4</sup>, F. Vanhoutte<sup>2</sup>, P. Scalliet<sup>1</sup>, V. Remouchamps<sup>6</sup>

<sup>1</sup>UCL Cliniques Universitaires St Luc, Department of Radiation Oncology, Brussels, Belgium; <sup>2</sup>Ghent University Hospital, Department of Radiation Oncology, Ghent, Belgium; <sup>3</sup>University Hospital of Liège, Department of Radiation Oncology, Liège, Belgium; <sup>4</sup>AZ Groeninge, Department of Radiation Oncology, Kortrijk, Belgium; <sup>5</sup>Institut Jules Bordet, Department of radiation oncology, Brussels, Belgium; <sup>6</sup>CHU-UCL Namur - Site Saint Elisabeth, Department of radiation oncology, Namur, Belgium

#### Purpose or Objective

Quality indicators (QI) are measurement tools that can be used as guides to evaluate and improve overall quality of patient care. Monitoring QIs amongst departments allows for clinical practice benchmarking leading to exchange of best practice and the delivery of best-quality care. Mandated by the Belgian Federal Government, radiotherapy (RT) specific structural, process and outcome indicators were defined in a collaboration of the College for Physicians in Radiation Oncology (RO) in Belgium and the Belgian Quality Managers (QM) in radiotherapy Association (QMRT.be). Subsequently, a voluntary national QI data collection started, with the aim of generating benchmarking reports and supporting departmental and national quality improvement projects.

#### Material and Methods

The QI were defined through a simplified Delphi approach by a panel of RO, QM and medical physics experts following the national requirement to collect quantitative data annually (e.g. number of treatments) but also based on established guidelines or good practice. As such, 18 structural (e.g. number of equipment and treatment activities), 30 process (e.g. timely delivery) and 6 outcome QIs (recorded acute toxicity related to treatment for breast, head-and-neck and prostate cancer patients) have been defined. To evaluate the feasibility of data collection in all Belgian RT departments, a test phase was launched in 2015, collecting the full set of structural QIs, but limiting the number of patient-specific QIs (n=5 per pathology/department). Upon validation of this dummy run, as of 2016, a broader capture of process and outcome QIs was started (n=25 patients/pathology/department).

#### Results

A high department participation rate to this national QI project was obtained, with 100% of departments participating in 2015 and 2016 and 92% in 2017. This success rate is highly attributed to the presence of QM in each RT department. Over the 3 year-period, 33.993 data points were collected contributing to the establishment of the 54 QIs. The analysis of the collected QIs gave insight into national activity levels, resource availability, clinical practice and acute toxicity levels. This resulted in a yearly global report but also in the generation of individualized benchmarking documents in which each department is able to identify its performance as compared to other departments which are anonymously identified (see fig 1).

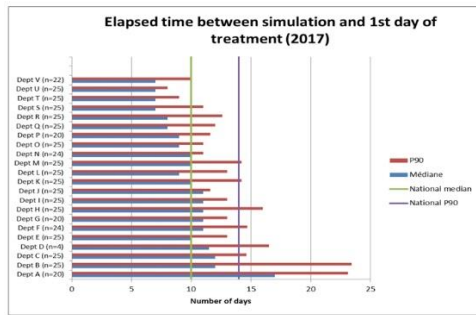


Fig. 1 - Process QI – Elapsed time between simulation and treatment for H&N cancer patients (n=509)

**Conclusion**

The development of a RT-QI project has been demanded by the Belgian national government as a potential tool to help RT departments to further optimise the quality of patient care. Although participation of each individual department is on voluntary basis, it has been shown feasible to collect defined QIs at national level with an almost complete participation rate. The analysis and generation of benchmarking documents guide centres in their quality improvement initiatives at departmental level and support national quality improvement initiatives.

**OC-0598 Estimating the need for palliative radiotherapy for breast cancer: A benchmarking approach**

C.J. Jin<sup>1</sup>, W. Kong<sup>1</sup>, W.J. Mackillop<sup>1</sup>  
<sup>1</sup>Queen’s Cancer Research Institute- Queen’s University, Cancer Care and Epidemiology, Kingston, Canada

**Purpose or Objective**

Palliative radiotherapy (PRT) benefits many patients with breast cancer, but optimal utilization rates remain undefined. The objective of this study was to estimate the appropriate PRT rate for the general breast cancer population.

**Material and Methods**

Ontario’s population-based cancer registry identified patients who died of breast cancer between 2009 and 2013. Multivariate analysis identified health systems factors affecting the use of PRT for breast cancer, enabling us to define a benchmark population with unimpeded access to PRT. Proportion of cases treated in the last 5 years of life (PRT<sub>5y</sub>) was standardized to overall population characteristics. Benchmarks were compared to province-wide PRT<sub>5y</sub> rates.

**Results**

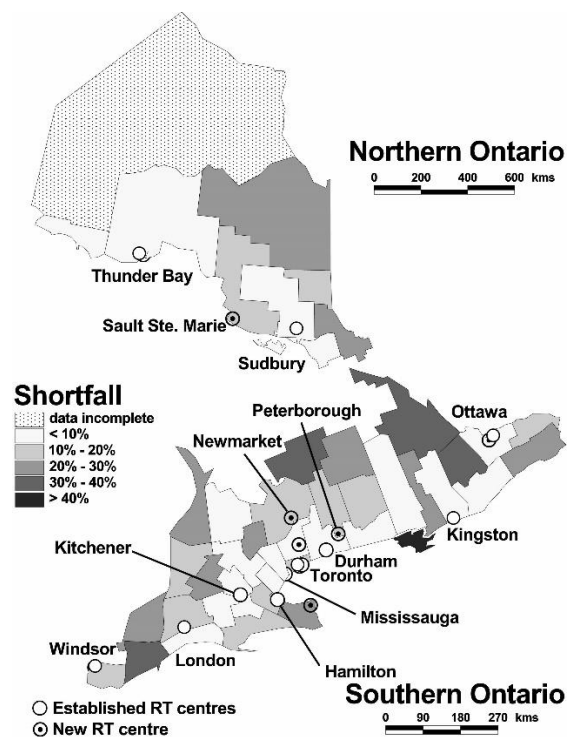
Overall, 36.2% of 11,075 patients who died of breast cancer between 2009 and 2013 received PRT at least once in the last 5 years of life. Availability of RT at the diagnosing hospital was the dominant determinant of increased PRT use; socioeconomic status and residential distance to nearest RT centre did not have a significant effect. Patients diagnosed at hospitals with on-site RT were therefore designated the benchmark population. The standardized benchmark for PRT<sub>5y</sub> was 40.7%, compared to the province-wide rate of 36.2%. Indication-specific benchmarks demonstrated that shortfalls in PRT use were highest for locoregional RT, followed by brain and bone metastases (Table). Age-specific benchmarks demonstrated that shortfalls in PRT use were >3 times greater in patients >70 vs ≤70 years. The extent of the shortfall varied widely amongst Ontario regions (Figure).

**Table: Benchmark Rates and Shortfalls in the Use of PRT<sub>5y</sub>**

	Standardized Benchmark Rate <sup>1</sup> (95% CI)	Actual Provincial Rate (95% CI)	Shortfall <sup>2</sup>
<b>Body</b>	8.8% (7.4%, 10.1%)	7.3% (6.8%, 7.8%)	16.8%
<b>Region</b>			
Bone	26.4% (24.0%, 28.8%)	23.7% (23.0%, 24.5%)	10.0%
Brain	14.4% (12.7%, 16.1%)	12.9% (12.3%, 13.6%)	10.2%
Other	7.5% (6.2%, 8.7%)	5.6% (5.2%, 6.1%)	24.4%
<b>Age</b>			
≤70	55.7% (50.5%, 60.8%)	52.3% (50.9%, 53.7%)	6.1%
>70	28.4% (25.0%, 31.7%)	22.9% (21.8%, 23.9%)	19.4%
<b>Total</b>	40.7% (37.8%, 43.6%)	36.2% (35.3%, 37.0%)	11.1%

*t*PRT<sub>5y</sub> rate among patients whose cancer was diagnosed at a hospital with RT on site, standardized to the distribution of life expectancy in the overall population;  
<sup>2</sup>Shortfall =  $(\text{Unmet Need} / \text{Total Need}) = (\text{Benchmark rate} - \text{Actual rate}) / \text{Benchmark rate} \times 100\%$

**Figure: Inter-county variations in shortfalls in the use of PRT for breast cancer in Ontario**



**Conclusion**

In a standardized benchmark Ontario population with unimpeded access to RT, 40.7% of patients who died of breast cancer received PRT, compared to 36.2% of the overall population. The gap between actual and optimal PRT rates was greatest in the elderly and varied widely across regions. An effort should be made to reduce the large age-related and regional differences in PRT use for patients with advanced breast cancer. This method provides a rational estimate of appropriate treatment rates required for monitoring and improving access to cancer care.

**OC-0599 Survival and local control deficits due to radiotherapy under-utilisation in NSW, Australia.**  
 G. Delaney<sup>1,2,3</sup>, G.S. Gabriel<sup>2,3</sup>, J. Shafiq<sup>2</sup>, R. Merie<sup>1</sup>, S. Vinod<sup>1,2,3</sup>, V. Batumalai<sup>1</sup>, M.B. Barton<sup>1,2</sup>  
<sup>1</sup>Liverpool Hospital, Area Cancer Services Radiation Oncology, Liverpool, Australia; <sup>2</sup>University of NSW,

*Medicine, Sydney, Australia ; <sup>3</sup>Ingham Institute of Medical Research, Liverpool Hospital, Sydney, Australia*

#### **Purpose or Objective**

Optimal radiotherapy utilisation rates suggest that approximately 48% of patients should receive radiotherapy based on evidence-based guideline recommendations and that 44% of cancer patients should receive radiotherapy within their first year of diagnosis (1). It has been widely reported that actual rates are often significantly lower than optimal. The aim in this study was to estimate the local control and overall survival shortfall that occurs as a result of radiotherapy under-use and to identify factors that predict under-use in NSW.

#### **Material and Methods**

All cases of registered cancer diagnosed in NSW, Australia, between 2009-2011 were identified from the NSW Cancer Registry and linked with data from all public and private radiation oncology departments. The actual Radiation Therapy utilisation (RTU) rate was calculated and compared with published evidence-based optimal rates (1). The deficit in radiotherapy use for each evidence-based radiotherapy indication was used to estimate the impact on 5-year local control (LC) and overall survival (OS). These were compared to the published estimates of radiotherapy benefits in the setting of optimal use (2). OS and LC shortfall in person number - defined as the number of people not achieving LC and OS benefit due to RT underutilisation - was then calculated. Univariate and multivariate analyses were performed to identify factors that contributed to reduced RTU.

#### **Results**

110 645 patients were diagnosed with cancer in NSW during the study period. The overall RTU rate was 25% within the first year of diagnosis compared to the reported optimal rate of 44% within the first year of diagnosis (2). The 5-year OS shortfall was 2.2% and 5-year LC shortfall was 10.9%. It is estimated that 1757 and 361 patients per year not receiving radiotherapy in NSW had local failure and poorer survival respectively during this study period. Male gender, older age, localised disease and longer travel distance were factors predicting radiotherapy under-utilisation on multivariate analysis. When compared with our analysis of NSW data from 2004, the current study shows an estimated overall survival improvement of 9% (3).

#### **Conclusion**

Under-use of recommended radiotherapy for cancer has been identified in this study, with a negative impact on patient outcomes. While improving, further work needs to be done to reduce this shortfall further. Older age, male gender and longer travel distance were predictors for sub-optimal RTU. These findings would assist in health service planning for radiotherapy and call for better adherence to treatment guidelines. Identification of the specific evidence-based indications with the greatest shortfall would assist with prioritising strategies to address the gap.

#### **References:**

1. Barton MB, et al. Radiotherapy and oncology. 2014;112(1):140-4.
2. Hanna TP, et al. Radiotherapy and oncology 2018;126(2):191-7.
3. Batumalai V., et al.. Radiotherapy and oncology 2018 (in press).

#### **OC-0600 Assessment of non-adherence to external radiotherapy treatment in cancer patients in Catalonia, Spain**

*J.M. Borràs<sup>1</sup>, R. Font<sup>2</sup>, J. Solà<sup>2</sup>, M. Macià<sup>3</sup>, M. Arenas<sup>4</sup>, R. Verges<sup>5</sup>, A. Eraso<sup>6</sup>, V. Tuset<sup>6</sup>, A. Bieta<sup>7</sup>, J.M. Solé<sup>8</sup>, N. Farré<sup>9</sup>, A. Pedro<sup>10</sup>, M. Mira<sup>11</sup>, J.A. Espinàs<sup>2</sup>*  
<sup>1</sup>University of Barcelona, Clinical Sciences, Catalonia, Spain; <sup>2</sup>IDIBELL, Pla Director d'Oncologia, Catalonia, Spain; <sup>3</sup>Catalan Institute of Oncology, Catalan Institute of Oncology, Catalonia, Spain ; <sup>4</sup>Hospital Sant Joan de

*Reus, Hospital Sant Joan de Reus, Catalonia, Spain ; <sup>5</sup>Hospital Universitari de la Vall d'Hebron, Hospital Universitari de la Vall d'Hebron, Catalonia, Spain ; <sup>6</sup>Institut Català d'Oncologia, Institut Català d'Oncologia, Catalonia, Spain; <sup>7</sup>Hospital Clínic de Barcelona, Hospital Clínic de Barcelona, Catalonia, Spain ; <sup>8</sup>Consorci Sanitari de Terrassa, Consorci Sanitari de Terrassa, Catalonia, Spain; <sup>9</sup>Hospital de la Santa Creu i Sant Pau, Hospital de la Santa Creu i Sant Pau, Catalonia, Spain ; <sup>10</sup>Hospital Clínic Plató, Hospital Clínic Plató, Catalonia, Spain ; <sup>11</sup>Hospital Arnau de Vilanova, Hospital Arnau de Vilanova, Catalonia, Spain*

#### **Purpose or Objective**

Non-adherence to external radiotherapy is an aspect of treatment which has not been fully explored. The objective of this study is to analyse the relevance of this problem and its impact on 1-year survival

#### **Material and Methods**

A Cohort study design was carried out with a prospective follow-up of cancer patients with indication of external radiotherapy. All patients with indication of treatment during year 2016 in the hospital of the public sector in Catalonia were included. Adherence was deemed acceptable if total dose received was over 90% of the dose prescribed. Statistical analysis was performed according to type of tumour, intention of treatment and age. Logistic regression was carried out to assess factors associated to adherence and Cox analysis was applied to assess their relationship with survival

#### **Results**

In total, 15.157 patients were included with an average age of 64.6 (± 14.0); 51.3% were males. Most frequent tumours were breast (27.4%), lung (16,1%) and prostate (12.4%). Radical intent was indicated in 69.2% of cases and 18.7% of patients received concomitant chemo. At least one day interruption of treatment, excluding public holidays, was observed in 41.8% of cases. The reasons (multiple choice) for these interruptions were, 75.8% due to problems with the equipment, 17.9% for medical reason, 7.9% due to the patient preference and 20.9% for others reasons. Patient adherence was of 95.5% of patients (receiving more than 90% of total dose). Radical intent was related (OR: 3.11; IC: 95%: 2.6-3.7) to better adherence. Older age was associated with lower probability of adherence. Head and neck, lung, digestive other than rectal and bone (including metastasis) cancers were associated with lower probability of adherence; while breast and prostate cancer patients were associated with significantly higher than average adherence. One-year survival was significantly higher among adherent patients, both in radical (HR: 4.5; IC95%:3.8-5.4) and palliative (HR: 2.1; IC95%:1.8-2.4) intent

#### **Conclusion**

Adherence of treatment is very high among this cohort of population based patients receiving treatment in the public sector in Catalonia. Lack of adherence is related to lower probability of survival and this factor should be considered in the follow-up of patients with radiotherapy treatment

#### **OC-0601 Stereotactic body radiotherapy for oligometastatic disease in belgium: costs and budgetary impact**

*D. Nevens<sup>1</sup>, I. Kindts<sup>2</sup>, N. Defourny<sup>3</sup>, M. Roskamp<sup>4</sup>, C. Mercier<sup>5</sup>, H. De Schutter<sup>4</sup>, C. Van de Voorde<sup>6</sup>, Y. Lievens<sup>7</sup>*  
<sup>1</sup>Department of Radiation Oncology, Iridium Kankernetwerk, University of Antwerp ; <sup>2</sup>KU Leuven-University Hospitals Leuven, Lab of Experimental Radiation Oncology, Leuven, Belgium ; <sup>3</sup>ESTRO, European Society for Radiotherapy and Oncology, Brussels, Belgium; <sup>4</sup>BCR, Belgian Cancer Registry, Brussels, Belgium; <sup>5</sup>University of Antwerp, Molecular Imaging-Pathology- Radiotherapy & Oncology MIPRO, Antwerp, Belgium; <sup>6</sup>KCE, Belgian Health Care Knowledge Centre,

Brussels, Belgium ; <sup>7</sup>Ghent University, Department of Radiation Oncology and Experimental Cancer Research, Ghent, Belgium

### Purpose or Objective

There is a steady rise in the use of Stereotactic Body RadioTherapy (SBRT) in oligometastatic disease (OMD). Besides a positive impact on patients' outcome, this may generate important financial consequences for radiotherapy budgets. Awaiting more clinical evidence, the Belgian compulsory health insurance system initiated a coverage with evidence development (CED) project for innovative radiotherapy, including SBRT, in 2011. Consequently, a provisional financing to treat OMD with SBRT was available in Belgium from 2013 onwards.

While analysis of the clinical and technical data captured between 9-2013 and 12-2017 is ongoing and inclusion in the formal reimbursement system pending, a cost-calculation and budget impact analysis (BIA) was carried out.

### Material and Methods

Using the CED data, the uptake of SBRT in patients with OMD in Belgium between 2013 and 2017 was reviewed. Based on these data, predictive growth scenarios for future uptake were developed. The cost of an SBRT treatment in the OMD setting in Belgium was calculated using the Health Economics in Radiation Oncology Time-Driven Activity-Based Costing (HERO TD-ABC) model developed by ESTRO, alimanted with national data on resources, treatments and operational parameters. Combining all this information, the future impact of this novel treatment indication on the radiotherapy budget in Belgium was evaluated.

### Results

The CED data showed a large increase in number of OMD treated with SBRT in Belgium: from 59 in 2013 to 459 in 2017. Based on this, three growth scenarios for uptake were developed: scenario 1, predicting a further linear increase; scenario 2, only accounting for demographic shift; and an 'intermediate' scenario 3 with linear increase for two more years, then plateauing to the demographic trends (Figure 1).

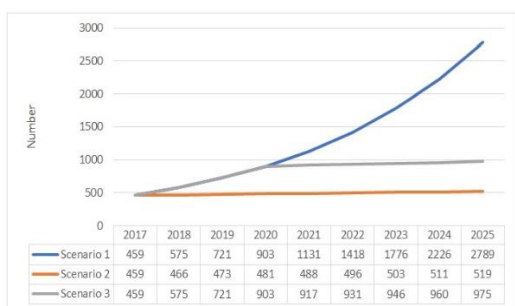


Figure 1

Using the HERO TD-ABC model, a real-life cost of 4,359 € per SBRT treatment was calculated, whereas the provisional financing within the CED program amounted to 3,802 €.

The 3 growth scenarios and the costs were combined to estimate the impact on the radiotherapy budget. For the TD-ABC costs, all OMD SBRT treatments were considered new indications, hence, additional SBRT courses and costs. For the CED financing data, 2 comparator scenarios were assumed. In the comparator 1 scenario, the SBRT courses for patients treated in the OMD setting are all considered additional SBRT courses. In the comparator 2 scenario, 50% of the SBRT courses are considered new cases and 50% are considered as previously treated with palliative intent, leading to a lower cost increment. Table 1 demonstrates the financial impact of the different scenarios.

		2017	Increase in 2020	Increase in 2025	
TD-ABC cost (€)	Scenario 1	2,000,781	1,935,396	8,155,689	
	Scenario 2	2,000,781	95,898	261,540	
	Scenario 3	2,000,781	1,935,396	2,249,244	
CED cost (€)	Scenario 1	Comparator 1	1,745,118	1,688,088	7,113,542
		Comparator 2	1,372,869	1,328,004	5,596,161
	Scenario 2	Comparator 1	1,745,118	83,644	228,120
		Comparator 2	1,372,869	65,802	179,460
	Scenario 3	Comparator 1	1,745,118	1,688,088	1,961,832
		Comparator 2	1,372,869	1,328,004	1,543,356

Table 1

### Conclusion

The possible impact on the radiotherapy budget of uptake of SBRT for OMD shows large variations. These data should be evaluated in the context of improved outcome and set against the background of the actual Belgian radiotherapy budget amounting to roughly 120 million €. Further real-life clinical and financial monitoring and prospective data gathering seems necessary.

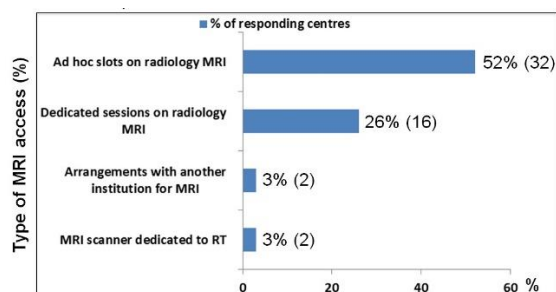
### OC-0602 Pattern of care of radiotherapy practice for EBRT patients in Spain

N. Defourny<sup>1</sup>, A.L. Medina<sup>2</sup>, J.L. Tarjuelo<sup>3</sup>, A. Rodríguez<sup>4</sup>, J. Giralt<sup>5</sup>, J.C. Novais<sup>6</sup>, M.M. Martín<sup>7</sup>, A.M. Luis<sup>8</sup>, J. Isern<sup>9</sup>, I.H. Lopez<sup>10</sup>, O. Leaman<sup>11</sup>, F. Arias De la Vega<sup>12</sup>, R. Morera<sup>13</sup>, L. Cerezo<sup>14</sup>, F.L. Campos<sup>15</sup>, S. Rodríguez<sup>16</sup>, A.J. Conde Moreno<sup>17</sup>, A. Lozano Borbalas<sup>18</sup>, N. Rodríguez de Dios<sup>19</sup>, M.E. Rodríguez-Ruiz<sup>20</sup>, P.C. Lara<sup>21</sup>, C. Ferrer<sup>22</sup>, J.M. Borrás<sup>23</sup>, C. Grau<sup>24</sup>, Y. Lievens<sup>25</sup>

<sup>1</sup>ESTRO A.I.S.B.L., HERO, Brussels, Belgium ; <sup>2</sup>Conselleria de Sanidade, Medical Physics and Radiation Protection, Coruña, Spain ; <sup>3</sup>Consorcio Hospitalario Provincial de Castellón, Medical Physics and Radiation Protection, Castelló de la Plana- Spain, Spain ; <sup>4</sup>Hospital Ruber Internacional, Radiation Oncology Department, Madrid, Spain ; <sup>5</sup>Vall d'Hebron University Hospital, Department of Radiation Oncology, Barcelona, Spain ; <sup>6</sup>Hospital Universitario Quirón Madrid, So Radiofísica y Protección Radiológica, Madrid, Spain ; <sup>7</sup>Hospital Universitario de la Princesa, Department of Radiation Oncology-, Madrid, Spain ; <sup>8</sup>Hospital Ramón y Cajal, Department of Radiation Oncology, Madrid, Spain ; <sup>9</sup>Hospital de la Santa Creu i Sant Pau, Radiotherapy, San Pau, Spain ; <sup>10</sup>Hospital Universitari Sant Joan de Reus, S.Oncologia Radioterápica, Reus, Spain ; <sup>11</sup>Hospital Duran i Reynals, Radiation Oncology Department, Hospitalet de Llobregat, Spain ; <sup>12</sup>Hospital de Navarra, Radiotherapeutic Oncology Department, Navarra, Spain ; <sup>13</sup>Clinica La Milagrosa, Tomotherapy Unit, Madrid, Spain ; <sup>14</sup>Hospital de la Princesa, Department of Radiation Oncology, Madrid, Spain ; <sup>15</sup>Fundación Instituto Valenciano de Oncología IVO, Servicio de Oncología Radioterápica, Valencia, Spain ; <sup>16</sup>Benidorm Hospital, Radiotherapy Department, Alicante, Spain ; <sup>17</sup>Instituto Oncológico de Castellón "Dr. Altava", Servicio de Oncología Radioterápica, Castellón, Spain ; <sup>18</sup>L'Hospitalet de Llobregat, Servicio de Oncología Radioterápica Institut Català d'Oncologia, Barcelona, Spain ; <sup>19</sup>Hospital de l'Esperança, Radiation Oncology Department, Barcelona, Spain ; <sup>20</sup>University of Navarra Clinic, Radiation Oncology Department, Pamplona, Spain ; <sup>21</sup>Hospital Universitario de Gran Canaria Dr. Negrín, Radiation Oncology Department, Las Palmas, Spain ; <sup>22</sup>Consorcio Hospitalario Provincial de Castellón, Servicio de Oncología Radioterápica, Castellón, Spain ; <sup>23</sup>L'Hospitalet de Llobregat, Cancer Prevention and Control Bellvitge Biomedical Research Institute - IDIBELL, Barcelona, Spain ; <sup>24</sup>Aarhus University Hospital, Department of Oncology-, Aarhus, Denmark ; <sup>25</sup>Ghent University Hospital, Department of Radiation Oncology, Ghent, Belgium

### Purpose or Objective

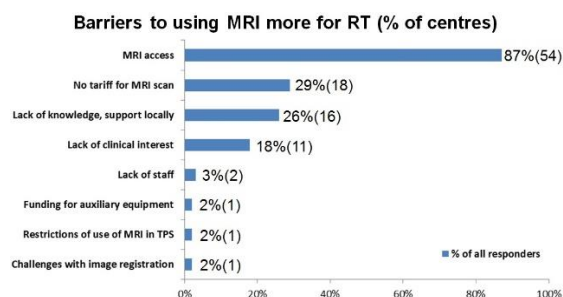




All centres using MRI in EBRT use rigid MRI to CT registration and two centres are currently using deformable image registration in addition. Commissioning and QA of image registration and MRI for EBRT showed large inter-centre heterogeneity caused by a lack of guidance.

Physics support for setting up a new MRI for EBRT service is varied across the UK with links with radiology being very important and 23% of centres reporting no support from physics staff with specialist MRI knowledge.

The largest reported barrier to utilising MRI further is a lack of MRI access (87% of centres) but a large proportion of all concerns are financially driven with a lack of tariff meaning centres do not get reimbursed for an MRI scan, see figure.



Looking forward, within the next five years, 37% of centres intend to use functional MRI, 38% of centres are planning for an MRI-simulator, 16% of centres are planning to utilise MRI-only radiotherapy and 10% are planning for an MRI-linac (on top of the 3% that currently have access).

### Conclusion

The current use of MRI for EBRT in the UK was audited. More than 2 in 3 of centres have some form of MRI access, but there are only 2 MRI-simulators at present. Collaboration with radiology departments is vital for both MRI access and staff support. The main barriers to fully integrate MRI are financially driven and a lack of tariff resulting in limited access. Knowledge gaps have been identified such as the lack of standardised QA guidance that will be addressed in the IPEM guidelines.

### OC-0604 The first UK survey of dose indices from radiotherapy treatment planning CT scans for adult patients

M. Williams<sup>1</sup>, T. Wood<sup>2</sup>, A. Davis<sup>3</sup>, J. Earley<sup>4</sup>, R. Plaistow<sup>5</sup>, R. Lindsay<sup>6</sup>, A. Palmer<sup>3</sup>, A. Nesbit<sup>4</sup>, S. Edyvean<sup>7</sup>, U. Findlay<sup>8</sup>

<sup>1</sup>Velindre University NHS Trust, Medical Physics, Cardiff, United Kingdom ; <sup>2</sup>Hull and East Yorkshire Hospitals NHS Trust, Radiation Physics, Hull, United Kingdom ; <sup>3</sup>Portsmouth Hospitals NHS Trust, Medical Physics, Portsmouth, United Kingdom ; <sup>4</sup>Royal Surrey County Hospital NHS Foundation Trust, Medical Physics, Guildford, United Kingdom ; <sup>5</sup>Cambridge University Hospitals NHS Foundation Trust, Medical Physics, Cambridge, United Kingdom ; <sup>6</sup>St James Institute of Oncology, Medical Physics, Leeds, United Kingdom ; <sup>7</sup>Public Health England, Radiation Dosimetry, Chilton,

United Kingdom ; <sup>8</sup>Public Health England, Medical Exposure, Chilton, United Kingdom

### Purpose or Objective

CT scans are an integral component of modern radiotherapy treatments, enabling the accurate localisation of the treatment target and organs-at-risk, and providing the tissue density information required for the calculation of dose in the treatment planning system. For these reasons, it is important to ensure exposures are optimised to give the required clinical image quality with doses that are as low as reasonably achievable. However, there is little guidance in the literature on dose levels in radiotherapy CT imaging either within the UK or internationally. The first UK wide dose survey for radiotherapy CT planning scans has been completed. The survey was initiated by a working party of the Institute of Physics and Engineering in Medicine (IPEM).

### Material and Methods

Patient dose metrics were collected for prostate, gynaecological, breast, 3D-lung, 4D-lung, brain and head & neck scans. Median values per scanner and examination type were calculated and national dose reference levels and 'achievable levels' of CT dose index (CTDI<sub>vol</sub>), dose-length-product (DLP) and scan length are proposed based on the third quartile and median values of these distributions, respectively.

### Results

A total of 68 radiotherapy CT scanners were included in this audit. The proposed national dose reference levels and achievable levels are shown in the table below. Significant variations in dose indices were noted, with head & neck and lung 4D yielding a factor of eighteen difference between the lowest and highest dose scanners. There was also evidence of some clustering in the data by scanner manufacturer, which may be indicative of a lack of local optimisation of individual systems to the clinical task.

Examination	Proposed reference level				Achievable level		
	PD (cm)	CTDI <sub>vol</sub> (mGy)	DLP (mGy·cm)	Scan length (mm)	CTDI <sub>vol</sub> (mGy)	DLP (mGy·cm)	Scan length (mm)
Breast	32	10	390	360	8	280	330
Gynaecological	32	16	610	400	12	510	380
Lung 3D	32	14	550	390	10	410	370
Lung 4D	32	63	1750	340	36	1170	330
Prostate	32	16	570	340	13	420	310
Brain	16	50	1500	290	42	1110	250
Head and neck	16	49	2150	420	26	1080	400

### Conclusion

The first UK wide audit of dose indices for adult patients undergoing CT scans for radiotherapy planning has been completed, and the results published (Tim J Wood et al 2018 Phys. Med. Biol. 63 185008). Reference values and achievable levels for CTDI<sub>vol</sub>, DLP and scan length have been proposed for seven common types of CT scan. It is anticipated that providing this data to the UK and wider radiotherapy community will aid the optimisation of treatment planning CT scan protocols.

### OC-0605 Is DIBH more robust than FB in VMAT left breast irradiation? Multicenter and multivendor analysis

S. Russo<sup>1</sup>, M. Esposito<sup>1</sup>, V. Hernandez<sup>2</sup>, J. Saez<sup>3</sup>, G. Nicolini<sup>4</sup>, E. Vanetti<sup>4</sup>, F. Rossi<sup>5</sup>, L. Paoletti<sup>6</sup>, P. Bastiani<sup>5</sup>, G. Reggiori<sup>7</sup>, S. Tomatis<sup>7</sup>, M. Scorsetti<sup>8</sup>, P. Mancosu<sup>7</sup>  
<sup>1</sup>Azienda USL Toscana Centro, SC Fisica Sanitaria - Firenze, Florence, Italy ; <sup>2</sup>Hospital Universitari Sant Joan de Reus-Reus, Department of Medical Physics, Tarragona, Spain ; <sup>3</sup>Hospital Clinic de Barcelona, Department of Radiation Oncology, Barcelona, Spain ; <sup>4</sup>Radiqa Developments, Medical Physics Team, Bellinzona, Switzerland ; <sup>5</sup>Azienda USL Toscana Centro, SC Radioterapia- Firenze, Florence, Italy ; <sup>6</sup>Azienda USL Toscana Centro, SC Radioterapia - Firenze, Florence, Italy ; <sup>7</sup>Humanitas Research Hospital, Medical Physics

Unit of Radiation Oncology Dept, Milan, Italy;  
<sup>8</sup>Humanitas Research Hospital, Radiotherapy and  
 Radiosurgery Dept., Milan, Italy

### Purpose or Objective

VMAT usually increases the dose conformity to the target but enhance the mean dose to organs at risk, mainly for the heart. Deep Inspiration Breath Hold (DIBH) was demonstrated to help in reducing the mean heart dose (MHD) and might be required in some cases. This study systematically investigates the possible advantages of DIBH in comparison to standard Free Breathing (FB) for left breast VMAT.

### Material and Methods

DIBH and FB VMAT plans for ten left side breast patients were optimized by two different TPSs (Monaco5.1 and Eclipse11) and Linac devices (Elekta Synergy and Varian TrueBeam). Dose prescriptions were 40.5Gy to the  $PTV_{breast}$  and 48Gy to the  $PTV_{boost}$  in 15 fractions.  $PTV_{breast} 98\% > 38.5Gy$ ,  $PTV_{boost} 98\% > 45.7Gy$ , and maximum dose to  $PTV_{boost} < 107\%$  were asked. OARs constraints were  $MHD < 4Gy$ ,  $V_{18Gy} < 5\%$  for heart;  $D_{mean} < 10Gy$ ,  $V_{20Gy} < 10\%$  for left lung;  $D_{mean} < 3Gy$  for right lung and breast. Several dynamic plan parameters and complexity indices were computed from the DICOM RTPlan files by using an homemade program. The overall modulation index  $Ml_{tot}$  was scored to take into account in a single parameter the leaf speed and acceleration and the gantry speed (GS). A global quality parameter accounting for both dosimetric scoring and plan complexity was defined as  $GP = (Ml_{tot} \times MHD / PTV_{breast} 98\%)$ . Pre-treatment QA verifications were carried out in both centers using the EPID-based Epiqa5.0 software (EPIDOSsro, Bratislava). Gamma index ( $\gamma$ ) analysis was performed with 3%G-3 mm, 2%G-2 mm and 3%L/3 mm criteria. Statistical significance was examined using a Wilcoxon signed rank-test for related samples and set at  $p \leq 0.05$ .

### Results

A significant better PTV coverage was found for DIBH plans in both centers compared to FB plans. DIBH plans were associated with a lower value in all the OARs dose parameters with significant reduction in MHD and  $V_{heart18Gy}$  ( $p < 0.005$ ). For FB plans  $MHD > 4Gy$  was observed in 30% of the cases. The plan complexity was generally slightly lower for DIBH plans than for FB ones, but differences were statistically significant only in few cases. The GP resulted significant lower in DIBH plans (Fig.1).

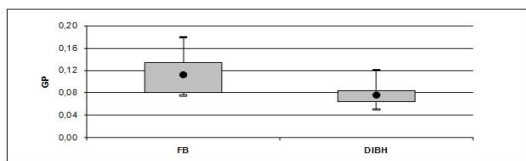


Fig.1 : Box plot for GP evaluated for DIBH and FB plans.

Regarding the plan delivery parameters, Eclipse used smaller and more complex MLC apertures, while Monaco further modulated the DoseRate and the GS than Eclipse, providing higher  $Ml_{tot}$  values. Both DIBH and FB optimizations yielded good results for QA verification with  $\gamma(3\%G-3mm) > 95\%$  in all cases (Fig.2); no significant difference was found. Higher  $\gamma(2\%G-2mm)$  values for DIBH plans than for FB were found for the Elekta institution with significant differences ( $p < 0.02$ ).

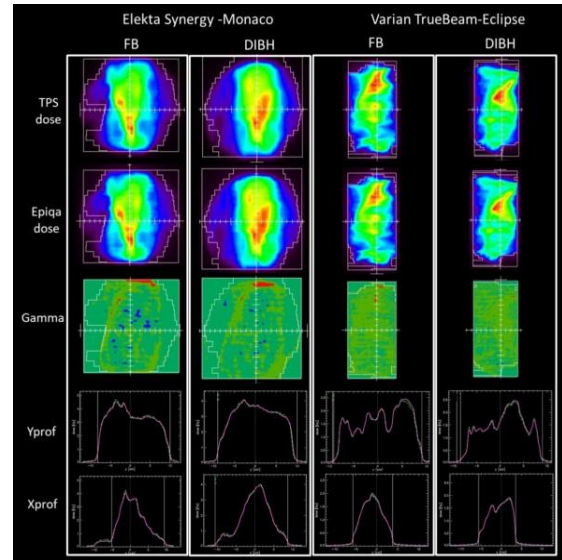


Fig.2: TPS and Epiqa dose distributions,  $\gamma(3\%G-3mm)$  results and isocenter dose profiles for FB and DIBH plans of same patient.

### Conclusion

VMAT DIBH technique is more robust than FB when the heart needs further sparing, because it allows an overall reduction of the OAR doses with a slightly lower level of plan complexity and without compromising plan deliverability.

### OC-0606 IMRT QA: comparing independent recalculation against measurement based methods

S. Kry<sup>1</sup>, M. Glenn<sup>1</sup>, C. Peterson<sup>1</sup>, D. Branco<sup>1</sup>, H. Mehrens<sup>1</sup>, A. Steinmann<sup>1</sup>, D. Followill<sup>1</sup>

<sup>1</sup>UT MD Anderson Cancer Center, Radiation Physics, Houston- TX, USA

### Purpose or Objective

To directly compare independent recalculation of the treatment plan against measurement-based IMRT QA to see which performed better at detecting unacceptable plans.

### Material and Methods

Acceptability of IMRT delivery was assessed with 337 IROC head and neck phantoms previously irradiated as part of clinical trial credentialing, 18 of which failed to meet IROC's 7%/4mm acceptability criteria. For each of the 337 cases, the institution's IMRT QA result, based on the method employed by the institution, was abstracted to determine how well their clinical QA (conducted on the phantom plan at the time of phantom irradiation) predicted the phantom irradiation result (i.e., did the phantom pass or fail). Each case was also independently recalculated by IROC using the institution's DICOM data and Mobius 3D (with linac class-specific beam models) to determine how well the recalculation predicted the phantom irradiation results (i.e., pass or fail). Comparisons between measurement-based IMRT QA and independent recalculation were made using truth tables to determine sensitivity and specificity of each, including subdivision by IMRT QA device (EPID, ArcCheck, ion chamber, or MapCheck). ROC analysis was also performed to evaluate the accuracy of measurement-based IMRT QA and independent recalculation as the strictness of the criteria for flagging failures varied.

### Results

For the 18 failing phantoms in the total cohort, measurement-based IMRT QA had a sensitivity of 6% (i.e., only 1 unacceptable plan was flagged based on clinical measurement-based IMRT QA methods). In contrast, the independent recalculation approach had a sensitivity of 72% (flagging 13 unacceptable plans). Overall, and when

the results were subdivided by IMRT QA device, the recalculation had a significantly higher sensitivity than any specific device examined (Table). Specificity was lower for the independent recalculation, but overall, incorporating both sensitivity and specificity, ROC analysis found superior performance (statistically significant) for the independent recalculation over clinical measurement-based IMRT QA. The area under the curve was 0.79 for the independent recalculation but only 0.60 for the measurement based approaches. Based on the ROC curves, the independent recalculation could detect 80% of unacceptable plans using a dose disagreement criteria (between the recalculation and the TPS value) of 3.8%. In order for measurement based IMRT QA methods to detect 80% of unacceptable plans, a clinically unrealistic criteria of 99.7% of pixels would need to pass a 3%/3mm criterion.

Device	# tests	#failing results	Measurement sensitivity (%)	Recalculation sensitivity (%)	Measurement specificity (%)	Recalculation specificity (%)
All	337	18	6	72	98	68
EPID	58	7	0	71	100	57
ArcCheck	93	4	0	100	100	70
Ion Chamber	44	1	0	100	91	67
MapCheck	121	5	20	40	100	67

### Conclusion

A simple independent recalculation using linac class-specific beam models had much better sensitivity at detecting unacceptable plans as compared to existing clinical measurement-based IMRT QA methods.

### OC-0607 IAEA supported national 'end-to-end' IMRT audit in Portugal

T. Santos<sup>1</sup>, M.D.C. Lopes<sup>2</sup>, E. Gershkevitch<sup>3</sup>, J. Izewska<sup>4</sup>  
<sup>1</sup>Faculty of Sciences and Technology, Physics Department, Coimbra, Portugal ; <sup>2</sup>Instituto Portugues de Oncologia de Coimbra Francisco Gentil E.P.E., Medical Physics Department, Coimbra, Portugal ; <sup>3</sup>North Estonia Medical Centre, Medical Physics Department, Tallinn, Estonia; <sup>4</sup>International Atomic Energy Agency, Dosimetry and Medical Radiation Physics Section, Vienna, Austria

### Purpose or Objective

IAEA has developed an IMRT audit programme to review physical aspects of IMRT H&N treatments through on-site visits. The audit was carried out in Portugal between April and September 2018. This abstract presents the results.

### Material and Methods

All radiotherapy centres performing IMRT treatments in Portugal, 20 out of 24 centres, have voluntarily participated. The centres equipment to perform IMRT is shown in Table 1.

Using a specially designed anthropomorphic H&N phantom - SHANE (CIRS Norfolk, VA) - and a set of contours, the audit methodology simulates all steps of a nasopharynx IMRT treatment, from CT scanning to treatment delivery, following the local protocol. To guide the planning optimization, a list of dose objectives and constraints was provided.

As part of the auditing process, pre-visit activities were performed concerning small field dosimetry and MLC performance which were also checked during the on-site visit. Beam output fluctuation on the audit day was taken into account.

The dosimetric verification of the H&N IMRT plan was performed with a dedicated dosimetry set including a small volume ionization chamber placed inside the phantom at four different locations (three PTVs and spinal cord) and an EBT3 film to assess the dose distribution in a coronal plane.

The agreement between the dose distributions in EBT3 film and calculated by the TPS was evaluated with FilmQA Pro software using triple channel dosimetry.

Table 1 – Audited radiotherapy equipment sets and techniques

Linac	TPS	Algorithm	Technique	Nr of Centres
Varian	Eclipse	AAA	Sliding Window	2
		AcurosXB	VMAT	10
		Monaco	VMAT	1
Elekta	Monaco	MC	Sliding Window	1
		MC	VMAT	4
Tomotherapy	VoLo	Fast Superposition	Step & Shoot	1
		CCC Superposition	Helical IMRT	1

### Results

Analysis of small field output factors calculated in the pre-visit phase showed that differences between participants' data and the Imaging and Radiation Oncology Core, IROC - Houston QA Centre reference dataset were generally within the tolerance of 3% for all field sizes. Good agreement was found between calculated and film measured profiles for the 2x2 cm<sup>2</sup> field in all centres. MLC QA test results were within 0.5 mm for the leaf positioning bias in all participating institutions.

All treatment plans have met the proposed plan constraints except three plans where at least one of the constraints was not accomplished.

The differences between ionization chamber measurements and calculated doses were on average -0.1 ± 2.0 % in PTVs and 0.2 ± 2.2% in the spinal cord, with the individual results of all centres within the established tolerances of ± 5% for PTVs and ± 7% for the spinal cord. One follow up visit was required to resolve a major deviation in the spinal cord.

Considering the results of film analysis, for global gamma criteria of 3%/3mm 20% TH, passing rates ranged from 90.3% to 99.1%, again all above the limit of acceptability of 90%.

### Conclusion

The IMRT audit supported by the IAEA carried out in Portugal showed an overall good agreement between planned and delivered doses although the IMRT treatment planning exercise was considered demanding.

### OC-0608 Credentialing of spine stereotactic ablative body radiotherapy in a multi-centre trial

N. Hardcastle<sup>1</sup>, O. Cook<sup>2</sup>, P. Mitchell<sup>3</sup>, S. Siva<sup>4</sup>  
<sup>1</sup>Peter MacCallum Cancer Centre, Physical Sciences, Melbourne, Australia ; <sup>2</sup>Trans-Tasman Radiation Oncology Group, Quality Assurance, Newcastle, Australia ; <sup>3</sup>Olivia Newton John Cancer and Wellness Centre, Medical Oncology, Melbourne, Australia ; <sup>4</sup>Peter MacCallum Cancer Centre, Radiation Oncology, Melbourne, Australia

### Purpose or Objective

The NIVORAD trial (ALTG14/002, ACTRN12616000352404) involves administration of immunotherapy with or without Stereotactic Ablative Body Radiotherapy (SABR) to a single extracranial lesion in metastatic non-small cell lung cancer (NSCLC). Treated lesions receive a single fraction of 18-20 Gy and can include lung, soft tissue and bone including spine. Given the multi-disciplinary and complex nature of SABR delivery in particular with spine, a credentialing approach was created focusing on review of SABR treatment processes and measurement of a spine case.

### Material and Methods

Credentialing was split into two streams. Centres with a previous SABR site visit through TROG were required to perform an axial film measurement of a benchmarking spine plan in an appropriate local phantom and submit raw radiochromic film images for analysis. Remaining centres had an on-site review of SABR processes based on international guidelines, followed by an axial film measurement of the spine benchmarking plan. Films were

analysed for dosimetric and positional accuracy: up to 5% global scaling was allowed, followed by gamma analysis at 2%/2mm/10% threshold. Positional accuracy at target-cord interface and target-cord dose gradient (80%-20% width) was required to be within 1 mm of planned.

#### Results

A total of 18 centres have been credentialed; eight centres had previous site visits and submitted film and 10 centres had an on-site SABR process review and measurement. Delivery devices included linear accelerator, TomoTherapy and Cyberkife systems. Five centres were not able to achieve 90% gamma passing rate (Figure 1). Of these, three failed in low (< 5 Gy) dose regions and were > 80% passing rate thus were deemed acceptable. Two failed over the full dose range; one resubmitted a new plan, with the original fail attributed to inappropriate MLC constraints. The remaining centre elected not to have spine remeasured. One centre had positional discrepancy greater than 1 mm, and all centres were able to deliver the planned dose fall off from 80% of prescription dose to 20% of prescription dose within 1 mm at the target-cord interface. Figure 2 shows consistency in the dose gradient between planned and measured dose at the target-cord interface.

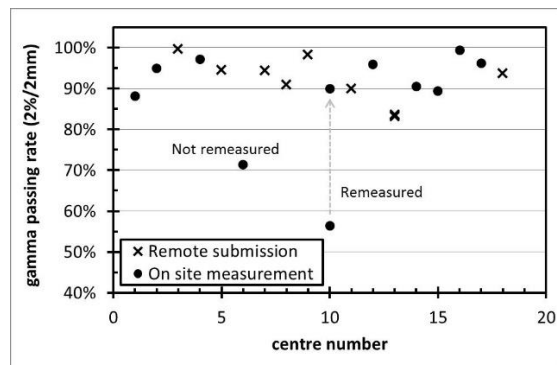


Figure 1: Gamma passing rate at 2%/2mm for all centres

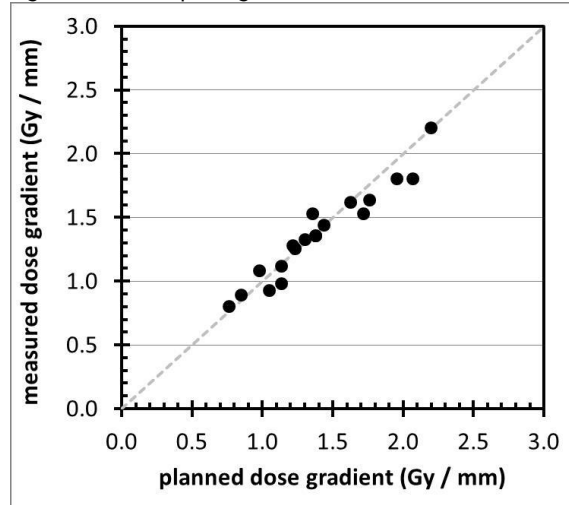


Figure 2: Dose gradient between the 80% and 20% of prescription dose at the target-cord interface

#### Conclusion

Credentialing measurements for spine SABR in a multi-centre trial have shown the majority of centres, independent of treatment modality can deliver spine SABR according to the treatment plan. The measurement process detected one centre with inappropriate MLC constraint setting that was rectified upon a repeat visit.

#### OC-0609 Urethra-sparing SBRT for prostate cancer: quality assurance of a randomized phase II trial

M. Jaccard<sup>1</sup>, T. Zilli<sup>1</sup>, A. Dubouloz<sup>1</sup>, L. Tsang<sup>2</sup>, S. Zvi<sup>2</sup>, N. Linthout<sup>3</sup>, S. Bral<sup>3</sup>, W. Verbakel<sup>4</sup>, A. Bruynzeel<sup>4</sup>, M. Björkqvist<sup>5</sup>, H. Minn<sup>5</sup>, L. Escude<sup>6</sup>, S. Jorcano<sup>6</sup>, J. Lencart<sup>7</sup>, A. Oliveira<sup>7</sup>, Z. Ozen<sup>8</sup>, U. Abacioglu<sup>8</sup>, J.M. Pérez-Moreno<sup>9</sup>, C. Rubio<sup>9</sup>, M. Rouzard<sup>1</sup>, R. Miralbell<sup>1</sup>  
<sup>1</sup>Geneva University Hospital, Radiation Oncology, Geneva, Switzerland; <sup>2</sup>Sheba Medical Center, Radiation Oncology, Ramat Gan, Israel; <sup>3</sup>Onze-Lieve-Vrouwenziekenhuis, Radiation Oncology, Aalst, Belgium; <sup>4</sup>VU University Medical Center, Radiation Oncology, Amsterdam, The Netherlands; <sup>5</sup>University Hospital Turku, Radiation Oncology, Turku, Finland; <sup>6</sup>Teknon Oncologic Institute, Radiation Oncology, Barcelona, Spain; <sup>7</sup>Portuguese Institut of Oncology, Radiation Oncology, Porto, Portugal; <sup>8</sup>Neolife Medical Center, Radiation Oncology, Istanbul, Turkey; <sup>9</sup>Hospital Universitario Sanchinarro, Radiation Oncology, Madrid, Spain

#### Purpose or Objective

To present the radiotherapy quality assurance (RTQA) results from a prospective multicenter phase II randomized trial of short vs. protracted urethra-sparing stereotactic body radiotherapy (SBRT) for localized prostate cancer (PCa).

#### Material and Methods

From 08/2012 through 12/2015, 165 patients (pts) from nine institutions with localized PCa were randomized and treated according to two different overall treatment time schedules: either 9 days (arm A, 82 pts), or 28 days, once-a-week, the same week-day (arm B, 83 pts). The prescribed dose was 36.25 Gy in 5 fractions of 7.25 Gy to the prostate planning target volume (PTV) with ( $n=92$ ) or without ( $n=73$ ) inclusion of the seminal vesicles (SV) (5-mm isotropic expansion, with a 3-mm posterior margin). The urethra planning risk volume (uPRV=prostatic urethra+3-mm margin) was planned to receive 32.5 Gy. Patients were treated either with a volumetric modulated arc therapy (VMAT) ( $n=112$ , 72 with SV) or intensity modulated RT (IMRT) ( $n=53$ , 20 with SV) technique under stereotactic conditions using Novalis linacs and ExacTrac image-guided technology.

Dosimetric results, PTV homogeneity index (HI), Dice similarity coefficient (DSC), number of monitor units (MU), as well as deviations from protocol dose constraints were retrospectively analyzed and compared between pts treated with a VMAT vs. IMRT technique.

#### Results

Major protocol deviations occurred for 52 pts (32%), mostly for uPRV (12%) and PTV (5%) coverage, and for the rectal (RW) and bladder wall (BW)  $V_{90\%}$  (7%, each) (Table 1), while minor deviations occurred for 67 pts (41%). For PTV and uPRV coverage, deviations were more frequent in the IMRT group ( $p=0.001$  and  $p<0.0001$ , resp.). As compared to IMRT, treatment planning with VMAT resulted in a slightly better uPRV coverage ( $D_{98\%}=31.1$  vs. 30.6 Gy,  $p<0.0001$ ), less MU (2335 vs. 3454,  $p<0.0001$ ), and better HI (0.09 vs. 0.11,  $p<0.0001$ ) and DSC (0.85 vs. 0.75,  $p<0.0001$ ) values. Moreover, VMAT yielded better dosimetric parameters for the BW  $V_{50\%}$  (26.1% vs. 33.3%,  $p=0.0001$ ) and the penile bulb (PB)  $D_{mean}$  (30.7 vs. 31.1 Gy,  $p=0.008$ ), while other dosimetric parameters were similar. The inclusion of the SV in the PTV impacted negatively on the RW  $V_{90\%}$  (9.1% without vs. 10.4% with,  $p=0.0003$ ) and RW  $V_{80\%}$  (13.2% without vs. 15.7% with,  $p=0.0003$ ). The PTV volume was found to mildly linearly correlate with the BW  $V_{50\%}$  ( $r=0.523$ ,  $p<0.0001$ ) and the femoral heads (FH)  $D_{2\%}$  ( $r=0.572$ ,  $p<0.0001$ ).

Table 1: Means and standard deviations (SD) of dosimetric parameters, protocol dose constraints, and number of plans with protocol deviations.

	Mean $\pm$ SD	Protocol constraints (acceptable deviations)	Major (minor) protocol deviations
PTV D <sub>98%</sub> (Gy)	34.4 $\pm$ 0.4	$\geq$ 34.4 Gy (33.7 Gy)	9 (32)
PTV D <sub>2%</sub> (Gy)	38.1 $\pm$ 0.6	< 38.8 Gy (39.9 Gy)	0 (10)
RW V <sub>100%</sub> (%)	1.7 $\pm$ 1.5	< 5% (10%)	0 (4)
RW V <sub>90%</sub> (%)	10.2 $\pm$ 3.3	< 10% (15%)	11 (66)
RW V <sub>80%</sub> (%)	14.5 $\pm$ 4.2	< 20% (25%)	0 (16)
BW V <sub>100%</sub> (%)	6.6 $\pm$ 3.4	< 10% (15%)	1 (20)
BW V <sub>90%</sub> (%)	12.6 $\pm$ 4.9	< 20%	11
BW V <sub>50%</sub> (%)	28.4 $\pm$ 11.2	< 50% (60%)	1 (3)
PB D <sub>mean</sub> (Gy)	8.8 $\pm$ 7.5	< 27.2 Gy	3
uPRV D <sub>98%</sub> (Gy)	31.0 $\pm$ 0.9	$\geq$ 30.9 Gy (30.2 Gy)	19 (15)
uPRV D <sub>2%</sub> (Gy)	34.6 $\pm$ 0.5	< 35.8 Gy	2
FH <sub>right</sub> D <sub>2%</sub> (Gy)	13.1 $\pm$ 3.2	< 18.1 Gy	7
FH <sub>left</sub> D <sub>2%</sub> (Gy)	13.1 $\pm$ 3.0	< 18.1 Gy	4

### Conclusion

The retrospective QA analysis of this prospective SBRT trial showed up to a 32% rate of dosimetric variations with potential impact on tumor control and/or toxicity profile. Use of an IMRT technique and inclusion of SV in the PTV were the major causes of protocol deviations. Integration of prospective RTQA protocols is encouraged for future PCa SBRT clinical trials to prevent and correct protocol violations before start of treatment.

### Proffered Papers: PH 13: Proffered paper: Modelling toxicity

#### OC-0610 Modelling of xerostomia after radiotherapy for head and neck cancer: a registry study

E. Onjukka<sup>1</sup>, C. Mercke<sup>2</sup>, A. Discacciati<sup>3</sup>, G. Alexandersson von Döbeln<sup>2</sup>, E. Björgvinsson<sup>2</sup>, H. Carstens<sup>2</sup>, S. Friesland<sup>2</sup>, G. Gagliardi<sup>1</sup>, C. Lenneby Helleday<sup>2</sup>, H. Sjödin<sup>2</sup>, G. Wickart Johansson<sup>2</sup>, I. Lax<sup>1</sup>  
<sup>1</sup>Karolinska University Hospital, Medical Radiation Physics and Nuclear Medicine, Stockholm, Sweden ;  
<sup>2</sup>Karolinska University Hospital, Oncology, Stockholm, Sweden ;  
<sup>3</sup>Karolinska Institute, Institute of Environmental Medicine, Stockholm, Sweden

#### Purpose or Objective

The purpose of this study is to model the incidence of late xerostomia in patients treated with radiotherapy (RT) for head-and-neck (H&N) cancer, based on data from a local quality registry.

#### Material and Methods

Since 2013 patients followed up after RT for Head and Neck cancer at Karolinska University Hospital are entered into a quality registry and scored for toxicity of the skin, mucosa, larynx, and mandible, as well as xerostomia, dysphagia and trismus, according to a modified RTOG/LENT-SOMA scale. Also patient- and treatment-related factors are recorded, including RT dose/volume parameters for external-beam RT, concomitant drug therapy, performance status, gender, age, tumour location, tumour stage, HPV association and smoking status. The registry has a compliance of 70% and currently includes records of 1400 patients.

The treatment technique is predominantly IMRT/VMAT (87%) with 6 MV. Prescribed dose to primary target volume

is; >73 Gy in 12%, 68 Gy in 69%, 66 Gy in 8% and 50 Gy in 9%. The dose/fraction is 2.2 Gy for the highest dose group and 2.0 Gy for the other groups. The number of fractions/week is 6 in 51% and 5 in 45% of the patients. The dose per fraction to elective volumes is 2.0 Gy or 1.52 Gy for two sequential dose plans and simultaneous integrated boost plans, respectively.

A logistic regression model of grade  $\geq 2$  late xerostomia was fitted for patients who had at least one follow-up scoring late toxicity, and no missing values for the included variables. Re-irradiated patients were excluded from the analysis. Forward selection of model parameters was used and discrimination and calibration were assessed with AUC and calibration curves. An internal validation with bootstrap was performed to correct the performance measure for optimism.

### Results

Out of the 673 patients included in the study 43% had a maximum score of grade  $\geq 2$  late xerostomia. The cohort characteristics are listed in the table. The following variables were selected when fitting the model: mean dose to the total parotid volume (ipsilateral + contralateral), tumour type, gender and concomitant drug therapy. A greater odds ratio was associated with higher parotid dose, oropharynx tumours, female gender and concomitant cisplatin treatment, respectively. The optimism corrected AUC was 0.638 (95%CI: 0.597; 0.678) and the calibration slope was 0.798 (95%CI: 0.535; 1.061). The model performance did not improve when forcing the inclusion of the mean dose to each parotid separately, and the odds ratios for the two parotids were equivalent.

	Grade <2 xerostomia	Grade $\geq 2$ xerostomia	p-value
N	384	289	
Female gender	114 (30%)	112 (39%)	0.014
Age (year), median (IQR)	63.5 (54, 70)	62 (56, 70)	0.75
Tumour type			<0.001
Oropharynx	176 (46%)	190 (66%)	
Oral cavity	97 (23%)	54 (19%)	
Larynx	36 (9.4%)	7 (2.4%)	
Other	75 (20%)	38 (13%)	
T stage			0.92
0	20 (5.2%)	15 (5.2%)	
1	94 (25%)	63 (22%)	
2	140 (37%)	110 (38%)	
3	65 (17%)	47 (16%)	
4	65 (17%)	54 (19%)	
N stage			<0.001
0	163 (42%)	84 (29%)	
1	46 (12%)	31 (11%)	
2, 2a, 2b	149 (39%)	139 (48%)	
2c	21 (5.5%)	33 (11%)	
3	5 (1.3%)	2 (0.7%)	
Smoking status			0.046
Never	74 (19%)	78 (27%)	
Smoker	87 (23%)	53 (18%)	
Previous	223 (58%)	158 (55%)	
Concomitant therapy			<0.001
No	183 (48%)	94 (33%)	
Cisplatin	111 (29%)	115 (40%)	
Eribitux	90 (23%)	80 (28%)	
Induction chemotherapy			
No	278 (72%)	197 (68%)	
Yes	106 (28%)	92 (32%)	
Fractions/week			0.011
5	154 (40%)	84 (29%)	
6	220 (57%)	194 (67%)	
10	10 (2.6%)	11 (4%)	
Median dose (Gy)			
ipsilateral parotid (IQR)	31.4 (22.1, 42.0)	37.6 (27.3, 45.2)	<0.001
Median dose (Gy)			
contralateral parotid (IQR)	17.5 (10.3, 21.9)	19.8 (16.2, 23.2)	<0.001
Median dose (Gy)			
total parotid (IQR)	24.4 (18.6, 30.7)	28.6 (23.1, 33.0)	<0.001

### Conclusion

This large registry study showed that for the patients treated with RT for H&N cancer, the strongest risk factor for late xerostomia is the dose to the total parotid volume. There does not seem to be any benefit in *predominantly* sparing the contralateral parotid.

#### OC-0611 Planned and delivered DVHs of the skin predict acute cutaneous toxicity after IGRT for HN cancer

M. Mori<sup>1</sup>, S. Foti<sup>2</sup>, I. Dell' Oca<sup>2</sup>, M. Branchini<sup>1</sup>, S. Broggi<sup>1</sup>, G.M. Cattaneo<sup>1</sup>, N. Di Muzio<sup>2</sup>, C. Fiorino<sup>1</sup>  
<sup>1</sup>San Raffaele Scientific Institute, Medical Physics, Milan, Italy ; <sup>2</sup>San Raffaele Scientific Institute, Radiotherapy, Milan, Italy

#### Purpose or Objective

To explore the ability of skin dose-volume histograms (DVH) to predict the risk of acute cutaneous toxicity (ACT) after Radio-chemotherapy for Head and Neck (HN) cancer patients (pts) and to test if DVHs recalculated during therapy may improve prediction.

#### Material and Methods

Seventy HN pts were treated with Helical Tomotherapy (HT) with radical intent (SIB technique: 54/66 Gy to PTV1/PTV2 in 30fr) and concurrent chemotherapy (excluding Cetuximab). The skin was defined as a superficial body layer 2mm thick (SL2). Prospectively evaluated CTCAE v4.0 ACT data were available. Average absolute DVH of SL2 for pts who developed severe (G3) and severe/moderate (G3/G2) ACT were assessed. The differences against DVHs of patients without ACT (G0/G1/G2 and G0/G1 respectively) were analyzed by two-tails t-test; univariable logistic analyses were performed selecting DVH values corresponding to the lowest p-values at t-tests. Multivariable logistic analyses were also performed considering CTV volume, age, sex, chemotherapy as potential predictive factors. In addition, the effect of dose changes during therapy was quantified in 32/70 pts, by recalculating DVHs at half and end therapy with a previously validated dose-of-the-day calculation method. The association between therapy DVHs and G3/G2 ACT was tested and compared against the one using planning DVH.

#### Results

Sixty-one % of pts experienced G2/G3 ACT (rate of G3=19%). As reported in Fig 1 (left), differences in skin DVHs (G2/G3 vs G0/G1) were significant in the range 53-68Gy. V56 was the most predictive parameter (OR= 1.12, 95%CI= 1.03-1.21, p= 0.001), with a best cut-off of 7.7cc. The logistic model for V56 was well calibrated (slope/R<sup>2</sup> of calibration plot: 0.97/0.99). When considering G3 ACT (Fig 1, right), V64 was the best predictor (OR= 1.13, 95%CI= 1.01-1.26, p= 0.027) with a best cut-off of 2.7cc. Average V64 were 2.2cc and 6cc for the two groups (G3 vs G0-G2); the logistic model for V64 also showed good calibration (slope/R<sup>2</sup>: 0.99/0.60). The association between DVHs and G2/G3 ACT was significant also in the subgroup of 32 pts with dose-of-the-day calculations available; t-tests on average DVHs at planning, half and end of treatment (Fig 2), showed none improvement of the association with ACT when considering therapy DVHs in place of planning DVHs.

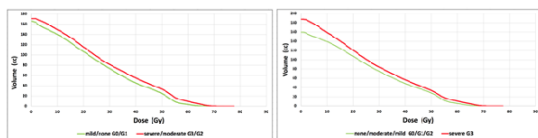


Figure 1: Average absolute DVH of SL2 for pts who developed severe/moderate (G3/G2) Vs mild/none (G0/G1) on the left. Only severe (G3) Vs moderate/mild/none (G2/G1/G0) on the right.

#### Conclusion

The relationship between SL2 DVH and ACT after HT of HN pts with a SIB approach was quantified. The results should help in identifying pts at risk and in implementing more effective skin-sparing planning strategies. In particular,

constraining V64 < 3cc (corresponding to 4x4cm<sup>2</sup> skin surface) should keep the risk of G3 ACT below 10%. Considering therapy DVHs in place of planning DVHs does not seem to improve prediction.

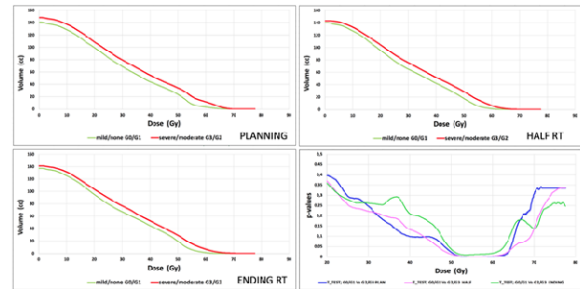


Figure 2: Average absolute DVH of SL2 for pts who developed severe/moderate (G3/G2) Vs mild/none (G0/G1) at planning on the left top, at half RT on the right top and at ending RT on the left bottom. On the right bottom the t-test average DVHs comparison of three RT phases shows none improvement of the association with ACT when considering therapy DVHs in place of planning DVHs.

#### OC-0612 A case-control study of brainstem substructures and morbidity following pediatric proton therapy

C. Stokkeväg<sup>1</sup>, D.J. Indelicato<sup>2</sup>, L.F. Fjæra<sup>3</sup>, Y. Lassen-Ramshad<sup>4</sup>, K.S. Ytre-Hauge<sup>3</sup>, Z. Li<sup>2</sup>, L. Toussaint<sup>5</sup>, O. Casares-Magaz<sup>3</sup>, S. Flampouri<sup>2</sup>, R. Mikkelsen<sup>6</sup>, C. Pedro<sup>7</sup>, O. Dahl<sup>1</sup>, L.P. Muren<sup>5</sup>  
<sup>1</sup>Haukeland University Hospital, Department of Oncology and Medical Physics, Bergen, Norway ; <sup>2</sup>University of Florida, Department of Radiation Oncology, Jacksonville, USA ; <sup>3</sup>University of Bergen, Department of Physics and Technology, Bergen, Norway ; <sup>4</sup>Aarhus University Hospital, Danish Centre for Particle Therapy, Aarhus, Denmark ; <sup>5</sup>Aarhus University Hospital, Department of Medical Physics, Aarhus, Denmark ; <sup>6</sup>Aarhus University Hospital, Department of Neuroradiology, Aarhus, Denmark ; <sup>7</sup>Portuguese Institute of Oncology Francisco Gentil de Lisboa, Department of Radiotherapy, Lisbon, Portugal

#### Purpose or Objective

Brainstem toxicity is a rare but severe condition that can follow treatment of pediatric brain tumors. Dose received by the brainstem is one of the treatment-specific causes of brainstem morbidity. Current data on brainstem toxicity are limited and the brainstem is often regarded as a single organ with dose constraints determined without considering potential regional sensitivity within the brainstem. The brainstem core has in some studies been found more radiosensitive than the outer surface, and diffusion tensor imaging has recorded non-uniform changes across different substructures of the organ. In order to investigate if outcome could be explained by different radio-sensitivities across the brainstem, dose/volume parameters in different anatomical brainstem regions were evaluated for pediatric brain tumor patients with brainstem toxicity vs. patients with no toxicity.

#### Material and Methods

A matched case-control was performed within a cohort of 954 pediatric brain tumor patients treated with proton therapy from 2006 to 2017. Ten patients presenting with symptomatic grade 2+ brainstem toxicity were each matched to three controls based on diagnosis, age within  $\pm 1.5$  years and by whole brainstem dose metrics (D0.1cc within  $\pm 2$  Gy, and D10% within  $\pm 2$  Gy). The brainstem core (brainstem cropped by 3 mm) and the regions medulla oblongata, midbrain, pons were segmented on T1/T2 MRI sequences fused with the CT scan used for treatment planning. The pons was further divided into four transversal zones (posterior, middle posterior, middle anterior and anterior) to approximate fiber tracts (Figure 1). Dose/volume metrics (obtained using an RBE of 1.1) for

each segmented structure were compared between cases and controls using two-way ANOVA tests with significance level 0.05.

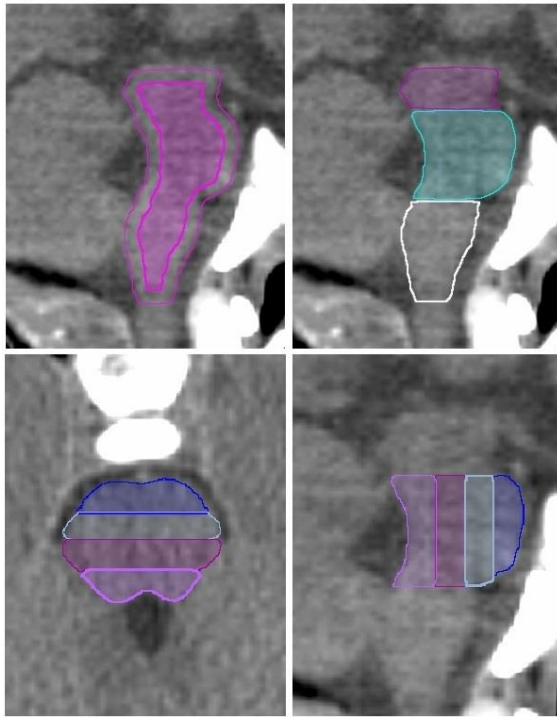


Figure 1. Brainstem structures: full brainstem and core (upper left), midbrain, pons and medulla oblongata (upper right), posterior, middle posterior, middle anterior and anterior pons (lower panels: left in transvers; right in sagittal).

## Results

Average D0.1cc, D10% and D50% of each brainstem substructure were not statistically significant different between cases and controls (Figure 2). Significant difference was also not found between the dose/volume parameters for the full brainstem. For both cases and controls, the medulla oblongata and anterior pons had the largest variance in all dose/volume parameters, whereas the variance of D50% was also high for the posterior pons.

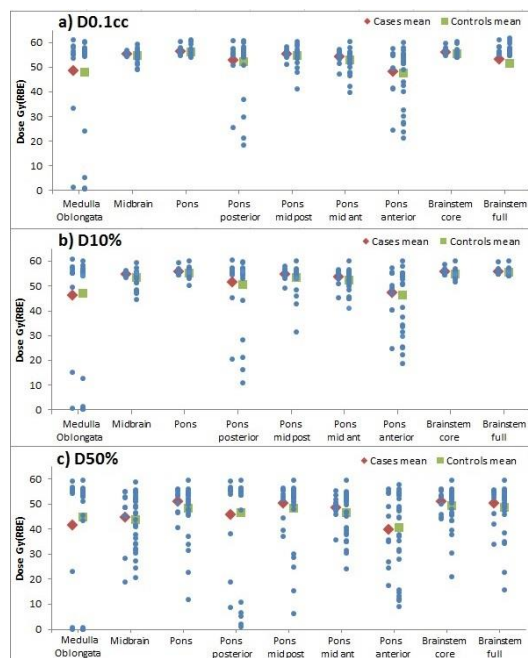


Figure 2: Dose/volume metrics for cases (shifted left) and controls (shifted right). Medulla oblongata, midbrain, pons, and the four transversal zones of the pons: posterior, middle posterior, middle anterior, anterior pons and brainstem core. The full brainstem dose metrics were used for matching.

## Conclusion

The brainstem morbidities manifested in the ten cases could not be explained by the investigated dose metrics, including the specific brainstem substructures. The variations in radio-sensitivity may therefore be due to other patient-specific factors not controlled for in this study, or may be better explained by other metrics including variable RBE doses.

### OC-0613 Spatial dose patterns of radiation pneumonitis in lung cancer patients treated by photons or protons

G. Palma<sup>1</sup>, S. Monti<sup>2</sup>, T. Xu<sup>3</sup>, E. Scifoni<sup>4</sup>, P. Yang<sup>3</sup>, S. Hahn<sup>3</sup>, M. Durante<sup>5</sup>, R. Mohan<sup>6</sup>, Z. Liao<sup>3</sup>, L. Cella<sup>1</sup>  
<sup>1</sup>National Research Council, Institute of Biostructures and Bioimaging, Napoli, Italy ; <sup>2</sup>Ircs SDN, Image Processing Department, Napoli, Italy ; <sup>3</sup>MD Anderson Cancer Center, Department of Radiation Oncology, Houston, USA ; <sup>4</sup>Istituto Nazionale di Fisica Nucleare, Trento Institute for Fundamental Physics and Applications, Trento, Italy ; <sup>5</sup>GSI Helmholtz Centre for Heavy Ion Research, Department of Biophysics, Darmstadt, Germany ; <sup>6</sup>MD Anderson Cancer Center, Department of Radiation Physics, Houston, USA

### Purpose or Objective

Radiation pneumonitis (RP) is a common side effect of thoracic Radiation Therapy (RT), and its incidence has been reported similarly in both Intensity-Modulated RT (IMRT) and Passive Scattering Proton Therapy (PSPT) [Liao *et al.*, JCO 2018]. Aim of this study is to investigate the spatial pattern of pulmonary and cardiac radiosensitivity (RS) to RP in patients enrolled in a prospective randomized trial of IMRT versus PSPT for locally advanced Non-Small-Cell Lung Cancer (NSCLC).

### Material and Methods

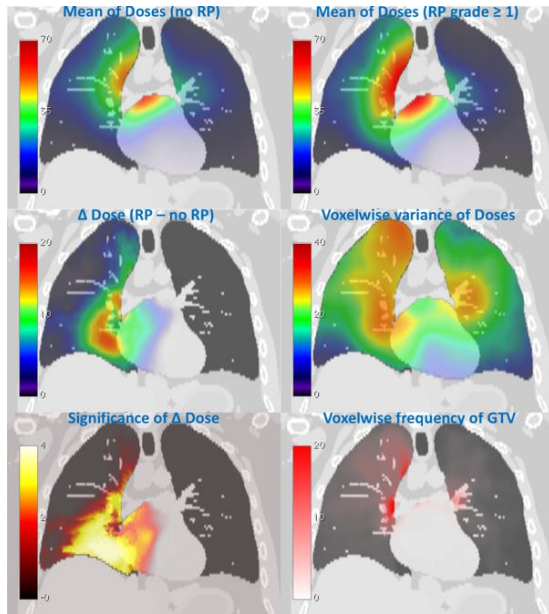
We analyzed data of 178 prospectively treated at a single institution with PSPT (64 patients) or IMRT (114 patients) for NSCLC. All patients were treated to a prescribed dose of 60 to 74 Gy in conventional daily fractionation with concurrent chemo-radiotherapy. Median patient age was 66 years (range: 33-85 years). Fifty-five patients (31%) in the trial developed RP of any grade scored according to CTCAE v. 3.0.

Each planning CT and dose map was spatially normalized to a common anatomical reference using a B-spline inter-patient registration algorithm after masking the gross tumor volume. A Voxel-Based Analysis (VBA) was performed according to a non-parametric permutation test accounting for multiple comparison, based on a cluster analysis method [Monti *et al.*, SciRep 2018]. The underlying general linear model of RP was designed to include dose maps and potential non-dosimetric variables significantly correlated with RP. A 3D significance map was derived and the clusters of voxels with dose differences that significantly correlated with RP at a  $p$ -level of 0.05 ( $S_{0.05}$ ) were generated accordingly.

The VBA was performed on the Entire Cohort (EC) and, separately, on the sub-cohorts of IMRT and PSPT. In order to quantify the match between the significance  $p$ -maps obtained on a sub-cohort ( $p_{IMRT}$  or  $p_{PSPT}$ ) and the  $p$ -map obtained on EC ( $p_{EC}$ ), the metrics DIV was computed as the Dice Index between the sublevel sets of  $p_{IMRT}$  or  $p_{PSPT}$  and  $p_{EC}$  with same relative volume  $V$  [Monti *et al.*, SciRep 2018].

### Results

The VBA on EC highlighted extended areas of significant dose differences between patients with and without RP in the lower part of the right lung and in the heart (Figure).



The mean dose in  $S_{0.05}$  for RP patients was 26 Gy, and for patients without RP was 11 Gy. The maps  $p_{IMRT}$  and  $p_{PSPT}$  showed a similar spatial pattern of  $p_{EC}$ , quantified by both the Areas Under the  $DIV[p_{EC}, p_{IMRT}]$  and  $DIV[p_{EC}, p_{PSPT}]$  Curves of 0.86.

#### Conclusion

Similar significance patterns highlighted by the 3 VBAs justify the choice to analyze the 2 sub-cohorts as a whole in search of valuable insights into the thoracic RS. The completely different dose patterns of PSPT provide an unprecedented chance to look at the results of a VBA, with a sensible reduction of a potential bias related to the spatial correlation of IMRT dose distributions. This lays more robust foundations to the previously reported hypotheses that the lower parts of the lungs and the heart play a prominent role in the development of RP [Monti *et al.*, SciRep 2018].

#### OC-0614 NTCP models of late rectal morbidity after proton therapy in 1036 prostate cancer patients

J. Pedersen<sup>1</sup>, S. Flampouri<sup>2</sup>, C. Bryant<sup>2</sup>, Z. Li<sup>2</sup>, N. Mendenhall<sup>2</sup>, L.P. Muren<sup>1</sup>

<sup>1</sup>Aarhus University Hospital, Department of Medical Physics, Aarhus, Denmark ; <sup>2</sup>University of Florida Health Proton Therapy Institute, University of Florida Health Proton Therapy Institute, Jacksonville- Florida, USA

#### Purpose or Objective

Normal tissue complication probability (NTCP) models may be used to guide patient selection and treatment evaluation for proton therapy (PT), but current models are derived from outcomes following photon-based radiotherapy. Since photons and protons have fundamentally different properties (reduced dose bath with PT and a higher relative biological effectiveness, RBE), NTCP models for photons might not be applicable to PT. The aim of this study was therefore to derive parameters of an established NTCP model when using prospectively recorded late morbidity data from PT, focusing on rectal morbidity and prostate cancer.

#### Material and Methods

Dose volume histogram data for the rectum and rectal wall from 1036 prostate cancer patients (with no pre-treatment anti-coagulation medication) treated with PT between 2006 and 2010 were used. Patients were prescribed target doses of 78-82 Gy (RBE = 1.1) in 2 Gy fractions. Lyman-Kutcher-Burman model parameters were derived for two alternative late grade 2 rectal bleeding endpoints (CTCAE v3.0): Grade 2A (GR2A) was classified as

medical (e.g. prescribed suppositories) and Grade 2B (GR2B) was classified as procedural (included minor cauterization and topical formalin application). Model parameters were derived for both the rectum and the rectal wall by maximum likelihood estimation, and profile likelihood estimation was used to calculate confidence intervals for the parameters. Patients were also sorted by NTCP values (low to high), and divided into 12 groups of 86-87 patients to allow for a comparison between the calculated NTCP and the clinically observed frequency of morbidity.

#### Results

Late GR2A+2B rectal bleeding was observed in 155/1036 patients (15%) and GR2B in 45/1036 patients (4%). The volume parameter  $n$  was low (0.04-0.14) both for GR2A+2B and GR2B, and lowest for GR2B for the rectum. For uniform irradiation of one-third of the rectum ( $V = 1/3$ ) an NTCP of 5% was found at 59 Gy for GR2A+2B and at 75 Gy for GR2B (Fig. 1). There was a close to 1:1 relation between the calculated NTCPs and the observed morbidity across the 12 groups (Fig. 2). However, there were large variations between the groups, most pronounced for GR2B (Fig. 2). The area under the curve values ranged between 0.62-0.63 for GR2A+2B and 0.54-0.55 for the GR2B.

Figure 1:

NTCP models for grade 2B + 2A and grade 2B only morbidity, for both the rectum and the rectal wall, showing the dose response for uniform irradiation of the whole organ (blue), 2/3 of the organ (green) and 1/3 of the organ (red). Note that the volume effect is smallest for the GR2B endpoint, and also smaller for the volume than the rectal wall. The best fit LKB parameters including their confidence intervals are summarised in the legends, for both morbidity endpoints and both the rectum and rectal wall. Note that the y-axis is not same scale.

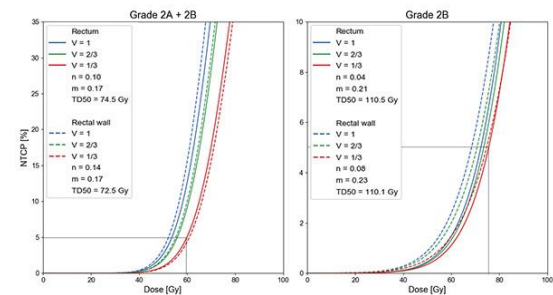
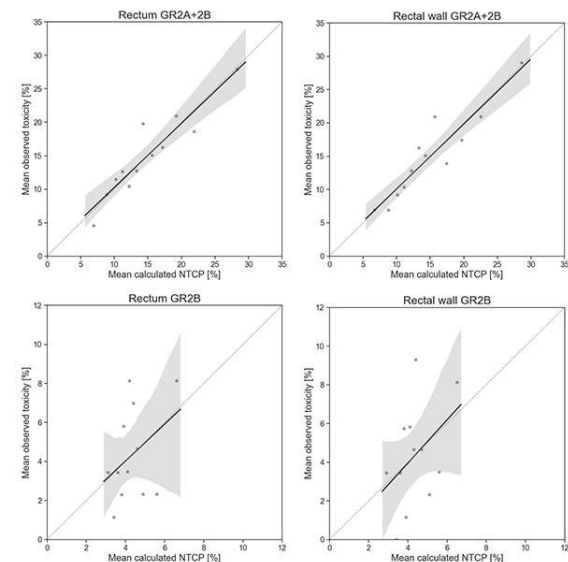


Figure 2:

Mean calculated NTCP values (based on best fit LKB parameters) vs. the actually observed frequency of morbidity for the twelve groups, both morbidity endpoints (GR2A+2B and GR2B), and both the rectum and rectal wall. Each data point shows the mean calculated NTCP (sorted from low to high) vs. observed frequency of morbidity for groups of 86-87 patients. Black solid lines are the best fit regression lines for the points, while the grey dotted lines are the identity line. As can be seen, the fitted lines and the identity line are almost identical indicating that the derived parameters fit the data.



## Conclusion

PT specific NTCP model parameters for prospectively recorded late rectal morbidity in more than 1000 patients were derived. The volume parameter was generally small indicating a weak volume effect, most pronounced for the GR2B endpoint. There was a difference of >15 Gy between the doses resulting in 5% morbidity for the two alternative endpoints. The models were internally validated, showing the appropriateness of our methodology. However, the predictive power on an individual level was moderate, in particular for GR2B due to fewer events. Further optimization of model performance will be explored, incorporating also spatial measures of the dose distributions.

## OC-0615 Predicting urinary toxicity via 2D and 3D dose map analyses in prostate cancer radiotherapy

E. Mylona<sup>1</sup>, A. Cicchetti<sup>2</sup>, T. Rancati<sup>2</sup>, F. Palorini<sup>2</sup>, S. Supiot<sup>3</sup>, N. Magné<sup>4</sup>, G. Crehange<sup>5</sup>, O. Acosta<sup>1</sup>, R. De Crevoisier<sup>1,6</sup>

<sup>1</sup>INSERM U1099 - University of Rennes, Laboratoire Traitement du Signal et de l'Image, Rennes, France ; <sup>2</sup>IRCCS Istituto Nazionale dei Tumori, Prostate Cancer Program, Milan, Italy ; <sup>3</sup>Institut de Cancérologie de l'Ouest - René Gauducheau, Radiotherapy Department, Nantes, France ; <sup>4</sup>Lucien Neuwirth Cancer Institute, Radiotherapy Department, St Priest en Jarez, France ; <sup>5</sup>Centre Georges François Leclerc, Radiotherapy Department, Dijon, France ; <sup>6</sup>Centre Eugène Marquis, Radiotherapy Department, Rennes, France

### Purpose or Objective

Risk estimation of urinary toxicity after prostate radiotherapy is generally based on bladder DVH, disregarding any spatial dose-distribution information. The objectives of the study were:

- To identify bladder subregions associated with urinary toxicity via pixel-wise and voxel-wise statistical analysis on 2D dose-surface maps (DSM) and 3D dose-volume maps (DVM), respectively.
- To evaluate their prediction capabilities with respect to the DVH of the whole bladder.

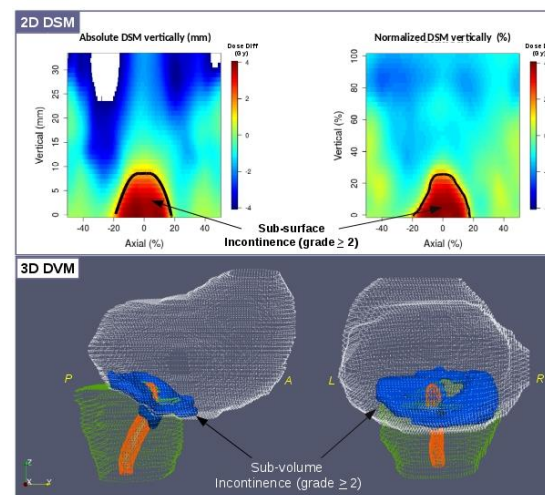
### Material and Methods

In total 272 prostate cancer patients treated with IMRT/IGRT from two multicentric phase III trials (STIC-IGRT and PROFIT), were prospectively analyzed. Local relationships between dose and specific urinary endpoints were investigated via 2D DSMs and 3D DVMs, by analyzing the planning dose distribution at pixel and voxel scales, respectively. DSMs were generated by anteriorly cutting and virtually unfolding the bladder surface. Maps were laterally normalized and aligned at the most inferior-posterior point. Normalized DSMs (nDSM) both laterally and vertically were also computed. DVMs were produced by first non-rigidly registering the population to a common coordinate system and then propagating the 3D dose distribution according to the transformation beforehand obtained. Pixel and voxel-wise non parametric analyses were performed, for DSMs and DVMs respectively, to identify regions of statistically significant dose differences between patients with/without toxicities. The spatial correlation between the regions found with the nDSMs and DVMs for each symptom was evaluated with the Jaccard score (intersection surface divided by union surface). Prediction capability was estimated by the area under the ROC curve (AUC) from logistic regression, performed at each dose bin of the DVH of the sub-volumes, the dose-surface histogram (DSH) of the sub-surfaces, and the DVH of the whole bladder.

### Results

A local dose-effect relationship was found for three late toxicity endpoints: incontinence (grade $\geq$ 2), retention (grade $\geq$ 1) and dysuria (grade $\geq$ 1). The 5-year toxicity rates were 4%, 23% and 13%, respectively. The subregions found with the two methods are mostly located in the inferior

and posterior bladder. The Jaccard scores were 0.3 (dysuria), 0.42 (retention) and 0.7 (incontinence). Figure 1 shows the identified sub-surface (top) and sub-volume (bottom) for urinary incontinence. Table 1 shows the prediction capabilities, for each endpoint, of the sub-volume's DVH, sub-surface's DSH and whole bladder's DVH. The dose bin with the highest significant AUC is reported.



Endpoint (late toxicity)	Method	Most predictive bin	AUC (p-value)	OR (95% CI)
Incontinence (grade $\geq$ 2)	Sub-surface DSH	S78	77.5 (0.01)	1.03 (1.01-1.06)
	Sub-volume DVH	V79	79.7 (0.01)	1.04 (1.01-1.07)
	Whole bladder DVH	V80	70.2 (0.01)	1.21 (1.05-1.41)
Retention (grade $\geq$ 1)	Sub-surface DSH	S62	62 (0.05)	1.01(1-1.02)
	Sub-volume DVH	V37, V62	68 (<0.01)	1.02 (1.01 - 1.04)
	Whole bladder DVH	-	NS	-
Dysuria (grade $\geq$ 1)	Sub-surface DSH	S77	70 (<0.01)	1.18 (1.07-1.3)
	Sub-volume DVH	V53	78.7 (<0.01)	1.06 (1.02-1.09)
	Whole bladder DVH	V63	70.1 (0.02)	1.04 (1.01-1.07)

Abbreviations: DVM= dose-volume map, DSM=dose-surface map, OR= odds ratio, AUC= area under the ROC curve, CI= confidence interval, NS = non significant

### Conclusion

Specific bladder subregions were identified by the two methods as more predictive of urinary toxicity than the whole bladder. Particularly, the DVM method highlights the importance of volumes near the bladder surface, but inside bladder volume, underlining the influence of variable bladder filling and, thus, entailing the need of optimizing dose even in "non-obvious" regions (i.e. what appears to be urine at planning CT).

## OC-0616 Introducing information on gut microbiota into toxicity modeling: preliminary results from a trial

T. Rancati<sup>1</sup>, N. Bedini<sup>2</sup>, L. De Cecco<sup>3</sup>, B. Avuzzi<sup>2</sup>, S. Morlino<sup>2</sup>, B. Noris Chiorda<sup>2</sup>, M. Dispinzieri<sup>2</sup>, S. Villa<sup>2</sup>, T. Di Florio<sup>1</sup>, F. Badenchini<sup>1</sup>, F. Palorini<sup>1</sup>, T. Giandini<sup>4</sup>, A. Cicchetti<sup>1</sup>, E. Mancinelli<sup>3</sup>, M.S. Serafini<sup>3</sup>, A. De Vecchi<sup>3</sup>, E. Orlandi<sup>5</sup>, R. Valdagni<sup>6</sup>

<sup>1</sup>Fondazione IRCCS Istituto Nazionale dei Tumori, Prostate Cancer Program, Milan, Italy ; <sup>2</sup>Fondazione IRCCS Istituto Nazionale dei Tumori, Radiation Oncology 1, Milan, Italy ; <sup>3</sup>Fondazione IRCCS Istituto Nazionale dei Tumori, Platform of Integrated Biology- Department of Applied Research and Technology Development, Milan, Italy ; <sup>4</sup>Fondazione IRCCS Istituto Nazionale dei Tumori, Medical Physics, Milan, Italy ; <sup>5</sup>Fondazione IRCCS Istituto Nazionale dei Tumori, Radiation Oncology 2 and Radiation Oncology 1, Milan, Italy ; <sup>6</sup>University of Milan and Fondazione IRCCS Istituto Nazionale dei Tumori, Oncology and Hemato-oncology / Prostate Cancer Program / Radiation Oncology 1, Milan, Italy

**Purpose or Objective**

A mono-institutional trial was set up in 2017 to investigate the role of gut/saliva microbiota (MB) in driving radio-induced toxicity (tox) after RT for prostate (PCa) and head&neck cancers.

We here focus on introduction of information on gut MB into a normal tissue complication probability model (NTCP) for acute gastro-intestinal (GI) tox in the PCa cohort.

**Material and Methods**

130 consecutive PCa patients (pts) receiving conventional (78Gy @2Gy/fr) or moderately hypofractionated (65Gy @2.6Gy/fr) VMAT+IGRT in 5 fr/week were enrolled.

A detailed evaluation was done pre-RT, during RT and at RT end, including gut MB measurement. Stool samples were collected using gut-OMNIgene devices (Oragene). DNA extraction was carried out using the QIAamp-DNA-Stool-Mini-Kit (Qiagen). The bacterial 16S ribosomal-RNA reads were analyzed with the QIIME software and pooled in Operational Taxonomic Units (OTUs) with Uclust software.

Grade 2 (G2) CTCAE acute G ltox was the primary endpoint.

For this preliminary evaluation 20 pts were selected: 10 with G0 and 10 with G2 tox. Unsupervised clustering (fuzzy c-means algorithm) was used to separate the pts into 2 MB clusters, based on relative abundance of OTUs at bacterial class level in MB before RT start. Information on MB clustering was introduced as a dose-modifying factor (dmf) into a logit NTCP model (characterized by D50=dose associated to 50% tox probability and steepness parameter k). Mean dose to the rectum was chosen as dosimetric predictor (as already found in the literature).

**Results**

Unsupervised clustering identified 13 pts included in a first MB cluster (A) and 7 in a second cluster (B), average OTU composition for pts in clusters A and B are presented in figure 1.

4/13 (31%) and 6/7 (86%) pts with tox were found in clusters A and B, respectively (p=0.019). MB clustering resulted in AUC=0.75 (95%CI=0.51-0.91) for tox discrimination. NTCP model including only mean rectal dose had D50=49Gy, k=16 (AUC=0.85, 95%CI=0.62-0.97). When clustering was introduced, k=20.5, D50=42Gy for cluster A vs D50=32Gy for cluster B were found: MB clustering dmf (B vs A)=0.76 (AUC=0.87, 95%CI=0.65-0.98), with significant improvement in goodness of fit and calibration. Model curves are reported in figure 2.

Figure 1: average Operational Taxonomic Unit composition at Class level for patient in microbiota clusters A and B

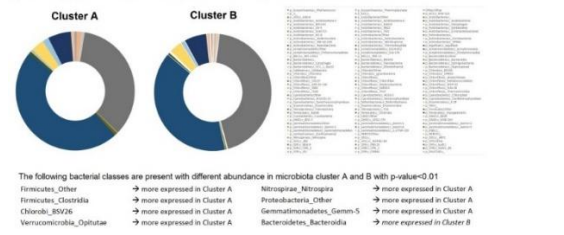
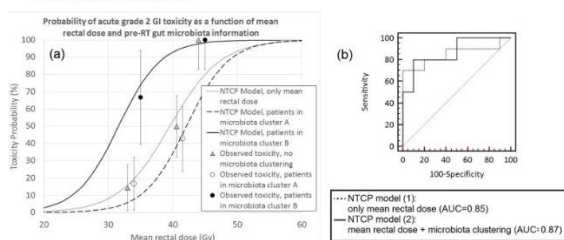


Figure 2. (a) Probability of acute grade 2 gastro-intestinal toxicity as a function of mean rectal dose and gut microbiota clustering. Observed complication rates are also reported (symbols with error bars representing the 68% confidence interval in observed frequencies as calculated from proportions in the study population and based on normal distribution of event). (b) ROC curves for NTCP models with and without inclusion of gut microbiota clustering as dose-modifying factor.



**Conclusion**

This preliminary study demonstrates the possibility of introducing patient-specific MB information into NTCP model, through use of unsupervised clustering to exploit the whole MB information (176 classes) without dramatically increasing the number of features to be included in the model.

Results obtained in a small sample of PCa pts seem promising in indicating that pts with/without radio-induced acute tox have different constitutional gut MB profiles.

Introduction of MB clustering into NTCP highly improves model performance. If confirmed in the whole accrued population, this could represent an important finding, not only for prediction of tox but also for design of possible interventional trials to reduce tox by modification of gut microbiota before RT start.

**Proffered Papers: RTT 6: Education and quality management for optimising patient care**

**OC-0617 Work interruptions in radiotherapy and their impact on patient safety.**

S. Cucchiaro<sup>1</sup>, M. Delgaudine<sup>2</sup>, N. Gourmet<sup>1</sup>, P. Coucke<sup>1</sup>  
<sup>1</sup>C.H.U. - Sart Tilman, Radiotherapy Department, Liège, Belgium ; <sup>2</sup>C.H.U. - Sart Tilman, STA Quality Department, Liège, Belgium

**Purpose or Objective**

Task Interruptions (TI) are common in hospitals and especially in Radiation Therapy (RT) Department. The main objective is to evaluate the number and characteristics of those interruptions in our RT department in order to propose solutions to reduce them to a minimum. There are many TI sources (phone calls, talk, noise,...), often of short duration and most often induced by team members. They affect attention, can generate stress, as well as treatment errors. The idea is to understand the TI, when they occur, where and who produces them and how the work is resumed. The goal is to implement prevention barriers to tasks identified as critical in the process and to allow a safe recovery of the task.

**Material and Methods**

Following an adverse event where an identified root cause was TI, we decided to carry out an exploratory study whose main objective is to be able to identify the sources of TI in the treatment unit as well as the timing of these interruptions. We used an observation grid (figure 1) with several items such as time, duration, nature, reason and consequence of the interruption. The TI were observed at the 5 service treatment units. The collected data has been analyzed in order to confirm that there are TI at the Radiation Therapists (RTTs) during a radiotherapy treatment, and that these TI can be a source of errors.

TI Hour	Step processing	Source of TI	Nature of TI	Reason for TI	Reaction to TI	Task recovery	Impact on activity	Duration of TI
1	Reception of the patient	1) Phone call	1) Professional of the sector	1) Contribution of information	1) Suspends action and treats the 2nd Action	1) Resume at the beginning of the task	1) No apparent consequence	1) Less than 1 min
2	Patient positioning	2) Patient	2) Professional of other sectors	2) Information search	2) Suspends action and delegates the 2nd	2) Resuming at TI	2) Loss of time in the task	2) Between 1 to 5 min
3	Imaging	3) Ambient noise	3) Professional non-service	3) Request for help	3) Continues the action in multitasking mode	3) Recovering from a period after the TI	3) Forgetting a task part	3) Between 5 and 10 min
4	Irradiation	4) Other	4) Patient	4) Request for help	4) Stop interrupting TI	4) Error in the activity	4) Error in the activity	4) Greater than 10 min
5	Check patient chart / administration		5) Ambulance / Volunteer	5) Other	5) Stop interrupting TI	5) No recovery		

Figure 1: Observation Items

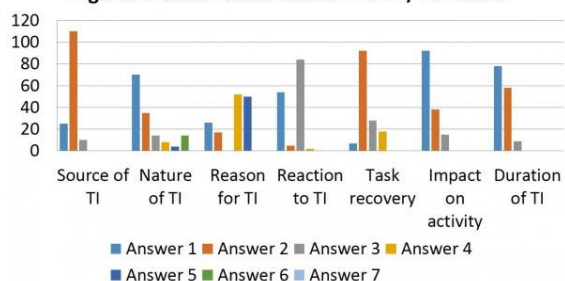
**Results**

A 5-hour observation at each treatment unit was performed for a total of 25 hours. 145 TI have been recorded. We were able to highlight an interruption every

10 minutes on average, that is, one interruption per treatment.

Moreover, these TI are characterized as a physical disturbance, on the part of a health professional, of a duration less than a minute and intervening mainly when the RTT is at the linac console, so during its activity of registration (image matching) and treatment delivery. In terms of impact on activity, we found that the TI lead to a break in the progress of the activity, and when they undergo one or more interruptions in their treatment activity, the RTTs react in different ways depending on the type of interruption. We observed 2 types of reactions: they can either stop their action and process the second, then return to the first task when the second is over or continue their 2 actions simultaneously, so in pure multitasking mode. Results in figures 1 and 2.

Figure 2: Observation results 145 TI / 25 Hours



## Conclusion

There are many TI in a RT department. This study allows us to highlight that TI can be a source of error and that there are a large number of elements on which it would be possible to act to limit risks.

RTT activity is impacted by many TI, attention is diverted, activities are performed in multitasking mode. It is important to limit TI, to optimize the work environment, to set up a formalized task recovery. Multiple solutions are discussed: awareness of RTT to refuse to be interrupted, identify people who should not be interrupted and recover the interrupted task in a safe way. The next step will be to extend the observation of TI to all those involved in the RT workflow.

## OC-0618 Clinical audits as a quality improvement tool in radiotherapy departments: the Belgian experience

A. Vaandering<sup>1</sup>, P. Scalliet<sup>1</sup>, F. Vanhoutte<sup>3</sup>

<sup>1</sup>UCL Cliniques Univ. St. Luc, Academic Department of Radiation Oncology, Brussels, Belgium ; <sup>2</sup>Belgian College for Physicians in Radiation Oncology, Brussels, Belgium ;

<sup>3</sup>Ghent University Hospital, Department of Radiation Oncology, Ghent, Belgium

## Purpose or Objective

The potential benefits of clinical audits are multiple and have the overall aim of encouraging continuous quality improvement through the implementation of corrective actions based on the recommendations emitted by the audits. A national project carried by the Belgian College of Radiotherapy brought about the instauration of systematic clinical audits of all radiotherapy (RT) departments using the IAEA QUATRO (Quality Assurance Team for Radiation Oncology) methodology from 2011 to 2015 included. The impact of these audits was then evaluated and the emitted recommendations were analysed to identify areas of weakness on a national basis.

## Material and Methods

The QUATRO methodology is a peer-review based audit covering all parts of the RT process that gives rise to a report containing a detailed account of the audit including a list of recommendations that the department is encouraged to implement (1). The recommendations extracted from all 25 audit reports were classified using

the coding key proposed by Izweska et al. (2). This taxonomy categorises these into four main divisions: issues pertaining to staffing, infrastructure, process or organisational factors. These are further subdivided into a 3-level categorisation code. Departments were also sent a questionnaire listing their recommendations and in which they were asked to evaluate the overall usefulness of the these as well as the usefulness and the actual impact of each individual recommendation based on an ordinal rating scale (see table 1).

Relevancy scale	Evaluation	The recommendation was not relevant at all to the department's situation/context	The recommendation was little relevant to the department's situation/context	The recommendation was moderately relevant to the department's situation/context	The recommendation was very relevant to the department's situation/context	The recommendation was primordial to the department's situation/context
		Score 0	1	2	3	4
Impact scale	Evaluation	The recommendation had no impact on the department's organisational/infrastructural situation	The recommendation had little impact on the department's organisational/infrastructural situation	The recommendation had a moderate impact on the department's organisational/infrastructural situation	The recommendation had a big impact on the department's organisational/infrastructural situation	The recommendation had a primordial impact on the department's organisational/infrastructural situation
		Score 0	1	2	3	4

Table 1 – Usefulness and impact score of the recommendations

## Results

Of the total of 381 emitted recommendations, 34% concerned process optimization. Twenty-seven percent of the recommendations concerned infrastructure (30% concerned the quality of the facility or the equipment). Finally, 19% and 20% of recommendations concerned organisational and staff issues respectively (e.g. RTT training and professional development). Twenty-three out of the 25 departments responded to the questionnaires. Fifty-four percent of the departments found the recommendations very useful. When scoring the usefulness of the individual recommendations, 42.7% were found to be very relevant with those pertaining to staff and organisation issues scored as being most relevant. When scoring the impact of the individual recommendations, 23.5% were deemed to have an important impact, the majority having a moderate impact (30.6%). Recommendations deemed to have the most impact were those pertaining to process optimisation.

## Conclusion

Revisions of the emitted recommendations have allowed the auditors to identify, on a national basis, common areas of improvement. Similarly, the questionnaires have been able to demonstrate that the recommendations were globally deemed very relevant. However, the global impact of these on the department's organisational/infrastructural situation was scored lower and this in majority due to factors outside of the department's control. Encouraged by this analysis, a second cycle of audits has started in Belgium with a modified QUATRO document (B-QUATRO).

1. International Atomic Energy Agency. *Comprehensive Audits of Radiotherapy Practices: A tool for Quality Improvement*. Vienna : IAEA, 2007.

2. Izweska J, Coffey M, Scalliet P, Zubizarreta E, Santos T, Vouldis I, Dunscombe P. Improving the quality of radiation oncology: 10 year's experience of QUATRO audits in the IAEA Europe region. *Radiation Oncology*. 2017, p. in press.

## OC-0619 Using continuous quality improvement to improve safety and reduce imaging errors in radiotherapy

D. Tan<sup>1</sup>, L. Davies<sup>1</sup>, M. Williams<sup>1</sup>, S. Jones<sup>1</sup>, N. Bales<sup>1</sup>, C. Beswick<sup>1</sup>, P. Wheeler<sup>1</sup>

<sup>1</sup>Velindre Cancer Centre, Radiotherapy, Cardiff, United Kingdom

## Purpose or Objective

A quality improvement (QI) project was implemented to facilitate the transition from standard two-dimensional megavoltage (2DMV) electronic portal imaging (EPI) to 2D kilovoltage (kV) imaging for the geometric verification of palliative indications within a radiotherapy (RT) department. Utilising QI methodologies, the aim of this work was to develop an image optimisation programme to ensure suitable image quality (using 2DKV imaging) whilst keeping doses as low as reasonably practicable (ALARP). It

was expected that the embedment of QI processes within the practice would enable both the delivery of accurate and meaningful radiation dose as well as the reduction in the number of imaging related radiotherapy errors (RTE).

#### Material and Methods

The Institute for Healthcare Improvement's Model for Improvement framework utilising plan, do, study, act (PDSA) cycles was employed to help structure and drive quality within this project. Four project measures were identified to monitor progress against the QI aim: subjective image quality, image dose, RTE and staff feedback. The QI programme was initiated in May 2017 and is still ongoing. During this period an RTE audit, frontline staff survey, subjective image quality audit, and a 'live' staff and RTE feedback was initiated to inform our intervention strategy, which consisted of 6 PDSA cycles (Figure 1). Following each intervention, relevant project measures were monitored to establish efficacy of the intervention.

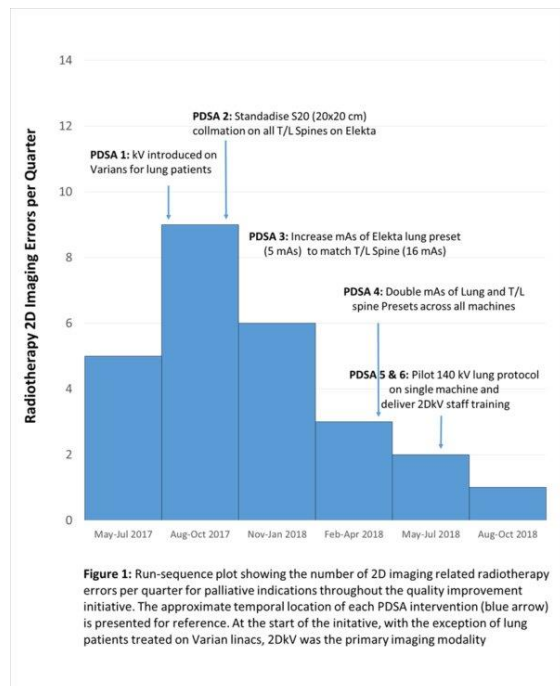


**Figure 1:** Run-sequence plot showing the number of 2D imaging related radiotherapy errors per quarter for palliative indications throughout the quality improvement initiative. The approximate temporal location of each PDSA intervention (blue arrow) is presented for reference. At the start of the initiative, with the exception of lung patients treated on Varian linacs, 2DkV was the primary imaging modality

#### Results

During the QI period the 'live' feedback from staff and RTE identified collimation and image quality as key areas for improvement, which was consistent with the image quality audit. For the staff survey 31 out of 52 therapeutic radiographers responded, with 80% of respondents being involved in some aspect of 2DkV imaging  $\geq 5$  times per month. There was a good level of confidence in all aspects of 2DkV imaging, however poor digitally reconstructed radiograph (DRR) quality was identified by 35% of staff as a major issue in the image guidance process. Other factors affecting quality related to the imaging workflow, inadequate collimation, and lack of confidence with utilising higher dose protocols. These findings were congruent with the RTE audit results (Figure 2), which also identified inadequate record keeping as a significant contributory factor to RTE. Figure 1 presents a run-sequence plot of RTE per quarter, alongside the timeframe of each PDSA cycle. Across the course of the QI initiative a steady and sustained reduction in RTE was observed, with current quarterly error rates running at one fifth of their pre QI values.

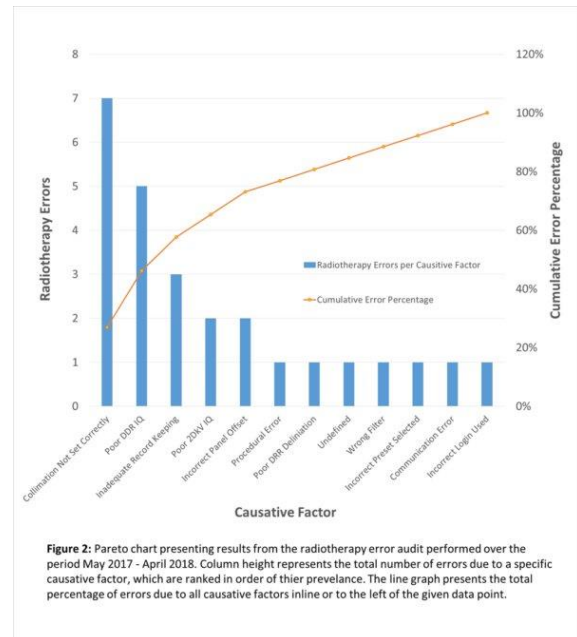


**Figure 2:** Pareto chart presenting results from the radiotherapy error audit performed over the period May 2017 - April 2018. Column height represents the total number of errors due to a specific causative factor, which are ranked in order of their prevalence. The line graph presents the total percentage of errors due to all causative factors inline or to the left of the given data point.

#### Conclusion

The use of a QI model to drive continuous improvement within this setting has been highly successful and has resulted in a clear reduction in imaging related RTE. Utilising the PDSA cycles has highlighted that whilst improvements have been made, a key number of interventions remain and require continual development and monitoring.

#### OC-0620 Stop: No! Take Action: Yes! A new approach to act on anatomical changes seen on CBCT

M. Buijs<sup>1</sup>, F. Pos<sup>1</sup>, M. Frantzen-Steneker<sup>1</sup>, F. Koetsveld<sup>1</sup>, P. Remeijer<sup>1</sup>

<sup>1</sup>Netherlands Cancer Institute, Radiotherapy, Amsterdam, The Netherlands

#### Purpose or Objective

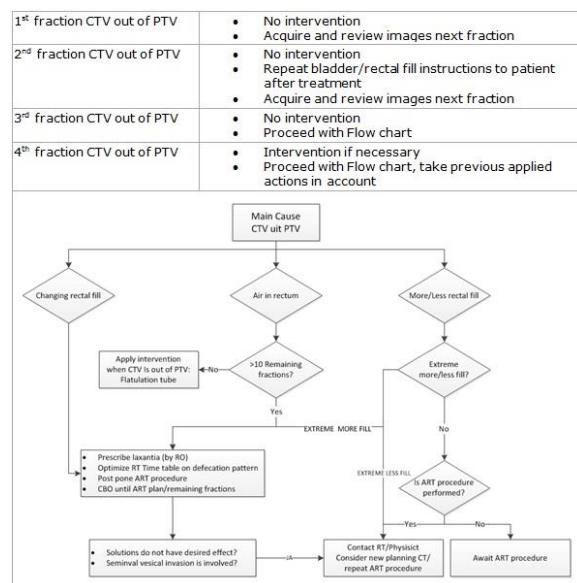
Currently for the most common treatment sites Traffic Light Protocols (TLP) have been developed to recognize and react to anatomical changes seen on CBCT scans. For the RO's as well as the RTT's this method proved to be quite labor-intensive, as it involves alerting the RO, handover of the findings, and finally decision making by the RO. Therefore a new approach was developed to act on anatomical changes: the Take Action Protocol (TAP). In this approach the RTT's do not only have a role in detecting anatomical changes, but are also deciding on the appropriate action and follow up in a standardized way, resulting in a significant shift in responsibility. The aim of this study was to evaluate the implementation of this "Take Action Protocol" and assess its impact on workload, burden of the RTT's responsibility, and the accuracy of the reviewing and decision making.

#### Material and Methods

During a pilot period from Sept 2017 to Febr 2018 the TAP, designed in collaboration with RO's and Medical Physicists, was applied for bladder and prostate patients. The protocol consists of a primary decision to act on the anatomical change seen on the online CBCT. When the anatomical change appears to be systematic, a flow chart guides the decision regarding the follow up of the treatment, see figure 1.

To evaluate the use of the TAP, CBCT images were retrospectively reviewed by an IGRT specialist to assess the accuracy of the reviewing and decision making. Also the impact on the workload was evaluated by scoring the amount of contact moments with an RO. Two surveys were

performed to assess the impact on workload for both RTT's and RO's, the burden of the responsibility for the RTT's and the involvement of the RO's by comparing one for the standard TLP and one for the TAP.



## Results

In 16 out of 22 bladder and 18 out of 56 prostate patients anatomical changes were seen on CBCT, that required a decision of the RTT's (see table 1). For the TAP, in only 2 bladder and 6 prostate patients further decision making of an RO was required (compared to all 34 for the TLP). 99% of the CBCT's were reviewed accurately by the RTT's. In 5 out of 34 patients additional instruction in the decision making by an IGRT specialist was required.

The results of the surveys showed that for both the RTT's and the RO's, the TAP provided a better balance between workload and efficiency in relation to the clinical relevance of acting on anatomical changes. The perceived involvement of the RO's and burden of the responsibility for the RTT's was comparable between the two protocols. Also acting appropriately on clinical relevant anatomical changes, was found to be improved by applying the TAP.

Table 1

	Anatomical changes on CBCT		Online interventions	Flow Chart actions	
	$N_{age}$	$N_e$	$N_e$	RTT	RT/PA
Bladder	16	38	15	6	2
Prostate	18	42	7	8	6

## Conclusion

The Take Action Protocol for anatomical changes provides an accurate method to act on anatomical changes, and gives RTT's more responsibility in the decision making, with an improved balance in efficiency and workload in relation to the clinical relevance of adapting on these anatomical changes.

### OC-0621 Changing responsibilities for RTTs on the MR-linac

A. Betgen<sup>1</sup>, J. Bilderbeek<sup>1</sup>, T. Janssen<sup>1</sup>, J. Kaas<sup>1</sup>, M. Nowee<sup>1</sup>, T. Vijlbrief<sup>1</sup>, L. Wiersema<sup>1</sup>, U. Van der Heide<sup>1</sup>

<sup>1</sup>Netherlands Cancer Institute, Department of Radiation Oncology, Amsterdam, The Netherlands

### Purpose or Objective

The current set-up of patients for irradiation on a conventional linac consists of positioning the patient, acquiring verification images with cone-beam CT,

registration of the images to the planning CT and correcting the setup with an automatic couch shift. In our department this entire procedure is performed by RTTs. Traffic light protocols guide fast decision making in case of anatomical deviations and prevent the necessity of a physician or physicist. With the clinical introduction of the MR-linac (Unity, Elekta AB), a linear accelerator with an integrated MRI scanner, workflow has changed. At the Unity MR-linac, set-up errors are always corrected by a plan adaptation based on the pre-beam MRI. Therefore, a new radiation plan is computed for each fraction, which has to be evaluated and approved online, which necessitates the presence of a physician and physicist. Our aim is to implement similar traffic light protocols on the MR-linac for decision making by RTTs only, which will alleviate the need for a physician and physicist to be present for all fractions.

### Material and Methods

In the pre-clinical phase, MRI scans were acquired at the MR-linac of patients with different tumor sites after informed consent. Based on a maximum of 5 MRI scans per patient, an MR-linac workflow, which included plan adaptation, was simulated. For anatomical changes we used our existing anatomical traffic light protocol, in which it is indicated when a physicist or physician should be contacted offline. Furthermore, isocenter shifts in LR, AP and CC direction were simulated within Monaco (v5.19.03) to analyze the differences between the reference plan and the adapted plans and to define limits in which the differences would be clinically acceptable. This resulted in a dosimetric traffic light protocol to judge whether the adaptation is better (green), worse but acceptable (orange) or unacceptable (red). 'Orange' plans can be approved by the RTTs, where 'red' plans need to be judged by a physician and/or physicist (an example is presented in table 1). An independent check of the adapted plan was performed for Monitor Units (MU), MU-fluence, largest aperture and area weighted MUs.

### Results

Currently, four prostate cancer patients and one rectum cancer patient started their treatment on the MR-linac, with 60 fractions given. For one patient, the anatomical traffic light protocol resulted in an off-line replanning, which is part of our routine adaptive procedure. In two fractions the dosimetric criteria for the PTV coverage were not met, which resulted in a red traffic light. In these two cases the physician and physicist decided to continue treatment. Limits were only exceeded by 7 and 14 cGy. In one case the independent MU check was not within the boundaries, but also accepted by the physicist.

	anatomic	dosimetric PTV coverage	dosimetric organs at risk	physics	accepted by
fr. 1	green	yellow	green	green	RTT
fr. 2	green	red	green	green	physician/physicist
fr. 3	green	yellow	green	green	RTT
fr. 4	green	yellow	green	green	RTT

Table 1. Example of decision making with traffic light protocols. Fraction 1, 3 and 4 are accepted by RTTs only.

### Conclusion

After a learning period and multidisciplinary discussions, the expectation is that RTTs at the MR-linac can perform online plan adaptation without the presence of a physician or physicist.

### Poster Viewing : Poster viewing 12: GI and Urological Cancers

### PV-0622 NCTP model for postoperative pulmonary complications after trimodality therapy in esophageal cancer

M. Thomas<sup>1,2</sup>, G. Defraene<sup>1,2</sup>, M. Lambrecht<sup>1,2</sup>, W. Deng<sup>3</sup>, J. Moons<sup>4</sup>, P. Nafteux<sup>4</sup>, S.H. Lin<sup>3</sup>, K. Haustermans<sup>1,2</sup>  
<sup>1</sup>KU Leuven - University of Leuven, Department of Oncology - Laboratory Experimental Radiotherapy, B-3000 Leuven, Belgium ; <sup>2</sup>UZ Leuven - University Hospitals Leuven, Department of Radiation Oncology, B-3000 Leuven, Belgium ; <sup>3</sup>The University of Texas MD Anderson Cancer Center, Department of Radiation Oncology, Houston - Texas, USA ; <sup>4</sup>UZ Leuven - University Hospitals Leuven, Department of Thoracic Surgery, B-3000 Leuven, Belgium

### Purpose or Objective

To develop a normal tissue complication probability (NTCP) model for postoperative pulmonary complications after neoadjuvant chemoradiotherapy (nCRT) followed by surgery in esophageal cancer (EC) patients. The added value of dosimetry to clinical information was verified.

### Material and Methods

We analyzed data from 697 patients with EC treated with nCRT followed by surgery at two major institutions between 2002-2017 (287 patients) and 2007-2017 (410 patients, including 134 patients treated with proton beam therapy (PBT)). A multivariable (forward stepwise built) logistic regression analysis studied the predictive value of clinical and treatment-related variables (gender, age, body mass index, smoking behavior, chronic obstructive pulmonary disease, histology and tumor and nodal stage) and additionally dosimetric variables (absolute and relative lung and heart volumes receiving 5Gy (V5) to 55Gy (V55), mean dose and radiation technique: 3D-CRT (reference category), IMRT, VMAT and PBT) for the presence of a postoperative pulmonary complication, which were extracted from prospectively obtained databases. Model performance was assessed by the Area Under the Curve (AUC) of the receiver operating characteristic curve. Model validation was performed using a nonrandom split-sample (TRIPOD type 2B study) of 90 patients selected based on treatment date (last 30 patients of each institution treated with photons and last 30 patients treated with PBT).

### Results

In total, 221 of 607 patients (36.4%) developed a pulmonary complication. Dosimetric information significantly improved the apparent AUC from 0.67 (95%CI 0.63-0.71) to 0.77 (95%CI 0.73-0.81) (likelihood ratio test  $p < 0.001$ ). In the optimal multivariable logistic regression model (Table 1 and Figure 1), the mean lung dose (OR 1.066), increasing age (OR 1.022), squamous cell carcinoma (OR 2.072) and radiotherapy technique (IMRT: OR 0.326; VMAT: OR 2.372; PBT: OR 0.276) were selected as predictors associated with the development of a pulmonary complication. In the validation set, the NTCP model had an AUC of 0.64, which increased to 0.71 after a refit of the model coefficients.

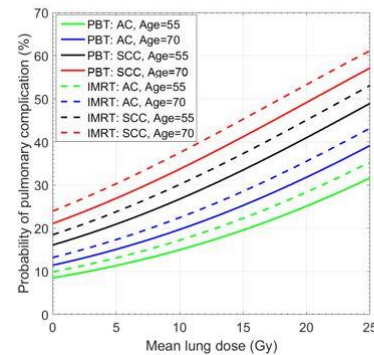
Table 1: Optimal multivariable logistic regression model for postoperative pulmonary complications (221 events).

95%CI = 95% confidence interval; AC = adenocarcinoma; SCC = squamous cell carcinoma; 3D-CRT = 3-dimensional conformal radiation therapy; IMRT = intensity modulated radiation therapy; VMAT = volumetric modulated arc therapy; PBT = proton beam therapy

Pulmonary complications		Odds ratio (95%CI)	p-value
Age (year)		1.022 (1.002-1.042)	0.029
Histology	AC	reference	
	SCC	2.072 (1.319-3.254)	0.002
Mean Lung Dose (Gy)		1.066 (0.999-1.139)	0.054
Radiotherapy technique	3D-CRT	reference	
	IMRT	0.326 (0.194-0.546)	<0.001
	VMAT	2.372 (1.054-5.337)	0.037
	PBT	0.276 (0.122-0.622)	0.002

Figure 1: Graphical representation of the optimal multivariable logistic regression model for patients treated with proton beam therapy and IMRT

PBT = proton beam therapy; IMRT = intensity modulated radiation therapy; AC = adenocarcinoma; SCC = squamous cell carcinoma



### Conclusion

Based on 697 patients with EC treated with nCRT followed by surgery at two major institutions, a useful NTCP model for the development of a postoperative pulmonary complication was obtained. Model validation suggests that updating the model is necessary when applied in a different patient cohort. The radiation technique variable was selected as a predictor independently from the mean lung dose, indicating the need to continuously update and adapt dose-volume models to new treatment conditions. By applying this NTCP model, we can select EC patients at high risk of treatment-induced complications in which we can further investigate the benefit of PBT.

### PV-0623 Tumor-stroma ratio for predicting pathologic response after chemoradiotherapy in esophageal cancer

I. Lips<sup>1</sup>, G.W. Van Pelt<sup>2</sup>, F.P. Peters<sup>1</sup>, J.A. Krol<sup>1</sup>, D. Van Klaveren<sup>3</sup>, J.J. Boonstra<sup>4</sup>, W.O. De Steur<sup>2</sup>, A. Farina Sarasqueta<sup>5</sup>, W.E. Mesker<sup>2</sup>, M. Slingerland<sup>6</sup>

<sup>1</sup>Leiden University Medical Center LUMC, Radiation Oncology Department, Leiden, The Netherlands ; <sup>2</sup>Leiden University Medical Center LUMC, Department of Surgery, Leiden, The Netherlands ; <sup>3</sup>Leiden University Medical Center LUMC, Medical Statistics, Leiden, The Netherlands ; <sup>4</sup>Leiden University Medical Center LUMC, Gastroenterology and Hepatology, Leiden, The Netherlands ; <sup>5</sup>Leiden University Medical Center LUMC, Pathology, Leiden, The Netherlands ; <sup>6</sup>Leiden University Medical Center LUMC, Medical Oncology, Leiden, The Netherlands

### Purpose or Objective

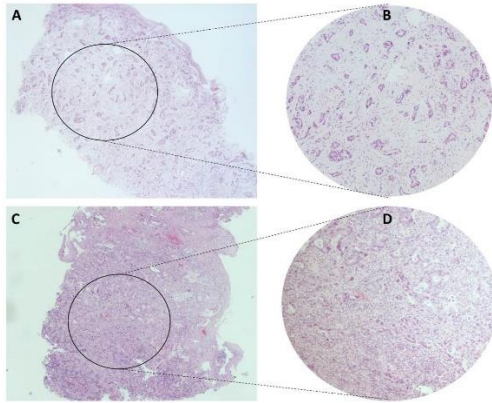
Standard treatment for patients with resectable esophageal cancer (EC) is neoadjuvant chemoradiotherapy (nCRT) followed by surgery. Treatment with nCRT leads to a pathologic complete response (pCR) in approximately 30% of patients. Surgery might be safely omitted in this selected group of patients, however with the current available options, predicting pCR after nCRT is insufficient.

The tumor micro-environment, including the supportive stromal component, plays a crucial role in the progression and spread of cancers. The amount of stroma in direct relation to the tumor has been proven to be a prognostic factor for survival in breast cancer, colon cancer and EC. For esophageal adenocarcinoma (EAC) scoring tumor-stroma ratio (TSR) in biopsy specimens was proven to be representative, reproducible and easy. In addition, in patients with EAC TSR was proven to correlate with response to neoadjuvant chemotherapy. The main focus of this study was to investigate the value of TSR in the prediction of pathologic response (PR) after nCRT in EC.

### Material and Methods

Patients with adenocarcinoma or squamous cell carcinoma of the esophagus who received nCRT followed by a resection between May 2010 and Sept 2015 were evaluated. Haematoxylin and eosin stained sections of pre-treatment biopsies were collected and TSR was independently assessed by two investigators. Patients were categorized in stroma-low ( $\leq 50\%$  stroma) and stroma-high ( $> 50\%$  stroma) groups for further analyses (Figure 1). The tumor regression grade (TRG) of the primary tumor was assessed to determine favorable (TRG 1-2) and non-favorable (TRG 3-5) PR. Univariate and multivariate logistic regression analyses were performed to investigate the relationship between TSR and PR.

Figure 1. Haematoxylin and eosin stained biopsy sections of EC. (A) Tumor with large spots of stromal tissue (stroma-high). Magnification (B) shows evident stromal proliferation between tumor cells. (C) Tumor with low stromal proliferation (stroma-low). As shown by the magnification (D) there is almost no stroma between the tumor cells.



## Results

A total of 94 patients were included in this study; 76 tumors were categorized as stroma-low and 18 as stroma-high. Median age was 64 years (range 25-82), 76% were men, 80% of the tumors were adenocarcinoma, most patients (77%) had cT3 stage and differentiation grade was well in 12%, moderate in 35% and poor in 53%.

A pCR (TRG 1) was found in 28 patients; 14 patients showed a near pCR (TRG 2). Non-favorable PR was seen in 31 (TRG 3), 19 (TRG 4) and 2 patients (TRG 5), respectively.

In univariate analysis patients with a stroma-low tumor had an approximately three-and-a-half times higher likelihood of a favorable response (TRG 1-2) on nCRT compared to patients with a stroma-high tumor (OR 3.50, 95%CI 1.06- 11.61,  $p = 0.04$ ). After adjustment for known predictive factors (gender, histology, cT-status and differentiation grade) a stroma-low tumor proved to be an independent predictive factor for a favorable PR (TRG 1-2) (OR 3.64, 95%CI 1.05-12.68,  $p = 0.04$ ).

**Conclusion**  
Tumor-stroma ratio was found to be a predictor of pathologic response in esophageal cancer patients receiving neoadjuvant chemoradiotherapy. Larger validation studies are needed to verify these results.

**PV-0624 pathologic response in pancreatic cancer treated with neoadjuvant MRI-guided radiation therapy**  
S. Rudra<sup>1</sup>, R. Brenneman<sup>1</sup>, S. Badiyan<sup>1</sup>, A. Wang-Gillam<sup>1</sup>, W. Hawkins<sup>1</sup>, R. Fields<sup>1</sup>, S. Strasberg<sup>1</sup>, M. Roach<sup>1</sup>, H. Kim<sup>1</sup>  
<sup>1</sup>Washington University in St. Louis, Radiation Oncology, Saint Louis, USA

## Purpose or Objective

The objective was to report the outcomes of patients diagnosed with initially unresectable pancreatic cancer who receive MR-guided adaptive radiation therapy (MRgRT) and chemotherapy then subsequently received surgical resection.

## Material and Methods

We retrospectively reviewed our institutional pancreatic cancer treatments to identify patients who received MRgRT and then subsequently underwent surgery. Patients were treated with dose-escalated RT regimens of either 50 Gy in 5 fractions (BED=100) or 67.5 Gy in 15 fractions (BED=97.9). Pathology reports from patients who received surgery were reviewed to identify response to neoadjuvant therapy. Grade 3 or higher abdominal toxicities were recorded. Overall survival (OS) was calculated using Kaplan-Meier analysis from date of starting RT.

## Results

A total of 88 patients (48 locally advanced pancreatic cancer patients, 21 borderline resectable pancreatic cancer patients, and 19 medically inoperable patients) received MRI-guided RT for unresectable pancreatic cancer from 2015 to 2018. Of this cohort, 17 patients (19%) received surgical resection after neoadjuvant therapy [8 (17%) patients with locally advanced pancreatic cancer and 9 (43%) patients with borderline resectable pancreatic cancer]. Median follow up after RT for this subgroup was 12 months. Median time from RT to surgery was 3 months. Pathologic response was found to be complete response in 3 patients (18%), partial response in 13 patients (76%) and progressive disease in 1 patient (6%). No acute toxicities were noted. Late grade 3+ abdominal toxicities were noted as follows: 2 patients with gastrointestinal bleeding due to ulcers at anastomotic sites, 1 patient developed cholangitis after surgery requiring hospitalization, and 1 patient developed a pseudoaneurysm of the celiac artery. The patient with progressive disease on the surgical specimen survived for 11 months after RT. The 2-year OS rate for the entire resected cohort was 60%.

## Conclusion

Neoadjuvant chemoradiation using adaptive MRgRT and dose-escalation generally resulted in at least partial response and in a few cases, complete pathologic response of the original unresectable pancreatic tumor. Prospective clinical trials evaluating adaptive MRgRT with dose escalation in borderline resectable and locally advanced pancreas cancer are in progress.

## PV-0625 Biological factors influencing outcomes in SBRT for colorectal cancer oligometastases (OM)

S. O' Cathail<sup>1</sup>, T. Smith<sup>2</sup>, R. Owens<sup>3</sup>, Y. Tsang<sup>4</sup>, M. Harrison<sup>2</sup>, M. Hawkins<sup>1</sup>

<sup>1</sup>CRUK/MRC Institute for Radiation Oncology University of Oxford, Oncology, Oxford, United Kingdom ; <sup>2</sup>Mount Vernon Cancer Centre, Oncology, London, United Kingdom; <sup>3</sup>Oxford University NHS Foundation Trust, Oncology, Oxford, United Kingdom ; <sup>4</sup>Mount Vernon Cancer Centre, Radiotherapy, London, United Kingdom

## Purpose or Objective

Stereotactic ablative body radiotherapy (SBRT) is offered to patients who have oligometastatic (OM) disease and are not suitable for surgical or other ablative treatments. OM Colorectal (CRC) cancer has been identified as potentially having worse outcomes compared to other histology types. We hypothesise that tumour biology impacts outcome in OM CRC.

## Material and Methods

A multi institution of prospective OM CRC patients treated with SBRT. Patients had  $< 3$  metastases, in  $< 2$  organs on multimodality imaging and exhausted local treatments options. PS 0-1. SBRT was delivered in 3-8 fractions depending on location.  $\alpha/\beta = 10$  was used to estimate biological effective dose. Location of primary and KRAS status was recorded. Progression was defined by imaging criteria as local (within field), locoregional (same organ but outside RT field) or distant. Univariate analysis was performed with log rank tests of Kaplan Meier curves and cox proportional hazard models. Significant variables on univariate testing were entered into a multivariate cox proportional hazard model.

## Results

Between 05/13 -05/18 132 CRC OM cases were treated and 95 patients had complete data for analysis. 70 (74%) metachronous OM. The median age was 67 years (range 36-89). 51 (54%) patients were male. Primary site of disease was rectum in 53 (56%), left colon in 22 (23%) and right colon in 15 (16%). OM sites treated: 27 liver, 56 lymph nodes (LN), 9 lung and 3 other. Median BED<sub>10</sub> was 79.2 Gy (range 37.5 - 151.2). Median FU was 13.7 mo (IQR 4.6 - 25.3). In-field local control at 1 year was 85.5% (95% C.I 76% - 96.2%). Median PFS for the cohort was 10.7 mo (95% C.I 8.1 - 15.2). The median PFS for the liver, lung and LN metastases were 6, 13 and 19 mo respectively. There was a significant difference in PFS based on metastasis location, with lymph node disease being associated with improved PFS (HR 0.34, 95% C.I 0.19 - 0.626, p = 0.0004; overall log rank, p = 0.0019). Lung was borderline. KRAS status was available for 47 patients (50%), 34 wild type and 13 mutant. WT KRAS status was associated with improved PFS (HR 0.44, 95% C.I 0.19 - 0.97, p = 0.04). No significant difference in PFS was seen when comparing groups by primary site, colon side, age, gender or whether presentation was with synchronous or metastatic disease. On MVA, metastasis location of lung and lymph node and KRAS WT or unknown status, remain statistically significant predictors of improved PFS.

## Conclusion

In this cohort lymph node metastases appear to be associated with improved PFS compared to lung, bone or liver sites independent of KRAS status. KRAS WT is a good prognostic factor for PFS in treatment with SABR. These findings could be used to further refine the selection of CRC OM for treatment with SABR and incorporating systemic treatment. The excellent local control, regardless of KRAS subtype, suggests that OM PFS is driven by locoregional or widespread failure highlighting need for exploring biological differences.

## PV-0626 Mismatch Repair System Deficiency increases response to neoadjuvant chemoradiation in rectal cancer

N. Meillon<sup>1</sup>, D. Vernerey<sup>2</sup>, J.H. Lefèvre<sup>3</sup>, G. Manceau<sup>4</sup>, M. Svrcek<sup>5</sup>, J. Augustin<sup>6</sup>, J. Fléjou<sup>3</sup>, O. Lascols<sup>7</sup>, J. Simon<sup>1</sup>, R. Cohen<sup>8</sup>, P. Maingon<sup>1</sup>, J. Bachet<sup>9</sup>, F. Huguet<sup>10</sup>

<sup>1</sup>Groupe Hospitalier Pitié-Salpêtrière-Charles-Foix-APHP, Radiation Oncology, Paris, France ; <sup>2</sup>University Hospital of Besançon, Methodology and Quality of Life Unit in Oncology, Besançon, France ; <sup>3</sup>Hôpital Saint-Antoine- APHP, Digestive Surgery, Paris, France; <sup>4</sup>Groupe Hospitalier Pitié-Salpêtrière-Charles-Foix- APHP, Digestive and Hepato-Pancreato-Biliary Surgery, Paris, France ; <sup>5</sup>Hôpital Saint-Antoine- APHP, Pathology, Paris, France ; <sup>6</sup>Groupe Hospitalier Pitié-Salpêtrière-Charles-Foix- APHP, Pathology, Paris, France; <sup>7</sup>Hôpital Saint-Antoine- APHP, Biology and Molecular Genetics, Paris, France ; <sup>8</sup>Hôpital Saint-Antoine- APHP, Medical Oncology, Paris, France; <sup>9</sup>Groupe Hospitalier Pitié-Salpêtrière-Charles-Foix- APHP, Hepato-Gastroenterology, Paris, France; <sup>10</sup>Hôpital Tenon- APHP, Radiation Oncology, Paris, France

## Purpose or Objective

Defective mismatch repair system (MMR) has been shown to have a favorable impact on outcome in colorectal cancer patients treated with surgery or immunotherapy, adjuvant chemotherapy being discouraged unless there is nodal involvement. Its impact on radiosensitivity is unknown in rectal cancer patients.

## Material and Methods

Patients treated for locally advanced rectal cancer between 2000 and 2016 were studied. MMR status was studied on the histological sample through PCR and immunohistochemistry. Reported points included age, sex, clinical and radiological tumor stages at diagnosis, modalities of neoadjuvant treatment, post-treatment

pathological staging, tumor regression score, and local, distant relapse-free, and overall survivals. An inverse probability of treatment weighting (IPTW) analysis was performed to evaluate the association of MMR proficiency on surgical and clinical outcomes. The primary endpoint was downstaging defined as a lower T and/or N after than before neoadjuvant treatment.

## Results

Among the 307 patients included, 21 (6.8%) had defective MMR (dMMR). Median follow-up was 36.7 months (95%CI: 34,7-39,7). dMMR patients were significantly younger than proficient MMR patients (pMMR) (60.4 y.o. (52.8-69.8) vs 45.4 y.o. (41.8-56.2), p<.0001) and trended towards a higher N stage (N1 patients: 14 (87.5%) for dMMR vs. 178 (64.0%) for pMMR, p=0.055).

In an unmatched analysis, dMMR patients had a higher pathological downstaging rate (17 (85.0%) vs. 137 (52.7%), p=0.005) and had a lower rate of recurrence (10.0% vs. 30.5%, p=0.12).

After IPTW matching, dMMR patients had a higher pathological downstaging rate (OR=5.77, 3.24-10.26, p<0.0001) and a longer recurrence-free survival (OR=0.29 (0.16-0.54), p<0.0001), although local recurrence free survival and overall survival did not differ significantly (HR=1.038 (0.475-2.27), p=0.925 and HR=0.65 (0.34-1.22), p=0.176 respectively).

Table. Survival endpoints IPTW analysis

	Hazard Ratio	95%CI	p-value
Overall survival	0.65	0.34-1.22	0.176
Recurrence free survival	0.34	0.19-0.60	0.0002
Disease free survival	0.30	0.17-0.53	<.0001

	Odds Ratio	95%CI	p-value
Downstaging	5.77	3.24-10.26	<.0001
Resection status	1.45	0.70-3.00	0.318
Recurrence	0.29	0.16-0.54	<.0001
Local recurrence	1.03	0.48-2.27	0.925
Metastatic recurrence	0.30	0.16-0.58	0.0003
Death	0.68	0.35-1.33	0.261

Abbreviation: CI, confidence interval.

## Conclusion

MMR deficiency was associated with tumor downstaging after neoadjuvant chemoradiation as well with increase recurrence-free survival. dMMR patients could be good candidates for rectal preservation strategy.

## PV-0627 IL17F-rs641701 polymorphism as prognostic factor in rectal cancer after preoperative chemoradiation

E. Palazzari<sup>1</sup>, E. Dreussi<sup>2</sup>, I. Maretto<sup>3</sup>, F. Navarra<sup>1</sup>, R. Innocente<sup>1</sup>, C. Belluco<sup>4</sup>, F. Matrone<sup>1</sup>, G. Fanetti<sup>1</sup>, A. Revelant<sup>5</sup>, M. Montico<sup>6</sup>, G. Toffoli<sup>2</sup>, S. Pucciarelli<sup>3</sup>, E. Cecchin<sup>2</sup>, A. De Paoli<sup>1</sup>

<sup>1</sup>IRCCS Centro di Riferimento Oncologico Aviano-National Cancer Institute, Radiation Oncology Department, Aviano, Italy ; <sup>2</sup>IRCCS Centro di Riferimento Oncologico Aviano-National Cancer Institute, Experimental and Clinical Pharmacology, Aviano, Italy ; <sup>3</sup>Padova University, Department of Surgical- Oncological and Gastroenterological Sciences- Section of Surgery, Padova, Italy ; <sup>4</sup>IRCCS Centro di Riferimento Oncologico Aviano-National Cancer Institute, Surgical Oncology Department, Aviano, Italy ; <sup>5</sup>IRCCS Centro di Riferimento Oncologico Aviano-National Cancer Institute and Padova University, Radiation Oncology Department, Aviano-Padova, Italy ; <sup>6</sup>IRCCS Centro di Riferimento Oncologico

### Purpose or Objective

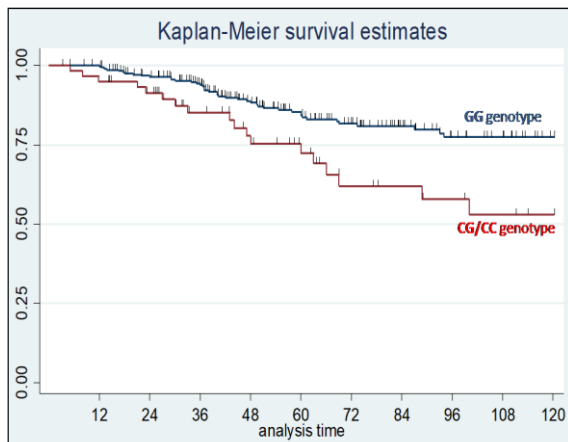
Patients (pts) with locally advanced rectal cancer (LARC) exhibit heterogeneous responses to Preoperative Chemoradiotherapy (preopCRT) and prognosis. Risk stratification based on clinical and biologic factors is an area of active investigation in order to personalize treatment. Immunogenetics, the study of polymorphisms (SNPs) in genes involved in immune system activity, could detect biomarkers virtually involved in tumor response to treatment and in prognosis. The aim of this study was to identify immunogenetic biomarkers of early recurrence and long term survival in LARC pts treated with preopCRT and radical surgery.

### Material and Methods

From December '93 to November '15, LARC pts undergoing preopCRT and surgery were consecutively enrolled at the National Cancer Institute-IRCCS Aviano and IOV-IRCCS Clinica Chirurgica I of Padova University. According to study purposes, pts were split in a training set and in a replication set. Firstly, 147 SNPs in 34 immune-related genes were analyzed in germline DNA samples of the training set. The potential association between these SNPs and the 2yrDFS was analyzed with logistic regression model. Significant SNPs arisen in the training set ( $p < 0.05$  after bootstrap analysis) were analyzed in the replication set with logistic regression. Secondly, replicated variants ( $p < 0.10$ ) were tested in the entire population in terms of 5yrMFS, 5yrDFS, and 10yrOS by multivariate Cox regression.

### Results

Clinical and pathological parameters of the 371 LARC pts were well balanced between the discovery ( $n=234$ ) and the replication set ( $n=137$ ). Three prognostic biomarkers were significantly associated with the 2yrDFS in the training set (*IL17F*-rs641701, *IL17F*-rs9463772, and *STAT3*-rs8069645:  $p=0.010$ ,  $p=0.020$ , and  $p=0.048$ , respectively), but only *IL17F*-rs641701 was significant in the replication set ( $p=0.099$ ). In the merged population of pts, this SNP was still significantly associated to both 5yrDFS (HR (95%CI)=1.84 (1.01-3.25),  $p=0.035$ ), and 5yrMFS (HR (95%CI)=2.11 (1.11-4.01),  $p=0.023$ ). *IL17F*-rs641701 was also significantly associated with 10yrOS (HR (95%CI)=2.66 (1.51-4.70),  $p=0.001$ ) (Fig.1), highlighting its pivotal prognostic role. To note *IL17F*-rs641701 effect on prognosis is independent from Tumor Regression Grade (TRG), as a matter of fact, when stratifying pts according to different TRG, *IL17F*-rs641701 marker identified subgroups of pts with significantly different prognosis within the same TRG group.



### Conclusion

The role of host immune system in the tumor control and its interaction with commonly used chemo-radio treatment is challenging. In this scenario, the assessment of *IL17F*-rs641701 as new potential prognostic biomarker in LARC pts could represent a link between immunity and disease control after preopCRT. Its independency from the already acknowledged prognostic factors as TRG, should encourage its use in the clinical practice to improve pts stratification according to the risk of disease progression to better tailor therapeutic approaches in LARC.

### PV-0628 Association of androgen deprivation duration and cardiovascular mortality in prostate cancer men

A. Yorozu<sup>1</sup>, S. Sutani<sup>1</sup>, K. Toya<sup>1</sup>, Y. Shiraishi<sup>1</sup>, S. Saito<sup>2</sup>

<sup>1</sup>Tokyo Medical Centre- NHO, Department of Radiation Oncology, Tokyo, Japan; <sup>2</sup>Tokyo Medical Centre- NHO, Department of Urology, Tokyo, Japan

### Purpose or Objective

To investigate whether duration of androgen deprivation therapy (ADT) is associated with an increased risk of cardiovascular mortality (CVM) in men treated with brachytherapy and/or external beam radiotherapy (EBRT) for intermediate and high-risk prostate cancer.

### Material and Methods

This is a retrospective analysis of prospectively collected data from men treated between 2003 and 2012 at one institution. Data on 1,628 patients treated for intermediate ( $n=1,234$ ) or high-risk ( $n=394$ ) prostate cancer with iodine-125 brachytherapy ( $n=486$ ), EBRT ( $n=196$ ), and a combination of brachytherapy and EBRT ( $n=946$ ) were included. In total, 1,005 patients (61.7%) received neoadjuvant ADT, concurrent with or in the absence of adjuvant ADT. Patients were divided into two groups according to the total duration of ADT: a short course group ( $n=803$ ) received  $\leq 12$  months (median duration: 6 months), and a long course group ( $n=202$ ) received  $>12$  months (median duration: 24 months) of ADT. The primary endpoint of this study was a CVM, which was defined as a death from myocardial infarction, sudden cardiac arrest, coronary artery disease, cardiac ischemia, malignant arrhythmia, or cerebrovascular stroke. Statistical analysis was conducted using a Kaplan-Meier estimator, a Cox regression model, and a competing risk model.

### Results

After a median follow-up time of 7.6 years (interquartile range: 5.6-10.2 years), overall survival was 92.1% at 7 years. In total, 194 men died; there were 53 cardiovascular deaths, 41 prostate cancer deaths, 67 other malignancy deaths, 31 other benign disease deaths, and two deaths due to unknown causes. The 7-year CVM rate was 1.2% in the non-ADT group, 2.1% in the short course ADT group, and 5.3% in the long course ADT group ( $p < 0.001$ ). In terms of baseline patient characteristics, long course ADT was significantly associated with elderly patients, EBRT treatment, high-risk group, and total androgen blockade. Univariate analysis revealed that older age, baseline cardiovascular disease, baseline diabetes, and long course ADT were significantly associated with increased CVM. Competing risk analysis revealed that duration of ADT was significantly associated with CVM, as well as age, baseline cardiovascular disease, and baseline diabetes. The 7-year overall survival rate was 94.3% in the non-ADT group, 92.1% in the short course ADT group, and 84.9% in the long course ADT group ( $p=0.008$ ). The Cox regression model revealed age and risk group as significant factors associated with overall survival; the duration of ADT was not significantly associated with overall survival.

### Conclusion

Long course ADT is associated with an increased risk of CVM in patients undergoing brachytherapy and/or EBRT for intermediate and high-risk prostate cancer. Age, baseline comorbidities, and duration of combined ADT

should all be considered to minimize the risk of CVM, when treatment options of brachytherapy and/or EBRT are discussed according to risk groups.

#### PV-0629 Late toxicity and PROMs in pelvic or prostate RT in high risk prostate cancer: A randomized trial.

V. Murthy<sup>1</sup>, J. Bhatia<sup>2</sup>, S. Kannan<sup>3</sup>, P. Gurav<sup>2</sup>, R. Krishnatry<sup>2</sup>, D. Chourasiya<sup>3</sup>, G. Prakash<sup>4</sup>, G. Bakshi<sup>4</sup>, S. Menon<sup>5</sup>, U. Mahantshetty<sup>2</sup>

<sup>1</sup>Advanced Center for Treatment- Research and Education in Cancer, Radiation Oncology, Mumbai, India; <sup>2</sup>Tata Memorial Center- HBNI, Radiation Oncology, Mumbai, India ; <sup>3</sup>Advanced Center for Treatment- Research and Education in Cancer, Cancer Research Secretariat, Mumbai, India ; <sup>4</sup>Tata Memorial Center- HBNI, Surgical Oncology, Mumbai, India ; <sup>5</sup>Tata Memorial Center- HBNI, Pathology, Mumbai, India

#### Purpose or Objective

The benefit of whole pelvis radiotherapy in node negative, high-risk prostate cancer is uncertain. While oncological outcomes of whole pelvis (WPRT) and prostate only (PORT) radiotherapy are awaited from ongoing trials, we present the toxicities and patient reported outcomes measures (PROMs) from a randomized controlled trial.

#### Material and Methods

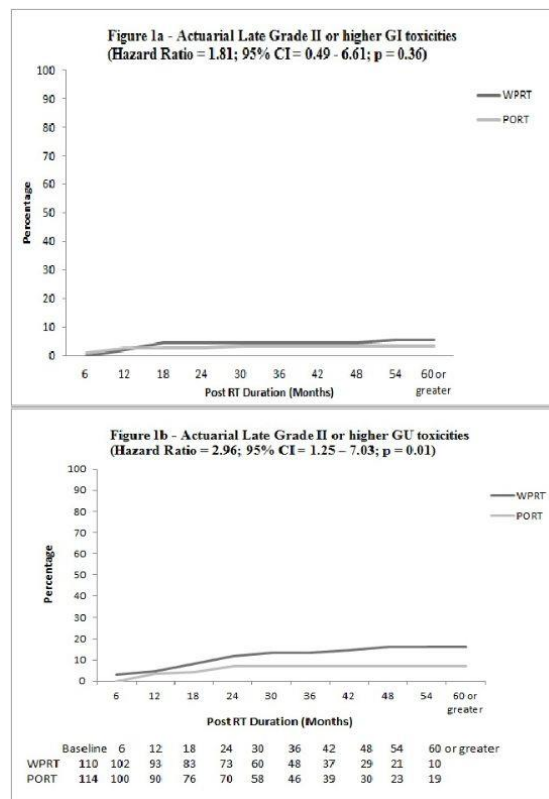
This single institution randomized controlled trial was conducted in node negative, high-risk adenocarcinoma prostate with an estimated nodal risk (Roach) of over 20%. Patients were randomized using stratified block randomization based on history of TURP (yes vs no), Gleason score (6-7 vs 8-10) and PSA levels (<50 vs >50). All patients received at least 2 years of androgen deprivation therapy and hypofractionated, daily image guided, intensity modulated radiotherapy to a dose of 68Gy in 25 fractions to prostate (2.72Gy/#) with 50Gy in 25 fractions to the pelvic nodes including the common iliac region in WPRT arm using simultaneous integrated boost. Late gastrointestinal (GI) and genitourinary (GU) toxicities (RTOG scale), PROMs (EORTC QLQ C-30 and PR 25) were documented at pre-treatment and every 3-6 months post treatment.

#### Results

A total of 224 patients were randomized to WPRT (n=110) and PORT (n=114) arms. Both the arms were well balanced for patient and disease characteristics. Median follow up was 37 months. Both the treatment arms were well tolerated with less than 3% actuarial grade III GI and GU toxicities and no grade IV toxicities (Table 1). Actuarial grade II or higher late GI toxicities were similar in both arms (Hazard Ratio = 1.81; 95% CI = 0.49 -6.61; p = 0.36), whereas late GU toxicities (grade II or higher) were significantly worse in WPRT arm (Hazard Ratio = 2.96; 95% CI = 1.25 - 7.03; p = 0.01) (Table 1; Figure 1a and 1b). A total of 217 patients (WPRT = 112; PORT = 105) completed 1068 questionnaires, with a median assessment time of 11 months (Range = 2 - 73 months). Each patient completed a mean of 5 assessments. Mean scores for global, bowel, urinary symptoms or any other domain were clinically or statistically no different between the two arms.

Table 1 - Actuarial Late Toxicities

	GI	- GI	- GI	- p	GU	- GU	- GU	- p
Overall - n	WPRT - n	PORT - n	WPRT - n	PORT - n	WPRT - n	PORT - n	WPRT - n	PORT - n
	224 (%)	110 (%)	114 (%)	value	224 (%)	110 (%)	114 (%)	value
I	52 (23.3)	28 (26.7)	24 (23.1)	0.92	86 (38.6)	39 (37.1)	47 (45.2)	0.02
II	9 (4)	5 (4.8)	4 (3.8)		22 (9.9)	16 (15.2)	6 (5.8)	
III	1 (0.4)	1 (1)	0 (0)		5 (2.2)	3 (2.9)	2 (1.9)	



#### Conclusion

This is the first randomized trial addressing the question of pelvic RT in patients with high risk, node negative prostate cancer using modern image guided radiotherapy and moderate hypofractionation. At a median follow up of 3 years, there were low grade III toxicities in both arms. Grade II GU toxicity was higher with WPRT while the GI toxicities and the PROMs were similar in the two arms.

#### PV-0630 10-year multi-centre experience of adjuvant radiotherapy in pN3 squamous cell carcinoma of the penis

Abstract withdrawn

#### Award Lecture: Donald Hollywood award lecture

#### OC-0631 Stem cell sparing IMRT for head and neck cancer patients: a double-blind randomized controlled trial

R. Steenbakkers<sup>1</sup>, M. Stokman<sup>1</sup>, R. Kierkels<sup>1</sup>, M. Schuurman<sup>1</sup>, A. Van den Hoek<sup>1</sup>, H. Bijl<sup>1</sup>, M. Dieters<sup>1</sup>, R. Coppes<sup>2</sup>, J. Langendijk<sup>1</sup>, P. Van Luijk<sup>1</sup>

<sup>1</sup>UMCG University Medical Center Groningen, Radiation Oncology, Groningen, The Netherlands ; <sup>2</sup>UMCG University Medical Center Groningen, Radiation Oncology - Cell Biology, Groningen, The Netherlands

#### Purpose or Objective

Head and neck cancer patients treated with radiotherapy often suffer from xerostomia. Critical for the radiation response of the parotid glands are the parotid gland stem cells, mainly located in the main salivary gland ducts (van Luijk, 2015). Reducing dose to these High Stem Cell Density (HSCD) regions may prevent xerostomia. This double-blind randomized controlled trial (RCT) aimed to determine the impact of dose reduction to the HSCD regions on parotid gland stimulated salivary flow

(FLOW12M) and patient-rated xerostomia 12 months (XER12M) after treatment.

#### Material and Methods

Patients with HNC treated with definitive bilateral radiotherapy (70 Gy in 35 fractions) with or without systemic treatment were eligible for the study. Target volumes and organs at risk (OARs) were delineated according to international guidelines. The parotid gland HSCD regions were contoured using in-house made software. Next, for every patient a standard parotid gland sparing IMRT plan (ST-IMRT) was generated. Second, a HSCD region sparing IMRT (HSCD-IMRT) plan was generated by reducing dose at the HSCD region as much as possible while keeping the whole mean parotid gland dose the same (Figure 1). Finally, patients were randomized between ST-IMRT (arm 1) and HSCD-IMRT (arm 2). Primary and secondary end-points were FLOW12M and XER12M, respectively.

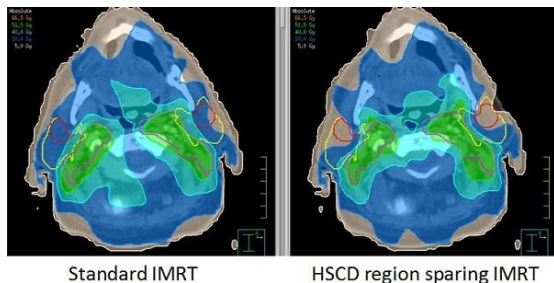


Figure 1. Dose distributions depicted on a CT of a patient with cT3N0 laryngeal cancer using standard IMRT and HSCD region sparing IMRT. The yellow lines are the parotid glands and the red lines are the HSCD regions. With standard IMRT the mean HSCD region dose is 15.8 Gy (right) and 20.6 Gy (left) and with HSCD region sparing IMRT this is 7.4 Gy (right) and 10.8 Gy (left).

#### Results

The study population was composed of 102 patients. 54 were assigned to receive ST-IMRT (arm 1) and 48 HSCD-IMRT (arm 2). The mean parotid gland dose was similar in both arms (contralateral: 24.2 and 23.8 Gy ( $p = 0.801$ ) for arm 1 and 2, and ipsilateral: 31.7 and 30.8 Gy ( $p = 0.659$ ), respectively). HSCD region sparing significantly reduced the dose to the HSCD region (contralateral: 16.4 to 12.6 Gy ( $p = 0.007$ ) for arm 1 and arm 2, respectively, and ipsilateral: 25.0 to 17.4 Gy ( $p = 0.005$ ), respectively). Baseline xerostomia and other OARs (oral cavity and submandibular glands) dose were similar in both arms. Compared to baseline, FLOW12M was reduced with 16.8% and 8.5% ( $p = 0.621$ ) for arm 1 and arm 2, respectively and XER12M was 50.0% and 45.9% ( $p = 0.720$ ), respectively. Multivariate analysis showed that the mean ipsilateral HSCD region dose and baseline xerostomia (none vs. any) were the most important predictors for XER12M. Subset analysis on patients without baseline xerostomia ( $n = 57$ ) showed that the rate of XER12M was markedly lower, i.e. 40.0% v. 23.8% ( $p = 0.253$ ) in arm 1 and arm 2, respectively. Furthermore, in this subgroup the only significant different dose parameter between patients with or without XER12M was ipsilateral HSCD region dose (28.9 v. 19.1 Gy,  $p = 0.007$ ).

#### Conclusion

In this double-blind RCT, stem cell sparing IMRT did not significantly improve salivary flow or reduce xerostomia 12 months after radiotherapy. However, the ipsilateral HSCD region dose was the most important dosimetric predictor for xerostomia, suggesting that dose to the HSCD region is more important for the development of xerostomia than dose to the entire parotid gland.

Award Lecture: Highlights of proffered papers

#### OC-0632 Radiotherapy-related lymphopenia affects overall survival in patients with lung cancer

A. Abravan<sup>1</sup>, C. Faivre-Finn<sup>1</sup>, J. Kennedy<sup>2</sup>, A. McWilliam<sup>1</sup>, M. Van Herk<sup>1</sup>

<sup>1</sup>The University of Manchester\ The Christie NHS Foundation Trust, Division of Cancer Sciences\ Radiotherapy Related Research, Manchester, United Kingdom; <sup>2</sup>The Christie NHS Foundation Trust, Radiotherapy Related Research, Manchester, United Kingdom

#### Purpose or Objective

Lymphopenia during radiotherapy (RT) has an adverse effect on patient's quality of life and can be life threatening. However, the relationship between RT dose and lymphopenia is still unknown. This work utilized data mining to identify anatomical regions where the received dose is correlated with lymphopenia. A predictive model of lymphopenia is also proposed.

#### Material and Methods

562 lung cancer patients treated with curative intent RT were used as a development set. All patients had baseline lymphocytes  $\geq 0.5 \times 10^9/L$ . A Cox model was used to assess prognostic factors of overall survival. Next, two matched groups were defined - patients with and without lymphopenia  $\geq G3$  (lymphocytes at nadir  $< 0.5 \times 10^9/L$  according to CTCAE v4.0) - based on planning target volume (PTV), baseline lymphocytes, prescribed dose, and histology. The purpose of matching was to eliminate tumor effects and improve data mining sensitivity. Following matching, 386 patients remained and image-based data mining was used to identify regions where dose correlates significantly with lymphopenia  $\geq G3$ . For that purpose, dose matrices (equivalent dose at 2 Gy/fraction,  $\alpha/\beta=10$ ) were aligned using registration of the planning CT images to one reference patient. Then, mean dose distributions were obtained for the two groups and organs of significance were detected. For these organs, various dose parameters were collected and those having the highest correlation with lymphocytes at nadir were selected for analysis. Multivariate analyses were conducted for the full development set by employing the identified dose parameters, along with non-dosimetric parameters significant in univariate analysis ( $p < 0.05$ ). Finally, the model was validated on 301 esophageal cancer patients.

#### Results

Cox regression showed that lymphopenia  $\geq G3$  in addition to age, PTV, performance status, and RT duration was an independent factor predicting overall survival in lung cancer (Figure 1). The heart, lung, and thoracic vertebrae showed regions where the difference in dose between the matched groups, with and without lymphopenia  $\geq G3$ , was significant. Mean dose to the heart and lung, and  $V_{20}$  of the thoracic vertebrae (volume receiving  $>20$  Gy) correlated most with lymphocyte counts at nadir in the matched set. A model including RT duration, baseline lymphocytes, vertebrae  $V_{20}$ , and mean heart dose was then chosen following backward elimination (Table 1). The Hosmer-Lemeshow test, based on deciles of risk, indicated that the model was a good fit. Accuracy and C-statistics of the model in the development set was 75% and 0.82 and in the validation set was 75% and 0.76, respectively.

Figure 1. Gross (left) to right Kaplan-Meier curves show overall survival, stratified by lymphopenia G3 in the matched and development lung cancer set.

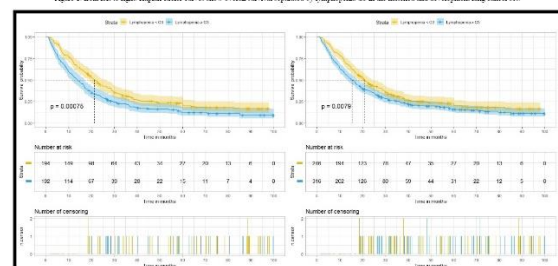


Table 1: Logistic regression results for patients/cancer characteristics and selected dosimetric parameters associated with lymphopenia  $\geq$  G3

Lymphopenia $\geq$ G3	n (%/median (range))	Univariate Logistic Regression		Multivariate Logistic Regression	
		OR	P value	OR	P value
<b>Patients parameters</b>					
Gender					
Female	257 (46%)	ref			
Male	305 (54%)	1.04	0.800		
Age (yr)	64 (22-93)	1.00	0.800		
Baseline lymphocytes ( $\times 10^9/L$ )	1.7 (0.5-12.4)	0.70	<0.001	0.40	<0.001
log(PTV)	2.6 (1.4-3.2)	7.90	<0.001		
PS					
0	135 (24%)	ref			
1	316 (56%)	1.00	0.900		
2	83 (15%)	0.60	0.070		
3	19 (3%)	0.80	0.600		
Histology					
LUAD	127 (22%)	ref			
LUSQ	168 (30%)	1.20	0.400		
SCLC	189 (34%)	0.50	0.003		
NoS	78 (14%)	1.10	0.600		
N Stage					
0	122 (22%)	ref			
1	51 (9%)	1.10	1.000		
2	275 (49%)	1.80	0.005		
3	75 (13%)	1.40	0.200		
<b>Therapeutic parameters</b>					
Chemotherapy status					
RT only	88 (16%)	ref			
pre Sequential RT	148 (26%)	0.80	0.400		
Concurrent	326 (58%)	1.50	0.100		
<b>RT dose parameters</b>					
RT duration (days)	28 (17-57)	1.11	<0.001	1.13	<0.001
Lung mean (EQD2 Gy)	14.7 (2.4-29.1)	1.15	<0.001		
Heart mean (EQD2 Gy)	10.2 (1.1-32.7)	1.06	<0.001	1.04	0.010
Thoracic Vertebrae $V_{20}$ ( $r_{EQD2}$ )	31.7 (0.02-81.3)	1.03	<0.001	1.02	0.030

OR: odds ratio; PTV: planning target volume; LUAD: lung adenocarcinoma; LUSQ: lung squamous carcinoma; SCLC: small cell lung cancer; NoS: not otherwise specified; RT: radiotherapy; EQD2: equivalent dose at 2 Gy/fraction ( $\alpha/\beta=10$ )

### Conclusion

Lymphopenia  $\geq$  G3 during RT is a significant risk factor for survival in lung cancer patients and careful management is thus required e.g. by minimizing vertebrae  $V_{20}$  and mean heart dose in order to limit irradiation of stem cells and blood pool. If dose constraints cannot be met, more frequent monitoring of lymphocyte counts during therapy and use of prophylactic antibiotics are recommended.

### OC-0633 Single dose high dose-rate (HDR) brachytherapy as monotherapy for localised prostate cancer

H. Tharmalingam<sup>1</sup>, Y.M. Tsang<sup>2</sup>, P. Hoskin<sup>1</sup>

<sup>1</sup>Mount Vernon Cancer Centre and The Christie NHS Foundation Trust, Clinical Oncology, London, United Kingdom; <sup>2</sup>Mount Vernon Cancer Centre, Radiotherapy, London, United Kingdom

*This abstract is part of the media programme and will be released on the day of its presentation*

### OC-0634 Implementation of plan of the day adaptive radiotherapy: Compliance to guidelines

A. Webster<sup>1</sup>, S. Hafeez<sup>2</sup>, E. Hall<sup>2</sup>, V. Hansen<sup>3</sup>, H. McNair<sup>4</sup>, R. Lewis<sup>2</sup>, H. Robert<sup>2</sup>

<sup>1</sup>National Radiotherapy Trials Quality Assurance RTTQA, Mount Vernon Cancer Centre, London, United Kingdom; <sup>2</sup>The Institute of Cancer Research, 15 Cotswold Road, Sutton- SM2 5NG, United Kingdom; <sup>3</sup>Laboratory of Radiation Physics, Odense University Hospital, Odense,

Denmark ; <sup>4</sup>The Royal Marsden, The Royal Marsden, Downs Road- Sutton, United Kingdom

### Purpose or Objective

RAIDER (CRUK/14/016) is the first international multicentre trial of tumour focused radical bladder radiotherapy delivered with plan of the day (PoD). A quality assurance (QA) programme, led in the UK by the National Radiotherapy Trials Quality Assurance (RTTQA) Group, was implemented to support participating centres. The pre-trial questionnaire identified only a third (11/33) UK centres had prior PoD experience. Therefore the QA programme initially included pre-trial education and assessment for Therapeutic Radiographers (RTTs) and on-trial retrospective feedback. Here we report initial findings on guideline compliance with respect to agreement of RTT led online plan selection with the offline plan selection of RTTQA reviewers. The strategy adopted to sustain compliance is outlined.

### Material and Methods

RAIDER is a two-stage phase II clinical trial randomising bladder cancer patients undergoing 20 fraction (f) or 32f radiotherapy to standard planning versus tumour focused PoD. Plan selections (small, medium, large) for 36 patients treated with PoD in Stage 1 (technical feasibility) were reviewed remotely offline by a single blinded observer from RTTQA. Plan selections were categorised, as per guidelines, using a traffic light approach:

Green = Acceptable

Amber = Acceptable variation

Red = Unacceptable variation

Green and amber cases were defined as guideline compliant.

The proportion of compliant plans was compared between groups by chi-squared tests.

Deviations from guidelines were assessed and plan selection guidance reviewed. Following updated guidance, online plan selections have so far been assessed for 17 Stage 2 patients.

### Results

439 CBCTs were reviewed from 19 centres. 318/439 (72%) plan selections by RTTs were guideline compliant. In the non-guideline compliant cases, the plan selections by RTTQA were smaller (87%), and larger (3%) and in 10% of cases the action taken would have been different e.g. remove the patient from treatment couch. 13% (n=16) of the non-compliant cases were deemed to require real-time active intervention by RTTQA. Compliance was greater in the 32f cohort, in centres with no previous PoD experience, in centres which previously employed weekly CBCTs for bladder patients, and for plan selections made in 2017, Table 1.

Table 1: Chi-square test comparing compliance in fractionation, PoD experience, bladder CBCT frequency and year of randomisation

Variable	Description	Frequency (n=439)	Guideline compliant cases		p value
			N	%	
Fractionation	32 fraction	206	135	77.5	0.03
	20 fraction	239	183	88.2	
PoD experience	Previous PoD experience	180	122	67.8	0.044
	No previous PoD experience	259	196	75.7	
Bladder CBCT frequency	Daily CBCT	58	33	56.9	0.004
	Weekly CBCT	381	285	74.8	
Year of randomisation	2015 + 2016	15 (2015) + 182 (2016)	133	66.5	0.012
	2017	242	187	77.3	

Expected count are projected frequencies if the null hypothesis is true, e.g. there is no association between fractionation and compliance

Based on these Stage 1 results the QA programme was revised to include:

1. Updated trial documentation detailing plan selection steps
2. Formal PoD reports for all centres
3. An interactive workshop with RTTs
4. A plan selection presentation
5. One-to-one training sessions

Since the implementation of these revisions for Stage 2, 102 CBCTs have been reviewed, from 16 centres. 98/102 (96%) plan selections were guideline compliant.

### Conclusion

In the Stage 1 feasibility study 72% plan selections were guideline compliant. To develop this compliance the trial's QA programme was revised. Initial results indicate that guideline compliance has improved as a result; thus, to support RTTs to deliver PoD, pro-active continuous QA is recommended.

### OC-0635 Targeting TEMPRSS2:ERG fusion to achieve a tumor-specific radiosensitization in prostate cancer

S. Köcher<sup>1</sup>, B. Beyer<sup>2</sup>, T. Lange<sup>3</sup>, L. Nordquist<sup>1</sup>, S. Burdak-Rothkamm<sup>1</sup>, T. Schlomm<sup>2</sup>, C. Petersen<sup>4</sup>, K. Rothkamm<sup>1</sup>, W. Mansour<sup>1</sup>

<sup>1</sup>University Medical Center Hamburg - Eppendorf UKE, Lab of Radiobiology and Experimental Radiation Oncology, Hamburg, Germany ; <sup>2</sup>Prostate Cancer Center-University Medical Hamburg Eppendorf, Martini-Klinik, Hamburg, Germany; <sup>3</sup>University Medical Center Hamburg-Eppendorf, Institute of Anatomy, Hamburg, Germany ; <sup>4</sup>University Medical Center Hamburg - Eppendorf UKE, Department of Radiotherapy and Radiooncology, Hamburg, Germany

### Purpose or Objective

Radiotherapy (RT) is one of the mainstay treatments for prostate cancer (PCa). Despite all technological advances in RT delivery over the recent years, improvements in molecular characterization of PCa have not changed clinical practice. Decision-making in RT for PCa is still guided by conventional clinical-pathological factors such as PSA-levels and Gleason scores. Local recurrence after RT is thought to occur predominantly in regions bearing higher histological tumor burden. Consequently, PCa is still the third-leading cause of cancer-related death in males. Therefore, there is a great need for development of strategies that improve both local control at the tumor site and eradicate occult metastasis in PCa patients.

### Material and Methods

ERG negative (DU145 and PC3) and positive (VCaP, DU145-ERG) cell lines were used to conduct the in vitro experiments. Plasmid assay was used to monitor a repair switch to PARP1-EJ. Immunofluorescence technique was employed to monitor  $\gamma$ H2AX, 53BP1 and RAD51. Ex vivo assay was established to monitor DSB repair in (i) xenografts established from DU145 or PC3 cells and (ii) 100 tumor biopsies freshly collected from 50 PCa patients. FISH was used to analyze ERG status in TMA from PCa patients.

### Results

Cells overexpressing ERG (VCaP or DU145-ERG) show a deregulation in DSB repair with a repair switch to PARP1-EJ. Consequently, PARP inhibition significantly increased the number of residual  $\gamma$ H2AX/53BP1 foci after IR exclusively in ERG overexpressing cells. HR defect was excluded by (i) plasmid assay, Rad51 foci formation and sensitivity to PARPi alone. We employed a functional ex-vivo assay, which allows the analysis of DSB repair in fresh tumor tissues. We confirmed the repair switch to PARP1-EJ in xenografts of ERG overexpressing cells as evidenced by elevated residual  $\gamma$ H2AX/53BP1 foci after PARP inhibition. We analyzed ERG fusion in (i) 14,000 PCa patients, who underwent radical prostatectomy and (ii) 1,426 PCa patients, who underwent salvage radiotherapy. Multivariable Cox proportional hazards model did not show any statistically significant differences between ERG status and PSA-recurrence free survival in both cohorts (p=0.35 and p=0.24, respectively). Next, tumor tissues from 50 PCa patients were collected, sliced in 100-300 $\mu$ m to prevent hypoxia, treated with or without the PARPi olaparib 2h-pre 2Gy and  $\gamma$ H2AX and 53BP1 foci were monitored. Our data showed no difference in the induction of DSBs but significantly higher number of residual  $\gamma$ H2AX/53BP1 foci in ERG-overexpressing patients compared to ERG low expressers.

### Conclusion

Collectively, these data indicate that ERG-overexpression is not a predictive marker for the response after RT in PCa but drives a switch to PARP1-EJ which in turn render cells radiosensitized by PARP inhibition. Clinically, this would rationalize the combination of PARP inhibitor olaparib with radiotherapy in ERG-positive PCa patients.

---

**Teaching Lecture: The DNA damage response to radiotherapy: mechanisms and therapeutic opportunities**

---

**SP-0636 The DNA damage response to radiotherapy: mechanisms and therapeutic opportunities**

M. Morgan<sup>1</sup>

<sup>1</sup>University of Michigan, Department of Radiation Oncology, Ann Arbor, USA

**Abstract text**

Cellular responses to radiation-induced DNA damage include cell cycle arrest, a transient delay in DNA synthesis, and activation of DNA repair pathways. In addition, emerging data suggest that DNA damage response (DDR) pathways may also modulate innate immunity. Research characterizing the vital role these pathways play in determining tumor cell survival has led to tremendous enthusiasm for the development of small molecule inhibitors which target critical proteins within DDR pathways, many of which are in clinical development in combination with radiation. This talk will provide an overview of current strategies designed to maximize the therapeutic efficacy of DDR inhibitors in combination with radiation, including incorporation with standard-of-care chemoradiation, novel combinations of DDR inhibitors targeting multiple steps in the DDR pathway, and integration of DDR inhibitors with immune checkpoint therapy.

---

**Teaching Lecture: Are adolescents and young adults (AYA) a specific patients' population?**

---

**SP-0637**

D. Walker<sup>1</sup>

<sup>1</sup>University Hospital, Queens Medical Center, Department of Radiotherapy, Nottingham United Kingdom

Abstract not received

---

**Teaching Lecture: Hypofractionation; Is there rationale from biology (a/b ratio)?**

---

**SP-0638 Hypofractionation: can the DNA damage response deliver a biological rationale?**

K. Rothkamm<sup>1</sup>

<sup>1</sup>University Medical Center Hamburg - Eppendorf UKE, Department of Radiotherapy / Laboratory of Radiobiology and Experimental Radiation Oncology, Hamburg, Germany

**Abstract text**

The delivery of large radiation doses in a reduced number of fractions is becoming more and more popular in the treatment of primary tumours such as breast and prostate cancer as well as in stereotactic body radiotherapy (SBRT) of oligometastases. While clinical trials data provide increasingly robust evidence supporting hypofractionation in certain therapeutic settings, the underlying biology is still poorly understood. Vascular damage, immunogenic and dose volume effects as well as the "Rs" of classical radiobiology may shape the overall response of tumours and normal tissues to altered fractionation. Cell cycle checkpoint control and DNA damage repair have recently been proposed as important biological modulators of cellular fraction size sensitivity. These recent mechanistic insights may help us establish predictive biomarkers of tumour fractionation sensitivity.

---

**Teaching Lecture: Recent insights into radiotherapy tolerance from the REQUITE Consortium**

---

**SP-0639 Recent insights into radiotherapy tolerance from the REQUITE Consortium**

C. West<sup>1</sup>

<sup>1</sup>The University of Manchester, Translational Radiobiology, Manchester, United Kingdom

**Abstract text**

Logic dictates that the needs of the many outweigh the needs of the few. Radiotherapy is given to maximise the probability of local control while accepting that a small proportion of patients might suffer with long-term side-effects that impact negatively on their health-related quality-of-life. Although toxicity is reduced with modern radiotherapy techniques, it is increased with multi-modality treatment. Worldwide, the total number of people who are alive within 5 years of a cancer diagnosis was estimated to be 43.8 million in 2018. If 40% of survivors received radiotherapy as part of their treatment, many people could be suffering with late effects even if the overall percentage is small. The importance of survivorship issues is increasingly recognised and includes the need for research to identify patients at risk of long-term side-effects. Many models and biomarkers have been reported and few validated. Some are starting to be implemented clinically. The ability to develop and validate models requires insights into radiotherapy tolerance. Accurate insight is only possible with high-quality data.

The EU funded REQUITE consortium established a high-quality resource for multi-national validation of models and biomarkers that predict risk of late toxicity following radiotherapy. An international, prospective cohort study recruited patients in 26 hospitals in eight countries. Eligible patients had breast, prostate or lung cancer and planned potentially-curable radiotherapy. To reflect real-world patients versus patients selected for inclusion in randomised trials, radiotherapy was prescribed according to local regimens, but centres used standardised data collection forms.

Between April 2014 and March 2017 REQUITE recruited 2,069 breast, 1,808 prostate and 561 lung cancer patients. Patients were followed for up to 2 years. The data highlight heterogeneity in patients and treatments across centres/countries that might pose a challenge when attempting to validate predictive models and biomarkers. For example, cancer patients tended to have a higher body mass index in Spain and the UK than in the other countries; the percentage of breast cancer patients who received intensity modulated radiotherapy ranged from <20% (France, Italy, Spain, US) to >80% (Belgium, UK); and the percentage of prostate patients having hormones ranged from 13% (Germany) to ~80% (Belgium, UK). The pre-radiotherapy baseline adverse effect data highlight that across all cancers and toxicities healthcare professional graded scores were lower than patients' grades. Baseline patient-reported grade  $\geq 2$  adverse effects varied between 12% (USA) and 41% (UK) for breast pain (breast patients); between 1% (Netherlands) and 13% (Belgium) for urinary incontinence (prostate patients); and 9% (Italy) to 38% (France) for dyspnoea (lung patients). Example prevalences of 2-year (1-year for lung) grade  $\geq 2$  CTCAE toxicities are 13% atrophy (breast), 3% rectal bleeding (prostate) and 27% dyspnoea (lung). Data from the REQUITE consortium highlight differences in patient characteristics and treatments that will affect radiotherapy tolerance.

---

**Teaching Lecture: Integration of PET imaging in radiation treatment planning**

---

#### SP-0640 Integration of PET imaging in radiation treatment planning

U. Nestle<sup>1</sup>

<sup>1</sup>Medical Center- Faculty of Medicine- University of Freiburg, Department of Radiation Oncology, Freiburg im Breisgau, Germany

Abstract not received

---

#### Teaching Lecture: Implementation and practice of SRS and SBRT: Consensus guidelines and protocols

---

#### SP-0641 Implementation and practice of SRS and SBRT: Consensus guidelines and protocols

J. Seuntjens<sup>1</sup>, E. Lartigau<sup>2</sup>

<sup>1</sup>McGill University Health Centre, Cedars Cancer Centre- Medical Physics, Montreal, Canada; <sup>2</sup>centre Oscar Lambret, Radiothérapie, Lille, France

##### Abstract text

Stereotactic Radiation Therapy (SRT) is a widely used radiation therapy technique relying on accurate delivery of highly conformal, sharply delineated high doses in few fractions to small target volumes and an accurate avoidance of critical risk organs. SRT is used intracranially (a.k.a. SRS) or extracranially (SBRT or SABR). SRT places major demands on clinicians with respect to peculiarities about the physics and dosimetry of small photon beams and the planning algorithm's limitations. Image guidance and quality assurance procedures are also more stringent. Finally, the radiation biology of hypofractionated radiation treatment for tumors and normal tissues must ideally be considered.

ICRU Report 91 (2017) arose from the lack of guidelines consistent with previous ICRU Reports about prescription, recording and reporting including Report 50 (ICRU, 1993), 62, (ICRU, 1999), and 83, (ICRU, 2010) for these types of clinical treatments. The Report provides a historical background and definitions of SRS and SBRT, emphasizing the characteristics stereotactic localization, hypofractionation, small beams and small targets, inverse optimization, image guidance; and the need for precise volume definition. Clinical prescriptions and dose tolerances for hypofractionation are still the subject of investigation and clinical debate and, aside from stating the limitations of LQ models and alternative models in this context, the Report is not prescriptive on this matter. Three main features that dominate the dosimetry of small beams from accelerators are a lack of charged-particle equilibrium, partial source occlusion and the importance of size and construction details of the detector used. In the Report, IAEA-AAPM TRS-483 (2017) recommendations are retained for reference dosimetry in a machine-specific reference field (*msr*) and for small fields, more than a single detector is recommended to determine relative output factors where the measured data should be corrected with the detector type-specific field output correction factor data. For reasons of dose accuracy required in extracranial situations, ICRU Report 91 mandates the use of advanced type-b model-based dose calculation algorithms. As SRT is characterized by high gradients in the dose distribution and hypofractionation it comes with the need to perform daily correction and verification of target location at a sub-mm precision using IGRT and appropriate QA procedures. ICRU 91 maintains the definition of prescription and risk volumes consistent with previous ICRU documents and the report discusses imaging modalities for GTV definition.

The Report maintains prescription of absorbed dose to the isodose surface  $D_v$  that covers an optimal percentage volume of the PTV while optimally restricting dose to the planning risk volume (PRV). With regards to recording and

reporting, the quantities SRT near maximum and SRT near minimum dose are introduced that take into account that for small volumes a minimum absolute volume is required in the assessment of the quantities.

This educational lecture will present a review of ICRU Report 91 (2017) including its rationale, small field dosimetry, volume definition, dose calculation, IGRT and QA as well as the prescription guidelines. The discussion will integrate this with the IAEA TRS-483 recommendations on small field calibration as well as with ongoing work by the AAPM Work Group on SBRT on the extraction of clinical and radiobiological information from the published SBRT outcomes literature.

Educational objectives:

1. to understand the implication of small photon radiation beams in calibration, relative dose measurement and treatment planning dose calculations in the context of Report 91 and TRS-483;
2. to learn about the ICRU Report 91 recommendations on volumes definition and dose-volume prescription, recording and reporting.

---

#### Teaching Lecture: How to select patients for radiotherapy with protons instead of photons

---

#### SP-0642 How to select patients for radiotherapy with protons instead of photons

J. Balosso<sup>1</sup>, J. Thariat<sup>2</sup>, J.L. Habrand<sup>2</sup>, T. Tessonnier<sup>3</sup>, P. Lesueur<sup>2</sup>, A. Chaikh<sup>4</sup>, D. Stefan<sup>5</sup>, J.M. Fontbonne<sup>4</sup>

<sup>1</sup>Centre François Baclesse and University Of Grenoble-Alpes, Radiation Oncology / Archade, Caen, France;

<sup>2</sup>University Unicaen- Centre François Baclesse And Archade, Radiation Oncology, Caen, France;

<sup>3</sup>Centre François Baclesse, Medical Physics, Caen, France;

<sup>4</sup>laboratory of Corpuscular Physics- CNRS- and ARCADE, Ami, Caen, France; <sup>5</sup>Centre François Baclesse, Radiation Oncology, Caen, France

##### Abstract text

Epidemiology of eligible cases for protontherapy, as well as selection criteria, are very controversial. Actually, the size of the eligible population is more a question of care offer than a true scientific question, since protons allow almost constantly a better dose distribution than photons for rather the same biological efficiency, thus assuming fewer side effects.

On the other hand, western European states as typical "providence states" are committed to provide to every patient the best possible cares. To be sustainable, this extremely costly policy needs a careful selection of the medical procedures that are the most "cost efficient". Protontherapy is at best ten times more expensive than X-rays, this is the point.

Thus, for a given patient and a given tumour, what is the most cost-effective procedure between X-rays and protontherapy? Raw physical dosimetric data cannot fully address this question. A difference of dose may not always translate in better outcomes and cost-effectiveness and, thus, may not be meaningful clinically. Nevertheless, radiation oncologists are aware of a benefit of proton therapy in given situations because of the better dose distribution of protons.

These situations are : when dose differences can lead to reduction of toxicities or side effects in a significant health cost sparing way and can improve QOL; when proton therapy results in dramatic reduction of integral dose, which is a critical advantage regarding second cancers for young patients or even of vital importance for genetically radiosensitive patients; when protons allow significant dose escalation for radioresistant tumours; when dose sparing with protons preserves options to irradiate future tumours in case they occur in the same anatomical region (rectal cancer years after cervix

cancer, prostate cancer years after rectal cancer, lung cancer after another lung cancer...); finally when re-irradiation might be curative but over toxic with X-rays. With such different endpoints, the benefit of protons requires different investigational methods. Their common principle is to translate a physical dose difference into a difference of risk that must be translated in differences of either medical outcome, QOL or health costs. All these situations are raising the concern to define what is a “significant” difference, in terms of human utility and economical sustainability.

Moreover, one must also take account of the potential medical drawbacks of protontherapy, namely a series of uncertainties that are not fully mastered yet: the range uncertainties, the lack of possibilities to check the anatomical accuracy of dose delivery, and certainly the underestimated question of the high RBE at the deep end of the beams... necessarily out of the GTV and possibly in sensitive tissues we aim at sparing. Some specific toxicities have been described that might be related to this question of RBE uncertainties. The scientific methods to address these endpoints deserve discussion. Only the classical phase III prospective controlled randomized clinical trials, for comparisons, can provide accurate contemporary comparative real measures of effects. However, they are rather expensive, unsuitable for rare situations or very late endpoints and results are delayed and short lasting. On the other hand, modelling appears as an attractive solution for immediate application and medical choice of protons vs photons. However it is not so easy either. As the assessment process is built on physical dose, several successive rounds of modelling are required to calculate the different endpoints. In particular, this needs many parameters related to the patient / tumour / treatment / outcomes that are as many sources of uncertainties. Thus a careful association of these two approaches is advisable.

First, clinical trials, with randomization, either of phases II or III, should produce a strong basis of high level of proof to allow the vital funding of protontherapy by health insurances. Randomized studies have also the valuable advantage to allow meta-analysis of studies of individual insufficient power. Meanwhile, they can provide initial values of model parameters.

Second, protontherapy can be continually modelled to estimate the expected gain and its cost effectiveness for each individual patient in the “real life” beyond the restrictive frame of clinical trials. All medical cases can feed cumulative databases to back statistically analysis to constrain and refine the models as a continuous improving process, relying in particular on machine learning, which is a kind of artificial intelligence. Finally, large interconnected databases will allow data mining and in-silico clinical trials, using modelling, to explore new applications and medical strategies. But, of course a critical and necessary input is the careful and shared follow-up of patients to identify early and late toxicities by the referent physician of the patient as well as by the protontherapy specialist.

---

#### Teaching Lecture: MR-guided radiotherapy in the pelvic region

---

##### SP-0643 MR-guided radiotherapy in the pelvic region

A. Tree<sup>1</sup>

<sup>1</sup>Royal Marsden Hospital Trust & Institute of Cancer Research, Uro-Oncology, London, United Kingdom

##### Abstract text

MR-guided radiotherapy is now a reality with two platforms, MRIdian and Unity, in clinical use in multiple centres. Daily adaptive replanning to online MR images is

now implemented routinely in these centres. Many dosimetric and machine-related hurdles have been surmounted to deliver MR-guided radiotherapy to date, but our clinical experience is still in its infancy. There are potential pitfalls and specific complexities of MR-guided radiotherapy from a dosimetric and clinical perspective. The changes in anatomy presented daily are unpredictable and their clinical relevance is uncertain. This lecture will outline clinical experience to date and explain some of the lessons learned so far with MR-guided radiotherapy.

The potential future advantages of MR-guided adaptive radiotherapy will be explored, sharing a vision of where this technology may take us in the next 5-10 years.

---

#### Symposium: Radiotherapy biomarkers: a confluence of imaging, genetics and pathology

---

##### SP-0644 Advances in imaging to predict and monitor radiation response

U. Van der Heide<sup>1</sup>

<sup>1</sup>Netherlands Cancer Institute, Radiation Oncology, Amsterdam, The Netherlands

##### Abstract text

A vast body of literature exists on a range of imaging biomarkers predicting response after radiotherapy. Functional techniques such as PET with FDG or hypoxia tracers and various forms of functional MRI have been shown to have prognostic value. Increasingly, combinations of texture features from anatomical and functional images are proposed that predict outcome. These methods can potentially be applied in radiotherapy to stratify patients between different treatment options before the onset treatment or at a later time point. A drawback in the adoption of functional imaging techniques in clinical practice is the substantial variability in methodology, both with respect to acquisition and analysis. Quantitative imaging techniques may be a way to resolve this issue. It will facilitate comparison of imaging data from longitudinal studies as well as multicenter trials.

To strengthen the evidence on biomarkers, single center as well as multi-center studies using functional imaging techniques, need to show that within their trial protocol consistent quantification of imaging is ensured. Quality assurance programs need to be part of trial protocols and can help broad implementation of quantitative techniques in the community.

Repeated imaging during the course of fractionated radiotherapy informs on anatomical and functional changes of the disease and creates the prospect of adaptation of treatment plans. Trials that modify the treatment several weeks into the treatment based on functional imaging, are ongoing. Also, the value of functional imaging for stratification of patients after neoadjuvant radiotherapy is being investigated. The analysis of longitudinal data can however be challenging. Deformations of tissue or shrinking of the tumor over time, make a voxel-by-voxel comparison of quantitative images acquired at different time points impossible. Descriptive statistics over the entire tumor volume may reflect response to the treatment, but in this approach the changes in spatial heterogeneity are lost. Frequent, preferably daily imaging may be beneficial in this context as from day to day the effect of tumor regression will be limited. Up to now, daily quantitative imaging was not feasible in clinical practice. However, with the introduction of MR-guided radiotherapy, patients receive an MRI exam during each treatment fraction. We recently showed that functional imaging is also feasible in this setting, creating the prospect of monitoring functional response to the treatment in unprecedented detail.

**SP-0645 New approaches to Radiotherapy biomarkers, the data has gotten big**E. Medico<sup>1</sup><sup>1</sup>University of Turin, Turin, Italy

Abstract not received

**SP-0646 Translation of biomarker signatures in daily clinical use?**M. Krause<sup>1</sup><sup>1</sup>TU Dresden- Med. Faculty Carl Gustav Carus, Department of Radiotherapy and Radiation Oncology, Dresden, Germany**Abstract text**

During the past decades, cancer treatment has been improved in a technically and medically manner. Nonetheless, the 5-year overall survival rate for head and neck squamous cell carcinoma (HNSCC) is still at about 50%. Currently, most patients with functionally inoperable HNSCC are treated with primary radiochemotherapy (RCTx). In contrast to radiotherapy alone, clinical trials showed that patients who received RCTx benefit in terms of increased overall survival and loco-regional control as well as freedom of distant metastases. However, concomitant chemotherapy is leading to increased toxicity. Another obstacle is the heterogeneity of tumor response to this treatment. Therefore, biomarkers are urgently needed to identify patient groups who require de-escalated or intensified treatment schedules based on their tumor biology in addition to established clinical parameters. Currently, a panel of promising biomarkers is tested in numerous clinical studies, such as human papilloma virus (HPV) status. A positive HPV infection status may be a suitable biomarker for patient stratification towards de-escalation treatment regimens. However, additional biomarkers are needed for further stratification of patients with HPV-negative tumors. This talk will give an overview about the results of biomarker studies and ongoing clinical trials.

**OC-0647 Analysis of biomarkers for late radiotherapy toxicity in the REQUITE project**

C. Talbot<sup>1</sup>, D. Azria<sup>2</sup>, T. Burr<sup>3</sup>, J. Chang-Claude<sup>4</sup>, A. Dunning<sup>5</sup>, M. Farcy Jacquet<sup>6</sup>, C. Herskind<sup>7</sup>, D. De Ruyscher<sup>8</sup>, R. Elliott<sup>9</sup>, S. Gutiérrez-Enriquez<sup>10</sup>, P. Lambin<sup>8</sup>, A. Müller<sup>4</sup>, T. Rancati<sup>11</sup>, T. Rattay<sup>1</sup>, B. Rosenstein<sup>12</sup>, P. Seibold<sup>4</sup>, R. Valdagni<sup>13</sup>, A. Vega<sup>14</sup>, L. Veldeman<sup>15</sup>, M. Veldwijk<sup>7</sup>, F. Wenz<sup>7</sup>, A. Webb<sup>1</sup>, C. West<sup>9</sup>

<sup>1</sup>University of Leicester, Department of Genetics, Leicester, United Kingdom ; <sup>2</sup>Institut du Cancer de Montpellier, Radiation Oncology, Montpellier, France ; <sup>3</sup>Source Bioscience, Research & Development, Nottingham, United Kingdom ; <sup>4</sup>German Cancer Research Center DKFZ, Division of Cancer Epidemiology, Heidelberg, Germany ; <sup>5</sup>University of Cambridge, Centre for Cancer Genetic Epidemiology, Cambridge, United Kingdom ; <sup>6</sup>Centre Hospitalier Universitaire de Nîmes CHU, Radiotherapy, Nîmes, France; <sup>7</sup>Medical Faculty Mannheim at Heidelberg University, Radiation Oncology, Mannheim, Germany; <sup>8</sup>Maastricht University Medical Center, Radiotherapie, Maastricht, The Netherlands ; <sup>9</sup>University of Manchester, Division of Cancer Sciences, Manchester, United Kingdom ; <sup>10</sup>Vall d'Hebron Institute of Oncology-VHIO, Oncogenetics, Barcelona, Spain; <sup>11</sup>Fondazione IRCCS Istituto Nazionale dei Tumori, Programma Prostate, Milan, Italy ; <sup>12</sup>Mount Sinai Medical School, Radiation Oncology, New York, United Kingdom ; <sup>13</sup>Fondazione IRCCS Istituto Nazionale dei Tumori, Programma Prostate, Milan, France ; <sup>14</sup>CHUS - Complejo Hospitalario Universitario de Santiago, Fundación Pública Galega de Medicina Xenómica, Santiago de Compostela, Spain ; <sup>15</sup>UZ Gent, Radiotherapy, Ghent, Belgium

*This abstract is part of the media programme and will be released on the day of its presentation*

**SP-0648 Criteria for choosing dose and irradiation techniques for palliative treatment**Y. Van Der Linden<sup>1</sup><sup>1</sup>Leiden University Medical Center Lumc, Department Of Radiotherapy, Leiden, The Netherlands**Abstract text**

Radiotherapy is an important treatment modality for advanced cancer patients who experience clinical symptoms caused by metastatic disease or the primary tumour itself. And times are changing, with the possibility to treat oligometastatic disease using stereotactic techniques and ablative doses with the goal of prolonged symptom control, and maybe, even prolonged survival. When considering the use of palliative radiotherapy it is therefore recommendable to think about some important issues

1- How do we select our patients for palliative

radiotherapy? Where in the disease trajectory is the individual patient?

2- What are the goals of palliative radiotherapy from the perspective of the patient? And how do we match these goals with the expected toxicity and clinical outcome?  
3- How do we choose between different radiation techniques and dose schedules? What is the evidence to support these choices?

During the talk these issues will be discussed

#### SP-0649 Uncertainties in single fraction treatment

J. Dhont<sup>1</sup>

<sup>1</sup>Vrije Universiteit Brussel, IMEC-SMIT-VUB ETRO, Brussels, Belgium

##### Abstract text

Uncertainties, possible differences between the planned and delivered therapy, enter the radiotherapy treatment workflow at every step of the process. Proper identification and understanding of the extent of each uncertainty, on both a patient and treatment system level, are crucial to enable precise and accurate radiotherapy delivery. Not only to ensure sufficient target dose and minimal dose to organs at risk, but also to be certain of the dose delivered; a prerequisite for further optimization to advance radiation oncology. In case of standard fractionation, most uncertainties such as organ motion become random, blurring the planned dose around the target. Only few uncertainties are systematic after multiple fractions, often caused by wrong calibration of set-up equipment, inducing a shift of the planned dose relative to the target. To be certain of sufficient dose to the CTV despite uncertainties, PTV margins are applied. Proposed margin recipes rightly make a distinction between random and systematic errors, with higher contribution coming from the latter. However, in case of single fraction treatment, an uncertainty shift occurs. Errors such as inaccurate patient set-up no longer become random but induce a single shift in the dose with respect to the target, as systematic errors do. Only few random uncertainties remain when the total dose is delivered at once, significantly altering the PTV margin when the treatment confidence level is to remain the same.

#### SP-0650 The Role of the RTT in the Palliative Patients Journey

K. Moore<sup>1</sup>

<sup>1</sup>Beatson West of Scotland Cancer Centre, radiotherapy, Glasgow, United Kingdom

##### Abstract text

As radiographers become more autonomous within radiotherapy we are taking on roles that have traditionally been undertaken by the medical staff or by clinical nurse specialists.

While nurses have had many years experience in consulting with the palliative patient, and many publications that describe how well this is done by our nursing colleagues there is very little in the way of evidence where a non medic/non nurse health care professional leads this type of consultation. This presentation will explore the RTT role within the palliative radiotherapy aspect of patient care and communicating the purpose of treatment.

Breaking bad news to a patient or discussing where they are with regard to end of life care takes experience, confidence and most of all knowledge of treatment options and outcomes. There are models for us to refer to such as the SPIKES model, however these 3 cases will demonstrate that providing the answers to the patient questions is often fraught with more questions than answers.

#### SP-0651 Healthy tissue response to a single fraction treatment : Impact of the individual radiosensitivity

N. Foray<sup>1</sup>

<sup>1</sup>U1052 Inserm - Radiobiology group- Lyon- France, Radiobiology, Lyon, France

##### Abstract text

The ATM protein is a major stress response factor involved in the DNA double-strand breaks (DSB) repair and signaling. We have recently provided evidence that the rate of the nucleo-shuttling of ATM protein was a good predictor of tissue radiosensitivity: irradiation triggers the monomerization of the abundant cytoplasmic ATM dimers, which allows the ATM monomers to diffuse in the nucleus. Once in nucleus, the ATM monomers phosphorylate the variant H2AX histone protein, which triggers the recognition of DSB and their repair via non-homologous end-joining (NHEJ) pathway. From hundreds fibroblasts derived from patients suffering from genetic disease or post-radiotherapy radiosensitivity, we have shown that delay in the nucleo-shuttling of ATM may cause lack of DSB recognition, incomplete DSB repair and radiosensitivity (1-4). A classification of radiosensitivity in three groups was proposed (5, 6): group I: radioresistance and low cancer risk, fast ATM nucleo-shuttling; complete DSB repair; group II: moderate radiosensitivity and high cancer risk, delayed ATM nucleo-shuttling; incomplete DSB repair; group III: gross DSB repair defect whatever the rate of the ATM nucleo-shuttling, hyper-radiosensitivity and high cancer risk with two sub-groups : sub-group IIIa (delayed ATM nucleo-shuttling, e.g. ataxia telangiectasia (ATM mutations)); sub-group IIIb (normal ATM nucleo-shuttling, e.g. the LIG4 syndrome (LIG4 mutations)) (1, 6). This model permits a relevant biological interpretation of the linear-quadratic model that links cell survival and radiation dose (7). We will ask from which threshold of DNA repair defect and ATM nucleo-shuttling, a palliation in RT can be deleterious.

##### References

1. Granzotto, A., et al (2016). *International journal of radiation oncology, biology, physics* 94, 450-460
2. Belkacemi, Y. et al (2016) *International journal of radiation oncology, biology, physics* 96, 629-636
3. Pereira, S., et al. (2018) *International journal of radiation oncology, biology, physics* 100, 353-360
4. Vogin, G., et al (2018) *International journal of radiation oncology, biology, physics* 101, 690-693
5. Joubert, A., et al. (2008) *International journal of radiation biology* 84, 1-19
6. Bodgi, L., et al (2013) *Journal of theoretical biology* 333, 135-145
7. Bodgi, L., and Foray, N. (2016) *International journal of radiation biology* 92, 117-131

---

#### Symposium: Mechanisms of treatment resistance in glioma

---

#### SP-0652 The role of DNA replication stress in glioma stem cell radiation resistance

R. Carruthers<sup>1</sup>, S. Ahmed<sup>2</sup>, K. Strathdee<sup>3</sup>, A. Chalmers<sup>4</sup>

<sup>1</sup>Beatson West of Scotland Cancer Centre, Clinical Oncology, Glasgow, United Kingdom; <sup>2</sup>University Of Sunderland, Faculty of Health Sciences and Wellbeing, Sunderland, United Kingdom; <sup>3</sup>University Of Glasgow, Institute of Cancer Sciences, Glasgow, United Kingdom ; <sup>4</sup>University of Glasgow, Institute of Cancer Sciences, Glasgow, United Kingdom

##### Abstract text

Radiation resistance and tumour recurrence are hallmarks of glioblastoma, which is one of the most aggressive human malignancies. Despite advances in the treatment of many other solid tumours, survival in glioblastoma has remained unchanged for many years, and many promising novel agents have failed to alter outcome in large phase 3

clinical trials. One contributing factor is thought to be the failure of many therapeutics to target glioblastoma stem-like cells (GSC) which exhibit DNA damage response (DDR) activation and enhanced DNA double strand break (DSB) repair. Although DDR activation and radiation resistance in GSC were documented many years ago the underlying reasons for this have remained enigmatic. Elucidation and understanding of this phenomenon would have significant implications for efforts to increase the efficacy of radiotherapy in the clinic. In this presentation we will provide an overview of DDR activation observed in GSC and explore its implications for radiation resistance. We will describe a unique DNA replication phenotype in GSC that predisposes them to high levels of DNA replication stress as an underlying mechanism for DDR activation and discuss possible sources of elevated replication stress in this cell population. Finally, we will examine targeting of DNA replication stress response as a promising therapeutic and radiation sensitisation strategy for clinical translation.

#### SP-0653 Tumor cell connections causing radiation resistance

F. Winkler<sup>1</sup>

<sup>1</sup>University of Heidelberg, Neurology, Heidelberg, Germany

##### Abstract text

The recent discovery of ultra-long and thin membrane protrusions of glioma cells, called tumor microtubules (TMs), has added to our understanding of these incurable tumors (Osswald et al., Nature 2015). Astrocytoma (including glioblastoma) cells extend these highly functional structures to colonize the brain, and to interconnect to one large communicating multicellular network. Glioma cells integrated into this TM network resist the cytotoxic effects of radiotherapy and chemotherapy. This talk will cover how our understanding of the disease "glioma" has changed, and how novel therapies are developed to tackle this basic cellular mechanism of resistance against radiotherapy, chemotherapy, and surgery.

#### SP-0654 Transcriptional response to temozolomide in Glioblastoma reveals critical role of long non-coding RNAs

S. Niclou<sup>1</sup>, S. Fritah<sup>1</sup>, M. Sarmini<sup>1</sup>, W. Jiang<sup>2</sup>, A. Muller<sup>1</sup>, M. Dieterle<sup>1</sup>, R. Mitra<sup>2</sup>, A. Golebiewska<sup>1</sup>, Z. Zhao<sup>2</sup>, F. Azuaje<sup>1</sup>

<sup>1</sup>Luxembourg Institute of Health, Department Of Oncology, Luxembourg, Luxembourg; <sup>2</sup>Vanderbilt University, Bioinformatics, Nashville, USA

##### Abstract text

Resistance to the alkylating agent temozolomide (TMZ) is a major cause of Glioblastoma (GBM) recurrence and dismal prognosis. To date, the epigenetic regulation of the O6-methylguanine methyltransferase (MGMT) promoter is the only TMZ-predictive marker with clinical relevance, but there is little knowledge of regulatory transcriptional pathways involved in therapy resistance. Here, we provide a comprehensive overview of the transcriptional response to TMZ in patient-derived cellular GBM models, with a special focus on the contribution of non-coding RNAs as novel markers of chemoresistance. Using RNA-Seq and small RNA-seq, we have uncovered a complex transcriptional response to TMZ and identified a subset of long non-coding RNAs (lncRNAs) mediating regulatory circuits. Interestingly, lncRNAs were mapped to processes linked to drug sensitivity, cell cycle regulation and/or developmental pathways. Among these lncRNAs, we characterized a novel lncRNA termed RADAR (RNA associated with DNA Damage and Replication) and show that RADAR is a chromatin-associated lncRNA involved in cell cycle control, apoptosis and sister chromatid cohesion. Altogether, this integrative analysis of RNA-seq

data provides new RNA-based predictors of chemoresistance, as well as potential targets to counteract this resistance in GBM.

#### SP-0655 Irradiation and targeted inhibition of the PI3K/AKT and MAPK pathways in glioma

P. Sminia<sup>1</sup>, R. Narayan<sup>1</sup>, A. Gasol<sup>1</sup>, F. Cornelissen<sup>2</sup>, J. Theys<sup>3</sup>, T. Lagerwei<sup>4</sup>, E. De Vries<sup>5</sup>, F. Bikhezari<sup>1</sup>, A. Denkova<sup>6</sup>, R. De Kruijff<sup>6</sup>, B. Slotman<sup>1</sup>, L. Stalpers<sup>7</sup>, B. Baumert<sup>8</sup>, B. Westerman<sup>2</sup>

<sup>1</sup>VU University Medical Center, Radiation Oncology, Amsterdam, The Netherlands; <sup>2</sup>VU University Medical Center, Neurosurgery- Neuro-Oncology Research Group, Amsterdam, The Netherlands; <sup>3</sup>Maastricht University Medical Center, Radiation Oncology, Maastricht, The Netherlands; <sup>4</sup>VU University Medical Center, Neurosurgery- Neuro-Oncology Research, Amsterdam, The Netherlands; <sup>5</sup>VU University Medical Center, Molecular Cell Biology and Immunology, Amsterdam, The Netherlands; <sup>6</sup>Delft University of Technology, Radiation Science and Technology, Delft, The Netherlands; <sup>7</sup>Academic Medical Center Amsterdam, Radiation Oncology, Amsterdam, The Netherlands; <sup>8</sup>University Hospital Bonn, Radiation Oncology, Bonn, Germany

##### Abstract text

Commonly defective core signaling pathways in glioma contributing to radioresistance include the tumor protein p53 (TP53) pathway, the retinoblastoma (RB) pathway and receptor tyrosine kinase (RTK) pathway. Combined treatment of irradiation, the key component of the current standard treatment of glioblastoma (GBM) patients, with drugs that selectively target these pathways, might improve the outcome of therapy.

Studies were performed on GBM cell lines and patient derived primary cultures grown as monolayer and multicellular spheroids with endpoints cell proliferation, clonogenic cell survival, spheroid growth rate, - volume reduction and - time to regrow. We investigated the single agent efficacy and radiosensitizing potential of a panel of novel targeted small molecule drugs including MK2206, RAD001, BEZ235, MLN0128 and MEK162. Effects on cell cycle distribution and expression of key target proteins were evaluated.

Out of the panel of drugs, both the allosteric AKT inhibitor MK2206 and MEK162 (binimetinib), which is an allosteric inhibitor of MEK1/2, were found to act as radiosensitizer. MK2206 delayed the growth of spheroids and sensitized to both irradiation and temozolomide via reduced phosphorylation of Thr308 and Ser473 residues of AKT. MEK162 was found to down-regulate and dephosphorylate the cell cycle checkpoint proteins CDK1/CDK2/WEE1 and DNA damage response proteins p-ATM/p-CHK2. When combined with radiation this led to a prolonged DNA damage signal. Next, the combination of MEK162 (50 mg/kg) and irradiation (3 x 2 Gy) was studied on orthotopic GBM8 brain tumor xenografts. The data showed a significantly reduced growth rate, increased growth delay and prolonged survival time of the animals. In addition, RNA expression of responsive cell cultures correlated to mesenchymal stratification of patient expression data. However, the delivery of MEK162 to the tumor site, like most chemical compounds, is abrogated by the blood-brain barrier (BBB). First in vitro data on BBB crossing demonstrated effective passaging of the drug when loaded in polymeric nanocarriers.

In conclusion, both the AKT inhibitor MK2206 and the MAPK inhibitor MEK162 demonstrated radiosensitizing potential in GBM spheroids in vitro and in orthotopic GBM xenografts in vivo. We identified a patient subgroup that might benefit from MEK inhibition combined with radiotherapy. This combinatorial treatment approach opens a novel therapeutic avenue for GBM patients.

Supported by the Dutch Cancer Foundation (KWF), grant

#VU2010-4874 and STOPHersentumoren.nl, grant #2015-009.

---

**Debate: This house believes that there is still a role for radiotherapy in pancreatic cancer**

---

**SP-0656 For the motion: resectable pancreatic cancer**  
T. Brunner<sup>1</sup>

<sup>1</sup>*Otto-von-Guericke-Universität Dept. Radiation Oncology, Magdeburg, Germany*

Abstract not received

**SP-0657 Against the motion: resectable pancreatic cancer**

M. Falconi<sup>1</sup>

<sup>1</sup>*San Raffaele Hospital, Pancreas Surgery, Milano, Italy*

**Abstract text**

The management of resectable pancreatic cancer is challenging and different strategies can be applied including upfront surgery followed by adjuvant therapy or neoadjuvant treatment followed by surgical resection. This decision is based on the presence of an anatomical and/or biological borderline resectable tumor. In the setting of neoadjuvant treatment, there is a lack of evidence that support the routine use of preoperative radiation therapy with chemotherapy, especially when considering multi-agents chemotherapy regimens (i.e. FOLFIRINOX; gemcitabine plus nab-paclitaxel). The rationale for preoperative chemoradiation is related to a lower rate of R1 resection rate following radiation therapy, but actually no RCT showed a real advantage of this approach over chemotherapy alone. In the setting of adjuvant treatment, there is an unclear role for adjuvant radiotherapy, that is most likely recommended for patients with a R1 resection. Most studies did not find any advantage in the survival rate following chemoradiation compared to adjuvant chemotherapy alone. However, several studies administered suboptimal and obsolete schedule of radiotherapy and/or included small cohorts of patients, and as a consequence this represents a major limitation of any comparison of chemoradiation versus chemotherapy alone, both in the adjuvant and neoadjuvant setting. Novel radiotherapeutic approaches including stereotaxic body radiation therapy should be evaluated in powered randomized clinical trial considering specific aims (local recurrence, overall survival, toxicity).

**SP-0658 For the motion: locally advanced pancreatic cancer**

F. Huguet<sup>1</sup>

<sup>1</sup>*Hôpital Tenon, Department of Radiotherapy, Paris Cedex 20, France*

**Abstract text**

At diagnosis, about 25% of patients with pancreatic adenocarcinoma presents with a locally advanced (non-metastatic but unresectable due to vascular invasion) or borderline resectable tumor. Despite the technical progress made in the field of radiation therapy and the improvement of the efficacy of chemotherapy, the prognosis of these patients remains poor. Recently, the role of radiation therapy in this setting has been much debated. However, some arguments support the use of radiation therapy for these patients. First, as shown in LAP07 trial, radiation therapy delivered after a phase of induction chemotherapy increases local control. Second, it allows a time without treatment for patients longer than chemotherapy alone. Third, patients who receive neoadjuvant radiation therapy have a higher chance to achieve a R0 resection and a major pathological response

(ypT0-1 ypN0). Moreover, new radiation techniques such as SBRT allow dose escalation to the target volume while improving sparing of nearby normal structures. Combined with more effective chemotherapy regimens, it should improve the outcome of these patients.

**SP-0659 Against the motion: locally advanced pancreatic cancer**

E. Van Cutsem<sup>1</sup>

*University Hospital Gasthuisberg, Leuven, Belgium*

Abstract not received

---

**Symposium: New developments in Head and Neck Cancer treatment**

---

**SP-0660 p16+ oropharyngeal cancer: new disease, new staging - what about treatment?**

P. Lassen<sup>1,2</sup>

<sup>1</sup>*Aarhus University Hospital, Department Of Oncology and Experimental Clinical Oncology, Aarhus, Denmark;*  
<sup>2</sup>*Princess Margaret Cancer Centre, Radiation Oncology, Toronto, Canada*

**Abstract text**

The incidence of Human papillomavirus (HPV) associated oropharyngeal carcinoma (OPC) is increasing in developed countries, and HPV positive OPC is a distinct disease entity from HPV negative OPC characterized by a unique epidemiology, molecular biology and oncogenesis. In addition, patients with HPV positive disease tend to be younger and healthier than their HPV negative counterpart due to differences in risk profiles, especially less heavy smoking and alcohol consumption, which again results in less significant comorbidity.

HPV positive squamous cell carcinoma is more sensitive to radiotherapy than HPV negative disease, and the highly significant prognostic impact of tumor HPV-status on treatment outcome and survival has led to the inclusion of HPV-associated p16 expression in the eighth edition of the AJCC/UICC TNM classification system. The overall general favorable prognosis in HPV positive OPC is however heterogeneous, and it is well known, that advanced disease-stage (T3-4N2) and smoking (>10packyears) negatively impacts prognosis, which have resulted in the definition of a group of intermediate risk patients with HPV positive disease.

Traditional treatment of advanced stage OPC consists of concurrent chemo-radiation, which is associated with substantial acute toxicity and long term morbidity, ultimately impacting quality of life for long-term survivors. As patients with HPV positive disease are typically younger, they will have to live longer with potential long term effects from treatment. This, combined with the general good prognosis, has led to the initiation of clinical trials investigating de-intensified therapies in HPV positive disease, in order to reduce toxicity without compromising outcome. Various strategies are presently being investigated within clinical trials including de-intensification of treatment by substituting Cisplatin with the EGFR-inhibitor Cetuximab, radiotherapy alone, reduction in adjuvant radiotherapy following primary surgery with minimally invasive surgical techniques based on pathology features and reduction in radiotherapy dose following induction chemotherapy in good responders.

Given the somewhat dismal prognosis of the intermediate risk HPV positive patients, trials have been initiated focusing on optimizing outcome for this group of patients also, for instance by incorporation of concurrent immunotherapy into primary radiotherapy. The first groundbreaking results have been published regarding the substitution of Cisplatin with Cetuximab

from two large-scale randomized trials (De-ESCALate and NRG Oncology RTOG1016), both showing significantly worse tumor control and survival outcomes for patients treated with Cetuximab, with comparable frequency and severity of acute toxicity and late morbidity. In this light, Cisplatin continues to be the standard of care for radiosensitization in all eligible patients with advanced HPV positive OPC, and treatment de-intensification strategies should only be evaluated within the frames of well-designed clinical trials.

The focus of this talk will be to summarize the current understanding of how to optimally treat HPV positive OPC integrating an overview of the design and rationale of ongoing clinical trials and a presentation of lessons learned from completed clinical trials.

#### SP-0661 Predictive models in treatment of head and neck cancer

H. Langendijk<sup>1</sup>

<sup>1</sup>UMCG University Medical Center Groningen, Department of Radiation Oncology, Groningen, The Netherlands

##### Abstract text

The relationship between 3-dimensional dose distributions and risks on radiation-induced side effects can be described by Normal Tissue Complication Probability (NTCP) models. NTCP-models may contain only one dose-volume predictor (dose metrics), but generally the performance of these model significantly improve when adding multiple other predictors (multivariable NTCP-models). According to the so-called model-based approach, next to outcome prediction, NTCP-models can be applied for dose optimization, selecting the best radiation technology, plan adaptation and even technology validation. For many side-effects, the risk may depend on more than one dose metrics to different organs at risk (OARs). To produce treatment plans that eventually result in adequate target dose coverage with the lowest probability on side effects, dose distributions to OARs should be translated into NTCP-profiles using NTCP-models (model-based dose optimization). For the selection of the best treatment plan, or even for the selection of patients for more advanced radiation technologies, like protons, information on NTCP-profiles next to dose profiles are essential to ultimately obtain the best clinical result, i.e. local control with the lowest rates of radiation-induced side effects. Currently, adaptive radiotherapy is mainly guided by dose deviations compared to the nominal plan. However, depending on the shape of the NTCP-curve, apparently large dose deviations do not necessarily translate into clinically relevant changes in the risks of side effects. Vice versa, relatively small dose deviations may result in major changes in the risk of side effects when they appear in the dose range with the steepest dose-effect relationship. Also here, NTCP-guided adaptations, also referred to as biologically-driven adaptive radiotherapy (BIOART) is more likely to result in the best clinical result. Many radiation technologies aiming at reduction of side effects are introduced in routine clinical practice, based on the ALARA-principle without any proper clinical validation. An alternative for RCT's is the so-called model-based validation, testing the null-hypothesis that observed toxicity rates obtained with the new RT technology is similar to that expected (based on NTCP-models) from the old technology. In summary, the model-based approach allows for a continuous improvement and validation of newly introduced radiation techniques and ultimately the most optimal outcome for patients treated with radiotherapy.

#### SP-0662 Immunotherapy in HNC - when and for whom, biomarkers of response

L.Licitra<sup>1</sup>

<sup>1</sup>Fondazione IRCCS Istituto Nazionale dei Tumori, Milan, Italy

Abstract not received

---

#### Symposium: New detector developments

---

#### SP-0663 Update on compact graphite calorimeter for absolute dosimetry measurements

T. Russell<sup>1</sup>

<sup>1</sup>National Physical Laboratory, Teddington United Kingdom

Abstract not received

#### SP-0664 Update on commercial scintillators

S. Beddar<sup>1</sup>

<sup>1</sup>The University of Texas MD Anderson Cancer Center, Radiation Physics, Houston- TX, USA

##### Abstract text

Within the last two decades, there has been a substantial research directed towards the use of scintillators to measure absorbed dose in radiation dosimetry in general and particularly in radiation therapy. The evolution of the many studies that focused on these new type of detectors followed 3 phases: 1) identifying suitable clinical applications where scintillation detectors would offer additional advantages over the commonly used detectors or dosimeters, 2) optimization of detector designs and component's system depending on the application of interest and 3) transfer and translation to the industry to commercialize these new detectors. A brief introduction to scintillation dosimetry, including a summary of their advantages and disadvantages will be presented.

The lecture will focus on commercial scintillators and an update on their present status including new scintillation detector developments that are ongoing. At the present time there are two commercial systems available on the market. One designed for absorbed dose and dose characterization for external beam radiation therapy (EBRT) commercialized by Standard Imaging. The second one designed for in vivo dosimetry and dose monitoring commercialized by Radiadyne. A third commercial system is in the development and clinical trial testing phase for HDR brachytherapy to be commercialized soon by Dosilab. Their first system is targeted at the QA of HDR brachytherapy equipment.

Finally, current and on-going research to respond to future needs such as brachytherapy in the domain of in vivo dosimetry and dose-tracking, including electromagnetic (EM) tracking will be presented.

#### SP-0665 Multichannel film dosimetry

I. Mendez Carot<sup>1</sup>

<sup>1</sup>Institute of Oncology Ljubljana, Department of Radiation Physics, Ljubljana, Slovenia

##### Abstract text

The dosimetry system composed of radiochromic films and a flatbed scanner is a dosimeter of choice in many radiotherapy and radiology applications. Upon irradiation, films polymerize, becoming increasingly dark with the absorbed dose. Variations in the visible absorption spectrum can be measured with a scanner, which yields three different signals (R, G and B), one for each color channel. Multichannel film dosimetry consists of the combination of the information provided by several color channels in order to obtain more accurate dose distributions. Various multichannel film dosimetry methods have been proposed in the literature. Each of them based on different assumptions regarding the

behavior of the dosimetry system. This lecture will describe some of the most employed multichannel methods: its assumptions, formulas, uncertainties, and weaknesses. Multichannel film dosimetry can deliver more accurate doses, mainly by mitigating spatial heterogeneities in the film-scanner response, in particular, variations in the active layer thickness. This lecture will also explain which sources of uncertainty are reduced by using multichannel methods and what other corrections can we apply to improve radiochromic film dosimetry.

#### SP-0666 Developments in time-resolved detectors

A. Rozenfeld<sup>1</sup>

<sup>1</sup>Centre for Medical Radiation Physics, University of Wollongong, University of Wollongong, Australia

##### Abstract text

A range of silicon-based dosimeters has been made available to address the challenges of ensuring an ever safer and more accurate treatment delivery in radiotherapy. These dosimeters, extensively used in the clinic, possess a set of convenient features: a response which is stable and linear with deposited dose, and the possibility of manufacturing sensitive volumes sufficiently small while retaining relatively high sensitivity. The present lecture reviews, in terms of design, applications and limitations, innovative silicon dosimeters able of high-spatial and temporal resolution which are being developed at the Centre for Medical Radiation Physics (CMRP).

Monolithic diode arrays with spatial resolution better than 2mm and temporal resolution better than 0,1ms are discussed for dose QA in a heterogeneous fully customized phantom for IMRT and VMAT treatments with small photon fields that dynamically track the tumor motion using dynamic multi-leaf collimator (DMLC). Diode arrays with spatial resolution as high as 0.05 mm for in body application for *in vivo* real time source dwelling position and time verification in high dose rate (HDR) and immediate source position as dropped in low dose rate (LDR) brachytherapy with submillimetre spatial resolution are discussed. Finally, the use of a MOSkin, a metal-oxide-semiconductor field-effect transistor (MOSFET) and innovative epi-diode detectors for time resolved rectal wall dosimetry and source tracking in gynaecological multi catheter applicator respectively in HDR brachytherapy are presented

---

Proffered Papers: PH 14: Proffered paper: Treatment planning of proton therapy

---

#### OC-0667 Experimental assessment of inter-centre variation and accuracy in SPR prediction within the EPTN

N. Peters<sup>1,2</sup>, P. Wohlfahrt<sup>1</sup>, A. Bolsi<sup>3</sup>, C.V. Dahlgren<sup>4</sup>, L. De Marzi<sup>5</sup>, M. Ellerbrock<sup>6</sup>, F. Fracchiolla<sup>7</sup>, J. Free<sup>8</sup>, C. Gomà<sup>9</sup>, J. Góra<sup>10</sup>, T. Kajdrowicz<sup>11</sup>, R. MacKay<sup>12</sup>, S. Molinelli<sup>13</sup>, O. Nørrevang<sup>14</sup>, I. Rinaldi<sup>15</sup>, V. Rompokos<sup>16</sup>, P. Van der Tol<sup>17</sup>, X. Vermeren<sup>18</sup>, C. Richter<sup>1,2,19,20</sup>

<sup>1</sup>OncoRay - National Center for Radiation Research in Oncology, Faculty of Medicine and University Hospital Carl Gustav Carus- Technische Universität Dresden-Helmholtz-Zentrum Dresden - Rossendorf, Dresden, Germany; <sup>2</sup>Helmholtz-Zentrum Dresden-Rossendorf, Institute of Radiooncology - Oncoray, Dresden, Germany; <sup>3</sup>Paul Scherrer Institut, Center for Proton Therapy, Villigen, Switzerland; <sup>4</sup>The Skandion Clinic, Skandionkliniken, Uppsala, Sweden; <sup>5</sup>Institut Curie, Centre de protonthérapie, Orsay, France; <sup>6</sup>Heidelberg Ion-Beam Therapy Center HIT, Department of Radiation Oncology - Heidelberg University Hospital, Heidelberg, Germany; <sup>7</sup>APSS Trento, Centro di Protonterapia di

Trento, Trento, Italy; <sup>8</sup>University of Groningen- University Medical Center Groningen, Department of Radiation Oncology, Groningen, The Netherlands; <sup>9</sup>KU Leuven, Department of Oncology, Leuven, Belgium; <sup>10</sup>EGB MedAustron GmbH, Medizinische Strahlenphysik, Wiener Neustadt, Austria; <sup>11</sup>Institute of Nuclear Physics, Polish Academy of Sciences, Krakow, Poland; <sup>12</sup>University of Manchester, Faculty of Life Sciences, Manchester, United Kingdom; <sup>13</sup>Centro Nazionale di Adroterapia Oncologica, Department of Medical Physics, Pavia, Italy; <sup>14</sup>Danish Centre for Particle Therapy, Aarhus University, Aarhus, Denmark; <sup>15</sup>Maastricht, Maastricht, The Netherlands; <sup>16</sup>University College London Hospitals, Department of Radiotherapy, London, United Kingdom; <sup>17</sup>HollandPTC, Protonen Therapie Centrum, Delft, The Netherlands; <sup>18</sup>Universitätsklinikum Essen, Westdeutsches Protonentherapiezentrum Essen, Essen, Germany; <sup>19</sup>Faculty of Medicine and University Hospital Carl Gustav Carus- Technische Universität Dresden, Department of Radiotherapy and Radiation Oncology, Dresden, Germany; <sup>20</sup>German Cancer Consortium DTK-partner site Dresden, German Cancer Research Center DKFZ- Heidelberg, Dresden, Germany

##### Purpose or Objective

The standard approach for CT-number to stopping-power-ratio (SPR) conversion in particle therapy is the use of a heuristic stepwise translation, a so-called Hounsfield look-up table (HLUT). It is defined by each treatment facility individually and depends on both the calibration method and CT scan protocol. A recent survey has shown broad variability in these parameters [1], making a simple comparison on HLUT level unfeasible. Hence, we present a comprehensive experimental evaluation of inter-centre variation and absolute accuracy in SPR prediction within the European Particle Therapy Network (EPTN).

##### Material and Methods

A head and a body phantom with 17 tissue surrogate inserts were scanned consecutively at the participating centres using their individual clinical scan protocol. The inserts were tissue-equivalent concerning particles; their composition and SPR were blinded for the participants. The SPR calculation was performed using each centre's CT scan and HLUT (Fig.1). The inter-centre variation and absolute accuracy in SPR prediction were quantified for each tissue surrogate individually and then summarised into the relevant tissue groups: lung, soft tissues and bones. Finally, to evaluate the integral effect on range prediction for typical clinical beams traversing different tissues, for three simplified beam paths the determined SPR deviations were accumulated according to their respective tissue distribution. So far, data from 9 out of 17 participating centres was available.

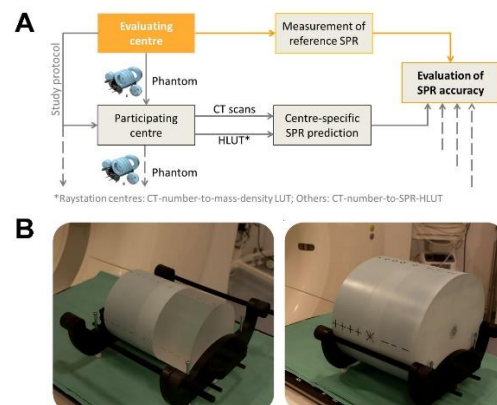
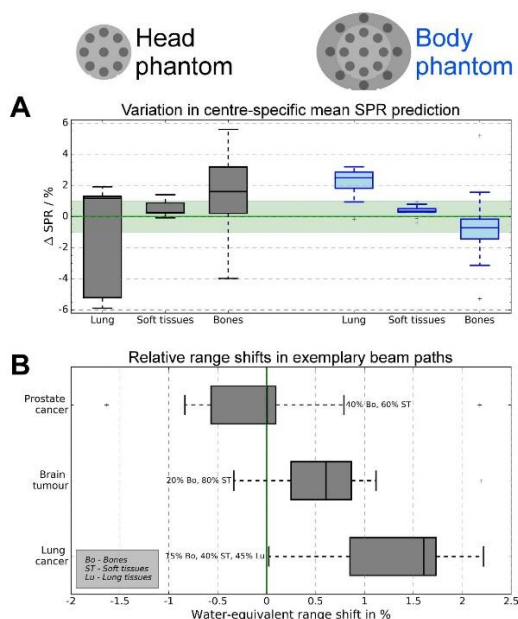


Figure 1: (A) Scheme of the study design. SPR: Stopping power ratio; HLUT: Hounsfield look-up table. (B) Experimental setup of the head (left) and body phantom (right) with the tissue surrogate inserts placed in the centre part of each phantom.

## Results

A  $2\sigma$  inter-centre variation in SPR prediction of 5.7% and 5.5% relative to water was determined for the bone inserts in the head and body setup, respectively. Comparable results were achieved for the lung tissue surrogates (6.4% and 2.2%). In the soft tissue region an overall higher accuracy was achieved with a variation below 0.9% in both setups and a mean SPR prediction accuracy below 0.5%. In the head setup, both lung tissues and bones were overestimated in most centres, while in the body setup the bones were underestimated (Fig. 2A). For the three exemplary beam paths, inter-centre variations in relative range were 1.5% on average. In specific centres, range deviations from reference exceeded 1.5% (Fig 2B).



**Figure 2:** (A) Variations in stopping-power-ratio (SPR) prediction between 9 centres. The 17 tissue surrogates were classified into the relevant tissue groups lung (2), soft tissues (11) and bones (4) and then averaged centrewise. (B) Resulting range shifts relative to water along three simplified beam path scenarios, resulting from an accumulation of the SPR deviations in the three tissue groups weighted with their relative contribution in the beam path. Whiskers in boxplot are defined by last values within 1.5x interquartile range.

## Conclusion

Large inter-centre variations in SPR prediction were observed in low- and high density tissue surrogates. The differences in deviation for bone between the two setups indicate a strong influence of scanning parameters such as the level of beam hardening correction, potentially resulting in range shifts of clinical relevance. As the study allows for a direct attribution of the measured deviations to the calibration methods and scan protocols used by the individual centres, it stresses the need for inter-centre standardisation. While this work addresses the accuracy in SPR prediction under idealised study conditions, a direct conclusion on overall range accuracy in patients is not possible. The study is currently still ongoing.

[1] Taasti et al. 2018, *phiRO* 6 25-30

## OC-0668 MRI-only proton therapy treatment planning with synthetic CT images generated using deep learning

A.M. Barragán Montero<sup>1,2</sup>, K. Souris<sup>1</sup>, S. Kazemifar<sup>2</sup>, R. Timmerman<sup>3</sup>, S. Jiang<sup>2</sup>, X. Geets<sup>1</sup>, E. Sterpin<sup>1</sup>, A. Owrang<sup>2</sup>

<sup>1</sup>Université Catholique de Louvain- Institute of Experimental & Clinical Research, Molecular Imaging-Radiotherapy and Oncology MIRO, Brussels, Belgium ; <sup>2</sup>UT Southwestern Medical Center, Medical Artificial Intelligence and Automation MAIA, Dallas, USA ; <sup>3</sup>UT

Southwestern Medical Center, Radiation Oncology, Dallas, USA

## Purpose or Objective

To evaluate the dosimetric accuracy of proton therapy treatment planning using synthetic CT images generated from magnetic resonance images (MRI) with a generative adversarial network (GAN).

## Material and Methods

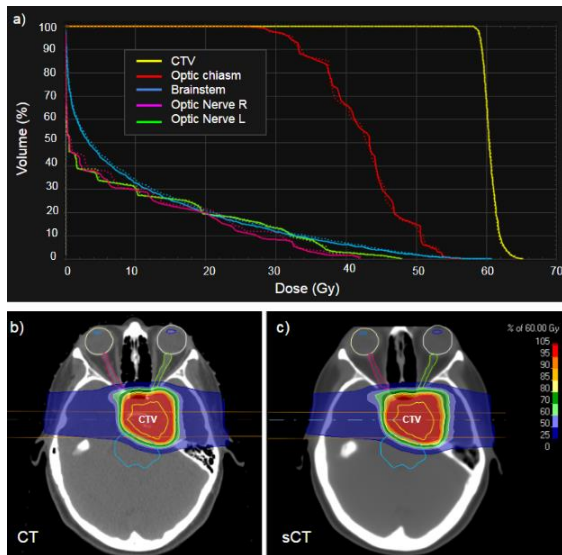
The GAN is a type of unsupervised deep learning algorithm that uses two neural networks that compete against each other: one network generates synthetic CT (sCT) candidates (generator), while the other evaluates them by comparison with real CT images (discriminator). This process is repeated until the discriminator cannot distinguish anymore between the real and synthetic CT, which entails that the generator learnt to accurately transform MR to CT images. The model was trained with (T1-weighted) MRI and CT slices from 63 brain cancer patients, and tested separately in 12 different patients. Synthetic CT images of the same patients were rigidly registered to the CT images using mutual information. Proton pencil beam scanning plans were created on the real CT of the 12 test patients, using RayStation v5.99 (RaySearch Laboratories AB), and recomputed on the sCT for dosimetric comparison. Robust optimization on the CTV with 3% range uncertainty and 3mm accounting for setup error was used to create the plans.

## Results

The average absolute error between the dose computed on the CT and sCT for the 12 test patients, and its standard deviation (SD), on the mean (Dmean) and maximum dose (Dmax) for relevant organs in the nominal case is presented in Table 1. For the CTV, the error on the dose delivered at 95% (D95) and 5% (D5) of the volume is also reported. Overall, the error remained below 2.5% of the dose prescription (60 Gy in all patients), for all considered metrics. Figure 1.a shows the DVH for one of the test patients, with overlapping lines for the dose on the CT (solid line) and sCT (dotted line). Figure 1.b and 1.c show the dose distribution on the same patient for CT and sCT, respectively, for a slice on the center of the target volume. The generation of a full 3D sCT for a given set of MRI slices took only 9 s.

		Average (%)	SD
CTV	D95	0,43	0,41
	D5	0,52	0,40
	D <sub>mean</sub>	0,28	0,21
Brainstem	D <sub>max</sub>	1,29	1,69
	D <sub>mean</sub>	0,40	0,43
Optic chiasm	D <sub>max</sub>	0,86	0,63
	D <sub>mean</sub>	1,36	1,10
Optic Nerve L	D <sub>max</sub>	2,43	2,34
	D <sub>mean</sub>	1,38	1,29
Optic Nerve R	D <sub>max</sub>	1,81	2,38
	D <sub>mean</sub>	0,46	0,66

**Table 1.** Average absolute error between the dose on CT and sCT for the test patients, and its standard deviation (SD), expressed as % of the dose prescription.



### Conclusion

The GAN model was able to generate high-quality synthetic CTs from MR images, which can directly be used for MRI-only treatment planning. Given the sensibility of scanned proton beam dose distributions on small differences along the beam path, our model shows a superior dosimetric accuracy that competes very closely to more conventional methods, such as atlas-based approaches, but requires no hand-crafted features and beats them in terms of computational speed. Our next task involves a complete evaluation of the plans robustness against multiple source of errors.

### OC-669 Development of a novel MRI-only treatment planning approach for ocular proton therapy

E. Fleury<sup>1,2</sup>, P. Trnková<sup>1,2</sup>, E. Erdal<sup>1</sup>, K. Hassan<sup>3</sup>, J. Beenakker<sup>4</sup>, J. Herault<sup>5</sup>, J. Pignol<sup>6</sup>, M. Hoogeman<sup>1,2</sup>

<sup>1</sup>Erasmus Medical Center, Radiation Oncology, Rotterdam, The Netherlands; <sup>2</sup>Holland Proton Therapy Center, Radiation Oncology, Delft, The Netherlands; <sup>3</sup>Leiden University Medical Center, Division of Image Processing, Leiden, The Netherlands; <sup>4</sup>Leiden University Medical Center, Department of Ophthalmology, Leiden, The Netherlands; <sup>5</sup>Centre Antoine Lacassagne, Radiation Oncology, Nice, France; <sup>6</sup>Dalhousie University, Radiation Oncology, Halifax, Canada

### Purpose or Objective

Proton therapy (PT) for Uveal Melanomas (UM) is often employed to lower the risk of irreversible side-effects such as vision impairment, loss or even enucleation. However, a main shortcoming is that high-resolution 3D image data for target volume definition and treatment planning is not used in clinical practice. Instead, the target volume is defined by 2D fundus photography or ultrasound and demarcated by tantalum clips stitched to the sclera. Moreover, the sole commercial treatment planning system (TPS) uses a simplistic eye model, and fails to account for detailed 3D information to accurately characterize the tumor and organs-at-risk (OARs). Besides, the optimal gazing angle for each patient needs to be manually defined and is not objectively optimized. To overcome these limitations, we aim to develop an MRI-only workflow for PT of UM in a multidisciplinary and multicenter approach. This project is to develop an MRI-based planning method with dose-based gaze-angle optimization.

### Material and Methods

5 patients referred to a single academic center for UM treatment were prospectively included into the study after signing an informed consent. High-resolution ocular images were acquired on a 7T Philips Achieva MRI (Best,

Netherlands) using a dedicated eye coil and sequences to reduce eye-motion artefacts. UM and OARs were automatically segmented, and subsequently, a 3D model of the eye was created (Figure 1). A TPS was developed in-house using a semi-analytical broad beam algorithm for passive scattering, in which the 3D eye-model was integrated. Human eye motion was mimicked through an Euler-sequence of rotations around the optical axis (abduction/adduction, elevation/depression and possible torsion). These rotations were used to simulate various clinically feasible gazing angles. For tumor coverage a safety margin was set by adjusting the range and modulation width of the Spread-Out-Bragg Peak proximal and distal edges. Lateral conformation was achieved by a collimator adjusted to the tumor contour. To optimize dose to OARs, a weighted-sum objective function was computed for each gazing angle, which also included an objective to penalize extreme gazing angles. Weights could be adjusted to prioritize sparing of specific OARs.

### Results

The novel treatment planning approach has been tested on 5 patients. Tumor coverage was reached for all cases ( $D_{95\%} > 95\%$ ). Figure 2 shows an example of the weighted-sum objective function for one patient for the clinical feasible gazing angles. Fig 2.A shows the map if optic nerve is prioritized. It shows that the half right's patient side should be avoided, while for the left half most angles are optimal. Fig 2.B shows the objective values for equally weighted sparing of OARs. This tool has great prospects for improving decision-making.

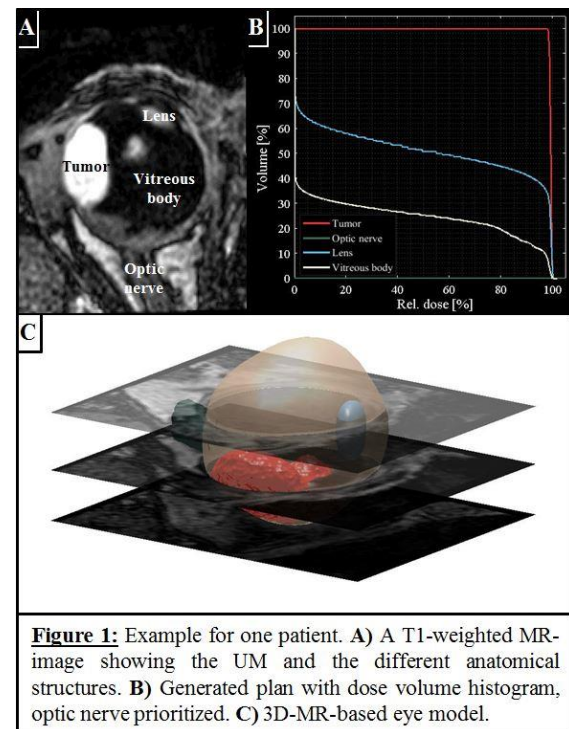
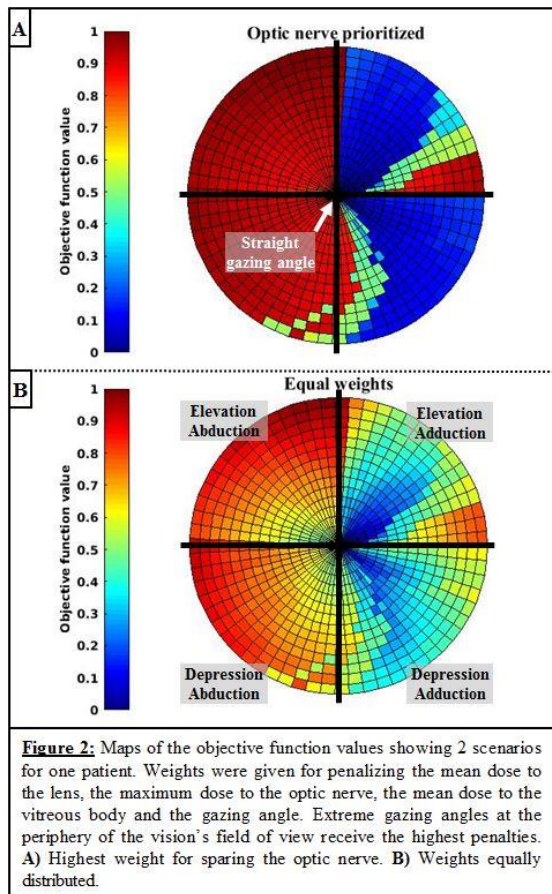


**Figure 1:** Example for one patient. A) A T1-weighted MR-image showing the UM and the different anatomical structures. B) Generated plan with dose volume histogram, optic nerve prioritized. C) 3D-MR-based eye model.



### Conclusion

A MRI-based TPS for ocular proton therapy was developed. For the first time in eye proton therapy treatment planning, a trade-off for OARs sparing was implemented, while maintaining the tumor coverage.

### OC-0670 Temporal lobe sparing radiotherapy for cognitive preservation in pediatric brain tumor patients

L. Toussaint<sup>1</sup>, D.J. Indelicato<sup>2</sup>, L.P. Muren<sup>1</sup>, Z. Li<sup>2</sup>, Y. Lassen-Ramshad<sup>3</sup>, K. Kirby<sup>2</sup>, C. Pedro<sup>4</sup>, R. Mikkelsen<sup>5</sup>, M. Di Pinto<sup>2</sup>, M. Høyer<sup>3</sup>, C.H. Stokkevåg<sup>6</sup>

<sup>1</sup>Aarhus University Hospital, Department of Medical Physics, Aarhus, Denmark; <sup>2</sup>University of Florida Health Proton Therapy Institute, Department of Radiation Oncology, Jacksonville, USA ; <sup>3</sup>Danish Center for Particle Therapy, Department of Oncology, Aarhus, Denmark; <sup>4</sup>Instituto Português de Oncologia Francisco Gentil, Department of Radiotherapy, Lisbon, Portugal; <sup>5</sup>Aarhus University, Department of Biomedicine, Aarhus, Denmark; <sup>6</sup>Haukeland University Hospital, Department of Oncology and Medical Physics, Bergen, Norway

*This abstract is part of the media programme and will be released on the day of its presentation*

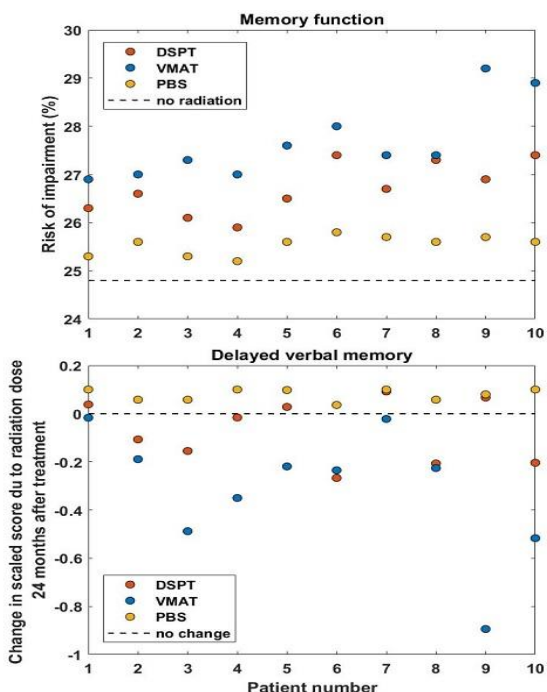


**Figure 2:** Memory impairment estimates based on temporal lobe doses (top) or left hippocampus V20Gy (bottom). For the bottom panel, a positive score (higher than the 'no change' line) represents improved delayed verbal memory. Patients are sorted by increasing CTV volume, and results are presented for the three treatment modalities.

**Conclusion**

The irradiated volumes of temporal lobe BSCs were consistently the lowest with PBS, predicting better post-treatment memory in children with centrally located brain tumors.

**OC-0671 Which planning strategy is better for Head and Neck Cancer: PTV based or CTV based robust IMPT ?**

W.G. Wang<sup>1</sup>, A. Qin<sup>1</sup>, P. Kabolizadeh<sup>1</sup>, X. Li<sup>1</sup>, D. Yan<sup>1</sup>, G. Liu<sup>1</sup>, R. Deraniyagala<sup>1</sup>, I. Grills<sup>1</sup>, C. Stevens<sup>1</sup>, D. Krauss<sup>1</sup>, X. Ding<sup>1</sup>  
<sup>1</sup>Beaumont Health, Proton Therapy Center, Royal Oak, USA

**Purpose or Objective**

A comprehensive plan evaluation platform was established based on the daily Cone-Beam Computed Tomography(CBCT) to assess the treatment robustness quality between PTV based IMPT(PTV-IMPT) and CTV based robust optimized IMPT(ro-IMPT) planning strategies in bilateral Head and Neck Cancer (HNC) treatment.

**Material and Methods**

9 bilateral HNC patients' CT structure sets were used in this study. Daily CBCT were converted into synthetic-CT (sCT) for dose reconstruction. The accuracy of the proton dose calculation in sCT is cross-validated via the same day's verification-CT sim (vCT) with 3D gamma index comparison. PTV-IMPT and ro-IMPT were generated on the initial planning CT. CTV high-risk volume(CTV\_high) received 70Gy and CTV low/intermediate-risk(CTV\_low) received 60Gy. For PTV-IMPT, the PTVs were expanded 3mm from the CTV; For ro-IMPT, robust optimization used 3mm setup and 3.5% range uncertainties. Dose accumulations were then calculated on the 35 sets of daily sCT and the target coverages were compared to the initial plans.

**Results**

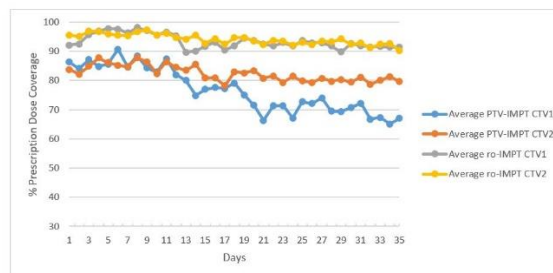
The 3D gamma index dose comparison (3mm/3%) showed an average pass rate of 98.2%+/-1.5% comparing the same day's pair of sCT and vCT with both plans (total 38 pairs). Through the dose accumulation of 35 treatment fractions, the PTV-IMPT plan group's mean V100 of CTV\_high/CTV\_low coverage degraded to 80.70%/85.73%

compared to 96.72%/96.13 of the ro-IMPT group (p<0.002). There was no significant difference in the OAR dose between the two planning strategies. One patient did have suboptimal coverage (CTV\_low <90%) even with ro-IMPT. Significant weight loss was noted for this patient during the treatment course (>5 lbs).

Table 1. Dose comparison between initial plan and dose accumulation from 35 fraction.

OAR	Planning Method	Initial Plan Mean (Range)	Accumulated Plan Mean (Range)
Brainstem max (cGy)	PTV-IMPT	1939 (703-2840)	2093 (1052-2714)
	ro-IMPT	1809 (933-2406)	1999 (1286-2682)
Spinal Cord max (cGy)	PTV-IMPT	2004 (1236-3258)	2516 (1283-3761)
	ro-IMPT	2204 (1489-3349)	2586 (1433-3655)
Ipsilateral Parotid mean (cGy)	PTV-IMPT	2943 (2104-3761)	3272 (2101-4276)
	ro-IMPT	2829 (2213-3465)	3178 (1903-3994)
Contralateral Parotid mean (cGy)	PTV-IMPT	1397 (862-1990)	1814 (1167-2697)
	ro-IMPT	1362 (983-2075)	1802 (1242-2979)
Mandible D0.1cc (cGy)	PTV-IMPT	6964 (6867-7007)	6986 (6708-7227)
	ro-IMPT	6993 (6865-7151)	7014 (6704-7132)
Larinx mean (cGy)	PTV-IMPT	4662 (3037-6152)	5030 (3327-6565)
	ro-IMPT	4674 (3100-6245)	4997 (3331-6288)
Oral Cavity mean (cGy)	PTV-IMPT	3391 (2102-4335)	3694 (2720-4703)
	ro-IMPT	3501 (2630-4917)	3749 (2736-5407)
Constrictor mean (cGy)	PTV-IMPT	5854 (5289-6266)	6003 (5377-6451)
	ro-IMPT	5699 (5152-6129)	5869 (5234-6385)
Constrictor V70Gy (%)	PTV-IMPT	23.3% (0-43.2%)	23.9%(10.9%-36.5%)
	ro-IMPT	19.7% (0-39.2%)	21.86%(0-40.6%)

Table 2. Average Dose Coverage to the target on the daily basis.



**Conclusion**

A comprehensive plan robustness evaluation platform based on the CBCT is established in our clinical workflow and enables dose accumulation and plan robustness evaluation on a daily basis. ro-IMPT demonstrated an optimal planning strategy over PTV-IMPT for bilateral HNC treatment. However, special cautions are needed for patients with significant weight or geometry changes.

**OC-0672 Proton radiotherapy for left-sided breast cancer in patients with pectus excavatum anatomy**  
 S. Korreman<sup>1</sup>, S. Andreassen<sup>2</sup>, J.B.B. Petersen<sup>1</sup>, B. Offeren<sup>3</sup>

<sup>1</sup>Aarhus University Hospital, Department of Oncology and Danish Center for Particle Therapy, Aarhus C, Denmark ;  
<sup>2</sup>Aarhus University, Department of Physics and Astronomy, Aarhus C, Denmark; <sup>3</sup>Aarhus University Hospital, Department of Oncology, Aarhus C, Denmark

**Purpose or Objective**

For breast cancer patients with challenging anatomy, such as pectus excavatum, it can be impossible to cover the entire breast and IMN without exceeding dose limits to the organs at risk using standard techniques. Proton therapy

may present a solution to this, and warrant referral of this subgroup of breast cancer patients for protons.

#### Material and Methods

Five patients with left-sided breast cancer, and visually confirmed pectus excavatum, were included in the study. Three treatment techniques were compared: Standard two-field tangential plans (forward planned using dynamic wedges and field-in-field techniques, plus occasional use of low-weight patch fields from other angles), VMAT with two arcs with separate isocenters, and IMPT using two or three fields (see figure 1). All treatment planning was done in the Eclipse TPS vs 13.7 (Varian Medical Systems). For all plans, the objective was to cover the PTV (whole breast plus IMN) within 95-107% of prescription dose 50Gy, with dose limits to whole heart ( $V_{40Gy}<5\%$ ,  $V_{20Gy}<10\%$ ), left anterior descending coronary artery (LAD,  $V_{20Gy}=0\%$ ,  $V_{10Gy}<5\%$ ) and lung ( $V_{20Gy}<25\%$ , mean dose  $<18Gy$ ).

#### Results

Target coverage was generally better in proton plans than in photon plans - see figure 2a - and was more consistent between patients for protons than for photons. For none of the patients could the minimum target dose of 95% be achieved for the entire PTV, however for proton plans  $V_{90\%}>99\%$  could be achieved for all patients, and  $V_{95\%}$  was always above 93%.

For organs at risk, proton plans could achieve doses below the dose limit levels for all patients and for all considered OAR. In figure 2b dose to LAD is shown for all plans. For whole heart, the mean[range]  $V_{40Gy}$  for the five patients was 1.2[0;5.6] for protons, 1.2[0.2;3.1] for VMAT and 9.2[0.8;16.7] tangential photon plans. The mean[range]  $V_{20Gy}$  was 1.7[0.7;2.3], 13.6[8.4;27.4] and 16.4[4.2;28.2] for protons, VMAT and tangential plans. Mean heart dose was 1.6[0.9;3.1]Gy, 11.4[7.5;15.1]Gy and 9.2[3.6;14.4]. For LAD,  $V_{20Gy}$  was 0 for all proton plans and  $V_{10Gy}$  was 1.4[0;3.7]. For VMAT photon plans LAD  $V_{20Gy}$  was 6.2[0;19.3], and  $V_{10Gy}$  was 46.5[16.9;80.8]. For tangential photon plans  $V_{20Gy}$  was 50.2[23.4;67.2] and  $V_{10Gy}$  was 56.3[28.8;75.5].

For lung, the mean[range]  $V_{20Gy}$  for the five patients was 15.6[14.3;17.7] for protons, 30.9[25.8;39.4] for VMAT and 34.7[24.3;51] for tangential photon plans. The mean[range] mean lung dose was 7.6[7;9.6]Gy, 17.2[15.6;21]Gy and 17.3[12.3;24.4]Gy.

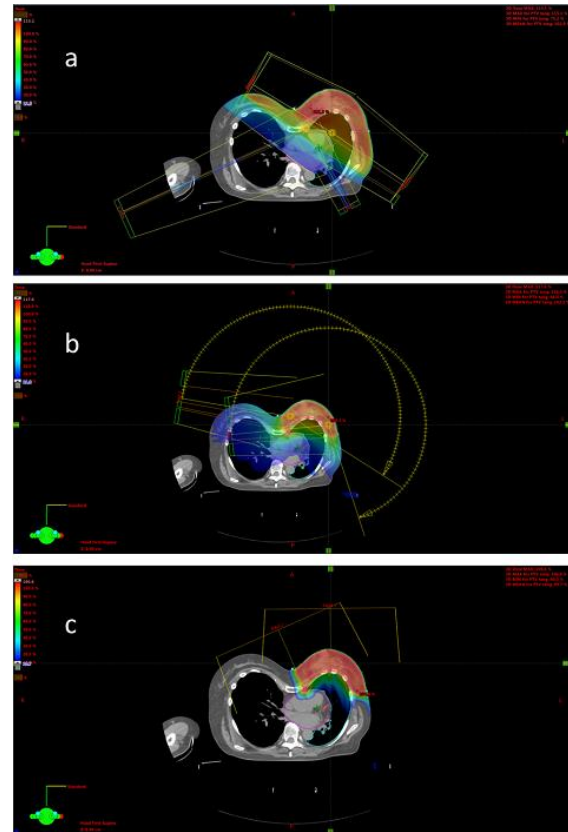


Figure 1:

The three planning techniques tested. (a) Tangential forward planned photon treatment using dynamic wedges and field-in-field, (b) Two-arc VMAT with separate isocenters, and (c) two-field proton IMPT.

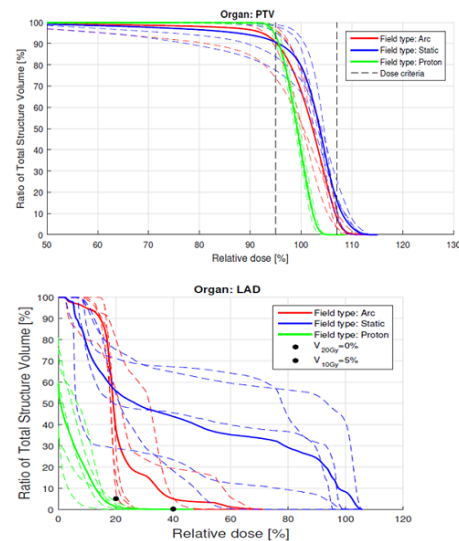


Figure 2:

DVHs for (a) target coverage and (b) LAD doses for the three planning techniques used. The dotted lines are for the separate patients, the solid lines are average DVHs over all patients.

#### Conclusion

For patients with left sided breast cancer, and the challenging anatomy pectus excavatum, proton therapy could advantageously be used to achieve adequate target coverage without compromising doses to organs at risk, for all patients included in this study. This could not be achieved for any of the patients using photon therapy with

any technique tested. For this subgroup of breast cancer patients the benefit from proton therapy is so large that it should be considered as an immediate indication for referral.

### OC-0673 LET variation as a function of different optimization approaches in proton beam therapy

G. Martino<sup>1</sup>, N. Van Lobenstein<sup>1,2</sup>, A. Carlino<sup>1</sup>, A. Resch<sup>3,4</sup>, M. Stock<sup>1</sup>, G. Kragl<sup>1</sup>

<sup>1</sup>MedAustron Ion Therapy Center, Medical Department, Wiener Neustadt, Austria; <sup>2</sup>Delft University of Technology, Faculty of Mechanical- Maritime- and Materials Engineering, Delft, The Netherlands; <sup>3</sup>Christian Doppler Laboratory for Medical Radiation Research for Radiation Oncology, Medical Radiation Research, Vienna, Austria; <sup>4</sup>Medical University of Vienna Austria, Department of Radiotherapy, Vienna, Austria

#### Purpose or Objective

Compared to photons, protons allow for decreased integral dose and an enhanced biological effectiveness, typically set to a constant value of 1.1. Amongst other factors, RBE depends on the LET of the projectile, which is increasing with decreasing proton energy. This creates concerns that a constant RBE might not sufficiently describe clinical situations where it is unavoidable to use beams stopping in front of critical OARs. In mixed particle fields, a dose-averaged LET ( $LET_d$ ) over the entire particle spectrum is a meaningful quantity to correlate to biological effect. In this work the computation of  $LET_d$  was performed with an MC algorithm available in a research version of the TPS RayStation. The  $LET_d$  computed in RS was benchmarked against Gate/Geant4. The aim of this work is to set up a validated tool to evaluate  $LET_d$  distributions resulting from different optimization strategies for cases with critical beam incidences.

#### Material and Methods

For LET benchmarking two regular shaped fields (box of  $5 \times 5 \times 5 \text{ cm}^3$ ) centered at a depth of 6 and 30 cm in water were optimized in RS and forward calculated in Gate/Geant4. All the plans were computed in a  $1 \times 1 \times 1 \text{ mm}^3$  dose grid. We compared depth  $LET_d$  profiles at the central axis of the two SOBPs and transverse  $LET_d$  profiles at three different depths corresponding to the distal part, central and proximal part of each SOBP. Plans were generated for a pediatric skull base case in RS using different optimization strategies (Single Field Optimization (SFO) and Multiple Field Optimization (MFO)), different number of beams (1 and 2), different maximum spot weights and number of distal energy layers (1 to 3).

#### Results

The benchmarking of RS against Gate/Geant4 showed an agreement within  $\pm 5\%$  for all depth  $LET_d$  profiles and transverse  $LET_d$  profiles analyzed (Fig. 1). The evaluation of Dose-Volume and LET-Volume Histograms within and around the PTV in our pediatric case showed that different optimization strategies lead to different dose and  $LET_d$  distributions in concentric rings around the PTV. Fig. 2 shows that the DVHs for a ring of 0.5 cm diameter around the PTV is similar for all optimization strategies. Here, the 2-fields SFO plan showed slightly higher integral doses. In all cases, the maximum value is the prescribed dose of 54 Gy(RBE). The corresponding  $LET_d$  showed lower values in the single-field plan in 60% and higher values in 40% of the ring volume. Very similar  $LET_d$  values were obtained in the SFO and MFO plans. The maximum  $LET_d$  value of the single-field plan is almost double if compared to the SFO and MFO plans.

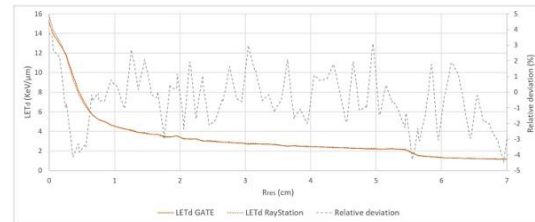


Figure 1: Depth  $LET_d$  profile computed with Gate/Geant4 (solid line) and with RS (dotted line) as function of residual range ( $R_{res}$ ) for the box placed at shallow depth (6 cm in water). The relative deviation in percent of the  $LET_d$  computed with RS from the  $LET_d$  computed with Gate/Geant4 is also shown.

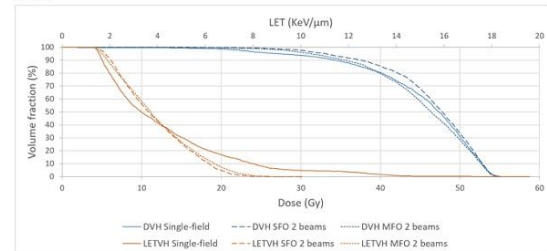


Figure 2: Dose-Volume histograms and LET-Volume histograms in a ring of 0.5 cm lateral distance from the PTV. The plans corresponding to three different optimization strategies are displayed: Single-field (solid line), two-fields SFO (dashed line) and two-fields MFO (dotted line).

#### Conclusion

$LET_d$  calculated by RS is in good agreement with Gate/Geant4 and offers a reliable tool for LET distribution display. Preliminary results suggest that 2-fields plans offer a better balance between  $LET_d$  and integral dose outside the target if compared to single-field plans. Altering the number of distal energy layers and the spot weight has an inferior impact (maximum 3% in the  $LET_d$ ) compared to increasing the number of beams.

#### Symposium: Focus on the Pelvic Region

### SP-0674 Status on adaptive strategies in the pelvic region - how far are we?

Y. Seppenwoolde<sup>1</sup>

<sup>1</sup>Medizinische Universität Wien, Department of Radiotherapy, Vienna, Austria

#### Abstract text

Despite the increased accuracy of irradiation techniques like IMRT and VMAT, sparing all organs at risk (OAR) in the pelvic area is still challenging because large changes in shape and position can be present due to variations in filling. With the introduction of cone-beam CT scanners and other on-board imaging systems, it became possible to observe these changes of internal organ configurations during each treatment fraction. Theoretically, this enables re-adaptation of plans according to tumour shrinkage and changes in OAR morphology, resulting in reduction of toxicity and better target coverage. Full online plan adaptation requires that re-delineation, re-optimizing of dose distributions and repetition of all legally required quality assurance steps should be performed in less than a few minutes. These workload intensive procedures would require a high degree of automation and workflow-integration that is still largely absent in off-the-shelf products.

Nonetheless, by finding a well-balanced compromise between full automation and degree of plan adaptation, it is possible to apply simplified schemes of adaptation that provides improved treatment. In clinical practice, different on- and offline methods are used. For cervix, bladder and rectum, volumetric imaging based library of plans, library of margins, 'ITV' with different steps of integration, (daily) reoptimisation or 'CBCT-guided evolutive library' are most appropriate,

often combined with an off-line way to detect tumor shrinkage. For cervix and bladder, inter/extrapolated motion prediction models can be generated based on pre-treatment imaging, though generation of these extra structures is still not straightforward and often based on in-house developed software.

For prostate, different ways of motion measuring are possible (i.e. implanted markers, RFID or ultrasound) because the prostate volume and shape remains primarily constant, just its global position varies, depending on surrounding organ filling/muscle motion. Tracking and gating can be used for the faster (intra-fraction) prostate motion.

For the library-based methods, plan selection is found to be robust: most studies show good correlation between online plan selection and offline clinician/expert panel plan selection; even with reduced image quality it is still possible to determine whether a target is within the pre-defined contours of the library. Reporting trustworthy dose-volume parameters to correlate with outcome is more of a challenge, as for the large and uncorrelated motion patterns in the pelvic region, DIR and dose warping algorithms are not well validated and re-delineation is too laborious (and not robust) on CBCT images to be used in clinical routine. Recent developments on CBCT based dose calculation are promising to improve this topic. An important aspect is patient safety: clinical (non-research) versions of commercial R&V software are not optimal for handling multiple plans of which only one is selected and the others disregarded, meaning that check and double check remains necessary to avoid mistakes. Robust and back-up procedures are necessary in case no decision can be made or if imaging fails.

#### SP-0675 Bladder filling - does it matter?

D. Bodusz<sup>1</sup>

<sup>1</sup>*Maria Skłodowska-Curie Memorial Cancer Center and Institute of Oncology, Radiotherapy Department, Gliwice, Poland*

##### Abstract text

Contemporary radiotherapy techniques of pelvic tumors may reduce normal tissue dose by conforming closely to target volumes. This allows reducing the toxicity of the treatment. To achieve this goal, it is necessary to reproduce the patient's position, the position of internal organs and their volume in accordance with the treatment plan performed in TPS (Treatment Planning System). The image guided radiation therapy techniques enable checking the position of internal organs as well as their volume. The protocol of preparation for radiotherapy includes obtaining the reproducibility of the bladder or rectum filling through the application of guidelines for patients. Many publications have shown the importance of bladder filling on CT images performed for treatment planning and bladder volume variations compared to the treatment plan during the whole course of radiotherapy. The main aim of this lecture is to summarize the available data in this topic, present our own experiences and give recommendations. This presentation will also focus on the discussion about various bladder preparation protocols, image guided radiotherapy techniques and on the impact of bladder volume on acute genitourinary toxicity.

#### SP-0676 MR-based treatment planning for prostate cancer

E. Persson<sup>1</sup>

<sup>1</sup>*Skåne University Hospital, Hematologi- Oncology and Radiation physics, Lund, Sweden*

##### Abstract text

MRI has today a given place in the radiotherapy workflow for several diagnoses. The superior soft tissue contrast of MRI makes it optimal for definition of the target area for radiotherapy. CT are traditionally used in the remaining

parts of the radiotherapy workflow, including delineation of organs at risk (OAR), treatment planning and reference images for patient positioning at treatment. For prostate cancer patients, MRI is optimal to differentiate between the prostate and surrounding soft tissues and OAR. To use the MRI for target definition requires a registration between the MRI and CT, often performed based on patient anatomy or fiducial markers in the prostate. This registration between two different image modalities are however associated with registration uncertainty. To avoid these registration uncertainties, which may occur when combining modalities, a radiotherapy workflow with MRI as the single modality has been proposed - called MRI-only. The reduction of uncertainty is especially important when radiotherapy is moving towards more precise techniques for treatment delivery and shrinking margins. An MRI-only radiotherapy workflow has great value for the patient, reducing the number of imaging sessions. To the clinic an efficient and possibly cost-reduced workflow are offered with simplified logistics.

To use MR as the single imaging modality in the radiotherapy workflow introduces technical obstacles. The systems used today in radiotherapy are traditionally based on CT-information and tasks such as treatment planning and patient positioning are not a straightforward procedure using MRI. Building an MRI-only workflow includes several changes of the current practice, where new tasks and new methods for quality assurance are needed. This includes quality assurance of the MRI for the purpose of treatment planning, generation of electron density information from the MRI referred to a synthetic CT or a pseudo CT to be used for treatment planning, identification of fiducial markers in the MRI and patient positioning strategies based on the MRI or synthetic CT information etc. Training and education plays also an important role of the implementation of new techniques and the introduction of new methods need to be performed in a safe way. The clinical implementation of MRI-only has been limited to a few centers, but recently the interest has increased and new clinics have started to adapt their own radiotherapy workflows to MRI-only. The clinical implementations covers both commercial solutions as well as in-house developed methods.

---

#### Joint Symposium: ESTRO-RANZCR: Radiotherapeutical management of oligometastatic disease

---

#### SP-0677 Oligometastatic Prostate SBRT: The How, What, Where and When

J. Martin<sup>1</sup>, P. Blanchard<sup>2</sup>, P. Greer<sup>1</sup>, P. Keall<sup>3</sup>, D. Pryor<sup>4</sup>, M. Sidhom<sup>5</sup>, S. Siva<sup>6</sup>, S. Supiot<sup>7</sup>, S. Turner<sup>8</sup>

<sup>1</sup>*Calvary Mater Newcastle, Radiation Oncology, Newcastle- Nsw, Australia*; <sup>2</sup>*Institute Gustave Roussy, Radiation Oncology, Villejuif, France*; <sup>3</sup>*University Of Sydney, Acrf Image X Institute, Sydney, Australia*; <sup>4</sup>*princess Alexandra Hospital, Radiation Oncology, Brisbane, Australia*; <sup>5</sup>*Liverpool Hospital, Radiation Oncology, Sydney, Australia*; <sup>6</sup>*peter Maccallum Cancer Centre, Radiation Oncology, Melbourne, Australia*; <sup>7</sup>*Institut De Cancérologie De L'ouest René-Gauducheau, Radiothérapie, Nantes, France*; <sup>8</sup>*Westmead Hospital, Radiation Oncology, Sydney, Australia*

##### Abstract text

Oligometastatic prostate cancer is a variably defined target, and an area of growing interest. One key question is how best to define this state, as prognosis will be dependent on the imaging modality used (conventional v functional), the tissues involved (nodal v bone v visceral), tempo of disease and the number of lesions detected (1 v 3 v 5 v more). Timing is also critical, given that the oligometastatic state can be detected either at diagnosis or following local treatment. There are options to

consider regarding the integration with systemic therapy. When detected at diagnosis, we also have an evolving understanding on the management of the primary tumour. The technical issues of delivering ablative or potentially immuno-stimulatory radiotherapy to such lesions raise their own challenges. Here we will explore the biology, technology and ongoing clinical trial activity in the oligometastatic state of prostate cancer.

#### SP-0678 SBRT for oligometastatic NSCLC

S. Senan<sup>1</sup>

<sup>1</sup>VU University Medical Center, Radiation Oncology, Amsterdam, The Netherlands

##### Abstract text

The oligometastatic paradigm suggests that patients with a limited number of metastases should be amenable to a curative treatment approach. The existence of an oligometastatic disease state in NSCLC is gaining acceptance. In the eighth edition of the American Joint Committee on Cancer staging system for lung cancer, a single extrathoracic metastasis (M1b) is staged as a separate disease entity than are patients with more widespread metastases (M1c). New insights in tumour biology also support the concept of aggressive treatment for oligometastases in order to improve outcomes [Turajlic S, Science 2016]. Metastatic spread can take place through multiple routes and in different directions, with metastases continuing to evolve after they have disseminated from the primary tumour. Potentially, metastases can re-infiltrate the primary tumour or surgical bed, a process called self-seeding. In addition, cross-metastatic seeding can occur, resulting in complex subclonal mixtures in the metastases themselves. Metastases present at the time a primary tumour is diagnosed are termed synchronous, whereas lesions presenting later (generally >3 months) are referred to as metachronous metastases.

In contrast to the considerable body of evidence in support of ablative stereotactic radiosurgery in patients with brain metastases, evidence in support for SBRT to oligometastases at any extracranial site was poor until recently. In metastatic NSCLC with so-called druggable mutations, the advent of effective systemic treatments has led to changes in ESMO and NCCN guidelines, both of which now recommend the ablative treatment of isolated lesions that grow after an initial response (oligorecurrence), or which fail to respond completely (oligopersistence). An individual patient data meta-analysis in 757 patients with 1-5 synchronous or metachronous metastases identified 3 prognostic risk groups by recursive partitioning analysis [Ashworth A, Clin Lung Cancer 2014]. A good prognostic group identified were patients presenting with metachronous metastases (5-year Overall Survival 48%), an intermediate risk group presenting with synchronous metastases and no nodal metastases (5-year Overall Survival 36%), and a poor prognostic group with synchronous metastases and regional nodal disease (5-year Overall Survival 14%). Direct evidence for SBRT in metachronous disease has come from the SABR-COMET trial, which randomly assigned 99 patients who had a controlled primary malignancy and 1-5 metastatic lesions to receive either palliative standard of care (SOC) treatments alone [control arm] or with SABR to all metastatic lesions [SABR arm] [Palma DA, ASTRO 2018]. Of these, 19 patients had a diagnosis of lung cancer. Median overall survival was 28 months in the control arm (95% CI 19-33 months) versus 41 months in the SABR arm (95% CI: 26 months to 'not reached'; p=0.09). Median progression-free survivals were 6.0 months (95% CI: 3.4-7.1 months) versus 12 months, respectively (95% CI: 6.9-30 months; p=0.001). Although grade 3 and higher toxicities were commoner with SBRT, no decreases in quality of life were observed. These findings represent the strongest clinical evidence

available in support of SBRT in the metachronous oligometastatic state across many tumor types. In synchronous oligometastases, the findings from 3 small studies, including 2 randomized trials, suggested that adding local ablative therapy (including SBRT) in such patients could improve progression-free survivals (ranging from 9.7-11.9 months) versus only standard of care (range 3.5-3.9 months) [Gomez DR, Lancet Oncol 2016; Iyengar P, JAMA Oncol 2017; Petty WJ, IJROBP 2018]. An update from one such study suggested that the overall survival was also improved by the addition of local ablative therapy [Gomez DR, ASTRO 2018]. However, there is a clear need to perform adequately powered, prospective randomized clinical trials to address this issue, especially given recent improvements in systemic therapy of NSCLC patients without any driver mutation. Recently, a multi-disciplinary group recommended guidelines for conducting trials of synchronous oligometastases, which could serve to have ensure more uniform trial eligibility criteria [Dingemans A, WCLC 2018]. The key elements of this document were as follows: (i) The definition, based on a systematic review, is to have a maximum number of 5 metastases, and limited to 3 organs. (ii) Eligible patients should have disease where a radical treatment is technically feasible with acceptable toxicity, taking into account all sites, that may modify the course of disease leading to a long-term disease control. (iii) All disease sites must be technically and safely treatable aiming for long-term control. (iv) Mediastinal lymph node involvement must be considered as locoregional disease in this definition. Other issues relating to trial design, as well as technical challenges in SBRT delivery, will be addressed during the talk.

#### SP-0679 Challenges in SBRT physics

T. Kron<sup>1</sup>

<sup>1</sup>Peter MacCallum Cancer Center, Physical Sciences, Melbourne, Australia

##### Abstract text

Background: Stereotactic Body Radiation Therapy (SBRT) has become in very short time an accepted treatment approach within radiation oncology. SBRT utilizes many features of modern radiotherapy technology, such as image guidance, motion management and small often intensity modulated fields, to deliver high biologically effective doses of radiation in very few fractions. It is the purpose of this presentation to highlight technological challenges in this context.

##### Argument

From a physics perspective challenges in SBRT can broadly be divided into three groups related to: i) equipment and software, ii) patient selection and set-up, and iii) target definition and re-identification during image guidance. Commissioning of equipment, such as 4DCT and small field dosimetry, has traditionally the first hurdle for the implementation of SBRT. For most of these tasks there are now standard solutions, protocols and recommendations that provide guidance for this work. While there are always emerging issues such as the combination of contrast injection and motion management, technical progress with equipment and the emergence of audits specifically designed for SBRT delivery contribute to generally safe implementation pathways. Patient positioning and immobilization may be more challenging as each patient is different. Long treatment times and various motion management options add to the complexity. Reproducibility of set-up feeds directly into decisions as to what image guidance method is appropriate and how frequently it would need to be applied. A particular challenge is the fast and reliable interpretation of the acquired images, which in many institutions leads to the requirement of radiation oncologists being present during image guidance.

Automation, and computer aided image interpretation are emerging to address these issues.

#### Conclusion

SBRT has enriched the practice of radiation oncology. This has not been without challenges and technical and workflow issues highlight the need to engage the whole multidisciplinary team for successful SBRT implementation.

#### SP-0680 Hints on optimal dose and fraction number from lung SBRT

R. Ruggieri<sup>1</sup>

<sup>1</sup>Sacro Cuore Don Calabria Hospital, Radiation Oncology, Negrar, Italy

#### Abstract text

Initial lung SBRT treatments [1] suggested that the LQ-model for cell survival (CS) might be inadequate at as high doses per fraction ( $d$ ) as 20 Gy. However, when compared with more complex LQL-models, the LQ-model produced equivalent goodness-of-fit for in vitro CS data even at high  $d$ -values, if a dose-range dependence from  $\alpha$  and  $\beta$  parameters was recognised [2]. When different CS-models were next used for BED, and hence TCP, computations, equivalence in goodness-of-fit resulted also for local-control data of early-stage NSCLC [3]; thus supporting the LQ-model, given its least number of free parameters, as the most appropriate CS-model for fitting TCP from SBRT of early-stage NSCLC. Further, when intra-tumour  $\alpha$ -heterogeneity was also included in TCP modeling of local-control data from lung SBRT, to deal with the hypothesis that tumor response is determined from the most radioresistant tumour clonogen sub-population, the goodness-of-fit from the LQ-model was even superior to the alternative LQL-models [4].

Once meta-analyses supported the existence of a dose-response relationship for SBRT of early-stage NSCLC [5], and then for oligometastatic lung lesions [6], with saturation of the effects over some threshold dose, the prescription of a minimum total BED of 100Gy<sub>10</sub> became the golden rule. Such threshold, however, might be modulated according to the tumour volume [7]: by reducing the dose to the smaller tumours (<3cm), so as by increasing the dose to the larger ones (>5 cm). Further, already from the Metha's analysis [5] it was deducible a wide increase in the necessary dose to get from the 3-fractions schedule the same level of local-control of the schedules with 4-5 fractions.

The above two observations, that a radioresistant clonogen sub-population might play a key role in severe hypofractionation, and that schedules with 4-5 fractions may be isoeffective although the use of a reduced dose (BED) with respect to 3-fractions schedules, strongly suggest that tumor hypoxia and its reoxygenation may be pivotal to lung SBRT. In support of this hypothesis, *in vivo* evidence was reported since 1975 of an 'inverse' dose behaviour between 3 and 5 fractions: i.e.,  $D_{50}(n=5)$  lower than  $D_{50}(n=3)$  [8]. Models including tumour hypoxia were able to reproduce such 'inverse' dose behaviour [9-10], by the re-sensitizing effect of reoxygenation, thus supporting the use for lung SBRT of schedules with  $\geq 5$  fractions, instead of 3 fractions [11]. By modeling reoxygenation in terms of a mono-exponential time factor [11], it is also possible to explain the wide (30%) observed difference in 3-year local control after lung SBRT, if alternate instead of consecutive days for treatment were used [12]. In conclusion, without the need to invoke any different cell-killing effect of radiation as a function of the  $d$ -value, tumour hypoxia seems to be the likely determinant of the optimal dose, number of fractions, and inter-fractions time-interval for lung SBRT.

#### References:

1. Timmerman R, et al. *Chest* 2003;124:1946-55
2. Wang JZ, et al. *Science Transl Med* 2010;2(39):39ra48. doi: 10.1126/scitranslmed.3000864

3. Guckenberger M, et al. *Radiother Oncol* 2013;109:13-20
4. Shuryek I, et al. *Radiother Oncol* 2015;115:327-334
5. Metha N, et al. *Pract Rad Onc* 2012;2:288-95
6. Guckenberger M, et al. *Radiother Oncol* 2016;118:485-91
7. Ohri N, et al. *Int J Rad Onc Biol Phys* 2012;84:e379-e384
8. Fischer JJ, Moulder JE. *Radiology* 1975;117(1):179-84. doi: 10.1148/117.1.179
9. Stavreva NA, et al. *Med Phys* 2005;32(3):720-5
10. Ruggieri R. *Phys Med Biol* 2004;49:4811-23
11. Ruggieri R, et al. *Phys Med Biol* 2013;58(13):4611-20.
12. Alite F, et al. *Radiother Oncol* 2016;121:9-14

---

#### Symposium: Plan of the day - present status and future aims

---

#### SP-0681 Online adaptive planning in pancreatic cancer

O. Bohoudi<sup>1</sup>

<sup>1</sup>VUMC, Radiotherapy, Amsterdam, The Netherlands

#### Abstract text

In recent years there has been growing interest in using stereotactic body radiotherapy for treatment of pancreatic cancer. Upper abdominal tumours such as pancreatic cancer are particularly suitable for performing adaptive treatment planning, because of the dynamic nature and proximity of several critical normal organs such as the duodenum, stomach and bowel. Recently, MR-guided RT systems have been clinically implemented, offering exceptional options for stereotactic and adaptive radiotherapy which necessitates fast and robust online planning. The aim of this talk is to describe and discuss an adaptive online strategy which can be performed within minutes, and only requires limited (re-)contouring by the physician.

#### SP-0682 Future developments in adaptive strategies

U. Oelfke<sup>1</sup>

<sup>1</sup>The Institute of Cancer Research, Joint Department of Physics, Belmont, United Kingdom

Abstract not received

#### SP-0683 Clinical results of PotD strategies

S. Hafeez<sup>1</sup>

<sup>1</sup>The Institute of Cancer Research and The Royal Marsden NHS Foundation Trust, Radiotherapy and Imaging, London, United Kingdom

#### Abstract text

Radiation technologies permitting high quality on-line imaging have demonstrated that the target for radiotherapy is dynamic. Many dosimetric studies have illustrated that accommodating for the individual's actual anatomical change offers opportunity for margin reduction with subsequent improved target coverage and normal tissue sparing. Clinical feasibility of this approach has also now been shown.

There are many examples in medicine where pressures and demands for high-tech treatment have led to widespread implementation of innovation before, or even without, robust evidence has been generated. Arguably, well-designed clinical trials remain the optimal method to demonstrate outcome benefit for patients. At present, how best to utilise this adaptive strategy in order to maximise the clinical gains for our patients remains to be determined. Head to head comparative studies of adaptive techniques may not be ambitious enough to demonstrate true potential. Instead it may be necessary to leverage the improved therapeutic ratio to deliver radiotherapy in circumstances that would have been otherwise challenging.

The aim of this talk is to present an overview of the current clinical evidence base, to discuss the trials in development that will provide future evidence base, and the challenges associated with clinical evaluation of technological innovation.

**SP-0684 MRI online ART: opportunities and pitfalls**  
**V. Valentini<sup>1</sup>**

<sup>1</sup>*Policlinico Universitario Agostino Gemelli-, Dipartimento di Diagnostica per immagini- Radioterapia Oncologica ed Ematologia, Roma, Italy*

**Abstract text**

The recent introduction of the magnetic resonance guided radiotherapy (MRgRT) delivery units leads to the possibility to reduce most of the sources of uncertainty that currently influence radiation therapy treatments delivery. The more reliable visualization of the therapy volumes, achieved through the higher soft-tissue contrast provided by the MR imaging and the possibility to monitor the tumour and organs at risk (OARs) position during the treatment fraction using a high-temporal resolution MR cine imaging, address indeed the main pitfalls of standard delivery approaches.

Besides these technological advances, the main advantage offered by the MRgRT is the possibility to online adapt the RT treatment plan, changing the dose distribution while the patient is still in treatment position and successfully taking into account the anatomy of the day. Aim of this talk is to describe and discuss the opportunities and pitfalls of this innovative approach, highlighting its role in managing the inter and intrafraction motion variability, the segmentation strategies to date available and the dosimetric aspects of this technique.

---

**Debate: This house believes that immunotherapy is really changing radiation oncology**

---

**SP-0685 For the motion: This house believes that immunotherapy is really changing radiation oncology**  
**E. Deutsch<sup>1</sup>**

<sup>1</sup>*Institut Gustave Roussy, Radiation Oncology, Villejuif, France*

**Abstract text**

RT has been used for more than a century for the clinical management of virtually all cancers with extraordinary results, both in terms of side effects and efficacy. Immunotherapy is revolutionizing the clinical management of patients affected by an increasingly wide array of tumors. However, a limited percentage of patients achieve long-term clinical benefits from immunotherapy employed as a standalone treatment, calling for the development of combinatorial regimens. Radiation therapy (RT) stands out as a particularly promising candidate in this setting, reflecting not only its established safety profile, but also the potential ability of RT to mediate robust immunostimulatory effects that may synergize with immunotherapy in systemic tumor control. Combining RT with immunotherapy is a logical approach to enhance local and systemic anti-tumour immunity in locally advanced and metastatic cancers to improve outcomes in previously incurable cancer. However, optimal radioimmunotherapy regimens may call for the redefinition of conventional RT doses and fractionation schedules. We will have to redesign RT regimens for radioimmunotherapy to mediate superior efficacy in the presence of limited side effects. Revisiting doses and fractionation schedules, reducing delivery volumes, sparing both draining lymph nodes, limiting the use of cytotoxic chemotherapeutics, employing radiomics to longitudinally monitor responses.

**SP-0686 Against the Motion: This house believes that immunotherapy is really changing radiation oncology**

**Michael Baumann<sup>1</sup>, Nadja Ebert<sup>2</sup>**

<sup>1</sup>*German Cancer Research Center Dkfz, Radiobiology/ Radiooncology, Heidelberg, Germany*

<sup>2</sup>*German Cancer Research Center Dkfz,*

*Radiobiology/ Radiooncology, Heidelberg, Germany*

**Abstract text**

In this debate arguments will be given against the motion that immunotherapy is really changing radiation oncology. In particular, it will be pointed out that clinical evidence for a breakthrough by combining radiotherapy with immunotherapy is shaky. Worse, no good biomarkers are available to predict response of immunotherapy alone, not to speak about biomarkers in the context of radioimmunotherapy. Ideas on rationales and mechanisms are plentiful, however supportive data for these ideas are rare and weak. Further details will be revealed during the debate.

**SP-0687 Combining Radiotherapy with Immunotherapy: focus on immunocytokines**

**Philippe Lambin<sup>1</sup>, R. Lieverse<sup>2</sup>, E.J. Van Limbergen<sup>3</sup>,**

**V. Olivo Pimentel<sup>1</sup>, D. Marcus<sup>2</sup>, A. Van Der Wiel<sup>1</sup>,**

**J. Theys<sup>1</sup>, A. Yaromina<sup>1</sup>, L.J. Dubois<sup>1</sup>, A. Hoeben<sup>4</sup>,**

**A.M. Dingemans<sup>5</sup>**

<sup>1</sup>*Maastricht University, Department of Radiotherapy, Maastricht, The Netherlands*

<sup>2</sup>*Maastricht University, Department of Radiotherapy, Maastricht, The Netherlands*

<sup>3</sup>*Maastricht University, Grow-School for Oncology And Developmental Biology, Maastricht, The Netherlands*

<sup>4</sup>*Maastricht University, Department of Medical Oncology, Maastricht, The Netherlands*

<sup>5</sup>*Maastricht University, Department of Pneumology, Maastricht, The Netherlands*

**Abstract text**

The advent of immunotherapy is currently revolutionizing the field of oncology, where different drugs are used to stimulate different steps in a failing cancer immune response chain. Radiotherapy modifies the tumor microenvironment, causes the release of tumor (neo)antigens and immunostimulatory signals, which can enhance the effect of immunotherapy. This talk will explore the possibility of bimodal treatment combining radiotherapy with immunotherapy, in particular immunocytokines (“push the accelerator approach”) rather than checkpoint inhibitors (“release the break approach”). L19 targets the extra domain B (ED-B) of fibronectin, a marker of tumor neoangiogenesis, and can be used as immunocytokine when coupled to Interleukin 2 (IL2). We hypothesized that radiotherapy in combination with L19-IL2 provides an enhanced antitumor effect, which is in particular dependent on ED-B expression. In summary, we have shown in several preclinical models that radiotherapy (RT) combined with L19-IL2 can induce a long-lasting antitumor effect (including a “memory effect”), dependent on ED-B expression and infiltration of cytotoxic T cells. We have shown that this effect is comparable if not superior to anti-tumor effect of checkpoint inhibitors (e.g. anti PD(L)-1) combined with single dose radiotherapy. Having recently completed a phase I safety clinical trial (NCT02086721), these promising preclinical studies will be translated to a multicentric, H2020 funded, randomized Phase II clinical study in NSCLC patients with less than 10 metastases ([www.immunosabr.info](http://www.immunosabr.info), see this link for the Youtube animation: <https://youtu.be/6wDE6RkriKA>).

References: In Press.2. Van Limbergen EJ, De Ruyscher DK, Olivo Pimentel V, Marcus D, Berbee M,

Hoeben A, Rekers N, Theys J, Yaromina A, Dubois LJ, Lambin P. Combining radiotherapy with immunotherapy: the past, the present and the future. *Br J Radiol.* 2017 May 25;20170157.3. Rekers NH, Zegers CM, Germeraad WT, Dubois L, Lambin P. Long-lasting antitumor effects provided by radiotherapy combined with the immunocytokine L19-IL2. *Oncoimmunology.* 2015 Apr 2;4(8):e1021541.4. Nicolle. H. Rekers, Catharina. M. L. Zegers, Ala Yaromina<sup>1</sup>, Natasja. G. Lieuwes, Rianne Biemans, Birgit L.M.G. Senden-Gijsbers, Mario Losen, Evert Van Limbergen, Wilfred T.V. Germeraad, Dario Neri, Ludwig Dubois, Philippe Lambin. Combination of radiotherapy with the immunocytokine L19-IL2: additive effect in a NK cell dependent tumour model. *Radiother. Oncol.* 20155. Rekers NH, Catharina. M. L. Zegers, Ala Yaromina<sup>1</sup>, Natasja. G. Lieuwes, Rianne Biemans, Birgit L.M.G. Senden-Gijsbers, Mario Losen, Evert Van Limbergen, Wilfred T.V. Germeraad, Dario Neri, Ludwig Dubois, Philippe Lambin. Combination of radiotherapy with the immunocytokine L19-IL2: additive effect in a NK cell dependent tumour model. *Radiother. Oncol.* 20156. Zegers CM, Rekers NH, Quaden DH, Lieuwes NG, Yaromina A, Germeraad WT, Wieten L, Biessen EA, Boon L, Neri D, Troost EG, Dubois LJ, Lambin P. Radiotherapy combined with the immunocytokine (L19-IL2) provides long-lasting anti-tumor effects. *Clin Cancer Res.* 2014 Dec 31.

**SP-0688 Against the motion: we don't need Costalotamab when we have SBRT**

M.Joiner<sup>1</sup>

<sup>1</sup>*Karmanos Cancer Institute Wayne State University, Detroit, USA*

Abstract not received

---

**Debate: This house believes that patients with squamous cell cancer of the esophagus no longer need surgery**

---

**SP-0689 For the motion**

F.Cellini<sup>1</sup>

<sup>1</sup>*Università Cattolica del Sacro Cuore, Radiation Oncology Gemelli ART, Rome Italy*

Abstract not received

**SP-0690 Against the motion**

B. Wijnhoven<sup>1</sup>

<sup>1</sup>*Erasmus Medical Center Rotterdam, Rotterdam, The Netherlands*

Abstract not received

**SP-0691 For motion**

M. Hulshof<sup>1</sup>

<sup>1</sup>*Academic Medical Center, Dept Radiation Oncology, Amsterdam, The Netherlands*

**Abstract text**

Longterm locoregional recurrences (LR) after definitive CRT in SCC still occurs in about 35% and is significantly worse compared LR rates after pCRT + S (13%). Even in patients with a good initial clinical response LR is in favour of surgery although overall survival is comparable. Treatment morbidity, quality of life and treatment costs are generally considered in favour of dCRT. Thus there is a need for application of more organ sparing treatment. Studies will be discussed that on one hand are trying to improve the outcome of dCRT (dose escalation, endoscopic resection, new drugs) and on the other hand will improve

the selection of good responding patients by histological or radiological response assessment.

**SP-0692 Against the motion This House believes that patients with Squamous Cell Carcinoma (SCC) of Oesophagus no longer need surgery**

W. Allum<sup>1</sup>

<sup>1</sup>*Royal Marsden Hospital Trust and Institute of Cancer Research, Surgery, London, United Kingdom*

**Abstract text**

The management of oesophageal SCC is a fully multidisciplinary process. There are options for treatment and the selection for an individual patient requires careful discussion in the context of each individual's health, stage of disease and personal wishes. The availability of options stimulates significant differences in opinion amongst all oncology disciplines, not only reflecting available evidence but also the pattern of disease epidemiologically. Across Europe there are significant variations with surgery, usually with neoadjuvant treatments, in some centres and definitive chemoradiotherapy in others. In the UK there is an apparent 50:50 split between surgery and chemoradiotherapy. National audit data show similar results stage for stage. Furthermore many UK patients have significant co-morbidity precluding radical surgery. Despite the sensitivity of oesophageal SCC to combination chemoradiotherapy, the rates of recurrence vary. This can occur as residual disease at the end of treatment or recurrent disease some time after treatment. Past series have indicated that salvage surgery was hazardous with limited survival. However more recent series have shown that although complication rates are greater than primary surgery, in experienced centres these rates are manageable. Furthermore 5 year survival rates show similar outcomes for planned surgery after neoadjuvant treatment and for salvage surgery. As a result the option of more selective surgery needs further investigation with not only the evaluation of surveillance programmes but also to address patient preferences based on careful discussion of all evidence. There is therefore still a definite place of surgery in the treatment of oesophageal SCC.

---

**Symposium: Controversies in the management of brain metastases**

---

**SP-0693 Whole brain irradiation with hippocampal avoidance**

A. Grosu<sup>1</sup>

<sup>1</sup>*Universitätsklinik Freiburg, Dept. of Radiation Oncology, Freiburg, Germany*

**Abstract text**

In patients with multiple brain metastases of solid tumors a whole brain radiotherapy (WBRT) is the most widely used treatment option. WBRT is associated with considerable neurotoxicity and may reduce the patients' quality of life. It is known that neural stem cells are located in the hippocampal region, supporting lifelong neurogenesis. The reduction of hippocampal functions like learning and memory as a consequence of WBRT is explained by damage to neural stem cells and by a lower ability for regeneration of neuron populations. Avoidance of neural stem cells in hippocampus may help to reduce the neurotoxicity of WBRT. Several studies have shown that a dose escalation to the brain metastases contribute to better local tumor control and putatively longer overall survival. By the use of new irradiation techniques a WBRT with hippocampal sparing and concomitant boost to the metastases (HA-WBRT) is feasible. The HIPPORAD - NOA 14 project aims to investigate the benefits of HA-WBRT compared to WBRT

without hippocampal avoidance on memory performance of patients treated for brain metastases. On a second level, structural and functional changes of the brain will be investigated which underly the neurocognitive side-effects of both treatments applying state-of-the-art neuroimaging techniques. It is hypothesized that the novel, recently established technique of WBRT with dose escalation to brain metastases and hippocampal avoidance minimizes the side-effect of cognitive deterioration while at the same time providing an optimal treatment for brain metastases.

**SP-0694 Radiosurgery alone in multiple brain metastases**

J. Zindler<sup>1</sup>

<sup>1</sup>*Erasmus MC, Radiotherapy, Rotterdam, The Netherlands*

**Abstract text**

Stereotactic radiosurgery (SRS) alone is a promising treatment strategy in the multimodality treatment of brain metastases (BM). Especially in low volume BM high local control rates can be achieved. Compared to whole brain radiotherapy (WBRT) it is assumed that the risk of side effects such as alopecia, fatigue, and neurocognitive damage is less and thereby quality of life is better preserved. Disadvantages of radiosurgery alone is the relatively high risk of development of new brain metastases during follow-up and a risk of symptomatic radionecrosis, especially in high volume BM. These disadvantage may impair quality of life of the patient. In the setting of more than 3 BM there is no level I evidence for the use of SRS in both low as high volume BM. Also for the use of WBRT, there is a general lack of level I evidence, especially since the publication of the QUARTZ trial in the primary setting (Mulvenna 2016), but also after the EORTC-trial (Kocher 2011/Solfiotti 2013) in the elective setting. Nowadays SRS is generally accepted as a treatment option for patients with a maximum of 3 BM. The main question is if SRS preserves better quality of life than WBRT in the setting of more than 3 BM, taking into account both the advantages as the disadvantages of SRS. This question is addressed in the Dutch NCT02353000 trial (Zindler 2017). Another potential value of SRS in the setting of a multimodality treatment with immunotherapy (Schoenfeld 2015) is the induction of a so called abscopal effect. Also upfront SRS in the setting of targeted agents is a promising treatment strategy to enhance penetration of the blood-brain barrier (Magnuson 2017). In conclusion, SRS is a promising treatment strategy for patients with more than 3 BM, but also in a multimodality approach with immunotherapy and targeted agents. In a rapidly changing field with more and more systemic treatment options, both the use of SRS as WBRT needs to be redefined in the setting of BM.

**SP-0695 Systemic treatment as alternative or addition to radiotherapy**

Nicolaus Andratschke<sup>1</sup>

<sup>1</sup>*University Hospital Zürich, Department of Radiation Oncology, Zurich, Switzerland*

**Abstract text**

Brain metastases are common events in the natural course of many metastasized solid cancers like breast, lung and renal cancer or melanoma with a cumulative risk of 10-30% in adults. Radiotherapy has been the mainstay of treatment and cytotoxic systemic therapy was not considered a viable option as sole treatment strategy.

Still in recent years, complex treatment strategies have been developed and this has impacted on the general management of brain metastases, although formal comparative level I evidence is still missing.

As a prime example, management of NSCLC patients with brain metastases has changed significantly since the

introduction of potent TKI drugs targeting specific driver mutations with significant CNS efficacy. The role of immunotherapy in treating BM is less clear, but initial reports tend to challenge upfront local brain directed treatment as well. Regardless of the recent advances CNS failure remains a significant challenge in these patients and there is a clear need to precisely define the role and optimal timing of local therapies. This will be critically reviewed in the context of BM from NSCLC as we.

Finally, a quick look to BM from melanoma and breast cancer will reveal similarities and differences in the management of BM compared to NSCLC.

**SP-0696 Integration of surgery and radiosurgery**

S. Blamek<sup>1</sup>

<sup>1</sup>*Maria Skłodowska-Curie Institute and Cancer Center-Gliwice Branch, Department of Radiotherapy, Gliwice, Poland*

**Abstract text**

The results of recently published randomized clinical trials indicate that radiosurgery should be preferred over whole brain radiotherapy (WBRT) in patients with resected brain metastases. Along with the results of the studies showing the advantages of SRS as opposed to WBRT in patients with intact metastases, they put radiosurgery in the position of the first choice treatment in patients metastatic disease in the brain. Nevertheless, there is still a number of patients who will benefit from neurosurgical resection of the metastatic tumor. Patients with large lesions, tumors with cystic component, presenting symptoms of mass effect and compression of neural structures are pointed out as potential candidates for surgery. On the other hand, there is emerging evidence that good outcome in patients with large metastases treated with hypofractionated radiosurgery can be achieved even in patients harboring tumours exceeding 4 cm in diameter. It is now commonly accepted that the limiting factor for the use of radiosurgery is not the number of metastases but rather the total volume of the tumours in the brain. It is true for single fraction treatment but in case of fractionated treatment the total volume of the neoplasm may play less important role. Consequently, the indications for surgical treatment in case of single and multiple metastases both in the setting of primary management and salvage after treatment failure are evolving. There is also much controversy about target definition for radiosurgery in case of postoperative treatment. Cavity shape and volume change over time which makes timing of postoperative radiosurgery one of the factors influencing outcome. Alternatively, preoperative radiosurgery emerges as a solution, potentially allowing for combination of benefits of surgery and radiosurgery without jeopardizing outcome, especially in the context of postulated association between surgical procedure and the risk of leptomeningeal disease. Finally, the issue of differentiation between radiation necrosis and tumour progression is gaining importance. The patients are followed up with MRI after the initial treatment which allows for detection of tumor volume increase far before clinical symptoms become apparent. It results with more effective salvage treatment but at the same time the risk of unnecessary intervention is increased and the first choice salvage treatment less obvious.

---

**Symposium: Improving delineation in RT: not only for the doctor**

---

**SP-0697 How to handle clinical inter-observer variation in contouring assessment**

M. Gooding<sup>1</sup>

*<sup>1</sup>Mirada Medical Limited, Science and Medical Technology, Oxford, United Kingdom*

#### Abstract text

“You don't learn to walk by following rules. You learn by doing, and by falling over” - Richard Branson.

To learn from our mistakes, we need to understand that we have made them first, and then find ways to address them. In this talk, we will look at the ways through which we can assess contouring accuracy, including quantitative, qualitative and dosimetric approaches, giving examples from published literature. However, such assessment is often confounded by clinical inter-observer variation, so we will also consider how we can address this in our assessments and consider its potential clinical implications. We will summarise by discussing what approaches can be taken to help us improve contouring quality.

#### SP-0698 CT-based delineation: What can we gain from state-of-the-art CT image acquisition and reconstruction techniques

C. Richter<sup>1,2,3,4</sup>, F. Negwer<sup>1</sup>, E.C. Troost<sup>1,2,3,4,5</sup>, P. Wohlfahrt<sup>1,2</sup>

<sup>1</sup>Oncoray - National Center For Radiation Research in Oncology, Faculty of Medicine and University Hospital Carl Gustav Carus- Technische Universität Dresden-Helmholtz-Zentrum Dresden - Rossendorf- Dresden-Germany, Dresden, Germany; <sup>2</sup>Helmholtz-Zentrum Dresden-Rossendorf, Institute Of Radiooncology, Dresden, Germany; <sup>3</sup>Department of Radiotherapy and Radiation Oncology, Faculty Of Medicine and University Hospital Carl Gustav Carus- Technische Universität Dresden, Dresden, Germany; <sup>4</sup>German Cancer Consortium Dktk, Partner Site Dresden, Dresden, Germany; <sup>5</sup>National Center for Tumor Diseases NCT, Partner Site Dresden, Dresden, Germany

#### Abstract text

X-ray computed tomography (CT) has been the standard imaging modality in radiation oncology for both, treatment planning and delineation of targets and organs at risk for decades. For further improvement, especially for delineation, magnetic resonance imaging (MRI) and positron emission tomography (PET) are being extensively investigated and more often included into clinical routines. They can provide better soft tissue contrast and functional information. Still, also in the field of CT imaging relevant improvements have been made, that are not so much in the spotlight. Hence, this talk will focus on novel CT image acquisition and reconstruction techniques and their potential benefit for radiation oncology applications.

First, the potential value of dual-energy CT (DECT) for delineation will be discussed. DECT has already been proven to allow for a more accurate treatment planning, especially in particle therapy. It provides additional tissue information compared to conventional CT imaging. Furthermore, DECT enables the reconstruction of different CT datasets with varying image contrasts. Currently, it is unproven whether this additional information translates into improvement of the segmentation and delineation quality. The exploration of this benefit in combination with machine learning approaches is envisioned. First studies will be presented. Second, the potential of iterative CT reconstruction methods will be highlighted. They allow for a substantial reduction of imaging dose to reach a similar noise level as conventional filtered back projection. Hence, iterative reconstruction is of high relevance for adaptive protocols as it reduces the dose burden from more frequent CT imaging during treatment.

Third, the value and challenges of metal artefact reduction algorithms will be covered. It has been shown that the visual image impression can be substantially

improved for regions suffering from metal artefacts in conventional CT reconstruction, suggesting a direct benefit for delineation purposes. However, as these algorithms can also quantitatively alter the image in regions not influenced by metal artefacts, great care should be taken - especially in particle therapy planning. In summary, state-of-the-art CT imaging can provide additional value for radiation oncology purposes. This talk aims to increase awareness of this potential. By revisiting the institutional imaging protocol, one can potentially improve the image quality for delineation and/or safe dose to patients.

#### SP-0699 Development of MR techniques focused on improved delineation

M. Philippens<sup>1</sup>

<sup>1</sup>UMC Utrecht, Department of Radiation Oncology- Q.00.3.11, Utrecht, The Netherlands

#### Abstract text

Tumor delineation and delineation of organs at risk is an important but still difficult step in steering the dose in the treatment planning. Contouring of the tumor is mostly guided by changes in anatomy, asymmetry, and contrasts in the images. Also for the delineation of OAR contrast is needed to distinguish the organ from the background. As CT contrast of soft tissues is limited even after contrast administration, MRI is a logical choice to improve contrasts. The MR signal originates from the protons in water or fat. By manipulating the signal in a MR sequence the contrast can be adjusted. The delineation of gross tumor tissue (GTV) is in conventional radiotherapy mostly restricted to the pretreatment phase or when large changes have been recognized during therapy. However, with the introduction of MR linacs in the radiotherapy, MR delineation of both the GTV and OAR will become daily practice during treatment.

Conventional MR contrasts are T1 and T2 weighted (T1w and T2w, respectively), which can be combined with fat suppression as fat has a high signal intensity on both T1 weighted as T2 weighted MRI. Generally, observers do agree better on delineation of OAR on MRI than on CT. Also for prostate and nasopharynx tumors, MRI has shown to decrease the target volume. For other tumor sites, increase of tumor volume is very common. This might be due to tumor induced changes in the vicinity of the tumor, which are included by the observers. This shows that although the soft contrast is much better on MRI, the interpretation might be more difficult. Therefore, clear guidelines are needed to improve tumor delineation or MR contrasts which are easier to interpret. Both dynamic contrast MRI and diffusion weighted MRI are widely used. These techniques, also referred to as functional imaging, reflect the status of the microvasculature and the microanatomy. The drawback of DCE-MRI is that rigorous post-processing is needed to effectively use it for contouring. Diffusion weighted MRI gives high contrast, but is frequently inadequate due to deformations which are inherent to the acquisition method used, echo planar imaging (EPI). Recently, several advances have been made to mitigate these distortions. One approach is to decrease the distortions in the EPI using acquisition acceleration methods. Another approach is to replace the EPI acquisition with a fast spin echo or steady state free precession method, which are both used for standard clinical MR acquisition. The disadvantage is that the acquisition is slower and motion artefacts have to be tackled.

The role of DCE-MRI in delineating the gross tumor volume (GTV) has been studied in prostate, head and neck, cervical cancer and brain.

Diffusion weighted MRI has been more frequently studied as a tool to improve the delineation. The high contrast between tumor and background might even allow automatic delineation. Also diffusion tensor imaging (DTI)

has been applied in the brain, where it might help contouring glioma invading the white matter. Although different MR imaging contrasts might give different GTVs, we know that in imaging we will never see all tumor tissue. Therefore, CTV margins are used in daily clinical practice. The better the imaging resembles the histology of a tumor, the smaller the CTV margin that has to be applied. The extent of the tumor outside the delineated volume can be determined using pathological validation of the tumor using histology. As MR imaging develops, the historical CTV margins might be too large as was illustrated for laryngeal cancer [20]. For brain tumors also blood oxygen level dependent MRI also referred to as functional MRI (BOLD fMRI) can be used to avoid functional regions in the brain. This technique shows the vascular response to neuronal activity. Besides contrast also high resolution can help to better define small structures, such as cranial nerves in case of perineural growth or small lymph nodes. Besides MR imaging, also MR spectroscopy has played a role, but never became a widely spread method, probably due to the demanding level of expertise. Particularly for brain and prostate, 1H MR spectroscopic imaging has shown its value.

Due to the emerging MR guided radiotherapy, highly accelerated techniques for motion characterization, tracking and gating in combination with sufficient contrast to distinguish the tumor and OAR are being developed. As response monitoring during treatment is important for adaptation of radiotherapy, especially DWI is being further developed.

In summary, the use of MRI in radiotherapy will increase in the near future as delineation will not only be part of the pre-treatment imaging but also of the treatment guidance. Therefore, the choice of MR imaging techniques which give a high contrast and allow fast acquisition are desired to make improve delineation accuracy and variation.

#### SP-0700 The future of margins in the era of new (multi-modality) imaging technology

J. Stroom<sup>1</sup>, S. Vieira<sup>1</sup>, C. Greco<sup>1</sup>

<sup>1</sup>Fundação Champalimaud, Radiation Oncology, Lisboa, Portugal

##### Abstract text

A large part of technical development in radiotherapy this century has concentrated on improving treatment accuracy through use of new imaging technology. During planning, MRI and PET imaging techniques have been applied to add precision to target delineation. During treatment, off-line correction strategies based on MV portal images have been gradually replaced by online corrections and plan adaptations using cone-beam CT. On-line MRI capabilities are now being introduced to refine treatment setup even further, and several systems for intra-fraction monitoring of moving patient anatomy are available.

However, in this presentation we will try to make the point that even with all the new imaging techniques, it might be worthwhile to hold on to safety margins for standard fractionated treatments for a while. Whereas systematic and random uncertainties, often denoted by standard deviations  $\Sigma$  and  $\sigma$ , should diminish when applying the above-mentioned imaging techniques, they will not reduce to zero. So, for fractionated radiotherapy, margin recipes of e.g. the form  $A\Sigma + B\sigma$  might still be applied, albeit with smaller values for  $\Sigma$  and  $\sigma$  as before. On the other hand, even though they are widely used, there still are several unresolved issues regarding margin recipes. To start, no randomized clinical studies have proven one margin recipe over another. Then, the added value of using ITV for breathing motion is highly debatable and delineation uncertainties are frequently ignored, just like uncertainties in microscopic disease. Moreover, it is

assumed that margins for microscopic disease (CTV) and geometrical uncertainties (PTV) should be kept separated. These issues will all be discussed.

Finally, the main effect of the new imaging modalities on radiotherapy safety margins might be indirect. The improved accuracy and smaller margins allow for ever higher treatment and fraction doses. There is now evidence that a different radio-biology applies to single-dose radiotherapy (SDRT). Apart from the standard radiation mechanism that targets misrepair of double strand breaks, higher fraction doses (> 12Gy) are believed to also induce tumor cell kill by injuries to the tumor microvasculature. We will discuss the possible consequences of SDRT on safety margins; margin factors A and B might change and even negative margins are not unthinkable.

---

#### Symposium: A new era for radiotherapy (anthropomorphic) phantoms

---

#### SP-0701 Personalized phantoms through 3D printing

S. Crowe<sup>1</sup>

<sup>1</sup>Royal Brisbane and Women's Hospital, Cancer Care Services, Herston, Australia

##### Abstract text

The application of 3D printing (or additive manufacturing) technologies and techniques in medical physics has exploded in the past five years. 3D printing has been widely used for treatment equipment, including bolus, compensators, shielding, immobilisation devices and brachytherapy applicators. These bespoke patient-specific solutions can be precisely fabricated, in a cost-effective way, with limited expertise.

For the medical physicist, 3D printing allows the fabrication of a wide variety of tools for quality assurance, of varying complexity. The simplest applications include ancillary dosimetry equipment such as jigs or build-up caps; followed by simple phantoms for mechanical, dosimetric and imaging QA; and custom inserts for existing QA phantoms.

Perhaps the most exciting application is the fabrication of anthropomorphic phantoms, suitable for evaluating new treatment and imaging technologies and techniques, end-to-end audits, trial accreditations, and answering research questions. 3D printed phantoms can include (and have included) variable density media, radionuclides, programmable motion, deformable components and embedded 3D gel dosimeters.

This presentation summarizes the scientific literature surrounding 3D printing as applied to medical physics phantoms; provides advice for design, fabrication and QA; and describes the local experience of a radiotherapy department attached to a 3D printing and biofabrication research institute.

#### SP-0702 Do we need to touch? Latest developments in physical and digital phantoms for 4D radiotherapy

C. McGarry<sup>1,2</sup>

<sup>1</sup>Belfast Health and Social Care Trust, Northern Ireland Cancer Centre, Belfast, United Kingdom; <sup>2</sup>Queen's University Belfast, Centre for Cancer Research AqD Cell Biology, Belfast, United Kingdom

##### Abstract text

Physical and digital anthropomorphic phantoms have been developed to represent the human body's anatomy and attenuation characteristics for imaging and dosimetric studies in radiotherapy over many years. With the advancement of multimodality imaging used to capture intra-fractional motion at the pre-treatment and delivery stages of the radiotherapy process, dynamic phantoms have emerged with varying levels of complexity for

imaging and dosimetry purposes. Dynamic phantoms require the addition of organ motion correlated with breathing traces to ensure that they are patient mimicking.

Digital or 'computational' anthropomorphic phantoms are typically created from acquired tomographic images, segmentation of organs, and specification of organ densities / chemical composition before a final registration of the segmented images into a 3D volume. Computer simulations are extremely adaptable; allowing control of anatomical features using physics based algorithms. Organ trajectory, shape and density do not always truly represent the patient in computational simulations as intended. Moreover, instead of representing patient specific characteristics, most available anthropomorphic phantoms are created using population-averaged characteristics. However, due to the versatility of computational phantoms, multiple phantoms have emerged which represent a wider population without the cost of manufacturing.

Physical phantoms have the added steps of manufacturing the organs and placing them inside a body securely. A plethora of in-house and commercial dynamic radiotherapy phantoms have been developed for imaging and dose verification. These range from simple homogeneous phantoms, placed on unidirectional moving platforms, to phantoms with 6 degrees of freedom motion with lung and cardiac deformations. Physical phantoms can be used in Institution-specific protocols and can include pre-treatment imaging, dose delivery and pre-treatment verification including local set-up procedures. Trade-offs between reproducibility and the magnitude of organ deformations are inherent in the manufacture of physical dynamic phantoms. Emerging phantoms will need to account for the increasingly diverse methods of external tracking which must be accurately correlated with internal tumour motion.

With the advent of 3D printing technology and advanced material development, it is clear that improvements in physical dynamic anthropomorphic 4D phantoms will follow for radiotherapy validation. Similarly, computational phantoms will advance significantly with improved resolution, texture and deformation models. This presentation will summarize the advantages and limitations of each dynamic phantom type and will discuss if future 4D radiotherapy research should be in the digital or physical domain, or both.

#### SP-0703 MR Linac anthropomorphic end-to-end QA phantoms: IROC-Houston's experience

A. Steinmann<sup>1</sup>, D. Followill<sup>2</sup>

<sup>1</sup>Ohio State University Wexner Medical Center, Radiation Oncology, Columbus- Oh, Usa ; <sup>2</sup>University Of Texas Md Anderson Cancer Center, Outreach Physics, Houston- Tx, Usa

##### Abstract text

The National Cancer Institute (NCI) requires participating institutions intending to use IMRT in NCI-sponsored clinical trial to first become credentialed by demonstrating their ability to accurately deliver radiation. The Imaging and Radiation Oncology Core at Houston (IROC-Houston) has developed various site-specific anthropomorphic phantoms that are used in the credentialing process. These conventional phantoms were originally designed as end-to-end QA tests for traditional CT-only radiotherapy workflow.

Unlike conventional linear accelerators, magnetic resonance imaging guided radiotherapy MRIGRT systems use CT images to capture electron density information for treatment planning and MR images to verify treatment setup, treatment guidance and online adapted radiotherapy. Using a single phantom to perform an end-to-end QA test means the phantom must be used and visualized in both CT and MR imagers. IROC-Houston's

conventional phantoms are constructed of rigid materials that lack MR signal. This lack of signal causes the tumor and surrounding tissue to be indistinguishable in MR imagers. Therefore, IROC-Houston's conventional phantoms are not adequate for MR/CT workflows and new end-to-end QA head and neck (H&N) and thorax phantoms must be constructed for MRIGRT systems. The main purpose of this study was to design and manufacture a stationary H&N and dynamic thorax anthropomorphic QA phantom that could be used as an end-to-end tool to credential institutions for MRIGRT systems. These phantoms were designed for MRIGRT systems that have a magnetic field ranging from 0.35T to 1.50T and were constructed with MR/CT visible and dosimetrically tissue equivalent materials. An MR conditional pneumatic system was also designed for the MRIGRT thorax phantom to enable lung motion during CT simulation and treatment.

With the purpose of these phantoms being used as a remote end-to-end auditing tool for credentialing institutions in NCI-sponsored clinical trials, these phantoms were also evaluated through a reproducibility and miniature feasibility study. The reproducibility study was conducted by irradiating each phantom three times on a Unity MR Linac system (7MV/1.5T). The miniature feasibility study was performed by sending both MRIGRT H&N and thorax phantom to three institutions and were irradiated on either an MRIdian (Co-60/0.35T) or an MRIdian Linac (6MV/0.35T) MRIGRT system. The phantoms were evaluated using EBT3 radiochromic film and TLDs and used the same dose constraints and passing criteria as IROC-Houston's conventional H&N and thorax phantoms. This lecture will discuss the designs, constructions and treatment evaluations for both IROC-Houston's MRIGRT H&N and dynamic thorax phantom.

#### SP-0704 Phantoms in particle therapy to verify Monte Carlo dose calculation

P. Wohlfahrt<sup>1,2,3</sup>

<sup>1</sup>Massachusetts General Hospital and Harvard Medical School, Department Of Radiation Oncology, Boston, Usa ;

<sup>2</sup>Oncoray - National Center for Radiation Research In Oncology, Faculty of Medicine and University Hospital Carl Gustav Carus - Technische Universität Dresden - Helmholtz-Zentrum Dresden-Rossendorf, Dresden, Germany; <sup>3</sup>Helmholtz-Zentrum Dresden - Rossendorf, Institute Of Radiooncology - Oncoray, Dresden, Germany

##### Abstract text

High-conformal treatment techniques, such as intensity-modulated radiotherapy or volumetric arc therapy in photon therapy as well as pencil-beam scanning in particle therapy, have been developed in the last decades to achieve a high tumor coverage while sparing healthy tissue more effectively. These technological achievements already led to an improved clinical outcome. Further sophisticated developments in imaging for tumor detection and treatment planning (e.g., dual-energy computed tomography, quantitative and functional magnetic resonance imaging as well as targeted positron emission tomography), and dose calculation (e.g., robust optimization and Monte Carlo algorithm) recently enter the routine clinical workflow. These continuous improvements in treatment precision and accuracy are associated with challenges for medical physicists in the verification of its proper functionality and assessment of its remaining uncertainty. Simplified phantoms, which not adequately simulate the geometrical complexity and tissue heterogeneity of patients, are often not sufficient to represent realistic clinical scenarios and to demonstrate the benefits of new advanced technologies. The use of anthropomorphic phantoms of known composition are suitable for such an experimental validation but require measurement setups close to the physical limits. Here, the generation and experimental

verification of a ground-truth anthropomorphic head phantom as well as its application for treatment planning, Monte Carlo dose calculation and range verification in particle therapy will be presented.

---

**Debate: Workload/clinic logistics, and not technical uncertainties, are the main barrier to widespread implementation of adaptive RT practice**

---

**SP-0705 Practicalities and Not Technical Uncertainties Limit the Clinical Implementation of Adaptive Radiotherapy**

M. Velec<sup>1</sup>, E. Forde<sup>2</sup>

<sup>1</sup>Princess Margaret Cancer Centre, Radiation Medicine Program, Toronto, Canada ; <sup>2</sup>Trinity College Dublin, Discipline Of Radiation Therapy, Dublin, Ireland

**Abstract text**

Image-guided radiotherapy has revealed the dynamic nature of patients who can unexpectedly exhibit positioning variations, substantial organ motion and deformation, weight loss and tumour responses. This motion degrades the planned dose, decreases treatment quality and may impact clinical outcomes. Systematically adjusting for these patient-specific variations through adaptive plan modification can improve the therapeutic ratio in individual patients and enable planning target volume reduction thereby reducing dose to nearby radiosensitive structures. However, widespread clinical implementation of adaptive radiotherapy including evaluation in clinical trials has been slow. This is in part due to ongoing technical issues, including the accuracy of tools vital to adaptive radiotherapy; such as auto-segmentation, auto-planning, deformable registration, and uncertainty in defining responding clinical target volumes. Appropriate commissioning and QA of these processes combined with conservative adaptation for targets can potentially overcome these safely. Another more palpable barrier to implementation is that clinical workflows are not yet streamlined enough for patients and staff to be practicable. Routine radiotherapy processes that are required for adaptation, including repeat imaging, planning and QA, can increase workload and create bottlenecks in the clinic. These logistics may potentially be overcome with adequate clinical experience, which may include RTTs assuming greater responsibility and independence in decision making and developing expertise in adaptive tools. Debate on whether practicalities or technical uncertainties limit the clinical implementation of adaptive radiotherapy will provide the community with direction on where future efforts should be focused. Widespread use of adaptive strategies will ultimately improve the effectiveness of radiotherapy by accounting for dynamic patient changes, and ensuring tumour control while minimizing toxicities.

**SP-0706 Against the motion**

E. Forde<sup>1</sup>

<sup>1</sup>TCD Discipline of Radiation Therapy, Dublin, Ireland

Abstract not received

---

**Plenary Session: Closing debate: Data mining or data farming?**

---

**SP-0707 For the motion**

TBC

**SP-0708 Against the motion**

TBC

# POSTERS

---

**ESTRO 38 Clinical Posters**

---

**Poster: Clinical track: Head and Neck**

---

**PO-0709 External beam radiotherapy for metastatic lesions of differentiated thyroid cancer**

M. Kenji<sup>1</sup>, Y. Hamamoto<sup>2</sup>, Y. Urashima<sup>1</sup>, N. Takata<sup>2</sup>, K. Kikuchi<sup>1</sup>, M. Miyagawa<sup>2</sup>, T. Mochizuki<sup>2</sup>  
<sup>1</sup>Matsuyama Red Cross Hospital, Radiology, Matsuyama city, Japan ; <sup>2</sup>Ehime University Graduate School of Medicine, Radiology, Toon City, Japan

#### Purpose or Objective

To evaluate the outcomes of external beam radiotherapy (EBRT) for metastatic lesions (MLs) of differentiated thyroid cancer (DTC).

#### Material and Methods

Between August 1997 to March 2018, 73 lesions in 36 patients (male/female = 15/21; age 35-87 years, median 62 years) received EBRT and were followed up by CT, MR images, and/or FDG-PET/CT in our institution. Median follow-up time was 14 months (range, 1-110 months). Among assessed 73 lesions, 56 lesions were distant metastases (bone/lung/other sites = 45/5/6) and 17 lesions were neck/mediastinal lymph-node metastases. Doses of EBRT were 8-70 Gy (median 40 Gy). Seventeen patients received radioactive iodine therapy (RAIT) after EBRT.

#### Results

One- and 3-year overall survival rates were 87% and 63%, respectively. One- and 3-year control rates of lesions received EBRT were 79% and 45%, respectively. Three-year control rates were 0% for lesions received <30 Gy (n=7), 35% for lesions received 30-49 Gy (n=38), and 82% for lesions received 50 Gy (n=28). There were statistically significant differences of control rates between <30 Gy and 30-49 Gy (p=0.0002), and <50 Gy and >50 Gy (P=0.00374). Three-year control rates according to sites of lesions were as following; 55% for neck/mediastinal lymph-nodes, 33% for the bone metastasis, and 65% for the lesions in other organs (P = 0.2201). Three-year control rates were 67% for lesions received RAIT after EBRT (27 lesions), and 30% for lesions received no RAIT after EBRT (46 lesions) (p=0.0093). There were no significant differences in control rates by age, sex, and pathological subtype (papillary carcinoma vs. follicular carcinoma). EBRT doses of >50 Gy and addition of RAIT after EBRT were statistically significant independent factors for the good control of lesions received EBRT on multivariate analysis.

#### Conclusion

Because a significant proportion of patients with MLs of DTC requiring EBRT survived for a long time, long-term control of irradiated lesions is required even in palliative intent radiotherapy. EBRT doses of >50 Gy and addition of RAIT after EBRT seemed to be useful for long-term control of lesions received EBRT.

#### PO-0710 IMRT+Carbon Ion Boost for Adenoid Cystic Carcinoma of the Minor Salivary Glands of the Oral Cavity

K. Lang<sup>1</sup>

<sup>1</sup>University Hospital Heidelberg- Radiooncology, Radiooncology Heidelberg, Heidelberg, Germany

#### Purpose or Objective

Adenoid cystic carcinomas (ACCs) are more frequently located in the minor salivary glands (MiSGs) of the oral cavity than in the major salivary glands and they are characterized by slow tumor progression and frequently local recurrence. Main treatment option is surgery followed by combined radiotherapy. This study summarizes our institution's experience with bimodal postoperative RT in ACCs of the minor salivary glands of the oral cavity to evaluate survival and toxicity.

#### Material and Methods

The retrospective analysis contained 67 patients with ACC of MiSGs of the oral cavity who underwent surgery followed by radiotherapy. The median cumulative IMRT

dose was 50 Gy followed by 24 Gy for C12 boost. Median follow-up was 40 months.

#### Results

Median 5-years overall survival (OS), progression free survival (PFS) and local disease free survival (LDFS) rates were 85.5%, 57.4% and 74.9%. Median time until progression was detected was 32 months (range: 2 - 205 months). Early grade > 3 mucositis, dermatitis and dysphagia were detected in 52.2%, 7.5% and 11.9%. Besides common toxicities two patients (3.0%) developed grade 3 toxicities with osteoradionecrosis of the jaw after 18 and 66 months. Higher-grade late toxicity (CTCAE grade 4) was not detected. There was no treatment related death.

#### Conclusion

Our results demonstrate that postoperative bimodal radiotherapy with IMRT plus C12 boost seem to be feasible and effective treatment method in ACC of MiSGs of oral cavity with good control and survival rates and tolerable toxicity.

#### PO-0711 Second Primary Cancer in Salivary gland cancer in South Korea: A Nationwide Population-based Study

J. Heo<sup>1</sup>, Y. Oh<sup>1</sup>, O.K. Noh<sup>1</sup>, M. Chun<sup>1</sup>, O. Cho<sup>1</sup>

<sup>1</sup>Ajou University School of Medicine, Radiation Oncology, Suwon, Korea Republic of

#### Purpose or Objective

The aim of this study was to evaluate the prevalence of second primary cancer (SPC) among salivary gland cancer (SGC) patients by using nationwide claims data in South Korea.

#### Material and Methods

The nationwide cohort assessed in this study patients who were diagnosed with SGC from January 1, 2010, to December 31, 2014. We analyzed cancer incidence according to the time sequence. Additionally, we evaluated standardized incidence ratios (SIRs) to estimate the risk of SPC in SGC patients.

#### Results

A total of 1,614 patients (868 male and 746 female subjects) who were diagnosed with SGC and received surgery were confirmed, and 829 patients received radiotherapy. Of these patients, one-hundred and fifty-five patients (9.6%) developed an SPC, and the most common cancer site was the thyroid (13.5%). Patients with SGC had a high risk of SPC (SIR 4.39, 95% CI: 3.73 - 5.14), particularly nasopharynx cancer (SIR 79.43), Non-Hodgkin lymphoma (SIR 14.95) and tonsillar cancer (SIR 66.67). Female had a higher risk of malignancy than male (SIR 5.14 for women and SIR 3.73 for men). Age was a significant predictive factor for SPC (P = 0.024) among clinical factors, and patients over 54 years were at a higher risk for mental disorders (hazard ratio: 1.43, P = 0.031).

#### Conclusion

SGC patients with surgery had a longer life expectancy and a higher risk of SPC than the general population did. Therefore, close surveillance for SPC is important in elderly patients with SGC.

#### PO-0712 A new prediction model for patient reported xerostomia; external validation in postoperative setting

H.P. Van der Laan<sup>1</sup>, L. Van den Bosch<sup>1</sup>, A. Van der Schaaf<sup>1</sup>, R.J.H.M. Steenbakkers<sup>1</sup>, H.P. Bijl<sup>1</sup>, M. Dieters<sup>1</sup>, J.G.M. Van den Hoek<sup>1</sup>, S. Both<sup>1</sup>, E. Schuit<sup>2</sup>, J.A. Langendijk<sup>1</sup>

<sup>1</sup>University of Groningen- University Medical Center Groningen, Department of Radiation Oncology, Groningen, The Netherlands ; <sup>2</sup>Utrecht University- University Medical Center Utrecht, Julius Center for Health Sciences and Primary Care, Utrecht, The Netherlands

#### Purpose or Objective

A new model for patient-reported moderate-to-severe xerostomia at 6 months ( $XER_{M6}$ ) after treatment was previously developed in a unique, high quality dataset of 750 patients who received definitive radiotherapy for head and neck cancer (HNC) and externally validated in datasets from two other institutions. The aim of the current research was to validate this NTCP-model in a cohort of HNC patients who received postoperative radiotherapy (PORT) with or without chemotherapy (CT).

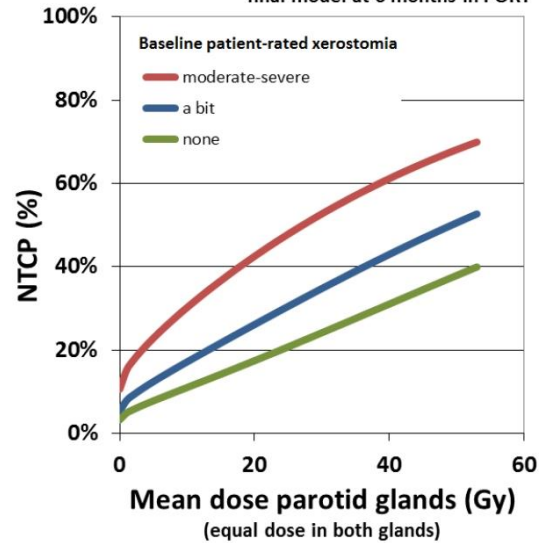
#### Material and Methods

The population of this prospective cohort study was composed of 218 HNC patients treated with PORT  $\pm$  CT. Baseline patient- and treatment characteristics, as well as acute and late toxicity and patient-rated outcome measures (i.e. EORTC QLQ-C30 and EORTC QLQ-HN35) were prospectively scored and linked to dose-volume parameters from both parotid and submandibular glands. The salivary glands were delineated according to the international guidelines (Brouwer et al. Radiother Oncol 2015) similar to those used in the development set. Multiple imputation was used to deal with missing data to avoid the bias of a complete case analysis. The original xerostomia model comprises baseline patient-reported xerostomia complaints, the summed square root transformation of the mean dose in both parotid glands ( $SSQ-D_{mean}$ ) and  $D_{mean}$  of both submandibular glands. A closed testing procedure was used to validate and, if necessary, update the xerostomia model for use in the postoperative setting.

#### Results

The prevalence of  $XER_{M6}$  was 27%, as compared to 41% (95%CI: 34.4% - 47.5%) as predicted by the model. A closed testing procedure to validate this model revealed that a model revision was necessary for use in the postoperative setting (Figure 1). Particularly, the association with the submandibular glands was weaker than described by the original model. In the current dataset, in contrast to the development dataset, patients often underwent neck dissections and had zero, one or two remaining submandibular glands post-surgery in 26%, 53% and 21% of the cases, respectively. Therefore, we tested whether a revised model including a variable for the number of post-surgery remaining submandibular glands or interaction terms including this factor, would better fit to the current dataset. However, this was not the case. Subsequently, we reduced our initial model, by excluding the mean dose in the combined submandibular glands, which did not change significantly the goodness of fit. The closed testing procedure then revealed that an update of the model intercept, to compensate for the lower response rate, was sufficient for this reduced model (ROC-AUC = 0.66, Nagelkerke  $R^2$  = 0.11) to be used in the postoperative setting (Figure 2).

#### Patient-rated moderate-severe xerostomia final model at 6 months in PORT



#### Conclusion

A new model for  $XER_{M6}$  was externally validated in the postoperative setting and established after excluding the variable describing the  $D_{mean}$  of both submandibular glands and an update of the model intercept.

#### PO-0713 PDRN-based cream in the prevention and treatment of radiodermatitis in Head and neck cancer: our experience.

F. Pastore<sup>1</sup>, A. Rese<sup>1</sup>, G. Panelli<sup>1</sup>, A. Pepe<sup>1</sup>, D. Toledo<sup>1</sup>, V. Iorio<sup>1</sup>

<sup>1</sup>Emicenter, Radiation Oncology, Mondragone, Italy

#### Purpose or Objective

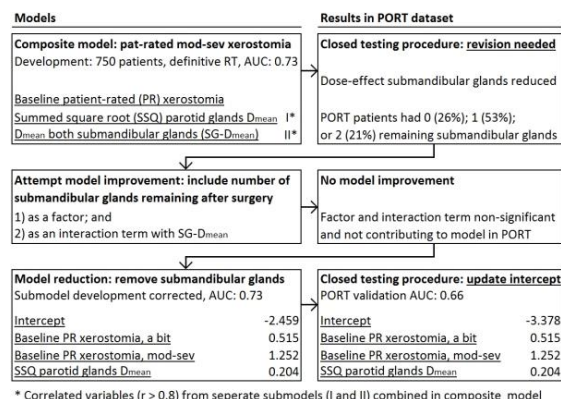
This study was designed to assess the efficacy and tolerability of a PDRN (Polideoxyribonucleotides)- based cream formulation in the prevention and treatment of radiodermatitis in patient with head and neck cancer treated with CRT (concomitant chemo-radiotherapy). PDRN is a well-known registered drug with tissue repairing, anti-ischemic and anti-inflammatory properties and we already tested it in a previous study on breast cancer patients.

#### Material and Methods

Patients with head and neck cancer has been randomized to use a cream, standard of care in our institution or a PDRN-based cream, throughout the duration of radiotherapy and for two weeks afterwards. Patients were monitored before therapy, weekly during therapy, and for 2 weeks after radiotherapy was completed, using RTOG skin toxicity grading scale. Patients were treated with Helicoidal Tomotherapy, choosing appropriate RT dose and fractionation according to disease presentation and with concomitant chemotherapy, using both conventional than hypofractionation schedules. We assessed on these patients several clinical variables as tumor histology, skin phototype, concomitant chemotherapy and medical conditions.

#### Results

Between december 2016 and march 2018, 102 consecutive patients, were enrolled in this study. Median age of the patients was 62.5 (range 46-84). 50/60 (83%) patients in the PDRN group vs. 57/62 (91%) patients in the control group had some grade of skin toxicity at the end of the treatment. At 4th week, 19/60 patients (31%) in the PDRN group vs. 37/62 (60%) patients in the control group had G2 grade of skin toxicity (p=0.0095). After 15 days from the end of the treatment, 5/60 patients (8%) in the PDRN group vs. 11/62 patients (18%) in the control group had some grade of skin toxicity (p=0.049). After 60 days from



the end of the treatment, 1/60 patients in the PDRN group vs. 4/60 patients in the control group had G1 grade of skin toxicity ( $p=0.047$ ). No differences were seen regarding other variables examined.

#### Conclusion

PDRN based cream improves the acute skin toxicity profile of head and neck cancer patients undergoing CRT. In these patients, the maximum skin toxicity grade is lower and the complete skin healing is faster. We need more patients and a longer follow up to assess late toxicity as fibrosis.

#### PO-0714 Toxicity profile of a SBRT boost as first-line treatment in oropharyngeal cancer patients

W. Heemsbergen<sup>1</sup>, S. Baker<sup>1</sup>, S. Petit<sup>1</sup>, J. Nuytens<sup>1</sup>, G. Verduijn<sup>1</sup>

<sup>1</sup>Erasmus MC Cancer Institute, Radiation Oncology, Rotterdam, The Netherlands

#### Purpose or Objective

To date, stereotactic body radiotherapy (SBRT) for head and neck cancer has been used primarily for re-irradiation of recurrent malignancies, despite the potential advantages in the setting of newly diagnosed disease and a growing interest internationally. There is sparse literature on long-term toxicity patterns in large patient series in the setting of a first-line treatment. In the current study we determined the late Grade  $\geq 3$  toxicity rates of a SBRT boost as primary treatment in the largest patient series to date.

#### Material and Methods

We performed a retrospective cohort study in 195 consecutive oropharyngeal squamous cell carcinoma patients collected from a prospective planning database. Eligible patients had T1-small T3 disease for which they were treated between 2009-2016 with a SBRT boost (3 x 5.5 Gy) to the primary tumor after accelerated 46 Gy IMRT to the primary tumor and neck, plus additional neck dissection in case of N positive disease (Table). The boost was delivered with a frameless robotic radiosurgery system. The GTV-CTV margin was 1 cm and the CTV-PTV margin was 5 mm for the IMRT phase and 3 mm for the boost. Main OAR dose constraints for the total plan (EQD2) were: spinal cord  $D_{max} < 50$  Gy and brain stem  $D_{max} < 60$  Gy (both hard planning constraints), parotid glands  $D_{mean} < 26$  Gy, submandibular glands  $D_{mean} < 39$  Gy, oral cavity  $D_{mean} < 50$  Gy, swallowing structures  $D_{mean} < 55$  Gy (where achievable). We determined Grade  $\geq 3$  toxicity rates ( $G_{\geq 3}$ ) as well as locoregional control (LRC), disease-specific survival (DSS), and overall survival (OS). Prognostic factors were assessed in Cox regression models. Sufficient follow-up (disease-free survival  $> 3$  months post-RT) for late toxicity assessment was available for 182 patients.

#### Results

Median follow-up was 4.3 years. Treatment compliance (100%) was high. Rates of cumulative 5-year (5Y) late  $G_{\geq 3}$ , LCR, DSS, and OS were 26%, 84%, 85%, and 67%, respectively. The most frequently observed  $G_{\geq 3}$  toxicities were mucosal ulceration or soft tissue necrosis ( $n=29$ , 5Y 17%), dysphagia or weight loss ( $n=15$ , 5Y 10%) and osteoradionecrosis (ORN) ( $n=11$ , 5Y 9%). At multivariable analysis, current smoker status was associated with increased  $G_{\geq 3}$  risks ( $HR=3.3$ ,  $p<0.01$ ), and pre-RT tooth extraction was associated with increased ORN risk ( $HR=6.5$ ,  $p<0.01$ ) Figure. Median interval extraction-start RT was 18 days and was not associated with ORN ( $n=63$ ,  $HR=1.9$ ,  $p=0.4$ ). Charlson Comorbidity Index  $\geq 2$  was associated with increased risks of dysphagia/weight loss ( $HR=6.6$ ,  $p=0.01$ ). These risk factors appeared to be more pronounced than reported in literature for conventional treatment.

#### Conclusion

Grade  $\geq 3$  toxicity profiles showed relatively high rates of soft tissue necrosis and osteonecrosis. LCR rates were

comparable with literature on conventional schedules for small tumors and survival was good in this population with 60% of advanced stage III-IVa disease. Strategies to mitigate severe toxicity risks are under investigation to improve the tolerability of the SBRT boost.

Baseline variables	N	%
Age (mean, range)	61(34-86)	
Male/female	122,73	63%,37%
ECOG 0/1	151,44	77%,23%
BMI $\leq 22$	43	22%
Pre-RT teeth extraction	63	32%
Packyears $\geq 10$	147	75%
Charlson Comorb Index $\geq 2$	97	50%
History or current alcohol abuse	59	30%
Smoker at diagnosis	103	53%
Stage grouping I-II / III-IVa	79,116	41%,59%
Subsite BOT / tonsil / other	35,113,47	18%,58%,24%
P16 pos / neg / unknown	63,30,102	32%,15%,52%
With concurrent chemo	12	6%
Neck RT uni-/bilateral	82,113	42%,58%
Additional neck dissection	101	52%

Table: patient, tumor, treatment characteristics

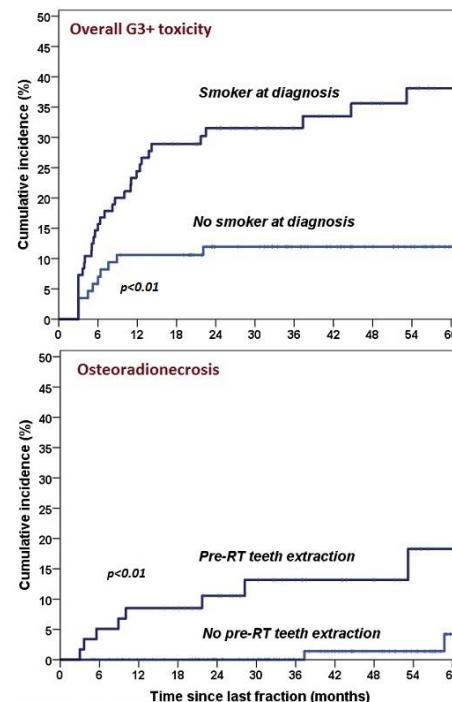


FIG. Grade  $\geq 3$  toxicity after SBRT boost

#### PO-0715 Nutritional intervention in head and neck cancer patients undergoing radiotherapy

L. Gutierrez Bayard<sup>1</sup>, M.D.C. Salas Buzón<sup>1</sup>, S. Garduño Sánchez<sup>1</sup>, M.J. Macías Lozano<sup>1</sup>, R. Rodríguez Sánchez<sup>1</sup>, S. Sayago Gil<sup>1</sup>, V. Díaz Díaz<sup>1</sup>, E. González Calvo<sup>1</sup>, I. Villanego Beltrán<sup>1</sup>, A. Ruiz Herrero<sup>1</sup>, M. Lorente Sánchez<sup>1</sup>, J. Jaén Olasolo<sup>1</sup>

<sup>1</sup>Hospital Universitario Puerta del Mar, Radiation Oncology, Cadiz, Spain

#### Purpose or Objective

To evaluate the benefit of motivational interviewing in addition to nutritional counseling in head and neck cancer (HNC) patients undergoing radiotherapy (RT)(+/- systemic treatment), to improve patients' nutritional behaviours.

#### Material and Methods

Sixty-one intervention patients received motivational interviewing and cognitive behavioural therapy compared

to 67 historical controls who received treatment as usual. The intervention is based on behaviour change counselling methods, including motivational interviewing to improve motivation to eat despite a range of barriers ( pain, mucositis, nausea, salivary toxicity , taste changes and appetite loss), and to provide patients with practical behaviour change strategies.

Assessments will be conducted at 5 time points (first, third and final week of radiotherapy, 4 and 12 weeks post-radiotherapy).

The primary outcome was nutritional status at the end of RT as measured by the Patient Generated Subjective Global Assessment (PG-SGA). Secondary endpoints: quality of life (EORTC QLQ-C30) and anticancer treatment tolerance.

#### Results

Intervention patients resulted in smaller loss of body weight than control group (mean difference, 1.8 kg [95%CI, 0.65-2.5];  $P = 0.005$ ), and a clinically important reduction on the PG-SGA (34% of controls vs. 17% intervention;  $P = 0.04$ ) in favor of the intervention condition. Secondary endpoints: reduced the need for changes in planned anti-cancer treatments (i.e. RT and/or systemic treatment dose reduction, interruptions or complete suspension)  $HR=0.38$  [95%CI, 0.2-0.89],  $P = 0.03$ ), and global QoL ( $P < 0.002$ )

#### Conclusion

HNC patients undergoing RT (+/- systemic treatment), receiving motivational and nutritional intervention resulted in better weight maintenance, and was associated with better anti-cancer treatment tolerance and improved quality of life .

#### PO-0716 Skull-base chordoma treated with proton and carbon ion radiotherapy : CNAO clinical experience

A. Iannalfi<sup>1</sup>, E. D'Ippolito<sup>1</sup>, V. Vitolo<sup>1</sup>, B. Vischioni<sup>1</sup>, M.R. Fiore<sup>1</sup>, M. Bonora<sup>1</sup>, S. Ronchi<sup>1</sup>, A. Barcellini<sup>1</sup>, R. Petrucci<sup>1</sup>, S. Molinelli<sup>1</sup>, A. Mirandola<sup>1</sup>, S. Russo<sup>1</sup>, A. Facchetti<sup>1</sup>, A. Vai<sup>1</sup>, E. Mastella<sup>1</sup>, G. Viselner<sup>2</sup>, G. Magro<sup>1</sup>, M. Ciocca<sup>1</sup>, L. Preda<sup>2</sup>, F. Valvo<sup>1</sup>, R. Orecchia<sup>1,3</sup>

<sup>1</sup>National Center of Oncological Hadrontherapy, Radiotherapy Unit, Pavia, Italy ; <sup>2</sup>National Center of Oncological Hadrontherapy, Diagnostic Image Unit, Pavia, Italy ; <sup>3</sup>European Institute of Oncology, Radiation therapy Unit, Milan, Italy

#### Purpose or Objective

Skull-base chordomas are rare and malignant tumors that originate from remnants of the chorda dorsalis (notochord). Particle radiotherapy provides dosimetric advantages and higher biological effective dose especially for radioresistant tumors . The aim of the study was to evaluate local control (LC) and toxicity profile of patients (pts) with skull-base chordoma treated with exclusive or adjuvant particle therapy (proton therapy -PT- and carbon ion therapy -CIRT-)

#### Material and Methods

Between September 2011 and July 2017, a total of 134 pts (79 men and 55 women) with a median age of 57 years (range 14-86) with histologically proven skull-base chordoma were treated with particle therapy at National Center of Oncological Hadrontherapy -CNAO. One-hundred and two (76%) pts had previous surgery and complete macroscopic resection was achieved only in 15 pts (20%). Sixty-one pts were treated with PT and 73 with CIRT. The particle choice (proton or carbon ion) was made on personalized basis. Median prescribed total dose was 70,4 Gy RBE (range 35,2-70,4 Gy RBE) in 8-22 fractions (median 16 fractions) of 3-4,4 Gy RBE (median 4,4 Gy RBE) for CIRT, and 74 Gy RBE (range 70-74 Gy RBE) in 27-37 fractions (median 37 fractions) of 2 Gy RBE for PT. Clinical outcome (LC, 3 year local relapse free- LRF5 and overall -survival - OS-) and toxicity profile in according with CTCAE criteria was evaluated

#### Results

The median follow-up was 32 months (range, 2-64 months). LC was 83%. In pts that underwent complete macroscopic surgery followed by PT, LC was 100%, in pts with incomplete resection/only biopsy and PT/CIRT, LC was 79%. The 3-year LRF5 and OS were 80% and 90% respectively. In field recurrence occurred in 13% (18 pts). In 16 out of 18 cases of recurrences the tumor was in close contiguity to the brainstem. Out of field recurrence was found in 5 pts: 2 cases occurred within surgical way, attributable to surgical seeding, One case of histologically confirmed cervical lymph-node relapse, 2 cases of newly appeared nodules of recurrence. Six pts (4%) developed distant metastasis after a mean interval of 12 months. The toxicity profile was favorable. Only 2 pts developed acute radiation induced high grade toxicity: with oral mucositis (grade 3). High grade (G3-G4) late toxicity occurred in 4% of pts: 1 case of complete visual loss (G4) expected because of optic nerve in field, 1 case of soft tissue necrosis, 2 cases of cranial nerve neuropathy and 2 cases of pituitary dysfunction

#### Conclusion

Particle therapy is the most innovative and conformal RT for treatment of skull base chordomas. It allows to deliver higher (biologically effective) dose levels and to obtain higher tumor control rates, minimizing radiation-related side effects

#### PO-0717 Addition of chemotherapy to hyperfractionated radiotherapy in advanced head and neck cancer

H. Jan<sup>1</sup>, T. Balint<sup>1</sup>, E. Boelke<sup>1</sup>, D. Freddy Noel<sup>1</sup>, B. Wilfried<sup>1</sup>, K. Kai<sup>2</sup>, M. Christiane<sup>1</sup>

<sup>1</sup>University Hospital Düsseldorf, Radiation Oncology, Düsseldorf, Germany ; <sup>2</sup>Johns Hopkins University School of Medicine- Baltimore- USA, Division of Biostatistics and Bioinformatics- Department of Oncology, Düsseldorf, Germany

#### Purpose or Objective

Adding chemotherapy (CTx) simultaneously to primary radiation therapy (RT) results in improved overall survival in patients with locally advanced tumors of the head and neck region (HN). A comparable effect has likewise been reported for hyperfractionated radiotherapy (HFX-RT) without concurrent CTx. Yet, the addition of CTx to HFX-RT has also been investigated in multiple trials. However a clear effect on oncological outcomes and toxicity profile has not been established and reported.

#### Material and Methods

We performed a literature search for randomized controlled trials comparing HFX-RT alone to HFX-RT + concurrent CTx in patients with locally advanced cancer of the head and neck region undergoing definitive radiotherapy. A meta-analysis was performed using the event rates and effect-sizes for overall survival (OS), cancer-specific survival (CSS) and disease-free survival (DFS) as well locoregional (LRC) and distant recurrence (DMR) as investigated endpoints. Additionally we compared selected acute and late toxicities in the included studies. Statistical analysis was performed using the Microsoft Excel add-in MetaXL 5.3 utilizing the inverse variance heterogeneity model.

#### Results

We identified six studies (n=1280 patients) randomizing between HFX-RT alone and the concurrent addition of CTx. OS was significantly improved in HFX-RT + CTx group ( $HR=0.77$  CI95%=0.66-0.89;  $p<0.001$ ). We found similar results in CSS ( $HR=0.72$  CI95%=0.60-0.88;  $p=0.001$ ) and DFS ( $HR=0.74$  CI95%=0.63-0.87;  $p<0.001$ ). The analysis also revealed improvements in the rate of locoregional and distant recurrences with CTx. Acute toxicities ( $\geq 3^\circ$  mucositis,  $\geq 3^\circ$  skin,  $\geq 3^\circ$  dysphagia) were not statistically different between both groups. Analysis of late adverse events included  $\geq 3^\circ$  xerostomia,  $\geq 3^\circ$  subcutaneous,  $\geq 3^\circ$  bone,  $\geq 3^\circ$  skin,  $\geq 3^\circ$  mucosal atrophy and

≥3<sup>rd</sup> dysphagia which were also not significantly different between the treatments.

#### Conclusion

The addition of chemotherapy to hyperfractionated RT schedules in definitive treatment of advanced HN-cancers improves all studied endpoints without a significant increase in the investigated high-grade acute and late toxicities.

#### PO-0718 Patterns of care for local recurrence of NPC after definite IMRT - a study by the HKNPCSG

W.T. Ng<sup>1</sup>, E.C. Wong<sup>1</sup>, L.L. Chan<sup>1</sup>, A.K. Cheung<sup>2</sup>, J.C. Chow<sup>3</sup>, D.M. Poon<sup>4</sup>, J.W. Lai<sup>5</sup>, C.L. Chiang<sup>6</sup>, K.H. Au<sup>3</sup>, A.W. Lee<sup>7</sup>

<sup>1</sup>Pamela Youde Nethersole Eastern Hospital, Clinical Oncology, Hong Kong, Hong Kong SAR China ; <sup>2</sup>Tuen Mun Hospital, Clinical Oncology, Hong Kong, Hong Kong SAR China ; <sup>3</sup>Queen Elizabeth Hospital, Clinical Oncology, Hong Kong, Hong Kong SAR China ; <sup>4</sup>Prince of Wales Hospital, Clinical Oncology, Hong Kong, Hong Kong SAR China ; <sup>5</sup>Princess Margaret Hospital, Clinical Oncology, Hong Kong, Hong Kong SAR China ; <sup>6</sup>Queen Mary Hospital, Clinical Oncology, Hong Kong, Hong Kong SAR China ; <sup>7</sup>The University of Hong Kong and The University of Hong Kong-Shenzhen Hospital, Departments of Clinical Oncology, Hong Kong, Hong Kong SAR China

#### Purpose or Objective

This retrospective study evaluated the patterns of care for patients with local recurrence of nasopharyngeal carcinoma (NPC) after intensity modulated radiotherapy (IMRT) treated in all public hospitals in Hong Kong from 2001 to 2010.

#### Material and Methods

Eligible patients were identified through the Hong Kong Cancer Registry data base. Patients with biopsy proven/radiologically documented local recurrence without concomitant distant metastasis were included. All patients received IMRT as the primary course of treatment. Patient demographics, tumour characteristics and treatment details were retrieved and verified. Survival outcomes after local recurrence were analysed.

#### Results

272 patients were identified. The median follow-up time was 31.5 months. Median time from primary diagnosis to local relapse was 29.6 months. The rT stage distribution was rT1: 30.5%, rT2: 9.6%, rT3: 25.4% and rT4: 34.6%. 74.3% had rN0 disease. Thirty one percent of patients received surgery, 35.7% received re-irradiation (RT), 23.2% received palliative chemotherapy alone and 10.3% had no active treatment. Early local recurrence was mostly treated with surgery (82.3% of Stage I, 38.1% of Stage II), while late recurrence was commonly treated non-surgically (52.1% of Stage III managed with re-RT; 42.3% of Stage IVA managed with chemotherapy alone). Adjuvant RT was commonly given in case of involved resection margin after radical resection (65.4%). Surgery was associated with 2.4% perioperative mortality, while re-RT was associated with 16.7% grade 5 late complications.

The 5-year overall survival (OS) for the whole group was 30.2%. Older age and advanced rT stage were adverse prognostic factors, while the use of surgery as primary treatment (mainly in early local recurrence) was associated with favourable outcome. The 5-year OS rates for patients who received surgery, re-RT, chemotherapy and no active treatment were 56.3%, 21.8%, 15.0% and 11.1% respectively. For the surgery group, resection margin status was the most important prognostic factor. Adjuvant RT did not improve local control and OS when compared with surgery alone and was associated with 28.5% of grade 4 toxicities or above. For the re-RT group, OS were adversely affected by older age and larger gross tumour volume. **Conclusion**

This study reflects the current patterns of care for local recurrent NPC in Hong Kong. Early detection of local recurrence is of paramount importance as surgery for resectable tumours is associated with the most favourable outcomes. Re-RT could be considered in selected patients with unresectable disease but favourable prognostic features.

#### PO-0719 head and neck contour peer review improves quality of radiotherapy targets

L. MCGEE<sup>1</sup>, J. Rwigema<sup>1</sup>, M. Halyard<sup>1</sup>, T. DeWees<sup>1</sup>, J. Gagneur<sup>1</sup>, S. Patel<sup>1</sup>

<sup>1</sup>Mayo Clinic Arizona, Radiation Oncology, Phoenix, USA

#### Purpose or Objective

Head and neck (HN) radiotherapy contour quality can directly impact local control and survival. However, few departments peer review (PR) contours prior to radiotherapy planning (RP). In an effort to further improve radiotherapy quality at our institution, we implemented a formal HN contour PR process. This series reports results of the first 7 months after initiation of this workflow.

#### Material and Methods

A formal HN contour PR process was implemented within our department. Contours were reviewed by radiation oncologists (RO) who specialize in HN cancer and revised prior to initiation of RP. A PR task item was built into the care path of the electronic medical record (EMR) to track the PR process. Dosimetry was not allowed to initiate RP until the PR task in the care path had been completed by the RO HN team.

RO participated in a weekly meeting to review contours. Together, the RO evaluated factors pertinent to individual patient contours including pretreatment imaging, physical examination photographs, recorded flexible scope examination, operative notes and surgical pathology. Contours were assessed by the RO HN team, and feedback was provided to the treating physician if contour revision was recommended. Contour revisions were graded by the RO present as follows: R0 (no change), R1 (minor revision, not deemed high risk) or R2 (major revision, deemed to have potential to negatively impact patient outcomes). The PR task was completed and grading of contours recorded in the EMR. The Cochran-armitage trend test was performed to determine if contour grade trend was significant over time.

#### Results

From February to August 2018, 110 HN cancer patients had the contour PR task completed in the EMR; 88 (80%) had grade recorded for contour revision. Four RO participated in the first 3 months; 3 RO participated all 7 months. Contours were graded as follows: R0 (N=50), R1 (N=20) and R2 (N=18). Over time the number of major revisions (R2) decreased (p=0.0001); month 1 (N=7) month 2 (N=3), month 3 (N=5) month 4 (N=2) and months 5-7 (N=0). Each individual RO who participated the entire time demonstrated reduction in R2 revisions; Oncologist A: month 1 (N=2), month 2 (N=1), month 3 (N=2), month 4 (N=1) and month 5-7 (N=0). Oncologist B: month 1 (N=2), months 2-4 (N=1) and months 5-7 (N=0). Oncologist C: month 1 and 3 (N=1) and months 2, 4-7 (N=0). The total number of RO revisions improved over time (p=0.0203); month 1 (N=5), months 2-3 (N=9), month 4 (N=5) month 5 (N=8), month 6 (N=12) and month 7 (N=3).

#### Conclusion

HN contour PR can be implemented into routine clinical workflow. The collective experience of multiple high volume RO led to improved contour quality over time for each RO. This improvement in contour quality may result in improved plan quality which in turn could lead to improved disease control and toxicity in patients treated after implementation of this process.

**PO-0720 Tumor volume/metabolism improve prognostication of anatomy-based stage for nasopharyngeal cancer?**

Y. Jeong<sup>1</sup>, K.K. Lee<sup>1</sup>, S.R. Moon<sup>1</sup>, S.Y. Noh<sup>2</sup>, J. Kwak<sup>2</sup>, S. Lee<sup>2</sup>

<sup>1</sup>Wonkwang University Hospital- Wonkwang University School of Medicine, Radiation Oncology, Iksan, Korea Republic of ; <sup>2</sup>Asan Medical Center- University of Ulsan College of Medicine, Radiation Oncology, Seoul, Korea Republic of

**Purpose or Objective**

We evaluated the prognostic value of the 8<sup>th</sup> edition of the AJCC/UICC staging system and investigated whether tumor volume/metabolic information refined the prognostication of current anatomy based staging system in nasopharyngeal cancer.

**Material and Methods**

The 133 patients with nasopharyngeal cancer who were staged with MRI and treated with IMRT between 2004 and 2013 were retrospectively reviewed, and all patients were re-staged according to the 8<sup>th</sup> edition of the AJCC/UICC staging system. The survival rates were estimated from the date of the start of radiotherapy, and univariate and multivariate analyses were performed to evaluate prognostic value of the 8<sup>th</sup> edition of the AJCC/UICC staging system and other factors including gross tumor volume and maximum standardized uptake value of primary tumor (GTV-T and SUV-T).

**Results**

The follow-up period was median 63 months (range, 7.2-155.8 months), and the 5-year OS was 80.8%. The stage group as well as age, pathology, GTV-T, and SUV-T were significant prognostic factors for OS in univariate analysis. In multivariate analysis, stage group (stage I-II vs. III-IVA) was the only significant prognostic factor (HR, 11.062, p=0.017), but, OS rates were not significantly different between stage I and II (5-year OS, 100% vs. 96.2%, p=0.347), and between stage III and IVA (5-year OS, 80.1% vs. 71.7%, p=0.673). Although SUV-T and GTV-T were not significant prognostic factors for OS in multivariate analysis, the incorporation of SUV-T and GTV-T into stage group improved prognostication of stage group. The OS rates were significantly different between stage I-II, III-IV (SUV-T ≤ 16), and III-IV (SUV-T > 16) (5-year OS, 97.2% vs. 78% vs. 53.8%, p < 0.001), and between stage I, II-IV (GTV-T ≤ 33ml), II-IV (GTV-T > 33ml) (5-year OS, 100% vs. 87.3% vs. 66.7%, p=0.021).

**Conclusion**

The current anatomy based staging system have limitations on prognostication for nasopharyngeal cancer even though that was based on the most accurate assessment of tumor extent by MRI. The tumor volume/metabolic information seems to improve the prognostication of current anatomy based staging system, and further studies are needed to confirm its clinical significance.

**PO-0721 Prognostic Value of Inflammatory Markers in Patients with Head and Neck Cancer.**

J. Mrochem-Kwarciak<sup>1</sup>, T. Rutkowski<sup>2</sup>, A. Wygoda<sup>2</sup>, A. Chmura<sup>1</sup>, K. Skłodowski<sup>2</sup>

<sup>1</sup>Maria Skłodowska-Curie Memorial Cancer Center and Institute of Oncology, Analytics and Clinical Biochemistry Department, Gliwice, Poland ; <sup>2</sup>Maria Skłodowska-Curie Memorial Cancer Center and Institute of Oncology, I Radiation and Clinical Oncology Department, Gliwice, Poland

**Purpose or Objective**

Inflammation is generally accompanied cancer disease. Evaluation of the inflammatory biomarkers in the treatment of head and neck cancer (HNC) patients is of potential prognostic value. The aim of present study was

to assess the prognostic value of indicators calculated on the basis of initial hematology parameters: neutrophil-to-lymphocyte ratio (NLR), lymphocyte-to-monocyte ratio (LMR), platelet-to-lymphocyte ratio (PLR), leukocyte count (WBC) and modified Glasgow Prognostic Score (mGPS) in patients with HNC after Radiotherapy alone or combined with chemotherapy.

**Material and Methods**

Between 01/2009 and 08/2013 191 patients with squamous cell carcinoma of nasopharynx (4%), oropharynx (39%), hypopharynx (13%), larynx (36%) or oral cavity (8%) were treated with curative intent with RT alone or combined with platinum-based chemotherapy. There were 47% patients with T1/2 and 53% with T3/4 of primary tumor stage and 31% and 69% of patients with N0 and N+ nodal stage disease, respectively. Complete blood counts (CBC), C-reactive protein (CRP) and albumin were estimated in blood or serum before the treatment. Patient mGPS was scored: as 0 when there were normal levels of albumin (≥35 g/l) and CRP (≤10 mg/l), as 1 when CRP was elevated (>10 mg/l) but albumin was normal and as 2 when CRP was elevated (>10 mg/l) and albumin was decreased (<35 g/l). Treatment outcome was defined as complete remission (CR - no evidence of disease) or treatment failure (TF - residual disease or recurrence).

**Results**

Median follow-up was 40 months. There was CR, and TF respectively in 69% and 31%. Second primary tumor or distant metastasis were observed in 12% of patients. Patients had significantly longer disease free-survival (DFS) when counts of WBC (< 6,77 G/l) and NLR (<2,01) were low (p=.002 and p=.03), respectively. Significantly longer overall survival (OS) was found for patients with low counts of WBC (<6,77 G/l) (p=.001), NLR (<2,01) (p=.01), or mGPS score (=0) (p=.04). No correlation was observed between LMR or PLR and DFS and OS.

**Conclusion**

In patients with head and neck cancer after radiotherapy alone or combined with chemotherapy high initial levels of NLR and WBC seems to predict worse treatment results. Low levels of inflammatory indicators like WBC, neutrophils count, mGPS, and high lymphocytes count may be associated with longer OS in this group in patients.

**PO-0722 Carbon ion radiotherapy for adenoid cystic carcinoma in the head-and-neck**

A. Hasegawa<sup>1,2,3,4</sup>, B. Vischioni<sup>3</sup>, M. Bonora<sup>3</sup>, S. Ronchi<sup>3</sup>, S. Molinelli<sup>3</sup>, M. Ciocca<sup>3</sup>, A. Facchetti<sup>3</sup>, F. Valvo<sup>3</sup>, P. Fossati<sup>5</sup>, B. Alicja Jereczek<sup>4</sup>, M. Koto<sup>2</sup>, T. Kamada<sup>2</sup>, J. Mizoe<sup>1</sup>, R. Orecchia<sup>3,4</sup>

<sup>1</sup>Osaka Heavy Ion Therapy Center, Radiation oncology, Osaka, Japan ; <sup>2</sup>National Institutes of Radiological Sciences Hospital, Radiotherapy, Chiba, Japan ; <sup>3</sup>National Center for Oncological Hadrontherapy CNAO, Radiation Oncology, Pavia, Italy ; <sup>4</sup>European Institute of Oncology IEO, Radiotherapy, Milan, Italy ; <sup>5</sup>MedAustron, Radiotherapy, Wiener Neustad, Austria

**Purpose or Objective**

The National Institutes of Radiological Sciences (NIRS)\* reported the clinical results of carbon ion radiotherapy (CIRT) for various types of head and neck malignancies, including acute and late morbidities, local control, and survival rates. In clinical protocols of the National Center for Oncological Hadrontherapy (CNAO), Fossati P et al \*\* demonstrated a practical method to translate NIRS RBE-weighted doses and the prescription doses of CIRT were applied based on this method. This study aims to evaluate the optimum dose of CIRT for adenoid cystic carcinoma (ACC) in the head-and-neck at CNAO compared to NIRS.

**Material and Methods**

Between December 2013 and June 2018, a total of 146 patients with adenoid cystic carcinoma of the head-and-neck were treated with carbon ion radiotherapy at CNAO. The prescribed tumor doses were 65.6 or 68.8 Gy (RBE) in

16 fractions over four weeks. Of 146 patients, 12 patients were irradiated with 65.6 Gy (RBE) and 134 patients were irradiated with 68.8 Gy (RBE). Each dose level is the dose equivalent to 57.6 and 60.8 Gy (RBE) of NIRS.

### Results

The patients consisted of 68 males and 78 females aged from 19 to 86 years with an average age of 54 years. The most frequent primary site was the nasal and paranasal sinus. Median follow-up time was 24.4 months (range, 4.2-60.9 months). Fourteen patients died because of local recurrence and/or distant metastasis, and 97 patients were alive without local recurrence at the time of this analysis. Median local control time was 21.4 months (range, 4.2-60.7 months). The 2-year local control and overall survival rates were 82% and 88%, respectively. The most frequent acute toxicity of 146 patients, grade 2 (G2) and grade 3 (G3) mucosal reactions were observed in 53 (36%) patients and 34 (23%) patients, respectively. No G3 mucosal reaction was observed in the 65.6 Gy (RBE) group. G2 acute skin reaction of all patients was observed in 30 (21%) patients. In the analysis of late toxicities, 8 (5%) patients showed G3 osteonecrosis and 5 (3%) patient showed G2 brain reaction. Only one patient needed the surgical intervention due to G3 encephalitis. All of these late toxicities were observed in the 68.8 Gy (RBE) group.

### Conclusion

The review article by Mizoe et al.\* reported the 2-year local control rate as about 95% and G2 and G3 mucosal reactions as 36% and 6%. Although our results were slightly inferior to this article, they showed acceptable toxicities and therapeutic effectiveness for adenoid cystic carcinomas. It is necessary to evaluate a large number of patients and a long follow up period.

\*Mizoe J et al. *Radiother Oncol* 2012; 103(1): 32-7.

\*\*Fossati P et al. *Phys Med Biol* 2012; 57: 7543-7554.

Acknowledgment: This study was partially supported by Associazione Italiana per la Ricerca sul Cancro (AIRC, project IG-14300).

### PO-0723 Benefits of deep learning for delineation of organs at risk in head and neck cancer

J. Van der Veen<sup>1,2</sup>, S. Willems<sup>3</sup>, D. Robben<sup>3</sup>, W. Crijs<sup>2</sup>, F. Maes<sup>3</sup>, S. Nuyts<sup>1,2</sup>

<sup>1</sup>KU Leuven - University of Leuven, Department of Oncology, Leuven, Belgium; <sup>2</sup>UZ Leuven - University Hospitals Leuven, Department of Radiation Oncology, Leuven, Belgium; <sup>3</sup>KU Leuven - University of Leuven, Medical Image Computing ESAT/PSI, Leuven, Belgium

#### Purpose or Objective

Delineation of organs at risk (OARs) is necessary for correct treatment planning and for comparison of dose-volume histograms between doctors, centres and studies. Although guidelines exist, manual delineation shows significant inter-observer variability. The aim was to develop a 3D convolutional neural network (CNN) that allows automated delineation of OARs resulting in more efficient and consistent contouring of head and neck cancer (HNC) patients.

#### Material and Methods

OARs from 70 HNC patients were manually delineated using the international consensus guidelines by Brouwer et al. (2015). The planning CT scans together with the delineations were used to train a single 3D CNN to delineate 16 different OARs. The 3D CNN is based on the work of Kamnitsas et al. (2017) and has four pathways. Each pathway operates on a different resolution and region of interest (ROI), allowing both a broader ROI and fine details to be processed simultaneously. These pathways are concatenated, followed by extra convolutional layers to predict the final delineation. Next, the automated delineation (Auto) of OARs was performed on planning CT images of 15 new patients. Then, the automated delineations were subsequently corrected by a senior resident and supervised by the treating physician

prior to treatment planning (Auto+Corr). Two weeks later the same OARs were manually delineated by the same two radiation oncologists (Manual). To quantify efficiency of automated delineation, the time taken for correction of the automated delineation was compared to manual delineation time. Dice similarity coefficients (DSCs) were calculated to quantify overlap between different contours (Auto, Auto+Corr, Manual) where a value of "1" represents perfect and "0" no overlap (Figure 1).

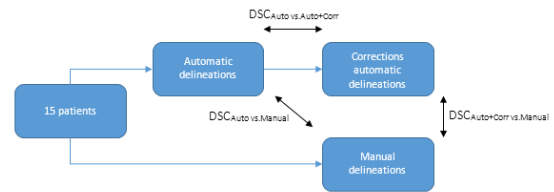


Figure 1: Overview of delineation process and DSCs relationships

$DSC_{Auto+Corr vs Manual}$  represents the overlap between manual delineation and corrected automated delineation

$DSC_{Auto vs Manual}$  represents the overlap between automated delineation and manual delineation

$DSC_{Auto vs Auto+Corr}$  represents the overlap between automated delineation and corrected automated delineation

### Results

Average correction time was significantly shorter than the average time needed for complete manual delineation (21 versus 34 minutes respectively,  $p < 6.5E-4$ ). The CNN performed best for spinal cord, oral cavity, mandible, brainstem and parotid glands with median  $DSC_{Auto vs Manual}$  of 0.92, 0.91, 0.91, 0.87 and 0.86 respectively. Median  $DSC_{Auto vs Auto+Corr}$  for these same OARs was 0.99, 0.96, 0.99, 0.94 and 0.97 respectively and this was in general significantly higher compared to  $DSC_{Auto vs Manual}$  ( $p < 1.1E-6$ ). For all OARs except supraglottic larynx, median  $DSC_{Auto vs Auto+Corr}$  was higher than  $DSC_{Auto+Corr vs Manual}$ , indicating that the corrections applied were smaller than the intra-observer variability (figure 2).

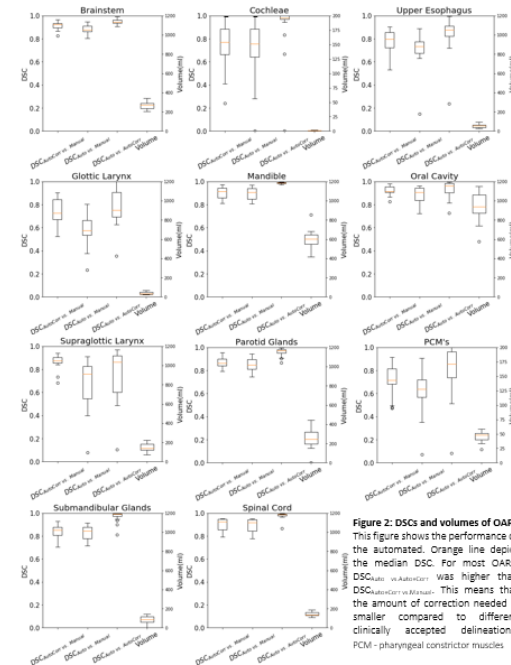


Figure 2: DSCs and volumes of OARs. This figure shows the performance of the automated. Orange line depict the median DSC. For most OARs,  $DSC_{Auto vs Auto+Corr}$  was higher than  $DSC_{Auto+Corr vs Manual}$ . This means that the amount of correction needed is smaller compared to different clinically accepted delineations. PCM - pharyngeal constrictor muscles

### Conclusion

We developed a CNN that allows more time efficient delineation of OARs in HNC patients. The CNN is able to produce automated delineations that only need small alterations in most OARs and it has therefore been implemented in clinical practice in our hospital.

### PO-0724 Texture analysis for predicting laryngeal preservation in advanced laryngo-pharyngeal cancers

Abstract withdrawn

**PO-0725 Multimodality imaging employing FDG-PET/CT paves the way for de-escalation of the elective dose**  
**S. Van den Bosch<sup>1</sup>, P.A.H. Doornaert<sup>2</sup>, C.H.J. Terhaard<sup>2</sup>, J.H.A.M. Kaanders<sup>1</sup>**

<sup>1</sup>Radboud University Medical Center, Radiation Oncology, Nijmegen, The Netherlands ; <sup>2</sup>University Medical Center Utrecht, Radiation Oncology, Utrecht, The Netherlands

**Purpose or Objective**

Modern multimodality imaging has improved the detection threshold of small nodal metastases in head and neck squamous cell carcinoma (HNSCC). This influences the tumorload in elective nodal target volumes and may have consequences for the radiotherapy dose required to control disease in this volume. This study investigates the effects of the introduction of FDG-PET/CT for radiotherapy planning on neck recurrence in HNSCC.

**Material and Methods**

A patient cohort that was treated for HNSCC with definitive (chemo)radiotherapy using IMRT/VMAT techniques in two tertiary head and neck clinics in The Netherlands from 2008-2016 was retrospectively analyzed. The focus of this analysis was on regional recurrence in the elective nodal target volume. For this purpose, co-registration was performed of the scans acquired during follow-up demonstrating the neck recurrence and the initial radiotherapy planning (FDG-PET)CT-scan. Actuarial rates of recurrence were calculated using the Kaplan-Meier method and multivariate analyses were performed using the Cox proportional-hazards model.

**Results**

A total of 633 patients with all stages HNSCC were included. A pre-treatment FDG-PET/CT-scan was acquired in 46% (290/633) and concomitant chemotherapy was administered in 38% (238/633) of the patients. Median follow-up was 32 months (IQR: 20-41). Two years after treatment, recurrence in the elective nodal target volume was observed in 3.9% (95% CI: 2.3-5.5) (24/633) of all patients. This was only 2.0% (95%CI: 0.2-3.8) in patients that had a FDG-PET/CT-scan for treatment planning ( $n=290$ ) versus 5.6% (95% CI: 3.1-8.2) in patients without ( $n=343$ ) ( $p=0.01$ ). The majority of these recurrences occurred synchronously with local recurrence: 17.4% (95% CI: 9.6-25.2) and were isolated in only 1.1% (95% CI: 1.0-1.2) ( $p<0.001$ ). For patients free of local recurrence, no recurrences in the elective nodal target volume occurred when a FDG-PET/CT-scan was acquired prior to treatment ( $p=0.01$ ). No differences in the rate of recurrence in the elective nodal target volume occurred in patients treated with concomitant chemotherapy 3.9% (95% CI: 1.2-6.6) versus 3.9% (95% CI: 1.9-5.9) ( $p=0.65$ ). In multivariate analyses, both local recurrence ( $p<0.001$ ) and acquisition of FDG-PET/CT-scan prior to treatment ( $p=0.03$ ) were significant predictors for recurrence in the elective nodal target volume, concomitant chemotherapy was not ( $p=0.59$ ).

**Conclusion**

The vast majority of nodal recurrences in the elective nodal target volume occur synchronously with local recurrence. Further, concomitant chemotherapy does not reduce this recurrence rate. Both observations indicate that most of these nodal manifestations are new seedings from the local recurrent tumor. Isolated recurrences in the elective nodal target volume are extremely rare (1.1%) and none occurred when FDG-PET/CT-scan was used for radiotherapy planning. This strongly supports the notion that elective neck dose can be safely de-escalated resulting in reduced toxicity of HNSCC radiotherapy.

**PO-0726 Lower toxicity incidence after SPECT/CT-guided elective nodal irradiation for head and neck cancer**

**P. De veij mestdagh<sup>1</sup>, W.V. Vogel<sup>2</sup>, M.L. Donswijk<sup>2</sup>, E. Lamers<sup>1</sup>, C. Carbaat<sup>1</sup>, W.H. Schreuder<sup>3</sup>, M.W.M. Van den Brekel<sup>3</sup>, A. Al-Mamgani<sup>1</sup>**

<sup>1</sup>Netherlands Cancer Institute / Antoni van Leeuwenhoek, Radiotherapy, Amsterdam, The Netherlands ; <sup>2</sup>Netherlands Cancer Institute / Antoni van Leeuwenhoek, Nuclear Medicine, Amsterdam, The Netherlands ; <sup>3</sup>Netherlands Cancer Institute / Antoni van Leeuwenhoek, Head and Neck surgery, Amsterdam, The Netherlands

**Purpose or Objective**

The great majority of patients with lateralized head and neck squamous cell carcinoma (HNSCC) treated with radiotherapy routinely undergo bilateral elective nodal irradiation (ENI), even though the incidence of contralateral regional failure after unilateral ENI is low. Excluding the contralateral neck from elective irradiation could reduce radiation-related toxicity and improve quality of life. The SUSPECT study (NCT02572661), a prospective fase 2 trial, investigates the feasibility, safety and clinical benefits of a novel, image-guided approach, in which lymph drainage mapping guides the elective irradiation of the neck in HNSCC patients. While we await data maturation for evaluation of oncologic safety, we report on the incidence, severity and duration of acute and late toxicity.

**Material and Methods**

Patients with lateralized cT1-3N0-2bM0 HNSCC were eligible for treatment with selective SPECT/CT-guided ENI (SSG-ENI). In case no contralateral drainage was visualized on SPECT/CT, patients received ipsilateral ENI only. If contralateral drainage to one "hot spot" was visible, the elective irradiation to the contralateral neck would be limited to the level containing the hot spot. In case of  $\geq 2$  contralateral hot spots on SPECT/CT, the patient was treated with conventional bilateral ENI, and not evaluable for the study endpoints. A matched historical cohort was formed that received conventional bilateral ENI (B-ENI) according to international guidelines. Matching was done based on tumor subsite, T- and N-classification, whether the patient received chemotherapy, and (for oropharyngeal tumors) HPV-status. Planning and treatment technique were identical to the study cohort.

**Results**

Fifty patients were treated with SSG-ENI, and were matched to 50 patients treated with B-ENI. Aside from follow-up time and CTV-PTV margin, baseline characteristics between the cohorts did not significantly differ. Mean irradiation doses to organs at risk were lower in the SSG-ENI cohort vs. the B-ENI cohort (contralateral parotid: 5 vs. 19 Gy; contralateral submandibular: 20 vs. 46 Gy; larynx: 39 vs. 52 Gy; constrictor muscles: 39 vs. 53 Gy; all tests  $p<0.001$  [Mann-Whitney-U]). The SSG-ENI cohort had a lower incidence of acute dysphagia, including tube feeding incidence (SSG-ENI: 10%, B-ENI: 50%,  $p<0.001$  [ $\chi^2$ ]), and a shorter median duration of acute mucositis and dysphagia. In the first year after treatment, incidences of grade $\geq 2$  late xerostomia and grade $\geq 2$  late dysphagia were significantly lower in the SSG-ENI cohort, including tube feeding incidence (3% vs. 26%,  $p=0.002$  [ $\chi^2$ ]). On multivariate logistic regression, bilateral ENI (OR 7.89, 95% CI 2.17-28.61,  $p=0.002$ ) and concurrent chemotherapy (OR 4.58, 95% CI 1.33-15.76,  $p=0.016$ ) were predictive for feeding tube placement.

Table 1: Comparison of acute and late toxicity between groups

	Incidence: n (%)			Duration: median (range) in days		
	SSG-ENI	B-ENI	p-value	SSG-ENI	B-ENI	p-value
Acute toxicity						
n=50/50						
Dermatitis grade ≥2	28 (56)	33 (66)	n.s.	21 (12-51)	25 (10-154)	n.s.
Dermatitis grade 3	11 (22)	7 (14)	n.s.	14 (10-21)	21 (5-29)	n.s.
Mucositis grade ≥2	40 (80)	44 (88)	n.s.	40 (14-120)	50 (14-206)	0.010
Mucositis grade 3	22 (44)	22 (44)	n.s.	26 (14-89)	51 (14-133)	0.023
Dysphagia grade ≥2	27 (54)	41 (82)	0.003	37 (13-150)	110 (12-155)	<0.001
Dysphagia grade 3 (tube feeding)	5 (10)	25 (50)	<0.001	45 (34-118)	102 (15-155)	n.s.
Late toxicity (90 days - 1 year)						
n=40/42						
Soft tissue fibrosis grade 2*	1 (2.5)	1 (2.4)	n.s.			
Xerostomia grade 2*	3 (7.5)	22 (52.4)	<0.001			
Dysphagia grade ≥2	1 (2.5)	17 (40.5)	<0.001			
Dysphagia grade 3 (tube feeding)	1 (2.5)	11 (26.2)	0.002			

Toxicity incidences: chi-squared test; toxicity duration: Mann-Whitney U test. All tests two-sided. \* no patients with grade 3 toxicity.

## Conclusion

Selective SPECT/CT-guided ENI decreased acute dysphagia, feeding tube placement, and late xerostomia, compared to conventional bilateral ENI. Additionally, it resulted in shorter duration of acute toxicity in general.

## PO-0727 Voice outcome following radiotherapy or laser microsurgery in patients with early glottic cancer

A. Allajbej<sup>1</sup>, F. Patani<sup>2</sup>, S. Di Biase<sup>2</sup>, D. Fasciolo<sup>2</sup>, C. Di Carlo<sup>2</sup>, C. Rosa<sup>2</sup>, L. Gasparini<sup>2</sup>, M. Di Francesco<sup>3</sup>, G. Falcone<sup>4</sup>, G. Quaternato<sup>5</sup>, A. Croce<sup>5</sup>, A. Di Pilla<sup>2</sup>, M. Trignani<sup>2</sup>, L. Caravatta<sup>2</sup>, D. Genovesi<sup>2</sup>

<sup>1</sup>SS. Annunziata, Radiotherapy, Chieti, Italy; <sup>2</sup>SS Annunziata, Radiotherapy, Chieti, Italy; <sup>3</sup>Papa Paolo VI Foundation, Speech rehabilitation, Chieti, Italy; <sup>4</sup>Papa Paolo VI Foundation, Phoniatrics, Chieti, Italy; <sup>5</sup>SS Annunziata, Otorhinolaryngology, Chieti, Italy

## Purpose or Objective

Oncological outcome of patients affected by early glottic cancer (EGC) treated with radiotherapy (RT) either Laser Microsurgery (LM) is similar, but it is not clear if and how these treatment modalities could differ in terms of voice quality (VQ) outcome and voice handicap. Prospective randomized studies comparing vocal outcomes following RT vs LM are lacking and voice evaluation methodology during follow-up is often not well structured. The aim of our study is to report clinical outcomes, focalizing on voice quality of patients who received either RT or LM.

## Material and Methods

We evaluated 45 EGC patients (Tis, T1 and T2 stages) submitted to primary RT or LM between 2008-2017. Overall survival (OS), progression free survival (PFS) and radiation induced toxicities according to CTCAE v. 4.0 scale were evaluated. For a subsample of this EGC population a multi-modality VQ analysis was performed. Voice evaluation includes: Voice Handicap Index (VHI-30), objective analysis using PRAAT software and perceptual rating performed by speech therapist (GRBAS scale). A clinical examination was performed jointly with radiation oncologist, otolaryngologist and speech pathologist, involving laryngeal evaluation with videostroboscope (VS) and laryngoscope

## Results

A total of 30 patients, average age of 74 years (range 54-86), received RT with a total dose of 66-70 Gy, 2 Gy/day, using 3-dimensional conformal technique. 15 patients received LM. Overall tumor stage distribution was: Tis (8.9%), T1 (86.7%), and T2 (4.4%). The median follow-up was 40.5 months (range 6-115 months). OS and PFS were 96.6% and 96.6% for RT group and 93.3% and 86.7% for LM group; from the original sample of 45 patients, in the context of ongoing VQ analyses 16 patients were evaluated to date. VHI-30 scores showed a mild (25.5) and severe (73.6) voice disability for RT and LM groups, respectively. Regarding GRBAS scale voice dysfunction in the LM group tends to be more moderate (67%) than severe (33%) whereas in the RT group tends to be more mild (40%) than moderate (20%).

VS evaluation showed reduced vocal cord motion in 50% of LM group and 10% of RT group and incomplete glottic closure in 100% of LM group and 40% of RT group. In the table we reported the vocal acoustic analysis and VS evaluation in both groups.

Table . Summary of videostroboscopy evaluation and vocal acoustic analysis of RT and LM groups

Laryngeal videostroboscopy evaluation		
Variable	RT (%)	LM (%)
Vocal cord motion		
Normal	80	50
Reduced	10	50
Amplitude vibration		
Normal	50	33,3
Increased	40	66,7
Mucosal wave		
Normal	80	33,3
Edema	10	66,7
Glottic closure		
Complete	50	0
Incomplete	40	100
Vocal acoustic analysis		
Variable	RT (mean ± SD)	LM (mean ± SD)
F <sub>0</sub> (Hz)	131,6 ± 23,8	206,8 ± 85,02
MPT (sec)	10,9 ± 3,21	7,44 ± 3,92
Jitter (%)	1,1 ± 1,52	1,86 ± 2,5
Shimmer (%)	10,35 ± 5,49	11,51 ± 5,58
HNR (dB)	13,48 ± 5,65	13,87 ± 5,60

\* For 1 patient in the RT group cordal examination was not possible due to important vagovagal reflex

MPT: Maximum phonation time, F<sub>0</sub> (Hz): Fundamental frequency, Jitter (%): Frequency variation, Shimmer (%): amplitude variation, HNR (dB): Harmonic s-to-Noise ratio. Threshold for pathologic voice: Jitter ≥ 1.04%, Shimmer ≥ 3.81%

## Conclusion

EGC patients can benefit from LM or RT both aimed to obtain organ and function preservation; as patients submitted to RT or LM can achieve similar OS and PFS rates, it is all about vocal "performance". Preliminary results from the recorded data (VHI-30, GRBAS scale and PRAAT analysis) seem to show a more favorable voice outcome in RT patients vs LM. The study is still ongoing; we attempt to recruit more patients, so then statistical analysis will be performed in order to compare clinical and voice outcome in two treatment modalities (RT and LM) and to confirm these results.

## PO-0728 Irradiation of salivary gland tumors with carbon ion radiotherapy (CIRT) at CNAO

B. Vischioni<sup>1</sup>, B. Dhanireddy<sup>2</sup>, M. Bonora<sup>1</sup>, S. Ronchi<sup>1</sup>, V. Vitolo<sup>1</sup>, M.R. Fiore<sup>1</sup>, E. D'Ippolito<sup>1</sup>, R. Petrucci<sup>1</sup>, C. Severo<sup>3</sup>, E. Ciurlia<sup>4</sup>, A. Hasegawa<sup>5</sup>, A. Iannalfi<sup>1</sup>, F. Valvo<sup>1</sup>, R. Orecchia<sup>1,6</sup>

<sup>1</sup>National Center of Oncological Hadrontherapy, Radiotherapy Unit, Pavia, Italy; <sup>2</sup>Post Graduate Institute of Medical Education and Research PGIMER, Department of Radiation Oncologist, Chandigarh, India; <sup>3</sup>University of Messina, Radiation therapy Unit, Messina, Italy; <sup>4</sup>Ospedale Vito Fazzi, Radiation therapy Unit, Lecce, Italy; <sup>5</sup>Osaka Heavy Ion Therapy Center, Radiation therapy Unit, Osaka, Japan; <sup>6</sup>European Institute of Oncology, Radiation therapy Unit, Milan, Italy

## Purpose or Objective

to report oncologic and functional outcomes of carbon ion radiotherapy (CIRT) in re-radiation setting for recurrent salivary gland tumors at CNAO.

## Material and Methods

From november 2013 to december 2016 patients (pts) with recurrent salivary gland tumors were enrolled in a phase-II protocol (CNAO-S14) to evaluate outcome of CIRT in the setting of carbon ions head and neck re-radiation in terms of toxicity and tumor control.

## Results

A total of 51 pts enrolled on the protocol were recurrent salivary gland tumors. Pts median age was 60 years (± 14.34), 53% males and 47% females. Majority of pts (74.5%) had adenoid cystic carcinoma, rT4a (51%) and rT4b (37%) stage, 90% without clinically diagnosed nodal

disease. Median dose of prior photon based radiation was 60Gy ( $\pm$  SD: 10.4, range: 24-78Gy). Median time interval between prior radiation and recurrence was 6.33 years (SD: 3.67, range: 1.08 to 20 years). Median dose of CIRT at the time of re-radiation was 60GyE at 3 GyE per fraction. During re-radiation, 11 pts (21.6%) had G0 toxicity (no toxicity), 19 pts (37.3%) had G1, 19 pts (37.3%) had G2 and 2 pts (3.9%) had G3 toxicity. Median follow-up was 19 months (SD: 14.42, range: 2-57). Twenty one (41.2%) pts had stable disease and 30 pts (58.8%) tumor progression at the time of last follow up. Furthermore, 14 pts (27.5%) had no late toxicity, 9 (18%) pts had G1, 19 pts (37%) had G2 and 9 pts (17.5%) had G3 late toxicities. Using Kaplan Meier method, estimated PFS (actuarial) at one, two and three years were 80%, 65.1% and 43.5% respectively. Estimated OS (actuarial) at one, two and three years were 90.2%, 69.1% and 54.5% respectively. The estimated mean and median PFS was 28.89 (SD: 3.06) and 25.00 (5.95) months respectively. In receiver operating curve (ROC) analyses, there was significant difference of median survival time after CIRT between the cut-off value of 34 cc of GTV in treated pts. The estimated median PFS in pts with GTV less than 34 cc and more than 34 cc were 34.00 ( $\pm$ 3.37) and 13 months ( $\pm$ 7.13) respectively (log rank test,  $p=0.038$ ).

### Conclusion

In re-radiation setting, CIRT is effective in controlling local progression of recurrent salivary gland tumors along with acceptable rates of acute and late toxicity.

### PO-0729 Prognostic factors analysis in a cohort of Nasopharyngeal cancer patients with 5-year follow-up

N.A. Iacovelli<sup>1</sup>, A. Cavallo<sup>2</sup>, A. Cicchetti<sup>3</sup>, L. Ferella<sup>1</sup>, N. Facchinetti<sup>1</sup>, T. Giandini<sup>2</sup>, S. Meroni<sup>2</sup>, D.A. Romanello<sup>1</sup>, P. Bossi<sup>4</sup>, L. Licitra<sup>4</sup>, E. Pignoli<sup>2</sup>, C. Fallai<sup>1</sup>, E. Orlandi<sup>1</sup>  
<sup>1</sup>Fondazione IRCCS Istituto Nazionale dei Tumori di Milano, Radiotherapy Unit 2, Milan, Italy; <sup>2</sup>Fondazione IRCCS Istituto Nazionale dei Tumori di Milano, Medical Physics Unit, Milan, Italy; <sup>3</sup>Fondazione IRCCS Istituto Nazionale dei Tumori di Milano, Prostate Cancer Program, Milan, Italy; <sup>4</sup>Fondazione IRCCS Istituto Nazionale dei Tumori di Milano, Head and Neck Medical Oncology Unit, Milan, Italy

### Purpose or Objective

To evaluate clinical outcome and prognostic factors in a consecutive series of non-metastatic nasopharyngeal carcinoma (NPC) patients (pts) treated curatively with intensity modulated radiotherapy (RT) techniques (IMRT, Intensity Modulated Radiation Therapy or VMAT, Volumetric Modulated Arc Therapy) and chemotherapy (CT) with a minimum follow-up of 5 years.

### Material and Methods

A retrospective analysis of consecutive non-metastatic NPC pts treated between 2005 and 2013 was conducted. According to WHO, 123 patients (89.8%) were suffering from undifferentiated NPC, 5 patients (3.6%), 2 patients (1.5%) and 7 patients (5.1%) were respectively affected by squamous cell carcinoma G1, G2 or G3. Two pts were in stage I (1.5%), 23 pts (16.8%) were in stage II, 38 pts (27.7%) in stage III, 29 pts (21.2%) in stage IVA and 45 pts (32.8%) in stage IVB. Five pts (3.6%) received RT alone: 1 pt in stage I and 4 pts in stage II. Of the remaining 132 pts (96.4%) (9 pts with stage II and 123 pts with stage III and IV) 30 patients (21.9%) received CT concomitant to RT and 102 patients (74.4%) were treated with induction CT followed by RT-CT. IMRT was given with standard fractionation at a total dose of 70 Gy. A dedicated software (VODCA, www.vodca.ch) was used to collect and analyze dosimetric parameters. Clinical outcomes investigated in the study were local control (LC), disease-free survival (DFS) and overall survival (OS). Kaplan-Meier analysis was performed for the outcomes considering dose and coverage parameters, staging, CT and RT technique.

### Results

Overall, 137 pts were eligible for this retrospective analysis. With a median follow up of 70 months (range 12 - 143) actuarial rates at 2 and 5 years were respectively: LC 92.2% and 90.4%, DFS 83.1% and 77.2% and OS 92.4% and 82.8%. The median follow-up period was 70 months (range 12-143 months). T stage was dichotomized as T1-T2-T3 vs T4. At 5 years the group T1-T2-T3 reported a LC of 93%, a DFS of 79% and a OS of 88%, whereas T4 pts reported a LC, DFS and OS respectively of 56%, 50% and 78%. All outcomes (LC, DFS and OS) were significantly better with VMAT compared to conventional IMRT (Table 1). In particular T4-stage pts treated with VMAT fared similarly compared to pts with T1-T2-T3 stages treated with conventional IMRT (Figure 1). Regardless of RT technique, pts with a V95% > 95.5% had better LC ( $p=0.006$ ). Pts with a D99% > 63.8 Gy had better LC ( $p=0.034$ ) and OS ( $p=0.005$ ). The threshold value of 43.2 cc of GTV T was prognostic for LC ( $p = 0.016$ ). At multivariate analysis GTV T, RT technique (VMAT) and D99% resulted prognostic for LC ( $p=0.04$ ).

Parameter	Patients	LC	LC stat.	DFS	DFS stat.	OS	OS stat.
T1-T2-T3	98	93%	HR=5.67	79%	HR=2.36	88%	HR=2.15
T4	39	56%	$p<0.001$	50%	$p=0.014$	78%	$p=0.09$
VMAT	64	95%	HR=3.75	89%	HR=3.01	97%	HR=6.81
IMRT	73	78%	$p=0.027$	63%	$p=0.007$	77%	$p=0.03$

Tab1. Statistical values of Kaplan-Meier analysis for the three outcomes: survival rate, hazard ratios (HR) and p-value.

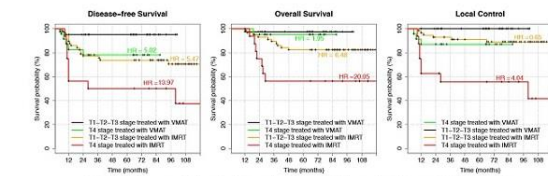


Fig. 1. Kaplan-Meier curves for the analyzed outcomes. Patients were stratified according to T stage and radiotherapy modality. (In black) Control (no late toxicity) and (in red) late toxicity (G1, G2, G3). HR= Hazard Ratio. OS= Overall Survival. DFS= Disease-free Survival. LC= Local Control.

### Conclusion

Although in a retrospective series, we demonstrated the prognostic value of some dose-volume parameters, potentially useful to improve planning procedure. In addition, for the first time in a non-endemic area, a threshold value of GTV T, prognostic for LC, has been confirmed.

### PO-0730 NTCP model for penetration/aspiration after (chemo)radiation including DVH parameters.

A. Gawryszuk<sup>1</sup>, H.P. Van der Laan<sup>1</sup>, R.J.M. Steenbakkers<sup>1</sup>, J.G.M. Van den Hoek<sup>1</sup>, H.P. Bijl<sup>1</sup>, J.A. Langendijk<sup>1</sup>  
<sup>1</sup>University Medical Center Groningen- Groningen, Department of Radiation Oncology, Groningen, The Netherlands

### Purpose or Objective

Late aspiration, especially silent, is one of the most hazardous complications after (chemo)radiation ((CH)RT) for head and neck cancer, resulting in 3-year morbidity rates of approximately 20% and increased mortality. However, limited data exists on dose-effect relationship for late aspiration. Radiation doses to some of the swallowing organs at risk (SWOARs), such as pharyngeal constrictor muscles, are associated mainly with the subjective dysphagia measurements. The purposes of this analysis was to identify the best predictors of penetration/aspiration (as assessed on videofluoroscopy (VF)), after (CH)RT, using clinical data as well as DVH parameters.

### Material and Methods

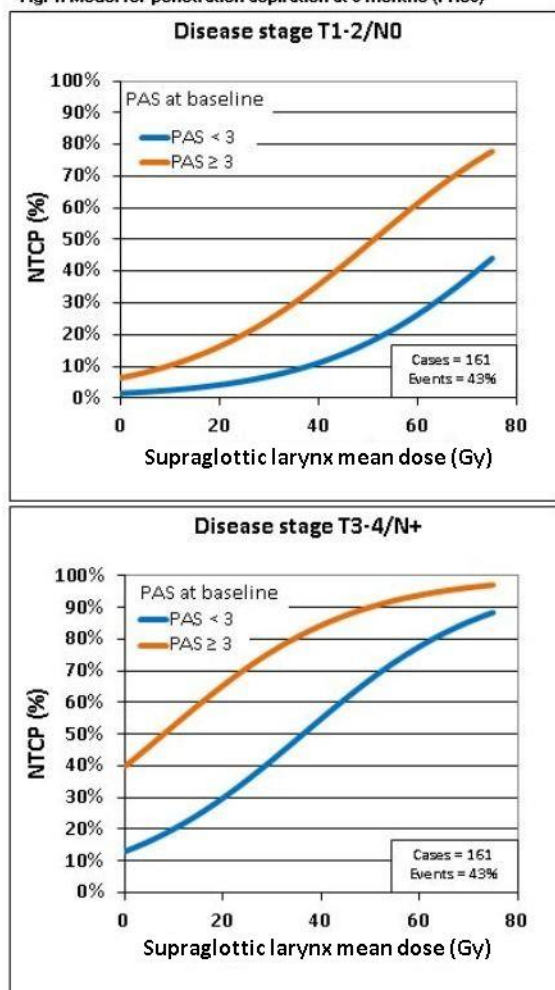
This prospective cohort study included 186 head and neck cancer patients receiving definitive (CH)RT. Patients underwent a comprehensive dysphagia assessment (including VF) at baseline and 6 months after treatment. 161 patients underwent VF at both time points and were included in this analysis. The primary endpoint was a Penetration Aspiration Scale (PAS) score  $\geq 3$

(penetration/aspiration) at 6 months after treatment, scored with VF (PAS6). From all baseline features, a set of candidate variables was selected based on plausible relevance in relation to PAS6. Average doses ( $D_{\text{mean}}$ ) to SWOARs were collected. Additionally, univariable analysis with correction for cross correlation of candidate variables was performed. Multivariable logistic regression with stepwise forward elimination and internal validation, using bootstrapping, was performed to correct for optimism of the model for PAS6.

### Results

The prevalence of PAS6 was 43% (73 patients). The best performing model included 4 independent prognostic factors for PAS6: PAS at baseline, T-stage, N-stage and  $D_{\text{mean}}$  to the supraglottic larynx. Figure 1. After internal validation using bootstrapping the model performance (Nagelkerke  $R^2$ : 0,398; ROC-AUC: 0.818) and calibration were good.

Fig. 1. Model for penetration aspiration at 6 months (PAS6)



### Conclusion

Patients with more advanced disease are at the highest risk of penetration/aspiration after (CH)RT. This risk increases substantially in case of penetration/aspiration observed at baseline VF. Moreover, increasing dose to supraglottic larynx contributes to further escalation of the risk of penetration/aspiration 6 months after (CH)RT.

### PO-0731 Transition from anatomical to geometric expansion modality for high-risk CTV in oropharyngeal cancer

P. Bonomo<sup>1</sup>, I. Desideri<sup>1</sup>, C. Becherini<sup>1</sup>, L. Visani<sup>1</sup>, V. Salvestrini<sup>1</sup>, M. Mariotti<sup>1</sup>, P. Garlatti<sup>1</sup>, L. Dominici<sup>1</sup>, L.

Livi<sup>1</sup>

<sup>1</sup>Azienda Ospedaliero-Universitaria Careggi, Radiation Oncology, Florence, Italy

### Purpose or Objective

The definition of primary tumor clinical target volume (CTV) for HNSCC has been recently reviewed in international guidelines. The aim of our work was to assess the impact of two different delineation approaches (anatomical vs geometric expansion) on the clinical outcome of patients with oropharyngeal cancer (OPC).

### Material and Methods

We performed a retrospective analysis of consecutive patients treated at our institution for OPC between January 2010 and April 2018. In 2014, our local policy to delineate high risk (HR) CTV for both primary (CTV-p) and nodal (CTV-n) GTVs shifted from an anatomical expansion (AE) to a geometric expansion (GE) modality, described as follows:

- AE: CTV-p consisted of the primary GTV plus the whole oropharyngeal anatomical compartment, edited for air cavities and anatomical barriers; CTV-n consisted of the nodal GTVs plus the corresponding lymph node level (delineated according to Gregoire's classification), including also the level immediately adjacent to it

- GE: CTV-p consisted of the primary GTV plus an isotropic 5 mm margin, manually edited for air cavities and anatomical barriers; CTV-n consisted of the nodal GTVs plus an isotropic 7 mm margin, manually edited to take into account anatomical barriers (i.e. sternocleidomastoid muscle, if not infiltrated). Of note, an additional 5 mm margin to the CTV-p was not added.

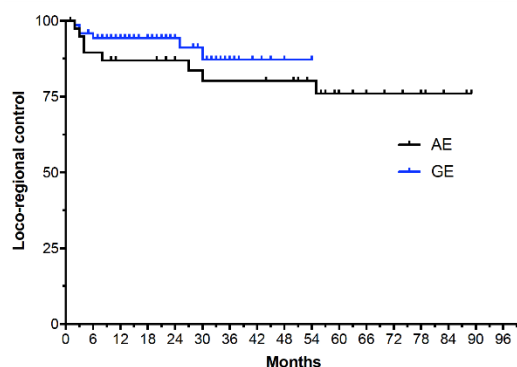
All patients received IMRT with 3 dose levels: the high, intermediate and low risk CTVs received 70, 60 and 50 Gy or 69.9, 59.4 and 52.8 Gy in 35 or 33 fractions, respectively, depending on whether a sequential or SIB technique was employed. A 3-5 PTV margin was added to CTV's (3 mm in case of daily image guidance). HPV status was not routinely available until 2015.

Locoregional control (LRC) was defined as the time from the last treatment day to local or nodal failure or both. Progression-free survival (PFS) was defined as the time from the last treatment day to disease progression or death from any cause. Overall survival (OS) was defined as the time from OPC diagnosis to death from any cause. Median LRC, PFS and OS were calculated. The relative estimates of LRC and PFS at 24 months were estimated by the Kaplan-Meier method.

### Results

A total of 116 patients were included (table 1). In terms of HR CTV expansion modality, 43 (37.1%) were treated with AE and 63 (62.9%) with GE, respectively. One patient in the AE cohort was lost to follow-up after first evaluation, therefore 115 patients are evaluable for outcome analysis. At a median follow-up of 26 months (range: 1-86), 87 patients were alive (75.6%). The median LRC, PFS and OS for the whole group were 24 (95% CI: 25.3-33.8), 24 (95% CI: 24.6-33.2) and 31 (95% CI: 30.7-38.6) months, respectively. There was no difference between the AE and GE cohorts in terms of 2-year LRC (86.9% vs 94.3%;  $p=0.28$ ) (figure 1) and PFS (68.8% vs 80.9%,  $p=0.56$ ).

Characteristic	No. of patients (%), n = 116	AE (%), n = 43	GE (%), n = 73
Median age, years (range)	62.5 (43-88)	60 (43-81)	63 (43-88)
Sex			
Male	84 (72.4%)	28 (65.1%)	56 (76.7%)
Female	32 (17.6%)	15 (34.9%)	17 (23.3%)
ECOG Performance Status			
0	97 (83.6%)	37 (86%)	60 (82.1%)
1	19 (16.4%)	6 (14%)	13 (17.9%)
Charlson Comorbidity index (age-adjusted)			
<4	49 (42.2%)	22 (51.2%)	27 (36.9%)
4-7	63 (54.3%)	19 (44.1%)	44 (60.3%)
≥8	4 (3.5%)	2 (4.7%)	2 (2.8%)
Smoking history (packyears)			
0	23 (19.8%)	6 (13.9%)	17 (23.3%)
<10	19 (16.3%)	12 (27.9%)	7 (9.5%)
10-20	27 (23.3%)	5 (11.6%)	22 (30.2%)
>20	47 (40.6%)	20 (46.6%)	27 (37%)
HPV status			
Positive	52 (44.9%)	7 (16.3%)	45 (61.6%)
Negative	20 (17.2%)	7 (16.3%)	13 (17.8%)
Unknown	44 (37.9%)	29 (67.4%)	19 (26%)
AJCC stage (Vilth ed)			
II	11 (9.5%)	4 (9.3%)	7 (9.5%)
III	23 (19.8%)	7 (16.3%)	16 (22%)
IVA	72 (62.1%)	30 (69.7%)	42 (57.6%)
IVB	10 (8.6%)	2 (4.7%)	8 (10.9%)
Treatment modality			
RT alone	23 (19.8%)	16 (37.2%)	7 (9.2%)
conc. cisplatin-RT	88 (75.9%)	25 (58.2%)	63 (86.4%)
TPF followed by CRT	5 (4.3%)	2 (4.6%)	3 (4.14%)
IMRT schedule			
sequential	22 (18.9%)	6 (14%)	16 (22%)
SIB	94 (81.1%)	37 (86%)	57 (78%)



### Conclusion

The adoption of a GE expansion modality with resulting smaller HR CTVs was not associated with a detrimental impact on outcome in OPC.

### PO-0732 NTCP model for osteoradionecrosis after definitive radiotherapy in head and neck cancer patients.

N. Den Haan<sup>1</sup>, L. Van den Bosch<sup>1</sup>, A. Van den Hoek<sup>1</sup>, H. Bijl<sup>1</sup>, R. Steenbakkers<sup>1</sup>, M. Dieters<sup>1</sup>, H.P. Van der Laan<sup>1</sup>, H. Langendijk<sup>1</sup>

<sup>1</sup>University Medical Center Groningen, Radiation Oncology, Groningen, The Netherlands

### Purpose or Objective

The purpose of this prospective cohort study was to develop a normal tissue complication probability (NTCP) model for predicting the risk of mandibular osteoradionecrosis (ORN) in patients with head and neck cancer (HNC) treated with definitive (chemo)radiotherapy.

### Material and Methods

The population of this study was composed of 740 patients with HNC treated with definitive (chemo)radiotherapy in the period from January 2007 to June 2016. Mandibular ORN was scored prospectively as part of a standard follow-up program according to CTCAEv4.0. Mandibular dose-volume histograms (DVH) were extracted from the treatment planning system. Dosimetric parameters were compared using the Wilcoxon rank-sum test. The model

was developed using a multivariate logistic regression analysis with backward selection.

### Results

The median follow-up time for all patients was 36 months. In total 18 out of 740 cases (2.4%) developed ORN grade ≥ 2 and the median time to ORN was 12 months. The cumulative incidence of ORN over 6, 12, 18 and 24 months was 1.2, 2.1, 2.6 and 3.1%, respectively.

To identify the most important DVH-parameter, the mean values of the DVH-parameters between cases and non-cases were compared first. The mean and maximum dose to the mandible were higher among patients with ORN vs. non-cases (31.7 vs 45.3 Gy,  $p = 0.003$  and 53.1 vs 71.8 Gy,  $p < 0.001$ , respectively). DVH bins from V25 to V70 were all significantly higher in the ORN cohort compared with controls (figure 1). The best predictor for mandibular ORN was the V60 (volume receiving 60 Gy). No other significant prognostic factors or confounders for ORN were identified. The p-value for this model was 0.002, with an OR of 16.21 (95% CI 2.79-94.28) and an AUC of 0.78 (95% CI 0.71-0.85). See figure 2 for the NTCP model.

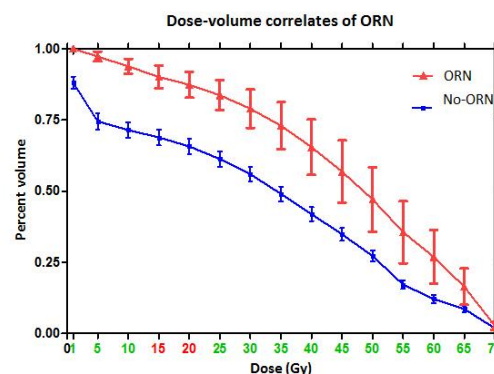


Figure 1. Comparison of the DVHs between the plans for ORN cases vs non-cases; each error bar is constructed using a 95% confidence interval of the mean. The numbers in green at the X-axis represent p-values <0.05, the numbers in red represent p-values >0.05.

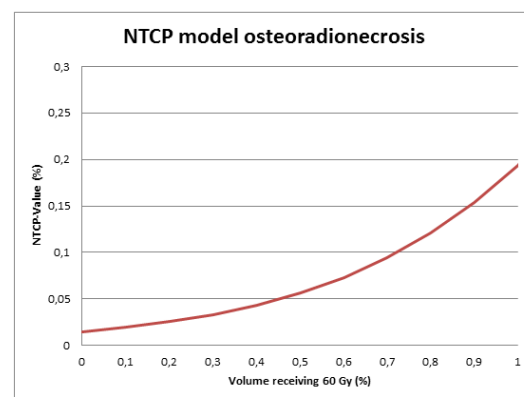


Figure 2. NTCP model osteoradionecrosis

### Conclusion

This is the largest prospective cohort study ever done on the development of mandibular ORN in patients treated with definitive radiotherapy or chemoradiation. In comparison to the incidence of ORN in the postoperative setting, the incidence of ORN is relatively low. The main risk factor is the dose to the mandible and in particular the high dose volume. The V60 turned out to be the most important prognostic factor.

### PO-0733 Non-invasive imaging for tumor hypoxia: a novel validated CT and FDG-PET-based Radiomic signature.

S. Sanduleanu<sup>1</sup>, A. Jochems<sup>2</sup>, T. Upadhaya<sup>3</sup>, A. Even<sup>2</sup>, R. Leijenaar<sup>2</sup>, F. Dankers<sup>4</sup>, R. Klaassen<sup>5</sup>, H. Woodruff<sup>2</sup>, M.

Hatt<sup>3</sup>, H. Kaanders<sup>4</sup>, O. Hamming-Vrieze<sup>6</sup>, H. Van Laarhoven<sup>7</sup>, R. Subramiam<sup>8</sup>, S. Huang<sup>9</sup>, B. O'Sullivan<sup>9</sup>, S. Bratman<sup>9</sup>, L. Dubois<sup>10</sup>, R. Miclea<sup>11</sup>, D. Di Perri<sup>12</sup>, X. Geets<sup>12</sup>, D. De Ruyscher<sup>13</sup>, F. Hoebbers<sup>14</sup>, P. Lambin<sup>2</sup>  
<sup>1</sup>Maastricht University, The-D Lab: Decision Support for Precision Medicine-, Maastricht, The Netherlands ;  
<sup>2</sup>Maastricht University, The-D Lab: Decision Support for Precision Medicine, Maastricht, The Netherlands ;  
<sup>3</sup>Université Brest, 3.Laboratory of Medical information processing, Brest, France ;  
<sup>4</sup>Radboud University Nijmegen Medical Centre, Department of Radiation Oncology, Nijmegen, The Netherlands ;  
<sup>5</sup>Academic Medical Centre, 7.Department of Medical Oncology, Amsterdam, The Netherlands ;  
<sup>6</sup>Antoni van Leeuwenhoek Medical Centre, Department of Radiation Oncology, Amsterdam, The Netherlands ;  
<sup>7</sup>Academic Medical Centre, Department of Medical Oncology, Amsterdam, The Netherlands ;  
<sup>8</sup>Johns Hopkins Medical Centre, Division of Nuclear Medicine-, Baltimore, The Netherlands ;  
<sup>9</sup>Princess Margaret Cancer Center, Department of Radiation Oncology, Toronto, Canada ;  
<sup>10</sup>Maastricht University, Department of Radiotherapy, Maastricht, The Netherlands ;  
<sup>11</sup>Maastricht University Medical Centre+, Department of Radiology, Maastricht, The Netherlands ;  
<sup>12</sup>Université catholique de Louvain, Center of Molecular Imaging, Brussels, Belgium ;  
<sup>13</sup>Maastricht Clinic, 2.Department of Radiation Oncology, Maastricht, The Netherlands ;  
<sup>14</sup>Maastricht Clinic, Department of Radiation Oncology, Maastricht, The Netherlands

#### Purpose or Objective

Tumor hypoxia increases resistance to radiotherapy and systemic therapy as well as promoting tumor metastasis. Our primary aim was to develop and validate a CT- and FDG-PET-based hypoxia classification signature based on radiomic features.

#### Material and Methods

A total of 131 patients (78 head and neck squamous cell carcinoma, 61 non-small cell lung cancer, 13 pancreatic carcinoma and 13 esophageal carcinoma) with low dose [<sup>18</sup>F]-HX4-PET/CT and 61 patients with [<sup>18</sup>F]-FDG-PET from 5 imaging centers were included. One dataset with [<sup>18</sup>F]-FAZA PET/CT (36 NSCLC) and another dataset (40 HNSCC) with pimonidazole stained tumor biopsies were used as additional external validation datasets. The primary gross tumor volumes (GTV) were manually delineated on CT. In order to create three dichotomized groups between hypoxic and well-oxygenated tumors, [<sup>18</sup>F]-HX4-derived hypoxic fractions (HF) were thresholded at 10%, 20% and 30%. The HX4-derived HF was defined as the ratio of the hypoxic region (tumor-to-background ratio > 1.4) to the total GTV. A random forest (RF)-based classifier was trained to stratify patients into hypoxia-positive/ negative cohorts based on radiomic features.

#### Results

In the 20% HF threshold group, the area under the receiver operating characteristic curve (AUC) for an RF model combining 5 CT-derived radiomic features achieved 0.79±0.16 in the Boston/ NKI and 0.76±0.18 in the UCL validation sets respectively. In the same threshold group, an RF model combining 10 radiomic features derived from FDG-PET reached an AUC of 0.74±0.23 to classify hypoxia in an external validation dataset (Boston/ Maastricht).

#### Conclusion

Our hypoxia signatures derived from CT and FDG-PET have the potential to inform interventional trials studying hypoxia-targeting agents by identifying patients with tumors likely to be hypoxic.

---

Poster: Clinical track: CNS

---

PO-0734 Patterns of Care in the Management of WHO Grade II and III Spinal Ependymomas

D. Yebo<sup>1</sup>, K. Liao<sup>2</sup>, B.A. Guadagnolo<sup>1</sup>, G. Rao<sup>3</sup>, A. Bishop<sup>4</sup>, C. Chung<sup>4</sup>, J. Li<sup>4</sup>, C.E. Tatsui<sup>3</sup>, L. Rhines<sup>3</sup>, S. Ferguson<sup>3</sup>, A. Paulino<sup>4</sup>, A. Ghia<sup>4</sup>  
<sup>1</sup>MD Anderson Cancer Center, Radiation Oncology- Joint appointment Health Services Department, Houston, USA ;  
<sup>2</sup>MD Anderson Cancer Center, Health Services Department, Houston, USA ;  
<sup>3</sup>MD Anderson Cancer Center, Neurosurgery, Houston, USA ;  
<sup>4</sup>MD Anderson Cancer Center, Radiation Oncology, Houston, USA

#### Purpose or Objective

Spinal ependymomas are rare with an incidence of 1 per 100,000. The management and patterns of care for spinal cord ependymomas require further investigation given the paucity of data for high grade disease.

#### Material and Methods

A National Cancer Database (NCDB) was searched for eligible patients >18 years old with a diagnosis of spinal ependymoma at a Commission on Cancer facility from 2004 through 2014. Chi-square test, simple logistic regression, and multivariable logistic regressions were used to assess the potential significance of associations between patient characteristics and treatment received. Facility volume characteristics were assessed in relation to survival by evaluating the number of patients diagnosed and the facility volume was organized by relative quartiles. We assessed the average number of patients seen at each facility within a 1-year timeframe and over an equivalent 10-year timeframe.

#### Results

Our study of 1,345 patients with high-grade spinal ependymoma and almost one decade of follow-up data uniquely describes practice patterns and long-term overall survival (OS) independent of treatment received for grade II and grade III ependymoma. The majority of grade II patients received surgery alone (81.1%). In contrast, 36.8% of grade III patients received surgery alone. Only 56.3% of grade III spinal ependymomas received adjuvant therapy with either radiation therapy (RT) or combination RT and chemotherapy after surgery. Over 60% percent of patients with grade III disease received initial adjuvant RT, in contrast to only 15.3% of patients with grade II ependymoma (P< 0.001). Patients living ≤20 miles from a RT facility were more likely to receive RT (P<0.001) than those living further away. On multivariable logistic regression, grade (grade III: OR 8.6, P<0.001) and facility distance were significantly associated with receipt of RT (P<0.0001). Among all patients, the 5 and 10-year OS rates were 94.7%/ 85.1% for patients with grade II disease and 58.2%/46.4% for those with grade III disease (P<0.0001). The OS rates were higher at facilities treating at least 1.5 patients per year (i.e., an average of 15 patients over 10 years), which corresponds to the top 81st percentile in facility volume. The 5-year OS rates were 96.7% for patients treated at high-volume facilities, followed by 93.4% at facilities treating 6-14 patients, 92.5% for 2-5 patients, and 86.8% for <2 patients over 10 years (P<0.0019).

#### Conclusion

In conclusion, our study is the largest series to date reporting observational patterns of care for grade II and III spinal ependymomas. Despite guideline recommendations for adjuvant therapy in all grade III ependymomas regardless of extent of resection, approximately 2 in 5 do not receive immediate adjuvant therapy and our data suggests this may be related to distance lived from a CoC facility. Facilities at which larger numbers of patients with spinal ependymomas are treated may experience better long-term outcomes.

---

PO-0735 Cognitive function after radiation therapy for brain tumours

L. Haldbo-Classes<sup>1</sup>, A. Amidi<sup>2</sup>, L. Wu<sup>3</sup>, S. Lukacova<sup>1</sup>, G. Von Oettingen<sup>4</sup>, R. Zachariae<sup>2</sup>, J. Kallehauge<sup>3</sup>, M. Hoyer<sup>5</sup>  
<sup>1</sup>Aarhus University Hospital, Department of Oncology,

Aarhus, Denmark ; <sup>2</sup>Aarhus University Hospital and Aarhus University, Department of Oncology and Department of Psychology and Behavioral Sciences, Aarhus, Denmark ; <sup>3</sup>Northwestern University Feinberg School of Medicine, Department of Medical Social Sciences, Chicago, USA ; <sup>4</sup>Aarhus University Hospital, Department of Neurosurgery, Aarhus, Denmark ; <sup>5</sup>Aarhus University Hospital, Danish Center for Particle Therapy, Aarhus, Denmark

### Purpose or Objective

To assess cognitive function in patients with a primary brain tumour treated with radiotherapy (RT). The extent of RT-induced changes in cognitive function is unknown. RT with protons instead of photons spares more healthy brain tissue and may reduce the risk of cognitive dysfunction; however, existing knowledge regarding the parts of the brain that need to be spared to prevent cognitive dysfunction, is limited. To determine the cognitive domains most affected by RT, we compared cognitive functioning in brain tumour patients treated with neurosurgery and RT with brain tumour patients treated with neurosurgery only. Furthermore, we investigated the correlations between cognitive scores and RT dose-volume parameters in specific areas of the brain.

### Material and Methods

A cross-sectional study assessing cognitive function in 110 patients with a primary brain tumour grade I-III or medulloblastoma (grade IV) treated at Aarhus University Hospital (AUH), Denmark, between 2006 and 2016. Two cohorts were established: A cohort of 81 brain tumour patients who had received neurosurgery followed by RT (RT+) and a cohort of 29 brain tumour patients who had only received neurosurgery (RT-). The patients completed questionnaires and underwent neuropsychological assessment with standardized tests. RT dose-volume histogram (DVH) of specific areas in the brain were extracted from the treatment plans to explore correlations between dose-volume parameters and cognitive scores.

### Results

Mean age was 53.5 years with an average time since diagnosis of 7.3 years. Compared with normative data, lower average scores were observed for the entire group in the following domains: verbal learning and memory ( $p < 0.001$ ), attention and working memory ( $p < 0.001$ ), processing speed ( $p < 0.001$ ), and executive functioning ( $p < 0.001$ ). Compared to RT- patients, RT+ patients scored lower on domains concerning processing speed ( $p = 0.04$ ) and executive function ( $p = 0.05$ ) and had higher impairment frequency on verbal fluency ( $p = 0.02$ ) with 16% of patients exceeding 1.5 SD below the normative mean. At time of analysis, 52 RT+ patients' DVH of the left hippocampus was extracted. When examining scores on Hopkins Verbal Learning Test (HVLT), a test assessing verbal learning and memory, higher RT dose to the hippocampus was correlated with the number of people with impaired scores on HVLT.

### Conclusion

Our results indicate that treatment, including RT, for a primary brain tumour may have negative long-term impact on cognitive function, especially on processing speed and executive function. Preliminary data suggest that higher RT dose to the left hippocampus is associated with greater verbal learning and memory impairment.

### PO-0736 Radiation necrosis after a combination of EBRT and iodine-125 brachytherapy in gliomas

I. Hadi<sup>1</sup>, D. Reitz<sup>1</sup>, R. Bodensohn<sup>1</sup>, O. Roengvoraphoj<sup>1</sup>, M. Niyazi<sup>1,2</sup>, C. Belka<sup>1,2</sup>, F. Kreth<sup>3</sup>, S.B. Nachbichler<sup>1</sup>

<sup>1</sup>University Hospital- LMU Munich, Department of Radiation Oncology, Munich, Germany ; <sup>2</sup>German Cancer Consortium DKTK, Department of Radiation Oncology,

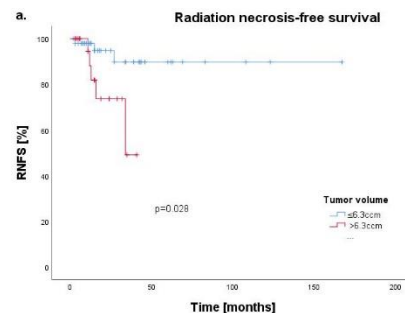
Munich, Germany ; <sup>3</sup>University Hospital- LMU Munich, Department of Neurosurgery, Munich, Germany

### Purpose or Objective

The frequency and the risk profile of radiation necrosis in patients with glioma undergoing either upfront stereotactic brachytherapy (SBT) and additional salvage external beam radiotherapy (EBRT) after tumor recurrence or vice versa remains unknown.

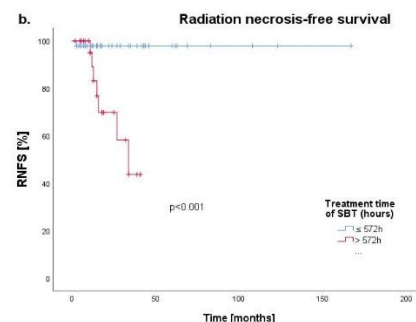
### Material and Methods

Patients with glioma treated with low-activity temporary iodine-125 SBT between 1999 and 2016 who had either additional upfront or salvage EBRT were included. Biologically effective doses were calculated. Radiation necrosis was diagnosed using stereotactic biopsy and/or metabolic imaging. The rate of radiation necrosis was estimated with the Kaplan Meier method. Risk factors were obtained from logistic regression models. ROC and AUC analyses were used to determine optimal cut-off values for identified risk factors.



### Results

Eighty-six patients (49 male, 37 female), with a median age of 47 years were included. Median follow-up was 15.0 months after second irradiation treatment. Fifty-eight patients received upfront EBRT (median total dose: 60 Gy), and 28 patients upfront SBT (median reference dose: 54 Gy, median dose rate: 10.0 cGy/h). The median time interval between both treatments was 19 months. In 8/75 (10.7%) patients a radiation necrosis was diagnosed. The one- and two- year risk of radiation necrosis was 5.1% and 11.7%, respectively. The logistic regression models indicated tumor volume of SBT (Fig.a), irradiation time of SBT (Fig.b), number of implanted seeds, and salvage EBRT as significant risk factors for radiation necrosis. Neither of the BED values nor the time interval between both treatments gained prognostic influence.



### Conclusion

The combination of upfront EBRT and salvage SBT or vice versa is feasible for glioma patients. The risk of radiation necrosis is mainly determined by the treatment volume but not by the interval between the therapies.

### PO-0737 Retrospective analysis of hypofractionated stereotactic radiotherapy for tumors larger than 2 cm

Y. Koide<sup>1</sup>, T. Kodaira<sup>1</sup>, H. Tachibana<sup>1</sup>, H. Tanaka<sup>1</sup>, N. Tomita<sup>2</sup>

<sup>1</sup>Aichi Cancer Center, Radiation oncology, Nagoya, Japan ; <sup>2</sup>Nagoya City University Graduate School of Medical Sciences, Department of Radiology, Nagoya, Japan

#### Purpose or Objective

Large brain metastases (BM) are associated with limited local control and neurotoxicity. Some recent studies reported that hypofractionated stereotactic radiotherapy (HFSRT) is a reasonable option for such tumors, relative to single-fraction therapy. We evaluated the efficacy and the safety of HFSRT for BM larger than 2 cm.

#### Material and Methods

From 2006 to 2016, 61 patients with BM larger than 2 cm were treated with HFSRT in our institution. The exclusion criteria were: (1) no available magnetic resonance imaging or computed tomography, (2) prior brain radiotherapy or surgery, and (3) combination with whole brain radiotherapy. All patients were treated using helical tomotherapy. The planning target volume (PTV) was set as the gross tumor volume plus a 2-mm margin in all dimensions. The prescription dose was 35 Gy in 5 fractions, and assigned to the 90% isodose surface used PTV coverage of 95%, normalized to 100% dose at the isocenter. Eligible patients were divided according to maximum BM diameter (group A [23 patients]:  $\geq 3$  cm, group B [22 patients]:  $< 3$  cm) to assess the relationship between tumor size and prognosis or safety. The primary endpoint was local control rate (LCR), and secondary endpoints were response rate (RR), brain progression-free survival (BPFS), median survival time (MST), and radionecrosis (RN). Univariate and multivariate analyses for LCR were conducted using Cox's proportional hazards model.

#### Results

A total of 45 patients with 58 lesions were eligible in this study. All patients completed planned HFSRT schedule without delay or discontinuation. At the last follow-up, 7 patients (15.6%) were alive, 34 patients (75.6%) had died, and 4 patients (8.9%) were lost to follow-up. The median follow-up period for all patients were 11.3 months (range: 1.7-93.9 months) and 15.2 months (range: 6.9-93.9 months) among patients who had not died. The median tumor volume for all lesions was 19.3 mL (range: 6.21-115.4 mL). The RR was 86.4% with an overall LCR of 64.7% at 12 months (67.1% for group A and 61.5% for group B [ $p = 0.45$ ]). The median BPFS and MST were 11.6 and 14.2 months, respectively. Univariate analyses revealed that female patients and gynecological cancer patients had poorer LCR, but they were not significantly independent prognostic factors in multivariate analyses ( $p = 0.06, 0.09$ , respectively). Two patients with breast cancer experienced RN (4.4%). One patient (group A) underwent resection 5 years after the HFSRT, and the other patient (group B) underwent resection 6 years after HFSRT.

#### Conclusion

HFSRT is safe for large BM but further studies are needed to determine optimal doses and fractions.

#### PO-0738 Extent of resection is potent prognostic factor next to molecular subtype in low-grade glioma

J. Choi<sup>1</sup>, S.H. Kim<sup>2</sup>, J.H. Chang<sup>3</sup>, S.H. Park<sup>1</sup>, C. Suh<sup>4</sup>

<sup>1</sup>Jeju National University Hospital, Radiation Oncology, Jeju, Korea Republic of ; <sup>2</sup>Yonsei University College of Medicine, Pathology, Seoul, Korea Republic of ; <sup>3</sup>Yonsei University College of Medicine, Neurosurgery, Seoul, Korea Republic of ; <sup>4</sup>Yonsei University College of Medicine, Radiation Oncology, Seoul, Korea Republic of

#### Purpose or Objective

We aimed to evaluate treatment outcomes and identify prognostic factors of low-grade glioma (LGG) patients according to the new 2016 WHO classification.

#### Material and Methods

The record of 153 patients diagnosed as WHO grade II LGG between March 2003 and November 2015 were retrospectively reviewed. Based on the 2016 WHO classification, 80 patients (52.3%) had diffuse astrocytoma (DA), IDH mutant; 45 patients (29.4%) had oligodendroglioma (ODG), IDH mutant and 1p/19q codeleted; and 28 patients (18.3%) had DA, IDH wild-type.

#### Results

The median age at diagnosis was 41 years (range, 22-74). Gross total resection (GTR) was performed in 71 patients (46.4%), subtotal resection in 31 (20.3%), partial resection in 43 patients (28.1%), and biopsy in 8 patients (5.2%). One hundred two patients (66.7%) received postoperative radiotherapy (RT). The median follow-up time was 69.9 months (range, 5.3-171.3). The 5-year and 10-year progression free survival (PFS) were 72.7% and 51.5%, and 5-year and 10-year overall survival (OS) were 82.5% and 63.5%, respectively. GTR and molecular subtype of IDH mutant and/or 1p/19q codeletion were favorable prognostic factors for both PFS and OS. Patients with tumoral IDH wild-type had significantly decreased OS than those with IDH mutation and 1p/19q codeletion. Among patients with ODG underwent GTR, no failure was observed after RT. Patients with IDH mutant and wild-type performed non-GTR had high recurrent rates after RT (47.6% and 57.9%). Regarding OS, age ( $< 40$  years), tumor location (frontal lobe), chemotherapy, and RT were not significant prognostic factors on multivariate analysis.

#### Conclusion

Molecular classification in LGG was of prognostic relevance, with the tumors that do not have IDH mutations and/or 1p/19 codeletion having a particularly poor outcome regardless of treatment. The favorable results were observed in patients who undergone GTR. Prospective study is needed to demonstrate the role of adjuvant treatment in LGG.

#### PO-0739 Sense and radiosensitivity - CyberKnife® stereotactic radiotherapy in patients with meningiomas.

H. Grzbiela<sup>1</sup>, R. Tarnawski<sup>1</sup>, E. Nowicka<sup>1</sup>, M. Gawkowska<sup>1</sup>, S. Owczarek<sup>1</sup>, M. Stapor-Fudzinska<sup>2</sup>

<sup>1</sup>Centrum Onkologii-Instytut im. M. Skłodowskiej-Curie Warsaw, III Radiotherapy and Chemotherapy Clinic, Gliwice, Poland ; <sup>2</sup>Centrum Onkologii-Instytut im. M. Skłodowskiej-Curie Warsaw, Radiotherapy Planning Department, Gliwice, Poland

#### Purpose or Objective

The objective of the study was to assess the effects of CyberKnife® stereotactic radiotherapy in patients diagnosed with meningiomas, and to evaluate, whether this technique, due to high conformality and steep dose fall-off, leads to a lesser degree of CNS toxicity, in particular concerning visual pathway toxicity.

#### Material and Methods

157 patients diagnosed with meningiomas, aged 20 - 79 (median 54), were treated in our Clinic between 2011 and 2014. 43 patients (27.4%) underwent neurosurgery at the time of diagnosis (pathology was meningothelial or psammomatous meningioma WHO grade 1), but during follow-up recurrence or progression of the tumor was observed. For 114 patients (72.6%), in whom surgery was not possible (due to tumor location or poor performance status), radiation therapy was primary treatment. All patients underwent CyberKnife® stereotactic radiation therapy. Tumor volume ranged from 1.5 to 37.5 cm<sup>3</sup>. Total dose received was 18 Gy (in 3 fractions), 21 Gy (in 3 fractions) or 16 Gy (in 2 fractions) - depending on tumor volume and location (especially in regard to the distance between tumor and visual pathway).

#### Results

All patients completed the treatment. 16 patients (10.2%) suffered from mild or moderate nausea (CTCAE grade 1 or 2), 37 patients (23.6%) reported headache CTCAE grade 1

or 2. No grade 3 or 4 acute toxicity was observed. Follow-up time was 38 - 75 months (median 58 months). To assess the results, MRI was performed every 6 months in the first two years of follow-up, then every 12 months. Partial tumor regression was observed in 28 patients (17.8%). In majority of patients (77.1%) the presence of a stable mass was confirmed. In 8 patients (5.1%) MRI scans revealed tumor progression (all of them underwent re-irradiation). None of the patients showed any severe neurological toxicity during follow-up. Most importantly, in patients with tumors located close to visual pathway, no visual impairment or loss of visual field was observed.

#### Conclusion

With the use of relatively low total dose we managed to achieve and maintain local control in 94.9% of patients and reduce the risk of CNS toxicity. Furthermore, it also allowed us to use re-irradiation in patients with tumor progression.

#### PO-0740 Can HSRS on tumor bed replace WBRT in resected brain metastases? Results of a phase II study

P. Navarria<sup>1</sup>, E. Clerici<sup>1</sup>, C. Franzese<sup>1</sup>, G.R. D'Agostino<sup>1</sup>, T. Comito<sup>1</sup>, F. De Rose<sup>1</sup>, D. Franceschini<sup>1</sup>, C. Iftode<sup>1</sup>, A. Tozzi<sup>1</sup>, F. Pessina<sup>2</sup>, L. Bello<sup>2</sup>, S. Cozzi<sup>1</sup>, I. Renna<sup>1</sup>, L. Di Brina<sup>1</sup>, M. Scorsetti<sup>1</sup>

<sup>1</sup>Humanitas Clinical and Research Hospital, Radiotherapy and Radiosurgery, Rozzano Milan, Italy ; <sup>2</sup>Humanitas Clinical and Research Hospital, Neurosurgery, Rozzano Milan, Italy

#### Purpose or Objective

The local control of large brain metastases is a crucial issue. Treatment options include whole-brain irradiation (WBRT), surgery, and stereotactic radiosurgery (SRS). As single-modality, none of these treatments are effective in controlling large brain metastases and a combined treatment is recommended. Surgery followed by WBRT was the standard treatment but it is burdened by a high risk of decline in neurocognitive functions. More recently surgery followed by SRS on the tumor bed is under investigation, but results are still poor. Based on this background we designed a prospective phase II study aimed to assess the benefit of surgical resection followed by hypofractionated radiosurgery (FSRS) on the tumor bed, instead of postoperative WBRT, for patient with single large brain metastases from solid tumor. Primary endpoint was local control rate; secondary endpoints toxicity, brain distant failure, and patients overall survival.

#### Material and Methods

Adults patients with primary diagnosis of solid tumors, KPS  $\geq 70$ , controlled extracranial disease, single brain metastasis  $\geq 2.1$ , or smaller but conditioning mass effect and/or neurological deficits and/or massive edema, and estimated survival  $\geq 3$  months were enrolled. Patients underwent previous WBRT were excluded. Surgical resection was performed with the aim to maximally (>95%) remove the tumor. Within 1 month from surgery, a fractionated SRS was performed on the tumor bed for a total dose delivered of 30 Gy in 3 daily fractions. Response was assessed according to RANO criteria, and toxicity using CTCAE scale. Incidence of radionecrosis was evaluated employing perfusion MRI and neurocognitive function with Milano Biccoca battery.

#### Results

Between 2014 and September 2018, 135 patients were enrolled, 63 female and 72 male with a median age of 49 years. The most common primary tumor was Non-Small Cell Lung Cancer (47%), followed by breast cancer (27%) and melanoma (10%). The median follow-up was 25 months (range 7-52 months). The 1,2-year LC rate were 98%, and 98%. Forty-two (34%) patients had new BDP at a median time of 19 months.

The median 1,2-year overall survival were 24 months, 91.3% and 73%. At the last observation time, 30 patients

(22%) were dead and 105 patients (78%) were alive. No detrimental effect on neurocognitive functions was recorded. Grade II radionecrosis occurred in 13% of patients and grade III 6% of cases treated.

#### Conclusion

Fractionated SRS after surgical resection is a safe and feasible option in patients with large brain metastases and oligometastatic disease.

#### PO-0741 Active spot-scanning proton therapy for intracranial meningiomas: CNAO experience

E. D'ippolito<sup>1</sup>, A. Iannalfi<sup>1</sup>, M. Bonora<sup>1</sup>, B. Viscioni<sup>1</sup>, M.R. Fiore<sup>1</sup>, S. Ronchi<sup>1</sup>, V. Vitolo<sup>1</sup>, A. Barcellini<sup>1</sup>, R. Petrucci<sup>1</sup>, A. Mirandola<sup>1</sup>, D. Maestri<sup>1</sup>, G. Magro<sup>1</sup>, A. Facoetti<sup>1</sup>, G. Viselner<sup>2</sup>, M. Ciocca<sup>1</sup>, L. Preda<sup>2</sup>, F. Valvo<sup>1</sup>, R. Orecchia<sup>1,3</sup>

<sup>1</sup>National Center of Oncological Hadrontherapy, Radiotherapy Unit, Pavia, Italy ; <sup>2</sup>National Center of Oncological Hadrontherapy, Diagnostic Imaging Unit, Pavia, Italy ; <sup>3</sup>European Institute of Oncology, Radiation therapy Unit, Milan, Italy

#### Purpose or Objective

Meningiomas are the most common primary intracranial tumors. If therapy is necessary, the standard treatment is gross total surgical resection. Proton therapy (PT) is an alternative therapeutic option for unresectable meningiomas, mostly located in the skull-base that are difficult to access, and a complementary treatment for complex and irregular tumors and lesions located in close proximity of critical organs at risk (OAR) as optic-pathways and brainstem where only subtotal or partial resection is possible. Aim of the study was to evaluate treatment results and toxicity in patients (pts) with meningiomas treated with active spot-scanning PT

#### Material and Methods

79 pts (29 men and 50 women) with a median age of 54 years (range 15-85) with intracranial meningioma (histologically proven 50/79) were treated with PT between October 2012 to December 2017 at CNAO. Pts, tumor and treatment characteristics were summarized in Tab 1. 59 pts had skull-base lesions. 44 pts were treated as primary treatment (exclusively PT= 32 pts, postoperative PT = 12 pts), 35 pts were treated for recurrence after surgery. For pts with histological diagnosis, 33 pts had a diagnosis of World Health Organization (WHO) Grade I, 13 of WHO Grade II and 4 of WHO Grade III respectively, while 29 pts had radiological diagnosis (28/29 skull-base lesions) and in all these cases <sup>68</sup>Ga-DOTATOC-PET was performed before treatment. All pts were treated using pencil-beam active scanning PT. The median administered dose was 55.8 Gy (relative biological effectiveness -RBE) (range, 50.4- 66) at 1.8-2.0 Gy RBE per fraction. Gross tumor volume (GTV) ranged from 2.3-205.71 cm<sup>3</sup> (median 22.8, mean 36.5). Late toxicity was assessed according to Common Terminology Criteria for Adverse Events -CTCAE- V4.03 scale

Tab 1. Patients, tumor and treatment characteristics

Characteristics	N. of patients (%)
<b>Total</b>	79 (100)
<b>Sex</b>	
Male	29 (37)
Female	50 (63)
<b>Age (years): median (range)</b>	57 years (range, 14-86)
<b>Histologic classification</b>	
WHO Grade I	33 (42)
WHO Grade II	13 (16)
WHO Grade III	4 (5)
No histology	29 (37)
<b>Clinical timing</b>	
Newly diagnosed tumors	44 (56)
Post surgery recurrence	35 (44)
<b>Tumor site</b>	
Skull-base meningioma*	59 (75)
Non-skull-base meningioma	20 (25)
<b>GTV (cm<sup>3</sup>): median (range)</b>	22.8 (2.3-205.71)
<b>Total (and fraction) doses (Gy RBE)</b>	
50.4 (L8)	3 (4)
54 (L8)	11 (14)
55.8 (L8)	31 (39)
56 (2)	2 (3)
57.5 (L8)	4 (5)
59.4 (L8)	9 (11)
60 (2)	7 (9)
64 (2)	1 (1)
66 (2)	11 (14)

## Results

Median follow-up was 17 months (range, 4.8-62.3). Very low rates of side-effects developed, including headaches, nausea and dizziness during treatment. No high-grade (grade 3-4) treatment-related toxicity was observed. Local control was 99%. Only one patient, affected by atypical meningioma, had local recurrence 22 months after the end of the treatment. Two pts with atypical and anaplastic meningioma respectively had "out-of-field" recurrence 20 and 8 months after the end of the treatment

## Conclusion

PT is a safe and effective treatment for pts with intracranial meningiomas, and it allows to deliver high local doses even in complex anatomy (as skull-base lesions) while sparing critical OARs

## PO-0742 The survival impact of the time between surgery and chemo-radiotherapy in Glioblastoma patients

O. Kaidar-Person<sup>1</sup>, I. Zur<sup>1</sup>, T. Tzuk-Shina<sup>1</sup>

<sup>1</sup>Rambam Health Care Campus - Faculty of Medicine, Oncology Institute, Haifa, Israel

## Purpose or Objective

Glioblastoma multiforme (GBM) is the most common primary CNS malignancy. Although multimodality therapy, it is bears grave prognosis. While importance of current treatment protocol is well-known and practiced, it is still unclear what is the optimal waiting time between surgery and the initiation of radio-chemotherapy (CRT). The aim of the current study is to evaluate the impact of the waiting time of initiation of CRT after surgery on disease outcome.

## Material and Methods

After IRB approval, we conducted a retrospective study of all medical records of GBM patients treated at our institution between 2005-2014. Data collected included: demographics, degree of surgical resection, performance status, dates and treatment protocols, and outcome. For data analysis, patients were divided into 3 groups according to the time-gap from surgery to initiation of CRT: < 4 weeks (47 patients), 4-6 weeks (72) and > 6 weeks (84). Univariate and multivariate analysis were performed. Overall survival (OS) and progression free survival (PFS) were analyzed using the Kaplan-Meier method and Cox proportional hazard model.

## Results

A total of 465 high-grade Glioma cases were reviewed, 261 were excluded. Only patients who were diagnosed with

GBM (not grade III) and were treated with surgery followed by CRT (temozolomide, TMZ) were included in the analysis. Median age was 60 years (23-79 years) with predominance male gender (61.7% vs. 38.3%). On a multivariate analysis: ischemic heart disease, degree of surgical resection, total radiation dose, number of TMZ cycles, and CRT waiting-time were significant for survival. A significant difference in OS (HR=0.49, p-value=0.002, 95% CI: 0.32-0.78) and PFS (HR=0.51, p-value= 0.003, 95% CI: 0.33-0.79) in the group who were CRT was initiated > 6 weeks after surgery, compared with the other two groups tested, favoring longer waiting times.

## Conclusion

According to our study, a time-gap of > 6 weeks for initiation of CRT after surgical resection was associated with better survival outcome. As our study represents retrospective "real-world data" from a tertiary hospital, the full report of the study analyzes the potential factors and biases that might have influenced our results and have significance in the daily practice.

## PO-0743 Single dose versus FSRT for brain metastases: a retrospective study.

C. De la Pinta Alonso<sup>1</sup>, E. Fernández<sup>1</sup>, M. Martín<sup>1</sup>, R. Hernandez<sup>1</sup>, C. Vallejo<sup>1</sup>, M. Martín<sup>1</sup>, A.B. Capúz<sup>2</sup>, J.A. Rojo<sup>3</sup>, I. Villodre<sup>3</sup>, S. Sancho<sup>1</sup>

<sup>1</sup>Ramon y Cajal Hospital, Radiation Oncology, Madrid, Spain ; <sup>2</sup>Ramon y Cajal Hospital, Medical Physics, Madrid, Spain ; <sup>3</sup>Ramon y Cajal Hospital, Radiotherapist, Madrid, Spain

## Purpose or Objective

Radiosurgery is increasing being employed for the treatment of brain metastases, both as an adjuvant to surgical resection, and also as a primary treatment modality. The aim of this study is to evaluate the efficacy and tolerability of radiosurgery in patients with brain metastases comparing two different treatment regimens, single-dose radiosurgery(SRS) and fractionated stereotactic radiotherapy(FSRT).

## Material and Methods

Between 2004-2018 we analyzed 97 patients with 135 brain metastases. Fifty-six patients were treated with SRS, and forty-one were treated with FSRT. The median doses were 16 Gy(12-20Gy) for the SRS group and 30 Gy in 5 fractions for the FSRT group. FSRT was used for large lesions or lesions located near critical structures. Kaplan Meier curves were constructed for overall survival and local control.

## Results

Median age was 61,9 years(32- 89 years). Patients had Karnofsky-performance status>70 in 72,8%. Median survival was 10 months for all patients(1-68). With a median of 10 months no significance differences between overall survival between groups(p=0,21). Local control for all patients was 67%. Local progression-free survival(LPFS) at 6 months and 1-year were 71% and 60%, respectively, for the SRS group and 80% and 69%, respectively, for the FSRT group(p = 0.129). Despite the fact that FSRT was used for large lesions and lesions in adverse locations LPFS was not inferior to SRS. We observed acute toxicities grade 1-2 consisted of brain edema(22p) and crisis without sequels(3p). Late complications consisted of radionecrosis(3p), post-radiation syndrome(1p), chronic crisis(5p), pan-hypopituitarism(1p) and insipid diabetes(1p). Acute toxicity was more frequently observed in the FSRT-group than in the SRS-group(29% vs. 23%, p=0.63) and chronic toxicity was more frequently observed in the FSRT-group than in the SRS-group(19,5% vs. 7,1%, p=0.11). Brain recurrence occurred in 37,5% and 14,6% FSRT vs SRS-group respectively(p=0.06).

## Conclusion

Because patients treated with FSRT exhibited similar survival times and LPFS rates with a lower risk of toxicity in comparison to those treated with SRS, despite the fact

that FSRT was used for large lesions and adverse locations, we find that FSRT can particularly be beneficial for patients with large lesions or lesions located near critical structures. Further investigation is warranted to determine the optimal dose/fractionation.

**PO-0744 Efficacy of single-fraction or fractionated SRS combined with CPIs in melanoma brain metastases**

G. Minniti<sup>1</sup>, D. Arzellini<sup>2</sup>, C. Reverberi<sup>2</sup>, F. Bianciardi<sup>1</sup>, B. Tolu<sup>1</sup>, C. Scaringi<sup>1</sup>, M. Osti<sup>2</sup>, P. Gentile<sup>1</sup>

<sup>1</sup>UPMC San Pietro FBF, Radiation Oncology, Roma, Italy ; <sup>2</sup>Sant' Andrea Hospital- University Sapienza- 00100 Rome, Radiation Oncology, Rome, Italy

**Purpose:** to investigate efficacy and safety of concurrent stereotactic radiosurgery (SRS), either single-fraction SRS s-fSRS; 18-22 Gy) or fractionated (fSRS; 3x9 Gy) SRS and ipilimumab or nivolumab in patients with untreated melanoma brain metastases.

**Patients and Methods:** Eighty consecutive patients with 326 melanoma BM, receiving SRS in combination with ipilimumab or nivolumab, were analyzed. Concurrent systemic treatment was generally started within 5 days before SRS and consisted of intravenous nivolumab or ipilimumab until disease progression or unacceptable toxicity. Primary endpoint of the study was intracranial progression-free survival (PFS). Secondary endpoints were extracranial PFS, overall survival (OS), and toxicity.

**Results:** Eighty patients were analyzed. Forty-five patients received SRS and ipilimumab (SRS+ipilimumab), and 35 patients SRS and nivolumab (SRS+nivolumab). With a median follow-up of 15 months, the 6-month and 12-month intracranial PFS rates were 69% (95%CI,54-87%) and 42% (95%CI,24-65%) in SRS+nivolumab group and 48% (95%CI,34-64%) and 17% (95%CI,5-31%) in SRS+ipilimumab group ( $p=0.02$ ), respectively. Similarly, patients treated with SRS and nivolumab had better 6-month extracranial PFS and 12-month OS (SRS+nivolumab, 57% and 37%; SRS+ipilimumab, 42% and 17%). Stratification for type of SRS showed that combined CPIs and fSRS were associated with better intracranial PFS; 6-month and 12-month rates were 70% and 40%, respectively, for patients receiving fSRS and 46% and 10%, respectively, for those undergoing sf-SRS ( $p=0.01$ ). As for intracranial PFS, fSRS resulted in better extracranial PFS. Grade 3 treatment-related adverse events occurred in 24% of patients receiving SRS and ipilimumab and 17% of patients receiving SRS and nivolumab.

**Conclusions:** In conclusion, concurrent SRS and CPIs show meaningful intracranial activity and acceptable toxicity in patients with either asymptomatic and symptomatic melanoma BM, particularly when fSRS is combined with nivolumab. Further studies need to investigate the potential stronger synergistic effect of fractionated radiation schedules and CPIs.

**PO-0745 Fractionated SRS (fSRS) or surgery plus fSRS to resection cavity for NSCLC large brain metastases**

G. Minniti<sup>1</sup>, C. Scaringi<sup>1</sup>, D. Arzellini<sup>2</sup>, F. Bianciardi<sup>1</sup>, B. Tolu<sup>1</sup>, R. Morace<sup>3</sup>, M. Osti<sup>2</sup>, P. Gentile<sup>1</sup>

<sup>1</sup>UPMC San Pietro FBF, Radiation Oncology, Roma, Italy ; <sup>2</sup>Sant' Andrea Hospital- University Sapienza, Radiation Oncology, Roma, Italy ; <sup>3</sup>IRCCS Neuromed-, Neurosurgery, 86077 Pozzilli IS, Italy

**Purpose or Objective**

To investigate clinical outcomes in patients with NSCLC brain metastases <4 cm in size undergoing complete surgical resection plus fractionated stereotactic radiosurgery to the resection cavity (fSRS) or fSRS alone.

**Material and Methods**

Two hundred and twenty-seven patients with 246 brain metastases receiving surgery plus fSRS (S+fSRS) or fSRS alone were analyzed. All lesions evaluated in the study were treated with a dose of 27 Gy given in 3 fractions over

three consecutive days. Cumulative incidence analysis was used to compare local control (LC), distant brain failure (DBF), and radiation-induced brain necrosis (RN) between groups from the time of SRS.

**Results**

At a median follow-up of 13 months, median OS and 1-year survival rates were comparable: S+fSRS, 13.5 months and 59%; fSRS, 15.2 months and 68% ( $p=0.2$ ). Median DBF did not differ significantly, being 12 and 14 months for S+fSRS and fSRS, respectively. Eighteen patients undergoing S+fSRS and 17 patients treated with fSRS recurred locally ( $p=0.4$ ). Six-month and 1-year LC rates were 92% and 85% in S+fSRS group and 96% and 91% in fSRS group, respectively ( $p=0.1$ ). Stable extracranial disease, systemic therapy with TKIs, a single brain metastasis, adenocarcinoma histology and KPS >70 emerged as significant independent indices of prolonged OS. Controlled extracranial disease and TKI therapy resulted to be the most significant independent prognostic factors.

**Conclusion**

In conclusion, fSRS is an effective treatment option for large NSCLC brain metastases, resulting in a similar local control and reduced risk of RN compared to S+fSRS.

**PO-0746 The utility of functional magnetic resonance imaging in target delineation of high-grade gliomas**

L. Qian<sup>1</sup>, Q. Fei<sup>1</sup>, Y. Zhang<sup>1</sup>, W. Guo<sup>1</sup>, X. Bian<sup>1</sup>, L. Yin<sup>1</sup>, P. Yan<sup>1</sup>, T. Wang<sup>1</sup>, P. Qian<sup>1</sup>, Z. Guo<sup>2</sup>, X. He<sup>1</sup>

<sup>1</sup>Jiangsu Cancer Hospital & Jiangsu Institute of Cancer Research & The Affiliated Cancer Hospital of Nanjing Medical University, Department of Radiation Oncology, Nanjing, China ; <sup>2</sup>Jiangsu Cancer Hospital & Jiangsu Institute of Cancer Research & The Affiliated Cancer Hospital of Nanjing Medical University, Department of Radiology, Nanjing, China

**Purpose or Objective**

This study explored the different survival outcomes and failure patterns of high-grade glioma (HGG) patients by comparing the combination of functional imaging technology (fMRI: perfusion weighted imaging (PWI), diffusion-tensor imaging (DTI)) and contrast-enhanced MRI (CE-MRI) imaging (enhanced T1) with CE-MRI alone in guiding the delineation of radiotherapy target area.

**Material and Methods**

102 patients with postoperative HGG between 2012 and 2016 were included in our study. All patients were treated with IMRT in combination with the standard STUPP regimen. MRI (plain scan + enhancement), MR spectroscopy (MRS), DTI and PWI were performed before radiotherapy for postoperative patients. 50 (cohort A) were delineated based on fMRI (PWI, DTI) and CE-MRI (enhanced T1). The other 52 (cohort B) were delineated based on CE-MRI (enhanced T1, FLAIR/T2) as controlled. Survival analysis was performed using the Kaplan-Meier method, and the difference between two groups were evaluated by log-rank test.  $p < 0.05$  was considered statistically significant.

**Results**

All clinical characteristics were comparable between the two cohorts. At a median follow-up of 20 months, 80 (78%) patients had died. The median survival benefit was 6 months. The median survival was 24 months in cohort A and 18 months in cohort B. The 2-year OS, PFS, and LRC rates were 48% vs 25% ( $p = 0.005$ ), 42% vs 13.46% ( $p = 0.0003$ ), and 40% vs 13.46% ( $p = 0.0007$ ) for cohort A and cohort B, respectively. Two cohorts had similar rates of disease progression and recurrence (62% vs 63.5%,  $p = 0.879$ ), while the proportion of failure patterns was different. In cohort A, 28 (90.3%) patients experienced recurrence within the irradiated field (50-60Gy); 4 (9.7%) experienced out-field failure (2 cases of marginal failure, 1 case of pituitary metastasis, 1 case of cerebrospinal fluid metastasis). In cohort B, 26 (78.8%) patients experienced

recurrence within the irradiated field (50-60 Gy); 7 (21.2%) experienced out-field failure (2 cases of marginal failure, 2 cases of corpus callosum metastasis, 1 case of pineal gland metastasis, 1 case of contralateral brain metastasis, 1 case of distant intraparenchymal metastasis).

#### Conclusion

This study was the first to explore the clinical value of fMRI in the delineation of radiotherapy target volume for HGG. It suggested that combination of fMRI and CE-MRI may improve the survival outcome compared to the traditional guidelines, and may reduce the risk of distant metastasis for HGG patients.

#### PO-0747 Results at long-term after linac-based radiosurgery of vestibular schwannomas

P. Anselmo<sup>1</sup>, M. Casale<sup>1</sup>, F. Trippa<sup>1</sup>, F. Arcidiacono<sup>1</sup>, S. Fabiani<sup>1</sup>, A. Di Marzo<sup>1</sup>, L. Draghini<sup>1</sup>, S. Terenzi<sup>1</sup>, E. Maranzano<sup>1</sup>

<sup>1</sup>Ospedale Santa Maria, Radiotherapy Oncology Centre, Terni, Italy

#### Purpose or Objective

Vestibular Schwannomas (VS) are benign tumors generally arising from vestibular component of the vestibulocochlear nerve. Hearing loss is the most common initial presenting symptom. This report regards patients with sporadic VS undergone linac-based radiosurgery (SRS) with a follow-up > 10 years.

#### Material and Methods

Between August 2002 and January 2008, 53 patients with 53 sporadic VS were treated. Patients not able to discriminate words or not hearing at all, were scored as 'non-serviceable hearing'. Trigeminal and facial nerve functions were assessed asking the patient about facial pain/paraesthesia. Median dose of SRS was 16.5Gy (range, 13-20Gy).

#### Results

Male/female ratio was 27/26. The median age was 59 years (range, 23-83). The median tumor volume was 1,7 cc (range, 0.09-7.4). Surgery has been performed before SRS in 14 (26%) patients (total or subtotal resection 5-9% and 9-17% patients, respectively). In these cases SRS was performed as salvage therapy for recurrent or progressive tumors. Other 39 (74%) patients underwent SRS alone. Fifty (94%) of patients had hearing loss as an initial symptom and 27 (51%) a "non-serviceable" hearing function. Ataxia, tinnitus, trigeminal neuralgia and facial pain/paraesthesia were presenting symptoms in 10 (19%), 8 (15%), 4 (7.5%) and 10 (19%) of the patients, respectively. Considering that 5 patients were lost to follow up, 48 (92%) patients were evaluable. At a median follow-up of 12 years (range, 2-16), 10 patients (21%) had an objective improvement of their initial symptoms with a MRI response classifiable as stable, partial or complete remission in 6, 3 and 1 patient, respectively. Twenty-one (44%) patients had stable symptoms, with a MRI showing stable disease, transient enlargement due to central tumor necrosis, or partial remission in 10, 3, 8 patients, respectively. Seventeen (35%) patients worsened their pre-treatment symptoms. This deterioration was transient in 12 patients and persistent in 5. In "serviceable-hearing" patients, 10-year hearing preservation rate was 92%. Four of 38 (11%) patients without pre-SRS facial toxicity, developed incomplete facial nerve palsy, that regressed in a median time of 6 months. Eleven of 44 (25%) patients without pre-SRS trigeminal neuralgia developed trigeminal toxicity which was transient or stable/mild during follow-up in 10 (23%) patients (median tumor size 18mm, median dose of 17Gy). In only 1 case (2%) trigeminal toxicity was severe and appeared 12 months after SRS (tumor size was 18.8mm and prescribed dose 16,5Gy). Crude radiologic tumor control rate was 100%.

#### Conclusion

Long-term follow-up confirmed the excellent tumor control associated to SRS of VS. Although the median administered dose was rather high, iatrogenic toxicity was acceptable and similar to that reported in literature.

#### PO-0748 Prognostic factors of distant brain failure free survival after stereotactic RT for brain metastasis

Y. Pin<sup>1</sup>, M. Loo<sup>1</sup>, A. Paix<sup>1</sup>, P. Meyer<sup>2</sup>, D. Antoni<sup>1</sup>, F. Proust<sup>3</sup>, G. Noël<sup>1</sup>

<sup>1</sup>Centre de Lutte Contre le Cancer, Radiation Oncology, Strasbourg, France ; <sup>2</sup>Centre de Lutte Contre le Cancer, Medical Physic, Strasbourg, France ; <sup>3</sup>Strasbourg University Hospital, Neurosurgery, Strasbourg, France

#### Purpose or Objective

Brain metastasis (BM) is a frequent evolution in patients with solid cancer. Treatments with whole brain radiotherapy (WBRT) demonstrated a benefit in overall survival (OS) but their indications are becoming controversial due to the induced cognitive impairment. The reduction of the use of WBRT is for the benefit of the stereotactic radiation therapy (SRT). Nevertheless, SRT rarely improved significantly the OS provided by the WBRT and suffers of higher distant metastasis rates. In this study, we tried to find prognosis factors of distant brain failure free survival (DFS) that might permit to refine the indications of the use of WBRT in patients treated for BM with SRT.

#### Material and Methods

Clinical, biological and imaging factors were retrospectively recorded from patients referred for upfront stereotactic radiotherapy of one to three BMs. Those factors included a new edema descriptor, the *Edema Theoretical Thickness* (ETT) defined by the difference of radius between a first perfect sphere which volume corresponds to the sum of BMs volumes and a second perfect sphere which volume corresponds to the sum of brain edemas volumes. DFS was studied in function of these factors with the Cox proportional hazards regression model. Relevant factors were selected by an univariate analysis. The most relevant non-colinear factors were selected using the Farrar-Glauber test. Then, the multivariate analysis was performed to find the significant factors predicting the DFS.

#### Results

Between January 2012 to December 2017, 182 patients were included. Factors found significant by the multivariate analysis on the DFS were the ETT (HR = 0.92,  $p = .022$ ) with a better DFS in patients with an ETT > 7.5 mm ( $p$  logrank = .011), the melanoma histologic type (2.67,  $p = .034$ ) and the BM local relapse after SRT (2.65,  $p = .018$ ).

#### Conclusion

In this study, we found that the survival free of distant brain failure is independently correlated to the melanoma histologic type, the local failure after SRT and the ETT. ETT appeared to reflect a potential abscopal-like effect in case of SRT for BM and should be included in further studies. The combination of BMs SRT with immunotherapy could be a further way of research.

#### PO-0749 New aspects regarding the treatment of glioblastoma

C. Matuschek<sup>1</sup>, B. Tamaskovics<sup>1</sup>, E. Boelke<sup>1</sup>, W. Budach<sup>1</sup>, F. Djiepmo<sup>1</sup>, J. Hausmann<sup>1</sup>, A. Kumar<sup>2</sup>, H. Pokhylevych<sup>2</sup>, D. Schomer<sup>2</sup>, A. Hayman<sup>2</sup>

<sup>1</sup>University Hospital Düsseldorf, Radiation Oncology, Düsseldorf, Germany ; <sup>2</sup>MD Anderson, Neuroradiology, Houston, USA

#### Purpose or Objective

Since 60 years no accurate classification system exists for glioblastoma. Furthermore, the treatment results are still very poor with a low survival rate. To understand the

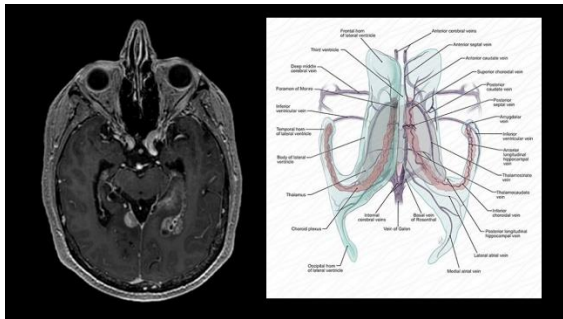
spread patterns of glioblastoma will help to define the clinical target volume for radiation therapy.

#### Material and Methods

After receiving IRB approval from MD Anderson, Houston Teys, the clinical MR imaging of 1250 cases of glioma were studied for 10 years using an anatomic software program developed by the authors (Anatom-e, Houston Texas). The final 3 years of the project was devoted to reorganizing venous anatomy to make it responsive to clinically relevant consultations and data mining. This was accomplished by developing deformable anatomic templates (DAT) which could overlay the venous territory maps on the clinical scans. The system also contained a drawing tool which embed the tumors shape into a DAT template. The software was also able to store and compare the shape and location of a single glioma between exams or across a group of tumors.

#### Results

The highly variable MR appearance of glial tumors and their complicated spread patterns strongly infer the existence of previously undescribed perivenous compartment in the cerebral hemispheres.



The only natural anatomic structure of the brain that is compatible with the shape and location of gliomas, regardless of their histology, is venous anatomy. The otherwise inexplicable tumor spread of certain multicentric gliomas to the contralateral hemisphere reflects perivenous spread along the deep venous network. Multicentric gliomas with corresponding venous maps will be presented. For example, we analyzed the case of a multicentric GBM (Figure 1) that spreads along the inferior chorooidal vein to the basal vein and then crosses the midline along the peduncular vein

#### Conclusion

DAT is capable of correctly explaining the complicated spread patterns of glioblastoma. It seems that the superficial and deep peri-venous compartments are responsible for the spread patterns of glioblastoma. Clinical imaging of gliomas strongly supports the existence of perivenous space which is capable of storing and spreading glial tumor cells throughout the brain. This new concept can be used to develop a new classification system for glial tumors and can be used to predict tumor growth

#### PO-0750 VMAT for CNS Tumors and alopecia: results of an observational study and new constraints for the SCALP

S. Scoccianti<sup>1</sup>, R. Grassi<sup>1</sup>, P. Marco<sup>1</sup>, F. Terziani<sup>1</sup>, G. Simontacchi<sup>1</sup>, C. Talamonti<sup>2</sup>, G. Caramia<sup>1</sup>, M. Lo Russo<sup>1</sup>, M.A. Teriaca<sup>1</sup>, E. Scoccimarro<sup>1</sup>, C. Saieva<sup>3</sup>, L. Cosi<sup>1</sup>, S. Pallotta<sup>2</sup>, L. Livi<sup>1</sup>

<sup>1</sup>Azienda Ospedaliera Universitaria Careggi, Radiation Oncology, Firenze, Italy ; <sup>2</sup>Azienda Ospedaliera Universitaria Careggi, Medical Physics Unit, Firenze, Italy ; <sup>3</sup>Istituto per lo Studio- la Prevenzione e la rete Oncologica, SC Epidemiologia of Risk Factors and Lifestyles, Florence, Italy

#### Purpose or Objective

To define a dose-response relationship for alopecia when using conventionally fractionated VMAT.

#### Material and Methods

The scalp was defined as a region of interest. At the moment of the end of RT and during the follow-up, the areas of scalp where alopecia developed were defined. Grade of alopecia was assessed according to CTCAE version 4.0. A treatment planning system-based dosimetric evaluation of areas of acute alopecia was performed. The following dosimetric parameters were registered for the whole scalp and the areas of alopecia: dose received by 0.1 cc ( $D_{0.1cc}$ ), mean D ( $D_{mean}$ ), volumes that received 16, 20, 25, 30, 35, 40 and 43 Gy ( $V_{16 Gy}$ ,  $V_{20 Gy}$ ,  $V_{25 Gy}$ ,  $V_{30 Gy}$ ,  $V_{35 Gy}$ ,  $V_{40 Gy}$  and  $V_{43 Gy}$ ). Receiver operating characteristics (ROC) curve analysis was used to identify dosimetric parameters associated with high risk of acute and chronic hair loss. Time from end of radiotherapy to alopecia recovery was analyzed. Kaplan Meier analysis and Cox regression analysis were performed in order to assess clinical and dosimetric factors impacting on the recovery probability.

#### Results

A total of 101 patients were included in the study. All the patients received a limited-volume RT with conventionally fractionated VMAT technique. 5 patients who were treated for deep tumors did not develop any area of alopecia. Their scalp received very low doses (mean  $D_{mean}$  3.1 Gy; mean  $D_{0.1cc}$  19.7 Gy). At the end of RT, 96/101 patients developed acute alopecia (G1 only n=11; G2 only n=52; G1+G2 n=33). The whole scalp of the patients with G1 and G2 alopecia received mean  $D_{mean}$  equal to 10.6 Gy and 11.8 Gy with mean  $D_{0.1cc}$  equal to 40.2 and 47.3 Gy, respectively.  $D_{0.1cc}$ ,  $D_{mean}$ ,  $V_{16 Gy}$ ,  $V_{20 Gy}$ ,  $V_{25 Gy}$ ,  $V_{30 Gy}$ ,  $V_{35 Gy}$ ,  $V_{40 Gy}$  and  $V_{43 Gy}$  were significantly different if compared with the same parameters of patients who did not developed acute alopecia ( $p < 0.05$ , Mann-whitney test). Mean  $D_{mean}$  in areas of alopecia G1 and alopecia G2 at end of RT was 16.5 Gy and 20.3 Gy, respectively ( $p < 0.05$ , Mann-whitney test). Mean  $D_{0.1cc}$  in areas of alopecia G1 and alopecia G2 at end of RT was 33.4 Gy and 44.6 Gy, respectively ( $p < 0.05$ , Mann-whitney test). Trichological follow-up was available for 74/101 patients. 65 patients (92.8%) had an intact scalp. Median time to recover was 5,9 months. The actuarial rate of hair recovery was 87.0% and 98.1% at 9, and 18 months after the end of RT. At ROC curve analysis,  $V_{16 Gy} \geq 16.7 cc$  and  $V_{20 Gy} \geq 5.2 cc$  were the strongest predictors of risk of acute alopecia, whereas  $V_{40 Gy} \geq 5.4 cc$  and  $V_{43 Gy} \geq 2.2 cc$  were the strongest predictors of risk of chronic alopecia. Kaplan Meier analysis and Cox regression showed that age,  $D_{0.1cc}$ ,  $D_{mean}$ ,  $V_{30 Gy}$ ,  $V_{35 Gy}$ ,  $V_{40 Gy}$  and  $V_{43 Gy}$  are related to recovery probability.

#### Conclusion

By treating patients with this scalp-sparing approach, in most patients complete recovery from alopecia was obtained within some months. By maintaining the doses lower than the dosimetric cut-off values we identified, further reduction of the risk of alopecia may occur.

#### PO-0751 Neutrophil lymphocyte ratio and Platelet lymphocyte ratio as a prognostic factor in brain metastases

A. Niiya<sup>1</sup>, K. Murakami<sup>2</sup>, R. Kobayashi<sup>2</sup>, K. Toyofuku<sup>2</sup>, E. Nishimura<sup>3</sup>, M. Kato<sup>2</sup>, Y. Ozawa<sup>4</sup>, H. Shinjo<sup>4</sup>, K. Miyaura<sup>2</sup>, M. Morota<sup>1</sup>, T. Serizawa<sup>5</sup>, Y. Ito<sup>2</sup>, A. Imai<sup>4</sup>, Y. Kagami<sup>2</sup>

<sup>1</sup>Showa University Koto Toyosu Hospital, Radiation Oncology, Koto-ku, Japan ; <sup>2</sup>Showa University Hospital, Radiation Oncology, Shinagawa-ku, Japan ; <sup>3</sup>Showa University Hospital, Radiology, Shinagawa-ku, Japan ; <sup>4</sup>Showa University Fujigaoka Hospital, Radiation Oncology, Yokohama, Japan ; <sup>5</sup>Tokyo Gamma Unit Center- Tsukiji Neurological Clinic, Neurosurgery, Chuo-ku, Japan

### Purpose or Objective

Brain metastases (BM) occurs in 10-30 % in adult cancer patients, and it is an important factor affecting patient survival rate and quality of life.

In recent years, neutrophil lymphocyte ratio (NLR) and platelet lymphocyte ratio (PLR) have been reported to correlate with overall survival (OS) in various cancers. However, few reports have verified the NLR and PLR in patients with BM. The purpose of this study is to evaluate whether NLR and PLR is a prognostic factor for OS, using in Japanese BM patients our hospital.

### Material and Methods

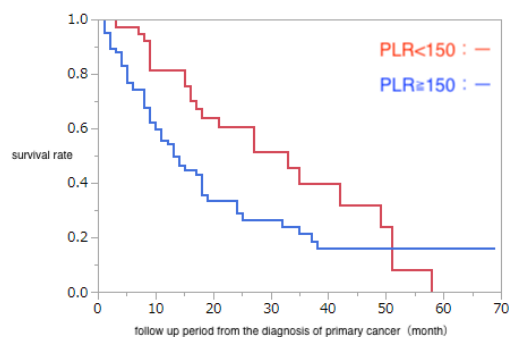
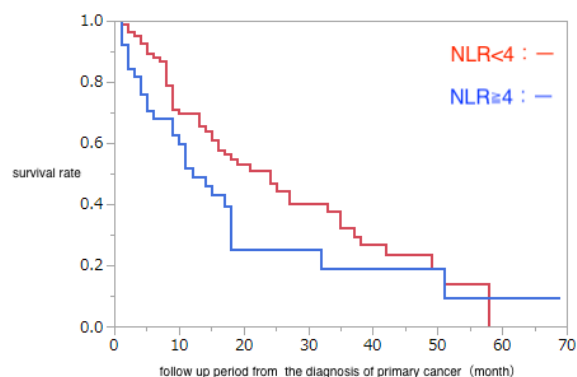
We retrospectively compiled the NLR and PLR in patients who received radiotherapy in our hospital from March 2011 to December 2017. Neutrophils, platelet and lymphocytes were calculated based on absolute values and analyzed with the OS. The absolute values of neutrophils, platelet and lymphocytes were obtained at the time of diagnoses of primary cancer and BM. For the data of BM, we didn't exclude patients who underwent chemotherapy or molecular targeted drugs for primary tumor.

### Results

The number of patients is 256, and primary sites were 150 lung, 66 breast, 15 gastrointestinal, 7 urological, and 18 others. The median age of the patient cohort at diagnosis of primary cancer was 65 years (range: 20-87 years), and BM was 66 years (range: 24-87 years). The patient group contained 136 males and 120 females, median KPS of BM detection was 70 (range: 10-100). Radiation therapy was 227 patients of whole brain irradiation (20-40 Gy) and 29 patients of stereotactic radiotherapy (15-32 Gy). The median follow up period was 19 months (mo.) from cancer diagnosis (range: 1-236 mo.), and 5 mo. from BM detection (range: 1-83 mo.). The median survival time (MST) from cancer diagnosis was 33 mo. and MST from BM detection was 9 mo.

Patients with NLR <4.0 at the diagnosis of primary cancer had better MST compared with patients with NLR  $\geq$ 4.0 (24 mo. vs. 12 mo.;  $P=0.0116$ ). Patients with PLR <150 at the diagnosis of primary cancer had better MST compared with patients with PLR  $\geq$ 150 (33 mo. vs. 13 mo.;  $P=0.0012$ ). Patients with NLR <4.0 at the time of BM detection had better MST compared with patients with NLR  $\geq$ 4.0 (12 mo. vs. 4 mo.;  $P<0.001$ ). Patients with PLR <150 at the time of BM detection had better MST compared with patients with PLR  $\geq$ 150, but there was no significant difference (15 mo. vs. 7 mo.;  $P=0.0538$ ).

Utilizing Multivariate analysis, age  $\geq$ 65 and PLR  $\geq$ 150 at the diagnosis of primary cancer were significantly correlated with survival (HR2.30;  $P=0.0008$ , HR2.17;  $P=0.0043$ ). KPS and NLR  $\geq$ 4 at the time of BM detection were significantly correlated with survival (HR1.53;  $P=0.0201$ , HR2.28;  $P<0.001$ ).



### Conclusion

NLR and PLR at the diagnosis of primary cancer might be prognostic factors. Furthermore, this tendency was also showed at the time of BM detection. To our knowledge, our study was the first report about NLR and PLR with BM patients who underwent radiation therapy. We are planning a prospective study to validate the results.

### PO-0752 Hypofractionated stereotactic radiotherapy for inoperable arteriovenous malformations

T. Takahashi<sup>1</sup>, T. Yamano<sup>2</sup>, K. Nishimura<sup>1</sup>, S. Ueno<sup>2</sup>, K. Washizu<sup>1</sup>, R. Soda<sup>1</sup>, S. Kondo<sup>1</sup>, N. Utsumi<sup>1</sup>, M. Shimbo<sup>1</sup>, S. Hatanaka<sup>1</sup>, M. Hariu<sup>1</sup>  
<sup>1</sup>Saitama Medical Center- Saitama Medical University, Radiation Oncology, Kawagoe, Japan ; <sup>2</sup>Saitama Medical Center- Saitama Medical University, Radiation Oncology, Kawagoe, Japan

### Purpose or Objective

In our institute, we performed hypofractionated stereotactic radiotherapy (HSRT) for inoperable arteriovenous malformations (AVM) whose Spetzler-Martin grade was mainly more than grade III. In this time, we investigated therapeutic efficacy and obliteration rate of our HSRT from the view point of prescription doses and dose fractionations, retrospectively.

### Material and Methods

We examined 23 patients of inoperable AVM who underwent HSRT at our institute between 2003 and 2014. Spetzler-Martin grade III was 90 % in patients. Mean nidus volume was 7.95 ml. At the beginning of HSRT, patients' median age was 30.5 years old (4 - 68 years old). Median observation periods were 56 months (4 - 117 months). A median dose was 33.8 Gy (20 - 40 Gy). Median fractionations were 6.8 fractions (4 - 13 fractions).

### Results

The occlusion rate at 2 years after HSRT was 57.1%, and 4 years 87.5 %, respectively. There is no evidence of obvious late adverse events of more than 3 grade. No significant difference in the occlusion rate of nidus volume was found between more than 14 ml and less than 14 ml. There was no significant difference in the occlusion rate between patients who received more than 7 Gy and less than 7 Gy, in a fractional dose. On the other hand, significant difference of obliteration rate of the nidus was found between patients who received more than 100 Gy and less than 100 Gy, in biological effective doses (BED) with  $\alpha/\beta=3$ . Patients who received more than 100 Gy in BED 3 resulted in favourable outcome ( $p=0.02$ ).

### Conclusion

In the past, stereotactic radiosurgery (SRS) has been mainly reported about radiotherapy for inoperable AVM. Although the therapeutic results of SRS is favorable, there is a tendency to reducing prescription doses for the patients who have large nidus volume, in consideration of adverse events. Our results suggest that HSRT also have been performed favorably and safely for patients whose nidus volumes were larger than 14 ml. Recently, some studies about HSRT occur in various reports, however suitable doses remain a subject of future investigation.

**PO-0753 radiotherapy quality assurance-POLCA trial-patients with anaplastic oligodendroglial tumors**

L. Feuvret<sup>1</sup>, H. Douzane<sup>2</sup>, C. Jenny<sup>1</sup>, A. D'Hombres<sup>3</sup>, L. Padovani<sup>4</sup>, M. Aumont<sup>5</sup>, G. Noel<sup>6</sup>, J. Jacob<sup>1</sup>, F.G. Riet<sup>1</sup>, C.H. Canova<sup>1</sup>, C. Dehais<sup>2</sup>, F. Fauchon<sup>7</sup>, Y. Meng<sup>8</sup>, F. Dhermain<sup>9</sup>

<sup>1</sup>Hôpital Pitié-Salpêtrière, RADIATION THERAPY, Paris, France ; <sup>2</sup>Hôpital Pitié-Salpêtrière, Neuro Oncology, Paris, France ; <sup>3</sup>Hôpital Lyon Sud, Radiation Therapy, Lyon, France ; <sup>4</sup>APHM, Radiation therapy, Marseille, France ; <sup>5</sup>René Gauducheau, Radiation Therapy, Saint Herblain, France ; <sup>6</sup>Paul Strauss, Radiation Therapy, Strasbourg, France ; <sup>7</sup>Centre des Hautes Energies, Radiation Therapy, Nice, France ; <sup>8</sup>Hôpital d'Argenteuil, Radiation Therapy, Argenteuil, France ; <sup>9</sup>Gustave Roussy, Radiation Therapy, Villejuif, France

**Purpose or Objective**

The ongoing phase III POLCA trial (NCT02444000) was designed to determine whether treating patients with newly diagnosed 1p/19q-codeleted anaplastic gliomas with PCV alone can increase overall survival without neurocognitive deterioration as primary endpoint. The control group treatment is intensity-modulated radiation therapy (IMRT) followed by 6 cycles of PCV chemotherapy and the experimental group treatment 6 cycles of PCV chemotherapy (radiotherapy being deferred at the time of progression) (October 2018: 60 patients in each arm). We report the results of retrospective individual case reviews (ICRs) for the first patients randomized to assess the study protocol compliance.

**Material and Methods**

All institutions were required to submit the radiotherapy plan of their first randomized patients. Full digital datasets uploaded to the CD rom were assessed by three independent reviewers through the "POLCA quality assurance" ANOCEF group (GRANOCEF). The software Artiview® (Aquilab SAS, France) package allowed experts to review and assess multimodality imaging and radiotherapy treatments.

**Results**

Forty-four ICRs from 14 centers were received and assessable. Twenty-three were evaluated as per protocol (53%), 5 as acceptable variation (11%) and 16 as unacceptable variations (36%). Most common unacceptable variations were related to the target volumes delineation (11 cases; 25%), OARs delineation (5 cases; 11%), dosimetric process (4 cases; 9%), dosimetric MRI (1 case; 2%) and no using IMRT (1 case; 2%).

**Conclusion**

The ICR analysis showed a significant number of major deviations with potential impact on toxicity profile and/or tumor control. OARs delineation dummy-run, guide book "list of main deviations", participation to "POLCA quality assurance" ANOCEF group, customized confidential reports may improve quality of radiotherapy technique. Prospective ICRs could prevent and correct protocol violations before starting treatment for future studies.

**PO-0754 Radiation-induced nausea and vomiting: how to delineate the Dorsal Vagal Complex ?**

A. Beddok<sup>1</sup>, J. Faivre<sup>2</sup>, A. Coutte<sup>3</sup>, J. Le Guévelou<sup>4</sup>, J. Welmant<sup>5</sup>, J. Clavier<sup>6</sup>, S. Guihard<sup>6</sup>, G. Janoray<sup>7</sup>, V. Calugaru<sup>8</sup>, Y. Pointreau<sup>9</sup>, A. Lacout<sup>10</sup>, J. Salleron<sup>11</sup>, M. Lefranc<sup>12</sup>, D. Hasboun<sup>13</sup>, H. Duvernoy<sup>14</sup>, J. Thariat<sup>4</sup>

<sup>1</sup>Curie Institute, Radiation Oncology, Paris / St Cloud, France ; <sup>2</sup>Lorraine Institute of Cancerology - Alexis-Vautrin Comprehensive Cancer Center, Academic Radiation Oncology & Brachytherapy, Vandœuvre-lès-Nancy, France ; <sup>3</sup>University hospital of Amiens, Radiation Oncology, Amiens, France ; <sup>4</sup>François Baclesse Center, Radiation Oncology, Caen, France ; <sup>5</sup>Montpellier Institute of Cancer, Radiation Oncology, Montpellier, France ; <sup>6</sup>Strasbourg Institute of Cancerology, Radiation Oncology,

Strasbourg, France ; <sup>7</sup>Tours Regional University Center, Radiation Oncology, Tours, France ; <sup>8</sup>Curie Institute, Radiation Oncology, Paris / Orsay, France ; <sup>9</sup>Jean Bernard Radiation Oncology Center, Radiation Oncology, Le Mans, France ; <sup>10</sup>Centre médico-chirurgical - ELSAN, Radiology, Aurillac, France ; <sup>11</sup>Lorraine Institute of Cancerology - Alexis-Vautrin Comprehensive Cancer Center, Statistic, Vandœuvre-lès-Nancy, France ; <sup>12</sup>University hospital of Amiens, Neurosurgery, Amiens, France ; <sup>13</sup>Pitié-Salpêtrière University Hospital, Neuroradiology, Paris, France ; <sup>14</sup>Besançon Regional University Hospital Center, pathology, Besançon, France

**Purpose or Objective**

Intensity-modulated radiation therapy (IMRT) treatment plans for head and neck cancer typically use a high number of radiation fields and may be associated with new beam-path non-target tissue toxicities, particularly nausea and vomiting. The dorsal vagal complex (DVC), including the area postrema, the nucleus of the solitary tract and the dorsal motor nucleus of the vagus, is a little known structure of the brainstem which may be implicated in the radiation-induced nausea and vomiting (RINV). The objective of our project was to define consensus guidelines for delineating the DVC.

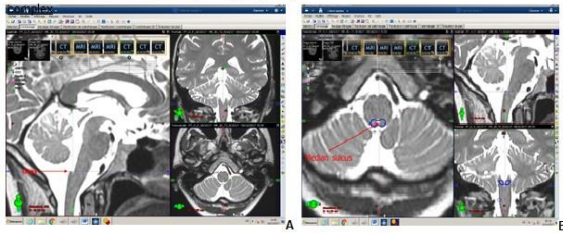
**Material and Methods**

The DVC was identified on autopsy sections and endoscopic descriptions. Anatomic landmarks and boundaries were used to establish radio-anatomic correlations on CT and Magnetic Resonance Imaging (MRI). The DVC delineation was performed on MRI images and reported on CT scans. Next, guidelines were provided to eight radiation oncologists (the working group, WG) for delineation guidance of this structure on DICOM-RT images of two patients being treated for a nasopharyngeal carcinoma. The evaluation of the variability of contours was benchmarked using a "experts' reference contour" (delineated with the help of three experts of the brainstem: HMD, DH, and ML). Firstly, each volume submitted by the eight radiation oncologists was compared with the reference volume. Secondly, different indices reflecting the correlation of the volume with the "experts' reference contour" were calculated: the Volume Ratio (VR), the Common Delineated Volume (CDV), and the Additional Delineated Volume (ADV). Then, the kappa index (KI) and the Overlap Volume (OV) were calculated.

**Results**

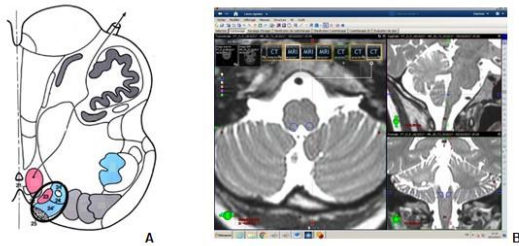
The DVC was defined with a concise description of its main anatomic boundaries. The caudal limit of the DVC is easily determined on a MRI sagittal view of the brainstem and must be delineated in the transversal plane of the obex, which is also in the plane of the central canal aperture (Fig 1). The DVC is located on both sides of the median sulcus of the medulla oblongata. In order to be more reproducible, we proposed delineating a 4-mm diameter circle which included the different parts of the DVC (Fig 2). The craniocaudal length of the DVC is 5 mm. The interobserver analysis showed that the DVC delineation was reproducible. The average volume and height of the DVC delineated by the WG were not significantly different from that of the expert with a result of 0.13 cm<sup>3</sup> (95% CI: 0.12-0.14) ( $p = 0.5$ ) and 0.5 cm ( $p = 1$ ), respectively. The different indices obtained by the WG compared to the expert were 0.98 (95% CI: 0.64-1.08) for the VR, 71% (95% CI: 44-87) for CDV, 27% (95% CI: 16-38) for the ADV, 0.58 (95% CI: 0.33-0.84) for the OV and 0.72 (CI 95%: 0.50-0.91) for the KI.

Fig. 1 Caudal limit of the dorsal vagal complex (DVC)



1 A: Sagittal view of the medulla oblongata showing the obex plane (red arrow). 1 B: The caudal limit of the DVC is a unique volume.

Fig. 2 Transversal view of the medulla oblongata at the level of the Dorsal Vagal Complex (DVC)



2 A: Diagram of a transversal plane of the medulla oblongata at the level of the DVC (Adapted from Duvernoy HM. Human brain stem vessels. Springer, Berlin Heidelberg New York Tokyo 1999; Published with permission). This structure includes the area postrema (25), the nucleus of the solitary tract (24) and the dorsal motor nucleus of the vagus (23). 21: median sulcus. 2 B: Transversal view of the medulla oblongata at the level of the DVC in our atlas. The DVC was indicated by a circle of 4 mm in diameter such that the delineation was reproducible.

## Conclusion

This atlas was feasible and reproducible for the delineation of DVC on planning CT using fused MRI. It will be used to prospectively assess dose-volume relationship for DVC and occurrence of nausea vomiting during intracranial or head and neck irradiation.

## PO-0755 Patterns of Re-irradiation for Recurrent Gliomas and Validation of a Prognostic Score

J. Verhoeff<sup>1</sup>, C. Post<sup>1</sup>, M. Kramer<sup>2</sup>, E. Smid<sup>1</sup>, H. Van der Weide<sup>2</sup>, K. Kleynen<sup>1</sup>, M. Heesters<sup>2</sup>

<sup>1</sup>UMC Utrecht, Radiation Oncology, Utrecht, The Netherlands ; <sup>2</sup>UMC Groningen, Radiation Oncology, Groningen, The Netherlands

## Purpose or Objective

Re-irradiation (ReRT) is a generally accepted method for salvage treatment in patients with recurrent glioma. However, no standard radiation regimen has been defined. This study aims to compare the efficacy and safety of different treatment regimens and to independently externally validate a recently published ReRT risk score introduced by Niyazi et al. (2018).

## Material and Methods

We retrospectively analyzed a cohort of patients with recurrent malignant glioma treated with salvage conventionally fractionated (CFRT; fractional dose <3 Gray), hypofractionated (HFRT; fractional dose 3-5 Gray) or stereotactic radiotherapy (SRT; fractional dose ≥5 Gray) between 2007 and 2017 at the University Medical Centers of Utrecht and Groningen.

## Results

Of the 121 patients included, 60 patients (50%) underwent CFRT, 22 (18%) HFRT and 39 (32%) SRT. The primary tumor was grade II-III in 52 patients and grade IV in 69 patients with median Overall Survival (mOS) since first surgery of 113 [Interquartile range: 53.2-137] and 39.7 [24.6-64.9] months respectively and mOS from first day of ReRT of 8.5 [6.5-11.6] and 11.3 [6.3-28.5] months respectively. Overall, mOS post ReRT was 9.7 months [6.5-14.6]. No significant difference in mOS was found between the treatment groups using log-rank test (p=0.17) and multivariate Cox regression (p=0.79) (mOS CFRT: 10.0

[6.9-17.6], HFRT: 7.7 [5.7-10.3] and SRT: 9.7 [6.2-14.9] months (Figure 1)). In multivariate analysis, Karnofsky performance scale ≥70% (p<0.01), ReRT for first recurrence (p=0.02), longer time interval between RT start dates (p<0.01) and smaller planning target volume (p<0.05) were significant favorable prognostic factors (Table 1). Eight patients (12.5%) developed severe, hospitalization required, acute toxicity and five cases (7.7%) of radionecrosis were reported in the UMC Utrecht dataset (n=65). The ReRT risk score showed good calibration by corresponding results of the Cox regression and Kaplan-Meier estimators (mOS of the prognostic groups in our cohort: 14.6, 9.76, 5.32 months versus Niyazi's development cohort 14.2, 9.1 and 5.3 versus Niyazi's validation cohort 13.8, 8.8 and 3.8 months). Discrimination performance of the score is modest (c-index: 0.65).

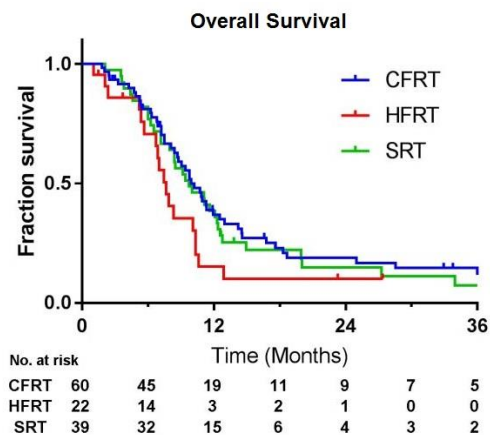


Figure 1. Kaplan-Meier curves showing overall survival from first day of re-irradiation (time in month) according to SRT (green line), HFRT (red line) and CFRT (blue line). Log-rank test was not significant (p=0.173). Pairwise comparison was also not significant (CFRT vs HFRT p=0.060; CFRT vs SRT p=0.735; SRT vs HFRT p=0.162).

Table 1. Univariate and multivariate Cox regression analysis of prognostic factors for overall survival in 121 patients receiving re-irradiation (16 censored, 20 cases with missing values). Data are expressed as hazard ratios and p-values.

Variable	Univariate analysis			Multivariate analysis		
	HR	95% CI	P-value	HR	95% CI	P-value
Age at ReRT	1.015	0.997-1.033	0.112	1.012	0.990-1.031	0.280
Sex (♂ vs ♀)	0.964	0.643-1.444	0.857	-	-	-
KPS at ReRT (<70% vs ≥70%)	3.434	1.954-6.034	<0.001*	3.138	1.730-5.692	<0.001*
WHO Grade initial (<IV vs IV)	0.525	0.347-0.794	0.002*	0.807	0.403-1.613	0.543
Initial Surgery (Gross total <sup>a</sup> )	-	-	-	-	-	-
Subtotal	0.956	0.627-1.458	0.835	-	-	-
Biopsy	0.670	0.362-1.237	0.200	-	-	-
Tumor side (lateral vs central)	1.725	0.751-3.961	0.199	-	-	-
TMZ (no vs yes)	1.822	1.185-2.801	0.006*	-	-	-
Number of recurrence <sup>b</sup> (≥2 vs 1)	0.887	0.601-1.311	0.548	1.801	1.096-2.957	0.020*
WHO Grade recurrence (<IV vs IV)	0.487	0.309-0.768	0.002*	-	-	-
Surgery prior to ReRT <sup>b</sup> (no vs yes)	0.716	0.398-1.288	0.265	-	-	-
Time interval <sup>c</sup>	0.982	0.974-0.989	<0.001*	0.981	0.969-0.993	0.002*
PTV	1.002	1.000-1.004	0.027*	1.002	1.000-1.004	0.047*
EQD2 <sub>app-10</sub> <sup>d</sup> cumulative	0.992	0.971-1.014	0.476	-	-	-

Abbreviations: CI: Confidence interval; EQD2: equivalent dose at fractionation of 2 Gy; HR: Hazard ratio; KPS: Karnofsky performance scale; NS: not significant; PTV: planning target volume; RT: radiotherapy; ReRT: re-irradiation; TMZ: temozolomide concurrent at initial therapy.

\*p value of <0.05 was considered significant; <sup>a</sup>Reference group: <sup>b</sup>Number of recurrences occurred before re-irradiation; <sup>c</sup>Surgery within 2 months prior to re-irradiation; <sup>d</sup>Time interval between start date of initial radiotherapy and start date of re-irradiation; <sup>e</sup>Calculated with  $\alpha/\beta = 10$  for tumor tissue.

## Conclusion

In our series, mOS after ReRT was sufficient to justify use of this modality. Until a reliable treatment decision tool is developed based on larger retrospective research, the decision for ReRT schedule should remain personalized and based on a multidisciplinary evaluation of each patient.

**PO-0756 Evaluating the DS-GPA in patients with 1-10 brain metastases treated with stereotactic radiosurgery**

S. Nagtegaal<sup>1</sup>, A. Claes<sup>1</sup>, T. Snijders<sup>2</sup>, J. Verhoeff<sup>1</sup>  
<sup>1</sup>UMC Utrecht, Radiation Oncology, Utrecht, The Netherlands ; <sup>2</sup>UMC Utrecht, Neurology, Utrecht, The Netherlands

**Purpose or Objective**

There are multiple prognostic models for predicting survival after treatment for brain metastases. One of them, the diagnosis-specific Graded Prognostic Assessment (DS-GPA), has been developed to predict the median survival for brain metastases from the most frequent primary sites. Our objective is to compare the survival predicted by the DS-GPA to actual survival in patients treated with SRS for 1-10 brain metastases. We will both evaluate the ability of the DS-GPA to predict the survival on an individual level, as well as its success in dividing a group of patients into different prognostic strata.

**Material and Methods**

We identified a consecutive cohort of patients treated with SRS for brain metastases in our institute. DS-GPA scores were calculated for each patient, and the median survival for each DS-GPA group was calculated. Differences in survival between DS-GPA groups were tested with Kaplan-Meier curves.

**Results**

Out of a total of 401 patients treated with SRS from 2012-2017, 366 patients with calculable DS-GPA were identified. Waterfall plots showing the difference between predicted median and actual survival per patient are shown in Figure 1, stratified by the number of brain metastases. The proportion of the survival times within each predicted quartile was 26.6%, 30.7%, 24.9% and 17.8% (for Q1-Q4, respectively). Figure 2 shows the Kaplan-Meier curves of the disease groups with a statistically significant difference between the DS-GPA strata.

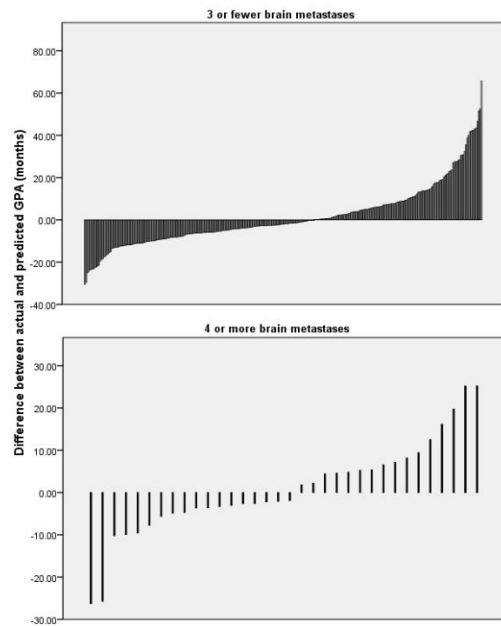


Figure 1 Waterfall plots showing the differences between the predicted and the actual survival on an individual level, stratified by the number of brain metastases

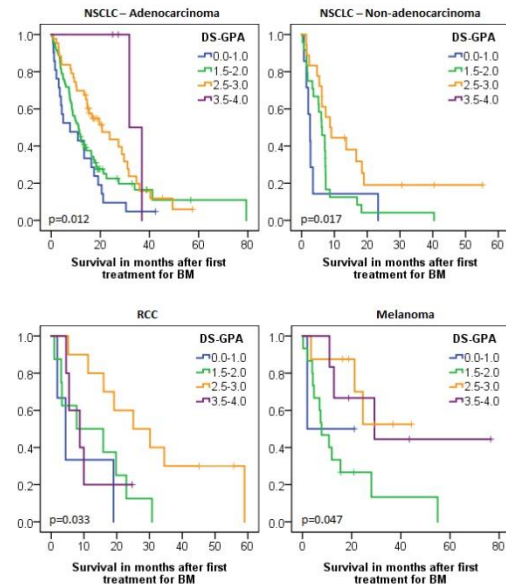


Figure 2 Survival curves for the disease subgroups with a statistically significant difference between the DS-GPA strata

**Conclusion**

DS-GPA seems to be a reliable tool for brain metastases patients treated with SRS. Although the differences between the predicted median and the actual survival difference can be large, the distribution of the actual survival within the predicted quartiles is as expected. This means that, although the DS-GPA doesn't give a point prediction of survival, it is able to accurately predict the range in which the survival will fall.

Furthermore, the DS-GPA is also useful in dividing the renal cell carcinoma, melanoma and both NSCLC disease groups into strata with different survival. This allows physicians to place a patient in a certain prognostic group, which may help to determine the most optimal treatment and the duration and frequency of follow-up.

The way physicians and other health professionals discuss the results of the DS-GPA score is important. The fact that it results in a median survival and not a point-predicted survival is an important distinction. Patients should not be told that the DS-GPA gives a precise prediction of the expected survival. Instead, a patient needs to be told that around half of the patients with similar clinical characteristics reach the median age, but that the other half dies before that time. This corresponds with our findings. Additionally, the window of survival that applies to half of the patients, i.e. the interquartile range, is another important message for patients, which is also something we have found in this study.

**PO-0757 Radiosurgery for cranial and spinal haemangioblastomas: monoinstitutional analysis.**

V. Pinzi<sup>1</sup>, A. Viola<sup>2</sup>, E. De Martin<sup>3</sup>, C. Iezioni<sup>4</sup>, M. Cerniauskaite<sup>1</sup>, M. Marchetti<sup>1</sup>, L. Fariselli<sup>1</sup>  
<sup>1</sup>Fondazione IRCCS Istituto Neurologico C. Besta, Neurosurgery- Unit of Radiotherapy, Milan, Italy ; <sup>2</sup>University of Milan, Radiation Oncology, Milan, Italy ; <sup>3</sup>Fondazione IRCCS Istituto neurologico C. Besta, Health Department, Milan, Italy ; <sup>4</sup>Fondazione IRCCS Istituto Neurologico C. Besta, Neurosurgery-Radiotherapy Unit, Milan, Italy

**Purpose or Objective**

Hemangioblastomas (HB) of the central nervous system are rare indolent WHO grade I vascular tumors of controversial origin that may occur sporadically or in association with von Hippel-Lindau (VHL) disease. Though primary therapy for HB is surgical resection, for patients

with subtotally excised or unresectable lesions and for patients with poor clinical status who are not good candidates for surgery, as well as those wishing a minimally invasive approach, radiotherapy (RT) or radiosurgery (SRS) can be an effective alternative. RT and SRS have been associated with good rates of local control in a 60-90% range, especially in patients with VHL. The aim of this study is to evaluate the efficacy and safety of SRS for patients with diagnosis of intracranial and spinal HB in terms of local control and toxicity.

#### Material and Methods

We conducted a retrospective analysis of 22 patients with a total of 37 HB: 23 intracranial HB and 14 spinal HB treated at our Institute from January 2012 until February 2017.

A regular clinical and radiological follow-up with MR imaging was scheduled at 4-6 month intervals after SRS procedure. The toxicity was recorded based on CTCAE 3.0v. The radiosurgical procedures were performed using a CyberKnife system, characterized by a 6MV linac mounted on a robotic arm for multiple, non-isocentric, non-coplanar beams sets delivery. Statistical analysis was carried out using SPSS 21.

#### Results

Twenty-two patients were followed for a median of 42 months (range 3-72 months). Median age at the time of SRS was 44 years (range 19-79), 8 patients were female and 14 male.

The diagnosis of HB was based on the histological findings, except in 7 patients without surgical removal. Seven patients had multiple lesions and 30 patients had a single lesion. The median tumour volume pre-SRS was 417 mm<sup>3</sup> (range, 40-15779 mm<sup>3</sup>). The mean prescription dose was 18 Gy (range, 10-25 Gy) in 1-5 fractions with median isodose line of 81% (range, 73-88%).

Two patients (9%) developed a recurrence, 12 patients (55%) showed stable disease and 8 (36%) partial response. There was no significant toxicity after treatments.

**Conclusion**  
SRS, both in single and multi-fractions settings, is potentially attractive for patients with VHL disease where multiple HB may develop either concurrently or sequentially and may be difficult to treat or retreat with repeated surgery and/or conventional radiation techniques without the risk of toxicity. Our results show that SRS can be considered a safe and effective treatment for intracranial and spinal HB.

---

#### Poster: Clinical track: Haematology

---

#### PO-0758 Whole brain RT plus concomitant Temozolamide in PCNSL after MTX-HD: a prospective phase II study

F. Catucci<sup>1</sup>, S. Chiesa<sup>2</sup>, M. Giraffa<sup>2</sup>, E. Maiolo<sup>3</sup>, F. Beghella<sup>2</sup>, T. Zinicola<sup>2</sup>, S. Hohaus<sup>3</sup>, V. Rufini<sup>4</sup>, V. Valentini<sup>2</sup>, M. Balducci<sup>2</sup>

<sup>1</sup>Istituto di Radiologia- Fondazione Policlinico Universitario A. Gemelli IRCCS, Dipartimento di Scienze Radiologiche- Radioterapiche ed Ematologiche, Roma, Italy; <sup>2</sup>Istituto di Radiologia- Fondazione Policlinico Universitario A. Gemelli IRCCS- Università Cattolica del Sacro Cuore, Dipartimento di Scienze Radiologiche- Radioterapiche ed Ematologiche, Roma, Italy; <sup>3</sup>Istituto di Ematologia - Fondazione Policlinico Universitario A. Gemelli IRCCS- Università Cattolica del Sacro Cuore, Dipartimento di Scienze Radiologiche- Radioterapiche ed Ematologiche, Roma, Italy; <sup>4</sup>Istituto di Medicina Nucleare - Fondazione Policlinico Universitario A. Gemelli IRCCS- Università Cattolica del Sacro Cuore, Dipartimento di Scienze Radiologiche- Radioterapiche ed Ematologiche, Roma, Italy

#### Purpose or Objective

To evaluate the overall survival (OS) in patients affected by primary cerebral lymphoma (PCNSL) treated with radiotherapy (RT) plus Temozolamide (TMZ) after treatment with high dose methotrexate (HD-MTX).

#### Material and Methods

Patients with an histological diagnosis of PCNSL, previously treated HD-MTX, were enrolled to receive TMZ concomitant to RT. The whole brain up to C2 leptomeninges received 30 Gy (2 Gy/die), while the total dose to initial site of disease or residual mass, if present, was modulated according to the response to HD-MTX (Complete response = 6 Gy, partial response = 10 Gy, progression disease = 16 Gy). According to our previous dose escalation study, concomitant TMZ was administered at a safety dose level of 75 mg/mq.

#### Results

From March 2004 to December 2017, 33 patients were enrolled: 18 males and 15 females. The median age was 64.5 yrs (range 50-76). Twenty-two patients received two cycles of HD-MTX, while 9 only one cycle (because of hematological toxicity) and 2 patients did not received any cycle (due to poor performance status). Nine patients were subjected to macroscopic surgical excision while the remaining patients were only subjected to biopsy. Twenty-five patients were treated with RT plus concomitant TMZ. The median follow up was 80 months (range 3-169), currently, 9 out of 33 patients (27%) are alive (7 without disease and 2 with stable disease), 22 patients died because of disease and 2 patients because of other causes. The median OS of the whole group was 23.1 months with at 1 years OS of 64% and at 3 years OS of 43%. The concomitant use of TMZ showed a significant impact on OS (p = 0.004).

#### Conclusion

Although with a limited patients selection, this prospective study demonstrated that the use of TMZ at a dose of 75 mg/mq concomitant to radiotherapy shows better results in terms of OS than radiotherapy alone.

---

#### Poster: Clinical track: Breast

---

#### PO-0759 Radiotherapy After Primary CHEMotherapy (RAPCHEM): protocol adherence in a Dutch registration study

L. Boersma<sup>1</sup>, P. Elkhuizen<sup>2</sup>, R. Houben<sup>3</sup>, E. Van Leeuwen<sup>4</sup>, S. Linn<sup>5</sup>, L. De Munck<sup>6</sup>, R. Pijnappel<sup>7</sup>, L. Strobbe<sup>8</sup>, T. Van Dalen<sup>9</sup>, J. Verloop<sup>6</sup>, A. Voogd<sup>10</sup>, J. Wessling<sup>11</sup>, P. Poortmans<sup>12</sup>

<sup>1</sup>Maastricht University Medical Centre+, Radiation Oncology Maastricht- GROW School for Oncology and Developmental Biology-, Maastricht, The Netherlands; <sup>2</sup>The Netherlands Cancer Institute, Radiotherapy, Amsterdam, The Netherlands; <sup>3</sup>Maastricht Clinic, Radiotherapy, Maastricht, The Netherlands; <sup>4</sup>BOOG study Center, not applicable, Amsterdam, The Netherlands; <sup>5</sup>The Netherlands Cancer Institute, Medical oncology, Amsterdam, The Netherlands; <sup>6</sup>Comprehensive Cancer Centre Netherlands, Breast cancer, Utrecht, The Netherlands; <sup>7</sup>University Medical Centre Utrecht, Radiology, Utrecht, The Netherlands; <sup>8</sup>Canisius Wilhelmina Hospital, Surgery, Nijmegen, The Netherlands; <sup>9</sup>Diakonessen Hospital, Surgery, Utrecht, The Netherlands; <sup>10</sup>Maastricht University Medical Centre+, GROW School for Oncology and Developmental Biology-, Maastricht, The Netherlands; <sup>11</sup>The Netherlands Cancer Institute, Pathology, Amsterdam, The Netherlands; <sup>12</sup>Institut Curie, Radiotherapy, Paris, France

#### Purpose or Objective

The indications for post-operative radiation therapy (PORT) after primary systemic treatment (PST) for stage I-

II breast cancer (BC) are unclear. Therefore, we conducted a prospective cohort study from 2011-2014 in the Netherlands (RAPCHEM: NCT01279304), to evaluate the 5-year locoregional recurrence rate for BC patients treated with PST, surgery, and PORT given according to strict study-guidelines (SG). The aim of the current analysis is to evaluate adherence to these SG.

#### Material and Methods

Between January 2011 and January 2015, all patients with cT1-2N1 (four or more suspicious nodes at imaging excluded) BC, treated with PST in the referral area of 18 Dutch RT centres were included. Trained clerks of the Dutch Cancer Registry registered tumour and treatment characteristics. Surgery consisted of breast conserving therapy (BCT) or mastectomy with a sentinel node (SN) biopsy and/or an axillary lymph node dissection (ALND). SG recommended whole breast RT for patients treated with BCT and adapted chest wall/nodal RT based on three risk categories, mainly based on the ypN status:

1. Low-risk (ypN0): breast RT in case of BCT/no chest wall RT in case of mastectomy;
2. Intermediate-risk (ypN1): chest wall/breast RT;
3. High-risk (ypN2): chest wall/breast RT with regional RT (level I-IV).

In 2013, an amendment was developed taking into account new insights in axillary treatment: in case of a positive SN, additional ALND could be replaced by axillary RT.

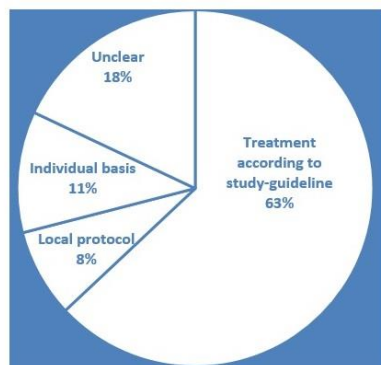
#### Results

From 2011-2014 we included 853 patients: 291 in the low-, 378 in the intermediate-, and 184 in the high-risk groups, respectively. 160 (19%) patients did not undergo an ALND. Overall, 63% of the patients were treated according to the SG (66% after BCT, 60% after mastectomy). Almost 10% received RT to fewer target volumes than recommended in the SG, and almost 25% received RT to more extensive target volume (Table). These percentages remained stable over the inclusion period. The largest variation was seen in the intermediate risk group (ypN1), where only 54% were treated according to the SG and where 16% received less and 27% received more RT than the SG. In half of the patients not treated according to the SG, the reason for deviation was unclear; in the other half, 60% deviated on an individual basis, whereas 40% were treated according to the local institutional protocol, since the radiation-oncologists did not agree with the SG (Figure).

Table showing percentage of patients treated according to study-guidelines, receiving more or less extensive RT than study-guidelines or just different than study-guidelines.

Risk group	RT according to study-guideline	Less RT than study-guideline	More RT than study-guideline	Different RT than study-guideline	Total
Low risk (ypN0)	61.5%	0.3%	37.5%	0.7%	100%
Intermediate risk (ypN1)	54%	16.4%	27%	2.7%	100%
High risk (ypN2)	85.3%	11.4%	0%	3.3%	100%
Total	63.3%	9.9%	24.7%	2.1%	100%

Figure showing reasons for not adhering to study-guidelines



#### Conclusion

The SG of the RAPCHEM study were followed in only 63% of patients. The largest variation in applied post-operative RT was observed in patients with ypN1 disease (intermediate risk group); deviation of the SG more often

resulted in more extensive RT than recommended by the SG. Future analyses will be aimed at evaluating the outcome of these patients in relation to risk factors and the actual RT given.

#### PO-0760 Heterogeneity of Radiosensitivity, Recurrence, and PD-L1 in Breast Tumor Single Cell RNA-Seq Data

B. Jang<sup>1</sup>, W. Han<sup>2</sup>, I.A. Kim<sup>3</sup>

<sup>1</sup>Seoul National University Hospital, Radiation Oncology, Seoul, Korea Republic of ; <sup>2</sup>Seoul National University-College of Medicine, Surgery, Seoul, Korea Republic of ; <sup>3</sup>Seoul National University-College of Medicine, Radiation Oncology, Seoul, Korea Republic of

#### Purpose or Objective

Tumor heterogeneity has been recently revealed in an advent of single-cell RNA sequencing. At a single cell level, heterogeneity of intrinsic tumor radiosensitivity, recurrence-risk, and their relationship remain unknown in breast cancer. In this study, we investigate the heterogeneity of intrinsic tumor radiosensitivity and recurrence risk in breast cancer patients.

#### Material and Methods

We investigated single cell mRNA sequencing data from GEO database (GSE75688) to profile 281 primary breast tumor cells. Subtypes of each tumor cell were classified by using PAM50 gene signature. OncoType DX and Endopredict gene signatures were used to estimate enrichment score and to assess the recurrence risk for each cell. To explore radiosensitivity, Gene Set Variation Analysis (GSVA) were performed across cells using radiosensitivity gene signatures including both RSI (Radiosensitivity Index) and 31-gene. PD-L1 expressed tumor cells were profiled as well.

#### Results

GSVA analysis showed that mean recurrence risk score of cells were different according to PAM50 breast cancer subtype, and cells were classified as basal subtype demonstrated higher risk recurrence score compared to those of other subtypes ( $P < 0.001$ ). Heterogeneity of recurrence risk was observed more frequently in luminal A subtype compared to basal/HER2 positive subtypes. Radioresistant tumor cells, representing high enrichment score of RSI, were more commonly found in basal type compared to those of other subtypes ( $P = 0.029$ ). RSI score was varied among cells from patient to patient, indicating the heterogeneity of intrinsic tumor radiosensitivity. There were significant correlations in a single cell resolution between RSI and 31-gene radiosensitivity (Pearson's  $r = 0.25$ ), between RSI and Endopredict risk score ( $r = 0.26$ ), and between OncoType DX and Endopredict enrichment scores ( $r = 0.61$ ), respectively. Most of the PD-L1 expressed cells were classified into high-risk recurrence group (92.8% for Endopredict and 100% for OncoTypeDX).

#### Conclusion

Tumor cells having various subtype or recurrent-risk coexisted regardless of individual pathologic subtype in a single cell level. Most radioresistant tumor cells showed basal subtype or PD-L1 expression. PD-L1 expressed cells were enriched in the high-risk or basal/HER2/luminal B subtype. Our results demonstrated the heterogeneity of intrinsic tumor radiosensitivity and recurrence risks in breast cancer patients.

#### PO-0761 Hypofractionated whole breast irradiation safety after breast-conserving surgery for young patients

I. Meattini<sup>1</sup>, Y. Kirova<sup>2</sup>, C. Saieva<sup>3</sup>, L. Visani<sup>1</sup>, E. Olmetto<sup>1</sup>, V. Salvestrini<sup>1</sup>, J. Kim<sup>4</sup>, W. Jung<sup>4</sup>, I. Desideri<sup>1</sup>, A. Fourquet<sup>2</sup>, P. Poortmans<sup>2</sup>, L. Livi<sup>1</sup>, K. Kim<sup>4</sup>  
<sup>1</sup>University of Florence - Azienda Ospedaliero Universitaria Careggi, Radiation Oncology Unit - Oncology Department, Florence, Italy ; <sup>2</sup>Institut Curie, Department of Radiation Oncology, Paris, France ;

<sup>3</sup>Institute for cancer research- prevention- and clinical network ISPRO, Cancer Risk Factors and Lifestyle Epidemiology Unit, Florence, Italy ; <sup>4</sup>Ewha Womans University College of Medicine, Department of Radiation Oncology, Seoul, Korea Republic of

### Purpose or Objective

Whole breast irradiation (WBI) ± boost on the primary tumour bed is the standard of care after breast-conserving surgery (BCS). For decades, conventionally fractionated WBI (CF-WBI) has been widely used. Pivotal phase 3 trials on hypofractionated-WBI (HF-WBI) showed comparable results in terms of efficacy with lower rates of acute side effects in favour of hypofractionation. However, due to the relatively low proportion of younger patients enrolled in these studies, HF-WBI is not broadly adopted for these patients. The aim of this retrospective case-control study is to confirm the safety of hypofractionation in younger patients.

### Material and Methods

Between 2007 and 2016, a total of 786 patients aged less than 60 years old with early stage breast cancer was treated with WBI after BCS in three leading breast cancer centres: 340 underwent HF-WBI while 446 cases were treated with CF-WBI. All patients were homogeneously scored following the acute and late RTOG/EORTC scales by treating expert physicians. Acute side effects were evaluated by scoring the maximum grade of oedema, erythema/pigmentation, and wet desquamation at the end of the WBI. Late toxicity was evaluated by scoring the maximum grade of oedema, erythema/pigmentation, desquamation, and breast fibrosis at 6, 12, 24, and 36 months.

### Results

At univariate analyses, hypofractionation showed a significant protective effect in terms of acute oedema (p=0.0001), acute wet desquamation (p=0.009), chronic oedema (p=0.0001), chronic erythema/pigmentation (p=0.0001), and chronic fibrosis (p=0.0002). Main results are summarized in Figure 1. At multivariate analysis independent factors for acute oedema were hypofractionation (HR 0.09, 95%CI 0.02 to 0.48; p=0.005), and adjuvant chemotherapy (HR 2.09, 95%CI 1.10 to 3.97; p=0.024); independent factors for chronic fibrosis were breast volume (HR 2.64, 95%CI 1.50 to 4.65; p=0.001), extensive intraductal component (HR 2.15, 95%CI 1.17 to 3.98; p=0.014), and tumour grade (HR 0.29, 95%CI 0.11 to 0.74; p=0.01). Major results are summarized in Figure 2.

Figure 1. Significant association between individual characteristics and toxicity in 786 breast cancer cases. P-values from univariate logistic models.

Toxicity	N	Protective factor	p-value	Risk factor	p-value
Acute Oedema (grade ≥2)	43	Hypofractionation Dmax/Prescribed dose (cut-off 107%)	0.0001 0.001	Chemotherapy	0.002
Chronic Oedema	50	Hypofractionation HER2 positive Dmax/Prescribed dose (cut-off 107%)	0.0001 0.037 0.003	EIC Boost dose Breast volume	0.0001 0.0001* 0.003
Acute Hyperpigmentation (grade ≥2)	163	HER2 positive Trastuzumab	0.0001 0.022	Smoke habits Boost dose Breast volume	0.001 0.01* 0.002
Chronic Erythema	110	Hypofractionation Dmax/Prescribed dose (cut-off 107%)	0.0001 0.001	EIC Margins Boost dose Breast volume	0.0001 0.008 0.0001* 0.034
Acute Wet Desquamation (grade ≥2)	20	Hypofractionation Dmax/Prescribed dose (cut-off 107%)	0.009 0.047	-	-
Chronic Fibrosis	117	Hypofractionation Tumour grade Ki67 index Dmax/Prescribed dose (cut-off 107%)	0.0002 0.022 0.023 0.017	EIC Boost dose Breast volume	0.0001 0.0001* 0.0001

\* ≥10 Gy or equivalent tumour bed boost dose

Figure 2. Univariate and multivariate analysis of acute oedema (grade ≥2) and chronic fibrosis.

Feature	n	Univariate		Multivariate	
		HR (95% CI)	p	HR (95% CI)	p
<b>ACUTE OEDEMA</b>					
Hypofractionation					
No	446	1		1	
Yes	340	0.09 (0.03-0.30)	0.0001	0.09 (0.02-0.48)	0.005
Chemotherapy					
None	509	1		1	
Adjuvant	259	2.63 (1.42-4.90)	0.002	2.09 (1.10-3.97)	0.024
Neoadjuvant	18	not evaluable	-	not evaluable	-
Dmax/Prescribed dose					
>107%	273	1		1	
≤107%	455	0.16 (0.06-0.46)	0.001	1.17 (0.26-5.27)	0.84
<b>CHRONIC FIBROSIS</b>					
Hypofractionation					
No	446	1		1	
Yes	340	0.44 (0.29-0.68)	0.0002	0.88 (0.35-2.22)	0.79
EIC					
Absence	548	1		1	
Presence	169	3.03 (1.99-4.62)	0.0001	2.15 (1.17-3.98)	0.014
Tumour grade					
1	176	1		1	
2	315	0.67 (0.42-1.07)	0.19	0.54 (0.29-0.99)	0.048
3	211	0.53 (0.31-0.92)	0.038	0.29 (0.11-0.74)	0.01
Ki67 index					
<20%	327	1		1	
≥20%	299	0.60 (0.38-0.93)	0.023	1.23 (0.61-2.51)	0.56
Boost dose					
None	51	1		1	
<10 Gy or equivalent	506	1.60 (0.48-5.34)	0.45	not evaluable	-
≥10 Gy or equivalent	229	6.76 (2.04-22.45)	0.022	not evaluable	-
Breast volume (cc)					
<492 (median)	365	1		1	
≥492	364	2.84 (1.83-4.41)	0.0001	2.64 (1.50-4.65)	0.001
Dmax/Prescribed dose					
>107%	273	1		1	
≤107%	455	0.58 (0.37-0.91)	0.017	1.00 (0.44-2.27)	0.99

### Conclusion

HF-WBI showed significantly better outcome in terms of main acute and late skin side effects. Longer follow-up is needed to confirm efficacy results. In line with recently updated international guidelines, the use of HF-WBI after BCS should be strongly encouraged and may largely replace CF-WBI independently of age.

### PO-0762 Low predictive value of mean heart dose for coronary artery dosimetry in breast cancer radiotherapy

S. JACOB<sup>1</sup>, J. Camilleri<sup>2</sup>, S. Derreux<sup>3</sup>, V. Walker<sup>1</sup>, O. Lairez<sup>4</sup>, M. Lapeyre<sup>5</sup>, E. Bruguière<sup>5</sup>, A. Pathak<sup>6</sup>, M. Bernier<sup>1</sup>, D. Laurier<sup>7</sup>, J. Ferrières<sup>8</sup>, D. Broggio<sup>9</sup>, G. Jimenez<sup>2</sup>

<sup>1</sup>Institut de Radioprotection et de Sureté Nucléaire IRSN, Laboratory of Epidemiology, Fontenay-aux-Roses / Toulouse, France ; <sup>2</sup>Clinique Pasteur, Radiotherapy Oncorad, Toulouse, France ; <sup>3</sup>Institut de Radioprotection et de Sureté Nucléaire IRSN, Unit of expertise in medical radiation protection, Fontenay-aux-Roses, France ; <sup>4</sup>Rangueil University Hospital, Cardiology, Toulouse, France ; <sup>5</sup>Clinique Pasteur, Radiology, Toulouse, France ; <sup>6</sup>Clinique Pasteur, Cardiology, Toulouse, France ; <sup>7</sup>Institut de Radioprotection et de Sureté Nucléaire IRSN, Department of health and biological effects of ionizing radiation, Fontenay-aux-Roses, France ; <sup>8</sup>National Institute of Medical Research INSERM, Cardiovascular Epidemiology, Toulouse, France ; <sup>9</sup>Institut de Radioprotection et de Sureté Nucléaire IRSN, Dosimetry, Fontenay-aux-Roses, France

### Purpose or Objective

In many studies that investigated radiation-induced cardiac toxicity of breast cancer radiotherapy, doses are described as those received by the entire heart and the mean heart dose is used as the reference dose for analyzing dose-response relationship. However the specific relationships between doses to cardiac sub-structures, in particular coronary arteries, and subsequent toxicity have not been well defined. Detailed individual dosimetry information for the heart and its sub-structures is required to better understand cardiac damage from radiation exposure. The aim of this dosimetric study was to analyze the distribution of individually-determined radiation exposure, in a population of breast cancer patients treated with three dimensional conformal radiation therapy (3D-CRT), and clarify whether mean heart dose is a good surrogate parameter for the dose to coronary arteries, in particular the left anterior descending artery.

### Material and Methods

Patients with left or right unilateral breast cancer (BC) treated with 3D-CRT between 2015 and 2017 were included (BACCARAT clinical study). Before RT, a coronary computed tomography angiography (CCTA) was performed. Registration of the planning CT and CCTA images allowed precise delineation of the coronary arteries on the planning CT images. Using the 3D dose matrix generated during treatment planning and the added coronary contours, dose distributions were generated for the following cardiac structures: whole heart, left main coronary artery (LMCA), left anterior descending artery (LAD), left circumflex artery (LCX) and right coronary artery (RCA). A descriptive analysis of the physical doses in Gray (Gy) was performed.

#### Results

Dose distributions were generated for 89 left-sided BC and 15 right-sided BC patients. The treatment schedule with tangential beams was either 50 Gy delivered in 25 fractions of 2 Gy or 47 Gy in 20 fractions of 2.35 Gy, with or without irradiation of regional lymph nodes. Additional beams to tumor bed (boost) were used, if clinically indicated. The mean heart dose (Dmean Heart) was  $2.9 \pm 1.5$  Gy for left-sided BC and  $0.5 \pm 0.1$  Gy for right-sided BC. For left-sided BC patients, the mean ratio Dmean LAD/Dmean Heart was around 5. All other ratios were below 1 except for RCA in right-sided BC patients (ratio=2.7). However, the coefficients of determination  $R^2$  indicated that the proportion of the variance in Dmean LAD or Dmean RCA predictable from Dmean Heart was low ( $R^2=0.45$  and  $0.36$  respectively). For left-sided BC patients with lower exposure (Dmean Heart < 3Gy), 56% of patients received doses > 40Gy to 20% of the LAD volume on average (V40Gy).

#### Conclusion

Our study illustrates that the predictive value of the mean heart dose was not good enough for coronary arteries, in particular for LAD, illustrating the importance of considering the distribution of doses within these cardiac substructures rather than just the mean heart dose to enhance knowledge on the risk of radiation-induced cardiotoxicity in breast radiotherapy.

#### PO-0763 Prognostic role of platelets-to-lymphocytes and neutrophil-to-lymphocytes ratio in breast cancer

I.R. Scognamiglio<sup>1</sup>, M. Tirozzi<sup>1</sup>, A. Romano<sup>1</sup>, M. Caroprese<sup>1</sup>, E. Zanella<sup>1</sup>, E. Scipilliti<sup>1</sup>, R. Mancuso<sup>1</sup>, A. Farella<sup>1</sup>, R. Solla<sup>2</sup>, C. Oliviero<sup>1</sup>, S. Clemente<sup>1</sup>, R. Pacelli<sup>1</sup>, M. Conson<sup>1</sup>

<sup>1</sup>University "Federico II" School of Medicine, Department of Advanced Biomedical Sciences, Napoli, Italy ;

<sup>2</sup>National Research Council, Institute of Biostructure and Bioimages, Napoli, Italy

#### Purpose or Objective

Breast cancer (BC) is the most common cancer and the first leading cause of cancer related death among women. Nowadays, many prognostic factors are available in clinical practice for BC patients, but ongoing efforts are made by the scientific community to identify new biomarkers for prognostic models' improvement. Inflammation is a hallmark of cancer and in the tumor-microenvironment it contributes to many cancer-promoting effects. Platelet-to-lymphocyte ratio (PLR) and neutrophil-to-lymphocyte ratio (NLR) are related to systemic inflammation and associated with prognosis in many solid tumors. The aim of this study is to verify the prognostic role of PLR and NLR in no metastatic BC patients who underwent radiotherapy (RT).

#### Material and Methods

Between January 2010 and December 2012, 229 consecutive BC patients treated in our department with adjuvant RT were analysed. 3D conformal RT with conventional fractionation schedule was administered. Clinical, pathological, and treatment characteristics of all patients are reported in Table 1. PLR and NLR were

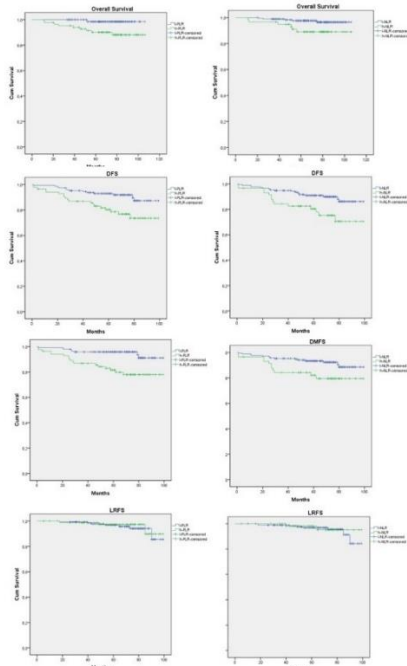
calculated as the absolute platelet count divided by the absolute lymphocyte count, and absolute neutrophil count divided by absolute lymphocyte count, respectively. The blood-count values were collected before RT. PLR and NLR were dichotomized and the cut-off values were 180 (namely, h-PLR $\geq$ 180, l-PLR<180) and 3 (namely, h-NLR $\geq$ 3, l-NLR<3), respectively. Actuarial 5 years overall survival (OS), disease free survival (DFS) were calculated. The impact of PLR and NLR along with patients clinical, pathological, and treatment characteristics on survival endpoints was evaluated. To this end, univariate and multivariate analyses were performed.

	number (%)
Site of disease	
Right	107 (47%)
Left	117 (51%)
Bilateral	5 (2%)
Histology	
CIS	11 (5%)
Ductal	176 (77%)
Lobular	29 (12%)
Other	13 (6%)
AJCC stage	
0	13 (6%)
IA	109 (47%)
IIA	49 (21%)
IIB	27 (12%)
IIIA	17 (7%)
IIIB	15 (7%)
Grading	
1	13 (7%)
2	104 (45%)
3	102 (44%)
Missing data	10 (4%)
Receptor status	
Luminal A	116 (51%)
Luminal B	71 (31%)
Basal Like	18 (8%)
Her2 Like	8 (3%)
Missing data	16 (7%)
Ki67	
<20	118 (52%)
$\geq$ 20	90 (39%)
Missing data	21 (9%)
Surgery	
Conservative surgery	221 (92%)
Mastectomy	18 (8%)
Chemotherapy	
Yes	119 (52%)
No	109 (47.6%)
Missing data	1 (0.4%)
Hormonal therapy	
Yes	194 (85%)
No	31 (13%)
Missing data	4 (2%)

Table1 Patient characteristics

#### Results

Median age was 55 years (range 25-84). At a median follow-up time of 70 months (range 5-99), 218 patients (95.2%) were alive. Eight patients (3.5%) died for disease progression, while 3 deaths (1.3%) were non-cancer related. There were 32 (14%) relapses of disease. At the univariate analysis, 5y-OS was 98.4% for l-PLR patients and 90.1% for h-PLR ( $p<0.002$ ). 5y-DFS was 98.4% for l-PLR patients and 88.9% for h-PLR ( $p<0.001$ ). h-PLR and h-NLR resulted significantly associated with higher distant recurrence rates, while it was not observed for locoregional recurrence rates. The results are reported in Figure 1. Among patients clinical, pathological, and treatment characteristics, stage III age < 55 years, triple negative status negatively affected 5y-OS and DFS. At multivariate analysis, only h-PLR and stage III resulted associated with poorer prognosis, with a significantly higher rate of distant recurrences.



DMFS and LRFS of 229 patients divided into l-PLR (PLR<180) and h-PLR (PLR≥180) group

### Conclusion

High PLR is associated with poor prognosis in breast cancer patients. This biomarker might be implemented in clinical practice to improve recurrence risk estimation.

### PO-0764 The effect of automatic heart contouring on model performance in predicting acute coronary events

D. SPOOR<sup>1</sup>, F. Peters<sup>1</sup>, V. Van den Bogaard<sup>1</sup>, A. Van der Schaaf<sup>1</sup>, B. Ta<sup>1</sup>, R. Vliegthart<sup>2</sup>, R. Kierkels<sup>1</sup>, H. Langendijk<sup>1</sup>, J. Maduro<sup>1</sup>, M. Sijtsema<sup>1</sup>, A. Crijs<sup>1</sup>  
<sup>1</sup>University Medical Center Groningen, Radiation Oncology, Vroomshoop, The Netherlands ; <sup>2</sup>University Medical Center Groningen, Radiology, Vroomshoop, The Netherlands

### Purpose or Objective

Breast cancer irradiation is associated with an increased risk of cardiac toxicity. The relationship between cardiac dose and toxicity was described by prediction models with the mean heart dose (MHD) as predictive variable. To determine the MHD the heart volume has to be delineated. Delineation of the heart can be done manually, but this is a time consuming method. Alternatively, methods for automatic contouring of the heart have been developed and the geometric overlap with manual contours has been studied. However, the effect of the contouring method on model performance has never been studied. In this study, the performances of NTCP models containing MHD based on automatic and manual generated contours of the heart were analyzed.

### Material and Methods

The study cohort consisted of 927 consecutive female breast cancer patients treated with radiotherapy after breast-conserving therapy. Manual contours of the whole heart were made routinely by technicians. Automatic contouring was performed with an in house developed multi-atlas based automatic segmentation (MABAS) tool for the heart. This tool has previously been proven to be an accurate and efficient method for automatic contouring of the heart on non-contrast planning CT scans. The NTCP model for acute coronary events (ACE) 9 years after radiotherapy by van den Boogaard et al. was refitted based on individual reconstructed MHD based on auto-contours (MABAS fit) and manual-contours (manual fit)

using Cox regression. Model performance was evaluated for both model fits by the -2 log likelihood and the c-statistic. The correlation between predicted risks of an ACE for both model fits was calculated. Calibration of both model fits was performed by plotting predicted risk of an ACE against observed ACE rates for different subgroups. These subgroups were created by stratification of patients by predicted risk of an ACE (0-5%, 5-10%, 10-15%, 15-20% and >20%) in both groups.

### Results

Model performance of the MABAS fit was comparable to the manual fit. The -2 log likelihood of the MABAS fit was 1.4 lower than the manual fit (323.2 vs. 324.6 respectively). The c-statistic of the MABAS fit and the manual fit were 0.82 (0.63-0.91) and 0.81 (0.72-0.90) respectively. Figure 1 shows that predicted risks for both model fits are highly correlated ( $r=0.994$ ). Despite an overestimation of the risk of an ACE due to limited follow-up, Figure 2 shows that the accuracy of the predictions for the MABAS fit and the manual fit are similar.

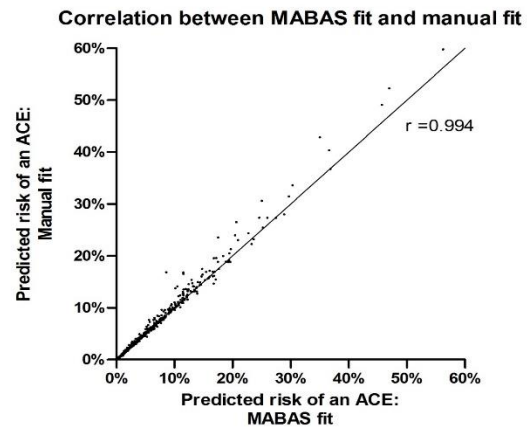


Figure 1: Correlation between predicted risks of an ACE for MABAS fit and manual fit

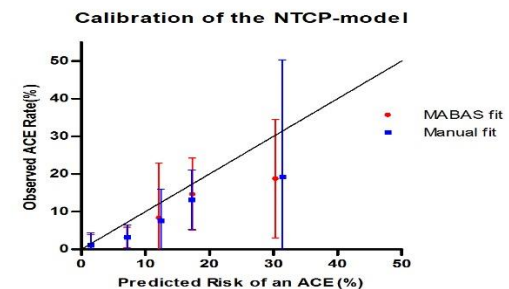


Figure 2: Calibration plot showing the predicted ACE rates 9 years after breast cancer radiotherapy as a function of observed ACE rates for two model fits; one dataset using MABAS derived MHD and the other using manual derived MHD.

### Conclusion

Refitting of the model by van den Bogaard et al. with datasets using MABAS and manual derived MHD results in highly correlated predictions and a comparable model performance.

### PO-0765 Oncological and cosmetic outcome after IOERT as a boost in a large cohort of breast cancer patients.

M. Machiels<sup>1</sup>, R. Weytjens<sup>1</sup>, K. Erven<sup>1</sup>, J.M. Westerhoff<sup>1</sup>, S. Amrouch<sup>1</sup>, J. Bosiers<sup>1</sup>, L. Verkinderen<sup>2</sup>, J. Hauspy<sup>2</sup>, P. Van Dam<sup>3</sup>, P. Dirix<sup>1</sup>, M. Vos<sup>1</sup>, P. Huget<sup>1</sup>, L. Dirix<sup>4</sup>, P. Meijnders<sup>1</sup>, S. Van Laere<sup>4,5</sup>, P.B. Vermeulen<sup>4,5</sup>, C. Billiet<sup>1,6</sup>  
<sup>1</sup>Iridium Kankernetwerk, Radiation Oncology, Antwerp,

Belgium ; <sup>2</sup>GZA Hospitals, Gynaecology, Antwerp, Belgium ; <sup>3</sup>Antwerp University Hospital, Multidisciplinary Oncologic Centre Antwerp MOCA, Edegem, Belgium ; <sup>4</sup>GZA Hospitals, Oncology, Antwerp, Belgium ; <sup>5</sup>University of Antwerp, Center for Oncological Research, Antwerp, Belgium ; <sup>6</sup>Oncology Center GZA, Translation Cancer Research Unit, Antwerp, Belgium

### Purpose or Objective

Advantages of using intraoperative radiotherapy with electrons (IOERT) as a boosting modality in breast-conserving therapy, include the direct visualization of the tumor bed, patient convenience, and allows a reduced dose to the skin, which may lead to a more favorable cosmetic outcome. We aimed to report oncological outcome, postoperative complication rate, mammographic changes on follow-up imaging, late toxicity and cosmetic outcome in women treated at our institution with IOERT as a boost modality in breast-conserving therapy for early invasive breast carcinoma or ductal carcinoma in situ (DCIS).

### Material and Methods

Between January 2007 and June 2018, 763 unselected patients of any risk group with early breast carcinoma or DCIS, treated at the GZA Hospitals were enrolled. During breast-conserving surgery, an IOERT boost of 9 Gy (90% reference dose) was applied, followed by whole breast irradiation (WBI). In a subset of patients (n=230) late toxicity and cosmetic outcome were scored prospectively using the LENT-SOMA breast questionnaires.

### Results

At a median follow-up of 62.2 months (range: 0.5 - 135), only 12 in-breast recurrences were observed, yielding a local tumor control rate of 98.4% at 5 years. A DFS of 95.1% at 5 years and OS of 97.2% at 5 years were noted. In univariate analysis, negative ER status, adjuvant hormonal therapy and interval between IOERT and EBRT predicted ipsilateral locoregional recurrence (Figure 1), albeit in multivariable analysis none reached significance. From the 12 patients with an in-breast recurrence, 9 were located within the initially involved quadrant and 3 outside this quadrant.

A total of 27 (3.5%) patients developed postoperative complications (e.g. hematoma, infection, wound dehiscence). None of the tumor characteristics nor any of the IOERT technical parameters were predictive for postoperative complications.

Ninety-nine percent of patients received follow-up imaging with a frequency < 2/year (median 0.92/y, range: 0 - 5.5). On follow-up imaging, 179 patients with mammographic changes were found of which 57% (n=102) required a biopsy.

After a median follow-up of 35 months (range: 22-64), the most prevalent G2 toxicities were breast fibrosis (29.5%) and breast pain (6.9%). Only 5.4% of patients reported any kind of G3 toxicity. A total of 78.8% patients had an excellent to good cosmetic outcome.

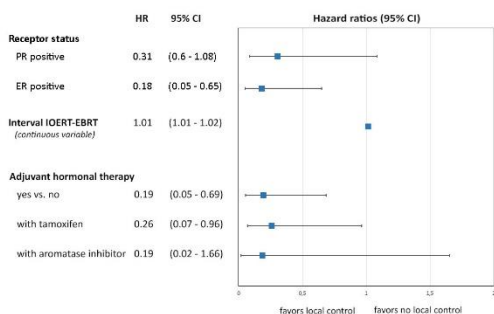


**Figure 1.** Forest - Plot: Hazard ratios (HR) and 95% confidence intervals (CI) obtained from univariable Cox

proportional hazards regression model of ipsilateral locoregional recurrences. Only significant characteristics are presented. Abbreviations: PR = progesterone receptor; ER = estrogen receptor.

### Conclusion

A 9 Gy IOERT boost combined with post-operative WBI provided outstanding local control rates, comparable to all trials with similar length of follow up. Furthermore, this is the largest cohort reporting on late toxicity and cosmetic outcome; our results demonstrate IOERT boost to be well-tolerated, with limited late toxicity and an excellent cosmetic outcome.

### PO-0766 The Italian Society of Radiation and Clinical Oncology (AIRO): snapshot on breast cancer management

F. Gregucci<sup>1</sup>, A. Fozza<sup>2</sup>, S. Falivene<sup>3</sup>, D. Smaniotto<sup>4</sup>, A. Morra<sup>5</sup>, A. Daidone<sup>6</sup>, R. Barbara<sup>7</sup>, A. Ciabattini<sup>8,9</sup>  
<sup>1</sup>Sacro Cuore Don Calabria - IRCCS, Radiation Oncology, Negrar, Italy ; <sup>2</sup>ASO S.S. Antonio e Biagio e Cesare Arrigo, Radiation Oncology, Alessandria, Italy ; <sup>3</sup>P.O. Ascalesi, Radiation Oncology, Napoli, Italy ; <sup>4</sup>Policlinico Universitario A. Gemelli IRCCS - Università Cattolica del Sacro Cuore - Istituto di Radiologia, Radiation Oncology, Roma, Italy ; <sup>5</sup>Istituto Europeo di Oncologia - IRCCS, Radiation Oncology, Milano, Italy ; <sup>6</sup>P.O. Abele Ajello, Radiation Oncology, Mazzara del Vallo, Italy ; <sup>7</sup>AO San Giovanni Addolorata, Radiation Oncology, Roma, Italy ; <sup>8</sup>Ospedale San Filippo Neri, Radiation Oncology, Roma, Italy ; <sup>9</sup>on the behalf of Italian Society of Radiation and Clinical Oncology AIRO Breast Group, Radiation Oncology, Italy, Italy

### Purpose or Objective

To investigate the actual attitude of the Italian Radiation Oncologists in the management of breast cancer (BC) concerning some controversial issues.

### Material and Methods

A nationwide, 21-points questionnaire was distributed online via Survey Monkey to the Italian Radiation Oncologists.

### Results

78 Centers answered the Survey for 34164 patients (pts) affected by BC. In most centers, the pts number treated was superior to 200/year and in almost all cases an experts multidisciplinary discussion was performed to choose the best treatment for each patient. 16734 (49%) pts were treated with hRT. The 95% of centers used this treatment approach as clinical practice after breast-conserving surgery (BCs) for early stage BC, mostly in women older than 50 years (40%) affected by invasive ductal carcinoma (IDC) (89%). Dose prescription ranged between 34-45Gy with high use of moderate hRT (40Gy/15fr and 42.4Gy/16fr in 62% of cases). In locally advanced BC, the post-mastectomy or regional nodal hRT was still rarely applied, 13% and 15% respectively. In early stage BC, the 60% of centers used partial breast RT (PBI) with different techniques. 216 (0.6%) pts received rRT after BC recurrence. In 80% of cases, the rRT was given more than 5 years after primary RT. The age factor was not related with the rRT choice (68% of answer were "all age") and the most frequent histological type was IDC (82%) alone or associated with other histology. Regarding RT volumes are so representative below: 54% total rRT (WBI/chest wall irradiation) and 94% PBI (including 42% of tumor bed RT). 3879 (11%) pts received RT after NAC. In the 55% of cases a clinical disease evaluation was performed at the end of NAC and in 40% before. Disease staging included sentinel node biopsy before and after NAC in 40% and 60% respectively. The chest wall and the ipsilateral lymph nodes RT is a shared choice by most of the Italian Radiation Oncologists in case of locally advanced BC at the disease onset (cT3-T4 and/or cN2-N3), regardless of the kind of response obtained after NAC (complete response vs partial response) and also independently by the axillary

surgical approach (SLB vs axillary lymph node dissection-ALND). In case of disease onset with limited lymph node involvement (cN1), the same therapeutic option is chosen based on the response obtained after NAC but not based on the axillary surgical approach: in case of residual disease after NAC (ypN+), post-mastectomy RT is performed in the 79% and 76% of cases after SLB or ALND, respectively. In this setting, breast RT was administered in 97% of pts after BCs, with hRT in 49% of cases.

#### Conclusion

This survey demonstrated the high interest for breast RT in the majority of Italian Centers. Some practices as rRT and RT omission in particular clinical settings need further verification before entering in current clinical practice. Future national clinical collaborative studies are advocated in order to investigate these controversial topics about BC RT.

#### PO-0767 Long-term results of adjuvant hypofractionated radiotherapy for breast cancer in elderly patients.

M.J. García Anaya<sup>1</sup>, I. García Ríos<sup>1</sup>, S. Segado<sup>1</sup>, Á. Fernández Forné<sup>1</sup>, C. Jódar López<sup>1</sup>, J.A. Medina Carmona<sup>1</sup>

<sup>1</sup>Hospital Universitario Virgen de la Victoria, Radiation Oncology, Malaga, Spain

#### Purpose or Objective

Radiotherapy is an important treatment for the local control of breast cancer. More than 30% of breast cancer cases occur in women 70 years of age or older, but adjuvant radiation therapy is often omitted in older women due to comorbidities, sociofamilial problems or difficulty to attend the radiotherapy sessions. Traditionally, whole-breast radiation therapy (WBRT) after surgery has been delivered over 5 weeks using a conventionally fractionated schedule (2 Gy daily) to a total dose of 50 Gy. This is a logistic issue, particularly for an elderly population, which affects radiotherapy accessibility and comprises a major determinant of its eventual underutilization. We need radiotherapy fractionation schedules adapted to elderly patients. Hypofractionation (HFRT) allows to administer a lower total dose delivered in fewer although larger fractions. The objective of this study is to evaluate local control, acute and late toxicity and disease-free survival of elderly breast cancer patients treated with once-weekly adjuvant whole-breast radiation therapy.

#### Material and Methods

A consecutive series of 240 breast cancer elderly patients underwent once-weekly hypofractionated WBRT after breast conservative surgery, mastectomy or only *biopsy*, from January 2006 to September 2017. Patients were primarily selected to take into account older age, poor medical condition and/or logistic issues. They were given 32.5 Gy in 5 fractions (6.5 Gy once a week) until October 2011. Subsequently, they were administered 28,5 Gy in 5 fractions (5,7 Gy once a week). The modification of the fractionation to a lower dose per fraction was chosen according to the approach of the UK FAST randomized trial.

#### Results

The median aged was 78 years (35-89). 204 (85%) patients underwent breast-conserving surgery, 34 (14.2%) radical surgery and 2 (0.8%) no surgery. The clinical stage distribution was as follows: I in 92 (38.3%), II in 98 (40.8%), III in 49 (20.4%). Axillary lymph nodes were positive in 40.3 % of cases. Adjuvant hormone therapy and chemotherapy was given in 83.3% and 16.7% respectively. There was no interruption of the treatment. Early skin reactions were tolerable. Late effects, mainly subcutaneous fibrosis, were recorded in 115 patients; they were classified as grade 1 in 94 cases, grade 2 in 24 cases and grade 3 in 7 patients (figure 1). No late toxicity in 115 patients. The patients with 32.5 Gy showed a worse cosmetic result

what the patients with 28.5 Gy. There were no differences in locoregional control between both treatment schedules. Locoregional control was 94.2% at 5 years (figure 2) and progression-free survival was 84.5% at 5 years. At a median follow-up of 46.3 months, 178 patients (74.2%) was alive and disease free and 30 (12,5%) patients die and disease free.

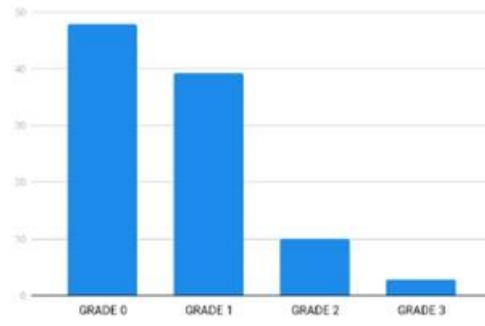


Figure 1: late toxicity (RTOG)

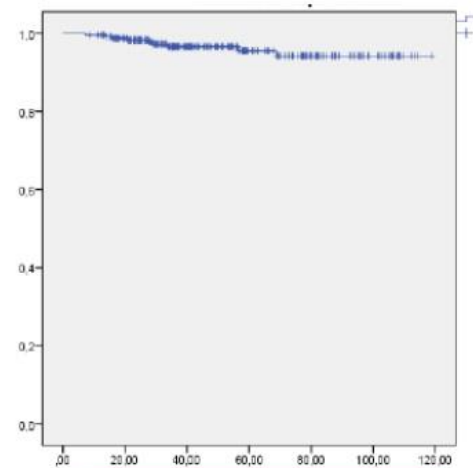


Figure 2: 5-years locoregional control: 94.2%

#### Conclusion

According to the findings from this retrospective study, HFRT schedule is effective and well tolerated in the elderly patients, with toxicity equivalent to other schemes of radiotherapy treatment and with a high level of compliance.

#### Poster: Clinical track: Lung

#### PO-0768 High Heart Dose Affects Overall Survival in Lung Cancer Patients Undergoing Radiation Therapy.

M. Fatyga<sup>1</sup>, S. Schild<sup>1</sup>, J. Niska<sup>1</sup>, M. Herman<sup>2</sup>, J. Li<sup>3</sup>, X. Liu<sup>3</sup>

<sup>1</sup>Mayo Clinic Arizona, Radiation Oncology, Phoenix, USA ;

<sup>2</sup>Mayo Clinic Rochester, Radiation Oncology, Rochester, USA ;

<sup>3</sup>Arizona State University, School of Computing-Informatics- Decision Systems Engineering, Tempe, USA

#### Purpose or Objective

To determine if radiation induced cardiac toxicity influences overall survival (OS) in stage III lung cancer patients undergoing radiation therapy (RT).

#### Material and Methods

A single institution database of 134 stage III Non Small Cell Lung Cancer patients, treated with RT, was retrospectively analyzed in this study. Survival status was obtained for each patient from the institutional tumor registry. Patients were treated with conventionally fractionated 3D Conformal and Intensity Modulated Radiation Therapy. The heart structure was contoured for each patient within the Varian Eclipse Treatment Planning System. A range of dose volume histogram (DVH) indices was computed from the whole heart cumulative DVH, and used together with patient specific characteristics in a family of Multivariate Cox Regression models. Each model used a single DVH index and all patient specific characteristics. The Akaike Information Criterion was used to find significant predictors in each model. We used this methodology to systematically search within a wide range of DVH indices for indices which may be predictive for a decrease in overall survival. Only one DVH index was used in each model because of strong correlations between indices. Subsequently, each heart was digitally subdivided into four segments along sup-inf and left-right axes. The same analysis was repeated using cumulative DVHs in each sub-part separately. Prescription dose, age before RT, mean lung dose, V20 lung dose, tumor location and laterality, stage, chemotherapy and surgery were used as patient specific characteristics.

#### Results

80 (60%) patients presented with stage IIIA and 54 (40%) with stage IIIB cancer. Doses prescribed were  $61.9 \pm 6.8$  Gy in 2Gy fractions, and 113 (77%) patients also received chemotherapy. 53 (40%) patients were alive at the last followup, while 81 (60%) were not. High doses to the heart were found to be significant predictors for the decreased overall survival, specifically: V%<sub>55Gy</sub> ( $p=0.01$ ) and V%<sub>60Gy</sub> ( $p=0.04$ ). Three patient characteristics were also found to be predictive for overall survival in all models: cancer stage (IIIA/IIIB,  $p=0.02$ ), chemotherapy ( $p<0.01$ ) and age before RT ( $p=0.02$ ). The analysis of digitally subdivided heart structures showed that V%<sub>55Gy</sub> ( $p=0.01$ ) and V%<sub>60Gy</sub> ( $p=0.02$ ) in the right-superior portion of the heart were significant predictors for the overall survival, while doses to the remaining three segments of the heart were not predictive. The index V%<sub>D</sub> indicates the percentage of the volume receiving dose 'D', or greater.

Whole Heart DVH index	V%5	V%10	V%15	V%20	V%25	V%30
p-value	0.63	0.613	0.648	0.531	0.446	0.554
Whole Heart DVH index	V%35	V%40	V%45	V%50	V%55	V%60
p-value	0.98	0.611	0.257	0.051	<b>0.011</b>	<b>0.039</b>

#### Conclusion

High doses to the heart in radiation therapy for lung cancer were associated with decline in overall survival, especially doses to the superior right segment of the heart. Minimizing high doses to the superior-right segment of the heart may potentially improve the overall survival for lung cancer patients and permit higher therapeutic doses.

#### PO-0769 Lung Organ-at-Risk volumes - The need for a better definition in the era of 4DCT

S. Vinod<sup>1</sup>, C. Choong<sup>1</sup>, P. Vial<sup>1</sup>, T. Kron<sup>2</sup>, D. Ball<sup>2</sup>  
<sup>1</sup>SWSLHD Liverpool Hospital, Cancer Therapy Centre, Liverpool BC, Australia ; <sup>2</sup>Peter MacCallum Cancer Centre, Radiation Oncology, Melbourne, Australia

#### Purpose or Objective

Accurate volume delineation is crucial to correct interpretation of lung dose volume histograms (DVHs). However the studies on which current lung DVH constraints are based were all conducted in the 3DCT era with varying definitions for lung volume for DVH calculation ie Lungs alone, Lungs - PTV, Lungs - GTV. These volume definitions have not been updated in the era of 4DCT.

#### Material and Methods

We undertook a survey of all Australian departments in 2018 to evaluate how lung OAR risk volumes were being defined in clinical practice. To assess the clinical impact of different volume subtractions, we calculated lung DVHs on a cohort of 10 consecutive patients who had completed IMRT for Stage II-III NSCLC to a dose of 60-66Gy/30-33 fractions. We calculated mean lung dose (MLD), V20 and V30 for "Lungs - PTV", "Lungs - CTV", "Lungs - ITV" and "Lungs - GTV\_EX (expiratory phase)", where "Lungs" were delineated on the average of the 4DCT. These parameters were also calculated for "Lungs - ITV" where "Lungs" were delineated on the average, inspiratory and expiratory phases.

#### Results

Of the 27/88 responses received, 1 department used "Lungs alone", 6 used "Lungs - PTV", 2 used "Lungs - CTV", 6 used "Lungs - ITV", 5 used "Lungs - GTV in one phase of the respiratory cycle" and 7 departments stated the volumes used varied according to individual radiation oncologists.

The different tumour volume subtractions resulted in a difference in MLD ranging from 0.9Gy to 4.15Gy (Figure 1), V20 from 1.5% to 6.6% (Figure 2) and V30 from 1.34% to 7.11%. Four patients had a difference in MLD greater than 2Gy, 7 patients a difference in V20 greater than 2% and 8 patients in V30 greater than 2%. Subtraction of the PTV resulted in the lowest DVHs. The largest difference between subtraction of GTV\_EX and ITV was 0.32Gy, 0.43% and 0.46% for MLD, V20 and V30 respectively.

Subtraction of the ITV from the lungs as defined on different datasets resulted in a difference in MLD ranging from 0.2Gy to 2.88Gy and V20 from 0.37% to 5.61%. One patient had a difference in MLD greater than 2Gy and 4 patients a difference in V20 greater than 2%. There was no consistent dataset for lung volume definition which was associated with lower DVHs.

Figure 1 - Mean lung dose (Gy) calculated for different tumour volume subtractions in 10 patients

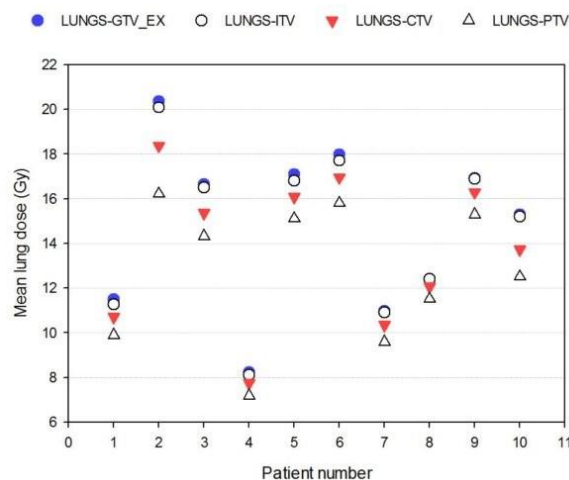
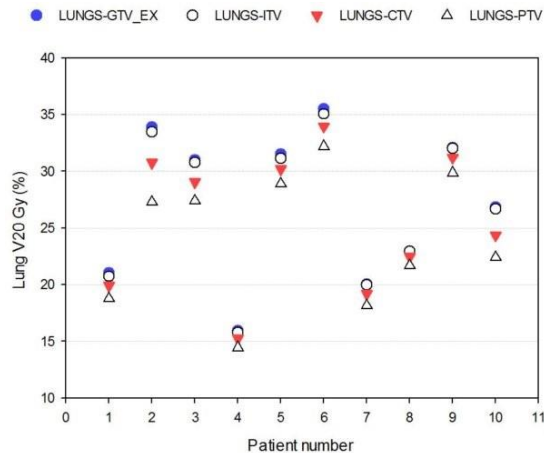


Figure 2 - Lung V20Gy (%) calculated for different tumour volume subtractions in 10 patients



### Conclusion

There is variability in definition of Lung OAR volumes. Clinically significant differences in lung DVH parameters are seen depending on the volume being subtracted. A robust definition of lung OAR volumes, applicable to both 3DCT and 4DCT simulation is needed. We suggest using “Lungs (average) - ITV” for 4DCT and “Lungs - GTV” for 3DCT simulation for Lung DVH calculation. Ideally these definitions should be used in clinical trial protocols to clarify the association between lung DVHs and toxicities and aid in translation of trial results into clinical practice.

### PO-0770 Clinical Outcomes of Concurrent Chemoradiation vs RT alone in Elderly Patients with Stage III NSCLC

D.Y. Kim<sup>1</sup>, J. Kim<sup>2</sup>, C. Song<sup>2</sup>, J.S. Lee<sup>3</sup>

<sup>1</sup>Seoul national university hospital, Radiation oncology, Seoul, Korea Republic of ; <sup>2</sup>Seoul National University Bundang Hospital, Radiation oncology, Seongnam, Korea Republic of ; <sup>3</sup>Seoul National University Bundang Hospital, Internal Medicine, Seongnam, Korea Republic of

### Purpose or Objective

In elderly patients with stage III Non-Small Cell Lung Cancer (NSCLC), there are no solid conclusions about which treatment modality is better for concurrent chemoradiotherapy (CCRT) or radiotherapy (RT) alone, considering combined comorbidity or poor treatment tolerance. This study evaluated clinical outcomes between CCRT and RT alone in patients  $\geq 70$ -year old in a single institution clinical practice

### Material and Methods

A total of 94 patients with unresectable stage III NSCLC treated with at Seoul National University Bundang Hospital between 2004 and 2016 were reviewed. We analyzed 82 patients with curative intent to compare the tolerance ( $\geq$  EQD2 54Gy and no unplanned break of RT more than 5days or no hospitalization due to severe toxicities) by chi-square test and overall survival (OS), locoregional recurrence (LRR) and distant metastasis (DM) between two treatments using Kaplan-Meier method. Also, we evaluated patients who had died within 4 months after RT and causes of deaths. Furthermore, we performed subgroup analyses of factors which affect OS and 4-month survival in each treatment group by stepwise cox regression model.

### Results

Median follow-up time was 20.1 months. Patients received CCRT (65.9%) and RT alone (34.1%), and induction chemotherapy was done in 68.5% and 50.0%, respectively. Treatment tolerance was significantly worse in CCRT (87.0%) compared to RT alone (100.0%) (P=0.046). Median survival was 21.1 months and 18.1 months for CCRT and RT alone group, which was not statistically significant. LRR

and DM also showed no significantly difference between two treatment modalities. Though there was no statistical significance, deaths within 4 months after RT (4-month death) were higher in CCRT than RT alone group. Most of 4-month deaths in CCRT were related to non-cancer related mortality, such as pneumonia. In toxicity analysis, acute esophagitis of grade 2 or higher occurred more frequently in CCRT than in RT alone (P=0.017). On multivariate analysis, OS was significantly associated with Charlson comorbidity index (CCI) of 5 or greater (HR 2.00, 95% CI 1.10-3.61, P=0.022) and weight loss of 5% or more after treatment (HR 2.46, 95% CI 1.33-4.54, P=0.004). The factors affecting 4-month survival were also CCI score $\geq$ 5 (HR 6.46, 95% CI 2.18-19.21, P=0.001) and treatment modality (HR 0.26, 95% CI 0.07-0.98, P=0.047). Furthermore, in patients with CCI score 5 or greater, RT alone showed significantly better survival than CCRT at 4 months of follow up (P=0.038).

### Conclusion

We found that there were no significant differences in OS, LRR and DM between CCRT and RT alone, rather poorer tolerance and higher incidence of acute esophagitis grade 2 or higher in CCRT group. In case of the elderly patients with CCI score 5 or more, RT alone seems to be favorable with low possibility of early death after the treatment, mostly due to non-cancer related mortality.

### PO-0771 Cardiac event after radical radiotherapy for lung cancer - initial results from a multi-centre study

F. Sun<sup>1</sup>, K. Banfill<sup>2</sup>, S. Falk<sup>2</sup>, M. Alan<sup>2</sup>, L. John<sup>1</sup>, W. Robert<sup>1</sup>, A. Azadeh<sup>2</sup>, S. Matthias<sup>2</sup>, V.H. Marcel<sup>2</sup>, F. Corinne<sup>2</sup>, F. Kevin<sup>1</sup>

<sup>1</sup>St James Institute of Oncology, Oncology, Leeds, United Kingdom ; <sup>2</sup>Christie Hospital- Manchester, Clinical Oncology, Manchester, United Kingdom

### Purpose or Objective

Lung cancer is the leading cause of cancer mortality worldwide. Radical radiotherapy plays a pivotal role in the management of early and locally advanced disease. Recent studies suggest adverse cardiac events post treatment may worsen survival outcome for patients. This study aims to identify risk factors which predispose patients to cardiac events post radiotherapy and we present the initial results from the initial 107 patients.

### Material and Methods

All patients who received radical dose of radiotherapy for lung cancer between 01/01/2010 to 30/12/2016 in Leeds and Manchester are to be included. 1709 patients have been identified. From these cohorts patients were excluded if they had multiple courses of radiotherapy to the chest. Individual patient clinical information was retrieved from the hospitals electronic patient record (EPR). Patient and cancer demographics have been collected. Pre-existing cardiac conditions, Charlson's Comorbidity index and Qrisk 3 scores were calculated. Post radiotherapy cardiac events were recorded, survival times were calculated.

### Results

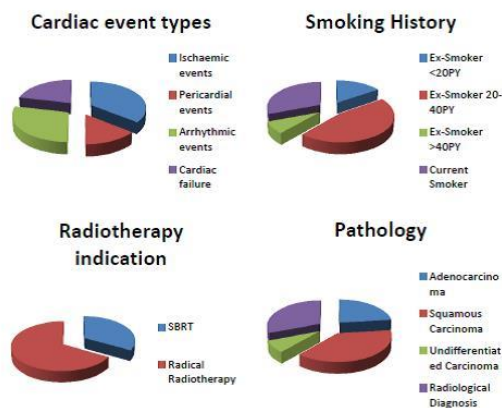
107 patients have been analysed so far. Median follow up is 26 months. Patient, tumour and radiotherapy characteristics are summarised in table 1. In the patients studied 30% had pre-existing cardiac conditions and 13% of patients experienced a cardiac events following radiotherapy (83% of these patients had pre-existing cardiac conditions). The median time from treatment to cardiac event was 13 months post radiotherapy. Patient characteristics of those who experienced cardiac toxicity are summarized in charts 2.

Table 1

Sex	Male	58(54%)
	Female	49(46%)
Age at RT treatment	Median =73	Range(45-90)
PS	0	6(5%)
	1	55(51%)
	2	43(40%)
	3	3(4%)
Smoking Status	Never smoked	2(2%)
	Ex-Smoker <10 PY	0(0%)
	Ex-smoker <20 PY	20(18%)
	Ex-Smoker 20-40PY	31(29%)
	Ex-Smoker >40 PY	17(16%)
	Current Smoker	37(35%)
Charlson Score	Median = 6 (2% estimated 10 year survival)	Range(3-10)
Qrisk3 Score	Median = 22.7% (%risk of stroke/MI in next 10 years)	Range(5.8-40.7)
Known pre-existing cardiac condition	= 32(30%)	Previous MI = 8 IHD = 12 Heart Failure = 1 Arrhythmia = 6 Valve defect = 2
RT indication	Adjuvant RT	10
	SBRT	48
	Concurrent ChemoRT	15
	Sequential ChemoRT	5
	Radical RT	26
	Radical RT for local recurrence	3
Pathology	Adeno	24
	Squam	29
	Adenosquam	0
	Undifferentiated NSCLC	4
	Small Cell	6
	Large Cell	3
	Radiological diagnosis	41

Charts 2

Patients who had cardiac toxicity following radiotherapy



### Conclusion

A substantial proportion of patients had a cardiac event following radical radiotherapy for lung cancer. A large proportion of these patients had pre-existing cardiac conditions. Cardiac events occur much sooner after lung cancer radiotherapy than post-radiotherapy for breast cancer or lymphoma. Further work is on-going to expand

the patient numbers, examine risk factors and correlate cardiac events/survival with radiotherapy dosimetry.

### PO-0772 Role of Prophylactic Cranial Irradiation in Extensive Disease Small Cell Lung Cancer

J. Chung<sup>1</sup>, S.Y. Kang<sup>2</sup>, G.J. Cheon<sup>2</sup>, H. Wu<sup>1</sup>, Y.S. Weo<sup>1</sup>, D. Kim<sup>3</sup>, H.J. Kim<sup>1</sup>

<sup>1</sup>Seoul National University Hospital, Department of Radiation Oncology, Seoul, Korea Republic of ; <sup>2</sup>Seoul National University Hospital, Department of Nuclear Medicine, Seoul, Korea Republic of ; <sup>3</sup>Seoul National University Hospital, Department of Internal Medicine, Seoul, Korea Republic of

### Purpose or Objective

The role of prophylactic cranial irradiation (PCI) remains controversial in extensive disease small cell lung cancer (ED-SCLC). This study is performed to identify the risk factors of symptomatic brain metastasis and to evaluate the impact of PCI on brain metastasis-free survival (BMFS) and overall survival (OS) according to the risk of symptomatic brain metastasis in ED-SCLC.

### Material and Methods

From 2006 to 2017, a total of 190 patients diagnosed with ED-SCLC who underwent FDG-PET and brain MRI prior to treatment were enrolled in this retrospective study. Among these patients, 53 (27.9%) received PCI and 137 (72.1%) did not. Prognostic index predicting a high risk of symptomatic brain metastasis was calculated in the observation group (137/190) on Cox regression model and the prognostic index was generated by summing significant factors weighted by hazard ratio of each. The role of PCI in each risk group was analyzed by using Kaplan-Meier survival analysis.

### Results

Median follow-up time was 10.6 months. 1-year and 2-year symptomatic BMFS and OS were 86.9%, 52.5% and 49.8%, 12.7%, respectively. Multivariate Cox regression analysis showed that 4 risk factors were associated with high risk of symptomatic brain metastasis: presence of extrathoracic metastases ( $P=0.005$ ), FDG-PET uptake in bone marrow (BM) or spleen ( $P < 0.001$ ), progressive disease (PD) after chemotherapy ( $P=0.010$ ), and high hemoglobin (Hb) level ( $P=0.006$ ). The prognostic index significantly divided patients into two subgroups of high and low-risk of symptomatic brain metastasis ( $P < 0.001$ ). PCI significantly improved BMFS in high-risk patients ( $P=0.002$ , 1-year rate 95.5% vs. 61.8%), but not in low-risk patients ( $P=0.522$ , 1-year rate 100.0% vs. 91.9%). However, PCI did not improve OS in patients at a high risk for symptomatic brain metastasis ( $P=0.736$ , 1-year rate 45.0% vs. 50.0%).

### Conclusion

Four prognostic factors are associated with a high risk of symptomatic brain metastasis in ED-SCLC: presence of extrathoracic metastases, FDG-PET uptake in BM or spleen, PD after chemotherapy, and high Hb level. PCI is beneficial for patients at a high risk of symptomatic brain metastasis in terms of BMFS, but not OS. Therefore, selective use of PCI in ED-SCLC according to risk stratification is recommended.

### PO-0773 CBCT is not valid for response evaluation after chemoradiotherapy for locally advanced NSCLC

G. Persson<sup>1,2,3</sup>, M. Pøhl<sup>2</sup>, L. Nygård<sup>2</sup>, S.R. De Blanck<sup>2</sup>, J. Scherman<sup>2,4</sup>, S.W. Langer<sup>2</sup>, K. Richter Larsen<sup>3,5</sup>, P.F. Clementsen<sup>6,7</sup>, L. Specht<sup>2,3</sup>, B.M. Fischer<sup>3,8</sup>, M.C. Aznar<sup>2,9</sup>, M. Josipovic<sup>2</sup>

<sup>1</sup>Herlev Hospital- University of Copenhagen, Department of Oncology, Herlev, Denmark ; <sup>2</sup>Rigshospitalet University of Copenhagen, Department of Oncology, Copenhagen, Denmark ; <sup>3</sup>Faculty of Health and Medical Sciences- University of Copenhagen, Department of Clinical Medicine, Copenhagen, Denmark ; <sup>4</sup>Lund University Hospital, Department of Radiation Oncology,

Lund, Sweden ; <sup>5</sup>Bispebjerg Copenhagen University, Department of Pulmonology, Copenhagen, Denmark ; <sup>6</sup>Roskilde Zealand University Hospital, Department of Internal medicine, Roskilde, Denmark ; <sup>7</sup>Faculty of Health and Medical Sciences- University of Copenhagen, Copenhagen Academy for Medical Education and Simulation CAMES, Copenhagen, Denmark ; <sup>8</sup>Rigshospitalet University of Copenhagen, Department of Nuclear Medicine- Cyclotrone and PET, Copenhagen, Denmark ; <sup>9</sup>Manchester Cancer Research Centre, University of Manchester, Manchester, United Kingdom

### Purpose or Objective

The PACIFIC trial showed a remarkable overall survival benefit with the adjuvant immune checkpoint inhibitor durvalumab after concomitant chemoradiotherapy (cCRT) for stage III non-small cell lung cancer (NSCLC). Inclusion criteria in the study were performance status (PS) 0-1 and no progression after cCRT. The adjuvant therapy was initiated within 42 days after the last radiotherapy (RT) fraction. There was a statistically significant advantage of starting adjuvant treatment early versus late within the 42 days, emphasizing the value of early response evaluation. We examined if response evaluation based on cone beam CT scans (CBCT) can be used to select patients for adjuvant therapy after cCRT. Furthermore, we assessed the fraction of patients eligible for adjuvant treatment with immune checkpoint inhibitor.

### Material and Methods

Patients with stage III NSCLC who received cCRT with cis- or carboplatin and vinorelbine in two prospective studies (2014-17) on deep inspiration breath-hold (DIBH) radiotherapy (RT) were included in the analysis. PS was prospectively registered at baseline and at completion of cCRT. CBCT response evaluation was performed retrospectively comparing the CBCT of the last fraction to the planning CT. Clinical response evaluation was done with contrast enhanced CT and compared to the planning CT. To avoid bias, CBCT evaluation was performed prior to assessing the CT evaluation. RECIST 1.1 criteria were used to evaluate if there was progression.

### Results

Ninety-four patients were included in the two trials. After the planning FDG-PET/CT, 18 patients were upstaged and received palliative treatment, two patients were downstaged and had stereotactic body RT or resection, and one patient died. Seventy-three patients proceeded to cCRT. Two patients progressed during cCRT (both brain metastases) and four patients were lost to follow-up before the evaluation CT, leaving 67 patients (46% men / 54% women), for analysis.

Median age was 65 (range 49-85) years and median baseline PS was 1. Pathology was adenocarcinoma (58%), squamous carcinoma (36%) and others (4%). Fifty-one (76%) patients received RT in DIBH and 16 (24%) patients in free breathing.

CBCT response evaluation revealed local progression in one patient and CT response evaluation found progression in seven patients. Furthermore, two patients were diagnosed with brain metastases on MR between end of RT and CT evaluation. Table 1 summarizes the progressing patients. CT evaluation was performed at median 57 (range 0-123) days after end of treatment.

Seventeen (25%) patients were in PS0, 41 (61%) patients in PS1 and nine (13%) patients in PS 2 at end of RT.

### Conclusion

CBCT cannot be recommended for treatment evaluation as most progressions (67%) were outside the CBCT field of view. Fifty (75%) patients were in PS 0-1 and without progression on CT evaluation after cCRT and thus candidates for adjuvant immune checkpoint inhibitor therapy.

Patient nr	Site of progression	Found on CBCT	Found on CT	Within CBCT FOV <sup>1</sup>	RT to CT time span <sup>2</sup> (days)
7	Primary tumour	Yes	Yes	Yes	93
14	Brain	No	No	No	50
16	Pleura, lungs	No	Yes	No	64
23	Lymph nodes (groin)	No	Yes	No	95
27	Lungs, lymph nodes, bones, kidney	No	Yes	Yes (bones)	65
28	lymph nodes (retroperitoneal)	No	Yes	No	67
44	Brain	No	No	No	90
46	lymph nodes (mediastinal)	No	Yes	Yes	34
63	liver	No	Yes	No	48

<sup>1</sup> Field of view (FOV), <sup>2</sup> Time from end of radiotherapy (RT) to CT acquisition

### PO-0774 Outcomes of IMRT/VMAT vs 2D/3D-conformal thoracic radiation in limited stage small-cell lung cancer

T.S. Toh<sup>1</sup>, A. Bang<sup>2</sup>, D. Pinto<sup>3</sup>, H. Katrina<sup>4</sup>, C. Brown<sup>4</sup>, W. Xu<sup>5</sup>, G. Liu<sup>4</sup>, B. Lok<sup>2</sup>

<sup>1</sup>University of Sheffield, Faculty of Medicine- Dentistry and Health, Sheffield, United Kingdom ; <sup>2</sup>Princess Margaret Cancer Centre, Radiation Medicine Program, Toronto, Canada ; <sup>3</sup>McMaster University, McMaster Faculty of Health Sciences, Hamilton, Canada ; <sup>4</sup>Princess Margaret Cancer Centre, Division of Medical Oncology and Hematology, Toronto, Canada ; <sup>5</sup>Princess Margaret Cancer Centre, Department of Biostatistics, Toronto, Canada

### Purpose or Objective

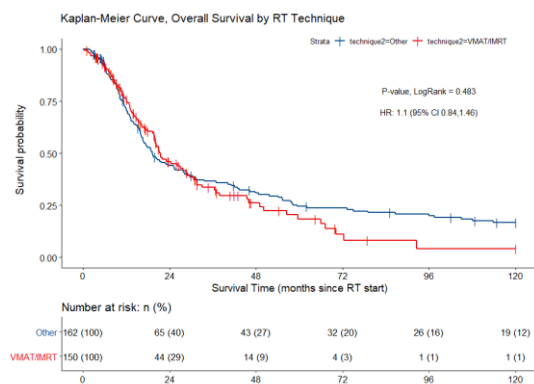
To compare the efficacy and toxicity between IMRT/VMAT and 2D/3D-conformal radiation techniques in limited-stage small-cell lung cancer (LS-SCLC) patients treated with curative intent.

### Material and Methods

A retrospective cohort of LS-SCLC patients treated with curative intent chemoradiation at the Princess Margaret Cancer Centre (1997-2018) were reviewed for patterns of efficacy/toxicity by radiation technique. Efficacy of different radiation techniques utilized overall survival (OS) from date of treatment initiation, censored at 10 years post-treatment start. The logrank test and Cox model were used to compare differences in survival by radiation technique. Toxicity rates (Grade  $\geq 2$  and  $\geq 3$  pneumonitis or esophagitis) were compared in a subset of patients (n=178) using logistic regression.

### Results

Of 312 LS-SCLC patients, the median age was 66 years (range: 39-85 years); 56% were males. 150 patients received IMRT (n=146) or VMAT (n=4). 162 received other forms of radiotherapy (27 3D conformal and 135 opposed AP/PA). Median follow-up was 16.6 months for all patients and 22.2 months for all living patients. Median OS was 20.5 months (95% CI: 18.8-25.3 months). The unadjusted hazard ratio comparing IMRT/VMAT versus other radiation techniques was 1.11 (95% CI: 0.84-1.46; p=0.48) for OS. Of the 178 patients in the toxicity-analyzable subset, 53% experienced Grade  $\geq 2$  esophagitis (9% Grade  $\geq 3$ ) and 10% experienced Grade  $\geq 2$  radiation pneumonitis (5% Grade  $\geq 3$ ). The unadjusted odds ratios comparing IMRT/VMAT vs. other radiation techniques were 0.69 (95% CI: 0.35-1.34; p=0.27) for grade 2+ esophagitis and 0.69 (95% CI: 0.24-1.98; p=0.49) for grade 2+ pneumonitis.



### Conclusion

With the advent of highly conformal radiotherapy techniques for the treatment of LS-SCLC patients, no difference in OS was identified. Lower rates of esophagitis and pneumonitis was observed, but this was not statistically different. Future work will be conducted to correlate dosimetric parameters with toxicity and outcomes.

### PO-0775 Palliative lung radiotherapy: audit of prescribing practice and survival analysis

T. Lewis<sup>1</sup>, J. Kennedy<sup>1</sup>, G. Price<sup>1</sup>, T. Mee<sup>2</sup>, K. Kirkby<sup>2</sup>, N. Kirkby<sup>2</sup>, D. Woolf<sup>1</sup>, N. Bayman<sup>1</sup>, C. Chan<sup>1</sup>, J. Coote<sup>1</sup>, C. Faivre-Finn<sup>1</sup>, M. Harris<sup>1</sup>, A. Hudson<sup>1</sup>, L. Pemberton<sup>1</sup>, A. Salem<sup>1</sup>, H. Sheikh<sup>1</sup>, H. Mistry<sup>1</sup>, D. Cobben<sup>1</sup>

<sup>1</sup>The Christie NHS Foundation Trust, Radiotherapy Related Research, Manchester, United Kingdom ;

<sup>2</sup>University of Manchester, Division of Cancer Sciences- School of Medical Sciences- Faculty of Biology- Medicine & Health, Manchester, United Kingdom

### Purpose or Objective

Choosing the optimal palliative lung radiotherapy (RT) regimen is challenging. The Royal College of Radiologists (RCR) guidance recommends treatment stratification based on patients' performance status (PS). The aim of palliative treatment is to alleviate symptoms, but evidence suggests higher radiotherapy doses are associated with survival benefits. Here, we present the effects of fractionation regimen and additional factors on the survival of palliative lung cancer radiotherapy patients.

### Material and Methods

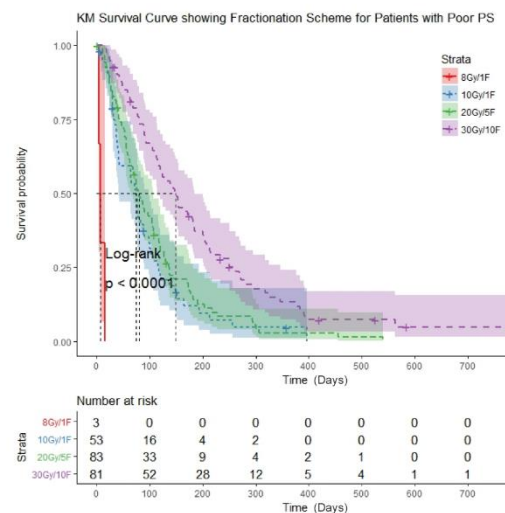
An audit comparing palliative non-small cell lung cancer (NSCLC) radiotherapy prescription with RCR guidance was conducted in a retrospective patient cohort (N=664) treated between 2013 and 2018 at a large cancer centre. Multivariable analysis of the prognostic significance of baseline patient characteristics and treatment prescription on overall survival was performed on a combined NSCLC and small cell lung cancer patient cohort (N=422). The percentage of patients dying within 30 days of treatment was calculated. Covariates investigated included: sex, age, PS, histology, comorbidities, stage, tumour location, tumour side, smoking status, pack year history, primary RT technique and fractionation scheme (8Gy/1F, 10Gy/1F, 20Gy/5F, 30Gy/10F).

### Results

80.8% of patients were treated according to RCR guidance. 2.6% good PS patients were under-dosed (i.e. lower dose and/or fractionation compared to RCR recommendations) and 16.6% poor PS patients were over-dosed. 85 patients (9.2%) died within 30 days of treatment.

Univariable analysis revealed that PS ( $p < 0.0001$ ), fractionation scheme ( $p < 0.0001$ ) and comorbidities ( $p = 0.03$ ) were significantly associated with survival. Univariable subset analysis results are displayed in Graph 1.

Multivariable analysis: better PS ( $p = 0.003$ ) and increased dose/fractionation regimens of up to 30Gy/10F ( $p < 0.0001$ ) were the only covariates that significantly correlated with increased survival.



Graph 1. Univariable subset analysis revealed that increased fractionation was associated with longer survival through every PS strata. Median overall survival (OS) of poor PS strata patients increased by 74 days when comparing those who received 30Gy/10F to 10Gy/1F.

### Conclusion

RCR guidance for palliative lung radiotherapy was followed for the majority of patients. Increased fractionation regimens (up to and including 30Gy/10F) were associated with better survival regardless of performance status.

### PO-0776 Neutrophil-to-lymphocyte ratio dynamics predict for survival in lung cancer treated with SBRT

M. Chowdhary<sup>1</sup>, R. Dhawan<sup>1</sup>, J. Switchenko<sup>2</sup>, S. Tian<sup>2</sup>, K. King<sup>1</sup>, M. Batus<sup>3</sup>, M. Fidler<sup>3</sup>, P. Bonomi<sup>3</sup>, N. Sen<sup>1</sup>, K. Patel<sup>4</sup>, M. Khan<sup>2</sup>, M. Gaurav<sup>1</sup>

<sup>1</sup>Rush University Medical Center, Radiation Oncology, Chicago, USA ;

<sup>2</sup>Emory University School of Medicine, Radiation Oncology, Atlanta, USA ;

<sup>3</sup>Rush University Medical Center, Medical Oncology, Chicago, USA ;

<sup>4</sup>Yale School of Medicine, Therapeutic Radiology, New Haven, USA

### Purpose or Objective

Systemic inflammation is known to play an important role in cancer progression. Neutrophil-to-lymphocyte ratio (NLR) may be a surrogate for systemic inflammatory response and tumor microenvironment. Indeed, high baseline levels of NLR has been shown to be a poor prognostic factor in various malignancies. Stereotactic body radiotherapy (SBRT) has been linked to systemic antitumor T-cell response via immune stimulation. The aim of this study is to assess percent (%) change in NLR, before and after SBRT, as a prognostic factor for survival in patients with early-stage lung cancer.

### Material and Methods

After IRB approval, patients treated with SBRT for Stage I-II lung cancer from 2012-2018 were retrospectively identified. Pre- and post-treatment NLR were calculated from blood counts obtained in closest proximity to SBRT delivery. Percent change in NLR was defined as  $([pre - post-SBRT NLR] / [pre-SBRT NLR])$ .

Overall survival (OS) was calculated using the Kaplan-Meier method. Intra- and extra-thoracic outcomes were calculated using the cumulative incidence model with competing risks for death. Multivariable Cox models were applied to adjust for confounders.

## Results

A total of 62 patients with evaluable % change NLR were available for analysis. The median time interval between blood draw and SBRT was 33 and 55 days for pre- and post-SBRT NLR, respectively. The overall median follow-up was 25.4 months.

Of the 62 patients, 38 (61.3%) demonstrated an increase in NLR following SBRT. Key patient characteristics (age, gender, race, KPS, smoking, comorbidities, steroid use, peripheral/central location, stage, mutation status) were well balanced, except for higher rates of hyperlipidemia and less involvement of right upper lobe in the NLR % change >0 cohort. Treatment characteristics (number of fractions, dose/fraction, total dose, BED) did not differ by cohort.

A statistically significant OS advantage was seen in patients when stratified by NLR % change: 12-, 24- and 36-month OS rates were 100% vs. 78.1%, 95.7% vs. 50.0%, and 87.7% vs. 45.0%, amongst patients with NLR % change ≤0 vs. >0, respectively. On univariate analysis, NLR % change (p=0.001), female gender (p=0.047), KPS (p=0.047), COPD (p=0.031), and total dose (p=0.013) were significant factors for OS. NLR % change >0 remained significant for predicting inferior OS (Hazard Ratio: 6.16 [95% CI: 1.70-22.28], p=0.006) on multivariable analysis confirmed; all other factors were not significant.

Other disease outcomes were not significantly associated with % change NLR: 2-year lobar recurrence (0% vs. 7.0%), nodal recurrence (4.4% vs. 18.2%), second primary (0% vs. 7.1%), or distant recurrence (13.3% vs. 22.7%) [all NLR % change ≤0 vs. >0].

## Conclusion

The percent change in NLR after SBRT, a potential marker for radiation-induced inflammatory response, is inversely related to OS in patients with early-stage lung cancer. If prospectively validated, NLR is a simple, systemic marker that can be easily used to guide subsequent management.

## PO-0777 Predicting overall survival after radiotherapy for brain metastases in patients with NSCLC

N. Knotter<sup>1</sup>, N. Horeweg<sup>1</sup>, I. Coremans<sup>1</sup>, R. Wiggeraad<sup>2</sup>, Y. Van der Linden<sup>1</sup>

<sup>1</sup>Leiden University Medical Center LUMC, Department of Radiotherapy, Leiden, The Netherlands; <sup>2</sup>Haaglanden Medical Center, Department of Radiotherapy, Leidschendam, The Netherlands

## Purpose or Objective

Brain metastases (BM) are common in non-small cell lung cancer (NSCLC) patients. The current standard treatment is palliative radiotherapy (RT), although its effect on symptoms and survival is debatable. The QUARTZ study suggested that only patients with a good performance status and expected prolonged survival benefit [1]. To aid in predicting overall survival (OS), recursive partitioning analysis (RPA) and Diagnosis specific graded prognostic score (DS-GPA), based on USA trial patients, were developed. Their use is currently widespread [2, 3, 4]. A recent Dutch study reported that OS in patients outside of trials is worse than these models suggest [5]. We therefore investigated whether these models correctly predict OS, and searched for additional prediction factors. Subsequently, a prognostic model was constructed to fit NSCLC patients with BM.

## Material and Methods

Retrospective cohort study of all patients with NSCLC treated with RT for BM at Leiden University Medical Center (2011-2018). Patient characteristics, data concerning fractionation schemes and follow-up were extracted from electronic patient charts. Kaplan-Meier's methodology was used to estimate OS. Uni- and multivariable Cox regression analyses were performed to identify significant prognostic factors and to define our prediction model. Performance of the three models was compared using the log-rank test.

## Results

188 patients were included. Mean age was 65 years, 50% was male, 69% had adenocarcinoma. Seventy percent received whole-brain RT (95% 20Gy/5#, 2% 25Gy/10# and 3% 39Gy/13#) and 30% underwent stereotactic RT (84% a single fraction of 15, 18, 20 or 21Gy). Ninety-one percent had a KPS ≥70, 70% had extracranial metastases at the time of brain metastases diagnosis. Forty-one percent had 1-2 BM, 46% 3-10 and 13% had >10 BM. Median OS was 4.9 months. The RPA and DS-GPA models did not show significant differences in OS between the risk groups (fig 1). Independent significant risk factors for mortality were non-adenocarcinoma, KPS <70, brain metastases (1-2 vs. 3-10 or >10) and age ≥65 years. Treatment type (whole-brain or stereotactic RT), fractionation schemes, extracranial metastases or mutation status (EGFR, KRAS, ALK/Ros) were not prognostic. Next, the LUMC-BM score was composed using these risk factors and classified patients into three risk groups (tab 1). The median OS for groups 1 (n=94), 2 (n=52) and 3 (n=26) were 6.9, 3.9 and 1.9 months (log rank p<0.0001), respectively. The hazard ratio's for mortality in group 2 and 3, relative to group 1, were 2.1 (95% CI 1.4-3.1) and 5.9 (95% CI 3.6-9.8) respectively.

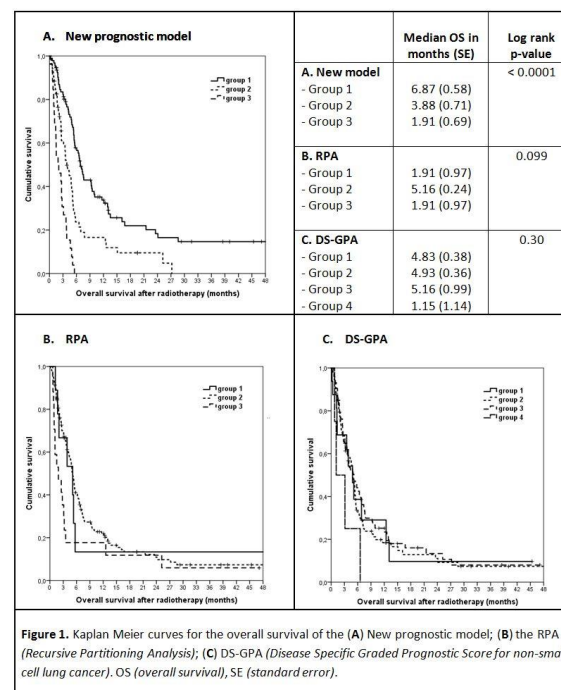


**Figure 1.** Kaplan Meier curves for the overall survival of the (A) New prognostic model; (B) the RPA (Recursive Partitioning Analysis); (C) DS-GPA (Disease Specific Graded Prognostic Score for non-small cell lung cancer). OS (overall survival), SE (standard error).

**Table 1.** New prognostic model for overall survival in patients with NSCLC and brain metastases

Prognostic factor	Scoring criteria		
	0	1	2.5
Histology	Adenocarcinoma	Non-adenocarcinoma	N.A.
KPS	≥ 70	< 70	N.A.
No. of BM	1 - 2	3 - 10	> 10
Age, years	< 65	≥ 65	N.A.

Risk Groups: 1 = 0 - 1 points; 2 = 2 - 2.5 points; 3 = 3 - 5.5 points  
N.A. (not applicable)

## Conclusion

Our new prognostic model more accurately predicts OS in NSCLC patients with brain metastases outside of trials than current widespread used RPA and DS-GPA prediction models. The validation study of our model is currently being performed.

**PO-0778 New prognostic factors in the SBRT treatment of early stage non-small cell lung cancer**

J. Di Muzio<sup>1</sup>, S. Badellino<sup>1</sup>, M. Levis<sup>1</sup>, L. Delsedime<sup>2</sup>, C. Mantovani<sup>1</sup>, M. Volante<sup>2</sup>, M. Papotti<sup>2</sup>, U. Ricardi<sup>1</sup>  
<sup>1</sup>University of Turin - Città della Salute e della Scienza, Radiation Oncology, Torino, Italy ; <sup>2</sup>University of Turin and Città della Salute e della Scienza Hospital, Pathology Unit- Department of Medical Sciences, Torino, Italy

**Purpose or Objective**

The indication of SBRT in operable patients affected by early stage NSCLC who refuse surgery is always increasing, with the need to identify prognostic factors for disease control. Our study aims to identify histological and molecular biology factors for a prognostic stratification of these patients.

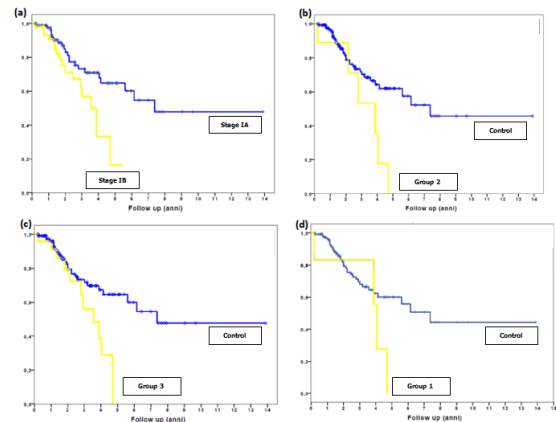
**Material and Methods**

The database of the radiotherapy institute of the University of Turin was retrospectively reviewed in search of patients underwent SBRT for early stage NSCLC from January 2003 to October 2017. Only patients with histological typing performed at the Pathology Unit of the University of Turin were included in the analysis. Patient and tumor data were collected together with immunohistochemistry and molecular biology data. Molecular biology data detected were EGFR mutation, ALK translocation, KRAS, ROS1 and BRAF mutation. The patients were analysed according to the subdivision into 3 groups. The first with the only KRAS positive, the second (unfavorable) with KRAS positive, ROS1 negative and BRAF positive, the third (very unfavorable) with the presence of the previous factors but EGFR and ALK negative. Total dose of treatment was prescribed at 80% isodose and risk-adapted treatment schedules were used. All patients were treated with a minimum BED of 100 Gy.

**Results**

142 patients were included in the analysis with a median follow-up of 22 months. Patient characteristics are listed in Table 1. Median progression free survival was 49 months. Stage ( $p = 0.008$ ) and molecular biology factors (KRAS  $p = 0.007$ , unfavorable  $p = 0.004$  and very unfavorable  $p < 0.001$ ) were statistically significant with univariate analysis. Stage ( $p = 0.02$ ) and the very unfavorable group ( $p < 0.001$ ) were confirmed at the multivariate analysis. Median cancer specific survival was 73.7 months. Stage ( $p = 0.02$ ) and molecular biology factors (KRAS  $p = 0.009$ , unfavorable  $p = 0.025$ , very unfavorable  $p = 0.027$ ) were statistically significant in the univariate analysis as clinical predictors. Stage ( $p = 0.03$ ) and the unfavorable group ( $p = 0.06$ ) were confirmed in multivariate analysis. Local control at 12, 24 and 36 months was 95.8%, 83.6%, 80.1%, respectively. Stage ( $p = 0.005$ ) and the very unfavorable group ( $p = 0.001$ ) proved to be predictive for univariate analysis. Both factors were confirmed in multivariate analysis ( $p$  respectively of 0.01 and 0.008). Systemic control at 12, 24 and 36 months was 90.1%, 72.5% and 67.7%, respectively. Stage ( $p < 0.001$ ), histology ( $p = 0.04$ ) and molecular biology factors (KRAS  $p < 0.001$ , unfavorable  $p < 0.001$  and very unfavorable  $p < 0.001$ ) proved to be predictive for univariate analysis. Only stage and the very unfavorable group were confirmed at the multivariate analysis ( $p$  of 0.03 and 0.002, respectively).

**Cancer Specific Survival**



	Number (%)	Media (range)
<b>Sex</b>		
Male	114 (80,3)	
Female	28 (19,7)	
<b>Age</b>		75 (52 - 86)
<b>Stage</b>		
Ia	88 (62)	
Ib	50 (35)	
<b>PTV Volume</b>		46,6 (4 - 143)
<b>Mean Lung Dose</b>		11,9 (2,50 - 19,80)
<b>BED</b>		114,4 (100 - 151,2)
<b>Diagnosis</b>		
Adenocarcinoma	83 (58,4)	
Squamous cell carcinoma	42 (29,6)	
NSCLC NOS	14 (9,8)	
Others	3 (2,1)	
<b>Pattern</b>		
Papillary	6	
Acinary	8	
Lepidic	2	
Micropapillary	1	
Solid	0	
Mixed	3	
<b>TTF1</b>		
Undetermined	93 (65,5)	
Negative	15 (10,5)	
Positive	34 (24)	
<b>P40</b>		
Undetermined	108 (76)	
Negative	13 (9,5)	
Positive	21 (14,5)	
<b>KRAS</b>		
Undetermined	136 (95,8)	
Mutated	6 (4,2)	
Not Mutated	0 (0)	
<b>EGFR</b>		
Undetermined	116 (81,7)	
Mutated	23 (16,2)	
Not Mutated	3 (2,1)	
<b>ALK</b>		
Undetermined	126 (88,7)	
Translocated	1 (10,5)	
Not Translocated	15 (10,7)	
<b>ROS1</b>		
Undetermined	140 (98,6)	
Mutated	0 (0)	
Not Mutated	2 (1,4)	
<b>B-RAF</b>		
Undetermined	141 (99,3)	
Mutated	1 (0,7)	
Not Mutated	0 (0)	

**Conclusion**

Molecular biology and histological parameter, such as KRAS, could select a population of patients with more aggressive tumor. These patients may be deserving of greater personalization of therapy by dose intensification or integration with systemic therapies.

**PO-0779 Current management of limited-stage SCLC and CONVERT trial impact: an EORTC LCG survey**

A. Levy<sup>1</sup>, L.E.L. Hendriks<sup>2</sup>, C. Le Pêchoux<sup>1</sup>, S. Falk<sup>3</sup>, B. Besse<sup>4</sup>, S. Novello<sup>5</sup>, A.C. Dingemans<sup>2</sup>, B. Hasan<sup>6</sup>, M. Reck<sup>7</sup>, T. Berghmans<sup>8</sup>, C. Faivre-Finn<sup>3</sup>  
<sup>1</sup>Gustave Roussy, Radiation Oncology, Villejuif, France ; <sup>2</sup>Maastricht University Medical Center, Pulmonary Diseases, Maastricht, The Netherlands ; <sup>3</sup>The Christie NHS Foundation Trust, Radiation Oncology, Manchester, United Kingdom ; <sup>4</sup>Gustave Roussy, Medical Oncology, Villejuif, France ; <sup>5</sup>AOU San Luigi, Oncology Department, Turin, Italy ; <sup>6</sup>European Organisation for Research and Treatment of Cancer, Statistics, Brussels, Belgium ; <sup>7</sup>LungenClinic Grosshansdorf, Pulmonology,

Grosshansdorf, Germany ; <sup>8</sup>Jules Bordet, Intensive Care and Oncological Emergencies & Thoracic Oncology, Brussels, Belgium

### Purpose or Objective

The CONVERT trial (NCT00433563: once-daily (OD) vs. twice-daily (BD) thoracic chemoradiotherapy (CRT)) confirmed that BD radiotherapy (RT) should continue to be considered the standard of care but impact on CRT regimens in daily care is unknown. A European survey was launched to evaluate current practice in good performance status (PS) limited-stage small-cell lung cancer (LS-SCLC) patients suitable for chemo-radiotherapy (CRT) to 1) assess the impact of the CONVERT trial and 2) identify relevant research questions for future clinical trials

### Material and Methods

An European Organisation for Research and Treatment of Cancer (EORTC) Lung Cancer Group (LCG) survey containing 28 questions on LS-SCLC was distributed between April 2018 and October 2018 to the EORTC LCG and several European thoracic oncology societies' members.

### Results

188 responses were analyzed (radiation oncologists: 50% [n=94], pulmonologists: 15% [n=28], medical oncologists: 23% [n=35]); 84% with >5 years' experience of treating SCLC. Italy (18%, n=34), Spain (16%, n=31), and the UK (15%, n=28) contributed the most. 87% (n=164) were aware of the CONVERT trial and 20% (n=38) included patients in the trial. Concurrent CRT is favoured (n=169, 90%) compared to sequential treatment. OD is the most commonly used regimen, but the use of BDRT increased after the CONVERT publication (n=120, 64% prior to and n=107, 57% after the publication) (Table 1). 60-66 Gy in 30-33 fractions is the most commonly prescribed OD RT regimen (n=73/120, 61%). The main reasons for not implementing BD after the CONVERT publication are logistical issues (n=84, 45%) and inconvenience for patients (n=55, 29%). 139 respondents (74%) deliver 4 cycles of chemotherapy and 45 deliver 6 cycles (24%) routinely in the context of CRT. G-CSF (granulocyte colony-stimulating factor) is used by 39%, either routinely or as secondary prophylaxis. Prophylactic cranial irradiation (PCI) is routinely used in patients who have not progressed after CRT (n=178, 95%). The most commonly prescribed PCI dose is 25 Gy in 10 fractions (n=150, 80%) and more than half of respondents do not apply an upper age limit (n=100, 53%). The main research questions of interest for LS-SCLC are 1) integrating novel targeted therapies-immunotherapies (151, 80%) and 2) PCI (+/- hippocampal sparing) vs. MRI surveillance (134, 71%).

Table 1: Type of preferred radiotherapy delivered in the concurrent setting.

	Before CONVERT Total=176* N (%)	After CONVERT Total=180* N (%)
<b>OD</b>	120 (68)	107 (59)
Preferred regimen	60-66 Gy: 73/120 (61)	60-66 Gy: 70 (65)
Preferred regimen	45 Gy: 55/56 (98)	45 Gy: 72 (99)

\*excluding respondents that never used concurrent CRT

### Conclusion

Although the CONVERT trial confirmed that BD radiotherapy should be considered the standard of care, OD (60-66 Gy in 30-33 fractions) remains the most prescribed radiotherapy fractionation.

### PO-0780 Prognostic value of PD-L1 expression in locally advanced NSCLC treated with chemoradiotherapy

K. Gennen<sup>1</sup>, L. Käsmann<sup>1</sup>, C. Eze<sup>1</sup>, M. Dantes<sup>1</sup>, O. Roengvoraphoj<sup>1</sup>, J. Taugner<sup>1</sup>, J. Neumann<sup>2</sup>, E. Mille<sup>3</sup>, A. Tufman<sup>4</sup>, R.M. Huber<sup>4</sup>, M. Orth<sup>1</sup>, S. Reu<sup>5</sup>, M. Niyazi<sup>1</sup>, C. Belka<sup>1</sup>, F. Manapov<sup>1</sup>

<sup>1</sup>LMU University Hospital Grosshadern, Department of Radiation Oncology, Munich, Germany ; <sup>2</sup>LMU University Hospital Grosshadern, Department of Pathology, Munich, Germany ; <sup>3</sup>LMU University Hospital Grosshadern, Department of Nuclear medicine, Munich, Germany ; <sup>4</sup>Thoracic Oncology Centre Munich Ludwig-Maximilians University, Division of Respiratory Medicine and Thoracic Oncology Department of Internal Medicine V, Munich, Germany ; <sup>5</sup>University Hospital Wuerzburg, Department of Pathology, Wuerzburg, Germany

### Purpose or Objective

Immune checkpoint inhibitors (CPIs) are an integral part of multimodal treatment approach in locally-advanced stage non-small cell lung cancer (LA-NSCLC). Purpose of the present study was to investigate prognostic value of PD-L1 expression on tumor cells and tumor-infiltrating lymphocytes (TILs) in a single-center patient cohort treated with chemoradiotherapy.

### Material and Methods

We collected tumor tissue samples and clinical characteristics of 37 LA- NSCLC patients treated with chemoradiotherapy between 2000 and 2004. The analyzed tissue was taken before therapy and immunostaining was performed by experienced pathologist. VENTANA PD-L1 (SP263) Rabbit Monoclonal Primary Antibody was used to detect PD-L1 in formalin-fixed, paraffin-embedded tissue through the OptiView CC1. The samples were pretreated for 64 minutes, the antibody incubation time measured 16 minutes. Dilution was not necessary (Ready-to-use, RTU). The histological staining was carried out by the Benchmark Ultra. Tumor cells and lymphocytes were analyzed separately. Based on PD-L1 expression (0%, 1-5%, >5%) 3 groups were defined.

### Results

All patients were treated with definitive chemoradiotherapy (CRT). Follow-up data of all patients until death was available. One patient was diagnosed in UICC stage II, 31 patients in stage III and 5 patients in stage IV. Absolute majority (35 patients, 95%) were treated with concurrent cisplatin- and taxane-based CRT. 23 patients (62%) received consolidative chemotherapy. A total of 30 males (81%) and 7 females (19%) were evaluated, 11 of which (30%) were non-smokers, 26 (70%) had at least 20 pack years. Patients without (0%) and very low expression (1-5%) of PD-L1 on tumor cells showed a significantly better overall survival compared to the subgroup showing PD-L1 expression over 5% with 13.8 versus 6.6 months as well as one-year survival rate of 67.7 versus 33.3%, respectively (p=0.039). Expression of PD-L1 on the TILs showed no significant impact on overall survival (p=0.808).

### Conclusion

PD-L1 expression on tumor cells correlates significantly with reduced overall survival in patients with LA-NSCLC treated with CRT. In contrast, PD-L1 expression on tumor-infiltrating lymphocytes has no impact on overall survival in our study.

### PO-0781 30 Gy single dose SBRT: Outcome in a large series of patients with lung oligometastatic disease

L. Nicosia<sup>1</sup>, L. Agolli<sup>2</sup>, M. Valeriani<sup>3</sup>, C. Reverberi<sup>3</sup>, S. Bracci<sup>3</sup>, L. Marinelli<sup>3</sup>, V. De Sanctis<sup>3</sup>, E. Cortesi<sup>4</sup>, M. Martelli<sup>5</sup>, C. De Dominicis<sup>6</sup>, M.F. Osti<sup>3</sup>  
<sup>1</sup>Ospedale Sacro Cuore "Don Calabria", Radiation Oncology, Negrar, Italy ; <sup>2</sup>Faculty of Medicine and University Hospital Carl Gustav Carus- Technische Universität Dresden- Germany. OncoRay - National Center for Radiation Research in Oncology, Department of Radiation Oncology, Dresden, Germany ; <sup>3</sup>Sant'Andrea Hospital- "Sapienza" University of Rome, Department of Radiation Oncology, Rome, Italy ; <sup>4</sup>Policlinico Umberto I "Sapienza" University of Rome, Department of Radiology- Oncology and Human Pathology, Rome, Italy ; <sup>5</sup>Carlo Forlanini Hospital- Rome, Thoracic Surgery Unit, Rome, Italy ; <sup>6</sup>Sant'Andrea Hospital- "Sapienza"

University of Rome, Department of Radiology, Rome, Italy

### Purpose or Objective

To evaluate local control (LC), long term adverse effects and survival in a series of patients with oligometastatic to the lung disease who received 30Gy in single dose with stereotactic technique.

### Material and Methods

Between December 2008 and April 2017, a total of 160 lung metastases in 123 patients affected by oligometastatic disease were treated, at our Institution, with stereotactic body radiotherapy (SBRT) delivered in a single dose of 30 Gy. The primary tumors in most cases were non small-cell lung cancer and colon-rectum cancer (46.3% and 29.2%, respectively). Prognostic factors were also assessed.

### Results

The median follow-up was 38 months. Twenty-three (14.3%) lesions in 20 patients progressed locally. Intra-thoracic progression (new lung lesions or thoracic lymph node metastases) occurred in 58 (47.1%) patients. Distant progression occurred in 43 (34.9%) patients after a median time of 14 months. The 3- and 5-year local relapse-free survival (LPFS) were 80.3% and 79.5% (median not reached), respectively. Late toxicity was evaluated in 148 patients (follow-up >6 months): 50 (33.7%) had grade  $\leq 2$  fibrosis, 10 (6.7%) experienced grade 3 fibrosis. Two (1.3%) cases of rib fracture occurred. One case of toxic death (grade 5) has been reported. Median OS was 39 months. Prognostic factor at the univariate analysis was: lesion diameter  $\leq 18$  mm correlated significantly with a longer LPFS ( $p=0.001$ ). Prognostic factors at the multivariate analysis were: lesion diameter  $< 18$  mm was predictive for longer LPFS ( $p=0.006$ ); oligometastases from primary colon cancer predicted significantly for worse LPFS ( $p=0.041$ ) and progression-free survival ( $p=0.04$ ).

### Conclusion

To our knowledge, the current study represents the largest series on the use of SBRT 30 Gy single dose for lung metastases. The proposed schedule showed to be effective and safe, when administered in selected oligometastatic patients. These results could be evaluated in further prospective series with the aim of investigating the safety of this schedule in selected candidates.

### PO-0782 External validation of NTCP models for pneumonitis in lung cancer patients receiving proton therapy

A. Niezink<sup>1</sup>, V. Jain<sup>2</sup>, O. Chouvalova<sup>1</sup>, R. Wijsman<sup>1</sup>, C. Muijs<sup>1</sup>, M. Frick<sup>2</sup>, A. Doucette<sup>2</sup>, C. Simone<sup>3</sup>, C. Chinniah<sup>2</sup>, J. Widder<sup>4</sup>, J. Langendijk<sup>1</sup>, A. Van der Schaaf<sup>1</sup>, A. Berman<sup>2</sup>

<sup>1</sup>University Medical Center Groningen, Radiation Oncology, Groningen, The Netherlands; <sup>2</sup>University of Pennsylvania, Radiation Oncology, Philadelphia, USA; <sup>3</sup>University of Maryland School of Medicine, Radiation Oncology, Baltimore, USA; <sup>4</sup>Medical University of Vienna, Radiation Oncology, Vienna, Austria

### Purpose or Objective

Concurrent chemo-radiotherapy (CRT) is the standard of care for patients with locally advanced non-small cell lung cancer (LA-NSCLC). Pneumonitis is the most frequently observed treatment related toxicity which can have significant impact on quality of life. Proton beam therapy (PBT) offers advantages over photon beam therapy by reducing radiation dose to healthy tissues. However, not all dose reductions are clinically relevant. Therefore a method to select patients that are most likely to benefit from this modality is warranted. One such approach is using normal tissue complication probability (NTCP) models for plan comparison. However, the currently available models are exclusively based on photon data. In this study, we investigated the validity of three photon

based NTCP models for radiation pneumonitis (RP) in patients that underwent CRT using PBT for LA-NSCLC.

### Material and Methods

The validation cohort consisted of 99 consecutive patients with LA-NSCLC (Stage III) treated with definitive CRT using PBT (pencil beam scanning and double scattering) between 2011-2016. Patients were treated to a total dose of 56-74cGy, assuming an RBE of 1.1 for PBT. RP was scored at 3 and 6 months post treatment (CTCAE v4.0). We evaluated the performance of the QUANTEC pneumonitis (QP) model, the QUANTEC model adjusted for clinical risk factors (AQP), as well as a newer and updated QP (NQP) model (ESTRO 2017, which has a steeper slope and includes current smoking). A closed testing procedure (CTP) was performed to test the need for model updating, either by calibration-in-the-large (re-estimation of model intercept), recalibration (re-estimation of intercept and slope) or model revision (re-estimation of all coefficients).

### Results

There were 21 events (21%) of Grade  $\geq 2$  RP in the PBT cohort. On univariable analysis, mean lung dose was significantly associated with RP ( $p=0.01$ ), as well as several DVH parameters ranging from V5 to V50, with the strongest association for V40 ( $p<0.01$ ). The CTP did not detect major deviations of the data from the models, but recommended adjustment of the intercept only for the photon-based AQP and NQP models. The apparent steepness of the dose-response relationship was larger in the PBT data than in the QP and AQP models, but lower than in the NQP model. However, these deviations were not significant, therefore the CTP did not recommend updating the slope or other model parameters. Redeployment of a new model using mean lung dose, V40, and smoking status (current smoking is a protective factor) did not improve the existing models (with update after validation).

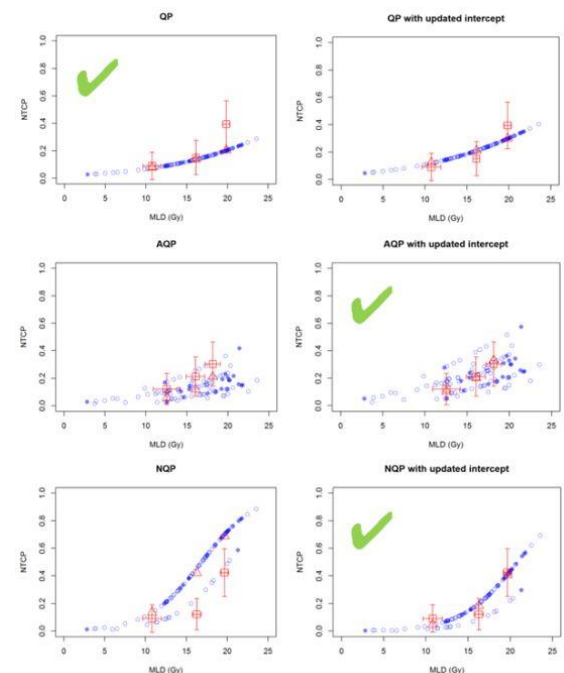


Figure 1: Predicted and observed NTCP as a function of mean lung dose (MLD) for three different models. Left = original models. Right = models with updated intercept. Blue circles = NTCP prediction for individual patients. Filled circle = patient with observed complication (pneumonitis). Red squares with error bars = average observed toxicity in 3 risk groups (grouped according to NTCP of the corresponding model). Red triangle = predicted average toxicity for each risk group. The green mark indicates recommended models by CTP.

### Conclusion

Three photon based NTCP models for RP were externally validated in a cohort of patients with LA-NSCLC treated

with PBT. The models performed well in this cohort and only small adjustments of the model intercepts were needed. This study indicates that photon based NTCP models are applicable among patients treated with protons.

### PO-0783 Standardizing mediastinal nodal CTV delineation in Stage III NSCLC: results of a two-phase dummy run

F. Chartier<sup>1,2,3</sup>, V. Remouchamps<sup>3,4</sup>, M. Lambrecht<sup>5</sup>, X. Geets<sup>3,6</sup>, E. Hortobágyi<sup>3,5</sup>, Y. Lievens<sup>3,7</sup>, L. Moretti<sup>1,3</sup>  
<sup>1</sup>Institut Jules Bordet, Department of Radiation Oncology, Brussels, Belgium ; <sup>2</sup>Université Libre de Bruxelles, Radiation Oncology, Brussels, Belgium ; <sup>3</sup>on behalf of the Belgian College for Physicians in Radiation Oncology, Radiation Oncology, Brussels, Belgium ; <sup>4</sup>CHU UCL Namur - site Ste Elisabeth, Department of Radiation Oncology, Namur, Belgium ; <sup>5</sup>University Hospitals Leuven, Department of Radiation Oncology, Brussels, Belgium ; <sup>6</sup>Cliniques Universitaires Saint-Luc, Radiotherapy Department, Brussels, Belgium ; <sup>7</sup>Ghent University Hospital, Department of Radiation Oncology, Ghent, Belgium

#### Purpose or Objective

Lymph node delineation in stage III non-small cell lung cancer (NSCLC) remains the subject of discussion as the inclusion or omission of a lymph node or station can have an important impact on both oncological outcome and toxicity. The Belgian College for Physicians in Radiation Oncology aims to improve the quality of radiotherapy in Belgium. Within this framework the Project on Cancer of the Lung (ProCaLu) focuses on standardizing delineation for locally advanced NSCLC. A two-phase contouring dummy-run on a single test case was performed to analyze the baseline interobserver variability on target definition and delineation and evaluate the effects of a national consensus before the start of a peer-review program for routine clinical practice.

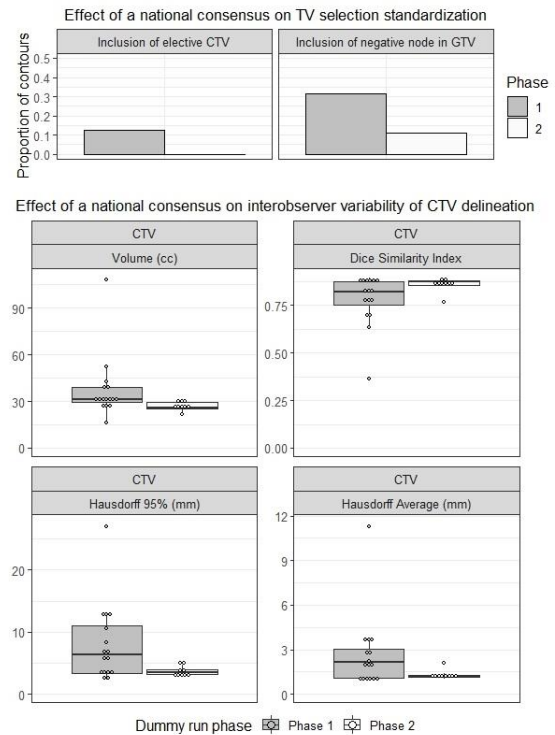
#### Material and Methods

All 25 radiotherapy centers in Belgium and Luxembourg were invited to take part in a delineation dummy-run by sending contours from at least one radiation oncologist (RO) dedicated to lung cancer treatments. The case consisted of a squamous cell carcinoma of the right upper lobe with nodal extension to station 4R staged cT1bN2M0 (TNM 7). The results of chest CT, PET/CT and endoscopic samplings were provided to participants and the planning CT was made available through a secure transfer platform. RO's were asked to delineate and upload back the GTV and CTV for the nodal disease. More than a year later and after the formulation of a national consensus based on current ESTRO guidelines (inclusion of only involved nodes with a 5 mm CTV margin) [Maarten L1] the case was resent to all centers with the same purpose. On all received contours, a description of the TV definition and delineation was obtained through visual inspection. Using an open-source software (3D Slicer with SlicerRT), the DICE Similarity Index and Hausdorff distances were analyzed to compare the delineations. To allow an evaluation of uniformity with these metrics, independent GTV and CTV contours by the first author were used as reference.

#### Results

At the first phase, 16 contours sent by 14 RT centers were analyzed. Important variations were due to the inclusion of a negative node in GTV (n=5) or elective CTV (n=2). The median volumes and interquartile ranges (IQR) were 11.9cc (10.4-14.1) for GTV and 31.2cc (29.3-39) for CTV. A preliminary analysis of the second phase was performed on 9 contours from 9 centers, 4 of which did not participate in phase 1. Median GTV and CTV volumes were 9.3cc (8.2-11.1) and 25.7cc (25.4-29.1) resp. One center included a negative node and none included elective CTV. The reference volumes were 11.4cc for GTV and 27.7cc for CTV. The volume comparisons demonstrated a reduction

in IQR for all metrics ranging from 22% to 90%. Most variations are due to target definition (GTV or CTV). Cropping patterns to other structures is also associated with variability.



	Phase 1 (n=16)		Phase 2 (n=9)		Difference IQR <sup>*</sup> reduction
	Median	IQR <sup>*</sup>	Median	IQR <sup>*</sup>	
<b>GTV</b>					
Volume (cc)	11.9	[10.4 - 14.1]	9.3	[8.2 - 11.1]	22%
DICE Similarity coefficient*	0.84	[0.76 - 0.87]	0.83	[0.79 - 0.87]	27%
Hausdorff Average (mm)*	1.4	[0.9 - 1.9]	1	[0.9 - 1.2]	70%
Hausdorff 95% (mm)*	4.4	[2.9 - 11.3]	3.2	[2.8 - 4.3]	82%
Hausdorff Maximum (mm)*	9.9	[6.2 - 20.3]	6.6	[6.5 - 8.6]	85%
<b>CTV</b>					
Volume(cc)	31.2	[29.3 - 39]	25.7	[25.4 - 29.1]	62%
DICE Similarity coefficient*	0.82	[0.75 - 0.88]	0.87	[0.86 - 0.88]	85%
Hausdorff Average (mm)*	2.1	[1.1 - 3]	1.2	[1.1 - 1.3]	89%
Hausdorff 95% (mm)*	6.3	[3.4 - 11.1]	3.5	[3.2 - 4]	90%
Hausdorff Maximum (mm)*	11.5	[7.4 - 20.3]	7.7	[6.4 - 8.8]	81%

\* Independent contour used as reference to evaluate uniformity.

<sup>\*</sup> Interquartile range (1st and 3rd quartiles)

Table 1: Uniformity of delineations through dummy run phases

#### Conclusion

The preliminary results of this dummy run hint that uniformity in target definition and delineation in NSCLC can reasonably be pursued. Full results will be reported.

### PO-0784 Repeat Stereotactic Body Radiation Therapy for Salvage of Local Failure after Definitive Lung SBRT

W. Kennedy<sup>1</sup>, P. Gabani<sup>1</sup>, J. Nikitas<sup>1</sup>, C. Robinson<sup>1</sup>, J. Bradley<sup>1</sup>, M. Roach<sup>1</sup>

<sup>1</sup>Washington University School of Medicine, Radiation Oncology, St. Louis, USA

#### Purpose or Objective

Stereotactic body radiation therapy (SBRT) for early-stage non-small cell lung cancer (NSCLC) provides high rates of local control. However, the optimal management of local failures after SBRT is unknown, and data describing the role of reirradiation with additional courses of SBRT for isolated local recurrences after previous lung SBRT are sparse. The purpose of this study is to investigate the safety and efficacy of repeat lung SBRT as salvage for patients with local failures after previous definitive SBRT for NSCLC.

## Material and Methods

Patients with primary NSCLC treated with salvage SBRT for local recurrence after previous definitive SBRT for early-stage NSCLC were identified using a prospective institutional review board-approved SBRT registry. Both initial and salvage SBRT courses were given in 3 to 5 fractions with a biologically effective dose (BED) of at least 100 Gy. Local failure was defined as either failure in the involved lobe within 1 cm of the initial planning target volume (PTV) or with significant treatment overlap of the  $\geq 25\%$  isodose lines. Lobar failures  $>1$  cm beyond the PTV, without overlap of at least the 25% isodose lines, or with other sites of recurrence were excluded from this study. Kaplan-Meier analysis was used to estimate survival outcomes.

## Results

We identified 21 patients who received salvage SBRT for salvage of local recurrence after initial SBRT for non-metastatic NSCLC treated between 2008 and 2017. Interval from initial to salvage SBRT was a median of 23 months (range, 7 - 52 months). The median age at salvage was 75 years (range, 59 - 89), median Karnofsky performance status was 80 (range, 60 - 100), and median age-adjusted Charlson comorbidity index was 6 (range, 2 - 11). Median tumor diameter was 1.4 cm (range, 1.0 - 2.5 cm). Median follow-up from time of salvage SBRT was 23 months (range, 2 - 59 months). Median survival after salvage SBRT was 24 months (range, 3 - 60 months). After salvage SBRT, two-year primary tumor control was 81%, distant control was 75% and overall survival was 68%. Four patients developed new lung primaries; 3 of these were new NSCLC while 1 patient developed small cell lung cancer. Grade 2 pneumonitis was observed in 2 patients (9%) and grade 2 chest wall toxicity was observed in 3 patients (14%). No grade 3+ toxicity was observed in this cohort.

## Conclusion

Reirradiation with SBRT for salvage of local failures after initial definitive SBRT for early-stage, medically-inoperable NSCLC appears to be a safe treatment modality associated with low rates of treatment-related toxicity and encouraging rates of tumor control observed in our series.

## PO-0785 Clinical significance of treatment related lymphopenia in lung SBRT and a method to ameliorate them

K. Wijesooriya<sup>1</sup>, J. Colen<sup>2</sup>, T. McMullen<sup>2</sup>, S. Liyanage<sup>3</sup>, C. Alonso<sup>1</sup>, K. Romano<sup>1</sup>, S. Peach<sup>1</sup>, P. Read<sup>1</sup>, J. Larner<sup>1</sup>

<sup>1</sup>University of Virginia, Radiation Oncology, Charlottesville, USA ; <sup>2</sup>University of Virginia, Physics, Charlottesville, USA ; <sup>3</sup>Albemarle High School, High School, Charlottesville, USA

## Purpose or Objective

Treatment related lymphopenia (TRL) is a side-effect of radiation therapy. Moderate to severe TRL decreases immunological function, causing suppression of immunoresponse to tumors as well as increased susceptibility to infection. Severity of TRL has been shown to correlate with inferior outcomes for patients in multiple prior studies. Even though SBRT provides over 90% local tumor control for patients with early stage inoperable non-small cell lung cancer (NSCLC), long-term OS at 3 years post SBRT remains suboptimal at 38%. Thus there is opportunity for improvement. This work focusses on TRL due to lung SBRT, and its effects on hospitalizations, and overall survival. This work also describes the first algorithm for predicting TRL for lung SBRT treatments as a potential strategy to minimize TRL.

## Material and Methods

We conducted an Institutional Review Board (IRB) approved retrospective analysis of 92 patients treated with Lung SBRT in the absence of chemotherapy where, RT treatment plans met all dosimetric criteria from RTOG

0915 and 0813. Kaplan-Meier curves, log-rank analysis and cox regression were performed to assess for survival differences associated with severe TRL in SPSS. We have developed a simulation for thorax RT to model circulating blood in treatment planning. In this we considered radiation dose to circulating blood by coupling the time-dependence of the radiation delivery with a blood flow transport model that considers the transient time in the regional structures as well as the mixing of irradiated and non-irradiated blood volumes.

## Results

On average, the patients saw a sharp decrease in absolute lymphocyte counts from 0- 25 days following SBRT to lung. By day 30, the mean ALC was only 58% of baseline. When the post RT lymphocyte count reduction falls in to (0.75 - 1.0)  $\times 10^9$  cells/L category, hospitalization within 5 months of SBRT increased by a factor of two compared to the lower lymphocyte depletion cohorts. Patients with severe TRL (less than  $0.5 \times 10^9$  cells/L) had worse overall survival (log rank,  $\chi^2=7.62$ ,  $p=0.006$ ). On multi-variate cox regression, minimum absolute lymphocyte count was directly related to survival, with a hazard ratio of 0.613 ( $p=0.034$ ). Predictive model results: a) predict the post treatment absolute lymphocyte value to better than 16% across all variables of interest: age, pre-Tx LYA value, post Tx blood draw day, treatment delivery time, tumor volume size, and location of the tumor. b) model has a sensitivity and a specificity to predict a patient having a post RT lymphocyte value of  $<0.8 \times 10^9$  cells/L with an the area under the curve (AUC) of Receiver Operating Characteristic (ROC) of 0.83 .

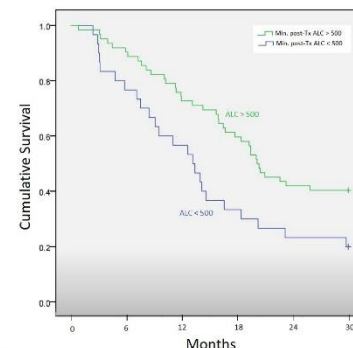


Figure 1 Overall survival up to 30 months post lung SBRT: Kaplan-Meier curve stratified by post lung SBRT absolute lymphocyte count of  $0.5 \times 10^9$  cells/L.

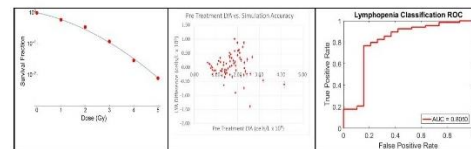


Figure 2: (left): simulation predicted cell survival compared to Nakamura data, (middle): difference of simulation predicted and measured post Tx lymphocyte count, (right): ROC curve for the preliminary simulation to predict post Tx LYA  $<0.8 \times 10^9$  cells/L.

## Conclusion

TRL due to lung SBRT treatments can have a clinically significant impact on overall survival and frequency of hospitalizations due to immune suppression. The predictive algorithm we have developed has an accuracy that could enable treatment plan design and optimization to reduce TRL.

Poster: Clinical track: Upper GI (oesophagus, stomach, pancreas, liver)

**PO-0786 Hemostasis radiotherapy for inoperable gastric cancer: A prospective study**

O. Tanaka<sup>1</sup>, A. Sugiyama<sup>2</sup>, T. Omatsu<sup>3</sup>, T. Taniguchi<sup>1</sup>, K. Ono<sup>1</sup>, Y. Kunishima<sup>4</sup>, M. Matsuo<sup>5</sup>

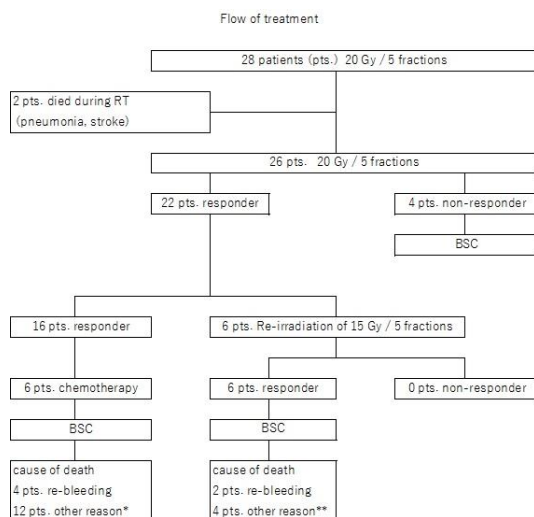
<sup>1</sup>Asahi University Hospital, Department of Radiation Oncology, Gifu, Japan ; <sup>2</sup>Gifu Municipal Hospital, Department of Radiation Oncology, Gifu city, Japan ; <sup>3</sup>Asahi University Hospital, Department of Gastroenterology, Gifu, Japan ; <sup>4</sup>Asahi University Hospital, Division Of Nursing, Gifu, Japan ; <sup>5</sup>Gifu University Hospital, Department of Radiology, Gifu city, Japan

**Purpose or Objective**

Standard treatment for progressive gastric cancer with bleeding includes hemostasis radiotherapy (RT). However, no prospective study of the ideal dosage has been conducted. We thus clarified the utility of RT for gastric cancer at a fixed dose and field.

**Material and Methods**

A total of 28 patients with gastric cancer with bleeding were enrolled in this study. The flow of treatment was shown in Figure 1. The initial RT plan was whole stomach irradiation. Although the examination indicated tumor spread, it was difficult to determine the border between normal tissue and malignancy tissue. We contoured the outer wall of the stomach with an injection of butylscopolamine on an empty stomach. The initial dose was 20 Gy / 5 fractions for full stomach. Hemostasis was achieved when hemoglobin levels in the blood tests stabilized within two weeks of irradiation. If re-bleeding occurred, patients decided whether or not to undergo re-irradiation. The salvage re-irradiation dose was 15 Gy / 5 fractions. Before RT, three or four clips were placed near the gastric tumor by endoscopy. The radiation oncologist contoured the tumor, CTV and PTV under guidance with clips. CTV was not for the whole stomach and only the partial stomach was irradiated. We scored the adverse events (AEs) each day during RT and one week after treatment.



\* reasons (pneumonia, DIC, liver disfunction, hear fairure, renal fairure, unknown)

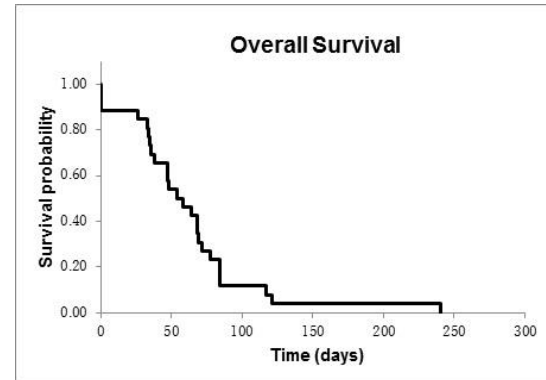
\*\* reasons (pneumonia, liver disfunction, unknown)

BSC: Best Supportive Care

**Results**

Two patients were excluded because they did not complete RT due to stroke and pneumonia. The response ratio of initial RT was 85% (22/26 patients). Six patients underwent re-irradiation, all of which responded (100%).

The median overall survival (OS) was 52 days (Figure 2). The median OS values of the non re-irradiation (one-time) and re-irradiation groups were 54 days and 36 days, respectively, which was not a statistically significant difference. There were no grade three or higher adverse events.



**Conclusion**

Re-irradiation followed by initial RT was effective for reducing adverse events and did not cause adverse events. OS did not differ between the one-time irradiation and re-irradiation groups. No predictive factors were identified. It may be necessary to determinate the ideal dose and fraction number of initial irradiation, which is preferably lower than 20 Gy.

**PO-0787 Adjuvant chemoradiation in resected gallbladder cancer: A prognostic model for overall survival**

C. Solé<sup>1</sup>, L. Vargas<sup>2</sup>, V. Solé<sup>2</sup>, F. Larsen<sup>2</sup>, S. Solé<sup>2</sup>

<sup>1</sup>Instituto de Radiaciones Médicas, Radiotherapy, Santiago, Chile ; <sup>2</sup>Clinica IRAM, Santiago, Chile

**Purpose or Objective**

Patients with gallbladder cancer (GBC) have a dismal prognosis. We investigated outcomes and risk factors for overall survival (OS) in patients treated with radical surgery and adjuvant chemoradiotherapy (CRT).

**Material and Methods**

A total of 212 patients with LAGC ( $\geq$ pT3 59% and/or pN+ 52%) were studied. The primary endpoint of the analysis was OS. We constructed a risk scoring system in which points were assigned to each risk factor by dividing each  $\beta$  coefficient in the final model by the lowest  $\beta$  coefficient and rounding to the nearest integer. A risk score was assigned to each subject by adding up the points for each risk factor present. Subjects were then divided into three risk groups based on their risk scores (0 points=low risk, 1-2 points= intermediate risk, 3-6 points= high risk).

**Results**

Median follow-up was 46.2 months (2-235). Five-year OS for the entire cohort was 53%. In multivariate analysis higher pT stage [HR: 2.43 (1.29-3.68),  $p = 0.01$ ], R1 resection [HR 5.06 (3.12-8.19),  $p < 0.001$ ], and number of surgical procedures [HR 1.41 (1.01-2.16),  $p = 0.05$ ] were associated with an increased risk of death. Five-year OS for patients with low (n=63), intermediate (n=94) and high (n=55) risk was 79.1%, 51.2% and 9.5%, respectively.

**Conclusion**

Overall results after multimodality treatment of GBC are promising. A risk model was generated to determine a prognostic index for individual patients with GBC. Classification of risk factors for death has contributed to propose a prognostic index that could allow us to guide risk-adapted tailored treatment.

**PO-0788 Preliminary analysis of PET/CT imaging on radiation field and relapse rates in esophageal cancer**

E. Jimenez-Jimenez<sup>1</sup>, P. Mateos<sup>2</sup>, N. Aymer<sup>3</sup>, R. Roncero<sup>3</sup>, I. Ortiz<sup>3</sup>, J. Pardo<sup>3</sup>, S. Sabater<sup>1</sup>

<sup>1</sup>Complejo Hospitalario Universitario de Albacete, Radiation Oncology Department, ALBACETE, Spain ;

<sup>2</sup>Clinica IMQ Zorrotaurre, Medical Physics Department, Bilbao, Spain ; <sup>3</sup>Hospital Universitari Son Espases, Radiation Oncology Department, Palma de Mallorca, Spain

#### Purpose or Objective

Our study analyzed the impact of pretreatment PET/CT uptake on pattern of relapse with respect to the volume encompassed by the radiotherapy field among patients with esophageal cancer.

#### Material and Methods

Fifty-six patients with stage II-IIIc esophageal cancer who received definitive or neoadjuvant radio/chemotherapy were analyzed. Patients underwent standard follow-up every 4 to 6 months.

Loco/regional failures were classified as "in-field", "borderline-field" and "out-field". The exact site of the disease recurrence was noted and accurately compared with the volume encompassed by the radiotherapy field.

#### Results

All patients underwent PET/CT scan before treatment. The median of follow-up was 23 months. The first site of relapse was metastatic recurrence and, secondly, local recurrence of primary tumor. The most frequent were "in-field" local (30.4%) and regional (17.9%) recurrence.

We observed a statistically significant relationship between patients classified-N1 by PET/CT and out-field nodal recurrence ( $p = 0.024$ ). In addition, there was a relationship between patients -N2 by PET/CT and in-field nodal recurrence ( $p=0.024$ ). However, no relationship was observed between location of involved nodes by PET or SUVmax values of the metastatic lymph nodes and regional recurrences.

The total number of relapses and location of relapses within the RT field were also analyzed. However, only the number of PET-positive nodes was an independent significant prognostic predictor for relapse (hazard ratio = 4.87,  $p < 0.001$ ).

#### Conclusion

Our results show that only FDG-PET/CT can provide useful information and it could modify radiation treatment. A larger number of enrolled patients with a longer follow-up is needed.

#### PO-0789 Evaluation of Hepatic Toxicity after Repeated Stereotactic Body RT for Hepatocellular Carcinoma

S.M. Yoon<sup>1</sup>, S. Lee<sup>2</sup>, H. Kim<sup>2</sup>, J. Jung<sup>2</sup>, J. Kwak<sup>2</sup>, B. Cho<sup>1</sup>

<sup>1</sup>Asan Medical Center- University of Ulsan College of Medicine, Radiation Oncology, Seoul, Korea Republic of ;

<sup>2</sup>Asan Medical Center, Radiation Oncology, Seoul, Korea Republic of

#### Purpose or Objective

This study aimed to evaluate the hepatic toxicity after repeated stereotactic body radiation therapy (SBRT) for recurrent hepatocellular carcinoma (HCC) using deformable image registration (DIR).

#### Material and Methods

Between January 2007 and December 2015, 85 patients who received two sessions of SBRT for HCC treatment were retrospectively analyzed. A DIR technique was used to calculate the cumulative dose of the first and second SBRT to the normal liver by matching the two computed tomography simulation images. The Dice similarity coefficient (DSC) index was calculated to evaluate the DIR accuracy. Radiation-induced liver disease (RILD) was defined as the worsening of the Child-Pugh score by  $\geq 2$  or elevation of transaminases or alkaline phosphatase of at least 5-fold or that of bilirubin of at least 3-fold compared to either the upper normal limit or the pretreatment

levels without an evidence of disease progression within 3 months of completing each SBRT.

#### Results

Median follow-up time was 45 months and median interval time between two SBRT sessions was 15 months (interquartile range [IQR], 7-24). Before the first and second SBRT, 6 (7.1%) and 12 (14.1%) patients were Child-Pugh class B, respectively. Median tumor size was both 1.7 cm before both SBRT treatments. Mean DSC index value was 0.93, being  $>0.9$  in 79 (92.9%) registrations. Median cumulative mean liver dose (MLD) was 9.3 Gy (IQR, 7.6-11.7). RILD was developed in three patients, and two of them, with Child-Pugh class B, experienced irreversible liver function deterioration following the second SBRT. Grade 3 or higher biliary stricture was not observed during the follow-up period.

#### Conclusion

The DIR method provided reliable information regarding cumulative doses to the liver. In patients with Child-Pugh class A liver function, repeated SBRT for small recurrent HCC could be safely performed with acceptable hepatic toxicity. The safety of repeated SBRT at a cumulative MLD around or above 13 Gy in patients with Child-Pugh class B hepatic function needs further evaluation.

#### PO-0790 A nationwide analysis evaluating a role of local treatment including external RT for BCLC C HCCs

C.H. Rim<sup>1</sup>, L. Jeongshim<sup>2</sup>

<sup>1</sup>Korea University Ansan Hospital, Radiation Oncology, Ansan- Danwon-gu, Korea Republic of ; <sup>2</sup>Inha University Hospital, Radiation Oncology, Incheon, Korea Republic of

#### Purpose or Objective

Sorafenib was recommended as a standard treatment for hepatocellular carcinoma (HCC) with Barcelona Clinic of Liver Cancer (BCLC) C. However, local treatment including radiation therapy (LRT) is also widely administered in practice. The aim of our study was to define the role of LRT among BCLC C patients using a nationwide cohort.

#### Material and Methods

From 2008 to 2014, 3401 patients with HCC BCLC C stage were identified from Korea Liver Cancer Study Group cohort. Among them, patients with information on initial therapy were extracted, and classified with 3 initial treatment groups: LRT, sorafenib, and no treatment.

#### Results

1486 HCC patients with BCLC C were inclusive in this study. Of these, 266 were assigned to LRT (17.9%), 316 to sorafenib (21.3%), and 904 to no treatment group (60.8%). Median survival time of the sorafenib group was shorter than that of the LRT group (3.8 vs. 7.6 months,  $p < 0.001$ ). In multivariable analysis, sorafenib group showed significantly higher risk related to mortality compared to RT group, not only among all patients (Hazard ratio [HR] 1.50, 95% confidence interval [CI] 1.23-1.84) but also between subgroups cohorts with portal invasions (1.55, 1.23-1.84), with lymph node metastases (2.42, 1.53-3.83), without distant metastases (1.43, 1.10-1.87) and with distant metastases (1.57, 1.13-2.19). Additionally, no treatment group showed the worst survival among three treatment groups not only in all patients, but also in all subgroup's patients (All  $P_s < 0.001$ ).

#### Conclusion

LRT as an initial treatment showed survival benefit as compared to sorafenib in HCC patients with BCLC C disease.

#### PO-0791 Neoadjuvant treatment potentially improves outcome in resectable pancreatic cancer: meta-analysis

E. Versteijne<sup>1</sup>, J.A. Vogel<sup>2</sup>, M.G. Besselink<sup>2</sup>, O.R. Busch<sup>2</sup>, J.W. Wilmink<sup>3</sup>, J.G. Daams<sup>4</sup>, C.H. Van Eijck<sup>3</sup>, B. Groot Koerkamp<sup>5</sup>, C.R. Rasch<sup>1</sup>, G. Van Tienhoven<sup>1</sup>

<sup>1</sup>Amsterdam UMC, Radiation Oncology, Amsterdam, The Netherlands ; <sup>2</sup>Amsterdam UMC, Surgery, Amsterdam,

The Netherlands ; <sup>3</sup>Amsterdam UMC, Medical Oncology, Amsterdam, The Netherlands ; <sup>4</sup>Amsterdam UMC, Medical Library, Amsterdam, The Netherlands ; <sup>5</sup>Erasmus MC, Surgery, Rotterdam, The Netherlands

### Purpose or Objective

Current standard treatment for patients with (borderline) resectable pancreatic cancer is resection followed by adjuvant chemotherapy. Several retrospective studies have suggested a benefit of neoadjuvant treatment, but suffer from selection bias as they only report the outcome of patients who ultimately underwent a resection. Evidence from randomized controlled trials reaching full accrual is lacking and the final results of the Dutch Pancreatic Cancer Group multicenter randomized PREOPANC trial are still awaited. The aim of this meta-analysis is to report survival by intention to treat in a comparison of upfront surgery versus neoadjuvant treatment in (borderline) resectable pancreatic cancer.

### Material and Methods

A systematic review of literature on Medline, EMBASE and the Cochrane Library was performed to identify studies reporting median overall survival (mOS) by intention to treat in patients with (borderline) resectable pancreatic cancer treated with or without neoadjuvant treatment. Two authors screened the articles independently for eligibility. Secondary outcomes included resection rate, reasons for no resection, R0 resection rate, positive lymph node rate and toxicity of the neoadjuvant treatment.

### Results

Overall, 3484 patients with (borderline) resectable pancreatic cancer were included from 38 studies, of whom 1738 (49.9%) received neoadjuvant treatment. The weighted mOS by intention to treat was 18.8 months after neoadjuvant treatment versus 14.8 months after upfront surgery. In the subset analysis among patients that actually underwent resection, the difference was larger (26.1 versus 15.0 months respectively). The overall resection rate was 66.0% with neoadjuvant treatment compared with 81.3% after upfront surgery ( $P < 0.001$ ), but the R0 rate was higher in (86.8 versus 66.9%;  $P < 0.001$ ) with neoadjuvant treatment. Positive lymph nodes were seen in 43.8% after neoadjuvant treatment versus 64.8% in the upfront surgery group ( $P < 0.001$ ). Of the patients who had neoadjuvant treatment, 17.8% did not undergo exploratory surgery, mostly due to progression of disease. Toxicity ( $\geq$ grade III) was reported in up to 64% of the patients receiving neoadjuvant therapy.

### Conclusion

This meta-analysis of neoadjuvant treatment versus upfront surgery by intention to treat suggests improved survival, R0 resection and less lymph node positivity with neoadjuvant treatment in patients with (borderline) resectable pancreatic cancer. The lower resection rate after neoadjuvant treatment suggests that this treatment selects patients who might not benefit from harmful large surgery because of early progression. The final results of the randomized PREOPANC trial are awaited.

**PO-0792 A randomized clinical trial on radiosensitizer effects of LMWH in Chemoradiation of esophageal SCC**  
S.A. Javadinia<sup>1</sup>, A. Taghizadeh Kermani<sup>2</sup>, S. Hosseini<sup>2</sup>, A. Fanipakdel<sup>2</sup>, M. Joudi Mashhad<sup>2</sup>, A. Gholami<sup>2</sup>

<sup>1</sup>Mashhad University of Medical Sciences, Student Research Committee, Mashhad, Iran Islamic Republic of ;

<sup>2</sup>Mashhad University of Medical Sciences, Department of Radiation Oncology- Omid Hospital, Mashhad, Iran Islamic Republic of

### Purpose or Objective

Current treatment approaches for esophageal cancer are associated with a poor survival, and there are ongoing efforts to find new and more effective therapeutic strategies. There are several reports on the anti-tumoral effects of low molecular weight heparin (LMWH). We have

assessed the possible survival benefit of LMWHs in esophageal malignancies.

### Material and Methods

This was a randomized, single blind, multi-center, phase II clinical trial on non-metastatic esophageal cancer candidate for neoadjuvant chemoradiotherapy. Patients were randomly assigned to the chemoradiotherapy-only arm (n=32) or chemoradiotherapy plus enoxaparin arm (n=37) using 1:1 allocation. Radiotherapy was delivered in 1.8-Gy daily fractions to a dose of 50.4 Gy in both groups. Paclitaxel 50 mg/m<sup>2</sup> and carboplatin (AUC2) were administered weekly concurrent with radiotherapy. In the intervention group, patients received enoxaparin (40 mg) daily as well as chemoradiation. Four to six weeks after treatment, all patients underwent esophagectomy.

### Results

Both groups were similar in term of age, gender, ECOG performance score, tumor grade, and location tumor (Table 1).

Table 1. Patient and tumor characteristics per treatment group

Variables	CRT+enoxaparin		CRT alone	P value
	Frequency (%)	Frequency (%)	Frequency (%)	
Age (years) <sup>1</sup>	60-61:	13 (35.1)	8 (25)	p=0.4
	61-:	24 (64.9)	24 (75)	
Gender <sup>2</sup>	Female:	18 (48.7)	13 (40.8)	p=0.8
	Male:	19 (51.3)	17 (53.2)	
ECOG PR <sup>3</sup>	0-I	37 (100)	32 (100)	-
	II	0 (0)	0 (0)	
Tumor location <sup>4</sup>	Upper thoracic:	1 (2.7)	2 (6.3)	p=0.3
	Middle thoracic:	21 (56.8)	13 (40.6)	
	Lower thoracic:	15 (40.5)	17 (53.1)	
Tumor grade <sup>5</sup>	T1:	29 (78.4)	25 (78.1)	p=0.8
	T1-IV:	8 (21.6)	7 (21.9)	

CRT: chemoradiation, ECOG PR: Eastern Cooperative Oncology Group (ECOG) performance status score. <sup>1</sup>Chi-Square test revealed no significant difference. <sup>2</sup>Fisher's exact test revealed no significant difference.

A Pathologically complete response in intervention and control group was 64.8% and 62.5%, respectively ( $p=0.9$ ) (Table 2).

Table 2. The difference of clinical and pathologic responses between two groups

Variables	CRT+enoxaparin		CRT alone	P value
	Frequency (%)	Frequency (%)	Frequency (%)	
Clinical response <sup>2</sup>	CCR	14 (38.9)	11 (35.5)	p=0.5
	SCR	21 (58.3)	17 (54.8)	
	PCR	1 (2.8)	3 (9.7)	
Classification of clinical response <sup>3</sup>	CCR	14 (38.9)	11 (35.5)	p=0.8
	RM	22 (61.1)	20 (64.5)	
Pathologic response <sup>4</sup>	pCR	24 (64.8)	20 (62.5)	-
	PD	13 (35.2)	12 (34.8)	
R staging <sup>5</sup>	R0 res	37 (100)	32 (100)	-
	R1 res	0 (0)	0 (0)	
	R2 res	0 (0)	0 (0)	

CCR: complete clinical response, SCR: significant clinical response, PCR: poor clinical response, pCR: pathologic complete response, PD: persistent disease, RM: residual mass, res: resection. Classification of clinical response based on CCR vs SCR+PCR. <sup>2</sup>Chi-Square test revealed no significant difference. <sup>3</sup>Fisher's exact test revealed no significant difference.

After a median follow up of 7 months, estimated one year disease free survival in the intervention and control groups was 78.9% and 70% respectively ( $p=0.5$ ). Toxicity from the experimental arm was minimal and there were no treatment-related deaths.

### Conclusion

Overall, the results of this study showed that the clinical and pathological response of squamous cell carcinoma of esophagus to the neoadjuvant chemoradiation was improved by the addition of enoxaparin to the treatment, although the difference was not significant. Also, there was an insignificant improvement in one year disease free survival of chemoradiotherapy patients receiving enoxaparin. Data from our study indicate that concurrent enoxaparin with radiotherapy and weekly paclitaxel/carboplatin chemotherapy was associated with minimal toxicity. The effects of LMWHs on survival of cancer patients, is probably due to a combination of direct anti-tumoral effects, antiangiogenic and immunomodulatory effects, beside indirect effects on the coagulation system. Most of these direct and indirect effects may have clinical efficacy in the treatment of SCC and gastroesophageal adenocarcinoma, although the

current data on this are contradictory and the observed benefits have been mostly from cellular and in-vitro investigations. Considering that treatment with LMWHs has few side effects, it is recommended that efforts to define the mechanisms of this group of these drugs in affecting tumor growth in the cellular level, and also clinical trials on the benefits of the anticoagulant and anti-tumoral effects, should be continued. However, it must be noted that the new generation of LMWHs lack the oligosaccharide segment and thus part of the antitumoral effects of these drugs may be limited.

**PO-0793 Nodal CTV selection according to primary tumor location and pT-stage for biliary tract cancers**

J. Socha<sup>1</sup>, D. Surdyka<sup>2</sup>, L. Kepka<sup>1</sup>  
<sup>1</sup>Military Institute of Medicine, Radiation Oncology, Warsaw, Poland ; <sup>2</sup>Cancer Center of the Lublin Region, Radiation Oncology, Lublin, Poland

**Purpose or Objective**

In adjuvant radiotherapy for biliary tract cancer there are no guidelines on nodal CTV selection in relation to primary tumor location and pT-stage. To assist radiation oncologists in determining the nodal CTV for each subsite of biliary tract, we aimed to formulate such recommendations based on the analysis of incidence and location of metastatic lymph nodes.

**Material and Methods**

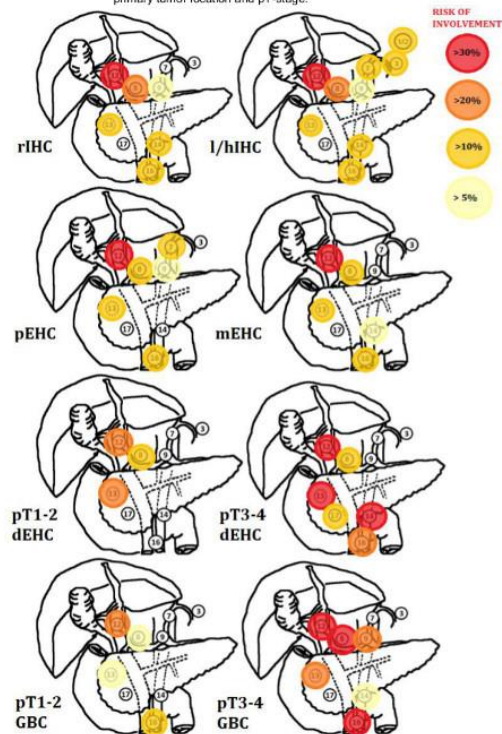
Systematic review was performed, using the “PubMed” and “Google Scholar” databases, to determine the rate of pathological nodal involvement of the respective lymph node stations (LNS) as a function of the primary tumor pT-stage (pT1-2 vs. pT3-4), separately for: right intrahepatic cholangiocarcinoma (rIHC), left/hilar intrahepatic cholangiocarcinoma l/hIHC), proximal extrahepatic cholangiocarcinoma (pEHC), middle extrahepatic cholangiocarcinoma (mEHC), distal extrahepatic cholangiocarcinoma (dEHC) and gall bladder cancer (GBC). A 5% or higher risk of involvement was assumed to justify inclusion of the LNS into CTV.

**Results**

Data on the rate of involvement for each LNS according to the pT-stage was available only for dEHC (6 studies, 522 patients) and GBC (5 studies, 338 patients); rate of involvement for each LNS was available separately for mEHC (5 studies, 132 patients) and pEHC (5 studies, 591 patients) and also separately for rIHC (4 studies, 74 patients) and l/hIHC (4 studies, 156 patients), Table 1. Based on the results, the following LNS should be included into nodal CTV (Figure 1):

1. pT1-2 dEHC: common hepatic artery (CHA), hepatoduodenal ligament (HDL) and posterior pancreaticoduodenal (PPD) LNS;
2. pT3-4 dEHC: CHA, HDL, pPD, superior mesenteric artery (SMA), paraaortic (Ao) and anterior pancreaticoduodenal (aPD) LNS; Celiac artery (CA) LNS risk of involvement in dEHC is below 5%, irrespective of the pT-stage.
3. pT1-2 GBC: CHA, HDL, pPD and Ao LNS;
4. pT3-4 GBC: CHA, HDL, pPD, Ao, CA, and SMA LNS;
5. mEHC: CHA, HDL, pPD, Ao and SMA LNS, risk of involvement for CA LNS is < 5%;
6. pEHC: CHA, HDL, pPD, Ao, CA and left gastric artery (LGA) LNS, risk of involvement for SMA LNS is < 5%;
7. rIHC: CHA, HDL, pPD, Ao, SMA and CA LNS;
8. l/hIHC: as for rIHC + additionally LGA, lesser curvature, and paracardial LNS - risk of involvement for these LNS is > 10%.

Figure 1. Risk of involvement of the respective lymph node stations in relation to primary tumor location and pT-stage.



Lymph node stations classification (according to JSHBPS - Japanese Society of Hepato-Biliary-Pancreatic Surgery):  
 8 - CHA: common hepatic artery, 9 - CA: celiac artery, 12 - HDL: hepatoduodenal ligament, 13 - pPD: posterior pancreaticoduodenal, 14 - SMA: superior mesenteric artery, 16 - Ao: paraaortic, 17 - aPD: anterior pancreaticoduodenal, 7 - LG: left gastric, 3 - LC: lesser curvature, 1/2 - PC: paracardial.  
 rIHC - right intrahepatic cholangiocarcinoma; l/hIHC - left/hilar intrahepatic cholangiocarcinoma; pEHC - proximal extrahepatic cholangiocarcinoma; mEHC - middle extrahepatic cholangiocarcinoma; dEHC - distal extrahepatic cholangiocarcinoma; GBC - gallbladder cancer; pT - pathological tumor stage.

Table 1. Risk of nodal stations involvement according to primary tumor location and pT-stage in biliary tract cancers

Location within	RISK OF LNS INVOLVEMENT													
	8 CHA	12 HDL	9 CA	13 pPD	14 SMA	16 Ao	17 aPD	7 LG	3 LC	1/2 PC	Total LNS+ pts (n)			
rIHC	100	100	100	100	100	100	100	100	100	100	100	100	100	100
l/hIHC	100	100	100	100	100	100	100	100	100	100	100	100	100	100
pEHC	100	100	100	100	100	100	100	100	100	100	100	100	100	100
mEHC	100	100	100	100	100	100	100	100	100	100	100	100	100	100
dEHC	100	100	100	100	100	100	100	100	100	100	100	100	100	100
GBC	100	100	100	100	100	100	100	100	100	100	100	100	100	100

All rates given are the pooled rates (random effect). \* significant heterogeneity; random model used for the proportion analysis  
 LNS - lymph node stations (according to JSHBPS - Japanese Society of Hepato-Biliary-Pancreatic Surgery Classification); 8 - CHA: common hepatic artery; 12 - HDL: hepatoduodenal ligament; 9 - CA: celiac artery; 13 - pPD: posterior pancreaticoduodenal; 14 - SMA: superior mesenteric artery; 16 - Ao: paraaortic; 17 - aPD: anterior pancreaticoduodenal; 7 - LG: left gastric; 3 - LC: lesser curvature; 1/2 - PC: paracardial.  
 rIHC - right intrahepatic cholangiocarcinoma; l/hIHC - left/hilar intrahepatic cholangiocarcinoma; pEHC - proximal extrahepatic cholangiocarcinoma; mEHC - middle extrahepatic cholangiocarcinoma; dEHC - distal extrahepatic cholangiocarcinoma; GBC - gallbladder cancer; pT - pathological tumor stage.

**Conclusion**

This systematic review provides evidence-based strategy for nodal CTV selection in biliary tract cancer according to primary tumor location and pT-stage. CA LNS that is usually included into CTV in clinical practice, has a low risk of involvement and can be omitted for pT1-2 GBC, for dEHC irrespective of pT-stage and for mEHC. Ao and SMA LNS that are usually omitted, have a high risk of involvement. Ao LNS should be routinely included for all the subsites except for pT1-2 dEHC, pT1-2 GBC and pEHC. LGA, lesser curvature, and paracardial LNS should be routinely included for l/hIHC.

**PO-0794 Postoperative Chemoradiotherapy in Gastric Cancer with Poor Response to Neoadjuvant Chemotherapy**

Y. Kundel<sup>1</sup>, B. Brenner<sup>1</sup>, G. Perel<sup>1</sup>, N. Gordon<sup>1</sup>, R. Levin<sup>1</sup>  
<sup>1</sup>Beilinson Hospital, Davidoff cancer center, Petach Tikva, Israel

**Purpose or Objective**

Current standard of care for patients (pts) with locally advanced gastric cancer (LAGC) includes perioperative

chemotherapy (CHT) and surgical resection. According to this approach, all pts receive the same CHT regimen in the neoadjuvant and postoperative setting, regardless of their tumors' pathological response. The CRITICS trial, comparing perioperative CHT with preoperative CHT followed by postoperative chemoradiotherapy (CRT), failed to demonstrate an improved overall survival (OS) with the addition of CRT, but subgroup analysis based on pathologic response to neoadjuvant CHT was not reported yet. The current study aims to evaluate treatment outcomes in pts with poor pathologic response to neoadjuvant CHT, who received postoperative CRT according to our institutional policy.

#### Material and Methods

A retrospective study on pts with LAGC in whom initial treatment strategy was perioperative CHT (ECX, EOX or ECF) and surgery (R0 or R1), but due to poor pathologic response, in their primary tumor and/or regional lymph nodes, to neoadjuvant CHT were treated with postoperative CRT. CRT consisted of 45 Gy in 25 fractions of 1.8 Gy, combined with capecetabine 825 mg/m<sup>2</sup> twice daily on radiotherapy days or continuous infusion of 5FU. Radiation treatment planning was IMRT.

#### Results

Between 2011-2017, 20 pts were treated. Median age was 60 years. Thirteen pts (65%) had proximal gastric tumors, 10 (50%) had diffuse subtype and 13 (65%) had signet ring cell histology. Clinical stages were IIA-III. All pts underwent surgery with D1-D2 lymphadenectomy. R0 resection was achieved in 10 pts (50%). Pathological stage was IIA in 2 pts (10%), IIB in 3 (15%), III in 14 (70%) and IVA in 1 (5%). Eighteen pts (90%) had pT3-T4 tumors and 14 (70%) had N2-N3 disease. Fifteen pts (75%) received also adjuvant chemotherapy before postoperative CRT (same or another regimen as in the neoadjuvant setting). Treatment was well tolerated; it was stopped in only one pt, due to grade 4 vomiting. With a median follow-up time of 32.0 months (range: 12-112 months), recurrences were documented in 11 pts (55%): 5 regional, 4 distant, and 2 combined regional and distant recurrences. Median progression-free survival (PFS) was 20 months (range: 18-21 months) and median OS has not been reached. Estimated 5-year PFS and OS were 42% and 56%, respectively.

#### Conclusion

In our small retrospective study, pts with LAGC assumed to have dismal prognosis due to poor pathologic response to neoadjuvant CHT, achieved a relatively good outcome following the addition of postoperative CRT, compared to reference arms in randomized trials (perioperative CHT arms in MAGIC and CRITICS). These results support the evaluation of an individualized treatment approach, tailored according to pathological response to neoadjuvant CHT, in future studies in this setting. Additional data, on more pts and longer follow-up, will be presented at the meeting.

#### PO-0795 Prediction of severe lymphopenia during chemoradiotherapy for esophageal cancer

P. Van Rossum<sup>1,2</sup>, W. Deng<sup>2</sup>, D. Routman<sup>3</sup>, A. Liu<sup>4</sup>, C. Xu<sup>2</sup>, Y. Shiraishi<sup>2</sup>, M. Peters<sup>1</sup>, K. Merrell<sup>3</sup>, C. Hallemeier<sup>3</sup>, R. Mohan<sup>4</sup>, S. Lin<sup>2</sup>

<sup>1</sup>UMC Utrecht, Radiation Oncology, Utrecht, The Netherlands; <sup>2</sup>The University of Texas MD Anderson Cancer Center, Radiation Oncology, Houston, USA; <sup>3</sup>Mayo Clinic, Radiation Oncology, Rochester, USA; <sup>4</sup>The University of Texas MD Anderson Cancer Center, Radiation Physics, Houston, USA

#### Purpose or Objective

In esophageal cancer patients, occurrence of grade 4 radiation-induced lymphopenia during chemoradiotherapy (CRT) has been associated with worse progression-free survival (PFS) and overall survival (OS). The aim of this study was to develop, internally and externally validate a

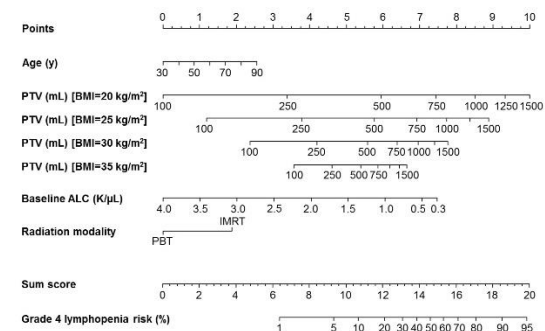
pretreatment clinical nomogram for the prediction of grade 4 lymphopenia to guide individualized treatment decision-making.

#### Material and Methods

Consecutive patients who underwent CRT for esophageal cancer at one center between 2004 and 2017 were identified. Absolute lymphocyte counts (ALCs) were obtained prior to, and weekly during CRT. Grade 4 lymphopenia was defined as ALC nadir <0.2 x10<sup>3</sup>/μL. Potential pretreatment predictors were selected based on literature and clinical reasoning. After multiple imputation, final predictors were selected using multivariable logistic regression with backward stepwise elimination. Internal validation of the final model was performed using bootstrapping. The model was evaluated in terms of calibration and discrimination, corrected for optimism, and presented as nomogram yielding 4 risk groups based on individual nomogram sum scores. External validation was performed by applying the model to an independent cohort of esophageal cancer patients who underwent CRT at another institution between 2015 and 2017. Finally, the relationships between nomogram-based risk groups and PFS and OS were assessed.

#### Results

Among 860 included patients, 322 (37%) experienced grade 4 lymphopenia during CRT. Higher age, larger planning target volume (PTV) in interaction with lower BMI, photon- rather than proton-based therapy, and lower baseline ALC were predictive for grade 4 lymphopenia in the final model yielding a corrected c-statistic of 0.76. The resulting nomogram is presented in Figure 1. External validation of the nomogram in 144 patients from another institution, in whom 58 (40%) had grade 4 lymphopenia, yielded a c-statistic of 0.72. Applying the nomogram sum score (0 to 20), patients were divided into 4 risk groups yielding predicted grade 4 lymphopenia risk rates of 10%, 24%, 43%, and 70%, respectively, which were in good agreement with observed incidences. Risk groups showed statistically significant associations with survival, with 5-year PFS rates of 54%, 50%, 41%, and 40%, respectively, and 5-year OS rates of 55%, 49%, 44%, and 37%, respectively.



#### Conclusion

A pretreatment clinical nomogram for the prediction of grade 4 radiation-induced lymphopenia during CRT for esophageal cancer with a good model performance was developed and validated, both internally and externally. The nomogram allows for prediction of the risk of grade 4 radiation-induced lymphopenia for each individual patient, which in turn is associated with PFS and OS. The nomogram can aid in the selection of patients suitable for mitigating treatment strategies or potential future therapeutic approaches, which may ultimately improve survival.

#### PO-0796 Carbotaxol definitive chemoradiotherapy for inoperable oesophageal cancer: UK multicentre study

R. Owens<sup>1</sup>, C. Cox<sup>2</sup>, S. Gombert<sup>3</sup>, S. Prince<sup>4</sup>, T. Bird<sup>5</sup>, N. Dorey<sup>6</sup>, U. MacGregor<sup>7</sup>, H. Al-Chamali<sup>8</sup>, C. Hurt<sup>2</sup>, S.

Mukherjee<sup>1</sup>

<sup>1</sup>Oxford University Hospital NHS Trust, Oncology, Oxford, United Kingdom ; <sup>2</sup>Cardiff University, Centre for Trials Research, Cardiff, United Kingdom ; <sup>3</sup>Guys and St Thomas Hospital, Oncology, London, United Kingdom ; <sup>4</sup>Univeristy Hospital Southampton, Oncology, Oxford, United Kingdom ; <sup>5</sup>Royal Marsden Hospital, Oncology, London, United Kingdom ; <sup>6</sup>Royal Devon and Exeter Foundation NHS Trust, Oncology, Exeter, United Kingdom ; <sup>7</sup>NHS Highland, Oncology, Inverness, United Kingdom ; <sup>8</sup>Royal Berkshire Hospital, Oncology, Reading, United Kingdom

### Purpose or Objective

The CROSS trial established weekly carboplatin (CP) based CRT as standard of care for pre-operative treatment of oesophageal cancer. Given the promising outcome and low toxicity profile, this regimen is being increasingly used internationally as a component of definitive CRT (dCRT) for inoperable oesophageal cancer, although no large studies demonstrate benefit or equivalence over standard cisplatin fluoropyrimidine (CF) based dCRT. In the UK, a national questionnaire demonstrated that although CF-dCRT remained treatment of choice, CP-dCRT was being offered to elderly patients, less fit patients and in those whom CF-dCRT was contra-indicated. We present the outcomes of CP-dCRT from a UK-wide national audit in this selective patient group.

### Material and Methods

Appropriate UK centres were identified through a national questionnaire. All patients were treated with weekly carboplatin (AUC2) and paclitaxel (50mg/m<sup>2</sup>) dCRT with curative intent between 2011-2018. Patient and tumour demographics, indication for CP-dCRT, toxicity, response rates (as per endoscopy and imaging), recurrence and overall survival were collected.

### Results

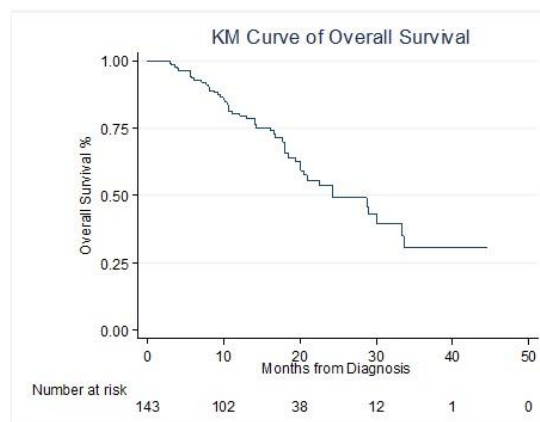
143 patients from 7 centres were included. Patient and tumour demographics are shown in Table 1.

Table 1

		n	%
Sex	Male	85	40.6%
	Female	58	59.4%
Age	Median (IQR, range)	73 ((64,78), 42-91)	
	70+	87	60.8%
	80+	25	17.5%
T stage	1	5	3.5%
	2	31	21.7%
	3	85	59.4%
	4	20	14.0%
	Missing	2	1.4%
N stage	0	59	41.3%
	1	59	41.3%
	2	21	14.7%
	3	4	2.8%
Site	Lower third	74	51.8%
	Middle third	58	40.6%
	Upper third	11	7.7%
Performance status	0	36	25.2%
	1	88	61.5%
	2	19	13.3%
Disease length (cm)	Median (IQR, range)	4.5 ((3.0, 6.1), 1-13)	
Histology	SCC	66	46.2%
	Adeno	77	53.8%

Median age was 73 years (range 42-91; 60.8% >70yrs; 17.5% >80 yrs). Indications for CP-dCRT included co-morbidities (48.3%), clinician choice (32.9%), poor tolerance/progression on induction chemo (18.9%). 43.4% received induction chemotherapy (commonly CF). 71.3% received IMRT, and 75.5% received 50Gy/25 fractions (dose range 41.4/23-64/32#). 96.5% completed RT and 85.3% completed ≥4 weekly infusions of CP. 36% of

patients experienced at least one grade 3+ toxicity (haematological-12%, non-hematological-34%). The most common grade 3 non-haematological toxicities were nausea and vomiting (8%). There were 2 recorded deaths during treatment (oesophageal hemorrhage, duodenal perforation). At the post-treatment response assessment, 91 patients had an endoscopy, 121 had imaging, and 12 patients died prior to this point. 69.2% had complete response (CR) on endoscopy, 86.0% had CR/Partial response (PR)/Stable disease (SD) on imaging and 70.3% had combined CR on endoscopy with CR/PR/SD on imaging. In all patients, median follow-up was 17.2 months (95% CI 14.7-20.5), median OS was 24.3 months (95% CI 20.0-33.5), median overall/local/distant relapse free survival were 16.8 (95% CI 14.2-24.3)/20.3 (95% CI 16.8-28.8)/24.3 (95% CI 16.8-33.1) months respectively, and 31% of patients had relapsed.



Median overall survival: 24.31 months (95% CI: 20.01, 33.45)

Median duration of follow up: 17.22 months (95% CI: 14.65, 20.47)

In patients that had a post-treatment endoscopy (n=91), treatment response (CR on endoscopy with CR/PR/SD on imaging) was associated with superior survival on multivariate cox regression (HR 4.79 (95% CI 1.83-12.55, p=0.001)).

### Conclusion

CP-dCRT is safe and deliverable in elderly and “poor performance” patients who would have otherwise received palliative treatment. The outcomes are comparable to CF based dCRT, and should be considered as the preferred treatment option in this patient group.

### PO-0797 Impact of <sup>99m</sup>Tc-GSA SPECT image-guided inverse planning on DFH parameters for SBRT planning for HCC

R. Toya<sup>1</sup>, T. Saito<sup>1</sup>, Y. Kai<sup>2</sup>, S. Shiraishi<sup>3</sup>, T. Matsuyama<sup>1</sup>, T. Watakabe<sup>1</sup>, F. Sakamoto<sup>3</sup>, N. Tsuda<sup>3</sup>, Y. Shimohigashi<sup>2</sup>, Y. Yamashita<sup>3</sup>, N. Oya<sup>1</sup>

<sup>1</sup>Kumamoto University Hospital, Radiation Oncology, Kumamoto, Japan ; <sup>2</sup>Kumamoto University Hospital, Radiological Technology, Kumamoto, Japan ; <sup>3</sup>Kumamoto University Hospital, Diagnostic Radiology, Kumamoto, Japan

### Purpose or Objective

A radiopharmaceutical tracer, <sup>99m</sup>Tc-labeled diethylene triamine pentaacetate-galactosyl human serum albumin (<sup>99m</sup>Tc-GSA), that binds specifically to the hepatic asialoglycoprotein receptor is used to assess hepatic function. Single-photon emission computed tomography (SPECT) using <sup>99m</sup>Tc-GSA provides three-dimensional information about regional liver function, and its findings suggest that regional function of patients with liver tumors is inhomogeneous because of previous treatments, such as radiofrequency ablation and transarterial

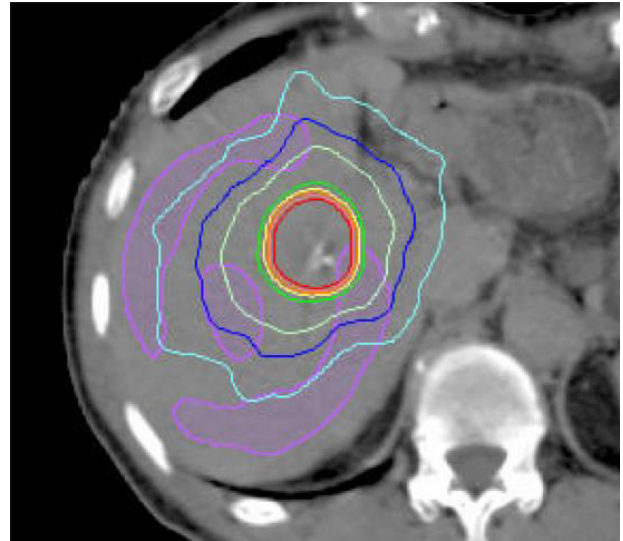
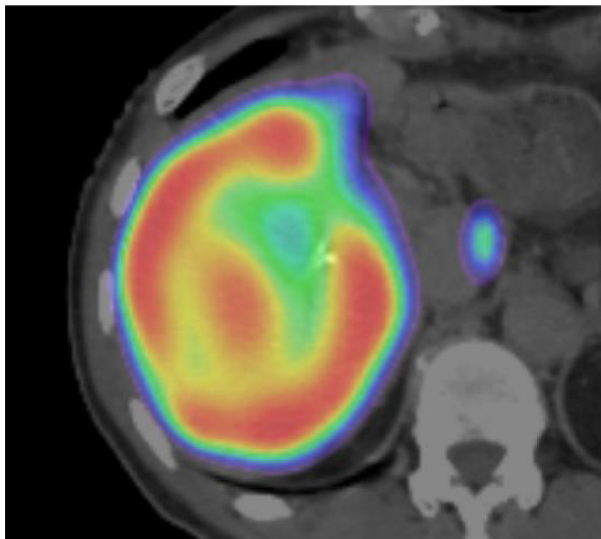
chemoembolization. A recent study revealed that a dose-function histogram (DFH) using  $^{99m}\text{Tc}$ -GSA SPECT provides dosimetric information of the liver function of HCC patients who underwent SBRT. Introduction of functional information of  $^{99m}\text{Tc}$ -GSA SPECT for use in inverse planning for IMRT might be a reasonable approach to spare liver function. We evaluated the impact of  $^{99m}\text{Tc}$ -GSA SPECT image-guided inverse planning on the DFH parameters of SBRT planning in HCC patients.

#### Material and Methods

Eleven patients with HCC were enrolled in this study. We used a SPECT/CT system (Symbia T16; Siemens Healthcare, Erlangen, Germany) for the SPECT/CT imaging. Attenuation-corrected SPECT and CT images and planning CT images were transferred to a Velocity AI (version 3.0.2; Varian Medical Systems, Palo Alto, CA, USA). We registered the SPECT/CT images onto the planning CT images: a rigid image registration followed by a non-rigid deformable registration. The functional liver structure (FLS) as an avoidance structure for optimization was derived from SPECT thresholds of 60%-80% of the maximum pixel value. Two treatment plans optimized without FLS (plan C) and with FLS (plan F) were designed for 50 Gy in 5 fractions to the planning target volume (PTV) by using a 2-arc RapidArc (Clinac iX; Varian Medical Systems, Palo Alto, CA, USA). DFH parameters were calculated as follows:  $F_x = (\text{sum of the counts within the liver volume receiving a dose } >x \text{ Gy} / \text{sum of the counts within the whole liver volume}) \times 100$ . Other parameters for the PTV included the absorbed dose received by 95% of the PTV ( $D_{95}$ ), mean dose, conformity index (CI), and homogeneity index (HI).

#### Results

In comparison with plan C, plan F significantly reduced the DFH parameters of  $F_5$  to  $F_{40}$  ( $p < 0.05$ ), and plan F did not significantly increase  $F_{45}$  and  $F_{50}$ . There were no significant differences in the DVH parameters of  $D_{95}$ , mean dose, CI, and HI for the PTV between plans C and F. There were no significant differences in the parameters of the OARs of the stomach, duodenum, spinal cord, and kidneys between plans C and F. There was no significant difference in the MUs between plans C and F.



#### Conclusion

DFH analyses revealed that  $^{99m}\text{Tc}$ -GSA SPECT image-guided inverse planning provided dosimetric benefits related to sparing of liver function while maintaining coverage of the PTV and may reduce hepatic toxicities.

#### PO-0798 Response assessment to neoadjuvant chemoradiotherapy for esophageal cancer using PET/CT and DW-MRI

A. Borggreve<sup>1</sup>, L. Goense<sup>1</sup>, P.S.N. Van Rossum<sup>2</sup>, S.E. Heethuis<sup>2</sup>, R. Van Hillegersberg<sup>3</sup>, J.J.W. Lagendijk<sup>2</sup>, A.L.H.M.W. Van Lier<sup>2</sup>, S. Mook<sup>2</sup>, J.P. Ruurda<sup>3</sup>, M. Van Vulpen<sup>4</sup>, F.E. Voncken<sup>5</sup>, B.M.P. Aleman<sup>5</sup>, A. Bartels-Rutten<sup>6</sup>, J. Ma<sup>7</sup>, P. Fang<sup>8</sup>, B.C. Musall<sup>7</sup>, S.H. Lin<sup>8</sup>, G.J. Meijer<sup>2</sup>

<sup>1</sup>UMC Utrecht, Radiation Oncology and Surgical Oncology, Utrecht, The Netherlands ; <sup>2</sup>UMC Utrecht, Radiation Oncology, Utrecht, The Netherlands ; <sup>3</sup>UMC Utrecht, Surgical Oncology, Utrecht, The Netherlands ; <sup>4</sup>Holland PTC, Holland Particle Center, Delft, The Netherlands ; <sup>5</sup>The Netherlands Cancer Institute - Antoni van Leeuwenhoek Hospital, Radiation Oncology, Amsterdam, The Netherlands ; <sup>6</sup>The Netherlands Cancer Institute - Antoni van Leeuwenhoek Hospital, Radiology, Amsterdam, The Netherlands ; <sup>7</sup>The University of Texas MD Anderson Cancer Center, Imaging Physics, Houston, USA ; <sup>8</sup>The University of Texas MD Anderson Cancer Center, Radiation Oncology, Houston, USA

#### Purpose or Objective

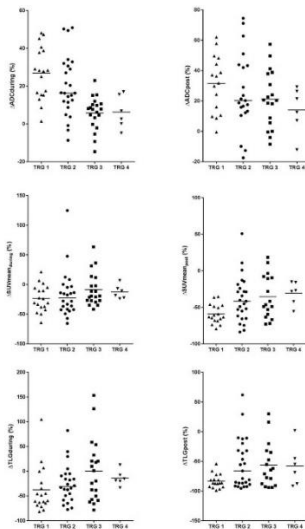
Around one third of the patients have a pathologic complete response (pCR) after neoadjuvant chemoradiotherapy (nCRT) for esophageal cancer. Accurate preoperative identification of this group could omit esophagectomy in these patients. The purpose of this prospective multicenter study was to evaluate the distinct and combined value of  $^{18}\text{F}$ -FDG PET/CT and DW-MRI during and after nCRT to predict pathologic response in esophageal cancer patients.

#### Material and Methods

In this prospective multicenter study, patients scheduled to receive nCRT followed by esophagectomy for resectable esophageal cancer underwent  $^{18}\text{F}$ -FDG PET/CT and DW-MRI scanning prior to start of nCRT, during nCRT and 0-2 weeks before esophagectomy. Response to nCRT was measured using the tumor regression grading system based on histopathological evaluation of the resection specimen (TRG1-4). Relative changes in  $^{18}\text{F}$ -FDG PET/CT ( $\Delta\text{SUV}$  and  $\Delta\text{TLG}$ ) and DW-MRI ( $\Delta\text{ADC}$ ) parameters were compared between patients with a pCR (TRG1) and non-pCR (TRG2-4) groups (Figure 1). Multivariable logistic regression analysis with bootstrapped 95% confidence intervals and

corresponding concordance measurements were calculated to evaluate the complementary value of <sup>18</sup>F-FDG PET/CT and DW-MRI.

Figure 1: Comparison of relative changes in <sup>18</sup>F-FDG PET/CT and DW-MRI imaging parameters during and after neoadjuvant chemoradiotherapy between histopathologic tumor regression grades (TRG). The solid horizontal lines represent group medians.



**Results**

A total of 69 patients with 203 <sup>18</sup>F-FDG PET/CT and 199 DW-MRI scans were eligible for analysis. A pCR was found in 26.1% (18/69). Relative changes in <sup>18</sup>F-FDG PET/CT parameters after nCRT ( $\Delta$ SUV<sub>mean,post</sub> [median, IQR] -63% (-68%, -49%) for pCR versus -42% [-58%, -16%] for non-pCR, p = 0.018 and  $\Delta$ TLG<sub>post</sub> [median, IQR] -86% [-93%, -81%] for pCR versus -65% [-88%, -32%] for non-pCR, p = 0.036), as well as changes in DW-MRI parameters during nCRT ( $\Delta$ ADC<sub>during</sub> [median, IQR] 28% [15%, 39%] for pCR versus 11% [3.7%, 17%] for non-pCR, p = 0.006) were significantly different between pathologic complete responders and non-responders in esophageal cancer (Table 1). A c-statistic of 0.74 for  $\Delta$ SUV<sub>mean,post</sub> alone, of 0.77 for  $\Delta$ ADC<sub>during</sub> alone and of 0.81 for the combination of  $\Delta$ ADC<sub>during</sub> with  $\Delta$ SUV<sub>mean,post</sub> was obtained in classifying patients as pCR and non-pCR.

Table 1. Relative changes in <sup>18</sup>F-FDG PET/CT and DW-MRI parameters between pathologic complete response (TRG 1) and non-pathologic complete response (TRG 2-4).

		Median (IQR)		p-value*	Holm-Bonferroni adjusted p-value	c-statistic
		pCR (TRG 1) (n=18)	non-pCR (TRG 2-4) (n=51)			
During treatment	$\Delta$ SUV <sub>mean,post</sub> (%)	-27 (-38, -8.8)	-19 (-33, -2.5)	0.246	0.492	0.59
	$\Delta$ SUV <sub>max</sub> (%)	-29 (-46, -8.1)	-23 (-35, -2.1)	0.408	0.492	0.57
	$\Delta$ TLG <sub>post</sub> (%)	-54 (-64, -23)	-20 (-50, 9.8)	<b>0.020</b>	0.100	0.69
	$\Delta$ ADC <sub>during</sub> (%)	28 (15, 39)	11 (3.7, 17)	<b>0.001</b>	<b>0.006</b>	0.77
Post treatment	$\Delta$ SUV <sub>mean,post</sub> (%)	-63 (-68, -49)	-42 (-58, -16)	<b>0.003</b>	<b>0.018</b>	0.74
	$\Delta$ SUV <sub>max</sub> (%)	-68 (-78, -58)	-54 (-71, -31)	<b>0.026</b>	0.103	0.68
	$\Delta$ TLG <sub>post</sub> (%)	-86 (-93, -81)	-65 (-88, -32)	<b>0.006</b>	<b>0.036</b>	0.72
	$\Delta$ ADC <sub>during</sub> (%)	34 (13, 46)	20 (10, 38)	0.139	0.417	0.63

\* p-value calculated based on Mann-Whitney U test

ADC apparent diffusion coefficient; c-statistic concordance statistic; IQR interquartile range; pCR pathologic complete response; SD standard deviation; SUV standardized uptake volume; TLG tumor lesion glycolysis; TRG tumor regression grade

**Conclusion**

This prospective multicenter study demonstrates that changes in <sup>18</sup>F-FDG PET/CT parameters after nCRT ( $\Delta$ SUV<sub>mean,post</sub> and  $\Delta$ TLG<sub>post</sub>) and early treatment-induced changes on DW-MRI during nCRT ( $\Delta$ ADC<sub>during</sub>) discriminate between pathologic complete responders from non-

responders in esophageal cancer. Moreover, <sup>18</sup>F-FDG PET/CT and DW-MRI are of complementary value in the assessment of histopathological response.

**PO-0799 Treatment outcomes of nodal positive unresectable thoracic esophageal carcinoma**

T. Huang<sup>1</sup>, S. Li<sup>2</sup>, Y. Chen<sup>2</sup>, H. Lu<sup>3</sup>, C. Lo<sup>3</sup>, F. Fang<sup>1</sup>, S. Chou<sup>1</sup>, Y. Wang<sup>1</sup>

<sup>1</sup>Kaohsiung Chang Gung Memorial Hospital and Chang Gung University School of Medicine, Proton and radiation therapy center, Kaohsiung, Taiwan ; <sup>2</sup>Kaohsiung Chang Gung Memorial Hospital and Chang Gung University School of Medicine, Department of Hematology-Oncology, Kaohsiung, Taiwan ; <sup>3</sup>Kaohsiung Chang Gung Memorial Hospital and Chang Gung University School of Medicine, Department of Thoracic & Cardiovascular Surgery, Kaohsiung, Taiwan

**Purpose or Objective**

The prognosis of unresectable (T4b) thoracic esophageal cancer (EC) is extremely poor and the optimal treatment strategy remains controversial. The present study investigated the treatment outcomes and prognostic factors of nodal positive (N+) T4b thoracic EC patients treated by curative intent concurrent chemoradiotherapy (CCRT).

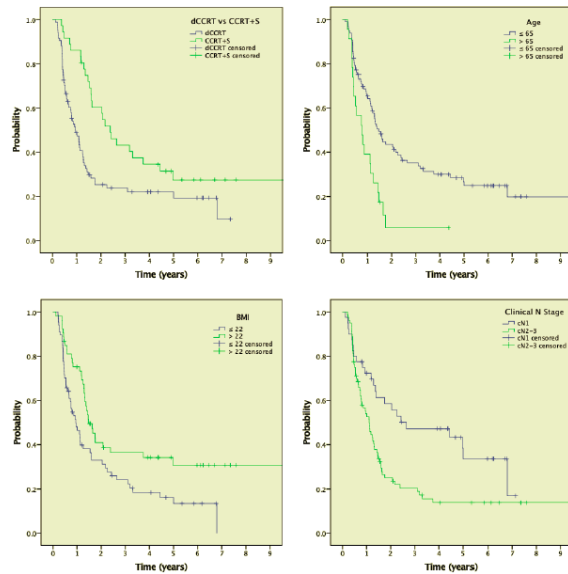
**Material and Methods**

A retrospective review of 1120 EC patients treated at our institution between 2009 and 2017 was conducted. One hundred and twenty T4b N+ thoracic EC patients without distant metastasis who underwent curative CCRT were identified for the following study. Among these patients, 84 patients were treated by definitive CCRT only (dCCRT) while salvage esophagectomy was performed in 36 patients (CCRT+S). All clinical factors were put into analysis. Survival analysis was calculated using Kaplan-Meier method with log-rank test, and prognostic factors were examined by Cox proportional hazards model.

**Results**

The median survival for the entire group of 120 patients was 15.5 months. The 1-year, 3-year, and 5-year overall survival (OS) was 60.2%, 29.5%, and 22.5%, respectively. Multivariable analysis revealed that CCRT+S (p = 0.014), age <= 65 (p = 0.001), Pre-CCRT body mass index (BMI) > 22 (p = 0.001), and clinical N1 (cN1) disease (p = 0.005) were significant independent prognostic factors. Tumor location (upper/middle/lower) and different invasion structures (great vessels, airway, or both) had no significant influence on OS.

Variable	Univariable analysis			Multivariable analysis		
	HR	95% CI	p value	HR	95% CI	p value
<b>Overall Survival</b>						
Surgery (No vs Yes)	1.976	1.236-3.160	0.004*	1.837	1.134-2.977	0.014*
Age (<=65 vs >65)	2.301	1.388-3.815	0.002*	2.504	1.449-4.325	0.001*
BMI (<=22 vs >22)	1.776	1.152-2.736	0.009*	2.166	1.372-3.419	0.001*
Lymph Node (cN2-3 vs cN1)	1.982	1.232-3.191	0.005*	2.018	1.232-3.304	0.005*
<b>Tumor Invasion</b>						
(Great Vessels/Airway/Both)				N.S.		
<b>Tumor Location</b>						
(Upper/Middle/Lower)				N.S.		



### Conclusion

Our study revealed that long-term survival is still achievable for patients with cT4b N+ EC. Patients with younger age, higher BMI, and cN1 disease tended to have better OS while salvage esophagectomy may further improve the outcomes.

### PO-0800 Radiation dose escalation in pancreatic cancer: a propensity-score matching study

X. Zhu<sup>1</sup>, C. Yangsen<sup>1</sup>, Z. Xianzhi<sup>1</sup>, S. Yuxin<sup>1</sup>, J. Xiaoping<sup>1</sup>, Q. Shuiwang<sup>1</sup>, C. Fei<sup>1</sup>, J. Zhen<sup>1</sup>, F. Fang<sup>1</sup>, G. Lei<sup>1</sup>, Z. Huojun<sup>1</sup>

<sup>1</sup>Changhai Hospital, Radiation Oncology, Shanghai, China

### Purpose or Objective

For patients with locally advanced pancreatic cancer, standard therapy consists of different combinations of chemotherapy and radiotherapy. Additionally, chemoradiotherapy may be the alternative option for those with resectable or borderline resectable but medically inoperable pancreatic cancer though there was no consensus about the optimal therapy. However, fewer studies have evaluated the association of radiation dose and survival or local control. Therefore, the aim of the study was to investigate the role of dose escalation in non-operable pancreatic cancer.

### Material and Methods

Consecutive patients with resectable or borderline resectable but medically inoperable due to comorbidities and locally advanced pancreatic cancer receiving SBRT and chemotherapy were included. Patient demographic and treatment information were stratified by a BED<sub>10</sub> of 60 to 70Gy versus a BED<sub>10</sub> >70Gy. Factors predictive of overall survival (OS), progression free survival (PFS) and local control (LC) were identified by multivariate analysis. OS, PFS and LC were further compared using propensity score matching.

### Results

Four hundred and thirty-three patients were included; 330 received 60 to 70Gy and 107 received doses >70Gy. Univariate analysis showed that tumor stage and CA19-9 response correlated with OS and PFS, while tumor stage, CA19-9 response and ECOG was associated with LC. After multivariate analysis, both tumor stage and CA19-9 response were predictive of OS, PFS and LC (P<0.001 for all analyses). Therefore, these two factors were used to develop matched cohorts. One hundred and seven patients in each group were included after propensity-score matching. Patients with a BED<sub>10</sub> >70Gy had a superior OS, PFS and LC compared with those with a BED<sub>10</sub> of 60 to 70Gy (OS: 13.7 months vs. 17.6 months, P<0.001; PFS: 9.4

months vs. 13.8 months, P<0.001; LC: 10.5 months vs. 15.0 months, P<0.001).

### Conclusion

BED escalation >70Gy may provide survival benefits and better local control in patients with pancreatic cancer but require further validation in prospective studies.

### PO-0801 Esophageal Cancer: One Organ, Two Histologies, One Treatment Strategy: Why?

M. Lamande<sup>1,2</sup>, L. Grandjean<sup>1</sup>, E. Gonne<sup>3</sup>, D. Van Daele<sup>4</sup>, J. Collignon<sup>3</sup>, M. Polus<sup>4</sup>, C. Loly<sup>4</sup>, J. Vanderick<sup>1</sup>, P. Coucke<sup>1</sup>, P. Martinive<sup>1,2</sup>

<sup>1</sup>C.H.U. - Sart Tilman, Department of Radiotherapy, Liège, Belgium ; <sup>2</sup>Institut Jules Bordet, Department of Radiotherapy, Brussels, Belgium ; <sup>3</sup>C.H.U. - Sart Tilman, Department of Medical Oncology, Liège, Belgium ; <sup>4</sup>C.H.U. - Sart Tilman, Department of Gastroenterology and Digestive Oncology, Liège, Belgium

### Purpose or Objective

Neoadjuvant radiochemotherapy (NRTC) is recommended for Adenocarcinoma (ADK) and Squamous Cell Carcinoma (SCC) of the esophagus for patients with good performance status and tumor located in the lower third of the esophagus. While often treated as a sole and unique entity, esophageal cancer could be viewed as two different pathologies based on tumor histology, pathogenicity and patient related co-morbidities. The aim of this study was to assess the Overall Survival (OS), median OS (mOS), Local and Distant Recurrences (LR/DR) in regard of tumor histology.

### Material and Methods

We retrospectively reviewed a cohort of patients with histological proven SCC or ADK esophageal cancer who received either definitive RTC or NRTC from 01/01/08 to 10/15/16. For definitive RTC patients received 50,4Gy in 28 fractions concomitantly with Cisplatin and 5FU or Carboplatin and Taxol. For NRTC they received 45Gy in 25 fractions with Carboplatin and Taxol. Patients who were not electable for NRTC due to co-morbidities, tumor stage or tumor location were treated by RCT and salvage surgery.

### Results

We identified 112 patients, 74 SCC and 38 ADK. NRTC was administrated to 9 SCC and 24 ADK, all the others received RTC. With a median follow up of 40 months, the 3 and 5y OS and mOS for all the cohort are for RTC 33%, 25,4% and 21,1 mo and for NRTC 38,5% 38,5% and 24,3mo, respectively (p=ns). Among 74 SCC (Ratio M/F=2), 85,1% were former smokers and 64% were still active and 71,6% had alcoholic habits at diagnosis. The 3 and 5y OS for RTC are 38% and 32% with 21,8mo mOS. For NRTC the 3y OS is 22,4% and 22,4mo mOS. Recurrences occurred in 40 % patients (LR alone 11%, LR and DR 5%, DR 24%). Most recurrences occurred (74%) during the first year after treatment and 70% of those patients died within the year of the relapse. Among 38 ADK (Ratio M/F=8,5), 65,8% were former and 47,4% were still active smokers and 26,3 % had alcoholic habits at diagnosis. Most of the patients (63%) were treated with NRCT. Recurrences occurred in 50 % patients (LR alone 5%, LR and DR 5%, DR alone 39%) and 58% of these relapses occurred within the first year. The mOS of RTC was 8,25 months without any survivors at 3 years. NRCT approach showed a mOS of 24,3 mo and 3 years OS of 40 %. Due to limited number of patients the 5 years OS is not reliable. More details are featured in Table

1.

Squamous cell carcinomas			Adenocarcinomas		
Items	Numbers	%	Items	Numbers	%
<b>Age</b>			<b>Age</b>		
Median	65,3	/	Median	64,5	/
Range	45-87	/	Range	47-83	/
<b>Sex</b>			<b>Sex</b>		
Male	51	68,92	Male	34	89,47
Female	23	31,08	Female	4	10,53
<b>Tumor localisation</b>			<b>Tumor localisation</b>		
Upper 1/3	22	29,72	Upper 1/3	1	2,63
Middle 1/3	34	45,94	Middle 1/3	4	10,53
Lower 1/3	17	22,97	Lower 1/3	18	47,37
Jonction	1	1,35	Jonction	15	39,47
<b>Tumor histological differentiation</b>			<b>Tumor histological differentiation</b>		
None	0	0	None	0	0
Poor	20	27,03	Poor	7	18,42
Middle	38	51,35	Middle	13	34,21
Well	12	16,22	Well	8	21,05
Other, in situ	1	1,35	Other, in situ	4	10,53
Unknown	3	4,05	Unknown	6	15,79
<b>Stage</b>			<b>Stage</b>		
Unknown	8	10,81	Unknown	8	21,05
Stage I	7	9,46	Stage I	0	0,00
Stage II	14	18,92	Stage II A	1	2,63
Stage III	38	51,35	Stage II B	2	5,26
Stage IV A	7	9,46	Stage III	24	63,16
Stage IV B	0	0	Stage IV A	2	5,26
			Stage IV B	1	2,63
<b>cTNM (v. 8)</b>			<b>cTNM (v. 8)</b>		
<b>T</b>			<b>T</b>		
cTx	5	6,8	cTx	4	10,8
cTis	0	0	cTis	0	0,0
cT0	0	0	cT0	0	0,0
cT1	7	9,6	cT1	1	2,7
cT2	7	9,6	cT2	5	13,5
cT3	48	64,9	cT3	24	64,9
cT4	7	9,6	cT4	3	8,1
<b>N</b>			<b>N</b>		
cNx	7	9,6	cNx	6	15,8
cN0	17	23	cN0	6	15,8
cN1	43	58,1	cN1	24	63,2
cN2	7	9,6	cN2	1	2,6
cN3	0	0	cN3	0	0,0
<b>M</b>			<b>M</b>		
cMx	5	6,8	cMx	6	15,8
cM0	65	87,8	cM0	30	78,9
cM1	4	5,4	cM1	1	2,6
Not assessed	0	0	Not assessed	1	2,6

### Conclusion

Both in ADK and SCC we achieved a good local control (>85%). There was no significant differences in OS between treatments. We showed that ADK were mostly treated with NRTC and SCC with RTC illustrating the difficulties of NRTC on SCC. Worth noticing, the OS of SCC treated with RTC demonstrated an OS as good as surgical series despite the advanced tumor stage of those patients (> 50% stage III) and tobacco / alcohol related comorbidities. These results, good tumor local controlled and OS for locally advanced tumors questioned the place of surgery as a standard of treatment for SCC.

### PO-0802 Lung dose was associated with severe lymphopenia in esophageal cancer undergoing trimodality therapy

J. Lin<sup>1</sup>, J. Lee<sup>2</sup>, C. Cheng<sup>3</sup>, T. Chang<sup>4</sup>, Y. Chen<sup>2</sup>  
<sup>1</sup>Changhua Christian Hospital, Radiation Oncology, Changhua, Taiwan ; <sup>2</sup>MacKay Memorial Hospital, Department of Radiation Oncology, Taipei, Taiwan ; <sup>3</sup>Changhua Christian Hospital, Department of Thoracic Surgery, Changhua, Taiwan ; <sup>4</sup>Changhua Christian Hospital, Department of Radiation Oncology, Changhua, Taiwan

### Purpose or Objective

Previous studies had reported lymphopenia was associated with poorer outcomes in esophageal cancer. The lung was reservoir of hematological stem cell. Radiotherapy and chemotherapy might destroy the hematological stem cells in the lung and could contribute to lymphopenia. This

study aimed to identify whether lung dosimetric parameters were predictive for severe lymphopenia in esophageal cancer patients.

### Material and Methods

A total 117 patients with esophageal cancer underwent neoadjuvant chemoradiotherapy followed by surgery during 2010 and 2015 in two academic centers were analyzed. With majority male gender, current smoker, squamous cell carcinoma histology, and clinical stage III disease, all patient underwent neoadjuvant therapy consisted of 2-3 course of cisplatin and 5-fluorouracil concurrent with radiotherapy (median dose 44 Gy). Patients with severe lymphopenia, defined as absolute lymphocyte count  $\leq 500$  during neoadjuvant therapy were compared to those without this toxicity. The logistic regression was used to identify predictive treatment-related and dosimetric factors for severe lymphopenia. Factors with a  $p$  value  $<0.05$  were considered significant. Further receiver-operating characteristic (ROC) curve was performed for these dosimetric parameters to obtain best cutoff values.

### Results

The mean heart dose of all patients was 18.06 Gy [standard deviation (SD): 6.67Gy]. The mean lung volume receiving 5 Gy or more (V5), lung V10, and lung V20 was 72.8% (SD: 21.1%), 52.2% (SD:17.8%), 20.3% (SD:6.5%), respectively. Lung V5 (odds ratio [OR]: 1.03, 95% confident interval [CI]: 1.00-1.06,  $p = 0.04$ ) and ECOG performance status (0 vs. 1, OR: 3.30, 95% CI: 1.15-9.44,  $p = 0.03$ ) were associated with severe lymphopenia when adjusting for pre-treatment feeding jejunostomy, cisplatin intensity, gross tumour volume, gross tumour dose, and lung V10. The ROC curve analysis generated best cutoff value of lung V5 of 75% (the area under the curve: 0.75,  $p < 0.001$ ). High probability of severe lymphopenia in patients with lung V5  $\geq 75\%$  compared to those with lung V5  $< 75\%$  (55.74% vs. 16.07%,  $p < 0.001$ ).

### Conclusion

Higher lung V5 was associated with severe lymphocyte declined in esophageal cancer patients underwent neoadjuvant chemoradiotherapy followed by surgery. Constraints for low dose lung volume may avoid severe lymphopenia in these patients.

### PO-0803 Endoluminal brachytherapy with induction chemotherapy and definitive chemoradiation in Ca. Esophagus

S. Raghunath<sup>1</sup>, R. Tiwari<sup>1</sup>, G. Narayanan<sup>1</sup>, B. Vishwanathan<sup>1</sup>, R. Sultana<sup>1</sup>  
<sup>1</sup>Vydehi Institute of Medical Sciences and Research Center, Radiation Oncology, Bangalore, India

### Purpose or Objective

#### Need for the Study:

Over 75% of people with cancer worldwide have no access to safe surgery. Access is worse in low income countries where 95% of people with cancer do not receive basic cancer surgery.

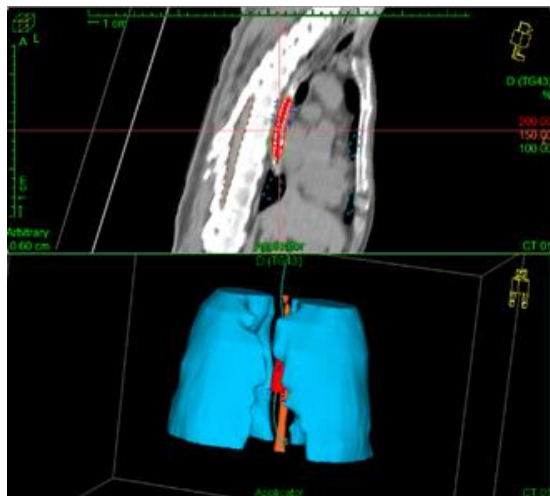
Patients in remote areas in Rural India, South Asia, Africa and Poorer EU Member States do not have access to surgical infrastructure or qualified personnel to deliver high quality surgery in locally advanced esophageal carcinoma. Further, Esophageal Cancer has an abysmal response despite multimodality treatment. Endoluminal Brachytherapy is an under-utilized modality in the curative setting and an elegant tool to escalate the dose to improve the clinical response and clinical symptoms.

This study examines if Dose Escalation with Endoluminal Brachytherapy after Induction Chemotherapy and Definitive Chemoradiation is feasible in the background of the above scenarios in underserved populations.

#### Objective:

To evaluate Dysphagia Free Interval (DFI), Disease Free Survival (DFS), Overall Survival (OS) and Toxicity Profile in

### Endoluminal Brachytherapy in Ca. Esophagus with Induction Chemotherapy and Definitive Chemoradiation. Material and Methods



31 patients with biopsy proven Esophageal Carcinoma Stage IIA-IVA with Node (-) Status were enrolled at our Institute from June 2007 to July 2018. ILRT 10Gy/2# was delivered following Definitive CTRT 50.4Gy/28# with 3-weekly CDDP/5-FU after 6-10 cycles of Paclitaxel/Carboplatin.

Proximal and Distal borders were marked from the Prechemotherapy tumor volume on OGD. Patients were simulated in a GE Multislice CT scanner to confirm accurate coverage of the pre-chemotherapy disease.

Positions were marked and secured on the Ryles Tube to prevent any shift in placement before and during treatment.

ILRT Dose was prescribed to 1 cm from the center of the source.

Swallowing Status was established on follow up. OS and DFS was censored at death or last follow up. Statistical Analysis was performed using SPSS.

#### Results

Patient Characteristics	
Total No. of Patients	31
Median Age of Recruitment	62.5 years
Distribution by Sex	
Male	20
Female	11
Distribution by Stage	
T2N0M0	3.22%
T3N0M0	87.09%
T4N0M0	9.6%
Histology	
Squamous Cell Carcinoma	87.09%
Adenocarcinoma	12.91%

- Median Age of Recruitment was 62.5 years. All 31 Patients completed treatment and were clinically stable at discharge. 83.97% Completed Chemotherapy, 96.77% completed Radiation Therapy according to protocol. 35.48% patients were alive on last follow up.
- Median OS was 21 months. OS at 2 years was 53.6%. Median DFI was 10.7 months. Those with a Cumulative EQD2 >60 Gy had a significant 5 year OS of 59.1% vs. 33.3% for those who received EQD2 <60 Gy (p=0.061, CI=76.3-91.4). 5 year DFS for EQD2 >60 Gy was 56.1% vs. 16.7% for those who received Cumulative EQD2 <60Gy (p=0.079, CI=74.2-93.8).
- There were no Grade III/IV acute toxicities. There were no Fistulas on follow up. 2 patients required stenting within 1 year of treatment and died within 2 months thereafter. 2 Patients developed CHF at 4 years. 1 Patient Developed Left Breast Fibrosis at 4.5 years.

#### Conclusion

Endoluminal Brachytherapy with Induction Chemotherapy and Definitive Chemoradiation is a feasible option in the absence of conventional alternatives.

#### PO-0804 Re-irradiation with SBRT for In-field Recurrence of Pancreatic Cancer After Prior SBRT

Y. Shen<sup>1</sup>, X. Zhu<sup>1</sup>, X. Ju<sup>1</sup>, Y. Cao<sup>1</sup>, S. Qing<sup>1</sup>, F. Cao<sup>1</sup>, H. Zhang<sup>1</sup>

<sup>1</sup>Changhai Hospital Affiliated to Second Military Medical University, Department of Radiation Oncology, Shanghai, China

#### Purpose or Objective

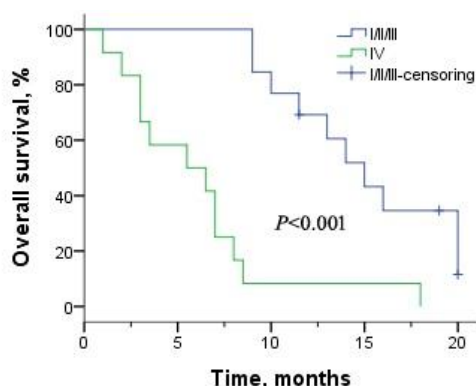
Stereotactic body radiation therapy (SBRT) is a promising alternative for pancreatic cancer with an excellent local control and acceptable toxicity. However, the safety and efficacy of SBRT for in-field recurrence after the initial SBRT remains unknown. Therefore, the aim of the study was to investigate the feasibility of re-irradiation with SBRT for local recurrent pancreatic cancer after the first SBRT.

#### Material and Methods

Twenty-six consecutive patients with pancreatic cancer received re-irradiation with SBRT after prior SBRT in our center between November 2013 and December 2016. One patient was lost to follow-up. Thirteen and twelve patients had limited disease (M0) and distant metastasis (M1) at the time of re-irradiation. Outcomes, including survival, disease control and toxicity, after treatment were evaluated in details.

#### Results

The median time between the first and second SBRT was 12.5 months (range, 6-29 months). The median prescription dose of the initial SBRT was 36Gy (range, 32-45Gy in 5-8 fractions), and of the re-irradiation with SBRT was 32Gy (range, 25-40 Gy in 5-8 fractions). The median OS of patients with M0 was 15 months (range, 9-20 months) from re-irradiation and 25 months (range, 12-42 months) from the first SBRT. Six months after re-irradiation, the percentage of disease control rate (DCR) was 77.3%. Whether patients received chemotherapy or not, CA19-9 levels declined dramatically after re-irradiation (P=0.002, 0.018). Thirteen of 18 patients (72.2%) had pain relief after re-irradiation. No Grade 4 or 5 toxicity was found during the whole treatment. One patient (4.2%) experienced late Grade 3 upper gastrointestinal hemorrhage.



### Conclusion

Re-irradiation with SBRT can provide effective analgesia and disease control with tolerable toxicity after prior SBRT for in-field recurrence, which is feasible for local relapsed pancreatic cancer. But it should be employed in highly selected patients with distant metastasis.

### PO-0805 Analysis of esophageal cancer patients treated with neoadjuvant therapy who never made it to surgery

M. Thomas<sup>1,2</sup>, L. Depypere<sup>3,4</sup>, J. Moons<sup>4</sup>, W. Coosemans<sup>3,4</sup>, T. Lerut<sup>3,4</sup>, H. Prenen<sup>5</sup>, K. Haustermans<sup>1,2</sup>, H. Van Veer<sup>3,4</sup>, P. Naftoux<sup>3,4</sup>

<sup>1</sup>KU Leuven - University of Leuven, Department of Oncology - Laboratory Experimental Radiotherapy, B-3000 Leuven, Belgium ; <sup>2</sup>UZ Leuven - University Hospitals Leuven, Department of Radiation Oncology, B-3000 Leuven, Belgium ; <sup>3</sup>KU Leuven - University of Leuven, Department of Chrometa, B-3000 Leuven, Belgium ; <sup>4</sup>UZ Leuven - University Hospitals Leuven, Department of Thoracic Surgery, B-3000 Leuven, Belgium ; <sup>5</sup>UZA - University Hospital Antwerp, Department of Oncology, B-2000 Antwerp, Belgium

### Purpose or Objective

Neoadjuvant treatment (NT) followed by esophagectomy is standard practice in patients with locally advanced resectable esophageal cancer (EC). However, not all patients who start NT will undergo esophageal resection. The aim of this study was to evaluate the group of patients, scheduled for NT followed by esophagectomy, who never made it to surgery.

### Material and Methods

We performed a retrospective institutional analysis of patients treated for locally advanced EC with NT (2002-2015), who did not undergo esophagectomy. Tumor (histology, cTNM, tumor location), patient (age, gender) and treatment related (NT regimen) characteristics were collected. The reason for cancellation of surgery and the proportion of patients with a clinical complete response (cCR) were reviewed. Subanalysis was performed according to the time period (2002-2010 vs 2011-2015) and histology (adenocarcinoma (AC) vs squamous cell carcinoma (SCC)). Median overall survival (OS) was calculated for the entire patient cohort and according to the two time frames and histology.

### Results

In 116 of 681 patients (17.0%), surgery was not performed after NT. NT treatment included chemoradiotherapy in 95 (81.9%) and chemotherapy alone in 21 (18.1%) patients. The median age of the patients not undergoing surgery was 66 years (IQR 60-70). The predominant clinical tumor stage was cT3 (75.9%) and most patients were clinically node positive (89.7%). A cCR was obtained in 23 patients (19.8%). Reasons for cancellation of surgery were disease progression in 50 (43.1%), poor general condition in 26

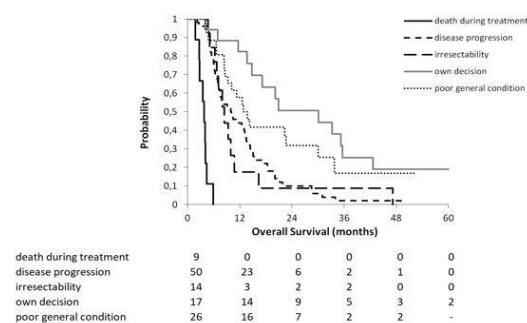
(22.4%), irresectability in 14 (12.1%), patients' own decision in 17 (14.7%); 10 of them had a cCR) and death during NT in 9 (7.8%) patients (Table 1). Patients refusing surgery had an improved median OS compared to those in whom esophagectomy was cancelled for other reasons (30.1 vs 13.8 months;  $p < 0.0001$ ) (Figure 1). In the second time period, irresectability decreased (17.4% vs 5.7%;  $p = 0.0279$ ). Median OS was not different over time (9.2 vs 12.6 months;  $p = 0.897$ ). Irresectability ( $p = 0.031$ ), patients' refusal ( $p = 0.015$ ) and poor general condition ( $p < 0.001$ ) were more frequent as reasons for cancellation in SCC patients. Median OS was 12.9 and 9.9 months for patients with an AC and a SCC ( $p = 0.485$ ), respectively. Median OS of patients in the surgery and non-surgery group was 36.5 and 10.8 months ( $p < 0.0001$ ).

Table 1: Reasons for cancellation of esophagectomy according to time period and histology.

AC = adenocarcinoma; SCC = squamous cell carcinoma

Reasons	2002-2010		2011-2015		Total (% of patient cohort without surgery)	Total (% of entire patient cohort)
	AC	SCC	AC	SCC		
Death during neoadjuvant treatment	0	4	4	1	9/116 (7.8)	9/681 (1.3)
Disease progression	14	13	15	8	50/116 (43.1)	50/681 (7.3)
Irresectability	3	8	2	1	14/116 (12.1)	14/681 (2.1)
Own decision	4	6	2	5	17/116 (14.7)	17/681 (2.5)
Poor general condition	3	8	6	9	26/116 (22.4)	26/681 (3.8)
<b>Total number of patients without surgery</b>	<b>24</b>	<b>39</b>	<b>29</b>	<b>24</b>	<b>116</b>	
<b>Total number of patients without surgery/with surgery</b>	<b>63/337 (18.7)</b>		<b>53/344 (15.4)</b>			<b>116/681 (17.0)</b>

Figure 1: Overall survival in the cohort of patients with cancelled esophagectomy



### Conclusion

One in six patients starting NT for EC never made it to surgery. Over time, irresectability as reason decreased. As a result, medical reasons became more important, indicating the paramount importance for upfront testing of medical operability. Cancellation of surgery was significantly more common in SCC patients. Reasons were medical inoperability and patients' own decision, besides a higher number of irresectable tumors. Patients who refused esophagectomy, often because of cCR, had a significant survival benefit compared to those who did not undergo esophagectomy because of other reasons.

### PO-0806 Impact of Hospital Volume and Trimodality in Survival Outcomes for Esophageal Cancer

M. Bringel oliveira duarte<sup>1</sup>, J. Barreto Campello Carvalheira<sup>2</sup>, E. Baldon Pereira<sup>1</sup>

<sup>1</sup>Hospital de Clinicas - Universidade Estadual de Campinas, Radiation Oncology, Campinas, Brazil ;

<sup>2</sup>Hospital de Clinicas - Universidade Estadual de Campinas, Clinical Oncology, Campinas, Brazil

### Purpose or Objective

Hospitals with a low volume of surgeries for esophageal cancer usually present a proportionally higher rate of complications for this procedure. However, it is unclear whether limited access to hospitals with a high volume of surgeries could influence the therapeutic plan for locally advanced esophageal squamous cell carcinoma (ESCC) in underdeveloped countries. Thus, in this population-based study, we assessed the influence of the number of treated

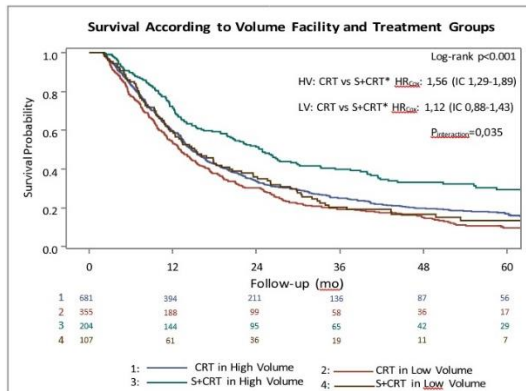
patients per hospital in the survival of patients with locally advanced ESCC submitted to chemoradiotherapy plus surgery (S+RCT) or definitive chemoradiotherapy (RCT).

#### Material and Methods

We used the Fundação Oncocentro de São Paulo (FOSP) database to identify 18 years old or older patients who received a diagnosis of stage II, or III (non-T4) ESCC between 2000 and 2013 (1347 patients and 64 hospitals). Treatments initiated 365 days after diagnosis, without T and N definition and with early mortality (until 60 days of diagnosis) were excluded. Descriptive variables were first accessed with chi-square test after categorizing hospitals as high (HH) or low volume (LH), 100 surgeries per year was used to divide the groups. Overall survival (OS) was compared with a log-rank test and with a Cox proportional hazards method, adjusting for all variables, then we tested the possible interaction between treatment type and volume facility.

#### Results

66% of patients were treated in HH hospitals, and 23% were treated with S+RCT without significative difference between facility's surgery volume and treatment performed ( $p=0,96$ ). There were more stage III ESCC treated in LH (46,1 vs 34,3%  $p<0,01$ ), more treatment initiated after 60 days of diagnosis in HH (61,0 vs 38,3%  $p<0,01$ ) and no significative age difference in volume facilities groups ( $p=0,48$ ). Median OS in months was 14,7 in HH/CRT, 24,9 in HH/S+RCT, 13,1 in LH/CRT and 15,1 in LH/S+RCT with positive association in log-rank test ( $P_{rank}<0,001$ ).



CRT: Chemoradiotherapy; HV: High Volume Hospital; LV: Low Volume Hospital; IC: Interval Confidence (accounting  $\alpha=0,05$ ); Log-rank test accounted treatment and facilities modalities; Cox Regression accounted for all variables, a Wald test was used for interaction.

In Cox analysis, female sex (HR 0,76  $p<0,01$ ) and treatment in HH (HR 0,82  $p<0,01$ ) were associated with better overall survival. Patients treated with RCT had worst OS (HR 1,38  $p<0,001$ ). After performing sensitivity analysis for treatment type and facility's surgery volume, we note a significative worst OS in those treated with CRT in HH (HR: 1,56; IC: 1,28-1,89) and no difference in that treated with CRT in LH (HR: 1,23; IC: 0,88-1,43), ( $P_{interaction}=0,035$ ).

Table 1. Multivariate analysis - Hazard Ratio for Death

Sex	HR	P
Male		
Female	0,76	0,002
Age		
18 to 50 years		
51 to 65 years	1,07	0,435
More than 65 years	0,97	0,785
Residency		
São Paulo State		
Outside São Paulo State	0,98	0,880
School Age		
Elementary Educ. Incomplete		
Elementary Educ. Complete	0,98	0,835
High School	0,85	0,171
Ignored	0,85	0,056
Time to Initiate Treatment		
Until 60 days		
After 60 days	0,99	0,902
Volume Facility		
High Volume	0,82	0,004
Low Volume		
Treatment and Diagnostic*		
Same Hospital		
Different Hospital	0,99	0,846
Year of Diagnostic*		
2000 to 2005		
2006 to 2010	0,88	0,104
2011 to 2013	0,80	0,009
Tumor Location		
Superior		
Middle	1,17	0,120
Inferior	1,24	0,095
Not Specified	1,25	0,031
Clinical stage		
II		
III	1,17	0,428
T stage		
1	0,88	0,666
2		
3	1,03	0,750
N stage		
0		
1	1,12	0,523
Treatment		
RCT	1,38	<0,001
Surgery + RCT		

\* Histologic Diagnostic; RCT: Radiochemotherapy

#### Conclusion

Although S+RCT is the gold standard for ESCC treatment, our data demonstrate different outcomes according to the facility's treatment volume. Suggesting that esophagectomy should be performed only in more experienced centers.

#### PO-0807 Heterogeneous FDG-guided dose escalation in definitive oesophageal radiotherapy: a feasibility study

H.R. Mortensen<sup>1</sup>, M. Nordsmark<sup>2</sup>, D.S. Møller<sup>3</sup>, S.N. Risum<sup>4</sup>, E. Holtved<sup>5</sup>, M. Nielsen<sup>6</sup>, B. Weber<sup>7</sup>, M. Josipovic<sup>8</sup>, L. Hoffmann<sup>9</sup>

<sup>1</sup>Aarhus University Hospital, Department of Oncology, Aarhus, Denmark ; <sup>2</sup>Aarhus University Hospital, Department of Oncology, Aarhus-, Denmark ; <sup>3</sup>Aarhus University Hospital, Department of Medical Physics, Aarhus, Denmark ; <sup>4</sup>Rigshospitalet Copenhagen University Hospital-, Department of Oncology, Copenhagen, Denmark ; <sup>5</sup>Odense University Hospital, Department of Oncology, Odense, Denmark ; <sup>6</sup>Odense University Hospital-, Laboratory of Radiation Physics, Odense, Denmark ; <sup>7</sup>Aarhus University Hospital-, Department of Oncology, Aarhus, Denmark ; <sup>8</sup>Rigshospitalet Copenhagen University Hospital-, Department of Oncology-, Copenhagen, Denmark ; <sup>9</sup>Aarhus University Hospital-, Department of Medical Physics-, Aarhus, Denmark

#### Purpose or Objective

Patients with localised esophageal and gastroesophageal junction (GEJ) cancer are offered definite chemoradiotherapy if considered non-resectable or medically inoperable. Despite treatment with curative intent a median survival of less than 20 months and a 5-year survival of 15-25% were found in clinical trials. Survival is affected by several factors, including lack of locoregional control with failures located in the treated target volumes.

A national randomized phase II study to investigate FDG-guided dose escalation in order to improve locoregional control and survival in this patient cohort is planned. Prior to final design of the randomized study, all centres participated in a delineation workshop and a treatment planning study; data from these are presented here.

#### Material and Methods

In the delineation workshop 5 patients were delineated by participants from all enrolment centres. For the treatment planning study, a common delineation was used. A homogenous dose of 50 Gy/25 fractions (fx) prescribed to the PTV is planned as the standard arm. In the experimental arm, the dose is escalated heterogeneously to the FDG-PET avid tumour volume (defined as 50% of SUV<sub>peak</sub>), with mean dose up to 63 Gy/25 fx for the most PET avid volumes of the primary tumour, and 60 Gy/25 fx for all malignant lymph nodes. The escalation dose is limited in favour of OAR constraints. A standard and an experimental treatment plan will be optimized for each patient prior to randomization. Mean dose to lungs and heart in the experimental plan must be kept within  $\pm 1$ Gy corresponding doses in the standard plan.

#### Results

Data from the target delineation workshop is presented in Table 1. Consistency of the delineated GTV-T, GTV-N and CTV volumes were acceptable. The two patients with the smallest target volumes had the largest relative range.

In the treatment planning study, the dose escalated FDG-PET avid part of tumour (PET<sub>GTV-T</sub>) constituted in median 45% (range 32% - 57%) of the GTV-T and received an average mean dose of 62.3 Gy. This resulted in an average mean dose to the GTV-T of 59.9 Gy. For the GTV-N, the average mean dose was 59.6 Gy. The combined clinical target volume (CTV-total) received an average mean dose of 55.3 Gy. Normal tissue doses were similar for the experimental and standard plan, with a difference in mean lung dose and mean heart dose in the two arms of 0.1 Gy and 0.2 Gy, respectively. The maximum dose for the standard plans was 55 Gy (110%). Higher doses up to 67 Gy were applied for the experimental plans, but only to small volumes respecting the strict normal tissue constraints (see figure)

Table 1: Median and range of target volumes for the five patients included in the delineation workshop

	GTV-T, median [range] cm <sup>3</sup>	GTV-N, median [range] cm <sup>3</sup>	CTV, median [range] cm <sup>3</sup>
Patient 1	121.7 [104.7–129.7]	4.9 [4.2–5.3]	406.1 [298.4–452.4]
Patient 2	109.0 [96.1–120.7]	No GTV-N	392.1 [337.0–466.2]
Patient 3	12.8 [11.0–40.1]	10.5 [5.9–14.1]	163.7 [129.6–313.0]
Patient 4	43.9 [41.0–43.3]	24.5 [20.6–33.0]	303.8 [246.5–326.3]
Patient 5	9.1 [7.0–14.1]	No GTV-N	71.5 [37.5–93.5]



#### Conclusion

Data from a target delineation workshop and a pilot treatment planning study suggest that FDG-guided dose

escalation in definitive radiotherapy for esophageal and GEJ cancer is feasible with similar normal tissue doses compared to standard treatment. A randomized dose escalation trial will be designed based on this knowledge.

#### PO-0808 Definitive involved-field radiotherapy for esophageal cancer: are we missing the target?

C. Viveiros<sup>1</sup>, G. Fernandez<sup>1</sup>, C. Pedro<sup>1</sup>, A. Pimenta<sup>1</sup>, L. Mirones<sup>1</sup>, M. Fortunato<sup>1</sup>, F. Santos<sup>1</sup>

<sup>1</sup>Instituto Português de Oncologia de Lisboa Francisco Gentil- EPE, Radiotherapy, Lisboa, Portugal

#### Purpose or Objective

Definitive concurrent chemoradiotherapy became the standard of care for patients with esophageal cancer not candidates to surgery. However, it is still controversial whether radiotherapy requires elective nodal irradiation (ENI) or only involved-field irradiation (IFI). The purpose of this study was to analyze failure patterns and survival in patients receiving IFI.

#### Material and Methods

Retrospective study of patients with pathologic proven esophageal cancer, not candidates to surgery, who have received IFI with curative intent, with or without concurrent chemotherapy, between January 2013 and December 2017. Comparing the target volume with radiological response, patterns of failure at the first recurrence were defined as in-field, regional out-of-field and distant failure. Response to treatment was also assessed and persistence disease was noted. Demographic data, tumor characteristics, imaging and treatment factors were recorded. Survival and disease-control outcomes were calculated from the first day of treatment with Kaplan-Meier method.

#### Results

105 patients were included, 95% with esophageal squamous cell carcinoma and 71.4% with lymph node involvement. All radiation treatments were delivered as three-dimensional conformal radiation therapy (3D-CRT) with standard fractionation (1.8Gy fraction). 93.3% with a total dose of 50.4Gy and a median overall treatment time of 39 days. 94.3% patients received concurrent chemotherapy.

With a median follow-up of 13.2 months, 33 patients (31.4%) had persistent disease, most of whom evolved with distant metastasis (11) and out-of-field recurrences (4). Amongst the patients with complete response (72), there were 5 cases of out-of-field recurrences (only 2 of which were isolated out-of-field relapses, and both were in regions that would not have been included in ENI), 9 with in-field recurrences and 22 with distant metastasis. The median dose at sites where out-of-field relapse occurred was 13.8Gy (1-44 Gy). 21 patients (20%) had mixed failure patterns on the first evidence of disease failure (persistence and/or recurrence).

Median overall survival (OS) was 11.6 months (95% CI 8.2-14.9 months). There were significant differences in OS for patients with and without disease persistence (median OS 10.2 months vs 13 months,  $p < 0.05$ ). Median time to in-field, out-of-field and distant recurrences was 17.3 months (CI 95% 0-38 months), 9.7 months (CI 95% 0-25months) and 8.2 months (CI 95% 6.8-9.7 months), respectively.

Table 1. Patient characteristics		
CLINICAL PARAMETERS		N (%)
Gender		
Male		96 (91.4)
Female		9 (8.6)
Age (years)		
Median		62
Range		40 - 82
Other malignant tumor history		
		35 (33.3)
Histology		
Squamous cell carcinoma		100 (95.2)
Adenocarcinoma		4 (3.8)
Undifferentiated carcinoma		1 (1)
Location		
Cervical		24 (22.9)
Upper thoracic		29 (27.6)
Mid-thoracic		27 (25.7)
Lower thoracic		25 (23.8)
T stage		
T1		5 (4.8)
T2		9 (8.6)
T3		50 (47.6)
T4		23 (22)
Unknown		18 (17)
N stage		
N0		30 (28.6)
N+		75 (71.4)
Tumor length (cm)		
Median		6
Range		1 - 14
<sup>18</sup> F-FDG PET-TC Staging		
		99 (94.3)
Esophageal Tumor SUV		
Median		12
Range		2 - 48
No FDG uptake		3 (2.9)
Concurrent chemotherapy		
		99 (94.3)
Cisplatin and fluorouracil		44 (41.9)
Paclitaxel and carboplatin		43 (41)
Cisplatin		8 (7.6)
Carboplatin		2 (1.9)
Unknown		2 (1.9)

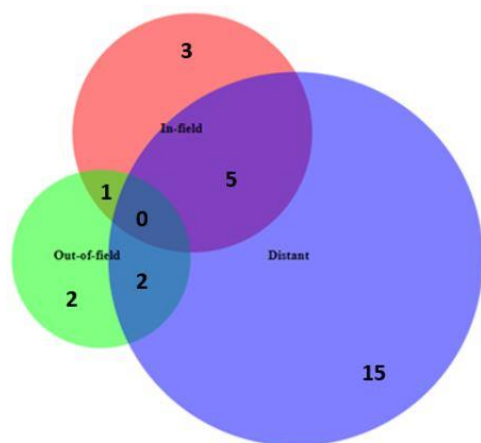


Figure 1. Failure patterns amongst patients with complete response

## Conclusion

Tumor persistence and distant recurrence were the main patterns of lack of disease control. Persistence after (chemo)radiotherapy negatively impacted survival. Out-of-field was the least frequent recurrence pattern. It is acceptable to maintain IFI technique.

## PO-0809 Gross Tumor Volume delineation in pancreatic cancer using MRI: final results of a multicenter study.

L. Caravatta<sup>1</sup>, F. Cellini<sup>2</sup>, N. Simoni<sup>3</sup>, C. Rosa<sup>1</sup>, R.M. Niespolo<sup>4</sup>, M. Lupattelli<sup>5</sup>, V. Picardi<sup>6</sup>, G. Macchia<sup>6</sup>, A. Sainato<sup>7</sup>, G. Mantello<sup>8</sup>, F. Dionisi<sup>9</sup>, M.E. Rosetto<sup>10</sup>, V. Fusco<sup>11</sup>, F. Navarra<sup>12</sup>, A. De Paoli<sup>12</sup>, A. Guido<sup>13</sup>, C. Vecchi<sup>14</sup>, R. Basilico<sup>15</sup>, R. Cianci<sup>16</sup>, A. Delli Pizzi<sup>17</sup>, M. Di Nicola<sup>18</sup>, G.C. Mattiucci<sup>2</sup>, V. Valentini<sup>2</sup>, A.G. Morganti<sup>13</sup>, D. Genovesi<sup>1</sup>

<sup>1</sup>"SS Annunziata" Hospital- "G. D'Annunzio" University, Radiation Oncology Unit, Chieti, Italy ; <sup>2</sup>Gemelli Advanced Radiation Therapy Center- Fondazione Policlinico Universitario "A. Gemelli"- Catholic University of Sacred Heart, Radiotherapy Unit, Rome, Italy ; <sup>3</sup>Azienda Ospedaliera Universitaria, Radiotherapy Unit, Verona, Italy ; <sup>4</sup>Azienda Ospedaliera S. Gerardo, Department of Radiation Oncology, Monza, Italy ; <sup>5</sup>University of Perugia and Perugia General Hospital, Radiation Oncology Section, Perugia, Italy ; <sup>6</sup>"Giovanni Paolo II" Foundation- Catholic University of Sacred Heart, Radiotherapy Unit- Department of Oncology, Campobasso, Italy ; <sup>7</sup>Azienda Ospedaliera Universitaria Pisana, Radiotherapy Unit, Pisa, Italy ; <sup>8</sup>State Hospital, Department of Radiotherapy, Ancona, Italy ; <sup>9</sup>Azienda Provinciale per i Servizi Sanitari- APSS-, Proton Therapy Unit- Department of Oncology, Trento, Italy ; <sup>10</sup>Ospedale Belcolle, Department of Radiation Oncology, Viterbo, Italy ; <sup>11</sup>Centro di Riferimento Oncologico Regionale, Department of Radiation Oncology, Rionero in Vulture-Potenza, Italy ; <sup>12</sup>Centro di Riferimento Oncologico-National Cancer Institute, Department of Radiation Oncology, Aviano, Italy ; <sup>13</sup>University of Bologna- S. Orsola-Malpighi Hospital, Radiation Oncology Center- Department of Experimental- Diagnostic and Specialty Medicine - DIMES, Bologna, Italy ; <sup>14</sup>Tecnologie Avanzate, Srl, Torino, Italy ; <sup>15</sup>"SS Annunziata" Hospital- "G. D'Annunzio" University, Department of Radiology, Chieti, Italy ; <sup>16</sup>"SS Annunziata" Hospital- "G. D'Annunzio" University, Department of Radiology, Chieti, Italy ; <sup>17</sup>"SS Annunziata" Hospital- "G. D'Annunzio" University, Department of Radiology, Chieti, Italy ; <sup>18</sup>"G. D'Annunzio" University, Laboratory of Biostatistics- Department of Medical- Oral and Biotechnological Sciences, Chieti, Italy

## Purpose or Objective

Variations in volume delineation in pancreatic cancer have been reported in previous studies. Thanks to the high soft tissue resolution, Magnetic Resonance Imaging (MRI) could improve the accuracy of tumor delineation in pancreatic cancer compared to Computed Tomography (CT). Since recommendations for pancreatic cancer contouring using MRI have been recently provided, a multi-institutional contouring dummy-run study was proposed to evaluate the impact of MRI on inter-observer agreement in Gross Tumor Volume (GTV).

## Material and Methods

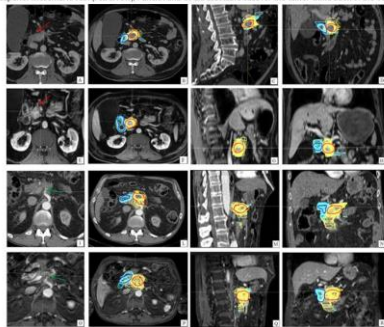
The study group for gastrointestinal cancers of the Italian Association of Radiation Oncologists (AIRO) proposed a multicenter contouring study to the centers interested in pancreatic cancer treatment. Two clinical cases of borderline resectable (Case 1) and locally advanced unresectable (Case 2) pancreatic cancer were selected by two radiologists and two radiation oncologists expert in pancreatic cancer. In two sequential steps, diagnostic contrast-enhanced CT scan and 1.5T MRI sequences were

sent to the participating centers. CT-GTVs were contoured while blinded to MRI data sets. Dice Similarity Index was used to evaluate the spatial overlap accuracy of both GTVs of all centers with respect to a national benchmark, identified on the basis of per-year high volume pancreatic cancer treatment center.

### Results

Thirty-one radiation oncologists from different Institutes joined the study and submitted the delineated volumes for both cases on CT scans and MRI images, respectively (Figure 1). CT- and MRI-GTV volumes were  $21.6 \pm 9.0 \text{ cm}^3$  and  $17.2 \pm 6.0 \text{ cm}^3$ , respectively for Case 1, and  $31.3 \pm 15.6 \text{ cm}^3$  and  $33.2 \pm 20.2 \text{ cm}^3$ , respectively for Case 2. MRI-GTV mean volume resulted significantly smaller than CT-GTV in the borderline resectable case ( $p < 0.05$ ), whereas no significant GTV differences between the two different imaging modalities were reported in Case 2. A substantial agreement was shown by the median DICE index for CT- and MRI-GTV resulting as 0.74 (IQR: 0.67-0.75) and 0.61 (IQR: 0.57-0.67) for Case 1; a moderate agreement was instead reported for Case 2: 0.59 (IQR: 0.52-0.66) and 0.53 (IQR: 0.42-0.62) for CT- and MRI-GTV, respectively.

Figure 1. Graphic representation on axial (Panels A, B, E, F, I, L, O and P), sagittal (Panels C, G, M and Q) and coronal (Panels D, H, N and R) planes of inter-observer variation between 31 Centers for CT (Panels A, B, C and D) and MRI (Panels E, F, G and H) GTV and duodenum of Case 1 (borderline resectable) and for CT (Panels I, L, M and N) and MRI (Panels O, P, Q and R) GTV and duodenum of Case 2 (unresectable). GTV and duodenum benchmark delineations are represented in red and blue solid outline, respectively. Yellow and light blue solid outlines represent GTVs and duodenum contours of the remaining 30 participating Centers. Panels A, E, I and O represent axial CT and MRI images of Case 1 (borderline resectable) and Case 2 (unresectable) without contours. Panels A and E: borderline resectable case for the encasement of the superior mesenteric vein (red arrow); Panels I and O: unresectable case for the tumor infiltration of the colon trunk (green arrow).



### Conclusion

DICE index for GTV delineation agreement was acceptable in the borderline resectable case, whereas a larger overlap deviations was recorded in the unresectable case, suggesting that the major issues in the outlining of macroscopic disease are present when vascular structures are more involved. Based on these results, CT scan, thanks to its high definition of tumor vessels infiltration, can still be considered as the gold standard for volume delineation in pancreatic cancer, especially in unresectable patients. Instead, since diagnostic MRI resulted in smaller GTV in borderline resectable case, the integration of the two imaging methods could offer an improved accuracy of target delineation when radiotherapy is delivered with more conformed techniques such as IMRT, VMAT and/or SBRT.

### PO-0810 Outcome following definitive radiotherapy in oesophageal cancer: A single UK centre experience.

S. Mehta<sup>1</sup>, A. Mcpartlin<sup>1</sup>, C. Hodgson<sup>1</sup>, G. Radhakrishna<sup>1</sup>, L. Bhatt<sup>1</sup>, H. Sheikh<sup>1</sup>

<sup>1</sup>The Christie NHS Foundation Trust, Clinical Oncology, Manchester, United Kingdom

### Purpose or Objective

Definitive chemo radiotherapy (dCRT) is the standard of care for inoperable oesophageal cancer patients, however, a large proportion are not suitable due to multiple factors such as co-morbidities or poor performance status. For this group definitive radiotherapy (dRT) alone may be considered. The consensus guidelines are lacking in this regards with wide variation in doses/ techniques of radiotherapy. Here we report our

experience of patients treated with dRT at one of the largest cancer centre in UK.

### Material and Methods

A total of 138 patients who received dRT for oesophageal cancer at the Christie hospital, Manchester, UK, from December 2009 to October 2013 were considered for the analysis. Radiotherapy was initially delivered using 3 field 3D conformal radiotherapy (3D-CRT) and subsequently 5-8-field intensity modulated therapy (IMRT) as practice evolved. Patients were followed up routinely in outpatient clinic after treatment at 3 monthly intervals for one year and then less frequently. Routine re-staging was not performed but investigations were carried out for concerning new or unresolving symptoms. Statistical analysis was performed using SPSS version 21. Survival was calculated from the first day of radiotherapy using the Kaplan-Meier technique and effect of disease characteristics tested using the log rank test. There was a minimum of 12 months follow up following completion of treatment.

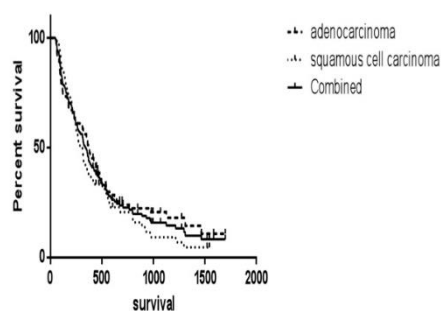
### Results

All patients commenced a course of 55 Gray (Gy) in 20 daily fractions over four weeks, with the exception of seven patients who received 50.4 Gy in 28 daily fractions over five and one half weeks due the volume of stomach involved by GOJ tumours. IMRT was received by 92.0% (127) of patients with the remaining 8.0% (11) treated with 3D-CRT. The demographics of patients and tumour characteristics are shown in table-1. The median follow up time was 22.9 months (range 11.9-55.8) in the 23 survivors at time of analysis and 11.1 months (range 1.5-55.8) in all patients. Post treatment swallow function was recorded at four to twelve weeks post radiotherapy in 78% (80) of patients with dysphagia at initial presentation. Improvement was noticed in 55% (44), stable swallow in 13% (11) and worsened swallow in 32% (26). Of the 138 patients treated, 4 failed to complete the intended radiotherapy course. The symptomatic oesophagitis was experienced by 81.6% (112) with strong opioid analgesics required during treatment or in the six weeks post treatment by 35.5% (49) of patients. Median overall survival (OS) from the start of radiotherapy was 11.1 months with a four year OS of 8.2%. There was no significant difference observed based on histology e.g. median OS for adenocarcinoma and squamous cell carcinoma was 12.1 vs. 9.8 months respectively (log rank,  $p = 0.27$ ) (figure-1).

Table 1: Patient characteristics

Characteristics	Squamous (N=56)	Adenocarcinoma (N=82)	Total (N=138)
Age	Median (range) 80 (49-92)	78 (55-91)	79 (49-92)
Gender	Male 24 (42.9%)	58 (70.7%)	82 (59.4%)
	Female 32 (57.1%)	24 (29.3%)	56 (40.6%)
Performance Status	0 5 (8.9%)	5 (6.1%)	10 (7.2%)
	1 27 (48.2%)	37 (45.1%)	64 (46.4%)
	2 20 (35.8%)	35 (42.7%)	55 (39.9%)
	3 4 (7.1%)	5 (6.1%)	9 (6.5%)
	4 15 (26.8%)	5 (6.1%)	20 (14.5%)
ACE-27 score	1 18 (32.1%)	26 (31.7%)	44 (31.9%)
	2 14 (25.0%)	33 (40.3%)	47 (34.1%)
	3 6 (10.7%)	16 (19.5%)	22 (15.9%)
	Not recorded 3 (5.4%)	2 (2.4%)	5 (3.6%)
	4 9 (16.1%)	26 (31.7%)	35 (25.4%)
O'Rourke dysphagia score	1 13 (23.2%)	17 (20.7%)	30 (21.7%)
	2 22 (38.2%)	28 (34.1%)	50 (36.3%)
	3 10 (17.9%)	8 (9.8%)	18 (13.0%)
	4 2 (3.6%)	3 (3.7%)	5 (3.6%)
	5 2 (3.6%)	3 (3.7%)	5 (3.6%)
Pre-treatment weight-loss	<10% 25 (44.6%)	48 (58.6%)	73 (53.0%)
	≥10% 17 (30.4%)	12 (14.6%)	29 (21.0%)
	Not recorded 14 (25.0%)	22 (26.8%)	36 (26.0%)
Nutritional support	None 23 (41.1%)	44 (53.7%)	67 (48.5%)
	Stent 7 (12.5%)	6 (7.3%)	13 (9.4%)
	RIG 25 (44.6%)	30 (36.6%)	55 (39.9%)
	RIG + stent 1 (1.8%)	2 (2.4%)	3 (2.2%)
Disease site within oesophagus	Upper 4 (7.1%)	0	4 (2.9%)
	Middle 24 (42.9%)	6 (7.3%)	30 (21.7%)
	Lower 27 (48.2%)	51 (62.2%)	78 (56.6%)
Stage	GOJ 1 (1.8%)	25 (30.5%)	26 (18.8%)
	IA 5 (8.9%)	10 (12.2%)	15 (10.9%)
	IB 5 (8.9%)	15 (18.3%)	20 (14.5%)
	IIA 3 (5.4%)	0	3 (2.2%)
	IIB 12 (21.4%)	27 (32.8%)	39 (28.3%)
	IIIA 27 (48.2%)	24 (29.3%)	51 (36.8%)
	IIIB 0	3 (3.7%)	3 (2.2%)
Radiotherapy technique	3D-CRT 2 (3.6%)	9 (11.0%)	11 (8.0%)
	IMRT 54 (96.4%)	73 (89.0%)	127 (92.0%)
Follow-up (months)	Median (range) 10.3 (2-51)	12.6 (2-56)	11.1 (2-56)

Figure 1: Kaplan Meier survival curve for histological sub-type



## Conclusion

High dose dRT alone appears to offer the chance of long-term survival in around 10% for oesophageal patients not fit for surgery or dCRT and should be considered instead of palliative measures only

## PO-0811 SBRT compared to sorafenib in locally advanced hepatocellular carcinoma: a propensity score analysis

E. Gkika<sup>1</sup>, T. Brunner<sup>2</sup>, N. Abbasi-Senger<sup>3</sup>, H. Alheit<sup>4</sup>, W. Baus<sup>5</sup>, O. Blanck<sup>6</sup>, S. Gerum<sup>7</sup>, M. Guckenberger<sup>8</sup>, D. Habermehl<sup>9</sup>, C. Ostheimer<sup>10</sup>, O. Riesterer<sup>8</sup>, J. Tamihardja<sup>11</sup>, D.J. Pinato<sup>12</sup>, L. Rimassa<sup>13</sup>, T. Pressiani<sup>13</sup>, M. Schultheiss<sup>14</sup>, R. Sharma<sup>12</sup>, M.E. Burlone<sup>15</sup>, M. Pirisi<sup>15</sup>,

M. Kudo<sup>16</sup>, J.W. Park<sup>17</sup>, C. Neumann-Haefelin<sup>18</sup>, A. Grosu<sup>19</sup>, R. Thimme<sup>18</sup>, D. Bettinger<sup>18</sup>

<sup>1</sup>Uniklinik Freiburg, Radiation Oncology, Freiburg, Germany ; <sup>2</sup>University of Magdeburg, Radiation Oncology, Magdeburg, Germany ; <sup>3</sup>University of Jena, Radiation Oncology, Jena, Germany ; <sup>4</sup>Radiotherapy Distler, Radiotherapy Distler, Bautzen, Germany ; <sup>5</sup>University Hospital of Cologne, Radiation Oncology, Cologne, Germany ; <sup>6</sup>University Medical Center Schleswig-Holstein- Campus Kiel, Department of Radiation Oncology, Kiel, Germany ; <sup>7</sup>Ludwig-Maximilians-University Munich, Department of Radiation Oncology, Munich, Germany ; <sup>8</sup>University Hospital of Zurich, Department of Radiation Oncology, Zurich, Switzerland ; <sup>9</sup>Klinikum Rechts der Isar- TU Munich, Department of Radiation Oncology, Munich, Germany ; <sup>10</sup>Martin Luther University Halle Wittenberg, Department of Radiation Oncology, Halle an der Saale, Germany ; <sup>11</sup>University Hospital of Würzburg, Department of Radiation Oncology, Würzburg, Germany ; <sup>12</sup>Imperial College London- Hammersmith Hospital, Department of Surgery and Cancer, London, United Kingdom ; <sup>13</sup>Humanitas Cancer Center- Humanitas Clinical and Research Center, Medical Oncology and Hematology Unit, Milan, Italy ; <sup>14</sup>Medical Center University of Freiburg, Department of Medicine II-, Freiburg, Germany ; <sup>15</sup>Università degli Studi del Piemonte Orientale "A. Avogadro", Department of Translational Medicine, Novara, Italy ; <sup>16</sup>Kindai University School of Medicine, Department of Gastroenterology and Hepatology, Osakasayama, Japan ; <sup>17</sup>National Cancer Center Hospital, Center for Liver Cancer, Goyang, Korea Republic of ; <sup>18</sup>Medical Center University of Freiburg, Department of Medicine II, Freiburg, Germany ; <sup>19</sup>Medical Center University of Freiburg, Department of Radiation Oncology, Freiburg, Germany

## Purpose or Objective

Stereotactic body radiation therapy (SBRT) has emerged as a safe and effective treatment for patients with hepatocellular carcinoma (HCC), but its role in advanced HCC is not well defined. In this study we aim to assess the efficacy of SBRT in comparison to sorafenib treatment in patients with advanced HCC.

## Material and Methods

We included 901 patients treated with sorafenib at six tertiary centers in Europe and Asia and 122 patients treated with SBRT from thirteen centers in Germany and Switzerland. Medical records were reviewed including laboratory parameters and treatment characteristics. Propensity score matching was performed to adjust for differences in baseline characteristics. The primary endpoint was overall survival (OS) and progression-free survival (PFS).

## Results

Median OS of SBRT patients was 18.1 [10.3 - 25.9] months compared to 8.8 [8.2 - 9.5] months in patients treated with sorafenib. After adjusting for different baseline characteristics, the survival benefit for patients treated with SBRT was still preserved with a median OS of 17.0 [10.8 - 23.2] months compared to 9.6 [8.6 - 10.7] months in patients treated with sorafenib. SBRT of intrahepatic lesions in patients with extrahepatic metastases was also associated with improved OS compared to patients treated with sorafenib in the same setting (17.0 vs 10.0 months,  $p=0.012$ ) whereas in patients with portal vein thrombosis (PVT) there was no survival benefit in patients with SBRT.

## Conclusion

In this retrospective comparative study, SBRT was superior compared to sorafenib in patients with advanced HCC.

## PO-0812 Pathological validation of endoscopically placed fiducials on tumor borders in esophageal cancer.

M. Machiels<sup>1</sup>, M.L. Van Montfort<sup>2</sup>, N.B. Thuijs<sup>2</sup>, M.I. Van Berge Henegouwen<sup>3</sup>, J.E. Van Hooft<sup>4</sup>, T. Alderliesten<sup>1</sup>, S.L. Meijer<sup>2</sup>, M.C.C.M. Hulshof<sup>1</sup>  
<sup>1</sup>Amsterdam UMC- locatie AMC, Radiation Oncology, Amsterdam, The Netherlands ; <sup>2</sup>Amsterdam UMC- locatie AMC, Pathology, Amsterdam, The Netherlands ; <sup>3</sup>Amsterdam UMC- locatie AMC, Upper GE Surgery, Amsterdam, The Netherlands ; <sup>4</sup>Amsterdam UMC- locatie AMC, Gastroenterology, Amsterdam, The Netherlands

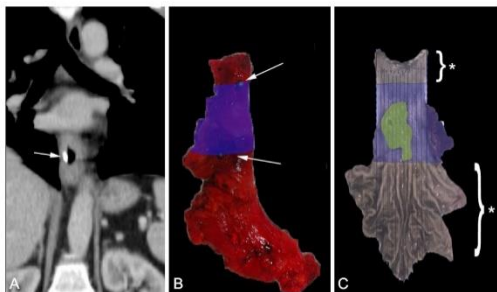
### Purpose or Objective

The microscopic tumor extension beyond the macroscopic tumor borders of esophageal cancer is scarcely investigated. Nonetheless this information is crucial for determining the clinical target volume (CTV) in radiation therapy [1]. Modern innovations in gross tumor volume (GTV) determination allow delineation with the aid of (echo)endoscopically placed fiducial markers on the tumor borders. The question arises whether the current voluminous clinical target volume (CTV) margins of 3-5 cm around the GTV to account for microscopic extension - based on one study solely - are still accurate [1]. In the present study, we analysed microscopic spread beyond the (echo)endoscopically determined tumor border (EDTB) with the use of fiducial markers at the tumor borders. Furthermore, we validated the use of fiducial markers placed on the EDTB as a surrogate for macroscopic tumor borders.

### Material and Methods

Thirty-two consecutive esophageal cancer patients were included in this study. All patients were treated with neoadjuvant chemoradiotherapy and fiducial markers were (echo)endoscopically implanted before treatment at the cranial and caudal tumor borders. The surgical specimens of all patients were collected from the operation room, fiducial marker positions were detected under CT guidance and demarcated with beads, and subsequently analysed at the pathology department for macroscopic and microscopic spread beyond the demarcations (EDTB) (Figure 1). Per specimen a shrinkage rate was calculated (i.e., distance between fiducial markers ex-vivo divided by distance between fiducial markers in-vivo). A logistic regression analysis was performed to determine predicting factors for microscopic spread beyond EDTB (significance level  $\alpha=0.05$ ).

**Figure 1.** A: Pre-operative CT scan of patient 3 in coronal view with caudal fiducial visible. Arrow indicates fiducial marker. B: Esophageal specimen exterior of patient 3 with blue inked area: (echo)endoscopically determined tumor area between both (echo)endoscopically determined tumor borders. Arrows indicate fiducial positions cranially and caudally, demarcated externally with green bead. C: Esophageal specimen interior of patient 3. Blue inked area: (echo)endoscopically determined tumor area. Green overlay: residual tumor left. Asterix indicates area examined for macroscopic and microscopic tumor spread.



### Results

A total of 60 EDTB were examined in 32 patients. As listed in Table 1, 16/32 (50%) of patients had a Mandard 3 or higher (i.e., residual tumor group) and were included for analysis of microscopic tumor spread analysis. In the residual tumor group, only 3/16 (19%) patients had microscopic spread beyond the cranial EDTB, and 4/16 (25%) had microscopic spread beyond the caudal EDTB. The mean microscopic spread beyond EDTB was 7 mm cranially (range: 6 - 9 mm) and 13.5 mm caudally (range:

5.8 - 20 mm). This extension was corrected for each individual determined shrinkage rate (mean: 93%). The presence of microscopic spread of cancer beyond EDTB was only significantly associated with initial tumor length ( $p = 0.028$ ). None of the patients had macroscopic tumor spread beyond the EDTB.

**Table 1.** Tumor, fiducial marker implantation and pathologic characteristics. Abbreviations: EDTB = (echo)endoscopically determined tumor border; GEJ = junctiontumor; EUS = echoendoscopy.

Tumor characteristics	N = 32 (%)	Microscopic tumor beyond EDTB N = 7 (%)
<b>Clinical T-classification</b>		
cT1	2 (6)	1 (14)
cT2	15 (47)	3 (43)
cT3	15 (47)	3 (43)
cT4	0	0 (0)
<b>Clinical N-classification</b>		
cN0	18 (56)	5 (71)
cN1	10 (32)	2 (29)
cN3	4 (13)	0 (0)
<b>Histology</b>		
adenocarcinoma	24 (75)	6 (86)
squamous cell carcinoma	8 (25)	1 (14)
<b>Location</b>		
mid-thoracic	6 (19)	1 (14)
distal	19 (59)	3 (43)
GEJ	7 (22)	3 (43)
<b>Implantation characteristics</b>		
<b>Technique</b>		
EUS	10 (32)	1 (14)
endoscopy combination	19 (59)	4 (57)
combination	3 (9)	2 (29)
<b>Fiducial on EDTB</b>		
yes	26 (81)	6 (86)
no	6 (19)	1 (14)
<b>Pathology characteristics</b>		
<b>Tumor regression grade</b>		
Mandard 1	9 (28)	0 (0)
Mandard 2	7 (22)	1 (14)
Mandard 3	11 (34)	4 (57)
Mandard 4	5 (16)	2 (29)
Mandard 5	0 (0)	0 (0)

### Conclusion

No macroscopic tumor was found beyond the EDTB. Only 19% and 25% of respectively the cranial and caudal EDTB, were traversed with a mean of 7 mm - 13.5 mm, and a maximum of 20 mm microscopic tumor. Our results indicate that current recommended CTV margins around the GTV to compensate for microscopic tumor along the esophageal wall can be reduced when the GTV is determined with the aid of fiducial markers.

[1]X.-S.Gao,et

al. *Int.J.Radiat.Oncol.Biol.Phys.* 2007;67:389-396.

### PO-0813 A Phase I/II Study of durvalumab and stereotactic radiotherapy in locally advanced pancreatic cancer

R. Tuli<sup>1</sup>, N. Nisen<sup>2</sup>, S. Lo<sup>3</sup>, V. Placencio<sup>1</sup>, G. Gresham<sup>3</sup>, A. Hendifar<sup>3</sup>

<sup>1</sup>Cedars-Sinai Medical Center, Radiation Oncology, los angeles, USA ; <sup>2</sup>Cedars-Sinai Medical Center, Surgery, Los Angeles, USA ; <sup>3</sup>Cedars-Sinai Medical Center, Medicine, los Angeles, USA

### Purpose or Objective

Previous studies targeting the PD-1/PD-L1 pathway in varying tumor types have shown blockade of this pathway can enhance the efficacy of radiotherapy (RT). However, no such data is available in pancreatic cancer (PC) and no significant responses have been seen in this disease with immune checkpoint blockade. Our group and others have observed the effect of both chemotherapy and RT is enhanced in PC by targeting the PD-1/PD-L1 pathway, and the degree of this response is dependent upon the native expression of PD-1/PD-L1. These data led us to hypothesize that the clinical efficacy of RT in PC can be enhanced with concurrent PD-L1 blockade. Herein, we report interim results of an ongoing phase 1/2 clinical trial in locally advanced (LA) and borderline resectable (BR) PC (NCT03245541).

### Material and Methods

Patients with LA or BR PC treated with standard of care gemcitabine and nab-paclitaxel for 3 to 6 cycles were enrolled. Treatment consisted of durvalumab (750 mg Q14

days) on D1. Stereotactic ablative radiotherapy (SABR; 6.6 Gy/fraction) was delivered every other day x 5 fractions beginning D8. Durvalumab continued as maintenance Q14 days until resection or progression. The run-in phase 1 utilized a standard 3+3 design prior to phase 2 expansion. Dose limiting toxicities (DLTs), adverse events (AEs) and serious adverse events (SAEs) were assessed during the first 10 weeks of study treatment. CT scans were obtained every 2 months for response assessment. Endoscopic research biopsies were obtained pre- and 6-8 weeks post-SABR, and weekly blood samples were obtained on D1, weekly for 10 weeks, and then every 2 months until resection or progression to assess for immune correlates of response.

### Results

Since 8/2017, 15 of 30 planned patients were enrolled of which 9 (60%) are LA and 6 (40%) were BR. Median age was 70 and 8 (53%) were female. No DLTs were identified in the phase 1 run in and enrollment in the phase 2 study continues. Grade 3 toxicities have been identified in 2 patients (nausea, anorexia). Ten patients have discontinued study treatment due to surgery (n=6) and disease progression (n=4; local = 1, distant = 2, local+distant = 1). All resections have been margin-negative. Objective response rates (RECIST 1.1) included SD (n=9) and PR (n=6). Two patients have died. Median PFS has not been reached.

### Conclusion

To our knowledge, this is the first report of a PD-L1 inhibitor-RT combination in LA PC. The regimen was safe, well tolerated and appears to be clinically active with high rates of margin-negative resection.

## Poster: Clinical track: Lower GI (colon, rectum, anus)

### PO-0814 Clinical target volume in radiation therapy for organ preservation in T2 rectal cancer

J. Socha<sup>1</sup>, L. Pietrzak<sup>2</sup>, A. Zawadzka<sup>3</sup>, A. Paciorkiewicz<sup>3</sup>, A. Krupa<sup>2</sup>, K. Bujko<sup>2</sup>

<sup>1</sup>Military Institute of Medicine, Department of Radiotherapy, Warsaw, Poland; <sup>2</sup>Maria Skłodowska-Curie Memorial Cancer Centre, Department of Radiotherapy I, Warsaw, Poland; <sup>3</sup>Maria Skłodowska-Curie Memorial Cancer Centre, Medical Physics Department, Warsaw, Poland

#### Purpose or Objective

There are no guidelines on clinical target volume (CTV) delineation for cT2 rectal cancer treated with organ preservation.

#### Material and Methods

A systematic review and meta-analysis were performed to determine the extent of distal mesorectal (DMS) and distal intramural spread (DIS), the risk of lateral lymph node (LLN) metastases in pT2 tumours, and regional recurrence pattern after organ preservation.

#### Results

The rate of DMS >1 cm was 1.9% (95% CI: 0.4%-5.4%), maximum extent: 1.3 cm. The rate of DIS >0.5 cm was 4.7% (95% CI: 1.3%-11.5%), maximum extent: 0.8 cm. The rate of LLN metastases was 8.2% (95% CI: 6.7%-9.9%) for tumours below or at peritoneal reflexion and 0% for higher tumours. Regional nodal recurrences alone (i.e. without concomitant intraluminal recurrences) were recorded in 1.1% (95% CI: 0.5%-1.7%) of patients after watch-and-wait and in 2.1% (95% CI: 1.2%-3.4%) after preoperative radiotherapy and local excision. Thus, the following rules for CTV delineation are proposed: caudal border 1.5 cm from the tumour to account for DMS or 1 cm to account for DIS, whichever is more caudal; cranial border at S2/S3 interspace; inclusion of LLN for tumours at or below peritoneal reflexion (see Table 1, Figure 1). A planning study was performed in eight patients to compare dose-

volume parameters obtained using these rules to that obtained using current guidelines for advanced cancers. The proposed rules led to a mean 18% relative reduction of planning target volume, which resulted in better sparing of at-risk organs.

### Conclusion

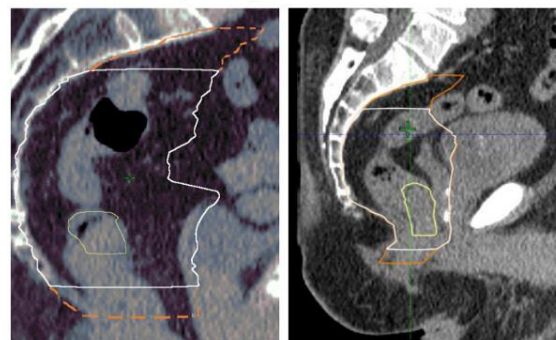
This meta-analysis suggests a smaller CTV for cT2 tumours than the current guidelines designed for advanced cancers.

Table 1. Proposed CTV borders in radiation therapy for organ preservation in patients with cT2 tumour.

Caudal border	1.5 cm caudally from the tumour to account for DMS or 1 cm caudally from the tumour to account for DIS, whichever is more caudal (see Figure 1).
Cranial border	S2/S3 interspace.
Lateral border	Pelvic wall for tumours with lower border located below or at the peritoneal reflexion to include LLNs. Mesorectal fascia for tumours with lower border located above the peritoneal reflexion.

DMS - distal mesorectal spread; DIS - distal intramural spread, LLN - lateral lymph node.

Figure 1. Comparison of clinical target volume (CTV) obtained after applying the proposed rules to that obtained after using the current guidelines.



A: cT2 cancer situated 6 cm from the anal verge. CTV<sub>proposed</sub>: white; CTV<sub>standard</sub>: orange.  
B: cT2 cancer situated 3 cm from the anal verge. CTV<sub>proposed</sub>: white; CTV<sub>standard</sub>: orange.

### PO-0815 Stereotactic radiation therapy in colorectal cancer brain metastasis: a multicentric cohort

A. Paix<sup>1</sup>, F. Thillays<sup>2</sup>, J. Biau<sup>3</sup>, N. Vulquin<sup>4</sup>, I. Pop<sup>5</sup>, K. Debbi<sup>6</sup>, A.L. Grosu<sup>5</sup>, G. Noël<sup>1</sup>

<sup>1</sup>Centre Paul Strauss, Radiothérapie, Strasbourg, France; <sup>2</sup>Institut Cancérologique de l'ouest, Radiothérapie, Saint Herblain, France; <sup>3</sup>Centre Jean Perrin, Radiothérapie, Clermont-Ferrand, France; <sup>4</sup>Centre Georges-François Baclesse, Radiothérapie, Dijon, France; <sup>5</sup>Universitätsklinikums, Klinik für Strahlenheilkunde, Freiburg, Germany; <sup>6</sup>Centre Henry Kaplan - CHU Tours, Radiothérapie, Tours, France

#### Purpose or Objective

Colorectal cancer (CRC) is the third most common cancer in western countries, but brain metastases only occur in 1% of CRC patients. Overall survival in CRC patients rises as new systemic drugs became available. Thus the incidence of brain metastases in CRC patients will likely increase. We conducted a multicentric analysis to evaluate and compare the outcomes of stereotactic radiosurgery (SRS) and hypofractionated stereotactic radiotherapy (HFSRT) in CRC brain metastasis management.

#### Material and Methods

On behalf of the association of French-speaking neuro-oncologist (ANOCEF), we retrospectively collected individual data of patients treated with SRS or HFSRT for CRC brain metastases in 6 hospitals in France and Germany.

The primary endpoint of the study was the radiological response rate define as a complete response, partial response or stability of the metastasis according to RANO

BM criteria. A Bayesian multivariate logistic regression was performed to evaluate the influence of several factors on the probability of response. Secondary endpoints included overall survival (OS) and brain progression-free survival (BPF5).

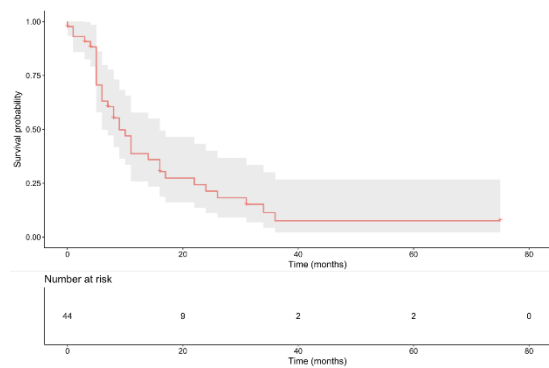
### Results

This international, multicentric retrospective analysis involved 58 patients and 69 metastases.

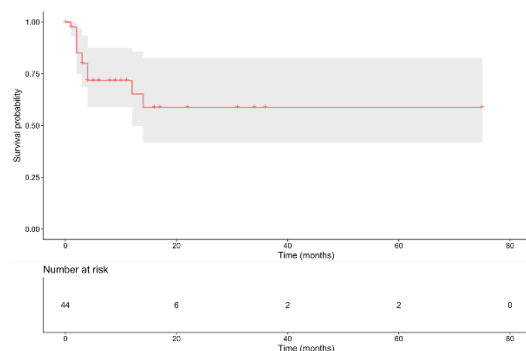
The median response rate for metastasis treated was 65.9% (CI 95% [51.9% - 79.9%]) and was positively influenced by SRS whereas multiple brain metastases were related to poorest response rates. The results of the Bayesian multivariate logistic regression are reported in Table 1.

	Odds Ratio	Standard deviation	2.5%	95%	p(OR<1)	p(OR>1)
Disease controlled	0.73	0.51	0.17	2.05	79%	21%
Multiple brain metastasis	0.72	0.52	0.16	2.05	80%	20%
PTV (mL)	0.99	0.03	0.94	1.04	70%	30%
SRS	3.27	4.12	0.36	13.5	21%	79%

The median follow-up from initial treatment was 31 months. The median overall survival (OS) from initial treatment was ten months (CI 95% [5 - 22]), the Kaplan-Meier survival curve is reported in Figure 1. OS was negatively influenced by extra-cranial metastases, male gender, whereas it influenced positively by brain progression-free survival (BPF5).



Median BPF5 was not met. BPF5 Kaplan Meier survival curve is reported in Figure 2.



### Conclusion

We report the results of one of the largest cohort of CRC brain metastasis treated with stereotactic radiotherapy.

This analysis suggests that CRC metastases have an overall poor response rate to stereotactic radiotherapy. However, it seems that SRS should prefer over HFSRT in patients with limited CRC brain metastases. Moreover, it demonstrates that BPF5 directly impact OS.

### PO-0816 Adaptive radiotherapy concomitant with chemotherapy as preoperative treatment for rectal cancer

P. Passoni<sup>1</sup>, N. Slim<sup>1</sup>, C. Fiorino<sup>2</sup>, C. Gumina<sup>1</sup>, M. Ronzoni<sup>3</sup>, V. Burgio<sup>3</sup>, A. Fasolo<sup>3</sup>, F. De Cobelli<sup>4</sup>, A. Palmisano<sup>4</sup>, U. Elmore<sup>5</sup>, P. De Nardi<sup>5</sup>, A.M. Tamburini<sup>5</sup>, A. Vignali<sup>5</sup>, R. Rosati<sup>5</sup>, R. Calandrino<sup>2</sup>, N. Di Muzio<sup>1</sup>  
<sup>1</sup>Ospedale San Raffaele IRCCS, Radiation Oncology, Milan, Italy ; <sup>2</sup>Ospedale San Raffaele IRCCS, Medical Physics, Milan, Italy ; <sup>3</sup>Ospedale San Raffaele IRCCS, Medical Oncology, Milan, Italy ; <sup>4</sup>Ospedale San Raffaele IRCCS, Radiology, Milan, Italy ; <sup>5</sup>Ospedale San Raffaele IRCCS, Surgery, Milan, Italy

### Purpose or Objective

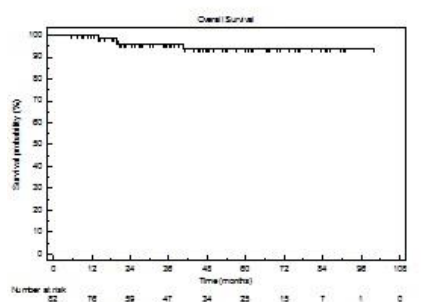
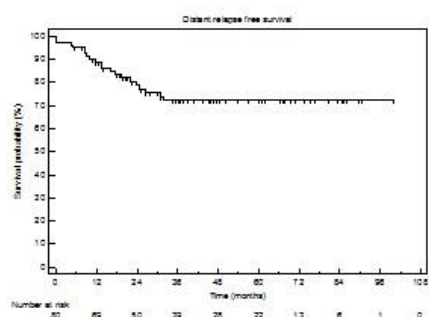
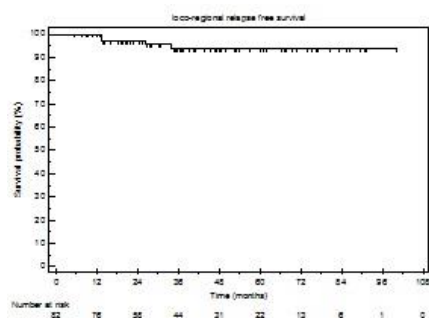
To report our clinical experience with hypofractionated, adaptive radiotherapy (RT) concomitant with chemotherapy (ChT) as preoperative treatment for rectal cancer.

### Material and Methods

Patients (pts) with T3/T4N0 or any TN+ rectal adenocarcinoma were included in an observational study. Chemotherapy consisted of Oxaliplatin 100mg/m<sup>2</sup> on days -14, 0, +14 and c.i. 5FU 200mg/m<sup>2</sup>/day or oral capecitabine 825mg/m<sup>2</sup>x2/day (from 2015 on) from day -14 to the end of RT. RT started on day 0, was delivered by Tomotherapy, and was divided into two phases of 12 and 6 fractions (Frs), respectively. Pts were positioned on Comby-Fix<sup>®</sup> and underwent a simulation CT and MR, subsequently matched. In the first RT phase CTV included mesorectum, perineum in case of tumor < 6cm from anal canal, and regional lymph-nodes. PTV was defined as CTV with a margin of 0.5 cm and received 27.6 Gy in 12 fractions (2.3 Gy/Fr). A simulation CT and MR were repeated after two cycles of ChT and 9 Frs of RT. Two new volumes were considered: GTVadaptive, defined as the residual tumour (T and N) visible on the intermediate MR images, and PTVadaptive, created from GTVadaptive with a margin of 0.5 cm. In the second RT phase, the adaptive phase, PTV again received 2.3 Gy/fr x 6 Frs (total dose 41.4 Gy in 18 Frs), while PTVadaptive received a simultaneous integrated boost of 3.1 Gy/Fr x 6 Frs (total dose 46.2 Gy in 18 Frs).

### Results

From 9/2009 to 5/ 2017, 82 pts were prospectively enrolled, T2=5, T3=72, T4=5, N+=67. Median distance from anal canal was 6.5 cm (0 cm in 18 pts), median cranium-caudal tumor length was 5 cm (1.2-11 cm). No G4 toxicity occurred; G3 toxicity consisted of diarrhoea in 10/82 pts (12%) and proctitis in 4 pts (5%). Diarrhoea always occurred before the adaptive phase. Eighty pts (97%) completed RT; median duration of RT was 25 days. Fifty-seven (70%) and 74 (84%) received > 75% of oxaliplatin and 5FU dose, respectively. Two pts achieved complete clinical response and refused surgery, 1 pt was lost, 1 pt had early distant progression. Seventy-eight pts were resected (73 R0, 5 R1), 72 pts had conservative surgery, 6 pts had abdominal-perineal amputation. Twenty-two pts (28%) had pathological complete response, 23 pts (29%) had TRG3 with 1-5% of residual vital cells. Fifty-two pts received adjuvant chemotherapy. At a median follow up of 30 months, calculated from the end of chemoradiotherapy to the last clinical check or death, 3 pts had local and 20 pts distant relapse. Local-regional-relapse free survival, distant metastasis free survival, and overall survival were 96.5%, 75.7% and 95.7%, respectively.



### Conclusion

Hypofractionated, adaptive RT concomitant with oxaliplatin and fluoropyrimidines is feasible with acceptable G3 toxicity and provides a very interesting response rate. There could be room for further dose escalation on the residual tumor with the aim of increasing pCR and/or cCR rates.

### PO-0817 PHASE II study about adaptive high dose radiotherapy in high risk rectal cancer

A. Guido<sup>1</sup>, V. Panni<sup>1</sup>, L. Fuccio<sup>2</sup>, L. Giaccherini<sup>3</sup>, D. Cuicchi<sup>2</sup>, P. Castellucci<sup>4</sup>, S. Fanti<sup>4</sup>, F. Coppola<sup>5</sup>, F. Di Fabio<sup>6</sup>, G. Poggioli<sup>2</sup>, G. Macchia<sup>7</sup>, F. Deodato<sup>7</sup>, V. Picardi<sup>7</sup>, M. Boccardi<sup>7</sup>, S. Cilla<sup>8</sup>, A. Arcelli<sup>1</sup>, G.P. Frezza<sup>9</sup>, A.G. Morganti<sup>1</sup>, S. Cammelli<sup>1</sup>

<sup>1</sup>Radiation Oncology Center- University of Bologna, Department of Experimental- Diagnostic and Specialty Medicine- DIMES, Bologna, Italy ; <sup>2</sup>S. Orsola-Malpighi Hospital- University of Bologna, Department of Medical and Surgical Sciences- DIMEC, Bologna, Italy ; <sup>3</sup>AUSL-IRCCS, Radiation Oncology Unit, Reggio Emilia, Italy ; <sup>4</sup>Nuclear Medicine Unit- University of Bologna, Department of Experimental- Diagnostic and Specialty Medicine- DIMES, Bologna, Italy ; <sup>5</sup>S.Orsola-Malpighi Hospital, Department of Diagnostic Medicine and of Prevention, Bologna, Italy ; <sup>6</sup>S. Orsola-Malpighi Hospital, Department of Medical Oncology, Bologna, Italy ; <sup>7</sup>Fondazione di Ricerca e Cura "Giovanni Paolo II",

Radiotherapy Unit, Campobasso, Italy ; <sup>8</sup>Fondazione di Ricerca e Cura "Giovanni Paolo II", Medical Physics Unit, Campobasso, Italy ; <sup>9</sup>Ospedale Bellaria, Radiotherapy Department, Bologna, Italy

### Purpose or Objective

Aim of this study was to evaluate the pathological complete response (pCR) rate in locally advanced rectal cancer (LARC) after adaptive high-dose neoadjuvant radiation therapy (RT) with concomitant plus sequential boost based on [18F]FDG-PET/CT performed two weeks after the start of RT.

### Material and Methods

Patients (pts) with biopsy proven LARC were included. Primary end-point was pCR rate. Secondary objectives included acute and late toxicity. The sample size was calculated based on the Simon's two-stage design. All pts underwent [18F]FDG-PET/CT at baseline (PET0) and after 2 RT weeks (PET1). Intensity modulated RT (IMRT) technique was delivered with concurrent capecitabine. The Gross Tumor Volume (GTV) was defined using a gradient-based delineation method and the maximal standardized uptake values (SUVmax) were recorded. The dose to rectum, mesorectum, and pelvic lymph nodes was 45 Gy (1.8 Gy/fr). A simultaneously integrated boost (SIB) was delivered to GTV+2 cm margin with a total dose of 50 Gy (2 Gy/fr). A sequential boost was delivered to GTV+5 mm margin with a total dose of 5 Gy in 2 fractions (2.5 Gy/fr) for a total dose of 55 Gy using cone-beam CT. Pathological response was scored based on the American College of Pathologist Tumor Regression Grading (TRG). Toxicity was scored according to the CTCAE v4.03 scale.

### Results

Eighteen pts (13 M, 5 F; median age 58.1 years) were enrolled. According to UICC TNM Staging (8th edition) classification the clinical stage was: T2N1M0 (2 pts), T3N1M0 (11 pts), T3N2M0 (2 pts), and T4N1M0 (3 pts). Nine-10 weeks since the end of neoadjuvant treatment all pts except one, who refused surgery after evidence of clinical complete response, underwent surgical resection. Six pts (35.3%) showed TRG=0 (pCR), 5 pts (29.4%) TRG=2, and 6 pts (35.3%) TRG 3. GTV measured at PET0 was 22 mL (range: 1.2-90.9) and at PET1 9.8 mL (range: 0-62.4) ( $p < 0.05$ ). Median GTV reduction was 60.2% (range: 0-100): 61.5% (range: 13.9-100) for responders (pCR) pts and 59.5% (range: 0-94.5) for non-responders ( $p = 0.91$ ). Median SUVmax of the rectal lesions was 15.1 (range 5.7-45) at PET0 and 8.3 (range: 0-20.4) at PET1 ( $p = 0.098$ ). Median SUVmax reduction was 40.4% (range: 0-100): 50% for responder pts and 35.2% for non-responders (both ranges: 0-100) ( $p = 0.39$ ). Most pts showed G1 GI and GU toxicity. Only one pt had acute GI G3 toxicity.

### Conclusion

Despite the delivery of the sequential boost on a reduced volume, adapted based on an early 18F-FDG-PET/CT, the pCR rate was 35.3%. This regimen was well tolerated.

### PO-0818 Comparison of three different approaches for bowel delineation in patients with rectal cancer.

E. Rijkmans<sup>1</sup>, B.B.D. Otto<sup>1</sup>, J.R.N. Van der Voort van Zyp<sup>2</sup>, R.Th. Zinkstok<sup>1</sup>, F.P. Peters<sup>1</sup>, C.A.M. Marijnen<sup>1</sup>  
<sup>1</sup>Leiden University Medical Center, Department of Radiation Oncology, Leiden, The Netherlands ;  
<sup>2</sup>University Medical Center Utrecht, Department of Radiotherapy, Utrecht, The Netherlands

### Purpose or Objective

Acute gastro-intestinal (GI) toxicity is one of the main dose-limiting toxicities in radiotherapy for rectal cancer. Previous studies showed a dose-response relationship for small bowel and acute GI toxicity. However, different contouring methods have been used, and there is no consensus on which is best suitable for clinical practice. This study aims to compare different bowel delineation

definitions and their association with toxicity in patients with locally advanced rectal cancer (LARC) treated with neo-adjuvant chemoradiotherapy.

**Material and Methods**

Data from a historical cohort study including all consecutive patients with LARC treated with chemoradiotherapy in our institute from 2003-2010 was used for this analysis. Patients were treated with a 3D conformal four-field technique. In all patients, bowel structures were delineated using three different techniques; individual small bowel loops (SBL), bowelbag following EMBRACE criteria and the RTOG bowel cavity (Fig 1). Delineations were performed by two observers (JVZ and BO) and checked by a second observer (ER/FP). An experienced radiologist was consulted if needed. Acute toxicity was scored according to CTCAE v4.0. Volumes receiving 5Gy-50Gy with an interval of 5Gy (V5-V50) of the different contours were correlated with occurrence of grade  $\geq 2$  acute diarrhea, using a Mann-Whitney U tests.

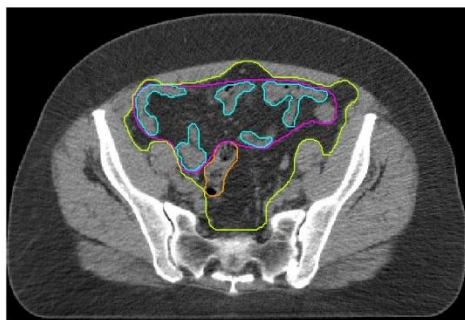


Figure 1. Example of different delineation contours. Small bowel (sky blue); Bowelbag (pink); RTOG (yellow green); Sigmoid (orange); Individual bowel loops (purple); Outer contour of small and large bowel, excluding rectosigmoid; All abdominal contents starting from the most inferior axial slice with small or large bowel loops or above the rectum.

**Results**

Planning CTs and acute toxicity data were available for 90 patients. Grade  $\geq 2$  acute diarrhea occurred in 33 out of 90 patients (36.7%) of which grade 3 in 10 patients (11.1%), no grade 4 or 5 diarrhea occurred. An association was found for all three techniques between irradiated bowel volume and the development of grade  $>2$  acute diarrhea. This association was most pronounced for low dose regions and for SBL and bowelbag compared to the RTOG bowel cavity (Fig 2). The strongest association was observed for the V15 of the bowelbag with a median V15 of 314cc for patients with  $<$  grade 2 diarrhea and a median V15 of 410cc in patients with grade  $\geq 2$  diarrhea ( $p=0.04$ ). Interestingly approximately 50% of volume of the bowelbag consisted of small bowel loops, while this was only approximately 13% for the RTOG bowel cavity (Fig 2).

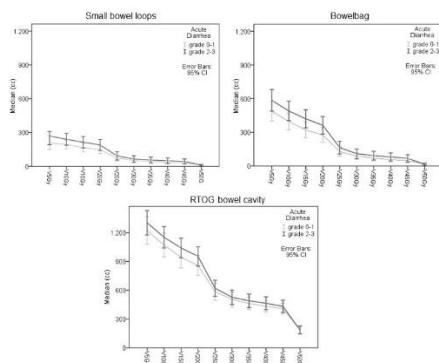


Figure 2. Association of V5-V50 of small bowel loops, bowelbag and RTOG bowel cavity with grade  $\geq 2$  acute diarrhea.

**Conclusion**

The bowelbag V15 was the best predictor for acute diarrhea grade  $\geq 2$  in patients treated with neo-adjuvant chemoradiation for rectal cancer. Further research is needed to assess the value of the bowelbag V15 in modern radiation techniques such as intensity modulated or volumetric arc therapy and in relation to late GI-toxicity.

**PO-0819 Stereotactic Radiation Therapy in Oligometastatic Colorectal Cancer: 102 patients and 150 lesions**

M.A. ZERELLA<sup>1,2</sup>, V. Dell'Acqua<sup>1</sup>, A. Surgo<sup>1</sup>, F. Kraja Pupuleku<sup>3</sup>, J. Kobiela<sup>4</sup>, P. Spsychalski<sup>4</sup>, C.M. Francia<sup>2</sup>, D. Ciardo<sup>1</sup>, C. Fodor<sup>1</sup>, F. Pansini<sup>5</sup>, S. Vigorito<sup>5</sup>, F. Cattani<sup>5</sup>, M.C. Leonardi<sup>1</sup>, B.A. Jereczek Fossa<sup>1,2</sup>

<sup>1</sup>IEO European Institute of Oncology- IRCCS, Division of Radiotherapy, Milan, Italy ; <sup>2</sup>University of Milan, Department of Oncology and Hemato-Oncology, Milan, Italy ; <sup>3</sup>University Hospital Centre "Mother Theresa", Department of Oncology, Tirana, Albania ; <sup>4</sup>Medical University of Gdansk, Department of General- Endocrine and Transplant Surgery, Gdansk, Poland ; <sup>5</sup>IEO European Institute of Oncology- IRCCS, Division of Medical Physics, Milan, Italy

**Purpose or Objective**

To evaluate local control (LC), progression free survival (PFS), overall survival (OS), toxicity and failure predictors in patients with oligometastatic colorectal cancer (CRC) treated with stereotactic radiation therapy (SRT) in a single institution.

**Material and Methods**

Patients with oligometastatic CRC disease (with 1-5 metastases) were analyzed retrospectively. Treatments were performed using VERO® (BrainLab) and CyberKnife® (Accuray) systems. The SRT prescribed dose was dependent on the volume of the lesions and its location. Treatment characteristics are summarized in table 1.

Table 1: SRT treatment characteristics (N=150 lesions)

	N-150	%
Region of lesions		
Chest	100	66.7
Upper abdomen	30	20
Pelvis	13	8.6
Head and neck	7	4.7
Site of lesions		
Lung	97	64.6
Other*	18	12
Liver	15	10
Lymph-node	13	8.7
Head and neck	7	4.7
PTV (cm <sup>3</sup> )	Median (q1, q3)	15.9 (9.1, 41.8)
Equivalent dose (BED) (Gy)	Median (q1, q3)	129 (45, 129)
Total dose (Gy)	Median (q1, q3)	45 (26, 45)
Dose/fraction (Gy)	Median (q1, q3)	15 (8, 15)

\*Other includes urinary bladder lesions, bone lesions, bronchus lesions, solid abdominal and pelvic lesions.

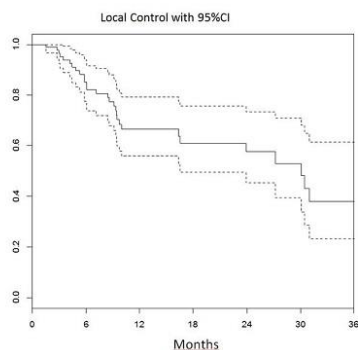
Legend: KPS: Karnofsky performance status; PTV: planning target volume; q1, q3: interquartile range

**Results**

102 consecutive oligometastatic CRC patients (150 lesions overall) were included for this study. They underwent SRT between February 2012 and December 2015. Median prescription dose was 45 Gy (median dose/fraction was 15 Gy delivered in 3 fractions and corresponding BED<sub>10</sub> was 112.5 Gy). Median follow-up was 11.4 months. Acute and late G1 toxicities were observed in 10% and 1.4% of patients, respectively. No patients experienced G3 and G4 toxicity. Considering the radiological response at 3 months and best radiological response, no progression was found in 82% and 85% out of 150 evaluable lesions, respectively.

Actuarial 6-month, 1-year, 2-year LC rates were 85%, 67%, 58% (image 1), respectively, whereas OS rates were 95%, 90% and 90%, respectively and PFS rates were 63%, 37% and 27% respectively. Pattern of failure was out-field in 35% and in-field in 31% of patients. Progressive disease was

significantly correlated with biological equivalent dose (BED) with a significant better LC when BED was  $\geq 75$  Gy ( $p < 0.0001$ ). Moreover, in multivariate analysis, LC was significantly higher in lesions with a Planning Target Volume (PTV) volume  $< 42$  cm<sup>3</sup> and treated with a BED  $\geq 75$  Gy. Patients with Karnofsky performance status (KPS)  $< 90$  showed a significantly higher out-field progression than the ones with KPS  $\geq 90$ .



### Conclusion

Patients with oligometastatic CRC are considered candidates for curative treatment because long-term survival can be expected. Recent studies have shown that SRT in oligometastatic CRC is an excellent option for local treatment of metastases with a good outcome and low toxicity profile. Our study confirms that SRT is an effective treatment with low treatment-associated morbidity. It should be considered as a valid option for properly selected patients. Further studies should be focused to clarify which patient subgroup will benefit most from this treatment modality. Furthermore, researchers should aim to define the optimal dose in order to improve tumor control while maintaining low toxicity profile.

### PO-0820 Effect of short-course radiotherapy on postoperative complications in locally advanced rectal cancer

S. Hoendervangers<sup>1</sup>, C. Sparreboom<sup>2</sup>, H. Van Grevenstein<sup>3</sup>, L. Verkooijen<sup>1</sup>, J. Lange<sup>2</sup>, P. Doornebosch<sup>4</sup>, M. Intven<sup>1</sup>

<sup>1</sup>UMC Utrecht, Radiotherapy, Utrecht, The Netherlands ;

<sup>2</sup>Erasmus MC, Surgery, Rotterdam, The Netherlands ;

<sup>3</sup>UMC Utrecht, Surgery, Utrecht, The Netherlands ;

<sup>4</sup>IJsselland hospital, Surgery, Capelle a/d IJssel, The Netherlands

### Purpose or Objective

Neoadjuvant short-course radiotherapy (5x5 Gy) with a prolonged interval to surgery (SCRT-delay) is regularly used as an alternative for neoadjuvant chemoradiation (CRT) in frail patients with locally advanced rectal cancer (LARC). However, evidence based data on management of LARC in the frail population is scarce. Consequently, there are no clear guidelines for the treatment of this group, and decision-making for the type of neoadjuvant therapy differs per center. With the increasing aging population, there is an urgent need for more evidence to justify the choice of neoadjuvant treatment in frail patients with LARC. Therefore, the aim of this study is to investigate the patient characteristics on which treatment deviation is based and to assess the effect on postoperative outcomes.

### Material and Methods

This is an observational study with data from the Dutch ColoRectal Audit (DCRA), a national audit in which clinical outcomes of patients undergoing primary colorectal surgery are registered. Non-metastatic LARC patients who

underwent surgery between May 2014 and May 2016 after an interval of  $\geq 6$  weeks were included. Missing values were replaced by multiple imputation. Differences in baseline characteristics between SCRT-delay and CRT were evaluated by  $\chi^2$ -test for categorical variables and t-test for continuous variables. The association between the different types of neoadjuvant treatment and postoperative complications was analyzed by multivariable logistic regression.

### Results

2,888 patients with LARC were included; 333 patients were treated with SCRT-delay and 2,555 with CRT. Mean age was higher in the SCRT-delay group compared to the CRT group (73.87 vs. 64.33,  $p < 0.001$ ). Also, prevalence of comorbidities was higher in the SCRT-delay group (81% vs. 66%,  $p < 0.001$ ). There were no statistically significant differences in tumor stage, surgical approach, the occurrence of postoperative complications, length of hospital stay or length of ICU stay. Patients in the SCRT-delay group more often received a permanent colostomy ( $p < 0.001$ ).

Table 1. Multivariable analysis of the association between neoadjuvant short-course radiotherapy with delayed surgery (SCRT-delay) or chemoradiation (CRT) and postoperative complications  $< 30$  days after surgery

	Adjusted OR (95% C.I.)	p-value
Age	1.006 (0.998-1.014)	0.17
Charlson Comorbidity Index	1.04 (0.96 - 1.13)	0.33
Distance from the anal verge (cm)	1.001 (0.98 - 1.02)	0.90
CT		
- 2	Ref.	
- 3	1.58 (1.03 - 2.47)	0.04
- 4	1.62 (1.02 - 2.61)	0.04
Distance to MRF $> 1$ mm	1.07 (0.88 - 1.31)	0.48
cN		
- 0	Ref.	
- 1	0.67 (0.45 - 0.98)	0.04
- 2	0.70 (0.49 - 1.01)	0.05
- cNx	1.27 (0.36 - 4.65)	0.71
Neoadjuvant therapy		
- Short course radiotherapy	0.99 (0.76 - 1.27)	0.91
- Chemoradiation	Ref.	
Interval to surgery (weeks)	1.01 (0.99 - 1.02)	0.21
ASA score		
- 1	Ref.	
- 2	1.31 (1.07 - 1.61)	0.01
- 3	1.36 (1.02 - 1.82)	0.03
- 4	2.56 (0.98 - 6.92)	0.06
Surgical approach		
- Transabdominal, open	Ref.	
- Transabdominal, scopic	0.87 (0.55 - 0.80)	$< 0.001$
- TEM	1.13 (0.04 - 32.8)	0.93
- Transanal, local excision	1.01 (0.04 - 25.7)	0.99
- Transanal and transabdominal, endoscopic (TaTME or TAMIS TME)	0.64 (0.43 - 0.96)	0.03
Surgical procedure		
- Local excision + TME	1.25 (0.001 - 2.66)	0.13
- Local excision + APR	4.43 (0.14 - 8.40)	0.82
- Partial Mesorectal Excision	0.37	0.23
- Total Mesorectal Excision	0.89	0.003
- Low anterior resection	Ref.	
- Abdominoperineal resection	0.86	0.37
- Proctocolectomy	2.07	0.24
- Other	3.45	0.02
Primary anastomosis	0.81	0.06

### Conclusion

Despite the higher age and the higher prevalence of comorbidities, postoperative complications were not significantly higher in the SCRT-delay group. Short-course radiotherapy was not associated with increased postoperative complications and seems to be a good alternative neoadjuvant treatment option for frail LARC patients.

### PO-0821 Long-term outcome of an organ preservation strategy following chemoradiotherapy in rectal cancer

E. Palazzari<sup>1</sup>, A. Lauretta<sup>2</sup>, F. Navarra<sup>1</sup>, R. Innocente<sup>1</sup>, C. Bellucco<sup>3</sup>, C. Bampo<sup>4</sup>, L. Balestreri<sup>5</sup>, F. Matrone<sup>1</sup>, G. Fanetti<sup>1</sup>, A. Revelant<sup>1</sup>, R. Cannizzaro<sup>6</sup>, V. Canzonieri<sup>7</sup>, A. Buonadonna<sup>8</sup>, J. Polesel<sup>9</sup>, G. Bertola<sup>10</sup>, A. De Paoli<sup>1</sup>

<sup>1</sup>Centro di Riferimento Oncologico CRO-IRCCS- Aviano-Italy,

<sup>2</sup>Centro di Riferimento Oncologico CRO-IRCCS- Aviano- Italy,

<sup>3</sup>Centro di Riferimento Oncologico CRO-IRCCS- Aviano- Italy,

<sup>4</sup>Centro di Riferimento Oncologico CRO-IRCCS- Aviano-Italy, Surgical Oncology,

<sup>5</sup>Centro di Riferimento Oncologico CRO-IRCCS- Aviano-Italy, Nuclear Medicine, Aviano, Italy ;

<sup>6</sup>Centro di Riferimento Oncologico CRO - IRCCS- Aviano-Italy, Radiology, Aviano, Italy ;

<sup>7</sup>Centro di Riferimento Oncologico CRO-IRCCS- Aviano-Italy, Gastroenterology,

<sup>8</sup>Centro di Riferimento Oncologico CRO-IRCCS- Aviano- Italy, Pathology, Aviano, Italy ;

<sup>9</sup>Centro di Riferimento Oncologico CRO - IRCCS- Aviano-Italy,

<sup>10</sup>Centro di Riferimento Oncologico CRO - IRCCS- Aviano-Italy,

Medical Oncology, Aviano, Italy ; <sup>9</sup>Centro di Riferimento Oncologico CRO - IRCCS- Aviano-Italy, Cancer Epidemiology, Aviano, Italy ; <sup>10</sup>Centro di Riferimento Oncologico CRO - IRCCS- Aviano-Italy, Surgical Oncology, Aviano, Italy

#### Purpose or Objective

Organ preservation strategy with local excision (LE) or watch and wait (W-W) in selected patients (pts) with locally advanced rectal cancer (LARC) who achieve a major (mCR) or complete clinical response (cCR) after preoperative chemoradiotherapy (CRT) may offer an opportunity to avoid major surgery and its effects on anorectal, sexual and urinary functions and quality of life. We report the long term outcome of pts undergoing pre-operative CRT and LE at our Institution

#### Material and Methods

Between January 1998 and July 2017 LE was proposed to pts as an alternative to TME after CRT when mCR or cCR were assessed at DRE, endoscopy with biopsy and MRI. CT-PET was used since 2002 in staging and restaging to characterize also metabolic response. LE was performed using either the traditional transanal approach or Transanal Micro Invasive surgery (TAMIS). Pathologic response was defined as pT stage and Mandard Tumor Regression Grade (TRG). Pts who achieved TRG1 or TRG2 were going to follow-up, whereas was planned for pT1-3, TRG3-5. Long term outcome was assessed by Log-Rank test in terms of 5 and 10yrs OS, DFS and local DFS (LDFS) and Colostomy Free Survival (CFS).

#### Results

Seventy-four pts (M/F: 47/27 ; median age 66 yrs, range 25-85) underwent to LE. Clinical stage at presentation was I in 10 pts, II in 39 and III in 25. Median distance from anal verge was 3.5 cm (range 2-8 cm). Radiotherapy (RT) consisted of 45-50.4 Gy in 25-28 frs in 50 pts and 45-54 Gy in 25 frs (IMRT-SIB) in 24 pts. Concomitant 5-FU or Capecitabine based chemotherapy was associated to RT in all pts. Pathologic T stage after LE was available for 70 pts; 4 pts with cCR entered in a W-W program. pT0 was achieved in 39 pts (56%), pT1-3 in 31 (44%). Overall 50 pts (71%) achieved TRG1 or TRG2 and 20 TRG3-5. Twelve of 20 TRG 3-5pts underwent to TME while 8 pts refused radical surgery. With a minimum follow up of 2 yrs (range 2-20yrs), the 5 and 10-yrs LDFS, DFS and OS in the overall 74 pts were 88.1% and 88.1%, 77.3% and 71.5%, and 88.2% and 74.4%, respectively. For the 43 T0 pts, including 39 pT0 and 4 cCR in W-W program, the 5 and 10-yrs LDFS, DFS and OS were 94.7% and 94.7%, 84% and 73.5%, and 91.6% and 73.2%, respectively. No significant difference of outcome were found between TRG1-2 and TRG3-5 pts, most receiving radical TME. At the same median follow up, 17 pts (24%) needed colostomy, 7 (14%) in TRG1-2 group and 10 (50%) in TRG3-5 respectively. The 10yrs CFS was 87.8% in TRG1-2 group and 52.7% in TRG3-5 and it was significantly different ( $p=0.001$ ) in these two subset of pts. No major complication were reported; 3 pT0 pts needed colostomy for fecal incontinence (2pts) or rectal stenosis (1pt) after LE.

#### Conclusion

Organ preservation with LE after CRT appears safe with favourable long-term outcome for selected LARC patients who achieve mCR or cCR. TME performed after LE don't get worse outcome in TRG3-5 pts. LE confirms a valid approach in organ preservation to improve quality of life in these pts.

<sup>1</sup>MacKay Memorial Hospital, Radiation Oncology, Taipei, Taiwan ; <sup>2</sup>Changhua Christian Hospital, Radiation Oncology, Changhua, Taiwan ; <sup>3</sup>MacKay Memorial Hospital, Obstetrics and Gynecology, Taipei, Taiwan

#### Purpose or Objective

Treatment-related toxicities and decreased levels of patient performance during cancer therapy might contribute to body composition changes and thereby impact outcomes. However, the effect of longitudinal body composition changes on outcomes in patients with advanced endometrial cancer is unknown. This study investigated the association between body composition changes during staging surgery and adjuvant chemoradiotherapy and outcomes in patients with stage III endometrial cancer.

#### Material and Methods

Pre- and post-treatment computed tomographic (CT) images of 131 patients with stage III endometrial cancer who were treated at 2 tertiary centers between 2008 and 2016 were analyzed. The skeletal muscle index (SMI), skeletal muscle radiodensity (SMD), and total adipose tissue index (TATI) were measured from 2 sets of CT images obtained at the level of the L3 vertebra. Patients with a reduction or increase in the SMD of  $\geq 5.0\%$  were classified as having 'SMD loss' or 'SMD gain', respectively. Predictors of overall survival (OS) and progression-free survival (PFS) were identified using Cox regression models.

#### Results

The median follow-up was 50.6 (range, 12.1-117.0) months. Overall, patients lost an average of 2.1% per 210 days (95% CI: -4.0 to -0.2;  $p = 0.03$ ) of SMD and 0.2% per 210 days (95% CI: -1.5 to 1.0;  $p = 0.70$ ) of SMI. Patients gained an average of 3.2% per 210 days (95% CI: -0.2 to 6.7;  $p = 0.07$ ) of TATI. Changes in SMD did not correlate with weight change (Spearman's  $\rho$  for SMD, -0.13;  $p = 0.13$ ). Changes in SMI and TATI positively correlated with weight change (Spearman's  $\rho$  for SMI, 0.20;  $p = 0.02$ ;  $\rho$  for TATI, 0.40;  $p = 0.001$ ). The 5-year OS for patients with SMD loss, stable SMD, and SMD gain were 59.7%, 94.0%, and 90.5%, respectively ( $p < 0.001$ ; Figure 1); the corresponding PFS were 55.9%, 92.8%, and 85.7%, respectively ( $p < 0.001$ ; Figure 1). On multivariable analysis, an SMD loss  $\geq 5.0\%$ /210 days of treatment was independently associated with poorer OS (hazard ratio: 10.20, 95% confidence interval: 2.24-46.42;  $p = 0.003$ ) and PFS (hazard ratio: 7.36, 95% confidence interval: 2.09-25.95;  $p = 0.002$ ). Pretreatment myosteatosis and sarcopenia, as well as changes in SMI and TATI during treatment, were not associated with survival. The pretreatment skeletal muscle gauge was associated with treatment modifications such as delays, dose reductions, and discontinuation of chemotherapy.

---

Poster: Clinical track: Gynaecological (endometrium, cervix, vagina, vulva)

---

PO-0822 Muscle density loss during cancer therapy for advanced endometrial cancer portends poor survival  
J. Lee<sup>1</sup>, J. Lin<sup>2</sup>, C. Chang<sup>3</sup>, M. Wu<sup>1</sup>, Y. Chen<sup>1</sup>

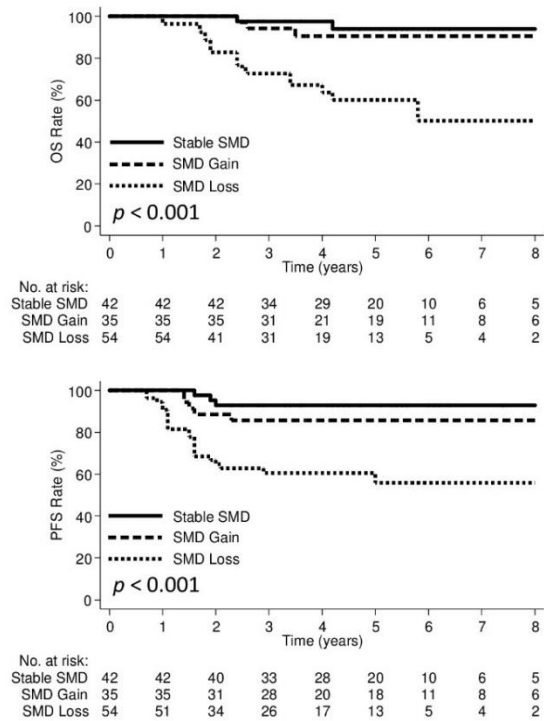


Figure 1 Kaplan-Meier curve demonstrating overall survival and progression-free survival according to skeletal muscle radiodensity change groups.

#### Conclusion

SMD decreased significantly during treatment and was independently associated with poorer survival in patients with stage III endometrial cancer who underwent staging surgery and adjuvant chemoradiotherapy. Furthermore, SMD loss was occult and occurred independently of weight change. Future studies are required to devise interventions aimed at preserving muscle based on individual body composition phenotypes to improve outcomes in advanced endometrial cancer.

#### PO-0823 Relevance of time interval and thermal dose for the clinical outcome of cervical carcinoma patients

M. Kroesen<sup>1</sup>, T. Mulder<sup>2</sup>, N. Holthe<sup>2</sup>, A. Aangeenbrug<sup>2</sup>, J.W. Mens<sup>2</sup>, L. Van Doorn<sup>3</sup>, M. Paulides<sup>4</sup>, E. Oomen-de Hoop<sup>2</sup>, R. Vernhout<sup>2</sup>, L. Lutgens<sup>5</sup>, G. Van Rhooen<sup>2</sup>, M. Franckena<sup>6</sup>

<sup>1</sup>Erasmus MC- University Medical Center Rotterdam, Radiation Oncology, Rotterdam, The Netherlands ;

<sup>2</sup>Erasmus MC- University Medical Center Rotterdam, Department of Radiation oncology, Rotterdam, The Netherlands ;

<sup>3</sup>Erasmus MC- University Medical Center Rotterdam, Department of Obstetrics and Gynaecology, Rotterdam, The Netherlands ; <sup>4</sup>Eindhoven University of Technology, Department of Electrical Engineering, Eindhoven, The Netherlands ;

<sup>5</sup>University Medical Centre Maastricht, Department of Radiation Oncology Maastricht, Maastricht, The Netherlands ; <sup>6</sup>Erasmus MC- University Medical Center Rotterdam, Department of Radiation Oncology, Rotterdam, The Netherlands

#### Purpose or Objective

Addition of deep hyperthermia to radiotherapy results in improved local control (LC) and overall survival (OS) compared to radiotherapy alone in locally advanced cervical carcinoma patients. Previously, we have shown that the thermal dose of hyperthermia significantly correlates with LC and disease specific survival (DSS). Besides thermal dose, the effect of the time interval

between radiotherapy and hyperthermia is expected to influence treatment outcome. Therefore, we investigated the effect of the time interval on treatment outcome. In addition, we investigated the effect of thermal dose in a more recent cohort, including patients treated with image guided brachytherapy (IGBT).

#### Material and Methods

We included all primary cervical carcinoma patients treated with thermoradiotherapy at our institute between 1996 and 2005. For these patients, patient and follow-up data, but not the time interval, were collected previously. In addition, we included all primary cervical carcinoma patients treated between 2005 and 2016. Data on patients, tumors and treatments, including thermal dose parameter TRISE and the use of IGBT, were collected. Follow-up data on LC, disease free survival (DFS), DSS, OS and late toxicity were collected or updated. Kaplan Meier and Cox proportional hazards analyses were used for statistical analyses.

#### Results

400 patients were included. Kaplan Meier and univariate Cox proportional hazard analysis showed no effect of the time interval (range 30-230 minutes) on any of the clinical outcome measures. In multivariate Cox analysis, the thermal dose parameter TRISE (HR 0.649; 95% CI 0.501-0.840) and the use of IGBT (HR 0.432; 95% CI 0.214-0.972), but not the time interval, were significant predictors of LC. In a more recent cohort of 227 patients, treated since our previous analysis of the effect of thermal dose, the independent effect of TRISE on LC in multivariate analysis (HR 0.43; 95% CI 0.28 - 0.68) could be replicated. Moreover, in the 66 patients treated with IGBT from 2012 onwards, the thermal dose parameter TRISE remained to have a significant effect (HR 0.33; 95% CI 0.12 - 0.96) on LC in univariate analysis. The 17 patients having a higher than median radiation dose to the High-Risk CTV in combination with a higher than median thermal dose (TRISE), experienced an excellent 5-year LC, DFS and DSS of 100 percent.

#### Conclusion

The time interval between radiotherapy and hyperthermia, up to 4 hours, has no effect on clinical outcome. The positive association between thermal dose and clinical outcome is replicated in an independent, more recent, cohort of cervical carcinoma patients. Importantly, in patients receiving state-of-the-art IGBT, the additive effect of thermal dose on clinical outcome remains.

#### PO-0824 Postoperative VBT vs EBRT/VBT in patients with early stage of uterine carcinoma - our update results

A. Masarykova<sup>1</sup>, D. Scepanovic<sup>1</sup>, M. Pobjakova<sup>1</sup>, A. Hanicova<sup>1</sup>, M. Fekete<sup>1</sup>

<sup>1</sup>National Cancer Institute, Radiation Oncology, Bratislava, Slovakia

#### Purpose or Objective

Background. - In different trials, like PORTEC-2, Vaginal Brachytherapy (VBT) alone did not make a significant difference in the overall or disease-free survival when compared to patients treated with External Beam Radiotherapy (EBRT) only. However, there are no randomized trials comparing VBT alone with EBRT plus VBT.

Purpose/Objective. - The purpose was to show our update results of VBT alone versus EBRT plus VBT in preventing the vaginal recurrences in patients with early stage of uterine carcinoma, as well as disease-free survival and overall survival of these patients.

#### Material and Methods

Total of 307 patients with early stages of the uterine carcinoma have performed postoperative radiotherapy during the period from 2006 to 2010. There were two groups of patients: 55 patients with VBT alone and 252

patients with combined of EBRT/VBT. In the group with VBT alone, 96% of patients received 5x6Gy HDR Ir-192, however, in the group with combined of EBRT/VBT, 52% of patients received 46Gy and 48% over 46Gy (up to 50.4Gy) by EBRT and the various fractionation regimens by VBT, the most of these patients received 3x6Gy (62%) and 2x6Gy (28%) HDR Ir-192.

#### Results

Ten-year risk of locoregional recurrence was 3.2% in the EBRT/VBT group and 2% in the group of patients with VBT alone ( $p=1$ , Fisher's exact test). However, the 10-year risk of distant metastases was 10.2% in combined EBRT/VBT group and 3% in VBT alone group of patients ( $p=0.2085$ ). During the median follow-up time of 72 months, 89% of patients with VBT alone lived and 79% of patients with combined of EBRT/VBT ( $p=0.1827$ ). The rate of late toxicity, in particular genitourinary was significantly lower in the VBT alone than in the combined of EBRT/VBT group (7.6% vs. 29%) ( $p=0.0057$ ). Ten-year DFS was 76% for the VBT alone group and 70% for group of patients with combined of EBRT/VBT and 10-year OS was 80% for VBT alone versus 77% for combined of EBRT/VT group of patients ( $p=0.8686$ ,  $p=0.7310$ , respectively).

#### Conclusion

Also, our update results showed that VBT alone is as effective as combined of EBRT/VBT in preventing the vaginal recurrences and achieving comparable survival rates as adjuvant settings in patients with early stage uterine carcinoma.

#### PO-0825 Differential impact of GLUT1 overexpression between HPV16-positive and -negative cervical cancer

B.H. Kim<sup>1</sup>, J.H. Chang<sup>1</sup>

<sup>1</sup>SMG-Seoul National University Boramae Medical Center, Radiation Oncology, Seoul, Korea Republic of

#### Purpose or Objective

Glucose transporter-1 (GLUT1) has been reported as a poor prognosticator associated with radioresistance and immune evasion through metabolic communication in various cancers, but little data is available on cervical cancer. Meanwhile, most cervical cancer is known to be caused by human papilloma virus (HPV), but treatment response and prognosis according to the HPV subtype are also unknown. This hypothesis-generating study was conducted to investigate the prognostic impact of GLUT1 in cervical cancer, in conjunction with HPV subtype.

#### Material and Methods

Clinicopathologic factors along with mRNA expression data were obtained using The Cancer Genome Atlas database. Tumor HPV status and immune cell abundance scores were extracted from previous publications. Total 298 patients with appropriate information were analyzed.

#### Results

High GLUT1 expression was associated with old age, squamous cell carcinoma, high tumor stage, pelvic lymph node metastases, and low hysterectomy rate. HPV16 positivity itself was not associated with other factors, except low tumor grade. Multivariate survival analysis revealed that high GLUT1 expression (HR 2.57,  $p = 0.002$ ) and HPV16 subtype (HR 0.56,  $p = 0.033$ ) were independent prognostic factors for OS. In the subgroup analysis, poor prognostic impact of high GLUT1 expression was maintained in the HPV16 (+) group ( $p < 0.001$ ), but not in the HPV16 (-) group ( $p = 0.495$ ). Decreased immune cell abundance scores of B cells, CD8 T cells, and Th1 cells by high GLUT1 expression were observed only in the HPV16 (+) group.

#### Conclusion

Despite of heterogenous treatments, our results suggested that GLUT1 expression and HPV16 subtype may have an independent prognostic value in cervical cancer. Especially in the HPV16 (+) group, GLUT1-mediated immunomodulation might be an important cause of treatment failure. Further proof-of-concept study is

warranted to identify novel immunometabolic targets to overcome radioresistance.

#### PO-0826 On the value of a prognostic tumour score in locally advanced cervical cancer

J.C. Lindegaard<sup>1</sup>, P. Petric<sup>1</sup>, A.M. Lindegaard<sup>1</sup>, K. Tanderup<sup>1</sup>, L.U. Fokdal<sup>1</sup>

<sup>1</sup>Aarhus University Hospital, Department of Oncology, Aarhus, Denmark

#### Purpose or Objective

Staging of cervical cancer is primarily based on clinical examination using the FIGO staging system. In early stage disease subjected to surgery pathology is included. However, imaging and particularly MRI may provide important additional prognostic information on local tumour extension not incorporated in FIGO. As these findings may be of significance in locally advanced cervical cancer (LACC) treated with definitive radiotherapy and brachytherapy, the aim of the present study was to investigate the feasibility of a simple but wide-ranging tumour score for methodical reporting and detailed prognostication.

#### Material and Methods

400 pts with LACC FIGO stage IB-IVA treated between 2005-2018 with external beam radiotherapy +/- concomitant cisplatin and image guided adaptive brachytherapy were included. The diagnostic work-up included clinical examination, FDG PET-CT and T2 weighted MRI. FIGO stage distribution was IB-IIA 9%, IIB 61% and III-IV 30%. The degree of involvement of 8 anatomical locations (cervix, left parametrium, right parametrium, vagina, bladder, ureter, rectum and uterine corpus) was scored according to a ranked ordinal scale with 0-3 points (Table 1). The total sum of points was calculated (T-score). Uni- and multi-variate analysis of the T-score in relation to age, performance status (WHO), comorbidity, histology, nodal-stage (PET-CT) and FIGO-stage was performed using Cox regression (SPSS). Endpoints were overall survival (OS), disease free survival (DFS), cancer specific survival (CSS) and local control (LC).

#### Results

The median T-score for all pts was 6 (range of 0-20). Potential prognostic findings not included in FIGO were involvement of the uterine corpus 41%, bladder wall 10%, and mesorectum/rectal wall in 12% (Table 1). Vaginal involvement was unaccounted for in 50% (IIB, IIB, IVA). In addition, bilateral parametrial invasion was found in 51% and bilateral hydronephrosis in 14%. Proximal only versus distal parametrial involvement was found in 41% and 27%, respectively. Based on the frequency distribution of the T-score, 4 equally sized risk groups were formed: 0-4, 5-6, 7-9 and >9 points (Table 1). The T-score was highly significant in both univariate and multivariate analysis and outperformed FIGO stage for all endpoints (OS, DFS, CSS and LC). When analysing the 245 pts with FIGO stage IIB (Figure 1) the T-score demonstrated a progressively worse OS with increasing score ( $p=0.021$ ). Similar results were obtained in 36 pts in stage IB-IIA ( $p<0.001$ ) and 119 pts in stage III-IV ( $p=0.041$ ).

#### Conclusion

The use of a tumour score based on both clinical examination and conventional MRI provided significant information capable of intra FIGO-stage prognostication. Confirmation of the results and tuning of the T-score in relation to the relative prognostic importance of the individual anatomical locations require analysis of an independent and larger cohort including especially more pts in stage IB-IIA.

**Table 1**

Anatomical locations used for scoring of local tumour extension in 400 patients with locally advanced cervical cancer. The degree of tumour involvement of the cervix, parametria, bladder, ureter, rectum, corpus uteri and vagina was scored from the integrated information obtained from gynaecological examination, endoscopy and MRI. The total score (T-score) was calculated by adding the points obtained from each location

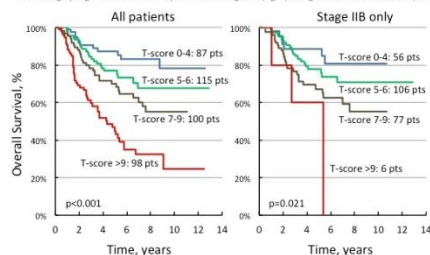
Location	Points	Scale	No of pts
Uterine cervix	0	Diameter <sup>§</sup> <20 mm	2 (0.5%)
	1	Diameter <sup>§</sup> 20-40 mm	7 (1.5%)
	2	Diameter <sup>§</sup> > 40 mm	4 (1%)
	3	Open*	387 (97%)
Parametrium left	0	Not involved	87 (22%)
	1	Proximal	161 (40%)
	2	Distal	99 (25%)
	3	To pelvic wall	53 (13%)
Parametrium right	0	Not involved	151 (38%)
	1	Proximal	132 (33%)
	2	Distal	71 (18%)
	3	To pelvic wall	46 (11%)
Bladder	0	Not involved	342 (86%)
	1	Bladder wall	29 (7%)
	2	Bullous oedema	12 (3%)
	3	Mucosa invaded	17 (4%)
Ureter#	0	Not involved	345 (86%)
	1	Unilateral	41 (10%)
	2	Bilateral	14 (4%)
Rectum	0	Not involved	349 (87%)
	1	Mesorectum	43 (11%)
	2	Rectal wall	5 (1%)
	3	Mucosa invaded	3 (1%)
Uterine corpus	0	Not involved	235 (59%)
	1	Lower third	82 (20%)
	2	Middle third	59 (15%)
	3	Upper third	24 (6%)
Vagina	0	Not involved	172 (43%)
	1	Upper third	161 (40%)
	2	Middle third	30 (8%)
	3	Lower third	37 (9%)
Total sum of points	T-score	0-4	87 (22%)
	T-score	5-6	115 (29%)
	T-score	7-9	100 (25%)
	T-score	>9	98 (24%)

<sup>§</sup>Maximal intra-cervical tumour diameter on MRI

\*Open cervical rim on MRI or evidence of tumour outside cervix (MRI and/or clinical)

#Ureteral stricture resulting in hydronephrosis

**Figure 1**  
Prognostic performance of the T-score in 400 pts with locally advanced cervical cancer (left) and for intra-stage prognostication in 245 pts in FIGO stage IIB (right) using overall survival as endpoint.



## PO-0827 Comparison of clinical examination and MRI for local cervical cancer staging (FIGO and T(NM))

J. Knoth<sup>1</sup>, R. Pötter<sup>1</sup>, I. Jürgenliemk-Schulz<sup>2</sup>, C. Haie-Meder<sup>3</sup>, L. Fokdal<sup>4</sup>, A. Sturdza<sup>1</sup>, P. Hoskin<sup>5</sup>, U. Mahantshetty<sup>6</sup>, B. Segedin<sup>7</sup>, K. Bruheim<sup>8</sup>, E. Wiebe<sup>9</sup>, B. Rai<sup>10</sup>, R. Cooper<sup>11</sup>, E. Van der Steen-Banasik<sup>12</sup>, E. Van Limbergen<sup>13</sup>, B. Pieters<sup>14</sup>, M. Sundset<sup>15</sup>, L.T. Tan<sup>16</sup>, R. Nout<sup>17</sup>, K. Tanderup<sup>4</sup>, C. Kirisits<sup>1</sup>, N. Nesvacil<sup>1</sup>, J.C. Lindegaard<sup>4</sup>, M. Schmid<sup>1</sup>

<sup>1</sup>Medical University Vienna, Department of Radiation Oncology, Wien, Austria ; <sup>2</sup>University Medical Centre Utrecht, Department of Radiotherapy, Utrecht, The Netherlands ; <sup>3</sup>Institut Gustave-Roussy, Department of Radiotherapy, Paris, France ; <sup>4</sup>Aarhus University Hospital, Department of Oncology, Aarhus, Denmark ; <sup>5</sup>Mount Vernon Cancer Centre, Department of Radiotherapy, Northwood, United Kingdom ; <sup>6</sup>Tata Memorial Hospital, Department of Radiation Oncology, Mumbai, India ; <sup>7</sup>Institute of Oncology Ljubljana, Department of Oncology, Ljubljana, Slovenia ; <sup>8</sup>The Norwegian Radium Hospital- Oslo University Hospital, Department of Oncology, Oslo, Norway ; <sup>9</sup>Cross Cancer Institute and University of Alberta, Department of Oncology, Edmonton, Canada ; <sup>10</sup>Postgraduate Institute

of Medical Education and Research, Department of Radiotherapy and Oncology, Chandigarh, India ; <sup>11</sup>St James's University Hospital, Leeds Cancer Centre, Leeds, United Kingdom ; <sup>12</sup>Radiotherapy Group, Radiation Oncology Department, Arnhem, The Netherlands ; <sup>13</sup>University Hospitals Leuven, Department of Radiation Oncology, Leuven, Belgium ; <sup>14</sup>Amsterdam University Medical Centers- University of Amsterdam, Department of Radiotherapy, Amsterdam, The Netherlands ; <sup>15</sup>St. Olavs Hospital, Clinic of Oncology and Women's Clinic, Trondheim, Norway ; <sup>16</sup>Cambridge University Hospitals NHS Foundation Trust- Addenbrooke's Hospital, Oncology Centre, Cambridge, United Kingdom ; <sup>17</sup>Leiden University Medical Center, Department of Radiation Oncology, Leiden, The Netherlands

## Purpose or Objective

To evaluate differences in local stage by using the FIGO system (only gyn examination, ± endoscopy) compared to the T(NM) system based only on MRI in pats. with locally advanced cervical cancer treated with primary CCRT and MR-based IGABT within the EMBRACE study and to assess the uncertainties of FIGO staging next to available MRI.

## Material and Methods

All 1416 pats. from EMBRACE I based on data dump (08/2017) were considered for analysis. Pats. were examined through gyn exam and MRI before treatment. Recto- and/or cystoscopy were optional. Tumour width, height and thickness in millimeter, infiltration of vagina, left and/or right parametrial tissue, pelvic wall, and rectum and/or bladder were reported as assessed through gyn exam ± endoscopy only and based on MRI only. For each pat. independent re-staging was performed through the investigators based on the database: (1) local FIGO stage (FIGO Cancer Report 2012/2015) based on clinical findings only; (2) T-stage (8<sup>th</sup> edition, 2017) on MRI only. Descriptive statistics were used to sum up FIGO- and T-stages and cross tables to evaluate the differences in local staging.

## Results

Data was available from 1338 pats.: FIGO stage was IB in 264 (19.7%) pats., IIA in 83 (6.2%), IIB in 755 (56.4%), IIIA in 15 (1.1%), IIIB in 191 (14.3%), and IVA in 30 (2.2%). T-stage was T1b in 207 (15.5%) pats., T2a in 75 (5.6%), T2b in 834 (62.3%), T3a in 12 (0.9%), T3b in 125 (9.3%) and T4a in 85 (6.4%) (table 1).

Differences in local tumour staging were found in overall 388 pats. (28.9%) (table 1): 141 pats. (10.5%) had a lower T-stage compared to FIGO, whereas 247 pats. (18.5%) had a higher T-stage. In FIGO IIB, 95/755 (12.5%) had a change in T-stage, ranging from T1b1 to T4a. In overall FIGO IB, 128/264 (48.5%) changed to another T-stage. For FIGO IB1, change of stage was in 50.4%, to T1b2 and T2b. For FIGO IB2, change was in 46.3%, mainly to T2b. For FIGO IIA (n=83), change of T-stage was in 66% (T2a1 to T2a2; and to T2b). For FIGO IIIB change of stage was in 100/191 (52.4%) with 62 classified as T2b and 35 as T4a. The small group of FIGO IVA pats. (n=30) changed in 13.3% to another T-stage (T2b/T3b). Change of stage between FIGO and T-stage varies considerably between the different FIGO stages from min 12.5% in FIGO IIB to max 69.2% in FIGO IIA1.

FIGO staging as performed primarily through the centers was different from FIGO re-staging through the investigators in 154/1338 pats. (11.5%).

	T stage									change of stage/total
	1b1	1b2	2a1	2a2	2b	3a	3b	4a		
IB1	70	24	4	0	43	0	0	0		71/141 (50,4%)
IB2	9	66	0	4	40	0	4	0		57/123 (46,3%)
IIA1	4	0	12	15	8	0	0	0		27/39 (69,2%)
FIGO IIA2	1	4	4	17	15	1	0	2		27/44 (61,4%)
stage IIB	22	8	7	8	660	2	28	20		95/755 (12,5%)
IIIA	0	0	1	1	3	8	0	2		7/15 (46,7%)
IIIB	0	0	0	2	62	1	91	35		100/191 (52,4%)
IVA	0	0	0	0	2	0	2	26		4/30 (13,3%)
										388/1338 (28,9%)

Table 1: Cross table showing all EMBRACE patients evaluable (n=1338) with FIGO and T-stages as re-staged through investigators based on clinical findings only and MRI findings only: stage and change of stage are indicated in absolute numbers in detail and overall when classified either based on FIGO (clinical exam) or on T-staging (MRI) criteria.

### Conclusion

When comparing FIGO based on gyn exam only and T-stages based on MRI only in the frame of a primarily unblinded FIGO assessment, about one third of pats. could be classified differently. Upstaging is more frequent than downstaging. To minimize these uncertainties, a comprehensive knowledge of the differential value of clinical and MRI findings for the different areas of tumour spread is necessary to integrate these findings into one comprehensive final local T-stage at diagnosis "T<sub>clinical, imaging</sub>" as suggested by the recent ESGO ESTRO ESP recommendations.

### PO-0828 Chronic Lower Extremity Lymphedema in Gynecologic Cancer Patients : EBRT versus Brachytherapy

W.L. Chang<sup>1</sup>, H. Kang<sup>1</sup>, H.J. Kim<sup>1</sup>, K.S. Seo<sup>2</sup>, H.S. Kim<sup>3</sup>  
<sup>1</sup>Seoul National University College of Medicine, Radiation Oncology, Seoul, Korea Republic of ; <sup>2</sup>Seoul National University College of Medicine, Rehabilitation Medicine, Seoul, Korea Republic of ; <sup>3</sup>Seoul National University College of Medicine, Obstetrics and Gynecology, Seoul, Korea Republic of

#### Purpose or Objective

The goal of this study is to compare the risks of chronic lower extremity lymphedema (LEL) between pelvic external beam radiation therapy (EBRT) and brachytherapy and further identify risk factors for chronic LEL in gynecologic cancer patients who underwent adjuvant radiotherapy after radical hysterectomy.

#### Material and Methods

FIGO stage I-III gynecologic cancer patients who underwent adjuvant RT between January 2013 and December 2017 after radical hysterectomy were reviewed retrospectively. After ruling out other causes of lower extremity edema, patients suspected for LEL were diagnosed as LEL when circumference difference between both legs was 2 cm or more. Patients diagnosed as LEL before RT were regarded as acute lymphedema. One-to-one case-matched analysis was conducted with propensity scores generated from patient, tumor and treatment characteristics.

#### Results

Of 252 patients who met the inclusion criteria, 216 (85.7%) patients were treated with pelvic EBRT with or without brachytherapy and 36 (14.3%) patients were treated with brachytherapy alone. Overall, 34 (13.5%) patients were diagnosed with LEL with a median follow-up of 30.6 months (range, 12.0 - 67.7 months). Median interval from surgery to the onset of LEL was 5.0 months (range, 1.1 - 31.7 months). The proportion of patients who were diagnosed with LEL in 6 months and one year was 55.9%

and 85.3%, respectively. In multivariate analysis, para-aortic lymph node dissection (HR, 2.537; 95% CI, 1.247 - 4.859; p=0.009), harvesting more than 30 pelvic lymph nodes (HR, 2.167; 95% CI, 1.050 - 4.472; p=0.037) and laparoscopic surgery (HR, 2.548; 95% CI, 1.127 - 5.760; p=0.025) were identified as independent risk factors for chronic LEL. After propensity score matching, EBRT group showed significantly higher chronic LEL rate than brachytherapy group (3-year LEL rate: 27.8% vs 10.8%, p=0.034).

### Conclusion

Chronic LEL was relatively common in patients with gynecologic cancer, especially during the first year after surgery. Para-aortic lymph node dissection, laparoscopic approach and harvesting more than 30 pelvic lymph nodes during surgery were risk factors for chronic LEL. Compared with brachytherapy, adjuvant pelvic EBRT was also significantly associated with an increased risk of chronic LEL.

### PO-0829 MRI-based texture analysis of lymph node for predicting clinical outcome in cervical cancer patients

S. PARK<sup>1</sup>, M.H. Hahm<sup>2</sup>, S. Na<sup>3</sup>, G.O. Chong<sup>4</sup>, S.Y. Jeong<sup>5</sup>, J.E. Lee<sup>1</sup>, M.K. Kang<sup>1</sup>, M.Y. Kim<sup>6</sup>, J. Kim<sup>1</sup>  
<sup>1</sup>School of Medicine- Kyungpook National University, Department of Radiation Oncology, Daegu, Korea Republic of ; <sup>2</sup>Kyungpook National University Hospital, Department of Radiology, Daegu, Korea Republic of ; <sup>3</sup>Kyungpook National University Chilgok Hospital, Department of Biomedical Engineering Center, Daegu, Korea Republic of ; <sup>4</sup>School of Medicine- Kyungpook National University, Department of Obstetrics and Gynecology, Daegu, Korea Republic of ; <sup>5</sup>School of Medicine- Kyungpook National University, Department of Nuclear Medicine, Daegu, Korea Republic of ; <sup>6</sup>Kyungpook National University Hospital, Department of Radiation Oncology, Daegu, Korea Republic of

#### Purpose or Objective

The aim of this study was to evaluate the feasibility of MRI-based texture analysis of metastatic lymph nodes for predicting survival of node-positive cervical cancer.

#### Material and Methods

We enrolled 89 patients with node-positive cervical cancer with initial magnetic resonance imaging (MRI) for staging. All patients were treated with definitive chemoradiotherapy in our institution, from 2006 to 2016. The criterion for a metastatic lymph node was defined as a maximum short axis diameter of  $\geq 8$  mm on pretreatment MRI. T2-weighted image (T2WI) and contrast-enhanced image (CE) of metastatic lymph nodes were segmented semi-automatically. Voxel based texture analysis of mathematical parameters in addition to first order statistics for semi-automatically segmented metastatic lymph nodes were done. The local progression-free survival (LRFS), regional progression-free survival (RPFS), distant metastasis-free survival (DMFS), disease-free survival (DFS), and overall survival (OS) were estimated using the Kaplan-Meier method, and the differences were compared using log-rank tests. P values of < 0.05 were considered statistically significant.

#### Results

First order statistics including median (p = 0.023), entropy (p = 0.021) and uniformity (p = 0.015) and parameters of gray level co-occurrence matrix including homogeneity (p = 0.023) and normalized inverse difference (p = 0.023) were significantly associated with RPFS. Entropy (p = 0.012) and uniformity (p = 0.030) were found to be associated with DFS. Median value from first order statistical method was associated with OS (p = 0.023).

#### Conclusion

MRI-based texture analysis of metastatic lymph node could provide quantitative and objective assessment for predicting clinical outcome in node-positive cervical

cancer patients treated with definitive chemoradiotherapy.

### PO-0830 Assessment of setup margins and additional subsite anisotropic margin expansions in cervical IGRT.

P. Naga CH<sup>1</sup>, U. Mahantshetty<sup>1</sup>, A. Nachankar<sup>1</sup>, Y. Ghadi<sup>1</sup>, L. Scaria<sup>1</sup>, D. Aravindakshan<sup>1</sup>, S. Sastri<sup>1</sup>, L. Gurram<sup>1</sup>, S. Shrivastava<sup>1</sup>, P. Naga CH<sup>1</sup>

<sup>1</sup>Tata memorial hospital, Radiation oncology, Mumbai, India

#### Purpose or Objective

The movements of utero-cervical complex, variation in organ filling (rectal and bladder), tumor regression and set-up uncertainties during the course of radiation pose a major challenge for the use of conformal radiation techniques in the treatment of cervical cancers. This prospective, observational study aimed to assess of set-up margins and further sub-site anisotropic margin expansions by quantifying set-up errors and organ motion, respectively in cervical cancer image-guided radiation therapy (IGRT).

#### Material and Methods

Patients with locally advanced cervical cancer undergoing definitive pelvic radio (chemo) therapy between April 2011 and April 2017 were included. Daily pre-treatment 3D-volumetric kilo-voltage, cone-beam computed tomography (kV-CBCT) of pelvic region was acquired. Initially co-registration of daily CBCT with the planning CT images was done to match pelvic vessels/CTV pelvic nodal region after initial rigid alignment based on bony anatomy. Subsequently, soft-tissue matching was done to record the residual set-up errors to assess organ motion at the levels of mid-cervical canal and uterine fundus, separately (Figure 1).

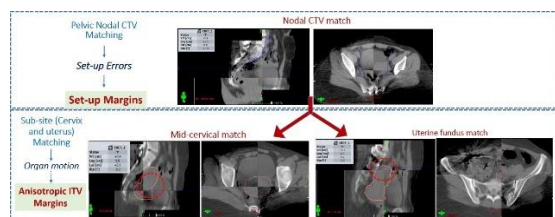


**Figure 1** : Representative sagittal and axial images illustrating CBCT matching at nodal-region CTV, mid-cervical and uterine fundus. Mean translational displacements, systematic, and random errors of the study population for matching at three levels were calculated. Set-up margins for clinical target volume (CTV) to planning target volume (PTV) and additional sub-site an-isotropic margin expansions for cervix and uterine region were derived separately using published margin recipes.

#### Results

Data acquired from 1389 kV-CBCT scans of 70 patients was considered for analysis. The recorded mean ( $\pm$ SD) displacements, systematic error ( $\Sigma$ ), random error ( $\sigma$ ) distribution along the six directions [left (X+) & right-lateral (X-), anterior (Y+) & posterior (Y-) directions and superior (Z+) & inferior (Z-)] in millimeter for pelvic nodal CTV region, mid-cervix, and uterine fundal matching is tabulated in Table 1. The calculated CTV-to-PTV margin and sub-site an-isotropic margin recipe for 95% coverage were 7.0 & 8.9 (bilaterally), 10.3 & 7.2 (antero-posteriorly) and 8.5 & 9.8 (supero-inferiorly), respectively. The obtained an-isotropic margin expansions for mid-cervix is 7.3 & 7.7, 8.5 & 6.7 and 9.5 & 8.5, respectively. Similarly, for uterine region, 7.3 & 7.6, 10.2 & 10.4 and 20.9 & 12.6, respectively (Table 1).

	Set-up errors (mm)				Organ motion (mm)									
	CTV pelvic nodal region				Cervix				Uterus					
	Mean ( $\pm$ SD)	$\Sigma$	$\sigma$	Margin	Mean ( $\pm$ SD)	$\Sigma$	$\sigma$	Margin	Mean ( $\pm$ SD)	$\Sigma$	$\sigma$	Margin		
X+	4.5 ( $\pm$ 3.4)	2.0	2.8	7.0	X+	4.5 ( $\pm$ 3.4)	2.1	3.0	7.3	X+	4.2 ( $\pm$ 3.1)	2.2	2.7	7.3
X-	4.5 ( $\pm$ 3.6)	2.7	3.3	8.9	X-	4.6 ( $\pm$ 3.4)	2.3	2.9	7.7	X-	4.6 ( $\pm$ 3.8)	2.3	2.7	7.6
Y+	5.3 ( $\pm$ 4.6)	3.0	4.1	10.3	Y+	5.4 ( $\pm$ 4.0)	2.3	4.0	8.5	Y+	6.6 ( $\pm$ 4.8)	2.7	4.8	10.2
Y-	4.9 ( $\pm$ 3.7)	1.9	3.5	7.2	Y-	5.1 ( $\pm$ 3.6)	1.8	3.1	6.7	Y-	7.4 ( $\pm$ 5.2)	3.0	4.3	10.4
Z+	5.1 ( $\pm$ 4.2)	2.4	3.5	8.5	Z+	5.5 ( $\pm$ 4.8)	2.7	3.9	9.5	Z+	12.1 ( $\pm$ 9.4)	6.6	6.2	20.9
Z-	4.7 ( $\pm$ 4.4)	2.9	3.6	9.8	Z-	4.7 ( $\pm$ 4.0)	2.3	3.8	8.5	Z-	6.6 ( $\pm$ 4.7)	4.0	3.8	12.6

**Table 1** : The mean, SD of target-motion along with systematic error ( $\Sigma$ ), random error ( $\sigma$ ) distribution and calculated margin (mm) recipe for 95% coverage in all three translational directions.

#### Conclusion

Our prospective study suggests set-up margins (CTV to PTV) to account for daily set-up uncertainties and an additional anisotropic margin for the cervical and uterine regions to account for organ motion during cervical cancer radiotherapy. Further research is warranted to evaluate various adaptive strategies for cervical cancer radiotherapy.

### PO-0831 Effect of pre-treatment hematological indices on survival in cervical cancer

U. Mahantshetty<sup>1</sup>, P. Naga CH<sup>1</sup>, L. Gurram<sup>1</sup>, R. Hawaldar<sup>2</sup>, S. Chopra<sup>3</sup>, S. Gupta<sup>4</sup>, J. Ghosh<sup>5</sup>, J. Bajpai<sup>5</sup>, S. Gulia<sup>5</sup>, J. Agarwal<sup>1</sup>

<sup>1</sup>Tata Memorial Hospital, Radiation Oncology, Mumbai, India ; <sup>2</sup>Tata Memorial Hospital, Clinical Research Secreteriat, Mumbai, India ; <sup>3</sup>ACTREC- Tata Memorial Centre, Radiation Oncology, Navi Mumbai, India ; <sup>4</sup>ACTREC- Tata Memorial Centre, Medical Oncology, Navi Mumbai, India ; <sup>5</sup>Tata Memorial Hospital, Medical Oncology, Mumbai, India

#### Purpose or Objective

Recent emerging evidences support that certain systemic indices of immune inflammation can act as independent prognostic factors for various cancers including cervical cancer. In this study, we investigate prognostic implications of pre-treatment hematological factors/indices in locally advanced cervical cancers treated with radical chemoradiation.

#### Material and Methods

The electronic medical records of 1051 cervical cancer patients of FIGO stage IB2 - IVA treated with chemoradiation in prospective studies between 2003 and 2017 were reviewed. All clinical parameters such as age, stage, histological type, nodal involvement and hematological parameters (haemoglobin, platelets, absolute neutrophil count, absolute lymphocyte count, absolute monocyte count) were recorded. Neutrophil/lymphocyte ratio (NLR), platelet/lymphocyte ratio (PLR) and lymphocyte/monocyte ratio (LMR) and prognostic nutritional index (PNI, defined as  $10 \times$  albumin concentration (g/dl)+0.005  $\times$  total lymphocyte count ( $\mu$ l)) were calculated. Univariate and multivariate (Cox regression) analyses was performed to evaluate impact of these factors on disease free survival (DFS) and overall survival (OS).

#### Results

With a median follow-up of 57 months (range, 3-169 months), the 5 years DFS and OS were 65% and 66.5%, respectively. **Table 1** shows in detail the outcome of univariate and multivariate analyses. On multivariate analysis, FIGO stage (HR, 1.57;  $p=0.000$ ) and LMR (HR: 0.92;  $p=0.007$ ) significantly affected DFS while FIGO stage (HR, 1.79;  $p=0.000$ ), LMR (HR, 0.92;  $p=0.008$ ), PNI (HR, 0.97;  $p=0.024$ ) and haemoglobin (HR, 0.93;  $p=0.039$ ) significantly affected OAS. Apart from FIGO Stage, LMR had a significant impact on both DFS and OAS.

Table 1: Univariate and multivariate survival analysis (n=1051).

		Univariate analysis (P-Value)		Multivariate analysis (P-Value)					
		DFS	OS	DFS			OS		
				P value	HR	95%CI	P value	HR	95%CI
<b>Clinico-pathological characteristics</b>									
Age (yrs)	≤50 Vs >50	0.272	0.471	0.088	0.99	0.97-1.00	0.33	0.99	0.98-1.00
FIGO Stage	IB2-IB Vs III-IVA	0.000*	0.000*	0.000*	1.57	1.28-1.93	0.000*	1.79	1.46-2.20
Histology	SCC Vs others	0.183	0.108	NS			NS		
Pelvic Node	Uninvolved Vs Involved	0.167	0.572	NS			NS		
<b>Hematological characteristics</b>									
Hb (g/dL)	≤11.5 Vs >11.5	0.020*	0.003*	0.249	0.96	0.90-1.03	0.039	0.93	0.87-1.00
Platelets(10 <sup>9</sup> /L)	≤300 Vs >300	0.130	0.060	0.190	1.00	1.00-1.002	0.288	1.00	0.99-1.001
NLR	≤2.5 Vs >2.5	0.050*	0.070	0.968	1.00	0.92-1.09	0.362	0.96	0.88-1.05
PLR	≤142 Vs >142	0.001*	0.000*	0.307	1.00	0.99-1.00	0.156	1.00	1.00-1.003
LMR	≤4.4 Vs >4.4	0.000*	0.000*	0.007*	0.92	0.86-0.98	0.008*	0.92	0.86-0.98
PNI	≤41 Vs >41	0.000*	0.000*	0.276*	0.99	0.96-1.01	0.024*	0.97	0.94-0.99

\*Statistically significance set at p ≤0.05

**Conclusion**

In cervical cancer patients treated with chemoradiation, LMR over and above established prognostic factors including FIGO Stage, hemoglobin and nutritional status seems to be an important independent prognostic factor for DFS and OAS. Further research to get more insights and clinical relevance is warranted.

**PO-0832 Para-aortic lymphadenectomy and recurrence patterns in locally advanced cervical cancer**

M.M. Soraya<sup>1</sup>, D.C. Moreno Santiago<sup>1</sup>, J. Giral Lopez de Sagredo<sup>1</sup>, R. Verges Capdevilla<sup>1</sup>

<sup>1</sup>Vall D'Hebron, radiation oncologist, Barcelona, Spain

**Purpose or Objective**

The aim of this study is to investigate the impact of primary para-aortic lymphadenectomy (PAL) on recurrence patterns in locally advanced cervical cancer patients.

**Material and Methods**

Data of all patients with cervical cancer treated in curative intent with external beam and brachytherapy +/- chemotherapy from 2001 to 2016 in our center were included in this retrospective study. Surgical staging was routinely performed before definitive treatment. However, there were some situations according to patient-related, tumor-related or logistic-related in which the surgical staging was not performed. Radiation was delivered to a clinical target volume comprising the uterus, cervix, vagina, parametrial tissues and pelvic nodes. Para-aortic region irradiation was performed only when there were prove of involved nodes by image or surgical staging.

**Results**

A total of 207 patients were included. The median follow-up was 39.6 months. Table 1 details clinical characteristics of the population according to surgical staging. Loco-regional and distant image staging was evaluated with MRI (97.1% of patients) and PET-CT (32.7% of patients, n=67), finding in MRI 46% of the patients with nodal affection and 55.2% (37) in PET-TC, without significative differences in the surgical vs non surgical groups. Para-aortic lymphadenectomy (PAL) via laparoscopic was done in 141 patients (68.1%). Globally 108 (54.5%) patients were diagnosed with pelvic positive and/or PA nodal involvement of which 35 received extended volume radiotherapy, 19% of them without surgical staging and 23% of those operated, without significant differences.

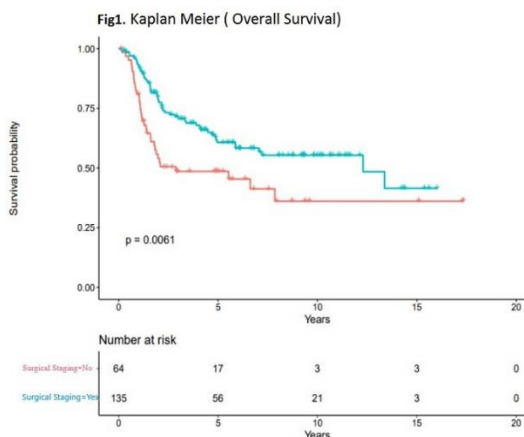
Recurrence happened in 68 patients (34%), 23 (35.4%) without surgical staging and 45 (33.3%) with PAL (p=ns). Local recurrence was described in 38.2% (39.1% and 37.8%, without and with PAL respectively; p=ns). The regional recurrence was 38.2%, 30.4% and 42.2 % respectively without significant differences between groups. The distance recurrence appeared in 52.9% to all group, 56.5%

for non-surgery group and 51% for surgery group, again without differences between the groups.

However overall survival (OS) was 46.87% in the non surgical group vs 60.75% in the surgical (p=0.0061) (Fig.1), probably due to the worse clinical features related with age, performance status and stage of tumor in the non surgical group (p<0.005).

Table 1: Main characteristics and recurrence patterns in patients with cervical cancer according to surgical staging

Characteristics	ALL n=206	Surgical Staging NO n=66	Surgical Staging YES n=141	p value
<b>Age</b>	52 (43.0-64.2)	65.5 (50.2-77.0)	49.5 (41.0-58.0)	<0.005
<b>ECOG</b>				<0.005
ECOG 0-1	193 (96.0%)	58 (87.9%)	135 (100%)	
ECOG 2-3	8 (4.0%)	8 (12.1%)	0 (0%)	
<b>FIGO stage</b>				<0.005
FIGO IB2-IIA2	80 (39.4%)	14 (21.2%)	66 (48.2%)	
Other FIGO stages	123 (60.6%)	52 (78.8%)	71 (51.8%)	
<b>Type of recurrence</b>	ALL n=68	Surgical Staging NO n=23	Surgical Staging YES n=45	p value
<b>Local failure</b>	26 (38.2%)	9 (39.1%)	17 (37.8%)	NS
<b>Regional failure</b>	26 (38.2%)	7 (30.4%)	19 (42.2%)	NS
Pelvic failure	17 (25%)	2 (8.7%)	15 (33.3%)	
PA failure	11 (16.2%)	5 (21.7%)	6 (13.3%)	
<b>Distant failure</b>	36 (52.9%)	13 (56.5%)	23(51.1%)	NS



**Conclusion**

In our group, those patients who underwent surgical staging had a better overall survival. However, Primary PAL does not demonstrate an improvement in loco-regional and distant control. This data suggest that PAL without prophylactic extended volume irradiation does not change the patterns of recurrence in patients with locally advanced cervical cancer.

**PO-0833 Development of a nomogram for predicting overall survival in patients with Cervical cancer**

A.B.A. Osong<sup>1</sup>

<sup>1</sup>Maastricht University, Maastr, Hasselt, Belgium

**Purpose or Objective**

The International Federation of Gynecologists and Obstetricians (FIGO) stage is a prominent prognostic factor for estimating patient's survival in cervical cancer. However, several studies have shown that additional clinical and pathologic variables further improve the prognostic performance of patient survival models. These survival models can be graphically represented in nomograms, enabling the estimation of a patient's overall survival (OS) probability based on these factors. However, these models should be contemporary to the additional routine clinical data. In this work, we developed and internally validated a nomogram to predict OS for cervical cancer patients treated with radiotherapy, optionally in combination with hyperthermia or chemotherapy.

**Material and Methods**

This study included a cohort of 494 patients treated primarily with radiotherapy between 1978 and 2015 with a curative intent. We analyzed five clinical variables, i.e. FIGO stage (IB - IIB), age, tumor diameter (<4cm and > 4cm), histologic type (squamous or adenocarcinoma), treatment (Radiotherapy (XRT), XRT and Chemotherapy, XRT and Hyperthermia). The outcome of interest is OS defined as the time between first treatment and death or last follow-up. Univariate analyses consists of Kaplan-Meier plots and log-rank test. The final multivariate Cox proportional hazard regression model used to build the nomogram included only variables with a statistical significance (p<0.05). The nomogram's performance was assessed by comparing the predicted values of the surviving and non-surviving patients to the observed values in a bootstrapped-internal calibration plots and the concordance index (C-index) where a C-index = 1 indicates a perfect prediction and C-index = 0.5 is comparable to a random guess.

**Results**

We excluded 64 patients with incomplete data reducing the cohort to 430 patients. The mean age in this cohort was 60 (29 - 93) years; Table 1 shows the variable distribution for this study cohort, including the univariate and multivariate statistical significance. The 5 and 10-year overall survival rate since first treatment was approximately 82% and 80% with a median survival period of 90 and 101 months respectively. The model had a C-index of 0.64 with a standard error of 0.024. Figure 1 shows the nomogram representation of the model and the bootstrapped calibration plot. The calibration plot shows an agreement between the models' predicted values and the observed values since most of the points are close to the diagonal line, which indicates perfect prediction.

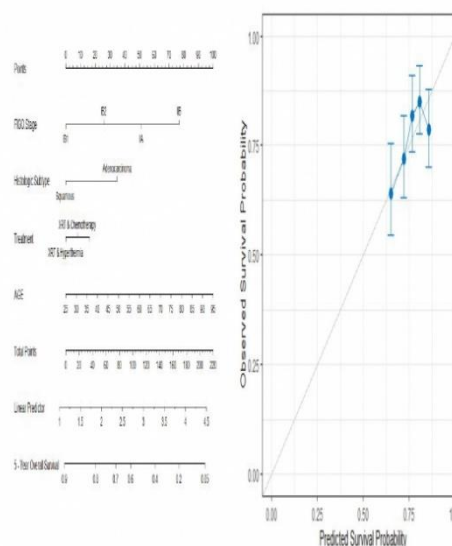


Figure 1: Nomogram for 5-year overall survival(Left) and Calibration curve of the nomogram for 5-year survival(Right)

**Conclusion**

We developed and internally validated a nomogram to predict 5 and 10 - year overall survival for patients with cervical cancer who were treated with radiotherapy, optionally combined with hyperthermia or chemotherapy.

Table 1: Univariate and multivariate analyses

Factors	Levels(n)	Univariate			multivariate		
		HR	95% CI	P-value	HR	95% CI	P-value
Age		1.02	1.01-1.03	<0.05	1.02	1.01-1.03	<0.05
Tumor size	>4 (248)	Ref			Ref		
	≤4 (205)	0.91	0.66-1.24	0.54	0.88	0.63-1.23	0.46
FIGO stage	IB1 (87)	Ref			Ref		
	IB2 (260)	1.32	0.84-2.09	0.21	1.19	0.76-1.84	0.43
	IIA (92)	2.22	1.34-3.66	0.00	1.89	1.15-3.11	0.01
	IIB (14)	3.13	1.27-7.71	0.01	3.61	1.55-8.41	<0.05
Histologic subtype	Squamous (406)	ref					
	Adenocarcinoma(41)	1.63	0.98-2.70	0.05	1.78	1.11-2.86	0.01
Treatment	XRT (262)	ref			ref		
	XRT / Chemotherapy(97)	0.75	0.45-1.24	0.27	0.76	0.47-1.22	0.26
	XRT / Hyperthermia(102)	0.77	0.50-1.18	0.23	0.73	0.47-1.11	0.04

**Poster: Clinical track: Prostate**

**PO-0834 Virtual imaging for patient information on radiotherapy planning and delivery for prostate cancer.**

J. Sulé-Suso<sup>1</sup>, J. Bisson<sup>1</sup>, S. Jassal<sup>1</sup>, M. Martínez<sup>2</sup>, N. Huxley<sup>1</sup>, C. Ellis<sup>1</sup>, D. Chambers<sup>1</sup>, K. Fields<sup>1</sup>, C. O'Donovan<sup>1</sup>, C. Edwards<sup>2</sup>, S. Vengalil<sup>1</sup>, R. Bhana<sup>1</sup>  
<sup>1</sup>University Hospital of North Midlands, Oncology Department, Stoke on Trent, United Kingdom ;  
<sup>2</sup>University Hospital of North Midlands, Physics- Oncology department, Stoke on Trent, United Kingdom

**Purpose or Objective**

To assess whether provision of information on RT planning and delivery with a virtual reality (VR) system (VERT) improves, apart from patient's satisfaction<sup>1</sup>, patient's compliance to RT (holding better their water prior to each RT session), and reduces side effects.

**Material and Methods**

This was a randomised study where patients were allocated to group 1 (information on RT planning and delivery using the VERT system was given prior to starting RT) or group 2 (information on RT planning and delivery using the VERT system was given after the last day of RT). Ninety-two patients with prostate cancer receiving radical RT were included in the study. The study was approved by the local ethics committee. For each study patient, their planning CT Scan images and RT plan were uploaded onto the VERT system using the Digital Imaging and Communication in Medicine (DICOM) standard. Patients and relatives were shown using VERT and on a one-to-one basis with a radiographer, a standard room where RT is given, a linear accelerator, and how RT is planned and delivered using their own planning CT Scans. Emphasis was put on the area to be treated and the organs around it. Bladder volumes were calculated from the planning CT Scan (prior to RT) and then on days 1, 2, 3 and then weekly

from the cone beam CT (CBCT) Scans. At the end of the exercise, patients were asked to fill in a quality of life questionnaire (EORTC QLQ-PR25) prior to RT, half-way through RT, on the day of the last fraction of RT and at 3 and 6 months after RT to assess side effects. Radiotherapy was performed using 10 or 6 MV photons delivered from a Varian 2100IX linear accelerator. Treatment planning was performed on the 'Eclipse' system using CT scans. A dose of 74 Gy in 37 fractions was delivered. Every patient completed the prescribed treatment.

#### Results

There were no differences in the number of CBCT scans between group 1 (39.0 CBCT scans per patient) and group 2 (38.5 CBCT scans per patient). No differences were seen either in the reduction of bladder volumes between groups 1 and 2. The percentages of the bladder volume for group 1 and group 2 patients when compared to the pre-RT bladder volume were 81.8 %  $\pm$  25.2 and 80.2 %  $\pm$  37.9 respectively at week 4, and 84.7 %  $\pm$  35.7 and 76.5 %  $\pm$  34.1 respectively on the last day of RT. Finally, based on the answers from the quality of life questionnaire, no differences in early or late side effects were seen between both groups of patients.

#### Conclusion

Providing information on RT planning and delivery using 3D imaging systems rather than 2D helped patients and relatives to better understand the complexity of RT planning and delivery<sup>1</sup>. However, no differences were seen regarding patients' compliance to RT or side effects from RT.

1. Sulé-Suso J., *et al.* Pilot study on virtual imaging for patient information on radiotherapy planning and delivery. *Radiography* 21: 273-277; 2015.

#### PO-0835 <sup>68</sup>Ga-PSMA11 PET/CT in prostate cancer patients with biochemical recurrence: PET positivity predictors

R. Parise<sup>1</sup>, S. Bartoncini<sup>1</sup>, A. Guarneri<sup>1</sup>, D. Deandris<sup>2</sup>, B. Lillaz<sup>3</sup>, S.D. Solla<sup>1</sup>, L. Spinelli<sup>1</sup>, D. Nicolotti<sup>2</sup>, E. Pilati<sup>2</sup>, M. Bellò<sup>2</sup>, R. Passera<sup>2</sup>, P. Gontero<sup>3</sup>, G. Bisi<sup>2</sup>, U. Ricardi<sup>1</sup>  
<sup>1</sup>A.O.U. Città della Salute e della Scienza, Oncology-Radiation Oncology, Torino, Italy; <sup>2</sup>A.O.U. Città della Salute e della Scienza, Medical Sciences- Nuclear Medicine Unit, Torino, Italy; <sup>3</sup>A.O.U. Città della Salute e della Scienza, Surgical Sciences- Division of Urology, Torino, Italy

#### Purpose or Objective

<sup>68</sup>Ga-PSMA-11 PET/CT is nowadays the most promising PET tracer in the detection of prostate cancer recurrence. The aim of this study is to assess the detection rate of this technique in patients with prostate cancer biochemical recurrence (BCR) with low PSA levels, and to evaluate which are the predictors of PET positivity.

#### Material and Methods

We prospectively enrolled patients referred to our Center between November 2016 and March 2018 with BCR, after primary treatment. All patients underwent <sup>68</sup>Ga-PSMA-11 PET/CT; in case of PSA >1.5 ng/ml the exam was performed only if previous choline PET/CT were negative. Clearly positive <sup>68</sup>Ga-PSMA-11 PET/CT findings were considered as true positive; dubious findings were explored by other imaging techniques and defined as true positive or true negative by a multidisciplinary consensus. Association between PET positivity and clinical patterns was evaluated by univariate and multivariate logistic regression models.

#### Results

A total of 140 <sup>68</sup>Ga-PSMA-11 PET/CT scans were performed; in 76 (54.3%) patients after radical surgical treatment only, in 3 (2.1%) patients after radiotherapy only and in 61 (43.6%) patients after radical surgery and adjuvant or salvage radiotherapy. Gleason Score (GS) was  $\leq$ 3+4 in 59 (42.1%),  $\geq$ 4+3 in 78 (55.8%) and not known in 3 (2.1%) patients, respectively. T stage was T1c-T2b-c in 69

(49.3%), T3a-b in 66 (47.1%) and not known in 5 (3.6%) patients, respectively. Median PSA value at the moment of PET/CT was 0.73 ng/ml (range 0.23-8.90); in particular, PSA was >0.2 and <0.5 ng/ml in 44 (31.5%), >0.5 e <1 ng/ml in 49 (35%), >1 and <1.5 ng/ml in 23 (16.4%) and >1.5 ng/ml in 24 (17.1%) patients, respectively. Median PSA doubling time and PSA velocity were 8.7 months (range 0.6-264.8) and 0.6 ng/ml/yr (range 0-30.2), respectively. <sup>68</sup>Ga-PSMA-11 PET/CT was considered positive in 57 cases (40.7%); recurrence was located in prostate bed (n=10), loco-regional lymph nodes (n=30), lymph nodes and bone (n=4), and distant sites (n=13). A significant association was observed for PSA velocity (median 0.9 in PET+ vs 0.35 ng/ml/yr in PET-, p<0.001), the 3 main risk factors for PET positivity were the last absolute PSA value before <sup>68</sup>Ga-PSMA PET/CT > 1 ng/ml (OR 5.64, 95% CI 2.23-14.26, p<0.001), a PSA doubling time  $\leq$ 8,7 month (OR 3.13, 95% CI 1.53-6.42, p 0.002) and a T3 stage (OR 4.33, 95% CI 2.06-9.10, p<0.001), both in univariate and multivariate logistic models. Patient management was modified in 29 cases (21%) on the basis of <sup>68</sup>Ga-PSMA-11 PET/CT findings.

#### Conclusion

Preliminary data suggest that <sup>68</sup>Ga-PSMA-11 PET/CT results may be clinically useful to detect prostate cancer recurrence at low PSA values, when dealing with the most aggressive disease patterns. In this setting, a proper selection of the patients that could really benefit of <sup>68</sup>Ga-PSMA-11 PET/CT is mandatory, in order to reach a more cost-effective profile. Larger prospective trials are needed.

#### PO-0836 Outcomes and factors by risk group after prostate brachytherapy: Cohort study in 2316 patients N. Katayama<sup>1</sup>, K. Nakamura<sup>2</sup>, A. Yorozu<sup>3</sup>, T. Kikuchi<sup>4</sup>, T. Magome<sup>5</sup>, S. Saito<sup>6</sup>, T. Dokiya<sup>7</sup>, M. Fukushima<sup>8</sup>, S. Kanazawa<sup>1</sup>

<sup>1</sup>Okayama University Hospital, Department of Radiology, Okayama, Japan; <sup>2</sup>Hamamatsu University School of Medicine, Department of Radiation Oncology, Hamamatsu, Japan; <sup>3</sup>National Hospital Organization Tokyo Medical Center, Department of Radiation Oncology, Tokyo, Japan; <sup>4</sup>Translational Research Center for Medical Innovation, Department of Statistics, Kobe, Japan; <sup>5</sup>Komazawa University, Department of Radiological Sciences- Faculty of Health Sciences, Tokyo, Japan; <sup>6</sup>National Hospital Organization Tokyo Medical Center, Department of Urology, Tokyo, Japan; <sup>7</sup>Kyoundou Hospital, Department of Radiology, Tokyo, Japan; <sup>8</sup>Translational Research Center for Medical Innovation, Director and Chairman, Kobe, Japan

#### Purpose or Objective

The nationwide prospective cohort study in Japan (J-POPS) resulted in excellent biochemical freedom from failure (bFFF) among all patients who were treated during the first 2 years. Here we report the bFFF by risk group and treatment modality and the associated factors of bFFF by risk group in those patients with prostate cancer undergoing permanent seed implantation (PI) with or without external beam radiation therapy (EBRT).

#### Material and Methods

A total of 2,316 patients in 42 institutes were evaluated. bFFF was evaluated using the Phoenix definition (prostate-specific antigen (PSA) nadir + 2.0 ng/mL). If the PSA subsequently fell to  $\leq$ 0.5 ng/mL without intervention, this was considered a PSA bounce. The scheduled follow-up assessments were conducted every 3 months for the first 2 years, and every 6 months thereafter for 5 years after completion of radiation therapy. We estimated the bFFF by the Kaplan Meier method. We also identified the factors associated with the bFFF by the Cox proportional hazard model.

#### Results

The median age was 69.0 (range, 45-89) years. Median PSA was 6.8 (range, 1.6-42.0) ng/ml. 2,103 patients (23.4%)

had clinical stage T2a or less and 1,309 (56.5%) had Gleason score (GS) less than 7. 542 patients (23.4%) received supplemental EBRT and 1,137 (49.1%) received hormonal treatment (HT). Median follow-up period was 60.0 months (interquartile range, 58.7-60.9 months). The 5-year bFFF rate in all patients, 1028 low risk (LR) patients, 1114 intermediate risk (IR) patients and 133 high risk (HR) patients were 93.6%, 94.9%, 92.7% and 91.1%, respectively (Fig. 1). The 5-year bFFF rate in PI group and EBRT combination therapy group were 93.7% and 93.3%, respectively. On multivariate analysis, older age, GS and the percent volumes of the prostate receiving 100% of the prescribed dose (prostate V100) ( $p = 0.0003$ ,  $<0.0001$  and  $0.0107$ , respectively) in all patients, older age, PSA and prostate V100 ( $p = 0.0002$ ,  $0.0048$  and  $0.0012$ , respectively) in LR patients, and GS and HT ( $p = 0.0003$  and  $0.0077$ , respectively) in IR patients were significantly associated with bFFF. There were no significant predictors in HR patients (Table 1).

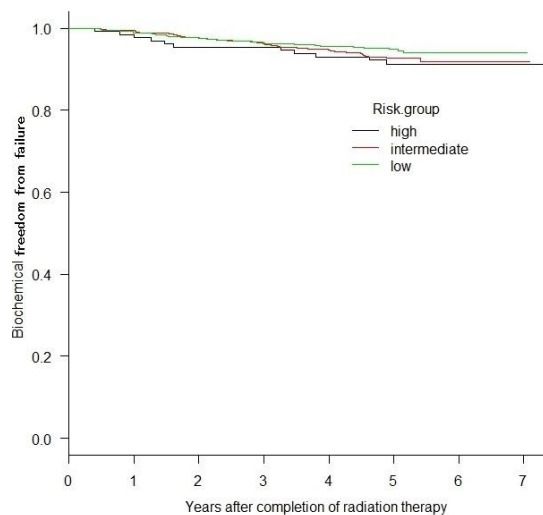


Table 1 Multivariate analyses for biochemical freedom from failure

Factors	Univariate analysis			Multivariate analysis			
	HR	95% CI	p	HR	95% CI	p	
<b>All cases</b>							
Age	0.960	0.936-0.985	0.0016*	0.954	0.929-0.979	0.0003*	
PSA	1.040	1.007-1.074	0.0161*	1.030	0.996-1.064	0.0803	
Gleason score	—	—	<0.0001*	—	—	<0.0001*	
	reference			reference			
6 or less	1.351	0.903-2.022	0.1435	1.432	0.954-2.151	0.0833	
7 (2+5, 3+4)	2.460	1.650-3.670	<0.0001*	2.562	1.685-3.894	<0.0001*	
7 (4+3), 8 to 10	0.968	0.943-0.995	0.0187	0.966	0.940-0.992	0.0107*	
Prostate V100 (%)							
<b>Low risk group</b>							
Age	0.928	0.891-0.967	0.0004*	0.926	0.889-0.964	0.0002*	
PSA	1.219	1.044-1.423	0.0123*	1.246	1.069-1.452	0.0048*	
Prostate V100 (%)	0.944	0.907-0.982	0.0044*	0.936	0.899-0.974	0.0012*	
<b>Intermediate risk group</b>							
Hormonal treatment	Yes	0.559	0.353-0.886	0.0133*	0.534	0.337-0.847	0.0077*
	No	—	reference	—	reference	—	
Gleason score	—	—	0.0005*	—	—	0.0003*	
	reference			reference			
6 or less	2.146	0.957-4.813	0.0640	2.092	0.932-4.693	0.0734	
7 (2+5, 3+4)	4.258	1.875-9.671	0.0005*	4.383	1.929-9.957	0.0004*	
7 (4+3), 8 to 10							
<b>High risk group</b>							
No significant factor							

HR = hazard ratio; CI = confidence interval; Other abbreviations as in Table 1.

\*: Significant risk factor

## Conclusion

PI with or without EBRT resulted in excellent short-term biochemical outcomes at all risks, especially in HR patients in Japan. Older age, PSA and prostate V100 in LR patients and GS and HT in IR patients independently affected bFFF.

## PO-0837 Dose-effect relationship for early late incontinence after IMRT in post-prostatectomy patients

P. Gabriele<sup>1</sup>, F. Munoz<sup>2</sup>, D. Cante<sup>3</sup>, B. Avuzzi<sup>4</sup>, C. Bianconi<sup>5</sup>, F. Badenchini<sup>6</sup>, B. Farina<sup>7</sup>, P. Farina<sup>8</sup>, E. Garibaldi<sup>9</sup>, T. Giandini<sup>9</sup>, G. Girelli<sup>10</sup>, V. Landoni<sup>11</sup>, A. Magli<sup>12</sup>, A. Maggio<sup>13</sup>, E. Moretti<sup>14</sup>, B. Noris Chiorda<sup>4</sup>, E.

Petrucchi<sup>15</sup>, P. Salmoiraghi<sup>16</sup>, E. Villa<sup>17</sup>, J.M. Waskiewicz<sup>18</sup>, N.G. Di Muzio<sup>5</sup>, T. Rancati<sup>6</sup>, C. Fiorino<sup>19</sup>, C. Cozzarini<sup>5</sup>  
<sup>1</sup>Istituto di Candiolo-Fondazione del piemonte per l'Oncologia IRCCS, Radiotherapy, Candiolo TO, Italy ;  
<sup>2</sup>Ospedale Regionale U Parini - AUSL Valle d'Aosta, Radiotherapy, Aosta, Italy ;  
<sup>3</sup>Ospedale di Ivrea- ASL TO4, Radiotherapy, Ivrea, Italy ;  
<sup>4</sup>Fondazione IRCCS Istituto Nazionale Tumori, Radiotherapy, Milano, Italy ;  
<sup>5</sup>San Raffaele Scientific Institute, Radiotherapy, Milano, Italy ;  
<sup>6</sup>Fondazione IRCCS Istituto Nazionale Tumori, Programma prostata, Milano, Italy ;  
<sup>7</sup>Ospedale degli infermi, Medical Physics, Biella, Italy ;  
<sup>8</sup>Comprendorio Sanitario di Bolzano, Medical Physics, Bolzano, Italy ;  
<sup>9</sup>Fondazione IRCCS Istituto Nazionale Tumori, Medical Physics, Milano, Italy ;  
<sup>10</sup>Ospedale degli infermi, Radiotherapy, Biella, Italy ;  
<sup>11</sup>Istituto Nazionale dei Tumori Regina Elena, Medical Physics, Roma, Italy ;  
<sup>12</sup>Ospedale di Udine, Radiotherapy, Udine, Italy ;  
<sup>13</sup>Istituto di Candiolo-Fondazione del piemonte per l'Oncologia IRCCS, Medical Physics, Candiolo TO, Italy ;  
<sup>14</sup>Ospedale di Udine, Medical Physics, Udine, Italy ;  
<sup>15</sup>Ospedale di Ivrea- ASL TO4, Medical Physics, Ivrea, Italy ;  
<sup>16</sup>Cliniche Gavazzeni Humanitas, Medical Physics, Bergamo, Italy ;  
<sup>17</sup>Cliniche Gavazzeni Humanitas, Radiotherapy, Bergamo, Italy ;  
<sup>18</sup>Comprendorio Sanitario di Bolzano, Radiotherapy, Bolzano, Italy ;  
<sup>19</sup>Fondazione Centro San Raffaele, Department of Medical Physics, Milano, Italy

## Purpose or Objective

Assessing predictors of patient-reported incontinence (INC) 1-year after post-prostatectomy IMRT, focusing on the impact of dose.

## Material and Methods

390 patients (pts) treated during 2012-2018 with adjuvant (ADV) or salvage (SALV) intent were enrolled in a registered (ClinicalTrials.gov) multi-centric cohort study aimed to assess predictors of intestinal, haematological and urinary toxicity. IMRT was delivered with conventional (n=228, 66-77.4Gy) or moderate hypo-fractionation (n=162, 65-75Gy, 2.2-2.7Gy/fr). Clinical and dosimetry data were prospectively collected including ICIQ-SF questionnaire for INC evaluation at baseline, half-RT, end-RT and every 6 months up to 5 years after IMRT. At the time of analysis, mature 1-year data were available; four ICIQ-based end-points were considered: a) "subjective" severe INC: ICIQ-SF>12; b) "subjective" moderate INC: ICIQ-SF>5; c) daily leakage: ICIQ3 (i.e. the score of question 3)>2; d) objective moderate INC: ICIQ3+4 (i.e. the sum of the scores of questions 3 and 4) >4. Predictors of 1-year prevalence were assessed through uni- (UVA) and multi-variable (MVA) logistic regression: potential clinical predictors included age, time from surgery, intent (ADV vs SALV), comorbidities and patient habits, type of surgery and baseline INC. The prescribed EQD2 (i.e.: PTV D<sub>mean</sub>) was also considered by applying alpha-beta values equal to 5 and 1Gy (EQD2\_5/EQD2\_1), reported in literature for late urinary toxicity. UVA/MVA were repeated excluding pts with the investigated symptoms at baseline.

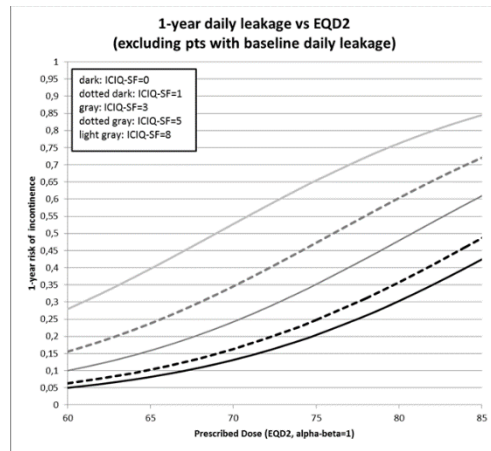
## Results

In total, 356/390 pts filled in baseline ICIQ-SF and 238/356 pts the 1-year ICIQ-SF. Pts experiencing a, b, c, d were 44 (18%), 131 (55%), 124 (52%) and 124 (52%) respectively. The corresponding baseline values were 33 (14%), 114 (48%), 102 (43%) and 103 (43%). For all end-points, baseline ICIQ-SF was the strongest predictor ( $p<0.0001$ , OR: 1.30-1.33), even excluding pts with baseline symptoms ( $p<0.0001$ , OR: 1.25-1.37). When excluding pts with symptoms at baseline, EQD2\_1 was predictive of both objective end-points c and d ( $p=0.02$ , OR: 1.089-1.090). At MVA, ICIQ-SF and EQD2\_1 were independent predictors: the resulting two-variable models well fit data (H&L test: 0.60-0.70) with good calibration (slope= 0.96,  $R^2=0.93$ ). The 1-year risk of daily leakage (n=132 patients, 42 daily leakage: 32%) is plotted in the figure against EQD\_1 for

few baseline ICIQ-SF values: ORs for EQD\_1 and ICIQ-SF were 1.11 ( $p=0.008$ ) and 1.28 ( $p=0.002$ ) respectively.

#### Conclusion

Baseline ICIQ-SF is the major predictor of 1-year INC. Despite the short follow-up, a dose-effect was found for objective INC when excluding pts with symptoms at baseline: the dose relationship was modulated by mild-moderate baseline symptoms. The association between EQD2\_1 and INC (not found for EQD2\_5,  $p>0.30$ ) is a confirmation of the previously reported high sensitivity to fractionation for INC, suggesting extreme caution in using moderate hypo-fractionation in the post-operative setting.



**PO-0838 Castrate testosterone predicts biochemical relapse free survival in non-metastatic prostate cancer**  
G. Ozyigit<sup>1</sup>, P. Hurmuz<sup>1</sup>, D. Yuze<sup>2</sup>, F. Akyol<sup>1</sup>  
<sup>1</sup>Hacettepe University- Faculty of Medicine, Department of Radiation Oncology, Ankara, Turkey ; <sup>2</sup>Hacettepe University- Faculty of Medicine, Department of Preventive Oncology, Ankara, Turkey

#### Purpose or Objective

We evaluated the effect of two different castrate testosterone levels, <50 and <20 ng/dL, on biochemical relapse free survival (BRFS) in patients with non-metastatic intermediate and high risk prostate cancers (PC) receiving definitive radiotherapy (RT) and androgen deprivation therapy (ADT).

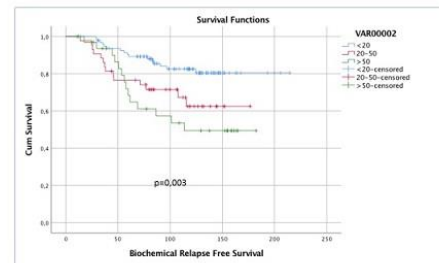
#### Material and Methods

We have a prospective treatment protocol for the definitive treatment of PC patients which was approved by the institutional ethical review board. Herein we included subset of patients with intermediate and high risk disease according to D'Amico risk group stratification. Between April 1998 and February 2011 173 patients with median age of 69 (range, 50-82 years) were treated. Radiotherapy was delivered by either three dimensional conformal technique (3DCRT) to a total dose of 73.4 Gy at the ICRU reference point or intensity modulated radiotherapy technique (IMRT) to a total dose of 76 Gy with daily fraction dose of 2 Gy. All the patients received 3 months of neoadjuvant ADT followed by RT and additional 6 months of ADT. ADT was delivered in the form of total androgen blockade (TAB): GnRH agonist plus antiandrogen. Testosterone levels were measured at each clinical follow-up visits. ASTRO Phoenix definition (nadir PSA+2 ng/dl) was used to define biochemical relapse. All patients should have at least 12 months of follow up.

#### Results

Median follow up duration was 125 months. Median initial PSA level was 14.2 ng/dL (range, 2-100 ng/dL) and median GS was 7 (range, 3-9). The characteristics of the patients

are shown in Table 1. All of the patients received 9 months of planned TAB. Nightly six patients (56%) had castrate testosterone level < 20ng/mL and 139 patients (80%) had castrate testosterone level < 50 ng/mL. Median testosterone recovery time after TAB cessation was 6 months (range, 6-30 months). Both cutoff values are valid at predicting BRFS. However patients with castration testosterone value <20 ng/dL have significantly better BRFS compared to other patient groups ( $p=0.003$ ) (Figure 1). When we compare two cutoff values using receiver operating characteristic curve (ROC) analyses, it was found that using 20 ng/dL is better than 50 ng/dL in predicting the BRFS (AUC= 0.63 versus 0.58, respectively).



Characteristics	Number (%)
AJCC 2010 T stage	
T1	3 (2%)
T2a	74 (43%)
T2b	14 (8%)
T2c	16 (9%)
T3a	40 (23%)
T3b	17 (10%)

Gleason score (median)	7 (3-9)
Initial PSA (median)	14 ng/dL (2-100 ng/dL)

D'Amico risk group	
intermediate	52 (30%)
High	121 (70%)
Perineural invasion	
Absent	103 (60%)
Present	56 (32%)
Unknown	14 (8%)
Percent positive core biopsy percentage	
≥50%	76 (44%)
>50%	59 (34%)
unknown	38 (22%)
Radiotherapy dose	
70 Gy	145 (84%)
75 Gy	16 (16%)

#### Conclusion

Castration testosterone level of less than 20 ng/dL achieved after primary RT plus ADT is associated with better BRFS. Using castration cut off value of 20 ng/dL is better in estimating the BRFS compared to 50 ng/mL. Further studies using current standard of care of high dose IMRT and longer ADT duration might support these findings.

**PO-0839 Correlation of recalculated-dose based on CBCT and toxicity in postoperative prostate cancer VMAT**

P. Buranaporn<sup>1</sup>, T. Jaikuna<sup>1</sup>, P. Dankulchai<sup>1</sup>  
<sup>1</sup>Faculty of Medicine Siriraj Hospital- Mahidol University, Division of Radiation Oncology- Department of Radiology, Bangkok, Thailand

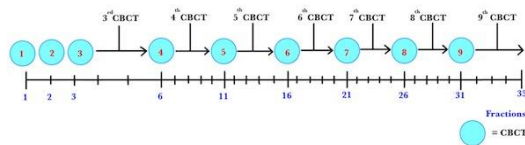
#### Purpose or Objective

To study relationship between GI and GU toxicity and estimated actual volume using recalculated-dose based on CBCT of deformable organs, rectum and bladder, receiving VMAT for postoperative prostate cancer patients.

#### Material and Methods

115 postoperative prostate cancer patients treated with VMAT technique from 2014-2017 were studied retrospectively. Rectum and Bladder were delineated on each CBCT image. Estimated actual dose on CBCT available fraction was recalculated on each CBCT image based on CBCT-calibration curve and was used as a

representative until next CBCT available fraction (as the figure shown). Recalculated dose was deformed into planning CT image by using deformable image registration from Velocity AI software version 3.2 to accumulate estimated actual dose in the treatment course. Dosimetric parameters were then studied, including V50, V60, V65, V70 and V75 for rectum and V65, V70, V75 and V80 for bladder based on QUANTEC study. Clinical toxicities of each case were reviewed from the patient records according to CTCAE version 5.0. Differences of mean volume between patients with grade 0-1 and grade 2-5 toxicities were compared using student T-test. Relationships between toxicities and volumes receiving doses were analyzed using logit analysis.



## Results

All patients with acute rectal toxicity grade 2 or more showed significant increase in volume receiving 50, 60, 65, 70, and 75 Gy radiation compared to those with acute rectal toxicity grade 0 and 1 ( $p=0.002$ ,  $0.007$ ,  $0.008$ ,  $0.021$ , and  $0.018$  respectively), while in late rectal toxicity grade 2 or more showed significant increase in volume receiving 50, 60, 70 and 75Gy radiation compared to group with late rectal toxicity grade 0 and 1 ( $p=0.011$ ,  $0.011$ ,  $0.011$ ,  $0.003$  respectively). For the correlation between rectal volume receiving 75 Gy and acute and late toxicities, the significant dose-response relationships were exhibited ( $p<0.001$ ). The probability for developing toxicities of 10%, 15% and 20% were related with volume receiving 75 Gy dose of 10.9, 15.7 and 19.3 cc in acute rectal toxicity and 10.9, 14.7 and 17.5 cc in late rectal toxicity. Acute and late bladder toxicity revealed no significant relationship with volume receiving radiation in all doses (65, 70, 75 and 80 Gy).

Probability of Grade 2-4 Acute Rectal Toxicity				
Volume (cc)	10%	15%	20%	p value
V50	46.5 (44.7 - 48.7)	51.8 (49.6 - 54.6)	55.8 (53.2 - 59.1)	1.000
V60	32.3 (31.0 - 33.8)	36.4 (34.8 - 38.3)	39.4 (37.6 - 41.7)	0.996
V65	24.0 (23.0 - 25.2)	27.3 (26.0 - 28.8)	29.7 (28.2 - 31.5)	0.650
V70	15.8 (14.5 - 17.6)	19.6 (18.0 - 21.7)	22.5 (20.5 - 24.9)	1.000
V75	10.9 (8.2 - 16.4)	15.7 (11.8 - 23.7)	19.3 (14.5 - 29.2)	0.000

Probability of Grade 2-4 Chronic Rectal Toxicity				
Volume (cc)	10%	15%	20%	p value
V50	45.5 (43.5 - 48.0)	52.226 (49.5 - 55.6)	57.2 (54.0 - 61.3)	0.920
V60	32.6 (30.8 - 34.8)	38.1 (35.8 - 41.0)	42.2 (39.5 - 45.8)	1.000
V65	25.2 (23.3 - 27.7)	30.8 (28.2 - 34.3)	35.0 (31.9 - 39.2)	1.000
V70	16.6 (15.0 - 18.8)	21.3 (19.1 - 24.2)	26.8 (22.1 - 28.4)	1.000
V75	10.9 (8.6 - 15.1)	14.7 (11.5 - 20.4)	17.5 (13.7 - 24.4)	0.000

## Conclusion

Estimated actual volume of rectum receiving high dose (V75) from CBCT-based recalculation was significantly related with grade 2-5 acute and late rectal toxicities in dose-response relationship. Adaptive planning should be considered for a novel approach in order to reduce toxicity.

## PO-0840 Two StereoTactic Ablative Radiotherapy Treatments for Localized Prostate Cancer (2STAR)

Y. Alayed<sup>1</sup>, P. Cheung<sup>1</sup>, W. Chu<sup>1</sup>, H. Chung<sup>1</sup>, M. Davidson<sup>2</sup>, A. Ravi<sup>2</sup>, J. Helou<sup>3</sup>, L. Zhang<sup>2</sup>, A. Mamedov<sup>2</sup>, A. Commisso<sup>2</sup>, K. Commisso<sup>2</sup>, A. Loblaw<sup>4</sup>

<sup>1</sup>Department of Radiation Oncology- Odette Cancer Centre- Sunnybrook Health Sciences Centre, Department of Radiation Oncology- University of Toronto, Toronto, Canada ; <sup>2</sup>Odette Cancer Centre- Sunnybrook health sciences centre, Department of Radiation Oncology, Toronto, Canada ; <sup>3</sup>Princess Margaret Cancer Centre,

Department of Radiation Oncology- University of Toronto, Toronto, Canada ; <sup>4</sup>Department of Radiation Oncology- Odette Cancer Centre- Sunnybrook Health Sciences Centre, Department of Radiation Oncology- University of Toronto- Institute of Health Policy-Measurement & Evaluation- University of Toronto, Toronto, Canada

## Purpose or Objective

Ultra-hypofractionation is appealing for prostate cancer (PCa) due to the low  $\alpha/\beta$  ratio, and increasing the dose per fraction could improve the therapeutic index. Here we report the outcomes of a phase II trial in prostate SABR using a two-fraction protocol.

## Material and Methods

Patients had low or intermediate risk prostate cancer. Three gold fiducials were implanted for image guidance. The clinical target volume (CTV) included the prostate only, and the planning target volume (PTV) was a 3mm expansion on the CTV, enabled through the use of a rectal immobilization device. The dose prescribed to D99 CTV was 26 Gy in 2 weekly fractions (EQD2 110 Gy<sub>1.4</sub>). The primary endpoint was quality of life using the EPIC questionnaire, and the minimal clinically important change (MCIC) was defined as an EPIC QOL decrease  $> 0.5$  SD. Biochemical failure (BF) was defined as nadir  $+2$ . Four-year PSA response rate (4yPSARR) was defined as  $< 0.4$  ng/ml.

## Results

30 patients were accrued in 2014 with a median follow-up of 49.3 months. 10% had low-risk, 33% had favourable intermediate-risk and 56% had unfavourable intermediate-risk PCa. Five patients received a short course of ADT. Median nPSA was 0.2 ng/ml. One patient had BF and is being observed. 56.6% of patients had a 4yPSARR. The mean EPIC QOL change from baseline was -1.1 for the urinary domain, -1.04 for the bowel domain, and -3.8 for the sexual domain. Six patients had a MCIC in the urinary or bowel domain, and 3 had a MCIC in the sexual domain. The cumulative rate of grade 3-4 late GI/GU toxicity was 3%, one patient had a grade 3 hemorrhoid and one had a grade 3 urinary retention.

## Conclusion

Two-fraction SABR in prostate cancer is safe and feasible, with a minimal change in QOL experienced by patients and a low rate of late grade 3-4 toxicity. The PSA kinetics and biochemical control rates are encouraging given that the majority had unfavourable intermediate-risk disease, although longer follow-up is required.

## PO-0841 Salvage SBRT for local prostate cancer recurrence after radiotherapy: a GETUG retrospective study

G. Martinage<sup>1</sup>, G. Janoray<sup>2</sup>, D.P. Rojas<sup>3</sup>, D. Zerini<sup>3</sup>, F. Goupy<sup>4</sup>, R. De Crevoisier<sup>4</sup>, E. Bogart<sup>5</sup>, G. Calais<sup>2</sup>, A. Toledano<sup>6</sup>, L. Chauveinc<sup>6</sup>, N. Scher<sup>6</sup>, P.Y. Bondiau<sup>7</sup>, J.M. Hannoun-Levi<sup>7</sup>, M. Silva<sup>8</sup>, E. Meyer<sup>8</sup>, P. Nickers<sup>1</sup>, T. Laceronerie<sup>9</sup>, E. Lartigau<sup>1,10</sup>, B.A. Jereczek-Fossa<sup>3</sup>, D. Pasquier<sup>1,10</sup>

<sup>1</sup>Centre Oscar Lambret, Academic Department of Radiation Oncology, Lille, France ; <sup>2</sup>CHRU de Tours, Oncology-Radiotherapy Department, Tours, France ; <sup>3</sup>European Institute of Oncology IRCCS- Istituto Europeo di Oncologia IRCCS Milano, Department of Radiotherapy- Department of Oncology and Hemato-oncology, Milan, Italy ; <sup>4</sup>Centre Eugène Marquis, Department of Radiotherapy, Rennes, France ; <sup>5</sup>Centre Oscar Lambret, Department of Biostatistics, Lille, France ; <sup>6</sup>Hartmann Radiotherapy Center, Department of Radiotherapy, Levallois-Perret, France ; <sup>7</sup>Antoine Lacassagne Cancer Center, Department of Radiation Oncology, Nice, France ; <sup>8</sup>Centre François Baclesse, Department of Radiation Oncology, Caen, France ; <sup>9</sup>Centre Oscar Lambret, Department of Medical Physics, Lille, France ; <sup>10</sup>Lille University, CRISAL UMR CNRS 9189, Lille, France

### Purpose or Objective

After external beam radiotherapy (EBRT) for prostate cancer, the most common site of recurrence is the prostate. The aim was to assess the efficacy and safety of salvage stereotactic body radiotherapy (SBRT) for local prostate cancer recurrence after radiotherapy.

### Material and Methods

We retrospectively reviewed patients with biopsy proven local prostate cancer recurrence after EBRT or brachytherapy in centers from the French Genito-Urinary Group (GETUG) and in the European Institute of Oncology in Milan. Disease extension was assessed by pelvic multiparametric MRI and choline PET in 87% and 94% of patients, respectively. Treatment was proposed by multidisciplinary team in each center and delivered every other day. Median SBRT dose was 36 Gy (range, 25-36.25 Gy) in 6 fractions (range, 5-6). The primary endpoint was second biochemical recurrence-free survival defined according to the Phoenix criteria. Toxicity was assessed according to CTCAE v.4.03.

### Results

Between April 2010 and January 2017, 99 patients were treated with salvage SBRT with a median follow-up of 22.8 months (range 2.4-88.8 months). Twenty-two, 36 and 41 patients presented with low, intermediate and high risk at first diagnosis according to D'Amico classification. All patients presented with biopsy proven recurrence. The median time interval between first radiotherapy and salvage SBRT was 7.5 years (range 2-18 years). Median age at salvage SBRT was 71.2 years (SD 6.4 years) and median PSA at recurrence was 4.3 ng/mL (range, 2-38 ng/mL). Thirty four percent of patients were treated with androgen deprivation therapy for a median duration of 12 months. Whole gland, half prostate and focal treatment was delivered in 48, 18 and 33 patients respectively. Median nadir PSA after salvage SBRT was 0.5 ng/mL, obtained after a median time interval of 10.7 months. Second biochemical recurrence-free survival rates at 2 and 3 years were 72% [95% CI: 60%-81%] and 52% [95% CI: 39%-64%], respectively. Overall survival rates at 2 and 5 years were 96% [95% CI: 87-99] and 87% [95% CI: 71-95], respectively.

The initial D'Amico prognostic group was the only prognostic factor of biochemical recurrence-free survival ( $p=0.025$ ).

No patient developed grade  $\geq 2$  acute gastro-intestinal toxicity; grade 2 and 3 acute genito-urinary toxicity were 8% and 1%, respectively. Late toxicity included urinary events (fifteen grade 2 and one grade 3) and rectal events (two grade 2). One patient presented a neuritis of grade 3.

### Conclusion

With a short follow up, this largest series shows that salvage SBRT allows for good biochemical control and acceptable toxicity, with the key advantage of non-invasiveness of SBRT. This treatment is not a standard, and has to be administered with caution in competent centers. Further prospective studies are necessary to confirm these preliminary results <sup>1</sup>

<sup>1</sup> <https://clinicaltrials.gov/ct2/show/NCT03438552>

### PO-0842 Real-Time tracking improves treatment: The TROG Stereo Prostate Ablative Radiotherapy with KIM trial

P. Keall<sup>1</sup>, D.T. Nguyen<sup>1</sup>, R. O'Brien<sup>1</sup>, E. Hewson<sup>1</sup>, H. Ball<sup>1</sup>, P. Poulsen<sup>2</sup>, J. Booth<sup>3</sup>, P. Greer<sup>4</sup>, P. Hunter<sup>4</sup>, L. Wilton<sup>4</sup>, R. Bromley<sup>3</sup>, J. Kipritidis<sup>3</sup>, T. Eade<sup>3</sup>, A. Kneebone<sup>3</sup>, G. Hruby<sup>3</sup>, T. Moodie<sup>5</sup>, A. Hayden<sup>5</sup>, S. Turner<sup>5</sup>, S. Arumugam<sup>6</sup>, M. Sidhom<sup>6</sup>, N. Hardcastle<sup>7</sup>, S. Siva<sup>8</sup>, K. Tai<sup>8</sup>, V. Gebiski<sup>9</sup>, J. Martin<sup>4</sup>

<sup>1</sup>University of Sydney, ACRF Image X Institute, Sydney, Australia ; <sup>2</sup>Aarhus University Hospital, Department of Oncology, Aarhus, Denmark ; <sup>3</sup>Royal North Shore Hospital, Northern Sydney Cancer Centre, Sydney,

Australia ; <sup>4</sup>Calvary Mater Newcastle Hospital, Department of Radiation Oncology, Newcastle, Australia ; <sup>5</sup>Westmead Hospital, Crown Princess Mary Cancer Centre, Sydney, Australia ; <sup>6</sup>Liverpool Hospital, Liverpool and Macarthur Cancer Therapy Centres, Sydney, Australia ; <sup>7</sup>Peter MacCallum Cancer Centre, Department of Physical Sciences, Melbourne, Australia ; <sup>8</sup>Peter MacCallum Cancer Centre, Department of Radiation Oncology, Melbourne, Australia ; <sup>9</sup>University of Sydney, NHMRC Clinical Trials Centre, Sydney, Australia

### Purpose or Objective

Kilovoltage Intrafraction Monitoring (KIM) is an emerging real-time target tracking technology for standard linear accelerators without the need for additional in-room hardware. In the TROG 15.01 Stereotactic Prostate Ablative Radiotherapy (SABR) with KIM (SPARK) trial, KIM was used to enable real-time target tracking in a multi-institutional setting. We test the primary hypothesis that real-time target tracking improves prostate dose distributions.

### Material and Methods

Forty-eight men with prostate cancer were treated with KIM-guided SABR delivering 36.25 Gy to the prostate in five treatments. During treatment the prostate (target) motion was corrected in real-time by implementing KIM-guided beam gating with couch shifts or multileaf collimator tracking. A dose reconstruction method was used to evaluate the dose to the target and organs at risk (OARs) with real-time KIM target tracking. The same dose reconstruction method was used to evaluate the dose that would have been delivered without real-time target tracking. Thus, all cases acted as their own internal controls. A treatment was considered a success if the target and rectal dose with real-time target tracking were closer to the planned dose than the target and rectal dose estimated without real-time target tracking. The prostate dose was represented by the dose to 95% of the planning target volume. The rectal dose was represented by the rectal volume receiving above 30 Gy. The trial was designed with 90% power and 95% confidence to rule in a KIM success rate of 2/3 in favour of the futility rate of 1/3.

### Results

Motion correction via beam gating or multileaf collimator tracking occurred in 51% (121/235) of the treatments where real-time target tracking was performed. The proportion of motion-corrected treatments with an improvement in dose distribution to both the prostate and rectum was 72% (87/121 treatments), significantly higher than the 33% prospectively defined futility cutpoint ( $p<0.0001$ ,  $\chi^2$ ). The prostate dose with KIM was closer to the plan by an average of 4.6% (range -1.7% to 41%). The rectal dose with KIM was closer to the plan by an average of 1.5% (range -1.2% to 9.7%). Waterfall plots of the prostate and rectal doses are shown in Figure 1.

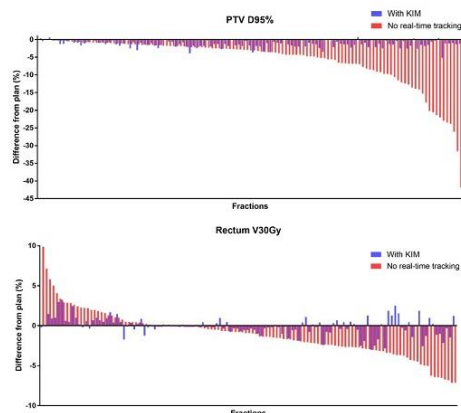


**Figure 1.** Waterfall plots of the difference in dose from the plan for the treatments with interventions with KIM (blue) and without KIM (red) (top) prostate (PTV D95%) and (bottom) rectum (V30Gy).

## Conclusion

The analysis of the SPARK trial primary outcome measure showed that the KIM real-time target tracking is clinically useful in improving the prostate and rectal dose in the presence of target motion.

## PO-0843 Toxicity of a brachytherapy boost for prostate cancer patients

L. Bokhorst<sup>1</sup>, S. Van der Pol<sup>2</sup>, C. Niël<sup>2</sup>, C. Hoekstra<sup>2</sup>  
<sup>1</sup>UMC Utrecht, Radiation Oncology, Utrecht, The Netherlands ; <sup>2</sup>Radiotherapiegroep, Radiation Oncology, Deventer, The Netherlands

### Purpose or Objective

To compare potency, urinary, and gastro-intestinal toxicity in men with prostate cancer receiving brachytherapy, external beam radiation therapy (EBRT), or EBRT with a brachytherapy boost (both low and high dose rate (LDR/HDR)).

### Material and Methods

From 2000-2018 all patients treated for prostate cancer in our institute were regularly followed and toxicity was prospectively collected at each follow-up visit using predefined questionnaires. For this analysis we compared IPSS score ( $\geq 20$  versus  $< 20$ ), potency score ( $\geq 5$  versus  $< 5$ ), on a 0 to 8 point scale with 8 being completely impotent and a score  $\geq 5$  being comparable with a CTCAE  $\geq 3$ ), urinary incontinence ( $> 1$  pad use per day), and rectal soiling (any pad use) between men receiving either brachytherapy alone (I-125, 145Gy), EBRT ( $\geq 76$ Gy), EBRT + LDR brachytherapy (50Gy + 100/110Gy), and EBRT + HDR brachytherapy (68Gy + 1x10-15Gy). Men receiving salvage treatment were excluded from this analysis.

### Results

During follow-up 3291 patients were treated (59% EBRT, 23% brachytherapy, 10% EBRT + LDR, 8% EBRT + HDR) received a total of 28877 follow-up visits (1000 patients were followed more than 7 years). Data completeness differed per questionnaire but ranged from 77% for urinary incontinence up to 86% for potency scores.

The largest difference in IPSS scores were seen in the first year after treatment, with more and longer urinary problems for men receiving LDR brachytherapy with or without EBRT versus EBRT alone of combined with HDR brachytherapy (figure 1).

After 2.5 and 4.5 years of follow-up overall urinary incontinence was 2.7% and 3.6% respectively, overall impotency (in men receiving no (neo)adjuvant hormonal therapy) was 38.3% and 49.9% respectively, and rectal soiling was reported by 0.5% and 0.5% respectively. There were no significant differences in potency score, urinary incontinence or rectal soiling between the different treatment groups during follow-up (table 1).

**Figure 1.** Percentage of men with IPSS score  $\geq 20$  during follow-up for the different treatment options.

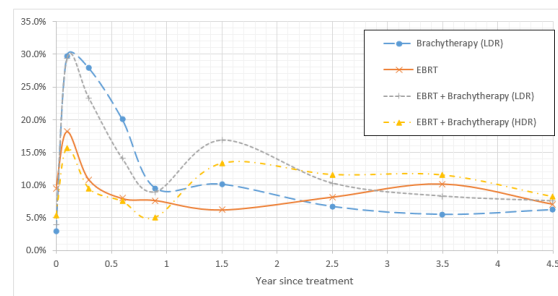


**Table 1.** Cox-proportional hazard models predicting impotency (potency score  $\geq 5$ ), urinary incontinence ( $> 1$  pad use per day), and rectal soiling (any pad use).

	Hazard ratio (95% CI)	p-value
<b>Impotency</b>		
<b>Treatment</b>		
EBRT	Reference	
Brachytherapy (LDR)	1.10 (0.93 - 1.30)	0.27
EBRT + LDR	0.99 (0.81 - 1.20)	0.90
EBRT + HDR	1.11 (0.93 - 1.32)	0.26
<b>Hormonal therapy (HT)</b>		
No HT	Reference	
Neo-adjuvant HT	1.04 (0.90 - 1.21)	0.57
Adjuvant HT	1.30 (1.06 - 1.60)	0.01
Potency score at baseline	1.26 (1.24 - 1.29)	<0.001
Age at baseline	1.01 (1.00 - 1.01)	0.02
	<b>Hazard ratio (95% CI)</b>	<b>p-value</b>
<b>Urinary incontinence</b>		
<b>Treatment</b>		
EBRT	Reference	
Brachytherapy (LDR)	1.20 (0.77 - 1.84)	0.42
EBRT + LDR	1.41 (0.84 - 2.37)	0.19
EBRT + HDR	1.50 (0.81 - 2.78)	0.20
<b>Hormonal therapy (HT)</b>		
No HT	Reference	
Neo-adjuvant HT	1.26 (0.92 - 1.73)	0.14
Adjuvant HT	1.19 (0.63 - 2.24)	0.59
TURP at baseline	4.45 (3.30 - 6.00)	<0.001
Age at baseline	1.00 (0.99 - 1.01)	0.77
IPSS score at baseline	1.02 (1.01 - 1.04)	<0.001
	<b>Hazard ratio (95% CI)</b>	<b>p-value</b>
<b>Rectal soiling</b>		
<b>Treatment</b>		
EBRT	Reference	
Brachytherapy (LDR)	0.80 (0.55 - 1.16)	0.24
EBRT + LDR	0.81 (0.51 - 1.30)	0.39
EBRT + HDR	0.68 (0.38 - 1.22)	0.20
<b>Hormonal therapy (HT)</b>		
No HT	Reference	
Neo-adjuvant HT	1.15 (0.86 - 1.54)	0.34
Adjuvant HT	1.26 (0.74 - 2.12)	0.39
Age at baseline	1.00 (1.00 - 1.01)	0.32

## Conclusion

Adding a brachytherapy boost (either LDR and HDR) did not increase long-term potency urinary, or gastrointestinal toxicity as compared to EBRT or brachytherapy (LDR) alone.

## PO-0844 Target motion mitigation and dose painting in prostate cancer SBRT: results from a Phase II study

C. Greco<sup>1</sup>, O. Pares<sup>1</sup>, N. Pimentel<sup>1</sup>, V. Louro<sup>1</sup>, B. Nunes<sup>1</sup>, J. Sroom<sup>1</sup>, S. Viera<sup>1</sup>, D. Mateus<sup>1</sup>, Z. Fuks<sup>1</sup>  
<sup>1</sup>Fundação Champalimaud, Radiation Oncology, Lisboa, Portugal

### Purpose or Objective

to report biochemical, MR response and patient-reported quality of life (QoL) after extreme SBRT (9Gyx5) in patients with histologically proven organ-confined adenocarcinoma of the prostate using target motion mitigation and OARs dose painting.

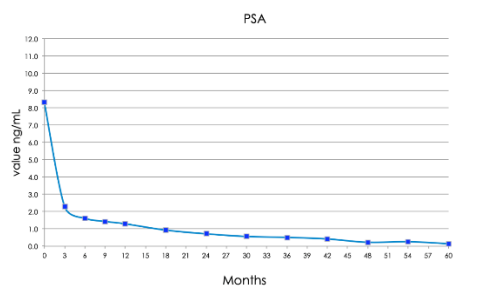
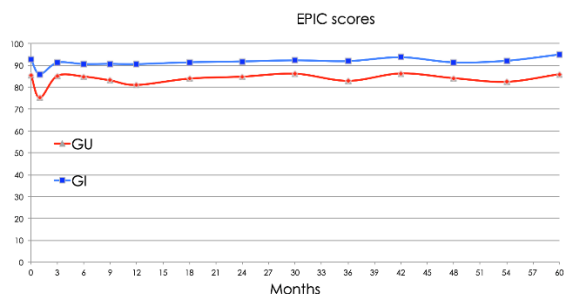
### Material and Methods

Between May 2013 and September 2017, 207 men were enrolled in an IRB-approved phase II prospective study to receive 45Gy in 5 consecutive daily fractions of 9Gy with critical tissue sparing (urethra, urogenital diaphragm and neurovascular bundles). Treatment planning was based on VMAT-IGRT with a negative dose-painting technique to fulfil organ-specific dose-volume constraints The CTV and

OARs were segmented on a fused CT/MR set acquired with organ motion-mitigation devices in place, namely, an endorectal air-filled balloon (150 cc) and a transponder-loaded Foley catheter. The CTV included the prostate gland and seminal vesicles and an isotropic 2 mm margin was added for the PTV. Validation a 2 mm margin expansion was performed in the first 60 patients. The urethral wall was anatomically identified through the catheter. All the other OARs were clearly identified on the MR image set. Strict QA procedures to validate the plan were carried out before final approval. At the time of treatment, anatomical reproducibility was achieved by recapitulating the positioning of the endoluminal devices. Precise PTV targeting was performed by CBCT and real-time motion management was obtained via beacon transponders, ensuring treatment delivery within the 2 mm PTV margin. Toxicities were graded according to the NCI CTCAE v.4, and QoL was assessed by EPIC and IPSS questionnaires. Tumor response was assessed by PSA and MRI at 6 and 12 months post-treatment.

### Results

On-line tracking with 2 mm motion tolerance was achieved in all cases. At a median follow-up of 33 months (range, 12-62), acute G2 GU and GI toxicities were 2% and 0%, respectively. Late G2 GU and GI toxicities were 1% and 0%, respectively. No G3 toxicity occurred. An initial 11% and 6% drop in the GU and GI EPIC domain scores, respectively, was observed at 1 month post treatment, returning to baselines by 3 months. Similarly, at one month median IPSS values increased from 7 to 11 also returning to baseline by 3-months. Post-treatment PSA kinetics show a rapid decline, reaching a median  $\leq 1$  ng/mL by 18 months. A total of 8 patients have relapsed biochemically (Phoenix definition). All relapses occurred in patients with intermediate risk disease between 24 and 36 months post-treatment. Actuarial probability of freedom from biochemical relapse at 48 months is 100% and 97% for low and intermediate risk patients, respectively. MR response at 6 months post-treatment correlated with long term bNED. 60 months bNED was 99% in patients with a negative DW-MR vs. 82% for those with persistent disease, respectively ( $p < 0.01$ ).



### Conclusion

These trial outcomes indicate that 5x9Gy SBRT can be consistently and safely delivered and is associated with excellent biochemical, imaging and QoL measures.

### PO-0845 What is the dosimetric benefit of daily position control imaging for prostate cancer radiotherapy?

M. Splinter<sup>1,2,3</sup>, T. Bostel<sup>2,4</sup>, C. Lang<sup>1,2,3</sup>, P. Häring<sup>1,2,3</sup>, N. Bougatf<sup>5</sup>, J. Debus<sup>2,3,6</sup>, N.H. Nicolay<sup>2,7</sup>

<sup>1</sup>German Cancer Research Center DKFZ, Division of Medical Physics in Radiation Oncology, Heidelberg, Germany; <sup>2</sup>German Cancer Research Center, Clinical Cooperation Unit "Radiation Oncology", Heidelberg, Germany; <sup>3</sup>Heidelberg Institute for Radiooncology, National Center for Radiation Research in Oncology, Heidelberg, Germany; <sup>4</sup>University Medical Center Mainz, Department of Radiation Oncology, Mainz, Germany; <sup>5</sup>Heidelberg Ion Beam Therapy Center, Department of Radiation Oncology, Heidelberg, Germany; <sup>6</sup>University Hospital Heidelberg, Department of Radiation Oncology, Heidelberg, Germany; <sup>7</sup>Freiburg University Medical Center, Department of Radiation Oncology, Freiburg, Germany

### Purpose or Objective

For prostate cancer patients, interfractional differences in bladder and rectum volumes as well as positioning inaccuracies result in dose deviations in the target volume (TV) and OARs; however, regarding the dose exposure associated with regular CT imaging, the optimal compromise between dose sparing and positioning accuracy remains to be elucidated. Therefore, the influence of daily vs. weekly CT-based positioning imaging on dosimetric deviations between accumulated applied and prescribed doses was analyzed.

### Material and Methods

The data of twenty prostate carcinoma patients (ten patients with primary radiation therapy for prostate cancer, ten patients with salvage treatments to the prostatic bed after previous prostatectomy), who underwent treatment (IMRT plan, 76.5Gy in 34fx for primary and 68Gy in 34fx for salvage treatments) were investigated (680 fractions in total). Prior to each daily fraction, position-control imaging (fx-CT) was carried out using a diagnostic in-room CT scanner (SOMATOM® Emotion Syngo, SIEMENS). For each patient, both daily and once-a-week (d1, d8, d15, d22, d29) fx-CTs were rigidly registered to the planning CT using the position correction vectors. TVs and all OARs were contoured and volumetrically compared to the structures of the planning CT. By using a deformable registration algorithm, doses were tracked, and applied dose were compared to the planned dose for each structure in dependence of the frequency of CT positioning imaging. Gamma analyses of the total dose distribution were performed at the tolerance level of 3%/3 mm for the  $\gamma < 1$  test, within the region receiving doses >10% of the maximum dose.

### Results

Volumetric changes and positional variations especially of the bladder revealed significant dose deviations between accumulated applied dose and planned dose for primary treatments and salvage treatments.

dose difference between applied dose and planned dose [Gy]	primary treatments		salvage treatments		
	daily fx-CTs	once a week fx-CTs	daily fx-CTs	once a week fx-CTs	
PTV	D50	-0.07±0.66	-0.61±0.77	0.11±0.65	-0.41±0.84
	D95	-8.94±6.14	-13.73±11.06	-2.88±4.70	-5.85±6.33
Bladder	D50	2.80±5.59	1.58±5.12	4.94±6.05	6.07±7.53
	D95	0.35±3.48	2.75±3.86	0.77±5.19	0.63±5.87

Doing once-a-week fx-CTs effected a decrease of the applied D<sub>50</sub> (0.54±0.45Gy; 4.79±7.84Gy) and D<sub>95</sub>

( $0.52 \pm 0.39$  Gy;  $2.97 \pm 2.88$  Gy) to the PTV compared to doing daily fx-CTs for primary and salvage treatments, which lead to a worse target volume coverage. For primary treatments, the applied  $D_{50}$  to the bladder was reduced ( $1.22 \pm 1.32$  Gy) by doing weekly fx-CTs instead of daily fx-CTs, while the applied  $D_{50}$  to the rectum was increased ( $2.40 \pm 2.21$  Gy). For salvage treatments, the applied  $D_{50}$  to the bladder was increased ( $1.13 \pm 3.64$  Gy) by doing weekly fx-CTs instead of daily fx-CTs, while the applied  $D_{50}$  to the rectum was reduced ( $0.14 \pm 1.47$  Gy). Doing once-a-week fx-CTs affected a decrease (3%) of the gamma passing rate compared to doing daily fx-CTs.

#### Conclusion

The observed variability resulted in significant dose increases and decreases of the  $D_{50}$  to the bladder and rectum, respectively. It could be shown that the dose decreases of the  $D_{50}$  and  $D_{95}$  to the PTV were statistically significant. Doing daily fx-CTs affected a higher gamma passing rate. Adaptive treatment planning may help to minimize the observed dosimetric deviations.

#### PO-0846 Dosimetric effects of a novel concept of adaptive radiotherapy for prostate cancer patients

M. Splinter<sup>1,2,3</sup>, T. Bostel<sup>2,4</sup>, C. Lang<sup>1,2,3</sup>, P. Häring<sup>1,2,3</sup>, J. Debus<sup>2,3,5</sup>, N.H. Nicolay<sup>2,6</sup>

<sup>1</sup>German Cancer Research Center DKFZ, Division of Medical Physics in Radiation Oncology, Heidelberg, Germany; <sup>2</sup>German Cancer Research Center, Clinical Cooperation Unit "Radiation Oncology", Heidelberg, Germany; <sup>3</sup>Heidelberg Institute for Radiooncology, National Center for Radiation Research in Oncology, Heidelberg, Germany; <sup>4</sup>Mainz University Medical Center, Department of Radiation Oncology, Mainz, Germany; <sup>5</sup>University Hospital Heidelberg, Department of Radiation Oncology, Heidelberg, Germany; <sup>6</sup>Freiburg University Medical Center, Department of Radiation Oncology, Freiburg, Germany

#### Purpose or Objective

Interfractional variations in bladder and rectal anatomy challenge current concepts of high-precision radiotherapy for prostate cancer patients, as the delivered dose may deviate from the planned dose. As the precise effects of these dose deviations are largely unknown and therefore plan adaptation strategies are difficult to evaluate, this analysis was aimed at investigating dosimetric consequences of a novel method for adaptive radiotherapy using an individualized plan database.

#### Material and Methods

The data of ten patients with prostate carcinoma (salvage radiotherapy to the prostatic bed, 68Gy in 34 fx, step-and-shoot IMRT) were investigated. Prior to each fraction, a diagnostic position-control-CT (fx-CT) was performed using a diagnostic in-room CT scanner (SOMATOM® Emotion Syngo, SIEMENS). Based on the daily fx-CT, the target volume and all OARs were contoured and volumetrically compared to the structures of the planning CT. One treatment plan was calculated based on the planning CT, and two additional plans were calculated based on the bladder filling observed using the first five fx-CTs, thereby creating a plan database that contained plans for low, intermediate and high bladder volume for each patient. Using a deformable registration algorithm for each daily fx-CT, applied doses were tracked and analyzed against the planned doses. The dosimetric effects were quantitatively compared.

#### Results

The use of a plan database did not result in significant benefits for all cases. In 9 of 10 cases, a better PTV coverage was reached. In 6 of these 9 cases, better sparing of the bladder and in 5 of these 6, better sparing of the rectum was achieved. A plan database was useful for 9, 6 or 5 cases of the cohort, depending on the maintained criteria. A plan database seemed particularly useful for patients with large or medium bladder volume (compared

to the first 5fx) at treatment planning. Interfractional variabilities resulted in an increase of  $D_{50}$  ( $0.40 \pm 0.38$  Gy) and a decrease of  $D_{95}$  ( $2.03 \pm 5.40$  Gy) to the PTV. The bladder volume showed the biggest interfractional volume variability ( $286 \pm 168$  ml), effecting a dose deviation of at mean  $7.76 \pm 6.05$  Gy of the  $D_{50}$ . By using a plan database, the applied dose of the bladder could be reduced by  $4.55 \pm 5.81$  Gy. The  $D_{50}$  of the PTV was marginally lower ( $-0.23 \pm 0.31$  Gy) and the  $D_{95}$  of the PTV was marginally higher ( $1.0 \pm 0.9$  Gy) than without using plan database and thus closer to the planning value.

#### Conclusion

The observed variability resulted in significant dose increases of the  $D_{50}$  to the bladder, whereas in the PTV, only small non-significant dose deviations could be detected. By including the bladder volume in the daily choice of the treatment plan - especially for patients with a challenging organ situation - a significantly lower dose to the OAR was achieved, while the target volume coverage was virtually unchanged. Further analyses will reveal a potential correlation of the observed dosimetric benefits with reduced clinical toxicities.

#### PO-0847 Rapid modulation of PSMA expression by ADT: Serial PSMA PET in men commencing androgen blockade.

L. Emmett<sup>1</sup>, V. Chalasani<sup>2</sup>, A. Kneebone<sup>3</sup>, G. Hruby<sup>3</sup>, A.M. Joshua<sup>4</sup>

<sup>1</sup>St Vincent's Hospital- Sydney- Australia, Department of Theranostics, Sydney, Australia; <sup>2</sup>Royal North Shore Hospital- Sydney, Urology, Sydney, Australia; <sup>3</sup>Royal North Shore Hospital, Radiation Oncology, Sydney, Australia; <sup>4</sup>St Vincent's Hospital Sydney, Oncology, Sydney, Australia

#### Purpose or Objective

Prostate specific membrane antigen (PSMA) can be targeted for both imaging and therapy purposes in the management of prostate cancer (PCa). In pre-clinical models, androgen blockade appears to increase expression of PSMA in both hormone sensitive and castrate resistant xenotypes. The aim of this study was to prospectively evaluate the effect on PSMA PET in men with measurable metastatic disease commencing initial androgen blockade in the hormone sensitive cohort or those commencing a novel antiandrogen (enzalutamide or abiraterone) in the castrate resistant cohort.

#### Material and Methods

Serial PSMA PET scans were performed at baseline, and days 9, 18 and 28 in 8 men with measurable metastatic hormone sensitive PCa commencing ADT (cohort 1) and 7 men with castrate resistant PCa commencing either enzalutamide or abiraterone (cohort 2). Gleason score (GS), age, time since diagnosis and prior treatments were documented. Testosterone and PSA (ng/ml) were measured at baseline and at all imaging time points. PET/CT was quantitatively analysed using MIM® software for number of lesions, SUV max, SUV mean and total tumour volume.

#### Results

**Cohort 1:** A mean 25% (IQR) reduction in intensity (SUV max) of PSMA by day 9 post androgen blockade (AB). This reduction in PSMA SUV max was seen in 88 % (7/8) men by day 9, with an associated PSA response in 100% men. There was more heterogeneity on day 18 and 28 PSMA with an increase in PSMA SUV max in 2/8 (25%) men, although overall tumour volume reduced in all men. **Cohort 2:** A mean 28% (IQR) increase in intensity of PSMA SUV was recorded by day 9 post AB. All men demonstrated an increase in both the intensity of uptake and volume on PSMA PET compared to baseline. This increase in quantitative parameters occurred by day 9 in all men, and had reduced by day 18 and 28 imaging. PSA responses were more delayed in cohort 2, with 2/7 men demonstrating PSA progression on the study.

	Baseline(Cohort 1)	Day 9(Cohort 1)	Baseline(Cohort 2)	Day 9(Cohort 2)
PSA (median)ng/m	52 ± 82	31 ± 23	53 ± 257	32 ± 407
SUV max	23 ± 14	14 ± 10	52 ± 23	87 ± 34
SUV mean	6 ± 3.6	4 ± 3.5	7.7 ± 2.2	10.5 ± 3.9
Total volume (mls)	28 ± 40	12 ± 48	290 ± 1141	290 ± 1585

### Conclusion

PSMA is a manipulable receptor with rapid dichotomous in-vivo response on PSMA PET to androgen blockade dependent on hormone sensitive versus castrate resistant PCa phenotype. This has important implications for the interpretation of PSMA PET imaging, and in the timing/sequencing of PSMA targeted therapy.

### PO-0848 Early mortality of prostatectomy vs. radiotherapy as a primary treatment for prostate cancer

D. Medenwald<sup>1</sup>, K. Medenwald<sup>1</sup>, A. Glowka<sup>1</sup>, D. Vordermark<sup>1</sup>, C. Dietzel<sup>1</sup>

<sup>1</sup>Martin Luther University Halle-Wittenberg, <sup>1</sup>Department of Radiation Oncology, Halle/Saale, Germany

### Purpose or Objective

To assess the extent of early mortality and its temporal course after prostatectomy and radiotherapy in the general population.

### Material and Methods

Data from SEER-database and German epidemiologic cancer registries were used for the years 2005-2013. Metastasized cases and deaths from bladder cancer were excluded (avoiding incidental cases after bladder cancer). Analysing overall mortality, year-specific Cox regression models were used for German and US-American data after adjusting for age (including age squared), risk stage and grading. To estimate temporal hazards we computed year-specific conditional hazards for surgery and radiotherapy after propensity-score matching and applied constant proportional hazard models.

### Results

In German and US-American populations we observed higher initial three-month mortality odds for prostatectomy (USA: 7.4-fold risk, 95% CI: 6.1-9.0; Germany: 8.5, 95% CI: 4.5-16.0) approaching the null effect value not before 20 months after diagnosis (used as a cut-off for the observational period defining early mortality).

During the observational period we observed an increasing hazard ratio for the 20-month mortality in the US-population (2005: 1.4, 95% CI: 1.2-1.6; 2013: 1.8, 95% CI: 1.4-2.1) for the surgery/radiotherapy comparison. In the German population the effect remained virtually constant (2005: 1.5, 95% CI: 1.0-2.3; 2013: 3.4, 95% CI: 2.1-5.7). Considering low-risk cases, the adverse surgery effect appeared stronger.

### Conclusion

There is strong evidence from two independent populations of a considerably higher early mortality after prostatectomy compared to radiotherapy extending the time of early mortality considered by previous studies up to 20 months.

### PO-0849 Pattern of Relapse After Metastases Directed Therapy in Oligorecurrent Prostate Cancer

I. San Miguel<sup>1</sup>, D. Büchser<sup>1</sup>, F. Suarez<sup>1</sup>, F. Casquero<sup>1</sup>, I. Fernandez<sup>2</sup>, E. Rodeño<sup>2</sup>, R. Ortiz de Zarate<sup>1</sup>, R. Llarena<sup>3</sup>, J. Garcia Olaverri<sup>3</sup>, L. Martinez-Indart<sup>4</sup>, P. Bilbao<sup>1</sup>, A. Gomez De Iturriaga<sup>4</sup>

<sup>1</sup>Cruces University Hospital, Radiation Oncologist, Baracaldo, Spain ; <sup>2</sup>Cruces University Hospital, Nuclear Medicine, Baracaldo, Spain ; <sup>3</sup>Cruces University Hospital, Urology, Baracaldo, Spain ; <sup>4</sup>Cruces University Hospital / Biocruces Health Research Institute, Radiation Oncologist, Baracaldo, Spain

### Purpose or Objective

A better knowledge of the pattern of recurrence after metastases directed therapy (MDT) in patients with oligometastatic disease might be useful to select the most appropriate candidates. The aim of this study is to report in a prospective cohort of oligorecurrent prostate cancer patients factors associated with the pattern of relapse and disease control after MDT.

### Material and Methods

From 2012 to 2017, 104 lesions diagnosed with Ch-PET in 53 consecutive oligometastatic-recurrence prostate cancer patients have been treated. Biochemical failure was defined using the nadir+2 ng/mL definition; a DFS event was defined as evidence of disease by any clinical, pathological or radiological method. Reassessment with Ch-PET imaging was performed in case of biochemical failure or if clinically indicated to rule out local or distant metastatic progression. Patterns of first progression following MDT were recorded. In case of an oligometastatic recurrence outside the previous PTV field, a retreatment with SBRT or IMRT was offered. Descriptive analyses were done. Chi-square and Fisher-exact tests were performed to evaluate the influence of patient, tumor, and treatment characteristics on the pattern of relapse. A p<0.05 considered statistically significant

### Results

The different subsites of metastatic involvement before 1<sup>st</sup> MDT were lymph-nodes in 67.9% and bone in 32.1% of patients. The treatments administered to the initial oligo-recurrence sites were IMRT (49%) and SABR (51%) +/- short course ADT. After a median follow-up of 28 months (6-54 months), 89% of the patients remain alive and only 3 deaths were related to prostate cancer. At last follow-up 34% of the patients were free from disease progression. Twenty-five patients with biochemical failure after 1<sup>st</sup> MDT presented distant recurrence on re-staging Ch-PET and 64% (16/25) were again oligometastatic relapses allowing for a 2<sup>nd</sup> MDT in 12 patients. In terms of relapse site, 7/7 (100%) patients with initial bone disease presented a subsequent bone relapse, 10/18 (56%) patients with initial nodal disease presented a nodal relapse and 8/18 (44%) a bone relapse. At diagnosis, a PSA pre-PET<4.5ng/mL was associated with higher probability of presenting with nodal oligometastases (p=0.049). The variables with significant association with nodal relapse after MDT were a pre-MDT PSA<10ng/mL (p=0.049) and initial nodal oligometastatic site (p=0.02). A PSADT>12 months before MDT was the only factor statistically associated with higher disease control (p=0.011).

### Conclusion

Long-term disease control is still possible in oligometastatic patients who receive MDT. At relapse, most patients are again oligometastatic allowing for repeated MDT. The pre-MDT PSA and initial nodal oligometastatic site are associated with a further nodal relapse. Patients presenting with a PSADT>12 months and a PSApre-PET<4.5ng/mL may have a better prognosis.

### PO-0850 Comparison of self-reported acute urinary incontinence in pts treated with adjuvant or salvage IMRT

F. Munoz<sup>1</sup>, D. Cante<sup>2</sup>, E. Garibaldi<sup>3</sup>, A. Peruzzo<sup>4</sup>, E. Petrucci<sup>5</sup>, E. Delmastro<sup>3</sup>, G. Sanguineti<sup>6</sup>, A. Faiella<sup>6</sup>, B.

Avuzzi<sup>7</sup>, B. Noris Chiorda<sup>7</sup>, T. Giandini<sup>8</sup>, V. Vavassori<sup>9</sup>, E. Villa<sup>9</sup>, G. Girelli<sup>10</sup>, B. Farina<sup>10</sup>, J.M. Waskiewicz<sup>11</sup>, A. Magli<sup>12</sup>, E. Moretti<sup>13</sup>, R. Valdagni<sup>14</sup>, C. Bianconi<sup>15</sup>, F. Badenchini<sup>16</sup>, N. Di Muzio<sup>15</sup>, T. Rancati<sup>16</sup>, C. Fiorino<sup>17</sup>, C. Cozzarini<sup>15</sup>

<sup>1</sup>Ospedale Regionale U.Parini-AUSL Valle d'Aosta, Radiotherapy, Aosta, Italy ; <sup>2</sup>Ospedale di Ivrea- A.S.L. TO4, Radiotherapy, Ivrea, Italy ; <sup>3</sup>Istituto di Candiolo-Fondazione del Piemonte per l'Oncologia IRCCS, Radiotherapy, Candiolo Torino, Italy ; <sup>4</sup>Ospedale Regionale U.Parini-AUSL Valle d'Aosta, Medical Physics, Aosta, Italy ; <sup>5</sup>Ospedale di Ivrea- A.S.L. TO4, Medical Physics, Ivrea, Italy ; <sup>6</sup>Istituto Nazionale dei Tumori "Regina Elena", Radiotherapy, Roma, Italy ; <sup>7</sup>Fondazione IRCCS Istituto Nazionale dei Tumori, Radiotherapy, Milano, Italy ; <sup>8</sup>Fondazione IRCCS Istituto Nazionale dei Tumori, Medical Physics, Milano, Italy ; <sup>9</sup>Cliniche Gavazzeni-Humanitas, Radiotherapy, Bergamo, Italy ; <sup>10</sup>Ospedale degli Infermi, Radiotherapy, Biella, Italy ; <sup>11</sup>Comprensorio Sanitario di Bolzano, Radiotherapy, Bolzano, Italy ; <sup>12</sup>Azienda Ospedaliero Universitaria S. Maria della Misericordia, Radiotherapy, Udine, Italy ; <sup>13</sup>Azienda Ospedaliero Universitaria S. Maria della Misericordia, Medical Physics, Udine, Italy ; <sup>14</sup>University of Milan- Department of Oncology and Hemato-oncology - Fondazione IRCCS Istituto Nazionale dei Tumori- Prostate Cancer Program - Fondazione IRCCS Istituto Nazionale dei Tumori- Radiation Oncology 1, Radiotherapy, Milano, Italy ; <sup>15</sup>Fondazione Centro San Raffaele, Radiotherapy, Milano, Italy ; <sup>16</sup>Programma Prostata- Fondazione IRCCS Istituto Nazionale dei Tumori, Radiotherapy, Milano, Italy ; <sup>17</sup>Fondazione Centro San Raffaele, Medical Physics, Milano, Italy

## Purpose or Objective

The fear of treatment induced urinary incontinence is one of the treatment sequelae mainly advising against post-prostatectomy. Purpose of this study was to compare the risk and trend over time of acute patient-reported urinary incontinence (PRUI) after adjuvant (ADV) or salvage (SALV) IMRT.

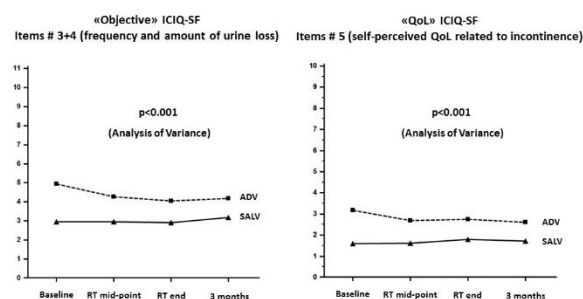
## Material and Methods

An ongoing multicentric observational trial, registered at ClinicalTrials.gov, is evaluating PRUI in pts treated with IMRT for prostate cancer. The ICIQ-SF questionnaire (ICIQ) has to be filled-in by pts at baseline, at RT mid-point and end, 3 and 6 months after RT end and thereafter every 6 months up to 5 years. IMRT is delivered at both conventional (CF) or moderate hypo-fractionation (HYPO). Complete ICIQ at baseline, RT mid-point and end were available for 316 pts (266 at 3 months). Pts characteristics in ADV (n=140) and SALV (n=176) cohorts were: time to RT (TTRT) 4 vs 24.4 months, EQD2 RT dose for a/b=10 Gy 72 vs 74 Gy, HYPO 53% vs 33%, median # of RT fractions 35 vs 37, hormonal therapy 58% vs 33%, Tomotherapy (TOMO) vs VMAT vs static-field IMRT (SS-IMRT) 46%/50%/4% vs 38%/48%/14%, open vs robotic vs laparoscopic surgery 68%/26%/6% vs 60%/28%/12%.

## Results

Two ICIQ-based end-points were considered: "objective PRUI" (OBJ=sum of the scores of items #3 and #4, frequency and amount of urine loss, respectively, score 0-11) and the impact on QoL as reported by pts (item #5, score 0-10). Overall, the mean and median scores for both end-points were significantly higher at baseline, during and immediately after irradiation in the ADV cohort (Table 1 and Figure 1). Nevertheless neither ADV nor SALV RT led to OBJ nor QoL worsening. Of the 266 with ICIQ at baseline and at 3 months, 2/55 (4%) and 12/107 (11%) with a baseline OBJ score <5 exhibited a corresponding score ≥5 at 3 months. The end-point for logistic regression analysis was set as an OBJ score ≥5 at 3 months. Among the variables investigated (age, BMI, TTRT, HORM, type of surgery, dose/fraction at PB, seminal vesicles bed, lymph-nodal PTV, EQD2 to PB, RT intent, baseline OBJ and RT

technique) only those with a p-value ≤0.20 were entered into a multivariable model. In the overall population the only two covariates predictive of OBJ ≥5 at 3 months were baseline OBJ (OR 2.65, p<0.0001) and RT intent (OR 0.35, reference ADV, p=0.008) (AUC: 0.92 95% 0.88-0.95%) while in the subset of pts with a baseline OBJ<5 only baseline OBJ retained the statistical significance (OR 3.01, p=0.003, AUC 0.83 95% 0.76-0.89%).



«Objective» ICIQ-SF (median scores)				
	Baseline	RT mid-point	RT end	3 months
Adjuvant	5	4	4	4
Salvage	3	3	3	3

«Objective» ICIQ-SF (mean scores)				
	Baseline	RT mid-point	RT end	3 months
Adjuvant	4.82	4.19	4.05	4.20
Salvage	3.02	3.02	3.01	3.17
p-value (t-student)	<math><0.0001</math>	0.0004	0.002	0.005

«QoL» ICIQ-SF (median scores)				
	Baseline	RT mid-point	RT end	3 months
Adjuvant	2	2	2	1
Salvage	0	1	1	1

«QoL» ICIQ-SF (mean scores)				
	Baseline	RT mid-point	RT end	3 months
Adjuvant	1.66	1.70	1.89	1.72
Salvage	3.10	2.68	2.76	2.60
p-value (t-student)	<math><0.0001</math>	0.001	0.007	0.009

## Conclusion

Baseline OBJ score was the major predictor of PRUI 3 months after post-prostatectomy RT. Pts receiving ADV IMRT exhibited significantly higher OBJ and QoL scores in the 3 months after RT start, but the overall levels of PRUI and QoL impairment were rather low. Contrarily to what commonly believed, neither ADV nor SALV RT led to any worsening of post-prostatectomy OBJ or QoL in the first 3 months after RT, despite the relatively high delivered dose.

**PO-0851 Quality of life after whole pelvis RT for prostate cancer: results from a prospective study**  
G. Sanguineti<sup>1</sup>, D. Cante<sup>2</sup>, F. Munoz<sup>3</sup>, A. Faiella<sup>1</sup>, E. Petrucci<sup>4</sup>, A. Peruzzo<sup>5</sup>, E. Garibaldi<sup>6</sup>, P. Gabriele<sup>6</sup>, B. Avuzzi<sup>7</sup>, T. Giandini<sup>8</sup>, B. Noris Chiorda<sup>7</sup>, V. Vavassori<sup>9</sup>, E. Villa<sup>9</sup>, P. Salmoiraghi<sup>10</sup>, G. Girelli<sup>11</sup>, J.M. Waskiewicz<sup>12</sup>, A. Magli<sup>13</sup>, E. Moretti<sup>14</sup>, R. Valdagni<sup>15</sup>, C. Bianconi<sup>16</sup>, F. Badenchini<sup>17</sup>, N. Di Muzio<sup>16</sup>, T. Rancati<sup>17</sup>, C. Fiorino<sup>18</sup>, C. Cozzarini<sup>16</sup>

<sup>1</sup>Istituto Nazionale dei Tumori "Regina Elena", Radiotherapy, Roma, Italy ; <sup>2</sup>Ospedale di Ivrea- A.S.L. TO4, Radiotherapy, Ivrea, Italy ; <sup>3</sup>Ospedale Regionale U.Parini-AUSL Valle d'Aosta, Radiotherapy, Aosta, Italy ; <sup>4</sup>Ospedale di Ivrea- A.S.L. TO4, Medical Physics, Ivrea, Italy ; <sup>5</sup>Ospedale Regionale U.Parini-AUSL Valle d'Aosta, Medical Physics, Aosta, Italy ; <sup>6</sup>Istituto di Candiolo-Fondazione del Piemonte per l'Oncologia IRCCS, Radiotherapy, Candiolo Torino, Italy ; <sup>7</sup>Fondazione IRCCS Istituto Nazionale dei Tumori, Radiotherapy, Milano,

Italy ; <sup>8</sup>Fondazione IRCCS Istituto Nazionale dei Tumori, Medical Physics, Milano, Italy ; <sup>9</sup>Cliniche Gavazzeni-Humanitas, Radiotherapy, Bergamo, Italy ; <sup>10</sup>Cliniche Gavazzeni-Humanitas, Medical Physics, Bergamo, Italy ; <sup>11</sup>Ospedale degli Infermi, Radiotherapy, Biella, Italy ; <sup>12</sup>Comprensorio Sanitario di Bolzano, Radiotherapy, Bolzano, Italy ; <sup>13</sup>Azienda Ospedaliero Universitaria S. Maria della Misericordia, Radiotherapy, Udine, Italy ; <sup>14</sup>Azienda Ospedaliero Universitaria S. Maria della Misericordia, Medical Physics, Udine, Italy ; <sup>15</sup>University of Milan- Department of Oncology and Hemato-oncology - Fondazione IRCCS Istituto Nazionale dei Tumori-Prostate Cancer Program - Fondazione IRCCS Istituto Nazionale dei Tumori- Radiation Oncology 1, Radiotherapy, Milano, Italy ; <sup>16</sup>Fondazione Centro San Raffaele, Radiotherapy, Milano, Italy ; <sup>17</sup>Programma Prostata- Fondazione IRCCS Istituto Nazionale dei Tumori, Radiotherapy, Milano, Italy ; <sup>18</sup>Fondazione Centro San Raffaele, Medical Physics, Milano, Italy

### Purpose or Objective

To determine the evolution of Quality of Life (QoL) within the 1st year after RT for prostate cancer (PC) and its relationship with RT-related urinary and bowel symptoms (symp).

### Material and Methods

Patients (pts) in a multicenter observational study aimed at evaluation of symp and QoL after WPRT were included. Bowel toxicity was scored by means of the Inflammatory Bowel Disease Questionnaire (IBDQ), including QoL scales evaluating both social (SWB) and emotional (EWB) wellbeing. In IBDQ scales (range 1-7) lower scores indicate worse outcome. Moreover, QoL was also measured through the Hospital Anxiety and Depression Scale (HADS), which scores anxiety (ANX) and depression (DEP) separately (range 0-21 for both, greater values mean increased severity, score  $\geq 8$  indicating ANX/DEP mood). Urinary toxicity was scored through both the IPSS (range 0-35) (range 0-21), with greater scores indicating increased symptom's severity for both questionnaires. Longitudinal evaluation of QoL in the 1st year after RT was analyzed by means of ANOVA for multiple measures. Associations between urinary/bowel symp and 1.worsening of SWB/EWB of at least 2 points compared to baseline and 2.presence of ANX/DEP mood at 1 year were evaluated by means of logistic regression (LR).

### Results

304 pts were available for longitudinal evaluation, 38% treated with conventional RT and 62% with moderate hypofractionation with radical (28%), adjuvant (33%) or salvage (39%) intent. Median EQD2Gy (a/b=3Gy) to prostate/prostatic bed was 74Gy, that to pelvic nodes 50Gy.

Evolution of QoL over time was characterized by a quadratic trend for SWB & EWB ( $p > 0.001$ ), with significant worsening at RT end and subsequent recovery after RT completion. Conversely, ANX & DEP could be described by a linear decreasing trend ( $p = 0.002/p = 0.01$ ), reaching the lowest average values at 1 yr (see Figures 1 and 2). At multivariate LR, SWB worsening (23 pts) was associated to urinary obstructive symp (OR=1.09 for 1-point IPSS increase,  $p = 0.006$ ), while EWB worsening (9 pts) was associated to bowel symp (OR=5 for 1-point IBDQ decrease,  $p = 0.001$ ).

ANX mood (30 pts) was independently associated with both urinary obstructive symp (OR=1.12 for 1-point IPSS increase,  $p = 0.001$ ) and bowel symp (OR=3.2 for 1-point IBDQ decrease,  $p = 0.0007$ ). DEP mood (18 pts) was associated to urinary incontinence (OR=1.14 for 1-point ICIQ increase,  $p = 0.001$ ).

ANX/DEP at 1 year were highly negatively correlated with EWB ( $r = -0.79/-0.71$ ,  $p < 0.001$ ).

Figure 1: Quality of life scores as a function of time.

Open circles represent all data points, solid squares represent mean values, while bars represent 68% confidence intervals for the mean.

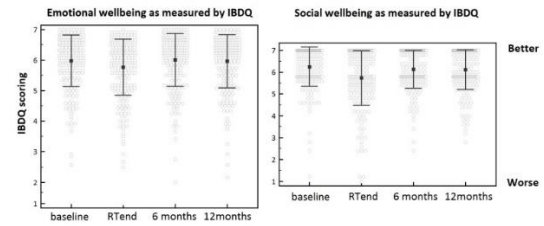
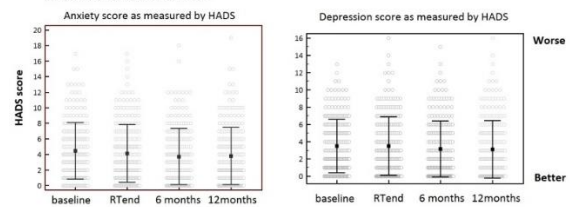


Figure 2: Anxiety and depression as a function of time.

Open circles represent all data points, solid squares represent mean values, while bars represent 68% confidence intervals for the mean.



### Conclusion

SWB & EWB after WPRT for PC are both decreased shortly after RT completion but recover within 1 year, with a limited number of pts reporting worsening SWB/EWB scores at 1 year, mainly associated with persistent bowel and obstructive urinary symp.

ANX/DEP decrease over time, suggesting their being more related to emotional upset following PC diagnosis rather than to treatment and side effects. Residual presence of ANX/DEP mood is significantly associated to both bowel and urinary symp.

### PO-0852 Stereotactic Body Radiation Therapy for Unfavorable Prostate Cancer: Large institutional experience.

N. Aghdam<sup>1</sup>, S. Katarian<sup>1</sup>, M. Danner<sup>1</sup>, M. Ayoob<sup>1</sup>, T. Yung<sup>1</sup>, S. Lei<sup>1</sup>, D. Kumar<sup>2</sup>, B.T. Collins<sup>1</sup>, J. Lischalk<sup>1</sup>, A. Dritschilo<sup>1</sup>, S. Suy<sup>1</sup>, J. Lynch<sup>3</sup>, S.P. Collins<sup>1</sup>

<sup>1</sup>Georgetown University Hospital, Department of Radiation Medicine, Washington DC, USA ; <sup>2</sup>North Carolina Central University, Julius L. Chambers Biomedical/Biotechnology Research Institute BBRI, Raleigh, USA ; <sup>3</sup>Georgetown University Hospital, Department of Urology, Washington DC, USA

### Purpose or Objective

External beam radiation therapy plus brachytherapy boost is a highly effective treatment for unfavorable prostate cancer. However, utilization of brachytherapy in the United States is declining and not all patients are ideal candidates for this treatment approach due to technical reasons. Stereotactic body radiotherapy (SBRT) has emerged as a standard high dose option for low and favorable intermediate risk prostate cancer patients. In this report, we present the biochemical disease free survival for unfavorable prostate cancer treated with SBRT in a large single institution cohort.

### Material and Methods

All patients with unfavorable intermediate risk (more than one intermediate risk factor, GS 4+3, or greater than 50% positive biopsy cores) and high risk prostate cancer treated with SBRT at a single institution were eligible for this study. Treatment was delivered using the robotic SBRT with doses of 35-36.25 Gy in five fractions or 19.5 Gy in three fractions followed by fiducial-guided supplemental IMRT (45-50.4 Gy). In general, patients with high grade, non-organ confined disease received supplemental IMRT. Patient's characteristics were

extracted from a prospective institutional quality of life trial (IRB 09-510). Biochemical failure free survival (BFFS) was determined using the Kaplan-Meier method.

#### Results

A total of 751 patients from 2008 to 2017 were eligible for analysis, of which 427 with UF-IR disease and 324 had HR disease. Fifty percent of the patients received short term ADT (81% HR, 24% UF-IR). At median follow up of 36 months BFFS was 89% for all patients, and 93% and 84% for UF-IR and HR patients respectively (p=0.015). Patients treated with SBRT alone had 91% BFFS as compared to those treated with supplemental IMRT with 86%.

#### Conclusion

SBRT plus or minus supplemental IMRT for high risk prostate cancer shows similar early biochemical responses as alternative dose escalated radiation therapy treatments. In the authors' opinions, SBRT is a reasonable option for unfavorable prostate cancer when a longer course of EBRT is not possible due to logistical challenges.

#### PO-0853 Bladder and urethra subregions predicting urinary toxicity after prostate cancer radiotherapy

E. Mylona<sup>1</sup>, O. Acosta<sup>1</sup>, T. Lizee<sup>1</sup>, J. Castelli<sup>2</sup>, C. Lafond<sup>2</sup>, G. Crehange<sup>3</sup>, N. Magne<sup>4</sup>, S. Chiavassa<sup>5</sup>, S. Supiot<sup>5</sup>, R. De Crevoisier<sup>1,2</sup>

<sup>1</sup>INSERM U1099 - University of Rennes, Laboratoire Traitement du Signal et de l'Image, Rennes, France ; <sup>2</sup>Centre Eugène Marquis, Radiotherapy department, Rennes, France ; <sup>3</sup>Centre Georges François Leclerc, Radiotherapy department, Dijon, France ; <sup>4</sup>Lucien Neuwirth Cancer Institute, Radiotherapy department, St Priest en Jarez, France ; <sup>5</sup>Institut de Cancérologie de l'Ouest, Medical Physics Department, Nantes, France

#### Purpose or Objective

To apply a voxel-based analysis on the planning 3D dose distribution in order to identify symptom-related subregions (SRSs) of the bladder/urethra associated with acute and late urinary toxicity in prostate cancer radiation therapy (RT).

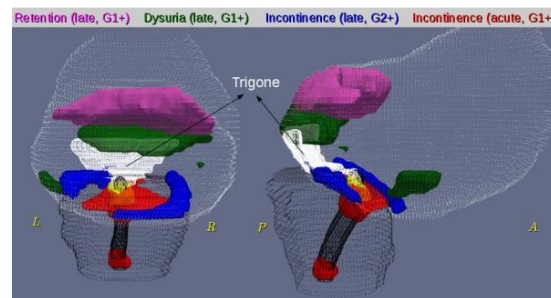
#### Material and Methods

Overall, 272 prostate cancer patients treated with IMRT/IGRT from two multicentric prospective phase III trials were analyzed. Each patient's organ contours (bladder, urethra and prostate) were spatially normalized to a common coordinate system (CCS) via non-rigid registration. The obtained 3D deformation fields were used to propagate the planning dose distributions from the native space of each patient to the CCS. A voxel-based statistical analysis was applied to generate 3D dose-volume maps for different urinary symptoms and identify corresponding SRSs with statistically significant dose differences between patients with/without toxicity. All the identified SRSs were propagated from the CCS back to the native space of each individual and DVHs for the SRSs and the whole bladder were computed. Dose bins of significant dose difference between patients with/without urinary toxicity were identified. Logistic regression was used to estimate the DVH prediction capability (1Gy bin-wise) of the SRSs compared to the whole bladder.

#### Results

A local dose-effect relationship was found in the bladder and the urethra. SRSs of significant dose differences (p-value<0.01) were identified for four endpoints: acute and late incontinence in the urethra and the trigone, late retention and dysuria in the posterior part of the bladder, with average dose differences ranging from 1.26 to 9.28 Gy. Figure 2 shows these SRSs on the template. The DVHs of the SRSs were significantly predictive of toxicity with maximum areas under the ROC curve (AUC): 71% for acute incontinence, 80% for late incontinence, 68% for late retention and 79% for late dysuria. The DVH of the bladder was predictive only for late incontinence and late dysuria (AUC=70%). Table 1 shows the prediction capability of the

DVH for the SRSs and the whole bladder in the native space.



A. Acute toxicity					
Symptom	Region	Most predictive DVH bin (Vx)	AUC	p-value	OR (95% CI)
Incontinence	Acute incontinence SRS	V81	70.9	<0.01	1.05 (1.02-1.09)
	Whole bladder	-	-	NS	-
B. Late toxicity					
Symptom	Region	Most predictive DVH bin (Vx)	AUC	p-value	OR (95% CI)
Incontinence	Late incontinence SRS	V79	79.7	0.01	1.04 (1.01-1.07)
	Whole bladder	V80	70.2	0.01	1.21 (1.05-1.43)
Retention	Late retention SRS	V37, V62	68	<0.01	1.02 (1.01-1.04)
	Whole bladder	-	-	NS	-
Dysuria	Late dysuria SRS	V53	78.7	<0.01	1.06 (1.02-1.09)
	Whole bladder	V63	70.1	0.02	1.04 (1.01-1.07)

Abbreviations: SRS= symptom-related subregion, OR= odds ratio, AUC= area under the ROC curve, Vx= volume receiving at least x Gy, CI= confidence interval, NS= Non-significant

#### Conclusion

The dose delivered to the urethra, the trigone and the posterior region of the bladder was predictive of acute and late incontinence, late retention and late dysuria. These SRSs appear more predictive than the whole bladder, suggesting that identification of radiosensitive subregions can improve the prediction capabilities for urinary toxicity and may be spared in order to decrease urinary symptoms. Additionally, this study provides the first evidence that explicitly correlate the true 3D dose to the urethra with urinary toxicity following EBRT.

#### PO-0854 Extreme vs moderate hypofractionation for localized Pca: a Propensity Score Matching Analysis

G. Marvaso<sup>1</sup>, D. Ciardo<sup>1</sup>, S. Gandini<sup>2</sup>, G. Riva<sup>1</sup>, E. Frigo<sup>3</sup>, D. Zerini<sup>1</sup>, S. Comi<sup>4</sup>, R. Cambria<sup>4</sup>, O. De Cobelli<sup>5</sup>, R. Orrecchia<sup>6</sup>, B.A. Jereczek-Fossa<sup>1,3</sup>

<sup>1</sup>IEO- European Institute of Oncology IRCCS, Radiotherapy, Milan, Italy ; <sup>2</sup>IEO- European Institute of Oncology IRCCS, Epidemiology and Biostatistics, Milan, Italy ; <sup>3</sup>University of Milan, Department of Oncology and Hemato-oncology, Milan, Italy ; <sup>4</sup>IEO- European Institute of Oncology IRCCS, Medical Physics, Milan, Italy ; <sup>5</sup>IEO- European Institute of Oncology IRCCS, Urology, Milan, Italy ; <sup>6</sup>IEO- European Institute of Oncology IRCCS, Scientific Directorate, Milan, Italy

#### Purpose or Objective

The aim of this study is to compare clinical outcome and toxicity of 2 cohorts of clinically localized prostate cancer (PCa) patients treated with 2 different radiotherapy (RT) regimens: Extreme hypofractionation (EH, 35Gy or 32.5Gy in 5 fractions) vs moderate hypofractionation (MH, Fox-Chase regimen, 70Gy in 26 fractions) both using image-guided intensity modulated RT (IG-IMRT).

#### Material and Methods

Radiation Therapy Oncology Group/European Organization for Research and Treatment of Cancer criteria (RTOG/EORTC) and Houston definition (nadir+2) were used for toxicity and biochemical failure evaluation, respectively. Multivariate proportional Hazard Cox

models, stratified for propensity score strata, were used to compare the 2 populations in term of overall survival (OS), clinical progression free survival (cPFS), biochemical PFS (bPFS) and gastro-intestinal (GI) toxicity and genitourinary (GU) toxicity. Propensity scores reflect the probability that a patient received MH or EH based on his baseline characteristics. Patients receiving MH were matched on a one-to-one basis with subjects receiving EH. Matching was performed based on nearest-neighbor matching. The analyses were applied on the matched cohorts and on the whole cohorts, stratifying the analyses by risk strata identified with the propensity scores (Table 1).

### Results

The analysis included 227 PCa patients treated in 2007-2015, receiving MH-IG-IMRT and 194 patients treated with EH-IG-IMRT in 2012-2015. Median age was 75 years (range: 50-89). Median follow-up was 43 months. A statistically significant difference in distribution regarding Gleason score (GS) and risk group was found between the 2 groups ( $p=0.004$  and  $p=0.002$ , respectively). 226 patients with good matching characteristics and balance (113 men per group) were selected after propensity score matching. A multivariate Cox analysis performed on the pre-matched cohort showed that bPFS, cPFS and OS were not statistically different between the 2 treatment groups ( $p=0.439$ ,  $p=0.317$ ,  $p=0.906$ , respectively), after adjusting for prognostic variables and confounding factors (Figure A,B,C). These results were confirmed in the matched population analysis. As concerning GI toxicity, compared with EH, in MH acute  $G>1$  events were significantly more (3% vs 9%,  $p=0.007$ ). As concerning GU toxicity, compared with EH, in MH, acute  $G>1$  events were registered in 11% vs 26% ( $p<0.001$ ). Multivariate Cox regression models showed no significant differences between the cohorts in term of late GI and GU toxicity. Acute GU/GI toxicities in the matched cohort were confirmed to be worse in the MH ( $p=0.002$  and  $p<0.001$ ). The GU/GI toxicity detected at last follow-up were both in line with those emerged from the pre-matched analyses ( $p=0.43$  and  $p=0.08$ ).

### Conclusion

Utilizing the Propensity Score Comparison there was no difference in terms of oncological outcome at a median follow-up of 43 months comparing the 2 RT modalities. Moreover, the 2 RT regimens were associated with similar toxicity profiles.

### PO-0855 Development and Validation of a Prostate Cancer Patient Decision Aid: Towards Participative Medicine

A. Ankolekar<sup>1</sup>, B. Vanneste<sup>2</sup>, E. Bloemen<sup>3</sup>, J. Van Roermund<sup>4</sup>, E. Van Limbergen<sup>2</sup>, K. Van de Beek<sup>4</sup>, V. Zamboni<sup>5</sup>, M. Oelke<sup>6</sup>, A. Dekker<sup>1</sup>, P. Lambin<sup>7</sup>, R. Fijtten<sup>1</sup>, A. Bertlang<sup>8</sup>

<sup>1</sup>Maastricht University, Knowledge Engineering, Maastricht, The Netherlands ; <sup>2</sup>Maastricht University, Radiotherapy, Maastricht, The Netherlands ; <sup>3</sup>Fontys University of Applied Sciences, n/a, Eindhoven, The Netherlands ; <sup>4</sup>Maastricht University Medical Centre+, Urology, Maastricht, The Netherlands ; <sup>5</sup>Zuyderland Medical Center, Urology, Sittard, The Netherlands ; <sup>6</sup>St. Antonius-Hospital Akademisches Lehrkrankenhaus der WWU Münster, Urology, Gronau, Germany ; <sup>7</sup>Maastricht University, The D-Lab- Research Institute GROW, Maastricht, The Netherlands ;

<sup>8</sup>Maastricht University, n/a, Maastricht, The Netherlands

### Purpose or Objective

Prostate cancer is the second most prevalent cancer in men in the Western world. Insufficient information on the different treatment options often results in suboptimal treatment choices that could lead to poor quality of life and additional costs. A Cochrane meta-analysis proved the value of patient decision aids (PDAs) in improving patient knowledge and enabling values clarification to facilitate shared decision making, yet poor design is a major

implementation barrier.

We develop an interactive web-based PDA based on user-centered design for better integration into the care pathway. In this approach, users are involved early and often in order to improve quality, reliability, usability of the PDA, and build ownership.

### Material and Methods

PDA development consisted of five rounds of semi-structured interviews and usability tests with, urologists (n=8), radiation oncologists (n=4), nurses (n=2), general practitioners (n=8), ex-patients (n=19), usability experts (n=4) and male test volunteers (n=11). The PDA was continuously tested and refined based on user feedback. Interview topics included informational needs, PDA requirements and possible implementation barriers. We tested usability with surveys and heuristic evaluation by experts.

### Results

Initial versions focused on clinical details (anatomy, complications, contra-indications) but as the rounds progressed the PDA was updated to reflect non-clinical factors that influenced patients' choices: treatment logistics, the impact of side-effects on daily life and uncertainty. Patients tended to choose aggressive surgery due to fear and lack of knowledge, underlining the need for more balanced information, particularly on radiotherapy. Usability experts suggested navigational and visual changes, e.g. a sidebar menu, neutral color palette, more white space and less textual clutter to improve readability (Fig. 1 and 2).

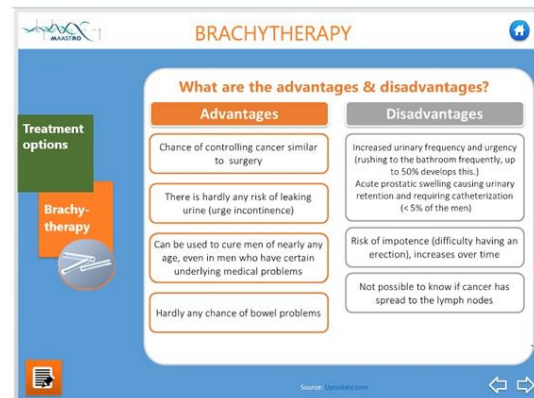


Figure 1: Treatment information about brachytherapy in the initial versions of the PDA

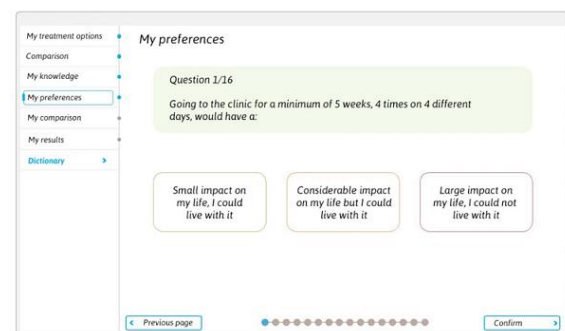


Figure 2: An example of values clarification in the final version of the PDA

The final PDA ([www.beslissamen.nl](http://www.beslissamen.nl)) contains seven sections:

1. **Introduction:** a 2-minute video priming patients for using the PDA.
2. **My treatment options:** textual and visual information (diagrams, videos) on each treatment option (brachytherapy, external radiation, surgery and active surveillance).

3. **Comparison:** a table listing pros and cons of each treatment side-by-side.
4. **My knowledge:** Ten true/false questions to confirm the patient's understanding.
5. **My preferences:** 16 values clarification questions about treatment experience, quality of life, and uncertainty.
6. **My comparison:** four questions asking the patient to select treatment aspects that are least desirable.
7. **My results:** a tabular overview of the values clarification. This can be printed for use in the consultation to guide the SDM talk in accordance with patient values.

### Conclusion

User-centered design provided valuable insights into PDA requirements but resulted in a time-consuming process and a diverse range of perspectives that were challenging to integrate. The PDA is currently being evaluated in a clinical trial (NCT03278197).

**PO-0856 Metastasis-directed therapy for oligoprogressive castration refractory prostate cancer**  
**C. Berghen<sup>1</sup>, S. Joniau<sup>2</sup>, P. Ost<sup>3</sup>, K. Poels<sup>1</sup>, W. Everaerts<sup>2</sup>, K. Haustermans<sup>1</sup>, G. De Meerleer<sup>1</sup>**  
<sup>1</sup>University Hospital of Leuven, Radiation Oncology, Leuven, Belgium ; <sup>2</sup>University Hospital of Leuven, Urology, Leuven, Belgium ; <sup>3</sup>University Hospital of Ghent, Radiation Oncology, Ghent, Belgium

### Purpose or Objective

In metastatic castration refractory prostate cancer (mCRPC) state-of-the-art treatment consists of a systemic treatment with second-line hormones, chemotherapy or bone seeking agent in addition to palliative androgen deprivation therapy (pADT). Clinical progression is the signal to switch to next-line systemic treatment (NEST). A subgroup of these progressive patients shows oligoprogression, defined as the progression of a limited number of metastatic spots while the majority of metastases are controlled by ongoing systemic therapy. We hypothesized that metastasis directed therapy (MDT) against these oligoprogressive lesions might defer the need for NEST. Therefore, we performed this retrospective analysis.

### Material and Methods

We analyzed the outcome of patients who were treated with MDT for mCRPC oligoprogressive disease, defined as either the progression of  $\leq 3$  existing oligometastatic sites and/or the appearance of  $\leq 3$  new metastasis and/or local recurrence. In total, the number of progressive/new lesions was  $\leq 3$ . All patients were under systemic therapy with pADT whether or not combined with second-line systemic treatment. The time frame of the study was from 1/2012 until 3/2018. Primary endpoint was NEST-free survival (NEST-FS). Secondary endpoints were progression-free survival (PFS) and toxicity scoring.

### Results

A total of 35 cases of oligoprogression were included who received MDT consisting of SBRT (n=22), metastasectomy (n=2), or local treatment with more conventionally fractionated radiotherapy (n=11). A total of 51% in the MDT-group had upfront metastatic disease, from which 61% had upfront oligometastatic disease. At the time of oligoprogression the majority had bone lesions (69%). Others had nodal disease or a combination of both or local recurrence. There were no patients with oligoprogressive visceral metastasis. Most patients were on systemic treatment with pADT only. The median follow-up time was 30 months (IQR 9-42). There was a median NEST-free survival (NEST-FS) of 16 months (CI 95% 12-31) and PFS of 12 months (CI 95% 7-18). SBRT or surgery-related toxicity was minor, with limited grade 1 and 2 toxicity and only one patient experiencing acute grade 3 toxicity after treatment for local relapse in the prostate.

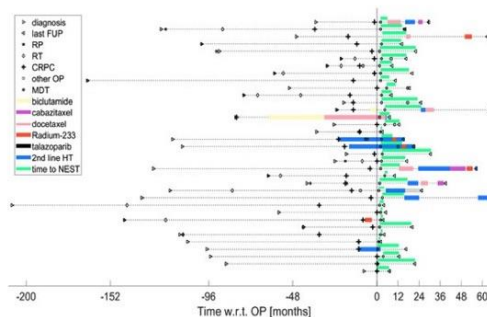


Figure 1. Overview of therapies pre- and post-diagnosis of oligoprogression  
 Oligoprogression is defined as the zero point on x-axis; FUP: follow-up; RP: radical prostatectomy; RT: radiation therapy; CRPC: castration refractory prostate cancer; OP: oligoprogression; MDT: metastasis-directed therapy; NEST: next-line systemic treatment.

Table 1: Patient Characteristics		MDT group (n=35)
<b>Time point: initial diagnosis prostate cancer</b>		
Median age in years (IQR)		64 (57-70)
Median PSA (ng/ml) (IQR)		12 (7-16)
Gleason 8-10 (%)		24 (69)
Metastatic disease (%)		18 (51)
Local treatment (%)		28 (80)
ADT (%)		19 (54)
<b>Time point: oligoprogression</b>		
Median age in years (IQR)		70 (66-76)
Median PSA (ng/ml) (IQR)		3 (1-10)
Time period being on ST (months) (IQR)		24 (22-52)
<b>Number of progressive lesions (including LCR)</b>		
1		20 (58)
2		10 (28)
3		5 (14)
<b>Type of lesion</b>		
Lymph node		5 (14)
Bone		24 (69)
Lymph node + bone		1 (3)
LCR		4 (11)
LCR + bone		1 (3)
<b>Toxicity</b>		
grade 1		5 (14%)
grade 2		2 (6%)
grade 3		1 (3%)
grade 4		0
grade 5		0
<b>Outcome</b>		
Median follow-up, months (IQR)		17 (8-25)
Median progression free survival, months (95% CI)		12 (7-18)
Median NEST-free survival		16 (12-31)

Legend: IQR: interquartile range; PSA: prostate specific antigen; ADT: androgen deprivation therapy; ST: systemic therapy; LCR: local recurrence; NEST: next-line systemic treatment

### Conclusion

Our data demonstrate an important deferral of NEST with a median NEST-FS of 16 months in 35 cases of patients treated with MDT. These data are unique and may induce a paradigm shift in the treatment of these patients. Prospective clinical trials are warranted to further define the patient characteristics and treatment outcomes.

**PO-0857 MRI-derived radiomics to select patients with high-risk prostate cancer for adjuvant radiotherapy**  
**V. Bourbonne<sup>1</sup>, M. Vallières<sup>2</sup>, F. Lucia<sup>1</sup>, G. Fournier<sup>2,3</sup>, A. Valéri<sup>2,3</sup>, D. Visvikis<sup>2</sup>, V. Tissot<sup>4</sup>, O. Pradier<sup>1,2</sup>, M. Hatt<sup>2</sup>, U. Schick<sup>1,2</sup>**

<sup>1</sup>CHRU Brest, Radiation Oncology, Brest, France ;

<sup>2</sup>Université de Bretagne Occidentale, LaTIM UMR 1101

INSERM, Brest, France ; <sup>3</sup>CHRU Brest, Urology Unit,

Brest, France ; <sup>4</sup>CHRU Brest, Radiology, Brest, France

### Purpose or Objective

Radical prostatectomy (RP) is one of the treatments of choice for patients with prostate cancer (PCa) but biochemical recurrence (BCR) after RP occurs in 50% of patients, particularly in those who harbor high risk features like locally advanced disease (T3-4), positive margins (R1) or high Gleason score. Adjuvant radiotherapy

(RT) has been proven effective to prolong biochemical control, but is associated with a higher risk of grade  $\geq 2$  toxicity. We aimed to develop and validate a magnetic resonance imaging (MRI)-based radiomics signature with prognostic value in patients with high risk PCa, in order to guide patients management especially regarding the use of adjuvant RT.

#### Material and Methods

One hundred-seven patients with histologically proven PCa with high-risk features namely pT3-4, and/or R1, and/or Gleason 8-10 and treated with RP with or without lymphadenectomy from 2010 to 2016 at our institution, and with available preoperative pelvic MRI were included. Adjuvant treatment, postoperative PSA > 0.04 ng/mL and c/pN1 were exclusion criteria.

Prostatic tumors were delineated on both the ADC and T2 MRI sequences using 3D Slicer® v4.8.0 and IBSI-validated radiomic features were extracted. The cohort was randomly split into training (n=70) and testing (n=37) sets. The selection of a subset of 10 radiomics features was performed in the training set using an aggressive false discovery reduction procedure relying on stability and correlation checks and robustness score. Correlation with BCR was assessed using ROC curves and Cox regression analysis was performed to identify independent predictive variables.

#### Results

After a median follow-up of 52.0 months, 17 (16.0%) patients experienced BCR. In the training set, none of the clinical features was significantly correlated with BCR. Amongst the 10 radiomic features pre-selected, an ADC feature outperformed the others with an AUC of 0.85 to predict biochemical relapse-free survival (bPFS) ( $p = 0.0001$ ).

In the testing set, this feature remained significantly predictive of BCR (AUC of 0.76) and prognostic of bPFS ( $p = 0.0236$ ).

#### Conclusion

One ADC radiomic feature appeared to be strongly predictive of BCR following RP. This feature could help in redefining the population who would mostly benefit from treatment intensification such as adjuvant RT.

#### PO-0858 Dosimetric correlation analysis of observed toxicities in prostate cancer patients treated with SBRT

N. Pienimäki<sup>1</sup>, K. Vuolukka<sup>2</sup>, J. Heikkilä<sup>2</sup>, J. Palmgren<sup>2</sup>, J. Seppälä<sup>2</sup>

<sup>1</sup>University of Eastern Finland, Department of Applied Physics, Kuopio, Finland ; <sup>2</sup>Kuopio University Hospital, Centre of Oncology, Kuopio, Finland

#### Purpose or Objective

The aim of this study was to investigate the correlation between dosimetric parameters and registered toxicities in ultra-hypofractionated radiotherapy of prostate cancer (PCa).

#### Material and Methods

Between the years 2012 and 2015 220 patients received ultra-hypofractionated radiotherapy (5x7.0 Gy / 7.25 Gy) delivered with CyberKnife robotic system for the radical treatment of PCa at Kuopio University Hospital, Finland. Toxicities were observed in 36 patients which were divided in four different groups; Intermediate-term Genitourinary toxicities (GU, n=19), intermediate-term rectal toxicity (GI, n=7), Infectious problems toxicity (INF, n=7) and Acute toxicity (ACUTE, n=4). Comparison groups of patients were formed for each toxicity group by selecting similar patients without any toxicity according to age, size of PTV and hormonal treatment. Average DVH curves (Fig.1) for rectum and bladder were produced for each group and were used to choose representative dose-volume parameters for correlation analysis. In correlation analysis the mean values of absolute volume doses, mean values of relative volume doses and relative volumes for

dose in percentage was studied. The results were further analysed by using Wilcoxon rank sum test. Analysis was done separately per each toxicity group and its comparison group.

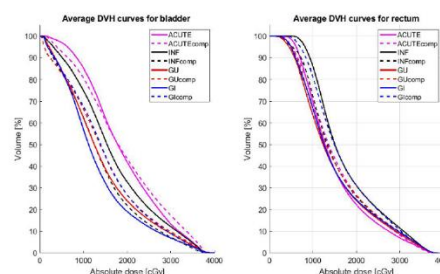


Figure 1: Average DVH curves of bladder and rectum for each toxicity group and comparison groups.

#### Results

For the INF patients significant differences between the groups were discovered for the higher doses of bladder (D5% ( $p=.007$ ) and D10% ( $p=.005$ )). In addition, for bladder the results between INF patients and comparison group differed significantly with V35 ( $p=.0006$ ) and somewhat notably with V30 ( $p=.07$ ). When investigating the doses delivered to rectum, significant differences were observed with medium dose value V10 ( $p=.038$ ). Also, with V15 ( $p=.07$ ) and D50% ( $p=.07$ ) some notable differences were observed.

For the GI patients in the analysis for rectum, it was observed that the doses of D5cc ( $p=.07$ ) and D10cc ( $p=.05$ ) differed remarkably between the groups. When analysing relative volumes for dose in percentage, it was observed that for rectum V15 ( $p=.07$ ) the volumes for doses were remarkably different. Further research is still needed in order to verify the significance of these observed values. Significant correlation between toxicity symptoms and dosimetric values were not found for the GU and for the ACUTE groups, respectively. All the notable results are presented in Table 1.

Toxicity Group	Structure	Variable	Toxicity patients Dose [Gy $\pm$ SD]	Comparing group Dose [Gy $\pm$ SD]	P value
GI	Rectum	D5cc	31.0 $\pm$ 2.5	28.6 $\pm$ 2.9	0.073
GI	Rectum	D10cc	25.2 $\pm$ 3.1	22.2 $\pm$ 3.1	0.053
INF	Bladder	D5%	35.5 $\pm$ 1.2	34.1 $\pm$ 1.7	0.073
INF	Bladder	D5%	34.2 $\pm$ 1.3	31.4 $\pm$ 2.2	0.007
INF	Bladder	D10%	30.5 $\pm$ 2.4	26.2 $\pm$ 4.0	0.053
INF	Rectum	D50%	15.1 $\pm$ 1.4	13.0 $\pm$ 2.8	0.073
Toxicity Group	Structure	Variable	Toxicity patients Volume [% $\pm$ SD]	Comparing group Volume [% $\pm$ SD]	P value
GI	Rectum	V15	39 $\pm$ 11	50 $\pm$ 13	0.073
INF	Rectum	V15	50 $\pm$ 8	42 $\pm$ 14	0.073
INF	Rectum	V10	86 $\pm$ 9	73 $\pm$ 15	0.038
INF	Bladder	V35	5 $\pm$ 2	2 $\pm$ 0	0.001
INF	Bladder	V30	12 $\pm$ 6	7 $\pm$ 3	0.073

Table 1: The most remarkable mean values of dose per volume and volumes for dose in percentage for bladder and rectum for GI and INF toxicity patients and their comparison group.

#### Conclusion

High maximum doses to critical organs was found to correlate strongly with observed INF and GI toxicities for the PCa patients treated with ultra-hypofractionated radiotherapy. For the GU and ACUTE groups no correlation between the groups in toxicity and dose distributions was found. For the medium range doses there were only slight differences between toxicity and control group, respectively. The daily variation of the treated anatomy could have an effect for the non-significance of the lower doses since dose received by the critical organs of may vary by fraction.

#### PO-0859 Validation of genetic variants associated to late severe toxicity after prostate cancer RT

A. Cicchetti<sup>1</sup>, T. Rancati<sup>2</sup>, F. Ballarini<sup>3</sup>, M. Dispinzieri<sup>4</sup>, T. Giandini<sup>5</sup>, B. Avuzzi<sup>4</sup>, C. Cozzarini<sup>6</sup>, C. Fiorino<sup>7</sup>, R. Valdagni<sup>8</sup>

<sup>1</sup>Fondazione IRCCS Istituto Nazionale dei Tumori and University of Pavia, Prostate cancer program/Department of Physics, Milan, Italy ; <sup>2</sup>Fondazione IRCCS Istituto Nazionale dei Tumori, Prostate cancer program, Milan, Italy ; <sup>3</sup>University of Pavia, Physics Department INFN-Section of Pavia, Pavia, Italy ; <sup>4</sup>Fondazione IRCCS Istituto Nazionale dei Tumori, Radiation Oncology 1, Milan, Italy ; <sup>5</sup>Fondazione IRCCS Istituto Nazionale dei Tumori, Medical Physics, Milan, Italy ; <sup>6</sup>San Raffaele Scientific Institute, Radiation Oncology, Milan, Italy ; <sup>7</sup>San Raffaele Scientific Institute, Medical Physics, Milan, Italy ; <sup>8</sup>University of Milan and Fondazione IRCCS Istituto Nazionale dei Tumori, Department of Oncology and Hemato-oncology / Prostate cancer program & Radiation Oncology 1, Milan, Italy

### Purpose or Objective

To validate the impact of single nucleotide polymorphisms (SNPs) on radio-induced toxicity (tox) after curative RT for prostate cancer (PC).

### Material and Methods

Comprehensive literature search for SNPs associated to increased risk for tox after PC RT was carried out. A panel of 8 SNPs was established.

A cohort of PC patients (pts) from a prospective trial on RT-induced toxicity was identified.

They were treated with radical IMRT to a total dose of 78Gy at 2Gy/fr or to 65-74.2Gy with 2.55-2.65Gy/fr.

Blood samples were collected during the follow up (fup) for DNA extraction (Oct2016-May2017).

Selected endpoint was overall moderate-severe late tox assessed at 3 year-fup, i.e. scoring of at least one symptom among the following: grade $\geq$ 2 rectal bleeding (CTCAE), chronic faecal incontinence (FI) (CTCAE average grade $>$ 1 during whole fup), severe urinary dysfunction (15-point worsening in IPSS questions #1to#7), hematuria, stricture and moderate-severe urinary incontinence (by 2-point worsening in ICIQ question #3).

Association of selected SNPs with overall late tox was investigated through logistic regression (LR).

Confirmed SNPs (similar Odds Ratios) were later included into a LR model together with Equivalent Uniform Dose (EUD) for bladder and rectum, as computed from DVHs corrected with a/b=3Gy). For both bladder and rectum, volume parameters n for overall late tox were determined by literature search.

### Results

108 pts were included in the study. Overall late tox was scored in 37 pts (34%).

3/8 investigated SNPs were confirmed: rs3931914CG, rs2293054GA and rs845552AG (De Langhe Rad&Onc 2014, see Fig. 1 for details).

From literature search, we identified a volume parameter n=0.1 for bladder (p=0.003, i.e. bladder acting as serial organ for late urinary tox) and n=0.25 for rectum (p=0.007, i.e. relevance of medium to high doses is kept, correctly matching the presence of 2 distinct patterns in late rectal tox, which includes both bleeding, affected by small volumes receiving high doses, and FI, affected by mean rectal dose).

The final LR model included: bladder EUD (fitted OR=1.10), rectal EUD (fitted OR=1.09) and SNPs (literature OR=2.59, 0.23 and 5.3 for rs845552AG, rs2293054GA and rs3931914CG ). Total p=0.015, calibration slope=0.83 and AUC=0.70, details on calibration in fig 2b.

Fig 2a presents the nomogram derived from LR model, where the genetic risk score is reported as the number of SNPs harboured by the single patient. The nomogram highlights that given the same dose to organs at risk (i.e. same bladder EUD+rectal EUD) presence of 1 SNP is increasing tox risk by 5%, while presence of 2 or 3 SNPs increases tox risk by more than a factor 2.

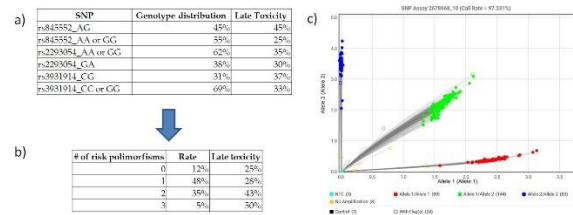


Fig. 1: Panel a) Genotype distribution among the patients and rate of late toxicity in the dichotomized categories, panel b) patients classification by number of risk polymorphisms, panel c) example of rs845552 distribution before the dichotomization.

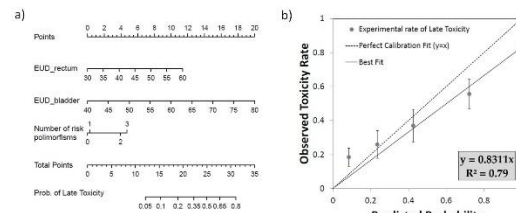


Fig. 2: Panel a) Predictive nomogram of Late Overall Toxicity with genetic risk score reported as number of risk polymorphisms, panel b) Calibration Plot for the predictive model with EUD+SNPs (with coefficients showed in De Langhe et al.)

### Conclusion

3 SNPs previously identified as associated with increased risk of RT-induced tox were confirmed in this validation study. **Late overall tox incidence was well described by a data+literature driven model** (effect size of SNPs and volume parameters for EUD calculations from literature, effect size for bladder and rectal EUD fitted on data).

### PO-0860 Improving consistency of proximal seminal vesicle delineation for prostate SBRT

K. Morrison<sup>1</sup>, N. Van As<sup>1</sup>

<sup>1</sup>Royal Marsden NHS Trust, Radiotherapy, London, United Kingdom

### Purpose or Objective

Accurate and consistent clinical target volume (CTV) delineation is important in stereotactic body radiotherapy (SBRT). The proximal 1 - 2 cm seminal vesicles (pSV) are included in the CTV for low/ intermediate risk prostate cancer, however there is no clear consensus on how this should be defined. Within the PACE SBRT trial, inconsistent pSV delineation has been demonstrated between centres. The aim of this study is to investigate a delineation method which will improve consistency in further trials.

### Material and Methods

21 experienced prostate radiotherapy clinicians (consultants and trainees), were identified at a national uro-oncology conference, and invited to participate in a contouring exercise. Using fused CT and MRI imaging from one selected intermediate-risk prostate cancer case, participants were instructed to contour: superior prostate (partial contour provided); full seminal vesicles (SV); and proximal 1cm SV as defined by the clinician (pSV method A). A further pSV contour was defined by creating a 1cm circumferential prostate margin, and including the section of SV within this region (pSV method B). For each method, investigational contours were compared to a set of reference contours, using measured volume (cc) and calculated conformity indices: DICE similarity coefficient; Geographical Miss Index (GMI); and Discrepancy Index (DI). Results for methods A and B were compared to analyse differences in consistency, using paired t-test to measure statistical significance.

### Results

19 sets of contours were complete and analysable. For pSV method A, the mean investigational contour volume was 11.07 cc (95% CI 9.04 - 13.11) compared to the reference contour 8.65 cc. For method B, the mean investigational

volume was 5.91 cc (95% CI 5.49 - 6.34) compared to the reference contour volume of 6.46 cc. The mean DICE similarity coefficient (ideal value 1) for method A was 0.67 (95% CI 0.63 - 0.71), and was significantly higher for method B at 0.81 (95% CI 0.78 - 0.84,  $p < 0.0001$ ), demonstrating greater concordance with the reference contour. The mean DI (ideal value 0) was 0.35 (95% CI 0.28 - 0.43) for method A, and was significantly lower for method B at 0.15 (95% CI 0.11 - 0.18,  $p < 0.0001$ ) indicating a lower possibility of excessive contouring with this method, in comparison to the reference contour. The was not a significant difference in mean GMI (ideal value 0), at 0.24 (95% CI 0.16 - 0.32) for method A, and 0.23 for method B (95% CI 0.18 - 0.27,  $p = 0.7$ ).

#### Conclusion

Consistency of pSV delineation is improved by the use of a circumferential prostate margin to define the extent of the seminal vesicles to be included in the target volume. This method is recommended for use in future prostate radiotherapy trials, and will be adapted for the PACE C trial which will compare SBRT with conventional radiotherapy in higher risk patients, including 2cm pSV within the CTV.

#### PO-0861 Analysis of nodal and prostatic bed RT in oligorecurrent PC patients treated with PSMA-PET-guided RT

S. Kirste<sup>1</sup>, S. Kroeze<sup>2</sup>, C. Henkenberens<sup>3</sup>, N. Schmidt-Hegemann<sup>4</sup>, M. Vogel<sup>5</sup>, J. Becker<sup>6</sup>, H. Christiansen<sup>7</sup>, S. Combs<sup>8</sup>, A. Müller<sup>9</sup>, C. Belka<sup>10</sup>, M. Guckenberger<sup>2</sup>, A. Grosu<sup>11</sup>

<sup>1</sup>University Hospital Freiburg, Radiooncology, Freiburg, Germany ; <sup>2</sup>University Hospital Zürich, Department of Radiation Oncology, Zürich, Switzerland ; <sup>3</sup>Medical School Hannover, Department of Radiooncology and Special Oncology, Hannover, Germany ; <sup>4</sup>University Hospital LMU Munich, Department of Radiation Oncology, Munich, Germany ; <sup>5</sup>Technical University Munich, Department of Radiation Oncology, Munich, Germany ; <sup>6</sup>University Hospital Tübingen, Department of Radiooncology, Tübingen, Germany ; <sup>7</sup>Medical School Hannover, Department of Radiotherapy and Special Oncology, Hannover, Germany ; <sup>8</sup>Technical University Munich, Department of Radiooncology, Munich, Germany ; <sup>9</sup>University Hospital Tübingen, Department of Radiation Oncology, Tübingen, Germany ; <sup>10</sup>University Hospital LMU Munich, Department of Radiooncology, Munich, Germany ; <sup>11</sup>University of Freiburg, Department of Radiooncology, Freiburg, Germany

#### Purpose or Objective

Patients with prostate cancer and PSMA-PET/CT detected oligo-recurrent disease are a very heterogeneously treated group of patients. Various treatment regimens are currently practiced in different institutions in an individual approach to this patient group; in particular, there are no clear recommendations concerning doses, treatment fields and radiation techniques (conventional versus hypofractionated versus stereotactic body radiotherapy). This study's aim is to investigate treatment patterns at different institutions and to analyze the influence of target volume concepts on progression-free-survival (PFS).

#### Material and Methods

Data of 305 patients from 6 different academic centers that were treated with definite radiotherapy (RT) because of oligorecurrent 68Ga-PSMA -positive prostate cancer between 04/2013 and 01/2018 were evaluated. To describe treatment regimen at different institutions descriptive statistics was used. PFS was analyzed using Kaplan-Meier survival curves and log rank testing. Uni-, and multivariate analyses were performed to determine influence of treatment parameters on PFS.

#### Results

According to the pretreatment PSMA-PET/CT 92 patients (30.2%) had a recurrence in the prostate bed only, 134 (43.9%) had recurrence in the lymphatics with or without prostate bed recurrence and 79 patients (25.9%) had distant metastasis. RT was directed to the PET/CT-positive lesions only, without elective RT in 85 patients (27.9%). The prostate bed was irradiated in 234 patients (76.7%) either electively (103 patients) or because of a PSMA-PET/CT detected recurrence (131 patients). 71 patients (23.3%) received treatment to other lesions without irradiation of the prostate bed. If the prostate bed was electively irradiated the median dose was 66.6 Gy (range, 48 - 70 Gy) in single doses of 1.8 - 2 Gy. If pelvic lymphatics were electively irradiated median dose was 47.5 Gy (range, 42-56 Gy) in single doses of 1.8 Gy (1.5 - 2 Gy). Most patients were treated with conventional RT 155 (50.8%) or conventional RT with a simultaneous integrated boost (SIB) technique 122 (40%). SBRT was used in 18 (5.9%) and combined SBRT and conventional RT in 10 (3.3%) patients. Patients who did not receive elective RT of the prostate bed had a 3- year biochemical free survival of 38% compared to 57% of patients who received RT of the prostate bed. Median biochemical free survival was 24 vs. 32 months ( $p=0.03$ ). Dose to the prostate bed or lymph nodes had no influence on PFS. Elective RT to the pelvic or paraaortic lymph nodes did not result in a statistically significant difference in PFS (25 vs. 30 months). In multivariate analysis location of recurrence and type of radiotherapy (conventional RT vs. SBRT and combined conventional/SBRT) were significantly associated with PFS.

#### Conclusion

Treatment regimens for PSMA-positive oligorecurrent prostate cancer in 6 academic institutions vary substantially in terms of treatment fields and technique. Patients who did not receive elective irradiation of the prostate bed had a significantly worse PFS than patients who received elective irradiation of the prostate bed.

#### PO-0862 P2 RCT of Home-based physical activity in pts treated by ADT and EBRT for localised prostate carcinoma

C.P. Doyle<sup>1</sup>, P. Thirion<sup>2</sup>, B. O'Neill<sup>2</sup>, M. Dunne<sup>2</sup>, V. Curtis<sup>3</sup>  
<sup>1</sup>Trinity Biomedical Science Institute, Medicine, Dublin, Ireland ; <sup>2</sup>St Lukes Radiation Oncology Network, Radiation Oncology, Dublin, Ireland ; <sup>3</sup>The London School of Hygiene and Tropical Medicine, Disease Control, London, United Kingdom

#### Purpose or Objective

To assess the feasibility and efficacy of a home-based moderate-to-vigorous physical activity walking exercise intervention (MVPA-WEI) in patients (pts) with localised prostate cancer treated by protracted (6-8 weeks) fractionated External Beam Radiotherapy (EBRT) and short-term (< 1 year) Androgen Deprivation (ADT).

#### Material and Methods

A Phase 2 randomised trial compared standard of care versus home-based MVPA-WEI, consisting of a prescription of 3000 steps in 30 minutes on 5 days each week, i.e. a cadence of 100 steps/minute (in addition to patient pre-determined habitual step/day) for the duration of radiotherapy (7-8 weeks).

Patients treated radically for localised prostate carcinoma by a combination of AD and EBRT, having completed a minimum of 3 month of induction and requiring concomitant AD during EBRT, in addition to having a sedentary life style were eligible for recruitment.

Intervention feasibility was evaluated through quantitative and qualitative methods. The efficacy endpoints were: **Adherence to exercise prescription** (pedometer and logbook [walking frequency, intensity and time]), **Fatigue** (Brief Fatigue Inventory [0-90]), **Health Related Quality of Life** (FACT-P [0-156]), **Anthropometric measures** (Weight [kg], % Body fat, % Muscle mass, Waist

circumference [cm]) and Functional Fitness [2 minute step test and 30 second sit-to-stand test]).

Patient were recruited at planning CT scan and randomised at fraction 6 of EBRT. Assessments were conducted at baseline (planning CT), mid EBRT, end of EBRT, and at 1 month post EBRT.

#### Results

From 02/2014 to 04/2014, 24 pts were recruited (12 per arm). All pts were evaluable. The overall MVPA-WEI adherence rate in the intervention group was 81.8%. 33% of pts in the control group increased their average daily step count. When compared to baseline, pts allocated to the intervention group experienced at 1 month post EBRT, greater and persistent improvements in 1) fatigue [mean Fatigue score difference: -20.17 vs. +5.75], 2) quality of life [Improved FACT-P score only noted in the intervention group], 3) anthropometric measurements [mean weight difference: -1.7 Kg vs. + 1.7 Kg, mean % body fat difference: - 1.1% vs. +1.1%, mean waist circumference difference: -0.9 cm vs. + 3.4 cm, mean % muscle mass difference: +0.5% vs. - 0.8%] and 4) physical performance [2min step performance difference: +55.8% vs. + 30%, Sit-to-stand test performance difference: +25.3% vs. 9.0%]

#### Conclusion

This preliminary evidence suggests that a pragmatic home-based MVPA-WEI is feasible and has potential clinical benefits in pts treated by EBRT+ADT, and thus provides a strong rationale for a Phase 3 randomised trial.

---

#### Poster: Clinical track: Urology-non-prostate

---

#### PO-0863 Adaptive radiotherapy for carcinoma of the urinary bladder: Long term outcomes with dose escalation

P. Gupta<sup>1</sup>, V. Murthy<sup>1</sup>, K. Baruah<sup>1</sup>, R. Krishnatry<sup>1</sup>, G. Bakshi<sup>1</sup>, G. Prakash<sup>2</sup>, M. Pal<sup>2</sup>, A. Joshi<sup>3</sup>, K. Prabhaskar<sup>3</sup>  
<sup>1</sup>Tata Memorial Centre, Dept of Radiation Oncology, Mumbai, India ; <sup>2</sup>Tata Memorial Centre, Dept of Urology, Mumbai, India ; <sup>3</sup>Tata Memorial Centre, Dept of Medical Oncology, Mumbai, India

#### Purpose or Objective

This study was done to assess the clinical outcomes with dose escalated, image guided adaptive radiation therapy (ART) in patients of muscle invasive bladder cancer (MIBC), as a part of trimodality treatment approach for bladder preservation.

#### Material and Methods

Patients with non-metastatic MIBC treated with ART were analysed. After maximal resection of bladder tumor, they were treated with radical chemoradiation. For ART, 3 anisotropic planning target volumes were concentrically grown (PTVs small, medium and large) around the bladder. A library of intensity modulated radiotherapy (IMRT) plans was created for each patient. A dose of 64 Gy in 32 fractions to the whole bladder and 55 Gy to the pelvic nodes was planned. In selected patients with solitary tumor or two tumors in close proximity, without any in situ carcinoma component, dose escalation to tumor bed to 68 Gy (equivalent dose for 2-Gy fractions assuming  $\alpha/\beta$  of 10 [EQD2]<sub>10</sub> = 68.7 Gy) was planned. Simultaneous integrated boost was used for dose escalation and these patients were treated with a comfortably full bladder. On-board daily megavoltage imaging was used every day to choose the most appropriate PTV encompassing the bladder ('Plan-of-the-day' approach) for each fraction.

#### Results

A total of 106 patients were analysed. Most patients had T2 (68%) or T3 (19%) disease. Twenty three patients (22%) received neoadjuvant chemotherapy and 76% received concurrent weekly chemotherapy (platinum-based in 63%, gemcitabine-based in 35%). Ninety two patients (87%) completed the planned dose of 64 Gy to the whole bladder

while sixty three patients (59%) received 68 Gy to the tumor bed as boost. With a median followup of 26 months, 3-year locoregional control (LRC), disease-free survival (DFS), and overall survival (OS) were 74.3%, 62.9%, and 67.7% respectively. 82% retained a disease-free bladder, while another 8.5% had non muscle invasive recurrences managed conservatively. Patients receiving dose escalation to 68 Gy showed no difference in OS and DFS compared to those receiving <68 Gy. Acute and late Radiation Therapy Oncology Group (RTOG) grade III/IV genitourinary (GU) toxicity was seen in 7.5% and 6.5% patients respectively. Acute and late RTOG grade III gastrointestinal (GI) toxicity was seen in 0% and 3.8% patients respectively. The incidence of grade III/IV acute or late GU or GI toxicity was not found to be associated with dose escalation.

#### Conclusion

Dose escalation with adaptive plan-of-the-day approach for bladder irradiation is clinically safe and effective. A high bladder preservation rate can be achieved without compromising on survival or toxicities using plan of the day ART.

#### PO-0864 Normal tissue sparing with diffusion weighted MRI informed tumour boost in bladder radiotherapy

K. Chan<sup>1</sup>, K. Warren-Oseni<sup>2</sup>, H. Abdel-Aty<sup>3</sup>, A. Dunlop<sup>2</sup>, D. McQuaid<sup>2</sup>, M. Koh<sup>3</sup>, A. Sohaib<sup>3</sup>, R. Huddart<sup>3</sup>, S. Hafeez<sup>3</sup>

<sup>1</sup>The Royal Marsden NHS Foundation Trust, Radiotherapy and Imaging, London, United Kingdom ; <sup>2</sup>The Institute of Cancer Research and The Royal Marsden NHS Foundation Trust, Joint Department of Physics, London, United Kingdom ; <sup>3</sup>The Institute of Cancer Research - The Royal Marsden NHS Foundation Trust, Radiotherapy and Imaging, London, United Kingdom

#### Purpose or Objective

Partial bladder radiotherapy for the radical treatment of muscle invasive bladder cancer (MIBC) can be utilized with no adverse effect on local control [1, 2]. Studies however have failed to show improved toxicity. This may be due in part to uncertainty in CT based GTV delineation. DWI has an established diagnostic role in local MIBC staging with improved accuracy over CT. Here we evaluate the use of DWI to inform GTV delineation and its impact on normal tissue sparing.

#### Material and Methods

Twenty-one patients with unifocal T2-T3N0M0 MIBC recruited to an ethics approved phase I dose escalation radiotherapy protocol (NCT01124682) were evaluated. For treatment the tumour boost volume (GTV) was delineated on the radiotherapy planning CT (GTV<sub>CT</sub>). Pre-radiotherapy DWI was performed on a 1.5T system using b values 0, 50,100, 250, 500 and 750s/mm<sup>2</sup>. GTV was drawn on 750 s/mm<sup>2</sup> image (GTV<sub>DW-MRI</sub>) using in-house software (Adept, Institute of Cancer Research, London), was imported into the TPS (Raystation 6.99, RaySearch Laboratories, Stockholm, Sweden) and registered to the radiotherapy planning CT scan (using anatomical information from T2 and b0 image). The GTV and CTV (whole bladder) was expanded anisotropically (1.5cm anteriorly and superiorly, 1.0cm posteriorly and 0.5cm laterally and inferiorly) to create PTV<sub>boost-CT</sub>, PTV<sub>boost-DW-MRI</sub>, and PTV<sub>bladder</sub>. Two VMAT plans were created (for five patients), each treating PTV<sub>bladder</sub> to 52Gy and PTV<sub>boost</sub> to 70Gy in 32 fractions using the two different PTV<sub>boost</sub> volumes. Target volumes and dose to normal structures between were compared using Wilcoxon signed rank test where possible.

#### Results

All tumours seen on T2 image were identified on DWI. In 3 patients no tumour was seen on either T2 or DWI. Mean GTV<sub>CT</sub> was 34.1cm<sup>3</sup> (SD 21.1; range 6.7-78.7). Mean GTV<sub>DW-MRI</sub> was 15.6cm<sup>3</sup> (SD 23.4; range 0-104.4). GTV<sub>DW-MRI</sub> was significantly smaller than GTV<sub>CT</sub> (p=0.001).

Table below summaries normal tissues constraints achieved at planning.

Organ at risk	Constraint	*Plan using PTV <sub>boost,CT</sub>			*Plan using PTV <sub>boost,DWI</sub>		
		Median	Range	Median	Range	Median	Range
Rectum	V30<80%	39.2	27.5	44.0	37.6	21.7	43.4
	V50<60%	1.1	0.8	6.4	2.0	0.8	6.7
Other bowel	V30<178 cm <sup>3</sup>	146.5	0.0	352.7	141.8	0.0	316.6
	V45<139 cm <sup>3</sup>	62.9	0.0	144.1	94.2	0.0	206.1
	V50<127 cm <sup>3</sup>	50.5	0.0	115.1	62.6	0.0	137.1
	V55<115 cm <sup>3</sup>	34.2	0.0	66.9	5.2	0.0	24.1
	V60<98 cm <sup>3</sup>	11.9	0.0	39.2	3.1	0.0	17.8
	V65<40 cm <sup>3</sup>	7.1	0.0	31.4	1.1	0.0	13.4
Normal bladder outside PTV <sub>boost</sub>	V60<80%	22.3	15.2	63.9	22.1	8.4	77.9
	V65<50%	33.0	7.9	91.6	11.0	3.6	53.3

\*Where n=5, and corresponding median GTV<sub>CT</sub> was 43.6 cm<sup>3</sup> (range 19.3-76.1), median GTV<sub>DWI</sub> was 10.1 cm<sup>3</sup> (range 4.3-30.7)

## Conclusion

DWI informed boost delineation for bladder radiotherapy planning improved normal tissue sparing at high dose bowel and bladder constraints by >60% compared to CT based GTV delineation. Acquiring DWI for radiotherapy planning may therefore complement target volume delineation and inform non-uniform dose delivery to biological sub-volumes for bladder radiotherapy dose escalation trials. Work is on-going to demonstrate this.

## Poster: Clinical track: Skin cancer / malignant melanoma

### PO-0865 Curative HDR brachytherapy (HDR-BT) for non-melanoma skin cancers (NMSC)

B. Emami<sup>1</sup>, C. Hentz<sup>1</sup>, I. Rashed<sup>1</sup>, K. Stang<sup>1</sup>, A. Gliniewicz<sup>1</sup>, M. Mysz<sup>1</sup>, D. Eilers<sup>1</sup>, R. Tung<sup>1</sup>

<sup>1</sup>Loyola University Medical Center, Radiation Oncology, Maywood, USA

#### Purpose or Objective

NMSC is the most common malignancy. Standard treatments are surgery; radiotherapy: external beam radiotherapy (EBRT) and brachytherapy with HDR-BT and electronic brachytherapy (e-BT) sources.

With some treatment modalities, incompatibility with certain anatomical sites (surgery and e-BT), operational/wound complications (surgery), dosimetric limitations (e-BT), and cosmetic/functional complications (surgery) often result in suboptimal cure rates or unacceptable sequela. In order to overcome these issues, we have used HDR-BT in treatment of selected NMSC patients.

#### Material and Methods

From July 2015 to June 2018, 105 NMSC lesions of basal cell carcinoma (BCC), squamous cell carcinoma (SCC), cutaneous T cell lymphoma (CTCL), or Merkel cell carcinoma in 75 patients were treated using HDR-BT (Iridium-192) using an Elekta Freiburg flap surface applicator according to an internal review board approved prospective protocol.

Targeted lesions with 5-10mm margins were delineated at the time of CT simulation using radiopaque wires attached to thermoplastic mesh. The Freiburg flap is affixed to the mesh surface. A dose of 32-40 Gy in 8-10 fractions was delivered to a depth of 3-5 mm depending on lesion thickness. Patient and treatment characteristics, pain level and medication use, early (<3 month) and late toxicities (CTCAE v4.03), physician- and patient-reported cosmesis, and cancer outcomes were recorded in a prospective manner. Univariate generalized linear mixed effects models were used to estimate odds of suboptimal cosmesis (fair-poor vs. excellent-good).

#### Results

Median age of patients was 82 (range 74-88). Fifty-eight percent of lesions were SCC, 42% BCC. The median lesion size was 4mm (range 4mm - >5cm). Patient comorbidities were also recorded, with 51% of patients with vascular

disease, 26% current or former smokers, and 20% with autoimmune disease. The median follow-up time is 15 months. Results are shown in Table 1 and Figure 1.

Site	Histology	n	Tumor Control (%)	RFS (%)	Acute Skin Toxicity (≥ grade 2)	Late Skin Toxicity (≥ grade 2)	Physician Reported Cosmesis	Patient Reported Cosmesis
H&N	BCC	24	100%	100%	4/30%	0%	Good-Excellent in 100%	Good-Excellent in 95.8%
	SCC	19	100%	100%	0%	0%	Good-Excellent in 100%	Good-Excellent in 100%
Skull	BCC	1	100%	100%	0%	0%	Good-Excellent in 100%	Good-Excellent in 100%
	SCC	17	94%	94%	0%	0%	Good-Excellent in 100%	Good-Excellent in 100%
Extremities	BCC	8	100%	100%	1 of 6	0%	Good-Excellent in 100%	Good-Excellent in 100%
	SCC	24	96%	96%	4%	0%	Good-Excellent in 94%	Good-Excellent in 92%
Other	BCC	1	100%	100%	0%	0%	Excellent 100%	Excellent 100%
	SCC	1	100%	100%	0%	0%	Excellent 100%	Excellent 100%

Table 1. Treatment of selected subtypes, basaloid and squamous. \*Single SCC recurrence in immunosuppressed patient who died of her aggressive metastatic disease.



Figure 1. (a) Pre-treatment tumor (scalp), (b) HDR-BT Treatment Setup, (c) Outcome at completion of treatment, (d) Outcome at 1 year follow-up. Note: After completion of treatment patient underwent hair coloring.

## Conclusion

HDR-BT with surface applicators has important dosimetric and time advantages over other radiation modalities for NMSC. Based on our results, HDR-BT also offers excellent tumor control with exceptional cosmetic results in properly selected patients with NMSC. Future directions include a multi-institutional randomized trial comparing HDR-BT with EBRT.

### PO-0866 Cost-effectiveness analysis of stereotactic radiotherapy in melanoma brain metastases.

A. Paix<sup>1</sup>, F. Thillays<sup>2</sup>, F. Courtault-Deslandes<sup>3</sup>, I. Pop<sup>4</sup>, J. Biau<sup>5</sup>, O. Briard<sup>6</sup>, A.L. Grosu<sup>4</sup>, E.A. Sauleau<sup>7</sup>, G. Noël<sup>1</sup>

<sup>1</sup>Centre Paul Strauss, Radiothérapie, Strasbourg, France ;

<sup>2</sup>Institut Cancérologique de l'Ouest, Radiothérapie, Saint-Herblain, France ;

<sup>3</sup>Centre Georges-François Leclerc, Radiothérapie, Dijon, France ;

<sup>4</sup>Universitätsklinikum Freiburg, Klinik für

Strahlenheilkunde, Freiburg, Germany ;

<sup>5</sup>Centre Jean Perrin, Radiothérapie, Clermont-Ferrand, France ;

<sup>6</sup>Centre Henry Kaplan - Centre Hospitalier Universitaire de Tours, Radiothérapie, Tours, France ;

<sup>7</sup>Centre Hospitalier Universitaire de Strasbourg, Groupe de

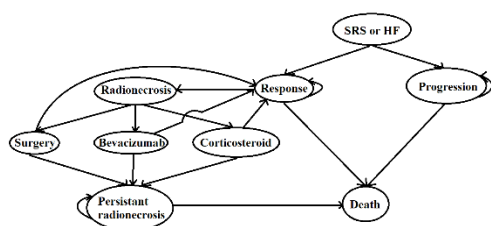
méthodologie et recherche clinique GMRC, Strasbourg, France

#### Purpose or Objective

Melanoma is the third cancer responsible for brain metastases in frequency. To treat these metastases, when a safe surgery could not be performed, there is a global agreement to prefer stereotactic radiotherapy, performed in either one single fraction (SRS) or several fractions (HFSRT), over whole brain irradiation, to preserve cognitive function with a better metastases response to treatment.

#### Material and Methods

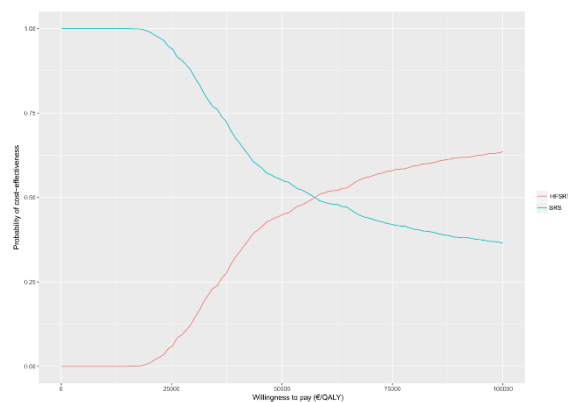
We developed a Markov model, reported in Figure 1, based on retrospectively collected data of treatment delivered in 6 hospitals in France and Germany, to describe survival and treatment-related complications of patients treated for a single melanoma brain metastasis. This analysis was conducted from the French payer perspective on a lifetime horizon. Utility values, recurrence risks, and costs were adapted from the literature. Deterministic (DSA) and probabilistic (PSA) sensitivity analyses were performed to assess the influence of the assumptions made.



## Results

In the base case analysis, SRS and HFSRT total costs were 5,444.68€ and 7,349.83€, and the quality-adjusted life expectancies were 1.4641 and 1.4763.

In the probabilistic sensitivity analysis, SRS and HFSRT were associated with a mean total cost of 5,258.77€ and 7,138.91€, and a quality-adjusted life expectancy of 1.4709 and 1.4928 QALYs, respectively. SRS appeared to be 1,880.14€ cheaper than HFSRT with a decrease of quality-adjusted life expectancy of 0.0219 QALYs. The acceptability curves reported a probability of cost-effectiveness of nearly 85.1% and 36.5% for SRS for willingness thresholds of 30,000 and 100,000€/QALY respectively, as represented in the acceptability curves reported in Figure 2.



## Conclusion

This is the first medico-economic evaluation of SRS and HFSRT in melanoma brain metastases and its results suggest that HFSRT is cost-effective over SRS.

## Poster: Clinical track: Sarcoma

### PO-0867 Prognostic impact of the "Sekhar Grading System for Cranial Chordomas" - an attempt at validation

A. Hottinger<sup>1,2</sup>, B. Bojaxhiu<sup>1</sup>, M. Walser<sup>1</sup>, B. Bachtary<sup>1</sup>, A. Pica<sup>1</sup>, D.C. Weber<sup>1</sup>

<sup>1</sup>Paul Scherrer Institute, Center for Proton Therapy, Villigen, Switzerland ; <sup>2</sup>University Hospital Basel, Radiotherapy and Radiation Oncology, Basel, Switzerland

#### Purpose or Objective

Skull base chordomas (SBCs) are rare and heterogeneously behaving tumors. Though still classified as benign they can grow rapidly and are locally aggressive. To adapt the treatment to the specific needs of patients at higher risk of recurrence, a preoperative grading system would be useful.

The aim of this retrospective analysis was to assess the prognostic impact of the "Sekhar Grading System for Cranial Chordomas" (SGSCC; Brito da Silva et al. *Cranial Chordoma: A New Preoperative Grading System*.

*Neurosurgery* 2017;0:1-13) looking at the cohort of patients treated at our institution as to determine if the SGSCC is reproducible in a larger cohort and ultimately to ensure more risk adapted local treatments for these challenging tumors.

#### Material and Methods

Searching our database, we identified patients (n = 142) treated for SBC between 2004 and 2016 with surgery and pencil beam scanning proton therapy. We analyzed the patient specific data focusing on the 5 criteria proposed for the SGSCC (recurrence after prior treatment, tumor size, number of anatomic regions and vessels involved as well as intradural invasion) and sorted them according to their scores (ranging from 2 to 25 points) into three prognostic groups (0-7 points low-risk, 8-12 points intermediate-risk and 13-25 points high-risk). The three groups were then analyzed in regards of local control (LC), local recurrence free survival (LRF5) and overall survival (OS).

#### Results

The mean clinical follow up was 53.7 (range, 3.2-152.3) months; of the entire cohort, 34 (23.9%) patients had a local recurrence (LR), resulting in a LC of 75% at 5 years. OS was 83% at 5 years, 12 (8.5%) patients died due to local progression. The LRF5 at 5 years was 70%. When split into the three SGSCC prognostic groups, the observed LC was 90%, 72% and 64% (p = 0.07) in the low-, intermediate- and high-risk group, respectively. A similar correlation existed for LRF5 with 93%, 89% and 66% (p = 0.05) and for OS with 89%, 83% and 76% (p = 0.65) for the same SGSCC prognostic groups.

#### Conclusion

After splitting our patient cohort into three SGSCC risk groups we found a trend towards better outcome for those SBC patients treated with proton therapy with lower as opposed to higher scores.

### PO-0868 Total Marrow Irradiation in Myeloma Multiple patients candidate to allogeneic transplant

A. Chiara<sup>1</sup>, S. Broggi<sup>2</sup>, M. Pasetti<sup>1</sup>, I. Dell'oca<sup>1</sup>, M. Azizi<sup>1</sup>, G. Salvadori<sup>1</sup>, S. Selli<sup>1</sup>, M. Marcatti<sup>3</sup>, A. Assanelli<sup>3</sup>, J. Peccatori<sup>3</sup>, M. Cattaneo<sup>2</sup>, F. Ciceri<sup>3</sup>, N. Di muzio<sup>1</sup>

<sup>1</sup>Ospedale San Raffaele, Radioterapia, Milano, Italy ;

<sup>2</sup>Ospedale San Raffaele, Fisica Sanitaria, Milano, Italy ;

<sup>3</sup>Ospedale San Raffaele, Ematologia, Milano, Italy

#### Purpose or Objective

Total Body Irradiation (TBI) is as part of the conditioning regimen for haematopoietic stem cell transplantation in haematological diseases. Higher doses of radiation reduce the relapse rate but increase Treatment Related Mortality (TRM). Total Marrow Irradiation (TMI) using Helical Tomotherapy (HT) showed to enhance the therapeutic ratio ( Target dose/Organ At Risk dose) reducing TRM. We report the first results of feasibility, safety and toxicity of myeloablative Treosulfan-based conditioning chemotherapy (cTreoCT) combined with dose-escalating TMI in patients (pts) affected by advanced Multiple Myeloma (MM).

#### Material and Methods

Twelve patients (pts) (5 males and 7 females with a median age 59 yrs), affected by advanced MM, were treated from December 2012 to January 2018. All pts received a cTreoCT combined with TMI using HT. 2 Gy (2 times a day) was delivered with a dose escalation approach from 8 to 14 Gy; the total dose is increased in a triplet approach only if extra-hematological (G<sub>2</sub> ≥ 4 grade) toxicities don't appear in the previous dose patient's group. The treatment was delivered with two different plans: an upper plan from head to half leg (Head First Supine Setup) and with a low plan included the complete legs (Feet First Supine Treatment). Both plans were delivered in helical mode. For each pt a personalized immobilization device, including head, thorax/pelvis and foot masks, was builded.

## Results

All pts received the planned TMI dose (95% of PTV received almost 90% of prescription dose) with a good Organ At Risk (OAR) sparing (the dose at OAR was < 50% of prescription dose); all pts, after the transplant, achieved engraftment with no secondary graft failure. No grade 3-4 extra-hematological toxicity has been registered in the first 30 days. Five deaths have occurred, 2 due to TRM and 3 due to progression disease. With a median follow-up time of 39 months, 3-yr PFS was 38% and 3-yr OS was 48%. Day +100 incidence of grade II-IV aGVHD was 36%; grade III-IV 9%; 1-year incidence of cGVHD was 39%. 3-year relapse incidence was 39%. 7 pts have experienced an extensive/severe cGVHD with significant involvement the lower legs and ankles. This toxicity seems more evident for patients treated with higher doses (>10 Gy), probably correlated also to the skin higher dose delivered with HT technique, in particular at the pretibial level for patients with poor adipose pannicle. The combination effect with the type of cTreoCT and with the type of used GvHD prophylaxis regimen should be better investigated.

## Conclusion

These data show that TMI addition to cTreoCT is feasible and has not demonstrated an addition of at least short-term toxicities. The late toxicity found in the limbs leads us to find solutions to avoid such side effects in patients irradiated at doses above 12 Gy, such as reviewing the PTV contouring at the tibia level or as using different techniques in legs irradiation (like tomodirect) and as improving GvHD prophylaxis regimen.

---

## Poster: Clinical track: Paediatric tumours

---

### PO-0869 Reducing pulmonary and renal toxicity in children receiving TBI with forward planned IMRT

M. Bishr<sup>1</sup>, E. Nicholson<sup>2</sup>, E. Durie<sup>3</sup>, M. Potter<sup>2</sup>, M. Ethell<sup>2</sup>, C. Anthias<sup>2</sup>, C. Messiou<sup>4</sup>, I. Johnson<sup>5</sup>, S. Eagle<sup>3</sup>, W. Ingram<sup>3</sup>, F. Saran<sup>3</sup>, H. Mandeville<sup>5</sup>

<sup>1</sup>Children's Cancer Hospital Egypt, Department of Radiotherapy, Cairo, Egypt; <sup>2</sup>Royal Marsden NHS Foundation Trust, Department of Haematology, London, United Kingdom; <sup>3</sup>Royal Marsden NHS Foundation Trust, Department of Radiotherapy, London, United Kingdom; <sup>4</sup>Royal Marsden NHS Foundation Trust, Department of Radiology, London, United Kingdom; <sup>5</sup>Royal Marsden NHS Foundation Trust, Children and Young People's Unit, London, United Kingdom

#### Purpose or Objective

Total body irradiation (TBI) is an integral part of conditioning regimens prior to haematopoietic stem cell transplantation (HSCT). However, there is a risk of both short term and long term side effects, especially in children. This study evaluates the pulmonary and renal toxicity of a novel forward planned (FP) intensity modulated radiation therapy (IMRT) TBI technique.

#### Material and Methods

We retrospectively identified 65 paediatric patients (≤ 16 years old) who received TBI-based full intensity allogeneic HSCT between July 2009 and March 2018. The whole body was the specified target volume and the dose was prescribed to the 100% with a reduction of the median lung dose by approximately 15% compared to the whole body. All dose modulations were multi-leaf collimator-based and treatment was delivered twice a day using 10 MV photons and a dose rate of 14-19cGy/min. Pulmonary toxicity was subdivided into infective pneumonia (IP), based on the identification of a causative agent in blood or bronchoalveolar lavage, and idiopathic pneumonitis syndrome (IPS) when no organism could be detected. The estimated glomerular filtration rate (eGFR) was calculated using Schwartz's formula and chronic kidney disease (CKD) was defined as eGFR <60 mL/min/1.73m<sup>2</sup> for ≥ 3 months.

## Results

All patients were treated for haematopoietic malignancies, most commonly acute lymphoblastic leukemia (78.5%), at a median age of 8.7 years (range 2-16). TBI doses were 14.4Gy (63%), 13.2Gy (5%) or 12Gy (32%). Patients were followed up for a median of 1.7 years (range 13 days - 8.3 years) and the mean overall survival (OS) was 58 months (95% CI 45.9 - 70). The 2-year OS was 68% (95% CI 54 - 78) and the 2-year progression-free survival (PFS) was 54% (95% CI 40 - 66). The 100 day non-relapse mortality (NRM) in our patients was 14% (95% CI 7 - 23) and 2-year NRM was 23% (95% CI 13 - 35). None of the patients developed CKD at 5 years and a total of 31 patients (47.7%) developed pulmonary toxicity. Only one patient (1.5%) developed grade 1 IPS, while 30 patients (46.2%) had IP, of whom five patients died accounting for 41.6% of NRM. One patient developed bronchiolitis obliterans organizing pneumonia (BOOP) 4 months post-HSCT and another patient developed pulmonary inflammatory myofibroblastic tumor 6.4 years post-HSCT. Compared to males, females had a lower risk of developing pulmonary toxicity (OR 0.25, p-value 0.037). Patients who were cytomegalovirus (CMV)-mismatched from their donors exhibited 3.4-times higher risk of developing pulmonary toxicity as compared to CMV-matched recipients with a trend for significance (p-value 0.08).

## Conclusion

Compared to parallel opposed technique in literature, our novel FP-IMRT-TBI technique for paediatric full intensity HSCT yields lower rates of renal and pulmonary toxicity, specifically IPS. This favourable safety profile supports the adoption of highly conformal radiotherapy techniques to further improve quality of life of long-term survivors after HSCT in childhood.

### PO-0870 Treatment Outcomes for Pediatric Basal Ganglia Germinomas: A single institute experience in Taiwan

Y. Kang<sup>1</sup>, S. Lin<sup>2</sup>, Y. Lee<sup>3</sup>, F. Chang<sup>4</sup>, M. Liang<sup>3</sup>, H. Chen<sup>3</sup>, Y. Liu<sup>1</sup>, T. Wong<sup>3</sup>, Y. Chen<sup>1</sup>

<sup>1</sup>Taipei Veterans General Hospital, Division of Radiation Oncology- Department of Oncology, Taipei, Taiwan; <sup>2</sup>National Yang-Ming University, Faculty of Medicine, Taipei, Taiwan; <sup>3</sup>Taipei Veterans General Hospital, Division of Pediatric Neurosurgery- Neurological Institute, Taipei, Taiwan; <sup>4</sup>Taipei Veterans General Hospital, Department of Radiology, Taipei, Taiwan

#### Purpose or Objective

Pediatric basal ganglia germinoma is a rare and unique disease. Our purpose was to evaluate the clinical outcomes of pediatric basal ganglia germinomas after treatment.

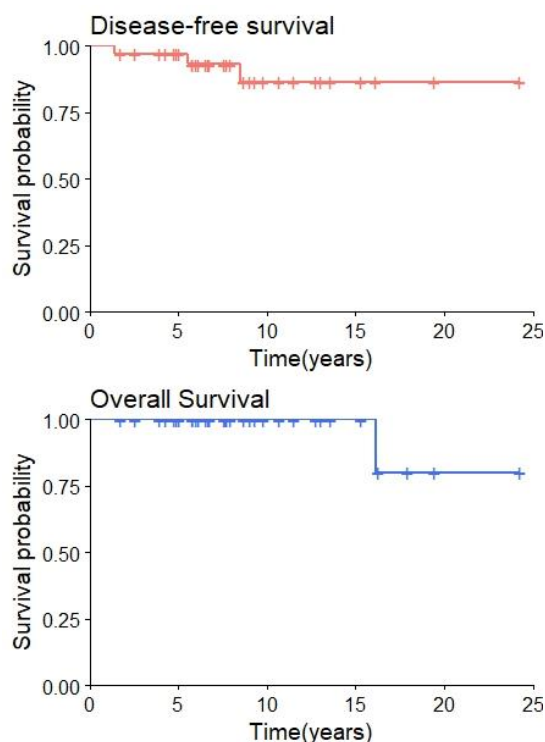
#### Material and Methods

The medical records of 33 children with pediatric basal ganglia germinomas treated at Taipei Veterans General Hospital between 1994 and 2015 were retrospectively reviewed. There were 1 female (3.03%) and 32 males (96.97%) with a median age at diagnosis of 12.18 years (range, 7-19 years old). Age, sex, symptoms, pathological findings, treatment modalities, recurrence patterns, recurrence date, death date, and toxicities were recorded. Survival curves were estimated with the Kaplan-Meier method, and univariate Cox proportional hazards models were used to identify possible risk factors.

#### Results

The median overall survival was 7.77 years (range, 1.76-24.28 years), with 2- and 3-year disease-free survival rates of 97% and 94%, respectively. Thirty patients (90.9%) were treated successfully without recurrence. Three patients (9.1%) suffered from recurrence during follow up, and all of them were treated successfully by salvage treatment. Only one patient (3.0%) died during follow-up because of radiotherapy related sarcoma over scalp. Focal irradiation

showed a trend of lower disease-free survival rate in Kaplan-Meier survival curves ( $p=0.12$ ) when compared to irradiation to whole ventricle, whole brain, or cranial spinal area. There is no disease-free survival difference in risk factors analysis in univariate Cox proportional hazards models, including age, metastatic status at diagnosis, tumor diameter, chemotherapy, and BHCG detection. Patients who received irradiation only to whole ventricle showed lower treatment toxicity and better quality of life during follow-up compared to irradiation to whole brain and cranial spinal area.



### Conclusion

Our results showed excellent disease-free survival and high rate of success of salvage treatment among pediatric basal ganglia germinomas after radiotherapy with or without chemotherapy. Focal irradiation showed a trend of lower disease-free survival, and whole ventricle irradiation showed lower treatment toxicity and better quality of life.

### PO-0871 Efficacy of radiotherapy boost in incompletely resected paediatric ependymoma: a retrospective study

M. Ramos Albiac<sup>1</sup>, B. Gutiérrez<sup>1</sup>, N. Mestre<sup>2</sup>, M. Mota-Foix<sup>3</sup>, S. Pérez-Hoyos<sup>3</sup>, A. Llort<sup>4</sup>, P. Cano<sup>5</sup>, J. Giralt<sup>1</sup>  
<sup>1</sup>Hospital Universitario Vall d'Hebron, Radiation Oncology Department, Barcelona, Spain ; <sup>2</sup>Centro de Regulación Genómica, Centro de Regulación Genómica, Barcelona, Spain ; <sup>3</sup>Vall d'Hebron Institut de Recerca, Unitat d'Estadística i Bioinformàtica, Barcelona, Spain ; <sup>4</sup>Hospital Universitario Vall d'Hebron, Pediatric Oncology, Barcelona, Spain ; <sup>5</sup>Hospital Universitario Vall d'Hebron, Neurosurgery, Barcelona, Spain

### Purpose or Objective

The main objective of the study is to determine whether a radiotherapy boost to residual tumour in incompletely resected paediatric ependymoma confers the same local control (LC) and overall survival (OS) than a complete resection.

### Material and Methods

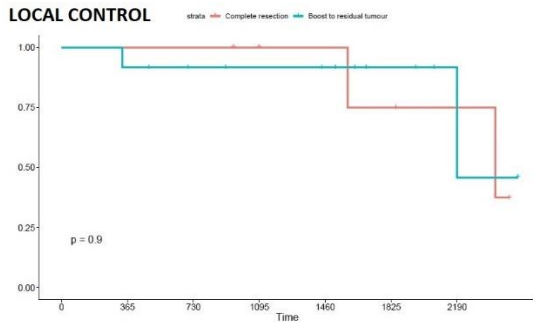
We retrospectively analyzed 23 patients diagnosed with ependymoma and treated with upfront post-operative

radiotherapy in our institution between April 2003 and April 2017. We registered age, sex, location of primary tumour, extent of resection, histological grade, radiation dose to tumour bed, boost dose to residual tumour and radiation technique. We have follow-up data of all patients, having also registered date of first relapse, date of death and/or date of last follow-up. We divided patients in 4 groups according to radiotherapy target volumes: surgical bed in patients with complete resection ( $n=6$ ), surgical bed plus boost to residual tumour ( $n=12$ ), residual tumour only ( $n=4$ ) and tumour bed without boost in one patient with residual tumour. We then compared OS, DFS and LC only for the first two groups using the Kaplan-Meier method. For age and radiotherapy dose, Cox univariate analysis was applied.

### Results

Median follow-up was 4.2 years. The characteristics of the patients are summarized in table 1. Of all 23 patients, 18 of them were alive at the moment of last follow-up, 14 of which were free of disease. 2 patients presented distant failure and 7 patients presented local relapse. We observed non-significant differences in OS, DFS and LC between the complete resection group and the boost group. 2-year OS was 100% and 100% respectively, DFS 100% and 91.7% respectively and LC 100% and 91.7% respectively. 4-year OS was 100% and 87.5% respectively, DFS 100% and 80.2% respectively and LC 100% and 91.7% respectively. We observed statistically significant differences only in DFS for histological grade, response to upfront treatment and age.

Patients characteristics	ALL (N=23)
Age	8.0 [5.75-13]
Sex	
F	11 (47.8%)
M	12 (52.2%)
Location	
Posterior Fossa	14 (60.9%)
Spinal Cord	3 (13%)
Supratentorial	6 (26.1%)
Resection	
Complete	6 (26.1%)
Incomplete	17 (73.9%)
Histological grade	
I	1 (4.3%)
II	6 (26.1%)
III	16 (69.6%)
RT technique	
3DCRT	14 (60.9%)
IMRT	8 (34.8%)
Unknown	1 (4.3%)
Boost (N=12)	
SFRT	7 (58.3%)
SIB	5 (41.7%)
Response	
NER	6 (26.1%)
CR	9 (39.1%)
PR	2 (8.7%)
SD	6 (26.1%)
Relapse location (N=9)	
Local	7 (77.8%)
Distant	2 (22.2%)



### Conclusion

No statistically significant differences in OS, DFS and LC were observed between the complete resection group and the boost group, considering that it is a small series with limited follow-up of some patients. These results are consistent with other published data considering the potential benefit in LC and OS of a radiation boost to residual tumour in incompletely resected ependymoma patients, although further investigation is necessary.

### PO-0872 Hematological toxicity of 3DCRT and VMAT craniospinal irradiation in pediatric medulloblastoma

B. Diletto<sup>1</sup>, E. Pecori<sup>1</sup>, O. Alessandro<sup>2</sup>, S. Meroni<sup>3</sup>, T. Giandini<sup>3</sup>, C. Stucchi<sup>3</sup>, C. Cavatorta<sup>3</sup>, E. Schiavello<sup>4</sup>, V. Biassoni<sup>4</sup>, M. Massimino<sup>4</sup>, E. Pignoli<sup>3</sup>, L. Gandola<sup>1</sup>

<sup>1</sup>Fondazione IRCCS Istituto Nazionale dei Tumori, Radiation Oncology 1, Milan, Italy ; <sup>2</sup>Università degli Studi di Milano, Residency Program in Radiation Oncology, Milan, Italy ; <sup>3</sup>Fondazione IRCCS Istituto Nazionale dei Tumori, Medical Physics, Milan, Italy ; <sup>4</sup>Fondazione IRCCS Istituto Nazionale dei Tumori, Pediatric Oncology, Milan, Italy

### Purpose or Objective

Craniospinal irradiation (CSI) is a milestone of the postoperative treatment of pediatric standard risk (SR) and high risk (HR) medulloblastoma (MB). Advantages of VMAT technique for CSI in term of target coverage and organ sparing have been documented, but it causes exposition of red bone marrow to low doses, worsening hematopoiesis. Aim of the study was the evaluation of hematological toxicity of pediatric SR and HR MB pts treated with 3DCRT or VMAT-CSI.

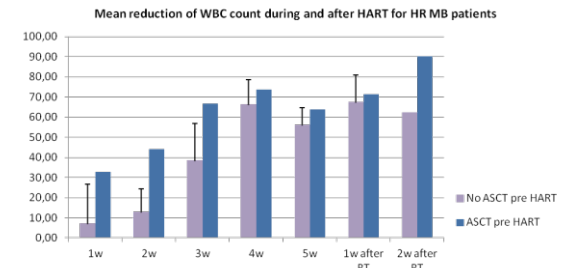
### Material and Methods

RT and clinical details of SR and HR MB pts treated in our Institution were collected. Prescription doses to SR patients: 23.4 Gy/1.8 Gy daily to craniospinal axis, followed by a tumor bed boost up to a total dose of 54 Gy. All SR children then received a standard maintenance chemotherapy (CT). Prescription doses to HR patients: hyperfractionated accelerated RT (HART) with CSI doses of 39 Gy or 31.2 Gy/1.3 Gy bid, depending on age, followed by a boost to the tumor bed up to a total dose of 59.8 Gy when indicated. Before HART all HR pts received high-dose sequential CT. HR pts with persistent disease before HART, were consolidated with 2 courses of myeloablative CT and autologous stem cell transplant (ASCT) before irradiation, while the remaining received standard maintenance CT after HART. Hematological changes were recorded weekly during RT and scored according to RTOG system. Mean RT doses to iliac bones were collected to evaluate dose to red bone marrow.

### Results

Data from 26 patients (SR: 11,HR: 15) were collected (median age 10 y,4-33): 10 pts received 3DCRT (SR: 5,HR: 5), 16 pts VMAT (SR:6,HR:10). 4 HR pts were consolidated with 2 ASCT before HART (3DCRT:1,VMAT:3). Within SR

groups no hematological toxicity differences were observed (4 G3 leuko-neutropenia,3DCRT:2/5,VMAT:2/6). G3 toxicity occurred in all HR pts.G4 (leuko-neutropenia, thrombocytopenia) was recorded in 4 VMAT pts, 3 of whom received ASCT before HART. More use of G-CSF and transfusions during and after RT was required for VMAT pts, and 1 ASCT-VMAT child stopped earlier HART due to hematological toxicity. Pts irradiated with VMAT and undergoing ASCT showed a more pronounced and persistent leukopenia during and after HART (Figure). Evaluation of mean absorbed doses by iliac bones showed a significant difference in pts treated with 3DCRT (0.9 Gy) or VMAT (5.8 Gy).



### Conclusion

Low doses irradiation of red bone marrow during VMAT-CSI has the potential to interfere with hematopoiesis implying a more severe hematological toxicities in HR pts who received ASCT before HART. Hence, to reduce toxicity during VMAT-CSI, at least in this subgroup, iliac bones should be contoured as OAR and a planning effort is strongly recommended to lower mean dose to these structures. Nevertheless, hematological toxicity in our series was never life threatening and always reversible and we continue to recommend VMAT for CSI due to the documented advantages of this technique in sparing higher RT doses to other vital organs such as heart, lungs and liver.

### PO-0873 Associations between vessel volume and neurocognition In children treated with proton therapy

A. Srivastava<sup>1</sup>, J. Contreras<sup>1</sup>, H. Heimos<sup>1</sup>, S. Perkins<sup>1</sup>  
<sup>1</sup>Washington University School of Medicine, RADIATION ONCOLOGY, Saint Louis, USA

### Purpose or Objective

Vasculopathy is a well-recognized late side effect of radiotherapy (RT) in the pediatric population, and RT-induced cerebrovascular injury is thought to induce neurocognitive impairment. In this study we sought to further characterize this relationship by evaluating the effects of proton beam RT (PBT) on volumetric changes in the cerebral vasculature and corresponding changes in neurocognitive function.

### Material and Methods

In this prospective study, we evaluated 13 children, ages 4-21, with a primary CNS malignancy treated with PBT. Magnetic resonance imaging of the brain (bMRI) was obtained pre-treatment and at scheduled follow-up visits post-RT every 3-6 months, and substructures were auto-segmented on MPRage sequences using a well-validated auto-segmentation program. Patients completed neurocognitive testing using the National Institutes of Health Toolbox Cognitive Battery (NIH-TCB) at baseline and during follow-up visits within three months of their bMRIs. Using linear mixed effects models, we evaluated the effects of age, time since PBT, and RT dose on cerebral vessel volumes and TCB metrics.

### Results

The median age at RT was 14 years (range 4-19), and median follow-up time was two years (range 0.5-2.9). The plurality of patients was treated for medulloblastoma

(n=5). Following PBT, cerebral vessel volume (CVV) decreased with time ( $p=0.02$ ), and this effect was more notable in younger patients undergoing RT (interaction variable,  $p<0.01$ ). CVV was also found to be positively associated with language-related TCB domains [composite cognitive function ( $p<0.01$ ), crystallized function ( $p=0.02$ ), and picture vocabulary tests ( $p=0.05$ )], which all decreased from baseline during follow up ( $p<0.01$  for each test) in these patients. On dosimetric analysis, total brain volume receiving 10 Gy (V10) was found to be the strongest predictor of TCB testing with worse outcomes found with higher values of V10.

#### Conclusion

Based on this prospective study, use of RT is associated with decreases in performance in neurocognitive testing, and this may be mediated through declines in cerebral vessel volume. Ultimately, limiting dose to total brain volume and maintaining a low V10 may help to mitigate these changes, though further follow-up and studies are needed.

#### PO-0874 The feasibility of MR-Linac treatment planning in childhood abdominal Neuroblastoma

M. Llewellyn<sup>1</sup>, G. Smyth<sup>2</sup>, N. Lavan<sup>1</sup>, S. Nill<sup>2</sup>, U. Oelfke<sup>2</sup>, H. Mandeville<sup>1</sup>

<sup>1</sup>The Royal Marsden NHS Foundation Trust, Clinical Oncology, London, United Kingdom ; <sup>2</sup>The Institute of Cancer Research and The Royal Marsden NHS Foundation Trust- Sutton- London- UK, Joint Department of Physics, London, United Kingdom

#### Purpose or Objective

Radiotherapy plays an important role in the management of paediatric abdominal malignancies. Treatment planning techniques are often highly complex due to large target volumes, the close proximity of OARs, and the challenge of ensuring uniform future vertebral bone growth. The Elekta Unity MR-Linac (Elekta AB, Stockholm, Sweden) enables highly detailed real-time imaging while avoiding the concomitant doses of daily kV imaging. However, the dosimetric effects of a magnetic field on treatment plan quality for paediatric abdominal radiotherapy are unknown.

This study aims to explore the feasibility of IMRT planning with the presence of a magnetic field for abdominal malignancies. Dosimetric comparisons of target volumes and OARs between conventional linac and MR-Linac based treatment plans are made.

#### Material and Methods

Ten postoperative paediatric patients with abdominal Neuroblastoma were identified and two nine-field IMRT plans were produced for each child. One plan was produced for the MR-Linac, accounting for the effects of the 1.5T magnetic field, and another for a conventional linac (Monaco V5.19, Versa HD, Elekta AB, Stockholm, Sweden). All plans were produced to deliver a median PTV dose of 21 Gy in 14 fractions and were planned to observe clinical dose constraints. Dose calculation was performed using a Monte Carlo dose engine and a calculation uncertainty of 2%, grid size 3x3x3mm. Doses to PTV, adjacent vertebral bodies and OARs were compared and Homogeneity Index (HI) and Conformity Number (CN) were measured for each technique.

#### Results

All plans met required dose objectives and were clinically acceptable; Mean PTV volume was 259.1 cm<sup>3</sup> (range 143-498 cm<sup>3</sup>). There were no significant differences in PTV near maximum (D<sub>2%</sub>) or near minimum (D<sub>98%</sub>) doses between MR-Linac and conventional linac. For those tumour sites where there was a component of lung irradiation (n=7), MR-Linac treatment plans achieved a small but significant reduction in the volume of lung receiving 15 Gy ( $p=0.03$ ) compared to the conventional linac. There were no other statistically significant

differences in dose to OARs and no significant differences in PTV homogeneity or conformity were observed.

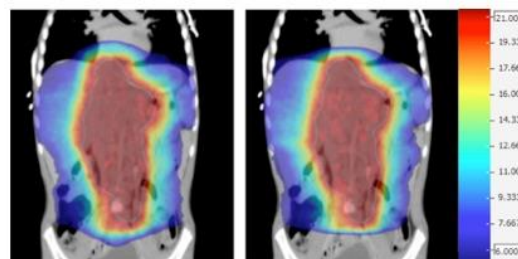


Figure 1. A example of a conventional treatment plan (L) and MRL treatment plan (R)

Metric	Clinical objective	Value mean $\pm$ standard deviation		p-value
		MR-Linac	Conventional Linac	
PTV D <sub>2%</sub> (Gy)	< 22.5	21.7 $\pm$ 0.1	21.6 $\pm$ 0.1	0.4
PTV D <sub>98%</sub> (Gy)	> 18.9	20.1 $\pm$ 0.4	20.1 $\pm$ 0.3	0.7
HI	N/A	0.08 $\pm$ 0.02	0.07 $\pm$ 0.2	0.7
CN	N/A	0.65 $\pm$ 0.05	0.65 $\pm$ 0.03	0.9
Adjacent vertebral body V <sub>15 Gy</sub> (%)	> 95%	98 $\pm$ 0.8	98.3 $\pm$ 1.5	0.6
Combined Kidney V <sub>14 Gy</sub> (%)	< 40%	37.2 $\pm$ 7.6	33.1 $\pm$ 4.9	0.1
Combined Kidney Mean (Gy)	< 15	13.3 $\pm$ 3.3	11.8 $\pm$ 0.6	0.2
Heart Mean (Gy)	< 15	4.1 $\pm$ 2	3.6 $\pm$ 1.7	0.2
Liver V <sub>21 Gy</sub> (%)	< 50%	1.7 $\pm$ 1.1	2 $\pm$ 1.4	0.1
Lung V <sub>15 Gy</sub> (%)	< 10%	4.6 $\pm$ 2.5	5.3 $\pm$ 3	0.03
Lung V <sub>12 Gy</sub> (%)	< 25%	7.4 $\pm$ 8	8 $\pm$ 4.8	0.2
GI Tract (%)	< 100%	3 $\pm$ 2.6	3.1 $\pm$ 2.8	0.8

Table 1. Dose statistics and plan quality metrics for both techniques. Values were judged to be statistically significant for p-values < 0.05

#### Conclusion

MR-Linac treatment planning for upper abdominal malignancies in children is feasible and produces clinically acceptable plans. Achieved dose distributions were comparable to a conventional linac, despite large treatment volumes and the high complexity of plans. Combining plan quality with more accurate visualisation of abdominal soft tissues and improved delineation of target volumes, the MR-Linac has the potential to reduce setup errors and further decrease normal tissue radiation exposure/ integral dose compared with radiotherapy on a conventional linac.

#### PO-0875 Development of pituitary deficits after radiotherapy in pediatric patients after long follow-up.

C. Satragno<sup>1</sup>, E. Tornari<sup>1</sup>, S. Barra<sup>2</sup>, F. Giannelli<sup>2</sup>, L. Belgioia<sup>1</sup>, M. Giaccardi<sup>3</sup>, N. Di Iorgi<sup>3</sup>, M.L. Garre<sup>4</sup>, R. Haupt<sup>5</sup>, R. Corvò<sup>1</sup>

<sup>1</sup>University of Genoa and San Martino Hospital, Health Science Department DISSAL and Radiation Oncology, Genoa, Italy ; <sup>2</sup>San Martino Hospital, Radiation Oncology, Genoa, Italy ; <sup>3</sup>Istituto Giannina Gaslini, Department of Pediatrics, Genoa, Italy ; <sup>4</sup>Istituto Giannina Gaslini, Department of Neurooncology, Genoa, Italy ; <sup>5</sup>Istituto Giannina Gaslini, Epidemiology and Biostatistics Unit, Genoa, Italy

#### Purpose or Objective

To evaluate the risk of developing pituitary deficits in pediatric patients with central nervous system (CNS) tumors treated by radiotherapy.

#### Material and Methods

We retrospectively analyzed patients with brain tumors, younger than 16 years, with a minimum follow up of 2 years after the end of radiotherapy. In this study, we evaluated GH, ACTH and TSH deficiency and if endocrine deficit correlate with pituitary gland and hypothalamic dose.

#### Results

Between 1996-2015, 88 consecutive patients have been identified. Among them, we had to exclude 20 patients because they presented hormone deficiency before starting RT, and 4 more because they had the

endocrinological follow-up in less than 2 years. Therefore, 64 patients were evaluated: 32 medulloblastomas (50.0%), 17 gliomas (26.5%), 7 germinomas (10.9%), 3 ependymomas (4.6%), and 5 other histological types (7.8%) (2 Ewing sarcomas, 1 PNET, 1 pinealoblastoma, 1 ATRT). 61 pts also underwent to chemotherapy and 42 to surgery. The mean pituitary dose in patients with GHD was  $36.5 \pm 9.78$  Gy ( $p < 0.01$ ), TSHD  $38.0 \pm 6.0$  Gy, ACTHD  $34.6 \pm 10.5$  Gy. Patients treated with 3DCRT had a higher risk of developing GHD, ACTHD, and TSHD when compared to those treated with IMRT techniques ( $p < 0.05$ ). The "safe dose" to under which no patient has shown GH deficiency is  $< 10$  Gy while for TSH and ACTH deficit is  $< 20$  Gy.

#### Conclusion

Our data underline the role of pituitary dose on endocrine deficits; IMRT should be the preferred technique in the treatment of paediatric CNS.

---

#### Poster: Clinical track: Palliation

---

#### PO-0876 Stereotactic Body Radiation Therapy for thoracic nodes metastases, a multi-institutional experience

D. Franceschini<sup>1</sup>, F. Bianciardi<sup>2</sup>, R. Mazzola<sup>3</sup>, F. De Rose<sup>1</sup>, P. Gentile<sup>2</sup>, F. Alongi<sup>3,4</sup>, M. Scorsetti<sup>1,5</sup>

<sup>1</sup>Humanitas Research Hospital, RADIO THERAPY AND RADIOSURGERY, Rozzano Milan, Italy; <sup>2</sup>San Pietro Fatebenefratelli Hospital, Radiation Therapy Department, Rome, Italy; <sup>3</sup>IRCCS Sacro Cuore Don Calabria Hospital, Radiation Oncology Department, Negrar-Verona, Italy; <sup>4</sup>University of Brescia, Radiation Oncology Department, Brescia, Italy; <sup>5</sup>Humanitas University, Department of Biomedical Sciences, Rozzano-Milano, Italy

#### Purpose or Objective

To evaluate safety and efficacy of Stereotactic Body Radiation Therapy (SBRT) in patients with thoracic nodes oligometastases

#### Material and Methods

The present study is a multicenter analysis. Oligometastatic patients, affected by a maximum of 5 active lesions in 3 or less different organs, treated with SBRT to thoracic nodes metastases between 2012 and 2017 were included in the analysis. Primary end point was local control (LC), secondary end points were overall survival (OS), progression free survival (PFS), acute and late toxicity. Univariate and multivariate analysis were performed to identify possible prognostic factors for the survival endpoints.

#### Results

76 patients were included in the analysis. Different RT dose and fractionation schedules were prescribed according to site, number, size of the lymph node(s) and to respect dose constraints for relevant organs at risk. Median BED delivered was 75 Gy (interquartile range: 59-86 Gy). Treatment was optimal; one G1 acute toxicity and 7 G1 late toxicities of any grade were recorded. Median follow up time was 23.16 months. Sixteen patients (21.05%) had a local progression, while 52 patients progressed in distant sites (68.42%).

Median LC was not reached, LC at 6, 12 and 24 months was 96.05% (CI 88.26-98.71%), 86.68% (CI 75.86-92.87) and 68.21% (CI 51.89-80.00%), respectively. Median OS was 28.3 months (interquartile range 16.1-47.2). OS at 6, 12, 24 and 36 months was 98.68% (CI 91.03-99.81%), 86.34% (CI 76.07-92.42%), 55.98% (CI 42.61-67.40%) and 41.61% (CI 27.85-54.80%), respectively. Median PFS was 9.2 months (interquartile range 4.1-17.93). PFS at 6, 12 and 24 months was 63.16% (CI 51.29-72.89%), 34.99% (CI 24.22-45.94%) and 16.84% (CI 8.91-26.92%), respectively.

At multivariate analysis, RT dose, colorectal histology, systemic therapies were correlated with LC. Performance

status and the presence of metastatic sites other than the thoracic nodes were correlated both with OS and PFS. Local response was a predictor of OS.

#### Conclusion

SBRT for thoracic nodes was safe and feasible. Higher RT doses were correlated to better LC and should be taken in consideration at least in patients with isolated nodal metastases and colorectal histology.

#### PO-0877 Utilization of short course palliative radiation therapy in breast cancer bone metastasis

P. Gabani<sup>1</sup>, B. Fischer-Valuck<sup>2</sup>, W. Kennedy<sup>1</sup>, L. Ochoa<sup>1</sup>, M. Thomas<sup>1</sup>, M. Daly<sup>1</sup>, I. Zoberi<sup>1</sup>, C. Abraham<sup>1</sup>

<sup>1</sup>Washington University in Saint Louis, Radiation Oncology, Saint Louis, USA; <sup>2</sup>Emory School of Medicine, Radiation Oncology, Atlanta, USA

#### Purpose or Objective

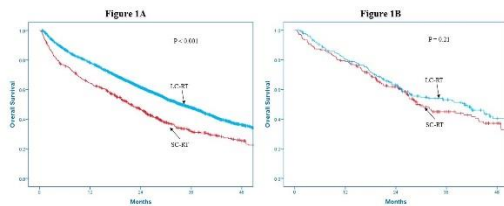
Breast cancer is one of the most common malignancies associated with bone metastasis. Recent evidence suggests equivalent palliative efficacy between short course RT (i.e.  $\leq 5$  fractions) and long course RT ( $\geq 10$  fractions) for the palliation of bone metastasis. Despite this, the uptake of short course RT remains low. This is an observational study of a large national cohort evaluating the patterns of care associated with various palliative RT fractionation schemes for the treatment of breast cancer bone metastases.

#### Material and Methods

Patients with metastatic breast cancer bone metastasis from 2010 - 2015 were obtained from a national cancer database. Patients who were treated with palliative RT to bone lesions with 8 Gy in 1 fx or 20 Gy in 5 fx were categorized as short course RT (SC-RT). Patients who were treated with palliative RT to bone lesions with 30 Gy in 10 fx or 37.5 Gy in 15 fx were categorized as long course RT (LC-RT). Patients receiving other RT fractionation schemes were excluded. Patients receiving RT to the spine for cord compression were excluded. Multivariable logistic regression analysis was used to evaluate factors associated with the receipt of SC-RT. Exact match using propensity score was used to balance the baseline patient characteristics between SC-RT and LC-RT. Overall survival (OS) was estimated with Kaplan-Meier method. Multivariable Cox proportional hazards model was used to evaluate factors associated with OS. Significance was defined at a value of  $p < 0.05$ .

#### Results

A total of 4816 patients were included in the analysis: 737 (15.3%) received SC-RT and 4079 (84.7%) received LC-RT. The median follow up was 24.3 months (range: 0.8 - 84.7). The utilization rate of SC-RT increased significantly from 10.7% in 2010 to 20.7% in 2015 ( $p < 0.01$ ). On multivariable analysis, factors that were associated with a higher likelihood for the receipt of SC-RT were age  $\geq 60$  (ref = age  $< 60$ , OR 1.27 (1.06 - 1.52),  $p = 0.01$ ), treatment to extremities (ref = spine, OR 2.15 (1.69 - 2.74),  $p < 0.01$ ), treatment to ribs (ref = spine, OR 3.15 (1.76 - 5.63),  $p < 0.01$ ), treatment at an academic/research program (ref = community cancer program, OR 1.78 (1.47 - 2.17),  $p < 0.01$ ), and triple negative breast cancer (ref = hormone positive, OR 2.29 (1.72 - 3.04),  $p < 0.01$ ). On multivariable analysis, SC-RT was associated with a worse OS compared to LC-RT (HR 1.38 (1.20 - 1.59),  $p < 0.01$ ). The 3-yr OS was 31.9% in SC-RT vs 47.9% in LC-RT group (Fig 1A,  $p < 0.01$ ). However, after exact match using propensity score, there was no difference in the 3-yr OS between the two groups (53.1% vs. 45.0%, Fig 1B,  $p = 0.21$ ).



### Conclusion

LC-RT remains the most common RT fractionation scheme for palliative treatment of breast cancer bone metastases. However, the use of SC-RT is increasing, particularly in more recent years, and for older patients and treatments at academic/research centers. As observed in multiple randomized trials, we also demonstrate equivalent OS between SC-RT and LC-RT after propensity matching.

### PO-0878 Implementing a dedicated inpatient radiation team with multidisciplinary palliative care rounds

D. MARK<sup>1</sup>, P. Gilbo<sup>1</sup>, S. Joseph<sup>1</sup>, A. Goenka<sup>1</sup>, B. Bloom<sup>1</sup>  
<sup>1</sup>Northwell Health, Radiation Medicine, Lake Success, USA

#### Purpose or Objective

To improve inpatient radiation care in our academic tertiary center, we have initiated a two pronged approach: we implemented daily inpatient multidisciplinary palliative care rounds (MPCR) including radiation oncology, medical oncology, and palliative care to improve interdisciplinary communication, and then started a dedicated inpatient radiation oncology team consisting of an attending and physician assistant to enhance continuity of care. We analyzed the impact of both interventions on number of inpatient treatment courses, recommended number of fractions, treatment completion rates, and length of inpatient stay.

#### Material and Methods

We initially implemented MPCR in July 2017 and then implemented our dedicated inpatient radiation team in January 2018. We retrospectively reviewed records for patients treated at our inpatient facility from 1/2017-6/2018 and recorded demographic data, treatment details, and length of inpatient stay after a radiation oncology consultation. We compared 6 months of baseline data (1/2017-6/2017), to data after the implementation of MPCR (7/2017-12/2017) and after the implementation of a dedicated inpatient care team (1/2018-6/2018).

#### Results

307 inpatient treatment courses were administered during this 18 month interval. There was a 35% increase in number of inpatient radiation treatments courses in the 6 months after development of MPCR (77 compared to 104) and a 63% year-to-year increase in the 6 months after both interventions (77 compared to 126). Number of fractions recommended after both interventions decreased from a mean of 6.1 (1/2017-6/2017) to 4.9 (1/2018-6/2018) which was significant (p=0.02). There was an increase of single fraction treatment courses offered from 7 (1/2017-6/2017) to 21 (1/2018-6/2018), and this trended toward significance (p=0.09). Treatment terminations did not significantly differ between time periods (11.7% initially, 13.5% after MPCR, and 11.1% after implementation of the dedicated team). Lastly, we noted a significant decrease of length of stay after a radiation oncology consultation from a mean of 16.2 days at baseline (1/2017-6/2017), to 14.7 days after the implementation of MPCR (7/2017-12/2017), to 12.3 days after the implementation of a dedicated inpatient radiation oncology team (p=0.004 when comparing 1/2017-6/2017 to 1/2018-6/2018).

#### Conclusion

Through the implementation of daily inpatient multidisciplinary rounds and a dedicated inpatient

radiation oncology team to enhance continuity of care, we noted significant changes in practice patterns. In addition to a continued increase in the number of inpatients treated with radiation, we noted a significant decrease in number of fractions prescribed to our palliative patients and a significant decrease in length of inpatient stay after a radiation oncology consultation. We hypothesize that this is due to enhanced communication between our dedicated inpatient radiation oncology team and allied medical oncology and palliative care providers.

### PO-0879 Mobile health for monitoring of health status in palliative care patients: a feasibility study

M. Pavic<sup>1</sup>, V. Klaas<sup>2</sup>, G. Theile<sup>1</sup>, J. Kraft<sup>1</sup>, G. Tröster<sup>2</sup>, M. Guckenberger<sup>1</sup>

<sup>1</sup>University Hospital Zürich, Radiooncology, Zurich, Switzerland ; <sup>2</sup>Swiss Federal Institute of Technology, Wearable Computing Laboratory, Zurich, Switzerland

#### Purpose or Objective

Discharge from hospital is a vulnerable phase in palliative patients' trajectories resulting in frequent unplanned readmissions. We examined the feasibility of remote monitoring of palliative patients using wearables in form of a smart-phone and a bracelet, aiming to detect deterioration of health status early and to prevent emergency readmissions.

#### Material and Methods

Patients treated with palliative intent in an inpatient setting were recruited for this prospective single-center observational feasibility study. Inclusion criteria were age >18, a severe medical condition (metastatic cancer or severe cardiac/pulmonary disease), ECOG performance status ≤2, no relevant cognitive impairment and good knowledge of German language. Patients were provided with two mobile health devices, an Android smartphone with a pre-installed activity monitoring app developed for this study and a sensor-equipped bracelet that recorded physical and social activity, vital signs and daily subjective ratings of pain and distress. Quality of life was assessed weekly by means of the EORTC QLQ-C30. The follow-up period was 12 weeks and started at discharge from hospital.

#### Results

Between February 2017 and February 2018 68 patients were eligible, of which 31 (46%) patients with a median age of 64 years (range 39-85) consented to participate. All included patients had a cancer diagnosis. Twenty-five patients completed the study period of 12 weeks, 3 died in between, 3 discontinued. On average, the bracelet was worn on 53 % of the study days. Wearing time per study day was on average 63 % (time considered between 8:00 and 20:00). The smartphone was worn at 85 % of the study days and wearing time was 50 % per day (8:00 to 20:00). Completion rate of digital questionnaires for patient reported outcome/subjective ratings (of pain and distress) was 73%. During the study period 8 unplanned hospital readmissions occurred. Patient reported ratings of pain, distress and QLQ-C30 scores were not associated with emergency readmission, whereas heart rate variability (HRV) while resting (root mean square of the successive differences), resting heart rate and speed of steps differed significantly between groups of patients with emergency readmissions versus no readmission.

#### Conclusion

Monitoring of palliative cancer patients using wearables is feasible. First results indicate that features of resting HRV, resting heart rate and speed of steps might be promising mobile health biomarkers to predict unplanned hospital readmission and are more significant than subjective ratings

### PO-0880 Validation of a predictive model for survival in patients receiving radiotherapy for bone metastases

K. Yasui<sup>1</sup>, H. Katagiri<sup>2</sup>, T. Onoe<sup>1</sup>, H. Ogawa<sup>1</sup>, H. Harada<sup>1</sup>, H. Asakura<sup>1</sup>, S. Maki<sup>1</sup>, A. Nakura<sup>1</sup>, Y. Ito<sup>1</sup>, M. Hirata<sup>1</sup>, S. Murayama<sup>1</sup>, Y. Honda<sup>2</sup>, M. Miyagi<sup>2</sup>, J. Wasa<sup>2</sup>, H. Murata<sup>2</sup>, M. Takahashi<sup>2</sup>, T. Nishimura<sup>1</sup>

<sup>1</sup>Shizuoka Cancer Center, Radiation oncology, Nagaizumi - Cho- Shizuoka, Japan ; <sup>2</sup>Shizuoka Cancer Center, Orthopedic surgery, Nagaizumi - Cho- Shizuoka, Japan

#### Purpose or Objective

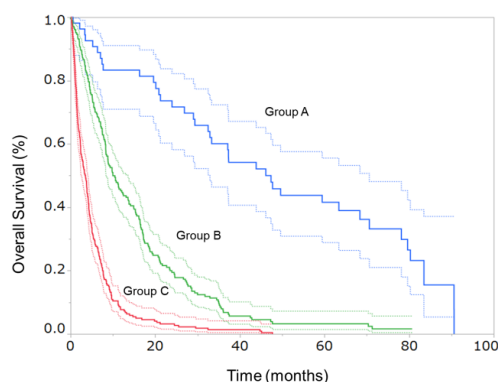
To validate a predictive model for survival in patients with bone metastases who are receiving radiation therapy.

#### Material and Methods

We previously constructed a predictive model for patients' survival using six prognostic factors: the primary lesion, visceral or cerebral metastases, abnormal laboratory data, poor performance status, previous chemotherapy, and multiple skeletal metastases. Each prognostic factor was assigned scores. Each patient was scored from 0-10 and classified into one of three groups: group A (those with scores 0-3), group B (those with scores 4-6), and group C (those with scores 7-10). This model was constructed from the records of 808 patients with bone metastases from 2005 to 2007. To validate the model, we evaluate 497 patients with bone metastases receiving radiotherapy from 2010 to 2012. Survival was estimated by the Kaplan-Meier method. The log-rank test was used to compare the survival times.

#### Results

The median survival was 6.1 months; group A (n = 54) 47.4 months (95% CI, 32.5-68.4 months); group B (n = 207) 10 months (95% CI, 8.4-13.1 months); and group C (n = 236) 3.5 months (95% CI, 2.6-4.0 months). The survival probability at 6, 12, and 24 months was 91%, 83%, 72%, respectively for group A; 70%, 45%, 19%, respectively for group B; and 28%, 8%, 3%, respectively for group C ( $p < 0.001$ ).



#### Conclusion

Our predictive model can be utilized to predict prognosis for patients with bone metastases receiving radiation therapy. External validation is needed in order to confirm our findings.

#### PO-0881 Outcomes of oligometastatic bone disease treated with conventional or stereotactic radiotherapy

S. Van de Ven<sup>1</sup>, J.M. Van der Velden<sup>1</sup>, W.S.C Eppinga<sup>1</sup>, D.H.J.G Van den Bongard<sup>1</sup>, H.M. Verkooijen<sup>1</sup>

<sup>1</sup>UMC Utrecht, Radiation Oncology Department, Utrecht, The Netherlands

#### Purpose or Objective

Stereotactic body radiotherapy (SBRT) has become a widely adopted treatment for patients with oligometastatic bone disease, despite limited evidence of superiority. We compared patient-reported pain, quality of life (QoL) and survival outcomes of patients with oligometastatic bone metastases within the prospective

PRESENT cohort, treated with conventional radiotherapy or SBRT.

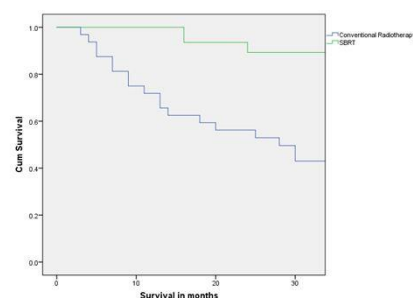
#### Material and Methods

We included all patients with oligometastatic bone disease ( $\leq 5$  metastatic lesions within  $\leq 3$  different organs) enrolled in the PRESENT cohort between June 2013 and September 2017. Since SBRT was only available as a treatment option at our department since December 2014, all patients before that date were treated with conventional radiotherapy (3D-CRT, IMRT or VMAT). Main outcomes were pain response (duration of pain response and best response defined as 'complete', 'partial' or 'stable response'), QoL (EORTC QLQ-BM22 and QLQ-C15-PAL), overall survival (OS), progression free survival (PFS), and time to start of, or switch in systemic treatment (FFSS) after radiotherapy. To control for potential confounders, patients were stratified into bone metastases only yes/no, histology (e.g. 'favorable histology' (breast or prostate) or 'other histology'), interval between diagnoses of the primary tumor and detection of oligometastatic disease  $\leq 12 > 12$  months with correction for age and WHO performance.

#### Results

Of the 131 patients, 66 patients were treated with conventional radiotherapy (1x8 Gy (44%), 5x4 Gy (12%), 10x 3 Gy (36%)) and 65 patients were treated with SBRT (1x 18Gy (35%), 3x10 Gy (30%) and 5x7 Gy (20%)). The median duration of follow-up was 46 and 25 months for the conventional radiotherapy and SBRT group respectively. There was no difference in best reported pain response within the first 12 months after treatment (pain response 81% vs. 84 %,  $p=0.79$ ) or duration of the response (23 weeks (95% CI 1-58) versus 25 weeks (95% CI 0-50),  $p=0.79$  in the SBRT group). All quality of life domains were similar, with the exception of physical functioning which was better in the SBRT group. The SBRT group demonstrated superior median OS (median OS not reached vs. 18 months) and PFS rates (median PFS 12 months (95% CI 5.3-18.6) versus 5 months (95% CI 3.5-6.5,  $p= 0.002$ ), figure 1). After correction for age and WHO performance, treatment with SBRT significantly prolonged OS and PFS in patients with an interval between primary tumor and oligometastatic disease  $>12$  months (table 1). Treatment with SBRT did not affect FFSS in any subgroup within our cohort.

Figure 1. Overall Survival



Numbers at risk:  
 Conventional radiotherapy: 66 44 30 24  
 SBRT: 65 45 30 13

Table 1. OS and PFS according to subgroups, with correction for WHO and age.

	1 Year OS			1 Year PFS		
	CRT (N)	SBRT (N)		CRT (N)	SBRT	
<b>Total</b>	65% (66)	85% (65)	p=0.00 HR 0.44 CI <b>0.237-0.81</b>	19% (62)	54% (64)	p=0.02 HR 0.63 CI <b>0.41-0.95</b>
<b>Type of oligometastases</b>						
• Bone metastases only	75% (40)	85% (62)	p=0.01 HR 0.59 CI 0.26-1.31	26% (37)	62% (61)	p=0.65 HR 0.65 CI 0.39-1.08
Bone+ other metastases	50% (26)	84% (13)	p=0.01 HR 0.28 CI <b>0.10-0.79</b>	80% (25)	23% (13)	p=0.45 HR 0.73 CI 0.34-1.56
<b>Histology</b>						
Favorable	94% (32)	100% (38)	p=0.02 HR 0.273 CI 0.06-1.28	94% (31)	78% (37)	p=0.02 HR 0.54 CI <b>0.29-1.00</b>
Other	38% (34)	63% (27)	p=0.004 HR 0.48 CI <b>0.24-0.91</b>	32% (31)	20% (27)	p=0.06 HR 0.67 CI 0.30-1.14
<b>Interval primary tumor and detection of metastases</b>						
≤12 months	59% (34)	53% (22)	p=0.88 HR 0.70 CI 0.55-2.40	18% (32)	14% (22)	p=0.71 HR 1.1 CI 0.59-1.93
>12 months	72% (32)	100% (43)	p=0.00 HR 0.139 CI <b>0.04-0.49</b>	21% (29)	73% (42)	p=0.00 HR 0.47 CI <b>0.26-0.85</b>

OS= Overall Survival, CRT= conventional radiotherapy, SBRT= stereotactic radiotherapy, HR= hazard ratio, CI= confidence interval, N=number of patients

**Conclusion**

SBRT to oligometastatic bone metastases did not improve QOL or pain response compared to conventional radiotherapy. Only patients with an interval between primary tumor and oligometastatic disease >12 months showed prolonged OS and PFS after treatment with SBRT.

**PO-0882 Outcome and Toxicity of Hypofractionated Image-Guided SABR for Spinal Oligometastases**

C. Billiet<sup>1</sup>, C. Mercier<sup>1,2</sup>, F. Vandaele<sup>1</sup>, P. Vermeulen<sup>3</sup>, S. Van Laere<sup>3</sup>, P. Huget<sup>1</sup>, D. Verellen<sup>1</sup>, P. Dirix<sup>1</sup>

<sup>1</sup> Department of Radiation Oncology, Iridium Kankernetwerk, University of Antwerp, Belgium; <sup>2</sup> University of Antwerp, Molecular Imaging- Pathology- Radiotherapy & Oncology MIPRO, Antwerp, Belgium; <sup>3</sup> Oncologisch Centrum GZA, Translation Cancer Research Unit, Antwerp, Belgium

**Purpose or Objective**

To evaluate tumor control and toxicity after high-dose stereotactic hypofractionated intensity modulated radiation therapy for patients with spinal oligometastases.

**Material and Methods**

Between March 2015 and March 2018, 40 consecutive patients with a localized spine metastasis (C1 to sacrum) from a histologically confirmed solid tumor received stereotactic ablative radiotherapy (SABR) to a total of 44 lesions and were followed for at least 6 months. SABR was delivered in three fractions of 8-10 Gy following international consensus delineation guidelines. All patients were treated with linac-based rotational SABR using cone-beam CT image-guidance and online correction of set-up errors in six degrees of freedom. An optical surface monitoring system (OSMS) was used to ensure patient immobilization. Factors associated with progression-free survival were retrospectively investigated by multivariate analysis. Local recurrence was defined as regrowth within the irradiated field or clear exacerbation of symptoms such as pain and motor deficits.

Table 1 : Patient and tumor characteristics

Patient related factors (N=40)	
<b>Sex</b>	
Male	28 70%
Female	12 30%
<b>Performance status</b>	
WHO 0	29 72.5%
WHO 1	11 27.5%
WHO 2	0 0%
<b>Median age (start treatment)</b>	69.5 (28-86)
<b>Primary tumor</b>	
Prostate	24 60%
Breast	7 17.5%
Other	9 22.5%
<b>RPA class</b>	
1	14 35%
2	21 52.5%
3	5 12.5%
<b>Systemic treatment</b>	
Yes	28 70%
No	12 30%
Tumor related factors (N=44)	
<b>Solitary lesion</b>	
Yes	22 50%
No	22 50%
<b>Extent of disease</b>	
Oligometastatic (n ≤5)	41 93.1%
Poly	3 6.9%
<b>Location</b>	
Cervical	0 0%
Thoracic	23 52.2%
Lumbar	18 40.9%
Sacral	3 6.8%
<b>Imaging at diagnosis</b>	
MR	35 79.5%
PET/PSMA/choline scan	19 43.2%
Bone scan +/- SPECT	20 45.5%
<b>Timing</b>	
Synchronous	14 31.8%
Metachrone	29 65.9%
Primary	1 2.2%
<b>Time interval</b>	36 (0-228)

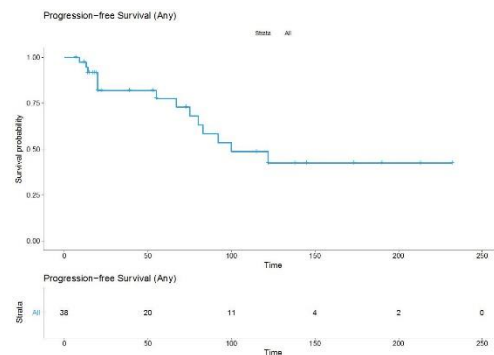
WHO: World health organization; RPA: Recursive partitioning analysis; MR: magnetic resonance; PET: Positron emission tomography; PSMA: Prostate-specific membrane antigen; SPECT: Single Photon Emission Computed Tomography

**Results**

Mean follow up was 69 months for all patients. Patient and tumor characteristics are depicted in Table 1. The 1-year progression free survival (PFS) was 97% for all patients (median PFS 92 months)(Figure 1) . In three patients (6,8%) a local recurrence was observed. No radiation-induced myelopathy was observed. Vertebral compression fractures developed de novo in 4.5% (2/44) of patients. In multivariate analysis, synchronous (vs. metachronous) lesions (p< 0.001; HR= 113.5), older age (p= 0.01; HR= 1.1) and no systemic therapy (p= 0.02; HR= 8.1), were correlated with worse PFS. In subgroup analysis for prostate cancer patients only, synchronous lesions were confirmed as significant predictive factor for PFS in multivariate analysis.

The mean volume of the gross target volume (GTV) was 11 cc and for the clinical target volume (CTV) 32cc. Mean dosimetric parameters D2%, D50% and D98% for the CTV and planning target volume (PTV) were 32.0 Gy, 18.6 Gy, 29.0 Gy and 33.1 Gy, 21.7 Gy, 30.7 Gy respectively.

Figure 1 : Progression free survival for all patients



**Conclusion**

These results show high rates of efficacy and minimal toxicity in patients treated with high-dose stereotactic hypofractionated RT for spinal metastases. Oligometastatic patients with metachronous lesions, younger age and additional systemic therapy seem to

benefit the most from SABR for spinal metastases. Probably, these metachronous lesions are the main reflection of a true oligometastatic state. However, these findings need to be investigated further in larger and prospective trials.

**PO-0883 Phase II trial of stereotactic body radiation therapy for abdomino-pelvic lymph node oligometastases**

C. Franzese<sup>1</sup>, T. Comito<sup>1</sup>, A. Tozzi<sup>1</sup>, F. De Rose<sup>1</sup>, P. Navarra<sup>1</sup>, P. Mancosu<sup>1</sup>, S. Tomatis<sup>1</sup>, M. Scorsetti<sup>1</sup>  
<sup>1</sup>Humanitas Research Hospital, Radiotherapy and Radiosurgery, Rozzano Milan, Italy

**Purpose or Objective**

Stereotactic body radiotherapy (SBRT) is nowadays considered an effective approach for the management of oligometastatic patients. Few data exist on radiotherapy in the context of isolated or limited lymph node metastases. We analyzed clinical results of oligometastatic patients treated with high dose SBRT for lymph node metastases in abdomen and pelvis.

**Material and Methods**

This is a prospective, phase 2 trial. Primary end-point was the assessment of acute and late toxicity; secondary end-points were local control (LC), progression free survival (PFS) and overall survival (OS) The schedule of SBRT was 48 Gy delivered in 4 fractions of 12 Gy each. Inclusion criteria were: Histologically-proven carcinoma of gastro-intestinal, genito-urinary of gynecological primary site, WHO performance status  $\leq 2$ , maximum 3 lymph node sites of disease, maximum diameter  $\leq 5$  cm, abdomen-pelvic site. Physical examinations and toxicity assessments were performed during and after SBRT according to CTCAE v4.0. Tumour response was evaluated on CT-MRI-PET scans using the RECIST modified criteria.

**Results**

From 2015 to 2018, 41 patients with 52 lymph nodes were enrolled. Median age was 69.2 years and 87.8% of patients were male. Most common primary tumour was located in genito-urinary tract (70.7%), and in particular prostate adenocarcinoma (58.8%), followed by gastro-intestinal (26.8%) and gynecological (2.5%) disease. One single lymph node was treated 32 patients, while 2 and 3 lymph node in 7 and 2 patients, respectively. Systemic therapy was administered before SBRT in 43.9% of patients and during SBRT in 14.6%. Median clinical target volume diameter was 15 mm (6 - 49). With a median follow-up of 16.7 months, only 3 patients reported grade 1 acute toxicity, in the form of pain, dysuria and fatigue. In the late setting, chronic pain was observed in 1 patient. In-field progression was observed in 5 (12.2%) patients with a 1- and 2- years rate of 96.4% and 77.1%. Systemic therapy during SBRT was associated with worse LC (HR 8.6, 95%CI 1.41 - 52.7,  $p=0.020$ ). Out-field lymphnodal progression was observed in 17 (41.4%) of cases and distant progressions in 8 (19.5%) cases. Median PFS was 12.8 months. At time of analysis all patients were alive except one with 1- and 2-years OS of 100% and 94.7%.

**Conclusion**

Treatment of lymph node metastases with high dose SBRT can be considered a safe option with high rates of local control in the context of multidisciplinary management of oligometastatic patients.

**PO-0884 Predicting 30-day mortality for palliative radiotherapy**

A. Witztum<sup>1</sup>, S. Wu<sup>1</sup>, E. Gennatas<sup>1</sup>, G. Valdes<sup>1</sup>, T. Solberg<sup>1</sup>, S. Braunstein<sup>1</sup>  
<sup>1</sup>Department of Radiation Oncology, University of California- San Francisco, San Francisco, USA

**Purpose or Objective**

Decision support for cancer patients at end of life is needed to optimize outcome for this population. Currently

there are a limited number of mortality prediction tools such as the TEACHH and Chow models. Here we build a model incorporating multiple factors to predict 30-day mortality for patients treated with palliative radiotherapy (RT) for advanced cancer.

**Material and Methods**

A cohort (n=518) of patients treated with external beam RT to a site of metastatic disease between 2012-2016 was included. Factors that may be associated with death within 30 days of RT treatment, including demographics and clinical and laboratory data were retrospectively collected. Generalized linear models (GLMNET package) were built with no regularization (logistic regression), and with regularization (Lasso and Elastic Net). Random forest (RANGER) and gradient boosting machine (GBM) models were also built to assess non-linearity in the response. Missing data was imputed by replacing values with either the mean or the mode, and adding a variable which indicated which patients had missing data for each variable. All models were built in R using cross validation withholding 25% of the data (test set), and stratified subsampling to account for unbalanced outcome. Each model was seeded in order to enable a pairwise t-test to compare the distribution of test balanced accuracies of each model. The area under the ROC curve (AUC) was also reported. The variable importance for linear models was calculated by multiplying the coefficient with the standard deviation of that variable for normalization.

**Results**

Lung, breast, and prostate cancer accounted for 55% of primary malignancies, with bone and brain accounting for 85% of treatment sites. 125 patients (24%) died within 30 days of RT. A logistic regression model resulted in a mean balanced accuracy (MBA) of 0.76 (AUC = 0.83). Adding Lasso or Elastic Net regularization offered a small improvement in MBA of 0.78 for both models ( $p=0.07$ ,  $p=0.09$ ) and an AUC of 0.83 and 0.84 (Figure 1) respectively. The non-linear models proved worse than logistic regression with random forest having an MBA of 0.74 ( $p=0.01$ , AUC = 0.82) and GBM having an MBA of 0.75 ( $p=0.08$ , AUC = 0.83). The most important variables in the logistic regression model are those indicative of missing data in other variables. Both Lasso and Elastic Net (Figure 2) regularizations, however, result in more interpretable variables such as TEACHH score, performance score, and hospice status. These features also have high importance in both non-linear models. For comparison, the AUC when using TEACHH score alone was 0.69.

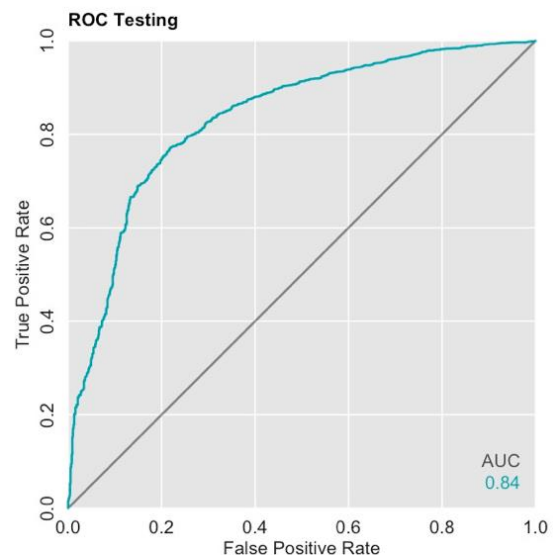


Figure 1: Area under the ROC curve for a generalized linear model with ElasticNet regularization (alpha tuned over 0, 0.3, 0.5, 0.7, 1).

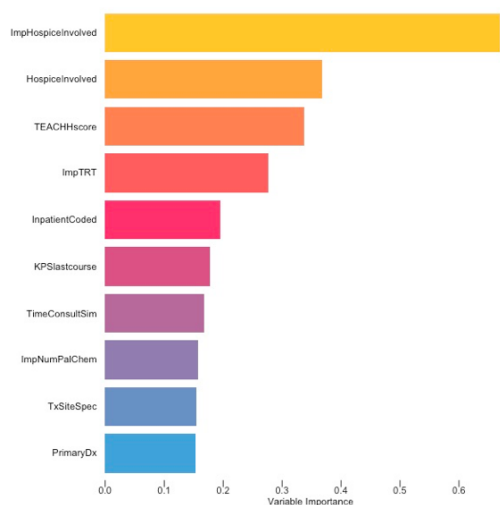


Figure 2: Variable importance for a generalized linear model with ElasticNet regularization (alpha tuned over 0, 0.3, 0.5, 0.7, 1). TRT = Time from referral to treatment, KPS = Karnofsky performance status, NumPalChem = Number of palliative chemo courses, InpatientCoded = Inpatient status at time of consult, TEACHHscore = Score according to TEACHH mortality prediction model, Imp prefix = Variable indicating if data was imputed.

### Conclusion

A linear prediction model was built to predict 30-day mortality for palliative RT patients with advanced cancer. An AUC of 0.84 was obtained (0.15 higher than TEACHH) proving that the problem is well characterized by the features selected. This encourages us to prospectively validate the model with the hope that it can be informative in the physician/patient decision process.

### Poster: Clinical track: Elderly

**PO-0885 Comprehensive geriatric assessment tools for elderly patients with early NSCLC treated with SBRT**  
 F. Cuccia<sup>1</sup>, A. Donofrio<sup>1</sup>, V. Valenti<sup>1</sup>, A. Tripoli<sup>1</sup>, N. Luca<sup>1</sup>, A. Palmeri<sup>1</sup>, G. Terranova<sup>1</sup>, E. Quartuccio<sup>1</sup>, G. Napoli<sup>1</sup>, G. De Gregorio<sup>1</sup>, D. Cespuglio<sup>2</sup>, G. Mortellaro<sup>2</sup>, G. Ferrera<sup>2</sup>, A. Lo Casto<sup>3</sup>

<sup>1</sup>Radiation Oncology School - University of Palermo, Radiotherapy Department - ARNAS Civico Hospital, Palermo, Italy ; <sup>2</sup>ARNAS Civico Hospital, Radiotherapy Department, Palermo, Italy ; <sup>3</sup>Radiation Oncology School - University of Palermo, Section of Radiological Sciences - DIBIMED, Palermo, Italy

### Purpose or Objective

The constant increase of life expectancy is associated to a higher incidence of cancer diagnosis in the elderly population. For aged patients with early stage Non Small Cell Lung Cancer (es-NSCLC), surgery is not often proposable, so Stereotactic Body Radiotherapy (SBRT) represents an attractive option for elderly subjects unfit or refusing resection, leading to a reduced percentage of untreated patients. In the effort to offer the best tailored approach to this subset of more vulnerable patients, several authors suggest the use of geriatric comprehensive assessment tools in order to facilitate a more customized treatment. Here we report our single-center experience of SBRT for es-NSCLC in  $\geq 65$  years patients, who were evaluated in the pre-treatment setting using G8 screening tool and Charlson Comorbidity Index (CCI).

### Material and Methods

From March 2014 to June 2018 we retrospectively evaluated 42 patients  $\geq 65$ -years with es-NSCLC who were assessed with G8 screening tool and CCI. Median age was 74 years (range, 65-91), 38 were stage I and 4 stage II.

Adenocarcinoma was the most frequent histological subtype, detected in 18 pts, undifferentiated in 3, squamous cells in 8; in 13 cases histological confirmation was not available and diagnosis was made on the evidence of pathological uptake recorded on PET scan. SBRT was performed with Helical Tomotherapy delivering 60-70 Gy in 8-10 fractions for peripheral lesions and 50-60 Gy in 10 fractions for central and ultra-central lesions. Acute and late toxicity assessment was conducted using CTCAE v4.0 scale; for the first year after RT, follow-up was based on quarterly chest CT scans and PET scans if needed. Any clinical correlation was evaluated with Fisher's exact test and Kaplan-Meier method and log-rank test were performed for Local Control (LC) and Overall Survival (OS) estimates.

### Results

Median CCI and G8 scores were 6 (4-11) and 14 (12-17). Median treatment time was 15 days (10-24), with 29 patients treated daily, and 13 every other day. BED<sub>10</sub> $\geq 100$ Gy schedules were administered in 53% (n=22) of cases, for a median BED<sub>10</sub>=105 Gy (75-119). With a median follow-up of 14 months (3-37) we observed 3 cases of acute G2 radiation pneumonitis, resolved after steroids therapy. As regards late toxicity, we reported only one case of G2 non-cardiac chest pain and one case of G2 radiation pneumonitis treated with steroids. At statistical analysis, G8 scores $\leq 14$  were significantly associated with late toxicity rates (p=0.049), no other statistical correlation was found. At the time of the analysis, we detected 4 local failures resulting in 1- and 2-yrs LC rates of 91% and 86%. 12 patients out of 42 died, 6 for non-cancer related causes, resulting in 1- and 2-yrs OS rates of 93% and 80%.

### Conclusion

In our experience the use of the G8 screening tool, for the pre-treatment evaluation of elderly patients candidate to SBRT for es-NSCLC, revealed a predictive power for late toxicity patterns, suggesting its implementation for a more tailored approach.

### Poster: Clinical track: Other

**PO-0886 Partial tumor irradiation exploiting immunomediated effects: tumor microenvironment as a new oar.**

S. Tubin<sup>1</sup>

<sup>1</sup>KABEG Klinikum- Landeskrankenhaus, Strahlentherapie und Radioonkologie, Klagenfurt, Austria

### Purpose or Objective

In a pre-clinical phase of this translational oncology research, it was proved for the first time that the hypoxic tumor cells show higher potential for induction of the bystander (BE) and abscopal effects (AE) than the normoxic cells: single high-dose irradiation of the hypoxic tumor exclusively resulted in significantly stronger radiation-hypoxia-induced BE and AE. These finding were translated to a clinic. Since BE and AE are mediated by the immune-system cells, we hypothesized that high-dose partial tumor irradiation (PTI), targeting exclusively the hypoxic tumor segment, and leaving the tumor microenvironment intact, would generate an effective tumor-abscopal signaling and antigen release leading to immune-mediated regression of whole partially-irradiated tumor (due to BE) but also of unirradiated metastases (due to AE). Primary endpoint included BE and AE response rates. Secondary endpoints included assessment of toxicity, overall (OS) and disease-specific survival (DSS).

### Material and Methods

Clinical study involved 32 patients whose bulky tumors of the lung, H&N, pancreas, kidney, skin and adrenal glands were partially irradiated. "Bystander Tumor Volume (BTv)" (hypoxic segment) was defined using PET-CT, as a

hypovascularized-hypometabolic junctional zone between the central necrotic and peripheral hypervascularized-hypermetabolic tumor segment. Based on tumor site and volume, BTV was irradiated with 1-3 fractions of 10 or 12 Gy prescribed to 70% isodose, avoiding the tumor microenvironment (Fig.1, 2). No patient received systemic therapy. Immunohistochemistry was performed on the available tissue samples after neoadjuvant PTI and surgery to explore for the modifications within the tumor microenvironment.

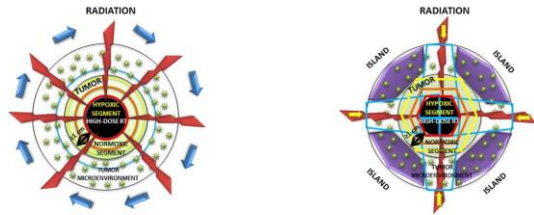


Figure 1A DYNAMIC RADIATION ARCS: Figure shows how a desired high radiation dose (red ring) is delivered by the means of dynamic arcs very precisely and conformally to the hypoxic tumor segment (red/black area). Moving from that high-dose region through the necrotic tumor towards outside of the tumor, the dose will sharply fall off (orange ring-moderate dose, yellow ring-low dose) reaching a very low dose-level (blue ring) outside the tumor at the level of the tumor microenvironment, being at that level very steady and homogeneously distributed. In this case, an acceptably low radiation dose will cover a small volume of the tumor microenvironment closer to the tumor's periphery leaving it viable and functional.

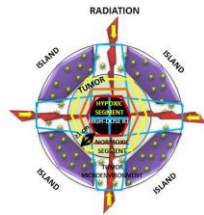
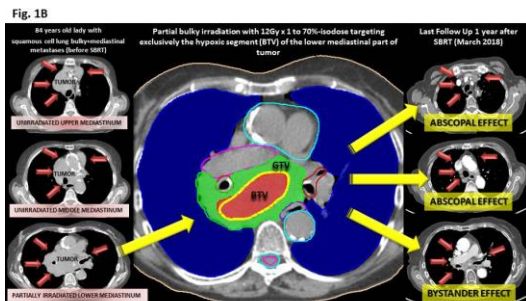


Figure 1B LOW NUMBER OF STATIC RADIATION FIELDS: Figure shows how a desired high radiation dose (red ring) is delivered by the means of a static radiation fields to the hypoxic tumor segment (red/black area) whereby a significant volume of the tumor microenvironment is constantly spared from radiation dose. Moving from that high-dose region through the necrotic tumor towards outside of the tumor, the dose will fall off (orange ring-moderate dose, yellow ring-low dose) reaching a very low dose-level (blue area) outside the tumor, covering a smaller volume of the tumor microenvironment. In this case, a larger volume of the tumor microenvironment remains intact in a form of the islands.



## Results

On an average, the BTV corresponded to 30% of the bulky tumors. With median follow-up of 11 months (range: 2-22) OS and DSS were 71% and 84%, respectively. BE response rate was 95%. Average bulky shrinkage was 60%, with 20% complete responses. AE response rate was 47% with mean reduction of unirradiated metastases of 50% (range: 30-100%). No patient experienced acute or late toxicity of any grade. The immunohistochemical findings after neoadjuvant PTI showed that apoptosis-inducing factor was massively upregulated in the partially irradiated bulky and also at unirradiated-abscopal tumor sites, whereas a dense immune reaction was observed only at the border of the partially irradiated tumor but not at the abscopal site indicating an important role for the tumor-abscopal signaling.

## Conclusion

PTI for bulky tumors was feasible, effective and safe, showing high potential for induction of BE and AE, that could be translated in improved therapeutic ratio.

**Relevance:** PTI showed high *neoadjuvant* potential to convert unresectable into resectable lesions; very convenient *palliative* 1-3 days treatment for patients in poor general conditions, offering an *improved cost-effectiveness profile*; safe *salvage re-irradiation* option in case of relapses.

**PO-0887 Radiation toxicity in patients with collagen vascular disease: Meta-analysis of case-control studies**

P. Shaikh<sup>1</sup>, F. Alite<sup>2</sup>, V. Bakalov<sup>3</sup>, B. Emami<sup>4</sup>, J. Vargo<sup>5</sup>, M. Wu<sup>6</sup>, G. Jacobson<sup>5</sup>, W. Small<sup>4</sup>, M. Harkenrider<sup>4</sup>  
<sup>1</sup>West Virginia University, Radiation Oncology, Kentwood, USA ; <sup>2</sup>Geisinger Medical Center, Radiation Oncology, Danville- PA, USA ; <sup>3</sup>Allegheny General Hospital, Internal Medicine, Pittsburgh- PA, USA ; <sup>4</sup>Loyola University Chicago, Radiation Oncology, Maywood- IL, USA ; <sup>5</sup>West Virginia University, Radiation Oncology, Morgantown- WV, USA ; <sup>6</sup>Loyola University Chicago, Radiation Oncology, Chicago- IL, USA

## Purpose or Objective

Several retrospective matched-pair series have reported on late effects of radiotherapy(RT) in patients with collagen vascular disease(CVD). Results have been conflicting and concern remains that patients are at greater risk for late toxicity.

## Material and Methods

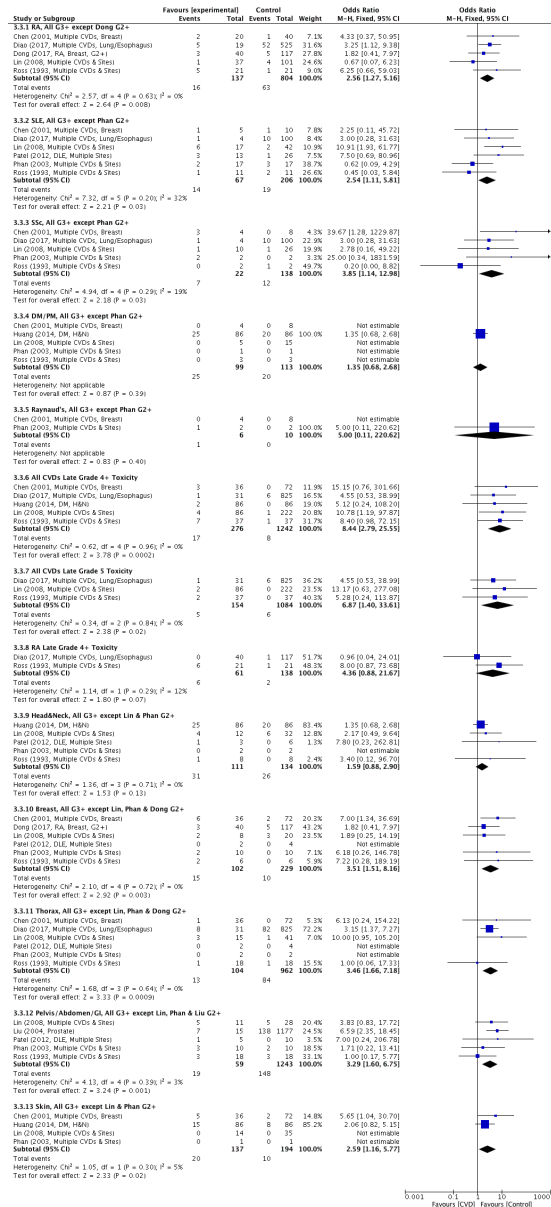
A comprehensive EMBASE and Medline search was performed to identify case-control series reporting RT toxicity in patients with CVDs. Results were synthesized from studies reporting at least grade 2 or 3 (G2/3+) acute and/or late toxicities in patients with rheumatoid arthritis(RA), systemic lupus erythematosus(SLE), scleroderma (SSc), Dermatomyositis/Polymyositis (DM/PM), Raynaud's, Mixed connective tissue disease(MCTD)/Sjogren's. Results were analyzed on the random-effects(RE) model if there was evidence of between-study heterogeneity, otherwise the fixed-effects model(FE) was used. Hazard ratio(HR) was used for overall late toxicity for all CVDs and survival endpoints and odds ratio(OR) for subgroup toxicity analysis.

## Results

10 studies were identified with 4112 patients (CVD=380, control=3732). Grade 2/3+late toxicity was seen in 18.4% (68/370) RT courses in CVD patients vs. 10.1% (262/2588) in control patients (Fig). Pooled data showed significantly worse grade 2/3+ late toxicity in patients with CVD vs. control (HR=2.37; 95% CI 1.71-3.28, p<0.00001, FE). Subgroup analysis showed RA patients had 16/137 (11.7%) RT courses complicated by grade 2/3+ late toxicities vs. 63/804 (7.8%) in control patients (OR=2.56; 95% CI 1.27-5.16, p=0.008). SLE patients had 14/67 (20.9%) RT courses complicated by grade 2/3+ late toxicities vs. 19/206 (9.2%) in control patients (OR=2.54; 95% CI 1.11-5.81, p=0.03, FE). SSc patients had 7/22 (31.8%) RT courses complicated by grade 2/3+ late toxicities vs. 12/138 (8.7%) in control patients (OR=3.85; 95% CI 1.14-12.98, p=0.03, FE). No significant differences were found in late grade 2/3+ toxicity for subgroups of DM/PM or Raynaud's. Late grade 4 and 5 toxicity was significantly higher in CVD patients, 6.2% vs. 0.64% (HR=8.44, p=0.0002) for Grade 4 and 3.2 vs. 0.55% (HR=6.87, p=0.02) for Grade 5. Abdomen/Pelvis had the highest probability of late grade 2/3+ toxicity (32.2%, bowel toxicity) followed by head & neck (27.9%, likely reflecting higher dose) compared to breast, thorax and skin (<15%) anatomic sites. Overall acute G2/3+ was also significantly worse in CVD group (OR 2.0, p<0.0001) and in the subgroups of patients with SLE (OR=2.25, p=0.05) and DM/PM (OR=3.39, p<0.0001). There was statistically significant worse disease-free-survival in CVD patients vs. controls (HR=1.46, p<0.01) but no difference in overall, loco-regional or distant metastases free survival.

## Conclusion

Metanalysis demonstrated significantly higher RT induced late toxicity, including risk of death in irradiated CVD patients, especially in RA, SLE and SSc subgroups and in abdomen/pelvis and head/neck anatomic sites. These findings support further validation in prospective manner.



Material and Methods

Enrolled patients suffered from recurrent VT or electrical storm (ES) refractory to CA and AADs. Before the procedure, an electroanatomic mapping (EAM) was performed to localize the VT substrate (VT-sub). All patients underwent a planning CT co-registered with a cardiac MRI or a cardiac CT to help in volume definition. For each case, the cardiologist delineated the VT-sub according to the EAM data. The distal dipole of the ICD lead was used as a fiducial marker for tracking. The median dose of 25 Gy (range, 20-25 Gy) was delivered to the VT-sub using the Cyberknife® system.

Results

Since September 2017, five patients with VT or ES refractory to AADs and CA were treated. Four patients were elective, while another one, hospitalized in the intensive care unit (ICU), was intubated because of an ES with multiple ICD shocks refractory to CA. VT was due to an ischemic cardiomyopathy in two patients and to a non-ischemic cardiomyopathy in the three others. In all patients, SBRT was successfully delivered using near real-time ICD lead tracking with an average time of 54 minutes. The median ablation volume was 22 cc (range, 19-35 cc). After a median follow-up of 5 months (range, 4-11), the elective patients did not experience any VT recurrence. The ICU patient, suffering from a non-ischemic cardiomyopathy, was extubated 3 days after SBRT and remained free of ICD shocks during 4 months; he presented, however, a new ES episode 19 weeks after the procedure related to a new VT-sub successfully treated by CA. In all patients, the ICD interrogation confirmed that no sustained VT episodes arose from the irradiated site after SBRT. Importantly, no SBRT-related toxicity occurred.

Conclusion

SBRT appears as an efficient tool for the treatment of refractory VT caused by myocardial scarring. Recurrence was observed only in non-ischemic cardiomyopathy remote from the irradiated site.

**PO-0889 Breathing modulation in patients treated for mobile tumours: moving forward to clinical integration**  
 G. Van Ooteghem<sup>1,2</sup>, D. Dasnoy-Sumell<sup>3</sup>, G. Liistro<sup>4</sup>, E. Sterpin<sup>5</sup>, G. Xavier<sup>1,2</sup>

<sup>1</sup>Institut de Recherche Expérimentale et Clinique, Molecular Imaging- Radiotherapy and Oncology MIRO, Brussels, Belgium; <sup>2</sup>Cliniques Universitaires Saint Luc, Radiation Oncology, Brussels, Belgium; <sup>3</sup>Université Catholique de Louvain, ImagX-R, Louvain-La-Neuve, Belgium; <sup>4</sup>Cliniques Universitaires Saint Luc, Pneumology, Brussels, Belgium; <sup>5</sup>Université Catholique de Louvain, Molecular Imaging- Radiotherapy and Oncology MIRO, Brussels, Belgium

Purpose or Objective

We previously demonstrated that mechanically-assisted and non-invasive ventilation (MANIV) can be used safely without sedation on healthy volunteers. MANIV can be used to regularise the breathing pattern by constraining the breathing rate (BR) and the tidal volume (Volume-controlled ventilation mode - VC). Breathing modulation can also be achieved by the shallow-controlled mode (SH) which reduces the breathing amplitude proportionally to the BR increase while the Slow-controlled mode (SL) mimics repeated end-inspiratory breath-holds. To allow the clinical integration of MANIV in radiotherapy, patients' tolerance and the intra- and inter-session reproducibility of the breathing-related tumour motion were thus evaluated.

Material and Methods

In lung or liver cancer patients (cohort A), the tumour motion was assessed with the VC and SH modes and compared to spontaneous breathing (SP). In left breast cancer patients (cohort B), the nipple motion was assessed with the SL mode and compared to spontaneous breath-

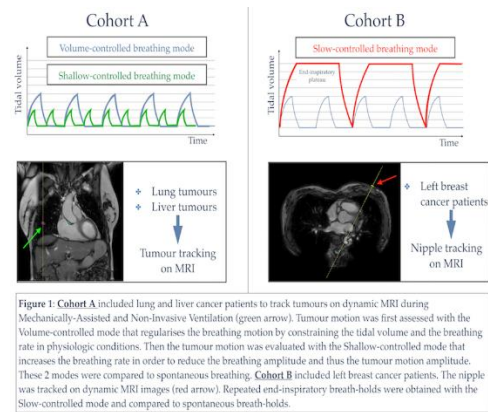
**PO-0888 Stereotactic body radiotherapy for refractory ventricular tachycardia: clinical outcomes**

R. Jumeau<sup>1</sup>, M. Ozsahin<sup>1</sup>, J. Schwitzer<sup>2</sup>, F. Duclos<sup>1</sup>, V. Vallet<sup>3</sup>, M. Zeverin<sup>3</sup>, R. Moeckli<sup>3</sup>, E. Pruvot<sup>4</sup>, J. Bourhis<sup>1</sup>  
<sup>1</sup>Centre Hospitalier Universitaire Vaudois, Department of Radiation Oncology, Lausanne Vaud, Switzerland; <sup>2</sup>Centre Hospitalier Universitaire Vaudois, Cardiac MR center, Lausanne Vaud, Switzerland; <sup>3</sup>Centre Hospitalier Universitaire Vaudois, Department of Radiation Physics, Lausanne Vaud, Switzerland; <sup>4</sup>Centre Hospitalier Universitaire Vaudois, Department of Cardiology, Lausanne Vaud, Switzerland

Purpose or Objective

Ventricular tachycardia (VT) caused by myocardial scarring bears a significant risk of mortality and morbidity that can be partially controlled by the implantation of a cardioverter-defibrillator (ICD). Recently, stereotactic body radiotherapy (SBRT) appeared as a promising tool for the management of VT refractory to antiarrhythmic drugs (AADs) and catheter ablation (CA). We present herein the outcomes of our series of patients treated under an institutional SBRT program for refractory VT.

holds (SPBH) (Figure1).



All the patients underwent one coaching session, one simulation session and then 2 dynamic MRI sessions. Each MRI acquisition lasted for 6 minutes with a first acquisition in SP/SPBH followed by those with MANIV. Patients' objective tolerance was assessed with oxymetric monitoring (SpO<sub>2</sub>, etCO<sub>2</sub>). Subjective tolerance was assessed through questionnaires fulfilled after each session. The motion of the tumour, or the nipple, was tracked and expressed in position, amplitude, period and plateau within each MRI (intra-session analysis) and between MRI (inter-session analysis).

### Results

Five lung cancer patients, 5 liver cancer patients (61-83 years old) and 10 left breast cancer patients (49-77 years old) were included (Table 1).

	Cohort A	Cohort B
Total (n)	10	10
Region of interest (n)	Lung tumour (5) Liver tumour (5)	Left breast nipple (10)
Sex ration (M/F)	8/2	0/10
Age (years)		
Median	66	58
Min - max	61 - 83	49 - 77
BMI (kg/m <sup>2</sup> )		
< 18	0	0
18-25	3	6
25,1 - 30	4	3
> 30	3	1
Tobacco use (n)		
no	7	8
former	3	1
active	0	1
COPD (n) (GOLD stage)	1 (GOLD II)	0
OAS With CPAP (n)	1	2
Performance status (n)		
ECOG 0	5	9
ECOG 1	4	1
ECOG ≥ 2	1	0
Previous chemotherapy (n)	4	3

Table 1: Demographic data of Cohort A and Cohort B  
(M = male; F = female; BMI = Body Mass Index; COPD = Chronic Obstructive Pulmonary Disease;  
OAS = Obstructive Sleep Apnea Syndrome; CPAP = Continuous Positive Airway Pressure device)

MANIV was well tolerated without any interruption, nor oxymetric changes. Main reasons of discomfort were the facial mask (47%) and the arms position (29%), before MANIV itself (18%).

In cohort A, the BR in VC and SH were all more stable than in SP in intra- and inter-session analysis. Switching from VC to SH led to a motion amplitude reduction of 0.6mm to 9mm proportional to the BR increase (1.5 to 3.4-fold increase).

The greatest effect was observed in a liver tumour with a spontaneous median amplitude of 28.7mm (IQR 12.8mm) reduced to 17.6mm (IQR 4.8mm) with SH.

In cohort B, the repeated breath-holds in SL were as stable as in SPBH in terms of range within a same plateau (0.7mm in SPBH and 0.9mm in SL) or position between plateaus (0.2mm of median variation for both). Plateaus in SL lasted 16,7sec (IQR=4.6) and 20sec in SPBH.

### Conclusion

This trial demonstrates that MANIV can be used safely in unsedated patients. MANIV may thus be proposed in

clinical practice to improve the current motion mitigation techniques such as margins reduction (SH mode), respiratory gating (SL mode) or tracking (VC mode). Indications still have to be refined and patients well-selected according to appropriate clinical situation.

### PO-0890 Abscopal effects in metastasized cancer patients treated with PD-1 inhibition and radiation therapy

M. Trommer<sup>1</sup>, S.Y. Yeo<sup>2</sup>, T. Persigehl<sup>2</sup>, A. Bunck<sup>2</sup>, M. Schlaak<sup>3</sup>, H. Gröll<sup>2</sup>, S. Theurich<sup>4</sup>, M. Von Bergwelt<sup>4</sup>, J.M. Herter<sup>1</sup>, E. Celik<sup>1</sup>, S. Marnitz<sup>1</sup>, C. Baues<sup>1</sup>

<sup>1</sup>University Hospital of Cologne, Department of Radiation Oncology, Köln, Germany; <sup>2</sup>University Hospital of Cologne, Department of Diagnostic and Interventional Radiology, Köln, Germany; <sup>3</sup>Ludwig Maximilian University, Department of Dermatology and Allergology, Munich, Germany; <sup>4</sup>Ludwig Maximilian University, Department III of Internal Medicine- Hematology and Oncology, Munich, Germany

### Purpose or Objective

Immune-checkpoint inhibitors targeting the programmed death receptor 1 (PD-1) have shown promising results in the fight against several malignancies. Radiation therapy (RT) induces the release of immunogenic targets and the secretion of damage-associated molecules. Subsequent systemic anti-tumor reactions can lead to a regression of non-irradiated lesions, which is called abscopal effect. The aim of this study was to evaluate abscopal effects based on radiological imaging of irradiated cancer patients receiving simultaneously anti-PD1 antibodies.

### Material and Methods

We analyzed 48 patients treated with PD-1 inhibitors and radiotherapy between August 2014 and December 2017. Inclusion criteria were at least one distant metastatic site outside V10% (volume of tissue receiving at least 10% of the prescribed irradiation dose) and start of RT after at least one month of anti-PD1 therapy (pembrolizumab 2 mg/kg every three weeks or nivolumab 3 mg/kg every two weeks) or within one month after the last application. Abscopal effect was defined as shrinkage of one or more non-irradiated lesions outside V10% with no additional treatment. To distinguish the abscopal effect from the systemic effects of immunotherapy alone, radiological imaging had to be performed twice before RT and at least once after completion of RT. In every radiological image taken during radio-immunotherapy, the largest diameter of the lesions was measured. A size change of more than 20 % was considered as significant decrease or enlargement.

### Results

11 patients met the inclusion criteria. We observed lesion shrinkage outside V10% in four out of 11 analyzed cases, one patient demonstrated as case example. In five patients, all lesions progressed during the analyzed period, whereas two patients showed already reduced or stable lesions after immunotherapy alone. Nivolumab was given in four cases and pembrolizumab in seven cases. Patients were irradiated with a mean of 50,67 Gy total dose (median 50 Gy) in the analyzed time period. Seven patients were treated stereotactically using Cyberknife® (20 Gy / 65 %). One out of those received three Cyberknife® treatments, one patient additionally received hypo-fractionated treatment (3 Gy single dose (SD)), two patients additionally hypo-fractionated and normo-fractionated treatment (3 Gy SD and 1,8 or 2 Gy SD). Two patients had only hypo-fractionated (3 Gy SD) and two only normo-fractionated (2 Gy SD) radiotherapy. Three out of four patients showing AE were treated stereotactically, all AE patients received a high total dose (mean: 77,6 Gy, median: 78 Gy).

### Conclusion

We demonstrated that four out of 11 patients who were considered for this analysis showed a regression of lesions

outside the irradiation field. Confirming the clinical evidence of a systemically mediated effect of radiotherapy, our study contributes to understanding the circumstances of its occurrence and assists in developing a setting for the effective use of the synergistic mechanisms of radioimmunotherapy.

## Physics Posters

### Poster: Physics track: Basic dosimetry and phantom and detector development

#### PO-0891 Radiochromic film based output measurement for radio-biological experiments at low energy photons

N. Tomic<sup>1</sup>, L. Lieng<sup>1</sup>, M. Lecavalier<sup>1</sup>, J. Seuntjens<sup>1</sup>, R. Aparidian<sup>1</sup>, S. Devic<sup>1</sup>

<sup>1</sup>Jewish General Hospital, Radiation Oncology, Montreal, Canada

#### Purpose or Objective

Purpose of radiobiological experiments with small animals is to provide information of the efficacy of dose delivered for the investigated new modalities, for which it is essential to determine exactly the delivered dose. If the experimental setup is simulated before the actual experiment, radiochromic film with high spatial resolution can be used as a calibration tool, providing the spatial output data for future experiments.

#### Material and Methods

We designed experimental setup for radiobiological studies in the irradiation of the mouse abdomen (Fig.1a). It consists of the polyactic acid mouse holder and the half cylinder phantom mimicking the mouse during output measurements, both created using 3D printer (MicroBOT). Irradiation was carried by the Axxent -Xoft (Xoft Inc. Sunnyvale, CA) electronic brachytherapy system and Vaginal Applicator. The applicator was covered with the lead collimator having the 7 mm diameter hole, aligned with the source position within the applicator. Dose range used in the described setup is from 2 to 30 Gy. The irradiator has the beam quality of 50 kVp and the measured HVL of 0.81 mm Al.

We used EBT3 model GAFCHROMIC™ film to estimate the output and the 2D dose distribution. Output of the irradiator at the reference point of measurement in terms of air kerma in air was measured using a calibrated parallel plate (Exradin A20) ionization chamber following AAPM TG-61 protocol. At the same reference point, film pieces were irradiated to create calibration curve for given beam quality in terms of air kerma in air as a function of film response to radiation:  $(PV_0/PV) \cdot -1$  [Aldelaijan et al. *Phys. Med.* **49**,112-118(2018)].

Output of irradiator at the phantom surface mimicking mouse was determined by employing previously described film reference dosimetry system, where dose to water is determined by multiplying air kerma in phantom by the mass-energy attenuation coefficient ratio water to air,  $(m_{en}/r)_{air}^{wat}$ , for a given beam quality [Tomic et al. *Med. Phys.* **37**,1083-1092(2010)].

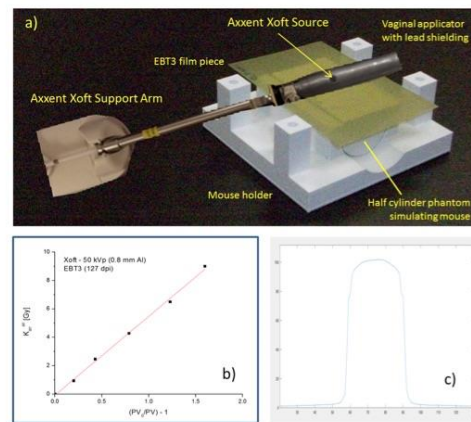


Figure 1: Calibration of the experimental setup for radiobiological studies of mouse irradiation: a) mouse holder with the half cylinder phantom to mimic the mice, Axxent-Xoft electronic brachytherapy system with Vaginal Applicator as an irradiator and the piece of EBT3 film between the irradiator and the surface of the mouse model phantom; b) calibration curves for EBT3 GafChromic™ film based reference dosimetry system at irradiator beam quality (50 kVp, 0.81 mm Al); c) dose profile extracted from the irradiated EBT3 film piece during the irradiation of the mouse model phantom with 7 mm diameter collimator opening aligned with the source position within the applicator.

#### Results

Figure 1.b presents calibration curve for measured beam quality showing linear response in wide dose range. Output of described irradiator at the surface of the animal model phantom in the center of lead opening was found to be  $8.4 \pm 0.1$  Gy/min, and obtained 2D dose distribution was found to be uniform. Profile through the region of irradiation (Fig 1.c) shows dose uniformity to be within 95% from dose in the middle of the profile over 80% of the field diameter defined at 50% of central axis dose. Due to significant energy dependence of the EBT3 film response for effective photon energies below 100 keV, the beam quality has to be determined before using described reference dosimetry protocol.

#### Conclusion

We described method to measure the output and the 2D dose distribution of low energy photons in radiobiological setups with small animals using the EBT3 radiochromic film dosimetry protocol with the uncertainty in measured dose of the order of 5%.

#### PO-0892 On the orientation of ionization chambers in dosimetry of small photon fields

B. Casar<sup>1</sup>, E. Gershkevitch<sup>2</sup>, I. Mendez<sup>1</sup>

<sup>1</sup>Institute of Oncology Ljubljana, Department for Dosimetry and Quality of Radiological Procedures, Ljubljana, Slovenia; <sup>2</sup>North Estonia Medical centre, Medical Physics Service, Tallinn, Estonia

#### Purpose or Objective

The new IAEA Code of Practice TRS - 483 for dosimetry of small static photon fields provides advice on the orientation of various detectors for measurements of beam profiles and field output factors (FOFs). For cylindrical ionization chambers (ICs), it is advised to place the IC with its stem perpendicular to the beam axis for the determination of FOFs, while for the measurement of lateral beam profiles, the recommended orientation is parallel to the beam axis. Accurate positioning of the IC in the center of the field is crucial to obtain accurate values for FOFs. As the most accurate location of the center of the field lies in the middle of two orthogonal lateral beam profiles at FWHM, which is supposed to be obtained in a parallel orientation, recommendations from TRS-483 are somewhat incoherent. We aimed to analyze differences in detector specific output correction factors (OCFs) between parallel and perpendicular orientations of IC and to resolve the ambiguity on how to perform measurements of FOFs with ICs.

### Material and Methods

The measurements were made on Elekta Versa HD linac for 6 and 10 MV beams with and without flattening filter. FOFs were acquired for nine small square fields ranging from 0.5 to 10.0 cm (nominal sizes) shaped with MLC and jaws, at SSD = 90 cm and 10 cm depth in a 3D water phantom. Nominal field sizes were converted to equivalent square field sizes ( $S_{clin}$ ) as  $S_{clin} = (AxB)^{1/2}$ , where A and B correspond to the measured field width and length defined at the FWHM.

Discrete values of FOFs were determined with two reference detectors, Exradin W1 plastic scintillator and EBT3 radiochromic films, fitted with the analytical function  $FOF(S_{clin})$  proposed by Sauer and Wilbert - Eq. (1). EBT3 films were irradiated in an RW3 Solid Water phantom under the same set-up as described above and analyzed with Radiochromic.com software. Four types of ICs - IBA Razor, IBA CC04, PTW 31022 3D PinPoint and PTW 31023 PinPoint - were used in parallel and perpendicular orientations to measure signal ratios  $M(S_{clin})/M(S_{ref})$  between clinical and reference ( $10 \times 10 \text{ cm}^2$ ) fields. The orientation was kept unchanged (parallel or perpendicular) for the scanning procedure and the point measurements. Discrete values of OCFs determined with Eq. (2) were fitted by the function shown in Eq. (3).

$$FOF(S_{clin}) = P_{\infty} \frac{S_{clin}^n}{l^n + S_{clin}^n} + S_{\infty} (1 - e^{-b \cdot S_{clin}}) \quad (1)$$

$$OCF(S_{clin}) = \frac{FOF(S_{clin})}{\frac{M(S_{clin})}{M(S_{ref})}} \quad (2)$$

$$OCF(S_{clin}) = \frac{1 - e^{-\frac{10-a}{b}}}{1 - e^{-\frac{S_{clin}-a}{b}}} + c \cdot (S_{clin} - 10) \quad (3)$$

### Results

For the smallest fields, OCFs were always lower (closer to unity) in parallel than in perpendicular orientation for all ICs, regardless of the beam energy used (Fig. 1).

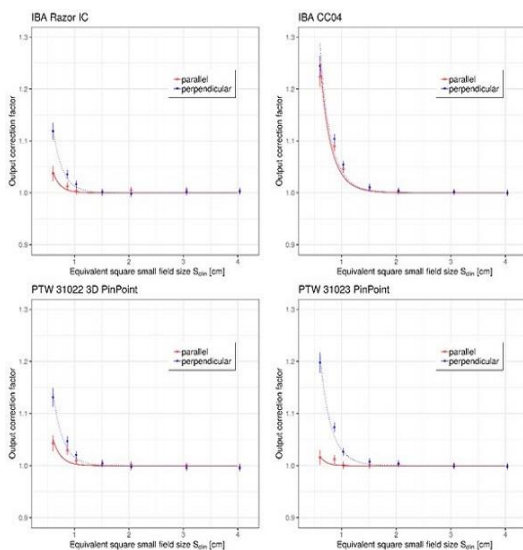


Fig 1: Output Correction Factors (OCF) for four IC obtained in 6 MV WFF photon beam from Elekta Versa HD linac, displayed as discrete points and as curves of analytical function from Eq. (3)

### Conclusion

For the determination of FOFs and OCFs for cylindrical IC, we recommend the orientation with its stem parallel to the beam axis. Our recommendation arises from two main

arguments: (i) the center of the radiation field can be determined from lateral beam profiles using the IC in a parallel orientation as recommended in TRS-483, (ii) OCFs were lower in parallel compared to perpendicular orientation for the smallest fields in all studied ICs.

### PO-0893 Absolute dosimetry with polymer gels - A TLD reference system

A. Schwahofer<sup>1</sup>, P. Mann<sup>1</sup>, C. Karger<sup>1</sup>

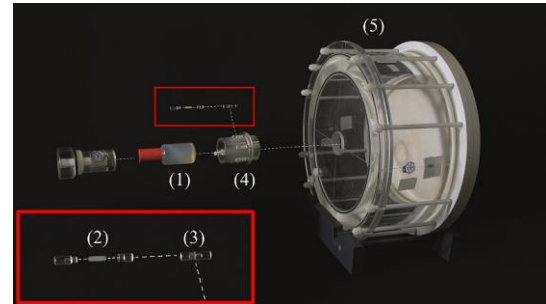
<sup>1</sup>German Cancer Research Center DKFZ, Department of Medical Physics in radiation therapy, Heidelberg, Germany

#### Purpose or Objective

Absolute dosimetry in 3D with polymer gels (PG) is generally complicated and usually requires a second independent measurement with conventional detectors. This is why, PG are often used only for relative dosimetry. To overcome this drawback, we combine PG with a 1D thermoluminescence (TL) detector within the same measurement. The TL detector information is then used as additional information for calibration of the gel.

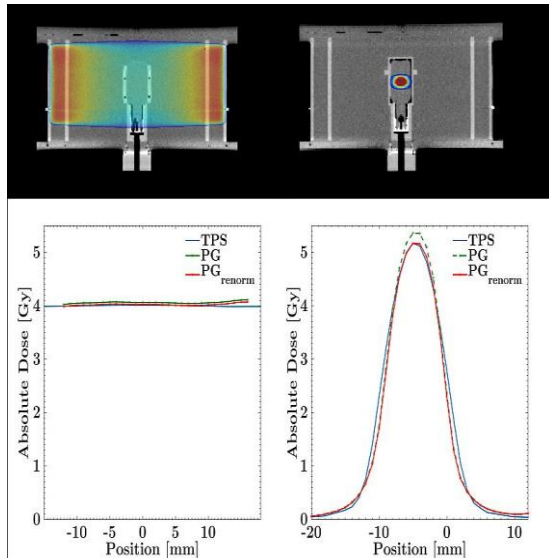
#### Material and Methods

The PAGAT dosimetry gel was used in combination with TLD600 (LiF:Mg,Ti). TL detectors were attached on the surface of the PG container placed inside a cylindrical Phantom (figure 1). To test the usability of this setup, two irradiation geometries were carried out: (a) homogeneous target coverage and (b) small-field irradiation. PG was evaluated with magnetic resonance imaging (MRI) and the TL detectors with a Harshaw 5500 hot gas reader.



### Results

PG dosimetry alone showed deviations of up to 4% as compared to calculations. Including additionally the dose information of the TL detectors for PG calibration, this deviation was decreased to less than 1% for both irradiation geometries (figure 2). This is also reflected by the very high -passing rates of >96% (3%/3mm) and >93 % (2%/2mm), respectively.



### Conclusion

This study presents a novel method combining 3D PG and TL dose measurements for the purpose of absolute 3D dose measurements that can also be applied in complex anthropomorphic phantoms using only a single measurement. The method was validated for two different irradiation geometries including a homogeneous large field as well as a small field irradiation with sharp dose gradients.

### PO-0894 Characterization of a multilayer ionization chamber for relative depth-dose curves in particle beams

A. Vai<sup>1</sup>, D. Maestri<sup>1</sup>, G. Magro<sup>1</sup>, A. Mairani<sup>1,2</sup>, E. Mastella<sup>1</sup>, A. Mirandola<sup>1</sup>, S. Molinelli<sup>1</sup>, S. Russo<sup>1</sup>, M. Togno<sup>3</sup>, S. La Civita<sup>3</sup>, M. Ciocca<sup>1</sup>

<sup>1</sup>National Center for Oncological Hadrontherapy CNAO, Medical Physics Department, Pavia, Italy; <sup>2</sup>Heidelberg Ion Beam Therapy Center HIT, Physics Department, Heidelberg, Germany; <sup>3</sup>IBA Dosimetry, Research and Development, Schwarzenbruck, Germany

### Purpose or Objective

To characterize a commercial multilayer ionization chamber (MLIC) detector primarily designed for measurements of integrated depth-dose (IDD) curves of both proton and carbon ion scanning beams, for QA purposes.

### Material and Methods

The commercial MLIC *Giraffe* (IBA Dosimetry, Schwarzenbruck, Germany) is a device developed for integrated depth-dose (IDD) curves measurements of a central axis pencil-beam, with FWHM ranging between 0.5 to 3 cm. Preliminary, water-equivalent calibration factory values were verified against the reference curves acquired with the Peakfinder water column (PTW GmbH, Freiburg, Germany). For both protons and carbon ion beams, the device was tested in terms of short- and long term repeatability, linearity and dose-rate independence. Accuracy of the detector was tested by evaluating range (distal  $R_{90}$ ) of IDD curves for a set of representative energies for both particle species against reference acquisitions in water. Two modulated proton spread-out Bragg peak (SOBP) were measured and range compared to theoretical values. To increase the native spatial resolution (approx. 2 mm), consecutive acquisitions were acquired respectively with and without build-up PMMA plates. The possibility of a double- (none + 1-mm WET thick) or triple-merge (none + 1-mm + 0.44-mm WET thick) was investigated in terms of accuracy.

### Results

Particle type dependent WET-offset values < 1 mm were measured, while chamber length was found in agreement to the value provided by the vendor. Measurements showed a high repeatability: mean relative standard deviation was within 0.5% for all channels and both particle types. Moreover, the detector response was linear with dose ( $R^2 > 0.99$ ) and independent on the dose rate. The mean deviation over the channel-by-channel readout respect to the reference beam flux was equal to 0.2% and 0.6% for protons and carbon ions respectively. The long-term stability of the gain calibration was very satisfying for both particle types, with values of channel mean relative standard deviation less than 1% for all the acquisitions performed at different times. Merging of measured data with and without 1-mm plate provided the right trade-off between accuracy and measurement time for QA purposes. Against reference curves in water, deviations in BP position were < 1 mm for both particle types in the whole investigated energy range. Similar results were found for modulated SOBPs against expected values.

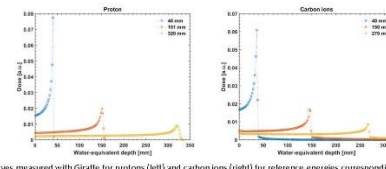


Figure. IDD curves measured with Giraffe for protons (left) and carbon ions (right) for reference energies corresponding to a nominal BP depth of 40-, 151-, 320-mm for protons and 40-, 150-, 270-mm for carbon ions. Curve values are normalized for equal integral dose.

Particle	Energy	Distal $R_{90}$ in water [mm]	Distal $R_{90}$ with Giraffe [mm]	$\Delta R_{90}$ [mm]	$\Delta R_{90}$ [%]
Mono-energetic pencil beam P	72.6 [MeV]	40.5	40.4	-0.1	-0.3%
Mono-energetic pencil beam P	148.8 [MeV]	152.4	152.3	-0.1	-0.1%
Mono-energetic pencil beam P	228.6 [MeV]	322.9	323.3	0.4	0.1%
Mono-energetic pencil beam C + ripple-filters	133.7 [MeV/u]	37.48	37.3	-0.2	-0.5%
Mono-energetic pencil beam C + ripple-filters	279.9 [MeV/u]	147.6	147.4	-0.2	-0.1%
Mono-energetic pencil beam C + ripple-filters	398.8 [MeV/u]	266.7	267.6	0.85	0.3%

Table. Distal  $R_{90}$  measured with the Giraffe device vs reference measurement in water with the Peakfinder for several IDD curves for both proton and carbon ion beams.

### Conclusion

To our best knowledge, this is the first time the detector has been used with carbon ion beams. The Giraffe was proved to be accurate, linearly responding with dose, precise and easy to handle for QA beam energy checks of both protons and carbon ion beams.

### PO-0895 Anthropomorphic breathing phantom with lung and liver components for testing MR-guided radiotherapy

E. Colvill<sup>1</sup>, M. Krieger<sup>1</sup>, Y. Zhang<sup>1</sup>, S. Safai<sup>1</sup>, D.C. Weber<sup>1</sup>, A.J. Lomax<sup>1</sup>, G. Fattori<sup>1</sup>

<sup>1</sup>Paul Scherrer Institute, Center for Proton Therapy, Villigen, Switzerland

### Purpose or Objective

Magnetic resonance (MR) imaging is widely recognised as a key element in many new frontiers of radiotherapy such as daily treatment adaptation and motion compensated dose delivery. Currently available phantoms for treatment quality assurance are however limited in realism and provide poor MR imaging texture. Therefore, renewed effort went to develop an anatomical model with good imaging contrast for testing new sequences and image-guided radiotherapy techniques.

### Material and Methods

We expand on an existing anthropomorphic breathing thorax phantom by making use of 3D printing to develop a new, anatomically correct, lung model with improved mechanical properties and tissue characteristics. The respiratory tract including trachea and main bronchi has been segmented from clinical data and used as inlet for ventilation. The lung infill modulated during printing to

mimic the lung parenchyma tissue, embedded with a solid region shaped from a patient's lung tumour and six nitroglycerine capsules as reference landmarks. The full internal mesh structure is covered with a thin layer of polyorganosiloxane gel making the complex pattern visible in MR imaging. The phantom is completed with a liver mould shaped by a thin casing of silicon, filled with gel and elastic plastic internal structures. Once fitted into a pre-existent rib-cage and skin models, stationary and 4D CT and T1 weighted MR imaging sequences were acquired to evaluate the structure visibility and mechanical properties of each component of the phantom.

### Results

Contrast of the 3D printed flexible material and the polyorganosiloxane gel was good on the T1 weighted MRI with image intensities of -500 - -400 and 0 - 100 respectively. The silicon liver casing had an image intensity range of 600 - 800. Good contrast is also confirmed on CT images with 0 - 150 HU for the printed plastic, 50 - 200 HU for gel and 650 - 800 HU for the silicon-based liver casing. The range of motion between exhale and inhale breathing phases evaluated as magnitude of the deformable image registration vector field was around 4 mm at the upper lobes and 15 mm in the inferiors. Similar deformation was seen for the liver and the surface skin, mechanically connected with the lung and ribcage (Figure 1.).

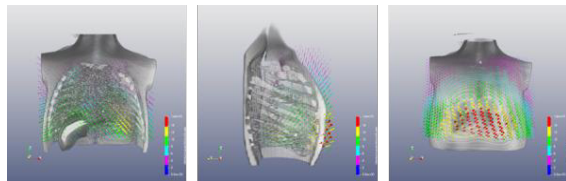


Figure 1 : Time resolved imaging of Lung Cancer phantom: volume rendering from lateral and frontal perspective of 4D MR images. Vector field describes the displacement of voxels between exhale and inhale breathing phases; scale in millimetres goes from no-motion (blue) to 16 mm (red). Coronal (left-hand panel), lateral (central panel) cuts and surface motion (right-hand panel).

### Conclusion

A ventilated thoracic dosimetry phantom has been updated to allow for enhanced imaging with MR and CT by the addition of new lung and liver models. These additions will allow for reliable validation of 4D imaging techniques and treatments as well as deformable image registration quality assurance.

### PO-0896 Motorised 3D printed water tank designed for measurements in MR linear accelerators

H.L. Riis<sup>1</sup>, P.F. Lange<sup>1</sup>, T.L. Schierbeck<sup>1</sup>, L. Gregorius<sup>1</sup>, F. Mahmood<sup>1,2</sup>, U. Bernchou<sup>1,2</sup>, C. Brink<sup>1,2</sup>, A.S. Bertelsen<sup>1</sup>  
<sup>1</sup>Odense University Hospital, Department of oncology, Odense, Denmark ; <sup>2</sup>University of Southern Denmark, Department of clinical research, Odense, Denmark

### Purpose or Objective

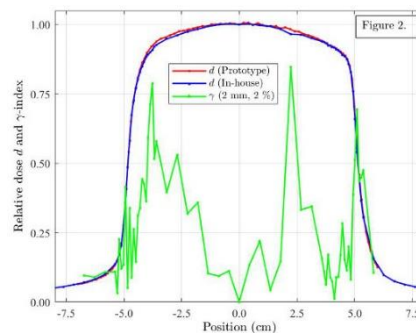
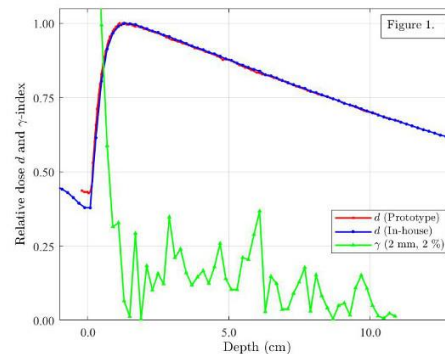
The recent introduction of MR linear accelerators (MR-linacs) for clinical treatment of patients opens new possibilities and challenges in radiotherapy. Beam data collection in a water tank for commissioning of dose planning systems for an MR-linac is more challenging compared to a conventional linear accelerator. The bore diameter, the isocentre height, the lack of room lasers, light field and cross-hair makes the setup of a water tank more complex on an MR-linac. The presence of a strong magnetic field in an MR-linac requires, for safety and handling, that water tanks to be used on MR-linacs are constructed of non-ferromagnetic materials. This work demonstrates that an MR-compatible motorized in-house designed water tank can be used at the high-field MR-linac Unity from Elekta based mainly on 3D printed parts.

### Material and Methods

An in-house designed and developed water tank was produced. The water tank consists of around 60 parts. Three ultrasonic motors manufactured by SHINSEI Corporation, toothed wheels, belts, aluminium spindlers, carbon rods and bearings were bought commercially. Arms and detector holders were printed in plastic using 3D printers. The outer dimension of the tank was 44×33×50 cm<sup>3</sup> with Perspex walls of 12 mm in thickness. Data collection uses Mephysto mc<sup>2</sup> (PTW) as interface in line with data collection on all our conventional accelerators. The data acquired using the in-house water tank was compared with data collected by Elekta, during commissioning, using a prototyped MR-compatible water tank developed in collaboration between Philips, Elekta and PTW. Scans in both water tanks were carried out using a PTW microDiamond detector as field detector and a reference detector. The scans were all performed on the same Elekta Unity MR-linac with 7 MV FFF x-ray energy characterised by a beam quality index of 0.70.

### Results

Depth dose as well as profile scans at gantry 0° at the depths 5 and 10 cm for the square field sizes 2×2, 5×5 and 10×10 cm<sup>2</sup> were carried out at a source-to-surface (SSD) distance of 133.5 cm (SAD=143.5 cm). In Figure 1 and 2, examples of the depth dose and cross-plane profiles at 10 cm are shown, respectively, for a 10×10 cm<sup>2</sup> field. The comparison is evaluated via  $\gamma$ -index calculations using the criteria 2 mm/2 %. The  $\gamma$ -index was found to be < 1 except in the build-up region of the depth dose curve, Figure 1. The two microDiamond detectors seem responding differently in the air to water region resulting in  $\gamma > 1$ . Figures show a good agreement between the data measured in the two water tanks.



### Conclusion

It is demonstrated that it is technically possible to replace a commercial non-MR-compatible water tank with an in-house MR-compatible printed water tank. This work also proves that the accuracy of an in-house built water tank is comparable to a prototyped MR-compatible tank. Furthermore, special requests on design and dimensions as well as an ability of repair and future improvements are in

our view an advantage of in-house fabrication of water tanks.

#### PO-0897 Development of an anthropomorphic lung phantom for imaging and radiotherapy

A. WEIDNER<sup>1,2,3</sup>, A. Runz<sup>1,4</sup>, W. Johnen<sup>1,4</sup>, G. Echner<sup>1,4</sup>

<sup>1</sup>DKFZ, Medical Physics in Radiation Oncology, Heidelberg, Germany ; <sup>2</sup>University of Heidelberg, Faculty of Medicine, Heidelberg, Germany ; <sup>3</sup>Mannheim University of Applied Sciences, Faculty of Informationtechnology, Mannheim, Germany ; <sup>4</sup>Heidelberg Institute for Radiation Oncology HIRO, National Center for Radiation Research in Oncology NCRO, Heidelberg, Germany

#### Purpose or Objective

Aim of this work is to develop an anthropomorphic, maneuverable and flexible lung phantom which can be used for end-to-end-tests in the radiation therapy. Furthermore, the lung phantom should be durable and the manufacturing process reproducible.

#### Material and Methods

As a basis for the lung phantom, anonymized CT image data of patients were used, which were downloaded from the following website

"<http://www.cancerimagingarchive.net/>". To achieve CT and MRI characteristics of human lung as well as the flexibility, a silicone is used which was optimized by means of its magnitude of elasticity, stability and imaging properties in MRI and CT. First, the DICOM data was opened in Medical Imaging Interaction Toolkit (MITK) and the lung was segmented and transformed into a virtual model. Based on this model the lung phantom could be constructed with the CAD software AutoCAD Inventor and the tool freeform. The internal structure of the lung, thus the bronchia and the alveola, were carried out by a grid structure. First an outer casting mold was constructed and 3D printed using the Objet30 Pro Polyjet 3D printer. To facilitate the internal structure, a core was constructed as an insertion for the outer casting mold. It consists of a grid structure with 5mm by 5mm by 5mm and was 3D printed with a water soluble polyvinyl alcohol (PVA) material by using the Ultimaker 3 Extended 3D printer (Fig. 1 (a) in red). To realize silicone model with an internal grid structure, the core was placed precisely in the outer casting mold and filed out with silicone. After the silicone was hardened, the silicone lung phantom can be removed from the outer casting mold and put into water to dissolve the core composed of water soluble PVA material (Fig. 1 (b)). Using a catheter, a tumor model was inserted into the lung phantom. Afterwards MRI and CT Imaging were performed using a T2 - sequence for the MRI respectively a thorax sequence for the CT imaging (Fig. 2).

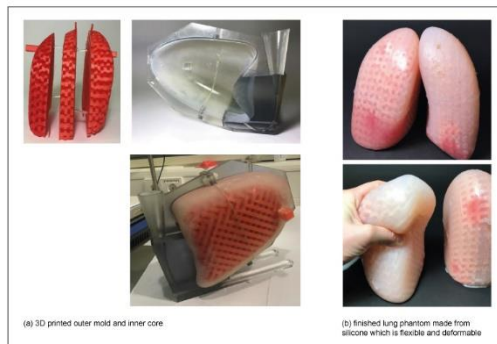


Figure 1: 3D print and finished lung phantom made of silicone

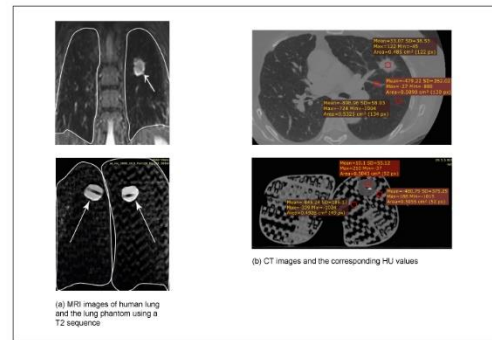


Figure 2: Comparison of human lung and lung phantom with the two imaging methods MRI and CT

#### Results

The HU values of the internal structure of the lung phantom indicate a deviation of 7% compared to the human lung (Fig. 2 (b)). The comparison of the MRI images ((Fig. 2 (a)) shows, that the contrast of the silicone lung phantom is the same as of a human lung.

#### Conclusion

A method to manufacture such an anthropomorphic lung phantom was developed, which allows a reproducible manufacturing process. In this manner the lung model can be used to perform experiments with an implanted tumor model. Due to the reproducibility determined by the steady geometry of the lung model and the consistent manufacturing process, it is possible to achieve constantly good requirements for experiments. Further on, a tumor model in the form of dosimetry gel could be inserted into the lung phantom and normal respiration could be simulated.

#### PO-0898 Advanced Diamond Dosimeter for quality Assurance in Radiotherapy

C. Talamonti<sup>1</sup>, K. Kanxheri<sup>2</sup>, S. Sciortino<sup>3</sup>, S. Lagomarsino<sup>4</sup>, L. Alunni Solestizi<sup>2</sup>, M. Caprai<sup>2</sup>, M. Ionica<sup>2</sup>, M. Casati<sup>5</sup>, S. Calusi<sup>1</sup>, M. Mangoni<sup>1</sup>, S. Pallotta<sup>1</sup>, L. Servoli<sup>2</sup>

<sup>1</sup>University of Florence, Dip Scienze Biomediche Sperimentali e Cliniche, Firenze, Italy ; <sup>2</sup>Istituto Nazionale di Fisica Nucleare, Sezione di Perugia, Perugia, Italy ; <sup>3</sup>University of Florence, Dip Fisica e Astronomia, Firenze, Italy ; <sup>4</sup>Istituto Nazionale di Fisica Nucleare, Sezione di Firenze, Firenze, Italy ; <sup>5</sup>Azienda Ospedaliera Universitaria Careggi, Fisica Medica, Firenze, Italy

#### Purpose or Objective

The aim of this study is to test a novel diamond device, 3DDOSE, to be used for high precision and high reliability machine quality assurance.

#### Material and Methods

3DDOSE is a polycrystalline chemical vapor deposited 3D diamond detector with graphitic in bulk electrodes, fabricated using a pulsed laser technique. Main advantages of such solution are the low voltage working point (tens of V), the all-carbon material presented to the photon beam, the relatively high sensitive volume with respect to the planar electrodes devices ( 0.125 mm<sup>3</sup> for 0.5 mm<sup>2</sup> area) allowing for an higher signal. Also being a volume detector, it should have small dependence from its orientation with respect to the beam. For these reasons it is a good candidate to a dosimeter for beam QA. Tests of the 3DDOSE diamond dosimeter, developed at University of Florence, were performed by means of an Elekta Synergy LINAC at the University Hospital of Florence with conventional 6MV photon beams. The 3DDOSE was placed at the isocenter and inserted in a precisely motorized PMMA phantom at a depth of 10cm with field size variable from 1.6x1.6cm<sup>2</sup> to 10x10cm<sup>2</sup> to be used for relative dose measurements. A very

preliminary dosimetric characterization was performed, the studied parameters were repeatability, response linearity versus absorbed dose and dose rate dependence. In-plane and cross-plane beam profiles were acquired with the setup configuration (SSD=90 cm and depth=10 cm). Beam profiles were acquired scanning the field with 0.1mm step. A comparison with single crystal diamond detector specifically developed for small field (PTW60019) was also performed. Signal ratios were obtained by considering the 3DDOSE charge value for different nominal field size. For each acquisition 100 cGy were delivered at a Dose rate of 430 cGy/min. The 3.2x 3.2 cm<sup>2</sup> FS was used as reference. Values were compared with PTW60019 and a plastic scintillator dosimeter.

**Results**

The 3DDOSE detector was tested for time stability and repeatability showing excellent performance with less than 0.6% signal variation. It also showed a linear response for low dose rates with a deviation from linearity of 2%. As an example in fig.1 the 0.8x0.8 cm<sup>2</sup> in-plane profiles for 3DDOSE, and the single crystal diamond PTW60019 were shown. In table1 the signal ratios as function of the nominal field size are reported and compared with PTW60019 and the plastic scintillator detector EXTRADIN W1 used as reference in the hospital. Even if this study is very preliminary and more works must be done, both on the detector contacts and in testing it for small fields measurements, the obtained results show a good agreement both with the single crystal diamond and the plastic scintillators and are good starting point for developing a new device for QA.

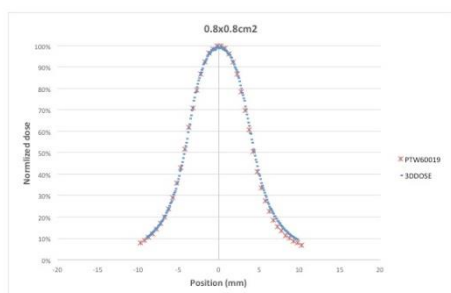


Fig.1 In-plane 0.8 x 0.8 cm<sup>2</sup> 3DDOSE (blue points) and PTW60019 (orange points)

Nominal field size	3DDOSE	PTW60019	W1	deviation 3DDOSE respect to W1	deviation PTW60019 respect to W1
1.6	0.901	0.915	0.910	-1.5%	0.5%
2.4	0.962	0.963	0.966	-0.1%	-0.3%
3.2	1.000	1.000	1.000	0.0%	0.0%
10.4	1.171	1.174	1.174	0.3%	0.0%

Tab.1 3DDOSE, PTW60019 and W1 Signal Ratios normalized to the FS 3.2 x 3.2 cm<sup>2</sup>. Values are compared with single crystal diamond PTW60019 and the plastic scintillator dosimeter Exradin W1

**Conclusion**

3DDOSE demonstrated its potentiality to be used as dosimeter for beam quality assurance, moreover a 3DDose array or a 2D matrix could be realized to speed up QA tests on clinical beams.

**Poster: Physics track: Dose measurement and dose calculation**

**PO-0899 Validation of dose calculation accuracy on daily cone-beam CT scans in the thoracic region**

L. Hoffmann<sup>1</sup>, M. Alber<sup>2</sup>, U.V. Elstrøm<sup>1</sup>, L.P. Kaplan<sup>1</sup>, D.S. Møller<sup>1</sup>

<sup>1</sup>Aarhus University Hospital, Department of Oncology-Medical Physics, Aarhus, Denmark ; <sup>2</sup>Heidelberg University Hospital, Department of Radiation Oncology-, Heidelberg, Germany

**Purpose or Objective**

Large anatomical changes may occur during RT of lung cancer. Daily image guidance combined with adaptive RT can correct for these changes. However, the quality of cone-beam CT (CBCT) is often regarded as problematic for dose computation. This study investigates the accuracy of daily dose calculation on CBCT using three different algorithms with the purpose of daily assessment of delivered dose.

**Material and Methods**

Stoichiometric calibration was performed for the CT and CBCT images. Twelve patients were set up using soft tissue matching based on daily CBCTs. All patients had a surveillance CT scan (sCT) at fraction 10. Target and OAR structures were delineated on the sCT and rigidly transferred to CBCT at fraction 10. The treatment plan was recalculated on the sCT and CBCT using the AAA, Acuros (Varian Medical Systems) and Monte Carlo SciMoCa (ScientificRT) algorithms. On CBCT, large regions with HU<950 were seen. Density overrides with HU=900 were performed for these regions followed by recalculation of dose (CBCTlift). Dose to 98% (D<sub>98</sub>), 2% (D<sub>2</sub>) and mean dose to CTV was analyzed in addition to dose to the hottest 1 cm<sup>3</sup> of the spinal cord and oesophagus (D<sub>1cc</sub>). Dose parameters were compared for the algorithms between sCT and CBCT or CBCTlift.

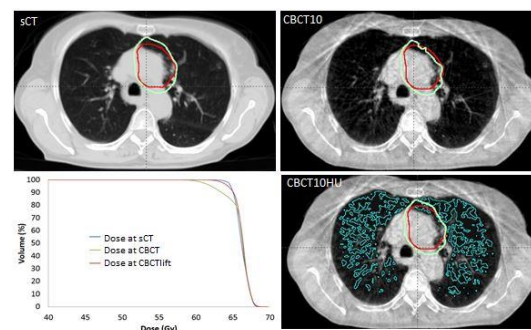


Fig 1. sCT and CBCT for one patient. CTV in red and the 95% isodose level in light green. The segmentation of all lung pixels with HU < 950 is shown in turquoise to the lower right. At sCT no lung pixels with HU < 950 was detected. Dose volume histogram for the CTV is shown to the lower right for dose calculated on sCT (blue), CBCT (green) and CBCT (red) with density override

**Results**

The CTV dose distribution calculated by Acuros is shown for one patient in Fig. 1. A very similar dose distribution is seen, except for underdosage of the CTV on the CBCT in the lung region with low HU density. Density override removes the discrepancy. In Fig. 2, a box plot for CTV dose difference between sCT and CBCT is shown for all 12 patients and all three algorithms. The median difference of the mean dose is <0.5% for all algorithms with a maximum deviation of 1.3%. The dose difference range between the 1<sup>st</sup> and 3<sup>rd</sup> inter quartile ranges (IQR) for D<sub>98</sub> is 6.4%, 5.0% and 2.7% for Acuros, SciMoCa and AAA, respectively. The deviations between sCT and CBCT mainly stem from lung regions with very low HU only in the CBCTs affecting primarily Acuros and SciMoCa. The density override in these regions reduces the IQR to 1.0%, 0.8%

and 0.9%, respectively, showing largest sensitivity to low HU numbers for the Acuros and SciMoCa algorithms. The IQR for  $D_2$  is nearly identical for all algorithms and <0.9% with median values <0.5%. Nearly no difference is seen between CBCT and CBCTlift for these near maximum doses. The median value of dose difference in  $D_{1cc}$  is <0.5% and the IQR is <1.6% for both oesophagus and spinal cord.

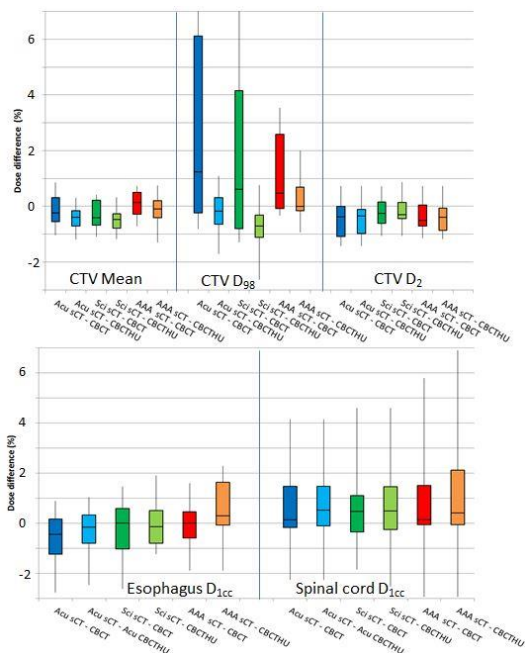


Fig 2: Difference in dose between sCT and CBCT presented as a boxplot. The box shows the range between 1<sup>st</sup> and 3<sup>rd</sup> inter quartile ranges, the vertical line in the middle indicates the median value and the whiskers range from minimum to maximum value.

**Conclusion**

Dose calculation on CBCT images calibrated by a stoichiometric metric and density override of HU values <950 results in clinically acceptable deviations for both target and OARs. A median deviation in target mean dose of <0.5% and IQR for  $D_{98}$  and  $D_2$  <1% was obtained for all algorithms. The lower quality in CBCT has a similar impact for all algorithms if HU override is applied. The CBCT calibration/modification method is readily implemented for automatic decision making for adaptive RT for all three dose computation algorithms

**PO-0900 The magnitude of dose calculation errors as a component of IROC phantom failures**

S. Edward<sup>1</sup>, M. Glenn<sup>1</sup>, P.A. Balter<sup>1</sup>, J.M. Pollard-Larkin<sup>1</sup>, C.B. Peterson<sup>2</sup>, R.M. Howell<sup>1</sup>, D. Followill<sup>1</sup>, S.F. Kry<sup>1</sup>  
<sup>1</sup>The University of Texas MD Anderson Cancer Center, Radiation Physics, Houston, USA ; <sup>2</sup>The University of Texas MD Anderson Cancer Center, Biostatistics, Houston, USA

**Purpose or Objective**

From 2012 to present, 17% of IROC SBRT spine and 15% of IROC moving lung phantom irradiations have failed to meet established acceptability criteria. In this study, we looked at the contribution of dose calculation errors to these failing results.

**Material and Methods**

We evaluated dose calculation errors by comparing the calculation accuracy of institutions' treatment planning systems (TPS) versus IROC-Houston's previously established [add reference] independent dose recalculation system (DRS). Each calculation was compared to the measured dose actually delivered to the phantom; cases where the recalculation was more accurate were interpreted as a deficiency in the

institution's TPS. 188 phantom irradiation plans (128 lung and 60 spine) were recomputed. The spine phantom simulates a highly modulated SBRT case; the lung phantom represents a low-to-none modulation moving target case.

**Results**

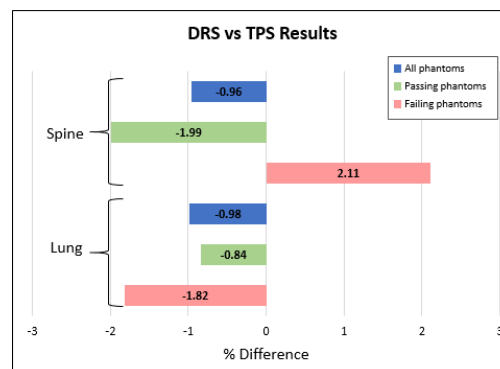
The results of the recalculation comparisons are shown in table 1. Overall, the DRS performed better than the TPS in about 52% of the spine cases. However, in the subset of phantoms that failed IROC criteria, the DRS was more accurate 93% of the time, indicating an error in the institution's dose calculation system. In contrast, the lung phantom DRS recalculations were better only 31% of the time for all cases and 28% of the time in failing lung phantoms, indicating that dose calculation errors were not substantially present.

More accurate calculation	Spine			Lung		
	Pass	Fail	Total	Pass	Fail	Total
DRS	17	14	31	35	5	40
TPS	28	1	29	75	13	88

Table 1. Performance of the dose recalculation system compared with institutions' TPS.

Figure 1 shows the differences between the accuracy of the DRS and TPS. These values represent the average percentage difference over all phantoms within each cohort. A positive difference % value indicates better DRS performance, meaning that the institution TPS is suboptimal. Correspondingly, a negative value indicates better TPS performance (which is the expected outcome if the TPS is well commissioned).

In terms of magnitude of average dose accuracy (instead of frequency), the overall TPS performance surpassed that of the DRS in all cases except the failing spine phantoms which were more than 2% more accurate with the DRS as compared to the institution's calculation. This reiterates the fact that for this phantom, a great majority of the error stems from the institutions' dose calculation systems.



**Conclusion**

For spine phantoms, the institutions' TPS performed better overall, but the DRS was remarkably better among the failing cohort. This indicates substantial room for improvement in many institutions' TPS calculations (likely beam models). In contrast, lung phantom calculations indicated no direct dependence of failure on dose calculation.

**PO-0901 2D solid-state array detectors: a technique for in-vivo dose verification at varying effective area**

G. Biasi<sup>1</sup>, K. Utitsarn<sup>1,2</sup>, M. Petasecca<sup>1</sup>, M. Carolan<sup>3</sup>, V.L. Perevertaylo<sup>4</sup>, W.A. Tomé<sup>3</sup>, M.L.F. Lerch<sup>1</sup>, T. Kron<sup>6,7</sup>, A.B. Rosenfeld<sup>1</sup>  
<sup>1</sup>University of Wollongong, Centre for Medical Radiation Physics, Wollongong, Australia ; <sup>2</sup>Lopburi Cancer Hospital, Department of Medical Services, Lopburi, Thailand ; <sup>3</sup>Wollongong Hospital, Illawarra Cancer Care Centre, Wollongong, Australia ; <sup>4</sup>SPA-BIT, n/a, Kiev,

Ukraine ; <sup>5</sup>Albert Einstein College of Medicine, Department of Radiation Oncology, New York, USA ; <sup>6</sup>Peter MacCallum Cancer Centre, Department of Physical Sciences, Melbourne, Australia ; <sup>7</sup>University of Melbourne, Sir Peter MacCallum Cancer Institute, Melbourne, Australia

### Purpose or Objective

In the present study, a novel technique for using a high-resolution (2 mm) 2D solid-state detector prototype 'MP512' in transmission mode (TM) is introduced. The technique aimed at using measurements in TM to calculate absolute dose at  $d_{max}$ , in a homogenous phantom of solid water, in effective area ( $A_{eff}$ ) which could be varied in size to best suit that of the monitored target.

### Material and Methods

The MP512 has 512 diode-sensitive volumes, 0.5 mm × 0.5 mm each, uniformly distributed with a pitch of 2 mm over a square area of 52 mm side. Measurements in TM were performed with the MP512 at a surface-to-detector distance (SDD) variable in the range from 0.3 cm to 24 cm and in dose mode (DM) at  $d_{max}$  in a homogenous phantom of solid water (Figure 1). We considered jaw-defined static square fields of 2 cm, 3 cm, 5 cm, 8 cm and 10 cm side produced by a 6 MV flattened beam delivered by a Varian Clinac® iX linear accelerator equipped with a Millennium 120-multi-leaf collimator (MLC). Measurements were used to derive a relationship between the response in DM and the response in TM as a function of SDD and field size. To verify the relationship, we calculated from measurements in TM at 4 cm and 24 cm SDD the response in DM in square fields of 1 cm and 4 cm side and in clinical step-and-shoot IMRT fields. For all IMRT plans, we used the Pinnacle's adaptive convolution-superposition (CS) algorithm implemented into the Pinnacle<sup>3</sup> treatment planning system (TPS) version 14 (Philips Medical Systems, Eindhoven, The Netherlands). Dose calculations were performed at  $d_{max}$  with a 2 mm grid. A gamma index analysis was used to cross-check our dose calculations with TPS calculations and with measurement in DM with the MP512 itself, with Gafchromic™ EBT3 films and with a Farmer ionization chamber.

### Results

Calculations in square fields of 1 cm and 4 cm side agreed with measured values within ±2%. Calculations in IMRT fields (Table 1) had, using acceptance criteria of 3%/3 mm, 2%/2 mm and 1%/1 mm respectively, gamma passing rates (%GP) greater than 96.89%, 90.50%, 62.20% at SDD 4 cm and greater than 97.22%, 93.80%, 59.00% at SDD 24 cm. When considering a 1%/1 mm acceptance criterion, lower %GP between our dose calculations and TPS calculations (Table 1) could be explained by factors such as sub-millimetre misalignments in detector positioning and dose averaging in TPS calculations over a 2 mm grid. This result emphasizes the importance of developing high-spatial resolution dosimetry detectors.

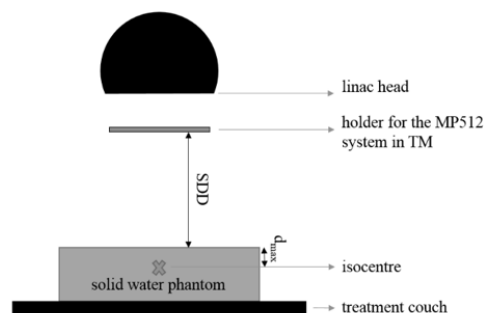


Figure 1. Use of the MP512 system in TM (not to scale).

Table 1. Gamma evaluation for IMRT plan dose calculation at SDD of 4 cm and 24 cm.

SDD [cm]	acceptance criteria											
	3%/3 mm				2%/2 mm				1%/1 mm			
	TPS	MP512, calc. vs EBT3	MP512, calc. vs MP512, meas.	MP512, calc. vs TPS	TPS	MP512, calc. vs EBT3	MP512, calc. vs MP512, meas.	MP512, calc. vs TPS	TPS	MP512, calc. vs EBT3	MP512, calc. vs MP512, meas.	MP512, calc. vs TPS
4	98.14%	96.89%	99.79%	90.50%	92.00%	98.59%	62.20%	69.40%	99.40%			
24	97.22%	97.53%	99.69%	93.80%	93.80%	97.69%	59.00%	71.00%	99.00%			

### Conclusion

We derived a relationship between the response of the MP512 in TM and in DM at  $d_{max}$ , as a function of SDD and field size. As at a different SDD corresponds a different  $A_{eff}$  at  $d_{max}$ , using this relationship measurement in TM could be performed at the SSD producing the  $A_{eff}$  which best fits the size of the monitored target. This study represented also a first step in the development of a real-time high-spatial resolution 3D dose reconstruction technique based on TM measurements with the MP512 prototype.

### PO-0902 The ACDS approach to measuring dose to bone and comparing to TPS reported dose to water and medium

J. Lye<sup>1</sup>, M. Shaw<sup>1</sup>, J. Lehmann<sup>2</sup>, A. Alves<sup>1</sup>, R. Brown<sup>1</sup>, C. Davey<sup>1</sup>, F. Kadeer<sup>1</sup>, J. Kenny<sup>1</sup>, J. Supple<sup>1</sup>

<sup>1</sup>Australian Radiation Protection and Nuclear Safety Agency, Australian Clinical Dosimetry Service, Melbourne- Victoria, Australia ; <sup>2</sup>Calvary Mater Hospital, Physics, Newcastle, Australia

### Purpose or Objective

In clinical dosimetry there is a difference in planned dose to a patient when dose to medium or dose to water is used. This is an issue that is particularly notable when looking at dose to bone treatments such as SABR/SBRT spine (4-12% differences depending on bone type and the definition of dose to water used by a particular TPS). It should also be considered when looking at the smaller (~1%) yet more widespread effect of using either dose to water or dose to muscle/adipose for soft tissue plans. The purpose of this work is to determine a consistent definition of dose and to apply this definition to report the differences between measurements in bone and calculated dose from TPS algorithms.

### Material and Methods

There are three commonly used definitions of dose:

Dose to medium as calculated by Monte Carlo algorithms (dose to medium-in-medium,  $D_{m,m}$ );

Dose to water with variable electron density as calculated by "conventional TPSs" (dose to water-in-water,  $D_{w,w}$ ); and

Dose to water converted from dose to medium using stopping powers: approximates dose to the water material of a cell in an otherwise non-water medium (dose to water-in-medium,  $D_{w,m}$ ).

Of importance is that the two different definitions of dose to water are not equivalent. Our main aim is for consistent definitions, and to use only one definition of absorbed dose to water. The ACDS defines absorbed dose as the dose to medium in a medium approximated by the average J/kg across a voxel (around 1-2mm<sup>3</sup>). Dose to water is then a particular case of this definition where the medium is water. Dose to water is defined as  $D_{w,w}$ . This gives a consistent definition of dose in TPS calculations and reference dosimetry and is closest to the previously used definitions of dose which clinical data is based on.

### Results

The ACDS measures dose to bone in the SABR spine audit with EBT3 film and microdiamond measurements in CIRS cortical and trabecular bone. These measurements are performed with a detector measuring in bone but

calibrated in dose to water in a water phantom. Monte Carlo modelling is required to convert the measurements to either dose to water ( $D_{w,w}$ ) or dose to medium ( $D_{m,m}$ ). The EGSnrc code was used to correct the raw measurements with a microdiamond in trabecular bone as shown in Figure 1. Before correction the measurements were higher than planned doses for both  $D_{w,w}$  and  $D_{m,m}$  with averages of -2.1% and -4.1% respectively. After correction the averages are -0.8% and +0.2% respectively.



**Figure 1** Summary of dose differences ((planned-measured)/measured) from spine point dose in trabecular bone.

For measurements in solid water, an algorithm dependent correction for dose to tissue is planned for TPS reporting dose to medium.

#### Conclusion

For measurements in bone, the ACDS applies Monte Carlo corrections to report  $D_{w,w}$  and  $D_{m,m}$  with a detector calibrated with dose to water. The ACDS does not calculate and report on Dose to water in medium, as determined by applying stopping power ratios to dose to medium calculations.

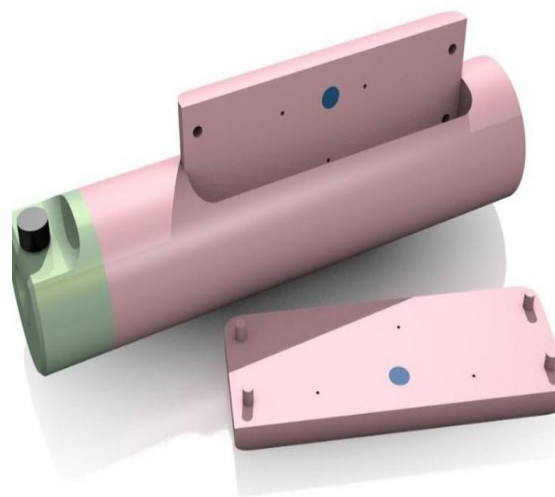
#### PO-0903 AcurosXB dose verification of ultra-small lung lesions with EBT-XD film in a heterogeneous phantom

M. Öllers<sup>1</sup>, A. Swinnen<sup>1</sup>, F. Verhaegen<sup>1</sup>

<sup>1</sup>Maastric Clinic, Medical Physics, Maastricht, The Netherlands

#### Purpose or Objective

Modern type 'c' dose calculation algorithms can predict dose for stereotactic treated lung tumors larger than 4cm<sup>3</sup> with an uncertainty up to 5% (Fogliata et al., 2017). However, the trend to treat tumors with volumes below 1cm<sup>3</sup> with hypofractionation poses a serious challenge even for type 'c' algorithms. Common recommendations for QA and dose verification in SBRT treatments are to use phantoms that are homogeneous: either water-equivalent (e.g. PTW RW3/Octavius, SunNuclear Delta4) or lung-equivalent materials (e.g. CIRS thorax). The CIRS4D thorax phantom provides a lung-equivalent film rod containing a water-equivalent spherical target (figure 1) that provides a more realistic verification set-up. Our aim was to evaluate the accuracy of the AcurosXB dose algorithm with EBT-XD film in a homogeneous and heterogeneous phantom for targets below 1cm<sup>3</sup>



#### Material and Methods

The PTW RW3 and CIRS4D thorax phantom were used to verify the dose distribution of 10 lung cancer patients with GTV volumes below 1cm<sup>3</sup>. EBT-XD film measurements were performed in the RW3 slab phantom at 5 cm depth. Treatment plan verification was performed in the CIRS4D phantom in a film rod containing a 0.1 cm<sup>3</sup> water-equivalent target. All measurements were performed on a 6MV Varian Truebeam STx linac for single fraction doses of 15 or 18Gy. Treatment plans were calculated in Eclipse 15.5 with the AcurosXB 15.5.11 dose algorithm. Films were analyzed using an EPSON 11000 XL film scanner and FilmQA Pro software (Ashland, USA), following a dedicated protocol (Lewis et al., 2012; Lewis et al. 2016).

#### Results

The average GTV volume for the 10 patients was 0.6±0.5 cm<sup>3</sup>. Regarding the homogeneous RW3 verifications, the average difference between maximum dose on film and maximum dose on the corresponding dose plane in the TPS was 2.6±1.6%. Recalculating the patient plans in the CIRS4D phantom in lung with an artificial lung tumor matching the patient tumor size yields differences between maximum dose on film and maximum dose on the corresponding dose plane in Eclipse up to 16.5% with an average overdose of 10.8±4.7%. In general, larger differences were found between measurement and predicted dose by the AcurosXB algorithm as tumor size decreased.

#### Conclusion

Dose verification of small lung tumors should be performed in a heterogeneous phantom incorporating a water-equivalent target that is of a comparable size to the original tumor to be treated. Current verification methods in homogeneous phantoms do not seem suitable for these challenging stereotactic lung treatments. The AcurosXB dose calculation consistently underestimates dose in (very) small lung tumors.

- Fogliata et al., Physica Medica, 44, 167-162, 2017
- Lewis et al., Med. Phys. 39(10), 6339, 2012
- Lewis et al., Med.Phys., 42(2), 643-649, 2016

#### PO-0904 Benchmarking of a module for Monte Carlo simulation of proton transport in the PENELPE code

N. Verbeek<sup>1,2,3</sup>, S. Smyczek<sup>1,3,4</sup>, J. Wulff<sup>1,3</sup>, C. Bäumer<sup>1,3,5</sup>, B. Timmermann<sup>1,3,5,6</sup>, L. Brualla<sup>1,2,3</sup>  
<sup>1</sup>University Hospital Essen, West German Proton Therapy Centre Essen WPE, Essen, Germany; <sup>2</sup>University of Duisburg-Essen, Faculty of Medicine, Essen, Germany; <sup>3</sup>University Hospital Essen, West German Cancer Center WTZ, Essen, Germany; <sup>4</sup>Heinrich Heine University

Düsseldorf HHU, Physics, Medical Physics, Germany ;  
<sup>5</sup>German Cancer Consortium DKTK, Radiation Oncology and Imaging, Heidelberg, Germany ; <sup>6</sup>University Hospital Essen, Department of Particle Therapy, Essen, Germany

### Purpose or Objective

PENH is a recently coded module for simulation of proton transport in conjunction with the Monte Carlo (MC) code PENELOPE [1]. The purpose of this work is to benchmark this module. PENH uses calculated differential cross sections for proton elastic collisions that include electron screening effects as well as nuclear structure effects. Proton-induced nuclear reactions are simulated from information in the ENDF-6 database [2], or from alternative nuclear databases in ENDF format (e.g., TENDL-2017).

### Material and Methods

Results from simulations with PENH are compared with simulation data obtained from TOPAS MC v3.1p2 [3] and RayStation 6 MC [4]. In all simulations a measurement-derived Fermi-Eyges [5] beam model, with nominal energy 225 MeV, was used. The beam model reproduced the phase-space of an IBA pencil beam (PB) scanning dedicated nozzle. The simulated geometry consisted of a water phantom with a 50 cm-thick layer of air upstream of it. Simulated dose results were compared to experimental data obtained with the MatriXX PT 2D detector (IBA Dosimetry) [6].

### Results

Depth dose profiles taken at varying radius from the central axis are shown in figure 1. The radial distance from the central axis at which the profiles are plotted appears above of each subfigure. All plots shown are normalized to the central axis dose at a depth of 3 cm. Excellent agreement is observed among the evaluated codes with the experimental data up to 3 cm from the central axis, that is, at the halo region where the dose drops three orders of magnitude from the maximum dose. Results from RayStation MC were smoothed with a moving average filter. Results from TOPAS MC coincide with experimental data up to six orders of magnitude below the maximum. Results from both RayStation and PENH qualitatively reproduce the experimental behavior in the low dose regions from three to six orders of magnitude below the maximum.

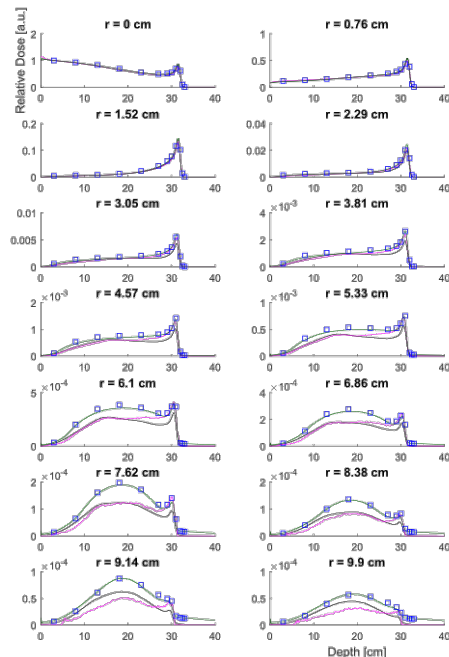


**Figure 1.** Dose Deposition of a 225 MeV Proton PB in a Water Phantom. Comparison between Measurement (squares), TOPAS MC (green line), RayStation MC (magenta) and PENH (black). The average standard statistical uncertainty of the dose distribution taking into account those bins that score more than 50% of the maximum dose is 0.02%, <0.1% and <0.02% for PENH/PENELOPE, RayStation and TOPAS MC, respectively. The combined uncertainty for the experimental data is 2.5%. In all cases uncertainty bars are smaller than the symbols used for experimental data.

### Conclusion

The outstanding agreement between TOPAS MC and experimental data is partly due to the fact that TOPAS MC takes into account neutron transport and PENH does not. However, the differences in the results produced by both codes cannot be fully ascribed to neutron simulation. They arise from the different physics models and tracking schemes. We conclude that the elaborate physics modeling of the PENELOPE/PENH code yields results consistent with measurements.

- [1] F. Salvat and J. M. Quesada, “Nuclear effects in proton transport and dose calculations” (to be published).
- [2] M. Herman and A. Trkov, ENDF-6 Formats Manual Nuclear Energy Agency July, 2010.
- [3] Perl J *et al.* TOPAS: an innovative proton Monte Carlo platform for research and clinical applications *Med. Phys.* 39 6818-37, 2012.
- [4] RaySearch Laboratories AB, Schweden. RAYSTATION 6 Reference Manual. RSL-DRS-6.0-REF-EN-1.0-2016-12-22, Dezember 2016.
- [5] B. Gottschalk. Techniques of proton radiotherapy: transport theory, *arXiv:1204.4470v2*, 2012.
- [6] IBA Dosimetry GmbH, Schwarzenbruck. MatriXX PT User's Guide. P-09-005-510-002 01, August 2012.

**PO-0905 Validation of a 4D Monte Carlo optimization and planning feature for CyberKnife lung treatment**  
 S. Trivellato<sup>1,2</sup>, E. Rondi<sup>1</sup>, S. Vigorito<sup>1</sup>, E. Miglietta<sup>3</sup>, F. Castellini<sup>3</sup>, G. Piperno<sup>3</sup>, A. Ferrari<sup>3</sup>, B.A. Jereczek-Fossa<sup>3,4</sup>, F. Cattani<sup>1</sup>

<sup>1</sup>IEO- European Institute of Oncology IRCCS, Unit of Medical Physics, Milan, Italy ; <sup>2</sup>University of Milan, Department of Physics, Milan, Italy ; <sup>3</sup>IEO- European Institute of Oncology IRCCS, Division of Radiation Oncology, Milan, Italy ; <sup>4</sup>University of Milan, Department of Oncology and Hemato-oncology, Milan, Italy

### Purpose or Objective

In thorax treatments, the management of respiratory motion is mandatory. An available treatment planning

system for the CyberKnife robotic radiosurgery system is offering a 4D treatment planning and optimization feature to take into account tissue motion recorded in a 4D computed tomography (4DCT). The aim of the study is to experimentally validate the 4D Monte Carlo (MC) dose calculation before its use in the clinical routine of not visible lung lesions when tracking is not feasible.

#### Material and Methods

A thorax-moving phantom was used to simulate 3 motion sets amounting to 9 patterns. Two of them were defined with a lesion velocity of 1 mm/s and 2.5 mm/s respectively. The last set was defined to simulate 3 patients' extracting surrogate motions from RPM files (Real-Time Position Management, Varian Medical Systems) while the superior-inferior lesion displacement was measured as the distance between the barycentre of the CTV in the full-inhale and full-exhale phases. The phantom was scanned for a static benchmark (SB) in absence of motion. An 8-respiratory phase binning was performed and images were imported in the Precision® Treatment Planning System (Accuray Inc.): 4D plans were optimized and calculated for all different motion patterns (MP Plans) with an 80% prescription to the PTV. All dose distributions were calculated with the Ray Tracing (RT) algorithm and then recalculated by a MC algorithm with a 1% uncertainty. Plans were delivered to the phantom with axial and sagittal films positioned in the lung insert. A local  $\gamma$ -analysis was performed with the FilmQA Pro software (Ashland) to quantitatively evaluate the agreement between the calculated and measured doses. Treatment plans were considered acceptable if the passing rate ( $P_\gamma$ ) was greater than or equal to 90%. Results for the 3 set of motions have been compared to evaluate the 4D module performances.

#### Results

$\gamma$ -analysis results for the SB plans are reported in Fig. 1. An acceptable  $P_\gamma$  is reached in axial and sagittal planes for the RT plan when the  $\gamma$ -criteria are 7%/3 mm and 8.5%/3 mm, respectively. The MC calculation showed an acceptable  $P_\gamma$  for 3%/3 mm  $\gamma$ -criteria in both directions. On the other hand, MP  $\gamma$ -analysis results are reported in Table 1 in terms of axial, sagittal and overall mean  $P_\gamma$ (3%/3 mm). The overall mean passing rate for the 3 motion sets are 85.3%, 59.9% and 66.2% for RT Plans; 92.7%, 95.9% and 84.1% for MC Plans.

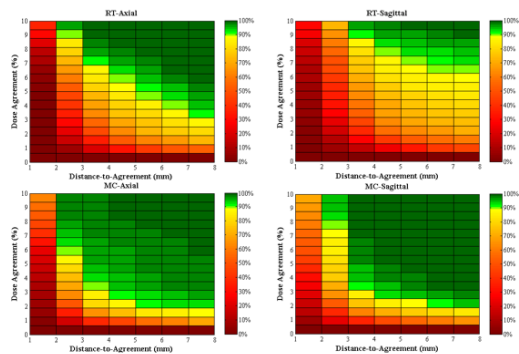


**Figure 1** Graphical representation of the passing rate in the axial and sagittal planes for the RT plan (top) and the MC plan (bottom). The color bar on the right associates the used colors with the percentage of gamma analysis passing pixels.

		RT	MC
Set 1	Axial	92.4%	93.9%
	Sagittal	78.1%	91.4%
	<b>Mean</b>	<b>85.3%</b>	<b>92.7%</b>
Set 2	Axial	68.4%	95.2%
	Sagittal	51.3%	96.5%
	<b>Mean</b>	<b>59.9%</b>	<b>95.9%</b>
Set 3	Axial	70.0%	83.3%
	Sagittal	62.3%	84.9%
	<b>Mean</b>	<b>66.2%</b>	<b>84.1%</b>

**Table 1** Percentage of pixels passing the 3%/3 mm criteria for various motion sets for RT and MC dose calculation.

#### Conclusion

The static benchmark has allowed a definition of minimum 3%/3 mm  $\gamma$ -criteria for following measurements because of the used experimental setup. The 4D feature allows obtaining an acceptable agreement between measured and calculated dose distributions in lung treatments when a MC calculation is performed. Future studies will follow to define a breathing-irregularity cut-off guaranteeing an acceptable passing rate for the third set. The RT calculation resulted in not acceptable accordance with measured dose distributions.

#### PO-0906 Perturbation techniques for optimizing IAEA phase spaces for different medical linacs

J.C. Martins<sup>1</sup>, R. Saxena<sup>1</sup>, S. Neppel<sup>2</sup>, A. Alhazmi<sup>1</sup>, M. Reiner<sup>2</sup>, C. Belka<sup>2</sup>, K. Parodi<sup>1</sup>

<sup>1</sup>Ludwig-Maximilians-Universität München, Chair of Experimental Physics - Medical Physics, Garching b. München, Germany ; <sup>2</sup>LMU Munich, Department of Radiation Oncology - University Hospital, München, Germany

#### Purpose or Objective

Monte Carlo techniques are very accurate for simulating dose distributions in radiotherapy, provided the model is based on detailed geometric information of the linac. Alternatively, validated phase space (PhSp) files (e.g. provided by IAEA) can be used, however these are available for a limited number of linac models. This work proposes a methodology to optimize an existing IAEA PhSp to produce fine-tuned machine-specific PhSp for an Elekta Synergy linac, by tuning the energy and momentum of the particles inside the PhSp.

#### Material and Methods

An Elekta Synergy linac coupled with an Agility collimator was modeled using Geant4. Due to unavailability of geometric information of the linac's head, the IAEA PhSp for Elekta Precise was used as surrogate. Percentage Depth Dose (PDD) and lateral profiles, for different field sizes and 6 MeV photon beams, were measured and simulated under the same conditions. The discrepancies between measurements and simulations were quantified in term of cost values. Initially, the information inside the PhSp was perturbed randomly, aiming at finding correlations with the simulated dose profiles. Subsequent perturbations were performed following identified correlations, in the direction of decreasing cost values. To

optimize the iterative process, the PhSp was cropped into smaller sections, depending on the field size and simulation configuration. The differences in the simulated results using cropped PhSp, in comparison to the corresponding results using the full PhSp, are under 3% (Figure 1), which assures no relevant information was disregarded. Small energy perturbations were applied to cropped PhSp and PDD were simulated. This process was repeated until a minimum cost value was reached and an optimal energy value was found. Next, the momenta of the particles in all three directions were perturbed, following identified constraints and statistical correlations between particle's momentum and lateral profiles. Two distinct optimal perturbation factors were found for particles' momentum in crossline and inline directions.

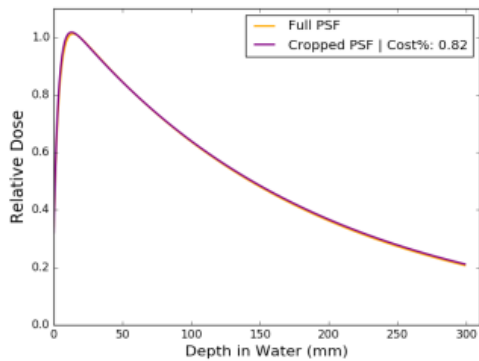


Figure 1 - Comparison of the PDD profiles simulated using the full PhSp (in orange) and the cropped PhSp (in purple), for the 10x10 cm<sup>2</sup> field. For this simulation, the cropping section corresponds to a 20 mm disc, meaning that only the particles positioned inside a 20 mm disc centered in the center of the full PhSp are included in the cropped PhSp. The cost value between both curves is 0.82%. If the cropping is performed correctly, the simulated curves performed with full and cropped PhSp should be similar, yielding a small cost value.

## Results

For validation, the optimal perturbation factors were finally applied to the entire PhSp for different field sizes. For the considered linac, an energy perturbation of 0.32 MeV results in PDD cost values under 1.5% for all fields considered, and improves cost values for lateral profiles in the inline direction (Figure 2). Perturbation factors of 0.61% and 0.05%, when applied separately to the momenta of particles in the crossline and inline direction respectively, yield cost values below 3%. Several approaches to merge both factors and investigate the method with different beam energies are under evaluation.

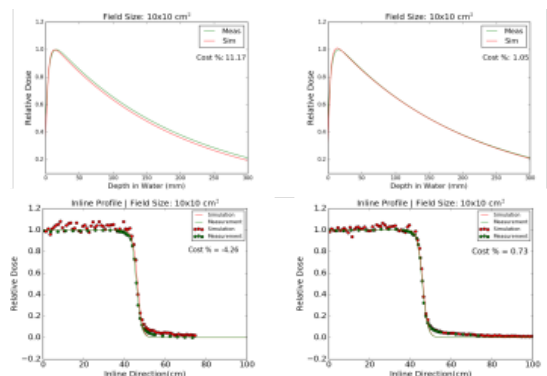


Figure 2 – Percentage Depth Dose (PDD) and Inline profile for a 10x10 cm<sup>2</sup> field (A) before energy optimization and (B) after energy optimization. A better agreement between measured and simulated profiles can be qualitatively seen after energy optimization. Quantitatively, cost values decreased from 11.17 to 1.05 % for PDD and from 4.26% to 0.73% for inline profile.

## Conclusion

A methodology for optimization of an existing PhSp was developed, enabling generation of machine-specific PhSp

based on validated IAEA PhSp. It offers an alternative when neither geometric details nor validated PhSp are available for a specific machine.

**PO-0907 Gafchromic EBT3 film for absolute dosimetry in proton therapy based on averaging of beam quality**  
 A. Resch<sup>1</sup>, P. Heyes<sup>1</sup>, H. Fuchs<sup>1</sup>, D. Georg<sup>1</sup>, P. Hugo<sup>2</sup>  
<sup>1</sup>Medizinische Universität Wien, Department of Radiotherapy and Christian Doppler Laboratory for Medical Radiation Research for Radiation Oncology, Vienna, Austria ; <sup>2</sup>MedAustron Ion Therapy Centre, Medical Physics, Wiener Neustadt, Austria

## Purpose or Objective

Gafchromic EBT3 films are a relevant dosimeter for proton therapy due to their high spatial resolution and near water equivalence. Currently their energy dependent relative effectiveness (RE) limits their usage for absolute dosimetry in particle therapy to the beam quality (e.g. the average linear energy transfer (LET)) at calibration. Previously, beam quality correction factors have been proposed based on a fluence averaging over the mixed charged particle field. In this study we investigate the RE for varying energy distributions to provide experimental evidence for a suitable averaging method.

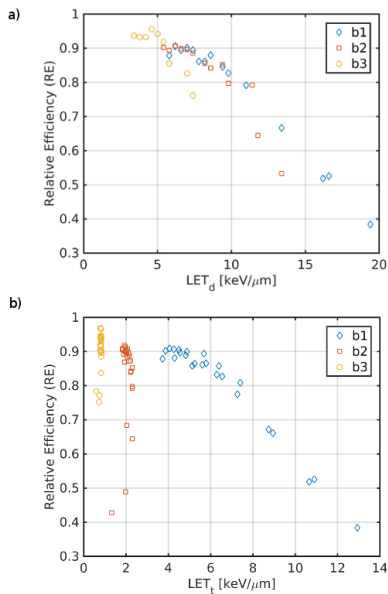
## Material and Methods

The RE as a function of depth was experimentally characterized for two beam types, mono-energetic (initial beam energy) and spread-out Bragg peaks (SOBPs). The initial beam energies ( $E_0$ ) of three single-energy fields were 62, 148 and 252 MeV. Three constant-dose SOBPs ( $E_0$  ranging from 62 to 68 MeV) were created with different energy distributions by superimposing a fraction of low LET protons ( $E_0 = 252$  MeV). Beam 1 (b1) consisted only of the SOBP. In beam 2 (b2) approximately 50% of the initial fluence and in beam 3 (b3) approximately 50% of the dose was contributed by the low LET beam. To ensure lateral charged particle equilibrium a field size of 7x7cm<sup>2</sup> was used.

EBT3 films were calibrated in a low LET region, in the entrance plateau region of a single-energy 179.2 MeV proton beam, for several dose levels. Gate/Geant4 Monte Carlo (MC) simulations employing a validated beam model were used to calculate the absorbed dose to water as well as dose- (LET<sub>d</sub>) and track-average LET (LET<sub>t</sub>). Dose simulated with MC was normalized to measurements with a plane parallel ionization chamber in the SOBP. The RE of the EBT3 response was calculated as the ratio of the film dose relative to MC simulated dose.

## Results

The RE was found to be below unity except for the 62 MeV beam at around LET<sub>d</sub> = 6 keV/μm (corresponding to points shortly before the Bragg peak). RE as a function of LET<sub>d</sub> of all beams was similar up to approximately 5 keV/μm. In Fig.1 the measured RE is shown as a function of LET<sub>d</sub> and LET<sub>t</sub> for the 3 SOBP beams. The RE of b1 to b3 was comparable but differed at high LET<sub>d</sub>. The same experimental RE (but with smaller LET binning) expressed as a function of LET<sub>t</sub> revealed the limitations of the concept of fluence averaging, as there was no one-to-one correlation of LET<sub>t</sub> and RE for beams b2 and b3. The LET<sub>t</sub> for b2 and b3 hardly increased over depth and hence could not reflect the decreasing RE over depth.



## Conclusion

Our experiments indicate that a fluence based beam quality correction function for EBT3 films may be limited in its applications for intensity modulated proton therapy. At high LET there was also a tendency of the RE-LET<sub>d</sub> relation to differ for different initial beam energies and fluences. A single parameter may not be sufficient to represent beam quality with respect to film response. Current work in progress is to develop a formalism for RE of EBT3 film response.

## PO-0908 Determination of surface dose in pencil beam scanning proton therapy

A. Kern<sup>1,2,3</sup>, C. Bäumer<sup>1,3,4</sup>, K. Kröninger<sup>2</sup>, L. Mertens<sup>2</sup>, B. Timmermann<sup>1,3,4,5</sup>, J. Walbersloh<sup>6</sup>, J. Wulff<sup>1,3</sup>

<sup>1</sup>University Hospital Essen, West German Proton Therapy Centre Essen WPE, Essen, Germany ; <sup>2</sup>Technical University Dortmund, Experimental Physics IV, Dortmund, Germany ; <sup>3</sup>University Hospital Essen, West German Cancer Center WTZ, Essen, Germany ; <sup>4</sup>German Cancer Consortium DKTK, Radiation Oncology and Imaging, Essen, Germany ; <sup>5</sup>University Hospital Essen, Department of Particle Therapy, Essen, Germany ; <sup>6</sup>Materialprüfungsamt NRW, Strahlenschutz, Dortmund, Germany

## Purpose or Objective

Quantification of surface dose within the first few hundred μm is challenging, albeit of large interest for proton therapy to study dose effects in the skin. Treatment planning systems are typically limited in their ability to calculate skin dose accurately. Experimental determination on the other hand is affected by the detectors' volume and in case of ionization chambers by the entrance wall. Aim of this study is the estimation of the absorbed dose at and around depth of 70 μm according to ICRU [1] with different dosimetric approaches for surface dose in proton pencil beam scanning.

## Material and Methods

Four different detectors were tested for determination of surface dose in water: EBT3 GAFCHROMIC®, LiF:Mg,Ti TLDs, IBA PPC05 plane-parallel and PTW 23391 extrapolation chamber. The irradiation setup consisted of a monoenergetic extended proton pencil beam with 100 MeV, 150 MeV and 226.7 MeV. Radiochromic films are used within a vertical stack and in wedge geometry and analyzed/calibrated with FilmQA Pro™ (triple channel dosimetry). The extrapolation chamber PTW 23391 was

used as a conventional ionization chamber with a fixed electrode gap of 2 mm. Three Kapton® entrance windows with the thicknesses of 25 μm, 50 μm and 75 μm were employed. TLDs provided as powder pressed onto a piece of aluminium. TOPAS [2] in version 3.1.2 was used to model an IBA PBS Nozzle and score dose to water in voxels of 5x5x5 mm<sup>3</sup> within a cubic phantom.

## Results

Both figures show the relative dose, normalized to a reference depth of 3 cm for the various detectors as a function of depth for 150 MeV. The results in figure 1 show the proton build-up effect. The two ionization chambers, the TLDs and the combination of film and wedge have good agreement with each other, whereas TOPAS and the film stack can deviate from these by up to 1 %. The errors of the mean value are within 1-2 ‰, except for the TLDs, which show larger deviations of up to 2.3 ‰. From the extrapolation chamber and TLD measurements and TOPAS calculations respectively, the skin dose at 70 μm amounted approx. 87 % of the dose at reference depth of 3 cm, see figure 2.

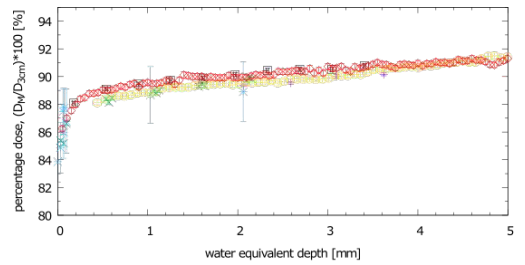


Figure 1: Percentage dose within the first 5 mm of water equivalent depth for 150 MeV

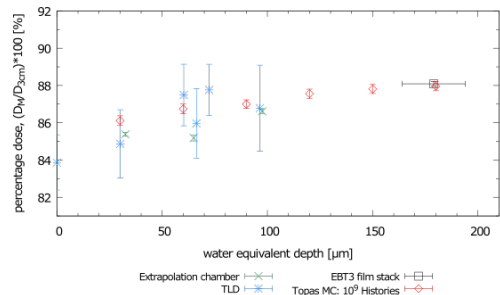


Figure 2: Percentage dose within the first 200 μm of water equivalent depth for 150 MeV

## Conclusion

All measurement methods show a good agreement within the first 5 mm. With the extrapolation chamber, the TLDs and the EBT3 film, data in the micrometer range can be measured. The extrapolation chamber shows the smallest uncertainties and the largest dynamic range. The TLDs have the largest uncertainty. TOPAS MC reproduces the experimental results. With regard to the skin dose, it can be noted that at 70 μm it amounts to approx. 87 % of the total dose from the reference depth in 3 cm. Furthermore, a dose increase of 4 % can be observed in the first 200 μm.

## References

- [1] ICRU. 1985. "Determination of dose equivalents resulting from external radiation sources." Report No. 39, International Commission on Radiation Units and Measurements
- [2] Perl J et al. 2012. "TOPAS: An innovative proton Monte Carlo platform for research," Med. Phys. 39 6818-37

## PO-0909 Development and experimental validation of a user code for time-resolved Monte Carlo simulations

P. Sibolt<sup>1</sup>, C.E. Andersen<sup>2</sup>, C.F. Behrens<sup>1</sup>, R.O. Cronholm<sup>3</sup>, E. Heath<sup>4</sup>

<sup>1</sup>Herlev & Gentofte Hospital, Radiotherapy Research Unit- Department of Oncology, Herlev, Denmark ;

<sup>2</sup>Technical University of Denmark, Center for Nuclear Technologies, Roskilde, Denmark ; <sup>3</sup>Skåne University Hospital, Department of Radiation Physics, Lund, Sweden ; <sup>4</sup>Carleton University, Carleton Laboratory for Radiotherapy Physics, Ottawa, Canada

#### Purpose or Objective

Due to intra-fractional motion in the abdominal and thoracic region of cancer patients, there is a need for solutions to accurately calculate external x-ray beam radiotherapy dose in four dimensions with synchronization between the dynamic beam configuration and deforming anatomy. In order to facilitate determination of time-dependent accuracy of advanced radiotherapy techniques, there is furthermore a need for the advanced dose calculation solution to be time-resolved. The aim of this project was to develop and experimentally validate a user code for time-resolved Monte Carlo (MC) calculations of dose delivered to a dynamic thorax phantom.

#### Material and Methods

Time-resolved Monte Carlo simulations were based on the previously developed 4DdefDOSXYZnrc/EGSnrc MC user code, which scores dose in a time-varying deformable geometry. To improve efficiency of the simulations, photon cross-section enhancement (XCSE) was implemented in a region surrounding the voxel in which dose was scored. One three-dimensional conformal radiotherapy (3DCRT) plan and one volumetric modulated arc therapy (VMAT) plan (both 6 MV) were optimized on and delivered to a set of static and dynamic configurations of an in-house developed dynamic thorax phantom. Time-resolved MC calculations using linac logfile based input files were synchronized with and compared to measurements using a fiber-coupled organic plastic scintillator detector (PSD). Measurements and calculations were conducted in the center of a spherical tumor (PMMA) embedded in a motion controlled cylindrical lung insert (balsa wood), laterally positioned in the body (PMMA) of the thorax phantom.

#### Results

Using the time-resolved MC code with a XCSE factor of 8 and binning the data to a resolution of 100 ms, a statistical uncertainty of approximately 2% was achievable. Comparison with PSD measurements revealed cases with disagreements in low-dose regions and narrow dose peaks, which are attributed to uncertainty in the position of the PSD and currently under investigation. However, a majority of the results indicated good agreement; first of all in the accumulated dose (in most cases within 2-3%) and secondly in the dose as a function of time as indicated by agreements in temporally resolved dose gradients. This applies for both the 3DCRT and VMAT techniques applied to the set of phantom configurations investigated.

#### Conclusion

A novel user code for time-resolved MC calculations of dose delivered to a deforming anatomy was developed and initial validation included indications of good temporal agreements in detecting dose gradients compared to PSD dosimetry in a dynamic thorax phantom. The solution has high potential in assisting in the detection of underlying causes to deviations detected in the accumulated dose as delivered by advanced motion managed radiotherapy techniques.

#### PO-0910 Lumbosacral proton therapy treatment of a patient with large spine metal implants

C. Peucelle<sup>1</sup>, A. Gérard<sup>1</sup>, D. Maneval<sup>1</sup>, M. Vidal<sup>1</sup>, A. Falk<sup>1</sup>, J. Héroult<sup>1</sup>

<sup>1</sup>Centre Antoine Lacassagne, Radiotherapy, Nice, France

#### Purpose or Objective

Metal implants complicate radiotherapy delivery by creating artifacts in CT images. Artifacts, as well as CT-number inaccuracy of very high-density material, may affect range calculation in the TPS for proton therapy and

result in major uncertainties in the delivered dose. Therefore, presence of metal implants is often a determining criterion in deciding to contraindicate proton therapy. This work reports the implemented strategy at the Mediterranean Institute for Proton Therapy (Nice, France) that allowed a patient with lumbosacral chordoma to benefit from proton therapy with the Proteus@ONE IBA system despite large metallic spine implants.

#### Material and Methods

The titanium alloy materials implanted in the patient (screws, nuts, rods) were provided by the manufacturer. The purpose was to quantify the shift in proton range when implants were placed in the beam and compare it to the shift calculated in the TPS used for proton pencil beam scanning treatments (RayStation). EBT3 Gafchromic films were interspersed among 1 cm-thick solid water slabs. The phantom was placed along the beam direction to assess depth dose distributions. Metal implants were positioned at the films entrance. The phantom was irradiated using a 120 MeV-proton scanned field covering a 20 cm<sup>2</sup> area (see figure 1). CT images of the set-up were obtained by scanning the phantom with and without the use of Smart Metal Artifact Reduction (MAR) reconstruction algorithm. In RayStation, irradiation conditions were reproduced based on the CT images. Bragg peak positions measured in the films for each implant were compared to the calculated ones in several configurations: using both uncorrected and MAR-corrected images; overriding or not the density of the delineated implants in the TPS; using both Pencil Beam and Monte Carlo algorithms.



Figure 1: EBT3 film irradiated parallel to the beam direction with a 120-MeV scanned proton field. The Bragg peak is shifted at the implants locations.

#### Results

In all cases, maximum error in TPS range calculation was 18.9 mm. In both CT series, the errors were minimized when implants density was overridden in RayStation. Although MAR-corrected images reduced beam hardening artifacts, they mis-reproduced implant dimensions. Hence, the following planning strategy was adopted: implants were delineated on uncorrected CT and contours were copied on MAR-corrected CT. The metal structure was overridden to a compound defined in RayStation based on Ti with a density of 4,42 g/cc. The range uncertainty parameter of robust optimization in the TPS was set to 5%. To account for maximal errors, 5 mm CTV-to-PTV margins were added to target and organs-at-risk near the implants.

#### Conclusion

In this work, evaluation of the maximum error in calculated proton range allowed to define adapted safety margins and create a robust treatment plan for a patient with lumbosacral chordoma with metal spine implants. The strategy implemented could be re-used in further proton therapy treatments. Besides, the use of a dual energy CT scan could improve the definition of high density structures CT-number, allowing reducing safety margins. Further investigations are ongoing, including absolute dose studies.

#### PO-0911 Choose before you measure. Setting gamma parameters for different QA devices on the basis of ROC.

M. Gizińska<sup>1,2</sup>, D. Błatkiewicz<sup>1</sup>, M. Bukat<sup>1</sup>, M. Gil-Ulkowska<sup>1</sup>, S. Maluszczyk<sup>1</sup>, A. Paciorkiewicz<sup>1</sup>, D.

Szałkowski<sup>1</sup>, A. Walewska<sup>1</sup>

<sup>1</sup> *Maria Skłodowska-Curie Memorial Cancer Center and Institute of Oncology, Medical Physics Department, Warsaw, Poland*; <sup>2</sup> *University of Warsaw Faculty of Physics, Department of Biomedical Physics, Warsaw, Poland*

### Purpose or Objective

An important question which should be answered prior to pre-treatment measurement is whether we want to check linac performance and detect all MLC errors or do we want to detect only those errors with clinically relevant impact on dose distribution. Some groups reported capability of different gamma parameters to detect clinically relevant errors. In our work we propose to use Receiver Operating Characteristic (ROC) in order to compare three different QA devices and choose gamma analysis parameters - especially tolerance level for percent of passing points (PPP).

### Material and Methods

Forty clinical IMRT plans (10 plans for each of tumor localizations: gynecology, prostate, brain, head and neck) were used in our study. All plans were clinically accepted and used for patients treatment. Sixteen known MLC errors of different magnitude were introduced for each plan. Dose distribution was recalculated in TPS (Eclipse AAA 13.6.23) on the patient CT. We created verification plan for all plans (original and with error) for three QA devices: ArcCHECK (SunNuclear), Octavius 729 (PTW), EPID (Varian). In order to do the bias-free evaluation, artificial measurements were created based on the dose calculations in TPS. Artificial measurement is a file created with a Python script on the basis of TPS dicom dose distribution which mimics the real measurement file. All artificial measurements were compared with original verification plan in adequate software (SNCPatient, Verisoft, Portal Dosimetry). Gamma analysis was performed with 5% threshold. Tested parameters were: 3mm/3%, 2mm/2%, 1mm/1% for both max and local evaluation. From dose comparison between the clinical plan and error plans we flagged each of 680 plans with Positive or Negative, where Positive meant clinically relevant change in PTV dose (i.e. D98%<95%, D2%>107% or  $\Delta D_{mean}>2\%$ ). While changing the gamma evaluation percent of passing points tolerance level we calculated sensitivity (True Positive Ratio) and specificity (True Negative Ratio) for all tested devices. ROC curves were evaluated for each site and gamma parameters.

### Results

In Figure 1 ROC curves for 3mm/3% max gamma evaluation are shown. Octavius 2D (with 729 array) performs slightly better than EPID. Area under ROC curve for ArcCHECK is smaller thus showing lower performance in detecting clinically relevant errors. It can be seen that 98% tolerance for Octavius and EPID does not balance between Sensitivity and Specificity. ROC curves obtained for 3mm/3% local gamma evaluation (Figure 2) show that ArcCHECK tolerance level should be set to 90% while EPID and Octavius tolerance levels should be 95%-98%. For these parameter all detectors performed similarly.

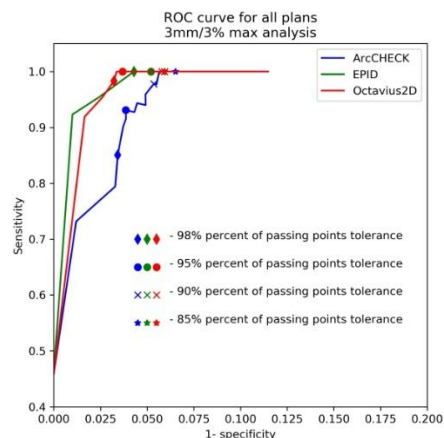


Figure 1. Comparison of ROC curves for 3 tested detectors for 3mm/3% max gamma parameters.

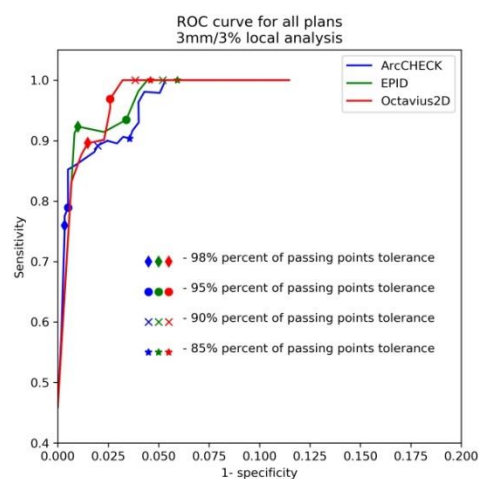


Figure 2. Comparison of ROC curves for 3 tested detectors for 3mm/3% local gamma parameters.

### Conclusion

ROC analysis for pre-treatment QA device can help in setting the tolerance level of PPP for gamma analysis aimed to detect clinically relevant dose distribution change. Our study showed that for 3mm/3% gamma evaluation ArcCHECK tolerance level should be set to lower value than that for Octavius and EPID.

### Poster: Physics track: Radiation protection, secondary tumour induction and low dose

#### PO-0912 Effect of Heart Anatomy on Radiation Related Cardiac Risk in the Childhood Cancer Survivor Study

R. Howell<sup>1</sup>, J. Bates<sup>2</sup>, L. Qi<sup>3</sup>, B. Hoppe<sup>2</sup>, C. Lee<sup>4</sup>, S.A. Smith<sup>1</sup>, K.C. Oeffinger<sup>5</sup>, L.S. Constine<sup>6</sup>, W.M. Leisenring<sup>7</sup>, D.A. Mulrooney<sup>8</sup>, T.M. Gibson<sup>8</sup>, G.T. Armstrong<sup>8</sup>, Y. Yasui<sup>8</sup>

<sup>1</sup>University of Texas at MD Anderson Cancer Center, Radiation Physics, Houston- TX, USA ; <sup>2</sup>University of Florida, Radiation Oncology, Gainesville- FL, USA ;

<sup>3</sup>University of Alberta-, Public Health Sciences, Edmonton- AB, Canada ; <sup>4</sup>Radiation Epidemiology Branch, National Cancer Institute, Bethesda- MD, USA ; <sup>5</sup>Duke University, Department of Medicine, Durham- NC, USA ;

<sup>6</sup>University of Rochester Medical Center, Department of Radiation Oncology, Rochester- NY, USA ; <sup>7</sup>Fred Hutchinson Cancer Research Center, Clinical Research Division, Seattle- WA, USA ; <sup>8</sup>St. Jude Children's Research Hospital, Department of Epidemiology and Cancer Control, Memphis- TN, USA

### Purpose or Objective

We previously estimated rates of severe/disabling, life-threatening, or fatal cardiac disease in 24,214 five-year survivors in the Childhood Cancer Survivor Study (CCSS). At doses  $\geq 10$ Gy, a linear dose-response relationship was observed between mean heart doses (MHD) and rates of any cardiac disease, coronary artery disease, and heart failure. For each individual, we reconstructed radiation-therapy-(RT)-treatments on age-specific phantoms. MHDs were calculated for a heart model located between thoracic vertebral bodies T5 and T9 (base heart model). Variability in heart anatomy was not considered, and its effect on the dose-response relationship is unknown. This study explored the impact of this variability on the dose response.

### Material and Methods

CCSS includes individuals diagnosed in 1970-1999 with median age at diagnosis and attained age of 7.0 (range 0-20.9) and 27.5 (range 5.6-58.9) years, respectively. Those treated with RT ( $n = 11,668$ ) received conventional RT without Computed-Tomography-(CT)-based planning; heart positions were unknown. To assess the possible range of heart positions, we documented the superior and inferior aspects of hearts from CT scans in a sample of contemporary pediatric RT patients ( $n=43$ ) and for International Commission on Radiological Protection (ICRP) reference phantoms (ages: 0,1,5,10,15). We classified ten unique heart positions (including that base heart). Nine hearts models were added to our age-specific phantoms. MHDs were calculated for heart models located in ten different positions for each individual. Dose-response relationships were evaluated using weighted piecewise-exponential models adjusting for attained age, sex, age at diagnosis, race, smoking history, year of diagnosis, treatment (alkylating agents, anthracycline, and an interaction between anthracycline and age at diagnosis) where individuals' MHDs were assigned in three ways: (1) base heart; (2) the 10 hearts weighted according to the distribution in the sample group; (3) age-based heart (the heart position of the ICRP phantom of the same age).

### Results

Shown in Figure 1(a-b) are scatter plots comparing the MHDs for the base heart model to the alternate dose-assignment methods; corresponding relative rate estimates of the three cardiac-disease rates by MHD are reported in Table I. The estimates are largely consistent between the established heart model using base heart model and the two alternate models. Consistent with our previous findings, here we report that the relative rates of cardiac toxicity increase with MHD  $\geq 10$  Gy monotonically ( $P<0.005$ ) and agree within 20% regardless of which heart model is used in the analyses.

Mean Heart Dose (Gy)	Any Cardiac Disease Relative Rate (95% CI)		
	Base Heart	10 Location	Age-based
None	Ref	Ref	Ref
0.1 – 9.9	0.8 (0.6 - 1.0)	0.8 (0.6 - 1.0)	0.8 (0.6 - 1.0)
10 – 19.9	2.0 (1.5 - 2.8)	2.1 (1.6 - 2.8)	2.3 (1.7 - 3.0)
20 – 29.9	2.8 (2.0 - 3.8)	3.1 (2.2 - 4.2)	2.8 (2.0 - 3.8)
> or = 30	6.2 (4.7 - 8.2)	6.2 (4.6 - 8.3)	6.8 (5.1 - 9.2)
Mean Heart Dose (Gy)	Coronary Artery Disease Relative Rate (95% CI)		
	Base Heart	10 Location	Age-based
None	Ref	Ref	Ref
0.1 – 9.9	1.0 (0.6 - 1.5)	1.0 (0.7 - 1.5)	1.0 (0.6 - 1.5)
10 – 19.9	2.8 (1.7 - 4.5)	2.9 (1.8 - 4.5)	3.2 (2.1 - 5.0)
20 – 29.9	3.3 (2.0 - 5.5)	3.7 (2.3 - 6.0)	3.3 (2.0 - 5.5)
> or = 30	7.2 (4.8 - 10.9)	7.1 (4.6 - 10.8)	7.3 (4.8 - 11.1)
Mean Heart Dose (Gy)	Heart Failure Relative Rate (95% CI)		
	Base Heart	10 Location	Age-based
None	Ref	Ref	Ref
0.1 – 9.9	0.7 (0.5 - 0.9)	0.7 (0.5 - 0.9)	0.7 (0.5 - 0.9)
10 – 19.9	1.6 (1.0 - 2.4)	1.8 (1.2 - 2.6)	1.8 (1.2 - 2.6)
20 – 29.9	2.9 (1.9 - 4.4)	3.4 (2.2 - 5.1)	3.3 (2.2 - 5.0)
> or = 30	6.5 (4.4 - 9.6)	6.2 (4.1 - 9.3)	6.8 (4.5 - 10.3)

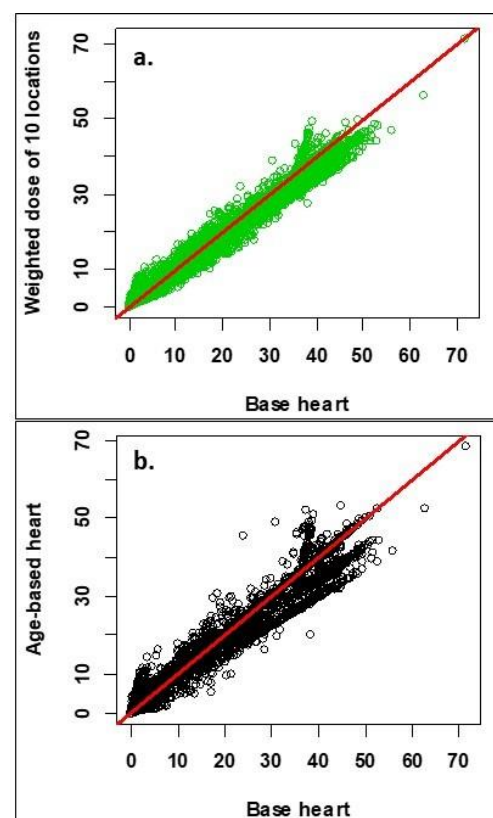


**Figure 1:** Scatter plots comparing mean heart doses (MHD) for base heart (red line) with MHDs for **a.** 10 hearts weighted based on sample group and **b.** age-based hearts (heart position of ICRP phantom of same age).

### Conclusion

These data indicate that the heart model used in our previous analysis is robust and representative of the various possible heart positions that may occur for patients in pediatric cohorts. Based on these data, we have confirmed the soundness of our dose response model for cardiac disease.

### PO-0913 Cancer risk after breast proton therapy considering physiological and radiobiological uncertainties

A. Raptis<sup>1</sup>, J. Ödén<sup>2</sup>, O. Ardenfors<sup>2</sup>, A. Flejmer<sup>1</sup>, I. Toma-Dasu<sup>3</sup>, A. Dasu<sup>1</sup>

<sup>1</sup>The Skandion Clinic, Radiotherapy, Stockholm, Sweden ; <sup>2</sup>Stockholm University, Department of Physics, Stockholm, Sweden ; <sup>3</sup>Stockholm University, Medical Radiation Physics, Stockholm, Sweden

#### Purpose or Objective

To investigate the risk of radiation induced second cancer following breast radiotherapy with protons, to evaluate the impact of the physiological movements and the radiobiological uncertainties and to compare the results with corresponding risks from photon treatments.

#### Material and Methods

Twelve thoracic patients who underwent CT scans in breath hold at inhalation, breath hold at exhalation and free breathing were included in this study. Photon and proton plans aiming at delivering 50 Gy (RBE) in 25 fractions to the delineated whole left breast were generated for all twelve patients assuming a constant RBE of 1.1 for protons. In order to evaluate the plans in terms of second primary cancer risk, two models were employed: a competition model and a plateau-shaped model. The impact of physiological breathing movement was assessed from the dose distributions corresponding to the different breathing phases. The proton treatment plans were evaluated assuming a RBE=1.1 or a variable RBE model, enabling an analysis of the proton radiobiological uncertainty and its influence on the calculated risk of radiation-induced second cancer. The influence of the uncertainty in  $\alpha/\beta$  values was also studied. The integral doses for both modalities and both risk models were calculated and their correlation with risk prediction was investigated.

#### Results

The oesophagus, the contralateral breast and the heart received practically 0 Gy (RBE) for all proton plans, whereas the photon plans resulted in mean doses less than 1.2 Gy to the organs. The lungs received the highest doses with both modalities, with an average of 1.45 Gy for the photon plans and 0.58 Gy (RBE) for the proton plans (RBE=1.1). The average risk of developing a second primary cancer in the lungs according to the competition model was estimated to 0.31% and 0.12% for the photon and proton plans, respectively. The calculated risk was lower for the proton plans compared to the photon plans for all OARs, risk models, breathing phases as well as when considering all the tested values of the parameters of the radiobiological models. The variable RBE model predicted slightly higher risks compared to the constant RBE of 1.1, although the risks were still lower than for the photon plans. The risks for the proton plans did not increase with the integral dose, this was however observed for the photon plans [Figure 1].

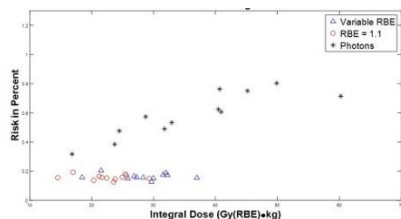


Figure 1: The relationship between integral dose and the total risk for second cancer predicted by the competition (bell-shaped risk) from the photon and proton plans for the patients included in the study.

#### Conclusion

The risk of radiation-induced second cancer following breast radiotherapy was lower for proton therapy in comparison to photon radiotherapy. The uncertainties in physiological movements and radiobiological parameters affected the absolute values of the risk estimates but not

the general trend of higher risk associated with photon therapy than for proton therapy.

### PO-0914 Patient specific organ dose evaluation in cone beam CT

A. Sardo<sup>1</sup>, F.R. Giglioli<sup>1</sup>, E. Gallio<sup>1</sup>, V. Rossetti<sup>1</sup>, C. Fiandra<sup>2</sup>, O. Rampado<sup>1</sup>

<sup>1</sup>A.O.U. Città della Salute e della Scienza di Torino, Medical Physics Department, Turin, Italy ; <sup>2</sup>University of Turin, Radiation Oncology Department, Turin, Italy

#### Purpose or Objective

Daily images from Cone Beam CT (CBCT) could deliver significant dose to the patient, which should be considered and evaluated. It is essential to associate the absorbed dose delivered by the imaging procedures to the treatment of each patient. Aim of this work is to calculate organ doses for patients undergoing CBCT when treated with radiotherapy.

#### Material and Methods

The system in use was an Elekta CBCT (XVI) and the protocols analysed were four: head, pelvis, chest and chest 4D with different parameters. The formula for organ dose calculation, was obtained from Rampado et al. (Med Phys 2016;43(5):2515-26), where dose to organs were evaluated by means of Monte Carlo simulation in phantom; the effect of patient size were also accounted for.

$$D_T = D_{W,1Ph} \cdot (D_T / D_{W,1Ph})_{tab} \cdot a \cdot e^{-bx}$$

In particular  $D_{W,1Ph}$  is the measured dose in a phantom for the specific protocol,  $x$  is the effective diameter of the patient,  $(D_T / D_{W,1Ph})_{tab}$ ,  $a$  and  $b$  are tabulated data from the article cited above. Patients were analyzed from march to june 2017. For each case were registered: the effective diameter from simulation CT, CBCT protocol, number of CBCT scans.

#### Results

Two hundred patients were considered and the mean doses and standard deviation for all the protocols are illustrated in the table .

Protocol	Organ	Mean ± SD [mGy]
H&N S20	Oralmucosa	28.9 ± 2.2
	Salivary glands	30.1 ± 2.3
	Respiratory airways	27.7 ± 2
	Spinal cord	18.8 ± 1.4
PELVIS M20 F1	Colon	425.6 ± 55.9
	Bladder	536.3 ± 57.2
	Ovaries	472.6 ± 84.2
	Prostate	401.0 ± 50.8
CHEST 4D SYMMETRY	Breast	66.4 ± 32.9
	Heart	45.5 ± 21.6
	Lung	38.8 ± 19.1
CHEST M20 F0	Breast	469.3 ± 119.8
	Heart	443 ± 111.0
	Lung	473.2 ± 118.5
CHEST M20 F1	Breast	439.2 ± 97.3
	Heart	550.6 ± 122.0
	Lung	477.3 ± 106.9

For head protocol, the mean CBCT doses were about 26.3±2.1 mGy for all organs. Instead, doses of about 458±60 mGy were evaluated for pelvis protocol. CBCT Doses for Chest 4D protocol were lower than other chest ones (about 50.3±25 mGy vs 461±115 mGy). This difference was due to number of CBCT scans/treatment fractions.

#### Conclusion

Dose from CBCT procedures should be accounted for; based on organ doses calculations, a program of dose optimization could be performed.

Poster: Physics track: Treatment plan optimisation: algorithms

PO-0915 Integral multi-scenario robustness evaluation of anatomical robust optimization in head and neck

M. Cubillos Mesías<sup>1</sup>, E.G.C. Troost<sup>1,2,3,4,5</sup>, F. Lohaus<sup>1,2,3</sup>, L. Agolli<sup>2</sup>, M. Rehm<sup>2</sup>, C. Richter<sup>1,2,3,4</sup>, K. Stützer<sup>1,4</sup>

<sup>1</sup>OncoRay - National Center for Radiation Research in Oncology, Faculty of Medicine and University Hospital Carl Gustav Carus- Technische Universität Dresden - Helmholtz-Zentrum Dresden - Rossendorf, Dresden, Germany; <sup>2</sup>Faculty of Medicine and University Hospital Carl Gustav Carus, Department of Radiotherapy and Radiation Oncology, Dresden, Germany; <sup>3</sup>German Cancer Consortium DKTK, Partner site Dresden, Dresden, Germany; <sup>4</sup>Helmholtz-Zentrum Dresden - Rossendorf, Institute of Radiooncology - OncoRay, Dresden, Germany; <sup>5</sup>National Center for Tumor Diseases NCT, Partner Site Dresden, Dresden, Germany

Purpose or Objective

Classical robust optimization considers uncertainties in patient setup and particle range. Usually plan robustness is evaluated from calculation of perturbed dose distributions based on the planning CT, without considering potential anatomical changes that may occur during the treatment course. Our aim was to compare the overall plan robustness of classical robust optimization (cRO) with the recently proposed anatomical robust optimization (aRO) based on an integral multi-scenario evaluation, considering all types of uncertainties including anatomical variations.

Material and Methods

Datasets for 20 head and neck cancer patients, including a planning CT and weekly control CTs, were analyzed. Two intensity-modulated proton therapy (IMPT) plans were calculated: cRO, using solely the planning CT, and aRO, including additionally the first two control CTs in the plan optimization. For the robustness analysis, perturbed dose distributions with random setup uncertainties and fixed range uncertainty values of -3.5%, 0% and +3.5% were generated, drawing for each fraction  $n$  a random number from a Gaussian distribution around 0 mm with a standard deviation of 2.5 mm for the isocenter shift in each cardinal direction ( $x_n, y_n, z_n$ ). Moreover, in each fraction  $n$  the correspondent weekly control CT was used to consider the anatomical changes during therapy. 33 single-fraction perturbed doses were calculated and summed to generate a perturbed whole-treatment dose distribution. The procedure was repeated 10 times for each of the three range uncertainty values, resulting in 30 perturbed dose distributions per plan (Figure 1).

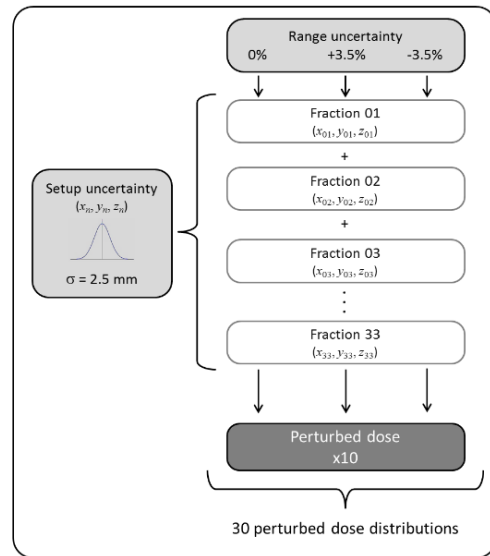


Figure 1. Workflow for the generation of perturbed dose distributions, generating random setup uncertainty values per fraction  $n$  with fixed range uncertainty values. In each fraction  $n$  the anatomy of the correspondent weekly control CT is considered.

Results

Both nominal plans fulfilled the clinical objective for target coverage ( $D_{98\%} \geq 95\%$  of the prescribed dose). The median values calculated from the 30 perturbed dose distributions for each patient showed a reduction in the target coverage for the cRO plan, with mean (minimum) values of 94.9% (88.1%) and 95.4% (89.3%) for the low- and high-risk CTV, respectively, in comparison with 96.6% (92.0%) and 96.8% (93.6%), respectively, for aRO (Figure 2a). The variation in CTV coverage between the 30 scenarios, i.e. the width of the perturbed dose distributions, was found to be larger for cRO plans, with median (maximum) values of 1.9 (8.3) and 1.4 (5.6) for low- and high-risk CTV, respectively, in comparison with 1.4 (3.4) and 0.9 (5.2) for aRO plans, respectively. Moreover, the cRO case showed reduced robustness in comparison with aRO for some patients, where certain scenarios violate the clinical objective, as shown in Figure 2b.

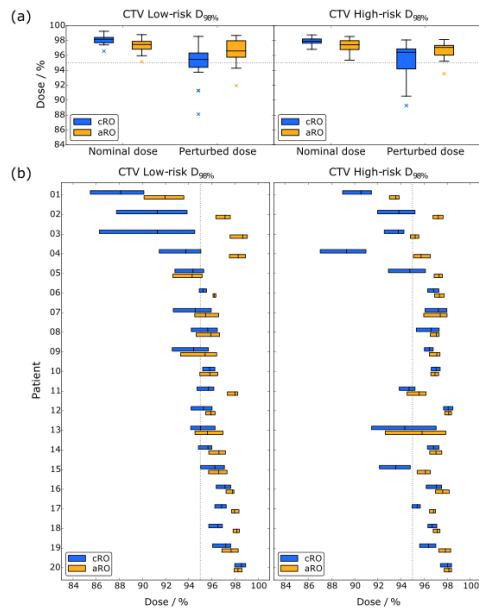


Figure 2.  
(a) Comparison of target coverage for cRO and aRO plans in nominal dose and medians of the perturbed dose distributions for all patients. The dashed line represents the clinical objective (95%).  
(b) Distribution of the generated perturbed dose distributions for target coverage per patient. Central line in each box represents the median value. The dashed line represents the clinical objective (95%).  
Abbreviations: cRO, classical robust optimization; aRO, anatomical robust optimization.

## Conclusion

Anatomical robust optimization showed superior plan robustness in comparison with the classical approach in a comprehensive multi-scenario evaluation. Anatomical variations play an important role in the overall plan robustness together with setup and range uncertainties, therefore their effect should not be underestimated or neglected.

## PO-0916 Energy layer switching sequence optimization algorithm for an efficiency proton arc therapy delivery

X. Ding<sup>1</sup>, X. Li<sup>1</sup>, G. Liu<sup>1</sup>, C. Stevens<sup>1</sup>, D. Yan<sup>1</sup>, P. Kabolizadeh<sup>1</sup>

<sup>1</sup>Beaumont Health, Proton Therapy Center, Royal Oak, USA

### Purpose or Objective

Spot-Scanning Proton Arc therapy (SPArc) has been a great interest of the society because of the improved dosimetric outcome. Due to the magnetic field hysteresis, it costs significant time in the energy layer switching especially switching from low energy to high energy layers. Thus, we presented a new energy layer and delivery sequence optimized SPArc algorithm (SPArc\_seq) to shorten the proton arc delivery time.

### Material and Methods

SPArc\_seq includes an energy layer sorting and control point re-sampling mechanism taking into account of proton arc delivery sequence through the gantry rotation. The SPArc\_seq plan is optimized for high to low energy delivery sequence instead of random layer switching which was introduced in the original SPArc algorithm. Both SPArc and the novel SPArc\_seq were tested on three kinds of disease sites: prostate, lung and brain cancer. Both plan group (SPArc and SPArc\_seq) were delivered at a fixed 0 degree gantry angle simulating the arc delivery sequence and energy switching in clock-wise gantry rotation. Total actual delivery time was recorded and dose measurements were performed using a 2D ion chamber array device, MatriXXONE, at 3cm depth.

### Results

With a similar proton arc plan quality, SPArc-seq optimized plan was able to successfully reduce 56% (beam-on time comparison: 330s vs 756s), 52% (beam-on time comparison: 305s vs 635s) and 55% (beam-on time

comparison: 256s vs 570s) of proton arc delivery time compared to SPArc in prostate, lung and brain cancer respectively. Absolute dose measurements showed within 2% difference compared to the plans. 2D Gamma Index (3%/3mm) showed more than 97% passing rate in both SPArc and SPArc\_seq.

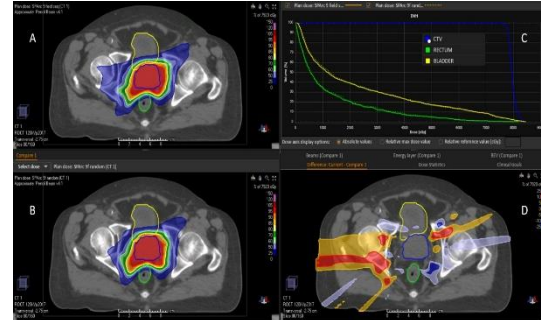


Figure 1. A representative axial view of the dose comparison. (A) SPArc\_seq; (B) SPArc; (C) DVH comparison. Solid line is the SPArc and dotted line is the SPArc\_seq; (D) dose difference between SPArc and SPArc\_seq

Table 1. SPArc Energy layer delivery sequence from gantry 0 to 360 clock-wise



## Conclusion

The new SPArc\_seq optimization algorithm is able to effectively reduce proton arc treatment delivery time by about half compared to the original SPArc algorithm. Such findings in the proton arc delivery efficiency improvement paves the road for future clinical implementations.

## PO-0917 Deep Convolutional Network with transfer learning for dose prediction in VMAT prostate treatments

P.G. Franco<sup>1</sup>, E.M. Ambroa<sup>2</sup>, J. Perez-Alija<sup>1</sup>, M. Ribas<sup>1</sup>, M. Colomer<sup>2</sup>

<sup>1</sup>Hospital de la Santa Creu i Sant Pau, Medical Physics, Barcelona, Spain; <sup>2</sup>Consorci Sanitari de Terrassa, Medical Physics Unit - Radiation Oncology, Terrassa, Spain

### Purpose or Objective

We believe that the use of Deep convolutional neural networks (DCNN) with transfer learning (widely used in other science fields with good results) offers tremendous opportunities in the field of Medical Physics. We propose its use in radiotherapy to identify suboptimal plans and guide plan optimization. We have focused the study in the prediction of rectum dose-volume histograms (DVH) for VMAT prostate patients.

### Material and Methods

We retrospectively collected data of 134 prostate patients treated with a simultaneous integrated boost VMAT technique (70 Gy and 50.4 Gy in 28 fractions to the prostate and lymph nodes respectively). QUANTEC dose-volume constraints were taken into account as a starting point for treatment planning. VGG-16 (DCNN, ImageNet Large Scale Visual Recognition Challenge 2014) was used as our network architecture. VGG-16 is a DCNN pre-trained with more than 1.2 million natural images of 1000 object categories (ImageNet image dataset). For image classification we dropped the last three fully connected

layers from the VGG-16 and added a new fully connected neural network to properly transfer learning to our data. Our data was split into training, validation and test sets (98, 26 and 10 patients in each set respectively). To apply this DCNN to our problem, for each patient we extracted the contour information included in the CT and feed this data to the modified VGG-16. The model was trained on single slices of the patient instead of a whole 3D image. DCNN output is a 2D rectum DVH for every slice. Rectum DVHs from our test set were compared to DVHs predicted by our model. An actual plan was considered suboptimal if the mean square error (MSE) of the prediction was greater than the MSE of the validation plus 2 standard deviations. If predicted DVH was better than the actual DVH a replan was carried out to study the cause of this discrepancy.

### Results

DCNN with transfer learning successfully predicted rectum DVHs for our test patients. The predicted DVH was comparable to the actual DVH except for two cases (20%) where the model predicted a substantially better DVH (Fig.1). In these two cases, replanning decreases doses to the rectum without worsening the PTVs or any organ at risk.

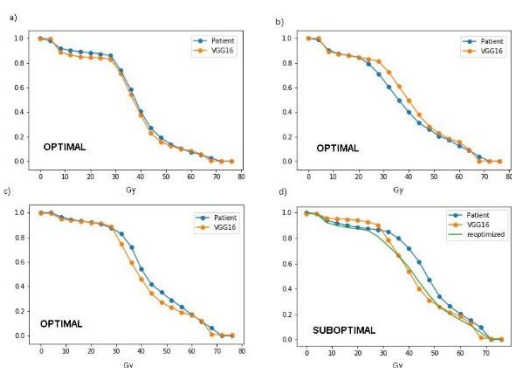


Figure 1. Predicted rectum DVH for 4 patients.

Table I shows a dosimetric comparison between the original plan (blue line), the predicted one (orange line) and the re-optimized plan (green line) for the suboptimal patients. Our replan strategy achieved an improvement of 28.7% and 15.0% in V40 for both patients.

		Dosimetric results comparison				
Patient	Plan	V40Gy (%)	V50Gy (%)	V60Gy (%)	V65Gy (%)	V70Gy (%)
1	Original plan	78.1	45.0	23.1	13.9	3.9
	VGG prediction	42.6	17.6	9.8	5.4	0.3
	Re-optimized plan	49.4	30.1	17.8	11.8	3.7
2	Original plan	71.8	40.4	20.1	13.7	4.8
	VGG prediction	48.0	23.7	14.4	8.2	0.5
	Re-optimized plan	56.8	30.1	15.5	9.8	2.8

Table I

### Conclusion

We successfully used a pre-trained DCNN to predict rectum DVH's for VMAT prostate patients, allowing for effectively detect suboptimal plans and guiding plan optimization to improve dose distribution. To our knowledge this is one of the first attempts to apply the transfer learning of DCNN to dose prediction in radiotherapy. Thus we demonstrate that transfer learning of DCNN is a feasible solution to the lack of training data in radiation oncology. Future work will include DVH prediction for the remaining organs at risk.

### PO-0918 Optimal parameters to perform the Pseudo Skin-Flash on VMAT on breast radiotherapy

M. Lizondo<sup>1</sup>, A. Latorre-Musoll<sup>2</sup>, N. Espinosa<sup>2</sup>, A. Coral<sup>2</sup>, C. Cases<sup>2</sup>, N. Jornet<sup>2</sup>, P. Carrasco<sup>2</sup>, P. Delgado-Tapia<sup>2</sup>, A. Ruiz-Martinez<sup>2</sup>, I. Valverde-Pascual<sup>2</sup>, M. Barcelo<sup>2</sup>, M. Ribas<sup>2</sup>

<sup>1</sup>Institut de Recerca Hospital de la Santa Creu i Sant Pau, Servei de Radiofísica i Radioprotecció, Barcelona, Spain ;

<sup>2</sup>Hospital de la Santa Creu i Sant Pau, Servei de Radiofísica i Radioprotecció, Barcelona, Spain

### Purpose or Objective

In breast radiotherapy, the use of dynamic techniques (IMRT, VMAT) usually include a skin flash region outside the body contour to ensure correct irradiation of CTV accounting for uncertainties in position, breathing or possible anatomical changes. In VMAT, the common approach consists in optimizing the VMAT plan on an extended CT including a virtual bolus out of the body contour in the area of the PTV.

We present a detailed method to obtain the optimal thickness and HU value assigned to this virtual bolus, regarding plan robustness and dosimetric impact of the strategy.

### Material and Methods

7 bilateral breast patients treated for whole breast radiotherapy were retrospectively selected for the study. For each patient, we defined 16 modified-CT (CT') by adding to the original CT (CT0) all combinations of width (0.5cm & 1.0cm) and HU (from -700 to 0, 100 HU steps) of the bolus.

We optimized a VMAT plan (RapidArc®, Varian Medical Systems, POv13.5.35, AAAv13.5.35) on the CT0 (*NoAction plan*) and on each CT' (*CT' plans*) by using the same optimization objective template per patient and a PTV excluding 5mm of skin. We recalculated CT' plans to CT0 by fixing MU (*CT0 plans*).

For the dosimetric impact of the strategy, CT' plans and CT0 plans were compared on the basis of doses to PTV (Dmean, D98 and D2) and doses to OARs, particularly to heart (Dmean, V30), lungs (V5) and liver (Dmean).

The robustness is assessed by shifting the isocenter 0.5cm and 1.0cm in the breathing direction, and recalculating CT0 plans and *NoAction plan* by fixing MU (*CT0-shifted plans*). *CT0-shifted plans* and *CT0 plans* were compared on the basis of D98 and D2 relative differences on the portion of the PTV in the buildup region (1cm-depth inner margin beneath the skin, PTV<sub>skin</sub>), which is likely to increase the sensitivity of the analysis.

Optimal parameters were those that maximized the plan robustness on CT0 and minimized dosimetric impact of this strategy.

### Results

All PTV dose indexes increased when the re-calculation was made on CT0. Minimum relative Dmean differences were found between -400 and -600 HU depending on the bolus thickness (Fig1). Doses to OARs are not significantly affected.

Regarding to robustness, for shifts of 1.0 cm there are significant differences between choosing a bolus thickness of 0.5 cm or 1.0 cm, which is not observed for shifts of 0.5 cm (Fig2). Best robustness is found for -500 HU and 1.0 cm thickness. It is worth noting that when no pseudo skin flash strategy is applied, relative dose differences up to 20% can be found.

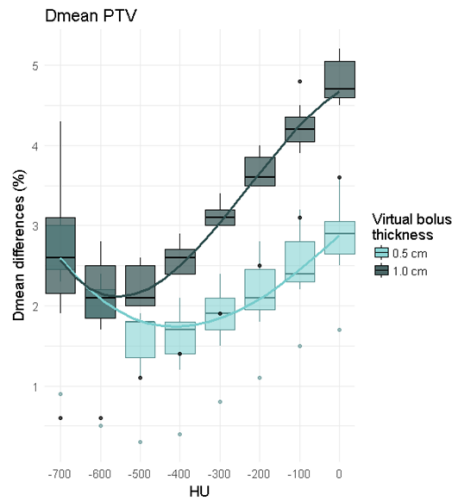


**Figure 1.** PTV Dmean relative variation between *CT* plans and *CT0* plans for each virtual bolus HU assignment.

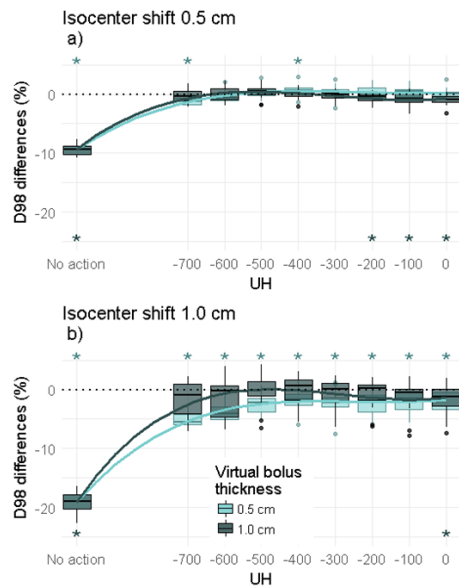


**Figure 2.** D98 relative variation between the *CT0*-shifted plans and *CT0* plans for each virtual bolus HU assignment and *NoAction* plan, evaluated on PTVskin. Asterisks on the top (related to 0.5 cm of virtual bolus width) and on the bottom (related to 1.0 cm width) inform when the corresponding boxplot is significantly different from zero (t-test, RStudio).

## Conclusion

A virtual bolus of 1.0 cm and a HU-value of approximately -500 HU would maximize plan robustness against movements up to 1.0 cm in the breathing direction. Additionally, this HU-value minimizes the dosimetric impact of the strategy. Therefore in most of the patients it will be no necessary to re-normalize the clinical treatment and if it was, it will be a minor change. The study has been focus at breast radiotherapy but same methodology could be applied on other locations.

## PO-0919 Automatic radiotherapy treatment planning using Particle Swarm Optimization

L.A. Künzel<sup>1</sup>, S. Leibfarth<sup>1</sup>, O.S. Dohm<sup>2</sup>, A. Müller<sup>2</sup>, D. Zips<sup>2,3</sup>, D. Thorwarth<sup>1,3</sup>

<sup>1</sup>Section for Biomedical Physics Department for Radiation Oncology, University Hospital Tübingen, Tübingen, Germany; <sup>2</sup>Department for Radiation Oncology, University Hospital Tübingen, Tübingen, Germany; <sup>3</sup>German Cancer Consortium DKTK partner site Tübingen,

and German Cancer Research Center DKFZ, Heidelberg, Germany

## Purpose or Objective

To investigate the potential of Particle Swarm Optimization (PSO) for automatic planning of VMAT radiotherapy (RT). The aim of this PSO is to formulate an optimal patient individual treatment planning problem, i.e. to define optimal planning constraints leading to the best achievable plan.

## Material and Methods

PSO is a statistical, collective and iterative optimization technique which uses the knowledge of each particle about its own best and the swarm's best position to update particle positions for each generation. For automatic RT planning, a particle is considered a plan with its position determined as a vector of planning constraints. To evaluate plan quality, i.e. determine the particle's best positions a scoring function was introduced, based on the sum of individual plan quality scores for dose-volume-histogram (DVH) parameters for planning target volume (PTV) and priority organs at risk (OAR). The plan quality score is defined in a way to increase if the DVH parameter fulfills planning goals and penalizes if the goals are violated.

Automatic treatment planning using PSO was tested for 8 postoperative prostate cases, with a prescribed dose of 66 Gy to the PTV in addition to two rectum and one bladder constraint. N=30 particles were initialized and the PSO was executed for m=100 generations. PSO and manually generated plans were compared dosimetrically with respect to the planning goals, visual inspection of dose distributions and DVHs.

## Results

PSO successfully proposed treatment plans comparable to manually optimized ones in all 8 cases. The mean (range) PTV *EUD* was 65.4 Gy (64.7-65.9) for manual and 65.2 Gy (64.8-65.6) for PSO plans, respectively. Also *D*<sub>98%</sub> for the PTV is slightly higher in manual plans, with 62.8 Gy (61.7-63.6) and 62.5 Gy (61.8-63.0), respectively. On the other hand, PSO plans achieve lower doses in rectum *D*<sub>2%</sub>, 67.0 Gy (66.6-67.5) vs. 66.2 Gy (65.8-66.5, p=0.008). Fig 1 provides an overview of all evaluated planning goals. On average, PSO proposed plans with better OAR sparing but inferior PTV doses. However, this compromise between PTV and OAR doses is directly related to the definition of the scoring function. According to the scoring function used in this study, manual plans had lower plan quality scores compared to PSO plans with -0.61 (-2.41-0.96) vs. 1.41 (-0.84-6.78).

Overall, good convergence of the planning goals and the plan quality score was observed with increasing particle generations (Fig 2a-b). As demonstrated by Fig 2c-d, PSO proposed comparable dose distributions.

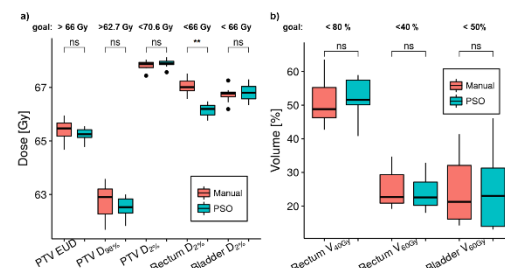


**Fig 1:** Boxplots and planning goals for all parameters evaluated by the plan quality score (Wilcoxon signed rank test, ns not significant, \* p < 0.05, \*\* p < 0.01, \*\*\* p ≤ 0.001).

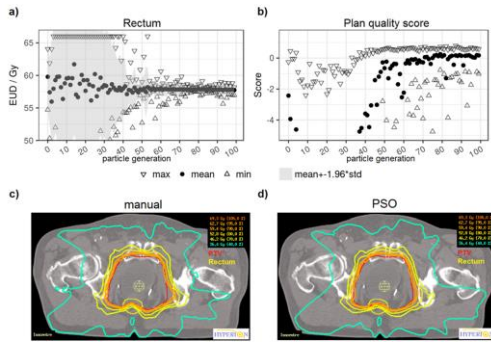


Fig 2: Case PC03: a) shows an example for the evolution of minimum, maximum and mean rectum constraint as a function of particle generation, with a shrinking search area and a stabilization of the mean constraint value. Similarly, the mean quality score converges towards a maximum value during PSO (b). Dose distributions of a representative slice for the manual and the PSO plan are provided in c) and d).

**Conclusion**

PSO allows for automatic generation of VMAT plans with comparable plan quality compared to manually optimized plans. However, further research is needed concerning optimization parameters and the optimal number of particles and generations to fully explore the potential of PSO for automatic planning. The plan quality score has to be further refined to find reasonable and clinical acceptable compromises between PTV and OAR doses.

**Poster: Physics track: Treatment planning: applications**

**PO-0920 Knowledge-based planning significantly reduces dose to organs at risk for lung cancer**

L. Hoffmann<sup>1</sup>, M.M. Knap<sup>2</sup>, D.S. Møller<sup>1</sup>  
<sup>1</sup>Aarhus University Hospital, Department of Oncology-Medical Physics, Aarhus, Denmark ; <sup>2</sup>Aarhus University Hospital, Department of Oncology, Aarhus, Denmark

**Purpose or Objective**

The introduction of knowledge-based planning has been shown to result in reduced variability in treatment plans and for some patient groups also reduced dose to organs at risk (OARs). RapidPlan (RP) has been introduced into the Eclipse treatment planning system (Varian Medical Systems). The aim of the present study was to investigate if a general reduction in dose to OARs was achievable by using a RP model. Furthermore, for all patients two different beam angle selections were compared.

**Material and Methods**

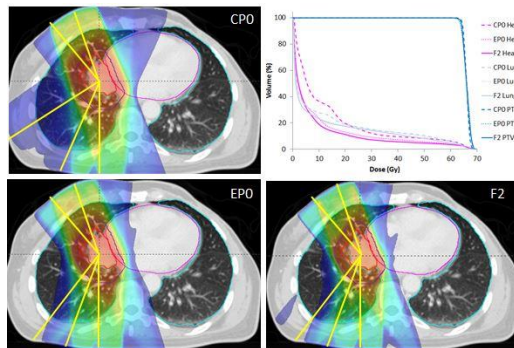


Fig. 1. Treatment plans CPO (clinical plan), EPO (experienced planner plan) and F2 (final plan) for one patient. Dose distributions are shown as dose colour wash for all doses > 10Gy. Yellow lines show beam angles. Upper right: Dose volume histogram showing dose to heart (pink), lung (light blue), esophagus (green) and PTV (dark blue). A clear reduction in dose to all OARs is seen between CPO and EPO. A further reduction is seen for the dose to the heart when applying the RP model (F2).

Seventy-four consecutive lung cancer patients were selected for configuration of the RP model. The patient group consisted of 49 NSCLC patients treated by 60-66 Gy in 30-33 fractions and 25 SCLC patients treated by 45 Gy

in 30 fractions. The median [range] gross tumour volume (GTV) was 29 cm<sup>3</sup> [4-472] and the planning target volume (PTV) was 259 cm<sup>3</sup> [51-1069]. The clinical plans (CPO) consisted of 4-8 IMRT fields. Beam angles were set individually for each patient plan by different dose planners. The plans should comply with constraints for spinal cord (D<sub>max</sub><45Gy), esophagus (D<sub>1cm3</sub><100%), body (D<sub>max</sub><110%), lungs (MLD<19Gy, V20Gy<35% and V5Gy<60%) and heart (V40Gy<30%, V25Gy< 50%). Retrospectively, an experienced planner made 74 new treatment plans (EPO). Beam angles and optimization constraints were selected so that dose to the lungs and heart was minimized, still securing full target coverage (V95%>99%) while minimizing conformity index (CI). These EPO plans were used to generate a RP model (RP1). For each patient, two new plans were made using RP1 (CP1 and EP1) based on the field configurations of CPO and EPO. A second RP model (RP2) was created from the optimal plan (CP1 or EP1) for each of the 74 patients. This final RP model was used to generate the final plan (F2) for each patient. Dosimetric parameters were compared using a Wilcoxon signed rank test. p< 0.05 was considered significant.

**Results**

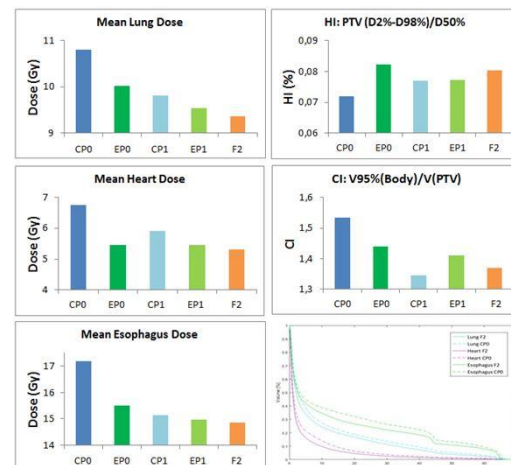


Fig. 2. Bar charts showing the median value of the mean lung/heart/esophagus dose for CPO (dark blue), EPO (dark green), CP1 (light blue), EP1 (light green) and F2 (orange). Lower right: Dose volume histogram showing mean dose for all 74 patients for lungs (light blue), heart (pink) and esophagus (green). The steep change at ~45Gy for esophagus stems from patients treated with 45Gy.

Beam angle selection and dose distribution is shown for one patient in Fig 1, where a clear reduction in dose to heart, lungs and esophagus is seen due to optimal beam directions for EPO vs CPO. Further reduction is obtained by applying the RP model. In Fig. 2, the median value of mean lung/heart/esophagus dose for all 74 patients decreases significantly from CPO to EPO due to optimal beam angle selection. The application of RP1 adds a significant reduction in mean doses to lungs and esophagus (D<sub>CP1</sub><D<sub>CPO</sub>; D<sub>EP1</sub><D<sub>EPO</sub>) and a further significant reduction is seen for all OARs for RP2. The heterogeneity index (HI) increases significantly between CPO and F2. However all plans fulfil PTV<sub>V95%</sub>>99% and Body<sub>D<sub>max</sub></sub><110%. The CI decreases significantly between CPO and F2 or EPO and F2, meaning that the RP model makes the plans more conformal in addition to OARs sparing.

**Conclusion**

Introduction of RapidPlan significantly reduces dose to lungs, heart and esophagus. The highest reduction is seen when RP is combined with optimal beam angles. The conformity index is significantly reduced, while PTV dose coverage is maintained for RP plans. Further reduction is seen by creation of a second RP model (RP2).

**PO-0921 Assessment of CT-based imaging biomarker of COPD in IGRT planning for lung cancer patient**

T. Shiiinoki<sup>1</sup>, Y. Yuasa<sup>1</sup>, K. Fujimoto<sup>1</sup>

<sup>1</sup>Yamaguchi University, Department of Radiation Oncology- Graduate School of Medicine, Ube, Japan

**Purpose or Objective**

One of the most severe complications in radiotherapy of lung cancer is radiation pneumonitis (RP). Chronic obstructive pulmonary disease (COPD) is a recognized risk factor for RP. COPD is a heterogeneous disorder that arises from pathological processes including emphysematous lung tissue destruction, gross airway disease and functional small-airways disease (fSAD) in varying combinations and severity within an individual. It is widely accepted that fSAD and emphysema are two main components of COPD and that a spectrum of COPD phenotypes with varying contributions of these components exists in individual patients. The purposes of this study were to quantify relative lung function using a parametric response map (PRM) as the imaging biomarker of COPD and to assess the dosimetric impact of its integration in treatment planning in volumetric modulated arc therapy (VMAT).

**Material and Methods**

Seven patients who underwent stereotactic body radiotherapy (SBRT) for lung cancer with COPD were enrolled in this study. Four-dimensional CT data sets were acquired around the whole lung with 20-slice CT scanner under free breathing. Next, the entire lung was scanned under breath-hold with a full inspiration. The PRM of quantitative CT as expressed in HU, a measure of tissue density, was determined by imposing two thresholds: (i) -950 HU on full inspiration scan, with values less denoting emphysema, and (ii) -856 HU on normal expiration scan, with values less denoting gas trapping. Therefore, deformable image registration (DIR) was performed from full inspiration to normal exhalation (50%). Classification of voxels with HU values characteristic of lung parenchyma representing normal, fSAD, or emphysema. PRM as imaging biomarker of COPD were calculated for each patient. The VMAT plan was designed based on the total lung. Dosimetric parameters (percent lung volume receiving 5 Gy [V5], V10, V20, and mean lung dose [MLD] to whole lungs (anatomical) versus functional lungs (normal and fSAD)) were compared.

**Results**

Figure 1 showed examples of PRM for two patients. PRM was able to visualize lung function. Red, yellow and green areas indicate emphysema, fSAD and normal lung regions. For all patients, the mean  $\pm$  standard deviation (S.D.) of relative volume of emphysema, fSAD, and normal volume for total lung volume were  $5.4 \pm 8.8\%$  (0.2%-24.6%),  $30.3 \pm 15.2\%$  (8.8%-50.2%) and  $62.5 \pm 20.6\%$  (39.1%-90.8%). Figure 2 indicated an example of dose distribution for patient 3 in coronal and sagittal plane and the mean in V5, V10, and V20 for whole lung, normal, and fSAD, respectively. Mean differences between anatomical and functional lung (normal, fSAD) were 1.9% (0.2%-3.9%), 3.5% (0.3%-10.7%), 1.5% (0.5%-3.5%), 3.6% (0.3%-10.2%), 0.7% (0.2%-1.7%), 1.8% (0.3%-4.1%) and 39 cGy (5.6-67 cGy), 87.5 cGy (22.2-252.2cGy) in V5, V10, V20, and MLD, respectively.

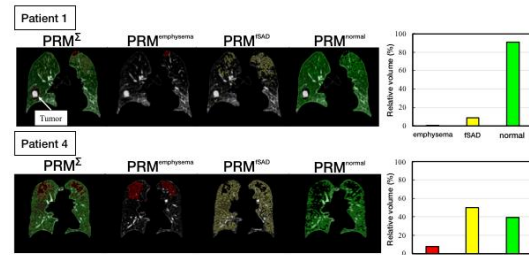


Figure 1. Examples of PRM for two patients

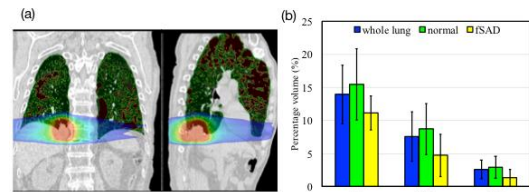


Figure 2. (a) An example of dose distribution for patient 3 in coronal and sagittal plane. (b) The mean in V5, V10, and V20 for whole lung, normal, and fSAD for all patients.

**Conclusion**

It is necessary to evaluate the weighted functional volume in the treatment planning with integration of PRM for functional lung-sparing VMAT.

**PO-0922 Knowledge-based optimization of an adaptive, early-regression-guided, technique for rectal cancer**

R. Castriconi<sup>1</sup>, C. Fiorino<sup>1</sup>, S. Broggi<sup>1</sup>, P. Passoni<sup>2</sup>, N. Di Muzio<sup>2</sup>, R. Calandrino<sup>1</sup>, G.M. Cattaneo<sup>1</sup>

<sup>1</sup>IRCCS San Raffaele Scientific Institute, Medical Physics, Milano, Italy ; <sup>2</sup>IRCCS San Raffaele Scientific Institute, Radiotherapy, Milano, Italy

**Purpose or Objective**

The aim of current study is to implement a knowledge-based (KB) optimization strategy to our adaptive (ART) early-regression guided boosting technique in neo-adjuvant radio-chemotherapy for rectal cancer.

**Material and Methods**

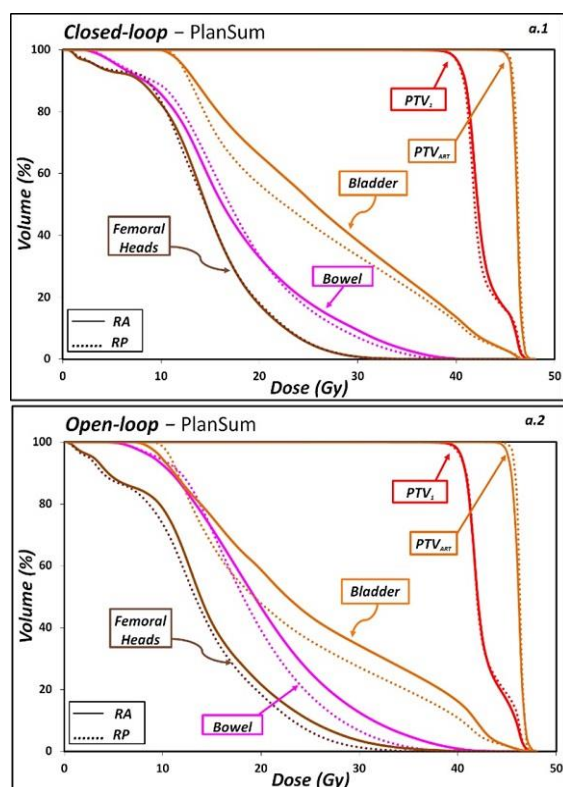
An ART approach for rectal cancer aiming to boost the residual tumor (GTV) in the last part of the treatment was developed and clinically implemented since 2009. The protocol consists of a first phase delivering 27.6Gy to tumor/lymph-nodes, 2.3Gy/fr (PTV<sub>1</sub>); followed by the ART phase concomitantly delivering 18.6Gy (3.1Gy/fr) and 13.8Gy (2.3Gy/fr) respectively to the residual tumor (PTV<sub>ART</sub>) and to PTV<sub>1</sub>. PTV<sub>ART</sub> is obtained by expanding GTV, as visible on MRI taken at fraction 9. Forty VMAT (Varian RapidArc) clinical plans were available and used to generate a KB-model for the first phase using the RapidPlan tool implemented in the Eclipse system (v13.5). Due to the large variability of the size and location of the residual tumor, a robust strategy in order to scale the KB-model of the first phase to the ART one was applied. Twenty clinical plans were retrospectively analysed in terms of PTV<sub>ART</sub> dose distribution: 2cm shell around PTV<sub>ART</sub> (1cm cranial-caudal) was generated for each ART plan. An automatic optimization template for the ART part was obtained by scaling the dose constraints of the first part and including constraints for the shell. An internal (closed-loop) and external (open-loop) validation were performed for both phases, in order to assess the potentiality of the method: all automatic plans (RP) were compared in terms of OARs/PTVs parameters against the original plans (RA).

**Results**

Before assessing best constraints for the shell, shell-DVHs of 20 ART plans were analysed and not found to be correlated with PTV<sub>ART</sub> volume or with the ratio between

PTV<sub>ART</sub> and PTV<sub>1</sub>. Then, the prescribed dose of the PTV<sub>1</sub> was chosen as soft-constraint for  $D_{\text{mean}}$  of the adaptive shell, with lower weight compared to PTV<sub>ART</sub> constraints, optimized to obtain a high dose gradient around PTV<sub>ART</sub> without losing its coverage. The resulting automatic plans were generally better than or equivalent to clinical plans. We reported the comparison of the plan sum (first+second phase) mean-DVH for both internal and external validation (figure 1).

In closed-loop, PTVs coverage and homogeneity were comparable; OARs sparing for RP was slightly improved. In open-loop, coverage and homogeneity of PTV<sub>ART</sub> were improved and OARs sparing for RP was always better with most of the improvements statistically significant ( $p < 0.05$ ): of note,  $V_{30\text{Gy}}$  for bowel was improved of 9% and  $V_{40\text{Gy}}$  for bladder of 8%. Moreover, a reduction of the planning time was obtained in RP plans.



### Conclusion

The suggested KB strategy for automatic planning in the case of ART early-regression guided boosting technique in neo-adjuvant radio-chemotherapy for rectal cancer was found to be satisfactory. The replacement of conventional planning is currently ongoing in our clinical activity.

### PO-0923 How can a limited number of proton slots be optimally used in combined proton-photon treatments?

S. Fabiano<sup>1</sup>, M. Bangert<sup>2</sup>, N. Andratschke<sup>1</sup>, M. Guckenberger<sup>1</sup>, J. Unkelbach<sup>1</sup>

<sup>1</sup>University Hospital Zurich, Department of Radiation Oncology, Zurich, Switzerland; <sup>2</sup>German Cancer Research Center, Department of Medical Physics in Radiation Oncology, Heidelberg, Germany

### Purpose or Objective

Currently, proton treatment slots are a limited resource. Combined proton-photon treatments, in which most fractions are delivered with photons and only a few with protons, may represent a solution to optimize the allocation of proton resources over a patient population. Nowadays, institutions performing combined treatments optimize intensity modulated radiation therapy (IMRT) and

proton therapy (IMPT) plans separately so that each modality delivers the prescribed dose per fraction to the target volume. The aim of this study is to demonstrate how both modalities can be combined to optimally exploit the protons' ability to reduce the integral dose in normal tissues, also addressing the issue of the robustness of combined treatments against proton range uncertainties.

### Material and Methods

We consider treatment sites (a spinal metastasis, a sacral chordoma, and an atypical meningioma) in which organs at risk (OARs) are located within or near the tumor. As an example, Figure 1 shows the spinal tumor case where the target volume entirely surrounds the cauda. Protection of the cauda requires fractionation in the planning risk volume (PRV). Hence, proton and photon fractions should deliver similar doses to this region. Meanwhile, the remaining target volume can be hypofractionated with protons. Such a proton-photon combination was planned by simultaneously optimizing IMRT and IMPT plans while accounting for the fractionation effect through the biologically effective dose (BED) model. A  $BED_{10}$  corresponding to 35.2 Gy in 5 fractions was prescribed to the target volume while limiting the maximum dose in the cauda to the  $BED_2$ -equivalent of 20 Gy in 5 fractions. Stochastic optimization was applied to mitigate range uncertainties.

### Results

Figure 1 illustrates an optimized combination with 1 IMPT and 4 IMRT fractions. Figures 1a and 1b show the IMRT and IMPT dose distributions per fraction. Figure 1c displays the cumulative equieffective dose (EQD) and shows that protons and photons together yield the prescribed BED to the target volume. Protons and photons deliver similar doses to the PRV to protect the cauda through fractionation. Meanwhile, parts of the tumor are hypofractionated with protons. Therefore, the total dose delivered with photons is reduced leading to a reduction of the integral dose to normal tissues. In fact, optimized combinations with 1 or 2 proton fractions achieve 63% and 84% of the integral dose reduction in normal tissues that a 5-fraction IMPT plan yields, compared to 20% and 40% for the simple combinations. However, combined treatments which are optimized without accounting for proton range uncertainties, are very sensitive to errors (Figure 2a). Stochastic optimization leads to robust combinations (Figure 2b) without compromising the benefit over simple combinations.

### Conclusion

A limited number of proton fractions is optimally used in combined proton-photon treatments if protons hypofractionate parts of the tumor while near-uniform fractionation is maintained in serial OARs.

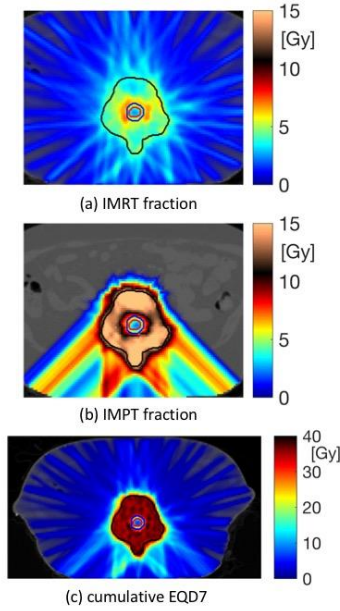


Figure 1: Optimized combined proton-photon treatment with 1 IMPT and 4 IMRT fractions. The contours show the target volume (black), the cauda (red), and the corresponding PRV (blue).

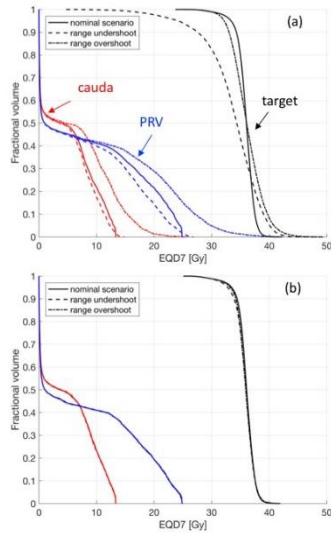


Figure 2: DVHs evaluated for EQD7 from the non-robust (a) and robust (b) optimized combinations with 1 IMPT and 4 IMRT fractions for 3 error scenarios. Range errors were modelled by uniformly scaling the CT Hounsfield units by  $\pm 5\%$ .

**PO-0924 Viability of standardized FFF VMAT TBI treatment plans for extended SSD delivery based on AP-width**

R. Frederick<sup>1,2</sup>, A. Hudson<sup>2,3</sup>, G. Pierce<sup>1,2,3</sup>  
<sup>1</sup>University of Calgary, Department of Physics and Astronomy, Calgary, Canada ; <sup>2</sup>Tom Baker Cancer Centre, Department of Medical Physics, Calgary, Canada ; <sup>3</sup>University of Calgary, Department of Oncology, Calgary, Canada

**Purpose or Objective**

Total body irradiation (TBI) treatments require a large radiation field that often necessitates delivery at an extended source-to-surface distance (SSD), resulting in supplementary set-up procedures that increase treatment

times and patient discomfort. This project aims to decrease planning and treatment time while attaining acceptable dose uniformity by designing stock TBI plans based on patient anterior-posterior (AP) width at umbilicus, and by evaluating the use of flattening filter free (FFF) delivery.

**Material and Methods**

Retrospective examination of 47 TBI patients receiving a prescription of 4Gy/2fx BID was completed using Varian Eclipse™. All patients were treated using our centre's clinical AP/PA VMAT technique at extended SSD with beam spoiler. Patients were stratified into 4 AP width categories: 17-19cm, 19-21cm, 21-23cm, and 23-25cm. The latter two groups were additionally sorted into either short or tall heights. To generate standard FFF VMAT TBI plans, the clinical TBI 6MV 40x10cm<sup>2</sup> open field arcs were used as the plan base with the beam energy substituted with 6MV FFF. Dose homogeneity was achieved through planning MLC leaf positions based on AP midplane lateral dose profiles at eight superior-inferior locations for three patients in each category, and calculated output factors. Custom Python™ code positioned the MLCs at their calculated locations. Two plans (supine, prone) were created for each category for a total of 12 standard plans, and applied to all patients depending on their categorization. The clinical and FFF TBI plans were compared by examining dose-volume histogram (DVH) parameters, dose rates, and beam-on times.

**Results**

Figure 1 presents DVH parameters for all patient categories for the clinical and FFF plans, and Table 1 lists the associated median (range) for each parameter. Significantly similar dose coverage (D98) is seen between the clinical and FFF plans, but the FFF plans have hotspot (D2) and mean lung dose (MLD) distributions that are significantly shifted higher compared to the clinical plans. This decreased dose uniformity still lies within acceptable clinical bounds, and is expected for the standardized FFF plans versus the clinical plans that are tailored to an individual patient. The presented DVH distributions and summarized plan parameters are representative of those for each AP-width category separately.

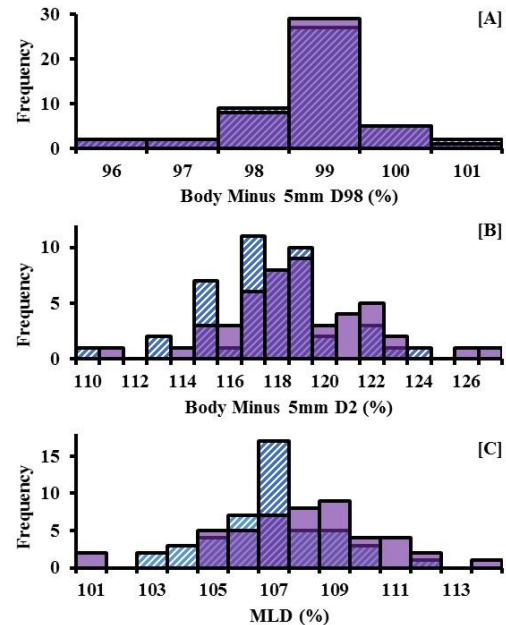


Figure 1. The distribution of clinical and FFF plan dose-volume histogram (DVH) parameters for all 47 patients. [A] Body Minus 5mm D98%, [B] Body Minus 5mm D2%, and [C] Mean Lung Dose (MLD) frequencies.

Table 1. Median (range) of dose-volume histogram (DVH) and various plan parameters for the clinical and FFF TBI plans. Statistical comparison between DVH parameter distribution medians was performed using the Wilcoxon Rank Sum Test. P-values indicating significantly different medians ( $\alpha = 0.05$ ) are bolded.

		Clinical TBI Plans	FFF TBI Plans	P-Value
DVH Parameters	Body Minus 5mm D98 (%)	98.200 (95.125 - 100.680)	98.200 (95.125 - 100.600)	0.9940
	Body Minus 5mm D2 (%)	117.525 (109.150 - 123.650)	118.375 (110.075 - 126.700)	<b>0.0434</b>
	MLD (%)	106.500 (102.275 - 111.350)	107.250 (100.800 - 113.350)	<b>0.0203</b>
Plan Parameters	Average Dose Rate at Midplane (cGy/min)	11.07 (9.85 - 12.24)	18.07 (15.78 - 20.66)	-
	Monitor Units (MU)	10837 (9803 - 12184)	15496 (13552 - 17744)	-
	Beam-On Time (min)	18.06 (16.34 - 20.31)	11.07 (9.68 - 12.67)	-

MLD: mean lung dose

Table 1 lists average dose rates, monitor units (MU), and beam-on times for the clinical and FFF plans for all patient categories. On average, the increase in dose rate and MU are 64.8% and 41.8% respectively for the FFF plans in comparison to the clinical plans. The decrease in beam-on time is 39.2% on average for the FFF plans.

#### Conclusion

The standard AP-width based FFF TBI plans yield a clinically acceptable dose homogeneity that is similar to our current clinical plans while reducing both planning and beam-on time. This technique therefore offers the possibility of decreasing the overall treatment time, and improving patient experience.

#### PO-0925 On the ability of a knowledge based planning process to improve itself

A. Fogliata<sup>1</sup>, G. Reggiori<sup>1</sup>, C. Franzese<sup>1</sup>, D. Franceschini<sup>1</sup>, S. Tomatis<sup>1</sup>, M. Scorsetti<sup>2</sup>, L. Cozzi<sup>2</sup>

<sup>1</sup>Humanitas Research Hospital, Department of Radiation Oncology, Milan-Rozzano, Italy; <sup>2</sup>Humanitas Research Hospital and Humanitas University, Department of Radiation Oncology and Faculty of Biomedical Science, Milan-Rozzano, Italy

#### Purpose or Objective

A knowledge based planning (KBP) engine generates a model from geometric and dosimetric data of a cohort of selected plans, in order to obtain mathematical parameters to estimate the possible DVHs of critical structures, according to the strategy adopted for the plans in the model. Those DVHs are used as optimization objectives for IMRT or VMAT planning for any new patient. As a machine learning process, the KBP is generally able to improve the plan quality. The aim of the present work is to determine if the KBP process RapidPlan (Varian, Palo Alto, CA) can improve itself, i.e. if plans generated by RapidPlan (improved in quality with respect to the clinical plans) can be the source to generate a new RapidPlan model to further improve the plan quality.

#### Material and Methods

Clinical VMAT plans from 83 patients presenting advanced head and neck cancer were selected to build a RapidPlan model. All the plans delivered prescription doses of 54.45 and 69.96 Gy to the elective and boost target volumes, respectively, in 33 fractions with simultaneous integrated boost. The optimization process was manual, using the PRO optimizer. The 83 clinical plans were used to generate a RapidPlan model, named HN-RP-1, using a defined and ad-hoc tuned list of objectives in the model. The HN-RP-1 model was then used to generate new plans for the same 83 patients as above, using the same plan geometry. Those new RapidPlan plans were the input of a new RapidPlan model, named HN-RP-2, having the same list of objectives as HN-RP-1.

A cohort of 20 patients was chosen from the institutional database to validate the two models, HN-RP-1 and HN-RP-2, to assess and compare their plan quality.

#### Results

The HN-RP-2 model presented an improved mathematical process relative to HN-RP-1, showing increased R<sup>2</sup> parameters: 0.634/0.541 (parotids), 0.866/0.599 (oral cavity), 0.756/0.534 (larynx), 0.731/0.204 (spinal cord) for HN-RP-2/HN-RP-1, respectively. Also the regression plots presented general improvements. Regarding the plan quality, D<sub>1%</sub> to the serial organs, spinal cord and brain stem, increased with HN-RP-2 model of 3-4%, not significant. All the parallel organs showed, on the contrary, an improvement with HN-RP-2 relative to HN-RP-1 model, in general around 1% (significant for some structures), with the larynx showing the highest mean dose reduction of 5% (p<0.01). The doses averaged over the 20 validation plans were: 26.3±0.8/26.5±0.8 Gy (parotid mean dose), 40.9±2.3/41.2±2.3 Gy (oral cavity mean), 27.5±2.1/29.0±2.0 Gy (larynx mean), 28.7±0.7/28.0±0.7 Gy (spinal cord D<sub>1%</sub>) for HN-RP-2/HN-RP-1.

#### Conclusion

A second model based on a previous model could improve the plan quality for the parallel organs at risk, and possibly the robustness of the model itself, considering the better mathematical parameters of HN-RP-2 relative to HN-RP-1.

#### PO-0926 A novel approach to automatic planning: robust templates for lung VMAT SBRT

L. Marrazzo<sup>1</sup>, C. Arilli<sup>1</sup>, S. Calusi<sup>2</sup>, M. Casati<sup>1</sup>, C. Talamonti<sup>1,3</sup>, P. Bonomo<sup>4</sup>, L. Livi<sup>3,4</sup>, S. Pallotta<sup>1,3</sup>

<sup>1</sup>Azienda Ospedaliera Universitaria Careggi, Medical Radiation Physics, Firenze, Italy; <sup>2</sup>Istituto Fiorentino di Cura e Assistenza, Medical Physics and Radiation Oncology, Firenze, Italy; <sup>3</sup>University of Florence, Department of Biomedical- Experimental and Clinical Sciences, Firenze, Italy; <sup>4</sup>Azienda Ospedaliera Universitaria Careggi, Radiation Oncology, Firenze, Italy

#### Purpose or Objective

To develop and validate a planning class solution for VMAT SBRT of lung lesions, that achieved target and organs-at-risk (OAR) doses within established constraints using the multicriterial optimization (MCO) of Monaco treatment planning system (Elekta-CMS Software, MO, USA).

#### Material and Methods

The template, containing a list of planning objectives, was first established on a population of 10 lung SBRT patients planned for 55Gy/5fr (peripheral lesions, near to or partly overlapped with the thoracic wall) and refined with a stepwise process. In order to account for anatomical changes between patients, so to achieve personalized results, stage 1 (ideal fluence optimization) was conducted giving priority to OARs and using the MCO. MCO further pushes OARs dose, stopping just before compromising target coverage. To improve gradient and conformity a ring structure around the PTV was set in the list of objectives. Stage 2 (segmentation) was conducted giving priority to PTV coverage. The template was then applied (with no manual intervention) on 20 further patients and the resulting plan was compared with the manual clinical plan. Dose distributions were compared in terms of dosimetric plan parameters (dose to PTV, conformity and gradient index and dose to OARs). Dosimetric verification was performed and evaluated in terms of  $\gamma$  passing rate and point dose measurements, in order to assess that the planned dose distribution could be reliably delivered. Statistical significance of differences between automatic and manual plans was evaluated using paired two-sided Wilcoxon signed-rank test.

#### Results

No statistically significant differences in PTV coverage (p=0.6) and PTV maximum dose (p=0.2) were observed,

while a statistically significant improvement was observed in gradient index ( $p < 0.01$ ) and Paddick conformity index ( $p = 0.01$ ). Data are presented in Table 1.

	PTV $V_{95}$ (%)	PTV $D_{95}$ (Gy)	GI	PCI	Chest wall $V_{30Gy}$	Total lung $V_{20Gy}$ (%)	Heart $D_{10cc}$ (Gy)	Esophagus $D_{50}$ (Gy)	Cord $D_{10cc}$ (Gy)	Cord $D_{1cc}$ (Gy)
MCO auto plan (AVG±SD)	98.0±1.2	59.6±0.4	4.9±0.6	0.83±0.08	22.6±12.7	5.6±3.1	10.5±7.9	9.0±6.0	8.7±4.9	8.1±4.4
Clinical plan (AVG±SD)	97.5±2.0	58.8±2.6	6.6±1.5	0.77±0.12	28.0±14.3	6.5±3.2	12.3±9.6	10.6±3.7	10.7±4.5	9.0±4.3
p	0.6	0.2	<0.01	0.01	<0.01	<0.01	0.2	0.3	0.02	0.2

Table 1. PTV parameters (dose, gradient and conformity) and OARs parameters for MCO auto and clinical manual plans.  $V_{95}$ =volume receiving 95% of the prescription isodose;  $V_{30}$ =volume receiving X Gy;  $D_{10cc}$ =dose to X cc of the considered organ; GI= Gradient Index= volume encompassed by the 50% of the prescription isodose/prescription isodose volume; PCI= Paddick Conformity Index= (target volume in the prescription isodose)/(target volume \* prescription isodose volume).

The improvement in gradient is due to the MCO effectively reducing the constraint on the ring around the PTV. An example of dose distribution is shown in Figure 1.

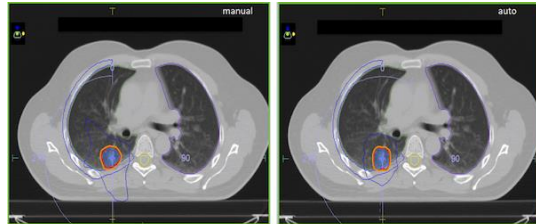


Figure 1. Comparison between manual (left) and automatic (right) dose distributions. In orange the prescription isodose, in blue the isodose relative to the 50% of the prescription isodose.

A general improvement in dose to OARs was observed (Table 1), that resulted to be statistically significant for chest wall  $V_{30Gy}$  and total lungs  $V_{20Gy}$  ( $p < 0.01$ ) and for cord  $D_{0.1cc}$  ( $p = 0.02$ ).

Even a small reduction in doses to OARs, although already below constraints, can be clinically significant in the light of patient retreatment.

Concerning dosimetric verifications, no statistically significant differences were observed in  $\gamma$  passing rates (3%, 3mm, TH10%, local), that were on average (95.4±0.1%) and (96.6±1.4%) for manual and MCO plans, respectively. No manual plan changes were required: all the 20 plans automatically generated were considered clinically acceptable. Average planning time was 10 minutes.

### Conclusion

This study describes a novel approach for automating the planning process and demonstrates the feasibility of developing a class solution for lung VMAT SBRT that produces clinically acceptable plans with a high conformity in a time-efficient manner.

### PO-0927 Lower dose to hippocampi and other OARs with IMPT than with VMAT and IMRT for skull-base meningiomas

M. Florijn<sup>1</sup>, A.W.M. Sharfo<sup>2</sup>, R.G.J. Wiggendaad<sup>3</sup>, J.P.C. Van Santvoort<sup>1</sup>, A.L. Petoukhova<sup>1</sup>, M.S. Hoogeman<sup>4</sup>, M.E. Mast<sup>3</sup>, M.L.P. Dirks<sup>2</sup>

<sup>1</sup>Haaglanden Medical Centre, Medical Physics, Leidschendam, The Netherlands; <sup>2</sup>Erasmus MC Cancer Institute, Radiation Oncology, Rotterdam, The Netherlands; <sup>3</sup>Haaglanden Medical Centre, Radiation Oncology, Leidschendam, The Netherlands; <sup>4</sup>Holland Proton Therapy Centre, Medical Physics & Informatics, Delft, The Netherlands

### Purpose or Objective

Meningiomas are considered benign in 90% of the cases. When surgery is not feasible radiotherapy (RT) is used, however potential late RT effects include neurocognitive impairment. Proton therapy might be beneficial, especially in case of larger target volumes, because of the steep dose fall-off beyond the target volume. In this study we applied fully automated treatment planning to systematically evaluate the dosimetric differences between intensity modulated proton therapy (IMPT), volumetric modulated arc therapy (VMAT) and intensity modulated radiotherapy (IMRT). The purpose of this study

was to minimize the dose in the organs at risk with specific focus on the hippocampi, while ensuring adequate target coverage.

### Material and Methods

Twenty skull-base meningioma patients with a target volume diameter of > 3 cm were included in this study. A dose of 28x1.8 Gy<sub>RBE</sub> was prescribed, in ten cases to the 100% isodose (conventional), in ten other cases to the 80% isodose (stereotactic). A system for fully automated plan generation was used to calculate a) a coplanar, dual arc VMAT plan, b) an IMRT plan with nine non-coplanar beams with optimized gantry and couch angle, c) an IMPT plan with three patient-specific selected non-coplanar beams. For all plans, the same set of constraints and prioritized objectives was used. The photon plans were generated with 2mm CTV-PTV margin; for IMPT a mini-max robust optimization was used with ±2mm setup and ±3.5% range robustness. For fair comparison, all plans were rescaled to the same target coverage, i.e., 98% of the PTV (IMRT/VMAT) and 98% of the CTV for the worst case robustness scenario (IMPT) should receive 47.88 Gy (conventional), or 50.4 Gy (stereotactic). For statistical comparison, a two-sided p-value ≤ 0.05 was considered statistically significant.

### Results

Compared to IMRT and VMAT, IMPT allowed for a much better dose conformity to the target volume (Figure 1). Consequently, large dose reductions in organs at risk were observed (Figure 2). In particular, with respect to IMRT, the mean dose and D40% in the bilateral hippocampus were on average reduced by 41% and 71% (conventional), and by 64% and 79% (stereotactic), respectively (ANOVA  $p \leq 0.02$ ). Emphasis on conformity during optimization led to a high benefit for the normal brain dose as well. With IMPT, the mean dose in the normal brain and the volumes receiving 10-30 Gy were 28-55% reduced (ANOVA  $p \leq 0.03$ ) compared to IMRT. Also the mean doses in the optic nerves, retina, cochlea, brainstem and cerebellum were significantly lower. When comparing IMPT and VMAT, even larger dose differences were observed, mainly due to the coplanar beam setup in VMAT.

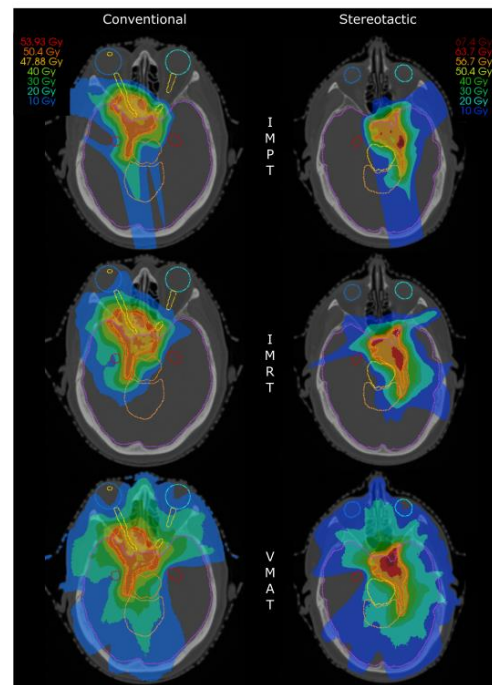
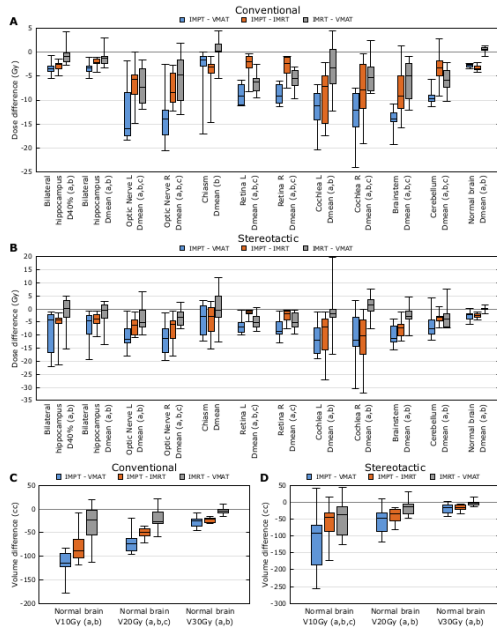


Figure 1. Example of dose distributions for one skull-base meningioma patient treated with conventional prescription (left) and one with stereotactic prescription (right) for IMPT, IMRT and VMAT.



**Figure 2** Differences in dosimetric values for organs at risk between IMPT and VMAT, IMPT and IMRT, and IMRT and VMAT. The central line of each box represents the median value for the 10 study patients with conventional prescription (A and C) and with stereotactic prescriptions (B and D), its upper and lower edge the 25th and 75th percentiles. The whiskers extend to the minimum and maximum differences per group. Negative values indicate lower dose for IMPT (blue/orange) or IMRT (grey); a, b and c indicate statistically significant differences ( $p < 0.5$ ) for IMPT vs VMAT, IMPT vs IMRT and IMRT vs VMAT, respectively.

**Conclusion**

For skull-base meningiomas IMPT allows for a considerable dose reduction in the hippocampi and normal brain compared to both IMRT and VMAT, which may lead to a clinically relevant reduction of late neurocognitive side effects.

**PO-0928 Treatment plan quality assessment for focal dose escalation in prostate cancer**

M. Van Schie<sup>1</sup>, T. Janssen<sup>1</sup>, D. Eekhout<sup>1</sup>, I. Walraven<sup>1</sup>, A. Kotte<sup>2</sup>, L. Kerkmeijer<sup>2</sup>, C. Draulans<sup>3</sup>, K. Haustermans<sup>3</sup>, R.J. Smeenk<sup>4</sup>, U. Van der Heide<sup>1</sup>

<sup>1</sup>Netherlands Cancer Institute, Radiation Oncology, Amsterdam, The Netherlands ; <sup>2</sup>University Medical Center Utrecht, Radiation Oncology, Utrecht, The Netherlands ; <sup>3</sup>University Hospitals Leuven, Radiation Oncology, Leuven, Belgium ; <sup>4</sup>Radboud University Medical Center, Radiation Oncology, Nijmegen, The Netherlands

**Purpose or Objective**

In a multicenter randomized trial of focal prostate dose escalation up to 95 Gy was prescribed to the tumor in the dose escalation arm, with 77 Gy to the entire prostate in both arms. However, as the dose constraints to normal tissue surrounding the target volume were leading, we investigated what extent of dose escalation to the tumor was achieved.

In clinical practice, it can be challenging to assess whether a treatment plan is optimal in terms of achieved boost dose and dose to organs at risk (OARs). Therefore we developed a predictive model to identify treatment plans in which a higher boost dose could be achieved for the specific patient's anatomy. **Material and Methods**

We analyzed planning CT scans and clinical delineations together with co-registered planned dose distributions of 531 patients from 4 institutions. We compared dose characteristics for the standard and dose-escalated arms. For the latter we determined the percentage of plans with an  $D_{50\%}$  and  $D_{98\%}$  above 82.4 Gy (107 % of 77 Gy), and quantified the correspondence with prescribed dose using the following parameters:

- Quality Factor<sup>[1]</sup>:  $QF = 1/n * \sum |1 - D_{planned}/D_{prescribed}|$ ,

- Homogeneity Index<sup>[2]</sup> (CTV - GTV only):  $HI = (D_{2\%} - D_{98\%}) / D_{50\%}$ ,
- Conformation Number<sup>[3]</sup> (GTV only):  $CN = GTV_{95\%}/GTV * GTV_{95\%}/V_{95\%}$ .

Plans with above-median QF and HI and below-median CN were selected to train a linear regression model to predict  $D_{98\%}$  in the GTV using a 5-fold cross validation scheme. Training was performed on the first 3 principle components (PCs) per Overlap Volume Histogram (OVH) of PTV, GTV, bladder and rectum (in total 10 OVHs). Subsequently, the model was applied to the remaining plans to identify treatment plans with more than 10 Gy difference between planned and predicted dose in the GTV. **Results**

Dose-volume parameters are shown in Table 1.  $D_{50\%}$  and  $D_{98\%}$  were above the threshold of 82.4 Gy in 99 and 71% of the GTVs, respectively. We observed comparable bladder and rectum dose-volume parameters between both arms of the trial. Median QF and HI of all dose-escalated plans were 5.4% and 26.9%, median CN of all GTVs was 0.25. Seventy-eight out of 374 GTVs were selected to train both models. For  $D_{98\%}$  the best predictive model included 5 PCs. Eleven GTVs were identified with a planned  $D_{98\%}$  more than 10 Gy lower than predicted, corresponding with 9 treatment plans. Figure 1 displays the predicted versus planned  $D_{98\%}$  in the GTVs of both training and test data.

**Table 1.** Dose-volume parameters (median and 95% confidence interval) for PTV, CTV, GTV, Bladder and Rectum in the standard and dose-escalated arm.

Structure	Dose-volume parameters	Standard Arm (n = 271)	Study Arm (n = 260)	Constraints
PTV	$V_{95\%}$ (%)	98.3 (90.9 – 99.5)	97.1 (86.9 – 99.0)	> 99%
CTV - GTV	$D_{2\%}$ (Gy)	79.3 (77.5 – 81.1)	91.3 (83.1 – 95.5)	
	$V_{125\%}$ of 77 Gy (%)	2.5 (0.0 – 21.7)	28.1 (11.4 – 59.9)	
	$D_{98\%}$ (Gy)		84.7 (77.1 – 91.4)	
GTV	$D_{50\%}$ (Gy)		93.1 (84.9 – 95.4)	
	$D_{98\%}$ (Gy)		84.7 (77.1 – 91.4)	
	$V_{95\%}$ of 95 Gy (%)		78.2 (0.00 – 99.6)	
	$D_{2\%}$ (Gy)	75.5 (73.2 – 78.5)	76.3 (73.4 – 80.4)	
Bladder	$D_{2\%}$ (Gy)	74.7 (72.0 – 78.1)	75.2 (72.7 – 78.7)	
	$V_{125\%}$ (%)	4.2 (1.0 – 10.7)	4.8 (0.9 – 11.0)	< 10%
	$V_{150\%}$ (cm <sup>3</sup> )	0.0 (0.0 – 0.0)	0.0 (0.0 – 0.7)	< 1 cm <sup>3</sup>
	$D_{2\%}$ (Gy)	74.1 (72.4 – 75.8)	75.2 (72.2 – 78.0)	
Rectum	$D_{2\%}$ (Gy)	73.5 (70.7 – 75.2)	73.7 (71.0 – 76.1)	
	$V_{150\%}$ (%)	33.7 (12.8 – 62.1)	33.0 (17.3 – 59.1)	< 50%
	$V_{125\%}$ (%)	4.1 (1.6 – 8.1)	4.0 (1.6 – 7.2)	< 5%
	$V_{175\%}$ (cm <sup>3</sup> )	0.0 (0.0 – 0.2)	0.3 (0.0 – 1.5)	< 1 cm <sup>3</sup>
	$D_{2\%}$ (Gy)	74.7 (72.0 – 78.1)	75.2 (72.7 – 78.7)	

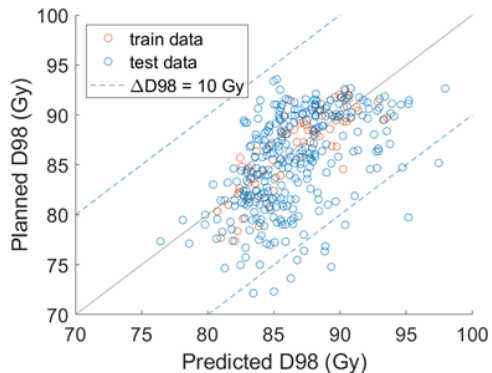


**Figure 1.** Predicted versus planned  $D_{98\%}$  of the training (orange) and test data (blue). Dotted lines indicate a dose difference of 10 Gy.

**Conclusion**

In this study we observed that a relevant dose escalation above 82.4 Gy was realized in the majority of patients. Meanwhile we showed no differences in OAR dose between both arms of the trial. Although limited dose escalation to a large extent can be assigned to unfavorable anatomy, we developed a model that identified treatment plans where nonetheless a higher boost dose was predicted to be achievable.

- [1] B. Vanderstraeten et al, PMB 2006  
 [2] Q. Wu et al, IJROBP 2003  
 [3] A. van 't Riet et al, IJROBP 1997

### PO-0929 Focal boost dose escalated prostate SBRT on the Halcyon fast-rotating O-ring linac

R. De Roover<sup>1</sup>, W. Crijns<sup>1</sup>, S. Michiels<sup>1</sup>, C. Draulans<sup>1</sup>, K. Poels<sup>1</sup>, K. Haustermans<sup>1</sup>, T. Depuydt<sup>1</sup>

<sup>1</sup>Catholic University of Leuven, Department of Oncology, Leuven, Belgium

#### Purpose or Objective

A commercially available fast-rotating O-ring linac, Varian Halcyon (HA), has been shown to improve the time-efficiency of conventionally fractionated volumetric modulated arc therapy (VMAT). The dual-layer multi-leaf collimator's (MLC) 10 mm leaf-width, however, may limit its use for stereotactic body radiotherapy (SBRT). In this study, HA is compared with a SBRT-dedicated C-arm linac for the planning and delivery of focal boost dose escalated prostate SBRT.

#### Material and Methods

Sixteen patients with intermediate or high risk prostate cancer were planned for whole-gland prostate SBRT with a focal boost to the macroscopic tumor using VMAT. Prescription was 35 Gy to the prostate (PTV<sub>prostate</sub>), 30 Gy to the seminal vesicles (PTV<sub>sv</sub>), and 40 Gy to the focal boost (GTV<sub>boost</sub>) in 5 fractions. The GTV<sub>boost</sub> should be aimed to receive up to 50 Gy as long as the organ at risk (OAR) sparing is not at risk. Plans were generated for HA using 6MV flattening filter free (FFF) dual arc (HA2) and triple arc (HA3) VMAT. Field shaping was performed by both MLC layers independently (10 mm leaf-width, with a 5 mm offset between the staggered layers). The collimator angles were 10°/80° and 10°/45°/80° for dual arc and triple arc respectively. For comparison, plans were generated on a Varian TrueBeam STx (2.5 mm leaf-width) using 6MV dual arc (TB2) VMAT, with collimator angles 10°/80°. The Photon Optimizer and Anisotropic Analytical Algorithm were used in Varian Eclipse (v15.6) for each plan. Identical optimization objectives were used for each plan within a patient. Plans were normalized to 35 Gy covering 95% of PTV<sub>prostate</sub>.

PTV coverage and OAR sparing were compared between HA2, HA3 and TB2 using a two-sided Wilcoxon matched-pairs signed-rank test. Pre-treatment quality assurance (QA) was performed using portal dosimetry using a 2%(local)/2mm gamma evaluation with a low dose exclusion threshold set to 20% of the prescribed dose. The time needed to deliver the plans in auto-sequencing mode was recorded.

#### Results

Median target coverage, OAR doses and plan properties are compiled in Table 1. Figure 1 shows the median dose-volume histogram for a selection of OARs. Both HA2 and HA3 achieved similar target coverage and focal boost dose escalation compared to TB2. All OAR doses were well within our clinical criteria. Similar urethral sparing was obtained for HA2 and HA3 compared to TB2. Increased D<sub>max</sub> to rectum and bladder was observed for HA2 and HA3 (median increase of 0.6 Gy and 0.4 Gy respectively). The median plan delivery time was reduced with of 34 sec and 16 sec for HA2 and HA3, respectively. All plans passed pre-treatment QA with gamma agreement scores above 94.6%.

**Table 1.** Target coverage, OAR doses and plan properties for the studied patient population (N = 16). The median values are shown together with the minimum and maximum value within brackets. HA2 and HA3-results yielding p < 0.05 for a two-sided Wilcoxon matched-pairs signed-rank test compared to TB2 are indicated in bold.

		TB2	HA2	HA3
<b>Target coverage</b>				
GTV <sub>boost</sub>	D <sub>95%</sub> [Gy]	40.9 [40.1, 49.9]	40.9 [40.2, 50.4]	40.9 [40.2, 50.0]
	D <sub>100%</sub> [Gy]	48.0 [42.0, 51.4]	47.4 [42.8, 52.5]	47.8 [43.0, 52.5]
PTV <sub>prostate</sub>	D <sub>95%</sub> [Gy]	33.9 [33.3, 34.6]	33.9 [33.3, 34.4]	33.9 [33.3, 34.5]
	D <sub>90%</sub> [Gy]	30.2 [29.3, 30.9]	<b>30.0</b> [29.4, 30.6]	30.2 [29.6, 30.8]
<b>OAR doses</b>				
Rectum	D <sub>max</sub> [Gy] <sup>a</sup>	35.3 [34.6, 37.9]	<b>35.9</b> [34.9, 38.8]	<b>36.0</b> [34.9, 38.7]
	D <sub>10%</sub> [Gy]	34.5 [31.1, 35.4]	<b>34.6</b> [32.5, 35.7]	<b>34.6</b> [32.1, 35.6]
	D <sub>mean</sub> [Gy]	12.8 [11.3, 14.3]	<b>13.1</b> [11.5, 14.5]	13.0 [11.4, 14.4]
Bladder	D <sub>max</sub> [Gy] <sup>a</sup>	38.6 [37.2, 41.8]	<b>38.7</b> [37.5, 44.1]	<b>38.6</b> [37.5, 42.4]
	D <sub>10%</sub> [Gy]	37.1 [35.4, 38.6]	36.8 [35.8, 38.6]	36.8 [35.6, 38.4]
	D <sub>mean</sub> [Gy]	16.3 [8.6, 25.7]	<b>17.3</b> [9.0, 26.3]	<b>16.4</b> [8.8, 26.1]
Urethra	D <sub>max</sub> [Gy] <sup>a</sup>	38.7 [37.6, 39.8]	39.0 [37.3, 39.8]	38.7 [37.5, 39.8]
<b>Plan properties</b>				
Monitor units [MU]		2605 <sup>b</sup> [2407, 2856]	<b>2232<sup>b</sup></b> [1938, 2798]	<b>2382<sup>b</sup></b> [2088, 2874]
Plan delivery time [min:sec]		4:27 [4:07, 4:52]	<b>3:53</b> [3:23, 4:51]	<b>4:11</b> [3:24, 4:59]
Pre-treatment QA γAS [%] <sup>c</sup>		99.2 [97.4, 100.0]	99.7 [94.6, 100.0]	98.9 [94.9, 100.0]

Abbreviations: OAR = organ at risk; TB2 = VMAT on a Varian TrueBeam STx using 2 arcs, HA2 & HA3 = VMAT on a Varian Halcyon using 2 and 3 arcs respectively; QA = quality assurance; γAS = gamma agreement score.  
<sup>a</sup>maximum point dose (D<sub>max</sub>) defined as the dose at 0.035 cc volume.  
<sup>b</sup>different absolute dose calibrations were used for both systems: 1 MU corresponds to 0.8 cGy for TB and 1.0 cGy for HA, both delivered at 10 cm depth by a 10 × 10 cm<sup>2</sup> field at 90 cm source-surface distance.  
<sup>c</sup>gamma analysis was performed using 2%(local)/2mm gamma criteria and a low dose exclusion threshold set to 20% of the prescribed dose.

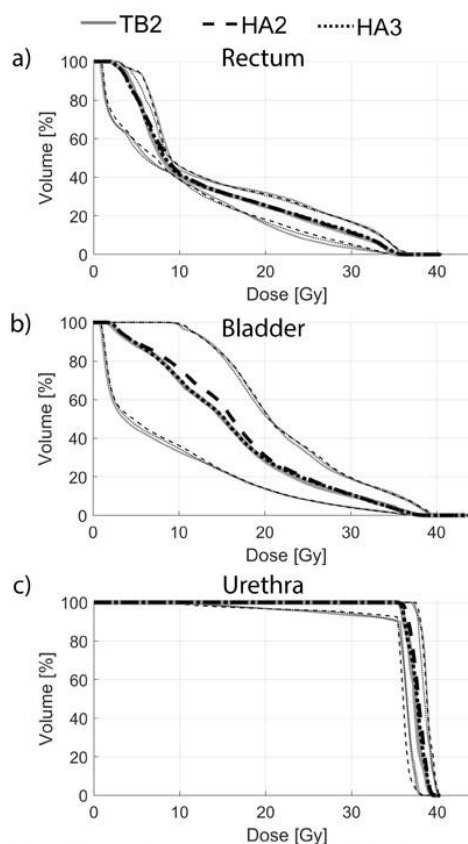


**Figure 1.** Dose-volume histogram for a selection of organs at risk for the three VMAT solutions. Median DVHs and the DVH range (minimum to maximum DVH) are computed over the whole studied patient population (N=16).

#### Conclusion

Compared to a SBRT-dedicated C-arm linac, HA achieved clinically comparable quality for focal boost dose escalated prostate SBRT planning. This study demonstrates the potential of a mainstream fast-rotating O-ring linac to deliver increasingly used prostate SBRT treatments.

### PO-0930 Knowledge-based planning of head and neck cancer; comparisons of target and normal tissue parameters

A.I.S. Holm<sup>1</sup>, L. Kaplan<sup>1</sup>, U.V. Elstrøm<sup>1</sup>, S.S. Korreman<sup>2</sup>  
<sup>1</sup>Aarhus University Hospital, Department of oncology, Aarhus C, Denmark ; <sup>2</sup>Aarhus University Hospital, Department of oncology and Danish Center for Particle Therapy, Aarhus C, Denmark

**Purpose or Objective**

Knowledge-based planning (KBP) has the potential to improve plan quality. We have recently implemented KBP (Rapidplan, Eclipse, Varian Medical Systems), in our clinic. Here we report on comparison between non-KBP and KBP treatment plans for advanced head and neck cancer (HCN) patients.

**Material and Methods**

The KBP model was validated on twenty HNC patients. Three target volumes (TV) are covered by a SIB plan, with prescribed doses (PD) of 66Gy (PTV1), 60Gy (PTV2) and 50Gy (PTV3). Two planning strategies were applied: one with optimization parameters from a generic HNC template and one with patient specific KBP optimization parameter. All plans were three-arc VMAT plans. The two plans were compared using quantitative metrics for target coverage, homogeneity and conformity, steep dose fall-off at PTV1, Integral dose, low-dose bath and mean doses to the brainstem, salivary glands, oral cavity, lips, thyroid, and swallowing structures. P-values were calculated using Wilcoxon signed rank test with  $p < 0.05$  considered significant.

**Results**

Target parameters are shown in fig. 1. No differences were observed for target coverage (data not shown). Target homogeneity was slightly higher for KBP than non-KBP plans. Three out of the four metrics for target conformity show that at least PTV1 and PTV3 are less conformal for KBP than non-KBP. The steep dose-fall of PTV1 is higher for KBP than non-KBP. Comparisons for normal tissues are shown in fig. 2. Using KBP decreases the mean doses to the pharyngeal constrictor muscles (PCM), the glottis larynx and the thyroid gland, whereas the remaining OAR mean doses remain unchanged. The volumes receiving 10 Gy and 15 Gy are decreased by KBP and the integral dose decreases slightly from 127.0J [min: 54.0J; max: 226.3J] to 126.0J [52.9J; 224.1J] by KBP (p-value: 0.018).

Fig. 1. Comparisons of target parameters. Non-KBP data are given in red and KBP data in blue. All values are mean values with error bars showing the maximum and minimum values. Between two bars the corresponding p-value is given and significant differences are framed by green boxes. The specific target parameter and its corresponding definition are given in the labels below.

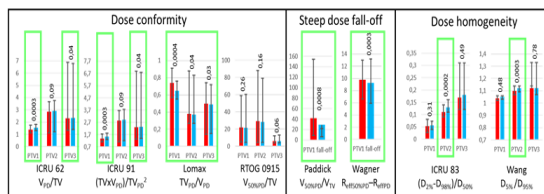
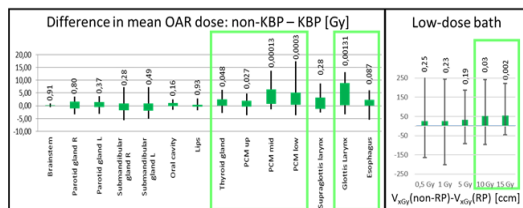


Fig. 2. Comparisons of normal tissue parameters: mean doses to OAR and low-dose bath. All data are given as differences between the non-KBP and KBP plans. Mean doses to OAR in a box-plot, with the 1<sup>st</sup> and 3<sup>rd</sup> quantile, and maximum and minimum values. For the low-dose bath values are given as mean values with error bars showing the maximum and minimum values. Above the data the corresponding p-value is given and significant differences are framed by green boxes.



**Conclusion**

KBP gives similar target coverage as previously accepted clinical plans, with the advantage of reducing the mean doses to a number of OAR, slightly lowering the volume receiving 10 Gy and 15 Gy as well as the integral dose. Since the conformity of PTV3 is decreased, the OAR benefits are due to the steeper dose gradient.

**PO-0931 Application of a thin, energy-layer specific multi-leaf collimator for proton pencil beam scanning.**  
C. Winterhalter<sup>1,2</sup>, G. Meier<sup>1</sup>, D. Oxley<sup>1</sup>, D.C. Weber<sup>1,3,4</sup>, A. Lomax<sup>1,2</sup>, S. Safai<sup>1</sup>

<sup>1</sup>Paul Scherrer Institute, Center for Proton Therapy, Villigen PSI, Switzerland ; <sup>2</sup>ETH Zurich, Physics Department, Zurich, Switzerland ; <sup>3</sup>University Hospital of Zurich, Radiation Oncology Department, Zurich, Switzerland ; <sup>4</sup>University Hospital of Bern, Radiation Oncology Department, Bern, Switzerland

**Purpose or Objective**

For pencil beam scanning (PBS) proton therapy, lateral fall-off has been shown to be inferior when compared to passive scattering proton therapy. For shallow tumours adjacent and close to critical structures, this might lead to unnecessary high doses to organs at risk. As such, collimation could potentially improve PBS proton dose distributions.

**Material and Methods**

For four patients with tumours located close to the brainstem, we have investigated the potential advantages of the use of a thin, multi-leaf collimator for energy-level specific collimation. By thin, we mean a collimator with a thickness just sufficient to stop protons with ranges in water of up to 15 cm, beyond which lateral penumbra is anyway determined by scattering in the patient. Additionally, two different pencil beam placement techniques - rectilinear grids (4 mm spacing, clinical approach) or contour scanning - have been analysed with and without collimation using different expansions for the contour scanning scenarios (0mm, 1mm, 2mm, 3mm, see Meier et al (Phys. 2017 Med. Biol. 62; 2398)). For the optimization process, both collimated and un-collimated pencil beams have been included in an analytical dose calculation, but all final dose distributions have been calculated using Monte Carlo (TOPAS).

**Results**

Figure 1 shows the improvement in penumbra when moving from grid to collimated contour scanning for an example patient field. For this case, grid scanning combined with collimation reduced the V30% outside the target by 20% in comparison to the un-collimated grid scenario. For contour scanning alone, a maximal V30% reduction outside the target of 26% was achieved (0mm contour expansion) which increased to 33% with collimation (2mm contour expansion). These improvements however come at the cost of reduced target dose homogeneity. As such, the best un-collimated/collimated dose distributions (i.e. scenarios retaining dose homogeneity while reducing dose to the normal tissue) were achieved with a 1mm/3mm contour expansion, without and with collimation respectively (c.f. figure 1). Finally, for four patients, collimated (shallow) and un-collimated (deep) fields have been combined and compared to the best un-collimated approach (Table 1), showing that the use of a collimator could reduce the V30% by 0.8-8.0% and the mean dose to the brainstem by 1.5-3.3% for such combined plans.

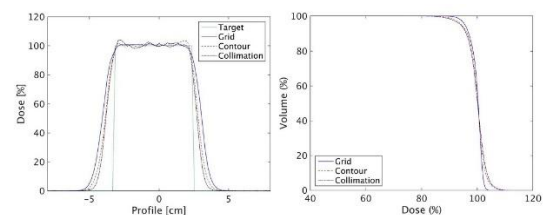


Figure 1: Example profiles in the patient geometry (a) and dose volume histogram for the target volume (b) for the clinical grid scanning (blue), the uncollimated contour scanning (contour extension 1 mm, red), and the collimated contour scanning (contour extension 3 mm, black)

	P 1	P 2	P 3	P 4
Collimated/total fields	3/3	2/3	1/3	2/4
V30	-7.9%	-8.0%	-0.9%	-0.8%
Mean dose to brainstem	-2.1%	-3.3%	-3.1%	-1.5%

**Table 1:** For four patients, V30 (doses outside the target) and mean dose to the brainstem are compared between the best collimated and the best uncollimated plan. All values are given in percentage of the uncollimated result, and negative values indicate a reduction when applying collimation.

### Conclusion

For patients treated in the cranium region, MC simulations of the use of a thin, energy-layer specific multi-leaf collimator have shown to lower doses to normal tissues in comparison to grid and un-collimated contour scanning, especially the brainstem. Best dose results are obtained when combining collimation with pencil beam placements following the target contour. Further improvements are expected either by improving the model in the optimization and/or by using different contour expansions within the same field, or even optimizing the expansion and beam placement itself.

### PO-0932 Identification of modes of tumour changes in NSCLC during radiotherapy

L.M. Amugongo<sup>1</sup>, E. Vasquez Osorio<sup>1</sup>, A. Green<sup>1</sup>, D.

Cobben<sup>1</sup>, V.H. Marcel<sup>1</sup>, A.M. Alan<sup>1</sup>

<sup>1</sup>University of Manchester, Division of Cancer Sciences- Faculty of Biology- Medicine and Health- University of Manchester, Manchester, United Kingdom

### Purpose or Objective

Cone-beam computed tomography (CBCT) is routinely used to set up and verify patient position during radiotherapy (RT) of non-small cell lung cancer (NSCLC) patients. CBCT images can be used to assess tumour changes during RT. This information is currently used qualitatively to inform treatment adaption. However, uncertainty exists regarding the mode of tumour change (elastic or non-elastic) and therefore the safety of adapting treatment. This study introduces a novel approach based on shells around the tumour boundary to automatically distinguish different modes of tumour change.

### Material and Methods

CBCT images of 80 NSCLC patients were collected and registered to the planning CT scan using a two-step alignment process. (1) Rigid registration of the bones to remove gross translation and rotations; (2) Localised soft tissue registration, translation only, on a slightly expanded gross tumour volume (GTV). Intensity normalisation was then applied to the CBCTs. Eight shells, 1mm thick and extending 4 mm inwards and outwards from the planning CT GTV surface, were created. The external shells were constrained to the lung/tumour boundary. Typically, shells 1-3 describe gross target volume changes, 4-5 tumour/lung boundary changes and 6-8 show changes to the local lung tissue. From each shell, the mean intensity was extracted across all normalized CBCTs. Linear fits of the mean intensities for each shell were plotted. Affinity propagation, an unsupervised clustering method, was used to explore whether modes of tumour change could be identified based on the gradients of these fits.

### Results

All CBCTs were successfully registered to the planning CT scan and shells were visually verified to ensure they avoided mediastinum/chest wall. Distinct modes of tumour changes could be seen in the intensity gradients of the CBCT. The majority of patients showed small density changes during the course of treatment (figure 1a), but some showed large changes (figure 1b). Affinity propagation clustered the patients into 7 groups, shown in

figure 2, suggesting definite modes of tumour shrinkage can be identified from our approach.

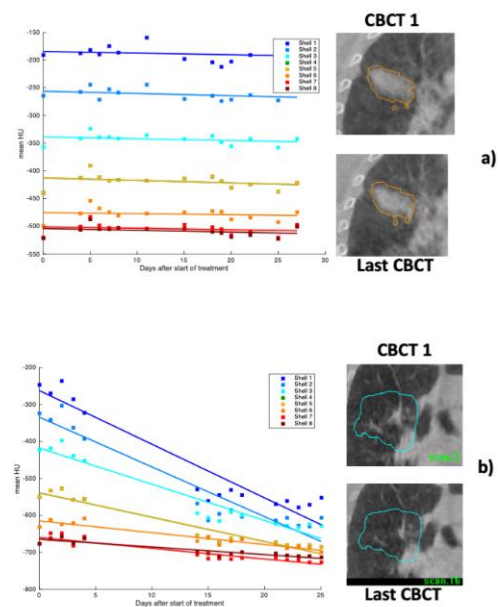


**Fig 1:** Example of patient with little changes a) and patient with major density changes b).

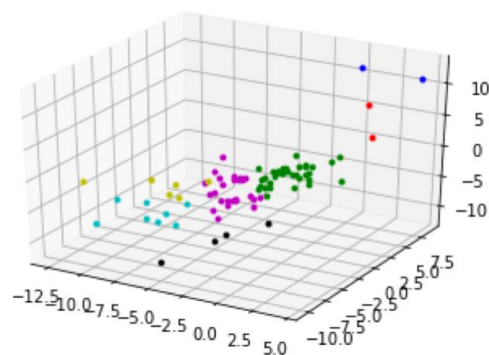


**Fig 2:** Clustering based on slope of density of shells inside, at the border and outside of the target volume as observed in different patients.

### Conclusion

Our novel methodology automatically identified distinct modes of tumour changes for lung cancer patients from routine on-treatment CBCT imaging. Future work will include more patients, to optimise the clusters, identify and validate the mode of change for each group, e.g., related to histopathology.

### PO-0933 Single isocenter SRS for multiple brain metastases: dosimetric comparison of DCAT and VMAT

J. Hofmaier<sup>1</sup>, R. Bodensohn<sup>1</sup>, S. Garny<sup>1</sup>, M. Reiner<sup>1</sup>, M. Eder<sup>1</sup>, Y. Dinc<sup>1</sup>, S. Corradini<sup>1</sup>, C. Belka<sup>1,2</sup>, M. Niyazi<sup>1</sup>  
<sup>1</sup>University Hospital LMU Munich, Department of Radiation Oncology, Munich, Germany; <sup>2</sup>German Cancer Consortium DKTK, partner site Munich, Munich, Germany

### Purpose or Objective

For a long time whole brain radiotherapy (WBRT) has been the only treatment option for multiple cerebral metastases whereas a few lesions (usually up to four) were treated with SRS. In the recent decade SRS has become an option also for patients with more lesions. The Elements™ Multiple Brain Mets SRS (MBMSRS) tool (Brainlab, Munich, Germany) enables the simultaneous treatment of up to 15 metastases on LINACs with a single isocenter using non-coplanar dynamic conformal arcs (DCAT). This study compares the dosimetric properties of this technique with non-coplanar volumetric modulated arc therapy (VMAT) (Elekta Monaco®).

### Material and Methods

Datasets of 20 patients with a total of 66 lesions who were treated with MBMSRS version 1.5 at an Elekta Versa HD™ were included in this comparison. A single fraction dose of 15-20 Gy was prescribed to the 80% isolevel encompassing 98% of the PTV (GTV plus a margin of 1mm). All patients were re-planned using VMAT in Elekta Monaco® 5.11. For all plans, the total number of monitor units and the volume of the brain receiving more than 4, 5 and 8 Gy were compared using the Wilcoxon signed rank test (WSRT). Using a density based clustering algorithm, dose clouds of 10 Gy, 12 Gy and half of the prescription dose were identified and assigned to the corresponding lesion. The V10Gy and V12Gy around each lesion were compared using WSRT. Targets with overlapping 10 Gy clusters were joined and treated as one lesion (2 lesions joined: 5 times, 3 lesions joined: once). Paddick conformity index and gradient index (GIPTV) were calculated and compared only for lesions which could be separated in the clusters corresponding to their half prescription dose. To identify a possible predictor for VMAT being superior, the correlation of the differences between V10Gy and V12Gy for both techniques with the sphericity (a measure of similarity to a perfect sphere) of the corresponding PTV was assessed using Spearman's rank correlation coefficient.

### Results

The MBMSRS plans showed superior results in all the investigated metrics (see Table 1). All differences were significant ( $p < 0.05$ ). A moderate correlation of the difference of the V10Gy and V12Gy between the two techniques with the PTV sphericity (Spearman's rho = 0.27 and 0.30, for V10Gy and V12Gy, respectively and  $p < 0.05$  for both parameters) was found. Lesions with higher sphericity tended to have a better healthy brain sparing with MBMSRS.

	MBMSRS DCAT median (range)	#plans MBMSRS superior	Monaco® VMAT median (range)	#plans VMAT superior	P (Wilcoxon SR)
<b>Plan data N=20</b>					
Cumulative MU	4569 (3543-7790)	17	5840 (4089-10769)	3	<0.05
V4Gy (brain) [ccm]	45.6 (18.5-215.9)	19	123.1 (37.5-418.6)	1	<0.05
V5Gy (brain) [ccm]	33.7 (13.0-120.5)	19	69.1 (26.0-273.6)	1	<0.05
V8Gy (brain) [ccm]	17.4 (6.3-52.6)	19	26.6 (10.6-86.4)	1	<0.05
<b>PTV data N=59</b>					
V10Gy (healthy brain) [ccm]	3.2 (0.4-19.3)	55	4.9 (1.0-19.9)	4	<0.05
V12Gy (healthy brain) [ccm]	2.1 (0.1-13.1)	53	3.1 (0.5-13.9)	6	<0.05
<b>PTV data without overlapping N=53</b>					
Paddick CI	0.75 (0.58-0.89)	30	0.73 (0.38-0.88)	22	<0.05
GIPTV	5.99 (3.50-15.73)	48	7.17 (3.35-33.00)	5	<0.05

Table 1 - Investigated metrics for the 20 treatment plans, the 59 lesions and the 53 lesions for which the target indices were computed.

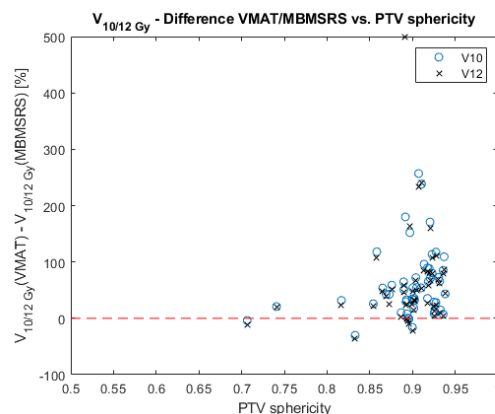


Fig. 1 - Difference in V10Gy and V12Gy scattered against the sphericity of the respective PTV. A sphericity value of 1 corresponds to a perfect sphere, values <1 to shapes deviating from a sphere.

### Conclusion

In most cases, MBMSRS can generate plans with steeper dose gradients, superior healthy brain sparing and less MU as compared to VMAT. In particular cases where the shape of the treated lesions deviates substantially from a sphere, VMAT can be superior.

**PO-0934 Physical and biological doses with increasing number of proton beams for pediatric brain irradiation**  
 L. Toussaint<sup>1</sup>, D.J. Indelicato<sup>2</sup>, K.S. Holgersen<sup>1</sup>, J.B.B. Petersen<sup>1</sup>, C.H. Stokkevaag<sup>3</sup>, Y. Lassen-Ramshad<sup>4</sup>, O. Casares-Magaz<sup>1</sup>, C. Pedro<sup>5</sup>, R. Mikkelsen<sup>6</sup>, A. Vestergaard<sup>4</sup>, H. Hasle<sup>7</sup>, L.P. Muren<sup>1</sup>

<sup>1</sup>Aarhus University Hospital, Department of Medical Physics, Aarhus, Denmark; <sup>2</sup>University of Florida Health Proton Therapy Institute, Department of Radiation Oncology, Jacksonville, USA; <sup>3</sup>Haukeland University Hospital, Department of Oncology and Medical Physics, Bergen, Norway; <sup>4</sup>Danish Center for Particle Therapy, Department of Oncology, Aarhus, Denmark; <sup>5</sup>Instituto Português de Oncologia Francisco Gentil, Department of Radiotherapy, Lisbon, Portugal; <sup>6</sup>Aarhus University, Department of Biomedicine, Aarhus, Denmark; <sup>7</sup>Aarhus University Hospital, Department of Pediatrics, Aarhus, Denmark

### Purpose or Objective

Dose conformity and normal tissue sparing of photon-based radiotherapy has improved considerably with the introduction of arc delivery techniques. The concept of proton arc therapy is just becoming commercially/clinically available. Besides the potential for improved physical dose conformity, proton arc therapy might also lessen the concern of elevated linear energy transfer (LET) and relative biological effectiveness (RBE) at the end of the proton range. The aim of this project was therefore to simulate the effects of proton arc therapy for pediatric brain irradiation with respect to dose coverage and conformity, including LET-weighted biological doses.

### Material and Methods

Two cylindrical phantoms were used to create a series of treatment plans with varying number of equiangular coplanar beams (2, 3, 4, 6, 8, 10 and 12), where a dose of 54 Gy was prescribed to a cylindrical target. CTs and target volume delineations of three pediatric brain tumor patients were used to construct plans with 3, 6 and 12 equiangular coplanar beams. Doses delivered to a large

number of manually segmented brain structures associated with cognition were evaluated. Conformity relative to the target was assessed by using both the Conformity Index (CI) and Hausdorff Distance (HD) for multiple isodose levels in both the phantoms and patients. Biologically corrected dose distributions were calculated and compared across plans using two RBE strategies: (1)  $RBE_{1,1}$ , corrected assuming uniformly 10% higher effectiveness of the proton plans, and (2)  $RBE_{LET}$ , calculated using a LET/RBE research script (Eclipse treatment planning system), with the LET distributions normalized to achieve an average  $RBE_{LET} = 1.1$  within the target.

### Results

The CI improved in the phantom plans with up to six beams while no further benefit was observed with larger number of beams. The 3-beam plans showed high-LET and high-RBE regions at the distal edge of each beam while the 12-beam plans resulted in a more uniform distribution of LET and RBE, with the RBE closer to 1.1 (Fig. 1). Similar patterns were seen in both phantoms and patients. Compared to the 3-beam plans, the 12-beam plans had approximately 2 mm lower HD between the target and the 45 Gy isodose surfaces in all directions. The plans with increased number of beams had a more uniform HD between the target and intermediate dose surfaces (10 and 20 Gy) across all directions while the corresponding HD for the 3-beam plans were highly depending on beam direction. The 3-beam plans had the smallest low-dose 'bath' (at 2 and 5 Gy; Fig. 2).

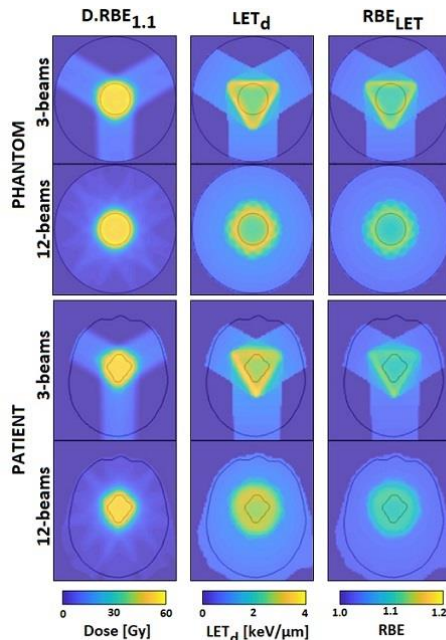


**Figure 1:** Biological dose distributions calculated using an RBE of 1.1 (left column), the LET distribution (central column) and the LET-based RBE distribution calculated as  $1 + c \times LET$ , for plans using three (first row) and twelve beams (second row) in both a phantom (top panel) and a patient (bottom panel). The high-LET patterns are more evident in the phantom plans since these were optimized with only generic normal tissue constraints while the patient plans were optimized using several specific constraints for a range of organs at risk.

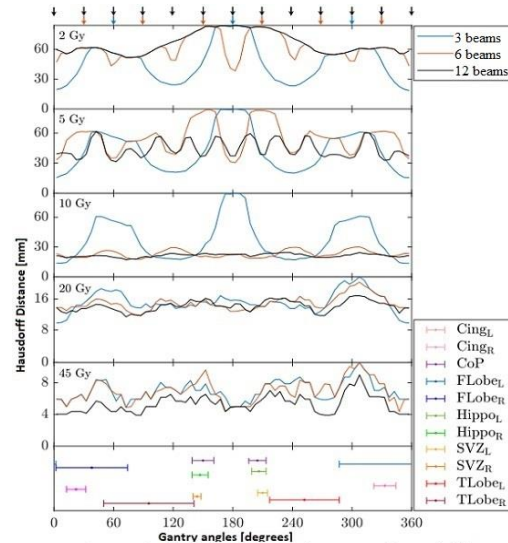


**Figure 2:** The Hausdorff Distance between the target surface and different isodose surfaces (2, 5, 10, 20 and 45 Gy) as a function of the gantry direction for the treatment plans indicated by the arrows on top of the panel: three beams (blue), six beams (orange) and twelve beams (black). The bottom panel shows the extensions of the different OARs in the central plane of the beam's eye view as a function of the gantry angles, showing e.g. the cingulum (Cing), Circuit of Papez (CoP), frontal lobes (FLobe), hippocampus (Hippo) and temporal lobes (TLobe).

### Conclusion

The *physical* conformity at high-dose levels in both phantom and patient plans improved when adding up to six fields, suggesting a potential for proton arc therapy. Increasing the number of beams also resulted in more uniform *biological* dose distributions, due to the reduced high-LET volumes. However, increasing the number of beams also enlarged the low-dose 'bath' (<5 Gy) with possible implications for secondary cancer risks.

### PO-0935 Implementation of an in-house solution for motion management-based treatment planning

D. Dechambre<sup>1</sup>, A. Delor<sup>1</sup>, F. Vanneste<sup>1</sup>, X. Geets<sup>1</sup>  
<sup>1</sup>Cliniques Universitaires Saint-Luc, Radiotherapy department, Brussels, Belgium

### Purpose or Objective

No commercial system provides an approach to 4DCT treatment planning with mid-ventilation (MidV) or mid-position (MidP) as respiration-induced target motion strategies. Therefore clinics have to develop their own and often complicated solution using mostly third party software (e.g. Reggui). The aim of this study was to evaluate the feasibility of using an in-house treatment planning system-based (TPS) script to replace, simplify and automatize our current and complex MidP workflow.

### Material and Methods

Scripting was edited in RayStation (RS) system v8 using IronPython v2.7. A graphical user interface (GUI) was designed using XAML which allows for flexible and interactive data visualization.

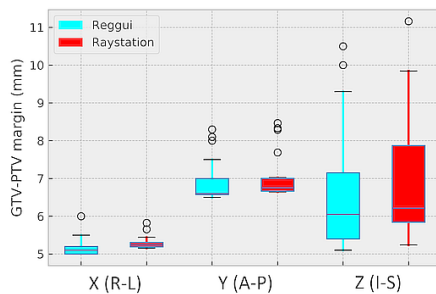
Prior GTV delineation was performed on a single 4DCT phase. Hybrid deformable registration was processed with the remaining phases and the resulting displacement fields were used to map the tumour contour. Given the impossibility to reconstruct the MidP CT from RS using diffeomorphic deformations, MidV-like approach was developed where the selected 4DCT phase minimizes the 3D vector between GTVs and MidP centers of mass (CoM). Chosen MidV\_GTV is then transferred onto the time-average CT and translated to the MidP CoM coordinates, correcting for the hysteresis movement within the GTV rigidity hypothesis. Corresponding 4DCT phase was used for the organs-at-risk delineation.

To validate the methodology, twenty consecutive lung SBRT cases treated in our institution were retrospectively

processed using the RS script. Spatial and volumetric comparison of the resulting PTV was performed against the Reggui-generated one. Statistical significance was assessed using a paired t-test at a 0.05 significance level.

### Results

Patient population consisted in 15 peripheral and 5 central lesions with average 3D motion vector of 10.2 (SD 6.6) mm. The spatial position of the gravity centre showed no statistical differences (<0.1mm) between the Reggui and RS-based PTV. While the script-generated target volume was systematically larger by an average value of 0.42 (0.85) cc ( $p<0.05$ ), the GTV to PTV margin was found significantly larger only in the right-left and anterior-posterior direction by an average of 0.1 (0.1) mm and by 0.2 (0.5) mm in inferior-superior (Figure 1).



### Conclusion

MidP-like solution was successfully integrated into the treatment planning system using built-in scripting capabilities. Hence, workflow was simplified while user inputs and manual interventions were minimized. The development of a tumour deformation handling solution is currently ongoing.

### PO-0936 To be or not to be homogeneous in SBRT plans? a systematic multi-planning study

P. Mancosu<sup>1</sup>, G. Reggiori<sup>1</sup>, A. Gaudino<sup>1</sup>, F. Lobefalo<sup>1</sup>, L. Paganini<sup>1</sup>, V. Palumbo<sup>1</sup>, A. Stravato<sup>1</sup>, S. Tomatis<sup>1</sup>, M. Scorsetti<sup>1,2</sup>

<sup>1</sup>Humanitas Research Hospital, Radiotherapy and Oncology, Rozzano Milan, Italy; <sup>2</sup>Humanitas University, Biomedical Sciences, Rozzano Milano, Italy

### Purpose or Objective

In stereotactic body radiation therapy (SBRT) delivered with modulated plans, two opposing approaches could be followed. ICRU 83 recommends to normalize modulated plans at mean dose to the target (homogeneous approach - HOM). AAPM WG 101 recommends to normalize SBRT plans at a specific isodose (inhomogeneous approach - INH). The new ICRU91 for stereotactic treatments does not recommend an explicit normalization but it advises to report doses at near maximum (D2%), minimum (D98%) and mean dose to the target. In this study, a systematic study on the dosimetric effect of the two approaches was performed.

### Material and Methods

Four patients were randomly selected by the internal database of candidates to lung SBRT. Internal Target Volume (ITV) was generated as the union of clinical target volumes (CTV) contoured on 4D-CT series. Planning target volume (PTV) was defined as ITV+5mm in the 3 directions. Volumetric modulated arc therapy (VMAT) plans were optimized by seven experts who performed two different plans on each patient: HOM (normalization at mean dose to PTV; objectives: CTV-V98%>98%, PTV-V95%>95%, PTV-V105%<5%, hotspots only inside ITV) and INH (normalization at PTV-V98%=98%; objectives: PTV-D2%<150%, PTV-D2%>140%). Plans were all prescribed to 48 Gy in 4 fractions. Daily image guided radiotherapy by CBCT

was performed before each fraction. Plans were recalculated on the maximum inspiration and expiration phases of the 4D-CT series, and on CBCTs. Statistical significance was examined using a Wilcoxon signed rank-test for related samples and set at  $p\leq 0.05$ . The computations were carried out with the STATA 13.0.

### Results

A total of 392 plans were calculated and analyzed. All plans fully accomplished the objectives. Example of dose distributions for the two approaches is reported in figure 1. A general higher variability between planners was found for INH (the highest differences for ITV-D50%). Excluding obvious results, HOM plans resulted in higher body V50% sparing ( $P=0.16$ ), lower total MU ( $P<0.001$ ), lower gradient index ( $GI=\text{body V50\%/V95\%}$ ) with  $GI_{\text{HOM}}=4.1\pm 0.3$  and  $GI_{\text{INH}}=3.8\pm 0.1$  ( $P<0.001$ ), lower PTV-D98% ( $95.1\pm 0.3\%$  vs  $98\%$  -  $P<0.001$ ). In the 4D-CT series, CTV-D98% was relatively reduced of  $2.1\pm 0.3\%$  and  $9.3\pm 3.5\%$  for HOM and INH ( $P<0.001$ ), however absolute CTV-D98% values were higher for INH. In the CBCT series, a similar behavior for both approaches was observed with patient and day-by-day variations.

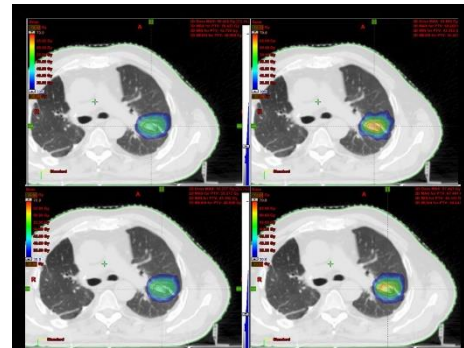


Figure 1: Axial views for (Left) HOM and (Right) INH approaches for two planners. Colorwash ranging between 30-70Gy

### Conclusion

The HOM approach resulted in more reproducible dose distribution between different planners and lower mean dose to the body. The INH approach, however, produced significantly higher mean doses to the target and steeper dose gradients. When defining a clinical protocol, physicians should be aware of advantages and drawbacks of the two approaches.

### PO-0937 Can butterfly VMAT in DIBH reduce dose of LAD in left breast cancer radiotherapy?

M. Maffei<sup>1</sup>, S. Bou Selman<sup>1</sup>, S. Hofer<sup>2</sup>, M. Haller<sup>2</sup>, P. Ferrari<sup>2</sup>

<sup>1</sup>Azienda sanitaria dell'Alto Adige, Servizio di radioterapia oncologica, Bolzano, Italy; <sup>2</sup>Azienda sanitaria dell'Alto Adige, Servizio di fisica sanitaria, Bolzano, Italy

### Purpose or Objective

to assess the feasibility of a multi partial arc in deep inspiration breath hold to minimize dose of left anterior descending coronary artery (LAD) and compare dose between conformal 3D and VMAT both in free breathing and deep inspiration breath hold conditions.

### Material and Methods

21 patients underwent left breast cancer radiotherapy were considered, prescribed dose was 56 Gy in 28 fractions. A total of four treatment combinations were compared (84 plans): 3D-conformal free-breathing (FB), 3D-conformal deep inspiration breath hold (DIBH), 2 partial arcs (from arc angle 290° to 160° clockwise and counterclockwise) free-breathing VMAT (VMAT) and 4 partial arcs using butterfly technique (20 sec per arc, from arc angle 290° to 350°, 120° to 160°, both clockwise and counterclockwise), in order to warranty the treatment

in deep inspiration breath hold (VMAT-DIBH). Conformity and Homogeneity index were calculated. Statistical analysis was performed. Data were expressed as mean  $\pm$  standard deviation. Unpaired Student's t-test was used to compare inter-group means. A P-value equal to or less than 0.05 was considered significant.

#### Results

Conformity and Homogeneity index were significantly better for VMAT compared to 3D plans. 4 partial arcs in VMAT-DIBH were appropriate for patients in breath hold, preserving efficacy of PTV coverage. Dose comparison showed a statistically significant reduction in heart and ventricle mean dose respectively from FB  $3.8 \pm 1.9$  Gy  $5.9 \pm 3.4$  Gy, to VMAT  $3.0 \pm 0.8$  Gy  $4.1 \pm 1.3$  Gy and DIBH  $1.6 \pm 0.8$  Gy  $2.0 \pm 1.3$  Gy. VMAT-DIBH was comparable with DIBH, heart  $1.7 \pm 0.5$  Gy and ventricle  $2.0 \pm 0.7$  Gy, but significantly reduced maximal dose in LAD (43%) and D2 LAD (42%).

#### Conclusion

DIBH reduced dose compared with FB in left breast cancer radiotherapy. VMAT showed to be the second choice in case of ineligible patient. VMAT-DIBH was feasible and comfortable for patients using small partial arcs in butterfly configuration, with a maximum delivery time of 20 sec per arc. VMAT-DIBH was efficacy adding LAD dose reduction (Dmean, Dmax and D2) to the DIBH advantages, at the expense of a small increase in the dose to the contralateral breast. Butterfly VMAT-DIBH improve heart protection in left breast cancer radiotherapy.

#### PO-0938 Spine SBRT plan comparison for Cyberknife and VMAT delivery incorporating intrafraction PTV margin

T. Oshea<sup>1</sup>, C. Jones<sup>1</sup>, C. Meehan<sup>1</sup>

<sup>1</sup>The Royal Marsden NHS Foundation Trust, Radiotherapy Physics, London, United Kingdom

#### Purpose or Objective

Stereotactic body radiotherapy is an effective method for treatment of spine metastases. At our institute the standard of care is treatment on the CyberKnife (CK) system with kV x-ray based intrafraction motion tracking. We investigate the ability to plan and verify the delivery of treatments using a Varian TrueBeam (TB) Linac with intrafraction motion accounted for in the PTV margin calculation.

#### Material and Methods

Intrafraction motion log data from nine previously treated CK patients (T1 - L2 vertebrae) was analysed and used to calculate PTV margins to account for delineation, phantom transfer and patient motion errors. Two-arc VMAT treatments were planned using the Varian Eclipse treatment planning system (with Acuros version 13.7.14 dose calculation) for 27 to 30 Gy in three fractions with 6FFF beams and 1400 MU/min dose-rate. Plans were compared with clinical CK plans which used a nominal 2.0 mm PTV margin. The deliverability of three plans (T1, T7 and L1) was verified by point dose measurement with a semiflex ionisation chamber in a solid water phantom.

#### Results

Mean ( $\pm$ SD) intrafraction motion using all CK log data was  $0.3 \pm 0.8$  mm (SI),  $0.2 \pm 1.3$  mm (RL) and  $0.7 \pm 0.7$  mm (AP) resulting in PTV margins of 4.0, 4.3, 3.7 mm (which also accounted for delineation, phantom transfer and set-up error estimates). The spinal cord PRV margin was 2.0 mm. The mean PTV coverage for VMAT plans with either 2 mm ( $87.6 \pm 2.7\%$ ) or 4 mm ( $84.3 \pm 2.2\%$ ) PTV margins was not significantly less than CK plans ( $85.9 \pm 4.8\%$ ). CTV coverage was significantly ( $p < 0.05$ ) better for VMAT plans. Risk organ doses were below UK NHS CTe guideline limits in all cases. The three verification plans were delivered to the solid water phantom on a TB Linac with an agreement between measured and calculated dose of  $3.5 \pm 0.1\%$ .

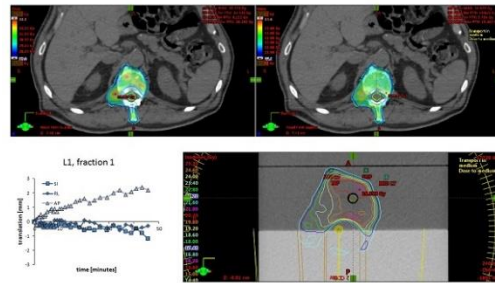


**Figure 1.** L1 vertebra: Comparison of CyberKnife (upper left) and TrueBeam (upper right) planning, example of log-file reconstructed intrafraction motion data used in PTV margin calculation (lower left) and solid water phantom plan verification (lower right).

#### Conclusion

A 4 mm PTV margin can be used to account for translational motion (and other error sources) in the absence of intrafraction motion compensation. PTV coverage for VMAT plans (with 4 mm PTV margin) was not significantly different to CK plans (with 2 mm PTV margin). 2-arc VMAT treatment fractions maintaining maximum dose-rate can be delivered in a much faster time (mean  $< 3.5$  minutes vs. CK  $\sim 40$  minutes) with deliverability verified within our institutes tolerance ( $< 5\%$ ).

#### PO-0939 Suspected impact of linear energy transfer on treatment related toxicities from proton therapy

J. Ödén<sup>1,2</sup>, E. Traneus<sup>2</sup>, P. Witt Nyström<sup>3,4</sup>, I. Toma-

Dasu<sup>1,5</sup>, A. Dasu<sup>3</sup>

<sup>1</sup>Stockholm University, Department of Physics, Stockholm, Sweden ;

<sup>2</sup>RaySearch Laboratories AB, Department of Research, Stockholm, Sweden ;

<sup>3</sup>The Skandion Clinic, The Skandion Clinic, Uppsala, Sweden ;

<sup>4</sup>The Danish Centre for Particle Therapy, The Danish Centre for Particle Therapy, Århus, Denmark ;

<sup>5</sup>Karolinska Institutet, Department of Oncology-Pathology, Stockholm, Sweden

#### Purpose or Objective

To analyse dose-averaged linear energy transfer ( $LET_d$ ) and relative biological effectiveness (RBE) distributions for three patients with suspected treatment related toxicity following intracranial proton therapy. Various planning strategies to reduce  $LET_d$ , RBE and normal tissue complication probabilities (NTCP) were also investigated.

#### Material and Methods

Plans for three patients treated with single-field uniform dose plans with fractionation doses of 1.8 Gy (RBE) to the target in 28 or 30 fractions (assuming RBE=1.1) were recalculated in an independent treatment planning system (TPS) with a Monte Carlo dose engine using the original CT-data, CT-calibration and beam data. The resulting physical dose distribution and  $LET_d$  were used as input to calculate the RBE-weighted dose ( $D_{RBE}$ ) using two  $LET_d$ - and  $\alpha/\beta$ -dependent variable RBE-models. For the targets,  $\alpha/\beta$  values of 3 or 10 Gy were used, whereas 2 Gy were assumed for the normal tissues. Resulting distributions of  $D_{RBE}$  and  $LET_d$  were analysed together with NTCP estimations. Following this, four intensity modulated proton therapy (IMPT) plans were generated in order to investigate the potential of  $LET_d$ , RBE and NTCP reductions in the critical structures: (1) IMPT with the clinical beam arrangements and only dose objectives, (2) alternative beam arrangements and only dose objectives, (3) clinical beam arrangements with dose and track-end objectives (penalized protons stopping in critical structures), (4) alternative beam arrangements with dose and track-end objectives.

#### Results

The recalculated dose distributions agreed well with the dose distributions calculated in the clinically used TPS. The variable RBE-models predicted an increase of 7-12 Gy (RBE) in the near-maximum  $D_{RBE}$  ( $D_{RBE, 2\%}$ ) for the structures with the observed toxicities resulting in not fulfilling the clinical goals. The NTCP for the structures with the observed toxicities increased from 0.8, 0.0 and 0.1% (RBE=1.1) to 15.5, 3.6 and 1.8% (Wedenberg RBE-model) for the three patients, respectively. All alternative plans produced physical dose distributions which were similar or better than the clinical plans, while also generally allowing for substantial  $D_{RBE}$ ,  $LET_d$ , and NTCP reductions in several critical structures assuming the variable RBE-models. In all cases, alternative plan 4 resulted in the lowest values, with a  $LET_d$  reduction of 50%, or more, compared to the clinical plan.

**Table 1.** Mean and near-max RBE-weighted dose ( $D_{RBE, mean}$ / $D_{RBE, 2\%}$  [Gy (RBE)]), mean and near-max  $LET_d$  ( $LET_{d, mean}$ / $LET_{d, 2\%}$  [keV/ $\mu$ m]) and NTCP [%] for the critical structure with the observed toxicity for each of the three patients. An  $\alpha/\beta=2$  Gy was assumed for all calculations.

Patient #	Plan	RBE = 1.1			Wedenberg RBE-model <sup>a</sup>		
		$D_{RBE}$	$LET_{d, 2\%}$	NTCP <sup>c</sup>	$D_{RBE}$	$LET_{d, 2\%}$	NTCP <sup>c</sup>
Patient 1 Brain-stem	Clinical	28.0/55.0	-	0.8	37.8/65.9	5.7/9.4	15.5
	Alt 1 <sup>d</sup>	25.1/54.6	-	0.7	34.4/66.8	6.0/10.5	15.7
	Alt 2 <sup>e</sup>	25.1/54.5	-	0.7	32.7/65.3	4.8/8.0	12.0
	Alt 3 <sup>f</sup>	25.3/54.6	-	0.6	31.4/63.9	3.9/5.7	8.0
	Alt 4 <sup>f</sup>	24.7/54.9	-	0.6	27.3/58.0	2.2/4.1	1.9
Patient 2 Optic Nerve L	Clinical	30.5/48.7	-	0.02	41.8/60.3	5.2/6.3	3.6
	Alt 1 <sup>d</sup>	20.6/44.9	-	0.00	30.8/56.9	5.8/6.7	1.2
	Alt 2 <sup>e</sup>	20.6/43.4	-	0.00	26.2/53.8	3.3/4.4	0.4
	Alt 3 <sup>f</sup>	19.1/46.7	-	0.00	27.2/55.7	5.0/6.2	1.1
	Alt 4 <sup>f</sup>	22.1/46.9	-	0.00	25.5/52.6	2.2/3.2	0.2
Patient 3 Optic Nerve R	Clinical	11.1/51.2	-	0.10	14.3/58.7	4.9/8.6	1.8
	Alt 1 <sup>d</sup>	8.7/48.9	-	0.04	11.4/57.2	5.1/7.5	1.5
	Alt 2 <sup>e</sup>	8.0/48.8	-	0.03	10.4/58.1	4.3/5.5	1.9
	Alt 3 <sup>f</sup>	8.2/48.5	-	0.05	9.9/53.4	3.2/5.5	0.4
	Alt 4 <sup>f</sup>	8.4/47.9	-	0.05	9.7/51.8	2.2/3.2	0.3

<sup>a</sup>Wedenberg et al. Acta Oncologica 2013;52:580-588

<sup>b</sup> $LET_{d, mean}$  and  $LET_{d, 2\%}$  was evaluated for voxels with  $\geq 5\%$  of the prescribed dose

<sup>c</sup>s-model. Brainstem:  $D_{50}=65.1$  Gy,  $\gamma=2.4$ ,  $s=1.0$ . Optic nerve:  $D_{50}=65.0$  Gy,  $\gamma=2.3$ ,  $s=1.0$

<sup>d</sup>Clinical beam arrangements. Only physical dose objectives

<sup>e</sup>Alternative beam arrangements. Only physical dose objectives

<sup>f</sup>Clinical beam arrangements. Physical dose objectives and proton track-end objectives

<sup>g</sup>Alternative beam arrangements. Physical dose objectives and proton track-end objectives

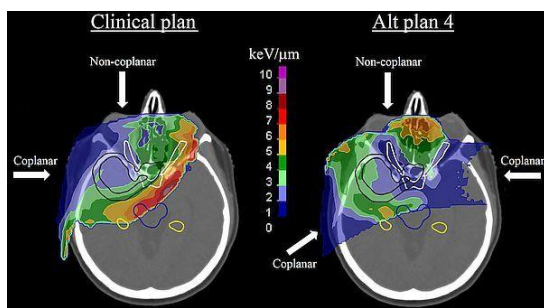


**Figure 1.** Representative transversal slice of patient 2 showing  $LET_d$  for the clinical plan and alternative plan 4, with the beam arrangements. The CTV, PTV (black lines), left optic nerve, right optic nerve, chiasm (white lines), brainstem (blue line) and left/right hippocampus (yellow lines) are shown. The  $LET_d$  is shown for doses  $>5\%$  of 54 Gy (RBE).

## Conclusion

Although a study of this size and design could not establish direct causality between RBE and toxicity, the analysis indicates that the enhanced RBE, due to high  $LET_d$ , could be a potential cause of the observed toxicities. Combining IMPT with alternative beam arrangements and/or objectives beyond physical dose allow for  $D_{RBE}$ ,  $LET_d$ , and NTCP reductions in several critical structures for intracranial lesion, without compromising the target dose. Such planning strategies might hence be a future tool in order to maximize the benefit of proton therapy.

## PO-0940 The effects of Bragg curve degradation in proton therapy of bronchial carcinomas

V. Flatten<sup>1,2</sup>, K. Baumann<sup>1,2</sup>, U. Weber<sup>3</sup>, S. Lautenschläger<sup>1</sup>, F. Eberle<sup>1</sup>, R. Engenhart-Cabillic<sup>1</sup>, K. Zink<sup>2</sup>

<sup>1</sup>University Medical Center Giessen-Marburg, Department of Radiotherapy and Radiooncology, Marburg, Germany ;

<sup>2</sup>University of Applied Sciences Giessen THM, Institute of Medical Physics and Radiation Protection, Giessen, Germany ;

<sup>3</sup>GSI Helmholtzzentrum für Schwerionenforschung, Biophysics Division, Darmstadt, Germany

### Purpose or Objective

Sub-millimetre-sized heterogeneities like lung parenchyma cause a degradation of the Bragg curve. State-of-the-art treatment planning systems are unable to consider the degradation in the treatment planning process ignoring the influence on the dose distribution. Potentially, this can result in an underdosage of the PTV and an overdosage of distal normal tissue.

In a previous study we presented a strategy to consider this Bragg peak degradation by applying a density modulation to the voxels associated with the lung [1]. In this study we use this tool to analyse the effects of this Bragg curve degradation on CT based phantoms, enabling a thorough investigation of the dependencies of parameters effecting the degradation and present data for five treatment plans on patient CTs.

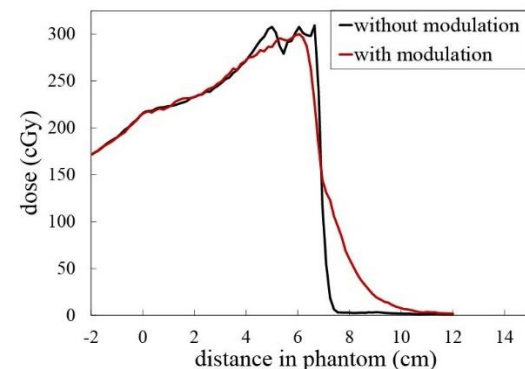
### Material and Methods

Stereotactical proton treatment plans were optimised using the treatment planning system Eclipse (VARIAN) on phantom and patient CTs. Each plan was then recalculated using the Monte Carlo toolkit TOPAS [2]. In a first scenario, the treatment plans were recalculated using the original density values from the treatment planning CT which correlates to the dose distribution predicted by the treatment planning system.

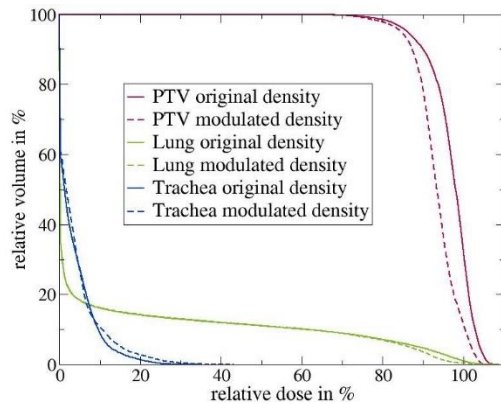
In a second scenario, the density values of each voxel within the lung were modulated using a mathematical model [1], thus giving the actual dose distribution in the patient.

The phantoms that were used covered a range of different distances of the treatment volume in lung as well as various tumour volumes.

### Results



In Figure 1 an exemplary depth-dose curve through one of the phantom dose distribution shows the effect of the Bragg peak degradation in comparison to the curve predicted by the treatment planning system.



In Figure 2 the dose-volume histograms of a patient plan with and without the modulation is presented. It shows an underdosage for the PTV (red) and an overdose in the distal tissue (here: the trachea in blue).

The results from the phantom study show an increase in the dose difference as the distance in lung increases and the volume decreases. Underdoses from a few percent up to 12% for distances up to 15cm in lung were found in a conservative approach. For patients plans, the PTV underdosage ranges between 1% and 5% in comparison to the plan calculated with the treatment planning system.

#### Conclusion

We are able to analyse the effects of Bragg curve degradation due to lung parenchyma in the treatment planning process of lung cancer patients. As the inclusion of this Bragg peak degradation cannot be easily implemented in treatment planning routines, this study gives a conservative approximation for the underdose in the PTV, when it is not accounted for.

[1] Baumann K-S, Witt M, Weber U, Engenhardt-Cabillic R and Zink K 2017 An efficient method to predict and include Bragg curve degradation due to lung-equivalent materials in Monte Carlo codes by applying a density modulation *Phys. Med. Biol.* 62 3997-4016

[2] Perl J, Shin J, Schuemann J, Faddegon B and Paganetti H 2012 TOPAS: an innovative proton Monte Carlo platform for research and clinical applications *Med. Phys.* 39 6818-37

#### PO-0941 Can dose gradient-based plan optimisations compete with autoplanning for optimal prostate plans?

D. Schuring<sup>1</sup>, A. Van Nunen<sup>1</sup>, F. Van Aarle<sup>1</sup>, T. Jongsmavan Nunen<sup>1</sup>, T. Budiharto<sup>1</sup>  
<sup>1</sup>Catharina Hospital, Department of Radiation Oncology, Eindhoven, The Netherlands

#### Purpose or Objective

Multiple studies have shown that autoplanning improves consistency and optimal OAR sparing for individual patients in treatment planning [1]. These inconsistencies in OAR sparing are often caused by the use of mean dose or DVH objectives in the inverse optimisation, which are sensitive to anatomical variations in patients and require adjustments by the treatment planner. By optimising on the dose gradients inside the OAR, more consistent results can be obtained as these objectives are less sensitive to these variations. This was tested by replanning clinical prostate patients using these gradient-based objectives and comparing the resulting OAR doses to the clinical plans using the "traditional" optimisation approach.

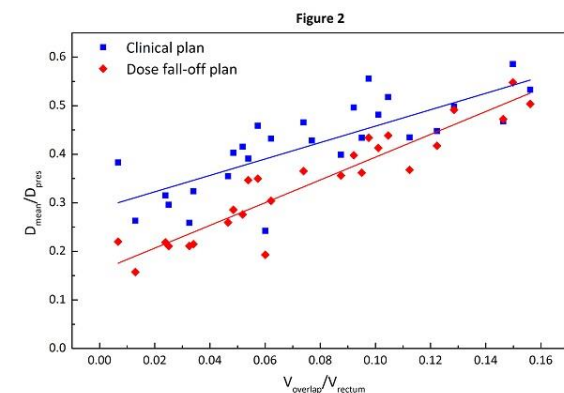
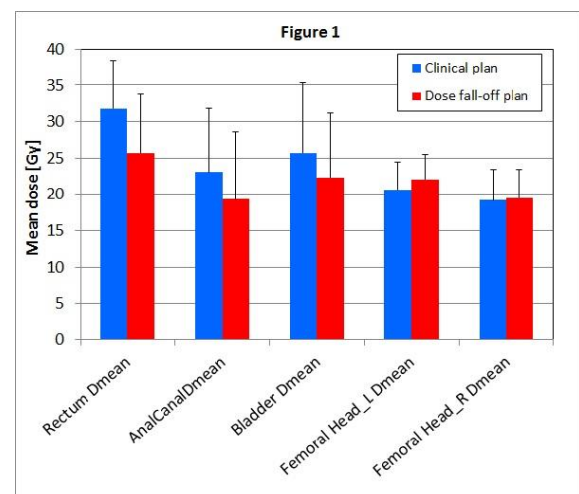
#### Material and Methods

27 patients with prostate cancer receiving a total dose of 76 Gy were randomly selected from the clinic. These patients were then replanned with a new class solution that uses dose fall-off objectives on the OAR in the RayStation TPS. During re-optimisation no manual adjustments to the objectives were allowed. For the

clinical as well as the dose fall-off plans, PTV and OAR dose parameters (rectum, anal canal, bladder, femoral heads) were evaluated to check if OAR sparing improved. In analogy to knowledge-based approaches, consistency of the the rectum sparing was analysed by plotting the mean dose against the fraction of rectum volume overlapping the PTV [1] for both the clinical and dose fall-off treatment plans.

#### Results

For all patients, the new optimisation approach resulted in clinically acceptable plans with a reduction of the dose in the rectum, anal canal and bladder (fig. 1), while maintaining similar PTV coverage and conformity and only a slight increase of the dose in the femoral heads. The largest improvement in OAR sparing was observed for the rectum and anal canal (an average reduction of the mean dose of 19.1 and 16.3% respectively). This was mostly achieved by a reduction of the intermediate dose to these OAR (< 45 Gy). Fig. 2 shows the normalized mean rectum dose as a function of the fraction of the rectum volume overlapping the PTV. Over the whole range of overlap a reduction of the mean rectal dose was achieved, with the largest gains at smaller overlaps fractions. For these patients, the dose constraints can be easily achieved, and larger manual adjustments are needed to achieve optimal sparing. The dose fall-off based optimisations furthermore resulted in a more consistent OAR sparing, reflected by a reduction of the spread of the rectum dose as a function of the overlap fraction.



#### Conclusion

When using a new class solution with dose-gradient objectives for the OAR, a significant improvement of rectum, anal canal and bladder sparing for prostate patients was achieved without manual adjustments of the planning objectives. Similar to autoplanning approaches, this results in more consistent sparing of the OAR with

varying patient anatomy, and less sensitivity to planner experience and skills.

[1] Powis et al., *Radiat Oncol* 12 (2017) 81

**PO-0942 Optimization of adaptive aperture margins in robustly optimized pencil beam scanning proton plans**  
G. Vilches Freixas<sup>1</sup>, M. Unipan<sup>1</sup>, I. Rinaldi<sup>1</sup>, J. Martens<sup>1</sup>,  
C. Ares<sup>1</sup>, G. Bosmans<sup>1</sup>

<sup>1</sup>*Maastric Clinic, Department of Radiation Oncology, Maastricht, The Netherlands*

**Purpose or Objective**

At the end of the beam line of the Mevion S250i proton therapy system there is an adaptive aperture to reduce lateral penumbra, especially at low energies, by laterally trimming the spots at the edge of the treatment field. The goal of this study was to determine the optimal aperture margin (AM) from the CTV in a robust optimized plan for different anatomical sites, treatment volumes, and number of beams.

**Material and Methods**

In a water phantom, a L-shaped volume simulating a CTV with 10 cm the largest x, y and z dimensions was placed at different depths from 1 up to 15 cm from the phantom surface. In the first phase of the study, nominal non-robust Monte Carlo (MC) 60 Gy(RBE) (2 Gy(RBE) x 30 fractions) plans were created. Using the scripting module in Raystation 8.A, plans varying from single-beam up to 4 beams were generated for every target volume depth. In each plan, the AM margins from the target volume were varied from 2 mm to 10 mm in 2 mm steps. In the second part of the study, 120 robust optimized MC plans taking into account 4 mm setup uncertainty (SU) and 3.5% range uncertainty were created with different AMs. In a robust optimized plan, the SU uncertainties should also be taken into account in the aperture margin. For this reason, the AM in a robust optimized plan (AM\_RO) are defined as the AM in a nominal plan plus the SU:  $AM_{RO} = AM_{nominal} + SU$ . Moreover, to check this hypothesis, extra 2 mm margins were added and subtracted to the AM\_RO in a robustly optimized plan.

Plan robustness, after plan optimization, was further evaluated with the previous robustness settings (4 mm setup and 3.5% range uncertainties, respectively) by calculating 28 different scenarios of combined uncertainties via an automated script. In both phases of the study, the following metrics were used to drive a decision: Homogeneity Index (HI), D98%, D2%, D95% and the Conformity Index (CI). The results were benchmarked against 6 head and neck and 9 central nervous system brain tumour patients.

**Results**

The effect of the AM was more predominant at shallow depths, as expected. More beams allow tighter AMs. The optimal AM was found to be: 4 mm + SU for 1 to 3 beams, 2 mm + SU for 4 beams, and 6 mm + SU for 1 to 2 beams in the case of shallow tumours (Fig. 1 and 2). For the last situation, AM had to be enlarged to improve target coverage. Furthermore, based on the clinical validation, an AM of 6 mm + SU was found to be optimal also for small tumours close to air cavities.

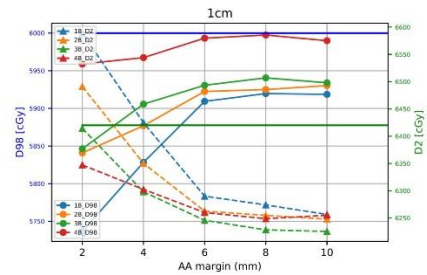


Figure 1. Results of the first phase of the study: nominal non-robust MC plans. D98 and D2 for the 1 cm depth tumour as a function of the AM. D98 (circles) is expected to be as close as possible to the prescribed dose (blue line) and, at the same time, D2 (triangles) below 107% of the prescribed dose (green line).

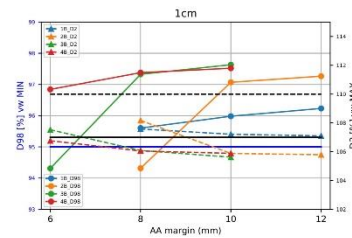


Figure 2. Results of the second phase of the study: robustly optimized and evaluated MC plans. D98 in the robust evaluation distribution (w/ MIN) and D2 in the robust evaluation distribution (w/ MAX) for the 1 cm depth tumour as a function of the AM. D98 (circles) is expected to be above 95% of the prescribed dose (blue line) and, at the same time, D2 (triangles) below 107% of the prescribed dose (black solid line). The discontinuous black line in the right axis represents the 107% of the prescribed dose.

**Conclusion**

Optimal AMs for robustly optimized pencil beam scanning (PBS) proton plans for the Mevion S250i were derived and validated for 15 patient cases. The use of apertures in PBS improves lateral penumbra and potentially reduces the dose to the organs at risk.

**PO-0943 Harmonization of proton planning for head and neck cancer using PBS: First report of the IPACS collaboration**

M. Stock<sup>1</sup>, J. Gora<sup>1</sup>, A. Perpar<sup>2</sup>, P. Georg<sup>2</sup>, G. Kragl<sup>1</sup>, E. Hug<sup>2</sup>, V. Vondracek<sup>3</sup>, J. Kubes<sup>4</sup>, C. Algranati<sup>5</sup>, M. Cianchetti<sup>6</sup>, M. Amichetti<sup>6</sup>, T. Kajdrowicz<sup>7</sup>, R. Kopeck<sup>7</sup>, P. Olko<sup>7</sup>, K. Skowronska<sup>7</sup>, U. Sowa<sup>7</sup>, E. Gora<sup>8</sup>, K. Kisielwicz<sup>8</sup>, B. Sas-Korczynska<sup>8</sup>, T. Skora<sup>8</sup>, A. Bäck<sup>9</sup>, M. Gustafsson<sup>10</sup>, M. Sooar<sup>10</sup>, P. Witt Nyström<sup>11</sup>, T. Björk Eriksson<sup>12</sup>

<sup>1</sup>MedAustron Ion Therapy Center, Medical Physics, Wiener Neustadt, Austria; <sup>2</sup>MedAustron Ion Therapy Center, Radiation Oncology, Wiener Neustadt, Austria; <sup>3</sup>Proton Therapy Center Czech, Medical Physics, Prague, Czech Republic; <sup>4</sup>Proton Therapy Center Czech, Radiation Oncology, Prague, Czech Republic; <sup>5</sup>U.O. di Protonterapia- Azienda Provinciale per I Servizi Sanitari Trento, Medical Physics, Trento, Italy; <sup>6</sup>U.O. di Protonterapia- Azienda Provinciale per I Servizi Sanitari Trento, Radiation Oncology, Trento, Italy; <sup>7</sup>Institute of Nuclear Physics Polish Academy of Sciences- Cyclotron Centre Bronowice, Medical Physics, Krakow, Poland; <sup>8</sup>Maria Skłodowska-Curie Memorial Cancer Center and Institute of Oncology, Radiation Oncology, Krakow, Poland; <sup>9</sup>University of Gothenburg, Radiation Physics, Gothenburg, Sweden; <sup>10</sup>Sahlgrenska University Hospital, Therapeutic Radiation Physics, Gothenburg, Sweden; <sup>11</sup>The Skandion Clinic, Radiation Oncology, Uppsala, Sweden; <sup>12</sup>Sahlgrenska University Hospital, Oncology, Gothenburg, Sweden

**Purpose or Objective**

Clinical evidence for the advantage of proton therapy (PT) is still limited. To show superiority larger scale clinical trials in a collaborative network must be performed. A collaborative network between PT centres in Trento in Italy, Poland, Austria, Czech Republic and Sweden (IPACS) was founded to implement those trials and harmonize PT.

This is the first report of IPACS with focus on proton therapy treatment planning of head-and-neck patients.

### Material and Methods

CT-data sets of five patients were included. During several face-to-face and online meetings a common treatment planning protocol was developed having objectives for target coverage and organ at risk (OAR) sparing together with their mutual prioritization as well as a definition of robustness evaluation. Each centre used its own treatment planning system (TPS) and planning approach with some restrictions specified in the treatment planning protocol. In addition, volumetric modulated arc therapy (VMAT) photon plans were created.

### Results

For CTV1 the average  $D_{98\%}$  was  $54.6 \pm 2.3$  Gy(RBE) for protons and  $54.9 \pm 0.5$  Gy(RBE) for VMAT (aim was 56 Gy(RBE)). For CTV2 the average  $D_{98\%}$  was  $60.8 \pm 5.7$  Gy(RBE) for protons and  $61.6 \pm 3.4$  Gy(RBE) for VMAT (aim was 70 Gy(RBE)). The average  $D_{2\%}$  for the spinal cord was  $25.1 \pm 8.5$  Gy(RBE) for protons and  $47.6 \pm 1.4$  Gy(RBE) for VMAT (see also Figure 1). The average  $D_{2\%}$  for chiasm was  $46.5 \pm 4.4$  Gy(RBE) for protons and  $50.8 \pm 1.4$  Gy(RBE) for VMAT respectively. Robust evaluation was performed and showed the least robust plans for plans with a low number of beams (see Figure 2).

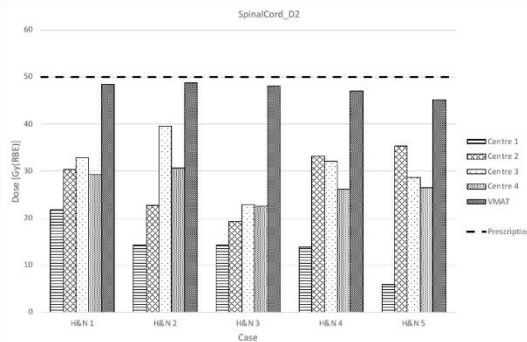


Figure 1: For the nominal plans, the  $D_{2\%}$  for the spinal cord for all 5 head and neck cases from each centre and the VMAT plan is shown. The planning aim was achieved by all plans. The dashed line shows the objective for spinal cord  $D_{2\%}$  which was  $< 50$  Gy (RBE).

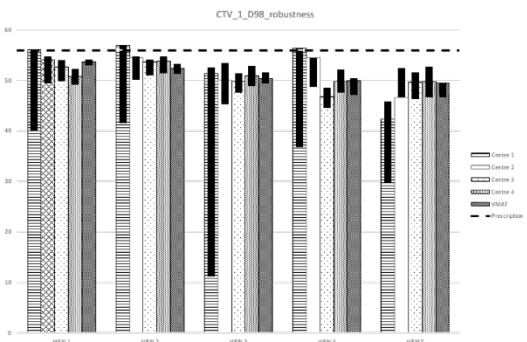


Figure 2:  $D_{98\%}$  for CTV1 in the first treatment phase for the nominal plans and the results of the robustness analysis for all 5 head and neck cases from each centre and the VMAT plan is shown. The black bars show the band width (max and min) of  $D_{98\%}$  for all the robustness scenarios. The dashed line shows the planning aim for CTV1  $D_{98\%}$  which was 56 Gy (RBE) respectively.

### Conclusion

Despite the detailed treatment planning protocol, differences in dose distribution and reported parameter were still identified. Although VMAT is more robust than PT, OAR sparing at intermediate distance from CTVs and

integral dose is worse. In future all OARs that should be included in the optimization need to be specified in order to further harmonize treatment planning.

### PO-0944 Proton therapy for esophageal cancer; variable relative biological effect and heart dose

C. Skinnerup Byskov<sup>1</sup>, A. Ivalu Sander Holm<sup>1</sup>, S.S. Korreman<sup>1</sup>, L. Hoffmann<sup>1</sup>, M. Nordmark<sup>2</sup>, D. Sloth Møller<sup>1</sup>  
<sup>1</sup>Aarhus University Hospital, Medical Physics, Aarhus C, Denmark ; <sup>2</sup>Aarhus University Hospital, Oncology, Aarhus C, Denmark

### Purpose or Objective

For patients with esophageal cancer the standard treatment is radiotherapy (RT) and concomitant chemotherapy, possibly followed by surgery. Dose to the organs at risk (OAR) can be substantially reduced by proton therapy (PT), and a recent study has shown that posterior field directions constitute the most robust beam configuration for PT [Møller et al., RO 2018]. These PT studies were based on a constant proton relative biological effect (RBE) of 1.1 which disregards data suggesting that RBE varies with linear energy transfer (LET), physiological and biological factors. Heart dose has been found to increase the risk of heart toxicity [Darby et al., NEJM 2013]. The aim of this study was therefore to investigate the effect of variable RBE on dose to the heart in PT for patients with esophageal cancer using posterior field directions.

### Material and Methods

Previously reported robustly optimized proton plans for 23 patients with esophageal cancer were used as baseline plans [Møller et al., RO 2018]. Two field configurations were applied for each patient, using one posterior field (I-plans) or two oblique posterior fields (V-plans) (Figure 1). The linear energy transfer (LET) and relative biological effect (according to the RBE model by McNamara et al. [PMB 2015]) were calculated in Eclipse using an Eclipse script developed by Sanchez-Parcerisa et al. [PMB 2016]. Mean heart dose (MHD), heart volumes receiving 25 Gy (V25Gy) and 40 Gy (V40Gy) and the near maximum dose (D2ccm) were measured and compared for the two different field configurations. Differences were tested using the Wilcoxon signed rank test, with  $p < 0.05$  considered significant.

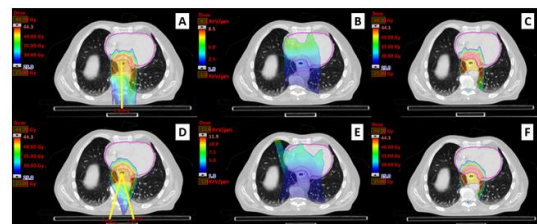


Figure 1: Dose comparisons between the I-plans (top row) and V-plans (bottom row). Field angles shown in yellow. For the RBE = 1.1 dose (A + D) and the McNamara RBE dose (C + F), the minimum dose displayed on the color wash is 25 Gy and all doses above 107% of the prescribed dose (44.3 Gy) are displayed in red. For the RBE weighted dose, only structures that are delineated on the CT scan have calculated doses. In the middle column, the LET distributions are displayed (B + E), the minimum is set to 1 keV/μm and here the maximum values calculated are 6.5 keV/μm for the I-plan and 11.9 keV/μm for the V-plan.

### Results

For the I-plans and the V-plans respectively, the population median MHD was reduced with 7.4 Gy and 6.9 Gy compared to the IMRT plans (Figure 2). When applying the variable RBE model, doses to the heart increased compared to using RBE 1.1. For the I-plans and [V-plans], respectively, the MHD was increased by  $1.0 \pm 0.5$  Gy [ $1.3 \pm 0.7$  Gy], V25Gy was increased by  $1.9 \pm 1.0\%$  [ $2.4 \pm 1.2\%$ ], V40Gy was increased by  $2.3 \pm 1.3\%$  [ $2.9 \pm 1.6\%$ ] and D2ccm was increased by  $3.5 \pm 1.0$  Gy [ $5.0 \pm 1.5$  Gy] (population mean  $\pm$ SD). Significant differences were found between the I-plans and V-plans for V25Gy and D2ccm.

	IMRT	I-plan RBE = 1.1	I-plan McNamara RBE	p-value RBE = 1.1 vs. McNamara RBE	V-plan RBE = 1.1	V-plan McNamara RBE	p-value RBE = 1.1 vs. McNamara RBE	p-value I-plan vs V-plan McNamara RBE
MHD (Gy)	17.0	6.4	9.6	<0.001	8.7	10.1	<0.001	>0.05
V25Gy (%)	23.3	15.9	18.3	<0.001	16.0	18.8	<0.001	<0.05
V40Gy (%)	7.3	6.5	9.2	<0.001	5.9	9.5	<0.001	>0.05
D2ccm (Gy)		42.4	46.2	<0.001	41.9	47.4	<0.001	<0.05

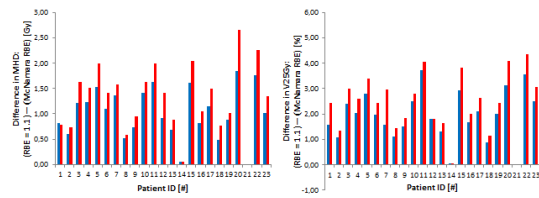


Figure 2: Top: Selected dosimetric parameters for the heart for IMRT, RBE = 1.1 doses and McNamara RBE doses. All values are median values and grey columns are previously published data. Bottom: Differences in dose between McNamara RBE dose and RBE = 1.1 dose for the individual patients. I-plans are shown in blue and V-plans in red.

## Conclusion

Accounting for the variable RBE effect in PT planning with only posterior fields for esophageal patients increases the dose to the heart. The heart exposure is, however, still considerably decreased compared to IMRT. Heart V25Gy and D2ccm were significantly increased when using the two-field configuration compared to the one-field configuration.

## PO-0945 Stochastic Frontier Analysis to predict sparing of organs-at-risk for VMAT-treated prostate cancer

A. Kroshko<sup>1</sup>, O. Morin<sup>2</sup>, L. Archambault<sup>1</sup>

<sup>1</sup>Université Laval, Physique- génie physique et optique, Quebec, Canada ; <sup>2</sup>University of California San Francisco, Department of Radiation Oncology, San Francisco, USA

## Purpose or Objective

Treatment planning of advanced radiation therapy techniques often require compromises between the delivery of the prescribed dose to the volume of interest and the sparing of the neighbouring organs-at-risk (OAR). A novel knowledge-based model was developed based on Stochastic Frontier Analysis (SFA) to predict achievable dosimetric indices for the bladder and the rectum for prostate cancer treated with VMAT.

## Material and Methods

SFA is modeled as an optimum frontier with dosimetric parameters degradation following a normal-half normal distribution. Model can converge into two extremes, a regression or an absolute frontier, otherwise a stochastic frontier is obtained. Seven parameters were used to describe the geometry between each OARs and PTV (e.g. the overlap volume and the Hausdorff distance). They are extracted with an automatized python routine within the 3D Slicer platform. Estimators of the model are determined using a maximum likelihood technique to obtain stochastic frontiers for 9 dosimetric indices (ex. V60Gy) only in terms of the geometric parameters. The model was developed with a database of 152 patients treated between October 2014 and May 2017 with prescribed dose to the PTV between 60 and 78 Gy with the treated volume being prostatic bed or prostate with seminal vesicles. A validation cohort of 20 random patients treated between December 2017 and April 2018 was then used to compare the planned dose to the predicted dose to the OAR. A metric quantifying the similarity between the predicted and the clinical plan is then calculated. It is defined as the sum of the dose difference between predicted and planned divided by the number of dosimetric indices predicted for an OAR. A negative value means that the predicted dose is lower than the one planned. The overall score is the sum of the score for the bladder and the rectum.

## Results

75% of the validation plans have an overall score lower than 5% dose difference between the predicted and the

planned DVH. Thus, the majority of the predicted plans are close to the planned ones or even suggests that further dose reduction is possible for those plans. 68% (27 out of 40) of the organs-at-risk are within the  $\pm 3\%$  dose difference with the planned values. Figure 1 presents the comparison between the planned dose values and the one predicted by our SFA model. The model is well adapted to predict different dosimetric sparing for the OARs and for different dose prescriptions. Considering there is no mathematical relationship between the predicted dosimetric indices the obtained dose-volume curves are quite smooth.

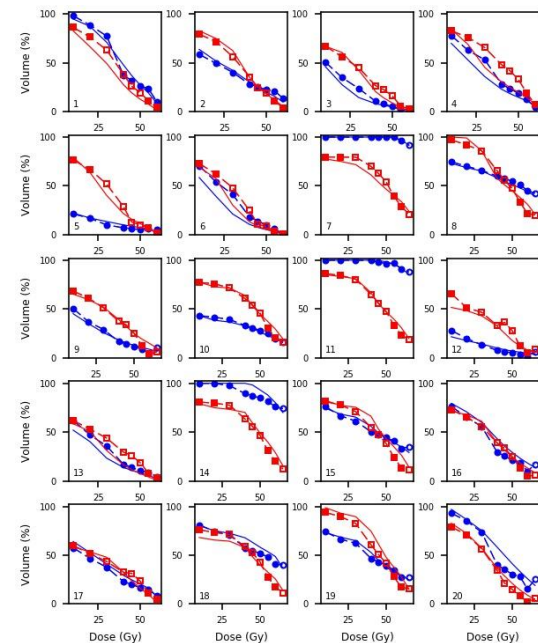


Figure 1: Comparison between the planned dose values (full line) and the predicted (dashed line) for the bladder (blue line - square) and the rectum (red line - circle) for the 20 patients in our validation cohort. Full marker represents a stochastic frontier for this dosimetric indice and an empty marker represents a regression.

## Conclusion

SFA is an adequate model to build a predictive model based on the morphological parameters of a retrospective database. The model is validated with a 20 patients cohort with different dose distribution. We wish to implement this technique into the clinical process of radiation therapy planning in order to maximise the sparing of the OARs.

## PO-0946 Inter-fraction robustness of DECT-based head and neck proton therapy with reduced range uncertainty margins

S. O'Reilly<sup>1</sup>, C. Cheng<sup>1</sup>, A. Lalonde<sup>2</sup>, B. Burgdorf<sup>1</sup>, W.J. Zou<sup>1</sup>, L. Yin<sup>1</sup>, S. Swisher-McClure<sup>1</sup>, A. Fotouhi Ghiam<sup>1</sup>, J.N. Lukens<sup>1</sup>, A. Lin<sup>1</sup>, L. Dong<sup>1</sup>, B.K.K. Teo<sup>1</sup>

<sup>1</sup>University of Pennsylvania, Radiation Oncology, Philadelphia, USA ; <sup>2</sup>Centre hospitalier de l'Université de Montréal, Radiation Oncology, Montreal, Canada

## Purpose or Objective

The Hounsfield unit (HU) to proton stopping power ratio (SPR) relative to water conversion is a source of uncertainty in proton therapy, with the generally accepted clinically applied range uncertainty for single energy computed tomography (SECT) being 3.5%. However, studies have shown that a range uncertainty of 2% is feasible when using SPR calculated with dual energy computed tomography (DECT). This decrease in range uncertainty leads to a reduction in margins, leading to decreased doses to organs at risk (OAR). This dose reduction can be substantial for head and neck cancer patients, who experience significant acute and late

toxicity. Robustly optimized head and neck plans using SPRs calculated using DECT and SECT were evaluated for OAR sparing and impact of inter-fraction setup variation.

#### Material and Methods

Ten post-operative head and neck patients (2 with SCC of the tongue, 1 parotid, 1 submandibular gland, 5 tonsil, and 1 unknown primary) were used for this study. Patients received a SECT scan followed by a DECT scan in sequential mode (80 kVp and 140 kVp) whereby  $p_e$  and  $Z_{eff}$  images were generated by the scanner software for SPR calculation. Both SECT and DECT calculated SPR images were used for robust optimization and dose calculation. Each plan consisted of 3 fields using multi-field optimization (MFO) to a CTV prescription of 60 or 63 Gy in 30 fractions. The proton plans were robustly optimized for CTV target coverage on SECT (3.5% range uncertainty) and DECT (2% range uncertainty) scans with 3 mm isocenter shifts. Comparison of treated volume outside of CTV- 50%, 70%, and 90% isodose volumes (minus the target volumes) were performed between SECT and DECT plans. Verification scans acquired during the course of treatment were used for forward calculation and evaluated for DECT plan robustness using a 1.5 mm isocenter shift and 2% range uncertainty. The 1.5 mm isocenter shift robustness parameter for the evaluation scans reflect the uncertainty in imaging and treatment isocenter coincidence as well as user dependent variability in image registration.

#### Results

The average reduction in the 50%, 70%, and 90% isodose volumes were 6.8%, 7.3%, and 13.3% respectively. An average decrease in esophagus max of 3.0 Gy (range -8.6 to 1.4 Gy), esophagus mean 0.6 Gy (-1.8 to 0.47 Gy), constrictor mean 1.2 Gy (-2.7 to 1.1 Gy), larynx mean 1.1 Gy (-2.7 to 0.6 Gy), and parotid mean 0.3 Gy (-3.9 to 1.7 Gy) were achieved with DECT plans. CTV coverage (at least 95%-95%) was maintained on each patient's verification scan in the second-to-worst case plan robustness analysis.

#### Conclusion

Using DECT for SPR calculation allows for reduced range uncertainty and margins leading to reduction of dose to regions outside target compared to SECT. Plans with reduced margins of 2% range uncertainty and 3 mm isocenter shifts were robust against inter-fraction setup variations.

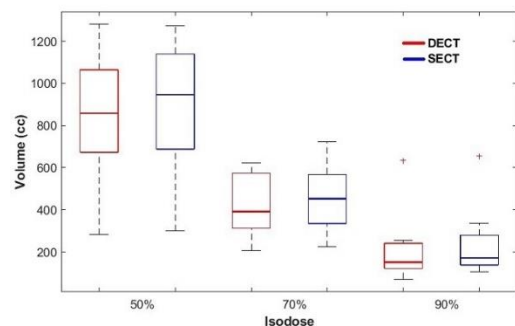


Figure 1. Comparison of treated volume outside of CTV- 50%, 70%, and 90% isodose volumes (minus the target volumes) between SECT (3.5% range uncertainty, 3 mm setup uncertainty) and DECT (2% range uncertainty, 3 mm range uncertainty) plans for ten post-operative head and neck patients.

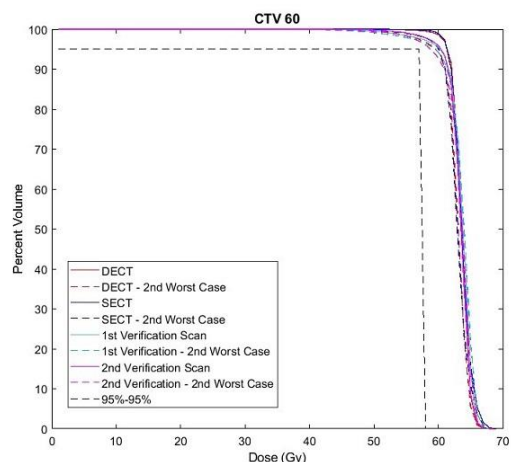


Figure 2. Representative CTV 60 coverage for robustly optimized DECT and SECT plans, compared with coverage for forward calculated plan on two separate verification scans (approximately two weeks apart) taken for a head and neck patient. The second-to-worst case scenario for CTV coverage is provided using 3 mm setup uncertainty for original DECT and SECT plans and 1.5 mm setup uncertainty for verification scans. DECT plans are calculated using 2% range uncertainty and SECT use 3.5% range uncertainty.

#### Poster: Physics track: Radiobiological and predictive modelling, and radiomics

##### PO-0947 The impact of dose deviations arising within the dosimetry chain on clinical outcomes

M. Bolt<sup>1</sup>, A. Nisbet<sup>2</sup>, T. Chen<sup>3</sup>, C. Clark<sup>4</sup>

<sup>1</sup>Royal Surrey County Hospital, Radiotherapy Physics, Guildford, United Kingdom ; <sup>2</sup>University of Surrey, Physics, Guildford, United Kingdom ; <sup>3</sup>University of Surrey, Chemical and Process Engineering, Guildford, United Kingdom ; <sup>4</sup>National Physical Laboratory, Radiation and Dosimetry, Teddington, United Kingdom

#### Purpose or Objective

Delivered radiotherapy dose may be compared between clinics due to the traceability of dose between Primary Standards Laboratories (PSL). Uncertainties arise at each point in the calibration chain and thus the actual delivered dose can deviate from that desired. These uncertainties have been quantified for each step; calibration transfer to a secondary standard instrument, transfer to field instruments, and subsequent QA measurement tolerances. Radiobiological modelling has been used to predict the clinical impact of these uncertainties.

#### Material and Methods

Uncertainty in the initial transfer of the calibration from PSL to the clinic was determined from on-site audits performed by the PSL over 2 decades and is normally distributed with a SD of 0.7% [1]. Data from over 24,000 multi-centre beam output measurements was used as a basis of the uncertainty following calibration and had a 0.7% SD [2]. Combining these uncertainties with daily fluctuations (0.2% SD) gives the overall measured uncertainty within the calibration chain of 1.0% SD.

Linear-Quadratic (LQ) and Lyman-Kutcher-Burman (LKB) models were implemented to model the effect of systematic and random deviations in delivered dose. Modelling was developed for prostate (10yr bPFS and grade 2 rectal bleeding) and head and neck (2yr survival and xerostomia induction) cases. The LQ model was used to calculate individual patient response and aggregated to provide population estimates. The clinical cases assessed cover a wide range of dose-response (even some prostate cancers have steep dose response [3]).

#### Results

A systematic dose shift of +2% through the course of treatment was estimated to change TCP by between 6.1-7.0% for the populations. Table 1 shows results for a range

of realistic systematic deviations in delivered dose existing throughout the treatment course.

Dose shift (%)	Modelled change in outcome prediction caused by							
	TCP				NTCP			
	Prostate		Head & Neck		Prostate		Head & Neck	
	RT01 Trial	Fox Chase	PARSPORT	PARSPORT	Rectum	Parotid		
	Ind.	Pop.	Ind.	Pop.	Ind.	Pop.		
-3	-22.2	-10.8	-28.7	-17.3	-26.1	-10.2	-12.8	-4.2
-2	-14.1	-7.2	-18.6	-10.7	-16.7	-6.2	-8.5	-2.8
-1	-6.7	-2.7	-9.0	-5.1	-8.0	-3.8	-4.2	-1.4
0	0	0	0	0	0	0	0	0
1	6.1	2.3	8.2	4.7	7.1	3.1	4.1	1.4
2	11.4	6.1	15.6	8.6	13.5	7.0	8.1	2.8
3	16.2	9.0	22.1	12.1	19.0	9.2	12.0	4.1

**Table 1:** Percentage change in outcome probability for different clinical cases. TCP was calculated for an individual patient with fixed alpha/beta ratio and a population included a variation in alpha/beta ratio across the patient cohort.

<sup>1</sup>RT01 was a randomised controlled trial comparing 64Gy and 74Gy for prostate cancer [Deaneley et al. 2014, The Lancet Oncology 15(4), 464-473].

<sup>2</sup>Fox chase assessed a range of delivered doses to the prostate between 70-76Gy for medium risk prostate cancer [Hanks et al. 2002, Int. Jour. Of Radiat. Onc. Biol. Phys. 54(2) 427-435].

<sup>3</sup>PARSPORT examined dose sparing of the parotid glands using conformal and IMRT. Here the doses from the IMRT plans are used as these are more comparable to modern treatment techniques [Nutting et al. 2011, The Lancet Oncology, 12(2) 127-136].

Based on treating patients on different machines within a clinic the Fox Chase case, shows the greatest variation in TCP with 5<sup>th</sup> and 95<sup>th</sup> percentiles of 71.0% and 80.7% (range 9.7%). The RT01 prostate case and head and neck case had 5<sup>th</sup> and 95<sup>th</sup> percentiles of 52.5% and 58.9% (range 6.4%), and 60.1% and 66.8% (range 6.7%) respectively. Figure 1 shows variation in predicted outcome for a cohort of patients due only to machine assignment.

Variation in TCP based on machine assignment: Population

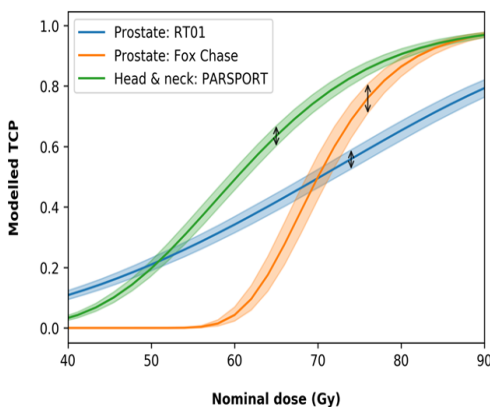


**Figure 1:** The simulated variation in TCP for a cohort of patients with spreads in alpha/beta values for the clinical cases detailed in Table 1. The solid line indicates the mean values and shaded regions indicate 5<sup>th</sup> to 95<sup>th</sup> percentiles. Variation in this simulation arises solely due to the machine to which a patient is assigned.

**Conclusion**

This analysis highlights the importance of accurate dosimetry, not only at initial calibration but also with QA. Current recommended action levels of 2% may require revision to reduce this potential difference in clinical outcome. Changes of this magnitude are readily detected; however this information is seldom used routinely. Clinical trials may benefit from reducing uncertainty in delivered dose to provide more robust assessments of response between trial arms, particularly in the context of reduced variation possible with modern treatment techniques.

**Refs**

- [1] Thomas et al. 2017 Phys. Imaging Radiat. Oncol. 3 21-7
- [2] Bolt et al. 2017 Phys. Imaging Radiat. Oncol. 4 39-43
- [3] Hanks et al. 2002 Radiat. Onc. Biol. Phys. 54(2) 427-435

**PO-0948 Predicting lung function post-RT in lung cancer using multivariate and principal component analysis**

Y. Dong<sup>1</sup>, M. Tawhai<sup>2</sup>, C. Veiga<sup>3</sup>, T. Doel<sup>4</sup>, D. Landau<sup>5</sup>, J. McClelland<sup>3</sup>, K. Burrowes<sup>1</sup>

<sup>1</sup>University of Auckland, Chemical and Material Engineering, Auckland, New Zealand ; <sup>2</sup>University of Auckland, Auckland Bioengineering Institute, Auckland, New Zealand ; <sup>3</sup>University College London, Department of Medical Physics & Biomedical Engineering, London, United Kingdom ; <sup>4</sup>University College London, Wellcome EPSRC Centre for International and Surgical Sciences, London, United Kingdom ; <sup>5</sup>University College London, Department of Oncology, London, United Kingdom

**Purpose or Objective**

Radiation therapy to treat lung cancer presents a trade-off between eradicating cancer cells and minimising radiation-induced lung damage (RILD). It is challenging to predict which patients will suffer from RILD due to the large variation in individualised response to RT, due to factors such as age, smoking status and baseline lung function. The ability to accurately predict this risk and the functional implications of RILD for an individual patient is lacking. Previous studies have typically used univariate analyses to predict lung function post-RT, with limited multivariate statistical analysis applied in this area. In this study, we apply statistical methods including principle component analysis (PCA) and multiple linear regression on a well-defined clinical dataset of patients with lung cancer before and after RT to develop a computational tool to improve RT planning and treatment in patients with lung cancer.

**Material and Methods**

Forty-four patients were selected from a Phase 1/2 trial of isotoxic dose-escalated RT and concurrent chemotherapy in patients with stage II/III non-small cell lung cancer, known as the IDEAL-CRT trial. All patients were treated with 63-73 Gy in 30 fractions over 6 weeks (daily). CT and pulmonary function data (FEV<sub>1</sub>, DLCO and FVC) were collected 12 months post-RT. We applied multivariate analysis, using PCA and multiple stepwise regression to develop a model to predict lung function post-RT. The dataset contained 14 variables, shown in Fig. 1. We used the PCAmix method which combines standard PCA for numerical data and multiple correspondence analysis for categorical data in the R software environment. PCAmix calculated the principal component scores (PCs) which were used as predictors to build a multiple linear regression model applying a stepwise method. Our results (PCAmix predicted) were compared with predictions using general multiple linear regression (MLR predicted) and measured values of lung function.

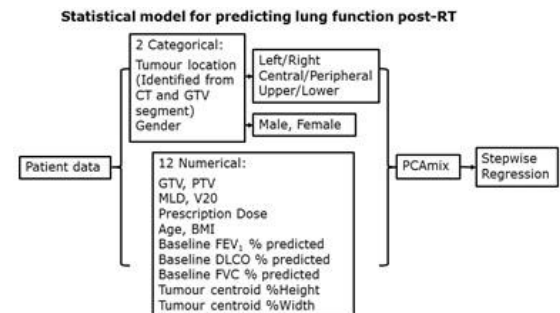


**Fig. 1:** Demonstration of the 14 variables used in our multivariate analysis.

**Results**

The r-squared value of the PCAmix regression model was 81%, compared to 55% when using the MLR model. The FEV<sub>1</sub> % predicted at 12 months post-RT measured/predicted were compared to assess how well

our model performed (Fig. 2). This method was also used to predict DLCO and FVC % predicted 12 months post-RT, with r-squared values of 71% and 74% respectively. A 10-fold cross-validation indicated that the model was over fitted using all 12 PCs, therefore 4 PCs with a p value greater than 0.05 were removed to resolve this issue.

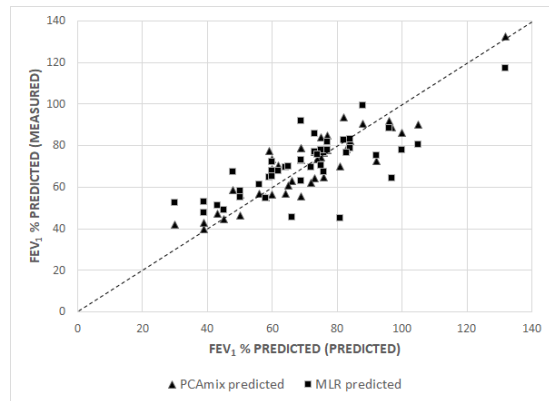


Fig. 2: Measured vs predicted FEV<sub>1</sub> % predicted 12 months post-RT. Predicted values were obtained using PCAmix regression (▲) and MLR regression (■) models.

#### Conclusion

The PCAmix regression method shows great potential in combining PFTs, dosimetry and demographic parameters for the prediction of lung function post-RT for lung cancer patients. This method must be validated with a larger sample size in the future.

#### PO-0949 Improved external validation performance of predictive radiomics models using statistical methods

A. Chatterjee<sup>1</sup>, M. Vallières<sup>1</sup>, A. Dohan<sup>2</sup>, I. Levesque<sup>1</sup>, Y. Ueno<sup>2</sup>, S. Saif<sup>2</sup>, C. Reinhold<sup>2</sup>, J. Seuntjens<sup>1</sup>

<sup>1</sup>McGill University, Medical Physics, Montreal, Canada ;  
<sup>2</sup>McGill University, Radiology, Montreal, Canada

#### Purpose or Objective

In radiomics, a predictive model may underperform on data from independent institutions. Region-of-interest contouring variability and image acquisition differences are two possible causes. While models can be made robust by inter-institutional data pooling, it is unlikely that the combined dataset reflects the global distribution of radiomic features. We aimed to create a statistical methodology to improve outcome prediction on external datasets of uterine adenocarcinoma patients with endpoints of (a) lymphovascular space invasion (LVSI), and (b) FIGO stage, grouped as early (IA) and advanced.

#### Material and Methods

The central idea, developed by us in earlier work, involves (a) creating balanced training and testing sets by under-sampling the majority class, and (b) standardizing training and testing sets separately. Standardization makes a feature distribution have zero mean and unit standard deviation. Standardizing features separately for each dataset reduces feature variability between datasets. Teaching set (used for training and validation) contained 94 samples (Hospital X) and testing set comprised 63 samples (Hospital Y). 6 different MRI sequences were available for each patient. Extracted features followed Image Biomarker Standardisation Initiative recommendations. They were divided into non-texture (e.g., morphological, histogram-based) and texture (e.g., matrix-based), to see if any benefit resulted from using texture features, which are harder to interpret. The 2 prediction approaches were: (i) using single features, and (ii) combining only three features, using basic machine learning tools (e.g., Naïve Bayes) to avoid over-training. Single feature selection focused on picking the strongest predictive features whereas combined feature selection

focused on predictors that were strong (but not necessarily the strongest) and did not have much redundancy. Feature selection was based on statistical stability of features in the teaching set. Corrections for multiple hypothesis testing were applied whenever appropriate.

#### Results

The table summarizes our findings. When including texture features in addition to non-texture features, the best AUC for a single feature improved in both the training set and the testing set. When combining three texture features into a model, the best AUC in the training set was better than for a single feature. However, this improvement was not seen in the testing set. The likely explanation is that while standardization reduces the differences between the two datasets, it cannot eliminate them.

Table: Summary of the best performing prediction models. First, we show a model with one feature (either non-texture or texture feature), and then a model with 3 features.

Outcome	Single non-texture feature	Training AUC (mean)	Testing AUC	Corrected p-value
FIGO	Least PCA axis length	0.78	0.78 [0.70,0.87]	0.004
LVSI	Area/Volume	0.75	0.75 [0.69,0.81]	0.016

Outcome	Single texture feature	Training AUC (mean)	Testing AUC	Corrected p-value
FIGO	NGLDM, dc_var	0.82	0.81 [0.72, 0.90]	0.01
LVSI	NGLDM, HDLGE	0.78	0.79 [0.73, 0.86]	0.01

FIGO (corrected p-value = 0.0017)	Training	Validation	Testing
Accuracy	0.79 [0.74,0.84]	0.78 [0.68,0.86]	0.78 [0.72,0.83]
Sensitivity	0.73 [0.62,0.83]	0.73 [0.64,0.86]	0.70 [0.63,0.77]
Specificity	0.85 [0.76,0.90]	0.82 [0.64,0.93]	0.87 [0.79,0.89]
AUC	0.88 [0.84,0.93]	0.87 [0.77,0.95]	0.79 [0.73,0.86]

LVSI (corrected p-value = 0.017)	Training	Validation	Testing
Accuracy	0.77 [0.69,0.82]	0.74 [0.60,0.87]	0.71 [0.65,0.76]
Sensitivity	0.74 [0.65,0.81]	0.72 [0.60,0.87]	0.69 [0.60,0.74]
Specificity	0.79 [0.71,0.84]	0.76 [0.60,0.93]	0.73 [0.65,0.82]
AUC	0.83 [0.78,0.89]	0.80 [0.69,0.92]	0.76 [0.68,0.85]

#### Conclusion

Our methodology yielded model performances that are statistically significant and match (FIGO stage) or surpass (LVSI) the performance of an expert radiologist. Due to the statistical nature of the approach, it can be applied to diverse scenarios. We are applying this technique when modeling the risk of distant metastasis in head and neck squamous cell carcinoma datasets collected from 6 different hospitals.

#### PO-0950 Determining the radiodensity range for data-driven quantification of radiation-induced lung fibrosis

L.M. Wang<sup>1</sup>, A. Chatterjee<sup>2</sup>, A. Semionov<sup>3</sup>, J. Tsui<sup>4</sup>, S. Lee<sup>5</sup>, I. Yang<sup>4</sup>, Y. Al Bulushi<sup>4</sup>, J. Seuntjens<sup>2</sup>, N. Ybarra<sup>6</sup>

<sup>1</sup>McGill University, Medical Physics Unit, Montreal, Canada ; <sup>2</sup>Cedar's Cancer Centre, Medical Physics Unit, Montreal, Canada ; <sup>3</sup>Royal Victoria Hospital, Radiology, Montreal, Canada ; <sup>4</sup>Cedar's Cancer Centre, Radiation Oncology, Montreal, Canada ; <sup>5</sup>Memorial Sloan Kettering Cancer Centre, Memorial Sloan Kettering Cancer Centre, New York, USA ; <sup>6</sup>Montreal University Healthcare Centre - Research Institute, Radiobiology, Montreal, Canada

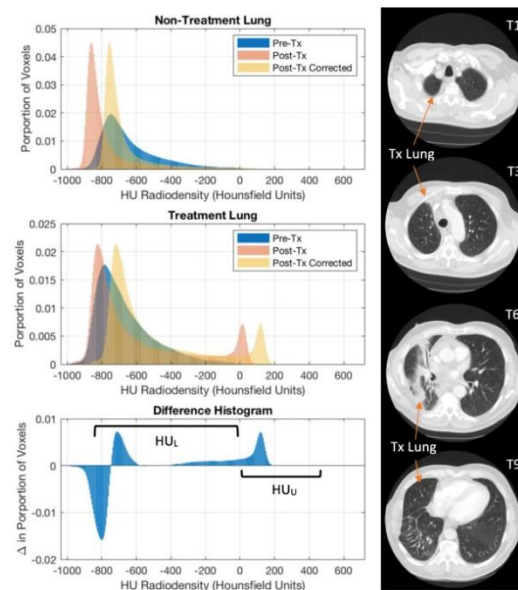
#### Purpose or Objective

Many data-driven strategies have been developed to quantify radiation-induced lung fibrosis (RILF) in patients after thoracic radiotherapy (RT). These methods make use of the unique distributions of voxel radio-densities, measured in Hounsfield Units (HU), in computed tomography (CT) images of the lung. These unique HU distributions can indicate the presence of certain interstitial diseases through measurable variations. However, to our knowledge, there is no empirical and quantitative evidence to support exact HU ranges that best characterize and delineate the radio-density

characteristics of RILF. This study aims to empirically test and propose an appropriate HU range which corresponds to RILF.

### Material and Methods

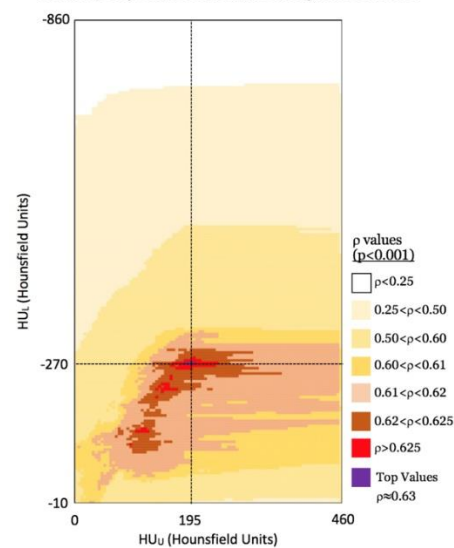
Voxel HU values were extracted from 68 patient lung CTs at pre-treatment (simulation CT) and 6-months post-treatment (diagnostic CT). A team of 2 radiation oncologists and 2 radiologists scored the patient population for RILF severity on a five-grade scale: 0 = no fibrosis, 1 = 1 pulmonary segment equivalent of fibrosis (PSEF), 2 = 2 PSEF, 3 = 3 PSEF, 4 = 4 PSEF, 5 = >5 PSEF. We defined PSEF as the volume of half the right middle lung lobe. Post-treatment images were deformably registered to pre-treatment CTs using an in-house algorithm developed in MevisLab™. The registered image was corrected using the non-irradiated lung to account for scanner differences between images acquired at baseline and follow-up. For the irradiated lung parenchyma (defined as total treated lung volume minus PTV) the voxel HU counts were binned as histograms. The difference between follow-up and baseline histograms was computed and its area normalized to unity. We then computed the integral ( $HU_{int}$ ) of the difference histogram between a lower ( $HU_L$ ) and upper ( $HU_U$ ) HU range.  $HU_L$  was varied between -860 HU (below which is health lung parenchyma) to -10 HU and  $HU_U$  was varied between 0 HU to 460 HU (above which is no longer soft tissues). Each combination of  $HU_L$  and  $HU_U$  yielded a unique  $HU_{int}$  for each patient. For the patient cohort, the Spearman correlation ( $\rho$ ) was calculated between these unique  $HU_{int}$  and the mode of the physician assigned scores. See Figure 1 for an illustration of the method.



### Results

As seen in Figure 2, for a fixed  $HU_U$  value of 200 HU, changes in the  $HU_L$  showed dramatic effects on  $\rho$ , with values of 0.07 ( $p < 0.001$ ) at -850 HU increasing to 0.63 ( $p < 0.001$ ) at -270 HU. With  $HU_L$  fixed at -270 HU, we observed no more than 20% variation in  $\rho$  when  $HU_U$  was varied. The best performance ( $\rho = 0.63$ ) was for  $HU_L = -270$  HU and  $HU_U = 195$  HU.

Heatmap of  $\rho$  between  $HU_{int}$  and Physician's Score



### Conclusion

For a quantitative analysis of RILF, we found a value of  $\approx -270$  HU to be appropriate for  $HU_L$ . We were unable to establish a  $HU_U$  recommendation given  $HU_U$  choice is less impactful on the predictive ability of  $HU_{int}$ . We suspect this is due to the reduced number of voxels that occupy the higher densities. These recommendations need to be externally validated on larger populations.

### PO-0951 How to build accurate prediction models without sharing patient data across hospitals?

I. Zhovannik<sup>1,2</sup>, Z. Shi<sup>1</sup>, F. Dankers<sup>1,2</sup>, T. Deist<sup>3</sup>, A. Traverso<sup>1</sup>, P. Kalendralis<sup>1</sup>, R. Monshouwer<sup>2</sup>, J. Bussink<sup>2</sup>, R. Fijten<sup>1</sup>, H. Aerts<sup>4,5,6</sup>, A. Dekker<sup>1</sup>, L. Wee<sup>1</sup>

<sup>1</sup>Maastricht University Medical Center +, Radiation Oncology - Maastricht, Maastricht, The Netherlands ; <sup>2</sup>Radboud University Medical Center, Radiation Oncology, Nijmegen, The Netherlands ; <sup>3</sup>Maastricht University, The D-Lab: Decision Support for Precision Medicine, Maastricht, The Netherlands ; <sup>4</sup>Harvard Medical School, Brigham and Women's Hospital, Boston, USA ; <sup>5</sup>Maastricht University Medical Center +, Radiology, Maastricht, The Netherlands ; <sup>6</sup>Dana-Farber Cancer Institute, Computational Imaging and Bioinformatics Laboratory, Boston, USA

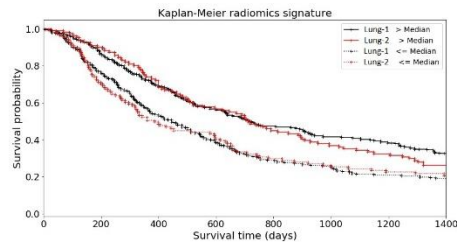
### Purpose or Objective

Imagine if you had an intelligent model that could select the most optimal treatment for a cancer patient, i.e. optimizing the tradeoff between tumor control and side effects. Are we close to having such a model? Patient data are unstructured and distributed in patient databases all over the world - that is the greatest challenge. In addition, there are bureaucratic and legal barriers to share (even anonymized) patient data. To avoid the difficulties of data-sharing we proposed to use a distributed learning approach where the privacy-sensitive data never leaves the hospital. In this approach, only a model is shared and optimized.

### Material and Methods

We used the pioneering approach of Aerts et al (2014) to build a model in a distributed fashion without data sharing between two hospitals. The developed Cox proportional hazards radiomic model splits a patient cohort into two groups by the median mortality risk. To train and validate the model we used two cohorts of non-small cell lung cancer patients of the two hospitals (441 and 221 patients respectively). We extracted radiomic image biomarkers from the Gross Tumor Volume (GTV) of both cohorts. Radiomics ontology (RO) and radiation oncology ontology

(ROO) were used to make radiomics and clinical data extracted in the hospitals intelligible for models. We validated the model distributedly using the Varian Learning Portal securing local patient data.



## Results

We found a significant split in both training (log-rank test  $p=0.009$ ) and validation cohorts (log-rank test  $p=0.03$ ).

## Conclusion

The original model was reproduced with the significant data split. This way we showed that imaging prediction models can be made in a distributed fashion without data-sharing.

## PO-0952 CT-based Radiomics Predicting HPV Status in Head and Neck Squamous Cell Carcinoma

Z. Shi<sup>1</sup>, C. Zhang<sup>2</sup>, M. Welch<sup>3</sup>, P. Kalendralis<sup>1</sup>, W. Leonard<sup>1</sup>, A. Dekker<sup>1</sup>

<sup>1</sup>GROW - School for Oncology and Development Biology-Maastricht University Medical Centre, Department of Radiation Oncology Maastricht Clinic, Maastricht, The Netherlands ; <sup>2</sup>Maastricht University, Department of Data Science and Knowledge Engineering, Maastricht, The Netherlands ; <sup>3</sup>University of Toronto, Department of Medical Biophysics, Toronto, Canada

## Purpose or Objective

Human papillomavirus (HPV) testing is an important prognostic factor for oropharyngeal squamous cell carcinoma (OPSCC). HPV-related OPSCC is now considered to be a separate tumour type from non-HPV related tumours with differential cancer prognosis. Conventionally, HPV status is determined via a minimally invasive needle biopsy. The aim of this study was to investigate whether CT image-derived radiomics are able to predict HPV status of patients diagnosed with primary OPSCC in a non-invasive approach.

## Material and Methods

Six independent cohorts, 255 patients in total were collected in this study, in which patients were treated with radiation only or chemo-radiation therapy as part of their treatment. HPV positive was defined as expression of the p16 gene variant. CT scans with visible artifacts (e.g., metallic dental fillings) within the GTV were excluded from further analysis. The data was randomly split into training ( $n=142$ ), tuning ( $n=48$ ) and test ( $n=65$ ) sets. CT images were resampled to isotropic voxels of 2 mm via linear interpolation. A total of 1105 radiomic features, consisting of histogram statistics, shape, texture and features by Wavelet and Laplacian of Gaussian filtering, were extracted from the GTV via an open-source radiomics package O-RAW that is an extension wrapper of PyRadiomics. Feature selection was based on: (i) feature stability ranking, (ii) Kolmogorov-Smirnov test of each feature between HPV positive and negative, and (iii) correction between the remaining features. For the model, a parsimonious yet optimally predictive set of features from the remaining candidates after selection

were determined by recursive feature elimination. The radiomic features were not normalized on any data sets. Multivariable logistic regression, SVM, and random forest, were applied for training classifier. The classification performance of HPV status was assessed by the area under the receiver operator curve (AUC). The Wilcoxon test was used to assess significance between AUCs and random ( $AUC=0.5$ ).

## Results

Out of 255 patients, 174 (68.2%) patients were with HPV positive and the rest 81 (31.8%) patients were with negative. After feature selection, 3 radiomic features, (i) original\_shape\_Sphericity, (ii) original\_firstorder\_Entropy, and (iii) log-sigma-3-0-mm-3D\_glszm\_SizeZoneNonUniformityNormalized, were selected to develop models. The multivariable logistic regression classifier achieved the highest AUC on both training and test sets, yielding mean AUCs of 0.79 (95% CI: 0.78 - 0.79,  $p$ -value  $< 10^{-4}$  Wilcoxon test) and 0.72 (95% CI: 0.71 - 0.72,  $p$ -value  $< 10^{-4}$  Wilcoxon test), respectively. The AUCs are shown in Figure 1. The performance of HPV status prediction of the three classifiers are shown in Table 1.

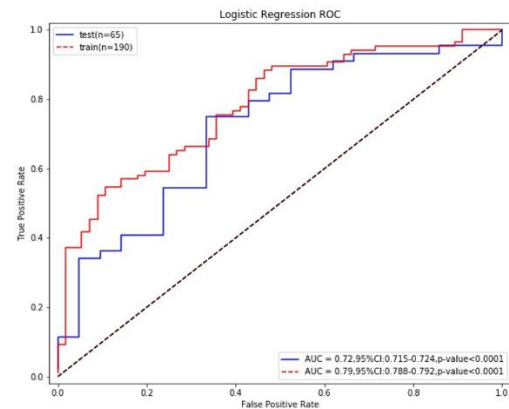


Figure 1: The receiver operator curve for HPV status classification using logistic regression.

Table 1: Classification of HPV status using three approaches.

	100 times 5-fold CV mean AUC on training set	1000 times bootstrapped AUC on test set
Logistic Regression	0.79, 95% CI: 0.78 - 0.79, $p$ -value $< 0.0001$ Wilcoxon test	0.72, 95% CI: 0.71 - 0.72, $p$ -value $< 0.0001$ Wilcoxon test
Linear SVM	0.76, 95% CI: 0.75 - 0.77, $p$ -value $< 0.0001$ Wilcoxon test	0.70, 95% CI: 0.70 - 0.71, $p$ -value $< 0.0001$ Wilcoxon test
Random Forest	0.68, 95% CI: 0.67 - 0.69, $p$ -value $< 0.0001$ Wilcoxon test	0.60, 95% CI: 0.59 - 0.61, $p$ -value $< 0.0001$ Wilcoxon test

\*CV: cross validation; CI: confidence interval

## Conclusion

It is possible to classify HPV status for HNSCC patients using CT image-derived features, which could lead to better precision treatment decision. However, the results should be further validated on larger and external datasets.

## PO-0953 Are quality assurance phantoms useful to assess radiomics reproducibility? A multi-center study

A. Traverso<sup>1</sup>, I. Zhovannik<sup>2</sup>, Z. Shi<sup>1</sup>, P. Kalendralis<sup>1</sup>, R. Monshouwer<sup>3</sup>, M. Starmans<sup>4</sup>, S. Klein<sup>5</sup>, E. Pfaehler<sup>6</sup>, R. Boellaard<sup>6</sup>, A. Dekker<sup>7</sup>, L. Wee<sup>1</sup>

<sup>1</sup>Maastricht Radiation Oncology Maastricht Clinic, Radiotherapy, Maastricht, The Netherlands ; <sup>2</sup>Radboud University Medical Centre, Radiation Oncology, Nijmegen, The Netherlands ; <sup>3</sup>Radboud University Medical Center, Radiation Oncology, Nijmegen, The Netherlands ; <sup>4</sup>Erasmus Medical Center, Medical Physics, Rotterdam, The Netherlands ; <sup>5</sup>Erasmus Medical Centre, Medical Physics, Rotterdam, The Netherlands ; <sup>6</sup>University Medical Centre Groningen, Medical Physics, Groningen, The Netherlands ; <sup>7</sup>Maastricht Radiation

*Oncology Maastricht Clinic, Radiation Oncology, Maastricht, The Netherlands*

### Purpose or Objective

To guarantee the generalizability and validity of radiomics-based models, only reproducible features should be used. "Reproducible" features refer to features that show marginal differences when imaged with different settings. Only a few expensive phantoms specially designed for radiomics studies are available on the market. In this study, we exploited the feasibility of performing radiomics reproducibility studies with a quality assurance phantom, commonly used in the clinics.

### Material and Methods

The dataset (available at <https://xnat.bmia.nl/>) consists of CT scans of the COPD Gene Phantom II (Phantom Laboratory, Greenwich, NY, USA) acquired in three Dutch medical centers. Acquisition parameters like slice thickness, or convolutional kernel were varied from the standard thorax protocols.

Textural and statistical first order (FO) features were extracted using Pyrex (<https://github.com/zhenweishi/Py-rex>) from a spherical region in the insert cavities of the phantom. The relative difference (RD) between features values on different scanners with different settings was used to evaluate features reproducibility, with the following thresholds: a)  $0 < RD \leq 10\%$ : high reproducibility, b)  $10\% < RD \leq 30\%$ : medium reproducibility; c)  $RD > 30\%$ : poor reproducibility. Agreement between centers were evaluated using the Spearman rank correlation coefficients ( $\rho$ ).

### Results

73 radiomics features were extracted. Slice thickness: around 50% of the features in all the centers ( $\rho = 0.8$ ) showed poor reproducibility. Most of the GLSZM (Gray Level Size Zone Matrix) features were poorly reproducible compared to the other textural features. FO features were in general more stable than textural features. Reconstruction kernels: almost all the FO features presented high reproducibility in all the centers ( $\rho = 0.75$ ). Again, textural features were more impacted, with GLSZM features the least reproducible in all the centers. Only a small percentage of features (14% for center1, 14% for center2, and 30% for center3 presented high reproducibility) were robust for all the perturbations. There is only small subset (12%, 9/73) of common features with high reproducibility between the centers (Figure1). However, it is possible to isolate a larger common subset of features presenting poor reproducibility in all the three centers. Again, the majority of textural features had overall poor reproducibility compared to FO features.

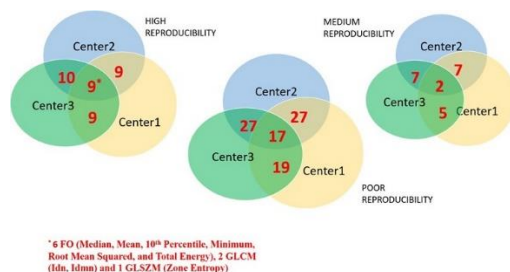


Figure1: results of the comparative analysis. A common subset of 19 features was found to be poor reproducible for all the centers. Only 9 features had high reproducibility

### Conclusion

Radiomics features are strongly affected by acquisition parameters. FO features were more robust than textural features. As Figure1 shows, the consensus is higher when using phantoms to identify features that present poor reproducibility. We showed that it is possible to use standard and common quality assurance phantoms to

investigate features reproducibility. In particular, as our results show, simple phantoms are mostly useful to define a list of "excluded" features due to their poor reproducibility even in the presence of inserts of simple shapes.

### PO-0954 A Prediction Model of Acute Esophageal Toxicity in Esophageal Squamous Cell Carcinoma Patients

L. Jiang<sup>1</sup>, S. Lu<sup>1</sup>, J. Lu<sup>1</sup>, W. Hu<sup>1</sup>, J. Wang<sup>1</sup>, Y. Chen<sup>1</sup>, K. Zhao<sup>1</sup>

<sup>1</sup>Fudan University Shanghai Cancer Center, Department of Radiation Oncology, Shanghai, China

### Purpose or Objective

This study sought to establish a multivariable normal tissue complication probability (NTCP) model for Grade  $\geq 2$  acute esophageal toxicity (AET) after definitive intensity-modulated radio(chemo)therapy in patients with esophageal squamous cell carcinoma (ESCC).

### Material and Methods

A cohort of 181 ESCC patients was enrolled in this study. The clinical and dosimetric parameters were analysed. Clinical parameters included age, gender, use of concurrent chemotherapy, T, N, M stage, and tumor location. Dosimetric parameters of the esophagus included the following: V5 to V65 with step of 5Gy, mean esophagus dose, maximum esophagus dose, GTV-L, PTVp-L. A Spearman's rank correlation coefficient matrix was calculated. A univariate logistic analysis was performed for each available predictor. The multivariate logistic regression model was achieved by least absolute shrinkage and selection operator (LASSO) logistic regression for predictor selection. The performance of the model was evaluated by the area under the curve (AUC) of the receiver operating characteristic (ROC) curve and calibration plot. The external validation of the model were carried out in a independent cohort.

### Results

A total of 42 patients (22.8%) developed Grade  $\geq 2$  AET. In the univariate logistic analysis, age  $> 65$  and length of planning target volume of primary esophageal cancer (PTVp-L) were significantly associated with risk of Grade  $\geq 2$  AET (Table 1). The final model (Table 2) enrolled age  $> 65$  (OR=0.59), PTVp-L (OR=1.03), and lower thoracic esophageal cancer (OR=0.53). The model parameters for the multivariable logistic regression model didn't correlate to each other. The AUC of the prediction model was 0.6837(95%CI: 0.5975-0.7699) (Figure 1), and the cross-validation optimism-corrected AUC was 0.64. The model showed moderate calibration (Figure 2). On validation in the external dataset, the prediction model showed moderate calibration and moderate discrimination (AUC 0.5901 (95%CI: 0.467-0.7132) for predicting Grade  $\geq 2$  AET.

**Table 1** Results from univariate logistic regression analysis for clinical and dosimetric parameters.

Clinical and dosimetric parameters	Coefficient	Standard error	Odds ratio (95%CI)	P-value
Age (years) (> 65 vs ≤ 65)	-1.141	0.413	0.32(0.14-0.72)	<b>0.006</b>
PTVp-L (per cm increase)	0.107	0.055	1.11(1.00-1.24)	<b>0.049</b>
No. of pack-years (>18 vs ≤ 18)	0.055	0.354	1.06(0.53-2.11)	0.877
Alcohol (yes vs no)	0.218	0.365	1.24(0.61-2.55)	0.550
Gender (female vs male)	0.249	0.386	1.28(0.60-2.73)	0.519

**Table 2** Predictive parameters from LASSO logistic regression analysis of the final model.

Predictor	Coefficient	Odds ratio
Age (> 65 vs ≤ 65)	-0.528	0.59
PTVp-L (per cm increase)	0.026	1.03
Lower thoracic ESCC constant	-1.254	

Figure 1

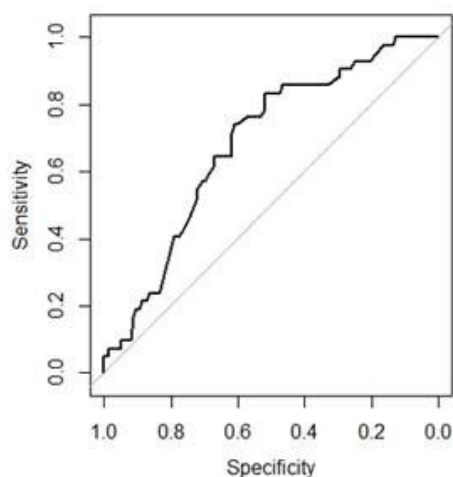
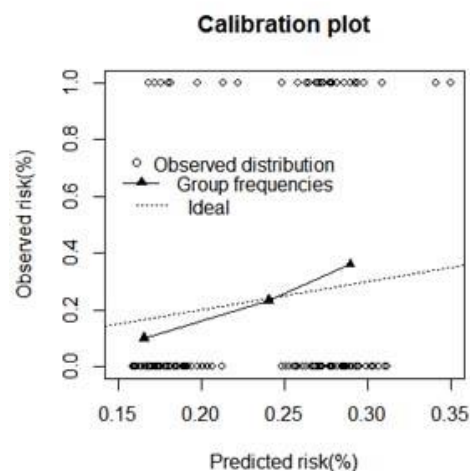


Figure 2



### Conclusion

A multivariate NTCP model including age, PTVp-L, and tumor location predicts Grade  $\geq 2$  AET after radio(chemo)therapy for ESCC. The results of this study suggest that the risk of Grade  $\geq 2$  AET decreased in elderly or lower thoracic esophageal cancer patients while increased in patients with longer PTVp-L.

### PO-0955 Radiomics signature as predictors of survival and local control after pancreatic carcinoma SBRT

L. Cozzi<sup>1</sup>, T. Comito<sup>2</sup>, A. Fogliata<sup>2</sup>, C. Franzese<sup>2</sup>, D. Franceschini<sup>2</sup>, C. Bonifacio<sup>3</sup>, A. Tozzi<sup>2</sup>, L. Di Brina<sup>2</sup>, E. Clerici<sup>2</sup>, S. Tomatis<sup>2</sup>, G. Reggiori<sup>2</sup>, F. Lobefalo<sup>2</sup>, A. Stravato<sup>2</sup>, P. Mancosu<sup>2</sup>, A. Zerbi<sup>4</sup>, M. Sollini<sup>5</sup>, K. Margarita<sup>3</sup>, A. Chiti<sup>6</sup>, M. Scorsetti<sup>1</sup>

<sup>1</sup>Humanitas Research Hospital and Humanitas University, Radiation Oncology Dept and Biomedical Science Dept, Milan-Rozzano, Italy; <sup>2</sup>Humanitas Research Hospital, Radiation Oncology Dept, Milan-Rozzano, Italy; <sup>3</sup>Humanitas Research Hospital, Radiology Dept, Milan-Rozzano, Italy; <sup>4</sup>Humanitas Research Hospital, Pancreatic Surgery Dept, Milan-Rozzano, Italy; <sup>5</sup>Humanitas Research Hospital, Nuclear Medicine Dept, Milan-Rozzano, Italy; <sup>6</sup>Humanitas Research Hospital and Humanitas University, Nuclear Medicine Dept and Biomedical Science Dept, Milan-Rozzano, Italy

### Purpose or Objective

Pancreatic adenocarcinoma has generally unfavorable prognosis. Combined chemio-radiotherapy is a frequently adopted treatment, especially for patients unfit to surgery, leading to possible overall survival at 2 years of about 30%. To better personalize the treatment, the ability of a radiomics signature to predict clinical outcome after stereotactic body radiation therapy has been explored.

### Material and Methods

One-hundred patients have been selected from the institutional database, presenting histologically proven, inoperable locally advanced pancreatic cancer and treated in our department with SBRT with a total dose of 45 Gy in 6 fractions. All patients underwent planning CT with no contrast agent, where the CTV was delineated and accurately cleaned from confounding regions. Radiomics texture features were extracted for these CTVs using the LifeX software tools. A total of 41 features were computed. The statistical analysis was conducted with dedicated routines on R scripts.

The cohort of 100 patients was separate in two groups of 60 and 40 patients, used for the training and validation processes, respectively. In the training phase, with the univariate Cox regression, the prognostic value of clinical and radiomic features was investigated to the predict

overall survival, OS, and the local control, LC. The quality of the models was appraised by means of the concordance index and the area under the curve, AUC. The significant predictors at univariate analysis were included in a multivariate Cox regression model including the uncorrelated significant features. The multivariate model was then verified on the validation group.

### Results

The analysis of clinical and textural data showed 9 predictors significant at univariate analysis for OS, and 4 predictors significant for LC. In the multivariate model, only two variables resulted significant predictors for OS: age and Homogeneity\_GLCM with  $p < 0.01$ , with AUC of 0.80 (95%CI: 0.66-0.94) and 0.73 (95%CI: 0.53-0.93) in the training and validation groups, respectively. Again in the multivariate model, two features were retained: short run low grey level emphasis and grey level non-uniformity, with AUC of 0.65 (95%CI: 0.52-0.81) and 0.61 (95%CI: 0.50-0.78) for the training and validation sets, respectively. In the low risk group, the median OS and LC in the validation group were 14.4 (95%CI: 12.2-21.2) and 28.6 (95%CI: 12.5-not reached) months, while in the high-risk group were 8.6 (95%CI: 7.0-18.0) and 17.5 (95%CI: 7.6-not reached) months, respectively.

### Conclusion

A CT based radiomic signature was identified which correlate with OS and LC after SBRT for pancreatic adenocarcinoma, and allowed to identify low and high-risk groups of patients.

### PO-0956 Non Invasive Grading of Non-Small Cell Lung Cancer Using Machine Learning Models Based on Radiomics

S. Aouadi<sup>1</sup>, R. Hammoud<sup>1</sup>, T. Torfeh<sup>1</sup>, N. Al-Hammadi<sup>1</sup>  
<sup>1</sup>National Center for Cancer Care & Research, Radiation Oncology, Doha, Qatar

#### Purpose or Objective

Grading of non-small cell lung cancer (NSCLC) is crucial for appropriate therapy decisions and prediction of prognosis. Traditionally, invasive histological methods are used. We propose non-invasive approaches for grading NSCLC by training machine learning models on radiomics.

#### Material and Methods

259 patients with NSCLC were collected from the dataset [NSCLC-Radiomics] in The Cancer Imaging Archive. For each patient, pretreatment CT scans, manual delineation of the GTV and histological classification (28 adenocarcinoma (AC), 85 squamous cell carcinoma (SCC), 93 large cell carcinoma (LCC), and 53 adenosquamous carcinoma (NOS) cases) were available. The dataset was randomized and divided into training and validation sets of 200 and 59 patients respectively.

CT scans were resampled to  $1 \times 1 \times 1 \text{ mm}^3$  voxels using three-dimensional Lagrangian polygon interpolation and intensities were divided into bins of 10HU from -1000 to 3000HU. 42 radiomic features were extracted from GTV's VOI, defined on each patient CT, using LIFEx software (v4.00). They were composed of 3 shape, 8 first order, and 31 texture features. Shape features describe the 3D geometric properties of the tumor. The first order features describe tumor intensity distribution. Texture features, which describe the intra-tumor heterogeneity, were extracted from the gray level co-occurrence (6), neighborhood grey-level different (3), grey-level run length (11), and grey-level zone length (11) matrices.

Machine learning models are composed of three blocs: preprocessing, selection and classification. Multiple configurations were benchmarked. Features preprocessing methods were QTRG (mapping data to have normal distribution), MINMAX\_SC (linear scaling to [0, 1]), or ROBUST\_SC (scaling to the interquartile range). The selection methods of the most representative features were based on elastic-net regularization (ELASTIC-NET), univariate statistical tests (Anova-F or mutual information

(MI)), or Support Vector Machine (SVM) model. The binary classifiers, trained to predict each histological class (AC, SCC, LCC, and NOS), were linear model or deep neural networks (DNN) (ReLU activation, dropout of 0.35, and 2 layers of 30 neurons each).

The performance of the machine learning models was assessed by the computation of the ROC curve, the area under the ROC curve (AUC; measure of separability between classes for any threshold) and the accuracy (the fraction of correct predictions) for each histological class.

### Results

Table 1 displays the AUC and Accuracy on training and validation sets using the best machine learning methods having linear or DNN classifiers. Figure 2 shows the ROC curves obtained for tumor grade prediction on validation set. DNN gave superior modeling of the training set whereas linear models gave better prediction on the validation set.

### Conclusion

We demonstrated that machine learning models trained on CT's radiomic features could potentially predict histological categorization of NSCLC tumors. Further investigations will be done.

**Table1.** The AUC and Accuracy obtained for the training (auc<sub>t</sub>, acc<sub>t</sub>) and validation sets (auc<sub>v</sub>, acc<sub>v</sub>) using the superior machine learning method with linear or DNN classifiers.

Histology	Machine Learning Model	auc <sub>t</sub>	auc <sub>v</sub>	acc <sub>t</sub>	acc <sub>v</sub>
AC	(ROBUST_SC, ELASTIC-NET, LINEAR)	0.52	0.63	0.89	0.86
	(QTRG, MI, DNN)	0.81	0.58	0.89	0.88
LCC	(ROBUST_SC, MI, LINEAR)	0.60	0.60	0.60	0.70
	(QTRG, MI, DNN)	0.80	0.60	0.70	0.61
NOS	(MINMAX_SC, SVM, LINEAR)	0.60	0.70	0.80	0.90
	(QTRG, MI, DNN)	0.77	0.59	0.77	0.86
SCC	(MINMAX_SC, MI, LINEAR)	0.59	0.70	0.69	0.61
	(QTRG, MI, DNN)	0.70	0.60	0.74	0.63

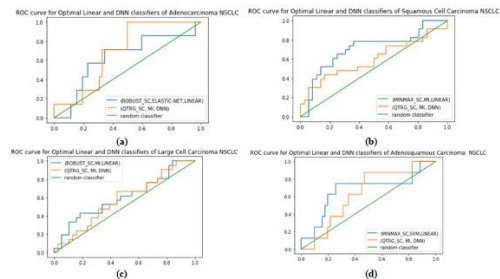


**Figure2.** The ROC curves obtained for the prediction of Adenocarcinoma (a), Squamous Cell Carcinoma (b), Large Cell Carcinoma (c), and Adenosquamous Carcinoma (d) histological grade on the validation set.

### PO-0957 Radiomics study from the dose-painting multicenter phase III trial on newly diagnosed glioblastoma

F. Tensaouti<sup>1,2</sup>, J. Bailleul<sup>1,2</sup>, E. Martin<sup>3</sup>, F. Desmoutin<sup>2</sup>, S. Ken<sup>4</sup>, J. Desrousseaux<sup>1</sup>, L. Vieilleveigne<sup>4</sup>, J. Lotterie<sup>2,5</sup>, V. Lubrano<sup>2,6</sup>, I. Catalaa<sup>2,7</sup>, G. Noël<sup>8</sup>, G. Truc<sup>9</sup>, M. Sunyach<sup>10</sup>, M. Charissoux<sup>11</sup>, N. Magné<sup>12</sup>, P. Auberdiac<sup>13</sup>, T. Filleron<sup>3</sup>, P. Peran<sup>2</sup>, E. Cohen-Jonathan Moyal<sup>1,14,15</sup>, A. Laprie<sup>1,2,15</sup>  
<sup>1</sup>Institut Claudius Regaud/Institut Universitaire du Cancer de Toulouse - Oncopôle, Radiation oncology, Toulouse, France ; <sup>2</sup>ToNIC- Toulouse Neuroimaging Center- Université de Toulouse- Inserm- UPS-, Inserm 1214, Toulouse, France ; <sup>3</sup>Institut Claudius Regaud/Institut Universitaire du Cancer de Toulouse - Oncopôle, Biostatistics, Toulouse, France ; <sup>4</sup>Institut Claudius Regaud/Institut Universitaire du Cancer de Toulouse - Oncopôle, Medical Physics, Toulouse, France ; <sup>5</sup>CHU Toulouse, Nuclear Medicine, Toulouse, France ; <sup>6</sup>CHU Toulouse, Neurosurgery, Toulouse, France ; <sup>7</sup>CHU Toulouse, Radiology, Toulouse, France ; <sup>8</sup>Centre Paul Strauss- EA 3430- University of Strasbourg, Radiation Oncology, Strasbourg, France ; <sup>9</sup>Centre Georges-François Leclerc, Radiation Oncology, Dijon, France ; <sup>10</sup>Centre Léon-Bérard-, Radiation oncology, Lyon, France ; <sup>11</sup>Institut du Cancer de Montpellier, Radiation Oncology,

Montpellier, France ; <sup>12</sup>Institut de Cancérologie de la Loire Lucien Neuwirth, Department of Radiation Oncology, Saint-Priest-en-Jarez, France ; <sup>13</sup>Clinique Claude Bernard, Radiation oncology, Albi, France ; <sup>14</sup>INSERM U1037- Centre de Recherches contre le Cancer de Toulouse, Radiation oncology, Toulouse, France ; <sup>15</sup>Université Toulouse III Paul Sabatier, Radiation oncology, Toulouse, France

### Purpose or Objective

Gliomics is a research project with the goal of extracting radiomics from multimodal imaging data of multicenter prospective phase III trial for newly diagnosed glioblastoma (NCT01507506) [1]. This study compares quantitative radiomics features extracted from the boost, ie. the high-dose volume (HDV) with the low-dose volume (LDV) on planning CT scan. The aim is to quantify increased aggressiveness of the tumor in area defined by MRI (the high dose).

### Material and Methods

Eighty Three patients included in the SPECTRO-GLIO trial presenting with and without local recurrence at the time of the radiomics analysis were analyzed in this study, Forty-one patients (49.4 %) were in Arm A, with Stupp protocol (3DCRT or IMRT 60 Gy/2Gy on contrast enhancement (GTV1)+ 2 cm margin with concomitant temozolomide (TMZ) and six months of TMZ maintenance); Forty-two patients (50.6 %) were in Arm B with the standard treatment with an additional simultaneous integrated boost of intensity-modulated radiotherapy (IMRT) of 72Gy/2.4Gy delivered on the MR spectroscopic imaging metabolic volumes of CHO/NAA>2 and contrast-enhancing lesions or resection cavity(GTV2)+ 1cm margin [2].

For each patient, the GTV1 and GTV2 were delineated in the participating centers following guidelines for arm A, delineated in the coordinating center for arm B and were all validated by central review. The CT and structure data in DICOM RT format were imported into IBEX (Imaging Biomarker Explorer software) [3] and automatically processed using in-house developed data analytics. As the majority of relapses were in the CTV, 116 features (GrayLevelCooccurrenceMatrix, GrayLevelRunLengthMatrix, Intensity, NeighborIntensityDifference, Shape) [3] were extracted from CTV1 and CTV2 volumes. The Wilcoxon signed-rank test was used for paired comparison and Bonferonni's correction was applied. Corrected p-value <0.05 was considered statistically significant. Statistical analyses were conducted using R version 3.5.1.

### Results

The statistics analysis showed that of the 116 features extracted, 39 of them proved to be significantly different between CTV1 and CTV2. As reported in table 1(below), 18 of significant features were RayLevelRunLengthMatrix, Intensity and NeighborIntensityDifference with a p value <0.0001.

	CTV 1	CTV 2	p
GrayLevelRunLengthMatrix25.GrayLevelNonuniformity			<0.0001
Median (range)	3976.73 (1970.48 ; 8099.2)	1315.91 (338.08 ; 3182.28)	
GrayLevelRunLengthMatrix25.LongRunEmphasis			<0.0001
Median (range)	206.71 (74.82 ; 713.94)	121.42 (52.19 ; 538.17)	
GrayLevelRunLengthMatrix25.LongRunHighGrayLevelEmpha			<0.0001
Median (range)	51.53e+5 (18.7e+5 ; 17.81e+05)	30.03e+5 (12.69e+5 ; 13.42e+05)	
GrayLevelRunLengthMatrix25.RunLengthNonuniformity			<0.0001
Median (range)	2558.45(257.16 ; 20059.46)	354.48(26.91 ; 2707.41)	
IntensityDirect.Energy			<0.0001
Median (range)	1.79E+11(7.7e+10 ; 4.4e+11)	3.45e+10(7.0e+9 ; 1.12e+11)	
IntensityDirect.LocalEntropyMax			<0.0001
Median (range)	3.16(1.68 ; 5.49)	2.9(1.4 ; 5.16)	
IntensityDirect.LocalEntropyMedian			<0.0001
Median (range)	0.88 (0.23 ; 1.22)	1.01(0.64 ; 1.37)	
IntensityDirect.LocalEntropyStd			<0.0001
Median (range)	0.67 (0.43 ; 1.1)	0.58 (0.35 ; 0.8)	
IntensityDirect.LocalRangeMean			<0.0001
Median (range)	210.36 (149.08 ; 361.78)	339.12 (232.91 ; 513.45)	
IntensityDirect.LocalRangeMedian			<0.0001
Median (range)	9(6 ; 18)	14(7 ; 30)	
IntensityDirect.LocalRangeStd			<0.0001
Median (range)	414.85 (361.68 ; 494.73)	486.86 (415.13 ; 531.63)	
IntensityDirect.LocalStdMax			<0.0001
Median (range)	583.38 (530.07 ; 598.68)	570.05 (527.96 ; 593.74)	
IntensityDirect.LocalStdMean			<0.0001
Median (range)	80.25 (57.29 ; 136.21)	133.08 (85.22 ; 203.02)	
IntensityDirect.LocalStdMedian			<0.0001
Median (range)	2.64 (1.79 ; 5.22)	3.94 (1.86 ; 9.8)	
IntensityDirect.LocalStdStd			<0.0001
Median (range)	169.29 (147.05 ; 198.53)	202.34 (174.05 ; 227.41)	
NeighborIntensityDifference25.Busyness			<0.0001
Median (range)	5.43E-05 (1.12E-05 ; 2.34E-04)	8.43E-05(1.58E-05 ; 1.15E-03)	
NeighborIntensityDifference3.Coarseness			<0.0001
Median (range)	1.36E-05(4.79E-06 ; 3.42E-05)	9.17E-05 (1.80E-05 ; 5.32E-04)	
NeighborIntensityDifference3.Contrast			<0.0001
Median (range)	6.01 (0.47 ; 17.95)	13.58 (0.9 ; 41.42)	

**Table 1: The 18 most significant radiomics features between CTV1 and CTV2**

### Conclusion

There was a significant difference of features between the two doses volumes which may be a reflection of tumor heterogeneity. To consolidate the findings of this study we will extend the radiomics analysis to multimodal MR imaging data [4] that was acquired longitudinally during this trial and correlate the features of interest to survival. [1] Laprie et al, BMC Cancer, under review after minor revision

[2] Ken et al, Radiat Oncol 2013

[3] Zhang et al, Medical Physics 2015

[4] Khalifa J et al. Eur Radiol. 2016

### PO-0958 Mortality Risk Stratification Model based on Radiomics Only: Analysis of Public Open Access HNC Data

Z. Shi<sup>1</sup>, C. Zhang<sup>2</sup>, T. Zhai<sup>3</sup>, M. Welch<sup>4</sup>, L. Wee<sup>1</sup>, A. Dekker<sup>1</sup>

<sup>1</sup>Maastricht University Medical Centre, Department of Radiation Oncology Maastricht Clinic- GROW - School for Oncology and Development Biology, Maastricht, The Netherlands ; <sup>2</sup>Maastricht University, Department of Data Science and Knowledge Engineering, Maastricht, The Netherlands ; <sup>3</sup>University of Groningen, Department of Radiation Oncology- University Medical Center Groningen, Groningen, The Netherlands ; <sup>4</sup>University of Toronto, Department of Medical Biophysics, Toronto, Canada

### Purpose or Objective

The primary aim of this study was to investigate whether CT image-derived radiomics are able to predict overall survival (OS) of patients diagnosed with primary Head and Neck Squamous Cell Carcinomas (HNSCC).

### Material and Methods

5 independent cohorts, 411 patients in total were collected in this study, in which patients were treated with radiation only or chemo-radiation therapy as part of their treatment. CT scans with visible artifacts (e.g., metallic dental fillings) within the GTV were excluded from further analysis. The dataset was split into training set (cohort 1, 2 and 3, n=308) and validation set (cohort 4 and 5, n=103) with the ratio of 3:1. CT images were resampled to isotropic voxels of 2 mm via linear interpolation. A total of 1105 features, consisting of

histogram statistics, shape, texture and features by Wavelet and Laplacian of Gaussian filtering, were extracted from the GTV via an open-source radiomics package O-RAW that is an extension wrapper of PyRadiomics. Radiomic features were pre-selected to reduce the probability of over-fitting. If the Spearman correlation between pairs of radiomic features was bigger than 0.85, then the feature with the lower univariable association with OS was eliminated from further analysis. All the pre-selected potential radiomic features were analysed for their prognostic power using the median value in the training set as the threshold value in the univariable analysis. The logrank test was used to assess whether the individual feature can stratify patients into high and low risk groups. The radiomic features were not normalized on any data sets. Multivariable Cox proportional hazards regression model was used to examine the association between survival and radiomic features. The concordance index (c-index) was determined to assess the models discrimination power. 100 times bootstrapping was performed to compute c-index and the Wilcoxon test was used to assess radiomics signature power, compared with random (c-index = 0.5).

### Results

After feature selection, 8 radiomic features were selected: (1) log-sigma-1-0-mm-3D\_glszm\_LowGrayLevelZoneEmphasis, (2) log-sigma-2-0-mm-3D\_gldm\_DependenceVariance, (3) log-sigma-2-0-mm-3D\_glszm\_SmallAreaLowGrayLevelEmphasis, (4) log-sigma-3-0-mm-3D\_gldm\_DependenceEntropy, (5) wavelet-LHH\_firstorder\_Median, (6) wavelet-LLH\_gldm\_DependenceVariance, (7) original\_firstorder\_Maximum, and (8) original\_glszm\_SmallAreaLowGrayLevelEmphasis. The Cox regression model resulted in a c-index of 0.70 (95%CI: 0.63-0.74) on the training set and a c-index of 0.65 (95%CI: 0.56-0.68) on the validation set. The Kaplan-Meier curves of training and validation sets are shown in Figure-1. The prognostic score demonstrated significant differences in OS between risk groups in both training ( $X^2$  17.0,  $p < 0.001$ ) and validation sets ( $X^2$  5.4,  $p = 0.02$ ).

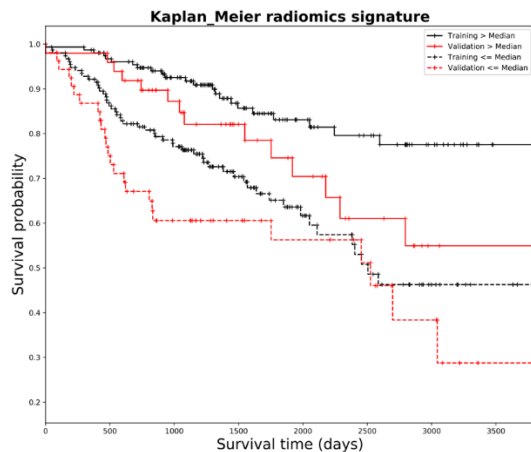


Figure 1: Kaplan-Meier curves for patients stratified by radiomics signature.

### Conclusion

The radiomics signature showed a promising performance to predict overall survival of HNSCC patient. The further study will investigate the prognostic performance models combining radiomics and clinical factors.

### PO-0959 Robust features selection in Apparent Diffusion Coefficient (ADC) maps of cervix cancer patients

A. Traverso<sup>1,2</sup>, M. Kazmierski<sup>1</sup>, Z. Shi<sup>1</sup>, J. Weiss<sup>3</sup>, S. Fiset<sup>4</sup>, L. Wee<sup>1</sup>, A. Dekker<sup>1</sup>, D. Jaffray<sup>2</sup>, K. Han<sup>4,5</sup>

<sup>1</sup>Maastricht Radiation Oncology Maastricht, Radiotherapy, Maastricht, The Netherlands ; <sup>2</sup>Princess Margaret Cancer Center, Department of Medical Physics, Toronto, Canada ; <sup>3</sup>Princess Margaret Cancer Center, Department of Biostatistics, Toronto, Canada ; <sup>4</sup>Princess Margaret Cancer Center, Radiation Medicine Program, Toronto, Canada ; <sup>5</sup>University Of Toronto, Department of Radiation Oncology, Toronto, Canada

### Purpose or Objective

Quantitative features (radiomics) extracted from computed tomography (CT) have shown promising prognostic and predictive power in radiation oncology. The extension of radiomics to Magnetic Resonance Imaging (MRI)/ Diffusion Weighted Imaging (DWI) is of interest to improve diagnostic performance and evaluate treatment response. However, several challenges apply: greater acquisition protocol differences compared to CT, presence of arbitrary units in the image (need for normalization), contouring inter-observer variability, and risk of redundant information (e.g. association of features with tumor volume). In this study, we investigated the aforementioned challenges, proposing a method for robust features extraction

### Material and Methods

This retrospective study was conducted using apparent diffusion coefficient (ADC) maps derived from DWI from 81 women with stage IB-IVA cervical cancer treated with definitive chemoradiation in 2009-2013. Two radiation oncologists independently delineated the gross tumour volume directly on the ADC maps with the aid of coregistered T2-weighted images (Median DICE 0.72±0.13). Radiomic features were computed with an open source software (PyRadiomics) for first-order intensity statistics (FO), shape metrics (SM) and textural analyses (TA) together with different imaging filters available (Table 1). To investigate the impact of normalization, five different normalizations were considered (Table1). Feature reproducibility with respect to inter-observer variability was assessed using concordance correlation coefficients (CCC). Association of features with tumor volume was investigated by using the Spearman Correlation Coefficient ( $\rho$ )

Table 1: Description of different normalizations and filters used in the analysis. The bin width corresponds to the width of the bins used to quantize the images values to create the histogram of their distributions. To avoid skewed distributions the bin counts should be between 60 and 300. The histogram is then used to compute statistical first order features used toward features. A filter is a pre-processing operation applied to the whole image before features extraction.

Normalization legend	Bin width / bin counts	Description
Raw	25 / 90	No normalization is applied. Only original values of the images are considered. The histogram of the image values is created with a bin width of 25 (e.g. 1 bin = 0.24 arbitrary units)
S1BW0.05	0.05 / 90	All the original values are centered creating a Gaussian distribution by centering the image values at the mean with standard deviation 1. A bin width of 0.05 is used
S333BW25	25 / 65	All the values are normalized between -1000 and +1 to make them similar to CT values. A bin width of 25 is used
S100BW5	5 / 85	Same as its normalization S1, but a scaling factor of 100 is applied to the values. This normalization was previously used by studies for ADC maps in prostate cancer. A bin width of 5 is used to create the histogram.
S100BW15	15 / 25	Same as S100BW5, but a bin width of 15 is used
S100BW20	20 / 25	Same as S100BW5, but a bin width of 20 is used
Filter Name	Description	
Exponential	Computes the exponential of the original image. The filter can enhance the present of signal in the ROI, compared to the background of other anatomical regions. However, in case of small ROIs the effect of noise can totally embed the importance of textural features	
Logarithm	Computes the logarithm of the absolute value of the original image + 1. Resulting values are rescaled on the range of the initial original image and negative intensities are made negative in resultant filtered image	
Square	Compute the square of the image intensities. Resulting values are rescaled on the range of the initial image, and negative values are kept negative	
Square Root	Computes the square root of the absolute value of the image intensities. Since the absolute values are computed, the importance of low intensity values (background) is reduced	
Gradient	Applies a gradient filter to the image before features extraction. The gradient filter is often used for edge detection. The goal of edge detection is to reveal particular patterns in the image. This filter can enhance the presence of particular textures in the ROI	

### Results

Figure 1C shows the Venn diagrams for the different normalizations applied to all 562 features. Overall, feature reproducibility was strongly affected by normalization; using a Gaussian distribution with no rescaling (S1) and a smaller bin width (BW005) resulted in best feature reproducibility (Figure 1A) Conversely, normalizing values to be as similar as in CT (S333BW25) led to the lowest reproducibility. The number of bin counts was too small for normalizations S100BW20 and BW15. There were no significant differences between filters except for the gradient filter, which increased both the number of reproducible features (Figure 1B) and

decreased the association with tumour volume. Finally, normalization and inter-observer variability had a larger impact on TA than SM and FO features.

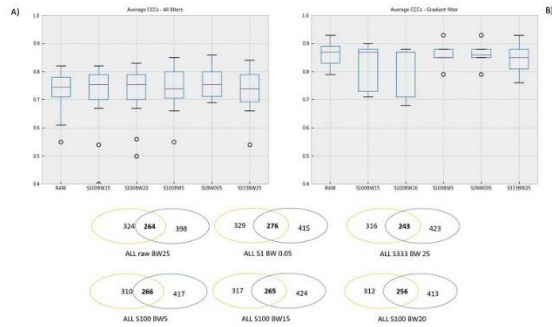


Figure 1: A) Average CCCs for all features for different normalizations. B) Average CCCs for gradient filtered features. C) Venn diagrams for features selection for the 562 features for different normalizations (see Table 1 for details on normalization). The orange circle contains all the features with CCC > 0.7 (reproducibility cut-off). The blue circle contains all the features with a Spearman correlation with volume < 0.0 (volume dependence cut-off). The intersection corresponds to both conditions verified. It is possible to see that the normalization S1 leads to more reproducible features, compared other normalizations and to non-normalized features.

## Conclusion

To reduce false discovery rates, only reproducible features with respect to inter-observer variability and acquisition settings should be used. Due to the presence of arbitrary units in MRI, normalization before feature extraction should be performed. A smaller bin width (0.05) together with Gaussian normalization is suggested when extracting radiomics features. Gradient filter reduces the dependence from volume and might provide additional valuable information to non-filtered features

## PO-0960 Automated sarcopenia assessment and its predictive power in lung cancer radiotherapy patients

A. Green<sup>1</sup>, C. Cipriano<sup>2</sup>, E. Vasquez Osorio<sup>1</sup>, J. Weaver<sup>2</sup>, M. Van Herk<sup>1</sup>, A. McWilliam<sup>1,3</sup>

<sup>1</sup>The University of Manchester, Department 58-Radiotherapy Related Research, Manchester, United Kingdom ; <sup>2</sup>The Christie NHS Foundation Trust, Medical Oncology, Manchester, United Kingdom ; <sup>3</sup>The Christie NHS Foundation Trust, Radiotherapy Related Research, Manchester, United Kingdom

### Purpose or Objective

Sarcopenia is a condition of progressive muscle wastage, and is typically assessed by measuring the properties of the skeletal muscle at the L3 vertebral level. Several studies have investigated the predictive power of sarcopenia assessment, particularly in conjunction with chemotherapy. In this work, we introduce an automated method to extract a slice from routine PET/CT close to the L3 vertebral level and segment the skeletal muscle. Several characteristics of the muscle were investigated for their predictive power in a large retrospective cohort of lung radiotherapy patients in a Cox survival model.

### Material and Methods

Skeletal muscle (SM), subcutaneous and visceral fat (SCF & VF) were manually delineated on 201 L3 slices from staging PET/CT images. A training (n=160) and validation (n=41) set was used to train an implementation of the well-known UNet convolutional neural network (CNN), configured to produce multi-label segmentation. This segmentation was followed by a dense conditional random field (CRF) to improve the results. The segmentation was validated using a 5-fold cross validation, with Distance To Agreement (DTA) calculated for each volume, see figure 1.

The L3 vertebrae were segmented in staging PET/CT for 95 lung cancer using ADMIRE v2.0 (10 atlases). Slices at the centre of the propagated structures were extracted and segmented using CNN+CRF. Areas and mean HU were extracted from the segmentations. These, along with log tumour volume, N stage, high/low performance status (PS), gender, and age were tested using an elastic net

regression, and those identified further analysed in a Cox model.

### Results

The mean DTA ranged between 0.7 and 1.6 mm for the SM segmentation, which was reduced to between 0.3 and 1.3 mm following the CRF. Elastic net regression selected log tumour volume, N stage, high/low PS and gender. Of the sarcopenia variables, only the mean HU in the SM was selected. These variables informed a multivariate Cox model, the result of which is shown in table 1. Mean HU in the skeletal muscle was found to be predictive (p=0.016), with a hazard ratio of 0.98 per HU: more sarcopenic patients would be predicted to have worse outcome. An optimum split value of 0 HU was found; those patients with mean HU greater than this value have median survival 13.5 months, whereas those in the low mean HU group have median survival of only 9 months. Survival curves, and the result of a Cox regression analysis for the two groups are shown in figure 2 and table 1 respectively.

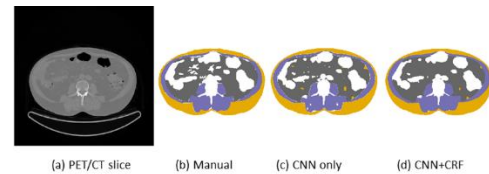


Figure 1: Example PET/CT slice (a) and manual segmentation (b) from the 201 images used to train the network. Automatic segmentations produced using the CNN alone (c) and with the additional CRF step (d) as part of the cross validation are also shown. Structures shown are the SCF in orange, SM in purple and VF in Grey. Characteristics extracted from these segmentations in the lung cohort include the area of all segmentations, and the mean HU of the SM.

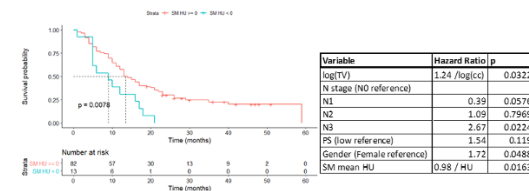


Figure 2: Kaplan-Meier curves for 95 patients split into high and low mean SM HU groups with a threshold value of 0 HU. Patients in the low group have median survival time of 9 months, while those with high mean HU have a median survival of 13.5 months. Low mean HU is indicative of fat infiltration in the SM, a sign of sarcopenia.

Table 1: Cox proportional hazard ratios for variables selected using elastic net regression on clinical variables and sarcopenia-related variables. Mean HU in the SM is identified as significant, with a HR < 1, indicating higher mean HU is protective.

### Conclusion

A fully automated sarcopenia assessment method has been developed and tested in a retrospective cohort of 95 lung cancer patients. This is the first analysis of the influence of sarcopenia on lung radiotherapy patient outcomes. In these patients, the mean HU of the SM has been found to be predictive, with an optimum cutoff of 0 HU. This can be explained as fat invasion in the SM is typical of sarcopenic patients, lowering the mean HU.

## PO-0961 MR-Δimage biomarkers to identify partial HNC responders that advance to complete responders

L.V. Van Dijk<sup>1</sup>, T. Zhai<sup>1</sup>, M. Van Dijk<sup>1</sup>, H.P. Bijl<sup>1</sup>, J.G.M. Vemer-van der Hoek<sup>1</sup>, M. Dieters<sup>1</sup>, N.M. Sijtsema<sup>1</sup>, R.J.H.M. Steenbakkers<sup>1</sup>, J.A. Langendijk<sup>1</sup>

<sup>1</sup>UMCG University Medical Center Groningen, Radiation oncology, Groningen, The Netherlands

### Purpose or Objective

Many head and neck cancer (HNC) patients have radiological partial tumour response assessed 2 months after definitive (chemo-)radiotherapy. Most of these

partial responders eventually advance in to complete responders (approximately 70%). To support decision-making in additional diagnostic and therapeutic interventions, it is crucial to identify those who develop a complete response from those who have residue or recurrence, i.e. persistent disease. Therefore, this study aims to identify  $\Delta$ image biomarkers from MRI scans 2 months after radiotherapy that may identify patients that will advance into persistent disease, and for which a more aggressive approach may be needed.

#### Material and Methods

This is a retrospective analysis in a prospective cohort of consecutive HNC patients treated between 10-2012 and 11-2014 at our department. Included were those who had a partial tumour response 2 months after treatment, and in whom pre- and post T1-TSE contrast enhanced MRI (T1ce-MRI) scan was acquired. These MRI scans were standardized to fat tissue. Subsequently, image biomarkers, representing geometric, intensity and textural characteristics of the primary tumour were extracted from the standardized pre- and post T1ce-MRI scans. Univariable logistic regression was performed to identify significant  $\Delta$ image biomarkers, where the Area Under the ROC Curve (AUC) gives an indication of the discriminative power. Pearson correlation (<0.80) was used to select independent variables. Unpaired t-test was performed to test a significant difference between the  $\Delta$ image biomarkers in patients with and without persistent disease.

#### Results

Out of the 51 partial responders, 12 (24%) patients progressed into persistent disease, including 8 residues and 4 recurrences. The median follow-up time was 44 months (range: 4-63 months). Univariable analysis showed that 26 of the in total 84  $\Delta$ image biomarkers were significantly associated with persistent disease. After the correlation analysis, 6 independent significant variables were identified (Table 1). The t-test showed that 5 of 6  $\Delta$ image biomarkers were significantly different in the patient with and without persistent disease (Table 1). The best performing  $\Delta$ image biomarker, the information correlation 1 (texture feature) suggests that tumours that show a large reduction in heterogeneity are more likely to result in persistent disease than tumours that have increased heterogeneity (examples are shown in Figure 1).

#### Conclusion

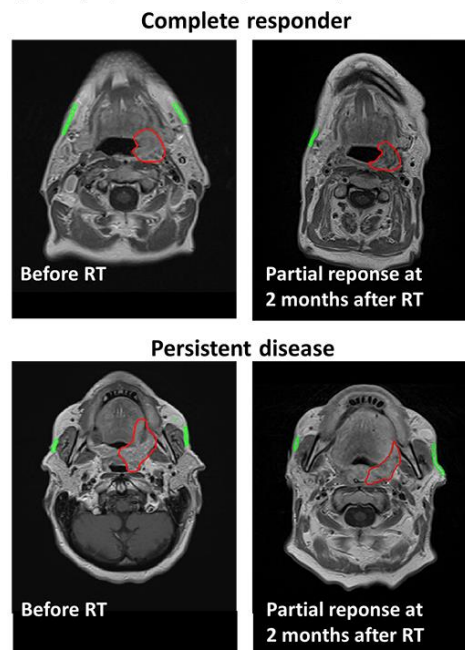
The results of this pilot study suggest that pre- and post-MRI information have potential to identify patients with radiological partial response at 2 months after radiotherapy will advance into complete responders or progress into persistent disease. This information may support clinical decision-making in cases with partial response at response evaluation using MRI.

Table 1. Independent significant univariable  $\Delta$ image biomarkers. Unpaired t-test: difference in  $\Delta$ image biomarker for patient with and without persistent disease.

	Univariable analysis			unpaired t-test		
	p-value	$\beta$ (95%CI)	AUC	p-value	$\mu 1$ (95%CI)	$\mu 2$ (95%CI)
$\Delta$ inf.corr1	0.007	1.36 (0.38-2.35)	0.79	0.007	-0.24 (-0.52-0.03)	0.79 (0.13-1.46)
$\Delta$ Kurtosis	0.015	1.15 (0.22-2.08)	0.72	0.022	-0.21 (-0.49-0.08)	0.67 (-0.02-1.36)
$\Delta$ LRHGE	0.020	-0.88 (-1.62-0.14)	0.72	0.028	0.19 (-0.11-0.49)	-0.62 (-1.27-0.04)
$\Delta$ Flattness	0.020	1.38 (0.21-2.54)	0.76	0.027	-0.17 (-0.49-0.15)	0.55 (-0.01-1.1)
$\Delta$ MAD <sub>robust</sub>	0.034	-0.79 (-1.51-0.06)	0.71	0.029	0.17 (-0.14-0.49)	-0.56 (-1.16-0.03)
$\Delta$ LRE	0.035	-0.84 (-1.62-0.06)	0.68	0.056	0.18 (-0.1-0.46)	-0.59 (-1.34-0.17)

inf.corr1: information correlation 1; LRHGE :Long Run High Graylevel Emphasis;  
MAD<sub>robust</sub>: Mean absolute deviation robust; LRE: Long Run length Emphasis

Figure 1. Example patients with a partial response at 2 months after radiotherapy that progress into a complete responder (top row) or persistent disease (bottom row).



PO-0962 Bladder changes during first week of RT for prostate cancer determine the risk of urinary toxicity  
O. Casares Magaz<sup>1</sup>, R. G. Raidou<sup>2</sup>, N. J. Petterson<sup>3</sup>, V. Moiseenko<sup>4</sup>, J. Einck<sup>4</sup>, A. Hopper<sup>4</sup>, R. Knopp<sup>4</sup>, L. P. Muren<sup>1</sup>

<sup>1</sup>Aarhus University Hospital, Medical Physics - Oncology, Aarhus, Denmark ; <sup>2</sup>TU Wien, Institute of Visual Computing & Human-Centered Technology, Wien, Austria ; <sup>3</sup>Sahlgrenska University Hospital, Medical Physics, Gothenburg, Sweden ; <sup>4</sup>University of California San Diego, Radiation Medicine and Applied Sciences, San Diego, USA

#### Purpose or Objective

Modern radiotherapy (RT) protocols for prostate cancer allow dose escalation to the prostate, however, the risk of late genitourinary (GU) toxicity is still dose-limiting. The associations between GU toxicity and dose/volume parameters in the bladder remain not fully understood. The weak associations may be due to considerable changes occurring in bladder volume, shape and position during the RT course. By using well-established methods for shape analysis and algorithms from machine learning for dimensionality reduction and clustering, we evaluated whether parameterized shape descriptors of the bladder from the first week of treatment better classify patients into exhibiting and not exhibiting late GU toxicity.

#### Material and Methods

A matched case-control study was performed within a cohort of 258 prostate cancer patients, where a previous analysis had not shown any differences in planned or actually delivered dose/volume endpoints between cases and controls. Patients were treated to prescription doses of 77.4-81.0 Gy using daily cone-beam CT (CBCT)-guidance. Twenty-seven patients (10.5%) presented late RTOG GU  $\geq$  Grade 2 toxicity and those without symptoms prior to treatment (N=8) were selected as cases. Each case was matched with three controls based on pre-treatment GU symptoms, age, Gleason score, follow-up time, and hormone therapy. CBCTs from the first week of treatment were rigidly registered to the planning CT using the recorded treatment shifts, and the bladder was manually contoured on each CBCT. Each bladder volume was described using seventeen shape descriptors. In order to

detect similarities across patients we performed dimensionality reduction using the t-distributed stochastic neighborhood embedding (t-SNE) followed by a Gaussian Mean Shift Clustering. ANOVA tests for each descriptor and each cluster were performed to find statistically significant differences. A repeated measurements model was fitted at each cluster to evaluate within-cluster trends for patients with and without toxicity (Fig. 1).

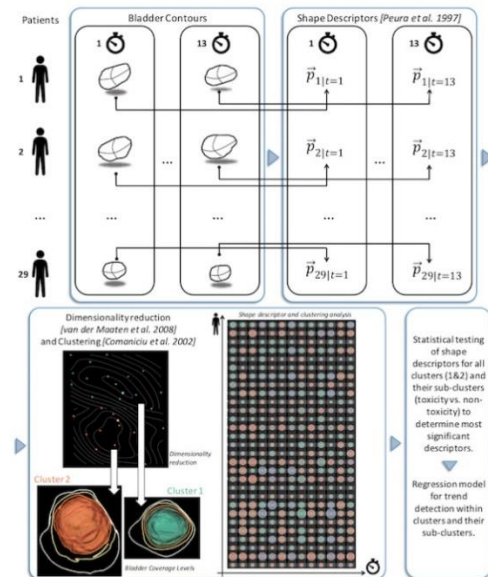


Figure 1. The workflow of our followed approach. Each patient bladder is described by 17 basic shape descriptors, and machine learning for dimensionality reduction and clustering is used to determine the two most important clusters (excl. outliers) in the data. Then, statistical testing and regression modelling is used to detect which of the 17 shape descriptors are more important.

## Results

Two clusters with distinct shape characteristics comprised 85% of the patients while a third cluster (15%) included outliers. Clusters remained similar when data from the entire RT course was pooled in the t-SNE classification. Significant differences between cases and controls were observed at each cluster in seven descriptors (convexity and elliptic variance along the three principal axes, and compactness). In cluster 1 (small bladder volumes) more convex and round bladder shapes were associated with higher toxicity risk, while in cluster 2 (large bladder volumes) more concave and elliptical shapes were associated with higher risk of toxicity (Fig. 2).

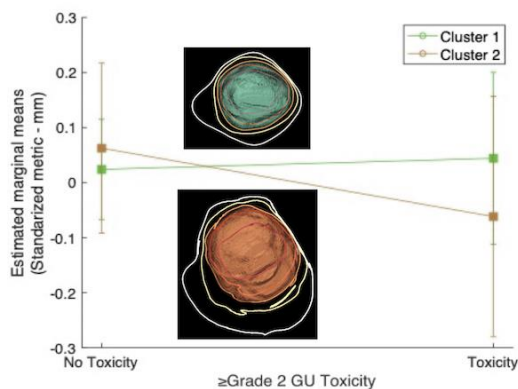


Figure 2. Fit to repeated measurements models using the data from each of the two clusters identified in the tSNE classification (only first week of treatment). The model for each cluster included the 7 shape descriptors not highly correlated (Pearson Coeff. < 0.6) and showing significant differences between patients presenting toxicity and those free from toxicity. For each cluster a sketch of the population average and quartiles bladder shape (at the central slice) are showed.

## Conclusion

Bladder shape changes occurring during the first week of treatment show potential to predict the risk of developing

late GU toxicity after RT for prostate cancer. Patient-specific changes in bladder shape might be related to the exposure of the most radiosensitive areas of the bladder to high doses.

## PO-0963 A novel normalisation technique for voxel size dependent radiomic features in oesophageal cancer

P. Whybra<sup>1</sup>, C. Parkinson<sup>1</sup>, K. Foley<sup>2</sup>, J. Staffurth<sup>2</sup>, E. Spezi<sup>1</sup>

<sup>1</sup>Cardiff University, School of Engineering, Cardiff, United Kingdom ; <sup>2</sup>Cardiff University, School of Medicine, Cardiff, United Kingdom

### Purpose or Objective

In oncology, radiomic studies hope to identify quantitative imaging features that predict survival and therapy response. To be clinically useful, features need to be robust. For 3D features that measure tumour heterogeneity, isotropic voxels are advised to ensure no directional bias [1]. Normally, PET/CT scans are not isotropic and require interpolation. The voxel size chosen is important; resampling a scan to smaller dimensions increases the number of voxels in a region of interest (ROI). An intrinsic dependency between common features and number of voxels in a ROI has been found [2]. This study evaluates methods to improve feature robustness and introduces a novel normalisation technique for voxel size dependent radiomic features in oesophageal cancer (OC).

### Material and Methods

18F-FDG PET images (scanned and segmented with the same protocol) from 441 OC patients (training=353, validation=88) were included [3]. Standardised and validated [1] in-house feature extraction algorithms were used. Voxel intensities were discretised with a fixed bin width (0.5 SUV). Five selected features recommended for voxel normalisation [2] were extracted from the original scan dimension and 5 isotropic sizes. Patients were ranked based on the feature result of the original dimension. Surface models were generated on the training dataset to normalise each feature using the voxel size and feature value. A concordance correlation coefficient (CCC) was used to determine reproducibility between features extracted from the original dimension and a range of interpolated voxel sizes.

### Results

Fig.1 shows development of a surface model and results for a selected feature, run length non-uniformity (RLNU). Fig.2 is a feature heatmap of the CCC results for each voxel dimension for the validation dataset. There are 3 versions of each feature; standard (CCC 0.16-0.96), voxel number normalised (CCC 0.08-0.99), and surface model normalised (CCC 0.95-0.99). Features normalised with a surface model performed the best in each case.

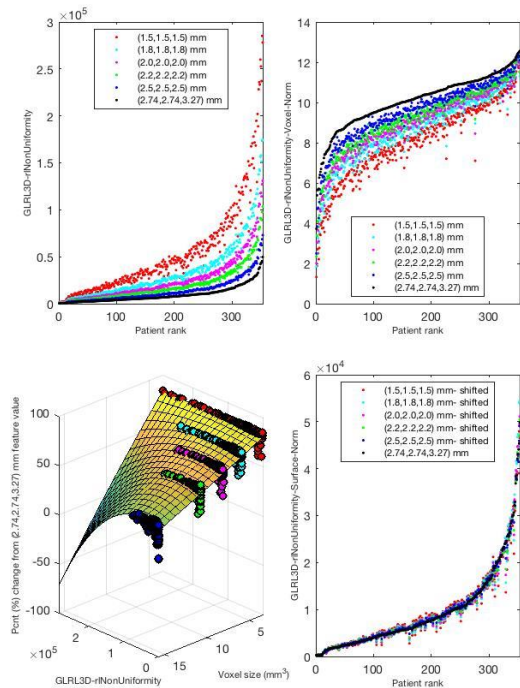


**Fig. 1:** Results for RLNU (training). TOP: (left) feature calculated at each voxel dimension against patient rank. (right) Feature normalised by voxel number in ROI. BOTTOM: (left) Surface model to calculate feature change. (right) Surface model shifted result.

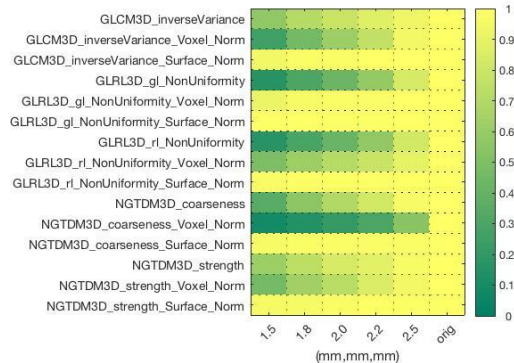


**Fig. 2:** CCC heatmap for each feature (validation dataset)

**Conclusion**

We developed, tested and validated a novel normalisation technique for voxel size dependent radiomic features. Ongoing work aims at validating the proposed approach on other imaging modalities.

**References**

- [1] A. Zwanenburg *et al.*, "Image biomarker standardisation initiative" -arXiv:1612.07003
- [2] M. Shafiq-Ul-Hassan *et al.*, "Voxel size and gray level normalization of CT radiomic features in ESTRO\_lung cancer," *Sci. Rep.* 2018.
- [3] K. G. Foley *et al.*, "Development and validation of a prognostic model incorporating texture analysis derived from standardised segmentation of PET in patients with oesophageal cancer," *Eur. Radiol.*, 2017.

**PO-0964 Stability and prognostic significance of CT radiomic features from oesophageal cancer patients**  
 C. Piazzese<sup>1</sup>, P. Whybra<sup>1</sup>, R. Carrington<sup>2</sup>, T. Crosby<sup>3</sup>, J. Staffurth<sup>4</sup>, K. Foley<sup>5</sup>, E. Spezi<sup>1</sup>  
<sup>1</sup>Cardiff University, School of Engineering, Cardiff, United Kingdom ; <sup>2</sup>Velindre Cancer Centre, Medical

Physics, Cardiff, United Kingdom ; <sup>3</sup>Velindre Cancer Centre, Department of Oncology, Cardiff, United Kingdom ; <sup>4</sup>Velindre Cancer Centre, Radiotherapy & Clinical Trials, Cardiff, United Kingdom ; <sup>5</sup>Cardiff University, School of Medicine, Cardiff, United Kingdom

**Purpose or Objective**

Radiomics aims at extracting quantitative features from medical images. Several studies focussed on the potential value of radiomic analysis in predicting tumour response for oesophageal cancer (OC) patients using contrast enhanced CT images. However, in clinical practice contrast agents are not always administrable, making the development of a new radiomic model necessary. In this work, we investigated the usefulness of radiomic features extracted from contrast and non-contrast enhanced CT scans in the development of a prognostic model in OC.

**Material and Methods**

CT images and radiotherapy volumes of 213 patients from a clinical trial in OC<sup>1</sup> were processed with the CERR package<sup>2</sup>. Patients were divided into 3 groups: mixed group (MG) with contrast and non-contrast enhanced CT images (n=213), contrast group (CG) with contrast enhanced CT scans (n=138) and non-contrast group (nCG) with non-contrast enhanced CT data (n=75). Radiomic features were automatically extracted in 2D and 3D in compliance with the IBSI<sup>3</sup>, using in-house developed data analytics software<sup>4</sup>. Stable features were selected as the ones with similar intra-groups distributions (Kruskal-Wallis test). Corresponding 2D and 3D stable features within each group were evaluated for differences (Wilcoxon signed rank test). Remaining filtered features and clinical characteristics were used to develop a prognostic model with the Cox regression method.

**Results**

A total of 119 2D and 3D features were computed from each group. The Kruskal-Wallis test excluded 82, 3 and 6 unstable features obtained from MG, from CG and from nCG, respectively (Fig. 1). Some stable features (6 for MG, 15 for CG and 17 for nCG) did not show a significant difference if extracted considering 1 tumour layer at a time or considering the whole tumour volume. Among stable features, 4 features showed no difference if obtained from 3D or 2D data and were stable in all the 3 groups. The Cox regression model, constructed with 8 clinical and radiomic variables, identified 1 feature (GLDZM zone distance variance) associated with survival (Table 1).

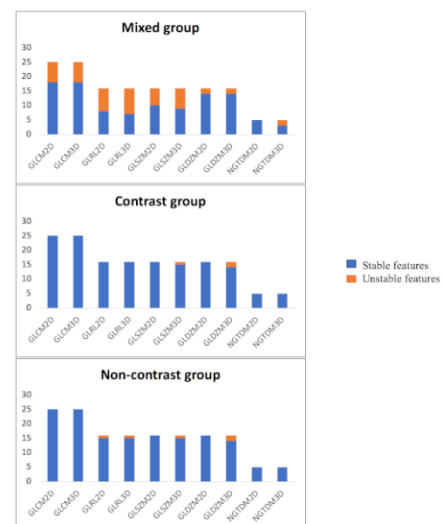


Figure 1. Stable and unstable features extracted from the different groups.

**Conclusion**

The prognostic model has identified 1 texture significantly and independently correlated with overall survival. This

feature can add value over and above currently known prognostic factors if computed in 2D or 3D and independently from administration of CT contrast agents.

Prognostic variable	p-value	Parameter estimate	Hazard Ratio	95% Confidence Intervals	
				Lower	Upper
GLDZM zone distance variance	0.005	0.274	1.315	1.085	1.593

Table 1. Results of the Cox regression model

**References:**

1. Hurt CN et al.SCOPE1:a randomised phase II/III multicentre clinical trial of definitive chemoradiation,with or without cetuximab,in carcinoma of the oesophagus.BMC Cancer.2011 Oct 28;11:466
2. Deasy JO et al.CERR:a computational environment for radiotherapy research.Med Phys.2003 May;30(5):979-85
3. Zwanenburg A et al.Image biomarker standardisation initiative. <https://arxiv.org/abs/1612.07003v7>
4. Gwynne S et al.Toward semi-automated assessment of target volume delineation in radiotherapy trials:the SCOPE1 pretrial test case.Int J Radiat Oncol Biol Phys.2012 Nov 15;84(4):1037-42

**PO-0965 How to find the best radiomics features for prediction of overall survival in SBRT for HCC?**

P. Fontaine<sup>1</sup>, O. Acosta<sup>1</sup>, F. Riet<sup>2</sup>, J. Castelli<sup>2</sup>, K. Gnep<sup>2</sup>, A. Simon<sup>1</sup>, A. Depeursinge<sup>3</sup>, R. De Crevoisier<sup>2</sup>

<sup>1</sup>Univ Rennes- CLCC Eugne Marquis- INSERM- LTSI - UMR 1099- F-35000 Rennes- France, Ltsi, Rennes, France ;

<sup>2</sup>Univ Rennes- CLCC Eugne Marquis- INSERM- LTSI - UMR 1099- F-35000 Rennes- France, CLCC Eugène Marquis, Rennes, France ; <sup>3</sup>University of Applied Sciences Western Switzerland HES-SO- TechnoArk 3- CH-3960 Sierre-Switzerland, Hes-SO, Sierre, Switzerland

**Purpose or Objective**

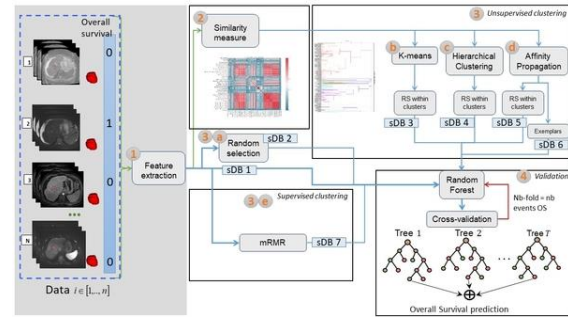
One of the major issues in radiomics is the very large amount of tested extracted features, compared to the often-reduced sample size and the low number of events. Reduction of dimensionality may be therefore an important preliminary step to improve the prediction capability of the predictive models. The aims of the study were:

- to propose methods for reducing redundancy by selecting the more informative features from -multimodal images;
- to evaluate and compare the prediction capability of the models when using these methods.

The considered example was MRI based radiomics to predict overall survival after SBRT for hepatocellular carcinoma (HCC).

**Material and Methods**

Eighty-one patients underwent SBRT for inoperable HCC. For each patient, 7 modalities of MR images were acquired. A total of 273 features were extracted from manually delineated tumours belonging to 4 radiomics categories (geometrical, first order, gradient-based and second order) in each modality. As we follow the workflow [Figure 1]



, a similarity measure based on Spearman correlation was computed across the features. Four methods for feature selection were then assessed namely three unsupervised (K-means, Hierarchical clustering (HC) and Affinity propagation (AP)) and a supervised (mRMR) clustering and compared random selection (RS) and no selection (using all the features). Affinity propagation clustering yields a set of exemplars which better represented each cluster. Finally, in order to assess the predictive capabilities of each one of the feature selection method, a random forest classifier was trained and tested via a stratified-K-fold (K=19 the occurrence of decease event) cross-validation. This process was repeated 1000 times. Feature importance as assessed by aggregation of the performance at each try. The performance is evaluated by computing the precision (True positive / True positive + True negative) of prediction.

**Results**

The table displays the selected predictive feature depending on the selection methods. Unsupervised clustering algorithms allowed to select a non-redundant set of features able to significantly better predict HCC overall survival [Exemplars from AP: Precision= 0.76 ± 0.01, (p-value < 0.001)], in comparison to the other methods [All features: Precision = 0.73 ± 0.001; RS from all features : Precision = 0.71 ± 0.3 ; RS from K-means clustering : Precision = 0.715 ± 0.1; RS from HC: Precision = 0.74 ± 0.02; RS from AP clustering: Precision = 0.735 ± 0.01 and exemplars from mRMR: Precision = 0.735 ± 0.01] . The most reproducible predictive features are related with the shape of the tumour [Figure 2]

All features		Random selection	Random Selection HC
1	T1_Tardif_Flatness	T1_Gado_Least_Axis_Length	T1_Gado_Least_Axis_Length
2	T1_Gado_Least_Axis_Length	T1_Tardif_Flatness	T1_Tardif_Flatness
3	T1_Tardif_Least_Axis_Length	T1_Tardif_Least_Axis_Length	T1_Tardif_Least_Axis_Length
4	T1_Tardif_Canny_std	T2_Log_mean	T2_Log_mean
5	T2_Log_mean	T1_Tardif_Canny_std	T1_Tardif_Canny_std
6	T2_Sobel_mean	T2_Log_std	T2_Sobel_mean
7	T2_Log_std	T2_Sobel_mean	T2_Log_std
8	T2_mean	T2_mean	T2_mean
9	T2_max	T2_max	T2_max
10	ADC_skeness	T1_Gado_Compactness1	T1_Gado_Sphericity

Exemplars AP		Random selection Kmeans	Random selection AP
1	T1_Tardif_Flatness	T1_Gado_Least_Axis_Length	T1_Gado_Least_Axis_Length
2	T2_mean	T1_Tardif_Flatness	T1_Tardif_Flatness
3	ADC_mean	T1_Tardif_Least_Axis_Length	T1_Tardif_Least_Axis_Length
4	T1_Gado_Compactness1	T2_Log_mean	T2_Log_mean
5	Diffusion_DWI_1_Sphericity	T1_Tardif_Canny_std	T1_Tardif_Canny_std
6	T1_Gado_Information_Measures_of_Correlation_2	T2_Log_std	T2_Sobel_mean
7	T2_Sum_Average	T2_Sobel_mean	T2_Log_std
8	T1_Tardif_Elongation	T2_mean	T2_mean
9	Diffusion_DWI_1_Elongation	T2_max	T2_max
10	T2_Sphericity	T1_Gado_Sphericity	T1_Gado_Compactness1

**Conclusion**

A framework for feature selection in a radiomics workflow is presented. Unsupervised methods allow to cluster together groups of features increasing the prediction capabilities and reducing redundancy. AP outperforms the other features selection method suggesting the use of the exemplars as representative feature of each cluster.

**PO-0966 Prediction of Locoregional Control in Hepatocellular Carcinoma After SBRT with Deep Learning**

I. El Naqa<sup>1</sup>, R. Ten Haken<sup>1</sup>

<sup>1</sup>University of Michigan, Radiation Oncology, Ann Arbor, USA

### Purpose or Objective

Despite high local control in patients with hepatocellular carcinoma (HCC) who receive liver stereotactic body radiotherapy (SBRT), locoregional control (LRC) remains dismal and is associated with long-term failures and poor survival. The purpose of the current study is to evaluate deep learning models for predicting LRC and personalization of HCC treatment.

### Material and Methods

Data from 146 HCC patients who received SBRT from 2005-14 were analyzed retrospectively. Tumor doses (median prescribed = 49.8 Gy, delivered in 3 or 5 fractions) were bio-corrected to 2 Gy equivalents. Patient demographics (age, sex, stage, etc) dosimetric (dose-volume metrics of tumor and surrounding normal tissue), and toxicity information ((ALBI, Child-Pugh, enzymatic changes) were extracted from the patients' records. Despite local control of greater than 90%, the locoregional failure rate was 54.7% with a median follow-up of 11 months. Predictive models based on deep machine learning techniques for predicting LRC were developed using the open source neural network library (Keras). The deep learning network architectures included dense and dropout layers with ReLU activation functions. The loss function was defined in terms of cross-entropy and the weights for the network were estimated using an adaptive stochastic gradient algorithm (Adam). These models were compared with traditional statistical techniques based on variable shrinkage analysis with logistic regression (Lasso-logistic). The data were normalized using z-scoring (mean-centered) prior to modeling. To avoid overfitting pitfalls, 10-fold cross-validation resampling was used to evaluate prediction, and performance was assessed using the area under the receiver-operating characteristics curve (AUC).

### Results

When modeling with Lasso-logistic regression the predictive LRC achieved an AUC = 0.57 on cross-validation with functional toxicity (ALBI) as the highest contributor. When deep learning was applied, the prediction of LRC improved by 17.5%, and the prediction of the algorithm reached an AUC = 0.67 on cross-validation. The performance seemed to be affected by the dropout layer rates, which act as a regularization process to prevent neural network overfitting, with a dropout rate of 20% providing stable results.

### Conclusion

Machine learning methods based on deep learning can provide a robust framework for estimating locoregional failure risk in HCC patients post-SBRT. However, proper tuning of parameters is necessary to avoid overfitting and evaluation on independent data is needed to further assess generalizability. These new LRC models show promise for personalizing new regimens for combining local and systemic therapy in HCC patients.

### PO-0967 Prediction of treatment outcome for head and neck cancers using radiomics of PET/CT images

A. Rosvoll Groendahl<sup>1</sup>, A.D. Midtved<sup>1</sup>, G.S. Elvatun Rakh Langberg<sup>1</sup>, O. Tomic<sup>1</sup>, U.G. Indahl<sup>1</sup>, I. Skjei Knudtsen<sup>2</sup>, E. Malinen<sup>3</sup>, E. Dale<sup>4</sup>, C.M. Futsaether<sup>1</sup>

<sup>1</sup>Norwegian University of Life Sciences NMBU, Faculty of Science and Technology, Ås, Norway ; <sup>2</sup>Oslo University Hospital, Department of Medical Physics, Oslo, Norway ; <sup>3</sup>University of Oslo / Oslo University Hospital, Department of Physics / Department of Medical Physics, Oslo, Norway ; <sup>4</sup>Oslo University Hospital, Department of Oncology, Oslo, Norway

### Purpose or Objective

The objective of this study was to evaluate the usefulness of radiomics for predicting locoregional relapse in head and neck cancer patients using PET/CT images.

### Material and Methods

This retrospective study includes 182 head and neck cancer patients, who underwent a combined 18F-FDG-PET/CT scan prior to radiotherapy. Patients were divided into two classes according to locoregional control; 47 with failures and 135 with control. The radiomics approach was used to extract features characterizing the primary tumour from both PET and CT images. First order statistical features such as median values and interquartile range, shape features including sphericity and tumour surface area as well as texture features describing intensity non-uniformity, busyness and coarseness were calculated. Features were also calculated from PET and CT images transformed using point and two-dimensional transformations to emphasize particular aspects of the tumour. Clinical factors (age, sex, ECOG status, Charlson comorbidity status, HPV-status, TNM stage, pack years of smoking, days on the hypoxic radiosensitizer nimorazole and number of weekly cisplatin doses) were also included as features. Seven feature selection methods were tested to select the most relevant features for classification among the more than 2 500 features. Classification of the patients according to outcome was performed using 14 different algorithms. The performance measure ROC-AUC (Receiver Operating Characteristics - Area Under the Curve) of the classification models was estimated using nested cross-validation and was used to assess and compare the models.

### Results

The classification models with the highest performance gave a mean AUC of  $0.66 \pm 0.10$ . The models were obtained using ReliefF for feature selection and either Partial Least Squares Regression (PLSR), logistic regression, Linear Discriminant Analysis (LDA) or AdaBoost as classifiers (Figure 1). These models were based on tumour shape and heterogeneity features such as busyness, which characterises rapid intensity changes between neighbouring voxels within the tumour. Interestingly, the feature selection methods consistently chose image features over clinical factors when these were included in the same classification. Classification models based solely on clinical factors gave poorer performance with a mean AUC of  $0.57 \pm 0.10$ .

### Conclusion

Characteristics of primary head and neck tumours extracted from PET and CT images were better predictors of treatment outcome than clinical factors alone. Particularly tumour shape and tumour heterogeneity were selected as relevant features for treatment outcome prediction. Future efforts should be directed at improving classification performance by exploring other feature engineering and feature selection approaches.

	ReliefF	LDA	RF	LOG-1	M	PCA	ICA
PLSR	0.66	0.60	0.60	0.57	0.57	0.57	0.57
LOG-2	0.66	0.60	0.60	0.57	0.56	0.57	0.56
LDA	0.66	0.60	0.60	0.57	0.56	0.56	0.56
LOG-1	0.66	0.60	0.60	0.57	0.58	0.55	0.55
QDA	0.65	0.62	0.59	0.53	0.56	0.58	0.57
AdaBoost	0.66	0.60	0.59	0.57	0.56	0.54	0.54
LinearSVC	0.63	0.60	0.60	0.57	0.54	0.54	0.54
Neural Networks	0.64	0.60	0.58	0.58	0.53	0.54	0.54
SVC	0.65	0.60	0.57	0.57	0.54	0.51	0.51
GNB	0.65	0.62	0.60	0.54	0.54	0.49	0.49
MARS	0.63	0.58	0.55	0.57	0.53	0.51	0.51
KNN	0.61	0.59	0.58	0.55	0.53	0.50	0.50
RF	0.62	0.58	0.56	0.53	0.51	0.52	0.52
Decision Tree	0.61	0.59	0.54	0.50	0.52	0.51	0.50

Figure 1. Mean AUC obtained using classification models based on radiomics features for outcome prediction. Fourteen classification algorithms (rows) and seven feature selection methods (columns) were compared. Abbreviations are as follows. Partial Least Squares Regression (PLSR), logistic regression with L2 (LOG-2) or L1 regularization (LOG-1), Linear Discriminant Analysis (LDA), Quadratic Discriminant Analysis (QDA), Support Vector Classifiers (SVC), Gaussian Naïves Bayes (GNB), Multivariate Adaptive Regression Splines (MARS), K-Nearest Neighbours (KNN), Random Forest (RF), Mutual Information (MI), Principal Component Analysis (PCA), Independent Component Analysis (ICA).

### PO-0968 Prostate-specific phantom for radiomic features quality assurance

S. Osman<sup>1,2</sup>, E. Russell<sup>1</sup>, R.B. King<sup>2</sup>, A.J. Cole<sup>1,3</sup>, C. McGrath<sup>4</sup>, S. Jain<sup>1,3</sup>, A.R. Hounsell<sup>1,2</sup>, K.M. Prise<sup>1</sup>, C.K. McGarry<sup>1,2</sup>

<sup>1</sup>Queen's University Belfast, Centre for Cancer Research

& Cell Biology, Belfast, United Kingdom ; <sup>2</sup>Belfast Health & Social Care Trust- Northern Ireland Cancer Centre, Radiotherapy Physics, Belfast, United Kingdom ; <sup>3</sup>Belfast Health & Social Care Trust- Northern Ireland Cancer Centre, Department of Clinical Oncology, Belfast, United Kingdom ; <sup>4</sup>Belfast Health & Social Care Trust- Forster Green Hospital, Radiological Sciences and Imaging, Belfast, United Kingdom

### Purpose or Objective

A phantom study to assess the repeatability, reproducibility and robustness of radiomic features in the presence of fiducial marker (FM) induced artefacts on multi-modality imaging.

### Material and Methods

An in-house developed pelvis water phantom containing boxes filled with gelatine and FMs (6 boxes) or without FMs (2 boxes), was used in this study. Three FMs were placed in each box in a spatial distribution similar to that for PCa patients. The boxes were placed at the centre of the water phantom and scanned using several imaging modalities typically used to image prostate cancer patients; MRI (2 scanners), CT (2 scanners), CBCT (3 different scanning protocols), Table 1. Four setup arrangements were used to place the 2 boxes of interest at the centre of the phantom for each scan. After contouring the boxes, and before features extraction, several image pre-processing settings (i.e. resampling and discretization) were tested. Radiomic features extracted were the first order gray-level (GL) statistics from intensity histograms, and features based on; GL co-occurrence matrix (GLCM), GL run length matrix (GLRLM), GL size zone matrix (GLSZM), GL distance zone matrix (GLDZM), neighbourhood gray tone difference matrix (NGTDM) and neighbouring GL dependence matrix (NGLDM). 1642 features were extracted from each box, including textural and statistical features after applying different image filtering methods. Intra-class correlation coefficient (ICC) was computed to provide an estimation of the test-retest reliability and consistency of the features extracted (ICC = 0 non-reproducible, ICC = 1 perfectly reproducible features). In this analysis, a threshold of ICC > 0.8 was considered to identify robust features.

Table1: Specifications of scanners, protocols and tests performed.

Modality	Model	Test-retest	Intra-scanner	Inter-scanner
CT1	GE Optima CT580	120 kV, 200 mA	120 kV, 200 mA	CT1 vs CT2
CT2	GE Discovery CT590 RT	120 kV, 200 mA	120 kV, 400 mA	120 kV, 200 mA
CBCT1	ver 2.5.16 on Varian TrueBeam	125 kV, 1080 mAs	CBCT1 vs CBCT2 vs CBCT3	
CBCT2		125 kV, 855 mAs		
CBCT3		140 kV, 1687.5 mAs		
MRI1	Siemens Magnetom Aera 1.5T	T1w T2w		T1w: MRI1 vs MRI2
MRI2	GE Optima MR450w 1.5T	T1w T2w		T2w: MRI1 vs MRI2

### Results

In the test-retest repeatability experiment (Figure 1 rows 1-9), a relatively high proportion of CT-based radiomic features were reliable (CT1= 78% and CT2= 86%). CBCT features showed the highest repeatability with (CBCT1=93%, CBCT2= 95%, CBCT3= 87%) of the features having ICC > 0.8 for different CBCT scanning protocols. Reduced reliability was observed for MRI-based features with MRI1 =53% and MRI2=74% reliable features for T1 scans and 73% and 85% T2 scans on MRI1 and MRI2, respectively.

The intra-scanner study of robustness of features against scanning parameters variation, table 1 showed that 72% and 89% of the features were robust, for CT1 and CT2, respectively. Using different CBCT scanning protocols 66% of the features were robust. Inter-scanner reproducibility was 48% for CT although only 2% and 4% of features were reproducible for T1 and T2 MRI scans, respectively, possibly due to different manufacturers.

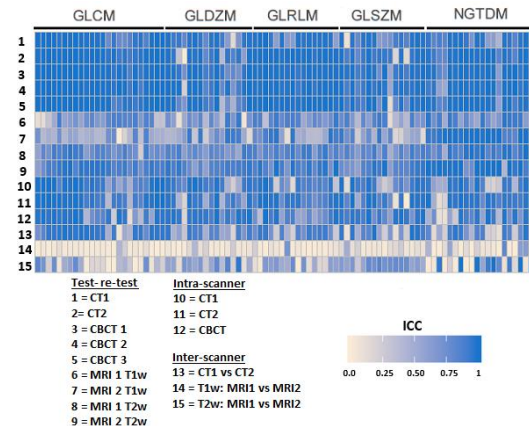


Figure1: a heat map showing a subset of the features' interclass correlation coefficients (ICC) for: test-retest (rows 1-9), intra-scanner (10-12) and inter-scanner (13-15) analysis. All scans were re-sampled to 2.5mm isotropic voxels before features extraction and grey level values discretised with 10 Hounsfield Units (HU) bin width.

### Conclusion

Despite significant FM artefacts on CT and CBCT, preliminary results from this study show that CT and CBCT features are more reliable and reproducible than MRI features. The very poor inter-scanner reproducibility of MRI-based features can have a drastic impact on the results of radiomics studies.

### PO-0969 Sensitivity analysis of an in silico model of prostate tumour growth and response to radiotherapy

C. Sosa marrero<sup>1</sup>, Ó. Acosta<sup>1</sup>, M. Castro<sup>1</sup>, A. Hernández<sup>1</sup>, N. Rioux-Leclercq<sup>1</sup>, R. Mathieu<sup>1</sup>, F. Paris<sup>2</sup>, R. De Crevoisier<sup>1</sup>

<sup>1</sup>Univ Rennes-CHU Rennes-CLCC Eugène Marquis-INSERM, Ltsi - UMR 1099- F-35000, Rennes, France ; <sup>2</sup>Université de Nantes, Crcina, Nantes, France

### Purpose or Objective

*In silico* models are appealing tools to understand and predict tumour growth and response to RT. A major issue of computational models is the large number of variables they may contain. The objective of this work was to perform a Morris sensitivity analysis on a prostate tumour growth and response to RT model, to identify the most relevant parameters and determine which ones can be negligible

### Material and Methods

Histopathological specimens from 7 patients with localized prostate cancer, treated with radical prostatectomy, were used to initialise 21 computational tissues with different tumour and vascular densities. Tumour foci were delineated by a pathologist on the HES axial slides (figure 1.a) and a CD31 staining (figure 1.b) was carried out to identify the blood vessels. A multi-scale *in silico* model was generated, considering the prostate computational tissues, where each voxel corresponded to a cell of the following 7 types: healthy glandular/endothelial, tumour glandular/neo-created endothelial and dead (by apoptosis, hypoxic necrosis or mitotic catastrophe). Figure 1.c shows the corresponding initial computational tissue. The model integrated 5 biological processes: oxygenation of the tissue (Oxy.) using a reaction-diffusion equation (Espinoza *et al.*, *Med Phys* 2013); proliferation of tumour cells, considering their life-cycle (Prolif.); angiogenesis based on the VEGF diffusion (Angio.) (Harting *et al.*, *Phys. Med. Bio* 2007); phase-and-oxygen-dependent response to irradiation, using the linear-quadratic model and considering cycle arrests and death by mitotic catastrophe (RespTolrr.) and resorption of dead cells (Resor). The table presents the 34 parameters of the model, indicating the process they intervene in. Every simulation considered a total dose of 80 Gy, administered every 24 h, from Monday to Friday.

Figure 1.d shows the computational prostate tissue after 80 Gy. The tumour density (number of tumour cells divided by the total number of cells) at the end of the treatment was used as output of the model. The Morris sensitivity method calculated, on the 21 computational tissues (73500 simulations in total), the mean and standard values ( $\mu_i^* \pm \sigma_i$ ) of 100 elementary effects for each parameter. The Euclidean distance of the point ( $\mu_i^*$ ,  $\sigma_i$ ) to the origin was the indicator of the impact of parameter  $i$ .

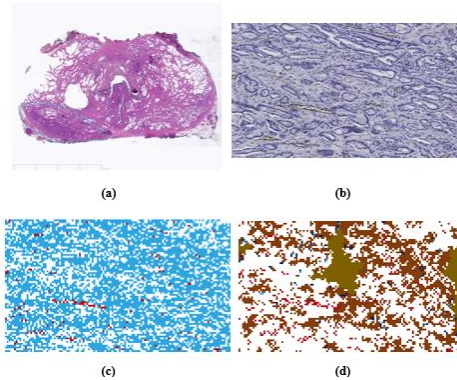


Figure 1. Example of an (a) histopathological cut; (b) CD31 staining; (c) initial computational tissue, where healthy cells are represented in white; tumour, in light blue and pre-existing endothelial in light red and (d) computational tissue after a 40 x 2 Gy RT treatment, where tumour cells with DNA damaged by irradiation are represented in dark blue; neo-created endothelial, in dark red and dead by hypoxic necrosis, in ochre and by mitotic catastrophe, in brown

## Results

The table shows a ranking of the 34 parameters of the model, according to their mean Euclidean distances over the 21 tissues.

Parameter of the model	Biological process	Mean Euclidean distance
Duration of cycle of tumour cells	Prolif.	41.68 ± 3.90
Dose per fraction	RespToIrr.	41.62 ± 4.47
Dose threshold of immediate death by apoptosis	RespToIrr.	21.51 ± 4.45
Duration of arrest at checkpoints G1/S and G2/M due to irradiation	RespToIrr.	11.23 ± 2.10
O <sub>2</sub> Michaelis constant	Oxy.	7.53 ± 4.36
O <sub>2</sub> Michaelis-Menten maximum rate	Oxy.	7.25 ± 3.75
pO <sub>2</sub> threshold of hypoxia	Oxy.	6.64 ± 3.14
α of tumour cells in phase G1	RespToIrr.	5.52 ± 4.87
α of tumour cells in phase G2	RespToIrr.	4.43 ± 2.98
α of tumour cells in phase M	RespToIrr.	3.56 ± 1.17
pO <sub>2</sub> of pre-existing endothelial cells	Oxy.	3.26 ± 1.96
O <sub>2</sub> diffusion coefficient	Oxy.	2.66 ± 2.04
α of tumour cells in phase S	RespToIrr.	2.13 ± 1.55
α of tumour cells in phase G0	RespToIrr.	1.77 ± 1.52
αβ of tumour cells in phase G0	RespToIrr.	1.74 ± 1.09
αβ of tumour cells in phase M	RespToIrr.	1.70 ± 0.53
αβ of tumour cells in phase G1	RespToIrr.	1.52 ± 0.82
αβ of tumour cells in phase G2	RespToIrr.	1.47 ± 0.94
Duration of cycle of healthy cells	Resor.	1.29 ± 0.87
α of healthy cells	RespToIrr.	1.29 ± 1.12
VEGF of hypoxic cells	Angio.	1.28 ± 1.20
pO <sub>2</sub> of neo-created endothelial cells	Oxy.	1.26 ± 1.03
αβ of healthy cells	RespToIrr.	1.25 ± 0.70
αβ of neo created endothelial cells	RespToIrr.	1.24 ± 1.25
αβ of pre-existing endothelial cells	RespToIrr.	1.21 ± 0.67
pO <sub>2</sub> threshold of hypoxic necrosis	Oxy.	1.18 ± 0.45
αβ of tumour cells in phase S	RespToIrr.	1.10 ± 0.22
α of neo-created endothelial cells	RespToIrr.	1.09 ± 0.35
Duration of cycle of neo-created endothelial cells	Angio.	1.06 ± 0.34
VEGF threshold to trigger angiogenesis	Angio.	1.04 ± 0.22
α of pre-existing endothelial cells	RespToIrr.	1.02 ± 0.17
VEGF Michaelis-Menten maximum rate	Angio.	0.99 ± 0.15
VEGF Michaelis constant	Angio.	0.99 ± 0.24
VEGF diffusion coefficient	Angio.	0.98 ± 0.21

**Table. Ranking of the 34 parameters of the model, according to their mean Euclidean distance to the origin**

**Conclusion**  
The Morris sensitivity analysis identified the duration of the cycle of tumour cells and the dose per fraction as the parameters having the greatest effect on the final tumour density after 80 Gy. The VEGF Michaelis-Menten maximum rate, the VEGF Michaelis constant and the VEGF diffusion coefficient had the lowest impact.

## Poster: Physics track: Intra-fraction motion management

### PO-0970 Advances in intra-fraction movement detection during stereotactic radiosurgery

O. Semeniuk<sup>1</sup>, P. Sadeghi<sup>1,2</sup>, J.D. Farah<sup>1</sup>, J. Robar<sup>1,2,3</sup>

<sup>1</sup>Nova Scotia Health Authority, Medical Physics, Halifax, Canada ; <sup>2</sup>Dalhousie University, Department of Physics & Atmospheric Science, Halifax, Canada ; <sup>3</sup>Dalhousie University, Department of Radiation Oncology, Halifax, Canada

#### Purpose or Objective

Detection of cranial position during stereotactic radiosurgery (SRS) is crucial for correcting for intrafractional motion. This abstract describes a novel technology that takes advantage of capacitive motion sensing (CMS) for real-time, 3D motion detection during SRS. The CMS system senses the capacitive signal from the cranium and provides advantages over systems that are based on x-ray imaging or use skin as the surrogate. Here, we report our progress on performance optimization for the CMS system with an emphasis on advances in sensitivity, detection precision and dynamic range.

#### Material and Methods

The performance of two capacitive-to-digital converters was evaluated to determine the most suitable candidate for practical applications. We compared the MPR121 (Adafruit Industries) converter performance (used in the proof-of-concept study [1]) against FDC1004 (Texas Instruments) - a device possessing an active shield technology. The active shield enables whole-system noise minimization, thus boosting sensitivity. Here, sensitivity was our primary performance metric, defined as capacitance change per unit of displacement; detection precision was defined as ratio of noise amplitude to sensitivity; and dynamic range was defined as the largest distance from the target at which we were able to detect a sub-millimeter displacement. CMS prototypes were tested with 5x5 cm<sup>2</sup> sensors in a parallel plate set-up and a head phantom made in-house. The phantom was 3D printed from a CT scan of a volunteer's thermoplastic mask, layered with a copper foil to provide a capacitive signal, and subsequently grounded. A micro-stage and 6D Hexapod were used to simulate subjects' motion with millimeter steps.

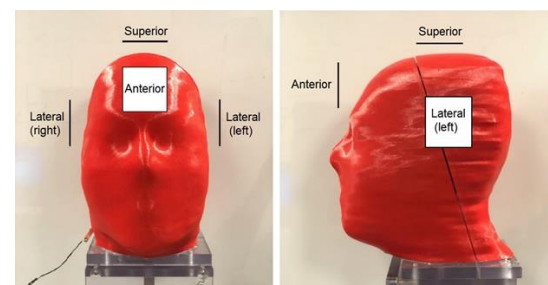


Figure 1. Diagram of CMS sensor positions with respect to the head phantom.

## Results

The sensitivity and detection precision of FDC1004-based CMS system were found to be at least an order of magnitude greater than the MPR121-based CMS system. A precision of 0.1 mm was reached with the FDC1004 sensors even at a large separation distance (34 mm) between the sensor and the ground plate, outperforming the MPR121 sensor which achieved precision of ~5 mm. When tested with the head phantom, the FDC1004 system also showed superior performance with submillimeter detection precision in all directions including anterior motion (reported to be most challenging orientation to detect

[1]). To provide the sensitivity of FDC1004, the MPR121-based system would necessitate sensors with areas larger by a factor of six. In addition, larger sensors would have to be two times closer to the target in order to provide similar performance [1].

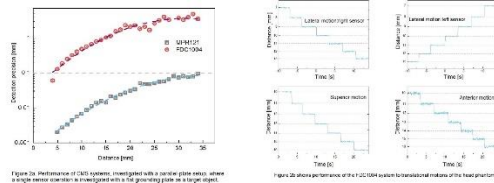


Figure 2a. Performance of 1200 capacitors investigated with a custom data logger. Average sensor capacitance is measured with a 100 pF generating plate at a larger depth. Figure 2b. Shows performance of the FDC1004 system for translational motions of the head phantom.

## Conclusion

These advances in CMS technology offer significant performance improvements in terms of sensitivity, detection precision, sensor size and the dynamic range relative to the system previously described [1], thus making it more attractive and practical for clinical use.

## References

1. P. Sadeghi *et al* 2018 *Phys. Med. Biol.* **63** 165019

## PO-0971 Capacitive monitoring system for intrafraction rotation detection during frameless radiosurgery

P. Sadeghi<sup>1</sup>, O. Semeniuk<sup>1</sup>, R. James<sup>1,2</sup>

<sup>1</sup>Dalhousie University, Physics & Atmospheric Sciences, Halifax, Canada ; <sup>2</sup>Dalhousie University, Department of Radiation Oncology, Halifax, Canada

### Purpose or Objective

This work presents a novel, non-ionizing technique for continuous intra-fraction patient position monitoring during stereotactic radiosurgery. The system provides real-time cranial positioning information without relying on surrogates such as skin.

### Material and Methods

The system is comprised of an array of conductive sensors arranged around the cranium. Capacitance of the sensor array is monitored continuously. The system is unique in that it is not sensitive to the position of the thermoplastic mask but registers the motion of the cranium within. The system has been shown previously (Sadeghi, Lincoln *et al.* 2018) to demonstrate 0.1 mm sensitivity in detection of cranial translation, and in this work is assessed for rotation detection. A cranial phantom with a hollow space modelling the average human brain was 3D printed provided a signal for evaluation of the optimal sensor arrangement for rotation detection (figure 1). The brain cavity walls were covered with thin copper foil (0.025 mm thickness) to replicate the conductivity of human brain. The cranial phantom was attached to a hexapod stage capable of performing 6D motion with respect to any pre-defined origin in space. Three plates were arranged around the phantom at 1 cm distance in superior, left lateral, and right lateral directions. Each plate was comprised of three sensors, each made from 0.025 mm thick copper film on 3D printed PLA backing. The middle sensor was 2.7 cm in diameter, the anterior and posterior sensors (sensors 1 & 3) were half rims with inner and outer diameters of 9 cm and 12 cm, respectively (figure 1). Pitch and roll rotations were introduced as the phantom was rotated in 1 degree steps in both positive and negative directions. The axes and origin for head rotation were defined based on Fick convention (Kunin, Osaki *et al.* 2007). Sensitivity was defined as change in average signal per degree rotation. The range (noise band) was the difference between maximum and minimum data points under stationary conditions. When the sensitivity was higher than the noise band, the sensor was considered to be detecting the respective motion.

## Results

Our experiments show that posterior sensors on right and left lateral plates detect cranial roll (figure 2) with average sensitivity of 0.04 and 0.06 pF per degree, respectively. Posterior and anterior sensors on the superior plate detect cranial pitch (figure 2) with average sensitivity of 0.13 and 0.06 pF per degree, respectively.

## Conclusion

We had previously shown (Sadeghi, Lincoln *et al.* 2018) the capability of this system to detect translation motion. The current results show potential for rotation detection with this technology by monitoring the cranium without the need for ionizing radiation or the use of skin as a surrogate.



Figure 1. (a) The 3D printed phantom with copper layered brain cavity. (b) The array arrangement consisting of superior, left lateral, and right lateral plates. (c) Each plate is comprised of three sensors.

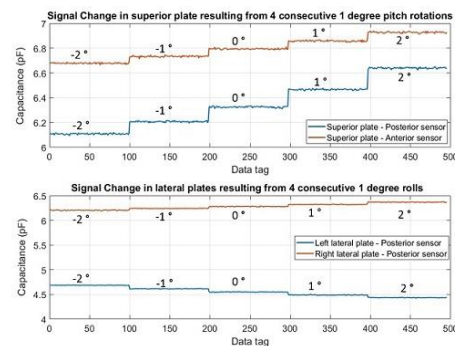


Figure 2. (Top) Detection of cranial pitch. Rotation ranging from -2 degrees (chin rotating away from the chest) to +2 degrees (chin rotating toward the chest) in 1 degree steps. (Bottom) Detection of cranial roll. Rotation ranging from -2 degrees (rotation toward the right) to +2 degrees (rotation toward the left) in 1 degree steps.

## PO-0972 Intrafraction prostate motion effects with or without ERB in highly hypofractionated proton therapy

L.G.M. Zwart<sup>1,2</sup>, C.L. Brouwer<sup>1</sup>, P. Klinker<sup>1</sup>, C.H. Slump<sup>2</sup>, K.K. Wang<sup>3</sup>, N. Vapiwala<sup>4</sup>, J.A. Langendijk<sup>1</sup>, S. Both<sup>1</sup>, S. Aluwini<sup>1</sup>

<sup>1</sup>University of Groningen- University Medical Center Groningen, Department of Radiation Oncology, Groningen, The Netherlands ; <sup>2</sup>University of Twente, MIRA Institute for Biomedical Technology and Technical Medicine, Enschede, The Netherlands ; <sup>3</sup>Johns Hopkins University, Department of Radiation Oncology and Molecular Radiation Sciences, Baltimore, USA ; <sup>4</sup>University of Pennsylvania, Department of Radiation Oncology, Philadelphia, USA

### Purpose or Objective

Pencil beam scanning (PBS) technology allows the use of superior beam properties of protons to potentially improve outcomes with extreme hypofractionated radiotherapy for prostate cancer (PCa) patients. One of the technical challenges is the increased sensitivity to range uncertainties and intrafraction prostate motion. We have evaluated the robustness of extreme hypofractionated PBS proton plans to intrafraction prostate motion with (wERB) and without endorectal balloon (nERB) in PCa patients.

### Material and Methods

Intrafraction motion measurements were available from 59 patients treated in  $\geq 30$  fractions in the department of radiation oncology of the University of Pennsylvania. Motion was recorded in left, right, superior, inferior, anterior and posterior direction for up to 6 minutes using a real-time electromagnetic tracking system. Patients (five wERB and six nERB) with the largest magnitudes of

motion were selected. The time-weighted average motion for each direction was calculated for all fractions of each patient. Thereafter, the mean intrafraction motion for each direction was calculated for both wERB and nERB groups. Planning CTs (pCTs) of 4 representative PCa patients treated at our institution were used to create virtual proton plans, using an extreme hypofractionated regimen of 4 fractions of 9.5 Gy(RBE), applying robust optimization using 5 mm setup and 3% range uncertainty to fulfill V100>95% for the clinical target volume (CTV). The calculated mean intrafraction motion for both groups was applied to the pCTs of those 4 patients and 44 synthetic CTs (sCTs) were created using deformable image registration in RayStation 6.99 as a surrogate to real time 4D calculations. Differences in CTV coverage and max dose to the organs at risk between the sCTs and pCTs were compared.

### Results

Mean and standard deviation of intrafraction motion of both groups are listed in Table 1. The influence of intrafraction motion was negligible for CTV coverage which was maintained (V100>95%) in both groups. No detectable dose differences were found for the bladder. Posterior prostate motion resulted in a median max dose decrease to the anorectum of 61 cGy (wERB) and 65 cGy (nERB); inferior prostate motion resulted in a median max dose decrease of 53 cGy (wERB) and 57 cGy (nERB), respectively (Fig. 1A). A median max dose decrease to the anal canal of 0 cGy (wERB) and 158cGy (nERB) was found for posterior prostate motion and 92 cGy (wERB) and 184 cGy (nERB) for inferior prostate motion, respectively (Fig. 1B).

Table 1: Mean and standard deviation of intrafraction prostate motion with and without ERB in left, right, superior, inferior, anterior and posterior direction recorded using a real-time electromagnetic tracking system.

	Left (mm)	Right (mm)	Superior (mm)	Inferior (mm)	Anterior (mm)	Posterior (mm)
With ERB	0.31 ± 0.16	0.32 ± 0.12	0.67 ± 0.20	0.94 ± 0.22	0.77 ± 0.26	0.99 ± 0.20
Without ERB	0.57 ± 0.61	0.43 ± 0.22	1.09 ± 0.40	1.34 ± 0.47	1.40 ± 0.80	1.49 ± 0.45

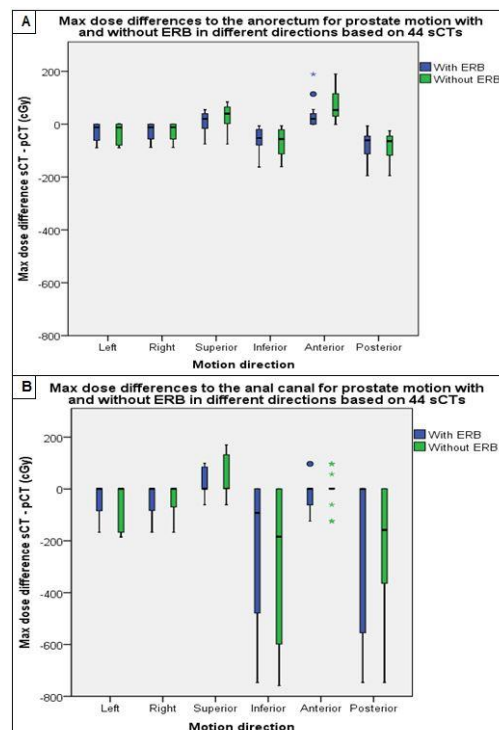


Figure 1: Max dose differences to the anorectum (A) and anal canal (B) for prostate motion with and without ERB in different directions based on 44 sCTs.

### Conclusion

Worst-case intrafraction prostate motion for both wERB and nERB groups did not negatively influence the

robustness of our extreme hypofractionated optimized proton plans, with negligible effect on target coverage and bladder dose. Doses to the anorectum and anal canal were most sensitive to posterior and inferior prostate motion. Our results suggest that ERB has no additive value on plan robustness. Further investigation with a larger patient cohort is needed to confirm our results.

### PO-0973 Residual intra-fraction error in non-immobilized patients treated with tracked robotic spinal SBRT

E. Rossi<sup>1</sup>, C. Fiorino<sup>1</sup>, A. Fodor<sup>2</sup>, G.M. Cattaneo<sup>1</sup>, C. Deantoni<sup>2</sup>, A. Sbalchiero<sup>2</sup>, A. Tavilla<sup>2</sup>, N.G. Di Muzio<sup>2</sup>, R. Calandrino<sup>1</sup>, S. Broggi<sup>1</sup>

<sup>1</sup>San Raffaele Scientific Institute, Medical physics, Milan, Italy ; <sup>2</sup>San Raffaele Scientific Institute, Radiotherapy, Milan, Italy

### Purpose or Objective

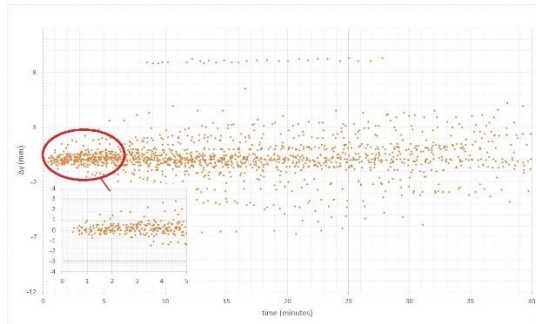
To assess residual intra-fraction patient motion in the delivery of spinal radiosurgery with CyberKnife (CK, Accuray, Inc.) using spine tracking in non-immobilized patients. Moreover, the intra-fraction motion with respect to the first alignment (i.e. tracking not available) is quantified and its relationship with time is assessed.

### Material and Methods

The Xsight Spine tracking technique with CK enables to track skeletal structures near the spine, avoiding the implantation of fiducial markers and, possibly, immobilization systems, allowing comfortable set-ups for, often, painful patients. X-ray images are taken to correctly align the patient on the treatment couch, then images are regularly acquired during treatment to correct for patient motion. Residual error during tracking deals with the shifts between consecutive images and may be safely quantified considering the registered shifts between them. We collected delivery data from 20 patients previously treated with tracking for spinal lesions without immobilization (51 fractions, 1615 images): 16-30 Gy (median 24Gy) in 1-5 fractions (10/20 with single fraction, 3/20 with multiple lesions) were delivered. The time between images for tracking varies between 30'' and 2' (median 1' ± 30''). Residual error is quantified for each image as the difference between measured translational and rotational corrections and the previous values. The error distribution for each fraction, patient and the whole population is assessed, including a possible relationship with time. Similarly, for intra-fraction motion in absence of tracking, we consider the shifts from the alignment coordinates (at time 0).

### Results

Residual intra-fraction error after tracking is limited: translational shifts >0.5mm are detected in only 2.5%, 6.8% and 4.8% of 1615 acquired images for cranio-caudal, left-right and anterior-posterior translations respectively; shifts >1mm in 0.8%, 2%, 1.4%; shifts >1.5mm in 0.2%, 0.5%, 0.3%; shifts >2mm in 0.2%, 0.2% and 0.1%. As for roll, 0.7% of shifts are >1°, 0.1% for pitch and yaw. No time dependence is found and the overall mean errors are close to 0 with SD (systematic error on the overall population) within 0.1 mm (table). About the "no-tracking" scenario, a time dependence is found (figure), especially for left-right ( $\Delta y$ ) translations. Up to 3' after starting the delivery no shifts larger than 2mm are observed, up to 5' they vary within a 3mm range. Then, major shifts appear mostly due to large (up to 9 mm) patient motion and time-related continuous shifts: after 10' and 20'  $\Delta y$  was > 3mm in respectively 4 and 10 fractions out of 51.



Without tracking		
	Mean	SD
$\Delta x$ (mm)	-0,19	0,81
$\Delta y$ (mm)	0,24	1,57
$\Delta z$ (mm)	0,15	0,62
$\Delta roll$ (°)	0,00	0,37
$\Delta pitch$ (°)	-0,03	0,29
$\Delta yaw$ (°)	-0,07	0,37
With tracking		
	Mean	SD
$\Delta x$ (mm)	-0,01	0,05
$\Delta y$ (mm)	0,02	0,06
$\Delta z$ (mm)	0,01	0,04
$\Delta roll$ (°)	0,00	0,02
$\Delta pitch$ (°)	0,01	0,02
$\Delta yaw$ (°)	0,00	0,02

### Conclusion

Spine tracking with CK is highly efficient also for non-immobilized patients: the residual error seems to be time independent and is close to 0. If tracking is not employed (i.e.: with other delivery modalities), shifts show a dependence on time. For delivery times exceeding 5' in the considered non-immobilized patient scenario, tracking seems to be highly recommendable.

**PO-0974 Intra-fractional stability of Deep Inspiration Breath Hold during RT for lung and lymphoma cancer**  
 D. Sloth Møller<sup>1</sup>, M.L. Schmidt<sup>1</sup>, T. Ravkilde<sup>1</sup>, P.R. Poulsen<sup>1</sup>, J. Hansen<sup>1</sup>, E.S. Worm<sup>1</sup>, H.H. Schmidt<sup>2</sup>, M.M. Knap<sup>2</sup>, A. Safwat<sup>2</sup>, H.K. Rose<sup>2</sup>, L. Hoffmann<sup>1</sup>  
<sup>1</sup>Aarhus University Hospital, Department of Medical Physics, Aarhus C, Denmark ; <sup>2</sup>Aarhus University Hospital, Department of Oncology, Aarhus C, Denmark

### Purpose or Objective

Deep Inspiration Breath Hold (DIBH) during thoracic RT is attractive as it may reduce dose to the lungs and heart compared to free breathing RT. However, intra-fractional geometric instability during several breath holds may decrease the target coverage. We investigate intra-fractional uncertainties during planning, before/after each fraction delivery, and during actual field delivery.

### Material and Methods

Twenty-two patients (15 lung cancer (LC) and 7 sarcoma/lymphoma (SL)) were treated with DIBH-RT. The RPM system with an external marker (EM) placed caudally on the thoracic cage was used as a surrogate for the DIBH level. For all scans and treatments, the DIBH level measured by EM was < 2mm. Four DIBH planning-CT (pCT) scans were acquired: one for RT planning and three to

assess the inter-DIBH uncertainty (Fig1a). To assess inter-DIBH uncertainty during treatment, pre-treatment CBCT scans were acquired for daily setup (CBCT1) and post-treatment (CBCT2) at the first three fractions and once a week afterwards. For LC with tumour (T) and lymph node (N) involvement, T and N were analysed separately. SL targets were mostly mediastinal (M) and grouped with the mediastinal N targets. Systematic ( $\Sigma$ ) and random ( $\sigma$ ) errors were calculated using the van Herk formalism. Intra-DIBH uncertainty was measured by intra-treatment 5Hz fluoroscopic kV imaging of gold markers implanted at N-site for LC (Fig1b) and motion trajectories were derived (Fig1c). The interquartile motion range (IQR) was determined for each treatment field.

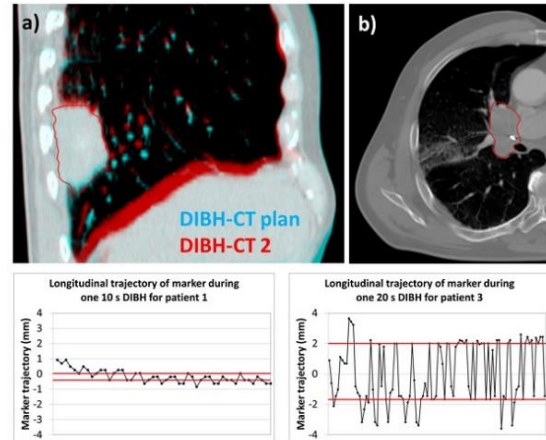


Figure 1 a) Inter-DIBH analysis. Comparison of two DIBH-CTs acquired for planning. Same comparison is made for CBCT acquired before and after treatment. b) DIBH-CT with gold marker implanted in lymph-node. c) Intra-DIBH analysis. Full motion trajectory of implanted gold marker for patient with intra-DIBH uncertainty below 2 mm and for patient with more than 4 mm intra-DIBH uncertainty. The red lines indicate the interquartile range for these two DIBHs.

### Results

The inter-DIBH uncertainty analysis (Fig 2) for LC T sites showed low stability in longitudinal position and poor correspondence between the uncertainties derived from DIBH pCTs and inter-DIBH CBCT1/2. In some patients, only minor overlap between motion ranges was seen and the mean value of the range was shifted from zero. For M sites the stability was higher and the correspondence better due to target location closer to EM, but the DIBH pCTs were still poor predictors of the actual inter-DIBH uncertainty during treatment. Errors in mm for the LC T sites were  $\Sigma_{LR}, \Sigma_{AP}, \Sigma_{CC}=0.7, 1.5, 2.3$ ,  $\sigma_{LR}, \sigma_{AP}, \sigma_{CC}=0.8, 1.5, 1.4$  (by CT) and  $\Sigma_{LR}, \Sigma_{AP}, \Sigma_{CC}=0.8, 1.1, 1.6$ ,  $\sigma_{LR}, \sigma_{AP}, \sigma_{CC}=1.2, 1.8, 2.9$  (by CBCT). For M sites  $\Sigma_{LR}, \Sigma_{AP}, \Sigma_{CC}=1.1, 1.1, 2.0$ ,  $\sigma_{LR}, \sigma_{AP}, \sigma_{CC}=0.9, 0.9, 1.7$  (CT) and  $\Sigma_{LR}, \Sigma_{AP}, \Sigma_{CC}=0.7, 1.2, 1.1$ ,  $\sigma_{LR}, \sigma_{AP}, \sigma_{CC}=0.9, 1.3, 1.6$  (CBCT). These errors do not reflect the difference between CT and CBCT observed for the individual patients (Fig 2).

Fig 1c shows examples of the intra-DIBH uncertainty. The mean IQR over all DIBH's for each patient ranged from 0.4mm to 1.9mm, in good agreement with the 2mm allowed EM window. The max IQR, however, ranged from 2.8mm to 16.4mm and 1%-23% of all DIBH's of each patient had IQR>2mm.

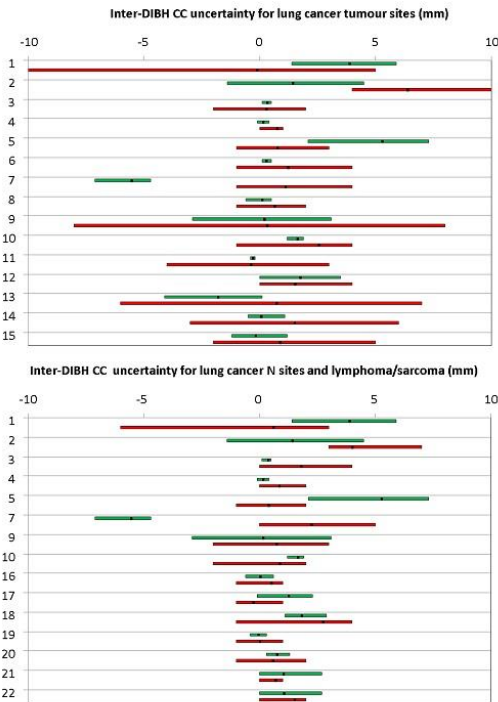


Figure 2: Upper panel: Inter-DIBH uncertainty for lung cancer primary tumour sites. Lower panel: Mediastinal targets (lymphoma/sarcoma patients (16-22) and lung cancer lymph node sites). For each patient the green bar indicates the range in uncertainty measured by DIBH-CTs, while the red bar indicates the range in uncertainty measured by comparison of CBCT1 and CBCT2. The black line in each bar indicates the mean value for the corresponding range.

### Conclusion

Inter-DIBH and intra-DIBH uncertainties varies greatly between patients. For some patients, the size of the uncertainties will undermine the advantages of DIBH. DIBH-CTs acquired before treatment do not predict the inter-DIBH uncertainty observed during treatment.

### PO-0975 Feasibility of single-camera intra-bore surface scanning in an O-ring linac

L. Delombaerde<sup>1</sup>, S. Petillion<sup>1</sup>, C. Weltens<sup>1,2</sup>, T. Depuydt<sup>1,2</sup>

<sup>1</sup>University Hospital Gasthuisberg, Department of Radiation Oncology, Leuven, Belgium ; <sup>2</sup>KU Leuven - University of Leuven, Department of Oncology, Leuven, Belgium

### Purpose or Objective

Patient surface scanning inside closed-bore linacs or imaging systems is difficult using ceiling-mounted projector/camera assemblies. A compact single camera surface scanning system (SCSS) for motion monitoring inside an O-ring linac is proposed and characterized.

### Material and Methods

A Microsoft Kinect depth camera is mounted on a movable rack placed at the back-end of the bore of a Halcyon (Varian Medical Systems, USA) (fig. 1). A transformation to the linac coordinate system retrieved from a cube detection calibration, is applied to the surface point cloud data acquired by the SCSS. The real-time surface data is registered using an Iterative Closest Point algorithm to a region-of-interest (a) of a 3D CAD-model or (b) of a reference surface acquisition from the first fraction. The positioning accuracy is investigated using anthropomorphic 3D printed phantoms with clinically relevant surface complexity: a head, hand and breast (fig. 2). Each phantom was placed 24 times to within 0 - 11 mm and 0 - 7.6° from the planned position to emulate clinically observed positioning errors. At every position a CBCT is acquired and a surface registration is performed. The surface registration result is compared to a CBCT-to-

planning-CT fiducial marker registration with 6 degrees of freedom. The performance of the SCSS for positioning accuracy for these specific phantoms was also benchmarked against a commercial surface scanning system (AlignRT, VisionRT Ltd., UK) on a C-arm system.

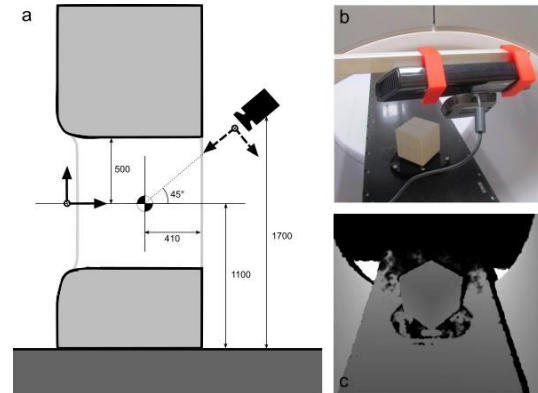


Figure 1: (a) Illustration of the depth camera's position relative to the linac isocenter. Distances (in mm) indicated as a reference. Sensor's dimensions not to scale. The camera's coordinate system is indicated with dashed arrows, the couch axes with solid arrows. (b) Photograph of the Kinect mounted on the movable rack. (c) View of the calibration cube from the sensor's position.

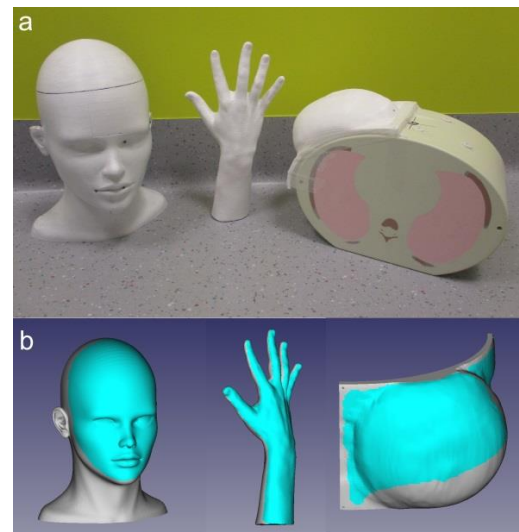


Figure 2: (a) Photograph of the 3 anthropomorphic phantoms used in the accuracy evaluation of the closed-bore surface scanning prototype. Head, hand and breast phantom were painted white and 10 lead markers inserted in evenly distributed cavities. The breast phantom is taped to the CIRS Thorax SBRT EZE phantom to simulate a realistic position. (b) The region-of-interest (cyan) selected on the 3D CAD-model.

### Results

The registration errors of the SCSS, compared to CBCT of the 3 phantoms combined were: Lat:  $0.30 \pm 0.76$  mm, Vert:  $-0.25 \pm 0.17$  mm, Long:  $0.31 \pm 0.48$  mm and Yaw:  $-0.31 \pm 0.83^\circ$ , Pitch:  $0.10 \pm 0.26^\circ$ , Roll:  $0.51 \pm 0.59^\circ$  for the CAD-model reference, and Lat:  $-0.65 \pm 0.74$  mm, Vert:  $0.32 \pm 0.15$  mm, Long:  $0.21 \pm 0.50$  mm and Yaw:  $-0.49 \pm 0.46^\circ$ , Pitch:  $0.13 \pm 0.25^\circ$ , Roll:  $-0.66 \pm 0.65^\circ$  for the surface acquisition reference. The AlignRT system had combined registration errors of: Lat:  $0.74 \pm 0.64$  mm, Vert:  $-0.57 \pm 1.40$  mm, Long:  $0.61 \pm 0.82$  mm and Yaw:  $-0.33 \pm 0.31^\circ$ , Pitch:  $-0.15 \pm 0.34^\circ$ , Roll:  $0.38 \pm 0.29^\circ$ . No correlation between displacement magnitude from the planned position and SCSS registration errors were found,  $p > 0.14$ .

### Conclusion

The prototype single camera intra-bore surface system is capable of accurately detecting displacements from the planned position of the phantoms. The compact system, proposed in this work, will allow surface guided radiotherapy and monitoring of intra-fraction motion inside the bore of O-ring gantries.

### PO-0976 Validation of respiratory motion modeling through repeated 4DMRI in the abdomen: preliminary results

G. Meschini<sup>1</sup>, C. Paganelli<sup>1</sup>, G. Fontana<sup>2</sup>, A. Pella<sup>2</sup>, A. Mancin<sup>3</sup>, A. Vai<sup>4</sup>, M. Riboldi<sup>5</sup>, F. Valvo<sup>6</sup>, G. Baroni<sup>1</sup>  
<sup>1</sup>Politecnico di Milano, Department of Electronics Information and Bioengineering, Milan, Italy ; <sup>2</sup>National Centre of Oncological Hadrontherapy, Bioengineering Unit, Pavia, Italy ; <sup>3</sup>National Centre of Oncological Hadrontherapy, Medical Radiology Technicians Unit, Pavia, Italy ; <sup>4</sup>National Centre of Oncological Hadrontherapy, Medical Physics Unit, Pavia, Italy ; <sup>5</sup>Ludwig-Maximilians-Universität, Chair of Experimental Physics - Medical Physics, Munich, Germany ; <sup>6</sup>National Centre of Oncological Hadrontherapy, Radiation Oncology Unit, Pavia, Italy

#### Purpose or Objective

Respiratory motion modeling in radiotherapy provides the estimation of anatomical changes induced by breathing, when continuous 3D imaging feedback is not available. However, the evaluation of the model performance in case of intra- and inter-fraction variability of the respiratory pattern is still a challenge. In this study, we exploited repeated 4DMRI acquisitions to create the training and testing datasets for respiratory motion model validation.

#### Material and Methods

Repeated 4DMRI of a pancreas (P\_pan) and a liver cancer patient (P\_liv) were acquired. Patients underwent two scans, one after the other, before irradiation and another scan after irradiation, in order to image intra- and inter-fraction variations, respectively (Table). Specifically, multi-slice acquisition of sagittal images (pixel size: 1.33mm×1.33mm, slice thickness: 5mm) during free breathing and retrospective 4DMRI reconstruction<sup>1</sup> were performed. The motion model<sup>2,3</sup> was trained on the first 4DMRI, thus establishing a correlation between a respiratory surrogate (here image-based) and motion information extracted through deformable image registration (DIR). The model was tested on the subsequent intra- and inter- 4DMRI, estimating the motion by means of the surrogate only. Inter-fraction baseline shifts were compensated<sup>3</sup> (Table). The estimated and the imaged ground truth (GT) motions were finally compared.

#### Results

The tumor center of mass (COM) distance between GT and model output had median values below 2.2mm both for P\_pan and P\_liv (Figure). Median errors below 2mm were observed consistently for the considered organs at risk (kidney and liver, respectively). For P\_liv, higher variability of tumor COM distances was quantified in the inter-fraction scenario, with errors up to 6.5mm for respiratory phases close to end-inhale. This is likely due to the baseline shift, the higher range of motion with respect to the training dataset (Table) and to DIR uncertainty.

Table.

	Tumor range of motion [mm]			Inter-fraction baseline shift [mm]
	Training 4DMRI	Intra-4DMRI	Inter-4DMRI	
P_liv	14.3	10.0	19.0	9.5
P_pan	10.5	9.2	10.9	2.7

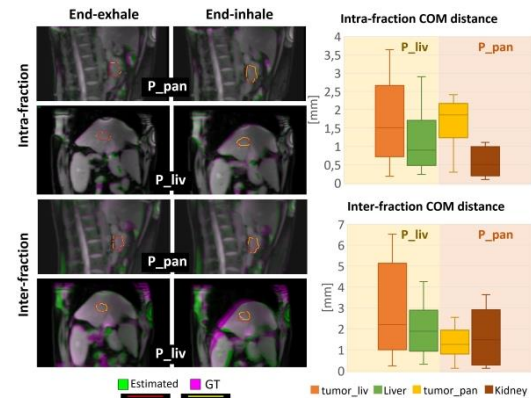


Figure. Left: sagittal slices showing the overlay between estimated and GT volumes, with the corresponding tumor contours. Right: boxplot of the COM distances between estimated and GT structures position.

#### Conclusion

A validation framework based on repeated 4DMRI is proposed for motion modeling in presence of intra- and inter-fraction changes. Preliminary results suggest the feasibility of motion modeling in the abdomen, with median residual errors comparable to the voxel size. The compensation of inter-fraction variations by re-training the model on a newly acquired dataset could improve its performance. Patient acquisitions is currently ongoing, aiming at extending the validation to a larger patient cohort and assessing the impact of DIR error.

<sup>1</sup>Meschini et al 2017 A multi-dimensional approach for retrospective 4DMRI sorting, 4D Treatment Planning Workshop

<sup>2</sup>Meschini et al 2017 Evaluation of residual abdominal tumour motion in carbon ion gated treatments through respiratory motion modelling, Phys Med

<sup>3</sup>Fassi et al 2015 Surrogate-driven deformable motion model for organ motion tracking in particle radiation therapy, PMB

### PO-0977 Improved 4D proton dosimetry via correlation with beam delivery details using log-files

N. Kostikhina<sup>1</sup>, H. Palmans<sup>2</sup>, S. Waid<sup>3</sup>, M. Stock<sup>2</sup>, D. Georg<sup>1</sup>, B. Knäusl<sup>1</sup>

<sup>1</sup>Medical University of Vienna / AKH Vienna, Department of Radiotherapy and Christian Doppler Laboratory for Medical Radiation Research for Radiation Oncology, Vienna, Austria ; <sup>2</sup>EBG MedAustron GmbH, Medical Physics, Wiener Neustadt, Austria ; <sup>3</sup>EBG MedAustron GmbH, Therapy Accelerator- Commissioning and Development, Wiener Neustadt, Austria

#### Purpose or Objective

For implementing pencil beam scanning treatment in the presence of target motion, detailed insight in the treatment delivery sequence is essential. In this work, a 4D framework was implemented and applied for different scenarios, allowing to study the correlation between time-resolved dosimetry and beam delivery (BD) log files.

#### Material and Methods

A pulsed scanned proton beam with varying intensity was employed for the experiments. To represent target motion in a realistic human anatomy, an anthropomorphic breathing phantom, dedicated to proton dosimetry, was used. Two patient-specific parameters were varied: tumor volume (TV) and motion pattern. For TVs of 12cm<sup>3</sup> (TV1) and 97cm<sup>3</sup> (TV2) static and sinusoidal (0.6cm and 2.0cm amplitude) tumor motions were investigated. For both TVs a CT based treatment plan was created with the phantom in static position and delivered for all motion scenarios. The dose was determined in the target volume and the penumbral region with 0.5s time intervals using four (for TV1) and five (for TV2) pinpoint (PP) ionization chambers. The start of the phantom's motion was triggered by a pre-

defined beam extraction event enabling reproducible measurements. BD parameters, recorded with a time-resolution of 5.0 $\mu$ s, were retrospectively correlated time-wise with the dosimetric data (figure 1 (top)).

### Results

Comparing corresponding spills of the treatment deliveries, the intensity variation was up to 8% for TV1 and up to 24% for TV2 (see table 1). This resulted in accumulated treatment time differences of up to 11 and 39 sec, respectively. The total dose differences (DDs) between deliveries of the same plan were within 0.3% for individual PPs for static measurements for both TV sizes. 0.6cm target motion resulted in DDs of up to 1% for TV1 and up to 2% for TV2. Motion of 0.6cm did not introduce much larger contributions to the dose perturbations within tumor region than those coming from accelerator dependent intensity fluctuations. DDs were more pronounced for a target motion of 2 cm. The dose deviated more for the smaller volume, i.e. by 16, 7, 5 and 16 % for PP1-4 (figure 1 (bottom)), while for TV2 it remained below 9% for PPs within the tumor volume (PP1-4). Measurements in the penumbral region (PP5) for TV2 showed a high sensitivity to motion for both amplitudes (15% relative SD for 0.6cm motion and 42% for 2.0cm motion).

Table 1 - beam delivery parameters and resulting dose measurements for the considered tumor volumes and motion scenarios

Treatment plan specification:		Tumor volume 1 (12 cm <sup>3</sup> )	Tumor volume 2 (97 cm <sup>3</sup> )
Energy layers		34 (76.0 - 102.5 MeV)	46 (67.5 - 115.0 MeV)
Spot weight range		0.9-47.1 *10 <sup>6</sup> NP/fx	0.9-47.5 *10 <sup>6</sup> NP/fx
Number of spots		5643	7735
Beam intensity variation (relative SD), mean (min, max) [%]		3.7 (1.2, 8.4)	6.0 (2.0, 23.6)
Accumulated treatment time difference [sec]		11	39
Total dose differences between deliveries of the same plan for PP1-PP4(5) (relative SD) [%]	Phantom static	0.1, 0.0, 0.1, 0.0	0.0, 0.1, 0.1, 0.2, (0.3)
	Motion scenario - moving 0.6 cm	0.5, 0.3, 0.2, 1.2	2.3, 0.9, 1.5, 1.4, (15.4)
	Motion scenario - moving 2.0 cm	16.3, 6.8, 4.7, 15.7	4.7, 5.5, 8.5, 3.9, (41.9)

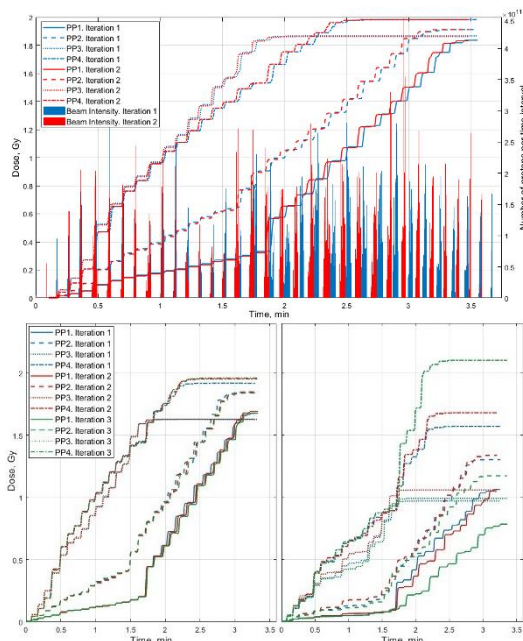


Figure 1 - (top) time-resolved dose measurements in the static phantom (2 iterations) for TV1 by means of four PPs, correlated in time with beam intensity. (bottom) time-resolved dose measurements for TV1 by means of four PPs in the presence of 0.6cm (right) and 2.0cm (left) target motion (3 iterations each).

### Conclusion

Time-resolved dose measurements and their correlation with the BD log files showed the relation of the BD time structure and the spill intensity, which is the basis for 4D

dose calculation. The application of 4D dosimetry in combination with the log file analysis underlined the dependence of the dosimetric accuracy of an individual plan delivery on beam delivery variations and patient-specific parameters.

### PO-0978 Accurate positioning with decreased treatment time using surface guided tomotherapy

A. Haraldsson<sup>1,2</sup>, S. Ceberg<sup>2</sup>, C. Crister<sup>2</sup>, S. Engelholm<sup>1</sup>, S.Å.J. Bäck<sup>1,2</sup>, P.E. Engström<sup>1</sup>

<sup>1</sup>Skåne University Hospital, Department of Hematology-Oncology and Radiation Physics, Lund, Sweden ; <sup>2</sup>Lund university, Medical Radiation Physics, Lund, Sweden

### Purpose or Objective

Accurate, reproducible, and fast setup of the patient is important for a successful radiotherapy treatment, especially for complex treatment techniques such as helical tomotherapy. Daily imaging with mega voltage computer tomography (MVCT) is accurate but increases the imaging dose and the total patient time on the treatment couch. Thereby additional intra-fraction position uncertainty caused by patient movements are introduced. In this study, we quantified the setup deviation and time gain when using surface scanning for daily setup with weekly MVCT imaging for reference as compared to daily MVCT. We analysed 16 835 treatment fractions from our TomoTherapy HD (Accuray Inc., Madison, USA) installed with a Sentinel optical surface scanning system (C-RAD Positioning AB, Uppsala, Sweden).

### Material and Methods

The surface of the patient was used to calculate the position using rigid registration against a reference surface. The patient setup was performed using in-room lasers, surface scanning and MVCT for the first three fractions. A new reference surface was acquired on the third fraction after a MVCT-based couch correction. On the following fractions, we used in-room lasers for setup, followed by daily surface scanning and weekly MVCT. The *MVCT image setup correction vector*, which was defined as the 3D translational correction as assessed by image registration, was used to evaluate the setup based on surface scanning. For each plan, the correction vector for one randomly selected fraction was used for the analysis. The *imaging time*, which was the time from imaging start to beam-on including any following procedures. The imaging time for one fraction was randomly selected per plan and imaging modality and multiplied with the number of fractions. Typical PTV margins at our clinic are 5 mm for head and neck patients and 10 mm for targets in the thorax and abdomen.

### Results

A total of 894 plans were analysed with a treatment date from 2012 to 2018. Of the setup correction vectors, 90 % were within 2.3 mm for CNS (N=284), 2.9 mm for H&N (N=254), 8.7 mm for thorax (N=144) and 10.9 for abdomen (N=134) patients. The setup deviations were divided in a random and a systematic component according to Yan et al. 1997 (Table 1). The difference in imaging time was assessed as total imaging time per treatment plan, modality, and treatment site (Figure 1). The difference in total imaging time per fraction was significant for all sites ( $p < 0.005$ ) as assessed by linear regression and the Mann-Whitney U test.

### Conclusion

The setup deviation was small compared to the standard PTV margins for all sites but the abdomen. In addition, daily surface scanning with weekly MVCT was significant faster than using daily MVCT. We therefore conclude that daily surface scanning with weekly MVCT is an accurate and fast alternative to daily MVCT for positioning of CNS, H&N and thorax patients receiving treatments on a TomoTherapy unit. For patients treated in the abdomen, daily surface scanning should proceed with caution.

Table 1: Mean systematic and mean random error (1SD) tabulated with the margin calculated for the PTV based on the deviations for surface scanning. Calculated from all MVCT setup correction vectors.

Site	Axis	Systematic error (mm)	Random error (mm)
H&N	Lateral	0.4	0.7
	Longitudinal	1.3	1.2
	Vertical	0.5	2.1
CNS	Lateral	0.2	0.5
	Longitudinal	0.3	0.6
Thorax	Lateral	0.8	1.4
	Longitudinal	1.2	4.0
	Vertical	1.0	2.5
Abdomen	Lateral	1.0	1.1
	Longitudinal	1.2	3.3
	Vertical	1.7	2.5

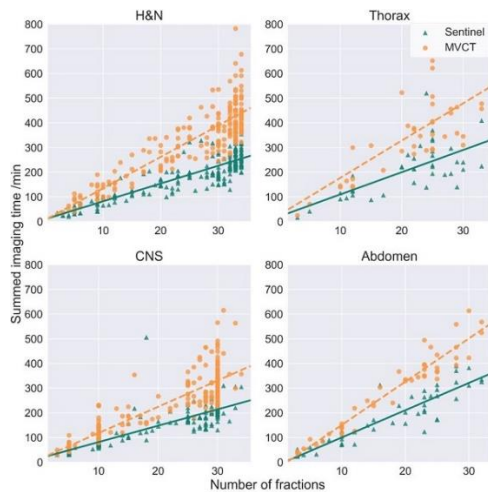


Figure 1: Summed imaging time against number of fractions per treatment plan, for imaging with Sentinel and with MVCT respectively. The imaging time for one fraction was randomly selected per plan and imaging modality and multiplied with the number of fractions.

### PO-0979 The Use of Triggered Imaging for Intrafraction Target Verification in Liver SBRT Breathhold

M. Walb<sup>1</sup>, K. Jethwa<sup>1</sup>, S. Park<sup>1</sup>, C. Hallemeier<sup>1</sup>, D. Pafundi<sup>1</sup>

<sup>1</sup>Mayo Clinic, Radiation Oncology, Rochester, USA

#### Purpose or Objective

Target localization in liver SBRT is challenging due to organ motion and target visualization difficulties using volumetric CBCT. To mitigate these concerns, respiratory gating techniques, such as breathhold (BH) with implanted fiducials, are used. The Varian TrueBeam RPM system uses external markers as a surrogate for internal motion to measure respiration amplitude. This assumes that a patient BH during treatment correlates with internal motion observed at simulation. A larger PTV expansion may address this uncertainty but at the cost of less normal tissue sparing.

To reduce uncertainty in target localization at treatment, we commissioned triggered imaging in the advanced imaging suite in TrueBeam 2.7. This allows for 2D kV images to be triggered at the beginning of each BH, before beam delivery, and verify that the internal fiducials are within an expanded contour overlay determined from simulation. A retrospective analysis was performed to determine the utility of triggered imaging for liver SBRT BH patients. **Material and Methods**

Target localization is initially performed with a 2D-2D kV match followed by 3D or 6D CBCT match to the fiducials. Then, prior to each beam delivery period, a 2D kV image acquisition is triggered when the patient holds their breath within the gating window. The acquired image

shows the overlay of a 5 mm radial expansion of each fiducial contour based on the planning CT coordinates to compare with the current location of the fiducials. The treatment team pauses the beam (1-2 s) for assessment of the contour overlay, and determines whether to resume beam delivery if the fiducials are inside the overlay or re-image if outside it. Re-imaging starts with repeating the triggered image and assessment, and re-evaluating if a full CBCT localization is warranted.

Retrospective analysis was performed on 129 fxs (30 pts) to quantify how frequently re-localization with CBCT was needed after commencing treatment, and how often the fiducials were not aligned in the initial BH attempt (false starts), but immediately repeating the triggered image with subsequent BH attempts (without shifting the patient) showed the fiducials within tolerance for treatment to proceed.

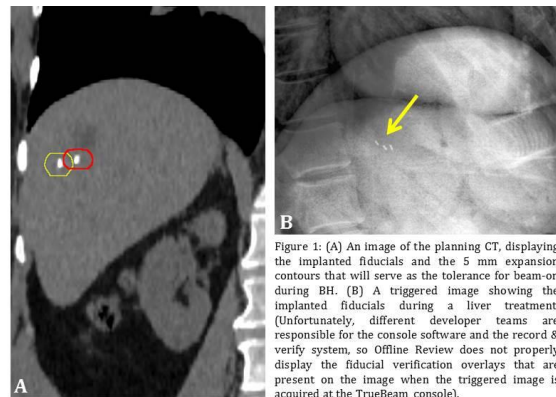


Figure 1: (A) An image of the planning CT, displaying the implanted fiducials and the 5 mm expansion contours that will serve as the tolerance for beam-on during BH. (B) A triggered image showing the implanted fiducials during a liver treatment. (Unfortunately, different developer teams are responsible for the console software and the record & verify system, so Offline Review does not properly display the fiducial verification overlays that are present on the image when the triggered image is acquired at the TrueBeam console).

#### Results

After initial localization, and treatment was either in progress or about to begin, 11.6% of fxs showed fiducials repeatedly outside of tolerance and required a new CBCT localization, requiring a mean vector ( $\pm$ SD) CBCT shift of  $5.8 \pm 2.7$  mm. In 27.1% of fxs, a false start was recorded, but re-imaging with another triggered image allowed treatment to proceed without a repeat CBCT.

Table 1: Frequency & Magnitude of Triggered Imaging-Guided Interventions

Total Fx with Triggered Imaging	Total Fx Re-CBCT	Total Fx False Starts		
129	15	35		
	11.63%	27.13%		
	Vertical	Longitudinal	Lateral	$\Delta r$
Mean Absolute Value of CBCT shifts $\pm$ SD	0.24 $\pm$ 0.21 cm	0.45 $\pm$ 0.27 cm	0.12 $\pm$ 0.13 cm	0.58 $\pm$ 0.27 cm

#### Conclusion

The results demonstrate a valuable role for intrafraction verification imaging for sites which rely on an external surrogate to gate the beam. Approximately 12% of patients required a second localization with a mean shift of 6 mm which can have a significant impact on a geographic miss. Plans include further analysis to guide liver margin expansions and assess the technology for additional SBRT sites, such as prostate.

#### Poster: Physics track: Adaptive radiotherapy and inter-fraction motion management

### PO-0980 Dosimetric comparison of library of plans and online MRI-guided radiotherapy of cervical cancer

J. Visser<sup>1</sup>, P. De Boer<sup>1</sup>, K.F. Crama<sup>1</sup>, Z. Van Kesteren<sup>1</sup>, C.R.N. Rasch<sup>1</sup>, L.J.A. Stalpers<sup>1</sup>, A. Bel<sup>1</sup>

<sup>1</sup>Amsterdam UMC- location AMC, Radiation Oncology, Amsterdam, The Netherlands

#### Purpose or Objective

Online MRI-guided radiotherapy of cervical cancer has the potential to further reduce dose to organs at risk (OAR) as

compared to a library of plans approach (LOP), which is currently the state of the art. However, intrafraction anatomical changes set a lower limit on the required PTV margin. The aim of this study is a dosimetric comparison of MRI-guided strategies with a LOP strategy taking intrafraction anatomical changes into account.

#### Material and Methods

The 14 patients included in this study were treated with chemoradiation at our institute and received weekly MRIs after informed consent. The weekly MRIs were considered to represent day-to-day anatomical changes that occur during the treatment. For the LOP strategy the plans were based on interpolations of the cervix-uterus on pretreatment full and empty bladder scans. The two MRI-guided strategies (MRI\_3mm and MRI\_5mm) consisted of treatment plans created on the weekly sagittal MRIs with 3 mm and 5 mm PTV margin around the cervix-uterus. All plans were VMAT dual arc plans with a prescribed dose of 45 Gy in 25 fractions. For the dosimetric evaluation of the different strategies targets and OARs were delineated on each weekly transversal MRI, which was acquired on average 10 minutes after the sagittal MRI. This way also the effect of intrafraction motion was taken into account. To enable comparison with DVH parameters for the whole treatment, for each weekly MRI the fraction dose was multiplied by 25, the total number of fractions. For the delineations on each transversal MRI the following DVH parameters were calculated: cervix-uterus CTV  $D_{98\%}$ , high-risk CTV  $D_{98\%}$ , bowel bag  $V_{40Gy}$  and  $V_{30Gy}$ , and bladder and rectum  $D_{mean}$  and  $V_{40Gy}$ .

#### Results

For the MRI\_5mm strategy  $D_{98\%}$  of the high-risk CTV was at least 95% for all weekly MRIs of all patients, while for the LOP and MRI\_3mm strategy this requirement was not satisfied for at least one weekly MRI for 1 and 3 patients, respectively. In Figure 1 an example is given where intrafraction anatomical changes resulted in insufficient coverage of the cervix-uterus CTV for the MRI\_3mm strategy. As compared to the LOP strategy the bowel bag  $V_{40Gy}$  was on average reduced by 148  $cm^3$  and 135  $cm^3$  for the MRI\_3mm and MRI\_5mm strategy, respectively, while for  $V_{30Gy}$  this was 136  $cm^3$  and 129  $cm^3$  (Figure 2). Bladder  $D_{mean}$  was reduced by 2.7 Gy and 1.8 Gy, for the MRI\_3mm and MRI\_5mm strategy, respectively, while bladder  $V_{40Gy}$  was reduced by 24% and 17% (percentage points). Rectum  $D_{mean}$  was reduced by 14.0 Gy and 11.9 Gy, while  $V_{40Gy}$  was reduced by 53% and 47% (percentage points). All differences were significant ( $p < 0.05$ ).

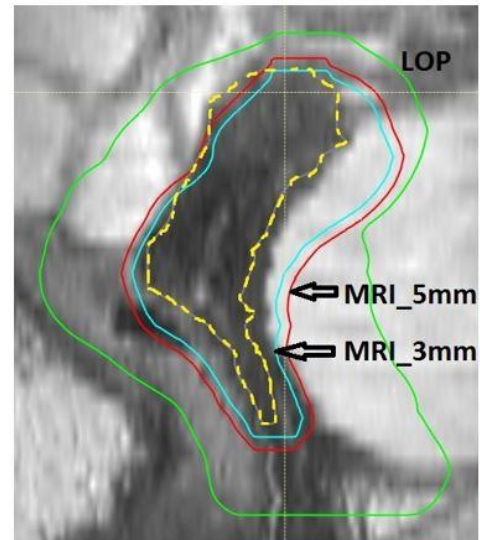


Figure 1: PTV of the selected plan in the LOP (green), and the PTVs of the MRI\_5mm (red) and the MRI\_3mm (blue) strategy overlaid on a transversal MRI. In this example, due to intrafraction bladder filling, the coverage of the cervix-uterus CTV (yellow dashed line) was insufficient for the MRI\_3mm strategy ( $D_{98\%} < 95\%$ ), while it was sufficient for the MRI\_5mm and LOP strategy

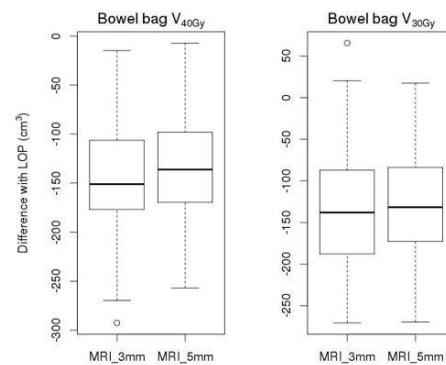


Figure 2: Bowel bag  $V_{40Gy}$  and  $V_{30Gy}$  for all weekly MRIs and all patients. The difference is shown between the MRI\_3mm and LOP strategy, and between the MRI\_5mm and LOP strategy. Negative values indicate more sparing for the MRI strategies.

#### Conclusion

With online MRI-guided radiotherapy of cervical cancer considerable sparing of OARs can be achieved. If a new treatment plan can be generated and delivered within 10 minutes, an online MRI-guided strategy with a 5 mm PTV margin for the CTV of the cervix-uterus is sufficient to account for intrafraction anatomical changes.

#### PO-0981 Role of on-table plan adaptation in MR-guided ablative radiation therapy for central lung tumors

T. Finazzi<sup>1</sup>, M. Palacios<sup>1</sup>, F. Spoelstra<sup>1</sup>, C. Haasbeek<sup>1</sup>, A. Bruynzeel<sup>1</sup>, B. Slotman<sup>1</sup>, F. Lagerwaard<sup>1</sup>, S. Senan<sup>1</sup>

<sup>1</sup>VU University Medical Center, Department of Radiation Oncology, Amsterdam, The Netherlands

#### Purpose or Objective

As patients with centrally located lung tumors are at increased risk of toxicity with SABR, we performed stereotactic MR-guided adaptive radiation therapy (or SMART) for such patients. We retrospectively analyzed the benefits of daily on-table plan adaptation.

#### Material and Methods

Twenty-four patients with central tumors underwent video-assisted, respiration-gated SMART on the MRIdian (ViewRay, Inc.). Tumors were sub-grouped as moderately central (PTV within 2 cm of proximal bronchial tree; n=18), ultracentral (PTV overlapping trachea / main stem

bronchi; n=1) or paracardial (PTV touching mediastinal or pericardial pleura; n=5). Risk-adapted fractionation was used to deliver 60Gy in 8 fx (n=19), 55Gy in 5 fx (n=4) or 60Gy in 12 fx using a GTV-PTV margin of either 3 mm (n=19) or 5 mm (n=5). For each fraction, daily MR-guided setup and on-table plan re-optimization based on PTV coverage and organ at risk (OAR) constraints was performed. Gated breath-hold delivery was performed under continuous MR-guidance. Of a total of 181 fractions, 167 were available for analysis. Benefits of daily plan re-optimization were studied by comparing 167 'predicted' plans, which are the calculated baseline plans on the anatomy-of-the-day, with the re-optimized treatment plans, using Wilcoxon signed-rank test after exclusion of normality.

#### Results

In baseline plans, median PTV was 30.5 cc (range 4.2-70.2), and 95% of PTV received a median dose of 60Gy (55.0-62.6) and a BED<sub>10</sub> of 105Gy (85.0-115.5 Gy). The mean interfractional volume change of clinician-contoured GTV and PTV were 0.4 cc (-3.2 - 6.8) and 0.7 cc (-3.3 - 11.7), respectively, with 75% of fractions showing a GTV/PTV variability  $\leq 1$ cc when compared to baseline. Clinicians had chosen re-optimized plans for treatment in 91% of fractions; reasons included better PTV coverage (62%), OAR sparing (5%), a combination of PTV coverage / OAR sparing (12%), or because institutional protocol for some other tumor sites routinely selected this option (12%). PTV coverage by the prescription dose improved in re-optimized plans (PTV V100% 87.7% vs. 92.2%; p<0.01), leading to an increase in fractions fulfilling the PTV V100%  $\geq 95\%$  objective from 24.6% to 85.6%. A benefit for adaptation persisted when the 40 fractions with a GTV/PTV change  $\geq 1$ cc from baseline were excluded from analysis (PTV V100% 87.7% vs. 91.6%; p<0.01). Median GTV and PTV doses, however, showed smaller improvements after re-optimization (GTV D50 69.0 vs. 69.3Gy, p<0.05; PTV D50 65.9 vs. 66.3Gy, p<0.01). Predefined OAR planning constraints were violated more often in predicted plans than in re-optimized plans (mean 0.73 vs. 0.53 violations per fx; p<0.05), and re-optimization allowed for better sparing of OARs in all cases when this was cited by the clinician as the reason for plan adaptation.

#### Conclusion

In central lung tumors treated using SMART, on-table plan adaptation improved PTV coverage, while avoiding excessive OAR doses.

#### PO-0982 The dosimetric impact of geometric image distortions in slice-based 4D-MRI on the MR-linac

M. Fast<sup>1</sup>, R. Keesman<sup>1</sup>, W. Van den Wollenberg<sup>1</sup>, C. Juan-Cruz<sup>1</sup>, T. Van de Lindt<sup>1</sup>, U. Van der Heide<sup>1</sup>, J. Sonke<sup>1</sup>  
<sup>1</sup>Netherlands Cancer Institute, Department of Radiation Oncology, Amsterdam, The Netherlands

#### Purpose or Objective

4D-MRI is the modality of choice for guiding online plan adaptation of thoracic and abdominal lesions treated on the MR-linac. Like other MRI sequences, 4D-MRI is subject to scanner-specific geometric image distortions caused by gradient non-linearity and main magnetic field inhomogeneity. Specifically for research 4D sequences based on multi-slice 2D acquisitions, no 3D correction is currently available on the Elekta Unity MR-linac (Elekta AB, Stockholm, Sweden). Instead, only a 2D in-plane correction is applied leaving residual through-plane distortions unchanged. This study compares the dosimetric impact of (residual) geometric distortions on the online plan adaptation workflow of the MR-linac for liver SBRT.

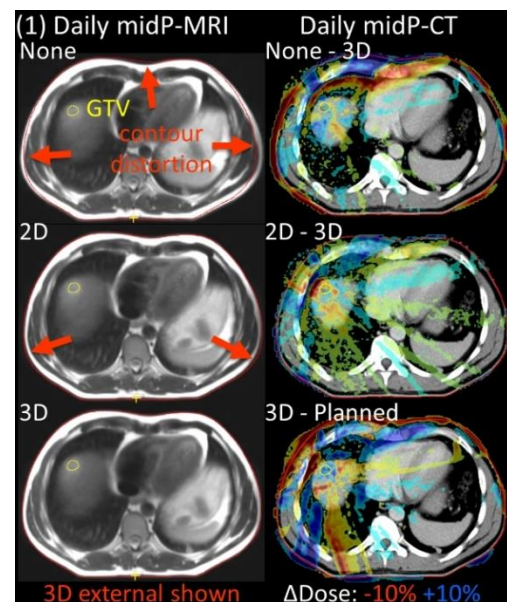
#### Material and Methods

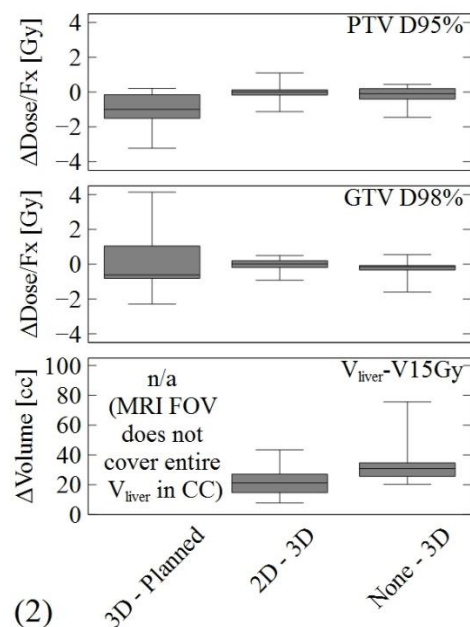
We investigated three different correction strategies for geometric image distortions on the Elekta Unity: A) None; B) 2D, in-plane distortion correction (current default); C) 3D, in-house developed full correction of the

retrospectively sorted 4D-MRI. The 3D-corrected images were considered as ground truth. All image corrections were derived from manufacturer-provided spherical harmonics coefficients. In this study, we included axial 4D-MRIs of three oligometastatic liver patients scanned on the MR-Linac (total: 10 imaging fractions). First, a step-and-shoot IMRT MR-linac plan (3x20 Gy, 10-13 beams) was created in Monaco 5.4 for each patient on the planning mid-position (midP)-CT. Next, each 4D-MRI was warped into a midP-MRI prior to applying the image corrections. The treatment plan was then adapted for each imaging fraction based on a rigid registration of the tumour mask in the planning midP-CT to the 3D-corrected midP-MRI ('adapt-to-position'). Last, the planning midP-CT was deformably registered to each version of the daily midP-MRIs. The adapted plan was then re-calculated and evaluated using these daily midP-CTs.

#### Results

Visual inspection of the daily midP-MRIs in the axial orientation revealed mostly consistent contours between 3D- and 2D-corrected images. Uncorrected images featured local distortions of the external patient contour of up to 2 cm (fig 1). For the tumours, which were always positioned within 10 cm of the machine isocentre, 3D distortions were below 1.5 mm and hardly visible. Dose on the daily midP-CT showed local differences of up to 4 Gy/Fx compared to the original plan. Importantly, the daily dose differences induced by anatomical variations (3D-Planned) were much larger than the dose differences of the correction strategies (2D-3D, None-3D) for the PTV D95% and GTV D98% (fig 2). For the liver, the median increase in volume receiving less than 15 Gy was 31 cc (None) and 21 cc (2D) compared to the 3D-corrected images.





## Conclusion

When evaluating delivered dose on the daily anatomy, the relatively simple 2D in-plane geometric distortion correction closely approximates the 3D correction for axial 4D-MRIs. Further research is needed to assess the impact of image distortions on contouring and plan re-optimisation ('adapt-to-shape').

## PO-0983 Accumulating delivered dose to the rectum using finite element analysis improves toxicity prediction

L. Shelley<sup>1,2</sup>, D. Noble<sup>3</sup>, M. Romanchikova<sup>4</sup>, K. Harrison<sup>5</sup>, A. Bates<sup>3</sup>, M. Sutcliffe<sup>1</sup>, S. Thomas<sup>2</sup>, N. Burnet<sup>6</sup>, R. Jena<sup>3</sup>  
<sup>1</sup>University of Cambridge, Department of Engineering, Cambridge, United Kingdom ; <sup>2</sup>Cambridge University Hospitals, Department of Medical Physics & Clinical Engineering, Cambridge, United Kingdom ; <sup>3</sup>Cambridge University Hospitals, Department of Oncology, Cambridge, United Kingdom ; <sup>4</sup>National Physical Laboratory, Data Science, Teddington, United Kingdom ; <sup>5</sup>University of Cambridge, Cavendish Laboratory, Cambridge, United Kingdom ; <sup>6</sup>University of Manchester, Manchester Academic Health Science Centre, Manchester, United Kingdom

## Purpose or Objective

In prostate cancer radiotherapy (RT), the rectum is a dose-limiting organ. Existing NTCP models are based on planned DVH data from the static pre-treatment CT scan. However, delivered dose to the rectum differs from planned due to interfraction motion.

Here we present a system for accumulating motion-inclusive delivered dose to the rectal wall, using biomechanical modelling and finite element analysis (FEA) to build voxel-by-voxel dose histories, and use this data to construct NTCP models incorporating spatial features.

## Material and Methods

185 prostate cancer patients treated with helical IGRT were split into training (n = 139) and validation groups (n = 46). Dose prescriptions were 74 Gy/37# and 60 Gy/20#, combined by converting to EQD in 37 fractions. Rectal position during treatment was identified from daily MVCTs using a locally developed autosegmentation algorithm. The auto-contours were used to generate a simulated rectal model in the FEA environment, Abaqus (Dassault Systèmes®). For each patient, the model was biomechanically grown and deformed to the planned and daily contours. Daily dose to the rectal wall was calculated

using the independent dose calculation system, CheckTomo. Total delivered dose was determined by accumulating daily dose at each finite element (or, voxel). 3D voxel-wise statistical analysis was performed for dose differences between patients with and without rectal bleeding (RB)  $\geq$ Gr2 at 2 years (prospectively collected; CTCAEv4.03; n = 15 ,training; n = 6, validation), for planned and delivered dose. Subregions were identified where  $p < 0.05$  ( $SRR_{0.05}$ ) and  $p < 0.01$  ( $SRR_{0.01}$ ) (Figure 1), and the equivalent uniform dose (EUD) was calculated for each SRR, as well as the full rectal wall (RW).

Univariate analyses were performed to identify the dose metrics and clinical prognostic factors to be included in a multivariable logistic regression model. NTCP was calculated as:  $NTCP = 1/(1+exp(-S))$ , where S is dependent upon the outcome of the logistic regression (Schaake et al., 2017).

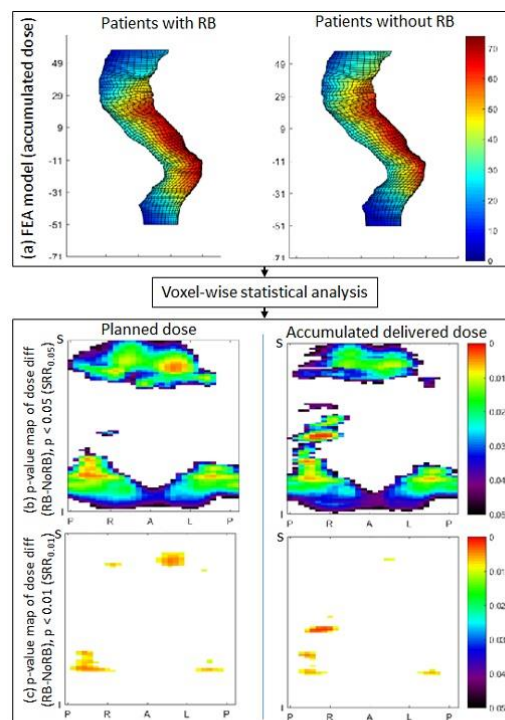


Figure 1 – (a) Delivered dose to rectum, accumulated using finite element analysis, split by patients with and without RB  $\geq$  G2. Voxel-wise statistical analysis was performed on dose differences (with/without RB) to generate p-value threshold maps (shown here virtually unfolded to 2D) to identify subregions where  $p < 0.05$  ( $SRR_{0.05}$ ), and  $p < 0.01$  ( $SRR_{0.01}$ ), for both planned and delivered dose. The EUD of each subregion was used to formulate a NTCP model.

## Results

Univariate analysis revealed that EUD of  $SRR_{0.01}$ ,  $SRR_{0.05}$ , and RW, from delivered dose, were discriminative of RB. No significant associations were observed for corresponding planned dose metrics. Pre-treatment status of hypertension (HTN) was associated with RB.

A NTCP model was generated for each dose metric. For the training set, all NTCP models were predictive of RB for both planned and delivered dose metrics (Figure 2), the strongest being  $SRR_{0.01}(\text{delivered})+\text{HTN}$ , with AUC 0.801 [95%CI: 0.697, 0.905]. The only model predictive of RB upon testing of the validation cohort was  $SRR_{0.01}(\text{delivered})+\text{HTN}$ , AUC 0.829 [0.693, 0.966].

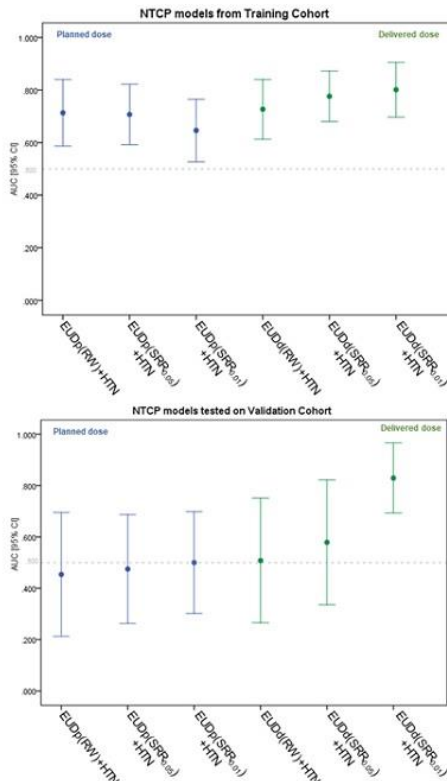


Figure 2 – Area Under the Receiver Operator Characteristic Curve (AUC) for NTCP models of RB ≥ G2. Results were considered significant if AUC > 0.6 and lower 95%CI > 0.5. Multivariable logistic regression models generated from the training cohort for dosimetric parameters (EUD of RW, SRR0.05, and SRR0.01) with HTN status, for planned and FEA-accumulated delivered dose, were all found to be good predictors. The only model predictive of RB upon testing with the validation cohort was based on delivered dose to SRR0.01+HTN, with AUC = 0.829 [95% CI: 0.693, 0.966].

**Conclusion**

A NTCP model based on delivered dose to SRR0.01 and HTN was generated and validated for RB. External validation would be desirable. FEA provides a more anatomically representative tool for dose accumulation than planar homogeneous expansion. Improved toxicity prediction based on delivered dose could be useful for decision making in adaptive RT.

**PO-0984 Univariate toxicity associations are stronger with delivered than planned dose in HNC patients.**

D. Noble<sup>1</sup>, K. Harrison<sup>2</sup>, A. Hoole<sup>3</sup>, M. Wilson<sup>4</sup>, S. Thomas<sup>3</sup>, A. Bates<sup>5</sup>, L. Shelley<sup>6</sup>, N. Burnet<sup>7</sup>, R. Jena<sup>1</sup>  
<sup>1</sup>University of Cambridge, Oncology, Cambridge, United Kingdom ; <sup>2</sup>University of Cambridge, Cavendish Laboratory, Cambridge, United Kingdom ; <sup>3</sup>Cambridge University Hospitals NHS Foundation Trust, Department of Medical Physics and Clinical Engineering, Cambridge, United Kingdom ; <sup>4</sup>University College London, Department of Medical Physics and Biomedical Engineering, London, United Kingdom ; <sup>5</sup>Cambridge University Hospitals NHS Foundation Trust, Cambridge Clinical Trials Unit- Box 401, Cambridge, United Kingdom ; <sup>6</sup>University of Cambridge, Engineering, Cambridge, United Kingdom ; <sup>7</sup>University of Manchester, Manchester Academic Health Science Centre, Manchester, United Kingdom

**Purpose or Objective**

Differences between planned (D<sub>P</sub>) and delivered (D<sub>A</sub>) dose to OARs in patients with HNC are well documented; adaptive strategies may reduce such differences, but lack an evidence base. To date, no data exists proving that patient toxicity associates more strongly with D<sub>A</sub>, compared to D<sub>P</sub>. This study aims to test that hypothesis.

**Material and Methods**

All HNC patients recruited to the VoxTox study (UK CRN ID 13716) were eligible. All were treated with standard radical protocols on TomoTherapy with daily IG. Swallowing OARs (ipsi & contralateral parotids - IPG & CPG, submandibular glands - ISMG & CSMG, superior & middle pharyngeal constrictors - SPC/MPC, oral cavity - OC and supraglottic larynx - SGL) were segmented on planning scans, according to published atlases. An open-source deformable image registration toolbox (Elastix), in-house dose calculation software (CheckTomo), planning kV and IG-MVCTs were used to compute D<sub>P</sub> and D<sub>A</sub> OAR DVHs. Mean dose was used for analysis. Toxicity was assessed with CTCAEv4.03 at baseline, and 1 year, using 3 endpoints: xerostomia (Xer), salivary duct inflammation (SDI), dysphagia (Dys). Baseline data on comorbidities, primary site (PDS), TNM staging, surgery, smoking, alcohol and systemic therapy (SACT) were collected. Univariate analysis was undertaken to examine relationships between baseline parameters, D<sub>P</sub>, D<sub>A</sub>, and Gr2+ toxicity. Odds ratios (ORs) were calculated for all variables. Dose differences between cases with and without Gr2+ toxicity were assessed with t-tests. AUC of ROC curves were calculated for dosimetric parameters.

**Results**

141 patients had full datasets available for analysis. PDS were: 90 oropharynx, 14 hypopharynx/larynx, 16 salivary gland/sinus/skin, 10 oral cavity, 5 nasopharynx, 6 CUP. Concomitant SACT: cisplatin 78, cetuximab 11, none 52. Mean dose differences (D<sub>A</sub> - D<sub>P</sub>, 95% CI) for each OAR were: IPG 1.58Gy (1.36-1.81), CPG 0.93Gy (0.71-1.15), ISMG 1.00Gy (0.84-1.15), CSMG 1.23Gy (1.07-1.39), SPC 0.92Gy (0.80-1.03), MPC 0.73Gy (0.55-0.92), OC 0.62Gy (0.46-0.79), SGL 0.95Gy (0.71-1.20) (Fig 1).

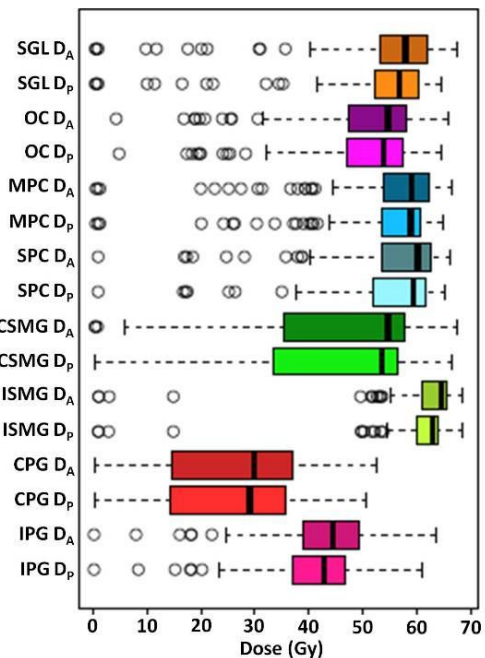


Figure 1: Planned (D<sub>P</sub>) and delivered (D<sub>A</sub>) mean dose to OARs. I = ipsilateral, C = contralateral. PG = parotid gland, SMG = submandibular gland, SPC/MPC = superior & middle pharyngeal constrictors, OC = oral cavity, SGL = supraglottic larynx. n = 141 patients.

Concomitant SACT increased the risk of all toxicity endpoints (ORs, 95% CIs); Xer 2.22 (1.10-4.52), SDI 3.16 (1.41-7.55), Dys 3.33 (1.04-14.1), as did baseline symptoms for Xer (2.10, 1.01-4.27) and SDI (5.06, 1.68-15.3), and higher N-stage (2+) for Xer (2.10, 1.04-4.27). Univariate relationships between dose to relevant OARs and toxicity are shown in Table 1.

	Planned dose (mean)			Delivered dose (mean)		
	t-test p (95% CI)	OR (95% CI)	AUC (95% CI)	t-test p (95% CI)	OR (95% CI)	AUC (95% CI)
OARs CTCAE v4.03 Grade 2+ Xerostomia						
IPG	0.70 -4.1 to 2.8	1.007 0.972 to 1.044	0.54 0.48 to 0.64	0.77 -4.0 to 3.0	1.005 0.971 to 1.041	0.53 0.43 to 0.63
CPG	0.018 -9.4 to -0.9	1.033 1.006 to 1.063	0.61 0.51 to 0.71	0.012 -10.0 to -1.2	1.034 1.007 to 1.063	0.62 0.52 to 0.71
ISMG	0.066 -8.7 to 0.3	1.039 0.999 to 1.108	0.65 0.54 to 0.76	0.058 -9.1 to 0.2	1.040 1.000 to 1.107	0.66 0.56 to 0.77
CSMG	<0.001 -16.7 to -4.8	1.035 1.015 to 1.058	0.64 0.54 to 0.73	<0.001 -17.0 to -4.8	1.034 1.014 to 1.056	0.64 0.54 to 0.73
OARs CTCAE v4.03 Grade 2+ Salivary duct inflammation						
IPG	0.75 -4.14 to 3.0	1.006 0.969 to 1.046	0.55 0.45 to 0.65	0.75 -4.2 to 3.1	1.006 0.970 to 1.045	0.55 0.45 to 0.65
CPG	0.038 -9.2 to -0.3	1.031 1.002 to 1.063	0.61 0.51 to 0.70	0.020 -10.1 to -0.9	1.034 1.005 to 1.065	0.62 0.52 to 0.71
ISMG	0.38 -6.8 to 2.7	1.019 0.982 to 1.079	0.56 0.45 to 0.68	0.37 -7.1 to 2.7	1.019 0.983 to 1.078	0.57 0.48 to 0.69
CSMG	0.011 -14.7 to -1.9	1.031 0.979 to 1.047	0.60 0.51 to 0.70	0.011 -14.9 to -1.9	1.030 1.007 to 1.058	0.61 0.51 to 0.70
OARs CTCAE v4.03 Grade 2+ Dysphagia						
SPC	0.012 -11.2 to -1.4	1.148 1.045 to 1.311	0.69 0.58 to 0.79	0.009 11.6 to -1.7	1.161 1.053 to 1.338	0.70 0.66 to 0.80
MPC	0.039 -10.9 to -0.3	1.113 1.023 to 1.259	0.65 0.53 to 0.76	0.035 -11.4 to -0.4	1.106 1.023 to 1.237	0.66 0.54 to 0.77
OC	0.049 -10.2 to 0	1.063 1.006 to 1.145	0.58 0.48 to 0.68	0.048 -10.5 to -0.1	1.063 1.007 to 1.142	0.58 0.47 to 0.68
SGL	0.059 11.3 to 0.2	1.079 1.010 to 1.187	0.61 0.50 to 0.73	0.052 -11.9 to 0.1	1.079 1.012 to 1.182	0.62 0.51 to 0.74

Table 1: Univariate analysis of late toxicity (1 year point prevalence) as a function of planned ( $D_p$ ) and delivered ( $D_d$ ) dose parameters to OARs (ipsilateral - I and contralateral - C parotid glands - PG and submandibular glands - SMG, superior - S and middle - M pharyngeal constrictor muscles PC, oral cavity - OC and supraglottic larynx - SGL). ORs indicate % increase in odds of Gr2+ toxicity/Gy increase to OAR. No relationship found - cells clear. No relationship between dose to OAR and toxicity endpoint - cells clear. Relationship stronger - cells green ( $D_d$  stronger = 15). Relationship weaker - cells red ( $D_d$  weaker = 2). Relationship equivalent or equivocal - cells blue (7).

## Conclusion

Clear associations with concomitant SACT, pre-treatment symptoms and toxicity were seen.  $D_A$  was higher than  $D_p$  to all OARs. Differences were small in most patients. Despite this, a trend for marginally stronger univariate associations between  $D_A$  parameters, compared to  $D_p$ , and toxicity was seen. Results should be interpreted with caution due to multiple testing, and comparison with multivariate models is required as a next step. Nonetheless, this data is the first to compare relationships between both  $D_p$  &  $D_A$  and toxicity in HNC, and to suggest stronger links with the latter.

## PO-0985 Online-adaptive proton therapy: assessing accuracy of robust dose restoration in lung patients.

E. Borderias<sup>1</sup>, E. Sterpin<sup>1</sup>, X. Geets<sup>2</sup>, K. Bernatowicz<sup>1</sup>, K. Souris<sup>1</sup>

<sup>1</sup>Université Catholique de Louvain, Center of Molecular Imaging- Radiotherapy and Oncology, Brussels, Belgium ;

<sup>2</sup>Cliniques universitaires Saint-Luc, Department of Radiation Oncology, Brussels, Belgium

## Purpose or Objective

Intensity-modulated proton therapy (IMPT) offers excellent dose conformity and reduces the integral dose in the OAR compared to conventional radiotherapy. During the treatment, density changes may alter planned proton ranges in the patient and compromise the accuracy of the plan. To take into account this effect, isovolume dose restoration (iDR) uses isodose contours generated from the initial dose distribution and their associated weighted objectives (maximum and minimum) to reoptimize the plan and reproduce the initial dose in repeated CTs. The objective of this work was to test the performance of iDR in lung cancer patients.

## Material and Methods

The provided database included planned and two repeated 4D-CTs (every two weeks) for fourteen patients. Twelve of them present lymph nodes in addition to the primary tumour. iDR was performed in the first series of repeated 4D-CTs. The prescribed dose ( $D_p$ ) to target was 66 Gy (33 fractions of 2 Gy). Robust optimization was used for the targets, with setup errors of 5mm, range errors of 3%, and

three phases of the respiratory cycle (end-exhale, end-inhale, and midV). Plans were optimized based on CTV coverage criteria (worst-case  $D95% > 95%D_p$  and  $D5% < 105%D_p$ ) in RayStation (RaySearch Laboratories, Sweden). For the evaluation of the results, two different metrics were calculated: 1)  $D95%$  and  $D5%$  dose values for the CTV in the nominal case; 2) dose differences between restored/distorted and initial dose distributions reported by  $DE(vol=2\%)$  values in four different volumes (prescribed, high, medium and low dose regions).  $DE(vol=2\%)$  represents the absolute dose errors (evaluation-initial dose) in at most 2% of the analysed region.

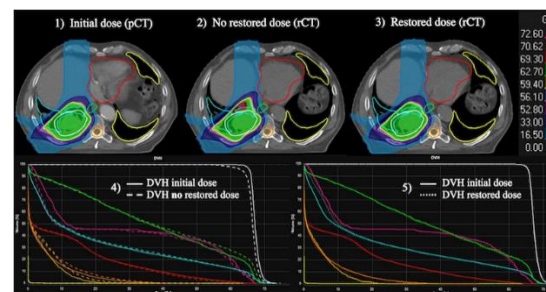
## Results

The evaluation of initial plans on repeated CTs showed large dose distortions, which were substantially reduced after restoration. No target underdosage was observed after restoration, whereas for 28% (4/14) of the patients, the CTV coverage criteria were not accomplished before restoration. In limit cases (21% or 3/14 patients), where  $D95%/D5%$  levels were reached (only  $\pm 1$ Gy), iDR improved considerably the DVH metrics (see Table 1). In the analysis of local dose differences, median  $DE(vol=2\%)$  decreased from 10.06 Gy in distorted plans to 3.23 Gy in the restored plans.

Patient	INITIAL		RESTORED		DISTORTED	
	D95% (Gy)	D5% (Gy)	D95% (Gy)	D5% (Gy)	D95% (Gy)	D5% (Gy)
1	65.74	67.99	65.85	67.91	65.55	68.60
2	65.26	70.02	65.42	70.08	63.10*	69.45*
3	65.24	68.79	65.35	68.85	64.52	69.73*
4	65.76	68.57	65.81	68.69	65.11	69.25*
5	65.74	68.14	65.03	67.83	65.41	67.62
6	65.48	68.62	65.45	68.94	62.26*	70.10*
7	65.36	68.04	65.57	68.10	60.68*	67.74
8	65.30	68.57	65.61	68.76	64.73	68.84
9	65.71	68.51	65.46	69.08	64.05	67.94
10	65.89	68.76	65.73	68.60	65.34	69.29
11	65.76	68.07	65.44	68.62	65.56	67.89
12	65.63	69.61	65.63	69.73	63.42*	68.84
13	65.79	68.30	65.63	68.52	65.67	68.55
14	65.58	68.97	65.57	69.18	64.54	68.78

## Conclusion

Restoring clinically-approved dose distribution on repeated CTs does not require new ROI segmentation and is compatible with an online adaptive workflow. With iDR, we are able to accurately reproduce the initial dose, despite density changes, maintaining stable the DVH-based parameters (see Figure.1). Hot spots and underdosage in the CTV can be corrected by implementing iDR in the clinical workflow.



## PO-0986 Inter-fraction anatomical changes in pediatric abdominal tumors during photon and proton therapy

F. Guerreiro<sup>1</sup>, E. Seravalli<sup>1</sup>, G.O. Janssens<sup>2</sup>, J.H. Maduro<sup>3</sup>, C.L. Brouwer<sup>3</sup>, E.W. Korevaar<sup>3</sup>, A.C. Knopf<sup>3</sup>, B.W. Raaymakers<sup>1</sup>

<sup>1</sup>UMC Utrecht, Department of Radiotherapy, Utrecht, The Netherlands ; <sup>2</sup>UMC Utrecht, Department of Radiation Oncology, Utrecht, The Netherlands ; <sup>3</sup>UMC Groningen, Department of Radiation Oncology, Groningen, The Netherlands

### Purpose or Objective

During radiotherapy treatment (RT) of abdominal pediatric tumors, inter-fraction anatomical changes such as patient's diameter variations due to weight loss/gain and different gastrointestinal gas volumes might occur. The goal of this study was to investigate the dosimetric impact of daily anatomical changes based on cone-beam computed tomography (CBCT) information in robust optimized photon and proton RT dose distributions.

### Material and Methods

Volumetric modulated arc therapy (VMAT) and pencil beam scanning proton therapy (PBS) dose distributions were calculated using the original planning-CT scan for 20 pediatric patients (average 3, range 1-8 years) treated for neuroblastoma (n=11) and Wilms' tumor (n=9). VMAT plans were based on a 6 MV full-arc while PBS plans on 2-3 posterior-oblique fields with prescribed doses (PD) ranging between 14.4-36 Gy. Treatment plans were robust optimized on the patient-specific internal target volume (ITV) using a uniform 5 mm set-up uncertainty. Moreover, for the PBS plans a 3% proton range uncertainty was accounted for. The plan robustness was evaluated using multiple dose distributions associated with various error scenarios: set-up (with the magnitude of 5 mm in 26 directions per VMAT and PBS plans) and range errors ( $\pm 3\%$  density scaling, resulting in 52 scenarios per PBS plan). Plans were accepted if the V95% of the ITV > 98% in the voxel-wise minimum evaluation dose. Fractional dose re-calculations were performed using clinical CBCT images. For the estimation of Hounsfield units (HUs) from the daily CBCT data, the gas volumes on the planning-CT were filled with a water equivalent density and the planning-CT was deformably registered to each CBCT. Gas volumes were delineated on the CBCTs and copied rigidly to the deformed CTs (dCTs). Fractional doses were re-calculated on the dCTs and accumulated rigidly. To compare planned and accumulated doses, dose-volume histogram (DVH) parameters were calculated for the clinical ITV and organs at risk (OARs).

### Results

For both techniques, the ITV coverage was fulfilled for the original planned dose distributions. For the ITV, mean differences between planned and accumulated doses ranged between [-0.1% - 0.8%] and [-0.1% - 0.1%] for the VMAT and PBS plans (Table 1), respectively. On the accumulated doses, the ITV coverage was not reached (V95% < 99%) for 2 patients, for the VMAT plans (Figure 1). For the OARs, mean differences between planned and accumulated doses ranged between [-0.4% - 0.2%] and [-0.2% - 0.0%] for the VMAT and PBS plans (Table 1), respectively.

**Table 1.** Mean  $\pm$  standard deviation (SD) differences (%) between planned and accumulated doses for selected DVH parameters for VMAT and PBS dose distributions.

Structure	Parameter	Planned - Accumulated Dose (%)			
		VMAT		PBS	
		Mean $\pm$ SD	Range	Mean $\pm$ SD	Range
ITV	D <sub>95%</sub>	0.8 $\pm$ 1.7	[-1.9; 7.2]	0.1 $\pm$ 0.5	[-0.5; 1.9]
	D <sub>mean</sub>	0.2 $\pm$ 0.9	[-2.4; 2.2]	0.1 $\pm$ 0.1	[-0.1; 0.3]
	D <sub>2%</sub>	-0.1 $\pm$ 1.0	[-2.8; 2.3]	-0.1 $\pm$ 0.6	[-1.7; 0.5]
	V <sub>95%</sub>	0.4 $\pm$ 1.5	[0.0; 6.8]	0.1 $\pm$ 0.3	[0.0; 0.7]
Kidney R		-0.4 $\pm$ 2.3	[-5.4; 3.1]	-0.1 $\pm$ 0.4	[-1.0; 0.9]
Kidney L		-0.2 $\pm$ 1.7	[-5.2; 3.8]	0.0 $\pm$ 0.6	[-1.1; 1.6]
Liver	D <sub>mean</sub>	0.2 $\pm$ 0.7	[-0.9; 2.5]	-0.2 $\pm$ 0.7	[-2.3; 1.1]
Spleen		0.0 $\pm$ 1.7	[-5.6; 4.0]	0.0 $\pm$ 0.5	[-1.0; 1.5]

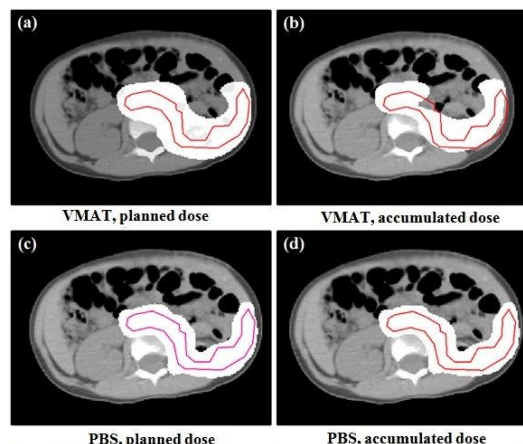


**Figure 1.** VMAT (a,b) and PBS (c,d) planned and accumulated dose distributions for one of the patients failing the ITV coverage (V<sub>95%</sub> < 99%) in the accumulated VMAT dose distribution (b). Dose distributions are overlaid on the planning-CT and the 95% isodose line is shown in white and the ITV in red.

### Conclusion

In this study, the need of performing re-planning during RT was evaluated for children treated for abdominal tumors. RT using PBS with posterior-oblique irradiation fields proved to be highly robust against anatomical inter-fraction changes. In photon therapy using a VMAT delivery, daily anatomical changes proved to affect the target coverage to a higher extent when compared to PBS.

### PO-0987 Rotational setup errors in breast cancer radiotherapy: the effect on treatment margins.

J. Seppala<sup>1</sup>, K. Vuolukka<sup>1</sup>, T. Viren<sup>1</sup>, J. Heikkilä<sup>1</sup>, J. Honkanen<sup>1</sup>, A. Pandey<sup>2</sup>, A. Al-Ghuri<sup>2</sup>, M. Shah<sup>2</sup>, S. Sefa<sup>2</sup>, T. Koivumäki<sup>3</sup>

<sup>1</sup>Kuopio University Hospital, Center of Oncology, Kuopio, Finland ; <sup>2</sup>University of Eastern Finland, Department of Applied Physics, Kuopio, Finland ; <sup>3</sup>Central Finland Central Hospital, Department of Medical Physics, Jyväskylä, Finland

### Purpose or Objective

Rotational errors might have a significant effect on radiotherapy (RT) target coverage if not considered in PTV margins. In this work, we investigated the residual rotational errors in breast cancer RT.

### Material and Methods

Daily low dose CBCT setup images of 93 breast cancer patients treated with RT were retrospectively investigated for rotational errors in patient setup. Patients were imaged with CT in supine position arms above the head on a breast board (C-Qual™ Breastboard, Civco, USA). 20 of the patients were imaged in deep inspiration breath hold (DIBH). With 50 patients, the treatment area included the whole breast and with 43 patients, the treatment area included also the axillary lymph nodes. A 3D image co-registration was conducted between 1731 CBCT images and the respective planning CT images (Mosaic system v2.62, Elekta AB) and image translation and rotations in coronal (COR), sagittal (SAG) and transversal (TRA) planes were recorded (Fig 1). Pearson correlation coefficient was used to determine the relation between the magnitude of rotational error and body mass index (BMI), age, side of a treatment, use of DIBH, chemotherapy, time between surgery and RT and the number of fractions (either 15 or 25).

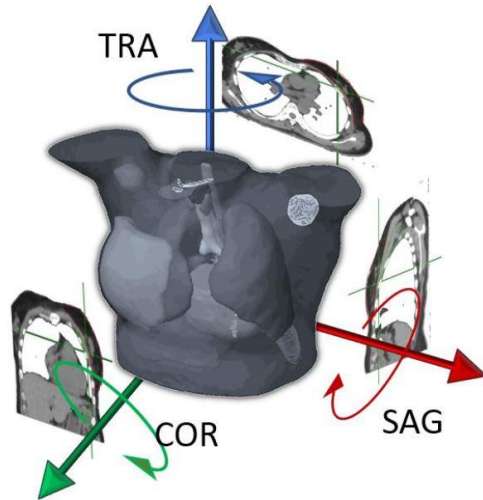


**Fig 1.** The directions of the rotations investigated in this study.

#### Results

The mean absolute translational shifts from skin marker-based patient setup were  $4 \pm 3$  mm,  $3 \pm 3$  mm and  $4 \pm 4$  mm in anterior-posterior, left-right and cranio-caudal directions, respectively. The residual rotational errors were on average  $0.0 \pm 1.4^\circ$  for COR,  $0.2 \pm 1.6^\circ$  for SAG and  $0.2 \pm 1.9^\circ$  for TRA directions (Fig 2). The mean absolute rotations were  $1.0 \pm 0.9^\circ$  for COR,  $1.2 \pm 1.0^\circ$  for SAG and  $1.4 \pm 1.3^\circ$  for TRA directions, respectively. Overall, 35% of the residual rotational errors were larger than  $2^\circ$ . In 244 fractions (14%) the rotational error was over  $3^\circ$ . A three-degree rotational error would result in a translational shift of 4 mm at the edge of a typical breast cancer PTV (radius 8 cm), and for a PTV with axillary lymph nodes involved (radius up to 12 cm), the translational error would increase up to 6 mm. Modest but statistically significant correlations were found between patient age ( $r=0.27$ ,  $p=0.01$ , smaller errors with younger age) and the use of DIBH ( $r=0.23$ ,  $p=0.02$ , smaller errors with DIBH) and the rotational errors.

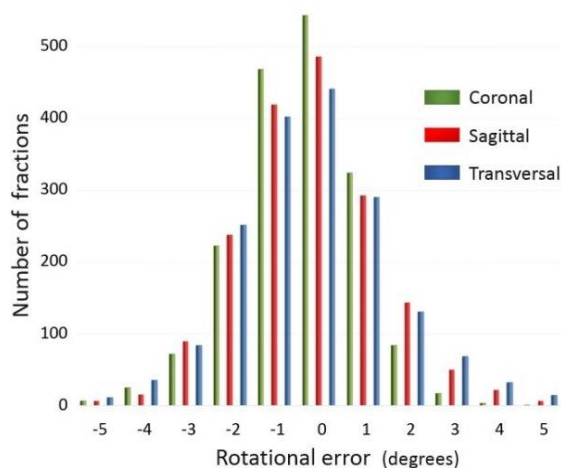


**Fig 2.** Histogram of the residual rotational errors in coronal, sagittal and transversal directions for all investigated setup images.

#### Conclusion

With online patient position correction methods, the translational setup deviations can be reduced to negligible values. However, the rotational residual setup errors should also be accounted when determine the PTV margins. Furthermore, the PTV margins taking into account the rotational errors should depend on the size

and shape of target volume. In whole breast RT with axillary lymph node involvement the clinical rotational setup errors can result in over 6 mm translational shifts at the edge of the PTV.

#### PO-0988 CBCT-based library of plans approach in gastric cancer radiotherapy: proof of concept

M. Bleecker<sup>1</sup>, K. Goudschaal<sup>1</sup>, A. Bel<sup>1</sup>, J. Sonke<sup>1,2</sup>, M.C.C.M. Hulshof<sup>1</sup>, A. Van der Horst<sup>1</sup>

<sup>1</sup>Amsterdam UMC- University of Amsterdam, Radiation Oncology, Amsterdam, The Netherlands ; <sup>2</sup>Netherlands Cancer Institute, Radiation Oncology, Amsterdam, The Netherlands

#### Purpose or Objective

Current protocols for gastric radiotherapy (RT) use one treatment plan only. A library of plans for gastric cancer may ensure adequate irradiation by adapting the treatment to large day-to-day anatomical changes in size, shape and position. Here, we assess the feasibility of CBCT-guided gastric cancer adaptive RT (ART) with a library of plans based on the planning CT (pCT) and the daily CBCTs of the first week of RT.

#### Material and Methods

Three patients, who had received single-plan pre-operative RT within the CRITICS-II trial (NCT02931890; 45 Gy; 25 fractions; PTV margin = 10 mm) with daily CBCT-guidance, were included. For this retrospective study, all CBCTs were rigidly registered to the pCT based on bony anatomy and if needed corrected in longitudinal direction for diaphragm position (Velocity 4.0, Varian). One expert radiation oncologist manually delineated CTV (i.e. entire stomach and regional lymph nodes) according to trial protocol on pCT and the first 5 CBCTs (Fig 1A). For delineation on CBCT, the CTV\_pCT was copied and subsequently adjusted. From these 6 CTVs, we created 3 Plan Selection Volumes (PSVs) (Fig 1B): PSV\_large = union of all 6 CTVs + 3 mm, PSV\_medium = volume occupied by 4 of 6 CTVs (i.e. volume with at least 4 overlapping CTVs) + 3 mm, and PSV\_small = smallest delineated CTV + 3 mm; 3 mm was used to preserve a 7 mm PTV margin to account for remaining uncertainties. A specially trained RTT selected the most appropriate PSV for the remaining 20 fractions (i.e. fractions 6-25). The selected PSV must encompass the CTV as visible on the CBCT.

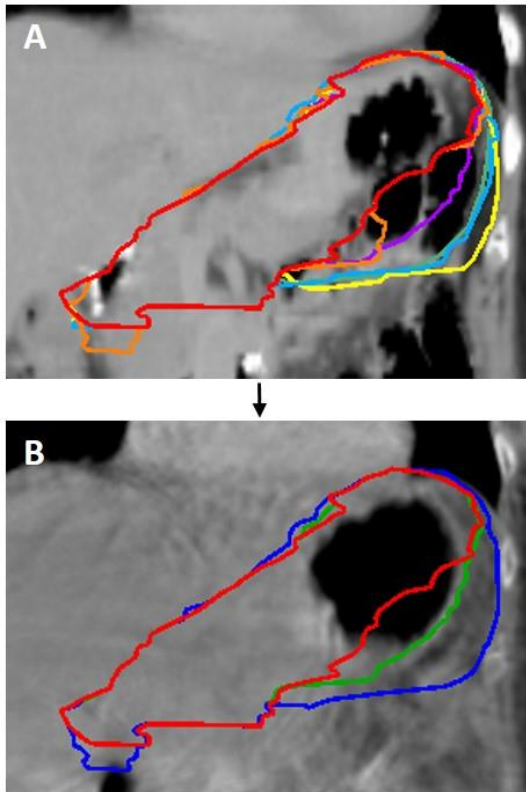


Fig 1: Example of ART approach in patient 3. A) Delineated CTV on pCT (red) and CBCTs; B) Generated PSVs for volume selection on CBCT.

## Results

For all patients, the CTV could be delineated on the first 5 CBCTs. However, often no adjustments with respect to CTV\_pCT were made in caudal, ventral and left-lateral direction because of poor visibility due to low image quality and changing volumes of gas in the stomach and colon (Fig 1A). All 15 CTV\_CBCTs were partially outside the pCT\_PTV, with on average 3.4% of the volume (range 0.0%-9.3%).

PSV selection showed no apparent pattern over time (Fig. 2A). Overall, PSV\_large was selected in 28 fractions (46.7%), PSV\_medium in 20 fractions (33.3%) and PSV\_small in 11 fractions (18.3%; Fig. 2B). For two patients, only PSV\_medium and PSV\_large were selected; for these patients, PSV\_small equaled CTV\_pCT. For only one fraction (1.7%), it was not possible to select a PSV.

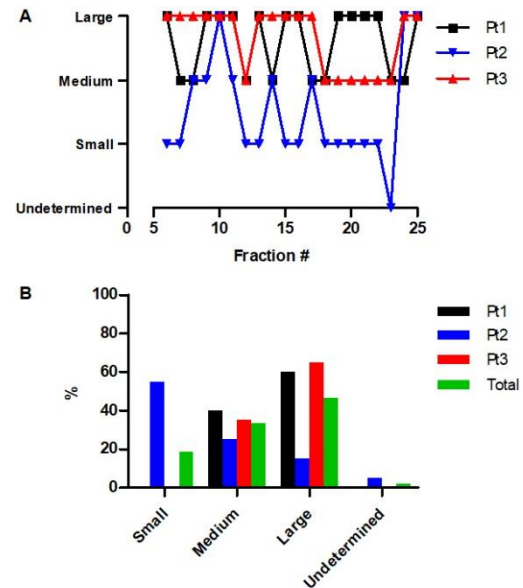


Fig 2: (A) Contour selection over time per patient. (B) Percentage of selected contours per patient and in total. For one fraction, no contour was selected.

## Conclusion

This study has demonstrated feasibility of CTV delineation and volume selection based on CBCT for certain anatomical regions of the stomach. The large variations in these regions showed the urgent need for improvement of the current clinical practice and these findings justify further research towards the development and implementation of gastric ART. However, for other regions of the stomach, CTV delineation and volume selection were unreliable due to poor visibility on CBCT. Consequently, the potential benefit of gastric fiducial markers will be explored in a follow-up study.

## PO-0989 Deep learning improves robustness of contour propagation for online adaptive IMPT of prostate cancer

M. Elmahdy<sup>1</sup>, T. Jagt<sup>2</sup>, R. Zinkstok<sup>3</sup>, C. Marijnen<sup>3</sup>, M. Hoogeman<sup>2</sup>, M. Staring<sup>1</sup>

<sup>1</sup>Leiden University Medical Center, Division of Image Processing- Department of Radiology, Leiden, The Netherlands ; <sup>2</sup>Erasmus MC Cancer Institute, Department of Radiation Oncology, Rotterdam, The Netherlands ; <sup>3</sup>Leiden University Medical Center, Department of Radiation Oncology, Leiden, The Netherlands

## Purpose or Objective

Online-adaptive radiotherapy holds the promise to mitigate daily anatomical uncertainties thereby increasing treatment precision. One of the major challenges here is the development and validation of sufficiently fast, accurate, and robust segmentation algorithms for target volumes and organs at risk. The purpose of this study is to improve contour propagation in the pelvic region by combining deep-learning based auto-segmentation with image registration and to validate it geometrically and dosimetrically for online-adaptive Proton Therapy (PT) for prostate cancer.

## Material and Methods

The proposed registration pipeline registers the daily CT scan to the planning, based on a combination of image intensities and, moreover, by an automatic segmentation of the bladder from the daily CT scan using a novel 3D convolutional neural network. The bladder was chosen for its influence on prostate motion. Registration performance is further enhanced by a digital inpainting of gas pockets with realistic bowel content, using a state-of-the-art generative adversarial network. We further

perform data normalization and in relevant cases digitally remove contrast agent from the bladder. Evaluation was performed on CT data from 18 prostate cancer patients, each with 7 to 10 repeat CT scans. Manual delineations of the prostate, lymph nodes, seminal vesicles, bladder and rectum were available for evaluation. Geometric performance was quantified using the Mean Surface Distance (MSD). The pipeline was validated dosimetrically on 11 out of 18 patients by simulating an online-adaptive PT workflow based on the propagated contours. To this end, for each repeat CT, a treatment plan was generated based on the propagated contours and the plan was evaluated using the manual delineations. A dose of 74 Gy was assigned to the high-dose PTV (prostate) and 55 Gy to the low-dose PTV (lymph nodes and seminal vesicles). The generated treatment plans were considered clinically acceptable if dosimetric coverage constraints derived from the manual contours were met (PTV  $V_{95\%} \geq 98\%$  and  $V_{107\%} \leq 2\%$ ).

### Results

The proposed pipeline achieved a MSD of  $1.29 \pm 0.33$ ,  $1.44 \pm 0.68$ , and  $1.52 \pm 0.45$  mm for the prostate, seminal vesicles, and lymph nodes, respectively (Fig. 1). The propagated contours met the dose coverage constraints in 85%, 91%, and 99% of the cases for the prostate, seminal vesicles, and lymph nodes, respectively (Fig. 2). 78% of the cases met all constraints at the same time, compared to 65% when using a standard registration approach. The average runtime for the proposed pipeline is 98 seconds per registration.

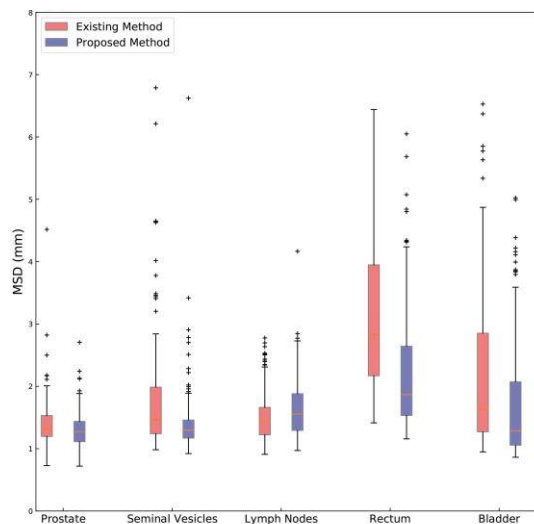


Figure 1. Boxplot comparison between an existing registrations method and the proposed method for image registration in terms of MSD for 161 registrations. Values closer to zero are better

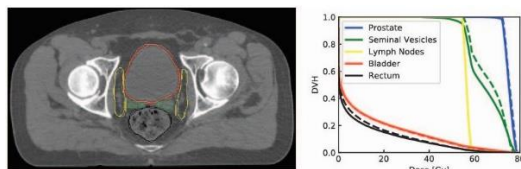


Figure 2. Example for the automatic contours propagation and the corresponding dose volume histograms. The solid line represents the manual contouring results while the dotted line is the automatically propagated one.

### Conclusion

The proposed registration pipeline obtained highly promising results for generating treatment plans adapted to the daily anatomy. With 78% of the automatically generated treatment plans directly usable without manual correction, a substantial improvement in system robustness was reached compared to an existing approach. The proposed method therefore facilitates more precise PT of prostate cancer.

### PO-0990 Positioning uncertainties for pediatric craniospinal irradiation and the impact of image guidance

D. Gasic<sup>1,2</sup>, A. Haraldsson<sup>3</sup>, N.P. Brodin<sup>4</sup>, K. Nysom<sup>5</sup>, T. Björk-Eriksson<sup>6,7</sup>, P. Munck af Rosenschöld<sup>3</sup>

<sup>1</sup>Rigshospitalet, Department of Oncology - Section of Radiotherapy, Nivå, Denmark ; <sup>2</sup>University of Copenhagen, Niels Bohr Institute, Copenhagen, Denmark ; <sup>3</sup>Skåne University Hospital, Department of Radiation Physics, Lund, Sweden ; <sup>4</sup>Albert Einstein College of Medicine, Institute for Onco-Physics, Bronx- NY, USA ; <sup>5</sup>Rigshospitalet - The Juliane Marie Center, Department of Pediatrics and Adolescent Medicine, Copenhagen, Denmark ; <sup>6</sup>Regional Cancer Centre, West, Gothenburg, Sweden ; <sup>7</sup>University of Gothenburg, Department of Oncology - Institute of Clinical Sciences - Sahlgrenska Academy, Gothenburg, Sweden

### Purpose or Objective

To investigate the setup errors for pediatric craniospinal irradiation (CSI) by following image guided correction protocols and explore how daily image-guided radiotherapy (IGRT) has impacted the positioning uncertainty. In particular, we wish to determine the use of six degree of freedom (DoF) couch corrections. Positioning uncertainty data may be used to estimate the uncertainty budget available for planning target volumes and organ-at-risk (OAR) margins, which is essential for the safe clinical implementation of hippocampal-sparing CSI for pediatric medulloblastoma. Patient alignment and setup errors become paramount when attempting to spare a critical organ such as the hippocampus during CSI.

### Material and Methods

In this multicenter study, a total of 14 pediatric patients treated with CSI were identified for whom treatment records and setup images were available. The setup images were registered offline to the reference image (digitally reconstructed from their pre-treatment computed tomography scan) using the automated tool and matching on bony anatomy. A 3 and 6 DoF match was performed, respectively, using both translational (superior-inferior (SI), anteroposterior (AP) and medial-lateral (ML)) and rotational (yaw = rotation around the AP axis, pitch = rotation around the ML axis and roll = rotation around the SI axis) information, ignoring the rotational deviation since only the 3 DoF couch shift was used for positioning these patients during treatment.

### Results

The residual errors should only include rotational deviation since only translational movement on the couch is used. However, rotational errors can affect the translational deviation as well (Table 1). When correcting the shifts according to a simulated IGRT-protocol, where the average of the first two fractions are used to correct the coming fractions, the results show large inter-fractional deviations especially for rotational deviations (Figure 1). Translational and rotational random uncertainty (RU) and systematic uncertainty (SU) were derived as well. If using an IGRT-protocol, such as the above mentioned, the translational residual setup error can be as high as 2.2 cm for an individual patient during a single fraction, and the rotational error as high as  $5.4^\circ$ . If using daily IGRT the maximum setup error was reduced to 0.8 cm translational and  $5.4^\circ$  rotational as well as 0.8 cm translational and  $2.4^\circ$  rotational setup error for 3 and 6 DoF couch shifts, respectively. The RU and SU of ML and roll worsens when only correcting for the first two fractions which further strengthens the indications for daily IGRT.

**Table 1:** Mean translational (superior-inferior (SI), anteroposterior (AP) and medial-lateral (ML)) and rotational positioning errors with corresponding range and uncertainties assuming setup based entirely on skin marks for both 3 and 6 degrees of freedom (DoF) and all isocenters (Units: cm and °/degrees).

3DoF	SI	Range	RU	AP	Range	RU	ML	Range	RU
Translational									
- Head	-0.08	(-1.0 - 2.2)	0.28	-0.20	(-1.1 - 1.0)	0.27	0.06	(-0.6 - 1.3)	0.21
- Thoracic	-0.07	(-0.9 - 2.4)	0.30	-0.04	(-0.9 - 0.8)	0.24	0.14	(-0.4 - 0.9)	0.21
- Lumbal	0.08	(-0.9 - 2.3)	0.29	0.27	(-0.8 - 2.1)	0.34	0.01	(-0.8 - 1.0)	0.27
6DoF	SI / Roll	Range	RU	AP / Yaw	Range	RU	ML / Pitch	Range	RU
Translational									
- Head	-0.10	(-0.9 - 2.2)	0.27	-0.19	(-1.3 - 1.0)	0.28	0.04	(-0.7 - 1.3)	0.30
- Thoracic	-0.07	(-0.9 - 2.4)	0.28	-0.08	(-0.9 - 0.8)	0.25	0.13	(-0.4 - 1.0)	0.29
- Lumbal	0.07	(-0.9 - 2.3)	0.29	0.27	(-0.8 - 2.0)	0.34	0.03	(-0.9 - 1.1)	0.33
Rotational									
- Head	0.03	(-2.5 - 2.7)	0.68	-0.04	(-1.9 - 3.6)	0.56	-0.38	(-5.4 - 3.8)	1.12
- Thoracic	0.02	(-3.6 - 2.0)	0.66	0.04	(-3.1 - 3.1)	0.40	0.68	(-0.8 - 3.7)	0.61
- Lumbal	-0.05	(-4.8 - 4.3)	0.60	0.00	(-2.1 - 3.3)	1.20	0.03	(-3.9 - 1.4)	0.66

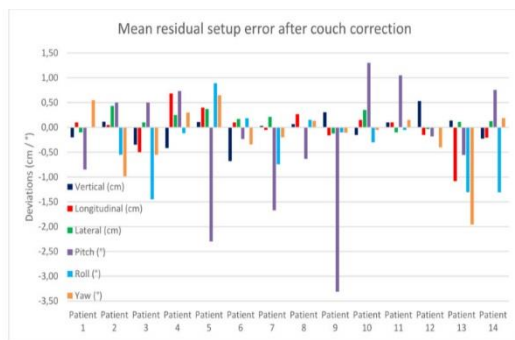


**Figure 1:** The mean residual setup error in 6 degrees of freedom for each patient after couch correction. Vertical describes the anteroposterior, longitudinal the superior-inferior and lateral the medial-lateral.

## Conclusion

Daily IGRT is the superior choice for pediatric CSI patients. However, following an IGRT-protocol is no insurance for a satisfactory alignment when only a 3 DoF couch is applied. There are still quite large residual errors some of which are the result of multiple isocenters and narrow field junctions even if a 6 DoF couch shift would be applied.

**PO-0991** A decision-support tool to select patients who may benefit from online adaptation in pancreatic SBRT  
 A. Magallón Baro<sup>1</sup>, P.V. Granton<sup>1</sup>, M.T.W. Milder<sup>1</sup>, M. Loi<sup>1</sup>, A.G. Zolnay<sup>1</sup>, J.J. Nuytens<sup>1</sup>, M.S. Hoogeman<sup>1</sup>  
<sup>1</sup>Erasmus MC Cancer Institute, Radiotherapy, Rotterdam, The Netherlands

## Purpose or Objective

At our institution, patients with Locally Advanced Pancreatic cancer (LAPC) responding to chemotherapy undergo SBRT on the Cyberknife using respiratory tracking via fiducial markers. SBRT plans exhibit conformal dose distributions with high dose gradients, sculpted to the anatomy of the planning CT scan (pCT) to protect the surrounding organs-at-risk (OAR). These OARs (stomach, duodenum and bowel) are also prone to receive additional dose due to daily anatomical variations that can result in dose-constraints violations. In our previous work, we developed a population-based motion model, which using principal component analysis, extracted common geometric variation patterns from a cohort of LAPC patients. Based on this model, we developed a tool to identify which LAPC patients may be at risk of exceeding the clinical dose-constraint of V35Gy<1ml due to daily anatomical changes, and hence, that may benefit from online adaptive strategies.

## Material and Methods

A total of 130 scans were collected for 35 LAPC patients, including the pCT scan and ideally 3 pre-fraction in-room CT scans (FxCT). The tool was validated by following a leave-one-out approach: each patient was tested on a model trained with the variations observed in the

remaining 34 subjects. For each case, the OAR pCT contours were registered non-rigidly to the model, which was used to sample N (~5000) random OAR deformations. The pCT dose volume was sampled inside each simulated organ yielding DVHs for each OAR. Next, we collected which percentage of simulated OAR had been detected to exceed the clinical dose-constraints on each patient. To validate the tool performance against real observed variations, simulated violation percentages were clustered in four risk groups (low risk-0/3Fx; mid-low risk-1/3Fx; mid-high risk-2/3Fx; high risk-3/3Fx) according to how many fractions exceeded the V35 when original plans were rigidly transferred to the FxCT. A threshold on each OAR was established by optimizing the discrimination of patients with higher risks.

## Results

Simulated violation percentages clustered per risk group are shown on Fig. 1. Pearson correlation coefficients of 0.5-0.8 were found between simulated risk and observed dosimetric changes, depending on the OAR. If all observed mid-high and high risk patient groups are combined into a high risk category, thresholds at 22, 57, 28% would maximally identify patients likely to violate OAR dose-constraints due to moving tissues for the simulated duodenums, stomachs and bowels; with a classification accuracy of 94, 71, 97%, respectively.

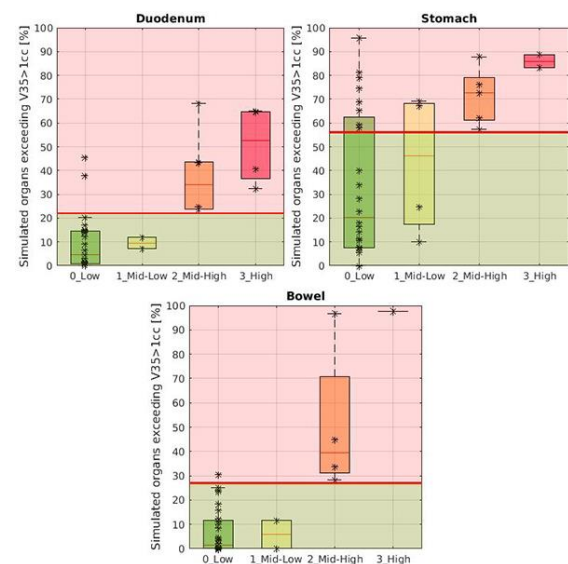


**Figure 1.** Percentage of simulated OARs exceeding the clinical dose-constraints (duodenum-upper left, stomach-upper right, bowel-bottom) clustered per risk group according to how many fractions resulted to exceed the dose-constraint in the clinic: 0/3 FxCT (low risk group), 1/3 FxCT (mid-low risk group), 2/3 FxCT (mid-high risk group), or 3/3 FxCT (high risk group). The thresholds established by the red horizontal line discriminate the patients (depicted in \*) who would be identified as mid-high or high risk (in the red region), and hence, that would be eligible for plan adaptation; against patients classified in the low or mid-low risk groups (in the green region), which would be discarded from applying this strategy.

## Conclusion

The positive relationship between the simulated probability of exceeding OAR dose tolerances and clinically observed dose-constraint violations is a promising tool to identify a high-risk patient suffering from the impact of daily variations. Established thresholds suggest patients can be stratified by making optimal use of available resources, and can prevent giving extra dose to low-risk patients not benefiting from plan adaptation.

**PO-0992** Investigating 4D Cone Beam CT reconstruction for moving targets at a scanned proton gantry system

L. Den Otter<sup>1</sup>, K. Chen<sup>2</sup>, G. Janssens<sup>3</sup>, A. Meijers<sup>1</sup>, S. Both<sup>1</sup>, J.A. Langendijk<sup>1</sup>, L.R. Rosen<sup>2</sup>, H.T. Wu<sup>2</sup>, A. Knopf<sup>1</sup>

<sup>1</sup>UMCG University Medical Center Groningen, Radiotherapy Oncology, Groningen, The Netherlands ;

<sup>2</sup>Willis-Knighton Cancer Center, Radiation Oncology, Shreveport, USA ; <sup>3</sup>Ion Beam Applications, Research and Development, Louvain-la-Neuve, Belgium

### Purpose or Objective

Scanned proton therapy is a highly conformal treatment technique and can provide increased healthy tissue sparing compared to photons or scattered protons. However, due to the time structure of the scanned beams this technique is highly sensitive to uncertainties and needs to be monitored when treating mobile tumors. Currently, only 3D Cone Beam CT (CBCT) acquisition is available on commercially available proton gantry systems. We investigate the possibility to use the same number of projections as for 3DCBCT acquisition to retrospectively reconstruct into 4D, with the goal to determine the inter-fraction tumor motion.

### Material and Methods

CBCT-projection data was acquired for eight patients at an IBA Proteus® ONE proton gantry system. Ten 4DCBCT images were reconstructed per patient. In order to compensate for the lower 4DCBCT quality due to the small amount of projections per phase, we applied a motion-aware temporal and spatial regularization method (MA-ROOSTER), by Mory *et al*<sup>1</sup>, to reconstruct with improved 4D-image quality. Corresponding 3DCBCT images were reconstructed using the conventional Feldkamp-Davis-Kress (FDK) algorithm. After importing the 4D-images into RayStation, the gross tumor volumes were deformably warped (ANACONDA algorithm) and centroid positions determined to calculate the 3D-vector motion[OLd(1)]. The contrast-to-noise ratio between tumor and lung tissue for the 4DCBCT images was calculated. Additionally, the structural similarity index (SSIM) between the 3DCBCT and 4DCBCT images were calculated to compare the quality of 3DCBCT vs. 4DCBCT images.

### Results

Figure 1 shows one phase of the reconstructed 4DCBCT images for three patients compared to 3DCBCTs. For the 4DCBCT images more noise is observed, and increased blurriness of anatomical features with more clearly present streak artefacts for some of the patients. Nevertheless, the tumor is visible and can be delineated to evaluate its motion. Table 1 shows the calculated 3D-vector centroid motion, the CNR, and SSIM for the 4DCBCT images. In all 8 patients motion variations could be tracked within all available ten scans. The CNR showed varying results for the different patients, confirming the observed variations in image quality when visually evaluating the reconstructed 4DCBCTs. The quality of the 4D-images according to the SSIM was around 30% of the 3DCBCT images (SSIM ~0.30).

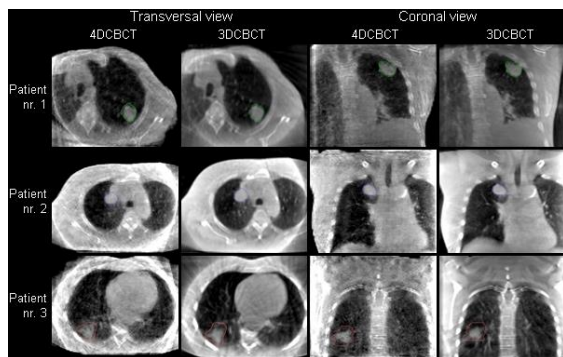


**Figure 1.** Transversal and coronal views of the reconstructed images in 3D and 4D (one phase) and the visual differences in image quality. The colored region in each image represents the tumor.

**Table 1.** Measured centroid motion of reconstructed 4DCBCT images and quality measure results of the contrast between tumor and lung tissue and differences in quality between 3DCBCT images and 4DCBCT images.

	Centroid motion (mm)	CNR (↑ better ratio)	SSIM (0-1)
		Median (range)	
Patient nr. 1	2.30 (1.19 - 3.89)	2.42 (1.68 - 3.02)	0.30 (0.25 - 0.34)
Patient nr. 2	2.42 (1.93 - 2.91)	2.20 (2.00 - 2.49)	0.34 (0.30 - 0.43)
Patient nr. 3	3.52 (2.27 - 4.60)	1.30 (0.76 - 2.45)	0.30 (0.21 - 0.32)
Patient nr. 4	1.43 (0.75 - 2.66)	2.47 (0.51 - 3.28)	0.24 (0.22 - 0.30)
Patient nr. 5	2.66 (1.90 - 3.54)	1.93 (1.74 - 2.17)	0.29 (0.17 - 0.31)
Patient nr. 6	1.49 (0.91 - 4.43)	2.96 (2.32 - 4.40)	0.30 (0.21 - 0.32)
Patient nr. 7	0.44 (0.14 - 2.00)	4.14 (1.62 - 5.11)	0.38 (0.21 - 0.40)
Patient nr. 8	0.69 (0.60 - 1.28)	3.54 (2.92 - 5.19)	0.30 (0.24 - 0.32)

Abbreviations: CNR = contrast-to-noise ratio

SSIM = structural similarity index ('1' represents identical images).

### Conclusion

It is possible to reconstruct 4DCBCT images with sufficient quality for tumor motion evaluation using the MA-ROOSTER algorithm. This is an important step towards an image guided adaptive proton therapy workflow for treating moving targets, however further work is warranted to improve 4DCBCT image quality.

### PO-0993 Uncertainty estimation of dose accumulation with deformable image registration in head and neck region

T. Kanehira<sup>1</sup>, S. Kranen<sup>1</sup>, J. Sonke<sup>1</sup>

<sup>1</sup>The Netherlands Cancer Institute, Radiation Oncology, Amsterdam, The Netherlands

### Purpose or Objective

The delivered dose distribution typically deviates from planned dose due to anatomical changes. Dose accumulation estimates the delivered dose over fractions using deformable image registration (DIR) to take anatomical changes into account. Registration errors, however, introduce an uncertainty in the dose mapping. This study estimates the uncertainty in the accumulated dose and compares it with differences between planned and accumulated dose for head & neck cancer (HNC) patients.

### Material and Methods

In this study, five HNC patients were included with a prescribed dose of 70 Gy in 35 fractions. Patients were positioned with daily CBCT guidance and received a repeat CT (rCT) mid-treatment for adaptive re-planning. CBCT-to-CT DIR was performed using an in-house implementation of bSpline deformations. To estimate the spatial uncertainty of the DIR, a modified version of the distance concordance metric (DDM) was implemented [1]. To that end, the deformable vector fields (DVF) deforming the plan CT (pCT) to the daily CBCT and the daily CBCT to the rCT were concatenated. Subsequently, the DDM for each voxel of the pCT was calculated as the standard deviation (SD) in all three directions over the typically 34 DVFs (we did not use the daily CBCT which was acquired on the same day as rCT) divided by the square root of 2. DDM was restricted to voxels within the patient external. To estimate accumulated dose, assuming the DIR uncertainty followed Gaussian distribution which had a SD of the DDM, we calculated the average dose over 35 samples from a 3D Gaussian distribution around each voxel. This was repeated 1000 times to calculate a confident interval of the accumulated dose. The dose uncertainty was calculated as a 95% confident interval (dose-CI) and any difference exceeding this dose-CI was considered as a true anatomical induced dose difference. For each patient, we calculated the accumulated dose, difference with planned dose ( $\Delta D$ , accumulated-planned), dose-CI, and the percentage of voxels with  $\Delta D$  exceeding the dose-CI.

### Results

DDM was larger in soft tissues and close to the field-of-view borders (Figure 1): median of 0.07 cm and 95<sup>th</sup> percentile of 0.37 cm within the external contour. These

registration uncertainties led to a median and 95<sup>th</sup> percentile dose-Cl of 0.0 Gy and 0.8 Gy, which were smaller than those of the difference between planned and accumulated dose: 1.1 Gy and 6.9 Gy respectively. The percentage of the voxels where the  $\Delta D$  was outside of the dose-Cl was 97.7 % (Figure 2).

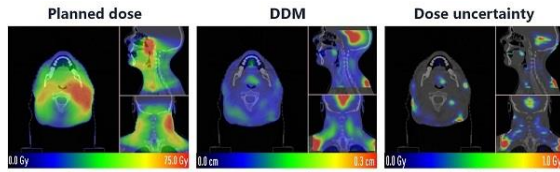


Figure 1. planned dose, DDM, and dose uncertainty for one of the patients. The left image shows the planned dose. The middle is the distribution of the norm of DDM. The right is the distribution of the width of the 95% confident interval of the dose uncertainty.

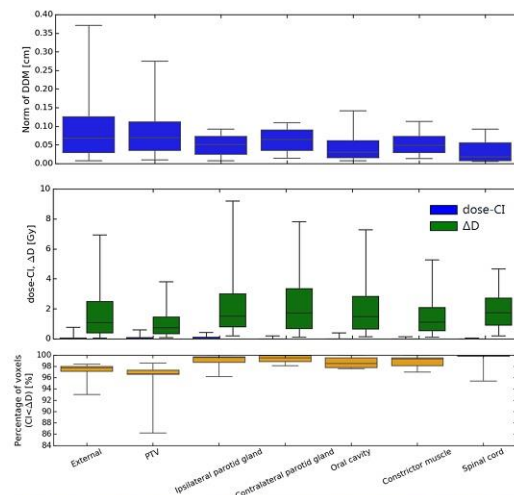


Figure 2. Boxplots of the norm of DDM and 95% confident interval of the dose uncertainty (dose-Cl), and differences between planned and accumulated dose ( $\Delta D$ ) and the percentage of the voxels with the  $\Delta D$  exceeding the dose-Cl for five patients. The box of the boxplots shows the interquartile, and the whisker shows 5/95 percentile for the top and middle boxplots and the minimum/maximum for the bottom.

## Conclusion

Small dose uncertainties were found. In the majority of voxels the uncertainties were smaller than the difference between planned and accumulated dose. This implies that DIR is sufficiently accurate to observe relevant changes in accumulated dose during treatments.

## PO-0994 Registration accuracy of 4D-MRI in lung acquired on the MR-linac

M. Rossi<sup>1</sup>, M. Fast<sup>1</sup>, T. Van de Lndt<sup>1</sup>, M. Nowee<sup>1</sup>, J. Belderbos<sup>1</sup>, F. Lalezari<sup>2</sup>, J. Sonke<sup>1</sup>

<sup>1</sup>Netherlands Cancer Institute, Radiotherapy Department, Amsterdam, The Netherlands ;

<sup>2</sup>Netherlands Cancer Institute, Radiology Department, Amsterdam, The Netherlands

## Purpose or Objective

Differential motion between the primary tumor and mediastinal lymph nodes requires considerable safety margins in locally advanced lung cancer patients. The Unity MR-linac (Elekta AB, Stockholm, Sweden) provides high soft-tissue contrast and thus the potential to adapt the treatment plan to account for such differential motion. We recently have developed a self-sorting 4D-MRI method for daily IGRT of liver patients. The aim of this study was to determine the registration accuracy in 4D-MRI scans of NSCLC lung patients acquired on the MR-Linac.

## Material and Methods

Six stage III NSCLC patients, receiving weekly 4D-MRI scans on the MR-linac were included in this study. Patients were treated on a conventional linac to a dose of 24x2.75 Gy.

To quantify local rigid registration accuracy, the first, third and last scans per patient were processed in a full circle method<sup>1</sup>. The 4D reconstructions of these scans were made with an in-house developed coronal 4D-MRI sequence. This is based on retrospective image sorting of 30 repetitions of a multi-slice turbo-spin echo acquisition with an image resolution of 2x2x5 mm<sup>3</sup>. The full circle either consisted of the mid-position planning CT(pCT) and two 4D-MRI scans or alternatively, the pCT was replaced by the mid-ventilation of the first 4D-MRI scan. A shaped region of interest of the primary tumour and of each individual lymph node was used for local rigid registration in both procedures. From the values obtained from the full circle method in each patient, the mean and SD were divided by  $\sqrt{3}$  to correct for the 3 registration steps in the circle. Patient characteristics were analyzed.

## Results

4D-MRI acquisition took about 4 minutes and showed adequate image quality (fig. 1) for 5 out of 6 patients. For the remaining 5 patients, all tumours were in the upper lobes and the average peak to peak amplitude of the primary tumour derived from the 4D-CT was 0.2, 0.4 and 0.2 cm in left/right, cranial/caudal and anterior/posterior respectively. The median GTV of the primary tumour was 88.3 cc and median GTV lymph nodes 49.9 cc. The corrected absolute mean of circle residuals was <0.11 cm for both primary tumor and lymph nodes in both methods. The corrected standard deviations are shown in table 1<sup>(1,2)</sup>.

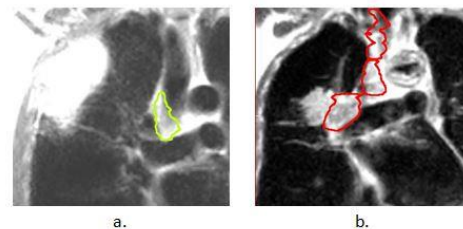


Fig. 1 a and b. a) 4D-MRI of lung showing primary tumour and lymph node 4R (in green) and b) 4D-MRI of lung showing lymph nodes 2R, 4R and 10R (in red)

Table 1. Registration inaccuracy in 4DMRI registration of MRI to pCT and MRI to MRI for primary tumour and lymph nodes calculated using the full circle method<sup>1,2</sup>

	Left/Right (cm)	Cranial/Caudal (cm)	Anterior/Posterior (cm)
Registration inaccuracy MRI to pCT			
Primary tumour	0.19	0.12	0.12
Lymph nodes	0.08	0.14	0.17
Registration inaccuracy MRI to MRI			
Primary tumour	0.08	0.15	0.10
Lymph nodes	0.12	0.17	0.10

## Conclusion

4D-MRI registration of primary tumor and lymph nodes seems feasible on the MR-Linac with local rigid registration inaccuracies <0.2 cm facilitating daily online IGRT for locally advanced lung cancer patients. Registration accuracy potentially increases following further optimization of 4D-MRI contrast and image resolution tailored to lung cancer patients.

<sup>1</sup>van Herk M et al. Med Phys 25:2054-2067, 1998

<sup>2</sup>Schaake et al. IJROBP 2014 Nov 15 90(4) 959-66

## PO-0995 An extension of van Herk's margin recipe to explicitly account for time trends in tumor set-up.

M. Giżyńska<sup>1,2</sup>, B. Heijmen<sup>3</sup>, P. Kukołowicz<sup>1</sup>

<sup>1</sup>Maria Skłodowska-Curie Memorial Cancer Center and Institute of Oncology, Medical Physics Department, Warsaw, Poland ; <sup>2</sup>University of Warsaw Faculty of Physics, Department of Biomedical Physics, Warsaw, Poland ; <sup>3</sup>Erasmus MC University Medical Center Rotterdam, Department of Oncology, Rotterdam, The Netherlands

## Purpose or Objective

The most applied CTV-PTV margin recipe is that proposed by van Herk et al.:  $M=2.5\sigma + 0.7\sigma$ , where  $\Sigma$  and  $\sigma$  describe

systematic and random setup errors [1]. This recipe does not explicitly account for interfraction time trends in tumor set-up, while such trends are observed for various tumor sites. In this work we propose 1) a novel characterization of set-up errors in a patient population with time trends, and 2) a margin recipe explicitly accounting for trends. The proposed formalism was evaluated for a large database of prostate cancer patients with time trends.

### Material and Methods

The database contains daily set-up errors of 839 prostate cancer patients, measured in their 39 treatment fractions using implanted gold fiducials.

Errors in a patient population with time trends are described by normal distributions characterized by  $\Sigma$ ,  $\alpha$  and  $\sigma'$ , with  $\alpha$  the standard deviation of observed time trend slopes (mm/fraction) in the population and  $\sigma'$  describing the true random errors, i.e. errors relative to the patient's trend line. Figure 1 shows the set-up errors for a single database patient with a time trend. For the analyzed database, population parameters were:  $\Sigma = [2.5, 3.4, 3.5]$  mm,  $\alpha = [-0.05, 0.07, 0.08]$  mm/fraction, and  $\sigma' = [1.9, 2.5, 2.6]$  mm for left-right, superior-inferior and anterior-posterior direction respectively.

Like in [1], the margin component for the random errors is given by  $0.7\sigma'$ . Similar to [1], we require for the margin component for the remaining errors (systematic and time trend errors) that 90% of the patients should be within the margin. The maximum set-up deviation during fractionated treatment,  $MD$ , of a patient with systematic set-up error,  $m$ , and time trend slope  $a$  is given by  $MD = |m| + 0.5(F-1)|a|$ , with  $F$  the total number of fractions (Fig. 1). To establish the required margin, the  $MD$  distribution is first determined by random sampling from the  $m$  and  $a$  distributions ( $10^7$  samples). The margin is then determined as the 90% cut-off point in the distribution. For validation of the novel margin recipe and for comparison with van Herk's recipe we established for both recipes the percentage of patients outside the margin. That was done with the ellipsoid test where we looked for patients not fulfilling  $\sum_i (MD_i/M_i)^2$  (with  $i$  denoting direction and  $M$  - margin size).

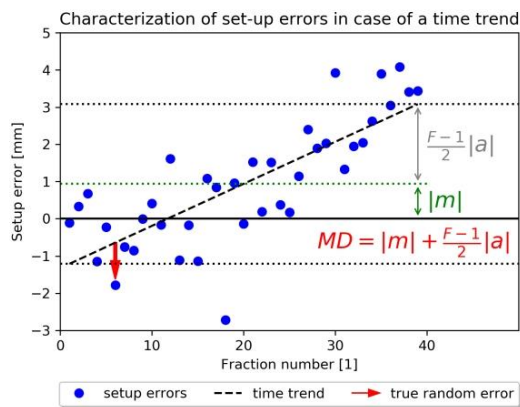


Figure 1. Maximum Deviation  $MD$  is derived from the middle position  $m$  and time trend slope  $a$  with the total number of fractions  $F$ .

### Results

For the prostate database, margins calculated with van Herk's recipe were 1-2mm smaller than those established with the novel recipe (Table 1). The percentage of patients outside the novel margin was 9.8% (compared to 10% expected), while for van Herk's margin this was almost 26%.

	Van Herk Approach	Time Trend Approach
Left-Right margin [mm]	6.3 (7.6)	7.6 (8.9)
Superior-Inferior margin [mm]	8.5 (10.2)	10.9 (12.7)
Anterior-Posterior margin [mm]	8.8 (10.6)	11.0 (12.9)
Percentage of patients outside	25.9%	9.8%

Table 1. Comparison of margins for three directions for the clinical database. Margins in brackets include the random error component given as  $0.7\sigma'$ . Percentage of patients outside the margin is calculated for the systematic margin component.

### Conclusion

Van Herk's CTV-PTV margin is not sufficient in case of time trends. We have proposed an extended recipe to fulfill the requirement that 90% of patients would indeed be irradiated with the prescribed dose when time trends are present. In case of no time trends, the modified recipe simplifies to van Herk's formula.

[1] van Herk et al., IJROBP 2000, Volume 47, Issue 4, Pages 1121-1135

### PO-0996 A knowledge-based tool to estimate the gain of re-planning strategy for Head and Neck (HN) ART

E. Cagni<sup>1</sup>, A. Botti<sup>1</sup>, M. Orlandi<sup>1</sup>, R. Sghedoni<sup>1</sup>, E. Spezi<sup>2</sup>, M. Iori<sup>1</sup>

<sup>1</sup>Azienda USL-IRCCS di Reggio Emilia, Medical Physics Unit, Reggio Emilia, Italy; <sup>2</sup>Cardiff University, School of Engineering, Cardiff, United Kingdom

### Purpose or Objective

This study aimed to investigate if a commercial knowledge-based tool for radiotherapy planning, RapidPlan (RP) (Varian Medical System, Palo Alto, CA), can be used to estimate the potential organ at risks (OARs) sparing in re-planning strategy for HN ART.

### Material and Methods

A database of 45 HN VMAT plans, were used as training set for RP model. A second evaluation set, of 10 advanced oropharyngeal HN patients were randomly selected from the department database. All VMAT plans in the evaluation set were generated by means of RP module to treat 3 targets at dose levels of 69.96Gy/59.4Gy/54.12 Gy in 33 fractions using a SIB technique.

For each evaluation patient 2 CBCTs were extracted corresponded to 16th and the 26th fraction. In Velocity AI v.3.2 (Varian Medical System), the planning CT was registered with each CBCT using deformable registration algorithm, generating an Adaptive CT (ART-CT). For each ART-CT, the plan was re-calculated in Eclipse (delivered DVH) and RP predictions (RP DVH) were performed.

The gain of the re-planning was evaluated by comparing RP DVH with the delivered DVH for left and right parotid glands (PG), spinal cord and oral cavity. As a surrogate for the RP DVH we considered the line running in the middle of the predicted range. The restricted sum of the residuals (RSR) [Appenzoller et al. Med Phys. 2012] is used to measure the discrepancy between DVHs. To evaluate the feasibility of the method, the range of RP DVH estimations (RP uncertainties) were compared with the gain of the re-planning. The absolute sum of residual (ASR), considering both positive and negative difference in the sum, was used for this analysis. Wilcoxon signed rank were used as statistical test.

### Results

The RP model showed an average chi square of  $1.06 \pm 0.04$  and coefficient of determination of  $0.51 \pm 0.11$ . Numerical values of RSR, that quantified the gain of re-planning, were reported in Table 1. The overall RSR (mean $\pm$ 1std), for all patient and both fractions, resulted  $2.8 \pm 2.9$  Gy,  $2.6 \pm 2.7$  Gy,  $2.7 \pm 2.8$  Gy for spinal cord, left and right PG and oral cavity respectively. For 95% of the cases,

RP predicted a gain in the re-planning (RSR>0). No statistically difference resulted in RSR values between the 2 fractions (p=0.82).

	fraction #16 RSR (Gy)									
	patient number									
spinal cord	1.1	2.5	0.0	7.1	8.7	3.6	2.5	1.4	4.4	3.9
left PG	2.0	4.4	0.5	1.6	4.4	0.6	0.1	0.0	0.0	0.4
right PG	4.6	5.5	0.0	1.2	2.7	0.4	0.1	0.9	0.0	6.7
oral cavity	0.3	7.5	0.0	0.0	3.5	0.1	0.1	0.0	0.0	5.5

	fraction #26 RSR (Gy)									
	patient number									
spinal cord	0.9	1.1	0.0	7.2	8.1	3.1	2.2	1.3	0.0	3.6
left PG	4.0	2.6	0.5	3.2	1.7	0.7	2.0	0.0	0.7	4.6
right PG	5.8	1.1	0.1	1.7	1.0	0.9	1.8	0.6	0.0	7.8
oral cavity	1.3	5.7	0.0	0.4	3.3	0.1	0.2	0.0	0.0	5.3

Table 1 RSR values between delivered DVH and RP DVH that represent the gain of re-planning for spinal cord, left and right PG and oral cavity.

RP prediction uncertainties (RP bound ASR) resulted higher than the gain of re-planning (delivered- RP ASR), as is showed in Figure 1 by means of a correlation graph.. Statistical test confirmed this result (p<0.01)

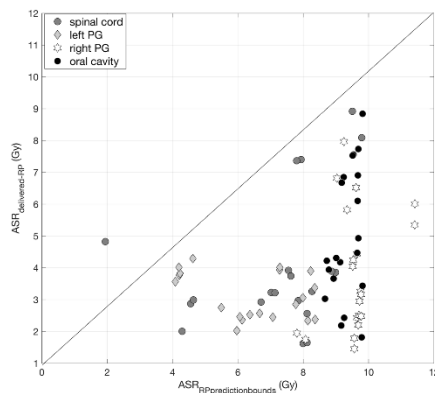


Figure 1 correlation graph, in term of ASR (Gy), between RP prediction uncertainties and the gain of re-planning (delivered - RP differences).

## Conclusion

In this study we have investigate the feasibility to use RP to estimate the potential gain of re-planning strategy for HN ART. Based on the analysis, DVHs predicted by RP can be used to estimate the potential OARs sparing when a new plan is performed. This information could be useful to assess the trigger point for a re-planning strategy. However, we found clinically relevant inaccuracies in RP predictions that limitate its application to HN ART. Therefore, further work is ongoing on RP model accuracy improvement.

## PO-0997 A Synthetic Generative Adversarial Network for Semantic Lung Tumor Segmentation

V. Kearney<sup>1</sup>, J.W. Chan<sup>1</sup>, S. Haaf<sup>1</sup>, S.S. Yom<sup>1</sup>, T. Solberg<sup>1</sup>  
<sup>1</sup>University of California UCSF, department of radiation oncology, San Francisco CA, USA

### Purpose or Objective

To demonstrate the feasibility of a novel generative adversarial network (GAN) for synthetic abnormal pulmonary CT generation and semantic lung tumor segmentation.

### Material and Methods

A 3D translational conditional GAN was implemented for synthetic image generation (label-to-CT) and segmentation (CT-to-label). Prior to synthetic image generation, a CT-to-label generator is given a CT image and trained to produce a binary mask of the left lung, right lung, heart, esophagus, spinal cord, and internal airways; a discriminator is trained to distinguish between “real” labels and synthetically generated “fake” labels. Once the network is conditioned, the label-to-CT synthetic image generator is trained by reversing the CT-to-label network and training the discriminator to perform the inverse task. The label-to-CT GAN is trained to generate arbitrary

abnormal pulmonary CTs with various tumor characteristics, which are used for synthetic data augmentation. A final CT-to-label GAN is trained to generate binary tumor masks from a 4 to 1 mixture of synthetic and real pulmonary CTs for 200 epochs, and fine-tuned for 20 epochs on real pulmonary CTs. Figure 1 shows the generator and discriminator components for all three GAN models. 208 stage I or stage II lung tumor patients previously treated with radiotherapy were used in this study. Patients with segmented hilar nodes were not included in this study. All algorithms were trained and hyperparameter tuned using 80% of the patients, and the remaining 20% were used to report final performance metrics. All models were distributed across two Nvidia V100 GPUs, and due to memory limitations, all images were resampled to 3x3x3 mm<sup>3</sup> and cropped to 128x128x64 voxels. To evaluate segmentation performance, all images were rescaled to their original dimensionality.

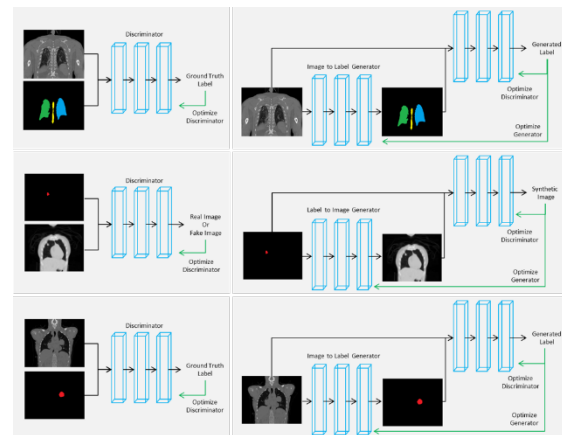


Figure 1. The preliminary GAN training workflow is shown for CT-to-label training of organs at risk (top). The label-to-CT workflow is shown which takes a binary tumor mask and generates arbitrary abnormal synthetic pulmonary CT variations (middle). The final CT-to-label GAN model is shown that generates realistic tumor masks given a CT image (bottom).

## Results

The synthetic GAN model (synthetic-GAN) was compared to a GAN model (real-GAN) and V-Net model (real-VNet) using only traditional data augmentation (rotation, random cropping, elastic deformation, and translation). Among the 20 patients analyzed, the average dice scores and standard deviations were  $0.82 \pm 0.15$ ,  $0.71 \pm 0.18$ , and  $0.69 \pm 0.16$  for synthetic-GAN, real-GAN, and real-VNet respectively.

## Conclusion

A synthetic conditional generative adversarial network was implemented that outperforms current state-of-the-art segmentation techniques for lung tumor segmentation. Furthermore, synthetically generated abnormal pulmonary images do not contain patient sensitive information and could be widely distributed to enhance cross institutional generalization.

## PO-0998 Setup and range robustness recipes for skull-base meningioma IMPT using Polynomial Chaos Expansion

C. Ter Haar<sup>1,2</sup>, S. Habraken<sup>2,3</sup>, D. Lathouwers<sup>1</sup>, R. Wiggenraad<sup>3,4</sup>, S. Krol<sup>3,5</sup>, Z. Perkó<sup>1</sup>, M. Hoogeman<sup>2,3</sup>  
<sup>1</sup>Delft University of Technology, Radiation Science & Technology, Delft, The Netherlands ; <sup>2</sup>Erasmus Medical Center Cancer Institute, Radiation Oncology, Rotterdam, The Netherlands ; <sup>3</sup>Holland Proton Therapy Center, Radiation Oncology, Delft, The Netherlands ; <sup>4</sup>Haaglanden Medical Center, Radiation Oncology, Leidschendam, The Netherlands ; <sup>5</sup>Leiden University

Medical Center, Radiation Oncology, Leiden, The Netherlands

### Purpose or Objective

To determine setup and range robustness settings for IMPT planning required to achieve a D98%-CTV of 95% of the prescribed dose in fractionated treatments in 98% of skull-base meningioma patients, for given systematic and random setup errors and systematic relative stopping-power prediction (range) errors.

### Material and Methods

Robust treatment plans to 50.4 Gy in 28 fractions were made for 9 patients using in-house developed software for multi-criteria optimization of treatment plans. Setup robustness settings from 0 to 5mm and relative range robustness settings from 0 to 5% were used in minimax robust optimization with 9 error scenarios: the nominal scenario, 6 shifted setup scenarios and 2 scenarios with range errors.

Polynomial Chaos Expansion (PCE) was applied to model the impact of setup and range uncertainties on dose. PCE provides a computationally efficient metamodel of the voxel doses. Normal distributions were assumed, and setup and range uncertainties were modeled as rigid shifts and scaling of CT values respectively. PCE was validated for beam and couch angles used in clinical IMPT planning on an independent dataset for the same treatment site. Required range and setup robustness settings were determined in two steps. First, the range uncertainty leading to adequate target and population coverage was determined for various range robustness settings and no setup robustness. To this end, a PCE for range uncertainties was constructed to simulate and evaluate 100.000 complete fractionated treatments. Subsequently, random and systematic setup uncertainties for given setup and range robustness settings were determined in the same fashion. All plans were scaled such that, in the worst optimization scenario, the D98%-CTV was equal to 95% of the prescribed dose. Final results were based on the worst performing patient and validated on the others.

### Results

Scaling all plans to the same target dose in the worst optimization scenario reduced the population variation of the D98%-CTV due to inter-patient variability from 2% to 0.4%. We found a linear relationship between range robustness (RR) and the actual range uncertainty ( $\rho$ ), see Fig. 1. The relationship between random ( $\sigma$ ) and systematic ( $\Sigma$ ) setup errors that just can be dealt with for given setup robustness (SR, different colors) is shown in Fig. 2. Nearby points of the same color correspond to different range uncertainties (and the corresponding range robustness from Fig. 1). The dashed line and curves are fits to the data points.

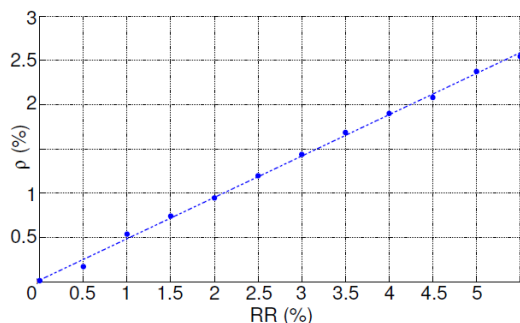


Figure 1: Required range robustness for varying range error.

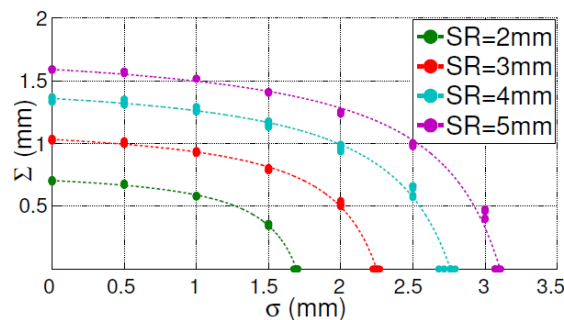


Figure 2: Random and systematic setup and range errors leading to adequate target and population coverage.

### Conclusion

With a population coverage of 98%, the required range robustness for range errors from 0 to 5mm is a factor 2 higher than the actual range error. Interference of setup and range error is negligible, and the required setup robustness does not depend on range robustness.

### Poster: Physics track: Quantitative functional and biological imaging

#### PO-0999 Functional Avoidance planning allows for lung dose reduction in radiotherapy of lung cancer

K. Farr<sup>1</sup>, K. West<sup>1</sup>, R. Yeghiaian-Alvandi<sup>1</sup>, D. Farlow<sup>2</sup>, R. Stensmyr<sup>3</sup>, A. Chicco<sup>2</sup>, E. Hau<sup>1,4,5</sup>

<sup>1</sup>Crown Princess Mary Cancer Centre- Westmead Hospital, Department of Radiation Oncology, Sydney West Radiation Oncology Network- Sydney, Australia ; <sup>2</sup>Westmead Hospital, Department of Nuclear Medicine-PET and Ultrasound, Sydney, Australia ; <sup>3</sup>Crown Princess Mary Cancer Centre- Westmead Hospital, Department of Medical Physics, Sydney West Radiation Oncology Network- Sydney, Australia ; <sup>4</sup>University of Sydney, Faculty of Medicine and Health, Sydney, Australia ; <sup>5</sup>Blacktown Hospital- Sydney West Radiation Oncology Network, Department of Radiation Oncology, Sydney, Australia

### Purpose or Objective

To evaluate the feasibility of functional avoidance radiotherapy planning for the definitive treatment of lung cancer. To characterize the achievable dosimetry of target and normal tissues of functional image-guided dose redistribution.

### Material and Methods

In all 15 consecutive patients with locally advanced non-small cell lung cancer (NSCLC) were included prospectively. Patients were planned to receive definitive (chemo)-radiation therapy (RT) of minimum 60 Gy. Perfusion SPECT/CT were performed prior to RT commencing. Functional lung, identified as 20-80% subvolumes of the maximum perfusion count (FL20-80), was segmented on SPECT/CT, and registered to planning CT. Two plans were optimized: 1) a reference CT-plan, blinded for functional structures, and 2) functional avoidance SPECT-plan, imposing higher priority on functional levels. The objective was to reduce dose to the highly perfused lung subvolumes without compromising PTV coverage, and respecting dose to other organs at risk (OAR) within the predefined constraints. Based on our previous study, dose constraint of 16 Gy to the FL40 sub volume, was used in functional dose planning to reduce the risk of radiation pneumonitis. For each patient a 3D-conformal, intensity modulated (IMRT) and volumetric arc (VMAT) plans were created for both reference and functional avoidance. In all six plans were produced per patient. Anatomical versus functional dose-volume parameters for functional lung subvolumes, and other OAR

were compared, as well as PTV coverage. All patients' treatment plans were delivered without the use of functional information.

### Results

Majority of patients had stage III disease (67%). Preliminary analysis of first eight patients showed the mean PTV volume of 375 cc, anatomical lung volume of 3595 cc. The mean volume for FL40 was 1144 cc. The ratio of functional lung to anatomical lung volume was 0.32. There was weak correlation between anatomical lung and FL volumes within patients (Pearson  $r=0.2$ ), due to perfusion defects variations (tumour, emphysema). The largest dose reduction was achieved with IMRT plans (Figure 1). Plans optimised to FL subvolumes resulted in a significant dose reduction by a mean of 2.1 Gy (20.2%) to the highest functional subvolume FL80 (CI 0.4-3.9  $p=0.02$ ). Dose reduction to FL40 and FL60 was 1.6 Gy (CI 0.6-2.7) and 1.5 Gy respectively (CI 0.3-2.8  $p=0.02$ ). Functional V20 improved by 5.4% (CI 1-10  $p=0.03$ ). Max dose to OAR (heart, oesophagus and spinal cord) and PTV coverage were not significantly different between plans. Detailed analysis of the whole patient cohort is underway.

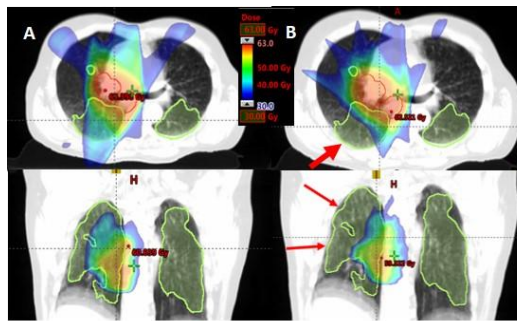


Figure 1. Differences in dose distribution with IMRT plan optimised to anatomical lung contour (A) and functional avoidance plan (B) optimised to FL40 sub volume, with FL40 volume spared for radiation dose as a result (arrows). CTV in red, FL40 in lime, dose in colour wash.

### Conclusion

Functional avoidance planning optimised to perfused lung volumes identified with SPECT resulted in improved dose volumetric outcomes for functional lung. This methodology may lead to potential reduction in radiation-induced lung toxicity in patients treated with definitive lung RT, and subsequently offers potential for target dose escalation.

### PO-1000 Vascular responses in normal brain tissue after combined immunotherapy and SRS to brain metastases

L. Nilsen<sup>1</sup>, E. Grøvik<sup>2</sup>, I. Digernes<sup>2</sup>, C. Saxhaug<sup>3</sup>, A. Latysheva<sup>4</sup>, O. Geier<sup>2</sup>, T.P. Hellebust<sup>5</sup>, D.O. Sætre<sup>6</sup>, B. Breivik<sup>7</sup>, K.D. Jacobsen<sup>8</sup>, Å. Helland<sup>8</sup>, K.E. Emblem<sup>2</sup>  
<sup>1</sup>Oslo University Hospital, Diagnostic Physics, Asker, Norway ; <sup>2</sup>Oslo University Hospital, Diagnostic Physics, Oslo, Norway ; <sup>3</sup>Oslo University Hospital, Radiology and Nuclear Medicine, Oslo, Norway ; <sup>4</sup>Oslo University Hospital, Radiology and Nuclear Medicine, Oslo, Norway ; <sup>5</sup>Oslo University Hospital, Medical Physics, Oslo, Norway ; <sup>6</sup>Østfold Hospital Trust, Radiology, Kalnes, Norway ; <sup>7</sup>Hospital of Southern Norway, Radiology, Kristiansand, Norway ; <sup>8</sup>Oslo University Hospital, Oncology, Oslo, Norway

### Purpose or Objective

Stereotactic radiosurgery (SRS) is a well-established treatment option for patients with brain metastases. Over the past few years, there has been a rapid increase in the additional use of immunotherapy. At present, there is limited understanding of the mechanisms behind the combined effects of immunotherapy and SRS. Our aim is to provide deeper insight into vascular responses of peri-

tumoral- and normal appearing brain tissue after combined immunotherapy and SRS.

### Material and Methods

Twenty-eight patients from our on-going prospective observational imaging study (*clinicaltrials.gov Identifier: NCT03458455*), with a total of 37 brain metastases from non-small cell lung cancer (N=14, n=17) or malignant melanoma (N=14, n=20), have so far been included. All patients received linear accelerator-based SRS (15-27Gy). The dose was prescribed to cover at least 99% of the PTV; contrast enhancing tumor on T1w post-contrast MRI+2 mm isotropic margin. The imaging protocol included pre-SRS MRIs and follow-up MRIs every third month for one year. Six patients (5 melanomas, 1 lung) received immunotherapy before and after SRS, and five patients (2 melanomas, 3 lung) started immunotherapy within 6 months post-SRS. Immunotherapy, pembrolizumab (2mg/kg) or ipilimumab (3mg/kg), or a combination, was given every third week. Relative cerebral vessel calibers (rVSI), and relative blood volume (rCBV) from micro- (spin echo) and macrovasculature (gradient echo), were calculated from perfusion MRI and Vessel Architectural Imaging. All values were normalized to normal appearing white matter receiving less than 2Gy. Normal brain tissue was defined as white- and gray-matter segmented from T1w pre-contrast images in SPM12 (Matlab), excluding tumor and edema which were drawn by experienced neuroradiologists. The normal appearing brain tissue was divided into five ROIs according to doses: >0-2Gy, 2->5Gy, 5->10Gy, 10->15Gy and >15Gy (peri-tumoral region) (Fig.1).

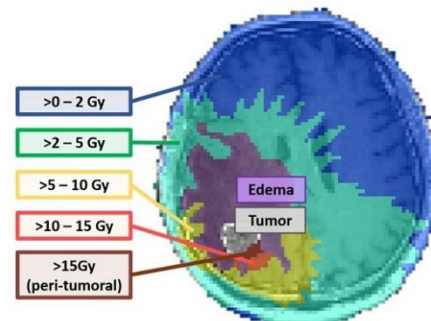
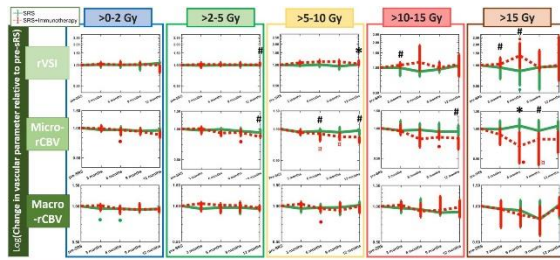


Fig. 1: The SRS dose distribution was divided into five distinct ROIs within normal appearing brain tissue (gray + white matter, excluding edema and tumor): >0-2Gy (blue overlay), >2-5Gy (green overlay), >5-10Gy (yellow overlay), >10-15Gy (orange overlay), and >15Gy; peri-tumoral region (brown overlay), excluding tumor and edema (purple overlay).

### Results

Before SRS, there were no significant differences in rVSI or micro- and macrovascular rCBV between the two treatment groups in any of the dose-level ROIs (Fig.2). However, six months post-SRS, patients treated with SRS and immunotherapy showed higher relative increase in rVSI (1.4;0.91-2.1 vs 0.82;0.51-0.97 ( $p<0.01$ )) together with greater reduction in micro-vascular rCBV (0.67;0.45-0.93 vs 1.1;0.98-1.3( $p<0.05$ )) in the peri-tumoral region. Median macro-vascular rCBV tended to decrease in both treatment groups, and there was no difference in the relative change (0.92;0.66-1.2 vs 0.85;0.68-0.96 ( $p=0.5$ )).



**Fig 2: Adding immunotherapy to SRS enhances treatment-induced effects in the peri-tumoral region (>15 Gy).** The three horizontal rows show log-transformed median change in rVSI (top), microvascular rCBV (middle) and macrovascular rCBV (bottom) relative to pre-SRS within the different dose ROIs at 3, 6, 9, and 12 months after SRS (error bars; interquartile range). No significant differences in any of the vascular parameters were present between the two treatment groups before SRS. Six months after SRS, peri-tumoral microvascular rCBV in patients treated with immunotherapy had increased relative to pre-SRS ( $p < 0.05$ ). In contrast, patients who had not received immunotherapy showed a decrease in rVSI ( $p < 0.05$ ), and at three- and six-months the relative change in peri-tumoral rVSI was different between the two treatment groups ( $p < 0.05$ ). While no significant changes in micro-vascular rCBV were present in patients treated with SRS only, patients on immunotherapy showed decrease in the microvascular blood volume 3-12 months after SRS in peri-tumoral regions as well as in regions receiving low doses (>2-5Gy) ( $p < 0.01-0.05$ ). Six and nine months post-SRS, the reduction on micro-rCBV was greater in the peri-tumoral region of patients treated with immunotherapy ( $p < 0.02/0.05$ ). Macrovascular rCBV tended to decrease in the high-dose regions for patients in both treatment groups, without any significant differences.

## Conclusion

Our preliminary data indicates that peri-tumoral regions are more susceptible to changes in vessel caliber and microvascular blood volume when immunotherapy is added to SRS. The relative decrease in microvascular rCBV, together with increase in rVSI in these patients, suggest that immunotherapy targets small and immature blood vessels in high dose regions.

## Poster: Physics track: Imaging acquisition and processing

### PO-1001 Combined image-based and biomechanical deformable image registration of extreme anatomical changes.

M. Nix<sup>1</sup>, S. Gregory<sup>1</sup>, M. Aldred<sup>1</sup>, L. Aspin<sup>1</sup>, B. Al-Qaisieh<sup>1</sup>, J. Lilley<sup>1</sup>, A. Appelt<sup>2</sup>, P. Dickinson<sup>3</sup>, L. Murray<sup>4</sup>  
<sup>1</sup>Leeds Cancer Centre, Radiotherapy Physics, Leeds, United Kingdom ; <sup>2</sup>Leeds Cancer Centre / University of Leeds, Radiotherapy Physics, Leeds, United Kingdom ; <sup>3</sup>Leeds Cancer Centre, Clinical Oncology, Leeds, United Kingdom ; <sup>4</sup>Leeds Cancer Centre / University of Leeds, Clinical Oncology, Leeds, United Kingdom

### Purpose or Objective

Deformable image registration (DIR) has long promised accurate fusion of radiotherapy (RT) images acquired with different geometry. However, with extreme tissue compression, e.g. reduced bladder/rectal filling, or post-surgical anatomy, where regularisation limits deformation, achieving acceptable accuracy has been challenging. The STRIDeR (Support Tool for Re-Irradiation Decisions guided by Radiobiology) project, required DIR of CTs, with bladder full at original RT and empty at reirradiation (reRT). In some cases, patient position changed from prone to supine and/or colorectal surgery had occurred in the interval. Accurate modelling of bladder filling is paramount for reRT as high original doses were typically delivered to the full bladder, not the bowel which moves into the previous RT field when the bladder is empty.

### Material and Methods

Commercially available tools (RayStation 7, RaySearch Laboratories, Stockholm, Sweden) were combined via scripting to develop an optimised automated method combining inverse hybrid<sup>1</sup> DIR, with biomechanical<sup>2</sup> DIR correction where necessary, which can accommodate large pelvic anatomical changes. Original and reRT CTs from 18 patients were registered using 1) Rigid registration, 2) Hybrid DIR, 3) Inverse hybrid DIR and 4) Optimised inverse hybrid + biomechanical DIR. Registration quality was assessed using Dice similarity (DSC) and mean distance to agreement (MDA).

Registration utility for reRT was also assessed by two expert oncologists using a 5-point Likert scale.

## Results

Optimised inverse hybrid + biomechanical DIR improved clinical utility for dose-summation in reRT considerably/moderately in 10/8 of 18 cases, with RIR never equivalent or preferred by clinician assessment. DSC was consistently improved (fig. 1) by optimised DIR, most notably for the critical bladder deformation (DSC >0.94 for all cases without compromising registration of other organs). Hybrid DIR alone completely failed in 7 cases, with bladder DSC <0.1, whilst achieving similar results to the optimised method for the remaining cases. MDAs were also smallest for the optimised method, achieving median MDA < 0.2 cm for bladder and bone. Colon, the most challenging organ to register due to sliding motion and interaction with bladder deformation, also showed improvement (median MDA = 0.3 cm (0.1-4.2 cm) relative to RIR and hybrid methods (median MDA > 1 cm).

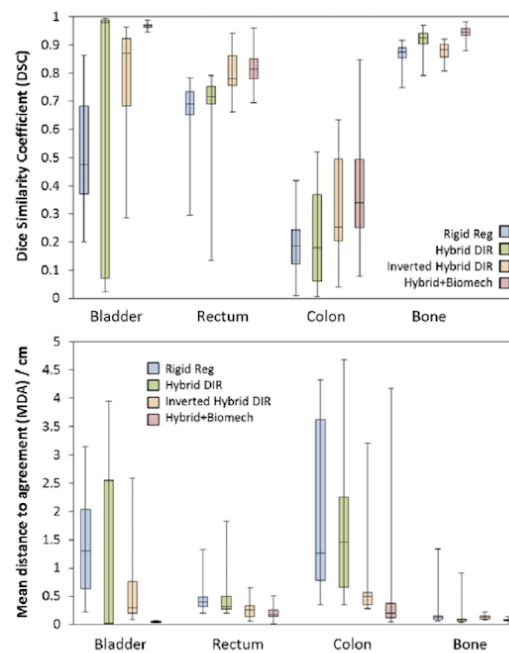


**Figure 1: Dice similarity coefficient (upper panel) and mean distance to agreement (lower panel) for bladder, rectum, colon and bone contours registered by four methods including the optimised method developed for this work (pink) which shows significant gains in registration quality over standard hybrid DIR (green). Median, interquartile range and extrema are shown by boxes and whiskers respectively.**

## Conclusion

Combination of image-based hybrid and biomechanical CT to DIR allows accurate modelling of extreme changes in bladder filling and associated soft tissue deformation, where even advanced hybrid algorithms fail.

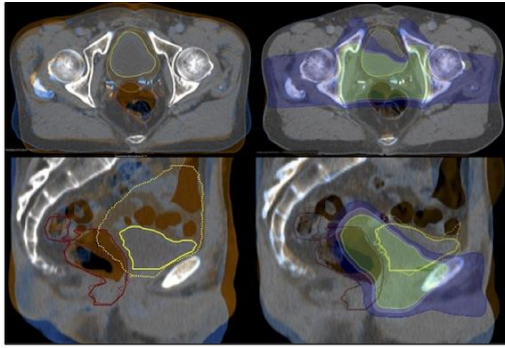


Figure 2: Example RIR (left) showing extreme bladder filling difference and DIR using the optimised method (right), showing final contour overlap and deformed dose. The dose originally delivered to the bladder is modelled correctly as having moved with the bladder. Bowel superior to the bladder at original RT is correctly modelled as having received minimal dose.

This accuracy is essential to realistically deform previously deposited dose (fig. 2), allowing accurate dose summation with radiobiological correction for planning of reRT. Combined image-based and biomechanical registration strategies may have application in dose-accumulation, adaptive re-planning, or summation of EBRT and brachytherapy doses.

#### PO-1002 Pseudo Computed Tomography generation using 3D deep learning - Application to brain radiotherapy

E. ALVAREZ ANDRES<sup>1,2</sup>, L. Fidon<sup>2,3</sup>, M. Vakalopoulou<sup>3</sup>, G. Noël<sup>4</sup>, S. Niyoteka<sup>1</sup>, N. Benzazon<sup>5,6</sup>, E. Deutsch<sup>1,5,7</sup>, N. Paragios<sup>2,3</sup>, C. Robert<sup>1,5,6</sup>

<sup>1</sup>U1030 Molecular Radiotherapy, Paris-Sud University - Gustave Roussy - Inserm - Paris-Saclay University, Villejuif, France ; <sup>2</sup>TheraPanacea, Radiotherapy, Paris, France ; <sup>3</sup>Centre for Visual Computing, Paris-Saclay University, Gif-sur-Yvette, France ; <sup>4</sup>Department of Radiotherapy, Paul Strauss Institute, Strasbourg, France ; <sup>5</sup>Paris-Sud University, Paris-Saclay University, Le Kremlin-Bicêtre, France ; <sup>6</sup>Department of Medical Physics, Gustave Roussy - Paris-Saclay University, Villejuif, France ; <sup>7</sup>Department of Radiotherapy, Gustave Roussy - Paris-Saclay University, Villejuif, France

#### Purpose or Objective

We used 3D convolutional neural networks designed for a high-resolution mapping of any T1-weighted Magnetic Resonance Imaging (MRI, with or without contrast agent) to a pseudo Computed Tomography (pCT). We conducted an evaluation using relevant metrics for radiotherapy based on the dose difference estimation from the Computed Tomography (CT) and the pCT. Our method achieves state of the art results and is robust to the potential use of a contrast agent.

#### Material and Methods

488 couples of brain 3D images including a CT and a T1-weighted or an enhanced T1-weighted MRI were used for training and validation of a 3D deep neural network architecture combined with a series of residual blocks containing dilated filter convolutions. All the network parameters were optimized based on the Mean Absolute Error (MAE) loss function (Figure 1).

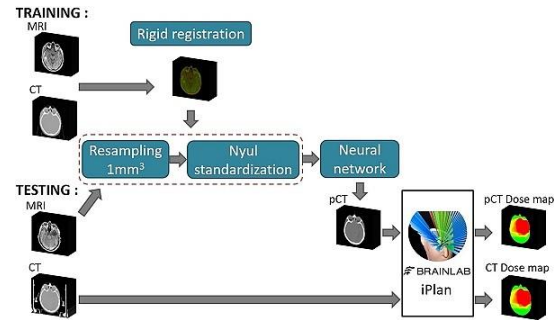


Figure 1: General workflow of the study.

For the evaluation step, we generated the pCTs of 10 grade 3 and 27 grade 4 new glioma patients (test cohort) who received either 3D conformational radiotherapy or Intensity Modulated Radiation Therapy. Prescribed doses ranged from 30Gy to 60Gy. The treatment plan based on the initial CT was transferred to the pCT. To evaluate the differences in the intensities between the initial CT and the pCT, the MAE was calculated. Global 1%/1mm, 2%/2mm and 3%/3mm gamma indexes and dose values extracted from the Dose Volume Histograms (DVHs) of the Planning Target Volume (PTV) were used to quantify the dose differences.

#### Results

Comparing the CT and pCT head regions of the 37 patients of the test dataset gave a MAE of 86 +/- 29 Hounsfield Units. Metrics based on the dose difference are more relevant for radiation therapy. Differences in DVHs were 0.13% +/- 0.08%, 0.14% +/- 0.10%, 0.15% +/- 0.17% for the doses corresponding to 50%, 95% and 98% of the PTV respectively. Global gamma indexes computed in the head region led to pass rates equal to 98.27% +/- 1.02%, 99.67% +/- 0.31% and 99.84% +/- 0.18% for the 1%/1mm, 2%/2mm and 3%/3mm criteria respectively (Figure 2).

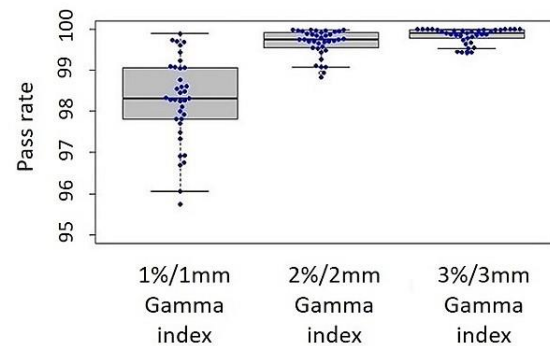


Figure 2: Gamma pass rates for the 1%/1mm, 2%/2mm and 3%/3mm global gamma index criteria.

#### Conclusion

To our knowledge, this is the first dosimetric study integrating 3D deep learning architectures. Promising pCT have been obtained with a high accuracy in terms of dose prediction. They outperform the state of the art dosimetric results (Dinkla et al., 2018), in which gamma pass rates of 91.1% +/- 3.0%, 95.8% +/- 2.1% and 99.3% +/- 0.4% for the 1%/1mm, 2%/2mm and 3%/3mm global gamma criteria were achieved and lead to a feasible application in clinics.

#### PO-1003 A deep learning based auto-segmentation for GTVs on NPC MR images

E. Xiangyu<sup>1</sup>, Y. Hongmei<sup>2</sup>, H. Weigang<sup>2</sup>, W. Jiazhou<sup>1</sup>  
<sup>1</sup>Shanghai Cancer Center- Fudan University, department of radiotherapy, Shanghai, China ; <sup>2</sup>Shanghai Cancer Center- Fudan University, department of radiotherapy, Shanghai, China

### Purpose or Objective

Segmentation of gross tumor volumes (GTVs) on nasopharyngeal carcinoma (NPC) MR images is an important basis for NPC radiotherapy planning. Manual segmentation of GTVs is a time-consuming and experience-dependent process in NPC radiotherapy. This study is aimed to develop a simple deep learning based auto-segmentation algorithm to segment GTVs on T1-weighted NPC MR images.

### Material and Methods

This study involved the analysis of 510 MR images from two datasets: (a) T1-weighted contrast-enhanced head and neck (H&N) MR images of 305 NPC patients and (b) T1-weighted H&N MR images of 205 patients without obviously abnormal regions in head. An FCN based on VGG16 was developed to perform automatic segmentation of GTVs. Data were randomly separated into training (90%) and validation (10%) datasets. Additionally, 15 patients were manually contoured by two oncologists for performance evaluation. Performance of the automated segmentation was evaluated the similarity of automated and manual segmentation on Hausdorff distance (HD), average surface distance (ASD), Dice index (DSC), and Jaccard index (JSC).

### Results

The HD, ASD, DSC, JSC (mean±std) were 16.18±7.93mm, 2.42±1.38mm, 0.71±0.12, 0.57±0.13 for validation dataset; and these indices were 14.21±4.73mm, 1.51±0.98mm, 0.83±0.08, 0.72±0.12 between two human radiation oncologists, respectively. The t-test indicated there was no statistically significant difference between automated segmentation and manual segmentation concerning HD(p=0.67), ASD(p=0.46), DSC(p=0.17), JSC(p=0.16).

### Conclusion

The results suggested that the performance of automated segmentation of GTV is close to manual segmentation's performance based on T1-weighted NPC MRIs. However, the manual segmentation performed better than automated segmentation. Thus, automated segmentation must be modified manually before being put into use.

### PO-1004 Simulation of tissue dependent magnetic field susceptibility effects in MRI guided radiotherapy

C. Kroll<sup>1</sup>, M. Opel<sup>2</sup>, C. Paganelli<sup>3</sup>, F. Kamp<sup>4</sup>, S. Nepl<sup>4</sup>, G. Baroni<sup>3</sup>, O. Dietrich<sup>3</sup>, C. Belka<sup>4</sup>, K. Parodi<sup>1</sup>, M. Riboldi<sup>1</sup>

<sup>1</sup>Ludwig-Maximilians-Universität Munich, Medical Physics, Garching, Germany; <sup>2</sup>Bayerische Akademie der Wissenschaften, Walther-Meißner-Institut, Garching, Germany; <sup>3</sup>Politecnico di Milano, Dipartimento di Elettronica- Informazione e Bioingegneria, Milano, Italy; <sup>4</sup>Ludwig-Maximilians-Universität Munich, Department of Radiation Oncology- University Hospital, Munich, Germany; <sup>5</sup>Ludwig-Maximilians-Universität Munich, Department of Radiology- University Hospital, Munich, Germany

### Purpose or Objective

The use of MRI for guidance in external beam radiotherapy needs to face the issue of spatial distortions, which may hinder accurate geometrical characterization. In this contribution, susceptibility values for different tissue types were measured, and tissue dependent effects simulated in a digital anthropomorphic CT/MRI phantom.

### Material and Methods

The simulation of the magnetic field distortion due to tissue dependent susceptibility effects relied on the iterative solution of Maxwell equations<sup>1,2</sup> in a multiple step procedure. The obtained magnetic field maps were then post-processed and values in parts per million (ppm) were converted into geometric distortion depending on the gradient strength. The simulation procedure was validated on test objects, for which an analytical solution can be

derived. For this purpose, a sphere and hollow shell were tested, varying the object susceptibilities from paramagnetic to diamagnetic and testing different convergence criteria. The digital anthropomorphic CT/MRI phantom CoBAT<sup>3</sup> was then used for simulation of tissue dependent effects. The input susceptibility values of liver, lung and muscle tissue were experimentally measured in porcine tissue samples, relying on SQUID (Superconducting Quantum Interference Device) magnetometry at normal pressure in the 0.35 - 3.0 T range (Figure A).

### Results

In the validation of the susceptibility algorithm, a RMS error between analytical and numerical solutions of 0.09 ppm for the sphere and of 0.35 ppm for the hollow shell was obtained, corresponding to a 10<sup>-12</sup> convergence tolerance. The tissue volume susceptibilities (expressed in SI units) remained constant in a physiological temperature range of 309.5 K - 313.5 K. The average ± standard deviation values over the temperature range were (-2.06 ± 0.02)·10<sup>-6</sup> for lung, (-9.91 ± 0.02)·10<sup>-6</sup> for liver and (-12.84 ± 0.08)·10<sup>-6</sup> for muscle tissue at 1.5 T (Figure A). Using the determined susceptibilities and values for bone, blood, fat, water and air as reported in the literature<sup>4,5</sup>, magnetic alterations stemming from susceptibility effects were simulated (Figure B). The ppm-differences ranged from -7.68 ppm to 4.36 ppm at 1.5 T, corresponding to 1.15 mm maximal distortion at a gradient strength of 10 mT/m.

### Conclusion

Different tissues create local magnetic changes, with enhanced effects at the boundaries (Figure B), which scale with the magnetic field strength. Through the determination of magnetic susceptibilities of different tissue types, a more realistic representation of susceptibility induced distortions is feasible. A phantom study, dealing with magnetic field alterations due to static field inhomogeneities and gradient non-linearities is currently ongoing, aiming at a comprehensive simulation of major effects in spatial distortion for MRI guidance.

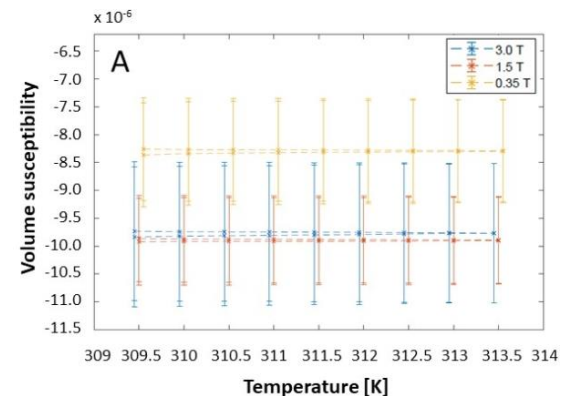
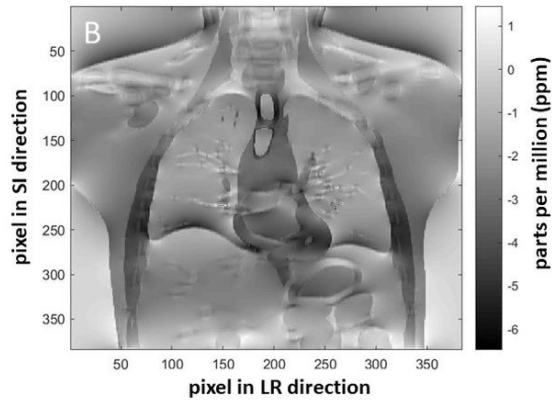


Figure A. Volume susceptibility measurements for liver tissue samples. Errors bars were calculated taking into account weight loss in the sample during measurements



**Figure B. Tissue dependent variations in the CoMBAT phantom at 1.5 T.**

- doi: 10.1016/0730-725X(92)90489-M
- doi: 10.1016/S0730-725X(02)00601-X
- doi: 10.1007/s11517-017-1646-6
- doi: 10.1118/1.4764481
- doi: 10.1118/1.597854

**PO-1005 Evaluating different generator networks of a conditional generative adversarial network**

L. Fetty<sup>1</sup>, P. Kuess<sup>1</sup>, N. Nesvacil<sup>1</sup>, T. Nyholm<sup>2</sup>, D. Georg<sup>1</sup>, H. Furtado<sup>1</sup>

<sup>1</sup>Medical University of Vienna, Department of Radiotherapy and Christian Doppler Laboratory for Medical Radiation Research for Radiation Oncology, Vienna, Austria ; <sup>2</sup>Umea University, Department of Radiation Sciences, Umea, Sweden

**Purpose or Objective**

The conversion of MR images to synthetic CTs (sCT) is of great importance for MR-only workflows. Deep learning has become a very popular and promising feature extraction technique which is used for many tasks in medicine. Image to image translations for MR-sCT conversions can be performed by classic convolutional neural networks and generative adversarial networks (GAN). For a better understanding of specific deep learning techniques and to identify the best suitable method on a quantitative basis, a systematic evaluation of different networks is of highest importance.

The aim of this study was to investigate the influence of different GAN generator structures on the image conversion and their impact on the mean absolute error (MAE). Further we transferred the learned features to different MRI scanners to identify whether the network-learned features can be applied globally. **Material and Methods**

4 different generator networks were implemented into an existing GAN structure (pix2pix). The generators were based on SE-ResNet (SN), DenseNet (DN), u-net (UN) and embedded net (EN). Pelvic T2-weighted MR (0.35T open MR) images of 40 patients (29 male and 11 female) were used, resulting in a training set of 1972 image pairs. The same settings for discriminator, loss function and learning cycles (epochs) were used for all tests. The test data set contained 12 patients. A gold atlas dataset (GA) was used to evaluate the impact of the trained networks on other MR scanners (1.5 and 3T). Finally, all networks were combined by calculating the median (ME) over all voxels of the converted images.

The performance of the networks was evaluated by the MAE in the outer patient contour and the bone region. **Results**

The best results for the training dataset were obtained using the SN and the DN. However, a divergence was observed between the training and test datasets with increasing epoch counts (Figure 1). EN and UN performed slightly worse, but training and test sets were always

within the standard deviation. The MAE at the 100<sup>th</sup> epoch count was about 47HU for DN and SN and 71HU for EN and UN for the whole body. During the testing phase the MAE of all 4 networks ranged between 61-70HU.

For the GA dataset, the EN performed worse with a MAE of 85-90HU. For both 3T systems the DN showed low ranges and a better performance than for the test data. ME produced the best results for bone regions in all datasets (Figure 2).

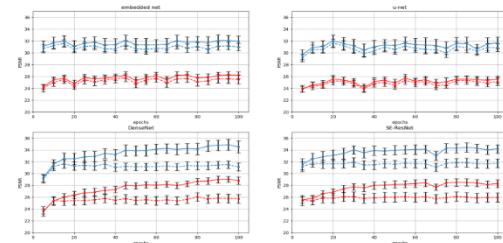


Figure 1: training and test loss of the GANs with the four different generator structures.

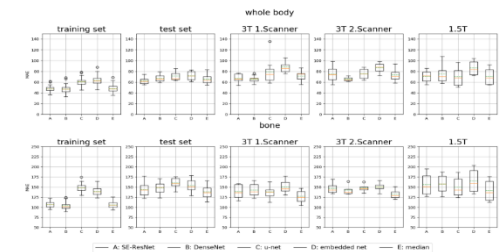


Figure 2: Metrical evaluation of the different datasets with the different network structures compared to the median calculated of all networks for the whole body and the bone

**Conclusion**

Differences between networks should be considered if applied to new data. Detailed information on the networks' performance should be reported in studies that utilize such methods. Our ME results suggest that a combination of multiple networks can increase overall performance. The results indicate that a comprehensive comparison between generator types is necessary when using deep learning methods on image post-processing with deep learning methods.

**PO-1006 Patient-specific stopping power calibration for proton therapy based on proton radiographic images**

Abstract withdrawn

**PO-1007 Comparison of deep learning with three other methods to generate pseudo-CT for MRI-only radiotherapy**

A. Largent<sup>1</sup>, A. Barateau<sup>1</sup>, J. Nunes<sup>1</sup>, C. Lafond<sup>1</sup>, P.B. Greer<sup>2,3</sup>, J.A. Dowling<sup>4</sup>, H. Saint-Jalmes<sup>1</sup>, O. Acosta<sup>1</sup>, R. De Crevoisier<sup>1</sup>

<sup>1</sup>Univ Rennes- CLCC Eugène Marquis- INSERM- LTSI - UMR 1099, Laboratoire du traitement du signal et de l'image, Rennes, France ; <sup>2</sup>Calvary Mater, Department of Radiation Oncology, Newcastle, Australia ; <sup>3</sup>University of Newcastle, School of Mathematical and Physical Sciences, Newcastle, Australia ; <sup>4</sup>Australian e-Health Research Centre, Commonwealth Scientific and Industrial CSIRO, Herston/Queensland, Australia

**Purpose or Objective**

Deep learning methods (DLM) have recently been developed to generate pseudo-CT (pCT) from MRI for radiotherapy dose calculation. The main advantage of these methods is the speed of pCT generation. The objective of this study was to compare a DLM to a patch-based method (PBM), an atlas-based method (ABM) and a

bulk density method (BDM) for prostate MRI-only radiotherapy.

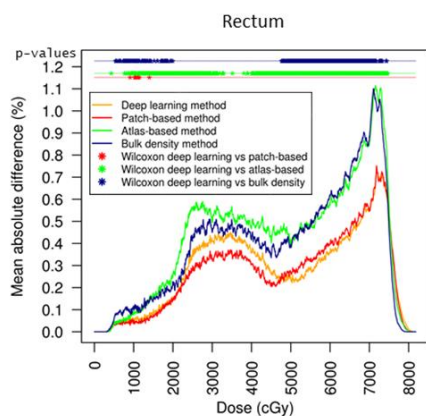
#### Material and Methods

Thirty-nine patients received VMAT for prostate cancer (78 Gy in 39 fractions). T2-weighted MR images were acquired in addition to the planning CT images. pCT were generated from MRI by four methods: a DLM, a PBM, an ABM and a BDM (water-air-bone density assignment). The DLM was a generative adversarial network (GAN) using a perceptual loss. The PBM was performed with feature extraction and approximate nearest neighbour search. DLM and PBM were trained with a cohort of 25 patients. The four methods were compared in a validation cohort of 14 patients. Imaging endpoints were mean absolute error (MAE) and mean error (ME) of Hounsfield units (HU) from voxel-wise comparisons between pCT and reference CT. Dose uncertainties of the methods were defined as the absolute mean differences between DVH parameters for the organs at risk and PTV calculated from the reference CT and from the pCTs for each method. 3D gamma index analyses (local, 1%/1mm) were also performed. The Wilcoxon test was used to compare the uncertainty of the DLM to those of the three other methods.

#### Results

In the whole pelvis, the DLM showed significantly lower MAE (mean value of 37 HU) compared to the PBM (41 HU), ABM (43 HU) and BDM (99 HU). The ME obtained from the PBM (-1 HU) was lower compared to those of the DLM (-9 HU), ABM (-8 HU) and BDM (-18 HU). The table shows the dose uncertainty of each pCT generation method for each volume-of-interest. The figure shows the dose uncertainty of each method along the whole DVH for the rectum. Significant differences are displayed with the use of the symbol \*. DVH differences were significantly lower when using the DLM and the PBM, than the ABM and BDM. All the mean gamma values were significantly lower with the DLM or the PBM, compared to the ABM and BDM.

Volumes of interest	Prostate CTV	Prostate PTV	Rectum	Bladder			
Dosimetric endpoints	D <sub>99%</sub> (cGy)	V <sub>95%</sub> (%)	V <sub>100%</sub> (%)	D <sub>max</sub> (cGy)	V <sub>50%</sub> (%)	D <sub>max</sub> (cGy)	
CT <sub>ref</sub> values	7150	96.4	5.9	7298	20.1	7770	
Absolute difference between the dose calculated on the reference CT and the pseudo-CT	Deep learning method	52	0.7	0.5	52	0.2	26
	Patch-based method	51	0.7	0.5	52	0.2	25
	Atlas-based method	79	1.3	0.8	81	0.5	61
	Bulk density method	79	1.3	0.8	80	0.5	67



#### Conclusion

In order to generate pCT from MRI for dose calculation, the four assessed methods provide clinically acceptable uncertainties (<1%). The DLM and PBM provide however

the lowest imaging and dosimetric uncertainties. The DLM appears particularly attractive due to its accuracy and the very fast calculation time (<1 min).

#### PO-1008 Image quality characterisation of a proton gantry-mounted cone-beam CT system

K. Andersson<sup>1</sup>, C. Vallhagen Dahlgren<sup>1</sup>, A. Dasu<sup>1</sup>

<sup>1</sup>The Skandion Clinic, Department of Medical Physics, Uppsala, Sweden

#### Purpose or Objective

Cone-beam computed tomography (CBCT) is an important tool for precise patient positioning and tracking of anatomical changes during the course of radiotherapy. For proton therapy, it is crucial to reduce such uncertainties due to the sharp distal dose fall-off. Proton gantry-mounted CBCT generally differ from linac systems, e.g., the source-to-isocenter distance (SID) may be larger and they may lack bowtie filters. Organ doses for a proton-gantry CBCT have recently been investigated by Ardenfors et al [1]. They concluded that posterior scans result in lower organ doses than anterior scans and should therefore be preferred if image quality could be preserved. The aim of the current project was to evaluate image quality for several scan protocols of the same proton gantry-mounted CBCT system.

#### Material and Methods

A Catphan® 600 phantom (The Phantom Laboratory, Salem, NY) was scanned with the CBCT system of a proton pencil-beam scanning gantry (Ion Beam Applications, Belgium) at the Skandion Clinic, Sweden. The system has SID=261.8 cm and no bowtie filter applied. Images were acquired for the head, thorax and pelvic protocols with rotations of 360°, 190° anterior or 190° posterior. Image quality was assessed several times over several months. Images were analyzed using ImageJ software (NIH, Bethesda, MD) using the image quality parameters recommended by the EFOMP-ESTRO-IAEA protocol [2]. The tolerance levels used for geometrical accuracy, CT number accuracy and uniformity were the same as during system acceptance. Contrast-to-noise ratios (CNR) and resolution were also evaluated.

#### Results

Geometrical accuracy was within tolerance for every protocol, while uniformity exceeded the tolerance for all series (see Table 1). CT number accuracy was generally within tolerance, but in some cases higher deviations were seen for a few contrast targets. CNR:s were considerably low for head scans, and were highest for pelvis protocols. Resolution was considered to be acceptable for all scans. Generally no relevant image quality differences between posterior and anterior scans were found.

Table 1. Summary of image quality parameters determined for the proton gantry-mounted cone-beam CT system.

Protocol	Tube voltage (kV)	Tube current (mAs)	Geometrical accuracy (Tolerance: 1%)	CT number accuracy (Tolerance: ΔHU < 40)	Uniformity (Tolerance: ΔHU < 40)	Low contrast (CNR)	Resolution (Line pair/cm)
Head, 190° A	100	569	✓	ΔHU <sub>max,sk</sub> > 40 HU	X	0.6	7
Head, 190° P	100	569	✓	ΔHU <sub>max,sk</sub> > 40 HU	X	0.7	7
Head, 360°	100	1082	✓	ΔHU <sub>max,sk</sub> > 40 HU	X	0.9	7
Thorax, 190° A	110	910	✓	ΔHU <sub>max,sk</sub> > 40 HU	X	1.2	8
Thorax, 190° P	110	910	✓	✓	X	1.4	8
Thorax, 360°	110	1732	✓	✓	X	1.9	8
Pelvis, 190° A	120	1820	✓	ΔHU <sub>max,sk</sub> > 40 HU	X	1.9	8
Pelvis, 190° P	120	1820	✓	ΔHU <sub>max,sk</sub> > 40 HU	X	2.2	8
Pelvis, 360°	120	3464	✓	ΔHU <sub>max,sk</sub> > 40 HU	X	2.8	8

A – anterior, P – posterior, HU – Hounsfield units, CNR – contrast-to-noise ratio

#### Conclusion

While geometrical accuracy was found to be acceptable, tests of CT number accuracy, uniformity and low resolution showed deviations. Therefore image quality based on these aspects needs to be further investigated. Posterior scans resulted in equal image quality as anterior scans, and could hence preferably be used since organ doses are reduced. The stability of the system will be assessed based on measurements repeated periodically for a longer time period.

## References

1. Ardenfors O, et al. Organ doses from a proton gantry-mounted cone-beam computed tomography system characterized with MCNP6 and GATE. *Phys Med.* 2018;53:56-61
2. de las Heras Gala H, et al. Quality control in cone-beam computed tomography (CBCT) EFOMP-ESTRO-IAEA protocol. *Phys Med.* 2017;39:67-72.

## PO-1009 Comparison of automatic tumour segmentation approaches for head and neck cancers in PET/CT images

A. Rosvoll Groendahl<sup>1</sup>, M. Mulstad<sup>1</sup>, Y. Mardal Moe<sup>1</sup>, I. Skjei Knudtsen<sup>2</sup>, T. Torheim<sup>3</sup>, O. Tomic<sup>1</sup>, U.G. Indahl<sup>1</sup>, E. Malinen<sup>4</sup>, E. Dale<sup>5</sup>, C.M. Futsaether<sup>1</sup>

<sup>1</sup>Norwegian University of Life Sciences NMBU, Faculty of Science and Technology, Ås, Norway; <sup>2</sup>Oslo University Hospital, Department of Medical Physics, Oslo, Norway; <sup>3</sup>University of Oslo / Oslo University Hospital, Institute for Cancer Genetics and Informatics, Oslo, Norway; <sup>4</sup>University of Oslo / Oslo University Hospital, Department of Physics / Department of Medical Physics, Oslo, Norway; <sup>5</sup>Oslo University Hospital, Department of Oncology, Oslo, Norway

### Purpose or Objective

The objective of this study was to assess methods based on PET thresholding, machine learning using a linear classifier, and deep learning for automatic tumour segmentation of head and neck cancers in PET/CT images.

### Material and Methods

This retrospective study examines 197 head and neck cancer patients who underwent a combined 18F-FDG-PET/CT scan prior to radiotherapy. Three tumour segmentation approaches with different levels of complexity were compared: (i) PET thresholding techniques, (ii) voxelwise classification using the machine learning algorithm Linear Discriminant Analysis (LDA), and (iii) deep learning using convolutional neural networks (CNNs). Manual gross tumour delineations made by an oncologist and a nuclear medicine specialist were considered as the ground truth. PET thresholding was conducted using either absolute thresholding or a percentage of maximum SUV, optimized using the Dice similarity coefficient (DSC) or the Receiver Operating Characteristics (ROC). The LDA approach used input features engineered using voxel intensities and voxel neighbourhood information extracted from the original PET/CT images and images transformed using CT windowing, as well as point and two-dimensional transformations to highlight different image characteristics. Training data was down-sampled to 50/50 class-balance prior to training the LDA model. The deep learning approach used a U-net architecture with a Dice loss function. Weights were initialised using the He initialisation scheme and optimised using Adam with a  $10^{-4}$  step size and default hyperparameters. Raw PET images and raw or windowed CT images without down-sampling were used for this approach.

The segmentation performance on validation data was assessed using the Dice similarity coefficient, sensitivity, specificity and the ROC-AUC (Receiver Operating Characteristics-Area Under the Curve).

### Results

For PET thresholding, optimizing the SUV threshold with respect to ROC rather than DSC resulted in somewhat better segmentation with higher and balanced sensitivity (0.83-0.87) and specificity (0.85-0.89) (Table 1). LDA segmentation based only on CT images performed poorly (DSC 0.17), whereas segmentation based on PET images gave high sensitivity, specificity, AUC and DSC (0.50). Thus, features engineered from CT images did not provide sufficient information for tumour segmentation using a linear classifier. CNN segmentation had the overall highest DSC (0.62) (Table 1, Figure 1). Interestingly, CNN

segmentation based only on CT images performed similarly to segmentation using PET images.

### Conclusion

All segmentation approaches based on PET images performed satisfactorily due to the high SUV of the tumour relative to other tissues. However, only the deep learning approach was able to discern the tumour in CT images, without the need of extensive feature engineering as required by the linear classifier.

**Table 1.** Mean performance measures for automatic tumour segmentation obtained using validation data for the methods PET thresholding, voxelwise classification using a linear classifier (LDA), and deep learning (CNN).

Method	Input images	DSC	Sensitivity	Specificity	AUC
Absolute threshold*	PET	0.58	0.62	0.98	NA
Percentage threshold*	PET	0.57	0.62	0.96	NA
Absolute threshold**	PET	0.44	0.87	0.89	NA
Percentage threshold**	PET	0.49	0.83	0.85	NA
LDA	CT <sub>w</sub> + CT <sub>w</sub>	0.17	0.80	0.63	0.81
LDA	PET <sub>w</sub>	0.50	0.87	0.93	0.97
LDA	PET <sub>w</sub> + CT <sub>w</sub> + CT <sub>w</sub>	0.50	0.88	0.93	0.97
Deep Learning	CT	0.51	0.58	0.98	NA
Deep Learning	CT <sub>w</sub>	0.56	0.65	0.99	NA
Deep Learning	PET	0.59	0.68	0.98	NA
Deep Learning	PET + CT	0.60	0.64	0.98	NA
Deep Learning	PET + CT <sub>w</sub>	0.62	0.66	0.98	NA

\* DSC optimal

\*\* ROC optimal

NA: Not Applicable

PET: Raw PET image

PET<sub>w</sub>: Raw PET image and transformations of PET

CT: Raw CT image

CT<sub>w</sub>: Raw CT and transformations of CT

CT<sub>w</sub>: Window setting transformation(s) of CT

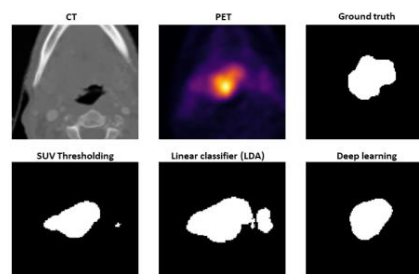


**Figure 1.** The PET/CT images and ground truth (top row) for one image slice and the segmentation results (bottom row) from SUV thresholding (ROC optimal percentage of maximum SUV), the linear classifier LDA (PET<sub>w</sub> + CT<sub>w</sub> + CT<sub>w</sub>, Table 1) and deep learning (PET + CT, Table 1).

## PO-1010 Clinical evaluation of deep learning delineation of head and neck OARs.

W. Van Rooij<sup>1</sup>, H. Ribeiro Brandao<sup>1</sup>, A. Delaney<sup>1</sup>, B. Slotman<sup>1</sup>, W. Verbakel<sup>1</sup>, M. Dahele<sup>1</sup>

<sup>1</sup>VUMC, Radiotherapy, Amsterdam, The Netherlands

### Purpose or Objective

Target and organ-at-risk (OAR) delineation is a key step in radiotherapy treatment planning and adaptive radiotherapy, but it is often time consuming and resource intensive. Additionally, it is subject to interobserver variability and may require considerable anatomical knowledge. Most available automated methods for delineation do not, in general, perform as well as desired, and/or are slow. Deep learning for automated delineation is promising, but its evaluation has typically only been presented in terms of similarity coefficients or observer ratings for a limited number of OARs. Therefore, this retrospective study evaluates (1) the geometric accuracy, and (2) the dosimetric (clinical) impact of using deep learning delineation on many OARs for head and neck cancer (HNC).

### Material and Methods

142 anonymized clinical datasets, consisting of clinically contoured CT scans and structure sets, were used to train a convolutional neural network (U-Net) and 15 were used as a test set. The objective was to automate the delineation of the following OARs: left and right submandibular gland, left and right parotid gland, larynx, cricopharynx, pharyngeal constrictor muscle (PCM), upper esophageal sphincter (UES), brain stem, oral cavity and esophagus. Each OAR was delineated both manually (MD,

the clinical contour) and with deep learning (DLD). No manual editing was performed on the DLD contours. In order to avoid plan optimization bias, treatment plans were created using knowledge-based planning, based on MD and DLD structures (MD-plans, DLD-plans) and the mean dose to the manually delineated OAR structures was compared.

### Results

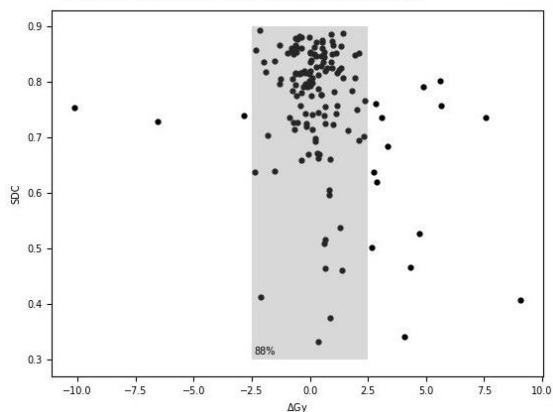
Generation of deep learning contours takes ~10 seconds for all OARs. The average dose was statistically significantly higher for DLD-plans for the lower larynx, the inferior PCM, and the esophagus (table 1). Average differences were not clinically significant, but differences in some individual cases could be. From the 209 OARs, 28 (13.4%) received an increase of more than 2Gy with the DLD-plans, and 7 (3.3%) a decrease of more than 2Gy. A full overview of the OARs' Sørensen-Dice coefficients (SDC) and their increase/decrease in Gy ( $\Delta$ Gy) for DLD-plans compared to MD-plans can be seen in figure 1. Low SDCs were generally the result of variability in the MD or the limited amount of training data.

Table 1. Averaged doses per OAR for MD-plans (MD-D) and DLD-plans (DLD-D) and the difference between them ( $\Delta$ Gy). \* implies statistical significance ( $p < 0.05$ ).

Structure	MD-D <sub>mean</sub> (Gy)	DLD-D <sub>mean</sub> (Gy)	$\Delta$ Gy
Brain stem	34.5 +/- 8.1	35.8 +/- 6.7	1.3 +/- 3.1
Spinal cord	42.0 +/- 1.2	41.7 +/- 1.4	-0.3 +/- 1.1
Oral cavity	31.1 +/- 8.7	31.6 +/- 8.5	0.4 +/- 1.2
Parotid (i)	31.1 +/- 11.1	31.0 +/- 11.4	-0.1 +/- 0.7
Parotid (c)	21.6 +/- 3.9	21.6 +/- 4.0	0.0 +/- 0.8
Submandibular (i)	50.9 +/- 11.5	51.8 +/- 11.1	0.9 +/- 3.4
Submandibular (c)	34.2 +/- 6.3	34.4 +/- 6.5	0.2 +/- 1.0
Cricopharynx	27.7 +/- 11.4	28.2 +/- 11.6	0.5 +/- 1.5
Lower larynx*	25.0 +/- 16.5	25.7 +/- 16.6	0.8 +/- 1.3
Upper larynx	42.4 +/- 15.8	42.2 +/- 15.8	-0.1 +/- 2.4
Inf PCM*	35.2 +/- 13.5	36.5 +/- 13.7	1.4 +/- 1.8
Med PCM	51.3 +/- 9.0	51.1 +/- 9.2	-0.1 +/- 0.9
Sup PCM	54.6 +/- 9.8	54.8 +/- 9.5	0.2 +/- 0.7
UES	21.5 +/- 11.3	22.0 +/- 11.7	0.5 +/- 2.1
Esophagus*	20.4 +/- 6.1	22.7 +/- 5.6	2.2 +/- 1.6

Figure 1. Scatterplot of the SDC (y-axis) and  $\Delta$ Gy (x-axis) of all OARs.

PCM and larynx are taken as composite structures here.



### Conclusion

Using a training set consisting of only a relatively limited number of OAR delineations without extensive curating, automated deep learning segmentation for head and neck OARs, is fast and for most organs it performs sufficiently

well for treatment planning purposes. Since some contours can deviate from the clinical contours, clinical inspection of automated contours is still required. The combination of automated DLD plus model-based automated planning has the potential to increase the efficiency of routine clinical care, and facilitate online adaptive radiotherapy.

### PO-1011 Calibration and validation of ion stopping power prediction with Philips IQon Spectral CT

F. Faller<sup>1</sup>, B. Ackermann<sup>2</sup>, G. Pahn<sup>3</sup>, M. Alber<sup>1</sup>, W. Stiller<sup>4</sup>, A. Mairani<sup>2</sup>

<sup>1</sup>University Hospital Heidelberg, Department of Radiation Oncology, Heidelberg, Germany; <sup>2</sup>Heidelberg Ion-Beam Therapy Center HIT, Department of Radiation Oncology, Heidelberg, Germany; <sup>3</sup>Philips Healthcare, Clinical Scientist CT, Hamburg, Germany; <sup>4</sup>University Hospital Heidelberg, Diagnostic Radiology, Heidelberg, Germany

### Purpose or Objective

This study presents for the first time an experimental validation of stopping-power ratio (SPR) prediction from Philips IQon Spectral CT data, exploring its benefit for improving radiotherapy (RT) treatment planning, especially in view of the accuracy requirements imposed by proton and heavy ion therapy. For this purpose, we investigated the added value of derived quantitative image data, such as three-dimensional maps of effective atomic number ( $Z_{\text{eff}}$ ) and electron density relative to water (ED) covering the whole acquisition field-of-view. The ultimate purpose of this study was the derivation of an accurate three-dimensional map of  $\text{SPR}_w$  based on maps of  $Z_{\text{eff}}$  and ED acquired with spectral CT imaging technique.

### Material and Methods

The accuracy of ED and  $Z_{\text{eff}}$  by Philips IQon Spectral CT was verified in phantoms with various tissue-equivalent inserts (Gammex 467, CIRS 062M).  $\text{SPR}_w$  values were determined following the Bethe equation and applying different approaches available in literature aiming to convert  $Z_{\text{eff}}$  maps in ionization potential (I) maps. The impact of spectral CT scanning settings, regarding acquisition and reconstruction parameters, namely tube potential, acquisition dose, and gantry rotation time, on  $Z_{\text{eff}}$  and ED maps was assessed. The derived  $\text{SPR}_w$  maps values were validated against experimentally determined  $\text{SPR}_{\text{meas}}$  of the same insert. Comparisons against  $\text{SPR}_w$  derived using spectral CT were performed, evaluating the accuracy of the methodology.

### Results

We calibrated and validated three-dimensional maps of  $Z_{\text{eff}}$  and ED from spectral CT data with phantom measurements (deviation within a few per cent compared to reference data). Using  $Z_{\text{eff}}$  data from spectral CT, tissue surrogates can be characterized more accurately than using standard HU-calibration. For the tissue surrogates  $\text{SPR}_w$  predicted from spectral CT images was within a mean accuracy of <1 % compared to  $\text{SPR}_{\text{meas}}$  (Figure 1). The experimental validation in defined materials is a mandatory step to show absolute  $\text{SPR}_w$  errors from spectral CT prediction before considering biological tissue samples. Furthermore, a method for efficient integration of  $\text{SPR}_w$  in the Monte Carlo treatment planning framework available at the Heidelberg Ion Beam Therapy center was developed.

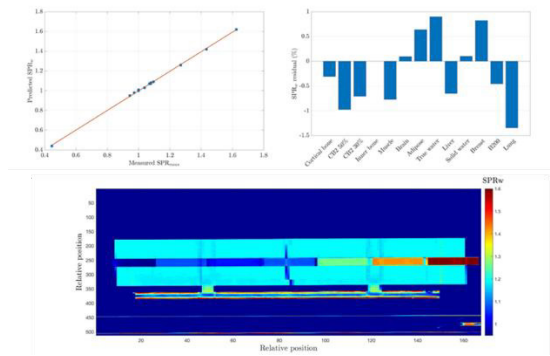


Figure 1: Upper left: Relation between predicted  $SPR_w$  and measured  $SPR_{meas}$ . Upper right:  $SPR_w$  residual for measured tissue surrogates. Bottom: Cross-section through a phantom with seven tissue-equivalent inserts showing predicted  $SPR_w$ .

### Conclusion

In this study we investigated the ability of Philips IQon Spectral CT imaging technique to predict the  $SPR_w$  for particle therapy more accurately using an image-based calculation of both ED and  $Z_{eff}$ . Further comparative studies of  $SPR_w$  maps derived from spectral CT to those determined by conventional CT imaging for RT planning and range measured in biological tissue samples will evaluate its potential in realistic tissue compositions. These results will be additionally presented at the conference.

### PO-1012 Dual-energy computed tomography for improved delineation in postoperative brain-tumor patients

P. Wohlfahrt<sup>1,2</sup>, L. Agolli<sup>3</sup>, M. Krause<sup>1,2,3,4,5</sup>, K. Pilz<sup>3</sup>, C. Richter<sup>1,2,3,4,6</sup>, E. G. C. Troost<sup>1,2,3,4,5,6</sup>

<sup>1</sup>OncoRay - National Center for Radiation Research in Oncology, Faculty of Medicine and University Hospital Carl Gustav Carus - Technische Universität Dresden - Helmholtz-Zentrum Dresden-Rossendorf, Dresden, Germany; <sup>2</sup>Helmholtz-Zentrum Dresden-Rossendorf, Institute of Radiooncology - OncoRay, Dresden, Germany; <sup>3</sup>Department of Radiotherapy and Radiation Oncology, Faculty of Medicine and University Hospital Carl Gustav Carus - Technische Universität Dresden, Dresden, Germany; <sup>4</sup>German Cancer Consortium DKTK, partner site Dresden and German Cancer Research Center DKFZ Heidelberg, Dresden, Germany; <sup>5</sup>National Center for Tumor Diseases NCT, partner site Dresden: German Cancer Research Center DKFZ Heidelberg - Faculty of Medicine and University Hospital Carl Gustav Carus at Technische Universität Dresden and Helmholtz Association / Helmholtz-Zentrum; <sup>6</sup>Both authors share last authorship, equal contribution, Dresden, Germany

### Purpose or Objective

The clinical use of dual-energy CT (DECT) contributes to an improved accuracy in proton treatment planning compared to single-energy CT (SECT) as demonstrated in recent studies. A precise delineation of tumor volumes and organs at risk (OARs) is essential in particular for emerging high-conformal treatment techniques. Since DECT provides additional tissue information and allows for the generation of various tissue contrasts, we assessed its influence on the intra- and inter-observer delineation variability.

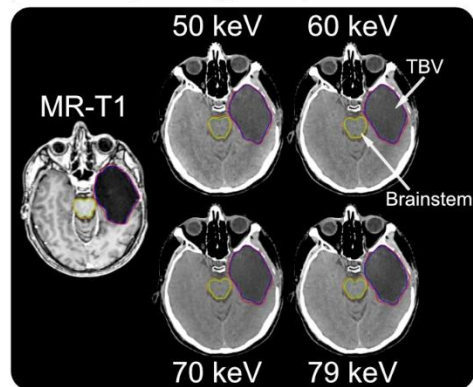
### Material and Methods

Two cohorts of 10 postoperative brain-tumor patients each, receiving either a 120kVp SECT or 80/140kVp DECT scan with identical total dose, were evaluated. Pseudo-monoenergetic CT (MonoCT) datasets of 50, 60, 70 and 79keV, representing several tissue contrasts, were derived

from DECT scans processed in syngo.via (Siemens Healthineers). Three radiation oncologists with different levels of experience in neuro-oncology delineated the postoperative tumor bed volume (TBV) and OARs (brainstem, parotid and lacrimal glands, eyes, lenses, optic nerves, and chiasm) on each dataset, at least two-weeks apart per patient. Relevant image information was blinded. The delineations on SECT datasets were repeated once to assess the intra-observer variability. Finally, the delineation was also performed on T1/T2 MR scans as clinical reference.

The contour conformity was quantified by the Jaccard index (JI) and Hausdorff distance (HD) between the intersection and union of the respective contours (Fig. 1).

### A Inter-observer variability - DECT (3 clinicians per energy & MR)



### B Intra-observer variability - DECT (4 different energies per clinician)



Fig.1: Assessment of inter- and intra-observer delineation variability for pseudo-monoenergetic CT (MonoCT) datasets derived from dual-energy CT (DECT). The tumor bed volume (TBV) and brainstem are exemplarily shown.

### Results

The median inter-observer TBV conformity (Fig. 2A) was almost independent from the CT dataset (HD=6-9mm, JI=61-66%) and comparable to MR scans (HD=6-7mm, JI = 66-67%). The consistency of brainstem contours (Fig. 2B) was best at the lowest energy of MonoCT datasets (median HD=2.8mm, JI=81%). In contrast, the contour conformity of the parotid glands (Fig. 2C) gained slightly from an increased energy (median HD reduction of 0.6mm, JI increase of 1%) and also led to better results as MR scans. For these OARs, using the most suitable MonoCT instead of SECT resulted in smaller inter-observer variations. No relevant differences between SECT and MonoCT were determined for the other OARs, potentially due to their small volume.

The intra-observer TBV variability obtained on SECT did not depend on clinical experience. However, the contouring of less experienced clinicians is more affected by different image contrasts introduced by MonoCT of different energies (Fig. 2D).

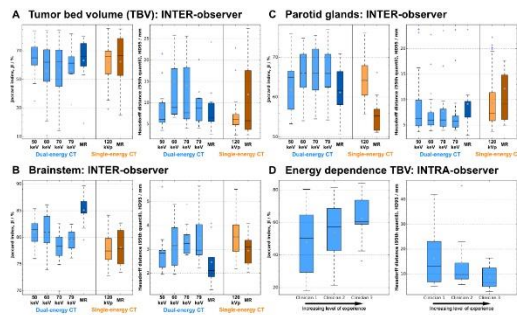


Fig.2: Inter-observer delineation variability of three radiation oncologists for TBV (A) and organs at risk such as brainstem (B) and parotid glands (C) as well as intra-observer variability of the TBV contour at different image contrasts (MonoCT of 50, 60, 70 and 79 keV).

### Conclusion

For postoperative brain-tumor patients, DECT-derived MonoCT datasets can improve the intra- and inter-observer delineation conformity compared to the currently used SECT. Moreover, they in part led to similar or better results as the gold standard MR. The most suitable image contrast to meet individual delineation requirements of anatomical structures can be chosen after CT acquisition. Future studies need to show whether the advantages can also be translated to other tumor entities and body regions.

Poster: Physics track: Implementation of new technology, techniques, clinical protocols or trials (including QA & audit)

### PO-1013 Unscheduled interruptions and total treatment time for VMAT prostate treatments

E.M. Ambroa Rey<sup>1</sup>, J. García-Miguel Quiroga<sup>1</sup>, A. Ramirez Muñoz<sup>1</sup>, D. Navarro Giménez<sup>1</sup>, R. Gómez Pardos<sup>1</sup>, M. Colomer Truyols<sup>1</sup>

<sup>1</sup>Consorci Sanitari de Terrassa, Medical Physics Unit-Radiation Oncology, Terrassa, Spain

#### Purpose or Objective

Treatment interruptions during radiotherapy may have a negative effect on patient outcome and uncompensated interruptions increase the risk of local recurrence. The causes of treatment interruptions may be preventive equipment maintenance, local and national public holidays, treatment toxicity, equipment breakdown, and also patient's private reasons.

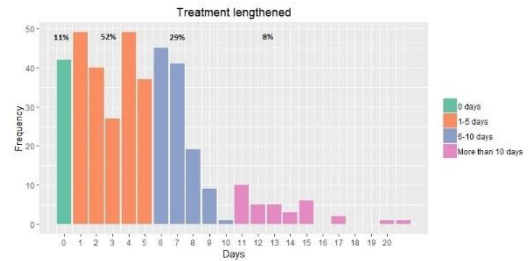
It is important to account for these interruptions and evaluate if the total treatment time (TTT) is within a reasonable margin.

#### Material and Methods

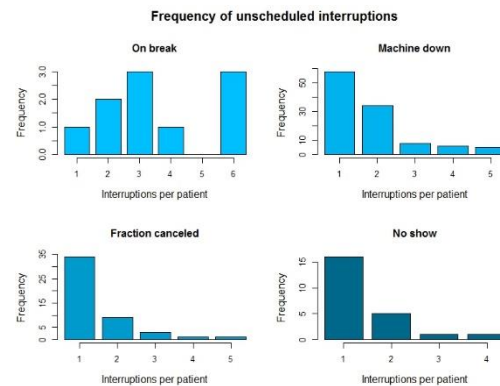
From April 2014 to July 2018, 392 patients with prostate cancer were analyzed for this study. VMAT plans were carried out using Monaco TPS (v5.10). There are 14 local/national holidays each year in our country. Although there is no consensus about what is the ideal treatment time for prostate cancer, most publications recommend not exceeding the TTT by more than 2 to 5 days. Some form of compensation should be introduced where the interruption results in a prolongation of overall treatment time of more than five days.

#### Results

Frequency of treatment lengthened is displayed in Figure I. If we consider scheduled treatment time plus 5 days at most, 63% of the treatments were completed on time (only 11% of them were completed with zero days of delay). Meanwhile, 29% had a delay between 6-10 days and approximately an 8% of the patients had a delay of more two weeks. That means that 37% of prostate patients must have treatment compensations.



Moreover, 73% of the patients started treatment on a Monday (38%) or Tuesday (35%); 16% started on a Wednesday, 10% on a Thursday and 1% on a Friday. Regarding the type of interruption (B= on break; M= machine down; X= canceled, N=no show), 37% of the patients suffered at least one type of unscheduled interruptions (one type 74%; combination of two types 23%; and combination of three types, 3%). Most frequent interruption is M, followed by X. Frequency of type of interruption is shown in Figure II. Also, 52% of the patients suffered scheduled interruptions like preventive machine maintenance or public holidays.



If we look the 'Machine down' histogram (Figure II), 58 patients had only one day of interruption because of a machine breakdown, meanwhile 34 patients had two days of interruption.

In the histogram 'Fraction cancelled' you can see that 34 patients suffered one day of interruption, meanwhile 8 patients suffered two days of interruption.

#### Conclusion

Unscheduled interruptions, like machine breakdown and patient illness, make difficult to complete the treatment in an ideal time. Although our institution has a protocol to deal with these interruptions, from the results we can conclude that this protocol should be reviewed. Also, due to the machine overload, it is difficult to compensate these unscheduled interruptions for every patient. Therefore the best option could be to open the facility to treat patients on weekend days and public holidays to cope with predictable and unpredictable interruptions to normal treatment.

### PO-1014 Novel independent dosimetry audit based on end-to-end testing in proton beam therapy.

A. Carlino<sup>1</sup>, H. Palmans<sup>1,2</sup>, C. Gouldstone<sup>2</sup>, P. Trnkova<sup>3,4</sup>, S. Vatnitsky<sup>1</sup>, M. Stock<sup>1</sup>

<sup>1</sup>MedAustron Ion Therapy Center, Medical Physics, Wiener Neustadt, Austria; <sup>2</sup>National Physical Laboratory, Medical Physics, Teddington, United Kingdom; <sup>3</sup>Erasmus MC, Medical Physics, Rotterdam, The Netherlands; <sup>4</sup>HollandPTC, Medical Physics, Delft, The Netherlands

#### Purpose or Objective

The purpose of end-to-end testing (EZE) is to confirm that the entire logistic chain of a radiation treatment starting from CT imaging, treatment planning, patient positioning and verification and beam delivery is adequately implemented resulting in sufficient accuracy of planned dose delivery. A novel methodology for dosimetric EZE based on customized anthropomorphic phantoms using alanine dosimetry, ionization chambers and radiochromic films was established at a scanned proton therapy facility (called A here). Based on this methodology an independent dosimetry audit was developed and applied, for the first time, to a starting proton therapy facility (called B here) equipped with a scanned beam delivery system. We present results of both proton facilities including overall 4 different beam lines.

#### Material and Methods

A homogeneous polystyrene phantom and two anthropomorphic phantoms (pelvis and head phantom) have been customized to allocate different detectors such as radiochromic films, Farmer chamber and alanine pellets. During testing, the phantoms were moving through the workflow as real patients to simulate the entire clinical procedure. The CT scans were acquired with pre-defined scan protocols used at the A and B proton therapy facility for cranial and pelvic treatments. All treatment planning steps were performed with RayStation (RS) v6.1 and v7.0 TPS available respectively at A and B institute. A physical dose of 10 Gy was planned to clinically shaped target volumes in order to achieve reproducibility better than 0.5% on the dose delivered to the alanine pellets. In the treatment rooms the plans were delivered to the phantoms loaded either with alanine pellets and radiochromic EBT3 films or a Farmer chamber (figure 1). The alanine pellets (5.0 mm diameter and 2.4 mm thickness) and their read-out were provided by NPL. Corrections for the alanine “quenching” were derived by a Monte Carlo dose calculation platform implemented in a non-clinical version of RayStation.



Figure 1: EZE audit procedures with the head phantom. Left: the phantom loaded with Farmer chamber at the B proton therapy facility. Right: the phantom loaded with 22 alanine pellets and EBT3 films at the A proton therapy facility.

#### Results

The measured absolute dose to water obtained with the Farmer chamber in all delivered plans was within 2% of the TPS calculated dose. A maximum lateral homogeneity index of 3.5% inside the treatment field was measured with EBT3 films. Doses derived with the alanine pellets after correction for the quenching effect showed a mean deviation within 2% and a maximum deviation below 5% in the homogeneous and anthropomorphic phantoms (figure 2). Several audits are planned to be performed in the near future and more results coming from other proton therapy facilities may be available at the time of the presentation.

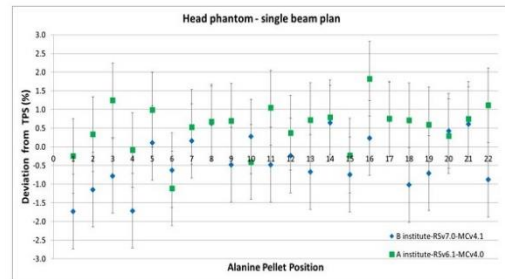


Figure 2: Relative differences between dose derived with alanine pellets and TPS planned dose for a single beam plan delivered to the head phantom. In blue symbols the comparison for the plan delivered at the B proton therapy center and in green symbols the comparison for the plan delivered at the A proton therapy center.

#### Conclusion

Our experience shows that alanine pellets are suitable detectors for dosimetric EZE test based audits and the developed procedures can be used to support implementation of upcoming new proton beam therapy facilities in Europe and may also serve as dosimetric credentialing for clinical trials in the future.

#### PO-1015 Design of 2.5 MeV electron beam applicator for < 5 mm thick superficial lesions

A. Valve<sup>1</sup>, H. Nurmi<sup>1</sup>, A. Kulmala<sup>1</sup>, S. Koskenmies<sup>2</sup>, M. Tenhunen<sup>1</sup>

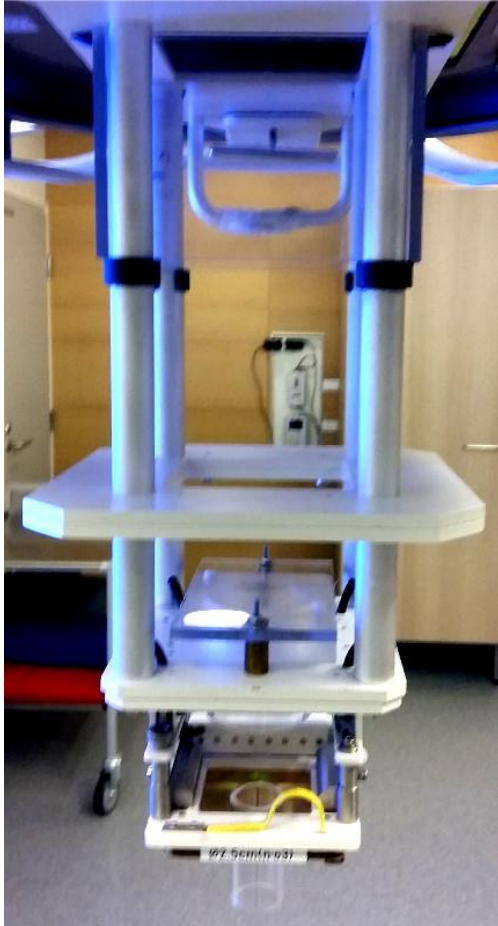
<sup>1</sup>Helsinki University Hospital, Cancer Center, Helsinki, Finland; <sup>2</sup>Helsinki University Hospital, Department of Dermatology, Helsinki, Finland

#### Purpose or Objective

Skin cancers are the most common of all malignant diseases. Many types of small cancerous skin lesions require only  $\leq 5$  mm treatment depth. Treating that kind of targets with any deeper penetration is unnecessary and may be harmful. We have modified a standard electron applicator to produce a set of well collimated circular fields, aiming nearly constant depth dose between 0 - 5 mm and a steep fall-off at depths  $> 6$  mm.

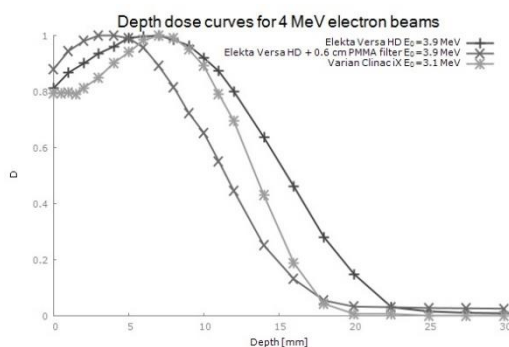
#### Material and Methods

The standard electron 6x6 cm square applicator of the Elekta Versa HD linear accelerator has been modified to reduce nominal 4 MeV electron beam suitable for the purpose. With a 6 mm thick polymethyl-metacrylate (plexiglas) filter slab bottom edge located 18.0 cm from the isocenter the energy was reduced from  $R50 = 1.8$  cm of the standard 4 MeV to  $R50 = 1.0$  cm. To achieve sharp edges the fields has been collimated with the plexiglas tubes from 2.5 to 5 cm inner diameters. In addition, lateral radiation through open sides of the applicator outside the field edges has been reduced with plexiglas plates. The final design of the applicator is presented in Fig 1.



## Results

With the modified applicator it is possible to achieve reasonably flat dose distribution in lateral and depth (< 6 mm) directions (Fig 2). After 6 mm depth there is a rapid dose fall-off with  $R50 = 1.0$  cm and  $R_p = 1.6$  cm. The penumbræ are sharp ( $\pm 6$  mm at depth of dose maximum). The energy filter plate reduces the dose output by a factor of 7.



## Conclusion

Our electron applicator has very favorable dose distribution characteristics for treating small superficial skin lesions, compared with either superficial x-ray devices or skin applicators of brachytherapy afterloaders. With x-rays < 100 kV tissues with higher density, like cartilage or bone, receive higher dose because of higher local absorption. Additionally, both x-rays and Ir-192 produce higher dose deeper than 5 mm in healthy tissue and higher dose inhomogeneity within the target depths  $\leq 5$  mm. Currently, we are initiating a clinical trial for testing the safety and efficacy of the new skin applicator.

## PO-1016 Segmentation of CT images with AI: compensating annotation uncertainties using contour augmentation

U. Javaid<sup>1</sup>, D. Dasnoy<sup>2</sup>, J. Lee<sup>1</sup>

<sup>1</sup>UCLouvain, IREC/MIRO, Brussels, Belgium ; <sup>2</sup>UCLouvain, ICTeam, Louvain-la-neuve, Belgium

### Purpose or Objective

Annotation of organs-at-risk (OARs) and target volumes (TVs) on CT scans is a key step in radiotherapy. Manual annotation is still in practice whereas to automate it, deep learning (DL) is currently being investigated. However, performance of DL networks (DLNs) depends highly on ground truth (GT) quality. For example, in radiotherapy, delineating TVs is of prime concern and proper care is taken while drawing them. OARs are not always a priority and sometimes roughly annotated. Rough annotation affects the predictive capabilities of DLNs in terms of organ localization. The network learning is thus sub-optimal, as it cannot improve over the given unique, possibly offset contour. Augmenting GT can address this issue. In this work, we propose **contour augmentation** to compensate the insufficient annotation quality by training a fully convolutional network (**dilated UNet**) with multiple GTs per image.

### Material and Methods

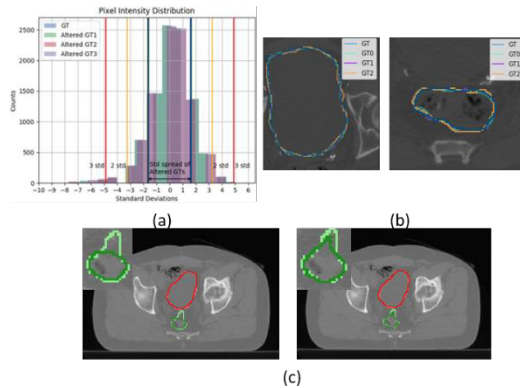
To address annotation uncertainties, we augment the input contours per image and produce multiple contours. Given a single GT, we apply random deformation within **4mm** to its x and y coordinates. A *Gaussian* smoothing is applied to smoothen the deformed contours to be qualitatively consistent with the original GT. Each deformed GT is considered as an additional GT. By incorporating multiple GT variations in the training phase, the model not only learns from a single ambiguous GT but from a sampled distribution of GTs, which can enhance its predictive capabilities, especially if some sampled GTs better correlate with features in the input image than the original GT. Our dataset consists of **pelvic** CT scans acquired from **67** patients (retrospective use). The CT images and their corresponding OAR annotations, in particular *bladder* and *rectum* were used for this study. We train our model on **1163** CT slices.

### Results

After training, our model is able to take into account the different variabilities in GT and thus is more robust to missing/wrong annotations as compared to a model trained with a single GT. In the example test case (Figure 1), we show that our model is able to correct the missing annotation. We report **Dice score**, **95th percentile Hausdorff distance** and **average symmetric surface distance** for bladder and rectum as  $0.91 \pm 0.12$  and  $0.89 \pm 0.09$ ,  $2.08 \pm 0.93$  and  $1.38 \pm 1.09$  mm,  $0.24 \pm 0.11$  and  $0.14 \pm 0.08$  mm respectively.

### Conclusion

We address insufficient annotation quality by augmenting the manual annotations in GT. We call it *contour augmentation*. The proposed framework enables the DLNs to capture variability in terms of localizing the organ boundaries, allowing to correct the missing annotations at inference time. Our framework offers good generalization ability as it can be trained on any semantic segmentation task. We believe that contour augmentation can lead to accurate organ localization as it can cope with the possible bias introduced by annotation uncertainty.



## PO-1017 Towards magnetically focused proton minibeam: investigating the limits of a clinical PBS nozzle

T. Schneider<sup>1</sup>, L. De Marzi<sup>2</sup>, A. Patriarca<sup>2</sup>, Y. Prezado<sup>1</sup>  
<sup>1</sup>Imagerie et Modélisation en Neurobiologie et Cancérologie IMNC, CNRS - Université Paris 11 - Université Paris 7, Orsay, France ; <sup>2</sup>Institut Curie - PSL Research University, Centre de Protonthérapie d'Orsay - Radiation Oncology Departmentn, Paris, France

### Purpose or Objective

Proton minibeam radiation therapy [1] is a novel and promising technique which already showed a remarkable widening of the therapeutic window for radioresistant tumours [2,3]. So far, this technique has been implemented at a clinical centre [4,5] by means of a multi-slit collimator. The goal of this work was to evaluate the feasibility of generating proton minibeam at a clinical beamline without the need of an external collimator. This would maximise the dose rate, reduce the neutron production and pave the way for 3D intensity-modulated treatment planning. The biological data obtained in recent experiments indicates that the tolerances of normal tissue can be increased when irradiated with narrower beams. In particular, in order to maximize the normal tissue sparing, beam widths narrower than 3 mm are preferred [2, 6]. However, in the current clinical configuration, the beam spot size at isocentre is 18 mm at 100 MeV and 10 mm at 200 MeV (values referring to the full width at half maximum [FWHM] of the lateral beam profile).

### Material and Methods

The Monte Carlo simulation toolkit TOPAS v.3.1.p02 [7] was used to model a complete pencil beam scanning nozzle (IBA Proteus PLUS) including the quadrupole and dipole magnets. The model was benchmarked against experimental data and the impact of different modifications of the beamline on the spot size and beam divergence was evaluated. Among others, the modifications included changing the magnetic field of the focusing elements, adding extra focusing magnets and reducing the distance between certain nozzle components.

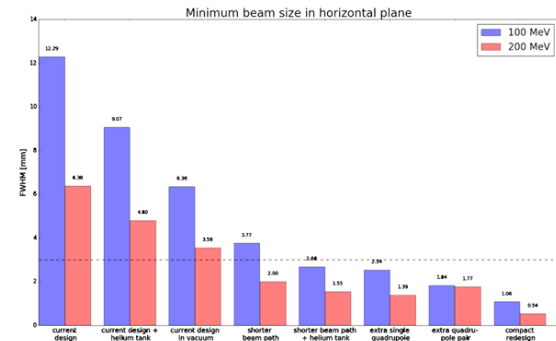
### Results

The limits of the current nozzle have been established: the beam widths cannot be made smaller than 12.3 mm at 100 MeV or 6.4 mm at 200 MeV by changing only the magnetic fields. The addition of extra focusing magnets at the exit of the nozzle allows to obtain widths as small as 1.8 mm at 100 MeV and 1.4 mm at 200 MeV. Furthermore, the reduction of nozzle dimensions, keeping only essential components allows to reach 1.1 mm at 100 MeV and 0.6 mm at 200 MeV.

### Conclusion

This is the first study evaluating a collimator-free generation of proton minibeam at a clinical centre. Our first results indicate that the implementation at current clinical beamlines will be challenging. However, we

propose different approaches that would enable the beam size reduction required to obtain proton minibeam.



### References

- [1] <https://doi.org/10.1118/1.4791648>
- [2] <https://doi.org/10.1038/s41598-017-14786-y>
- [3] [https://doi.org/10.1016/S0167-8140\(18\)30879-X](https://doi.org/10.1016/S0167-8140(18)30879-X)
- [4] <https://doi.org/10.1118/1.4935868>
- [5] <https://doi.org/10.1002/mp.13209>
- [6] Proton minibeam radiation therapy leads to a superior tumor control than standard proton therapy in RG2 glioma-bearing rats. Submitted to Int. J. Radiat. Oncol. Biol. Phys.
- [7] <https://doi.org/10.1118/1.4758060>

## PO-1018 Current status of pediatric image-guided radiation therapy in Europe: An international survey

C. Windmeijer<sup>1</sup>, A. Bel<sup>1</sup>, R. De Jong<sup>1</sup>, B. Balgobind<sup>1</sup>, G. Collaboration<sup>2</sup>, C. Rasch<sup>1</sup>, I. Van Dijk<sup>1</sup>  
<sup>1</sup>Amsterdam UMC- location AMC, Radiation Oncology, Amsterdam, The Netherlands ; <sup>2</sup>Participating institutions, Radiation Oncology, Various Europe, The Netherlands

### Purpose or Objective

Image-guided radiotherapy (IGRT) enables high precision tumor treatment while sparing healthy tissues. Particularly in pediatric radiotherapy the value of IGRT is widely acknowledged, but there is no consensus on the 'best practice'. With this survey we aim to evaluate clinical pediatric IGRT patterns in European radiotherapy institutes.

### Material and Methods

An eight-domain survey based on seven treatment sites was sent to members of the Pediatric Radiation Oncology Society and/or our IGRT project-based consortium in 70 European institutes. The domains include items on radiotherapy preparation, planning and delivery. Responses were collected from June-September 2018.

### Results

In total, 42/70 institutes (60%) responded; 33/42 (79%) treat children, one of which focuses exclusively on total body irradiation. The number of children treated annually varies between institutes and per site from 1 to 130 (Figure 1). Photon/electron therapy is used in 26/33 (79%) centers, and 3/33 (9%) use photon therapy only. Proton therapy (PT) is available in 5/33 (15%) institutes, whereas 7/28 (25%) of photon centers refer to proton centers; 2/33 (6%) use both photon and proton therapy. To immobilize patients, facial masks are used in 100% of brain, craniospinal axis (CSA) and head-and-neck (H&N) radiotherapy (all devices in Table 1). Most institutes (89% (thorax), 93% (abdomen), 96% (extremities) and 100% for other sites) use 3DCT scans to define the treatment target. Also MRI (range, 79% for thorax to 97% for brain), PET (range, 21% for CSA to 79% for H&N), and, for thorax and abdomen, 4DCT scans (by respectively 43% and 31% of institutes) are used. IMRT/VMAT is the most common treatment technique (range, 71% for CSA to 87% for brain), followed by 3DCRT (range, 36% for H&N to 69% for

extremities). Averaged over all sites, 3D conformal PT is used in 60% and IMPT in 80% of the proton centers. Averaged over all enquired indications, 70% of institutes follow (inter)national clinical treatment protocols, although varying protocols are used depending on indication and institute. Most institutes treat patients in supine position (range, 82% for CSA to 94% for brain). Regarding image guidance during treatment delivery, in-room 3D CBCT (kV) is used most frequently (range, 57% for CSA to 86% for thorax, Table 1). Daily online imaging is used by the majority (range, 85% for extremities to 90% for abdomen and pelvis), and offline imaging protocols (eNAL) are used by 14% (H&N) to 21% (thorax) of institutes.

Figure 1. Estimated number of patients treated annually across participating institutions, per treatment site.

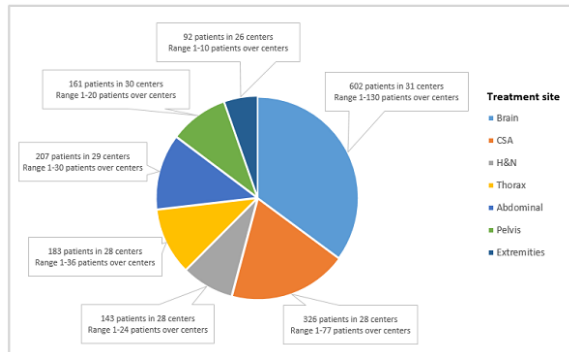


Table 1. Overview of immobilization and in-room IGRT practice for pediatric patients in the 33 responding institutes treating children

	Brain (N=31) N (%)	CSA (N=28) N (%)	H&N (N=28) N (%)	Thorax (N=28) N (%)	Abdomen (N=29) N (%)	Pelvis (N=30) N (%)	Extremities (N=25) N (%)
<b>Preparation</b>							
<b>Immobilization devices</b>							
Facial mask / head cast	31 (100)	28 (100)	28 (100)	9 (32)	3 (10)	0 (0)	1 (4)
(Partial) body cast	8 (26)	6 (21)	7 (25)	15 (54)	9 (31)	9 (30)	8 (31)
Vacuum mattress	14 (45)	16 (57)	7 (25)	18 (64)	23 (79)	21 (70)	20 (77)
Knee support	22 (71)	16 (57)	17 (61)	18 (64)	19 (66)	23 (77)	19 (75)
Foot support	7 (23)	7 (25)	4 (14)	8 (29)	8 (28)	15 (50)	19 (73)
<b>Treatment delivery</b>							
<b>In-room IGRT devices</b>							
MV planar imaging (2D); MV film or EPID	9 (29)	9 (32)	6 (21)	4 (14)	5 (17)	6 (20)	8 (31)
kV planar imaging (2D)	15 (48)	13 (46)	12 (43)	13 (46)	11 (38)	14 (47)	13 (50)
Stereotactic targeting (2D, 1kV and 1 MV image)	8 (26)	0 (0)	1 (4)	0 (0)	2 (7)	2 (7)	0 (0)
kV CBCT (3D)	23 (74)	16 (57)	22 (78)	24 (86)	24 (83)	24 (80)	19 (73)
MV CBCT (3D)	4 (13)	4 (14)	5 (18)	2 (7)	4 (14)	4 (13)	4 (15)
MR guidance	1 (3)	0 (0)	0 (0)	0 (0)	0 (0)	0 (0)	0 (0)
<b>IGRT protocols</b>							
Daily online	27 (87)	24 (86)	24 (86)	24 (86)	26 (90)	27 (90)	22 (85)
Offline	5 (16)	5 (18)	4 (14)	6 (21)	5 (17)	5 (17)	5 (19)
NAL	0 (0)	0 (0)	0 (0)	0 (0)	0 (0)	0 (0)	0 (0)
eNAL	5 (16)	5 (18)	4 (14)	6 (21)	5 (17)	5 (17)	5 (19)
SAL	0 (0)	0 (0)	0 (0)	0 (0)	0 (0)	0 (0)	0 (0)

Abbreviations: CSA, craniospinal axis; H&N, head and neck; 3DCT, 3D Computed Tomography; IMRT, Intensity Modulated Radiotherapy; VMAT, Volumetric Arc Therapy; IMPT, Intensity Modulated Proton Therapy; IGRT, Image-Guided Radiotherapy; EPID, Electronic Portal Imaging Device; CBCT, cone-beam CT; MR, Magnetic Resonance; NAL, non-action level; eNAL, extended non-action level; SAL, shrinking action level

## Conclusion

Our results show moderate agreement in clinical pediatric IGRT use in European institutes. The findings from this survey can help to define internationally acceptable standard quality criteria for 'best practice' guidelines for pediatric IGRT.

**PO-1019 The elephant plot: Differentiating between early recurrence and Benign Lung Injury after SABR**  
**I. Phillips<sup>1</sup>, H. Wang<sup>2</sup>, P. Evans<sup>2</sup>, V. Ezhil<sup>3</sup>, H. Saxby<sup>3</sup>, C. South<sup>3</sup>, M. Hussein<sup>4</sup>, A. Nisbet<sup>3</sup>, S. Alobaidli<sup>5</sup>, E. Chandry<sup>3</sup>**  
<sup>1</sup>Edinburgh Cancer Centre, Clinical Oncology, Edinburgh, United Kingdom; <sup>2</sup>University of Surrey, Centre for Vision- Speech and Signal Processing, Guildford, United Kingdom; <sup>3</sup>Royal Surrey County Hospital, St Lukes Cancer Centre, Guildford, United Kingdom; <sup>4</sup>National Physical Laboratory, Medical Radiation Physics, Teddington, United Kingdom; <sup>5</sup>Kuwait Cancer Control Centre, Radiotherapy Physics, Kuwait City, Kuwait

## Purpose or Objective

SABR (Stereotactic Ablative Body Radiotherapy) is an effective radiotherapy treatment for early stage lung tumours. Differentiating between the morphology of early recurrent/residual tumour and radiation induced lung injury (RILI) after SABR is challenging using both CT and PET-CT imaging. In this study we investigated whether CT

textural analysis of the whole lung can help differentiate between tumour and RILI after SABR.

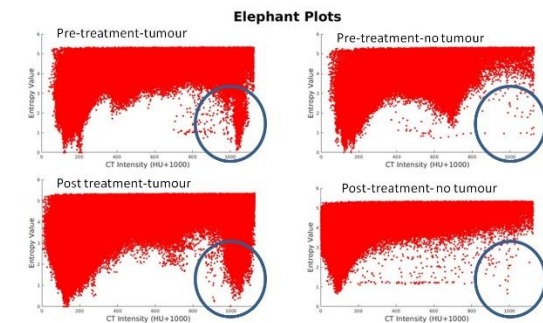
## Material and Methods

We compared the 6 month post SABR single phase CT scan of 25 patients (who had not recurred at 2 years), with 4 patients who had PET-CT proven recurrence 6 months after treatment.

The ipsilateral lung was segmented on the CT scan. A Grey Level Co-occurrence matrix (GLCM) for each lung containing tumour was created. Each voxel had a density and an entropy score assigned relative to the neighbouring 26 voxels. Previously we showed that a 2D data plot of each voxel (density vs entropy) showed an 'elephant plot' with the tumour corresponding to the elephant 'trunk' when comparing the lung ipsilateral to tumour with the contra-lateral lung. We performed a sub-region analysis on the elephant trunks, which included those voxels, which had a high density, but low entropy score. We performed 4 sub-analyses using different density and entropy thresholds, to include different parts of the elephant trunk.

## Results

The most statistically significant differences were found using an entropy score of 2 or less and density (HU) of 0-150. P values for Mann-Whitney test comparing recurrence vs non-recurrence was: number of voxels in sub-ROI (p=0.007) and Entropy Standard Deviation (p=0.048).



## Conclusion

CT texture analysis may be useful as a cost effective means of differentiating between tumour and RILI after SABR. This technique provides a promising model to track changes in lung parenchyma in malignant or benign lung disease. However, further validation in a prospective trial on a larger cohort of patients is required.

**PO-1020 The Sicily Dosimetric Project: a multi-institutional project on IMRT/VMAT lung treatment**  
**C. Marino<sup>1</sup>, E. Bonanno<sup>1</sup>, N. Cavalli<sup>1</sup>, G.R. Borzi<sup>2</sup>, A.**

**Brogna<sup>3</sup>, R. Costa<sup>4</sup>, V. D'Antoni<sup>5</sup>, I. Fazio<sup>6</sup>, G. Iacoviello<sup>7</sup>, S.I. Illari<sup>8</sup>, S. Mele<sup>9</sup>, A. Rabito<sup>10</sup>, N. Romeo<sup>11</sup>, V. Salamone<sup>12</sup>, L. B. Tonghi<sup>13</sup>**

<sup>1</sup>Humanitas - Centro Catanese di Oncologia, Medical Physics, Catania, Italy; <sup>2</sup>REM Radioterapia, Radiotherapy, Catania, Italy; <sup>3</sup>AOU Policlinico G. Martino, Medical Physics, Messina, Italy; <sup>4</sup>ASP 2 Caltanissetta, Radiotherapy, Gela, Italy; <sup>5</sup>Casa di Cura La Maddalena, Radiotherapy, Palermo, Italy; <sup>6</sup>Casa di Cura Macchiarella, Radiotherapy, Palermo, Italy; <sup>7</sup>ARNAS Ospedale Civico, Medical Physics, Palermo, Italy; <sup>8</sup>Freelance Physicist, Via D. Sanfilippo 1, Catania, Italy; <sup>9</sup>AOE Cannizzaro, Medical Physics, Catania, Italy; <sup>10</sup>ASP 7 Ragusa, Medical Physics, Ragusa, Italy; <sup>11</sup>ASP 5 Messina, Radiotherapy, Taormina, Italy; <sup>12</sup>AOU Policlinico Vittorio Emanuele, Medical Physics, Catania, Italy; <sup>13</sup>ARNAS Garibaldi, Medical Physics, Catania, Italy

## Purpose or Objective

Multi-Institutional dosimetric projects allow to share knowledges and to ensure adequate quality of practice

and treatment delivery; the Sicily Dosimetric Project was born with this aim, using an approach very similar to external audits procedure.

#### Material and Methods

Thirteen centers from Sicily with a good experience in lung IMRT/VMAT treatments and with a great heterogeneity in terms of technologies, have participated to the project. In the first step, shared CT images (with CT calibration curve), with Target and OARs defined for a thorax anthropomorphic phantom, have been used to perform a treatment plan using 6MV energy beam with a prescription dose of 66 Gy in 33 fractions. Imposed planning constraints have been: at least 98% of the PTV received 95% of the prescribed dose and 2% of the PTV received 107% as maximum value; Heart,  $V_{25Gy} < 10\%$ ,  $D_{average} < 26Gy$ ; Lungs ((Dx+Sx)-GTV):  $V_{20Gy} \leq 30\%$ ;  $V_{5Gy} \leq 65\%$ ;  $D_{average} \leq 20Gy$ . Dosimetric analysis of treatment plans have been performed considering cumulative DVH curves for PTV and OARs. In the second step, OSL detectors, commissioned and analyzed from a pilot center, have been used. Preliminary measurements have been performed using RW3 slab phantom ( $30 \times 30 \times 10 \text{ cm}^3$ ) and reference conditions. One OSLD, allocated in apposite slab, situated at depth of 5 cm, has been irradiated at 2 Gy dose, with  $10 \times 10 \text{ cm}^2$  field and using SAD set up; the average over three measurements has been compared with expected dose. Verification plans have been generated and delivered in the same RW3 slab phantom using both ionization chamber and OSL dosimeters (repeating measurements three times). Finally, treatment plans have been delivered on the anthropomorphic phantom with end-to-end approach and OSLD allocated in the apposite inserts. Dose has been verified in three points: PTV, Heart and Mediastinum. To check the positioning of the phantom, CBCT, MV or kV, have been used. The anthropomorphic phantom without OSLDs inside has been resealed over the couch 5 times and the average positions for all directions, longitudinal, vertical and lateral, have been taken into account to obtain corrected dose values from TPS.

#### Results

Results related to the first step of the project satisfy imposed constraints by most of all centers; mean values for PTV:  $D_{98\%} = 63,50Gy$  (61,25-65,83),  $D_{2\%} = 69,18Gy$  (67,10-70,85); Heart:  $V_{25Gy} = 9,33\%$  (7,60%-11,65%),  $D_{average} = 9,87Gy$  (8,45-11,45); Lungs:  $V_{20Gy} = 22,74\%$  (18,50-27,90),  $V_{5Gy} = 51,39\%$  (39,48-58,28),  $D_{average} = 12,77Gy$  (10,71-14,80). Results related to the second step of the project are showed in Tab.1. Fig.1 shows the correlation between algorithms involved in the project and final results related to the anthropomorphic phantom; as it is expected Monte Carlo based algorithms give better results respect to CCC and AAA algorithms.

Center	RW3 Slab Phantom			Anthropomorphic Phantom		
	2Gy Ref. Cond. (OSLD)	IC	OSLD	Mediastinum (OSLD)	PTV (OSLD)	Heart (OSLD)
1	1,02	1,00	0,98	0,98	1,05	0,90
2	1,01	1,03	0,99	1,04	1,03	0,93
3	0,97	1,00	0,98	0,96	1,02	0,98
4	0,96	0,99	0,94	0,95	1,03	0,92
5	1,01	1,04	0,93	0,95	1,04	1,12
6	0,99	1,01	0,99	0,99	0,99	0,96
7	0,98	1,02	0,96	0,94	0,96	0,93
8	0,97	0,98	0,96	0,94	0,99	1,00
9	0,94	1,02	0,98	0,94	0,96	1,01
10	1,02	0,99	0,98	1,04	0,98	1,03
11	0,97	0,99	0,95	0,97	0,99	0,89
12	0,95	1,02	0,97	1,02	1,08	1,12
13	1,00	0,99	0,98	1,00	1,02	1,01

Tab.1: Values are expressed in terms of ratio: measured values over expected ones

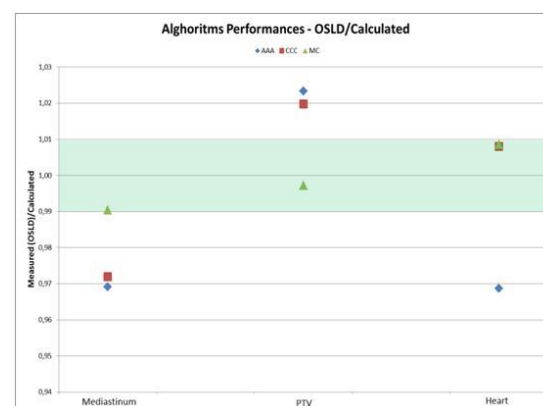


Fig. 1

#### Conclusion

The Sicily Dosimetric Project has been able to identify local problems for advanced treatments and could provide indications for future audit approach.

#### PO-1021 Influence of beamline and scanning magnets on the magnetic fringe field at a proton PBS nozzle

S. Gantz<sup>1,2</sup>, L. Riemann<sup>2</sup>, J. Smeets<sup>3</sup>, J. Pawelke<sup>1,2</sup>, A. Hoffmann<sup>1,2,4</sup>

<sup>1</sup>Helmholtz-Zentrum Dresden-Rossendorf, Radiooncology-OncoRay, Dresden, Germany; <sup>2</sup>OncoRay - National Center for Radiation Research in Oncology, Medical Center for Radiation Physics, Dresden, Germany; <sup>3</sup>Ion Beam Applications SA, Advanced Technology Group, Louvain-la-Neuve, Belgium; <sup>4</sup>Faculty of Medicine and University Hospital Carl Gustav Carus at the Technische Universität Dresden, Radiotherapy and Radiation Oncology, Dresden, Germany

#### Purpose or Objective

Real-time soft-tissue image guidance is a desirable concept to improve the targeting precision of proton therapy. In 2017, the first prototype of an MR-integrated proton therapy setup was realised at our horizontal fixed research beamline. Moving towards a clinical application this *in-beam* MRI system shall be transferred to a pencil beam scanning (PBS) research beamline that provides volumetric dose spot delivery. A magnetic survey was performed to quantify the effects of beamline and scanning magnets on the environmental magnetic field.

#### Material and Methods

The magnetic fringe field at the PBS nozzle was measured by a tri-axial Hall-probe magnetometer (THM 1176-LF, Metrolab) at two positions: (P1) at a lateral position 700 mm from the center of the scanning magnets, and (P2) at the planned magnetic isocenter of the *in-beam* MR

scanner, which is 2270 mm downstream from the last scanning magnet on the beam central axis. Measurement point P1 was chosen to be able to differentiate between magnetic field changes due to energizing the beamline (quadrupole) and the scanning (dipole) magnets. Two maps of PBS spots were delivered by the PBS nozzle: (M1) consisted of 16 energy layers ranging from 70 to 230 MeV (steps of 10 MeV) with a single central spot for each layer, and (M2) used a single energy of 200 MeV with a field size of (200 x 200) mm<sup>2</sup> and a step width of 5 mm, resulting in 41 x 41 spots. The magnets were energized to deliver maps M1 and M2 to study the magnetic field effects of changing beam energies and changing spot positions, respectively, but no beam was transported for radiation protection of the sensitive Hall-probe. All 3 magnetic field components were logged during spot map scanning by Labview-based software (THM1176 v4.0, Metrolab) at a sample frequency of 10 Hz.

### Results

For position P1, the magnetic field changes due to setting the beamline magnets to the 16 energy levels, as well as operating the scanning magnets to the 41 spot rows can be clearly observed (Fig. 1), with maximum amplitudes  $|\Delta B_{\max}|$  of up to 28.6  $\mu\text{T}$  and 55.3  $\mu\text{T}$ , for maps M1 and M2, respectively. For position P2, the  $|\Delta B_{\max}|$  was 9.0  $\mu\text{T}$  and 10.1  $\mu\text{T}$  for M1 and M2, respectively. This translates into an off-resonance frequency shift of 383.4 Hz and 430.3 Hz for <sup>1</sup>H-MR imaging, respectively.

### Conclusion

Significant changes in the environmental magnetic fringe field of a proton PBS beamline are measurable due to the operation of its beamline and scanning magnets. These changes translate into off-resonance frequency shifts that could cause significant MR image shifts in the frequency encoding direction. This needs to be confirmed by magnetic field mapping around the magnetic isocenter of the MRI scanner once it has been installed at the PBS nozzle. To counteract this effect, either the image shifts need to be compensated for or the PBS nozzle needs to be magnetically shielded from the MRI scanner.

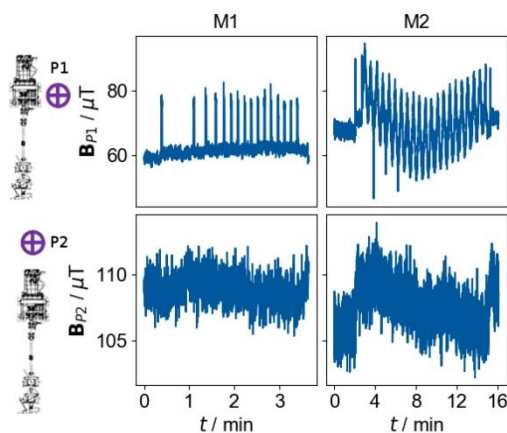


**Figure 1:** Schematic representation of PBS beamline with measurement positions P1 and P2 (left). Amplitude of magnetic fringe field measured during delivery of maps M1 and M2 at positions P1 (top row) and P2 (bottom row).

### PO-1022 A study on the image registration accuracy of intrafraction cone beam computed tomography images

S. Arumugam<sup>1</sup>  
<sup>1</sup>Liverpool and Macarthur cancer therapy centres-  
 Liverpool Hospital, Department of Medical Physics,  
 Liverpool, Australia

#### Purpose or Objective

Intrafraction (IF) cone beam computed tomography (CBCT) image acquisition procedure allows the CBCT image acquisition during treatment delivery and has the

potential to improve the treatment efficiency. However the quality of IF-CBCT images may be degraded due to scatter from treatment beam. The purpose of this study is to investigate the change in image quality between CBCT and IF-CBCT images and its impact on image registration accuracy.

#### Material and Methods

An Elekta linear accelerator with XVI imaging system (Elekta Limited, Crawley, UK) was used for this study. The image quality that resulting from Head and Neck (H&N), Lung and Spine pre-treatment and IF CBCT presets were quantified by imaging a Catphan-503 phantom (The Phantom Laboratory Inc, NY, USA). The IF-CBCT images were acquired with the delivery of both 6MV and 10 MV FFF VMAT arc of hypofractionated treatment plans. The number of projection images acquired for both CBCT and IF-CBCT are maintained constant for respective treatment site specific presets. The image quality metrics such as uniformity, low contrast visibility, spatial resolution and image geometry in horizontal, vertical and longitudinal directions were studied to characterise the quality of CBCT image data. To study the accuracy of image registration, the CBCT and IF-CBCT image data of H&N, lung and lumbar spine region of an anthropomorphic phantom were acquired and registered with the respective reference planning CT data. The baseline registration error for each treatment site was quantified by registering pre-treatment CBCT with respective reference CT using grey value registration. The image registration error resulting from 6D position offsets, ranging from 3mm to 10mm in translation and 0° to 3° in rotation, of the IF-CBCT data was studied with both bone and grey value registration methods available in XVI system to study the registration accuracy with IF-CBCT images.

#### Results

Table 1 shows the Catphan image quality results for both CBCT and IF CBCT imaging. The image uniformity, low contrast visibility and spatial resolution of the IF-CBCT images are relatively degraded compared to pre-treatment CBCT images. The geometry of both CBCT and IF-CBCT images are within  $\pm 0.5$  mm of the expected values. The image registration results of IF-CBCT images agreed within  $\pm 0.5$ mm and  $\pm 0.5^\circ$  in translation and rotation directions compared to baseline error with both bone and grey value registration for studied treatment sites.

**Table 1:** Image quality metrics and CBCT and IF CBCT images if Catphan 503

Imaging mode	Uniformity (%)	Low contrast visibility (%)	Spatial resolution (lp/cm)	Geometry agreement (mm)
CBCT	1.9(0.5)	2.4(0.6)	3(1)	0.1(0.2)
IF-CBCT	4.0(0.7)	3.6(1.7)	3(0)	0.1(0.3)

#### Conclusion

The registration accuracy of IF-CBCT images are not affected by its degraded image quality and it deemed clinically useful for the studied anatomical sites and registration methods.

**PO-1023 Continuous Positive Airway Pressure for respiratory gating in lymphomas: a workflow analysis**  
 F. Giglioli<sup>1</sup>, E. Gallio<sup>1</sup>, M. Levis<sup>2</sup>, P. Solidoro<sup>3</sup>, C. Fiandra<sup>2</sup>, S. Bartoncini<sup>2</sup>, V. De Luca<sup>2</sup>, C. Cavallin<sup>2</sup>, G. Iorio<sup>2</sup>, R. Parise<sup>2</sup>, G. Furfaro<sup>2</sup>, U. Ricardi<sup>2</sup>  
<sup>1</sup>A.O.U. Città della Salute e della Scienza di Torino, Medical Physics, Torino, Italy; <sup>2</sup>University of Turin, Radiation Oncology- Department of Oncology-, torino, Italy; <sup>3</sup>A.O.U. Città della Salute e della Scienza di Torino, Division of Pulmonology, Torino, Italy

### Purpose or Objective

Continuous positive airway pressure (CPAP) is a form of positive airway pressure ventilator, which applies mild air pressure on a continuous basis and has long been safely used in patients with obstructive sleep apnea to maintain airway patency. The aim of this study is to determine the efficacy of CPAP on lung volume and respiratory management in patients treated for Hodgkin and primary mediastinal lymphoma.

### Material and Methods

The CPAP consists in a small air pump, tubing, and facemask, providing a constant stream of pressurized air to the lungs. Some effects expected during CPAP are hyperinflation of the lungs, stabilization and flattening of the diaphragm. The CPAP pressure used for each patient was selected as 18 cm H<sub>2</sub>O; two CT were performed: one in the free breathing condition (FB) and the other with the CPAP. The patients were trained for wearing the mask before the CT mainly to test the compliance with the system. 4DCT was accepted if the percent variation of the phase amplitude was < 0.25. Median prescription dose to the PTV was 30 Gy in 2-Gy fractions and Lungs, female breasts, heart and cardiac structures (coronary arteries, valves, atria and ventricles) were all contoured as organs at risk. Planning were performed with Monaco tps ver. 5.1; CPAP series were planned comparing a full arc (FA) plus an anterior non coplanar one in a sagittal plan with a butterfly geometry (BF). The best plan between the two solutions was selected and replanned in FB condition. The final plan was then chosen by the physician based on the OARs doses. The intersection between PTV and the Heart was evaluated as a measure of the "stretching" of the organs in case of CPAP. The treatment was performed with an Elekta Synergy and a Cone Beam CT (CBCT) was acquired before each session. To check the Lungs filling, the CBCT were analyzed in terms of measured volume displayed in the CT field of view of the fifteen days of treatment.

### Results

24 patients were recruited; 22/24 (92%) were treated with the CPAP system. The mean percent standard deviation of the amplitude was 0.19 (sd 0.08) compared to 0.21 (sd 0.11) of the 4DCT population. CPAP increased mean lungs volume (4.21 vs 2.71, p<0.001) and the mean volume difference was 1498 (sd 417) cc. The intersection between PTV and the hearts was 12 (sd 24) cc for CPAP and 27 (sd 29) for FB (p<0.01). The plans selected were 58% FA and 42% BF. The use of CPAP resulted in lower doses for all the cardiac structures (p<0.01). The variation of the volume of the lungs measured in all the CBCT was < 4,5%.

### Conclusion

CPAP has demonstrated to be a useful method for respiratory management; the analysis of the amplitude of the 4DCT revealed an equal or minor lungs movement respect to the 4DCT patients population. The analysis of CBCT demonstrated that CPAP is a constant and reproducible way to fill the lungs. Effort has to be made in finding some geometric parameters to prospectively select patients benefiting the use of CPAP by analyzing the CT.

### PO-1024 Solutions for MR-based RT planning with an open low field scanner using neural network tools

L. Fetty<sup>1</sup>, M. Buschmann<sup>1</sup>, G. Heilemann<sup>1</sup>, P. Kuess<sup>1</sup>, T. Nyholm<sup>2</sup>, H. Herrmann<sup>3</sup>, D. Georg<sup>1</sup>, N. Nesvacil<sup>1</sup>  
<sup>1</sup>Medical University of Vienna, Department of Radiotherapy and Christian Doppler Laboratory for Medical Radiation Research for Radiation Oncology, Vienna, Austria ; <sup>2</sup>Umeå University, Department of Radiation Sciences, Umeå, Sweden ; <sup>3</sup>Medical University of Vienna, Department of Radiotherapy, Vienna, Austria

### Purpose or Objective

In radiation oncology CT information is essential for TPS dose calculation whereas MRI is utilized to increase the delineation accuracy. In the past years multiple methods were developed to create synthetic CT (sCT) information from MR images directly, and are starting to be implemented in pilot studies on MRgRT. However, limited FOV can truncate the patient's body contour, which is required for calculating the dose deposition from the skin border to the target region. The use of small FOV scanners e.g. 0.35T open MR, thus are posing new challenges in the field of MR-only planning. The aim of this project was to develop (1) an MRI-acquisition and post-processing protocol to overcome scanner limitations, (2) an MR-only RT workflow for our department and (3) auxiliary software to implement conversion in this setting.

### Material and Methods

An MRI-only workflow for combining multiple laterally shifted MR scans and a conversion technique were designed and tested for the 0.35T MAGNETOM C! open-MR scanner (Siemens, Erlangen) with a maximum FOV of 400mm. The lateral table movement of the open-MR was used to position the patient twice off-isocenter to ensure the coverage of the complete body contour. A third sequence was acquired in the central position for delineation purposes. In a post processing step the two off-center images were stitched and further resampled to the single acquisition MRI to provide a full body contour. For sCT conversion a neural network was trained with about 2000 transversal 2D pelvis images. The workflow is illustrated in figure1.

The stitching protocol was tested for four prostate carcinoma patients treated with a VMAT technique. The sCT of the stitched volume was compared to the planning CT. Dose distribution comparisons was performed for the rigidly (rCT), deformed registered (dCT) corresponding CT and the sCT.

**Results**  
 Dice coefficient were 92% for left and right femoral bone and above 99% for the whole body between MR and sCT. The gamma analysis (2mm/2%) resulted in a 99.9% and 94.9% average pass rate for the dCT and rCT in the outer body contour, respectively. The dCT showed a dosimetric error below 1% in the target region where the rCT showed an increased error in the low dose region (D98%) of the target (as illustrated in table 1). The biggest uncertainty (D2% above 6%) was observed in the rectum for the rCT which was below 1.5% for the dCT.

Table 1: Dose comparison in percentage of PTV, femoral heads, bladder, rectum and the whole body.

		deformed CT		rigid CT	
		Mean [%]	SD [%]	Mean [%]	SD [%]
PTV	D2%	-0.9	0.4	-0.1	0.4
	D50%	-0.8	0.3	0.2	0.6
	D98%	0.2	0.9	4.4	4.0
femoral head right	D2%	-0.3	0.2	-0.3	0.4
	D50%	-0.4	0.2	-0.4	0.8
femoral head left	D2%	-0.5	0.3	-0.2	0.3
	D50%	-0.3	0.1	0.1	1.0
bladder	D2%	-2.0	0.4	-1.1	0.8
	D50%	-0.3	0.5	-0.1	0.2
	V70Gy	-0.7	0.7	-0.3	0.4
rectum	D2%	1.2	1.8	6.0	3.3
	D50%	-0.8	0.8	-1.6	1.0
	V70Gy	0.2	0.4	1.5	0.8
whole body	D10%	-0.3	0.1	-0.6	0.2
	D50%	-0.0	0.0	0.0	0.0
	D90%	0.0	0.0	0.0	0.0

### Conclusion

This study shows the potential of clinically implementing sCTs generated from a low-field open MR for patients with body contours larger than the single scan FOV. The lateral table movement is a benefit of the open-MR compared to most diagnostic scanners. The method could help overcome dosimetric uncertainties due to geometric distortions at the FOV borders. The dosimetric analysis showed comparable accuracy with published results of alternative methods for dose parameters and gamma analysis.

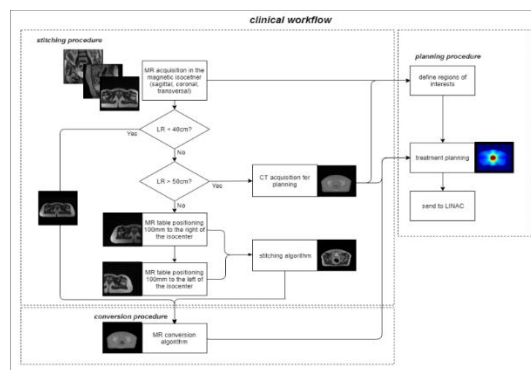


Figure 1: MR-only workflow description for the open 0.35T MR scanner

## PO-1025 The impact of dose to medium on the results of a national spine SBRT dosimetry audit

J. Lee<sup>1</sup>, R. Patel<sup>1</sup>, D. Eaton<sup>2</sup>, C. Clark<sup>3</sup>

<sup>1</sup>Mount Vernon Cancer Centre, National Radiotherapy Trials QA, Northwood, United Kingdom ; <sup>2</sup>Guy's Cancer Centre, Physics Department, London, United Kingdom ; <sup>3</sup>National Physical Laboratory, Teddington, London, United Kingdom

### Purpose or Objective

This national audit was carried out to verify the dosimetric and positional accuracy of spine SBRT treatment across a range of modalities and algorithm types. We investigated the impact of different algorithms for the calculation of dose in and around bone using film, Microdiamond (MD) and alanine dosimetry.

### Material and Methods

A modified CIRS E2E phantom was used; metal pins facilitated submillimetre registration between EBT3 GafChromic film and calculated dose grid. Bone and tissue equivalent alanine holders were used. The geometry of the detectors and target volumes is shown in figure 1. Centres were provided with a delineated CT dataset. Centres added their clinically used PTV and cord PRV margins. Planning constraints were prescription dose of 27Gy/3# to cover  $\geq 95\%$  of PTV, cord PRV  $D_{0.1cc} < 21.8\text{Gy}/3\#$  and cord  $D_{0.1cc} < 18\text{Gy}/3\#$ . Each centre scanned the phantom and re-calculated their optimised plan on their CT dataset with all locally available algorithm types; being of dose to medium (Dm,m), dose to water (Dw,w) and dose to water in a medium (Dw,m).

FilmQAPro software was used for analysis. Maximum distance-to-agreement (DTA) for the cord constraints and prescription isodoses were measured. The average dose to small areas-of-interest (AOIs)  $\sim 9\text{mm}^2$  at positions corresponding to the small volume dose detectors were also compared.

The Wilcoxon Signed Rank test was used to assess the difference between Dm,m and Dw,m algorithms.

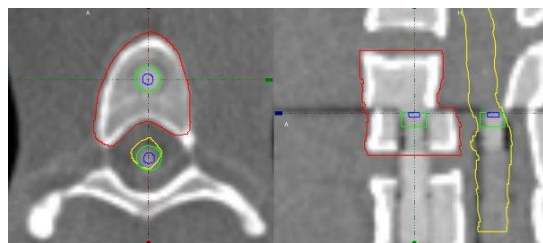


Figure 1. The geometry of the CTV (red), cord (yellow), alanine pellet (green), Microdiamond detector (blue). The film is inserted axially into the phantom 1mm superior of the alanine and MD detector. The small AOI film regions are at the same axial position as the MD detector and 1mm superior.

### Results

Measurements were made at 16 centres (1 Tomotherapy, 4 Cyberknife, 11 linac) which were treating SBRT spine routinely. Centres used PRV margins of 2mm and PTV margins of 2-3mm.

All centres achieved a DTA of  $\leq 2\text{mm}$  for the cord constraint isodose lines. The maximum distances between measured and calculated prescription isodoses was  $-2\text{mm}$  and  $+6\text{mm}$  (negative sign implying lower target coverage than planned). There was no significant correlation with algorithm type.

Small volume dose measurement results in the vertebra and cord for the different detectors and algorithms are shown in table 1. Particularly in the cord, differences between measured and calculated doses are higher than those normally reported in dosimetry audits, reflecting the contribution of the steep dose gradients in SBRT plans. For all plans, doses calculated in the vertebra with Dm,m were lower at all detector points than with Dw,m (average difference being 4.6% for MD, 4.0% for alanine, 3.4% for film,  $p=0.04$ ).

For all plans, Dm,m calculated cord doses were also lower than the Dw,m doses (average 0.9% for MD ( $p=0.08$ ), 0.7% for alanine ( $p=0.08$ ), 1.3% for film ( $p=0.04$ )).

	Dm,m (Acuros, MC), n=6	Dw,w (AAA, CC, Raytracing), n=14	Dw,m (Acuros, MC), n=5
Isodose DTA (mm)	average (min, max)	average (min, max)	average (min, max)
18Gy/3#	0.7 (-1.0, 2.0)	0.4 (-2.0, 1.5)	0.7 (-0.5, 2.0)
21.8Gy/3#	0.6 (-1.0, 1.5)	0.2 (-2.0, 1.5)	0.7 (-0.5, 1.5)
27Gy/3#	3.0 (1.5, 6.0)	1.5 (-2.0, 5.5)	2.6 (2.0, 3.0)
Film 9mm <sup>2</sup> area	average (min, max)	average (min, max)	average (min, max)
Vertebra (%)	5.0 (1.3, 9.6)	4.1 (-8.3, 10.3)	0.9 (-2.2, 6.1)
Cord VOI (%)	10.3 (4.8, 18.1)	4.6 (-19.9, 22.6)	7.8 (-5.6, 18.3)
Microdiamond	average (min, max)	average (min, max)	average (min, max)
Vertebra (%)	5.3 (1.1, 8.2)	3.9 (0.0, 9.0)	0.5 (-2.4, 3.4)
Cord VOI (%)	8.2 (0.1, 32.9)	-0.3 (-10.5, 12.5)	2.3 (-1.3, 8.5)
Alanine	average (min, max)	average (min, max)	average (min, max)
Vertebra (%)	4.2 (-1.0, 8.5)	2.4 (-1.4, 4.2)	1.3 (-2.1, 4.5)
Cord VOI (%)	9.7 (2.3, 35.1)	0.8 (-8.6, 8.2)	3.9 (-3.3, 8.7)

Table 1. Results of the isodose maximum distance-to-agreement, film small area-of-interest and MD and alanine dose comparisons. Positive values indicate measurements higher than calculated.

### Conclusion

The audit gathered evidence of safe implementation of spine SBRT; irrespective of algorithm type, all centres safely protected the cord and sufficiently covered the CTV with the prescription dose. Changing from Dm,m to Dw,m algorithms improved the agreement of point doses within vertebra and cord. This is assumed to be due to the water equivalence and calibration of the detectors.

## PO-1026 Evaluation of a microdiamond detector for a national spine SBRT end to end dosimetry audit

R. Patel<sup>1</sup>, J. Lee<sup>1</sup>, D. Eaton<sup>2</sup>, C. Clark<sup>3</sup>

<sup>1</sup>Mount Vernon Hospital, Radiotherapy RTTQA, Northwood Middlesex, United Kingdom ; <sup>2</sup>Guy's Cancer Centre, Radiotherapy, London, United Kingdom ; <sup>3</sup>Royal Surrey County Hospital, Radiotherapy, Guildford, United Kingdom

### Purpose or Objective

A national end to end audit of 16 centres (1 Tomotherapy, 4 Cyberknife, 7 Varian Linacs & 4 Elekta Linacs) was completed to assess the dosimetric accuracy of spinal SBRT. Spine SBRT plans are amongst the most complex currently delivered and the audit assessed the accuracy of treatment delivery by centres using a wide variety of equipment combinations. The audit utilised a microdiamond detector in addition to alanine and Gafchromic film. The results of the audit were analysed to determine the suitability of the microdiamond detector for future audits.

### Material and Methods

The audit required participating centres to deliver a clinically acceptable plan to an anthropomorphic spine phantom. Cyberknife centres had beam angles limited by  $40^\circ$  superiorly and  $20^\circ$  inferiorly from coplanar. Phantom alignment matched clinical practice for SBRT at each centre. Basic outputs were acquired in reference conditions using a PTW 0.125cc chamber and the microdiamond detector, with an additional output at the end of the audit to assess drift of the microdiamond detector. Delivered dose was measured at points in the

PTV vertebra and spinal cord, these measurements were compared with expected values from the TPS. Point doses were measured using alanine and the microdiamond detector. Detector output corrections were used for each centre based on measurements at standard output conditions. Centres also recalculated plans using all commissioned planning algorithms available on their TPS.

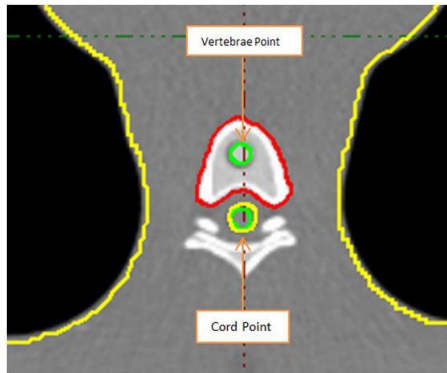


Figure 1 A CT image of the audit phantom with CTV (Red), Spinal Cord (yellow), Lungs (yellow) and measurement points (green) delineated

## Results

The output of the microdiamond detector had a mean deviation from the PTW 0.125cc chamber of 0.13% (S.D. 0.48%,  $P = 0.301$ ) at reference conditions for the 16 centres. The mean difference between outputs measured at the start and end of each audit visit was 0.07% (S.D. 0.32%,  $P = 0.929$ ).  $P$  values were calculated using a Wilcoxon sign rank test.

Results of the phantom measurement are given in Table 1. No significant difference was noted between the different detectors using a Wilcoxon sign rank test ( $P=0.926$ ). All linac treatments utilised coplanar VMAT delivery, while Cyberknife treatments utilised non-coplanar delivery.

Measurement Point	Delivery Equipment	No. Centres	Microdiamond Detector		Alanine	
			Mean Difference from TPS (%)	S.D. (%)	Mean Difference from TPS (%)	S.D. (%)
PTV Vertebra	Tomotherapy	1	5.8	-	1.8	-
	Cyberknife	4	3.2	1.5	0.7	1.7
	Varian	13	3.9	2.9	3.3	1.6
	Elekta	6	2.5	3.5	2.2	3.9
	All	24	3.5	2.8	2.6	2.5
Spinal Cord	Tomotherapy	1	-10.5	-	-8.6	-
	Cyberknife	4	-2.2	2.9	1.4	3.2
	Varian	13	2.3	5.9	2.2	5.1
	Elekta	6	8.6	12.2	11.3	12.3
	All	24	2.4	8.4	3.7	8.3

Table 1 Audit Results: The mean difference from TPS predicted values for the Microdiamond and Alanine phantom measurements, results are separated between the different delivery equipment.

## Conclusion

The results of the output measurements have shown that the microdiamond detector is consistent with the PTW 0.125cc chamber when measuring absolute dose. No drift was seen over the duration of any individual audits or the entire audit programme for the microdiamond detector. When measuring point doses during treatment delivery, the microdiamond detector was able to accurately measure dose independent of treatment equipment for both coplanar and non-coplanar delivery. The results were comparable with measurements with alanine, which has been widely used in national audit programmes. The results of this audit show that the microdiamond detector is suitable for future use in complex dosimetry audit, although further work is required to assess the long term stability of the detector and frequency of recalibration required.

## PO-1027 IMRT in breath hold for left breast cancer patients: surface tracking and clinical implementation

M. Cardoso<sup>1,2</sup>, S. Vieira<sup>1</sup>, A. Martins<sup>1</sup>, A. Soares<sup>1,2</sup>, M. Possanzini<sup>1,3</sup>, J. Morales<sup>1</sup>, C. Greco<sup>1</sup>  
<sup>1</sup>Champalimaud Foundation, Radiotherapy, Lisboa, Portugal ; <sup>2</sup>Mercurius Health, Radiotherapy, Lisboa,

Portugal ; <sup>3</sup>A.O. "G. Brotzu", Radiation Oncology, Cagliari, Italy

## Purpose or Objective

Deep inspiration breath hold (DIBH) for left breast cancer radiotherapy has shown beneficial dosimetric results on cardiac dose. Recently, DIBH was clinically implemented in our department for these cancer patients without lymph node (LN) involvement. This study reports on: a) validation of the optical surface tracking system used; b) aspects of treatment delivery with IMRT in DIBH.

## Material and Methods

We evaluated the static and dynamic performances of optical surface monitoring system (OSMS, Varian), which monitors patient surface, using a thorax phantom that can move periodically. To test system stability the phantom was continuously monitored during 90 minutes. Ten OSMS readings of the phantom position were done to test reproducibility. To evaluate the static accuracy, translational shifts from 1 to 20mm were manually applied to the couch and compared to OSMS shift readings. Dynamic tracking was analyzed, by comparing phantom surface markers position with pre-defined thresholds. Coincidence between linac beam hold signals, measured with an oscilloscope, marker positions and OSMS hold status, was analyzed.

Nineteen left breast patients were planned with IMRT (15 fractions, 2.7Gy to the whole breast with an integrated boost of 3.2Gy). CT scans were performed in free breathing (FB) and breath hold (BH) for each patient (fig1a) and contours were delineated in both by the radiation oncologist (RO). Similar plans were performed in Eclipse (Varian), with the same dose tolerances (fig1b). Doses to breast PTV, PTV and CTV boost, heart, left descending artery (LAD), right breast, right and left lung were analysed. The final delivery plan was chosen by RO. Before delivery a CBCT in FB was first acquired to verify patient position and a partial CBCT to evaluate BH. A beam hold threshold of 3mm was used for the OSMS (fig1c), given our CTV-PTV margin of 3mm. After delivery, a CBCT in BH was acquired.

Fig1. - Analysis of breath hold and imaging process for one patient.

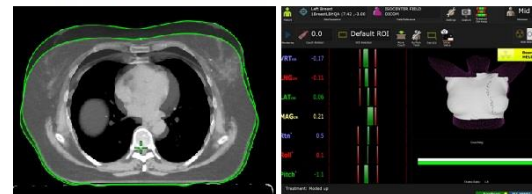


Fig1a. - Planning CT in free breathing (FB) and breath hold (BH).

Fig1c. - OSMS system during delivery. Red bars: beam hold threshold (3mm,<sup>39</sup>). Green bars: patient position within thresholds.

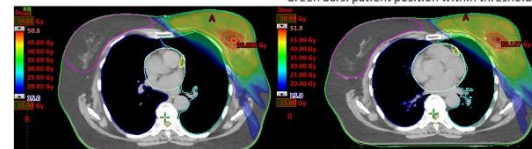


Fig1b. - Dose distribution: BH plan (left) and FB plan (right).

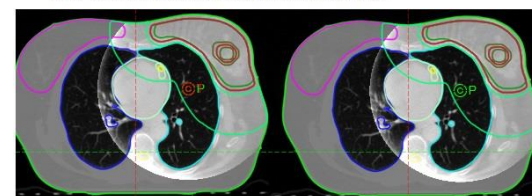


Fig1d. - Example of two CBCTs acquired in BH, during a treatment. Left: Initial CBCT before delivery (matching shifts: vrt=0.06cm, lng=0.00cm, lat=-0.08cm). Right: Final CBCT after delivery (matching shifts: vrt=0.01cm, lng=-0.08cm, lat=-0.06cm).

## Results

Concerning stability, a drift of 0.09mm was noted. The static reproducibility was found to be 0.04±0.01mm and

the agreement with 3D couch shifts was within 0.05 ±0.02mm. Beam hold can be achieved until threshold of 1mm and the gating coincidence between beam hold signals was estimated less than 1 second. Table 1 shows our planning data. In BH plans, as compared with FB, a decrease of 1.5±0.3Gy in mean heart dose and of 7.5±2.9Gy in maximum LAD dose was reported. Only for one patient the BH plan was not advantageous. On average, an extra CBCT in BH was acquired per session, due patient stability. On average, treatment delivery in BH was 26min, twice the FB value. Differences between BH CBCT before and after treatment delivery were well within the CTV-PTV margin (fig1d).

		FB Plan		BH Plan		Differences BH-FB		p value
		Mean	SD	Mean	SD	Mean	SD	
CTVBoost	V(100%) %	99,8	0,3	99,9	0,2	0,1	-0,1	0,67
	Volume (cc)	15,5	10,3	17,1	11,4	1,6	1,1	0,75
	Dmax (Gy)	50,8	0,8	50,6	0,7	-0,2	-0,1	0,48
PTVBoost	V(95%) %	99,5	0,6	99,5	0,6	0,0	0,0	0,76
	Volume (cc)	29,0	16,3	31,8	18,6	2,9	2,3	0,73
	Dmax (Gy)	50,9	0,9	50,6	0,7	-0,2	-0,2	0,39
PTVBreast	V(95%) %	99,2	0,5	99,4	0,5	0,2	-0,1	0,32
	Volume (cc)	683,2	252,0	702,3	248,8	19,2	-3,2	0,95
	Dmax (Gy)	50,9	0,9	50,6	0,7	-0,2	-0,2	0,40
Left Lung	V(18,07Gy)%	13,9	3,2	12,8	3,6	-1,1	0,4	0,34
	V(4,82Gy)%	47,9	4,7	43,9	5,9	-4,0	1,2	0,03
	Mean(Gy)	8,1	0,8	7,3	0,8	-0,8	0,0	0,01
	Volume (cc)	1205,3	292,3	2133,9	388,8	928,6	96,5	<<0,001
Right Lung	V(4,82Gy)%	1,8	2,4	1,8	2,7	0,0	0,3	0,95
	Mean(Gy)	1,6	0,4	1,4	0,5	-0,2	0,0	0,20
	Volume (cc)	1421,0	259,2	2404,9	329,6	983,9	70,4	<<0,001
Heart	V(9,38Gy)%	11,6	3,7	3,9	3,2	-7,7	-0,5	<<0,001
	V(30,6Gy)%	0,1	0,1	0,0	0,0	-0,1	-0,1	0,05
	Mean(Gy)	5,1	0,5	3,6	0,8	-1,5	0,3	<<0,001
	Volume (cc)	533,5	81,0	492,8	83,4	-40,7	2,4	0,14
Right Breast	V(4,82Gy)%	0,7	0,7	0,7	0,7	-0,1	-0,1	0,75
	Mean(Gy)	1,1	0,3	1,1	0,3	0,0	0,0	0,65
	Volume (cc)	663,7	235,1	667,5	232,3	3,8	-2,8	0,96
LAD	Dmax (Gy)	25,3	1,6	17,8	4,5	-7,5	2,9	<<0,001

**Table1** – Dose and volume differences calculated for the dosimetric plans in free breathing and breath hold for 19 patients. The statistical results, as calculated with the student t-test, are also shown (in green the values considered statistically significant, p<0.05).

## Conclusion

The OSMS system has been validated for continuous monitoring patient inspiration during treatment and is now being used clinically. DIBH with IMRT technique leads to better cardiac sparing as compared to FB. In the near future, we plan to extend DIBH to left breast patients with LN.

## PO-1028 Absolute validation of MR versus radiation iso-center on a high-field MR linac

U. Bernchou<sup>1</sup>, A. Bertelsen<sup>1</sup>, H.L. Riis<sup>1</sup>, H.R. Jensen<sup>1</sup>, C.R. Hansen<sup>1</sup>, F. Mahmood<sup>1</sup>, C. Brink<sup>1</sup>

<sup>1</sup>Odense University Hospital, Laboratory of Radiation physics, Odense, Denmark

### Purpose or Objective

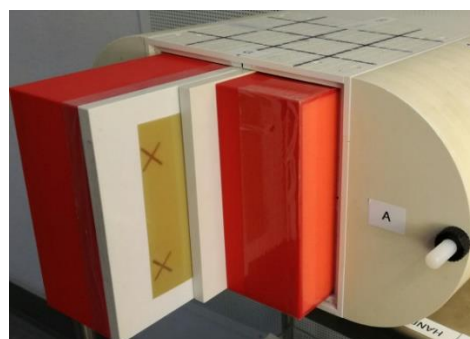
The superior soft-tissue contrast offered by the newly introduced MR linacs allows the localization of the tumour and surrounding normal tissue while the patient is on the treatment couch. However, in order to rely on the daily MR images for guidance of radiotherapy, there is a need to validate the positional accuracy between the planned and delivered dose distribution including all potential uncertainties of MR imaging and dose delivery. This abstract demonstrates a method to perform end-to-end validation of the dose delivery on a high-field MR linac based on an in-house 3D printed, MR visible phantom.

### Material and Methods

MR visible phantom inserts were created for the IMRT phantom (Scanditronix Wellhöfer). The MR visible parts were made of a bi-component silicone rubber (Eurosil 10 Orange) with added softener. The silicone is MR visible and the signal strength depends upon the amount of softener. Perspex rods were cast into silicone rubber with varying amounts of softener within 3D printed containers, creating an inhomogeneous MR visible phantom insert. Two such

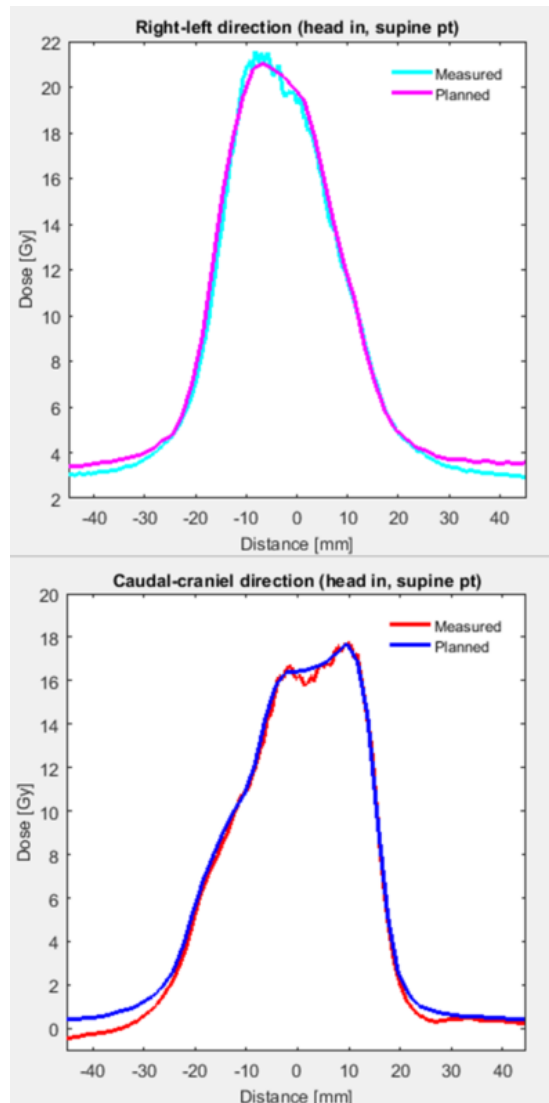
inserts were created and sandwiched around a radiochromic film supported by two solid water plates (see figure 1). The solid water plates contained copper crosses such that their positions were visible on the film after irradiation. The phantom supports both vertical and horizontal film alignment.

A seven beam stereotactic IMRT plan based on a CT scan of the entire phantom was created in the treatment planning system Monaco v 5.40 (Elekta AB, Sweden). At a high-field MR linac, T2 weighted 3D spin echo MR scans of the phantom were performed. Rigid registration of the MR position relative to the CT scan was performed in Online Monaco. The registration was used to calculate the current position of the treatment planning iso-center within the phantom as predicted by the entire treatment chain. After irradiation, the films were scanned in a flatbed scanner and gray levels were converted to dose (Lewis MedPhys 2012). The fixed copper crosses were visible on the film and were used to define the exact position of the film within the phantom.



## Results

An example of comparisons of relative profiles obtained from the film and the planned dose is shown in figure 2. The observable differences in dose are partly due to uncertainties in the conversion of optical density to dose. The high positional precision between the two dose profiles reflects the positional accuracy of the entire system. At our local MR linac, the end-to-end phantom measures a lateral offset of 0.4 mm, a longitudinal offset of 0.1-0.6 mm, and a vertical offset of 0.3 mm.



### Conclusion

Using 3D printed MR visible silicone inserts it was possible to create an end-to-end validation phantom for MR linacs. The phantom has been used in our department and the uncertainty of the dose positions is around half a millimeter, which is needed to make precise MR linac treatments.

### PO-1029 The use of Elekta Agility MLC Dynamic log files for VMAT QA

M. Picioli<sup>1</sup>, K. Torzsok<sup>1</sup>, A. Ruiz Plata<sup>1</sup>, F. Marangoni<sup>1</sup>, H. Broque<sup>1</sup>, J. Aponte<sup>1</sup>

<sup>1</sup>Fundacion Arturo Lopez Perez, Medical Physics, Santiago, Chile

### Purpose or Objective

The usage of massive dynamic parameters during VMAT treatments requires the implementation of new QA mechanisms. One major contributor potentially leading to mistreatments if not properly calibrated is the MLC. Following TG142 recommendations we have created a simple method in order to measure the constancy of leaf speed and positioning accuracy through Elekta Dynamic log files interpretation.

### Material and Methods

For MLC quality control a set of fields has been created using Elekta iComCAT V.13.0 software and loaded up in Linac Synergy console. In order to evaluate leaf speed

constancy a sweeping gap of 2cm x 24cm capable of sweeping 20 cm from X1 to X2 has been used. In order to calculate the theoretical MU value for this field, the following equation was applied:

$$UM = \frac{(\Delta UM / \Delta t)_{max}(x_f - x_i)}{(\Delta x / \Delta t)_{max}}$$

The MU above calculated took into consideration leaf banks at maximum nominal speed and maximum dose rate. Rising up the MU for this field in the software means that MLC should slow down. On the other hand, reducing this value means dose rate will slow down automatically. Once the desirable leaf speed has been calculated through a specific MU, it was compared against the logs from the machine. Regarding leaf positioning accuracy, a picket fence containing 3 segments of 6cm x 24cm was created and irradiated at 4 cardinal angles. For both field configurations, each leaf was analyzed individually and the actual values found in the logs were reported and compared against iComCAT theoretical values. Images for both field configurations were also acquired with IviewGT and compared against the logs providing a more reliable qualitative analysis than simple image visual inspection.

### Results

Figure 1 represents the real leaf speed constancy for both leaf banks obtained from the logs files. Leaf absolute positions were measured in 0,25 s time intervals and are represented by Y and X axis respectively. X1 bank starts moving at -10cm and bank X2 at -8cm (Elekta scale).



Figure 1 - MLC Speed Test

From Figure 1 we can see that both leaf banks have the same constant speed through the field. Any deceleration caused by lack of lubrication or issues with the motors could be easily recognized by deflections in the lines. The real leaf speed gathered from the graph differs less than 1% with respect to the calculated value in iComCAT. For the picket fence field, whilst irradiation of gantry 180 degrees, logs have shown maximum deviation of 0,4 mm for leaf 57 of X2 bank with respect of it nominal position. Leaf bank X2 also presented major differences in average for the same angle.

### Conclusion

Although the utilization of dynamic log files for Elekta linacs is not known in the clinical environment, this work shows it could be a very reliable and powerful tool for accuracy in positioning and speed constancy determination of the Agility MLC, also providing a quantitative complement of simple visual MLC Picket fence image inspection.

### PO-1030 Absolute validation of Multi Leaf Collimator (MLC) positions on a high-field MR linac.

A. Bertelsen<sup>1</sup>, U. Bernchou<sup>1</sup>, H.L. Riis<sup>1</sup>, C. Brink<sup>1</sup>

<sup>1</sup>Odense University Hospital, Laboratory of Radiation Physics, Odense, Denmark

### Purpose or Objective

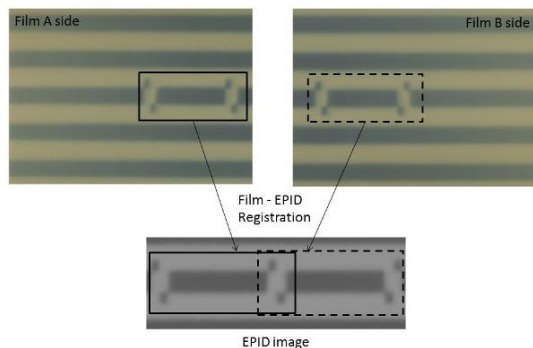
Use of MR guidance prior to each treatment delivery facilitates an improved target definition which has the potential to decrease the irradiated volume needed to ensure target dose coverage. In order to reduce the irradiated volume it is important that the MLC is well calibrated such that the dose is delivered as intended. On the high field MR linacs, that recently have started to treat patients, it is not possible to image all MLC positions on the EPID system (EPID cannot image all leaves and neither the full leaf range), which hinders full MLC validation using the EPID system. This abstract demonstrates a film-EPID combined method which can be used to make absolute validation of the full motion range of all MLC leaves.

### Material and Methods

Calibration of the Elekta Unity MLC was validated using film/EPID dosimetry. Two Gafchromic EBT3 films were placed with a ~7 cm overlap between two slabs of Perspex in the top of the bore so that the films covered the area of the largest possible area of a 56 cm wide field. MLC segments defined 2 cm wide fields offset by -9 cm, -4.5cm, 0cm, 4.5cm, and 9 cm from the isocentre, respectively. For the central segment three groups of adjacent pairs of MLC leaves, visible on the EPID, were deliberately offset to mark the position of these specific MLC leaves (Figure 1). While irradiating the films, the EPID system was used to measure the EPID-visible part of the field. The relation between the EPID system (positions and rotation) and the radiation isocentre is known from standard QA.

The films were scanned in a flatbed bed scanner and gray values converted to dose (Lewis et al MedPhys 2012). Data was evaluated using in-house developed MATLAB program. Based on the three groups of MLC offsets it was possible to perform an automated registration between the individual films and EPID image.

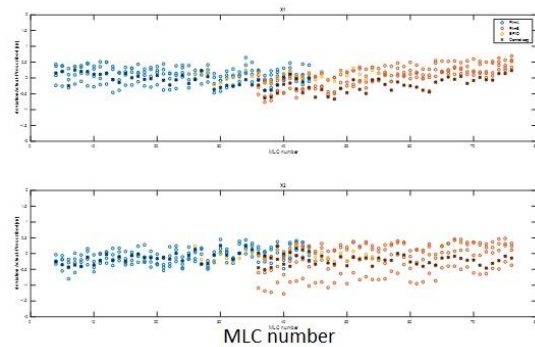
Based on the registration with the EPID it was possible to scale all detected film edges to actual positions. A linear fit per leaf between requested and observed leaf positions was made resulting in an amplitude/gain and offset correction need for an ideal calibration of the MLC.



### Results

The average amplitude/gain and offset for the two banks are (std. deviation): 0.995 (0.001), 0.994 (0.001), 0.133 mm (0.164mm), -0.017mm (0.189mm), respectively (deviations shown in figure 2). The average difference between actual and observed position for the individual leaves is 0.18 (0.39) mm and -0.07 (0.43) mm for the two banks, respectively. Except for offset of the second bank all the values do statistically significant deviate from

either one or zero with p values well below 0.001 (T-test).



### Conclusion

Validation of MLC positions of a high-field MR accelerator is possible by combining EPID and film. Small but likely clinically irrelevant systematic deviations are observed. The random error, standard deviation of the position errors, is below 0.5 mm which is needed in order to reduce irradiation volume based on MR imaging prior to each treatment fraction.

### PO-1031 Automated patient specific collision prevention: the future of noncoplanar SRS planning

T. Mann<sup>1</sup>, K. Thind<sup>2,3</sup>, N. Ploquin<sup>2,3</sup>

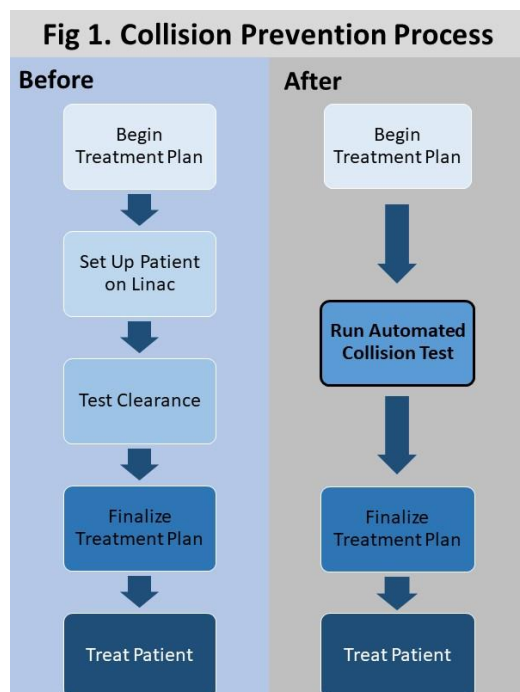
<sup>1</sup>University of Calgary, Physics and Astronomy, Calgary, Canada ; <sup>2</sup>University of Calgary, Oncology, Calgary, Canada ; <sup>3</sup>Tom Baker Cancer Centre, Medical Physics, Calgary, Canada

### Purpose or Objective

The use of noncoplanar treatment planning in Linac-based Stereotactic Radiosurgery (SRS) increases the likelihood of a collision between the gantry and the patient, immobilization device, or the couch. Treatment simulation is necessary prior to patient treatment which increases inefficiency due to implications on resource utilization. The goal of this project is the clinical implementation of an automated patient specific collision detection software during the treatment planning process, ultimately improving resource utilization and the process flow for SRS patients.

### Material and Methods

Eclipse Scripting Application Programming Interface (ESAPI) developed by Varian Medical Systems (Palo Alto, California, USA) was used to create patient specific collision detection software. This software uses patient contours, treatment plan parameters, and models of a Varian Edge Radiosurgery system to perform a clearance check. Previous validation with an anthropomorphic phantom demonstrated 100% collision detection accuracy of the software using a 5 cm expansion zone around the patient. During the planning process, the collision detection software was utilized for all frameless SRS patients planned over two months. In the implementation phase any potential collisions predicted by the software were further tested by treatment simulation on a Linac. The proposed change in treatment planning workflow post-implementation of the automated software is shown in figure 1.



## Results

A summary of the results for all fields tested can be seen in figure 2. The range of calculated minimum distances between the gantry and the patient or the treatment couch is shown for each couch angle. The average minimum distance was 16.6 cm and the median was 15.8 cm. One colliding field, using a 5 cm patient expansion zone, was detected by the software out of a total of 148 fields tested for 36 patients. This field was treatment simulated on a Linac and confirmed to be a collision risk. No undetected collisions occurred clinically during the implementation phase.

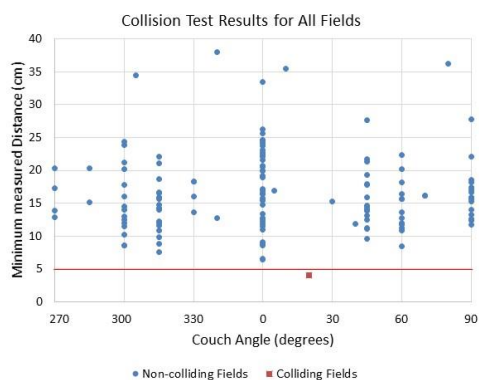


Fig 2. Minimum calculated distance between structures for each treatment field segmented by couch angle. Crossing the 5 cm safety margin outlined in red was defined as a collision.

## Conclusion

We successfully clinically implemented collision detection software for SRS. The software was capable of detecting all potential collision risks. Moving forward, using the automated software instead of performing treatment simulation on a Linac will result in clinical resources being utilized more effectively and help avoid any potential re-planning due to collision risk. While the current conservative gantry trajectory treatment planning approach is effective at avoiding most collisions, a planning approach that utilizes patient specific model based collision testing will allow for a larger number of control points to be used in treatment plan optimization.

The implications of this new method on SRS dosimetry are currently being explored.

## PO-1032 The potential of CBCT for setup and treatment verification in proton therapy for prostate cancer

E. Fura<sup>1</sup>, A. Dasu<sup>2</sup>, A. Ureba<sup>3</sup>, U. Isacson<sup>4</sup>, S. Johansson<sup>5</sup>  
<sup>1</sup>Stockholm University, Medical radiation physics, Stockholm, Sweden ; <sup>2</sup>Skandionkliniken, Medical radiation physics, Uppsala, Sweden ; <sup>3</sup>Karolinska University Hospital, Medical Radiation Physics, Stockholm, Sweden ; <sup>4</sup>Uppsala university hospital, Medical radiation physics, Uppsala, Sweden ; <sup>5</sup>Uppsala university hospital, Oncology, Uppsala, Sweden

### Purpose or Objective

Proton beam treatments (PBT) in the pelvic region can prove difficult due to the sensitivity of the particle tracks to changes in the medium and its implications on the dose distribution. Various registration approaches and stabilisation techniques are available for setup verification for pelvic treatments such as rigid registration to structures like bones and markers, but studies on the matter are scarce. Cone Beam Computer Tomography (CBCT) provides 3D information on the morphology of the patient and could be used daily in the clinic as an image-guided system to verify the patient positioning. However, CBCT images cannot generally be used directly to investigate the impact of inter-fractional changes on the dose distribution. Therefore, this study aimed at developing a method for assessing the impact of inter-fractional changes in proton therapy for prostate cancer by means of CT-to-CBCT deformable registration for various registration approaches.

### Material and Methods

Five prostate cancer patients with rectal rods, used as a stabilization technique, previously treated with photon therapy were included in this study. The patients were replanned with protons for a boost treatment aimed at delivering 4 fractions of 5 Gy, to a total of 20 Gy. The patients underwent a planning CT(pCT) before treatment and one CBCT before each fraction of the boost. The CBCTs were used to deform the pCT to four new deformed image sets representing each fraction. The newly deformed image sets were then rigidly registered to the pCT with two different registrations approaches, bones and markers. The robustness of these registrations was evaluated for two different plans on the pCT (a lateral field arrangement and an anterior oblique field arrangement). The plans were then copied and recalculated over to the bone or marker registered deformed CT sets. After deforming the dose distributions to the pCT, all fractions were then summed up, compared to the reference plan of the pCT and evaluated.

### Results

Bone and marker registrations for both plans resulted in close to 100% coverage of the CTV. The doses to nearby OAR on the summed plans were below the constraints. The coverage of the PTVs on the summed plans were up to 8% lower than for the reference plan. Interestingly, there was a trend for the PTVs where the registration to the bones for the lateral field arrangement had consistently higher coverage than the registration to the markers for all patients.

### Conclusion

The results show that it is possible to use deformable image registration of CBCTs to verify the coverage of the target with PBT. Registering the deformed CT to the bones of the pCT seems to be more robust than registration to the markers in the prostate when using a lateral field arrangement. However, both plans can be used clinically without compromising the coverage of the target.

**PO-1033 What is required to make logfile-based Monte Carlo a viable QA method for realtime plan adaptation?**  
 S. Klüter<sup>1,2,3</sup>, C.K. Spindelreier<sup>1,2,3</sup>, A. Fees<sup>1,2,3</sup>, G. Major<sup>1,2,3</sup>, J. Debus<sup>1,2,3,4,5,6</sup>, M. Alber<sup>1,2,3</sup>

<sup>1</sup>Heidelberg University Hospital, Radiation Oncology, Heidelberg, Germany ; <sup>2</sup>National Center for Tumor Diseases NCT, Radiation Oncology, Heidelberg, Germany ; <sup>3</sup>Heidelberg Institute of Radiation Oncology HIRO, Radiation Oncology, Heidelberg, Germany ; <sup>4</sup>German Cancer Consortium DKTK, partner Site Heidelberg, Heidelberg, Germany ; <sup>5</sup>Heidelberg Ion-Beam Therapy Center HIT, Radiation Oncology, Heidelberg, Germany ; <sup>6</sup>German Cancer Research Center DKFZ, Clinical Cooperation Unit Radiation Oncology, Heidelberg, Germany

#### Purpose or Objective

Real-time plan adaptation renders common means of treatment delivery QA infeasible. To date, the only available method appears to be linac logfile recording and a high-accuracy secondary dose computation (LOG2DOSE). Here, we explore the level of detail and accuracy required for Monte Carlo (MC) simulation of the MRIdian Linac (ViewRay Inc, USA) as well as the necessary stability and precision of linac and MLC to afford a sufficient level of accuracy and sensitivity for daily QA of real-time adapted treatment plans.

#### Material and Methods

In order to detect dose delivery errors with LOG2DOSE with high sensitivity, two prerequisites must be met:

1. the logfile information needs to be precise in all parameters, which relates to MLC properties as well as linac characteristics,
2. the MC model needs to be accurate in every aspect of source and collimator simulation, i.e. it is not acceptable that errors cancel out.

From the combination of logfile precision and MC accuracy we estimate the maximum 3D dose errors that would go unnoticed with LOG2DOSE.

The data presented here were obtained with a prototype of an MR-compatible motorized water phantom, various MR-compatible ionization chambers (Standard Imaging, PTW), a micro-diamond detector (PTW), and two different ionization chamber (IC) arrays (Sun Nuclear, PTW). A set of specific measurements was designed to investigate the MC model of the ViewRay TPS with respect to photon spectrum, energy fluence distribution and MLC model. Logfile precision was evaluated with respect to mechanical stability of the MLC and its calibration, beam start-up behaviour and MU-linearity.

#### Results

The MC source model proved extremely accurate, confirmed by output factors and depth dose curves within 0.5%. Transmission/leakage through single stacks of the double-stack MLC was initially off by 50% (mean) and up to 350% (peak), reducing the leaf width by 0.075 mm fixed this issue.

Differences between actual and recorded linac behaviour originated from two sources: during beam start-up, the linac output can be between 1% and 6% less for the first 10 monitorunits (MU), with associated energy-dependent fluctuations of the cross-profile. Further, the leaves show a mean hysteresis of 0.4 mm. Leaf calibration remained stable during 6 months. The 2D array was reliable down to a 3%/3mm gamma (G33) criterion but showed spurious disagreements for more sensitive criteria, caused by coarse spacing and large volume averaging of the ICs in the array.

#### Conclusion

Issues with MC originated from an overly idealized linac model. Precise adjustment to reality including manufacturing and calibration tolerances is required. Logfiles contain residual errors that could be considered in MC simulations, but for practical reasons very narrow fields (leaf hysteresis) and less than 10 MU per segment

(beam start-up) should be avoided. Given these constraints, the sensitivity of LOG2DOSE is higher (up to G11) than that of a 2D array (G33). Thus, LOG2DOSE can be a viable QA method for the MRIdian Linac.

**PO-1034 Development of predictive daily machine quality assurance system to predict forthcoming failures**

T. Fuangrod<sup>1</sup>, W. Puyati<sup>2</sup>, A. Khawne<sup>2</sup>, M. Barnes<sup>3</sup>, P. Greer<sup>3</sup>

<sup>1</sup>Chulabhorn Royal Academy, Faculty of Medicine and Public Health- HRH Princess Chulabhorn College of Medical Science, Bangkok, Thailand ; <sup>2</sup>King Mongkut's Institute of Technology Ladkrabang, Department of Computer Engineering, Bangkok, Thailand ; <sup>3</sup>Calvary Mater Hospital Newcastle, Department of Radiation Oncology, Waratah, Australia

#### Purpose or Objective

A predictive daily machine quality assurance (QA) system based on machine performance check (MPC) tests was developed. This system can be used for a proactive prevention procedure for estimating forthcoming machine failures.

#### Material and Methods

An integration between statistical process control (SPC) and autoregressive integrated moving average (ARIMA) forecast model was applied. Total of 490 daily MPC outputs between 2/2015 - 3/2017 were acquired and each parameter of MPC were arranged, which ordered by testing dates, to be a time series. The time-series optimal ARIMA forecast model and the SPC-based warning level (2 sigma) were calculated from 85% of overall data. The system predicted the one-step ahead of MPC outputs then compared with the warning level. The accuracy of forecast model between predicted and measured MPC tests was evaluated using 15% of overall data.

#### Results

Most results of one-step ahead forecasting of each parameter of MPC were measured by mean absolute error (MAE) were less than 0.05, excepted jaw collimation, relative gantry, tangential of kV imager, beam output and uniformity change. Overall average MAE was 0.03 for all MPC tests. The accuracy of predicted MPC tests versus the warning level was 83.83%. The table 1 shows results of accuracy tests for the predictive daily QA system.

Table 1. Results of accuracy tests for ARIMA forecast model and accuracy rate of warning stage for each MPC test parameter.

Type	MPC tests	Mean absolute error (MAE)	Average accuracy
Isocenter	Size	0.01	97.80%
	MV imager projection offset	0.02	79.12%
	kV imager projection offset	0.03	61.54%
	Maximal offset leaves A	0.02	100.00%
Collimation	Maximal offset Leaves B	0.03	98.97%
	Mean Offset Leave A	0.02	98.97%
	Mean Offset B	0.02	98.97%
	Individual MLC leaf A	0.02	98.56%
	Individual MLC leaf B	0.02	98.13%
	Jaw X1	0.06	47.42%
	Jaw X2	0.05	95.88%
	Jaw Y1	0.07	64.21%
Gantry	Jaw Y2	0.05	79.17%
	Rotation offset	0.02	100.00%
	Absolute	0.01	92.86%
	Relative	0.06	100.00%
Couch	Lateral	0.04	100.00%
	Longitudinal	0.02	64.86%
	Pitch	0.01	98.63%
	Roll	0.00	95.38%
	Rotation	0.01	48.10%
	Vertical	0.04	91.78%
kV imager	Rotation induced couch shift	0.02	100.00%
	In plane rotation	0.00	100.00%
	Source Axial	0.03	95.60%
MV imager	Tangential	0.10	98.90%
	In plane rotation	0.00	100.00%
	Source Axial	0.01	60.44%
Beam	Tangential	0.01	100.00%
	Center shift	0.04	89.52%
	Beam output change	0.12	94.29%
Overall	Uniformity change	0.07	93.33%
	Overall	0.03	83.83%

## Conclusion

A novel concept of predictive daily machine QA system was proposed that applied the historical MPC test data to develop the ARIMA forecast model and SPC-based warning level for each parameter. The system could detect the forthcoming errors where predict MPC test exceeds the SPC-based warning level for each parameter. This represents the likelihood of machine failure in the near future and requires for further investigation and/or calibration.

## PO-1035 Linac commissioning methodology for the Elekta Unity MR Linac

I. Hanson<sup>1</sup>, S. Nill<sup>2</sup>, J. Chick<sup>1</sup>, U. Oelfke<sup>2</sup>

<sup>1</sup>The Royal Marsden NHS Foundation Trust & The Institute of Cancer Research, Radiotherapy Physics, Sutton, United Kingdom ; <sup>2</sup>The Royal Marsden NHS Foundation Trust & The Institute of Cancer Research, Physics, Sutton, United Kingdom

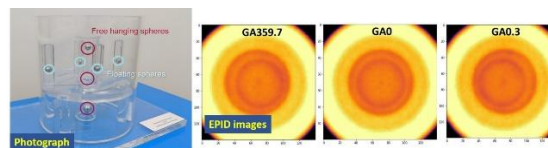
### Purpose or Objective

The Elekta Unity MR Linac (MRL) allows for daily adaptive radiotherapy based on high quality, real-time imaging. A commissioning program has been developed to ensure the safe and accurate operation of the MRL.

Measurements performed on the MRL have to overcome several challenges. Amongst these are the presence of the magnetic field and its influence and limitations on the measuring equipment that can be used, the lack of lasers and light field, the limited bore size and the lack of access to the linac head from the treatment room. We have developed novel methods and tools to address these issues. Consideration of the interdependencies of the MRL parameters was given when designing and ordering tests in order to eliminate any self-referencing loops.

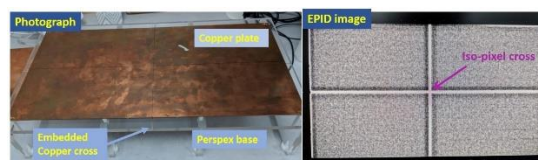
### Material and Methods

An in-house phantom was developed to provide a set of foundational measurements from which further dependent tests could be built upon (see figure 1). This phantom ensures the correct orientation of the radiation beam along the vertical and horizontal axis. The same phantom is used to measure the absolute position of the radiation beam with respect to the fixed EPID panel, and also the rotation of the EPID panel. Once this rotation had been determined the EPID panel could then be used to confirm the rotation of the collimating system.



The dose linearity & repeatability of the linac was confirmed using an ion chamber, with the same measurements used to assess the dosimetric characteristics of the EPID panel. This was necessary as the EPID will be used as a routine dosimeter for daily QA measurements.

Film was used to determine the absolute calibration of the MLCs and jaws using an in-house built copper jig. Copper is used to reduce the effect of the magnetic field on the secondary electron trajectories, such that the deposited dose more closely matches the photon fluence. The same jig was used to locate the films with respect to the absolute beam coordinate system defined by the EPID panel via a copper cross (see figure 2). Copper was also used in an in-house ring phantom used to measure the radiation isocentre radius of the MRL using a star-shot.



Finally, an end-to-end test was performed using the STEEV phantom. A reference plan was generated and adapted using a daily MRL. The difference between reference predicted dose and measured dose was recorded

### Results

The radiation beam was found to be within  $0.3^\circ$  in the horizontal and vertical plane. The EPID panel rotation was  $0.092^\circ$ . The collimator rotation averaged over all cardinal gantry angles was  $-0.01^\circ$ .

The average MLC positioning error was  $(-0.12 \pm 0.23)$ mm. The radiation isocentre radius was 0.32mm. Repeat 1MU exposures agreed dosimetrically to within 1.4%.

Finally, end-to-end testing of the adaptive workflow using the STEEV showed an excellent agreement of 0.018 %

### Conclusion

New methodologies and tools have been developed to commission the radiation delivery system of the Elekta Unity. Measurements showed that the MRL is operating within expectations.

## PO-1036 Deep Learning for automatic contouring of clinical target volumes in breast cancer patients.

P. Poortmans<sup>1</sup>, A. Henry Alexandre<sup>1</sup>, P. Aljabar<sup>2</sup>, R. Baggs<sup>2</sup>, M. Gooding<sup>2</sup>, M. Leclerc-Chalvet<sup>2</sup>, Y. Kirova<sup>1</sup>

<sup>1</sup>Institut Curie Ensemble Hospitalier, Department of Radiation Oncology, Paris cedex 05, France ; <sup>2</sup>Mirada Medical Ltd., Research & Development, Oxford, United Kingdom

### Purpose or Objective

To improve consistency and decrease workload, we introduced and evaluated a system for automated contouring of clinical target volumes (CTV) in breast cancer.

### Material and Methods

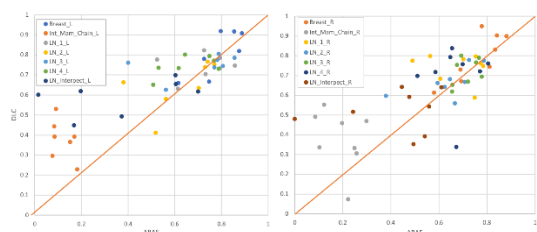
For 146 patients undergoing radiation therapy (RT) for breast cancer, CT-based images were acquired for treatment planning purposes. CTVs, including the breast, and the following lymph node regions: internal mammary chain, interpectoral and axilla levels one to four, were manually delineated on all slices following the ESTRO

guidelines. These delineations served as reference labels for evaluating the automated contours. The Deep Learning Contouring (DLC) model (DLCExpert™, WorkflowBox 2.0, Mirada Medical Ltd) was trained on 63 CTs for left-, and 52 for right-sided breast cancer. The remaining 15 and 16 CTs, respectively, served as a test set for evaluation. For the same test patients, atlas based automatic segmentation (ABAS) was also carried out using atlases formed by ten representative manually contoured pairs from each training set, i.e. two sets of auto-contours were generated for each patient: DLC and ABAS. The ABAS contours provide a benchmark for evaluating the DLC predictions. The accuracy of each method was assessed by quantitative measures against reference contours. Quantitative measures were obtained by comparing the automatic with the manual delineations, using the Dice similarity coefficient (DSC) and the median surface distance (SD).

### Results

The DSC for most CTV's, in both left and right patients, showed that DLC out-performed ABAS. The figure shows a scatter-plot comparing matched data and DSC. The surface distances for DLC were comparable or lower than for ABAS contours, again suggesting improved accuracy.

Figure: Scatter plots of Dice scores for ABAS and DLC.



### Conclusion

The tested deep learning contouring algorithm is a promising tool for improving clinical target volume delineation for breast cancer. To further validate this, we plan to assess the clinical acceptability of the automatic contours by using a modified version of the Turing Test to compare them against manually drawn contours ([www.autocontouring.com](http://www.autocontouring.com))

### PO-1037 In silico analysis of MR-only planning for simulation-free MR-guided spine SBRT

O. Green<sup>1</sup>, L. Henke<sup>1</sup>, S. Rudra<sup>1</sup>, A. Price<sup>1</sup>, S. Mutic<sup>1</sup>, C. Robinson<sup>1</sup>

<sup>1</sup>Washington University School of Medicine, Radiation Oncology- Physics Division, Saint Louis, USA

### Purpose or Objective

Spine SBRT is a proven treatment modality for primary and metastatic tumors. The proximity of the spinal cord necessitates the acquisition of either MR or CT myelography imaging. The time between diagnostic imaging, simulation, and treatment can stretch to upward of two weeks, potentially reducing the probability of favorable outcome. Application of an established online-adaptive radiotherapy workflow using a hybrid MR-linac system may allow for reduction in time to treatment. In this study, we sought to evaluate the dosimetric reliability of applying our current online adaptive radiotherapy method to enable a simulation-free workflow for spine SBRT patients, wherein the patient is imaged on the hybrid MR-linac unit, a pre-selected base plan is adapted, and treatment commences while the patient remains on-table, using a bulk density override MR-only planning approach.

### Material and Methods

Four patient datasets were chosen to be representative of typical patient habitus observed in the clinic (1 obese, 1 over-weight, 2 non-obese; 2 male, 2 female). For each, MRI datasets from previous MR-linac treatments as well as

simulation CT datasets were collected. For each dataset, six CTVs were contoured on MRI per International Spine Radiosurgery Consortium (ISRC) consensus guidelines. The bulk density override function of the integrated MR-linac treatment planning system was used to assign a tissue-equivalent density (1.02 g/cc) to all non-bony anatomy except lung-equivalent (0.25 g/cc) as appropriate. The spinal column and adjacent rib bones were assigned a standard bone density override value of 1.12 g/cc. Corresponding CT datasets were fused as secondary images to MRI datasets. For each PTV, three plans were created and compared by dose volume histogram analysis: (1) bulk density override plan, (2) bulk density override plan recalculated on the registered CT; (3) reoptimized plan using CT alone.

### Results

PTV coverage changed by an average of 2.5% when bulk density override plans were compared to plans using the real relative electron densities. The maximum dose to 0.035cc of the spinal cord changed by an average of 0.24 Gy (corresponding to 0.9% of the constraint dose of 28 Gy), with a maximum observed deviation of 0.83 Gy. All plans achieved maximum cord doses <28 Gy, with a maximum of 21.44 Gy). Similar differences were observed for 3, 5, 7, and 10 mm expansions around the cord and 100% and 50% conformity indices, indicating that bulk density overrides provided for robustness equivalent to CT-based plans (Figure 1).

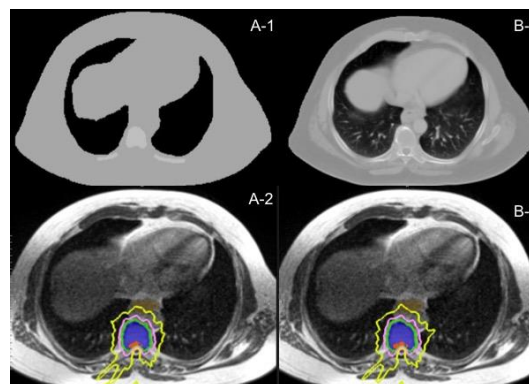


Figure 1. Bulk density (A-1) plan (A-2) compared to CT-based (B-1) plan (B-2), with 100%, 80%, and 50% isodoses (cyan, pink, and yellow) shown.

### Conclusion

Using a bulk density override for spine SBRT based on MR-linac images was found to have acceptable accuracy for a simulation-free, MR-only process. A Phase I clinical trial evaluating the feasibility and safety of simulation-free MR-guided spine SBRT is underway.

### PO-1038 MR-only Radiation Therapy: a silent patient-friendly workflow using a light-weight, flexible coil

C. Cozzini<sup>1</sup>, C. Bobb<sup>2</sup>, M. Engström<sup>3</sup>, S. Kaushik<sup>4</sup>, R. Molthen<sup>2</sup>, D. Rettman<sup>2</sup>, V. Goruganti<sup>5</sup>, W. Chiang<sup>5</sup>, F. Wiesinger<sup>1</sup>

<sup>1</sup>GE Healthcare, Applied Science Laboratory Europe, Garching bei München, Germany ; <sup>2</sup>GE Healthcare, Healthcare Imaging, Waukesha, USA ; <sup>3</sup>GE Healthcare, Healthcare Europe, Stockholm, Sweden ; <sup>4</sup>GEGlobal Research, GE Corporate, Bangalore, India ; <sup>5</sup>NeoCoil, MRcoil, Pewaukee, USA

### Purpose or Objective

The ability of using a single imaging system for tumor delineation and dose calculation for Radiation Therapy (RT) planning is highly appealing in terms of clinical workflow simplification and patient experience. MRI is known for its superior soft tissue contrast when compared to CT and silent Zero Echo Time (ZTE) MR imaging was

recently demonstrated suitable for both Attenuation Correction in PET/MR and for pseudo CT conversion for head and neck applications [1]. To achieve an optimized MR-only workflow however, dedicated RT coils are needed to allow patient positioning in the MRI including RT fixation devices. To reach the desired coverage and image quality, current clinical practice often results in a bulky and uncomfortable set-up typically in form of a composition of different coils. Here we present a novel RT coil based on GE lightweight Air technology [2] and demonstrate its performance for standard head and neck MR imaging and ZTE based pseudo CT conversion. This highly flexible Air coil greatly simplifies the RT workflow and well adapts to varying patient position and size.

#### Material and Methods

A 3-tesla GE SIGNA MR scanner (GE Healthcare, Chicago, IL) and a prototype coil were used for standard MRI and ZTE data acquisition in phantoms and healthy volunteers. The coil consists of 22 channels of which 15 located in the face, allowing for 3 different coil modes: head only, head and neck, and chest only. ZTE data were processed with a Deep Learning (DL) method where a 3D convolutional neural network of the U-net architecture with 8-layers, Adam optimizer and RMSE cost function was adapted to perform pseudo CT computation via image regression. This method was trained on N=50 patients using matched pairs of ZTE and CT patient data sets using standard product surface coils [3].

#### Results

Figure 1 shows the prototype coil and the coronal views of standard gradient echo (LAVA-Flex) and fast spin echo (FS) MR pulse sequences including Dixon type fat-water separation. The images clearly illustrate full head and neck coverage, including the shoulders, as required for RT planning.

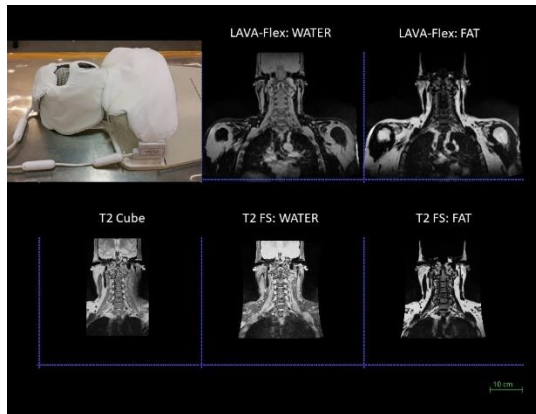


Figure 1 Top left: air coil prototype; Right: Water and Fat separation from LAVA-Flex for neck and shoulder coverage. Bottom: T2FS water; T2FS fat; T2cube acquisitions.

Figure 2 shows ZTE images acquired with 1.5 mm isotropic resolution with corresponding, DL computed pseudo CT at the bottom. The skull and the spine are correctly captured, while a few false positive bone voxels are present in the neck and in the sinus region. A proper training on data acquired with the prototype coil with matched resolution is expected to produce superior results



Figure 2: top ZTE images with 1.5 isotropic resolution. Bottom: DL derived pseudo CTs

#### Conclusion

A silent, patient-friendly MR-only RT workflow compatible with all types of fixation devices has been enabled by a new lightweight and flexible Air coil prototype. These first results show that the coil has appropriate coverage and image quality to achieve pseudo CT conversion paving the way for an efficient and patient friendly MR-only RT workflow

#### PO-1039 Spine SBRT with Halcyon™: Plan Quality, Delivery Accuracy, and Speed

H. Petrocchia<sup>1</sup>, I. Malajovich<sup>1</sup>, C. Wang<sup>2</sup>, K. Teo<sup>1</sup>, D. Lei<sup>1</sup>, T. Li<sup>1</sup>

<sup>1</sup>University of Pennsylvania, Radiation Oncology, Philadelphia, USA ; <sup>2</sup>Duke University, Radiation Oncology, Durham, USA

#### Purpose or Objective

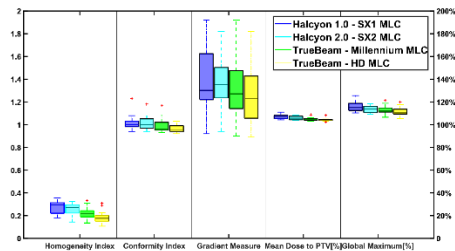
A new dual-layer staggered 1cm MLC in Halcyon™ treatment platform (Varian Medical, Palo Alto, CA) has improved speed, leakage, and DLG compared to 120-Millennium (0.5cm) and High Definition (0.25cm) MLCs in the TrueBeam platform. Halcyon 2.0 with SX2 MLC has the ability to modulate both upper and lower MLC banks; while previously in version 1.0 the SX1 MLC uses the lower MLCs to modulate the fluence and the upper MLCs function as a backup jaw by moving to the most distally extended lower leaf pair. It is not clear how these two newly designed MLCs perform for spine SBRT cases and when compared to TrueBeam MLCs. In this study, we investigate the effects of 4 different MLC designs on spine SBRT treatments.

#### Material and Methods

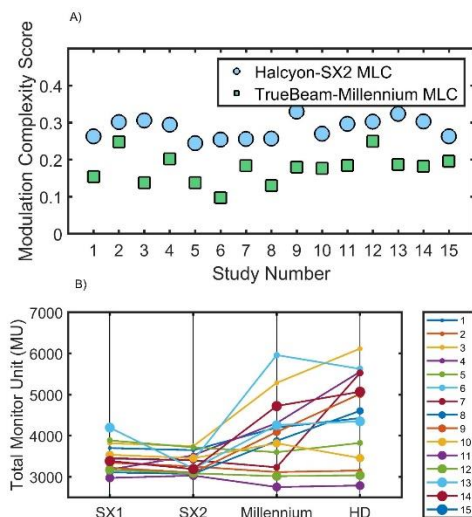
15 patients previously treated with spine SBRT were re-planned according to NRG-BR002 guidelines for all MLCs with a prescription of 3000cGy in 3 fractions, 6xFFF, 800 MU/min, and 3-arc VMAT technique. All plans were normalized to 90% of the target volume covered by prescription dose. Since the diameter of the spinal cord is comparable to the 1cm leaf width, this study evaluates the ability of the dual-layer staggered MLCs to modulate fluence using an 0.5cm effective leaf width by examining the percentage of shaping performed by the proximal MLC, the modulation complexity score (MCS), the total MU, and the gamma index passing rate based on delivery measurements using ArcCheck.

#### Results

Halcyon SX1 and SX2 plans are shown to have similar conformity and homogeneity index (SX2: CI 1.0±0.06, HI 0.27±0.05; SX1: CI 1.0±0.07, HI 0.29±0.05) as compared to the TrueBeam platform (HD: CI 0.95±0.03, HI 0.18±0.06; Millennium: CI 0.96±0.07, HI 0.21±0); however, the gradient measure as defined by Eclipse indicates the TrueBeam platform has steeper dose fall off than the Halcyon platform.



We investigate how much additional modulation is provided by the proximal MLC between SX2 and SX1 by analyzing the amount of leaf shaping for leading and trailing leaves. In Halcyon 2.0, the proximal MLC was found to shape the field on average by  $29.5 \pm 6.2\%$ . Despite the increase in modulation from SX1 to SX2, the MCS for the Millennium MLC is lower for all cases compared to SX2 plans. For delivery accuracy measurement, all TrueBeam plans were adjusted to be 1400 MU/min as compared to 800 MU/min available in the Halcyon platform to optimize delivery characteristics. The 2%/2mm gamma index passing rates for SX1 and SX2 are  $98.8 \pm 0.2\%$  and  $96.9 \pm 2.0\%$ , respectively. The delivery time for SX2 plans are  $4:19.0 \pm 25$  sec compared to  $3:59.46 \pm 24$  sec for the Millennium MLC.



### Conclusion

Halcyon SBRT plans are shown to have similar plan quality to plans generated with the Millennium MLC but inferior to HD MLC. Despite the increase in modulation between SX1 to SX2 and the theoretical modulation resolution of 0.5cm in the latter, the lower MCS implies SX2 is generating plans with less modulation than the 120-Millennium MLC with 0.5cm physical width. SX2 plans are superior in terms of heterogeneity and conformity than SX1.

## Posters Brachytherapy

### Poster: Brachytherapy: Breast

#### PO-1040 Partial breast irradiation with interstitial multicatheter HDR BT for breast cancer.

N. Cihoric<sup>1</sup>, A. Tsikkinis<sup>1</sup>, D. Terribilini<sup>1</sup>, D. M. Aebersold<sup>1</sup>, K. Lössl<sup>1</sup>

<sup>1</sup>Inselspital- Bern University Hospital- University of Bern, Department of Radiation Oncology, Bern, Switzerland

### Purpose or Objective

To evaluate the efficacy, toxicity profile and dosimetric parameters of accelerated partial breast irradiation (APBI) delivered with interstitial multicatheter HDR brachytherapy (HDR-BT) after breast-conserving surgery (BCS).

### Material and Methods

We analyzed a series of patients (pts) treated from 2005 to 2017 with HDR-BT APBI using multicatheter interstitial brachytherapy after BCS. HDR-BT APBI was offered to pts fulfilling the ESTRO criteria for APBI and to selected pts with high-risk features but with metastatic disease and/or significant comorbidities and a limited life expectancy. In total 419 pts were treated. 279 (66.6%) pts fulfilled the ESTRO criteria for APBI and 140 (33.4%) pts did not. Catheters were implanted during or 4 - 8 weeks after BCS. Dose-volume parameters and quality indices were reported according to the ICRU 58 recommendations. We assessed the locoregional control and survival. Toxicity profiles were evaluated according to CTCAE v4.0.

### Results

The median age at time of therapy was 68 years (range: 31 - 93 years). A total dose of 32 Gy was delivered in 8 fractions of 4 Gy twice daily. 289 (69%) pts received hormonal therapy, 99 (24%) pts did not, for 31 (7%) unknown. Chemotherapy was administered in 45 (11%), omitted in 343 (82%) and unknown in 31 (7%) pts. HER2 oriented therapy was given in 6 (1%) pts. Median follow-up time was 25 months (range 3 - 131 months). 29 (6.9%) pts developed disease relapse. Seven (1.7%) pts developed in-breast tumor relapse, 10 (2.4%) relapsed in the regional nodal area and 22 (5.3%) developed systemic metastases. We did not record any relapse within the planning target volume. During follow-up 50 (11.9%) pts died. 384 (91.6%) pts did not experience any acute toxicities, 32 (7.6%) developed Gr. I toxicity, 1 (0.2%) Gr. II and 2 (0.5%) Gr. III toxicity. Late toxicity was not recorded in 263 (62.8%) pts, 145 (34.6%) pts presented Gr. I toxicity, 9 (2.1%) Gr. II and 2 (0.5%) pts developed late Gr. III toxicity. There were no cases of acute or late Gr. IV or higher toxicity. The mean volumetric doses were: MCD 5.3 (range 3.2 to 6.1), V PTV (ccm): 62.6 (8.7 - 332.6), V100 (ccm): 72.7 (range 13.1 - 960.2), V100(%) = CI - 91.0 (47.4 - 99.0), V150 (lmp ccm): 19.9 (5.4 - 90.9) V150 (%): 27.1 (range 15.1 - 51.1). The mean DNR was 0.3 (range 0.2 - 0.5), while the DHI was 0.7 (0.3 - 0.8). The mean COIN was 0.7 (0.4 - 0.8).

### Conclusion

HDR-BT APBI achieves excellent local control with a favorable toxicity profile. In selected pts with high-risk features, HDR-BT APBI provides a viable alternative to conventional radiotherapy.

### Poster: Brachytherapy: Gynaecology

#### PO-1041 Benefit of interstitial needles supplementing the ring applicator in cervical cancer brachytherapy

J. Ståhl Kornerup<sup>1</sup>, E. Thorstensen Andersen<sup>2</sup>, S. Danielsen<sup>1</sup>, A. Dybdahl Wanderås<sup>1</sup>, M. Sundset<sup>3</sup>, K. Fjellanger<sup>2</sup>, M. Eidem<sup>1</sup>, A.B. Langeland Marthinsen<sup>1</sup>

<sup>1</sup>St Olav's University Hospital, Department of Radiotherapy- the Cancer Clinic, Trondheim, Norway ;

<sup>2</sup>Norwegian University of Science and Technology,

Department of Physics, Trondheim, Norway ; <sup>3</sup>St Olav's

University Hospital, Department of Gynaecological Oncology, Trondheim, Norway

### Purpose or Objective

How well can dose prescription for target coverage and dose limits for organs at risk (OARs) be fulfilled in

brachytherapy (BT) of cervical cancer using ring applicator, if supplementary interstitial needles are used?  
**Material and Methods**

36 BT fractions from 9 patients were studied retrospectively. Target volumes (CTV<sub>HR</sub>) and OARs (bladder, rectum and sigmoid colon) were delineated in MR image sets acquired before each fraction. The BT dose was prescribed to provide a total CTV<sub>HR</sub> dose of 90-95Gy (EQD<sub>2</sub>,  $\alpha/\beta=10$ ) in terms of D<sub>90%</sub> when combined with external radiation of 1.8Gyx25. The maxdose (D<sub>2cc</sub>) to bladder, rectum and sigmoid colon was restricted to 80, 65 and 70Gy (EQD<sub>2</sub>,  $\alpha/\beta=3$ ), respectively. The Hybrid Inverse Planning Optimization (HIPO) algorithm (Oncentra Brachy, Elekta version 4.3) was used.

The 1<sup>st</sup> set of 36 plans was generated to fulfil CTV<sub>HR</sub> dose prescriptions without needles, whereas the OAR doses had secondary priority. These plans revealed the most challenging OARs regarding violating of dose limits. The 2<sup>nd</sup> set of 36 plans was generated with the primary goal to fulfill the OAR dose limits. These plans revealed which parts of the CTV<sub>HR</sub> that were difficult to cover with adequate dose without needles. The unsuccessful fractions of the 2<sup>nd</sup> set were re-optimized with use of interstitial needles for the 3<sup>rd</sup> set of plans. The needles were thoughtfully placed where possible, with appropriate distances to the OARs.

**Results**

In the 1<sup>st</sup> and 2<sup>nd</sup> set of plans, the dose constraints for OARs and CTV<sub>HR</sub> were fulfilled in 19 of 36 fractions (53%). The remaining 17 fractions (47%) were regarded as failed. The plans that failed in the 1<sup>st</sup> set of plans in terms of OAR dose constraints also failed in the 2<sup>nd</sup> set of plans in terms of not fulfilling CTV<sub>HR</sub> dose. The OAR most frequently exceeding the dose constraint in the 1<sup>st</sup> set of plans was sigmoid colon (11 fractions, mean excess dose (MED): 0.37Gy), followed by bladder (9 fractions, MED: 0.32Gy) and rectum (4 fractions, MED: 0.38Gy). For 10 of the 17 failed BT fractions, the dose constraints became fulfilled when interstitial needles were added (see table). The mean volume of CTV<sub>HR</sub> was 31.8±8.9cc for the primary successful plans, 38.2±7.7cc for the plans fulfilled using needles and 37.1±10.1cc for the not fulfilled plans.

Table: The BT fractions with all dose constraints for CTV<sub>HR</sub> (D<sub>90%</sub> within 7.7-8.3 Gy) and OARs (D<sub>2cc</sub> of 5, 4, 3, 9 and 4.5 Gy for bladder, rectum and sigmoid colon, respectively) fulfilled are indicated with "Success". The non-successful BT fractions are presented with the reason for failing.

Patient nr ↓	Fraction nr →	Dose distribution for the different sets of plans							
		1 <sup>st</sup> and 2 <sup>nd</sup> set of plans (without needles)				3 <sup>rd</sup> set of plans (with needles)			
1	1	Bladder = 57 Gy Sigmoid = 47 Gy CTV <sub>HR</sub> = 7.3 Gy	Sigmoid = 5.1 Gy CTV <sub>HR</sub> = 7.0 Gy	Success	Success	Success	N/A	N/A	N/A
		Bladder = 5.8 Gy Rectum = 4.3 Gy CTV <sub>HR</sub> = 6.9 Gy	Success	Sigmoid = 5.2 Gy CTV <sub>HR</sub> = 6.6 Gy	Success	Success	N/A	N/A	CTV <sub>HR</sub> = 6.9 Gy
2	1	Bladder = 5.8 Gy Rectum = 4.3 Gy CTV <sub>HR</sub> = 6.9 Gy	Success	Sigmoid = 5.2 Gy CTV <sub>HR</sub> = 6.6 Gy	Success	Success	N/A	N/A	CTV <sub>HR</sub> = 6.9 Gy
		Rectum = 4.4 Gy Sigmoid = 4.7 Gy CTV <sub>HR</sub> = 7.2 Gy	Success	Success	Success	N/A	Success	N/A	N/A
3	1	Success	Success	Success	Success	N/A	N/A	N/A	N/A
		Success	Success	Success	Success	N/A	N/A	N/A	N/A
4	1	Success	Success	Success	Success	N/A	N/A	N/A	N/A
		Success	Success	Success	Success	N/A	N/A	N/A	N/A
5	1	Success	Success	Success	Success	N/A	N/A	N/A	N/A
		Bladder = 6.6 Gy Rectum = 4.2 Gy CTV <sub>HR</sub> = 7.0 Gy	Success	Success	Success	N/A	N/A	N/A	CTV <sub>HR</sub> = 7.0 Gy
6	1	Sigmoid = 4.7 Gy CTV <sub>HR</sub> = 7.6 Gy	Sigmoid = 4.9 Gy CTV <sub>HR</sub> = 7.5 Gy	Sigmoid = 4.7 Gy CTV <sub>HR</sub> = 7.5 Gy	Success	Success	N/A	Success	N/A
		Success	Success	Success	Success	N/A	N/A	N/A	Success
7	1	Success	Success	Success	Success	N/A	N/A	N/A	Success
		Sigmoid = 5.0 Gy CTV <sub>HR</sub> = 6.9 Gy	Bladder = 5.5 Gy CTV <sub>HR</sub> = 7.6 Gy	Success	Success	Bladder = 5.6 Gy CTV <sub>HR</sub> = 7.2 Gy	Success	Success	N/A
8	1	Bladder = 5.7 Gy Sigmoid = 5.0 Gy CTV <sub>HR</sub> = 7.0 Gy	Sigmoid = 5.3 Gy CTV <sub>HR</sub> = 6.8 Gy	Bladder = 5.7 Gy CTV <sub>HR</sub> = 7.5 Gy	Bladder = 5.5 Gy CTV <sub>HR</sub> = 7.0 Gy	N/A	N/A	N/A	N/A
		Success	Success	Success	Success	N/A	N/A	Success	N/A
9	1	Bladder = 5.7 Gy Sigmoid = 5.0 Gy CTV <sub>HR</sub> = 7.0 Gy	Sigmoid = 5.3 Gy CTV <sub>HR</sub> = 6.8 Gy	Bladder = 5.7 Gy CTV <sub>HR</sub> = 7.5 Gy	Bladder = 5.5 Gy CTV <sub>HR</sub> = 7.0 Gy	N/A	N/A	Success	N/A
		Success	Success	Success	Success	N/A	N/A	Success	N/A

For each non-successful fraction (without needles):  
 The row above the dashed line indicates which OAR dose constraints that were exceeded, and by how much, when CTV<sub>HR</sub> was fulfilled (1<sup>st</sup> set of plans). The row below the dashed line indicates the best achievable CTV<sub>HR</sub> with all the OAR dose constraints fulfilled (2<sup>nd</sup> set of plans).  
 For each non-successful fraction (with needles):  
 The row above the dashed line indicates which OAR dose constraints that were exceeded, and by how much, when CTV<sub>HR</sub> was fulfilled (1<sup>st</sup> set of plans). The row below the dashed line indicates the best achievable CTV<sub>HR</sub> values with all the OAR dose constraints fulfilled.  
 N/A = not applicable.

**Conclusion**

When utilizing needles as supplement to ring applicators, the total number of BT fractions which fulfilled the prescribed CTV<sub>HR</sub> and OAR doses increased from 53% to 81%. Although not all plans became successful using needles, the CTV<sub>HR</sub> D<sub>90%</sub> was always improved. Sigmoid colon and bladder were most frequently surpassing the dose limits in the failed plans. For each patient, it was not possible to predict whether the dose plan would be successful or not for the consecutive fractions. The CTV<sub>HR</sub> tended to be smaller for the plans that were primary fulfilled. The result implies that interstitial needles are a helpful tool for optimizing the dose distribution; however, they do not ensure complete success for every BT fraction.

**PO-1042 Toxicity results after Electronic Brachytherapy treatment in endometrial cancer patients**

A. Miranda Burgos<sup>1</sup>, A. Méndez Villamón<sup>1</sup>, M. Gascón Ferrer<sup>1</sup>, A. Campos Bonel<sup>1</sup>, B. Garcia Gimeno<sup>1</sup>, S. Lozares Cordero<sup>2</sup>, J.A. Font Gómez<sup>2</sup>, R. Ibáñez Carreras<sup>1</sup>, M. Tejedor Gutiérrez<sup>1</sup>

<sup>1</sup>Hospital Universitario Miguel Servet, Radiation Oncology, Zaragoza, Spain ; <sup>2</sup>Hospital Universitario Miguel Servet, Medical Physics and Radiation Protection, Zaragoza, Spain

**Purpose or Objective**

To analyse the toxicity outcomes after treatment with Electronic Brachytherapy (XB) in postsurgical endometrial cancer patients treated at our medical centre.

**Material and Methods**

Prospective study in which we selected 118 patients, between September/2015 and May/2018, that received treatment with XB (Axxent Xofter device) administered twice a week after endometrial cancer surgery, with IMRT planification. The patients were divided in two groups: Group 1 (73/118) considered high risk received external beam radiotherapy (46Gy) followed by XB (15Gy in 5Gy fractions) and group 2 (45/118) considered intermediate risk received exclusive XB (25Gy in 5Gy fractions). We analysed the median dose in bladder, rectum and sigmoid D2cc, V50, V35 with XB comparing the doses with Ir192. The vaginal mucosa, gastrointestinal (GI) and genitourinary (GU) toxicities were analysed with the Common Terminology Criteria for Adverse Events (CTCAE 4.0) scale.

Table: The BT fractions with all dose constraints for CTV<sub>HR</sub> (D<sub>90%</sub> within 7.7-8.3 Gy) and OARs (D<sub>2cc</sub> of 5, 4, 3, 9 and 4.5 Gy for bladder, rectum and sigmoid colon, respectively) fulfilled are indicated with "Success". The non-successful BT fractions are presented with the reason for failing.

Patient nr ↓	Fraction nr →	Dose distribution for the different sets of plans							
		1 <sup>st</sup> and 2 <sup>nd</sup> set of plans (without needles)				3 <sup>rd</sup> set of plans (with needles)			
1	1	Bladder = 5.7 Gy Sigmoid = 4.7 Gy CTV <sub>HR</sub> = 7.3 Gy	Sigmoid = 5.1 Gy CTV <sub>HR</sub> = 7.0 Gy	Success	Success	N/A	N/A	N/A	N/A
		Bladder = 5.8 Gy Rectum = 4.3 Gy CTV <sub>HR</sub> = 6.9 Gy	Success	Sigmoid = 5.2 Gy CTV <sub>HR</sub> = 6.6 Gy	Success	Success	N/A	N/A	CTV <sub>HR</sub> = 6.9 Gy
2	1	Bladder = 5.8 Gy Rectum = 4.3 Gy CTV <sub>HR</sub> = 6.9 Gy	Success	Sigmoid = 5.2 Gy CTV <sub>HR</sub> = 6.6 Gy	Success	Success	N/A	N/A	CTV <sub>HR</sub> = 6.9 Gy
		Rectum = 4.4 Gy Sigmoid = 4.7 Gy CTV <sub>HR</sub> = 7.2 Gy	Success	Success	Success	N/A	Success	N/A	N/A
3	1	Success	Success	Success	Success	N/A	Success	N/A	N/A
		Success	Success	Success	Success	N/A	N/A	N/A	N/A
4	1	Success	Success	Success	Success	N/A	N/A	N/A	N/A
		Success	Success	Success	Success	N/A	N/A	N/A	N/A
5	1	Success	Success	Success	Success	N/A	N/A	N/A	N/A
		Bladder = 6.6 Gy Rectum = 4.2 Gy CTV <sub>HR</sub> = 7.0 Gy	Success	Success	Success	N/A	N/A	N/A	CTV <sub>HR</sub> = 7.0 Gy
6	1	Sigmoid = 4.7 Gy CTV <sub>HR</sub> = 7.6 Gy	Sigmoid = 4.9 Gy CTV <sub>HR</sub> = 7.5 Gy	Sigmoid = 4.7 Gy CTV <sub>HR</sub> = 7.5 Gy	Success	Success	N/A	Success	N/A
		Success	Success	Success	Success	N/A	N/A	N/A	Success
7	1	Success	Success	Success	Success	N/A	N/A	N/A	Success
		Sigmoid = 5.0 Gy CTV <sub>HR</sub> = 6.9 Gy	Bladder = 5.5 Gy CTV <sub>HR</sub> = 7.6 Gy	Success	Success	Bladder = 5.6 Gy CTV <sub>HR</sub> = 7.2 Gy	Success	Success	N/A
8	1	Bladder = 5.7 Gy Sigmoid = 5.0 Gy CTV <sub>HR</sub> = 7.0 Gy	Sigmoid = 5.3 Gy CTV <sub>HR</sub> = 6.8 Gy	Bladder = 5.7 Gy CTV <sub>HR</sub> = 7.5 Gy	Bladder = 5.5 Gy CTV <sub>HR</sub> = 7.0 Gy	N/A	N/A	N/A	N/A
		Success	Success	Success	Success	N/A	N/A	Success	N/A
9	1	Bladder = 5.7 Gy Sigmoid = 5.0 Gy CTV <sub>HR</sub> = 7.0 Gy	Sigmoid = 5.3 Gy CTV <sub>HR</sub> = 6.8 Gy	Bladder = 5.7 Gy CTV <sub>HR</sub> = 7.5 Gy	Bladder = 5.5 Gy CTV <sub>HR</sub> = 7.0 Gy	N/A	N/A	Success	N/A
		Success	Success	Success	Success	N/A	N/A	Success	N/A

For each non-successful fraction (without needles):  
 The row above the dashed line indicates which OAR dose constraints that were exceeded, and by how much, when CTV<sub>HR</sub> was fulfilled (1<sup>st</sup> set of plans). The row below the dashed line indicates the best achievable CTV<sub>HR</sub> with all the OAR dose constraints fulfilled (2<sup>nd</sup> set of plans).  
 For each non-successful fraction (with needles):  
 The row above the dashed line indicates which OAR dose constraints that were exceeded, and by how much, when CTV<sub>HR</sub> was fulfilled (1<sup>st</sup> set of plans). The row below the dashed line indicates the best achievable CTV<sub>HR</sub> values with all the OAR dose constraints fulfilled.  
 N/A = not applicable.

## Results

The median dose in bladder with XB vs. Ir192 was: 2cc 64.01 vs. 69.9%, V50 7.2 vs. 12.6Gy, V35 15.2 vs. 28.1. In rectum XB vs. Ir192 was: D 2cc 65.17% vs. 67.7%, V50 7.9 vs. 10.9Gy, V35 16.7 vs. 31.8Gy. In sigmoid XB vs. Ir192 was: D 50% vs. 58.0%, V50 8.6 vs. 16.2Gy, V35 21.1 vs. 37.5Gy.

The median follow-up was 21 months (range 5 - 36 months).

In group 1, acute vaginal mucositis (G1) was observed in 32.91% of the patients, GI toxicity (G1) in 5.41% and GU toxicity (G1) in 8.11%. In group 2, we observed acute vaginal mucositis G1 in 34.09% of the patients and G2 in 4.55%, GI toxicity (G1) occurred in 6.52% and GU toxicity (G1) was present in 13.04%. There was no grade 3 or greater toxicity in any of the groups. Late toxicity was observed in only 4 patients: Mucositis (G1) in 3 patients, GI (G1) in 2 and GU toxicity (G1) in 3 patients.

## Conclusion

The dose received by the organs at risk with the XB is less compared to Ir192, with a good coverage of the PTV. The greater toxicity was observed immediately after the treatment was finished with an important reduction of the symptoms after 6 months. This technique shows excellent results as for toxicity.

**PO-1043 Vaginal Cuff treatment with Electronic Brachytherapy in Gynaecologic Cancer: Our experience**  
A. Miranda Burgos<sup>1</sup>, A. Méndez Villamón<sup>1</sup>, R. Ibáñez Carreras<sup>1</sup>, M. Gascón Ferrer<sup>1</sup>, A. Campos Bonel<sup>1</sup>, E. Muñoz Sanz<sup>1</sup>, S. Lozares Cordero<sup>2</sup>, A. Gandía Martínez<sup>2</sup>, M. Tejedor Gutierrez<sup>1</sup>

<sup>1</sup>Hospital Universitario Miguel Servet, Radiation Oncology, Zaragoza, Spain ; <sup>2</sup>Hospital Universitario Miguel Servet, Medical Physics and Radiation Protection, Zaragoza, Spain

## Purpose or Objective

To analyse the outcomes in terms of toxicity and survival analysis after treatment with Xofigo Electronic Brachytherapy (XB) in postsurgical gynaecologic cancer patients treated at our medical centre.

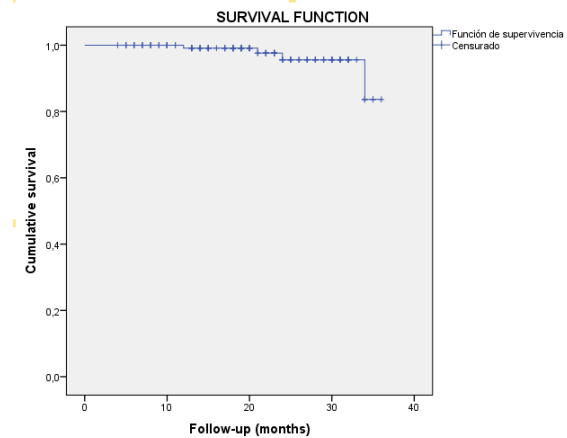
## Material and Methods

Prospective study in which we selected 140 patients that received treatment with Xofigo Electronic Brachytherapy administered twice a week after gynaecologic cancer surgery, with 3D planification. The patients were selected from September 2015 to July 2018. They were divided in two groups: Group 1 (91/140) considered high risk and group 2 (49/140) intermediate risk. Group 1 received external beam radiotherapy (46Gy) followed by XB (15Gy in 5Gy fractions) and group 2 received exclusive XB (25Gy in 5Gy fractions). We analyzed the median dose in bladder, rectum and sigmoid D2cc with XB. The vaginal mucosa, gastrointestinal (GI) and genitourinary (GU) toxicities were analyzed with the Common Terminology Criteria for Adverse Events (CTCAE 4.0) scale. We built a Kaplan-Meier curve to estimate the survival over time of follow-up.

## Results

The median follow-up was 20 months (range 3 - 36 months). Of all the patients treated, 87.14% were endometrial cancer patients, 7.86% cervical cancer, 2.86% vaginal cancer and 2.14% were vaginal recurrences. The median dose in bladder with XB was D2cc: 12,01Gy. In rectum median D2cc was 11,78Gy. In sigmoid median D2cc was 9,24Gy. In terms of toxicity, acute vaginal mucositis (G1) was observed in 21.29% of the patients and G2 in 1.43%, GI toxicity (G1) occurred in 4.28% and GU toxicity (G1) in 7.14%. There was no grade 3 or greater toxicity in any of the groups. At 6 months follow-up, all of the patients were asymptomatic. As for survival, 4 patients have died during the follow-up, 2 of them showed systemic progression and the other 2 had synchronous tumor. The

Kaplan Meier results, show that at 2 years follow-up, 95% of the patient are going to be alive. We have estimated that 97,1% of our patients are progression free and alive.



## Conclusion

The electronic brachytherapy is an alternative to high dose-rate brachytherapy. The XB obtains good coverage of PTV with lower doses in organs at risk. The greater toxicity was observed immediately after the treatment was finished with an important reduction of the symptoms after 6 months. It also shows an excellent rate of overall survival and progression free disease.

## Poster: Brachytherapy: Head and neck

**PO-1044 Salvage brachytherapy for oral or oropharyngeal tumor in a previously irradiated volume**  
P. Pierre-Marie<sup>1</sup>, M. Mounie<sup>2</sup>, B. Fleury<sup>3</sup>, S. Racadot<sup>1</sup>, J. Suchaud<sup>1</sup>, P. Pommier<sup>1</sup>

<sup>1</sup>Centre Léon Bérard, Radiotherapy, LYON, France ; <sup>2</sup>University Hospital of Toulouse, Inserm, Toulouse, France ; <sup>3</sup>Marie Curie Institute, Radiotherapy, Valence, France

## Purpose or Objective

To assess the outcome of salvage brachytherapy for oral and oropharyngeal squamous cell carcinoma in previously irradiated areas.

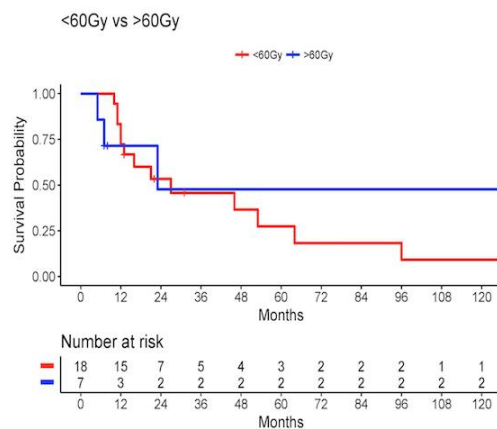
## Material and Methods

This is a retrospective study of 25 patients treated at the Centre Léon Bérard between 1997 and 2016 for primary (21) or recurrent (4) oral or oropharyngeal SCC in a previously irradiated area. Fifteen patients were treated with salvage brachytherapy alone, while 10 patients also received external radiotherapy. The median time between the first and the second irradiation was 56 months (range, 10-212 months). All but three patients had surgical resection and four patients received chemotherapy. The median brachytherapy dose was 45 Gy (range, 15-64 Gy) for a median total dose of 57 Gy (range, 40-70 Gy). Patient age, BMI, tumor stage, radiotherapy dose and time between the first treatment and recurrence were analyzed as prognostic factors.

## Results

The median overall survival was 16 months. Patients with less advanced (T1) tumors survived significantly longer (27 vs 14.5 months,  $p=0.046$ ). Five patients experienced a local recurrence, only one of which had been treated with a total dose greater than 60 Gy. In multivariate analysis, the risk of death was found to be 80% lower in patients who had received more than 60 Gy ( $p=0.072$ ). There was four grade 3 acute toxicities and no grade 3 or greater late toxicities.

Patients characteristics (n=25)		
Sex ratio (M/F)	N	20/5
Age	Median (min – max)	59 (45-84)
Performance Status (OMS)	0 1	13 12
BMI	Median (min – max)	22.2 (17.9-35.5)
<b>Primary tumor</b>		
Primary Tumor location	Oropharynx	8
	Occult primary	8
	Oral cavity	4
	Larynx	3
	Nasopharynx	1
	Hypopharynx	1
Primary treatment	EBRT alone	21
	EBRT + BT	4
	Chemotherapy	12
	Surgery	18
Primary RT dose (Gy)	EBRT alone: Median (min – max)	62 (50-70)
	EBRT + BT: Median (min – max)	65 (50-72)
Dose at the recurrent/2 <sup>nd</sup> tumor volume (Gy)	EBRT + BT: Median (min – max)	50 (50-70)
<b>Second or recurrent tumor</b>		
Recurrent/ new	Recurrent	4
	2nd cancer	21
Delay (1 <sup>st</sup> – salvage RT) (Months)	Median (min, max)	56 (10-212)
Tumor location	Base of tongue	12
	Mobile tongue	6
	Floor of the mouth	2
	Tonsil	2
	Vallecula	2
	Soft palate	1
T stage	T1 (<2 cm)	7
	T2 (2-4 cm)	11
	T3 (> 4 cm)	3
	T4 (adjacent organs)	1
	Tx	3
N stage	N0	21
	N+	2
	Nx	2
<b>Salvage Treatment</b>		
Surgery	Total	22
	R2	1
	R1	18
	R0	2
	RX	1
Chemotherapy	Neoadjuvant	3
	Concomitant with EBRT	1
Radiotherapy	BT alone	15
	EBRT + BT	10
Brachytherapy	LDR (N)	18
	- # loops: median (min, max)	3 (2, 5)
	PDR (N)	7
	- # of catheters: median (min, max)	6 (4,8)
RT dose (Gy)	BT alone: Median (min – max)	45(15-64)
	EBRT: Median (min – max)	36(12-60)
	EBRT + BT: Median (min – max)	57 (40–70)
	Cumulative dose: median (min, max)	110 (90-140)
Delay EBRT – BT (days)	Median (min, max)	16(-36-21)



### Conclusion

Salvage brachytherapy may offer a curative option for selected patients with an acceptable risk of severe toxicity for the treatment of primary or recurrent tumor in a previously irradiated area.

**PO-1045 Retreatment using Ru-106 or I-125 plaque in uveal melanoma locally recurrent after brachytherapy**  
 L. Tagliaferri<sup>1</sup>, M.M. Pagliara<sup>2</sup>, B. Fionda<sup>3</sup>, A. Scupola<sup>2</sup>, L. Azario<sup>4</sup>, M.G. Sammarco<sup>2</sup>, R. Autorino<sup>3</sup>, V. Lancellotta<sup>5</sup>, S. Cammelli<sup>6</sup>, C.G. Caputo<sup>7</sup>, R. Martinez-Monge<sup>8</sup>, G. Kovács<sup>9</sup>, M.A. Gambacorta<sup>10</sup>, V. Valentini<sup>10</sup>, M.A. Blasi<sup>2</sup>  
<sup>1</sup>U.O.C. Radioterapia Oncologica, Dipartimento di Diagnostica per immagini- Radioterapia Oncologica ed Ematologia- Fondazione Policlinico Universitario "A. Gemelli" IRCCS, Rome, Italy ; <sup>2</sup>UOC di Oncologia Oculare- Istituto di Oftalmologia, Università Cattolica del Sacro Cuore- Fondazione Policlinico Universitario "A. Gemelli" IRCCS, Roma, Italy ; <sup>3</sup>U.O.C. Radioterapia Oncologica, Dipartimento di Diagnostica per immagini- Radioterapia

Oncologica ed Ematologia- Fondazione Policlinico Universitario "A. Gemelli" IRCCS, Roma, Italy ; <sup>4</sup>U.O.C. Fisica Sanitaria- Istituto di Fisica, Università Cattolica del Sacro Cuore- Dipartimento di Diagnostica per immagini- Radioterapia Oncologica ed Ematologia- Fondazione Policlinico Universitario "A. Gemelli" IRCCS, Roma, Italy ; <sup>5</sup>Radiation Oncology Section, University of Perugia and Perugia General Hospital, Perugia, Italy ; <sup>6</sup>Radiation Oncology Center, Department of Experimental- Diagnostic and Specialty Medicine - DIMES- S. Orsola-Malpighi Hospital- University of Bologna, Bologna, Italy ; <sup>7</sup>Istituto di Oftalmologia, Fondazione Policlinico Universitario A. Gemelli IRCCS, Roma, Italy ; <sup>8</sup>Clinica Universidad de Navarra, Clínica Universidad de Navarra, Navarra, Spain ; <sup>9</sup>Interdisciplinary Brachytherapy Unit, University of Lübeck - University Hospital S-H, Lübeck, Germany ; <sup>10</sup>U.O.C. Radioterapia Oncologica- Istituto di Radiologia, Università Cattolica del Sacro Cuore- Dipartimento di Diagnostica per immagini- Radioterapia Oncologica ed Ematologia- Fondazione Policlinico Universitario "A. Gemelli" IRCCS, Roma, Italy

### Purpose or Objective

To present the results of a patient therapeutic approach using a second course of Interventional Radiotherapy (Brachytherapy) in a setting of patients with local recurrence of uveal melanoma.

### Material and Methods

Patients who had already undergone ocular brachytherapy at IOC (Interventional Oncology Center) of the "Gemelli ART" (Advanced Radiation Therapy) of Rome were considered. In this group, five patients with a local recurrence that received a second course of treatment with a plaque were included in our analysis. The reirradiation was performed with a plaque of Ruthenium-106 (dose prescribed to the apex 100 Gy) or of Iodine-125 (dose prescribed to the apex 85Gy).

### Results

All patients were in the first time treated with Ruthenium 106 plaque; the reirradiation was performed with Ruthenium 106 plaque in three cases and with Iodine in the remaining two cases. The mean time between the first and the second plaque was 56.8 months (range 25-93 months). After a median follow-up of 44.2 months (range 26-65 months) from retreatment the local tumor control rate was 100% and there was no patient who underwent secondary enucleation due to retreatment failure. Distant metastasis occurred in one patient after 6 months from retreatment. All patients evolved a worsening of the visual acuity (median visual acuity was 0.42 at time of recurrence and declined to 0.24 at the most recent follow-up); cataract occurred in two cases, no patient developed scleral necrosis.

### Conclusion

In well selected cases a retreatment strategy with plaque may offer a high probability of tumor control and organ preservation with a worsening in the visual acuity.

### Poster: Brachytherapy: Physics

#### PO-1046 Precision of source tracking in brachytherapy with scintillation detectors

J. Johansen<sup>1</sup>, H.M.L. Rosales<sup>2,3</sup>, M. Overgaard<sup>1</sup>, E.B. Jørgensen<sup>1</sup>, G. Kertzscher<sup>1</sup>, S. Beddar<sup>4</sup>, K. Tanderup<sup>1</sup>, L. Beaulieu<sup>2,3</sup>

<sup>1</sup>Aarhus University Hospital, Department of oncology, Aarhus C, Denmark ; <sup>2</sup>Université Laval, Département de physique- de génie physique et d'optique et Centre de recherche sur le cancer, Québec, Canada ; <sup>3</sup>CHU de Québec - Université Laval, Département de radio-oncologie et Axe Oncologie du CRCHU de Québec,

Québec, Canada ; <sup>4</sup>The University of Texas, MD Anderson Cancer Center, Houston, USA

### Purpose or Objective

The purpose of this study is to evaluate source tracking in brachytherapy using two state of the art detectors: 1) an inorganic scintillator detector (ISD) and a multipoint plastic scintillation detector (mPSD). The former is significantly energy dependent, while the latter is subject to the stem effect due to lower scintillation intensities. The hypothesis of this study is that source tracking with sub-millimeter precision can be obtained by accounting for these effects.

### Material and Methods

One ISD (Csl) and a mPSD composed by BCF-10, BCF-12, BCF-60 were placed in a 40x40x40cm<sup>3</sup> water phantom. The dosimeters were coupled to two independent data acquisition systems using optical fibers. The dose rates were read out at 40Hz (ISD) and 70kHz (mPSD). The dosimeters were surrounded by nine hollow plastic needles to provide a symmetric configuration for the two dosimeters, fig. 1. A treatment plan was used with ten source dwell positions in each needle and 5mm source steps. The dosimeters were placed in the center depth of the ten dwell positions. Irradiation was performed four times, two times with dwell times of 20s and two times with dwell times of 1s.

First, the distances between the individual source positions and the individual dosimeters were determined based on the relation between dose rate and distance (TG43 formalism). The distances were compared to the expected distances between dwell positions and dosimeters based on the phantom geometry.

For the ISD measurements, the distance offset was then separated in to a shift along the needle (z) and one radially away from the dosimeter (r). This was done by making a joint virtual shift of all the dwell positions in a single needle to best match the measured dose rates to TG43 as described in [1].

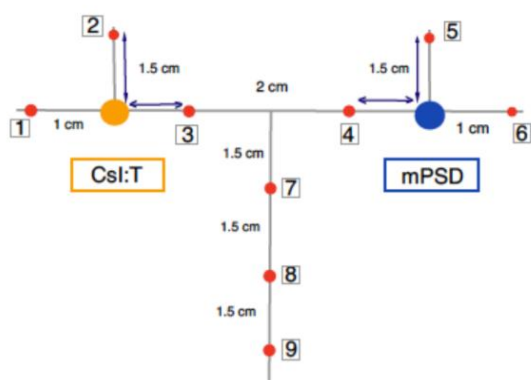


Fig. 1: Configuration of the phantom measurements.

### Results

The deviation between measured and expected distances for each dwell position were within 0.6mm (ISD) and 1mm (mPSD) at source-to-detector distances <40mm and within 1.1mm (ISD) and 1.8mm (mPSD) at larger distances (up to 58mm).

Table 1 shows the radial (r) and longitudinal (z) shifts determined for each needle individually using the ISD. The maximum offset was  $r=0.49\text{mm}$  and  $z=-0.79\text{mm}$ . The maximum differences between the four measurements for a single needle was  $r=0.29\text{mm}$  (Needle 6) and  $z=0.34\text{mm}$  (Needle 5). The mean $\pm$ SD offset across all needles and measurements were  $r=0.054\pm 0.21\text{mm}$ ,  $z=-0.22\pm 0.27\text{mm}$ . This precision corresponds to the precision of the source positioning of the afterloader.

Needle	Needle-to-ISD dist. (mm)	Run 1 (t=20s)		Run 2 (t=20s)		Run 3 (t=1s)		Run 4 (t=1s)	
		r (mm)	z (mm)	r (mm)	z (mm)	r (mm)	z (mm)	r (mm)	z (mm)
1	12	0.19	0.073	0.16	0.12	0.20	0.11	0.14	-0.013
2	15.1	-0.40	-0.14	-0.25	-0.15	-0.18	-0.084	-0.14	-0.21
3	13	0.12	-0.15	0.11	-0.16	0.015	-0.23	0.0093	-0.25
4	33	-0.12	0.15	-0.19	0.22	-0.32	0.26	-0.27	0.12
5	50.3	-0.074	-0.077	-0.0069	0.0032	-0.057	0.065	-0.23	-0.28
6	58	0.21	-0.47	0.056	-0.40	0.046	-0.55	-0.079	-0.72
7	27.5	0.37	-0.23	0.28	-0.22	0.20	-0.25	0.17	-0.34
8	37.8	0.25	-0.35	0.15	-0.32	0.24	-0.42	0.095	-0.41
9	50.5	0.49	-0.69	0.24	-0.71	0.29	-0.61	0.27	-0.79
Min		-0.40	-0.69	-0.25	-0.71	-0.32	-0.61	-0.27	-0.79
Mean (SD)		0.11 (0.27)	-0.21 (0.26)	0.061 (0.18)	-0.18 (0.28)	0.48 (0.20)	-0.19 (0.30)	0.0038 (0.19)	-0.32 (0.30)
Max		0.49	0.15	0.28	0.22	0.29	0.26	0.27	0.12

Table 1: The positional offset of each needle determined using the ISD and for each irradiation.

### Conclusion

Source tracking using state of the art scintillation dosimeters can be done with a precision comparable to the free space of the source and dosimeters inside the needles (-0.2mm). The tracking methodology can be transformed into a real-time approach.

[1] Johansen et al. Time-resolved in vivo dosimetry for source tracking in brachytherapy, *Brachy.* 17 (2018) 122-132

### PO-1047 Evaluation of ACE dose calculation model on HDR treatments delivered with a multichannel applicator

M. Carrara<sup>1</sup>, P. Caricato<sup>1</sup>, T. Giandini<sup>1</sup>, C. Tenconi<sup>2,3</sup>, A. Cerrotta<sup>4</sup>, B. Papalardi<sup>4</sup>, F. Piccolo<sup>4</sup>, C. Fallai<sup>4</sup>, E. Pignoli<sup>1</sup>  
<sup>1</sup>Fondazione IRCCS Istituto Nazionale dei Tumori, Medical Physics, Milan, Italy ; <sup>2</sup>Fondazione IRCCS Istituto Nazionale dei Tumori, Radiation Oncology 1, Milan, Italy ; <sup>3</sup>University of Milan, Oncology and Haemato-oncology, Milan, Italy ; <sup>4</sup>Fondazione IRCCS Istituto Nazionale dei Tumori, Radiation Oncology 2, Milan, Italy

### Purpose or Objective

To investigate the performance of the Advanced Calculation Engine (ACE) (Oncentra Brachy 4.5) in comparison to the AAPM-TG43 calculations for 24 HDR vaginal brachytherapy treatments delivered with a multichannel vaginal applicator (MVA), since patient's anatomy and heterogeneities are not considered with the latter algorithm.

### Material and Methods

After the commissioning of ACE according to the indications of the AAPM TG-186 recommendations, this dose calculation model was retrospectively applied on 24 vaginal HDR brachytherapy treatments delivered at our Institution with MVAs of two different diameters (i.e., 25 and 30 mm). The following volumes were all contoured: applicator, free air catheters, sigma, rectum, bladder, cortical bone, adipose tissue and remaining soft tissue, and their corresponding materials and priorities were assigned. Patient plans were then computed using both uniform and HU-based densities and compared with the TG-43 calculations in terms of relative differences between D0.1cc, D1cc and D2cc to rectum, sigmoid and bladder. D90%, D95%, D100%, V90%, V95%, V100% and V150% to the target were all compared, as well as the dose to a point P placed 5 mm above the applicator central tip.

### Results

The average relative differences between the calculated parameters for the 24 patients are shown in figure. All mean differences resulted within  $\pm 2\%$ , except the dose to the point P and the V150% to the target. In particular, the dose to P resulted higher if calculated with ACE, most probably due to the reduced attenuation by the air cavity of the central catheter. In some cases (i.e., sigmoid close over the applicator), this increased dose might result in a

higher dose to the sigmoid, as also demonstrated by the wider error bars of the sigmoid parameters plotted in figure. In the opposite, the V150% to the target resulted lower with ACE, probably in light of the higher attenuation of the applicator material if compared to water. Differences between uniform densities and HU-based calculations were all negligible, as well as dose distributions resulting with the use of MVAs of two different diameters.

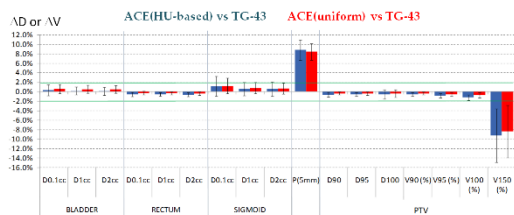


Figure 1: Mean relative differences between the dosimetric parameters evaluated for the target and the different organs at risk. In blue, comparison between HU-based ACE calculation and TG-43; in red, comparison between uniform density ACE calculation and TG-43. Error bars: one standard deviation.

### Conclusion

In general, on the 24 investigated treatments the ACE dose calculation model results in similar dose distributions as the commonly used AAPM-TG43 algorithm, both for targets and organs at risk, with the exception of the V150% to the target and the dose at 5 mm above the applicator tip.

### PO-1048 Variability in catheter reconstruction for multi-catheter interstitial brachytherapy

K. Kallis<sup>1</sup>, T. Kaltsas<sup>1</sup>, S. Kreppner<sup>1</sup>, M. Lotter<sup>1</sup>, V. Strnad<sup>1</sup>, R. Fietkau<sup>1</sup>, C. Bert<sup>1</sup>

<sup>1</sup>University Hospital Erlangen, Radiation Oncology, Erlangen, Germany

### Purpose or Objective

Accelerated partial breast irradiation of the tumor bed using interstitial brachytherapy is a common treatment option for selected breast cancer patients. Reconstruction of the source path is a time consuming manual procedure during treatment planning that influences the planned dose delivery. The aim of this study is to evaluate inter-observer variabilities for catheter reconstruction. Further, we explored the feasibility of an automated catheter reconstruction using an electromagnetic tracking (EMT) system, integrated into an afterloader prototype.

### Material and Methods

The catheter reconstructions of three physicists were compared for 26 patients, in total 426 catheters, see figure 1. Keeping constant the CT data, contours, dwell times, dwell positions (DPs), plan optimization and normalization settings, the geometrical deviations between the corresponding DPs of the repeated reconstruction and the reference plan were evaluated. Also, the effects on coverage index (CI), dose non-uniformity ratio (DNR), conformal index (COIN), and the dose to the organs at risk were analyzed. The clinical approved plan served as reference.

In addition, the catheter traces were reconstructed with the help of EMT data. The EMT measurement was conducted directly after CT imaging using a Flexitron prototype (Elekta, Veenendaal, The Netherlands) equipped with an EMT sensor. In combination with an Aurora EMT system (NDI, Waterloo, Canada) all catheters can be automatically digitized, which takes 6-9 minutes depending on the number of implanted catheters. Using an in-house routine, the measured catheter traces were rigidly registered to the catheter button centers defined on the CT image and automatically imported to the treatment planning system within one minute.

### Results

Over all patients and all manual catheter reconstructions a mean deviation between corresponding DPs of

0.58±0.49 mm was detected. Mean deviations to the reference plan of 0.48±0.31 mm and 0.58±0.35 mm were found for the first and second observer, respectively. The length of the catheter traces varied 0.45±0.39 mm on average. The mean deviation of CI varied by 0.25±0.29%, variations in DNR, COIN, mean heart dose and mean lung dose were all <0.01%. The skin dose changed in the maximum by 4.10%. Nevertheless, manual reconstruction of the catheter paths is a time consuming (3-5 minutes per catheter) procedure in treatment planning. Evaluation of magnitude and implication on the geometrical deviations and the dose distribution using the EMT measurements is still ongoing.

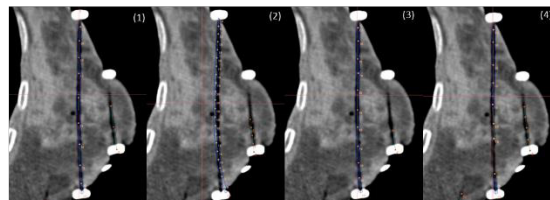


Figure 1 Comparison of different reconstruction techniques. Four different reconstruction techniques are presented. All images show the same slice of one patients CT image. In blue the projected catheter is visualized. The defined control points, defining the path are presented in red. Figure (1) shows the reconstruction of the approved clinical plan. Figure (2) shows the catheter reconstruction using the EMT measurement. Figure (3) presents the reconstruction of observer one and figure (4) the catheter path of observer two.

### Conclusion

The study proved that a repeated reconstruction of the catheter traces does not lead to a large change in dose exposure or large geometrical deviations. However, lack of ground truth poses a challenge to reliable quality assessment of the reconstruction. Using EMT measurements seems to be a feasible, dose free and quick option for catheter reconstruction.

### PO-1049 Assessing PTV margin adequacy in permanent breast seed implant for complex target geometries

A. Guebert<sup>1,2</sup>, A. Frederick<sup>1,2</sup>, M. Roumeliotis<sup>1,2,3</sup>, T. Meyer<sup>1,2,3</sup>, S. Quirk<sup>1,2,3</sup>

<sup>1</sup>University of Calgary, Department of Physics and Astronomy, Calgary, Canada; <sup>2</sup>Tom Baker Cancer Centre, Division of Medical Physics, Calgary, Canada; <sup>3</sup>University of Calgary, Department of Oncology, Calgary, Canada

### Purpose or Objective

Permanent breast seed implant (PBSI) brachytherapy presents a convenient, single day alternative to standard whole breast radiotherapy. For widespread adoption, robust treatment planning recommendations are required. Clinical PBSI treatment plans recommend a 10-15 mm expansion of the clinical target volume (CTV) to the planning target volume (PTV). The PTV margin is cropped to the chest wall muscle and 5 mm from the skin surface as these structures present anatomic boundaries. For patients where the target is located in close proximity to the skin and chest wall, significant cropping of the PTV is required on both sides. For this subset of patients, accounting for approximately 25% of our cohort, poor coverage has been observed on the post-implant CT. This simulation study aims to investigate PTV cropping in the skin-chest wall direction and the impact on post-implant dosimetry.

### Material and Methods

Four typical CTV volumes (6.6, 10.1, 15.6, and 30.5 cm<sup>3</sup>) were modelled as ellipsoids. The PTV margin for each volume was modelled as isotropic expansions of 10 mm in the direction parallel to the needle, and the template left-right direction, and 0, 4, 7, or 10 mm in the skin-chest wall direction (Figure 1). Treatment plans were generated with 15 mm seed spacing for needles passing through the CTV, and 10 mm seed spacing for needles passing through only the PTV. The prescription dose was 90 Gy. For each margin combination, 1500 implants were simulated by application of a seed delivery error sampled from our reported clinical

seed placement accuracy, treated as a normal distribution. In the three needle directions, the mean displacement ( $\pm$  standard deviation) was: 6.7 mm ( $\pm 7.8$  mm) in the shallow-deep direction, 0.75 mm ( $\pm 4.4$  mm) in the template left-right direction, and 0.10 ( $\pm 4.0$  mm) in the skin-chest wall direction. The skin and chest-wall were imposed as boundaries for seed placement in the simulation. Resultant CTV coverage was assessed using the  $V_{100\%}$ .

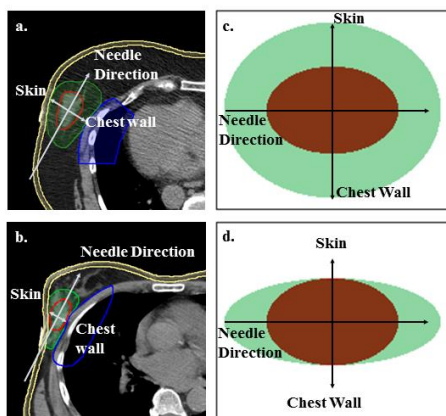


**Figure 1:** Axial patient CT scans (a. and b.) with contoured CTVs (red) and PTVs (green). The PTV in b. is cropped closely to the CTV due to proximity to the skin and chest wall. This is shown in ellipsoidal geometry in c. and d, where the CTV (red) is expanded isotropically to the PTV (green) in c., indicating no cropping, and anisotropically to the PTV in d, indicating cropping. The coordinate system is shown in all four panes, with left-right being the direction into and out of the page.

## Results

In general, PTV cropping has a larger effect on dosimetry for small volume CTVs. In this simulation, large decreases in  $V_{100\%}$  coverage are observed for the smallest PTV (0 mm skin-chest wall margin) on the three smallest CTVs, particularly in comparison to the largest CTV. For these CTV/PTV combinations, the mean  $V_{100\%}$  was 46%, as opposed to 89% for the largest CTV. For all CTVs, a cropping to a 7 mm skin-chest wall margin likely does not substantially affect coverage compared to the 10 mm uncropped PTV. Overall, the results show that the volume of the CTV is important when considering resultant  $V_{100\%}$  coverage when seed delivery error is taken into account, particularly when patient anatomy requires severe cropping to the skin and chest wall.

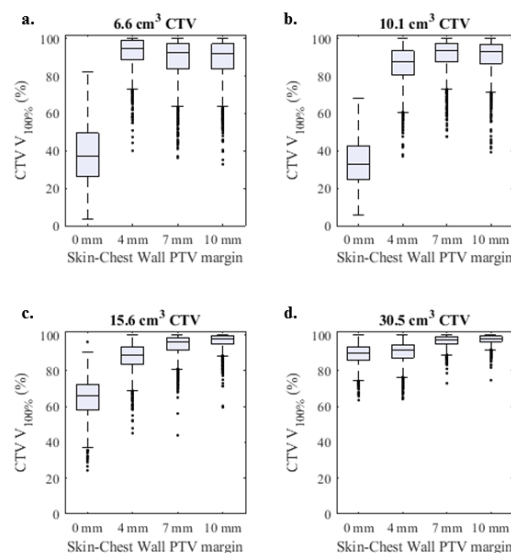


**Figure 2:** Resultant  $V_{100\%}$  for 1500 simulated implants for a. 6.6 cm<sup>3</sup>, b. 10.1 cm<sup>3</sup>, c. 15.6 cm<sup>3</sup>, and d. 30.5 cm<sup>3</sup> CTVs, for four skin-chest wall PTV margins. Boxes correspond to 25 and 75 percentiles of the data, with the line indicating median. Whiskers represent the 95% confidence interval. Outliers are indicated by dots.

## Conclusion

Simulations of an idealized target geometry reveal an interplay between CTV/PTV size and post-implant dosimetry when seed delivery error is accounted for. This motivates the necessity of considering CTV size and the extent of PTV cropping when assessing PBSI treatment plans.

### PO-1050 A gynecological multichannel applicator including a real-time treatment verification system

A. Romanyukha<sup>1</sup>, M. Carrara<sup>2</sup>, T. Giandini<sup>2</sup>, M. Petasecca<sup>1</sup>, T. Al-Salmami<sup>1</sup>, D. Cutajar<sup>1</sup>, A. Cerrotta<sup>3</sup>, B. Pappalardi<sup>3</sup>, F. Piccolo<sup>3</sup>, E. Pignoli<sup>2</sup>, A. Rosenfeld<sup>1</sup>  
<sup>1</sup>University of Wollongong, Centre for Medical Radiation Physics CMRP, Wollongong, Australia; <sup>2</sup>Fondazione IRCCS Istituto Nazionale dei Tumori, Medical Physics, Milan, Italy; <sup>3</sup>Fondazione IRCCS Istituto Nazionale dei Tumori, Radiation Oncology 2, Milan, Italy

### Purpose or Objective

To develop, calibrate, and test an innovative prototype of a vaginal multichannel applicator with an embedded system for real-time verification of source dwell position and time in HDR <sup>192</sup>Ir brachytherapy, to ensure that planned treatments are delivered in accordance to the original treatment plans.

### Material and Methods

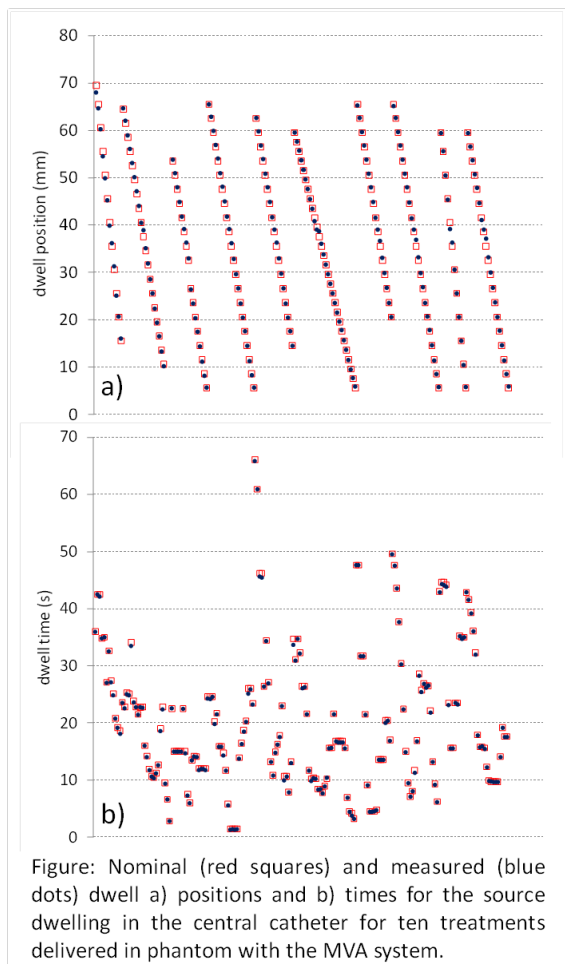
The applicator prototype is modeled based on a multichannel vaginal applicator (MVA) that is 30 mm in diameter and contains seven peripheral and one central catheter(s). Three p-type epi diodes are placed around the upper region of the MVA and were selected due to their efficiency in the measurement of high-energy photons associated with the <sup>192</sup>Ir source. The readout system is an AFE and FPGA system capable of 100  $\mu$ s online readout for up to four diodes at a time. The *ad hoc* detectors and electronics have been all developed and optimized according to the specific task.

In this study, a prototype of the MVA system was characterized, and an efficient method for real-time source localization and dwell time measurement was established. Once the method was defined and tested, the accuracy of the MVA system was then quantified in

phantom on ten vaginal treatments previously delivered at our Institution.

## Results

The characterization of the MVA system showed no significant dependence on radiation intensity for a range of Air Kerma Strengths between 34 and 13 mGy<sup>2</sup>h<sup>-1</sup>. After its characterization and calibration, the MVA system demonstrated the ability to resolve the HDR BT source position and dwelling time along the first 70 mm of the applicator, encompassing the most clinically relevant region for HDR BT vaginal treatments. 95% of measurements showed positional discrepancies between nominal and measured values within 0.8 mm and 1.5 mm for the source dwelling in the central and in the peripheral catheters, respectively. 95% of the measured dwell times for the central and peripheral catheters were within 0.4 s and 0.2s, respectively, if compared to the nominal values. Nominal and measured values for the source dwelling in the central catheter are shown in the figure.



## Conclusion

The proposed intracavitary MVA system has demonstrated the ability to simultaneously deliver and verify the HDR BT treatment with, in general, sub-mm and sub-second accuracy. Once improved, the system will provide essential information in real time to help ensure that the treatment is delivered in accordance with the planned treatment plan. Further studies may help to further increase spatial and time resolution.

## PO-1051 quality analysis automation of a prostate low dose rate seed implant using clustering methods

D. Rodríguez Latorre<sup>1</sup>

<sup>1</sup>Hospital Universitario Central de Asturias, Radiofísica, Oviedo, Spain

## Purpose or Objective

I-125 seed implants are a reference treatment for low risk prostate tumors. The quality of this treatment depends on the precision in the placement of these seeds in the planned points to achieve the proper dose distribution. Post-implant dosimetry is based on the need to evaluate the quality of the implant once the forces applied by needles and by the ultrasound probe have disappeared and once the edema caused in the implant process has gone. In many places post-implant dosimetry is not done because it is time-consuming and also because of the difficulty to have reliable image modality to simultaneously define the position of the seeds and volumes: prostate and OARs. We developed a fast and reliable method to identify strands and individual seeds that would give geometric quality index of the implant, which allows us to check the robustness of the implantation method and if any cold spot is to be expected.

## Material and Methods

The treatment planning system PSID™ 5.0 (Eckert & Ziegler BEBIG GmbH) is used, that allows us to extract the positions of the seeds of the planning in real time (online planning), as well as the positions after a month (postplanning).

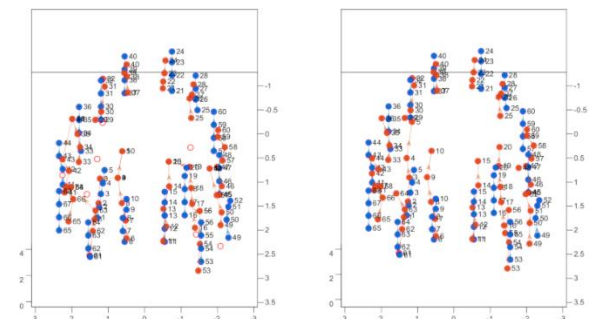
The MATLAB Statistics and Machine Learning Toolbox (MATLAB R2018a, MathWorks®) was used to write a code for seeds and strands identification using clustering techniques following the next steps:

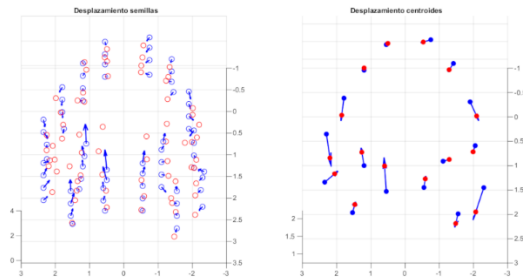
1. Rigid registration with Iterative Closest Point, which uses an affine transformation to get rid of the differences between imaging datasets (online and postplan) due to its different reference systems.
2. Hierarchical clustering with the dataset online using the MATLAB linkage function.
3. Assignment using KDTreeSearcher and knnsearch MATLAB functions, first to generate a binary tree and then the subsequent k nearest neighbor search.

## Results

The assignment is correct in most cases and it considerably reduces the time to obtain a visualization of the geometric differences between online and postplan datasets. Nevertheless the assignment is not completely when: there are seeds too far away from their original position in the XY plane, and when some strands appear bended in the Z direction.

Once the assignment problem was solved we calculated the displacement vector for each seed, the strand centroid displacement vector, and the separation between consecutive seeds in the same strand to see if the 1 cm metric remains, which is the theoretical separation between seeds. We saw that in average the postplan consecutive seed separation was 0.9 cm.





### Conclusion

We have developed a fast method to solve the assignment problem between two seed datasets which does not need any adjustable parameter to work. This allows us to calculate some metrics to assess the quality of the implant.

### PO-1052 Is there a clinically meaningful change in anatomy during planning of US HDR prostate brachytherapy?

A. David<sup>1</sup>, V. Brennan<sup>2</sup>, G. Cohen<sup>1</sup>, A. Damato<sup>1</sup>

<sup>1</sup>Memorial Sloan Kettering Cancer Center, Medical Physics, New York, USA ; <sup>2</sup>Memorial Sloan Kettering Cancer Center, Radiation Oncology, New York, USA

#### Purpose or Objective

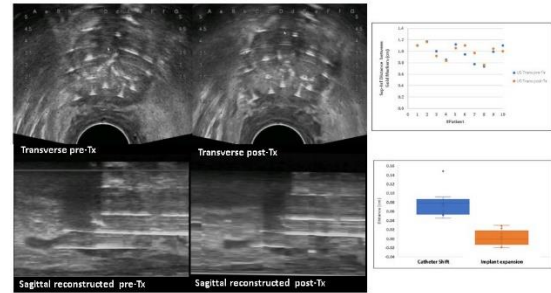
To investigate the role of anatomical and implant geometry changes during planning time in final delivered dose for US-based HDR prostate brachytherapy

#### Material and Methods

The record of 13 patients who received US-based HDR prostate brachytherapy at our institution was retrospectively reviewed. All patients receive a single dose fraction brachytherapy boost treatment, 2 weeks before external beam treatment. Gold fiducial markers were positioned at the apex and base of the prostate at the beginning of the procedure. A set of static US images were acquired using transverse transducer pre-treatment (pre-Tx) after needle insertion and used for contouring, final digitization, and dose optimization. Post-treatment (post-Tx) transverse images were acquired immediately after treatment delivery. Targets were re-contoured and the clinical plans (dwell pattern and times on the newly digitized catheters) was replicated on the post-Tx images. The DICOM plans were analyzed using MATLAB routines to assess **catheter shift** (average distances between reciprocal dwell source positions pre- and post- treatment after rigid registration between all dwell positions is performed) and **implant expansion** (average of the difference between the distances from each dwell source position to the center of mass of the dwell sources system). **Superior-inferior swelling** (difference between the post- and pre-Tx distance between fiducial markers) was assessed on 10 patients. Differences in target volumes are also reported.

#### Results

The number of needles (average  $\pm$  1 standard deviation) was  $13 \pm 2$  needles. No meaningful catheter shift ( $0.08 \pm 0.03$  cm), implant expansion ( $0.003 \pm 0.02$  cm) and sup-inf swelling ( $-0.01 \pm 0.09$ ) were observed. Changes in target volume, were  $0.26 \pm 3.41$  cm<sup>3</sup>.



### Conclusion

Geometric assessment of single catheter shift, implant expansion and superior-inferior swelling indicate that no clinical meaningful change occurred in the time between planning scan and treatment. Further analysis will be performed to assess the role of contouring uncertainty on the patient-by-patient results. More patients and dose distributions are being analyzed to validate these results, which suggest high fidelity between planned and delivered dose.

### Poster: Brachytherapy: Prostate

### PO-1053 Efficacy/toxicity after high dose rate brachytherapy as monotherapy for localized prostate cancer

S. Novikov<sup>1</sup>, S. Kanaev<sup>1</sup>, M. Gotovchikova<sup>1</sup>, R. Novikov<sup>1</sup>, D. Ilin<sup>1</sup>, M. Girshovitch<sup>1</sup>

<sup>1</sup>Prof. N.N. Petrov Research Institute of Oncology, Radiotherapy, St. Petersburg, Russian Federation

#### Purpose or Objective

to present toxicity profile and biochemical control rates of a prospective single center trial comparing 2 fractions of 13 Gy and three fractions of 11.5 Gy high dose rate brachytherapy as sole treatment for localized prostate cancer.

#### Material and Methods

Between 01.06.2013 and 01.06.2017, 198 men with clinically localized prostate cancer T1-T3aNOm0, Gleason score below 8 and PSA less than 20 ng/ml were included in the study. Sixty-seven patients received TRUS guided HDR brachytherapy in 2 fractions of 13 Gy, 131 men - in 3 fractions of 11.5 Gy. Qmax below 10 ml/sec and IPSS above 20 were excluding criteria. Biochemical failure was registered according to the Phoenix definition, and toxicity was scored according CTCAE-5.

#### Results

Median follow-up was 40.9 (range 15.1-71.1) months. The 36 month's biochemical control (BC) was 95.5% for 121 patients with follow-up of 36-56 months: 100% - in low-risk, 94.2% - in intermediate risk and 90.5% - in high risk groups. We found comparable BC rates for patients that received 2 fractions (BC-93.2%) and 3 fractions (BC-98.5%) HDR-BT.

Grade 2 late genitourinary toxicity manifested by urgency in 4 (2%) cases; grade 3 late toxicity was detected in 2 (1%) men with urethral stenosis and another 1 (0.5%) - with severe urgency. Median International Prostate Symptom Score raised from 8 [4; 12] (0-21) (before HDR-BT) to 12 [7;16] (1,0-28,0) 3 months after the treatment with subsequent decrease to 10 [9;16] (1-25) and 7 [7;8] (6-12) after 12 and 36 months of follow-up (p=0,001).

In the same manner median Q<sub>max</sub> decreased from 15,0 [12,7;18,0] (9,0-36,0) ml/sec to 14,3 [12,0; 17,0] (7,0-30,0) ml/sec 3 months after treatment (p=0,001) and subsequently reached 14,9 [13,1;17,0] (7,0-25,0) and 14,1 [13,0;16,0] (6,0-29,0) ml/sec 1 and 3 years after the end of HDR-BT.

Median International Index of Erectile Function score before treatment was 15 [10;20] (1-25) and decreased to 10 [4; 10] (1-21) 3 months after HDR-BT. Surprisingly it increased to 12 [4;16] (1-22) after 12 months of follow-up: at that time in 57.6% cases it was above 11 points. Grade I-II late gastrointestinal toxicity detected in 12 cases (6.1%), without any patient with grade III toxicity. Fractionation scheme has no significant impact on early and late toxicity.

#### Conclusion

this single center comparative study demonstrated that in patients with localized prostate cancer both fractionation regimes demonstrated high 36-months biochemical control with very limited early and late toxicity.

#### PO-1054 LDR versus HDR brachytherapy boost in prostate cancer patients - a retrospective analysis

S. Rodda<sup>1</sup>, L. Murray<sup>1</sup>, D. Bottomley<sup>1</sup>, P. Bownes<sup>2</sup>, C. Wilkinson<sup>3</sup>, E. Adiotomre<sup>4</sup>, B. Al-Qaisieh<sup>2</sup>, E. Dugdale<sup>1</sup>, O. Hulson<sup>4</sup>, J. Mason<sup>2</sup>, J. Smith<sup>4</sup>, A. M Henry<sup>1</sup>  
<sup>1</sup>St.James institute of Oncology, Clinical Oncology, Leeds, United Kingdom ; <sup>2</sup>St.James institute of Oncology, Brachytherapy Physics, Leeds, United Kingdom ; <sup>3</sup>St.James institute of Oncology, Brachytherapy, Leeds, United Kingdom ; <sup>4</sup>St.James institute of Oncology, Radiology, Leeds, United Kingdom

#### Purpose or Objective

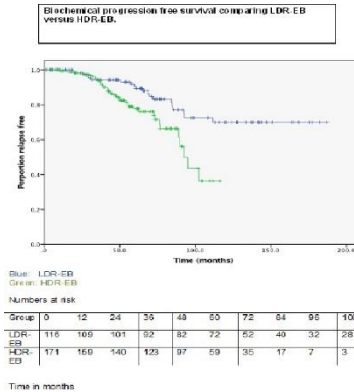
In the absence of randomised comparison, to report biochemical Progression Free Survival (bPFS) and morbidity outcomes in men with non-metastatic prostate cancer treated with LDR or HDR brachytherapy boost (BT) techniques combined with external beam radiotherapy(EBRT).

#### Material and Methods

347 men consecutively treated with combination of BT boost and EBRT from 1996 - 2012 from a single centre were included. All were staged using prostate MR and bone scan. Data was extracted from a prospectively maintained database and electronic case records. Patients with no record of post implant PSA were excluded from the analysis. 287 patients were evaluable. 116 had LDR (I-125) BT to a dose of 110 Gy in combination with EBRT 45Gy in 20 Fractions (LDR-EB) treated from 1996 to 2007. 171 had HDR BT (17 Gy in 2 fractions or 15 Gy in 1 fraction) in combination with EBRT 35.75Gy in 13 or 37.5Gy in 15 fractions respectively (HDR-EB) treated from 2007-2012. Duration of androgen deprivation was at clinician discretion. Nadir+2 definition was used to define bPFS and toxicity scored using RTOG.

#### Results

Median FU was 74.1 and 57.0 months for the LDR-EB and HDR-EB groups respectively. Both groups were relatively well balanced (Table 1). The LDR-EB group were slightly younger than HDR-EB group (63 vs 65 years: p=0.02) and had significantly larger proportion of high risk disease (p=0.02). At 5 years there was a significant improvement in bPFS in LDR-EB compared to HDR-EB groups (90.5% vs. 77.6%, p=0.003). On MVA Gleason grade  $\geq 8$  vs 6 (HR: 5.47) and treatment group LDR-EB vs HDR-EB (HR: 2.33) both predicted bPFS. The 5-year cumulative incidence of G3 and above GU and GI toxicity was higher in LDR -EB (8% and 5%) compared to HDR-EB groups (4% and 1%) but did not reach statistical significance.



	LDR N=128	-EB N=219	-EB N=219	P-Value
Evaluable patients	116	171		
Missing Data	12(9.5%)	48(22%)		
Median f/u(Range) months	74.1(1.0-187)	57.0(1.8-116)		
Median Age (Range) years	10.7(1.6-59)	10(1.4-131)		0.02
Median PSA ng/mL	10.7(1.6-59)	10(1.4-131)		ns
Gleason Score N (%)				
6	17 (15%)	20 (12%)		
7	76 (65%)	121 (71%)		ns
8-10	21 (18%)	29 (17%)		
Unknown	2 (2%)	1 (<1%)		
T category N (%)				
T1c-T2c	50 (43%)	69 (40%)		
T3a-T3b	56 (48%)	97 (57%)		ns
Unknown	10 (9%)	5 (3%)		
NCCN Risk group N (%)				
Low	2 (2%)	2 (1%)		
Intermediate	28 (24%)	68 (40%)		0.02
High	80 (69%)	94 (55%)		
Unknown	6 (5%)	7 (4%)		
Hormone Duration N (%)				
≤12 Months	74 (64%)	126 (74%)		0.06
>12 months	7 (6%)	27 (16%)		
Unknown	35 (30%)	18 (10%)		

#### Conclusion

The risk of biochemical failure was more than double in men treated with HDR-EB compared to LDR-EB. There was higher grade 3+ GU and GI toxicity in the LDR-EB group although this has not reached statistical significance. LDR-EB may provide the most effective PSA control at 5 years. The results of this study should be regarded as hypothesis generating in view of its retrospective design, lack of randomization and missing data.

#### PO-1055 High-dose rate brachytherapy boost for T3 prostate cancer patients: a single institution experience

M. XU<sup>1</sup>, D. Diao<sup>1</sup>, A. Lazar<sup>1</sup>, K. Shinohara<sup>2</sup>, A. Chang<sup>3</sup>, A. Cunha<sup>1</sup>, I. Hsu<sup>1</sup>

<sup>1</sup>University of California San Francisco, Radiation Oncology, San Francisco, USA ; <sup>2</sup>University of California San Francisco, Urology, San Francisco, USA ; <sup>3</sup>University of California Los Angeles, Radiation Oncology, Los Angeles, USA

#### Purpose or Objective

Treating prostate cancer with extraprostatic extension (stage T3a) or seminal vesicle invasion (stage T3b) using brachytherapy boost after external beam radiotherapy (EBRT) enables dose escalation and is technically challenging. Treatment outcomes associated with high-dose rate (HDR) brachytherapy boost for T3 disease have not been well described. This study sought to assess disease control rates among patients treated with HDR brachytherapy boost for T3 disease.

#### Material and Methods

Retrospective chart review was performed to identify patients with T3 prostate cancer treated with combination EBRT and HDR brachytherapy boost between July 1997 and September 2014. Biochemical recurrence (BCR), defined as prostate specific antigen (PSA) nadir + 2 ng/mL, locoregional recurrence (LRR), distant metastases (DM), and prostate-cancer specific mortality (PCSM) were estimated using cumulative incidence and subdistribution hazard ratio (SHR) competing risk analysis. Overall survival (OS) was estimated using Kaplan Meier product limit estimator, with Cox proportional hazards modeling used to analyze associations between pre-treatment characteristics and survival outcomes.

#### Results

Of 185 patients, 139 (75.1%) had T3a and 46 (24.9%) had T3b disease. Gleason 8-10 disease was present in 87 (47.3%) patients and the median PSA was 9.3 (interquartile range [IQR] from 25th to 75th percentile, 5.8-19.4). Nearly all patients received whole pelvis EBRT (178, 96.2%) and androgen deprivation therapy (95.7%, median duration 11 months).

The median follow-up time was 89 months (IQR 49-122). The 8-year BCR rate was 29%; 26.1% for T3a and 38.3% for T3b (SHR 1.5, 95% CI 0.9-2.7,  $p = 0.15$ ). The 8-year LRR rate was 7.9%, 5.2% for T3a and 16.8% for T3b (SHR 2.3 95% CI 0.9-6.1,  $p = 0.09$ ). The 8-year DM rate was 11.9%, 9.2% for T3a and 21.3% for T3b (SHR 3.0, 95% CI 1.5-6.2,  $p = 0.003$ ). The 8-year PCSM rate was 3.6%, 1.9% for T3a and 9.1% for T3b (SHR 6.1, 95% CI 1.6-23.7,  $p = 0.008$ ). The 8-year OS rate was 90.1%, 91.5% for T3a and 85.7% for T3b disease (Cox HR 2.1, 95% CI 0.9-4.7,  $p = 0.07$ ). Grade 3 or higher gastrointestinal and genitourinary (GU) toxicities were rare; only one patient had a grade 3 chronic GU toxicity (0.6%).

**Conclusion**  
HDR brachytherapy boost for T3 prostate cancer was well tolerated. Patients with T3b disease had higher rates of LRR and statistically significantly higher rates of DM and PCSM. This suggests HDR brachytherapy boost is safe and efficacious for T3 disease, but combination chemohormonal agents may be necessary to address the high metastatic risk in patients with locally advanced prostate cancer, particularly for T3b disease.

#### PO-1056 Ultra-Focal Salvage HDR-brachytherapy for recurrent prostate cancer: a single institution experience

C. Salembier<sup>1</sup>, A. Rijnders<sup>1</sup>, C. Assenmacher<sup>2</sup>, M. Debecker<sup>1</sup>, I. Tshiakatumba<sup>1</sup>, A. Gulyban<sup>1</sup>, O. Michel<sup>1</sup>  
<sup>1</sup>Europe Hospitals - Site St Elisabeth, Department of Radiation Oncology, Brussels, Belgium; <sup>2</sup>Europe Hospitals - Site St Elisabeth, Department of Urology, Brussels, Belgium

#### Purpose or Objective

To evaluate the clinical outcome of ultra-focal salvage brachytherapy (UFSBT) after primary external beam radiotherapy or LDR-brachytherapy in terms of toxicity and efficacy, based on a single institution experience.

#### Material and Methods

Between June 2016 and June 2018 twenty patients underwent UFSBT. Patients were initially treated for primary prostate cancer with external beam radiotherapy or LDR brachytherapy. Following the development of biochemical failures (based on the Phoenix criteria), the presence of exclusive local recurrences was confirmed using Ga-68-PSMA-PET/CT and multi-parameter MRI. Treatment procedure consisted of an ultrasound guided catheter placement followed by the definitive planning using dedicated CT with co-registered PET/CT and MRI datasets. Gross tumor volume (GTV) delineation was performed on these datasets, following cognitive co-registration focusing on the region of the treatment. A margin of 5 mm (constrained to the prostatic urethra and the anterior rectal wall) was added to generate the Clinical target volume (CTV). All patients were treated

using a MicroSelectron HDR (Elekta AB, Stockholm, Sweden). The prescription dose was a single fraction of 19 Gy to the CTV. The dose distribution was graphically optimized for maximal CTV coverage while respecting the pre-defined dose constraints for the organs at risk: Bladder\_D1cc  $\leq 12$  Gy, Rectum\_D1cc  $\leq 12$  Gy and Urethra\_D10  $\leq 17.7$  Gy. Patients were followed up every 3 months for Prostate Specific Antigen (PSA) and toxicity assessment using CTCAE version 4.0.

#### Results

Sixteen patients received external beam radiotherapy and four LDR-brachytherapy as primary treatment. The mean interval between the primary treatment and salvage brachytherapy was 9.2 years (range 4-16). At presentation for UFSBT, three patients received already a hormonal treatment for their biochemical recurrence. This treatment was stopped at the day of intervention. So none of the patients received concomitant or adjuvant hormonal treatment in association with the salvage brachytherapy procedure. The mean age at time of UFSBT was 72 years (range: 56-88). On average nine (range 6-12) needles were inserted. The mean CTV was 9.4 cc (range: 4.7-24.0). All relevant dose constraints were respected (average  $\pm$  standard deviation): CTV\_D95: 19 $\pm$ 2.1 Gy, Bladder\_D1cc: 5.5 $\pm$ 3 Gy, Rectum\_D1cc: 9.2 $\pm$ 2.2 Gy, Urethra\_D10: 10.8 $\pm$ 3.3 Gy.

Median follow-up after UFSBT was 12 months (range: 3.9-28.0), with two biochemical recurrences to date. One of these 2 recurrent patients refused additional investigation and was put under hormonal treatment, while the other one remained locally uncured (persistent and identical prostate lesion at 12 months follow-up). Toxicity was limited to GU and GI grades I in all treated patients.

#### Conclusion

Ultra-focal salvage brachytherapy using HDR with a single fraction of 19 Gy offers an effective treatment option with promising local control and limited toxicity.

#### PO-1057 Salvage high-dose-brachytherapy for recurrent prostate cancer patients: 10 years of experience.

P. Lelek<sup>1</sup>, M. Stankiewicz<sup>1</sup>, T. Krzysztofciak<sup>1</sup>, S. Kellas-Slecza<sup>1</sup>, M. Fijałkowski<sup>1</sup>, P. Wojcieszek<sup>1</sup>  
<sup>1</sup>Maria Skłodowska-Curie Memorial Cancer Center and Institute of Oncology Gliwice, Brachytherapy Department, Katowice, Poland

#### Purpose or Objective

The analysis of mature results of salvage high-dose-rate brachytherapy (sHDRBT) for recurrent prostate cancer.

#### Material and Methods

This retrospective study on sHDRBT analyses prostate cancer patients suffering local failure (biopsy confirmed) after primary irradiation. They were included in this research consecutively from the introduction of this method to achieve median follow-up >5 years. Planned treatment schedule was interstitial sHDRBT in three fractions of 10 Gy, every two weeks. Acute and late toxicity of the treatment was assessed using the RTOG/RTOG grading criteria. Biochemical relapse was defined according to the Phoenix consensus. 5-year biochemical failure-free survival was calculated.

#### Results

83 men were enrolled in our study, treated from 2008 to 2012. Median follow - up time was 61 months (11- 111 months). Median age was 70 years (55 - 80). Median relapse peak PSA was 3,1 ng/ml (0,065 - 19,9 ng/ml). Median PSA at last follow-up was 0,358 ng/ml (0,008-2470,74 ng/ml). 80 patients suffered from urinary toxicity grade 2 or below. 11 patients developed late urinary toxicity grade 3. 6 patients had late rectal toxicity grade 1. There were 34 biochemical relapses. 25 patients suffered from metastases. 5- year biochemical failure-free survival was 59%.

## Conclusion

There is a place for salvage HDRBT in the efficient treatment of localised prostate cancer relapse after prior radiotherapy due to its ability to deliver the significant radiation dose to the prostate while minimising normal tissue exposure. The toxicity rates of the procedure are acceptable although the selection of candidates for salvage HDRBT should be carried out carefully with the consideration of the individual risk of distant failures.

## PO-1058 Long-term outcomes of LDR compared to hypofractionated EBRT for intermediate-risk prostate cancer

N. Sanmamed Salgado<sup>1</sup>, L. Joseph<sup>1</sup>, J. Crook<sup>2</sup>, J. Borg<sup>1</sup>, P. Chung<sup>1</sup>, P. Warde<sup>1</sup>, A. Di Tomasso<sup>1</sup>, A. Berlin<sup>1</sup>, M. Patel<sup>1</sup>, A. Bayley<sup>1</sup>, C. Catton<sup>1</sup>, J. Helou<sup>1</sup>

<sup>1</sup>Princess Margaret Cancer Center, Radiation oncology, Toronto, Canada ; <sup>2</sup>BC Cancer Center for the Southern Interior, Radiation oncology, Kelowna, Canada

### Purpose or Objective

Low dose-rate brachytherapy (LDR) and hypofractionated external beam radiotherapy (EBRT) are accepted standard treatments in the setting of intermediate-risk (IR) prostate cancer. As yet, none of these options have been tested against one another in a randomized trial. We aim to compare the long-term oncologic outcomes of IR prostate cancer patients treated with LDR or EBRT at a single institution.

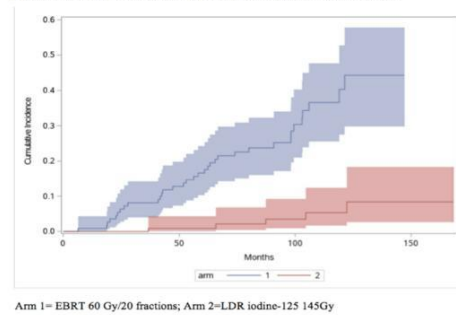
### Material and Methods

Between January 2005 and December 2013, 248 patients diagnosed with IR prostate cancer ( $\leq T2c$ , Gleason  $\leq 7$  and PSA  $\leq 20$  ng/mL) were treated with LDR or EBRT; 123 patients received a permanent implant of iodine-125 seeds prescribed to 145 Gy as a minimum peripheral dose and 125 patients were treated with EBRT to a total dose of 60 Gy in 20 fractions. The "nadir +2 ng/mL" PSA threshold (Phoenix definition) was used to define biochemical relapse (BR). To account for the competing risk of death, the cumulative incidence function (CIF) of BR and metastases for each group, and the 95% confidence intervals were reported. To test whether the difference between the groups is significant, Gray's method was applied. The Kaplan-Meier (KM) method was used to estimate overall survival (OS) and prostate cancer specific survival (PCSS), and log-rank test was used to compare treatment groups. A two-tailed p-value  $\leq 0.05$  was considered statistically significant.

### Results

Median follow-up was 95 [interquartile range (IQR): 79-118] and 96 (IQR: 63-123) months in the LDR and EBRT groups, respectively. In the LDR group, mean age was 65 ( $\pm 7$ ) with a median PSA at baseline of 6.8 ng/mL (IQR: 5.3-9.6); for the EBRT group, mean age was 71 ( $\pm 5$ ) years and median PSA at baseline was 7.4 ng/mL (IQR: 5.9-9.7). Neoadjuvant androgen deprivation therapy was used for cytoreduction in 4 patients treated with LDR and none with EBRT. BR was observed in 5 patients treated with LDR and 34 treated with EBRT. At 60 months and 90 months, the CIF of BR was 0.9% (0.1-4.4) and 3.5% (0.9-9.2) vs. 16.6% (95% CI: 10.3-24.2) and 23.7% (16.0-32.3) ( $p < 0.001$ ) in the LDR and EBRT groups (Figure 1). The median time to develop metastases was 99 months (IQR: 70-121) in the entire cohort with no statistical significant difference between groups. At 90 and 108 months, the CIF of metastases was 0% and 1.6% (95% CI: 0.1-7.5) compared to 3.4% (95% CI: 0.9-8.9) and 9.1% (95% CI: 3.5-18.2) in the LDR and EBRT groups ( $p = 0.003$ ), respectively. At the last follow-up, 24 patients were deceased in the cohort. Amongst those, 3 died from their cancer in the EBRT group [PCSS of 96.4% (95% CI: 89.3-98.8)] and none died in the LDR group ( $p = 0.09$ ).

Figure 1: Cumulative incidence function of biochemical recurrence with 95% CI



## Conclusion

Permanent iodine-125 seed implant was associated with higher biochemical and distant failure control in our cohort when compared to moderately hypofractionated EBRT. In the absence of a randomized trial, LDR when feasible should be offered to patients with a life expectancy of  $>7$  years.

## PO-1059 Separation and rectal dosimetry with a hydrogel spacer inserted during prostate HDR brachytherapy

R. DAVDA<sup>1</sup>, D. Pendsé<sup>2</sup>, A. Mitra<sup>1</sup>, M. Prentice<sup>1</sup>, L. Melcher<sup>3</sup>, N. Rosenfelder<sup>4</sup>, M. Singhera<sup>3</sup>, R. Patel<sup>5</sup>, M. Boutros<sup>5</sup>, C. Allen<sup>2</sup>, H. Payne<sup>1</sup>

<sup>1</sup>University College London Hospitals NHS Foundation Trust, Oncology, London, United Kingdom ; <sup>2</sup>University College London Hospitals NHS Foundation Trust, Radiology, London, United Kingdom ; <sup>3</sup>North Middlesex University Hospital NHS Trust, Oncology, London, United Kingdom ; <sup>4</sup>Royal Free London NHS Foundation Trust, Oncology, London, United Kingdom ; <sup>5</sup>University College London Hospitals NHS Foundation Trust, Radiotherapy Physics, London, United Kingdom

### Purpose or Objective

Pre-rectal spacers have been shown to reduce high dose radiation to the rectum and late patient reported toxicity for men treated with external beam radiation (EBRT). The ICEMAN trial is investigating the insertion of a pre-rectal spacer in men with high risk localised or locally advanced prostate cancer undergoing high dose rate (HDR) brachytherapy boost followed by EBRT to the pelvis. We report initial findings using a novel technique to insert hydrogel spacer (SpaceOAR) during the HDR procedure.

### Material and Methods

Trial participants underwent multi-parametric prostate MRI  $< 2$  weeks prior to the HDR brachytherapy and spacer insertion procedure, with a second MRI 5 days after the procedure. Brachytherapy procedures were via a transperineal approach under transrectal ultrasound guidance. Immediately prior to brachytherapy catheter implantation, a 15 cm Kellett needle was inserted in the midline between Denonvillier's fascia and the anterior rectal wall to the prostate midgland and the 5Fr Kellett sheath left in-situ. After HDR implant catheter placement hydrodissection of the pre-rectal space was achieved by injecting saline via this sheath with subsequent injection of 10 cc hydrogel spacer.

A CT planning scan was used to contour PTV, organs at risk and spacer. Brachytherapy plans were produced using graphical (GRO) and inverse planning by simulated annealing (IPSA). HDR prescription was 15 Gy to the prostate and seminal vesicles followed by 46 Gy in 23 fractions EBRT to the pelvis. Separation between posterior prostate and anterior rectal wall was measured by a Uro-radiologist on the MRI prior to, and MRI after the procedure on T2 axial 3 mm slices using sagittal planes for reference at the apex, mid-gland, base and seminal

vesicles. HDR rectal dosimetry in a cohort of men with hydrogel spacer inserted as described is reported, as well as for 10 patients contemporaneously treated without a spacer.

### Results

Complete 10cc hydrogel injection was successful in 6/7 patients and incomplete (<10 cc) in 1 case due to concerns of sheath placement. All men received 15 Gy HDR boost as planned. No complications have been observed. Initial results suggest separation between the prostate and anterior rectal wall was greater after the procedure compared with pre-procedure at all levels (Table 1).

Participant	separation prostate - anterior rectal wall pre-procedure (mm)					separation prostate - anterior rectal wall post-procedure (mm)				
	Apex	Mid-gland	Base	SV	Mean	Apex	Mid-gland	Base	SV	Mean
1	0	0	2	7	2.3	1	5	9	10	6.3
2	0	0	2	1	0.8	2	2	2	7	3.3
3	0	0	0	2	0.5	3	3	7	9	5.5
4	0	1	2	3	1.5	7	9	9	13	9.5
5	0	0	1	1	0.5	0	3	4	3	2.5
6	3	2	2	4	2.8	6	7	9	8	7.5
7	0	1	2	1	1	3	5	7	8	5.8

On comparison to contemporarily treated cohort without a hydrogel spacer, initial results suggest spacer reduces the volume of rectum receiving clinically significant moderate / high isodose levels  $\geq V30$  (4.5Gy) (Table 2).

Patient	PTV Volume (cc)	Absolute Rectum volume(cc) receiving dose (% of 150y)								
		V <sub>100</sub>	V <sub>95</sub>	V <sub>90</sub>	V <sub>85</sub>	V <sub>80</sub>	V <sub>75</sub>	V <sub>70</sub>	V <sub>65</sub>	V <sub>60</sub>
Participant1	32.7	26.6	12.4	4.9	1.8	0.6	<0.2	<0.2	<0.2	<0.2
Participant2	36.3	28.4	11	3.9	1.1	<0.2	<0.2	<0.2	<0.2	<0.2
Participant3	56.3	46.3	15.5	2.8	<0.2	<0.2	<0.2	<0.2	<0.2	<0.2
Participant4	35.8	26.6	9.4	3.3	1.1	0.4	<0.2	<0.2	<0.2	<0.2
Participant5	52.4	28.4	9.4	3.2	0.8	<0.2	<0.2	<0.2	<0.2	<0.2
Participant6	32.5	28.5	13.1	4.8	1.4	0.2	<0.2	<0.2	<0.2	<0.2
Participant7	64.1	38.8	9.4	1.5	<0.2	<0.2	<0.2	<0.2	<0.2	<0.2
Non Trial	26.5	26	16.1	6.4	2.1	0.4	<0.2	<0.2	<0.2	<0.2
Non Trial	27.4	24.5	10.9	4.7	2	0.8	0.2	<0.2	<0.2	<0.2
Non Trial	33.3	33	22.8	13.3	6.7	2.9	0.79	<0.2	<0.2	<0.2
Non Trial	35.5	32.4	16.8	9.1	4.4	1.8	0.5	<0.2	<0.2	<0.2
Non Trial	38	31.8	12.9	5.1	2	0.7	0.1	<0.2	<0.2	<0.2
Non Trial	40.8	29.8	16.2	7.9	3.8	1.7	0.4	<0.2	<0.2	<0.2
Non Trial	42.5	28.6	14.8	7.2	3.2	1.3	0.3	<0.2	<0.2	<0.2
Non Trial	46.9	37.4	19.7	8.3	3.2	1	<0.2	<0.2	<0.2	<0.2
Non Trial	55.5	50.2	19.9	7.2	2.3	0.6	<0.2	<0.2	<0.2	<0.2
Non Trial	78.7	71.2	34.5	16.4	7.7	3.5	1.3	0.2	<0.2	<0.2

### Conclusion

Initial experience using an adapted, novel technique of hydrogel injection at the time of HDR brachytherapy suggests that this procedure is feasible and results in greater separation between the prostate and rectum, associated with improved rectal dosimetry. Further work will be reported in a larger cohort of study participants and clinical impact of any dosimetric improvement using patient reported outcome measures.

### Poster: Brachytherapy: Miscellaneous

#### PO-1060 Role of intraluminal brachytherapy as palliative treatment in advanced esophageal cancer

V. Pareek<sup>1</sup>, R. Bhalavat<sup>2</sup>, M. Chandra<sup>2</sup>, C. Bakshi<sup>3</sup>, N. Bhambhani<sup>4</sup>

<sup>1</sup>Jupiter Hospital, Radiation Oncology, Mumbai, India ;

<sup>2</sup>Jupiter Hospital, Radiation Oncology, Thane, India ;

<sup>3</sup>Jupiter Hospital, Medical Oncology, Thane, India ;

<sup>4</sup>Jupiter Hospital, Surgical Oncology, Thane, India

#### Purpose or Objective

This study aims to assess the improvement in dysphagia, associated complications and overall and disease free survival with intraluminal brachytherapy (ILRT) as palliative care in advanced esophageal cancer

#### Material and Methods

Thirty-four patients were treated with high dose rate ILRT with or without external radiation therapy from 2009 to 2017 at our institute. Patients were assessed for various

parameters including disease stage, length of lesion, KPS and as per grade of dysphagia at presentation. The patients received median dose of 6Gy at 1 cm off axis for 2 fractions one week apart. Fourteen patients were treated radically and 20 patients post EBRT. Multivariate analysis was used to assess the predictors for dysphagia improvement. Remissions of dysphagia and other clinical and radiological factors were assessed in the first month post-treatment, and then in the third, sixth, and twelfth months. The survival rate was compared with some chosen clinical factors using a log-rank test and the Kaplan-Meier method.

### Results

Patients were followed up as per standard institute protocol. Median dysphagia free survival was 12 months. Stricture was seen in 3 patients and ulceration noted in another 2 patients. However, no tracheoesophageal fistula or procedure related complications were noted. Complications were seen with the post EBRT group. The overall survival in the cohort was 12 months and was better post EBRT as compared to radical ILRT ( $p < 0.001$ ). On multivariate analysis, stage of disease ( $p=0.02$ ), size of lesion ( $p=0.018$ ) and grade of dysphagia ( $p=0.023$ ) were found to be predictors for improved outcomes with use of ILRT in palliation.

### Conclusion

Brachytherapy in the form of ILRT in advanced esophageal cancer provides good palliation with minimal complications and improved survival and quality of life to patients.

#### PO-1061 Brachytherapy For Bladder Rhabdomyosarcoma In Children: Initial Single Institutional Experience

A. Slocker Escarpa<sup>1</sup>, E. Iraolagoitia Lasa<sup>2</sup>, J. Mases Rosines<sup>3</sup>, D. Najjari Jamal<sup>4</sup>, M. Vancells<sup>5</sup>, J. Mora<sup>6</sup>, F. Pino<sup>7</sup>, C. Gullón<sup>7</sup>, C. Gutierrez Miguez<sup>4</sup>

<sup>1</sup>Institut Català d'Oncologia, Brachytherapy, Barcelona, Spain ;

<sup>2</sup>Hospital Universitario Donostia, Radiation Oncology, Donostia - San Sebastián, Spain ;

<sup>3</sup>Institut Català d'Oncologia, Radiation Oncology, Barcelona, Spain ;

<sup>4</sup>Institut Català d'Oncologia, Brachytherapy, Barcelona, Spain ;

<sup>5</sup>Sant Joan de Déu - Esplugues, Paediatric Surgery, Barcelona, Spain ;

<sup>6</sup>Sant Joan de Déu - Esplugues, Medical Oncology, Barcelona, Spain ;

<sup>7</sup>Institut Català d'Oncologia, Medical physics, Barcelona, Spain

#### Purpose or Objective

As total cystectomy is mutilating, evidence has been published about the possibility of bladder conservation with macroscopic complete gross tumour resection followed by immediate High Dose Rate brachytherapy (HDR-BT). The aim of this abstract is to communicate our initial experience in multimodal approach of treating non-metastatic paediatric bladder rhabdomyosarcoma (RMS) with HDR-BT at Catalan Oncology Institute (ICO).

#### Material and Methods

3 children referred to our paediatric hospital have been treated until July 2018. In all cases, plastic tubes were placed during the surgery of tumour resection, following the HDR-BT technique described by Gustave Roussy Institute. They received 10 fractions (4Gy each, 2 times per day) with a total dose of 40Gy, completing it in the 15 days after surgery.

Patient 1: a 2 year-old boy diagnosed in 2009 of bladder neck botryoidal rhabdomyosarcoma classified at intermediate risk group was treated with induction chemotherapy. Protocol evaluation evidenced tumour persistence, and total tumour resection with HDR-BT was performed in December 2009. Afterwards, he received 6 cycles of adjuvant chemotherapy, finishing all the treatment in May 2010.

Patient 2: a 12 year-old girl initially treated with radical concomitant chemoradiotherapy (50Gy, standard fractionation) had tumour persistence. She was referred

to perform a salvage surgery of the tumour located at the limit of bladder trigone - output of the right ureter, followed by postoperative HDR-BT in November 2011.

Patient 3: a 11 months-old female affected with alveolar rhabdomyosarcoma at vesical neck classified at high risk group was initially treated induction chemotherapy in December 2017, resulting in partial tumour response after 2 different systemic lines. She underwent complete tumour resection and HDR-BT in July 2018.

#### Results

Patient 1 suffered from acute myeloblastic leukaemia in 2014; nevertheless, he currently is cured of both processes. Patient 2 relapsed locally after a year of treatment completion, so salvage total cystectomy needed to be done. Although the treatment of patient 3 has been very recent, she is free of disease at the first radiology control 3 months after treatment (follow-up is needed to see further results).

#### Conclusion

Multimodal approach in bladder conservative treatment with HDR - BT is a feasible alternative to total cystectomy in children. Although our experience is limited, the results could be comparable to those reported by the series of cases published in literature.

#### PO-1062 brachytherapy in patients with bowen disease

J.L. Munoz Garcia<sup>1</sup>, M.A. Gonzalez Ruiz<sup>2</sup>, J. Quiros Rivero<sup>1</sup>

<sup>1</sup>Badajoz University Hospital, Radiation Oncology, Badajoz, Spain ; <sup>2</sup>Punta de Europa Hospital, Radiation Oncology, Algeciras, Spain

#### Purpose or Objective

**Purpose/Objective:** High-dose-rate (HDR) brachytherapy, plesiotherapy modality, is a treatment option for Bowen disease (BD) patients with good oncologic outcomes. The objective of our study was to evaluate the initial results of BD patient treated in our centre in terms of local and cosmetic control.

#### Material and Methods

**Material/methods:** Observational, retrospective study of 12 BD lesions (12 patient) treated in our hospital from May 2015 to October 2017 with HDR brachytherapy using Valencia applicators, flaps and hand-made custom moulds (plesiotherapy). The treatment for all patients was delivered in 6 Gy fractions over seven sessions, two times a week, to a total dose the 42 Gy (EQD2 56 Gy; a/b10).

#### Results

**Results:** With a median follow-up of 32 months (range 19-48), all patients had complete response and are alive (LC 100%). Only one patient presented a new lesion in a different area from the first location treated (DFS 90%). Most of the patients (67%) did not have acute toxicity; 4 patients (33%) developed erythema grade 2 and one patient (8.33%) developed conjunctivitis. One patient presented Ectropion as a late adverse event with regular cosmetic result (8.33%). 91% of patients had good or excellent cosmetic result with high level of satisfaction.

#### Conclusion

**Conclusion:** Our initial results in Bowen disease patient treated with High-dose-rate brachytherapy, plesiotherapy modality, shown and excellent local control, and disease free survival and cosmetic results. Brachytherapy hypofractionated regimen is a simple and cost-effective non-surgical attractive treatment option for the treatment of BD patients.

#### PO-1063 Single-fraction low-energy electronic brachytherapy for conjunctival lymphoma

G. Sarria<sup>1</sup>, C. Cabrera<sup>2</sup>, G.J. Sarria<sup>2</sup>, M. Buitrago<sup>3</sup>, P. Fuentes Rivera<sup>2</sup>, S. Serpa<sup>3</sup>, F. Giordano<sup>1</sup>

<sup>1</sup>Universitätsklinikum Mannheim, Strahlentherapie, Mannheim, Germany ; <sup>2</sup>Instituto Nacional de Enfermedades Neoplásicas, Radiotherapy, Lima, Peru ;

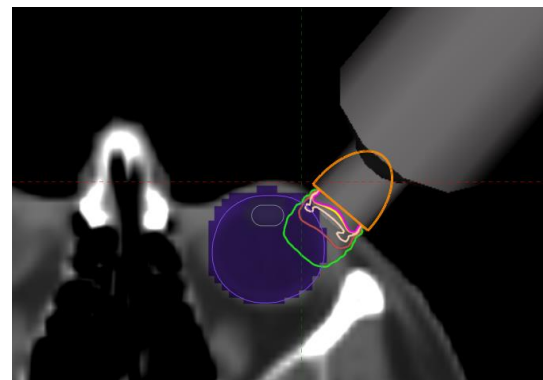
<sup>3</sup>Instituto Nacional de Enfermedades Neoplásicas, Ophthalmic Oncology, Lima, Peru

#### Purpose or Objective

Conjunctival lymphoma represents an uncommon tumor accounting for 5-10% of total extranodal lymphomas. Although radiotherapy is a frequent treatment option, limited capacities and lack of specialized centers are common problems in Peru, forcing radiation oncologists to apply short courses of radiotherapy. We here report a case series of patients treated with a novel single-shot scheme and also reviewed the literature for current short-course irradiation strategies.

#### Material and Methods

Three cases of conjunctival marginal zone (B-cell) lymphoma (MZL/MALT) of the fornix are presented. Following biopsy and sonographic assessment of the lesion thickness the application procedure was then carried out under topical anesthesia, blocking of the ocular musculature and fixing of the eyelids with a blepharostat. The head was then fixed in a thermoplastic mask, which was fenestrated over the affected eye. For brachytherapy, a low-energy X-ray device (50 kV maximum energy; Intrabeam, Carl Zeiss Meditec AG) equipped with a flat applicator was placed on the lesion, with light pressure to flatten the tumor. A focused single dose of 14 Gy kilovoltage brachytherapy, prescribed to the maximum thickness of the lesion was applied. This dose was chosen after calculating the equivalent dose of a 2 Gy fraction scheme ( $EQD2 = BED/[1 + \{2/\alpha/\beta\}]$ ) which, taking into account an approximate relative biological effectiveness (RBE) of 1.3 and a tumor  $\alpha/\beta$  ratio of 10 Gy, resulted in an EQD2 of 36.4 Gy. Follow-up was scheduled in quarterly intervals.



#### Results

Due to the absorption properties of low-energy x rays, the dose to the lens was less than 4 Gy in the worst case scenario. After 16, 19 and 28 months of follow-up, none of the three patients treated exhibited acute or chronic toxicities and remained local or distant disease-free.

#### Conclusion

Single-dose kilovoltage brachytherapy was effective and safe in this small collective. Based on the literature, there

is evidence that local treatment in short-course radiotherapy is effective and should be considered amongst the therapeutic options for these patients; however this should be evaluated prospectively in a larger patients cohort.

**PO-1064 Reducing dysphagia with palliative 2D HDR brachytherapy improves survival in esophageal cancer**

W. Burchardt<sup>1</sup>, A. Chyrek<sup>1</sup>, J. Skowronek<sup>1</sup>

<sup>1</sup>Greater Poland Cancer Centre, Department of Brachytherapy, Poznan, Poland

**Purpose or Objective**

The goal of this study was to assess the effectiveness of dysphagia relief and overall survival in patients with advanced esophageal cancer treated with palliative high-dose-rate (HDR) 2D brachytherapy (BT).

**Material and Methods**

The study was conducted using data from medical reports of Cancer Center from January 2010 to December 2016. 133 patients with advanced or incurable esophageal cancer were treated with palliative purpose with 2D HDR BT. Median dose was 22,5 Gy in 3 fractions as primary treatment. The dysphagia was assessed in 93 patients and these patients were further analyzed. Median age was 65 years (45-88). 17,2 % of patients were female and 82,8 % male. Squamous cell carcinoma was diagnosed in 59,4 %, adenocarcinoma in 22,6% and other tumors in 6,7% cases. In 11,3 % of patients, the histopathological report was unknown. 19 patients were treated with chemotherapy and 4 with external beam radiotherapy after BT.

**Results**

Median follow up was 2,8 months (range 0,2-42,7). Median tumor length was 7,5 cm. Patients before treatment present following grades of dysphagia: I - 57 %, II - 33,3 %, III - 6,5 %, IV - 3,2 %; grades dysphagia after BT were significantly lower: 0- 38,7 %, I - 31,2 %, II - 20,4 %, IV - 1,1 % (p<0,001, Wilcoxon test). Mean time of dysphagia relief was 4,6 months and was achieved in 55 %, stabilization occurred in 31 %, and worsening of symptom was reported in 14% of cases. The patients with dysphagia relief (4,2 vs 2,2 months, p<0,01) or age <= 65 lived longer (3,7 vs 2,0 months p<0,01). The length of the tumor, primary localization, and primary grade of the dysphagia weren't factors which influenced the survival of patients. The logistic regression model didn't find any predictors for treatment response.

**Conclusion**

HDR 2D BT reduces dysphagia and prolongs survival especially in younger patients who response the treatment. HDR 2D BT meets the assumption of palliative treatment for advanced esophageal cancer.

---

**Poster: Radiobiology track: Radiobiology of normal tissues**

---

**PO-1065 Multiparametric radiobiological parameters implementation to predict radiation-induced side effects**

M. Ben Kacem<sup>1</sup>, M. Benadjaoud<sup>2</sup>, F. Soysouvanh<sup>1</sup>, M. Dos Santos<sup>3</sup>, G. Tarlet<sup>1</sup>, V. Buard<sup>1</sup>, A. François<sup>1</sup>, O. Guipaud<sup>1</sup>, F. Milliat<sup>1</sup>, V. Paget<sup>1</sup>

<sup>1</sup>National Insitute for Radiobiological Protection and Nuclear Safety IRSN, Radiobiology of Medical Exposure Laboratory LRMed, Fontenay aux Roses, France ;

<sup>2</sup>National Insitute for Radiobiological Protection and Nuclear Safety IRSN, Radiobiology and Regenerative Medicine Research Service SERAMED, Fontenay aux Roses, France ; <sup>3</sup>National Insitute for Radiobiological Protection and Nuclear Safety IRSN, Radiobiology of Accidental Exposure Laboratory LRAcc, Fontenay aux Roses, France

**Purpose or Objective**

Radiotherapy (RT) is used to treat more than half of cancers. Despite the development of practices and devices that precisely deliver radiation dose to tumor with high dose rate, the biological effects on healthy tissue remain poorly studied.

To predict radiation-induced biological effects, radiobiologists use the Relative Biological Effectiveness (RBE) concept to compare doses between two ionizing radiations given the same biological effect. RBE is essentially based on clonogenic assay to determine the impact of a defined ionizing radiation. Survival clonogenic curves are modelled by the linear quadratic model, and, according to several studies, this assay is insufficient to predict effects on healthy tissues after radiation. Based on the various effects known after irradiation, it is necessary to develop multiparametric RBE measures to predict the biological effects of emerging radiation therapy protocols.

**Material and Methods**

Human Umbilical Vein Endothelial Cells (HUVECs) were irradiated with a linear accelerator using two different dose rates (0.63 and 2.5 Gy/min). Endothelial cells (EC) were chosen for their involvement in radiation induced damages on healthy tissue. To predict accurately the adverse effects on healthy tissues, we have measured multiple *in vitro* biological readouts (clonogenic assay, viability, cell cycle, senescence and gene expression) at 3, 7, 14 and 21 days post-irradiation. The biological measures are already modelled on Matlab for each assay and will be integrated all together in a unique predictive model. Finally, total body irradiations and localized irradiations were conducted on preclinical mice models (C57BL/6J) to validate the *in vitro* data.

**Results**

Our *in vitro* results show a significant dose rate effect on cellular morphology of HUVECs. After irradiation at the lowest dose rate, clonogenic survival (RBE = 0.8) and cell viability (RBE < 1) are higher. Furthermore, we have measured less B-galactosidase activity (related to radio-induced senescence) after irradiation at 0.63 Gy/min compared to 2.5 Gy/min (RBE = 0.5). Moreover, the proportions of cells in the cell cycle phases and a 44 genes expression involved in senescence process were found modified according to the dose rate. *In vivo*, after the irradiation of an exteriorized segment of small intestine (19 Gy) on mice, a significant higher loss of weight was measured at the higher dose rate.

**Conclusion**

These data show a deleterious effect of the highest dose rate. The mathematical model will be consolidated by supplemental *in vitro* measures on Human Lung Microvascular Endothelial Cells (HMVEC-L) to validate the impact of the dose rate.

To complete this study, we also focus our work on biological effects of different fractionated irradiation protocols both *in vitro* (on HUVECs) and *in vivo* (whole thorax irradiations on a preclinical mice model). These biological measures will be modelled and integrated within the predictive model in the future.

---

**Poster: Radiobiology track: Radiobiology of stem cells (cancer and normal tissue)**

---

**PO-1066 The unique DDR mechanisms of human induced pluripotent stem cells (hiPSC)-derived chondrocytes**

E. Stelcer<sup>1,2,3</sup>, K. Katarzyna<sup>1,2</sup>, S. Wiktoria M.<sup>1,2</sup>

<sup>1</sup>Poznan University of Medical Sciences, Department of Electroradiology, Poznan, Poland ; <sup>2</sup>Greater Poland Cancer Centre, Radiobiology Lab, Poznan, Poland ;

<sup>3</sup>Medical University of Warsaw, Postgraduate School of Molecular Medicine, Warsaw, Poland

### Purpose or Objective

Human induced pluripotent stem cells (hiPSCs) constitute a real breakthrough in regenerative medicine. We differentiated hiPSCs towards chondrocytes (hiPSC-derived chondrocytes, hiPSC-DCHs) as a real hope for patients diagnosed with osteoarthritis. However, it is still a research area that must be more precisely investigated to ensure safety of patients. Thus, we investigate the DDR mechanisms of these cells exposed to IR. Previously, we demonstrated results concerning  $\gamma$ H2AX, DNA repair, apoptosis and senescence. In this study, we aim to show the analyses of cell cycle, ROS level and changes in mitochondrial membrane potential of irradiated cells.

### Material and Methods

We differentiated of hiPSCs into chondrocyte-like cells. The hiPSC-derived chondrocytes were treated with IR (0; 1; 2 and 5 [Gy]). Then, we performed analysis of cell cycle using propidium iodide (9h after IR as a most sensitive time point that we previously selected). Immediately after IR, we investigated level of generated ROS taking advantage of CellROX Green Flow Cytometry Assay Kit (TBHP served as a positive control). Finally, the analysis of mitochondrial membrane potential was based on JC-1 staining (CCCP served as a positive control).

### Results

The irradiated hiPSCs demonstrated accumulation of cells in S phase. On the contrary, both mature chondrocytes and hiPSC-DCHs revealed arrest of cell cycle in G2 phase. Furthermore, chondrocyte-like cells obtained from hiPSCs revealed characterization of cell cycle similar to fully differentiated cells (hiPSC-DCHs vs chondrocytes). In that case the majority of cells were noticeable in G1 phase. In contrast, non-irradiated hiPSCs as highly proliferative type of cells demonstrate the highest percentage of S phase. The IR did not cause a dramatic differences in the ROS level in all investigated types of cells (hiPSCs, hiPSC-DCHs and mature chondrocytes). However, there was a significant dissimilarity between overall profile of hiPSCs and differentiated cells (both hiPSC-DCHs and chondrocytes). The non- and irradiated hiPSCs showed the relatively high level of ROS- that was shifted to the positive control- in contrast to differentiated cells. In turn, the most notable changes of mitochondrial membrane potential was observed as hiPSC-DCHs (above 30% of stained cells) revealing - in this aspect - their high radiosensitivity.

### Conclusion

We provided a new knowledge concerning hiPSC-derived cells. We can observe that radioresistance of hiPSC-DCHs significantly differ from both "parental" hiPSC and mature chondrocytes generating a unique, individual and specific DDR of these cells. It may have an influence on their genetic stability. In further part of research we plan to focus on testing hiPSC-DCHs in *in vivo* model.

Funding: National Science Centre (2012/E/NZ3/01819) and (2016/23/N/NZ7/01892)

### PO-1067 High expression of CCND2 in glioblastoma is associated with an increased risk of early mortality.

C. Bouchart<sup>1</sup>, A. Trépant<sup>2</sup>, M. Hein<sup>3</sup>, D. Van Gestel<sup>1</sup>, P. Demetter<sup>4</sup>

<sup>1</sup>Institut Jules Bordet - Université Libre de Bruxelles, Department of Radiation-Oncology, Brussels, Belgium ;

<sup>2</sup>Erasme University Hospital - Université Libre de Bruxelles, Department of Pathology and DIAPATH-Center of Microscopy and Molecular Imaging CMMI, Brussels, Belgium ; <sup>3</sup>Erasme University Hospital - Université Libre de Bruxelles, Department of Psychiatry and Sleep Laboratory, Brussels, Belgium ; <sup>4</sup>Institut Jules Bordet - Université Libre de Bruxelles, Department of Pathology, Brussels, Belgium

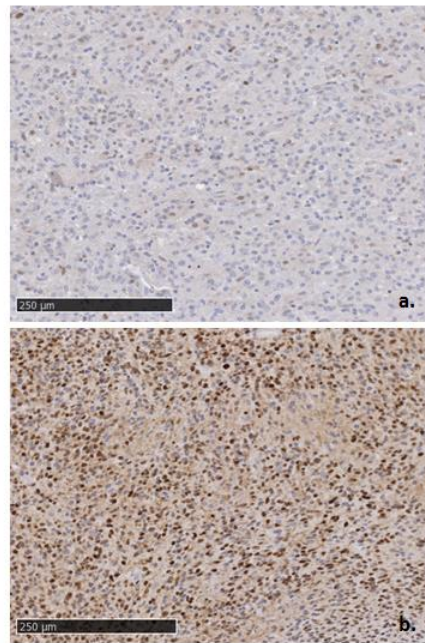
### Purpose or Objective

Glioblastomas (GBM) are highly radio- and chemoresistant tumors associated with poor outcome. Cyclin D2 (CCND2) is known to play a critical role in cell cycle progression, tumorigenicity and radioresistance in GBM, particularly in the subpopulation of glioma stem cells. The aim of our study is to better understand the evolution of CCND2 expression during treatments and to investigate its clinical significance in GBM.

### Material and Methods

Immunohistochemical expression analysis of CCND2 was carried out on paired GBM samples of 72 patients, comparing initial resections with recurrent tumors after radiation therapy alone (RT) (n=36) or radio-chemotherapy with temozolomide according to the Stupp regimen (RT-TMZ) (n=36). Semi-quantitative analysis of CCND2 nuclear staining was performed by two independent observers. Every tumor was scored according to the number of stained cells (low nuclear expression < 30% and high nuclear expression  $\geq$  30%). (Figure 1) Multivariate logistic regression analysis was conducted to investigate clinical and demographic risk factors of early mortality in GBM patients.

Figure 1. CCND2 expression profile in glioblastoma.



CCND2 presents a nuclear and a cytoplasmic expression in glioblastoma. a. Low nuclear expression of CCND2 (<30% of tumour cells nuclei stained). b. High nuclear expression of CCND2 ( $\geq$ 30% of tumour cells nuclei stained).

### Results

Compared to the primary tumor, CCND2 expression was decreased in GBM recurrences after treatment with RT ( $32.00 \pm 19.00$  vs  $20.00 \pm 19.00\%$ ,  $p = 0.013$ ) or RT-TMZ ( $31.00 \pm 20.00$  vs  $19.00 \pm 18.00\%$ ,  $p = 0.001$ ). The decrease in CCND2 expression did not differ significantly according to the treatment used ( $p = 0.731$ ). Multivariate logistic regression analysis revealed that significant risk factors predicting early mortality (<12 months) in GBM patients are: time to recurrence  $\leq$  6 months [OR 23.88 (CI 95% 4.36 to 130.68)], subtotal surgery at recurrence [OR 10.58 (CI 95% 1.81 to 62.01)] and high nuclear expression of CCND2 ( $\geq$  30%) at initial surgery [OR 7.97 (CI 95% 1.35 to 46.98)]. The following variables were not included in the model because they were not significant: gender, age, preoperative use of corticosteroids, type of initial surgery,

type of adjuvant treatment, and nuclear expression of CCND2 at recurrence. (Table 1)

**Table 1: Summary of logistic regression for screening variables predicting early mortality in glioblastoma patients (n=72).**

Variables	Adjusted OR (CI 95%)	P-value
Time to recurrence (months)		<0.001
>6 (n=42)	1	
≤6 (n=30)	23.88 (4.36 to 130.68)	
Type of surgery at recurrence		0.009
Total (n=31)	1	
Subtotal (n=41)	10.58 (1.81 to 62.01)	
CCND2 nuclear expression (%)		0.022
At initial surgery	1	
<30 (n=30)		
≥30 (n=42)	7.97 (1.35 to 46.96)	

Not included in the model because not significant: gender, age, preoperative corticosteroids, type of initial surgery, type of adjuvant treatment, and nuclear expression of CCND2 at recurrence.  
Adequacy of model: Hosmer-Lemeshow chi2 (p=0.927)  
Specificity of model: Linktest (linear component p<0.001 and nonlinear component p=0.260)  
OR = Odds Ratio, CI = Confidence Interval

## Conclusion

Adjuvant treatments globally reduce expression of CCND2. To our knowledge, we are the first to demonstrate that high nuclear CCND2 expression at initial surgery is associated with higher risk of early mortality for GBM patients. These results confirm preclinical data observed in immunocompromised mice suggesting that targeting CCND2 could be promising for GBM therapy.

## Poster: Radiobiology track: Radiobiology of particles and heavy ions

### PO-1068 Very high yield of double strand breaks found at the distal end of the proton Bragg peak

N.F.J. Edin<sup>1</sup>, A.M. Rykkelid<sup>1</sup>, A. Görgen<sup>1</sup>, A. Baker<sup>1</sup>, S. Siem<sup>1</sup>, K. Ytre-Hauge<sup>2</sup>, E. Malinen<sup>1</sup>

<sup>1</sup>University of Oslo, Physics, Oslo, Norway ; <sup>2</sup>University of Bergen, Department of Physics, Bergen, Norway

#### Purpose or Objective

While protons can be delivered more precisely with less radiation to the normal tissue than X-rays, emerging reports indicate that X-rays and protons affect cellular response pathways in different ways. The involved mechanisms include DNA repair, epigenetic modulation, immunogenicity, and regulation of cytokines and protein phosphorylation. It is therefore not possible to predict biological effects of proton irradiation from dose-response data from X-ray irradiation. In this study, we use low energy protons of 16 MeV with a high dose-averaged linear energy transfer (LET) to measure differential cellular responses at different positions in the proton Bragg Peak (BP) with varying LET. We compare measured clonogenic survival to H2AX-phosphorylation at 3 different time points after proton irradiation using an experimental setup ensuring accurate dosimetric depth positioning of T98G glioblastoma cells.

#### Material and Methods

A horizontal 16 MeV proton beam line for in vitro cell irradiation was constructed. The beam line consisted of a single scattering foil, a monitor chamber type 7862 (PTW, Freiburg, Germany) and an Advanced Markus ionization chamber (PTW) with a 30 micron entrance window for absolute dosimetry. T98G glioblastoma cells plated on dishes were irradiated with protons in a cylindrical heater at different depths, corresponding to different position before and in the BP. Clonogenic survival was measured and the number of DNA double strand breaks was assessed by an H2AX-phosphorylation-antibody using flow cytometry at 3 different time points to measure initial damage as well as repair. LETs varied from 7.5 to 44 keV/um and 220 kV X-rays were used as reference radiation.

## Results

Clonogenic survival of T98G cells followed a linear-quadratic response for X-irradiation and irradiation at the front of the BP. At the distal end of the BP, cell survival per dose was much lower and a log-linear response function was found to be a better fit. Comparing with X-ray response at 37 % survival, RBE values at frontal and distal end of the BP were  $1.7 \pm 0.1$  and  $4.9 \pm 0.4$ , respectively. The initial H2AX phosphorylation was found to be up to 4 times higher at the distal end of the BP compared to the front as measured 0.5 h after 5 Gy irradiation using the same dose-rate and proton fluence in both positions. When the cells were irradiated at the top of the BP with the same proton fluence, the dose was 22 Gy and induced similar amounts of H2AX-phosphorylation as in the distal end of the BP with 5 Gy (figure 1). While most damage was repaired for cells irradiated in the front of the BP, high amounts of residual damage were seen after 5 Gy in the distal end and for 22 Gy at the top of the BP.

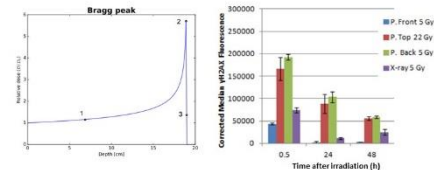


Figure 1. Left panel: T98G cells were irradiated at 3 different positions in the Bragg peak: 1: Front of the BP; 2: Top of the BP; 3: Back or distal end of the BP. Right panel: The amount of DNA double strand breaks was measured using flow cytometry and +H2AX antibody at 3 time points after proton irradiation in 3 different positions in the BP as well as X-ray irradiation. The proton fluence, as measured by a monitor chamber, was kept constant for the 3 positions in the BP.

## Conclusion

A higher amount of more complex DNA double strand breaks is induced by high LET relative to low LET protons. This is consistent with a change in shape of the survival curves with the presence of a “shoulder” for the lower LET, which is strongly reduced for the higher LET.

### PO-1069 RBE calculation for hadrontherapy by the BIANCA biophysical model

M.P. Carante<sup>1</sup>, F. Ballarini<sup>2</sup>

<sup>1</sup>Istituto Nazionale di Fisica Nucleare INFN, Physics Department, Pavia, Italy ; <sup>2</sup>University of Pavia, Physics Department, Pavia, Italy

#### Purpose or Objective

The main purpose of the present work consists of comparing RBE values calculated by the BIANCA model for V79 cells (often used for hadrontherapy beam characterization) and AG01522 cells (considered as representative of normal tissues) exposed to different charged particles (protons, C-ions and He-ions) with the corresponding experimental values, and showing examples of applications to hadrontherapy beams.

#### Material and Methods

BIANCA (Biophysical Analysis of Cell death and chromosome Aberrations) is a two-parameter biophysical model that calculates the probability of radiation-induced cell death as well as chromosome aberrations, which can be regarded as indicators of normal tissue damage. The model is based on the idea that some DNA damage types (“Cluster Lesions”, where by definition each CL produces two independent chromosome fragments) lead to chromosome aberrations following distance-dependent (mis-)rejoining, or un-rejoining, of chromosome fragments, and that some aberrations lead to (clonogenic) cell death. The yield of CLs, which depends on radiation

quality (i.e. particle type and energy), is an adjustable parameter; the probability that a chromosome fragment remains unrejoined, which depends on cell type but is independent of radiation quality and thus can be adjusted basing on photon data, is the second parameter.

#### Results

Up to now, the model has been tested against experimental data on V79 cells and AG01522 cells exposed to protons, C-ions and He-ions of different energy, as well as photons for comparison. The good agreement between simulations and data allowed validating the model; furthermore, a database of CL yields was produced that allows predicting cell survival curves for different ions, in principle for any LET value. By fitting these curves, tables of alpha and beta coefficients were produced for different ion types and energies for both considered cell types, and the corresponding RBE were calculated. The RBE values predicted this way were in good agreement with experimental data taken from the literature. Since these tables can be read by a radiation transport codes, an interface was developed between BIANCA and FLUKA, which allows producing "biological" profiles for hadrontherapy beams.

#### Conclusion

These results show that BIANCA can produce RBE values to be used in hadrontherapy.

---

### Poster: Radiobiology track: Radiation-induced signalling pathways

---

#### PO-1070 Identification of biologically active factors in ionizing radiation regulated secretome

M. Pruschy<sup>1</sup>

<sup>1</sup>University of Zurich, Applied Radiobiology, Zurich, Switzerland

#### Purpose or Objective

Ionizing radiation (IR) leads to DNA damage and genome instability. In addition, IR also leads to stress responses in tumor cells by activating signal transduction pathways and inducing secretion of numerous auto- and paracrine factors. As part of an exhaustive IR-dependent secretome analysis, which was previously performed in our laboratory, placental growth factor (PLGF) was identified to be secreted in response to IR. It is a homodimeric protein, belongs to vascular endothelial growth factor (VEGF)-family and binds to VEGFR1. PLGF expression is low to undetectable in most tissues in healthy subjects, but becomes significantly upregulated in disease.

#### Material and Methods

PLGF expression and secretion were analyzed across multiple cancer cell lines and at different time points after irradiation with increasing doses of IR (0, 5 and 10Gy) by qRT-PCR and ELISA, respectively. Two medulloblastoma cell lines (p53 wildtype vs. p53-mutated) were chosen for further experiments with siRNA and the HIF1-alpha inhibitor BAY 87-2243 under normoxic and hypoxic (1% O<sub>2</sub>) conditions to investigate the downstream targets of BAY 87-2243.

#### Results

PLGF expression and secretion was already upregulated at 4h and 24h, respectively, in p53 wild-type cancer cells. Interestingly, only minimal or delayed PLGF expression could be detected in p53-mutated cell lines. PLGF is also upregulated under hypoxic condition. Therefore, cells were treated with the HIF1-alpha inhibitor BAY 87-2243 under normoxic and hypoxic condition (1% O<sub>2</sub>). Interestingly, BAY 87-2243 attenuated PLGF-secretion only in p53-mutated cells. These results suggest that PLGF is differentially regulated by either p53 or HIF1-alpha. To further link p53 and PLGF, p53 wildtype cells were treated with p53 inhibitor Pifithrin-α or MDM-2 inhibitor MI-773. PLGF secretion was decreased after Pifithrin treatment

and increased in MI-773 treated cells further linking p53 and PLGF.

In order to investigate the paracrine effect of PLGF, we have developed PLGF knock out cells using a CRISPR-Cas9 approach. These cells will be used for *in vitro* and *in vivo* experiments to study the paracrine effect of IR-induced PLGF secretion on tumor and endothelial cells and for tumor radiosensitivity.

#### Conclusion

In conclusion, PLGF, which has so far not been investigated in response to IR, might play a relevant role for the radiation response on the level of tumor angiogenesis.

#### PO-1071 RIBE alters biological properties of the wound fluids

K. Kulcenty<sup>1</sup>, I. Piotrowski<sup>2</sup>, D. Murawa<sup>3</sup>, W. Suchorska<sup>2</sup>

<sup>1</sup>Poznan University of Medical Sciences- Greater Poland Cancer Centre, Department of Electroradiology- Radiobiology Lab, Poznan, Poland ; <sup>2</sup>University of Medical Sciences- Greater Poland Cancer Centre, Department of Electroradiology- Radiobiology Laboratory, Poznań, Poland ; <sup>3</sup>Poland Baptism Monument Hospital, Department of General and Minimally Invasive Surgery, Gniezno, Poland

#### Purpose or Objective

After breast cancer surgery, more than 90% of local recurrences occur in the same quadrant as the primary cancer. Wound fluids (WF) are believed to play a role in this process by inducing an inflammatory process in the scar tissue area. Given that most local relapse occur within the scar tissue area, researchers have investigated whether localized radiotherapy, such as intraoperative radiotherapy (IORT), could be more effective than postoperative RT in inhibiting local tumor recurrence. Despite the availability of strong clinical data demonstrating the benefits of IORT, the biological basis underlying this process is still not well- understood. It is known that ionizing radiation (IR) directly affects the cells by damaging DNA and consequently changing the phenotype of the cell. In addition to a direct action, the effect of IR may also be observed in cells that were not irradiated, but were in a close proximity to irradiated cells - a phenomenon called radiation induced bystander effect (RIBE). It was also showed that RIBE significantly modifies the tumor microenvironment. Given this background we assume that postoperative fluid from patients after intraoperative radiation therapy acts through bystander effect (RIBE, radiation induced bystander effect) that induces the radiobiological response in unirradiated cells and modify their phenotype.

#### Material and Methods

To confirm this hypothesis, WF collected from patients after breast conserving surgery (BCS) alone (WF) (i.e., without IORT), after BCS followed by IORT treatment (RT-WF) or WF from BCS patients together with conditioned medium from irradiated cells (WF+RIBE) were incubated with MDA-MB-468 cells. Using microarray analysis we compared cells incubated with collected fluids. The GSEA analysis was performed to demonstrate biological processes characteristic for treated cells. RT-qPCR and flow cytometry analysis were used to confirm obtained results.

#### Results

The microarray analysis of wound fluids stimulated MDA-MB-468 cells indicated common biological processes for RT-WF and WF+RIBE group. Overrepresentation of processes involved in cell cycle regulation, DNA repair and oxidative phosphorylation was observed in RT-WF and WF+RIBE group while WF group was characterized by overrepresentation of pathways involved in INF-α response, INF-γ response, inflammatory response and IL6 JAK/STAT3 signaling pathway.

### Conclusion

In the present study we indicated a common biological processes activated in MDA-MB-468 cell line stimulated with WF collected from patients after IORT treatment and cells treated with WF collected from BCS patients together with RIBE medium. Therefor we confirmed the role of the radiation-induced bystander effect in altering the biological properties of the wound fluids.

---

### Poster: Radiobiology track: Immuno-radiobiology

---

#### PO-1072 INTRABEAM: precision hypo-fractionated radiotherapy with a systemic immune response.

I. Linares<sup>1</sup>, M.Á. Berenguer<sup>1</sup>, E. Martínez<sup>1</sup>, M. Laplana<sup>1</sup>, R. Cañas<sup>2</sup>, S. Comas<sup>3</sup>, H. Pérez-Montero<sup>1</sup>, M. Ventura<sup>1</sup>, F. Guedea<sup>1</sup>

<sup>1</sup>Institut Català d'Oncologia, Radiation Oncology, Barcelona, Spain ; <sup>2</sup>Institut Català d'Oncologia., ONCOBELL Program-IDIBELL., Barcelona, Spain ; <sup>3</sup>Institut Català d'Oncologia, Radiation Oncology, Badalona, Spain

#### Purpose or Objective

To evaluate the changes in immune-cell phenotype in peripheral blood following intraoperative radiotherapy (IORT) in breast cancer patients.

#### Material and Methods

45 patients were classified in three groups of treatment as follows: Group A (Lumpectomy and Intrabeam exclusive), Group B (Lumpectomy and Intrabeam followed by EBRT 40.05 Gy in 15 fractions of 2.67 Gy) and Group C (Lumpectomy and EBRT 40.05 Gy in 15 fractions of 2.67 Gy +/- EBRT boost 9 Gy in 3 fractions). For each group, peripheral blood mononuclear cells (PBMCs) were isolated from heparinized venous blood samples collected before treatment and during different time points after treatment: before lumpectomy, 48 hours after IORT or EBRT, and 3 and 10 weeks after radiation treatment was completed. Peripheral blood populations of cytotoxic T-cells (CTL), helper T-cells, Natural Killer cells (NK), regulatory T-cells (Treg) and Myeloid Derived Suppressor cells (MDSC) were measured using flow cytometry. Cell phenotypes were evaluated using the FACS Navios system (BeckmanCoulter). Data were analyzed using FlowJo software (Tree Star Inc., Ashland, OR, USA).

#### Results

30 patients were included: 11, 15 and 4 patients for Group A, B and C respectively. For group A and B, the number of CTL increased three weeks after IORT (60.20% basal vs 67.10%) and EBRT (66.50% basal vs 71.30%) respectively. In contrast, for the control group (group C), a decrease in CTL was seen (64.35% vs 61.50%). In group A the number of NK cells increased after treatment (46.20% basal vs 59.20%), while in group B (42.90% basal vs 36.35%) and group C (56.80% basal vs 38.40%), we observed a NK decrease. For Treg we had mixed results which were hard to interpret. For Group A we saw a decrease during treatment (1.54% basal vs 1.44%) while for Group B we observed an increase of these cells (2.0% basal vs 2.75%). After 3 weeks, this tendency was reverted. For Group C, we observed an increase during treatment (1.45% basal vs 2.87%). For the MDSC panel, for granulocytes we observed a decrease in group A (6.44% basal vs 5.78%) and an increase in both group B (7.90% basal vs 10.31%) and group C (7.65% basal vs 10.20%) after 10 weeks. For Monocytes, in group A we observed the number of activated monocytes stable (8.95% basal 9.13%), whereas in group B and C we saw an increase after EBRT.

#### Conclusion

These results suggest that high doses per fraction would play an important role in CT, NK cells but not on the Treg and monocytes immunosuppression cells. Deciphering immune responses to treatment in breast cancer patients

might introduce new useful biomarkers for treatment choices in the future.

#### PO-1073 Biomathematical modeling of fractionated irradiation on immunogenic cell death induction in vitro

F. Eckert<sup>1</sup>, L. Bardoscia<sup>1,2</sup>, P. Hausmann<sup>1</sup>, Z. Daniel<sup>1</sup>, D. Thorwarth<sup>3</sup>, S.M. Huber<sup>4</sup>

<sup>1</sup>University Hospital Tübingen, Radiation Oncology, Tübingen, Germany ; <sup>2</sup>University of Brescia, Radiation Oncology, Brescia, Italy ; <sup>3</sup>University Hospital Tübingen, Section for Biomedical Physics- Department of Radiation Oncology, Tübingen, Germany ; <sup>4</sup>University Hospital Tübingen, Experimental Radiation Oncology, Tübingen, Germany

#### Purpose or Objective

Immunogenic cell death (ICD) is counted among the crucial steps of eliciting effective anti-tumor immune responses after irradiation. Most publications argue in favor of hypofractionated regimens. However, systematic analyses of radiobiological parameters such as fractionation sensitivity are scarce for ICD induction. Several clinical settings such as the treatment of glioblastoma including large volumes of normal brain tissue rely on normofractionated radiotherapy regimens. Thus, we aimed to evaluate ICD induction systematically after different radiation regimens and modeled the data with biomathematical methods.

#### Material and Methods

A standard glioblastoma cell line (U87MG) and two patient-derived, stem cell enriched glioblastoma cell lines (LKVII and LKXVII) were analyzed for their membrane exposure of Calreticulin (CRT) 24h after irradiation (determined as a suitable time point in an initial experiment for the kinetics of CRT exposure after irradiation with 15 Gy) with single doses (2-24 Gy) and daily fractionated treatment (5 x 2 Gy, 3 Gy and 4 Gy, respectively). Percentage of cells with irradiation-induced CRT exposure after single dose irradiation was fitted with a non-linear least square fit to a Hill function. Equivalent single fraction irradiation doses were calculated for membranous CRT after fractionated irradiation using the equation derived from the data fit. Immunogenic cell death induction was confirmed by HMGB1 release (ELISA), normalized to number of viable cells 48h after single dose irradiation for U87MG and LKVII.

#### Results

The three cell lines showed a vast difference in basal CRT positivity in unirradiated controls of 6.9±0.24%, 9.5±0.09% and 15.3±0.18% for U87MG, LKVII and LKXVII, respectively. All cell lines showed significant ICD induction after irradiation with ≥8Gy single dose and 5 x 3 Gy and 4 Gy. The data were well fitted by a Hill function (R<sup>2</sup>>0.98). For both patient-derived cell lines, normofractionated irradiation of 10 Gy significantly increased membrane exposure of CRT. Corresponding single doses for fractionated regimens were higher for LKVII and LKXVII compared to U87MG. Significant HMGB1 release into the medium was observed for 8 Gy irradiation for LKVII and for 16 Gy for both tested cell lines (8.9±0.9 pg/10<sup>6</sup> cells vs. 21.1±1.5 pg/10<sup>6</sup> cells, 4.0±0.7 pg/10<sup>6</sup> cells vs. 47.4±9.35 pg/10<sup>6</sup> cells for LKVII and U87MG, respectively).

#### Conclusion

Glioblastoma cells, a highly radioresistant tumor entity, shows ICD after single dose of 8 Gy or higher and fractionated irradiation. Daily fractionated irradiation seems to lead to accumulation of cellular damage leading to immunogenic cell death. Even a clinically low dose of 5 x 2 Gy induces ICD in patient-derived, stem cell enriched cultures. Thus, at least concerning the initial step of effective anti-tumor immune response, normofractionated radiotherapy might be a possible partner for immunotherapy strategies in the clinic.

**PO-1074 Radiotherapy and immuno-check point inhibitors for brain metastases. A mono-institutional analysis.**

C. Di Carlo<sup>1</sup>, F. Patani<sup>1</sup>, D. Fasciolo<sup>1</sup>, S. Di Biase<sup>1</sup>, C. Rosa<sup>1</sup>, A. Allajbeji<sup>1</sup>, L. Gasparrini<sup>1</sup>, P. Di Marino<sup>2</sup>, M. De Tursi<sup>2</sup>, L. Caravatta<sup>1</sup>, M. Trignani<sup>1</sup>, D. Genovesi<sup>1</sup>  
<sup>1</sup>Department of Radiation Oncology- SS Annunziata Hospital, G. D'Annunzio University, Chieti, Italy ;  
<sup>2</sup>Medical Oncology Unit- SS Annunziata Hospital- Chieti, Department of Medical- Oral and Biotechnological Sciences- University G. D'Annunzio, Chieti-Pescara, Italy

**Purpose or Objective**

As suggested by the literature, immunotherapy (IT) combined with radiotherapy (RT) could be a promising strategy to enhance treatment efficacy, but the safety and timing of their association remains unclear. The aim of our analysis is to assess the safety of IT concomitant or close to RT in patients with brain metastases.

**Material and Methods**

From November 2016 to September 2018, 13 patients with brain metastases from renal cells carcinoma (2 patients), non-small cell lung cancer (6 patients) and melanoma (5 patients) were treated in our Institute and retrospectively analyzed. The radiation treatment was defined concomitant when it was performed after the beginning of IT course. Acute and late toxicities were evaluated according to CTCAE v 4.0 scale. After RT, patients were reevaluated with total body CT scan. MRI was also performed in case of FSRT after 3 months from RT.

**Results**

Median age was 71 years (range: 54-78 years). All patients reported a performance status  $\geq 70\%$  according to Karnofsky scale, except one with 60%. Median follow up was 12 weeks (range: 2-60 weeks). Patients received IT with anti-PDL1 (12 patients) or anti-CTLA4 (1 patients) that was concomitant in 10 cases, while 2 patients started immunotherapy within two months from RT. Whole brain radiotherapy (WBRT) with a total dose of 20 Gy (4 Gy/fraction) was administered in 11 patients, while the remaining 2 patients underwent fractionated stereotactic radiotherapy (FSRT) with a total dose of 24 Gy (8Gy/fraction). Median number of IT cycles was 9 and it is still ongoing in 3 cases. All patients received concomitant corticosteroids therapy (dexamethasone, at ranging dose between 2 mg/die and 12 mg/die).

Combination IT-RT was well tolerated without unexpected toxicities. The 92% of patients had G0 acute toxicities according to CTCAE scale. Only in one case, radiotherapy was interrupted for poor clinical condition. Late toxicities were collected in 7/13 patients and it was G0 in the 70%. The remaining 30% of patients, showed G1-G2 neurological toxicity. No case of radionecrosis was detected. At the time of analysis, 5 patients were died for disease complications, non-related to the treatment.

**Conclusion**

From our data, IT resulted to be safe in patients treated with concomitant RT for brain metastases without G3-G4 acute toxicities and radionecrosis. Longer follow-up and a higher number of patients are necessary to confirm these data.

**Poster: Radiobiology track: Radiation and tumour metabolism**

**PO-1075 CBX4 contributes to radioresistance of esophageal squamous cell carcinoma by targeting autophagy**

H. Zhu<sup>1</sup>, L. Chu<sup>1</sup>, Q. Liu<sup>1</sup>, H. Zhu<sup>1</sup>, S. Lai<sup>1</sup>, K. Zhao<sup>1</sup>  
<sup>1</sup>Fudan University Shanghai Cancer Center, Radiation Oncology, Shanghai, China

**Purpose or Objective**

We investigated the effects of Chromobox 4 (CBX4) in esophageal squamous cell carcinoma (ESCC) and its role in radiosensitivity.

**Material and Methods**

We used quantitative real-time polymerase chain reaction and immunohistochemistry analyses to compare expression of CBX4 between radioresistant and radiosensitive ESCC samples. Lentivirus was used to knockdown of CBX4 gene and stable transmitted cell line of KYSE150 and TE13 were made. In vitro cell counting kit 8 and clone formation assay were used to detect cell viability and proliferation. Radioresponse was primary examined by clone formation assay after exposure of 0, 2, 4, 6, 8 Gy X-ray by a medical accelerator of different stable cell lines. Then autophagy as well as apoptosis, cell-cycle arrest, and  $\gamma$ -H2AX expression were examined in 0 Gy and 8 Gy by flow cytometer and immunofluorescence. Gene-chips and western blot were used to investigate molecular mechanism. In vivo experiments of xenografts were used to confirm the results.

**Results**

Levels of eEF2K were increased in radioresistant ESCC samples compared with radiosensitive tissues, as well as ESCC cell lines. Increased levels of CBX4 were associated with ESCC survival times of patients ( $P < 0.05$ ). CBX4 promotes ESCC proliferation and tumorigenicity in vitro and in vivo. An improved radioresponse was detected in CBX4 knockdown cells. Affymetrix GeneChip was used in CBX4 knockdown TE13 and control cells in normal conditions and 8 Gy of irradiation and autophagy pathways were detected by bioinformatic analysis. Improved protein expression of Atg5, mTOR, LC3, and TP53 were confirmed by western blot. In xenograft radiosensitivity experiments, improved radioresponse with a reduction of tumor doubling time was observed. Immunohistochemistry and immunofluorescence of tumor tissue confirmed the molecular mechanism of autophagy pathway.

**Conclusion**

CBX4 is overexpressed in ESCC and associated with progression and shorter survival times of patients. Decreased expression of CBX4 correlated with a reduction of malignancy in biological behavior and an improvement of radioresistance in ESCC, which may be mediated by autophagy signaling pathway. Targeting CBX4 may be a potential therapeutic approach of ESCC in the future.

**PO-1076 Concomitant association of T-DM1 and radiation: An in vitro study on HER2 breast cancer cells**  
M. Fabien<sup>1</sup>, Y. Kirova<sup>1</sup>, P. Verrelle<sup>1</sup>, M. Teulade-Fichou<sup>2</sup>, F. Mègnin-Chanet<sup>2</sup>

<sup>1</sup>Institut Curie, Radiotherapy, Paris, France ; <sup>2</sup>Institut Curie-Recherche, inserm U1196/CNRS UMR 9187 - CMIB, Orsay, France

**Purpose or Objective**

The better understanding of the EGFR receptors involved in the oncogenesis of HER2 positive breast cancers has led to the emergence of new therapeutic classes: the Antibodies Drug-Conjugate (ADC). T-DM1 is an ADC combining the anti-HER2 monoclonal antibody trastuzumab with molecules of DM1, a powerful mitotic spindle inhibitor. In HER2 positive breast cancer, T-DM1 is a validated treatment but the effects of concomitant association with radiation are not known. The objective of this study is to determine *in vitro* the effects of concomitant irradiation with T-DM1 on five different HER2 positive breast cancer cell lines.

**Material and Methods**

Five cell lines of human breast cancer with different levels of HER2 expression (HCC-1954, BT-474, SKBR-3, MDA-MB-453, ZR-75). T-DM1 was provided by Roche®/Genetech upon MTA. Expression levels were determined by western blot. T-DM1 toxicity was assessed using the CellTiter-Glo®

assay. Cell cycle analysis was performed by flow cytometry after incorporation of BrdU. HER2 cells were irradiated (GSR  $^{137}\text{Cs}$  662 keV) at different dose levels (from 1 to 8 Gy) after exposure to T-DM1. Survival fractions were determined based on clonogenic assays or on cell survival after 5 doubling times. Radiosensitivity parameter ( $D_{10}$  and  $D_{37}$ ) were calculated using the mean values of a and b determined from the curves drawn for best fit to the experimental data.

### Results

The action of T-DM1 on HER2 cells showed significant lethality by deprivation of the HER2 signaling pathway and intracellular DM1 action on the cell cycle with significant G2/M phase blocking. After 72h treatment with T-DM1 alone, the median effective dose ( $ED_{50}$ ) determined for the six cell lines used is function of the expression of the receptor HER2 except for one cell line (BT474). Using sub-toxic doses of T-DM1 and short-term drug exposure (6 or 12h), the cell viability still decreases dramatically after several days. After irradiation alone,  $D_{37}$  and  $D_{10}$  were significantly higher for the three high-HER2 expressing cells lines (HCC1954, BT474 and SKBr3) compared to the low-HER2 expressing cells (MDA-453 and ZR-75-1), with a linear increasing relationship between the radioresistance and the level of HER2 expression ( $D_{37}$ :  $r^2=0.9$ ;  $p<0.0001$  and  $D_{10}$ :  $r^2=0.7$ ;  $p<0.0001$ ).

In combination with radiation, T-DM1 elicited strictly additive interaction. There was no significant difference on  $D_{10}$  compared to control for all cell lines. HCC1954 :  $D_{10}$  T-DM1 =  $6.15\pm 0.64$  vs  $6.0\pm 0.24$  for control; BT-474:  $D_{10}$  T-DM1 =  $7.86\pm 0.22$  vs  $7.6.0\pm 0.43$  for control; SKBr3 :  $D_{10}$  T-DM1 =  $5.68\pm 0.29$  vs  $5.43\pm 0.14$  for control; MDA-MB-453 :  $D_{10}$  T-DM1 =  $4.82\pm 0.07$  vs  $4.02\pm 0.17$  for control and ZR-75-1 =  $D_{10}$  T-DM1 =  $3.3\pm 0.3$  vs  $3.02\pm 0.3$  for control.

### Conclusion

Although HER2 expression is a radioresistant factor, T-DM1 did not have any radiosensitizing impact on HER2 positive breast cancer cells in this *in vitro* study. The major toxicity of T-DM1 alone could explain this phenomenon but further explorations are needed.

### PO-1077 The heterogeneous metabolic and mutational landscape of non-small cell lung carcinomas

T. Van Zon - Meijer<sup>1</sup>, W. Peeters<sup>1</sup>, M. Looijen-Salamon<sup>2</sup>, R. Biemans<sup>3</sup>, L. Dubois<sup>3</sup>, P. Span<sup>1</sup>, J. Bussink<sup>1</sup>

<sup>1</sup>Radboud university medical center, Radiotherapy and Oncology Laboratory- Department of Radiation Oncology, Nijmegen, The Netherlands ; <sup>2</sup>Radboud university medical center, Pathology, Nijmegen, The Netherlands ; <sup>3</sup>Maastricht Comprehensive Cancer Centre- Maastricht University Medical Centre, Department of Precision Medicine- The M-Lab- GROW - School for Oncology and Developmental Biology, Maastricht, The Netherlands

### Purpose or Objective

Both hypoxia and oncogenic mutations rewire tumor metabolism causing treatment resistance. Metabolic inhibition might therefore sensitize tumors to radiation. We explored glucose and glutamine metabolism-related markers and mutation status in stage I-IIIa NSCLC in relation to histology and tumor aggressiveness characteristics. Furthermore, we examined the effect of lonidamine (hexokinase inhibitor) and/or 968 (glutaminase inhibitor) on metabolism, cell growth, cytotoxicity and radiosensitivity in NSCLC cell lines *in vitro*.

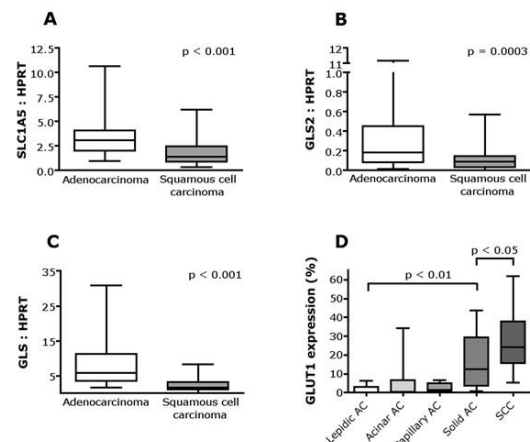
### Material and Methods

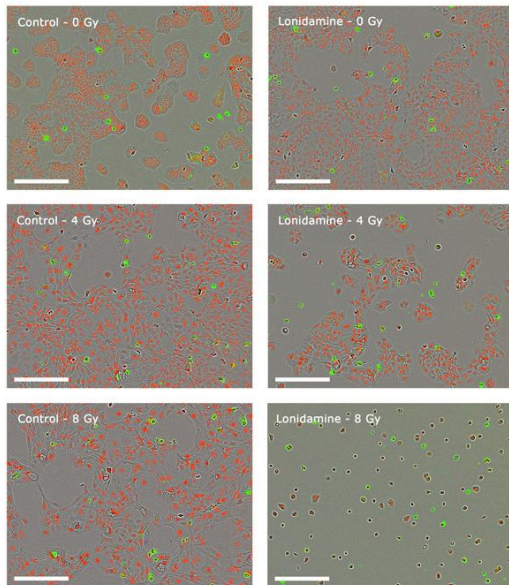
Mutation analysis was performed for 97 tumors. Metabolic marker expression was measured by immunofluorescent staining (protein) and qPCR (mRNA) (n=81). Adeno- (H23, HCC827, H1975) (AC) and squamous cell carcinoma (H520, H292, SW900) (SCC) NSCLC cells were treated with lonidamine and/or 968 for 72 hours under physiological levels of glucose (1.5 mM). Cells were irradiated with 0, 4

or 8 Gy. Cell growth of H2B-mCherry transduced cells and cytotoxicity (CellTox™ Green Cytotoxicity Assay) were measured using live cell imaging (IncuCyte). Inhibitory effects on metabolic profiles were determined using Seahorse XF96 extracellular Flux analyzer.

### Results

Glutamine metabolism-related markers were significantly higher in AC than SCC (Figure 1A-C). Glucose transporter 1 (GLUT1) protein was higher in solid than lepidic AC ( $p<0.01$ ), but was highest in SCC ( $p<0.05$ ) (Figure 1D). In AC, GLUT1 protein correlated with poor differentiation grade ( $p<0.001$ ), lymph node metastases ( $p=0.003$ ) and worse disease-free survival ( $p=0.008$ ). Glutamine transporter (SLC1A5) protein was higher in AC with worse pTNM stage ( $r(s)=0.39$ ,  $p=0.009$ ). *TP53* and *PIK3CA* mutations were more often found in SCC than AC (97.4% versus 71.2%,  $p=0.001$ ; 10.5% versus 0%,  $p=0.011$  respectively), while *EGFR* and *KRAS* mutations were more frequently observed in AC (10.2% versus 0%,  $p=0.042$ ; 35.6% versus 5.3%,  $p=0.001$  respectively). NSCLC cell lines responded differently to lonidamine and/or 968, largely corresponding with changes in glycolytic and mitochondrial metabolism upon treatment. 968 was cytotoxic in cell lines with high glutaminase C expression (H1975 and H520), whereas combination treatment was cytotoxic in *KRAS* mutated cell lines (SW900 and H23). H292 and HCC827 were resistant to combination treatment. Treatment with 968 and especially lonidamine resulted in radiosensitization of H292 and HCC827 in terms of decreased relative cell growth and increased cytotoxicity (Figure 2).





### Conclusion

NSCLC is a heterogeneous disease, with differences in mutational status, expression of metabolism-related markers between AC and SCC but also within AC subtypes, and response to metabolic inhibition. GLUT1 and SLC1A5 expression correlated with aggressive tumor behavior only in AC. So, these markers could select a group of AC patients that require intensification of treatment. Only a part of NSCLC patients may benefit from the combination of radiation therapy and metabolic inhibition, making stratification necessary.

### PO-1078 Superparamagnetic Iron Oxide Nanoparticle Mediated Radiosensitization at Megavoltage Radiation

E. Korkmaz Kıraklı<sup>1</sup>, G. Takan<sup>2</sup>, S. Hoca<sup>3</sup>, F.Z. Biber Müftüleri<sup>2</sup>, A. Yurt Kılçar<sup>2</sup>, S. Arun Kamer<sup>3</sup>, Y. Anacak<sup>3</sup>  
<sup>1</sup>DR. Suat Seren Chest Diseases and Surgery Research and Educational Hospital, Radiation Oncology, Izmir, Turkey; <sup>2</sup>Ege University Institute of Nuclear Sciences, Department of Nuclear Applications, Izmir, Turkey ; <sup>3</sup>Ege University, Radiation Oncology, Izmir, Turkey

### Purpose or Objective

Superparamagnetic Iron Oxide Nanoparticles (SPIONs) in combination with radiotherapy have been representing themselves as novel radiosensitizers in recent years. The purpose of this study was to assess SPION's *in vitro* radiosensitizer effect at clinically utilized 6MV energies which remains relatively as an unexplored issue and to calculate Nanoparticle Enhancement Ratio (NER) of SPIONs.

### Material and Methods

Human breast adenocarcinoma (estrogen receptor positive) (MCF-7), human breast adenocarcinoma (triple negative) (MDAMB-231) and human ovarian carcinoma (MDAH-2774) cell lines were used. Citrate coated-SPION's were synthesized.

Morphology and size analysis of *cit*-SPIONs were performed by transmission electron microscopy (TEM). The size distribution of nanoparticles was determined by dynamic light scattering (DLS).

The effect of the *cit*-SPIONs on cell viability was evaluated using trypan blue exclusion test. MTT assay was applied to determine the safe SPION dose to perform radiation treatment experiments.

To achieve full scatter conditions, a special type of solid water phantom was designed which 96 well-plates can be placed in, at 5cm depth along the central axis. Cells were then irradiated with various doses (2,4,6,8Gy). Cells were

left to grow to form clones. At 14<sup>th</sup> day of colonization, colonies containing  $\geq 50$  cells were scored. The whole procedure was repeated three times independently. Clonogenic survival curves were plotted as the log of the surviving fraction as a function of the dose. Dose Modifying Factor (DMF) which can be called as Nanoparticle-mediated Enhancement Ratio (NER- very similar to well-known oxygen enhancement ratio) based on clonogenic assays for each single radiation dose, was derived from cell survival curves.

### Results

By TEM images, dimensions of *cit*-SPION's were measured between 6-25nm and they were spherical in shape.

Cell viability (trypan blue) and MTT assay were carried out and it was proven that *cit*-SPION's at 0.1mg/mL concentration and after 24 hours of incubation did not exhibit cytotoxic effect on all three cell lines .

NER values were cell line specific and depended on radiation dose.

The highest radiosensitization effects were seen in MCF-7 and MDAH 2447 cells at 2Gy (NER: 1.49 and 1.39 respectively), in MDA-MB-231 cells at 4Gy (NER:1.20). Cell survival fraction was also significantly lower in MDAH 2447 cells at 4Gy (p=0.019). While at 6Gy there was radiosensitization effect only in MCF-7 cells (NER:1.10), at 8Gy there wasn't any radiosensitization in any cell line (NER:1.03-1.08)

### Conclusion

These results raise the possibility that synergistic effects of SPIONs may cause dose dependent and cell line specific radiosensitization at 6MV X-ray energies. Since there has been scarce data inquiring information on the "Z" and the X-ray energy dependence and *in vitro* radiosensitizer effect of SPIONs at high MV energy levels relevant in clinic, our study might be accepted as important.

### PO-1079 Metabolic changes with the administration of radiotherapy in lung, head and neck cancer patients

E. Rodríguez-Tomás<sup>1</sup>, M. Murcia<sup>2</sup>, M. Arguís<sup>2</sup>, I. Dolz<sup>2</sup>, M. De Abreu<sup>2</sup>, G. Baiges-Gaya<sup>1</sup>, N. Cabré<sup>1</sup>, F. Luciano-Mateo<sup>1</sup>, L. Torres-Royo<sup>2</sup>, M. Arquez<sup>2</sup>, J. Gómez<sup>2</sup>, J. Acosta<sup>2</sup>, D. Gómez<sup>2</sup>, C. Jordi<sup>1</sup>, J. Jorge<sup>1</sup>, S. Sabater<sup>2</sup>, M. Arenas Prat<sup>2</sup>

<sup>1</sup>Hospital Universitari Sant Joan de Reus, Unitat de Recerca Biomèdica, Reus, Spain ; <sup>2</sup>Hospital Universitari Sant Joan de Reus, Radiation Oncology, Reus, Spain

### Purpose or Objective

Radiotherapy treatment can produce metabolic changes in cancer patients. The application of metabolomics to the study of energy metabolism in cancer is an underdeveloped issue, and only a few studies have investigated this in lung (LC) and head and neck cancer (HNC) patients exposed to radiotherapy (RT), despite its potential relevance in clinical practice. The aims of our study were to analyze the changes produced by RT on the activity and concentration of serum PON1 and the variations in the lipoprotein profile and metabolites of low molecular weight in LC and HNC patients and to correlate these changes with the clinical and pathological characteristics of patients and tumors, and their response to treatment.

### Material and Methods

The study included LC patients (n=33) and HNC patients (n=28) treated with RT. Control group (n= 50) was formed by Mediterranean health people. Blood samples for analyses were obtained before and after 8one month later) the irradiationtreatment. Lipoprotein profile and the metabolites of low molecular weight carried out by nuclear magnetic resonance. Statistical analysis was performed with SPSS 22.0 statistical package.

### Results

Mean ages were 72 (65.50-79.0) and 65 (56.25-73.0) years old in LC and HNC patients, respectively. The most prevalent histologic type was squamous carcinoma in both groups. Even though, the frequency of tumor relapse was

similar in both groups (LC 14%; HNC 9%), the deaths were higher in LC patients (19%). The schedule of RT treatment was 45-60 Gy (2-2.6 Gy/day, 5 days/week). Relative to control, both groups had significantly lower serum PON1 concentration, and arylesterase activity ( $p < 0.001$ ). We observed that after RT not only increased PON1 concentration in cancer patients but also arylesterase activity decreased. Intermediate density lipoprotein (IDL), triglycerides linked with different lipoprotein profiles and the VLDL particles size were significantly higher in cancer groups in comparison to control group. Whereas leucine, isoleucine, tyrosine, acetate, glutamine and formate metabolites were significantly lower in cancer groups, alanine, glucose and glutamate were significantly higher in the same groups. Only in HNC group showed significantly differences in glutamine and glutamate metabolites between before and after RT treatment.

**Conclusion**

Our study demonstrates that RT treatment can modulate anti-oxidant defense mechanisms and metabolites in cancer patients. These results could be useful as a biomarker to predict RT response and the prognosis of patients.

**Poster: Radiobiology track: DNA damage response**

**PO-1080 Does hyperthermia clinically alter the  $\alpha/\beta$ ? Insights from thermoradiotherapy vs. radiotherapy trials**

N.R. Datta<sup>1</sup>, S. Bodis<sup>1</sup>

<sup>1</sup>Kantonsspital Aarau, Radio-Onkologie, Aarau, Switzerland

**Purpose or Objective**

Hyperthermia at 39-43°C is a known potent radiosensitizer, primarily due to its ability to radiosensitize hypoxic tumor cells and inhibit post radiation repair of the potentially lethal DNA damage. This should be expected to alter the  $\alpha/\beta$  values of the linear-quadratic (L-Q) model. The present study has been carried out to clinically estimate the  $\alpha/\beta$  from randomized studies of thermoradiotherapy (HTRT) vs. radiotherapy (RT) in recurrent breast (RBRT), head and neck (stages III/IV) (LAHNC) and cervix cancers (stages IIB-IVA) (LACC).

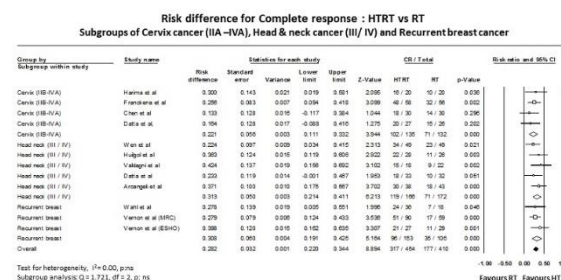
**Material and Methods**

Three recently published meta-analyses (2016) for HTRT vs. RT in RBRT, LAHNC and LACC, totaling 20 studies with 1,505 patients were evaluated for their complete response (CR). Only those studies with a specified RT dose (D), dose per fraction (d) and corresponding CRs in both groups were selected. Effect measures - odds ratio, risk ratio, risk difference (RD), tests for heterogeneity ( $I^2$ ) and subgroup analysis were carried out for the included trials. The biological effective dose with RT ( $BED_{RT}$ ) in these studies were individually computed using the L-Q equation without any time factor correction and assuming an  $\alpha/\beta_{RT}$  of 10 Gy for all sites. Since all trials had a positive outcome with HTRT over RT, the resultant enhanced thermoradiobiological BED for HTRT ( $BED_{HTRT}$ ) was correspondingly computed as a product of the  $BED_{RT}$  and %difference in CR between HTRT and RT. With the "D" and "d" of both HTRT and RT arms in each trial being similar, the  $\alpha/\beta$  following HTRT ( $\alpha/\beta_{HTRT}$ ) was estimated as,  $\alpha/\beta_{HTRT} = Dd / (BED_{HTRT} - D)$ , derived from the L-Q model.

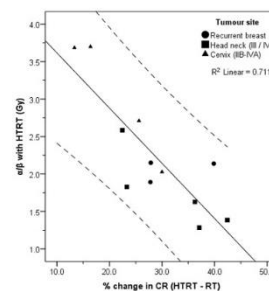
**Results**

12 studies with 864 patients were shortlisted - RBRT (3 studies, n=259), LAHNC (5 studies, n=267) and LACC (4 studies, n=338). Mean RT dose was 53.4 Gy (SD:  $\pm 14.3$ ) delivered in 2.2 Gy/fraction (SD:  $\pm 0.74$ ). Mean temperature was 42.4°C (SD:  $\pm 0.9$ ) and most patients received 2 sessions of HT per week for an average duration of 50 minutes, delivered mostly following RT. The overall risk difference of 0.28 was in favour of HTRT ( $p < 0.001$ ).

There was no significant difference in outcomes for the three sites on subgroup analysis (Fig.1).



Mean  $BED_{RT}$  was 64.7 Gy (SD:  $\pm 15.5$ ) while the mean  $BED_{HTRT}$  was estimated as 109.5 Gy (SD:  $\pm 32.1$ ). The overall computed  $\alpha/\beta_{HTRT}$  was 2.25 Gy (SD:  $\pm 0.79$ ) and it revealed an inverse relation with the %improvement in CR with HTRT ( $r^2: 0.71, p=0.001$ ) (Fig.2).



The  $\alpha/\beta_{HTRT}$  for RBRT, LAHNC and LACC were 2.05 Gy, 1.74 Gy and 3.03 Gy ( $p=0.027$ ), reflecting a reduction in  $\alpha/\beta$  by HTRT (range: 69.7% - 82%). On regression analysis, none of the treatment variables except %improvement in CR predicted for  $\alpha/\beta_{HTRT}$  (coeff: -0.74,  $p=0.001$ ).

**Conclusion**

The reduction in the clinically estimated  $\alpha/\beta_{HTRT}$  corroborates with the *in vitro* studies. HT inhibits repair of RT induced DNA double strand breaks resulting in enhancing the  $\beta$  component of cell kill, consequently leading to a fall in  $\alpha/\beta$ . This should be of practical use in optimizing RT time-dose-fractionation schedules with HT in the clinics.

**PO-1081 Biological interaction of a static magnetic field (SMF) with ionizing irradiation**

T. Schmid<sup>1,2</sup>, F. Hellmund<sup>2</sup>, S. Lemmer<sup>2</sup>, K. Illicic<sup>1</sup>, M. Melzner<sup>2</sup>, S. Bartzsch<sup>1</sup>, J.J. Wilkens<sup>2</sup>, S.E. Combs<sup>1,2</sup>

<sup>1</sup>Helmholtz Zentrum München, Institute of innovative Radiotherapy, Neuherberg, Germany ; <sup>2</sup>Klinikum rechts der Isar - Technical University of Munich, Radiooncology, Muenchen, Germany

**Purpose or Objective**

During the last decade there have been several technical developments in radiotherapy, like the development of integrated magnetic resonance imaging (MRI) in a linear accelerator. However, in literature the interaction of a static magnetic fields (SMFs) with radiation as part is still controversially discussed. Interactions could lead either to

aneugenic damages, induced by alteration in the mitotic spindle, as well as clastogenic damages produced by chromosome breaks. In this study, a clonogenic cell survival assay was performed to measure the interaction of a static magnetic field with radiation. Additionally, the mechanism of a possible biological interaction was analyzed using multicolor fluorescence in situ hybridization (mFISH).

#### Material and Methods

Human glioblastoma cells (LN-18) as well as human peripheral blood T-cell lymphocytes were seeded in petri dishes, which were placed inside a phantom. The irradiation for cell survival test was performed with a 6 MV linac with doses of 0, 1, 2, 4, 6, and 8 Gy in the presence and absence of a SMF of 1 Tesla produced by a permanent magnet. For the chromosome aberration test, irradiations with 2 and 4 Gy in the presence and absence of a SMF of 1 Tesla were performed. Chromosome aberrations were analyzed in at least 300 metaphases per treatment group using Metafer4 software. For both experiments three technical as well as three biological replicates were performed.

#### Results

The survival curves were fitted using the linear quadratic model. The survival fractions in absence of an SMF exceed the ones in presence of an SMF for all dose points between 1 and 8 Gy by 12% to 31%. The statistical analysis showed a significant decline ( $p \leq 0.05$ , ANOVA test) of the overall cell survival when irradiation was combined with a static magnetic field. However, the chromosome aberration test did not show an induction of chromosome aberrations in general or a shift in the complexity or completeness of damages. The number of all chromosome aberrations was  $0.71 \pm 0.05$  without and  $0.73 \pm 0.05$  with a SMF during the 2 Gy irradiation.

#### Conclusion

Up to now, there are only very few studies that have investigated the combinational effect of a static magnetic field and radiation. Most of these studies were in line with our results showing that a static magnetic field increases the efficiency of the radiotherapy. Additionally, our study showed evidence that the altered cell survival is not caused by clastogenic DNA damages, which leads us to the hypothesis that aneugenic effects may cause the change in cell survival. Further experiments, including a micronucleus assay with centromere FISH and staining of the mitotic spindles by immunohistochemistry are proposed.

#### PO-1082 Dihydroouabain is a novel radiosensitizer identified by high throughput screening.

Z. Li<sup>1</sup>, K. Tamari<sup>1</sup>, Y. Seo<sup>1</sup>, K. Minami<sup>1</sup>, Y. Takahashi<sup>1</sup>, K. Otani<sup>1</sup>, O. Suzuki<sup>1</sup>, F. Isohashi<sup>1</sup>, K. Ogawa<sup>1</sup>

<sup>1</sup>Osaka University Graduate School of Medicine, Radiation Oncology, Suita-Osaka, Japan

#### Purpose or Objective

Radiosensitizers have had only limited success in clinic. High throughput screening (HTS) is a popular method to identify candidate compounds from a large number of compounds for drug discovery, however it has not been used to establish a method to identify new radiosensitizers so far. The aims of this study were identifying potential radiosensitizers by HTS and clarifying the specific mechanisms of new radiosensitizers in combination with radiotherapy (RT).

#### Material and Methods

We performed HTS by using 1280 compounds. The parental HeLa human cervical cancer cells were pre-treated with compounds and exposed to gamma-irradiation under normoxic and hypoxic conditions. After incubating the cells for 4 days, cellular viabilities were measured by using MTS assay. Then, the radiosensitizing effect of candidate compounds was validated by clonogenic survival assays. The radioresistant cell line (HeLa-RT) was established

from HeLa cell line. Apoptosis assay and western blot analysis were examined in 0Gy and 8Gy with or without a candidate compound in HeLa and HeLa-RT cell lines. Sphere formation assay was utilized to detect tumor sphere forming capacity.

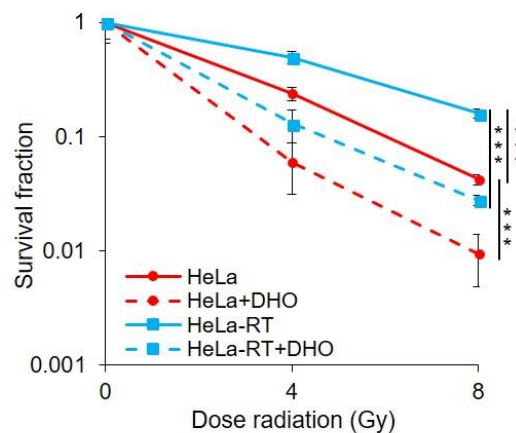


Figure 1: Clonogenic survival assays of HeLa and HeLa-RT cells treated with DHO, n=3 wells per group. \*\*\*P-value < 0.001.

#### Results

HTS identified 22 compounds as candidates for radiosensitizers. Among them, we selected Dihydroouabain (DHO) which was known as an inhibitor of  $\text{Na}^+/\text{K}^+$  ATPase and was not reported as a radiosensitizer. Clonogenic survival assays showed significant radiosensitizing effect of DHO in HeLa cells and in HeLa-RT cells (Figure 1). The combination of DHO and RT enhanced radiation-induced apoptosis. Western blot showed that  $\gamma\text{-H2AX}$  and pS345-Chk1 significantly increased and prolonged in combination treatment with DHO and RT compared with RT alone or DHO alone group. In addition, DHO treatment inhibited the capability of tumor spheres forming in HeLa and HeLa-RT cells. Taken together, DHO enhanced radiosensitivity through inhibition of DNA repair pathway, and induction of cancer cell apoptosis.

#### Conclusion

HTS is an efficient method for identifying new radiosensitizers. We identified DHO as a novel radiosensitizer by HTS.  $\text{Na}^+/\text{K}^+$  ATPase might be a novel target for radiosensitization.

#### PO-1083 The dual inhibitor BEZ235 radiosensitizes HNSCC cells due to impairment of the DSB repair

A. Arenz<sup>1</sup>, V. Balzer<sup>1</sup>, K. Dreffke<sup>1</sup>, T. Rieckmann<sup>2</sup>, S. Köcher<sup>3</sup>, E. Dikomey<sup>1,3</sup>, R. Engenhart-Cabillic<sup>1</sup>, A. Wittig<sup>4</sup>, U. Schötz<sup>1</sup>

<sup>1</sup>Philipps-University Marburg, Department of Radiotherapy and Radiooncology, Marburg, Germany ;

<sup>2</sup>University Medical Center Hamburg Eppendorf, Laboratory for Radiobiology & Experimental Radiooncology and Department of Otolaryngology and Head and Neck Surgery, Hamburg, Germany ; <sup>3</sup>University Medical Center Hamburg Eppendorf, Laboratory for Radiobiology & Experimental Radiooncology, Hamburg, Germany ; <sup>4</sup>Friedrich-Schiller-University Jena, Department of Radiation Oncology, Jena, Germany

#### Purpose or Objective

The Phosphatidylinositol-3-kinase (PI3K) pathway is the sixth most frequent mutated oncogenic pathway in head and neck squamous cell carcinoma (HNSCC) presenting in 60% of HPV-positive (HPV pos) and 31% of HPV-negative (HPV neg) tumors. The following study examines the

impact of PI3K pathway inhibition by the dual inhibitor BEZ235 on radiation sensitization of HPV pos and HPV neg HNSCC cell lines.

#### Material and Methods

The effect of BEZ235 in combination with radiation was determined for five HPV pos and five HPV neg HNSCC cell lines. Therefore, assays were used to identify alterations in the PI3K pathway and the DNA damage response (DDR), specifically ATM and DNA PKcs by Western Blot. Flow cytometric analysis was used to examine the cell cycle by Nicoletti staining and apoptosis by AnnexinV-staining. Repair of DNA double strand breaks (DSB) was visualised by gamma-H2AX foci formation and repair efficiency of homologous recombination (HR) and non-homologous end joining (NHEJ) was examined with repair plasmids. Survival after treatment was determined by colony formation assay.

#### Results

Treatment of cells with BEZ235 (50 nM) suppressed activation of Akt via Ser473 phosphorylation. Single use of BEZ235 does not interfere with cell cycle progression. In combination with irradiation, BEZ235 induces a significant increase in G1 arrest with a similar effect for both HPV pos and neg cell lines. Radiation-induced apoptosis was unaffected after the dual treatment. However, for all HNSCC cell lines DNA DSB repair was notably impaired in a way which is independently from HPV- or Akt- status but restricted to G1 cells, while clearly less effects were seen for S or G2 phase cells. These results suggest an inhibition of NHEJ, but not HR, which could be validated using repair-specific plasmids. The reduction of NHEJ could be attributed to a strong inhibition of DNA PKcs at S2056. In accordance with these data, colony formation assay revealed a significant increase of cellular radiosensitivity, which was especially pronounced for G1-phase cells.

#### Conclusion

The dual PI3K-inhibitor BEZ235 can be used to increase the radiation response of HNSCC independently from HPV- and Akt-status.

#### PO-1084 Poly ADP-ribose polymerase-1 inhibitors enhance soft tissue sarcoma radiosensitivity: in vivo study.

M. Mangoni<sup>1,2</sup>, M. Sottili<sup>1</sup>, G. Salvatore<sup>1</sup>, D. Pezzulla<sup>1</sup>, S. Lucidi<sup>1</sup>, M.A. Teriaca<sup>1</sup>, V. Maragna<sup>1</sup>, A. Peruzzi<sup>1</sup>, M. Perna<sup>1</sup>, G. Stocchi<sup>1</sup>, F. Terziani<sup>1</sup>, G. Caramia<sup>1</sup>, R. Grassi<sup>1</sup>, C. Talamonti<sup>3</sup>, G. Beltrami<sup>4</sup>, D. Campanacci<sup>4</sup>, D. Greto<sup>1</sup>, L. Livi<sup>1</sup>

<sup>1</sup>University of Florence, Radiotherapy Unit, Firenze, Italy

<sup>2</sup>Istituto Toscano Tumori, Itt, Florence, Italy ;

<sup>3</sup>University of Florence, Medical Physics Unit, Firenze, Italy ;

<sup>4</sup>University of Florence, Orthopedic Oncology Unit, Firenze, Italy

#### Purpose or Objective

Soft-tissue sarcomas (STS) are aggressive tumors with a poor prognosis and limited effective therapeutic options, thus there is a major clinical need for novel strategies. Poly-ADP ribose polymerase (PARP)-1 promotes base excision repair and DNA strand break repair. Inhibitors of PARP (PARPi) have shown to enhance the cytotoxic effect of irradiation, and evidences suggest that PARPi could be used to selectively kill cancers defective in DNA repair. Tumorigenesis in sarcomas is linked to aberrant biological pathways and some STS have defect in DNA repair systems, so there is a rationale for using PARPi in STS.

We previously demonstrated that PARPi are potent radiosensitizers on human STS in vitro models: they reduced cell survival, inhibited DNA damage repair and pro-survival ERK signaling when used in combination with irradiation.

The aim of the present study was to investigate the effect of PARP inhibition and irradiation on tumorigenesis of irradiated tumor cells in a xenograft model of rhabdomyosarcoma in mice.

#### Material and Methods

Rhabdomyosarcoma cells were irradiated with 3 Gy, with or without a 24 hours olaparib (1 µM) pre-treatment. Non-irradiated cells were used as controls. Four group of mice were compared: 1) control; 2)olaparib; 3)irradiation; 4)irradiation+olaparib.

Rhabdomyosarcoma xenograft was obtained by s.c. injection of 6×10<sup>6</sup>cells in the flank of CD1 nude mice. Tumor volume was measured twice a week for 30 days by the formula  $[\text{lenght} \times (\text{width} \times \text{width})]/2$ . Immunofluorescence and western blotting analysis have been performed.

#### Results

Olaparib alone reduced tumor growth compared to control, but without reaching a statistical significance. Irradiation alone showed an effect on tumorigenesis with a significant reduction of tumor volume compared to control. The association of olaparib and irradiation showed an even higher decrease in tumor volume compared to irradiation alone, reaching the statistical significance vs. irradiation or olaparib alone after 8 days. The mean immunofluorescence of gamma H2AX on rhabdomyosarcoma cells was significantly increased after treatment with olaparib and with radiation alone; a significantly higher intensity of fluorescence was obtained with combined treatment. Tumor growth was inversely proportional to the mean immunofluorescence of gamma H2AX. Further biomolecular analysis are ongoing.

#### Conclusion

In this study we confirmed previous in vitro data and showed that olaparib enhances the therapeutic effect of radiation on rhabdomyosarcoma xenograft, with significant reduction of tumorigenesis. These preliminary data encourage to further study association of PARPi with IR as a promising treatment for STS.

#### PO-1085 Prolonged trifluridine/tipiracil treatment radiosensitises colorectal cancer cells

K. Rothkamm<sup>1</sup>, T. Rieckmann<sup>2</sup>, S. Christiansen<sup>1</sup>, A. Brinker<sup>1</sup>, A. Stein<sup>3</sup>, U. Schumacher<sup>4</sup>, T. Frenzel<sup>5</sup>, C. Petersen<sup>6</sup>, S. Burdak-Rothkamm<sup>6</sup>

<sup>1</sup>University Medical Center Hamburg - Eppendorf UKE,

Department of Radiotherapy and Radio-Oncology / Laboratory of Radiobiology & Experimental Radiation Oncology, Hamburg, Germany ;

<sup>2</sup>University Medical Center Hamburg - Eppendorf UKE, Department of Otorhinolaryngology- Head and Neck Surgery /

Laboratory of Radiobiology & Experimental Radiation Oncology, Hamburg, Germany ;

<sup>3</sup>University Medical Center Hamburg - Eppendorf UKE, Department of

Oncology- Hematology and Bone Marrow

Transplantation, Hamburg, Germany ;

<sup>4</sup>University Medical Center Hamburg - Eppendorf UKE, Institute of

Anatomy and Experimental Morphology, Hamburg,

Germany ;

<sup>5</sup>University Medical Center Hamburg - Eppendorf UKE, Department of Radiotherapy and Radio-

Oncology / Institute of Anatomy and Experimental

Morphology, Hamburg, Germany ;

<sup>6</sup>University Medical Center Hamburg - Eppendorf UKE, Department of

Radiotherapy and Radio-Oncology, Hamburg, Germany

#### Purpose or Objective

Trifluridine/ Tipiracil (TFTD) has shown clinically relevant activity in colorectal cancer after fluoropyrimidine failure and may be of increased efficacy in combination with radiotherapy (RT) compared to current standard capecitabine chemoradiotherapy (RChT). As the underlying molecular mechanisms are still poorly understood, we aimed to determine the response of four colorectal cancer cell lines to TFTD alone and in combination with RT in order to provide a preclinical rationale for TFTD-based RChT treatment of rectal cancer.

#### Material and Methods

HT29 (MSS, CIN+, Ras wt, BRAF mut (V600E), p53 mut), HCT116 (MSI, CIN-, Ras mut, BRAF wt, p53 wt), SW48 (MSI,

CIN-, Ras wt, BRAF wt, p53 wt) and CaCo2 (MSS, CIN+, Ras wt, BRAF wt, p53 mut) colorectal cancer cells were analysed for cell viability (beta-hexosaminidase assay), trifluridine incorporation (anti-BrdU immunofluorescence), DNA damage induction (H2AX phosphorylation), cell cycle dynamics (5-ethynyl-2'-deoxyuridine pulse labelling & flow cytometry) and colony formation following treatment with TFTD and/or X-rays.

#### Results

While treatment with 1-10 µM TFTD for three days only moderately affected cellular metabolic activity, 5-day treatments showed significant effects at all concentrations in all cell lines except CaCo2. All cell lines incorporated similar amounts of trifluridine during S phase, irrespective of TFTD concentration and duration of treatment. Cells arrested in S phase and appeared to undergo endoreplication, resulting in polyploidy. TFTD treatment for 2, 6 and 24 h induced gamma-H2AX mainly in S/G2, while G1 phase cells remained mostly unaffected. Interestingly, levels subsided close to controls at 6 h in TFTD-resistant CaCo2 cells. Colony assays performed for 4 µM TFTD and X-rays alone as well as in four different treatment combination schedules demonstrated purely additive effects when cells were treated with X-rays and TFTD within 6 hours of each other. However, 24 h TFTD treatment prior to irradiation caused marked radiosensitisation in all cell lines analysed so far, with dose enhancement factors of 1.5-3. Corresponding xenograft studies using the same cell lines are underway.

#### Conclusion

Cell cycle arrest and endoreplication resulting in polyploidy may contribute to the cytotoxicity of TFTD. The observation of a strong radiosensitising effect after prolonged treatment with TFTD provides a robust argument for a daily fractionated combined regime of TFTD and RT in rectal cancer treatment.

---

**Poster: Radiobiology track: Biological therapies (e.g. viruses, vaccines)**

---

#### PO-1086 Antitumor Efficacy of Combined Gene and Radio - Therapy in Animals

O. Bezborodova<sup>1</sup>, I. Alexeenko<sup>2</sup>, A. Gevorkov<sup>3</sup>, E. Nemtsova<sup>1</sup>, A. Boyko<sup>3</sup>, E. Khmelevskiy<sup>3</sup>, R. Yakubovskaya<sup>1</sup>, A. Pankratov<sup>1</sup>, A. Kaprin<sup>4</sup>, E. Sverdlov<sup>5</sup>  
<sup>1</sup>Moscow Research Gerzen Oncology Institut, Laboratory of Modifiers and Protective Agents in Anti-Cancer Therapy, Moscow, Russian Federation ; <sup>2</sup>Shemyakin and Ovchinnikov Institute of Bioorganic Chemistry Institute of Molecular Genetics, Laboratory of Structure and Functions of Human Genes, Moscow, Russian Federation ; <sup>3</sup>Moscow Research Gerzen Oncology Institut, Radiation oncology, Moscow, Russian Federation ; <sup>4</sup>Moscow Research Gerzen Oncology Institut, Director of the Institute, Moscow, Russian Federation ; <sup>5</sup>Shemyakin and Ovchinnikov Institute of Bioorganic Chemistry Institute of Molecular Genetics, Laboratory of Structure and Functions of Human Genes, Moscow, Russian Federation

#### Purpose or Objective

Objective of the research was to study the anti-tumor activity of gene therapeutic constructs (GTC) used in combination with radiotherapy.

#### Material and Methods

*Gene therapeutic constructs*: bicistronic constructs of HSVtk-hGM-CSF plasmid DNA with HSVtk (thymidine kinase of herpes simple virus) and human hGM-CSF (granulocyte-macrophage colony stimulating factor) genes and HSVtk-mGM-CSF plasmid DNA with HSVtk and murine mGM-CSF genes. Every construct is included into a non-viral vector of PPT (Polyethylene glycol-Polyethylenimine-TAT peptide) block-copolymer. *Prodrug*: ganciclovir (GCV) (Cymeven, Roche Products

Ltd, Switzerland). *Animals*: mice BALB/c and nude mice. *Lines of the human* (KB oral mucosa carcinoma) *and murine* (C26 colon carcinoma) *tumor cells*. *Irradiation* of the animals was performed once in a single focal dose (RPM) of 5 Gy for every mouse using Elekta Precise linear accelerator (nude mice, KB tumor) or Theratron Equinox gamma-therapeutic apparatus (60Co, γ-radiation, BALB / c mice, C26 tumor) after its intratumoral injection GTC. *The efficacy of the combined gene and radiotherapy* was evaluated by the grade of tumor growth inhibition (T/C, u), and the treatment was considered to be efficient (synergistic effect) at T/C[combined therapy] < T/C[GENE THERAPY] x T/C[RADIOTHERAPY]. *Statistical analysis* was performed using Statistica ver. 10.0 programme.

#### Results

The combined treatment using GTC and the local irradiation in a single dose of 5 Gy on the model of subcutaneous KB xenograft or on the transplanted C26 murine tumor demonstrated a pronounced antitumor effect. The indices of efficiency of the combined therapy demonstrated the synergism of GTC/GCV and radiation impacts. The obtained synergism of the experimental therapeutic effects of the suicide gene therapy and radiotherapy opens up good prospects of further study of the combined therapy with the inclusion of these components of treatment.

#### Conclusion

The revealed spectrum of the anti-tumor activity of GTC/GCV systems may be used as the basis for choice of cancer diseases in early clinical trials. The synergy between suicidal gene therapy and radiation therapy proves to be prospective for further study of the combined therapy with an inclusion of these components of treatment. The reported study was funded by RFBR according to the research project No. 16-34-60185.

---

**Poster: Radiobiology track: Radiation response biomarkers**

---

#### PO-1087 The interaction between miR-221 overexpression and radiosensitivity in mamma carcinoma cell lines

E. Hirmer<sup>1,2,3</sup>, R. Kell<sup>3</sup>, S. Winkler<sup>3</sup>, K. Winkler<sup>3</sup>, L. Mutschelknaus<sup>3</sup>, S. Mörtl<sup>3</sup>, M. Atkinson<sup>1,2,3</sup>, S. Combs<sup>1,2</sup>, T. Schmid<sup>1,2</sup>, N. Anastasov<sup>3</sup>  
<sup>1</sup>Klinikum rechts der Isar, Radiooncology, München, Germany ; <sup>2</sup>Helmholtz Zentrum München, Institute of innovative Radiotherapy, Neuherberg, Germany ; <sup>3</sup>Helmholtz Zentrum München, Department of Radiation Sciences, Neuherberg, Germany

#### Purpose or Objective

Despite the steady improvement of breast cancer therapy, the prognosis for certain subgroups like triple negative breast cancer (TNBC) remains poor. In order to identify new therapeutic targets, it is important to analyze the pathogenesis of TNBC on a molecular level. TNBC shows significant overexpression of miR-221, which is associated with poor prognosis. By regulating cellular processes like proliferation, migration and cell survival, miR-221 is heavily involved in tumor pathogenesis. The interaction of miR-221 overexpression with radiation and its influence on migration, proliferation and colony formation were further investigated.

#### Material and Methods

The mammary carcinoma cell lines SKBR3 and MDA-MB-231 were transduced with lentiviral vectors to ensure miR-221 overexpression in SKBR3 cells or miR-221 knock-down in MDA-MB-231, naturally overexpressing miR-221. In order to analyze the interaction between radiation and miR-221 expression, the miR-221 or anti-miR-221 cells were compared to the empty vector controls (EV co-expressing

GFP), whose miR-221 expression levels equal the non-transduced cells. The cells were irradiated at doses of 0 to 8 Gy using a Cs<sup>137</sup> gamma irradiation source. Clonogenic cell survival with respect to radiation and miR-221 overexpression was examined using colony formation assays. Effects of miR-221 expression combined with irradiation on proliferation (cell counting) and migration (wound scratch assays) were analyzed. qRT-PCR was performed to determine miR-221 expression changes upon irradiation.

#### Results

miR-221 overexpressing cells showed significantly higher migration capacity in both cell lines. Remarkably, the migration capacity remained constant even upon 8 Gy ionizing radiation treatment. In parallel, miR-221 overexpressing cells showed elevated proliferation in both cell lines 72 hours after radiation. The reduction of cell numbers upon radiation was more pronounced in MDA-MB-231 than in SKBR3. The clonogenic survival assays confirmed that miR-221 overexpressing SKBR3 cells were more radioresistant than the control. In MDA-MB-231, no significant effect of miR-221 knock-down on clonogenic survival was observed. Additionally, irradiation did not alter the miR-221 expression levels significantly.

#### Conclusion

The results of our experiments show reproducibly increased migration and proliferation of mammary carcinoma cell lines SKBR3 and MDA-MB-231 upon miR-221 overexpression. The effect of miR-221 on migration remains constant upon irradiation whereas proliferation decreases after radiation treatment. Additionally, the proliferation assays show a drastic reduction of viable cells upon irradiation, whereas no strong reduction of migration upon radiation can be observed. This leads to the assumption that irradiation might increase migration levels. Regarding the consequences for a personalized radiotherapy in the future, miR-221 overexpression in TNBC patients indicates a higher risk of metastasis development.

#### PO-1088 DNA repair genes polymorphisms as biomarkers of tumor control in LDR BT prostate cancer patients

D. Carignan<sup>1</sup>, É. Vigneault<sup>2</sup>, L. Villeneuve<sup>3</sup>, S. Desjardins<sup>4</sup>, S. Magnan<sup>2</sup>, P. Després<sup>3</sup>, A. Martin<sup>2</sup>, W. Foster<sup>2</sup>, C. Guillemette<sup>6</sup>, É. Lévesque<sup>7</sup>

<sup>1</sup>CHU de Québec-UL Research Center, Oncology, Quebec, Canada ; <sup>2</sup>CHU de Québec-UL, Radio-Oncology, Quebec, Canada ; <sup>3</sup>CHU de Québec-UL Research Center and Faculty of Pharmacy- Laval University, Pharmacogenomics Laboratory, Quebec, Canada ; <sup>4</sup>CHU de Québec-UL Research Center, Endocrinology and Nephrology, Quebec, Canada ; <sup>5</sup>CHU de Québec-UL Research Center, Physics- Physical Engineering and Optics Department- Laval University, Quebec, Canada ; <sup>6</sup>CHU de Québec-UL Research Center and Faculty of Pharmacy- Laval University, Pharmacogenomics Laboratory and Canada Research Chair in Pharmacogenomics, Quebec, Canada ; <sup>7</sup>CHU de Québec-UL Research Center, Endocrinology and Nephrology and CHU de Québec-UL Hemato-Oncology department, Quebec, Canada

#### Purpose or Objective

To evaluate the association of inherited germline variations in DNA repair associated genes with tumor control in patients treated with permanent implant prostate brachytherapy (PIPB).

#### Material and Methods

The cohort consists of 478 I-125 PIPB patients with a median follow-up of 51 months after seeds implantation. Upon consent of patients, DNA was prepared from mononuclear cells and genotyped for 215 haplotype tagging single nucleotide variations (htSNPs) in genes of DNA damage response and repair pathways. Their

association with biochemical recurrence (BCR) was assessed using Cox regression models and Kaplan-Meier survival curves with log-rank tests.

#### Results

After adjustment for the established risk factors including age, PSA at diagnostic, Gleason score and androgen-deprivation therapy use; 17 htSNPs in ACVRL1, ERCC1 and 3, MGMT, MSH6, RAD51A, TP53BP1 and XRCC6, were initially found to be associated with an altered risk of BCR, with adjusted hazard ratios (HR<sub>adj.</sub>) ranged between 0.27 - 12.39 ( $P \leq 0.05$ ). Upon adjustment for multiple testing, one marker remained significant ( $q < 0.001$ ). Compared to carriers of the ERCC3 rs4150499 T allele, patients homozygous for C allele ( $n = 23$ ) had a significant higher risk of BCR with a HR of 12.39 (IC<sub>95%</sub> 4.22-36.39;  $p < 0.0001$ ;  $q < 0.001$ ). The Kaplan-Meier survival curve revealed a median BCR-free survival time reduced from  $213 \pm 7$  to  $99 \pm 12$  months (log-rank  $P < 0.00001$ ) for homozygous carriers of the ERCC3 rs4150499 C allele compare to non-carriers.

#### Conclusion

This study suggests an association of the rare intronic variant (Frequency=0.05 in the study) of the ERCC3 with an elevated risk of BCR after PIPB. An independent validation is required whereas the underlying biological mechanism remained to be assessed.

#### PO-1089 Improvement and optimization of $\gamma$ H2AX foci assay as a predictive tool for radiation sensitivity

T. Rassamegevanon<sup>1</sup>, S. Löck<sup>1,2</sup>, M. Baumann<sup>1,2,3,4,5</sup>, M. Krause<sup>1,2,3,4,5</sup>, C. Von Neubeck<sup>1,4</sup>

<sup>1</sup>OncoRay - National Center for Radiation Research in Oncology, Faculty of Medicine and University Hospital Carl Gustav Carus- Technische Universität Dresden-Helmholtz-Zentrum Dresden - Rossendorf, Dresden, Germany ; <sup>2</sup>Department of Radiotherapy and Radiation Oncology, Faculty of Medicine and University Hospital Carl Gustav Carus- Technische Universität Dresden, Dresden, Germany ; <sup>3</sup>Helmholtz-Zentrum Dresden - Rossendorf, Institute of Radiooncology - OncoRay, Dresden, Germany ; <sup>4</sup>German Cancer Consortium DKTK-Partner Site Dresden, and German Cancer Research Center DKFZ, Heidelberg, Germany ; <sup>5</sup>National Center for Tumor Diseases NCT- Partner Site Dresden- Germany: German Cancer Research Center DKFZ- Heidelberg- Germany- Faculty of Medicine and University Hospital Carl Gustav Carus- Technische Universität Dresden- Dresden- Germany, and- Helmholtz-

#### Purpose or Objective

Prediction of tumor radiation response using molecular biomarkers has been considered as a promising approach for treatment individualization to improve therapeutic outcome. Phosphorylation of histone H2AX ( $\gamma$ H2AX) is one of the earliest response to DNA double strand break induction. Detection of  $\gamma$ H2AX focus formation on *ex vivo* irradiated solid tumor biopsies demonstrated a high potential as a predictive assay for intrinsic radiosensitivity [1]. We aim to further optimize and develop the *ex vivo*  $\gamma$ H2AX foci assay to increase clinical relevance.

#### Material and Methods

Tumor xenograft models of human head and neck squamous cell carcinoma were used in this study. Tumor-bearing mice (*in vivo*) and xenograft-derived biopsies (*ex vivo*) were irradiated with 0 - 8Gy; fixed and paraffin embedded 24 h post irradiation. The  $\gamma$ H2AX foci were visualized by immunostaining. Manual quantification of  $\gamma$ H2AX foci was performed solely in perfused regions determined by pimonidazole (hypoxic marker) and BrdU (proliferation marker) staining.

#### Results

This study is focused on two aspects: a) Tumor heterogeneity: To study the effect of tumor heterogeneity in the *ex vivo*  $\gamma$ H2AX foci assay, we analyzed multiple equally treated xenograft tumor specimens (sham- and 4 Gy irradiated). The outcome

suggested a strong intratumoral heterogeneity with a slight intertumoral heterogeneity [2]. We studied degree of heterogeneity in  $\gamma$ H2AX foci between experimental set-ups (*in vivo* and *ex vivo*) by subjecting two published *in vivo* and *ex vivo* datasets to a statistical model. A lesser degree of heterogeneity was found in the *in vivo* dataset relative to *ex vivo* dataset [3]. These results confirmed the necessity of multiple biopsies, regions of interest, and nuclei to obtain an accurate prediction. We currently characterize  $\gamma$ H2AX foci in different chromatin distributions to gain deeper insight into the heterogeneity of foci in both set-ups.

b) Reflectiveness of *ex vivo* biopsies to *in vivo* tumors: We investigated whether *ex vivo* tumor biopsies can reflect radiation response of the corresponding *in vivo* tumors. Dose response curves of  $\gamma$ H2AX foci showed a comparable radiation response between biopsies and tumors in most of evaluated tumor lines. The slopes of dose response curves could classify tumors according to intrinsic radiosensitivity.

#### Conclusion

Overall, our results support the clinical applicability of the *ex vivo*  $\gamma$ H2AX foci assay as a predictive method for radiation sensitivity. To minimize inter-observer variations, a semi-automated foci-counting algorithm is under development.

This work was supported by a grant of the Federal Ministry of Education and Research (BMBF 02NUK035C).

#### Reference

- [1] Menegakis, A. et al., *Radiother. Oncol.* 116(3), 473-479 (2015)  
 [2] Rassamegevanon, T. et al., *Radiother Oncol.* 124(3), 379-385 (2017)  
 [3] Rassamegevanon, T. et al., *Int J Mol Sci.* 19(9). pii: E2616 (2018)

#### PO-1090 A second (third, fourth...) look at the In Vitro Clonogenic Assay

R. KOCH<sup>1</sup>, C. Harmel<sup>2</sup>, I. Dokic<sup>2</sup>, A. Abdollahi<sup>2</sup>, M. Alber<sup>1</sup>, E. Bahn<sup>1,3</sup>

<sup>1</sup>Department of Radiation Oncology, Heidelberg University Hospital, Heidelberg, Germany ;

<sup>2</sup>Translational Radiation Oncology, German Cancer Research Center DKFZ, Heidelberg, Germany ; <sup>3</sup>Clinical Cooperation Unit Radiation Oncology, German Cancer Research Center DKFZ, Heidelberg, Germany

#### Purpose or Objective

The *in vitro* clonogenic assay (IVCA) presents the standard *in vitro* experimental method in radiobiology: the cell survival curve lays the foundation for most biological models in radiotherapy. Since its introduction in 1956, the IVCA has remained basically unchanged: irradiated cells are incubated to form colonies, which are subsequently scored as either doomed or vital, based on their size. Here, we suggest to record the colony growth and show by temporally resolved statistical analysis of colony formation that the underlying basic assumptions of the *in vitro* IVCA are often not fulfilled, which may lead to systematic errors in cell radiation response parameters  $\alpha$  and  $\beta$ .

#### Material and Methods

Cells of different strains were seeded onto 96 well plates, irradiated with single doses of 0-7 Gy X-Rays and immediately placed into an incubator with automated acquisition of phase-contrast images in 3 h intervals for up to 9 days (IncuCyte® Live-Cell Analysis System). Image-treatment and automated colony scoring were performed in R/ImageJ with the use of self-developed routines. Colonies were scored and tracked over time based on combined position and shape parameters. Cell survival curves were calculated from the acquired database for different combinations of scoring parameters. A biomathematical colony growth model was developed that numerically simulates the entire experimental procedure:

stochastic radiation damage, colony growth via proliferation, size-dependent colony scoring.

#### Results

We analysed the effects of time-of-scoring and of scoring threshold on cell survival curves and on extracted parameters. These thresholds should have no influence on the outcome within a reasonable range. However, we made contrary observations: cell survival curves undergo an apparent shift when scored at subsequent time points, with (logarithmic) slope decreasing and curvature increasing over time (Fig. 1a). As a result, cell survival parameters and shift considerably when a linear/quadratic formula is fitted to the cell survival curves, the derived  $\alpha/\beta$  ratio varies over a large range (Fig. 1b). Analysis of colony growth curves suggests that this effect is connected to a dose-dependent proliferation rate.

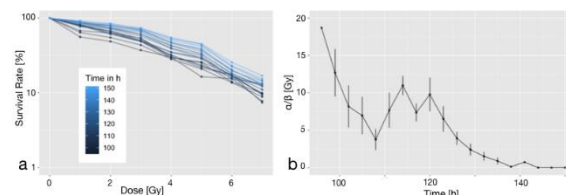


Fig. 1: Effect of time-of-scoring in the clonogenic assay of H3221 cells. a) Cell survival curves when scored at different time points. b)  $\alpha/\beta$  ratio at each time-of-scoring.

#### Conclusion

The clonogenic assay rests on the working hypothesis that irradiated cells will either perish after few mitoses, or proliferate constantly to form vital colonies. We observe that, since this condition is not generally fulfilled, systematic errors arise. We propose a temporally and statistically resolved analysis of colony size distributions. This removes the scoring bias by separating cell survival from the effects of colony growth. Additionally, a biomathematical model can be employed for in-depth analysis of the underlying colony formation.

#### Poster: RTT track: Patient preparation, positioning and immobilisation

#### PO-1091 Multimedia assisted information to patients with prostate cancer undergoing curative radiotherapy.

S. Rahbek<sup>1</sup>, I. Nordentoft<sup>1</sup>

<sup>1</sup>Herlev Hospital, Radiotherapy, Herlev, Denmark

#### Purpose or Objective

To reduce side effects, it is important for patients with prostate cancer, treated with curative radiotherapy, to have an empty rectum and a moderately filled bladder. To ensure that, they need to follow a bladder/bowel protocol.

The purpose of this study is:

- To use multimedia assisted information in preparing of the patient before radiotherapy treatment to increase the patient awareness of how to follow the instructions of the bladder/bowel protocol.
- To improve patient understanding of organs anatomical placement in the treatment area.

#### Material and Methods

Semi-structured individual interviews of a sample of 10 men undergoing radiotherapy were conducted. Each interview covered 5 topics: Information, understanding, experience, knowledge and improvement. At the end of each interview we showed two images: an animated image, and an x-ray image of the pelvic organs. Additionally, three of the patients were also shown an animated movie.

The data was taped, transcribed and analyzed within the 5 topics.

### Results

Through the analysis of the interviews it was clear that most of the patients, despite the information provided, had a misconception about how the organs are placed inside the small pelvic - including the prostate. The patients claimed that they understood the protocol presented to them, but most of them were not able to explain why it was important to follow. Some patients had formed their own alternative understanding of why the protocol was important to make sense of it. Almost all patients pointed out that beside side effects from the treatment itself, external factors such as finding a parking lot and different time of treatment appointments, had a negative impact on their ability to follow the protocol. All the patients, who were shown the two images, pointed out that the animated image helped them to a better understanding of the bowel/bladder protocol. The three patients who were shown the animated movie all preferred the movie and the animated image as a combination. All the patients felt that the use of multimedia as an information tool had a great impact on their understanding of the protocol and why it is important to comply.

### Conclusion

The use of multimedia assisted information to patients undergoing curatively intended radiotherapy treatment for prostate cancer can support and improve the understanding of the importance of complying with the bladder/bowel protocol - as well as the understanding of organs anatomical placement in the treatment area. The results of this study are going to be used for further investigation of patient ability, and an animated movie is created as well as animated images are implemented in the department.

Even though this study only focuses on patients with prostate cancer, we presume that data can be applied to similar diagnostic groups, that also need to follow a bowel/bladder protocol.

### PO-1092 The influence of a 6D couch and an individual head support on positioning in head-and-neck cancer

M. Rodrigue<sup>1</sup>, S. Veen<sup>1</sup>, J. Van Egmond<sup>2</sup>, M. Van Hameren<sup>1</sup>, T. Van Oorschot<sup>1</sup>, S. De Vet<sup>1</sup>, J. Van Santvoort<sup>2</sup>, R. Wiggenraad<sup>1</sup>, M. Mast<sup>1</sup>  
<sup>1</sup>Haaglanden Medical Center, Radiation Oncology, Leidschendam, The Netherlands ; <sup>2</sup>Haaglanden Medical Center, Medical Physics, Leidschendam, The Netherlands

#### Purpose or Objective

Accurate patient positioning in head and neck radiotherapy is of utmost importance because of the enhanced risk of overdosage to radiation-sensitive tissues. A six degrees of freedom couch permits optimization of set-up by enabling correction of rotational errors. Improved patient immobilization can be achieved by adding an individual head support to the immobilization system. No previous study has compared different treatment couches and head supports in combination with online cone-beam CT-based position verification in head and neck radiotherapy. Therefore, the aim of this comparative study was to evaluate the benefit of a six degrees of freedom couch and an individual head support using online cone-beam CT position verification and correction in head-and-neck cancer patients.

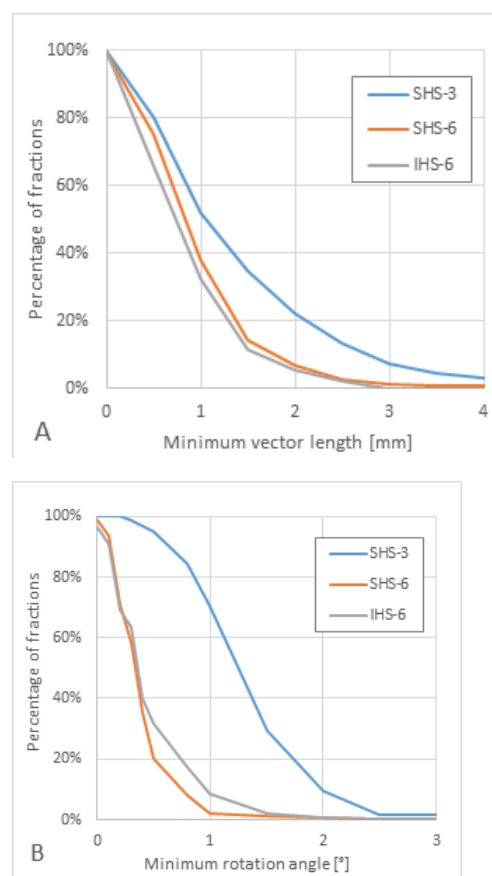
#### Material and Methods

This prospective study analysed 30 patients in three cohorts. Patients were either treated with a standard head support and conventional three degrees of freedom couch (SHS-3), a standard head support and six degrees of freedom couch (SHS-6), or an individual head support and six degrees of freedom couch (IHS-6). All set-up errors

were corrected online using cone-beam CT. Interfraction and intrafraction clipbox translations and rotations were assessed. Linear mixed models were used to calculate differences between cohorts.

### Results

A total of 1,605 matches were performed derived from 827 cone-beam CT's in 413 fractions. Interfraction mean translation vectors of the clipbox were <1.5 mm for all cohorts. These vectors were significantly lower for IHS-6 compared to SHS-3 ( $0.8 \pm 0.3$  vs.  $1.4 \pm 0.7$  mm,  $P=0.001$ ). Interfraction translation vectors of  $\geq 2$  mm were seen in 22%, 7%, and 5% of fractions for SHS-3, SHS-6 and IHS-6, respectively (Figure A). Interfraction rotation angles of  $\geq 1$  degree were seen in 71% of all fractions for SHS-3, as opposed to <8% of all fractions in the other cohorts (Figure B). Intrafraction clipbox translations and rotations did not differ between cohorts.



### Conclusion

A six degrees of freedom couch and an individual head support in head and neck radiotherapy yields less interfraction clipbox translations and rotations. The use of these tools could be of importance in reducing radiation-related toxicity of organs at risk in head-and-neck cancer patients.

### PO-1093 Comparison of conventional dark tattoo ink versus invisible tattoo ink for breast radiotherapy

L.H. Lim<sup>1</sup>, P.P.E. Pang<sup>1</sup>, F.Y. Wong<sup>1</sup>  
<sup>1</sup>National Cancer Centre Singapore, Division of Radiation Oncology, Singapore, Singapore

#### Purpose or Objective

Reproducibility is critical in radiotherapy (RT). In addition to immobilization, patients are usually tattooed. Occasionally, female breast cancer patients have refused permanent tattoos due to cosmetic reasons and a wish not to be reminded of their disease. Henna was used as a non-permanent alternative. Sometimes, these markings are

lost, ensuing repeated CT simulations and planning, incurring treatment delays, increased costs and impact on logistics and manpower.

An invisible ultraviolet (UV) tattoo ink has been used as an alternative to tattoos. Landeg et al. [1] previously reported no significant inter-fraction setup reproducibility deviation and improved patients' personal body image. However, the acceptability and reproducibility of UV tattoo ink on Asians who differ in skin pigmentation and cultural sensitivity as compared to Caucasians is unknown. We conducted a pilot study to assess the feasibility of replacing Indian ink with UV ink in our female breast cancer patients undergoing RT.

#### Material and Methods

5 patients were enrolled in this prospective study. Each patient was given 2 conventional dark ink and 2 invisible UV ink tattoos. During treatment, the given tattoos were used to align to setup treatment field borders. Routine X-ray verification was used to confirm RT position. The visibility of UV tattoos were assessed during each RT fraction. A body image survey [2] was used to assess patients' acceptance of each ink type. This was administered at 3 time points (CT simulation, last week of RT and 6 weeks post-RT). An in-house staff satisfaction survey was administered once to the Radiation Therapists (RTTs) to assess their perception of the UV tattoos and their use in RT positioning.

#### Results

At 'CT simulation', 3 out of 5 (60%) patients were apprehensive about the impact of the tattoos on their body image and felt conscious about their appearance. However, post-RT, 100% of the patients were satisfied with the appearance of the UV tattoos and did not feel less attractive physically/sexually or less feminine. At post-RT, 4 out of 5 (80%) patients were satisfied with their body with respect to the UV tattoo and did not feel conscious about their appearance, found no difficulties looking at their naked self and did not intentionally avoid people. The UV tattoo ink posed minimal risk of infection or allergy as none of these events were observed. 12 RTTs responded to the staff satisfaction survey. All of them found it easy to locate the UV tattoos and recommended its use in future breast cancer patients. Although 92% of RTTs felt that UV tattoos did not affect the total time taken for patient setup, 42% indicated more time is needed to locate them. Nonetheless, most commented that invisible ink is aesthetically acceptable and can improve patients' confidence. In addition, some felt that it would be valuable for patients with darker skin pigmentation.

#### Conclusion

From this feasibility study, we conclude that the invisible ink is well accepted by the breast cancer patients and RTTs.

#### PO-1094 Use of an individual abdominal corset in patients with upper-GI tumors treated with proton therapy

J. Thiele<sup>1</sup>, S. Schneider<sup>2</sup>, C. Valentini<sup>3</sup>, F. Lohaus<sup>3</sup>, S. Sarah<sup>4</sup>, D. Haak<sup>1</sup>, M. Krause<sup>5</sup>, A. Hoffmann<sup>6</sup>, E. Troost<sup>5</sup>  
<sup>1</sup>University Hospital and Faculty of Medicine Carl Gustav Carus- Technische Universität Dresden- Dresden- Germany, Department of Radiotherapy and Radiation Oncology, Dresden, Germany ; <sup>2</sup>University Hospital and Faculty of Medicine Carl Gustav Carus- Technische Universität Dresden- Dresden- Germany, OncoRay - National Center for Radiation Research in Oncology- Dresden- Germany- Helmholtz-Zentrum Dresden - Rossendorf- Institute of Radio, ; <sup>3</sup>University Hospital and Faculty of Medicine Carl Gustav Carus- Technische Universität Dresden- Dresden- Germany, Department of Radiotherapy and Radiation Oncology- OncoRay - National Center for Radiation Research in Oncology- Dresden- Germany, Dresden, ; <sup>4</sup>University Hospital and Faculty of Medicine Carl Gustav Carus- Technische

Universität Dresden- Dresden- Germany, OncoRay - National Center for Radiation Research in Oncology- Dresden- Germany- Helmholtz-Zentrum Dresden - Rossendorf- Institute of Radio, ; <sup>5</sup>University Hospital and Faculty of Medicine Carl Gustav Carus- Technische Universität Dresden- Dresden- Germany, Department of Radiotherapy and Radiation Oncology- OncoRay - National Center for Radiation Research in Oncology- Dresden- Germany- Helmholtz, ; <sup>6</sup>University Hospital and Faculty of Medicine Carl Gustav Carus- Technische Universität Dresden- Dresden- Germany, Department of Radiotherapy and Radiation Oncology- OncoRay - National Center for Radiation Research in Oncology- Dresden- Germany- Helmholtz,

#### Purpose or Objective

The irradiation of tumors, which are subject to respiration-induced motion is challenging for pencil beam scanning (PBS) based proton therapy due to the interplay effect and the temporally varying tissue densities along the beam path. Here, we report on the feasibility, tolerability and setup reproducibility of an individualized immobilization device for patients with tumors in the upper abdomen, who are treated with PBS.

#### Material and Methods

Since January 2018, nine patients with tumors in the upper abdomen (pancreas, liver and gall bladder) have been treated with PBS at our department. All patients eligible for this study underwent the following procedure within 10-days: (1) intra-tumoral implantation of three fiducial markers for target localization, (2) design of an individualized abdominal corset for motion reduction by abdominal compression, (3) abdominal MRI scan with intravenous contrast agent (c.a.) for target volume definition and tumor motion quantification, and (4) 4D-CT scan with c.a. for treatment planning. CT simulation and irradiation was performed with a vacuum mattress (Fig.1). Before each treatment fraction, the position of the target volume was verified with orthogonal X-ray imaging. First, a 2D/2D match with the DRRs was performed and then the position of the fiducial markers was verified (tolerance level: 3-5mm). In case this tolerance level was exceeded, a CT scan was performed in-room and the dose distribution was recalculated for plan comparison; in case of clinically relevant changes in the dose distribution, a new plan was calculated.

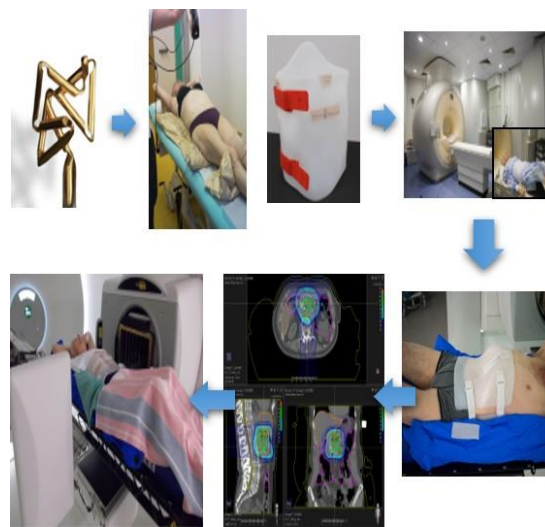


Fig.1 Workflow: fiducial marker (GoldAnchor®) implantation, individual abdominal corset, diagnostic MRI in treatment position; planning dual-energy CT; treatment volume delineation and planning; delivery of PBS.

## Results

All patients tolerated the marker implantation, the abdominal corset and the treatment well with no treatment interruptions. In 4 out of the 300 applied fractions (1,3%) the tolerance level of the fiducial markers was exceeded. For these fractions, the recalculated dose distribution nevertheless showed sufficient target coverage (Fig. 2). The entire treatment fraction (including patient positioning, setup verification and dose delivery) did not exceed the standard time slot of 30 minutes.

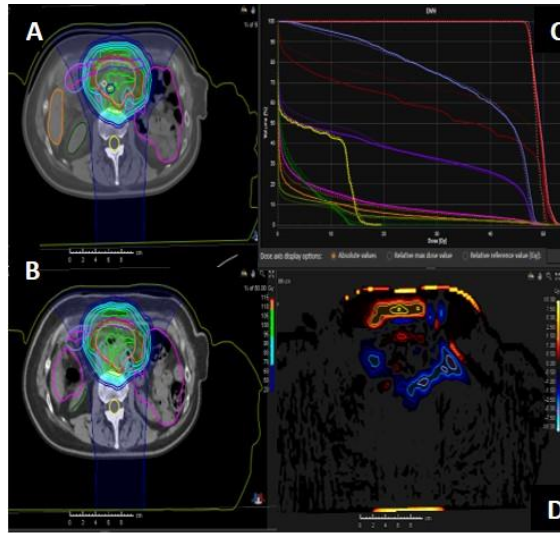


Fig. 2 Plan comparison during treatment. A: original dose distribution on treatment planning dual energy CT; B: dose distribution recalculated during treatment; C: the DVH highlighting the differences between the two plans (solid line: planning CT, dotted line: repeated CT); D: difference in dose distribution.

## Conclusion

This study demonstrates that PBS-based proton therapy with an abdominal corset to reduce breathing motion of GI-tumors is feasible, well-tolerated by patients and provides a reproducible setup without prolonging the daily treatment time.

### PO-1095 Time management and hands-on experience with ELEKTA Unity 1.5T MRI-Linac

C. Marks<sup>1</sup>, A. Stolte<sup>1</sup>, D. Thorwarth<sup>2</sup>, L.H. Braun<sup>1</sup>, S. Boeke<sup>1</sup>, D. Wegener<sup>1</sup>, J. Boldt<sup>1</sup>, C. Ortinau<sup>1</sup>, M. Kammler<sup>1</sup>, B. Holl-Henkel<sup>1</sup>, C. Gani<sup>1</sup>, D. Zips<sup>3</sup>, M. Nachbar<sup>4</sup>, O. Dohm<sup>4</sup>, D. Mönnich<sup>4</sup>

<sup>1</sup>University Hospital Tübingen, Department of Radiation Oncology, Tübingen, Germany; <sup>2</sup>Section for Biomedical Physics Tübingen- Eberhard Karls University Tübingen, Department of Radiation Oncology, Tübingen, Germany; <sup>3</sup>University Hospital Tübingen- Eberhard Karls University Tübingen, Department of Radiation Oncology, Tübingen, Germany; <sup>4</sup>Section for Biomedical Physics Tübingen, Department of Radiation Oncology, Tübingen, Germany

### Purpose or Objective

MR-Linac (MRL) hybrid devices are a new development in radiation oncology. Workflow and time management represent a challenge for all involved professions. Herein we present our initial experience with the ELEKTA Unity. Despite longer treatment times at MRL, patients may benefit from MRL and could be treated more accurately with hypofractionated radiotherapy. MRI allows better soft tissue contrast of the tumor and adjacent OARs. The mobility of the tumor and the patient movement can be detected online and adaptive response may be considered. In addition, the MRI, unlike a CBCT, does not generate additional radiation exposure to the patient.

## Material and Methods

The first patient treated with MRL had oligometastatic prostate cancer and was treated for a pararectal lymph node metastasis.

The workflow consisted of: CT planning with MRL table top and acquisition of an MRI at the MRL. An 8 beam step-and-shoot IMRT plan was created. The staff consisted of RTTs, Radiation Oncologists and Medical Physicists.

The daily MRL workflow included a pretreatment MRI. Based on this, plans were optimized with the "adapt to position" algorithm in order to adjust the plan of the daily anatomy. The patient received real time MRI (4D) during plan optimization and beam-on to confirm sufficient target volume coverage. Post-treatment MRI was performed for in-silico studies after treatment. Time required for individual steps (CT planning, patient positioning, MRI, plan optimization and daily treatment) of the treatment process were recorded.

## Results

At Unity the total duration for planning was 395 minutes on average, for IMRT at a conventional linac it was 330 minutes for CT (no additional MRI). An average of 46 minutes was required for daily treatment on MRL, 16 minutes for the linac. The radiation delivery time is comparable on both devices with approximately 2-3 minutes.

The total time required for planning, radiation and post-MRI and offline verification of the adapted and treated plan was 503 minutes at MRL and 357 minutes at linac (CBCT, no MRI).

The daily pre-treatment scans took 3-7 minutes at MRL and 2-3 minutes for linac with CBCT.

## Conclusion

Due to the new workflow and the involvement of all professional groups for daily radiation, each individual step took more time than with conventional linac treatment (IMRT). With each additional patient, we expect significantly reduced treatment times. With increasing experience, the planning and treatment times can be further reduced to enhance efficiency.

### Poster: RTT track: Imaging acquisition and registration, OAR and target definition

### PO-1096 Geometrically correct MR imaging with optimal Signal to Noise Ratio for Hippocampus delineation

S. Takken<sup>1</sup>, M. Frantzen-Steneker<sup>1</sup>, T. Vijlbrief-Bosman<sup>1</sup>, L. Ter Beek<sup>1</sup>, M. Kwint<sup>1</sup>, J. Belderbos<sup>1</sup>, U.A. Van der Heide<sup>1</sup>

<sup>1</sup>Netherlands Cancer Institute, Radiotherapy, Amsterdam, The Netherlands

### Purpose or Objective

Following the RTOG0933 contouring atlas [1], the hippocampus is visualized with a T1-weighted 3D gradient TFE sequence. Unfortunately, this can have a Water Fat Shift (WFS) in the order of 2mm. When matching the fatty skull bone tissue to the planning-CT, this may result in a 2mm mismatch of the hippocampus (fig.1a). For Radiotherapy (RT), scanning in an immobilization mask is debated as the benefit to obtain the scan in RT position and minimize motion artifacts comes at the cost of a reduced Signal to Noise Ratio (SNR). Patients can be scanned with flexible coils at either side of the mask combined with Anterior and Posterior (A&P) coil arrays to regain SNR.

Purpose of this study is to obtain a geometrically correct MR sequence with sufficient image quality to use for delineation of the hippocampus, in head coil or in RT position.

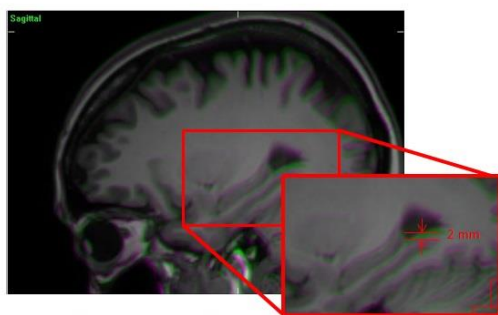


Fig 1a. Hippocampus displacement due to WFS

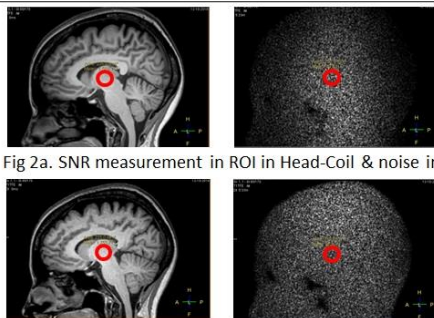


Fig 2a. SNR measurement in ROI in Head-Coil & noise image

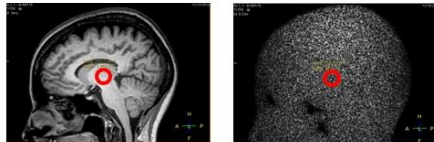


Fig 2b. SNR measurement in ROI in Flex-Coil & noise image

#### Material and Methods

A volunteer was scanned on a 3T Philips Ingenia MRI scanner. The 3D T1-TFE sequence had a field of view of 270x253x204mm, 1.1x1.1x1.2mm voxels (FHxAPxRL), TR/TE 6.8/3.1ms, Flip Angle 9°, Sense 1.8 (RL). A diagnostic sequence was scanned in head-coil with WFS 1.8 pixel, the optimal RT sequence with flexible and A&P and WFS of 1.0 pixel. Both coil set-up and WFS were varied separately.

A separate noise scan without RF was obtained with the same setting and scaling as the 3D T1-TFE. The SNR was obtained by taking the ratio of the mean signal and noise measured in a Region Of Interest (ROI) of 235mm<sup>2</sup> in two locations: a homogeneous part of the ventricle near the hippocampus and the right part of the brain (fig.2). Two trained observers were asked to give the scans a [1-4] score if the scan was suitable for hippocampus delineation (table 1).

#### Results

The SNR measurements are reported in table 1. Changing the WFS from 1.8 to 1.0 pixel results in a 25.9-30.8% decrease in SNR (head coil) and 26.0-26.1% (flex+A&P coils). The use of flex+A&P coils resulted in a reduction in SNR compared to the head coil of 23.1-42.2% depending on location and WFS. The flex+A&P coils give a homogeneous SNR over the image. When scanning in head coil a SNR increase by a factor 1.2-1.3 is seen from center to the right side of the brain. The SNR reduction from the diagnostic to the optimal RT sequence was 46.8% near the hippocampus and 57.1% in the right part of the brain. The observers gave all scans a sufficient score ( $\geq 3$ ) for delineation of the hippocampus, irrespectively which type of coils or WFS setting were used.

SNR = Signal/Noise				
Location	Headcoil WFS 1.8 pixel		Flexcoil WFS 1.0 pixel	
	HP*	RB**	HP	RB
Signal (mean)	1509.1	1309.5	1452.3	1277.4
Noise (mean)	40.4	28.5	56.2	37.5
SNR	37.4	45.9	25.8	34.1
			26.9	26.6
			19.9	19.7
Observer score [1 = not usable, 2 = recognisable anatomy, not sufficient, 3 = good/sufficient, 4 = excellent]				
	Headcoil WFS 1.8 pixel	Headcoil WFS 1.0 pixel	Flexcoil WFS 1.8 pixel	Flexcoil WFS 1.0 pixel
observer 1	3	3	3	3
observer 2	4	3	3	3

\*HP = near the hippocampus

\*\*RB = part of the right side of the brain

Table 1: measured SNR and observer score

#### Conclusion

Scans with a large WFS setting should not be used for RT delineation of the hippocampus, since shifts of 2mm can be found. Changing from head coil to flex+A&P coils, has more effect on SNR loss than changing to a smaller WFS. Scanning in RT position with flex+A&P coils and low WFS, the 3D TFE scan was considered suitable for delineation.

[1]

<https://www.rtog.org/corelab/contouringatlases/hippocampus/ampalsparing.aspx>

#### PO-1097 Interobserver variability in tumor bed contouring for breast cancer: comparison between RTO and RTT

E. La Rocca<sup>1,2</sup>, M. Dispinzieri<sup>1,2</sup>, T. Giandini<sup>3</sup>, V. Lici<sup>2</sup>, S. Frasca<sup>2</sup>, F. Bonfantini<sup>3</sup>, R. Valdagni<sup>1,4</sup>, L. Lozza<sup>2</sup>, E. Pignoli<sup>3</sup>, M.C. De Santis<sup>2</sup>

<sup>1</sup>University of Milan, Department of Oncology and Hemato-Oncology, Milano, Italy; <sup>2</sup>Fondazione IRCCS Istituto Nazionale dei Tumori, Radiotherapy Unit 1, Milano, Italy; <sup>3</sup>Fondazione IRCCS Istituto Nazionale dei Tumori, Medical Physics Unit, Milano, Italy; <sup>4</sup>Fondazione IRCCS Istituto Nazionale dei Tumori, Director- Radiation Oncology 1 and Prostate Cancer Program, Milano, Italy

#### Purpose or Objective

To evaluate the interoperator variability between radiation oncologist (RTO) and radiation therapist (RTT) in tumor bed (TB) contouring for patients (pts) with early breast cancer.

#### Material and Methods

We retrospectively analyzed pts undergoing breast conservative surgery who received a boost on the TB. The RTT contoured the TB independently of the RTO after a training course. In the group 1 CTV boost was the surgical bed, defined by adding 1 cm to the surgical clips placed in the lumpectomy cavity during surgery. In the group 2 the boost CTV was defined on the evaluation of preoperative mammography, medical history, intraoperative data and ultimate histological description. Moreover in this group the seroma cavity or a metallic find on the scar were used to identify the CTV boost. The CTVs were three dimension expanded of 0.5 cm creating a planning target volume. We compared the contours in terms of volume, number of slices, and DICE similarity coefficient (DSC).

#### Results

Forty pts were evaluated. Twenty pts had surgical clips (group 1), the other twenty had no clips (group 2). For each pts of group 1, no difference in the number of contoured slice was found between the two operators, but a statistically significant difference was found in terms of volumes, being RTT TB on average ~ 45% smaller than RTO TB (9.5±5.5 cm<sup>3</sup> vs. 17.4±10.5 cm<sup>3</sup>). For group 2, random variations between the two operators were found in terms of contour location, number of contoured slices, and volumes, with mean values of 24.7±16.3 cm<sup>3</sup> and 26.7±17.1 cm<sup>3</sup> for RTT TB and RTO TB, respectively. The TB delineated for this group were significantly bigger (p<0.05) than those delineated by the RTT for group 1. A difference was obtained by comparing the TB volumes delineated by both the operators in each group: 13.4±9.2 cm<sup>3</sup> in group1 vs. 25.7±16.5 cm<sup>3</sup> in group 2. The mean

DICE value between RTO TB and RTT TB was  $0.69 \pm 0.07$  (range 0.53-0.81) in group1 and  $0.37 \pm 0.18$  (range 0-0.58) in group2 ( $p < 0.05$ ).

### Conclusion

This study showed a decrease of the interoperator variability in the TB contouring with the use of surgical clips. The reduction of the volumes in the group with clips is closely related to the possibility of decrease side effects like fibrosis. The RTT following an appropriate training may become an important figure in the radiotherapy multidisciplinary team, able to support the RTO also in the contouring phase of the radiotherapy treatment.

### PO-1098 GTV definition agreement in brain metastasis radiosurgery using 1.5T MRI-sim: a multi-observer study

J. Yuan<sup>1</sup>, G.G. Lo<sup>2</sup>, Y. Zhou<sup>1</sup>, O.L. Wong<sup>1</sup>, W.W.K. Fung<sup>3</sup>, K.F. Cheng<sup>3</sup>, K.Y. Cheung<sup>1</sup>, S.K. Yu<sup>1</sup>

<sup>1</sup>Hong Kong Sanatorium & Hospital, Medical Physics and Research Department, Happy Valley, Hong Kong SAR China ; <sup>2</sup>Hong Kong Sanatorium & Hospital, Department of Diagnostic and Interventional Radiology, Happy Valley, Hong Kong SAR China ; <sup>3</sup>Hong Kong Sanatorium & Hospital, Department of Radiotherapy, Happy Valley, Hong Kong SAR China

### Purpose or Objective

We aim to assess the gross target volume (GTV) definition agreement in the treatment planning of frameless radiosurgery for brain metastasis by using 1.5T MRI-simulation data via a multi-observer study of MRI/CT registration and lesion delineation variability.

### Material and Methods

10 patients (brain metastases  $n=33$ ) received CT-simulation (no contrast,  $0.78 \times 0.78 \times 1 \text{mm}^3$ ) and 1.5T MR-simulation (3D-T1w-FSE with Gd contrast:  $1 \times 1 \times 1 \text{mm}^3$ ) scans in the identical thermoplastic mask fixed treatment position on the same day prior to their Cyberknife radiosurgery. Three observers were asked to blindly conduct rigid MRI/CT registration and then GTV contouring on the MRI fused CT images. Registration transformation matrix and the center position, volume, dice similarity coefficient (DSC) of the delineated lesions between the observers (obs) were compared using one-way ANOVA and intraclass correlation coefficient (ICC).

### Results

The inter-observer registration translational variability (RMS of the registration shift SD between 3 observers) was 0.07, 0.07, 0.1 and 0.08mm in LR, AP, SI and 3D, respectively. The GTV center position variability (RMS of GTV coordinate SD of 3 observers) was 0.18, 0.21, 0.18 and 0.23mm in LR, AP, SI and 3D. All individual rigid registration shifts relative to the mean registration shifts of all observers were well within 0.3mm in all translations (Fig. 1 upper row). All GTV center positions relative to their mean delineated position by all observers were all within 0.5mm (Fig. 1 lower row). The volumes of the delineated GTVs between three observers (obs1:  $1.23 \pm 1.51 \text{cc}$ , obs2:  $1.35 \pm 1.67 \text{cc}$ , obs3:  $1.30 \pm 1.59 \text{cc}$ ) showed insignificant difference (one-way ANOVA:  $p=0.955$ ); and excellent ( $\text{ICC} > 0.75$ ) agreement ( $\text{ICC}=0.9986$ , 95% CI = [0.9975, 0.9993]). The DSC between the observers were  $0.87 \pm 0.06$  (obs1vs2),  $0.85 \pm 0.07$  (obs1vs3) and  $0.85 \pm 0.12$  (obs2vs3). The inter-observer agreement was excellent ( $\text{ICC}=0.9546$ , 95% CI = [0.9076, 0.9797]) for the tumors with volume  $\geq 0.2 \text{cc}$ . However, large inter-observer variability in terms of DSC ( $\text{ICC}=0.2505$ , poor) was observed for the small targets with volume  $< 0.2 \text{cc}$  (Fig.2).

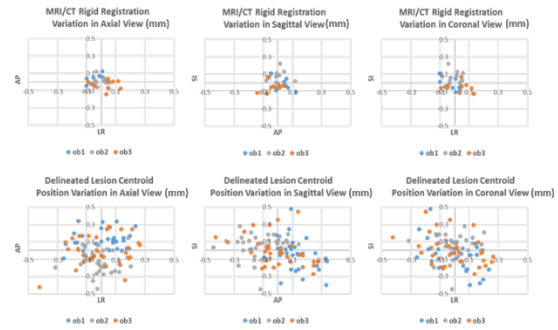


Fig. 1. The scatter plot of the rigid registration variability relative to the mean lesion volume of the whole cohort and the contoured lesion centroid position variability relative to each lesion's mean centroid position

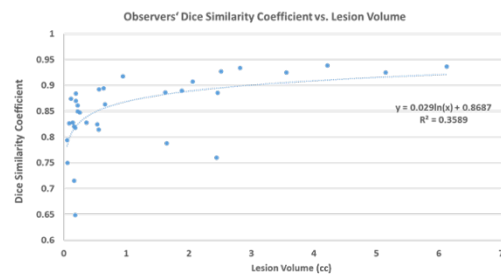


Fig. 2. The scatter plot of the observer's Dice Similarity Coefficient vs. mean tumor size. Excellent inter-observer agreement was found when the tumor size is larger than 0.25cc.

### Conclusion

Excellent inter-observer GTV definition agreement could be achieved in the frameless brain metastasis radiosurgery planning using 1.5T MR-sim data.

### PO-1099 A multi-center contouring study of spinal cord comparing myelo-CT and MRI fusion.

H. Tanaka<sup>1</sup>, H. Shimizu<sup>1</sup>, T. Aoyama<sup>1</sup>, H. Tachibana<sup>1</sup>, Y. Koide<sup>1</sup>, D. Katou<sup>1</sup>, S. Adachi<sup>1</sup>, R. Miyauchi<sup>1</sup>, Y. Ooshima<sup>2</sup>, T. Koidaira<sup>1</sup>

<sup>1</sup>Aichi Cancer Center, Radiation Oncology, Nagoya, Japan ; <sup>2</sup>Aichi Medical University, Radiation Oncology, 1-1 Yazakokarimata- Nagakute-Aichi, Japan

### Purpose or Objective

Spine stereotactic body radiotherapy (SBRT) is an emerging treatment for patients with spinal metastases and is rapidly being adopted in the clinic. Spinal cord is one of the most important organs at risk in Spine SBRT. To contour spinal cord, Myelo-CT or MRI fusion are used. To date, inter modality validation between Myelo-CT and MRI fusion in contouring spinal cord has not been evaluated. A multi-center contouring study was performed to evaluate inter modality variations between Myelo-CT and MRI fusion.

### Material and Methods

Six matured radiation oncologists from 2 centers joined this study. Plain CT, myelo-CT and MRI scans were performed on 12<sup>th</sup> thoracic to 5<sup>th</sup> lumbar vertebra of a patient who had bone metastases in 4<sup>th</sup> lumbar vertebra. The myelo-CT and MRI were registered to a plain CT by a radiation oncologist. Six radiation oncologists contoured lumbar 1<sup>st</sup> to 2<sup>nd</sup> spinal cord without metastases in vertebra on registered myelo-CT and MRI independently for this study. To avoid inter Radiation Treatment Planning system variations, all registration and contouring were performed on RayStation. Inter modality validation between myelo-CT and MRI fusion, inter observer variations in myelo-CT, and inter observer variations in MRI were evaluated with Dice similarity coefficient.

### Results

Inter modality Dice similarity coefficient between myelo-CT and MRI was  $0.801 \pm 0.026$ . (Average  $\pm$  SD) Inter observer Dice similarity coefficient in myelo-CT was  $0.873 \pm 0.030$ . (Average  $\pm$  SD) Inter observer Dice similarity coefficient in MRI was  $0.836 \pm 0.092$ . (Average  $\pm$  SD) Average volume spinal cord with MRI was  $1.874\text{ml} \pm 0.408$ . (Average  $\pm$  SD) Average volume spinal cord with Myelo-CT was  $1.682\text{ ml} \pm 0.221$ . (Average  $\pm$  SD). All contours were showed in Figure.

#### Conclusion

Inter modality variations between myelo-CT and MRI fusion, inter observer variations in myelo-CT and inter observer variations in MRI were evaluated and were larger than 0.7. The difference between myelo-CT and MRI fusion is small in contouring Spinal cord.

#### PO-1100 Validation of Atlas Based Segmentation for OAR in the brain.

A. Van Nunen<sup>1</sup>, A. De Graaf<sup>1</sup>, T. Budiharto<sup>1</sup>, D. Schuring<sup>1</sup>  
<sup>1</sup>Catharina hospital, Radiotherapy, Eindhoven, The Netherlands

#### Purpose or Objective

Manual delineation of organs at risk (OAR) is time consuming and possibly variable between observers. Atlas Based Segmentation (ABS) enables automatization of OAR delineation and can reduce workload and variability. Aim of this study was to investigate the accuracy of OAR delineation in the brain when using ABS.

#### Material and Methods

Delineations of OAR (brainstem, chiasm, cochlea, optic nerves, pituitary gland, retina, lacrimal glands, lenses and eyes) were generated using the ABS module in RayStation (Raysearch Laboratories, Stockholm, Sweden). OAR were segmented in 15 patients using four different atlases containing 10 CT scans, 25 CT scans, 10 MRI scans and 25 MRI scans. These were compared to the manual delineations. All OAR were reviewed by a radiation oncologist (RO) to determine whether they were clinically acceptable. Different parameters (volumes, specificity, sensitivity and Dice Similarity Coefficient (DSC)) were analysed and a Receiver Operating Characteristic (ROC) analysis was performed. A pairwise statistical analysis was performed to determine whether larger atlases could increase the accuracy of the automatic delineation and whether MRI atlases improve the delineation of the brainstem and chiasm.

#### Results

Highest median DSC (>0.8) was found for eyes and brainstem (figure 1). The median DSC was 0.5-0.7 for the cochlea, pituitary gland and optic nerves, and 0.4-0.5 for lenses, retina and chiasm (MRI). Lowest DSC was found for the chiasm based on the CT-atlas (figure 1). No statistically significant improvement was observed for atlases with 25 scans compared to atlases with 10 scans. The delineation of the brainstem and chiasm improved significantly by using an MRI atlas.

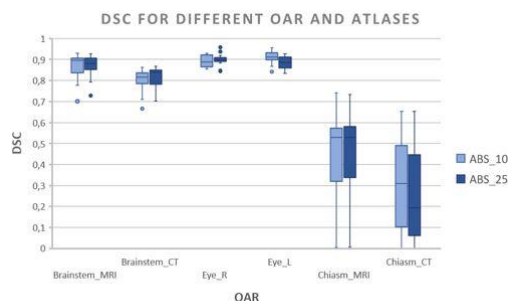


Figure 1: DSC for the evaluated atlases and OAR.

The ROC analysis shows that all points for the eyes and 14/15 points for the brainstem are plotted in the

“acceptable” quadrant (figure 2). This was confirmed by the RO who considered the delineations clinically acceptable. Most of the plotted points for the cochlea are in quadrant “acceptable” and some points were plotted in the “poor” quadrant, however the qualitative analysis shows that most ABS delineations were acceptable (13/15). Unacceptable results for pituitary gland, optic nerves, retina, lacrimal glands and lenses were found, which is in accordance with the DSC results. Despite the low DSC and the ROC analysis for the chiasm, the RO concluded that 11/15 ABS delineations were clinically acceptable.

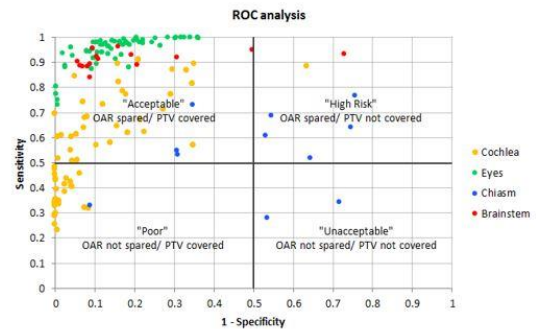


Figure 2: ROC analysis for different OAR.

#### Conclusion

Accurate delineation of the brainstem, cochlea and eyes was obtained by using ABS. Automatic delineations of optic nerves, retina, lacrimal glands, lenses and pituitary gland were not clinically acceptable. Automatic delineation of the chiasm with a MRI atlas is a good starting point, however manual corrections are needed for an accurate delineation. Increasing the number of scans in the atlas did not significantly improve the results, but caused an increase in computation time. Using an MRI atlas improved the accuracy of automatic delineations of the brainstem and chiasm.

#### PO-1101 Feasibility of PSMA PET/CT for evaluation of radiotherapy toxicity in salivary glands

N. Bruin<sup>1</sup>, V. Mohan<sup>2</sup>, J. Van de Kamer<sup>2</sup>, A. Al-Mamgani<sup>2</sup>, J. Sonke<sup>2</sup>, W. Vogel<sup>1</sup>

<sup>1</sup>Netherlands Cancer Institute, Departments of Radiation Oncology and Nuclear Medicine, Amsterdam, The Netherlands ; <sup>2</sup>Netherlands Cancer Institute, Department of Radiation Oncology, Amsterdam, The Netherlands

#### Purpose or Objective

Patients treated with high dose radiotherapy for head and neck cancer may suffer from a severe dry mouth (xerostomia) due to salivary gland damage. This toxicity has been difficult to evaluate with quantitative and gland-specific measurements. Functional imaging with prostate specific membrane antigen (PSMA) PET/CT is thought to indicate viable gland cells in salivary glands, and can theoretically be used to evaluate cell loss after radiotherapy. Our purpose is to investigate the technical and logistical feasibility of repeated PSMA PET/CT to evaluate salivary gland toxicity after radiotherapy.

#### Material and Methods

Seven patients have been included in an ongoing prospective study, that will include 20 head-neck cancer patients who are treated with 35 fractions of 2 Gy. Four PSMA PET/CT scans of the head-neck area were made at baseline, during treatment, and at 1 and at 6 months post treatment. Patients were scanned in treatment position using a flat table top, base, personalized mask and knee support, using a Philips Gemini TOF PET/CT scanner. A low dose of 50 MBq PSMA was administered, and the scan was acquired after an incubation period of 45 min. The field of view was from orbit to clavicles, in 2 bed positions of 6

minutes each. PET images were reconstructed to voxels of  $2 \times 2 \times 2 \text{ mm}^3$ . Low dose CT parameters included 2 mm slices and 40 mAs with dose optimization. PSMA PET images were co-registered to the original planning CT using rigid registration, based on the accompanying low dose CT. The image quality and image registration, along with the change in uptake were assessed visually.

### Results

At the time of this evaluation, all included patients had completed their scheduled scans successfully. 7 had received a baseline and mid-treatment scan, 5 had received a 1 month post-treatment scan and 3 had received a 6 month post-treatment scan. The radiation dose per scan was estimated at 3 mSv (1 mSv for PET, 2 mSv for CT). The image quality of the PSMA PET and low dose CT were visually good and without artefacts (figure 1). Image registration between the PSMA PET and the planning CT was visually good for the baseline scan, but was increasingly challenging during and after treatment due to anatomical changes caused by weight loss and gland regression. Areas of signal loss corresponded to the dose distribution (figure 2).

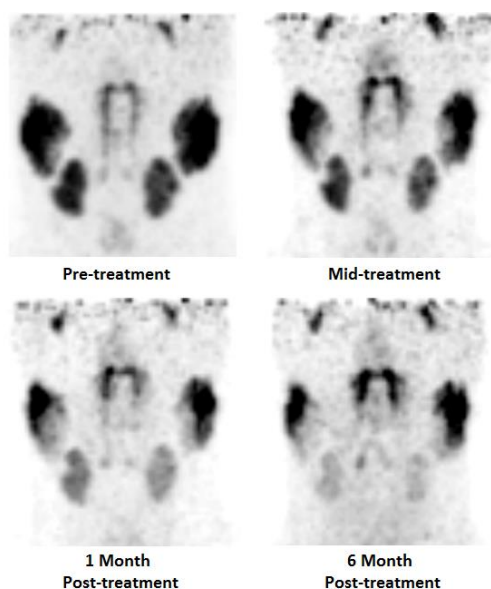


**Figure 1.** PET imaging results of patient 1. Coronal projections of four PSMA PET scans at progressive time points.

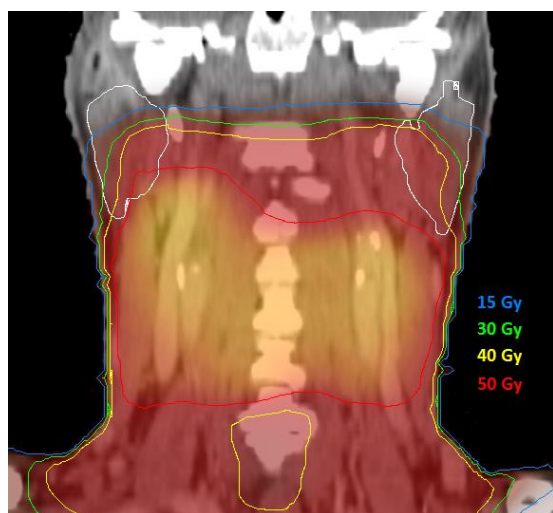


**Figure 2.** Dose distribution for patient 1, overlaid on planning CT with isodose lines. Parotid gland outlines visible in white.

PSMA PET/CT for monitoring of salivary gland cell loss is feasible, with acceptable patient burden, low radiation burden, and sufficient image quality for quantitative gland-based and voxel-based evaluations. Anatomical changes after treatment can complicate image registration.

### PO-1102 Multi-atlas vs. single-atlas auto-segmentation for Head and Neck OARs: time efficiency and accuracy

D. Gugyeras<sup>1</sup>, A. Farkas<sup>2</sup>, M. Csima<sup>3</sup>, Z. Cselik<sup>4</sup>, J.

Hadjiev<sup>2</sup>, A. Gulyban<sup>5</sup>, F. Lakosi<sup>2</sup>

<sup>1</sup>Kaposi Somogy County Teaching Hospital, Dr. József Baka Diagnostic- Radiation Oncology- Research and Teaching Center, Kaposvár, Hungary ; <sup>2</sup>Somogy County Kaposi Mor Hospital, Dr. József Baka Diagnostic- Oncoradiology and Research Center, Kaposvar, Hungary ; <sup>3</sup>Kaposvar University, Faculty of Pedagogy, Kaposvar, Hungary ; <sup>4</sup>Csolnoky Ferenc Hospital, Radiation Oncology, Veszprem, Hungary ; <sup>5</sup>Europa Hospitals, Radiation Oncology, Bruxelles, Belgium

### Purpose or Objective

to test and compare time efficiency and accuracy between single-atlas (SingleA) and multi-atlas (MultiA) based auto-segmentation in Head and Neck (H&N) organs at risk (OAR) delineation.

### Material and Methods

60 patients with hypopharynx/larynx cancer were selected and divided into two groups: ideal population (T1-T2/N0-1, n=30 pts) and clinical scenario ( $\geq T3/ \geq N2a$ , n=30 pts). All manual delineation was performed by an expert RTT, including semi-automated options (Ref). The baseline single- and multi-atlas for both groups consisted of 10 reference delineated cases with 20 OARs (Brain, Brainstem, Oral cavity, Mandible, Oesophagus, PharynxConstr, PituitaryGland, Spinal Cord, ThyroidGland, Trachea, L/R Submandgland, L/R Eye, L/R Lens, L/R OpticNerve and L/R Parotis). For the next 10 patients (11-20th) atlas contours were generated with both MultiA and SingleA, followed by manual corrections (MultiCor, SingleCor). For the remaining patients (21-30th) the extended atlas (consisting of 1-20th cases with "Ref" contour) was used to generate the same set of OARs. Time required for Ref, Multi, MultiCor ( $T_{MultiCor}$ ), Single, SingleCor ( $T_{SingleCor}$ ) were measured and compared using t-test. Delineations (Ref vs. Multi, MultiCor and Single, SingleCor) were compared using relative Dice Similarity Coefficient (DSC), Jaccard index (JI), commonly contoured volumes (CCV) and 95% of the Hausdorff distance (HD95%). Baseline vs. extended atlas performance was compared using two sided t-test with  $p < 0.05$  significance level.

### Results

MultiA outperformed in 57.5 % of the volumetric parameters the SingleA with significantly lower  $T_{Cor}$  as well (11min:19sec vs. 15:20,  $p < 0.001$ ) (Table1-2). By increasing the number of atlas cases a >7 min gain per patient (8:37 vs. 15:57,  $p < 0.001$ ) was achieved. Time saving ( $T_{MultiCor} - T_{SingleCor}$ ) did not differ between ideal and clinical population ( $p = 0.66$ ) and became more pronounced with advanced atlases (4:00 vs. 7:20,  $p < 0.001$ ). The extended atlas did not improve delineation performance compared to baseline atlas.

AtlasSet	Significant difference (No of metrics, %)		No significant difference (No of metrics, %)	
	MultiA better	SingleA better	MultiA better	SingleA better
MultiA vs. SingleA	92/160 (57.5)	1/160 (0.5)	30/160 (19)	37/160 (22)
Basic vs. Advanced	Basic	Adv.	Basic	Adv.
	0	5/320 (2)	0	1/320 (0.3)
per software, per stage				
			155/320 (48)	159/320 (49.7)
T1-2, N0-1 vs. T3-4, N2+	T1-2	$\geq T3, N+$	T1-2+	$\geq T3, N+$
per software	4 (2.5)	3 (2)	5 (3)	0
			73 (45.5)	75 (47)

### Conclusion

ROI	Relative Dice			Relative Jaccard		
	Mirada	Smart	p-value	Mirada	Smart	p-value
Brain	0.99 (0.01)	0.94 (0.03)	<0.001	1.00 (0.01)	0.96 (0.02)	<0.001
Brainstem	1.00 (0.02)	0.97 (0.05)	0.002	1.00 (0.02)	0.98 (0.04)	<0.001
Cavum Oris	0.94 (0.14)	0.68 (0.18)	<0.001	0.95 (0.12)	0.73 (0.16)	<0.001
L Submandgland	0.75 (0.20)	0.62 (0.26)	0.001	0.79 (0.19)	0.66 (0.25)	<0.001
Left Eye	0.90 (0.15)	0.78 (0.09)	<0.001	0.92 (0.13)	0.83 (0.07)	<0.001
Left Lense	0.56 (0.48)	0.32 (0.23)	0.01	0.58 (0.42)	0.36 (0.23)	<0.001
Left OpticNerve	0.59 (0.33)	0.47 (0.21)	0.13	0.62 (0.32)	0.52 (0.21)	0.01
Left Parotis	0.94 (0.06)	0.77 (0.12)	<0.001	0.96 (0.05)	0.82 (0.09)	<0.001
Mandible	0.82 (0.41)	0.96 (0.06)	0.04	0.83 (0.4)	0.97 (0.05)	0.002
Oesophagus	0.68 (0.20)	0.57 (0.19)	0.001	0.73 (0.18)	0.63 (0.18)	<0.001
PharynxConstr	0.73 (0.57)	0.25 (0.34)	<0.001	0.75 (0.49)	0.29 (0.32)	<0.001
Pituitary gland	0.70 (0.32)	0.50 (0.30)	0.01	0.73 (0.30)	0.54 (0.30)	<0.001
R Submandgland	0.83 (0.62)	0.63 (0.20)	0.08	0.86 (0.57)	0.69 (0.18)	0.01
Right Eye	0.91 (0.11)	0.76 (0.09)	<0.001	0.93 (0.09)	0.81 (0.06)	<0.001
Right Lense	0.68 (0.86)	0.34 (0.16)	0.04	0.66 (0.72)	0.39 (0.16)	0.002
Right OpticNerve	0.49 (0.35)	0.41 (0.23)	0.32	0.52 (0.34)	0.46 (0.23)	0.05
Right Parotis	0.94 (0.10)	0.79 (0.14)	<0.001	0.95 (0.08)	0.83 (0.11)	<0.001
Spinal Cord	0.99 (0.02)	0.94 (0.07)	<0.001	1.00 (0.02)	0.95 (0.05)	<0.001
ThyroidGland	0.69 (0.24)	0.42 (0.21)	<0.001	0.72 (0.22)	0.47 (0.21)	<0.001
Trachea	0.98 (0.05)	0.68 (0.17)	<0.001	0.99 (0.04)	0.74 (0.16)	<0.001

## Conclusion

Multi-atlas compared to single-atlas achieved significantly better segmentation accuracy and time efficiency for H&N OARs. Extended atlas did not improve accuracy, however clinically relevant time sparing was observed.

## PO-1103 Introducing contrast-delayed magnetic resonance imaging in radiosurgery treatment of glioblastoma.

F. Padelli<sup>1</sup>, E. De Martin<sup>2</sup>, Y. Mardor<sup>3</sup>, D. Last<sup>3</sup>, V. Pinzi<sup>4</sup>, M.G. Bruzzone<sup>1</sup>, L. Fariselli<sup>4</sup>, V. Cuccarini<sup>1</sup>, D. Aquino<sup>1</sup>  
<sup>1</sup>Fondazione IRCCS Istituto Neurologico Carlo Besta, Neuroradiology Unit, Milan, Italy ; <sup>2</sup>Fondazione IRCCS Istituto Neurologico Carlo Besta, Health Department, Milan, Italy ; <sup>3</sup>Sheba Medical Center, Advanced Technology Center, Tel Hashomer, Israel ; <sup>4</sup>Fondazione IRCCS Istituto Neurologico Carlo Besta, Radiotherapy Unit, Milan, Italy

### Purpose or Objective

Stereotactic radiosurgery (SRS) of intracranial lesions is based on the accurate delivery of very high doses of radiation in one or a few fractions to a well-defined volume, thus effectively sparing adjacent organs at risk (OARs). Milestone of this technique is therefore the acquisition of appropriate imaging for a really optimised treatment planning. Conventional magnetic resonance imaging (MRI) may not be able to differentiate tumor / non-tumor enhancing tissues. In this study we introduce treatment response assessment maps (TRAMs) [Zach et al. Neuro Oncol. 2015], based on the concept of delayed contrast extravasation MRI, into a radiosurgery treatment planning system (TPS) for target identification purposes.

### Material and Methods

Five patients presenting with disease progression of glioblastoma multiforme (GBM), previously treated according to our clinical practice, were enrolled in this study. For all patients an irradiation theoretical target volume was defined by contouring the enhancement area on a 3D T1-weighted MRI sequence (1-mm slice thickness, contiguous slices) acquired after contrast agent intravenous injection.

TRAMs were obtained subtracting the post-contrast 3D T1-weighted images from the same MRI sequence acquired about 75 minutes after. Tumor burden was then also identified and outlined on TRAMs images, specifically processed to be imported in the TPS (Figure 1). Maintaining the target coverage maximization as primary objective (prescription dose to 95% of the target) for comparison purposes, plan optimization tests were performed in two ways for each patient: considering only the conventionally delineated target or considering only the TRAMs delineated target. The plans obtained for each patient were compared in terms of target volume and dose volume histogram (DVH) data.

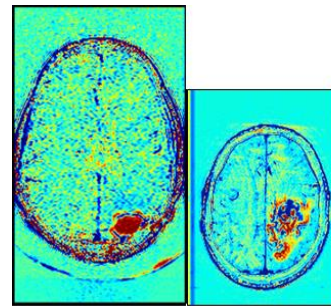


Figure 1.

Example showing one of the TRAMs used for radio-surgical planning. Difference values are colour code segmented. Blue pixels correspond to negative differences, i.e. complete contrast clearance (tumor areas), while red pixels represent the ones in which difference is positive, i.e. contrast medium accumulation during time (treatment-effect areas).

## Results

For all patients the target volume contoured on the TRAMs images was smaller than the one contoured on conventional MRI, with a fraction of approximately 1/2 in one case. Non-overlapping areas were also identified. Consequently, the percentage of healthy brain volume receiving 12 Gy was always in favour of the TRAM target case, with a reduction from 1.5 to 5%. Doses to other OARs adjacent to the target were also reduced.

## Conclusion

The addition of delayed contrast extravasation MRI information in the identification of the radiosurgery treatment target can affect the planning optimisation process in the re-irradiation scenario of relapsing glioblastoma multiforme. Further investigations on the actual clinical impact of this imaging modality seems appropriate.

## PO-1104 Implementing an automated target delineation service in multi-institutional environment in Finland

J. Heikkilä<sup>1</sup>, H. Virsunen<sup>1</sup>, L. Voutilainen<sup>1</sup>, K. Vuolukka<sup>1</sup>, A. Nevantaus<sup>2</sup>, M. Haatanen<sup>2</sup>, L. Sailas<sup>3</sup>, J. Seppälä<sup>1</sup>  
<sup>1</sup>Kuopio University Hospital, Centre of Oncology, Kuopio, Finland ; <sup>2</sup>Central Finland Central Hospital, Department of Radiotherapy, Jyväskylä, Finland ; <sup>3</sup>North Karelia Central Hospital, Department of Radiotherapy, Joensuu, Finland

### Purpose or Objective

According to many publications there are remarkable variations in radiotherapy (RT) target delineation. These publications conclude that interobserver variability in target delineation is the biggest source of uncertainty in RT process, potentially inducing systematic errors in radiation dose delivery. In some cases, this uncertainty could have an impact on clinical outcome of individual patients. [1]

Different tools to reduce variability in target volume delineation has been studied, such as training, guidelines, and autosegmentation methods. In this study we implemented fully automated target delineation service into multi-institutional environment, which should decrease the interobserver variability.

### Material and Methods

The developed delineation service consists of the following components (Fig 1): pseudonymization gateway in a hospital network, Ensemble integration platform between the hospital and delineation service,



interobserver variation in RTQA feedback and allow meaningful interpretation of RTQA results with associated outcomes. RTQA should implement prospective TVD review to identify deviations that require modification prior to treatment delivery.

---

**Poster: RTT track: Treatment planning and dose calculation / QC and QA**

---

**PO-1106 Comparison of hybrid IMRT techniques for breast SIB irradiation**

C. Van den Beemd<sup>1</sup>, J. Penninkhof<sup>1</sup>, N. Holtzer<sup>1</sup>, M. Baaijens<sup>1</sup>, B. Heijmen<sup>1</sup>  
<sup>1</sup>Erasmus MC, Radiotherapy, Rotterdam, The Netherlands

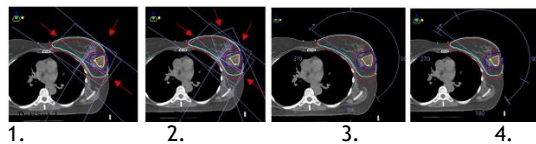
**Purpose or Objective**

Intensity modulated radiotherapy (IMRT) significantly reduces target dose heterogeneity in curative breast treatments. However, it is associated with an increase in whole body exposure to low doses from scattered and leakage radiation, and the reproducibility of the planned dose distributions during delivery (robustness) may become more challenging. To mitigate these problems, hybrid IMRT has been proposed, combining open fields with an overall low dose contribution of IMRT. This study compares four different techniques for hybrid planning of simultaneous integrated boost (SIB) treatment, using either a static-gantry Dynamic Multi-Leaf Collimation (DMLC) or VMAT beams in combination with two open beams.

**Material and Methods**

Plans were created for a dose prescription of 45.57 Gy to the whole breast and 55.86 Gy to the tumor bed volume in 21 fractions. All hybrid techniques employed two open tangential beams encompassing the whole breast, together contributing at least 70-80% of the prescribed dose. This dose was used as bias dose in optimization of the full dose while adding 1) three DMLC beams (hDMLC3), 2) four DMLC beams (hDMLC4), 3) one partial arc of 200 degrees (hVMAT1), or 4) three partial arcs (hVMAT3: 30, 200, 30 degrees). See Figure 1 for graphical presentations of the four treatment approaches.

Figure 1: Beam arrangements of the DMLC/VMAT beams in the four investigated hybrid techniques.



Five patients were included with scans both in breath hold and in free breathing. Target coverage, dosimetric parameters for organs at risk, conformity indexes and delivered Monitor Units are evaluated. All plans were created using Monaco version 5.11.01 (Elekta AB, Stockholm). **Results**

Relative rankings of the hybrid approaches were similar for free breathing and breath hold planning CT-scans. For all patients, target coverage and homogeneity in the 4 hybrid approaches were clinically acceptable and comparable. The best conformality was always observed with VMAT. For the organs at risk hybrid plans with DMLC fields were superior to VMAT. Particularly the mean dose to the contralateral lung and contralateral breast was higher for VMAT plans with average differences of 0.6 Gy and 0.5 Gy, respectively. Differences between three or four DMLC beams were clinically insignificant. The hybrid DMLC technique with three beams (hDMLC3) resulted in the lowest amount of MU (374 MU), compared to 408 MU for hDMLC4, 426 MU for hVMAT1 and 593 MU for hVMAT3, respectively.

**Conclusion**

Because of lower doses in the organs at risk, hybrid DMLC plans are preferred over hybrid VMAT plans. The differences between three or four DMLC beams were small in this study. During the clinical implementation we found that in some individual cases the use of four DMLC beams resulted in a better plan quality, in particular the conformality. Therefore, the use of four DMLC beams is preferred and currently used in our clinic.

**PO-1107 Institutional experience of adaptation from IMRT to VMAT in post-operative cases of carcinoma tongue**

K. Jain<sup>1</sup>, P. Patel<sup>2</sup>  
<sup>1</sup>GCRI- civil hospital - Ahmedabad, Radiotherapy, Ahme, India ; <sup>2</sup>GCRI, Radiotherapy, Ahmedabad, India

**Purpose or Objective**

Intensity modulated radiation therapy (IMRT) and volumetric modulated arc therapy (VMAT) are being used for treatment of head and neck cancers with discrepancy regarding superiority of one technique over the other. Our aim was to analyse various dosimetric parameters of IMRT and VMAT plans, to compare between the two techniques for treatment of operated cases of Ca. Tongue

**Material and Methods**

The study included 50 patients of IMRT and 50 patients of VMAT with patients matched with respect to the pathological stage and volume of PTV to minimise selection bias. Following parameters were assessed for comparison: Target coverage Dose to Organ at Risk (OAR), conformity index (CI) Homogeneity index (HI) Monitor Unit (MU) delivered Treatment time

**Results**

There was no significant difference regarding PTV coverage, HI and CI in both plans ( $p > 0.05$ ). Significantly more MUs were delivered in IMRT with average difference of about 30% more MUs as compared to VMAT ( $p < 0.001$ ). Treatment delivery time was reduced by around 8.5 +/- 4 minute for VMAT. No significant difference was found in dose to OAR like larynx, Parotid, brain stem and pharyngeal constrictor muscles. Spinal cord maximum dose was about 1 +/- 0.4 Gy less in VMAT plans.

**Conclusion**

VMAT is emerging as mainstream treatment option for various sites like pelvis, lung and head and neck. No sufficient data is available for a specific sub site in head and neck cancers. In our study, we found that both VMAT and IMRT plans had comparable coverage of PTV. Sparing of OAR was marginally better with VMAT. But there was marked reduction in treatment delivery time with VMAT. Risk of intrafraction motion was reduced with VMAT with improved patient compliance. VMAT has become an institutional policy for patients of Ca. Tongue receiving adjuvant radiotherapy at our centre. We are exploring role of VMAT in other sub sites too.

**PO-1108 Comparison of VMAT plans for spine SABR according to optimization algorithm PRO and PO**

S. Son<sup>1</sup>  
<sup>1</sup>Seoul national university hospital, Radiation Oncology, Seoul, Korea Republic of

**Purpose or Objective**

To evaluate the quality of volumetric modulated arc therapy (VMAT) plans for stereotactic ablative radiotherapy (SABR) by optimization algorithm of progressive Resolution Optimizer (ver.13. 7.16, PRO) and Photon Optimizer (ver.13.7.16, PO).

**Material and Methods**

20 cases of VMAT plans for spine SABR were retrospectively selected for this study. For each case, 2 kinds of VMAT plans with coplanar 2 full arcs were generated using Eclipse (Ver.13.7) and optimized with 2 different optimization algorithms the PRO and PO

respectively. Every condition was applied identically to both plans except optimization algorithms for fair comparison. The dose distributions were calculated using the AcurosXB (ver.13.7) with the calculation grid of 0.2 cm. All VMAT plans were normalized that the target volume irradiated by 18Gy the prescription dose ( $V_{100\%}$ ) would be 80%. For organs at risk (OARs),  $D_{10\%}$ , of spinal cord, dose received at 0.03 cc of spinal cord ( $D_{0.03cc}$ ) and mean dose to the spinal cord were calculated. The homogeneity indices (HIs) of target volumes and total monitor units (MUs) for each VMAT plan were calculated. High-definition MLC<sup>TM</sup> (HD MLC) and 10 MV flattening filter free (FFF) photon beams of TrueBeam STx<sup>TM</sup> were used for VMAT plans.

#### Results

The average values of  $D_{10\%}$ ,  $D_{0.03cc}$  and mean dose to spinal cord of PRO plans were  $896.62 \pm 59.66$  cGy,  $1004.67 \pm 65.70$  cGy,  $619.83 \pm 67.23$  cGy and PO were  $981.2 \pm 76.89$  cGy,  $1116.3 \pm 80.94$  cGy,  $655.01 \pm 64.87$  cGy, respectively. ( $p < .001$ ) The average value of HIs of PRO plans were  $1.13 \pm 0.09$  while that was  $1.17 \pm 0.1$  for PO plans, showing better homogeneity of target volumes. ( $p < .001$ ) The average values of total MU of PRO and PO plans were  $6146 \pm 576.79$  and  $5156 \pm 627.29$ , respectively. ( $p < .001$ )

#### Conclusion

Using PRO with higher MU for spine SABR VMAT plans are showing better results for the spinal cord doses while maintaining better target volume coverage as PO.

#### PO-1109 Plan quality and treatment time comparison between DCA and VMAT for cranial SRT

Y. Kato<sup>1</sup>, D. Watanabe<sup>1</sup>, R. Wakabayashi<sup>1</sup>, M. Inohira<sup>1</sup>, S. Itoya<sup>1</sup>, J. Okubo<sup>1</sup>, K. Miyamoto<sup>1</sup>, S. Shimizu<sup>2</sup>, Y. Oshiro<sup>2</sup>  
<sup>1</sup>Tsukuba Medical Center Hospital, Radiological Technology, Tsukuba, Japan ; <sup>2</sup>Tsukuba Medical Center Hospital, Radiation Oncology, Tsukuba, Japan

#### Purpose or Objective

Dynamic conformal arc therapy (DCA) and intensity modulated radiotherapy (IMRT) are major techniques of cranial stereotactic radiotherapy (SRT). Some reports have suggested that IMRT using step and shoot and dynamic techniques improved dose concentration and homogeneity, but increases low dose area and treatment time compared to DCA. In this study, we compare DCA and volumetric modulated arc therapy (VMAT) techniques for cranial IMRT, and compare dosimetry parameters and treatment time.

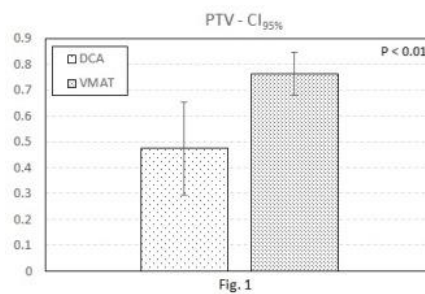
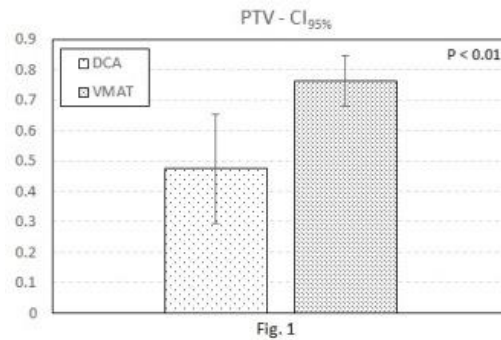
#### Material and Methods

Each 10 clinically-used treatment plans with DCA and VMAT for a single brain metastatic lesion were randomly selected for this study. The DCA treatment was re-planned with VMAT techniques, therefore total of 30 treatment plans were evaluated. In the DCA plans, 6 non-coplanar arcs with couch rotations ranged from  $285^\circ$  to  $75^\circ$  generally spaced at  $30^\circ$  interval were used. In the VMAT plans, 4-arcs with couch rotation ranged from  $270^\circ$  to  $45^\circ$  spaced at  $45^\circ$  interval were used. Conformity index (CI) and homogeneity indexes (HI) were calculated to compare dosimetry for target lesion, and V10 was calculated to evaluate low dose extent. The objective for each plan was to mean dose of the PTV covered by 100% of prescribed dose while minimizing the dose to the normal brain. All plans were generated using a single isocenter. A dose of 42 Gy in 7 fraction was prescribed and normalized to the isocenter. CI and HI were compared between clinically used DCA and VMAT. Also between clinically used and re-planned plan for each patient, CI, HI, and V10 were compared. Actual value was evaluated for treatment time.

#### Results

In comparison of the clinically-used plans, the mean CI was  $0.479 \pm 0.177$  and  $0.773 \pm 0.095$  for DCA and VMAT, respectively ( $p < 0.01$ ), and the mean HI was  $1.585 \pm 0.321$  and  $1.172 \pm 0.046$  for DCA and VMAT, respectively ( $p <$

$0.01$ ) (Fig.1). Also in the comparison of the plans of each patients, better CI and HI were observed in VMAT plans (CI:  $0.582 \pm 0.193$  vs.  $0.810 \pm 0.087$ ,  $p < 0.01$ , HI:  $1.237 \pm 0.150$  vs  $1.121 \pm 0.045$   $p < 0.05$ ). V10 was  $14.57\% \pm 8.02\%$  and  $17.24\% \pm 9.32$  respectively ( $p = 0.35$ ) for DCA and VMAT, respectively. The mean treatment time was 4 minutes 53 seconds ( $\pm 1.4$  seconds) and 3 minutes 56 seconds ( $\pm 2.8$  seconds) for DCA and VMAT, respectively ( $p < 0.01$ ) (Fig.2).



#### Conclusion

VMAT significantly improved dose concentration and homogeneity to the target compared to DCA and reduced treatment time. Also, there was no significant difference in low dose spreading.

#### PO-1110 CT-based HDR brachytherapy for salvage prostate cancer: the way to avoid or delay hormonal treatment

N. Dunnewold<sup>1</sup>, E. Kouwenhoven<sup>1</sup>, P. Koper<sup>1</sup>, S. Van den Berg<sup>1</sup>, J. Van der Klein<sup>1</sup>, J. Noordermeer<sup>1</sup>, N. Tak-Nobel<sup>1</sup>, K. Van Wingerden<sup>1</sup>, M. Mast<sup>1</sup>, H. De Jager<sup>1</sup>  
<sup>1</sup>Haaglanden Medical Center, Radiotherapy, The Hague, The Netherlands

#### Purpose or Objective

Despite ongoing technical improvements, about 40% of the patients will experience a PSA relapse after external radiotherapy [1]. Many recurrences are confined to the prostate and burdensome androgen deprivation therapy is prescribed frequently. In the era of mpMRI and PSMA-PET, early local recurrences can be diagnosed and treated locally using HDR salvage brachytherapy. This treatment has been described using MRI in the operating room (OR) [2]. However, many departments do not have access to such imaging equipment, making it challenging to adopt this procedure. We describe an adapted CT-based workflow in our department.

#### Material and Methods

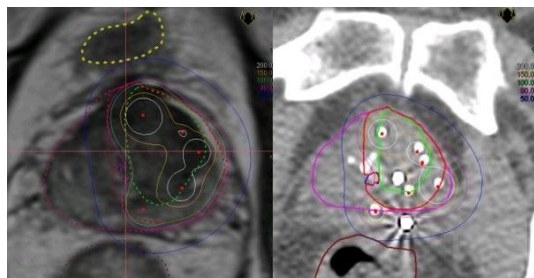
Up until now we treated eight patients, 4 - 11 years after their primary radiotherapy treatment, with mpMRI and PSMA-PET proven local recurrence. Mean PSA by diagnosis of recurrence was 3.3 ug/l (range 1.5-5.8). For GTV delineation the PSMA-PET, T2 weighted SPACE MR and T2W TSE MR were co-registered. The CTV was obtained from the GTV, applying a margin of 5mm, avoiding the urethra and removing the parts outside the prostate. Defining the

needle configuration was one of the pre-plan goals. A single dose of 19 Gy was prescribed. Sparing of critical organs (OARs) is a prerequisite, with specific focus on the urethra constraint (max. 17.7 Gy in 10% volume). A slight underdosage of the target was accepted when necessary. When the primary goal of target coverage (100% dose in 95% volume) could not be met, a second requirement (17 Gy in 90% volume) was used. The implantation of needles in the OR was performed using TRUS imaging co-registered with mpMRI / PSMA-PET. In the radiotherapy department a CT scan was obtained for catheter reconstruction and contouring of OARs. The final treatment plan was calculated. Prior to treatment the position of the needles was verified against gold fiducials or seeds from the primary treatment using fluoroscopy.

### Results

The defined workflow has proven to be feasible. The primary coverage goal for the pre-plan was met in 3 out of 8 cases. The secondary coverage requirement for the pre-plan was met in all cases. For the treatment plan these numbers are the same, except for two cases:

1. Primary goal was met at treatment, not for pre-plan;
2. Primary goal was not met; secondary requirement was met for the pre-plan but failed for treatment (13.1 Gy for 90% volume).



Example of MR-based pre-plan and CT-based treatment plan. Shown are CTV (red), GTV (green), urethra (blue), rectum (brown), bladder (yellow). Coverage was 87% and 86%, respectively.

Mean urethra dose was 16.8 Gy in 10% volume; mean rectal dose 7.9 Gy in 1 cc. Acute toxicity was limited so far with only one patient needing a catheter for 2 weeks (calculated risk: initial IPSS score 18; Qmax 6ml/s).

### Conclusion

This single fraction treatment of prostate recurrences is feasible using CT only for treatment planning. Dose constraints can be met, tumour coverage is in general adequate and acute toxicity limited. This seems to be a way to delay or even avoid androgen ablation. The treatment effect needs to be evaluated after sufficient follow-up.

1. Zumsteg et al. Eur Urol. 2015;67:1009
2. Maenhout et al. Technol Cancer Res Treat. 2017;16:1194

### PO-1111 Knowledge-Based Planning as a Real Time Review QA Feedback Tool in the TROG 1501 SPARK trial

O. Cook<sup>1</sup>, A. Moore<sup>1</sup>, R. Kaderka<sup>2</sup>, K. Moore<sup>2</sup>, P. Keall<sup>3</sup>, J. Martin<sup>4</sup>

<sup>1</sup>TROG Cancer Research, Radiation Therapy Quality Assurance, Newcastle, Australia ; <sup>2</sup>University of California- San Diego, Radiation Medicine and Applied Sciences, California, USA ; <sup>3</sup>University of Sydney, Faculty of Medicine and Health, Sydney, Australia ; <sup>4</sup>Calvary Mater Newcastle, Radiation Oncology, Newcastle, Australia

### Purpose or Objective

Quality assurance (QA) in radiotherapy (RT) clinical trials is essential to ensure protocol compliance, patient safety and trial quality. However, protocol compliance does not necessarily ensure optimal plan generation. This study aimed to demonstrate the feasibility and impact of

Knowledge-Based Planning (KBP) feedback as part of the Real Time Review (RTR) process for the Stereotactic Prostate Adaptive RT Utilising Kilovoltage Intrafraction Monitoring (SPARK) trial.

### Material and Methods

A knowledge based dose-volume histogram (DVH) estimation model and automated planning routine were created using 34 SPARK RT plans that had previously been submitted as part of the clinical trial QA program. The KBP routine was applied to 6 subsequent patients pre-treatment. A feedback report comparing the KBP generated DVH versus the initial plan was collated using a customised script and sent to the site within 24 hours. Centres were asked to review the report and decide whether they would amend their clinical plan. A patient specific questionnaire (PSQ) was also supplied to each centre to gauge implementation and interpretation of the KBP information.

### Results

Of the 6 patients, 5 were protocol compliant and 1 case was replanned due to a major protocol deviation. As a result of KBP feedback 2/5 (40%) cases which were originally protocol compliant, were nevertheless replanned (Figure 1). Protocol dose constraints for all 6 cases were calculated and an average for each metric was generated. The mean dose-volume metrics were then compared between the initial submission, resubmission and KBP generated plans. Overall, the rectum, bladder, penile bulb and urethra planning risk volume (PRV) demonstrated that an improved dose-volume relationship could be achieved compared to the initial submission and was implemented in practice for the 3 resubmitted cases. Variable results were observed for the femoral heads, demonstrating a potential dose trade off (Table 1).

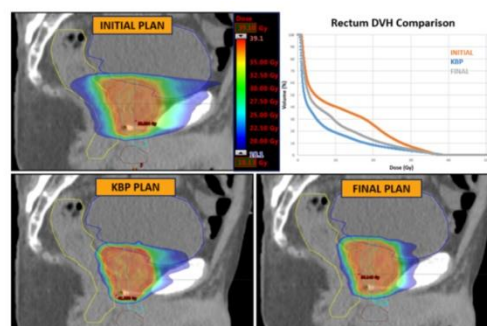


Figure 1. Case Study: Sagittal slice and DVH comparison of initial, KBP and final plans

Table 1

Organ at Risk (OAR)	Trial Constraint	Initial D (Gy)	KBP D (Gy)	Initial (Resubmitted) D (Gy)	Resubmitted D (Gy)
Rectum	V18.13Gy ≤50%	21.7 (15.5 - 29.3)	13.7 (8.8 - 20.9)	23.1 (15.5 - 29.3)	15.0 (10.8 - 19.2)
	V32.63Gy ≤5%	2.6 (0.4 - 4.9)	1.7 (0.0 - 3.9)	2.0 (0.4 - 4.8)	1.4 (0.1 - 3.1)
Bladder	V18.13Gy ≤50%	16.1 (3.5 - 29.6)	14.9 (4.4 - 32.2)	21.1 (16.1 - 29.6)	19.5 (9.4 - 32.4)
	V32.63Gy ≤10%	4.5 (0.9 - 8.5)	4.57 (1.0 - 10.4)	5.8 (3.6 - 8.5)	5.4 (2.0 - 9.1)
Urethra PRV	D0.1cc ≤38.78Gy	37.6 (37.1 - 37.9)	37.0 (36.6 - 37.7)	37.4 (37.1 - 37.5)	37.2 (37.0 - 37.5)
Penile Bulb	D0.1cc ≤36.25Gy	14.8 (3.7 - 25.3)	12.9 (3.5 - 21.5)	14.4 (4.9 - 25.3)	12.1 (6.3 - 20.1)
Lt FemHead	D0.1cc ≤30Gy	16.4 (12.1 - 20.8)	16.6 (13.6 - 21.9)	14.8 (12.1 - 16.5)	16.7 (14.3 - 20.0)
Rt FemHead	D0.1cc ≤30Gy	17.1 (14.3 - 21.9)	17.7 (14.4 - 22.0)	16.2 (14.3 - 18.1)	18.4 (13.5 - 21.5)

The PSQ was completed for 3 patients and open ended email response was received for the remaining 3 cases. All centres indicated that the KBP feedback process was a valuable tool for quality improvement in clinical trials and that the KBP feedback report provided enough information to make meaningful changes to their plans. In 2 cases the centres felt the turn-around time and resources were not sufficient if they were to make the suggested changes.

### Conclusion

KBP feedback was successfully incorporated into the RTR process for the SPARK trial and demonstrated that both improvements to and validation of plan quality for OAR dosimetry could be achieved. KBP feedback was received well with centres seeing value of this novel QA tool. There is potential to continue to build and improve on the model for future SBRT prostate trials, whether it be used as a QA

feedback tool or utilised at a site level during initial planning. Further prospective investigation of the role of KBP in radiotherapy clinical trials is planned.

---

**Poster: RTT track: Image guided radiotherapy and verification protocols**

---

**PO-1112 Real-time online matching in high dose treatments: Do RTTs perform as well as physicians?**

D. Levin<sup>1</sup>, G. Grinfeld<sup>1</sup>, V. Greenberg<sup>1</sup>, Y. Lipsky<sup>1</sup>, S. Zalmanov-Faermann<sup>1</sup>, Y. Tova<sup>1</sup>, R. Pfeffer<sup>1</sup>

<sup>1</sup>Assuta Medical Centers, Radiation Therapy, Tel Aviv, Israel

**Purpose or Objective**

For high dose per fraction treatments such as stereotactic body radiotherapy (SBRT) we require a physician to perform the pre-treatment on board imaging (OBI) match. The purpose of this study was to determine if patient matching positioning performed by radiation therapists (RTTs) is as accurate as physician matching.

**Material and Methods**

Sixteen RTTs and five physicians participated in this study. Data were collected from 113 patients totaling 324 measurements. 60 patients were treated for bone lesions, 53 for soft tissue lesions such as lung and liver. Matching was performed using kV-kV imaging for bones, and cone beam CT (CBCT) for soft tissue. All treatments were delivered on Varian linear accelerators (Palo Alto, CA). The initial match was performed by the RTTs and the shifts noted. The match was then reset, and the physician performed an independent match without prior knowledge of the RTT match. Physician couch shifts were applied for treatment. We used the Mann-Whitney rank sum test to determine statistical significance.

**Results**

The differences in patient shifts between physicians and RTTs were calculated in three translational and one rotational axis. The average vector shift was  $0.88 \pm 0.57$  cm vs.  $0.91 \pm 0.57$  cm for RTTs vs. physicians respectively. Neither the average vector nor the individual axis shifts were statistically significantly different ( $p > 0.2$ ). There was no significant difference when testing for bony or soft lesion matches separately.

**Conclusion**

RTT OBI matching is as accurate as physician matching for both bone and soft tissue lesions. Based on these results, RTTs are as qualified as physicians to perform a pre-treatment match. Thus, it may be feasible for the RTTs to perform the match, and the physician to review it off-line, without being present at the machine during treatment. When the RTT team is well-trained this does not compromise patient safety.

**PO-1113 Evaluation of CBCT and Orthogonal X-ray for Position verification in Radiotherapy of Prostate Cancer**

S.Y. Ng<sup>1</sup>, V.W.C. Wu<sup>2</sup>, G. Chiu<sup>1</sup>

<sup>1</sup>Hong Kong Sanatorium & Hospital, Department of Radiotherapy, Happy Valley, Hong Kong SAR China ; <sup>2</sup>The Hong Kong Polytechnic University, Department of Health Technology and Informatics, Hong Kong, Hong Kong SAR China

**Purpose or Objective**

In routine practice of modern radiotherapy, cancer patients are scanned with a computer tomography (CT) scanner to obtain a set of CT images (planning CT) for treatment planning. Before treatment delivery, the patient position is verified by using Cone Beam Computed Tomography (CBCT) or conventional orthogonal planar image (OPI), for matching with the planning CT or the digitally reconstructed radiographs (DRR) generated from

the planning CT respectively. This study aims at evaluating the dosimetric impact and the matching time of using CBCT and OPI in position verification in radiotherapy of prostate cancer.

**Material and Methods**

Fifteen prostate cancer patients positioned with CBCT during radiotherapy were recruited retrospectively. OPI were simulated by generating DRR using CBCT in Eclipse™ treatment planning system (Varian Medical Systems, Palo Alto, CA). 3D-3D matching on CBCT/planning CT and 2D-2D matching on simulated OPI/DRR were performed in MIM Maestro™ (MIMSoftware, inc., Cleveland, OH, USA). Time spent on matching was recorded. Treatment plans were created on CBCT and the matching results were applied for dose calculation in Eclipse™. The two position verification methods were compared in terms of Iso-displacement vector (IDV), conformity index and homogeneity index of targets, dose-volume parameters of bladder and rectum in the resultant dose distributions, and matching time consumption. The results were tested using two-tailed Wilcoxon matched pairs signed rank test with a significance level of 0.005.

**Results**

Largest differences in IDV of CBCT-based and OPI-based position verification were found in antero-posterior direction (average 1.6 mm) and were statistically significant. The conformity index and homogeneity index of targets, the dose-volume parameters of bladder and rectum of the two position verification methods are summarized in Table 1. The use of CBCT resulted in a better conformity and homogeneity of the targets. Dosimetrically, CBCT was superior than OPI in terms of bladder dose but slightly inferior than OPI in terms of rectum dose for position verification. The scatter plot for matching time consumption in CBCT-based and OPI-based position verification in each fractions are shown in Figure 1. The time spent on performing 3D-3D matching and 2D-2D matching were  $4.2 \pm 0.5$  minutes and  $1.7 \pm 0.3$  minutes respectively and the differences were statistically significant.

	CBCT-based positional verification		OPI-based positional verification		Difference is statistically significant? (p<0.005)
	Mean	SD	Mean	SD	
Conformity Index (PTV)	0.654	0.088	0.628	0.100	Yes
Homogeneity Index (Prostate bed)	0.053	0.033	0.062	0.043	Yes
D <sub>max</sub> (bladder) [Gy]	71.724	1.274	71.941	1.251	Yes
V <sub>max</sub> (bladder) [cc]	20.416	13.936	21.824	14.699	Yes
D <sub>max</sub> (rectum) [Gy]	70.573	1.477	70.079	1.883	No
D <sub>0</sub> (rectum) [Gy]	22.924	16.829	22.216	16.018	No

Table 1: Summary of the conformity and homogeneity of the targets and the dose-volume parameters of bladder and rectum in the resulted dose distributions of the CBCT-based and OPI-based positional verifications

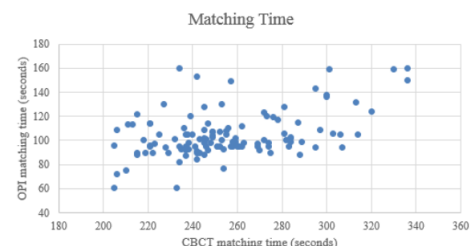


Figure 1: Scatter plot for matching time consumptions in CBCT-based and OPI-based positional verifications.

**Conclusion**

CBCT-based position verification yields a significant different IDV and is dosimetrically beneficial comparing with OPI-based position verification in radiotherapy treatment of prostate cancer. However, in addition to CBCT acquisition time, CBCT-based position verification requires a longer matching time than OPI-based position verification. Therefore, the choice of position verification

methods should depend on the availability of resources in the radiotherapy department and the tolerance on the treatment accuracy.

**PO-1114 Organ motion characterization by a novel fiducial marker in esophageal cancer radiotherapy**

H. Gripsgård<sup>1</sup>, K.C.D. Pham<sup>2</sup>, N.I. Glenjen<sup>1</sup>, G.M. Engeseth<sup>1</sup>, B.K. Abelseth<sup>1</sup>, T.H. Sulen<sup>1</sup>, U.Ø. Sølsvik<sup>3</sup>, L.B. Hysing<sup>4</sup>

<sup>1</sup>Haukeland University Hospital, Cancer Treatment and Medical Physics, Bergen, Norway ; <sup>2</sup>Haukeland University Hospital, Department of Medicine, Bergen, Norway ; <sup>3</sup>University of Bergen, Department of Global Public Health and Primary Care- Faculty of medicine, Bergen, Norway ; <sup>4</sup>Haukeland University Hospital/University of Bergen, Cancer Treatment and Medical Physics/ Department of Physics and Technology, Bergen, Norway

**Purpose or Objective**

A novel fiducial marker was explored for use in image-guided radiotherapy (IGRT) of esophageal cancer patients by characterizing inter- and intra-fractional organ motion.

**Material and Methods**

Twelve esophageal cancer patients proposed for radiotherapy participated in this pilot-study. Markers (1-6 per patient) were implanted EUS- guided prior to radiotherapy planning CT (CT<sub>p</sub>) with additional 4DCT, and the patients received IGRT (23-33 fractions, 41.4-66.0 Gy) with daily cone beam computed tomography (CBCT, n=302) and/or orthogonal planar images (2D/2D, n=61) and a repeated CT- and 4DCT the last treatment week. Marker presence, planning target volume (PTV) coverage, centroid position and extreme positions on CBCT were recorded per patient and -treatment fraction. Inter- and intra-fractional motion were characterized, in all patients and grouped according to marker location.

**Results**

At treatment end, 92% of markers visible at CT<sub>p</sub> were still present. The PTV accounted for marker variation in >95% of treatment fractions for 92% of the patients. Overall 3D inter-fractional variation was >1cm in 23% and >0.5cm in 58% of the markers. Median (IQR) intra-fractional motion of all markers was 1.2 cm (0.4 cm) in the longitudinal, 0.11 cm (0.51 cm) in the ventral and 0.0 cm (0.13 cm) in the lateral direction.

**Conclusion**

The use of the investigated fiducial marker may be beneficial for IGRT in esophageal cancer as the marker loss during radiotherapy was limited. Inter- and intra-fractional variation was substantial with largest motion in the longitudinal direction and more pronounced in the caudal part of esophagus.

**PO-1115 The UK lung SABR survey on behalf of the Advanced Radiotherapy Technologies Network**

S. Brown<sup>1</sup>, M. Beasley<sup>2</sup>, H. McNair<sup>3</sup>, C. Faivre-Finn<sup>4</sup>, K. Franks<sup>2</sup>, L. Murray<sup>5</sup>, M. Van Herk<sup>4</sup>, A. Henry<sup>5</sup>

<sup>1</sup>The Christie NHS Foundation Trust, Radiotherapy Related Research, Manchester, United Kingdom ; <sup>2</sup>Leeds Cancer Centre, Radiotherapy Research Group, Leeds, United Kingdom ; <sup>3</sup>The Institute of Cancer Research and Royal Marsden Hospital, Division of Radiotherapy and Imaging, Sutton, United Kingdom ; <sup>4</sup>University of Manchester and The Christie NHS Foundation Trust, Radiotherapy Related Research, Manchester, United Kingdom ; <sup>5</sup>University of Leeds- Leeds Institute of Cancer and Pathology and Leeds Cancer Centre, Radiotherapy Research Group, Leeds, United Kingdom

**Purpose or Objective**

SABR has become the standard of care for patients with medically inoperable early stage non-small cell lung cancer or for patients who decline surgical resection. In the UK a limited number of centres are commissioned by the NHS to provide this treatment. The delivery of large

doses of radiotherapy is potentially associated with serious toxicity. Therefore strict image guidance protocols are required to ensure its safe delivery.

To build a comprehensive national picture of SABR provision, and the barriers faced by centres attempting to implement SABR, a survey was conducted on behalf of the UK Advanced Radiotherapy Technologies Network (ART-NET). In particular this focused on image guidance and the management of anatomical changes.

The aim was to identify any variation in current practice and areas where guidance may require updating. This work will inform the development of adaptive protocols for novel treatment platforms.

**Material and Methods**

An online survey was created and piloted amongst ART-NET member centres. This was then disseminated electronically to radiotherapy service managers in all UK NHS centres.

**Results**

100% of NHS centres responded to the survey. 36/62 UK centres deliver lung SABR. Of these, 6 English centres provide SABR despite not being commissioned to do so. 56% of SABR centres treat 20-100 patients per year, and 19% treat fewer than 20 patients per year. Lack of national commissioning was cited as the most common barrier to implementation by non-SABR centres (86%). These centres will refer appropriate patients to a SABR centre, although 62% also provide conventionally fractionated radiotherapy as a local alternative.

Most variation was seen in the frequency of cone-beam computed-tomography (CBCT); 8 different CBCT workflows were reported. Only 52% of centres have a protocol for addressing the impact of anatomical changes. Overall, 67% of centres planning to develop a service in the next year believe image guidance protocols require updating. The most commonly suggested topic was the frequency of image guidance including the necessity of pre or post-treatment scans.

**Conclusion**

Eligible patients may face difficulty accessing SABR due to a lack of commissioning in some centres. This issue should be investigated further to ensure there is equitable access to lung SABR in the UK. There is a need to update existing guidelines, as evidenced by the heterogeneity in image guidance practice across the UK. These should also incorporate advice on the management of anatomical changes and will inform future adaptive IGRT protocols on novel radiotherapy platforms such as the MR-linac.

**PO-1116 Set-up in locoregional breast irradiation: reduced margins for subclavicular and axillar lymph nodes.**

M. Admiraal<sup>1</sup>, S. Hoek<sup>1</sup>

<sup>1</sup>VU University Medical Center, Department of Radiation Oncology, Amsterdam, The Netherlands

**Purpose or Objective**

For locoregional irradiation of the breast, tangential fields to the breast were combined with VMAT to achieve steep dose falloff around the lymph node levels I-IV. After introduction of this new planning technique, setup instructions were adapted with additional focus on these lymph node regions. This allowed for reduction of the CTV-PTV margin in the lymph nodes, from 8mm to 5mm in all directions.

**Material and Methods**

21 breast cancer patients with 47 sessions were included in this study. Treatment plans consisted of tangential, ventrally open fields which delivered most of the dose to the breast and VMAT which delivered most of the dose to the nodal area.

Setup was performed based on 2 orthogonal 2D kV images. Instructions for this setup defined a maximum misalignment of 5mm in the bony anatomy in the lymph node regions, and 8mm in the humeral head and the

ventral bony anatomy. Online, CBCT's and tangential MV images were acquired for verification of adequate positioning of the lymph node region and breast tissue. Offline, the CBCT's and MV portal images were used to evaluate the misalignment in lymph node regions, thoracic wall, breast and humeral head after the online match. Accurate quantification of these misalignments was obtained by performing separate CBCT matches offline, focusing on each of these structures individually.

#### Results

For lymph nodes level I-II, 2D-2D kV setup lead to adequately positioning in all sessions. Levels III-IV were adequately positioned in 46 out of 47 sessions. In only one session setup lead to a 6mm misalignment in vertical direction which was larger than the CTV-PTV margin. Average misalignments were 0.2, 0.19 and 0.13 in vertical, longitudinal and lateral directions respectively (fig.1) Verification with CBCT and tangential MV images shows that misalignment of the thoracic wall was less than 8mm in all sessions. The breast contour deviated more than 8mm in 5 out of 47 sessions. This was related to seroma change. With the tangential field approach, breast contour deviations had a minimal effect on the breast dose coverage. Misalignment of the humeral head exceeded the limit of 8mm in 5 of the 47 sessions, but none resulted misalignment of the lymph nodes larger than 5mm.

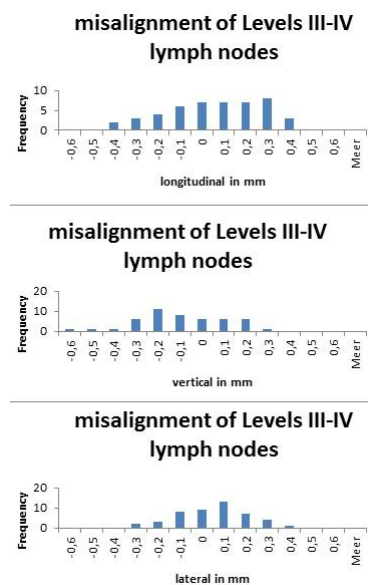


Fig 1. Misalignment of lymphnodes level III-IV after 2D/2D kV setup with additional setup instructions.

#### Conclusion

For locoregional breast irradiation, this study has shown that 2D-2D kV setup with additional setup instructions results in adequate positioning of the lymph nodes having a 5 mm CTV-PTV margin. Accurate positioning of bony anatomy in the lymph node region and the humeral head remains important, and misalignments of more than 5mm resp 8mm should result in repositioning or CBCT verification of the lymph nodes.

Poster: RTT track: Motion management and adaptive strategies

#### PO-1117 Dosimetric effect of parotid glands geometric modifications during the IMRT for NPC

W. Mnejja<sup>1</sup>, H. Daoud<sup>1</sup>, L. Farhat<sup>1</sup>, N. Fourati<sup>1</sup>, T. Sahnoun<sup>1</sup>, W. Siala<sup>1</sup>, J. Daoud<sup>1</sup>

<sup>1</sup>Hbib Bourguiba Hospital, radiotherapy, sfax, Tunisia

#### Purpose or Objective

During the treatment of nasopharyngeal carcinoma (NPC), the use of intensity modulated radiotherapy (IMRT) showed positive therapeutic effects on irradiated patients by reducing xerostomia. We proposed in this work to evaluate the dosimetric impact of parotids anatomic variation during the IMRT for the NPC.

#### Material and Methods

Patients with NPC receiving IMRT treatment were included. For each patient, a second dosimetric CT was performed at a dose of 38 Gy, which was fused with the initial planning dosimetric CT. Manual contouring of the parotids was performed on the second scanner. We recorded the volume and the isocenter position in the three planes of space (X, Y, Z), and the average dose at parotids (right and left) on both scanners. We calculated the volume percent change. Statistical mean differences were calculated using Wilcoxon signed-rank' test and SPSS 20 software was used for data analysis.

#### Results

Twenty consecutive patients were enrolled in this study. We observed a significant decrease of right parotid volume of 28 % [5%-48%] with  $p = 10^{-3}$ , and a decrease of 27.9% for the left parotid [0-54%] with  $p = 10^{-3}$ . Parotid migration averages in the medial direction (X) were of 2.1 mm [-2,3\_15](right) and 2,2 mm [-60\_2,8] (left). Moreover, It was only 0.9 mm (right) and 0.2 mm (left) in the postero-anterior direction (Y) , also in cranio-caudal direction with 0.9 mm (right) and 0.4 mm (left). Regarding dosimetry results, we observed an increase in the mean dose. This increase was significant for the left parotid with an average value of 3.23 Gy more ( $p = 0.02$ ), and no significant for the right parotid with an average value of 0.82 Gy more ( $p = 0.35$ ).

#### Conclusion

The moving of the parotid after nodal tumor falling, and also the decrease of its volume cause the migration of parotid to the higher dose areas. This can explain the dose increase noted on the scanner during treatment. It seems that a careful adaptation of the treatment plan should be considered during therapy.

#### PO-1118 Verification of new respiratory gating device for clinical use in proton therapy wobbler method

I. Maeshima<sup>1</sup>

<sup>1</sup>Suwa Red Cross Hospital, Radiation Therapy Center, Fujimi, Japan

#### Purpose or Objective

In recent years, a new respiratory synchronizer (AbchesET) has been developed that allows the patient's own respiratory control to be more easily performed. By using AbchesET, respiratory control by the patient himself can be easily and accurately reproduced by directly seeing indication of rotation angle of pointer displayed on a small monitor. In this study, we compared the conventional respiration synchronizer (ANZAI) as a comparative subject and made various investigations on the usefulness of respiratory synchronous irradiation of proton beam wobbler method using a new respiratory synchronizer (AbchesET).

#### Material and Methods

Verification of proton beam characteristics and delay time at respiratory synchronized irradiation was performed for each of ANZAI and AbchesET. With regard to verification of beam characteristics, verification of synchronism with no synchronization (stopped state) (Gate width: 12%, 25% when maximum expiration is 0%) is performed using a moving body phantom and a two dimensional detector for a rectangular radiation field. We evaluated each beam characteristics (Flatness, Symmetry, Penumbra, Field size and Dose) of the irradiation field. We also evaluated the dose distribution by gamma analysis. The breathing waveform of the moving body phantom was evaluated with respect to three types of respiration rates (Breath per

Minute, BPM), two kinds of amplitudes ( $\pm 1$  cm,  $\pm 2$  cm) with reference to the sinusoidal wave, and the breathing waveform of the respiratory synchronizer. The delay time from the gating signal until the proton beam is generated and cut off was measured by our own measurement system.

#### Results

Flatness and Symmetry were confirmed to be within  $\pm 2\%$  in all conditions, within the range of  $\pm 3\%$  with respect to the field size and Dose, and clinically no problem. On the other hand, with regard to Penumbra, BPM tends to increase as BPM gets bigger, especially with amplitude of  $\pm 2$  cm, it was necessary to consider both AbchesET and ANZAI for clinical use. Regarding the evaluation of the dose distribution, the gamma pass rate tends to decrease as the Gate width increases and as BPM increases, particularly when the amplitude is  $\pm 2$  cm, it shows a remarkable drop in the pass rate. Regarding measurement of delay time, the delay time of AbchesET is  $36.7 \pm 27.2$  msec,  $46.8 \pm 28.7$  msec with beam ON and OFF, the delay time of ANZAI is  $48.6 \pm 24.8$  msec,  $57.2 \pm 25.2$  msec with beam ON and OFF respectively there were. In beam ON and OFF, the delay time tends to be less for AbchesET, and clinical use is considered to be no problem.

#### Conclusion

Although respiratory synchronous irradiation of proton beam wobbler method using AbchesET has some use restrictions, it was confirmed that it can be sufficiently used clinically. We conclude that respiration synchronized irradiation of proton beam wobbler method with higher accuracy is achieved by using AbchesET.

#### PO-1119 Strategies to maintain bladder and rectum volumes do not reduce the GTV movement for rectal cancer rt

N. Espinosa<sup>1</sup>, A. Coral<sup>1</sup>, M. Lizondo<sup>2</sup>, J. Balart<sup>3</sup>, S. Bermejo<sup>3</sup>

<sup>1</sup>Hospital de la Santa Creu i Sant Pau, Servei de Radiofísica i Radioprotecció, Barcelona, Spain ; <sup>2</sup>Institut de Recerca Hospital de la Santa Creu i Sant Pau, Servei de Radiofísica i Radioprotecció, Barcelona, Spain ; <sup>3</sup>Hospital de la Santa Creu i Sant Pau, Servei d'Oncologia Radioteràpica, Barcelona, Spain

#### Purpose or Objective

The aim of our study is to determine whether the variability of rectal volume diminishes when bladder and rectum filling preparation instructions are followed by patients who undertake preoperative rectal IMRT.

#### Material and Methods

Thirty patients that received preoperative IMRT (45 Gy in 5 weeks, 1.8 Gy/day) for a rectal cancer between May 2016 and May 2017 were evaluated. Patients were treated in supine position. Fifteen patients without (group A) and 15 with bladder and rectum filling preparation instructions (group B) were evaluated. Group B patients were required to urinate and drink 330 mL of water 1 hour before planning CT and each fractional treatment. In addition, they were required to empty the rectum just before planning and treatment with probiotics help. Radiation was delivered using a 2100CD Clinac linear accelerator equipped with on-board Imager System (Varian). A no-action level offline setup protocol was employed by taking and averaging first 5r images and at least a cone beam CT (CBCT) was weekly undertaken. Two staff members delineated the GTV on each slice of CBCT (weekly\_GTV). As well, CBCTs were co-registered (Eclipse, Varian) with its respective planning CT to determine whether any weekly\_GTV was 1.5 cm or more beyond the planningGTV according to the Figure 1. The results were reported as percentages (%), and the chi-square test (SPSS) was used to examine differences between groups.

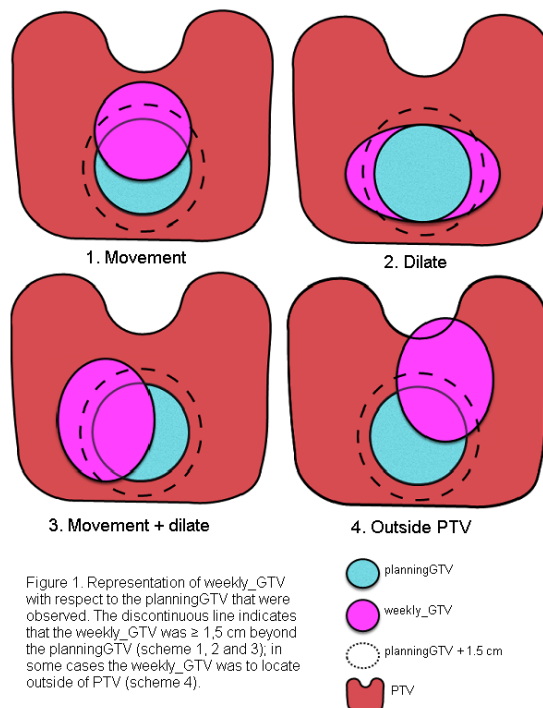


Figure 1. Representation of weekly\_GTV with respect to the planningGTV that were observed. The discontinuous line indicates that the weekly\_GTV was  $\geq 1.5$  cm beyond the planningGTV (scheme 1, 2 and 3); in some cases the weekly\_GTV was to locate outside of PTV (scheme 4).

#### Results

In total, 72 CBCT per group were analyzed. It was found that the weekly\_GTVs meet the criteria of the Figure 1 in 23 CBCTs (31.9%) of the patients in the group A and in 19 CBCTs (26.4%) of the group B; p-value = 0,58. Per each patient, weekly\_GTVs were found  $\geq 1.5$  cm beyond planningGTV in 28% times in the group A and 22.7% in the B; p-value = 0.39 (Figure 2). However, variations in the group B were lower than group A in which there were patients that every weekly\_GTV were  $\geq 1.5$  cm beyond, whereas this scenery was not found in group B (Figure 2). Weekly\_GTVs meet the criteria 4 of the Figure 1, in which GTV bring outside PTV, in 9 CBCTs (12.5%) in the group A and in 6 (8.3%) in B.

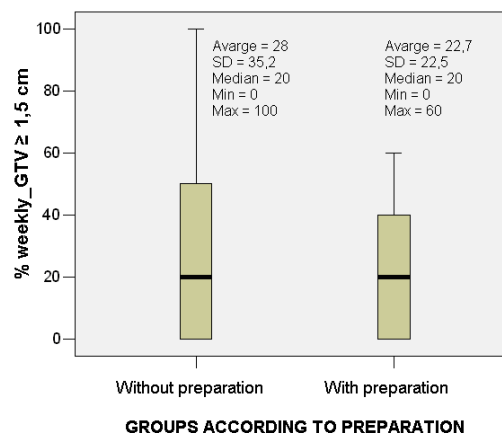


Figure 2. Percentage of the weekly\_GTV that was  $\geq 1.5$  cm of the planningGTV for each patient in particular according to the preparation. The differences are not significant (p=0,39)

### Conclusion

These findings suggest that the strategies used to keep bladder and rectum volumes constant in these cohort of patients were useless to prevent GTV movement, sometimes beyond the PTV. This conclusion could be translated to the CTV. We highly recommended complementing these strategies with daily image guided IMRT. Our results support the notion of having plan libraries for preoperative rectal IMRT to adapt anatomic variations.

### PO-1120 Deformable-image-registration-based Adaptive Radiotherapy on Halcyon's MV CBCT system

Y. Huang<sup>1</sup>, H. Qiaoqiao<sup>1</sup>, W. Hao<sup>1</sup>, Z. Yibao<sup>1</sup>

<sup>1</sup>Peking University Cancer Hospital & Institute, Department of Radiation Oncology, Beijing, China

### Purpose or Objective

Imaging dose integration as enabled by the MV CBCT system of Varian's new Linac Halcyon can avoid extra dose in image guidance as encountered by routine adaptive therapy(ART). To investigate benefits of ART on the new system, this work performed deformable image registration algorithm to reconstruct daily dose, validated the dosimetric accuracy and indicated appropriate time of replanning.

### Material and Methods

A historical Nasopharyngeal Cancer patient treated by 33 fractions of one full-arc VMAT on Halcyon was studied. CT rescanning and replanning was conducted after 18<sup>th</sup> fraction due to macroscopic tumor shrinkage. Planning CT(pCT) and replanning CT(rCT) along with pre-treatment MV CBCT images were retrieved from Varian's ARIA system. Reconstructed dose of second plan (Ddir) based on pCT deformed to MV CBCT at 21<sup>st</sup> fraction was compared with original dose of second plan(Dgold) through a 3mm/3%/10%threshold global gamma analysis. With the DIR algorithm provided by Velocity AI, pCT was registered to MV CBCT at each fraction and produced a series of reconstructed dose of initial plan (rDp), which were further accumulated and compared with original dose of initial plan (Dp) scaled with fraction number. Taking replanning into account, reconstructed dose(rDr) of second plan based on rCT deformed to MV CBCT was used in place of rDp in the last 13 fractions and further accumulated with rDp in the first 20 fractions, which was compared with accumulation of second plan's original dose (Dr) in the last 13 fractions with Dp in the first 20 fractions. The accumulated dose comparison was restricted within the FOV of MV CBCT.

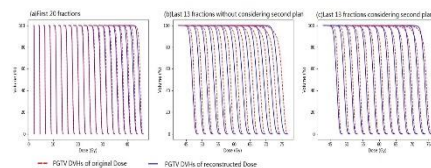
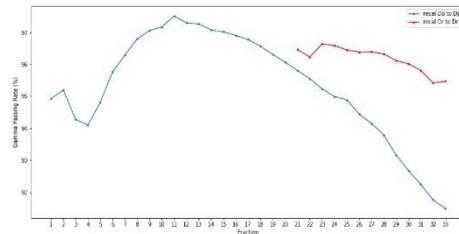
### Results

91.01% of the dose grid points fall within 3mm/3% criteria of 10% threshold global gamma analysis with Ddir as evaluation and Dgold as reference, with over half of the dose grid points having a gamma index below 0.2. Using accumulated Dp as reference and accumulated rDp as evaluated dose distribution, gamma passing rates gradually increase from 95% to 97% due to averaging of random dose deviation, but decrease continuously after one third of the course, down to less than 92% in the end, indicating when anatomical variation began to take the major effect (Fig 1). In comparison, using Dr accumulated with Dp as reference and rDr accumulated with rDp as evaluated dose distribution, gamma passing rates maintain steadily above 95% (Fig1). In accordance, planned and recalculated DVHs of PGTV are largely overlapped in the first 20 fractions(Fig2(a)) but the disparity between DVHs gradually increase without replanning in the last 13 fractions (Fig2(b)), while high DVHs similarity is maintained when considering replanning in the last 13 fractions (Fig2(c)).

### Conclusion

This study validates the dosimetric feasibility of dose reconstruction based on CT-to-MV CBCT deformable

registration as conducted on the MV CBCT imaging modality provided by Halcyon that enforces image guidance at each fraction and takes imaging dose into account, providing guidance on time to replan.



### PO-1121 Characterizing Dosimetric Uncertainties to Tumour Volume and Organs at Risk in Rectal Cancer

O. Babatunde<sup>1</sup>, S. O'Cathail<sup>1</sup>, R. Cooke<sup>1</sup>, B. George<sup>1</sup>, M. Robinson<sup>1</sup>, F. Van den Heuvel<sup>1</sup>, M. Hawkins<sup>1</sup>

<sup>1</sup>University of Oxford, Department of Oncology, Oxford, United Kingdom

### Purpose or Objective

Avoiding adverse toxicities in rectal cancer is dependent on a high degree of accuracy and precision in treatment. However, the daily uncertainty with position and volume of the Organs at Risk (OAR) can result in an increased dose to these organs. In this study, we sought to characterize the inter-fractional uncertainties in target volume and OAR, and identify factors that might predict patients most likely to benefit from online plan adaptation.

### Material and Methods

10 patients treated with neoadjuvant intensity modulating radiation therapy (IMRT) for locally advanced rectal cancer were retrospectively analysed. All patients received 45 Gy/25 fractions with simultaneous integrated boost (SIB) to GTV of 52 Gy total five times a week. The presence or absence of rectal gas was subjectively assessed in each patient's planning computed tomography (CT) and treatment cone beam CT (CBCT) images. Bladder volumes were re-contoured for all patients and mean bladder dose was calculated. Increased small bowel dose was assessed by a Yes/No criteria: Increased small bowel volume in the greater than 5Gy isodose region than was planned and/or increased dose to the small bowel of greater than 5Gy.

### Results

30% of patients had rectal gas changes in greater than 50% of their CBCT images. Rectal gas changes were as common in the first week of treatment as during the remaining treatment course and no clear time trend was seen (36% versus 32.43%). Relative change in bladder volume varied extensively between and within patients. Average planning bladder volume was 399.51 ml (SD ± 273.93) versus 254.95 (SD ± 112.49) for the treatment CBCT bladder volume. No significant difference was seen in bladder volumes over the course of treatment (t statistic: -0.382; DF: 85; p value: 0.410), but 74% of treatment volumes were smaller overall for the duration of treatment in comparison to the initial planning bladder volumes. The mean bladder dose was correlated with the relative change in bladder volume (Regression coefficient: -0.68; Pearson coefficient: -0.67; p value < 0.0001). 64% of treatment scans met criteria for increased bowel

dose. A relative decrease in bladder volume was predictive of meeting criteria for increased dose to the small bowel ( $\beta$  estimate: -4.7; Odds Ratio: 0.0091;  $p$  value < 0.0001).

#### Conclusion

Volume variability in the bladder suggests that the planned dose is not equivalent to the dose delivered to the OAR for the majority of rectal cancer patients. Early changes in bladder and rectal gas volume do not predict for late changes. Large decreases in bladder volume result in a dose increase to the bladder and small bowel dose metrics, which are in the clinically significant range.

---

#### Poster: RTT track: Patient care, side effects and communication

---

#### PO-1122 Assessment of bladder volume and urinary symptoms for patients undergoing prostate radiotherapy.

E.P.P. Pang<sup>1</sup>, M. Lian Chek Wang<sup>1,2</sup>, J.K.L. Tuan<sup>1,2</sup>, T.W.K. Tan<sup>1,2</sup>, M.L.K. Chua<sup>1,2</sup>, E.T. Chua<sup>1,2</sup>, W.S. Looi<sup>1</sup>, W.L. Nei<sup>1</sup>, A. Hussain<sup>1</sup>

<sup>1</sup>National Cancer Centre Singapore, Division of Radiation Oncology, Singapore, Singapore; <sup>2</sup>Duke-NUS, Graduate Medical School, Singapore, Singapore

#### Purpose or Objective

Patients undergoing prostate radiotherapy have been routinely instructed to obtain a full bladder. However, the achieved bladder volumes during treatment were often sub-optimal due to persistent issues of incontinence, frequency and side effects of treatment. Some of these patients undergoing radiotherapy to the prostate alone would have limited radiation dose to the bowels by default. This study investigated the achieved mean bladder volume in relations to pre-existing urinary functions and side effects after prostate (+/- seminal vesicles) volumetric modulated arc therapy (VMAT).

#### Material and Methods

20 patients undergoing prostate (+/- seminal vesicles) VMAT (74Gy, 37# over 7.5 weeks) were recruited in a prospective observational study to evaluate the impact of their urinary functions on bladder volume. 736 cone-beam computed tomography (CBCT) scans were used to analyse the overall bladder consistency. All the patients were routinely instructed to obtain a full bladder (150cm<sup>3</sup> as threshold) by voiding, followed by drinking 400-600ml of water and wait 30-60 minutes before CT simulation and daily treatment. No specific rectal preparations were given but all the patients were encouraged to empty their bowels before each procedure. Treatment planning constraints to the bladder ( $V_{70}$ ,  $V_{65}$ ,  $V_{60}$ ) were routinely evaluated based on the Quantitative Analyses of Normal Tissue Effects in the Clinic (QUANTEC) guidelines and approved for treatment. Spearman correlation test was conducted to analyse the mean bladder volume of each patient in relations to their respective urinary functions that were assessed using the Common Terminology Criteria for Adverse Events (CTCAE, version 3) and International Prostate Symptom Score (IPSS) at three timepoints (pre-treatment, mid-treatment and post-treatment). A further Mann-Whitney U test was performed to analyse pre-treatment urinary functions between the patients with mean bladder volume <150cm<sup>3</sup> versus  $\geq$ 150cm<sup>3</sup>.

#### Results

The mean (range) population bladder volume was 152.2cm<sup>3</sup> (79.6cm<sup>3</sup>-336.2cm<sup>3</sup>). There was a moderate positive correlation between mean bladder volume with incomplete bladder emptying symptoms during mid-treatment ( $r_s=0.498$ ,  $p=0.025$ ) and post-treatment urinary straining ( $r_s=0.491$ ,  $p=0.028$ ) respectively for the IPSS sub-scores. Patients with pre-treatment incontinence tend to

achieve mean bladder volume <150cm<sup>3</sup> (n=11) versus those without  $\geq$ 150cm<sup>3</sup> (n=9) ( $p=0.023$ ). However, none of the CTCAE-assessed radiation-induced urinary side effects had showed significant correlation with the mean bladder volume.

#### Conclusion

This study suggests a further review on patient selection to be instructed with full bladder protocol as those with pre-existing urinary incontinence tend to sustain a smaller mean bladder volume during treatment. In addition, patients with larger bladder volumes sustained throughout the treatment may experience post-treatment urinary straining compared to those with smaller bladder volumes.

#### PO-1123 Could patient-related outcome measures help us in radiotherapy review clinics?

M. Sivanandan<sup>1</sup>, C. Sharma<sup>1</sup>, J. Christian<sup>1</sup>

<sup>1</sup>Nottingham University Hospitals NHS Trust, Oncology and Radiotherapy, Nottingham, United Kingdom

#### Purpose or Objective

Common Terminology Criteria for Adverse Events (CTCAE) are widely used in radiotherapy (RT) review clinics to assess severity of acute toxicities. No clinical intervention is generally indicated in those with no toxicity (grade 0) or mild toxicity (grade 1) in contrast to those with higher grades of toxicity.

Toxicity symptom monitoring is an area in which patient self-reporting could be used to inform clinical interventions: If those with no or mild toxicity from RT could be identified through appropriate patient-related outcome measures (PROMs), this cohort could potentially be spared a face-to-face review in a RT clinic whereas those with greater toxicity could be identified for clinical review.

The aim of our retrospective analysis was to ascertain the frequency of different acute toxicity grades for patients on RT for breast and prostate cancer, which represent the highest volume tumour sites in our tertiary centre, to inform the usefulness of PROM collection.

#### Material and Methods

The trust's RT database was used to identify adjuvant breast RT and radical prostate RT patients between April and May 2018 inclusive. The RT clinic annotations for those patients were analysed and appropriate CTCAE toxicity grades were extracted for appropriate adverse events relevant for tumour site.

#### Results

116 breast and 91 prostate RT patients were identified. In the breast cohort, 89 patients suffered grade 0/1 toxicity at worst, representing 76.7% of the cohort. In the prostate cohort, 52 patients suffered grade 0/1 toxicity at worst, representing 57.1% of the cohort. No grade 3/4 toxicity was seen in either group. The most common grade 1 toxicity in the breast patients was skin toxicity (44.7%) and in prostate patients was urinary frequency (45.6%). Grade 2 toxicity in the breast cohort was largely skin toxicity (76.7%) and in the prostate group was principally urinary frequency (44.4%). In the prostate cohort, grade 2 toxicity was more commonly seen in those that received nodal RT versus those that did not (76.9% vs.37.2%), reaching statistical significance ( $p = 0.01$ ); in the breast cohort, grade 2 toxicity was more common in those that received a boost versus no boost (35.3% vs. 21.2%) but not reaching statistical significance ( $p=0.20$ ). Both the prostate nodal and breast boost RT groups represented a small proportion of their overall tumour-site groups (14.3% and 14.7% respectively).

#### Conclusion

A large proportion of patients on adjuvant breast and radical prostate RT suffer minimal acute toxicity with potential subgroups more likely to suffer toxicity. If appropriate PROM tools were developed to reliably identify these groups, both those who could safely avoid attending a clinic appointment in person and those who

require a face-to-face review could be identified. This serves as a proof of concept for the work of the digital technology team in our department and we are developing a pilot programme incorporating electronic PROM measures in RT review clinics to explore this in further detail.

**PO-1124 A pilot study: Utilization of PROMs in hypofractionated radiotherapy for localized prostate cancer**  
K. Crowther<sup>1</sup>, P. Shiels<sup>1</sup>, A. Cole<sup>1,2</sup>, P. Shepherd<sup>3</sup>, S. Jain<sup>1,2</sup>, D. Mitchell<sup>1</sup>

<sup>1</sup>Belfast Health and Social Care Trust, Cancer Centre-Radiotherapy, Belfast, United Kingdom ; <sup>2</sup>Queen's University, Centre for Cancer Research and Cell Biology, Belfast, United Kingdom ; <sup>3</sup>Ulster University, School of Health Sciences, Belfast, United Kingdom

**Purpose or Objective**

Patient Reported Outcome Measures (PROMS) are a useful metric in evidence-based clinical care and translational research. Recording treatment toxicities and Quality of Life (QoL) scores can provide useful information in counseling future patients to aid decision-making and inform consent. Real time PROMS have the ability to improve patient care and guide changes to therapy. Curative treatment options for prostate cancer (PCa) include prostatectomy, brachytherapy, external beam radiotherapy (EBRT) and combination therapy utilizing EBRT followed by High Dose Rate Brachytherapy (HDR-BT). There is limited published evidence comparing PROMS for modern day radiotherapy techniques. This prospective study tested the feasibility of collecting multiple PROMS from PCa patients comparing HDR-BT combined with hypofractionated EBRT (hEBRT) (Combination Group) and hEBRT alone (Monotherapy Group).

**Material and Methods**

Between June and August 2017, 20 men with localised PCa with confirmed treatment regimen, consented to participate. Ten patients received combination therapy (37.5Gy/15f + 15Gy HDR implant) and ten received hEBRT (60Gy/20f). Urinary, bowel, sexual, hormone problems and QoL were examined before, during and after treatment, using validated PROMS questionnaire methods and analysed as specified by developers. The results presented using descriptive statistics including the Mann-Whitney U test to exam statistical significance.

**Results**

All participants completed treatment without interruption with 100% response rate to PROMS. SF-12 assessed QoL and results are summarized in Figure 1.

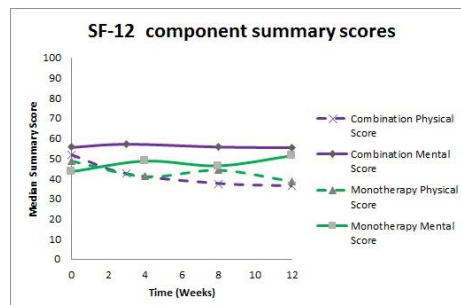


Figure 1: Summary of SF-12 results for Physical and Mental Component Summary Scores

International Index of Erectile Function (IIEF-5), International Prostate Symptom Score (IPSS) and Expanded Prostate Index Composite-26 (EPIC-26) assessed treatment-related symptoms. IIEF-5 demonstrated severe erectile dysfunction (ED) occurrence at baseline at 20% this increased to 80% at Week 12 within both groups. All men reported some ED symptoms at Week 12. IPSS results

showed a significant difference at the end of hEBRT; Combination (M=12, SD=4.58) and Monotherapy (M=20.5, SD=9.97); p=0.041. EPIC-26 results are presented in Table 1.

Time point/ Measure		Urinary Summary Score				Bowel Summary Score			
		MP	SD	MID**	P	MP	SD	MID**	P
Baseline	Combination Group	90.28	8.08	4.04	0.43	100	7.45	3.72	0.97
	Monotherapy Group	90.28	18.83	9.32		100	6.05	3.03	
Final RT	Combination Group	80.56	13.72		0.27	85.42	18.01		0.03
	Monotherapy Group	89.44	19.62			64.59	25.89		
8 weeks	Combination Group	83.87	9.14		0.45	91.87	19.48		0.17
	Monotherapy Group	77.78	16.42			75.00	16.64		
12 weeks	Combination Group	93.05	14.23		0.16	97.5	5.36		0.005
	Monotherapy Group	78.73	19.23			75.00	14.23		
Time point/ Measure		Sexual Summary Score				Hormone Summary Score			
		MP	SD	MID**	P	MP	SD	MID**	P
Baseline	Combination Group	47.00	22.93	11.47	0.05	82.50	15.71	7.86	0.82
	Monotherapy Group	20.00	13.99	7.00		82.50	16.29	9.14	
Final RT	Combination Group	31.48	25.76		0.12	82.50	21.36		0.4
	Monotherapy Group	10.42	9.99			72.50	32.16		
8 weeks	Combination Group	6.25	17.65		0.11	82.50	25.48		0.25
	Monotherapy Group	2.09	9.29			75.00	24.55		
12 weeks	Combination Group	17.34	13.82		1.0	85.00	22.81		0.79
	Monotherapy Group	15.28	11.7			80.00	18.33		

\*Median; \*\* minimum important difference (MID) = 0.5 SD

Table 1: Summary of EPIC-26 results for Combination and Monotherapy groups

Final fraction of hEBRT bowel summary demonstrated a clinically relevant difference and statistically significant difference; Combination (M=85.42, SD=18.01) and Monotherapy (M=64.59, SD=25.89); p=0.03 this remained at Week 12 (p=0.005).

**Conclusion**

This small study showed excellent patient compliance with completion of PROMS. Both treatment groups tolerated treatment well and there was minimal impact on QoL. In relation to treatment-related symptoms, the monotherapy group reported a higher incidence of bowel toxicity compared to the combination group. The feasibility of collecting multiple PROMS is evidenced in this study, streamlining of these tools into integrated technology applications and real time PROMS measurement has the ability to benefit patients and guide clinicians in adapting therapies based on individual need.

**PO-1125 Helical Tomotherapy for patients with pectus excavatum treated for early stage breast cancer.**

A. Alexandre<sup>1</sup>, P. Dominique<sup>1</sup>, F. Alain<sup>1</sup>, K. Youlia M.<sup>1</sup>

<sup>1</sup>Institut Curie Ensemble Hospitalier, Radiothérapie, Paris cedex 05, France

**Purpose or Objective**

To evaluate our experience with Helical Tomotherapy (HT) for patients with pectus excavatum (PE) who received adjuvant radiotherapy (RT) for early stage breast cancer (BC).

**Material and Methods**

A retrospective study of all patients with PE treated by intensity modulated radiation therapy (IMRT) using HT between 2009 and 2015 was done. All patients received breast +/- boost or chest wall irradiation and most of them received lymph nodes (LN) irradiation. Dose constraints for organs at risk (OAR) were defined using optimization scale developed in our Department. Evaluation of early and late toxicity was done using Common Terminology Criteria for Adverse Events v.4.0 (CTCAE).

**Results**

Between 2009 and 2015, 179 patients were treated with adjuvant HT when conventional radiation therapy techniques cannot ensure an optimal dose distribution. Among them, 40 patients (7.8%) were presented with PE and were included in this study. Median age was 53 years (range 30-75). Twenty-nine patients (72.5%) received

adjuvant or neoadjuvant anthracycline and taxans based chemotherapy and 28 (70%) received adjuvant hormonal treatment. Thirty-six patients were treated with breast conserving surgery and 4 by mastectomy. All patients were treated with normofractionated radiotherapy with a dose of 50Gy to breast or chest wall and LN if indicated, and a dose of 63Gy to the boost volume in case of indication. There were 15 (45%) left side and 22 (55%) right side breast cancers. Median follow-up was 47 months. Among them, 27 patients (67.5%) received irradiation to regional LN including internal mammary chain (IMC). Every patient received optimal CTV and PTV coverage of 96-98%. The mean heart dose was: 8Gy (3.5-10.8). The mean lung V20Gy was 20.8% (7.2-29.2) to ipsilateral lung. The contralateral breast received mean dose of 4.7Gy (2.5-6.1). The HT was well tolerated with grade 1 (67.5%) and 2 (30%) acute skin reactions and only 1 (2.5%) grade 1 acute esophagitis. Concerning late toxicities, we observed only 4 cases (10%) with grade 1 fibrosis. No cardiac toxicity was observed. At last follow-up, there was only 1 local recurrence, no regional LN recurrence and 3 (7.5%) metastatic progressions.

#### Conclusion

HT is useful for this very much selected group of PE breast cancer patients for whom the conventional radiation therapy techniques cannot ensure an optimal homogeneous dose distribution or cannot respect the constraints to the OAR. Longer follow-up is necessary to confirm and validate these results in this population of patients.

---

#### Poster: RTT track: Education and training/role development

---

#### PO-1126 Caring for Patients with Dementia Undergoing Radiation Therapy - A National Audit

A. O'Donovan<sup>1</sup>, J. Flood<sup>1</sup>

<sup>1</sup>Applied Radiation Therapy ARTT research group, Discipline of Radiation Therapy- Trinity College Dublin, Dublin, Ireland

#### Purpose or Objective

The number of people with dementia is increasing in conjunction with the rapid growth of the older aged population in many countries worldwide. More people with dementia will also be diagnosed with cancer and may require radiotherapy at some stage of their disease trajectory.

It is therefore necessary that care is taken to ensure that the Radiation Therapy (RT) department practice environment meets criteria for good practice in dealing with patients with dementia, in order to limit distress whenever practically possible.

The primary aim of this national audit was to investigate Irish radiation therapy departments, with regard to dementia care in the areas of the department environment, clinical practice and staff training.

#### Material and Methods

The audit was conducted according to recommendations for best practice and universal design, particularly those of the Society and College of Radiographers (UK), the dementia friendly environment/dwelling guidelines and the King's Fund. The audit took place between September and November 2017.

The environmental assessment consisted of six standards encompassing orientation, mobility, security, continence, wellbeing, and meaningful interaction. Clinical practice consisted of four standards encompassed by patient rights, informed consent, holistic care, and patient autonomy. Staff education and training was divided into the standards of training and support.

#### Results

Nine RT departments were assessed during the course of this audit, representing a 75% response rate. The national mean level of compliance with current best practice was 67%, with overall compliance to the recommendations for environmental layout (65%), clinical practice (67%) and staff training (75%). Only the latter achieved the target level of compliance.

#### Conclusion

Improvement of areas such as environmental layouts, dementia-focused protocols and education, as well as establishing links with other healthcare professionals and departments, will enable centres to meet all current standards of best practice in the future.

#### PO-1127 The development and initial evaluation of a simulated clinical radiotherapy training centre.

S. Ketterer<sup>1</sup>, P. Bridge<sup>1</sup>

<sup>1</sup>University of Liverpool, Department of Radiotherapy-School of Health Sciences, Liverpool, United Kingdom

#### Purpose or Objective

While the radiotherapy clinical environment is a source of rich learning for therapeutic radiography students, workload pressure on clinical departments can impact on implementation and support of placements as well as restrict learning opportunities. Although evidence supports use of simulation for health profession training, much of this is based on students' self-assessment of enjoyment and perceived learning. Simulation activities are also generally restricted to specific aspects of the role and rarely provide a realistic representation of the daily workload. This study aimed to determine the feasibility of developing and evaluating an integrated simulation placement capable of simulating a real radiotherapy department. The project also aimed to scope the potential to reduce the clinical training burden by directly replacing some clinical weeks with simulation.

#### Material and Methods

The project commenced with a scoping exercise that identified the range of activities, tasks and skills development expected from a first year student on their clinical placement. This was then mapped to existing and potential simulation equipment and activities. Realism was provided by "branding" of the facility as a virtual department, while actors and service users provided a range of patients for students to engage with. Students were randomised to simulation or clinical placement and then their assessment scores following placement were compared.

#### Results

A two-week integrated simulation placement was successfully developed and implemented within an academic department. The core simulation workspaces comprised a couch with alignment lasers, mould room water-bath, computed tomography scanner, virtual linear accelerator, radiotherapy planning consoles and virtual reality headsets. The placement was populated with academic and clinical staff, with actors and service users providing "patient" contact. Initial evaluation indicated that students valued the structured approach of the placement and the opportunity to gain familiarity with techniques in a safe unpressured environment. The ability to learn from mistakes was perceived to be particularly valuable. Comparison of assessment scores demonstrated equivalence of learning for the simulated placement. The integrated and prospectively designed learning experience of the simulation placement is targeted to the specific learning outcomes of the placement and in some cases led to improved learning compared to clinical placement.

#### Conclusion

Results from this study indicate that an integrated radiotherapy simulation placement can be undertaken successfully in a dedicated academic facility. The placement can be used to prepare students for more

efficient clinical placement and reduce overall clinical placement time. In turn, this can increase student throughput and capacity.

#### PO-1128 Clinical implementation of deformable image registration (DIR)

C. Callie<sup>1</sup>, G. Dinsdale<sup>1</sup>, S. Deshpande<sup>1</sup>, M. Jameson<sup>2</sup>  
<sup>1</sup>SWSLHD Radiation Oncology, Liverpool and Macarthur Cancer Therapy Centres, Liverpool BC, Australia ;  
<sup>2</sup>Ingham Institute for Applied Medical Research, Ingham Institute, Liverpool, Australia

##### Purpose or Objective

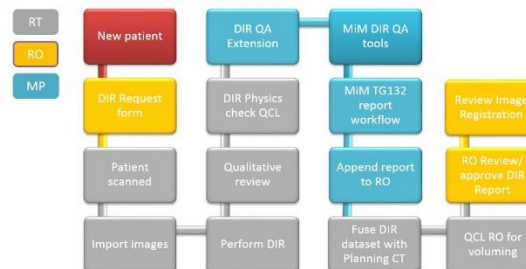
Deformable Image Registration (DIR) is increasingly used worldwide in adaptive radiotherapy scenarios, although local knowledge and experience within Australia is limited. DIR is a complex technique and clinical use of it brings many uncertainties, potential risks and workflow considerations. A recent publication by AAPM Task Group 132 (TG-132) addresses this and has outlined recommendations for mitigating potential risks associated with image registration. DIR involves significant collaboration between the multidisciplinary team, therefore governance around responsibilities and communication is essential. Training and education amongst all staff groups is also important. The purpose of this presentation is to discuss our departments' experience in the clinical implementation of DIR for pre-planning head and neck PET fusions. This will cover workflow, quality assurance procedures, education and incorporation of TG-132 recommendations.

##### Material and Methods

MiM Maestro software V6.8.5 was used as the platform to perform DIR before the data was transferred to either Tomotherapy or Pinnacle for planning. Multidisciplinary stakeholder meetings were held between radiation oncologists, radiation therapists and medical physicists to determine the clinical workflow and governance of data management. An in-house quality assurance tool was developed to provide quantitative information on the results of the deformation in user defined regions of interest. The TG-132 report was reviewed, and processes were developed to incorporate the recommendations into clinical practice. A comprehensive multidisciplinary competency package was developed to address training and education requirements. Radiation oncologists, radiation therapists and medical physicists were trained using our competency based system. The requirements to be deemed competent were tailored for each group. This involved: watching training videos, completing quizzes, performing practice cases and attending DIR registrations.

##### Results

A DIR request was developed and added to our existing booking process in Mosaic Oncology Information System. Quality Checklist items (QCLs) were created in Mosaic to manage workflow and facilitate communication between the multidisciplinary team (figure 1). Processes were established to combine the report generated from the in-house QA tool with a modified MiM report to meet TG-132 recommendations. DIR training cases were loaded into a training database. Radiation therapists performing DIR completed three cases of varying difficulty as part of their competency requirements. Radiation oncologists were required to attend three DIR registrations to understand the process before being able to freely request the technique for their patients. Medical physicists received training and performed initial cases under close supervision by lead physicist.



##### Conclusion

DIR was successfully implemented for head and neck pre-planning PET and PETCT within our department.

#### PO-1129 An analytical approach to aggregate patient workflows for system dynamics modelling of radiotherapy

J. Lindberg<sup>1</sup>, P. Holmström<sup>1</sup>, S. Hallberg<sup>2</sup>, T. Björk-Eriksson<sup>3</sup>, C. Olsson<sup>1</sup>  
<sup>1</sup>Clinical Sciences, Radiation Physics, Gothenburg, Sweden ; <sup>2</sup>Templog, Gothenburg, Sweden ; <sup>3</sup>Clinical Sciences, Oncology, Gothenburg, Sweden

##### Purpose or Objective

Radiotherapy (RT) is one of the most technology-intense and complex disciplines of health care and understanding departmental responses to various changes are challenging. Simulation models, as suggested by system dynamics (SD) methodology, can help to increase this understanding by allowing scenarios to be tested *in-silico* before implementation. To this end, patient inflows to RT departments constitutes the first step of the RT process and must be thoroughly understood to create the initial parts of the model. Patients are treated with different intents for numerous diagnoses, typically leading to over 100 possible workflows for a large RT department. In this work, we investigate to what extent individual workflows can be reduced (aggregated) based on similarity in resource use to meet requirements of an SD-model where the aim is to keep the data input format small.

##### Material and Methods

We used real data for patients treated with curative and palliative intent at a seven-linac RT department in Sweden during 2015-2016. Workflow similarity was investigated by Mann-Whitney U tests and pair-wise correlations ( $r$ ) between all possible combinations of workflows, with and without consideration of treatment intent. Similarity was quantified by averaged absolute pair-wise utility rate differences (%) and correlation analysis ( $r$ ). Grouping of workflows was decided using two customized algorithms: 1. All elements correlate with one main element; 2. All elements correlate with each other. Both algorithms were applied to five correlation coefficient cutoffs ( $r=0.75/0.80/0.85/0.90/0.95$ ) to identify the smallest number of workflow groups.

##### Results

During the studied period, 128 workflows could be distinguished for 3209 patients (72 workflows for 2094 patients with curative intent/56 workflows for 1115 patients with palliative intent). Workflow dissimilarity was indicated for <1%; correlations were generally  $\geq 0.87$  (median). For grouping algorithm 1, median number of groups (maximum within-group differences) for workflows with curative intent only were in the range 10-33 (107-279%), for palliative intent only 5-14 (37-63%), and without consideration of treatment intent 11-39 (30-123%). For grouping algorithm 2, corresponding numbers were 10-45 (41-279%), 5-39 (32-92%), and 11-87 (60-252%). Detailed results in Table 1.

TABLE 2. Results of the self-perceived didactic value of the e-learning program for experienced radiation therapists (RTT) working only with treatment delivery. The results are presented in the table below. The results are presented in the table below. The results are presented in the table below.

Grouping	Learner's self-perceived didactic value				Learner's self-perceived didactic value				Learner's self-perceived didactic value			
	Strongly agree	Agree	Disagree	Strongly disagree	Strongly agree	Agree	Disagree	Strongly disagree	Strongly agree	Agree	Disagree	Strongly disagree
1	80	10	10	10	80	10	10	10	80	10	10	10
2	80	10	10	10	80	10	10	10	80	10	10	10
3	80	10	10	10	80	10	10	10	80	10	10	10
4	80	10	10	10	80	10	10	10	80	10	10	10
5	80	10	10	10	80	10	10	10	80	10	10	10
6	80	10	10	10	80	10	10	10	80	10	10	10
7	80	10	10	10	80	10	10	10	80	10	10	10
8	80	10	10	10	80	10	10	10	80	10	10	10
9	80	10	10	10	80	10	10	10	80	10	10	10
10	80	10	10	10	80	10	10	10	80	10	10	10
11	80	10	10	10	80	10	10	10	80	10	10	10
12	80	10	10	10	80	10	10	10	80	10	10	10
13	80	10	10	10	80	10	10	10	80	10	10	10
14	80	10	10	10	80	10	10	10	80	10	10	10
15	80	10	10	10	80	10	10	10	80	10	10	10
16	80	10	10	10	80	10	10	10	80	10	10	10
17	80	10	10	10	80	10	10	10	80	10	10	10
18	80	10	10	10	80	10	10	10	80	10	10	10
19	80	10	10	10	80	10	10	10	80	10	10	10
20	80	10	10	10	80	10	10	10	80	10	10	10
21	80	10	10	10	80	10	10	10	80	10	10	10
22	80	10	10	10	80	10	10	10	80	10	10	10
23	80	10	10	10	80	10	10	10	80	10	10	10
24	80	10	10	10	80	10	10	10	80	10	10	10
25	80	10	10	10	80	10	10	10	80	10	10	10
26	80	10	10	10	80	10	10	10	80	10	10	10
27	80	10	10	10	80	10	10	10	80	10	10	10
28	80	10	10	10	80	10	10	10	80	10	10	10
29	80	10	10	10	80	10	10	10	80	10	10	10
30	80	10	10	10	80	10	10	10	80	10	10	10
31	80	10	10	10	80	10	10	10	80	10	10	10
32	80	10	10	10	80	10	10	10	80	10	10	10
33	80	10	10	10	80	10	10	10	80	10	10	10
34	80	10	10	10	80	10	10	10	80	10	10	10
35	80	10	10	10	80	10	10	10	80	10	10	10
36	80	10	10	10	80	10	10	10	80	10	10	10
37	80	10	10	10	80	10	10	10	80	10	10	10
38	80	10	10	10	80	10	10	10	80	10	10	10
39	80	10	10	10	80	10	10	10	80	10	10	10
40	80	10	10	10	80	10	10	10	80	10	10	10
41	80	10	10	10	80	10	10	10	80	10	10	10
42	80	10	10	10	80	10	10	10	80	10	10	10
43	80	10	10	10	80	10	10	10	80	10	10	10
44	80	10	10	10	80	10	10	10	80	10	10	10
45	80	10	10	10	80	10	10	10	80	10	10	10
46	80	10	10	10	80	10	10	10	80	10	10	10
47	80	10	10	10	80	10	10	10	80	10	10	10

**Conclusion**

Regardless of grouping approach, number of patient workflows could be aggregated into a tenth of initial number of individual workflows for the least conservative correlation coefficient. Even fewer groups could be identified when treatment intent was disregarded, but only for a reduced criteria of group similarity. It seems feasible to create an SD-model over the RT-process with a manageable number of aggregated workflows of high similarity without having to compromise on treatment intent. Having such reduced number of workflows at hand may also be of assistance when scheduling RT.

**PO-1130 Development of an e-learning program to enhance and maintain the knowledge of experienced RTT's**

J. Gornitzka<sup>1</sup>, L. Aksebo<sup>1</sup>, M. Torp<sup>2</sup>, V. Matthäi<sup>2</sup>, T. Bjørn<sup>3</sup>, K.L. Gottlieb<sup>3</sup>

<sup>1</sup>Odense University Hospital, Department of Oncology, Odense, Denmark ; <sup>2</sup>Unit for E-learning, Region of Southern Denmark, Vejle, Denmark ; <sup>3</sup>Laboratory of Radiation Physics, Odense University Hospital, Odense, Denmark

**Purpose or Objective**

Radiotherapy Planning (dosimetry) is a highly specialized area of radiotherapy and clinical oncology ensuring accurate radiation treatment to cancer patients. In the radiotherapy clinic it is difficult to find time and space to enhance and maintain knowledge about dosimetry among the experienced radiation therapist (RTT) working only with treatment delivery. The lack of daily experience with dosimetry can potentially impact their confidence and clinical skills. The aim of this project was to develop an e-learning program for experienced RTT's and evaluate the impact on the program on their clinical work.

**Material and Methods**

An e-learning program was developed in collaboration between department physicists, RTT's and the regional unit for e-Learning. The e-learning program consists of four main topics: Patient simulation, image modalities (CT, MR, PET), dose planning and plan control (see example in Figure 1). The four topics explain the pre-treatment-workflow.

The self-perceived didactic value of the program was evaluated using a face validated (5 persons) questionnaire with a 4-point Likert scale, which was sent immediately after completion of the e-learning. The questionnaire referred to the applicability of the course within the four topics, as well as their degree of understanding the workflow among the different professions in the pre-treatment. The evaluation questionnaire was repeated three months after to measure whether the RTT's used their knowledge from the course in their clinical work.

Figure 1: Example from the e-learning program



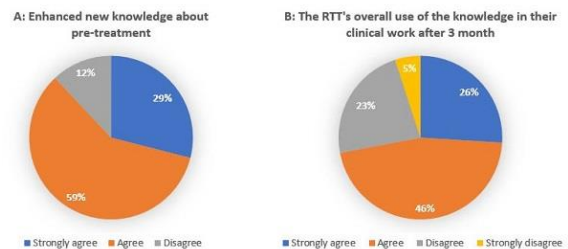
**Results**

The response rate among the 47 RTT's in the first questionnaire was 87 %, and 83 % at follow up questionnaire 3 month after.

88 % of the responders strongly agreed or agreed in having enhanced new knowledge about pre-treatment (Figure 2 A). In the group of RTT's with 0-10 years of experience (n=10) 50 % strongly agreed that the e-learning had given them new knowledge, while 22 % of the group with more than 10 years of experience (n=31) strongly agreed in this question.

The RTT's responded that the two chapters about image modalities and dosimetry had the highest applicability to their clinical work. 98 % strongly agreed or agreed to this. All responders (100 %) strongly agreed or agreed that the e-learning gave them an understanding of the pre-treatment workflow. After three months 79 % had used this knowledge about workflow in their clinical work. After three month 72 % of the responders used their overall enhanced knowledge about pre-treatment in their clinical work (Figure 2 B). In the group with 0-10 years of experience 70 % had used this knowledge, compared to 78 % in the group of the more experienced RTT's .

Figure 2: The responders evaluation of the e-learning program



**Conclusion**

The use of an e-learning program for experienced RTT's in the treatment site is an effective method to enhance and maintain knowledge about dosimetry and the pre-treatment workflow.

**Poster: RTT track: Risk management/quality management**

**PO-1131 Quality assurance of the pretreatment plan review in radiotherapy**

S.F. Huang<sup>1</sup>, H.W. Cheng<sup>1</sup>, C.Y. Kuo<sup>1</sup>, C.C. Chang<sup>1</sup>, L.J. Chen<sup>1</sup>, J.T. Tsai<sup>1</sup>

<sup>1</sup>Shuang Ho Hospital- Taipei Medical University, Radiation Oncology, New Taipei City, Taiwan



## E-posters Clinical

---

Electronic Poster: Clinical track: Head and Neck

---

### EP-1133 SPECT-CT visualization of lymph flow pattern for radiotherapy planning in patients with tongue cancer

S. Novikov<sup>1</sup>, P. Krzhivitsky<sup>2</sup>, Z. Radzhabova<sup>3</sup>, M. Girshovitch<sup>4</sup>, M. Kotov<sup>3</sup>, O. Ponomareva<sup>4</sup>, R. Nazhmutdinov<sup>3</sup>, J. Melnik<sup>4</sup>, S. Kanaev<sup>4</sup>

<sup>1</sup>Prof. N.N. Petrov Research Institute of Oncology, Radiotherapy, St. Petersburg, Russian Federation ; <sup>2</sup>Prof. N.N. Petrov Research Institute of Oncology, Nuclear Medicine, St Petersburg, Russian Federation ; <sup>3</sup>Prof. N.N. Petrov Research Institute of Oncology, Head and Neck Surgery, St Petersburg, Russian Federation ; <sup>4</sup>Prof. N.N. Petrov Research Institute of Oncology, Radiotherapy, St Petersburg, Russian Federation

#### Purpose or Objective

to determine topography of sentinel and second echelon lymph nodes (LNs) in patients with tongue cancer and to analyze how this information can be used for radiotherapy planning.

#### Material and Methods

SPECT-CT visualization of lymph-flow patterns was performed in 26 primary patients with tongue cancer. Data acquisition was started 60-90 min after 4 peritumoral injections of 99mTc-nannocolloids (100-150MBq in 0.3-0.4ml). On SPECT-CT images we determined topography of all sentinel and second echelon LNs according to standard LN levels and the type (mono- or bilateral) of lymph-flow from the primary tumour. All patients underwent MRI and US examinations of regional LNs and in 17 cases LNs status was verified by histological examination.

#### Results

In 14 of 26 (54%) patients SPECT-CT determined bilateral pattern of lymph flow from tongue cancer. In most of these patients (10 cases, 71%) distance from medial border of the primary lesions to medial sulcus of the tongue was less than 5 mm. On the contrary, in 10 of 12 patients with lateralized lesions (distance to medial sulcus 5 and more mm) we detected monolateral lymph-flow pattern.

In 5 of 26 patients (19%) LNs with 99mTc-nannocolloids uptake were localized only on Ib-IIa levels. In another 16 cases (62%) sentinel and second echelon LNs were visualized on level Ib-IIa-III. Wide distribution (Level Ia-IIa-III-IV-VI) of LNs with tracer uptake was mentioned in 5 (19%) cases.

One of 13 cT1-2N0M0 operated patients had non-signal LN metastasis on the same level with signal LN. None of the 2 non-operated cT1-2N0M0 patients demonstrated signs of LN recurrence. On the contrary, at least 2 of 9 patients with cT1-3N1M0 disease had metastatic LNs distally from LNs with uptake of radiocolloids.

In 12 patients with monolateral lymph flow we didn't find cases with contralateral LN involvement. According to proposed strategy of lymph flow guided radiotherapy we plan radiotherapy to regional LNs that localized on the same levels as visualized sentinel and second echelon LNs. Finally we compared standard treatment plans with radiation portals that were designed according to topography of sentinel and second echelon LNs. Preliminary data indicated that lymph flow guided strategy can significantly (1.6-3.3 times) reduce clinical treatment volume and absorbed dose in contralateral parotid gland (1.1-3.3 times).

#### Conclusion

In patients with tongue cancer and clinically negative regional lymph nodes SPECT-CT visualization of lymph flow from the primary tumour can significantly influence the

# E-POSTERS

decision about optimal clinical treatment volume. Lymph flow guided strategy can significantly reduce radiation exposure to normal tissues.

#### EP-1134 Head and neck cancer management in Chinese hospitals: a multicentre questionnaire-based survey

C. Wu<sup>1</sup>, G. Li<sup>2</sup>

<sup>1</sup>The 4th Affiliated Hospital of China Medical University, Radiotherapy, Shenyang, China ; <sup>2</sup>1st hospital of China Medical University, Radiotherapy, Shenyang, China

##### Purpose or Objective

The treatment modalities for head and neck cancer (HNC) may vary in different departments of tertiary care hospitals. This survey was conducted to demonstrate the diagnosis and management practices for HNC in radiotherapy (RT) and other departments (OTH) in various tertiary care hospitals across China.

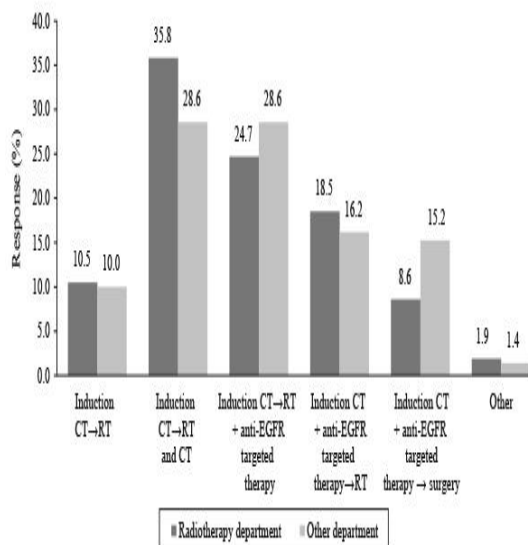
##### Material and Methods

This study was a real-world, multicentre, questionnaire-based survey, conducted between October, 2017 and January, 2018. The survey included oncologists working in RT and OTH from 100 randomly selected tertiary care hospitals in 21 cities of China. A questionnaire developed after consulting 9 HNC experts and pre-tested by 40 oncologists was used for formal investigation with oncologists. The evaluated outcomes consisted of the most prevalent stage and type of HNC treated, treatment strategies used and effect of human papilloma virus (HPV) test and age on HNC prognosis. The results were presented as percentages.

##### Results

Of the 272 oncologists included, 120 (44.1%) and 152 (55.9%) were from RT and OTH, respectively. Of the 120 oncologists from RT, 91 (75.8%) oncologists reported presence of HNC multidisciplinary team for HNC management in their institution. Locally advanced (LA) non-resectable HNC and LA HNC was the mostly reported tumour type and stage of HNC on the 1<sup>st</sup> visit of the HNC patients across both the departments as shown in Table 1. A greater percentage of oncologists reported metastatic/recurrent stage of HNC at the 1<sup>st</sup> visit in OTH compared to RT, Table 1. The most commonly treated type of HNC in both RT and OTH was reported to be nasopharyngeal carcinoma followed by laryngeal cancer, oropharyngeal and nasal cancers, as indicated in Table 1. Almost all the oncologists in RT and >93% in OTH, considered induction therapy for large tumours requiring shrinkage in HNC management. Induction chemotherapy (ICT) with radiotherapy and radiotherapy + anti EGFR were the preferred algorithms in both RT and OTH, as shown in Figure 1. In RT, 36.7% and 35.8% oncologists considered adding anti-EGFR to combined radical radiotherapy + chemotherapy during induction and post induction respectively, with a similar trend observed in OTH (40.8% and 27.6%). HPV testing was performed via polymerase chain, fluorescence in situ hybridization and P16 immunochemistry reaction as responded by 49.1%, 28.3% and 22.5% oncologists, respectively in the RT. Compared with OTH, higher proportion of oncologists in RT (64.5% Vs 81.7%) agreed that HPV testing could guide HNC prognosis. According to 75.8% and 71% oncologists in RT and OTH, age >70 years affected treatment decision for HNC. Additionally, >70% and 60% oncologists in RT and OTH agreed that patients aged >75 years had poorer prognosis for HNC than patients aged <65 years.

Figure 1. Treatment modalities followed by oncologists in radiotherapy and other departments



→ Followed by; + Combined with; CT Chemotherapy; RT Radiotherapy

Table 1. Type of tumour and stage of HNC on the first visit in Radiotherapy and other departments

Characteristics	Oncologists Response (%)	
	Radiotherapy	Other
<b>Type of tumour for HNC</b>		
Early stage and surgery allowed	15.0	17.8
Locally advanced (resectable)	15.8	19.7
Locally advanced (Non-resectable)	63.3	44.1
Metastatic/recurrent	5.8	18.4
<b>Stage of HNC</b>		
Early Stage	6.7	12.5
Locally advanced stage	90.0	69.1
Metastatic/recurrent	3.3	18.4
<b>Type of HNC</b>		
Nasopharyngeal carcinoma	70.8	60.5
Laryngeal cancer/hypopharyngeal carcinoma	18.3	25.0
Oropharyngeal cancer/oral cancer	6.7	9.9
Nasal tumour/ethmoid sinus tumour/ maxillary sinus tumour	4.2	4.6

##### Conclusion

The findings revealed that most Chinese oncologists in RT recommend induction therapy primarily with induction chemotherapy and radiotherapy which was in accordance with NCCN guidelines for HNC management.

#### EP-1135 Effect of Primary Treatment on Neck Dissection Choice in Nasopharyngeal Carcinoma Regional Failure

R. SIM<sup>1</sup>, S. Mueller<sup>2</sup>, G. Iyer<sup>3</sup>, N.C. Tan<sup>3</sup>, K.C. Soo<sup>3</sup>, R.S. Mahalakshmi<sup>3</sup>, H.K. Tan<sup>4</sup>

<sup>1</sup>Yong Loo Lin School of Medicine- National University of Singapore, Medicine, Singapore, Singapore ; <sup>2</sup>National Cancer Centre Singapore, Department of Surgical Oncology, Singapore, Singapore ; <sup>3</sup>SingHealth Duke-NUS Head and Neck Centre, Surgical Oncology, Singapore,

Singapore ; <sup>4</sup>Singapore General Hospital, Division of Surgery, Singapore, Singapore

### Purpose or Objective

Regional failure in nasopharyngeal carcinoma (NPC) is managed by salvage treatment in the form of neck dissection. Radical neck dissection (RND) is preferred over modified radical neck dissection (MRND), since it is traditionally believed to offer better long term disease control. However, with the advent of more advanced imaging modalities like high-resolution Magnetic Resonance Imaging, Computed Tomography and Positron Emission Tomography-CT scans, earlier detection is achieved. Additionally, concurrent chemotherapy also contributes to reduced tumour burden. Hence, there may be a lesser need for a RND and a greater role for MRND. With this retrospective study, the primary aim is to ascertain whether MRND, as opposed to RND, has similar outcomes and hence, whether there would be more grounds to offer a less aggressive procedure to achieve lower patient morbidity.

### Material and Methods

This is a retrospective study of 66 NPC patients treated at Singapore General Hospital between 1994 to 2016 for histologically proven regional recurrence, of which 41 patients underwent RND and 25 who underwent MRND, based on surgeon preference. The type of ND performed, primary treatment mode, adjuvant treatment and pattern of recurrence was reviewed. Overall survival (OS) was calculated using Kaplan-Meier estimate and compared.

### Results

Overall, the disease parameters such as nodal involvement and extranodal extension were comparable between the two groups. Comparing MRND and RND, the median (IQR) OS is 1.76 (0.58 to 3.49) and 2.41 (0.78 to 4.11) respectively. However, the p-value found is 0.5301 and hence not statistically significant.

### Conclusion

RND is more aggressive and has been associated with greater morbidity. Hence, with similar outcomes, MRND could be an alternative salvage procedure for regional failure in selected NPC patients, allowing similar salvage rates with lesser mortality and morbidity.

### EP-1136 Management SCC unknown primary with contemporary diagnostic and radiotherapy techniques

C. Paterson<sup>1</sup>, R. Crosbie<sup>2</sup>, P. McLoone<sup>3</sup>, D. Grose<sup>1</sup>, A. James<sup>1</sup>, C. Lamb<sup>1</sup>, M. Rizwanullah<sup>1</sup>, S. Schipani<sup>1</sup>, C. Wilson<sup>1</sup>, F. Campbell<sup>4</sup>, F. Easton<sup>4</sup>, M. Thomson<sup>5</sup>

<sup>1</sup>Beatson WoSCC, Clinical Oncology, Glasgow, United Kingdom ; <sup>2</sup>NHS Greater Glasgow & Clyde, Ear Nose & Throat, Glasgow, United Kingdom ; <sup>3</sup>Beatson WoSCC, Radiotherapy, Glasgow, United Kingdom ; <sup>4</sup>Beatson WoSCC, Nursing, Glasgow, United Kingdom ; <sup>5</sup>Beatson WoSCC, Therapeutic Radiography, Glasgow, United Kingdom

### Purpose or Objective

No randomised evidence exists to guide treatment of squamous cell carcinoma of unknown primary (SCCUP) of the head and neck. Two main approaches with RT exist - treating involved neck only (INO) or the addition of an elective dose to potential primary sites and contralateral neck (MUC). The rationale for this is to reduce the likelihood of the primary tumour emerging in the future but results in increased toxicity. If the frequency of mucosal primary emergence remains low without elective irradiation, we may be able to spare our patients toxicity. As SCCUP in the head and neck has a much better prognosis than unknown primary cancers presenting below the clavicles, the avoidance of late and permanent toxicity is highly relevant.

The purpose of our study was to evaluate disease related outcomes and doses to organs at risk in a contemporary

cohort of patients investigated, diagnosed and treated for SCCUP.

### Material and Methods

This was a retrospective cohort study; patients with histologically confirmed SCCUP with unilateral neck disease staged with FDG PET-CT scan were eligible. Patients were identified from the radiotherapy database and electronic case records reviewed.

### Results

26 patients with unilateral neck disease from SCCUP were treated between August 2012 and April 2016. All patients underwent investigation with FDG PET-CT and EUA.

All patients underwent radiotherapy with volumetric modulated arc therapy (VMAT). Patients receiving radiotherapy as primary treatment received 65Gy/30# to areas of gross disease and entirety of that involved nodal level and 54Gy/30# to areas considered at risk of harbouring microscopic disease. Patients who received adjuvant RT following neck dissection received either 65Gy/30# (if ECS) or 60Gy/30# to involved nodal levels (if no ECS) and 54Gy/30# to areas at risk of microscopic disease.

16 patients received INO RT, 10 patients received MUC RT. 37.5% patients receiving INO RT had HPV/p16 positive disease. 50% patients receiving MUC RT had HPV/p16 positive disease. 56.3% patients in INO group received concurrent cisplatin, 50% in the MUC cohort.

Median follow up is 35 months (range 30-46mths). No mucosal primaries in either group have emerged. 1 patient in the MUC group relapsed in contralateral neck in the elective dose volume. 2 year OS is 81.3% in INO group, 80% in MUC group.

Dose to organs at risk are shown in table below.

	INO RT (n=16)	MUC RT (n=10)	
Mean dose contralateral parotid	1217cGy	3336cGy	p<0.01
Maximum dose brain stem	3270cGy	4191cGy	p<0.01
Maximum dose spinal cord (	3686cGy	4023cGy	p=0.056
Mean dose midline mucosa (thyroid-cricoid)	4040cGy	5068cGy	p<0.01
Mean dose midline mucosa (cricoid - sternum)	2658cGy	3324cGy	p=0.07

### Conclusion

This is the only contemporary series of SCCUP head and neck where all patients have undergone a PET-CT as part of their diagnostic work up and the first series to compare outcomes from unilateral neck radiotherapy with VMAT to irradiating potential mucosal primary sites with VMAT.

RT to INO does not result in more frequent emergence of mucosal primary or contralateral recurrence in SCCUP. The observed reduction in dose to OARs with INO approach may represent an opportunity to spare patients toxicity and would support further research to confirm the benefits of RT to INO.

### EP-1137 DW MRI as biomarker of response during RT for intermed/high risk SCC oropharynx: a feasibility study

C. Paterson<sup>1</sup>, I. McCrea<sup>2</sup>, L. Hay<sup>3</sup>, S. Allwood-Speirs<sup>4</sup>, L. Devlin<sup>3</sup>, M. Sankaralingam<sup>4</sup>, P. McLoone<sup>1</sup>, C. Wilson<sup>1</sup>, D. Grose<sup>1</sup>, A. James<sup>1</sup>, C. Lamb<sup>1</sup>, M. Rizwanullah<sup>1</sup>, S. Schipani<sup>1</sup>, I. Nixon<sup>1</sup>, M. Thomson<sup>3</sup>, M. McJury<sup>4</sup>, J. Foster<sup>4</sup>, A. Duffton<sup>3</sup>

<sup>1</sup>Beatson WoSCC, Clinical Oncology, Glasgow, United Kingdom ; <sup>2</sup>NHS Greater Glasgow & Clyde, Radiology, Glasgow, United Kingdom ; <sup>3</sup>Beatson WoSCC, Therapeutic Radiography, Glasgow, United Kingdom ; <sup>4</sup>NHS Greater Glasgow & Clyde, Medical Physics, Glasgow, United Kingdom

### Purpose or Objective

Despite radical chemo-radiotherapy (CRT), many patients with intermediate and high risk SCC oropharynx (OPSCC) relapse. Treatment related toxicity limits further uniform

intensification across the patient group. If a predictive biomarker for outcomes from CRT can be identified during treatment, individualised and adaptive treatment strategies may be employed for the non-responders. This is the 1<sup>st</sup> study to use DW MRI for early response assessment in a specific H&N sub-site with sub-type of similar biological behaviour. The primary aim of this study was to determine the feasibility of:

- Recruiting patients
- Carrying out DW MRI at baseline (MRI 1) and week 3 (MRI 2) of RT
- Measuring apparent diffusion coefficient (ADC) on each scan for each target lesion, as per study protocol (Paterson et al, Clinical and translational radiation oncology, Feb 2017, Vol 2, p 13-18)

#### Material and Methods

Patients with intermediate and high risk, locally advanced OPSCC receiving radical RT/CRT were recruited to this prospective observational imaging study with national REC approval (15/WS/0159);

A feasibility study was carried out to evaluate the viability of this approach in the 1<sup>st</sup> 20 patients recruited.

Patients underwent DW- MRI immediately prior to #1 and #11. 3D target lesions were defined on each MRI by a clinical oncologist and radiologist. ADC measurements were obtained for each target lesion (primary and lymph nodes), and % change in ADC calculated. Disease status for each target lesion is noted at follow up at 6, 12, 18 and 24 months.

#### Results

71 patients have been recruited to date. The first 20 patients were recruited over a 10 month period, with a high recruitment up-take of approximately 62.5% of those screened.

Of the first 20 patients recruited 16 patients (80%) completed both MRI scans. One patient underwent MRI-1 and declined MRI-2 as they felt unable to tolerate the scan. Three of the patients were unable to undergo the 1<sup>st</sup> MRI therefore were withdrawn before being scanned (1-poor IV access for contrast, 1- unable to tolerate the scan, 1 - MRI unavailable).

All 16 scanned patients had at least one target lesion that was measurable on DW MRI baseline and repeat image for the purposes of recording ADC.

#### Conclusion

Feasibility work has demonstrated good patient compliance with scanning requirements and the ability to measure ADC in target lesions suggesting this is a viable approach to identifying the sub-group of non-responders during RT which may ultimately allow individualised and adaptive treatment intensification.

Establishing ADC thresholds that predict for local failure is an essential step towards using DW-MRI to improve the therapeutic ratio. The MeRInO study will help establish these thresholds in OPSCC

#### EP-1138 Non-invasive imaging of tumour hypoxia using EF5 and PET-CT in head and neck cancer: A pilot study.

E. Tran<sup>1</sup>, S. Hamilton<sup>1</sup>, D. Wilson<sup>2</sup>, F. Benard<sup>2</sup>, A. Tran<sup>2</sup>, F. Lacroix-Poisson<sup>2</sup>, E. Berthelet<sup>1</sup>, J. Wu<sup>1</sup>  
<sup>1</sup>BC Cancer Agency - Vancouver, Radiation Oncology, Vancouver, Canada ; <sup>2</sup>BC Cancer Agency - Vancouver, Functional Imaging, Vancouver, Canada

#### Purpose or Objective

Tumour hypoxia is an important factor in treatment failure following radiation therapy for locally advanced head and neck squamous cell carcinoma (HNSCC). This pilot study was performed to evaluate the feasibility of using

[18F]EF5 for clinical PET imaging of tumour hypoxia in HNSCC planned for radical radiotherapy.

#### Material and Methods

Fourteen patients with Stage III/IV HNSCC undergoing radical radiotherapy were enrolled between 2012 and 2016. Patients were imaged before and 2 weeks into radiation treatment with EF5-PET. All patients had an FDG-PET CT prior to treatment. On the FDG-PET CT, standardized uptake values (SUV) were calculated using a region of interest drawn around the target area images for suspicious primary and nodal disease separately where  $SUV = (\text{peak activity/mL in region of interest}) / (\text{injected activity/g of body weight})$ . These lesions were evaluated for corresponding EF5 uptake on the EF5-PET. After injection of 185 to 370 MBq of [18F]EF5, PET data was obtained in three-dimensional mode. EF5 uptake was evaluated by the tumour-to-muscle activity ratio (TMR) and a ratio of >1.5 was considered EF5 positive. Paired t-test was used to determine whether there is a significant difference between the TMR before and during treatment, based on the 2 EF5-PET scans.

#### Results

Median follow up was 26 months. All patients except one had 2 EF5-PET and 1 FDG-PET CT scan. One patient declined the second EF5-PET scan. No adverse pharmacological reactions were observed after administration of [18F]EF5. 13 patients had oropharyngeal cancer (all except 1 was p16+) and 1 had nasopharynx cancer. All patients were treated with 70Gy and 12 received concurrent chemotherapy.

38 lesions were identified on pre-treatment FDG-PET CT imaging. EF5 was positive in 22 lesions (8 primary and 14 nodal sites) before treatment. 6 lesions (3 primary and 3 nodal) remained EF5 positive during radiation, although 4 had borderline TMR ranging between 1.5-1.62. Mean TMR difference pre and during treatment was 0.30 for primary (p=0.003) and 0.53 for nodal disease (p=0.001). One patient with p16- oropharynx cancer had EF5+ persistence during treatment and subsequently had local recurrence. Two patients with p16+ oropharynx cancer died of metastatic relapse, one of which was EF5+ pre-treatment which did not persist during treatment.

#### Conclusion

PET imaging with [18F]EF5 was feasible, and adequate image quality was achieved. The single p16- oropharynx cancer patient who had no resolution of tumour hypoxia in lymph node and primary disease had locoregional recurrence requiring salvage therapy. In this study, EF5+ persistence was not predictive recurrence in p16+ oropharynx cancer, however, larger scale studies to further assess the impact of EF5-PET detected hypoxia prior and during radiation treatment is warranted to evaluate its ability to predict treatment outcomes.

#### EP-1139 Prognostic impact of hematological profile in oropharyngeal cancer treated with chemoradiotherapy

G. Fanetti<sup>1</sup>, D.P. Rojas<sup>2</sup>, G. Marvaso<sup>2</sup>, A. Daniela<sup>2</sup>, S. Gandini<sup>3</sup>, A. Ferrari<sup>2</sup>, C. Gobitti<sup>1</sup>, E. Palazzari<sup>1</sup>, E. Coassin<sup>1</sup>, F. Navarra<sup>1</sup>, A. De Paoli<sup>1</sup>, M. Cossu Rocca<sup>4</sup>, F. Nolè<sup>4</sup>, E. Vaccher<sup>5</sup>, M. Ansarin<sup>6</sup>, V. Lupato<sup>7</sup>, C. Furlan<sup>8</sup>, D. Ciardo<sup>2</sup>, R. Orecchia<sup>9</sup>, G. Franchin<sup>1</sup>, B.A. Jerezczek-Fossa<sup>2</sup>

<sup>1</sup>IRCCS Centro di Riferimento Oncologico CRO National Cancer Institute, Division of Radiation Oncology, Aviano, Italy ; <sup>2</sup>IRCCS European Institute of Oncology, Division of Radiation Oncology, Milano, Italy ; <sup>3</sup>IRCCS European Institute of Oncology, Division of Epidemiology and Biostatistics, Milano, Italy ; <sup>4</sup>IRCCS European Institute of Oncology, Division of Medical Oncology of Urogenital and Head and Neck Tumours, Milano, Italy ; <sup>5</sup>IRCCS Centro di Riferimento Oncologico CRO National Cancer Institute, Division of Medical Oncology and Immunorelated Tumors, Aviano, Italy ; <sup>6</sup>IRCCS European Institute of Oncology, Division of Otolaryngology and Head and Neck Surgery, Milano, Italy ; <sup>7</sup>S. Maria degli Angeli, Division of

Otolaryngology, Pordenone, Italy ; <sup>8</sup>S. Martino Hospital, Division of Radiation Oncology, Belluno, Italy ; <sup>9</sup>IRCCS European Institute of Oncology, Scientific Directorate, Milano, Italy

#### Purpose or Objective

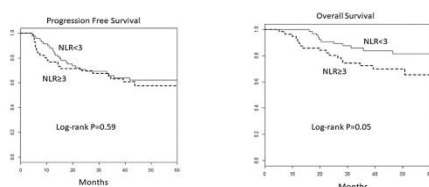
To evaluate the role of baseline neutrophil-to-lymphocyte ratio (NLR) and other haematological biomarkers and ratios such as neutrophil, lymphocyte, platelet and monocyte count, Lymphocyte to monocyte ratio (LMR) and Platelet to Lymphocyte ratio (PLR) as prognostic markers in locally advanced squamous cell carcinoma of the oropharynx (OPC) treated with definitive chemoradiotherapy (CxRT).

#### Material and Methods

A retrospective analysis of 125 patients, affected with locally advanced OPC and treated between 2010 and 2015 at two tertiary cancer centers in Northern Italy (European Institute of Oncology, Milan and Centro di Riferimento Oncologico, Aviano) was performed. Inclusion criteria were: age > 18 years, stage III or IV (TNM 7<sup>th</sup> ed.), definitive CxRT. Progression-free survival (PFS) and overall survival (OS) curves were evaluated using the Kaplan-Meier method. Multivariate Cox proportional hazard models were applied to obtain hazard ratios adjusted for other prognostic factors and confounders.

#### Results

Median age was 61 (42-77) years and 94 (75.2%) patients were male. HPV status was available in 102 (81.6%) patients and among them 77 (61.6%) pts had HPV/p16+ related OPC. Therapeutic choice consisted in sequential, concurrent and induction followed by concurrent CxRT schedule was delivered to 43 (34.4%), 71 (56.8%) and 11 (8.8%) pts, respectively. Median follow up was 50 months (range 5 - 95 months). A value of  $NLR \geq 3$  was associated with poorer OS with almost a triple increased risk of death: HR=2.7 (95%CI:1.2, 6.2; p=0.02, adjusted for age, gender, chemotherapy, HPV status and ECOG performance status). Two-years OS was 91% and 81% in pts with  $NLR < 3$  and  $\geq 3$ , respectively (figure 1). No correlation was found between other haematological parameters and prognosis. When restaged with TNM 8<sup>th</sup> edition, NLR confirmed prognostic role with increased significance (p=0.03).



#### Conclusion

In our cohort, a baseline  $NLR \geq 3$  at treatment initiation represented a negative prognostic marker for OPC treated with definitive CxRT. Our results are in line with literature data and confirmed after re-staging with last TNM. Therefore, this inexpensive and readily available marker could be considered for risk stratification of pts with locally advanced OPC.

#### EP-1140 Retropharyngeal Lymph Node Metastasis in Hypopharyngeal Carcinoma: Analysis from Multi-center Data

Z. Yin<sup>1</sup>, X. Zhang<sup>2</sup>, Y. Sun<sup>3</sup>, S. Miao<sup>4</sup>, C. An<sup>5</sup>

<sup>1</sup>Tianjin Medical University Cancer Institute & Hospital, Radiotherapy, tianjin, China ; <sup>2</sup>Cancer Institute Hospital-Chinese Academy of Medical Sciences- Peking Union Medical College, Head and Neck Surgery, Beijing, China ; <sup>3</sup>Sun Yat-sen University Cancer Center- State Key Laboratory of Oncology in South China, Department of

Radiation Oncology, Guangzhou, China ; <sup>4</sup>Harbin Medical University Cancer Hospital, Department of Radiation Oncology, Harbin, China ; <sup>5</sup>Cancer Institute Hospital-Chinese Academy of Medical Sciences- Peking Union Medical College, Department of Head and Neck Surgery, Beijing, China

#### Purpose or Objective

This study aimed to determine the prevalence, risk factors and prognostic significance of retropharyngeal lymph node (RPLN) in hypopharyngeal squamous cell carcinoma based on magnetic resonance image (MRI).

**Purpose** This study aimed to determine the prevalence, risk factors and prognostic significance of retropharyngeal lymph node (RPLN) in hypopharyngeal squamous cell carcinoma based on magnetic resonance image (MRI).

#### Material and Methods

A total of 259 patients diagnosed with hypopharyngeal carcinoma (HPC) from three cancer institutions in China were retrospectively analyzed. The MRIs of all patients were reviewed by two senior radiologists and the RPLNs were identified. 250 patients (96.5%) were male, with a median age of 57 years old (range: 36-85 years old). Most (85.7%) of them presented advanced diseases (stage III or IVa-b).

#### Results

RPLN metastasis was discovered in 44 patients (17%). Logistic analysis showed that primary tumor site located in posterior pharyngeal wall (PPW), PPW invasion, N2-3 stage, multiple LNs, and Level II/III LN involvement were identified as independent factors associated with RPLN metastasis in HPC. The rates of RPLN metastasis in patients with primary site located in posterior pharyngeal wall (PW), PW invasion and N2-3 were 37%, 30% and 31%, respectively, compared to those with primary disease located in pyriform sinus, T1-2 and N0-1 were 13%, 10% and 3%, individually. Patients with RPLN metastasis had a significant lower 5-year overall survival rate and 5-year disease-free survival rate than non-RPLN metastasis group (OS: 28% vs. 48%, p=0.001; DFS: 25% vs. 41%, p=0.040).

#### Conclusion

metastasis was not uncommon in hypopharyngeal carcinoma, with a prevalence of 17% in this study. Primary tumor located in PW, PW invasion, and cervical LN nodes are risk factors for RPLN metastasis. RPLN metastasis is a poor prognosticator for survival in hypopharyngeal carcinoma.

#### EP-1141 Marginal local failure in nasopharyngeal carcinoma in the era of intensity modulated radiotherapy

K. REN<sup>1</sup>, Z. Yin<sup>2</sup>

<sup>1</sup>Tianjin Medical University Cancer Hospital & Institute, Department of radiation oncology, Tianjin, China ; <sup>2</sup>Tianjin Medical University Cancer Hospital & Institute, Department of Radiation Oncology, Tianjin, China

#### Purpose or Objective

This study makes a detailed analysis of the initial irradiated dose of the recurrent site and local failure patterns after intensity-modulated radiation therapy (IMRT). Based on this analysis, further improvement of delineation recommendations may be made in order to reduce the local recurrence in nasopharyngeal carcinoma (NPC).

#### Material and Methods

In total, 253 newly diagnosed non-metastatic NPC patients between Jan. 2012 and Dec. 2014 were retrospectively enrolled. For patients with local failure, the location and extent of local failures were transferred to the pretreatment planning computed tomography (CT) for dosimetric analysis. The dose of radiation received by GTVr (gross tumor volume of recurrence) was calculated and analyzed with dose-volume histogram (DVH). Failures

were classified as: "in field" if 95% of GTVr was within the 95% isodose, "marginal" if 20%-95% of GTVr was within the 95% isodose, or "outside" if less than 20% of GTVr was inside the 95% isodose.

#### Results

With a median follow-up time of 61.3 months, the 5-year local control was 89%. 21 patients developed local recurrence. Dose conformity with IMRT was excellent, and the recurrence was mainly within 2 years after the first treatment. The dosimetric analysis showed that 14 failures were classified as "in-field", 1 out-field failure, and only 6 failures as "marginal" failure. Of these 6 marginal failures, two failures occurred in the site of sinus cavernosus, two presented failure in jugular foramina, one was nasal cavity and one in oropharynx wall.

#### Conclusion

In the era of intensity-modulated radiotherapy, in-field failures are still the main patterns for local recurrence. However, there were also 6 marginal recurrences, these recurrence patterns may help presenting us some data when delineation the target volume.

#### EP-1142 Death from aspiration after definitive radiotherapy for hypopharyngeal or supraglottic cancer

N. Kanayama<sup>1</sup>, T. Ikawa<sup>1</sup>, K. Wada<sup>1</sup>, T. Hirata<sup>1</sup>, M. Morimoto<sup>1</sup>, K. Hayashi<sup>1</sup>, K. Konishi<sup>1</sup>, T. Teshima<sup>1</sup>  
<sup>1</sup>Osaka International Cancer Institute, Radiation Oncology, Osaka, Japan

#### Purpose or Objective

The aim of this study is to identify predictors of death from aspiration after definitive radiotherapy for hypopharyngeal or supraglottic cancer, retrospectively.

#### Material and Methods

A total of 391 patients were identified from our institutional data base as started definitive radiotherapy for hypopharyngeal and supraglottic cancer between 2006 and 2014. Eighty one patients had a history of malignancy and 76 patients were diagnosed synchronous malignancy. Thirty six patients had a history of surgery for esophageal cancer and 16 patients received simultaneous radiotherapy for synchronous esophageal cancer. The primary site of tumor was hypopharynx in 277 patients and supraglottis in 114. Clinical stages were 0 in 4 patients, I in 28, II in 94, III in 92, IVA in 153, and IVB in 20. Treatment modality were RT alone in 157 patients, CCRT in 222, others in 12. Radiation modality were 3DCRT in 307 patients, IMRT or VMAT in 84. Median total dose was 70 Gy/35 fr. To explore the cause of death, cause of death was divided into 5 categories. "cancer under study", "other malignancy", "complication of treatment", "no data", and "others". "Others" include aspiration pneumonia and other comorbid illness. Clinical factors (age, performance status, tumor location, clinical T and N stage, treatment modality, radiation modality, history of malignancy, synchronous malignancy, history of surgery for esophageal cancer, simultaneous radiotherapy for synchronous esophageal cancer) were investigated for death from aspiration. Multivariate analysis (MA) was performed by using Cox proportional hazard model and  $p < 0.05$  was considered significant.

#### Results

Median follow up for survivors was 6.4 (range: 1.6-12.2) years. The 5-year overall survival and laryngectomy free survival rate were 61.1% and 53.9%. Fifty six patients received total laryngectomy in the follow up. The cause of total laryngectomy were severe dysphagia in 3 patients, laryngeal necrosis in 3, recurrence or second malignancy in 50. In the follow up time, 175 patients died. Eighty six patients (49%) died from "cancer under study", 46 (26%) from "other malignancy", 2 (1%) from "complication of treatment", 9 (5%) from "no data" and 32 (18%) from "others". Eleven patients died from aspiration. The median survival for patients who died from aspiration was

1.3 (range: 0.3-6.4) years. In MA, history of surgery for esophageal cancer (HR: 5.55, 95% confidence interval: 1.33-23.33;  $p = 0.019$ ) and simultaneous radiotherapy for synchronous esophageal cancer (HR: 8.07, 95% confidence interval: 1.93-33.78;  $p = 0.004$ ) was risk factor for death from aspiration.

#### Conclusion

History of surgery for esophageal cancer and simultaneous radiotherapy for synchronous esophageal cancer was predictor for death from aspiration after definitive radiotherapy for hypopharyngeal and supraglottic cancer.

#### EP-1143 Regional nodal failure after primary treatment for differentiated thyroid cancer.

G. Fanetti<sup>1</sup>, E. Borsatti<sup>2</sup>, T. Baresic<sup>2</sup>, C. Bampo<sup>2</sup>, A. Esposito<sup>3</sup>, S. Mazzone<sup>3</sup>, C. Mazzon<sup>4</sup>, E. Minatel<sup>1</sup>, A. Revelant<sup>1</sup>, S. Pisu<sup>1</sup>, A. Nappo<sup>1</sup>, E. Casanova Fuga<sup>5</sup>, M. Burello<sup>5</sup>, V. Giacomarra<sup>3</sup>, G. Franchin<sup>1</sup>, C. Gobitti<sup>1</sup>  
<sup>1</sup>IRCCS Centro di Riferimento Oncologico CRO National Cancer Institute, Division of Radiation Oncology, Aviano, Italy; <sup>2</sup>IRCCS Centro di Riferimento Oncologico CRO National Cancer Institute, Division of Nuclear Medicine, Aviano, Italy; <sup>3</sup>S. Maria degli Angeli Policlinic Hospital, Division of Otolaryngology, Pordenone, Italy; <sup>4</sup>S. Maria degli Angeli Policlinic Hospital, Unit of Endocrinology and Metabolic Diseases, Pordenone, Italy; <sup>5</sup>IRCCS Centro di Riferimento Oncologico CRO National Cancer Institute, Division of Medical Physics, Aviano, Italy

#### Purpose or Objective

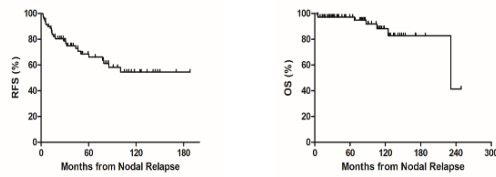
To evaluate the management and outcome of patients experiencing regional nodal relapse after primary treatment for differentiated thyroid cancer (DTC).

#### Material and Methods

Data of all consecutive patients treated at our Institution for DTIC were prospectively collected. All patients (at the time of first diagnosis) underwent surgery for non-metastatic DTC and received adjuvant radioiodine (I-131), if indicated. Regular follow up was performed with Thyroglobulin (Tg) and anti-Tg antibodies level and neck ultrasound (US). In case of suspicious nodes cytological proof of relapse was required and restaging was performed. Treatment of nodal failure was decided on the basis of clinic-radiological features and patient preference. After that, follow up examination with Tg and anti-Tg antibodies level as well as US was performed every 6 months for 5 years, then yearly. Restaging with Total body scan with radioiodine or 18FDG TC/PET was prescribed in case of raise of Tg level and/or positive US. Informed consent for use of anonymized data for scientific purpose was expressed.

#### Results

After primary treatment for DTC, 70 out of 1222 patients experienced a first locoregional nodal recurrence after a median time follow up of 21.6 months (range 3-334 months). Patients characteristics are shown in table 1. Treatment consisted of surgical (with or without adjuvant treatment) and non-surgical approach in 65 (93%) and 6 (7%) patients, respectively. Median follow up was 81.8 months (range 4.5-248.7 months) during which we observed a second relapse in 24 (34%) patients. Pattern of failure consisted in locoregional lymph nodes and distant sites in 19 (79%) and 5 (21%) patients, respectively. Five years-Relapse Free (RFS) and Overall Survival (OS) were 68.5% and 97.1%, respectively as shown in figure 1. At the last follow up 56 (80%), 7 (10%), 3 (4%) and 4 (6%) patients were alive with no evident disease, alive with disease, dead of disease and dead for other causes, respectively. Of the 6 patients treated with non-surgical approach (i.e. I-131 in 4 pts, external beam radiotherapy in 1 patient and TSH suppression in 1 case), only 1 patient had a second recurrence and is alive with disease at the last follow up. The remaining 5 patients are alive with no evident disease.



### Conclusion

Savage treatment of locoregional failure is effective in disease control for DTC with high percentage of RFS and OS. Surgical approach represents the treatment of choice. In patients ineligible for surgery, I-131 and external beam radiotherapy offered a valid option of cure.

### EP-1144 Is volumetric staging an alternative to TNM staging system in radiotherapy of tongue cancer?

M. MISZCZYK<sup>1</sup>, A. Napieralska<sup>2</sup>, B. Maciejewski<sup>2</sup>  
<sup>1</sup>Centrum Onkologii - Instytut im. Marii Skłodowskiej-Curie Oddział w Gliwicach, Zakład Planowania Radioterapii, Gliwice, Poland ; <sup>2</sup>Centrum Onkologii - Instytut im. Marii Skłodowskiej-Curie Oddział w Gliwicach, Zakład Radioterapii, Gliwice, Poland

### Purpose or Objective

The purpose of this study is to evaluate the prognostic value of GTV-based volumetric staging system (VS) in tongue cancer patients and compare it with the results based on the TNM staging system.

### Material and Methods

The clinical material consists of 99 consecutive patients with anterior or base of tongue cancers, aged 25-83 (median 58,2), treated with radical radiotherapy or chemoradiotherapy as a primary treatment between 2003 and 2014 in a single institution (Table I). The study excluded patients with prior surgical treatment. Total dose of 64-78 Gy was delivered to the primary site. Neoadjuvant chemotherapy was administered in 7 cases, concurrent in 15 cases and both in 8 cases. Efficacy of the irradiation was evaluated using 5-year overall survival (5yOS) and 3-year disease-free survival (3yDFS). The study group was retrospectively assessed using TNM classification (7<sup>th</sup> edition) and VS. The latter divided patients according to the gross tumor volume (GTV), that is combined total volume of the primary lesion and volume of metastatic lymph nodes. The cut-off values were 15 and 70 cubic centimeters (cc). The thresholds for volumetric staging system were adapted from works by Studer et al. based on retrospective analysis of the frequency of local failures in particular GTV ranges. The statistical analysis employed basic statistical tools and following tests: Shapiro-Wilk test, Kruskal-Wallis H test, Gehan-Wilcoxon test, logrank test, Chi-square test, Kaplan-Meier estimator and Cox proportional hazards model for single and multiple predictor analysis.

### Results

TNM stage groups correlated well with mean GTV ( $p=0.0001$ ) but the standard deviation of GTV overlapped between patients with TNM stage I-III, II-IVa and III-IVc. TNM stage groups did not correlate well with 5yOS ( $p=0.1$ ). At 5 years patients with TNM stage group III presented highest OS and patients with TNM stage IVa-IVc proved to have only marginally worse 5yOS than patients with TNM stage I-II disease.

The volumetric stage correlated well with 5yOS as presented in attached figure ( $p=0,001$ ). There was no statistically significant correlation between 3yDFS and TNM stage group ( $p=0,05$ ). On the other hand, VS correlated well with 3yDFS ( $p=0,0001$ ). The 3yDFS significantly decreased with increasing GTV and it was 69%

for patients with  $GTV < 15cc$ , 32% for patients with  $GTV$  between 15 and 70cc and 0% for patients with  $GTV > 70cc$ . In Cox regression model, both volumetric staging, addition of chemotherapy and BED reached statistically significant  $p$ -value of  $p=0.00006$  for VS,  $p=0.004$  for BED and  $p=0.017$  for addition of chemotherapy.

### Conclusion

Volumetric staging could be used as a prognostic tool in tongue cancer patients treated with radical radiotherapy and proved to be more accurate than TNM staging system at predicting 5-year overall survival and 3-year disease-free survival.

### EP-1145 Xerostomia and volume and CT number changes of parotid glands during IMRT for head and neck cancer

S. Ishikura<sup>1</sup>, T. Nakabayashi<sup>2</sup>, F. Kobayashi<sup>2</sup>, H. Fukuma<sup>3</sup>, Y. Shibamoto<sup>1</sup>

<sup>1</sup>Nagoya City University Graduate School of Medical Sciences, Department of Radiology, Nagoya, Japan ; <sup>2</sup>Accuray Japan K.K., Division of Tomotherapy Physics & Clinical Support, Tokyo, Japan ; <sup>3</sup>Nagoya City University Hospital, Department of Radiology, Nagoya, Japan

### Purpose or Objective

The purpose was to quantify and analyze the volume and CT number changes of the parotid glands during helical tomotherapy (HT) using daily MVCT images and to evaluate the correlation among these changes, xerostomia grades, and doses to the parotid glands.

### Material and Methods

Between September 2014 and February 2018, 34 patients (pts) with oropharyngeal squamous cell carcinoma were treated with HT at our institution. Patient characteristics were as follows: male/female, 28/6; median age, 68 years (range, 41-84); subsites anterior/lateral/posterior, 7/25/2; T1/2/3/4a, 4/17/8/5; N0/1/2a/2b/2c, 5/7/2/14/6; Stage II/III/IVA, 4/8/22. We used simultaneous integrated boost (n=18: 66 Gy/30 fr in 16; 70 Gy/35 fr in 2) and conventional cone-down boost (n=16: 70 Gy/35 fr in 13; others in 3). Therapies were induction chemotherapy (n=17: paclitaxel/cisplatin/fluorouracil, 15; others, 2) and concurrent biotherapy or chemotherapy (n=26: cetuximab, 20; cisplatin, 4; others, 2). During HT, pts underwent MVCT-guided radiotherapy at each session. We used an Accuray Precision™ research workstation with PreciseART™ Adaptive Radiation Therapy to analyze the volume and CT number changes of the parotid glands during HT. We examined correlations among the dose-volume histogram (DVH) values of the parotid glands, the volume and CT number changes for the first 20 fractions, and the grades of acute xerostomia (dry mouth, CTCAE version 4.0). For pts with a conventional cone-down boost, the DVH values of the initial plan were scaled to 70 Gy/35 fr. We analyzed the correlations of the xerostomia grades and the volume and CT number changes by box plots (significance level,  $p < 0.05$ ). We analyzed the correlations between the doses to the parotid glands and the volume and CT number changes by scatter plots and calculated correlation coefficients. This study was approved by our institutional review board.

### Results

The median follow-up was 1.2 years. The 2-year overall survival was 89%. Eight pts had acute grade 2 xerostomia; none had grade 3. Of these 8 pts, 7 had stage IV disease; 6 received induction chemotherapy, and 6 received concurrent biotherapy. The average of the median dose to the right and left parotid glands was 33.7 Gy (range, 10-63.6 Gy) and 26.2 Gy (7.6-56.9 Gy), respectively. There was no significant difference in the average of the median dose, the volume change, and CT number change between pts with grade 0-1 and 2 xerostomia. Weak-to-moderate correlations existed between the median dose to the parotid glands and both the volume change (Fig. 1,  $R =$

0.38) and CT number change (Fig. 2,  $R = 0.45$ ).

Fig. 1

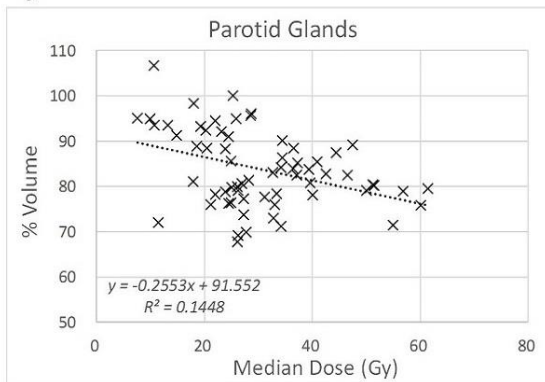
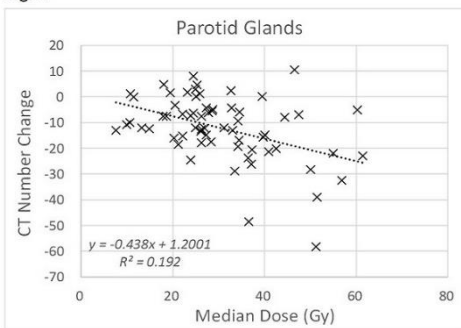


Fig. 2



### Conclusion

The volume and CT number of the parotid glands decreased as a function of the median dose to the parotid glands but were not significantly related to the grade of xerostomia. Further investigation is needed to determine if these changes would predict moderate-to-severe xerostomia and if adaptive radiotherapy could reduce acute and late toxicities.

### EP-1146 Prognostic Value of Hypoxia for Locally Advanced Hypopharynx Squamous Cell Carcinoma

F. Sert<sup>1</sup>, G. Serin<sup>2</sup>, A. Veral<sup>2</sup>, M. Esassolak<sup>1</sup>  
<sup>1</sup>Ege University Medical School&Hospital, Radiation Oncology, Izmir, Turkey; <sup>2</sup>Ege University Medical School&Hospital, Pathology, Izmir, Turkey

### Purpose or Objective

Head and neck squamous cell carcinoma (HNSCC) is the 6th common malignancy worldwide. As one of HNSCC, hypopharyngeal squamous cell carcinoma (HPSCC) only constitutes approximately 3-5% of HNSCC, but it is usually diagnosed in the advanced stage with poor treatment outcome. In the past decades, different treatment options, including surgery, chemotherapy (CT), radiotherapy (RT), and immunotherapy, have been developed and utilized for HPSCC, but any of those options could not achieve a promising results and the survival rate has not been improved significantly. We should both investigate and understand the resistance mechanisms of this group of patients in order to obtain more promising treatment outcomes. We aim to compare the relationship between the expression of hypoxia-associated marker HIF-1 $\alpha$  and proliferation with Ki-67 and clinical outcome after definitive CRT for locoregionally advanced p16 (-) HPSCC

### Material and Methods

Between January 2005 and December 2016, patients diagnosed with T3-4 HPSCC treated with curative intent by (chemo)radiation were identified using the radiation therapy. Clinicopathologic and outcomes data were

collected retrospectively. Pretreatment biopsy formalin-fixed paraffin-embedded tumor blocks were used for reevaluation in terms of related immune markers. Totally 44 patients were evaluated for this analysis. Pretreatment HIF-1 $\alpha$  and Ki-67 expressions, clinicopathologic data, and tumor volume were analyzed and compared with treatment outcomes.

### Results

Median age was 56 (range, 25-79), and 39% of them were female. Patient characteristics are shown in table 1. The median follow-up duration for all patients and surviving patients was 22.5 months (range, 4-213 months) and 93.0 months (range, 14-213 months), respectively. Ten patients (23%) developed distant metastases, and 15 (34%) had local/locoregional failure. At the time of the last follow-up, 11 patients (25%) were alive. Only 5 patients had p16 positivity, others had p16 (-) tumors. We could not find any significant effect of p16 status over treatment outcome. Median overall survival (OS), locoregional recurrence-free survival (LRFS), and metastasis-free survival (MFS) times were 24.5, 22, and 22.5 months, respectively. Two-years OS, LRFS, and MFS rates were 52%, 64%, and 75%, respectively. Ten of 44 tumor specimens were HIF-1 $\alpha$ -negative with a significantly better 5-year survival ( $92 \pm 8\%$ ) versus 34 patients who were HIF-1 $\alpha$ -positive ( $45 \pm 10\%$ ;  $p < 0.02$ ). patients with hemoglobin levels  $<12$  g/dl showed elevated HIF-1 $\alpha$  expression compared to patients with hemoglobin levels  $\geq 12$  g/dl ( $p=0.02$ ). Additionally, HIF-1 $\alpha$  correlated with Ki-67 proliferation marker ( $p = 0.01$ ).

### Conclusion

This is the first study to evaluate specifically at T3-4 HPSCC for a relationship between hypoxia-associated marker expression and clinical treatment outcomes. Pretreatment immunohistochemical HIF1 $\alpha$  and Ki67 expression are adverse prognostic factors for LRFS and OS, indicating HIF-1 $\alpha$  and Ki-67 expressions may show a more treatment resistant tumor type. However, we could not give p16 as a prognostic marker T3-4 HPSCC.

### EP-1147 Local control rate in patients with skull-base chondrosarcoma treated with particle therapy

E. D'ippolito<sup>1</sup>, A. Iannalfi<sup>1</sup>, B. Vischioni<sup>1</sup>, V. Vitolo<sup>1</sup>, M.R. Fiore<sup>1</sup>, S. Ronchi<sup>1</sup>, M. Bonora<sup>1</sup>, A. Barcellini<sup>1</sup>, R. Petrucci<sup>1</sup>, A. Mirandola<sup>1</sup>, A. Vai<sup>1</sup>, E. Mastella<sup>1</sup>, G. Viselner<sup>2</sup>, M. Ciocca<sup>1</sup>, L. Preda<sup>2</sup>, F. Valvo<sup>1</sup>, R. Orecchia<sup>1,3</sup>  
<sup>1</sup>National Center of Oncological Hadrontherapy, Radiotherapy Unit, Pavia, Italy; <sup>2</sup>National Center of Oncological Hadrontherapy, Diagnostic Image Unit, Pavia, Italy; <sup>3</sup>European Institute of Oncology, Radiation therapy Unit, Milan, Italy

### Purpose or Objective

Chondrosarcoma is a rare bone tumor that arise from the cartilage. Skull-base location is reported in about 6% of cases. The therapeutic approach to chondrosarcoma of the skull-base is still controversial and clinical experience is limited because of the relative rarity of this tumor. The aim of the study was to assess the local failure rate and overall survival (OS) of patients treated with particle therapy (Proton therapy -PT and Carbon Ion radiotherapy -CIRT) after maximal surgery or in the exclusive setting.

### Material and Methods

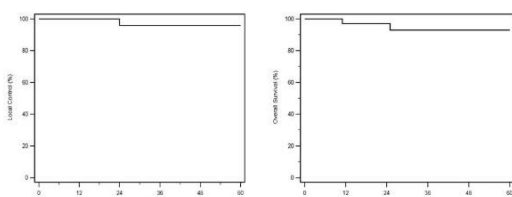
between September 2011 to May 2017 35 patients (pts) (17 male, 18 female) with a median age of 45 years (range, 13-78) with histologically proven skull-base chondrosarcoma were treated with PT or CIRT at National Center of Oncological Hadrontherapy (CNAO). 17 pts (49%) underwent previous surgery. A total of 13 pts had grade I (well differentiated), 20 pts had grade II (moderately differentiated) and 2 pts had grade III (poorly differentiated) chondrosarcoma. 6 pts had brainstem involvement, 1 pts optic pathway involvement. 17 pts were treated with CIRT, 18 pts with PT. Median gross tumor volume (GTV) was 16,4 cm<sup>3</sup> (range, 1,64 - 28,28).

Median prescribed total dose was 70,4 Gy RBE (range 66-70,4 Gy RBE) in 15-16 fractions (median 16 fractions) of 4,4 Gy RBE for CIRT, and 74 Gy RBE (range 70-74 Gy RBE) in 35-37 fractions (median 35 fractions) of 2 Gy RBE for PT. Clinical outcome (local control -LC- and overall survival -OS-) and toxicity profile (according to Common Terminology Criteria Adverse Events -CTCAE V4.03- scale) were evaluated

#### Results

The median follow-up was 34 months (range, 5-70 months). Only 1 patient had local progression 24 months after the end of the treatment. The LC rate was 97%. The 1-year, 3-year and 5-year LC rates were 100%, 96% and 96% respectively; the corresponding OS rates were 97%, 93% and 93% respectively (Fig 1). The toxicity profile was favorable. No pts developed late G4 treatment-related toxicity. G3 late toxicity occurred in 2 (5.7%) of pts: 1 case of hearing impairment and 1 case of ocular toxicity (sight reduction)

Fig.1 Local control and Overall Survival in pts with skull base chondrosarcoma treated with particle therapy



#### Conclusion

particle therapy is a safe and effective treatment in pts with chondrosarcoma of the skull-base

#### EP-1148 Long-term outcome of IMRT with simultaneous integrated boost in nasopharyngeal carcinoma

I. Linares<sup>1</sup>, M. Taberna<sup>2</sup>, J. Nogués<sup>3</sup>, R. Mesía<sup>2</sup>, D. Najjari<sup>1</sup>, J. Mases<sup>1</sup>, I. Guix<sup>1</sup>, M. Plana<sup>2</sup>, A. Lozano<sup>1</sup>  
<sup>1</sup>Institut Català d'Oncologia, Radiation Oncology, Barcelona, Spain ; <sup>2</sup>Institut Català d'Oncologia, Medical Oncology, Barcelona, Spain ; <sup>3</sup>Hospital Universitario de Bellvitge, Otorhinolaryngology, Barcelona, Spain

#### Purpose or Objective

To report the long-term clinical outcomes of nasopharynx cancer patients treated with IMRT-simultaneous integrated boost (SIB) in a non-endemic area.

#### Material and Methods

We retrospectively reviewed the data from 70 patients with non-metastatic nasopharyngeal carcinoma who received IMRT-SIB from January 2007 to December 2015. High-risk PTV was treated with a daily dose of 2.12 Gy and a total dose of 69.96Gy. Low-risk PTV was treated with a daily dose of 1.64 Gy and a total dose of 54.12 Gy. Patients received concurrent chemotherapy during the course of the RT with intravenous administration of 100 mg/m<sup>2</sup> cisplatin every 3 weeks or 30-40 mg/m<sup>2</sup> weekly. The induction chemotherapy regimen was TPF (docetaxel/cisplatin/5-fluorouracil) or PF every 3 weeks for 2-3 cycles. Post-radiation adjuvant chemotherapy with PF (two-three cycles) also was used as option treatment. We analyzed the survival outcome and late toxicity outcome (scale CTCAE v4.03).

#### Results

73% of all cases were men; median age was 51 years (range 15 - 79). Non-keratinizing carcinoma was the most common histological type (76.9%) and EBV was positive in 44 (62.9%). According to the AJCC 7<sup>th</sup> Edition staging system 94.3% of cases were locally advanced disease, stage III-IVB. Only 7 patients (10%) were treated exclusively with RT, while the rest received

chemotherapy, mainly concurrent (88.4%). 29 (41.5%) patients received induction chemotherapy. 25 (35.7%) patients received neoadjuvant and adjuvant chemotherapy. Response rate 8 weeks after ending radiotherapy were: complete response 65.7%, partial response 29.9%, stable disease 1.5% and progressive disease 2.9%. At a median follow-up of 62 months (range 4-136), 9 patients experienced local regional failure and distant metastasis occurred in 12 patients. 1-ys, 3-ys and 5- ys Disease Free Survival were 90%, 79% and 67%, respectively while 1-ys, 3-ys and 5- ys Overall Survival were 98%, 86% and 74% respectively. The most common late adverse effects were: xerostomia, dysphagia, and fibrosis. Grade 3 dental damage and xerostomia occurred in 1 case (16%) and 1 (2.1%) respectively. No case of grade IV toxicity was observed.

#### Conclusion

IMRT-SIB combined with concurrent chemotherapy or plus neoadjuvant or adjuvant chemotherapy resulted in promising rates of local regional control with acceptable rates of late side effects in patients with nasopharyngeal carcinoma.

#### EP-1149 Albumin-to-alkaline phosphatase ratio in nasopharyngeal cancer: a propensity score matching analysis

J.S. Kim<sup>1</sup>, B. Keam<sup>2</sup>, D.S. Heo<sup>2</sup>, D.H. Han<sup>3</sup>, C. Rhee<sup>3</sup>, J. Kim<sup>4</sup>, K.C. Jung<sup>5</sup>, H. Wu<sup>1</sup>

<sup>1</sup>Seoul National University Hospital, Department of Radiation Oncology, Seoul, Korea Republic of ; <sup>2</sup>Seoul National University Hospital, Department of Internal Medicine, Seoul, Korea Republic of ; <sup>3</sup>Seoul National University Hospital, Department of Otorhinolaryngology, Seoul, Korea Republic of ; <sup>4</sup>Seoul National University Hospital, Department of Radiology, Seoul, Korea Republic of ; <sup>5</sup>Seoul National University Hospital, Department of Pathology, Seoul, Korea Republic of

#### Purpose or Objective

We first analyzed the prognostic power of albumin-to-alkaline phosphatase ratio (AAPR) before radical radiotherapy (RT) in non-metastatic nasopharyngeal cancer (NPC) patients.

#### Material and Methods

The records of 170 patients with biopsy-proven, non-metastatic NPC treated by radical RT between 1998 and 2016 at our institution were retrospectively reviewed. Median follow-up duration was 50.6 months. All patients received intensity-modulated RT and cisplatin based chemotherapy before, during, or after RT. The major treatment of patients were based on concurrent chemoradiotherapy (92.4%). The AAPR was calculated by the last value of both albumin and alkaline phosphatase within 1 month immediately preceding RT. The optimal cut-off level of AAPR was determined by using *Cutoff Finder*, a web-based system. Propensity score matching (PSM) analysis was performed.

#### Results

The optimal cut-off level of AAPR was 0.4876. After PSM analysis of whole cohort, an AAPR was not related to survival outcomes. In PSM analysis for patients with locoregionally advanced nasopharyngeal cancer (LA-NPC), an AAPR  $\geq 0.4876$  was related to better overall survival (OS), progression free survival (PFS) and locoregional relapse free survival (LRRFS) (OS, HR: 0.341, 95% CI: 0.144-0.805, p=0.014; PFS, HR: 0.416, 95% CI: 0.189-0.914, p=0.029; LRRFS, HR: 0.243, 95% CI: 0.077-0.769, p=0.016, respectively).

#### Conclusion

The AAPR, inexpensive and readily derived from a routine blood test, could be an independent prognostic factor for patients with LA-NPC. And it might help physicians determine treatment plans by identifying the patient's current status. Future prospective clinical trials to validate its prognostic value are needed.

**EP-1150 Dosimetric benefit on adaptive IMPT for patients with locally advanced nasopharyngeal carcinoma**

W.W. Lam<sup>1</sup>, H.F.V. Lee<sup>2</sup>, K.Y. Cheung<sup>1</sup>, S.K. Yu<sup>1</sup>

<sup>1</sup>Hong Kong Sanatorium & Hospital, Medical Physics & Research Department, Happy Valley, Hong Kong SAR China ; <sup>2</sup>The University of Hong Kong, Department of Clinical Oncology- Li Ka Shing Faculty of Medicine, Hong Kong, Hong Kong SAR China

**Purpose or Objective**

To evaluate the dosimetric impact and benefit on adaptive IMPT (APT) for locally advanced NPC patients due to anatomical changes.

**Material and Methods**

11 NPC patients (AJCC stage III & IV) were planned with IMPT using 3 beams with MFO and SIB technique in Eclipse proton TPS. PTVs (PTV<sub>70</sub> and PTV<sub>66</sub>) were aimed to achieve a V<sub>95%</sub> covered by 70 and 66 Gy(RBE), respectively. Patients were scanned by PETCT (ReCT) at 3<sup>rd</sup> week additionally to initial planning CT. DIR were performed between the two CT image sets and all deformed contours on ReCT were verified. To quantify the dosimetric impact due to anatomical changes, a non-adaptive IMPT plan was created by recalculating the initial IMPT plan on ReCT while an adaptive plan was created by reoptimizing on ReCT to evaluate the dosimetric benefit on APT. D<sub>99.5%</sub> and D<sub>95%</sub>, CN and HI of PTVs, D<sub>max</sub> and D<sub>2%</sub> of brainstem, spinal cord, optic chiasm, left and right optic nerves and D<sub>mean</sub> of left and right parotid glands were reported. gEUD and NTCP of OARs were calculated using LKB model. Wilcoxon signed-rank test was used for statistical analysis. A 2-tailed p<0.05 was considered significant.

**Results**

No statistically significant difference were found in D<sub>99.5%</sub>, D<sub>95%</sub>, CN and HI of all PTVs between adaptive and original plan although both PTVs were reduced by 11%(p=0.001) on ReCT. The mean D<sub>99.5%</sub>, D<sub>95%</sub>, CN and HI of PTV<sub>66</sub> were deteriorated by 9.8%(p=0.003), 3.1%(p=0.003), 23.0%(p=0.001) and 120.4%(p=0.001) in non-adaptive vs original plan. The mean CN and HI of PTV<sub>70</sub> were worsen by 50.9%(p=0.001) and 120.5%(p=0.001) in non-adaptive vs original plan. No significant difference were found in D<sub>max</sub>, D<sub>2%</sub>, gEUD and NTCP of brainstem, spinal cord, optic chiasm and optic nerves between adaptive and original plan. Significant increase in mean D<sub>max</sub>, D<sub>2%</sub>, gEUD of brainstem by 8.1%(p=0.019), 10.1%(p=0.014) and 10.7%(p=0.014) were found in non-adaptive vs original plan. The mean NTCP of brainstem was increased from 0.06 to 0.14% (p=0.01). Significant increase in mean D<sub>max</sub>, D<sub>2%</sub>, gEUD of spinal cord by 25.4%(p=0.001), 26.7%(p=0.001) and 26.2%(p=0.001) were found in non-adaptive plan. The mean NTCP of spinal cord was increased from 0.08 to 1.3%(p=0.001). Significant increase in mean D<sub>max</sub>, D<sub>2%</sub>, gEUD of optic chiasm by 5.1%(p=0.002), 5%(p=0.003) and 9.2%(p=0.032) were found in non-adaptive vs original plan. The mean NTCP of optic chiasm was increased from 1.4 to 9.4%(p=0.019). No statistically difference were found in D<sub>max</sub>, D<sub>2%</sub>, gEUD and NTCP of optic nerves in non-adaptive vs original plan. Significant increase in D<sub>mean</sub>, gEUD and NTCP of parotid glands were found in adaptive and non-adaptive vs original plan. D<sub>mean</sub>, gEUD and NTCP were significantly reduced by 5.4%, 5.8% and 5.5% for left parotid gland while 9.1%, 9.2% and 18.3% for right parotid gland in adaptive vs non-adaptive plan.

Table 1. Summary of dosimetric results for original, adaptive and non-adaptive IMPT plan

Target volume/ OARs	Parameters	Original Plan (mean ± SD)	Adaptive Plan (mean ± SD)	Non-Adaptive Plan (mean ± SD)	% Difference (%) (Original vs Adaptive)	P	% Difference (%) (Original vs Non-Adaptive)	P
PTV <sub>70</sub>	D <sub>99.5%</sub> [Gy(RBE)]	68.54 ± 0.67	60.66 ± 0.71	66.85 ± 1.29	0.18	0.570	-7.47	0.083
	D <sub>95%</sub> [Gy(RBE)]	70.94 ± 0.31	70.14 ± 0.31	69.45 ± 1.60	0.36	0.658	-0.89	0.438
	CN	8.69 ± 0.13	6.68 ± 0.11	7.34 ± 0.11	-3.11	0.016	-50.86	0.001*
	HI	3.93 ± 0.09	3.93 ± 0.04	3.74 ± 0.08	9.81	0.002	120.50	0.001*
	Volume	118.56 ± 98.86	150.47 ± 97.72	150.47 ± 97.72	11.50	0.001*	11.50	0.001*
PTV <sub>66</sub>	D <sub>99.5%</sub> [Gy(RBE)]	62.02 ± 1.68	65.81 ± 0.22	63.03 ± 0.81	2.27	0.148	-9.77	0.003*
	D <sub>95%</sub> [Gy(RBE)]	66.12 ± 0.12	65.26 ± 0.23	64.05 ± 2.14	0.21	0.175	-3.97	0.003*
	CN	8.80 ± 0.04	6.80 ± 0.04	6.67 ± 0.06	6.67	0.185	-31.00	0.001*
	HI	8.11 ± 1.70	4.98 ± 0.98	5.79 ± 0.50	3.95	0.405	175.40	0.001*
	Volume	898.95 ± 150.65	817.96 ± 149.09	817.96 ± 149.09	11.33	0.001*	11.33	0.001*
Brainstem	D <sub>max</sub> [Gy(RBE)]	59.44 ± 4.00	47.52 ± 1.90	43.80 ± 4.31	9.69	0.067	11.06	0.014*
	D <sub>2%</sub> [Gy(RBE)]	37.59 ± 1.66	33.64 ± 2.09	33.54 ± 3.08	10.31	0.004	16.69	0.001*
	gEUD	3.56 ± 0.94	6.11 ± 0.58	5.14 ± 0.11	65.15	0.067	132.92	0.010*
	NTCP (%)	0.06 ± 0.01	0.25 ± 0.10	0.21 ± 0.02	3.79	0.240	29.00	0.001*
	Volume	35.84 ± 3.01	33.25 ± 1.70	48.21 ± 7.59	6.98	0.175	26.70	0.001*
Spinal Cord	D <sub>max</sub> [Gy(RBE)]	51.61 ± 2.51	44.61 ± 2.87	41.81 ± 2.25	6.13	0.133	26.68	0.001*
	D <sub>2%</sub> [Gy(RBE)]	28.66 ± 2.71	30.73 ± 2.47	34.55 ± 5.77	6.08	0.175	28.73	0.001*
	gEUD	0.98 ± 0.09	0.93 ± 0.03	1.12 ± 0.10	74.83	0.268	184.99	0.001*
	NTCP (%)	48.41 ± 2.63	48.41 ± 6.76	50.88 ± 13.83	0.37	0.898	5.06	0.682*
	Volume	465.18 ± 1.09	46.81 ± 1.00	46.84 ± 1.48	-7.73	0.999	4.95	0.892*
Optic Chiasm	D <sub>max</sub> [Gy(RBE)]	38.48 ± 0.28	38.81 ± 7.82	39.81 ± 13.30	6.46	0.175	9.17	0.032*
	D <sub>2%</sub> [Gy(RBE)]	5.88 ± 1.64	7.21 ± 9.58	11.05 ± 9.37	22.59	0.287	348.09	0.001*
	gEUD	49.77 ± 11.48	53.82 ± 14.74	49.36 ± 11.91	4.15	0.209	-0.41	0.846
	NTCP (%)	49.77 ± 11.22	47.61 ± 12.27	47.77 ± 12.64	1.79	0.999	-2.23	0.462
	Volume	117.55 ± 13.02	11.86 ± 12.11	11.86 ± 12.11	9.21	0.765	7.66	0.217
Left Optic Nerve	D <sub>max</sub> [Gy(RBE)]	4.91 ± 2.14	4.66 ± 1.53	3.75 ± 2.70	34.83	0.445	1.91	0.618
	D <sub>2%</sub> [Gy(RBE)]	20.91 ± 15.51	21.59 ± 14.63	20.76 ± 14.93	2.27	0.113	1.22	0.536
	gEUD	48.87 ± 15.81	47.58 ± 15.17	47.46 ± 15.88	1.01	0.818	1.01	0.411
	NTCP (%)	1.22 ± 2.33	0.89 ± 1.77	1.15 ± 2.74	27.59	0.377	-7.63	0.763
	Volume	48.85 ± 15.58	27.46 ± 6.63	46.79 ± 7.25	17.76	0.001*	24.77	0.001*
Right Optic Nerve	D <sub>max</sub> [Gy(RBE)]	49.77 ± 11.22	47.61 ± 12.27	47.77 ± 12.64	1.79	0.999	-2.23	0.462
	D <sub>2%</sub> [Gy(RBE)]	20.91 ± 15.51	21.59 ± 14.63	20.76 ± 14.93	2.27	0.113	1.22	0.536
	gEUD	48.87 ± 15.81	47.58 ± 15.17	47.46 ± 15.88	1.01	0.818	1.01	0.411
	NTCP (%)	1.22 ± 2.33	0.89 ± 1.77	1.15 ± 2.74	27.59	0.377	-7.63	0.763
	Volume	48.85 ± 15.58	27.46 ± 6.63	46.79 ± 7.25	17.76	0.001*	24.77	0.001*
Left Parotid Gland	D <sub>max</sub> [Gy(RBE)]	65.29 ± 36.03	66.11 ± 17.16	60.81 ± 17.47	12.08	0.001*	39.29	0.001*
	D <sub>2%</sub> [Gy(RBE)]	46.85 ± 2.16	51.67 ± 7.78	48.34 ± 5.71	14.13	0.001*	24.52	0.001*
	gEUD	47.63 ± 0.78	34.08 ± 7.13	39.61 ± 5.71	13.77	0.001*	73.16	0.001*
	NTCP (%)	44.63 ± 16.81	76.83 ± 15.52	60.86 ± 8.04	36.11	0.001*	60.94	0.001*
	Volume	47.63 ± 0.78	34.08 ± 7.13	39.61 ± 5.71	13.77	0.001*	73.16	0.001*

\*Indicated as statistically significant

**Conclusion**

Anatomical changes had a significant dosimetric impact on IMPT plan quality and APT showed dosimetric benefits in both targets and OARs for locally advanced NPC patients.

**EP-1151 Effects of Continued Smoking in Head and Neck Cancer Patients: A Systematic Review and Meta-Analysis**

J. Smith<sup>1</sup>, D. Nastasi<sup>1</sup>, R. Tso<sup>1</sup>, V. Vangaveti<sup>1</sup>, B. Renison<sup>2</sup>, M. Chilkuri<sup>3</sup>

<sup>1</sup>James Cook University, College of Medicine and Dentistry, Townsville, Australia ; <sup>2</sup>The Townsville Hospital, Townsville Health Library, Townsville, Australia ; <sup>3</sup>The Townsville Hospital, Radiation Oncology, Townsville, Australia

*This abstract is part of the media programme and will be released on the day of its presentation*

### EP-1152 Tumor volume as a prognostic factor in irradiated patient for locally advanced oral cavity cancer

N. Janmune<sup>1</sup>

<sup>1</sup>Songklanagarind hospital, Radiation Oncology, Hatyai, Thailand

#### Purpose or Objective

To determine the effect of the pretreatment tumor volume, in locally advanced oral cavity squamous cell carcinoma, on the survival in patients treated with concurrent chemoradiotherapy.

#### Material and Methods

Review of 74 patients, with histologically confirmed stage III-IV (AJCC 8<sup>th</sup> edition) squamous cell carcinoma of oral cavity, receiving treatment at a tertiary radiation oncology center between January 2009 and March 2016. The patients were treated with either primary radiation or concurrent chemoradiation therapy. This study excluded patients with lip cancer, metastatic disease, and those who diagnosed with other second primary cancer, except non-melanoma cancer of skin. Pretreatment computed tomography (CT) scans were reviewed by experienced neurological diagnostic radiologist for TNM staging. For tumor volume delineation process, the pretreatment CT was delineated by consensus of at least three researchers with Eclipse Planning System (version 10). For statistical analysis, the survival analysis was determined by a Kaplan-Meier estimator. The optimal cutoff tumor volume was evaluated by receiver-operating curve analysis. In the associations of predictor variables, univariate and multivariate analysis were performed with Cox proportional hazards regression models. A p-value of less than 0.05 was considered significant.

#### Results

From 74 patients, 67 patients who received treatment with concurrent chemotherapy were analyzed. The majority of the patient were male (82%), age 59±12.6 years with ECOG score 0-1 (89%). Almost all of them had T stage 3-4 and N stage 2-3. A half of primary tumors site were oral tongue. The median Total Tumor Volume (TTV) was 73.25 cm<sup>3</sup> (IQR 41.9, 132.3). The median survival was 1.04 years (95% CI 0.91 - 1.69). The optimal cutoff TTV that significantly affect the overall survival rate was ≥ 59.8 cm<sup>3</sup> (p < 0.001) (Figure 1). Multivariate analysis showed TTV ≥ 59.8 cm<sup>3</sup> (HR 3.19; 95% CI 1.59-6.4; P < 0.001) and IMRT/VMAT radiation technique (HR 3.5; 95% CI 1.38-9.08; P = 0.002) were considered to be the factors influencing the overall survival outcome.

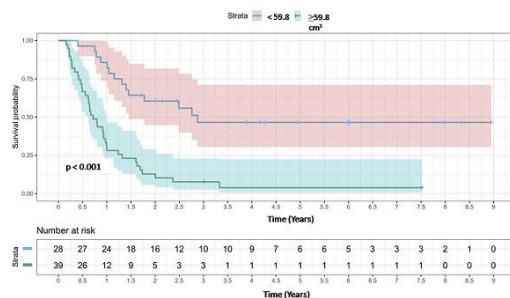


Figure 1. Kaplan-Meier of overall survival according to total tumor volume

#### Conclusion

TTV influenced on the overall survival of locally advanced oral cavity squamous cell carcinoma. In addition, TTV may be considered as a factor to select the appropriate treatment option for these patients.

### EP-1153 A retrospective single institutional analysis of 175 elderly head and neck squamous cell carcinoma

A.K. Gandhi<sup>1</sup>, M. Rastogi<sup>1</sup>, S.S. Nanda<sup>1</sup>, R. Khurana<sup>1</sup>, R. Hadi<sup>1</sup>, K. Sahni<sup>1</sup>, A. Srivastava<sup>1</sup>, A. Bharati<sup>1</sup>, S. Mishra<sup>1</sup>

<sup>1</sup>Dr Ram Manohar Lohia institute of Medical Sciences, Radiation Oncology, Lucknow, India

#### Purpose or Objective

We aimed to retrospectively analyze the demographics, clinical outcome and compliance to treatment of elderly (≥ 65 years) head and neck squamous cell carcinoma (HNSCC) at our institution

#### Material and Methods

Data of 175 consecutive patients of HNSCC presenting to the radiation oncology clinic from February 2013-June 2017 were retrieved and analyzed. Patients with primary in nasopharynx/ para-nasal sinuses, those with metastatic disease at presentation and patients who underwent surgery were excluded from analysis. Following patient details were retrieved from the medical charts: patient demographics, co-morbidities, primary site, stage (AJCC 7th edition), radiation dose parameter, compliance and disease free survival (DFS). DFS was calculated from the date of diagnosis till the time of recurrence. Statistical analysis was done using SPSS (version 21.0). Kaplan Meier method was used for survival analysis and p<0.05 was considered significant

#### Results

Patient characteristics are summarized in Table 1. 76% of patients were ≥ 70 years of age. After registration and initial evaluation, 11 patients (6.3%) defaulted before initiation of treatment. Of remaining 164 patients, 128 (78%) were planned for a radical and 36 (22%) for palliative intent of therapy. Of 128 patients planned for definitive radiotherapy (107 patients) /chemoradiotherapy (21patients); 97 patients (75%) received ≥ 60 Gray of radiation dose. Neo-adjuvant chemotherapy (NACT) was administered in 70/107 patients receiving definitive radiotherapy alone. Median number of NACT cycles was 2 (range 2-3). Median number of concurrent chemotherapy (CCT) cycles was 5 (range 3-6). Median radiotherapy dose was 60 Gray (range 20-70 Gray). Regimens used during NACT were mainly taxane/platinum/5-Fluorouracil based and during CCT was weekly cisplatin (35-40 mg/m<sup>2</sup>). Of 36(22%) patients planned for palliative intent therapy, palliative radiotherapy (median dose 20 Gray in 5 fractions) was delivered in 25 patients; palliative chemotherapy in 20 patients and 9 patients received both. Median follow up was 13 months (range 4-26 months). Median DFS for entire cohort was 17.9 months. Median DFS for patients treated with radical intent was 26.7 months versus 5.5 months for palliative intent (p<0.001). On univariate analysis, site of disease (p=0.10; Oral cavity primary worse), stage of disease (p<0.001; stage IV worse) and radiation dose ≥ 60 Gray (p<0.001; better outcome) were significant predictors of DFS. Karnofsky performance score, age and presence of co-morbidities did not impact DFS (p=NS).

Patient Characteristics	
Median Age (Range)	72 years (65-98)
Male: Female ratio	159:16
<b>Site of disease</b>	
<b>Oral Cavity</b>	<b>41 (23.4%)</b>
Tongue	15
Buccal Mucosa	14
Others	12
<b>Oropharynx</b>	<b>58 (33.15%)</b>
Base of tongue	43
Tonsil	12
Others	03
<b>Larynx</b>	<b>51 (29.14%)</b>
Supraglottic	38
Glottic	11
Others	02
<b>Hypopharynx</b>	<b>25(14.3%)</b>
Pyrimiform Sinus	13
Others	12
<b>T Stage</b>	
T2	33(18.8%)
T3	87(49.7%)
T4	50(28.6%)
Unknown	05
<b>N Stage</b>	
N0	46(26.2%)
N1	54(30.8%)
N2	65(37.1%)
N3	07(4%)
Unknown	03
Co-morbidities	68(38.8%)
Median KPS	70 (60-90)

### Conclusion

Approximately, 3/4<sup>th</sup> of the patients of elderly HNSCC are offered radical intent therapy in our clinical setup. Of these, 75% of patients complete sufficient dose of radiation therapy ( $\geq 60$  Gray of radiation dose). Oral cavity primary and stage IV disease portend dismal outcome.

### EP-1154 Definitive RT and Postoperative RT of adenoid cystic carcinoma: a propensity score analysis

T.H. Lee<sup>1</sup>, B. Jang<sup>1</sup>, J.H. Kim<sup>1</sup>, H. Wu<sup>1</sup>, Y.S. Seo<sup>1</sup>, S.H. Oh<sup>2</sup>, D. Kim<sup>2</sup>, S.K. Kwon<sup>2</sup>, T. Won<sup>2</sup>, E. Chung<sup>2</sup>

<sup>1</sup>Seoul National University Hospital, Department of Radiation Oncology, Seoul, Korea Republic of ; <sup>2</sup>Seoul National University Hospital, Department of Otorhinolaryngology, Seoul, Korea Republic of

### Purpose or Objective

The mainstay radical treatment of adenoid cystic carcinoma in the head and neck (HNACC) is surgery. The outcome of definitive radiotherapy (RT) and surgery combined with postoperative radiotherapy (PORT) has not been properly compared due to the rarity of disease and imbalances of characteristics between patients receiving either treatment. The present study aims to compare outcomes of definitive RT versus surgery + PORT for HNACC using adjustment with propensity scores (PS).

### Material and Methods

A retrospective review of medical records was performed in patients who underwent definitive RT (n=47) or surgery + PORT (n=145) for newly diagnosed nonmetastatic HNACC between January 1981 and December 2016. A median follow-up period was 4.9 years (range, 0.34 to 27.6 years). PS was estimated using factors including age, sex, T stage, N stage, radiotherapy techniques and primary sites. Propensity score (PS) matching and inverseprobability of treatment weighting (IPTW) were used to estimate and compare survival outcomes.

### Results

Five-year overall survival (OS), disease-free survival (DFS), locoregional control (LRC), distant metastasis-free survival (DMFS) of unmodified cohort were 75.7%, 31.4%, 66.3%, 34.2% (definitive RT) and 86.8%, 49.5%, 79.7%, 55.9% (surgery + PORT). These treatment outcomes were significantly different between two groups (p<0.05). In the PS-matched cohort, differences between the treatment outcomes were not significant. Five-year OS, DFS, LRC, DMFS of PS-matched cohort were 72.6%, 37.8%, 74.4%, 39.5% (definitive RT) and 89.3%, 48.2%, 79.0%, 52.1% (surgery + PORT). Also in the IPTW-adjusted cohort, the differences were not significant. Five-year OS, DFS, LRC,

DMFS of IPTW-adjusted cohort were 77.9%, 51.7%, 81.9%, 53.6% (definitive RT) and 86.8%, 48.9%, 79.9%, 53.7% (surgery + PORT).

### Conclusion

Two analyses using PS showed there were no differences in treatment outcomes after balancing patient characteristics. Definitive RT would actually give better treatment results than those reported in previous studies. These results ultimately need be explored in a randomized trial.

### EP-1155 Rare entities in head-and-neck cancer: A single institutional experience of carbon-ion reirradiation

T. Held<sup>1</sup>, P. Windisch<sup>1</sup>, S. Akbaba<sup>1</sup>, K. Lang<sup>1</sup>, D. Bernhardt<sup>1</sup>, P. Plinkert<sup>2</sup>, S. Kargus<sup>3</sup>, K. Freier<sup>3</sup>, S. Rieken<sup>1</sup>, K. Herfarth<sup>1</sup>, J. Debus<sup>1</sup>, S. Adeberg<sup>1</sup>

<sup>1</sup>Heidelberg University Hospital, Department of Radiation Oncology, Heidelberg, Germany ; <sup>2</sup>Heidelberg University Hospital, Department of Otorhinolaryngology-Head and Neck Surgery, Heidelberg, Germany ;

<sup>3</sup>Heidelberg University Hospital, Department of Oral and Maxillofacial Surgery, Heidelberg, Germany

### Purpose or Objective

The objective of this investigation was to evaluate outcome and toxicity of carbon-ion reirradiation (CIR) in patients with rare tumor entities of head-and-neck cancer. There are no guidelines for the treatment of these indications, therefore we want to increase the body of evidence.

### Material and Methods

Thirty-two consecutive patients with infrequent head-and-neck cancer entities treated at our clinic between 2010 and 2017 were retrospectively analyzed regarding progression free survival (PFS), overall survival (OS), patterns of failure and toxicity. Acute (initial 90 days after CIR) and late toxicity were assessed using NCI CTCAE v4.03.

### Results

The median age prior to CIR was 63 years (range 27 - 79 years) and the median time between initial irradiation and CIR was 5.2 years (range 0.6 - 46.5 years). On average, patients received 4 (range 1 - 6) tumor-specific treatments before CIR. 22% of primary tumors were mucoepidermoid carcinomas, 19% were acinar cell carcinomas, 16% were esthesioneuroblastomas, 13% were lymphoepithelial carcinomas and 9% myoepithelial carcinomas. Other entities included sinonasal undifferentiated carcinoma, salivary duct carcinoma and neuroendocrine carcinoma. Most common tumor sites were salivary glands (47%), nasopharynx (22%) and paranasal sinus (19%). 28 patients (87.5%) had T4-tumors and 4 patients (12.5%) had distant metastases prior to CIR. The median PTV and CTV of CIR were 137.1 ccm (range 23.1 - 714.89 ccm) and 98.3 ccm (range 13.3 - 550.6 ccm) respectively. Patients received a median dose of 51 Gy (RBE) (range 36 - 66 Gy (RBE)) in 3 Gy (RBE) fractions and the median cumulative applied dose after CIR was 128.6 BED 2Gy (range 105.8 - 146.5 BED 2Gy). 22% underwent surgical resection prior to CIR. Median overall survival after CIR was 24.1 months (95% CI 16.1 - 32.0 months). 11 patients (34%) survived at least 2 years after CIR. Local and distant control one year after CIR were 66% and 72% respectively. 92% of local recurrences after CIR were in-field. Patients with tumors infiltrating the skull base had a significantly worse OS compared to patients with salivary gland tumors (p=0.012). In addition, patients with two prior irradiation treatments compared to one prior course of radiation therapy had a significantly worse OS (p=0.001). No serious acute or late toxicity ( $\geq$  grade 3) after CIR was observed. Late toxicities of grade 2 included middle ear inflammation (n=3; 9.4%), dysgeusia (n=3; 9.4%), trismus (n=3; 9.4%) and impaired hearing (n=3; 9.4%). 18 months

after CIR, one patient developed a brain necrosis (grade 2) which was treated with bevacizumab.

#### Conclusion

In patients with rare tumor entities of locally advanced, recurrent head-and-neck cancer, CIR is an effective and safe treatment alternative to salvage surgery or palliative systemic therapy in carefully selected patients with good performance status. Further prospective studies are merited to confirm these findings.

#### EP-1156 Radical radio-chemotherapy in head and cancer: retrospective comparison between weekly and 3-weekly CDDP.

M. Buglione<sup>1</sup>, M. Gerardi<sup>2</sup>, D. Greco<sup>1</sup>, M. Maddalo<sup>1</sup>, A. Daniela<sup>2</sup>, M. Bonù<sup>1</sup>, M. Augugliaro<sup>3</sup>, A. Alghisi<sup>1</sup>, L. Pegurri<sup>1</sup>, A. Ferrari<sup>2</sup>, D. Tomasini<sup>1</sup>, G. Marvaso<sup>2</sup>, R. Orecchia<sup>4</sup>, B. Jereczek<sup>3</sup>, S.M. Magrini<sup>1</sup>  
<sup>1</sup>University and Spedali Civili - Brescia, Radiation Oncology Unit, Brescia, Italy ; <sup>2</sup>IEO- European Institute of Oncology IRCCS, Division of Radiation Oncology, Milano, Italy ; <sup>3</sup>IEO- European Institute of Oncology IRCCS and University of Milano, Division of Radiation Oncology and Oncology and Hemato-Oncology Department, Milano, Italy ; <sup>4</sup>IEO- European Institute of Oncology IRCCS, Scientific Direction, Milano, Italy

#### Purpose or Objective

Even if three weekly (3w) CDDP is considered the standard chemotherapy given concurrently with radiotherapy in the treatment of head and neck cancer, the alternative use of weekly (w) CDDP is widely adopted, because is thought to be less toxic and more manageable. This retrospective analysis aims to compare toxicity and survival of these two schedules.

#### Material and Methods

Patients eligible for the analysis had meso/hypopharyngeal or laryngeal locally advanced disease and were treated with radical radio-chemotherapy. Patient, disease and treatment characteristics were analysed and related with toxicity and survival, using  $\chi^2$ -test, log-rank test and propensity score (age, T, N, M) analysis (SPSS®).

#### Results

Between Jan 2010 and Jan 2017 166 patients were treated in two large reference Italian Centres, 52 pts with 3w (100mg/m<sup>2</sup>) and 114 pts with w-CDDP (40mg/m<sup>2</sup>). Patients treated with w-CDDP had a statistically significant older age (p=0.005), worse Karnofsky performance (p=0.000); higher smoking and alcohol consumption (p=0.000). Moreover, in this group there were less meso-pharyngeal (65% vs 90%; p=0.001) and N2-3 disease (71% vs 84.7% p=0.02) and more T3-4 disease (54% vs 38%; p=0.05). All patients were treated with equivalent RT doses. The CDDP cumulative doses were equivalent in both groups (p=0.10); the rate of RT interruption was higher in the w group. Clinical response was similar in the two groups (p=0.081 and p=0.984 in relation to N and T response, respectively). Local relapse rate is higher in w-group (17.65% vs 11.5%) while metastases occurrence is worse in 3w-group (4.4% vs 19.2%) (p=0.01).

Anaemia, leukopenia, renal toxicity, mucositis and dysphagia rates were similar in the two groups. Thrombocytopenia, nausea and vomiting were more frequent in the w-group (p=0.01 and 0,007 respectively). Overall survival was influenced by tumour site (better for meso-pharyngeal disease p=0.04), nodal stage (better for N0-1 p=0.01), and nodal response to treatment (better for CR p=0.004) but not by the CDDP schedule (p=0.433). Relapse free survival was influenced only by the nodal response to treatment (better for CR, p=0.015). All survival data were confirmed after propensity score analysis.

#### Conclusion

With the limits of a retrospective analysis the study showed the equivalence of the two CDDP schedules in

terms of survival outcomes. The higher rates of some toxicities and the higher rates of treatment interruptions in the w group could be explained by the worse patients and disease characteristics at baseline. A prospective randomised study comparing these two schedules is desirable to define the optimal chemotherapy association for patients treated with radical intent.

#### EP-1157 Elective nodal dose of 40 Gy is sufficient for locally advanced oropharyngeal carcinoma.

K. Asai<sup>1</sup>, S. Ohga<sup>1</sup>, S. Nomoto<sup>1</sup>, T. Yoshitake<sup>1</sup>, M. Shinoto<sup>1</sup>, K. Matsumoto<sup>1</sup>, H. Hirata<sup>1</sup>  
<sup>1</sup>Kyushu University, Clinical Radiology, Fukuoka, Japan

#### Purpose or Objective

To clarify the optimal dose of elective nodal irradiation for locally advanced oropharyngeal squamous cell carcinoma.

#### Material and Methods

We enrolled 119 locally advanced oropharyngeal carcinoma patients treated at our institution between April 2003 and October 2017. The inclusion criteria were followings: 1) over 6 months of follow-up period, 2) treated with definitive chemoradiotherapy or bioradiotherapy. In our institution, elective nodal regions were received 40 - 41.4 Gy with fraction size of 1.8 - 2 Gy. Gross lesions were prescribed with 65 - 70 Gy. We evaluate the pattern of failure, overall survival rate, and progression free survival rate. Incidence of regional failure within the elective nodal region is also evaluated.

#### Results

The median age of the patients was 63 years old, and the median follow up period was 44 months. Clinical Stage (according to AJCC 7th) was Stage III in 21, Stage IVa in 86, Stage IVb in 12. HPV status was p16 positive in 21, negative in 15, unknown in 83. Smoking status was  $\geq 10$  pack-years in 79, <10 pack-years in 35, unknown in 5. Treated with chemoradiotherapy in 115, bioradiotherapy in 4. Treatment method was 3D-CRT in 99, IMRT in 20. Recurrence was observed in 39 cases. The 5-year Overall survival rate and progression free survival rate was 76.6% and 63.2%, respectively. The pattern of failure was local in 21, regional in 17, distant in 11. Among the regional recurrence cases, nodal recurrence within the elective nodal regions was observed only in one case.

#### Conclusion

Dose of 40 Gy is sufficient for elective nodal region in locally advanced oropharyngeal cancer.

#### EP-1158 Impact of postoperative target volumes in management of head and neck carcinoma of unknown primary

F. Pondeur<sup>1</sup>, P. Pommier<sup>2</sup>, J. Ton Van<sup>3</sup>, E. Monchet<sup>3</sup>, D. Girodet<sup>1</sup>, M. Poupart<sup>1</sup>, P.E. Roux<sup>1</sup>, P. Zrounba<sup>1</sup>, M. Julieron<sup>3</sup>, S. Deneuve<sup>1</sup>

<sup>1</sup>Centre Léon Bérard, Head and Neck, LYON, France ;

<sup>2</sup>Centre Léon Bérard, Radiotherapy, Lyon, France ;

<sup>3</sup>Centre Oscar Lambret, Head and Neck, Lille, France

#### Purpose or Objective

We aimed to compare the outcomes of postoperative unilateral radiotherapy (UL-RT) versus bilateral radiotherapy plus total mucosal irradiation (COMP-RT) in management of head and neck carcinoma of unknown primary (HNCUP).

#### Material and Methods

Retrospectively, 69 patients with unilateral HNCUP treated in 2 cancer institutes between 2004 and 2014 were included. Diagnosis work-up included for all patients a positron emission tomography-computed tomography. The proportion of p16 positive HNCUP was similar in both centers. All patients were treated with curative intent by initial ipsilateral neck dissection. In one center, all 23 patients underwent UL-RT while in the other center, all 46

patients received a COMP-RT. The long-term quality of life (QOL) of the patient was evaluated using the Quality of Life Questionnaire for Head and Neck 35.

#### Results

After a median follow up of 6.3 years, primary tumour emerged in 3 (13%) patients in UL-RT group and in 4 (9%) patients in COMP RT group ( $p=0.68$ ). There were no differences ( $p=0.34$ ) in cervical node recurrence rate between UL-RT group (4%) and COMP-RT group (22%). The locoregional recurrence free survival rate at 5-years was 81% in UL-RT group and 68.6% in COMP-RT group ( $p=0.21$ ). When comparing it with COMP-RT, UL-RT had a trend to an improvement of the QOL related to teeth problems, swallowing, troubles with social contact and use of pain killers.

#### Conclusion

Unilateral postoperative radiotherapy provides similar outcomes as COMP-RT in unilateral HNCUP management. This radiotherapy modality seems to improve radiation morbidity and long term QOL of patients without compromising re-irradiation possibilities.

#### EP-1159 To compare outcome of Intensive nutritional support with standard practise in head and neck cancer.

T. Shahid<sup>1</sup>, N. Kalyani<sup>1</sup>, S. Modak Das<sup>2</sup>, M. Mukherjee<sup>1</sup>, J. Bhattacharya<sup>1</sup>, A. De<sup>1</sup>, R. Talukdar<sup>1</sup>, A. Samanta<sup>1</sup>, T. Ghosh<sup>1</sup>, D. Barman<sup>1</sup>, S. Sadhukhan<sup>1</sup>, P. Vijayaraghavan<sup>1</sup>, R. Rajan<sup>1</sup>

<sup>1</sup>Apollo Gleneagles Hospital, Radiotherapy, Kolkata, India ; <sup>2</sup>Apollo Gleneagles Hospital, Nutrition and Dietetics, Kolkata, India

#### Purpose or Objective

A randomized control study to evaluate the effect of Nutritional support following the American Dietetic Association Medical Nutrition Therapy (ADA MNT) protocol with standard practise (SP) for patients of head and neck cancer undergoing radiotherapy either alone or with chemotherapy. To determine the impact of nutritional intervention (NI) compared with standard practice (SP). Malnutrition related to persistent poor oral intake during radiation has significant adverse impact on clinical outcome and quality of life. Nothing much can be done in majority of our patients due to resource and financial crunch in our country. Henceforth, after radiotherapy, the nutritional status of the patients is poor and the curative effect is often unsatisfactory.

#### Material and Methods

60 patients, previously untreated and biopsy proven squamous cell carcinoma histology to be treated with either radical radiotherapy or radical concurrent chemo radiation with curative intent were included. (50 Male and 10 Female). Mean age being 51 years. Patients were randomized to receive either NI ( $n=31$ ) (nutrition counseling following the American Dietetic Association Medical Nutrition Therapy (ADA MNT) protocol for radiation oncology) or SP (general nutrition talk and booklet)( $n=29$ ). Main outcome measure was dietary intake (protein and kilocalorie) assessed at baseline, 4, 8 and 12 weeks after starting radiotherapy. Statistical analyses repeated measures ANOVA performed on an intention to treat basis.

#### Results

The NI group had a higher mean total kilocalorie ( $p=0.02$ ) and protein intake ( $p<0.001$ ) compared with the SP group. Mean intake per kilogram of body weight for the NI group ranged from 29 to 32 kcal/kg/day compared with 24 to 28 kcal/kg/day for the SP group ( $p=0.02$ ). The NI group had a higher mean protein intake (1.2-1.4g/kg/day) compared with the SP group (1.0-1.1g/kg/day) ( $p=0.001$ ). Treatment breaks were seen in 10 % of patients in NI group as compared to 30 % in SP group. Even the Health related Quality of Life (HRQOL) was better in the NI group. HRQOL was measured by the European Organization for Research

and Treatment for Cancer (EORTC) QLQ-C30 and EORTC HN35.

#### Conclusion

Intensive NI following the ADA MNT protocol results in improved dietary intake compared with SP and appears to beneficially impact on nutrition related outcome in patients receiving radiotherapy. All patients undergoing radiotherapy either alone or with concurrent chemotherapy should receive thorough nutrition assessment, adequate nutritional counselling and nutritional support for a meaningful clinical outcome.

#### EP-1160 Quantifying the impact of radiologic revision in head and neck cancer: monoinstitutional experience

D. Alterio<sup>1</sup>, L. Preda<sup>2</sup>, S. Volpe<sup>1,3</sup>, C. Giannitto<sup>2</sup>, G. Riva<sup>1,3</sup>, A.F. Pounou Kanga<sup>1,3</sup>, M. Atac<sup>4</sup>, G. Giugliano<sup>4</sup>, A. Ferrari<sup>1</sup>, G. Marvaso<sup>1</sup>, S. Durante<sup>1,3</sup>, S. Arculeo<sup>1,3</sup>, I. Turturici<sup>5</sup>, M. Cossu Rocca<sup>6</sup>, M. Ansarin<sup>4</sup>, M. Bellomi<sup>2</sup>, B.A. Jereczek-Fossa<sup>1,3</sup>, R. Orecchia<sup>7</sup>

<sup>1</sup>European Institute of Oncology IRCCS, Department of Radiation Oncology, Milan, Italy ; <sup>2</sup>European Institute of Oncology IRCCS, Department of Radiology, Milan, Italy ;

<sup>3</sup>University of Milan, Department of Oncology and Hemato-Oncology, Milan, Italy ; <sup>4</sup>European Institute of Oncology IRCCS, Department of Head and Neck Surgery, Milan, Italy ;

<sup>5</sup>University of Rome- Tor Vergata, Department of Radiation Oncology, Rome, Italy ;

<sup>6</sup>European Institute of Oncology IRCCS, Department of Head and Neck and Urogenital Medical Oncology, Milan, Italy ; <sup>7</sup>European Institute of Oncology IRCCS, Scientific Directorate, Milan, Italy

#### Purpose or Objective

Although the role of the radiologist as a core member of the multidisciplinary team (MDT) for Head and Neck (HN) cancer management has been increasingly advocated, a quantitative analysis on the impact of imaging revision is not available in currently published works. To address this unmet need, the current study provides a full report of MDT meetings held at a tertiary care cancer center at the presence of expert dedicated HN radiologists.

#### Material and Methods

Retrospective revision of cases discussed at MDT meetings from April 2014 to March 2017 for whom a radiologic revision was required. All cases were revised by two dedicated HN radiologists (LP and GC having 15 and 5 years experience in HN cancer imaging, respectively). Inclusion criteria were: 1) clinical and/or radiological suspicion or histologically-proven diagnosis of HN cancer, 2) availability of a written medical record of the MDT discussion and final radiological report 3) follow-up length of at least 12 months, 4) written informed consent for the use of personal data for educational and scientific purposes. Exclusion criteria were: adjuvant treatment (i.e. radiation treatment alone or in association with systemic therapies) and/or diagnosis of thyroid cancers. Both malignant and benign tumors were included. Only computed tomography (CT) and magnetic resonance (MR) imaging were considered. The following descriptors were used: 1) any changes of radiological staging (per Tumor Node Metastasis, TNM, staging system 7th ed.) 2) any changes in treatment strategy. The latter were categorized as either "major modifications" (i.e. MDT non indication to surgery in favor of radiotherapy± systemic therapy) or "minor modifications" (i.e. MDT indication to an alternative approach: open versus minimally-invasive surgery). Accuracy of MDT indication-to-treatment was verified through follow-up data (pathological specimens and/or subsequent imaging and/or clinical information).

#### Results

Five-hundred forty cases were retrieved, mainly at the time of tumor diagnosis (57%) and locally-advanced tumors (69%). The most represented HN subsite was the oropharynx (28%). MR-only was the most commonly reviewed type of imaging (46%), followed by CT-only

(43%). **Table 1** represents the clinical aim to radiologic imaging revision. Cases' stratification according to radiologic indication is represented in **Fig. 1**. Follow-up showed that radiology-driven MDT decision was correct in 117 of the 118 cases with available follow-up (99%), with 43 patients having a histological confirmation.

#### Conclusion

Data emerging from our work strongly support the inclusion an expert radiologist in the core of each institutional HN MDT. Further efforts of prospective nature are warranted in order to assess whether imaging revision translates into improved oncological outcomes in this clinical setting.

#### EP-1161 Clinical response and toxicity of VMAT low-dose RT with intravenous steroids for Graves' Orbitopathy

B. Salas<sup>1</sup>, R. Cabrera<sup>1</sup>, L. Ferrera<sup>1</sup>, M. Lloret<sup>1</sup>, M. Zajac<sup>1</sup>, J. Rutllan<sup>2</sup>, F. Medina-Rivero<sup>2</sup>, P.C. Lara<sup>3</sup>

<sup>1</sup>Hospital Universitario de Gran Canaria Doctor Negrin., Radiation Oncology, Las Palmas de Gran Canaria, Spain ;  
<sup>2</sup>Hospital Universitario de Gran Canaria Doctor Negrin., Ophthalmology, Las Palmas de Gran Canaria, Spain ;

<sup>3</sup>Hospital Universitario San Roque/Universidad Fernando Pessoa Canarias, Oncology, Las Palmas de Gran Canaria, Spain

#### Purpose or Objective

Radiotherapy has been considered an alternative to high doses glucocorticoids in progressing GO. Low doses (LD-RT) produce an anti-inflammatory effect and seemed to be equally effective than the old common fractionation protocol of 20 Gy, in 10 daily doses over a two-week period. Lower doses of 10 Gy fractionated in 1 Gy a week over 10 consecutive weeks, have been not studied under the new techniques as volumetric modulated arc therapy (VMAT) or Intensity-modulated radiation therapy (IMRT). Furthermore, there is no publications about the efficacy and toxicity of the combined use of LD-RT VMAT/IMRT and high doses glucocorticoids. The aim of this study is to analyze for the first time the clinical response and toxicity of a LD-RT VMAT/IMRT schedule plus high doses glucocorticoids in moderate to severe GO.

#### Material and Methods

33 patients (59 orbits) with diagnosis of moderate to severe Graves' ophthalmopathy (GO) according to EUGOGO were included in this prospective cohort study under our RT Quality Assurance programmed from March 2013 to February 2018. Treatment schedule consisted in retro-orbital LD-RT with VMAT or IMRT (Total Dose 10Gy, 1Gy/fraction/week) and concurrent high dose intravenous glucocorticoids therapy (Methylprednisolone 6 doses of 500mg/week, followed by 4 doses of 250 mg/week). The treatment response was evaluated by clinical activity score (CAS: Range 0-7), considering active GO CAS  $\geq 3$  and inactive GO CAS  $<3$ . Toxicity was scored by the CTC4.0 criteria. Clinical evaluation was jointly done by the ophthalmologist and the radiation oncologist at 3 months intervals. Follow-up was closed in October 1, 2018.

#### Results

All patients completed the irradiation and concurrent steroids therapy schedule. 29 orbits (49.2%) had active GO symptom score (CAS  $\geq 3$ ) before treatment and a mean pretreatment-CAS of 4,1. Three months after treatment all 59 orbits (100%) had inactive GO symptom score (CAS  $<3$ ). A marked reduction from mean pretreatment-CAS of 4,1 to posttreatment-CAS of 1,6 was observed ( $p=0.003$ ) (Figure 1). During follow-up 1 patient (1 orbit) required posterior decompression surgery, and 3 patients (4 orbits) required strabismus surgery due to reactivation and progression of GO symptoms. Three-year freedom from surgery was 81.5 $\pm$ 9.5% (Figure 2). Acute toxicity was very mild (only grade I): eye dryness: 18 orbits (30,5%) eye redness in 9 orbits (15,25%), and photophobia 1 orbit (1.69%). Toxicity from glucocorticoids therapy was G0. No

cataracts or other late toxicity was found.

Figure 1

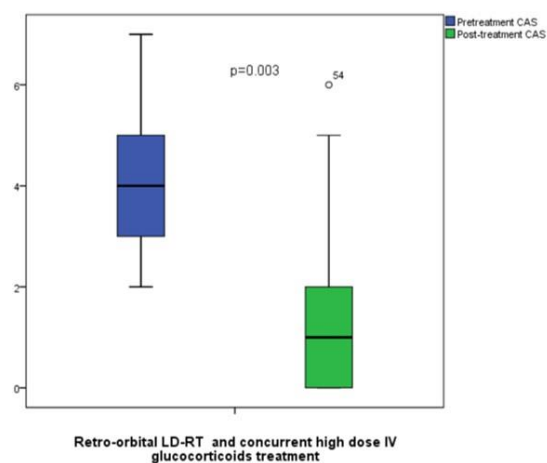
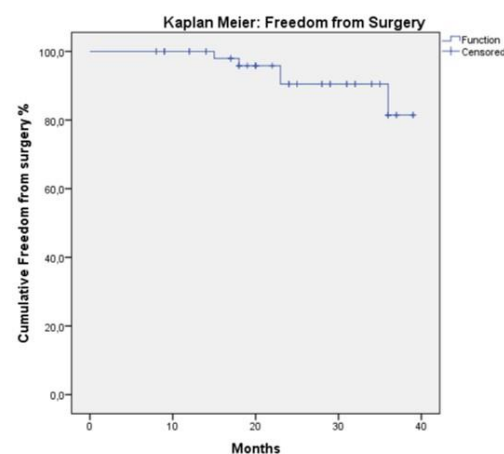


Figure 2



#### Conclusion

Highly-conformation techniques (VMAT/IMRT) retro-orbital LD-RT (10Gy, 1Gy/fraction/week) and concurrent high dose intravenous glucocorticoids is a very active treatment for Moderate to Severe Graves' Orbitopathy. Acute toxicity was very low and no cataracts appeared in the follow-up period. Rescuing surgery was needed in very few cases with a 3-year freedom from surgery of 81.5 $\pm$ 9.5%.

#### EP-1162 Post-radiotherapy sarcopenia: a new prognostic factor in oropharyngeal cancers?

C. Dupin<sup>1</sup>, R. Poncin<sup>1</sup>, A. Daste<sup>2</sup>, C. Majoufre<sup>3</sup>, V. Castetbon<sup>3</sup>, E. De-Mones<sup>3</sup>, R. Trouette<sup>1</sup>, V. Vendrely<sup>1</sup>  
<sup>1</sup>Bordeaux University Hospital, Radiation Oncology, Bordeaux, France ; <sup>2</sup>Bordeaux University Hospital, Medical Oncology, Bordeaux, France ; <sup>3</sup>Bordeaux University Hospital, Head Neck Surgery, Bordeaux, France

#### Purpose or Objective

Sarcopenia, or loss of muscle mass, is common in oncology, and is associated with survival in some retrospective studies. The objective of this study was to evaluate pre- and post-radiotherapy (RT) sarcopenia in patients treated for oropharyngeal cancer and its impact on survival.

#### Material and Methods

All consecutive patients treated for oropharyngeal cancer by irradiation without surgery with curative intent at

Bordeaux University Hospital, , with pre- and post-RT PET-scan were included. During RT, the variation in weight and the lumbar skeletal muscle index (SML) were studied according to oral nutrition, or use of feeding tube with preventive or curative intent. Sarcopenia was evaluated by SML calculated as the ratio of (L3 muscle surface) / (size)<sup>2</sup>, on pre- and post-RT PET scans. Overall and progression free survival have been estimated by the Kaplan-Meier method and evaluated according to pre- and post-RT sarcopenia and type of nutrition.

### Results

From 2011 to 2017, 124 patients were irradiated for oropharyngeal cancer and 116 (93%) had chemoradiotherapy. Median follow-up was 18.2 months [1.7-71.6]. At diagnosis, 55 patients (44%) were sarcopenic compared to 80 patients (65%) 3 months after RT ( $p < 10^{-6}$ ). Patients were less sarcopenic before treatment with p16+ oropharynx cancer than when with p16- oropharynx cancer: 28% vs 63% ( $p < 0.001$ ). Overall Survival was not significantly associated with pre-RT sarcopenia, [Hazard Ratio = 1.6; 95% CI = 0.77-3.2;  $p = 0.12$ ], as well as PFS [HR = 0.57; 0.32-1.03;  $p = 0.052$ ]. Patients lost less weight during RT with preventive feeding tube (mean weight loss :1.6 kg) compared to curative feeding tube (5.6 kg) or exclusive oral nutrition (4.2 kg) ( $p = 0.003$ ). The SML decreased significantly less in the case of preventive feeding tube (-4%) versus curative feeding tube (-12%) or exclusive oral nutrition (-8%) ( $p < 0.001$ ). Finally, OS [HR = 0.38; 0.18-0.81;  $p = 0.03$ ] and PFS [HR = 0.45; 0.26-0.82;  $p = 0.02$ ] were significantly associated with post-RT sarcopenia. At 2 years overall survival was 85% in non-sarcopenic patients after radiotherapy compared with 69% in sarcopenic patients after radiotherapy.

### Conclusion

Evaluation of sarcopenia is relevant in oropharyngeal cancers. Preventive enteral nutrition, associated with decreased muscle mass or post-RT sarcopenia, is predictive of OS and PFS.

### EP-1163 Hypo vs conventional radiotherapy for T1 glottic cancer: A prospective cohort study

B. Salas<sup>1</sup>, D.J. Domínguez Nuez<sup>2</sup>, R. Cabrera<sup>1</sup>, L. Ferrera<sup>1</sup>, M. Lloret<sup>1</sup>, P.C. Lara<sup>3</sup>

<sup>1</sup>Hospital Universitario de Gran Canaria Doctor Negrín., Radiation Oncology, Las Palmas de Gran Canaria, Spain ;

<sup>2</sup>Universidad de Las Palmas de Gran Canaria, Medicine School. Radiation Oncology, Las Palmas de Gran Canaria, Spain ; <sup>3</sup>Hospital Universitario San Roque/ Universidad Fernando Pessoa Canarias, Oncology Department, Las Palmas de Gran Canaria, Spain

### Purpose or Objective

The aim of the present study is to evaluate the clinical outcomes and toxicity rates of a series of prospectively followed patients suffering from squamous T1N0M0 glottic cancers treated either with conventional or hypofractionated radiotherapy schedules.

### Material and Methods

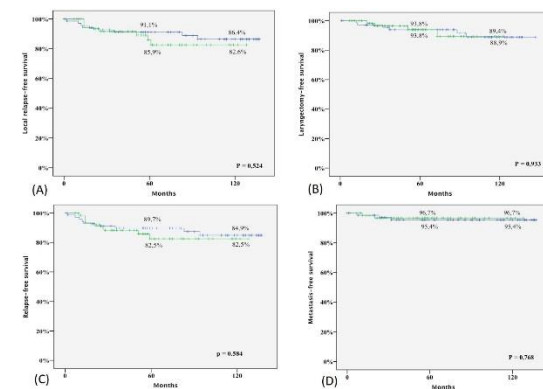
From Jan 1<sup>st</sup>, 2005 to August 1<sup>st</sup>, 2017, T1N0M0 squamous glottic cancers treated by exclusive curative radiotherapy were included in this study. Patients were followed prospectively under our programme for Radiotherapy Quality Assurance. Curative radiotherapy was administered daily, 5/fr/week, either as a conventional fractionation schedule, with doses ranging from 1,8 to 2Gy per day, total dose of 70,2/70 Gy in 7 weeks or hypofractionated schedule with a dose from 2,2 to 2,25Gy per day, total dose 63,8/63Gy in 5,5 weeks. Fractionation schedule was chosen by the treating physician, according to his/her best knowledge. Stratification for fractionation schedule (conventional or hypofractionated) was predetermined in the study. Follow-up was performed by the referring otorhinolaryngologist and the treating

radiation oncologist by clinical examination and laryngoscopy. CT-scan was used when needed.

### Results

One hundred thirty-eight (138) patients were included in this prospective cohort study from January 2005 to August 2017. Follow-up was closed in April 2018 (mean follow-up 78,11 ± 39,85 months, range 7 to 137 months, median 77 months). No one of the patients included were lost of follow-up until last visit or death. Seventy-one patients were treated by conventional schedules and sixty-seven by hypofractionated schedules. Patients characteristics for age, sex, alcohol and tobacco consumption were similar in both cohorts. All patients showed a complete clinical response after radiotherapy according to RECIST criteria. No differences were found for local relapse free survival ( $p=0,524$ )(Fig 1A), larynx preservation rate ( $p=0,933$ )(Fig 1B), disease recurrence ( $p=0,584$ )(Fig 1C) metastases ( $p=0,768$ )(Fig 1D) second primary tumours ( $p=0,895$ ) or Overall Survival rates ( $p=0,70$ ) between the two cohorts. Acute laryngopharyngeal toxicity was higher in the hypofractionation group ( $p = 0,004$ ), mainly due to an increase in mild and moderate toxicity. Severe late laryngeal toxicity (oedema) was similar in both cohorts ( $p=0,714$ ).

Figure 1



### Conclusion

In the present study, the hypofractionated schedule seems to be a feasible treatment option that have similar results than conventional fractionation treatment. Total treatment time saved (1.5w) at a cost of a moderate increase in mild toxicity is convenient for the patient and families.

### EP-1164 Estimated benefit of proton therapy and dose de-escalation in HPV p16-positive oropharyngeal cancer

P. Brodin<sup>1</sup>, R. Kabarriti<sup>2</sup>, V. Gondi<sup>3</sup>, M. Pankuch<sup>3</sup>, M. Garg<sup>2</sup>, W. Tomé<sup>2</sup>

<sup>1</sup>Montefiore Medical Center/Albert Einstein College of Medicine, Radiation Oncology, Bronx, USA ; <sup>2</sup>Montefiore Medical Center, Radiation Oncology, Bronx, USA ;

<sup>3</sup>Northwestern Medicine Chicago Proton Center, Radiation Oncology, Warrenville, USA

### Purpose or Objective

Dose de-escalation strategies are being explored for oropharyngeal cancer (OPC) patients with good prognoses through human papilloma virus (HPV) p16-positive tumor biopsies. Here, we estimate the quality of life (QoL) benefit of proton therapy (PT) for different dose de-escalation levels for OPC, using a data-driven approach for estimating the QoL burden from normal tissue complications.

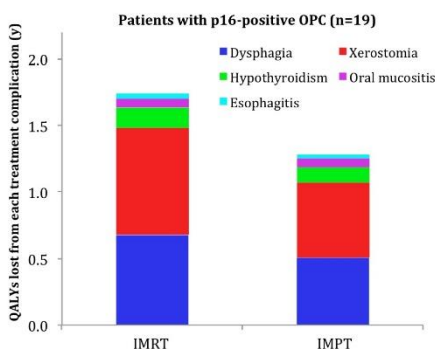
### Material and Methods

The most recent normal tissue complication probability (NTCP) models for dysphagia, xerostomia, esophagitis,

oral mucositis and hypothyroidism were identified through a systematic literature review. The NTCP for these endpoints was estimated in a cohort of 33 OPC patients, of which 19 had HPV p16-positive tumors. NTCP estimates were based on delivered photon intensity-modulated radiation therapy (IMRT) plans, and comparative intensity-modulated PT (IMPT) plans generated from clinical protocols in a collaborating PT center. Equal target coverage and robustness optimization was used in PT plans to account for setup uncertainty. Latencies and durations of complications were modeled based on NTCP estimates while accounting for OPC-specific age-, sex-, and smoking status-adjusted conditional survival probability. The quality-adjusted life years (QALYs) lost attributable to each treatment complication were then calculated by assigning quality-adjustment factors based on severity of complications. Monte Carlo sampling 10,000 times for each patient case was done to account for the uncertainty in underlying modeling parameters and quality-adjustment factors.

### Results

Mean age was 61y, 73% were male, 61% had stage IV disease and 70% had >10 pack-year smoking history. For all patients the average QALYs lost from all modeled complications were 1.52 with IMRT and 1.15 with IMPT, with average 0.37 QALYs spared with PT. The estimated QALYs spared varied considerably between patients and was significantly greater for patients with p16-positive tumors (0.45 vs. 0.25 QALYs,  $p=0.004$ ). Estimated QALYs lost from each complication are shown in the figure for patients with p16-positive tumors, illustrating how long-term complications dysphagia and xerostomia dominate the QoL burden. The table shows estimated QALYs spared with PT for different levels of dose de-escalation to the primary disease for p16-positive tumors, assuming that treatment efficacy remains at the lower dose levels. The combination of dose de-escalation and IMPT results in the lowest estimated QALYs lost.



De-escalation dose level	Average QALYs lost from IMRT	Average QALYs lost from IMPT	Average QALYs spared with proton therapy	Range in QALYs spared with proton therapy among patients
Planned dose	1.73	1.29	0.45	0.18 – 0.81
60 Gy	1.51	1.12	0.40	0.16 – 0.81
50 Gy	1.21	0.91	0.30	0.13 – 0.61
40 Gy	0.95	0.74	0.22	0.09 – 0.41

### Conclusion

The estimated QALYs spared with PT varies greatly even among p16-positive oropharyngeal cancer patients and identifying those who would benefit most using this data-driven approach could improve resource allocation and patient selection for PT. Since PT delivered with dose de-escalation protocols is estimated to have the least QoL burden it is imperative that this be tested prospectively, especially in regards to treatment efficacy.

### EP-1165 Failure Patterns of Cervical Lymph Nodes in Metastases of Unknown Primary according to Target Volume

D.Y. Kim<sup>1</sup>, D.S. Heo<sup>2</sup>, B. Keam<sup>2</sup>, S. Ahn<sup>3</sup>, J. Kim<sup>4</sup>, K.C. Jung<sup>5</sup>, J.H. Kim<sup>1,6,7</sup>, H. Wu<sup>1,6,7</sup>

<sup>1</sup>Seoul National University College of Medicine, Radiation Oncology, Seoul, Korea Republic of ; <sup>2</sup>Seoul National University College of Medicine, Internal Medicine, Seoul, Korea Republic of ; <sup>3</sup>Seoul National University College of Medicine, Otorhinolaryngology, Seoul, Korea Republic of ; <sup>4</sup>Seoul National University College of Medicine, Radiology, Seoul, Korea Republic of ; <sup>5</sup>Seoul National University College of Medicine, Pathology, Seoul, Korea Republic of ; <sup>6</sup>Seoul National University, Cancer Research Institute, Seoul, Korea Republic of ; <sup>7</sup>Seoul National University, Institute of Radiation Medicine- Medical Research Center, Seoul, Korea Republic of

### Purpose or Objective

To analyze the clinical outcomes in patients with metastatic carcinoma of cervical lymph nodes from an unknown primary (MUO) according to the radiation target volume, and suggest an optimal radiation field

### Material and Methods

A total of 62 patients with MUO at Seoul National University Hospital between 1998 and 2016 were reviewed. We compared the overall survival (OS), locoregional recurrence (LRR) and primary site failure depending on radiation target volume. The target volume was classified according to whether the head and neck mucosal sites were included and whether the neck node was treated unilaterally or bilaterally.

### Results

Median follow-up time was 44.1 months. 37.1% (n=23) of patients received mucosa RT and 62.9% (n=39) didn't. Mucosa RT showed no significant effect on OS and LRR. Though mucosa RT had borderline significance with primary site failure, only 4 patients (10.3%) who had not treated mucosa developed a subsequent mucosal head and neck carcinoma. Moreover, the location of primary site failure was found to be unpredictable and 75% of recurred patients received successful salvage therapies. When analyzing the unilateral (n=35) or bilateral neck irradiation (n=21), there were no significant differences in OS and LRR between the two radiation fields. When treated bilaterally, there were 2 patients who recurred at ipsilateral in-field and 1 patient found out recurrence at contralateral neck. In case of the unilateral irradiation, there were 4 recurrences at ipsilateral in-field and 2 cases at ipsilateral out-field, especially neck node level I. In addition, when treated both neck, more mucositis occurred significantly.

### Conclusion

We found that there were no benefits in OS and LRR in patients with MUO when treating head and neck mucosal sites and bilateral neck node in radiation target volume. Primary site failure was hard to predict and salvage therapy could be performed in case of incidence of subsequent mucosal carcinoma.

### EP-1166 Optimal timing for salvage surgery after definitive radiotherapy in hypopharyngeal cancer.

S. Chun<sup>1</sup>, B. Keam<sup>2</sup>, D.S. Heo<sup>2</sup>, K.H. Kim<sup>3</sup>, M. Sung<sup>4</sup>, E. Chung<sup>4</sup>, J. Kim<sup>5</sup>, K.C. Jung<sup>6</sup>, J.H. Kim<sup>1</sup>, H. Wu<sup>1</sup>

<sup>1</sup>Seoul National University Hospital, Department of Radiation Oncology, Seoul, Korea Republic of ; <sup>2</sup>Seoul National University Hospital, Department of Internal Medicine, Seoul, Korea Republic of ; <sup>3</sup>Bundang Jesaeng Hospital, Department of Otorhinolaryngology, Seongnam, Korea Republic of ; <sup>4</sup>Seoul National University Hospital, Department of Otorhinolaryngology, Seoul, Korea Republic of ; <sup>5</sup>Seoul National University Hospital, Department of Radiology, Seoul, Korea Republic of ; <sup>6</sup>Seoul National University Hospital, Department of Pathology, Seoul, Korea Republic of

**Purpose or Objective**

Use of radiotherapy combined with chemotherapy is increasing in hypopharyngeal cancer. However, many show residual tumor after radiotherapy. Timing for treatment evaluation and salvage therapy is essential. However, optimal timing for salvage surgery has not been suggested. In this study, we tried to evaluate optimal timing for tumor response assessment.

**Material and Methods**

Patients who were diagnosed with hypopharyngeal squamous cell carcinoma between 2006 and 2015 were retrospectively analyzed. All patients received definitive radiotherapy with or without chemotherapy. Response of all treated patients were analyzed at 1, 3, and 6 months after radiotherapy. Any patients with progression before 6 months were excluded.

**Results**

A total of 54 patients were analyzed. Complete remission (CR) rates at 1 month (CR1), 3 months (CR3) and 6 months (CR6) were 66.7%, 81.5% and 90.7%, respectively. Non-CR at 1 month (NCR1), 3 months (NCR3), and 6 months (NCR6) showed poor locoregional recurrence-free survival rates (1-year rates of 63.7%, 66.7% and 0.0%, respectively) compared to CR1, CR3 and CR6 (1-year rates 94.3%, 88.0% and 91.5%, respectively). Particularly significant differences were seen between CR6 and NCR6 ( $p < 0.001$ ). Of 10 patients with NCR3, 5 showed CR at 6 months (NCR3/CR6). There was no statistical difference in locoregional recurrence-free survival between CR3 and NCR3/CR6 group ( $p = 0.990$ ).

**Conclusion**

Our data suggest half of patients who did not show CR at 3 months eventually achieved CR at 6 months. Waiting until 6 months after radiotherapy may be appropriate for avoiding additional salvage therapy.

**EP-1167 Sparing of high retropharyngeal lymph node irradiation in patients with oropharyngeal carcinoma**

B. Kang<sup>1</sup>, J.H. Kim<sup>1</sup>, H. Wu<sup>1</sup>, I.A. Kim<sup>2</sup>, K. Eom<sup>2</sup>

<sup>1</sup>Seoul National University College of Medicine, Radiation Oncology, Seoul, Korea Republic of ; <sup>2</sup>Seoul National University College of Medicine- Seoul National University Bundang Hospital, Radiation Oncology, Seongnam, Korea Republic of

**Purpose or Objective**

In radiotherapy for head and neck cancer, it is very important to define the appropriate treatment volumes that determine the treatment outcome and toxicity. We examined the feasibility of omitting elective retropharyngeal (RP) nodal irradiation in oropharyngeal cancer.

**Material and Methods**

We performed a retrospective review from 2009 to 2016; 197 patients with oropharyngeal squamous cell carcinomas were treated with definitive or postoperative radiation therapy at the Seoul National University Hospital or Seoul National University Bundang Hospital. Of these patients, 151 patients (76.6%) were treated ipsilateral RP nodal areas up to the upper edge of C1 vertebral body, while the other 46 patients (23.4%) were not. We reviewed patterns of failures, disease free survival, and patient-reported chronic xerostomia status in each patient group.

**Results**

During follow-up period, two patients developed RP nodal recurrences (4-108 months, median =46 months). There was no RP nodal recurrences in patients with a distance >1cm from gross tumor volume (GTV) to high RP nodal areas. There was no significant between-group difference in disease free survival, with a rate of 80.7% in the high RP nodal-irradiation group and 87.2% in the RP nodal spared group ( $P=0.22$ ). Patients in the high RP nodal-irradiation group had higher mean ipsilateral parotid gland dose (mean 28.7Gy vs 21.3Gy,  $P<0.001$ ) and higher rates of chronic xerostomia (72.2% vs. 58.7%,  $P=0.03$ ).

**Conclusion**

Omission of ipsilateral high RP irradiation in oropharyngeal squamous cell carcinoma patients seems safe and improves the patients' quality of life, especially for xerostomia.

**EP-1168 Early radiation induced changes in salivary glands in nasopharyngeal cancer patients after IMRT**

W.V. Wu<sup>1</sup>, M.T. Ying<sup>2</sup>, D.L. Kwong<sup>3</sup>, G.K. Wong<sup>4</sup>, P. Khong<sup>5</sup>

<sup>1</sup>Hong Kong Polytechnic University, HTI, Kowloon- Hong Kong- SAR, China ; <sup>2</sup>Hong Kong Polytechnic University, Health Technology & Informatics, Hong Kong, Hong Kong SAR China ; <sup>3</sup>University of Hong Kong, Clinical Oncology, Hong Kong, Hong Kong SAR China ; <sup>4</sup>Queen Mary Hospital, Clinical Oncology, Hong Kong, Hong Kong SAR China ; <sup>5</sup>University of Hong Kong, Diagnostic Radiooogy, Hong Kong, Hong Kong SAR China

**Purpose or Objective**

Parotid and submandibular glands are the main source of saliva. Both glands are irradiated to high dose by radical external beam radiotherapy (EBRT) in nasopharyngeal cancer (NPC) patients. Xerostomia is one of the common radiation induced complications in NPC patients caused by damaged of parotid and submandibular glands after RT. Persistent xerostomia causes difficulties in mastication and swallowing and enhances the risks of dental problems. The aims of this study were to assess the changes of the salivary glands after 6 months of post-RT using magnetic resonance imaging (MRI), ultrasonography (US), saliva flow rate and contents.

**Material and Methods**

25 NPC patients with stage I to III (UICC) treated by routine EBRT using 6 MV 9-field intensity modulated radiotherapy and with no previous history of salivary glands disorder were recruited. Each subject underwent US and MRI examinations, saliva test before the start of radiotherapy (RT) and at 6 months after RT. The US assessment was conducted by the same operator in which the haemodynamics including the blood flow velocity and vascular resistance of the salivary glands were measured. The MRI, which was performed using T1 and T2 axial and sagittal scans with slice thickness of 3 mm, provided the salivary glands' morphological information. The saliva test included the measurement of mean saliva flow rate (SFR) and the main contents of the saliva including alpha-amylase and immunoglobulin A (IgA). The mean values of each measured parameters were calculated and paired t-test was conducted to assess their differences between the two time intervals.

**Results**

The mean volumes of parotid and submandibular glands were significantly reduced by about 30% at 6-month after RT ( $p < 0.001$ ). The two glands also demonstrated lower vascular velocity, resistive and pulsatility indices ( $p < 0.05$ ) when compared to the pre-RT condition. This indicated that the blood flow in the post-RT glands was slower and the blood vessels experienced lower pressure than those of the pre-RT. In addition, the post-RT mean SFR was reduced by more than 9 times when compared with that in pre-RT ( $p < 0.001$ ). The levels of the salivary alpha amylase and IgA were also significantly reduced at the 6-month post-RT interval.

**Conclusion**

Our study demonstrated that there were substantive impacts on the physiological and morphological aspects of the salivary glands after radical EBRT in NPC patients. The side effects were relatively early in which most measured parameters demonstrated significant changes at 6-month post-RT interval.

### EP-1169 Evaluation of swallowing function with PSSHN scale for head and neck cancer patients undergoing IMRT

S. Agarwal<sup>1</sup>, P. Mukherjee<sup>1</sup>, M. Roy<sup>1</sup>, S. Kommineni<sup>1</sup>, N. Kalyani<sup>1</sup>

<sup>1</sup>Jaslok Hospital and Research Centre, Radiation Oncology, Mumbai, India

#### Purpose or Objective

Head neck radiotherapy is associated with significant swallowing and speech dysfunction. Intensity modulated radiotherapy may allow us to reduce the doses to swallowing structures and decrease associated morbidity. Aim of present study is to prospectively assess change in swallowing function using PSSHN questionnaire.

#### Material and Methods

This is a prospective; ethics approved protocol for assessment of change in swallowing functions for head neck carcinoma patients undergoing curative intent radiotherapy with or without concurrent chemotherapy. Patients were asked to fill up PSSHN questionnaire at baseline, at conclusion of radiation and at 3 months post radiation. Change in PSSHN scores were evaluated for all patients. CTRI Registration No is CTRI/2017/11/010378.

#### Results

Between August 2017 to April 2018, 61 patients were enrolled in the study and written informed consent was obtained. Primary sites were: Buccal mucosa 21, Oral Tongue 12, Oropharynx 10, Hypopharynx 5, Larynx 5 and Naopharynx 4. All patients were treated with IMRT with median RT dose of 60 Gy. Thirty seven patients received concurrent chemotherapy. Three patients were excluded from analysis (One died, two withdrew consent). The mean weight loss was 5 kg (range: 3-12 kg). Seventeen patients needed nasogastric tube / PEG tube during radiation. At 3 month follow up, 1 patients had persistent nasogastric tube. Mean PSSHN score at baseline was 228. The mean score at completion of RT was 142 with mean decline in score was 86 (Range 10-225). The mean score at 3 months post RT was 225. Normacy of diet was worst affected domain in PSSHN at completion of RT. There was no significant correlation between ipsilateral or bilateral nodal irradiation and decline in PSSHN scores. Buccal mucosa primary site had less decline in scores as compared to other sites however difference was not significant.

#### Conclusion

There is significant decline in PSSHN score at completion of radiation with normalcy of diet being worst affected domain. There was almost recovery of PSSHN scores after 3 months post completion of radiation.

### EP-1170 Predictive factors of chemoradiation induced oral mucositis in head and neck cancer patients.

F. Arcadipane<sup>1</sup>, E. Olimpo<sup>2</sup>, R. Ragona<sup>2</sup>, G.C. Iorio<sup>2</sup>, S. Martini<sup>2</sup>, E. Gallio<sup>1</sup>, P. Franco<sup>2</sup>, U. Ricardi<sup>2</sup>

<sup>1</sup>Città della Salute e della Scienza, Department of Oncology- Radiation Oncology, Torino, Italy; <sup>2</sup>University of Turin, Department of Oncology- Radiation Oncology, Torino, Italy

#### Purpose or Objective

Radiation-induced oral mucositis (OM) is a major dose-limiting toxicity in head and neck cancer (HNC) patients. It is a normal tissue injury caused by chemotherapy (CT) and/or radiotherapy (RT), which has marked adverse effects on patient quality of life and cancer therapy continuity. We prospectively evaluated a cohort of patient affected with HNC and treated with CT/RT in order to identify dosimetric parameters and clinical characteristics predictive for OM occurrence

#### Material and Methods

We proposed a series of questionnaires, concerning pain (VAS score), quality of life and functional endpoints (OMWQ-HN, FACT-HN) to a total of 41 HNC patients. To define OM, both WHO and OMAS scores were used. Patient

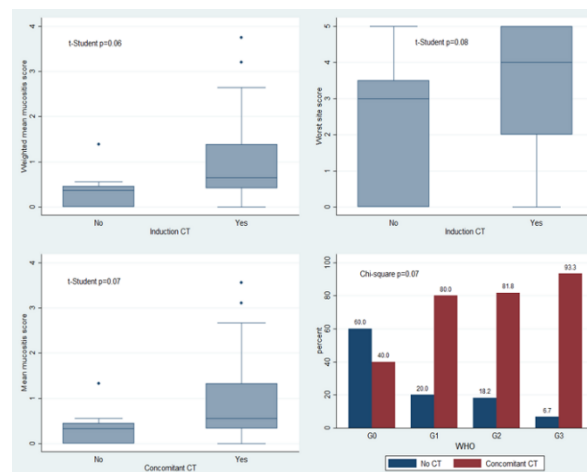
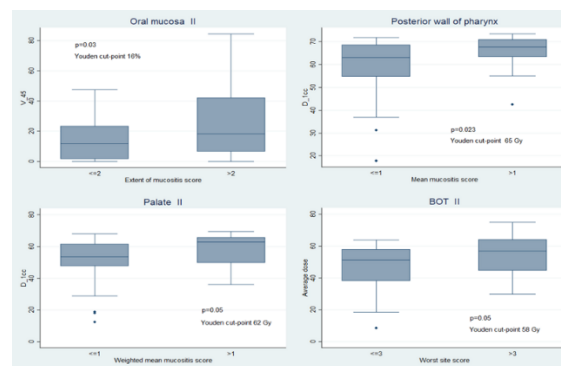
and treatment characteristics were considered. The whole oral mucosa was divided in 4 subsites: palate, base of tongue (BOT), oral cavity (OC) and posterior wall of pharynx (PWP). Planning target volumes were subtracted from the whole oral mucosa and from each subsite and dose-volume histogram (DVH) data were extracted.

DOSIMETRIC PARAMETERS	PALATE	BOT	OC	PWP	ORAL MUCOSA
Average dose	37,72 [15,62]	53,87 [15,28]	42,50 [13,69]	53,28 [14,86]	43,90 [12,57]
D 1cc	56,43 [16,40]	61,54 [12,86]	61,45 [13,36]	60,63 [12,25]	65,90 [10,87]
V20	78,65 [30,95]	94,23 [20,15]	87,70 [21,64]	90,73 [19,43]	87,56 [20,67]
V30	64,70 [33,03]	89,96 [24,27]	72,77 [26,44]	86,00 [24,22]	75,30 [23,78]
V45	37,04 [30,09]	75,74 [35,47]	45,96 [30,03]	77,14 [33,16]	50,69 [25,75]
V50	28,63 [27,92]	69,71 [37,38]	38,53 [29,79]	72,37 [35,22]	42,97 [25,50]

Table 1 Dosimetric Parameters; [Standard Deviation]

#### Results

A similar trend during treatment and follow-up was found both for the OMAS and PRO scores. In our analysis patient's age ( $p=0,02$ ), V30 ( $p=0,02$ ) and V45 ( $p=0,03$ ) of the oral mucosa, resulted to be significantly related to OM. The maximum dose (Dmax) received from PWP was related to Mean Mucositis Score (MMS) ( $p=0,023$ ), Weighted Mean Mucositis Score (WMMS) ( $p=0,022$ ) and Extent of Mucositis Score (EMS) ( $p=0,05$ ). Palate Dmax was related to MMS ( $p=0,05$ ), WMMS ( $p=0,05$ ). For BOT, the average dose was correlated to Worst Site Score (WSS) ( $p=0,05$ ). (Fig.1) OM was found to be significantly related to induction CT (WMMS  $p=0,06$  and WSS  $p=0,08$ ) and concomitant CT (MMS  $p=0,07$ ). Among patients with G3 OM, 93,3% were given concomitant CT while 6,7% underwent exclusive RT ( $p=0,07$ ). (Fig.2)



### Conclusion

In our prospective cohort, we observed a correlation between acute toxicity and pain, impairment in global health status and general QoL. DVH analysis of oral mucosa and its subsites accurately predicts acute oral mucosa toxicity. We were also able to assess the predictive value of clinical parameters for OM. Further studies will be needed to understand clinical relevance, implement daily practice and improve results.

### EP-1171 Toxicity profile of locally advanced head and neck cancer patients treated in 30 or 33 fractions RT

C. Franzese<sup>1</sup>, A. Fogliati<sup>1</sup>, D. Franceschini<sup>1</sup>, F. De Rose<sup>1</sup>, T. Comito<sup>1</sup>, P. Navarria<sup>1</sup>, L. Cozzi<sup>1</sup>, S. Tomatis<sup>1</sup>, M. Scorsetti<sup>1</sup>

<sup>1</sup>Humanitas Research Hospital, Radiotherapy and Radiosurgery, Rozzano Milan, Italy

### Purpose or Objective

Shortening the overall treatment time without increasing acute reactions is one of the major aims in radiotherapy for locally advanced head and neck cancer (LAHNC). Volumetric modulated arc therapy (VMAT) with Simultaneous Integrated Boost (SIB) showed improvements in the outcome and pattern of toxicity. Aim of this work is to evaluate the toxicity of patients presenting LAHNC, after VMAT-SIB treatment in two fractionation schemes of 30 and 33 fractions.

### Material and Methods

Two groups of LCHNC patients were selected: the first, named 33fx, of 98 patients who received 69.96 and 54.45 Gy in SIB in 33 fractions, between April 2009 and November 2015; the second, named 30fx, of 48 patients who received 66.0 and 54.0 Gy in SIB in 30 fractions, between March 2016 and January 2018. All the patients were treated with VMAT-SIB. Target volumes were delineated as CTV adding 1 cm margin to GTV for primary tumour, and according to the international guidelines for nodal regions; a CTV to PTV 5 mm isotropic margin was added for the 33fx group, and 3 mm margin for the 30fx group. Acute toxicity was graded according to CTCAE 3 for skin, salivary, mucosal, dysphagia. Doses from DVHs for each patient were recorded and analysed to determine possible correlations between dose to critical structures (parotids, oral cavity, submandibular glands and constrictor muscles) and toxicity grade.

### Results

The dosimetric results showed a significant reduction of the mean doses to the main critical structures when reducing the number of fraction (and the total dose) as well as the CTV to PTV margin. To the parotids, the mean doses were assessed as 28.0±0.7 and 21.8±0.9 Gy for 33fx and 30fx groups, respectively; to the oral cavity they were 46.3±0.9 and 40.9±1.4 Gy; for the constrictor muscles 59.5±0.5 and 52.1±0.9 Gy. Errors are the standard error of the mean.

Acute mucosal toxicity was reported as G1 in 28.6/27.1% (33fx/30fx) of the cases, G2 in 45.9/41.7%, G3 in 8.2/4.2%. Acute dysphagia was recorded as G1 in 22.4/18.8% of the patients in the 33fx/30fx groups, G2 in 25.5/56.3%, and G3 in 7.1/4.2%. Acute salivary toxicity was G1 in 25.5/8.3% of the cases, G2 in 3.1/6.3%, and G3 in 1.0/0.0%. The toxicity profile, in favour of the 30fx group, was significant only for dysphagia (p<0.01, test t). The highly significant difference in the mean doses was not translating to the same high degree of significance in the toxicity profile.

### Conclusion

Treatment of LAHNC with 30 fractions radiotherapy and 3 mm of margin seems to be advantageous for the decreased mean doses to the major organs at risk. However, significant toxicity benefit was only demonstrated in the reduction of dysphagia.

### EP-1172 Microstructural and physiological changes of parotid glands after RT for head and neck cancer

M. Bruvo<sup>1</sup>, C. Behrens<sup>2</sup>, R. Hvass<sup>3</sup>, H. Hjorth Johannesen<sup>3</sup>, A.M. Lynge Pedersen<sup>4</sup>, C. Maare<sup>2</sup>, E. Samsøe<sup>2</sup>, F. Mahmood<sup>5</sup>

<sup>1</sup>University College Copenhagen, Radiography, Copenhagen N, Denmark ; <sup>2</sup>Herlev Hospital, Radiotherapy Research Unit, Herlev, Denmark ; <sup>3</sup>Herlev Hospital, Department of Radiology, Herlev, Denmark ; <sup>4</sup>University of Copenhagen- School of Dentistry, Department of Odontology, Copenhagen N, Denmark ; <sup>5</sup>Odense University Hospital, Department of Oncology, Odense C, Denmark

### Purpose or Objective

Salivary gland hypofunction and xerostomia are prominent complications of conventional radiotherapy (RT) of head and neck cancer (HNC), having considerable negative impact on the patients' quality of life. It is therefore important to assess the salivary gland function in these patients for diagnostic and management purposes.

The aim of this study is to investigate use of diffusion-weighted magnetic resonance imaging (DWI) in the assessment of radiation-induced microstructural changes of the parotid glands in terms of apparent diffusion coefficients values (ADC), compared to physiological changes in terms of measurements of whole salivary flow rates. It is hypothesized that use of combined methods for assessment of parotid gland function, provides further insight into the factors that can predict xerostomia.

### Material and Methods

Five patients with HNC who have completed their RT course were assessed in this pilot study. The patients were examined before the first RT fraction (scan 1), after completion of the RT course (scan 2) and one year after completion of the RT course (scan 3). Unstimulated (at rest) and gustatory-stimulated DWI examinations were performed on a 1T MRI system using the DWIBS sequence. Whole-volume region of interest (ROI) method was used for delineation of parotid glands. To suppress perfusion and salivary flow effects high b-values (400, 600 and 800 s/mm<sup>2</sup>) were used for ADC calculation using a mono exponential fit. Unstimulated and chewing-stimulated whole saliva were collected and the flow rates were calculated. The degree of xerostomia was evaluated using the Radiation Therapy Oncology Group/European Organization for Research and Treatment of Cancer (RTOG/EORTC) morbidity score. Mean radiation dose (Gy) was registered for both contra- and ipsilateral parotid glands.

### Results

Mean ADC (ADC<sub>Mean</sub>) values and salivary flow rates were higher in the stimulated than in the unstimulated state (Figure 1a). An increase in ADC<sub>Mean</sub> from scan 1 to scan 3 both in unstimulated and gustatory-stimulated state is observed. Further, the unstimulated salivary flow tended to decrease, while chewing-stimulated salivary flow decreased between scan 1 and 2 and increased from scan 2 to scan 3. The ADC<sub>Mean</sub> tended to increase (R<sup>2</sup> = 0.29-0.37), and the salivary flow rates to decrease (R<sup>2</sup> = 0.01-0.12), with increasing mean radiation dose to the glands (Figures 1b). Mean radiation dose to the ipsilateral parotid gland was used for the correlation between saliva flow rates and mean dose. Figure 1c shows a strong correlation between both ADC<sub>Mean</sub> and saliva flow, and the degree of xerostomia (R<sup>2</sup> = 0.66-0.97).

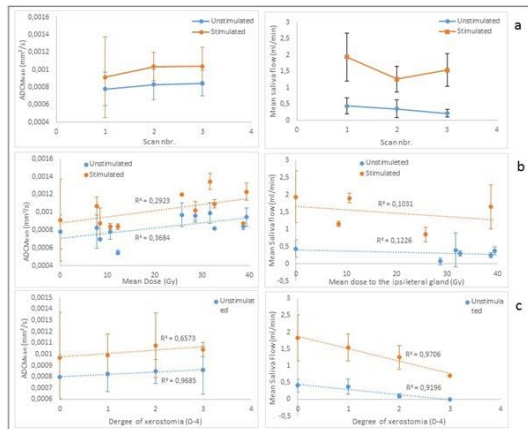


Figure 1. a) Mean ADC (Mean) values and mean salivary flow rates changes from scan 1 to scan 3 both in unstimulated and stimulated state; b) Correlation (R<sup>2</sup>) between mean ADC (Mean) values and mean radiation dose as well as correlation (R<sup>2</sup>) between mean salivary flow rates and mean dose to the ipsilateral parotid gland; c) Correlation (R<sup>2</sup>) between mean ADC (Mean) values and mean salivary flow rates and the degree of xerostomia; d) Unstimulated and stimulated state; e) Correlation (R<sup>2</sup>) between mean ADC (Mean) values and mean salivary flow rates and the degree of xerostomia; f) Unstimulated and stimulated state.

### Conclusion

The results of this pilot study indicate that the severity of microstructural and physiological changes of the parotid glands after RT is dependent on the mean radiation dose to the glands. It also suggests that DWI and salivary flow measurements can be used for assessing parotid gland function after RT and are associated with degree of xerostomia.

### EP-1173 Changes in blood pressure in patients undergoing radiotherapy for head and neck cancers

A. Nachankar<sup>1</sup>, P. Dandekar<sup>1</sup>

<sup>1</sup>Sir H N Reliance Foundation Hospital and Research Center, Radiation Oncology, Mumbai, India

### Purpose or Objective

Head and neck cancer patients undergoing radiotherapy often complain of fatigue, generalized weakness, light headedness associated with poor nutrition, weight loss, dehydration and vasomotor changes. Various theories are proposed for vasomotor imbalance including neurochemical causes, direct damage to carotid body due to radiation or effect on vasomotor centers in brainstem, effect of chemotherapy. Hence, we studied pattern of blood pressure (BP) changes in head and radiotherapy patients.

### Material and Methods

Patients with head and neck cancer, with ECOG 0-1 receiving radiotherapy to head and neck region to a dose of 60-70 Gy over period of 6-7 weeks from December 2016 to Feb 2018. We recorded blood pressure of patients, pre-radiotherapy, weekly during radiotherapy and postradiotherapy at 3-6 monthly interval. Patient symptoms were documented at the same time. We also contoured carotid body region to see document doses.

### Results

We analyzed 60 patients of head and neck cancers receiving radiotherapy to head and neck region, 34 patients received concurrent chemotherapy. Thirty-two patients received radiotherapy to bilateral neck. Twenty four out of 60 patients were hypertensive at baseline and were on antihypertensive medications and all patients continued their antihypertensive treatment. Only one patient had history of hypotension in the past. Average weight loss during radiotherapy was 4.1%. We found that there was statistically significant decline in blood pressure from 3<sup>rd</sup> to 6<sup>th</sup> week of radiotherapy in both systolic and diastolic blood pressure. Maximum average BP decline till 5<sup>th</sup> week of radiotherapy from baseline 132 +/-13 / 78 +/-7 mm of Hg to 115 +/-16 / 71 +/-9 mm of Hg (P<0.05). Compared baseline there was significant decline in blood pressure from 132 +/-13 / 78 +/-7 mm of Hg to 121 +/-14 / 75 +/-7 at 3 to 6 months post radiotherapy (P<0.05). Very

few patients complained of orthostatic hypotension. Mean doses to carotid body region were 62.45 +/- 4 Gy.

### Conclusion

There is a significant decline in BP recorded during in patient undergoing head and neck radiotherapy the effect of which was persistent upto 6 months after radiotherapy. Maximum decline observed upto 5<sup>th</sup> week of treatment. Hence, it is worthwhile to monitor BP during and after treatment and appropriate intervention to be taken.

### EP-1174 Assessment of nausea and dysgeusia in head and neck cancer patients undergoing radiotherapy

C.G. Iorio<sup>1</sup>, S. Martini<sup>1</sup>, F. Arcadipane<sup>2</sup>, E. Olimpio<sup>1</sup>, P. Franco<sup>1</sup>, U. Ricardi<sup>1</sup>

<sup>1</sup>University of Torino, Department of Oncology- Radiation Oncology, Torino, Italy ; <sup>2</sup>Città della Salute e della Scienza, Department of Oncology- Radiation Oncology, Turin, Italy

### Purpose or Objective

Nausea (N) and dysgeusia (Dg) are common side effects occurring during treatment in HN cancer patients, in case of either exclusive radiotherapy (RT) or combined modality treatment (CMT). Patients' daily living can be significantly affected by N/Dg, with a subsequent worsening of treatment compliance. We prospectively scored nausea and we employed an 18-item CiTAS (chemotherapy (CT)- induced taste alteration scale) questionnaire to evaluate 4 taste dimensions identified through factor analysis: decline in basic taste, discomfort, phantogeusia-parageusia, and general alterations.

### Material and Methods

Between 2016 and 2018, 31 patients were treated with Volumetric Modulated Arc Therapy (VMAT) in the HN region within a definitive or adjuvant setting (RT or CMT, 6 or 7 weeks overall treatment time). All patients were given 'Naumix/Naugin' (GAMfarma, Milan, Italy) a spray, containing ginger, anise and vitamin B6 as a prophylactic approach to prevent N/Dg. CiTAS scale was evaluated at baseline (Bs), every week of treatment and during follow-up at 2 adjunctive time-points (1 week and 1 month after RT end).

### Results

Patients were aged 64 (range 34-83) with mostly male sex (61.3%). Most represented tumor subsite was oropharynx (25.9%). Most common histology was SCC (77.4%). Patients were mainly staged as T1-T2 disease (58%); N0(19%), N1-3(71%). RT was delivered as definitive (38.7%) or adjuvant (61.3%) treatment with prescribed doses ranging from 54 to 70 Gy. Acute toxicities were generally mild. Grade 1 nausea was reported by 6.5% of patients at Bs, reaching the maximum value during the VI week (38.7%). No patient referred ≥ G2 nausea at Bs, while this endpoint peaked up at III week (13% of patients) with an optimal recovery in most of the patients with antiemetic drugs (Tab.1).

Tab 1- Worst events (Nause)- Note: Frequencies (Percentages) - Scale (1-3)

Grade	Baseline (n=31)	I week (n=31)	II week (n=31)	III week (n=31)	IV week (n=31)	V week (n=31)	VI week (n=31)	VII week (n=20)	I week post (n=31)	I month post (n=31)
1	2 (6.45)	6 (19.35)	10 (32.26)	6 (19.35)	10 (32.26)	8 (25.81)	12 (38.71)	5 (25.00)	5 (16.13)	2 (6.45)
2	0	1 (3.23)	0	4 (12.90)	1 (3.23)	1 (3.23)	2 (6.45)	0	1 (3.23)	0

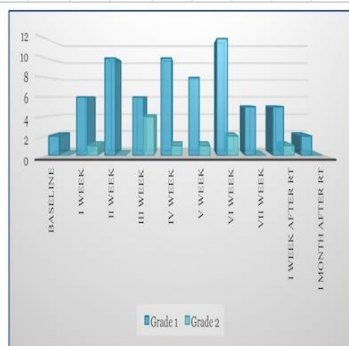


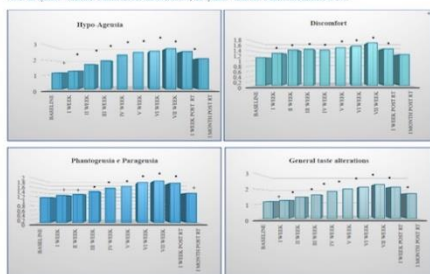
TABLE 1

For detailed CiTAS score results see Tab.2. Mean Hypo-Ageusia score was 1.14(±0.4) at Bs progressively increasing during RT and reaching the maximum values during the VII week at 2.82(±1.4) and decreasing after RT down to 2.13(±1.23) at 1 month from the end of treatment. The same could be observed for discomfort score which was 1.14(±0.47) at Bs, increased up to 1,74(±0.98) at week VII and decreased at 1.27(±0.45)1 month after treatment. The phantogeusia/parageusia score, which was 1.16(±0.60) at Bs, increased to 1.92(±1.08) at week VII and decreased to 1.36(±0.7) at week I after RT. A similar pattern was observed for general taste alterations score: 0.17(±0.43) at Bs, 2.35(±1.04) at week VII of RT and 1.73(±0.87) after 1 month from RT end.

TABLE 2

Scale trend

Note: the symbol \* indicates a difference at the level of 5%, the symbol † indicates a difference inferior to 1%.



Mean values and standard deviation CiTAS Scale

Note: only 20 patients of the overall study population (n=31) have attended a treatment schedule including a seventh week of treatment, according to the adjusted or definitive treatment setting.

Scale	Baseline	I week	II week	III week	IV week	V week	VI week	VII week	I week post	I month post
Hypo-Ageusia	1.14 (0.40)	1.26 (0.52)	1.73 (0.86)	1.99 (0.93)	2.38 (1.18)	2.57 (1.33)	2.64 (1.37)	2.82 (1.40)	2.62 (1.37)	2.13 (1.23)
Discomfort	1.14 (0.47)	1.32 (0.67)	1.45 (0.70)	1.48 (0.72)	1.45 (0.66)	1.55 (0.75)	1.61 (0.86)	1.74 (0.98)	1.50 (0.63)	1.27 (0.45)
Phantogeusia and Parageusia	1.16 (0.60)	1.27 (0.69)	1.31 (0.50)	1.45 (0.59)	1.60 (0.72)	1.68 (0.92)	1.85 (1.04)	1.92 (1.08)	1.82 (1.04)	1.36 (0.70)
General taste alterations	1.17 (0.43)	1.28 (0.50)	1.49 (0.66)	1.64 (0.69)	1.88 (0.74)	2.05 (0.99)	2.17 (1.03)	2.15 (1.04)	2.17 (1.03)	1.73 (0.87)

Conclusion

In conclusion our prospective clinical data point out the N/Dg trend during RT or CMT in HN cancer patients. We provided a quantitative and qualitative assessment of N/Dg, potentially useful for future comparison.

EP-1175 Use of different RBE-models in carbon ion RT - saving OAR constraints from being lost in translation

J.E. Dale<sup>1,2</sup>, S. Molinelli<sup>3</sup>, V. Vitolo<sup>3</sup>, B. Vischioni<sup>3</sup>, M. Bonora<sup>3</sup>, G. Magro<sup>3</sup>, A. Mairani<sup>3,4</sup>, A. Hasegawa<sup>5</sup>, O. Dahl<sup>2</sup>, F. Valvo<sup>3</sup>, P. Fossati<sup>3,6</sup>

<sup>1</sup>Haukeland University Hospital, Department of Oncology, Bergen, Norway ; <sup>2</sup>University of Bergen, Department of Clinical Science- Faculty of Medicine, Bergen, Norway ; <sup>3</sup>National Center for Oncological Hadrontherapy, Clinical department, Pavia, Italy ; <sup>4</sup>Heidelberg Ion-Beam Therapy Center, Medical physics unit, Heidelberg, Germany ; <sup>5</sup>Osaka Heavy Ion Therapy Center, Clinical department, Osaka, Japan ; <sup>6</sup>MedAustron, Carbon ion radiotherapy unit, Wiener Neustad, Austria

Purpose or Objective

In order to optimize carbon ion radiotherapy (CIRT) there is a need to validate dose constraints for important organs at risk. For the optic nerve (ON), constraints have been validated by the National Institute of Radiobiological Sciences (NIRS), Japan, in which the Relative Biological Effectiveness (RBE) of the CIRT has been predicted by the mixed beam model (RBE<sub>NIRS</sub>). These constraints are not immediately useful for centers where the Local effect model (RBE<sub>LEM</sub>) is used, because comparative studies show that RBE<sub>LEM</sub> can predict a 60% higher RBE in the entrance region of the beam, and 5-15% higher RBE in the spread-out Bragg peak, relative to RBE<sub>NIRS</sub>. At the National Center for Oncological Hadrontherapy (CNAO), Italy, current dose constraints for ONs comply with the NIRS constraints: D1% < 40 Gy(RBE) and D20% < 28Gy(RBE), although RBE<sub>LEM</sub> is used in treatment plan optimization. This is a conservative approach, possibly resulting in excessive underdosage to tumors close to the optic pathways. The aim of this work is to improve CNAO's ON dose constraints by analyzing institutional toxicity and by relating the results to RBE<sub>NIRS</sub>.

Material and Methods

A total of 65 optic nerves from 38 patients treated at CNAO with CIRT to the head and neck region in the period 2013-14 were analyzed. The physical dose of the patients' treatment plans was reproduced. Subsequently, both the RBE<sub>LEM</sub> and RBE<sub>NIRS</sub> was applied as RBE model, thus relating CNAO clinical toxicity to the NIRS constraints in RBE<sub>NIRS</sub>-weighted dose. Prediction of doses to selected volumes of the ONs giving x% probability of toxicity (TDx%) was derived using logistic regression.

Results

Median follow-up time was 47 (26-67) months. No toxicity occurred in the 56 ONs in which the current constraints were obeyed. Three ONs developed visual decline at doses D1%≥71 Gy(RBE<sub>LEM</sub>)/68 Gy(RBE<sub>NIRS</sub>) and D20%≥68 Gy(RBE<sub>LEM</sub>)/62 Gy(RBE<sub>NIRS</sub>). Table 1 presents patient characteristics and results of NTCP modelling. TD50 was comparable to the NIRS publication, while TD5 was substantially higher in our results, probably due to a scarcity of ONs receiving mid- to high doses relative to the ONs in NIRS publication. Figure 1 presents DVHs of all ONs in both RBE<sub>LEM</sub>- and RBE<sub>NIRS</sub>-weighted doses and demonstrates that potential new CNAO D1% and D20% constraints should be maximum 49 and 40 Gy(RBE<sub>LEM</sub>), substantially lower than the predicted TD5 doses, in order to comply with the respective NIRS constraints of 40 and 28 Gy(RBE<sub>NIRS</sub>).

TABLE 1					
PATIENT AND DISEASE CHARACTERISTICS CNAO PATIENTS (n=38)					
<b>Gender</b>	Female : Male		18:20		
<b>Age</b>	Median (range), years	59	(16-81)		
<b>ON volume</b>	Median (range), cm <sup>3</sup>	0.92	(0.45-1.57)		
<b>Total dose</b>	Median (range), Gy(RBE)	70.4	(68.8-76.8)		
<b>Fraction dose</b>	Median (range), Gy(RBE)	4.4	(4.3-4.8)		
<b>Site</b>	Clivus	12	31.6%		
	Paranasal sinus	9	23.7%		
	Skull base	9	23.7%		
	Nasal cavity	4	10.5%		
	Nasopharynx	2	5.2%		
<b>Histology</b>	Other	2	5.2%		
	Adenoid cystic carcinoma	14	36.8%		
	Chordoma	14	36.8%		
	Chondrosarcoma	3	7.9%		
	Other sarcoma	5	13.2%		
	Acinar cell carcinoma	1	2.6%		
	Mucosal malignant melanoma	1	2.6%		
COMPARISON NTCP		CNAO		NIRS <sup>1</sup>	CNAO/NIRS-1
CNAO vs NIRS		(RBE <sub>LEM</sub> )	(RBE <sub>NIRS</sub> )	(RBE <sub>NIRS</sub> )	(RBE <sub>NIRS</sub> )
<b>TD5, Gy(RBE)</b>	D1%	62	49	n.s.	
	D10%	61	45	30*	50,0 %
	D20%	55	42	28*	50,0 %
	D30%	47	37	24*	54,2 %
	D50%	41	30	12*	150,0 %
<b>TD50, Gy(RBE)</b>	D1%	71	68	n.s.	
	D10%	69	63	63	0,0 %
	D20%	66	60	n.s.	
	D30%	64	57	59	-3,4 %
	D50%	61	53	51	3,9 %

n.s.= not specified. \*=approximated from NTCP curves<sup>1</sup>

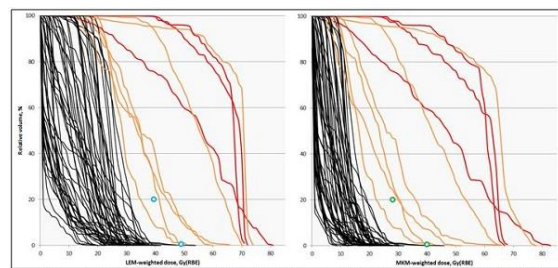


Figure 1: Cumulative DVHs of 65 ONs in RBE<sub>LEM</sub>-weighted dose (left panel) and RBE<sub>NIRS</sub>-weighted dose (right panel), showing the 3 ONs that developed visual decline (red), the DVHs that did (orange and red) or did not (black) breach NIRS D1% and/or D20% constraints (green circles) in RBE<sub>LEM</sub>-weighted dose. Blue circles illustrate possible new RBE<sub>LEM</sub>-weighted dose constraints that would comply with RBE<sub>NIRS</sub>-weighted dose constraints.

### Conclusion

This analysis confirms that the current constraints used at CNAO are safe, but suggest that the D1% and D20% constraints could be increased to about 49 and 40 Gy(RBE<sub>LEM</sub>), respectively. However, due to uncertainties in the recalculation method applied, and differences in the physical beam model of original NIRS and CNAO treatment planning system, only a partial and step-wise escalation of dose constraints should be done within protocols providing careful observation and revalidation.

### EP-1176 Comparison of patient and physician reported acute toxicities during head and neck cancer radiotherapy

J. Bhattacharya<sup>1</sup>, A. Jawade<sup>1</sup>, P. Vijayaraghavan<sup>1</sup>, T. Shahid<sup>1</sup>, M. Mukherjee<sup>1</sup>, R. Talukder<sup>1</sup>, A. Samanta<sup>1</sup>, C. Saikia<sup>1</sup>, A. De<sup>1</sup>, D. Barman<sup>1</sup>, T. Ghosh<sup>1</sup>, S. Sadhukhan<sup>1</sup>  
<sup>1</sup>Apollo Gleneagles Hospital- Kolkata, Radiation Oncology- Cancer Block- 1st Floor, Kolkata, India

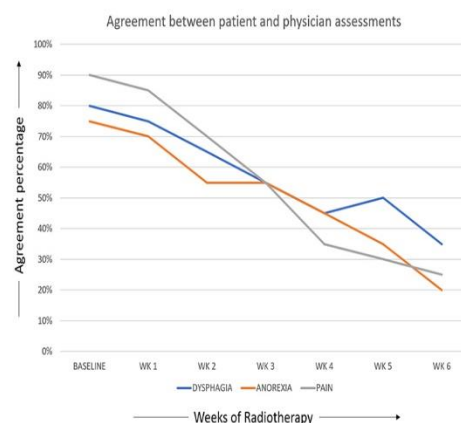
### Purpose or Objective

The purpose of our study was to prospectively assess and compare acute toxicities reported by radiation oncologists and patient reported outcome measures (PROM) during concurrent chemoradiation for locally advanced squamous cell carcinoma of head and neck. The aim was to find discordance between subjective and objective assessments and its characteristics.

### Material and Methods

Twenty patients of locally advanced head and neck squamous cell carcinoma on radical concurrent chemoradiation were included. Acute toxicities were assessed at baseline, weekly and at the end of treatment by the radiation oncologists and patients themselves independently. National Cancer Institute's Common Terminology Criteria for Adverse Events (CTCAE version 5.0) for 12 domains was used by the radiation oncologists while PROM for the same were recorded using PRO-CTCAE. At each point of assessment, the toxicity grades were compared in terms of agreement or disagreement between patients and physicians. The incidence, pattern and degree of disagreement between patients and physicians were analysed statistically. The relation between severity of toxicity and degree of disagreement were studied and plotted with Bland Altman Analysis.

### Results



20 male patients with mean age of 59 years with locally advanced carcinoma of oral cavity, oropharynx, hypopharynx and larynx were assessed. 6 (30%) and 12 (60%) patients presented with T4 disease and Node positive disease respectively. All patients were treated with cisplatin based chemoradiation. 3DCRT or IMRT were used. 30-35% patients developed grade 3 acute toxicity in terms of dysphagia, mucositis or dermatitis as per CTCAE. No grade 4 or above toxicity was noted. Some degree of disagreement existed at baseline for symptoms like pain (10%), dysphagia (20%), anxiety (25%) and depression (20%). The agreement between physician assessments and PROM demonstrated a decreasing trend from 80-100% at baseline to 20-35% at week 6 of treatment for all domains. Maximum disagreement was observed with pain (80%) and Anorexia (20%) at 6<sup>th</sup> week. The degree of disagreement (by one or two points) was found to be increasing with severity of toxicity grades (mean toxicity grade). The patient reported toxicity grades always remained higher across all domains towards the end of treatment. 3 patients required hospitalisation for toxicity management and treatment was interrupted for 4 patients.

### Conclusion

The study found that a significant amount of disagreement exists between physician and patients and the gap increases with the severity of toxicity. The result evokes the thought that there is a possibility of under-assessment by the physician or over-assessment of acute toxicities by the patients which may ultimately affect the final clinical outcome. These two scales can be used as complementary tools to assess acute toxicities more accurately so that an early intervention can be done. This is an ongoing prospective study in our department.

### EP-1177 Comparative study assessing QoL in HNSCC patients treated with Radical Radiation with IMRT vs 3DCRT

M. Mukherjee<sup>1</sup>, J. Bhattacharya<sup>1</sup>, T. Shahid<sup>1</sup>, A. Samanta<sup>1</sup>, L.N. Biswas<sup>1</sup>, A. Jawade<sup>1</sup>, A. De<sup>1</sup>, D. Barman<sup>1</sup>, T. Ghosh<sup>1</sup>, S. Sadhukhan<sup>1</sup>, P. Vijayaraghavan<sup>1</sup>, R. Talukdar<sup>1</sup>, C. Saikia<sup>1</sup>, R. Rajan<sup>1</sup>, R. Raj<sup>1</sup>  
<sup>1</sup>Apollo Gleneagles Hospital, RADIATION ONCOLOGY, Kolkata, India

#### Purpose or Objective

The purpose of the study is to assess and compare health-related quality of life (HRQOL) in patients with HNSCC, treated with radical radiotherapy with IMRT versus 3D-CRT.

#### Material and Methods

From January 2018 to May 2018, 40 patients of squamous cell carcinoma of oropharynx, larynx and hypopharynx (cT1-3 N0-2b except cT1N0 glottic cancer) undergoing radical radiotherapy either alone or with concurrent chemotherapy were included in this study. Patients were treated with radical doses with conventional fractionation using either IMRT or 3DCRT. EORTC QLQ-C30 and HN35 were used to study the HRQOL and assessed for each patients at baseline i.e. before the commencement of radiation, at 3<sup>rd</sup> week of RT, after completion of treatment, at 1 month and at 3 months of follow up. Radiation induced acute toxicities were assessed by RTOG acute toxicity criteria, every week during radiotherapy. For comparison, QOL data collected at different point of time were analyzed using unpaired 't' test and for acute radiation induced toxicities chi-square test was used.

#### Results

40 patients were evaluated in the study. The mean age of the sample population was 60 years with predominant male population (90%). Larynx was the commonest site (18 patients, 45%). 13 patients (32.5%) had T3 disease and 10 (25%) patients had node positive disease. 14 (35%) patients received cisplatin based concurrent chemotherapy. The number of patients treated with 3DCRT and IMRT were 19 and 21 respectively. HRQOL scores of various components deteriorated during and after treatment in both the arms. HRQOL scores of fatigue (24 vs 17, p=0.041), appetite loss (73 vs 44, p<0.001) and sense problems (31 vs 15, p<0.001) were significantly worse in IMRT group during and after completion of treatment. However, these differences were not evident at 3 months of follow up. Dryness of mouth and sticky saliva were significantly more in 3D-CRT group (HR-QoL score for dryness of mouth 60 vs 0, p<0.001 and for sticky saliva 9.52 vs 0, p=0.24) during radiation and 3 months after completion of treatment. Insomnia and ill feeling were found to be significantly more in 3DCRT arm. Other parameters like global health, physical, emotional and social functions, speech and swallowing, nutritional parameters remained comparable in both arms. There was no grade 4 or above acute toxicities. No significant difference was observed in acute toxicities e.g. mucositis, dysphagia, skin toxicities between IMRT and 3DCRT arm during RT.

#### Conclusion

Our study shows that technique of radiation (3D-CRT and IMRT) affects QoL in HNSCC, treated radically. Though there was no difference in terms of acute toxicity in between groups but IMRT did significantly better considering dryness of mouth and sticky saliva, not only during treatment but at 3 months after completion of treatment. More number of patients and long term follow up is required to validate these findings. This is an ongoing study in our department.

### EP-1178 Prognostic role of FDG-PET/CT during radiotherapy in patients with hypopharyngeal carcinoma

T. Mase<sup>1</sup>, Y. Toyomasu<sup>1</sup>, Y. Watanabe<sup>1</sup>, T. Kawamura<sup>1</sup>, A. Takada<sup>1</sup>, S. Ochiai<sup>2</sup>, Y. Yamashita<sup>3</sup>, N. Ii<sup>4</sup>, H. Sakuma<sup>1</sup>, Y. Nomoto<sup>1</sup>

<sup>1</sup>Mie University Hospital, Department of Radiology, Tsu, Japan ; <sup>2</sup>Saiseikai Matsusaka General Hospital, Department of Radiation Oncology, Matsusaka, Japan ; <sup>3</sup>Matsusaka Central Hospital, Department of Radiation Oncology, Matsusaka, Japan ; <sup>4</sup>Ise Red Cross Hospital, Department of Radiation Oncology, Ise, Japan

#### Purpose or Objective

Our study aimed to investigate the prognostic effects of <sup>18</sup>fluoro-2-deoxy-D-glucose positron emission tomography/computed tomography (PET/CT) during definitive radiotherapy (RT) in patients with hypopharyngeal squamous cell carcinoma.

#### Material and Methods

The pretreatment and interim PET/CT images of 38 patients with hypopharyngeal squamous cell carcinoma, receiving definitive RT between February 2014 and June 2018, were evaluated prospectively. RT was delivered 5 days a week using a single daily fraction of 1.8 Gy, to a total dose of 70.2 Gy. The interim PET/CT images were taken at a cumulative RT dose ranging from 36.0 to 45.0 Gy. The maximum standardized uptake value (SUV<sub>m</sub>) of primary tumor both pretreatment PET/CT and interim PET/CT and the reduction ratio of the SUV<sub>m</sub> (SRR) between the two images were measured. Progression-free survival (PFS) was calculated using the Kaplan-Meier method. Univariate and multivariate analyses were performed to evaluate the prognostic value of pretreatment SUV<sub>m</sub>, interim SUV<sub>m</sub>, SRR, age, sex, primary tumor site, T classification, and stage for prediction of PFS.

#### Results

The median follow-up time was 18 months (range, 6-55 months). The 1-year and 2-year PFS rates were 75.6% and 68.6 %, respectively. Eleven (29%) of 38 patients experienced disease recurrence (n=10, 26%) or death (n=4, 11%). In univariate analysis, a higher interim SUV<sub>m</sub> and a lower SRR were associated with the inferior PFS (Figure 1, Figure 2). Conducting a multivariate analysis revealed that an interim SUV<sub>m</sub> of primary tumor was an independent prognostic factor for PFS (Hazard ratio (95% CI), 12.5(1.59-98.21); p=0.016).

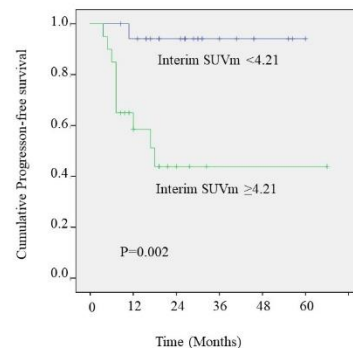


Figure.1 Progression-free survival according to interim SUV<sub>m</sub>. SUV<sub>m</sub>=maximum standardized uptake value.

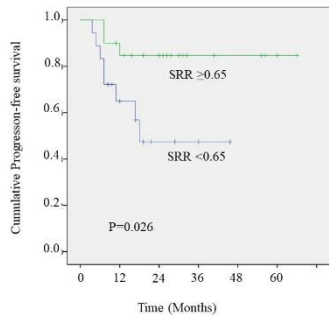


Figure 2 Progression-free survival according to SRR.  
SRR=reduction ratio of the maximum standardized uptake value of primary tumor.

### Conclusion

A higher interium SUVm of primary tumor was founded to be the prognostic indicator of oncological outcome.

### EP-1179 Primary concurrent chemoradiotherapy for locally advanced laryngeal squamous cell carcinoma

D. Adjogate<sup>1</sup>, F. De Felice<sup>1,2</sup>, Y. Suh<sup>1</sup>, J. Jeannon<sup>3</sup>, R. Oakley<sup>3</sup>, R. Simo<sup>3</sup>, M. Lei<sup>1</sup>, T. Guerrero Urbano<sup>1</sup>

<sup>1</sup>Guy's and St Thomas' NHS Foundation Trust, Department of Clinical Oncology, London, United Kingdom ;

<sup>2</sup>Policlinico Umberto I "Sapienza" University of Rome, Department of Radiotherapy, Rome, Italy ; <sup>3</sup>Guy's and St Thomas' NHS Foundation Trust, Head and Neck Unit, London, United Kingdom

### Purpose or Objective

Treating locally advanced laryngeal squamous cell carcinoma (SCC) with primary chemoradiotherapy (CRT) can preserve the larynx without compromising survival. However, whether this is associated with good functional outcomes remains up for debate. The aim of this study was to evaluate survival and functional outcomes in patients with locally advanced laryngeal SCC treated with primary CRT, with a focus on T3 disease.

### Material and Methods

We retrospectively analysed data from all consecutive patients with stage III-IV (M0) disease treated with primary CRT in our centre between January 2007 and December 2016.

Study endpoints were overall survival (OS), disease free survival (DFS), laryngectomy free survival (LFS), laryngo-oesophageal dysfunction free survival rate (LEDFS) and functional preservation rates (defined by freedom from tracheostomy or feeding tube at 2 years). Prognostic factors were assessed by univariate and multivariate analysis.

### Results

76 patients who underwent primary radical CRT were analysed. 25 patients received induction chemotherapy prior to CRT. 64 patients (89%) received concomitant platinum-based chemotherapy, and 8 (11%) concomitant Cetuximab. 74% of patients were treated with IMRT. All patients received elective nodal irradiation. The median follow-up was 42 months (range 3-109).

Median OS was 62 months. OS rates were 73.6% and 51.5% at 2- and 5 years, respectively. The 2- and 5-year DFS rates were 68.3% and 62.8%. For patients with T3 disease, the 2-year OS rate was 79.5% and DFS rate was 70.2%. Patients with positive nodal status, N2b or above disease, stage IV disease and age greater than 60 years demonstrated poor OS on univariate analysis. Older age (HR 3.13; 95% CI 1.39-6.98, p=0.005) and positive nodal status (HR 3.81; 95% CI 1.15-12.62, p=0.029) remained poor prognostic factors for survival on multivariate analysis.

Functional preservation was 67.3% at 2 years in all patients alive (64.8% in T3 patients). 70% of patients treated with IMRT had a preserved larynx at 2 years versus 58.3% for 3D-conformal RT. The 2-year LEDFS rate was 47.4%. The

2-year LFS rate was 85.8% for all patients and 89.9% for T3 patients. Salvage laryngectomies were performed in 11 patients; of which 10 were performed within 2 years of CRT. Use of induction chemotherapy had no effect on LFS or OS. There was also no demonstrated difference in LFS rate between RT technique (IMRT vs. 3D-conformal), primary tumour localization (Supraglottic vs. Glottic) or T3 subgroup (fixed vs. mobile larynx or cartilage invasion vs. no cartilage invasion).

### Conclusion

Our study illustrates high rates of OS, DFS and LFS. Functional preservation was highest in patients treated with IMRT. LEDFS rate was moderately low due to the inclusion of all-cause deaths, as per international consensus. The survival rates suggest that carefully selected patients with locally advanced laryngeal carcinoma can successfully be treated with larynx-preserving primary CRT without compromise on survival.

### EP-1180 Re-radiation in head and neck malignancies: experience from a tertiary care centre in eastern india

J. Bhattacharya<sup>1</sup>, M. Mukherjee<sup>1</sup>, V. Kumar K<sup>1</sup>, R. Rajan<sup>1</sup>, T. Shahid<sup>1</sup>, S. Goswami<sup>1</sup>, L. Naha Biswas<sup>1</sup>, P. Chatterjee<sup>1</sup>, S. Saha<sup>1</sup>

<sup>1</sup>Apollo Gleneagles Hospital- Kolkata, Radiation Oncology- Cancer Block- 1st Floor, Kolkata, India

### Purpose or Objective

Recurrent and second primary (RSP) of head-and-neck squamous cell carcinomas (HNSCC) arising within or close to previously irradiated areas are of significant clinical challenge. Salvage surgical resection is the standard of care, but reirradiation is often needed as an adjunct treatment and also needed when surgery is not feasible. The therapeutic ratio of reirradiation for RSP of HNSCC may be improved in the intensity modulated radiation therapy (IMRT) era. However, patient selection for reirradiation remains challenging. The aim of the study is to investigate outcomes after IMRT based reirradiation and to assess toxicity and median survival after re-irradiation in recurrent head and neck cancer patients treated at our institution since January 2013 till December 2017.

### Material and Methods

All patients were treated after confirming prior radiation dose, treatment portal and treatment technique or by assuming patients got a full radical dose of prior radiation. Minimum gap of 6 months after prior radiation, PS ECOG 1-2, Age < 75 years, no prior grade 4 late toxicity were taken as the inclusion criteria.

### Results

43 patients were included of which 37 were male and 6 were female. Recurrent disease was local in 70% and second primary in 30%. Minimum and maximum radiation free interval was 6 months and 196 months respectively with a mean interval being 58 months. 44% were treated radically and 56% treated post-operatively. All the patients were treated with IMRT/VMAT with conventional fractionation. Target volumes in 30 patients included nodal volumes only and in 13 patients primary disease was the target. (Depending on the recurrence pattern). Mean dose to PTV was 58.6 Gy with a minimum dose of 36 Gy and maximum 66 Gy was prescribed according to the clinical scenario and disease free interval. 6 patients received concurrent chemotherapy. The rates of grade 3 and grade 4 acute toxicities were 18% and 4.2% respectively. Median survival was 33 months, with 61% of the 43 patients alive at the time of this analysis. Poor nutritional status, weight loss, speech and swallowing difficulty was the other toxicity seen almost in every patient.

### Conclusion

Outcomes of our study reflect an efficient way of utilizing technology in combination with stringent patient selection criteria. IMRT technique must be applied with high priority to the limited target volume to reduce acute and late

morbidities and to reduce inevitable radiation related complications such as dysphagia, speech issue and neurological damage. In spite of all, the prognosis remains uncertain.

### EP-1181 Structure delineation using a deformable image registration-based contour propagation in HNC

B. Ng-Cheng-Hin<sup>1</sup>, D. McQuaid<sup>2</sup>, A. Dunlop<sup>2</sup>, S. Court<sup>2</sup>, I. Petkar<sup>1</sup>, C. Nutting<sup>1</sup>, K. Harrington<sup>1</sup>, S. Bhide<sup>1</sup>, K. Newbold<sup>1</sup>

<sup>1</sup>The Institute of Cancer Research and Royal Marsden NHS Trust, Head and Neck Radiotherapy and Imaging, Sutton, United Kingdom ; <sup>2</sup>The Institute of Cancer Research and Royal Marsden NHS Trust, Joint Department of Physics, Sutton, United Kingdom

#### Purpose or Objective

Delineation of head and neck structures and target volumes on planning CT is an essential but time-consuming process for the radiation oncologist (RO). Repeat delineation as part of adaptive radiotherapy substantially increases clinical workload, therefore there is interest in facilitating this process in a safe and efficient manner.

The aim of this study is to assess the benefit of the contour propagation component of a commercial adaptive planning workflow and the potential to save RO delineation time.

#### Material and Methods

5 head and neck cancer patients underwent a pre-treatment and repeat planning CT during treatment as part of the INSIGHT trial (CCR3926). The organs at risk (OARs) and target volume were delineated on the pre-treatment and repeat CT using RayStation 7.0 (RaySearch Laboratories, Stockholm, Sweden). The delineated structures from the pre-treatment scan were propagated to the repeat CT using an intensity-based Deformable Image Registration (DIR). This involved an initial rigid registration followed by DIR of the pre-treatment CT onto the repeat CT. The propagated structures were independently reviewed, modified and compared to the RO-delineated structures on the repeat scan. All contours were delineated by a single RO and reviewed by 2 experienced RO.

RO delineation was compared to the DIR propagated group using time factors and qualitative analysis using Dice similarity coefficient (DSC) and mean distance to agreement (MDA). **Results**

The mean time taken by the RO to delineate on the repeat CT was 87.34 minutes (SD 13.32). The mean time to propagate and amend the contours was significantly reduced (Paired t-test,  $p = 0.0039$ ) to 34.46 minutes (SD 7.02).

Compared to RO delineation, the mean MDA were 1.10 mm (SD 1.10) and 0.77 mm (SD 0.38) for unmodified and modified contours respectively. The mean DSC were 0.76 (SD 0.17) and 0.82 (SD 0.13) for the unmodified and modified contours respectively.

DSC for the unmodified structures were  $<0.8$  for the GTV and small OARs such as the lens, optic nerves and chiasm. All DSC either improved or remained unchanged following RO amendment.

Table 1. DICE and MDA scores reflecting the volumetric overlap and mean surface distance between 2 contours on registered images respectively. These scores compare clinician recontoured structures to clinician modified or unmodified propagated structures. A DSC tolerance of 0.8 to 0.9 and MDA between 2 to 3 mm were used tolerance as suggested by the AAPM Radiation Therapy Committee Task Group 132.

		DSC		MDA	
		Mean	Standard Deviation	Mean (mm)	Standard Deviation (mm)
GTV Node	RO Modified	0.82	0.06	0.62	0.29
	Unmodified	0.63	0.12	1.89	1.50
GTV Primary	RO Modified	0.73	0.07	1.23	0.29
	Unmodified	0.52	0.27	3.56	2.84
Right Parotid	RO Modified	0.89	0.03	0.91	0.25
	Unmodified	0.87	0.03	1.03	0.29
Left Parotid	RO Modified	0.89	0.02	0.78	0.17
	Unmodified	0.87	0.03	0.90	0.17
Spinal Cord	RO Modified	0.86	0.03	0.62	0.16
	Unmodified	0.85	0.03	0.63	0.14
Brain Stem	RO Modified	0.87	0.02	1.15	0.17
	Unmodified	0.86	0.01	1.21	0.16
Chiasm	RO Modified	0.55	0.21	0.88	0.47
	Unmodified	0.50	0.15	1.24	0.50
Right Optic Nerve	RO Modified	0.80	0.02	0.50	0.17
	Unmodified	0.72	0.12	0.62	0.33
Left Optic Nerve	RO Modified	0.77	0.02	0.59	0.29
	Unmodified	0.67	0.07	0.83	0.32
Right Lens	RO Modified	0.74	0.09	0.28	0.11
	Unmodified	0.73	0.08	0.33	0.12
Left Lens	RO Modified	0.70	0.19	0.50	0.37
	Unmodified	0.64	0.17	0.56	0.34
Right Globe	RO Modified	0.92	0.03	0.55	0.33
	Unmodified	0.92	0.03	0.61	0.35
Left Globe	RO Modified	0.93	0.01	0.52	0.13
	Unmodified	0.92	0.03	0.59	0.24
High dose CTV	RO Modified	0.91	0.03	1.1	0.31
	Unmodified	0.91	0.03	1.1	0.33
Prophylactic CTV	RO Modified	0.84	0.01	1.28	0.23
	Unmodified	0.81	0.05	1.45	0.42

#### Conclusion

Contour propagation using DIR significantly reduces RO delineation time. Although volumetric overlap did not perform well for small organs and the GTV, the mean MDA for each structure showed a high level of agreement for all structures apart from the unmodified GTV. This suggests that DSC overestimates the errors for small structures. RO modifications led to an improvement in volumetric overlap of the majority of the organs and target volume, but did not match perfectly. This may be accounted for by intra-observer variability or a bias towards making minimal changes to the propagated structures. A larger patient database is required to confirm the findings of this study and further work on the dosimetry impact of RO modification versus no modifications should be made.

### EP-1182 Selective neck irradiation for oropharynx cancer in relation with human papilloma virus status

S. Park<sup>1,4</sup>, D. Oh<sup>1</sup>, J.M. Noh<sup>1</sup>, Y.C. Ahn<sup>1</sup>, Y.H. Ko<sup>2</sup>, M.K. Chung<sup>3</sup>, H.S. Jeong<sup>3</sup>, Y.I. Son<sup>3</sup>, C. Baek<sup>3</sup>

<sup>1</sup>Samsung Medical Center, Radiation Oncology, Seoul, Korea Republic of ; <sup>2</sup>Samsung Medical Center, Pathology, Seoul, Korea Republic of ; <sup>3</sup>Samsung Medical Center, Otorhinolaryngology-Head and Neck Surgery, Seoul, Korea Republic of ; <sup>4</sup>Keimyung University Dongsan Medical Center, Radiation Oncology, Daegu, Korea Republic of.

#### Purpose or Objective

To evaluate the feasibility of selective neck irradiation (SNI) policy during definitive radiation therapy (dRT), in relation with human papilloma virus (HPV) status, for oropharyngeal cancer (OPC).

#### Material and Methods

From January 2008 to December 2017, 214 OPC patients received dRT, mainly by Helical Tomotherapy. HPV status was known in 150 patients (HPV+ in 115 and HPV- in 35), and the majority (138/150, 92.0%) received concurrent systemic therapy. Between HPV+ and HPV- patients, there

was no difference in the characteristics of demography, tumor burden (according to the 7th edition AJCC stage), and treatment. The same dose schedule, according to our SNI policy, was applied regardless of HPV status: 66-68.4 Gy in 30 fractions to the gross tumor volume (GTV); 60 Gy in 30 fractions to the high-risk clinical target volume (HR-CTV) that included immediately adjacent lymphatic level; and 36 Gy in 18 fractions to the low-risk CTV (LR-CTV) that included 1 additional lymphatic level, respectively.

#### Results

The median follow-up period was 35 (3-120) months. Grade  $\geq 3$  mucositis, dermatitis, weight loss, and soft tissue necrosis developed in 35 (16.4%), 7 (3.3%), 14 (6.5%), and 11 patients (5.1%), respectively, with no difference according to HPV status. The 3-year rates of locoregional control (LRC), distant control (DC), and overall survival (OS) of all patients were 91.7%, 89.6%, and 89.1%, respectively. HPV+ patients achieved significantly better LRC (93.3% vs. 78.6%,  $p=0.013$ ), but no difference was apparent in DC (89.1% vs. 85.8%,  $p=0.542$ ) and OS (90.6% vs. 81.6%,  $p=0.110$ ), respectively. Among 14 patients who developed regional failure, the failure sites in relation to the target volume were inside the GTV/HR-CTV in 11 (78.6%), both inside and outside the GTV/HR-CTV in two (14.3%), and outside the GTV/HR-CTV in one (7.1%), respectively.

#### Conclusion

Based on favorable LRC in HPV+ patients with the equivalent acute side effect profile, coupled with infrequent outside the GTV/HR-CTV failure, the current SNI policy seems successful, both in HPV+ and HPV- patients, and additional effort to improve LRC in HPV- patients may be necessary.

#### EP-1183 Proton therapy boost in locally advanced head and neck cancer: toxicity and clinical outcome

E. D'Ippolito<sup>1</sup>, B. Vischioni<sup>1</sup>, M. Bonora<sup>1</sup>, S. Ronchi<sup>1</sup>, V. Vitolo<sup>1</sup>, D. Alterio<sup>2</sup>, M.R. Fiore<sup>1</sup>, R. Petrucci<sup>1</sup>, A. Iannalfi<sup>1</sup>, A. Barcellini<sup>1</sup>, A. Mrandola<sup>3</sup>, E. Mastella<sup>1</sup>, G. Magro<sup>1</sup>, G. Viselner<sup>4</sup>, A. Facoetti<sup>1</sup>, M. Ciocca<sup>1</sup>, L. Preda<sup>4</sup>, M. Krengli<sup>5</sup>, G. Ivaldi<sup>6</sup>, P.F. Franco<sup>7</sup>, U. Ricardi<sup>7</sup>, M.F. Palazzi<sup>8</sup>, B.A. Jereczek-Fossa<sup>2,9</sup>, F. Valvo<sup>1</sup>, R. Orecchia<sup>1,2</sup>

<sup>1</sup>National Center of Oncological Hadrontherapy, Radiotherapy Unit, Pavia, Italy ; <sup>2</sup>European Institute of Oncology, Division of Radiation Therapy, Milan, Italy ; <sup>3</sup>National Center of Oncological Hadrontherapy, Radiation therapy Unit, Pavia, Italy ; <sup>4</sup>National Center of Oncological Hadrontherapy, Diagnostic Imaging Unit, Pavia, Italy ; <sup>5</sup>University Hospital- Novara, Division of Radiation Oncology, Novara, Italy ; <sup>6</sup>ICS Maugeri Pavia, Unit of Radiation Oncology, Pavia, Italy ; <sup>7</sup>University of Turin, Department of Oncology- Radiation Oncology, Turin, Italy ; <sup>8</sup>Niguarda Ca' Granda Hospital, Unit of Radiotherapy, Milan, Italy ; <sup>9</sup>University of Milan, Department of Oncology and Hemato-oncology, Milan, Italy

#### Purpose or Objective

evaluation of feasibility, acute toxicity and early clinical outcome in patients (pts) with locally advanced head and neck cancer (LAHNC) treated with exclusive sequential mixed beam (MB) approach: intensity modulated radiation therapy (IMRT) followed by proton therapy (PT) boost on high risk areas.

#### Material and Methods

between July 2012 to January 2018, 41 pts (29 male, 12 female), median age 51 years (range, 18-74), with histologically proven LAHNC (stage III and IV) were treated using a MB approach: IMRT of the neck and macroscopic disease, followed by PT boost on the pre-treatment macroscopic disease. Tumor sites were: nasopharynx 28 pts (69%), oropharynx 5 pts (12%), larynx 1 patient (2%), sinonasal 4 pts (10%) and oral cavity 3 pts (7%). The histology was: squamous cell carcinoma for 11 pts (28%), neuroendocrine tumor for 2 pts (5%);

nasopharynx tumor were classified according to World Health Organization (WHO) classification (2005): I type 4 pts (10%), II type 19 pts (47%) and III type 4 pts (10%). IMRT prescription dose was 54-60 Gy (elective irradiation of the neck and macroscopic disease), PT prescription dose was 10-20 Gy Relative Biological Effectiveness (RBE), for a total dose up to 70-74 Gy RBE. Local control (LC) and toxicity profile (according to Common Terminology Criteria Adverse Events -CTCAE V4.03- scale) were evaluated

#### Results

Twenty-three pts (56%) received platinum based induction chemotherapy, 39 pts (95%) received concurrent chemoradiation therapy. The median follow-up was 12 months, (range, 4-57). Treatment was well tolerated, 11 (27%) pts developed grade 3 acute radiation-related toxicity: 2 pts (5%) mucositis, 1 patient (2%) skin reaction and 5 pts (12%) dysphagia. No pts had high grade (grade 3-4) late toxicity. Grade 2 late toxicity was xerostomia found in 12 (29%) pts. Two pts (5%) developed G1 brain radionecrosis at 14 and 16 months after the end of the treatment, respectively, in both cases it was resolved at least follow-up. LC was 83%. Four pts had local recurrence at 12, 11, 8 and 8 months after treatment, respectively. Three pts developed distant metastases at 6, 18 and 25 months after the end of the treatment. Three pts died for tumor specific-causes.

#### Conclusion

for pts with LANHC a MB approach was feasible and our results showed good short-term outcome and limited radiation-related side effects. Preliminary results are encouraging but a longer follow-up and large patient accrual are required.

#### EP-1184 Target volume delineation for adaptive treatment in HNSCC is highly variable among experts

R. Apolle<sup>1,2</sup>, H.P. Bijl<sup>3</sup>, P. Blanchard<sup>4</sup>, A. Laprie<sup>5</sup>, I. Madani<sup>6</sup>, A. Ruffier<sup>4</sup>, W. Van Elmpt<sup>7</sup>, E.G.C. Troost<sup>1,2,8,9,10</sup>

<sup>1</sup>OncoRay - National Center for Radiation Research in Oncology, Faculty of Medicine and University Hospital Carl Gustav Carus- Technische Universität Dresden-Helmholtz-Zentrum Dresden - Rossendorf, Dresden, Germany ; <sup>2</sup>Helmholtz-Zentrum Dresden-Rossendorf, Institute of Radiooncology - OncoRay, Dresden, Germany ; <sup>3</sup>University Medical Center Groningen, Department of Radiation Oncology, Groningen, The Netherlands ; <sup>4</sup>Gustave Roussy Cancer Campus, Department of Radiation Oncology, Villejuif, France ; <sup>5</sup>Institut Claudius Regaud, Department of Radiotherapy, Toulouse, France ; <sup>6</sup>University Hospital Zürich, Department of Radiation Oncology, Zürich, Switzerland ; <sup>7</sup>Maastricht University Medical Centre, GROW - School for Oncology and Developmental Biology- Department of Radiation Oncology Maastricht, Maastricht, The Netherlands ; <sup>8</sup>Faculty of Medicine and University Hospital Carl Gustav Carus- Technische Universität Dresden, Department of Radiotherapy and Radiation Oncology, Dresden, Germany ; <sup>9</sup>German Cancer Consortium DKTK, Partner Site Dresden- and German Cancer Research Center DKFZ-Heidelberg, Dresden, Germany ; <sup>10</sup>National Center for Tumor Diseases NCT, Partner Site Dresden- German Cancer Research Center DKFZ- Heidelberg- Faculty of Medicine and University Hospital Carl Gustav Carus- Technische Universität Dresden- and- Helmholtz Association / Helmholtz-Zentrum,

#### Purpose or Objective

Inter-observer variability (IOV) in target volume delineation is a well-documented phenomenon and a major source of uncertainty in radiation treatment (RT) planning. The increasing adoption of adaptive RT adds a dynamic component to IOV, which is largely unknown. We analysed IOV in the pre- and mid-treatment (PT and MT) setting using expert primary gross tumour volume (GTV)

and clinical target volume (CTV) delineations in locally advanced HNSCC.

#### Material and Methods

Five patients from routine clinical practice, who underwent repeat imaging, were selected such that a variety of features likely to prompt adaptation were included. Brief case reports and CT imaging data were sent to five observers, the latter supplemented with pre-therapeutic FDG-PET in four cases. Observers received PT and MT imaging data at least one week apart and were asked to delineate the GTV and CTV in their own treatment planning system and to comment on their delineation process, i.e. on how GTV to CTV expansion and adaptation were performed. Delineations were rasterised on a 1mm<sup>3</sup> grid and their compatibility assessed with the Generalised Conformity Index (Cl<sub>gen</sub>). Differences in IOV between PT and MT were probed with Wilcoxon signed-rank tests and the correlation between GTV and CTV IOV evolution with Spearman rank correlation. While it is respectively impossible and very difficult for these tests to show two-sided  $\alpha=0.05$  significance at  $n=5$ , more powerful parametric alternatives cannot credibly be employed. Delineations were processed with ITK and statistical analyses performed in R.

#### Results

A total of 82/100 delineations were received and analysed. Figure 1 shows an overview of IOV in terms of volume overlap. All cases and volumes suffered a reduction of Cl<sub>gen</sub> when transitioning from PT to MT ( $p=0.063$  for both CTVs and GTVs). There was generally better agreement in CTV than GTV delineations at individual time points, and the correlation between GTV and CTV Cl<sub>gen</sub> changes was very weak ( $p=0.5$ ,  $p=0.45$ ). This comparative robustness of CTV delineations might stem from GTV to CTV expansion practices, which overwhelmingly employed sizeable isotropic margins (mean: 7.6 mm) and additional editing for anatomical boundaries at both time points. Figure 2 shows a case in which Cl<sub>gen</sub> for CTVs remains stable despite deteriorating IOV in the primary GTV. MT GTV delineations were often based on PT delineations after image registration (14/24 analysed observers and cases), the remainder contoured *de novo*. Post-transfer adaptation to changed anatomy was performed by two observers and inclusion of the PT GTV in the MT CTV by one. Shortcomings of this contouring challenge are a lack of MRI and contrast-enhanced CT at both time points.

#### Conclusion

IOV in target volume delineation increases during treatment, where a disparity in institutional adaptation practices adds to the static causes of IOV. Consensus guidelines are urgently needed and should recommend scope, frequency, and quality of MT imaging alongside adaptation strategies.

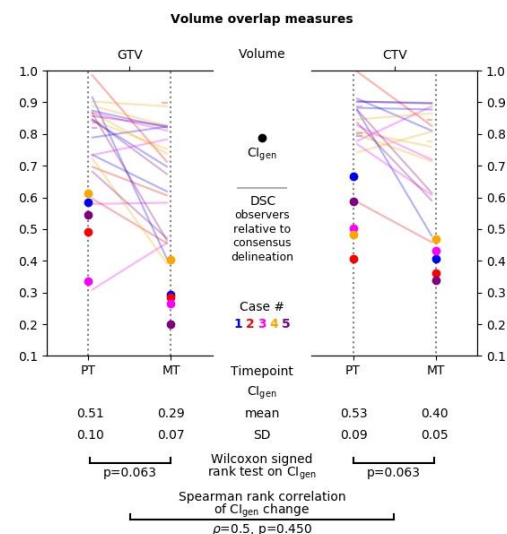


**Fig. 1:** Statistical overview of delineation overlap metrics. The Generalised Conformity Index (Cl<sub>gen</sub>) is shown for each case and time point for Gross Tumour Volume (GTV) and Clinical Target Volume (CTV) delineations. Its summary statistics are printed below, alongside the results of 1) hypothesis tests for a non-zero change in Cl<sub>gen</sub> when transitioning from pre- to mid-treatment time points (PT to MT), and 2) the correlation of those Cl<sub>gen</sub> changes between GTV and CTV delineations. The changes in Dice Similarity Coefficients (DSC) for each observer relative to a median consensus delineation (i.e. the collection of voxels delineated by at least half the observers) are depicted for comparison. Only a stub at either PT or MT is shown for observers who did not provide delineations for both.

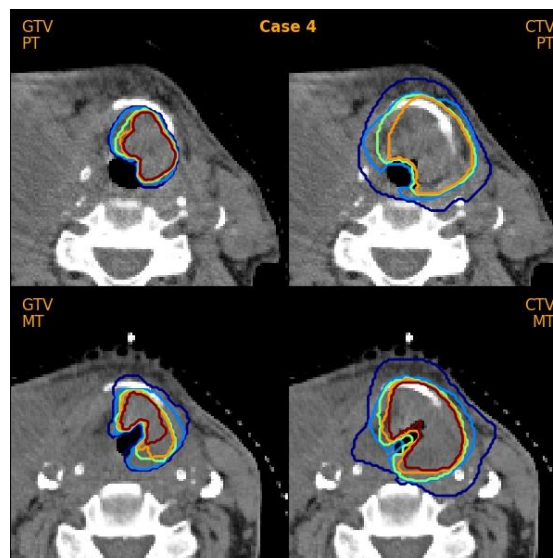


**Fig. 2:** Illustration of inter-observer variability in target volume delineation for a case of cT3N2cM0 laryngeal carcinoma. Central axial slices are superimposed with contours representing the fraction of observers who included the contained voxels in their delineation (from the exterior inwards: dark blue: 1/5 observers, maroon: 5/5 observers). Despite a reduction of agreement in GTV delineation (left column), CTV variability remains relatively stable (right column).

**Abbreviations:** PT, pre-treatment; MT, mid-treatment.

**Note:** only 4 PT CTV delineations received for this case.

#### EP-1185 QOL for HPV+ SCC of the oropharynx treated with transoral laser microsurgery and postoperative IMRT

T. DeWees<sup>1</sup>, J. Rwigema<sup>2</sup>, L. McGee<sup>2</sup>, T. Nagel<sup>3</sup>, M. Golafshar<sup>4</sup>, S. Patel<sup>2</sup>

<sup>1</sup>Mayo Clinic Arizona, Biomedical Statistics and Informatics, Scottsdale, USA ; <sup>2</sup>Mayo Clinic Arizona, Radiation Oncology, Phoenix, USA ; <sup>3</sup>Mayo Clinic Arizona, Otorhinolaryngology ENT/Head and Neck Surgery, Phoenix, USA ; <sup>4</sup>Mayo Clinic Arizona, Health Sciences Research, Scottsdale, USA

#### Purpose or Objective

Upfront surgical management of oropharyngeal tumors with adjuvant radiation therapy is becoming a more common treatment paradigm. Low morbidity has been

reported in head and neck cancer patients treated with transoral laser microsurgery (TLM) rather than open procedures. We sought to characterize patient reported quality of life outcomes in patients treated with TLM and adjuvant radiotherapy.

#### Material and Methods

HPV positive oropharyngeal squamous cell carcinoma patients treated at a single institution from February 2013 through March 2015 were included in the study. The patients prospectively completed the University of Washington Head and Neck Quality of Life Surveys (UW-QOL) at baseline and every 3 months after therapy. The UW-QOL survey evaluated QOL in 12 domains specific to head and neck cancer and 3 domains of global health status, assigning scores on 0-100 scale.

Initial analysis was conducted utilizing repeated measures mixed models, with underlying unstructured covariance, utilizing all survey data to determine if significant differences existed in QOL over time for each of the 15 scored questions. Comparisons between paired time-points was conducted via T-tests utilizing Tukey's adjustment for multiple comparisons. Similarly, univariate mixed models were fit utilizing clinical and demographic variables in order to determine their association with QOL outcomes with statistical significance considered for  $p < 0.05$ . Kaplan-Meier methods estimated Locoregional control, distant control and overall survival. **Results**

Of the 26 patients participating, 25 of the patients completed at least two of the assigned surveys and are included in this analysis. Forty-four percent received concurrent chemotherapy. Median follow up was 44 months, with the respective 1-year and 2-year LRC, DC, and OS of 100%/100%, 100%/87%, and 96%/96%. Within 9 months after IMRT, 100% of patients QOL scores were not significantly worse than pre-treatment for all QOL questions. Saliva quantity and consistency was the only question in which QOL was significantly lower than baseline at any time-point, however, within 9 months patients had recovered to within a non-significant statistical and clinical difference. The average measures of Pain, Recreation, Mood, Anxiety, health-related QOL, and overall QOL were all significantly higher for all patients at 12 months than baseline, with Mood and Anxiety achieving significant improvement at 6 and 9 months, respectively. Mixed Modelling identified worse QOL associated with primary base of tongue treatment, bilateral neck surgery, advanced pathological T Stage, no PNI, higher dose, and a distant recurrence needing salvage treatment ( $p < 0.05$ ).

#### Conclusion

QOL for HPV positive oropharyngeal carcinoma after TLM and IMRT returns to pre-RT levels within 9 months of treatment, with most patients achieving a clinically significant increase in QOL within 12 months of treatment. This treatment approach appears to provide excellent disease control while preserving their quality of life.

**EP-1186 The new target delineation impact on carotid and bulb sparing for T1 glottic cancer: VMAT vs 3DCRT**  
L. Ferella<sup>1</sup>, F. Vittorini<sup>2</sup>, E. Varrassi<sup>3</sup>, P. Franzese<sup>3</sup>, M. Di Staso<sup>3</sup>, F. Marampon<sup>4</sup>, C. Sorce<sup>5</sup>, A. Chalaszczyk<sup>5</sup>, G. Grimaldi<sup>5</sup>, E. Di Cesare<sup>6</sup>, E. Orlandi<sup>7</sup>, V. Tombolini<sup>4</sup>, C. Masciocchi<sup>8</sup>, G.L. Gravina<sup>5</sup>

<sup>1</sup>Fondazione IRCC Istituto Nazionale dei Tumori Milan-University of L'Aquila, Radiotherapy 2 Unit. Department of Biotechnological and Applied Clinical Sciences- Division of Radiotherapy. Laboratory of Radiobiology L'Aquila, Milano, Italy ; <sup>2</sup>San Salvatore Hospital, Service of Medical Physics., L'Aquila, Italy ; <sup>3</sup>San Salvatore Hospital- University of L'Aquila, Department of Radiation Oncology, L'Aquila, Italy ; <sup>4</sup>Policlinico Umberto I Hospital- Sapienza- University of Rome, Department of Radiation Oncology, Rome, Italy ; <sup>5</sup>University of L'Aquila, Department of Biotechnological and Applied Clinical Sciences- Division of Radiotherapy. Laboratory of

Radiobiology, L'Aquila, Italy ; <sup>6</sup>University of L'Aquila, Department of Biotechnological and Applied Clinical Sciences- Division of Radiotherapy., L'Aquila, Italy ; <sup>7</sup>Fondazione IRCC Istituto Nazionale dei Tumori, Radiotherapy 2 Unit- Radiotherapy 1 Unit, Milano, Italy ; <sup>8</sup>University of L'Aquila, Department of Biotechnology & Applied Clinical Science., L'Aquila, Italy

#### Purpose or Objective

To investigate whether Volumetric Modulated Arc Therapy (VMAT) maintains its superiority on 3D-conformal-radiotherapy (3DCRT) in reducing dose to carotid arteries (CA) and carotid bulbs (CB) using a target sparing contouring approach in cT1 glottic cancer (GC).

#### Material and Methods

CTV of 10 cT1a0 GC patients were retrospectively contoured according to the new contouring recommendations proposed by Gregoire and colleagues. The CAs were separately outlined along their extracranial course. Since CB is the most critical structure involved in atherosclerosis, it was also outlined including two cm superior and inferior to carotid bifurcation according to Framingham Heart study. A 1 mm isotropic margin was applied to account for anatomical changes during cardiac cycle. 3DCRT and VMAT plans specifically optimized for carotid sparing were generated. The prescribed dose was 63 Gy in 28 fractions. In all plans at least 95% of the PTV was requested to receive  $\geq 95\%$  of the prescription dose and a spinal cord maximum dose of 25 Gy was allowed. Ipsilateral and contralateral CB and CA Dmax, Dmean, V35, V50 were determined. The two techniques were also compared for OAR doses and plan quality indices (V95, V107, D2, D98, Conformity index and Heterogeneity Index). T test for paired data with logarithmic transformation for continuous variables was used to compare dosimetric parameters. Mean and confidence interval of 95% were used to summarize continuous variables. A Two-sided  $\alpha$  error of 5% was used as significance threshold.

#### Results

Mean ipsilateral CB and CA Dmax significantly decreased from 51,8 Gy to 32,8 Gy ( $p < 0.0001$ ) and from 54 Gy to 44 Gy ( $p = 0,0005$ ) for 3DCRT and VMAT, respectively. VMAT significantly lowered ipsilateral CB Dmean ( $p = 0,0001$ ) and V35 ( $p = 0,0052$ ) and ipsilateral CA V35 ( $p = 0,0002$ ). Similarly, contralateral CB ( $p < 0,0001$ ) and CA Dmax ( $p < 0,0001$ ) were lower in VMAT than in 3DCRT. Moreover, contralateral CB ( $p = 0,0002$ ) and CA Dmean ( $p < 0,0001$ ) and contralateral CB ( $p = 0,02$ ) and CA V35 ( $p = 0,0052$ ) were higher with 3DCRT. VMAT significantly reduced the dose to pharyngeal constrictor muscles, thyroid gland and supraglottic larynx. Spinal cord Dmax was lower in 3DCRT plans (Table 1). No significant difference was found in terms of plan quality indices except for the better Conformity Index of VMAT plans (0,7 vs 0,6 of 3DCRT,  $p = 0,0197$ ). As regards hot-spots volumes, no sensitive structures out of target volumes such as contralateral arytoids were involved. For both VMAT and 3DCRT hot-spots fell inside the PTV. In particular, ipsilateral arytoid was involved in the 30% of 3DCRT and in 40% of VMAT plans, while ipsilateral supraglottic space in the 20% of 3DCRT and in 20% of VMAT plans.

Table 1: Dosimetric data for OAR in 3DCRT and VMAT.

OAR	3DCRT MEAN (CI 95%) (Gy)	VMAT MEAN (CI 95%) (Gy)	Mean difference (Gy)	P value
Spine (Dmax)	19,6 (18,9 to 20,2)	21,5 (20,9 to 22,1)	1,9	<0,0001
Spine PRV (Dmax)	19,2 (16,5 to 21,8)	18,8 (10,6 to 26,8)	0,4	0,92
Medium PCM (Dmean)	7,8 (5,4 to 11,2)	3,6 (2,1 to 6,0)	4,2	0,0006
Inferior PCM (Dmean)	51,9 (47,3 to 57,0)	42,4 (38,6 to 46,5)	9,6	0,0048
Supraglottic larynx (Dmean)	37,9 (33,0 to 43,5)	27,2 (22,1 to 33,5)	10,3	0,0012
Cricopharyngeal inlet (Dmean)	40,7 (33,4 to 49,6)	28,8 (23,8 to 34,8)	12,3	0,0026
Cervical oesophagus (Dmean)	2,1 (1,1 to 4,1)	1,4 (0,5 to 3,6)	0,7	0,6526
Thyroid gland (Dmean)	16,2 (11 to 23,9)	7,4 (4,3 to 12,8)	9,0	0,0003

OAR: organ at risk; 3DCRT: 3-Dimensional Conformal Radiotherapy; VMAT: Volumetric Modulated Arc Therapy; CI 95%: confidence interval of 95%; PRV: planned risk volume; PCM: pharyngo-constrictor muscle.

## Conclusion

Even with the new target delineation method, VMAT provides dosimetric advantages in carotids, bulbs and in the most of OARs sparing respect to 3DCRT in T1 GC.

## EP-1187 Different carotid contouring results in dosimetric variability and significant anatomical missing

L. Ferella<sup>1</sup>, F. Vittorini<sup>2</sup>, E. Varrassi<sup>3</sup>, P. Franzese<sup>3</sup>, M. Di Staso<sup>3</sup>, F. Marampon<sup>4</sup>, C. Sorce<sup>5</sup>, A. Chalaszczyk<sup>5</sup>, G. Grimaldi<sup>5</sup>, E. Di Cesare<sup>6</sup>, E. Orlandi<sup>7</sup>, V. Tombolini<sup>4</sup>, C. Masciocchi<sup>6</sup>, G.L. Gravina<sup>5</sup>

<sup>1</sup>Fondazione IRCC Istituto Nazionale dei Tumori Milan-University of L'Aquila-, Radiotherapy 2 Unit. Department of Biotechnological and Applied Clinical Sciences-Division of Radiotherapy. Laboratory of Radiobiology L'Aquila, Milano, Italy ; <sup>2</sup>San Salvatore Hospital- L'Aquila, Service of Medical Physics, L'Aquila, Italy ; <sup>3</sup>S. Salvatore Hospital- University of L'Aquila, Department of Radiation Oncology, L'Aquila, Italy ; <sup>4</sup>Policlinico Umberto I Hospital- Sapienza- University of Rome, Department of Radiation Oncology, Rome, Italy ; <sup>5</sup>University of L'Aquila, Department of Biotechnological and Applied Clinical Sciences- Division of Radiotherapy. Laboratory of Radiobiology, L'Aquila, Italy ; <sup>6</sup>University of L'Aquila, Department of Biotechnological and Applied Clinical Sciences, L'Aquila, Italy ; <sup>7</sup>Fondazione IRCC Istituto Nazionale dei Tumori, Radiotherapy 2 Unit- Radiotherapy 1 Unit, Milano, Italy

## Purpose or Objective

Carotid Artery (CA) sparing approach is a field of increasing interest owing to long life expectancy of patients with early glottic cancer (EGC). A CA delineation consensus lacks with no internationally recognized dose constraints for this structure. Here we compare, in terms of anatomical and dosimetric variability, three of the most common CA delineation methods found in literature.

## Material and Methods

CA of 10 cT1a N0 EGC patients were outlined using 3 different approaches: 1) the whole CA from its origin up to the internal carotid entry into skull base (Contour 1); 2) the tract of CA from its origin up to at least 2.5 cm above the hyoid bone (Contour 2); 3) the tract of CA 1 cm superior and inferior to PTV (Contour 3). The carotid bulb (CB) was contoured 2 cm inferiorly and superiorly to carotid bifurcation according Framingham Heart definition due to its role in the radio-induced atherosclerosis. A 1 mm isotropic carotid and bulb margin was added to compensate the changes during cardiac cycle. Thirty VMAT carotid sparing plans were generated and CA Dmax, Dmean, V35 and V50 were compared across the different contouring approaches. T-test for paired data with logarithmic transformation was used to compare dosimetric parameters. A two-sided p-value < 0.05 was the significance threshold

## Results

In terms of carotid structures missing, Contour 3 did not include the entire bulb in 100% of contoured carotids while Contour 1 and 2 always included it entirely. A significant variability in ipsilateral and contralateral CA Dmean and ipsilateral CA V35 were found among the three contouring approaches with the lowest, intermediate and highest mean values found for Contour 1, Contour 2 and Contour 3, respectively (Table 1). No consistent variability was found for bilateral CA Dmax and V50 and for contralateral CA V35 across the three contouring approaches (Table 1).

Table 1: Dosimetric comparison of three different carotid artery delineation approaches in VMAT planning.

Dosimetric parameter	Contour 1 Mean (95% CI)	Contour 2 Mean (95% CI)	Contour 3 Mean (95% CI)	P value		
				Contour 1 vs 2	Contour 1 vs 3	Contour 2 vs 3
<b>Ipsilateral carotid</b>						
Dmax (Gy)	40,2(36,7 to 44,2)	39,6(35,8 to 43,7)	39,6(35,8 to 43,7)	1	1	1
Dmean (Gy)	8,5 (7,0 to 10,3)	10,5 (8,6 to 12,8)	20,9(18,2 to 23,9)	<0,0001	<0,0001	<0,0001
V35 Gy (%)	1,9 (0,1 to 3,6)	2,3 (0,1 to 4,5)	4,6 (0,1 to 9,2)	0,0545	0,0603	0,0568
V50 Gy (%)	0	0	0	NA	NA	NA
<b>Contralateral carotid</b>						
Dmax (Gy)	17,4(14,3 to 21,1)	17,4(14,3 to 21,1)	17,4(14,3 to 21,1)	0,5667	0,5449	0,3434
Dmean (Gy)	3,8 (3,1 to 4,6)	4,6 (3,7 to 5,7)	8,4 (6,4 to 10,9)	<0,0001	<0,0001	<0,0001
V35 Gy (%)	0	0	0	NA	NA	NA
V50 Gy (%)	0	0	0	NA	NA	NA

Contour 1: whole carotid from its origin to skull base entry; Contour 2: from carotid origin to at least 2.5 cm above hyoid bone; Contour 3: 1 cm superiorly and inferiorly to PTV; V35: volume percentage receiving  $\geq$  35 Gy; V50: volume percentage receiving  $\geq$  50 Gy; NA: not assessable.

## Conclusion

Here we document the need for a standardized CA delineation since a relevant dosimetric variability and a significant missing of important structures has been documented among the three most frequent used contouring approaches. Based on our Institutional preference, we suggest to delineate the whole bulb and whole CA from its origin up to the skull base entry to decrease interobserver variability among clinicians.

## EP-1188 Carbon ion radiotherapy for recurrent pleomorphic adenoma at CNAO: preliminary results.

S. Ronchi<sup>1</sup>, B. Vischioni<sup>1</sup>, V. Vitolo<sup>1</sup>, M. Bonora<sup>1</sup>, A. Hasegawa<sup>2</sup>, M.R. Fiore<sup>1</sup>, A. Iannalfi<sup>1</sup>, E. D'Ippolito<sup>1</sup>, R. Petrucci<sup>1</sup>, A. Barcellini<sup>1</sup>, S. Molinelli<sup>1</sup>, D. Maestri<sup>1</sup>, G. Viselner<sup>3</sup>, A. Facchetti<sup>1</sup>, M. Ciocca<sup>1</sup>, L. Preda<sup>3</sup>, F. Valvo<sup>1</sup>, R. Orecchia<sup>1,4</sup>

<sup>1</sup>National Center of Oncological Hadrontherapy, Radiotherapy Unit, Pavia, Italy ; <sup>2</sup>Osaka Heavy Ion Therapy Center, Radiation therapy Unit, Osaka, Japan ; <sup>3</sup>National Center of Oncological Hadrontherapy, Diagnostic Imaging Unit, Pavia, Italy ; <sup>4</sup>European Institute of Oncology, Radiation therapy Unit, Milan, Italy

## Purpose or Objective

To evaluate response and toxicity of carbon ion radiotherapy (CIRT) for recurrent pleomorphic adenoma patients (pts).

## Material and Methods

Inclusion criteria based on the CNAO phase II clinical protocol CNAOS10/2012/C were: (1) prior histological diagnosis of pleomorphic adenoma; (2) relapse after at least one previous surgical approach; (3) further surgery excluded (due to high risk of facial nerve damage/medical contraindications/refusal of the patient); (4) no previous radiotherapy. CIRT prescription dose was 65.6 Gy[RBE] in 16 fractions (4.1 Gy[RBE]/fraction). Local response and toxicity (tox) were respectively evaluated using RECIST and CTCAE v.4.0 criteria. MRI was performed after treatment every 3-4 months (mo.) in the first 2 years, every 6 mo. in the third year, then once a year.

## Results

Between November 2012 and May 2017, 24 pts were treated. Median age was 47 years (range 20-68). Median time from first diagnosis to CIRT was 17.4 years (range 1-33.5). Median number of previous surgeries was 3 (range 1-6). Median time from last surgery to CIRT was 16.8 mo. (range 9.8-274.4). Two and 22 pts were treated for unimodular and plurimodular recurrence, respectively. Mean GTV was 19.8 cc (range 1.1-91.1). Mean CTV was 83.5 cc (range 25.6-148.6). Median follow-up (FU) time was 23.3 mo.(range 7.8-64.4). Radiological response at first FU was partial response and stabilization in 2 and 22 pts, respectively. At last FU, all pts were alive with local control maintained. Only 1 patient treated for plurimodular tumor had out-field recurrence at 4.5 years after CIRT. Tox during/at the end of treatment was G0, G1, G2 for 3 (12.5%), 9 (37.5%), and 12 (50%) pts, respectively. Acute tox within 3 months was G0, G1, G2 for 10 (41.7%), 11 (45.8%), and 3 (12.5%) pts, respectively.

Maximum late tox was G0, G1, G2 for 3 (12.5%), 13 (54.2%), and 8 (33.3%) pts, respectively. No G3-G4 late tox was observed. Among pts with late tox, 11 (45.8%) had peripheral neuropathy (G1 and G2 in 8 (33.3%) and 3 (12.5%) pts, respectively). No patient experienced facial nerve damage as treatment-related tox.

#### Conclusion

In our experience, CIRT in recurrent pleomorphic adenoma pts has shown excellent local control and good toxicity profile. It might be a good alternative to invasive surgery especially when the latter is judged to be at high risk of facial nerve damage. However, a larger series of patients and a longer follow-up are needed to better investigate outcomes, especially in terms of late toxicity.

#### EP-1189 Adenoid Cystic Carcinoma Of The Head And Neck Treated With Carbon Ion Radiotherapy At CNAO

M. Bonora<sup>1</sup>, B. Vischioni<sup>1</sup>, D. Caivano<sup>2</sup>, A. Hasegawa<sup>3</sup>, V. Vitolo<sup>1</sup>, S. Ronchi<sup>1</sup>, E. D'Ippolito<sup>1</sup>, A. Iannalfo<sup>1</sup>, M.R. Fiore<sup>1</sup>, A. Barcellini<sup>1</sup>, R. Petrucci<sup>1</sup>, S. Russo<sup>1</sup>, S. Molinelli<sup>1</sup>, A. Vai<sup>1</sup>, G. Viselner<sup>4</sup>, A. Facoetti<sup>1</sup>, M. Ciocca<sup>1</sup>, L. Preda<sup>4</sup>, F. Valvo<sup>1</sup>, R. Orecchia<sup>1,5</sup>

<sup>1</sup>National Center of Oncological Hadrontherapy, Radiotherapy Unit, Pavia, Italy ; <sup>2</sup>University of Turin, Department of Oncology- Radiation Oncology, Turin, Italy ; <sup>3</sup>Osaka Heavy Ion Therapy Center, Radiation therapy Unit, Osaka, Japan ; <sup>4</sup>National Center of Oncological Hadrontherapy, Diagnostic Imaging Unit, Pavia, Italy ; <sup>5</sup>European Institute of Oncology, Radiation therapy Unit, Milan, Italy

#### Purpose or Objective

To evaluate preliminary results of carbon ion radiotherapy (RT) in patients (pts) with adenoid cystic carcinoma (ACC) of the head and neck (H&N) region treated with curative intent

at the National Center for Oncological Hadrontherapy (CNAO) according to the phase II clinical study CNAO S9/2012/C.

#### Material and Methods

Between March 2013 and September 2016, 135 patients (M/F = 61/74) with ACC of the H&N were treated with active scanning carbon ion RT. Pts average age was 54 (range 19 -

82). Tumour site was minor salivary gland in 90 (67%) and major salivary gland in 45 (33%) pts. In 20 pts (15%) treatment was at disease recurrence, 115 (85%) pts were treated after first

diagnosis. Before carbon ion RT, 83 (62%) pts received surgery, of these 60 (45%) pts had positive margins (R1), 13 (10%) pts had no status of margins on histological report, and 9 (7%)

pts received debulking surgery (R2). No pts received previous RT. In all the cases prescribed total dose was of 68.8 Gy(RBE) in 16 fractions, 4 fractions/week. Toxicity was

evaluated according to the CTCAE v.4.0. Pts were followed up every three months after RT with clinical evaluation and MRI. For all patients C11 methionine PET-TC was used for target delineation.

#### Results

Median follow-up time was 23 months (range: 1 - 51 months). Local Control was reached in 101 out of 135 (75%) patients, with 12 and 24-months local control rates of 91% and

81% respectively. The Progression-Free Survival at 12 and 24 months was 81% and 67%, respectively. The Distant Metastasis Free Survival at 12 and 24 months was 86% and 81%,

respectively. Median overall survival (OS) time was 24 months and the rates of OS were 95% and 85% at 12 and 24 months respectively. At the end of treatment toxicity was G0 in 2%, G1 in

20%, G2 in 52% and G3 in 26% of the patients. At 3 months toxicity was G0 in 36%, G1 in 43%, G2 in 19% and G3 in 2% of the patients. Acute G3 was always mucositis, in the long FU the late

maximum toxicity was G3 for 20 (15%) pts and G4 for 2 (1%) pts. There were no G5 events. **Conclusion** CNAO preliminary data show encouraging outcome results and acceptable toxicities but longer follow-up is needed.

#### EP-1190 Preliminary evaluation of salivary cytokines in patients treated with IMRT for head and neck cancer

A. Cavallo<sup>1</sup>, N.A. Iacovelli<sup>2</sup>, T. Rancati<sup>3</sup>, N. Facchinetti<sup>2</sup>, T. Di Florio<sup>3</sup>, V. Doldi<sup>4</sup>, E. Campi<sup>4</sup>, N. Zaffaroni<sup>4</sup>, T. Giandini<sup>1</sup>, L. Ferella<sup>2</sup>, D.A. Romanello<sup>2,5</sup>, C.T. Delle Curti<sup>2,5</sup>, P. Bossi<sup>6</sup>, E. Pignoli<sup>1</sup>, C. Fallai<sup>2</sup>, R. Valdagni<sup>3,7,8</sup>, E. Orlandi<sup>2,8</sup>

<sup>1</sup>Fondazione IRCCS Istituto Nazionale dei Tumori, Medical Physics Unit, Milan, Italy ; <sup>2</sup>Fondazione IRCCS Istituto Nazionale dei Tumori, Radiation Oncology 2, Milan, Italy ;

<sup>3</sup>Fondazione IRCCS Istituto Nazionale dei Tumori, Prostate Cancer Program, Milan, Italy ; <sup>4</sup>Fondazione IRCCS Istituto Nazionale dei Tumori, Molecular

Pharmacology Unit, Milan, Italy ; <sup>5</sup>University of Milano-Bicocca, School of Medicine and Surgery, Milan, Italy ;

<sup>6</sup>Fondazione IRCCS Istituto Nazionale dei Tumori, Head and Neck Medical Oncology Unit, Milan, Italy ;

<sup>7</sup>University of Milan, Department of Oncology and Hemato-oncology, Milan, Italy ; <sup>8</sup>Fondazione IRCCS Istituto Nazionale dei Tumori, Radiation Oncology 1, Milan, Italy

#### Purpose or Objective

The role of salivary inflammatory markers and their early variation in predicting increased risk radiation-induced acute toxicities in head and neck cancer (HNC) patients (pts) is under investigation within a prospective observational clinical trial. Preliminary evaluation is here reported.

#### Material and Methods

A series of HNC pts curatively treated with intensity modulated RT (prescribed dose  $\geq 66$  and  $\geq 54$  Gy for definitive and post-operative setting, respectively; 2-2.12 Gy/fraction; 5 fractions/week) with or without chemotherapy was considered.

Saliva samples for inflammatory marker levels evaluation were collected before RT (T0) and in the third week (T1), i.e. between the 10<sup>th</sup> and 15<sup>th</sup> RT fraction. The concentration (pg/ml) of IL-1B and IL-6 cytokines was measured using ELISA assays.

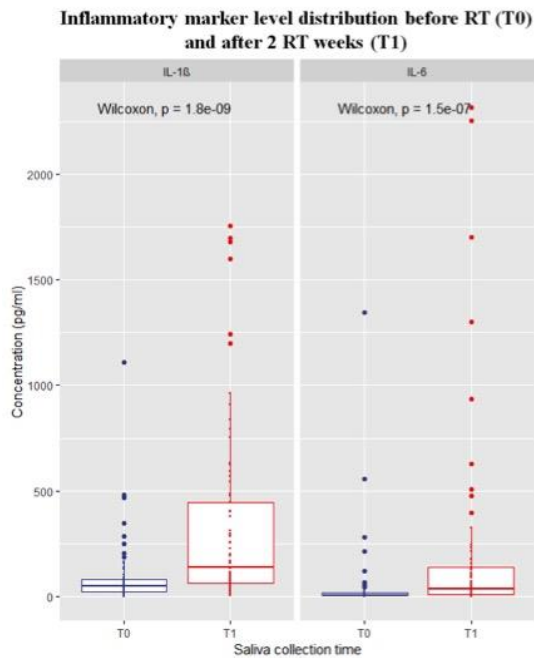
Acute toxicity profiles were assessed according to CTCAE v4.0 at baseline and weekly during RT. The following endpoints were considered: maximum oral mucositis (OM) grade (G) $\geq 3$ , mean OM G $\geq 1.5$  during RT, maximum dysphagia G3 and maximum dry mouth G $\geq 2$ . Early cytokines variation and its possible association with toxicity were evaluated with Wilcoxon signed-rank and Mann-Whitney tests, respectively.

#### Results

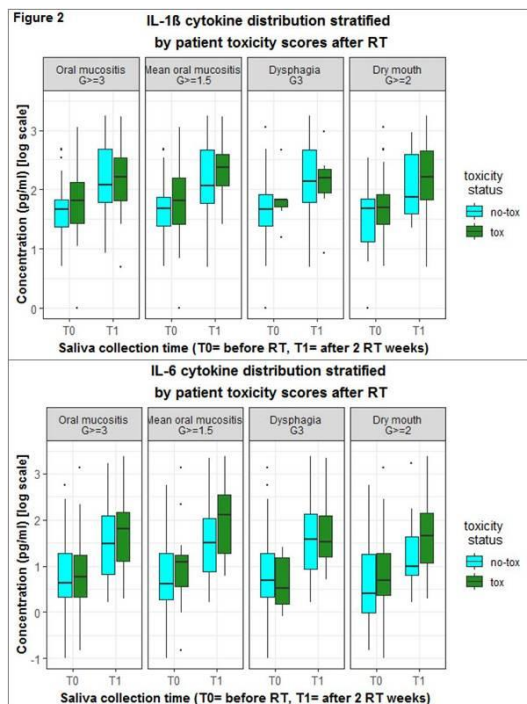
81 pts were available for this analysis; only 73/81 had saliva samples collected for both time points. Collection of saliva at T1 was difficult in many cases, due to an already present salivary flow alteration in the third week of RT.

OM G $\geq 3$  was reported in 27 pts (37%), mean OM G $\geq 1.5$  in 14 pts (19%), dysphagia G3 in 7 (10%) and dry mouth G $\geq 2$  in 60 pts (82%).

Salivary levels of both cytokines significantly varied between T0 and T1 (p<0.001). Figure 1 reports marker level distributions and early changes after 2 weeks of RT. The variation in IL-1B and IL-6 concentration was: <0 pg/ml (i.e. decrease in concentration) for 12 and 13 pts, in the range 0-300 pg/ml (i.e. mild to moderate increase) for 42 and 52 pts, higher than 300 pg/ml (i.e. large increase) for 19 and 8 pts, respectively.



No significant association was found between inflammatory marker levels and the selected toxicity endpoints ( $p > 0.05$  in all cases). Figure 2 shows the distribution of cytokine levels at both time points stratified by pts who showed (label “tox”) or did not show (label “no-tox”) the selected toxicity endpoints.



## Conclusion

RT for HNC induced a significant increase in salivary cytokine levels of IL-1 $\beta$  and IL-6 already after 20 Gy. Unlike some recent published results though, this preliminary analysis did not detect any association between the inflammatory marker concentration changes and the most impairing acute toxicities commonly arising throughout the treatment. Of note, collection of saliva during treatment was difficult in many cases and density

of saliva collected at T1 was usually high, with this probably impacting the absolute concentration of inflammatory markers. This points out the need to develop protocols for corrections of concentrations for saliva density.

## EP-1191 Effect on local control of addition of chemotherapy to radiotherapy for T2 cancer of the hypopharynx

S. Gaito<sup>1</sup>, S. Mehta<sup>1</sup>, A. McWilliam<sup>2</sup>, R. Almond<sup>3</sup>, L.W. Lee<sup>4</sup>, K. Garcez<sup>4</sup>, D. Thomson<sup>4</sup>, J. Price<sup>1</sup>, K. Mais<sup>4</sup>, A. McPartlin<sup>4</sup>

<sup>1</sup>The Christie NHS Foundation Trust, Clinical Oncology, Manchester, United Kingdom ; <sup>2</sup>University of Manchester, Radiotherapy Related Research, Manchester, United Kingdom ; <sup>3</sup>The Christie NHS Foundation Trust, Clinical Outcomes Unit, Manchester, United Kingdom ; <sup>4</sup>The Christie NHS Foundation Trust, Head and Neck Clinical Oncology, Manchester, United Kingdom

## Purpose or Objective

A benefit from chemo-radiotherapy (CRT) for bulky stage II hypopharyngeal squamous cell cancer (HPSCC) has proponents but limited supporting evidence. We investigate the effect on local control (LC) of the addition of chemotherapy (CT) to radiotherapy (RT) for T2 HPSCC.

## Material and Methods

A retrospective analysis was performed of patients with T2 (node negative or positive) HPSCC receiving definitive RT or CRT at a single academic cancer centre. Patient and disease characteristics were obtained from electronic records. Primary gross tumour volumes were calculated from CT planning scans or diagnostic imaging. LC analysis was censored at time of first failure or death. The logrank test was used for correlation between tumour volume and LC. Cox proportional hazard modelling of LC by treatment received was performed to account for competing risks.

## Results

62 patients were identified, treated from April 2007 to July 2016. Patient demographics, treatment received and site of first failure are shown in table 1. Median follow-up in patients not experiencing failure was 25 months (range 1-107 months) and 20 months (3-85 months), and median time to first failure 12.2 months (2 - 58 months) and 6.4 months (3-77 months), after RT or CRT respectively. Initial local failure occurred in 10% (3) and 39% (12) of those patients receiving CRT or RT ( $p = 0.047$ , HR = 0.272, 95% C.I. 0.075-0.982). After RT, a significant negative correlation was identified between primary tumour volume and local control (spearman rho -0.59,  $p = 0.008$ ). Patients with primary tumour volumes  $> 8 \text{ cm}^3$  vs  $\leq 8 \text{ cm}^3$  had significantly worse local control rates ( $p = 0.01$ ) after RT.

		RT	CTRT
Number of patients		31	31
Male (n (%))		23 (74)	24 (77)
Age (yrs) (Median(range))		68 (45-85)	60 (37-77)
PS (n (%))	0	5 (16)	12 (39)
	1	14 (45)	15 (48)
	2	12 (39)	4 (13)
Smoking status (n (%))	Never	1 (3)	3 (10)
	Ex	9 (29)	15 (48)
	Current	13 (42)	9 (29)
	Not known	8 (26)	4 (13)
T2 (n (%))		31 (100)	31 (100)
Subsite (n (%))	Piriform sinus	23 (74)	25 (81)
	Posterior pharyngeal wall	3 (10)	2 (6)
	Post cricoid	5 (16)	4 (13)
Node positive (n (%))		9 (29)	27 (87)
Prior neck dissection (n (%))		4 (13)	1 (3)
Radiotherapy (n (%))	55 Gy/20 #	13 (42)	6 (19)
	66 Gy/30 #	18 (58)	25 (81)
Technique (n (%))	3D CRT	5 (16)	6 (19)
	IMRT/VMAT	26 (84)	25 (81)
Disease relapse (n (%))		15 (52)	14 (48)
Site of first failure (n (%))	Local	12 (39)	3 (10)
	Regional	0 (0)	8 (26)
	Distant	4 (13)	5 (16)

### Conclusion

In this cohort the addition of CT to RT is associated with improved LC for T2 HPSCC. Patients with larger tumours were more likely to experience local failure after RT, and for this group treatment intensification with CTRT may be of benefit, even in node negative patients. Competing risk analysis has been used to account for the risk of early distant failure or death and censure in node positive patients receiving CTRT. Moreover, local failure is known to remain the predominant site of first recurrence, and risk of local failure is known to be increased, in node positive patients after CTRT. Tumour biology or first site of failure variation between the two groups is therefore unlikely to explain the significant difference in LC identified.

### EP-1192 Hair loss during intensity modulated radiotherapy for nasopharyngeal carcinoma

N. Fourati<sup>1</sup>, Z. Fessi<sup>1</sup>, W. Mnejja<sup>1</sup>, L. Farhat<sup>1</sup>, T. Sahnoun<sup>1</sup>, W. Siala<sup>1</sup>, J. Daoud<sup>1</sup>

<sup>1</sup>Hopital Habib Bourguiba, Radiation Oncology, Sfax, Tunisia

### Purpose or Objective

Hair loss is a common complication of brain tumor radiotherapy but has not been reported following conventional radiotherapy of nasopharyngeal carcinomas (NPC). The use of posterior fields during intensity modulated radiotherapy (IMRT) of NPCs made hair loss common. The aim of this study was to evaluate all patients treated with IMRT for NPC to determine correlation between scalp doses and hair regrowth.

### Material and Methods

Twenty-one patients treated with IMRT for NPC were prospectively followed during the radiotherapy period and up to 6 months after the end of the irradiation. All patients had 7 fields irradiation including a posterior field. A simultaneous boost technique was used to deliver 69.96 Gy in 33 Fractions to the nasopharynx and involved lymph nodes. The scalp was not considered as an organ at risk during radiotherapy planning. To evaluate the doses received, we have delineated the tissue between the skin and the skull taking as an upper limit 6 mm above the upper edges of the posterior field. We then reported the maximum dose (Dmax), the minimum dose (Dmin), the

mean dose (Dmean), the percentage of volume receiving more than 10 Gy (V10Gy), the percentage of volume receiving more than 20 Gy (V20Gy) and the dose received by 50% of the scalp (D50%).

After the end of treatment, patients were followed in consultation at 1 month, 3 months and 6 months to determine the hair regrowth. Mann-Whitney test was used to compare doses between patients with total and partial regrowth at 3 months.

### Results

The median Dmax, Dmin and Dmean were 42.77 (31.86-63.98), 1.32 (0.9-1.96) and 16.11 (12.42-20.66) respectively. The median D50%, V10Gy and V20Gy were 16.91 Gy (9.74-19.85), 69.07% (49.02-80.19) and 35.36% (21.25-49.5) respectively. All patients had hair loss during the treatment phase. After 1 month of the end of treatment, all patients had partial hair regrowth. At 3 months, 7 patients (33.3%) had total hair regrowth. Median Dmean, V10Gy and V20Gy for patients with total regrowth were 16.11Gy (12.48-17.67), 68.81% (49.02-74.3) and 35.36 (21.25-45.79) respectively versus 16 Gy (14.09-20.31), 72.03% (58.32-79) and 34.86% (25.19-49.5) respectively for patients with partial regrowth (p not significant in all cases). At six months, only one patients did not have complete hair regrowth (Dmean: 19.53, V10Gy : 78% and V20Gy: 48.8%).

### Conclusion

During IMRT for NPC a Mean dose of 16 Gy is responsible for acute hair loss in 100% of cases. However, this loss is only transient with partial regrowth from 1 month of the end of treatment and a total regrowth at 6 months in almost all cases. The consideration of scalp as an organ at risk during treatment planning would be necessary. Since the dose limits to be respected are not reported in the literature for the irradiation of the NPC, we propose, through the results of our study, a Dmean < 16 Gy, V10Gy < 68% and V20Gy < 35%.

### EP-1193 Analysis of competing and tumor deaths and predictors factors in advanced head and neck cancer.

I. Zapata Martínez<sup>1</sup>, I. Navarro Doménech<sup>1</sup>, M. Álvarez Pérez<sup>2</sup>, M.J. García Anaya<sup>1</sup>, B.I. Pajares Hachero<sup>3</sup>, M.D. Toledo Serrano<sup>1</sup>, I. Jerez Sainz<sup>1</sup>, R. Ordoñez Marmolejo<sup>1</sup>, A. Otero Romero<sup>1</sup>, R. Correa Generoso<sup>1</sup>, I. García Ríos<sup>1</sup>, A. Román Jobacho<sup>1</sup>, J.A. Medina Carmona<sup>1</sup>, J. Gómez-Millán Barrachina<sup>1</sup>

<sup>1</sup>Hospital Virgen de la Victoria, Radiation Oncology, Málaga, Spain ; <sup>2</sup>University of Málaga, Pathological Anatomy, Málaga, Spain ; <sup>3</sup>Hospital Virgen de la Victoria, Medical Oncology, Málaga, Spain

### Purpose or Objective

Non-cancer deaths or competing mortality (CM) in locoregionally advanced head and neck cancer (LAHNC) contribute importantly to the poor outcomes of these patients. The objective was to analyze the incidence of CM and tumor mortality (TM) in LAHNC patients and to determine possible prognostic factors.

### Material and Methods

Cohort study of 292 patients with LAHNC treated in our hospital between 2005- 2015 with radiotherapy (RT) in combination with systemic therapy. Nonparametric test was used to analyze the incidence of each death. A Fine and Gray regression model was used to investigate factors associated with CM and TM.

### Results

Median follow-up was 60 months. Performance status, as measured by the Eastern Cooperative Oncology Group (ECOG), which was 0 in 57% (n= 167) of patients. Comorbidity was classified by head and neck comorbidity index (HN-CCI). Moderate or severe grade comorbidity was seen in 18% (n= 53) of cases. Most of the patients (65.5%, n=191) were treated with concurrent chemo-radiotherapy (CRT) treatment and 3D conformal RT technique was used in 74.5% (n=217).

Regarding to toxicity, 55% (n= 160) of the patients presented acute pharyngo-esophageal toxicity grade 3 to 5 (CTCAE v4.0). Chronic toxicity greater or equal to grade 3 (RTOG escale) was presented in 15.5% of patients.

The 5-year cumulative incidence of TM was 39.7%: 36.4% corresponding to primary tumor-death and 3.3% to second tumor-death. The predictors factors of TM were: poor performance status (ECOG 1-2 vs 0; HR 1.52), advanced stage (IVA-B versus III; HR 1.8) and non-CRT treatment versus concurrent CRT regimens (HR 1.76).

The 5-year cumulative incidence of CM was 11.8%. The incidence to CM secondary to acute and chronic toxicity were 5.5% and 1.5%, respectively. The cumulative incidence of death related to comorbidity was 4.4% (Figure 1).

In the multivariate analysis the predictors factors of CM were increased age (HR 1.05) and comorbidity (HR 3.03). Patients with moderate to severe comorbidity presented a CM risk three times higher than those patients with mild or without comorbidity (Table 1). Acute mucositis grade 3 to 5 was associated with CM in the bivariate analysis but not in the multivariate analysis.

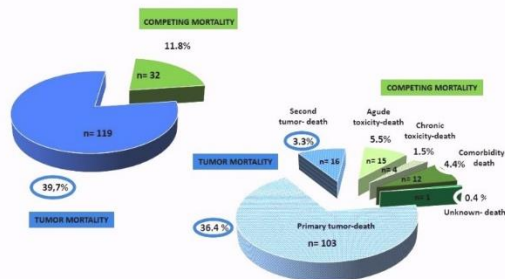


Figure 1: 5-year cumulative incidences of causes of death.

Characteristic	TUMOR DEATH			COMPETING DEATH		
	Hazart Ratio	95% CI	p	Hazart Ratio	95% CI	p
Age	0.99	0.97-1.01	0.23	1.05	1.07-1.09	0.023
HN-CCI (0-1 vs 2-6)	0.8	0.41-1.55	0.5	3.03	1.13-8.08	0.03
ECOG (0 vs 1-2)	1.52	1.03-2.25	0.03	0.97	0.44-2.13	0.94
Stage (III vs IV)	1.8	1.16-2.72	0.008	0.63	0.29-1.39	0.25
Treatment (RCT vs non-RCT)	1.76	1.17-2.6	0.007	0.68	0.29-1.55	0.36

Table 1: Multivariate analyses of predictors factors of competing and tumor mortality.

### Conclusion

This study demonstrates an important incidence of competitive deaths in patients with LAHNC treated with combined treatments. Among the factors that predict these deaths, age and, especially, moderate-severe comorbidity have been identified. Tumor deaths were associated with poor performance status, stage IV, and concurrent RT plus anti-EGFR. All these factors must be considered especially in the choice of the combined treatment of patients with LAHNC.

### EP-1194 Acute toxicity in nasopharyngeal cancer patients treated with IMRT followed by proton therapy boost

D. Alterio<sup>1</sup>, E. D'Ippolito<sup>2</sup>, B. Vischioni<sup>2</sup>, R. Ricotti<sup>2</sup>, S. Gandini<sup>3</sup>, M. Bonora<sup>2</sup>, V. Vitolo<sup>2</sup>, E. Mastella<sup>2</sup>, G. Magro<sup>2</sup>, S. Ronchi<sup>2</sup>, P.F. Franco<sup>4</sup>, U. Ricardi<sup>4</sup>, M. Krengli<sup>5</sup>, S. Comi<sup>1</sup>, E. Verri<sup>6</sup>, G. Ivaldi<sup>7</sup>, B.A. Jereczek-Fossa<sup>1,8</sup>, F. Valvo<sup>2</sup>, R. Orecchia<sup>1,2</sup>

<sup>1</sup>European Institute of Oncology, Division of Radiation Oncology, Milan, Italy ; <sup>2</sup>National Center of Oncological Hadrontherapy, Radiotherapy Unit, Pavia, Italy ;

<sup>3</sup>European Institute of Oncology, Division of Epidemiology and Biostatistics Unit, Milan, Italy ; <sup>4</sup>University of Turin, Department of Oncology- Radiation Oncology, Turin, Italy ; <sup>5</sup>University Hospital- Novara, Division of Radiation Oncology, Novara, Italy ; <sup>6</sup>European Institute of Oncology, Division of Oncology, Milan, Italy ; <sup>7</sup>ICS Maugeri- I.R.C.C.S, Unit of Radiation Oncology, Pavia, Italy ; <sup>8</sup>University of Milan, Department of Oncology and Hemato-oncology, Milan, Italy

### Purpose or Objective

To compare radiation-induced acute toxicity in patients (pts) affected by locally advanced nasopharyngeal cancer (NPC) treated with sequential intensity modulated radiotherapy (IMRT) and proton therapy boost (mixed beam-MB approach) with an historic cohort of pts treated with a full course of only IMRT.

### Material and Methods

From June 2012 to November 2017, 27 consecutive pts with locally advanced NPC (cT3-4, any N, M0) were treated with MB approach. It consisted in a first phase of treatment performed with IMRT up to 54-60 Gy followed by a second phase performed by proton therapy boost (with pencil beam scanning) up to 70-74 Gy RBE (Relative Biological Effectiveness) prescribed to the macroscopic disease according to the pre-treatment radiologic images. This cohort were compared to an historic cohort of 17 consecutive pts treated with only IMRT only. Pts treated with IMRT only received a total dose of 69.96 Gy. A standard fractionation schedule (1.8-2.12 Gy/fraction, 1fraction/day, 5 fractions/week) was used in both cohorts. Concurrent (with or without induction) platinum-based chemotherapy was administered in all pts. The acute-toxicity profile was considered as the worst event occurred during the entire course of treatment according to Common Terminology Criteria Adverse Events V4.03 scale.

### Results

The 2 cohorts of pts were comparable with no significant differences regarding clinical parameters. The prescribed total dose was significantly higher (p=0.02) in pts treated with MB compared to those treated with only IMRT only. Acute grade 3 mucositis and grade 2 xerostomia were found in 11% and 76% (p=0.0002) and 7% and 35% (p=0.02) of pts treated with MB and IMRT, respectively. No other significant differences were found among the analyzed parameters. For MB cohort median follow-up was 25 months. All but one pts achieved complete tumor response and no patients developed local and/or regional recurrences. At last follow up, 22 pts were still alive with no evidence of disease. For IMRT only cohort median follow-up was 51 months. One patient died one week after the end of radiotherapy for treatment-related toxicity. One patient did not achieve a complete response to treatment on the primary tumor. He progressed on both primary tumor and neck lymph node and died 19 months from the end of treatment. Three patients experienced tumor local progression after 19, 51 and 82 months, respectively; 2 pts experienced also lymph node recurrences and 1 patient also lymph node metastasis

### Conclusion

Our results suggest that sequential MB approach for locally advanced NPC pts is safe with an excellent acute toxicity profile. Preliminary results on clinical outcome are encouraging but need to be confirmed in larger cohort of pts with a longer follow-up

### EP-1195 Functional assessment of late toxicity and quality of life after IMRT for sinonasal carcinoma

M.B. Sharma<sup>1</sup>, K. Jensen<sup>2</sup>, S.F. Urbak<sup>3</sup>, M. Funding<sup>3</sup>, A. Amidi<sup>4</sup>, C. Grau<sup>5</sup>

<sup>1</sup>Aarhus University Hospital, Department of Oncology, Aarhus, Denmark ; <sup>2</sup>Aarhus University Hospital, Danish Center for Particle Therapy, Aarhus, Denmark ; <sup>3</sup>Aarhus University Hospital, Department of Ophthalmology,

Aarhus, Denmark ; <sup>4</sup>Aarhus University Hospital, Unit for Psychooncology and Health Psychology- Department of Psychology and Behavioural Sciences, Aarhus, Denmark ; <sup>5</sup>Aarhus University Hospital, Department of Oncology- Danish Center for Particle Therapy, Aarhus, Denmark

#### Purpose or Objective

Proton therapy (PT) may be beneficial in the treatment of sinonasal carcinomas (SNC) as normal tissue may be spared and radiation-induced sequelae, thus, reduced. Evaluation of late toxicity is important for patient selection and evaluation of PT. Therefore, we aimed to objectively assess late toxicity and quality of life (QoL) in patients treated with intensity modulated radiotherapy (IMRT) for SNC.

#### Material and Methods

All patients who were alive, without recurrence, and who had received IMRT for SNC between January 2008 - January 2017 were eligible for this cross sectional study. Out of 26 eligible patients, 18 consented to participate. All participants had been treated with primary or postoperative IMRT with or without concomitant chemotherapy. Late toxicities were evaluated with a battery of standardized neurocognitive tests assessing different cognitive domains, comprehensive objective ophthalmological examination, blood samples and synacthen test evaluating pituitary function, and olfactory assessment with the Brief Smell Identification Test (BSIT). QoL was evaluated with EORTC QLQ-C30, EORTC QLQ-BN20, Sinonasal Outcome Test-22 (SNOT-22) and Hospital Anxiety and Depression Scale (HADS). In addition, diffusion-weighted magnetic resonance imaging of the brain was performed. These results are not included here.

#### Results

Thirteen males and five females were enrolled; median age was 70.5 years (range 47-83). Participants were treated with a prescribed dose of 60-68 Gray to T-sites in the nasal cavity (n=11) or the maxillary sinus (n=7). Compared with normative data, patients evidenced poorer neurocognitive functioning in several cognitive domains including processing speed ( $p<0.05$ ), verbal learning and memory ( $p<0.01$ ), attention and working memory ( $p<0.05$ ), and verbal fluency ( $p<0.01$ ). Assessment of vision revealed a significant correlation between max radiation dose to the chiasm and grade 3 visual acuity impairment ( $p=0.046$ ) (CTCAE ver. 4.0). The function of the pituitary gland did not present any significant dose response correlations; however, there was an indication of a relationship between higher doses and more affected hormone levels in all axes. Olfactory functioning was impaired (BSIT  $\leq 8$  points) in 15/18 patients. In the global QoL analyses, the most affected domains were social-, emotional-, and physical functions, whereas drowsiness and fatigue were the highest scoring symptoms. No abnormal depression scores were found, but 15/18 participants reported increased anxiety. Anxiety was related to a poorer outcome in the global QoL score ( $p=0.029$ ). SNOT-22 evaluated the impact of sinonasal symptoms on the QoL. The areas that affected the QoL most were lack of smell or taste, thick nasal discharge, need to blow the nose, and blocked nose.

#### Conclusion

The results of the present study indicate considerable toxicity subsequent to IMRT with a substantial influence on patient QoL. Due to these initial findings, the study group intent to perform a larger nationwide study.

#### EP-1196 Treatment of elderly head and neck cancer patients: Update on comorbidity impacts and complications

H. HA<sup>1</sup>, S.E. Combs<sup>1</sup>, S.U. Pigorsch<sup>1</sup>

<sup>1</sup>Klinikum rechts der Isar- TUM Munich, Dept. of RadioOncology and Radiation Therapy, Munich, Germany

#### Purpose or Objective

The management of elderly patients with head and neck cancer (HNC) still remains a challenge with no clear guidelines. Selection criteria for treatment decision are yet elaborative and based on specific factors impacting the patient's performance status. The aim of this retrospective study is to derive recommendations for daily practice and to develop the optimized individual treatment concept for elderly patients  $\geq 70$  years.

#### Material and Methods

146 patients with HNC treated by any kind of radiotherapy (RT) aged  $\geq 70$  years at diagnosis (median age 77.9 years, SD +6.37) at the Dept. of RadioOncology and Radiotherapy at the Technical University Munich between February 2009 and December 2016 were analyzed. The data collection is based on patient's medical records, tumor registry and the department's internal database. Kaplan-Meier Analysis, log rank test and univariate analysis were utilized to compare the outcome survival (OS) stratified by age, treatment, treatment intention, TNM staging and comorbidity impacts via Age-adjusted Charlson Comorbidity Index (ACCI) differentiated in groups: Low (3-5): n = 89 (61.0%); medium (6-8) n = 41 (28.1%); high (9-11) n = 16 (11.0%).

#### Results

Patients with all radiotherapy approaches (definitive, adjuvant or palliative) were included in this analysis. The median OS of all patients was 41.7 mo. (95%CI: 34.2-49.2 mo.). The single dose of RT varied between 1.7-2.7 Gy and the total doses between 4-70.4 Gy depending on the treatment concept. There are significant differences of OS in all categories: Age category (70-79 yrs.: 50.0 months (95%CI: 40.7-59.4mo) vs. 80-89 yrs.: 25.0 months (95%CI: 16.6-33.3mo) vs.  $\geq 90$  yrs.: 13.0 months (95%CI: 1.2-24.8mo) and ACCI Groups (Low ACCI: 50.1 mo. (95%CI: 40.6 - 59.7 mo.) with a mortality of 34 (37.4%) pts. vs. Medium ACCI: 20.9 mo. (95%CI: 10.0 -29.8 mo.) with a mortality of 25 (61.0%) pts. vs. High ACCI: 24.8 mo. (95%CI: 9.8 - 39.7 mo.) with a mortality of 10 (62.5%) pts.), and treatment (RT alone med. OS 31.9 mo. (95%CI: 24.7-39.0 mo.) vs. CRT med. OS 73.9 mo. (95%CI: 60.4-87.4 mo.). Most benefit for younger patients with the best survival prognosis after CRT and a lower ACCI. Therapy-induced complications were detected such as radiomucositis n = 72 (49.3%), radiodermatitis n = 60 (41.1%), dysphagia n = 50 (34.2%), nausea n = 20 (13.7%), PEG complication n=18 (12.3%), additional chemotherapy induced anemia n = 10 (6.8%), mouth dryness n = 8 (5.5%). Required supportive placements included PEG tube n = 52 (35.6%), tracheostomy n = 32 (21.9%), port catheterizations n = 24 (16.4%).

#### Conclusion

Analyzing ACCI groups within the CRT collective was to assess a possible influence on OS. The evaluation is skewed due to a small number of patients with a high ACCI Score who underwent CRT. The impact of therapy-induced complications on the outcome survival and therapeutical process needs to be put into consideration. The assessment of required supportive placements can be a useful predictor to measure the severity of adverse events.

#### EP-1197 Pattern, timing, and detection of recurrence in HPV positive oropharyngeal cancer

M. Echevarria<sup>1</sup>, L. Harrison<sup>1</sup>, A. Trotti<sup>1</sup>, J. Caudell<sup>1</sup>

<sup>1</sup>H. Lee Moffitt Cancer Center and Research Institute, Radiation Oncology, Tampa, USA

#### Purpose or Objective

HPV positive oropharyngeal cancer has a new staging system, reflecting their higher cure rates. Given high cure rates, the most efficient surveillance scheme and optimal post treatment monitoring tools for this patient population have not been established. We therefore sought to evaluate the pattern, timing, and detection of

recurrence in HPV positive oropharyngeal cancer to identify optimal post-treatment diagnostic tools.

#### Material and Methods

After institutional review board approval, records of patients with non-metastatic HPV-associated oropharyngeal cancer were retrospectively reviewed. We identified 406 patients with biopsy-proven, HPV positive oropharyngeal cancer treated with definitive radiotherapy. Patients were followed at intervals of 3 months and all patients underwent imaging 2-3 months post treatment in the form of PET/CT or neck CT. Locoregional control (LRC) and freedom from distant metastasis (FFDM) were estimated according to Kaplan-Meier method and comparisons were made by log rank test.

#### Results

The median follow up for all patients was 40 months. The 3 year LRC for the entire cohort was 91.3%. Patients with AJCC 8<sup>th</sup> edition stage I, stage II, and stage III had a LRC of 94.9%, 85.7%, and 82.3% respectively. There were a total of 30 locoregional recurrences, 28 (93.3%) of which presented with either symptoms or persistent disease on 2-3 month post treatment imaging. Of these 28 patients, 13 patients were found to have recurrent disease on the initial 2-3 month post treatment imaging and 15 patients presented with symptoms that led to the identification of recurrent disease. 3-year FFDM for the entire cohort was 88.4% and when stratified by stage patients with stage I, II, and III had a FFDM of 91.6%, 87.6%, and 74.1%, respectively. There were a total of 31 distant recurrences, 25 (80.6%) of which were identified due to symptoms or on 2-3 month post treatment imaging. Of these 25 patients, 15 patients were found to have recurrent disease on the initial 2-3 month post treatment imaging and 10 patients presented with symptoms that led to the identification of recurrent disease.

#### Conclusion

Our results showed that identification of the majority of locoregional and distant recurrences was either symptom driven or identified in the initial post treatment imaging performed 2-3 months after completion of radiation. Based on these results it is reasonable to follow patients clinically with a history and physical examination with direct visualization and to forgo further imaging after the initial post treatment imaging shows a complete response.

#### EP-1198 Knowing the oropharyngeal cancer associated with the human papillomavirus

L. Gutierrez Bayard<sup>1</sup>, M.D.C. Salas Buzón<sup>1</sup>, S. Garduño Sánchez<sup>1</sup>, M.J. Macías Lozano<sup>1</sup>, R. Rodríguez Sánchez<sup>1</sup>, S. Sayago Gil<sup>1</sup>, V. Díaz Díaz<sup>1</sup>, E. Gonzalez Calvo<sup>1</sup>, I. Villanego Beltrán<sup>1</sup>, A. Ruiz Herrero<sup>1</sup>, M. Lorente Sánchez<sup>1</sup>, J. Jaén Olasolo<sup>1</sup>

<sup>1</sup>Hospital Universitario Puerta del Mar, Radiation Oncology, Cadiz, Spain

#### Purpose or Objective

For resected HPV-positive oropharynx squamous cell carcinoma (HPV+ OPSCC) high node number is a critical determinant of survival, based on the 8th edition American Joint Committee on Cancer staging system. In our study, we analyzed the relationship between the number of affected lymph nodes (LNs), neck level and the pattern of failure (local, regional, and distant recurrences).

#### Material and Methods

We retrospectively studied 28 HPV+ OPSCC patients treated with neck dissection (ND) and either resection or radiotherapy of the primary tumor between 2014 and 2017. External beam radiation (+/- chemotherapy) was given based on the pathologic findings.

#### Results

Metastatic pathologic LNs were the following : 0% (0/5) in level I, 78.5% (22/28) in level II, 25% (7/28) in level III,

9.1% (2/22) in level IV, and 9% (1/11) in level V. The level V LN was clinically evident preoperatively. 24.2% elective neck dissection contained occult LNs, all of which were in level II and without extranodal extension. 18 (64.28%) patients underwent adjuvant radiation; 7 (25%) patients underwent adjuvant chemoradiation. With a mean follow-up of 25 months on multivariate analysis, >5 involved lymph nodes was significantly associated with worse progression free survival (PFS) (P=0.001). Rates of 3-year locoregional recurrence (LRR) in patients with ≤5 vs > 5 were 8% and 23% (P=0.1). Rates of 3-year distant metastases (DM) were 14% and 52% between ≤5 and >5 (P<0.001).

#### Conclusion

For p16+OPSCC, therapeutic NDs should include any levels bearing suspicious LNs and levels II, III, and IV, while elective NDs should be encompass at least levels II and III, followed by indicated adjuvant treatment, are associated with a low nodal recurrence rate. Patients with more than 5 involved lymph nodes appear to have worsened rates of disease recurrence. While these patients appear to be at high risk of both LRR and DM, the predominant mechanism of failure is distant (over 50%). More ambitious studies are necessary that allow to enlarge our knowledge in this entity.

#### EP-1199 Metastatic lymph node features with and without extracapsular extension in head and neck Squamous Cell Carcinoma

J. Zheng<sup>1</sup>, A. Flaman<sup>2</sup>, D. Yegendorf<sup>3</sup>, B. Purgina<sup>2</sup>, S. Chakraborty<sup>4</sup>, M. Gaudet<sup>1</sup>, H. Alain<sup>1</sup>

<sup>1</sup>The Ottawa Hospital Regional Cancer Centre, Radiation Oncology, Ottawa, Canada ; <sup>2</sup>The Ottawa General Hospital, Anatomical Pathology, Ottawa, Canada ; <sup>3</sup>University of Ottawa, Science, Ottawa, Canada ; <sup>4</sup>The Ottawa General Hospital, Radiology, Ottawa, Canada

#### Purpose or Objective

In Head and Neck Squamous Cell Carcinoma (HNSCC) patients with metastatic involved cervical lymph nodes, extra-capsular extension (ECE) carries with it increased risks of local recurrence and distant metastases. ECE is an indication for chemo-radiation after neck dissection which adds significant toxicity. This can potentially be avoided if patients could be risk stratified for ECE prior to surgery. We aim to analyze clinical, pathological and pre-operative radiological features of these patients to better risk stratify for presence of ECE.

#### Material and Methods

HNSCC patients aged 18 years and older diagnosed between October 2010 and May 2017 at a single institution. Patients had pathological positive metastatic lymph nodes and undergone neck dissection without neo-adjuvant treatment. The patients' clinical information, pathological reports and pre-operative CT scans were obtained from the Ottawa Hospital electronic medical record and clinical imaging software. In cases of incomplete pathology data, slides were re-examined by a pathologist. Suspicious lymph nodes from each CT scan were matched to metastatic lymph nodes from dissection specimens based on corresponding level, size and morphological features. Statistical analyses were done through Chi-squared testing.

#### Results

Clinical and pathological data of 142 patients were analyzed in this study. ECE was present in 45 patients (32%) and absent in 90 (63%) while unknown for 7 (5%) patients. An association was found between the number of positive lymph nodes and the presence of ECE. For patients with 1-2 metastatic lymph nodes and 3 or more metastatic lymph nodes, the rate of ECE was 18% and 60% respectively (p<0.001). p16 status was only reported for 63 patients but was also associated with ECE. It was present in 19% of p16 positive and 46% of p16 negative

patients ( $p=0.03$ ). There were no significant associations between ECE and gender, age at diagnosis and pathological tumour grade.

Pre-operative CT scans of 80 patients were examined and 136 metastatic lymph nodes were matched to pathological data. Of this data set, 30 (22%) lymph nodes were positive for ECE. There was a non-statistically significant trend towards more incidence of ECE seen in matted nodes against discrete nodes (27% vs. 15%,  $p=0.14$ ) and those with necrosis (27% vs. 14%,  $p=0.11$ ). No association was found between ECE and size or eccentricity of LN as well as smoothness or distinctness of LN borders. Radiological features such as calcified and cystic lymph nodes were too rare to have statistical significance.

#### Conclusion

We were able to demonstrate a statistically significant association between presence of ECE and number of metastatic lymph nodes as well as p16 status. Analysis of radiological features did not reveal any associations with ECE. Further analysis will be required to see if a combination of clinical and radiological features is best at predicting presence of ECE.

#### EP-1200 Is skin dose distribution a predictive factor for the development of severe radiation dermatitis?

P. Bonomo<sup>1</sup>, C. Talamonti<sup>2</sup>, L. Marrazzo<sup>2</sup>, I. Desideri<sup>1</sup>, D. Pezzulla<sup>1</sup>, L. Dominici<sup>1</sup>, A. Rampini<sup>3</sup>, S. Bertocci<sup>3</sup>, R. De Majo<sup>3</sup>, C. Gasperi<sup>4</sup>, A.S. Curion<sup>4</sup>, L. Lastrucci<sup>3</sup>, S. Pallotta<sup>2</sup>, L. Livi<sup>1</sup>, S. Caini<sup>5</sup>

<sup>1</sup>Azienda Ospedaliero-Universitaria Careggi, Radiation Oncology, Florence, Italy; <sup>2</sup>Azienda Ospedaliero-Universitaria Careggi, Medical Physics, Florence, Italy; <sup>3</sup>Ospedale San Donato, Radiation Oncology, Arezzo, Italy; <sup>4</sup>Ospedale San Donato, Medical Physics, Arezzo, Italy; <sup>5</sup>Cancer Research and Prevention Institute ISPO, Cancer Risk Factors and Lifestyle Epidemiology Unit, Florence, Italy

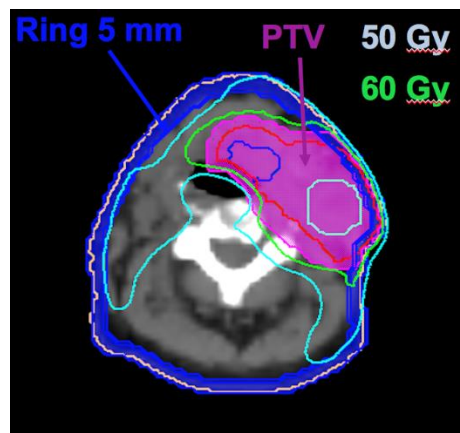
#### Purpose or Objective

In the context of locally advanced HNSCC, no biomarkers are available to predict the development of radiation dermatitis (RD). In the absence of putative skin dose constraints, large variability exists in IMRT planning optimization to avoid the potential risk of undue toxicity. The aim of our work was to assess whether skin dose-volume parameters may be predictive of severe RD.

#### Material and Methods

We retrospectively reviewed consecutive patients treated at two fellow institutions between Oct. 2011 and Nov. 2017 for locally advanced HNSCC. A 2:1 frequency-matched cohort analysis was performed to identify patients with similar demographic and disease-features who received cisplatin or Cetuximab. On the native planning CT scans, 3 skin ring structures were semi-automatically delineated by subtracting 2, 3 and 5 mm below the external patient surface (figure 1: 5 mm example), extending between the upper and lower limits of PTV plus a fixed 1 cm margin. For all 3 skin ring ROI's, the following dosimetric parameters were collected: V50, V60, maximum absolute dose expressed in terms of point value and percentage of total prescription dose. Acute toxicity was prospectively recorded according to CTCAE v. 4.1. A total dose of 66-70.5 Gy was delivered in 30-35 fractions with conventional or accelerated fractionation (dose per fraction, 2/2.12/2.35 Gy, respectively). A 3-5 PTV margin was added to CTV's (3 mm in case of daily image guidance). HPV status was not routinely available until 2015. To assess whether any patient, disease, treatment and skin dose distribution - related characteristics correlated with the development of G3/G4 RD, categorical and continuous variables were tested with Fisher's exact chi-square test and Mann-Whitney test, respectively. A multivariate Poisson regression analysis was performed when multiple risk factors with a p value <0.05 were identified in the univariate analysis. A ROC

curve analysis was applied to estimate the predictive accuracy of dosimetric threshold values for G3/G4 RD.



#### Results

Ninety-patients were evaluated (table 1). G3/G4 RD, oral mucositis and dysphagia developed in 37 (41.1%), 40 (44.4%) and 24 (24.4%) patients, respectively. As expected, the G3/G4 RD was numerically higher in the cetuximab group (50% vs 36.6% in the cisplatin cohort;  $p=0.122$ ). In univariate analysis, PS >1, weight loss at end of RT > 10 Kgs, mean relative dose intensity of Cetuximab, 2 mm skin ring V50 and V60 were significantly correlated with G3/G4 RD. In multivariate analysis, PS >1 and marked weight loss were the only 2 factors that retained significance ( $p=0.028$  and  $0.030$ , respectively). The best predictive accuracy of skin ring ROI's for G3/G4 RD was provided by 19.9 cc of 2 mm skin ring at 50 Gy and 5.8 cc of 2 mm skin ring at 60 Gy (both AUC 0.61).

Characteristic	No. of patients (%), n = 90	Cisplatin cohort (%), n = 60	Cetuximab cohort (%), n = 30
Median age years (range)	62 (19-88)	62 (19-78)	65 (44-88)
Sex			
Male	73 (81.1%)	47 (78.3%)	26 (86.6%)
Female	17 (18.9%)	13 (21.7%)	4 (13.4%)
ECOG Performance Status			
0	56 (62.3%)	48 (80%)	8 (26.7%)
1	32 (35.5%)	12 (20%)	20 (66.6%)
2	2 (2.2%)	0 (0%)	2 (6.7%)
Primary tumor			
Oropharynx	47 (52.3%)	31 (51.7%)	16 (53.4%)
Larynx	18 (20%)	12 (20%)	6 (20%)
Hypopharynx	13 (14.4%)	9 (15%)	4 (13.3%)
Other	12 (13.3%)	8 (13.3%)	4 (13.3%)
HPV status			
Positive	30 (33.3%)	22 (36.7%)	8 (26.7%)
Negative	10 (11.1%)	7 (11.7%)	3 (10%)
Unknown	7 (7.8%)	2 (3.3%)	5 (16.7%)
AJCC stage (Vilth ed)			
III	25 (27.8%)	18 (30%)	7 (23.3%)
IVA	54 (60%)	37 (61.7%)	17 (56.7%)
IVB	11 (12.2%)	5 (8.3%)	6 (20%)
Mean relative dose intensity (%; SD)			
Cisplatin	77.4% (14.8)	77.4% (14.8)	/
Cetuximab	84.2% (15.2)	/	84.2% (15.2)
IMRT technique			
static	24 (26.7%)	16 (26.7%)	8 (26.7%)
rotational	3 (3.3%)	2 (3.3%)	1 (3.3%)
helical	63 (70%)	42 (70%)	21 (70%)
IMRT schedule			
sequential	27 (30%)	18 (30%)	9 (30%)
SIB	63 (70%)	42 (70%)	21 (70%)

#### Conclusion

Along with known risk clinical factors occurring during RT such as a marked weight loss, the extent of a 2 mm skin ring ROI receiving 50 and 60 Gy may help predict beforehand the development of severe RD.

### EP-1201 Outcomes in young patients (<math>\leq 40</math>) treated for oral cavity squamous cell carcinoma in the modern era

A. Billfalk Kelly<sup>1</sup>, L. Lin<sup>2</sup>, W. Xu<sup>2</sup>, S.H. Huang<sup>1</sup>, R. Wu<sup>1</sup>, A. Bayley<sup>1</sup>, S. Bratman<sup>1</sup>, J. Kim<sup>1</sup>, M. Giuliani<sup>1</sup>, J. Ringash<sup>1</sup>, J. Waldron<sup>1</sup>, B. O'Sullivan<sup>1</sup>, J. Cho<sup>1</sup>, D. Goldstein<sup>3</sup>, A.A. Hosni<sup>1</sup>, A. Hope<sup>1</sup>

<sup>1</sup>Princess Margaret Cancer Centre, Radiation Oncology, Toronto, Canada ; <sup>2</sup>Princess Margaret Cancer Centre, Biostatistics, Toronto, Canada ; <sup>3</sup>Princess Margaret Cancer Centre, Surgery, Toronto, Canada

#### Purpose or Objective

Outcomes of oral cavity squamous cell carcinoma (OSCC) tend to be worse than other head and neck squamous cell carcinomas (HNSCC) despite modern surgical and radiation techniques and the use of postoperative concurrent chemotherapy in high risk OSCC. Anecdotal evidence has suggested that OSCC patients under the age of 40 have aggressive disease. We evaluated the outcomes of OSCC patients <math>< 40</math> treated in the modern IMRT era at our institution.

#### Material and Methods

After obtaining REB and institutional approval, OSCC patients under 40 were identified from our prospectively collected database. Details were collected in relation to tumor and treatment factors. Oncologic outcomes including overall survival, disease free survival, and loco-regional control were determined for this sub-set. Overall survival (OS) and disease-free survival (DFS) were analyzed using Kaplan Meier method and loco-regional control was evaluated using competing risk analysis.

#### Results

From 1183 consecutive patients with OSCC treated with curative intent between 2005 and 2017, 57 patients (5%) under the age of 40 were identified. The median age was 33 years (range 18-39). In the study cohort 42% of patients were female and 58% male; 61% of patients were lifelong non-smokers, with only 23% current smokers, and 16% ex-smokers; 44% were non-drinkers. ECOG performance status was 0-1 in 92.9% (one 2, 3 missing data). Surgery was to the primary lesion only in 26%, to the primary with an ipsilateral neck dissection in 53%, and 21% had surgery to the primary with bilateral neck dissections. Only 5% of patients had positive microscopic resection margins. Lymph node involvement with extra-nodal extension was seen in 17% of patients, 5% had LVI and 37% had PNI. Almost 60% received definitive surgery alone, while in 40% surgery was followed by adjuvant radiotherapy; among these, 65% received concurrent chemotherapy. The adjuvant radiotherapy dose received ranged from 56Gy in 40 fractions to 70.72Gy in 35 fractions; 26% of patients received 60Gy in 30 fractions, and 52% receiving 66Gy in 33 fractions. Almost half, 44%, had stage I disease, 10.5% stage II, 16% stage III, 28% stage IV; 1 patient's biopsy showed CIS despite a large tumor. Serious comorbidity was present in 8 patients: 6 with previous malignancies (10.5%), 1 with Fanconi's Anaemia, and 1 with severe SLE causing renal failure. With a median follow-up of 4.27 (5.03 in survivors) years, 1-year OS was 94% (0.88-1), 3-year OS 84% (0.75-0.95) and 5-year OS 82% (0.71-0.93). DFS was 84% (0.74-0.94) at one year, and 66% (0.54-0.81) at 5 years. Event free survival was 87% at 1 year (94-74), 79% at 3 years (88-65) and 74% at 5 years (84-57).

#### Conclusion

The clinical impression of poor outcomes for patients aged under 40yrs may represent recall bias. Such treated curatively for OSCC in our institution appear to have acceptable OS and DFS.

### EP-1202 Associations between smoking cessation after radiotherapy for larynx cancer and patient outcomes

A. Srivastava<sup>1</sup>, J. Contreras<sup>1</sup>, M. Daly<sup>1</sup>, H. Gay<sup>1</sup>, W. Thorstad<sup>1</sup>, A. Apicelli<sup>1</sup>

<sup>1</sup>Washington University School of Medicine, Radiation Oncology, Saint Louis, USA

#### Purpose or Objective

Continued tobacco use is known to be a poor prognostic factor among patients undergoing radiation therapy (RT) for cancers of the head and neck. However, this relationship is not well characterized for carcinomas of the larynx/hypopharynx (LNX/HPX), which are almost exclusively associated with tobacco use. Therefore, in this study we sought to evaluate whether there was a disease control and survival benefit to smoking cessation after RT for cancers of the LNX/HPX.

#### Material and Methods

An institutional database of patients with squamous cell carcinoma of the LNX/HPX treated with definitive intent RT between 2012 and 2017 was reviewed. Patients were eligible for inclusion if they had a documented history of tobacco use at the beginning of RT and were planned to undergo definitive therapy. Following completion of therapy, patients were stratified into two cohorts based on continued tobacco use. The student's t-test and Fisher exact test were utilized to compare baseline clinical and demographic covariates. The Kaplan-Meier method and log-rank test were used to estimate and compare locoregional control (LRC), distant control (DC), and overall survival (OS) between the cohorts, and Cox regression tests were used to identify predictors of these outcome metrics.

#### Results

A total of 102 patients were eligible, and 34 (33.3%) continued smoking following definitive therapy. Most patients (52/102, 51%) underwent surgery, and the majority (71/102, 70%) received concurrent chemotherapy with RT. Median follow-up time was 26 months (range 1-64). Baseline demographic and clinical characteristics were similar between the groups, but smoking cessation was less common among African Americans ( $p=0.03$ ). At two years of follow up, actuarial LRC rates were 63% for patients who continued to smoke and 79% for patients who stopped ( $p=0.02$ ) while DC rates were 86% and 90%, respectively ( $p=0.53$ ). There was a survival benefit in patients who stopped smoking (92% v. 78%,  $p=0.01$ ). On multivariate analysis, smoking status post RT (hazard ratio [HR]: 2.6, 95% confidence interval [CI]: 1.8-3.9;  $p=0.01$ ), higher performance status (HR: 2.3, 95% CI: 1.4-4.2,  $p=0.03$ ), and advanced tumor stage (HR: 2.9, 95% CI: 1.7-5.8,  $p=0.02$ ) were predictive of worse OS. Notably there was no association between number of pack-years previously smoked and disease outcome ( $p=0.21$ ).

#### Conclusion

Smoking cessation after definitive treatment of larynx/hypopharynx cancer is associated with a significant increase in OS regardless of extent of smoking history, underscoring the importance of smoking cessation.

### EP-1203 Characterization of DCE-MRI parameters associated with advanced mandibular osteonecrosis

A.S.R. Mohamed<sup>1</sup>, R. He<sup>1</sup>, Y. Ding<sup>1</sup>, J. Wang<sup>1</sup>, B. Elgohari<sup>1</sup>, H. Elhalawani<sup>1</sup>, J. Johnson<sup>1</sup>, J. Stafford<sup>1</sup>, J. Bankson<sup>1</sup>, V. Sandulache<sup>2</sup>, C. Fuller<sup>1</sup>, S. Lai<sup>1</sup>

<sup>1</sup>The University of Texas- MD Anderson Cancer Center, Radiation Oncology, Houston, USA ; <sup>2</sup>Baylor College of Medicine, Otolaryngology, Houston, USA

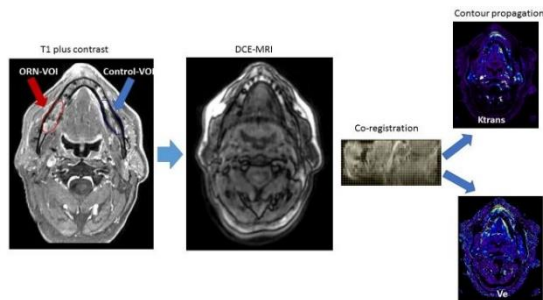
#### Purpose or Objective

We aim to characterize the quantitative DCE-MRI parameters associated with advanced mandibular ORN following definitive radiotherapy for head and neck cancer patients.

#### Material and Methods

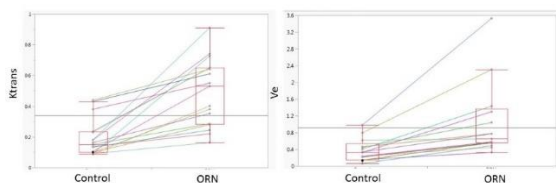
Patients with advanced ORN after curative-intent radiation treatment of head and neck cancer were prospectively enrolled in an observational imaging study after institutional-review board approval and study-

specific informed consent. Eligibility criteria included; age > 18 years, pathological evidence of head and neck malignancy with a history of curative-intent external beam radiotherapy; patients with clinically confirmed high-grade ORN requiring surgical intervention; and no contraindications to MRI. Prior to DCE-MRI, T1 mapping was performed using a total of 6 variable flip angles. The DCE-MRI acquisition consisted of a 3D SPGR sequence to gain a sufficient signal-to-noise ratio (SNR), contrast, and temporal resolution. Images were acquired every 5.5 s for a total of 5 minutes. Extended Toft's pharmacokinetic model was used for analysis. Motion correction was applied to enhance the quality of map computation. Manual segmentation of advanced ORN 3-D volume was done using anatomical sequences (T1, T2, and T1+contrast) to create ORN volumes of interest (ORN-VOIs). Subsequently, normal mandibular VOIs were segmented on contralateral healthy mandible of similar volume and anatomical location (i.e. mirror image) to create self-control VOIs. Finally, anatomical sequences were co-registered to DCE sequences and contours were propagated to respective Ktrans and Ve quantitative parameter maps. The workflow is summarized in Figure 1.



## Results

Seventeen patients with advanced ORN requiring surgical resection of the mandible were analyzed. Median age at diagnosis was 59 years (range 38-72), and 88% were men. Primary tumors were localized to the oropharynx (n=9), oral cavity (n=4), salivary glands (n=2) and nasopharynx (n=2). All patients were treated with intensity modulated radiotherapy (IMRT) to a median dose of 70 Gy in 33 fractions. Using matched pairs analysis, we measured higher Ktrans and Ve values in ORN-VOIs compared with control regions (0.49 vs 0.19 min<sup>-1</sup>, p<0.0001 and 1.2 vs 0.6, p=0.01; respectively). The median relative increase of Ktrans in ORN-VOIs was 2.7 fold greater than that of healthy mandibular control VOIs (range 1.4-7.8); the relative increase of Ve in ORN-VOIs was 2.6 fold greater than that of healthy mandibular control VOIs (range 1.1-8). Figure 2 depicts boxplots of ORN vs Control VOIs parameters.



## Conclusion

Our results confirm there is a quantitatively significant higher degree of leakiness in the mandibular vasculature as measured using DCE-MRI parameters of areas affected with advanced grade of ORN versus healthy mandible. We were able to measure significant increases in both parameters (2.7 fold Ktrans, 2.6 fold Ve) compared to values from non-ORN mandibular bone. Further efforts are ongoing to validate these findings and to establish DCE-

MRI parameter thresholds for early detection of subclinical cases of ORN.

## EP-1204 Quantitative signal intensity kinetics of normal tissues of the head and neck on the MR-Linac.

F. Gregucci<sup>1,2</sup>, H. Bahig<sup>1</sup>, A.S. Mohamed<sup>1</sup>, R. He<sup>3</sup>, B.A. Elgohary<sup>1</sup>, H. Lee<sup>4</sup>, Y. Ding<sup>4</sup>, J. Wang<sup>4</sup>, H. Elhalawani<sup>1</sup>, G.S. Ibbott<sup>4</sup>, M. Chetvertkov<sup>4</sup>, G. Bosco<sup>4</sup>, S. Ikner<sup>4</sup>, S.P. Ng<sup>4</sup>, D.C. Fuller<sup>1</sup>

<sup>1</sup>University of Texas MD Anderson Cancer Center, Radiation Oncology, Houston, USA ; <sup>2</sup>University of Padova, Radiation Oncology, Padova, Italy ; <sup>3</sup>University of Texas Medical School, Diagnostic and Interventional Imaging, Houston, USA ; <sup>4</sup>University of Texas MD Anderson Cancer Center, Radiation Physics, Houston, USA

## Purpose or Objective

The MR-Linac, a hybrid device combining a magnetic resonance with a linear accelerator, holds the promise of online anatomic and functional imaging which would allow daily radiotherapy adaptation. In this study, we sought to quantitatively assess the repeatability and reproducibility of signal intensity (SI) over time from serial T1- and T2-weighted magnetic resonance imaging (MRI) acquired on the MR-Linac with standardized acquisition parameters and under stable conditions.

## Material and Methods

6 healthy volunteers underwent 7 serial, immediately consecutive T1- and T2-weighted MRI studies of the head and neck (H&N) region using a 3 Tesla MR-Linac. Normal tissue volume of interest (VOI) were defined based on spin-echo sequences T1- and T2-weighted imaging. For a total of 42 MRI studies, we performed manual segmentation using T2-spin-echo sequence, for the following VOI: mandible, parotid glands, submandibular glands, sternocleidomastoid muscles, spinal cord and vertebral body. Deformable image registration was performed between the different MRI time points in T1 and T2 sequences, all VOI were then propagated and reviewed by expert radiation oncologists. From these serial MRI studies, a collection data concerning the VOI has been created bringing out a quantitative analysis of the following SI parameters: mean, max and min values. For the statistical analysis the VOI were grouped in the following 4 tissue categories: gland (G), bone (B), muscle (M) and nerve (N).

## Results

The mixed model estimates on T1-MRI showed that max, min and mean values of SI were for G group -1002.88 (t=0.0014), -161 (t=0.0005) and -394.56 (t<0.0001), respectively; for B group -384.73 (t=0.178), -202.41 (t<0.0001) and -442.24 (t<0.0001), respectively; for M group -1008.08 (t=0.0013), 26.69 (t=0.513) and -91.18 (t=0.283), respectively; for N group 1962.63 (t=0.0004), 230.41 (t=0.0029) and 603.68 (t=0.0003), respectively. The mixed model estimates on T2-MRI showed that max, min and mean values of SI were for G group -9.97 (t=0.03), 11.39 (t<0.0001) and 6.49 (t=0.04), respectively; for B group -0.59 (t=0.89), 3.43 (t=0.12) and 12.44 (t=0.0008), respectively; for N group 66.75 (t<0.0001), 17.00 (t<0.0001) and 27.35 (t<0.0001), respectively. The F-test in T1- and T2-weighted MRI showed differences between the different VOI groups in max, min and mean SI values (f<.0001 for all) but no SI differences inside the same VOI group and between the different time points for each VOI groups.

## Conclusion

The SI kinetics for analyzed tissue categories on T1 and T2-spin-echo sequences are reproducible and repeatable between different subjects and over the time, keeping unchanged the MRI acquisition parameters. These results could be an helpful tool for future studies of correlation between SI kinetics deviation and observed toxicity profile for the purpose of developing predictive models in H&N cancer.

**EP-1205 A new alpha particle treatment for recurrent or aggressive head and neck squamous cell carcinoma**  
A. Popovitzer<sup>1</sup>

<sup>1</sup>Rabin Med. Ctr. Beilinson Campus, Department of Radiation Oncology, Petah-Tikva, Israel

**Purpose or Objective**

The first clinical trial in humans with skin and oral cavity squamous cell carcinoma was performed in order to evaluate the effect of a unique intra-tumoral alpha radiation based tumor ablation treatment termed Diffusing Alpha emitters Radiation Therapy (DaRT). DaRT relies on alpha particles and thus, effective against hypoxic tumors. DaRT seeds can be produced with various intensities, sizes, and shapes and enable custom designed seeds. In our prior animal studies, we demonstrated the effectiveness of the treatment in mice for many tumors. In this first Human study, we evaluated its role for Skin and Oral Cavity Squamous cell Carcinoma.

**Material and Methods**

Materials/Methods: A Radium-224 loaded sources (DaRT seeds) were inserted into solid tumors and released by recoil short-lived alpha-emitting atoms (Rn-220, Po-216, Pb-212, Bi-212, Po-212, Tl-208). These atoms disperse in the tumor and spray it with highly destructive alpha radiation. The decay products diffuse in the tumor mass to a distance of at least 5 mm. Thus, a sizable fraction of the tumor is irradiated by alpha particles, and because of their short half-life, only small amounts of the isotopes disperse in the body.

**Results**

Results: A feasibility and safety clinical study is ongoing and currently, 18 patients were treated. All patients were radiation resistant recurrent histopathological confirmed skin or head and neck SCC, and tumor size  $\leq 5$  centimeters in the longest diameter, were enrolled. Treatment was delivered based on a CT-simulation pre-treatment plan. The Ra-224 Alpha DaRT Seeds were inserted under local anesthesia using a specially designed Alpha DaRT Applicator. The seeds (1 cm long and 0.7 mm in diameter) each carrying a dose of 2  $\mu$ Ci were placed 6 millimeters from each other. CT was used to check the position of the radioactive seeds. Two to four weeks after implantation the seeds were removed, and six weeks after treatment CT was performed to assess the effect of treatment. Blood tests and urinalysis were performed during the treatment. The Age of the patients ranged between 70 to 94 (median 81). Eleven patients had recurrent oral cavity SCC and seven diagnosed with aggressive skin SCC. All were treated within radiation failure fields (Radiation dosage  $>60$  Gy). With a median follow up of 5 months, All tumors responded to the treatment; 13 tumors had a complete response, five tumors showed a partial response. No major toxicity was noted. The areas around the treated tumors were not necrotic and no radionecrosis developed

**Conclusion**

Conclusion: In this feasibility and safety human study we demonstrated that alpha particles based DaRT exhibit enhanced radiobiological potential. The treatment was effective against radio-resistant SCC tumors without major toxicity.

---

Electronic Poster: Clinical track: CNS

---

**EP-1206 SRS/SRT for patients with brain Metastasis RPA Class II disease: Results from Single institution**

M. El-Haddad<sup>1</sup>, O. AlSalih<sup>2</sup>, L. Eley<sup>1</sup>, E. Johnson<sup>1</sup>, M. Chandrasekaran<sup>1</sup>, K. Nyathi<sup>1</sup>, H. Trieu<sup>1</sup>, S. Kumar<sup>1</sup>, C. Birch<sup>1</sup>, F. Sheikh<sup>3</sup>, H. Joy<sup>3</sup>, P. Grundy<sup>4</sup>, J. Ching<sup>1</sup>, J. Duffill<sup>1</sup>, S. Geoff<sup>1</sup>

<sup>1</sup>University hospital southampton, Clinical Oncology, Southampton, United Kingdom ; <sup>2</sup>St Thomas' Hospital

Guy's Hospital, Cancer Center, London, United Kingdom ; <sup>3</sup>University hospital southampton, Department of Radiology, Southampton, United Kingdom ; <sup>4</sup>University hospital southampton, Wessex Neurosurgery Center, Southampton, United Kingdom

**Purpose or Objective**

Recursive partitioning analysis is one of the important factor that determine patients' prognosis and choice of our treatment. The aim of this study is to emphasize the role of stereotactic radiosurgery (SRS)/radiotherapy (SRT) in patients with brain metastasis RPA class II.

**Material and Methods**

Hundred and twenty-four patients treated for brain metastasis at University hospital Southampton between November 2016 and June 2018. Eighty-eight (71%) patients were treated with SRS, 36 (29%) patients treated with SRT, choice of SRS/SRT was chosen depending on tumour size and dose to normal brain tissue or proximity to normal risk structures e.g. brain stem. Median dose for SRS patients was 18Gy single fraction (range: 12-21Gy), and for SRT 21Gy in 3-5 fractions (range: 21-25Gy). All patients treated on linear accelerator ELKTA® with Agility™MLC and Exactrac™ system. Dose prescription ranged between 60% and 72% isodose line. <sup>TM</sup>. OAS calculated from the date if treatment till date of last follow-up.

**Results**

Median age at referral was 65 year, with 50% of the patients aged between 56 and 71 year. Fourteen patients were between 76 and 80 year. Sixty-seven female (54%) and 57 (46%) male. Fifty patient (40%) had lung cancer diagnosis, 19 patients (15%) diagnosed with melanoma the rest were between, Breast 14 patients (11%), renal cell 12 patients (10%), colorectal 8 patients (6%) others 21 patients (18%). Main toxicity profile was brain oedema and need for steroid longer than our defined protocol of 8 days, one patient had brain stem necrosis following single fraction 15Gy for 2.5cm lesion, improved on steroids for 8 weeks without evidence of recurrence. Survival analysis was done for 81 patients only, 10 patients didn't have follow up data, the rest of patients were enrolled at a later time and did not have a minimum follow-up of 6 months at the time of the last data cutoff. Median overall survival for the whole group was 15 months (95% CI 10.05 -19.94), progression free survival 12 months (95% CI 8.88 -15.11). Majority of our patients 65% classified as Class II disease OAS for this group was 11 months (95% CI 8.17-13.8) and PFS was 10 months (95% CI 8.07 -11.7).

**Conclusion**

SRS/SRT is effective in patients with brain metastasis Class II RPA longer follow-up is still needed.

**EP-1207 Fractionated stereotactic radiation therapy for resected brain metastases: a preliminary report**

A. Di Marzo<sup>1</sup>, F. Trippa<sup>1</sup>, P. Anselmo<sup>1</sup>, F. Arcidiacono<sup>1</sup>, S. Terenzi<sup>1</sup>, L. Draghini<sup>1</sup>, M. Italiani<sup>1</sup>, M. Casale<sup>1</sup>, M. Muti<sup>1</sup>, S. Fabiani<sup>1</sup>, E. Maranzano<sup>1</sup>

<sup>1</sup>"S. Maria" Hospital Terni, Radiotherapy Oncology Centre, Terni, Italy

**Purpose or Objective**

Cavity stereotactic radiosurgery (SRS) or fractionated stereotactic radiation therapy (FSRT) are emerging treatment options after surgical resection of brain metastases (BM). Recent randomized trials, aimed to clarifying the adverse effects of postoperative whole-brain radiation therapy (WBRT) for BM have confirmed the association of neuro-cognitive and quality of life decline with WBRT. The recent phase 3 NCCTG study comparing SRS and WBRT for resected BM showed comparable overall survival and superior preservation of cognitive function after SRS, supporting the rationale for limiting WBRT to only patients where it is clinically essential. We present a preliminary report of our experience on surgical cavity FSRT.

### Material and Methods

Between May 2011 and August 2018, 19 patients (pts) with surgical resected BM were irradiated with FSRT in 5 fractions. Median age was 66,5 years (range 50-74); primary tumor was non-small cell lung cancer (7 pts), breast cancer (4 pts), gastrointestinal cancer (5 pts), others (3 pts). All patients were evaluated by Karnofsky performance status (KPS) and neurologic functional score (NFS). Localization was obtained using fusion imaging from computed tomography (CT) and magnetic resonance imaging (MRI) of the brain. Gross tumor volume (GTV) was defined as radiologically visible surgery cavity in contrast-enhancing T1-weighted MRI sequences, clinical target volume (CTV) was coincident with GTV and planning target volume was GTV/CTV plus an additional 2-3 mm in all directions (average PTV 28.6 cc). Pts were treated with a 6-MV linear accelerator fitted with a dynamic micro-multileaf collimator. Ten pts received 5x6 Gy and eight 5x7 Gy. All pts were followed by MRI and clinical examination 3 months after FSRT and at 3 months intervals thereafter. Local control (LC) was defined as a lack of relapse of the irradiated surgical cavity, and brain control (BC) as LC in absence of other documented BM. A brain failure at the site of FSRT was defined "in-field relapse", whereas appearance of new BM "out-field relapse".

### Results

After a median follow-up of 16 months (range 4-79), 17 of 19 pts were evaluable because one was lost to follow up and one too early. 9 pts (52,9%) had LC and BC, seven (41,1%) reached LC without BC, one (6%) had in- and out-field relapse. So, in 16 (94,1%) pts, postoperative FSRT reached a LC and in more than one-half LC and BC. All pts in progression were re-irradiated, four with SRS, two with WBRT and two with WBRT plus SRS to a second progression. Altogether, after cavity stereotactic radiotherapy, 19 new lesions were treated with SRS. No acute neither late toxicity was registered, no treatment-related NFS decline was observed.

### Conclusion

Our preliminary report showed that surgical cavity FSRT for resected BM was effective in more than one half of pts with a good neuro-cognitive outcome. WBRT and/or SRS can be reserved to pts with brain progression of disease.

### EP-1208 Twenty years experience in treating Childhood medulloblastoma: Between the past and the present .

J. Khalil<sup>1</sup>

<sup>1</sup>National Institute of Oncology Sidi Mohamed Ben Ab, Radiotherapy, Rabat, Morocco

### Purpose or Objective

Medulloblastoma (MB) is the most common primary malignant central nervous system tumor of childhood. These last decades, treatment modalities have largely evolved resulting in better survival rates. Nevertheless, long term toxicities are a major concern in this setting.

### Material and Methods

Our study is a retrospective one conducted at Xinhua Hospital in Shanghai, China. It included 121 patients treated for medulloblastoma from 1993 to December 2013.

### Results

Mean age at diagnosis was 6.7 years (range 1-14.3 years). Total surgical resection was achieved in 60% of the cases. Classic medulloblastoma was found in 59% of the cases. Adjuvant radiotherapy was delivered in all cases and chemotherapy concerned 70.2% of the studied cohort. The median follow-up time of the study was 84 months (range, 24-120months). 5 and 10 years Progression free survival (PFS) were 83.2% (95% CI), 69.5% (95% CI) and 5 years and 10 years Overall survival (OS) were 82.5% (95% CI), and 72.5% (95% CI). Patient's age significantly influenced survival; patients under 3 years old had the worse outcomes (P=0.01). T and M stages also significantly

impacted survival rates, advanced stages were associated with lower rates (P= 0.08 and 0.05 respectively). Finally, patients receiving Temozolomide had bad outcomes when compared to the new standard protocol used in the department (P=0.03). The most commonly reported late toxicity was growth suppression in 35 patients (52.2%).Hypothyroidism requiring hormone replacement was recorded in 29% of the cases. Hearing loss, and problems including poor concentration, poor memory and learning difficulties were reported in 19% and 25% of the cases respectively. Second cancers were noted in three cases.

### Conclusion

Overall, our results are comparable to those reported in the literature; nevertheless efforts should be made to ensure longer follow ups and correctly assess treatment related toxicities.

### EP-1209 First clinical results using HyperArc™ and Linac-based VMAT radiosurgery in brain metastases.

F. Alongi<sup>1,2</sup>, F. Gregucci<sup>1</sup>, R. Mazzola<sup>1</sup>, N. Gajj-Levra<sup>1</sup>, M. Rigo<sup>1</sup>, V. Figlia<sup>1</sup>, L. Nicosia<sup>1</sup>, S. Corradini<sup>3</sup>, F. Ricchetti<sup>1</sup>, R. Ruggeri<sup>1</sup>

<sup>1</sup>Hospital Sacro Cuore Don Calabria- Cancer Care Center, Radiation Oncology, Negrar, Italy ; <sup>2</sup>University of Brescia, Radiation Oncology, Brescia, Italy ; <sup>3</sup>LMU University Hospital, Radiation Oncology, Munich, Germany

### Purpose or Objective

The use of Stereotactic Fractionated Radiotherapy (SFRT) or Radiosurgery (SRS) is increasing in the treatment of brain metastases (BMs), also for multiple BMs. Aim of the present study is to evaluate safety and effectiveness of SRS/SFRT for BMs, using a new non-coplanar mono-isocenter technique (HyperArc™ Varian Medical System).

### Material and Methods

Patients with a diagnosis of BMs with a diameter inferior to 3 cm, a life expectancy more than 3 months and good performance status, were eligible for Linac-based volumetric modulated arc therapy (VMAT) SFRT/SRS with HyperArc™. Clinical evaluation and MRI were requested after 45-60 days by the SRS/SFRT, and every 2-3 months during follow-up (FU). A retrospective analysis of patients, BMs, treatment characteristics and outcomes included toxicity, local control (LC), overall survival (OS) and intracranial time to progression (iTTP), were performed.

### Results

From August 2017 to May 2018, 381 BMs in 64 patients were treated. Two hundred forty-six BMs (43 patients) were evaluated, 73 BMs (10 patients) were excluded due to Karnofsky performance status (KPS) < 60 and died before first control and 62 BMs (11 patients) did not yet perform FU visit at the time of the analysis. The median BMs number for each patients was 5 (range 1-21). With a median FU time of 6 months (range 1-10), 244 out 246 (99%) BMs were controlled (18% complete response; 41% partial response, 40% stable disease), only 2 BMs (1%) showed a progression disease, at the first control. No acute (within 3 months) and late (above 3 months) toxicities were reported. At the time of analysis, median OS has not yet been achieved, while median iTTP was 5 months. In univariate analysis, statistically negative prognostic factors for OS were histology of primary tumor (P=0.009): lung/breast cancer had better survival rates as compared to melanoma/other; cumulative volume of intracranial disease  $\geq 15$ cc (P=0.04) and systemic progression disease (P=0.005). At multivariate analysis, cumulative volume of intracranial disease  $\geq 15$ cc (P=0.04) and systemic progression disease (P=0.009) were confirmed independent negative prognostic factors for OS. Considering CR/PR as "local treatment response", while SD/PD as "not local treatment response", the analysis of LC profile stratified by histology, PTV and BED, using Chi-square test, showed that melanoma/other histological

type ( $P=0.0001$ ), PTV $>1$  cc ( $P=0.041$ ) and BED $<47.2$  Gy ( $P=0.0001$ ) were negative predictive factors of response.

#### Conclusion

The present data showed that SFRT/SRS with HyperArc™ is safe and effective for multiple BMs, mostly in appropriately selected patients. The utilization of SFRT/SRS for BMs is promising and should be explored in randomized trial.

#### EP-1210 Local control and toxicity of IORT with low energy X-rays after resection of brain metastasis

H. Kahl<sup>1</sup>, S. Sabine<sup>2</sup>, M. Heiko<sup>3</sup>, G. Ute<sup>3</sup>, K. Ina<sup>3</sup>, H. Volkmar<sup>3</sup>, M. Christoph<sup>4</sup>, B. Ansgar<sup>4</sup>, K. Jürgen<sup>2</sup>, S. Georg<sup>1</sup>  
<sup>1</sup>Klinikum Augsburg, Strahlenklinik, Augsburg, Germany ;  
<sup>2</sup>Klinikum Augsburg, Stabsstelle Medizinphysik, Augsburg, Germany ;  
<sup>3</sup>Klinikum Augsburg, Neurochirurgische Klinik, Augsburg, Germany ;  
<sup>4</sup>Klinikum Augsburg, Klinik für Diagnostische Radiologie und Neuroradiologie, Augsburg, Germany

#### Purpose or Objective

The paradigm of adjuvant radiotherapy after resection of brain metastasis is changing from whole brain irradiation (WBI) to localized brain radiotherapy (LBRT). Improving survival of stage IV patients, puts neurologic late toxicity more and more into focus. IORT with low energy is a promising method to apply LBRT for brain metastasis as it maximally shortens the resection radiation interval as well as the time to the start of mostly needed systemic treatment compared to external beam radiation.

#### Material and Methods

We performed a retrospective analysis of patients treated with low energy X-ray IORT after resection of brain metastasis (mamma carcinoma 6, colorectal cancer 5, melanoma 4, NSCLC 4, renal cell carcinoma 2, other 2) between 2013 and 2018 at the Klinikum Augsburg. In total 25 metastases were resected in 22 patients (9 males/13 females) and treated with IORT using the Intrabeam system. Four patients had recurrent disease, of which 3 were pretreated with WBI. All patients fitted to RPA class 1 and 2 (8 and 14 patients). Median age was 60.8 years (44-82 years), median applied dose 20Gy (16-20Gy) on the surface of the applicator and median applicator size 2.5 cm (1.5 -4cm). None of the patients received additional planned WBI. Actuarial overall survival (OS), local control rate (LC), distant brain control (DC) were calculated by the Kaplan-Meier method and put into context with published and own data of adjuvant LBRT with radiosurgery (SRS) or hypofractionated stereotactic radiotherapy (HSRT).

#### Results

With a median follow up (FU) of 12.1 months (1 to 48 months), actuarial overall survival (OS) @ 1 year (2 years) was 73% (60%). The LC (actuarial LC @1year/@2years) of all 25 lesions was calculated 88% (85%/53%). DC of the 22 patients @1year (@2years) was 44% (44%). Only 3 patients received WBI as salvage after IORT (14%), all other distant recurrences were treated and controlled with SRS. We found a symptomatic brain necrosis rate of 4% (1 lesion/pre-treated with WBI+SRS boost), but found asymptomatic radiotherapy induced MR alterations also in the FU of 2 other patients (8%/cumulative 12%). One air embolism occurred during the IORT procedure. One patient developed a lethal infarction of the a. cerebri media 14 days post surgery. One patient with 2 consecutive resections and IORT procedures developed a bacterial meningoencephalitis and one postoperative thrombopenic bleeding requiring surgery occurred. No other healing complications were observed. There was no increased use of steroids post operatively compared to patients with brain metastasis resection only.

#### Conclusion

IORT with low energy is a feasible option to apply LBRT after resection of brain metastasis providing comparable local control with no increased toxicity compared to

postoperative external beam LBRT. It provides the chance of earlier start of systemic treatment after resection of brain metastasis compared to external beam LBRT.

#### EP-1211 Radiation necrosis after SRS for intracranial metastases from lung cancer: A retrospective review

A. Sharma<sup>1</sup>, L. Mountjoy<sup>2</sup>, R. Butterfield<sup>3</sup>, N. Zhang<sup>3</sup>, H. Ross<sup>2</sup>, S. Schild<sup>4</sup>, J. Ashman<sup>4</sup>, T. Daniels<sup>4</sup>, H. Paripati<sup>2</sup>, M. Mrugala<sup>1</sup>, S. Vora<sup>4</sup>, N. Patel<sup>5</sup>, R. Zimmerman<sup>5</sup>, T. Sio<sup>4</sup>, A. Porter<sup>1</sup>

<sup>1</sup>Mayo Clinic Arizona, Neuro-Oncology, Phoenix, USA ;  
<sup>2</sup>Mayo Clinic Arizona, Hematology/Oncology, Phoenix, USA ;  
<sup>3</sup>Mayo Clinic Arizona, Research Biostatistics, Phoenix, USA ;  
<sup>4</sup>Mayo Clinic Arizona, Radiation Oncology, Phoenix, USA ;  
<sup>5</sup>Mayo Clinic Arizona, Neurosurgery, Phoenix, USA

#### Purpose or Objective

Radiation therapy is the primary treatment of intracranial metastasis (ICM) from lung cancer. Radiation necrosis (RN) occurs post-treatment with an incidence of 5-24%. Radiographically, RN remains a diagnostic quandary that can appear indistinct from tumor progression. We reviewed the spectrum of imaging changes in patients with SRS-treated ICM from lung cancer (LC) in an effort to classify potential risk factors for RN and to identify radiographic differentiators of RN versus tumor progression.

#### Material and Methods

Patients with LC and ICM who received stereotactic radiosurgery (SRS) for treatment between 2013 and 2018 at our institution were retrospectively reviewed at our institution. Sixty-three patients were identified. Demographics, tumor type, ICM burden and location, chemotherapy, surgery, and SRS details as well as outcomes were recorded. Magnetic resonance imaging (MRI) was reviewed and evaluated using the Response Assessment in Neuro-Oncology criteria (RANO).

#### Results

Of the 63 patients included in this study, clinical and radiographic criteria for RN were seen in 24 (38%) as early as 2 months and as late as 5 years post-RT. Six were taken to the OR because of refractory symptoms and were found to have pathology-proven RN. Patients with RN were significantly more likely to have had resection of an ICM (45.8%) prior to radiation than patients who did not have RN (20.5%,  $p=0.04$ ). No significant differences were found in location, size, or genetic profile of lesions, but a non-significant trend for RN was seen in younger patients (average age 64 vs 68,  $p=0.08$ ). Twenty patients received treatments directed towards RN - steroids, surgery, laser ablation or bevacizumab. The 4 remaining Patients who did not receive treatment had clinical/functional decline and lower overall survival (OS) of 13 months, vs 21.5 months if they did receive treatment. 85% of patients treated for RN experienced radiographic and clinical benefit. When steroids were used alone, the rate of improvement was 85.7% (6/7). There was 100% improvement with laser ablation (4/4) and bevacizumab (4/4). Surgical resection of RN resulted in improvement in 4/6 patients (66%), however the remaining two were left with increased neurologic morbidity that likely hastened death. All surgical specimens collected showed necrotic changes with only one revealing a mix of RN and tumor.

#### Conclusion

We present one of the larger case series of ICM in LC and their treatment outcomes. Our observation of RN as late as 5 years post-RT for ICM necessitates clinician awareness and early intervention to reduce morbidity. Younger age and prior surgical resection are potential risk factors for RN. Providers should keep a high index of suspicion for RN as development can occur several months after treatment for ICM. Several treatment options showed benefit without increased morbidity and improved survival in this cohort,

and should be considered if tissue diagnosis is not available.

#### EP-1212 Clinical outcome in brain metastases from breast cancer treated with stereotactic radiotherapy

G. Riva<sup>1</sup>, A. Ferrari<sup>1</sup>, S. Durante<sup>1</sup>, D. Ciardo<sup>1</sup>, G. Piperno<sup>1</sup>, M.C. Leonardi<sup>1</sup>, S. Vigorito<sup>2</sup>, E. Rondi<sup>2</sup>, R. Orecchia<sup>3</sup>, B.A. Jereczek-Fossa<sup>1</sup>

<sup>1</sup>Istituto Europeo di Oncologia - IEO, Radiotherapy, Milan, Italy ; <sup>2</sup>Istituto Europeo di Oncologia - IEO, Medical Physics, Milan, Italy ; <sup>3</sup>Istituto Europeo di Oncologia - IEO, Scientific Director, Milan, Italy

#### Purpose or Objective

The objective of this study was to report our institutional experience with CyberKnife in the stereotactic radiation treatment (SRT) of patients with brain metastases.

#### Material and Methods

One-hundred and two consecutive patients with brain metastases from breast cancer (199 lesions) were treated with brain SRT with CyberKnife from 02/2012 to 11/2017 as first brain radiation treatment and reviewed retrospectively for patient, tumor, and imaging characteristics. Parameters included demographics, histology and primary tumor characteristics, presence and control of extracranial disease, number of lesions and tumor volume. The imaging characteristics assessed were complete response (CR), partial response (PR), stable disease (SD), local (LF) and distant brain failure (DBF). Overall survival (OS) and local control (LC) at 2 years were evaluated

#### Results

After a median follow-up of 11.6 months (range 2.6-65.6), at least one radiological evaluation was available for 152 brain metastases (76 patients, all women). Most of the lesions (41%) were treated with a single session of SRT with a total dose of 21 Gy, other fractionations (24 Gy in 2 or 3 sessions) were preferred in case of two or more concomitant metastases or in case of greater volume of the target.

CR, PR and SD as best response were reported in 67 (44%), 56 (37%) and 26 (17%) of 152 lesions respectively, while 3 (2%) lesions had a progression disease at first control.

Fifteen out of 149 (10%) lesions showed LF after a median of 12.5 months (range 1.2-63.4).

Forty-seven (61%) women out of 76 developed DBF after a median of 7.0 months (range 1.0-39.6).

Radionecrosis was radiologically (11c-methionine Positron Emission Tomography and/or Nuclear Magnetic Resonance with gadolinium) diagnosed for 14 lesions (13 patients, 17%) in a median time of 7.3 months (range 2-20.4). Seven (9%) women referred neurological symptoms (such as seizures), a neurosurgical treatment was needed for 3 of them in order to control symptoms.

At the time of assessment, 36 (47%) patients are still alive, 32 (42%) died for tumor progression and 8 (11%) were lost to follow-up. OS after 2-years is 52%, LC after 2-years is 63%.

Table 1: Characteristics of patients and treatment outcomes

Characteristics	Value
Patients treated	102
Lesions treated	199
Patients with radiological evaluation	76
Lesions with radiological evaluation	152
Median age, years	52.8 (range, 32 – 82)
Sex, patients (% of 76)	
F	76 (100%)
M	0 (0%)
Histology of primary tumor, patients (% of 76)	
Luminal A	10 (13%)
Luminal B	41 (54%)
Triple negative	13 (17%)
Erb-B2 overexpression	12 (16%)
Maximum radiological response, lesions (% of 152)	
CR	67 (44%)
PR	56 (37%)
SD	26 (17%)
PD at first radiological control	3 (2%)
Local failure, lesions (% of 149)	
Yes	15 (10%)
No	134 (90%)
Distant brain failure, patients (% of 76)	
Yes	47 (62%)
No	29 (38%)
Radionecrosis, lesions (% of 152)	
Yes	14 (9%)
No	138 (91%)

#### Conclusion

Our results showed the efficacy in the treatment of brain metastases from breast cancer with CyberKnife SRT. Correlation between clinical (volume of brain disease) and histological parameters with favorable outcome is under investigation.

#### EP-1213 Prediction of new brain metastases after radiosurgery: validation of two nomograms in our serie.

C. De la Pinta Alonso<sup>1</sup>, R. Hernández<sup>1</sup>, E. Fernández-Lizarbe<sup>1</sup>, M. Martín<sup>1</sup>, C. Vallejo<sup>1</sup>, M. Martín Martín<sup>1</sup>, A.B. Capúz<sup>2</sup>, S. Barrio<sup>3</sup>, M. Torres<sup>3</sup>, S. Sancho<sup>1</sup>

<sup>1</sup>Ramón y Cajal Hospital, Radiation Oncology, Madrid, Spain ; <sup>2</sup>Ramón y Cajal Hospital, Medical Physics, Madrid, Spain ; <sup>3</sup>Ramón y Cajal Hospital, Radiotherapist, Madrid, Spain

#### Purpose or Objective

Prediction of patients at highest risk for brain recurrence after radiosurgery remains a clinical concern. The aim of our study was to evaluate two published nomograms (Ayala et al and Rodrigues et al) to predict the risk of brain recurrence in a Spanish-population treated with radiosurgery in our institution.

#### Material and Methods

We retrospectively identified 85 patients diagnosed of brain metastases who had undergone radiosurgery from 2006 through 2018 at the Ramón y Cajal University Hospital (Madrid). Clinical factors and performance status of the nomograms for prediction of brain recurrence were assessed.

#### Results

Median follow-up time was 9 months. Among the 85 patients, 13 (15.3%) developed brain recurrence. We evaluated our data set with the nomograms models. Because of missing data, 12 of the 85 patients were excluded. We analyzed 3, 6, 9-months probabilities of recurrence in Ayala nomogram and 1-year with the Rodrigues nomogram. Only patients with brain recurrence were included in our validation. Calibration for 3, 6, 9-months to and 1-year probability of free brain recurrence for the nomogram showed good model calibration with intermediate correlation of nomogram-predicted probability of brain recurrence and observed probability of brain recurrence as estimated by the Kaplan-Meier method. The best correlation was in terciles in Ayala nomogram and deciles in Rodrigues nomogram. We have stratified patients in three groups in Ayala nomogram: low risk of recurrence (11-79points), intermediate risk (80-140points) and high risk (140-260points). We have stratified patients in two groups in Rodrigues nomogram:

low risk of recurrence (0-150 points), and high risk (151-350 points).

#### Conclusion

The Ayala nomogram shows validity in our population and allows users to integrate the information from different variables to provide precise risk stratification. The Rodrigues nomogram don't show validity in our population. We have validated these nomograms in our Spanish population and we are considering new lines of study.

#### EP-1214 Patterns of care: Treatment of glioblastoma in elderly patients

C. Straube<sup>1</sup>, S. Antoni<sup>2</sup>, P. Schaffer<sup>3</sup>, J. Gempt<sup>4</sup>, C. Zimmer<sup>5</sup>, B. Meyer<sup>6</sup>, S.E. Combs<sup>1</sup>, F. Schmidt-Graf<sup>2</sup>  
<sup>1</sup>Klinikum rechts der Isar- TU München, Department of Radiation Oncology, München, Germany ; <sup>2</sup>Klinikum rechts der Isar- TU München, Department of Neurology, München, Germany ; <sup>3</sup>MVZ InnMed Oberaudorf, Praxis für Strahlentherapie, Oberaudorf, Germany ; <sup>4</sup>Klinikum rechts der Isar- TU München, Department of Neurosurgery, München, Germany ; <sup>5</sup>Klinikum rechts der Isar- TU München, Department of Neuroradiology, München, Germany ; <sup>6</sup>Klinikum rechts der Isar- TU München, Department of Neurosurgery, München, Germany

#### Purpose or Objective

The optimal treatment for elderly glioblastoma patients is certainly unknown. We surveyed the pattern of care and the outcome of elderly glioblastoma (GBM) patients treated with varying adjuvant treatments, including radiotherapy (RT), temozolomide regimens, best supportive care (BSC).

#### Material and Methods

Patients older than 65 years who underwent surgery for GBM between 2010 and 2016 at the Klinikum rechts der Isar, Munich, and who were treated with adjuvant therapies or underwent BSC were eligible. We analysed the median overall survival (mOS) by the Kaplan-Meier method and extracted prognostic factors with Cox regression modeling.

#### Results

200 patients (106 female, 94 male) with a median age of 74 years (65-91 years) and a median Karnofsky performance status before adjuvant therapy of 80 (20-100) met the criteria. MGMT promotor was evaluated in 109 patients and was methylated in 40 cases, 123 were IDH wild type and 77 unknown. 45 patients underwent biopsy (8 got resection afterward), 92 partial and 63 gross total resections.

mOS of the entire cohort was 5.5 months. 76 patients underwent RT only (mOS 4.96 months), 10 received chemotherapy (CT) (mOS 9.90 months) and 54 RT and concomitant CT (mOS 13.73 months). Active adjuvant treatments with radiation therapy (HR 1.52 if no RT), MGMT promotor methylation (HR 0.49 if present), as well as the presence of paresis (HR 0.28 if no present), were significant prognostic factors in a multivariate model.

52 patients underwent treatment for progressive disease (mOS 13.77 months), including 23 patients undergoing second surgery, 14 patients (mOS 13.77 months) salvage RT or RCT and 15 patients (mOS 11,45 months) salvage CT. Patients undergoing BSC were generally in a worse physical condition (KPS 60 vs. KPS 80,  $p < 0.001$ ) and older (77.5y vs. 73.8y,  $p < 0.001$ ).

#### Conclusion

Our data underline the efficacy of active adjuvant treatment for GBM, optimally with RCT, even in an elderly cohort. As expected, the performance status after surgery is the most important predictor for BSC.

#### EP-1215 Fibroblast Activating Protein specific PET for advanced target volume delineation in Glioblastoma

P. Windisch<sup>1</sup>, M. Röhrich<sup>2</sup>, S. Regnery<sup>1</sup>, E. Tonndorf-Martini<sup>1</sup>, T. Held<sup>1</sup>, K. Lang<sup>1</sup>, D. Bernhardt<sup>1</sup>, S. Rieken<sup>1</sup>, U. Haberkorn<sup>2</sup>, J. Debus<sup>1</sup>, S. Adeberg<sup>1</sup>  
<sup>1</sup>Heidelberg University Hospital, Department of Radiation Oncology, Heidelberg, Germany ; <sup>2</sup>Heidelberg University Hospital, Department of Nuclear Medicine, Heidelberg, Germany

#### Purpose or Objective

To assess target volume alterations when contouring is based on PET-CT with 68Ga-radiolabeled ligands of Fibroblast Activating Protein, FAPI-02 and FAPI-04, versus conventional pretreatment imaging with contrast enhanced CT and MRI.

#### Material and Methods

Fourteen Glioblastoma (GBM) patients treated between 10/2017 and 08/2018 received an additional FAPI-PET prior to treatment. As one patient's tumor, the only one with an IDH-mutation, showed very low FAPI-enhancement compared to healthy appearing normal tissue, analysis was carried out with the remaining 13 patients. Three different FAPI-GTVs were created using a 5-, 7- and 10-fold threshold of increased uptake compared to normal tissue (FAPIx5, FAPIx7, FAPIx10). Following GTV delineation, according to the EORTC guidelines, based on thresholds the volumes were corrected for false-positive enhancement.

MRI-GTVs were created based on T1-weighted Gd-enhancement. Based on these GTVs, MRI-CTVs were created by adding a 20 mm margin. Applying another 3-5 mm margin to the MRI-CTV resulted in the MRI-PTV.

#### Results

GTVs based on MRI resulted in a median volume of 33.8 ml (range: 0.5 - 88.2 ml) while GTVs based on FAPIx5, x7 and x10 resulted in volumes of 49.6 ml, 33.7 ml and 23.8 ml respectively (ranges: 3.5 - 115.6 ml, 2.1 - 99.7 ml and 1.4 - 76.7 ml). FAPI-GTVs were significantly different from MRI-GTVs for FAPIx5 ( $p = 0.022$ ) and FAPIx10 ( $p = 0.068$ ) but not FAPIx7 ( $p = 0.95$ ).

As MRI- and FAPI-GTVs were not congruent, adding FAPI-GTVs to MRI-GTVs to create a combined MRI/FAPI-GTV resulted in an increase of the median volume of 17.7 ml, 8.9 ml and 3.9 ml (ranges: 2.9 - 49.3 ml, 1.6 - 32.4 ml and 0.8 - 18.7 ml) for FAPIx5, x7 and x10 respectively which corresponds to increases of the MRI-GTV by 55.6%, 27.3% and 17.2% (ranges: 20.0 - 586.3%, 12.4 - 311.8% and 3.9 - 164.7%). Changes to the MRI-GTVs caused by adding FAPI-GTVs were highly significant for all FAPI-PET thresholds ( $p < 0.001$ ).

Median MRI-PTV was 271.5 ml (112.4 - 490.9 ml). To determine whether FAPI-GTVs were included in the MRI-PTV, we calculated the overlap between both volumes. While in almost all patients PET-GTVs were completely included in the much larger MRI-PTVs as expected, one patient's FAPI-GTV was not entirely covered by the MRI-PTV (30.9 ml, 21.3 ml and 13.5 ml of uncovered FAPI-GTV respectively).

No complications occurred during either MRI or FAPI-PET.

#### Conclusion

FAPI-PET can provide additional insight into GBM spread compared to conventional pretreatment imaging and might therefore prove to be especially useful for treatment planning in radiation oncology but also for surgical interventions. Further research is warranted to assess appropriate thresholds for different patients and possible prognostic significance of tracer uptake.

#### EP-1216 Single- versus 2-session Gamma Knife surgery for symptomatic midsize brain metastases

S. Yomo<sup>1</sup>

<sup>1</sup>Aizawa Hospital, Division of Radiation Oncology- Aizawa Comprehensive Cancer Center, Matsumoto, Japan

### Purpose or Objective

Two-session Gamma Knife surgery (GKS) has been recently demonstrated as an effective and less invasive alternative for large metastases (BM) not amenable to microsurgical resection. Taking these results, a clinical question arises as to whether this treatment strategy further improve treatment outcome of symptomatic midsize BM (2-10mL). The aim of the present study was to compare the local therapeutic effects and toxicities of single-session and 2-session GKS in the treatment of symptomatic midsize BM.

### Material and Methods

Patients with focal neurological deficits attributable to midsize BM who underwent upfront GKS from 2011 to 2018 were retrospectively identified from an institutional database. Patients both with post-GKS imaging studies and neurological evaluation on outpatient visit were eligible. The combined endpoint, imaging and/or functional worsening of the lesion treated, was compared between the 2 treatment arms after 1:1 propensity score matching.

### Results

A total of 214 symptomatic midsize BM in 183 cancer patients were identified, including 145 and 69 tumors treated with single-session and 2-session GKS, respectively. After propensity score matching, 63 pairs of tumors were obtained. Gray test showed that two-session GKS achieved a longer local progression-free interval compared with single-session GKS ( $p = 0.035$ ). Two-session GKS was also associated with greater immediate improvement in KPS scores ( $18 \pm 15$  vs  $11 \pm 13$ ,  $p = 0.008$ ). Overall survival time in single- and 2-session GKS were 13.4 months and 15.0 months, respectively ( $p = 0.47$ ).

### Conclusion

Two-session GKS could achieve more durable local tumor control and functional improvement than single-session SRS for patients with symptomatic midsize BM, although overall survival advantage did not become evident.

**EP-1217 Reirradiation of recurrent gliomas with CyberKnife® SRS/SRT: a monoinstitutional experience**  
V. Borzillo<sup>1</sup>, E. Scipilliti<sup>2</sup>, R. Di Franco<sup>1</sup>, F. Cammarota<sup>1</sup>, P. Muto<sup>1</sup>

<sup>1</sup>Istituto Nazionale Tumori Fondazione Pascale, UOC Radioterapia, Napoli, Italy; <sup>2</sup>Università Federico II, Dipartimento di scienze biomediche avanzate, Napoli, Italy

### Purpose or Objective

The aim of our study was to retrospectively evaluate the efficacy and toxicity of reirradiation with Cyberknife (CK) stereotactic radiosurgery (SRS)/ stereotactic radiotherapy (SRT) in patients with recurrent gliomas pre-irradiated.

### Material and Methods

Between May 2013 and August 2018, 33 patients (56 lesions) with recurrent gliomas (RGs), previously treated with standard Radiotherapy (RT) (50-60 Gy; 1.8-2Gy/fx) with or without concomitant and adjuvant temozolomide (TMZ), were reirradiated with CyberKnife®SRS/SRT. The median time interval between primary RT and reirradiation was 22 months (range 2-116). Twenty patients had a grade IV (GBM), eleven grade III and 2 grade II gliomas. Median Karnofsky performance status was 80 (range 30-100). The total prescription dose of CyberKnife®SRS/SRTretreatment was 20-30 Gy in 5 fractions (fs), 20-26Gy in 4 fs, 15-24 Gy in 3 fs, and 12-24 Gy in single fraction (fx) at isodose line of 80% (range 75-80%). We calculate median overall survival (OS) from the diagnosis date and median OS from reirradiation. Acute and late toxicities were graded according to Radiation Therapy Oncology Group scale.

### Results

Median follow-up was 8 months (range 0-41). 28/33 patients were evaluable for the FU, because 5 patients died before the first FU. Median OS after SRS/SRT was 8 months (range 0.16-43) for all patients, 6 months (range 0.16-41) for GBM and 15 months (range 0.23-43) for grade

II-III. Median OS from the diagnosis was 37 months (range 12-168) for all patients, 28 months (range 14-80) for GBM and 103 months (range 12-168) for grade II-III. No toxicity during treatment was observed, and all patients completed the CK treatment. No patient developed severe (> grade 3) toxicity. Radiation necrosis was observed in 5 patients (15%).

### Conclusion

Our retrospective experience demonstrates that CK® SRS/SRT retreatment is a feasible and well tolerated option for recurrent Gliomas previous irradiated. In these patients the better treatment choice remains individual and based on a multidisciplinary evaluation. However, a longer follow-up and enrolment of more patients are needed to confirm our results and to guide us in choosing the most appropriate treatment.

**EP-1218 Upfront stereotactic radiosurgery in patients with brain metastases from small cell lung cancer**

S. Yomo<sup>1</sup>

<sup>1</sup>Aizawa Hospital, Division of Radiation Oncology- Aizawa Comprehensive Cancer Center, Matsumoto, Japan

### Purpose or Objective

Because of the high likelihood of multiple brain metastases (BM) from small cell lung cancer (SCLC), the role of focal treatment using stereotactic radiosurgery (SRS) has yet to be determined. We aimed to evaluate the efficacy and limitations of upfront SRS for patients with BM from SCLC.

### Material and Methods

Patients with BM from SCLC who received upfront SRS from 2009 to 2018 without prophylactic or therapeutic whole brain radiotherapy (WBRT) were retrospectively identified from an institutional database. Overall survival (OS), neurological death-free survival, remote and local tumor recurrence rates were analyzed.

### Results

None of 86 consecutive patients were lost to follow-up and the median follow-up for censored observations was 10.3 months. The median age was 69 years, and the median Karnofsky performance status was 90. One- and 2-year OS rates were 37% and 11%, respectively. The median OS time was 8.7 months. One- and 2-year neurological death-free survival rates were 11% and 18%, respectively. In total, 240/301 tumors (80%) in 70 patients (81 %) with radiological follow-up data were evaluated. One- and 2-year rates of remote BM relapse were 57% and 62% (per patient), respectively. One- and 2-year rates of local control failure were 16% and 21% (per lesion), respectively. Repeat SRS, salvage WBRT and microsurgery were subsequently required in 36, 14 and 2 patient, respectively. Symptomatic radiation injury, treated conservatively, developed in 3 patients.

### Conclusion

The present study suggested upfront SRS to be a potentially effective and minimally invasive treatment option for BM from SCLC. Although repeat salvage treatment was needed in nearly half of patients to achieve control of distant BM, such continuation of radiotherapeutic management might contribute to reducing the rate of neurological death.

**EP-1219 Prognostic factors of salvage stereotactic radiotherapy for recurrent high-grade glioma.**

K. Takehana<sup>1</sup>, M. Uto<sup>1</sup>, K. Ogura<sup>2</sup>, Y. Arakawa<sup>3</sup>, Y. Mineharu<sup>3</sup>, T. Mizowaki<sup>1</sup>

<sup>1</sup>Kyoto University Hospital, Department of Radiation Oncology, Kyoto, Japan; <sup>2</sup>Kobe City Medical Center General Hospital, Department of Therapeutic Radiology, Kobe, Japan; <sup>3</sup>Kyoto University Hospital, Department of Neurosurgery, Kyoto, Japan

### Purpose or Objective

The treatment of recurrent high-grade glioma (HGG) is challenging. Various treatments including salvage stereotactic radiotherapy (SRT), salvage surgery, bevacizumab (BEV) or chemotherapy are used, but optimal treatment strategy is still unknown. We reviewed patients with recurrent HGG treated with salvage SRT to analyze feasibility, safety and prognostic factors.

### Material and Methods

We retrospectively analyzed patients with histologically proven recurrent HGG who received salvage SRT from October 2007 to February 2018 at our hospital. Patients younger than 18 years old or who received no follow-up MRI were excluded. Overall survival (OS) and progression-free survival (PFS) were calculated by Kaplan-Meier method from the start date of salvage SRT. Cox proportional hazard model was used for multivariate analysis. Toxicity was evaluated by CTCAE version 4.0. A p-value < 0.05 considered to be significant.

### Results

A total of 86 eligible patients were identified. Patient characteristics were as follows; male/female=54/32, median age 52 years old (range, 19-88), latest WHO grade before salvage SRT III/IV=29/57. Initial recurrence pattern was local/diffuse/distant/multiple=46/22/6/12. Clinical target volume was defined as only contrast-enhancing lesion for 27 patients, and contrast-enhancing lesion and high-intensity area on fluid-attenuation inversion recovery image for 59 patients. Median interval between initial radiation and initial recurrence was 12.2 months (range, 1.0-447.3). Median planning target volume was 40.8cc (range, 1.4-491.1). Median prescribed dose of salvage SRT was 25Gy (range, 22.5-35Gy). BEV was administered to 70 patients, of which 51 patients were BEV naïve at salvage SRT and 19 patients were BEV failed at salvage SRT. Median follow-up period was 8.1 months from the start date of salvage SRT. The median OS was 10.4 months (95% confidence interval [CI]: 8.8-12.8) and the median PFS was 6.5 months (95% CI: 4.6-8.3). By multivariate analysis, more than 1 year interval between initial radiation and initial recurrence (HR 0.44, 95% CI: 0.25-0.79, p<0.01) and BEV naïve at salvage SRT (HR 0.37, 95% CI: 0.18-0.75, p<0.01) were identified as favorable factors of OS. Diffuse pattern at initial recurrence (HR 2.35, 95% CI: 1.18-4.68, p=0.04) and WHO grade IV (HR 2.26, 95% CI: 1.20-4.28, p=0.01) were unfavorable factors for OS. Diffuse pattern at initial recurrence (HR 1.80, 95% CI: 1.02-3.17, p=0.04) and WHO grade IV (HR 1.78, 95% CI: 1.05-3.01, p=0.03) were unfavorable factors for PFS.

Grade 2 or higher radiation necrosis developed in 7 patients. Six of them were improved with corticosteroid or BEV but 1 patient required surgery.

### Conclusion

Salvage SRT was feasible and safe treatment for recurrent HGG. Further prospective trials are needed to determine optimal sequencing or combination with BEV.

### EP-1220 Initial Clinical Experience of Carbon Ion Re-Irradiation of Recurrent High-Grade Glioma

Abstract withdrawn

### EP-1221 Palliative cranial irradiation improves survival in PCNSL patients ineligible for systemic therapy

J. Song<sup>1</sup>, R. Samant<sup>1</sup>, X.Y. Fan<sup>2</sup>, M. Jay<sup>3</sup>, H. Chaudry<sup>3</sup>, D. MacDonald<sup>3</sup>, I. Bence-Bruckler<sup>3</sup>, V. Nair<sup>1</sup>

<sup>1</sup>The Ottawa Hospital, Radiation Oncology, Ottawa, Canada ; <sup>2</sup>The Ottawa Hospital, Pathology and Laboratory Medicine, Ottawa, Canada ; <sup>3</sup>The Ottawa Hospital, Hematology, Ottawa, Canada

### Purpose or Objective

Primary central nervous system lymphoma (PCNSL) is a very rare type of cancer representing only 3% of all CNS

malignancies and 1% of non-Hodgkin lymphomas (NHL). Prognosis is generally poor with a median survival of less than 3 months if untreated. Standard of care for PCNSL is upfront high-dose methotrexate-based chemotherapy, with or without whole brain radiotherapy (WBRT). However, in recent years, the role of WBRT in a primary management has been questioned due to its toxicity and lack of convincing data for survival benefit. Even its role in a palliative setting remains to be clearly elucidated. In this retrospective study, data on WBRT for patients who are ineligible for systemic therapy were analyzed and correlated to patient outcomes, compared to the supportive care only.

### Material and Methods

Patients diagnosed with PCNSL between 2002 and 2017 were selected. Patients were excluded if they received systemic therapy or focal radiation only. Data on patient demographics and WBRT (total dose, fractionation, tumor biologically effective dose [a/b=10, BED<sub>10</sub>]) were collected and correlated with clinical outcomes. Survival curves were generated with the Kaplan-Meier method and compared using the log-rank test. Multivariate analysis was performed where prognostic variables and patient outcomes were correlated with the Cox proportional hazard model.

### Results

A total of 48 patients were selected for analysis. Median age at diagnosis was 74 years (range 30-89 years) and median follow up among survivors was 4.4 years. The majority (85.4%) of tumors were identified as diffuse large B-cell lymphoma (DLBCL) on histology. Among all patients, 29 (60.4%) patients completed WBRT, 2 (4.2%) patients did not complete WBRT and 17 (35.4%) patients received no treatment. Median time interval between diagnosis and WBRT was 34 days (range 7-359 days). Median overall survival (OS) was 4.4 months. Patients who received WBRT had significantly better OS (8.8±1.8 months) compared to those with no WBRT (3.3±1.0 months) (p=0.003). In multivariate analyses, the addition of WBRT was associated with improved OS (hazard ratio [HR] 0.37, 95% CI 0.18-0.76, p=0.006). Among patients who received WBRT, whole brain dose higher than 30Gy was not associated with survival outcomes (p=0.43). However, a higher dose (35Gy, p=0.051) and BED<sub>10</sub>(45Gy, p=0.017) to gross tumor were associated with improved OS.

### Conclusion

PCNSL patients who are ineligible for systemic therapy may still benefit from WBRT with a significant improvement in survival outcomes, compared to the best supportive care. Dose escalation through the addition of a gross tumor boost in these patients was associated with an improved overall survival. Future prospective studies are necessary to test the validity and confirm the significance of our study results.

### EP-1222 Simultaneous Integrated Boost in Anaplastic Astrocytoma: a propensity score matching analysis

W.C. You<sup>1</sup>, C. Chen<sup>1</sup>, J. Lin<sup>1</sup>

<sup>1</sup>Taichung Veterans General Hospital, Department of Radiation Oncology, Taichung City, Taiwan

### Purpose or Objective

Local recurrence remains a major cause of disease progression in anaplastic astrocytoma (AA). Escalation of radiation dose may lead to better results. The aim of this study is to evaluate the impacts of temozolomide chemoradiation with simultaneous integrated boost (CCRT-SIB) on clinical outcomes in the AA patients.

### Material and Methods

We retrospectively searched all AA patients who had received surgical resection followed by chemoradiation in our institute from September 2004 to June 2015. Exclusion criteria is histology of oligodendroglioma or the oligodendroglial component was >10%. In CCRT-SIB protocol, a field-in-field escalation of 2.3 Gy per fraction

to tumor bed was applied in addition to 54-60 Gy/30 fractions chemoradiation with temozolomide, with a total of 69 Gy/30 fractions. Univariate and multivariate analyses were utilized for the possible prognostic factors of overall survival (OS).

#### Results

A total of 51 AA patients were identified and 42 patients were enrolled in final analysis by using 1:2 propensity score matching of Karnofsky performance status and extent of resection among the AA patients. The median follow up time is 41 months. CCRT-SIB is associated with better OS (hazard ratio HR: 0.32, 95% CI: 0.11-0.96;  $p=0.042$ ) in univariate analysis. On the contrary, contrast-enhanced AA had worse OS (HR: 6.12, 95% CI: 1.33-28.22;  $p=0.02$ ). The 3-year PFS rate and OS rate in CCRT-SIB was 59.1% and 75%. Acute and long term neurotoxicity was similar.

#### Conclusion

Our study revealed better OS and PFS in the AA patients treated with CCRT-SIB. Further prospective randomized trial is encouraged to define the role of CCRT-SIB.

#### EP-1223 Clinical experience and outcomes of radiosurgery with a single isocentre for 2-10 brain metastases.

S. Rogers<sup>1</sup>, N. Lomax<sup>1</sup>, S. Alonso<sup>1</sup>, B. Eberle<sup>1</sup>, S. Gomez Ordonez<sup>1</sup>, J. Schürkens<sup>1</sup>, E. Rabe<sup>1</sup>, J. Fandino<sup>2</sup>, O. Riesterer<sup>1</sup>, G. Lutters<sup>1</sup>, S. Bodis<sup>1</sup>

<sup>1</sup>Kantonsspital Aarau, Radiation Oncology- KSA-KSB, Aarau, Switzerland ; <sup>2</sup>Kantonsspital Aarau, Neurosurgery- KSA-KSB, Aarau, Switzerland

#### Purpose or Objective

Commercial software has recently become available to facilitate radiosurgery (RS) treatment planning and delivery by using a single isocentre for multiple brain metastases (BMs). Patients with multiple BMs represent 38% of our BM RS case load and have increased by 50% in the last 2 years. We have reviewed our initial experience of the feasibility and efficacy of the single isocentre dynamic conformal arc (SIDCA) technique.

#### Material and Methods

**Methods:** 51 patients, each with 2-10 BMs, have been treated on a Novalis STx Linac in our centre to date. 20 consecutive patients, planned with SIDCA (Elements Multiple Metastases v1.5, Brainlab), were included in the analysis. The standard dose prescription was 1 x 20 Gy, (V20Gy = 99%, with Dmax 115-130%), a 1 mm planning margin with a maximum of 10 cm<sup>3</sup> brain-GTV to receive 10 Gy per metastasis.

#### Results

The 20 patients had a total of 72 BMs. 70% of patients had NSCLC, the female to male ratio was 11:9 and the median age was 70 years (51-81 yrs). In 8/20 patients, BMs were grouped into 2-3 isocentres for either clinical indications (e.g. fractionated RS due to volume or postoperatively) or rotational uncertainties (> 4cm from isocentre) rather than increase the planning margin. Dose prescriptions were 52/72 BMs: 1 x 20 Gy, 7/72: 1 x 15-18 Gy, 13/72: 5 x 5-6 Gy according to patient and tumour factors. Mean single fraction PTV dose (59 BMs) was 22.1 Gy (15.8-23.95 Gy) and mean fractionated PTV dose (13 BMs) was 32.93 Gy (27.41-33.85 Gy). For single fractions, median PTV volume was 0.29 cm<sup>3</sup> (0.09-2.78 cm<sup>3</sup>) with a median total PTV volume of 1.08 cm<sup>3</sup> (0.36-7.74 cm<sup>3</sup>) per patient. For fractionated RS, these median volumes were 3.95 cm<sup>3</sup> (2.36-11.9 cm<sup>3</sup>) and 10.2 cm<sup>3</sup> (6.3-22.9 cm<sup>3</sup>) respectively. 5/20 patients had previous or simultaneous RS to single metastases or a surgical cavity, which increased the irradiated volumes and therefore sum plans were generated (Eclipse, Varian). At 6 week clinical follow-up, 3 patients still required steroids. 5 patients developed distant brain failure 3-6 mths after RS, of whom 3 received further SIDCA RS to the new BMs. 11 patients have died (med OS 6 mths, 2-13 mths); of these 9/11 patients (82%),

showed control of the irradiated BMs (3 CR, 3 PR, 4 SD according to the RANO criteria) at last follow-up.

#### Conclusion

SIDCA has been successfully implemented for patients with multiple BMs (and is also in routine use for patients with single BMs, as it can considerably decrease the duration of RS planning, verification and reporting). The irradiation of multiple BMs up to 4cm from the isocentre with the same fractionation scheme and a 1 mm margin is feasible, efficient and effective in daily practice. Local control rates > 80% are equivalent to those achieved in our centre with RS for single BMs.

#### EP-1224 Re-Irradiation in Recurrent Gliomas:

##### Treatment outcome and Prognostic factors

M. Mukherjee<sup>1</sup>, J. Bhattacharya<sup>1</sup>, T. Shahid<sup>1</sup>, V.

Kontham<sup>1</sup>, R. Rajan<sup>1</sup>, R. Talukdar<sup>1</sup>, A. De<sup>1</sup>

<sup>1</sup>Apollo Gleneagles Hospital, Radiation Oncology, Kolkata, India

#### Purpose or Objective

Gliomas have diverse prognoses that differ primarily depending on histologic subtype, grade and molecular marker expression. Even after aggressive multimodal treatment, most gliomas eventually recur. Treatment options for recurrent gliomas include surgery, chemotherapy, and re-irradiation. We sought to review our institutional experience with re-irradiation in the management of recurrent gliomas.

#### Material and Methods

We retrospectively reviewed 31 patients with recurrent or progressive gliomas who received re-irradiation between January 2012 and December 2016. Majority (20 patients) constituted High Grade Glioma. (Grade III and IV). Though the recurrence was more in Grade IV Glioma but these patients were not included in our analysis because of their poor performance status and Re-RT was not feasible in them. All the patients were assessed for Re-Surgery. Re-irradiation was offered to recurrent glioma patients with good performance status and at least 6 months had passed after initial radiotherapy (RT). All the patients were treated after doing planning CT Scan (Non-Contrast) and MRI of Brain (3 D FSPGR sequence) with I.V contrast and images were fused for target delineation. Target volume was delineation was kept conservative and the mean volume was 80 cc (50 to 140 cc). Technique of Radiotherapy was IMRT/VMAT and fractionation used was conventional. 11 patients were treated with concurrent oral Tab TMZ and 1 patient was treated with Inj Bevacizumab, 2 weekly cycle.

#### Results

Out of 31 patients, 11 patients were found to be fit for Re-Surgery but only 8 patients agreed to do so. All the patients received Re-Radiation. Median doses of re-irradiation and initial RT were 45.0 Gy and 59.4 Gy, respectively. The median time interval between initial RT and re-irradiation was 18 months. The median PFS and OS after re-irradiation were 3 and 7 months respectively. 12-month OS rate was 40%. 3 patients developed radiation necrosis and needed prolonged steroid therapy. In univariate analysis, Karnofsky performance status (KPS)  $\geq 70$  ( $p < 0.001$ ), re-irradiation dose  $\geq 45$  Gy ( $p = 0.040$ ), and longer time interval between initial RT and re-irradiation ( $p = 0.040$ ) were associated with improved OS. In multivariate analysis, KPS ( $p = 0.030$ ) and length of time interval between initial RT and re-irradiation ( $p = 0.048$ ) were important predictors of OS. Use of TMZ did not show any benefit. Molecular markers were not available for most of the patients and hence correlation could not be done.

#### Conclusion

Re-irradiation in conjunction with surgery could be a salvage treatment for very selected recurrent glioma patients with good performance status. Re-irradiation was associated with only modest palliative and survival

benefits in this retrospective review. Difficulties separating toxicity due to retreatment versus tumor progression and limited patient survival following retreatment preclude definite conclusions. Radiation necrosis was infrequent. In spite of multimodality treatment, the treatment outcome remains dismal.

#### EP-1225 Stereotactic Radiotherapy for Spine metastases using Brainlab® Elements Spine: preliminary results

N. Gaj Levra<sup>1</sup>, M. Rigo<sup>1</sup>, V. Figlia<sup>1</sup>, R. Mazzola<sup>1</sup>, L. Nicosia<sup>1</sup>, F. Ricchetti<sup>1</sup>, R. Ruggieri<sup>1</sup>, F. Alongi<sup>1,2</sup>  
<sup>1</sup>IRCCS Ospedale Sacro Cuore-Don Calabria, Radiation Oncology, Negrar, Italy ; <sup>2</sup>University of Brescia, Radiation Oncology, Brescia, Italy

#### Purpose or Objective

Stereotactic body radiation therapy is an emerging treatment option in several anatomical sites. Recently a new dedicated software (Brainlab® Elements Spine SRS™) has been developed in order to optimize the stereotactic body radiation treatment (SBRT) workflow in oligometastatic patients with spinal lesions. The prescription of ablative radiation dose to spine allows to potentially increase the probability to eradicate the metastatic disease and consequently improved local control. We report the initial experience of SBRT in spine metastases.

#### Material and Methods

Between March and September 2018, 27 spinal metastases on 16 patients underwent to spinal SBRT. The clinical target volume (CTV) was automatically generated on CT scan with fusion-image magnetic resonance imaging (MRI) and or PET-CT according to international spine radiosurgery consortium consensus<sup>1</sup>. A margin of 1 mm in all directions was added for the planning target volume (PTV). Dose prescription varied between 12 Gy to 30 Gy in 1 to 3 fractions. The dose-volume constraints for spinal was  $D_{1cc} < 13$  Gy in single fraction and  $D_{1cc} < 20$  Gy in 3 fractions. SBRT was delivered with volumetric modulated arc technique (VMAT) using multiple Arcs. Daily CBCT was performed. The patients were evaluated at the end of treatment, 3 months for toxicity and treatment response with MRI or PET-CT.

#### Results

The main patients' and lesions' characteristics are summarized in Table 1. In 4 patients a previous conventional radiation treatment to the vertebra was performed and a SBRT re-treatment was proposed. Before SBRT treatment median Numerical Rating Scale (NRS) was 2 (range 0-7). This value was confirmed at the end of SBRT. At the time of follow-up, we evaluated 10 patients out of 16. Median follow-up was 3 months (range 2-6 months). Local control of the spinal metastatic site was observed in all cases and at the time of follow-up NRS was 0 (range 0-3). No cases of  $\geq 3$  toxicity were reported.

Table 1 Summary of patients' and lesions' characteristics

Patients' and lesions' number	16 and 27
Mean age (range) [years]	66 (45-83)
Gender (M:F)	11:5
Primitive cancer (lesions' number)	
Prostate	9
Breast	9
Lung	4
Pancreas	1
Melanoma	1
Renal	3
Metastatic vertebra	
Cervical	5
Dorsal	18
Lumbar	4

#### Conclusion

SBRT by means of Brainlab® Elements Spine SRS™ seems to be a feasible, safe and effective treatment in oligometastatic patients with spinal metastases. A higher accrual and longer follow-up are necessary to establish its role in spinal oligometastatic patients.

#### EP-1226 Survival in patients with melanoma brain metastases treated by stereotactic radiotherapy

S. Lambert<sup>1</sup>, A. Huchet<sup>1</sup>, R. Trouette<sup>1</sup>, V. Karahissarlian<sup>1</sup>, C. Pouypoudat<sup>1</sup>, V. Atallah<sup>1</sup>, C. Dutriaux<sup>2</sup>, V. Vendrely<sup>1</sup>  
<sup>1</sup>CHU Bordeaux, Radiotherapy, Bordeaux, France ; <sup>2</sup>CHU Bordeaux, Dermatology, Bordeaux, France

#### Purpose or Objective

The development of immunotherapy or targeted therapies improved survival of patients treated for melanoma in last decade. Brain is one of the most frequent site of metastases in melanoma, treated by stereotactic radiotherapy (SR) whenever possible. The main side effect of this treatment is the development of radionecrosis in the irradiation field. The objective of this retrospective study is to evaluate the Overall Survival (OS), the event-free survival (EFS) (progression or radionecrosis) inside the radiation field, and the progression-free survival outside the radiation field, in patients treated for melanoma's brain metastases by SR.

#### Material and Methods

Ninety Four patients treated by SR, in our center, between first January 2011 and 31 december 2017 were included. Patients's prognostics characteristics before irradiation: number of metastases, Karnofsky Performance status (KPS), and the Graded prognostic assessment (GPA) score were collected for all of them. Datas about progression or radionecrosis were registered from radiologist's reports of follow-up's MRI after SR. Survival was calculated from the last irradiation day, with a Log-Rank method.

#### Results

With a median follow up of 11, 2 months. The KPS was at least 80% for 87 patients (93%), the number of brain metastasis was less than 3 for 88 patients (94%), and 69 patients (74%) had a GPA score of 3 or 4. The median OS was 12,2 months, with a 1-year OS and a 2 years OS respectively of 51% and 38%. The median EFS inside the radiation field was 14,9 months with a 1-year EFS and a 2 years-EFS of respectively 56% and 36%. The median progression-free survival outside the radiation field was 50% with a 1-year and 2-years progression-free survival of respectively 37% and 30%.

#### Conclusion

With an OS, at one and two years of respectively 51% and 38%, our results are similar to recent studies and confirm an improve of survival for melanoma patients with brain metastases treated by stereotactic radiotherapy.

#### EP-1227 The impact of first MR in clinical decision making of patients with HGG treated with RTCT

M. Cantarella<sup>1</sup>, F. Pasqualetti<sup>2</sup>, A. Gonnelli<sup>2</sup>, A. Molinari<sup>2</sup>, F. Paiar<sup>2</sup>  
<sup>1</sup>Casa di Cura San Rossore, Radiotherapy, Pisa, Italy ; <sup>2</sup>Azienda Ospedaliera Universitaria Pisana, Radiotherapy, Pisa, Italy

#### Purpose or Objective

Standard up-front therapy of high grade glioma (HGG) is focused on the so called Stupp protocol, that includes surgical resection followed by radiotherapy (RT) combined with concomitant and adjuvant chemotherapy with temozolomide (TMZ). As supported by several international guidelines, disease assessment is performed using magnetic resonance (MR) one month since the end of RT and then every 3 months: in case of tumour progression the administration of temozolomide (the most active agent against glioma) is interrupted and salvage therapy or best supportive care are recommended. The aim of this study is to investigate in a retrospective

manner the real value of first MR following RT and its relevance in clinical decision making about up-front therapy.

#### Material and Methods

Between April 2005 and July 2017, data of 78 patients (pts) with a proven diagnosis of HGG and treated with Stupp protocol at the University Hospital of Pisa were collected. Tumor progression was defined according to Mac-Donald's Criteria. Considering the potential presence of pseudo-progression (PSP) and the evolutionary pattern of the suspected recurrences, lesions suggestive for tumor progression inside the radiotherapy field were investigated with a new MR after 6-8 weeks. Otherwise, the presence of new lesions outside the radiotherapy field was interpreted as disease progression (PD) and patient's therapy was changed. Presence or absence of symptoms, extent of surgery and MGMT methylation status were recorded.

#### Results

The first MR after RT-CT evidenced infield progression (interpreted as PSP) in 16 pts (20.5%) and outfield progression in 8 (10.2%). Three out of 8 patients with outfield progression were symptomatic for the tumor growth. The second MRI confirmed the presence of PSP in 10 pts out of 16 pts whereas in 6 patients a true progression (PD) was present since the first MR.

#### Conclusion

In absence of symptoms, the first MR after radiochemotherapy influenced clinical decision making (sending the patients to further salvage therapy or BSC) only in 5 out of 78 patients (6.4%). In 72 patients, even in presence of radiological signs suggestive for disease progression inside the RT field, clinical decision making did not change. Further studies involving a higher number of patients are required in order to confirm our findings.

#### EP-1228 Omission of WBI does not impair cerebral control in solitary brain mets treated with focal RT

H. Kahl<sup>1</sup>, H. Müller<sup>2</sup>, V. Heidecke<sup>2</sup>, G. Stüben<sup>1</sup>

<sup>1</sup>Klinikum Augsburg, Strahlenklinik, Augsburg, Germany ;

<sup>2</sup>Klinikum Augsburg, Neurochirurgische Klinik, Augsburg, Germany

#### Purpose or Objective

Does omission of whole brain irradiation (WBI) lead to inferior neuro-cerebral control (NC) in unselected patients with singular brain metastasis?

#### Material and Methods

This is a retrospective study of 166 consecutive patients treated for singular brain metastasis from 1.1.2010 to 31.7.2017 at the radiotherapy department of Klinikum Augsburg. As endpoints overall survival (OS), local (LC) and distant (DC) cerebral control rates as well as the definitive NC were analyzed. 45 patients had a neurosurgical resection and a whole brain irradiation (OP+WBI/ median FU 8.1 months), 23 patients received a percutaneous stereotactic irradiation of the tumor cavity after resection (OP+SX/ median FU 11.3 months). 13 patients had an intraoperative radiotherapy of the tumor cavity with 50kV X-rays (OP+IORT/median FU 13.9 months). 85 patients were treated with radiosurgery alone (SX/ median FU 8.1 months). 128 patients (OP+WBI 29/OP+SX 18/ OP+IORT 13/SX 68) with available MR FU were used for the Kaplan-Meier estimation of LC, DC and NC. The term neuro-cerebral control (NC) - was introduced to evaluate the efficiency of all treatment strategies including salvage therapies (SX/OP/WBI) with regard to tumor control in the brain during the total course of disease. In this context NC is not achieved, if the last MRI of the CNS shows progressive disease independent of the patient's definitive cause of death.

#### Results

1-year OS (2-years OS) for OP+ WBI was 46% (33%), for OP+SX 82% (67%), for OP+IORT 92% (82%) and for SX 62%

(41%). 1y LC for OP+WBI was 69.4%, for OP+SX 79.4%, for OP+IORT 82% and 84.4% for SX. As expected 1y-DC of the OP+WBI patients (88.7%) was better than the 1y-DC of the focally irradiated patients (72.7% OP+SX/ 40% OP+IORT/50.9% SX). All patients with cerebral recurrences were treated with salvage therapy according to their pattern of relapse (SX/ WBI/ OP+/- IORT or SX). As a result of all treatments following 1y-NC were achieved: 68.9% OP+WBI, 88.9% OP+SX, 78.8% OP+IORT and 88.2% SX. 2y-NC was: 63.6% OP+WBI, 71.1% OP+SX, 78.8% OP+IORT and 88.2% SX. WBI could be avoided for most of the patients within the first (2<sup>nd</sup>) year: OP+ SX 94.4% (85.0%), OP+IORT 72.9% (72.9%), SX 74.8 % (60.4%).

#### Conclusion

This data provides further evidence for safe omission of WBI even in an unselected patient group with singular brain metastasis. All focal forms of radiotherapy +/- surgery used at the Klinikum Augsburg lead to a good persistent cerebral control (NC), despite of inferior DC compared to patients treated with WBI. For 2 out of 3 patients WBI was never necessary in the whole course of disease. However, regular MR Imaging is essential to detect and treat frequent distant relapses before they get symptomatic for the patients.

#### EP-1229 Repeated intracranial radiotherapy/SRT-Analysis of efficacy and safety including EQD2 sum plans

C. Schröder<sup>1</sup>, I. Stiefel<sup>1</sup>, S. Tanadini-Lang<sup>1</sup>, I. Pytko<sup>1</sup>, M. Guckenberger<sup>1</sup>, N. Andratschke<sup>1</sup>

<sup>1</sup>University Hospital Zürich, Department of Radiation Oncology, Zürich, Switzerland

#### Purpose or Objective

The number of patients receiving cranial re-irradiation for primary or metastatic lesions is rapidly growing since the introduction of stereotactic radiation techniques. Hence, it is possible to deliver multiple treatments in a very localized way, therefore sparing organs at risk and allowing for repetitions. Still the effect of multiple stereotactic treatments has to be carefully evaluated regarding safety and efficacy. We therefore analyzed diametrical and clinical data of patients receiving repetitive cranial irradiation using EQD2 sum plans created with non-rigid-registration to allow for optimal dose summation.

#### Material and Methods

We retrospectively analyzed the data of 76 patients that received repeated cranial radiotherapy from February 2013 to September 2016. 34 of those patients suffered from primary brain lesions (e.g. Glioblastoma), 42 from brain metastases. Patients with primary brain tumors received stereotactic radiotherapy to the GTV defined in a treatment-planning MRI plus a 3mm margin to derive the PTV, those with brain metastases to the GTV plus a 1 mm (definite RT) or 2 mm (adjuvant RT) margin.

EQD2 sum plans using non-rigid registration were calculated for all courses of intracranial radiotherapy using Aria Eclipse (Varian Medical Systems, Version 10) and MIM (MIM Software Inc. Version 6.7.9). Dose parameter were calculated for common organs at risk (e.g. brainstem) and target volumes (PTV). Clinical and radiological data was collected at regular follow-up appointments including toxicity, local control and survival.

#### Results

In total 76 patients received at least 2 courses of intracranial radiotherapy. 23 a third, 8 a fourth and 3 a fifth course of radiotherapy. The median prescription dose was 30 Gy for all RT courses combined. The median Dmean of the brain was 35 Gy (range 0.9 - 57.7 Gy) with a median D(1cc) of 99.1 Gy (range 40.9 - 142.2). The median D(1cc) of the brainstem was 38.4 (range 0.1 - 94.6 Gy), the median D(0.1cc) of the Chiasm was 33.2 (range 0.04 - 72.2 Gy). 74 % of patients suffered from low grade (G1-G2) acute toxicity, usually in the form of headache (18.4

%) and fatigue (19.7 %). There were only 2 >G3 toxicities with one patient developing seizures and one fatal radionecrosis.

At the time of analysis, 40 patients are still alive. Median OS from the time of first re-irradiation was 57 months (range 4 - 186 months). When looking at all treatment courses combined up to 58 % of patients had an intracranial controlled disease after any course of radiotherapy.

#### Conclusion

Repeated radiotherapy appears both safe and efficient in patients with recurrent primary or secondary brain tumors. There were only few high grade treatment related toxicities.

#### EP-1230 Hippocampal sparing radiotherapy in patients with primary brain tumors (PBT)

M. Konopka-Filippow<sup>1,2</sup>, E. Sierko<sup>1,2</sup>, D. Hempel<sup>1,2</sup>, E. Szweczek<sup>3</sup>, M. Wojtukiewicz<sup>2</sup>

<sup>1</sup>Comprehensive Cancer Center in Bialystok, Department of Radiotherapy, Bialystok, Poland ; <sup>2</sup>Medical University of Bialystok, Department of Oncology, Bialystok, Poland ; <sup>3</sup>Comprehensive Cancer Center in Bialystok, Department of Physics, Bialystok, Poland

#### Purpose or Objective

Radiotherapy (RT) is an integral part of brain cancer treatment in patients with primary brain tumors (PBT), but is also associated with deteriorated cognitive and memory functions. The aim of study was to report a dosimetric profile of contralateral hippocampal sparing (HS) RT for the treatment of PBT.

#### Material and Methods

HS RT was delivered in 15 patients with PBT using the volumetric modulated arc therapy (VMAT) technique between May 2016 and February 2018 at Comprehensive Cancer Center in Bialystok, Poland. The medical records and dosimetric parameters of RT plans: volumes of hippocampi, planning target volume (PTV), mean dose (Dmean), maximum dose (Dmax), D98% on hippocampus, D2% and Dmean on other organs at risk (OARs) (optic nerves, optic chiasm, lenses, brainstem) expressed as equivalent to a 2-Gy dose (EQD2/2) were analyzed. RT plans were designed in Monaco Treatment Planning System, version 5.11.02, algorithm Monte Carlo Phantom.

#### Results

The median age was 55.4 (range 33-72) years and 62.5% were female. Eleven patients (73.3%) had WHO grade III or IV tumor, whereas 4 patients (26.6%) had grade II tumor. The median PTV volume was 428.01 (range 135-800) cm<sup>3</sup> and the median prescribed dose was 60 (range 40-60) Gy. Concurrent chemotherapy was administered to nine patients (60%). Dmean and Dmax to the contralateral hippocampus was 12.64 (range 2.7-40) Gy and 15.87 (range 1,7-51) Gy, respectively.

#### Conclusion

Effective HS was made possible with the development of sophisticated RT delivering techniques such as VMAT. The contralateral hippocampus could be effectively spared in patients with PBT via VMAT. Further investigation is needed to qualify patients who will most benefit from HS - RT of the PBT.

#### EP-1231 Immune checkpoint inhibitor and encephalic radiotherapy: Toxicity and Adverse events

P. Matteucci<sup>1</sup>, B. Santo<sup>1</sup>, E. Ippolito<sup>1</sup>, P. Zuccoli<sup>1</sup>, G.M. Petrianni<sup>1</sup>, P. Trecca<sup>1</sup>, S. Gentile<sup>1</sup>, M. Miele<sup>1</sup>, S. Palizzi<sup>1</sup>, L. Trodella<sup>1</sup>, R.M. D'Angelillo<sup>1</sup>, S. Ramella<sup>1</sup>

<sup>1</sup>Università Campus Bio-Medico Roma, Radioterapia Oncologica, Roma, Italy

#### Purpose or Objective

Recently, immune checkpoint inhibitors (ICIs) have shown highly promising responses in solid tumors. Intracranial metastases are a common cause of morbidity and

mortality in patients with tumor, and are frequently managed with radiation therapy (RT). The safety of cranial RT in the setting of treatment ICIs has not been established. We aimed to assess toxicity and adverse events (AEs) in a cohort of patients who received cranial RT and were treated with anti programmed cell death-1 (PD-1).

#### Material and Methods

We identified 12 patients with advanced solid tumors (10 Non Small Cell Lung Cancer (NSCLC) -83.3%-, 1 melanoma-8.3%- and 1 renal cell carcinoma-8.3%-) with brain metastases, who received cranial RT and were treated with anti PD-1. RT-related AEs were retrospectively evaluated and analyzed according to ICI treatment status, cranial RT type, and timing of RT with respect to ICI.

#### Results

We enrolled 12 patients, between July 2017 and May 2018: 7 (58.3%), 2 (16.7%), and 3 (33.3%) patients received stereotactic RT, whole brain RT or both, respectively. 33.3% of patients received more than one stereotactic course. We observed seizures in one patient during whole brain RT who was symptomatic before treatment; Levitaceram dose escalation and mannitol were used to control seizures. We observed only one radionecrosis (8.33%) occurring 2 months after the end of stereotactic RT. We observed no significant difference in acute neurological toxicity between patients who received whole brain RT or stereotactic RT. Additionally, there was no difference in AE rates on the basis of timing of ICI administration with respect to RT. Cognitive evaluation is in full swing. The median follow up was 5 months, but 2 patients (16.7%) died before follow up and 2 (16.7%) haven't reassessed yet. 6 patients (50%) had brain MRI after RT: 2 (33.3%) had brain progression after stereotactic RT, 3 (50%) complete response after stereotactic RT and 1 (16.7%) partial response after whole brain RT. 2 patients (16.7%) died before MRI evaluation for extracranial disease progression and 4 patients (33.3%) will have MRI in the next few months.

#### Conclusion

Treatment with an ICI and cranial RT was not associated with a significant increase in RT-related AEs, suggesting that use of anti PD-1 in patients receiving cranial RT may have an acceptable safety profile. Nonetheless, additional studies are needed to validate this approach.

#### EP-1232 Hypofractionated RT in very elderly patients (≥ 75 years) diagnosed with GBM

C. Cavallin<sup>1</sup>, C. Mantovani<sup>2</sup>, G.C. Iorio<sup>1</sup>, I. Chiovatero<sup>1</sup>, S. Martini<sup>1</sup>, V. De Luca<sup>1</sup>, C. Palladino<sup>1</sup>, M. Levis<sup>2</sup>, F. Franchino<sup>3</sup>, R. Rudà<sup>3</sup>, U. Ricardi<sup>1</sup>

<sup>1</sup>University of Turin, Department of Oncology- Radiation Oncology, Torino, Italy ; <sup>2</sup>AOU Città della Salute e della Scienza, Department of Oncology- Radiation Oncology, Torino, Italy ; <sup>3</sup>AOU Città della Salute e della Scienza, Department of Neuro-Oncology, Torino, Italy

#### Purpose or Objective

Glioblastoma (GBM) is a highly aggressive tumor with a very dismal prognosis. Elderly patients are at poorer prognosis compared to younger ones and in some cases the benefit of hypofractionated radiotherapy (HFRT) +/- temozolomide (TMZ) is questionable. In this study, We aimed to report the efficacy of a HFRT schedule (42 Gy/14 fr) in a very elderly population (≥ 75 years) and to identify any prognostic factor for this critical group of patients.

#### Material and Methods

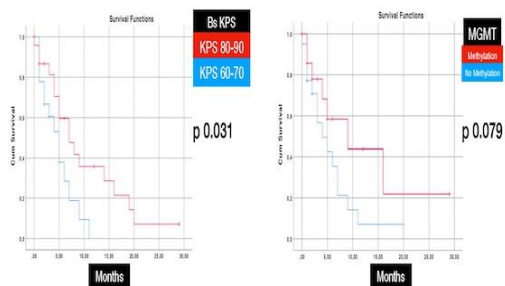
We retrospectively analysed the data of 45 very elderly patients ≥ 75 years affected with GBM, treated at our Institution between 2010 and 2018 with tridimensional conformal radiotherapy (3D-CRT). The median age at diagnosis was 76 years old (range 75-85). All patients underwent a multidisciplinary evaluation before treatment. Thirty-three patients (73,3%) underwent an upfront surgical approach: 17 (38%) underwent a

macroscopically radical resection while 16 (35,5%) received a partial resection. The remaining 12, deemed as non-surgical patients, had just a neuroradiological diagnosis of GBM in 10 cases, while 2 of them (4,4%) were biopsied. MGMT promoter was methylated in 33,3% (15/35 patients) of the surgical cohort. IDH-1 mutation was reported in just 1 patient (1/35, 2,2%). Oral temozolomide (TMZ) was given, either in the concomitant or in the adjuvant setting, to 15 (34,9%) and to 20 patients (50%) respectively. Overall survival (OS) was estimated since the last day of HFRT.

### Results

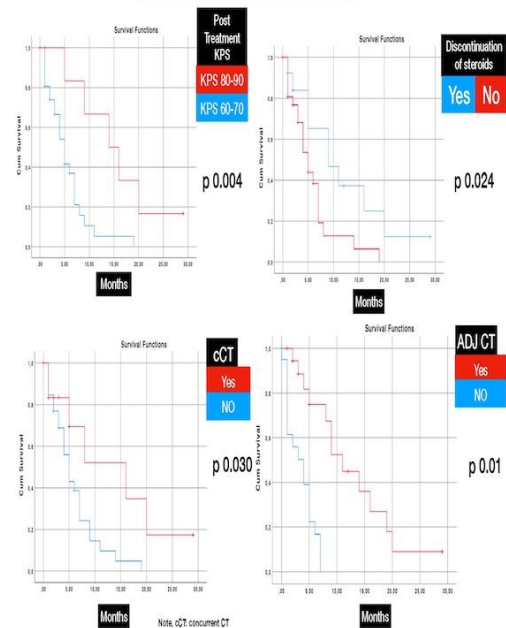
All patients completed the prescribed RT course of 42 Gy in 14 daily fractions (3 Gy/die), except one (2,2%) that was stopped at a total dose of 36 Gy, due to the worsening of neurological conditions. Median OS was only 6 months for the overall population. We observed that baseline (Bs) KPS was related to OS; in fact, patients with KPS >70 had a longer median survival time (7 vs 5 months,  $p$  0.031) compared to patients with KPS  $\leq$ 70. MGMT promoter methylation is related with a marginal OS benefit (median OS 9 vs 4 months,  $p$  0.079) (Fig1).

Fig.1 Pre-Treatment Prognostic Factors



Moreover, we observed that post-HFRT KPS >70 ( $p$  0.004), discontinuation of the steroid therapy ( $p$  0.024) and administration of concurrent ( $p$  0.030) or adjuvant CT ( $p$  0.01) were related to a better OS (Fig2).

Fig.2 Post-Treatment Prognostic Factors



At the multivariate analysis (MVA) administration of adjuvant CT was the only variable related to a better survival ( $p$  0.04; HR 0,268, CI 0,074-0,964), while KPS >70 post HFRT conferred a marginal survival benefit ( $p$  0.06; HR 0,125, CI 0,014-1,103).

### Conclusion

In the management of very elderly GBM patients, HFRT 3D-CRT, eventually combined with concurrent or adjuvant TMZ, appears to be a feasible and beneficial therapeutic option in patients with favorable features, such as good Bs KPS and MGMT promoter methylation. On the other hand, We suggest an accurate clinical and radiological multidisciplinary evaluation for patients at poorer prognosis (baseline KPS 60-70 and un-methylated MGMT promoter), in order to select the best treatment option (HFRT vs best supportive care) on a *case by case* strategy definition.

### EP-1233 Stereotactic radiosurgery to brain metastases using Varian HyperArc in the Beatson Cancer Centre

O. Kjartansdottir<sup>1</sup>, A. Williamson<sup>2</sup>, A. Patibandla<sup>1</sup>, S. Currie<sup>3</sup>, R. Carruthers<sup>4</sup>, A. Chalmers<sup>4</sup>, A. James<sup>1</sup>, S. Nowicki<sup>1</sup>

<sup>1</sup>Beatson West of Scotland Cancer Centre, Clinical Oncology, Glasgow, United Kingdom ; <sup>2</sup>Beatson West of Scotland Cancer Centre, Radiotherapy, Glasgow, United Kingdom ; <sup>3</sup>Beatson West of Scotland Cancer Centre, Physics, Glasgow, United Kingdom ; <sup>4</sup>Institute of Cancer Sciences- University of Glasgow, Clinical Oncology, Glasgow, United Kingdom

### Purpose or Objective

Stereotactic radiosurgery (SRS) has been established as an effective way of treating patients with metastases, delivering high doses to target lesions whilst sparing normal tissues in a highly conformal way. The Varian HyperArc VMAT treatment planning system utilizes several specialized functions to optimize a treatment plan, including 5 non-coplanar hemi-arc beam arrangements, automated settings for isocentre location and collimator angles, aiming to further increase conformity of target dose while reducing doses to surrounding normal tissues. HyperArc became available for clinical use in the Beatson Cancer Centre in October 2017. Prior to this we had already moved from a multi- to a single-isocentre

approach utilizing 2 co-planar full arcs 10X FFF (Flattening Filter Free) VMAT. The aim of this study was to review SRS treatment delivered via HyperArc in the Beatson Cancer Centre to determine if further optimization was achieved.

#### Material and Methods

We reviewed data on the first 36 patients treated using HyperArc planned SRS from October 2017 to September 2018, compared to a cohort of 105 patients treated with SRS with the previous technique. For treatment planning GTV was defined as the edge of the targeted contrast enhancing lesion on fused CT/MRI images. The PTV (there was no CTV) was generated by geometrically expanding the GTV by 2mm. Treatment was prescribed to the 80% isodose line. The evaluated parameters for PTV were dose, volume, number of lesions and gradient index (GI). Clinical records were reviewed to obtain information on age, gender, histology and adverse events reported within one week of SRS.

#### Results

36 patients were identified. Median age was 64 and 58% were female. Primary sites were 47% lung, 24% breast, 13% renal, 8% melanoma and 8% others. The most frequent radiosurgical dose delivered to the isocentre was 20Gy (58%) followed by 16Gy (31%). 75% had a single lesion, 17% had 2 lesions and 8% had 3 or more lesions treated. The median GI for single metastases was 2.98 (range 2.48-3.81) compared to a median GI of 3.47 (range 2.58-4.87) for the previous cohort ( $p < 0.01$ ). Median GI for multiple metastases was 3.33 (range 2.35-3.95) compared a median GI of 4.06 (range 2.76-5.17) for the previous cohort ( $p < 0.01$ ). The median PTV was 4.69cm<sup>3</sup> (range 0.45-16.74) compared to 6.0cm<sup>3</sup> (range 0.46-28.63) for the previous cohort. The only reported toxicity was one patient who had a seizure post SRS. Treatment response was assessed using MRI at 6 weeks and was similar for the 2 cohorts.

#### Conclusion

For patients with brain metastases, treatment with SRS delivered via HyperArc planning results in better conformity compared to the previous treatment planning system, with a more rapid fall-off in dose outside the treated lesion reducing the brain volume receiving significant dose. With the increasing use of SRS to treat patients with multiple metastases, this will potentially reduce the morbidity of the treatment.

#### EP-1234 Salvage radiotherapy and radiosurgery for first progression of supratentorial glioblastoma.

K. Nikitin<sup>1</sup>, A. Belyashova<sup>1</sup>, A. Golanov<sup>1</sup>, S. Zolotova<sup>1</sup>  
<sup>1</sup>Burdenko Neurosurgical Institute, Department of Radiation Oncology, Moscow, Russian Federation

#### Purpose or Objective

radiosurgery, hypofractionated and conventional fractionated irradiation was delivered for patients with first progression of supratentorial primary glioblastoma in Burdenko Neurosurgical Institute in 2009-2018. Authors presented a retrospective analysis of clinical data.

#### Material and Methods

130 patients (74 man and 56 women) with histologically confirmed primary glioblastoma (NOS - 115, IDH-wild type - 15 patients) were included in the study. Patient age was 18 - 74 years, mean age was 46 years. All patients underwent tumor removal (total, subtotal or partial) followed by conformal radiotherapy (58-63 Gy in 29-33 fractions) to primary tumor site with temozolomide. After completion of radiotherapy all patients received adjuvant chemotherapy with temozolomide. Mean time from completion of radiotherapy to first progression was 9.3 months.

First progression as single growing lesion in primary tumor region (locally) was observed 102 (78.5%) patients. Single distant new lesion in brain parenchyma with absence of progression in primary site had 17 (13%) patients. Multifocal progression (multiple new lesions) occurred in 11 (8.5%) patients. At the time of progression patients

started second-line chemotherapy or salvage irradiation or its combination.

13 patients with lesions smaller than 11 cm<sup>3</sup> received stereotactic radiosurgery with single dose of 15-24 Gy delivered with CyberKnife or Novalis (6 MeV LINAC). 69 patients with bigger tumors (8 - 48 cm<sup>3</sup>, median volume - 12.7 cm<sup>3</sup>) were irradiated with 3 to 7 fractions every day or every other day up to total dose of 21 - 39.5 Gy with CyberKnife. 48 patients with large lesions (63 - 382 cm<sup>3</sup>, median - 213 cm<sup>3</sup>) received 54-60 Gy in 30 fractions with Novalis or Primus (6 MeV LINAC).

#### Results

Mean follow-up was 13.3 months. Mean time from salvage irradiation to second progression was 6.2 months, mean overall survival after salvage irradiation was 18 months. Preliminary results showed better survival in patients received bevacizumab-based chemotherapy.

In 12 of 152 irradiated lesions (8%) clinically significant radiation necrosis developed, all were successfully treated with bevacizumab.

#### Conclusion

salvage irradiation with bevacizumab is an appropriate option for non-invasive treatment for first progression of supratentorial glioblastoma.

#### EP-1235 Response to re-RT helps deciding dose and predicts survival in Diffuse Intrinsic Pontine Glioma

J. Manjali<sup>1</sup>, T. Gupta<sup>1</sup>, J. Goda Sastri<sup>1</sup>, G. Chinnaswamy<sup>2</sup>, V. M Patil<sup>3</sup>, R. Krishnatry<sup>1</sup>

<sup>1</sup>Tata Memorial Hospital, Radiation Oncology, Mumbai, India ; <sup>2</sup>Tata Memorial Hospital, Paediatric Oncology, Mumbai, India ; <sup>3</sup>Tata Memorial Hospital, Medical Oncology, Mumbai, India

#### Purpose or Objective

Retrospective review for re-irradiation(reRT) in Diffuse Intrinsic Pontine Glioma (DIPG).

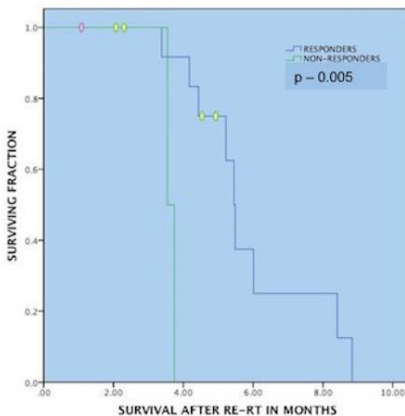
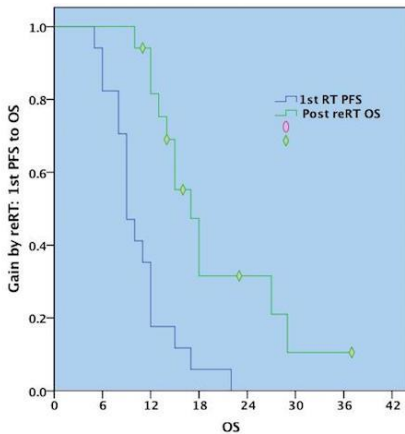
#### Material and Methods

Retrospective review of patients who underwent reRT since April 2016. The demographic, clinical and treatment details (descriptive statistics) are reviewed. The outcomes (progression-free survival; PFS, Overall Survival; OS: using Kaplan Meier and Log-rank test) and steroid use rates (descriptive statistics) is determined. OS difference for non-responders vs responders on reRT (at 10<sup>th</sup> -15<sup>th</sup> fraction clinical improvement determining total reRT dose <30.6 vs 39.6-45Gy respectively) using log-rank test.

#### Results

All consecutive 17 patients who received reRT were included. Their median age-at-initial diagnosis was 8 years, mean Lansky play-performance scale (LPS) of 65, diagnosed with >2/3 clinical criteria + all radiological criteria (100%) and received initial radiotherapy (RT) 54Gy/30# using 3DCRT resulting in >50% clinical improvement in all patients. The median PFS post-RT was 9.8 months (m). The progression defined as clinical and radiological criteria of diagnosis; all patient had >2/3 clinical criteria where five (29.4%) satisfied all three, mean LPS of 60 and mean post-RT time: 9.2 (4-20.5) m (Fig 1). ReRT was done using 3DCRT in all but one patient (IMRT) to a dose ranging 30-45 Gy. Four patients received <30Gy while rest between 39-43.2Gy. Four patients who received <30Gy, three either deteriorated or did not show any clinical improvement at 10<sup>th</sup> -15<sup>th</sup> fraction (18-27 Gy) despite suitable steroid doses, while one had extensive infiltrative disease limiting the reRT dose (30.6Gy). Remaining 13 patients showed clinical improvement mild to modest and were continued to pre-decided clinician dose (39.6-45Gy). The patient with extensive disease received 30.6Gy also showed good clinical improvement at the end of reRT (40%). The steroid dependency was reviewed in all 13 responders; all were on steroids at the time of reRT initiation, 46.2% were completely off, 38.5% were tapering 41.7% at the end of reRT. Later at one-month post reRT, 61.5% were able to get completely off

steroids. Two patients with good improvement post reRT developed intra-tumoral bleed on day 15 & 45 and succumbed. The post reRT 13 progression were noted where local and disseminated were 10 and 3 respectively. The median OS of the whole group was 15.3 m with OS at 12, 18 and 24 m of 81.6+9.6, 39.1+13.1 and 20.9+12% respectively. The median survival addition with reRT was 4.6 m (Fig 1,  $p < 0.001$ ). The median OS for patients receiving  $< 30\text{Gy}$  versus  $39.6\text{-}45\text{Gy}$  was 3.6 and 4.9 m respectively ( $p = 0.14$ ). The median OS for reRT responders vs non-responders was 4.9 vs 3.5 m ( $p = 0.005$ , Fig 2).



### Conclusion

ReRT can be considered in appropriately selected patients with DIPG at progression with good symptomatic benefit, modest toxicity, and acceptable survival. Clinical improvement on reRT by the 10-15<sup>th</sup> fraction can guide reRT dose in patients already on reRT.

### EP-1236 Volumetric assessment of cerebral edema after fractionated SRT for multiple brain metastases

H. Inokuchi<sup>1</sup>, Y. Ishihara<sup>1</sup>, K. Okano<sup>1</sup>, A. Kawamura<sup>1</sup>, K. Tsutsui<sup>1</sup>, M. Hiraoka<sup>1</sup>

<sup>1</sup>Japanese Red Cross Society Wakayama Medical Center, Department of Radiation Oncology, Wakayama, Japan

### Purpose or Objective

Fractionated stereotactic radiotherapy (FSRT) is emerging new technology which enables simultaneous irradiation for multiple, large brain metastases using linear accelerator (LINAC). The aim of this study was to evaluate local control and peritumoral cerebral edema after LINAC based FSRT as a first line therapy for multiple brain metastases.

### Material and Methods

We performed an IRB-approved retrospective analysis of patients underwent LINAC-based, image-guided, frameless FSRT consisting of 35Gy/5 fractions for lesions 1-15 cc and 30Gy/5 fractions for lesions 15cc< at our institution from August 2015 to August 2018. MRI were recorded at the initial time as a baseline and 2 months after the FSRT. Volumetric assessment of tumor regression and its relations to peritumoral edema were performed using contrast enhanced T1MRI, T2 weighted-MRI and perfusion-MRI.

### Results

We have treated 32 patients with 104 multiple brain metastases ranging 2 to 14 metastases (median 5). Primary cancer sites were lung (27), breast (3), cervix (1), and kidney (1). The mean metastases volume decreased from  $4.67 \pm 5.22$  cc to  $2.54 \pm 2.48$  cc ( $p = 0.001$ ), and the mean edema volume decreased from  $20.11 \pm 20.23$  cc to  $11.35 \pm 20.47$  cc ( $p = 0.02$ ). Cumulative tumor volumes were 2.5-39.6cc (median 22.4cc). The pre-existing edema was reduced in 78% ( $n=25$ ), stable in 22% ( $n=7$ ) at the time of first 2-months follow-up. Reduction of  $>75\%$  in existing edema was associated with the cumulative tumor volumes  $< 10$  cc ( $p = 0.03$ ) and primary adeno lung cancer ( $p = 0.02$ ). In 9/104 (8.6%) metastases, local failure was diagnosed with a mean follow-up time of 7.4 months (range 1-34 months). Estimated 1-year local control was 90.6%. Overall, 24/27 (88%) patients suffered from symptomatic edema was improved. No patients who were without symptoms at baseline developed signs of intracranial pressure following LINAC based FSRT.

### Conclusion

LINAC based stereotactic radiotherapy for multiple metastatic brain lesions demonstrated a relatively safe and effective treatment outcome with early shrinkage of lesions and peri-tumoral edema. Further investigation is needed to clarify the optimal dose fractionations.

### EP-1237 Vestibular schwannoma: Results of hypofractionated stereotactic radiotherapy

P. Pierre-Marie<sup>1</sup>, S. Tringali<sup>2</sup>, G. Beldjoudi<sup>1</sup>, P. Pommier<sup>1</sup>, R. Tanguy<sup>1</sup>

<sup>1</sup>Centre Léon Bérard, Radiotherapy, Lyon, France ;

<sup>2</sup>Centre Hospitalier Lyon Sud, Head and Neck, Lyon, France

### Purpose or Objective

Vestibular schwannomas (VS) are rare and symptoms commonly include unilateral hearing deficiencies, tinnitus and loss of balance. The management of VS may involve surgery, radiotherapy or watchful waiting. In our institution, the required attitude is defined in a multi-disciplinary staff with neurosurgeons, radiologists, head and neck surgeons and radiation therapists. For patients addressed to radiation therapy, we chose to use hypofractionated stereotactic radiotherapy (HFSRT) in 3 or 5 fractions to benefit the radiobiological advantages of fractionation. This study assesses the outcome of HFSRT for VS at a single institution.

### Material and Methods

We analyzed a retrospective case series. Patients were identified from patient records and a retrospective review of case notes and imaging reports was undertaken. All treatment was performed on a Cyberknife device. Two dose protocols were provided: 21 Gy in 3 fractions classically for stage II and for some stage III schwannomas and for the largest stage III 25 Gy in 5 fractions. All treatments were completed on a seven-day period. We assessed tumor response and recorded toxicity.

### Results

From November 2010 to December 2016, 64 patients were treated in our institution for their VS with an HFSRT protocol. Ten (15.6%) patients had a previous surgery and were treated on a progressing schwannoma with a mean 50 months between surgery and radiation therapy (range:

7-202 months). They mainly had Koos's stage II (N=37) and stage III (N=22) VS treated with 3 x 7 Gy (N=47) or 5 x 5 Gy (N=17) dose protocols. We reached a median follow-up of 28 months (range: 7-80 months).

The treatment was well tolerated with only four grade III acute toxicities (loss of balance for all this four, associated with a headache and tinnitus for one of these) and no grade IV or V. All of them were resolute with symptomatic treatment (corticosteroids). As late toxicity grade III or more we noticed one Bell's palsy, which was resolute with symptomatic treatment and one trigeminal neuralgia occurring 16 months after radiation therapy.

More than 50% of the population had a stable hearing after treatment.

Thirty three patients presented VS necrosis, appearing with a median delay of 7 months (range: 3-16 months). On the 64 patients we noted only 2 recurrences leading to a control rate of 97.1%. These recurrences occurred after 3 and 40 months.

These two patients benefited from salvage surgery and were free of any recurrence at the last consultation. They both were treated with upfront radiotherapy with a 3-fractions protocol on Koos's stage III VS. With few recurrences, the analyze of recurrence factors was narrow but we found as clinical factors influencing the risk of relapse the maximum size of more than 20 mm ( $p=0.003$ ) and on dosimetrical factors a conformal index  $<1.1$  ( $p < 0.0001$ ).

#### Conclusion

Our results suggest that our HFSRT using 21 Gy in 3 fractions or 25 Gy in 5 fractions is a well-tolerated and effective regimen.

#### EP-1238 Inter-observer variability in target delineation for brain metastases in stereotactic radiotherapy

S. Di Biase<sup>1</sup>, F. Patani<sup>1</sup>, D. Fasciolo<sup>1</sup>, C. Rosa<sup>1</sup>, C. Di Carlo<sup>1</sup>, A. Allajbeji<sup>1</sup>, L. Gasparini<sup>1</sup>, A. Delli Pizzi<sup>2</sup>, M. Trignani<sup>1</sup>, L. Caravatta<sup>1</sup>, D. Genovesi<sup>1</sup>

<sup>1</sup>SS. Annunziata" Hospital, Department of Radiotherapy - G. D'Annunzio University, Chieti, Italy ; <sup>2</sup>SS. Annunziata" Hospital, Department of Radiology - G. D'Annunzio University, Chieti, Italy

#### Purpose or Objective

In stereotactic radiotherapy for brain metastases (BM), target delineation is based on MRI co-registered with simulation-CT and involves a well-defined volume represented by enhancing area on T1 weighted sequences, defined as gross tumor volume (GTV). In these conditions, a limited inter-observer variability (IOV) could be expected. However, studies found significant differences in shape, size, and location in radiosurgery targets showing also an impact in plan conformity. The aim of this study was to quantify the IOV of target delineation in BM.

#### Material and Methods

A case of brain metastasis was proposed to 11 Radiation Oncologists (RO) of our Department. RO delineated GTV on T1 MRI co-registered with planning-CT using MIM Maestro software (MIM Software Inc). GTVs were analyzed and compared to a benchmark volume performed by a Neuroradiologist and a RO with expertise in brain radiotherapy jointly. The analysis of the obtained volumes was based on: DICE similarity index, Jaccard index, mean distance to agreement (MDA), Hausdorff distance, GTVs volumes, common volume (AV100), encompassing volume and centroids.

#### Results

The lesion had a well-defined small spheric appearance with a homogeneous contrast enhancement and without edema. The reference GTV volume was 1.04 cc. Mean participants volume was 1.14 cc (range 0.88-1.34 cc). Volumetric analysis of GTVs and similarity and discordance analysis of targets are reported in Table 1. Mean distance

of centroids (MDC) from the reference centroid was 0.27 mm. Mean DICE was 0.90 (range 0.85-0.92).

	cc
Mean volume	1,14
Median volume	1,13
Min volume	0,88
Max volume	1,34
Common volume, AV100	0,84
Encompassing volume	1,48
Reference volume	1,04
Similarity and discordance parameters	
Mean HD	1,96 mm
Mean MDA	0,28 mm
Mean DICE	0,90
Mean Jaccard	0,74
MDC	0,27 mm

Table 1. Volumetric and similarity/discordance analyses of targets.

HD: Hausdorff distance; MDA: Mean distance to agreement; MDC: Mean distance of centroids

#### Conclusion

In contrast to studies reporting IOV in SRT, our work pointed out a little variability. The peculiar appearance of the considered metastasis could have contributed to the agreement obtained. Anyway, our result need to be confirmed taking into account metastases of heterogeneous appearance and in this direction further evaluations are ongoing. Moreover, it should be evaluated the dosimetric implications of small IOV, due to the high dose ad rapid fall-off of stereotactic radiotherapy.

#### EP-1239 Role of perilesional edema in patients with glioblastoma undergoing adjuvant chemo-radiation

V. Nardone<sup>1</sup>, M. Gaetano<sup>1</sup>, M.G. Calvanese<sup>1</sup>, A. Di Biase<sup>1</sup>, I. Nuzzo<sup>2</sup>, L. Di Rienzo<sup>1</sup>, I. D'Onofrio<sup>1</sup>, M.G. Calvanese<sup>1</sup>, P. Pastina<sup>3</sup>, C. Guida<sup>1</sup>, C. Vitale<sup>2</sup>, P. Tini<sup>1</sup>, S. Cappabianca<sup>2</sup>, L. Pirtoli<sup>3</sup>

<sup>1</sup>Ospedale del Mare, Radiation Therapy Unit, Napoli, Italy ; <sup>2</sup>University of Campania "Luigi Vanvitelli", Department of Precision Medicine, Naples, Italy ; <sup>3</sup>Unit of Radiation Therapy, University Hospital of Siena, Siena, Italy

#### Purpose or Objective

The present study was designed to evaluate the role of perilesional edema calculated on pre-surgery MRI as a prognostic factor in patients with glioblastoma undergoing adjuvant chemo-radiation.

#### Material and Methods

We performed a retrospective analysis on 140 patients with glioblastoma undergone surgery and adjuvant chemo-radiation (C-RT) between January 2010 and December 2015.

Both perilesional edema (PE) and gross tumor volume (GTV) were contoured on MRI. We also calculated PE/GTV ratio, and PE + GTV (TV). Cut-offs were calculated with the software X-Tile. We correlated progression free survival (PFS) and overall survival (OS) with these parameters and the known prognosticators (surgery, KPS, age, MGMT status), with Kaplan Meier method (univariate) and Cox Regression Analysis (multivariate).

#### Results

A total of 140 patients were included in the analysis (mean age 61 years, median 64 years, range 35-84 years, 91 males and 49 females). Ninety-nine (70%) developed recurrence, whereas 90 patients (64%) died during the follow up.

We weren't able to calculate a cut-off value for both PE and GTV, but the found a cut-off for the PE/GTV ratio ( $>4$ ) for OS survival analysis.

The significant parameters at univariate analysis were KPS ( $p < 0,001$ ), surgery ( $p < 0,001$ ) and MGMT status ( $p < 0,001$ )

for PFS analysis, KPS ( $p < 0.001$ ), surgery ( $p: 0.005$ ), MGMT ( $p: 0.001$ ) and PE/GTV ratio ( $p: 0.005$ ).

At multivariate analysis of OS, the only significant parameters were MGMT ( $p: 0.011$ ), KPS ( $p: 0.008$ ) and PE/GTV ( $p: 0.034$ ).

#### Conclusion

Our results suggest that the PE/GTV ratio, together with the known clinical parameters, could play a role in the prognosis of glioblastoma patients.

#### EP-1240 Hypofractionated radiotherapy for non resectable glioblastoma multiforme patients

I. Nieto Regueira<sup>1</sup>, O. Virginia<sup>1</sup>, M. Victor<sup>1</sup>

<sup>1</sup>Hospital Meixoeiro VIGO, Radiation Oncology, Vigo, Spain

#### Purpose or Objective

Glioblastoma multiforme is one of the worst prognosis tumor of the central nervous system.

The first step in the treatment is complete surgical resection and it is a good medium and long term prognosis factor when performed.

In fact, when complete surgical resection is not possible, disease free survival and global survival decline significantly.

Radiotherapy is the other treatment that improves survival and local control. 1- year overall survival is observed in operated and irradiated patients and decreases to 3-4 months in non-resectable patients. Temozolomide, as concomitant treatment to radiotherapy, increases an average of 3 months the survival. Standard radiotherapy dose is 60 Gy in 2 Gy /fraction.

In the past higher doses have not shown a benefit in trials. Brachytherapy or radiosurgery have not shown any benefit either.

The aim of this prospective trial is to evaluate altered fractionation in these patients.

#### Material and Methods

Between 2014 January and 2017 December we treated 48 patients with non-resectable Glioblastoma multiforme with hypofractionated radiotherapy. 53% were males. The average age was 54 years-old. The media total dose administered was 70 Gy (66-74 Gy) The media dose per fraction was 2,45 Gy ( 2,2-2,6) 38 patients were treated with IMRT (79%).

Brain stem, optic pathways, pathway and motor cortex were protected, with a prescribed maximum dose of 54 Gy to brain stem and optic pathway and 60 Gy to motor pathway and cortex respectively.

#### Results

6 patients didn't finish radiotherapy treatment due to neurological clinical worsening caused by disease progression, observed on CT scan (12%).

In the remaining patients an increased acute side effects were not observed during the radiotherapy treatment. On the one-month follow-up MRI an increased of edema and contrast enhancement were observed in 31 patients (64%). These radiological findings improved in successive MRI in 25 patients (52%)

Media overall survival observed were 14 months. 9 patients underwent surgery after radiotherapy treatment. Radionecrosis was observed in 6 anatomopathological studies. The media overall survival in these patients were 18 months (14-23 months).

#### Conclusion

Hypofractionated radiotherapy is a well-tolerated treatment for unresectable Glioblastomas patients.

The contrast enhancement on the 1-month follow-up MRI was due to Pseudoprogression, and associated to a good prognosis.

Radionecrosis after surgical resection is associated to a better prognosis too.

Hypofractionated radiotherapy treatment improves overall survival in these patients.

#### EP-1241 Radiosurgery reirradiation of brainstem: clinical evaluation and its radiobiological correlation.

V. Pinzi<sup>1</sup>, D.M. Elena<sup>2</sup>, M. Marchetti<sup>1</sup>, L. Fariselli<sup>1</sup>

<sup>1</sup>Fondazione IRCCS Istituto Neurologico C. Besta, Neurosurgery- Unit of Radiotherapy, Milan, Italy ;

<sup>2</sup>Fondazione IRCCS Istituto Neurologico C. Besta, Health Department, Milan, Italy

#### Purpose or Objective

The main studies focused on radiosurgery-induced toxicity to the brainstem are only few. One of the largest studies by Trifiletti et al. analyzed 547 patients with 596 brainstem metastases treated with SRS. The authors found that brainstem tumor location or volume of tissue receiving 12 Gy were not correlated to a severe toxicity. On the other hand, Foote et al. analyzed 149 patients and concluded that doses  $\geq 15$  Gy to the brainstem conferred a significant increase in risk for cranial nerve complications and that the dosimetric factors predictive of cranial nerve palsy included  $D_{max} \geq 17.5$  Gy and prescribed dose  $\geq 12.5$  Gy. However, there are even less studies about radiosurgery re/irradiation of brainstem, unless for the impact of previous WBRT on the toxicity rate after SRS for brainstem metastases. The objective of the study was to analyse the radiation-related toxicity of the brainstem radiosurgery re-irradiation and its correlation with radiobiological parameters.

#### Material and Methods

We analyzed 12 patients who underwent re-irradiation for progression or relapse of tumors of the brainstem or close to it. The toxicity was recorded based on CTCAE scales. The clinical results were correlated with radiobiological parameters through the linear-quadratic model to express the re-irradiation tolerance in cumulative equivalent total doses when applied in 2Gy fractions (EQD2cumulative). We used  $\alpha/\beta$  values of 2.1 and 3.3Gy.

#### Results

The histology was high-grade glioma in 4 patients, metastases in 5, meningioma in 2 and unknown in 1 patient. Three patients underwent 5 radiation treatments (1 3Dconformal RT, 4 SRS), 1 patient received 4 RT treatments (1 3DCRT and 3 SRS), 1 patient received 3 RT treatments (3 SRS), 6 patients received one 3DCRT and 1 SRS course, 1 patient received two SRS treatments. The cumulative EQD2 (3,3) ranged 26.5-116.2Gy (mean  $\pm$  S.D:  $73 \pm 26.9$ Gy). The cumulative EQD2 (2,1) ranged 30.5-130Gy (mean  $\pm$  S.D:  $79.5 \pm 29.4$ Gy). The mean time interval between radiotherapy courses was  $18.7 \pm 20$  months (range 0-72 months; median 12 months; n = 23). The mean PTV was  $119.9 \pm 369.5$ cc (range 0.1- 1455.6). The mean follow-up was 44 months (range 10-145 months). At the time of analysis 7 patients were alive. No radionecrosis was reported. Only 1 patient developed G1 ataxia and dysphagia and only 1 patient developed a G2 ataxia. Both patients showed a neurological improvement after 1 month of corticosteroid therapy.

#### Conclusion

The overall outcome in the twelve described patients seems to be encouraging. Modern irradiation systems make it reasonable to administer successive irradiation treatments. Involving only 12 patients, this analysis cannot be expected to provide ground for us to draw definitive conclusions. However, the retrospective EQD2 values reported in this study can be used as starting point for a study focused on dose-reference for safe re-treatments.

#### EP-1242 Multisession radiosurgery re-irradiation for glioblastoma recurrence: a retrospective analysis.

V. Pinzi<sup>1</sup>, A. Viola<sup>2</sup>, M. Marchetti<sup>1</sup>, P. Gaviani<sup>3</sup>, E. Anghileri<sup>3</sup>, L. Fariselli<sup>1</sup>

<sup>1</sup>Fondazione IRCCS Istituto Neurologico C. Besta, Neurosurgery- Unit of Radiotherapy, Milan, Italy ;

<sup>2</sup>University of Milan, Radiation Oncology, Milan, Italy ;

<sup>3</sup>Fondazione IRCCS Istituto Neurologico C. Besta, Neuro-oncology, Milan, Italy

#### Purpose or Objective

Despite being various treatment strategies available, recurrent multiforme glioblastomas (rGBM) are difficult to manage. Limited evidence exists to suggest the superiority of any treatment modality for rGBM. The aim of this study is to evaluate the effectiveness of multisection radiosurgery (mRS) reirradiation as salvage treatment in terms of overall survival (OS) and progression free survival (PFS).

#### Material and Methods

Patients previously treated with surgery and chemoradiotherapy and re-irradiated with radiosurgery for rGBM from January 2014 to December 2016 were considered eligible. Global OS (gOS) was defined as the time between first surgery and death, OS as the time between the end of reirradiation and death, PFS as the time between reirradiation and disease progression. The statistical analysis was conducted using the Kaplan-Meier method.

#### Results

Forty-six patients were included in the analysis. Median time from primary treatment to recurrence was 14 months (range 1-79 months). Median follow-up was 4 months (range 2 days-32 months). All patients were treated with robotic radiosurgery (CyberKnife®). At the time of the analysis six of the 46 patients were alive. The median survival from initial diagnosis was 26 months (range 12-107 months). The 1-, 2-, and 3-years actuarial survival rates from diagnosis were 100, 70, and 50% respectively. Median survival following mRS was 7 months (range 1-24 months). The 1-, and 2-years actuarial survival rate following mRS were 29, and 11% respectively. The acute toxicity rate was 17%.

#### Conclusion

Our data suggest that mRS is a safe and effective treatment option for patients with rGBM. Further research and prospective studies are needed to better define the parameters of re-irradiation in this subset of patients.

#### EP-1243 Bevacizumab as treatment option for cerebral radiation necrosis A case series of 22 patients

R. Bodensohn<sup>1</sup>, I. Hadi<sup>1</sup>, D.F. Fleischmann<sup>1</sup>, C. Belka<sup>1</sup>, M. Niyazi<sup>1</sup>

<sup>1</sup>University Hospital- LMU Munich, Department of Radiation Oncology, Munich, Germany

#### Purpose or Objective

Radiation necrosis is one of the most serious adverse effects after cranial radiation therapy. The VEGF inhibitor Bevacizumab might be a feasible therapeutic option for symptomatic radiation necrosis when traditional treatments such as dexamethasone or mannitol fail. However, so far only few randomized studies with small cohorts (such as Levin et al with n=14) exist to show a beneficial effect for patients. Therefore, real life data is needed in order to support the data. This retrospective monocentric case study evaluates patients who received bevacizumab due to radiation necrosis in relation to clinical development.

#### Material and Methods

Using the internal database for cytostatic medication all patients who received bevacizumab in our department were identified. Only patients who received bevacizumab for radiation necrosis were included. Next to general patient characteristics symptoms before, during and after treatment and use of dexamethasone were evaluated using medical reports and internal documentation. The symptoms were coded with the CTCAE code for general neurological symptoms. Each patient received a code directly before each cycle and after the treatment (approximately 6 weeks). Additionally, the daily dose of dexamethasone was collected at these times. The patients that either improved in the symptoms or received less

dexamethasone after treatment or both were considered having benefitted a form the therapy.

#### Results

22 patients who received bevacizumab due to radiation necrosis were identified. For 10 patients (45,5%) the symptoms improved, 11 patients (50,0%) did symptomatically not improve during the treatment, 1 patient (4,5%) worsened. With 14 patients (63,6%) the dexamethasone dose could be reduced during therapy, 5 patients (22,7%) received the same dose of dexamethasone before and after treatment and 3 patients (13,6%) received a higher dose after treatment. According to this analysis 18 patients (81,8%) were able to benefit from the treatment with bevacizumab. No severe adverse effects e.g. bleedings were reported.

#### Conclusion

Bevacizumab is a good therapeutic option for patients with radiation necrosis as a complication after cranial radiation therapy. Patients could benefit from this treatment by improving symptomatically or through reduction of dexamethasone.

#### EP-1244 The impact of multidisciplinary tumor board in brain tumor management: the OMNYBuS Project

S. Chiesa<sup>1</sup>, C. Mazzeola<sup>2</sup>, G. Sabatino<sup>3</sup>, S. Gaudino<sup>1</sup>, M. Iezzi<sup>1</sup>, S. Luzi<sup>1</sup>, F. Beghella Bartoli<sup>1</sup>, G. La Rocca<sup>3</sup>, G.F. D'Onofrio<sup>3</sup>, C. Colosimo<sup>1</sup>, A. Olivi<sup>3</sup>, V. Valentini<sup>1</sup>, M. Balducci<sup>1</sup>

<sup>1</sup>Istituto di Radiologia-Fondazione Policlinico A. Gemelli IRCCS- Università Cattolica Sacro Cuore, Dipartimento Scienze Radiologiche- Radioterapiche ed Ematologiche, Rome, Italy; <sup>2</sup>Istituto di Radiologia-Fondazione Policlinico A. Gemelli IRCCS, Dipartimento Scienze Radiologiche- Radioterapiche ed Ematologiche, Rome, Italy; <sup>3</sup>Istituto di Radiologia-Fondazione Policlinico A. Gemelli IRCCS- Università Cattolica Sacro Cuore, Dipartimento Scienze dell'invecchiamento- neurologiche- ortopediche e della Testa-Collo- UOC Neurochirurgia, Rome, Italy

#### Purpose or Objective

A shared decision making in multidisciplinary context has become the standard practice for cancer care worldwide. The aim of the OMNYBuS project is to investigate the impact of tumor board in brain tumor management in order to obtain the best personalized treatment plan.

#### Material and Methods

Neurosurgeons, radiation oncologist, radiologist, anatomic pathologists and residents were involved in the multidisciplinary discussion. In this first phase of the study, we collected data retrospectively obtained from one year experience of multidisciplinary tumor board in order to arrange a strategy of the prospective phase. The primary endpoint was the evaluation of management change rate in terms of exchange, addition, or subtraction of treatment modality. The secondary endpoints were the delay considering treatment starting time, extra diagnostic work-up and time needed for academic discussion.

#### Results

Between March 2017 and March 2018, 148 consecutive cases were presented and discussed: 33,3% high grade gliomas, 10,8% anaplastic astrocytomas, 6,5% oligodendrogliomas, 2,2% low grade gliomas, 14% meningiomas, 14% single metastases, 8,6% multiple metastases, 5,4% other type of lesion. The multidisciplinary discussion focused on diagnostic imaging results and interpretation, medical, surgical, and/or radiation treatment planning, and pathology results and interpretation. The median time for case discussion was 10 minutes with a median tumor team members presence of 22 clinicians. The therapeutic plan change rate was 9.2%, mostly for high grade gliomas. A reduction of diagnostic work-up accounted for 65,7%. No delay was observed in treatment starting time.

### Conclusion

Almost all respondents indicated that these meetings were "very beneficial" to their own practice and these data emphasize the fact that in a relevant number of cases the initial treatment strategy could be modified after a multidisciplinary discussion. The retrospective phase allows us to elaborate case report form for data collection in order to prospectively analyze the adherence to guidelines, the reduction of diagnostic work-up and the patients related outcomes. We are using the new schedule for data collection in our multidisciplinary clinical practice.

### EP-1245 Evolution of non functioning pituitary adenoma after first surgery : long follow-up of 256 patients.

T. Charleux<sup>1</sup>, V. Vendrely<sup>1</sup>, A. Huchet<sup>1</sup>, R. Trouette<sup>1</sup>, A. Tabarin<sup>2</sup>, V. Jecko<sup>3</sup>, H. Loiseau<sup>3</sup>, C. Dupin<sup>1</sup>  
<sup>1</sup>Bordeaux University Hospital, Radiation Oncology, Bordeaux, France ; <sup>2</sup>Bordeaux University Hospital, Endocrinology and Metabolism, Bordeaux, France ; <sup>3</sup>Bordeaux University Hospital, Neurosurgery, Bordeaux, France

### Purpose or Objective

Pituitary adenomas account for 14 to 18% of all primary brain tumours. Our objective was to evaluate therapeutic outcome after the first surgery in non functioning pituitary adenomas (NFPA).

### Material and Methods

Between January 1978 and 2018 all patients treated by surgery for NPFA with at least 2 MRI in the follow-up and an endocrinologic follow-up in our hospital were included in this retrospective study. Evaluation concerned patients and tumor characteristics, radiation therapy data, time between each surgical procedure. Analysis of survival was done according to Kaplan Meier method.

### Results

Between 1978 and January 2018, 256 patients were treated by surgery for NPFA at our institution. Mean age at surgery was 55 [18 - 86] with 59% male. Mean tumor size was 29 mm [12 - 60] and post-operative MRI found residual tumor in 87 % of patients. Mean follow up was 10,2 years [0,6 - 40,1]. Median time to second treatment (second surgery or radiation therapy) was 10.3 years and only 32% did not need second treatment at 15 years. First event at 5, 10 and 15 years, was second surgery for 11%, 18% and 32% of patients and radiation therapy for 26%, 32% and 36%. After a second surgery, half of the patients were irradiated within 1,8 years and only 27% of patients did not receive radiotherapy within 5 years. All together, 32%, 43% and 61% of patients received radiation therapy within 5, 10 and 15 years after surgery for NPFA. After radiation therapy, 7% of patients had another surgery at 5 years and 9% at 10 and 15 years.

Patients treated by radiation therapy following surgery have a risk to suffer from gonadotropic, corticotropic and/or thyrotropic deficiencies in 65%, 66% and 73% of the cases. At least 14 to 38% of these are induced by the RT. Two patients had cerebral tumors : 1 meningioma present at first surgery, and a glioblastoma appeared after 13 years after radiation therapy. Six percent of patients had stroke both in the group treated with radiation therapy (6/107) or than without radiation therapy (9/149)

### Conclusion

After a first surgery for NPFA, most of patients needed another treatment (surgery or radiotherapy). In case of a second surgical resection, 73% of them received radiation therapy within the next 5 years, whereas in case of radiation therapy as second treatment, 8% needed surgery within the next 5 years.

### EP-1246 Outcomes and health-related quality of life in large skull base meningiomas treated with protons

D. Amelio<sup>1</sup>, D. Scartoni<sup>1</sup>, S. Lorentini<sup>1</sup>, L. Widesott<sup>1</sup>, R. Righetto<sup>1</sup>, I. Giacomelli<sup>1</sup>, M. Schwarz<sup>1</sup>, M. Amichetti<sup>1</sup>  
<sup>1</sup>Centro di Protonterapia, U.O. Protonterapia- Azienda Provinciale per i Servizi Sanitari - Trento, Trento, Italy

### Purpose or Objective

To report preliminary results of active beam scanning proton therapy (PT) for large skull base benign meningiomas (LSBM)

### Material and Methods

Thirty-three patients (pts) with LSBM were treated with PT between January 2015 and June 2018. Median age was 53 years (range, 28-82) while KPS ranged between 60 and 100 (median 90); 26 were female (79%), and 7 were male (21%). Twelve pts (36%) had histologically proven World Health Organization (WHO) Grade I tumors. In remaining pts diagnosis was based on the typical imaging appearance of benign meningioma. All patients received PT for residual, progressive or non-operable lesions. Newly diagnosed tumors received total dose of 50 GyRBE (RBE: relative biologic effectiveness) while progressing meningiomas 54 GyRBE. All the treatments were delivered at 2 GyRBE per fraction. Treatment planning was based on morphological magnetic resonance imaging (MRI) with contrast enhancement medium administration and 68-Ga-DOTATOC-PET. GTV ranged from 21 to 107 cc. Toxicity was assessed according to Common Terminology Criteria for Adverse Events version 4.0. Health-related (HR) quality of life (QoL) was assessed by the European Organization for Research and Treatment of Cancer Quality of Life Questionnaire (EORTC QLQ)--C30 and EORTC Quality of Life Questionnaire Brain Cancer Module (QLQ-BN20). Median follow-up (FU) time was 12 months (range, 3-41)

### Results

All pts completed the treatment without breaks. Registered acute side effects include grade 1 (12%) and grade 2 (9%) skin erythema, grade 1 (9%) and grade 2 (9%) alopecia, grade 1 (48%) fatigue, grade 1 (6%) and grade 2 (15%) conjunctivitis, grade 1 (15%) pain, grade 1 (15%) blurred vision, grade 1 (15%) headache, and grade 2 (9%) skin hyperpigmentation. One pts experienced grade 3 pain. There were no further grade 3 or higher acute toxicities. Registered late side effects include grade 1 (9%) and grade 2 (9%) alopecia, grade 1 (12%) fatigue, grade 1 (9%) and grade 2 (6%) headache, grade 1 (6%) dizziness, grade 1 (6%) blurred vision, grade 1 (6%) and grade 2 (6%) pain, grade 1 (6%) dry eye, and grade 1 (9%) skin hyperpigmentation. One pts experienced grade 3 pain. There were no further grade 3 or higher late toxicities. During follow-up one pts (3%) with cavernous sinus meningioma experienced complete obstruction of intracavernous carotid artery with mild transient symptoms that resolved in few days and brain tissue ischemia detected at MRI (grade 2). Before irradiation this pts already had a meningioma-related near-complete obstruction of the intracavernous carotid artery and received a vascular surgery evaluation. Currently, absolute tumor control is 100%. Moreover, relief of symptoms recorded before irradiation occurred in 27% of pts. The treatment was associated with improvement or stability in most of the preselected HRQoL domains

### Conclusion

PT is feasible and safe treatment for pts with LSBM with a favorable effect on HRQoL. Longer FU is necessary to assess definitive efficacy

### EP-1247 The patterns of care and management of brain metastases in a large Oncology centre

M. O' Cathail<sup>1</sup>, R. Bentley<sup>1</sup>, V. Crosby<sup>2</sup>, L. Aznar-Garcia<sup>1</sup>, A. Wilcock<sup>2</sup>, J. Christian<sup>1</sup>

<sup>1</sup>Nottingham University Hospital, Oncology and radiotherapy, Nottingham, United Kingdom ;

<sup>2</sup>Nottingham University Hospital, Palliative care, Nottingham, United Kingdom

### Purpose or Objective

Brain metastases (BM) affect up to 40% of patients with metastatic disease. Recent advances in systemic therapy means patients are living longer whilst the widespread availability of stereotactic radiosurgery (SRS) for brain metastases provides a realistic expectation of local control in suitable patients. There is a lack of data on the prevalence of treatment modalities used and the patterns of care these patients experience. We aim to quantify the proportion of patients receiving SRS, Whole brain radiotherapy (WBRT), neurosurgery and best supportive care (BSC) in a tertiary oncology centre.

### Material and Methods

Over a two year period (1<sup>st</sup> Jan 2016 - 31<sup>st</sup> Dec 2017), adult patients with a new radiologically confirmed diagnosis of BM were identified by retrieving all MRI and CT head scans that contained the words 'metastases', 'metastasis' or 'met' in the report. Only patients with a confirmed primary cancer were included. Patients who underwent SRS, WBRT or surgery were considered to have received 'treatment' for their BM. Receiving systemic anticancer treatment or steroids were not considered to be 'treatment'. Patients who did not receive 'treatment' for their BM were identified as BSC.

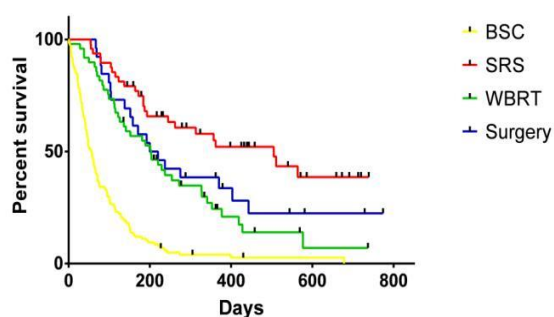
### Results

Of 2,422 scans, reviewed, there were 236 cases of newly diagnosed BM. The median age at diagnosis was 65 years (range 30-87). The median survival across all groups was 115 days (range 1-829). There were more females (58%) than males (42%). Lung cancer was the most common primary site (49%), followed by breast (20%) and melanoma (13%). At the time of diagnosis, 47% had controlled extracranial disease. Lung primaries carried the worst prognosis (median survival 95 days) with breast (202 days) the best.

Half of the cases received some form of treatment for their BM with the other half receiving BSC. There were 127 treatments delivered to 118 patients. WBRT (39.5%) and SRS (39.5%) were the most common with surgery used in 21%. Treatment modality varied according to primary tumour site. In breast WBRT (54%) was the most common treatment followed by SRS (15%). In lung and melanoma, this was reversed with SRS (21% & 53% respectively) more commonly used than WBRT (14% & 6% respectively). Patients who received SRS lived the longest; their median survival was not reached at assessment, compared to surgery (210 days) and WBRT (202 days). We identified 7 cases who received WBRT where an opportunity to give SRS may have been missed.

Of the 50% of patients who did not receive any treatment; median survival was 55 days. Of these, 62% had contact with palliative care services. Amongst treated patients, 54% were seen by palliative care.

Survival by treatment modality



### Conclusion

Half of all patients receive no brain directed therapy. Radiotherapy is the most common treatment though SRS may have been to 7 others who WBRT. We suggest a well resourced and dedicated dedicated BM MDT would provide

more consistent decision making as which was established this year in our centre. We will reassess the patterns of care after a year.

### EP-1248 Stereotactic radiotherapy for brain metastasis and systemic therapies: a safe combination?

M. Manicone<sup>1</sup>, M. Galaverni<sup>1</sup>, I. Renna<sup>1</sup>, P. Ciammella<sup>1</sup>, L. Giaccherini<sup>1</sup>, F. Bellafiore<sup>1</sup>, G. Timon<sup>1</sup>, F. Vigo<sup>1</sup>, A. Rosca<sup>1</sup>, D. Ramundo<sup>1</sup>, M. Galeandro<sup>1</sup>, M.P. Ruggieri<sup>1</sup>, T. Palmieri<sup>1</sup>, A. Botti<sup>2</sup>, R. Sghedoni<sup>2</sup>, E. Cagni<sup>2</sup>, M. Orlandi<sup>2</sup>, M. Russo<sup>3</sup>, C. Bonelli<sup>4</sup>, M. Pagano<sup>4</sup>, C. Iotti<sup>1</sup>  
<sup>1</sup>Azienda USL-IRCCS di Reggio Emilia, Radiation Oncology Unit, Reggio Emilia, Italy; <sup>2</sup>Azienda USL-IRCCS di Reggio Emilia, Medical Physics Unit, Reggio Emilia, Italy; <sup>3</sup>Azienda USL-IRCCS di Reggio Emilia, Clinical Neurology, Reggio Emilia, Italy; <sup>4</sup>Azienda USL-IRCCS di Reggio Emilia, Medical Oncology Unit, Reggio Emilia, Italy

### Purpose or Objective

Stereotactic Radiotherapy (SRT) is an effective treatment for brain metastases (BM) and is generally safe. Aim of this retrospective study was to compare toxicities and efficacy of SRT alone and in combination with systemic therapies in patients with BM.

### Material and Methods

We analyzed all patients treated between 2010 and 2017 at our institution with SRT for BM, with or without concurrent systemic therapy (defined as administered within four weeks of SRT).

We evaluated in this cohort of patients the haematological and neurological toxicities, brain progression free survival (bPFS) and overall survival, stratifying patients for yes/no systemic therapy.

### Results

Data on 45 patients were obtained. Median age at diagnosis of BM was 66 years (range 37-90 yrs). At the time of initial presentation, the majority of patients had ECOG performance status of 0-2.

The most common primary tumors were lung, breast, melanoma and kidney. Sixty percent of SRT treatments were delivered concurrently with systemic therapy, of which 56% were with conventional chemotherapy and 44% with targeted and immunotherapy agents. Patients were divided in two groups: SRT alone and SRT/systemic therapy. No differences between the two groups in terms of clinical and treatments characteristics were found. Median follow up was 10 months (range 1-65). Myelosuppression was minimal after treatment, with 9% grade 2-4 toxicity; grade  $\geq 2$  neurological symptoms were reported in 11% of patients, with one grade 5 neurological toxicity. There was no difference in haematological ( $p=0.79$ ) and neurological ( $p=0.96$ ) toxicities between the two groups. Histologically confirmed radionecrosis was reported in 2 patients (one in SRT alone and one in SRT/systemic therapy group) and radiologically suspected radionecrosis in 2 patients both in the group of concurrent therapy (one with chemotherapy and one with target therapy).

Median bPFS was 12.1 months, without any significant difference between the two groups ( $p=0.49$ ). To date 29 patients have died, of which 3 for brain progression, 13 for systemic progression and two for both systemic and brain progression. Nine patients were died for no tumor related causes and 2 patients for unknown causes. Median OS for entire group was 8.13 months without any difference between the two groups of patients. ( $p=0.37$ ).

### Conclusion

SRT for BM can be safely delivered concurrently with systemic therapy without significant increase in toxicity.

### EP-1249 Impact of retreatment or chemotherapy on survival in patients affected by a recurrent Glioblastoma

C. Mazzarella<sup>1</sup>, S. Chiesa<sup>1</sup>, S. Bracci<sup>2</sup>, T. Zinicola<sup>2</sup>, S. Longo<sup>2</sup>, F. Beghella Bartoli<sup>2</sup>, S. Luzi<sup>2</sup>, G. Sabatino<sup>3</sup>, A.

Albanese<sup>3</sup>, A. Olivi<sup>4</sup>, V. Valentini<sup>2</sup>, M. Balducci<sup>2</sup>  
<sup>1</sup>Fondazione Policlinico Universitario A. Gemelli IRCCS, Diagnostica per immagini- Radioterapia Oncologica ed Ematologia, Rome, Italy ; <sup>2</sup>Fondazione Policlinico Universitario A. Gemelli IRCCS-Università Cattolica del Sacro Cuore, Diagnostica per immagini- Radioterapia Oncologica ed Ematologia, Rome, Italy ; <sup>3</sup>Fondazione Policlinico Universitario A. Gemelli IRCCS, Scienze Neurologiche, Rome, Italy ; <sup>4</sup>Fondazione Policlinico Universitario A. Gemelli IRCCS-Università Cattolica del Sacro Cuore, Scienze Neurologiche, Rome, Italy

#### Purpose or Objective

Optimal management for recurrent glioblastoma (GBM) has not been established. Many therapies have been assessed with limited results and without significant increase in progression-free survival (PFS), or overall survival (OS). The object of this retrospective analysis was to evaluate the impact on OS with different salvage therapies, including systemic therapy, or re-irradiation plus systemic therapy or supportive care in patients affected by recurrent GBM to generate new hypotheses for future trials.

#### Material and Methods

Patients (pts) affected by GBM's recurrence and treated with according to EORTC 26981-22981-NCIC trial, were included. Those who died less a month after progression or with a poor performance status were excluded. Patients were subdivided into 3 groups: reirradiation plus chemotherapy (group A), chemotherapy alone (group B), supportive care (group C). Overall Survival was estimated using the Kaplan-Meier method and compared between three groups.

#### Results

The analysis included 217 pts with GBM who developed relapse from January 2009 to May 2016. Among them, 153 patients were evaluable for this analysis; 64 patients were excluded because they died less than one month after progression or for a poor performance status. Sixty-nine out of 153 patients (45%) belonged to Group C, 63 (41%) to group B, and 21 (14%) to group A. Median follow-up was 48 months in all patients. Median survival time from diagnosis was 18 months for the entire cohort: 14 months for patients of Group C, 28 months for group B, and 30 months for those of group A. The kind of treatment at recurrence time proved to significantly impact on OS ( $p=0.0001$ ).

#### Conclusion

Patients who did not receive any treatment had poorer survival than those who received chemotherapy alone or in combination with radiotherapy. Latter had a significantly better survival than chemotherapy group. Further investigations are needed to define the optimal choice of therapy, and in particular the role of re-irradiation and systemic treatment in patients with recurrent GBM.

#### EP-1250 Outcomes of Multiple Brain Metastases Radiosurgery with Gantry-Based Linac

P. Castro Peña<sup>1</sup>, C. Nino de Guzman<sup>1</sup>, D. Venencia<sup>1</sup>, L. Suarez Villasmil<sup>1</sup>, J. Suarez<sup>1</sup>, S. Zunino<sup>1</sup>  
<sup>1</sup>Instituto Zunino - Fundacion Marie Curie, Radiation Oncology, Cordoba, Argentina

#### Purpose or Objective

To evaluate tolerance, toxicity and survival in patients with multiple brain metastases treated Novalis-BrainLab SRS platform.

#### Material and Methods

Between Nov'16&Dec'17, 24patients were treated with SRS of multiple brain metastases(2 to 23). Seven patients had previously received WBRT; . The brain was the only organ with metastases in 13/24 patients. Nineteen patients showed neurologic symptoms prior to diagnosis. For CT simulation a Frameless Brainlab System was utilized. Treatment planning was performed using Elements TPS

v1.5 (BrainLab). The patients were positioned on a 6D couch and snap verification in each angle was done. Radiosurgery was given by Novalis Tx accelerator HDMLC-IGRT with ExacTrac V6 using 6 MV photon beam with dose rate 1000 MU/minute. Early and late toxicities as well as survival were evaluated in all the patients. Patients with up to 5 metastases were compared with te ones with 6 or more, and the ones with a tumor volume <10cc were compared with the rest with >10cc tumor volume. OS from SRS until last follow up or death, and progression-free survival (PFS) from SRS until first brain progression or last follow up, were estimated by the Kaplan-Meyer method.

#### Results

Mean age:54.2years [10.3-73.9] and mean follow-up 8.16 months [3.2-16.6].The mean number of lesions per patient was 7 [2-23] while the average volume of irradiated metastases was 1.34 cc [0.02-20.8].The prescribed dose was 22.2Gy[20.0-35.0] in1-5 fractions. The brain volume receiving 12Gy=53.7cc[4.3-600.0].5 patients were re-irradiated because of tumor regrowth (22 lesions) or new lesions (12 lesions); Of the 24 patients, 19 showed no symptoms of early toxicity whereas the remaining 5 presented G1-2 toxicity .Late toxicity was evaluated in 19 patients who survived for more than 3 months. Of the 19 patients, 12 did not show any toxicity while the remaining group presented G1-2 toxicity .No differences were found in patients with 5 or more metastases regarding the presence or absence of toxicities, or related to fractioning.The overall survival (OS) for the 24 patients at 6 months was 71%, and at one year 59%. No differences were found in the OS of patients with five or more metastases when compared with patients with less than five lesions (Cox-Mantel test,  $p = 0.806$ ); There were no differences when comparing patients with a total volume of metastases <10 cc and  $\geq 10$  cc (Cox-Mantel test,  $p = 0.865$ ). The progression-free survival (PFS) at 6 months was 89% and at one year 62%. No differences were found in PFS related to the number of metastases (Cox-Mantel test,  $p = 0.982$ ) or to the total volume of metastases (Cox-Mantel test,  $p = 0.296$ ).

#### Conclusion

Despite the number of patients limiting the statistical comparison of subgroups, results suggest that irradiation to multiple metastases is safe with Novalis Plataform and Elements SRS, showing acceptable toxicity and survival. If well in literature a detrimental in OS is described with a total tumor volume >10cc, we didn't find these difference.

#### EP-1251 focal hypofractionated stereotactic radiation therapy for brain metastases

H.J. Rosales Gonzalez<sup>1</sup>, H. Perez Montero<sup>2</sup>, A. Alvarez<sup>1</sup>, A. Mañes<sup>1</sup>, S. Comas Anton<sup>1</sup>, E. Luguera<sup>3</sup>, G. Antelo<sup>1</sup>, E. Baena<sup>1</sup>, M. Villalobos<sup>1</sup>, S. Villà<sup>1</sup>  
<sup>1</sup>Catalan Institute of Oncology, Radiation Oncology, Badalona, Spain ; <sup>2</sup>Catalan Institute of Oncology, Radiation Oncology, Hospitalet, Spain ; <sup>3</sup>Catalan Institute of Oncology, Medical Physics, Badalona, Spain

#### Purpose or Objective

Patients diagnosed with brain metastases have been traditionally treated with surgery, stereotactic radiosurgery (SRS) or whole-brain radiotherapy (WBRT). Focal Hypofractionated Stereotactical Radiation Therapy (FHSRT) may offer an alternative approach to conventional treatments for central nervous system metastases. Our objective was to analyze FHSRT outcomes at our institution.

#### Material and Methods

We retrospectively reviewed the records of 93 patients who were treated at our institution between 2014 and 2017. Eighty-two were diagnosed with a single metastasis, 19 patients with 2 metastases and 9 patients with 3 or more metastases. A total of 110 treatments were performed. Twenty-seven patients were treated with

surgical resection followed by FHSRT and 83 with FHSRT only. Most frequent histology of primary site was lung cancer in 62.72% of patients and breast cancer in 13.63%. Planning CT scans were performed with patient in supine position using high precision head mask-fixation system. Gross tumor volume (GTV) was defined using the planning CT scan registered with the diagnostic MRI. A 3 mm expansion was given to the GTV for defining the planning target volume (PTV). Treatments were performed using dynamic conformal arches (VMAT) with 6 MV energy photons. Dose prescribed was 27 Gy in 3 fractions for 67 treatments. Other dose schemes were: 24 Gy in 3 fractions for 20 treatments; 30 Gy in 10 fractions for 8 treatments; 35 Gy in 5 fractions for 7 treatments, 30 Gy in 5 fractions for 7 treatments and 30 Gy in 3 fractions for 1 treatment. Kaplan-Meier actuarial method was used for the analysis of the overall survival, disease free survival and the correlation of the dose scheme and time to progression.

### Results

Local progression was observed in 54 of the 110 treatments, among these, there were 26 patients who had one single lesion and 28 who had 2 or more lesions. In the local progression group, 42 patients receive further treatment. Twenty-two receive re-irradiation using FHSRT, 13 with WBRT, 5 where treated with SRS and 2 with surgical resection. Twelve patients did not receive any further treatment. Median overall survival was 8.36 months (r: 1-45). The median disease free survival was 6.7 months (r: 1-43). Grade 2 toxicity (CTCAE v4) was observed in 3 patients, and 10 patients presented neurological symptoms during FHSRT. Radiation necrosis was confirmed in 3 patients, 2 by RMI and 1 with coline PET-TC. When analyzing by subgroups the different dose schemes used, no statistically significant differences were found with respect to the time of recurrence.

### Conclusion

FHSRT is an effective alternative treatment for non-multiple brain metastases with high local control and acceptable tolerance. There were no differences regarding the prescribed doses and the time to progression. More data is needed in order to establish the optimal fractionation and dose scheme to be used.

### EP-1252 Brain metastases postoperative stereotactic RT: WBRT free survival predicted by an external nomogram

A. Mousli<sup>1</sup>, B. Bihin<sup>2</sup>, T. Gustin<sup>3</sup>, G. Koerts<sup>4</sup>, M. Mouchamps<sup>5</sup>, J. Daisne<sup>1</sup>

<sup>1</sup>Université Catholique de Louvain- CHU-UCL-Namur- site Sainte-Elisabeth, Radiation Oncology, Namur, Belgium ; <sup>2</sup>Université Catholique de Louvain- CHU-UCL-Namur- site Godinne, Biostatistics Unit, Yvoir, Belgium ; <sup>3</sup>Université Catholique de Louvain- CHU-UCL-Namur- site Godinne, Neurosurgery, Yvoir, Belgium ; <sup>4</sup>Centre Hospitalier Régional, Neurosurgery, Namur, Belgium ; <sup>5</sup>Centre Hospitalier Régional, Neurosurgery, Liège, Belgium

### Purpose or Objective

Patients with brain metastases (BM) represent an extremely diverse group with substantial variability in risk of intra-cranial failure and survival. Patient selection for stereotactic radiotherapy (SRT) alone is complex and requires considering multiple predictive factors. Given that the ultimate goal of SRT is to prolong survival without whole brain radiotherapy (WBRT), a nomogram based on multi-institutional data was developed by another team to display 6 and 12 months WBRT-free survival (WBFS) probabilities (Gorovets, al. IJROBP 2018). The aim of this study was to externally validate this nomogram.

### Material and Methods

We retrospectively reviewed the data of 70 patients treated between 2008-2017 by SRT for resected BM. The primary endpoint was the WBFS. Two subgroups of 35 patients were constructed with respect to the patient score in the nomogram (superior and inferior to the

median). In each group, the observed WBFS was plotted against the predicted WBFS. The ROC curve and AUC were calculated for both 6 and 12 months time points.

### Results

After a median follow up of 16.8 months, the 1-year local and distant brain failure rates were 14.3% and 35.0 %, respectively. The median time to salvage WBRT was 9.6 months. Median time to the first intracranial failure was 7.7 months. At the time of first recurrence, 90 % received local salvage therapy. We performed repeated SRT for 34% and salvage WBRT in 56%. After median time of 8.5 months, 10 patients experienced a second intracranial failure. Eight of 10 patients received further salvage therapy (5 WBRT, 3 SRT). The WBFS rates at 6 and 12 months were 87 % [IC<sub>95%</sub> = 79-95 %] and 56 % [IC<sub>95%</sub> = 45-69%], respectively. In terms of calibration, the 6 months rates were overestimated while they were accurate at 12 months (Fig. 1). It is reflected by the evolution of the cumulative proportion of WBRT or death in both subgroups with observed rates inferior to expectations at 6 months while they superimpose at 12 months (Fig. 2). A ROC curve was plotted for the 6 and 12 months nomogram predictions. AUC values were 0.47 and 0.62, respectively.

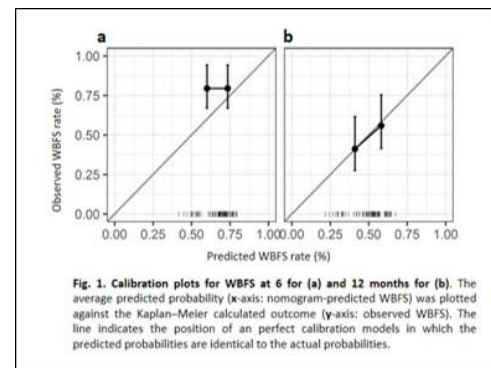


Fig. 1. Calibration plots for WBFS at 6 for (a) and 12 months for (b). The average predicted probability (x-axis: nomogram-predicted WBFS) was plotted against the Kaplan-Meier calculated outcome (y-axis: observed WBFS). The line indicates the position of an perfect calibration models in which the predicted probabilities are identical to the actual probabilities.

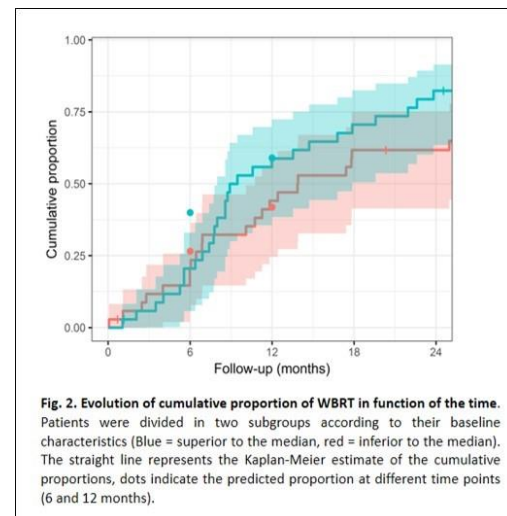


Fig. 2. Evolution of cumulative proportion of WBRT in function of the time. Patients were divided in two subgroups according to their baseline characteristics (Blue = superior to the median, red = inferior to the median). The straight line represents the Kaplan-Meier estimate of the cumulative proportions, dots indicate the predicted proportion at different time points (6 and 12 months).

### Conclusion

In our population of patients with operated BM and then stereotactically irradiated, the nomogram predicted correctly the WBFS at 12 months but not at 6 months. The median time to salvage WBRT was 9.6 months in our series while it was 6.2 months in the series by Gorovets. The fact that one third of our patients were treated with SRT as first salvage treatment may have played a role. Patients were operated and this may also be a confounding factor. All in all, it reflects the inherent limitation of applying prediction models to highly heterogeneous populations. Including more patients and characteristics

(e.g. molecular data) may improve the concordance index.

### EP-1253 Biological target volume using DTI-MRI in postoperative chemoradiotherapy for glioblastoma

A. Trip<sup>1</sup>, M.B. Jensen<sup>2</sup>, J.F. Kallehauge<sup>3</sup>, S. Lukacova<sup>4</sup>  
<sup>1</sup>Aarhus University Hospital and Netherlands Cancer Institute, Radiation Oncology, Amsterdam, The Netherlands ; <sup>2</sup>Aarhus University Hospital, Medical Physics, Aarhus, Denmark ; <sup>3</sup>Aarhus University Hospital, Danish Centre for Proton Therapy, Aarhus, Denmark ; <sup>4</sup>Aarhus University Hospital, Oncology, Aarhus, Denmark

#### Purpose or Objective

Glioblastoma (GBM) is a highly aggressive malignant brain tumour with a median overall survival of only 15 months. After postoperative chemoradiotherapy, most recurrences occur within or at the margin of the treatment volume. The standard clinical target volume (CTV) is typically defined as an isotropic 2 cm expansion around the surgical cavity and the area of contrast enhancement. This isotropic margin is not taking into account the preferential tumour growth along the white matter tracts of the brain. Diffusion tensor imaging (DTI) MRI can be used to model white matter tracts. The aim of this phase 1 feasibility study is to evaluate DTI-MRI diffusion growth models in the biological CTV definition of GBM.

#### Material and Methods

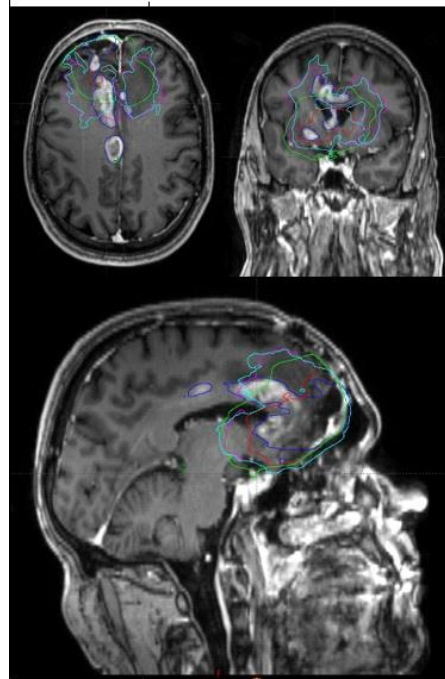
Adult GBM patients referred for postoperative RT were included, and underwent an additional pre-treatment DTI-MRI; actual treatment wasn't altered. The standard CTV was defined as described above, respecting anatomical barriers. DTI-MRI was used to create two biological CTVs, iso-volumetric to the standard CTV, using anisotropic margins based on tensor directionality of  $\gamma_0$  (bCTV $\gamma_0$ ) and  $\gamma_{20}$  (bCTV $\gamma_{20}$ ; higher  $\gamma$  meaning a higher assumed probability of tumour spread along white matter tracts). The similarity of the CTV and the bCTVs was assessed using the Dice similarity score (DSC; 0=no overlap, 1=complete overlap). Treatment effect was assessed by 3-monthly MRI and described by RANO criteria. Progression was defined as central, in-field/marginal and distant with respective  $\geq 95\%$ , 20-95%, or  $< 20\%$  of the recurrence volume (RV) located within the  $D_{95\%}$ . Only patients with an in-field/marginal or distant recurrence were selected for comparison of the bCTVs to the RV. The overlap or minimal distance between the bCTVs and the delineated RV was calculated.

#### Results

Between 10/2016 and 06/2018 38 patients were included. One patient went off-study and one was lost to follow-up, leaving 36 for analyses. Gross total resection was performed in 42% of patients, and 89% completed irradiation to 60 Gy in 30 fractions (Table). At a median follow-up of 9.5 (range 3-21) months, 23 patients had disease progression; 2 clinical, 19 central, 1 in-field/marginal, 2 distant. The median PFS was 7.0 (range 4.5-9.5) months. The mean DSC between CTV and bCTV $\gamma_0$  was 0.75 (range 0.65-0.85), and CTV and bCTV $\gamma_{20}$  was 0.72 (range 0.62-0.81) (bCTV $\gamma_0$  vs bCTV $\gamma_{20}$   $p < 0.001$ ). For patient 1 with a non-central recurrence the CTV/bCTV $\gamma_0$ /bCTV $\gamma_{20}$  overlapped with the RV by 87/90/89% (Figure). For patient 2 the CTV/bCTV $\gamma_0$ /bCTV $\gamma_{20}$  overlapped with the RV by 19/21/25%.

For patient 3 (no overlap) the shortest distance from the CTV/bCTV $\gamma_0$ /bCTV $\gamma_{20}$  to the RV was 4.6/3.6/3.3 cm.

Figure. DTI-MRI based biological target volume in postoperative chemoradiotherapy for GBM.



The standard pre-treatment GTV (red) and CTV (green) are depicted together with the bCTV $\gamma_0$  (magenta) and bCTV $\gamma_{20}$  (cyan) at the co-registered follow-up MRI at time of progression (blue). This example shows the improved overlap of the bCTVs to the recurrence volume at the corpus callosum compared to the standard CTV.

Table. Patient and treatment characteristics for the total study population, patients with a central recurrence and patients with a non-central recurrence.

Characteristic	Total (n=36)	Central recurrence (n=19)	Non-central recurrence (n=3)
	No. (%)	No. (%)	No. (%)
Age			
Median (range)	64 (25 – 76)	63 (44 – 75)	55 (52 – 63)
Gender			
Male	26 (72)	13 (68)	2 (67)
Female	10 (28)	6 (32)	1 (33)
KPS			
100	14 (39)	9 (47)	0
80-90	19 (53)	8 (42)	3 (100)
60-70	2 (6)	1 (5)	0
Unknown	1 (3)	1 (5)	0
Tumour localization			
Frontal	7 (19)	3 (16)	1 (33)
Temporal	15 (42)	7 (37)	1 (33)
Parietal	3 (8)	3 (16)	1 (33)
Occipital	3 (8)	2 (11)	0
Multiple areas	7 (19)	4 (21)	0
Extent of resection			
Biopsy only	9 (25)	4 (21)	0
Partial resection	12 (33)	5 (26)	1 (33)
Gross total resection	15 (42)	10 (53)	2 (67)
MGMT status			
Methylated	20 (56)	9 (47)	1 (33)
Non-methylated	14 (39)	9 (47)	2 (67)
Unknown	2 (6)	1 (5)	0
Radiation dose			
40 Gy in 15 fractions completed	2 (6)	1 (5)	0
60 Gy in 30 fractions completed	32 (89)	18 (95)	3 (100)
stopped/preliminary*	2 (6)	0	0
Temozolomide			
Concurrent			
never started	1 (3)	1 (5)	0
completed	30 (83)	17 (89)	3 (100)
stopped/preliminary	5 (14)	1 (5)	0
Adjuvant			
never started	7 (19)	5 (26)	0
completed	11 (31)	5 (26)	1 (33)
stopped/preliminary	15 (42)	9 (47)	2 (67)
ongoing	3 (8)	0	0

\*one patient received 50 Gy in 25 fractions, and one patient received 54 Gy in 27 fractions.

#### Conclusion

Biological DTI-MRI based CTV showed marginal improvement in a limited number of GBM patients with non-central recurrence. Further investigation in a larger cohort including non- iso-volumetric approaches is needed for further improvement in CTV definition.

### EP-1254 When could we spare hippocampus in the WB radiation for the primary central nervous system lymphoma?

F. Beghella Bartoli<sup>1</sup>, T. Zinicola<sup>1</sup>, S. Chiesa<sup>1</sup>, F. Catucci<sup>1</sup>, M. Giraffa<sup>1</sup>, C. Mazzarella<sup>1</sup>, D. Marchesano<sup>1</sup>, N. Dinapoli<sup>1</sup>, F. D'Alò<sup>2</sup>, S. Hohaus<sup>2</sup>, V. Valentini<sup>1</sup>, M. Balducci<sup>1</sup>  
<sup>1</sup>Policlinico A.Gemelli, Radiation oncology department-

*Gemelli ART, Roma, Italy ; <sup>2</sup>Policlinico A.Gemelli, Hematology Department, Roma, Italy*

#### **Purpose or Objective**

One of the main limiting factor of a whole brain radiation therapy (WBRT) is the neurocognitive functions (NCFs) decline, which is mainly caused by the radiation-induced injury to the hippocampus. This study evaluates the correlation between the site of (Primary Central Nervous System Lymphoma) PCNSL lesions and the hippocampal region to generate evidence to routinely spare of the hippocampus during a WBRT.

#### **Material and Methods**

Patients with pathologically proven PCNSL and MRI image pre-treatment were retrospectively reviewed. T1-weighted, axial MR image were imported on Varian Eclipse treatment planning system and registered with the simulation CT. The hippocampus as well as each PCNSL lesions were contoured. Three dimensional envelopes surrounding the hippocampus were generated adding 5, 10, and 15 mm. The minimum margin of 5 mm was considered for systematic setup error and dose fall-off between whole brain clinical target volume and the hippocampus.

#### **Results**

Between 2005 and 2018, 36 pts with 57 lesions were eligible for this study. PCNSL lesions' locations were: deep brain structures (26%), parietal lobe (23%), frontal lobe (19%), temporal lobe (14%), occipital lobe (7%), brainstem (5%), other sites (6%). In 18/57 lesions (31.6%) the distance from the hippocampus region was less than 5 mm and seven of them (12.3%) involved the hippocampus. Lesions over 15 mm from the hippocampus were observed in 30 cases (52.6%), while only the 15,8% was between 5 and 15 mm.

#### **Conclusion**

Our data don't support the routinely sparing of the hippocampal region in PCNSL. It could be considered in selected patients, when the spatial distribution of lesions is far more than 5 mm from the hippocampus.

#### **EP-1255 Health-Related Quality of Life in large recurrence Glioblastoma treated with protontherapy**

*D. Scartoni<sup>1</sup>, D. Amelio<sup>1</sup>, F. Fellin<sup>1</sup>, I. Giacomelli<sup>1</sup>, M. Schwarz<sup>1</sup>, M. Amichetti<sup>1</sup>*

*<sup>1</sup>Centro di Protonterapia, Protontherapy, Trento, Italy*

#### **Purpose or Objective**

Protontherapy (PT) could minimize the risk of side effects compared to conventional photon therapy and therefore reduce the possible detrimental effect on QoL of re-irradiation.

We report the effect of re-irradiation with active scanning PT of large recurrence GBM in terms of quality of life scored by the European Organization for Research and Treatment of Cancer Quality of Life Questionnaire (EORTC QLQ)-C30 and EORTC Quality of Life Questionnaire Brain Cancer Module (QLQ-BN20).

#### **Material and Methods**

Between January 2015 and October 2018 thirty patients with recurrence GBM were re-irradiated with active scanning PT. All patients had been previously treated with photon radiotherapy (60 Gy) with concomitant and adjuvant temozolomide (TMZ). Median age and Karnofsky performance status at re-irradiation were 53 years (range, 30-68 years) and 80%, (range, 60-100%), respectively. Target definition was based on CT, MR, and 18F-DOPA PET imaging. Median CTV (clinical target volume) was 69 cc (range, 11-259 cc). All patients received 36 GyRBE (RBE: relative biologic effectiveness) in 18 fractions, with concomitant TMZ in 7 patients (25%). Subscales within the EORTC QLQ-C30 include five functional scales (physical, role, emotional, cognitive, and social), three symptoms scales (nausea, vomiting, and fatigue), six single-item scales (insomnia, appetite loss, constipation, diarrhea,

dyspnea, and financial effect of tumor/treatment) and global QoL. The BN20 is specifically developed for brain patients and assessed visual disorders, motor function, communication deficit, various disease symptoms, treatment, toxicity and future uncertainty. The patients completed the EORTC questionnaires before starting PT, the day of the end of PT and every follow-up consult (1-month, 3-months) until progression of disease.

#### **Results**

The treatment was associated with stability in most of the preselected HRQOL domains. Global health improved over time with a maximum difference of 6 points between baseline and 3-months follow-up. Social functioning and motor dysfunction improved over time with a maximum difference of 8 and 2 points, respectively. We showed only a small not significance decrease in cognitive and emotional functioning. Interestingly, fatigue remained stable during the analysis such as the other preselected domains. Increase of CTV, use of steroids before protontherapy and concomitant chemotherapy are associated with a statistically significant worse QLQ C30\_Social, QLQ C30\_Physical and BN20\_Motor values.

#### **Conclusion**

Re-irradiation with PT for a large recurrence Glioblastoma is a safe treatment without a negative effect on HRQOL until the time of disease progression.

#### **EP-1256 Influence of PET-imaging during treatment planning on outcome in meningioma patients**

*K. Kessel<sup>1,2,3</sup>, H. Fischer<sup>1</sup>, T. Voglhuber<sup>1</sup>, C. Diehl<sup>1,2</sup>, C. Straube<sup>1,2</sup>, W. Weber<sup>1</sup>, S.E. Combs<sup>1,2,3</sup>*

*<sup>1</sup>Klinikum rechts der Isar- TU München, Department of Radiation Oncology, München, Germany ; <sup>2</sup>Deutsches Konsortium für Translationale Krebsforschung DKTK, Partner Site Munich, München, Germany ; <sup>3</sup>Helmholtz Zentrum München, Institute for Innovative RadiotherapyIRT, München, Germany*

#### **Purpose or Objective**

Radiotherapy (RT) is an alternative treatment to surgery for low-grade meningiomas or applied in an adjuvant setting. In high-grade cases, RT after resection is the treatment of choice.

RT improved over the years, and modern techniques such as IMRT combined with IGRT increase safety and precision. However, during treatment planning, definition of the planning target volume (PTV) remains challenging, and differentiation between healthy tissue, i.e. meninges, post-operative changes, and residual tumor can be difficult using MR and CT imaging alone. In this study, we evaluated the influence of additional PET-imaging on progression-free (PFS) and overall survival (OS).

#### **Material and Methods**

We analyzed 353 patients with primary RT of meningiomas treated between 1994 and 2017. For analyses, we divided the patients in low-grade (n=282) and high-grade (n=71) meningiomas. Table 1 shows the patient characteristic. Previous resection was performed in an adjuvant setting due to subtotal resection or later due to recurrent tumor growth.

Patients were treated with either fractionated stereotactic radiotherapy with a median dose of 54.0 Gy and median single dose of 1.8 Gy, or with radiosurgery with a median dose of 16 Gy. An advanced radiation oncologist delineated PTV based on diagnostic CT and MRI and, if available, additional PET-imaging with either <sup>68</sup>Ga-Dotanoc/Dotatoc, <sup>18</sup>F-FET (fluoroethyltyrosine) or C11 Methionin tracer.

	Low-grade (n=282)	High-grade (n=71)	OS	
			Univariate	Multivariate
Gender				
M	73 (25.9%)	41 (57.7%)		
W	209 (74.1%)	30 (42.3%)		
Age (median, range) [years]	60 (11-86)	62 (24-84)		
Resection				
Yes	179 (63.5%)	70 (98.6%)		
No	103 (36.5%)	1 (1.4%)		
Resection status				
Complete	17 (6%)	24 (33.8%)		
Incomplete	149 (52.8%)	39 (54.9%)		
n/a	13 (4.6%)	7 (9.9%)		
Time resection - RT (median, 95% KI) [months]	8.7 (19.8-31.2)	3.8 (6.3-16.3)		
PET-imaging for RT planning				
Yes	160 (56.7%)	42 (59.2%)		
No	122 (43.3%)	29 (40.8%)		
PET tracer				
68Ga-Dotanoc/Dotatoc	68 (42.5%)	31 (73.8%)		
F-18 FET	23 (14.4%)	5 (11.9%)		
C11 Methionin	69 (43.1%)	6 (14.3%)		

## Results

Median follow-up was 6.2 years (95%-KI: 6.6-7.6). For low-grade meningiomas, mean OS was 15.5 years (95%-KI: 14.7-16.2) and mean PFS was 15.2 years (95%-KI: 14.3-16.0) (median was not reached); for high-grade cases median OS was 12.0 years (95%-KI: 3.8-20.2), and median PFS was 5.0 years (95%-KI: 2.4-7.6).

PET imaging had significant influence on OS (p=0.035) and PFS (p=0.044) for low-grade meningiomas; however, in the multivariate analysis, it remained only significant for PFS. For high-grade cases, PET had no influence.

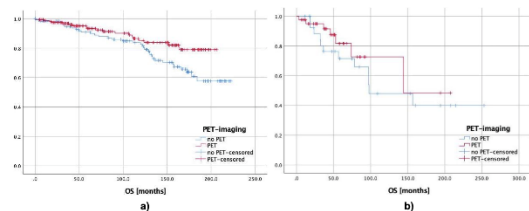


Figure 1: Survival curves of a) low-grade and b) high-grade meningiomas regarding PET based RT planning.

Table 2: Prognostic factors on OS and PFS for both low- and high-grade meningiomas.

	OS		PFS	
	Low-grade (n=282)	High-grade (n=71)	Low-grade (n=282)	High-grade (n=71)
	Univariate	Multivariate	Univariate	Multivariate
PET imaging (yes vs. no)	0.035*	0.382	0.413	-
PET Tracer (68Ga vs. F-18 vs. C11)	0.494	-	0.156	-
Previous resection (yes vs. no)	0.836	-	0.687	-
Resection status (complete vs. incomplete)	0.888	-	0.116	-
Time resection - RT	0.059	-	0.199	-
Age at diagnosis [years]	0.001*	0.001*	0.016*	-
PTV [ml]	0.001*	0.076	0.280	-
Gender (male vs. female)	0.001*	0.002*	0.940	-
	Univariate	Multivariate	Univariate	Multivariate
PET imaging (yes vs. no)	0.044*	0.047*	0.549	-
PET Tracer (68Ga vs. F-18 vs. C11)	0.132	-	0.096	-
Previous resection (yes vs. no)	0.087	-	0.018*	0.036
Resection status (complete vs. incomplete)	0.250	-	0.070	-
Time resection - RT [months]	0.673	-	0.496	-
Age at diagnosis [years]	0.294	-	0.023*	0.104
PTV [ml]	0.041*	0.046*	0.101	-
Gender (male vs. female)	0.214	-	0.403	-

## Conclusion

PET-imaging improves the detection of tumor cells, especially during treatment planning. It showed a significant influence on OS and PFS.

Further sub-analyses will investigate the influence of PET for resected patients, and large tumor volumes and establish cut-off values for which tumor sizes additional PET imaging might be beneficial. For low-grade meningiomas the time between resection and RT was borderline significant. With the factors age, PTV and gender a weighted scoring system will be developed for prognostic assessment.

## EP-1257 Post-operative hypo-fractionated SBRT in a large series of patients with brain metastases

G. Martinage<sup>1</sup>, J. Geffrelet<sup>2</sup>, D. Stefan<sup>2</sup>, E. Bogart<sup>3</sup>, E. Rault<sup>4</sup>, N. Reyns<sup>5</sup>, E. Emery<sup>6</sup>, S. Martinage Makhloufi<sup>7</sup>, R. Mouttet Audouard<sup>1</sup>, L. Basson<sup>1</sup>, X. Mirabel<sup>1</sup>, E. Lartigau<sup>1,8</sup>, D. Pasquier<sup>1,8</sup>

<sup>1</sup>Centre Oscar Lambret, Academic Department of Radiation Oncology, Lille, France ; <sup>2</sup>Centre François Baclesse, Department of Radiation Oncology, Caen, France ; <sup>3</sup>Centre Oscar Lambret, Department of Biostatistics, Lille, France ; <sup>4</sup>Centre Oscar Lambret, Department of Medical Physics, Lille, France ; <sup>5</sup>CHRU Lille, Department of Neurosurgery, Lille, France ; <sup>6</sup>CHU Côte de Nacre, Neurosurgery department, Caen, France ; <sup>7</sup>Centre Oscar Lambret, Department of Clinical Research and Innovation, Lille, France ; <sup>8</sup>Lille University, CRISTAL UMR CNRS 9189, Lille, France

## Purpose or Objective

The aim of this study was to assess, in a large series, the efficacy and tolerance of post-operative adjuvant hypofractionated stereotactic radiation therapy (HFSRT) for brain metastases (BMs).

## Material and Methods

Between July 2012 and January 2017, 160 patients with 167 surgical cavities from 2 centers were operated for BM and treated by HFSRT. Patients had between 1-3 BMs, no brainstem lesion or carcinomatous meningitis. CT scan and gadolinium contrast-enhanced MRI were used for treatment planning. HFSRT was delivered using a CyberKnife®-type robotic accelerator. The primary endpoint was local control. Secondary endpoints were distant brain control, overall survival (OS) and tolerance to HFSRT.

## Results

Seventy-three patients (46%) presented with non-small cell lung cancer (NSCLC), 23 (14%) had melanoma and 21 (13%) breast cancer. Median age was 58 years (range, 22-83 years). BMs were synchronous in 50% of the cases. Median tumor size was 32 mm (range, 7-78 mm) and 75% of the cases (n=124) BMs were supratentorial. Planning MRI was performed in 151 patients (94%).

The most frequent prescription regimens were 24 Gy in 3 fractions (n=52, 33%) and 30 Gy in 5 fractions (n=37, 23%). Local control rates at 6 months, 1 year and 2 years were

91% [95% CI, 85%-95%], 88% [95% CI, 81%-93%] and 81% [95% CI, 70%-88%], respectively. Distant control rate at 1 year was 48% [95% CI, 81%-93%]. In multivariate analysis, primary NSCLC ( $p=0.007$ ), the number of extra-cerebral metastatic sites ( $p=0.003$ ) and planning target volumes ( $p=0.012$ ) were associated with OS. There was no factor predictive of time to local progression. Median OS was 15.2 months [95% CI, 12.0-17.9 months] and the OS rate at 1 year was 58% [95% CI, 50%-65%]. Salvage radiotherapy was administered to 72 patients (45%), of which 49 received new HFSRT. Five patients underwent re-irradiation of the surgical bed by stereotactic radiation therapy. Ten (7%) patients presented late grade 2 and 4 (3%) patients late grade 3 toxicities. Thirteen (8.9%) patients developed radiation necrosis (all grades).

#### Conclusion

This large multicenter retrospective study shows that HFSRT allows for good local control of metastasectomy tumor beds and that this technique is well-tolerated by patients.

#### EP-1258 Predicting Brain V12Gy for Single-Isocenter Multi-Target Stereotactic Radiosurgery (SRS)

H. LIU<sup>1</sup>, T. Li<sup>1</sup>, H. Zhang<sup>2</sup>, W. Shi<sup>1</sup>

<sup>1</sup>Thomas Jefferson University Hospital, Radiation Oncology, Philadelphia, USA ; <sup>2</sup>Monte Vista Christian School, n/a, Watsonville, USA

#### Purpose or Objective

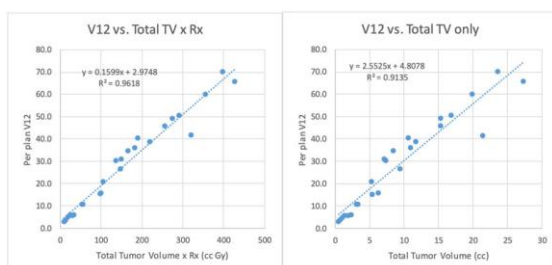
Stereotactic radiosurgery (SRS) for multiple brain metastasis has been shown to provide excellent local control with reduced cognitive impact. For this type of treatment, the volume of brain receiving 12Gy (V12Gy) has been shown to correlate with the occurrence of radionecrosis following SRS. This study aimed to determine a simple and efficient model for predicting V12Gy for patients undergoing stereotactic radiosurgery (SRS) for multiple brain tumors in a single session prior to treatment planning.

#### Material and Methods

30 single-isocenter-multi-target SRS cases planned with Brainlab Elements™ treatment planning system were retrospectively analyzed. A total amount of 221 tumors were prescribed to 15-24 Gy. V12Gy for each individual tumor and for each plan were extracted. Three methods were used to model V12Gy based on anatomy and prescription: a linear regression model on per-plan V12Gy combining all targets, a linear regression model on per-target V12Gy followed by summation per plan, and 3D geometric per-target expansion model that assumes V12Gy occurs at a certain distance outside each target. Actual-vs-predicted graphs and root-mean-square errors for per plan V12Gy were used to assess the prediction accuracy of each model.

#### Results

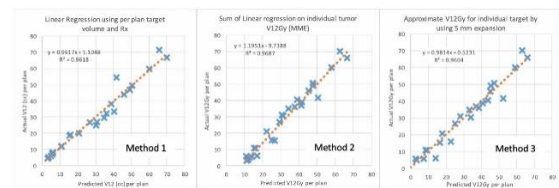
(1) Linear correlation analysis showed improved correlation when using the prescription-weighted sum of tumor volumes per plan (R-square = 0.9618) as input instead of using only total tumor volume (R-square = 0.9135). Using this simple linear model, the predicted V12Gy resulted an RMSE of 3.8 cubic-cm.



(2) The linear fitting model used prescription-weight

individual tumor volume as input to predict individual V12 Gy. Regression using 16-patient training data yielded an R-square of 0.9498. This model was then applied to the whole 30 patients to predict individual V12Gy for each tumor, which was then summed within each patient to give predicted per-plan V12Gy. The predicted V12Gy using this method resulted an RMSE of 5.9 cm<sup>3</sup>, and on average over-predict by 3.4±4.8 cm<sup>3</sup>.

(3) The geometric expansion method showed that a 5 mm expansion from each tumor's equivalent sphere provided most stable prediction of actual V12Gy volumes with a fixed offset of 13.7 cm<sup>3</sup> for nearly all tumor sizes. Using 5 mm expansion minus 13.7 cm<sup>3</sup> as prediction, the predicted V12Gy showed an RMSE of 4.0 cm<sup>3</sup>. This result was not substantially improved over simple linear regression method.



#### Conclusion

In this study we compared three empirical models to predict brain V12Gy using only tumor size and prescription information, which is readily available before planning. The results showed that the simple linear model performed reasonably well and offered very similar goodness of prediction compared to more complicated 2-step or 3D-based models. This linear model used prescription-weighted total tumor volume for a particular patient as input, and could help clinicians decide how many tumors and what prescription should be given without exceeding desired V12Gy limit even before treatment planning, therefore save clinical resources and improve patient throughput.

#### EP-1259 Retrospective Analysis of radiosurgery for ≥ 4 brain metastases from oncogene-addicted NSCLC

Y. Wang<sup>1</sup>, C. Calbat<sup>1</sup>, P. Allen<sup>1</sup>, N. Guha<sup>1</sup>, D. Gomez<sup>1</sup>, J. Li<sup>1</sup>

<sup>1</sup>University of Texas- MD Anderson Cancer Center, Radiation Oncology, Houston, USA

#### Purpose or Objective

The prolonged survival in NSCLC patients with EGFR-mutation or ALK-rearrangement treated with target agents calls for treatment of their brain metastases (BMs) with minimal toxicity and less systemic interruption. Although stereotactic radiosurgery (SRS) without whole brain radiation therapy (WBRT) is the preferred initial strategy for patients with 1-3 BMs, the paradigm remains elude for those with more than 3 cerebral lesions, particularly given the CNS penetration of available target therapies. The current study aims to investigate the overall survival, CNS progression and the rate of salvage WBRT in patients of EGFR-mutated or ALK-rearranged NSCLC with 4 or more BMs treated with SRS.

#### Material and Methods

We retrospectively reviewed NSCLC patients with EGFR-mutation or ALK-rearrangement who received Gamma Knife (GK) radiosurgery for 4 or more BMs in a single radiosurgery session at MD Anderson cancer center between 2009 and 2018. Overall survival, intracranial progression and freedom from WBRT were estimated using Kaplan-Meier analysis.

#### Results

Thirty-two patients, including 25 patients with EGFR mutation and 7 with ALK re-arrangement were identified and included in the current study with a total of 405 lesions treated with SRS. The median follow-up time was

22.8 months (range 1 to 71.4 months). The maximum number of BMs treated in a single GK radiosurgery per patient ranged from 4 to 18 (median 7), and the median number of total BMs treated over 1-5 courses of GK was 9 (range 4 to 37). The median overall survival for all patients was 33.4 months from the time of BM diagnosis. Overall survival was better in patients with fewer total number of lesions developed /treated (70.8 months for patients with 4-10 lesions, 34.5 months for those with 11-19 lesions and 27.7 months for those with >20 lesions), although this difference was not statistically significant ( $p=0.37$ ). The overall survival was not affected by the number of GK courses or the maximum number of BMs treated in a single GK session. Patients who received CNS-active TKIs had longer median survival (53.4 months) than those who received non-CNS active TKIs (33.4 months) ( $p=0.8$ ), and in this population receiving immunotherapy did not influence overall survival. Time to CNS progression after 1<sup>st</sup> course of GK radiosurgery was 10.1 months, and 6.2 and 6.3 months after the 2<sup>nd</sup> and 3<sup>rd</sup> course of GK, respectively ( $p=0.002$ ). Six patients received WBRT after the initial GK (crude rate of 18.8%), and the median time to WBRT was 13.6 months (range 10 to 23.9). Radiosurgery was well tolerated. Symptomatic radiation necrosis (RN) was observed in 4 of 405 treated BMs (0.98%) or 4 of 32 patients (12.5%).

#### Conclusion

In patients with multiple BMs from EGFR-mutated and ALK-rearranged NSCLC, the optimal initial management remains controversial. The results from our current retrospective study support the use of initial radiosurgery without WBRT as an effective and safe strategy for metastatic NSCLC patients with driven mutation and more than 4 BMs.

#### EP-1260 Outcomes of Local Control and CNS Toxicity with Single and Hypofractionated SRS for Brain Metastases

M. Patel<sup>1</sup>, S.R. Marcrom<sup>1</sup>, R.A. Popple<sup>1</sup>, A.M. McDonald<sup>1</sup>, K.O. Riley<sup>2</sup>, B.L. Guthrie<sup>2</sup>, J.M. Markert<sup>2</sup>, C.D. Willey<sup>1</sup>, M. Bredel<sup>1</sup>, J.B. Fiveash<sup>1</sup>

<sup>1</sup>University of Alabama-Birmingham, Department of Radiation Oncology, Birmingham, USA ; <sup>2</sup>University of Alabama-Birmingham, Department of Neurosurgery, Birmingham, USA

#### Purpose or Objective

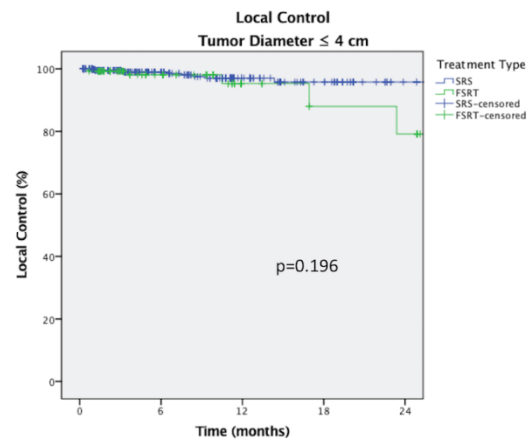
Radiosurgery is a standard management strategy of brain metastases in select patients. The role of single-fraction stereotactic radiosurgery (SRS) and hypofractionated stereotactic radiation therapy (FSRT) is currently evolving, with significant variability in utilization across institutions. We sought to retrospectively evaluate the impact of tumor size and treatment type (SRS vs. FSRT) on local control (LC) and CNS toxicity.

#### Material and Methods

All brain metastases from 2015-2017 treated with single-isocenter volumetric modulated arc therapy (VMAT) LINAC radiosurgery with a 6 DOF couch were captured. Tumors were included for analysis if they received SRS, FSRT, had no prior surgery or radiation, and had available follow-up imaging. The dose was prescribed to the edge of the GTV with no PTV margin. Local failure was defined as a 25% increase in tumor diameter on follow-up MRI or pathologic confirmation of tumor recurrence. Locally controlled tumors were censored at the time of last MRI follow-up, death, or whole brain radiation for distant brain failure. Significant CNS toxicity was per the RTOG definition as irreversible Grade 3 or higher toxicity. LC and CNS toxicity were evaluated by the Kaplan-Meier (KM) method with the log-rank test utilized to compare subgroups. A multivariable analysis (Cox Proportional Hazards model) of potential factors affecting LC was performed.

#### Results

A total of 688 tumors were included, 530 treated with SRS and 158 treated with FSRT. The median radiographic and clinical follow up was 5 months and 7 months, respectively. All subsequent comparisons are given as SRS versus FSRT. The median tumor diameter was 0.82 cm and 1.65 cm ( $p<0.001$ ). The KM estimate of 12-month LC among tumors  $\leq 4$ cm was 97% and 95% ( $p=0.196$ ). KM estimates of 12-month LC for tumors  $\leq 2$ cm was 98% and 100% ( $p=0.352$ ),  $>2$  to  $\leq 3$ cm was 91% and 100% ( $p=0.439$ ), and  $>3$  to  $\leq 4$ cm was 80% and 74% ( $p=0.863$ ). Additionally, KM estimate of 12-month freedom from significant CNS toxicity was 99% and 97% ( $p=0.308$ ) overall and 89% and 100% ( $p=0.128$ ) for tumors  $>3$  to  $\leq 4$  cm. Only tumor volume (HR 1.141;  $p<0.001$ ) was predictive of local failure in a multivariable analysis that included treatment type (HR 0.927;  $p=0.909$ ).



#### Conclusion

SRS and FSRT appear to have a high rate of local tumor control with a low rate of significant CNS toxicity. LC and CNS toxicity outcomes appear to be driven by tumor volume without being significantly affected by treatment type. FSRT appears to offer a safe and effective alternative to SRS in both large and small tumors. In patients with multiple metastases in which a large target requires fractionation, utilizing the same dose and fractionation across all treated targets, regardless of target size, offers an opportunity for improved efficiency in treatment planning and treatment delivery without compromising outcomes.

#### EP-1261 MRI-guided SABR of spinal metastases: comparison of Co-60 and linac treatments

R. Llorente<sup>1</sup>, C. Takita<sup>1</sup>, R. Yechieli<sup>1</sup>, J.C. Ford<sup>1</sup>, K. Brown<sup>1</sup>, M. Samuels<sup>1</sup>, E.A. Mellon<sup>1</sup>

<sup>1</sup>University of Miami/Sylvester Comprehensive Cancer Center / Jackson Memorial Hospital, Radiation Oncology, Miami, USA

*This abstract is part of the media programme and will be released on the day of its presentation*

procedures, which included surgery (12 patients), repeat gamma knife alone (5 patients), or a combination of repeat gamma-knife and surgery (3 patients). Of the patients receiving additional treatments, 14 experienced pain relief at their most recent follow up.

#### Conclusion

Complete pain control following GK treatment for TG neuralgia at one year was found to be 56% in our cohort. It is difficult to discern the actual control rate from the 1999-2006 cohort due to significant loss to follow-up, perhaps due to symptom resolution. 66% of patients in our cohort required additional procedures for pain management, including surgery and repeat GK. Future directions include reviewing more recent cases from 2006-2018, which may have improved follow up and documentation due to implementation of the electronic medical record.

#### EP-1263 Hippocampal avoidance in WBRT for Metastases - Comparative Neurocognitive and Dosimetric Assessment

V. Pareek<sup>1</sup>, R. Bhalavat<sup>1</sup>, M. Chandra<sup>1</sup>

<sup>1</sup>Jupiter Hospital, Radiation Oncology, Mumbai, India

#### Purpose or Objective

Hippocampus is associated with formation and storage of new memory and irradiation of the same during whole brain radiotherapy in brain metastases leads to decline in the neurocognitive function. Recent advancements in radiation delivery in form of IMRT, Hippocampal avoidance has been made possible. We analyze feasibility of hippocampal sparing and associated neurocognitive and dosimetric assessment.

#### Material and Methods

Between June 2016 to December 2017, 125 patients diagnosed radiologically and clinically with brain metastases were included in the study. Mini Mental State Examination (MMSE) and quality of life assessment with EORTC BN20 questionnaire were assessed along with dosimetry. Patients were assessed at baseline and followed by at 1, 3 and 6 months respectively. Factors were compared with the historical group with relation to quality of life especially neurocognitive functioning. Wilcoxon test for multiple comparisons was calculated to detect significant differences in global QoL scores. Dose received in WBRT was 30Gy in 10 fractions in both arms with boost of 9Gy in single metastases.

#### Results

Median age of accrued 125 patients was 48 years. Median D100% and Dmax to contralateral hippocampus was 7.1Gy and 16.7Gy. With IMRT, the doses to other critical structures were reduced. Patients treated with IMRT were found to have achieved desired dose constraints to hippocampus. Assessment of neurocognitive function between two groups, there was no difference at 1 month after treatment, however, difference was seen at 3 and 6 months favouring hippocampal avoidance. No difference noted in other aspects of quality of life between two groups. No severe toxicities (Grade 3 and 4) were noted in either group. Median survival in the HA-WBRT arm was found to be 10.1 months.

#### Conclusion

Conformal avoidance of hippocampus during WBRT is associated with improved neurocognitive function and quality of life. IMRT has found to provide better dosimetric outcomes in HA-WBRT

---

Electronic Poster: Clinical track: Haematology

---

#### EP-1262 Use of Gamma Knife Radiosurgery for Treatment of Trigeminal Neuralgia

D. Fabian<sup>1</sup>, J. Palmer<sup>2</sup>

<sup>1</sup>The Ohio State University, Radiation Oncology, Columbus, USA ; <sup>2</sup>Palmer, Radiation Oncology, Columbus, USA

#### Purpose or Objective

Gamma Knife radiosurgery (GK) has been shown to relieve symptoms of trigeminal neuralgia (TN). Success rates have been reported to range between 70-90% at a follow up of 19-75 months. Our objective was to evaluate the success rate of GK for TN treatment in our institution and to evaluate the need for additional procedures. Our hypothesis was that the need for additional treatments would be high.

#### Material and Methods

We identified 50 cases of refractory TG treated with GK at our institution from 1999-2006. These patients were retrospectively chart-reviewed and assessed for subjective pain control and need for medical management. Average GK dose was 38 Gy to the 50% isodose; the median dose was 40 Gy to the 50% isodose. Of these 50 cases, only 30 patients had adequate follow up at 1 year.

#### Results

Of the patients with adequate one-year follow up, 17 reported adequate control of their pain following the procedure (56%). 10 (33%) patients reported control at 2 years post first gamma knife treatment and 6 patients (13%) reported control at 5 years post first gamma knife treatment. 20 patients were reported to have additional

---

EP-1264 Patterns of care for orbital MALToma in Korea throughout 2016: a multicenter cross-sectional study

---

J. Lee<sup>1</sup>, D. Oh<sup>2</sup>, B.O. Choi<sup>3</sup>, K.Y. Eom<sup>4</sup>, J.H. Lee<sup>5</sup>, J.H. Kim<sup>6</sup>, S.W. Lee<sup>7</sup>, Y.K. Suh<sup>8</sup>, C. Suh<sup>9</sup>  
<sup>1</sup>Inha University Hospital, Radiation Oncology, Incheon, Korea Republic of ; <sup>2</sup>Samsung Medical Center-Sungkyunkwan University College of Medicine, Department of Radiation Oncology, Seoul, Korea Republic of ; <sup>3</sup>Seoul St. Mary's Hospital, Department of Radiation Oncology, Seoul, Korea Republic of ; <sup>4</sup>Seoul National University Bundang Hospital, Department of Radiation Oncology, Seongnam, Korea Republic of ; <sup>5</sup>St. Vincent's Hospital, Department of Radiation Oncology, Suwon, Korea Republic of ; <sup>6</sup>Kunyang University Hospital, Department of Radiation Oncology, Seoul, Korea Republic of ; <sup>7</sup>Asan Medical Center- Ulsan University College of Medicine, Department of Radiation Oncology, Seoul, Korea Republic of ; <sup>8</sup>National Cancer Center, Department of Radiation Oncology, Ilsan, Korea Republic of ; <sup>9</sup>Yonsei Cancer Center- Yonsei University College of Medicine, Department of Radiation Oncology, Seoul, Korea Republic of

### Purpose or Objective

Radiotherapy (RT) is an effective primary treatment for orbital mucosa-associated lymphoid tissue (MALT) lymphoma historically. Recent few studies reported the association between Chlamydia psittaci infection and orbital MALT lymphoma. We aimed to assess the current patterns of care in clinical practice for orbital MALT lymphoma in South Korea.

### Material and Methods

We performed a multicenter, cross-sectional cohort study of patterns of care for orbital MALT lymphoma in South Korea throughout 2016, and overall 8 institutions with 90 patients were participated. All patients diagnosed with orbital MALT lymphoma based on a pathologic confirmation.

### Results

The survey showed that most frequent upfront treatment for orbital MALT lymphoma was RT (80/90, 90%). Other treatments were given to a limited number of orbital MALT lymphoma patients as follows: wait and watch (6/90, 7%), antibiotics (3/90, 3%), and chemotherapy (1/90, 1%). Generally, RT was administered to the entire involved site such as entire conjunctiva/eyelid or entire orbit (96%), with a median total dose of 25.2 Gy. Lens shielding was performed for most patients with conjunctival and eyelid tumors (93%).

### Conclusion

Our findings revealed that RT was the mainstream of orbital MALT lymphoma treatment. Currently, for patients with orbital MALT lymphoma, RT has been performed to the entire involved subsites with a lower dose compared to the past, and lens shielding is applied to minimize the orbital complication.

### EP-1265 Total Skin Irradiation - 15 years of Gliwice experiences

G. Wozniak<sup>1</sup>, T. Latusek<sup>1</sup>, Z. Kaniszewska-Dorsz<sup>1</sup>, W. Mista<sup>1</sup>, B. Jochymek<sup>1</sup>, K. Lukasz<sup>1</sup>, W. Jerzy<sup>1</sup>, S. Blamek<sup>1</sup>  
<sup>1</sup>Maria Sklodowska-Curie Memorial Cancer Center and Institute of Oncology, Radiotherapy, Gliwice, Poland

### Purpose or Objective

Evaluation of effectiveness and early toxicity of total skin radiation for patients with primary skin lymphoma

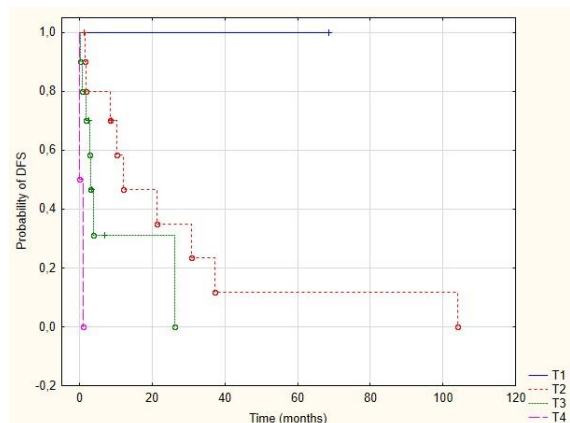
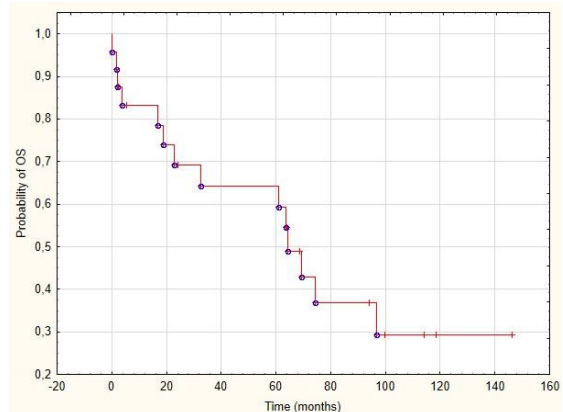
### Material and Methods

Between 2002 and 2017 25 patients with pathological diagnosed primary skin lymphomas were treated with electron radiotherapy using total skin irradiation technique. Male to female ratio was 14 to 11. In almost all patients (22) mycosis fungoides were confirmed. Median age was 66 years. One patient was staged as T1, 11 as T2, 10 as T3 and 3 as T4. Only three patients did not undergo any oncological therapy before radiation. All patients were irradiated 6MeV electron beams using linac. Total

dose ranged between 6 to 36 Gy (median 32) given in 1,5-2 Gy per fraction. In 6 cases additional boost fields for residual disease were used after the end of total skin treatment. Skin reactions and haematological toxicity were assessed with WHO score. OS and PFS were estimated using Kaplan Maier method.

### Results

Median follow up was 20 months. Two patients have not completed treatment. Each patient had skin reaction: 18 were scored as 1st, 4 as 2nd and 1 as 3rd grade. There was not any haematological toxicity observed within the group. Other adverse effects included: alopecia 6pts, conjunctivitis 4pts, general weakness 3pts. In 79% pts disease symptoms regression were observed, including complete response in 20%. Progression was documented in 3 cases. Median time to progression was 7 months, and OS was 64 months. One year PFS was 36% and 5yrs OS was 67%. (Fig1) There was significant differences in PSF depending of T stage (p=0,028) (Fig2). No other factors influencing the OS and PFS were proven. Cox hazard analysis showed that clinical stage and disease regression 6 weeks after radiotherapy are independent risk factors for progression.



### Conclusion

TSI in skin lymphomas using 6MeV electrons is a safe treatment method yielding satisfactory yet short term response rate. Only clinical stage has impact on time to disease progression

### EP-1266 Combination radiotherapy with Nivolumab for refractory classic Hodgkin lymphoma : about two cases

L. De Forceville<sup>1</sup>, B. Deau-Fischer<sup>2</sup>, P. Franchi<sup>2</sup>, A. Arsene-Henry<sup>3</sup>, T. Cassou Mounat<sup>4</sup>, D. Bouscary<sup>2</sup>, Y. Kirova<sup>3</sup>

<sup>1</sup>Hopital Tenon, oncologie médicale, Paris, France ; <sup>2</sup>Hopital Cochin, Hématologie, Paris, France ; <sup>3</sup>Institut Curie, Radiothérapie, Paris, France ; <sup>4</sup>Institut Curie, Médecine Nucléaire, Paris, France

### Purpose or Objective

For patients who experience relapse or refractory Hodgkin Lymphoma (R/R HL), the standard treatment option is high-dose chemotherapy followed by autologous stem cell rescue or transplant (HDT/ASCR). However about 50% of patients will have recurrence after HDT/ASCR and have worse prognosis. The anti-PD1 checkpoints inhibitors have remarkably improved outcomes of patients with R/R HL after HDT/ASCT. On the other hand, radiotherapy is an entire component of salvage therapy and its efficacy is now well established in term of local disease control in sites of R/R HL. Defining the optimal modality and timing of radiotherapy as these new agents arrive is a challenge. The purpose of our paper is to add at the literature two new cases of combination of radiotherapy with immunotherapy in patients who relapse after HDT/ASCT and consolidation with Brentuximab Vedotin (BV).

### Material and Methods

Clinical data were retrospectively collected using the computerized medical records available at the Curie Institute and Cochin Hospital. All imaging have been integrated into the local imaging software and re-read at Institut Curie.

### Results

Case 1: a 27 year-old man was diagnosed in 2015 with stage IV classic Hodgkin Lymphoma, with sus and under diaphragmatic lymph nodes and multiple bone lesions. After 4 cycles of BEACOPP, there was a persistence of a cervical lymph node and mediastinum uptake (Deauville score 4). The patient received a second line with BV-DHAX followed by autologous stem cell transplant (ASCT) in April 2016, resulting in complete metabolic response. A consolidation treatment with BV was initiated. The patient relapsed in June 2017 with cervical and mediastinal lymph nodes (confirmed by biopsy). It was decided an involved sites radiotherapy (30 Gy in IMRT) followed with nivolumab. The patient had now 26 cycles of nivolumab and is in complete response since the third injection.

Case 2: A 21 year-old woman was diagnosed in 2015 with classic Hodgkin Lymphoma stage IIAa, Bulky +. After 2 cycles of BEACOPP, Deauville score was 3. The treatment was de-escalated with ABVD. After 4 cycles, there was a marked increase of the mediastinum uptake. The multidisciplinary team of Cochin opted for a salvage chemotherapy by Brentuximab-DHAX, followed by ASCT and resulting in complete metabolic response. The patient then received a consolidation treatment with BV. The patient relapsed in may 2015 with supra-dipahragmatic nodes and reappearance of the mediastinal mass confirmed by biopsy. The patient received a localized radiotherapy of the mediastinum followed by Nivolumab. After 30 cycles of nivolumab, complete response was maintained, nivolumab was stopped since October 2017 and the patient is still in complete response.

### Conclusion

Involved sites radiotherapy followed by nivolumab is an interesting option for patients with RR/HL who experience a localized relapse after ASCT. This combination may increase the response to checkpoint inhibitors and allow to stop them.

### EP-1267 Deep Inspiration Breath-Hold versus free breathing radiotherapy in mediastinal lymphoma

A. Iversen<sup>1</sup>, H.R. Mortensen<sup>1</sup>, Hanne Krogh Rose<sup>1</sup>, Jolanta Hansen<sup>1</sup>

<sup>1</sup>Aarhus University Hospital, Department of Oncology and Medical Physics, Aarhus C, Denmark

### Purpose or Objective

Radiotherapy plays an important role in the treatment of mediastinal lymphomas as part of combined modality treatment. However, late effects, e.g. cardiac and lung toxicity as well as secondary cancers due to radiotherapy,

are of great concern especially for mediastinal tumors. It is therefore important to reduce normal tissue dose. Our aim was to evaluate local experience of radiotherapy for mediastinal tumors comparing deep inspiration breath-hold (DIBH) and free breathing (FB) technique with intensity-modulated radiotherapy (IMRT) in regards to normal tissue doses.

### Material and Methods

Since October 2017 12 patients have been planned with both DIBH and FB technique for mediastinal lymphomas according to IROG guidelines. Data on histology, chemotherapy, prior cardiac or lung malfunction and radiotherapy was obtained from the patient files. Target delineation was based on current international guidelines and patients were treated with 24-36 Gy; 2 Gy per fraction. Two IMRT plans were calculated and compared for each patient: one for FB and one for DIBH. All plans were simulated in Eclipse (version 13.7.14, Varian Medical Systems) with the AcurosXB 13.7.14 algorithm using 6-MV photon beams. The IMRT plans consisted of 5 to 7 fixed fields. The dosimetric parameters retrieved for the statistical analysis were PTV coverage, mean heart dose, mean lung dose, and lung V5 and heart V20.

### Results

12 patients were planned with both DIBH and FB IMRT. The patient cohort consisted primarily of men (8 male, 4 female) with a median age of 37 years (range 10-62). All patients received chemotherapy as initial treatment according to national guidelines. Seven patients were treated with radiotherapy in FB and five patients were treated in DIBH. There was no difference in age, total dose, CTV volume or CTV relation to the heart between patients treated with DIBH and patients treated in FB. Patients treated with DIBH had significantly reduced mean dose to total lung,  $V5_{total\ lung}$ , mean heart dose and  $V20_{heart}$  when comparing DIBH IMRT and FB plan IMRT ( $p < 0.5$ ). For three patients, plan robustness and DIBH instability contributed to treatment choice.

### Conclusion

The experience with DIBH IMRT is still limited in our department. Surprisingly, in the first 12 patients, DIBH IMRT was the treatment of choice in only five patients based on reduced doses to lungs and heart. The remaining seven patients were treated with FB IMRT, since no gain in normal tissue doses was obtained with DIBH IMRT. Further data is needed to properly select patients for DIBH IMRT and thereby individualize the radiation plan for the individual patient.

### EP-1268 Primary radiation therapy in stage I/II indolent orbital lymphoma: a single-center analysis

C. Eze<sup>1</sup>, I. Friedrich<sup>1</sup>, D. Reitz<sup>1</sup>, C. Belka<sup>1</sup>, M. Li<sup>1</sup>

<sup>1</sup>University Hospital LMU Munich, Department of Radiation Oncology, Munich, Germany

### Purpose or Objective

Non-Hodgkin Lymphoma is a heterogenic group of malignant diseases, which originate from the lymphatic system. They can be subdivided into B- and T-Cell-Lymphoma and classified into indolent/low-grade and high-grade/aggressive lymphoma. Radiotherapy is well-established in the management of stage I/II (Ann Arbor classification) indolent lymphoma. We conducted this retrospective analysis to evaluate the outcomes of patients with localized indolent orbital lymphoma who were treated at our center with definitive radiotherapy.

### Material and Methods

We retrospectively reviewed the medical charts of 47 patients (12 males, 35 females) with 52 lesions treated at our center from 1994- 2012 for histologically confirmed indolent orbital lymphomas. Median age at diagnosis was 63.5 years (range: 20-92) with 25 lesions on the right and 27 on the left. Five patients presented with bilateral involvement. The predominant histological subtype was mucosa-associated lymphoid tissue lymphoma in 84.6% of

cases. Most lymphomas were located in the conjunctiva (34.6%) and the lower or upper eyelids (34.6%). The majority of patients presented with stage I disease (76.9%). Radiation dose ranged from 21.6-45.0 Gy (median 39.8 Gy) in 1.8-2.0 Gy daily fractions. Median follow-up duration was 83 months.

#### Results

All but one patient achieved local complete remission. The 5- year progression-free survival rate was 77.5% (95% CI: 71.2 - 83.8) (Fig. 2). In addition, 5- and 10-year overall survival rates were 84.0% (95% CI: 78.4 - 89.6) and 77.1% (95% CI: 70.2 - 84.0), respectively. Of all patients who died within 5 or 10 years, there was only one documented case of progression. Treatment was in general well tolerated with acute toxicity, e.g. conjunctivitis (42.3%), ophthalmalgia (13.5%) and Keratitis (3.8%) with convalescence in the majority of cases. Late toxicity included all degrees of cataract, 31 patients (59.6%) and of xerophthalmia, 36 patients (69.2%).

#### Conclusion

Our retrospective analysis showed that moderate radiotherapy is an effective treatment modality with excellent local control and moderate late complication rates in the management of stage I/II indolent orbital Non-Hodgkin lymphoma.

---

### Electronic Poster: Clinical track: Breast

---

#### EP-1269 Local review of lung doses in simultaneous integrated boost (SIB) radiotherapy breast plans

J.F. Calvo Ortega<sup>1</sup>, J. Fernández-Ibiza<sup>1</sup>, S. Moragues

Femenia<sup>1</sup>, C. Laosa-Bello<sup>1</sup>, J. Casals<sup>1</sup>

<sup>1</sup>Hospital Quirónsalud Barcelona, Radiotherapy, Barcelona, Spain

#### Purpose or Objective

To perform a review of the lung radiation doses from breast cancer radiotherapy plans for a specific SIB scheme used in our department.

#### Material and Methods

Lung doses in 185 SIB treatment plans were included in this study. The whole breast ± axillary or supraclavicular lymph nodes and the tumor bed were planned to simultaneously receive 45.57 Gy and 55.86 Gy in 21 fractions, respectively. Supine radiotherapy with no breathing adaptation was performed. Plans were computed using the AAA algorithm of the Eclipse TPS v 13.0 and IMRT technique, modeled for 6 MV photon beams of a Varian Clinac 2100 CD. All plans fulfilled the organ-at-risk dose constraints used in our department for this 21 fraction radiotherapy scheme.

The following metrics were analyzed:  $V5_{ips}$ ,  $V20_{ips}$ , and mean lung dose ( $MLD_{ips}$ ) for the ipsilateral lung, and mean dose to both lungs ( $MLD_{whole}$ ).  $Vx_{ips}$  is the percentage volume of the ipsilateral lung receiving  $\geq x$  Gy. The values of these metrics collected in our plans were compared with the multicentric data recently reported by Aznar et al. in *Radiother Oncol.* 2018 Jan;126(1):148-154, as a way of assessing the quality of our breast plans.

#### Results

For breast plus regional lymph nodes (37 cases), comparison of our values vs. Aznar's values was (average ± standard error): 43.8% ± 2.1% vs. 46.6% ± 6.0% for  $V5_{ips}$ ; 14.3% ± 0.3% vs. 22.8% ± 1.3% for  $V20_{ips}$ ; 9.1 Gy ± 0.4 Gy vs. 11.2 Gy ± 0.5 Gy for  $MLD_{ips}$ ; and 4.8 Gy ± 0.2 Gy vs. 7.3 Gy ± 0.4 Gy for  $MLD_{whole}$ .

For simple breast (148 cases), comparison of our values vs. Aznar's values was (average ± standard error): 29.8% ± 0.8% vs. 40.2% ± 2.2% for  $V5_{ips}$ ; 9.9% ± 0.3% vs. 13.8% ± 0.4% for  $V20_{ips}$ ; 6.2 Gy ± 0.1 Gy vs. 8.6 Gy ± 0.2 Gy for  $MLD_{ips}$ ; and 3.2 Gy ± 0.1 Gy vs. 5.7 Gy ± 0.2 Gy for  $MLD_{whole}$ .

#### Conclusion

Inclusion of the regional lymph nodes considerably increased the metric values relative to irradiation of the whole breast only. Lung average doses attained with the 21 fraction SIB scheme used in our department were always smaller than the reported ones by Aznar et al. This can be considered as a quality test for our designed treatment plans.

#### EP-1270 Outcomes and toxicity of stereotactic radiotherapy for metastatic breast cancer - a retrospective study

M. AL-Hanaqta<sup>1</sup>, M. Niglas<sup>2</sup>, C. Jiang<sup>3</sup>, P. Cheung<sup>2</sup>, W. Chu<sup>2</sup>, H. Chung<sup>2</sup>, S. Myrehaug<sup>2</sup>, I. Poon<sup>2</sup>, A. Sahgal<sup>2</sup>, H. Soliman<sup>2</sup>

<sup>1</sup>Royal medical services, Radiation oncology, Amman, Jordan ; <sup>2</sup>Sunnybrook HSC, Radiation oncology, Toronto, Canada ; <sup>3</sup>University of Toronto, School of medicine, Toronto, Canada

#### Purpose or Objective

Technological advances in radiotherapy have allowed for the delivery of ablative doses to sites of disease in most parts of the body. In this trial, we describe the outcomes of a group of breast cancer patients treated to sites of metastatic disease with stereotactic radiotherapy (SBRT). Predictors of treatment outcomes are also investigated in this cohort.

#### Material and Methods

After institutional research ethics board approval, patients with metastatic breast cancer who received SBRT to metastatic disease from 2011 to 2016 were identified by electronic chart review. Patient demographics, histologic information and clinical data were collected from the electronic patient record and the radiation treatment planning system. Outcomes of interest included local control (LC), overall survival (OS), and progression free survival (PFS). In addition to Kaplan-Meier estimates, univariate analysis using the log-rank test, and multivariate analysis with cox regression was used to assess covariates, which were identified a priori.

#### Results

120 patients between the ages of 25 to 82 (median 54.8 years) with 193 treated lesions were identified. Median follow-up was 9.8 months (range 0.03 to 72.31 months). Patients' estrogen receptor (ER), progesterone receptor (PR) and Her-2 status were 83.9%, 70.7% and 18.4% respectively (maybe better to describe subtype here, e.g. luminal a). 70.3% had lymph node positive disease at diagnosis. The majority of treated lesions were in the spine (45%), followed by liver (20%), lung (18%) and non-spine bone (14%). There were no recorded grade 4 or 5 toxicities, with only 5.3% of patients reporting side effects (most commonly mild pain). 1-year LC, PFS and OS was 88%, 45% and 84% respectively. On univariate analysis, PFS varied depending on treatment indication (oligometastasis, oligoprogression or salvage) with a median PFS of 24.4 months, 5.6 months and 8.1 months respectively ( $p < 0.001$ ). Similarly, a difference in OS by treatment indication was also seen with 1-year survival of 91%, 82% and 57% respectively ( $p < 0.001$ ). Survival was influenced by molecular subtype, with the worst survival seen in patients with triple negative disease ( $p = 0.001$ ).

#### Conclusion

Local control rates remain excellent after SBRT to sites of metastatic disease in this population of breast cancer patients. The most significant risk for these patients remains distant failure, with significantly longer PFS in those being treated for oligometastatic disease in comparison to other indications. Favourable PFS observed in the oligometastases subgroup would support further randomized evaluation of the potential benefit of SBRT in this population, as is currently being performed in other tumour histologies.

### EP-1271 Effects of regular bra-wearing on acute skin toxicity in breast-conserving radiotherapy women

P. Thongkhao<sup>1</sup>, T. Peerawong<sup>1</sup>, R. Jiratrachoo<sup>1</sup>, J. Pruetkitti<sup>1</sup>, A. Geater<sup>2</sup>

<sup>1</sup>Faculty of Medicine- Prince of Songkla University., Radiology, Hat Yai- Songkhla, Thailand ; <sup>2</sup>Faculty of Medicine- Prince of Songkla University., Epidemiology Unit, Hat Yai- Songkhla, Thailand

#### Purpose or Objective

At present, the instruction of wearing bra in daily life during radiotherapy treatment course in breast conserving therapy (BCT) patients is unclear. This study aimed to evaluate the effect of regular bra-wearing during radiotherapy on acute skin toxicity and the quality of life in women with BCT.

#### Material and Methods

This study is a preliminary prospective non-inferiority cohort study. Women with any stage breast cancer who underwent BCT were enrolled from June 2017 to July 2018 at a single tertiary center in the Southern Thailand. The exclusion criteria included patients who underwent an immediate reconstruction, patients with pre-existing skin lesions in the treatment area, and patient with known systemic skin diseases, even not directly affecting irradiated fields. After informed consent was obtained, participants were instructed to wear appropriate bra, record the hours per day of wearing bra in a patient record form, and were told they could freely decide to wear the bra or not. Then all participants were classified by total hours of wearing bra during the radiotherapy treatment course into non-bra-wearing (0 hr.) and bra-wearing groups (>0 hr.). The acute skin toxicity was assessed weekly and one week after treatment end by CTCAE version 4 and the quality of life was assessed before and one week after treatment end by FACT-B Thai version 4. All participants were treated with a dose of 50Gy in 25 fractions over 5 weeks. An addition boost 10-16Gy was given, depending on clinical judgement. Differences in acute skin toxicity grade between the two groups were assessed using Chi-square test or a Fisher's exact test and the quality of life scores were compared using Student's t-test or Wilcoxon rank-sum test.

#### Results

A total of 99 patients were eligible, which 66 patients were in bra-wearing group and 33 patients were in non-bra-wearing group. Baseline patient characteristics were well balanced except for T-stage and median maximum dose. Overall rate of  $\geq$  G2 acute skin toxicity was 29% and began to appear after 4<sup>th</sup> week of treatment in both groups (Figure 1). The rate of  $\geq$  G2 acute skin toxicity was lower in bra-wearing group compared to non-bra-wearing group (16.7% vs. 54.5%,  $p < 0.001$ , respectively). In the multivariate analysis, the statistically significant factors that associated with increased the risk of  $\geq$  G2 acute skin toxicity were non-bra-wearing (0 hr.) ( $p < 0.001$ ), high body mass index ( $p = 0.002$ ), and high percentage of maximum dose ( $p = 0.022$ ) (Table 1). There was no difference in all five parts and total mean scores of after treatment FACT-B Thai between the bra-wearing and non-bra-wearing groups (118.4 vs. 114.7,  $p = 0.256$ , respectively).

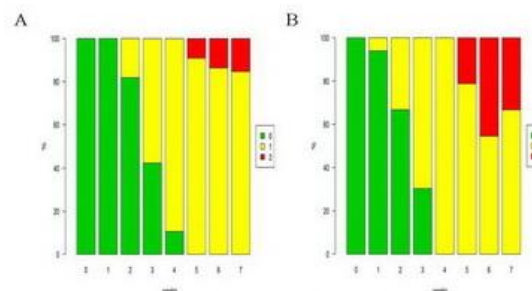


Figure 1. Proportions of acute skin toxicity in each week. (A) bra-wearing group and (B) non-bra-wearing group

Table 1. Multivariate analysis of the predictors for increased  $\geq$  G2 acute skin toxicity

	Adj. OR (95%CI)	P (Wald's test)	P(LR-test)
Total hour wearing bra (hr.)			< 0.001
Ref.= 0			
1-350	0.16 (0.04,0.58)	0.005	
>350	0.08 (0.02,0.43)	0.003	
Body mass index (kg/m <sup>2</sup> )			0.002
Ref.= <18.5			
18.5-24.9	0.46 (0.05,4.19)	0.493	
25-29.9	1.96 (0.2,18.94)	0.56	
$\geq 30$	9.48 (0.82,109.44)	0.072	
Maximum dose (%)			0.022
Ref.= $\leq 107$			
>107-110	1.21 (0.15,9.59)	0.859	
>110	5.62 (0.84,37.53)	0.075	

#### Conclusion

Regular bra-wearing during radiotherapy is not associated with increased the risk of  $\geq$  G2 acute skin toxicity and does not affect the quality of life compared to non-bra-wearing.

### EP-1272 Is hypofractionated nodal radiotherapy safe in the treatment of breast cancer patients?

C. Matthieu<sup>1</sup>

<sup>1</sup>CHU, Radiotherapy, BESANCON, France

#### Purpose or Objective

We retrospectively evaluated safety and efficacy of hypofractionated locoregional radiotherapy (HLRT) in breast cancer (BC) patients. We compared them patients treated, in the same period, with hypofractionated radiotherapy on the breast/wall chest only (HRT).

#### Material and Methods

We reviewed the charts of patients with biopsy-proven BC treated with postoperative HLRT (n= 275, 63%) or HRT (n= 160, 37%) between 2008 and 2011. Incidence of acute and late toxicity was the primary endpoint. Five-year locoregional-free survival (LRR-FS), disease-free survival (DFS) and overall survival (OS) were also analyzed and reported.

#### Results

Median follow-up was 61.7 months. Treatment was globally well-tolerated. Severe acute toxicity was found in 4.4% of the HRT cohort and 3.1% of the HLRT one ( $p = 0.79$ ), usually as dermatitis. HLRT patients presented more frequently G1-2 dysphagia (30.6% vs 0.4%,  $p < 0.001$ ) and/or G1-2 lymphedema (5.6% vs 0.4%,  $p = 0.002$ ). At multivariate analysis, tabagism was the only independent factor statistically influencing the risk of acute toxicity ( $p = 0.047$ ). Concerning late toxicity, HLRT patients presented more frequently G1-2 lymphedema (6.2% vs 0.7%,  $p = 0.003$ ). Five-year LRR-FS was 96.3% in the HRT and 92% in the HLRT population, respectively ( $p = 0.004$ ). Five-year DFS was 92.2% in the HRT and 83.4% in the HLRT population, respectively ( $p = 0.004$ ). Five-year OS was 96.4% in the HRT and 92.6% in the HLRT group, respectively ( $p = 0.027$ ).

### Conclusion

HLRT is safe and the clinical outcomes of our patients are comparable to the results of available randomized trials on hypofractionation for breast cancer. Further, prospective randomized trials are warranted to confirm our data and consider HLRT a standard of care.

### EP-1273 Increasing negative lymph node count prolong survival in breast cancer with neoadjuvant chemotherapy

X. Wang<sup>1</sup>, P. Wang<sup>1</sup>

<sup>1</sup>Tianjin Medical University Cancer Hospital & Institute, Department of Radiation Oncology, Tianjin, China

### Purpose or Objective

Adequate lymph node evaluation is recommended many malignant tumors including breast cancer. However, the role of negative lymph nodes (LNs) remains unclear in breast cancer (BC), especially in the setting of neoadjuvant chemotherapy. A retrospective analysis of BC treated with mastectomy after NAC in our institution was conducted.

### Material and Methods

A total of 435 patients diagnosed with BC who were treated with mastectomy after NAC were included in this analysis. The median age was 49 years old (22-76 years old). The clinical stage distributions were cT1-2 in 245 patients and T3-4 in 190 patients, cN0 in 82 cases, cN1 in 309 cases, and cN2 in 44 cases. The pathological stage distributions were ypT0-2 in 385 patients, ypT3-4 in 187 patients, ypN0 99 cases, ypN1 in 99 cases, ypN2 in 108 cases, and ypN3 in 129 cases.

### Results

With a median follow-up time of 61 months. The 5 year overall survival (5y-OS), 5 year locoregional failure free survival (5y-LRFS), 5 year distant metastasis free survival (5y-DMFS) were 74.8%, 84.1%, and 71.4%, respectively. The median number of dissected LNs is 22, and median positive LNs is 4. In multivariate analysis, negative LN count, estrogen receptor status, pathological T and N stage were independently prognostic factors associated with 5y-LRFS. A critical relationship was observed between negative LNs and 5y-LRFS, with a HR of 0.948 (95% CI: 0.917-0.981),  $p=0.002$ . Patients with negative LN counts more than 10 showed significantly superior 5y-LRFS than those with negative LN count no more than 10 (5y-LRFS were 90.6% in >10 negative LNs vs. 64.8% in  $\leq 10$  negative LNs,  $p=0.000$ ). Interestingly, similar survival trends were showed in patients with N-positive diseases (5y-LRFS were 87.4% in >10 negative LNs vs. 64.0% in  $\leq 10$  negative LNs,  $p=0.000$ ), but not in the N0 disease (5y-LRFS were 96.9% in >10 negative LNs vs. 100% in  $\leq 10$  negative LNs,  $p=0.724$ ). And more importantly, postmastectomy radiotherapy seems to only improved 5y-LRFS in patients with  $\leq 10$  negative LNs (5y-LRFS were 69.0% vs. 27.6% with or without PMRT,  $p=0.002$ ), but not patients with >10 negative LNs (5y-LRFS were 88.4% vs. 85.1% with or without PMRT,  $p=0.257$ ).

### Conclusion

This is the first study to confirm the relationship between negative lymph node count and prognosis of breast cancer in the setting of NAC. More negative lymph nodes imply longer survival, which may help to predict prognosis and make treatment recommendation.

### EP-1274 neoplastic brachial plexopathy in breast cancer survivors: diagnosis traps, RT-VMAT faisibility

S. Delanian<sup>1</sup>, P. Ding<sup>2</sup>, H. Huet de Froberville<sup>2</sup>, C. Boguszewski<sup>3</sup>, P. Pradat<sup>4</sup>

<sup>1</sup>Hopital Saint-Louis- APHP, Oncologie-Radiotherapie-Radiopathologie, Paris, France ; <sup>2</sup>Centre Clinique Porte de Saint-Cloud- Hôpital Americain de Paris, Radiophysique, Boulogne, France ; <sup>3</sup>Centre Clinique Porte de Saint-Cloud- Hôpital Americain de Paris, Radiotherapie, Boulogne, France ; <sup>4</sup>Hopital Pitié-

Salpêtrière- APHP, Oncologie-Radiotherapie-Radiopathologie, Paris, France

### Purpose or Objective

Neoplastic brachial plexopathy (NBP) is a carcinomatous peripheral neuropathy in the axillary-supraclavicular region, often misdiagnosed as a radiation-induced (RI) complication, even when node areas have not been irradiated. The literature is old and limited: series of 5 to 78 cases have been reported in 11 articles over 40 years (1968-2009), while histology, imaging and RT have undergone deep mutations.

### Material and Methods

330 long-survivor patients treated for breast cancer have been referred to Hôpital Saint-Louis (2004 -17), for brachial RI plexopathy round the inclusion period of our therapeutic phase III trial (NCT01291433): 12 % of the patients were finally diagnosed with a neoplastic origin. NBP was established after expertise based on the following arguments: delayed then progressive development of arm lymphedema (75%), intense arm pain, quite fast progressing motor symptoms, ptosis, slight inflammatory signs on MRI and PET-scan imaging (re-interpretation), and axillary volume exclusion of the primary RT volume (dosimetric check).

Fortywomen (65  $\pm$  9y), treated 14  $\pm$  7 years before by surgery (5 N0, 14 N-, 14  $\leq 2N+$ , 7  $\geq 6N+$ ) then radiotherapy (1974-2013), were diagnosed with NBP after 1 to 4 years of neurological evolution.

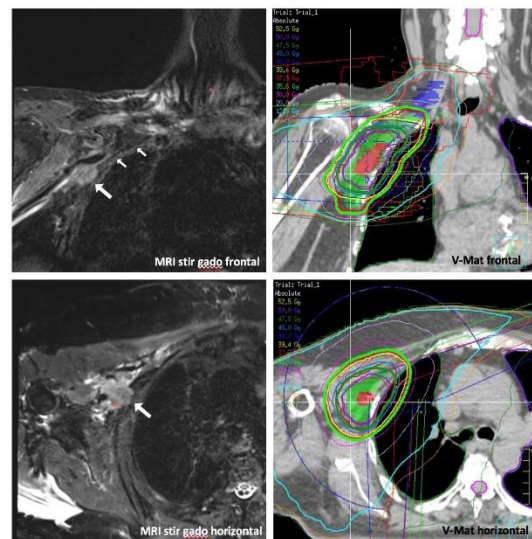
Patients had salvage chemotherapy-hormonotherapy, and for some of them, plexus RT by conformal then V-mat technique.

### Results

According to previous breast RT, 3 NBP prognostic groups were analyzed: 16 [R<sub>0</sub>] (40%) without any node RT, 11 [R<sub>1</sub>] supraclavicular RT only (without axillar), and 13 [R<sub>2</sub>] axillary and supraclavicular RT.

MRI and PET-scan were mis-interpreted either as very slow kinetic tumor (hormono-dependant) or inflammatory NBP. A triangular axillary fixation in the border of previous supraclavicular RT beam, SUV 2-5, was pathognomonic of R<sub>1</sub>NBP group (figure). The time BC-NBP was R<sub>1</sub>14 $\pm$ 7; R<sub>2</sub>12 $\pm$ 6; R<sub>3</sub>16 $\pm$ 7 years.

Plexus RT was done using a classical fractionation in 10 R<sub>0</sub>patients /16; or a salvage fractionation by Vokes protocol (every two weeks), because partial irradiated volume, in 3 R<sub>1</sub>patients/11 (figure); and not in R<sub>2</sub> patients. Radiotherapy allowed controlling pain and reducing motor signs of NBP.



### Conclusion

We describe here one of the largest published series of NBP patients. Diagnosis is often difficult and delayed but necessary, to possibly treat them: chemotherapy in irradiated R<sub>2</sub> patients; usual RT in never irradiated R<sub>0</sub> patients. Salvage plexus RT in R<sub>1</sub> patients was possible. RT was better performed by Vmat technique helping dose/volume homogeneity and sustainable efficiency. Best volume and dose (50Gy) have to be defined for these hyperalgesic and paretic patients.

#### EP-1275 Hypofractionated whole breast irradiation and IOERT in breast cancer: Toxicity and cosmetic outcome

G. Fastner<sup>1</sup>, R. Reitsamer<sup>2</sup>, K. Peter<sup>1</sup>, Z. Ingrid<sup>1</sup>, C. Fussl<sup>1</sup>, F. Zehentmayr<sup>1</sup>, B. Grambozov<sup>1</sup>, W. Hitzl<sup>3</sup>, D. Murawa<sup>4</sup>, A. Karzewska<sup>5</sup>, P. Milecki<sup>5</sup>, B. Urbański<sup>5</sup>, E. Hager<sup>6</sup>, J. Reiland<sup>7</sup>, A. Ciabattoni<sup>8</sup>, C. Matuschek<sup>9</sup>, W. Budach<sup>9</sup>, R. Brimmer<sup>10</sup>, C. Schumacher<sup>11</sup>, A. Ricke<sup>11</sup>, U. Ricardi<sup>12</sup>, V. Fusco<sup>13</sup>, F. Sedlmayer<sup>1</sup>

<sup>1</sup>Paracelsus Medical University- University Hospital Salzburg- Landeskrankenhaus, Radiotherapy and Radio-Oncology, Salzburg, Austria ; <sup>2</sup>Paracelsus Medical University- University Hospital Salzburg- Landeskrankenhaus, Gynecology, Salzburg, Austria ; <sup>3</sup>Paracelsus Medical University, Research Office - Biostatistics, Salzburg, Austria ; <sup>4</sup>Wielkopolska Cancer Centre, Oncological Surgery Clinic, Poznań, Poland ; <sup>5</sup>Wielkopolska Cancer Centre, Oncological Radiotherapy Clinic, Poznań, Poland ; <sup>6</sup>Landeskrankenhaus Klagenfurt, Radiotherapy/Radiooncology, Klagenfurt, Austria ; <sup>7</sup>Avera Regional Medical Center, Institut Breast Surgery, Sioux Falls, USA ; <sup>8</sup>San Filippo Neri Hospital, Radiotherapy, Rome, Italy ; <sup>9</sup>Heinrich Heine University, Medical Faculty- Dep. of Radiation Oncology, Düsseldorf, Germany ; <sup>10</sup>St. Lukes Hospital, General Surgery, Cedar Rapids, USA ; <sup>11</sup>St.-Elisabeth Hospital, Breast center/Dep. of Senology, Cologne-Hohenlind, Germany ; <sup>12</sup>University of Turin, Oncology- Radiation Oncology, Turin, Italy ; <sup>13</sup>IRCCS CROB Reference Cancer Center Basilicata, Radiation Oncology, Rionero in Vulture, Italy

#### Purpose or Objective

To prospectively assess the role of an intraoperative electron tumor-boost (IOERT) in combination with hypofractionated whole breast irradiation (HF-WBI) after breast conserving surgery (BCS) in terms of in breast recurrence (IBR), treatment tolerance and cosmetic outcome.

#### Material and Methods

Patient recruitment within the study protocol (NCT01343459) started in 2011. Treatment consisted of BCS, IOERT of 11.1 Gy and HF-WBI up to total dosages of 40.5 Gy in 15 fractions. Acute toxicity, late reactions and cosmesis were evaluated by CTC-scoring (Vers. 2), LENT-SOMA criteria and by a 5-point-Scoring System (van Limbergen et al), respectively. 5-year IBR will be analyzed in 3 different age groups (35-40y, 41-50y, >50y) and tested against predefined benchmarks by the sequential probability ratio test (SPRT).

#### Results

Of 627 eligible patients 583 were evaluated. For acute effects CTC-score 0-1 was observed in 91-92% at the end of HF-WBI and 4 weeks later. Late toxicity Grading 0-1 (mean values) by LENT-SOMA criterions occurred in 92.7% (89.6-97.3) at 4/5 months up to 96.5% (91-100) at 6 years after HF-WBI. Baseline cosmesis was first assessed after wound healing prior to HF-WBI. Of 583 patients cosmesis was scored as satisfactory (excellent/good) in 84% by subjective (patient) and in 67% by objective (doctor) assessment with no impairment thereafter. After a median follow-up of 45 months (range 0 - 74), no in-breast recurrence was noted.

#### Conclusion

Acute and late treatment tolerance of a combined IOERT/HF-WBI regimen is excellent in mid-term

assessment. With regard to postoperative appearance, early cosmetic results are not impaired

#### EP-1276 A Comparison of Breast Cosmetic Evaluation Methods in Hypofractionated Whole Breast Irradiation

M. Nozaki<sup>1</sup>, Y. Kagami<sup>2</sup>, M. Takahashi<sup>3</sup>, R. Machida<sup>4</sup>, T. Shibata<sup>5</sup>, Y. Ito<sup>2</sup>, Y. Nishimura<sup>6</sup>, Y. Kawaguchi<sup>7</sup>, Y. Saito<sup>8</sup>, Y. Nagata<sup>9</sup>, Y. Matsumoto<sup>10</sup>, T. Akimoto<sup>11</sup>, M. Hoiraoka<sup>12</sup>

<sup>1</sup>Dokkyo Medical University Saitama Medical Center, Radiology, Koshigaya, Japan ; <sup>2</sup>Showa University School of Medicine, Department of Radiation Oncology, Shinagawa, Japan ; <sup>3</sup>Kiryu Kosei General Hospital, Department of Radiology, Kiryu, Japan ; <sup>4</sup>National Cancer Center Hospital, Japan Clinical Oncology Group Data Center, Chuo, Japan ; <sup>5</sup>National Cancer Center Hospital, Japan Clinical Oncology Group Data Center, Chuo, Japan ; <sup>6</sup>Kindai University Faculty of Medicine, Department of Radiation Oncology, Osaka-sayama, Japan ; <sup>7</sup>International Cancer Institute, Department of Radiation Oncology, Osaka, Japan ; <sup>8</sup>Saitama Cancer Center, Division of Radiation Oncology, Kitaadachi, Japan ; <sup>9</sup>Hiroshima University Graduate School of Biomedical and Health Sciences, Department of Radiation Oncology, Hiroshima, Japan ; <sup>10</sup>Niigata Cancer Center Hospital, Department of Radiation Oncology, Niigata, Japan ; <sup>11</sup>National Cancer Center Hospital East, Division of Radiation Oncology and Particle Therapy, Kashiwa, Japan ; <sup>12</sup>Kyoto University Graduate School of Medicine, Department of Radiation Oncology and Image-applied Therapy, Kyoto, Japan

#### Purpose or Objective

A favorable cosmetic outcome has been defined as an important endpoint in breast-conserving therapy. Various evaluation methods have been studied, but the optimal evaluation method has yet to be identified. The present ancillary analysis of JCOG0906 focused on comparing three methods for evaluating breast cosmetic outcomes after hypofractionated whole breast irradiation (HF-WBI).

#### Material and Methods

Between February 2010 and August 2012, 312 Japanese women were registered in a Japanese HF-WBI trial, JCOG0906 (UMIN000003200), and 306 received HF-WBI. Of them, 292 were evaluated for breast cosmetic outcomes before and three years after HF-WBI using three evaluation methods: an institutional evaluation (IE), a panel evaluation (PE), and a computer-program evaluation (CE), on a scale of 4-points (excellent/good/fair/poor). IEs were performed using a check sheet by individual institutional radiation oncologists who directly saw each patient and took a frontal-breast photograph with all personal information masked. PEs and CEs were performed using the 584 photographs of the 292 patients. PEs were assessed by consent of two experts twice, with a three-year interval between the first and second PEs. CE was performed using BCCT. core software individually by two radiation oncologists (A and B). The intra-observer variability of PE, the inter-observer variability of CE, and the degree of agreement between IE and PE or CE were calculated using the kappa (k) and weighted kappa (wk) statistics. The degree of agreement was considered to be poor for kappa values < 0.21, fair for 0.21-0.40, moderate for 0.41-0.60, substantial for 0.61-0.80, and excellent for 0.81-1.00.

#### Results

The agreement between the first and second PEs using 292 photographs before HF-WBI was moderate (k=0.5974, wk=0.6405), and that using 292 photographs three years after HF-WBI was similar (k=0.5303, wk=0.6032). The agreement between A and B on CE using photographs before HF-WBI was substantial (k=0.7210, wk=0.7569), and that using photographs after HF-WBI was similar (k=0.7174, wk=0.7656). The agreement between IE and the second PE using photographs before HF-WBI was fair (k=0.3002, wk=0.3865), and that using photographs after

HF-WBI was similar ( $k=0.3465$ ,  $wk=0.4514$ ). The agreement between IE and CE of A using photographs before HF-WBI was poor ( $k=0.1306$ ,  $wk=0.2158$ ), and that using photographs after HF-WBI was similar ( $k=0.1180$ ,  $wk=0.2240$ ).

#### Conclusion

Although the agreement between IE and CE was poor both before and after HF-WBI, the inter-observer variability of CE was smaller than the intra-observer variability of PE. CE using BCCT. core was considered a reproducible evaluation method when cosmetic changes of breasts that had received HF-WBI were evaluated comparing the photographic appearances before and after treatment.

#### EP-1277 Locoregionally recurrent breast cancer treated with postoperative or salvage radiotherapy

B.H. Kim<sup>1</sup>, K.H. Shin<sup>2</sup>, E.K. Chie<sup>2</sup>, J.H. Kim<sup>2</sup>, K. Kim<sup>3</sup>, S. Kim<sup>1</sup>

<sup>1</sup>SMG-Seoul National University Boramae Medical Center, Radiation Oncology, Seoul, Korea Republic of ; <sup>2</sup>Seoul National University College of Medicine, Radiation Oncology, Seoul, Korea Republic of ; <sup>3</sup>Ewha Womans University College of Medicine, Radiation Oncology, Seoul, Korea Republic of

#### Purpose or Objective

The purpose of this study was to investigate the treatment patterns and outcomes of patients receiving radiotherapy (RT) for isolated locoregional recurrence (ILRR) of breast cancer.

#### Material and Methods

We retrospectively analyzed the medical records of 125 patients who were diagnosed with ILRR after initial curative resection (mastectomy or breast-conserving surgery) and underwent RT from 2006 to 2016 at two institutions. The median time from initial operation to ILRR was 38 months. After ILRR, 96 (77%) patients underwent curative resection followed by postoperative RT and 29 (23%) underwent salvage RT. Ninety-eight (78%) patients received systemic chemotherapy. Median RT dose was 51.0 Gy (range: 18.0-70.4).

#### Results

The sites of recurrences were classified as follows: local in 42 (34%) patients, regional lymph nodes in 64 (51%), and combined local and regional sites in 19 (15%). Twenty-eight (22%) patients had received RT for primary breast cancer, but only 10 (8%) underwent re-irradiation. The patterns of treatment were very heterogeneous according to the patient and disease presenting features, and partial breast irradiation or hyperthermia was not performed. Overall, 5-year locoregional progression-free survival, distant metastasis-free survival, progression-free survival (PFS), and post-recurrence overall survival (OS) were 78.4%, 59.0%, 55.0%, and 69.7%, respectively. On multivariate analysis, initial pN0-1 stage, disease-free interval ( $\geq 36$  months), and curative resection for recurrent disease were found to be independently associated with better PFS and OS. When we divided patients into four groups based on the number of prognostic factors, pairwise significant differences in PFS and OS were found. Grade 3 dermatitis and grade 2 lymphedema were observed in 2 (1.6%) and 6 (4.8%) patients, respectively.

#### Conclusion

Most patients with ILRR of breast cancer referred for RT were radiation-naive and re-irradiation was not actively carried out. RT following curative resection could achieve favorable PFS in these potentially salvageable patients without causing severe toxicity. Initial pN stage, disease-free interval, and curative resection for recurrent disease were important prognosticators.

#### EP-1278 Effect of heart's dose reduction by IMRT in postoperative radiotherapy for left-sided breast cancer

K. Ono<sup>1</sup>, T. Taniguchi<sup>1</sup>, K. Shiraki<sup>1</sup>, Y. Itou<sup>1</sup>, O. Tanaka<sup>1</sup>  
<sup>1</sup>Asahi University Hospital, Department of Radiation Oncology, Gifu, Japan

#### Purpose or Objective

To reduce the Heart's dose for patients undergoing postoperative radiotherapy for left-sided breast cancer is critical for the heart disorder. Deep inspiration breath hold and intensity modulated radiation therapy (IMRT) are reported as methods for reducing the cardiac dose, especially for the left anterior descending artery (LAD). We compared the radiation methods of various degrees and examined the details of the difference between static IMRT and volumetric modulated arc therapy (VMAT).

#### Material and Methods

Overall, 20 patients underwent postoperative radiotherapy for left-sided breast cancer from July 2016 to June 2018 at our institute. We conducted the following five treatment plans: 2 field-static IMRT (2 F-S-IMRT), 4 field-static IMRT (4 F-S-IMRT), 40 degrees dual partial arc VMAT (40d VMAT), 80 degrees dual partial arc VMAT (80d VMAT), and 210 degrees partial VMAT (210p VMAT). The prescription dose was 50 Gy/25 fractions for the planning target volume (PTV) in all treatment plans. The dosimetric calculation was optimized to achieve a coverage of 50 Gy prescribed for 95% of PTV by inverse treatment planning using the Monte Carlo algorithm. Each of the five treatment regimens was analyzed by the dose volume histogram (DVH), and the multiple comparison test was performed. The evaluation items were compared on Heart's V10 (coverage of 10% of the volume of the heart), LAD's V10, PTV's D95, and homogeneity index (HI).

#### Results

The coverage of 40d VMAT for the prescribed dose of PTV's D95 was significantly lower than that of the other treatment plans. The D95 of the breast of PTV was approximately 46 Gy. HI was also high, and uniformity within PTV was decreased. For the other treatment plans, D95 showed high PTV coverage, i.e., 48 Gy or higher. 4F-S-IMRT became the best dose distribution (D95 = 49.2 Gy, HI = 1.08 and PTV). As for the dose of Heart and LAD, 2 F-S-IMRT, 40 dV MAT, 80 dV MAT was highly effective in reducing the dose. As for the OAR dose, 2F-S-IMRT was the highest in a reduction effect for the Heart and LAD (the value was V10 = 9.3% of the Heart, V10 = 45.3% of LAD). Table Dose comparison of the PTV, Heart and LAD in the Five plans.

Structure	Dose parameter	2F-S-IMRT	4F-S-IMRT	40dVMAT	80dVMAT	210pVMAT
PTV	D95 (Gy)	48.0 ± 0.9	49.2 ± 0.6	46 ± 1.3	48.3 ± 0.7	48.5 ± 0.6
	HI	1.10 ± 0.02	1.08 ± 0.01	1.15 ± 0.03	1.10 ± 0.02	1.09 ± 0.01
Heart	V10 (%)	9.3 ± 6.1	15.0 ± 6.8	9.6 ± 6.7	10.0 ± 6.7	15.7 ± 10.3
	V10 (%)	45.3 ± 10.7	52.5 ± 14.2	47.3 ± 14.2	46.0 ± 17.7	54.2 ± 16.4

#### Conclusion

2 F-S-IMRT and 40d VMAT had advantage for lowering the dose of OAR, because the number of fields and the irradiation range angle are small. 4F-S-IMRT and 80d VMAT increase an X-ray beam from multiple directions, which ensured not only sufficient coverage of PTV but also reduced the heart's dose. In these methods, dispersion of D95 in PTV may be reduced. The shape of the mammary gland differs in each patient; these methods ensure the possibility of administering optimum dose prescription and thereby have clinical applications.

#### EP-1279 M1 neck lymph node positive without distant metastasis in breast cancer: comparison with stage IIIC

J.S. Klim<sup>1</sup>, K. Kim<sup>2</sup>, K.H. Shin<sup>1</sup>, J.H. Kim<sup>1</sup>, S.S. Kim<sup>3</sup>, T.H. Kim<sup>4</sup>, Y.B. Kim<sup>5</sup>, W. Park<sup>6</sup>, J.H. Kim<sup>7</sup>  
<sup>1</sup>Seoul National University Hospital, Department of Radiation Oncology, Seoul, Korea Republic of ; <sup>2</sup>Ewha Womans University College of Medicine, Department of Radiation Oncology, Seoul, Korea Republic of ; <sup>3</sup>Asan Medical Center, Department of Radiation Oncology, Seoul, Korea Republic of ; <sup>4</sup>National Cancer Center,

Center for Proton Therapy, Goyang, Korea Republic of ; <sup>5</sup>Yonsei Cancer Center, Department of Radiation Oncology, Seoul, Korea Republic of ; <sup>6</sup>Samsung Medical Center, Department of Radiation Oncology, Seoul, Korea Republic of ; <sup>7</sup>Dongsan Medical Center, Department of Radiation Oncology, Daegu, Korea Republic of

#### Purpose or Objective

To analyze the treatment outcomes of ipsilateral cervical lymph node (LN)-positive breast cancer in the absence of other distant metastases, and to compare these outcomes with those of supraclavicular LN (SCL)-positive breast cancer.

#### Material and Methods

Seventy-nine breast cancer patients with involvement of ipsilateral cervical LN above the supraclavicular fossa (cervical LN(+) group) were treated with curative intent from 2000 to 2014 at 7 institutions. Most patients (n=75) received systemic chemotherapy (neoadjuvant and/or adjuvant) and breast surgery followed by locoregional radiotherapy. Outcomes of the cervical LN(+) group were evaluated and compared with those of 183 patients with SCL involvement (SCL(+) group) from the KROG 16-14 study.

#### Results

Median follow-up duration was 51.2 months (range, 5.9-138.0). Twenty-two regional failures were found in 15 patients: axillary LN in 8, SCL in 6, internal mammary LN in 3, involved cervical LN in 4, and uninvolved cervical LN in 1. The 5-year overall survival (OS), disease-free survival (DFS), locoregional relapse-free survival (LRRFS), and distant metastasis-free survival (DMFS) rates were 64.9%, 44.8%, 68.9%, and 55.2%, respectively. Neck dissection failed to improve LRRFS and DFS (p=0.901 and 0.366, respectively). After propensity score matching, survival outcomes of the cervical LN(+) and SCL(+) groups were not statistically different (5-year OS, 62.6% vs. 72.2%, p=0.560; DFS, 45.7% vs. 52.2%, p=0.620; LRRFS, 64.7% vs. 78.1%, p=0.110; DMFS, 57.4% vs. 53.2%, p=0.590, respectively).

#### Conclusion

Based on comparable clinical outcomes, breast cancer patients with ipsilateral cervical LN metastases without other distant metastases might benefit from aggressive locoregional and systemic treatments as those with N3c disease.

#### EP-1280 Identification of gene profiles associated to increased risk of acute toxicity in breast cancer

M.C. De Santis<sup>1</sup>, I. Salido<sup>2</sup>, P. Gandellini<sup>3</sup>, A. Cicchetti<sup>4</sup>, T. Rancati<sup>4</sup>, M. Dispinzieri<sup>5</sup>, M. Carrara<sup>6</sup>, T. Giandini<sup>6</sup>, E. Pignoli<sup>6</sup>, E. La Rocca<sup>5</sup>, N. Zaffaroni<sup>2</sup>, R. Valdagni<sup>7</sup>, L. Lozza<sup>8</sup>

<sup>1</sup>Fondazione IRCCS Istituto Nazionale dei Tumori, Radiotherapy Department, Milan, Italy ; <sup>2</sup>Fondazione IRCCS Istituto Nazionale dei Tumori, Molecular Pharmacology, Milan, Italy ; <sup>3</sup>Fondazione IRCCS Istituto Nazionale dei Tumori, Molecular Pharmacology-, Milan, Italy ; <sup>4</sup>Fondazione IRCCS Istituto Nazionale dei Tumori, Prostate Cancer Program, Milan, Italy ; <sup>5</sup>Fondazione IRCCS Istituto Nazionale dei Tumori- Milan University, Radiotherapy Unit 1- Oncology and Hemato-Oncology University, Milan, Italy ; <sup>6</sup>Fondazione IRCCS Istituto Nazionale dei Tumori, Medical Physics, Milan, Italy ; <sup>7</sup>Milan University- Fondazione I.R.C.C.S Istituto nazionale Tumori, Radiotherapy Unit 1- Prostate Cancer Program-Oncology and Hemato-Oncology University, Milan, Italy ; <sup>8</sup>Fondazione IRCCS Istituto Nazionale dei Tumori, Radiotherapy Unit 1, Milan, Italy

#### Purpose or Objective

To identify gene expression profiles (GEP) associated to increased risk of grade 2+ acute skin erythema after adjuvant breast cancer (BCa) radiotherapy (RT).

#### Material and Methods

BCa pts treated with 3DCRT after breast conserving surgery were considered: 50Gy (2Gy/fr) whole breast photon RT followed in some cases by 10 or 16Gy photon or electron boost to the tumour bed. Acute skin erythema (AE) was assessed using RTOG scoring system before RT and every 5 fractions. Grade 2+ AE before boost was considered as the primary endpoint. Relevant clinical risk factors were prospectively recorded, dosimetric features were extracted from skin dose-volume histogram, with skin defined as the difference between the body contour and a 5mm inner isotropic contour from the body. Peripheral blood was obtained, RNA extracted from mononuclear lymphocytes (after in vitro expansion) and GEP determined using Illumina HumanHT-12 v4 Expression BeadChip (=47000 probes, =37000 genes). Unsupervised clustering was used to reduce the dimensionality of data (partition around medoids). Dosimetric, clinical and genetic variables were included into logistic regression.

#### Results

147 pts were available, 35/147 (24%) pts with grade2+ AE before boost, 82/147 pts had GEP information. Unsupervised clustering selected 208 genes identifying 3 clusters of pts: 38% toxicity in cluster A, 19% and 14% in clusters B and C, respectively (OR=5 for A vs "B OR C", p=0.01). Cluster A was mainly characterized by underexpression of genes involved in immunoregulation, inflammatory processes, antioxidant activity, cell cycle progression and differentiation. Multivariable regression resulted in a 3 variable clinical/dosimetric/genetic model including dose to 20cc of skin (p=0.02, OR=1.4 for 1Gy increase), skin phototype (p=0.05, OR=1.9 1+2 vs >2), GEP cluster (p=0.01, OR=5 A vs B+C). Inclusion of GEP clustering improved likelihood (-86.6 vs -78.9, p=0.05), calibration slope (0.86 and R<sup>2</sup>=0.01 vs 0.93 and AUC (0.62 vs 0.83, p=0.01). The figure shows details on study population, GEP clustering and predictive model curves.

#### Conclusion

Gene expression profiling resulted in the identification of a signature of enhanced radiosensitivity for acute toxicity after BCa RT. This signature was included in a predictive model leading to significant improvement in calibration, likelihood and discrimination.

#### EP-1281 New aspects regarding the treatment of multicentric compared to unifocal breast cancer

C. Matuschek<sup>1</sup>, B. Tamaskovics<sup>1</sup>, W. Budach<sup>1</sup>, J. Haussmann<sup>1</sup>, E. Boelke<sup>1</sup>, F. Djiepmo<sup>1</sup>, T. Fehm<sup>2</sup>, E. Ruckhaeberle<sup>2</sup>, M. Fleisch<sup>2</sup>, S. Roth<sup>1</sup>

<sup>1</sup>University Hospital Düsseldorf, Radiation Oncology, Düsseldorf, Germany ; <sup>2</sup>University Hospital Düsseldorf, Gynecology, Düsseldorf, Germany

#### Purpose or Objective

This study compares retrospectively from 1991-1998 the Overall survival (OS), five year disease related survival (DRS), relapse free and overall survival (RFS) in multicentric breast cancer compared to unifocal breast cancer.

#### Material and Methods

From our cohort including n=482 patients n= 85 (17,6%) presented with multicentric and 397 with unicentric breast cancer. 45% of the 85 multicentric patients and 34% of the 397 unicentric patients were ≤50 years. N=254 patients received breast conserving therapy and n=228 underwent mastectomy. 392 patients received chemotherapy and in n=90 patients no chemotherapy was administered. In the multicentric group n=74 received chemotherapy and n=11 not. N=383 patients were irradiated (n=56 in the multicentric group) and n=99 patients were not irradiated (n=29 in the multicentric group).

#### Results

The five-year OS in the multicentric group was: 78.5%, the RFS was: 75.1%, DRS: 91.8%, compared to the unicentric group: OS: 91.8%, RFS: 91.1%, DRS: 96.1%. In the 85

patient group with multicentric tumors the five year OS was significantly worse than in the 397 for patients with unicentric tumors. P=0,01, HR 3,34. The RFS and DFS were also significantly worse (p=0.000, p=0.012)

#### Conclusion

In our cohort OS, RFS and DFS were statistically significant better in patients with unifocal breast cancer than in multicentric breast cancer. The only significant parameter in the multivariate analysis was the ER-Status. Regarding this, more aggressive treatment (chemotherapy, targeted therapy and radiotherapy) may be necessary.

#### EP-1282 Postmastectomy radiation therapy using VMAT for breast cancer patients with expander reconstructions

F. De Rose<sup>1</sup>, A. Fogliata<sup>1</sup>, D. Franceschini<sup>1</sup>, C. Iftode<sup>1</sup>, S. Cozzi<sup>1</sup>, A. Stravato<sup>1</sup>, G. Masci<sup>2</sup>, R. Torrissi<sup>2</sup>, A. Testori<sup>3</sup>, C. Tinterri<sup>3</sup>, A.V.E. Lisa<sup>4</sup>, A. Veronesi<sup>4</sup>, S. Giannasi<sup>4</sup>, M. Klinger<sup>4</sup>, M. Scorsetti<sup>1</sup>

<sup>1</sup>Humanitas Research Hospital, Radiotherapy and Radiosurgery, Rozzano Milan, Italy ; <sup>2</sup>Humanitas Research Hospital, Medical Oncology, Rozzano Milan, Italy ; <sup>3</sup>Humanitas Research Hospital, Breast Surgery, Rozzano Milan, Italy ; <sup>4</sup>Humanitas Research Hospital, Plastic Surgery, Rozzano Milan, Italy

#### Purpose or Objective

The use of post-mastectomy radiotherapy (PMRT) following immediate breast reconstruction has increased over the past decade, and this integration is becoming crucial in the management of breast cancer patients. We aimed to retrospectively evaluate the complication rates of PMRT to immediate tissue-expander-based reconstructions and the improvement of radiation delivery using VMAT technique.

#### Material and Methods

We retrospectively reviewed clinical data of patients who underwent immediate expander breast reconstruction and received PMRT. All patients underwent VMAT technique to irradiate the reconstructed breast and supraclavicular region. The total dose was 50 Gy delivered in 25 fractions over 5 weeks. Neoadjuvant or adjuvant systemic therapy was administered in all patients. Protective lipofilling was routinely performed at the time of second-stage reconstruction.

#### Results

Between December 2014 and June 2017, PMRT was delivered to 46 consecutive patients with expander reconstruction. Median age was 49 years (range 36-73). Median follow-up was 27.7 months (range 10.8-42.6 months). Only two patients (4.6%) experienced reconstruction failure, in one case due to expander rupture and in the other one due to infection, following the first and the second-stage reconstruction, respectively. In most cases expanders were completely inflated before PMRT (79%). Median expander volume before PMRT was 450 cm<sup>3</sup> (range 140-690 cm<sup>3</sup>). The amount of expander inflation did not significantly affect dosimetry, except for skin dose, with a surface receiving more than 30 Gy of 36.6±0.9 cm<sup>2</sup> and 47.0±2.5 cm<sup>2</sup> for a volume expander below or above the median volume of 450 cm<sup>3</sup>, respectively. However, this variable was not a predictor for complications. Disease progression (local or distant) was recorded in 10.8% of patients.

#### Conclusion

Postmastectomy radiation therapy using VMAT technique for breast cancer patients with expander reconstructions is associated with a very low complication rate after both first and second-stage reconstruction. The expander volume before PMRT does not significantly compromise target coverage or increase dose to organs at risk.

#### EP-1283 Three-dimensional versus four-dimensional dose calculation for breast IMRT

J. Chung<sup>1</sup>, M. Chun<sup>1</sup>, J.M. Park<sup>1</sup>, J. Kim<sup>1</sup>, K. Shin<sup>1</sup>  
<sup>1</sup>Seoul National University Hospital, Department of Radiation Oncology, Seoul, Korea Republic of

#### Purpose or Objective

This study was performed to analyze the effect of intra-fractional motion caused by free-breathing during breast IMRT by using newly generated "four-dimensional (4D) calculated plan".

#### Material and Methods

From 2017 to 2018, twenty patients diagnosed with left breast cancer from Seoul National University Hospital (SNUH) were enrolled. Every patient was eligible for regional lymph node irradiation including internal mammary node (IMN). After the 3D-CT for the initial plan was taken, 4D-CT comprised of 0% to 90% respiratory phases was taken for every patient. Target contouring was performed on 3D-CT and on all ten respiratory phases of 4D-CT. After IMRT planning on 3D-CT, the plan parameters were copied to all ten respiratory phases of 4D-CT sets. One-tenth of the total dose (43.2 Gy / 16 fx) was applied to each phase, and the dose distribution was re-calculated. Ten re-calculated doses were then summated into one to generate "4D-calculated plan" which was compared with "3D-original plan".

#### Results

Mean PTV volume was 1253.8 ± 575.6 ml. Mean IMN volume was 76.5 ± 16.6 ml. There were no significant differences in conformity and heterogeneity index between the 3D-original plan and the 4D-calculated plan. Mean heart dose was significantly lower in the 4D-calculated plan by 1.7 ± 0.8 Gy (p=0.041), whereas a mean dose of ipsilateral lung did not differ between two plans. When PTV was subdivided into the breast, supraclavicular lymph node (SCL), and IMN, both breast and SCL had no significant differences in mean dose between two plans. However, the mean IMN dose was significantly higher by 2.2 ± 1.8 Gy (p=0.023) in the 4D-calculated plan, compared to the 3D-original plan.

#### Conclusion

The interplay effect between the free-breathing motion and the multi-leaf collimator modulation may have caused a discrepancy in dose distribution, especially in heart and IMN. Therefore heart and IMN doses should be optimized when calculating the delivery dose for the free-breathing left breast IMRT.

#### EP-1284 Older age and comorbidity in breast cancer: is radiotherapy alone the new therapeutic frontier?

E. La Rocca<sup>1,2</sup>, M. Dispinzieri<sup>1,2</sup>, E. Meneghini<sup>3</sup>, A. Fiorentino<sup>4</sup>, F. Bonfantini<sup>5</sup>, S. Di Cosimo<sup>6</sup>, M. Gennaro<sup>7</sup>, V. Cosentino<sup>5</sup>, M. Sant<sup>3</sup>, E. Pignoli<sup>5</sup>, R. Valdagni<sup>1,8</sup>, L. Lozza<sup>2</sup>, M.C. De Santis<sup>2</sup>

<sup>1</sup>University of Milan, Department of Oncology and Hemato-Oncology, Milan, Italy ; <sup>2</sup>Fondazione IRCCS Istituto Nazionale dei Tumori, Radiotherapy Unit 1, Milan, Italy ; <sup>3</sup>Fondazione IRCCS Istituto Nazionale dei Tumori, Analytical Epidemiology and Health Impact Unit, Milan, Italy ; <sup>4</sup>Regional General Hospital "F. Miulli", Department of Radiation Oncology, Acquaviva delle Fonti Ba, Italy ; <sup>5</sup>Fondazione IRCCS Istituto Nazionale dei Tumori, Medical Physics Unit, Milan, Italy ; <sup>6</sup>Fondazione IRCCS Istituto Nazionale dei Tumori, Department of Applied Research and Technological Development DRAST, Milan, Italy ; <sup>7</sup>Fondazione IRCCS Istituto Nazionale dei Tumori, Breast Surgery Unit, Milan, Italy ; <sup>8</sup>Fondazione IRCCS Istituto Nazionale dei Tumori, Director- Radiation Oncology 1 and Prostate Cancer Program, Milan, Italy

#### Purpose or Objective

To assess the impact of age, comorbidities and hormonotherapy (HT) use in

elderly breast cancer (BC) patients (pts) treated with hypofractionated radiotherapy (Hypo-RT).

#### Material and Methods

From June 2009 to December 2017, 734 ER-positive BC pts (stage pT1-T2, pNx-1, M0 and age over 65 years) receiving Hypo-RT and followed until September 2018, were analyzed. Hypo-RT consisted of 42.4 Gy in 16 daily fractions (2.65 Gy per fraction), while a sequential boost was administered in cases of grade 3 tumor and close or positive margins. Baseline comorbidities included in the hypertension-augmented Charlson Comorbidity Index (hCCI) were retrospectively retrieved. Baseline pts and tumour characteristics were analyzed in relation to HT status (never/discontinued, ongoing) at last contact by chi-2 test. Five-year disease-free survival (DFS) and overall survival (OS) were estimated by Kaplan-Meier method. The log-rank test was used to compare groups. Adjusted hazard ratios (HRs) were estimated by Cox proportional hazards models. In survival analysis, HT use was treated as time-dependent variable. A subgroup analysis was performed on pts aged  $\geq 70$  with a pT1 luminal A BC.

#### Results

The comorbidity was present in about 70% of pts (median age: 74 years). HT has been prescribed in 653 (88.9%) out of 734 analyzed pts. Most of them assumed the prescribed HT and 51 pts (7.8%) discontinued the treatment. Current HT use was less frequent for pts aged  $\geq 80$  ( $p < 0.001$ ) and pts with high comorbidity burden ( $hCCI \geq 2$ ) ( $p = 0.001$ ). At the time of the analysis, 673 (91.7%) pts were still alive and 33 pts (4.5%) experienced a disease progression (local or nodal recurrences and metastases). At a median follow-up 46.8 months (range 4-115 months), the overall 5-year DFS was 86.8% (95% CI 83.2-89.6%) varying between 89.5% for current HT use and 76.6% for no/discontinued HT use (log-rank  $p < 0.001$ ). The prognostic effect of HT was confirmed for pts aged  $\geq 70$  with a pT1 luminal A BC: 5-year DFS were 91.3% and 79% for ongoing HT user and no/discontinued HT user, respectively (log-rank  $p < 0.018$ ). The hazard of disease progression was significantly increased for pts with  $hCCI \geq 2$  and with tumour size  $\geq 1$  cm and strongly decreased for currently ongoing HT users. HT did not impact on OS neither in the whole group nor in pts pT1 luminal A  $\geq 70$  years.

#### Conclusion

This study shows that disease progression was strongly increased for pts with  $hCCI \geq 2$  and tumor size  $> 1$  cm and decreased for HT users. In elderly pts, HT assumption did not show a benefit in terms of survival. Further studies with tailored treatment approaches (RT alone versus RT+HT versus HT alone) are needed on elderly women with BC.

#### EP-1285 Hypofractionated irradiation in elderly breast cancer patients: an observational study

E. La Rocca<sup>1,2</sup>, M. Dispinzieri<sup>1,2</sup>, E. Meneghini<sup>3</sup>, A. Fiorentino<sup>4</sup>, F. Bonfantini<sup>5</sup>, S. Di Cosimo<sup>6</sup>, M. Gennaro<sup>7</sup>, V. Cosentino<sup>5</sup>, M. Sant<sup>3</sup>, E. Pignoli<sup>5</sup>, R. Valdagni<sup>1,8</sup>, L. Lozza<sup>2</sup>, M.C. De Santis<sup>2</sup>

<sup>1</sup>University of Milan, Department of Oncology and Hemato-Oncology, Milan, Italy; <sup>2</sup>Fondazione IRCCS Istituto Nazionale dei Tumori, Radiotherapy Unit 1, Milan, Italy; <sup>3</sup>Fondazione IRCCS Istituto Nazionale dei Tumori, Analytical Epidemiology and Health Impact Unit, Milan, Italy; <sup>4</sup>Regional General Hospital "F. Miulli", Radiation Oncology Department, Acquaviva delle Fonti Ba, Italy; <sup>5</sup>Fondazione IRCCS Istituto Nazionale dei Tumori, Medical Physics Unit, Milan, Italy; <sup>6</sup>Fondazione IRCCS Istituto Nazionale dei Tumori, Department of Applied Research and Technological Development DRAST, Milan, Italy; <sup>7</sup>Fondazione IRCCS Istituto Nazionale dei Tumori, Breast Surgery Unit, Milan, Italy; <sup>8</sup>Fondazione IRCCS Istituto Nazionale dei Tumori, Director- Radiation Oncology 1 and Prostate Cancer Program, Milan, Italy

#### Purpose or Objective

To assess efficacy, acute and late toxicity of hypofractionated radiotherapy (Hypo-RT) and impact of age and comorbidities in elderly breast cancer (BC) patients (pts).

#### Material and Methods

From June 2009 to December 2017 we analyzed 808 pts receiving 42.4 Gy in 16 daily fractions (2.65 Gy per fraction). A boost was only administered in cases of grade 3 primary tumor and close or positive margins. Acute and late toxicity was prospectively assessed during and after hypo-RT, based on the RTOG scale. Baseline comorbidities included in the hypertension-augmented Charlson Comorbidity Index (hCCI) were retrospectively retrieved. Five-year disease-free survival (DFS) and overall survival (OS) were assessed by Kaplan-Meier method and log-rank test was used to compare groups of age and comorbidity. Hazard ratios (HRs) were estimated by Cox proportional hazards models adjusting for tumor size, lymph node status, molecular subtype, grading, chemotherapy. Odds ratios (ORs) and 95% confidence intervals (CIs) of acute and late toxicity by of age, comorbidity and boost administration were estimated by ordinal or multinomial logistic models.

#### Results

The median age was 74 years (range 65-91 years), and 76.1% of the pts were over 70 years old. The median follow-up was 46.8 months (range 4-115 months). At baseline, 70.4% of pts were affected by at least one comorbidity. Invasive ductal carcinoma was the most common histological type (81.2%), and the most common subtype was luminal A (46.5%). 21.5% of pts underwent chemotherapy with anthracycline and taxane. Hormonotherapy has been prescribed in 657 (81.4%) pts. At the latest follow-up date, 730 (90.4%) pts were still alive, 47 (5.8%) experienced disease progression (local or nodal recurrences, contralateral BC, metastases), 18 died of BC and 60 died of other causes.

Older age and baseline comorbidity burden were associated with worst prognosis. Five-year DFS was 92.6, 87.2, 83.5 and 71.3% for 65-69, 70-74, 75-79 and  $\geq 80$  years, respectively (log-rank  $p < 0.001$ ). Five-year OS for increasing age-class was 94.7, 93.0, 86.7 and 80.9% (log-rank  $p = 0.002$ ). Five-year DFS and OS were 91.9% and 94.3% for pts without comorbidity and 74.3% and 84.5% for pts with high comorbidity burden ( $hCCI \geq 2$ ) (DFS log-rank  $p < 0.001$ , OS log-rank  $p = 0.017$ ).

Elderly pts had significantly higher odds of increasing score in acute asthenia. Pts with  $hCCI \geq 2$  had significantly increased odds of late edema and late fibrosis. Boost administration was significantly related to increasing score of acute skin toxicity and late fibrosis and edema.

#### Conclusion

Hypo-RT in elderly BC pts aged  $\geq 65$  years is effective and well-tolerated. This study also shows that age and comorbidities negatively impact DFS and OS. Further studies focusing on a better selection of elderly BC pts based on genomic and biological features and with tailored treatment approaches are warranted.

#### EP-1286 StrataXRT is non inferior to Mepitel Film in preventing radiation induced moist desquamation

M.W.T. Chao<sup>1</sup>, S. Spencer<sup>1</sup>, C. Kai<sup>1</sup>, C. Baker<sup>2</sup>, S. Jassal<sup>3</sup>, M. Law<sup>4</sup>, M. Cheng<sup>4</sup>, N. Zantuck<sup>4</sup>, V. Yu<sup>4</sup>, D. Stoney<sup>4</sup>, S.W. Loh<sup>3</sup>, E. Bevington<sup>3</sup>, G. Chew<sup>3</sup>, A. Hyett<sup>3</sup>, M. Guerrieri<sup>1</sup>, H. Ho<sup>1</sup>, M. Ng<sup>1</sup>, J. Wasiak<sup>5</sup>, F. Foroudi<sup>5</sup>

<sup>1</sup>Ringwood Radiation Oncology Centre, Department of Radiotherapy, Ringwood, Australia; <sup>2</sup>St Vincents Hospital, Surgical Oncology, Melbourne, Australia; <sup>3</sup>Austin Hospital, Surgical Oncology, Melbourne, Australia; <sup>4</sup>Maroondah Hospital, Surgical Oncology, Melbourne, Australia; <sup>5</sup>Austin Hospital, Department of Radiation Oncology, Melbourne, Australia

### Purpose or Objective

A within patient non inferiority randomised study was conducted to test whether StrataXRT (SX) was as effective as Mepitel film (MF) in reducing the severity and duration of acute radiation dermatitis (ARD) in breast cancer patients receiving post mastectomy radiation therapy (PMRT).

### Material and Methods

Breast cancer patients undergoing chest wall with or without nodal irradiation radiation therapy were eligible. Lateral and medial halves of the skin areas to be irradiated were randomized to MF or SX. Bolus was applied to the half of the course of radiation therapy (50-50.4Gy). ARD was assessed using the Common Terminology Criteria for Adverse Events scale (version 4.03) weekly for 10 weeks. The outcome measures were occurrence of moist desquamation in each half of the irradiated area, time weighted average (TWA) grade of radiation dermatitis and worst grade of radiation dermatitis over 10 weeks.

### Results

A total of 44 breast cancer patients receiving post mastectomy radiation therapy were recruited between January 2017 and December 2017. Of those, 43% had pathologic stage II and 57% had pathologic stage III disease. Seventy three percent received tangent based inverse planned intensity modulated therapy and 27% received volumetric arc therapy. For the 40 assessable patients (minimum of 6 weekly observations), the maximum grade of ARD in the SX halves were CTCAE grade 1 (30%) and grade 2 (70%) compared with grade 0 (5%), grade 1 (42.5%), grade 2 (50%) and grade 3 (2.5%) in the MF halves. The rate of moist desquamation was 12.5% for SX versus 20% for MF ( $p=0.099$ ).

The TWA of radiation dermatitis in the chest wall halves up to 10 weeks is 0.16 higher for SX vs MF (95% CI: 0.09-0.23). The upper limit of the CI is  $<0.25$  (criterion for non-inferiority set in protocol), it is concluded that SX is not inferior to MF at the 95% level. Although the difference between SX vs MF is statistically significant ( $p=0.0001$ ), it was not clinically significant.

The worst grade of radiation dermatitis in the halves within 10 weeks is 0.15 higher for SX vs MF (95% CI: -0.02-0.32). The upper limit of the CI is  $<0.50$  (criterion for non-inferiority set in protocol), it is concluded that SX is not inferior to MF at the 95% level. The difference between SX vs MF is not statistically significant ( $p=0.075$ ).

### Conclusion

The occurrence of moist desquamation, TWA grade of ARD and the worst grade of ARD for StrataXRT was not inferior to MF.

### EP-1287 Preliminary results of anthocyanin supplementation in breast cancer RT: impact on skin side effects

M. Boccardi<sup>1</sup>, F. Bracone<sup>2</sup>, F. Deodato<sup>1</sup>, A. De Curtis<sup>2</sup>, G. Macchia<sup>1</sup>, S. Cilla<sup>3</sup>, A. Di Castelnuovo<sup>2</sup>, A. Ianiro<sup>3</sup>, C. Cerletti<sup>2</sup>, A.G. Morganti<sup>4</sup>, M.B. Donati<sup>2</sup>

<sup>1</sup>Fondazione di Ricerca e Cura "Giovanni Paolo II"-Università Cattolica del Sacro Cuore, Radiotherapy Unit, Campobasso, Italy ; <sup>2</sup>IRCCS Neuromed, Dipartimento di Epidemiologia e Prevenzione, Pozzilli, Italy ; <sup>3</sup>Fondazione di Ricerca e Cura "Giovanni Paolo II"-Università Cattolica del Sacro Cuore, Medical Physics Unit, Campobasso, Italy ; <sup>4</sup>Radiation Oncology Center, Department of Experimental- Diagnostic and Specialty Medicine DIMES- University of Bologna, Bologna, Italy

### Purpose or Objective

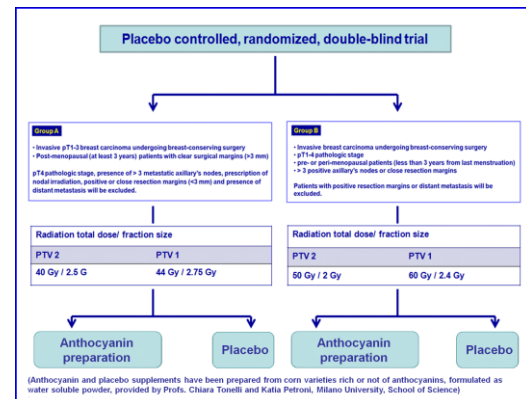
The role of anthocyanins has been studied in the prevention of radiotherapy (RT) side effects. In a prospective randomized study (Athena Project-FP7 European Union), we verified the impact of anthocyanin supplementation on acute and medium-term skin side effects of RT in breast cancer (BC) patients.

### Material and Methods

A double-blind randomized clinical trial with 2 parallel arms (A and B) was designed. BC patients were randomized to assume a preparation containing 125 mg anthocyanins (3 times a day) versus placebo. Supplementation started 1 week before and lasted till the end of RT. One group of patients (MARA3) received 44 Gy simultaneous integrated boost (SIB) over 16 fractions in 3 weeks by an hybrid IMRT class solution; the other group (MARA4) received 60 Gy SIB over 25 fractions in 5 weeks. Patients used a moisturizing cream (® Atonderma) during RT. Clinical evaluation was performed at the end of treatment and skin toxicity was graded according to RTOG score. Moreover, skin parameters, as elasticity (R0, R2 and R5 values), erythema (Mexa\_Er) and pigmentation (Mexa\_M), were measured in predefined areas of the irradiated breast and in the contra-lateral one through a specific device (Cutometer® dual MPA 580), before (T0), at the end (T1) and 1, 6 and 12 months after RT.

### Results

242 patients were eligible and 195 were randomized to groups A and B (Figure 1). Both clinical and cutometer evaluations failed to show differences in terms of skin toxicity (elasticity, erythema and pigmentation) between groups A and B. The elasticity parameters R0 ( $p=0.54$ ) and R2 ( $p=0.27$ ) similarly decreased from T0 in both arms, while Mexa\_M ( $P=0.74$ ) and Mexa\_Er ( $P=0.25$ ) similarly increased in both groups, suggesting no protective effect of anthocyanin supplementation. Neither RT protocol seemed to differently affect elasticity parameters. However, the increase in Mexa\_M and Mexa\_Er was greater in MARA4 (5 week RT) than in MARA3 (3 week RT) ( $p=0.0027$  and  $p=0.0087$ , respectively). Comparing irradiated and contra-lateral breast no differences were observed for R0 ( $p=0.48$ ) and Mexa\_M ( $p=0.14$ ) variations from T0 to T1 in groups A and B. On the contrary, decrease of R2 and increase of Mexa\_Er were observed only in irradiated but not in contra-lateral breast ( $p<0.0001$ ). Clinical toxicity RTOG data did not correlate with variations in parameters recorded by cutometer.



### Conclusion

Preliminary data failed to demonstrate that an anthocyanin supplementation can effectively protect BC patients from skin side effects of two different RT regimens.

### EP-1288 Dosimetric Comparison of Protons and Photons in Musculoskeletal Sparing During Breast Irradiation

A. Prescott<sup>1</sup>, J. Strauss<sup>1</sup>, E. Donnelly<sup>1</sup>, M. Gentile<sup>1</sup>, R. Patel<sup>1</sup>, D. Lipps<sup>2</sup>, S. Oza<sup>3</sup>

<sup>1</sup>Northwestern University, Radiation Oncology, Chicago, USA ; <sup>2</sup>University of Michigan, Kinesiology, Ann Arbor, USA ; <sup>3</sup>Memorial Sloan Kettering, Physical Medicine & Rehab, New York, USA

### Purpose or Objective

Radiotherapy (RT) to the breast has a functional impact on the upper extremity, especially when regional lymphatics are irradiated. This may be mediated in part through RT dose to the adjacent musculature. This study set out to compare the muscle doses deposited with protons vs. photons using 3D conformal RT.

### Material and Methods

Five consecutive patients diagnosed with node positive left-sided breast cancer were included. For a prior dosimetric study, plans were created with pencil beam scanning proton RT at free breathing and 3D conformal RT at DIBH. The plans were optimized for cardiac and pulmonary dose. For this study, the muscle volumes for eleven shoulder muscles anatomically located within or near the treatment field were contoured separately. The volume of each muscle receiving at least 30 Gy (V30 Gy) were calculated for each muscle and compared between treatment modalities using the two-tailed paired Student T test.

### Results

**Table 1: Muscle Dose**

	Photon (mean)	Proton (mean)	p value
Anterior Deltoid	0.6	0.0	0.1165
Infraspinatus	34.6	0.0	0.0251
Latissimus Dorsi	42.7	17.3	0.0406
Pectoralis Major	78.4	79.7	0.5688
Pectoralis Minor	99.9	93.2	0.0042
Posterior Deltoid	12.5	0.0	0.0182
Subscapularis	71.5	30.8	0.0191
Supraspinatus	82.2	0.0	0.0003
Teres Major	67.3	20.8	0.0118
Teres Minor	51.5	0.1	0.0204
Trapezius	28.6	0.0	0.0036

### Conclusion

Pencil beam scanning proton RT delivers less dose to most of the adjacent musculature as compared to 3D conformal RT during irradiation of the breast and draining lymphatics. The largest absolute differences are in the posterior shoulder muscles in the exit of the nodal field. The smallest differences in dose are noted in the pectoralis muscles which receive high dose in both plans. The reduction in muscle dose associated with protons may have implications for upper extremity function, although additional research is required.

### EP-1289 Phase I dose escalation trial using single fraction Stereotactic PBI for early stage breast cancer

A. Rahimi<sup>1</sup>, N. Kim<sup>2</sup>, A. Spangler<sup>2</sup>, M. Leitch<sup>3</sup>, P. Alluri<sup>2</sup>, X. Gu<sup>2</sup>, C. Ahn<sup>4</sup>, S. Goudreau<sup>5</sup>, S. Seiler<sup>5</sup>, D. Farr<sup>3</sup>, R. Woodridge<sup>3</sup>, B. Haley<sup>6</sup>, S. Bahrami<sup>2</sup>, D. Chen<sup>2</sup>, R. Rao<sup>7</sup>, R. Timmerman<sup>2</sup>

<sup>1</sup>University Texas Southwestern Medical Center, Radiation Oncology, Dallas, USA ; <sup>2</sup>University of Texas Southwestern Medical Center, Radiation Oncology, Dallas, USA ; <sup>3</sup>University of Texas Southwestern Medical Center, Surgery, Dallas, USA ; <sup>4</sup>University of Texas Southwestern Medical Center, Biostatistics, Dallas, USA ; <sup>5</sup>University of Texas Southwestern Medical Center, Radiology, Dallas, USA ; <sup>6</sup>University of Texas Southwestern Medical Center, Medical Oncology, Dallas, USA ; <sup>7</sup>Columbia University Medical Center, Breast Surgery, New York City, USA

### Purpose or Objective

To evaluate tolerability of escalating doses of single fraction stereotactic partial breast irradiation (S-PBI) in treating early stage breast cancer after partial mastectomy. We conducted a phase 1 dose escalation trial testing 3 dose levels, 22.5Gy, 26.5Gy and 30 Gy. The primary objective was to escalate the S-PBI single fraction dose utilizing a robotic stereotactic radiation system treating the lumpectomy cavity without exceeding the maximum tolerated dose (MTD) in patients with early stage breast cancer. We report on the first dose cohort.

### Material and Methods

Eligible patients included DCIS or invasive epithelial histologies, AJCC clinical stage 0, I, or II with tumor size <3cm, and negative margins. Prior to simulation 3-4 four gold fiducials were placed around the lumpectomy cavity for real-time respiratory tracking. Dose limiting toxicity (DLT) equaled grade  $\geq 3$  toxicity by CTCAE (version 4) deemed definitely related to treatment for: skin, rib bone(fracture), pulmonary (radiation pneumonitis), or neurological (intercostal or brachial plexus nerves) or any grade 4 or 5 toxicity definitely attributed to therapy. Both patients and physicians completed baseline and subsequent cosmesis outcome questionnaires using a four point scale of - excellent, good, fair, poor. Adjuvant endocrine or chemotherapy was permitted. Starting dose was 22.5 Gy in 1 fraction, dose cohort two is 26.5 Gy and third cohort is 30 Gy. Dose was escalated provided two or fewer of nine patients experienced a DLT within 90 days of treatment within each dose group. If more patients had DLT in a given dose cohort, the MTD would be exceeded.

### Results

11 patients enrolled on cohort one and had a median age of 66 years. All patients had ER/PR+ and Her2/neu- tumor profile. Median follow-up was 18 months. 80% of patients received endocrine therapy and 0% chemotherapy. MTD was not reached in cohort one and dose was escalated to cohort two. There were 19 grade 1 toxicity events, 2 grade 2 toxicities, and 1 grade  $\geq 3$  toxicity (which was breast pain that lasted for two days and resolved after antibiotics). There have been no recurrences or distant metastases. One patient developed fat necrosis and it was diagnosed 12 months after radiation treatment. Physicians scored cosmesis excellent or good in 100%, 100%, 100% and 100% (p=1.00) respectively, at baseline, 3, 6 and 12 months post SBRT, while patients scored the same periods 90.9%, 100%, 100% and 90.0% (p=1.00).

### Conclusion

Dose was escalated to 22.5 Gy in 1 fraction without a DLT and the majority of patient had good or excellent cosmesis. We are currently completing dose escalation for subsequent cohorts of 26.5Gy and 30 Gy in 1 fraction of S-PBI hoping to increase the likelihood of long term tumor control while evaluating toxicity and cosmesis.

### EP-1290 Impact of patient and treatment factors on heart and lung dose in left-sided breast radiotherapy

V.T. Nguyen<sup>1</sup>, T. Finazzi<sup>1</sup>, A. Papachristofilou<sup>1</sup>, F. Zimmermann<sup>1</sup>

<sup>1</sup>University Hospital Basel, Clinic of Radiotherapy and Radiation Oncology, Basel, Switzerland

### Purpose or Objective

The heart and lung are routinely exposed to incidental irradiation during adjuvant radiotherapy (RT) of breast cancer. We analyzed the impact of patient characteristics and treatment factors on heart and lung radiation dose in patients receiving adjuvant radiotherapy for left-sided breast cancer.

### Material and Methods

We identified patients who were treated with adjuvant RT for left-sided breast cancer in our institution between 2013 and 2018. The mean radiation doses to the heart (mean heart dose; MHD) and left lung (mean lung dose;

MLD) as well as V20Gy for both organs were collected from treatment plans. Patients were classified according to RT technique used (3DCRT, IMRT or VMAT) and target volumes treated. Group comparisons were performed to analyze heart and lung doses for different techniques and for RT with and without irradiation of regional lymph nodes (LN). The relationship between patient characteristics (body mass index (BMI), heart and total lung volume) and radiation exposure of the heart and lung was assessed using correlation analyses.

#### Results

A total of 344 female patients treated with adjuvant radiotherapy for left-sided breast cancer were eligible for analysis. Patients received a median dose of 50 Gy to the breast or chest wall +/- regional LN. Two-third (n=227) were treated with 3DCRT, whereas one third (n=117) received IMRT/VMAT. Regional LN irradiation was performed in 32% of patients and more often involved usage of IMRT/VMAT (55.8% of treatments vs. 23.6% for cases without LN irradiation). Overall, IMRT/VMAT showed a higher MHD (4.8Gy vs 3.5Gy;  $p<0.01$ ), left MLD (12.5Gy vs 8.6Gy;  $p<0.01$ ) and V20Gy of the left lung (25% vs 16.9%,  $p<0.01$ ) compared to 3DCRT. In a subgroup analysis of patients without LN irradiation (n=233), a difference remained for left MLD (IMRT/VMAT vs. 3DCRT 9.0Gy vs 7.2Gy;  $p<0.01$ ) and V20Gy of the left lung (18.0% vs 13.6%;  $p<0.01$ ). Inclusion of regional LN increased MHD (5.2Gy vs 3.4Gy;  $p<0.01$ ) and left MLD (14.8Gy vs 7.6Gy;  $p<0.01$ ) as well as V20Gy of the heart (5.3% vs 3.4%;  $p<0.01$ ) and left lung (30.2% vs 14.6%;  $p<0.01$ ) compared to treatment without regional LN. In particular, RT involving the internal mammary LN further increased heart and lung doses compared to RT involving only supraclavicular +/- axillary LN ( $p<0.01$  for all values; MHD 8.3Gy vs. 4.6Gy). Assessment of patient characteristics revealed a weak negative association between total lung volume and both MHD ( $r=-0.38$ ;  $p<0.01$ ) and heart V20Gy ( $r=-0.36$ ;  $p<0.01$ ). In addition, a weak positive correlation of BMI and MHD ( $r=0.25$ ;  $p<0.01$ ) was observed.

#### Conclusion

While IMRT/VMAT has been shown to improve dose homogeneity and conformity in RT for breast cancer, this has to be weighed against an increase in radiation exposure of the lung and potentially the heart. Similarly, the impact of regional LN irradiation on heart and lung dose needs to be considered in clinical decision making. These observations may help tailor personalized RT for patients with left-sided breast cancer.

#### EP-1291 Radiation Treatment Standards and Techniques in Breast Cancer in German speaking countries

M. Mayinger<sup>1</sup>, C. Straube<sup>2</sup>, D. Habermehl<sup>2</sup>, S.E. Combs<sup>2</sup>  
<sup>1</sup>Universitätsspital Zürich, Radiation Oncology, Zürich, Switzerland ; <sup>2</sup>Technical University of Munich, Radiation Oncology, Munich, Germany

#### Purpose or Objective

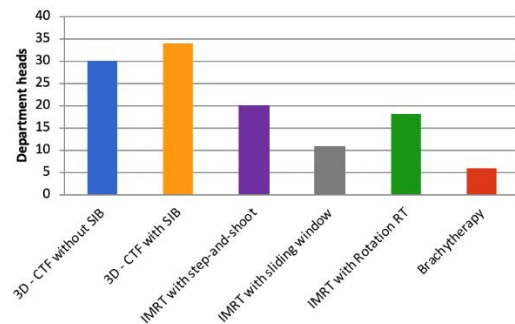
The large amount of prospective trials in early breast cancer has caused a wide variety in possible treatment techniques in early-stage breast cancer. Therefore the aim of this study is to assess radiation treatment standards and techniques in early-stage breast cancer in German speaking countries.

#### Material and Methods

Between July 2017 and August 2017, an email-based survey was sent to all 1408 physicians that are members of the German society of radiation oncology (DEGRO). The survey was completed by 180 physicians including 10 private practice owners and 52 heads of departments of community-hospital or university-hospital based radiation oncology services. The majority (82.1%) of the participants had >15 years of experience in radiation therapy (RT).

#### Results

In the adjuvant treatment of early-stage breast cancer the majority of departments (54.8%) used 3D - conformal tangential fields with a simultaneous integrated boost. 32.3% of the departments used intensity modulated radiation therapy (IMRT) with step-and-shoot, 29.0% with Rotation RT and 17.7% with sliding window (Figure). For internal mammary radiation the majority of participants (74.4%) used image guided radiation therapy (IGRT) with IMRT or volumetric modulated arc therapy (VMAT). When asked in which case participants would perform an irradiation of neck, supraclavicular and infraclavicular lymph nodes 67.2% indicated a case with 1-3 affected lymph nodes, with 100% treating a patient with >3 affected lymph nodes. Several questions focused on the participants' standard treatment plans for various clinical situations.



#### Conclusion

Our patterns of care survey showed that the majority of departments and radiation oncologists in German speaking countries align with the new S3 and AGO guidelines. For the adjuvant treatment of early-stage breast cancer 3D - conformal tangential fields with a simultaneous integrated boost is the preferred treatment technique. The use of IMRT is still limited to a specific patient cohort, although the majority of participants selected IGRT - IMRT / VMAT for irradiating the internal mammary lymphatic chain.

#### EP-1292 Zinc-L-Carnosine prevents dysphagia in breast cancer patients treated with adjuvant radiotherapy

S. Saldi<sup>1</sup>, E. Perrucci<sup>1</sup>, V. Lancellotta<sup>2</sup>, I. Palumbo<sup>2</sup>, L. Falcinelli<sup>1</sup>, C. Mariucci<sup>2</sup>, S. Chierchini<sup>2</sup>, V. Bini<sup>3</sup>, C. Aristei<sup>2</sup>

<sup>1</sup>Santa Maria della Misericordia Hospital, Radiation Oncology, Perugia, Italy ; <sup>2</sup>University of Perugia, Radiation Oncology, Perugia, Italy ; <sup>3</sup>University of Perugia, Internal Medicine Section of Internal Medicine and Metabolic and Endocrine Disease, Perugia, Italy

#### Purpose or Objective

Irradiation of level III and IV draining nodes in breast cancer patients is often associated with dysphagia, requiring treatment with FANS and/or steroids. The present randomized phase III trial determined whether Zinc-L-Carnosine (ZLC, Hepilor®), prevents or delays the onset of dysphagia in these patients.

#### Material and Methods

December 2015-October 2017: 40 breast cancer patients undergoing radiation therapy (RT) to the breast or chest wall and level III and IV lymph-nodes were randomized to receive ZLC or placebo. All underwent RT with Tomotherapy at a total dose of 50 Gy in 25 fractions. 11/40 (27,5%) women who had received conservative surgery were given a 10 Gy boost to the tumor bed, using a simultaneous instantaneous boost technique. The primary end-point was no dysphagia, as evaluated by the CTCAE v 4.0 and EAT-10 questionnaire. The trial was approved by the Regional Ethics Committee and all

patients gave signed informed consent. The Chi-square and Mann-Whitney tests analyzed differences between ZLC and placebo arms. The Kaplan-Meier test estimated the cumulative incidence of dysphagia and the log-rank test compared results. Univariate Cox regression analysis tested relations between toxicity and prognostic factors.

#### Results

All patients completed RT. Treatment arms were matched for age, chemotherapy (CT) and administration of Trastuzumab and hormonal therapy (HT). Overall, the median age was 56 years (range 28-82); 93% received CT before RT, 35% and 70% received, respectively, Trastuzumab and HT during RT. The esophagus median maximum dose (Dmax) was significantly higher in the placebo arm ( $p=0.005$ ). The median dose to the esophagus was similar in both groups ( $p=0.76$ ). Nine (45%) patients in the ZLC arm and 20 (100%) receiving placebo developed G1-G2 dysphagia during RT ( $p<0.0001$ ). No patient developed >G2 dysphagia. Five ZLC patients (25%) and 17 (85%) placebo patients with dysphagia required steroid treatment. ZLC was associated with a later onset and lower risk of G1-G2 dysphagia during RT (cumulative incidence 55.2%, 95%CI: 29.4-81.1 vs 100%, 95%CI: 85.4-100,  $p<0.0001$ ). Univariate analysis showed esophagus Dmax was not a significant risk factor for dysphagia.

#### Conclusion

In our phase III trial ZLC significantly prevented or delayed the incidence of dysphagia in breast cancer patients undergoing RT to the draining nodes. Consequently, the need for steroid therapy was significantly reduced.

#### EP-1293 Hybrid intensity modulated radiation therapy for treatment of cancer of left breast after mastectomy

Abstract withdrawn

#### EP-1294 Prognosis of patients with breast ductal carcinoma-in-situ who underwent breast-conserving surgery

S. Kuo<sup>1</sup>, S.H. Cheng<sup>2</sup>, L. Tseng<sup>3</sup>, Y. Chang<sup>4</sup>, F. Ou-Yang<sup>5</sup>, Y. Kuo<sup>6</sup>, Y. Chang<sup>7</sup>, H. Yeh<sup>8</sup>, C. Hsieh<sup>9</sup>, M. Yeh<sup>10</sup>, H. Chen<sup>11</sup>, W. Chang<sup>12</sup>, S. Chen<sup>13</sup>, C. Huang<sup>14</sup>

<sup>1</sup>National Taiwan University Hospital, Division of Radiation Oncology- Department of Oncology, Taipei, Taiwan ; <sup>2</sup>Koo Foundation Sun Yat-Sen Cancer Center, Department of Radiation Oncology, Taipei, Taiwan ; <sup>3</sup>Taipei Veterans General Hospital, Department of Surgery, Taipei, Taiwan ; <sup>4</sup>Mackay Memorial Hospital, Department of Surgery, Taipei, Taiwan ; <sup>5</sup>Kaohsiung Medical University Chung-Ho Memorial Hospital, Department of Surgery, Kaohsiung, Taiwan ; <sup>6</sup>National Cheng Kung University Hospital, Department of Surgery, Tainan, Taiwan ; <sup>7</sup>Taipei Tzu-Chi Hospital, Department of Surgery, New Taipei City, Taiwan ; <sup>8</sup>Lotung Poh-Ai Hospital, Department of Surgery, Yilan, Taiwan ; <sup>9</sup>Taiwan Adventist Hospital, Department of Surgery, Taipei, Taiwan ; <sup>10</sup>Chung Shan Medical University Hospital, Department of Surgery, Taichung, Taiwan ; <sup>11</sup>Taipei City Hospital Fuyou Branch, Department of Surgery, Taipei, Taiwan ; <sup>12</sup>Taipei Municipal Wanfang Hospital, Department of Surgery, Taipei, Taiwan ; <sup>13</sup>Changhua Christian Hospital, Department of Surgery, Changhua, Taiwan ; <sup>14</sup>National Taiwan University Hospital, Department of Surgery, Taipei, Taiwan

#### Purpose or Objective

We recently demonstrated that California/Van Nuys Prognostic Index (USC/VNPI) score 4-6, Eastern Cooperative Oncology Group (ECOG) E5194 cohort 1 criteria (tumor size  $\leq 2.5$  cm, low-to-intermediate grade disease/without necrosis, and surgical margins  $\geq 3$  mm), estrogen receptor-positive status, and tamoxifen administration were closely associated with lower ipsilateral breast tumor recurrence (IBTR) in our patients

(National Taiwan University Hospital cohort) who were treated with breast-conserving surgery (BCS) for ductal carcinoma in situ (DCIS). This study aimed to whether aforementioned prognostic factors predicted lower IBTR in breast DCIS patients from the other 12 hospitals of Taiwan (Taiwan cohort) who underwent BCS alone.

#### Material and Methods

Data for 910 women with breast DCIS who underwent BCS at Taiwan cohort between January 2004 and December 2011 were analyzed. The patients were divided into different categories according to the recurrence risk predicted using the USC/VNPI score (4-6, 7-9, and 10-12), ECOG E5194 criteria (cohort 1, and non-cohort 1). The IBTR (included DCIS and invasive cancer of the ipsilateral breast area) was calculated by the Kaplan-Meier method. The prognostic effects of age, estrogen receptor status, USC/VNPI score, ECOG E5194 cohort 1 criteria, and tamoxifen use were evaluated by log-rank tests.

#### Results

Of the patients, 549 were treated with breast irradiation after BCS and 361 were not. The patients who were treated with radiotherapy (RT) tended to have higher USC/VNPI scores (7-11) ( $p < 0.001$ ), and to have a trend to meet the ECOG E5194 non-cohort 1 criteria ( $p = 0.091$ ). With a median follow-up of 6.3 years (95% confidence interval 6.1 to 6.5), the 7-year risk of IBTR rate was 3.4% ( $n = 16$ ) in the patients who received RT and 8.3% ( $n = 27$ ) in those who did not ( $p = 0.002$ ). Among the 361 patients who underwent BCS alone, patients with USC/VNPI scores of 4-6 had a lower 7-year IBTR rate than those with USC/VNPI scores of 7-11 (6.6% vs. 14.5%,  $p = 0.015$ ). Similarly, patients in ECOG E5194 cohort 1 criteria had a lower 7-year IBTR rate than those in ECOG E5194 non-cohort 1 (6.5% vs. 14.2%,  $p = 0.001$ ). Furthermore, estrogen receptor-positive status ( $p=0.007$ ) and tamoxifen use ( $p = 0.024$ ) predicted lower IBTR rate in patients who underwent BCS alone.

#### Conclusion

Our results indicate that patients with low USC/VNPI scores (4-6) or meeting the ECOG E5194 cohort 1 criteria of breast DCIS who undergo BCS alone may have a lower IBTR rate. The administration of tamoxifen may reduce IBTR in patients with ER-positive breast DCIS who undergo BCS alone.

#### EP-1295 Impact of Alternative Positioning on Heart/Lung Dose: A Dosimetric Follow-up to the IMPORT LOW Trial

K. Petras<sup>1</sup>, E.D. Donnelly<sup>1</sup>, J.P. Hayes<sup>1</sup>, P. Rino<sup>1</sup>, W. Matthew<sup>1</sup>, J.B. Strauss<sup>1</sup>

<sup>1</sup>Northwestern University, Radiation Oncology, Chicago, USA

#### Purpose or Objective

As outcomes for early-stage breast cancer patients continue to improve, there has been a focus on reducing treatment-associated toxicity. Recently, the IMPORT LOW trial showed that in select low-risk patients, limiting the treated volume to the surgical bed and surrounding tissue was non-inferior to whole breast radiotherapy (RT) with regard to local control and was associated with small improvements in cosmetic results. All patients were treated in the supine position at free breathing. This analysis aimed to evaluate the impact on heart and lung dose when the field design of the IMPORT LOW trial was paired with an alternative positioning technique of either the prone position or deep inspiratory breath hold (DIBH).

#### Material and Methods

The planning CT scans of 30 consecutive early-stage breast cancer patients with available paired image sets at a single institution were identified. The paired image sets were: 1) 10 patients with right-sided breast cancer treated prone and supine; 2) 10 patients with left-sided breast cancer treated prone and supine; 3) 10 patients with left-sided breast cancer treated supine free breathing or

supine DIBH. The parameters of the partial breast RT arm of the IMPORT LOW trial were applied to each available scan and several dosimetric parameters were collected for comparison including mean heart dose, heart V25 Gy, mean ipsilateral lung dose, ipsilateral lung V20 Gy, and PTV coverage.

## Results

Results Table						
	Heart (mm)	p-value	Lung (mm)	p-value	Lung V20	p-value
R Breast Prone	0.35		1.43		2.01	
R Breast Supine	0.19	p=0.006	1.77	p=0.01	2.77	ns
L Breast Prone	0.89		0.71		0.60	
L Breast Supine	0.64	ns	2.19	p=0.001	3.24	p=0.01
L Breast DIBH	0.36		1.47		1.73	
L Breast FB	0.61	p=0.015	1.90	ns	2.58	ns

All doses expressed in Gy  
 mn=mean  
 ns=non-significant

Among patients with right-sided breast cancer, the supine position was associated with lower mean heart dose while the prone position was associated with lower mean ipsilateral lung dose. In left-sided breast cancer patients, the prone position yielded lower ipsilateral mean lung dose and lung V20 Gy values; while DIBH was associated with a lower mean heart dose and a trend towards lower lung V20 Gy (p=0.058).

## Conclusion

For well-selected women with early breast cancer, the IMPORT LOW trial showed that reducing the treated breast volume is equivalent in efficacy to treating the whole breast. Our results show that incremental reductions in heart and lung dose can be achieved by pairing this approach with alternative patient positioning techniques. Overall, the prone position yields the lowest lung dose, while in left-sided disease, DIBH provides optimal cardiac avoidance.

## EP-1296 Breast reconstruction and hypofractionated adjuvant radiotherapy: dosimetric and aesthetic analysis.

E. Bonzano<sup>1</sup>, M. Guenzi<sup>1</sup>, R. Corvò<sup>1</sup>

<sup>1</sup>IRCCS Policlinico San Martino and University, Department of Radiation Oncology, Genoa, Italy

## Purpose or Objective

The aim of our study was to analyze dose distribution, target coverage and doses to organs at risk(OAR) in patients(pts) who underwent Postmastectomy Radiotherapy (PMRT) following tissue expander-implant(TE) breast reconstruction and compare different RT techniques: Three Dimensional Conformal Radiation Therapy(3DCRT) and Helical Tomotherapy(HT). The second endpoint was to evaluate patient's outcome: capsular contracture and aesthetic result.

## Material and Methods

This study was conducted on 53 pts treated from April 2012 to June 2016. PMRT was delivered in a hypofractionated regime of 46 Gy in 20 fractions, 4 times per week. Pts median age was 49y.o.(range 31-78).TE was positioned after mastectomy, progressively inflated, then replaced by a permanent implant, almost 6 months after PMRT. The majority of patients (79.24%) received chemotherapy. Pts started PMRT 3weeks after adjuvant chemotherapy. According to the tumor overexpressed Human Epidermal Growth Factor-2(HER-2) receptor, 24.52% of patients received trastuzumab, as a PMRT concurrent treatment.PMRT was delivered in supine position; 33pts were treated by HT (according to the major complexity to spare OAR), 20pts by 3DCRT. Chest-wall, supraclavicular lymph-nodes, heart, left coronary artery, ipsilateral and contralateral lung, spinal cord, thyroid, contralateral breast and esophagus was delineated. The capsular contracture was evaluated by using the four-

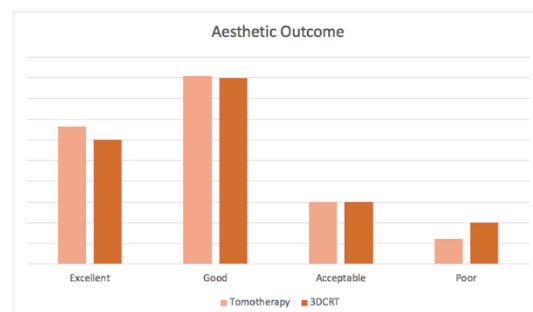
grade Baker scale, the aesthetic result was established according to the Harvard scale.

## Results

The treatment plans were compared using dose-volume histograms(DVHs) for planning target volume(PTV) and different OARs. The PTV minimum, mean and maximum doses, V95 (relative volume of breast PTV receiving 95% of the dose), and the dose at OAR were compared between 3DCRT and HT as reported in table 1. PTV coverage with the 95% isodose as expected was better for HT, as this curve fits best to the concave shape of the PTV compared to the 3DCRT(p<0.0001). A deeper analysis, only on the HT group, demonstrated that the more recent tomotherapy planning had a better dosimetry report than a few years ago. It meant a dose reduction in Dmax for ipsilateral lung and heart (p<0.0374 and p<0.0039). Capsular contracture Baker grade1-2: 1patient (HT) and 2pts (3DCRT). As regard, Baker grade3-4, 4pts (HT) and 2pts (3DCRT). An increased contracture rate was observed in patients who underwent 3DCRT (20%) instead of HT (15.15%). The aesthetic result has been classified as follow: "excellent", "good", "acceptable" and "poor".(Figure1)

	3DCRT ±SD	range	HT ±SD	range	p-value
<b>TARGET VOLUME</b>					
Dmax	48.19±0.68	46.09-48.9	49.34±1.11	47.02-50.21	0.0001
Dmin	16.71±12.63	1.16-34.07	34.87±4.11	27.14-42.32	0.0001
Dmean	43.54±1.73	40.29-45.71	45.83±0.79	45.12-49.39	0.0001
V95	72.26±9.66	47.57-84.6	97.00±2.77	88.61-99.59	0.0001
<b>SPC</b>					
Dmax	47.67±0.79	45.03-48.4	47.73±1.88	41.46-49.33	0.7922
Dmin	28.61±9.93	14.32-41.5	40.77±4.07	28.24-46.99	0.0003
Dmean	44.82±1.17	43.23-46.6	45.97±0.90	45.31-49.93	0.0221
<b>OAR</b>					
<b>HEART</b>					
Dmax	37.47±6.11	26.6-42.83	36.90±6.23	21.97-46.14	0.8357
Dmin	3.24±3.26	0.38-7.2	3.48±0.69	2.14-5.04	0.6222
Dmean	3.69±3.27	1.6-10.27	9.99±2.20	6.65-14.68	0.0022
V25	0.55±0.72	0-2	0.79±0.66	0-2.14	0.3192
<b>IPSILATERAL LUNG</b>					
Dmax	46.67±1.00	45.10-48.4	46.41±0.73	44.48-47.82	0.6212
Dmin	0.71±0.94	0.12-3.02	1.98±1.04	0.49-3.76	0.0001
Dmean	10.56±2.39	4.00-13.79	10.87±1.17	9.21-13.69	0.8645
V20	20.53±6.19	5.28-28.93	14.51±4.17	2.4-20.97	0.0009
V5	33.20±10.28	13.92-60.07	73.57±12.11	51.51-96	0.0001
<b>CONTRALATERAL LUNG</b>					
Dmax	2.95±0.41	2.68-3.43	20.93±5.05	14.21-33.3	0.0058
Dmin	0.68±0.55	0.09-1.2	1.19±0.54	0.43-2.14	0.2029
Dmean	1.91±2.32	0.56-4.6	4.96±0.70	4.08-7.37	0.0307
<b>LADCA</b>					
Dmax	17.90±3.81	11.26-22.3	18.85±3.13	10.87-26.59	0.8415
Dmin	2.66±1.00	1.3-3.79	4.30±1.33	2.63-8.25	0.0106
Dmean	6.41±2.27	3.81-10.28	8.48±1.88	5.4-12.5	0.0619
V25	0.11±0.28	0-0.7	0.13±0.32	0-1.05	0.9156
V20	0.16±0.39	0-0.96	0.01±0.03	0-0.12	1.0000
<b>THYROID</b>					
Dmax	42.85±7.53	26.83-48.2	47.16±1.18	46.11-52.05	0.0039
Dmin	1.45±1.99	0.49-7.73	5.97±3.65	1.57-14.89	0.0001
Dmean	18.45±5.21	9.92-27.17	24.00±5.41	14.15-34.43	0.0172
V15	44.90±9.00	31.92-59.87	60.84±18.88	30.53-99.58	0.0105
<b>ESOPHAGUS</b>					
Dmean	6.87±5.91	1.32-18.6	12.37±4.31	6.43-24.82	0.0095
V15	15.04±5.88	4.75-25.59	22.17±13.46	4.82-53.06	0.2617
<b>Spinalcord</b>					
Dmax	22.18±12.85	4-38.9	15.96±10.05	0.33-32.74	0.1658
Dmin	0.83±1.33	0.2-4.7	1.04±1.46	0.36-6.05	0.0240
Dmean	3.29±2.22	1.08-7.63	6.82±1.87	3.47-11.03	0.0004
<b>CONTRALATERAL BREAST</b>					
Dmax	21.75±7.62	16.3-27.14	23.61±9.40	11.9-52.13	0.7728
Dmin	1.05±1.22	0.19-1.92	1.79±0.45	1.19-3.56	0.5636
Dmean	2.98±2.39	1.29-4.67	5.50±2.34	3.94-15.95	0.1235

Table.1 Abbreviations: D<sub>max</sub> = maximum dose; D<sub>min</sub> = minimum dose; D<sub>mean</sub> = mean dose; V<sub>x</sub> = volume (%) receiving x dose (5y) or higher; SD = standard deviation. The unpaired t-test is used to compare the data.



### Conclusion

This hypofractionated regimen confirmed to be a feasible and safe treatment in reconstructed patients with both techniques. HT was associated with best target dose coverage, but at the cost of a greater OAR exposure to low doses and to higher mean doses. A longer follow-up is needed to assess the impact of low doses to healthy tissues. Both techniques allowed to achieve a good outcome, with a low failure rate.

### EP-1297 Heart of the Matter: A study of 112 left breast cancer patients treated with DIBH

J. Windsor<sup>1</sup>, T. Ramanarasiah<sup>1</sup>, M. Burke<sup>2</sup>, J. Mitchell<sup>2</sup>  
<sup>1</sup>Genesis CancerCare Queensland, Gold Coast, Tugun, Australia ; <sup>2</sup>Genesis CancerCare Queensland, Brisbane, Brisbane, Australia

### Purpose or Objective

To quantitatively compare the dose cardiac structures, including the Left Anterior Descending (LAD) artery, receive when Deep Inspiration (DIBH) technique is employed compared with Free Breathing (FB) technique in a cohort of 112 patients with left sided breast cancer.

### Material and Methods

In 2015, DIBH was first implemented across the 5 centres in our hospital network located in South-East Queensland, Australia. To assess the efficacy of the DIBH method, the first 112 patients with left sided breast cancer were analysed to quantitatively compare cardiac dose between FB and DIBH techniques. Each patient underwent two CT scans, one using standard FB technique and the second scan using Varian Real-time Position Management (RPM) respiratory gating system for DIBH technique. Treatment planning was performed per departmental protocol with tangential fields on each CT scan, using either IMRT or 3D conformal technique and dose fractionation at the discretion of the treating Radiation Oncologist (RO). Subsequent dose-volume histograms were calculated and compared using a paired t-test to evaluate mean dose to heart and Left Anterior Descending (LAD) coronary artery. All doses were compared at 2Gy per fraction equivalent.

### Results

112 patients were assessed for suitability to employ the DIBH technique. 10 patients were excluded from the study due to inability to breath hold or other technical reasons. A total of 102 patients, 101 female and 1 male, between the ages of 36 and 80 (mean 59) with left sided breast cancer were included for comparison. DIBH showed significant reduction in maximum cardiac dose (25.82Gy vs 38.29Gy,  $p < 0.001$ ), mean cardiac dose (1.21Gy vs 1.92Gy,  $p < 0.001$ ), cardiac V25Gy (1.78cc vs 8.46cc,  $p < 0.001$ ) and maximum LAD dose (15.8Gy vs 27.05Gy,  $p < 0.001$ ) compared to FB. A statistically significant increase in volume of lung receiving  $> 50\%$  of the prescribed dose in patients treated with DIBH (168.54cc vs 106.3cc,  $p < 0.001$ ) was noted compared to FB however all DIBH lung doses were within acceptable dose limitations for Organs at Risk (OAR).

Patient Demographics			
Mean Age	59		
Gender	Female	101	
	Male	1	
Radiation Dose To Organs at Risk			
	Free Breathing	DIBH	p-value
Cardiac Maximum Dose (Gy)	38.29	25.82	<0.001
Cardiac Mean Dose (Gy)	1.93	1.21	<0.001
Cardiac V25Gy (cc)	8.67	2.06	<0.001
LAD Maximum Dose (Gy)	27.05	15.8	<0.001
Left Lung V>50% Prescribed Dose (cc)	107	168.53	<0.001

Table 1.1 Comparison of dose to organs at risk between FB and DIBH techniques

### Conclusion

DIBH provides a significant reduction in the mean cardiac dose and LAD dose in patients undergoing left sided breast irradiation. It was possible to implement this technique in majority of the patients and this technique has now been successfully integrated into routine clinical practice.

While it is still early to assess differences in toxicity we are continuing follow up of patients in this cohort and hypothesise reduction in cardiotoxicity in the DIBH group.

### EP-1298 MR-guided delineation of target volumes in internal mammary lymph node radiotherapy

M. Groot Koerkamp<sup>1</sup>, A.C. Houweling<sup>1</sup>, M.E.P. Philippens<sup>1</sup>, M. Albrechts<sup>1</sup>, I.E. Van Dam<sup>1</sup>, J.M. Tjink-Felderhof<sup>1</sup>, E.M. Aalbers<sup>1</sup>, G.G. Sikkes<sup>1</sup>, J.J.W. Lagendijk<sup>1</sup>, H.J.G.D. Van den Bongard<sup>1</sup>  
<sup>1</sup>UMC Utrecht, Radiotherapy, Utrecht, The Netherlands

### Purpose or Objective

In breast cancer patients with tumorpositive internal mammary lymph nodes (IMN) internal mammary chain irradiation is indicated. Target delineation requires visualization of the internal mammary (IM) vessels. On standard planning-CT (pCT) scans without intravenous (IV) contrast these vessels can be difficult to distinguish. The purpose of this evaluation was to assess if additional non-contrast MR imaging facilitates delineation of IM vessels.

### Material and Methods

Since July 2017, all breast cancer patients with an indication for IMN irradiation at our department underwent 1.5T MR imaging. Patients were scanned in supine RT position, on a 5° wedge and an MR compatible arm support. The anterior receive coil was placed upon height adjustable coil bridges to avoid body contour deformation (Figure 1). Three fat-suppressed MR scans were acquired: a 3D T<sub>1</sub>-weighted spoiled gradient echo (T1w), a T<sub>2</sub>-weighted spin echo (T2w) and a respiratory gated and cardiac-triggered 3D balanced gradient echo (3Dcor) scan. The scans were registered to the pCT based on the region around the manubriosternal joint.



Figure 1: MRI scanning set-up at the 1.5T MRI scanner: flat table top, MR-compatible thorax-arm support, coil bridges and receive coils.

Breast radiation oncologists (ROs) and an RO in-training supervised by a breast RO delineated the IM vessels on the pCT. The use of the MR scans was up to the RO. In September 2018, the ROs filled in a short questionnaire to evaluate the delineation process using the MR images in addition to the pCT. Furthermore, we evaluated the workflow with RTTs that performed the MR scanning and MR-to-pCT registration.

### Results

Eighteen breast cancer patients underwent MR imaging for IM vessel visualization. MR scanning took  $\pm 30$  minutes per patient, including patient set-up. Scan quality was high in all patients, except in one patient due to patient motion caused by pain. According to the RTTs, the 3Dcor scan was most difficult to acquire due to gating and triggering settings to be entered manually. Registration of the T1w and T2w scans to the pCT went well, whereas the 3Dcor scan could not always be matched because the sternum is not clearly visible in this scan.

Six breast ROs and one RO in-training who delineated the scans of these patients evaluated their delineation process. All of them used the T1w scan and four ROs also used the T2w and/or 3Dcor scans. Five ROs (in training) reported that the MR scans (Figure 2) facilitated delineation of the IM vessels, provided that the scans were correctly matched to the pCT. However, three ROs reported no additional value of the MR scans when the IM vessels were already clearly visible on the pCT. One RO

reported no additional benefit of the MR scans at all due to patient motion during scanning.

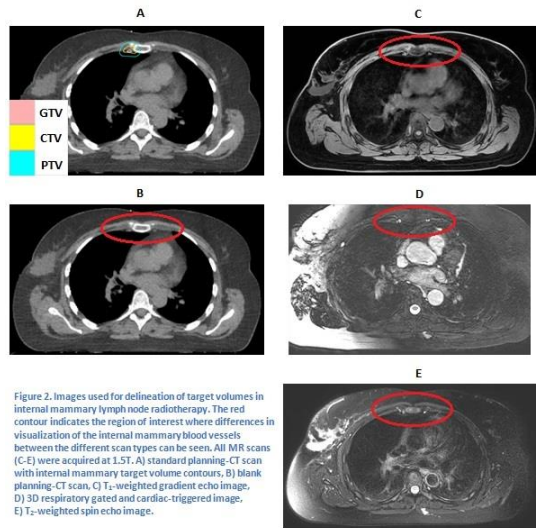


Figure 2. Images used for delineation of target volumes in internal mammary lymph node radiotherapy. The red contour indicates the region of interest where differences in visualization of the internal mammary blood vessels between the different scan types can be seen. All MR scans (C-E) were acquired at 1.5T. A) standard planning-CT scan with internal mammary target volume contours, B) blank planning-CT scan, C) T<sub>2</sub>-weighted gradient echo image, D) 3D respiratory gated and cardiac-triggered image, E) T<sub>2</sub>-weighted spin echo image.

**Conclusion**

MR-guidance facilitated delineation of IM vessels due to the improved visualization of the IM vessels when visualization on pCT was poor. Using a T1w scan only already provided adequate visualization. Our recommendation is to use non-contrast MR imaging for IMN target volume delineation when MR scanning facilities are readily available.

**EP-1299 Lymphatics in breast cancer: healthy nodes versus metastatic nodes**

L. Ernst<sup>1</sup>, K.J. Borm<sup>1</sup>, S.E. Combs<sup>1</sup>, M. Oechsner<sup>1</sup>, M. Düsberg<sup>1</sup>, M.N. Duma<sup>1</sup>

<sup>1</sup>Klinikum rechts der Isar- TU München, Department of Radiation Oncology, München, Germany

**Purpose or Objective**

Recently, a comprehensive study on PET positive lymph node (Ln) metastases in breast cancer patients has been published (Borm KJ et al. , IJROBP 2018). Nonetheless it is unclear if healthy Ln follow the same distribution pattern. The aim of this study was to detect all visible non pathological Ln in CT data sets in the same patient collective and compare them to the Ln metastases .

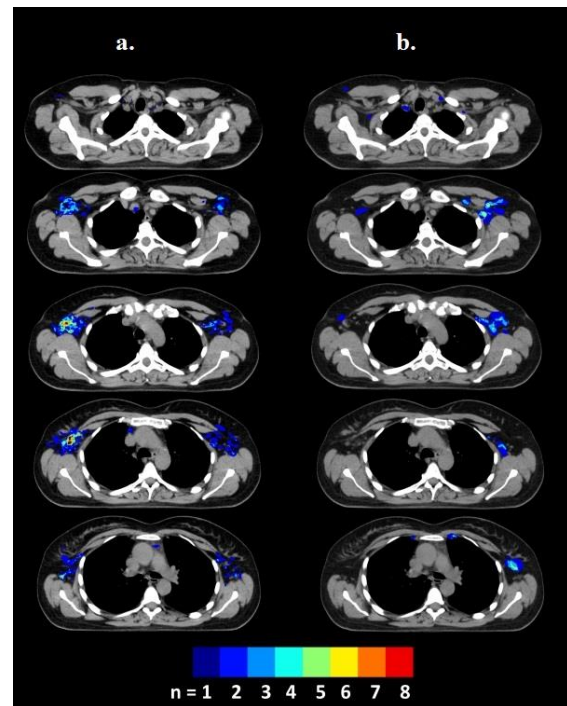
**Material and Methods**

The recently published dataset included 235 patients. Herein we report the (non pathological) contralateral lymph node distribution on the first patients from the same collective. For 34 patients we contoured all visible axillary/paraclavicular and internal mammary Ln contralateral to the primary tumor site. Patients with contralateral (or bilateral) lymph node metastases were excluded from this study. A total of 400 Ln were contoured. The size and localization of the Ln was recorded. The Ln were transferred to a standard patient using rigid and non-rigid registrations to create a “healthy Ln atlas”. Out of 400 Ln, 380 could be successfully transferred to the standard patient. This atlas was compared to the pattern of Ln metastases and to the ESTRO clinical target volume (CTV) contouring guidelines.

**Results**

The average diameter of the healthy Ln was 0.85 ± 0.37 cm and the mean volume was 0.20 cm<sup>3</sup> ± 0.30 cm<sup>3</sup>. Most healthy Ln were found in level I (n = 277; 69.25%), level IV (n = 63; 15.75%) and level II (n = 39; 9.75%), followed by the internal mammary region (n = 17; 4.25%) and level III (n = 4; 1.00%). Similar to this, pathological Ln were also predominantly found in level I (54.5%) and level IV (13.8%). Nonetheless, metastases were more often localized in

level III (10.0%) than in level II (9.8%) or in the internal mammary region (9.5%) compared to the healthy Ln. Figure 1 depicts a comparison of healthy Ln (a) vs pathological Ln (b) in the analyzed 34 patients.



Of 380 healthy Ln 124 (32.6%) were completely within , 128 in partly within (33.7%) and 128 outside (33.7%) the ESTRO CTV , respectively. The largest differences with regard to the CTV coverage (compared to the previous analysis of pathological lymph nodes) were found in the supraclavicular and internal mammary region (see table 1).

	Ln Metastases	partly inside		Healthy Ln	
		outside	inside	outside	inside
Level I	16.5%	48.7%	34.8%	25.3%	38.3%
Level II	14.0%	59.6%	26.3%	10.8%	43.2%
Level III	15.5%	62.1%	22.4%	0.0%	0.0%
supraclavicular region	31.3%	62.5%	6.3%	80.0%	7.3%
internal mammary region	29.1%	67.3%	3.6%	70.6%	29.4%
total	21.2%	53.8%	25.0%	33.7%	33.7%

**Conclusion**

Similar to Ln metastases, healthy lymph node accumulate in certain “hot spots” within the lymphatic drainage system. Even though these hot spots seem to be located in similar regions, there are relevant differences (ESTRO CTV coverage) between the lymph node pattern in healthy and pathological tissue that need to be further investigated.

### EP-1300 Beware of IMRT axillary dose reduction in non-axillary-dissected breast cancer patients

J. Gadea<sup>1</sup>, I. Ortiz<sup>1</sup>, D. Morera<sup>2</sup>, F. Sansaloni<sup>2</sup>, R. Roncero<sup>1</sup>, M. Hernández<sup>2</sup>, L. Valencia<sup>1</sup>, M.J. Sánchez<sup>2</sup>, J.E. Maturana<sup>1</sup>, J. Font<sup>2</sup>, P. José<sup>1</sup>

<sup>1</sup>Hospital Universitari Son Espases, Radiation Oncology, Palma de Mallorca, Spain ; <sup>2</sup>Hospital Universitari Son Espases, Medical Physics, Palma de Mallorca, Spain

#### Purpose or Objective

Classically the standard radiotherapy (RT) treatment in breast cancer has been tridimensional conformal radiotherapy (3D-CRT) with two tangential fields. In the IMRT era, homogeneity and conformity of the dose and target coverage has been improved in RT treatments. However, this fact could minimize the incidental irradiation of the axilla with potential clinical consequences. The aim of this study is to compare incidental axillary dose in breast cancer patients treated with IMRT vs 3D-CRT.

#### Material and Methods

Twenty female patients with breast cancer treated with breast-conserving surgery and adjuvant hypofractionated RT were evaluated in this study. Two dose groups were made for the analysis, one no-boost and one boost group for each patient. The total prescribed dose in the boost group was 40.05 Gy in 15 fractions (fx) to the whole breast and a 13.35 Gy/5fx photon boost to tumor bed sequentially in the 3D-CRT treatment and 40.05 Gy in 15fx to the whole breast and a 48 Gy/15fx photon integrated boost in the IMRT treatment. The total prescribed dose in the no-boost group was 40.05 Gy in 15fx for both techniques. Treatment plans were evaluated using cumulative dose-volume histogram data. Breast tissue, axillar node levels I, II and III and Rotter nodes and a sum of all were delineated. For the statistical analysis a T-student test was performed.

#### Results

In the no-boost group, IMRT technique showed significantly lower axillary irradiation compared with 3D-CRT ( $D_{\text{mean}}$  for total axilla: 23.84±6.57 Gy vs 30.53±8.44 Gy,  $p<0.05$ ) (Image 1). In the boost group, IMRT also showed significantly lower axillary irradiation compared with 3D-CRT ( $D_{\text{mean}}$  for total axilla: 25.34±7.07 Gy vs 31.23±8.80 Gy,  $p<0.05$ ). However, the boost location (upper quadrants vs lower quadrants) did not cause statistically significant differences in axillary dose with any of the two techniques. Details of each axillary level are shown in Table 1. When differences between the boost group and no-boost group treated with IMRT were evaluated, a significantly lower axillary irradiation was observed in the no-boost group ( $D_{\text{mean}}$  for total axilla: 25.34±7.07 Gy vs 23.84±6.56 Gy,  $p<0.05$ ). In contrast, although this difference was also seen with 3D-CRT between both groups, it was not statistically significant.

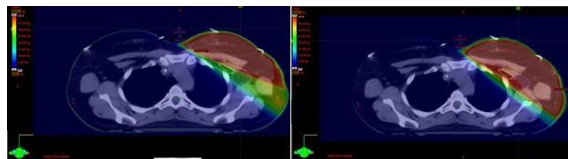


**Image 1** (Left): IMRT plan for a left-sided breast cancer patient with 40.05Gy prescription dose showed in color wash. Axillary levels I (purple), II (green), III (pink) and Rotter (gold) are delineated. (Right): The same patient with a 3D-CRT plan.

**Table 1.** Differences between both techniques in each axillary level separately

BOOST GROUP			
Node level		$D_{\text{mean}}$ (Gy) ± standard deviation	p
I	IMRT	29.63 ± 6.61	<0.05*
	3D	36.24 ± 8.19	
II	IMRT	14.86 ± 8.78	<0.05*
	3D	23.00 ± 12.71	
III	IMRT	8.88 ± 8.26	<0.05*
	3D	14.77 ± 14.05	
NO-BOOST GROUP			
Node level		$D_{\text{mean}}$ (Gy) ± standard deviation	p
I	IMRT	29.00 ± 5.28	<0.05*
	3D	34.77 ± 7.60	
II	IMRT	14.09 ± 8.71	<0.05*
	3D	22.53 ± 12.30	
III	IMRT	8.18 ± 7.59	<0.05*
	3D	14.37 ± 13.54	

\* Statistically significant p-value.

#### Conclusion

Incidental irradiation of the axilla was significantly lower with IMRT compared to 3D-CRT. Therefore, IMRT should be cautiously used in patients with limited positive sentinel lymph node disease who undergo breast conserving treatment without complete axillary lymph node dissection. There is a risk of leaving untreated microscopic node disease in these patients if we do not include axillary levels in the target volume.

### EP-1301 Postoperative EBRT in breast cancer: an analysis on 768 patients about predictors of late toxicity

A. Zamagni<sup>1</sup>, M. Buwenge<sup>1</sup>, M. Ferioli<sup>1</sup>, S. Bisello<sup>1</sup>, I. Capocaccia<sup>1</sup>, I. Ammendolia<sup>1</sup>, G. Macchia<sup>2</sup>, F. Deodato<sup>2</sup>, M. Boccardi<sup>2</sup>, D. Smaniotto<sup>3</sup>, S. Cilla<sup>4</sup>, A. Ianiro<sup>4</sup>, A. Di Stefano<sup>5</sup>, E. Cucci<sup>6</sup>, G.P. Frezza<sup>7</sup>, A.G. Morganti<sup>1</sup>, S. Cammelli<sup>1</sup>

<sup>1</sup>University of Bologna- Sant'Orsola-Malpighi Hospital, Radiation Oncology Center- Department of Experimental- Diagnostic and Specialty Medicine - DIMES, Bologna, Italy ; <sup>2</sup>Fondazione di Ricerca e Cura "Giovanni Paolo II", Radiotherapy Unit, Campobasso, Italy ; <sup>3</sup>Policlinico Universitario "A. Gemelli"- Università Cattolica del Sacro Cuore, Department of Radiotherapy, Roma, Italy ; <sup>4</sup>Fondazione di Ricerca e Cura "Giovanni Paolo II", Medical Physics Unit, Campobasso, Italy ; <sup>5</sup>Fondazione di Ricerca e Cura "Giovanni Paolo II", Gynecologic Oncology Unit, Campobasso, Italy ; <sup>6</sup>Fondazione di Ricerca e Cura "Giovanni Paolo II", Radiology Unit, Campobasso, Italy ; <sup>7</sup>Bellaria Hospital, Radiation Oncology Unit, Bologna, Italy

#### Purpose or Objective

To retrospectively evaluate risk factors for skin and subcutaneous late toxicity in 768 patients (pts) conservatively treated for breast cancer.

#### Material and Methods

We analysed 5-year  $G \geq 2$  skin and subcutaneous late toxicity-free survival (LTFS) stratifying pts based on potential risk factors: hypertension, diabetes, smoking habit, alcohol consumption, chemotherapy, hormonotherapy, stage, PTV volume, and EQD2.

#### Results

Univariate analysis results are shown in table 1. No correlation was found between  $G \geq 2$  LTFS and diabetes, smoking habit and alcohol consumption. Small but statistically significant correlations were found between

hypertension and G3 cutaneous 5-y-LTFS (98.5 vs 100%) and between chemotherapy and G3 subcutaneous 5-y-LTFS (98.4 vs 100%). A trend suggesting an impact of taxan-based chemotherapy schedules on G2 subcutaneous late toxicity was observed. Hormonotherapy with Aromatase Inhibitors (AI) was significantly ( $p < 0.0001$ ) associated with worse G2 subcutaneous 5-y-LTFS (75.6% vs 84.6% and 89.1% for Tamoxifen plus LH-RH analogue and Tamoxifen alone respectively). EQD2 was also related to G2 subcutaneous toxicity: in particular, better outcomes were observed in the group of pts treated with 50.4 Gy in 28 fractions (fr) with sequential electron boost of 10 Gy in 4 fr (EQD2 PTV 48.4 Gy, EQD2 BOOST 59.4 Gy). This was probably related to the used technique for boost delivery (electrons vs concomitant boost with tangential fields in the other two groups). In the two groups treated with IMRT and concomitant boost, G2 subcutaneous toxicity was higher in the one with higher EQD2, as expected. An interesting correlation ( $p = 0.001$ ) was also found between nodal status and G2 subcutaneous toxicity: pts with N2-3 disease, who underwent regional lymphadenectomy (with consequent alteration of lymphatic drainage) had a worse outcome compared to pts with N1 disease, where lymphadenectomy rate was lower. This could also be explained by the different technique (hemi-fields) used for pts who needed lymph nodes irradiation (typically pN2-3). Finally, PTV volume was correlated with G2 skin LTFS ( $p < 0.0001$ ), with a significant difference between values below and above the median (5y-LTFS: 98.4% vs 80.1%).

Table 1: Univariate analysis of risk factors for late toxicity

Factor	No.	n (%)	SIB		SUBCUTANEOUS	
			Rate (%)	HR (95% CI)	Rate (%)	HR (95% CI)
Age (years)	216	100	0.94	0.99	0.98	0.99
Chemotherapy	216	100	1.28	1.08	1.08	1.08
Radiotherapy	216	100	1.58	1.53	1.54	1.53
Hormonotherapy	216	100	1.20	1.05	1.05	1.05
EQD2	216	100	1.05	1.05	1.05	1.05
Nodal status	216	100	1.20	1.05	1.05	1.05
PTV volume	216	100	1.20	1.05	1.05	1.05

**Conclusion**

Our preliminary data confirm that some factors could be related to higher rates of late toxicity in pts treated for breast cancer. This analysis may represent the basis to develop predictive models of late toxicity.

**EP-1302 long-term clinical outcomes of IMRT with simultaneous integrated boost for breast cancer**

H. Lee<sup>1,2</sup>, M. Huang<sup>2,3</sup>  
<sup>1</sup>Ph.D. Program in Environmental and Occupational Medicine- Kaohsiung Medical University and National Health Research Institutes, Radiation Oncology, Kaohsiung, Taiwan ; <sup>2</sup>Kaohsiung Medical University Hospital, Radiation Oncology, Kaohsiung, Taiwan ; <sup>3</sup>Kaohsiung Medical University, Faculty of Medicine-College of Medicine, Kaohsiung, Taiwan

**Purpose or Objective**

To report the long-term survival outcomes and late toxicities resulted from intensity modulated radiotherapy (IMRT) with simultaneous integrated boost (SIB) for breast cancer patients after breast conserving surgery (BCS).

**Material and Methods**

The study included 216 patients with pathologically proven breast cancer who underwent BCS between 2010 and 2013. The median age was 52 years (Range: 21 to 81). All patients received IMRT-SIB to 2 dose levels simultaneously. They received 50.4 Gy at 1.8 Gy per fraction to the whole breast and 60.2 Gy at 2.15 Gy per fraction to the tumor bed by integral boost. The fractionation scheme was biologically equivalent to the sequential boost-technique comprising 25 fractions of 2 Gy

to the whole breast PTV followed by a boost irradiation in 6 fractions, using an alpha/beta ratio of 4 Gy for tumor response, based on the linear-quadratic cell survival model. Dermatological toxicities were assessed and documented in agreement with the Common Toxicity Criteria Adverse Events version 3 (CTCAE v.3.0). Cox regression model and Kaplan-Meier curves were calculated, and the log-rank test was used to evaluate the differences of overall (OS) and disease free (DFS) survival rates between two different modalities of radiotherapy.

**Results**

Among 216 patients, 174 received post-operative radiotherapy with Rapid-Arc and 42 patients had Tomotherapy after BCS. All patients tolerated IMRT-SIB without any interruption. The median follow-up was 6.4 years. Four patients (1.85%) in the entire cohort developed late skin complication after IMRT-SIB. For the entire cohort, the 5-year and 7-year OS rates were 94.4% and 93.1% respectively. The 5-year and 7-year DFS rates were 94.9% and 94.0 % respectively.

**Conclusion**

There exists no statistically significant difference in the rates of locoregional recurrence and overall survival when comparing RapidArc with Tomotherapy. IMRT-SIB was well tolerated with small late skin complication and good survival rates.

**EP-1303 Hypofractionated adjuvant radiotherapy in elderly low risk breast cancer patients: loss or gain?**

A. Fodor<sup>1</sup>, M. Pasetti<sup>1</sup>, P. Mangili<sup>2</sup>, B. Longobardi<sup>2</sup>, F. Zerbetto<sup>1</sup>, L. Perna<sup>2</sup>, I. Dell'Oca<sup>1</sup>, P. Signorotto<sup>2</sup>, R. Tummineri<sup>1</sup>, F. Borroni<sup>1</sup>, C.L. Deantoni<sup>1</sup>, A.M. Deli<sup>1</sup>, N. Slim<sup>1</sup>, A. Chiara<sup>1</sup>, P. Passoni<sup>1</sup>, S. Foti<sup>1</sup>, M. Azizi<sup>1</sup>, C. Fiorino<sup>2</sup>, A. Bolognesi<sup>1</sup>, N.G. Di Muzio<sup>1</sup>  
<sup>1</sup>San Raffaele Scientific Institute, Department of Radiotherapy, Milan, Italy ; <sup>2</sup>San Raffaele Scientific Institute, Medical Physics, Milan, Italy

**Purpose or Objective**

The PRIME II trial (Lancet Oncol 2015) and a recent meta-analysis (Radiother Oncol 2017) suggested that adjuvant radiotherapy does not impact overall survival in elderly patients (pts) with low risk breast cancer (LRBC), and therefore could be omitted. We report here the 5-year outcomes in elderly pts with LRBC treated with whole breast hypofractionated adjuvant radiotherapy (RT).

**Material and Methods**

One hundred forty five pts 70 years or older, with hormonal receptors positive, Her2-negative status (Luminal A/Luminal B Her2-negative) early stage (pTis-pT1c pN0-1a ≤ 3 positive lymph nodes) breast cancer, treated from 02/2009-05/2013, were included in this analysis. The patients were treated with whole breast radiotherapy to 40 Gy/15 fractions with a multiple-segments 3D-CRT technique, without tumor bed boost. Median age was 73 (70-90) years, 8 pts had ductal carcinoma in situ, 25 lobular invasive carcinoma or combination, 98 ductal invasive carcinoma and 14 other histology (mucinous, tubular, papillary); 70 were right sided and 75 left sided tumors. Hormonal therapy was prescribed in 133/ 145 pts. For possible side effects follow up visits were scheduled for 5 years. Acute toxicity during RT was evaluated with RTOG scale, late toxicity with SOMA-LENT score.

**Results**

A median number of 4 (2-6) segments were used to obtain a homogeneous dose distribution. Acute toxicity was: 24.1% G0, 69.0% G1 and 24.1% G2. Half of G2 toxicities were delayed, 7-15 days after RT, and concerned only the inframammary fold; 70% of them had breast volume > 600 cc. Two G2 toxicities were observed in low breast volume pts but with bolus for half therapy. Late toxicity was available for 131 pts: 16 % were G1 edema/dyschromia, rarely persistent over three years, while 7.6% G1 fibrosis/teleangiectasia, starting generally from the third

year after RT. Only one G2 fibrosis/teleangiectasia was observed, but maintaining a good cosmetic result. Four pts were dead at the last follow up: one of head and neck tumor, one of stroke and two of heart attack. The treatment plans of the two pts died of heart attack (one left sided tumor) were revised, but heart dosimetry was very good in both: V95%= 0 cc for both, V 20 Gy 0 for right sided, 0.76 cc for left sided pts and D 5 1.5 Gy for the right sided and 2.03 Gy for left sided patients, respectively. Two pts (1.52%) presented local relapse (4.4 and 7.9 years after HRT), 1 patient lymph-nodal relapse and 4 pts (3.02%) distant relapse.

### Conclusion

Elderly pts with LRBC treated with adjuvant RT showed a good treatment tolerance and low local relapse (LR) rate, lower than the up to 9% reported without RT. Thus, a short, convenient HRT could be prescribed even in the absence of a survival benefit, due to the improvement of the quality of life by the reduction of the LR rate to a very low level.

### EP-1304 What is the benefit of using more beams and/or non-coplanar beams in breast PBS proton therapy?

K. Verhoeven<sup>1</sup>, R. Houben<sup>1</sup>, K. Limpens<sup>1</sup>, M. Velders<sup>1</sup>, F. Visser<sup>1</sup>, G. Vilches-Freixas<sup>1</sup>, C. Ares<sup>1</sup>, G. Bosmans<sup>1</sup>, L. Boersma<sup>1</sup>

<sup>1</sup>GROW School for Oncology and Developmental Biology- Maastricht University Medical Centre, Radiation-Oncology Maastricht Clinic and ZON-PTC, Maastricht, The Netherlands

### Purpose or Objective

Pencil Beam Scanning (PBS) proton therapy (PT) has dosimetric advantages over photon therapy (PhT) in decreasing the dose to the organs at risk (OAR), which potentially leads to a reduction in late toxicity. To reimburse PT in breast cancer (BC) patients in our country a delta normal tissue complication probability (NTCP) of  $\geq 2\%$  for cardiac toxicity should be demonstrated based on the delta mean heart dose (MHD)[Darby et al, 2013] coming from the planning comparison between the PhT plan and the PBS PT plan.

The use of more beams (B) and/or of non-coplanar beams (NCB) will increase the treatment delivery time. Therefore, the aim of this study is to investigate the dosimetric added value of increasing the number of beams as well as the use of NCB in PBS PT for BC patients.

### Material and Methods

Fifteen BC patients (6 right and 9 left-sided) were selected for this dosimetric study. In 9/15 patients the internal mammary lymph node region was included in the target volume and 9/15 patients had an indication for a simultaneous integrated boost (SIB) on the tumor bed or on a macroscopic lymph node. The fractionation schemes used were 15 x 2.67Gy (1/15), 16 x 2.66Gy (5/15) and for SIB: 20 x 2.67Gy (1/15), 21 x 2.66Gy (3/15) or 23 x 2.66Gy (5/15). Six PBS PT plans were calculated for each patient: 2B, 2NCB, 3B, 3NCB, 4B and 4NCB using the RayStation treatment planning system with the Mevion beam characteristics and with the Monte Carlo calculation algorithm. PBS PT plans were made around the planning target volume (PTV). Target coverage and doses to the OARs (MHD, mean lung dose (MLD), contralateral breast (CLB) volume receiving  $\geq 2$ Gy (V2)) were registered. Statistical analysis was performed using the one-sample Wilcoxon rank-signed test with a significance level of  $<0.05$ .

### Results

Four out of 15 (27%) patients would have been accepted for PT according to the delta NTCP criteria. PTV coverage was fulfilled in all the plans (PTV V95%  $\geq 99\%$ ). The increase from 2B to 3B resulted in a small but significant reduction in the MHD (p=0.041) as well as a decrease in the MLD (p=0.001). The addition of an extra beam, thus 4B

instead of 3B, further decreased the MLD (p=0.001) and had a positive impact on the V2 CLB (p=0.009)(table 1). No added value in reducing the dose to the OARs has been observed by using NCB (2B vs 2NCB, 3B vs 3NCB and 4B vs 4NCB), except for the MLD when comparing 3B with 3NCB. The difference in OAR doses with increasing the number of beams or by using NCB did not translate in a delta NTCP of  $\geq 2\%$ .

Table 1. Median MHD, MLD and V2 CLB averaged over 15 patients with the range between brackets for photon plans and PBS PT plans with 2B, 2NCB, 3B, 3NCB, 4B, 4NCB. V2 CLB for photon plans was not available.

	Photon	PBS-PT 2B	PBS-PT 2NCB	PBS-PT 3B	PBS-PT 3NCB	PBS-PT 4B	PBS-PT 4NCB
MHD (Gy)	2.30 (0.50-12.00)	0.82 (0.10-4.83)	1.82 (0.08-4.45)	0.58* (0.09-3.87)	0.62 (0.08-3.74)	0.38 (0.12-3.24)	0.39* (0.11-3.67)
MLD (Gy)	7.96 (2.90-13.00)	6.11 (2.36-10.42)	5.59 (2.03-10.04)	5.87** (2.04-10.05)	5.44** (1.56-9.66)	5.01* (1.51-10.23)	4.82 (1.42-8.71)
V2 CLB (%)		2.49 (0.00-132.40)	0.10 (0.00-126.00)	2.08 (0.00-136.00)	1.56 (0.00-96.31)	0.56* (0.00-90.40)	0.67 (0.00-88.97)

\*p-value  $< 0.05$  between 2B and 3B

\*\*p-value  $< 0.05$  between 3B and 3NCB

\*p-value  $< 0.05$  between 3B and 4B

### Conclusion

Increasing the number of beams in BC PBS PT from 2 to 4 reduces significantly the doses to the OARs (MHD, MLD and V2 CLB), however with questionable clinical relevance. The use of non-coplanar beams does not improve the quality of the PBS proton plans. The perfect balance between reducing the dose to the OARs by using more beams and the time efficiency during PBS PT delivery is not clear and should be balanced out in a one by one basis.

### EP-1305 Long-term results up to 15 years after IORT boost in breast cancer patients

E. Sperk<sup>1</sup>, M. Pez<sup>1</sup>, G. Welzel<sup>1</sup>, A. Keller<sup>1</sup>, Y. Abo-Madyan<sup>1</sup>, M. Ehmann<sup>1</sup>, B. Tuschy<sup>2</sup>, S. Berlit<sup>2</sup>, M. Sütterlin<sup>2</sup>, F.A. Giordano<sup>1</sup>, F. Wenz<sup>1</sup>

<sup>1</sup>University Medical Center Mannheim, Department of Radiation Oncology, Mannheim, Germany; <sup>2</sup>University Medical Center Mannheim, Department of Gynecology and Obstetrics, Mannheim, Germany

### Purpose or Objective

Intraoperative radiotherapy (IORT) given as a boost during breast conserving surgery (BCS) is one of the standard boost methods for breast cancer. This is the first report of a mature and detailed toxicity and outcome follow-up after IORT boost with 50 kV x-rays up to 15 years.

### Material and Methods

Patients undergoing BCS plus IORT boost (med. 20Gy) and subsequent whole breast radiotherapy (WBRT, med. 46Gy) were included in this analyses. Follow-up was done twice yearly for 2 years and then yearly. Toxicity was evaluated according to a modified LENT SOMA scale (mod.: telangiectasia 0=no, 1=present). Cumulative (permanent  $>1=3$  events during follow-up) toxicity rates were calculated using the Kaplan-Meier method. Cumulative outcome (local/axillary recurrence, second breast cancer, metastasis, overall survival) were assessed with the Kaplan-Meier method.

### Results

Between 2002-2014, 400 breast cancers in 398 patients were treated with IORT boost (median age 63 years (30-85y), median follow-up 78 months (2-180)). Median interval between IORT - WBRT was 48 days (13-377), main type was ductal/NST in 70.5%, lobular 24%, T0/1/2: 0.5%/73%/26%, N0/1/2/3: 76%/19%/4%/1%, M0/1: 99%/1%. Chemotherapy/endocrine therapy was given in 35%/83%. Permanent moderate/severe fibrosis was seen in 18.3/19.1/21.2% at 3/5/10y, permanent breast edema  $>1$  in 2.4% at 5/10y, permanent ulceration  $>1$  in 0.3% at 5/10y, permanent lymph edema of the arm  $>1$  in 0.6/1.3% at 5/10y, permanent hyperpigmentation  $>1$  in 0.5% at 5/10y, permanent pain  $>1$  in 8.6% at 5/10y. Severe pain as first event was seen in 4% at 5/10y. Any telangiectasia as first event was seen in 18.3/23.2% at 5/10y. Our results

are in line with historical data (Bartelink JCO 2007, Lancet Oncol 2015: moderate/severe fibrosis 28.1/30.4% at 10/20y). Local recurrence rate was 1.7/2.0/6.6/10.1% at 3/5/10/15y, second breast cancer rate was 3.8/6/10.4% at 5/10/15y, axillary recurrence rate was 0.5/1.5% at 5/8-15y, metastasis rate was 4.1/6.7/14% at 3/5/10-15y and overall survival was 95.7/92.1/81.8/80.7% at 3/5/10/15y, which compares favorably to historical data (Bartelink JCO 2007, Lancet Oncol 2015: Local recurrence as first event 6.4/12/15% at 10/12/15y, metastasis 26% at 20y, overall survival 82/-73/59.7% at 10/15/20y).

#### Conclusion

IORT boost with low kV x-rays is a safe boost method for (high risk) breast cancer patients with a good local and distant control and acceptable toxicity rates during long-term follow-up.

#### EP-1306 Gated treatment of left-sided breast cancer: evaluation of lung movement, irradiated volume and mass

M. Oechsner<sup>1</sup>, M. Duesberg<sup>1</sup>, K. Borm<sup>1</sup>, J.J. Wilkens<sup>1</sup>, S.E. Combs<sup>1,2,3</sup>, M.N. Duma<sup>1,2,3</sup>

<sup>1</sup>Klinikum rechts der Isar- TU München, Department of Radiation Oncology, Munich, Germany; <sup>2</sup>Deutsches Konsortium für Translationale Krebsforschung DKTK, Partner Site Munich, Munich, Germany; <sup>3</sup>Institute of Innovative Radiotherapy, Department of Radiation Sciences- Helmholtz Zentrum München, Munich, Germany

#### Purpose or Objective

Treatment of left-sided breast cancer in deep inspiration breath-hold (DIBH), compared to free breathing (FB), was proved to reduce the dose to the heart and mostly also to the lung. For the evaluation of lung dose the dose mass histogram (DMH) seems to be more adequate than the dose volume histogram (DVH). The aim of this study was to compare DVH and DMH parameters for the left lung between treatment in FB and DIBH. Additionally, lung motion between FB and DIBH was analyzed.

#### Material and Methods

31 left-sided breast cancer patients were retrospectively selected. Treatment plans were optimized on CT datasets in FB and DIBH with the Eclipse treatment planning system (Varian Medical Systems, Palo Alto, CA). The CT datasets, structures and dose were transferred to the Matlab software (The MathWorks, Natick, MA) and DVH and DMH were calculated using self-written programs. Mean doses (Dmean) and volumes and masses receiving a certain dose (V5-45 and M5-45) were evaluated.

Using deformable image registration of the open source software Plastimatch we calculated deformation vector fields to analyze the movement of the left lung between FB and DIBH. Mean values for the movement in left-right, antero-posterior and cranio-caudal direction and a 3D vector were calculated and correlated to dose parameters. Data were statistically analysed using the wilcoxon test.

#### Results

The mean lung volume was 1432 ± 290 ml (mean ± standard deviation) in FB and 2581 ± 321 ml in DIBH. The mean lung density changed between FB and DIBH from 0.31 ± 0.05 g/cm<sup>3</sup> to 0.17 ± 0.03 g/cm<sup>3</sup>. Irradiation in DIBH resulted in a significantly reduced Dmean of the left lung: 10.0 ± 1.7 Gy in FB and 8.3 ± 1.5 Gy in DIBH (p<0.01). Relative volumes V5-45 were always smaller in DIBH than in FB (-12% to -51%, Table 1). In contrast to that, absolute volumes V5-45 were larger in DIBH (29% to 63%), except for V45 (-11%). For the irradiated lung mass the mean M5-45 were always larger in DIBH than in FB for both relative and absolute mass. However, some patients had an increased irradiated lung mass in DIBH (e.g. 4 patients for M20) or a decreased absolute irradiated lung volume in DIBH (e.g. 3 for V20).

The mean movement of the left lung between FB and DIBH was 1.5 ± 2.4 mm to the left, 16.0 ± 4.0 mm in anterior, 12.2 ± 4.6 mm in caudal direction with a mean 3D movement of 20.8 ± 4.1 mm (Fig 1). Depending on the individual patients, the ratio between movements in anterior and caudal varied from 89% to -54%, but that had no effect on the resulting dose. Increased lung movement correlated only with an increase in irradiated lung volume.

	FB		DIBH	
	absolut [cm <sup>3</sup> ]	relativ [%]	absolut [cm <sup>3</sup> ]	relativ [%]
V5	449.2 ± 99.2	31.7 ± 5.4	719.1 ± 152.1	28.0 ± 5.5
V10	331.2 ± 81.8	23.3 ± 4.3	480.9 ± 110.7	18.8 ± 4.1
V20	267.5 ± 67.0	18.9 ± 3.6	367.2 ± 86.6	14.4 ± 3.3
V30	232.0 ± 57.2	16.4 ± 3.2	315.2 ± 73.8	12.3 ± 2.9
V40	179.1 ± 49.9	12.6 ± 2.8	225.8 ± 62.2	8.8 ± 2.4
V45	108.1 ± 44.3	7.6 ± 2.5	98.9 ± 55.0	3.8 ± 2.0
	absolut [g]	relativ [%]	absolut [g]	relativ [%]
M5	107.6 ± 23.6	24.8 ± 4.7	102.1 ± 27.6	23.2 ± 5.0
M10	79.6 ± 19.9	18.3 ± 3.7	69.8 ± 20.5	15.8 ± 3.6
M20	65.3 ± 16.0	15.0 ± 3.0	55.7 ± 16.4	12.6 ± 2.9
M30	57.2 ± 13.4	13.1 ± 2.6	48.9 ± 14.2	11.0 ± 2.5
M40	46.0 ± 12.0	10.5 ± 2.3	38.1 ± 11.8	8.6 ± 2.1
M45	31.1 ± 11.0	7.1 ± 2.1	22.3 ± 9.6	5.0 ± 1.8

Table 1

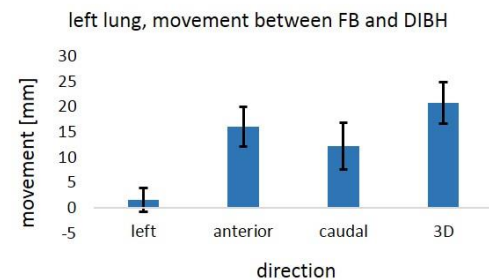


Figure 1

#### Conclusion

Treatment of left-sided breast cancer in DIBH resulted mostly in lower doses to the lung. Despite an increase in absolute irradiated lung volume in DIBH the irradiated lung mass is reduced. But for some patients there can also be a reverse effect. The amount of lung movement depends on the individual patient and correlated only to the absolute irradiated lung volume.

#### EP-1307 Deep inspiration breath-hold technique versus free breathing in RT treatment of left-sided breast

N. Jankarashvili<sup>1</sup>, I. Sikharulidze<sup>2</sup>, R. Sreseli<sup>3</sup>, N. Kartvelishvili<sup>4</sup>, M. Topeshashvili<sup>1</sup>

<sup>1</sup>Academician F. Todua Medical Center-Research Institute of Clinical Medicine, Radiation Oncology, Tbilisi, Georgia; <sup>2</sup>Tbilisi Cancer Center, Oncological Surgery, Tbilisi, Georgia; <sup>3</sup>S. Khechinashvili University Hospital, Chemotherapy Department, Tbilisi, Georgia; <sup>4</sup>S. Khechinashvili University Hospital, Oncological Surgery, Tbilisi, Georgia

#### Purpose or Objective

This study evaluates heart dose for deep inspiration breath hold (DIBH) versus free breathing (FB) technique in patients with left-sided breast cancer. For left-sided breast cancer patients, the heart, major coronary arteries, and left lung tend to be co-irradiated due to their proximity to the anterior chest wall. Therefore, radiotherapy can result in severe complications, and many

epidemiological studies have shown cardiac morbidity and mortality as major complications of left-sided breast/chest wall irradiation

#### Material and Methods

In Academician F. Todua medical center, Research Institute of Clinical Medicine from October 2017 88 patients under 55 underwent radiation therapy to evaluate LAD and heart doses using DIBH (Deep Inspiration Breath-Hold) technique and FB (Free Breathing). Patients were divided in 3 groups: only breast, with regional LNs and with IM chain.

#### Results

##### Target Volume Coverage

The target coverage was  $97.0 \pm 1.5\%$  and  $96.6 \pm 1.2\%$  (for V95) for the FB and DIBH plans, respectively. Other parameters HI and CI were also comparable.

##### Ipsilateral Lung Doses

The ipsilateral lung volumes were analyzed using 4 different dose volume parameters, i.e., V5, V20, V30, and Dmean. While DIBH increases volume of ipsilateral lung about 2 times, we did not find parameters V5, V20, V30 and Dmean appropriate for evaluation, although according to statistical parameters there was slight improvement in DIBH plans comparing with FB plans, but this was not considered comparable.

##### Heart Doses

It was observed, that V25 for the heart, one of the most useful parameter for heart dose evaluation, was almost near to zero in DIBH plans. Our statistical analysis showed that there was a significant reduction in dose to the heart in the DIBH plans for all other parameters too. Table 1 shows the heart dose observed from the FB and DIBH plans.

**LAD Doses** It is known, that the doses received by the LAD are directly proportional to the risk of development of radiation-induced ischemic heart disease. We evaluated LAD doses in the FB and DIBH plans with 4 different dose volume parameters (V5, V10, V25, and Dmean). Table 2 shows the LAD dose observed from the FB and DIBH plans. Very few studies in the literature dealt with doses to the LAD and no standard protocols for the estimation of LAD doses and tolerances have been defined, so we present our statistical data just for comparison in dose difference, which is quite large in the value. For the first group (only breast or chest) the dose is almost negligible in DIBH plans, while for FB plans we have very high doses for all statistical parameters. Furthermore, in the FB plans, there was lot of fluctuation in doses to the LAD due to respiratory motion, which could be avoided in the DIBH plans.

	V5		V10		V25		V30		Dmean	
	DIBH	FB	DIBH	FB	DIBH	FB	DIBH	FB	DIBH	FB
Only Breast	2.1min 0.00-0.03	1.9min 0.00-0.03	1.1min 0.00-0.03	1.0min 0.00-0.03	0.47min 0.00-0.03	0.47min 0.00-0.03	0.00min 0.00-0.03	0.00min 0.00-0.03	0.00min 0.00-0.03	0.00min 0.00-0.03
With LN	4.6min 0.00-0.04	3.0min 0.00-0.04	1.1min 0.00-0.03	1.0min 0.00-0.03	0.47min 0.00-0.03	0.47min 0.00-0.03	0.00min 0.00-0.03	0.00min 0.00-0.03	0.00min 0.00-0.03	0.00min 0.00-0.03
With IM Chain	5.7min 0.00-0.04	3.2min 0.00-0.04	1.1min 0.00-0.03	1.0min 0.00-0.03	0.47min 0.00-0.03	0.47min 0.00-0.03	0.00min 0.00-0.03	0.00min 0.00-0.03	0.00min 0.00-0.03	0.00min 0.00-0.03

Table 1: Heart Dose parameters for DIBH and FB plans

	V5		V10		V25		Dmean	
	DIBH	FB	DIBH	FB	DIBH	FB	DIBH	FB
Only Breast	1.7min 0.00-0.03	0.7min 0.00-0.03	0	0	0	0	0.00min 0.00-0.03	0.00min 0.00-0.03
With LN	2.1min 0.00-0.03	0.7min 0.00-0.03	0.3min 0.00-0.03	0.3min 0.00-0.03	0	0	0.00min 0.00-0.03	0.00min 0.00-0.03
With IM Chain	4.6min 0.00-0.04	2.3min 0.00-0.04	0.3min 0.00-0.03	0.3min 0.00-0.03	0.3min 0.00-0.03	0.3min 0.00-0.03	0.00min 0.00-0.03	0.00min 0.00-0.03

Table 2: LAD Dose parameters for DIBH and FB plans

#### Conclusion

DIBH considerably reduced radiation doses to the heart, lung, and LAD artery without compromising target coverage. For our study patients, the probability of a major coronary event within 10 years will be significantly reduced.

**EP-1308** positional analysis of a personalized breast immobilization technique for whole breast irradiation T. Chen<sup>2</sup>, M. Chung<sup>3</sup>, D. Tien<sup>3</sup>, R. Wang<sup>1</sup>, J. Chiou<sup>1,4</sup>, T. Kuo-Hsiung<sup>3</sup>, L. Long-Sheng<sup>1,5</sup>

<sup>1</sup>Taipei Medical University Hospital, Radiation Oncology,

Taipei, Taiwan ; <sup>2</sup>Taipei Medical University, School of Biomedical Engineering- College of Biomedical Engineering, Taipei, Taiwan ; <sup>3</sup>National Taipei University of Technology, Department of Electrical Engineering, Taipei, Taiwan ; <sup>4</sup>Taipei Medical University, Department of Radiology- School of Medicine- College of Medicine, Taipei, Taiwan ; <sup>5</sup>Taipei Medical University, Graduate Institute of Biomedical Materials and Tissue Engineering- College of Biomedical Engineering, Taipei, Taiwan

#### Purpose or Objective

Breast-conserving surgery followed by whole breast irradiation (WBI) is the standard treatment for patients with early-stage breast cancers. However, radiation dose to the heart and to the left anterior descending artery (LAD) during WBI is a risk factor of radiation-induced heart disease (RIHD). We developed PERSBRA (PERsonalized BReAst holder) technique to improve cardiac dosimetric profile during left sided WBI. PERSBRA involves a 3D-printed thermoplastic holder that adjusts breast position close to that could be achieved at the prone position. Previously we have reported a significant heart and lung dosimetric profile improvement with this technique. Here we further analyzed interfractional positional stability of the left breast.

#### Material and Methods

Fifteen participants with left-side early stage breast cancer were enrolled in our study. Lead markers were placed on participant's left side, right side and anterior side. Three sets of CT simulation images were acquired in treatment positions (set 1: no PERSBRA; set 2: with PERSBRA; set 3: with PERSBRA and was acquired at 6th day after set 2). The difference of markers' positions between the set 2 CT scans and the set 3 CT scans was recorded to evaluate the changes of breast position. The shape and volume changes were also evaluated from the contours on the set 2 CT scans and the set 3 CT scans. Target volumes and normal organs on all 3 sets were contoured by one radiation oncologist, and treatment plans were calculated with Pinnacle.

#### Results

With this device, the mean dose of heart and LAD in tangential fields was decreased by 28% ( $p < 0.01$ ) and 19% ( $p < 0.05$ ) respectively. The average errors of breast position with PERSBRA were  $0.23 \pm 0.14$ ,  $0.54 \pm 0.15$  and  $0.67 \pm 0.16$  cm in left-right (LR), craniocaudal (CC), and anteroposterior (AP) directions, respectively. The breast shape and volume difference between the set 2 CT and the set 3 CT was less than 1%. When applying set 2 CT-calculated treatment plans on set 3 CT, the PTV coverage ( $V_{95\%}$ ) was  $95.1 \pm 2.7\%$ , and  $D_{max}$  was  $109.4 \pm 0.5\%$ .

#### Conclusion

The radiation dose to the heart during left-sided WBI is a significant issue for early-stage breast cancer patients. Our analysis show that PERSBRA has good interfractional positional stability for breast immobilization and therefore supports its potential as a new option for cardiac sparing.

**EP-1309** Are OAR dose constraints for radical 3DCRT breast plans achievable? A one-year retrospective review.

S. McCauley<sup>1</sup>, B. O'Connell<sup>2</sup>, C. Lyons<sup>3</sup>, R. Evans<sup>3</sup>  
<sup>1</sup>Northern Ireland Cancer Centre, Clinical Oncology, Belfast, United Kingdom ; <sup>2</sup>North West Cancer Centre, Physics, Derry, United Kingdom ; <sup>3</sup>North West Cancer Centre, Clinical Oncology, Derry, United Kingdom

#### Purpose or Objective

Within our centre, a number of 3DCRT (3D Conformal Radiotherapy) breast cancer plans were exceeding mandatory dose constraints to achieve optimal 95% PTV (planning target volume) breast coverage. We performed a one-year retrospective review to ascertain our rate of non-conformity as well as identifying which treatment

plans and which OAR (organ at risk) dose constraints were most at risk of compromise.

#### Material and Methods

With the ARIA System we identified all patients who had radical 3DCRT for breast cancer from March 2017 to March 2018. All plans were peer reviewed, each with their respective PTV and OAR doses and volumes documented. The standards set were by Trust guidelines derived from the RTOG, ESTRO and RCR consensus target volume delineation for breast cancer.

#### Results

A total of 228 3DCRT breast treatments were planned. 88 (38.6%) plans were non-conformal, with 165 OAR dose constraint occurrences.

All 26 (100%) breast plans that included the SCF (supraclavicular fossa) (Breast +SCF +/-Boost) breached OAR dose constraints: 100% exceeded optimal V18Gy dose constraints whilst 80.8% exceeded mandatory V18Gy dose constraints. The mean ipsilateral lung dose of these 26 Breast +SCF plans was 8.76Gy, exceeding mean dose constraint set at <7.5Gy; and the mean ipsilateral V18Gy volume was 19% (mandatory dose constraint <15%). However five of the Breast +SCF +/-Boost plans that did not exceed mandatory OAR dose constraints also did not achieve optimal PTV coverage either (mean PTV95 breast: 92.1% coverage).

Treatment plans that included a boost (Breast + Boost) also had higher rates of OAR non-conformity. Right Breast +Boost: 47.3% compared to 20% of right Breast only plans; Left Breast +Boost: 40% compared with 21.6% of left Breast only plans.

Ipsilateral lung was the most non-conformal OAR dose constraint, with V18Gy exceeding tolerances in 33.3% of 3DCRT plans. The mean lung dose exceeded tolerances in 24.9% of 3DCRT plans.

Site	Left Breast			Right Breast			Total Exceeded (%)
	L Only	L +Boost	L-SCF +/- Boost	R Only	R +Boost	R-SCF +/- Boost	
Total	83	25	8	75	19	18	228
Lung Mean Dose Gy	6	6	6	3	4	16	41 (24.9)
Lung V18 Optimal %	17	9	2	15	9	3	55 (33.3)
Lung V18 Mandatory %	1	-	6	-	-	15	22 (13)
% Exceeding lung constraints	21.6%	40%	100%	20%	47.3%	100%	
Optimal PTV Breast 95% not met	-	-	3 (1-M)	-	-	5 (2-M)	
Optimal PTV SCF 90% not met	-	-	4 (2-M)	-	-	4 (4-M)	
Heart Mean Dose	3	4	1	-	-	-	8 (4.8)
Heart V13Gy %	12	8	7	1	-	-	28 (17)
Contralateral Lung	-	-	3	-	-	1	4 (2.4)
Contralateral Breast	1	-	1	-	2	3	7 (4.2)
Total all OAR exceeded (%)	40 (24)	27 (16)	26 (15)	19 (11.5)	15 (9)	38 (22.4)	165/165 (100)

#### Conclusion

Indubitably, the more radiotherapy that is delivered, the greater the risk of OAR dose constraint non-conformity. Concerning radical 3DCRT breast treatment plans, those necessitating an SCF field or boost will exceed constraints, despite greater allowances provided to achieve optimal PTV coverage. Thus are we asking too much of radiotherapy planning in achieving optimal PTV coverage, and should we consider planning margins to be tighter or relax dose constraints to OAR. On reflection, no patient who exceeded mandatory OAR dose constraints, namely ipsilateral lung V18Gy and mean lung dose, have encountered any pulmonary toxicity to date (range 9 months to 3 weeks), however we do plan to introduce pulmonary toxicity on post radiotherapy follow up assessment systemic questioning. Furthermore, we plan to

implement DIBH (deep inspiration breath hold) techniques and formally assessed set up margins with the use of daily imaging to allow us to reduce the current 1cm PTV margin to SCF, and improve dose constraint conformity.

#### EP-1310 Toxicity evaluation of a hypofractionated WBRT with SIB for breast cancer using TomoDirect

S. Dicuonzo<sup>1</sup>, M.C. Leonardi<sup>1</sup>, S. Raimondi<sup>2</sup>, E. Miglietta<sup>1</sup>, M.A. Gerardi<sup>1</sup>, A. Morra<sup>1</sup>, V. Dell'Acqua<sup>1</sup>, A. Surgo<sup>1</sup>, D.P. Rojas<sup>1</sup>, F. Pansini<sup>3</sup>, R. Luraschi<sup>3</sup>, F. Cattani<sup>3</sup>, C. Fodor<sup>1</sup>, P. Veronesi<sup>4,5</sup>, R. Orecchia<sup>6</sup>, B.A. Jereczek-Fossa<sup>1,5</sup>

<sup>1</sup>European Institute of Oncology, Division of Radiation Oncology, Milan, Italy; <sup>2</sup>European Institute of Oncology, Department of Epidemiology and Statistics, Milan, Italy; <sup>3</sup>European Institute of Oncology, Unit of Medical Physics, Milan, Italy; <sup>4</sup>European Institute of Oncology, Division of Breast Surgery, Milan, Italy; <sup>5</sup>University of Milan, Department of Oncology and Hemato-oncology, Milan, Italy; <sup>6</sup>European Institute of Oncology, Scientific Directorate, Milan, Italy

#### Purpose or Objective

To report tolerance of whole-breast radiotherapy (WBRT) with a simultaneous integrated boost (SIB) to the tumor bed (TB) using hypofractionated schedule delivered with intensity-modulated radiotherapy (IMRT) by means of Tomotherapy (Accuray Inc., Sunnyvale, CA) in Direct modality.

#### Material and Methods

A prospective cohort of patients with early breast cancer, operated on with breast conserving surgery, received 15-fraction schedule consisting of 40.05 Gy (2.67 Gy/fraction) to the whole breast and 48 Gy SIB (3.2 Gy/fraction) to the TB over the period 2013-2017.

The purpose of this analysis was to evaluate acute and intermediate toxicity assessed at the end of radiotherapy (RT) and within 6 months after RT, according to RTOG scale, and at 12 months using the LENT-SOMA scale, alongside cosmesis based on the Harvard criteria.

McNemar's test was used to compare any grade of toxicity, while univariate and multivariate analysis were used to examine predictive factors for severe toxicity at any time.

#### Results

Two hundred and eighty-three patients were analyzed. Acute toxicity was recorded at the end of RT for all patients and in 183 women within the next 6 months: Grade 2 toxicity occurred in 34% and 25% of the patients, respectively (Table 1). No Grade>2 was reported. A significant reduction of any grade toxicity was observed between the end of RT and the first assessment within the 6-month period (median time 3 months). At univariate analysis, age <40 years, breast volume >1000 cm<sup>3</sup> and D<sub>max</sub>≤115% of prescription dose were predictive factors of severe (Grade≥2) acute toxicity. At multivariate analysis, only age and breast volume were confirmed as predictive factors, with Relative Risks (95% Confidence Intervals): 2.02 (1.13-3.63) and 1.84 (1.26-2.67), respectively.

Twelve-month toxicity was available in 113 patients, who showed Grade 0-1 toxicity in 54% of cases (Table 2). Cosmetic evaluation, performed in 102 pts, revealed good-excellent outcome in 86% of the population.

**Table 1:** Acute skin toxicity according to the RTOG scale at two time points.

Toxicity/Grade	At the end of RT N = 287 (%)	Within 6 months N = 183 (%)	p-value	
Erythema	0	33 (11)	153 (84)	<0.0001
	1	203 (71)	27 (15)	
	2	51 (18)	3 (2)	
Desquamation	0	265 (93)	178 (97)	0.005
	1	17 (6)	4 (2)	
	2	4 (1)	1 (1)	
Edema	0	224 (78)	139 (76)	0.22
	1	63 (22)	44 (24)	
	2			
Any toxicity	0	24 (8)	118 (64)	<0.0001
	1	164(57)	19 (10)	
	2	98 (34)	46 (25)	

**Table 2:** Late skin toxicity according to the LENT-SOMA scale at 12 months.

Toxicity/Grade	At 12 months since the end of RT N = 113 (%)	
Pain	0	79 (70)
	1	26 (23)
	2	8 (7)
Edema	0	92 (81)
	1	13 (12)
	2	8 (7)
Hyperpigmentation	0	45 (40)
	1	58 (51)
	2	10 (9)
Hypopigmentation	0	88 (78)
	1	25 (22)
	2	2 (2)
Fibrosis	0	40 (35)
	1	55 (49)
	2	16 (14)
Breast Retraction	0	71 (63)
	1	30 (26)
	2	12 (11)
Breast Volume	0	47 (41)
	1	52 (46)
	2	14 (13)
Any Toxicity	0	12 (11)
	1	49 (43)
	2	50 (44)
	3	2 (2)

### Conclusion

Hypofractionated WBRT with SIB delivered with TomoDirect, is a safe and well-tolerated treatment both in terms of early and intermediate-term toxicity. Predictive factors of severe toxicity might be considered during treatment planning in order to further reduce side effects.

**EP-1311 POLO concept: salvage whole breast radiotherapy with Tomotherapy after intraoperative radiotherapy**

M.A. Gerardi<sup>1</sup>, M.C. Leonardi<sup>1</sup>, E. MIGLIETTA<sup>1</sup>, G. Riva<sup>1,2</sup>, A. Morra<sup>1</sup>, S. Dicuonzo<sup>1</sup>, A. Camarda<sup>1,2</sup>, A. Casbarra<sup>1,2</sup>, C. Fodor<sup>1</sup>, R. Orecchia<sup>3</sup>, B.A. Jereczek-Fossa<sup>1,2</sup>  
<sup>1</sup>European Institute of Oncology, Division of Radiation Oncology, Milan, Italy ; <sup>2</sup>University of Milan, Department of Oncology and Hemato-oncology, Milan, Italy ; <sup>3</sup>European Institute of Oncology, Scientific Directorate, Milan, Italy

### Purpose or Objective

To evaluate the dosimetric feasibility of salvage hypofractionated whole breast radiotherapy (WBRT) in patients who received intraoperative radiotherapy with electrons (IOERT) for breast cancer (BC). This approach, called POLO (Partially Omitted LObe), excludes the previous IOERT area from receiving the full prescription dose (Figure).

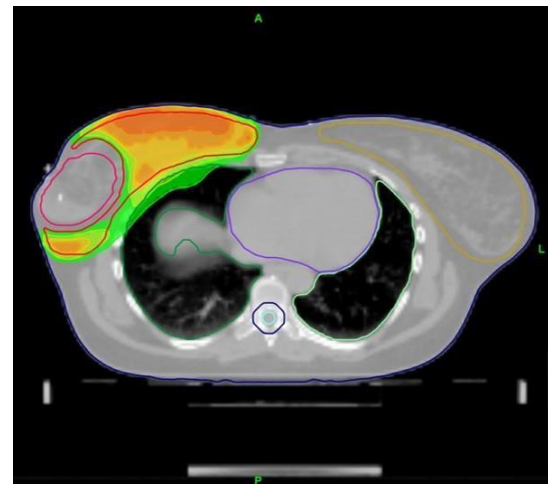


**Figure:** Transversal computed tomography view with the contouring of PTV, OARs and IOERT area and plan dose distribution.

### Material and Methods

Inclusion criteria were BC patients treated with IOERT full-dose (21 Gy at 90% isodose) who received WBRT as salvage treatment following either a local recurrence treated with repeat BCS (provided that IOERT area was left in place) or unfavorable features of the primary tumor on the final histologic report. All patients received hypofractionated schedules. The previous IOERT area was underdosed using the intensity-modulated radiotherapy (IMRT) by means of Helical Tomotherapy (Tomotherapy Inc., Madison, WI). The 5%, 25%, 50%, and 95% of IOERT volumes were planned to receive less than 20 Gy, 15 Gy, 10 Gy, and 5 Gy, respectively. All patients gave written informed consent.

### Results

From 2012 to 2014, 12 patients were treated with the POLO approach. Nine patients with local recurrence received 45 Gy in 20 fractions (2.25 Gy/fraction) in 4 weeks to the whole breast. Simultaneous integrated boost of 2.5 Gy in 20 fractions (50 Gy total dose) was delivered in 6/9 patients, whose local recurrence occurred distant from the IOERT area. Three patients, turned out to be not ideal candidates for IOERT as the sole treatment for the primary tumor, received WBRT up to 32 Gy in 8 fractions (n=2) and WBRT + irradiation of the infra/supraclavicular nodal region up to 40.05 Gy in 15 fractions (n=1). Median age was 65 years (range 47-76), 5 patients had left- and 7 right-sided BC, all but one had invasive carcinoma. Median tumor diameter was 0.85 cm. Regarding the IOERT volume, the median dosimetric parameters were D<sub>5%</sub>=20.8 Gy, D<sub>25%</sub>=14.3 Gy, D<sub>50%</sub>=9.7 Gy, D<sub>95%</sub>=4.3 Gy. The median values of V<sub>95%</sub>, V<sub>90%</sub>, D<sub>mean</sub> and D<sub>max</sub> of planning target volume (PTV) were 89%, 95%, 100% and 110% of prescribed dose, respectively; regarding boost, V<sub>95%</sub>, V<sub>90%</sub>, D<sub>mean</sub>, and

D<sub>max</sub> were 96%, 98%, 100% and 104% of the prescribed dose, respectively. All organs at risk (OARs) constraints were fulfilled (Table). No toxicity >G2 was reported either at the end of radiotherapy or at the 12-months examination. With a median follow-up time of 45 months (interquartile range 17-67), overall survival, disease-free survival and local control are 100%.

**Table:** Dose/volume constraints and planning values.

OARs	Constraints	Planning values [Gy]
Heart	D <sub>15%</sub> < 20 Gy	7.55 (4.7-17)
	D <sub>20%</sub> < 15 Gy	6.4 (4.4-14.3)
Ipsilateral Lung	D <sub>15%</sub> < 35 Gy	26.9 (19.5-32.2)
	D <sub>20%</sub> < 30 Gy	24.1 (17.6-29.3)
	D <sub>35%</sub> < 20 Gy	17.3 (11.9-20.3)
Contralateral Lung	D <sub>50%</sub> < 15 Gy	13.2 (7.7-14.5)
	D <sub>20%</sub> < 15 Gy	7.3 (4.0-13.1)
	D <sub>35%</sub> < 12 Gy	5.7 (3.0-11.1)
Contralateral Breast	D <sub>50%</sub> < 10 Gy	4.6 (3.0-10)
	D <sub>15%</sub> < 20 Gy	5.3 (3.4-7.0)
	D <sub>20%</sub> < 10 Gy	4.6 (3.2-6.6)
	D <sub>35%</sub> < 7 Gy	4.1 (2.8-5.7)
	D <sub>50%</sub> < 5 Gy	3.3 (2.6-4.8)

### Conclusion

The POLO approach is safe and technically feasible and resulted in high dose conformity of the target with a significant reduction of radiation dose delivered to the previous IORT area. A larger population and a longer follow-up are needed to better evaluate the clinical outcome.

### EP-1312 Evaluation of MRI-based guidelines for contouring tumors for preoperative partial breast irradiation

J. Vasmel<sup>1</sup>, M. Groot Koerkamp<sup>1</sup>, A. Kirby<sup>2</sup>, N. Russell<sup>3</sup>, S. Shaitelman<sup>4</sup>, D. Vesprini<sup>5</sup>, C. Anandadas<sup>6</sup>, A. Currey<sup>7</sup>, B. Keller<sup>8</sup>, L. Braunstein<sup>8</sup>, K. Han<sup>9</sup>, A. Kotte<sup>1</sup>, S. De Waard<sup>10</sup>, M. Philippens<sup>1</sup>, A. Houweling<sup>1</sup>, H. Verkooijen<sup>11</sup>, D. Van den Bongard<sup>1</sup>

<sup>1</sup>UMC Utrecht, Radiotherapy, Utrecht, The Netherlands ;

<sup>2</sup>The Royal Marsden NHS Foundation Trust, Radiotherapy, Sutton, United Kingdom ;

<sup>3</sup>The Netherlands Cancer Institute-Antoni van Leeuwenhoek Hospital,

Radiotherapy, Amsterdam, The Netherlands ;

<sup>4</sup>The University of Texas MD Anderson Cancer Center,

Radiation Oncology, Houston, USA ;

<sup>5</sup>Sunnybrook Health Sciences Centre, Radiation Oncology, Toronto, Canada ;

<sup>6</sup>Christie Hospital, Clinical Oncology, Manchester, United Kingdom ;

<sup>7</sup>Medical College of Wisconsin, Radiation Oncology, Milwaukee, USA ;

<sup>8</sup>Memorial Sloan Kettering Cancer Center, Radiation Oncology, New York, USA ;

<sup>9</sup>Princess Margaret Cancer Centre, Radiation Oncology, Toronto, Canada ;

<sup>10</sup>UMC Utrecht, Radiology, Utrecht, The Netherlands ;

<sup>11</sup>UMC Utrecht, Imaging, Utrecht, The Netherlands

### Purpose or Objective

The goal of this study was to evaluate recently developed expert consensus contouring guidelines in delineating primary breast cancers using MRI in a preoperative setting.

### Material and Methods

MRI-based contouring guidelines for target definition of primary breast tumors on dynamic contrast enhanced (DCE) MRI in supine position were developed by experienced breast radiation oncologists from the International MR-Linac Consortium and a dedicated breast radiologist. Using these guidelines, the gross tumor volume (GTV) was delineated by 6 breast radiation oncologists on 10 pre-treatment DCE-MRI scans from 10 cT1N0 breast cancer patients treated with single-dose preoperative partial breast irradiation (ABLATIVE trial, ClinicalTrials.gov: NCT02316561) in a first contouring

session. Clinical target volumes (CTV) were created by expanding the GTV by 2cm, while excluding skin and chest wall. After the first contouring session, the MRI-based guidelines were adapted, since the observers noted that the distinction between the contrast-enhanced tumor and surrounding vessels and glandular breast tissue was difficult in several cases. Therefore, the final guidelines recommended delineation on the DCE-MRI obtained after approximately 60-120 seconds vs. 300 seconds in the first guidelines. Guidelines did not change on using a diagnostic DCE-MRI (in prone position) to verify tumor spiculae and on including the fiducial marker in the GTV. After a 6-month interval, 5 breast radiation oncologists re-delineated 6 of the 10 cases using the updated guidelines. Three radiation oncologists were common to both meetings. We assessed the mean delineated volumes and the interobserver variation (IOV) during the two sessions. IOV was based on the generalized conformity index (CI). The CI was calculated using the following equation:  $CI = (\sum \text{pairs } ij |Ai \cap Aj|) / (\sum \text{pairs } ij |Ai \cup Aj|)$ .

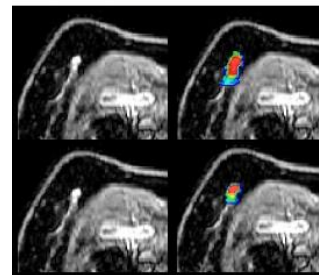
### Results

Following the first contouring session, the conformity indices of GTV varied between 0.28 and 0.77, and of CTV between 0.77 and 0.94 (Table 1). Following the second session, the conformity indices of GTV varied between 0.34 and 0.77, and of CTV between 0.78 and 0.94 (Table 1). The largest variation was observed in patients with increased glandular breast tissue enhancement, with a tumor close to large vessels or with large tumor spiculae (Figure 1).

**Table 1.** GTV and CTV conformity index per patient and moment of delineation. A CI of 1 indicates no interobserver variation, a lower CI indicates higher interobserver variation. \* = Was not delineated during this session. † = based on five observers, one observer delineated another structure than the tumor, this was considered an outlier and removed from the analysis.

Mean GTV volume (in ml)		Conformity index GTV		Mean CTV volume (in ml)		Conformity index CTV	
Session 1	Session 2	Session 1	Session 2	Session 1	Session 2	Session 1	Session 2
2.2	2.2	0.77	0.77	59.7	59.0	0.94	0.94
0.2	*	0.48	*	37.1	*	0.89	*
1.0	0.5	0.57	0.54	29.2	23.0	0.82	0.88
0.6	0.6	0.42	0.43	33.8	34.0	0.87	0.83
1.4	1.3	0.64	0.68	66.8	66.2	0.91	0.93
0.9	*	0.66	*	47.6	*	0.93	*
2.2	*	0.67	*	87.8	*	0.88	*
0.6	*	0.64	*	55.1	*	0.92	*
2.4	2.4	0.65	0.69	84.6	83.7	0.90	0.90
1.5 †	2.0	0.28 †	0.34	54.6 †	59.7	0.77 †	0.78

**Figure 1.** Coronal view of delineations of patient 3 during the first (upper row) and second (lower row) session, a blood vessel can be observed caudal of the tumor. Red= delineation by all observers, blue= delineation by 1 observer.



### Conclusion

Using expert-developed MRI-based contouring guidelines resulted in a relatively high interobserver variation in GTV and a low interobserver variation in CTV. The high interobserver variation in GTV can largely be attributed to small breast tumor volumes ( $\leq 1.5$  ml), and artifacts caused by markers and contrast-enhancement of surrounding vessels and breast tissue. In the context of 20mm expansion margins, small discrepancies in GTV contouring do not translate into significant variations in CTV.

### EP-1313 Adjuvant radiotherapy for primary squamous cell carcinoma of the breast

M. Ogita<sup>1</sup>, K. Shiraishi<sup>2</sup>, T. Chang<sup>3</sup>, J. Kawamori<sup>4</sup>, W. Takahashi<sup>1</sup>, T. Kiritoshi<sup>1</sup>, H. Yamashita<sup>1</sup>, K. Nakagawa<sup>1</sup>

<sup>1</sup>The University of Tokyo Hospital, Radiology, Tokyo,

Japan ; <sup>2</sup>Teikyo University Hospital, Radiology, Tokyo, Japan ; <sup>3</sup>National Institute of Radiological Sciences, Research Center Hospital for Charged Particle Therapy, Chiba, Japan ; <sup>4</sup>St. Luke's International Hospital, Radiation Oncology, Tokyo, Japan

### Purpose or Objective

Primary squamous cell carcinoma (SqCC) of the breast is a rare disease comprising only 0.1% of all breast cancer. Because of its rarity, the standard therapy for the breast SqCC has not been established, and the role of adjuvant radiotherapy is unclear.

### Material and Methods

We conducted a multicenter retrospective cohort study in four hospitals. Patients diagnosed with primary breast SqCC who received adjuvant radiotherapy as part of primary definitive treatment were included. Patients received radiotherapy for recurrence or palliative setting were excluded. Clinical outcome and the types of recurrence were examined. Overall survival (OS) and progression-free survival (PFS) were calculated using the Kaplan-Meier method.

### Results

From January 2002 to December 2017, seventeen breast SqCC patients who received adjuvant radiotherapy were included in the analysis. Median follow-up time was 33 months (range; 9-157). Median age was 54 years (range; 29-83). Two (12%), twelve (71%) and three (18%) patients had clinical stage I, II and III disease, respectively. Eleven (65%) patients underwent lumpectomy and subsequently had adjuvant radiotherapy to the conserved breast. Six (35%) underwent mastectomy and had post-mastectomy radiotherapy; five patients to the chest wall and regional lymph nodes and one patient to the chest wall only. Twelve (71%) had neo/adjuvant chemotherapy. Three (18%), ten (59%) and four (24%) patients had pathological stage I, II and III disease, respectively. Five (29%) had ER(+), two (12%) had PR(+) whereas none had HER2 overexpression. Twelve patients had triple negative breast cancer. Four patients (24%), 3 clinical stage II and 1 clinical stage III, had disease recurrence with a median progression-free interval of 292 days. The first site of recurrence was locoregional in 3 and concurrent local and distant metastasis in one. Two local recurrences occurred within the irradiated field. Five patients (37%) died, and four were due to breast cancer. Three-year OS rate was 69%, and three-year PFS rate was 73%.

### Conclusion

Breast SqCC carries a high risk of recurrence and worse prognosis. Multidisciplinary treatment may be required to prevent a recurrence, and further research is needed to clarify the best treatment approach.

### EP-1314 Cardiac structures doses and correlation with mean heart dose in breast radiotherapy treatment

M. Vázquez<sup>1</sup>, A. Giraldo<sup>1</sup>, S. Micó<sup>1</sup>, M. Altabas<sup>1</sup>, D. Sánchez<sup>2</sup>, J. Giralt<sup>1</sup>, V.M. Reyes Lopez<sup>1</sup>

<sup>1</sup>Hospital Universitario Vall d'Hebron, Radiation Oncology, Barcelona, Spain ; <sup>2</sup>Hospital Universitario Vall d'Hebron, Physics Department, Barcelona, Spain

### Purpose or Objective

Several authors have related the late cardiac toxicity in breast cancer (BC) patients to dosimetric parameters such as mean heart dose (MHD), and dose to left anterior descending artery (LAD) and the left ventricle (LV). Due to the difficulty in contouring these structures, we evaluated whether there was a significant correlation between the MHD and different parameters over LAD and LV.

### Material and Methods

We analysed female patients with BC treated with adjuvant Radiotherapy (RT) from January 2010 to December 2010 in our institution. Patients with previous thoracic RT were excluded. For analysis, the sample was

divided into two groups according to tumour laterality. All patients were treated on linear accelerator with 3-dimensional conformal RT technique, following our protocols: whole breast to a total dose of 50 Gy in 2 Gy fractions or 40.05-42.72 Gy in 15-16 fractions and a tumour bed boost of 16 Gy in 8 fractions, if indicated.

The heart, LAD, and LV were contoured retrospectively, according to RTOG guidelines. For each patient, the MHD and dose-distribution parameters of the LAD and LV were extracted from our treatment planning system. Differences were analyzed with two-tailed two-sample unpaired Mann-Whitney U-test ( $\alpha=0.05$ ).

### Results

The study cohort consisted of 117 patients (68 left(L)-sided and 49 right(R)-sided breast cancers) who had been treated in our institution. For analysis, the sample was divided into two groups according to tumour laterality. 89% were breast conserving patients. 33 patients received radiation on their axillary and/or supraclavicular nodes. Table 1 details clinical and dosimetric characteristics of the population according to the fractionation schedule.

For the entire cohort of L-sided patients, the MHD was higher compared to R-sided patients: 5.75 Gy (3.52; 7.4) and 1.25 Gy (1.07;1.5),  $p < 0.005$ , respectively. The mean dose to LAD was 26.4 Gy (9.6; 34.06) for L breast sided patients and 0.95 Gy (0.79;1.13) for R breast sided patients,  $p < 0.005$ . The mean dose to the LV was 9.84 Gy (5.88;12.53) for L-sided patients compared to 0.72 Gy (0.64;0.89) for R-sided patients,  $p < 0.005$ .

For L-sided patients a significant correlation was found between the MHD and the mean dose to the LAD, as shown in Fig.1. For every 1 Gy increase in MHD, mean LAD dose increased by 4.26 Gy. The MHD with the mean LV dose was also correlated (fig.1). A correlation between the dose to the LV and LAD was also demonstrated so that for every 1 Gy increase in mean dose to LV, mean LAD dose increased by 2.4 Gy (95% CI 2.08; 2.76)  $p < 0.001$ . In addition, a correlation between these dosimetric parameters was demonstrated in R-sided patients (Fig2).

	Left breast cancer n=68	Right Breast cancer n=49	p value
Age	57 (48, 66)	60 (47, 72)	NS
Type of fraction			
CFRT	57 (83.8%)	39 (78%)	NS
HFRT	11 (16.2%)	10 (20%)	NS
Target volume			
Chest wall	4 (5.9%)	8 (16.3%)	NS
Whole breast:	64 (94.1%)	41 (83.7%)	NS
- Boost			
Y	46 (71.9%)	31 (75.6%)	NS
N	18 (28.1%)	10 (24.4%)	NS
Regional nodes			
Y	17 (25%)	16 (32.7%)	NS
N	51 (75%)	33 (67.3%)	NS
Dosimetric values			
Mean heart dose (Gy)			
CFRT	5.921 (3.961, 7.513)	1.274 (1.121, 1.544)	<0.005
HFRT	3.958 (1.155, 6.701)	1.043 (0.908, 1.250)	<0.005
Mean LV dose (Gy)			
CFRT	10.619 (6.416, 13.142)	0.744 (0.663, 0.975)	<0.005
HFRT	5.801 (0.812, 12.008)	0.635 (0.551, 0.656)	<0.005
Mean LAD dose (Gy)			
CFRT	26.603 (12.448, 34.524)	0.984 (0.851, 1.178)	<0.005
HFRT	17.695 (1.049, 26.834)	0.811 (0.745, 0.899)	<0.005
Max LAD dose (Gy)			
CFRT	48.614 (36.163, 49.781)	1.244 (1.012, 1.431)	<0.005
HFRT	35.204 (1.261, 40.581)	1.008 (0.907, 1.087)	<0.005

Values of qualitative variables expressed in percentages and relative counts; values of quantitative variables expressed in median (25th percentile, 75th percentile). CFRT= conventional fractionated radiation therapy, HFRT= hypofractionated radiation therapy. Y=yes. N=no. LV= left ventricle. LAD= left anterior descending artery.

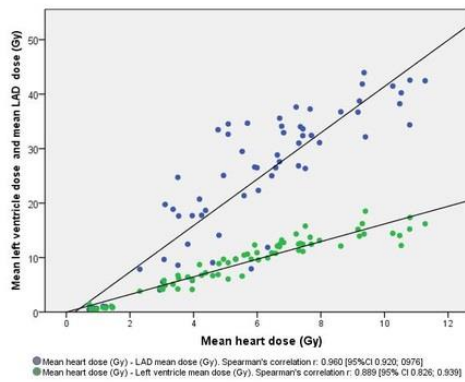


Figure 1. Correlation between MHD (Gy) and mean left ventricle and LAD doses (Gy) in left breast tumour patients.

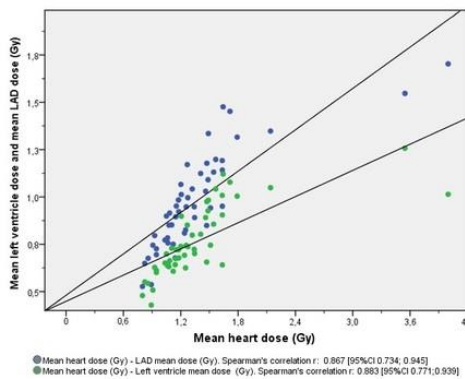


Figure 2. Correlation between MHD (Gy) and mean left ventricle and LAD doses (Gy) in right breast tumour patients.

## Conclusion

A strong correlation between the dose to the heart, LV and LAD was found. This correlation could allow us estimating the dose in LAD and LV through the MHD, being possible to avoid the contouring of the LAD and LV. We are currently working on the validation of a prediction model for acute/ischemic cardiac events in these patients.

## EP-1315 The FAST approach as adjuvant whole breast irradiation for frail breast cancer patients

M.A. Zerella<sup>1,2</sup>, S. Arculeo<sup>1,2</sup>, E. Miglietta<sup>1</sup>, A. Casbarra<sup>1,2</sup>, S. Dicuonzo<sup>1</sup>, V. Dell'Acqua<sup>1</sup>, M.A. Gerardi<sup>1</sup>, A. Morra<sup>1</sup>, C. Fodor<sup>1</sup>, F. Cattani<sup>3</sup>, V.E. Galimberti<sup>4</sup>, P. Veronesi<sup>2,4</sup>, R. Orecchia<sup>5</sup>, M.C. Leonardi<sup>1</sup>, B.A. Jereczek-Fossa<sup>1,2</sup>

<sup>1</sup>European Institute of Oncology IRCCS, Division of Radiation Oncology, Milan, Italy; <sup>2</sup>University of Milan, Department of Oncology and Hemato-oncology, Milan, Italy; <sup>3</sup>European Institute of Oncology IRCCS, Unit of Medical Physics, Milan, Italy; <sup>4</sup>European Institute of Oncology IRCCS, Division of Breast Surgery, Milan, Italy; <sup>5</sup>European Institute of Oncology IRCCS, Scientific Directorate, Milan, Italy

## Purpose or Objective

To evaluate the outcome in terms of toxicity, local control and survival of elderly breast cancer (BC) patients treated with adjuvant once-weekly hypofractionated radiotherapy (RT).

## Material and Methods

From 7/2011 to 4/2018, 271 BC patients were given received 5.7 Gy once a week for 5 weeks to the whole breast, without the boost to the tumor bed, after breast-conserving surgery. Data were extracted from a dedicated databank for research projects called "Adjuvant radiation treatments with intensity-modulated radiotherapy and/or hypofractionated schedules for breast cancer" which was notified to the IEO Ethical Committee. Patients were

eligible if affected by T1-T3 invasive BC, with no or limited axillary involvement. The scheme was offered to elderly women (age threshold of 65 years) and to those with commuting difficulties or disabling diseases.

## Results

Median age was 76 (45.5-86.4) years. Median follow-up was 24.6 (6.2-65.7) months. Most of BC were T1 (77%), while the remaining were T2 (22.2%), T3 (0.4%). Axillary status was negative in 68.3%, minimally involved in 14.4% (pN1) and not assessed in 17.3% of the cases (Nx). Most of the women received hormonal therapy (84%), while 10.7% received chemotherapy. The schedule was delivered either with three-dimensional conformal RT (n=133) or with intensity-modulated RT (n=138). No statistically significant difference was observed between the two techniques in terms of toxicity and efficacy. For 271 patients, maximum acute toxicity at the end of RT was as follows: grade (G) 1, 2 and 3 erythema in 63%, 7% and 0.4% of patients, respectively. G2 edema was detected in 10% of patients. Desquamation occurred in 4.4% as G1 and 1.5% as G2 of cases. At median 2-year follow up, LENT-SOMA assessment was available for 137 patients. Fibrosis (G1 and G2 in 46.7% and 9.5%, respectively) and skin changes (G1 and G2 hyper- or hypopigmentation in 29.2% and 2.2% respectively, G1 and G2 telangiectasia in 3 patients) were observed. A minority complained pain of G1 (n=26) and G2 (n=2) intensity. Two-year oncologic outcome was assessed for 257 patients. At the last follow-up examination, 244/257 patients were alive and free from any event. There was a total of 5 (1,9%) isolated locoregional recurrences: 4 involved the breast and 1 the axillary lymph nodes. Three women experienced a second cancer in other sites. Two died for other reasons (at 3 years, disease-free survival and overall survival were 100% and 99%) Predictive factors for toxicity were breast volume >500 cm<sup>3</sup> for acute toxicity, while none was correlated with severe late toxicity.

## Conclusion

Toxicity was mild and acceptable with high patients' satisfaction. Local control was acceptable, none died of BC and overall survival was 99% at 3 years.

## EP-1316 Radiotherapy in elderly breast cancer patients with hormone therapy: A population-based study

D. Medenwald<sup>1</sup>, A. Glowka<sup>1</sup>, D. Vordermark<sup>1</sup>, K. Medenwald<sup>1</sup>

<sup>1</sup>Martin Luther University Halle-Wittenberg, <sup>1</sup>Department of Radiation Oncology, Halle/Saale, Germany

## Purpose or Objective

For breast cancer patients above an age of 70 with a stage of pT1 and N0 receiving hormone therapy the value of additional radiotherapy has been challenged. The objective of this study is to analyze treatment patterns and outcomes of elderly female breast cancer patients above an age of 70 years in the general population.

## Material and Methods

This data set incorporates data on incident cancer cases and contains information on stage, histological features, and received treatment and survival outcomes. For this study, we excluded patients where the diagnosis of breast cancer was only available from autopsy/death certificates. Additionally, we only considered data from states with a high coverage of newly diagnosed cases (>70%, East Germany including Berlin, Bavaria, Rhineland-Palatine, Schleswig-Holstein). For subsequent analyses, we considered female breast cancer cases with recorded operative and hormone treatment, and histological confirmation of the cancer diagnosis.

For survival analyses, we used Cox proportional hazard models where we computed hazard ratios (HR) with respective 95 confidence intervals (CI). In order to respect

competing risks we used Fine-Gray models to assess tumor-specific survival. Models were adjusted for age and grading.

### Results

The application of radiotherapy in patients with hormone therapy increased from 71.4% in years before 2005 to 83.3% thereafter. In women aged 70 to 74 years 87.70 received radiotherapy. The figure decreased to 84.4% for patients between 75 and 79 years, and 57.6% in patients with 80 years or older. Considering all patients, only 2.6% were recorded to have died from breast cancer, while of all deaths breast cancer was the leading cause in 17.1%. Median survival was 51 months (95% CI: 45-55 months) for the radiotherapy group and 42 month for the hormone therapy (95% CI: 34-50 months)

Patients treated with additional radiotherapy had a better survival prospect when compared to women who received only hormone therapy (HR= 0.62, 95% CI: 0.52-0.73). Survival analyses revealed a benefit for patients with additional radiotherapy when compared patients with only hormone therapy (HR=0.41, 95% CI: 0.2-0.81) in terms of breast cancer-specific survival. Likewise, non-breast cancer-specific survival was more favorable in the radiotherapy group (HR=0.61, 95% CI: 0.44-0.86).

### Conclusion

Radiotherapy is widely applied in elderly breast cancer patients above an age of 70. However, due to the few deaths from breast cancer the benefit in terms cancer-specific survival remains unclear when population-based data are considered.

### EP-1317 Hyperthermic chest wall re-irradiation in recurrent breast cancer: a prospective observational study

C. De Colle<sup>1</sup>, N. Weidner<sup>1</sup>, V. Heinrich<sup>1</sup>, S. Brucker<sup>2</sup>, M. Hahn<sup>2</sup>, K. MacMillan<sup>1</sup>, U. Lamprecht<sup>1</sup>, S. Gaupp<sup>1</sup>, O. Voigt<sup>1</sup>, D. Zips<sup>1,3</sup>

<sup>1</sup>Eberhard Karls University Tübingen, Radiooncology, Tübingen, Germany ; <sup>2</sup>Eberhard Karls University Tübingen, Department of women's health, Tübingen, Germany ; <sup>3</sup>German Cancer Research Center DKFZ and German Cancer Consortium DKTK partner site Tuebingen, Radiooncology, Tuebingen, Germany

### Purpose or Objective

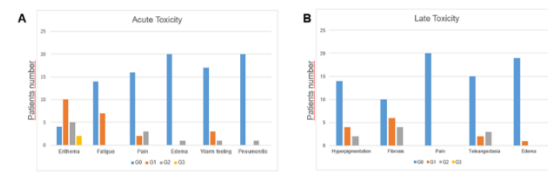
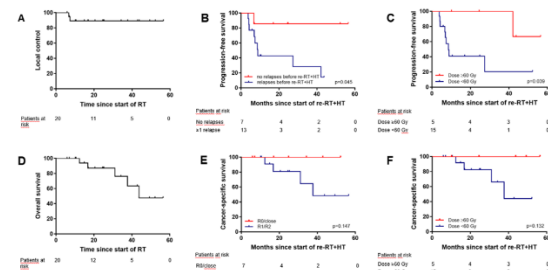
Surgical resection is the standard therapy for recurrent breast cancer (RBC). To increase local control (LC), especially after microscopically (R1) or macroscopically (R2) positive or close resection margins, re-irradiation is indicated. In these cases, radiotherapy (RT) must be carefully evaluated because re-RT might cause relevant toxicities. RT combined with hyperthermia (HT) as adjuvant treatment for RBC has been shown to improve LC compared to RT alone through a radiosensitizing effect. Despite the fact of level I evidence for re-RT+ HT, which was generated in the 1990s, it remains important to prospectively investigate this treatment because diagnosis and treatment of primary and RBC have continuously improved over the last 20 years.

### Material and Methods

Within the prospective registry HT03, patients with resected RBC (R1, R2 or close margins) and previously irradiated were included. Patients were treated with involved field RT to the chest wall limited to the region of recurrence with 50-50.4 Gy in 25-28 fractions followed by a boost up to a total dose of 60-60.4 Gy to the R1/R2 region. Concurrent superficial HT was performed twice per week with a therapeutic temperature of 40° - 42°C applied for 75 minutes. Primary endpoint was LC. In addition, acute and late toxicity according to CTCAE and RTOG criteria, overall survival (OS), cancer-specific survival (CSS) and progression-free survival (PFS) were evaluated.

### Results

Data from 20 patients and a total of 21 RBC were analyzed. Patients were treated with a median re-RT dose of 50.4 Gy (range, 39.6-60.4 Gy) and a median of 11 HT fractions (range, 2-23). Median time between RT and re-RT+HT was 66.2 months (range, 9.2-436.4). Re-RT+HT was well tolerated. Three patients experienced grade (G) 3 acute skin toxicity. No ≥ G3 late toxicity was observed. With a median follow up of 24.7 months (range, 5.8-56.5) two local relapses occurred. Ten patients experienced regional and/or distant disease progression. Five patients died, four of them from breast cancer. PFS was found to be favorable in patients treated with re-RT+HT for the first recurrence and with total doses of 60 Gy. A trend towards better CSS was found in patients with negative or close resection margins and after doses of 60 Gy.



### Conclusion

Re-RT+HT for RBC is well tolerated and provides good LC. Re-RT+HT seems to be more effective when applied at the time of the first relapse and after doses of at least 60 Gy. The registry will be continued for validation in a larger cohort and with longer follow up.

### EP-1318 Hypofractionated radiotherapy for breast cancer in elderly patients: 10 or 5 fractions?

E. Bonzano<sup>1</sup>, G. Polizzi<sup>1</sup>, M. Guenzi<sup>1</sup>, R. Corvò<sup>1</sup>  
<sup>1</sup>IRCCS Policlinico San Martino and University, Department of Radiation Oncology, Genoa, Italy

### Purpose or Objective

The aim of this study, was to compare 5 fractions (fx) one weekly hypofractionated Adjuvant Radiotherapy (RT) versus 10 fx four weekly hypofractionation in elderly patients (pts) affected by early breast cancer and to report clinical outcomes: skin toxicity profile, aesthetic result and treatment feasibility.

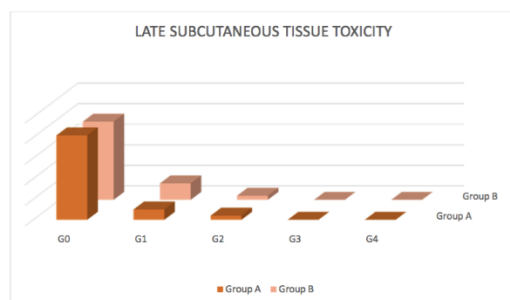
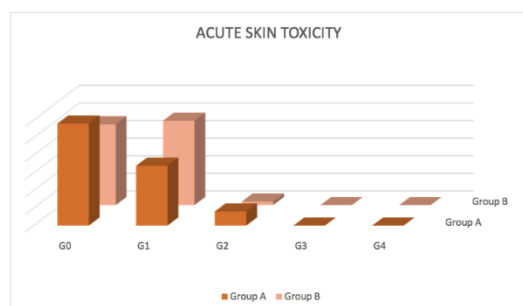
### Material and Methods

This retrospective study was conducted on 96 pts, aged over 70 years old (median age 79 y.o., range 72-95) with no severe comorbidities. From October 2016 to June 2017, pts underwent adjuvant radiotherapy, with two different hypofractionated schedules. The first group (groupA) underwent 28,5 Gray(Gy)/5fractions/1 fraction weekly plus/minus a 2.5 Gy Simultaneous Boost (SIB) on tumor bed in "high risk" cases, the second one (groupB) 35Gy/10 fractions/4 times a week with a concomitant boost of 3 or 4 Gy once a week, according to risk factors. Pts in both groups were pT1-2N0-1a, with different biologic patterns, laterality and size. Treatment was delivered in supine position, with tangential fields. Conventional 3DCRT constraints for lungs and heart were used; V20=0 for Left Anterior Descending Artery (LADCA) was translated to V12 for the one weekly hypofractionation and to V14 for the four weekly one, according to the radiobiological calculation. Acute skin toxicity and late subcutaneous

tissue toxicity were assessed respectively, at the end of RT and one year after treatment. The Radiation treatment tolerance was assessed using the acute and late radiation morbidity scoring criteria from the Radiation Therapy Oncology Group (RTOG) scale. Aesthetic result was evaluated according to the Harvard scale.

### Results

In groupA SIB was added in 22 pts(45%). In groupB a concomitant boost of 3 Gy was added in 31pts and a boost of 4Gy in the remaining 17pts. G3-G4 acute skin toxicity was not observed in both groups; G2 acute side-effects were significantly low: at the end of the treatment only 4 women in groupA and just one in groupB needed topic steroid therapy for G2 dermatitis, which ameliorated within 3 weeks after irradiation. 17 pts (groupA) and 24pts (groupB) showed G1 erythema. Concerning late subcutaneous tissue toxicity (12 months), fibrosis occurred in groupA as follow: G2 2 pts, G1 5pts, G0 41pts; furthermore 1 patient developed hyperpigmentation. As regard group B fibrosis G2 2 pts, G1 8 pts and G0 38pts, 2 patient showed a slight skin retraction. Aesthetic outcomes were from good to excellent in 94% and from fair to poor in 6% in groupA, and respectively 96% and 4% in groupB.



### Conclusion

Once weekly hypofractionated radiation therapy resulted comparable to ten fractions regimen without evidence of inferior treatment feasibility or higher adverse effects. Once weekly radiation therapy can be recommended as a safe and effective alternative for whole-breast adjuvant radiotherapy in elderly pts.

### EP-1319 Second primary lung cancer unlikely associated with irradiated breast cancer population in Taiwan

T.T. Ngo<sup>1</sup>, L. Chien<sup>2</sup>, L. Chen<sup>3</sup>, L. Lu<sup>4</sup>  
<sup>1</sup>Taipei Medical University, International PhD/Master Program in Medicine- College of Medicine, Taipei, Taiwan ; <sup>2</sup>Taipei Medical University, School of Health Care Administration- College of Management, Taipei, Taiwan ; <sup>3</sup>Taipei Medical University, Health and Clinical Data Research Center- College of Public Health, Taipei, Taiwan ; <sup>4</sup>Taipei Medical University, Graduate Institute of Biomedical Materials and Tissue Engineering- College of Biomedical Engineering, Taipei, Taiwan

### Purpose or Objective

Previous studies showed that second primary lung cancer (SPLC) is likely increased with the occurrence of ionizing radiation (RT) on BC patients (pts.). However, RT is not often used alone and SPLC is a rare event, therefore the risk of RT might be overestimated. To test the hypothesis that SPLC is associated with RT, we conduct this national population based, propensity score-matched (PSM) follow up study.

### Material and Methods

We reviewed all Taiwanese female, 20-80 years-old BC pts. in the databases of Taiwanese National Health Insurance and Taiwan Cancer Registry between 01 January 2002 to 31 December 2010. Exclusion criteria are: (1) missing or invalid demographic information; (2) had another cancer diagnosis before and six months post BC diagnosis date (index date, ID). To analysis the risk of RT alone, we excluded pts. (3) had received Cobalt 60 and other RT except linear accelerated RT; (4) had been treated with CT or died within a year after ID. To exclude patients who had uncompleted RT, we did not recruit pts. (5) had more than 1 fraction and less than 49 fractions of RT within one year after ID. We used PMS (1:2) to match pts. with RT (RT group) with those had no RT (non-RT group) to compare the incidence of SPLC later in both groups. The propensity scores for RT were formulated using 6 covariates: age, diagnostic year, social economic status (SES), residence, Charlson Comorbidity Index (CCI), and comorbidities. Standardize mean difference (SMD) and p-value (CI 95%) were used to compare the baseline characteristics of groups. End of follow up time is 31 December 2015 and subdistribution hazard ratio (sHR) was used in competing-risk regression models.

### Results

From 64758 BC recorded in the databases, 48996 pts. were excluded based on mentioned exclusion criteria. Among these 15762 eligible Taiwanese female primary BC pts., 4614 pts. had RT and 11148 pts. without RT. After matching, the differences between two group (age, diagnostic year, CCI and certain concurrent diseases) were reduced and the similarities were increased significantly. We revealed 29 SPLC in RT group (3539 pts., 29657 person-year follow up) and 57 SPLC in non-RT group (7078 pts., 56914 person-year follow up). Adjusted sHR was performed based on competing risk model adjusted for PMS covariates and we observed no difference between the two groups (p=0.949).

BC pts. who have lumpectomy are likely to have less radiation exposure to the lung than those have mastectomy. We divided RT group into two subgroups based on type of their surgery. Significant covariate differences were also observed at baseline. After matching, there were no statistical differences in the SPLC incidences between two groups (p=0.247).

### Conclusion

Our current results showed RT in the absence of CT does not increase the development of SPLC on Taiwanese female BC patients. We need further studies to identify specific agents using concurrent with RT is able to increase the risk of SPLC.

### EP-1320 Estimated survival benefit and cardiovascular risk due to radiotherapy for breast cancer in Chile

T. JP<sup>1</sup>, G. Martinez<sup>2</sup>, C. Sánchez<sup>3</sup>, R. Fernández<sup>2</sup>, L. Bravo<sup>4</sup>, M. Pinto<sup>4</sup>, E. Vinés<sup>1</sup>, T. Merino<sup>1</sup>  
<sup>1</sup>Pontificia Universidad Católica de Chile, Radiation Oncology, Santiago, Chile ; <sup>2</sup>Pontificia Universidad Católica de Chile, Cardiology, Santiago, Chile ; <sup>3</sup>Pontificia Universidad Católica de Chile, Medical Oncology, Santiago, Chile ; <sup>4</sup>Pontificia Universidad Católica de Chile, Oncology, Santiago, Chile

### Purpose or Objective

Improvements in oncologic treatments, including radiation therapy (RT), have decreased death due to breast cancer over the last decades. Up to 33% of deaths are attributed to cardiac causes in this treatment population, and mean heart dose (MHD) is associated with a relative increase in cardiovascular events (CVE) of 16% per Gray. The purpose of this study is to estimate potential survival benefit and cardiac risk of RT in a cohort of Chilean women with breast cancer.

### Material and Methods

Women with breast cancer who received adjuvant 3-D RT with curative intent between May 2017 and August 2018 were eligible for analysis. Predict® version 2.1 online tool and the American Heart Association (AHA) Predictive Score for cardiovascular disease were used to calculate the estimated overall survival and the CVE risk at 10 years. RT volumes and MHD were registered from their RT plans. The increase of CVE risk was estimated based on the model by Darby et al. Mortality from heart attack/stroke was estimated based on HeartScore® from the European Association of Preventive Cardiology, and the reduction on breast cancer mortality from RT based on the EBCTCG meta-analysis.

### Results

Seventy-two eligible women with breast cancer were analyzed, none had bilateral cancer. Mean age was 66 years (range: 43 to 87 yrs). Thirty-two patients (44%) had right breast cancer and 40 (56%) had left breast cancer. Mean baseline AHA 10-year CVE risk was 9.1% (0.2 to 44.6%), 38% were considered as high risk by AHA definition. The estimated mean 10-year mortality from heart attack and stroke was 2.38%. RT volume included the internal mammary chain in 7 (10%) patients, the mean dose to breast or chest wall was 41.6 Gy, the mean heart dose (MHD) was 2.37 Gy (0.6 to 12.9 Gy), 1.54 Gy (0.6 to 8.6 Gy) and 2.96 Gy (0.9 to 12.9 Gy) in whole cohort, right and left treatments, respectively. With RT, the mean 10-year estimated breast cancer survival increased from 64.6% to 68.4% (absolute mortality reduction 3.75%) and the mean the 10-year CVE risk increased from 9.14% to 12.3% (absolute 3.16%, range: 0.02 to 25.37%). If all patients had optimal management of their cholesterol, blood pressure and smoking habit, the 10-year CVE risk would be 7% without RT and 9.5% with RT (absolute increase 2.50%).

### Conclusion

RT for breast cancer increase the 10-year estimated overall survival in 3.75% and the CVE risk in 3.15%. An optimal management of cardiovascular risk and lowering the MHD will maximize the benefit of the treatment.

### EP-1321 Waiting times for breast cancer treatment in Chile according to public or private health insurance

T. IP<sup>1</sup>, C. Gabler<sup>2</sup>, C. Carvajal<sup>2</sup>, C. Osorio<sup>2</sup>, M. Camus<sup>3</sup>, C. Sánchez<sup>4</sup>, M. Silva<sup>2</sup>, T. Merino<sup>1</sup>

<sup>1</sup>Pontificia Universidad Católica de Chile, Radiation Oncology, Santiago, Chile ; <sup>2</sup>Instituto Nacional del Cáncer, Radiation Oncology, Santiago, Chile ; <sup>3</sup>Pontificia Universidad Católica de Chile, Surgical Oncology, Santiago, Chile ; <sup>4</sup>Pontificia Universidad Católica de Chile, Medical Oncology, Santiago, Chile

### Purpose or Objective

Chilean people can either have public or private health insurance. As breast cancer is the leading cause of cancer death in Chilean women, it has been prioritized in Chilean health system by law. It establishes that treatment should start within 30 days of being diagnosed and adjuvant treatment should start within 20 days from indication. The purpose of this study is to report stage of cancer and time from diagnosis to treatment in breast cancer patients according to health insurance system.

### Material and Methods

A retrospective review of the breast cancer database at the Centro del Cáncer of the Universidad Católica de Chile (CECA-UC) and at Instituto Nacional del Cáncer (INC) for patients treated from 2017 to 2018. All breast cancer patients treated at CECA-UC were included and a random sample of equal number of the patients treated at INC where included. Age, tumor size, neoadjuvant treatment, time to surgery and time to radiation were registered. Patients were analyzed according to health insurance (public or private). Student T test for continuous variables and Chi<sup>2</sup> for categorical variables were used.

### Results

Two hundred and seventy-nine women were included (168 public insurance, 111 private insurance), median age was 57 years (range 25-88). The median clinical tumor size (T) was 24.3 mm (2-100), pathologic T was 20.8 mm (0-116). Tumor status was T1 n=157, T2 n=94, T3 n=12. Nodal status was N0=170, N1=64, N2=21, N3=10. Neoadjuvant chemotherapy was received in n=55 and neoadjuvant radiotherapy n=2. By Insurance, public and private, clinical T was 29 and 21.5 mm (p=0.005), pathologic T 22.5 and 19.9 mm (p=0.5), nodal status was N0=92 and 78, N1=36 and 28, N2=18 and 3, N3 8 and 2 (p=0.02), received neoadjuvant chemotherapy 23.8% and 13.5% (p=0.034), respectively. Mean time from diagnosis to surgery in patients without neoadjuvant treatment was 66,4 and 30 days (p=0.001), time from diagnosis to radiotherapy was 263 and 128 days (p< 0.001), and time from surgery to radiotherapy was 153 and 80 days (p<0.001).

### Conclusion

Patients with public insurance have significantly more advanced cancer stage at diagnosis and have a longer time to surgery and to adjuvant radiotherapy than patients with private insurance.

### EP-1322 "Every breath you take": first results of INHALE (Inspiration Breath hold health related QoL) study

E. Ippolito<sup>1</sup>, S. Silipigni<sup>1</sup>, A. Sicilia<sup>1</sup>, S. Palizzi<sup>1</sup>, G.M. Petrianni<sup>1</sup>, B. Santo<sup>1</sup>, S. Gentile<sup>1</sup>, P. Zuccoli<sup>1</sup>, E. Molfese<sup>1</sup>, A. Iurato<sup>1</sup>, R.M. D'Angelillo<sup>1</sup>, S. Ramella<sup>1</sup>  
<sup>1</sup>Campus Biomedico University, Radiotherapy, Roma, Italy

### Purpose or Objective

Breath holding (BH) techniques enable clinicians to reduce radiation dose to the heart and the left descending artery (LAD) in left breast cancer patients. Despite such advantages, BH radiotherapy (RT) compared to free breathing RT (FB RT) has been shown to require more efforts during simulation and treatment delivery for both clinicians and patients. The aim of this study is to evaluate whether BH RT affects QoL and physical (fatigue) as well as psychological distress in breast cancer patients. Herewith we report the preliminary results.

### Material and Methods

All breast cancer patients aged less than 60 years old who were referred to our department of radiation oncology were asked to participate in this study. Patient-reported outcomes (PROMs) including EORTC QLQ CD30-BRC23 questionnaire (22 items), FACIT - Fatigue Scale vers. 4 (13 items), Hospital Anxiety and Depression Scale - HADS (14 items) were prospectively collected before the start of adjuvant radiotherapy (baseline) and at the end of treatment. All scores were square-root transformed (scale 0-10). Analysis of covariance (ANCOVA) was used with pre and post radiotherapy change in questionnaires scores as dependent variable, the treatment group (BH vs FB) as independent variable and the baseline measure as covariate.

### Results

Thirty-five consecutive breast cancer patients deemed to start radiotherapy treatment were asked to participate. All accepted to fulfill the questionnaires. Median age was

50 years (range 33-64 years)  
 Fourteen patients (40%) completed chemotherapy before radiotherapy, five patients (14.3%) had trastuzumab and twenty-five patients (80.6%) had hormone therapy during radiotherapy course. At the time of analysis pre and post radiotherapy questionnaires were available for 30 patients (13 left sided; 17 right sided). Depression scores, health related quality of life and fatigue did not change significantly during radiotherapy treatment for both groups (see table1). Patients reporting severe fatigue (FACIT - Fatigue Scale score >7) were 2/30 (6.6%) before and 3/30 (10%) after radiotherapy. Interestingly only one of these patients received BH radiotherapy. Anxiety and depression level was higher than mean score in all patients.

**Table 1**

Outcome	Treatment type	Mean (SD) T0	Mean (SD) T1	p
Overall QOL	FB	4,224 (0,961)	4,331 (0,953)	0,595
	BH	4,239 (0,804)	4,609 (1,851)	
Fatigue	FB	4,100 (1,631)	4,322 (1,637)	0,527
	BH	4,199 (1,590)	4,731 (1,620)	
Anxiety/depression	FB	6,015 (0,620)	5,268 (1,842)	0,392
	BH	6,235 (0,736)	4,568 (2,867)	

T0= pre radiotherapy; T1= post radiotherapy; FB= free breathing; BH= breath hold

**Conclusion**

The study is still ongoing. Preliminary results suggest that BH RT seems to not affect quality of life, psychological distress and fatigue in breast cancer patients undergoing radiotherapy.

**EP-1323 HeartSpare Plus: A comparison of the feasibility and acute toxicity of internal mammary chain RT**

A. Ranger<sup>1</sup>, A. Dunlop<sup>1</sup>, E. Donovan<sup>2</sup>, E. Harris<sup>1</sup>, N.M. DeSouza<sup>1</sup>, H. McNair<sup>1</sup>, A. Kirby<sup>1</sup>  
<sup>1</sup>ICR and Royal Marsden NHS Foundation Trust, Clinical Oncology, Sutton, United Kingdom ; <sup>2</sup>University of Surrey, Centre for Vision Speech and Signal Processing, Guildford, United Kingdom

**Purpose or Objective**

Inclusion of the internal mammary chain in the radiotherapy target volume (IMC\_RT) improves disease free and overall survival in higher risk breast cancer patients but increases radiation doses to the heart. The HeartSpare Plus dosimetry study demonstrated that the use of either modified wide-tangential fields (WT(vDIBH)) or volumetric modulated arc therapy (VMAT(vDIBH)) in combination with voluntary breath hold was capable of reducing mean heart dose to below 4Gy in the majority of patients. The subsequent HeartSpare Plus clinical trial aimed to compare set-up reproducibility, the time taken to deliver IMC-RT using WT(vDIBH) versus VMAT including planning time, dose to target volumes and organs at risk (OAR), and acute toxicities associated with each technique.

**Material and Methods**

Twenty left sided breast cancer patients requiring IMC-RT were randomised to receive WT(vDIBH) or VMAT radiotherapy. Treatment times were compared using unpaired two tailed t tests with a significance level of 0.05 to detect a difference of 5 minutes per fraction between techniques. The population mean displacement (MD), systematic error (Σ) and random error (σ) for CBCT chest wall matches in three planes of movement were

calculated for the two groups using the van Herk method. Dose statistics between groups were compared using a two tailed unpaired t test. Acute skin (RTOG), lung and oesophageal toxicity (CTCAE v 4.03) rates in the two groups were compared using the Mann-Whitney test.

**Results**

Eleven patients were treated with VMAT (three in free breathing (FB) and eight in vDIBH) nine patients were treated with WT(vDIBH). WT(vDIBH) required significantly longer total treatment times than VMAT (Table 1).

	WT(vDIBH) Mean (SD) (minutes)	VMAT Mean (SD) (minutes)	Mean difference (WT-VMAT) (minutes)	P value (95% CI, minutes)
Set up	10.0 (1.0)	6.4 (0.8)	3.6	<0.0001 (2.7 - 4.4)
Verification	1.5 (0.2)	1.6 (0.2)	-0.1	0.8468 (-0.5 - 0.5)
Shift	6.0 (0.8)	3.2 (1.2)	2.8	<0.0001 (2.2 - 3.9)
Treatment	11.2 (2.2)	2.6 (0.6)	8.6	<0.0001 (7.1 - 0.2)
Total	28.1 (3.3)	13.2 (1.7)	14.9	<0.0001 (12.4 - 17.4)

Table 1: Timings in minutes for the component parts of radiotherapy treatments in the two groups, WT(vDIBH) and VMAT

All techniques were equally reproducible. There was no statistically significant difference in MHD or Heart V<sub>17Gy</sub> between VMAT(vDIBH) and WT(vDIBH) (p=0.1269 and p=0.1490 respectively). There was no statistically significant difference in ipsilateral lung V<sub>17Gy</sub>, mean contralateral lung dose or mean contralateral breast dose between the VMAT and WT techniques. The humeral head, oesophagus and thyroid all received a statistically significantly higher dose in the VMAT group when compared to the WT(vDIBH) group (see table 2). There were no statistically significant differences in skin or lung toxicity within 3 months of treatment. Increased rates of oesophageal toxicity were seen during the third week of treatment and two weeks post treatment in the VMAT group but this was not statistically significant (see table 3). One year lung, shoulder and oesophageal toxicity will be presented.

OAR	WT(vDIBH) Mean (SD)		VMAT Mean (SD)		P value
	Mean (SD)		Mean (SD)		
MHD (Gy)	2.6 (1.2)		3.6 (0.7)		0.0422*
Heart V <sub>17Gy</sub> (%)	2.0 (2.3)		4.2 (2.0)		0.0369*
Maximum LAD dose (Gy)	31.2 (7.9)		35.2 (5.5)		0.2210
Ipsilateral lung V <sub>17Gy</sub> (%)	32.8 (3.3)		34.4 (1.4)		0.1604
Mean contralateral lung dose (Gy)	0.6 (0.2)		0.6 (0.1)		0.5889
Mean contralateral breast dose (Gy)	1.6 (1.2)		1.4 (0.5)		0.6830
Mean humeral head dose (Gy)	2.8 (1.0)		16.8 (6.2)		<0.0001
Maximum oesophageal dose (Gy)	20.1 (9.9)		37.3 (8.0)		<0.0001
Mean thyroid dose (Gy)	11.2 (3.1)		22.0 (6.1)		0.0032
Maximum brachial plexus dose (Gy)	40.4 (0.7)		40.1 (0.7)		0.3362

Table 2: Organ at risk dose statistics for WT(vDIBH) and VMAT treatments

\*MHD: acute radiation toxicity in the heart patients treated with VMAT (p=0.0422) and WT(vDIBH) (p=0.0369) respectively. There was no statistically significant difference in MHD (mean dose 1.45) or heart V<sub>17Gy</sub> (mean 3.7%) between VMAT(vDIBH) and WT(vDIBH) (p=0.1269 and p=0.1490 respectively).

OAR	Toxicity Grade	Percentage of patients								
		On treatment			2 weeks post treatment			3 months post treatment		
		WT (vDIBH)	VMAT	P value	WT (vDIBH)	VMAT	P value	WT (vDIBH)	VMAT	P value
Lung (CTCAE pneumonitis toxicity score)	Grade 0	100	80	0.47	89	80	>0.99	89	90	>0.99
	Grade 1	0	0		0	0		0	0	
	Grade 2	0	20		11	10		11	10	
Oesophageal (CTCAE oesophagitis toxicity score)	Grade 0	67	30	0.18	100	80	0.47			
	Grade 1	0	0		0	0				
	Grade 2	33	70		0	20				
Skin (RTOG skin toxicity score)	Grade 0	11	30	0.37	11	30	0.43			
	Grade 1	78	70		67	60				
	Grade 2	11	0		22	10				

Table 3: Acute toxicity for WT(vDIBH) and VMAT treatments. There was no Grade 3 or 4 toxicity in either group.

**Conclusion**

In patients undergoing IMC\_RT, VMAT(vDIBH) is quicker to deliver than WT(vDIBH) but is associated with more persistent acute oesophageal toxicity than WT(vDIBH).

**EP-1324 A Dosimetric Study of Heart and Lung Dose in Breast Radiotherapy-Our Institutional Experience**

C. Mccann<sup>1</sup>, E. Chow<sup>2</sup>, D. Vesprini<sup>2</sup>, L. Eric<sup>2</sup>, C. Paruag<sup>3</sup>, E. Lai<sup>3</sup>, M. Wronski<sup>1</sup>  
<sup>1</sup>Sunnybrook Health Sciences Centre, Odette Cancer Centre- Radiation Therapy Program- Medical Physics, Toronto, Canada ; <sup>2</sup>Sunnybrook Health Sciences Centre, Odette Cancer Centre- Radiation Therapy Program- Radiation Oncology, Toronto, Canada ; <sup>3</sup>Ryerson University, Medical Physics, Toronto, Canada

### Purpose or Objective

Adjuvant radiotherapy for breast cancer treatment has been long shown to reduce the risk of recurrence, but also results in incidental exposure of organs at risk (OAR) such as the heart and lungs. Several studies have reported on cardiac toxicity, showing an increase in the rate of ischemic heart disease after radiotherapy for left-sided breast cancer; and meta-analyses of women treated with breast radiotherapy have shown an increased risk of primary lung cancer, which is even more appreciable in the smoking population. Other potential lung complications from breast radiotherapy include pneumonitis and subsequent fibrosis, the risk of which further increases with the addition of chemotherapy. In this retrospective dosimetric study, we report on the cardiac and lung doses from over 400 breast cancer patients treated with radiotherapy at our centre, with the long-term goal of correlating dose to toxicity.

### Material and Methods

412 breast cancer patients treated with 50Gy in 25 fractions or 42.56Gy in 16 fractions were identified retrospectively. Cohorts were stratified based on the radiation technique including (i) 2-field tangential beam arrangement (n=256) (ii) 3- and 4-field techniques with standard tangents (n=92) and (iii) 4-field technique with wide tangents (n=64) to include the internal mammary chain (IMC), which was further stratified between treatment of right (n=34) and left-sided disease (n=30). Of the latter, patients simulated in free-breathing (n=8) and those simulated with a modified deep inspiration breath-hold technique (mDIBH) (n=22) were analysed separately. Standardized contouring based on the RTOG breast cancer atlas, in combination with standard field based planning was used. Dosimetric heart parameters evaluated included mean heart dose (MHD) and V(50%). Metrics for the combined lung volumes included V5Gy, V20Gy and Mean Lung Dose (MLD). ANOVA was also used to compare the dose between the techniques for statistical significance.

### Results

Dosimetric parameters for heart and lung are reported in table 1 for the different techniques, with the differences shown to be statistically significant. Breast cancer patients treated with radiotherapy which included regional nodal irradiation increased dose to both heart and lungs. mDIBH significantly reduced the dose to the heart as compared to the free-breathing technique.

HEART		Radiotherapy Technique	Standard Tangents (Left and Right)	3,4-Field Standard Tangents (left and Right)	4-Field Wide Tangents (Right side)	4-Field Wide Tangents (Left side, mDIBH)	4-Field Wide Tangents (Left side, free breathing)	One-Way ANOVA
Dosimetric Parameter	V(50%) %	Mean	0.12	0.48	0.28	0.91	2.8	p<<0.001
	Range	0-3.11	0-5.08	0-2.77	0-8.44	0.06-9.55		
MHD (Gy)	Mean	106.6	161.9	160.8	243.2	335.3		p<<0.001
	Range	2-350.2	2.9-398.9	8.2-364.2	149.6-373.7	185.8-648		

LUNGS (combined)		Radiotherapy Technique	Standard Tangents (Left and Right)	3,4-Field Standard Tangents (left and Right)	4-Field Wide Tangents (Right and Left)	One-Way ANOVA
Dosimetric Parameter	V20Gy (%)	Mean	5.47	13.54	17.04	p<<0.001
	Range	0.03-12.63	6.4-24.64	7.59-28.12		
V5Gy (%)	Mean	10.66	21.94	26.05	p<<0.001	
	Range	1.67-22.06	14.91-34.17	14.96-36.6		
MLD (Gy)	Mean	298.87	697.76	853.34	p<<0.001	
	Range	69.3-638.7	401.8-1393.8	421.0-1367.8		

### Conclusion

Standardized contouring and planning facilitates a meaningful dosimetric evaluation of OAR dose associated with breast radiotherapy, which in future studies can be correlated with toxicity. In an era where the benefits of breast radiotherapy well outweigh the risks in the majority of patients, it is important to consider the potential long-term effects of breast cancer radiotherapy from a survivorship lens.

### EP-1325 Personalized Medicine in breast cancer: a nomogram from prognostic score to deescalate radiotherapy

F. Marazzi<sup>1</sup>, A. Mulè<sup>2</sup>, V. Masiello<sup>1</sup>, R. Masetti<sup>3</sup>, R. Barone<sup>4</sup>, G. Franceschini<sup>3</sup>, F. Cacciatori<sup>2</sup>, F. Moschella<sup>3</sup>, C. Cannata<sup>1</sup>, L. Boldrini<sup>1</sup>, G. Mantini<sup>1</sup>, D. Smaniotto<sup>1</sup>, V. Valentini<sup>1</sup>

<sup>1</sup>Fondazione Policlinico Gemelli IRCCS, Radioterapia Oncologica, Roma, Italy; <sup>2</sup>Fondazione Policlinico Gemelli IRCCS, Department of Woman and Child Health-Pathology Unit, Roma, Italy; <sup>3</sup>Fondazione Policlinico Gemelli IRCCS, Multidisciplinary Breast Center, Roma, Italy; <sup>4</sup>Fondazione Policlinico Gemelli IRCCS, Università Cattolica Sacro Cuore- Dipartimento Scienze Radiologiche- Radioterapie ed Ematologiche- Istituto di Radiologia, Roma, Italy

### Purpose or Objective

OncotypeDX can enhance prediction of breast cancer recurrence (BRC), guiding adjuvant treatment options. Many studies showed a low local relapse for Recurrence Score (RS) < 18 and probably in these patients would be possible to deescalate adjuvant radiotherapy (RT). However, the opportunity to access this test is not always possible. The aim of this study is to investigate the correlation between classical immunohistochemistry (IHC) and RS in order to offer to clinicians a Decision Supporting System to be validated for deescalating RT

### Material and Methods

All patients who for ER+ HER2- breast cancer underwent Oncotype between 2014 and 2018 were retrospectively included in the study. The data selected for analysis were: age, menopausal status, pT, pN, PVI, IHC, RS and ER, PgR and HER2 expressed on Oncotype analysis. IHC was performed with standardized semi-quantitative method. Multivariable logistic regression analyses were applied to ascertain the associations between all these parameters and RS

### Results

The study comprised 407 patients who underwent Oncotype. Mean age was 53.7 (31-80) and 222 pts (54.55%) were > 50 years old. Oncotype results showed: 67 pts (16.5%) between 0-10, 173 pts between 11 and 18 (42.5%), 133 pts between 19 and 30 (32.7%), and 34 pts > 30 (8.3%). At the logistic regression analysis, RS score was significantly associated with ER (p=0.004), PgR (p<0.0001), and Ki67% (p<0.0001). Above pts with Oncotype ≤18 (0-18), a linear regression showed a model with AUC 0.814 (sensitivity 75%; specificity 75%) (Figure 1). Ten-cross fold validation of the model presented a mean AUC of 0,80 (0.7-0.9). A nomogram was generated for further prospective evaluation, predicting RS score < 18 for internal IHC prognostic factor (Figure 2).

### Conclusion

Prognostic factors present a good correlation with RS score in pts with RS ≤ 18 in our series. A nomogram for physician that enhance a good cost/effectiveness clinical practice need to be tested prospectively for deescalating adjuvant RT

### EP-1326 Assessment of rigorous dosimetry guidelines for a multi-institutional, phase II APBI clinical trial

S. Quirk<sup>1,2</sup>, P. Grendarova<sup>1</sup>, A. Guebert<sup>2</sup>, A. Frederick<sup>2</sup>, I.A. Olivetto<sup>1</sup>, M. Roumeliotis<sup>1,2</sup>

<sup>1</sup>University of Calgary, Oncology, Calgary, Canada;

<sup>2</sup>University of Calgary, Physics and Astronomy, Calgary, Canada

### Purpose or Objective

To compare the clinically achieved dosimetry of ACCEL trial with the trial's rigorous dosimetry guidelines in context with phase III multi-institutional accelerated partial breast irradiation (APBI) trials. These dosimetry guidelines were significantly stricter than dosimetry constraints formally imposed by trial protocol.

### Material and Methods

The ACCEL trial (<https://clinicaltrials.gov/NCT02681107>) is a Canadian, multi-institutional, phase II prospective

clinical trial investigating a new external beam APBI regimen, delivering 27 Gy in five consecutive daily fractions with *dosimetry constraints* consistent with major APBI trials such as ACCEL and NSABP B-39/RTOG-0413 (<https://clinicaltrials.gov/NCT00103181>). For the ACCEL trial, more rigorous *dosimetry guidelines* were established to ensure consistent and highly conformal dose distributions to address the hypothesis that poor dose conformity is important in causing cosmetic deterioration. These *dosimetry guidelines* were based on a retrospective planning study that required substantial APBI planning expertise to implement. In the current work, the clinical implementation of these *dosimetry guidelines* (recommendations and allowed variations) across multiple institutions is evaluated in the context of major APBI trial dosimetry constraints (Table 1). For 215 patients accrued to the ACCEL trial, dose-volume parameters were evaluated to determine the achievability of rigorous dosimetry guidelines in a heterogeneous clinical setting.

Table 1: Comparison of standard trial dosimetry constraints and ACCEL dosimetry guidelines recommendations and allowed variation. These *dosimetry guidelines* were significantly stricter than dosimetry constraints formally imposed by trial protocol.

	Trial Dosimetry Constraints		ACCEL Dosimetry Guidelines	
	NSABP B-39/ RTOG-0413	ACCEL	Recommendation	Allowed Variation
Lung				
V <sub>10%</sub> Rx	< 15%	< 10%	< 5%	5 - 10%
Heart				
V <sub>5%</sub> Rx	< 40%	< 5 - 15%	< 5%	5 - 10%
Ipsilateral Breast				
V <sub>50%</sub> Rx	< 60%	< 50%	< 35%	35 - 45%
V <sub>100%,95%</sub> Rx	< 35%	< 25%	< 10%	10 - 20%

## Results

215 patients planned by 12 dosimetrists and reviewed by 10 physicians and 10 physicists across three institutions were included. All APBI plans met NSABP B-39/RTOG-0413 and ACCEL trial *dosimetry constraints*. Normal tissue dosimetry guidelines for ipsilateral breast, lung, contralateral breast, heart, as well as high dose conformity, were satisfied by 95% of patients within the recommended or allowed variations. The mean ( $\pm$  standard deviation) of the ipsilateral breast V<sub>50%</sub> was 30.8 ( $\pm$ 7.8) % which is a significant improvement on the V<sub>50%</sub> less than 50% dose constraint of the NSABP B-39/RTOG-0413 and ACCEL trials (Figure 1). Similarly, the mean ( $\pm$  standard deviation) of the high dose (volume of 95% prescription dose) ipsilateral breast constraint was 10.5 ( $\pm$ 3.6) % as compared to the NSABP B-39/RTOG-0413 and ACCEL trial constraint of less than 25%.

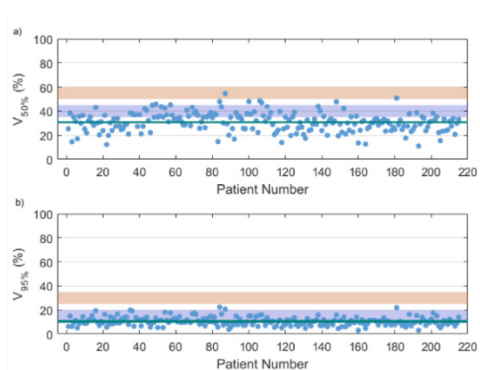


Figure 1: a) Ipsilateral Breast V<sub>50%</sub> and b) ipsilateral breast V<sub>95%</sub> are shown for all 215 patients. The shaded blue region is the acceptable variation of the rigorous ACCEL *dosimetry guidelines* and the shaded orange is the *dosimetry constraints* of the NSABP B-39/RTOG and ACCEL *dosimetry constraints*. The mean value is shown by the green line. For both metrics, the majority of patients, 98.4% and 96.2%, are well within the *dosimetry guidelines* and well below trial constraints.

## Conclusion

The *dosimetry guidelines* are stringent compared to major APBI trial constraints but this work demonstrated they are clinically achievable. These *dosimetry guidelines* provide a tangible means of ensuring consistency in plan quality

and high conformity across multiple institutions and clinicians, which demonstrate a substantial improvement over major APBI trial *dosimetry constraints*.

## EP-1327 Impact of neoadjuvant radiotherapy in locally advanced breast carcinoma

C. Sousa<sup>1</sup>, L. Pinto<sup>2</sup>, M. Cruz<sup>1</sup>, A. Neto<sup>1</sup>, J. Bastos<sup>3</sup>, C. Miranda<sup>1</sup>, G. Melo<sup>1</sup>, L. Khouri<sup>1</sup>, P. Figueiredo<sup>4</sup>, P. Alves<sup>5</sup>  
<sup>1</sup>Instituto Português de Oncologia de Coimbra, Radiotherapy, Coimbra, Portugal ; <sup>2</sup>Instituto Português de Oncologia de Coimbra, Medical Oncology, Coimbra, Portugal ; <sup>3</sup>Instituto Português de Oncologia de Coimbra, Regional Oncology Registry of the Centre, Coimbra, Portugal ; <sup>4</sup>Instituto Português de Oncologia de Coimbra, Anatomical Pathology, Coimbra, Portugal ; <sup>5</sup>Instituto Português de Oncologia de Coimbra- Faculty of Medicine - University of Coimbra, Radiotherapy, Coimbra, Portugal

## Purpose or Objective

The therapeutic approach in locally advanced breast carcinoma remains a clinical challenge. Standard treatment involves systemic therapy with chemotherapy (NACT) and / or hormone therapy (NAHT), surgery and radiation therapy when indicated. More than a third of patients are refractory to systemic cancer treatment, with maintenance of inoperability criteria. There are few data in the literature about alternative treatment when systemic therapy fails. With this study, we intend to evaluate the impact of neoadjuvant radiotherapy (NART) in the treatment of the locally advanced carcinoma.

## Material and Methods

We conducted a retrospective study including female patients, diagnosed with locally advanced invasive breast carcinoma, stages IIB to IIIC, submitted to NART between January 2014 and December 2015 at our institution. The radiotherapy regimens varied between 26Gy / 4Fr / 2,5weeks  $\pm$  30Gy / 10Fr / 2weeks, 50Gy / 25Fr / 5weeks and 60 Gy / 30Fr / 6weeks on the breast volume, supraclavicular and axillary lymph node region. The evaluation of pathological response (pR) was made based on Pinder criteria, divided into three groups: 1 - complete response, 2 - partial response > 90% and 3 - partial response  $\leq$  90%; Primary endpoint: pathological response (pR); Secondary endpoints: overall survival (OS), progression-free survival (PFS). Performed descriptive analysis and survival analysis with Kaplan-Meier method.

## Results

From a total of 51 patients submitted to NART, 42 were included, with a median age of 59 (32-86) years. The most frequent clinical stages were IIIA and IIIB, corresponding to 40.5% and 38.1%, respectively; 35 (83.3%) had lymph node involvement. 22 (52.4%) were basal like (n = 11) and luminal like (n = 11). 26 (61.9%) underwent NACT with anthracyclines and taxanes, 13 (30.9%) NAHT, 5 (11.9%) NART in monotherapy. All included patients underwent mastectomy. Our results: 6 (14.3%) had complete response, 2 of which had only NART. 87% of patients with pR > 90% were under 69 years old. 36 months OS was 64% and PFS was 60%. Subgroup analysis showed 36 months OS of 87% in group 2 versus 48% in group 3, 91% luminal A versus 27% basal like (p < 0.05). After surgery, 19 (45.2%) progressed, of which 17 had distant metastasis, correlated with a worse prognosis (p < 0.05).

## Conclusion

This retrospective study confirms that NART is an effective downsizing treatment in locally advanced breast carcinoma, allowing surgical resection regardless of systemic treatment performed. The pR > 90% is correlated with a better OS. These findings corroborate the literature, with the basal like intrinsic subtype and distant metastasis correlated with worse prognosis.

### EP-1328 A comparison of voluntary vs ABC breath hold in combination with VMAT for pan lymph node breast RT

A. Ranger<sup>1</sup>, A. Dunlop<sup>1</sup>, E. Donovan<sup>2</sup>, E. Harris<sup>1</sup>, N. DeSouza<sup>1</sup>, H. McNair<sup>1</sup>, A. Kirby<sup>1</sup>

<sup>1</sup>ICR and Royal Marsden NHS Foundation Trust, Clinical Oncology, Sutton, United Kingdom ; <sup>2</sup>University of Surrey, Centre for Vision Speech and Signal Processing, Guildford, United Kingdom

#### Purpose or Objective

Breath holding techniques reduce radiation dose to the heart for patients undergoing locoregional breast radiotherapy. This can be achieved either by using machine assisted techniques or voluntary breath hold with no apparent difference in reproducibility between techniques in the context of tangential treatments for the breast/ chest wall. This study aimed to compare the reproducibility of volumetric modulated arc therapy (VMAT) in combination with vDIBH in combination with the active breathing co-ordinator (ABC™, Elekta, Crawley, UK) device. We also aimed to test the feasibility of delivering radiotherapy using vDIBH in combination with VMAT and to patients who require wax bolus for treatment.

#### Material and Methods

Patients requiring locoregional breast radiotherapy including the internal mammary chain (IMC) either with wax bolus or with the combination of VMAT in breath hold were scanned in vDIBH and using the ABC device. Patients were randomised to receive one technique for fractions 1-7 and the other for fractions 8-15. Daily cone beam computer tomography (CBCT) was performed and matched to planning-CT data. Within patient comparisons of mean daily chest wall position were made using a paired t-test. Estimates of population, systematic and random errors were also made. Diaphragm positions in consecutive breath holds were measured and compared between techniques using the Wilcoxon signed-rank test. A novel couch mounted laser was developed to enable the use of vDIBH in combination with VMAT and for patients requiring wax bolus during treatment. Acute skin, lung and oesophageal toxicity was also recorded during and two weeks post treatment.

#### Results

16 patients completed treatment using both techniques. There was no statistically significant difference in mean chest wall displacement between techniques in any direction ( $\leq -1.3\text{mm}$  for ABC,  $\leq -1.5\text{mm}$  for vDIBH, all p non-significant). There was no difference in diaphragm position in consecutive breath holds between techniques (p=0.30, Figure 1) and treatment times were equivalent.



Figure 1: Comparison of diaphragm position using CBCT pre (image a) and post (image b) break in breath hold. Differences in diaphragm position were compared within patients for the vDIBH and ABC techniques.

Patients were successfully treated using VMAT in vDIBH including eleven who required wax bolus. Figure 2 demonstrates the use of the couch mounted laser.



Figure 2: The couch mounted laser (image c) developed for the trial to facilitate the combination of VMAT with vDIBH and the use of vDIBH in patients requiring a wax bolus for treatment. The laser attaches to the couch using suction pads. The laser is positioned using a ball mounted grip to shine the cross hairs onto the patients' skin (images a, b and d). The cross hairs with corresponding mark in free breathing (image a) and breath hold (image b).

Results for acute skin toxicity according to RTOG criteria, acute lung and oesophageal toxicity according to CTCAE criteria during the third week of radiotherapy and two weeks post treatment are presented in table 1. There was no grade 3 or 4 toxicity reported.

Toxicity	On treatment(% of patients)	2 weeks post treatment(% of patients)
Skin	Grade 0	31
	Grade 1	46
	Grade 2	23
	Grade 3	0
Pneumonitis	Grade 0	77
	Grade 1	0
	Grade 2	23
	Grade 3	0
Oesophagitis	Grade 0	92
	Grade 1	0
	Grade 2	8
	Grade 3	0

#### Conclusion

This study demonstrates that it is feasible to use vDIBH in combination with wax bolus or VMAT therapy for the treatment of breast cancer patients. Results support previous data that ABC and vDIBH are comparable in terms of positional reproducibility.

### EP-1329 A Single Pre-Operative Radiation Therapy (SPORT) Phase 1 Trial For Low Risk Breast Cancer

C. Pembroke<sup>1</sup>, M. Yassa<sup>2</sup>, C. Lambert<sup>3</sup>, V. Panet-Raymond<sup>3</sup>, S. Meterissian<sup>4</sup>, F. Tremblay<sup>4</sup>, D. Anderson<sup>5</sup>, P. Vavassis<sup>5</sup>, T. Hijal<sup>3</sup>

<sup>1</sup>Velindre Cancer Centre, Clinical Oncology, Cardiff, United Kingdom ; <sup>2</sup>University of Montreal, Radiation Oncology, Montreal, Canada ; <sup>3</sup>McGill University Health Centre, Radiation Oncology, Montreal, Canada ; <sup>4</sup>McGill University Health Centre, Surgery, Montreal, Canada ; <sup>5</sup>McGill University, Surgery, Montreal, Canada ; <sup>6</sup>University of Montreal, Surgery, Montreal, Canada

#### Purpose or Objective

A single-arm phase 1 feasibility trial offering a preoperative 20Gy fraction for low-risk breast cancer in the post-menopausal setting. We report on our primary objective; feasibility, surgical and cosmetic toxicity at 3 months.

#### Material and Methods

Eligibility criteria for low-risk disease included, age  $\geq 60$  years, unifocal invasive ductal carcinomas  $< 2\text{cm}$ , clinically

node negative, ER positive and HER2 negative. The gross tumour volume (GTV) was defined using mammography, ultrasonography and MRI and grown by 5mm to form the clinical target volume (CTV) and a further 10mm for the planning target volume (PTV). Patients were treated with a single 20Gy fraction to the PTV using volumetric arc therapy up to 72 hours prior to partial mastectomy and sentinel node biopsy. Toxicity was assessed, both subjectively and objectively, using the RTOG-EORTC radiation toxicity scale, NCIC CTCAE and EORTC cosmetic scale at baseline, 48 hours, 14 days and 3,6,9 and 12 months.

#### Results

A total of ten patients with clinical T1N0 invasive ductal carcinomas, with a median age of 69, were treated between October 2016 and March 2018. All patients were planned and treated successfully using pre-defined constraints to a mean PTV of 48.9 cc. Pathological review demonstrated an increase in tumour size by a mean of 2.06mm and all patients were node negative. Four patients had close (<1mm) margins to ductal carcinoma in-situ. Three patients required surgical revision of margins, one of whom chose a subsequent mastectomy and reconstruction following a further close margin. The fourth patient declined surgery and chose to have whole breast radiotherapy (42.56 Gy in 16 fractions). There were no surgical complications, all had grade 1 surgical scar pain and oedema 7 days following theatre but no delays in wound healing were demonstrated. At 3 months, 8 patients reported good (n=7) to excellent (n=1) cosmesis and 2 reported fair results. Six patients reported grade 1 hyperpigmentation and 1 patient had grade 2 and 3 pain and breast oedema respectively.

#### Conclusion

The preliminary results demonstrate feasibility and tolerability following a single pre-operative 20Gy fraction for early stage breast cancer. Continued follow-up is required to meet the secondary objectives including cosmesis at 12 months and ipsilateral breast recurrence.

#### EP-1330 Intraoperative electron radiotherapy (IOERT) boost in early breast cancer: toxicity analysis

C. Vidali<sup>1</sup>, Z. Pellin<sup>2</sup>, M. Severgnini<sup>3</sup>, S. Scomersi<sup>4</sup>, M. Bortul<sup>5</sup>

<sup>1</sup>ASUITS, Radiotherapy, Trieste, Italy ; <sup>2</sup>University of Trieste, Surgery, Trieste, Italy ; <sup>3</sup>ASUITS, Medical Physics, Trieste, Italy ; <sup>4</sup>ASUITS, Surgery, Trieste, Italy ; <sup>5</sup>University of Trieste, Surgery - Breast Unit, Trieste, Italy

#### Purpose or Objective

The clinical activity with IOERT as an anticipated boost in the treatment of early breast cancer started in October 2012 at the Breast Unit of the ASUITS of Trieste.

The aim of this study is to present the results of our experience with particular attention to acute and late toxicity.

#### Material and Methods

Patients with an invasive and unifocal breast tumor - cT1or T2 ≤ 2.5 cm - , cN0-N1 who underwent conservative surgery (quadrantectomy and sentinel node biopsy; axillary dissection only in case of macrometastasis) were eligible to IOERT boost, performed with the mobile LINAC Mobetron.

Two protocols were applied in our Center: 1) IOERT (dose: 10 Gy max. dose) followed by conventional whole breast radiotherapy (WBRT) (50 Gy in 25 fr.); 2) IOERT (11.1 Gy max. dose) followed by hypofractionated WBRT (40.5 Gy in 15 fr.), as in the HIOB Protocol schedule.

Acute toxicity was evaluated after IOERT and at the end of WBRT using the CTCAE 5.0 Toxicity Scoring system and late complications at 6 months and at every further follow-up, using the LENT-SOMA score.

#### Results

From November 2012 to July 2018, 103 IOERT procedures were carried out on 102 patients (one patient had a bilateral synchronous cancer and received the boost bilaterally): in 53 of them (51.46%) IOERT boost was followed by conventional WBRT (group 1) and in 50 of them (48.54%) by hypofractionated WBRT (group 2).

Median age was 67 years (range: 43-85 years); median follow-up was 40 months (range 6-73 months).

Acute toxicity after IOERT boost was present in 19 women (G1 in 14; G2 in 5 cases). Acute toxicity at the end of WBRT was evaluated in 97 patients (two patients refused WBRT; one patient underwent mastectomy and two were lost to follow-up): 74 of them (76.29%) experienced G1 and 7 of them (7.22%) G2 skin toxicity. No differences were observed between the two groups.

Late toxicity was evaluable in 89/97 patients (91.75%) with a minimal follow-up of 6 months (47 in group 1 and 42 in group 2): 19 of them (21.35%) reported G1 and 6 of them (6.74%) G2 toxicity. A statistically significant difference in late toxicity was observed in the two groups in favour of the group treated with hypofractionated WBRT (p=0.004) (Fig. 1).

No local recurrences were observed in the 97 women who concluded the whole treatment, while one patient who had refused WBRT developed a local relapse one year after IOERT. In addition two women developed distant metastases.

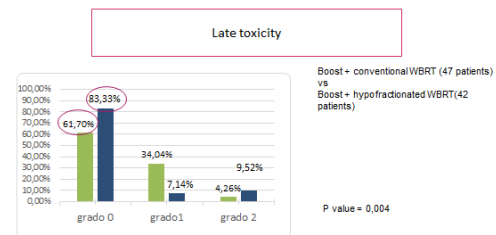


Fig. 1

#### Conclusion

In our experience recurrence rate was very low and acceptable acute and late toxicity were observed, especially in the group of patients who received hypofractionated WBRT after the intraoperative boost. Therefore the use of IOERT as an anticipated boost is encouraged in selected low-risk breast cancer women, even off- clinical trials.

#### EP-1331 Accelerated hypofractionated Whole Breast Irradiation with Concurrent TB Boost: Toxicity and cosmesis

S. Lasheen<sup>1</sup>, S. Shams El Din<sup>1</sup>, R. Moussa<sup>2</sup>, M. Hassan<sup>1</sup>, F. Hagag<sup>1</sup>

<sup>1</sup>NEMROCK Center- Kaser Al-AINI- Faculty of Medicine- Cairo University, Department of clinical oncology, Cairo, Egypt ; <sup>2</sup>NEMROCK Center- Kaser Al-AINI- Faculty of Medicine- Cairo University, Department of medical physics, Cairo, Egypt

#### Purpose or Objective

The safety and efficacy of accelerated hypofractionated WBI has been validated in several clinical trials, however tumor bed boost -when administered in these trials- was prescribed sequential to WBI. The safety of concomitant TB boost in this setting and its impact on cosmetic outcome is of great interest especially in high volume departments to reduce the work load as well as improve patient compliance. The aim of this study is to investigate the use of accelerated hypofractionated WBI with a concomitant TB boost in terms of toxicity and cosmetic outcome.

#### Material and Methods

In this prospective phase II study conducted at the department of clinical oncology, Cairo university, breast cancer patients indicated for post-operative WBI following BCS were recruited to receive an accelerated hypofractionated WBI schedule of 40 Gy/15 fractions over 3 weeks with a concurrent daily boost dose of 8.0 Gy/15 fractions. Dosimetric parameters were set using V38Gy & V36Gy for breast PTV coverage, V45.6Gy and V43Gy for tumor bed PTV coverage, while Dmax and Dmin were used to evaluate homogeneity. Sixty three patients were recruited accordingly, and were followed up for acute toxicity (using CTCAE v3.0 criteria), Late toxicity (reported at least 6 months after end of radiation course and thereafter) and cosmetic outcome (using Harvard score).

#### Results

The study was conducted during the period from June 2014 to June 2017. A total of 63 patients were recruited and followed for a median duration of 24 months (follow-up period ranged from 18 to 32 months). The recruited patients had a median age of 51 years (22-65 years), 24 patients had T1 tumors, 37 had T2 and only 2 recruited patients had T3 disease, and all were node negative. The dosimetric parameters for the coverage of target volumes and dose constrain for OAR were in compatible compliance with our protocol. The mean duration of the whole course of radiation (in days) was 22+/-2.1 days. About 20.63% of the patients had GII acute skin toxicity, while none developed GIII or more acute skin toxicity. As regard late skin toxicity (71.43%) of the patients had G0 late skin toxicity, and (28.57%) of the patients had G1 late skin toxicity no patients had G3 nor G4 late skin toxicity. Till last follow-up date, none of the recruited patients was documented to have >G0 heart nor lung toxicity. Also, none had documented loco-regional nor distant relapse. Regarding cosmetic outcome, 80.95% of the patients were reported as having excellent cosmetic score, while 19% were reported as good (as per Harvard criteria).

#### Conclusion

The proposed accelerated hypofractionated course of WBI with a concurrent TB boost shows acceptable acute toxicity and early cosmetic outcome, however longer follow up is required to better evaluate late toxicity, cosmetic & clinical outcomes.

#### EP-1332 An Urban Institution's Experience with the Oncotype DCIS Score: Predictors and Outcomes

T.Y. Andraos<sup>1</sup>, A. Orisamololu<sup>1</sup>, J. Fox<sup>1</sup>

<sup>1</sup>Montefiore Medical Center, Radiation Oncology, Bronx, USA

#### Purpose or Objective

The Oncotype DCIS Score<sup>®</sup> is a validated predictor of ipsilateral breast recurrence (IBR) in patients (pts) treated with lumpectomy for ductal carcinoma in-situ (DCIS). Criteria for its use are subjective and physician-dependent, and used to guide decision making for adjuvant radiation (RT). We evaluated possible predictors of the DCIS Score<sup>®</sup> and report on outcomes to date in our pt population.

#### Material and Methods

DCIS Scores<sup>®</sup> were available on 90 women who underwent lumpectomy between December 2011 and June 2018. DCIS Scores<sup>®</sup> were reported as low (score 0-38), intermediate (39-54), and high risk (>54). 10 pts' scores were the modified results accounting for age < or >50 and size < or > 1cm. Follow-up (F/U) was calculated from date of initial surgery to date of last mammogram or clinical exam. ANOVA, Chi-Square, and Pearson correlation tests were used to assess statistical comparisons between groups, with p <0.05 considered as statistically significant.

#### Results

Median age was 67 years (30-85). Median size on surgical pathology was 0.6 cm (0 - 4 cm), as measured on a single slide. Grade 1, 2, and 3 DCIS were present in 25 (27.8%),

47 (52.2%), and 18 (20%) of pts, respectively. Necrosis was observed in 46 cases (51.1%). All pts were estrogen receptor (ER) positive; 83 pts (92.2%) were progesterone receptor (PR) positive. Eleven pts (12.2%) underwent re-excision, and surgical margins were ultimately negative ( $\geq$  0.2 cm) in all. Median calculated Van Nuys Prognostic Index (VNPI) score was 6 (3-9). Median calculated Memorial Sloan Kettering (MSK) nomogram value for 10yr IBR risk was 8 (2 - 20). Median DCIS Score<sup>®</sup> was 11(0-79); 72 pts had low risk scores (80%). 26 pts (28.9%) received RT: 5/7 pts who had high risk scores, 6/11 with intermediate and 15/72 with low risk scores. 57 pts (63.3%) received hormonal therapy. High risk DCIS Score<sup>®</sup> correlated with higher nuclear grade (p<0.0001), necrosis (p=0.009), higher VNPI (P=0.002), and PR negativity (p=0.001). Pts with higher DCIS Scores<sup>®</sup> were more likely to have received RT (p=0.001). The MSK nomogram results did not correlate with the DCIS Score<sup>®</sup> results (Pearson correlation coefficient 0.464). Median MSK recurrence risks per Oncotype groupings were 8% in the low Oncotype DCIS risk group, 8% in the intermediate and 7% in pts within the high Oncotype risk group (p=0.256). At a median F/U of 2.13 years (0.04-6.45 years), there is no evidence of recurrence in any patient.

#### Conclusion

Pathologic factors including nuclear grade, necrosis, and PR status are strong predictors of DCIS Scores.<sup>®</sup> The VNPI correlated with DCIS Score<sup>®</sup>, whereas the more comprehensive and widely accepted MSK nomogram did not. Our results suggest a possible underestimation of risk by the MSK nomogram in those with intermediate-high risk DCIS Scores.<sup>®</sup> Long-term F/U is needed to confirm the validity of the DCIS Score<sup>®</sup> in our pt population, and to determine whether this assay versus the MSK nomogram can more accurately IBR risk.

#### EP-1333 Myocardial changes detected using Cardiac MRI in left breast patients treated with Radiation

S. Tang<sup>1</sup>, E.S. Koh<sup>1</sup>, R. Rai<sup>2</sup>, J. Otton<sup>3</sup>, D. Tran<sup>3</sup>, G. Delaney<sup>1</sup>, L. Holloway<sup>2</sup>, B. Schmitt<sup>4</sup>, G. Liney<sup>5</sup>

<sup>1</sup>Ingham Institute for Applied Medical Research, CCore, Liverpool, Australia ; <sup>2</sup>Ingham Institute for Applied Medical Research, Medial Physics, Liverpool, Australia ; <sup>3</sup>Liverpool Hospital, Department of Cardiology, Liverpool, Australia ; <sup>4</sup>Siemens Healthcare Pty Ltd, Siemens Healthcare, Sydney, Australia ; <sup>5</sup>Ingham Institute for Applied Medical Research, MRI Physics, Liverpool, Australia

#### Purpose or Objective

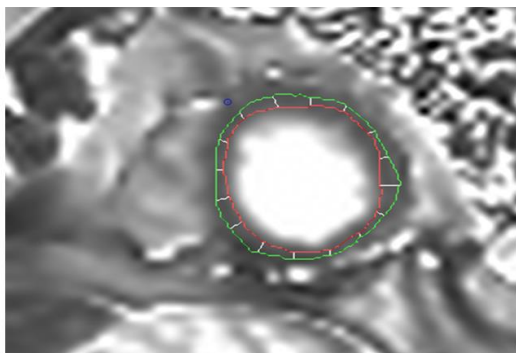
Acute cardiac changes following tangential breast radiation(RT) have been demonstrated using cardiac scintigraphic studies and advanced echocardiographic techniques. This study evaluates the prospective use of cardiac MRI (CMR) in detecting myocardial changes using serial cardiac mapping techniques over a 12 month period.

#### Material and Methods

For 21 left-sided female breast cancer patients (median aged 59 years(38-76)) receiving tangential RT(prospectively recruited between October 2015 and October 2016), three cardiac MRI scans were obtained; a baseline scan 2-3 days before adjuvant RT, 6 - 8 weeks and 12 months respectively following RT. No patients received chemotherapy. A clinical modified look-locker inversion(MOLLI) sequence was used to acquire myocardial short axis T1 maps, pre and 15 minutes post administration of gadolinium-based contrast agent(Gadovist), as well as T2 maps at 3Tesla. Myocardial partition coefficient( $\lambda$ ) was calculated according to ( $\Delta R1$ myocardium/ $\Delta R1$ blood), and extra cellular volume(ECV) was derived from  $\lambda$  by adjusting (1-haematocrit). Two independent T1/T2/ECV map segmentations of the left ventricle were obtained using cvi42, and averaged for analysis(see Figure 1). Single breath-hold SSFP cine acquisitions of the cardiac short axis

were used to determine end diastolic volume (EDV) and end systolic volumes (ESV), LVEF and myocardial mass (systolic and diastolic) indices. Paired t-tests were used to compare the baseline scan with the follow up (6-8 week) and 12 month post treatment scan. A p value of  $\leq 0.05$  was considered significant.

Figure 1 – Segmentation of the left ventricle in short axis (level of mid ventricle) on T1 map



## Results

Mean heart dose was 2.6Gy (1.5-3.9). LVEF, EDV, ESV were not significantly different 6 - 8 weeks, or 12 months following radiotherapy. LV myocardial mass index (LVMMI) (systolic), was significantly increased at 6-8 weeks follow up (53.6 vs 48.4g/m<sup>2</sup> p<0.001) and 12 months (55.5 vs 48.4g/m<sup>2</sup> p<0.001) following radiotherapy. LVMMI (diastolic) was significantly increased at 12 months (mean 58.5 vs 52.2g/m<sup>2</sup> p<0.001). T1 and T2 values were not significantly elevated at the 6-8 week follow up scan, but were significantly elevated at 12 months (T1(ms) - 1213 vs 1246ms p=0.02, T2(ms) - 43.2 vs 45.7ms p<0.01). There was no change in ECV values. Detailed results can be found in Table 1.

Table 1 – Baseline, follow (6-8 weeks) up and 12 month post left breast radiation values

Scan Metric	Baseline Scan	Follow up 6-8 week Scan	12 month Scan
Left ventricular ejection fraction (%)	63.6 (50.2-77.2)	64.7 (56.5-75.3)	64.6 (51.9-80.7)
End diastolic volume (mL)	104.7 (74.0-148.1)	106.0 (80.2-139.8)	107.1 (78.1-160.3)
End systolic volume (mL)	38.0 (23.2-29.3)	37.5 (22.0-51.5)	38.2 (15.8 - 59.3)
Myocardial Mass Index (diastolic) (g/m <sup>2</sup> )	52.2 (39.1-64.5)	57.5 (46.4-59.5) †	58.5 (50.6-75.7) †
T1 Relaxation time (ms)	1213 (1111-1291)	1230 (1165-1311)	1246 (1180-1311) †
T2 Relaxation time (ms)	43.2 (39.6 - 50.1)	42.4 (26.7 - 46.2)	45.7 (41.2-51.7) †
Extracellular Volume (%)	28.4 (23.6 - 32.9)	29.2 (25.3 - 33.0)	27.9 (24.7-37.0)

All reported values are median values (range). †denotes value statistically significant from baseline value with p<0.05.

## Conclusion

Preliminary results suggest that than the myocardial mass index (both systolic and diastolic) increases at 12 months following RT. T1 and T2 values were not significantly different at 6-8 weeks compared with baseline, however were increased at 12 months following radiotherapy. These results may suggest myocardial inflammation post RT occurs and may be detected utilising CMR.

## Electronic Poster: Clinical track: Lung

### EP-1334 Risk factors for esophagitis after hypofractionated palliative (chemo)radiotherapy for NSCLC

C. Nieder<sup>1</sup>, K. Imingen<sup>1</sup>, B. Mannsåker<sup>1</sup>, R. Yobuta<sup>1</sup>, E. Haukland<sup>1</sup>

<sup>1</sup>Nordlandssykehuset HF, Dept. of Oncology and Palliative Medicine, Bodø, Norway

#### Purpose or Objective

Esophagitis influences quality of life and might cause weight loss, treatment interruption and, in severe cases, hospitalization. Previous studies of risk factors mainly relate to curative treatment for non-small cell lung cancer (NSCLC), which often involves concomitant chemoradiation (CRT). Given the uncertainty around extrapolation of dose constraints, we analyzed risk factors in patients treated with hypofractionated palliative regimens, mainly for stage III and IV disease.

#### Material and Methods

A retrospective review of 106 patients treated with palliative 3-D conformal radiotherapy or CRT between 2009 and 2017 was performed. Inclusion criteria: prescribed total dose 30-54 Gy, dose per fraction 2.5-4 Gy (once daily, five fractions per week), esophageal dose >1 Gy. Uni- and multivariate analyses were performed to identify predictive factors for esophagitis grade  $\geq 1$  (CTCAE 5.0). Clinical information was abstracted from our electronic patient record system. All patients were followed during treatment by oncology nurses and physicians. Treatment plans were calculated with Varian Eclipse TPS.

#### Results

Forty percent of patients were treated with 15 fractions of 2.8 Gy (42 Gy) and 30% also received chemotherapy according to the CONRAD study regimen (induction and concomitant Carboplatin/Vinorelbine) published by the Norwegian Lung Cancer Group. Thirty-four percent were treated with 10 fractions of 3 Gy. Stage IV NSCLC was present in 47%. Esophagus Dmax was 39 Gy (population median) and Dmean 15 Gy. Overall 31% of patients developed esophagitis (26% grade 2-3, no grade 4-5). Several dosimetric parameters correlated with the risk of esophagitis (Dmax, Dmean, D5cc, V20, V30, V35, V40). Dmax outperformed other dosimetric variables in multivariate analysis. Furthermore, concomitant chemotherapy significantly increased the risk of esophagitis (for Dmax >39 Gy from 23 to 46%), while oral steroid medication reduced it (all p<0.05 in multivariate analysis). Age, gender and smoking were not significantly associated with esophagitis. When using general NSCLC dose constraints for mean esophagus dose the following rates of grade 2-3 esophagitis were observed: 29% for mean <34 Gy and 22% for mean  $\leq 28$  Gy. In contrast, mean <20 Gy resulted in 11% and mean <15 Gy in 5%. Median actuarial overall survival was 12 months in the CRT cohort and 7 months after RT alone (log-rank p=0.05).

#### Conclusion

In order to reduce the rates of grade  $\geq 2$  esophagitis after hypofractionated palliative treatment lower mean doses than those recommended in other NSCLC settings are preferable. Besides esophageal dose, CRT is the main risk factor for esophagitis. However, CRT also prolongs survival. Additional work is needed to confirm that steroids are able to modify the risk (or to rule out confounding effects of baseline variables not included in our database).

### EP-1335 Interaction of V20 and SUVmax as a predictor of lung toxicity

D. Scepanovic<sup>1</sup>, A. Masarykova<sup>1</sup>, P. Povinec<sup>2</sup>

<sup>1</sup>National Cancer Institute, Radiation Oncology, Bratislava, Slovakia ; <sup>2</sup>PET Centrum BIONT- a. s., Nuclear Medicine, Bratislava, Slovakia

#### Purpose or Objective

The present study aimed to determine if bilateral lung V20 (volume of the whole lung receiving  $\geq 20$  Gy) in connection with the standardized uptake value (SUV) determined with 18F-FDG PET/CT can be used to predict radiation pneumonitis (RP) in lung cancer patients who received radical radiotherapy.

#### Material and Methods

A total of 60 patients with non-small cell lung cancer received 18F-FDG PET/CT examination prior to

radiotherapy. All patients were treated with three-dimensional radiation therapy (3DRT). Radiotherapy was administered five times per week at 1.8-2.0 Gy per time, for a total dose of 60-66Gy. Consecutive eligible patients were assigned to cohorts of nine. SUVmax of each cohort was increased from 3.5 to 6.5, 9.5, 12.5, 15.5, and so on. The cut off value of V20 was 30%.

#### Results

There were 54 patients with V20 < 30% and 6 patients with V20 > 30%. There were no statistically significant differences in the different SUVmax cohorts between the non RP group and the RP group. Eighteen percent of all patients had lung toxicity grade 2. However, no one had severe toxicity. Among our patients there was no difference in the occurrence of lung toxicity either depending of the SUVmax or V20, or their interaction (p=1).

#### Conclusion

In conclusion, the FDG uptake in lung tissue prior irradiation was not associated with the V20 to predict radiation pneumonitis among our patients.

#### EP-1336 Immunogenic prognostic factors in patients with brain metastases from non-small cell lung cancer

H. Doi<sup>1</sup>, K. Nakamatsu<sup>1</sup>, S. Anami<sup>1</sup>, T. Uehara<sup>1</sup>, Y. Wada<sup>1</sup>, K. Fukuda<sup>1</sup>, M. Inada<sup>1</sup>, K. Ishikawa<sup>1</sup>, S. Kanamori<sup>1</sup>, H. Monzen<sup>1</sup>, Y. Nishimura<sup>1</sup>

<sup>1</sup>Kindai University Faculty of Medicine, Department of Radiation Oncology, Osaka-Sayama, Japan

#### Purpose or Objective

Immune checkpoint inhibitors have significantly improved survival outcomes among patients with recurrent and refractory non-small cell lung cancer (NSCLC). Whole brain radiotherapy (WBRT) might be useful for both intracranial tumor control and improving the immune response to systematic disease. This study aimed to identify prognostic factors for brain metastases (BMs) from NSCLC after WBRT. However, there are no clear prognostic factors for WBRT, especially among patients with BMs in terms of their potential immune response. Therefore, the present study aimed to identify prognostic factors for response to radiotherapy among patients with BMs from NSCLC.

#### Material and Methods

This study retrospectively evaluated 100 consecutive patients who underwent WBRT for BMs from NSCLC between December 2012 and October 2017. All patients had pathologically confirmed NSCLC (82 adenocarcinoma, 12 squamous cell carcinoma, and 6 others) and a diagnosis of BMs using images. Blood test data from between 4 weeks before WBRT and the first day of the WBRT course were available. All patients were typically treated using conventional external beam radiotherapy with opposed lateral treatment fields that encompassed the entire brain. The prescribed dose was calculated at the isocenter of the radiation fields based on daily treatments. Patients received a median dose of 30 Gy (range; 14- 45 Gy) in 10 fractions (5- 18 fractions). Clinical factors were tested for associations with overall survival after WBRT.

#### Results

The median follow-up time was 134 days (range: 14-1,395 days), and the median survival time was 143 days, and the 1-year survival rate was 30.4%. Univariate analyses revealed that better survival was associated with an Eastern Cooperative Oncology Group performance status (ECOG-PS) of 0-1, adenocarcinoma pathology, programmed death-ligand 1 (PD-L1) expression, no history of local therapy for BMs, no extracranial disease, LDH levels of <1.5 times the upper limit of normal, a neutrophil-to-lymphocyte ratio (NLR) of <5.0 (11-13), an RPA class of ≤2, and a GPA score of ≥1.5. In the multivariate analyses, better survival was independently associated with PD-L1 expression, no history of local

therapy for BMs, no extracranial disease, and an NLR of <5.0.

#### Conclusion

A low NLR and positive PD-L1 expression independently predict prognosis in patients with BMs from NSCLC after WBRT. These findings suggest that the potential immune response may influence survival among patients with BMs.

#### EP-1337 IMRT/VMAT vs. 3DCRT: the pathological and the clinical outcomes in LANSCLC treated with trimodality

S. Appel<sup>1</sup>, Y.R. Lawrence<sup>1</sup>, Z. Symon<sup>1</sup>, O. Haisraely<sup>1</sup>, M. Perlman<sup>2</sup>, E. Ofek<sup>2</sup>, D. Alezra<sup>1</sup>, T. Katzman<sup>1</sup>, N. Honig<sup>1</sup>, M. Ben-ayun<sup>1</sup>, T. Rabin Alezra<sup>3</sup>, S. Dubinsky<sup>1</sup>, J. Kraitman<sup>1</sup>, L. Tsvang<sup>1</sup>

<sup>1</sup>Chaim Sheba Medical Center, Radiation Oncology, Ramat Gan, Israel ; <sup>2</sup>Chaim Sheba Medical Center, pathology, Ramat Gan, Israel ; <sup>3</sup>Tel-Aviv Sourasky Medical Center, Radiation Oncology, Tel Aviv, Israel

#### Purpose or Objective

More advanced radiation techniques, such as Intensity-modulated radiotherapy (IMRT) and Volumetric Arc Therapy (VMAT) are associated with better normal-tissue sparing compared with traditional 3-dimensional conformal radiation (3DCRT). Conversely, these techniques require a high degree of technical expertise and may potentially inadvertently under-dose tumor due to interplay between beam intensity-modulation and tumor movement. We sought to assess the impact of different radiation techniques on pathological and clinical outcomes in non-small cell lung cancer (NSCLC).

#### Material and Methods

We conducted a retrospective analysis of LANSCLC patients treated with neoadjuvant chemoradiation followed by surgery between August 2012 and August 2018 at the Sheba Medical Center. We recorded the patient, stage, histology, and treatment details. Radiation dose was prescribed to cover 95% of PTV to high dose (60 Gy); contouring was according to the co-registered PET-CT, without elective nodal irradiation and delivered with daily on-board image guidance (IGRT including KV/KV or CBCT). Primary endpoints were pathologic regression scored according to College of American Pathologists recommendations, as well as the average percent of residual tumor cells.

Additional endpoints: surgical margins, the local control rates (LC), disease free (DFS) and overall survival (OS). For the purposes of analysis IMRT and VMAT were combined into a single category. Statistics included non parametric tests, Kaplan Meier estimates; and log rank test

#### Results

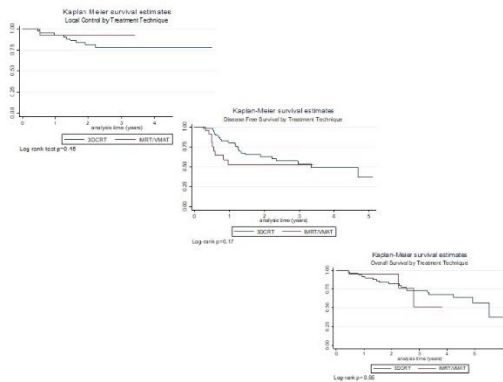
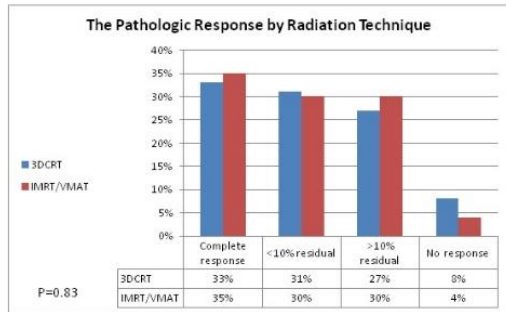
Our cohort included 74 pts, mean age 65.9 (45-79.7), males in 51/74 (69%) adenocarcinoma in 46/74 (62.1%) squamous in 21/74 (28.3%), stage 3 in 59/74 (79.7%), chemotherapy with platinum-based doublets in 72/74 (97.3%).

Radiation dose was 54 Gy and above in 90.5%, mode 59.2Gy. Radiation technique was 3DCRT in 51/74 (68.9%), IMRT in 5/74 (6.7%) and VMAT in 18/74 (24.3%). The use of IGRT-CBCT was in 14/23(61%) in IMRT/VMAT technique, compared to the 12/51(23.5%) in 3DCRT p<0.001.

Major pathologic response (including pCR and <10% residual cells) was similar between radiation techniques: for 3D: 32/51 (62.7%) and for IMRT/VMAT: 15/23 (65.2%) p=0.83. The rate of pCR was similar: for 3DCRT 17/51 (33.3%) and for IMRT/VMAT 8/23 (34.8%) p=0.9. Percent of pathological residual disease (mean±SD) was for 3DCRT: 16 % (SD±25.5) and for IMRT/VMAT: 22% (SD±27.2) p=0.36. Margins were negative in 90.1% (46/51) of patients treated with 3D vs. 89.4% (17/19) in IMRT/VMAT p=1.

At median follow-up of 3.2 years, 2 year local control of 83% (95%CI 70-91%), 2 yrs DFS was 59% (95%CI 46-70) and 3 yrs OS was 72.3% (95%CI 58-82). There was no difference

in LC (p=0.45) DFS (p= 0.17) and OS (p=0.9) between the techniques.  
 We found statistically significant improved in DFS in the major pathological response: HR 2.3 (95%CI 1.13-4.75) (p=0.02).



**Conclusion**

When used to treat NSCLC in the neoadjuvant setting, both IMRT/VMAT and 3DCRT produce comparable clinical and pathologic tumor-control outcomes.

**EP-1338 Hypofractionated Chemoradiotherapy for stage-3 Non-small cell Lung cancer- Single centre experience**

A. Patibandla<sup>1</sup>, N. Mohammed<sup>1</sup>, I. Brisbane<sup>1</sup>, P. McLoone<sup>2</sup>, J. Hicks<sup>1</sup>

<sup>1</sup>Beatson West of Scotland Cancer centre, Clinical Oncology, Glasgow, United Kingdom ; <sup>2</sup>University of Glasgow, Statistics, Glasgow, United Kingdom

**Purpose or Objective**

Concurrent chemoradiotherapy is standard of care for locally advanced stage-3 non-small cell lung cancer (NSCLC). Hypofractionated radical radiotherapy ( 5500cGy in 20 fractions over four weeks ) with chemotherapy (cisplatin & vinorelbine) has been proven safe and effective in a randomised phase -2 trial(SOCCAR trial). In this retrospective study we looked at our institutional experience of delivering this regimen.

**Material and Methods**

Electronic records were retrospectively reviewed for all stage-3 NSCLC patients who had SOCCAR regimen from January 2012 to December 2016. Data was censored on 31<sup>st</sup> March 2018. Kaplan-Meier analysis was used to estimate median survival.

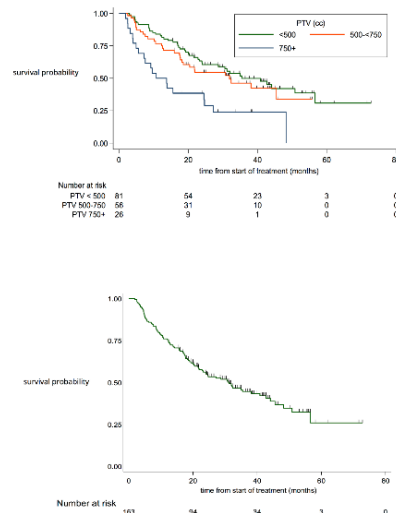
**Results**

Total of 163 patients, all the stage-3 NSCLC patients treated with SOCCAR regimen between January 2012 to December 2016. Median age- 63 years.

All patients except one were staged by PET-CT prior to starting treatment. All were either ECOG performance status of 0 or 1. Squamous cell carcinoma- 55%,

Adenocarcinoma- 31%, other- 14%.

Median follow up was 3.2 years. Median overall survival 31.2 months (95% CI 21.9- 42.8). On treatment toxicity was tolerable with no treatment related deaths. 20% had local recurrence, 23% had distant metastases and 7% had local recurrence & distant metastases. 77% of patients were treated by Volumetric modulated arc radiotherapy (VMAT) plan and 23% by conventional plan. The larger the planning target volume (PTV) lesser the median overall survival.



**Conclusion**

Hypofractionated radiotherapy with chemotherapy was well tolerated in stage -3 NSCLC patients. Toxicity was minimal and no non-cancer death within 90 days of treatment. Overall median survival was superior to all arms in recently published international phase 3 trials.

**EP-1339 Clinical outcomes of stereotactic radiotherapy using flattening-filter-free in lung cancers**

T. Taweesakulvashra<sup>1</sup>, S. Kitpanit<sup>1</sup>, A. Songthong<sup>1</sup>, C. Chakkabat<sup>1</sup>, N. Amornwicheit<sup>1</sup>, P. Alisanant<sup>1</sup>, C. Nantavithya<sup>1</sup>, C. Lertbutsayanukul<sup>1</sup>, K. Shotelersuk<sup>1</sup>, C. Khorprasert<sup>1</sup>, D. Kannarunimit<sup>1</sup>

<sup>1</sup>King Chulalongkorn Memorial Hospital- Chulalongkorn University, Division of Radiation Oncology- Department of Radiology, Bangkok, Thailand

**Purpose or Objective**

SBRT using FFF has been increasingly applied due to its benefits in escalating dose rate, short treatment time and less out-of-field dose, however, studies investigating outcomes and toxicities of this technique in lung cancers are lacking. Thus, we conducted a review to assess efficacy in terms of 2-year local control (LC), progression free survival (PFS), overall survival (OS) and treatment-related toxicities in patients with early-stage NSCLC and oligometastatic lung cancers.

**Material and Methods**

From February 2014 to July 2018, 101 patients underwent lung SBRT with FFF were retrospectively reviewed. All patients underwent SBRT with VMAT and unflatten beam using 6 and 10 MV photon. Patients with follow up period less than six months or lack of follow-up imaging were excluded. Dose and fractionation were selected from our institutional protocol. LC, PFS and OS were analyzed using Kaplan-Meier method. Early and late toxicities (6 months after SBRT) were evaluated. All target lesions were accounted for LC assessment.

## Results

101 patients and 143 lesions with median follow up time of 24 months were included for the analysis. 22 patients with 22 lesions were early NSCLC and 79 patients with 121 lesions were lung metastases in which 40% were from colorectal cancers and 21.4% were from primary lung cancers. SBRT fractionation ranged from 48-60 Gy in 3-5 fractions (10-18 Gy/fraction, BED 100-151 Gy10) and 25-60 Gy in 1-7 fractions (5-25 Gy/fraction, BED 36-180 Gy10) for early NSCLC and oligometastatic lung cancers, respectively. All patients completed treatment without any interruption. Mean tumor volume was 22.7 cc and mean PTV volume was 52.1 cc. 2-year LC, PFS and OS were 90.9%, 50.3% and 83.5% for early NSCLC, and 92.6%, 50% and 74.8% for metastatic lung cancers. Early toxicity was low with only five percent reporting CTCAE grade 2. The most common acute toxicity was pneumonitis (23.7%). No toxicity greater than grade 2 was found for early and late toxicity. BED>70 Gy10 was associated with better OS compared with less than 70 Gy for lung metastasis (HR 0.29, 95%CI = 0.09-0.84).

## Conclusion

Lung SBRT using FFF-technique provides promising clinical outcomes for both early-stage NSCLC and oligometastatic lung cancer patients. BED>70Gy10 in metastatic lung cancers may be adequate to yield good LC and OS. A prospective study is encouraged to confirm this result.

### EP-1340 Lactate dehydrogenase predicts survival in small cell lung cancer patients with brain metastases

S. Anam<sup>1</sup>, H. Doi<sup>1</sup>, K. Nakamatsu<sup>1</sup>, T. Uehara<sup>1</sup>, Y. Wada<sup>1</sup>, K. Fukuda<sup>1</sup>, M. Inada<sup>1</sup>, K. Ishikawa<sup>1</sup>, S. Kanamori<sup>1</sup>, Y. Nishimura<sup>1</sup>

<sup>1</sup>Kindai University Faculty of Medicine, Department of Radiation Oncology, Osaka-Sayama, Japan

## Purpose or Objective

Small-cell lung cancer (SCLC) represents < 20% of total lung cancer cases with poor survival outcome especially in patients with extensive disease. SCLC patients often develop brain metastases (BMs) over the course of the disease. However, specific predictors for outcomes associated with SCLC and BMs remain unclear.

## Material and Methods

Between February 2008 and December 2017, we identified 48 consecutive patients with BMs from SCLC who underwent WBRT at our institution. All patients had pathologically confirmed SCLC with a diagnosis of BMs, which was based on images. Blood test data between 4 weeks before the WBRT and the first day of WBRT treatment were available. When WBRT started, all patients had extracranial diseases except for one. The median age was 70 years; 42 (88%) and 6 (13%) patients were male and female, respectively. At the initial staging, 32 (67%) and 16 (33%) patients had extensive disease (ED) and limited disease (LD) SCLC, respectively. In addition, 22 (46%) patients had BMs at the time of the initial diagnosis of SCLC. All patients were typically treated with WBRT using conventional external beam radiotherapy and lateral-opposed treatment fields that encompassed the entire brain. Thirty-three (69%), 6 (13%), and 9 (19%) patients received the prescribed total dose of 30 Gy in 10 fractions, 37.5 Gy in 15 fractions, and 40 Gy in 16 fractions, respectively.

## Results

Forty patients died in the follow-up period. Symptoms due to BMs were observed in 25 (52%) patients. Among the 25 patients with symptomatic BMs, 16 (64%) showed symptom improvement after WBRT. The median survival was 232 days and the 1- and 2-year overall survival rates were 34.4% and 5.8%, respectively. The intracranial failures were found in 36% of patients. Univariate analyses revealed that longer survival was associated with 5 factors: Eastern Cooperative Oncology Group performance status (ECOG-PS) of 0-1 (p=0.0006), asymptomatic BMs

(p<0.0001), LDH levels in the normal range (p=0.0036), RTOG-RPA class 2 (p=0.0013), and a GPA score of ≥1.5 (p=0.0486). In patients with normal and elevated LDH values, the 1-year survival rate was 54.7% and 17.6%, respectively. No significant impact on survival after WBRT was observed for the clinical stage at the initial diagnosis, presence of BMs at the initial diagnosis, maximum diameter of BMs, number of BMs, prescription dose of WBRT (Gy), or the pre-WBRT serum levels of NLR and PLR. In multivariate analyses, elevated LDH levels (p=0.0133) and presence of symptoms due to BMs (p=0.0130) were found as significant independent predictors of poor survival.

## Conclusion

The present study revealed that high LDH level and the existence of BM-related symptoms predict a significantly poor survival after WBRT for BMs from SCLC. Elevated LDH may yield valuable information to identify patients with BMs who have poor survival outcomes.

### EP-1341 Evaluation of tumor motion variability with and without abdominal compression plate in lung SBRT

K. Talapatra<sup>1</sup>, V. Raturi<sup>1</sup>, R. Vadgaonkar<sup>1</sup>, S. Jadhav<sup>1</sup>, P. Chadha<sup>1</sup>, V. Mhatre<sup>1</sup>, S. Pilakkal<sup>1</sup>

<sup>1</sup>Kokilaben Dhirubhai Ambani Hospital and Medical Research Institute, Radiation Oncology -, Mumbai, India

## Purpose or Objective

To evaluate the significance of abdominal compression plate (ACP) with respect to variability in lung tumor motion and setup.

## Material and Methods

Fifteen consecutive lung cancer patients who received SBRT in our institute between January 2016 and December 2016 were enrolled prospectively. All patients were immobilized using Vacloc on SBRT base plate. Out of fifteen, six patients were treated with ACP and remaining nine were treated without plate. Cone beam CT scan was acquired before delivery of each fraction and appropriate shifts were applied after matching target volumes and OARs. Mean and standard deviation were calculated. Unpaired t test used for statistical analysis and all values p<0.05 was considered as statistically significant.

## Results

Tumor was located in upper lobe for 10 patients, in middle lobe for 2 and in lower lobe for 3 patients. Mean tumor motion was observed without ACP in comparison to with ACP is cranio-caudal (CC) direction 0.36±0.2cm versus 0.37±0.15 cm (p=0.28, CI: 0.32 to 0.1), in antero-posterior (AP) direction 0.34±0.2 cm versus 0.37±0.15 cm (p=0.879, CI: 0.19 to 0.22), in medio-lateral (ML) 0.38±0.14 cm versus 0.26 ±0.09 cm (p=0.1, CI: 0.25 to 0.02) and rotation motion observed was pitch 0.77°±0.46° versus 0.37° ± 0.1° (p=0.06, CI: 0.82 to 0.02), roll 1.24 °±0.8° versus 0.36°±0.21° (p=0.02, CI: 1.6 to 0.14), yaw 0.04°±0.43° versus 0.28°±0.18° (p=0.001, CI: 1.17 to 0.36).

	SBRT lung	Vertical (cm)	Lateral (cm)	Longitudinal (cm)	Pitch (°)	Roll (°)	Rotational (°)
N	Without ACP	9	9	9	9	9	9
	With ACP	6	6	6	6	6	6
Mean	Without ACP	0.338	0.377	0.358	0.767	1.24	1.05
	With ACP	0.237	0.267	0.375	0.370	0.368	0.282
Standard error mean	Without ACP	0.0673	0.0467	0.0679	0.155	0.267	0.144
	With ACP	0.0572	0.0395	0.0617	0.0437	0.0894	0.0759
Median	Without ACP	0.280	0.340	0.300	0.750	1	0.880
	With ACP	0.185	0.220	0.340	0.405	0.345	0.265
Standard deviation	Without ACP	0.202	0.140	0.204	0.465	0.801	0.433
	With ACP	0.140	0.0967	0.151	0.107	0.219	0.186
Variance	Without ACP	0.0408	0.0196	0.0414	0.217	0.642	0.187
	With ACP	0.0196	0.00935	0.0229	0.0114	0.0480	0.0346

## Conclusion

This study demonstrates the benefit of the abdominal compression plate in respiratory tumor motion to produce a high efficient decrease in breathing induced tumor motion especially the rotational movements (roll and yaw).

**EP-1342 SBRT for central lung malignancies using a Simultaneous Integrated Protection (SIP) approach**  
 R. Mazzola<sup>1</sup>, R. Ruggieri<sup>1</sup>, F. Vanessa<sup>1</sup>, R. Michele<sup>1</sup>, G.L. Niccolò<sup>1</sup>, R. Francesco<sup>1</sup>, N. Luca<sup>1</sup>, C. Stefanie<sup>2</sup>, A. Filippo<sup>1</sup>  
<sup>1</sup>Sacro Cuore Don Calabria Cancer Care Center, Radiation Oncology, Negrar, Italy; <sup>2</sup>University Hospital- LMU, Radiation Oncology, Munich, Germany

#### Purpose or Objective

It is recognized that Stereotactic Body Radiotherapy (SBRT) for centrally located lung malignancies is affected by high rates of severe toxicity. In the present study, we report the clinical outcomes following a novel intensity-modulated radiotherapy prescription dose, termed simultaneous integrated protection (SIP) for nearby organs at risk (OARs).

#### Material and Methods

The present study is a mono-institutional prospective observational study. The inclusion criteria were: single central lung lesion receiving SBRT; absence of extra-thoracic disease; Karnofsky performance status > 70; maximum tumor diameter < 5 centimeters (cm); at least 6 months of follow up after SBRT. Lung malignancies were defined as central according to the International Association for the Study of Lung Cancer (IASLC) recommendations (i.e., tumor within 2 cm to any mediastinal critical structure). The prescribed total doses of SBRT were: 70 Gy in 10 fractions and 60 Gy in 8 fractions. For ultra-central located lesions, a dose of 60 Gy in 10 fractions was delivered. The main planning instructions were: (1) to remain within the limits of the given dose constraints for an OAR; (2) to make use of the maximum possible dose to the OARs to minimize dose inhomogeneity for PTV. SBRT-related toxicity was prospectively assessed according to Common Terminology Criteria for Adverse Events (CTCAE) v4.0. The primary clinical end-point was the toxicity SBRT-related. Secondary endpoint was local control.

#### Results

According to the inclusion criteria of the present analysis, 40 patients affected by a single central malignancy were selected. The median follow up was 20 months (range 6-58 months). The median age was 72 years (range 30-81 years).

The median distance between tumor and mediastinal healthy structures was 0.6 cm (range 0- 1.8 cm). The one-year local control rate was 91%. The median time to local progression was 13 months (range 6-46 months). One-year distant progression free survival rate was 71.7%. At the time of the analysis, the 1- and 2- years overall survival rates were 86.9% and 72.6%, respectively. Acute and late clinical pulmonary toxicity  $\geq$  grade 2 were recorded in 2 out of 40 patients (5%) and 3 out of 40 patients (7%). No patient experienced cardiac toxicity. No narrowing or stenosis of any airway or vessel was registered.

#### Conclusion

SBRT using a PTV-SIP approach for single central lung malignancies allowed to achieve low toxicity SBRT-related with acceptable local control.

#### EP-1343 Multimodality Repeated-Ablative Therapies In Oligorecurrent Pulmonary Metastatic Disease

A. Macagno<sup>1</sup>

<sup>1</sup>Paoli-Calmettes Institute, Radiotherapy, Marseille, France

#### Purpose or Objective

Stereotactic radiotherapy (SBRT) and percutaneous thermal-ablation (TA) are surgery alternatives for the management of pulmonary oligometastases. In this collaborative work we analysed patients who undergone iterative focal ablative treatments on pulmonary oligometastases. We hypothesized that some of these

patients, although with progression with additional pulmonary oligometastases, would still have a potentially curable oligometastatic disease and repeated ablative therapies could delay systemic treatment.

#### Material and Methods

From October 2011 to November 2016, a retrospective analysis was performed at 2 academic centre including patients treated with SBRT and TA for pulmonary oligometastases.

#### Results

**Patient characteristics:** A total of 198 lesions were treated for 102 patients; 45 patients (44.1%) underwent repeated focal treatment at the pulmonary site for an oligorecurrent disease. The median follow-up of the cohort was 22.5 months. Respectively, 29 patients, 12 patients and 4 patients had 2, 3 and 4 treatment sequences. The median interval between the first and the 2<sup>nd</sup>, the 2<sup>nd</sup> and the 3<sup>rd</sup>, and the 3<sup>rd</sup> and the 4<sup>th</sup> sequence was respectively 13 months, 12.5 months and 10.5 months. A colorectal or renal primary cancer was found significantly more often in multi-treated oligorecurrent patients in contrast to a bronchopulmonary primary cancer.

**Treatment characteristics:** The number of lesions treated by TA, SBRT and surgery are respectively 95, 103 and 14 lesions. 31 patients had a treatment combining several types of ablative techniques either to treat several pulmonary lesions during the same sequence, or during different treatment sequences. Patients treated with SBRT had more significantly central topography lesions compared to those treated with TA (p <0.005). Lesions treated with SBRT were significantly larger in diameter than those treated with TA (p = 0.003).

**Patient outcome:** The 3-year overall survival rates of patients who had a single treatment sequence versus those with repeated treatments were respectively 73.9% and 78.8%, not significantly different (p = 0.86). The 3-year systemic therapy free survival of multi-treated oligorecurrent patients was 51.2%. In univariate analysis, only WHO status is significantly associated with OS (p=0.04).

Tolerance of repeated treatments was excellent, one grade 4 toxicity was observed.

#### Conclusion

We established the first series of repeated multimodal local treatment for oligometastatic or oligorecurrent disease. These repeated treatments are effective with acceptable pulmonary toxicity. OS of patients treated with curative intent on several oligometastatic events is similar of those treated for a single oligometastatic event. Ablative treatments of their oligometastases may delay the use of systemic treatments, with the clinician's main concern being the maintenance of quality of life.

#### EP-1344 Helical Tomotherapy based SBRT in early stage lung cancer: a mono-institutional study (2014-2018)

F. Pastore<sup>1</sup>, A. Rese<sup>1</sup>, F. Francomacaro<sup>1</sup>, F. Cammarota<sup>1</sup>, G. Ametrano<sup>1</sup>, D. Toledo<sup>1</sup>, V. Iorio<sup>1</sup>

<sup>1</sup>Emicenter, Radiation Oncology, Mondragone, Italy

#### Purpose or Objective

To evaluate the use of Helical Tomotherapy (HT) based SBRT in the treatment of early stage lung cancer patients. The HT system employs a compact 6 MV Linac-based on CT ring gantry to rotationally deliver intensity modulated fan beams. Patients are translated through-out the gantry on a treatment couch, resulting in helical irradiation geometry. The HT unit also contains a mega-voltage CT detector array located opposite the radiation source for pre-treatment verification, allowing accurate re-positioning. This technique permits to precisely target tumors while minimizing impact on surrounding healthy tissue.

### Material and Methods

45 patients with early stage lung cancer (cT1-T2, cN0) were treated in our institution from 2014 to 2017 with HT-SBRT. No patients had positive lymphnodes in previous CT or PET/CT scan. No patients were fit for surgical indication due to concomitant medical conditions. The patients was placed with arms above the head, while the hands held a support such as a handlebar. All the CT images were acquired from the skull base to 3 cm below the diaphragm. CT axial scanning was performed at 3-mm intervals: for this purpose a CT Multislice GE Healthcare Discovery 590HT was used. The radiation oncologists contoured the volumes of interest (CTV) according to the RTOG guidelines. The planning target volume (PTV) was generated from the CTV volume by adding a 3 mm margin in all directions. Accurate delineation of organ at risk was performed. Treatment plans were evaluated on a dedicated TPS. In these patients, we used several radiotherapy schedules, according to volume, site of the lesions and guidelines.

### Results

At 2-year follow-up, we observed complete response in 18 patients (40%), partial response in 14 (31%), stable disease in 9 (18%), progressive disease in 5 (11%). The median OS was 40 months. We analyzed acute and late toxicity: G1 Radiation Pneumonitis was seen in 10/45 patients (22%) and G2 was observed in 4/45 patients (8%). No patients need hospitalization. Moreover, G1 dyspnea was observed in 4 patients (11%) and G2 in 2 patients (5%). G1 radiation esophagitis was seen in 4/45 patients (8%). Other major complications (pain or hematologic) were not observed. Radiation-induced rib fracture was not seen in our group of patients.

### Conclusion

HT is a safe and feasible technique to treat patients with early stage lung cancer. Acute toxicity was acceptable. This study had several limitations: a small number of patients, an heterogeneous clinical and radiological presentation of treated lung cancer and an incomplete follow up. Also the use of different fractionation must be enrolled into the limits of these analysis.

### EP-1345 Serum Lactate Dehydrogenase: A Predictor of Therapeutic Response to Radiation Therapy in SCLC?

L. Ana Rita Carvalho da Costa<sup>1</sup>, G. Sofia<sup>1</sup>, A. Gonçalo<sup>1</sup>, R. Darlene<sup>1</sup>, F. Paula<sup>1</sup>, M. Margarida<sup>1</sup>, P. Gabriela<sup>1</sup>  
<sup>1</sup>Centro Hospitalar de São João, Radioterapia, Porto, Portugal

### Purpose or Objective

Increased values for serum lactate dehydrogenase (LDH) were significantly associated with a reduced duration of survival in patients with small cell lung cancer (SCLC) in several studies published in recent years. Although serum LDH has been reported as a prognostic biomarker in SCLC, it is not known whether this is due in part to a worse tumor response to radiation therapy. Little is known about how this factor influences prognosis, including the probability of long-term disease-free survival. The present retrospective study aims to analyze whether there is a correlation between the serum LDH and the radiation therapy response and prognostic significance of serum LDH in SCLC treated with thoracic irradiation.

### Material and Methods

This retrospective study included all patients diagnosed with SCLC and serum LDH levels at diagnosis and before radiation therapy, treated with thoracic irradiation at CHSJ, between January 2005 and April 2018. A database was created with information obtained from patients' clinical records. The serum LDH was registered at diagnosis and before radiation therapy and its possible association with treatment response, time to tumor relapse/progression, progression-free survival (PFS) and overall survival (OS) was assessed. Statistical analysis was performed with SPSSv24. The impact of the raised values

for serum LDH on cancer outcomes was evaluated using the Fisher Exact Test, Kaplan-Meier plots and the log rank test.

### Results

The study included 45 patients, 31 males and 14 females, with a median age of 66 years. Median follow-up time was 16 months. Sixteen patients diagnosed with localized disease, who underwent concurrent or sequential chemoradiation therapy, and 29 patients presented with disseminated disease at the diagnosis, having performed thoracic consolidation irradiation after a good response to chemotherapy. Of the 45 patients, 18 were in the high serum LDH group and 27 were in the normal serum LDH group. In comparison to a normal serum LDH, a high serum LDH was significantly associated with worse OS (11.8 months vs 20.6 months,  $p=0,049$ , CI 95%) and worse PFS, but not statistically significant (9.9 months vs 16.1 months,  $p=0.138$ , CI 95%). There was no relation between a high serum LDH and treatment response.

### Conclusion

Current knowledge about prognostic factors in SCLC includes serum LDH, with high serum LDH being a poor prognostic factor with shorter survival time. The mechanisms underlying this association are not fully understood, and the impact of serum LDH on the response to radiation therapy is not known. The present study showed that there is no association between an increased LDH value and a worse response to radiotherapy, although patients with increased LDH value had shorter PFS and OS. However, due to the small sample size, no definite conclusions can be drawn, and future studies are needed to safely assess a possible relationship between serum LDH and response to radiation therapy.

### EP-1346 A framework for systematic clinical evaluation of the MR-linac for treatment of lung cancer patients

D. Cobben<sup>1</sup>, H. Bainbridge<sup>2</sup>, J. Belderbos<sup>3</sup>, P. Cheung<sup>4</sup>, M. Dubec<sup>5</sup>, D. Gomez<sup>6</sup>, E. Gore<sup>7</sup>, E. Knowles<sup>8</sup>, F. Lalezari<sup>9</sup>, U. Oelfke<sup>9</sup>, J. Sonke<sup>3</sup>, R. Tijssen<sup>10</sup>, C. Van Es<sup>10</sup>, M. Van Herk<sup>11</sup>, A. Wetscherek<sup>9</sup>, F. McDonald<sup>2</sup>, C. Faivre-Finn<sup>1</sup>  
<sup>1</sup>Christie Hospital NHS-University of Manchester, Radiotherapy Related Research, Manchester, United Kingdom ; <sup>2</sup>The Royal Marsden NHS, Clinical Oncology, London, United Kingdom ; <sup>3</sup>The Netherlands Cancer Institute, Radiation Oncology, Amsterdam, The Netherlands ; <sup>4</sup>Sunnybrook Hospital, Radiation Oncology, Toronto, Canada ; <sup>5</sup>MD Anderson Cancer Centre, Radiation Oncology, Houston, USA ; <sup>6</sup>Medical College of Wisconsin, Radiation Oncology, Milwaukee, USA ; <sup>7</sup>Elekta, Real-Time Adaptive Treatment Portfolio, Crawley, United Kingdom ; <sup>8</sup>The Netherlands Cancer Institute, Radiology, Amsterdam, The Netherlands ; <sup>9</sup>ICR, Physics, London, United Kingdom ; <sup>10</sup>University Medical Centre Utrecht, Radiation Oncology, Utrecht, The Netherlands ; <sup>11</sup>University of Manchester, Radiotherapy Related Research, Manchester, United Kingdom

### Purpose or Objective

Our objective is to evaluate the introduction of the MR-linac (MRL) for the treatment of lung cancer patients via a systematic approach: R-IDEAL.

### Material and Methods

A recent innovation in radiotherapy is the MR-linac (MRL) developed by Elekta and Philips. The MRL combines a 1.5 T MRI with a 7 MV linac. It allows the acquisition of high resolution MR images for on treatment verification, adaption and response monitoring. Seven cancer institutions from Europe and North America, are working within the Elekta MR-Linac Consortium to evaluate the MRL within a framework called 'R-IDEAL' (Radiotherapy Idea Development Exploration Assessment Longterm Evaluation) (Verkooijen et al. Frontiers in Oncology 2017).

## Results

**STAGE 0:** We defined in 80 patients the optimal MRI sequences suitable for GTV and organ at risk (OAR) contouring: T2 Turbo Spin Echo (TSE), T2 TSE with fat sat, T1 radial gradient echo, and DIXON TSE. Two radiology-led workshops were organized and inter-observer agreement was assessed for OARs. These led to a consensus-based OAR atlas. A study is being prepared to compare the image quality of the current standard CBCT and MR images at baseline and mid-treatment for treatment verification and set-up correction.

**STAGE 1:** we will investigate the clinical feasibility of the MRL for standard of care radiotherapy and the scope for adaptive radiotherapy (margin reductions) and detecting changes in oxygenation during treatment on the MRL in patients with locally advanced (LA) Non-small Cell Lung Cancer (NSCLC).

**STAGE 2a/b :** Based on the results from stage 1 we will design a study aiming to reduce margins around the tumour and dose escalate in patients with LA NSCLC. Table 1. summarizes the ongoing and planned work within the Elekta MR-Linac Consortium.

	Pre-clinical studies	Idea	Development	Exploration	Assessment
	Stage 0	Stage 1	Stage 2a	Stage 2b	Stage 3
<b>Purpose</b>	Technical preparatory studies	Real time use of the MRL for treatment delivery in vivo	In vivo demonstration of the feasibility for treatment delivery	Pre-clinical proof of early clinical effectiveness and safety of the innovation	Final comparison of innovation against standard treatment
<b>Outcomes and planned work</b>	Development of MR-Linac sequences Development of a consensus atlas for MR-guided lung radiotherapy Comparison of quality of the pre-taken cone beam CT (CBCT) vs MR-Linac on image guidance	Investigation of the feasibility of standard RT on the MRL and real-time RT adaptation	Final answer to a cohort study of patients with reduced PTV margins	Investigation of dose escalation with hypofractionated RT in locally advanced NSCLC	Randomized controlled trial: standard of care vs dose escalated hypofractionated RT

## Conclusion

The aim of this programme of work is to generate robust evidence to support the introduction of the MRL and to improve outcomes of patients with LA NSCLC.

### EP-1347 “Risk adaptive” dose prescription in central NSCLC lesions in early stage NSCLC and lung metastases

M. Rigo<sup>1</sup>, N. Giaj-Levra<sup>2</sup>, V. Figliar<sup>2</sup>, R. Mazzola<sup>2</sup>, L. Nicosia<sup>2</sup>, F. Ricchetti<sup>2</sup>, R. Ruggieri<sup>2</sup>, F. Alongi<sup>3</sup>

<sup>1</sup>Istituto Oncologico Veneto - IRCCS Sacro Cuore Don Calabria Hospital, Radiation Oncology, Padova, Italy ;

<sup>2</sup>IRCCS Sacro Cuore Don Calabria Hospital, Radiation Oncology, Negrar-Verona, Italy ; <sup>3</sup>IRCCS Sacro Cuore Don Calabria Hospital - University of Brescia, Radiation Oncology, Negrar-Verona, Italy

### Purpose or Objective

Stereotactic ablative radiotherapy (SABR) is considered an innovative approach in early stage non-small cell lung cancer (NSCLC) and lung oligometastases. Initial experiences evaluated SABR in inoperable central (<2 cm from large bronchial tree) lung tumors located. Unacceptable levels of severe lung toxicity have been reported and “risk adaptive” dose prescription was considered an additional tool to overlap organs at risk (OAR). Aim of this study was to evaluate efficacy (local control) and tolerability in patients with a diagnosis of primary or metastatic central lung lesion, treated with a “risk adaptive” SABR approach.

### Material and Methods

Patients aged  $\geq 18$ -years with a histological or radiological proof of single central early stage NSCLC or lung oligometastases were enrolled. OAR were: homolateral lung, heart, spinal cord, esophagus, bronchial tree and chest wall. Total radiation dose was decided according to “risk adaptive” approach. In the case of overlap, sparing of the OAR was favoured to target volume coverage. A number of daily fractions between 4 and 10 was prescribed.

Radiological response was assessed according to RECIST, acute (<6 months) and late ( $\geq 6$  months) clinical and radiological toxicities were scored using Ickeoe et al. criteria and Common Terminology Criteria for Adverse Events version 4.0, respectively.

### Results

From January 2012 to September 2018, 29 patients with early stage or oligometastatic lung metastases received a SABR treatment. Median Biological equivalent dose prescription and fractions were: 105 Gy (range 96-119) and 10 (range 4-10), respectively. Median follow-up was 19 months. Local control was reported in 25 patients (86%), a local progression in 4 patients (14%). Early radiological abnormalities were identified as follows: no changes in 15 patients (52%), patch ground glass opacity in 9 (31%) and patchy consolidation and ground glass opacity in 5 (17%). Late radiological abnormalities were as follows: no changes in 5 cases (17%), scar-like pattern in 8 (28%), mass-like pattern in 10 (34%), not available in 6 cases (21%). Acute and late clinical pulmonary toxicity  $\geq$  grade 2 were recorded in 2 out of 29 patients (7%) and 3 out of 23 patients (13%).

### Conclusion

SABR “risk adaptive” prescription in inoperable central lung tumors is considered a safe and efficacy treatment. Higher accrual and follow-up are necessary to confirm these data.

### EP-1348 Clinical outcome of one-fraction early-stage lung SBRT: is it an option in selected patients?

I. Rodrigues<sup>1</sup>, T. Figueiredo<sup>1</sup>, J. Gagean<sup>1</sup>, C. Ferreira<sup>1</sup>, S. Conde<sup>1</sup>, L. Carvalho<sup>1</sup>, J. Cardia<sup>1</sup>

<sup>1</sup>Instituto Português de Oncologia do Porto Francisco Gentil, External Radiotherapy Department, Porto, Portugal

### Purpose or Objective

In our Institution, we follow an in-house protocol that encompasses fractionation schedules and constraints included in the RTOG 0813, 0236 and 0915 protocols (1x30Gy, 3x18-20Gy, 4x12-12.5Gy and 5x10Gy). Recently, ACROP-ESTRO guidelines suggested different fractionation schedules (3x15Gy and 4x12Gy), obtained by consensus among representatives from several European SBRT centers. The main purpose of this retrospective study was to evaluate the influence of fractionation on clinical outcome (global, specific and local progression-free survival) and toxicity in early-stage lung cancer patients in our Institution.

### Material and Methods

We retrospectively analysed all patients treated with SBRT for primary early-stage lung cancers in our department between 1st January 2012 and 31st December 2016. Treatments were carried according to RTOG protocols, and one-fraction schedules were selected for small peripheral tumors located away from the chest wall.

### Results

Between 2012 and 2016, 143 early-stage lung cancer patients (with 149 tumors) underwent SBRT. Most were males (79%) with a median age of 73 years (ranging from 51 to 91). Median follow-up was 22 months. Median maximum diameter was 2.3cm (from 0.7 to 5.5). Most tumors were adenocarcinomas (69%), followed by squamous carcinomas (28%). Thirty seven tumors were irradiated with 1 fraction of 30Gy, 18 with 3 fractions of 18-20Gy, 52 with 4 fractions of 12-12.5Gy and 39 with 5 fractions of 10Gy. As a result, 49.7% tumors remained stable, 24.8% exhibited a complete response and 19.5% a partial response. Disease progression was eventually observed in the treated area in 14 patients (9.8%), elsewhere in the lung in 16 patients (11.2%), in the lymph nodes in 15 (10.5%), and a distal progression was noted in 11 patients (7.5%). At 18 months, overall survival (OS) was 77.3%, disease-specific survival (DSS) was 91.9% and local progression-free survival (L-PFS) was 93.7%. The most

common acute toxicity was G1 fatigue (in 13 patients). The most frequently documented late side effect was G1 pneumonitis in 46 patients (followed by G1 dyspnea in 12, G1 thoracic pain in 11, and G1 cough in 10). Two ribs fractures occurred, and no toxicities greater than G3 were observed. Different fractionation schedules (including one-fraction) did not have an impact in OS, DSS or L-PFS, both in tumors  $\leq 2$ cm, and in tumors  $> 2$ cm, and no schedule exhibited a trend towards worse outcomes.

#### Conclusion

In our series, OS, DSS and L-PFS are in accordance with literature-reported outcomes. Although the low number of progressions may limit the analysis, one-fraction SBRT does not seem to be inferior to other fractionation schedules in appropriately selected patients. The low number of observed side effects (namely  $G \geq 3$ ) also did not allow us to infer any correlation with the fractionation schedule.

#### EP-1349 Three-d Surface Imaging as preferred tool for patients' set up in frameless SBRT for lung cancer

C.M.E. Perotti<sup>1</sup>, C. Pisani<sup>1</sup>, G. Loi<sup>2</sup>, A. Belli<sup>1</sup>, C. Bolchini<sup>1</sup>, Y. Huang<sup>3</sup>, J. Lyu<sup>3</sup>, M. Krengli<sup>4</sup>

<sup>1</sup>University Hospital "Maggiore della Carità", Department of Radiotherapy, Novara, Italy ; <sup>2</sup>University Hospital "Maggiore della Carità", Department of Medical Physics, Novara, Italy ; <sup>3</sup>Sichuan Cancer Center, Department of Radiation Oncology, Chengdu, China ; <sup>4</sup>University of "Piemonte Orientale"- University Hospital "Maggiore della Carità", Department of Translational Medicine- Department of Radiotherapy, Novara, Italy

#### Purpose or Objective

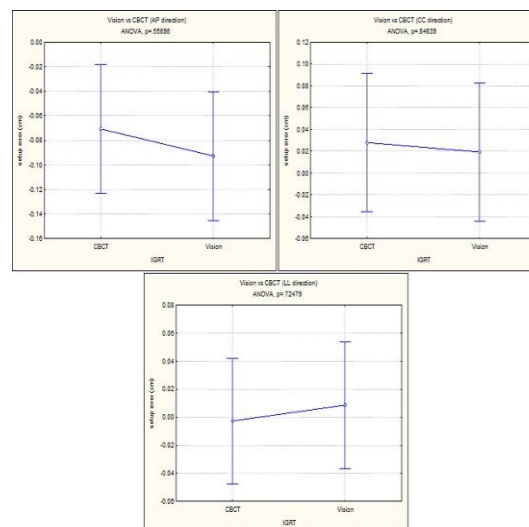
Surface-based image guided radiotherapy (IGRT) allows positioning and/or monitoring patients receiving radiation treatment in 3 dimensions (3D), without the use of ionizing radiation. The purpose of this study is to investigate the usage of 3D Surface Imaging, specifically the Vision RT's AlignRT system, as the primary tool for the set up of patients who are treated with frameless stereotactic body radiotherapy (SBRT) for lung cancer by comparison with cone-beam computed tomography (CBCT).

#### Material and Methods

Twenty patients (12 men and 8 women) were included in the study. For each fraction of treatment the patients were positioned using the AlignRT system and the vertical, longitudinal and lateral shifts were measured with the CBCT according the Cartesian axis system. Surfaces were captured just before CBCT acquisitions. The data were retrospectively retrieved, manually researching the medical records reporting the values of the shifts detected with CBCT. The mean, the range and the standard deviation relative to the shifts were calculated with respect to the X, Y and Z axes. The agreement between the two different procedures was then analyzed with the Bland-Altman test, which allows to evaluate the correlation between two systems that measure the same parameter.

#### Results

The mean of the shifts was found to be equal to -0.08 cm (range -0.3; 0.5) for the Z axis, equal to 0.01 cm (range -0.7; 0.5) for the X axis and 0.04 cm (range -0.8; 0.6) for the Y axis. The standard deviation was 0.21 cm for the Z axis, 0.22 cm for the Y axis and 0.23 cm for the X axis, respectively; these standard deviation values probably reflect the presence of some outliers values that are highly likely to represent data entry errors.



#### Conclusion

Three - dimensional surface imaging is confirmed to be a reliable method for patients' setup, able to guarantee high precision in the delivery of SBRT treatment.

#### EP-1350 DART-bid by VMAT for locally advanced NSCLC: Low toxicity, encouraging survival and tumor control

K. Wurstbauer<sup>1</sup>, R. Pinter<sup>1</sup>, M. Meinschad<sup>2</sup>, M. Kazil<sup>1</sup>, T. Hernler<sup>3</sup>, P. Cerkl<sup>3</sup>, T. Künzler<sup>2</sup>, A. De Vries<sup>1</sup>

<sup>1</sup>Academic Teaching Hospital, Radiation Oncology, Feldkirch, Austria ; <sup>2</sup>Academic Teaching Hospital, Medical Physics, Feldkirch, Austria ; <sup>3</sup>Academic Teaching Hospital, Pneumology, Hohenems, Austria

#### Purpose or Objective

Results of 60 Gy with concurrent chemotherapy for locally advanced NSCLC are disappointing. DART- bid (dose-Differentiated Accelerated RadioTherapy - 1,8 Gy twice daily) is a radiation dose-intensified approach, sequentially combined with chemotherapy. Our experience up to now is reported.

#### Material and Methods

55 widely unselected patients (85% in stages IIIA-C, 8<sup>th</sup> edition) were treated from 1/2015 until 5/2018. >5% weight loss/ 3 months in 31%, KI <80% in 24% of patients. Overall doses applied were as follows: Primary tumors 73.8 - 90.0 Gy, in positive correlation to tumor volumes; nodes 61.2 Gy; nodes electively 45 Gy (to sites about 6 cm cranial of macroscopically involved nodes); fractional doses 1.8 Gy bid; interval 8h.

GTV (ITV) to PTV: 7 mm; planning with the intention to spare as much as possible of the ipsilateral (tumorbearing) lung; application by VMAT; cone beam CT before every fraction.

Duration of radiotherapy 31 days median (28-37 days); in 89% of the patients 2 cycles platin-based chemotherapy were given before, with a target interval between chemotherapy and radiotherapy of < 8 days.

#### Results

With a median follow-up time of 12.6 months (3.9-37.5 m.) the 1-year overall survival rate is 72%, the median overall survival time 24.1 months; for the 21 patients (38%), matching with the RTOG 0617 inclusion criteria, the 1 year survival rate amounts to 78% and the median overall survival time is not reached.

7 local recurrences and 5 isolated regional recurrences occurred, resulting in local and regional tumor control rates at 1 year of 86% and 90%, respectively.

Acute adverse effects of pneumonitis grade 2 and 3 occurred in 4 and 1 patients, respectively; acute

esophagitis grade 1, 2, 3 in 18%, 53%, 2% of the patients, respectively. No acute toxicity grade 4 or 5 occurred. In 2 patients with central tumors and close vicinity to great vessels, a treatment relationship to lethal haemorrhages, 7 and 9 months after the end of radiotherapy, cannot be excluded. Besides that, no late toxicity >grade 1 was observed.

#### Conclusion

This accelerated, differentiated dose-intensified approach yields encouraging results for survival and tumor control; along with in general low toxicity up to now.

#### EP-1351 Long-term survival with FDG-PET directed therapy in NSCLC with synchronous solitary brain metastasis

S.J. Newman<sup>1</sup>, N. Bucknell<sup>1</sup>, M. Bressel<sup>1</sup>, P. Tran<sup>1</sup>, B. Campbell<sup>1</sup>, N. Haghighi<sup>1</sup>, D. Kok<sup>1</sup>, M. MacManus<sup>1</sup>, C. Phillips<sup>1</sup>, M. Shaw<sup>1</sup>, A. Wirth<sup>1</sup>, G. Wheeler<sup>1</sup>, D. Ball<sup>1</sup>, S. Siva<sup>1</sup>

<sup>1</sup>Peter MacCallum Cancer Centre, Radiation Oncology, Melbourne, Australia

#### Purpose or Objective

At diagnosis, approximately 10% of all patients with NSCLC have intracranial metastases, and 1% have synchronous solitary brain metastasis (SSBM). In similar cohorts treated radically to both sites published 5-year overall survival (OS) is 11-21%. Use of FDG-PET can significantly alter staging, treatment choices and intent. We investigate the outcomes of patients diagnosed with NSCLC and SSBM and treated with radical local therapies in the FDG-PET era.

#### Material and Methods

In this retrospective study, eligible patients had histologically-confirmed NSCLC and SSBM staged with FDG-PET and received radical treatment from 1/2/1999 to 31/12/2017. A lung-molecular graded prognostic assessment (lung-molGPA) score was assigned for each patient using age, ECOG score, and, if performed, molecular status. Overall survival (OS) and progression free survival (PFS) were calculated using Kaplan-Meier methods. Cox proportional hazard models determined prognostic factors for PFS.

#### Results

Forty-nine patients were eligible. Median age was 63 years (range: 34-76). Thirty (61%) were male. Nineteen patients (39%) were ECOG 0, 26 (53%) ECOG 1 and 4 (8%) ECOG 2. Sixty-seven percent were  $\geq$ T2 and 47% were  $\geq$ N2 (Table 1). Forty-six of 48 patients (1 unknown) (96%) had MRI brain. For intrathoracic disease, 10 patients (20%) had surgery, surgery and RT in 1 (2%), surgery and adjuvant chemoRT in 2 (4%), surgery and adjuvant chemotherapy in 2 (4%), chemoRT in 29 (59%), SABR in 4 (8%) and fractionated RT in 1 (2%). For intracranial disease, 20 patients (41%) had surgery, 7 (14%) definitive SRS and 22 (45%) had adjuvant RT. For adjuvant RT, 20 had whole brain RT and 2 had SRS cavity boost. Median follow up of all patients was 3.9 years. Median time to first relapse was 6 months (95%CI: 5-11). At 2 years, 45% of first failures were intracranial only (95%CI: 30-59). At 2 years PFS was 13% (95%CI: 6-28). At 2 and 5 years, OS was 56% (95%CI: 43-73) and 30% (95%CI: 18-51), respectively (Figure 1). In  $\geq$ N1 disease, 5 year OS was 34% (95%CI: 18-63). On univariable analysis, lower ECOG (HR 2.28, 95%CI: 1.17-4.43, p=0.014) and higher lung-molGPA scores (HR 0.26, 95%CI: 0.11-0.61, p=0.002) were associated with significantly longer OS. Higher lung-molGPA was associated with significantly longer PFS (HR 0.47, 95%CI: 0.24-0.94, p=0.031). On multivariable analysis, lung-molGPA (HR 0.33, 95%CI: 0.15-0.71, p=0.005) and N-stage (HR 1.56, 95%CI: 1.13-2.15, p=0.007) were significant positive and negative prognostic factors, respectively, for PFS.

Table 1: Tumour pathology and staging

Tumour type	
Adenocarcinoma	32 (65%)
Squamous cell carcinoma	5 (10%)
Large cell neuroendocrine carcinoma	3 (6%)
NSCLC NOS	9 (18%)
Differentiation	
Moderately	7 (21%)
Poorly	27 (79%)
Unknown	15
Mutation status	
EGFR	4 (44%)
KRAS	5 (56%)
Unknown	40
Tumour stage	
T0	1 (2%)
T1	15 (31%)
T2	20 (41%)
T3	8 (16%)
T4	5 (10%)
Nodal stage	
N0	22 (45%)
N1	4 (8%)
N2	20 (41%)
N3	3 (6%)

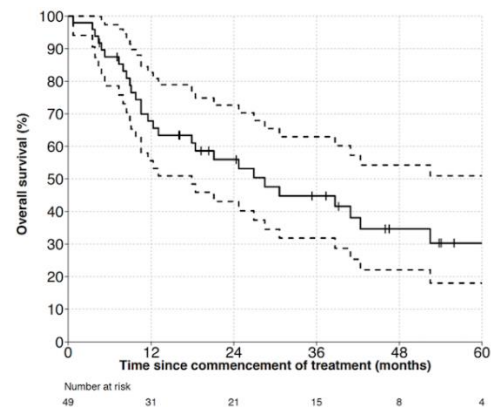


Figure 1: Five year overall survival

#### Conclusion

Patients with NSCLC and SSBM staged with FDG-PET had a 5 year OS of 30% when treated radically to both sites. This is greater than previously reported outcomes. For  $\geq$ N1 patients, the 5 year OS was 34%, which to our knowledge is the longest reported survival in similar populations. These results suggest that such patients should be treated with aggressive local therapy, as this can be associated with long-term OS and possible cure.

#### EP-1352 Locally advanced NSCLC: performance status based eligibility for adjuvant check point inhibitor

G. Persson<sup>1,2,3</sup>, T. Schytte<sup>4,5</sup>, A.L. Appelt<sup>6,7</sup>, S. Borissova<sup>1</sup>, C. Brink<sup>5,8</sup>, T.S. Hansen<sup>9</sup>, L. Hoffmann<sup>10</sup>, M. Josipovic<sup>3</sup>, A.A. Khalil<sup>11</sup>, M.M. Knap<sup>11</sup>, M.D. Lund<sup>12</sup>, C.M. Lutz<sup>10</sup>, D.S. Møller<sup>10</sup>, T.B. Nielsen<sup>8</sup>, M. Nielsen<sup>8</sup>, W. Ottosson<sup>1</sup>, M. Pøhl<sup>3</sup>, J.B. Thomsen<sup>3</sup>, O. Hansen<sup>4,5</sup>

<sup>1</sup>Herlev Hospital- University of Copenhagen, Department of Oncology, Herlev, Denmark ; <sup>2</sup>Faculty of Health and Medical Sciences- University of Copenhagen, Department of Clinical Medicine, Copenhagen, Denmark ;

<sup>3</sup>Rigshospitalet- University of Copenhagen, Department of Oncology, Copenhagen, Denmark ; <sup>4</sup>Odense University Hospital, Department of Oncology, Odense, Denmark ;

<sup>5</sup>University of Southern Denmark, Institute of Clinical Research, Odense, Denmark ; <sup>6</sup>St. James's University Hospital, Leeds Cancer Centre, Leeds, United Kingdom ;

<sup>7</sup>University of Leeds, Leeds Institute of Cancer and

Pathology, Leeds, United Kingdom ; <sup>8</sup>Odense University Hospital, Laboratory of Radiation Physics, Odense, Denmark ; <sup>9</sup>Vejle Hospital- University of Southern Denmark, Department of Oncology, Vejle, Denmark ; <sup>10</sup>Aarhus University Hospital, Department of Medical Physics, Aarhus, Denmark ; <sup>11</sup>Aarhus University Hospital, Department of Oncology, Aarhus, Denmark ; <sup>12</sup>Vejle Hospital- University of Southern Denmark, Department of Medical Physics, Vejle, Denmark

#### Purpose or Objective

The standard treatment of locally advanced non-small cell lung cancer (LA-NSCLC) has changed with the PACIFIC trial, stating that the addition of 1-year adjuvant immune checkpoint inhibitor therapy after completed concomitant chemoradiotherapy increases the 2-year survival rate compared to placebo. Inclusion criteria were a WHO performance status (PS) of 0-1 and no sign of progression. Adjuvant therapy should start within 42 days of completed chemoradiotherapy.

The aim of this analysis was to determine the fraction of patients with LA-NSCLC that have PS 0-1 within six weeks after completion of concomitant chemoradiotherapy and would hence be candidates for adjuvant immune checkpoint inhibitor therapy.

#### Material and Methods

We are currently recruiting patients with LA-NSCLC in a national multicenter randomized phase III isotoxic dose escalation trial. In the study the control arm receives 66 Gy in 33 fractions concomitantly with cis- or carboplatin every third week and fixed dose vinorelbine 50 mg three times weekly. The concomitant chemoradiotherapy is preceded by a single series of induction platinum-based combination chemotherapy. Radiotherapy is delivered with intensity modulated or volumetric arc modulated therapy. Daily image guidance with conebeam CT and treatment adaptation guidelines are used.

The trial inclusion criteria are cytology or histology proven LA-NSCLC and PS 0-1. Diagnostic procedures include FDG-PET/CT and endobronchial ultrasound (EBUS) with aspiration cytology from central mediastinal nodes. We are investigating the possibility of an amendment to allow for adjuvant immune checkpoint inhibitor therapy to enable continuous inclusion in the study. Thus, an unplanned interim analysis was performed within the trial, analyzing only baseline characteristics and PS at the first clinical follow-up six weeks post radiotherapy.

#### Results

Patients were included from January 2015 and forward. Data lock for the interim analysis was September 1<sup>st</sup>, 2018. 124 patients had completed their treatment and attended their first clinical follow-up. Clinical report form was filled out for 109 patients; PS data were missing for ten patients, leaving 99 for analysis. Patient characteristics are shown in Table 1. PS at start and six weeks after end of radiotherapy are shown in Figure 1. No patients were in PS 3 or 4 after radiotherapy.

#### Conclusion

The majority of patients (85%) with LA-NSCLC, who were staged with EBUS and PET/CT and received state-of-the-art concomitant chemoradiotherapy in a randomized dose escalation trial, remained in PS 0-1 after finished radiotherapy and were thus candidates for adjuvant immune checkpoint inhibitor therapy.

**Table 1: Patient characteristic (N=99)**

Age:	Median (range)	66 (38-80)
Sex:	Male	50
	Female	49
Histology:	Squamous	36
	Adeno	60
	Adenosquamous	2
	Other	1
Stage <sup>1</sup> :	IIB	5
	IIIA	55
	IIIB	39

<sup>1</sup> 7. IUCC

**Figure 1:**

Performance status (PS) at baseline vs. 6 weeks after radiotherapy (RT)

6 weeks after RT (no. of patients)	Baseline (no. of patients)		Total (N=99)
	PS 0	PS 1	
PS 0	31	12	44
PS 1	19	22	41
PS 2	6	8	14

#### EP-1353 Lung cancer extracerebral oligometastases/oligoprogression stereotactic irradiation

M. Kissel<sup>1</sup>, I. Martel-Lafay<sup>2</sup>, J. Lequesne<sup>3</sup>, J. Faivre<sup>4</sup>, C. Le Péchoux<sup>5</sup>, D. Stefan<sup>1</sup>, V. Barraux<sup>1</sup>, C. Loiseau<sup>1</sup>, J. Grellard<sup>3</sup>, S. Danhier<sup>1</sup>, D. Lerouge<sup>1</sup>, C. Chouaid<sup>6</sup>, R. Gervais<sup>7</sup>, J. Thariat<sup>1</sup>

<sup>1</sup>Centre François Baclesse, Radiotherapy, Caen, France ;

<sup>2</sup>Centre Léon Bérard, Radiotherapy, Lyon, France ;

<sup>3</sup>Centre François Baclesse, Clinical research, Caen, France ;

<sup>4</sup>Institut de Cancérologie de Lorraine, Radiotherapy, Nancy, France ;

<sup>5</sup>Institut Gustave Roussy, Radiotherapy, Villejuif, France ;

<sup>6</sup>Centre Hospitalier Intercommunal de Créteil, Pneumology, Créteil, France ;

<sup>7</sup>Centre François Baclesse, Pneumology, Caen, France

#### Purpose or Objective

While stereotactic irradiation (SBRT) of cerebral metastases is standard in oligometastatic lung cancer, the clinical benefit of SBRT in extracranial metastases depending on metastatic burden and aggressiveness awaits evidence. The aim was to assess feasibility and efficacy of a radical approach on all extracerebral metastatic sites among lung cancer patients with an "oligo" disease.

#### Material and Methods

This retrospective multicentric study in four French cancer centers included patients treated with SBRT on all their extracerebral metastatic sites corresponding to the following settings : extracerebral oligometastatic (one to five lesions at diagnosis), oligorecurrent (metastatic relapse with one to five metastases), oligoprogressive (1-5 progressive lesions with all other lesions controlled by systemic treatment) or oligopersistent (consolidative

radiotherapy with 1-5 residual lesions following systemic treatment) lung cancer.

#### Results

91 patients and 99 metastases were included. Local control was 91%, median progression free survival (PFS) was 6.3 months [4 ; 8.1] and median overall survival was 28.2 months [20.1 ; 35.5]. There were significant differences between metastatic settings : median overall survival was not reached in the oligometastatic group, 33 months in the oligorecurrence group, 28.2 months in the oligopersistent group and only 6.5 months in the oligoprogressive group. Metastatic site, nodal status and free interval for oligorecurrent patients were significant prognostic factors. Toxicities were moderate since only 5.5% of patients experienced grade 3 acute toxicities and none had late grade 3-4 toxicity. SBRT allowed delaying the administration of systemic treatments since more than half of the patients could remain free from systemic treatment for several months.

#### Conclusion

Optimal dose, fractionation and timing regarding association with systemic treatments remain to be defined. Aggressive metastatic management seemed feasible and appeared to delay reintroduction of systemic treatments. Larger scale randomized studies are necessary to demonstrate survival benefit.

#### EP-1354 Impact of Pulmonary SABR on Pulmonary Function Tests: Report of a single institution experience

M. Keys<sup>1</sup>, S. O'Sullivan<sup>1</sup>, R. Mc Dermott<sup>1</sup>, N. Wallace<sup>2</sup>, M. Dunne<sup>1</sup>, J. Armstrong<sup>1</sup>, P. Thirion<sup>1</sup>

<sup>1</sup>St. Luke's Radiation Oncology Network, Radiation Oncology, Dublin 6, Ireland ; <sup>2</sup>Cork University Hospital, Radiation Oncology, Cork, Ireland

#### Purpose or Objective

Pulmonary Stereotactic Body Radiotherapy (SABR) is a well established standard alternative therapy for patients (pts) diagnosed with inoperable early-stage Non Small Cell Lung Cancer (NSCLC). The impact of SABR on pulmonary function remains unclear. Results from retrospective studies suggest a minimal if any decline in post-SABR pulmonary function. The results were also mixed with regard to the Pulmonary Function Test (PFTs) parameter effected. We report here a single institution experience comparing prospectively acquired pre and post-SABR PFTs.

#### Material and Methods

From March 2014 to May 2018, 84 pts. with documented PFTs pre- and post-SABR (within 1 year post therapy) were identified. The main characteristics of the population included: median age of 75 years (from 59-91years), female predominant (57%), underlying COPD stage 3-4 (23.8%), and ex- or active smoker (87.6%). All pts. except for one were treated for NSCLC, pathologically proven in 86 pts. The tumour locations were mostly in the upper lobes (58.3%) and peripheral (88.1%). The median GTV and PTV volumes were 11.68cm<sup>3</sup> (from 1.04 to 52.58cm<sup>3</sup>) and 33.11cm<sup>3</sup> (from 6.39 to 116.72cm<sup>3</sup>) respectively. The protocol driven radiation schedules used were 54Gy/3 (11.9%), 60Gy/5 (73.8%) and 60Gy/8 (14.3%). Paired-samples t-tests were conducted to evaluate the Pre- and post-SABR PFT values and independent samples t-tests and ANOVA were conducted to compare the results between demographic characteristics.

#### Results

Pre- and post-SABR FEV<sub>1</sub> data was available for all 84 pts. The median pre- and post-SABR FEV<sub>1</sub> was 1.41L (from 0.4 to 2.9L) and 1.3L (from 0.45 to 2.8L) respectively. Overall There was a statistically significant post-SABR FEV<sub>1</sub> decrease, with a mean decrease of .05L [95% CI: 0.002 to 0.11, p=0.04]. Pre- and post-SABR DLCO was available in 68 pts. The median pre- and post-SABR DLCO was 9.1 ml/mmHg/min (from 0.6 to 20.7) and

9.5ml/mmHg/min (from 1.35 to 26.1) respectively. Overall there was a statistically significant post-SABR DLCO decrease, with a mean decrease of 2.5% [95% CI: 0.1-4.89, p=0.04]. However Individual variation was observed with a decrease observed in 40 pts, an increase in 22, and no change in 6. The only identified negative risk factor for post-SABR DLCO reduction was female gender.

#### Conclusion

The present study found a statistically significant post-SABR DLCO and FEV<sub>1</sub> decrease, however with significant inter-individual variation. Whether this is a temporary or permanent change, we were unable to assess this. Whether this decrease translates into a functional change is unlikely but not proven. The clinical significance and reversibility need to be further studied through large scale clinical trials and compared to other therapeutic alternatives.

#### EP-1355 Oligo-progressive status exhibits unfavorable survival in pulmonary oligo-recurrence treated by SABR

H. Lee<sup>1,2</sup>, J. Tsai<sup>3</sup>, S. Chen<sup>4</sup>, I. Lai<sup>5</sup>, C. Chen<sup>2,6</sup>, C. Ho<sup>7</sup>, J. Chiou<sup>1,2</sup>, Y. Kuo<sup>4</sup>

<sup>1</sup>Taipei Medical University Hospital- Taipei Medical University, Department of Radiation Oncology, Taipei, Taiwan ; <sup>2</sup>Taipei Medical University, Taipei Cancer Center, Taipei, Taiwan ; <sup>3</sup>Taipei Medical University-Shuang Ho Hospital, Department of Radiation Oncology, New Taipei City, Taiwan ; <sup>4</sup>China Medical University Hospital, Department of Radiation Oncology, Taichung, Taiwan ; <sup>5</sup>Taipei Veterans General Hospital, Division of Radiation Oncology- Department of Oncology, Taipei, Taiwan ; <sup>6</sup>Wan Fang Hospital- Taipei Medical University, Department of Radiation Oncology, Taipei, Taiwan ; <sup>7</sup>Camillians Saint Mary's Hospital Luodong, Department of Radiation Oncology, Yilan, Taiwan

#### Purpose or Objective

Oligo-progression exhibits distinct biological signatures during the evolution of cancer metastasis, but its clinical significance has not been clarified. We investigated the treatment outcome of stereotactic ablative radiotherapy (SABR) for pulmonary oligo-recurrence in metastatic cancer patients with controlled extrapulmonary diseases and evaluated the prognostic value of oligo-progressive status of targeted lung tumors.

#### Material and Methods

The patient inclusion criteria were pulmonary oligometastases with controlled primary and extrapulmonary disease, SABR as the primary local treatment for oligo-recurrent lung tumors, and consecutive imaging follow-up. Pulmonary oligo-recurrence was defined as ≤5 metastatic lung tumors with absent or controlled disease elsewhere. The status of targeted lung tumors were further classified into oligo-progressive and controlled status to indicate the drug resistance developing in lung or not, respectively. Overall survival (OS) and prognostic variables were evaluated using Kaplan-Meier analysis and Cox regression model.

#### Results

Thirty-two patients with sixty-seven lung tumors treated with SABR were enrolled. With a median follow-up period of 19.5 months, the median OS was 33.0 months. Oligo-progressive status (P = .0413) and an increased number of lung tumors (P = .0217) were independently associated with inferior OS. A higher biological effective dose (BED<sub>10</sub>) (P = .0423) was independently correlated with longer in-field radiographic progression-free survival. Synchronous metastases (P = .0133) and an Eastern Cooperative Oncology Group score of ≥1 (P = .0010) were significantly associated with inferior out-field radiographic progression-free survival. Grade 2 radiation pneumonitis occurred in six (18.8%) patients. No toxicity above grade 2 was recorded.

### Conclusion

Oligo-progressive status of lung tumors exhibits a less favorable survival outcome in metastatic patients with pulmonary oligo-recurrence treated by SABR.

### EP-1356 Targeted therapy with or without Radiotherapy in EGFR/ALK mutant NSCLC with Brain Metastases

I. Císcar García<sup>1</sup>, M. Martín Martín<sup>1</sup>

<sup>1</sup>Ramon y Cajal University Hospital, Radiation Oncology, Madrid, Spain

#### Purpose or Objective

The treatment of brain metastases of non-small cell lung cancer (NSCLC) especially those with EGFR and ALK mutation is controversial. TKIs may have more than 70% intracranial response rate in these patients, and delay radiotherapy until progression of disease has been proposed. The purpose of this study is to analyze the treatment and the results in our patients with brain metastasis of EGFR mutant or ALK positive NSCLC.

#### Material and Methods

Eligible patients were those diagnosed between January 2013 and December 2017 with brain metastases (found at diagnosis or at progression) from NSCLC. We registered the local and systemic progression and the type of treatment and moment received. We analyzed the brain progression free survival without radiation therapy (RT) and we compared the overall survival (OS) between patients treated with RT at diagnosis of the metastases and those who were treated at progression.

#### Results

43 patients with NSCLC and EGFR/ALK mutation, presented brain metastases throughout the disease evolution. 29 (67.5%) had EGFR, 13 (30%) ALK and 1 (2.3%) had ROS mutation. At diagnosis, those who had more than 3 brain metastases were 18 (62%) with EGFR mutation and 8 (57%) with ALK mutation. 21 patients (48.8%) were treated with initial radiotherapy and TKI, while in 16 patients (37.7%) the radiotherapy was delayed until the cerebral progression. 6 (14%) did not receive radiotherapy treatment: 3 of them because they died from the disease one month after diagnosis of brain metastases and were excluded for survival analysis. The type of radiotherapy used was holocraneal in 25 patients (58.1%), fractionated stereotactic in 4 patients (9.3%) and radiosurgery in 8 patients (18.6%). 5 received surgery and subsequent radiotherapy (2 fractionated and 3 radiosurgery). For patients with second-generation TKIs, the median lifetime of the communication of the cerebral results of diagnosis of brain metastasis was for 9 months and for the states with Erlotinib and Gefitinib or CT for 7 months. For patients with EGFR mutant tumors who were treated with delayed radiation therapy, the median time to brain progression was 7 months and 5 months for ALK and ROS. When they received radiotherapy at the diagnosis of brain metastases, the median to progression was the same for the two types of mutation, 13 months. The median overall survival for patients with EGFR mutation treated with RT at diagnosis of brain metastases was 16 months, while for patients as well as at 12 months, for ALK positive patients it was 21 and 23 months respectively, these differences were not significant.

#### Conclusion

Up front radiotherapy does not improve overall survival in patients with brain metastases of EGFR mutant or ALK positive non small cell lung cancer, but the potential benefit of delaying radiotherapy must be balanced with the short time of brain progression. We haven't found significant differences in the brain response between front and second-line TKIs.

### EP-1357 Spinal metastases from non-small cell lung cancer; is it a surrogate of bad outcome?

L. Krozkin<sup>1</sup>, I. Ospovat<sup>2</sup>, D. Machievsky<sup>2</sup>, E. Gez<sup>2</sup>, S. Soifer<sup>2</sup>, B. Corn<sup>2</sup>, Y. Natan Hoz<sup>2</sup>, O. Gutfeld<sup>2</sup>, D. Limon<sup>2</sup>  
<sup>1</sup>Soroka Medical Center, Radiotherapy, Beer Sheva, Israel ; <sup>2</sup>Tel Aviv medical center, Radiotherapy, Tel Aviv, Israel

#### Purpose or Objective

Bone metastases are a common event in patients with non-small cell lung cancer (NSCLC). One of the most common sites is the spinal column. The epidemiology of symptomatic spinal metastases in patients with NSCLC is not well described. The goal of this study was to describe this population of patients.

#### Material and Methods

Our database was retrospectively reviewed for patients treated with radiotherapy (RT) to spinal metastases from NSCLC, over a period of 2 years (2016-2017). From the database we documented patients, disease and treatment characteristics.

#### Results

78 patients were treated with RT for NSCLC spinal metastases over a period of 2 years. Of the patients, 68% were male, the median age was 64.4 years. 81% were diagnosed with adenocarcinoma, 17% with squamous cell carcinoma. 11.5% of the patients have EGFR mutation, none had ALK mutation. The location of the metastases was thoracic spine in 62% of patients, 47% in lumbar spine, 31% in sacrum and 13% in cervical spine. 40% presented with lesions in more than one spinal sub-site. Median time from diagnosis of metastatic disease to first treatment of spinal metastases was 1.9 months. The majority of patients (96%) were treated with a fractionation of 20-30Gy in 5-10 fractions, only 3 patients were treated with a single fraction of 8Gy, no patient was treated with stereotactic RT. About 10% were treated with a second course of RT, none to the same location. However, the two patients that required a third course of RT, were re-irradiated to previously treated lesions. Median survival was 5.5 months for the entire cohort. Patients with EGFR mutation had better survival (12.7mo vs. 4.4mo, p=0.046). Other tumor, treatment and patient parameters, didn't influence survival.

#### Conclusion

The most pronounced findings in our cohort of patients with metastatic NSCLC and spinal metastases, treated with RT, was the short time from disease diagnosis to spinal treatment and the relative short survival, when compared to known survival of stage IV NSCLC. This suggest that spinal metastases in NSCLC may predict a more aggressive course of disease.

### EP-1358 SBRT for de novo pulmonary tumors in patients with completely resected early stage NSCLC

Q. Zhao<sup>1</sup>, J. He<sup>1</sup>, Z. Zeng<sup>1</sup>

<sup>1</sup>Zhongshan Hospital- Fudan University, Department of radiation oncology, Shanghai, China

#### Purpose or Objective

Following surgery for early-stage non-small cell lung cancer (NSCLC), de novo pulmonary tumors are common. This study aimed to assess the efficacy, patterns of failure, and toxicity of stereotactic body radiotherapy (SBRT) in the treatment of de novo pulmonary tumors following curative resection of early stage NSCLC.

#### Material and Methods

We reviewed the medical data of patients who had received definitive intent SBRT for small lung cancer at Zhongshan Hospital, Fudan University, between June 2011 and December 2017. Patients who had experienced complete resection for prior early-stage NSCLC before SBRT were identified for further analysis. Incidences of loco-regional recurrence (LR) and distant metastasis (DM) were evaluated using the alternative cumulative incidence competing risk method. The probability of survival was estimated using the Kaplan-Meier method.

## Results

Thirty-three patients with 36 lesions were eligible and included in this study. The median follow-up time was 32 months. Estimated incidences of LR and DM were 37.62% and 15.92%, respectively, at 1 year and 48.02% and 21.23%, respectively, at 2 years. The progression-free survival and overall survival of all patients were 62.40% and 90.30%, respectively, at 1 year and 52.00% and 69.90%, respectively, at 2 years (Figure 1). Twenty-six patients experienced grade 1 SBRT-related toxicity, 11 patients experienced grade 2 SBRT-related toxicity, and 3 patients experienced grade 3 toxicity. There were no grade 4/5 toxicities or SBRT-related deaths during the follow-up period (Table 1).

## Conclusion

SBRT appears to be a safe and potentially effective alternative therapeutic option for de novo pulmonary tumors following early-stage NSCLC radical resection, despite impaired pulmonary reserve.

### EP-1359 Dosimetric Appraisal of VMAT for Stereotactic Radiosurgery in Lung Lesions in Comparison to Robotic Radiosurgery

E. Erdogan<sup>1</sup>, P. Boydak<sup>1</sup>, B. Eren<sup>1</sup>, F. Aksaray<sup>1</sup>  
<sup>1</sup>Okmeydani Training and Research Hospital, Radiation Oncology, Istanbul, Turkey

## Purpose or Objective

Role of stereotactic radiosurgery in the treatment of lung tumors has been well defined. Stereotactic radiosurgery techniques improvements are developing everyday. Comparisons of dosimetric quality has always been an ongoing subject of new conducting clinical trials. The aim of this study is to compare the dosimetric characteristics of robotic and conventional linac-based SBRT techniques for lung cancer.

## Material and Methods

Ten patients with lung patients were replanned with MONACO treatment planning system (ELEKTA Infinity Linac) which use MONTECARLO algorithm. Plans were created using 2 half arcs VMAT with CyberKnife (which use MONTECARLO algorithm) and dosimetric indices compared for both treatment platform. Identical image and contour sets were used for both modalities. Dose for organ at risk for SpinalCord, Oesofagus, R-L Lung for 1000cc, heart. PTVmax, treatment time, conformity index (CI), homogeneity index (HI), number of monitor units (MU). CI calculated for both platform manually as a ratio of total volume covered by reference isodose and the target volume ( $CI = VRI/TV$ ). D2-D98/D50 formula used for calculation HI (ICRU 62 reports) Statistical calculations were made by SPSS Statistics 22. The Shapiro-Wilk test used for normality in frequentist statistics. Paired sample t-test and Wilcoxon signed-rank test were used for normally and not normally distributed dependent samples. Differences were considered statistically significant if p values were < 0.05.

## Results

Robotic radiosurgery technique can achieve high degree of conformity (median CI=1.41) surrounding the inhomogeneous dose distribution (median HI= 0.27) at the cost of treatment time (mean 53 minutes). Volumetric modulated arc therapy technique improved this inhomogeneity (median HI= 0.05) and treatment time (estimated between 5 and 9 minutes) at the cost of conformity (median CI= 0,95). The number of MU necessary to deliver the prescribed dose was significantly greater in the case of CyberKnife system (p< 0.01). The dose to 1000 cc lung was well below institutional constraints for both modalities. Steep dose gradient near target volume were significantly better at CyberKnife system for all isodose volumes (80%, 60% and 40% isodose volumes) (p< 0.01)

## Conclusion

The dose distribution and dosimetric parameters of both the CyberKnife and VMAT plans are clinically acceptable lung treatment requirements. While the CyberKnife may deliver less lung dose than linac-based systems for tumors close to the anterior chest wall. Although there are some differences in dosimetric analysis, it is likely that robotic radiosurgery and volumetric modulated arc therapy plans would be clinically indistinguishable.

### EP-1360 Salvage SBRT for postoperative recurrence of NSCLC

S. Aoki<sup>1</sup>, H. Yamashita<sup>1</sup>, W. Takahashi<sup>1</sup>, K. Nawa<sup>1</sup>, T. Ota<sup>1</sup>, Y. Nozawa<sup>1</sup>, S. Ozaki<sup>1</sup>, T. Nakamoto<sup>1</sup>, K. Nakagawa<sup>1</sup>  
<sup>1</sup>University of Tokyo Hospital, Radiology, Tokyo, Japan

## Purpose or Objective

Standard treatment for patients with early-stage non-small cell lung cancer (NSCLC) who undergo surgery and subsequently develop local failure or intrathoracic oligo-recurrence remains controversial. We aimed to assess the feasibility of stereotactic body radiotherapy (SBRT) for these patients. We also evaluated factors associated with indices of survival.

## Material and Methods

Patients treated with SBRT for NSCLC recurrence who previously underwent curative surgical resection from October 2011 to October 2016 were evaluated. Post-recurrence survival and toxicity were analyzed, and prognostic factors for overall survival (OS), progression free survival (PFS) after salvage SBRT were identified by univariate and multivariate analysis.

## Results

A total of 51 patients and 58 tumors were analyzed. Median follow-up time was 25 months (35 months for surviving patients), and median OS after salvage SBRT was 32 months. The 1- and 3-year OS, PFS rate was 82.4% and 59%, 82.4% and 59%, respectively. Only 4 patients (7.8%) developed local failure. Median local control rate (LCR) was 71 months and the 1- and 3-year LCR was 97.8% and 94.9%. Four patients experienced grades ≤3 radiation pneumonitis and one experienced grade 5. Gender, location, type of surgery (lobectomy or limited suurgery), and operability of recurrent tumors were independent prognostic factors for OS.

## Conclusion

This study suggested that salvage SBRT is effective and well-tolerated in recurrent NSCLC patients with postoperative locoregional recurrence.

### EP-1361 Survival after two schedules of SBRT to centrally located lung tumors

M. Jelin<sup>1</sup>, C. Kristiansen<sup>1</sup>, S.S. Jeppesen<sup>1,2</sup>, M. Nielsen<sup>3</sup>, O. Hansen<sup>1,2,4</sup>

<sup>1</sup>Odense University Hospital, Dept. Oncology, Odense, Denmark ; <sup>2</sup>Odense University Hospital, AgeCare. Academy of Geriatric Cancer Research, Odense, Denmark ; <sup>3</sup>Odense University Hospital, Laboratory of Radiation Physics, Odense, Denmark ; <sup>4</sup>University of Southern Denmark, Institute of Clinical Research, Odense, Denmark

## Purpose or Objective

It is a challenge to apply stereotactic radiotherapy (SBRT) to centrally located non-small cell lung cancer (NSCLC). Initially we used 80 Gy/8F (BED10= 160 Gy), but changed the schedule to 50 Gy/5F (BED10=100 Gy). We here report the survival data for patients who were treated with either of the two schedules.

## Material and Methods

All patients have been prospectively registered. Additional data have been obtained retrospectively from patients files. Included patients were patients treated initially with one of the two schedules. Patients treated for recurrent disease, and patients treated in combination with

peripheral SBRT or conventional radiotherapy were excluded. The SBRT was given as 4-D VMAT. The 80 Gy/8 F or 50 Gy/5F was dosed centrally.

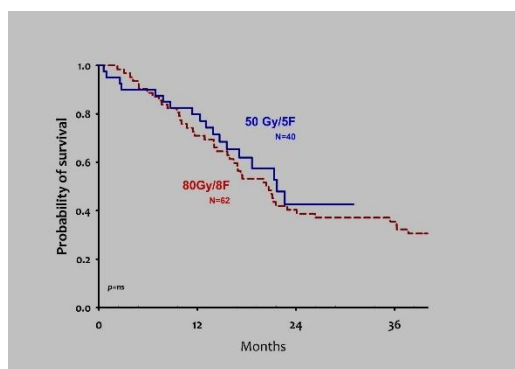
### Results

From 2012 to 2015 62 patients received 80 Gy and from 2016 to 2017 40 patients received 50 Gy.

**Table: Patient characteristics**

	50 Gy/5G N=40	80 Gy/8F N=62	Gy/8F
Age (yr.)	73.2 (86.4)	(46.8; 75.9; 90.5)	(50.0;
Sex			
Female	18 (45%)	35 (56%)	
Male	22 (55%)	27 (44%)	
Performance status			
0-1	20(50%)	32 (52%)	
2	12 (30%)	22 (36%)	
3	8 (20%)	8 (13%)	
FEV1% of predicted	59% (21-117%)	66% (22-123%)	
Stage (TNM7)			
I	15 (27.5%)	17 (27%)	
II	22 (55%)	35 (56.5%)	
III-IV	2(7.5%)	10 (16%)	
Histology			
Squamous carcinoma	19 (47.5%)	22 (35%)	
Adenocarcinoma	18 (45%)	24 (39%)	
Other histology	2(5%)	12 (19%)	
Unknown	1 (2.5%)	4 (6.5%)	

**Figure: Overall survival**



The median overall survival was 20.5 mo. in the 80 Gy group and 21.7 mo. in 50 Gy/5 (p=ns). The median cancer related survival was 59.7 mo. and not reached, respectively (p=ns).

### Conclusion

No difference was observed between the schedule groups in neither overall survival nor cancer specific survival.

### EP-1362 Re-Irradiation Of Whole Brain For Symptomatic Progression In Lung Cancer Patients

J.P. Agarwal<sup>1</sup>, S. Karmakar<sup>1</sup>, N. Mummudi<sup>1</sup>, A. Tibdewal<sup>1</sup>  
<sup>1</sup>Tata Memorial Hospital HBNI, Department of Radiotherapy, Mumbai, India

#### Purpose or Objective

Whole brain radiation therapy (WBRT) is an effective palliative measure and provides durable symptom relief in lung cancer patients with multiple brain metastases (BM). Clinico-radiological progression of BM after WBRT is a common and challenging scenario; treatment is tailored,

with various factors like driver mutation status, age, performance status, progression free interval and time since last irradiation influencing the treatment decision. Surgery or focal RT with stereotactic techniques may be an option for patients with oligo-metastases. However, they might not be a feasible option for patients with multiple BM. We aim to study the impact and outcome of patients with BM from lung cancer receiving WBRT for clinico-radiological progression.

#### Material and Methods

We retrospectively analyzed patients with BM from lung cancer who were registered at Tata Memorial Hospital, Mumbai, India between November 2012 to August 2017 and had undergone two courses of WBRT. Data of patients were retrieved from electronic medical records. Patients were treated using conventional or conformal technique with either tele-cobalt or Linear accelerator

#### Results

Out of 315 patients OF lung cancer, diagnosed and treated with WBRT for BM, 23 received re-WBRT. There were 12 men and 11 women with median age of 51 years (range 30 to 70yr with adenocarcinoma in 21 patients. Driver mutation status was positive in 65% patients (9 with EGFR and 6 with ALK mutation positive) and a majority of patients (83%) had BM at presentation. Clinico-radiological progression was the commonest indication of re-WBRT; only one patient had radiological progression alone. A majority of these patients had developed new symptoms while about 30% had recurrence of previous symptoms. Mean Karnofsky performance score (KPS) prior to re-WBRT was more than 70 in 13 patients (57%). Mean time interval between the two courses of WBRT were 17.1 months (range 5-33 months). Most patients received WBRT using a conventional technique (91%) and were treated in a tele-cobalt unit (83%). Re-WBRT fractionation schedule was 25 Gy/10 fractions (n=12, 52%) or 20 Gy/5 fractions (n=10, 44%). Mean biological effective dose (BED<sub>2Gy</sub>) for the first and second courses of WBRT were 63.75 Gy and 57.5 respectively. The average cumulative BED<sub>2Gy</sub> was 121 Gy (range 108-135 Gy). Almost all patients received short acting steroids during the course of re-WBRT. All patients completed the course of treatment. At the time of analysis, 7 patients were alive; median survival of patients after re-WBRT was 9 weeks (range 1-78 weeks).

#### Conclusion

In lung cancer patients with symptomatic progression of multiple BM and good prognostic features (driver mutation positive, good performance status and long time interval since last WBRT), re-WBRT is a safe and feasible option.

### EP-1363 Stereotactic Ablative Radiotherapy For Lung Cancer In Elderly Patients.

A. Revelant<sup>1</sup>, M. Emilio<sup>1</sup>, T. Marco<sup>2</sup>, D.P. Antonino<sup>1</sup>, G. Carlo<sup>1</sup>, F. Giuseppe<sup>1</sup>, P. Elisa<sup>1</sup>, M. Fabio<sup>1</sup>, N. Federico<sup>1</sup>, Z. Umberto<sup>3</sup>, P. Jerry<sup>4</sup>, F. Giovanni<sup>1</sup>  
<sup>1</sup>Centro di Riferimento Oncologico, Radiation Oncology, Aviano, Italy ; <sup>2</sup>Azienda Sanitaria Universitaria Integrata, Radiation Oncology, Udine, Italy ; <sup>3</sup>Azienda Ospedaliera Santa Maria degli Angeli, Pneumology, Pordenone, Italy ; <sup>4</sup>Centro di Riferimento Oncologico, Epidemiology, Aviano, Italy

#### Purpose or Objective

According to available evidences, stereotactic ablative radiotherapy (SABR) has been widely analyzed in elderly and appear to have similar benefits to their younger counterpart. However, for the definition of elderly often is used 70 years as threshold (as illustrated in International Society of Geriatric Oncology's Guidelines). The aim of this study is to demonstrate effectiveness and safety of using SABR in older patients (> 80 years old), with primary lung cancer, comparing the outcome in term of local control (LC), progression-free survival (PFS) and overall survival (OS) with younger patients at 1, 2 and 3 years. We didn't use the data at 5 years, because the event death is

influenced more by other factors (e.g. cardiac failure) than from lung cancer.

#### Material and Methods

We retrospectively reviewed clinical charts and treatment planning of early stage (Stage IA, IB) lung cancer patients treated with SABR between 2008 and 2016. We consider only patients  $\geq 65$  years old. All patients underwent at least one FDG-PET/CT exam before SABR. Total dose was 40-52 Gy in 5-8 fractions. The planning target volume was defined as the GTV, identified on CT simulation, plus 5 mm on axial plane and 10 mm on craniocaudal plane. We divided patients into two groups (group A:  $\leq 80$  years versus group B:  $> 80$  years) and clinical data were compared. LC, PFS and OS were analyzed with log-rank test. Acute and late toxicities were scored with CTCAE v. 4.03.

#### Results

A total of 88 patients were treated and analyzed (group A: 55 patients, M/F=38/17, median age= 73 years; group B: 33 patients, M/F=22/11, median age= 83 years). Median follow-up was 26 months (29 for Group A and 23 for Group B). LC at 1, 2 and 3 years was respectively 96%, 91% and 84% in group A vs. 96%, 81% and 81% in group B (p-value= 0.50). PFS at 1, 2 and 3 years was respectively 78%, 65% and 45% in group A vs. 76%, 51% and 39% in group B (p-value=0.59). OS at 1, 2 and 3 years was respectively 85%, 72% and 57% in group A vs. 88%, 58% and 45% in group B (p-value= 0.40).

No statistical significance was reached between Group A and B in terms of LC, PFS and OS. No differences in acute toxicity was shown among the two groups. We registered only two cases of late G3 pneumonitis (1 in group A and 1 in group B).

#### Conclusion

No significant difference in toxicity and compatible results in LC, PFS and OS were observed between patients younger or older than 80 years and this suggests that SABR is a feasible and effective treatment modality also in elderly population without risks of severe toxicity.

#### EP-1364 Haemoglobin and albumin levels, as clinical predictors in SBRT for early stage NSCLC

D.C. Moreno Santiago<sup>1</sup>, A. Giraldo Marin<sup>1</sup>, M. Ramos

Albiac<sup>1</sup>, J. Giralto Sagrera<sup>1</sup>

<sup>1</sup>Vall D'Hebron Hospital, Radiation Oncology, Barcelona, Spain

#### Purpose or Objective

The purpose of this study was to investigate serum albumin and haemoglobin levels as prognostic factors of stereotactic body radiotherapy (SBRT) for early stage NSCLC.

Numerous authors have reported that sex, age, Eastern Cooperative Oncology Group performance status (PS), tumour size, and T-stage are prognostic factors of early-stage NSCLC treated with SBRT. Following the steps of surgical series, many authors have tried to identify blood examination data commonly available in clinical settings and use that data to predict outcomes of SBRT.

#### Material and Methods

Retrospectively, we analyzed pre-treatment levels (considered up to one month prior to treatment) of haemoglobin and albumin to determine the impact on patient outcomes, such as: overall survival (OS); and event-free survival (EFS: local, regional or distance failures; and death), in patients with early stage NSCLC treated with SBRT in our centre, between February 2015 and January 2018.

Survival rates were estimated with Kaplan-Meier analysis, and multivariable analysis was completed using Cox proportional hazards model.

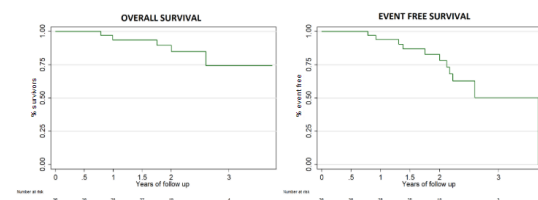
#### Results

Of all patients with diagnosis of early stage NSCLC treated with SBRT in our centre, 36 were included in this analysis (table 1). None of the patients had received previous

treatment with radiotherapy or chemotherapy in the past 5 years. Four patients were treated with SBRT after they refused surgery. The mean and median age was 72 years (range 54-89), with a mean follow up of 24 months (see Table1). The 2-year OS and EFS rates were 89.6% and 82.8%, respectively (fig. 1). In the multivariate analysis, significant factors for OS were albumin level HR= 0.05, 95% CI 0.00 - 0.50; p=0.01; and haemoglobin level HR= 0.43, 95% CI 0.22 - 0.83; p=0.01. The 2-year local, regional and distant control rates, were 93.1%, 93.1% and 95.8%, respectively. As expected, T stage was a significant predictive factor for local control (p=0.02). 5 patients died at the end of the follow up, none, however, related to treatment toxicity or tumour progression. In the multivariate analysis, the significant factors for EFS were as well: albumin level HR= 0.10, 95% CI 0.02 - 0.63; p=0.01; and haemoglobin level HR= 0.53, 95% CI 0.32 - 0.85; p=0.01.

Multivariate Cox proportional hazards regression was used to determine the optimal cut points: haemoglobin level  $>12.4\text{g/dL}$  was related with better OS and EFS, HR= 0.06, 95% CI 0.01 - 0.52; p=0.01 and HR= 0.17, 95% CI 0.05 - 0.64; p=0.01 respectively. Moreover, Albumin level  $>3.7\text{g/dL}$  was related too, with better OS and EFS HR= 0.13, 95% CI 0.02 - 0.78; p=0.03 and HR= 0.04, 95% CI 0.0 - 0.36; p=0.01 respectively.

Characteristics	No.	%	p	
Age	< 75 y	23	63.89	0.348
	$\geq 75$ y	13	36.11	
Gender	Male	31	86.11	0.559
	Female	5	13.89	
Histology	Squamous cell	8	22.22	0.631
	Adenocarcinoma	20	55.56	
	Others	8	22.23	
Smoke	Ex-smoker	26	72.22	0.280
	Smoker	7	19.44	
	Never	3	8.33	
KPS	>70	30	83.33	0.354
	$\leq 70$	6	16.66	
T stage	T1	27	75	0.006
	T2	9	25	
Failure	Local	4	11.11	0.001
	Regional	2	5.56	0.033
	Distance	4	11.11	0.001
	Death	5	13.89	1.000
Hemoglobin	Median	13,65g/dL		0.050
	25 <sup>th</sup> -75 <sup>th</sup> percentile	12,5 - 14,8g/dL		
Albumin	Median	4,11g/dL		0.021
	25 <sup>th</sup> -75 <sup>th</sup> percentile	3,88 - 4,24g/dL		



#### Conclusion

In the setting of SBRT for early-stage NSCLC, our results shows that, pre-treatment haemoglobin  $<12.4\text{g/dL}$  and/or serum albumin  $<3.7\text{g/dL}$ , are objective laboratory tests, feasible for estimation of prognosis of patients with early stage NSCLC.

**EP-1365 SBRT as salvage therapy for oligometastatic pleural mesothelioma after initial curative therapy**  
C. Schröder<sup>1</sup>, I. Opitz<sup>2</sup>, M. Guckenberger<sup>1</sup>, R. Stahel<sup>3</sup>, W. Weder<sup>2</sup>, R. Förster<sup>1</sup>, N. Andratschke<sup>1</sup>, O. Lauk<sup>2</sup>

<sup>1</sup>University Hospital Zürich, Department of Radiation Oncology, Zürich, Switzerland; <sup>2</sup>University Hospital Zürich, Department of Thoracic Surgery, Zürich, Switzerland; <sup>3</sup>University Hospital Zürich, Department of Medical Oncology, Zürich, Switzerland

**Purpose or Objective**

Patients with recurrent pleural mesothelioma after initial multimodal treatment presenting with very limited recurrences represent a challenge, as the optimal treatment strategy balancing toxicity and efficacy has not been defined yet. SBRT might be a promising option for these patients since it delivers a local ablative biologic dose of radiation. The intent of this retrospective analysis was to evaluate the feasibility of a novel strategy to integrate SBRT as first salvage therapy for limited pleural recurrences in pleural mesothelioma.

**Material and Methods**

Between 2005 and 2018, 21 patients with the histopathological diagnosis of malignant pleural mesothelioma (MPM) were treated with hypofractionated radiotherapy for oligometastatic progression. Most patients initially presented with stage III disease (57 %). Only one patient had distant metastases upon first diagnosis. The median age at first diagnosis was 65 years (range 33 - 75 years). Out of these 21 patients, 12 received induction chemotherapy prior to surgery, whereas in total 18 patients underwent macroscopic complete resection (MCR). 3 patients had additional intracavitary chemotherapy and 3 patients were treated with chemotherapy alone without any other treatment. Clinical and radiological data was collected at regular follow-up appointments including toxicity, local control and survival.

**Results**

A total of 50 lesions in recurrent MPM were treated with SBRT. A total of 21 patients received 1 course of radiation treatment, 10 of those received a second and 4 a third course of radiotherapy (RT). The median number of fractions at all courses was 5 (range 3 - 20) with a median dose per fraction of 5 Gy (range 2.5 - 12.5 Gy). The median total treatment dose was 30 Gy (20 - 50 Gy) with a median prescription isodose line (IDL) of 65 % (65 - 100 %). Median follow-up of all patients from diagnosis on was 124 weeks (range 32 - 662 weeks). At the time of analysis, 11 patients were still alive. Intrathoracic out-of-field or in-field recurrence after SBRT was observed in up to 62% of patients. After the first course of SBRT, a total of 13 patients had a thoracic recurrence (11 out-of-field, 2 in-field). After the second and third course the number of patients with thoracic recurrence was 6 and 2, respectively (each with 50 % in-field-recurrence). 12-months-local control was 85.2 % with a median time to local recurrence of 11 months. The median PFS after SBRT was 6 months (range 0 - 21 months) and the median OS from first diagnosis was 44 months (range 9 - 152 months). The OS at three years was 33 %. Overall, the radiation treatment was very well tolerated. Only 2 patients experienced above Grade 3 toxicities.

**Conclusion**

This analysis demonstrates the feasibility of an SBRT approach for recurrent MPM. SBRT with its few and low graded side effects was well tolerated even after multiple repetitions. Local control was excellent with a good median OS of 44 months.

**EP-1366 Repeated thoracic high-dose radiotherapy-Analysis of efficacy and safety including EQD2 sum plans**

C. Schröder<sup>1</sup>, I. Stiefel<sup>1</sup>, S. Tanadini-Lang<sup>1</sup>, I. Pytko<sup>1</sup>, M. Guckenberger<sup>1</sup>, N. Andratschke<sup>1</sup>

<sup>1</sup>University Hospital Zürich, Department of Radiation Oncology, Zürich, Switzerland

**Purpose or Objective**

Thoracic re-irradiation for primary or metastatic intrathoracic lesions remains a challenge regarding the balance between local efficacy and acceptable treatment related toxicity, as no firm data for safe guidance for re-treatment exists. In this retrospective analysis, we analyzed dosimetric data of patients that received re-irradiation of the thorax by generating EQD2 sum plans of all thoracic treatments. Furthermore, we looked at the clinical outcome of patients, including overall survival (OS) and toxicity.

**Material and Methods**

We retrospectively analyzed the data of 42 patients who received repeated high dose radiotherapy (RT) or stereotactic body radiotherapy (SBRT) for thoracic lesions from 12/2011 to 01/2017. Most patients had NSCLC (n=20), followed by esophageal cancer (n=6) and SCLC (n=4). Sum plans of 2Gy equivalent dose distributions (EQ2Gy) using non-rigid image registration to the latest planning CT scan were calculated for all courses of thoracic radiotherapy using Aria Eclipse (Varian Medical Systems, Version 10) and MIM (MIM Software Inc. Version 6.7.9). Dose parameter were calculated for common organs at risk (e.g. lung) and target volumes (PTV). Clinical and radiological data were collected at regular follow-up appointments.

**Results**

In total 42 patients received at least 2 courses of thoracic RT. 8 patients a third and 2 a fourth course of RT. For first treatment, 14 patients (33.3%) received an SBRT. For the second and third course 23 (54.8%) and 6 (75%) patients received treatment as SBRT. For the fourth course no patients received SBRT.

The median prescription dose (EQD2) was 42.2Gy<sub>10</sub> for all RT courses combined. The median volume of the combined PTV was 276cc (range 40-1115cc). The D1cc for the PTV ranges from 60.7-324.9 Gy<sub>10</sub> (median 108.4Gy<sub>10</sub>). Regarding organs at risk the median Dmean of both lungs was 10.1Gy<sub>3</sub> (range 1.9-17.9Gy<sub>3</sub>) with a median V(20Gy<sub>3</sub>) of 13.6% (range 0.5- 6.7%) and a maximum D1cc of 253.9Gy<sub>3</sub> (median 93.2Gy). The median Dmean of the esophagus was 20.7Gy<sub>3</sub> (range 2.78- 60.6Gy<sub>3</sub>) with a median D1cc of 58.7Gy<sub>3</sub> (range 7.9-100.6Gy<sub>3</sub>). The highest D1cc for the bronchial tree was 129.8Gy<sub>3</sub> (median 70.5Gy<sub>3</sub>) and 63.9Gy<sub>2</sub> for the spinal cord (median 35.6Gy<sub>2</sub>). The median follow-up was 33 months (range 3-191 months). Median OS of all patients after first re-irradiation was 19 months (range 1-45 months). At the time of analysis 18 patients were still alive 80% of patients suffered from mild G1-G2 toxicity, mostly in terms of coughing (20%). Only one patient suffered from a >G3 toxicity. This patient had a fatal esophageal rupture 16 months after re-irradiation of an NSCLC (esophagus D1cc=48.4 Gy).

**Conclusion**

Even though several organs at risk received a maximum D1cc of >100 Gy, thoracic irradiation proved to be safe with acceptable toxicities and effective with an excellent overall survival. Still, larger data sets with cumulative EQD2Gy dosimetric evaluation are necessary to define robust criteria for safe re-irradiation.

**EP-1367 Target volumes in adaptive treatment of NSCLC show large discrepancies among experts**

R. Apolle<sup>1,2</sup>, S. Appold<sup>1,3</sup>, J. Bussink<sup>4</sup>, C. Faviere-Finn<sup>5</sup>, J. Khalifa<sup>6</sup>, Y. Lievens<sup>7</sup>, D. De Ruyscher<sup>8</sup>, W. Van Elmpot<sup>8</sup>, E.G.C. Troost<sup>1,2,3,9,10</sup>

<sup>1</sup>OncoRay - National Center for Radiation Research in Oncology, Faculty of Medicine and University Hospital Carl Gustav Carus- Technische Universität Dresden-Helmholtz-Zentrum Dresden - Rossendorf, Dresden, Germany; <sup>2</sup>Helmholtz-Zentrum Dresden - Rossendorf, Institute of Radiooncology - OncoRay, Dresden,

Germany; <sup>3</sup>Faculty of Medicine and University Hospital Carl Gustav Carus - Technische Universität Dresden, Department of Radiotherapy and Radiation Oncology, Dresden, Germany; <sup>4</sup>Radboud University Medical Center, Department of Radiation Oncology, Nijmegen, The Netherlands; <sup>5</sup>The University of Manchester and The Christie NHS Foundation Trust, Division of Cancer Science, Manchester, United Kingdom; <sup>6</sup>Institut Claudius Regaud, Department of Radiotherapy, Toulouse, France; <sup>7</sup>Ghent University Hospital, Radiation Oncology Department, Ghent, Belgium; <sup>8</sup>Maastricht University Medical Centre, GROW - School for Oncology and Developmental Biology- Department of Radiation Oncology Maastricht, Maastricht, The Netherlands; <sup>9</sup>German Cancer Consortium DKTK, Partner Site Dresden and German Cancer Research Center DKFZ- Heidelberg, Dresden, Germany; <sup>10</sup>National Center for Tumor Diseases NCT, Partner Site Dresden- German Cancer Research Center DKFZ- Heidelberg- Faculty of Medicine and University Hospital Carl Gustav Carus- Technische Universität Dresden- and- Helmholtz Association / Helmholtz,

### Purpose or Objective

Target volume delineation is subject to inter-observer variability (IOV) and thus a major source of uncertainty in radiation treatment planning. IOV in the context of treatment adaptation is largely unknown. We analysed IOV of the primary gross tumour volume (GTV) and clinical target volume (CTV) in locally advanced NSCLC delineated by experts in the pre- and mid-treatment (PT and MT) setting.

### Material and Methods

Five patients from routine clinical practice, who underwent repeat imaging, were selected such that a variety of features likely to prompt adaptation, e.g. atelectasis, central primary tumour, was included. Brief case reports and CT imaging data were sent to six observers, supplemented with FDG-PET studies in two cases at PT and three at MT. Observers received PT and MT imaging data at least one week apart and were asked to delineate the GTV and CTV in their own treatment planning system and to comment on their delineation process, i.e. on how GTV to CTV expansion and adaptation were performed. Delineations were rasterised on a 1mm<sup>3</sup> grid and their compatibility assessed with the Generalised Conformity Index (Cl<sub>gen</sub>). Differences in IOV between PT and MT were probed with Wilcoxon signed-rank tests and the correlation between GTV and CTV IOV evolution with Spearman rank correlation. While it is respectively impossible and very difficult for these tests to show two-sided  $\alpha=0.05$  significance at  $n=5$ , more powerful parametric alternatives cannot credibly be employed.

### Results

A total of 109/120 delineations were received and analysed. Figure 1 shows an overview of IOV in terms of volume overlap. All but one case saw a reduction of Cl<sub>gen</sub> when transitioning from PT to MT ( $p=0.125$  for both GTVs and CTVs). Agreement in corresponding GTV and CTV delineations was generally comparable at individual time points, and there was a trend of a correlation between GTV and CTV Cl<sub>gen</sub> changes ( $p=0.9$ ,  $p=0.083$ ). This behaviour is consistent with almost all observers adopting an isotropic GTV to CTV expansion of 5 mm with rare editing for anatomical boundaries at either time point. MT GTV delineations were only occasionally adopted from PT after image registration (9/28 analysed observers and cases), the remainder contoured anew. Post-transfer adaptation to changed anatomy was performed by one observer, and inclusion of PT GTV in MT CTV by two. Figure 2 shows the two cases demonstrating the most extreme changes in IOV (improvement and deterioration). In both cases large volumes of consolidated lung lead to increased IOV, but at different time points. Shortcomings of this in

silico contouring challenge were incomplete FDG-PET availability and a lack of contrast-enhanced CT, both current clinical standard. Modern MRI would also have been welcomed by many.

### Conclusion

Differing approaches of reacting to intra-therapeutic changes further increase IOV in target volume delineation in the adaptive setting. Consensus guidelines and in-depth analysis of per-treatment tumour shrinkage patterns are urgently needed.

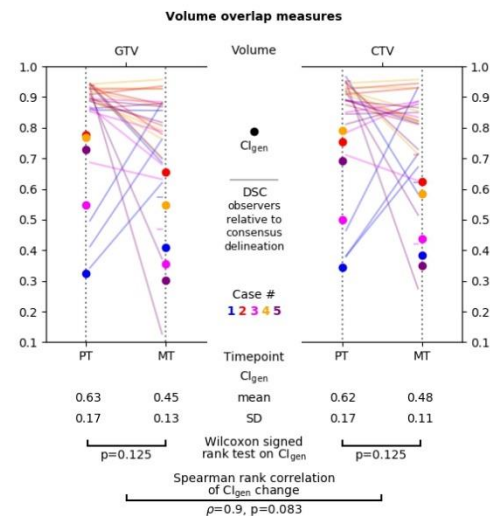


**Fig. 1:** Statistical overview of delineation overlap metrics. The Generalised Conformity Index (Cl<sub>gen</sub>) is shown for each case and time point for Gross Tumour Volume (GTV) and Clinical Target Volume (CTV) delineations. Its summary statistics are printed below, alongside the results of 1) hypothesis tests for a non-zero change in Cl<sub>gen</sub> when transitioning from pre- to mid-treatment time points (PT to MT), and 2) the correlation of those Cl<sub>gen</sub> changes between GTV and CTV delineations. The changes in Dice Similarity Coefficients (DSC) for each observer relative to a median consensus delineation (i.e. the collection of voxels delineated by at least half the observers) are depicted for comparison. Only a stub at either PT or MT is shown for observers who did not provide delineations for both.

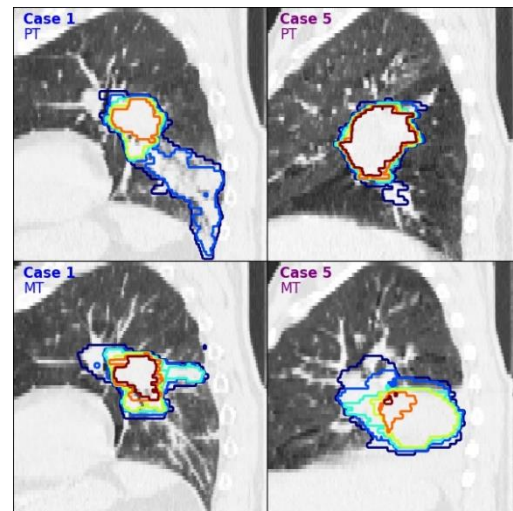


**Fig. 2:** Illustration of pre- and mid-treatment inter-observer variability in GTV delineation for two cases of NSCLC. Central sagittal slices are superimposed with contours representing the fraction of observers who included the contained voxels in their delineation (from the exterior inwards: dark blue: 1/6 observers, maroon: 6/6 observers). **Abbreviations:** (P/M)T, (pre/mid)-treatment. **Left:** Case 1 (cT4N2M0 NSCLC of the left pulmonary hilum with bronchial involvement) demonstrating dystelectasis and infiltrative changes at PT, which resolved during therapy. **Right:** Case 5 (cT3N0M0 NSCLC of the right lower lobe) developed pronounced atelectasis. **Note:** only 5 PT delineations received for Case 1.

**EP-1368 Circulating cell free DNA during chemo-radiotherapy in non-small cell lung cancer patients**  
 L. Nygaard<sup>1</sup>, L. Ahlborn<sup>2</sup>, G. Persson<sup>1,3</sup>, D. Chandrananda<sup>4</sup>, J. Langer<sup>5</sup>, B.M. Fischer<sup>3,5</sup>, M. Aznar<sup>1</sup>, S. Langer<sup>1</sup>, M. Gabrielaite<sup>2</sup>, A. Kjær<sup>3,5</sup>, N. Rosenfeld<sup>4</sup>, F. Mouliere<sup>4,6</sup>, O. Østrup<sup>2</sup>, I. Vogelius<sup>1,3</sup>, S. Bentzen<sup>7</sup>

<sup>1</sup>Rigshospitalet, Department of Oncology, Copenhagen, Denmark ; <sup>2</sup>Rigshospitalet, Center for Genomic Medicine, Copenhagen, Denmark ; <sup>3</sup>Faculty of Health Science-University of Copenhagen-, Department of clinical medicine, Copenhagen, Denmark ; <sup>4</sup>University of Cambridge, Cancer Research UK Cambridge Institute, Cambridge, United Kingdom ; <sup>5</sup>Rigshospitalet, Department of Clinical Physiology- Nuclear Medicine & PET and Cluster for Molecular Imaging, Copenhagen, Denmark ; <sup>6</sup>Amsterdam UMC- Vrije Universiteit, Department of Pathology- Cancer Center Amsterdam, Amsterdam, The Netherlands ; <sup>7</sup>University of Maryland Greenebaum Comprehensive Cancer Center and University of Maryland School of Medicine, Division of Biostatistics and Bioinformatics and Department of Epidemiology and Public Health-, Baltimore, USA

**Purpose or Objective**

To determine the change over time in circulating cell free DNA (cfDNA) in patients with locally advanced non-small cell lung cancer (NSCLC) during chemo-radiotherapy. Furthermore, the possibility for detection of circulating cell free tumor DNA (ctDNA) was assessed using shallow whole genome sequencing (sWGS) and size selection.

**Material and Methods**

Ten patients were included in a two-phase trial. The first four patients had blood samples taken prior to treatment and at 30 minutes, 1 hour and 2 hours after treatment to estimate the short-term dynamics of cfDNA after a therapy session. The remaining six patients had one blood sample taken on six treatment days 30 minutes post radiotherapy to measure the changes in cfDNA. Presence of ctDNA as indicated by chromosomal aberrations was investigated using sWGS. The sensitivity of the method was further enhanced using *in silico* size selection.

**Results**

The cfDNA concentration from baseline to 120 min after therapy was stable within 95% tolerance limits of +/- 2 ng/ml cfDNA. Changes in cfDNA were observed during therapy with an apparent qualitative difference between adenocarcinoma (average increase of 0.69 ng/ml) and squamous cell carcinoma (average increase of 4.0 ng/ml), see Figure 1. Silent chromosomal profiles were observed in 18 out of 23 samples across the two cancer types using sWGS. Size selection enhanced the detection rate from 22% to 74%. Tumor shrinkage on daily cone beam computer tomography scans during radiotherapy did not correlate with changes in concentration of cfDNA.

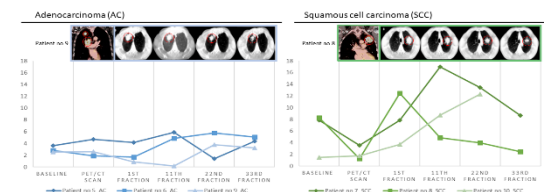


Figure 1. Representative PET/CT and CBCT scans and fluctuation in cfDNA concentration during radiation therapy in adenocarcinoma patients (AC) and patients with squamous cell carcinoma (SCC). Representative scans on corresponding time points are shown for AC (Patient 9) and for SCC (Patient 8).

**Conclusion**

cfDNA remain stable during the first 2 hours after a treatment fraction. However, based on the sWGS profiles, ctDNA represented only a minor fraction of cfDNA in this group of patients. The detection sensitivity of genomic alterations in ctDNA strongly increases by applying size selection.

**EP-1369 Heart delineations based on 3DCT, AVG and MIP scans: are they representative of the total motion?**  
 E. Vasquez Osorio<sup>1</sup>, H. McCallum<sup>2</sup>, S. Iqbal<sup>3</sup>, A. Bedair<sup>4</sup>, A. McWilliam<sup>1</sup>, G. Price<sup>1</sup>, J. Byrne<sup>2</sup>, D. Cobben<sup>5</sup>  
<sup>1</sup>University of Manchester, Radiotherapy Related Research, Manchester, United Kingdom ; <sup>2</sup>Northern Centre for Cancer Care- Freeman Hospital, Radiotherapy Physics, Newcastle upon Tyne, United Kingdom ; <sup>3</sup>Northern Centre for Cancer Care- Freeman Hospital, Radiotherapy, Newcastle upon Tyne, United Kingdom ; <sup>4</sup>North West Cancer Centre, Clinical Oncology, Derry-Londonderry, United Kingdom ; <sup>5</sup>Christie NHS-University of Manchester, Radiotherapy Related Research, Manchester, United Kingdom

**Purpose or Objective**

Evidence is emerging that the heart is more radiosensitive than previously assumed [1-2]. However, only delineations on the average projection or 3D CT scans are used for treatment planning. Therefore the motion of this organ due to respiration and contraction is not accounted for. In this pilot study, we assessed how representative the delineations based on the 3D CT scan, average (AVG) and maximum intensity projections (MIP) are.

**Material and Methods**

Both 3D and 4D CT scans for 10 lung cancer patients treated by SABR were used in this study. Median delineations, derived from 3 independent observers following a previously agreed protocol, were calculated on the 3D CT, AVG, MIP and 25% exhale scans. Delineations on each 4D phase scan (n=8) were created by propagating the median 25% exhale contours using RayStation v5.99. The volume representing the maximum extent of motion was estimated as the union of all 4D phase delineations (U4D), see figure 1 for an example. Surface distances from the U4D to 3D, AVG, MIP volumes were calculated. Distances in the most extreme surface points (1cm most superior/inferior, 10% most right/left/anterior/posterior) are reported.

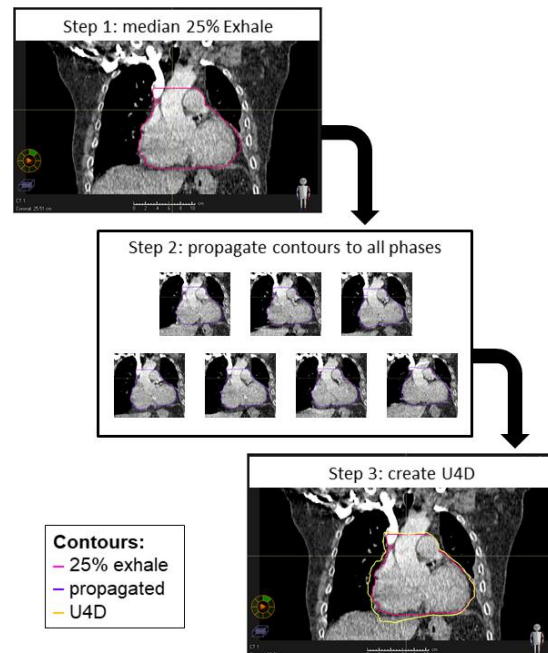
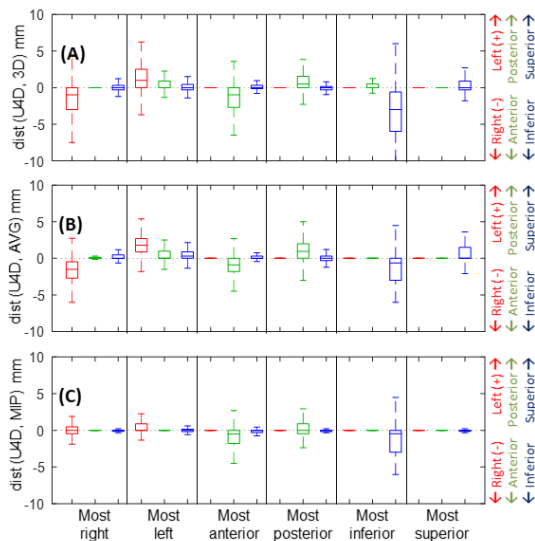


Fig 1: Creating the maximum extent of motion as the union of all 4D phase delineations (U4D).

**Results**

Figure 2 shows the distances for the most extreme surface points, for each delineation and direction (left-right, anterior-posterior and superior-inferior) summarized for

all patients. From the three delineations, MIP is the 'closest' to the maximum extent of motion, followed by AVG and 3D (smaller boxes and closer to zero).



**Fig 2:** Box plot reporting distances of the most extreme points from the maximum extent of motion volume (U4D) to the (A) 3D, (B) AVG and (C) MIP volumes, discriminated by direction. The lines inside the boxes represent the medians, the boxes extend between the 25 and 75 percentiles and the whiskers represent Tukey fences (1.5 x inter-quartile range).

### Conclusion

None of the delineations represented the heart's maximum extent of motion; the MIP was the 'most representative' volume. Current work includes determining the margin required for any of the delineations to better represent the maximum extent of motion. Research including dosimetric measurements and inter-observer variability is needed to determine the relevance of creating a planning organ at risk volume (PRV) of the heart.

[1] Johnson-Hart et al. *IJROBP*. 2018 Oct 1;102(2):434-442.

[2] Wang et al. *J Clin Oncol*. 2017. 35(13):1387-94.

### EP-1370 The impact of fractionation on lymphocyte counts in stage III NSCLC received chemoradiotherapy

Q. Zhao<sup>1</sup>, J. He<sup>1</sup>, Z. Zeng<sup>1</sup>  
<sup>1</sup>Zhongshan Hospital- Fudan University, Department of radiation oncology, Shanghai, China

### Purpose or Objective

Radiation-related lymphopenia (RIL) is associated with inferior clinical outcomes in lung cancer patients treated with radiation (RT) and immune checkpoint inhibitors (ICIs) following RT. This study was performed to investigate whether fractionation regime affects the peripheral total lymphocyte counts (TLCs) in definitive concurrent chemoradiotherapy (CCRT) for unresectable stage III non-small lung cancer (NSCLC).

### Material and Methods

We retrospectively reviewed 118 patients undergoing definitive CCRT for stage III NSCLC. Dose given to tumor and fractionation received determined by doctor and the intention from patients. The baseline of TLCs was defined as the value measured within one week before RT and a lymphocyte nadir was calculated as the minimum value measured during period of definitive RT. Patients were categorized into three groups. Group A received 2.0-2.2 Gy per fraction (ConRT), while group B received 2.3-2.8

Gy per fraction (moderately HypoRT, mHypoRT), and group C received 3 Gy per fraction Gy (HypoRT).

### Results

There were 52 (44.1%) patients in the ConRT group, 34 in mHypoRT (28.8%) and 32 (27.1%) in HypoRT. Median planning target volume was larger in ConRT (283.89 cm<sup>3</sup>) than in mHypoRT (154.35 cm<sup>3</sup>, P = 0.005) and in HypoRT (118.76 cm<sup>3</sup>, P = 0.001) while there were no difference in gross tumor volume between groups (P = 0.395). Three groups had similar median baseline of TLCs (P = 0.959). During radiation, 70.59% of mHypoRT patients had severe lymphopenia (ie, TLC <500 cells/μl) vs 48.08% of ConRT patients, and 37.50% of HypoRT patients (P < 0.021). Multivariate linear analyses demonstrated that lower baseline TLCs (P < 0.001), higher mean lung dose (P = 0.004) and mHypoRT (P = 0.014) were significantly risk factors of RIL. Higher post-RT TLCs was associated with improved progression-free survival (hazard ratio [HR]: 0.585; 95% confidence interval: 0.369-0.926; P = 0.022) regardless of fractionation regime.

### Conclusion

HypoRT may be more appropriate fractionation regime in definitive concurrent chemoradiotherapy for unresectable stage III non-small lung cancer (NSCLC) as it brings less severe RIL compared with mHypoRT and higher radiation dose compared with ConRT. Further large-scale studies are needed to confirm our findings.

### EP-1371 Impact of target volume delineation on weekly simulation CT during conformal radiotherapy in NSCLC

S. Silipigni<sup>1</sup>, A. Carnevale<sup>1</sup>, C.G. Rinaldi<sup>1</sup>, E. Ippolito<sup>1</sup>, A. Di Donato<sup>1</sup>, P. Matteucci<sup>1</sup>, G.M. Petrianni<sup>1</sup>, S. Palizzi<sup>1</sup>, P. Trecca<sup>1</sup>, B. Santo<sup>1</sup>, L. Trodella<sup>1</sup>, R.M. D'Angelillo<sup>1</sup>, S. Ramella<sup>1</sup>  
<sup>1</sup>Campus Biomedico University, Radiotherapy, Roma, Italy

### Purpose or Objective

Anatomical changes during radiotherapy in lung cancer might contribute to target missing and discrepancies between planned and delivered doses. Modern radiotherapy techniques manage the geometrical uncertainties of treatment planning and treatment delivery and thereby improve target coverage with a much steeper dose gradient and less irradiated normal tissue. The aim is to evaluate the shrinkage of target volume in patients with locally advanced NSCLC treated with concurrent radiochemotherapy (RCT) with an adaptive approach

### Material and Methods

Patients with locally advanced NSCLC treated with RCT were investigated. All patients had stage IIIA/IIIB or intrathoracic relapse after surgery. Treatment was performed with a linear accelerator (Varian Medical System) in a photon regimen, with a 6/15-MV nominal energy and three-dimensional conformal technique with multiple planar and nonplanar beams. Concurrent chemotherapy regimens were platinum-based doublets or monotherapy. All patients received a weekly CT simulation. On each weekly CT the CTV was delineated and in case of tumor's shrinkage, a new CTV was created and a new treatment plan outlined ("replanning")

### Results

From 2012 to 2014 replanning was outlined in 50 patients of 217 patients with locally advanced NSCLC treated with RCT and subjected to weekly simulation CT. Patients' characteristics were: mean age 69.6 years (range 38-92), squamous histology 56%, 32% adenocarcinoma, other 12%, stage IIIA 58% and IIIB 42%. The median total dose delivered was 66.6Gy (range 45-75.6) with standard fractionation. Median CTV at CT simulation was 125.2 cc. Contouring CTV on the weekly CT, we observed a progressive shrinkage of the target volume, in particular at the median dose of 19.8, 27, 36 Gy and 45 Gy we registered a reduction of 13%, 20%, 16%, and 43 %

respectively. The replanning has been performed at a median dose of 45Gy. Median CTV at replanning volume was 74.7 cc

#### Conclusion

Tumor shrinkage is common during RCT in NSCLC. There are points in time during the treatment course when it may be appropriate to adapt the plan to improve sparing of normal tissues. In our patients population in which an adaptive replanning was performed we early observed a tumor reduction (13% after 2 weeks of treatment). We are trying to understand if there are volume reduction patterns that can influence prognosis and therefore help to classify lung neoplasms in different groups

#### EP-1372 External Validation of a Survival Score for Limited Disease Small Cell Lung Cancer (LD-SCLC)

L. Käsmann<sup>1</sup>, R. Abdo<sup>1</sup>, C. Eze<sup>1</sup>, M. Dantes<sup>1</sup>, J. Taugner<sup>1</sup>, K. Gennen<sup>1</sup>, O. Roengvoraphoj<sup>1</sup>, D. Rades<sup>2</sup>, M. Niyazi<sup>1</sup>, C. Belka<sup>1</sup>, F. Manapov<sup>1</sup>

<sup>1</sup>LMU University Hospital Grosshadern, Department of Radiation Oncology, Munich, Germany; <sup>2</sup>University of Luebeck, Department of Radiation Oncology, Luebeck, Germany

#### Purpose or Objective

Definitive chemoradiotherapy is the standard treatment for limited disease small cell lung cancer (LD-SCLC). However, median survival in LD-SCLC ranges between 16 and 24 months due to early locoregional failure and metastases and not all patients can tolerate such intensive regimen. Defined subgroups such as patients in reduced health condition, with severe comorbidities or elderly need to be critical considered before treatment allocation. Patients with a poor survival prognosis should be offered a short course of treatment to avoid spending a substantial proportion of their limited remaining time with receiving chemoradiotherapy. In order to personalize treatment regimens a survival score for these patients was developed. The aim of this study is to validate the survival score for LD-SCLC in an independent patient collective.

#### Material and Methods

We collected data of all patients treated with chemoradiotherapy (CRT) for LD-SCLC between 2004 and 2015. The validation cohort of this study included 78 patients. 38% of all patients were treated with concurrent CRT. The survival score was calculated by independent prognostic factors namely gender, Karnofsky performance status (50-70 versus 80-100%), Tumor substage (very limited disease versus limited disease) and hemoglobin level before radiotherapy (< 12 mg/dl versus ≥ 12 mg/dl). Scoring points were derived from 2-year survival rates divided by 10 and added to scores for individual patients. Three groups were formed (9-13, 14-18 and 19-26 points). The 2-year survival rate of each group from the original study was compared to its corresponding group from this validation study.

#### Results

Median survival time in our patient collective is 17 months (range: 1-123months). 1- and 2-year-survival rates are 60% and 36%. In the current validation study, the 2-year survival rates were 0% in the 9-13 points group, 35% in the 14-18 points group and 43% in the 19-26 points group, respectively (p=0.018). The difference in 2-year survival between the 9-13 points and the 14-18 points group was significant in the complete cohort (p=0.007) as well after stratification of concurrent CRT in the validation cohort (p<0.001), whereas the difference between the 14-18 points and the 19-26 points group was not (p=0.602, p=0.770).

#### Conclusion

The score was reproducible and valid to estimate the 2-year survival rate of patients with LD-SCLC. In order to improve the differentiation between patients with an intermediate and a favorable survival prognosis, the scoring system needs further development.

#### EP-1373 Introducing PET CT in SBRT lung cancer follow-up: Preliminary results of our center protocol.

J. Luna<sup>1</sup>, D. Gonsalves<sup>1</sup>, L. Guzman<sup>1</sup>, M. Rincón<sup>2</sup>, M. Montero<sup>1</sup>, A. Ilundain<sup>1</sup>, W. Vasquez<sup>1</sup>, M.E. Lopez<sup>1</sup>  
<sup>1</sup>Fundación Jiménez Díaz, Radiation Oncology, Madrid, Spain; <sup>2</sup>Fundación Jiménez Díaz, Physics Radiation Oncology, Madrid, Spain

#### Purpose or Objective

To describe the preliminary results conducted for a follow-up protocol in primary lung cancer with stereotactic body radiation therapy in our center. The primary end point for this prospective study is to describe the morphologic and metabolic changes documented in the follow up with Positron emission tomography scan (PET CT) and the clinical decisions surrounding it.

#### Material and Methods

A multidisciplinary team consisted in radiation oncologist, radiologist and nuclear medicine specialist developed in 2014 a protocol for follow up in patients treated with SBRT for the lung cancer.

A Tomography (CT) and PETCT have to be present at the diagnoses.

SBRT treatment consisted in a 4D CT simulation scans with an Elekta frame based immobilization system and free breathing. The plan was delivered using Beam Modulator Linac with HEXA POD system and ELEKTA XVI CBCT system for quality assurance. Fractioning was determining by physician criteria.

Our follow-up included a CT scan at 2 months post treatment, then 2-3 months a PETCT and a second PETCT 2 month later for confirmation of results.

After these first three studies, if the patient presented a complete response (1° arm), as determine in the PERCIST 1.1 (PET Response Criteria in Solid Tumors), a CT every 6 months for the first 3 years were done.

If the patient presented a partial response or stable (2°arm), a follow up with PETCT was done every 6 months for the first 3 years. It was recommended in 1° arm that a progression had to be confirmed with a PET and in the 2° arm two possible options were available: a PETCT in 3 months or a biopsy.

We reviewed the clinical records from the patients involved in the study between April 2015 and November 2017 and analyzed local control rate (LC), loco regional progression (PLR) and systemic progression rate (PSR).

#### Results

We enrolled 31 patients. 77.4 % were men. The median age was 73 years (range 61-81 years). The localization for the tumor was 61 % peripheral, 22.5% central and 16.4% ultra central. The mean size of the tumor treated was 19.5 mm and with mean SUV max of 11.36 (sux max 1.4 - 31.7). The most frequent fraction prescription was 5 session of 10 Gy per session. The patients included in 1° arm follow up were 9.6%.

Median follow up of 19.22 months. LC was 96.8 %, PSR 16.4% and PLR 9.6%.

In 1° arm follow up, 2 patients presented a local progression with a complete response in PET CT.

In 2° arm, 3 patients went for lung biopsy because a disease progression with a negative results afterwards.

In both arms, 3 patients presented a radiological regional progression (lymph node ipsilateral) diagnosed in PET went for biopsy: 2 were negative and 1 positive

#### Conclusion

In our preliminary results, PET is useful to determine a morphologic and metabolic response in SBRT.

Developing a follow up protocol including PETCT for SBRT allows a homogeneity approach to clinical decisions.

#### EP-1374 ECOG-PS and its changes in inoperable stage III NSCLC patients treated with chemoradiotherapy

L. Käsmann<sup>1</sup>, J. Taugner<sup>1</sup>, C. Eze<sup>1</sup>, M. Dantes<sup>1</sup>, O. Roengvoraphoj<sup>1</sup>, K. Gennen<sup>1</sup>, M. Karin<sup>1</sup>, A. Tufman<sup>2</sup>, M.

Niyazi<sup>1</sup>, C. Belka<sup>1</sup>, F. Manapov<sup>1</sup>  
<sup>1</sup>LMU University Hospital Grosshadern, Department of Radiation Oncology, Munich, Germany; <sup>2</sup>Thoracic Oncology Centre Munich Ludwig-Maximilians University, Division of Respiratory Medicine and Thoracic Oncology Department of Internal Medicine V, Munich, Germany

#### Purpose or Objective

The Eastern Cooperative Oncology Group performance score (ECOG-PS) is widely used in clinical routine to quantify patients' general condition. We evaluated ECOG-PS before, after and its alteration in the course of chemoradiotherapy (CRT) in patients with stage III non-small cell lung cancer (NSCLC).

#### Material and Methods

The data of ninety-eight patients with NSCLC of UICC 7<sup>th</sup> edition stage IIIA/B and performance status ECOG 0-1 before treatment was evaluated. ECOG-PS before treatment, on first medical aftercare and the difference between, was examined for their impact on overall survival (OS) from initial diagnosis and time to local progression (TTLP), time to distant metastasis (TTDM) and event free survival (EFS) from the first day of irradiation.

#### Results

The majority of patients were treated with concurrent (79%) or sequential (11%) chemoradiotherapy, while 51% received induction chemotherapy. Median survival for the entire cohort was 20.8 (range: 15.3-26.2) months. Our cohort consisted of 62% males and 38% females. Before treatment ECOG-PS was 0 in 48% and 1 in 52% of patients, their median OS, one-year and two-year survival was 26.4 months, 85%, 53% and 18.9 months, 69%, 37% (p=0.108). After completion of CRT ECOG-PS was 0 in 34%, 1 in 46%, 2 in 18% and 3 in 2% of patients, median OS, one-year and two-year survival was 40.3 months, 88%, 64% for ECOG-PS 0, 19.3 months, 82%, 40% for ECOG-PS 1, 11.9 months, 50%, 28% for ECOG-PS 2 and 7.6 months, 0%, 0% for ECOG-PS 2 (p<0.001). During treatment ECOG-PS remained the same in 62%, was reduced by one in 3% and was increased by one in 30% and by two in 5% of patients. Taken together, 65% of patients had the same or better (=stable) and 35% of patients had worse ECOG-PS after CRT, with median OS, one-year and two-year survival of 29.3 months, 84%, 53% and 13.7 months, 62%, 29%, respectively (p<0.001). Increase of ECOG-PS during treatment impaired OS in both patient subgroups with initial ECOG-PS 0 (p=0.005, median OS 19.1 vs 31.4 months) and 1 (p=0.001, median OS 22.9 vs 11.1 months). Distant metastasis (DM) were diagnosed in 40 patients after completion of CRT. ECOG-PS before and after CRT did not predict occurrence of DM. Patients with an ECOG-PS increase during treatment however showed significantly more distant metastasis (53% vs 35%) with a median TTDM of 9.1 months (p<0.001). EFS was not affected by ECOG-PS before treatment but was impaired by ECOG-PS increase during CRT with median EFS of 9.4 vs 7.7 months (p=0.049) and by ECOG-PS after CRT with median EFS of 9.6 months, 9.0 months, 7.9 months and 3.5 months for ECOG-PS 0, 1, 2, 3, respectively (p=0.018). TTLP was not affected by ECOG-PS before and after treatment or ECOG-PS increase during treatment.

#### Conclusion

ECOG-PS and its changes have a strong impact on patients' outcome. Reduction of performance status was a significant negative factor for patients' probability to develop DM, for EFS and OS.

#### EP-1375 Heterogeneity score in inoperable stage III NSCLC patients treated with definitive chemoradiotherapy

J. Taugner<sup>1</sup>, L. Käsmann<sup>1</sup>, C. Eze<sup>1</sup>, M. Dantes<sup>1</sup>, O. Roengvoraphoj<sup>1</sup>, K. Gennen<sup>1</sup>, M. Karin<sup>1</sup>, A. Tufman<sup>2</sup>, M. Niyazi<sup>1</sup>, C. Belka<sup>1</sup>, F. Manapov<sup>1</sup>  
<sup>1</sup>LMU University Hospital Grosshadern, Department of Radiation Oncology- Munich- Germany., München,

Germany; <sup>2</sup>Thoracic Oncology Centre Munich Ludwig-Maximilians University, Division of Respiratory Medicine and Thoracic Oncology Department of Internal Medicine V, Munich, Germany

#### Purpose or Objective

Stage III non-small cell lung cancer (NSCLC) represents a very heterogeneous disease regarding principal patient- and tumor characteristics. In clinical routine, a simple heterogeneity score may further aid in personalizing multimodal therapy.

#### Material and Methods

The data of ninety-nine consecutive patients with performance status ECOG 0-1 treated until the end of 2016 with multimodal approach for inoperable NSCLC (UICC 7<sup>th</sup> edition stage IIIA/B) were evaluated. Patient- and tumor-related factors were examined for their impact on overall survival. Factors showing a significant negative association with patient prognosis were scored with one point each. Three subgroups with low, intermediate and high risk (0-1, 2-3 and 4-5 points) score were defined. The results were then validated in our own prospective cohort, which started January 2017 and includes 35 patients with at least one year of follow-up.

#### Results

The majority of patients were treated with concurrent (78%) or sequential (11%) chemoradiotherapy, while 53% received induction chemotherapy. Median survival for the entire cohort was 20.8 (range: 15.3-26.3) months. Age (p=0.020), gender (p=0.007), cumulative pack years (PY) (p=0.015), tumor-associated atelectasis (p=0.004) and histology (p=0.004) were shown to have a significant impact on survival. 12, 59 and 28 patients were defined to have a low, intermediate and high-risk heterogeneity score. Median survival, 1-, 2- and 3-year survival rates were distributed as follows: not reached, 100%, 83% and 67% in the low, 22.9 (16.3-29.5) months, 80%, 47% and 24% in the intermediate and 13.7 (11.1-16.3) months, 57%, 25% and 18% in the high-risk subgroup, respectively (p<0.001). Even though median survival was not yet reached in our validation cohort (low risk: 4; intermediate risk: 15; high risk: 16 patients), it has revealed a one-year survival trend with 100% for the low risk, 93% for the intermediate risk and 69% for the high risk subgroup (p=0.100).

#### Conclusion

A simple heterogeneity score was developed for inoperable stage III NSCLC patients with good performance status receiving multimodal therapy. The score may aid physicians to infer clinical outcomes and optimize everyday decision-making as well as planning of prospective studies.

#### EP-1376 Robotic SBRT with fiducial tracking for medically inoperable peripheral stage I NSCLC: final report

S. Kataria<sup>1</sup>, N. Aghdam<sup>1</sup>, M. Repka<sup>2</sup>, M. Marin<sup>3</sup>, L. Campbell<sup>1</sup>, S. Suy<sup>1</sup>, S. Collins<sup>1</sup>, E. Anderson<sup>4</sup>, J. Lischalk<sup>1</sup>, B. Collins<sup>1</sup>

<sup>1</sup>Georgetown University Hospital, Radiation Medicine, Washington DC, USA; <sup>2</sup>NYU Winthrop Hospital, Radiation Oncology, Mineola- New York, USA; <sup>3</sup>New York Medical College-Metropolitan Hospital, Internal Medicine, New York- NY, USA; <sup>4</sup>Georgetown University Hospital, Pulmonary & Critical Care Medicine, Washington DC, USA

#### Purpose or Objective

Published data have demonstrated robotic SBRT with fiducial tracking to be an effective alternative treatment for medically inoperable patients with peripheral Stage I NSCLC. Limited data, however, is available regarding the long term outcomes associated with using this technique. Here we report our institutional experience treating this patient population.

#### Material and Methods

Medically inoperable patients due to age or other comorbidities with biopsy proven peripheral Stage I NSCLC and a minimum follow up of 7 years were evaluated. PET/CT imaging was completed for staging. Three to five gold fiducial markers were implanted in or near tumors under CT guidance or via electromagnetic navigational bronchoscopy to serve as targeting references. Gross tumor volumes were contoured using lung windows. The margins were expanded by 5 mm to construct the planning treatment volume (PTV). Doses delivered to the PTV ranged from 45-60 Gy in 3 or 5 fractions. Treatments were delivered daily utilizing the CyberKnife system with fiducial tracking. Pulmonary function testing was completed a median 49 days prior to the start of SBRT and 1 year after completion. Clinical examination and PET/CT imaging were completed at 6 month follow up intervals.

#### Results

From August 2005 to August 2011, forty patients (median age 76 years) with a median maximum tumor diameter of 2.7 cm (range, 1.4-5.0 cm) were treated and followed for a minimum of 7 years or until death. A median dose of 50 Gy was delivered over a median 7 days (range, 3-13 days). The median follow up for all and alive patients was 4.6 and 8.9 years, respectively. There were 2 primary tumor failures, 1 involved lobe failure, and 1 nodal failure. The 5 year Kaplan-Meier primary tumor control, LC, LRC, distant control, and DFS estimates were 95%, 91%, 88%, 82%, and 70%, respectively. Overall survival (median 4.5 years) and cancer specific survival estimates at 5 and 8 years were 43% and 23%, and 79% and 62%, respectively. Nine patients, all whom had fiducials placed under CT guidance, developed a pneumothorax requiring chest tube placement: no pneumothoraces were observed following bronchoscopic fiducial placement. The 5 year cumulative incidence of radiation induced rib fracture (RIRF) was 53%, with a median time to fracture of 39 months. There was no difference in percent predicted FEV1 one year following SBRT; there was, however, a modest decline of 7.4% (p=0.02) in the percent predicted DLCO at one year.

#### Conclusion

Our institution's medically inoperable Stage I NSCLC outcomes compare favorably with conventional SBRT outcomes from RTOG 0618. Bronchoscopic fiducial placement minimizes the risk of pneumothoraces requiring chest tube placement. Although the RIRF rate was high, the majority of patients were asymptomatic, diagnosed via surveillance PET/CT imaging, and required only conservative management.

#### EP-1377 Role of psoas volume in locally advanced or metastatic NSCLC patients undergoing radiation therapy

V. Nardone<sup>1</sup>, S. Falivene<sup>1</sup>, Giugliano, Francesca Maria<sup>1</sup>, F. Scala<sup>2</sup>, Tini, Paolo<sup>3</sup>, Pirtoli, Luigi<sup>3</sup>, C. Guida<sup>1</sup>, S. Cappabianca<sup>2</sup>

<sup>1</sup>*Ospedale del Mare, Radiation Therapy Unit, Napoli, Italy*; <sup>2</sup>*University of Campania "Luigi Vanvitelli", Department of Precision Medicine, Naples, Italy*; <sup>3</sup>*Unit of Radiation Therapy, University Hospital of Siena, Siena, Italy*

#### Purpose or Objective

To evaluate the volume and median intensity of psoas muscle on CT imaging at the time of diagnosis as a prognosticator in patients with locally advanced or metastatic NSCLC undergoing chemotherapy or radio/chemotherapy.

#### Material and Methods

We included patients with NSCLC undergoing palliative radiation therapy at our Department between January 2010 and December 2017. We contoured on CT made at the diagnosis the volume of right and left psoas volume from the cranial border of L4 till the caudal border of L5. We calculated the median volume between the sides and we divided the median volume for the height of the muscle

(Median Area, MA), and we also divided the MA for the median intensity in Hounsfield Units (MA/I). We analyzed overall survival (OS) with these parameters (using the median value as cut-off) and the known prognosticators (age, ECOG, stage, previous surgery, number of metastases), with Kaplan Meier method (univariate) and Cox Regression Analysis (multivariate).

#### Results

We included 138 patients (97 males and 41 females), with a median age of 67 years (mean 64 years, range 30-84 years). At univariate analysis of OS, the significant parameters were the ECOG (p<0,001), the MA (p:0,001), MA/I (p:0,005), previous surgery (p:0,001), number of metastases (p<0,001). At multivariate analysis, only ECOG (p:0,004), MA (p:0,005), number of metastases (p:0,001) resulted significant.

#### Conclusion

MA and MA/I in NSCLC patients could represent an independent prognosticator of survival, and could help to stratify the patient's prognosis.

#### EP-1378 Brain imaging pre/post treatment in cN2 non-small cell lung cancer treated with chemo-radiation

C.W.E. Chan<sup>1</sup>, H.W.G. Gan<sup>1</sup>, P. Lyons<sup>1</sup>, P. Mcloone<sup>1</sup>, N. Mohammed<sup>1</sup>

<sup>1</sup>*Beatson West of Scotland Cancer Centre- Glasgow- UK, Clinical Oncology, Glasgow, United Kingdom*

#### Purpose or Objective

The incidence of brain metastases (BM) ranges from 10-47% and increases with more advanced non-small-cell lung cancer (NSCLC). Stage 3 NSCLC has 20% of patients diagnosed with BMs, and hence British Thoracic Society (BTS) guidelines state that brain imaging should be performed as part of pre-treatment staging. Asymptomatic BM identified on imaging may alter treatment. Therefore, the aims of this study are to assess pre-treatment imaging in radically treated cN2 NSCLC patients, the incidence of BM after definitive treatment and outcomes.

#### Material and Methods

Patients with stage cN2 NSCLC diagnosed between January 2013 to December 2016 and treated with chemo-radiation therapy (CRT) in the West of Scotland were analysed retrospectively using electronic patient records. Information of pretreatment investigations, treatment given, subsequent follow-up and outcomes were collated and analysed.

#### Results

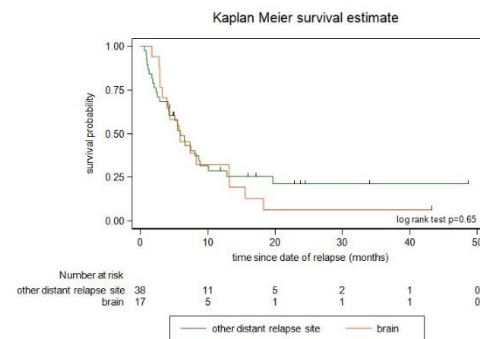
107 patients with stage cN2 NSCLC treated with CRT were identified and analysed. The median age was 65 years (26-84 years), 56(52%) female and 51(48%) male. ECOG performance status was recorded as 0, 1 and 2 in 55, 47 and 3 patients. TNM staging was T1(11%), T2(25%), T3(27%), T4(34%), Tx(2%) and all patients were cN2, M0(96%) and M1(4%). Pathology was squamous cell in 50%, adenocarcinoma 42% and other in 8%. 7 patients also demonstrated ALK or EGFR variants. Radiotherapy dose was 55Gy in 20 fractions over 4 weeks using volumetric modulated arc radiotherapy (VMAT) or 3DConformal radiotherapy. Nine patients received neoadjuvant chemotherapy and all patients had concurrent platinum doublet.

All patients underwent a positron emission tomography (PET) scan, but only 45 patients (41%) had a pre-treatment brain scan, of which 27 were CT scans and 18 were MRI scans. The proportion of brain scans performed increased over time:

Year	Imaged	No Image	Proportion
2013	5	17	0.23
2014	9	15	0.37
2015	16	27	0.37
2016	15	5	0.75

Chi-square for trend  $p=0.0015$

104 patients underwent follow-up imaging at a median of 49(IQR 22.5-87.5) days from end of treatment. During the follow-up period 56(51%) patients experienced distant relapse, of which 18(32%) had BM. Distant relapse occurred within 3 months of the end of treatment for 11 patients, of which 2 patients were diagnosed with BM. The median overall survival of patients relapsing with BM was 5.9 months(95% CI: 2.9-13.1) and with other site of relapse was 5.9 months(95% CI: 4.1-8.6). (See figure)



### Conclusion

Our study shows that clinicians have increasing awareness of the need for pre-treatment brain imaging in cN2 patients for radical treatment. This can still be improved further. After CRT, one third of patients relapsed with symptomatic BM for whom survival was poor. Progress in BM treatment warrants investigating the impact of routine follow up brain imaging after treatment.

### EP-1379 RE-STARTing after lung cancer: impact of a wellbeing event on global health status of survivors.

E. Ippolito<sup>1</sup>, M. Fiore<sup>1</sup>, C. Greco<sup>1</sup>, S. Silipigni<sup>1</sup>, B. Floreno<sup>1</sup>, M. Miele<sup>1</sup>, B. Santo<sup>1</sup>, L. Trodella<sup>1</sup>, R.M. D'Angelillo<sup>1</sup>, S. Ramella<sup>1</sup>

<sup>1</sup>Campus Biomedico University, Radiotherapy, Roma, Italy

### Purpose or Objective

Modern therapies led to an increased survival for patients with lung cancer. Therefore there is a need for dedicated survivorship care for these patients. The aim of this study was to investigate the impact of one day wellbeing event (RE-START initiative) on their health and QoL.

### Material and Methods

Patients with primary lung cancer treated in our institution, after the completion of cancer treatment and in clinical remission were asked to participate in the event. During the event, there were talks providing information on diet, keeping active and managing stress. During the event participants completed a survey package that included the Psychological General Well Being Index (22 items) for distress assessment, NCCN Survivorship Assessment for physical wellness evaluation (14 items), World Cancer Research Fund Cancer Risk derived questionnaire for Dietary and Lifestyle Habits (11 items). The same survey package was completed 3 months after the event by phone interviews.

### Results

From 2015 to 2017, 100 survivors were asked to participate in the event. 51 patients (51%) agreed to participate but only 19 (19%) patients were present. Baseline mean anxiety and depression level were 15.8 (scale 0-25, where the highest score corresponds to the lowest level of anxiety) and 11.83 (scale 0-15, where the highest score corresponds to the lowest level of depression) respectively. Only 25% of patients reported high level of anxiety. Only one patient (8%) showed severe depression. No change was detected three months after the event. Almost half of patients presented pain at baseline (56%) while 38% of patients experienced fatigue. Pain and fatigue improvement after the event occurred in 4 patients (27%). Most of patients reported healthy habits (67-100%). Improvement in dietary habits after the event was also reported (5-10%).

### Conclusion

Only few patients participated in the event. However information provided during the event led patients to modify their habits. Through the questionnaires we were able to identify subgroups of survivors with severe anxiety and depression to whom dedicate intervention strategies

### EP-1380 Intra-fractional Motion in Lung SBRT Treatments with Different IGRT Techniques

I.F. Durmus<sup>1</sup>, B. Tas<sup>1</sup>, A. Okumus<sup>1</sup>

<sup>1</sup>Yeni Yuzyil University Gaziosmanpasa Hospital, Department of Radiation Oncology, Istanbul, Turkey

### Purpose or Objective

Investigation of intra-fraction in 4D-CT and DIBH-CT techniques in lung SBRT treatments.

### Material and Methods

Intra-fraction motion was monitored in 76 fractions of 15 patients with lung SBRT. In 9 patients, 4D-CT scans were acquired into consideration in consideration of all phases of respiration, and ITV was created by adding a margin depending on the amount of motion of the GTV. PTV was created by including safety margins in ITV. Prior to the treatment, 4D-CBCT scanning was performed to ensure the accuracy of the target and patient position. Then, while the VMAT field was irradiated, CBCT scanning was performed simultaneously. After the treatment field was completed, the amount of motion in the target was determined. In this way, intra-fraction motion was monitored in 51 fractions of 9 patients. For the 6 patients with the catalyst surface scanning system, breath was restricted in the determined phase range (deep breath) of the respiration and a CT scan was performed. PTV was created by adding only one safety margin to the GTV, despite limited respiratory in patients scanned by DIBH-CT. Prior to the treatment, CBCT scanning was performed to ensure the accuracy of the target and patient position. Then, while the VMAT field was irradiated, CBCT scanning was performed simultaneously. After the treatment field was completed, the amount of motion in the target was determined. In this way, intra-fraction motion was monitored in 25 fractions of 6 patients.

### Results

The mean deviation ( $\pm$  direction) during treatment was 4 cm with 4D-CT and 0.13 cm with DIBH-CT. In 76 fractions of 15 patients, the maximum deviation was obtained smaller than 0.3 cm. A deviation of greater than 0.3 cm was obtained with the DIBH-CT on the vertical axis and 4D-CT on the longitudinal axis (Table1).

Intra-Fraction CBCT		Lateral (cm)	Longitudinal (cm)	Vertical (cm)
4D-CT (51)	Mean	0.07±0.07	0.10±0.08	0.10±0.09
	Maximum	0.3	0.35	0.29
DIBH-CT (25)	Mean	0.11±0.08	0.14±0.09	0.10±0.09
	Maximum	-0.23	-0.29	0.4

### Conclusion

When the intra-fraction deviation amounts in 76 fractions were examined by 4D-CT and DIBH-CT techniques, it was determined that treatment could be performed reliably with ITV 3 mm safety margin in both IGRT techniques.

In case of maximum deviation of  $\pm 2$  mm during treatment;

- With 4D-CT, safe treatment can be performed in 96.1% of all fractions in the lateral direction, in 90.2% of all fractions in the longitudinal direction, and in 90.16% of all fractions in the vertical direction.
- With DIBH-CT, safe treatment can be performed in 84% of all fractions in the lateral direction, in 76% of all fractions in the longitudinal direction, and in 92% of all fractions in the vertical direction.

Movement management was provided by DIBH-CT and 4D-CT techniques. However, there may be intra-fractional movement in the tumor. PTV should be created by adding 3-5mm safety margin to ITV.

### EP-1381 Stereotactic Body Radiotherapy for Unresectable Locally-Advanced Non Small Cell Lung Cancer

F. Arcidiacono<sup>1</sup>, M. Casale<sup>1</sup>, P. Anselmo<sup>1</sup>, F. Trippa<sup>1</sup>, L. Draghini<sup>1</sup>, S. Terenzi<sup>1</sup>, A. Di Marzo<sup>1</sup>, M. Italiani<sup>1</sup>, S. Fabiani<sup>1</sup>, E. Maranzano<sup>1</sup>  
<sup>1</sup>Radiotherapy Oncology Centre, Santa Maria Hospital, Terni, Italy

#### Purpose or Objective

Conventional fractionated radiotherapy (cRT) concurrent with chemotherapy (ChT) is the standard of care in unresectable locally-advanced non small cell lung cancer (LA-NSCLC). The majority of patients (pts) cannot tolerate this treatment due to its toxicity, so sequential ChT followed by cRT is the more frequent choice in clinical practice. Recently, stereotactic body radiotherapy (SBRT) has been used instead of cRT in early-stage NSCLC offering superior control with less toxicity. Few studies exist on SBRT in LA-NSCLC. We present our experience on this last topic.

#### Material and Methods

Between June 2015 and July 2018, 17 LA-NSCLC pts who underwent SBRT were analyzed. 13/17 (76%) pts received neoadjuvant ChT before SBRT. All pts had CT-PET before SBRT. In pts submitted to neoadjuvant ChT the target volume was the residual disease defined on the basis of CT-PET images. A specific treatment planning for primary tumor (T) and lymph-node/s (N) was done in 9 (53%) pts, while in remaining 8 (47%) the planning target volume (PTV) included both T and N. All pts repeated CT-PET 3 months after treatment and thereafter every 4-6 months. Response, cancer specific survival and toxicity were evaluated.

#### Results

Median age was 72 years (55-81). At diagnosis, 8 (47%), 7 (42%) and 2 (11%) pts had clinical N1, N2 and N3, respectively. Primary tumor was central in 12 (71%) and peripheral in 5 (29%) pts. Median PTV for T and N separately treated were 17.2 cc (8.7-67.96) and 15.02cc (9.9-72.3), while for T and N treated in the same target

median PTV was 91.86 cc (53.2-165.9). Median prescribed dose was 40 Gy (35-55) and 35 Gy (35-45) in 5 fractions to T and N, respectively. At the first follow up, all (100%) pts had a metabolic response at PET-CT. After a median follow-up of 7 months (range, 4-41) there were 3 (18%) local recurrences (LR), 2 (12%) regional node (RN) recurrences and 1 (6%) distant progression (DP). Median LR-free survival (FS), RN-FS and DP-FS were 6 (2-41), 7 (2-41) and 7 months (2-41), respectively. Median overall and cancer specific survival were 7 months (2-41). Of note, 2 pts who had hemoptysis before SBRT resolved the symptom after treatment. No patients developed > grade 2 CTCAE toxicity.

#### Conclusion

SBRT was a feasible, safe and effective treatment in selected unresectable LA-NSCLC pts. Although preliminary outcomes were promising in terms of results and toxicity, larger and more mature studies are needed before the routinely use in clinical practice.

### EP-1382 Texture analysis of FDG-PET in NSCLC treated with SBRT: a validation study of two prognostic features

M. Bertolini<sup>1</sup>, M. Galaverni<sup>2</sup>, M. Manicone<sup>2</sup>, I. Renna<sup>2</sup>, P. Ciammella<sup>2</sup>, L. Giaccherini<sup>2</sup>, F. Bellafiore<sup>2</sup>, G. Timon<sup>2</sup>, F. Vigo<sup>2</sup>, A. Rosca<sup>2</sup>, D. Ramundo<sup>2</sup>, M. Galeandro<sup>2</sup>, M.P. Ruggieri<sup>2</sup>, T. Palmieri<sup>2</sup>, A. Botti<sup>1</sup>, M. Orlandi<sup>1</sup>, R. Sghedoni<sup>1</sup>, E. Cagni<sup>1</sup>, E. Grassi<sup>1</sup>, F. Fioroni<sup>1</sup>, A. Filice<sup>3</sup>, M. Casali<sup>3</sup>, M. Iori<sup>1</sup>, C. Iotti<sup>2</sup>  
<sup>1</sup>Azienda USL-IRCCS di Reggio Emilia, Medical Physics Unit, Reggio Emilia, Italy; <sup>2</sup>Azienda USL-IRCCS di Reggio Emilia, Radiation Oncology Unit, Reggio Emilia, Italy; <sup>3</sup>Azienda USL-IRCCS di Reggio Emilia, Nuclear Medicine Unit, Reggio Emilia, Italy

#### Purpose or Objective

To validate the prognostic value of two textural features of 18F-FDG PET/CT in SBRT-treated early-stage NSCLC

#### Material and Methods

HISTO\_Kurtosis and Long-Run Low Gray-level Emphasis (GLRLM\_LRLGE) are textural features that predicted recurrence free survival (RFS) in a previous analysis on 18F-FDG PET/CT of patients with early stage NSCLC treated with SBRT at our center. We validated this findings in a wider patient population. Twenty-six patients with early stage NSCLC between 2010 and 2017 underwent a 18F-FDG PET/CT before SBRT treatment. In PET image sets of every patient a volume of interest was defined around the tumor by two experienced radiation oncologists. An automatic segmentation was performed inside this volume by using a fixed threshold of 40% of maximum SUV (standardized uptake value). For each volume 45 textural features were calculated using LIFEX software. For each patient clinical data about age, gender, Karnofsky Performance Status (KPS), initial stage, histology, location, prescribed biological effective dose, local recurrence, lobar recurrence, regional recurrence, distant recurrence and death were acquired. Study endpoint was recurrence free survival (RFS). Cut-off values were obtained using a support vector machine (SVM) based analysis and RFS were compared using log-rank test analysis.

#### Results

Median age of the population was 75 years (range 53-90) with 19 men and 7 women. The majority of patients (22) had KPS  $\geq$  80. Stage was T1N0M0 in 10 patients, T2N0M0 in 11, T3N0M0 in 5. Pathological diagnosis was achieved in 15 patients (7 adenocarcinomas and 8 squamous cell carcinomas). Tumor was located in upper lung field in 11 patients, in middle in 1 and in lower in 14. Most of the patients (20) were treated with BED  $\geq$  100 Gy, calculated using linear quadratic model with an  $\alpha/\beta$  ratio of 10 Gy. The median follow-up period was 17.5 months for the entire population and 20 months for the surviving patients. 1-year OS was 69% (CI 64-74). At final follow-up, 13

patients had recurrences: local (n=2), lobar (n=1), regional (n=2), distant (n=6), local and regional (n=1), local, regional and distant (n=1). SVM model found that HISTO\_Kurtosis and GLRLM\_LRLGE can describe patients with any disease recurrence (AUC=0.65). A cutoff of HISTO\_Kurtosis=2.5 obtained with log-rank test was able to classify the population in high and low recurrence risk (p=0.03).

#### Conclusion

Among baseline 18F-FDG PET/CT textural feature, HISTO\_Kurtosis and GLRLM\_LRLGE confirmed as predictors of RFS in our analysis. Although this needs further validation on a larger series of patients, it may reveal helpful in identifying patients who will benefit from closer surveillance or adjuvant therapy.

#### EP-1383 Cytokine profile of NSCLC patients treated with chemoradiotherapy regarding to radiation pneumonitis

Abstract withdrawn

#### EP-1384 Analysing stage III cN2 NSCLC treated with surgery or concurrent chemo-radiation

P. Lyons<sup>1</sup>, H.W.G. Gan<sup>1</sup>, C.W.E. Chan<sup>1</sup>, E. McCully<sup>1</sup>, S. Ansel<sup>1</sup>, M. Philip<sup>1</sup>, N. Mohammed<sup>1</sup>

<sup>1</sup>Beatson West Of Scotland Cancer Centre, Clinical Oncology, Glasgow, United Kingdom

#### Purpose or Objective

Non-small cell lung cancer (NSCLC) patients with stage 3 N2 disease are a heterogeneous group of patients who are offered surgery or chemo-radiotherapy. ESMO lung cancer guideline recommends consideration of surgery for early stage NSCLC - cT1-3 N0-cN2 M0. And inoperable, locally advanced patients are treated with radical chemo-radiation (CRT) if permissible. This study investigated the outcomes of stage 3 N2 patients either diagnosed after surgery or before CRT in order to compare their survival outcomes.

#### Material and Methods

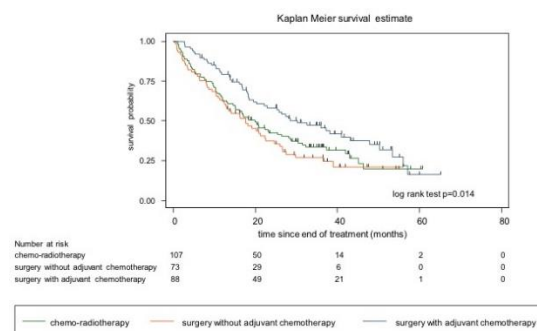
Patients with stage cN2 NSCLC diagnosed from January 2013 to January 2016, and treated with chemo-radiation or patients who underwent lung resection and had a diagnosis of pN2 in the West of Scotland were identified. A retrospective audit of patients was performed.

#### Results

We identified 161 patients with pN2 diagnosis after lung resection and 107 patients with cN2 diagnosis treated with concurrent chemo-radiation. The demographic data was similar between the surgical and CRT group except that the surgical pN2 group had prior clinical staging of cN0 (43%), cN1 (25%) and cN2 (31%) as opposed to CRT patients, which were all cN2.

In addition, only 88 patients (54%) of the surgical pN2 group were given adjuvant chemotherapy as opposed to all CRT cN2 patients.

The median overall survival (OS) of the surgical pN2 group was not significantly different compared with the more advanced cN2 CRT patients who had median survival 19.9 months (95% CI 14.6-26.4m), However, median OS in patients with surgical pN2 who received adjuvant chemotherapy had significantly higher overall survival than surgery alone - 30.2 months versus 17.6 months (95% CI 12.3-22.6m) (p=0.003) (Figure 1).



#### Conclusion

It is clear that NSCLC patients with pN2 disease (includes cN0-2) are not comparable with cN2 patients in terms of burden of disease. Yet our study demonstrated that median OS was not statistically different. This was because 43% patients were cN0 and were considered fit for surgery but not chemotherapy, resulting in 46% of pN2 patients not given adjuvant chemotherapy.

Hence, further investigation of the mediastinal nodal staging is warranted and possibly to reconsider mediastinal staging of PET negative nodes. In addition, patients considered for surgery should be assessed in terms of fitness for both surgery and chemotherapy or else be considered for chemo-radiation.

#### EP-1385 Does pneumonitis increase in irradiated lungs during immunotherapy? A generating hypotheses study

C. Mazzarella<sup>1</sup>, A. Martino<sup>2</sup>, A.R. Alitto<sup>1</sup>, F. Preziosi<sup>1</sup>, F. Catucci<sup>1</sup>, A. Petrone<sup>1</sup>, M. Campitelli<sup>1</sup>, F. Marazzi<sup>1</sup>, G.C. Mattiucci<sup>2</sup>, G. Palazzoni<sup>2</sup>, V. Valentini<sup>2</sup>, G. Mantini<sup>2</sup>  
<sup>1</sup>Fondazione Policlinico Universitario A. Gemelli IRCCS, Scienze Radiologiche- Radioterapiche ed Ematologiche, Rome, Italy ; <sup>2</sup>Fondazione Policlinico Universitario A. Gemelli IRCCS-Università Cattolica del Sacro Cuore, Scienze Radiologiche- Radioterapiche ed Ematologiche, Rome, Italy

#### Purpose or Objective

Immunotherapy with immune checkpoint inhibitors (ICIs) revolutionized therapy of advanced non-small-cell lung cancer (NSCLC). Nivolumab have been shown to improve overall survival in advanced, metastatic patients (pts) with NSCLC. Nevertheless, immune-related pneumonitis is a potentially fatal toxicity of anti-PD-1/PD-L1. This study investigates the role of chest radiotherapy (RT) and the development of immune-related pneumonitis in NSCLC treated with nivolumab.

#### Material and Methods

Consecutive patients with locally-advanced or metastatic NSCLC treated with nivolumab as second or third-line therapy for recurrent or progressive disease, between May 2017 and March 2018 were included. Patient demographics, treatment, adverse event and RT data including type of RT, volume of RT and number of courses were collected. Toxicity was evaluated according to the common terminology criteria for adverse events (CTCAE) version 4.0.

#### Results

Seventeen patients were treated, mostly male (65%), current or former smokers (76.5%) with Eastern Cooperative Oncology Group (ECOG) PS score <2 (88%). Median age was 67 years (range: 49-79). Previously 15/17 (88.2%) patients had undergone radiotherapy on the thoracic disease or for metastatic sites. Mean number of nivolumab cycles was 12 (range: 1-26). 11/17 (64.7%) patients had only locally-advanced disease. Of 15 patients who received any RT, we observed 3/15 (20%) G2/G3 pneumonitis and 1/15 (6.6%) G4. Only 1/4 (25%) pneumonitis occurred in RT field.

### Conclusion

Even if pneumonitis incidence is maybe higher in irradiated lung patients treated with nivolumab, the finding of clear factors that could cause this event needs to be identified. Moreover, research of preliminary predictive factors (functional tests, RT technique, patients intrinsic factors) could be useful to improve treatment option choices and also toxicity occurrence prevention.

### EP-1386 Stereotactic body radiation therapy for central early non small cell lung cancers- Yes! Its possible

R. Harjani Hinduja<sup>1</sup>, J. Zheng<sup>1</sup>, G. Cook<sup>1</sup>, R. MacRae<sup>1</sup>, J. Pantarotto<sup>1</sup>

<sup>1</sup>University of Ottawa, Radiation Oncology, Ottawa, Canada

### Purpose or Objective

Stereotactic Body Radiation Therapy (SBRT) is a standard treatment for early non small cell lung cancers. Concerns exist about its use in centrally located tumours. RTOG 0813 demonstrated the efficacy and tolerability of SBRT in centrally located tumours. However, there is a reluctance in many institutions regarding its widespread adoption into clinical practice. We report our institutional experience with treatment of central tumors.

### Material and Methods

We retrospectively reviewed consecutive medically inoperable early central NSCLC patients treated with SBRT in an ethics approved study. All tumours were biopsy proven and adequately staged by Positron Emission Tomography (PET) scan. The end points of interest were Local Recurrence Free Survival (LRFS) and Overall Survival (OS). The outcomes were compared based on ECOG status, left versus right sided tumours, histology, age adjusted Charlson Comorbidity index, SUVmax and pre-treatment Hemoglobin and Poly-Morpho-Nuclear (PMN) leucocytes.

### Results

92 patients who underwent SBRT for centrally located lung tumours were eligible. The median age was 75 years, (56 to 90 years). 40(43.5%) were males. The median age adjusted comorbidity index was 5. 86% were current/former smokers. 28, 34, 27 and 3 patients had ECOG 0, 1, 2 and 3 respectively. 52.2% had left and 47.8% had right sided tumours. 28.3% were squamous cell carcinomas, 50% were adenocarcinomas and remaining 21.7% included large cell and NSCLC-NOS. All patients were PET staged and the median SUVmax was 6.85. The most common dose schedule was 60Gy in 8 fractions. The dose fractionation was increased in 14 patients to deliver treatment in 15-20 fractions. The median BED was 105Gy. The median OS was 47 months as compared to 53 months for peripheral tumours in the database (p=0.08). The median local recurrence free survival (LRFS), Regional recurrence free survival (RRFS) and Distant relapse free survival (DRFS) was 40 months, 47 months and 45 months, respectively. Lower ECOG score patients had better OS as compared to higher ECOG score (median OS- 42, 61, 35 and 18 months, respectively p=0.05) and a trend towards better LRFS (P=0.07). Patients with pre-treatment hemoglobin >130g/L and PMN leucocyte count > 5\*10<sup>9</sup>/L were associated with improved OS (p= 0.03 and p= 0.003 respectively). Adenocarcinomas had a higher LRFS and OS as compared to squamous cell carcinomas, however this was not statistically significant (median OS- 65 and 47 months respectively, p= 0.2), (median LRFS of 47 and 35 months respectively, p= 0.10). There was no difference in LRFS or OS when stratified by age adjusted Charlson comorbidity score, SUVmax or location of left/right side.

### Conclusion

SBRT for centrally located tumours is feasible with outcomes comparable to published literature. Lower ECOG performance score, pre treatment hemoglobin >

130, PMNs > 5 and adenocarcinoma histology have a better outcome.

### EP-1387 Managing isolated local/regional recurrences after SBRT for inoperable early lung tumors - a dilemma

R. Harjani Hinduja<sup>1</sup>, J. Zheng<sup>1</sup>, J. Pantarotto<sup>1</sup>, R. MacRae<sup>1</sup>

<sup>1</sup>University of Ottawa, Radiation Oncology, Ottawa, Canada

### Purpose or Objective

Stereotactic Body Radiation Therapy (SBRT) is an accepted standard treatment for treatment of stage I medically inoperable non-small cell lung cancers (NSCLC). The most common mode of failure for these patients is distant failure. Among the few percentage of patients who fail locally or regionally, salvage treatment options are limited in this frail population. We aim to evaluate our experience in salvage treatments at local or regional isolated failures after SBRT.

### Material and Methods

We retrospectively reviewed failure patterns and subsequent treatments for our early NSCLC patients treated with SBRT/ hypo-fractionated radiation therapy between 2009 and 2015 in a research ethics board approved study. Local and regional recurrences were noted and then were categorized into isolated local/regional /loco-regional versus widespread progression (along with distant metastases). Salvage treatments offered to loco-regional recurrences were reviewed.

### Results

511 patients who received SBRT/hypo-fractionated radiation therapy were eligible for the study. 475 (92.95%) of the tumours were treated with SBRT. 395 (77.6%) were peripheral tumours and 114 (22.4%) were central. The median BED was 132Gy. With a mean follow up of 4.5 years, 47(9.2%), 47 (9.2%) and 85 (16.7%) experienced local, regional and distant failures respectively. Of these, 38 patients experienced isolated local and/or regional failure (21- local, 11- regional and 6 local and regional failure; with no distant failure). 21.05% (8) tumours received salvage treatment with modalities like RFA (3), re-irradiation with or without chemotherapy (5). Of the non-salvaged tumours (30), 16 (53.33%) received palliative treatments (7- palliative radiation, 9- palliative chemotherapy). The most common reason for non-salvaged tumors was poor performance score (Eastern Cooperative Oncology Group score 3 or 4), followed by dearth of local options. 13 additional patients developed loco regional failure with time-separated distant metastases (with distant failure at minimum 3 months after loco-regional failure), of which 6 were salvaged locally.

### Conclusion

Although, the outcomes for stage I medically inoperable patients are impressive with the advent of stereotactic body radiation therapy, management of local and regional recurrences remains a dilemma owing to poor performance status and overall frailty of this population.

### EP-1388 SABR Following Pneumonectomy: A Systematic Review of Clinical and Toxicity Outcomes

A. Louie<sup>1</sup>, A. Ariffin<sup>1</sup>, F. Al-Shafa<sup>1</sup>, R.G. Boldt<sup>1</sup>, A. Warner<sup>1</sup>, G. Rodrigues<sup>1</sup>, D. Palma<sup>1</sup>

<sup>1</sup>London Health Sciences Centre South West Regional Cancer Program, Department of Radiation Oncology, London, Canada

### Purpose or Objective

Survivors of lung cancer are at risk of second primary lung cancers (SPLCs), which are often curable. However, in patients who have previously undergone pneumonectomy, treatments options are limited. The aim of this study is to perform a systematic review of publications examining

treatment planning considerations, clinical outcomes, and toxicity rates of SABR following pneumonectomy.

#### Material and Methods

A systematic review of the literature was conducted in accordance with PRISMA guidelines using PubMed and EMBASE from inception to July 2018. A total of 220 entries were identified. Articles were limited to those published in the English language. 114 unique articles were assessed for eligibility. Inclusion criteria consisted of non-review articles involving at least 2 patients who received lung SABR post-pneumonectomy. Two reviewers independently performed abstract and full-text review, with discrepancies settled by a third reviewer.

#### Results

Of the 114 articles identified by the initial search, 10 articles comprising 108 patients who received lung SABR post-pneumonectomy met inclusion criteria. Median age was 70.8 (range 58.0-75.5), and most patients were male (median 77.0%, 73.9-100%, n=5). The weighted average incidence of grade 3 or higher toxicity was 11.7% (0-33.3%, n=9). There were 2 treatment-related deaths from one case series. Another death was reported that was infectious in nature, but the attributable effects of radiation could not be ruled out. The median 1-year rate of logoregional control was 90.2% (range 84.0-100%, n=6), which is consistent with previously published SABR data. Median BED<sub>10</sub> was 107.9 Gy (87.5-151.2 Gy, n=8), and the most common dose fractionation schemes were 54 Gy in 3 fractions (n=7), 48 Gy in 4 fractions (n=6), and 50 Gy in 5 fractions (n=5). The majority of studies used 4DCT image acquisition (9/10), a technique that captures a 3DCT volume over a period of time thereby describing the motion of a desired target. Respiratory gating was only employed in a single study.

#### Conclusion

SABR appears to be a safe and effective option for solitary pulmonary nodules in survivors of lung cancer with prior pneumonectomy. Multi-institutional and/or prospective studies would be helpful to determine the true risk and appropriateness of SABR in this high-risk patient population.

#### EP-1389 Lowered Whole Brain Irradiation Dose for Non-Small Cell Lung Cancer Patients with Brain Metastases

Y. Wang<sup>1</sup>

<sup>1</sup>Taipei Tzu Chi Hospital, Radiation Oncology, New Taipei City, Taiwan

#### Purpose or Objective

Non-small cell lung cancer (NSCLC) patients with brain metastases are traditionally treated with 30 Gy of whole brain irradiation (WBI). However, it has been reported to be correlated with neurocognitive function decline. In this study, we analyzed the survival of patients treated with different WBI dose to evaluate if lowered WBI dose provides comparable treatment outcome.

#### Material and Methods

We reviewed stage IV NSCLC patients with brain metastases who underwent brain irradiation at our hospital with the following exclusion criteria: 1) previous brain irradiation history; 2) brain metastases resected before irradiation; 3) poor medical condition with early termination of radiotherapy. The radiotherapy regimen for brain metastases varied from WBI only, WBI followed by metastatic tumor boost, to boost alone without WBI. The Graded Prognostic Assessment (GPA) score was calculated for each patient by their age, Karnofsky performance scores, number of cranial metastases, and if extracranial metastases were present. The survival time was calculated from the day radiotherapy completed. Kaplan-Meier survival analyses were performed separately for patients received WBI dose > 21 Gy (HWBI group) or ≤21 Gy (LWBI group) in each GPA class, and the difference between the groups was tested with the log-rank test.

#### Results

From Apr, 2010 to May, 2015, 77 patients were included in this study. Forty-two patients received WBI dose more than 21 Gy, and the other 35 received ≤21 Gy. In the GPA class 0-1, the median survival of HWBI group (n=21) was longer than the LWBI group (n=13) (2.26 vs. 1.03 months, p=0.075). In the GPA class 1.5-2.5, the median survival of HWBI group (n=20) was shorter than the LWBI group (n=20) (23.13 vs. 29.37 months, p=0.09).

#### Conclusion

With the potential of better neurocognitive function preservation, WBI dose ≤21 Gy showed a survival outcome non-inferior to 30 Gy. Although no significant difference detected, there is a trend encouraging to apply lower WBI dose to patients with higher GPA scores (1.5-2.5) for better survival benefit. Further prospective trials are required to confirm the optimal brain radiotherapy regimen for NSCLC patients with brain metastases.

#### EP-1390 Association between heart dose and survival for NSCLC patients underwent VMAT

C. XIE<sup>1</sup>, X. Jin<sup>1</sup>

<sup>1</sup>the 1st Affiliated Hospital of Wenzhou Medical University, Radiation and Medical Oncology, Wenzhou, China

#### Purpose or Objective

One critical finding of RTOG 0617 was that heart dose could impact the early overall survival (OS) of non-small cell lung cancer (NSCLC) patients underwent radiotherapy (RT), although mixed results were reported in studies trying to confirm this finding, studies all suggested that heart dose should be minimized during radiotherapy planning based on the known adverse effects of RT on vasculature and cardiac function. Intensity-modulated radiotherapy (IMRT) had been demonstrated to decrease the dose to lung and heart compared with 3D conformal radiotherapy. As an extended form of IMRT, volumetric modulated arc therapy (VMAT) is able to achieve similar dosimetric distribution while decreasing MU and treatment delivery time compared with IMRT. The purpose of this study is to investigate the efficacy and safety of VMAT, as well as the association of lung and heart dosimetry with OS in the NSCLC patients treated by VMAT.

#### Material and Methods

200 consecutive inoperable NSCLC patients treated by VMAT from March 2011 to September 2016 were retrospectively reviewed. OS rates were estimated with the Kaplan-Meier method. The Cox regression model estimated the hazard ratio (HR) and the corresponding 95% confidence interval (CI) for univariate (UVA) and multivariate (MVA) analyses. Multivariate model building was performed using stepwise regression (modification of the forward selection method) techniques utilizing significant univariate factors to avoid over-fitting the model.

#### Results

There were 174 NSCLC patients enrolled in this study with a median age of 63 years (range from 34-86 y). The average OS for these patients were 25.02 months with a median followup of 14.77 months. For an average prescribed dose of 55.90±0.50 Gy, the mean dose, V25, V30 and V 50 to heart were 16.03±0.63, 28.73%±1.51%, 25.80%±1.42%, and 8.38%±0.86%, and the mean dose, V5, V10, V13, V20 and V30 to lung were 13.78±0.31

Gy, 55.07%±1.54%, 40.68%±1.30%, 33.2%±1.09%, 23.03%±0.67%, and 15.22%±0.42%, respectively. Univariate analysis indicated that V30 of heart was associated with overall OS with a p value of 0.044, no other heart and lung dosimetric parameters was associated with OS. The V13 of lung was associated with acute radiation pneumonia with an RP rate of 9.78%. The dosimetric values of heart and lung were strongly correlated with each other.

#### Conclusion

Heart dose was associated with OS for advanced NSCLC treated by VMAT.

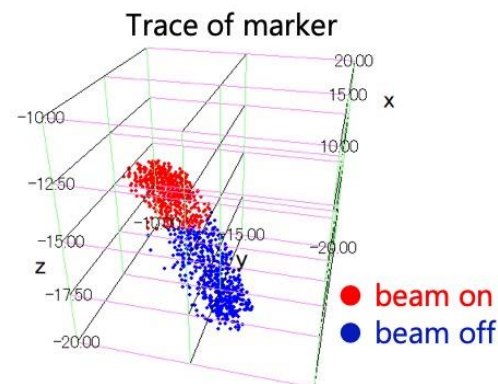
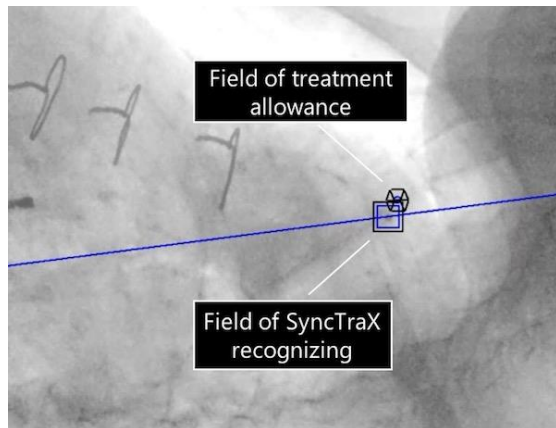
#### EP-1391 Stereotactic body radiotherapy using a new real-time tumor tracking system and fiducial markers

Y. Hiroshima<sup>1,2,3</sup>, K. Nitta<sup>1</sup>, T. Saitoh<sup>1</sup>, T. Ohno<sup>4</sup>, K. Shinoda<sup>1</sup>, Y. Tamaki<sup>1,5</sup>

<sup>1</sup>Ibaraki Prefectural Central Hospital, Radiation Oncology, Kasama, Japan ; <sup>2</sup>University of Tsukuba, Radiation Oncology- Faculty of Medicine, Tsukuba, Japan ; <sup>3</sup>University of Tsukuba Hospital, Radiation Oncology, Tsukuba, Japan ; <sup>4</sup>Dokkyo Medical University- Koshigaya Hospital, Radiology, Koshigaya, Japan ; <sup>5</sup>University of Tsukuba Hospital, Ibaraki Clinical Education and Training Center, Tsukuba, Japan

#### Purpose or Objective

A new fluoroscopic real-time tumor tracking radiotherapy (RTRT) system; the SyncTraX FX4 (Shimadzu Co., Kyoto, Japan) enables that transmits an irradiation permission signal to a treatment device while a fiducial marker is within a planned position and stops transmission when it comes off (Fig 1). In addition, while a system works, it can record a fiducial marker position quantitatively (Fig 2). Using this system, we can reduce the irradiation volume of normal tissue while guaranteeing the positional accuracy of the tumor even under free breathing and improve the patients' burden and adverse events. We report the safety and the feasibility of the stereotactic body radiotherapy (SBRT) using this system.



#### Material and Methods

Between October 2017 and June 2018, a total of 8 patients and 9 sites treated by SBRT with this system were retrospectively reviewed. This study included 7 men and 1 woman, whose age ranged from 66 to 86 (median 75). Treated sites of organ were lung (n=6) and liver (n=3). All of lung tumors were primary tumors and liver tumors were metastatic tumors. All patients were inserted several

fiducial markers, namely Visicoil to the liver and Disposable Gold Marker (Olympus Co. Tokyo, Japan) to the lung, on 1-2 weeks before CT. Patients planned as treated under free-breathing were taken CT with exhalation breath, and breath-hold were taken with inhalation breath. TrueBeam STX was used as the treatment device, and irradiation method was fixed multiple irradiation. Prescribed dose was 55.0 Gy/ 4 fr (n=8) or 66.0 Gy/ 10 fr (n=1), and all of them were D95 prescription, planned with RayStation. Average PTV volume treated was 33.9cc (range, 9.82-115cc). Conformity index in each irradiation field was 0.82-0.9, and the mean value was 0.86.

#### Results

Follow-up period was 2.3-8.8 months (median 5.1). As acute adverse event, radiation pneumonitis of grade 2 was observed in 1 patient in lung tumor patients. No serious adverse events related to radiotherapy and inserting fiducial markers were observed during the period. Local recurrence was observed in 1 patient, and distant metastasis was observed in 1 patient. Although treatment on free breathing was the basis, it was possible to shorten patient radiation exposure and treatment time by using in combination with respiratory arrest system. In the liver, to follow fiducial markers was difficult on the perspective direction, there were cases where a change was necessary in treatment plan.

#### Conclusion

SBRT using the SyncTraX FX4 system and fiducial markers was suggested as a safe and less burdensome treatment.

#### Electronic Poster: Clinical track: Upper GI (oesophagus, stomach, pancreas, liver)

#### EP-1392 Preoperative image-guided identification of response to nCRT in esophageal cancer (PRIDE study)

A. Borggreve<sup>1</sup>, I. Defize<sup>1</sup>, G. Meijer<sup>1</sup>, H. Van Laarhoven<sup>2</sup>, H. Langendijk<sup>3</sup>, V. Mul<sup>3</sup>, F. Voncken<sup>4</sup>, M. Verheij<sup>4</sup>, P.S.G. University Medical Center Utrecht<sup>1</sup>, P.S.G. The Netherlands Cancer Institute<sup>4</sup>, P.S.G. University Medical Center Groningen<sup>3</sup>, P.S.G. Amsterdam University Medical Centers<sup>5</sup>

<sup>1</sup>University Medical Center Utrecht, Radiation Oncology, Utrecht, The Netherlands ; <sup>2</sup>Amsterdam University Medical Centers, Department of Medical Oncology, Amsterdam, The Netherlands ; <sup>3</sup>University Medical Center Groningen, Radiation Oncology, Groningen, The Netherlands ; <sup>4</sup>The Netherlands Cancer Institute - Antoni van Leeuwenhoek Hospital, Radiation Oncology, Amsterdam, The Netherlands ; <sup>5</sup>Amsterdam University Medical Centers, Cancer Center Amsterdam, Amsterdam, The Netherlands

#### Purpose or Objective

Nearly one third of patients undergoing neoadjuvant chemoradiotherapy (nCRT) for locally advanced esophageal cancer have a pathologic complete response (pCR) of the primary tumor upon histopathological evaluation of the resection specimen. The primary aim of this study is to develop a model that predicts the probability of pCR to nCRT in esophageal cancer, based on diffusion-weighted magnetic resonance imaging (DW-MRI), dynamic contrast-enhanced magnetic resonance imaging (DCE-MRI), <sup>18</sup>F-fluorodeoxyglucose positron emission tomography and computed tomography (<sup>18</sup>F-FDG PET-CT). Accurate response prediction could lead to a patient-tailored approach with omission of surgery in the future in case of predicted pCR or additional neoadjuvant treatment in case of non-pCR.

#### Material and Methods

The PRIDE study is a prospective, single arm, observational multicenter study that will develop a multimodal prediction model for histopathological response to nCRT for esophageal cancer. A total of 200 patients with locally

advanced esophageal cancer - of which at least 130 patients with adenocarcinoma and at least 61 patients with squamous cell carcinoma - scheduled to receive nCRT followed by esophagectomy will be included. The primary modalities to be incorporated in the prediction model are quantitative parameters derived from MRI and <sup>18</sup>F-FDG PET-CT scans, which will be acquired at fixed intervals before, during and after nCRT. Secondary modalities include blood samples for analysis of the presence of circulating tumor DNA (ctDNA) at 3 time-points (before, during and after nCRT), and an endoscopy with (random) bite-on-bite biopsies of the primary tumor site and other suspected lesions in the esophagus as well as an endoscopic ultrasonography (EUS) with fine needle aspiration of suspected lymph nodes after finishing nCRT. The main study endpoint is the performance of the model for pCR prediction. Secondary endpoints include progression-free and overall survival.

#### Results

If the multimodal PRIDE concept provides high predictive performance for pCR, the results of this study will play an important role in the accurate identification of esophageal cancer patients with a pCR to nCRT. These patients might benefit from a patient-tailored approach with omission of surgery in the future. Vice versa, patients with non-pCR might benefit from additional neoadjuvant treatment.

#### Conclusion

**Trial registration:** The article reports on a health care intervention on human participants and was prospectively registered on March 22, 2018 under ClinicalTrials.gov Identifier: NCT03474341

#### EP-1393 Prospective fiducial placement in liver tumours: Effectiveness, placement 'quality' and toxicities

K. Katak<sup>1</sup>, S. G<sup>2</sup>, R. Madhavan<sup>1</sup>, T. Tatineni<sup>1</sup>, S. P. G<sup>3</sup>, J. J<sup>3</sup>, D. Dutta<sup>1</sup>

<sup>1</sup>Amrita Institute of Medical Sciences- Kochi, Radiation Oncology, Kochi, India ; <sup>2</sup>Amrita Institute of Medical Sciences- Kochi, Radiology, Kochi, India ; <sup>3</sup>Amrita Institute of Medical Sciences- Kochi, Radiation therapy, Kochi, India

#### Purpose or Objective

Fiducial placement in liver tumours (HCC) for Robotic Radiosurgery (Cyberknife, CK) treatment is considered crucial step of treatment and also associated with morbidity. Present prospective study evaluating the associated effectiveness, quality of fiducial placement and toxicities.

#### Material and Methods

Between Mar 2017-Mar 2018, 36 HCCs accrued in the ethical & scientific committee approved prospective study for CK treatment. Three fiducials were placed in liver (CT/USG guided) for tracking. Fiducials placed by radiologist (RD) with ideal fiducials will be equidistant from each other (max distance 5 cm, min distance 2 cm). Quality of fiducial placement as RD and radiation oncologist (RT) were assessed by "institution" defined scale. Placement time, pain score, complications, recovery time and factors influencing fiducial placement were analysed

#### Results

Thirty six patients (Male 92%, mean age 60.2 yrs, ECOG 0-1 92%, Child-Pugh A 89%, B&C 11%, majority in seg II & VI, PVT disease 64%) with HCCs underwent fiducial placement under guidance (CT scan 69%). 5, 4 & 3 fractions were in 29 (80%), 16 & 4%. Time for placement <20 min, within 45 min and >45 min were in 55%, 36% and 8% respectively. Three patients (8%) had gross displacement (2 in lung, 1 in abdomen) immediately after placement. One patient (4%) expired after fiducial placement (<72 hours) with decompensation. Five patients (15%) had minor complications (pain abdomen 2, pneumothorax 2). RD & RT Score values of poor, fair, good are 6%, 14%, 80% and

8%, 19%, 72% respectively. Correlation between RT & RD score was satisfactory (Pearson correlation test: 0.001). Placement time of 10-20 min, 20-45 min and more than 45 min were in 55%, 36% and 8% patients respectively. Poor pain score (3/4) was in 6% only. Good RT Score, good RD Score and poor pain score, in seg VII-VIII (n=12) and other segments (n=24) were 83% & 67% (p-value: 0.484); 83% & 79% (p-value: 0.186); nil & 8% (p-value: 0.69) respectively. In Child Pugh A (n=32) and B&C (n=4) were 78% & 25% (p-value: 0.08); 87% & 25% (p-value: 0.029) and 6% & 75% (p-value: 0.024) respectively. PS also influenced RT score (p-value: 0.014), RD score (p-value: 0.003), pain score (p-value: 0.016). Fiducial placement score improved from 30% in 1st 10 patients to 93% in last patient cohort (p-value: 0.023). Fiducial placement time reduced from 42.2 min to 14.3 min (p-value: 0.069) in the same cohort. Interfiducial distance, angle and distance from centre max and min are 4.7 & 2.4 cm; 82.7 & 28.5 degree and 5.1 & 2.1 cm respectively

#### Conclusion

Fiducial placement is safe and in experienced hands, quality of placement is 'good' in majority. Major complications and admission after fiducial placement is rare. Patients with poor Child Pugh Score, extensive liver involvement, poor PS have higher probability of complications. Segment of liver involved, BCLC stage do not influence fiducial placement quality.

#### EP-1394 Prognostication of HCC with PVT treated with SBRT: Early results from a prospective study in India

T. Tatineni<sup>1</sup>, K. Katak<sup>1</sup>, R. Madhavan<sup>1</sup>, S. G<sup>2</sup>, R. Das<sup>1</sup>, D. Dutta<sup>1</sup>

<sup>1</sup>Amrita institute of medical sciences, Radiation oncology, Kochi, India ; <sup>2</sup>Amrita institute of medical sciences, Radiologist, Kochi, India

#### Purpose or Objective

Present prospective study evaluating role of Radiosurgery (CK) in Indian patients and analyzed prognostic factors

#### Material and Methods

Inoperable HCC with PVT with good performance status, liver function were accrued after radiological diagnosis for CK (M6). Fiducial placement (3 number) done as per protocol. Triple phase contrast CT scan done, planning done with Multiplan. PVT categorized as Chen classification. GTV is gross contrast enhancing mass within the main portal vein, its tributaries and adjacent paranchymal disease. PTV margin was 2-3 mm. Dose as per established risk stratification protocol. Mean liver dose <15Gy & 800 cc liver <8Gy. Dosage was 22-50Gy/5fr. Prognostication done with Chen, Child Pugh (CP), AFP, CLIP score, GRETCH, BCLC classification and response to treatment, dosage

#### Results

: 27 HCC with PVT accrued in the study [mean age 59.1 yrs, 94% male; Child Pugh A 63%, B 30%; BCLC C 93% & D 7%; PS0-1: 89%, KPS>80: 81%; co-morbidities 40%; infective 15%, Alcohol intake 26%]. Patients presented with abdominal pain (44%), fatigue (30%), ascitis (15%) and melena (11%). CP Score 5,6,7 & 8 was in 37%,26%,19% & 19% respectively. 40% patients presented with abdominal pain, 30% with fatigue. 15% patients had focal disease with PVT, liver involvement >50% & <50% in 44% and 40%. 16% underwent TACE before SBRT. 56% received sorafenib after SBRT. PVT Chen classification VP2, VP3 & VP4 were in 22%, 33%, 41% respectively. CLIP score 1, 2, 3, 4, 5 was in 4%, 26%, 30%, 33% and 7% respectively. Mean follow up was 7 months (range 1.7-17.6 months). Mean actuarial OS was 10.8 months (SEM: 1.48; 95%CI: 7.8-13.7). At last follow up, 16/27(59%) were alive and 11/27(41%) were dead. 6(22%) had complete PVT response, 3(11%) had stable disease with partial PVT response, 7 (30%) have local progression, 3 (27%) had metastatic disease (1 lung, 2 spine) and 8 (73%) expired with local progression. No death due RILD. 6/27 (22%) patients had radiologically confirmed

re-canalization [5 in PVT & 1 in IVC]. Post-CK, 8% patient underwent TACE and 4% had TARE. Mild GI toxicities (Gr I-II) in 10 (40%), fatigue (Gr II-III) 7 (28%). One (4%) patient had Gr III GI toxicity and one (4%) patient had decompensation (<4wk) after treatment. Gender (p=0.542), infective etiology (p=0.356), alcohol intake (p=0.983), pre-CK AFP (p=0.581), BCLC stage (p=0.660), adjuvant Sorafinib (p=0.324) did not influence survival functions. Patients with PVT response (p=.003) had better survival. 1-yr actuarial OS in dose delivered (<39Gy Vs >39Gy: 65% vs 40%); CLIP Score (1-2 Vs 3-6: 75% Vs 40%); CP Score (5-7 Vs 8-9: 78% Vs 42%) & PVT Score (VP1-2 Vs 3-4: 67% Vs 56%) showed trend towards improved survival.

#### Conclusion

CyberKnife is safe & effective option in Indian HCC with PVT patients. Good PVT response, higher dose delivered, CP score, CLIP Score and PVT score have prognostic significance. RT dose and PVT response may be included in response assessment scoring system.

#### EP-1395 Radiation Dose to the Thoracic Vertebral Bodies is Associated with Acute Hematologic Toxicities

F. Lingli<sup>1</sup>, D. Xiaobo<sup>1</sup>

<sup>1</sup>Mianyang Central Hospital, Oncology, Mianyang, China

#### Purpose or Objective

Mean thoracic vertebral body(TVB) dose and low-dose parameters (V5-V20) are associated with severe acute hematologic toxicities(HT)during concurrent chemoradiotherapy (CRT) for lung cancer, in which optimal dosimetric cut-off points have been identified. Esophageal cancers are closer to TVBs than lung cancer and require longer radiation fields and different chemotherapy regimens. The optimal dosimetric cut-off points for TVBs in lung cancer maybe unsuitable for esophageal cancers. We aimed to explore factors associated with HT during CRT and optimal dosimetric cut-off points for TVBs in esophageal cancer.

#### Material and Methods

From January 2010 to June 2018, we selected patients with esophageal squamous cell carcinoma confirmed by pathology. We retrospectively examined radiotherapy plans for all patients who met the criteria and outlined the TVB dose for each patient. Average TVB dose and parameter data of V5-V60 were recorded on the dose-volume histogram diagram. Weekly blood routine results were recorded from the start of CRT to 2 weeks after the end of radiotherapy. At the same time, baseline data of age, ECOG score, body mass index, clinical stage, tumor length, induction chemotherapy, concurrent radiotherapy regimen, radiation dose, and radiotherapy modality were recorded. Simple logistic regressions were used to determine the correlation of all clinical and dosimetric parameters with HT. Multiple logistic regression models included dosimetric parameters and other variables with P<0.3 on univariate analysis. The receiver operating characteristic (ROC) curve was used to analyze optimal dose limiting points.

#### Results

A total 126 patients were included (90 males and 36 females), with average age 60 years. Only 7 (5.6%) patients received induction chemotherapy; the rest received CRT. A total 103 patients (81.7%) received intensity-modulated treatment. Of all patients, 53 (42.1%) received platinum plus taxane, 66 (52.4%) platinum plus fluorouracil, and 7 (5.5%) other regimens. The median radiotherapy dose was 60Gy (50-70Gy). Hematological toxicity grade 3 and above (HT3+) occurred in 34 of 126 patients, with incidence 27.0%. The average TVB dose was 32.65 Gy, V5 70.06%, V10 67.03%, V15 65.13%, V20 63.32%, V30 59.06%, V40 50.05%, V50 28.18%, and V60 8.48%. Age, concurrent chemotherapy regimens, TVB V30 and V40 were associated with HT(P<0.05). The threshold of TVB V40 was 35.75% for HT3+ occurrence; the incidence of HT3+ could be reduced from 29.7% to 15.9% by maintaining

the TVB dose below this threshold. The threshold of TVB V30 was 78.9%; the incidence of HT3+ could be reduced from 36.4% to 20.4% by maintaining the TVB dose below this threshold. Over age 61 years, concurrent chemotherapy with platinum plus taxane increased the incidence of HT3+.

#### Conclusion

The occurrence of HT in esophageal squamous cell carcinoma was associated with age, chemotherapy regimen, and TVB V30 and V40. Limiting the TVB dose and adjusting the chemotherapy regimen could reduce occurrence of HT3+.

#### EP-1396 the role of multidisciplinary team in radiotherapy for esophageal cancer

S. Zhao<sup>1</sup>, S. Wang<sup>1</sup>, F. Xu<sup>1</sup>, Y. Han<sup>1</sup>, W. Qi<sup>1</sup>, K. Youlia<sup>2</sup>, J. Chen<sup>1</sup>

<sup>1</sup>Ruijin Hospital- Shanghai Jiaotong University School of Medicine, radiation oncology, Shanghai, China ; <sup>2</sup>Institut Curie, radiation oncology, Paris, France

#### Purpose or Objective

To assess the effects of multidisciplinary team(MDT) on outcome of patients with esophageal cancer(EC) who had underwent radiotherapy, using propensity score matching. This is a retrospective cohort study

#### Material and Methods

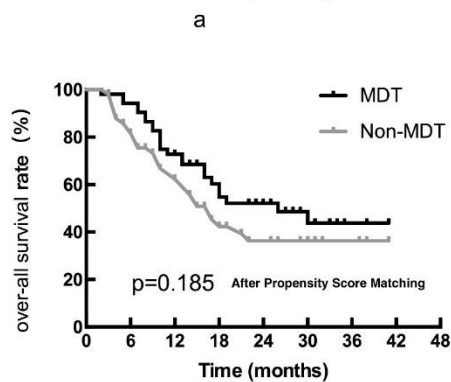
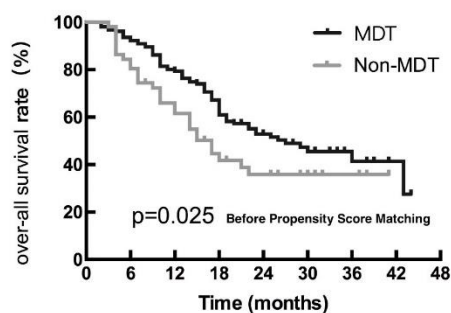
We collected all patients diagnosed with EC in radiation oncology department at our institution from January 2015 to May 2017. The patients were divided into groups by those who were presented and not presented at MDT meeting(MDT and non-MDT). Propensity-score matching was applied at a ratio of 1:1 comparing the two groups.

Variables	Before matching				After matching			
	All n=212	MDT n=87	Non-MDT n=125	X2 P	All n=166	MDT n=83	Non-MDT n=83	X2 P
Age(y)	66(44.8)	66(44.8)	66(44.8)	0.64 0.52	66(44.8)	66(44.8)	66(44.8)	0.58 0.58
<60	89(25.1)	44(25.1)	45(25.1)	3.92 0.14	89(25.1)	44(25.1)	45(25.1)	2.25 0.33
60-70	90(43.4)	44(43.4)	46(43.4)		90(43.4)	44(43.4)	46(43.4)	
>70	94(25.5)	29(24.5)	65(25.5)		94(25.5)	35(25.5)	59(25.5)	
Sex								
Male	102(85.8)	137(87.3)	45(81.8)	0.99 0.32	86(84.1)	45(84.9)	41(83.1)	0.07 0.79
Female	20(14.2)	20(12.7)	10(8.2)		17(15.9)	8(15.1)	9(17.0)	
PS								
0-1	197(92.9)	140(93.1)	57(92.7)	0.50 0.57	160(92.5)	48(92.5)	49(92.5)	1.00
2-3	15(7.1)	11(7.0)	4(7.3)		8(7.5)	4(7.5)	4(7.5)	
Location								
Neck-Upper	42(19.8)	30(19.1)	12(21.8)	3.41 0.33	21(18.8)	10(18.9)	11(20.8)	0.08 0.81
Middle-Lower	170(80.2)	127(80.9)	43(78.2)		85(80.2)	43(81.1)	42(79.2)	
Pathology								
SCC	198(92.5)	145(92.4)	53(92.7)	0.01 0.93	179(91.5)	48(92.5)	49(92.5)	1.00
Adeno or others	14(6.5)	12(7.6)	2(3.5)		9(8.5)	5(9.4)	4(7.5)	
Stage								
Ia	5(2.3)	3(2.8)	2(3.1)	1.31 0.52	3(2.8)	1(2.8)	2(3.1)	0.53 0.77
Ib	117(55.2)	112(71.3)	5(8.0)		66(62.5)	30(62.5)	36(62.5)	
IV	16(7.5)	11(7.0)	5(9.1)		15(14.5)	6(11.3)	9(17.0)	
Differentiation								
High	67(31.6)	54(34.4)	13(23.9)	2.22 0.33	27(25.9)	14(26.4)	13(24.9)	0.20 0.91
Mid	57(26.9)	41(26.1)	16(29.1)		28(26.4)	13(24.5)	15(28.3)	
Low	88(41.5)	62(39.5)	26(47.0)		51(48.1)	26(49.1)	25(47.8)	
Treatment modality								
With operation	154(48.1)	77(48.1)	77(48.1)	0.00 1.00	154(47.2)	74(48.3)	80(48.1)	0.15 0.70
non-operation	108(50.9)	80(51.9)	28(50.9)		66(52.8)	29(54.7)	27(50.9)	
With chemotherapy	171(80.7)	132(81.7)	39(80.8)	6.37 0.01	78(78.2)	40(75.5)	38(77.1)	0.19 0.66
non-chemotherapy	41(19.3)	24(18.3)	17(30.2)		26(24.4)	13(24.5)	13(25.1)	

patient, tumor, treatment characteristics before and after propensity score matching

#### Results

There were totally 212 patients analyzed, 157 with MDT and 55 non-MDT. In the unmatched population, there was no difference in patients and tumor characteristic between two group. In treatment options, the patients with MDT had significantly more in receipt of chemotherapy than non-MDT group(84.7% vs. 69.1%;  $\chi^2=6.373$ ;  $P=0.012$ ). In MDT group, there were longer median overall survival (OS) ( $P=0.025$ ) than in non-MDT group, as well as in subgroup analysis for the patients with PS status 0-1( $P<0.05$ ), with SCC( $P<0.05$ ), stage I-II( $P<0.01$ ), high-middle differentiation( $P<0.01$ ), with surgery( $P<0.01$ ). After propensity score matching for the similar characteristics including the treatment option, patients with phase I-II stage or high-middle differentiation had better survival in MDT group( $P<0.01$ ,  $P<0.05$ ). MDT was an independent predictor of receiving chemotherapy obtained in the regression analysis(OR, 2.827; 95% CI, 1.218-6.558).



Kaplan-Meier analysis of overall survival of MDT and Non-MDT groups

### Conclusion

MDT was associated more chemotherapy receipt in patients underwent radiotherapy for esophageal cancer, which may improve OS.

### EP-1397 S-1 versus S-1 plus cisplatin concurrent radiationtherapy for esophageal cancer: a mid-term report

Y. Wen<sup>1</sup>, Z. Zhao<sup>1</sup>, Y. Chen<sup>2</sup>, Y. Gui<sup>3</sup>, X. He<sup>4</sup>, Q. Yang<sup>5</sup>, M. Sun<sup>6</sup>, J. Miao<sup>7</sup>, Q. Jia<sup>8</sup>, H. Tian<sup>9</sup>, X. Du<sup>1</sup>

<sup>1</sup>Miayang Central Hospital, Oncology Department, Miayang, China; <sup>2</sup>Jiayang People's Hospital, Oncology Department, Jiayang, China; <sup>3</sup>Affiliated Hospital of North Sichuan Medical College, Oncology Department, Nanchong, China; <sup>4</sup>Langzhong people's Hospital, Oncology Department, Langzhong, China; <sup>5</sup>Ziyang People's Hospital, Oncology Department, Ziyang, China; <sup>6</sup>The first people's Hospital of Guangyuan, Oncology Department, Guangyuan, China; <sup>7</sup>Zigong Fourth People's Hospital, Oncology Department, Zigong, China; <sup>8</sup>The second people's Hospital of Jiangyou, Oncology Department, Jiangyou, China; <sup>9</sup>The first people's Hospital of Jiangyou, Oncology Department, Jiangyou, China

### Purpose or Objective

The chemotherapy regimens for concurrent chemotherapy and radiotherapy for esophageal cancer (EC) often comprise two drugs. However, retrospective studies have reported severe toxicity for patients with EC receiving radiotherapy combined with two-drug chemotherapy. While the incidence of side effects of single-drug chemotherapy is relatively low. Therefore, we designed a prospective, randomized, multicenter phase II trial to compare the efficacy and toxicity of combining S-1 or S-1 plus cisplatin with intensity-modulated radiation therapy for esophageal squamous cell carcinoma.

### Material and Methods

This randomized, controlled, multicenter trial compared S-1 versus S-1 plus cisplatin concurrent radiotherapy in patients with esophageal squamous cell carcinoma. Eighty-eight patients with unresectable or who were

medically unfit for surgery for esophageal squamous cell carcinoma (clinical stage I to III) were randomly assigned to receive four cycles (two concomitant and two postradiotherapy) of S-1 or S-1 plus cisplatin along with radiotherapy 60-66Gy/30 to 33 fractions. The primary outcome was the complete response rate of the primary tumor as measured by endoscopy and computer screening at three months after treatment completion. The secondary outcomes included survival and toxicity.

### Results

In August 2018, 88 patients were enrolled, 43 of which were evaluated by gastroscopy (45 cases have not yet been followed up by gastroscopy), including 25 cases in the experimental group receiving S-1 concurrent intensity-modulated radiotherapy treatment and 18 cases in the control group receiving concurrent S-1 plus cisplatin intensity-modulated radiation therapy. In the experimental group, 13 patients (52%) achieved complete remission, six (24%) achieved partial remission, four (16%) had stable disease, and two (8%) had progressed. In the control group, eight patients (44.4%) achieved complete remission, seven (38.9%) achieved partial remission, two (11.1%) had stable disease, and one (5.6%) had progressed. There was no significant difference in the rates of complete remission between the two groups ( $P > 0.05$ ). The radiotherapy completion rates were 95.6% and 88.9% in the experimental and control groups, respectively. The radiotherapy interruption rates in the two groups were 52% and 55.5%, respectively. The chemotherapy completion rates were 100% and 88.9% in the experimental and control groups, respectively. The chemotherapy interruption rate was 4% in the experimental group and 11.1% in the control group. The incidence of grade 2, 3, and 4 hematological toxicity was 56%, 4%, and 0%, respectively, in the experimental group and 66.6%, 16.6%, and 5.5%, respectively, in the control group.

### Conclusion

Conclusions: The mid-term data of this trial indicate that S-1 synchronous intensity-modulated radiation therapy is no significant differences in complete response rate to S-1 combined with cisplatin synchronous intensity-modulated radiation therapy, with fewer side effects. Therefore, patients are more likely to complete treatment with S-1 synchronous intensity-modulated radiation therapy alone.

### EP-1398 Lymphopenia and accidental splenic doses for locally advanced gastric cancer

F. Sert<sup>1</sup>, D. Yalman<sup>1</sup>, S. Ozkok<sup>1</sup>

<sup>1</sup>Ege University Medical School&Hospital, Radiation Oncology, Izmir, Turkey

### Purpose or Objective

Considering the high recurrence and mortality rates, additional predictive and/or prognostic factors have to be identified for the patients with locally advanced gastric cancer (LAGC). There is limited data evaluating the certain reason of lymphopenia and the relation between splenic doses and immunological response including NLR (neutrophil-to-lymphocyte ratio) and white blood cell counts over oncological outcomes for the patients with LAGC. The purposes of the present study are to determine the effect of CRT (chemoradiotherapy)-induced lymphopenia, and irradiated splenic volume and splenic doses on oncological outcomes in patients with LAGC.

### Material and Methods

A consecutive cohort of 52 patients with LAGC (pT3-4 and/or pN0-3b) treated with adjuvant CRT at our department between 2005 and December 2016 was identified for this trial. The absolute neutrophil, lymphocyte and platelet counts were recorded prior to any treatment (baseline), just after the completion of CRT, and 2-6 weeks after the completion of CRT (control evaluation).

## Results

The median clinical follow-up time from the beginning of first CT application was 30 months (range, 8-130 months). The incidence of severe lymphopenia was only 1% at control evaluation but it was 93% after CRT ( $p < .001$ ). The median OS time was 24 months (range, 8-126 months). The 2, 3, and 4-year OS rates were 65%, 59%, and 52%, respectively. There was no statistically significant difference in OS in patients with severe lymphopenia and SIR positivity after CRT ( $p = .75$ , and  $p = .31$ , respectively). Additionally, the severity of baseline lymphopenia or lymphopenia at the control evaluation had no effect on OS rates ( $p = .75$ , and  $p = .92$ , respectively). Median RFS time was 20 months (range, 6-120 months). The 2, 3, and 4-year RFS rates were 58%, 55%, and 50%, respectively. In univariate analysis, stage 3 disease ( $p < .001$ ) and MDLN ratio  $> 20\%$  ( $p < .001$ ) had negative effect on OS. In multivariate analysis for OS, stage III disease ( $p = .041$ ) and MDLN ratio  $> 20\%$  ( $p = .032$ ). In univariate analysis for RFS, stage 3 disease ( $p = .001$ ), and MDLN ratio  $> 20\%$  ( $p = .011$ ) had negative effect. MDLN ratio  $> 20\%$  was the only significant prognostic factor for RFS in multivariate analysis ( $p = .033$ ). In the ROC analysis, the AUC for mean splenic doses was 0.741 for OS ( $p = .042$ ) and 0.680 for RFS ( $p = .050$ ). Mean splenic dose  $\geq 35$  Gy was a significant poor prognostic factor for OS and RFS ( $p = .042$ , and  $p = 0.50$  respectively). Maximum splenic dose  $\geq 58$  Gy effected OS unfavorably ( $p = .050$ ). Volumetric modulated arc therapy (VMAT), intravenous CT, and age  $\geq 65$  years were significant predictors for severe lymphopenia.

## Conclusion

Severe lymphopenia could not be accepted as a predictive or prognostic factor for LAGC. Mean and maximum splenic doses should be kept on mind while evaluating the treatment DVHs. Age of patient, iv usage of concomitant CT agent and VMAT are the factors which can influence the ALCs of patients. Disease-related factors such as stage and metastatic lymph node ratio are seen the most important factors.

## EP-1399 A Pilot Study of Apatinib Combined with SBRT To Advanced Pancreatic Cancer

G. MA<sup>1</sup>, M. Shuo<sup>2</sup>, Z. Shuman<sup>1</sup>, X. Li-ang<sup>1</sup>

<sup>1</sup>4th Hospital Hebei Medical University, Radiotherapy, shijiazhang, China ; <sup>2</sup>Syracuse University, new York, USA

## Purpose or Objective

The primary endpoint: progression-free survival (PFS)

The secondary endpoint: overall survival (OS) and safety.

## Material and Methods

The study enrolled 10 patients with advanced pancreatic adenocarcinoma from Dec. 2015 to Apr. 2018. In the first week, all the patients were treated with Apatinib 500mg daily. At the same time, treatment plans of SBRT were finished. From the second week, Apatinib was taken 500mg daily and SBRT were going concomitantly. SBRT regimen was 50Gy/20F/4W. Same dosage of Apatinib was continued alone after SBRT to disease progression, death, or intolerable toxicity.

## Baseline Characteristics

Characteristic	n=10
Age(years)	
Median(range)	66(43-84)
Sex	
male	4(40%)
female	6(60%)
ECOG PS	
1	1(10%)
2	2(20%)
3	7(70%)
Stage	
III	9(90%)
IV	1(10%)

## Results

All patients were followed up for the tumor response evaluation. The median progression-free survival (PFS) was 4.5 months (95% CI, 3.47 to 5.53). The median overall survival (OS) was 7.5 months (95% CI, 5.95 to 9.05).

## Safety and Tolerability

Hypertension is one of the most frequent adverse events, which appeared in 3 of 10 pts. There also were some other AEs, Hand-food syndrome 2, proteinuria 1, diarrhea 1, fatigue 1, oral mucositis 1 and thrombocytopenia 1. AEs could be better controlled and no treatment-related hemorrhage occurred.

AE(%)	All Grade3/4
Hypertension	3 0
Hand-food syndrome	2 0
proteinuria	1 0
diarrhea	1 0
fatigue	1 0
oral mucositis	1 0
thrombocytopenia	1 0

## Conclusion

Our Results indicates that Apatinib combined with SBRT exhibits safety and efficacy to advanced pancreatic adenocarcinoma. More patients should be enrolled and observed

## EP-1400 Comparing Treatment Plans for Proximal and Middle/Distal Stomach Cancer: IMRT, VMAT, and Tomotherapy

Y. Chen<sup>1</sup>, J. Lin<sup>1,2</sup>, S. Huang<sup>1</sup>, Y. Chou<sup>3</sup>, M. Li<sup>1</sup>, J. Tsai<sup>1,2</sup>

<sup>1</sup>Shuang Ho Hospital- Taipei Medical University, Department of Radiation Oncology, New Taipei City, Taiwan ; <sup>2</sup>School of Medicine- College of Medicine- Taipei Medical University, Department of Radiology, Taipei, Taiwan ; <sup>3</sup>National Defense Medical Center, School of Public Health, Taipei, Taiwan

## Purpose or Objective

Adjuvant chemoradiotherapy is viewed as a definitive treatment after resection of stomach cancer (SC). To protect normal tissue, several highly conformal radiotherapy modalities evolved. Therefore, we aimed to compare dosimetric parameters of helical tomotherapy (TOMO), volumetric-modulated arc therapy (VMAT), and intensity-modulated radiotherapy (IMRT) in the adjuvant treatment of SC in different locations.

## Material and Methods

This retrospective study was conducted from January 2013 to May 2017 and included 11 patients with gastric cancer receiving adjuvant chemoradiotherapy after total

gastrectomy. Both IMRT and VMAT plans were generated on the Pinnacle treatment planning system and TOMO plans were generated using a helical tomotherapy system. Adjuvant radiotherapy was prescribed with a total radiation dose of 50.4 Gy in 28 fractions.

#### Results

In proximal SC, TOMO achieved a significantly lower dose for the heart, total kidney, left kidney, and liver than that of IMRT or VMAT ( $p < 0.05$ ). In middle/distal SC, lower total kidney mean dose and V20 were observed with TOMO compared with IMRT ( $p = 0.010$  and  $0.011$ , respectively) and VMAT ( $p = 0.049$ ;  $p = 0.014$ ).

#### Conclusion

For the adjuvant treatment of gastric cancer, TOMO not only provided superior dose sparing for total kidney, left kidney, and liver V30 in patients with proximal gastric cancer but also significantly lowered the heart dose in proximal SC when compared to IMRT or VMAT plan.

#### EP-1401 Practice-based clinical outcome of definitive radiation therapy for superficial esophageal cancer

T. Uno<sup>1</sup>, H. Kobayashi<sup>1</sup>, M. Watanabe-Nemoto<sup>1</sup>, R. Harada<sup>1</sup>, M. Saito<sup>1</sup>, A. Kanazawa<sup>1</sup>, Y. Iwai<sup>1</sup>, K. Murakami<sup>2</sup>, H. Matsubara<sup>2</sup>

<sup>1</sup>Chiba University Hospital, Department of Radiology, Chiba-City, Japan ; <sup>2</sup>Chiba University Hospital, Department of Esophageal-Gastro-Intestinal Surgery, Chiba-City, Japan

#### Purpose or Objective

To evaluate treatment patterns and clinical outcome of definitive radiation therapy for patients with T1b superficial esophageal cancer unfit for or refused definitive surgery in the Authorized Institute for Board Certified Esophageal Surgeon in Japan.

#### Material and Methods

Treatment chart of 51 patients (men/women: 44/7) with T1b superficial esophageal cancer treated with definitive radiation therapy between 2000 and 2017 were retrospectively reviewed. The median age was 77 years with a range of 52 to 88. The tumor length ranged from 2 to 15 cm (median, 5 cm). Thirty-eight patients did not have surgical candidate due to several reasons such as medical condition, high age, and preceding other cancer treatment. Thirteen patients including 5 with primary tumor located at the cervical esophagus refused surgery. All patients received external beam radiation therapy using linear accelerator with high-energy X-ray. The median total dose was 60 Gy. Field of radiation therapy was individualized considering patient and clinical factors such as age, performance status, primary tumor location and tumor length; local field with no lymph node prophylaxis was used in 11, long-I field in 17, long-T field in 18, and short-T field in 5. Every patient received computer-based adaptive 3D treatment. Seven patients underwent intracavitary brachytherapy using Ir-192 high-dose-rate remote after-loading system. Prescribed dose of brachytherapy was 10-12 Gy in 2 fractions of 5 mm submucosa. Concurrent chemotherapy (CDDP+5FU) was used for 32 patients.

#### Results

Eight patients had local recurrence and only 3 patients developed isolated regional recurrence outside the field of radiation therapy. At the time of data analysis, a total of 20 patients have died. Of those, however, esophageal cancer specific death was only 6 patients. Six patients had died of other cancer; HCC in 2, gastric cancer in 2, tongue cancer in 1 and pancreatic cancer in 1. The 3- and 5-year cause-specific survival rates were 83% and 69%. Among clinical factors such as age, gender, primary site, tumor length, tumor depth, use of concurrent chemoradiation (CCRT), field of RT and initial response, only the use of CCRT significantly influenced overall survival (OAS at 3 year, 56% and 70%,  $p=0.01$ ). Tumor location had marginal impact on OAS. None of 8 patients with Ce-Ut lesion had

died of esophageal cancer. Grade 3 or worse non-hematological toxicities were within acceptable range.

#### Conclusion

Treatment results of radiation therapy for patients with superficial esophageal cancer mainly unfit for surgery were retrospectively analyzed. Adaptive RT-field setting prevented isolated regional recurrence in superficial esophageal cancer.

#### EP-1402 Hypofractionated radiotherapy for patients with bulky unresectable biliary tract cancer

W. Kong<sup>1</sup>, J. Yang<sup>1</sup>, J. Yan<sup>1</sup>, J. Liu<sup>1</sup>, Z. Xia<sup>1</sup>, S. Li<sup>1</sup>, Y. Qiu<sup>2</sup>, B. Liu<sup>1</sup>

<sup>1</sup>Drum Tower Hospital- Medical School of Nanjing University & Clinical Cancer Institute of Nanjing University, The Comprehensive Cancer Centre, Nanjing, China ; <sup>2</sup>Drum Tower Hospital- Medical School of Nanjing University & Clinical Cancer Institute of Nanjing University, Department of General Surgery, Nanjing, China

#### Purpose or Objective

The treatment options are limited for the patients with unresectable biliary tract cancer (BTC), especially after the failure of the first-line chemotherapy. Although target therapy and checkpoint inhibitor therapy have improved the prognosis of a variety of advanced cancers in recent years, it has not been successful in treating advanced BTC. Unresectable advanced biliary tract cancers are often accompanied by extensive invasion or regional lymph node metastasis, and conventional radiotherapy can only achieve palliative effects. This study was the first to use helical tomotherapy-based hypofractionated radiotherapy to treat patients with bulky locally advanced and unresectable BTC (excluded diffuse metastatic disease).

#### Material and Methods

In total, we retrospectively analyzed 23 patients with bulky unresectable BTC (tumor size >10cm) treated by tomotherapy-based hypofractionated radiotherapy at Drum Tower Hospital between Feb 2015 and Oct 2017. The irradiated sites covered primary tumors and areas of local invasion, including metastatic lymph nodes that were confined to the abdominal or retroperitoneal space. Cox regression modal and Kaplan-Meier analysis were used to analyze the associations between patients' characteristics and overall survival (OS).

#### Results

The median total radiation dose was 54Gy (range 28-72Gy) and median biologically effective dose (BED) was 74.4Gy (range 37.8-115.2Gy). The median planning target volume (PTV) was 445.79cm<sup>3</sup>. Based on the various PTVs, patients received 2.4-6Gy/fraction with 8-28 fractions. After the radiotherapy, the local control rate was 65.2% and the median OS was 11.3 months (range 2.1-31.9 months). The most common cause of death was out-field failure and only three patients died of in-field failures. The longest survival was 31.9 months. BED  $\geq 70$ Gy significantly improved OS, compared to BED <70Gy (16.8 months vs. 5.05 months) (hazard ratio [HR] 0.146, 95% confidence interval [CI] 0.028-0.762,  $P=0.022$ ). No patients developed grade  $\geq 4$  toxicities.

#### Conclusion

Helical tomotherapy-based hypofractionated radiotherapy was effective and well tolerated for patients with bulky unresectable BTC. The dose escalation with higher BED could improve the survival for such patients. This might be a treatment option for patients with locally advanced biliary tract cancer, which cannot obtain benefit from the first-line chemotherapy.

#### EP-1403 Retrospective evaluation of usefulness of MR-guided adaptive radiotherapy of gastric MALT lymphoma

K. Okuma<sup>1</sup>, H. Okamoto<sup>1</sup>, K. Iijima<sup>1</sup>, F. Nishioka<sup>1</sup>, T. Kashiwara<sup>1</sup>, S. Shima<sup>1</sup>, M. Uematsu<sup>1</sup>, H. Igaki<sup>1</sup>, Y.

Nakayama<sup>1</sup>, J. Itami<sup>1</sup>, N. Murakami<sup>1</sup>, S. Nakamura<sup>1</sup>  
<sup>1</sup>National Cancer Center Hospital, Radiation oncology,  
 Tokyo, Japan

#### Purpose or Objective

It is well known that significant variations in stomach size, shape, and respiratory motion lead to uncertainties in target localization during treatment for stomach. For this reason, planning target volume (PTV) margin is large for the external beam radiation therapy (RT) of gastric mucosa-associated lymphoid tissue (MALT) lymphoma.

Magnetic-resonance (MR) -guided-online-adaptive-radiotherapy is a promising tool for gastric radiotherapy. Our online-adaptive-radiotherapy (On-line ART) process relies on daily image overview by the managing radiation-oncologist, who determines the need for creating a predicted plan if significant inter-fractional anatomical changes are noted.

In this study, the usefulness of MR guided adoptive radiation therapy of gastric MALT lymphoma was evaluated.

#### Material and Methods

Fifty-nine years old female patient with gastric MALT lymphoma underwent breath-hold radiotherapy on the MRI-cobalt system (ViewRay MRIdian system, Oakwood Village, OH, US). The prescribed dose to PTV (defined as a 5 mm expansion of the entire stomach) was 24 Gy in 12 fractions. The patient was instructed to not eat or drink starting four hours prior to treatment. Sagittal slice cine-MR images were acquired through the center of the stomach at 4 frames per second throughout the treatments. Clinical target volume (defined as the entire stomach) and organ at risks (OARs) were contoured on the first frame of the MR cine and tracked for the first 20 min of each treatment using offline optical-flow based deformable registration.

#### Results

The patient underwent RT as scheduled, without any significant adverse effects. MR-guided gating was performed with beam off when  $\geq 10\%$  of the stomach volume exceeded the 3.0-mm boundary expansion. Significant inter-fractional stomach variations on the order of 5.0 cm were observed. N = 12/12 fractions were adapted based on On-line ART. The mean dose of the CTV was 23.79 Gy (V100 = 99.13%).

#### Conclusion

Superior soft-tissue visualization combined with the MR-guided RT ability to dynamically adjust the treatment plan and/or gate the treatment delivery to account for intra-fractional anatomical changes offers great promise to further enhance treatment precision for gastric sites. This approach brings valuable opportunities to decrease overall toxicity profiles.

#### EP-1404 SBRT as definitive treatment of adrenal gland metastases: a single center experience

O. Hernando Requejo<sup>1</sup>, M. Peñacoba<sup>2</sup>, E. Sanchez Saugar<sup>1</sup>, M. Lopez Gonzalez<sup>1</sup>, X. Chen<sup>1</sup>, R. Alonso Gutierrez<sup>1</sup>, A. Montero Luis<sup>1</sup>, R. Ciervide Jurio<sup>1</sup>, J. Valero Albarran<sup>1</sup>, M. Garcia-Aranda Pez<sup>1</sup>, P. Fernandez Leton<sup>3</sup>, J.M. Perez Moreno<sup>3</sup>, J. Garcia Ruiz-Zorrilla<sup>3</sup>, D. Zucca Aparicio<sup>3</sup>, L. Alonso Iracheta<sup>3</sup>, M.A. De la Casa de Julian<sup>3</sup>, J. Marti Asenjo<sup>3</sup>, B. Alvarez Rodriguez<sup>1</sup>, A. Acosta Rojas<sup>1</sup>, J. Plama Delgado<sup>1</sup>, M.C. Rubio Rodriguez<sup>1</sup>

<sup>1</sup>Hospital Universitario Madrid Sanchinarro - Grupo Hospital de Madrid, Radiation Oncology, Madrid, Spain ;

<sup>2</sup>Hospital Universitario Marques de Valdecilla, Radiation Oncology, Madrid, Spain ; <sup>3</sup>Hospital Universitario Madrid Sanchinarro - Grupo Hospital de Madrid, Radiation Physics, Madrid, Spain

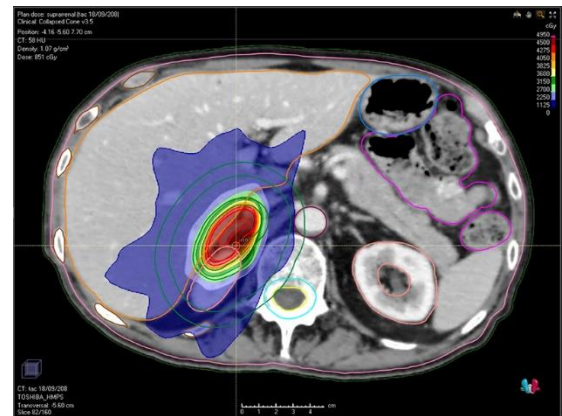
#### Purpose or Objective

Adrenal gland metastases are a common problem in oncology, causing abdominal pain, nausea and vomiting,

leading to patient discomfort. Classical treatment includes surgical resection or chemotherapy, being palliative conformal 3D Radiotherapy the only non-invasive local treatment available. Recently new definitive treatment modalities such as Radiofrequency ablation and SBRT have been developed with promising results. The aim of this study is to analyze the safety and efficacy of SBRT treatment for adrenal gland metastases.

#### Material and Methods

From April 2008 to September 2018 a total of 32 selected patients have been treated of adrenal gland metastases with SBRT at our Institution. Treatment techniques included fiducial-based Adaptive Respiratory Gating (7 patients), Dampening (19) and Active Breathing Coordinator (6). Treatment planning included 7 patients with VMAT, 11 with 3D Conformal Radiotherapy and 6 with IMRT (Fig1). Toxicity was evaluated with CTCAE v5.0. Statistical analysis included descriptive tests and Kaplan Meier curves for survival.

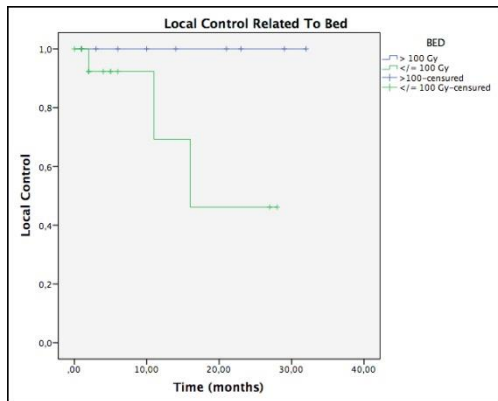


#### Results

All patients (18 males and 14 females) completed treatment as scheduled. The most common location of the primary tumor was lung (75%). Other locations were: gynecological (6%), colorectal, melanoma and sarcoma (3% each). Sixteen patients received SBRT for right adrenal gland, 15 for left gland and 1 for both glands. Median dose of 47 Gy (range 24-60 Gy) and median dose/fraction of 12 Gy (range 5-20 Gy) was administered. The median PTV size and volume was 31 mm and 57 cc respectively.

With a median follow up of 13.2 months local control crude rate was 88.89%. Five patients achieved a complete response, 11 partial response, 7 stable disease and 3 local progression. Estimated local control at 16 months was 77.3%. Median local failure free survival was not reached. Other distant metastases appeared in 85.2% of patients. Median overall survival was 12 months. Fifty seven percent of patients were alive at 12 months.

As prognostic factors we found that left adrenal metastases had statistically significant worse local control than right adrenal ones, which is straightly related with the total dose administered. Doses with BED above 100 Gy (BED- $\alpha/\beta_{10}$ ) had statistically significant better local control than those treated with BED of 100 Gy or below (Fig2). Local control after SBRT was not related with overall survival.



Tolerance to the procedure was generally good. Ten patients presented acute toxicity, being asthenia Grade 1 or 2 the most frequent in seven patients. Chronic toxicity was reported in two patients (6.25%), one Grade 3 enteritis and one Grade 3 abdominal abscess. No Grade 4-5 acute or chronic toxicity was reported.

#### Conclusion

In our experience SBRT for adrenal gland metastases is safe and effective, achieving good local control rates, which are directly related with the total dose administered. Further studies are needed to consolidate these results and evaluate the influence of SBRT in patient survival and quality of life.

#### EP-1405 Feasibility study of fiducial markers in oesophageal cancer radiotherapy

A. Morton<sup>1</sup>, D. McIntosh<sup>1</sup>, S. Currie<sup>2</sup>, A.J. Stanley<sup>3</sup>, S. Paterson<sup>4</sup>, D. Grose<sup>1</sup>, H. Marashi<sup>1</sup>, V. MacLaren<sup>1</sup>  
<sup>1</sup>Beatson West of Scotland Cancer Centre, Clinical Oncology, Glasgow, United Kingdom ; <sup>2</sup>Beatson West of Scotland Cancer Centre, Physics, Glasgow, United Kingdom ; <sup>3</sup>Glasgow Royal Infirmary, Gastroenterology, Glasgow, United Kingdom ; <sup>4</sup>NHS Forth Valley, Gastroenterology, Larbert, United Kingdom

#### Purpose or Objective

To determine whether insertion of 5mm radio-opaque gold fiducials (Cook Medical USA) during EUS impacts on inter- and intra-observer variability when defining oesophageal cancer GTV.

#### Material and Methods

14 patients with oesophageal cancer planned to undergo radical radiotherapy, with or without chemotherapy, underwent EUS to place 1-2 fiducials at the proximal and distal end of tumour unless stricturing prevented this. GTV of primary tumour was defined on a planning CT retrospectively 3 times by 3 separate clinicians using fiducials with CT-PET and EUS report.

#### Results

13 patients were imaged with 4 having superior/ inferior markers visible. 8 had only superior and 1 had no visible markers (4 due to stricturing tumours preventing placement, 5 due to marker migration). Unfortunately 1 patient died of mediastinitis secondary to oesophageal perforation following EUS at which stage the trial stopped early.

Intra-observer variability is shown in the attached table for clinicians 1, 2 and 3. Each clinician completed 3 separate contours and these were compared for all 13 cases. Inter-observer variability was assessed by comparing the first contours from each clinician, then the second contours separately followed by the third as shown in table as contour 1, 2 and 3.

For example in 'Contour 2' column, there were 3 contours for all 13 patients representing the second volume done by each of the 3 clinicians. For each patient the maximum difference between the 3 contours in the position of the

superior slice was established. The median and range of the final 13 differences in position in cm is documented. The same was done for the inferior slices. As the 13 tumours varied in size looking at cm<sup>3</sup> was less useful for difference in volume, instead percentage difference between the largest and smallest volume was used. E.g. if largest volume is 16cm<sup>3</sup> and smallest is 8cm<sup>3</sup> then there is a 50% difference in the volumes.

	Intra-observer Variability			Inter-observer Variability		
	Clinician 1	Clinician 2	Clinician 3	Contour 1	Contour 2	Contour 3
<b>Superior Slice</b>						
Median Variability (cm)	0	0.2	0.2	0.4	0.4	0.4
Range of Variability (cm)	0 - 1.2	0 - 0.8	0 - 2.4	0 - 2.4	0 - 2	0 - 2.4
<b>Inferior Slice</b>						
Median Variability (cm)	0.2	0.6	0.4	0.6	0.6	0.6
Range of Variability (cm)	0.2 - 1.4	0.2 - 1.0	0.2 - 3.4	0.2 - 1.4	0.2 - 3.4	0.2 - 1.4
<b>Volume</b>						
Median Variability (%)	8.8%	11.7%	17.2%	20.2%	25.9%	28.6%
Range of Variability (%)	4.1 - 32.4%	2.3 - 27.5%	3.1 - 59.1%	8.5 - 44.1%	6.7 - 56.4%	6.1 - 63.1%

#### Conclusion

Inter and intra-observer variability was significant despite markers; small variations at the inferior and superior border still contributed to considerable variation in the final volume.

Fiducial placement and retention at the inferior border was lower than would be anticipated, however inter-observer variability was similar to the superior slice. In the context of multi-modality imaging techniques to identify GTV, it is likely marker contribution has been restricted. Cases where they are most likely to contribute are tumours difficult to appreciate on imaging. Given the rare but recognised complication of death following perforation at EUS, identifying patients most likely to benefit is key.

#### EP-1406 Mapping Pattern of LNMs for Postoperative Radiotherapy in TESCC: Defining the Clinical Target Volume

J. Yu<sup>1</sup>, C. Li<sup>1</sup>, W. Ouyang<sup>1</sup>, Y. Xu<sup>1</sup>, J. Zhang<sup>1</sup>, C. Xie<sup>1</sup>  
<sup>1</sup>Zhongnan Hospital of Wuhan University, Radiation and Medical Oncology, Wuhan, China

#### Purpose or Objective

The clinical target volume (CTV) for postoperative radiotherapy for thoracic esophageal squamous cell carcinoma (TESCC) needs to be defined. The study aim was to map the first metastatic lymph nodes (LNMs) in a computed tomography (CT)-based atlas and to guide CTV delineation in postoperative radiotherapy for TESCC.

#### Material and Methods

Sixty-nine patients with primary regional LNMs after esophagectomy were included. The LNM epicenters were registered onto corresponding anatomic axial CT images of a standard patient in the treatment position, with reference to the surrounding vascular and bony structures. The LNM sites were based on lymph node map of esophageal cancer, AJCC 8<sup>th</sup>. Accordingly, regional lymph node stations 1 to 8M were defined as the upper-middle mediastinum region (UMMR); stations 8Lo, 9, and 15 were defined as the inferior mediastinum region (IMR); and stations 16 to 20 were defined as the upper abdominal lymph node region (UAR). The lymph metastasis risk for different segments was assessed.

#### Results

One hundred and seventy-nine LNMs were mapped onto standard axial CT images. The upper-middle mediastinum region (station 1 to 8M) was the most common site for LNMs. It contained 97% of metastases in the upper segment, 90% in the middle segment, and 66% in the lower one. Advanced pathological stage ( $\geq$ IIIB) might be a predictive factor for upper abdominal region (UAR) relapse in lower TESCC. Lower cervical para-tracheal LNMs were within a 4.3-cm bilaterally expanded area from the midline and a 2.2-cm expanded area from the anterior, from the superior border of the C7, to the inferior border of the first thoracic vertebra.

Table 1. Patient characteristics

Variable	Value	
Age (y), median (range)	56 (44-80)	
Sex		
Male	60 (87.0%)	9 (13.0%)
Female		
Surgical	type	
Ivor-Lewis	15 (21.7%)	
Sweet	41 (59.4%)	13 (18.9%)
Location	Upper	
Middle	11 (15.9%)	
Low	31 (44.9%)	27 (39.2%)
Grade		
Well	8 (11.6%)	
Median	32 (46.4%)	
Poor	24 (34.8%)	
Undifferentiated	5 (7.2%)	
Stage		
I	12 (17.4%)	
II	19 (27.5%)	
III	30 (43.5%)	8 (11.6%)
IVa		
Adjuvant chemotherapy		
Yes	17 (24.6%)	52 (75.4%)
No		

### Conclusion

A modified target from the upper border of C7 to the lower border of the carina of the trachea could cover the high-risk area of TESCC. UAR seems to be an elective irradiation target for lower TESCC at pathological IIIB stage or above.

### EP-1407 Sarcopenia is a weak prognostic factor before chemoradiotherapy of esophageal carcinomas

B. Bethsabée<sup>1</sup>, Q. Laurent<sup>1</sup>, C. Pierre<sup>2</sup>, H. Valerie<sup>1</sup>, G. Sophie<sup>1</sup>, A. Thomas<sup>3</sup>, L. Nelson<sup>3</sup>, G. Jean-Marc<sup>3</sup>, C. Hennequin<sup>1</sup>

<sup>1</sup>Hôpital Saint-Louis, Radiation Oncology, Paris, France ; <sup>2</sup>Hôpital Saint-Louis, Surgery, Paris, France ; <sup>3</sup>Hôpital Saint-Louis, Gastro-enterology, Paris, France

### Purpose or Objective

Sarcopenia seems to be an important prognostic factor of esophageal carcinoma (EC) before surgery. Data are less convincing before chemoradiotherapy (CRT) and this prompts us to review our experience in a recent cohort study.

### Material and Methods

Between 2010 and 2015, all patients with a locally advanced EC treated with upfront CRT and a CT-scanner at the time of CRT available were included. All patients had an 18-FDG-PET-CT to eliminate distant metastases. Decision of surgery was performed after CRT (40-50 Gy) according to tumor extension, performance status (PS), comorbidities and response to CRT. To evaluate sarcopenia, a single slice at the L3 level was identified and total skeletal muscle (TMA) and subcutaneous and visceral fat were measured. The skeletal muscle index (SMI) is calculated as follows: TMA/height<sup>2</sup> (m<sup>2</sup>). Sarcopenia was internationally defined as a SMI of  $\leq 39$  cm<sup>2</sup>/m<sup>2</sup> for women and  $\leq 55$  cm<sup>2</sup>/m<sup>2</sup> for men. We used also the definition given by Martin et al. (JCO, 2013): for patients with a body mass index (BMI) < 25, SMI < 41 cm<sup>2</sup>/m<sup>2</sup> for women and < 43 cm<sup>2</sup>/m<sup>2</sup> for men; if BMI  $\geq 25$ , SMI < 41 cm<sup>2</sup>/m<sup>2</sup> for women and < 53 cm<sup>2</sup>/m<sup>2</sup> for men.

### Results

104 patients were included: Mean age: 63 yrs. Men: n=72. PS 0: 32; PS 1: 59; PS 2: 13. T-stage: T2: 4; T3: 95; T4: 5. N stage: N1-2: 76. Weight loss >5%: n=74. Surgery after CRT: 39. Histology: Squamous cell cancer (SCC): 69. Mean SMI was 35 cm<sup>2</sup>/m<sup>2</sup> for women and 46 cm<sup>2</sup>/m<sup>2</sup> for men. According to the international definition, sarcopenia was found in 84 pts (81%). It was correlated to initial BMI, but not to age, weight loss, PS or T stage. According to the

Martin's definition, 64 pts (61.5%) had sarcopenia. 3-year overall survival (OS) was 34.6%. Prognostic factors for OS in univariate analysis were initial PS and surgery. Sarcopenia, using international or Martin's definition, was not significantly associated with OS. However, when using the median SMI for each sex as a cut-off (a lower level than the other definitions), sarcopenia is associated with OS (at 3 years: 43.3% vs 26.2%; p=0.02). However, in multivariate analysis, only PS remains statistically associated with OS. There was no correlation between fat measurements and OS.

### Conclusion

High level of sarcopenia is associated with OS in patients with EC treated with up-front CRT; but its prognostic value is low and disappears in multivariate analysis.

### EP-1408 Cardiac dose and treatment-elicited inflammation are related to poor survival in esophageal cancer

Y. Ho<sup>1</sup>, J. Lin<sup>1</sup>, T. Chou<sup>1</sup>, L. Hung<sup>1</sup>, C. Huang<sup>1</sup>, C. Pi<sup>1</sup>, T. Chang<sup>1</sup>, M. Liu<sup>1</sup>

<sup>1</sup>Changhua Christian Hospital, Radiation Oncology, Changhua City, Taiwan

### Purpose or Objective

Definitive concurrent chemoradiation (CCRT) is the standard treatment for esophageal cancer with cervical location or non-surgical candidate and able to tolerate chemoradiation. Studies have correlated cancer-related inflammatory response and treatment-related toxicities with worsening survival. The purpose of this study was to evaluate the prognostic factors and normal tissue dosimetric parameters affecting overall survival (OS), as well as the predictive values on OS of the levels of neutrophil to lymphocyte ratio (NLR) at baseline, during-CCRT and post-CCRT periods.

### Material and Methods

Between 2010 and 2015, 110 newly diagnosed stage II and III patients, with the majority of squamous cell carcinoma, were identified from our institution. Patients' clinical, dosimetric, and laboratory data at baseline, during and post-CCRT were collected by review of medical records. The Cox proportional hazard model was used to identify the potential risk factors for OS. Thresholds were chosen to increase specificity and to dichotomize continuous variables, as the median for heart mean dose and baseline NLR, and the upper quartile for increased NLR during-CCRT.

### Results

Median follow up was 21.0 months (range 3-95 months) and overall survival was 20.6 months. A total of 75% of patients had stage III disease and all patients completed definitive CCRT. Two-year OS and five-year OS were 27% and 16%. Univariate analysis showed that male gender (p = 0.035), stage (II vs. III, p = 0.058), ECOG performance status (0 vs.  $\geq 1$ , p = 0.031), mean heart dose (>2070.5 vs.  $\leq 2070.5$  cGy, p = 0.017), baseline NLR (>3.56 vs.  $\leq 3.56$ , p = 0.005) and increased NLR during-CCRT (>27.46 vs.  $\leq 27.46$ , p = 0.022) were significantly associated with poor OS. On multivariate analysis, stage (Hazard Ratio [HR] 1.71; 95% CI 1-2.9, p = 0.048), performance status (HR 5.89; 95% CI 2.21-15.67, p < 0.001), mean heart dose (HR 1.71; 95% CI 1.09-2.68, p = 0.02), baseline NLR (HR 1.9; 95% CI 1.19-3.04, p = 0.007) and increased NLR during-CCRT (HR 2.58; 95% CI 1.52-4.39, p < 0.001) remained significantly associations with reduced OS.

### Conclusion

Mean heart dose > 2070.5 cGy, baseline NLR > 3.56 and increased NLR during-CCRT > 27.46 were poor prognostic markers for OS in esophageal cancer patients receiving definitive CCRT. Minimal cardiac dose during radiotherapy and novel therapy targeting tumor or treatment-elicited inflammatory response might improve survival for patients with esophageal cancer underwent definitive CCRT.

**EP-1409 QoL for Gem and ABX plus SBRT versus Gem and S-1 plus SBRT in metastatic pancreatic cancer**

X. Zhu<sup>1</sup>, C. Yangsen<sup>1</sup>, Z. Xianzhi<sup>1</sup>, S. Yuxin<sup>1</sup>, J. Xiaoping<sup>1</sup>, Q. Shuiwang<sup>1</sup>, C. Fei<sup>1</sup>, J. Zhen<sup>1</sup>, F. Fang<sup>1</sup>, J. Zhen<sup>1</sup>, Z. Huojun<sup>1</sup>

<sup>1</sup>Changhai Hospital, Radiation Oncology, Shanghai, China

**Purpose or Objective**

Nearly 50% of patients had metastatic pancreatic cancer at initial diagnose. Therefore, priority may be given to quality of life, which required improvement of survival without simultaneously compromise of health-related quality of life (HRQOL) during treatment. Moreover, radiotherapy could be an option for amelioration of local symptoms in addition to potential abscopal effects, contributing to improvement of HRQOL. Hence, we sought to evaluate the HRQOL after SBRT and different chemotherapy regimens in the management of metastatic pancreatic cancer.

**Material and Methods**

Patients with biopsy-proven and radiographically metastatic pancreatic cancer were included and prospectively followed up from 2013 to 2017. Chemotherapy was delivered after SBRT with an interval of 3 weeks, which were required for 4 cycles. The regimens were gemcitabine plus nab-paclitaxel (GT group) or gemcitabine plus S-1 (GS group). The Chinese version of Brief Pain Inventory (BPI) and 5-level European quality of life 5-dimensions (EQ-5D-5L) were used in this study. Due to limited survival of patients with metastatic pancreatic cancer, questionnaires were completed before SBRT and right after the whole treatment. Patient-reported global changes and scores of questionnaires were assessed. To be simplified, all changes were stratified into "better", "no change" and "worse" in the analysis. Data were analyzed with Spearman's rank correlation, ordinal regression. Propensity score matched analysis were further performed to evaluate these two regimens.

**Results**

Seventy-five and eighty-nine patients received gemcitabine plus nab-paclitaxel and gemcitabine plus S-1, respectively. No differences of baseline characteristics were found between these two groups. No differences of BPI scores were found between pre- and post-treatment in each group, while only the post-treatment EQ-5D-5L score was higher than that at baseline in GS group ( $P < 0.001$ ). The response "better" of BPI was found in 15 and 38 patients in GT and GS group, respectively ( $P < 0.001$ ). On multinomial logistic regression, compared with GS group, the probability of GT group achieving "better" global change of BPI was 0.289 ( $P = 0.015$ ). The "better" change of EQ-5D-5L was found in 20 and 42 patients in GT and GS group, respectively ( $P < 0.001$ ). After multinomial analysis, compared with GS group, the probability of GT group gaining improvement of EQ-5D-5L was 0.334 ( $P = 0.031$ ). After propensity score matching analysis, more patients had improvement of BPI and EQ-5D-5L in GS group compared with GT group ( $n = 24$  vs.  $n = 12$ ,  $P = 0.002$ ;  $n = 28$  vs.  $n = 16$ ,  $P = 0.002$ ). No grade 3 or more radiation-induced toxicity occurred. More patients in GT group experienced grade 3 or more hematological and gastrointestinal toxicity than those in GS group ( $n = 25$  vs.  $n = 16$ ,  $P = 0.024$ ;  $n = 17$  vs.  $n = 10$ ,  $P = 0.049$ ).

**Conclusion**

GS may achieve better HRQOL than GT. Therefore, GS may be an alternative of GT for metastatic pancreatic cancer, especially for Asians.

**EP-1410 PET compared to CT in target delineation for SBRT of pancreas adenocarcinoma.**

C. De la Pinta Alonso<sup>1</sup>, J.D. García<sup>2</sup>, D. Sevillano<sup>2</sup>, A. Martínez-Lorca<sup>3</sup>, R. García<sup>4</sup>, M. Martín<sup>1</sup>, M. Martín<sup>1</sup>, R. Hernanz<sup>1</sup>, E. Fernández-Lizarbe<sup>1</sup>, T. Muñoz<sup>1</sup>, J.A. Domínguez<sup>1</sup>, J.F. Crespo<sup>5</sup>, C. Vallejo<sup>1</sup>, A. Hervás<sup>1</sup>, F. López<sup>1</sup>, S. Sancho<sup>1</sup>

<sup>1</sup>Ramon y Cajal Hospital, Radiation Oncology, Madrid, Spain ; <sup>2</sup>Ramon y Cajal Hospital, Medical Physics, Madrid, Spain ; <sup>3</sup>Ramon y Cajal Hospital, Nuclear Medicine Department, Madrid, Spain ; <sup>4</sup>Ramon y Cajal Hospital, Radiology Department, Madrid, Spain ; <sup>5</sup>Ramon y Cajal Hospital, Nursery Department, Madrid, Spain

**Purpose or Objective**

In SBRT quality control of target delineation pancreatic tumors is essential to deliver adequate doses of radiation to the primary tumor while preserving adjacent healthy organs. The purposes of this study was to evaluate the variability in contouring of these tumors in our center and our hypothesis is that PET allows better visualization of pancreatic tumours and will optimize the accuracy of tumor delineation for SBRT compared with CT only.

**Material and Methods**

A planning CT and PET/CT were performed in all patients. Gross tumor volume (GTV) in both CT and PET/CT were delineated. 8 physicians of Radiation Oncology Department performed the contours. Pancreatic locations included bed surgery recurrence, pancreatic body (2p) and pancreatic-head. The cases show different difficulty: low acquisition contrast, previously treated with chemotherapy or low SUV in PET/CT. In both CT and PET, the GTV volumes, conformity index (CI) and distance between the centers of mass (dCOM) were compared.

**Results**

Four patients were included. The GTV volume as defined on CT was in all cases larger or at least as large as the GTV volume on PET. The median GTV volume on PET was 7,1 mL (range, 1,7-14,9 mL), compared to 12,5 mL on CT (range 5-18,6 mL). Contouring of pancreatic adenocarcinoma on CT resulted in non-statistically significant larger lesions (mean increase 5,46mL) compared with PET ( $p = 0.254$ ). Variability between observers in CT was minor than PET (17,14 vs 23,45mL). Overlap ratio has not showed differences between CT and PET.

**Conclusion**

PET and TC seems to represent extend of the GTV in pancreatic tumors accurately. Contouring based on CT-only could result in an overestimation of the actual tumor volume, which may cause overdosage of the GTV in SBRT treatment plans by this combining CT and PET could be help in contouring. The interobserver variability in target delineation of pancreatic tumors GTV in this study is noteworthy. We consider need multi-institution studies involving abdominal SBRT require appropriate quality assurance programs for target delineation.

**EP-1411 What is the best imaging study to contouring liver metastases in SBRT?**

C. De la Pinta Alonso<sup>1</sup>, J.D. García<sup>2</sup>, D. Sevillano<sup>2</sup>, R. García<sup>3</sup>, A. Martínez-Lorca<sup>4</sup>, M. Martín<sup>1</sup>, E. Fernández-Lizarbe<sup>1</sup>, M. Martín<sup>1</sup>, J.A. Domínguez<sup>1</sup>, R. Hernanz<sup>1</sup>, T. Muñoz<sup>1</sup>, S. Sancho<sup>1</sup>

<sup>1</sup>Hospital Ramon y Cajal, Radiation Oncology, Madrid, Spain ; <sup>2</sup>Hospital Ramon y Cajal, Medical Physics, Madrid, Spain ; <sup>3</sup>Hospital Ramon y Cajal, Radiology Department, Madrid, Spain ; <sup>4</sup>Hospital Ramon y Cajal, Nuclear Medicine, Madrid, Spain

**Purpose or Objective**

In SBRT tumor delineation is essential to deliver adequate doses of radiation while preserving adjacent healthy organs. Defining liver metastases gross tumor volume (GTV) requires multimodal imaging, acquired in different perfusion phases. Most liver metastases can be imaged in the portal venous phase. The purposes of this study was to evaluate the variability in contouring of these tumors in our center and compare three studies: CT, MRI and PET

**Material and Methods**

Anonymous, multiphase-CT, MRI and PET/CT obtained from five patients (6 lesions) with liver metastases were

included and distributed to a panel of 8 radiation oncologists. Liver locations were segments II, IV (2) and VI (3). The cases show different difficulty: low acquisition contrast, previously treated with chemotherapy, inhomogeneous liver parenchyma or low SUV in PET/CT. The agreement was assessed using the kappa-statistic. Agreement interpretation was evaluated using Landis and Koch's interpretation. The institutional review boards approved the study.

#### Results

The median GTV volume on MRI was 2,8 mL (0,7-16,1 mL), compared to 3mL on CT (0,6-8,6 mL) ( $p=0,07$ ). The median GTV volume on PET was 6 mL (2,5-18mL), compared to 3mL on CT (0,6-8,6 mL) ( $p=0,15$ ). Variance between observers in CT was minor that MRI and PET (5,75 vs 9 vs 19,9). The index of agreement was low (0,083) between CT and MRI in all patients. The index of agreement was low ( $kappa=0,005$ ) between CT and PET in all patients.

#### Conclusion

In cases with well-defined tumor CT is more easy and reproducible. In cases with no defined tumor in CT we need other tools: MRI and/or PET/CT. The interobserver variability in target delineation in this study is noteworthy. Multi-institution consensus was necessary.

#### EP-1412 Excellent pCR rate in patients with HCC after SBRT +/- TACE as bridging to liver transplantation

S. Gerum<sup>1</sup>, C. Heinz<sup>2</sup>, C. Belka<sup>3</sup>, P.M. Paprottka<sup>4</sup>, J. Neumann<sup>5</sup>, E. De Toni<sup>6</sup>, M. Guba<sup>7</sup>, F. Roeder<sup>8</sup>

<sup>1</sup>Radiation Oncology- University of Munich LMU- Germany, Department of Radiation Oncology- University of Munich LMU- Germany, Munich, Germany ; <sup>2</sup>Radiation Oncology- University of Munich LMU- Physics, Department of Radiation Oncology- University of Munich LMU- Germany, Munich, Germany ; <sup>3</sup>Radiation Oncology- University of Munich LMU-, Department of Radiation Oncology- University of Munich LMU- Germany, Munich, Germany ; <sup>4</sup>Interventional Radiology- LMU, Department of interventional Radiology- LMU- University Hospital of Munich, Munich, Germany ; <sup>5</sup>Pathology- LMU, Department of Pathology- LMU- University Hospital of Munich- Germany, Munich, Germany ; <sup>6</sup>Gastroenterology, Department of Medicine II- Liver Center Munich- University Hospital- Munich- Germany., Munich, Germany ; <sup>7</sup>Visceral- Vascular- Transplantation Surgery, Department of General- Visceral- Vascular and Transplantation Surgery- Hospital of the LMU Munich- Germany, Munich, Germany ; <sup>8</sup>Radiation Oncology- University of Munich LMU-, Department of Radiation Oncology- LMU- University Hospital of Munich- Germany, Munich, Germany

#### Purpose or Objective

**Background:** To report histopathological response rate and overall outcome after stereotactic body radiotherapy (SBRT) +/-TACE (transarterial chemoembolisation) as bridging to orthotopic liver transplantation (OLT) in patients with hepatocellular carcinoma (HCC).

#### Material and Methods

**Patients and methods:** We retrospectively analyzed 6 patients with 7 HCC lesions, who had been listed for orthotopic liver transplantation and had received SBRT as bridging treatment. All patients fulfilled EASL criteria for diagnosis and Milan criteria for OLT eligibility. All patients were judged ineligible for other locally ablative treatments (except TACE) or surgical resection by multidisciplinary evaluation. 4 patients received SBRT within 6 weeks from TACE of the same lesion(s). Liver function was Child-Pugh class A in 3, B in 2 and C in 1 patient(s). Cause of underlying cirrhosis was toxic in 2, hepatitis viral infection in 2 and autoimmune in 2 patients. Dose and fractionation varied dependent on localisation, size, motion and liver function. 6/7 lesions were treated with 37.5 Gy prescribed to the surrounding 65% isodose in

3 fractions. Immobilization included a vacuum pillow in all and abdominal compression in 5 patients. Treatment planning was based on contrast-enhanced 4D-CT using an ITV concept with a PTV margin of 6 mm. Daily image guidance was performed with CBCT using fiducial markers or lipiodol enhancement after TACE.

#### Results

**Results:** Median interval between SBRT and OLT was 6 months (range 1-8 months). Median follow-up from SBRT was 24 months (range 7-79). All patients remained locally and distantly controlled until OLT. In 5/6 patients and 6/7 lesions no residual HCC (pathologic complete response) was found in the explanted liver. The only patient with residual disease had been treated with SBRT only (no TACE) and received OLT early (1 month) after SBRT. No acute toxicity from SBRT was observed, except deterioration of liver function in the CP C patient salvaged by OLT. One patient died shortly after OLT due to postoperative complications and one due to distant failure 9 months after OLT, resulting in a 2yr-OS rate of 66%.

#### Conclusion

**Conclusion:** SBRT with or without TACE is a locally effective and well-tolerated bridging treatment for HCC patients listed for orthotopic liver transplantation.

#### EP-1413 Correlation between N-L Ratio, P-L Ratio and Survival in patients with LAPC: A new prognostic factor?

P. Trecca<sup>1</sup>, M. Fiore<sup>1</sup>, C. Greco<sup>1</sup>, E. Ippolito<sup>1</sup>, R.M.

D'Angelillo<sup>1</sup>, L. Trodella<sup>1</sup>, S. Ramella<sup>1</sup>

<sup>1</sup>Campus-Bio Medico University, Radiotherapy Unit, Rome, Italy

#### Purpose or Objective

The aim of the study was to investigate the role of inflammatory markers such as neutrophil-lymphocyte ratio (NLR) and platelet-lymphocyte ratio (PLR) in predicting the prognosis of patients with locally advanced pancreatic cancer (LAPC) treated by radiochemotherapy (RCT)

#### Material and Methods

Fifty-two patients (F:30; M:22; median age 64 years, range 40-75 yrs) with histologically proven pancreatic ductal adenocarcinoma enrolled in a prospective one-armed phase II study were evaluated. All patients were treated with gemcitabine-based RCT after an accurate pre-treatment staging. NLR and PLR were calculated from data collected within 14 days before the start of the concurrent RCT. We stratified population into groups according to the cut-off values: NLR<3 (n=30 pts), NLR ≥3 (n=22 pts), PLR<200 (n=38 pts), PLR ≥200 (n=14 pts). Survival data among subgroups classified by each factor were analyzed via the Kaplan-Meier curve and compared by the log-rank test.

#### Results

For NLR<3 and NLR≥3 groups, respectively, median OS were 17.7 months and 13 months ( $p=0.15$ ), and median PFS were 12.4 months and 18.1 months ( $p=0.4$ ). For PLR<200 and PLR≥200 groups, respectively, median OS were 21.5 months and 12.4 months ( $p<0.001$ ), and median PFS were 20 months and 12.5 months ( $p=0.2$ ).

#### Conclusion

These data suggest that high NLR and high PLR could predict worst OS and PFS. More studies with a large population may be useful in order to validate NLR and PLR as predicting markers for prognosis of patients with LAPC.

#### EP-1414 SBRT for the treatment of hepatocellular carcinoma: a retrospective multicenter study

N. Scher<sup>1</sup>, F.G. Riet<sup>2</sup>, G. Janoray<sup>1</sup>, K. Debbi<sup>1</sup>, S. Levy<sup>1</sup>, P. Louisot<sup>1</sup>, E. Chajon<sup>2</sup>, E. Salame<sup>1</sup>, I. Barillot<sup>1</sup>, R. De Crevoisier<sup>2</sup>, G. Calais<sup>1</sup>, S. Chapet<sup>1</sup>

<sup>1</sup>Hopital Bretonneau, Centre, Tours, France ; <sup>2</sup>Centre Eugene Marquis, Bretagne, Rennes, France

#### Purpose or Objective

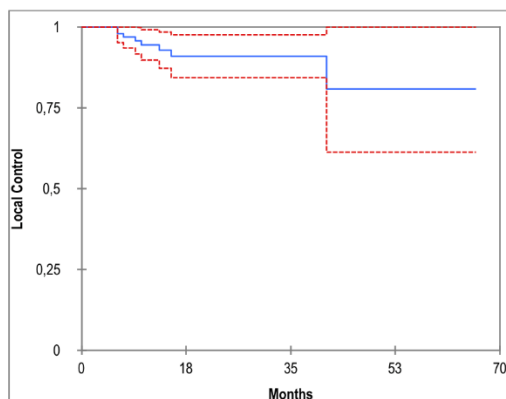
To describe local control, overall survival, progression-free survival and toxicities of Cyberknife® based stereotactic body radiation therapy (SBRT) in the treatment of hepatocellular carcinoma (HCC).

#### Material and Methods

The records of all the patients treated for HCC at the Eugene Marquis center, Rennes and the Bretonneau Hospital, Tours; between November 2010 and December 2016, were reviewed. The treatment was performed as a salvage treatment; as a bridge to liver transplantation or if no other treatment was possible.

#### Results

136 patients were consecutively included in the study. The median follow-up was 13 months. The median total dose prescribed, median fractionation and median overall treatment time were respectively 45 Gy, 3 fractions and 5 days. The overall survival, progression-free survival and local control rates at 1 year and 2 years were 79.8% and 63.5%; 61.3% and 39.4%; 94.5% and 91%. Two grade 3 acute toxicity events and two grade 4 late toxicity events corresponding to a duodenal ulcer have been reported. Seven patients underwent classic RILD (radio-induced hepatitis) and thirteen patients showed non-classical RILD. BCLC stage, WHO grade and PTV volume were correlated with overall survival in univariate Cox analysis.



#### Conclusion

SBRT is an effective and well tolerated in the treatment of inoperable HCC or as a bridge to liver transplantation. The toxicity is mainly related to cirrhotic background and requires a selection of patients and strict dose constraints.

#### EP-1415 Preliminary results of a phase II study of induction Folfirinox followed by chemoradiation in LAPC

P. Trecca<sup>1</sup>, M. Fiore<sup>1</sup>, R. Coppola<sup>2</sup>, L.E. Trodella<sup>1</sup>, R.M. D'Angelillo<sup>1</sup>, L. Trodella<sup>1</sup>, S. Ramella<sup>1</sup>

<sup>1</sup>Campus-Bio Medico University, Radiotherapy Unit, Rome, Italy ; <sup>2</sup>Campus-Bio Medico University, General Surgery, Rome, Italy

#### Purpose or Objective

The aim of this study was to evaluate the safety and efficacy of induction FOLFIRINOX followed by a high weekly dose of gemcitabine-based radiochemotherapy in patients with borderline resectable or unresectable locally advanced pancreatic cancer.

#### Material and Methods

This trial was performed as a single-center one-armed phase II study. From January 2015 we evaluated twenty-two patients with borderline resectable or unresectable pancreatic cancer (characteristics of patients are summarized in table 1). A pre-treatment staging was performed with CT scan, 18FDG PET-CT scan and laparoscopy. Patients with metastatic disease were excluded. Suitable patients received chemotherapy with

Folfirinox (four cycles every 14 days). Patients without disease progression after restaging received conformal radiation therapy with concurrent gemcitabine at the dose of 600 mg/mq weekly.

Characteristic	No of patients (N = 22)	%
<b>Age (years)</b>		
Median	63.5	
Range	48-79	
<b>Sex</b>		
Male	10	45,5
Female	12	54,5
<b>ECOG performance status</b>		
0	22	100
1	0	0
<b>CA 19-9 at diagnosis, U/mL</b>		
Median	4219	
Range	<2-8945	
<b>Tumorlocalization</b>		
Head	18	81,8
Body/Tail	4	18,2
<b>Resectability status</b>		
Borderline resectable	6	27,3
Locally advanced unresectable	16	72,7

#### Results

Further to the results of the pre-treatment workup, nine patients (40,9%) were excluded from the protocol because of the evidence of metastatic disease, and thus a total of thirteen patients were consequently enrolled. Five patients (38,5%) had a progression of disease after induction chemotherapy. Eight patients (61,5%) completed radiochemotherapy. Of these, four patients underwent surgical radical resection (30,8%). At the present, the median Overall Survival was 13,8 months and the median Progression Free Survival was 18,9 months. For the entire cohort of patients the treatment was well tolerated. Only haematological grade 3-4 toxicities were observed.

#### Conclusion

Although the follow-up time is limited, these preliminary data of the protocol treatment show promising results for patients with borderline resectable and unresectable pancreatic cancer. The enrollment is actually ongoing. Continued optimization in multimodality therapy and an accurate patient selection are crucial for the appropriate treatment of patients.

#### EP-1416 Palliative Oesophageal Chemoradiotherapy: A Phase 1 Clinical Trial

J. Martin<sup>1</sup>, D. Fiona<sup>2</sup>, J. Loh<sup>3</sup>, S. Ackland<sup>2</sup>, T. Bonaventura<sup>2</sup>, M. Fay<sup>1</sup>, M. Kumar<sup>1</sup>, J. Lynam<sup>2</sup>, G. Mallesara<sup>2</sup>, M. O'Neill<sup>1</sup>, J. Smart<sup>1</sup>, A. Van der Westhuizen<sup>2</sup>, V. Wills<sup>4</sup>, T. Wright<sup>4</sup>

<sup>1</sup>Calvary Mater Newcastle, Radiation Oncology, Newcastle- NSW, Australia ; <sup>2</sup>Calvary Mater Newcastle, Medical Oncology, Newcastle- NSW, Australia ;

<sup>3</sup>University of Malaya, Radiation Oncology, Kuala Lumpur, Malaysia ; <sup>4</sup>John Hunter Hospital, Department of Surgery, Newcastle- NSW, Australia

***This abstract is part of the media programme and will be released on the day of its presentation***

54.8%, and abdominal discomfort: 64.2%). Median time to symptom progression was 89 days (range: 12-392 days), in which patients with CR+PR at 1 month had more durable control of symptoms than those with SD+PD (median 114 days vs. 55 days, p=0.24). Treatment is well tolerated with only 2 patients (3.8%) developing grade 3 toxicities. (fatigue, n=1; vomiting, n=1). AFP response, radiological response rate, and disease control rate at 3 months were 38.6%, 15.2%, and 54.6% respectively.

**Table 1.** Bar Chart showing proportion of patients with clinical improvement of pain and abdominal discomfort at 1 month (CR+PR, SD, and PD)

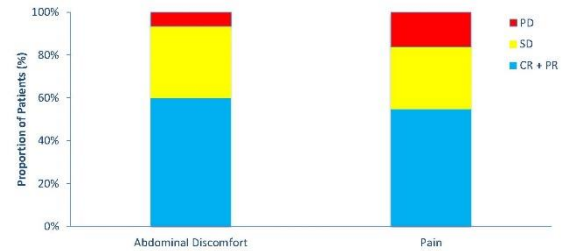


**Table 2.** Symptom response (CR, PR, SD & PD), response duration, and overall survival of patients



**EP-1417 Palliative Liver Radiotherapy (RT) of Advanced Hepatocellular Carcinoma (HCC) in Endemic Population**

C.L. Chiang<sup>1,2</sup>, C.S. Yeung<sup>3</sup>, N.S. Wong<sup>3</sup>, K.C. Tsang<sup>1</sup>, B.Y. Chan<sup>1</sup>, S.K. Ha<sup>1</sup>, C.H. Ho<sup>3</sup>, F.A. Lee<sup>3</sup>

<sup>1</sup>The University of Hong Kong, Department of Clinical Oncology, Hong Kong, Hong Kong SAR China ; <sup>2</sup>HKU-Shenzhen Hospital, Department of Clinical Oncology, Shenzhen, China ; <sup>3</sup>Tuen Mun Hospital, Department of Clinical Oncology, Hong Kong, Hong Kong SAR China

**Purpose or Objective**

This study aims at evaluating the symptom response, response duration, and toxicity of palliative liver radiotherapy (RT) in advanced HCC patients in endemic area.

**Material and Methods**

We reviewed the clinical records of unresectable HCC patients treated with palliative RT (8Gy single fraction) in our institution. Eligible patients were unsuitable or refractory to TACE and SBRT, with an index symptom of pain or abdominal discomfort. Physician reported symptoms [complete response (CR), partial response (PR), stable disease (SD), and progressive disease (PD)] were documented monthly at the first 3 months and every 3 months thereafter till death. The primary outcome was the percentage of patients with clinical improvement of index symptom (CR+PR) at 1 month. Secondary outcomes were symptom response duration, toxicities, alpha-feto protein (AFP) response (>20% drop from baseline), and radiological response.

**Results**

Fifty-two patients were included in the study. Thirty-eight (73%) were hepatitis B carriers; median size of the largest tumor was 13cm (range 3-24cm); 33 (63.5%) had tumor involvement >50% of total liver volume. Fifty-one (98.1%) were Barcelona Clinic Liver Cancer (BCLC) stage C and twenty-three of them (45.1%) received Sorafenib after radiotherapy. The index symptom was pain in 34 patients, and abdominal discomfort in 18 patients. At 1 month, 57.8% of patients had improvement of symptoms (pain:

**Conclusion**

Substantial patients had improvement of index symptoms after receiving palliative liver RT with median response duration of around 3 months. The treatment is well tolerated with minimal toxicities.

**EP-1418 Initial results of carbon ion radiotherapy combined with S-1 for locally advanced pancreatic cancer**

Y. Mori<sup>1</sup>, M. Okamoto<sup>1</sup>, H. Kiyohara<sup>2</sup>, H. Katoh<sup>3</sup>, K. Shibuya<sup>1</sup>, T. Kaminuma<sup>1</sup>, S. Shiba<sup>1</sup>, N. Okano<sup>1</sup>, T. Ohno<sup>1</sup>, T. Nakano<sup>1</sup>

<sup>1</sup>Gunma Heavy Ion Medical center, Radiation oncology, Maebashi-city, Japan ; <sup>2</sup>Maebashi red cross hospital, Radiation oncology, Maebashi-city, Japan ; <sup>3</sup>Kanagawa cancer center, Radiation oncology, Yokohama city, Japan

**Purpose or Objective**

Generally, patient with locally advanced pancreatic cancer (LAPC) is treated with chemotherapy alone or X-ray radiotherapy (RT) concurrent with gemcitabine (GEM). Median survival time (MST) of standard treatment is about 14 months. Recently, there was a report of carbon ion radiotherapy (C-ion RT) with concurrent usage of GEM for LAPC which showed 2-year overall survival (OS) rate and MST 48% and 22.5 months, that is better outcome compared with other treatment for LAPC. However, there is no report for C-ion RT combined with other chemotherapy. On the other hand, postoperative adjuvant chemotherapy with S-1 significantly extended both overall and relapse-free survival of Japanese patients with resected pancreatic cancer compared with GEM. [OM1] [Office2] Thus, we hypothesize that C-ion RT concurrent S-1 (tegafur/gimeracil/oteracil potassium) is more effective for LAPC and started prospective phase II study in our institute.

**Material and Methods**

Eligibility criteria: (1) Pathologic confirmation of pancreatic invasive ductal carcinomas or clinical diagnosis by imaging. (2) Absence of distant metastasis (patients with para-aortic lymph node metastasis were eligible) (3) Unresectable primary tumors due to T4 disease based on the 7th edition of TNM classification, involving either the celiac axis or the superior mesenteric artery. (4) Without gastrointestinal ulcer (stomach, duodenum) (excluding repaired ulcer) (5) Age at registration is from 20 to 80 years old (6) ECOG performance status (PS) of 0 to 2. (7) Without the surgical resection history to a pancreatic cancer. Without the radiotherapy to a pancreatic cancer. Treatment: Prescribed doses were 55.2 Gy [relative biological effectiveness (RBE)] in 12 fractions. Concurrent S-1 was administered orally during 28 days, the dose levels were 80 mg/-1.00 m<sup>2</sup>, 100 mg/1.00-1.50 m<sup>2</sup>, 120 mg/1.50- m<sup>2</sup> per day. Clinical outcome measures: The primary endpoint was overall survival (OS). The secondary endpoints were local control (LC) rate, progression free survival (PFS) rate and adverse effects. Toxicity was graded using Common Terminology Criteria for Adverse Events, version 4.0 (CTCAE 4.0).

**Results**

There were 13 patients enrolled this study from January 2016 to December 2017 in our institute. MST was 23.4 months. 1 and 2-year OS was 100% and 38%. 1 and 2-year LC are 80% and 28%. 1 and 2-year PFS rate are 60% and 49%. There were occurrences of acute toxicity, leukopenia grade 2 in 2 patients and grade 3 in 1 patient, anemia grade 2 in 2 patients and grade 3 in 1 patient, thrombocytopenia Grade 2 in 1 patient. There is no patient with Grade 4 or higher. There were no occurrences of late toxicity of grade 3 or higher.

**Conclusion**

Initial results show that C-ion RT combined with S-1 appears to be tolerated and not inferior compared with GEM for LAPC. Although there are still few cases, C-ion RT combined with S-1 is also considered to be one of the options of treatment for LAPC.

**EP-1419 Salvage concurrent chemoradiotherapy for postoperative locoregional recurrence of esophageal cancer**

T. Kiritoshi<sup>1</sup>, H. Yamashita<sup>1</sup>, W. Takahashi<sup>1</sup>, M. Ogita<sup>1</sup>, K. Nakagawa<sup>1</sup>, O. Abe<sup>1</sup>

<sup>1</sup>The University of Tokyo Hospital, Radiology, Bunkyo-ku, Japan

**Purpose or Objective**

The aim of this study was to evaluate clinical results of salvage CRT for locoregional recurrence after esophagectomy for squamous cell carcinoma of esophagus.

**Material and Methods**

We performed a retrospective review of 73 consecutive patients who received salvage chemoradiotherapy between 2001 and 2017 for locoregional recurrence of esophageal carcinoma after curative surgery. The intended radiotherapy regimen was 50-60 Gy in 25-30 fractions combined with concurrent platinum-based chemotherapy. The endpoints of this study were overall survival, progression free survival and prognostic factors. Survival rates were estimated using the Kaplan-Meier method, and statistical analysis was performed using the log-rank test. Univariate and multivariate analysis were performed using the log-rank test and the Cox proportional hazards model respectively.

**Results**

The median follow-up period for survivors was 42.7 months. The 1-, 2-, 3-year overall survival were 82.4%, 46.2% and 33.8% respectively with a median survival time of 21.6 months. Out of all 73 patients, 29 patients were alive beyond 2 years from salvage therapy. The median PFS time was 9.7 months. Ten patients survived for more than 5 years from the start of salvage chemoradiotherapy. Overall survival was significantly longer in the nedaplatin plus S-1 group (median 29.1 months, 95% CI 15.2-66.4) than other chemotherapy group (median 16.7 months, 14.0-24.6; hazard ratio 2.34; p=0.012). Re-recurrence within irradiated field was seen in 26 patients and was significantly correlated with shorter overall survival (hazard ratio 3.12; p<0.01).

**Conclusion**

Salvage chemoradiotherapy using nedaplatin plus S-1 could be a new treatment option for locoregional recurrence after esophagectomy for esophageal squamous cell carcinoma.

**EP-1420 Utility of FIB-4 index for hepatocellular carcinoma patients treated with proton beam therapy**

Y. Sekino<sup>1</sup>, T. Okumura<sup>1</sup>, N. Fukumitsu<sup>2</sup>, T. Iizumi<sup>1</sup>, D. Miyauchi<sup>1</sup>, N. Mizoguchi<sup>1</sup>, K. Murofushi<sup>1</sup>, K. Ohnishi<sup>1</sup>, M. Mizumoto<sup>1</sup>, T. Nonaka<sup>1</sup>, K. Nakai<sup>1</sup>, H. Ishikawa<sup>1</sup>, K. Tsuboi<sup>1</sup>, H. Sakurai<sup>1</sup>

<sup>1</sup>Faculty of Medicine- University of Tsukuba, Radiation Oncology & Proton Medical Research Center, Tsukuba, Japan ; <sup>2</sup>Kobe Proton Center, Radiation Oncology, Kobe, Japan

**Purpose or Objective**

The FIB-4 index is a simple noninvasive index for evaluating hepatic fibrosis which consists of age, aspartate aminotransferase (AST), alanine aminotransferase (ALT) and platelet count (PLT). This index is reported to be a significantly useful noninvasive surrogate marker for prognosis of hepatocellular carcinoma (HCC) patients received hepatectomy. However, the FIB-4 index has not been validated specifically in HCC patients receiving proton beam therapy (PBT). The purpose of this study is to evaluate the prognostic performance of the FIB-4 index for HCC patients treated with PBT.

**Material and Methods**

A total of 55 consecutive HCC patients treated with PBT at the University of Tsukuba between 2001 and 2013 were analyzed. Eligibility criteria included patients with a single lesion, tumor size of ≤5 cm and Child-Pugh (CP) A5. Patients with vascular invasion were excluded. The cutoff

value for the FIB-4 index was determined with the result from a receiver operating characteristic curve analysis. The effect of the FIB-4 index on overall and recurrence-free survival was retrospectively evaluated.

#### Results

Median age was 70 years old (range: 39-87). Median follow-up period was 64 months. Median tumor size was 30 (range: 12-50) mm. The cutoff value for the FIB-4 index was set to 3.5. The median FIB-4 index was 3.45 (range: 1.2-10.4) with 51% at  $\leq 3.5$  (low FIB-4 group) ( $n = 28$ ) and 49% at grade  $> 3.5$  (high FIB-4 group) ( $n = 26$ ). The PFS and OS rates for the entire cohort at 3 and 5 years were 57%, 45% and 85%, 66%, respectively. The PFS rate for the low FIB-4 group at 3 and 5 years were 59% and 50% and for high FIB-4 group 53% and 36%, respectively ( $p=0.259$ ). The OS rate for the low FIB-4 group at 3 and 5 years were 89% and 76% and for high FIB-4 group 80% and 53%, respectively. A statistically significant difference was recognized between the groups ( $p=0.011$ ).

#### Conclusion

The FIB-4 index appears to be a promising predictor of long-term outcomes for HCC patients treated with PBT.

#### EP-1421 Combined chemoembolization and radiotherapy for hepatocellular carcinoma with portal vein thrombosis

K. Treewatthanawong<sup>1</sup>, N. Amornwichee<sup>1</sup>, A. Prayongra<sup>1</sup>, P. Alisanant<sup>1</sup>, C. Khorprasert<sup>1</sup>, K. Shotetersuk<sup>1</sup>

<sup>1</sup>King Chulalongkorn Memorial Hospital, Division of Therapeutic Radiation and Oncology- Department of Radiology, Bangkok, Thailand

#### Purpose or Objective

Patients with hepatocellular carcinoma with portal vein thrombosis have limited choice of therapy due to extensive disease and poor underlying liver function. We conducted a retrospective analysis of patients with hepatocellular carcinoma (HCC) with portal vein thrombosis (PVT) who underwent transarterial chemoembolization (TACE) and radiotherapy (RT) to evaluate the efficacy and toxicity.

#### Material and Methods

In this study, non-metastatic HCC with PVT patients treated with TACE and RT from March 2010 to December 2017 were retrospectively reviewed. Primary outcome was response of PVT. Secondary outcomes included response of tumor, overall survival (OS), acute toxicities and prognostic factors for OS.

#### Results

80 patients were included for analysis. Median patient age was 61.71 years old (50.5-72.92). Mean of the tumor diameter was 7.12 cm (range, 1-20 cm). Fifty-nine (74.7%) patients had main or first branch PVT. Mean radiation dose was 41.35 Gy (range, 8-60 Gy) at 1.8-10 Gy per fraction. For PVT, the response rate was 32.4% and the complete response rate was 5.6%. For primary tumor, the response rate was 50% and the complete response rate was 2%. The median survival was 12 months (10.89-13.11). The 1, 2- and 3-year survival rates were 44.6%, 22.6% and 10%, respectively. On univariate analysis, age, Child-Pugh classification, MELD score, ECOG, serum level of AFP, HBV infection, tumor size, site of PVT and response of PVT were not significant prognostic factors for OS. The BED was insignificant associated with the response of PVT. Grade 3 and 4 hepatotoxicity occurred in 9.2% of patients. There was no treatment-related death.

#### Conclusion

TACE plus RT is a safe and practical treatment option for HCC with PVT. However, further prospective large-scale study is required to evaluate the optimal patient selection, dose/fractionation and prognostic factors related to response and toxicities.

#### EP-1422 Unresectable biliary cancer: results of a pooled analysis of combined CHEMORADIOTHERAPY

S. Bisello<sup>1</sup>, A. Palloni<sup>2</sup>, M. Buwenge<sup>1</sup>, R. Autorino<sup>3</sup>, F. Cellini<sup>3</sup>, L. Tagliaferri<sup>3</sup>, M. Gabriella<sup>4</sup>, F. Deodato<sup>4</sup>, V. Picardi<sup>4</sup>, S. Mignona<sup>5</sup>, S. Cilla<sup>6</sup>, V. Perri<sup>7</sup>, A. Tringali<sup>7</sup>, A. Galuppi<sup>1</sup>, G. Brandi<sup>2</sup>, A.G. Morganti<sup>1</sup>, S. Cammelli<sup>1</sup>, V. Valentini<sup>3</sup>, G.C. Mattiucci<sup>3</sup>

<sup>1</sup>S. Orsola-Malpighi Hospital, Department of Experimental- Diagnostic & Speciality Medicine DIMES- University of Bologna, Bologna, Italy ; <sup>2</sup>S. Orsola-Malpighi Hospital, Department of Medical and Surgical Sciences - DIMES- University of Bologna, Bologna, Italy ; <sup>3</sup>Sacred Heart Catholic University, Radiation Oncology Department, Rome, Italy ; <sup>4</sup>"Giovanni Paolo II" Foundation- Catholic University of the Sacred Heart, Radiation Oncology Unit, Campobasso, Italy ; <sup>5</sup>"Giovanni Paolo II" Foundation- Catholic University of the Sacred Heart, Medical Oncology Unit, Campobasso, Italy ; <sup>6</sup>"Giovanni Paolo II" Foundation- Catholic University of the Sacred Heart, Medical Physics Unit, Campobasso, Italy ; <sup>7</sup>Gemelli University Hospital- Università Cattolica del Sacro Cuore, Digestive Endoscopic Unit, Rome, Italy

#### Purpose or Objective

To retrospectively evaluate the outcome of a combined modality treatment based on chemoradiation (CRT) +/- brachytherapy (BRT) in a pooled analysis of 3 series from different institutions of patients with unresectable biliary cholangiocarcinoma (CC).

#### Material and Methods

Data of patients with intrahepatic CC (ICC), Klatskin's Tumor (KT), distal extrahepatic CC (ECC), and gallbladder cancer (GBC) diagnosed from 1991 to 2017 were retrospectively analyzed. The treatment was mainly based on concurrent chemotherapy (CT) plus external beam radiotherapy (EBRT), +/- BRT boost. The Kaplan-Meier method was used to calculate survival curves in terms of overall survival (OS). Log-rank test was used to compare survival curves.

#### Results

Seventy-eight patients were included in this analysis (59%: males; 41%: female; median age: 67 years). A minority of patients (7.7%) were treated for disease recurrence after surgery. According to TNM, 77.6% of patients had a T stage  $> 3$  and 79% of patients were treated with CRT while 21% received EBRT followed by sequential CT. Median EBRT dose was 50 Gy (range: 16-75 Gy) delivered with conventional fractionation. CT was based on Gemcitabine or 5-Fluorouracil. BRT was prescribed to 50% of patient with a median dose of 7 Gy. Reported Grade  $\geq 3$  acute GI and hematological toxicity were 13.0% and 7.9%, respectively. No other severe acute toxicities were reported. One- and 2-year OS were 60.1 % and 29.2%, respectively (median: 15 months), while 1- and 2-year PFS were 42.4% and 7.8%, respectively. Analyzing the impact of BRT on OS, 24-month OS was 22.9% for the BRT group, and 36.2% for EBRT alone, while at 48-months, OS was 9.8% for the BRT group, and 0.0% for the group without BRT ( $p = 0.68$ ).

#### Conclusion

Combined modality treatment (CRT + BRT) in unresectable biliary cancer was associated with acceptable toxicity and OS almost comparable to the actual standard (CT). Further prospective studies are needed to improve outcome by using advanced treatment techniques and innovative combined modality therapies.

#### EP-1423 SBRT in locally advanced pancreatic cancer: a real-life study (PAULA-1)

A. Arcelli<sup>1</sup>, G. Macchia<sup>2</sup>, A. Guido<sup>1</sup>, F. Dalla Torre<sup>2</sup>, S. Cilla<sup>3</sup>, V. Scotti<sup>4</sup>, M.E. Rosetto<sup>5</sup>, I. Djan<sup>6</sup>, S. Parisi<sup>7</sup>, G.C. Mattiucci<sup>8</sup>, M. Fiore<sup>9</sup>, P. Bonomo<sup>10</sup>, A. Bacigalupo<sup>11</sup>, R.M. Niespolo<sup>12</sup>, P. Gabriele<sup>13</sup>, D. Francesco<sup>2</sup>, N. Simoni<sup>14</sup>, R. Mazarotto<sup>14</sup>, A.G. Morganti<sup>1</sup>

<sup>1</sup>Radiation Oncology Center- University of Bologna, Department of Experimental- Diagnostic and Speciality Medicine - DIMES, Bologna, Italy ; <sup>2</sup>Fondazione di Ricerca

e Cura "Giovanni Paolo II", Radiotherapy Unit, Campobasso, Italy; <sup>3</sup>Fondazione di Ricerca e Cura "Giovanni Paolo II", Medical Physic Unit, Campobasso, Italy; <sup>4</sup>Radiosurgery Center Malzoni, Radiosurgery Center, Agropoli, Italy; <sup>5</sup>Ospedale Belcolle, Radiotherapy Unit, Viterbo, Italy; <sup>6</sup>Medical Faculty-University of Novi Sad, Institute of Oncology Vojvodina-Sremska Kamenica, Novi Sad, Serbia; <sup>7</sup>Ospedale Casa Sollievo della Sofferenza San Giovanni Rotondo, Radiotherapy Unit, San Giovanni Rotondo- Foggia, Italy; <sup>8</sup>Policlinico Universitario "A. Gemelli"- Università Cattolica del Sacro Cuore, Department of Radiotherapy, Rome, Italy; <sup>9</sup>Università Campus Biomedico, Department of Radiotherapy, Rome, Italy; <sup>10</sup>Azienda Ospedaliero Universitaria Careggi AOUC- Università di Firenze, Department of Radiotherapy, Florence, Italy; <sup>11</sup>IRCCS AOU San Martino- IST, Department of Radiotherapy, Genova, Italy; <sup>12</sup>Azienda Ospedaliera San Gerardo, Radiotherapy Unit, Monza Mi, Italy; <sup>13</sup>Fondazione del Piemonte per l'Oncologia FPO- IRCCS Candiolo, Department of Radiotherapy, Torino, Italy; <sup>14</sup>University Hospital, Radiotherapy Unit, Verona, Italy

### Purpose or Objective

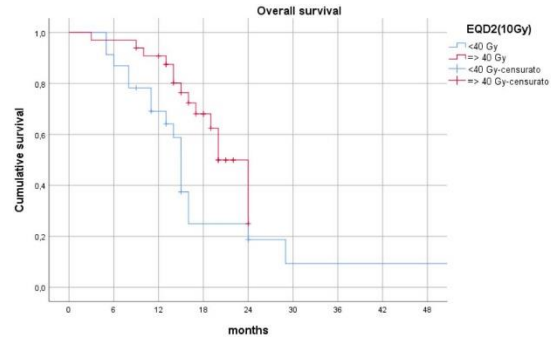
Locally advanced pancreatic cancer (LAPC) presents an intermediate prognosis between resectable and metastatic patients, with a median overall survival (OS) ranging from 9 to 13 months. A standard treatment approach is lacking with large variation between different institutions. We performed a real-life study retrospectively reviewing the experience of 6 different centers treating LAPC with stereotactic body radiotherapy (SBRT).

### Material and Methods

We included 56 pts with LAPC, undergoing SBRT +/- chemotherapy (CT) with multiagent CT regimens. Exclusion criteria were metastatic disease and radical surgical treatment. Only palliative surgery was allowed. Median total dose, median dose/fraction, and median equivalent dose (EQD<sub>2</sub>[ $\alpha/\beta$ ]<sub>10Gy</sub>) for SBRT were 30 Gy (range: 18-45), 6 Gy (range: 4-10), and 40 Gy (range: 23-65) respectively. Toxicity was evaluated by CTCAE version 5.0 scale. Overall survival, local control (LC), and disease metastasis-free survival (DMFS) were estimated and compared by Kaplan-Meier and log-rank methods, respectively.

### Results

We included 56 pts in this analysis (M/F: 31/25; median age: 68, range: 36-89). Median, 6 months, 1-year, and 2-year OS were: 19.0 months, 92.9%, 81.9%, and 27.1%, respectively. Six months, 1-year, and 2-year LC were: 92.5%, 76.3%, and 55.4% (median LC was not reached), respectively. Median, 6 months, 1-year, and 2-year DMFS were: 15.0 months (range 12.0-17.9), 87.3%, 59.5%, and 26.0%, respectively. A better prognosis was recorded in pts treated with both neoadjuvant (median OS: 15.0 vs 24.0 months, p=0.002) and adjuvant CT (median OS: 15.0 vs 29.0 months, p=0.017). Patients treated with a total SBRT dose  $\geq$ 30 Gy (p=0.030), with a fractionation dose  $\geq$  6 Gy (p= 0.014), and with a computed EQD<sub>2</sub>[ $\alpha/\beta$ ]<sub>10Gy</sub>  $\geq$ 40 Gy (p= 0.007) had a better OS. Total dose (p= 0.024) and EQD<sub>2</sub>[ $\alpha/\beta$ ]<sub>10Gy</sub> (p= 0.024) were significantly associated to higher local control. Gastrointestinal (GI) acute toxicity rates were as follows: G1: 24.4%, G2: 2.3%, G3: 0.0%. Only one case of G3 GI late toxicity (2.5%) was recorded.



### Conclusion

SBRT +/- CT resulted tolerable and effective in this "real-life" retrospective analysis. Further prospective studies are needed to define optimal radiation schedules and integration modalities with systemic therapies.

### EP-1424 SBRT vs chemoradiation: a case-control study (PAULA-2)

A. Arcelli<sup>1</sup>, F. Bertini<sup>1</sup>, A.G. Morganti<sup>1</sup>, A. Guido<sup>1</sup>, F. Deodato<sup>2</sup>, S. Cilla<sup>3</sup>, F. Dalla Torre<sup>2</sup>, V. Scotti<sup>4</sup>, M.E. Rosetto<sup>5</sup>, I. Djan<sup>6</sup>, S. Parisi<sup>7</sup>, G.C. Mattiucci<sup>8</sup>, M. Fiore<sup>9</sup>, P. Bonomo<sup>10</sup>, A. Bacigalupo<sup>11</sup>, R.M. Niespolo<sup>12</sup>, P. Gabriele<sup>13</sup>, N. Simoni<sup>14</sup>, R. Mazzarotto<sup>14</sup>, G. Macchia<sup>2</sup>  
<sup>1</sup>Radiation Oncology Center- University of Bologna, Department of Experimental- Diagnostic and Specialty Medicine - DIMES, Bologna, Italy; <sup>2</sup>Fondazione di Ricerca e Cura "Giovanni Paolo II", Radiotherapy Unit, Campobasso, Italy; <sup>3</sup>Fondazione di Ricerca e Cura "Giovanni Paolo II", Medical Physic Unit, Campobasso, Italy; <sup>4</sup>Radiosurgery Center Malzoni, Radiosurgery Center, Agropoli, Italy; <sup>5</sup>Ospedale Belcolle, Radiotherapy Unit, Viterbo, Italy; <sup>6</sup>Medical Faculty-University of Novi Sad, Institute of Oncology Vojvodina-Sremska Kamenica, Novi Sad, Serbia; <sup>7</sup>Ospedale Casa Sollievo della Sofferenza San Giovanni Rotondo, Radiotherapy Unit-, San Giovanni Rotondo FG, Italy; <sup>8</sup>Policlinico Universitario "A. Gemelli"- Università Cattolica del Sacro Cuore, Department of Radiotherapy, Rome, Italy; <sup>9</sup>Università Campus Biomedico, Department of Radiotherapy, Rome, Italy; <sup>10</sup>Azienda Ospedaliero Universitaria Careggi AOUC- Università di Firenze, Department of Radiotherapy, Firenze, Italy; <sup>11</sup>IRCCS AOU San Martino- IST, Department of Radiotherapy, Genova, Italy; <sup>12</sup>Azienda Ospedaliera San Gerardo, Radiotherapy Unit-, Monza MI, Italy; <sup>13</sup>Fondazione del Piemonte per l'Oncologia FPO- IRCCS Candiolo, Department of Radiotherapy, Torino, Italy; <sup>14</sup>University Hospital, Radiotherapy Unit, Verona, Italy

### Purpose or Objective

Treatment of locally advanced pancreatic cancer (LAPC) is controversial. SBRT is an emerging radiotherapy technique able to achieve high local control rates. We performed a case control study comparing outcome in terms of local control (LC), disease metastases-free survival (DMFS), and overall survival (OS) between two cohorts of patients treated with chemoradiation (CRT) +/- chemotherapy (CT) or SBRT +/- CT.

### Material and Methods

Patients (pts) treated with CRT +/- neoadjuvant CT, +/- adjuvant CT (control group: CG) were matched to pts treated with SBRT +/- neoadjuvant CT, +/- adjuvant CT (case group: SG) based on age ( $\leq$ / $>$  65years), tumor diameter (<3.0 cm; 3.0-3,9 cm; and  $\geq$  4.0 cm), clinical T stage, clinical N stage, neoadjuvant CT, adjuvant CT. Matching was performed without knowledge of outcomes. Median dose in pts treated with SBRT was 30.0 Gy (range: 18.0-35.0) and median dose in pts treated with EBRT was 50.4 Gy (range: 18.0-63.0). Survival curves were assessed

by Kaplan-Meier method and compared using longrank test.

### Results

Ninety-two LAPC patients were enrolled (CG/SG: 46/46 pts; M/F: 52/40; median age: 65.5 years, range: 36.0-89.0, median follow-up: 17.0 months, range: 3.0-70.0). At univariate analysis no significant differences between the two groups were recorded. Results in terms of OS, LC, DMFS are shown in the table.

	Groups	6 months (%)	12 months (%)	24 months (%)	Median (months)	p value
OS	CG	95.5	79.0	47.2	21	.702
	SG	91.5	82.8	33.1	19	
LC	CG	86.3	66.9	59.6	31	.271
	SG	93.2	75.8	53.5	NR*	
DMFS	CG	83.8	64.5	51.2	31	.084
	SG	87.0	53.9	16.9	14	

\*NR: not reached

### Conclusion

This case-control study shows that the two treatment approaches achieved comparable outcomes in patients with LAPC.

### EP-1425 MRI heterogeneity analysis for predicting response to neoadjuvant therapy in oesophageal cancer

K. Owczarczyk<sup>1</sup>, C. Kelly-Morland<sup>1</sup>, C. Yip<sup>2</sup>, M. Siddique<sup>1</sup>, N. Maisey<sup>3</sup>, A. Qureshi<sup>3</sup>, J. Gossage<sup>4</sup>, G. Cook<sup>1</sup>, V. Goh<sup>1</sup>  
<sup>1</sup>King's College London, Department of Cancer Imaging-Division of Imaging Sciences and Biomedical Engineering, London, United Kingdom ; <sup>2</sup>National Cancer Centre Singapore, Department of Oncology, Singapore, Singapore ; <sup>3</sup>Guy's and St.Thomas' Hospital NHS Foundation Trust, Department of Oncology, London, United Kingdom ; <sup>4</sup>Guy's and St.Thomas' Hospital NHS Foundation Trust, Department of Upper GI Surgery, London, United Kingdom

### Purpose or Objective

Response to neoadjuvant treatment has been shown to be a major predeterminant of survival in oesophageal cancer. The ability to predict response prior to oesophagectomy would allow for adaptive treatment approaches with potentially improved outcomes. We hypothesized that heterogeneity analysis of MRI may be predictive of response to neoadjuvant treatment.

### Material and Methods

Prospective IRB approved study of patients with oesophageal cancer undergoing neoadjuvant chemotherapy or chemoradiotherapy (CRT) followed by oesophagectomy. Three MRI scans including a 3D T2w ECG and respiratory-triggered sequence as well as Diffusion Weighted Imaging (DWI) sequence (b=0,100, 900) were carried out at baseline (T0), following first cycle of chemotherapy (or 10# of CRT, T1) and prior to surgery (T2).

VOIs were outlined in 3D on T2w sequences & ADC parametric maps, generating 6 VOIs per case (T2w and DWI at each timepoint). Heterogeneity analysis was carried out using in-house software. Highly correlated features ( $p > 0.8$ ) were excluded. Seven imaging features were analysed per case - Mean Intensity, Intensity SD, Intensity CoV, Entropy (Ent), Kurtosis (Kurt), Mean Fractal Lacunarity (MFL) and VOI volume (cm<sup>3</sup>). Primary outcome was Mandard tumour regression grade in the resected specimen (good response TRG1-2 (<10% residual tumour cells) vs no response TRG4-5 (>50%)).

Predictive value of imaging features was assessed in univariate analysis using false discovery rate (FDR) corrected cut-off of  $p < 0.05$  (Benjamini Hochberg correction for multiple testing). Huber method was used to minimise risk of model overfitting. Wilcoxon non-parametric test was used to compare values between subgroups. Selected features were assessed in a clinico-

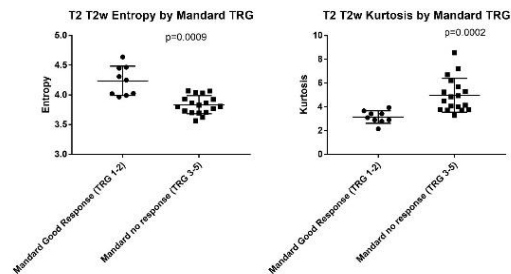
pathological multivariate model using Cox proportional hazard ratio.

### Results

Out of 41 patients recruited, 33 underwent surgery (27/33 male, median age 65±11, 30 adeno/ 3 SCC, 30 NACT/ 3CRT). 12/33 were good responders, 14/33 showed no response.

In univariate analysis, T2 T2w Kurt and T2 T2w Ent were predictive of good response (FDR  $p = 0.0001$  and  $0.0002$ , respectively), whilst T2 T2w MFL, T2 T2w Ent and T2 volume were predictive of no response (FDR  $p = 0.03$ ,  $0.04$ ,  $0.04$ , respectively). None of the DWI derived features met the predefined FDR cut-off.

T2 T2w Kurt was significantly lower whilst T2 T2w Ent was significantly higher in good responders ( $p = 0.0002$ ,  $0.0009$ , respectively). Spearman  $\rho$  between linear Mandard TRG and T2 T2w Kurt and Ent was  $0.55$  ( $p = 0.002$ ) and  $-0.62$  ( $p = 0.0005$ ), respectively. Dichotomised T2 T2w Kurt (>median vs  $\leq$  median) remained significantly predictive of good response in multivariate model including age, gender, cT (cT2 vs cT3-4), cN (cN0 vs cN+) and histopathology (SCC vs adeno) with an OR  $0.04$  ( $0.001-0.48$ ,  $p = 0.008$ )



### Conclusion

This prospective data shows that heterogeneity analysis has a role in predicting pathological response to treatment in oesophageal cancer and warrants investigation in a larger patient cohort.

### EP-1426 Postoperative Radiotherapy In Pancreatic Cancer Patients. A Single Institution Experience

M. Caroprese<sup>1</sup>, M. Tirozzi<sup>1</sup>, G. Porri<sup>1</sup>, I.R. Scognamiglio<sup>1</sup>, E. Toska<sup>1</sup>, L. Faraci<sup>1</sup>, A. Perillo<sup>1</sup>, F. Pati<sup>1</sup>, A. Farella<sup>1</sup>, R. Solla<sup>2</sup>, S. Clemente<sup>1</sup>, M. Consoni<sup>1</sup>, R. Pacelli<sup>1</sup>

<sup>1</sup>University "Federico II" School of Medicine, Department of Advanced Biomedical Sciences, Napoli, Italy ;

<sup>2</sup>National Research Council, Institute of Biostructures and Bioimages, Napoli, Italy

### Purpose or Objective

Pancreatic cancer is the fourth leading cause of cancer-related deaths worldwide. At present, the only chance for cure and prolonged survival is surgical resection with macroscopic tumor clearance. Even following potential curative resection more than 80% of the patients ultimately die of the disease due to local recurrence and/or distant metastasis. The high rate of local recurrence is predetermined by the microscopic frequently incomplete resections as a result of the anatomical location of the tumor and the growth pattern of pancreatic cancer cells. According to the Royal College of Pathologists (RCP), positive surgical margin status is defined as the microscopic presence of tumor cells within 1 mm of the resection margin. The aim of this study was to determine the impact of margin status on disease free survival (DFS) and overall survival (OS) in patients undergoing adjuvant radiotherapy.

### Material and Methods

Thirty-two consecutive patients treated by radiotherapy for M0 pancreatic adenocarcinoma at the Radiotherapy Department of the University "Federico II" (Naples, Italia)

between November 2011 and April 2018 were enrolled. Radiation treatment was delivered after surgery with or without neoadjuvant chemotherapy with doses ranging between 45 and 56Gy, concurrently with radiosensitizing chemotherapy. Clinical and pathological characteristics of all patients are reported in Table 1. Prognostic impact of surgical margin status were estimated by the Kaplan-Meier method. Log-rank test was used to compare survival between groups.

	PSM (n=11)	NSM (n=21)	p value	Overall (n=32)
Age	66 (48-78)	62 (51-74)	0.184	63 (48-78)
Sex				
Male	8 (72.7)	14 (66.7)	0.725	22 (68.8)
Female	3 (27.3)	7 (33.3)		10 (31.3)
Primary location				
Head/uncinated	6 (54.5)	16 (76.2)	0.246	22 (68.8)
Body/tail	5 (45.5)	4 (19.0)		9 (28.1)
Multiple	0 (0)	1 (4.8)		1 (3.1)
Largest tumor size (mm)	35 (20-90)	29 (15-52)	0.018	30 (15-90)
Stage				
1	1 (9.1)	1 (4.8)		2 (6.3)
2	9 (81.8)	13 (61.9)	0.312	22 (68.8)
3	1 (9.1)	7 (33.3)		8 (25.0)
Lymph nodes status				
Pos	6 (54.5)	18 (85.7)	0.053	24 (75.0)
Neg	5 (45.5)	3 (14.3)		8 (25.0)
RT technique				
3D-CRT	10 (90.9)	19 (90.5)	0.968	29 (90.6)
IMRT	1 (9.1)	2 (9.5)		3 (9.4)
Irradiation site				
T	1 (9.1)	2 (9.5)	0.968	3 (9.4)
T+N	10 (90.9)	19 (90.5)		29 (90.6)
RT dose				
45 Gy	4 (36.4)	9 (42.9)	0.369	13 (40.6)
50,4 Gy	6 (54.5)	12 (57.1)		18 (56.3)
54 Gy	1 (9.1)	0 (0)		1 (3.1)
Follow-up	35 (6-60)	27 (11-46)	0.244	28.5 (6-60)

Table 1 Clinical and pathological characteristics of all patients. PSM= positive surgical margins, NSM=negative surgical margins

## Results

Of 32 total patients, 11 (34.4%) had positive surgical margin (PSM) status and 21 (65.6%) negative surgical margin (NSM) status. The median follow-up period was 28.5 (IQR: 17.25-35.75) months; of the 20 (62.5%) observed deaths, all of these were directly tumor-related. Only six patients (18.8%) resulted free of recurrent disease. First recurrence was loco-regional for 9 patients (29.0%) and distant for 10 (32.3%) patients; 7 patients (22.6%) presented both. Median DFS among the PSM and NSM groups was 11 versus 13 months, respectively ( $P=.965$ ); no differences in OS were also seen between the two groups ( $P=.550$ ). The results are reported in Figure 1.

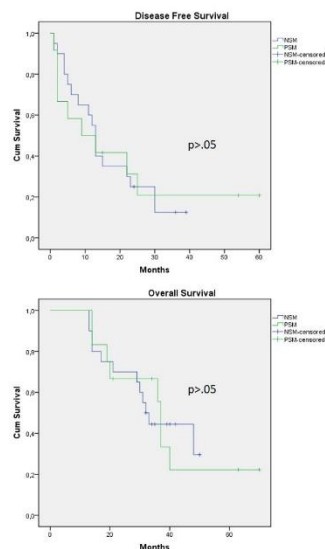


Figure1 Disease free survival (DFS) and Overall survival (OS). PSM= positive surgical margins, NSM=negative surgical margins.

## Conclusion

Although a positive surgical margin status may be suggestive of high local recurrence rate, in our small series of patients affected by locally advanced pancreatic cancer treated with adjuvant chemo-radiotherapy there were no DFS or OS difference between PSM and NSM groups.

## EP-1427 Prognostic role of neutrophil-to-lymphocytes ratio in pancreatic cancer

M. Caroprese<sup>1</sup>, I.R. Scognamiglio<sup>1</sup>, M. Tirozzi<sup>1</sup>, F. Piccolo<sup>1</sup>, E. Scipilliti<sup>1</sup>, A. Roscigno<sup>1</sup>, J. De Robbio<sup>1</sup>, M.V. Agbaje Olufemi<sup>1</sup>, M. Sorrentino<sup>1</sup>, A. Farella<sup>1</sup>, C. Oliviero<sup>1</sup>, M. Conson<sup>1</sup>, R. Pacelli<sup>1</sup>  
<sup>1</sup>University "Federico II" School of Medicine, Department of Advanced Biomedical Sciences, Napoli, Italy

## Purpose or Objective

Pancreatic cancer is one of the most aggressive malignancy with dismal 1- and 5-year survival rates of 21% and 3% respectively. Although a high neutrophil-to-lymphocyte ratio (NLR) has been reported to be a predictor of poor survival in patients with pancreatic cancers, its prognostic role in patients with locally advanced pancreatic cancer undergoing radiotherapy remains unclear. The aim of the present study was to determine the prognostic role of NLR in patients with locally advanced pancreatic cancer undergoing radiotherapy.

## Material and Methods

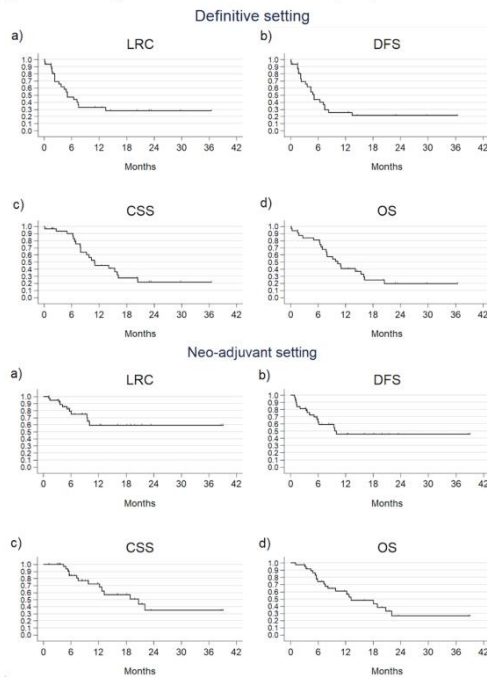
Fifty-three consecutive patients treated by radiotherapy for M0 pancreatic adenocarcinoma at the Radiotherapy Department of the University "Federico II" (Naples, Italia) between January 2011 and April 2018 were enrolled. Radiation treatment was delivered with a dose range between 45 and 56Gy, after a neoadjuvant chemotherapy or after neoadjuvant chemotherapy and surgery, concurrently with radiosensitizing chemotherapy. Two different contexts were defined with regard to target extension, namely tumor site only (T) irradiation, tumor site + prophylactic regional nodes irradiation (T+N). Univariate and multivariate analyses were performed to identify clinicopathological predictors of disease free survival and overall survival, including pre-radiotherapy NLR. NLR was defined as the absolute neutrophil count divided by absolute lymphocyte count. A low-NLR was defined as  $NLR < 1.2$  and a high-NLR was defined as  $NLR \geq 1.20$ .

## Results

Clinical and pathological characteristics of all patients are reported in Table 1. Median follow-up was 18 months. 47



Figure 1. Oncological results for definitive and pre-operative treatments



In DE cohort, 1-year LC (local control) and LRC (local-regional control) were 45.5% (SD:9.7;95%CI:26.3-62.9) and 32.58% (SD:8.9;95%CI:16.5-50.1). One-year DFS (disease-free survival), CSS (cancer-specific survival) and OS (overall survival) were 25.5% (SD:8.3;95%CI:11.3-42.4), 45.1% (SD:9.6;95%CI:26.1-62.4) and 40.6% (SD:8.9;95%CI:23.3-57.3), respectively. For patients who underwent a trimodality strategy, 1-year LC and LRC were 77.6% (SD:8.6;95%CI:55.2-89.8) and 59.4% (SD:10.1;95%CI:37.2-76.0), respectively. Finally, 1-year DFS, CSS and OS were 45.5% (SD:9.5;95%CI:26.5-62.7), 72.3% (SD:8.5;95%CI:51.7-85.3) and 60.7% (SD:8.6;95%CI:41.8-75.2).

#### Conclusion

Our retrospective clinical and dosimetric data show the feasibility of VMAT in the DE and PO treatment of oesophageal cancer patients for both SCC and adenocarcinoma histology, with a mild toxicity profile and robust dosimetric results for both target coverage and sparing of organs at risk.

#### EP-1429 IG-IMRT improves short-term survival for lymph node metastases from hepatocellular carcinoma

Z. Haige<sup>1,2</sup>, S. Jing<sup>1</sup>, C. Yixing<sup>1</sup>, Z. Zhaochong<sup>1</sup>  
<sup>1</sup>Zhongshan Hospital- Fudan University, Department of Radiation Oncology, Shanghai, China ; <sup>2</sup>Luoyang Central Hospital, Department of Radiation Oncology, Luoyang, China

#### Purpose or Objective

To evaluate the responses and toxicities in hepatocellular carcinoma (HCC) patients with abdominal lymph node metastasis (LNM) treated with either Image-guided Intensity-modulated radiotherapy (IG-IMRT) or non-IG-IMRT.

#### Material and Methods

We retrospectively reviewed 85 HCC patients with regional LNM treated with IG-IMRT or non-IG-IMRT (including IMRT and 3D-CRT) according to patients' intention at our institution between 2011 and 2016. They were identified as HCC by clinical diagnosis with LNM appeared synchronously or metachronously at the confirmation of HCC. The radiation dose to GTV arranged 44.3 to 75.9 Gy, which was limited by Organ At Risk (mainly limited by gastrointestinal tract). The tumor

responses, local control rate, overall survival and toxicities were evaluated.

#### Results

Mean dose of biological effective dose (BED) with  $\alpha/\beta = 10$  Gy delivered by IG-IMRT group was  $67.23 \pm 8.48$  Gy vs.  $63.43 \pm 5.01$  Gy ( $p = 0.008$ ) by non-IGRT group. The objective response rates (ORR) of IG-IMRT vs. non-IGRT was 95.3% vs. 80.9% ( $P = 0.085$ ). The actuarial local control rate of IG-IMRT vs. non-IGRT was 74% vs. 52.3% at one-year, and 69% vs. 47% at two-year. ( $p = 0.019$ ), which showed the advantage of IG-IMRT. Longer median overall survival was found in IG-IMRT group (15.3 months) than that in non-IGRT group (9.7 months), ( $p = 0.098$ ). One-year overall survival of IG-IMRT vs. non-IGRT was 69% vs. 38.1%, ( $P = 0.006$ ). However, two-year overall survival of them was 19.3% vs. 14.5% ( $p = 0.066$ ) with p-value was 0.098 which indicated no superiority of long-term survival of IG-IMRT. Number of lymph node  $\geq 2$ , previous treatment without surgery were negative independent prognostic factors, while  $BED_{10} \geq 65$  Gy was a protective factor. Toxicities were mild for both groups while IG-IMRT showed less late hepatic toxicity.

#### Conclusion

Dose delivered by IG-IMRT is slightly higher which appears to be more effective and shows a superiority of short-term survival and local control rate in HCC patients with LNM.

#### EP-1430 Can SBRT improve the prognosis of unresectable pancreatic cancer? Clinical results on 106 patients

T. Comito<sup>1</sup>, C. Franzese<sup>1</sup>, E. Clerici<sup>1</sup>, P. Navarria<sup>1</sup>, G.R. D'Agostino<sup>1</sup>, S. Carrara<sup>2</sup>, L. Rimassa<sup>3</sup>, S. Tomatis<sup>1</sup>, A. Zerbi<sup>4</sup>, M. Scorsetti<sup>1</sup>

<sup>1</sup>Humanitas Research Hospital, Radiotherapy and Radiosurgery, Rozzano Milan, Italy ; <sup>2</sup>Humanitas Research Hospital, Gastroenterology, Rozzano Milan, Italy ; <sup>3</sup>Humanitas Research Hospital, Oncology, Rozzano Milan, Italy ; <sup>4</sup>Humanitas Research Hospital, Pancreatic Surgery, Rozzano Milan, Italy

#### Purpose or Objective

Pancreatic cancer is characterized by a poor prognosis. Surgery is the gold standard of care, however more than 50% of patients are unresectable at the time of diagnosis. In patients with locally advanced pancreatic cancer (LAPC), the integration of chemotherapy (CT) and chemo-radiation treatment (CRT) is the current therapeutic option, associated with a significant toxicity rate and with a disappointing overall survival (OS). In the last years, the role of stereotactic body radiotherapy (SBRT) in the treatment of LAPC was investigated. Higher local control related to the high doses employed, short overall treatment time and sequential integration with systemic therapy, represent the crucial advantages of SBRT over conventional CRT. Objective of this study is to assess the efficacy of SBRT in patients with inoperable LAPC.

#### Material and Methods

Patients with unresectable LAPC with maximum tumor diameter  $\leq 5$ cm, without lymph node disease and without distant metastasis were treated with SBRT, after multidisciplinary board evaluation. Prescription dose was 45Gy in 6 fractions. Primary end-point was freedom from local progression (FFLP). Secondary end-points were overall survival (OS), progression-free survival (PFS) and toxicity. Local control (LC) was defined according to RECIST v1.1 criteria. Acute and late toxicity was scored according to the NCI Common Terminology Criteria for Adverse Events (CTCAE) v3.0.

#### Results

Between January 2011 and December 2017, 106 patients (49 male-57 female) with LAPC were treated with SBRT at Humanitas cancer Center. Median age was 68.5 years (range 41-88 years). 58 patients (55%) received CT before SBRT, for a median time of 5 months (range 3 - 10

months). Median follow-up was 86 months (range 2-88 months). FFLP was 83% and 67% at 1 and 2 years, respectively. At univariate ( $p < 0.03$ ) and multivariate analysis ( $p < 0.001$ ), lesion size was significant for LC. Median PFS was 11 months. Median OS from diagnosis was 17 month. CT administered before SBRT ( $p < 0.005$ ) and FFLP ( $p < 0.002$ ) were significantly correlated with OS. Grade 3 gastrointestinal toxicity was detected in 2% of patients.

#### Conclusion

SBRT is an effective and safe local therapy for selected patients with LAPC. Our results suggest that the stereotactic treatment may be a promising therapeutic option in the multi-modality treatment of these patients

#### EP-1431 Impaired health in long term survivors of esophageal cancer after neo-adjuvant chemoradiotherapy?

C. De Groot<sup>1</sup>, K. Muijs<sup>1</sup>, J. Plukker<sup>2</sup>, P. Van Luijk<sup>1</sup>, H. Langendijk<sup>1</sup>, J. Beukema<sup>1</sup>

<sup>1</sup>UMCG, Radiation Oncology, Groningen, The Netherlands ; <sup>2</sup>UMCG, Surgical Oncology, Groningen, The Netherlands

#### Purpose or Objective

Due to the clinical introduction of neo-adjuvant chemoradiotherapy (nCRT) prior to surgery, the number of long-term survivors of esophageal cancer (EC) is rising. Therefore, treatment-related toxicity, in particular cardiopulmonary toxicity, becomes increasingly important. The primary objective of this cross-sectional pilot study was to identify (subclinical) cardiopulmonary dysfunction in EC patients after nCRT followed by surgical resection as compared to surgery alone.

#### Material and Methods

EC survivors who were 5-15 years after curative resection with (n = 20) or without (n = 20) nCRT were enrolled. All patients underwent the following examinations; anamnesis (incl ACE-27), physical examination, quality of life (QoL) questionnaires, blood tests and a 6-minute walking test.

#### Results

Patient characteristics at baseline and at the time of the cross-sectional measurements are listed in *table 1*. Using the EORTC -C30, a trend towards impaired role functioning in the nCRT group was observed (89 v 95,  $p = 0.13$ ). Additionally, fatigue was more common after nCRT (14.9 v 9.2;  $p = 0.13$ ). Other domains, symptom scales and global QoL were similar in both groups. The 6-minute walking test showed reduced exercise tolerance in the nCRT group. In this group, 11 (55%) patients had poor scores (<80% of predicted; corrected for age, gender and BMI) compared to 5 (25%) in the surgery alone group ( $p = 0.07$ ). ACE-27 scores increased over time in both groups. Although statistically significance was not reached in this small cohort ( $p = 0.11$ ), the increase in ACE score was more pronounced in the nCRT group ( $\Delta$ ACE = 0.75) compared to those treated with surgery only ( $\Delta$ ACE = 0.30). Moreover, patients in the nCRT group were younger and had shorter (follow up) time to develop toxicity/comorbidity (average FU time: 88 v 126 months). Similar results were found for the cardiovascular subscale of the ACE-27, which showed again a marked increase after nCRT ( $\Delta$ ACE=0.80 v 0.35;  $p = 0.10$ ). This was in particular due to a higher incidence of de novo atrial fibrillation after nCRT (CTCAE v4.0  $\geq$  grade 2: 5 v 1 new cases,  $p = 0.08$ ).

Relatively high serum NT-proBNP levels were found in both groups (*table 1*). After excluding patients with known cardiovascular disease from the analysis, average NT-proBNP levels in the surgery alone group decreased to normal (115 ng/L) whereas levels in the nCRT group remained elevated (271 ng/L;  $p = 0.06$ ). Troponin-T levels are similar in both groups and all in the normal range.

Table 1: Patient characteristics

	Surgery (n = 20)	nCRT (n = 20)	
<b>General characteristics</b>			
<b>Sex</b>			P = 0.26
- Male	17 (85%)	14 (70%)	
- Female	3 (15%)	6 (30%)	
<b>Clinical T stage</b>			P < 0.01
- cT1	10 (50%)	0 (0%)	
- cT2	2 (10%)	6 (30%)	
- cT3	8 (40%)	14 (70%)	
<b>Clinical N stage</b>			P = 0.02
- cN0	14 (70%)	7 (35%)	
- cN1	6 (30%)	7 (35%)	
- cN2	0 (0%)	6 (30%)	
<b>Histology</b>			P = 0.71
- AC	15 (75%)	16 (80%)	
- SSC	5 (25%)	4 (20%)	
<b>Baseline (prior to nCRT and/or surgery)</b>			
<b>Age</b>	63.3 (SD 11.3)	60.0 (SD 7.6)	P = 0.29
<b>WHO PS</b>			P = 0.60
- 0	16 (80%)	17 (85%)	
- 1	3 (15%)	3 (15%)	
- 2	1 (5%)	0 (0%)	
<b>ACE-27<sup>1</sup></b>	0.60 (SD 0.75)	0.70 (SD 0.73)	P = 0.67
<b>ACE-27 CVD<sup>2</sup></b>	0.35 (SD 0.67)	0.35 (SD 0.67)	P = 1.00
<b>Coronary events</b>	2 (10%)	1 (5%)	P = 0.55
<b>At the time of cross-sectional measurements</b>			
<b>Age</b>	74.0 (SD 10.3)	67.8 (SD 7.6)	p = 0.04
<b>Months after surgery</b>	125.6 (SD 37.7)	88.3 (SD 22.1)	P < 0.01
<b>WHO PS</b>			P = 0.94
- 0	12 (60%)	11 (55%)	
- 1	6 (30%)	7 (35%)	
- 2	2 (10%)	2 (10%)	
<b>ACE-27<sup>1</sup></b>	0.90 (SD 1.00)	1.45 (SD 1.00)	P = 0.09
<b>ACE-27 CVD<sup>2</sup></b>	0.70 (SD 0.90)	1.15 (SD 1.04)	P = 0.15
<b>New atrial fibrillation</b>	1 (5%)	5 (25%)	P = 0.08
<b>New coronary events</b>	2 (10%)	1 (5%)	P = 0.55
<b>NT-ProBNP</b>	214.8 (SD 406.1)	267.0 (SD 305.4)	P = 0.66
<b>NT-proBNP excl CVD<sup>3</sup></b>	115.2 (SD 75.9)	270.8 (SD 313.8)	P = 0.06
<b>Troponin T</b>	13.9 (SD 8.6)	10.6 (SD 4.6)	P = 0.13

Abbreviations: AC = Adenocarcinoma; SCC = squamous cell carcinoma.

<sup>1</sup>Adult Comorbidity Evaluation Questionnaire. Scoring: 1=mild, 2=moderate, 3=severe.

<sup>2</sup>Sub score on cardiovascular disease section ACE-27.

<sup>3</sup>After exclusion of patients with known cardiac disease. Surgery n=15, nCRT n=18.

#### Conclusion

Despite younger age and shorter follow up, patients treated with neo-CRT showed more increase in (cardiac) comorbidity scores compared to patients who underwent surgery alone. In addition, their exercise tolerance seems to be worse as well. The results of this pilot study emphasizes the need for further research in larger cohorts of patients.

#### EP-1432 Re-irradiation of abdominal malignancies: toxicity, cumulative dose and outcome

L. Caravatta<sup>1</sup>, F. Fiorica<sup>2</sup>, F. Dionisi<sup>3</sup>, C. Rosa<sup>1</sup>, L. Boldrini<sup>4</sup>, M. Lupattelli<sup>5</sup>, D. Genovesi<sup>1</sup>, M. Massaccesi<sup>6</sup>  
<sup>1</sup>"SS Annunziata" Hospital- "G. D'Annunzio" University, Radiation Oncology Unit, Chieti, Italy ; <sup>2</sup>University Hospital Ferrara, Department of Radiation Oncology, Ferrara, Italy ; <sup>3</sup>Azienda Provinciale per i Servizi Sanitari- APSS, Proton Therapy Unit- Department of Oncology-, Trento, Italy ; <sup>4</sup>Fondazione Policlinico Universitario "A. Gemelli"- Catholic University of Sacred Heart, Radiology Department, Rome, Italy ; <sup>5</sup>University of Perugia and Perugia General Hospital, Radiation Oncology Section, Perugia, Italy ; <sup>6</sup>Fondazione Policlinico Universitario "A. Gemelli"- Catholic University of Sacred Heart, Department of Radiological- Radiotherapy and Hematology Sciences, Rome, Italy

#### Purpose or Objective

A systematic review about abdominal re-irradiation (Re-I) was performed, on behalf of the Association of Radiation Oncology (AIRO) study group for the re-irradiation, aiming to explore the toxicity, cumulative dose and outcome.

#### Material and Methods

A computerized search of the literature was performed by MEDLINE, EMBASE, OVID, and Cochrane database. The computer search was supplemented with hand searches of reference lists. Only studies analyzing reporting toxicity and/or safety as outcomes of patients re-treated where Re-I involved overlap with previous radiotherapy (RT) were taken into consideration. Retrospective and prospective studies with at least 10 patients were

included. To improve the comparability of the different Re-I regimens and to assess the relationship between RT dose and toxicity, when not reported in the study, equivalent dose in 2 Gy fractions was calculated according to the linear-quadratic model.

### Results

Nine studies met the inclusion criteria, published between 2002 and 2017. Only 2 were prospective trials. Overall, 203 patients were definitely re-irradiated within the abdomen. Patients presented recurrence of pancreatic (100 patients), liver (38 patients) and gastro-esophageal (14 patients) cancer. Median follow-up from Re-I ranged from 5.9 to 28 months. Previous RT was delivered with a median dose of 50.4 Gy (45 to 74.5 Gy) using conventional fractionation; in 1 study a stereotactic RT (SBRT) boost was delivered after conventional external beam RT. The mean time relapsed since previous RT ranged from 2 to 32 months (median time=18 months). Technique used for Re-I were SBRT (5 studies), intensity modulated RT (1 study), <sup>125</sup>I seed interstitial brachytherapy (1 study) and proton therapy (2 studies). Re-I prescription doses were variable (22.5 Gy in 3 fractions to 126,5 Gy with brachytherapy with <sup>125</sup>I). Regarding to toxicities, 29 episodes of G3 toxicity were reported: 15 episodes were acute (transient RILD, abdominal pain and bleeding, anorexia and fatigue), whereas 14 were late (RILD, bowel obstruction, gastric perforation). Relationship between cumulative dose and toxicities rate ( $\geq$ G3) is reported in Table 1. The 1-year overall survival rate was reported in 8 studies and resulted as 48.2% (95%CI:38.1-61%). The 1-year local recurrence free survival rate obtained from 7 studies was 70.7% (95% CI: 62.8-79.7%). Improvements in pain was evaluated in 5 studies, with 72.8% of patients experiencing pain relief.

Table 1: Relationship between cumulative dose for acute responding and for late responding tissue according to the linear-quadratic model and toxicities rate

Author et al.	Previous RT	EQD2 acute tissue and tumor (Gy)	EQD2 late tissue (Gy)	Cumulative acute dose (Gy)	Cumulative late dose (Gy)	Acute toxicities $\geq$ G3	Late toxicities $\geq$ G3
Daghighi et al. 2016	Previous RT	49.56 and 56 (SBRT)	48.38 and 52.8 (SBRT)	67.25(*) and 80.81	88.38 and 92.8 (*)	11% (3/27)	7% (2/27*)
	Re-I	31.25	40				
Haque et al. 2009	Previous RT	34.5 median dose	40.85 median dose	67.54	71.9	8% (1/13)	8% (the same pt)
	Re-I	33.04 median dose	31.05 median dose				
Huang et al. 2016	Previous RT	49.5 (no tox) and 52.5 (tox)	20.8 (no tox) and 20.1 (tox)	82.4 (no tox) and 95.1 (tox)	33.1 (no tox) and 50.3 (tox)	9.2% (4/36)	25% (9/36)
	Re-I	33.9 (no tox) and 40.6 (tox)	12.3 (no tox) and 10.2 (tox)				
Kooget al. 2017	Previous RT	49.56	48.38	80.81 and 129.48 (RS)	88.38 and 188.38 (RS)	8.7% (2/23)	-
	Re-I	31.25 and 79.92 (RS)	40 and 140 (RS)				
Yao et al. 2015	Previous RT	50.1	50.5	123.1	84.5	0	0
	Re-I	73	34				
Lomnicka et al. 2012	Previous RT	49.56	48.38	81.44	93.38	0	7.1% (2/28)
	Re-I	33.88	45				
Abuazam et al. 2012	Previous RT	48	48	156	138	0	0
	Re-I	88	90				
Boisard et al. 2017	Previous RT	49.56	48.38	108.96	107.78	20% (3/15)	0
	Re-I	59.4	59.4				
Fernandez et al. 2016	Previous RT	54	54	109.8	109.8	13% (2/14)	0
	Re-I	54	54				

RT: radiotherapy; Re-I: re-irradiation; EQD2: equivalent dose in 2 Gy fractions; SBRT: stereotactic radiation therapy; RS: radiosurgery; pt: patient \*previous SBRT

### Conclusion

Few studies, most of them retrospective, are actually available in the literature able to reach our requisites. Based on the results of our analysis, abdominal re-irradiation seems to be safe feasible in terms of severe toxicities with good local control and symptoms palliation. Prospective studies or large data collections seem to be necessary to define patients selection criteria to ensure maximal benefit of Re-I treatment approach.

### EP-1433 GTV contouring in hepatocellular carcinoma: a comparison between two imaging techniques

C. De la Pinta Alonso<sup>1</sup>, J.D. García<sup>2</sup>, D. Sevillano<sup>2</sup>, R. García<sup>3</sup>, M. Martín Martín<sup>1</sup>, M. Martín Sánchez<sup>1</sup>, T. Muñoz<sup>1</sup>, E. Fernández-Lizarbe<sup>1</sup>, R. Hernández<sup>1</sup>, J.A. Domínguez<sup>1</sup>, C. Vallejo<sup>1</sup>, S. Sancho<sup>1</sup>

<sup>1</sup>Hospital Ramon y Cajal, Radiation Oncology, Madrid, Spain ; <sup>2</sup>Hospital Ramon y Cajal, Medical Physics, Madrid, Spain ; <sup>3</sup>Hospital Ramon y Cajal, Radiology Department, Madrid, Spain

### Purpose or Objective

Definition of gross tumor volume (GTV) in hepatocellular carcinoma (HCC) requires dedicated imaging in multiple contrast medium phases. MRI has an important role in

evaluation of HCC. The aim of this study was to evaluate the interobserver agreement in GTV of HCC in a multicenter panel and compare MRI and CT in GTV delineation.

### Material and Methods

After the institutional review boards approved the study we analyzed anonymous, multiphase-planning CT, and MRI obtained from five patients with HCC. Eight radiation oncologist in our center using CT and MRI to delineate GTVs of hepatocellular carcinomas. Liver locations were segments II, IV, V, VI and VIII. The cases show different difficulty: low acquisition contrast, previously treated with transarterial-chemoembolization, arterial thrombosis, or inhomogeneous liver parenchyma due to cirrhosis. In both CT and MRI, the GTV volumes and distance between the centers of mass (dCOM) were compared. The index of agreement was evaluated according to Landis and Koch.

### Results

The GTV volume as defined on CT was in all cases larger or at least as large as the GTV volume on PET. The median GTV volume on MRI was 2 mL (0,4-85,6 mL), compared to 3,55mL on CT (0,2-64 mL) (p=0.09). Variance between observers in CT was minor than MRI (259,3 vs 332,4). The index of agreement was low (0,029) between CT and MRI in all patients.

### Conclusion

In cases with well-defined tumor CT is more easy and reproducible. In cases with no defined tumor in CT we need other tools as MRI. The interobserver variability in target delineation of HCC in this study was noteworthy.

### EP-1434 Neoadjuvant chemoradiotherapy in patients with esophageal or esophageal gastric junction cancer

N. Slim<sup>1</sup>, R. Tummineri<sup>1</sup>, P. Parise<sup>2</sup>, E. Mazza<sup>3</sup>, L. Albarello<sup>4</sup>, F. Puccetti<sup>2</sup>, A.M. Deli<sup>1</sup>, E. Incerti<sup>5</sup>, M. Azizi<sup>1</sup>, I. Dell'oca<sup>6</sup>, A. Cossu<sup>2</sup>, M. Reni<sup>3</sup>, R. Rosati<sup>2</sup>, P. Passoni<sup>1</sup>, N. Di Muzio<sup>1</sup>

<sup>1</sup>San Raffaele Scientific Institute- Milano- Italy, Radiation Oncology, Milan, Italy ; <sup>2</sup>San Raffaele Scientific Institute- Milano- Italy, Surgery, Milan, Italy ; <sup>3</sup>San Raffaele Scientific Institute- Milano- Italy, Clinical Oncology, Milan, Italy ; <sup>4</sup>San Raffaele Scientific Institute- Milano- Italy, Pathological Anatomy, Milan, Italy ; <sup>5</sup>San Raffaele Scientific Institute- Milano- Italy, Nuclear Medicine, Milan, Italy ; <sup>6</sup>San Raffaele Scientific Institute- Milano- Italy, Radiation Oncology, Milano, Italy

### Purpose or Objective

to report our experience in patients (pts) with esophageal (EC) or esophageal gastric junction (EGJ) cancer treated with neoadjuvant chemoradiotherapy IG-IMRT PET based.

### Material and Methods

from April 2014 to April 2018, 56 pts (m: 43, f: 13), with histologically proven EC or EGJ were treated according to CROSS study. Median age at diagnosis: 56 years (28-80), median KPS: 90 (80-100). Twenty-eight pts had adenocarcinoma (50%), 27 pts had squamous cell carcinoma (48.2%), 1 pt had adeno-squamous carcinoma (1.7%). All pts underwent c-e CT and PET simulation, repeated for restaging. Radiotherapy (RT) consisted in 41.4 Gy in 23 fractions combined to chemotherapy (ChT) with carboplatin and paclitaxel.

### Results

clinical stage was: T1: 1pt (2%), T2: 14 pts (25%), T3: 38 pts (68%), T4: 3 pts (5%), N0: 11 pts (20%), N+: 45 pts (80%). The site of tumor was proximal/middle third in 4 pts (8%), middle/middle-distal third in 34 pts (60%), distal third/distal-EGJ/ EGJ in 18 pts (32%). Median tumor length was 4 cm (0.8-15 cm). RT was delivered by Tomotherapy in 37 pts (66%) and by VMAT in 19 pts (34%). All pts completed RT. Median cycles of ChT was 5 (2-6 cycles), 70% pts received a full dose of ChT. G3 acute haemathological toxicity was: neutropenia in 3.5 % (2pts), lymphopenia in 67.8% (38 pts), anemia in 1.7% (1pt). G3

gastrointestinal toxicity occurred in 14.2% (8 pts). Three pts (5.3%) had bacterial pneumonia (1 pt G5). Responses: 55/56 pts were available (1 pt early lost). Median time to restaging was 42 days (14-87 d). CT/PET showed local RP in 27 pts, SD 9 pts, RC 18 pts, PD in 1pt. Median time from CT/RT to surgery was 61 days (15-148). Forty-three pts (75%) underwent surgery, 13 excluded (7 for PD, 3 for worsening clinical condition, 1 died, 1 lost, 1 pt had cCR). One pt underwent urgent surgery 15 days after CT/RT because of aorto-esophageal fistula. Post-surgery stage was T0: 7pts (16%), T1: 9 pts (22%), T2: 12 pts (28%), T3: 14 pts (32%), T4: 1 pt (2%); N0: 25 pts (58%), N+: 18 pts (42%). Forty-one/ 43 pts (95.3%) had R0. Mandard TRG was: TRG1: 7 pts (16.5%), TRG2: 8 pts (18.5%), TRG3: 22 pts (51%), TRG4: 6 pts (14%). At a median follow up of 17.4 months (4.1-49.4 m): 25/43 pts (58%) are free from disease, and 18/43 pts (42%) had a progression disease (2 of them had a local relapse concomitant to distant progression). Median time to progression was 20 months (1.5-96.9 m). Median OS of all pts was 17.4 months (3-49.4 m).

#### Conclusion

Our data seems to be comparable to CROSS data in term of R0 and toxicity profile. In patients treated with IG-IMRT and chemotherapy, lymphopenia was the major cause of not optimal tolerability of treatment and could explain the onset of pneumonia and the difference between TRG responses.

#### EP-1435 Impact of diabetes on outcome and toxicity of chemoradiation for esophageal squamous cell carcinoma

D. Bierbaumer<sup>1</sup>, S. Muench<sup>1</sup>, B. Haller<sup>2</sup>, D. Habermehl<sup>1</sup>, P.T. Pfluger<sup>3</sup>, K. Stemmer<sup>3</sup>, S.E. Combs<sup>1</sup>

<sup>1</sup>Klinikum rechts der Isar- Technical University Munich- Ismaninger Str. 22, Department of Radiation Oncology, 81675 Munich, Germany ; <sup>2</sup>Klinikum rechts der Isar- Technical University Munich- Grillparzerstr. 18, Institute of Medical Informatics- Statistics and Epidemiology- Medical School, 81675 Munich, Germany ; <sup>3</sup>Helmholtz Zentrum München- Ingolstädter Landstraße 1, Insitue for Diabetes and Obesity, 85764 Neuherberg, Germany

#### Purpose or Objective

For patients with locally advanced squamous cell carcinoma of the esophagus (SCC), international guidelines recommend neoadjuvant chemoradiation (nCRT) with subsequent surgery or definite chemoradiation (dCRT) for patients unsuitable for surgery. Until now, there are conflicting data regarding the impact of diabetes on the effectiveness and toxicity of chemoradiation in these patients. Aim of this study was to compare oncologic outcome and toxicity between patients with and without diabetes mellitus type 2 (DTM2) undergoing nCRT or dCRT for locally advanced SCC.

#### Material and Methods

In total, 108 patients with locally advanced SCC were included in this analysis. Within this cohort, we identified 25 patients with DMT2 with a median haemoglobin A1c (HbA1c) of 6.7%. Baseline and tumor characteristics, oncologic outcome and toxicity of these patients were compared to 83 patients without diabetes. For the analysis of toxicity, patients were stratified by therapy.

#### Results

Patients with DTM2 were had a significantly higher body mass index (BMI) than patients without DTM2 (median BMI 27.2 vs. 22.7 Kg/m<sup>2</sup>, p=0.001). However, no further differences regarding baseline and tumor characteristics were seen between both patient groups. In addition, there was no significant difference in terms of progression-free survival (median PFS 14.0 months (DTM2) vs 13.9 months (no DTM2), p=0.147). Concerning OS, there was a trend towards an increased OS in patients without DTM2 (median OS 23.3 months (DTM2) vs. 25.6 months (no DTM2), p=0.095). However, within a multivariable Cox regression

model, diabetes did not independently affect OS. After nCRT and surgery 25% (no DTM2) and 38% (DTM2) of patients had a pathologic complete tumor response (p=0.721). When stratifying patients by therapy, higher rates of anemia were seen in patients with DTM2 after nCRT (≥II° 60% vs. 34%, p=0.0001). However, this difference was not confirmed in patients undergoing nCRT. In addition, no significant differences were seen for the rates of leukopenia and thrombocytopenia between both groups.

#### Conclusion

While there was a small trend towards an increased OS in patients without DTM2, DTM2 did not affect PFS or histopathologic tumor response in patients undergoing neoadjuvant or definite chemoradiation for esophageal squamous cell carcinoma. However, higher rates of anemia were seen in diabetic patients undergoing nCRT.

#### EP-1436 SBRT for large hepatocellular cancer unsuitable for other therapies: Results from a clinical audit

K. George<sup>1</sup>, S. Chopra<sup>1</sup>, R. Engineer<sup>1</sup>, K. Rajamanickam<sup>1</sup>, S. Mehanery<sup>2</sup>, K. Joshi<sup>2</sup>, J. Swamidas<sup>2</sup>, S. Patkar<sup>3</sup>, P. Patil<sup>4</sup>, V. Ostwal<sup>5</sup>, S. Mehta<sup>4</sup>, M. Goel<sup>3</sup>

<sup>1</sup>Tata Memorial Hospital, Radiation Oncology, Mumbai, India ; <sup>2</sup>Tata Memorial Hospital, Radiation Physics, Mumbai, India ; <sup>3</sup>Tata Memorial Hospital, Surgical Oncology, Mumbai, India ; <sup>4</sup>Tata Memorial Hospital, Gastroenterology- Department of digestive diseases and clinical nutrition, Mumbai, India ; <sup>5</sup>Tata Memorial Hospital, Medical Oncology, Mumbai, India

#### Purpose or Objective

To evaluate the outcomes of liver stereotactic radiotherapy (SBRT) in the treatment of large hepatocellular carcinomas (HCC) that are unsuitable for, or refractory to prior liver-directed therapies.

#### Material and Methods

Between March 2015 and June 2018, patients with primary HCCs refractory or progressive to or unsuitable for treatment with loco-regional therapies were treated with SBRT. Only patients of Child status A5-B7 and with adequate normal liver reserve of 700 cc or higher were eligible. SBRT was delivered using IMRT or VMAT using video bio-feedback based deep inspiration breath-hold technique to a total dose of 25-54 Gy in 5-6 fractions. Overall survival (OS) and progression free survival (PFS) were determined by Kaplan-Meier analysis. In-field, out-of field recurrences and toxicities were also assessed. Univariate and multivariate analysis was performed to assess impact of various prognostic factors on outcome.

#### Results

Twenty one patients with large HCCs were treated. The median tumour diameter was 9.6 cm (5-21) and median GTV volume was 350 cc (32.9-2541.5 cc). Overall, 57.1 % patients were BCLC B and 42.9 % patients were BCLC C. Majority of the patients (80.9%) had some form of previous therapy (TACE, Sorafenib, RFA, PVE). The median SBRT dose prescription was 42Gy/6 fractions (24-54 Gy). The median normal liver volume was 1080 cc (423-1979 cc) and median normal liver dose was 15.3 Gy. At a median follow up of 9 months (1-26 mths), only 9.5% patients (n=2) had in-field tumour progression, 14.3% (n=3) had out of field new lesions and 33.3% (n=7) had extra-hepatic distant failure. The 1 year and 2 year local control rate was 88% and 43% respectively. The median overall survival for the entire cohort was 13 months (3-36) respectively. The 1- and 2 - year overall survival rates were 51% and 15% respectively. Overall rate of grade ≥ III toxicity attributable to SBRT was 14%. Patients with Child A 5 liver function status had a better overall survival (21 months) than Child A 6 and Child B7 patients (11 months and 8 months respectively) [p value = 0.01]. BCLC class B patients had a better overall survival (17 months) than BCLC C (8 months), however this was not significant [p

value = 0.184]. Also, tumours with GTV < 350 cc volumes had a better overall survival (24 months) compared to GTV of greater than 350 cc (8 months) [p value = 0.004]. On multivariate analysis tumour volume >350 cc remained the only predictor for adverse OS (p=0.005).

#### Conclusion

This study showed that SBRT can be used safely and effectively to treat large HCCs with or without prior loco-regional therapies, resulting in good local control and survival with acceptable toxicity.

#### EP-1437 The prognostic significance of neutrophil / lymphocyte ratio for SBRT of cholangiocellular carcinoma

N. Bartl<sup>1</sup>, S. Adebahr<sup>1</sup>, S. Kirste<sup>1</sup>, I. Popp<sup>1</sup>, H. Schäfer<sup>1</sup>, A. Grosu<sup>1</sup>, T.B.B. Brunner<sup>1</sup>, E. Gkika<sup>1</sup>

<sup>1</sup>Medical Center- Faculty of Medicine- University of Freiburg- German Cancer Consortium DKTK Partner Site Freiburg- German Cancer Research Center DKFZ- Heidelberg- Germany, Department of Radiation Oncology, Freiburg, Germany

#### Purpose or Objective

In this analysis, we evaluated the prognostic significance of the neutrophil / lymphocyte ratio (NLR) in patients treated with stereotactic body radiation therapy (SBRT) for cholangiocellular carcinomas.

#### Material and Methods

Consecutive patients (n = 26) with histologically confirmed cholangiocellular carcinoma who were treated with SBRT between 2007 and 2017 are included in this analysis. The majority of patients were treated for local recurrence after primary therapy or as primary therapy because there was no operative treatment option. Patients received a median total dose of 50 (range 21-66) Gy in 3-12 fractions.

#### Results

Median survival was 14 months with overall survival (OS) 1 year after SBRT of 61% with median progression-free survival (PFS) at 13 months and 51% at 1 year. The local control was 72% after 1 year. The median NLR was 3 (range 2-10) with a median CRP of 15 (3-96) mg / L with a median bilirubin of 1 (1-22) mg / dL and a median LDH of 233 (156-462) U / l. The OS did not correlate significantly with the NLR (HR 1.231, 95% CI 0.992-1.572, p = 0.059) neither was it correlated with NLR above the median (18 vs 14 months, p = 0.34). Furthermore, no correlation could be shown between CRP, LDH or bilirubin with overall Survival.

#### Conclusion

In this analysis, no correlation could be demonstrated between NLR and survival in patients with cholangiocellular carcinoma treated with SBRT.

#### EP-1438 Safety and tolerability of liver re-irradiation using high dose SBRT

D. Gabrys<sup>1</sup>, R. Kulik<sup>2</sup>, L. Dolla<sup>2</sup>, K. Trela-Janus<sup>1</sup>, A. Roch-Zniszczol<sup>1</sup>, S. Blamek<sup>1</sup>

<sup>1</sup>Maria Skłodowska-Curie Memorial Cancer Center and Institute of Oncology, Radiotherapy Department, Gliwice, Poland ; <sup>2</sup>Maria Skłodowska-Curie Memorial Cancer Center and Institute of Oncology, Department of Radiotherapy and Brachytherapy Planning, Gliwice, Poland

#### Purpose or Objective

The liver can tolerate a high dose of radiation if a sufficient volume of healthy liver tissue is spared. In the current paper we examined the safety and tolerability of liver reirradiation and dose volume histograms (DVH) of combined treatment plans.

#### Material and Methods

From patients who were treated with at least twice SBRT irradiation to the liver we choose 23 patients treated with high dose liver irradiation. The patients underwent retreatment for a primary (one patient with HCC) or metastatic recurrent or new liver tumour. With the use of

Velocity, a treatment planning evaluation system, we integrated imaging scans and treatments information from particular patient. Therefore, combined dose was associated with images for review of treatment plans using isodose curves and DVH. Furthermore we analysed blood parameters and patient performance status.

#### Results

Several fractionation schemes were used, for primary therapy of 12-15 Gy to the total dose 36-48 Gy, for second course of irradiation of 10-15 to the total dose 30-48, third (8 pts) of 3-15 Gy to the total dose 15-50. Median total dose was 90 Gy (range 72-209). Median highest total radiation dose to one GTV volume was 48 Gy (range 36-95).

Stereotactic radiotherapy is a good local therapy for liver tumours since in majority of cases (28 GTV) first liver re-irradiation was administered to previously non-irradiated area and only in 6 GTV to previously treated volume. Median interval from initial RT to first retreatment was 8.5 months (range 3.4-50.8). Patients who underwent third radiotherapy were irradiated for recurrent tumour after first treatment (4 GTV) and after second course (4 GTV), but also 3 patients underwent radiotherapy to previously not irradiated volume. Median time from first radiotherapy to last visit was 19.5 months (range 3.5-60). We did not notice significant decrease in mean liver volume which was 1516 cm<sup>3</sup> (range 947-2875) at the time of first radiotherapy and 1458 cm<sup>3</sup> (range 1047-2673) at last treatment, although it was irradiated with high doses. Median dose to the 700 cm<sup>3</sup> of functional liver was 16.8 Gy (range 3.7-33.7). The cumulative mean dose to the liver was 20.2 Gy (range 10.2-32.7). mean volume receiving 10 Gy was 61.5 % (range 26-80.2), and 21 Gy was 36.3 % (range 13.5-54.9). High doses used in our patients did not translate into significant liver dysfunction. Grade 1 increase in the level of AST was found in 5 patients, and only in one patients grade 2. Grade 1 ALT increase was found in 1 patients, and single patients experienced G1, and G2 increase of bilirubin level. The elevation of liver enzymes was related to the progression of the disease within and outside the liver.

#### Conclusion

High dose re-irradiation with SBRT to the liver tumors is a safe and tolerable option that allows prolongation of survival with advanced liver disease. Prospective studies are needed to establish accurate dose constraints and treatment guidelines.

#### EP-1439 The role of FDG PET / CT in SBRT of primary tumors in the upper abdomen

N. Bartl<sup>1</sup>, S. Adebahr<sup>1</sup>, S. Kirste<sup>1</sup>, I. Popp<sup>1</sup>, H. Schäfer<sup>1</sup>, A. Grosu<sup>1</sup>, T.B. Brunner<sup>1</sup>, E. Gkika<sup>1</sup>

<sup>1</sup>Medical Center- Faculty of Medicine- University of Freiburg- German Cancer Consortium DKTK Partner Site Freiburg- German Cancer Research Center DKFZ- Heidelberg- Germany, Department of Radiation Oncology, Freiburg, Germany

#### Purpose or Objective

In this analysis, we evaluated the role of FDG PET / CT in the planning of stereotactic body radiation therapy (SBRT) of primary tumors in the upper abdomen (pancreatic carcinoma, cholangiocellular carcinoma, hepatocellular carcinoma).

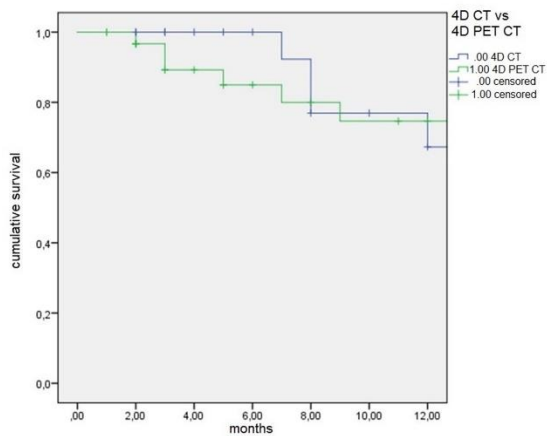
#### Material and Methods

Consecutive patients (n = 101) who were treated with SBRT for upper abdominal carcinoma [pancreas n = 17, cholangiocellular carcinoma (CCC), n = 37, hepatocellular carcinoma (HCC), n = 48] were included in this analysis. In total, 42 patients (41%) had FDG PET / CT or 4D FDG PET / CT available for defining the target volume and 59 patients (59%) had no FDG PET / CT.

#### Results

The local control (LC) was 75% for all treatments after 1 year. In the patients who had FDG PET / CT, the LC was

75% at 1 year and at 73% ( $P = 0.74$ ) in patients without FDG PET / CT. Overall survival was median at 13 months (95% CI 8,663-17,337) for the entire cohort and at 10 months for those without FDG-PET / CT versus 14 months for FDG-PET / CT, with no statistical relevance ( $p = 0.18$ ). For the CCC, the LC was 90% for the FDG-PET / CT ( $n = 20$ ) patients at 1 year and 76% for the FDG-PET / CT ( $n = 17$ ) patients ( $p = 0.4$ ). For pancreatic carcinoma, LC was 60% at 1 year in both groups (with FDG-PET / CT,  $n = 12$ , and without FDG-PET / CT,  $n = 5$ ), and LC was at 1 year for HCCs 75% in the group with FDG-PET / CT ( $n = 10$ ) and 82% in the group without FDG-PET / CT ( $n = 32$ ). FDG PET / CT did not affect survival in any of the subgroups. In Klatskin tumors and in pancreatic carcinomas, however, local congestion and inflammation revealed false positive findings.



### Conclusion

The FDG-PET / CT seems to play a role in the definition of the target volume for the CCCs in contrast to the HCCs (LC after 1 year 90% vs 76%). For pancreatic carcinoma, it is rather unclear because of the small number of patients who did not have FDG PET / CT at the time of the target volume definition. Furthermore, it has to be taken into account that Klatskin's tumors and pancreatic carcinomas may be falsely positive due to local congestion and Inflammation.

### EP-1440 Early and late toxicity of hypofractionated stereotactic radiotherapy in hepatic tumors

M. Le Bon<sup>1</sup>, B. Celine<sup>2</sup>, K. Fabrice<sup>3</sup>

<sup>1</sup>Centre Léon Bérard, Radiothérapie, Lyon, France ;

<sup>2</sup>Centre Jean Perrin, Radiothérapie, Clermont-Ferrand, France ;

<sup>3</sup>Centre Jean Perrin, Physique médicale, Clermont-Ferrand, France

### Purpose or Objective

To evaluate the outcomes of stereotactic radiation therapy for primary and secondary liver tumors in terms of efficacy and safety.

### Material and Methods

Between December 2013 and June 2016, 25 patients were included. Treatment was performed on a linear accelerator Novalis TX<sup>®</sup>. The prescription dose was 42 to 60 Gy in 3 to 5 fractions. Local control at 1 year was evaluated with mRECIST and RECIST criteria. Acute and late toxicity were evaluated with CTCAE v4.0 criteria.

### Results

Median follow-up was 10.5 months. Treatment tolerance was good with few side effect  $\geq 3$ , no acute toxicity and only one late toxicity.

We have highlighted that hepatic artery hemorrhage was associated with the presence of a biliary prosthesis in contact with the artery ( $p = 0.006$ ) and in the irradiation

field. There was no correlation with the dose delivered to the artery and hepatic artery hemorrhage.

Univariate analysis of predictive factor of late toxicity after stereotactic body radiotherapy in hepatic tumors in 25 patients

late toxicity	Gr 0-1	Gr 2-3-4	p-value
Sex (H/F)	73,7%	75%	$p=0,68$
Age (average, year)	70,6	61,6	$p=0,05$
OMS			$p=0,37$
0	10	5	
1	7	1	
2	2	2	
Larger diameter (average, cm)	27,6	38,2	$p=0,05$
GTV Volume (average, cm <sup>3</sup> )	32,3	49,6	$p>0,05$
PTV Volume (average, cm <sup>3</sup> )	143,5	169,9	$p>0,05$
EQD2 <sub>100</sub> (average, Gy)	68,3	78,4	$p>0,05$
Number of fractions (average)	4,5	4,6	$p>0,05$
Vrs 18 Gy/3F (average, mL)	1083,0	1096,5	$p=0,96$
Vrs 15 Gy/5F (average, mL)	1163,5	1177,0	$p=0,91$
V21 Gy / foie (average, mL)	281,1	398,9	$p=0,24$
Average dose to Liver-GTV (average, Gy)	10,1	10,9	$p>0,05$
Maximum dose to great vessels (average, Gy)	33,3	38,9	$p>0,05$
Ethical marker without / with	RR 1 [0,3-2,9]		$p=0,62$
Azotherapy/IMRT	RR 1,1 [0,4-3,4]		$p=0,61$
Prosthesis yes/no	all toxicities		$p=0,54$
	RR 1,9 [0,5-7,2]		
	hemorrhage		$p=0,006$
	RR		

M : man, F : female, EQD2<sub>100</sub>: biological equivalent dose at 2 Gy per fraction with an  $\alpha/\beta$  at 1 for the tumor.

GTV : Gross Tumor Volume, PTV : Planning Target Volume, Vrs 18 Gy/3F : volume of healthy liver receiving

18 Gy for treatments in 3 fractions, Vrs 15 Gy/5F : volume of healthy liver receiving 15 Gy for treatments in 5

fractions, V21 Gy : volume of liver receiving 21 Gy, Average dose to Liver-GTV : average dose received by the

healthy liver, RR : relative risk.

### Conclusion

Stereotactic radiation therapy for liver tumors allow a good local control with poor secondary effects. Be careful with patients with biliary prostheses in the vicinity of the target volume because there is a risk of hemorrhage of the hepatic artery in contact with the prosthesis.

### EP-1441 Chemoradiotherapy with weekly Carboplatin and Paclitaxel in elderly patients with oesophageal cancer

S. Pan<sup>1</sup>, M. Abraham<sup>2</sup>, L. Bhatt<sup>1</sup>, H. Sheikh<sup>1</sup>, G. Radhakrishna<sup>1</sup>

<sup>1</sup>The Christie NHS Foundation Trust, Clinical Oncology,

Manchester, United Kingdom ;

<sup>2</sup>The Christie NHS Foundation Trust, Dietetics, Manchester, United Kingdom

### Purpose or Objective

Definitive chemoradiation for oesophageal cancer preferentially utilises cisplatin and a fluoropyrimidine chemotherapy concurrent with 50Gy in 25 fractions of radiotherapy. However, this regimen can be challenging to deliver in the elderly or frail population. A phase II trial of concurrent chemoradiotherapy with weekly carboplatin and paclitaxel for advanced oesophageal cancer has shown comparable outcomes.

We report a single institution retrospective series utilising concurrent radiotherapy 50Gy in 25 fractions with weekly carboplatin and paclitaxel in the elderly population.

### Material and Methods

All patients of 70 years and above treated with concurrent chemoradiation with weekly carboplatin and paclitaxel from January 2016 to April 2018 were included in this retrospective analysis. Demographics and clinical information were obtained from the electronic system. Radiation was delivered using IMRT (intensity modulated radiation therapy) technique with a total dose of 50Gy in 25 fractions. Patients received weekly

concurrent paclitaxel (50mg/m<sup>2</sup>) and carboplatin (area under the curve, AUC 2). All patients had image-guidance using cone beam CT as per NRG guidelines.

#### Results

There were a total of 19 patients with a median age of 77 (range 70 -85). Sixty-eight percent (68%) of patients were male, 89% had performance status of 0-1 and 79% had an adenocarcinoma primary.

The median overall survival has not been reached. One year survival rate is 83%. Median time to clinical progression is 13 months (range 3 - 21). All patients had stable or improvement in their swallowing function following treatment.

A total of 17 patients (89%) completed 4 or more cycles of weekly chemotherapy. Reasons for early discontinuation of chemotherapy include Grade 2 neutropenia, Grade 2 thrombocytopenia and intercurrent infection. All 19 patients completed the course of 25 fractions of radiotherapy.

There was no Grade 3 or 4 toxicities. Grade 2 oesophagitis occurred in 7 patients (37%). Seven patients had prophylactic feeding tube inserted, which were removed within 3 months of treatment, apart from two patients. Of the other 12 patients, none required feeding tube insertion. Only 6 (32%) patients lost 5-10% of their baseline weight.

Sixteen patients had their initial three month follow-up with restaging CT scan of thorax, abdomen and pelvis, and endoscopic assessment to evaluate the disease response. The remaining three opted to have only clinical follow-up. Of the sixteen, 12 patients (75%) had biopsy confirmation of no residual disease present. The remaining four patients had persistent disease but no visceral metastatic disease at three months, apart from one patient who had new supraclavicular and paratracheal lymph node.

#### Conclusion

This retrospective study indicates that weekly concurrent regime is well tolerated, and may be considered for elderly patients. Further study into the efficacy of the regimen including the utility of induction Carboplatin and Paclitaxel is warranted.

#### EP-1442 Clinical and pathological response after neoadjuvant/radical CH-SBRT for pancreatic adenocarcinoma

X. Chen<sup>1</sup>, E. Sanchez<sup>1</sup>, M. Lopez<sup>1</sup>, O. Hernando<sup>1</sup>, A. Montero<sup>1</sup>, J. Garcia<sup>2</sup>, M.A. De la Casa<sup>2</sup>, M. Garcia Aranda<sup>1</sup>, R. Ciervide<sup>1</sup>, J. Valero<sup>1</sup>, J. Palma<sup>1</sup>, R. Alonso<sup>1</sup>, J.M. Perez<sup>2</sup>, D. Zucca<sup>2</sup>, L. Alonso<sup>2</sup>, P. Garcia de Acilu<sup>2</sup>, J. Marti<sup>2</sup>, P. Fernandez Leton<sup>2</sup>, C. Rubio<sup>1</sup>

<sup>1</sup>University Hospitals HM Sanchinarro - Puerta del Sur, Radiation Oncology, Madrid, Spain ; <sup>2</sup>University Hospitals HM Sanchinarro - Puerta del Sur, Medical Physics, Madrid, Spain

#### Purpose or Objective

Pancreatic adenocarcinoma (PA) remains one of the most lethal malignancies. Surgery is the only curative treatment. Chemotherapy (CH), radiotherapy or both are now being studied as neoadjuvant approaches. We are going to review feasibility and single centre experience with stereotactic body radiation therapy (SBRT) and a gating technique as a neoadjuvant or radical treatment in PA.

#### Material and Methods

Since February 2014, 36 patients (p) with a median age of 67 years (range 43-86) with histologically proven adenocarcinoma of the pancreas were enrolled on this protocol. Six p (16.7 %) were treated with a radical intent and 30 p (83.3 %) as a part of a neoadjuvant treatment. For all patients treated with neoadjuvant intent, CH had given before SBRT. Neoadjuvant CH schedule: 26 p received gemcitabine nab-paclitaxel, 4 p FOLFIRINOX, 1 p XELOX and 1 p unknown CH schedule. Prior to radiation,

at least 2 gold fiducials markers were located into the tumour guided by gastro-endoscopic ultrasound. All SBRT treatments included intravenous and oral contrast CT or PET-CT for GTV delineation. Intensity-modulated radiation therapy (IMRT) and daily image-guided radiation therapy (IGRT) with intrafraction control of tumour motion with a Novalis ExacTrac Adaptive Gating System were performed in all patients. Total dose: 50 Gy in 5 fractions were prescribed in all patients.

#### Results

With a median follow-up (FU) of 9.4 months (range 1 - 47.9 months), 12 p (33 %) are alive without tumour, 2 p (5.5 %) are alive with distance metastases and 17 p (47.2%) have died; median overall survival (OS) was 14.9 months (range 6.6 - 53.4 months) and the actuarial 12 and 24 months OS was 73% and 53% respectively. Thirty three p (91.7%) remain locally controlled and median time to local progression after SBRT was 9 months (range 0,33 - 47.9 months). For any kind of progression disease, the actuarial progression-free survival at 12 and 24 months were 82.2% and 61.8% respectively. Twenty one patients (58.3%) underwent surgery. Tumour-free margins were achieved in 18 p (85.7%). Twenty pathological evaluation were done: 14 p (70%) achieved tumour free lymph node status. Tumour regression grade (TRG) was analysed in 17 p: 7 p complete response or marked response (TRG 0 - 1: 41.2%), 9 p moderate response (TRG 2: 52.9%) and 1 p poor response (TRG 3: 5.9%). Pancreatic SBRT was well tolerated in our cohort of patients. No grade 3 or higher toxicity was observed.

#### Conclusion

In our experience, pancreatic SBRT is a feasible and well-tolerated treatment. As neoadjuvant treatment, increase tumour-free margins and induce tumour regression. Most patients are free from local progression. The benefit of survival will be evaluated with longer FU.

#### EP-1443 Real-time tumor tracking in pancreatic SBRT by percutaneous US-guide implantation of transponders

J.F. Castilla Martinez<sup>1</sup>, R. Chicas-Sett<sup>1</sup>, J. Godoy<sup>1</sup>, C. Hernandez<sup>2</sup>, I. Morales-Orue<sup>1</sup>, M. Zajac<sup>1</sup>, J. Zafra<sup>1</sup>, M. Lloret<sup>1</sup>, P.C. Lara<sup>3</sup>

<sup>1</sup>Dr. Negrin University Hospital of Gran Canaria, Radiation Oncology, Las Palmas, Spain ; <sup>2</sup>Dr. Negrin University Hospital of Gran Canaria, Radiology, Las Palmas, Spain ; <sup>3</sup>San Roque Hospital/Universidad Fernando Pessoa Canarias, Oncology, Las Palmas, Spain

#### Purpose or Objective

SBRT is gaining acceptance in locally advanced pancreatic cancer treatment. Anyhow critical surrounding organs and treatment toxicity makes crucial to tailor irradiation to the tumor volume sparing as much normal tissue as possible. The aim of this study is to assess for the first time the feasibility of percutaneous ultra sonogram (US)-guided implantation of electromagnetic transponders of the Calypso 4D Tracking System in locally advanced pancreatic cancer. As a secondary objective, to assess intra and inter-fractional pancreatic movement during SBRT treatment.

#### Material and Methods

Seven patients with locally advanced pancreatic cancer were included in this study between September 2017 and September 2018. Under percutaneous ultrasound guidance, 3 transponders were implanted in triangulated coordinates into the pancreas. The Calypso System's tracking mode was used to monitor inter and intra-fractional motion.

#### Results

Successful percutaneous US-guide implantations were achieved for all 21 transponders. No adverse events related to the implantation were reported. Transponder positioning was stable during the whole SBRT treatment (5 fractions/every other day) with a mean change in the geometrical inter-transponder position of 0.3 mm (SD 0.05

- 0.4; range, 0.1 - 0.5 mm;  $p=0.37$ ) in all 35 SBRT session among all patients.

Inter-fractional motion measurements were based on more than 25,000 registries for each patient. Pancreatic movement was scored in the left-right (X), superior-inferior (Y), and anterior-posterior (Z) axes in real time using Calypso's transponders tracking mode. There was a major pancreatic movement in the Y-axis:  $10\pm 1.2$ mm, compared to the X-axis:  $4\pm 0.4$ mm and Z-axis:  $5\pm 0.3$ mm. Mean intra-fractional motion was also found to be larger for the Y-axis:  $5\pm 3.6$ mm than X-axis:  $3\pm 2.3$  mm and Z-axis:  $4\pm 3.1$ mm.

#### Conclusion

Our results suggest that percutaneous US-guided implantation is feasible with limited side effects or risk of migration. Significant motion of the tumor was reported during and between treatments. Cranial-caudal movement (Y-axis) ranged 10mm representing a challenge for adequate tumor coverage. Standardized PTV margins for pancreatic SBRT should take this movement into consideration. Real-time tumor tracking may allow for a more accurate delivery of radiation therapy in pancreatic cancer.

#### EP-1444 Clinical results of proton beam therapy for unresectable intrahepatic cholangiocarcinoma

S. Shimizu<sup>1</sup>, T. Okumura<sup>1</sup>, N. Mizoguchi<sup>1</sup>, H. Numajiri<sup>1</sup>, K. Murofushi<sup>1</sup>, K. Onishi<sup>1</sup>, Y. Oshiro<sup>1</sup>, M. Mizumoto<sup>1</sup>, T. Nonaka<sup>1</sup>, H. Ishikawa<sup>1</sup>, H. Sakurai<sup>1</sup>

<sup>1</sup>Proton Beam Therapy Center-University of Tsukuba Hospital, radiation oncology, Tsukuba city, Japan

#### Purpose or Objective

Surgery is considered the only curative treatment for intrahepatic cholangiocarcinoma (ICC). However, most patients with ICC present with unresectable disease at the time of diagnosis, only approximately 30% of the patients with ICC have operable disease. The standard of therapy for unresectable ICC is chemotherapy, but the median survival time (MST) is less than 1 year. Recent progress of radiotherapy has made it possible to deliver high doses to the tumor, and some studies have suggested efficacy of radiotherapy for unresectable ICC. Proton beam therapy (PBT) can deliver much higher doses to the tumor while keeping dose constraint to surrounding normal tissues. In this study we evaluated the clinical outcome and prognostic factors of PBT for patients with unresectable ICC.

#### Material and Methods

From October 2001 to March 2017, 37 patients with unresectable ICC (Stage I, II, IVa, IVb: 4, 4, 19, 10) were treated with PBT. The reason of unresectable disease were medically inoperable (old age, poor performance status (PS)), tumor progression, and both for 5, 22, and 10 patients, respectively. The patients group included 22 male and 15 female, and the median age was 68 years old (range: 32-87 years old). Twelve, 19, and 6 patients had PS of 0, 1, and 2, respectively. Child-Pugh score was A for 27 patients, and B for 10 patients. Ten patients had multiple tumors, and 10 patients had distant metastases. Jaundice was observed in 11 patients. Patients were classified into curative group (25 patients) and palliative group (12 patients), depending on whether the planning target volume covered all the macroscopic tumors or not. The treatment dose was 66Gy in 10 fractions, 72.6 GyE in 22 fractions, and 74.0 Gy in 37 fractions for 1, 21, and 5 patients, respectively. Sixteen patients received concurrent chemotherapy.

#### Results

Median follow-up time for patients alive at time of analysis was 37.5 months. The MST for 37 patients was 15 months, and overall survival time was 60%, 41%, 31% at 1, 2, and 3 years, respectively. One- and 2- year local control rates were 94% and 69%, respectively. According to multivariate analysis, curative treatment ( $p=0.008$ ), lack of jaundice

( $p=0.039$ ), and chemotherapy after PBT ( $p=0.003$ ) were significant factor for favorable survival. The MST for curative and palliative group was 25 and 7 months, respectively. No severe (grade 3) acute toxicities were observed. As for late toxicity, 3 patients experienced grade 3 biliary tract infection, but the causal relationship with irradiation was unclear.

#### Conclusion

The PBT could deliver high doses to the tumor safely, and may contribute to improvement of local tumor control and survival for patients with unresectable ICC.

#### EP-1445 Gastroduodenal toxicity in patients having bile duct brachytherapy for perihilar cholangiocarcinoma

N. McDonnell<sup>1</sup>, C. Deufel<sup>1</sup>, K. Merrell<sup>1</sup>, M. Neben Wittich<sup>1</sup>, T. Whitaker<sup>1</sup>, W. Harmsen<sup>2</sup>, K. Fruth<sup>2</sup>, M. Haddock<sup>1</sup>, C. Hallemeier<sup>1</sup>

<sup>1</sup>Mayo Clinic, Radiation Oncology, Rochester, USA ; <sup>2</sup>Mayo Clinic, Biomedical Statistics and Informatics, Rochester, USA

#### Purpose or Objective

For patients with localized, unresectable perihilar cholangiocarcinoma (pCCA), an approach of neoadjuvant chemoradiotherapy (CRT), bile duct brachytherapy (BT), and orthotopic liver transplantation has shown favourable survival. This study aims to determine if there is a correlation between BT gastroduodenal (GD) dose and GD adverse events (AEs).

#### Material and Methods

This was a single institution retrospective review of all patients with localized, unresectable pCCA who received CRT and biliary high dose rate (HDR) BT as planned neoadjuvant therapy before liver transplant. Patients received external beam RT (EBRT, planned dose of 45 Gy in 30 fx, twice per day over 3 weeks) with concurrent 5-fluorouracil. Between 0 and 4 weeks after completion of EBRT, HDR BT (Iridium-192 remote afterloading system) was administered through 1-2 nasobiliary or percutaneous transhepatic catheter(s). CT-based BT treatment planning was utilized, with the target volume typically including a 1 cm radial expansion from the centre of the involved perihilar bile ducts. The duodenum/stomach was contoured and dose was converted to biologically equivalent dose (BED) using  $\alpha/\beta=3$ . Treatment was 1-4 fx administered over 1-2 days. Following completion of BT, patients received maintenance capecitabine until liver transplant. GD AEs were graded using NCI-CTCAE, v5.0. Cumulative incidence of grade 2+ and 3+ GD AEs was determined from date of BT, with death a competing risk. Univariable regression models were generated to examine for potential correlation between patient, disease, and treatment variables and GD AEs.

#### Results

The study included 120 patients treated from 2009-2018. Median age was 54 years (range 24-73) and 73% were male. 61% had primary sclerosing cholangitis and 45% had a history inflammatory bowel disease (IBD). Delivered EBRT dose was 45 Gy in 95% (range, 42-50 Gy). HDR BT schedule was 9.3 Gy/1 fx (74%), 16 Gy/4 fx (15%), 12.4 Gy/2 fx (6%), or other (5%). The median GD D0.1cc was 4.27 Gy and the median BED<sub>3</sub> was 12.67 Gy. Median follow up after BT was 14 months (range 1-99 months). Grade 2+ and 3+ GD AEs occurred in 38% (n=46) and 28% (n=34). Grade 3+ GD AEs were haemorrhage (n=17), stricture (n=11), ulcer (n=5), gastritis/duodenitis (n=4), and perforation (n=1). Median time from BT to first grade 3+ AE was 5.8 months (range 0.1-64). At 12 months, the cumulative incidence of G2+ and G3+ GD AEs were 33% (95% CI: 24-42%) and 23% (95% CI: 14-31%), respectively. On univariable analysis, there was no association between age, gender, PSC, history of IBD, or EBRT dose and risk of grade 2+ or 3+ GD AEs (all  $P>0.05$ ). BT GD D0.1cc (minimum dose to the 0.1 cc

receiving the greatest dose) was associated with risk of G2+ ( $p<0.01$ ) and G3+ ( $p=0.048$ ) GD AEs, as was BED<sub>3</sub> ( $<0.01$  and  $<0.01$ ).

#### Conclusion

For patients with pCCA receiving CRT and HDR BT, higher BT GD D0.1 cc and higher BED<sub>3</sub> were both associated with an increased risk of GD AEs.

---

**Electronic Poster: Clinical track: Lower GI (colon, rectum, anus)**

---

#### EP-1446 Clinical efficacy and safety of consolidative radiotherapy in the maintenance treatment of mCRC

Z. LIN<sup>1</sup>, Z. Danyang<sup>1</sup>, Y. Dandan<sup>1</sup>, W. Jing<sup>1</sup>, Z. Tao<sup>1</sup>

<sup>1</sup>Union Hospital- Tongji Medical College- Huazhong University of Science and Technology, Cancer Center, Wuhan, China

#### Purpose or Objective

For metastatic colorectal cancer (mCRC) patients responding to induction therapy, maintenance treatment prolongs the progression-free survival (PFS) while maintains quality of life. The purpose of this study was to evaluate the clinical efficacy and safety of local consolidative radiotherapy in maintenance treatment for patients with limited mCRC.

#### Material and Methods

Between October 2011 and June 2017, 19 mCRC patients (6 males and 13 females) who achieved a partial response (PR) or stable disease (SD) to induction chemotherapy and received subsequent consolidative radiotherapy of metastatic lesions and maintenance treatment were retrospectively enrolled.

#### Results

The median age was 57 years (range 33 to 70). Nine patients received local consolidative radiotherapy to liver (median BED=66.3 Gy), 6 patients to pelvis (median BED=60.0 Gy), 5 to lung (median BED=78.0 Gy), and others. The incidence of LR failure was 5.3% and 21.1% at 1 and 2 years, respectively. The incidence of distant failure was 47.4% and 68.4% at 1 and 2 years, respectively. The median OS was 35.5 months (95% CI, 13.41-57.59), and median PFS was 12.4 months (95% CI, 1.77-23.03). Main grade 3 or 4 toxicities were leukopenia ( $n=2$ , 10.5%). The most common adverse events were leukopenia ( $n=14$ , 73.7%), thrombocytopenia ( $n=7$ , 36.8%), anemia ( $n=5$ , 26.3%), transaminase elevation ( $n=5$ , 26.3%), and diarrhea ( $n=2$ , 10.5%).

#### Conclusion

Consolidative radiotherapy prior to maintenance treatment improved local control and prognosis of mCRC patients with acceptable toxicities. Despite the limited data of present study, it could be contemplated as an effective therapeutic alternative in selected patients.

#### EP-1447 Effect of waiting time to radiation on local control and overall survival in rectal cancer

A. Tangkananan<sup>1</sup>, R. Jiratrachu<sup>1</sup>

<sup>1</sup>Prince of Songkla University, Division of Radiation Oncology- Department of Radiology- Faculty of Medicine, Songkla, Thailand

#### Purpose or Objective

To evaluate the effect of waiting time to radiation after diagnosis on local control and overall survival in locally staged rectal cancer patients, and to show the cause of prolonged waiting time: referring pathway or internal radiation oncology division.

#### Material and Methods

A data of 275 patients with locally staged adenocarcinoma of rectum who were treated with radiation as neoadjuvant concurrent chemoradiation or definite concurrent chemoradiation between January 2011 and December

2016 were reviewed. Waiting time was defined as interval between the pathological diagnosed date until the first fraction of radiation delivered date. Referring pathway interval was defined as time from the pathological diagnosed date to the first date of radiation oncologist and patient meeting. Internal radiation oncology division interval was defined as time from the first date of radiation oncologist and patient meeting to the first fraction of radiation delivered date.

#### Results

The median waiting time was 41 days (IQR 25, 56.2); referring pathway interval 27 days (IQR 13, 44), internal radiation oncology division interval 11 days (IQR 8, 16). The estimated 5-year local control and overall survival were 76.8% (95%CI 68.4-86.2) and 61.7% (95%CI 54-70.5), respectively. In patients who had local recurrence, the median waiting time was 57 days (IQR 40, 78.8) compared with 42 days (IQR 27, 64) in patients who did not have (P-value 0.014). According to waiting time  $\leq 35$  days, 36-56 days and  $>56$  days, the estimated 5-year local control were 90%, 74%, 60% respectively as shows in figure 1. Using waiting time  $\leq 35$  days as the reference group, the HR of local recurrence were 4.49 (95%CI 1.2-16.83, P-value 0.026) with waiting time 36-56 days and 9.05 (95%CI 2.23-36.79, P-value 0.002) with waiting time  $>56$  days. Multivariate analysis showed that ECOG score, radiation dose and surgery were associated with local recurrence. We did not found the relationship between waiting time and overall survival.

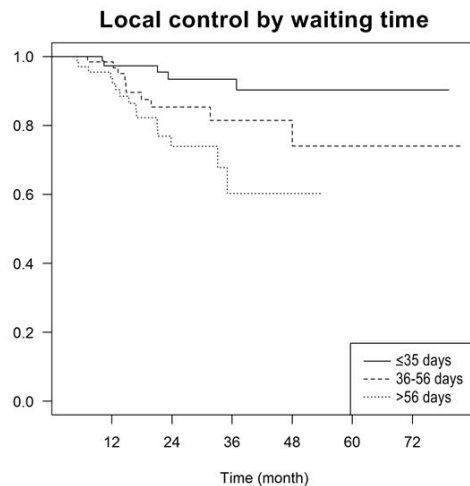


**Figure 1** Estimated local control by waiting time

#### Conclusion

Prolonged waiting time to radiation was strongly associated with poorly local control but not overall survival. The main duration of waiting time was referring pathway interval.

#### EP-1448 Preoperative VMAT with simultaneous integrated boost for locally advanced distal rectal cancer

Y. Yang<sup>1</sup>, Q. Liu<sup>2</sup>, P. Zhao<sup>1</sup>, J. Qian<sup>1</sup>, Q. Peng<sup>1</sup>, Y. Zhu<sup>1</sup>, L. Feng<sup>3</sup>

<sup>1</sup>the Second Affiliated Hospital of Soochow University, Radiotherapy & Oncology, Suzhou, China ; <sup>2</sup>Beijing Luhe Hospital Affiliated to Capital Medical University, Radiation Oncology, Beijing, China ; <sup>3</sup>Chinese PLA General Hospital, Radiation Oncology, Beijing, China

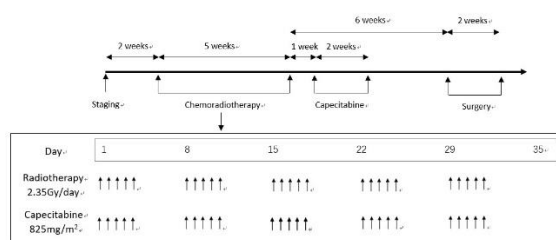
#### Purpose or Objective

The aim of this study was to evaluate the safety and clinical efficacy of a combined preoperative regimen consisting of volumetric modulated arc therapy-

simultaneous integrated boost and capecitabine chemotherapy for distal rectal cancer.

#### Material and Methods

A total of 26 patients with locally advanced distal rectal cancer were enrolled from March 2015 to May 2016. The tumor had to have evidence of cT3-T4 with any N, or any T with N1 or N2 disease on pelvic magnetic resonance imaging (MRI), staged according to the 2009 classification of the American Joint Committee on Cancer (7th edition). The radiation dose fractionation was 58.75 Gy/25 fractions (2.35 Gy/fraction) for rectal tumor and pelvic lymph node metastasis and 50 Gy/25 fractions for pelvic lymph node stations, accompanied with simultaneous capecitabine chemotherapy. Completion of the simultaneous chemotherapy was ensued by 1 week of rest and then another cycle of induction chemotherapy with capecitabine. A radical rectal cancer surgery was performed 6-8 weeks after the simultaneous chemoradiotherapy. The primary endpoints were the complete pathological response rate and the postoperative sphincter preservation rate. This study was a non-randomized, open-labeled, single-arm, single-institution, prospective, phase II trial. All patients provided written informed consent before they were recruited for the study.



#### Results

All 26 patients completed the neoadjuvant chemoradiotherapy, among which 25 received surgical treatment, and 1 patient declined the surgery due to severe perianal edema. The postoperative complete pathological response rate was as high as 32% (8/25), while the sphincter preservation rate was 60% (15/25); the overall T/N downstaging rate was 92% (23/25), and the R0 resection rate was 100%. During the chemoradiation, the occurrence rate of grade 1 adverse reactions was 85% (22/26), including 10 hematologic toxicities, 11 cases of diarrhea, 12 cases of excretory response, 9 cases of radiodermatitis, and 5 cases of hand-foot syndrome; the occurrence rate of grade 2 acute adverse reactions was 53.8% (14/26), including 7 cases of hematologic responses, 8 cases of diarrhea, and 2 cases of radiodermatitis. There were 2 cases of grade 3 acute adverse reactions, both of which were radiodermatitis. None of the acute adverse reactions were more severe than grade 4. After the surgery, there was one case of ureteral injury and one case of intestinal obstruction, but no perioperative deaths occurred.

#### Conclusion

In conclusion, the chemoradiation regimen of preoperative VMAT-SIB<sub>58.75Gy</sub> and a single cycle of induction chemotherapy with capecitabine for patients with distal rectal cancer is safe and feasible with a satisfactory complete pathological response rate, sphincter preservation rate, and R0 resection rate.

#### EP-1449 Prognostic Value of Volumetric PET Parameters in Patients with Locally Advanced Rectal Cancer

F. Sert<sup>1</sup>, A. Oral<sup>2</sup>, R. Savas<sup>3</sup>, D. Yalman<sup>1</sup>, S. Ozkok<sup>1</sup>  
<sup>1</sup>Ege University Medical School&Hospital, Radiation Oncology, Izmir, Turkey ; <sup>2</sup>Ege University Medical School&Hospital, Nuclear Medicine, Izmir, Turkey ; <sup>3</sup>Ege University Medical School&Hospital, Radiology, Izmir, Turkey

#### Purpose or Objective

For locally advanced rectal cancer (LARC) patients, preoperative neoadjuvant radiochemotherapy followed by total mesorectal excision (TME) is the standard treatment. The aim of our study is to determine the prognostic and/or predictive role of 18F-FDG PET/CT parameters such as SUVmax, SUVmean, Metabolic Tumor Volume (MTV) and Total Lesion Glycolysis (TLG=MTVxSUVmean) for the patients with LARC treated with neoadjuvant radiotherapy±chemotherapy(nCRT).

Characteristic	Number (%)
<b>Age (year)</b>	
Median	61
Range	29-86
<b>Sex</b>	
Female	49 (646)
Male	57 (654)
<b>Location</b>	
Proximal:Rectosigmoid	18 (617)
Middle	34 (632)
Distal	54 (651)
<b>Histopathology</b>	
Adenocarcinoma	102 (696)
Signet ring cell carcinoma	2 (62)
Mucinous adenocarcinoma	2 (62)
<b>Lymphovascular Invasion</b>	
+	20 (618)
-	86 (682)
<b>Perineural Invasion</b>	
+	20 (618)
-	86 (682)
<b>Clinical T Stage AJCC 2010</b>	
T2	6 (66)
T3	90 (685)
T4	10 (69)
<b>Clinical N Stage AJCC 2010</b>	
N0	24 (622)
N1	77 (673)
N2	5 (65)
<b>Concomitant Chemotherapy</b>	
+	88 (683)
-	18 (617)
<b>Radiotherapy Technique</b>	
3 Dimensional Conformal Intensity Modulated	12 (611)
	94 (689)
<b>Pathological Complete Response (ypT0N0)</b>	
+	46 (644)
-	60 (656)
<b>Metabolic Tumor Volume (MTV)</b>	
≥14.6 cm <sup>3</sup>	55 (652)
<14.6 cm <sup>3</sup>	51 (648)
<b>Total Lesion Glycolysis (MTVxSUVmean)</b>	
≥117	58 (654)
<117	48 (646)

#### Material and Methods

Between January 2005 and December 2016, a total of 106 patients with clinical T3-4 and/or N+ rectal cancer without distant metastasis were included this retrospective evaluation. Totally 106 patients met our criteria. Median age was 61 (range, 29-86) and 54% of them were female. Patient characteristics are shown in table 1. Correlation between metabolic and volumetric parameters and tumor characteristics was evaluated. Prognostic factors for overall survival (OS), local recurrence-free survival (LRF5), and distant metastasis-free survival (DMFS) were analyzed. All patients were treated with concurrent chemotherapy except 18 (17%) of them. Among the patients receiving concurrent chemotherapy 68 (64%) received oral capecitabine, and 20 (19%) received 5-Fluorouracil with leucovorin during RT.

#### Results

The median follow-up duration for all patients and surviving patients was 39.0 months (range, 6-103 months) and 40 months (range, 22-103 months), respectively. Sixteen patients (15%) developed distant metastases, and

5 (5%) had local/locoregional failure. Pathologic complete response (pCR) was defined as the absence of viable cancer cells in the resected specimen (ypT0N0). pCR was achieved in 17% of all cases (18/106). According to TRG system, grade 0-1 and grade 2-3 responders were 45 patients (42.5%) and 61 patients (57.5%), respectively. The mean  $\pm$  SD SUVmax, SUVmean, MTV and TLG were  $16.9 \pm 9.6$  (range, 3.6 - 60.2),  $9.6 \pm 6.3$  (range, 2.4 - 49.2),  $24.7 \pm 26.4$  cm<sup>3</sup> (range, 2.8 -160.5 cm<sup>3</sup>) and  $268.7 \pm 474.5$  (range, 21.8 -3,092.0) for the entire group, respectively. There was a weak correlation between SUVmax of primary rectal tumors and MTV (Pearson correlation coefficient [r] = 0.238; p < 0.001). On the other hand, SUVmax of primary rectal tumors and TLG were significantly correlated (r=0.538; p < 0.001). Neither SUVmax nor SUVmean were affected by patient and tumor characteristics. On the other hand, volumetric FDG-PET parameters, such as MTV and TLG, were significantly higher in patients with larger tumors ( $\geq 3$  cm) and middle rectum located tumors compared to the patients with smaller tumors (<3 cm), and proximal or distal rectum located tumors. Posttreatment extensive stage of disease (p=.013), absence of concomitant CT (p=.012), MTV  $\geq 14.65$  cm<sup>3</sup> (p=.008), and TLG  $\geq 117.00$  (p=.023) were unfavorable prognostic factors for OS on multivariate analysis.

#### Conclusion

Although FDG-PET is not a standard imaging modality for the treatment of rectal cancers a negative effect of high MTV and TLG on OS was shown in our study. We should consider more intense treatment approaches for tumors with high MTV and TLG values.

#### EP-1450 How smoking status impacts patients undergoing radiochemotherapy for anal canal carcinoma?

L. Grandjean<sup>1</sup>, M. Lamande<sup>1</sup>, E. Gonne<sup>2</sup>, D. Van Daele<sup>3</sup>, J. Collignon<sup>2</sup>, M. Polus<sup>3</sup>, C. Loly<sup>3</sup>, L. Seydel<sup>4</sup>, J. Vanderick<sup>1</sup>, P. Coucke<sup>1</sup>, P. Martinive<sup>5</sup>

<sup>1</sup>CHU de Liege, Radiation therapy, Liege, Belgium ; <sup>2</sup>CHU de Liege, Medical Oncology, Liege, Belgium ; <sup>3</sup>CHU de Liege, Gastroenterology and Digestive Oncology, Liege, Belgium ; <sup>4</sup>CHU de Liege, Biostatistics- SIME, Liege, Belgium ; <sup>5</sup>Institut Jules Bordet, Radiation therapy, Brussels, Belgium

#### Purpose or Objective

Radiochemotherapy (RCT) is the standard of care for Anal Canal Squamous Cell Carcinoma. Although, tobacco consumption during RTC decrease overall survival (OS), cancer specific survival (CSS) and disease-free survival (DFS) in many tumors but it has never been demonstrated in anal cancer. The aim of this study is to compare the results of a tertiary university hospital in terms of colostomy-free survival (CFS), OS, CSS, DFS and to identify prognosis factors in regards to tobacco consumption.

#### Material and Methods

We retrospectively identified 110 patients, with histologically proven SCC of anal canal treated with RCT in our institution between 01/2008 and 12/2017. Patients received 59.4Gy in 33 fractions concomitantly with 5FU and MMC either based on RTOG (45Gy to the pelvic + 14.4Gy for the boost) or EORTC (36Gy to the pelvic + 23.4Gy for the boost) protocol with one week gap before the boost.

#### Results

Most patients presented locally advanced tumor (57.3% of stage III, table 1). Patients benefit from the RTOG and EORTC treatments in 54% and 46 %, respectively. With a median follow-up of 40.6 months (0.3 - 114.7), the 3- and 5-year OS are 73.5% (95% CI, 63.3%-81.2%) and 63.4% (95% CI, 51.6%-73.1%) and for CSS, 81.7% (95% CI, 72.4%-88.1%) and 74.2% (95% CI, 62.7%-82.7%). The 3- and 5-year DFS are 72% (95% CI, 61.9%- 79.8%) and 68.6% (95% CI, 57.8%-77.2%) and for CFS, 81.9% (95% CI, 72.5%- 88.4%) and 79.9% (95% CI, 69.7%-87.1%). Local recurrence (LR) occurred in

20.9% patients, mean and median time to LR was 12.2 and 7.8 months. Males are more likely to have colostomy for LR (HR=3.59, P= 0.014). Tumor stage but not node stage is also associated with higher LR (HR=10.4 for T4 vs T1). There is no correlation between T and N stage with distant metastases. Active smokers at diagnosis/treatment are more likely to undergo a colostomy procedure for LR than former smokers or non-smokers (HR 7.793; P= 0.0053 and HR 2.99; P= 0.2719). Smoking status has no impact on distant failure. Elderly patients have a worse CSS (HR 1.08; P<0.0001) and a significantly higher risk of 90-day mortality after treatment (OR = 1.20; p< 0.0015) with a 26 folds increase risk (p= 0.0031) if patient is older than 71 years.

Characteristics	Number of patients (%)
Age, median (range), y	63.32 (36.4-92.4)
Male/Female	45 (40.9)/65 (59.1)
OMS status	
1	102 (92.7)
2	7 (6.4)
3	1 (0.9)
Smoking	
Current smokers	48 (43.6)
Ex-smokers	16 (14.5)
Non-smokers	46 (41.8)
T category	
Tis	2 (1.8)
T1	13 (11.8)
T2	40 (36.4)
T3	36 (32.7)
T4	18 (16.4)
TX	1 (0.9)
N category	
N0	50 (45.5)
N1	29 (26.4)
N2	14 (12.7)
N3	16 (14.5)
NX	1 (0.9)
Clinical node status	
Positive	50 (45.5)
Negative	60 (54.5)
AJCC stage	
0-I	14 (12.7)
II	33 (30.0)
IIIA	24 (21.8)
IIIB	39 (35.5)

#### Conclusion

For the first time in the SCC of anal cancer, we pointed out tobacco consumption as a negative prognosis factor for LR. We also identified a cut-off of 71 years old for treatment related mortality. Worth noting the homogeneity of the cohort in a retrospective study thanks to institutional treatment protocol. The vast majority of patients presented T3/T4 and positive clinical nodes explaining an OS slightly lower than those observed in clinical trials with less advanced tumors. The CSS and the CFS are in accordance with the literature. To conclude, we should advise patients to stop tobacco consumption during treatment, and we should submit all patients more than 71 years old to an oncologic geriatric evaluation.

#### EP-1451 Impact of tobacco smoking on patient's outcome after (chemo)-radiotherapy for anal cancer

L. Jacques<sup>1</sup>, H. Christophe<sup>1</sup>, E. Isabelle<sup>2</sup>, A. Laurent<sup>3</sup>, G. Gaël<sup>4</sup>, G. Jean-Marc<sup>5</sup>, G. Sophie<sup>1</sup>, A. Thomas<sup>5</sup>, V. Alain<sup>6</sup>, C. Pierre<sup>7</sup>, L. Quero<sup>1</sup>

<sup>1</sup>Saint-Louis Hospital, Radiation Oncology, Paris, France ; <sup>2</sup>Croix Saint Simon Hospital, Proctology, Paris, France ; <sup>3</sup>Bichat Hospital, Proctology, Paris, France ; <sup>4</sup>Bichat Hospital, Gastroenterology, Paris, France ; <sup>5</sup>Saint-Louis Hospital, Gastroenterology, Paris, France ; <sup>6</sup>Croix Saint

*Simon Hospital, Digestive Surgery, Paris, France ; <sup>7</sup>Saint-Louis Hospital, Digestive surgery, Paris, France*

#### **Purpose or Objective**

Squamous cell cancer of the anus is associated with multiple risk factors, including infection with human papillomavirus [HPV] and human immunodeficiency virus, immunosuppression, multiple sex partners, receptive anal sex and tobacco smoking. The aim of our study was to identify prognostic factors associated with poor outcome after radiotherapy for anal cancer.

#### **Material and Methods**

We analysed retrospectively the medical records of 171 patients treated by (chemo)-radiotherapy for a non-metastatic anal cancer in our institution from 2000 to 2015. Patients and tumor characteristics, treatments (chemotherapy (CT), radiotherapy (RT), and surgery) and outcomes were analyzed. Colostomy-free, disease-free and overall survivals at 5 years were studied. Univariate and multivariate analyses were performed by logistic regression in order to determine factors associated with poor progression free survival (PFS).

#### **Results**

Patients characteristics were as follow: median age: 62 years (range 36-89); gender: 45 males (26%) and 126 females (74%); HIV serology: positive 21 patients (12%), negative or unknown 150 patients (88%); tobacco smoking: 86 Pts (50%) among whom 28 Pts and 58 Pts were current and former smokers respectively. Tumors were classified as locally limited (T0-1-2, N0, M0) for 86 pts (50%) and locally advanced (T3-4 or N+, M0) for 85 pts (50%). Median total dose was 64.4 Gy (range 54-76.6), 146 patients were treated by concurrent chemoradiotherapy. Factors associated with poor PFS in univariate analysis were: tumor size >4cm, lymph node involvement; tobacco smoking, no initial surgical excision and anal warts at diagnosis. In multivariate analysis, only tobacco smoking status was significantly associated with poor PFS (HR=2.85 [1.25-6.50], p=0.013). 5-years-PFS for non-smokers, former smokers and current smokers was 88.1%, 76.7% and 73.8% respectively (p=0.038). Tobacco smoking was also associated with poor overall survival (p=0.03) and colostomy free survival (p=0.02).

#### **Conclusion**

Tobacco smoking status is associated with poor overall survival, PFS and colostomy free survival in patients treated for anal cancer by (chemo)-radiotherapy.

#### **EP-1452 Response after neoadjuvant radiochemotherapy as prognostic factor in locally advanced rectum cancer**

S. Couto Gonçalves<sup>1</sup>, A. Ponte<sup>1</sup>, M. Marques<sup>1</sup>, J. Casalta-Lopes<sup>1</sup>, I. Nobre-Góis<sup>1</sup>, T. Teixeira<sup>1</sup>, A. Barros<sup>2</sup>, M. Borrego<sup>1</sup>

<sup>1</sup>Centro Hospitalar e Universitário de Coimbra, Radiation Oncology, Coimbra, Portugal; <sup>2</sup>Centro Hospitalar e Universitário de Coimbra, Oncology, Coimbra, Portugal

#### **Purpose or Objective**

Locally advanced rectal cancer (LARC) treatment includes neoadjuvant (NA) radiotherapy (RT) to achieve downsizing and downstaging and subsequently increase loco-regional (LR) control. The well-known long-course (LC) associates pelvic RT, 45-50.4Gy/25-28F/5-5.5weeks (1,8Gy/F), and radiosensitizing chemotherapy (RTCT). This study aims to evaluate pathological response and survival of patients with LARC after LC.

#### **Material and Methods**

Patients with LARC cT3-4 treated with NA RTCT LC prior to surgery between 2002-2017 were included. Tumor response was evaluated by AJCC staging system; toxicity by CTCAE5.0; survival by Kaplan-Meier;  $\alpha=0.05$ .

#### **Results**

320 patients were included, median age of 65 years, 64.4% male, karnofsky >80% in 94.4%. At diagnosis the median

values for CEA and CA19.9 were 3.5 ng/mL and 8.6 U/mL. Tumors were located at inferior in 47.5% and at medial in 47.5%. Clinical staged cT3N+ in 72.5% and 87.8% was cN+. Acute toxicity was present in 81.6%, G3-4 in 10.0%. The majority was hematologic (44.7%; 1.9% G3-4), cutaneous (44.7%; 4.1% G3-4), diarrhea (24.7%; 3.4% G3-4). Following surgery, positive margins (R+) were obtained in 9.7%, more often in tumors of the inferior (p<0.001); lymphovascular invasion (LVI) was found in 9.7% of pathological specimens. Pathological assessment found ypT0N0 in 15.9%, ypT1-2N0 in 28.4% and ypT3-4 or ypN+ in 55.6%. Lower pre-treatment CEA was related to better response (median of 2.0ng/mL to ypT0N0, 3.05ng/mL to ypT1-2N0, 4.6ng/mL to ypT3-4/N+; p<0.001). Better response was linked to lower rate of R+ and LVI (for both ypT0N0: 0%, ypT1-2N0: 2.2%, ypT3-4/N+: 16.3%; p<0.001). With a median follow-up of 52 months, 5 years LR disease-free survival (LRDFS), disease-free survival (DFS), overall survival (OS) and cancer-specific survival (CSS) were 91.8%, 68.5%, 70.8% and 80.4%, respectively. Pathological response (data in 5 years, ypT0N0 vs ypT1-2N0 vs ypT3-4/N+) related to better LRDFS (100% vs 100% vs 84.9%; p<0.001), DFS (88.9% vs 85.4% vs 54.1%; p<0.001), OS (92.5% vs 82.5% vs 60.3%; p<0.001) and CSS (97.3% vs 88.7% vs 69.7%; p<0.001). Prognostic factors identified at univariate analysis were tumor location on DFS (p=0.012) and CSS (p=0.014), CEA at diagnosis on DFS (p=0.002), OS (p=0.002) and CSS (p=0.001), pre-treatment CA19.9 on LRDFS (p=0.036), DFS (p=0.027), OS (p=0.017) and CSS (p=0.001), LVI on LRDFS (p=0.004), DFS (p<0.001), OS (p=0.004) and CSS (p<0.001), R+ on LRDFS (p<0.001), DFS (p<0.001), OS (p<0.001) and CSS (p<0.001). In multivariate analysis R+ kept prognostic impact on LRDFS (p=0.009); pathological response (p=0.002), LVI (p=0.023) and R+ (p<0.001) on DFS; pathological response (p=0.023 and p=0.010, respectively) and R+ (p<0.001 for both) on OS and CSS.

#### **Conclusion**

RTCT LC in LARC is well-tolerated with manageable toxicities. Better response to treatment was related to better surgical and survival outcomes. Multivariate analysis identified R+, LVI and pathological response as prognostic factors.

#### **EP-1453 Machine learning prediction of early distant progression after SBRT for colorectal cancer**

H. Chung<sup>1</sup>, P. Lang<sup>1</sup>, M. Kayvanrad<sup>2</sup>, R. Thompson<sup>3</sup>, W. Chu<sup>1</sup>, E. Gennatas<sup>4</sup>, G. Valdes<sup>4</sup>, P. Cheung<sup>1</sup>

<sup>1</sup>Odette Cancer Centre- University of Toronto, Radiation Oncology, Toronto, Canada ; <sup>2</sup>University of Toronto, Rotman Research Institute, Toronto, Canada ; <sup>3</sup>Saint John Regional Hospital, Radiation Oncology, Saint John, Canada ; <sup>4</sup>University of California San Francisco, Radiation Oncology, San Francisco, USA

#### **Purpose or Objective**

While SBRT for oligo-metastases (OM) and oligo-progression (OP) has been increasingly utilized, it remains a challenge in identifying patients who would benefit from SBRT, due to complex interactions of patient, tumour and treatment factors. This study examines the ability of machine learning (ML) based classifiers to identify colorectal (CRC) patients who develop early distant progression (DP,  $\leq 90$  days since treatment completion) after completing SBRT for OM and OP, and thus received little benefit.

#### **Material and Methods**

All CRC patients treated with SBRT to any extracranial site at a single institution for OM/OP in 2009 - 2016 were retrospectively reviewed. Clinical characteristics included age, gender, pre-SBRT CEA, RAS status, ECOG performance, treatment indication (OM/OP), primary in situ, SBRT location, disease-free interval (DFI) since last treatment, number of prior lines of systemic of therapy, PTV volume and mean PTV BED. Univariable and

multivariable logistic regression was used to identify predictors of DP. Classification methods included: logistic regression (LR) gradient boosting (GBM), adaptive boosting (ADA), and random forest (RF). Patient characteristics with a high correlation ( $\rho > 0.6$ ) and factors in which missing data  $> 30\%$  were excluded from the models. 10-fold cross validation was used to assess the models. Classifier performance was assessed by receiver operating characteristic curves.

#### Results

113 patients with 226 treated lesions were included; 79 patients and 203 lesions treated for OM and 34 patients and 23 lesions for OP. 31 (27%) of the treated patients had DP within 90 days. 2 patients died within 90 days. In univariable analysis, SBRT location (non-lung/liver), higher CEA, shorter DFI, greater number of prior systemic therapy lines and lower mean PTV BED were significantly associated with early DP ( $p < 0.05$ ). In multivariable analysis, shorter DFI and higher CEA were significant predictors of DP ( $p < 0.05$ ). Performance of the various classifiers is shown in Table 1. All ML classifiers were significantly better at identifying patients with DP compared to the logistic regression model ( $p < 0.05$ ). There was no statistically significant difference in performance between the various ML classifiers.

Table 1. Classifier performance.

	LR	GBM	ADA	RF
Sensitivity	0.55	0.49	0.25	0.48
Specificity	0.73	0.87	0.96	0.92
PPV	0.22	0.31	0.51	0.51
NPV	0.92	0.90	0.93	0.93
AUC	0.61	0.70	0.74	0.76

#### Conclusion

The ability to predict patients at risk of DP would assist clinicians in identifying patients who may benefit minimally from SBRT for OM/OP disease. External validation would be of benefit.

#### EP-1454 Multi-parametric MRI as a biomarker in anal cancer: a prospective trial

M. Jones<sup>1</sup>, G. Hruby<sup>2</sup>, M. Kumar<sup>3</sup>, A. Capp<sup>3</sup>, S. Sridharan<sup>3</sup>, C. Coolens<sup>4</sup>, P. Stanwell<sup>5</sup>, J. Arm<sup>6</sup>, S. Gallagher<sup>3</sup>, C. Holder<sup>7</sup>, C. Oldmeadow<sup>7</sup>, J. Martin<sup>3</sup>

<sup>1</sup>Royal Hobart Hospital, Radiation Oncology, Hobart, Australia ; <sup>2</sup>Royal North Shore Hospital, Radiation Oncology, St Leonards, Australia ; <sup>3</sup>Calvary Mater Newcastle, Radiation Oncology, Waratah, Australia ; <sup>4</sup>Princess Margaret Cancer Centre, Radiation Oncology, Toronto, Canada ; <sup>5</sup>The University of Newcastle, School of Health Sciences, Callaghan, Australia ; <sup>6</sup>Calvary Mater Newcastle, Radiology, Waratah, Australia ; <sup>7</sup>Hunter Medical Research Institute, Statistics, New Lambton Heights, Australia

#### Purpose or Objective

To investigate the role of multi-parametric magnetic resonance imaging (MRI) as a potential biomarker in squamous cell carcinoma of the anal canal (AC).

#### Material and Methods

A multi-centre cohort of 20 patients with non-metastatic AC were enrolled on a prospective clinical trial. Multi-parametric MRIs, incorporating diffusion weighted (DW) and dynamic contrast enhanced (DCE) sequences, were performed at time of staging, during the second and fourth week of chemo-radiotherapy (CRT) and 8 weeks post treatment. MRI parameters were extracted from the primary tumour and correlated with recurrence.

#### Results

With a median follow up of 17 months, 3/20 patients had a local recurrence, and 5/20 had any recurrence. Apparent diffusion coefficient (ADC) skewness ( $p=0.04$ ,

AUC 0.9 and  $p=0.02$ , AUC 0.91) and standard deviation (SD) ( $p=0.2$ , AUC 0.9 and  $p=0.01$ , AUC 0.94) at baseline and week 2, kurtosis ( $p=0.01$ , AUC 0.92) and SD ( $p=0.01$ , AUC 0.96) at week 4 and change in minimum ADC between baseline and week 2 ( $p=0.02$ , AUC 0.94) and baseline and week 4 ( $p=0.02$ , AUC 0.94) significantly predicted for local recurrence. For prediction of any recurrence, ADC min ( $p=0.02$ , AUC 0.87) and SD ( $p=0.01$ , AUC 0.85) at baseline, max ( $p=0.03$ , AUC 0.77) and SD ( $p=0.02$ , AUC 0.81) at week 4 were significant. On LASSO logistic regression, ADC minimum and SD at baseline were retained for any recurrence. No DCE parameters were predictive of recurrence.

#### Conclusion

A number of ADC parameters at various time points appear predictive of local and any recurrence. No DCE parameters correlated with recurrence.

#### EP-1455 Post chemoradiotherapy FDG-PET parameters predict for recurrence in anal cancer: a prospective trial

M. Jones<sup>1</sup>, G. Hruby<sup>2</sup>, U. Metser<sup>3</sup>, S. Sridharan<sup>4</sup>, A. Capp<sup>4</sup>, M. Kumar<sup>4</sup>, S. Gallagher<sup>4</sup>, N. Rutherford<sup>5</sup>, C. Holder<sup>6</sup>, C. Oldmeadow<sup>6</sup>, J. Martin<sup>4</sup>

<sup>1</sup>WP Holman Clinic- Royal Hobart Hospital, Radiation Oncology, Hobart, Australia ; <sup>2</sup>Royal North Shore Hospital, Radiation Oncology, St Leonards, Australia ; <sup>3</sup>Princess Margaret Cancer Centre, Cancer Clinical Research Unit, Toronto, Canada ; <sup>4</sup>Calvary Mater Newcastle, Radiation Oncology, Waratah, Australia ; <sup>5</sup>Calvary Mater Newcastle, Nuclear Medicine, Waratah, Australia ; <sup>6</sup>Hunter Medical Research Institute, Statistics, New Lambton Heights, Australia

#### Purpose or Objective

To investigate the prognostic significance of serial F-18 fluorodeoxyglucose-positron emission tomography (PET) parameters in squamous cell carcinoma of the anal canal (AC).

#### Material and Methods

A multi-centre prospective trial of 19 patients with non-metastatic AC treated per protocol underwent PET imaging before and 12 weeks following chemo-radiotherapy (CRT). PET parameters from the primary tumour were extracted and correlated with recurrence.

#### Results

With a median follow up of 15.8 months, 3/19 patients relapsed locally and 5/19 had any recurrence. On post-CRT PET, the median standard uptake value (SUV) within a volume of interest (VOI) bounded by an SUV of 3 correlated with local recurrence ( $p$  value =  $< 0.01$ , AUC 1.0). The mean SUV 3 did not reach significance ( $p$  value = 0.06, AUC 0.91). On LASSO logistic regression, post-CRT SUVmax was retained on the grouped post model for both local and any recurrence, but not in the final model. No pre-CRT PET parameters reached significance.

#### Conclusion

Patients with a metabolic PET response had a very low risk of recurrence or progression. 12-week post-CRT PET parameters extracted from the primary tumour correlated with local recurrence. Further studies in larger cohorts are warranted to confirm this finding.

#### EP-1456 Clinical impact of re-irradiation with carbon ion radiotherapy for locally recurrent rectal cancer

F. Valvo<sup>1</sup>, A. Barcellini<sup>1</sup>, V. Vitolo<sup>1</sup>, M.R. Fiore<sup>1</sup>, A. Iannalfi<sup>1</sup>, B. Vischioni<sup>1</sup>, A. Facoetti<sup>2</sup>, M. Bonora<sup>1</sup>, S. Ronchi<sup>1</sup>, R. Petrucci<sup>1</sup>, E. D'Ipollito<sup>1</sup>, A. Mirandola<sup>3</sup>, S. Molinelli<sup>3</sup>, S. Russo<sup>3</sup>, G. Viselner<sup>3</sup>, G. Magro<sup>3</sup>, D. Maestri<sup>3</sup>, M. Ciocca<sup>3</sup>, L. Preda<sup>4</sup>, R. Orecchia<sup>5</sup>

<sup>1</sup>National Centre of Oncological Hadrontherapy CNAO, Radiation Oncology, Pavia, Italy ; <sup>2</sup>National Centre of Oncological Hadrontherapy CNAO, Radiobiology, Pavia, Italy ; <sup>3</sup>National Centre of Oncological Hadrontherapy CNAO, Department of Medical Physics, Pavia, Italy ;

<sup>4</sup>National Centre of Oncological Hadrontherapy CNAO- University of Pavia, Radiation Oncology- Department of Clinical Surgical- Diagnostic and Pediatric Sciences, Pavia, Italy ; <sup>5</sup>National Centre of Oncological Hadrontherapy CNAO- European Institute of Oncology, Radiation Oncology, Pavia- Milano, Italy

#### Purpose or Objective

The re-irradiation of locally recurrent rectal cancer presents challenges due to the proximity of critical organs such as bowel. Ion beam therapy, specifically carbon ions radiotherapy (CIRT) have some advantages for the favorable relative biological effectiveness and physical dose distribution providing a highly conformal dose distribution while minimizing normal tissue damage. The aim of this study is to report our experience on feasibility and toxicity of carbon-ion radiotherapy (CIRT) in previously irradiated patients with locally recurrent rectal cancer.

#### Material and Methods

Between August 2014 and February 2017, a total of 10 patients (M:F= 8:2) were treated with CIRT as re-irradiation for locally recurrent rectal cancer at National Centre of Oncological Hadrontherapy (CNAO). Patient ages ranged between 46 to 78 years (median 58.5 years). All patients had a history of surgery and pelvic radiotherapy. Specifically, the dose of previous radiotherapy ranged from 45 to 50.4 Gy in 9 patients one of which received a brachytherapy boost up to a total dose of 20Gy. One patient was irradiated with a total dose of 76 Gy for a prostatic cancer. One patient, at time of the first recurrence, underwent to re-irradiation with stereotactic radiotherapy (30 Gy in 6 fractions). They had 7 presacral, 1 perineal, 1 perianal and 1 pre-coccygeal relapses. Three patients received spacer implantation prior to CIRT to secure adequate distance between bowel and tumor. Toxicity was scored according CTCAE 4.0 scale.

#### Results

The median interval between the two courses of radiotherapy was 89.3 months (range: 13.8 - 138.2). Median total dose of CIRT was 60 GyRBE (range: 35-76.8) and was administered in a median number of 16 fractions (range: 15-20) over 4 weeks (from 3 to 4.8 Gy RBE/fraction). The GTV ranged from 7.21 to 300.8 cm<sup>3</sup> with a median of 28.42 cm<sup>3</sup>. The PTV ranged from 53.55 to 742.64 cm<sup>3</sup>. All patients completed the scheduled treatment course. Median follow-up was 13 months. Acute toxicity was mild and mainly neuropathic: grade 2 (G2) neuropathic pain in 1 (10%) and G1 in 2 (20%) patients. The major late toxicities were peripheral neuropathy (20%, G2). No G<sub>≥3</sub> acute/late reaction nor pelvic infections were observed. Four patients were diagnosed with local progression after carbon ion radiotherapy with a median disease free survival of 11.4 months (range: 2.4- 39.7). Three patients experienced systemic progression. The estimated 1-year-local control rate was 80%.

#### Conclusion

In our experience, CIRT for locally recurrent rectal cancer appears to be safe and effective with an acceptable rate of morbidity of normal tissue. More data and longer follow-up are required to investigate the long-term disease control and to determine late effects.

#### EP-1457 Moderate hypofractionation and SIB with volumetric modulated arc therapy (RapidArc) for anal cancer

A. Tozzi<sup>1</sup>, C. Iftode<sup>2</sup>, S. Cozzi<sup>2</sup>, G.R. D'Agostino<sup>2</sup>, C. Franzese<sup>2</sup>, L. Di Brina<sup>2</sup>, T. Comito<sup>2</sup>, F. De Rose<sup>2</sup>, I. Renna<sup>2</sup>, D. Franceschini<sup>2</sup>, P. Navarra<sup>2</sup>, E. Clerici<sup>2</sup>, P. Mancosu<sup>2</sup>, F. Lobefalo<sup>2</sup>, A. Stravato<sup>3</sup>, M. Scorsetti<sup>4</sup>  
<sup>1</sup>Humanitas Research Hospital, Radiotherapy and Radiosurgery, Rozzano Milan, Italy ; <sup>2</sup>Humanitas Research Hospital, Radiotherapy and Radiosurgery, Rozzano, Italy ; <sup>3</sup>Humanitas Research Hospital,

Radiothera and Radiosurgery, Rozzano, Italy ; <sup>4</sup>Humanitas University, Department of Biomedical Sciences, Rozzano, Italy

#### Purpose or Objective

This is a retrospective analysis of patients affected by anal squamous cell carcinoma treated with moderately hypofractionated radiotherapy and concurrent chemotherapy according to the Nigro schedule. End-point of the analysis were the assessment of acute and late toxicity and clinical response

#### Material and Methods

Data of Patients affected by locally advanced anal squamous carcinoma and submitted to exclusive chemoradiation were retrospectively analyzed. Radiotherapy was delivered in 28 daily fractions by Linear accelerators with the VMAT technique in its RapidArc form. Before each radiotherapy fraction a cone -beam CT was performed to verify the patient setup (IGRT). Physical examinations and toxicity assessments were performed during and after RT according to CTCAE v4.0. Tumour response was evaluated on CT-MRI-PET scans using the RECIST modified criteria

#### Results

From 2016 to 2018, 40 patients were treated in our Institution. Median age of patients was 65 years ; 93% had Stage II-III. Dose ranged from 61.6 to the primary tumor and nodes CT-PET positive to 50.4 Gy to the elective nodes. Thirty-eight (95%) patients were submitted to concomitant chemotherapy; two patients were submitted to radiotherapy only, because unfit for chemotherapy. Acute genitourinary toxicity was reported in the form of grade 1 by 11 patients (27.5%) and grade 2 by 3 patients (7.5%). Acute rectal toxicity was observed in 29 patients (72.5 %) as grade 1 and 4 patients (10%) as grade 2. Acute skin toxicity of grade 3 was diagnosed in 3 patients (7.5%). Acute gastrointestinal toxicity was reported by 31 patients (77.5%) as grade 1, 3 patients (7.5%) as grade 2 and 2 patient (5%) as grade 3. Late toxicity was represented by grade 1 genito-urinary toxicity in 4 patients (10%), and grade 1 and 2 rectal toxicity in 17 and 3 patients( 42.5% and 7.5%), respectively. Late skin toxicity was reported by 8 and 3 patients (20% and 7.5%) as grade 1 and 2, respectively. Late gastrointestinal toxicity was reported by 12 patients (40%) as grade 1 ; no late intestinal toxicity of grades 2 and 3 were recorded. At the restaging workup ,34 patients (85%) achieved a complete response and 6 patients (15%) a partial response. No patient had local progression during follow-up while one patients had metastatic progression of disease. All but one patient were alive at time of analysis

#### Conclusion

Moderate hypofractionation with SIB and RapidArc was shown to be safe, with acceptable toxicity. Longer follow-up is needed to assess clinical outcome

#### EP-1458 Acute toxicities comparing VMAT versus 3D-CRT in locally advanced rectal cancer

M. Zimmermann<sup>1</sup>, S. Weick<sup>1</sup>, F. Exner<sup>1</sup>, A. Richter<sup>1</sup>, M. Flentje<sup>1</sup>, B. Polat<sup>1</sup>

<sup>1</sup>University hospital Wuerzburg, Department of radiation oncology, Wuerzburg, Germany

#### Purpose or Objective

In locally advanced rectal cancer multimodal treatment including neoadjuvant radio(chemo)therapy is standard of care. The use of modern radiotherapy treatment techniques like IMRT and IGRT are becoming more common. Here, we analysed the impact of VMAT planning on bladder and small bowel sparing in comparison to conventional treatment planning.

#### Material and Methods

From 08/2015 to 01/2018, 35 patients with rectal cancer with UICC stage II and III were included in this retrospective analysis. All patients received long-term 5-

FU-based radio-chemotherapy with 50.4 Gy in 28 fractions followed by surgery and adjuvant chemotherapy. Radiation dose was delivered using conventional radiotherapy (3D-CRT) with posterior-anterior and opposed lateral field arrangement (with additional segments) in prone treatment position using a belly board. For CT-planning and each treatment fraction, a full bladder was required. Small bowel loops were individually contoured up to 3 cm above the cranial PTV border. The 3D treatment plans were compared to retrospectively calculated VMAT plans with equal dose prescription. Values for Dmean and Dmax for bladder and small bowel were calculated. Additionally the small bowel volume receiving doses between 5 and 50 Gy ( $V_{5-50}$ ) in 5 Gy intervals were recorded. Acute bladder and small bowel toxicities were classified according to CTCAE v4.03. Comparison of mean values was done by using t-test statistics, with p-values < 0.05 regarded as significant.

#### Results

Median patient age was 62.7 years. Nineteen patients were female and 16 male. Tumor stage was T3 100%, N0 3%, N1 14% and N2 83%. Nine patients (26%) developed acute cystitis Grade 1 and 18 patients (51%) acute diarrhea  $\geq 2$ . While occurrence of cystitis did not depend on bladder and PTV volume (p=0.442; p=0.943), there was a significant dependence on higher Dmean values to the bladder (grade 0: 25.2 Gy vs. grade 1: 29.4 Gy; p=0.009). Neither the PTV volume nor the bladder volume correlated with acute diarrhea (p=0.395 and p=0.303). If larger small bowel volumes were close to the PTV, higher grades of diarrhea occurred (grade 0-1: 648.8 ml vs. grade > 2: 846.1 Gy; p=0.021). This relation was also true for almost all dose levels ( $V_{5-50}$ ):  $V_5$  grade 1: 425.5 ml vs. grade 2: 606.6 ml; p=0.017. After re-planning the 3D plans with a VMAT technique dose to bladder and small bowel could be significantly reduced: Dmean bladder 26.3 Gy vs. 21.9 Gy (p<0.01) and Dmean small bowel 11.3 Gy vs. 7.7 Gy (p<0.01). Also, the other small bowel volumes receiving 5 to 45 Gy could be spared by VMAT (p<0.01).

#### Conclusion

Acute cystitis and gastrointestinal toxicities are dose and volume dependent. Irradiated volumes can be sufficiently reduced with VMAT planning compared to 3D-CRT. This effort might reduce urinary and gastrointestinal toxicities.

#### EP-1459 Impact of sentinel lymph-node biopsy and FDG-PET in staging and radiation treatment of anal cancer

N. Slim<sup>1</sup>, P. Passoni<sup>1</sup>, R. Tummineri<sup>1</sup>, C. Gumina<sup>1</sup>, G.M. Cattaneo<sup>2</sup>, P. De Nardi<sup>3</sup>, C. Canevari<sup>4</sup>, M. Ronzoni<sup>5</sup>, C. Fiorino<sup>2</sup>, E. Incerti<sup>4</sup>, A.M. Tamburini<sup>3</sup>, L. Gianolli<sup>4</sup>, L. Gianni<sup>3</sup>, R. Rosati<sup>3</sup>, N. Di Muzio<sup>1</sup>

<sup>1</sup>San Raffaele Scientific Institute- Milano- Italy, Radiation Oncology, Milan, Italy; <sup>2</sup>San Raffaele Scientific Institute- Milano- Italy, Medical physics, Milan, Italy; <sup>3</sup>San Raffaele Scientific Institute- Milano- Italy, Surgery, Milan, Italy; <sup>4</sup>San Raffaele Scientific Institute- Milano- Italy, Nuclear Medecine, Milan, Italy; <sup>5</sup>San Raffaele Scientific Institute- Milano- Italy, Medical Oncology, Milan, Italy

#### Purpose or Objective

To assess the role of sentinel lymph-node biopsy (SLNB) and FDG-PET in staging and radiation treatment (RT) of anal cancer patients (pts).

#### Material and Methods

80 pts (m:32, f:48), median age 61 years (38-87y) with anal squamous cell carcinoma were treated from 3/2008 to 3/2018. Twenty-seven/80 pts (34%) were HIV+. Pts without evident clinical inguinal LN metastases (mts) and/or with discordance between clinical and imaging were considered for SLNB. FDG-PET was performed in 69/80 pts. Pts with negative imaging in inguinal LNs and negative SLNB could avoid RT on groin. CTV included GTV (primary tumour and positive LNs) and pelvic  $\pm$  inguinal

LNs. PTV1 and PTV2 corresponded to GTV and CTV, respectively, adding 0.5 cm. RT dose was 50.4 Gy/28 fractions (fr) to PTV2 and 64.8 Gy/36 fr to PTV1, delivered with 3DCRT, VMAT (RA) or Tomotherapy, concomitant to NIGRO scheme chemotherapy.

#### Results

FDG showed inguinal uptake in 20/69 pts (29%) and in 11/20 pts lymphoscintigraphy was performed: SLNB confirmed inguinal mts in 4/11 (36%) pts, 6/11 (54.5%) pts were false positive and SLN not found in 1 pt. FDG-PET was negative in 49/69 pts (71%) and in 30/49 (61%) lymphoscintigraphy was performed: 6/30 (20%) showed mts, 23/30 (77%) were true negative and SLN not found in 1 pt. PET was false positive in 50% HIV- pts versus no HIV+ pts.

Fifty-four/80 pts (67.5%) received RT on groin (RA: 26 pts, 3DCRT: 14 pts, Tomotherapy: 14 pts); 19/54 pts were HIV+.

Pts treated vs no treated on groin showed more inguinal dermatitis toxicity (G1-G2: 27 (50%) vs 3 pts (11.5%) and G3-G4: 9 pts (17%) vs 0%. HIV+ pts treated on groin had more G3-G4 perineal dermatitis toxicity (9 (33.5%) vs 5 pts (18.5%). All pts treated on groin showed higher G3-G4 hematological toxicity vs not treated pts independently of HIV status.

RA better avoid inguinal region than 3DCRT. Tomotherapy was better than 3DCRT and RA in perineal toxicity (28.5% vs 43% and 42.5%, respectively), and was superior to 3DCRT in inguinal toxicity (14% vs 36%).

All pts were evaluated for responses, at a median follow-up of 36.8 months (5-128 m): 70 pts (87.5%) showed a complete response, 9 pts (11.25%) a partial response, 1 pt (1.25%) a stable disease, while 11 pts (13.75%) had a local relapse (3 with distant mts), median time to local relapse was 9.3 months (6.2-25.5). Twelve pts (5%) had a distant progression, median time to distant progression was 11.16 months (1.4-20.53). No pts treated or not on groin showed inguinal relapse.

#### Conclusion

SLNB improve FDG-PET inguinal LNs staging which has a large false positive and false negative rate, independently of HIV status and guides decision in inguinal RT. Inguinal irradiation could be avoided based on negativity of imaging and SLNB. Advanced RT techniques should better avoid toxicity especially in HIV+ pts.

#### EP-1460 Internal Margin evaluation in prone or supine rectal cancer patients using CBCT

C. Rosa<sup>1</sup>, L. Gasparini<sup>1</sup>, S. Di Biase<sup>1</sup>, C. Di Carlo<sup>1</sup>, A. Allajbej<sup>1</sup>, F. Patani<sup>1</sup>, D. Fasciolo<sup>1</sup>, A. Vinciguerra<sup>1</sup>, L. Caravatta<sup>1</sup>, D. Genovesi<sup>1</sup>

<sup>1</sup>Ospedale Clinicizzato S. S. Annunziata, Department of Radiation Oncology- SS. Annunziata Hospital- "G. D'Annunzio" University- Chieti- Italy, Chieti, Italy

#### Purpose or Objective

Due to a reported dose-response relationship in rectal cancer radiotherapy, a greater interest in dose intensification on small boost volume arises. When conformational techniques, as IMRT and VMAT, are used an accurate delineation of gross tumor volume (GTV) and an appropriate organ motion evaluation are suggested. Our previous study evaluated internal movement (IM) of GTV and mesorectum in patients in prone position on CBCTs. Now, this study aimed to use CBCT for GTV and mesorectal IM evaluation, in rectal cancer patient treated with neoadjuvant radiochemotherapy, examining the differences in prone and supine position.

#### Material and Methods

Thirty-two locally advanced rectal cancer patients (M:22, W:10) underwent CT scan simulation, 16 in prone and 16 in supine position, with controlled bladder filling. Co-registering MRI imaging with CT scan simulation, GTV (tumor site plus corresponded rectum) and mesorectum (from the sacral promontory to the level where the levator

ani muscle inserts into the rectal wall) were delineated. CBCTs were performed once a day during the first 5 fractions, then once or twice a week during all treatment, by Elekta X-Ray volume imaging system (XVI). All CBCTs were co-registered with CT scan simulation and the IM was estimated for GTV. Bladder was also delineated. Co-registrations were performed on RayStation platform (RaySearch Laboratories, Stockholm, Sweden) by bone landmarks and corrected for set-up error. IM evaluation was obtained for both prone and supine position, as mean shift in left and right (L-R), postero-anterior (P-A) and cranio-caudal (Cr-C) directions and volumes variability were calculated by DICE index.

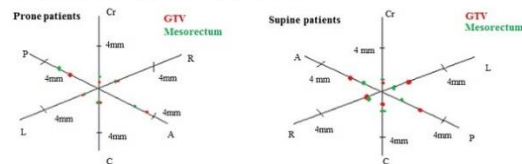
### Results

A total of 296 CBCTs were performed and retrospectively analysed: 147 in prone and 149 in supine position. Mean shift in left and right (L-R), postero-anterior (P-A) and cranio-caudal (Cr-C) directions for GTV and mesorectum were shown in Figure 1. Mean DICE index for GTV, mesorectum and bladder was 0.74, 0.86, 0.65, respectively in prone position, and 0.78, 0.89, 0.69 respectively in supine position. Detailed values are reported in Table 1.

Table 1. Mean shift in left-right (L-R), postero-anterior (P-A) and cranio-caudal (Cr-C) directions, mean volumes and DICE index for GTV, mesorectum and bladder in prone and supine position.

147 CBCT (prone pts)		L-R (cm)	P-A (cm)	Cr-C (cm)	Volume (cm <sup>3</sup> )	DICE index		
GTV	-0.14	0.14	0.23	-0.35	0.10	-0.19	38.45	0.74
Mesorectum	-0.13	0.13	0.29	-0.26	0.19	-0.19	339.46	0.86
Bladder	-0.26	0.22	0.39	-0.52	0.60	-1.00	226	0.65
149 CBCT (supine pts)		R-L (cm)	A-P (cm)	Cr-C (cm)	Volume (cm <sup>3</sup> )	DICE index		
GTV	-0.10	0.17	0.26	-0.23	0.09	-0.10	39.87	0.78
Mesorectum	-0.10	0.09	0.15	-0.12	0.12	-0.16	361.78	0.89
Bladder	-0.15	0.19	0.62	-0.37	0.76	-0.45	236.73	0.69

Figure 1. Mean shift in left-right (L-R), postero-anterior (P-A) and cranio-caudal (Cr-C) directions for GTV (tumor site plus corresponded rectum) and mesorectum



### Conclusion

In our study, GTV and mesorectum IM, evaluated in patients in prone and in supine position, were less than 4mm in all directions. Despite the small number of patients evaluated, we do not observe relevant variation in prone and supine position, even if, in the same deviations, supine position resulted in lesser movement compared to prone position. Our purpose is to increase our evaluation with more patients. Anyway, in both set-up, IM could be obtained with CBCTs and this could be an useful method for appropriate treatment intensification.

### EP-1461 SBRT Pelvic re-irradiation: 2cm "rind" around PTV and small bowel dosimetry of rectal recurrences

S. O'Cathail<sup>1</sup>, T. Smith<sup>2</sup>, Y. Tsang<sup>2</sup>, M. Harrison<sup>2</sup>, M. Hawkins<sup>1</sup>

<sup>1</sup>CRUK/MRC Institute for Radiation Oncology University of Oxford, Oncology, Oxford, United Kingdom ; <sup>2</sup>Mount Vernon Cancer Centre, Oncology, London, United Kingdom

### Purpose or Objective

Management of locally recurrent rectal cancer (LRR) with re-irradiation is challenging. SBRT is an alternative but concerns around small bowel (SB) tolerance remain. We hypothesise the sharp dose gradient of SBRT means that only SB within 2cm of the PTV would be relevant.

### Material and Methods

A prospective nationally maintained database for SBRT re-irradiation was interrogated. Eligibility criteria were

pelvic recurrence in a previously irradiated colorectal cancer, not eligible for exenteration, >6 month disease free survival, >6 month from previous RT, ≤3 metastases, PS 0-1. SBRT dose of 30Gy in 5 fractions in <10 days was specified. Anatomical compartments of site recurrence were mapped using a published atlas. A 2cm 'rind' was added to the PTV and overlapping volume with small bowel was assessed. Clinician reported CTCAE and patient reported Visual Analogue Scale (VAS). Linear regression was used to assess predictive factors of SB D<sub>0.5cc</sub>.

### Results

28 patients with 33 separate pelvic lesions were treated between 10/15 and 06/18. 22 patients had lateral pelvic compartment recurrence. All completed the SBRT. The median age was 64 years (range: 36-84). 27/28 had received 45-50.4Gy in 25-28F with concurrent Capecitabine, 1/28 received 25Gy/5F, all followed by surgery. Including SBRT, the cumulated effective dose received was >100Gy<sub>10</sub>. The median GTV volume was 14.9cc (range 0.47-121.73 cc). 23 lesions had overlap with SB. Median SB overlap volumes in the 2cm rind 12.5 cc (0-179.3). Dose to overlap volumes were median (max) D<sub>0.5cc</sub> =20.6 Gy (36Gy), D<sub>3cc</sub>=16.9Gy (33.6Gy), D<sub>5cc</sub>=17.1Gy (32.4Gy).

With a median FU of 10 months (range 5.4 - 23.4) local control at 1 year was 82.9% (C.I 66% -100%). No grade 3 toxicity was recorded. Median (range) VAS score before radiation was 75 (40-80) and 85 (45-90), a significant improvement (Wilcoxon signed rank, p=0.00861)

GTV volume and non-lateral location were significant predictors of increase overlap SB D<sub>0.5cc</sub> in a linear regression model (GTV p=0.0032, non-lateral, p=0.026; R<sup>2</sup> 0.2872, p=0.0062).

### Conclusion

SBRT in this inoperable re-irradiation cohort of patients produces initial acceptable local control at 1 year. Follow-up is continued for late toxicity events. Lateral pelvic disease, of small size will predicts that D<sub>0.5cc</sub> of small bowel volume within 2 cm of PTV will be lower than for larger non-lateral lesions. We propose limiting dose to 5cc of bowel within 2cm of PTV to 17.1 Gy as new parameter for SBRT re-irradiation.

### EP-1462 Stereotactic body radiation therapy (SBRT) in metastatic colorectal cancer (mCRC)

G.R. Mireia<sup>1</sup>, M.A. Marina<sup>2</sup>, H.M. Ana<sup>3</sup>, S.A. Maria José<sup>2</sup>, L.D.M. Miriam<sup>2</sup>, C.F. Silvia<sup>4</sup>, F.D. Amaya<sup>2</sup>, H.P. Alejandro<sup>5</sup>, L.T. José<sup>6</sup>, C.H. Carlos<sup>7</sup>

<sup>1</sup>Hospital General de Requena /Hopsital General de Valencia, Medical Oncology Department, Requena, Spain ; <sup>2</sup>Hospital General Universitario de Valencia, Medical Oncology, Valencia, Spain ; <sup>3</sup>Eresa Grupo Médico. Hospital General Universitario de Valencia, Radiotherapy, Valencia, Spain ; <sup>4</sup>Hospital General Universitario de Valencia- Universitat de València- Ciberonc, Molecular Oncology Laboratory, Valencia, Spain ; <sup>5</sup>Hospital General Universitario de Valencia- Ciberonc, Molecular Oncology Laboratory, Valencia, Spain ; <sup>6</sup>Eresa Grupo Médico. Hospital General Universitario de Valencia, Head of Radiotherapy, Valencia, Spain ; <sup>7</sup>Hospital General Universitario de Valencia- Universitat de València- Ciberonc, Head of Medical Oncology Department, Valencia, Spain

### Purpose or Objective

It is estimated that 25% of patients with CRC have metastases at diagnosis and up to 50% will develop them during the course of the disease. Although the multidisciplinary treatment in advanced disease has undergone a remarkable improvement in recent years, the median OS of the patients not candidates for surgery is approximately 30 months. Ablative therapies such as SBRT have helped to increase this survival with high local control rates in patients with visceral metastases in retrospective series.

The aim of this study is to analyze the efficacy and safety of treatment with SBRT on metastatic lesions in a cohort of patients with mCRC.

#### Material and Methods

Retrospective study of patients treated with SBRT on metastatic lesions in different locations between February 2012 and August 2016 at the General University Hospital of Valencia. The variables collected in the study were age, sex, location of the primary tumor, date of surgery, stage of the disease, RAS mutational status, location and number of metastases, type of relapse, treatment with SBRT, number of surgeries and previous chemotherapy lines. Statistical analysis was performed using the statistical package SPSS version 20.

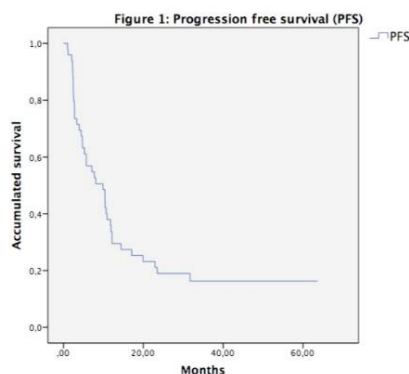
#### Results

A total of 49 patients were included (65.5% men). The average age was 70 years. 89.8% of the primary tumors were located in the left colon. 48% of the cases presented mutation in RAS. The distribution by stage at diagnosis was 10.2% for both stages I and II, 20.4% for III and 59.2% for IV. 83.7% of the metastases were metachronic. 46.9% of the patients were treated with more than 2 chemotherapy lines and 24.5% with  $\geq 2$  surgeries of metastases before the SBRT treatment. 53.1% of metastatic lesions were located in the lung and 30.6% in the liver. 28.6% of lesions treated with SBRT were the first relapse of the disease. 79.6% of the patients had no metastases in other sites at the time of treatment and 44.9% were treated in more than one lesion.

The total dose received in the treatment of SBRT was 45 Gy in 57.4% of the cases (fractionation of 1500cGy/session, 3 sessions, DEB 93.8 Gy) and 22.2% with a dose of 60 Gy. The most frequent adverse events are described in table 1. None of the patients had grade 3-4 events.

The median follow-up was 26.1 months. The PFS after treatment with SBRT was 9.9 months (95% IC 4.6 - 15.1) and the median OS was 28.9 months (95% IC 19.0 - 38.7). No relapses were observed in 20% of the patients after SBRT. Female sex and chemotherapy treatment before SBRT were significantly associated in the multivariate analysis with worse PFS (HR = 3.5,  $p = 0.001$  and HR = 4.81,  $p = 0.002$ ).

Type of toxicity	N (%)
Asthenia	12 (24.5)
Anorexia	4 (8.2)
Pulmonar	0
Cardiac	0
Cutaneous	1 (2)
Digestive	1 (2)



#### Conclusion

Treatment of CRC metastases with SBRT provides a meaningful benefit in PFS with low toxicity. Up to 20% of the patients achieves durable responses. This study supports the implementation of local therapy with SBRT in the multidisciplinary management of mCRC.

#### EP-1463 Radiation dose intensification in rectal cancer: a survey by the AIRO gastrointestinal study group

L. Caravatta<sup>1</sup>, M.A. Gambacorta<sup>2</sup>, G. Mantello<sup>3</sup>, M. Lupattelli<sup>4</sup>, M. Di Tommaso<sup>1</sup>, R. Consuelo<sup>1</sup>, G. Macchia<sup>5</sup>, A. De Paoli<sup>6</sup>, R.M. Niespolo<sup>7</sup>, F. Dionisi<sup>8</sup>, M.E. Rosetto<sup>9</sup>, F. Valvo<sup>10</sup>, M.F. Osti<sup>11</sup>, A.G. Morganti<sup>12</sup>, V. Valentini<sup>2</sup>, D. Genovesi<sup>1</sup>

<sup>1</sup>"SS Annunziata" Hospital- "G. D'Annunzio" University, Radiation Oncology Unit, Chieti, Italy; <sup>2</sup>Gemelli Advanced Radiation Therapy Center- Fondazione Policlinico Universitario "A. Gemelli"- Catholic University of Sacred Heart, Department of Radiotherapy, Rome, Italy; <sup>3</sup>State Hospital, Department of Radiotherapy, Ancona, Italy; <sup>4</sup>University of Perugia and Perugia General Hospital, Radiation Oncology Section, Perugia, Italy; <sup>5</sup>"Giovanni Paolo II" Foundation- Catholic University of Sacred Heart, Radiotherapy Unit- Department of Oncology, Campobasso, Italy; <sup>6</sup>Centro di Riferimento Oncologico- National Cancer Institute, Department of Radiation Oncology, Aviano, Italy; <sup>7</sup>Azienda Ospedaliera S. Gerardo, Department of Radiation Oncology, Monza, Italy; <sup>8</sup>Azienda Provinciale per i Servizi Sanitari- APSS, Proton Therapy Unit- Department of Oncology-, Trento, Italy; <sup>9</sup>Ospedale Belcolle, Department of Radiation Oncology, Viterbo, Italy; <sup>10</sup>Fondazione CNAO, Radiation Oncology Center, Pavia, Italy; <sup>11</sup>Sant'Andrea Hospital- Sapienza University of Rome, Department of Radiation Oncology, Rome, Italy; <sup>12</sup>University of Bologna- S. Orsola-Malpighi Hospital, Radiation Oncology Center- Department of Experimental- Diagnostic and Specialty Medicine - DIMES, Bologna, Italy

#### Purpose or Objective

Since a dose-response relationship in rectal cancer has been reported, a boost dose to macroscopic disease could represent a potential strategy to improve oncological outcomes in not responder patients after preoperative long-course radiotherapy (LCRT) or to select patients for which organ-preserving strategies might be possible. The Italian Association of Radiation Oncology (AIRO) study group of gastrointestinal malignancies proposed a national survey to investigate boost volume definition, doses and techniques used for dose intensification in preoperative LCRT for rectal cancer.

#### Material and Methods

In September 2018, an online survey was produced by a restricted group of recognized experts in rectal cancer. Members of AIRO gastrointestinal study group were individually contacted to request their participation to the survey. An expertise in rectal cancer treatment was required on the basis of the professional experience and their involvement in the multidisciplinary team for rectal cancer treatment. The questionnaire had 25 items focused on: center characteristics (5 items), simulation (3 items), imaging (4 items), volumes and doses (5 items), planning and treatment (8 items).

#### Results

Overall, 38 radiation oncologists from different Institutes (north Italy: 25, center: 8, south: 5) joined the study. Twenty-six declared to perform dose intensification preoperative LCRT. The characteristics of patients treated with dose intensification are reported in Table 1. Boost volume is defined as the Gross Tumor Volume (GTV) or as mesorectum area at the level of GTV, with or without additional margins, in 11 (42,31%) and 15 (57,69%) centers, respectively. Boost volume is delineated by

diagnostic imaging as magnetic resonance (MR: 85,71%), computed tomography (CT scan: 39,29%), and/or positron emission tomography (PET-CT: 35.71%). Co-registration with CT simulation is performed in 60.70% of the centers. An isotropic (73%), anisotropic (11,5%) or personalized (15,5%) margin is added for the for planning target volume. Doses are escalated by sequential boost in 6 centres up to 54-55Gy. Concomitant or simultaneous boost is delivered in 20 centers up to 55-60Gy (2.2-2.5Gy/fraction). Intensity-modulated radiotherapy (IMRT) is used in 76,92% of the centers. Intra-operative Radiotherapy or peri-operative Brachytherapy is used in one center. Image-gated RT (IGRT) protocols are used in 22 centers (84,61%). Concomitant chemotherapy based on Capecitabine (57,69%) or 5-FU (42,31%), is administrated in 25 centers (96,15%).

**Table 1.** Characteristics of patients treated with dose intensification preoperative long-course radiotherapy (multiple choice question type).

	N	%
cT4	17	65,38
cT3 MRF+	13	50,00
cN+, extra-mesorectal	9	34,62
cN2	7	26,92
cT3 N0-N+, low rectum	6	23,08
All patients	8	30,77
No-fit patients for surgery and/or CHT	2	7,69

MRF: mesorectal fascia; CHT: chemotherapy

### Conclusion

This survey illustrates the current status of dose intensification in preoperative LCRT in Italy. A high quality of dose escalation treatment was showed as highlighted by volume delineation in the majority of centers based on MR imaging, and on the delivery using IMRT in more than 75%. Future clinical trials are needed to standardize this treatment approach aiming to improve treatment outcomes among locally advanced rectal cancer patients.

### EP-1464 A systematic literature review of rectal re-irradiation: tolerance and outcomes

L. Caravatta<sup>1</sup>, F. Fiorica<sup>2</sup>, A.R. Alitto<sup>3</sup>, C. Rosa<sup>1</sup>, A. Nardangeli<sup>3</sup>, F. Munoz<sup>4</sup>, L. Bianco<sup>4</sup>, L. Giaccherini<sup>5</sup>, G. Timon<sup>5</sup>, F. Dionisi<sup>6</sup>, M. Massacesi<sup>3</sup>  
<sup>1</sup>"SS Annunziata" Hospital- "G. D'Annunzio" University, Radiation Oncology Unit, Chieti, Italy; <sup>2</sup>University Hospital Ferrara, Department of Radiation Oncology, Ferrara, Italy; <sup>3</sup>Fondazione Policlinico Universitario "A. Gemelli"- Catholic University of Sacred Heart, Department of Radiological- Radiotherapy and Hematology Sciences, Rome, Italy; <sup>4</sup>Azienda U. S. L. della Valle d'Aosta, Department of Radiotherapy, Aosta, Italy; <sup>5</sup>Arcispedale Santa Maria Nuova - IRCCS, Radiation Oncology Unit, Reggio Emilia, Italy; <sup>6</sup>Azienda Provinciale per i Servizi Sanitari- APSS, Proton Therapy Unit- Department of Oncology, Trento, Italy

### Purpose or Objective

Standard treatment for locally advanced rectal cancer includes pelvic radiotherapy (RT). Re-irradiation (Re-I) could be required in case of local relapse, that may cause significant morbidity and symptoms impacting quality of life. Unfortunately, Re-I could produce severe normal tissues complications, with variable rate of toxicities. A systematic review, on behalf of the Association of Radiation Oncology (AIRO) study group for the re-irradiation, was conducted aiming to report the toxicity and outcome of pelvic Re-I for rectal cancer recurrences, in terms of local and/or lymph node disease.

### Material and Methods

MEDLINE, EMBASE, OVID, and Cochrane database were used for the systematic search strategy. The computer search was supplemented with hand searches of reference lists. Only studies analyzing outcomes of patients re-treated where Re-I involved overlap with previous RT were taken into consideration. To determine the pooled toxicities rate ( $\geq$ G3), pain relief, overall survival (OS), and local recurrence free survival (LRF5), a meta-analysis technique over single arm study was performed.

### Results

Fourteen studies met the inclusion criteria, published between 2002 and 2017. Only four studies were prospective trials. Overall, 634 patients were analysed in the pelvis for Re-I within the pelvis for rectal cancer recurrences. Median follow-up from Re-I was 18.5 months (4.9 - 40 months). Four studies described the previous irradiation dose, delivered with a median dose of 50.4Gy (45-54 Gy) using a conventional fractionation. The mean time relapsed since previous irradiation was 28.8 months (22 - 47.4 months). Stereotactic RT technique was used for Re-I in 3 studies, carbon ions therapy in 1study, and external beam RT (EBRT) in the remaining studies (10 studies). Variable Re-I doses were prescribed: 25 Gy - 37.5 Gy. A hyper-fractionation schedule was employed in 8 of 10 EBRT studies. Concomitant chemotherapy was given in 501 patients (79%; 10 studies). Overall, 172 episodes of Grade  $\geq$ 3 toxicity were reported; 52 were acute (severe diarrhea, moist desquamation, mucositis) and 120 were late toxicities (chronic severe diarrhea, fistula, small bowel obstructions, pelvic abscess, ureteral stricture, skin ulcerations). Factors influencing toxicities could be identified in surgical resection after Re-I, anterior tumor location, and a shorter retreatment interval of  $\leq$  24months. Pain relief, was evaluated in 10 studies: 88.3% (95% CI: 83.9-92.9%) of patients experienced pain relief. The pooled 2-year OS rate (13 studies) was 54.6% (95%CI:47.8-62.3%). The pooled 2-year LRF5 rate (11 studies) was 49.4% (95% CI: 42.1-57.9%).

### Conclusion

Based on the results of our analysis, rectal Re-I reported moderate rates of acute and late toxicities, although symptoms palliation and local control could be obtained. Prospective studies or large data collections seem to be necessary to define patients selection criteria to ensure maximal benefit of Re-I treatment approach.

### EP-1465 Impact of diabetes on outcome and toxicity of neoadjuvant (chemo)radiation for rectal cancer

D. Bierbaumer<sup>1</sup>, S. Muench<sup>1</sup>, B. Haller<sup>2</sup>, D. Habermehl<sup>1</sup>, P.T. Pfluger<sup>3</sup>, K. Stemmer<sup>3</sup>, S.E. Combs<sup>1</sup>  
<sup>1</sup>Klinikum rechts der Isar- Technical University Munich- Ismaninger Str. 22, Department of Radiation Oncology, 81675 Munich, Germany; <sup>2</sup>Klinikum rechts der Isar- Technical University Munich- Grillparzerstr. 18, Institute of Medical Informatics- Statistics and Epidemiology- Medical School, 81675 Munich, Germany; <sup>3</sup>Helmholtz Zentrum München- Ingolstädter Landstraße 1, Institute for Diabetes and Obesity, 85764 Neuherberg, Germany

### Purpose or Objective

For patients with locally advanced rectal cancer, the German S3- guideline recommends neoadjuvant chemoradiation (nCRT) or short-course neoadjuvant radiotherapy (nRT) with before surgery to improve local control rates. While complete pathologic responses after neoadjuvant treatment are more commonly seen in patients without diabetes, there are conflicting results regarding the impact of diabetes on overall survival. Aim of this study was to compare oncologic outcome and toxicity between diabetic and non-diabetic patients undergoing neoadjuvant (chemo)radiation for rectal cancer.

### Material and Methods

In total, 73 patients with locally advanced rectal cancer who underwent surgery after neoadjuvant chemoradiation

or neoadjuvant short-course radiotherapy, were included in this analysis. Within this cohort, we identified 20 patients with diabetes mellitus type 2 (DMT2) with a median haemoglobin A1c (HbA1c) of 6.2%. Baseline and tumor characteristics, oncologic outcome and toxicity of these patients were compared to 53 patients without diabetes.

#### Results

Patients with DMT2 were significantly older than patients without diabetes (median age 68 vs. 60 years;  $p=0.006$ ). In addition there was a strong trend towards an increased body mass index (BMI) in patients with DMT2 (median BMI 26.8 vs. 24.6 Kg/m<sup>2</sup>,  $p=0.09$ ). After a median follow-up of 49.7 months, there were no significant differences regarding progression-free survival (PFS) between both groups. In contrast, median overall survival (OS) was significantly higher in patients without DMT2 (median OS not reached), compared to patients with DMT2 (45.2 months,  $p=0.006$ ). DMT2 was also confirmed to independently affect OS in a multivariable Cox regression model ( $p=0.029$ ). After nCRT, pathologic complete response was seen in 10% of patients with DMT2 and in 7% of patients without DMT2, ( $p=0.944$ ). Regarding toxicity, diabetic patients had a higher rate of anemia than patients without diabetes ( $\geq 11^\circ$  43% vs. 10%,  $p=0.004$ ). However, no significant differences were seen for the rates of leukopenia ( $\geq 11^\circ$  21% (DMT2) vs. 14% (no DMT2),  $p=0.377$ ) and thrombocytopenia ( $\geq 11^\circ$  0% (DMT2) vs. 0% (no DMT2)).

#### Conclusion

While there were no significant differences for PFS or the rate of complete pathologic remission after nCRT, median OS was significantly higher in patients without DMT2 than in diabetic patients. A significant difference was also seen for the rate of anemia after nCRT, but not for leukopenia or thrombocytopenia.

#### EP-1466 Preoperative chemoradiation with raltitrexid in locally advanced rectal cancer: a systematic review

E. Galofaro<sup>1</sup>, V. Panni<sup>1</sup>, M. Buwenge<sup>1</sup>, A. Guido<sup>1</sup>, G. Macchia<sup>2</sup>, F. Deodato<sup>2</sup>, V. Picardi<sup>2</sup>, M. Boccardi<sup>2</sup>, S. Mignogna<sup>3</sup>, C. Pozzo<sup>3</sup>, F. Di Fabio<sup>4</sup>, A.G. Morganti<sup>1</sup>, S. Cammelli<sup>1</sup>

<sup>1</sup>Policlinico Universitario S. Orsola Malpighi, Radiation Oncology Center- Department of Experimental-Diagnostic and Specialty Medicine - DIMES, Bologna, Italy ; <sup>2</sup>Fondazione di Ricerca e Cura "Giovanni Paolo II", Radiotherapy Unit, Campobasso, Italy ; <sup>3</sup>Fondazione di Ricerca e Cura "Giovanni Paolo II", Medical Oncology Unit, Campobasso, Italy ; <sup>4</sup>Policlinico Universitario S. Orsola Malpighi, Department of Medical Oncology, Bologna, Italy

#### Purpose or Objective

Neoadjuvant chemoradiotherapy with capecitabine followed by surgery is the standard therapy in patients with locally advanced rectal cancer (LARC). Raltitrexid (RTX) is a specific TS inhibitor with a radiosensitizing effect. No systematic reviews have been performed to analyze the efficacy of RTX based chemoradiotherapy in LARC. The aim of this study was to systematically review available literature to analyze the safety and efficacy of RTX based chemoradiation in terms of pathological CR.

#### Material and Methods

A systematic review of literature published from the earliest date possible to May 2018, using PubMed electronic database was conducted. Only articles reporting at least one of the following patients' outcome: toxicity and/or pathological complete response (pCR) or tumor downstaging were analyzed. Only studies of patients with diagnosis of locally advanced rectal cancer treated with neoadjuvant RTX based chemoradiotherapy alone or combined with other drugs were considered.

#### Results

Fourteen studies were included. All the studies had prospective study design. Median follow up was 40.3 months (range 15-91). Median G3/G4 toxicity and pCR were: 24,8% (range: 16.4-44.4%) and 34.8% (range: 27.7-50.0%), respectively. Moreover, tumor downstaging was reported in nine articles ranging between 53% and 85%.

#### Conclusion

Neoadjuvant chemoradiation with RTX in the preoperative treatment of LARC is reasonably tolerated and able to achieve high pCR rates.

#### EP-1467 KRAS mutation status as predictor factor in locally advanced rectal cancer

M. Campo<sup>1</sup>, S. Flamarique<sup>1</sup>, A. Gemma<sup>1</sup>, L. Alejandra<sup>2</sup>, G. David<sup>3</sup>, M. Fernando<sup>4</sup>, M. Ainara<sup>1</sup>, R. Maitane<sup>1</sup>, R. Lombardo<sup>1</sup>, A. Fernando<sup>1</sup>

<sup>1</sup>Hospital of Navarra, Radiation Oncology, Pamplona, Spain ; <sup>2</sup>Hospital of Navarra, Medical Oncology, Pamplona, Spain ; <sup>3</sup>Hospital of Navarra, Pathology, Pamplona, Spain ; <sup>4</sup>Hospital of Navarra, Physics, Pamplona, Spain

#### Purpose or Objective

Standard treatment of locally advanced rectal cancer (LARC) includes neoadjuvant chemo-radiotherapy followed by total mesorectal excision (TME). However, some patients have poor tumor response and long-term oncologic outcomes, indicating a lack of benefit from preoperative CRT. The mutation of Kirsten RAS (KRAS) is a molecular transducer and important component of the EGFR pathway and is now widely accepted as a predictor of poor response to anti-EGFR monoclonal antibodies in metastatic colorectal cancer. Nevertheless, few trials have investigated the KRAS status and clinical outcomes in LARC patients treated with neoadjuvant CRT followed by TME. Therefore, we evaluate the Tumor Regression Grade (TRG), Relapse-Free Survival (RFS) and Overall Survival (OS) according to the KRAS oncogene status in LARC.

#### Material and Methods

We evaluated retrospectively 23 patients with LARC treated at our Hospital between January 2013 and August 2018. Tumor DNA was obtained from pretreatment biopsy tissues. Standard polymerase chain reaction analysis was executed to detect specific mutations in KRAS using established primers. All patients received preoperative irradiation of 45Gy in 25 fractions to the whole pelvis at 1.8 Gy/day and 5,4 Gy in 3 fractions to the primary tumor and visible nodes, daily of 5 consecutive days per week. Concurrent chemotherapy was administrated as oral Capecitabine (825mg/m<sup>2</sup> twice daily during radiation time). All patients underwent TME 6-8 weeks after the end of preoperative completion CRT. Tumor regression grade after CRT was classified according to the Mandard grading system; good responders were defined as Mandard TRG1 and TRG2 and bad responders as Mandard TRG3, TRG4 or TRG5. Kaplan-Meier method and the log-rank test were used to compare survival distributions. The significance of correlations between mutation status and tumor regression was assessed by the Chi-square test. All statistical test were 2-sided, and  $p$ -values  $<0.05$  were considered statistically significant.

#### Results

The clinicopathological characteristics of the patients are summarized in *Table1*. KRAS mutation was found in 30,4% of the patients. TRG (1-2) after CRT were 56,2% and 42,8% ( $p= NS$ ), for wild-type and mutant KRAS groups (image1). After a median follow-up of 31 months, there was no difference in RFS (47,7 vs 23,3 months) or OS (51,5 vs 30 months) between wild-type and mutant-type KRAS groups, respectively (image2).

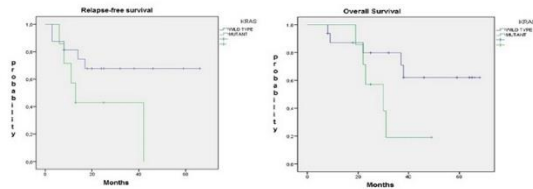


**TABLE 1.** Clinicopathological characteristics of locally advanced rectal cancer patients

Characteristics	No. of patients, %
<b>Gender</b>	
Male	18 (78,3)
Female	5 (21,7)
<b>Age (years)</b>	
Median (range)	63 (49-75)
≤60	11 (47,8)
>60	12 (52,2)
<b>Tumor localization (cm to anal margin)</b>	
High (11-15)	4 (17,4)
Medium (6-10)	13 (56,5)
Low (0-5)	6 (26,1)
<b>Clinical tumor classification</b>	
cT3	19 (82,6)
cT4	4 (17,4)
<b>Clinical nodal classification</b>	
cN0	1 (4,3)
cN1	7 (30,4)
cN2	15 (65,3)
<b>Histologic Grade</b>	
High	9 (39,1)
Moderate	11 (47,8)
Poor	3 (13,1)
<b>CEA level, ng/ml</b>	
≤5	12 (52,2)
>5	11 (47,8)
<b>Tumor regression grade (TRG)</b>	
TRG 1-2	12 (52,2)
TRG 3-4-5	11 (47,8)

**Conclusion**

Clinical trials over the KRAS oncogene status and treatment outcomes in LARC are limited, thus we focused on the potential of KRAS oncogene status as a biological predictive marker. Although KRAS status seems to have slightly better prognosis in patients treated with neoadjuvant CRT followed by curative surgery in LARC, it does not reach significant results (probably due to insufficient sample) in TRG, RFS or OS. It would be interesting to carry out prospective trials with longer follow-up examining KRAS mutation in locally advanced rectal cancer for an increased understanding.

**EP-1468 Radiomics versus volume reduction for rectal cancer response prediction in hybrid MR guided RT**

L. Boldrini<sup>1</sup>, D. Cusumano<sup>1</sup>, J. Lenkowicz<sup>1</sup>, G. Chiloiro<sup>1</sup>, C. Casà<sup>1</sup>, C. Masciocchi<sup>1</sup>, F. Cellini<sup>2</sup>, N. Dinapoli<sup>2</sup>, L. Azario<sup>1</sup>, S. Teodoli<sup>2</sup>, M.A. Gambacorta<sup>1</sup>, M. De Spirito<sup>1</sup>, V. Valentini<sup>1</sup>

<sup>1</sup>Università Cattolica del Sacro Cuore, Dipartimento di Diagnostica per immagini- Radioterapia Oncologica ed Ematologia, Rome, Italy ; <sup>2</sup>Fondazione Policlinico Universitario A. Gemelli IRCCS, Dipartimento di Diagnostica per immagini- Radioterapia Oncologica ed Ematologia, Roma, Italy

**Purpose or Objective**

Hybrid Magnetic Resonance guided Radiotherapy (MRgRT) represents an innovative therapeutic approach for locally advanced rectal cancer (LARC) patients (pts). Even if daily positioning MR imaging is characterized by low spatial resolution, its superior soft tissue contrast provides better visualization of therapy volumes and allows a direct and reliable visualization of tumor response throughout the treatment. The possibility to apply a radiomics approach to these images is however still under investigation.

Aim of this study was to extract radiomics parameters and compare their performance in complete clinical response (cCR) prediction with tumor volume reduction, known imaging biomarker of response.

**Material and Methods**

Patients affected by LARC undergoing neoadjuvant chemoradiotherapy on a hybrid 0.35 T MRgRT unit were considered for this analysis.

Prescribed dose was 55 Gy to primary tumor and corresponding mesorectum (PTV1) and 45 Gy to pelvic nodes and mesorectum (PTV2) delivered through a simultaneous integrated boost approach. The cCR was assessed with a MR acquired 6 weeks after chemoradiotherapy and digital examination (DE). An imaging acquisition protocol of 6 true fast imaging with steady state precession (TRUFI) MR scans per pt was performed: the first MR was acquired at first simulation (t0) and the remaining ones at fractions t5,t10,t15,t20 and t25. All the images had a spatial resolution of 1.5x1.5x1.5 mm<sup>3</sup> and an acquisition time of 175 sec. In order to investigate the variation of the radiomics parameters throughout the treatment, all features were normalized respect to the value obtained in simulation (t0).

A total of 52 radiomics features (morphological, statistical, textural and fractal) was firstly analyzed, while 254 ratios were calculated.

The Wilcoxon Mann Whitney test was performed to identify the feature whose variation can be more predictive of cCR.

**Fig. 1**

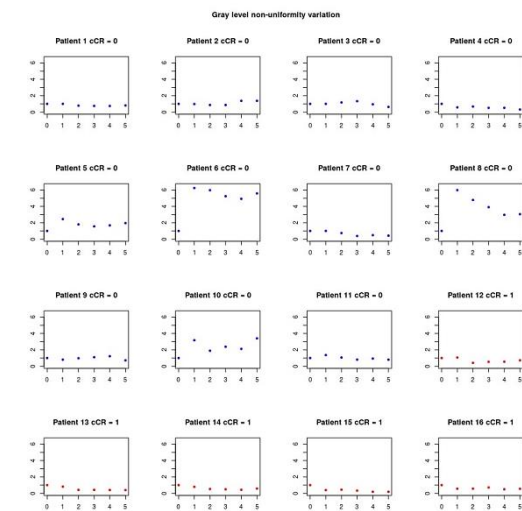
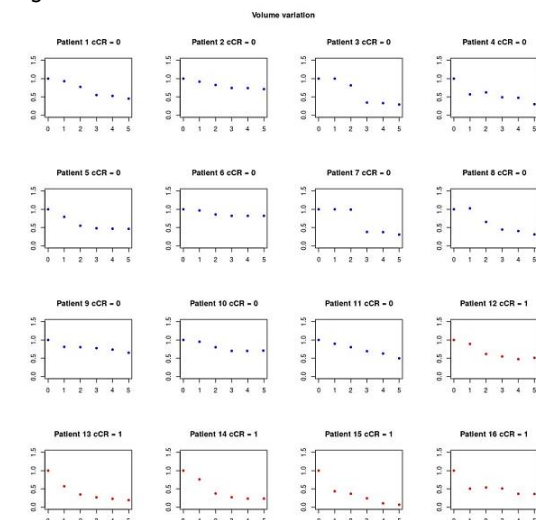


**Fig. 2**



## Results

16 pts (13 male and 3 female) were enrolled, out of which 5 pts (31%) showed cCR.

The most predictive radiomics feature was the “grey level non-uniformity” (*glnu*), whose variation resulted to be always significant in discriminating cCR pts from not responding ones ( $p=0,0375$  at t5;  $0,0005$  at t10;  $0,0133$  at t15;  $0,0032$  at t20;  $0,0380$  at t25).

Volume variation resulted to be significant in 4 of the considered time fractions ( $p=0,0490$  at t5;  $0,0032$  at t10;  $0,0636$  at t15;  $0,0055$  at t20;  $0,0275$  at t25). The trends of *glnu* and volume are reported in figure 1 and 2 respectively for all the pts.

## Conclusion

This hypothesis generating study suggests that hybrid 0.35 T MRgRT images could be suitable for radiomics analyses despite the low spatial resolution and that radiomics parameters may perform better than standard tumor shrinkage measurements in the prediction of cCR.

### EP-1469 Radiation dose to pelvic floor muscles and functional outcome after treatment for anal cancer

C. Kronborg<sup>1</sup>, P. Christensen<sup>2</sup>, B.G. Pedersen<sup>3</sup>, K.G. Spindler<sup>1</sup>

<sup>1</sup>Aarhus University Hospital, Oncology, Aarhus C, Denmark ; <sup>2</sup>Aarhus University Hospital, Surgery, Aarhus C, Denmark ; <sup>3</sup>Aarhus University Hospital, Radiology, Aarhus C, Denmark

#### Purpose or Objective

Chemoradiotherapy is the standard treatment for localized anal cancer. However, high dose pelvic radiation is associated with significant both acute and late toxicity. Late and persistent gastrointestinal dysfunction is among the most frequent, debilitating toxicities, with anal incontinence affecting up to 50 %. Radiation dose to the sphincter apparatus, but also to muscles of pelvic floor has been associated to functional gastrointestinal outcome in these patients.

The LARS (lower anterior resection syndrome) questionnaire is a patient reported outcome measure, which evaluates bowel dysfunction after rectal surgery. It consists of five items, all relevant to the late toxicities seen after pelvic radiotherapy: frequent bowel movements, gas and fecal incontinence, fragmentation, and urgency.

We aimed to: i: compare radiation dose to sphincters and pelvic floor muscles in patients with no LARS and major LARS. ii: correlate radiation dose to sphincters and pelvic floor muscles and the 5 individual items in LARS score.

#### Material and Methods

From 2009 to 2015, anal cancer patients were routinely asked to fill out LARS questionnaires at follow-up. For this project all patients with no LARS (score 0-19) were selected from the cohort and an equal number of patients with major LARS (score 30-42).

The Internal and external sphincter (contoured as sphincter complex), levator ani and puborectal muscles were delineated on planning MRI or CT-scans. Dose volume parameters: V50Gy, V60Gy, D90%, Dmean, and Dmax were obtained for each structure and for bowel bag V45Gy and V30Gy.

Differences between patients with no or major LARS were tested by Mann-Whitney U-test, correlations by Spearman’s rank correlation. **Results**

A total of 36 patients were included, 18 patients with no LARS (median 11, range 0-20) and 18 with major LARS (median 37 range 31-39). Gender, age, TNM stage, PTV, chemotherapy, time to LARS score (mean 692 and 749 days) were not statistically different in the two groups. Thirty-three patients were treated with 64 Gy/ 51,2 Gy in 32 fractions, (one with 46 Gy, one 45Gy, and one 54Gy). Thirty patients received therapy with 2 arc VMAT and six with 6-field IMRT.

Dose to sphincter complex (Dmean, V50Gy and D90%) differed significantly between patients with no and major LARS ( $p=0.049$ ,  $0.035$  and  $0.024$  respectively).

There was a significant correlation between D90% to the sphincter complex and the LARS sub-unit “Do you ever have accidental leakage of liquid stool?” (1: yes, 2: no),  $p=0.047$ , with higher risk of incontinence with higher dose. The same applied for V45Gy to the bowel bag and question “How often do you open your bowels?” (1: <1 time per day, 2: 1-3 times per day, 3: 4-7 times per day, 4: >7 times per day),  $p=0.029$ , with higher risk of frequent bowel movements with higher dose. **Conclusion** Specific doses to the sphincter complex could become a useful predictor of anal incontinence and high LARS, and dose to bowl bag a predictor of frequent bowel movements after radiotherapy for anal cancer

### EP-1470 Response assessment in rectal cancer patients treated with MRI-guided RT: preliminary results

A. Re<sup>1</sup>, G. Chiloire<sup>2</sup>, L. Boldrini<sup>2</sup>, F. Cellini<sup>2</sup>, M. Giraffa<sup>1</sup>, P. De Franco<sup>1</sup>, B. Corvari<sup>2</sup>, E. Meldolesi<sup>2</sup>, B. Fionda<sup>2</sup>, D. Cusumano<sup>3</sup>, S. Teodoli<sup>3</sup>, V. Valentini<sup>1</sup>, M.A. Gambacorta<sup>1</sup>  
<sup>1</sup>Università Cattolica del Sacro Cuore, Diagnostica per immagini- Radioterapia oncologica ed Ematologia, Roma, Italy ; <sup>2</sup>Fondazione Policlinico Universitario A. Gemelli IRCCS, Diagnostica per immagini- Radioterapia oncologica ed Ematologia, Roma, Italy ; <sup>3</sup>Fondazione Policlinico Universitario A. Gemelli IRCCS, Diagnostica per immagini- Radioterapia oncologica ed Ematologia - U.O.C. Fisica Sanitaria, Roma, Italy

#### Purpose or Objective

To evaluate the efficacy in terms of complete response (CR) of neoadjuvant magnetic resonance-guided radiotherapy (MRgRT) delivered with a hybrid 60Co-MRI unit in locally advanced rectal cancer (LARC) patients (pts).

#### Material and Methods

MRgRT includes daily MRI for setup and real-time cine MRI scans for target tracking.

Pts affected by LARC and clinically eligible for MRgRT were consecutively enrolled.

The clinical target volume (CTV)<sub>1</sub> included the tumor volume and the corresponding mesorectum received 55 Gy/2.2 Gy per fraction and the CTV<sub>2</sub>, including total mesorectum and draining lymph nodes, 45 Gy/1.8 Gy with a simultaneous integrated boost. CTV to PTV margins were 0.5 cm in all directions.

Fluoropyrimidine-based concomitant chemotherapy (CT) was planned, Oxalyplatin was added in selected cases. Acute adverse events were registered according to CTCAE v.4.0 scale.

Surgery was planned at least 8 weeks after the end of chemoradiotherapy (CRT) and pathological complete response (pCR) was defined as ypT0N0.

#### Results

From February 2017 to July 2018 20 LARC pts were enrolled.

Massive lymph nodal involvement (cN1 or cN2) or mesorectal fascia involvement were observed in 30%, 55% and 60% of the cases, respectively. Extra-mesorectal pathological nodes were detected in 30% of pts. Primary lesion was located in low rectum in 40% of the pts. Compliance to CRT was overall good: all pts completed the prescribed treatment.

Fifteen patients (75%) required at least one day of suspension from CRT (average 2,65 days, range 1-10). No patient reported grade 3 or 4 hematological, genitourinary or skin toxicity.

Overall GI adverse events were more commonly reported: 5 pts (25%) showed grade 3 diarrhea during CRT. Two pts (10%) did not undergo surgery as complete clinical response (cCR) was described at restaging exams and confirmed at early follow up assessments and were

addressed to watch and wait. The surgical interval was on average 14 weeks after the end of CRT (range 9-21). Total mesorectal excision was performed in 18 pts (with only 1 abdominal-perineal resection). 22.2% of the pts showed pCR, while the CR overall rate (4 pCR+2 cCR) was 30%. As reported in Tab.1, tumor and nodal downstaging was observed in 65% and 95% of pts, respectively.

Tab1: Tumor and nodal Response according to clinical staging

	ypT0/ycN0	ypT1	ypT2	ypT3	ypT4
cT2			1		
cT3	3	1	2	6	
cT4	3		1	3	
TOT	6	1	4	9	
	ypN0/ycN0	ypN1	ypN2		
cN0	9				
cN1	6				
cN2	8	2	1		
TOT	23	2	1		

All cases in whom there were some kind of response are highlighted

### Conclusion

These preliminary results suggest the possibility to treat LARC pts with MRgRT. Although the limited number, the results seem promising if compared to toxicity data available in literature. MRgRT may potentially support PTV margin reduction and dose-escalation in a tailored and personalized treatment perspective.

### EP-1471 Evaluating the safety and efficacy of neo-adjuvant chemotherapy in locally advanced rectal cancer

K. Saeed<sup>1</sup>, T. Sadaf<sup>1</sup>, A.S. Kazmi<sup>1</sup>, S. Butt<sup>1</sup>, A.A. Syed<sup>2</sup>, M.A. Yusuf<sup>3</sup>

<sup>1</sup>Shaukat Khanum Memorial Cancer Hospital & Research Center., Clinical & Radiation Oncology, Lahore, Pakistan ; <sup>2</sup>Shaukat Khanum Memorial Cancer Hospital & Research Center., Surgical Oncology, Lahore, Pakistan ; <sup>3</sup>Shaukat Khanum Memorial Cancer Hospital & Research Center., Internal Medicine, Lahore, Pakistan

### Purpose or Objective

Standard therapy for locally advanced rectal cancer (LARC) is pre-operative chemo radiotherapy and post-operative chemotherapy. Local recurrence rate for LARC is around 6% while distant recurrence rate is about 25%. Introducing systemic therapy early in the treatment can help control the micrometastasis. Adjuvant chemotherapy is difficult to tolerate due to morbidities of chemoradiation and surgery. We report the safety and efficacy of neo adjuvant chemotherapy before Chemoradiotherapy on tumor downsizing and pathologic complete response (pCR) in Locally advanced rectal cancer.

### Material and Methods

Records of 244 patients treated between April 2007 to November 2014 were retrospectively reviewed, using the hospital information system. Patients were treated by multi-modality approach. Neo adjuvant Chemotherapy used was 3 weekly cycles of Capecitabine 1000mg/m<sup>2</sup> Day 1-14 per oral and Oxaliplatin 130mg/m<sup>2</sup> on Day 1 I/V. Eastern co-operative oncology group (ECOG) performance scale was used to evaluate performance, before chemotherapy. Common terminology criteria for adverse events grades used to measure chemo toxicity.

### Results

226 out of 244 patients received neoadjuvant chemotherapy. Majority of the patients received 4 cycles before the chemoradiation. Patients were reviewed

clinically and via blood tests before each cycle for toxicity of chemotherapy. All of the patients were able to complete the treatment with no major toxicities (Hand-foot syndrome, hematologic, Skin, Neuropathy and diarrhea) of the chemo observed. Pathologic complete response was seen in 41 (23%) of the patients. R0 resection was observed in 70% of patients.

### Conclusion

Neo-adjuvant chemotherapy CapOx can safely be delivered before chemoradiation and planned surgery. It results in tumor regression, a high rate of delivery of planned therapy, and a substantial pathological CR rate. Chemotherapy is well tolerated in the neoadjuvant settings. Further randomized clinical trials are needed to support this evidence.

### EP-1472 Obesity and Colorectal Cancer: Impact of the Gut Microbiota

J. Gomez-Millan Barrachina<sup>1</sup>, L. Sanchez-Alcoholado<sup>2</sup>, A. Otero<sup>1</sup>, R. Ordoñez<sup>1</sup>, D. Castellano-Castillo<sup>2</sup>, Y. Lupiañez-Perez<sup>1</sup>, M.I. Queipo-Ortuño<sup>2</sup>, A. Román<sup>1</sup>

<sup>1</sup>Hospital Virgen de la Victoria, Radiation Oncology Department, Malaga, Spain ; <sup>2</sup>Hospital Virgen de la Victoria, Clinical Management Unit of Endocrinology and Nutrition- Laboratory of the Biomedical Research Institute of Málaga IBIMA- Virgen de la Victoria University Hospital- Universidad de Málaga- Málaga- Spain CIBER de Fisiopatol,

### Purpose or Objective

Obesity is considered an important factor in the increased risk of colorectal cancer (CRC) (up to 70%), but the role that the intestinal microbial population plays in this link is not well established. The aim of this study was to determine the intestinal microbiota composition in fecal samples from CRC patients with and without obesity compared to the microbiota present in normal-weight healthy controls, in order to unravel the possible association between gut microbiota, the inflammatory level and the intestinal permeability in the context of obesity-associated CRC.

### Material and Methods

The study was conducted over 50 CRC patients (25 patients with BMI < 30 kg/m<sup>2</sup> and 25 patients with BMI > 30 kg/m<sup>2</sup>) who were age and sex paired to 30 normal-weight healthy controls. Fecal bacterial DNA was extracted and analyzed by 16 S rRNA sequencing using an Ion S5 platform and followed by a bioinformatic analysis by QIIME II.

### Results

Patients with CRC had lower bacterial diversity and richness than normal-weight controls, being even lower in CRC subjects with obesity (BMI > 30 kg/m<sup>2</sup>). The microbiota of CRC patients was characterized by a reduction in butyrate and lactate producing bacteria (*Faecalibacterium prausnitzii*, *Roseburia*, *Butyrivibrio* and *Bifidobacterium*) and an increase in opportunistic pathogens (*Streptococcus*, *Fusobacterium nucleatum* and *Escherichia coli*). Moreover, the relative abundance of these opportunistic pathogens was significantly higher in obese CRC patients compared to normal-weight CRC patients and healthy controls. The serum levels of IL-1B (proinflammatory cytokine) and the gut permeability (determined by zonulin levels) were significantly increased in obese CRC patients than in normal-weight CRC patients and healthy controls. Additionally, zonulin levels were significantly correlated with the relative abundance of several microbial groups, being in a positive way with *Prevotella* in normal-weight CRC patients and with *Escherichia coli* in obese CRC patients, while negative associations were found with the relative abundance of *Ruminococcus* and *Faecalibacterium prausnitzii* in normal-weight controls.

### Conclusion

The presence of obesity in CRC patients is related to lower diversity of microbiota, higher gut permeability, higher

presence of opportunistic pathogens such as *Fusobacterium nucleatum*, which in turn could be responsible, at least in part, of the higher levels of inflammation found in these patients. These data point out the importance that gut microbiota could have in the appearance and development of CRC-associated to obesity and could give new clues for the development of new diagnostic tools for CRC prevention.

**EP-1473 Anal adenocarcinoma: a comprehensive review of management practices and clinical outcomes**

J. Lukovic<sup>1</sup>, J. Kim<sup>1</sup>, A. Liu<sup>2</sup>, J. Ringash<sup>1</sup>, J. Brierley<sup>1</sup>, R. Wong<sup>1</sup>, A. Barry<sup>1</sup>, L. Dawson<sup>1</sup>, B.J. Cummings<sup>1</sup>, M. Krzyzanowska<sup>3</sup>, E.X. Chen<sup>3</sup>, D. Hedley<sup>3</sup>, R. Prince<sup>3</sup>, F. Quereshy<sup>4</sup>, A. Easson<sup>4</sup>, C.J. Swallow<sup>5</sup>, R. Gryfe<sup>5</sup>, E. Kennedy<sup>5</sup>, A. Hosni<sup>1</sup>

<sup>1</sup>Princess Margaret Cancer Centre - University Health Network- University of Toronto, Department of Radiation Oncology, Toronto, Canada ; <sup>2</sup>Princess Margaret Cancer Centre, Department of Biostatistics, Toronto, Canada ; <sup>3</sup>Princess Margaret Cancer Centre - University Health Network- University of Toronto, Department of Medical Oncology, Toronto, Canada ; <sup>4</sup>University Health Network- University of Toronto, Department of Surgical Oncology, Toronto, Canada ; <sup>5</sup>Princess Margaret Cancer Centre - Mount Sinai Hospital- University of Toronto, Department of Surgical Oncology, Toronto, Canada

**Purpose or Objective**

Primary adenocarcinoma of the anal canal (ACC) is rare. There is a lack of consensus regarding the optimal treatment for these patients. The purpose of this retrospective cohort study was to evaluate the multidisciplinary management outcomes of patients with ACC to better define the optimal treatment paradigm.

**Material and Methods**

Patients with anal cancers treated at a tertiary cancer center from Jan 1995 to Dec 2016 were identified. Definitive treatment was either chemoradiation (CRT: 52-63 Gy with concurrent 5-fluorouracil [5FU] and mitomycin-C [MMC]) or trimodality therapy (TMT: abdominoperineal resection [APR] with adjuvant or neoadjuvant CRT [45-50Gy with concurrent 5FU or capecitabine]). Baseline characteristics were compared between the treatment groups. Local (LF) and regional failure (RF), and distant metastasis (DM) cumulative incidences were estimated. The Kaplan-Meier method was used to estimate progression-free survival (PFS) and overall survival (OS). Cumulative incidence and survival outcomes were compared between two treatment groups using the log rank test.

**Results**

There were 1007 cancer patients identified and 89(8.72%) had ACC histology. Eleven (12.4%) had distant metastases, 36(46.2%) were treated with TMT, 23(29.5%) received CRT, 8(8.99%) were treated with wide local excision, 7(7.87%) received palliative care, and 4(4.49%) were treated at outside cancer centers.

The 5-year LF was 9.4% in the TMT group vs 50.8% in the CRT group (p=0.003). (Figure 1a) In the TMT group, 3 patients (2/3 had a positive radial margin) failed locally 3, 8, and 22 months after definitive treatment and were treated palliatively. Out of the 23 patients treated with CRT, 7(30.4%) never achieved a complete response and 9(39.1%) experienced LF. The median time to LF was 4.2 years (CRT) and not reached for patients treated with TMT. Eight of the CRT patients had an isolated local recurrence and were treated with salvage APR. The 5-year cumulative incidence of colostomy was 53.6%. There was no difference in the 5-year RF cumulative incidence (TMT: 10.1% vs. CRT: 21.2%; p=0.231) or DM (TMT: 27% vs. CRT: 25.6%; p=0.734). (Figure 1b,c)

There was no difference in PFS at 5 years (TMT: 48% vs. CRT: 32.2%; p=0.178) and a borderline significant

improvement in OS in patients treated with TMT (TMT: 83.7% vs. CRT: 57.3%; p=0.052). (Figure 2a,b) The median time to death was 5.1 years (range: 0.9 to 15.7 years) in the TMT group and 4.1 years (range: 0.8 to 18.2 years) in the CRT group.

**Conclusion**  
Despite prior reporting, ACC continues to be a therapeutic dilemma for gastrointestinal oncologists. This retrospective cohort suggests a benefit of TMT over non-operative management for ACC although CRT may be considered a reasonable alternative for patients favouring functional organ preservation. The role of adjuvant chemotherapy remains to be elucidated.

**EP-1474 Preoperative RT-CT in locally advanced rectal cancer using different RT doses; our experience**

D. Delishaj<sup>1</sup>, I.C. Fumagalli<sup>1</sup>, A. Cocchi<sup>1</sup>, A. Vola<sup>1</sup>, G. De Nobili<sup>1</sup>, F. Gherardi<sup>1</sup>, F. Bonsignore<sup>2</sup>, F. Tagliabue<sup>3</sup>, J. Arnoffi<sup>4</sup>, R. D'Amico<sup>1</sup>, F. Declich<sup>2</sup>, A. Ardizzoia<sup>4</sup>, C.P. Soatti<sup>1</sup>

<sup>1</sup>Ospedale Manzoni di Lecco, Department of Radiotherapy, Lecco, Italy ; <sup>2</sup>Ospedale Manzoni di Lecco, Department of Medical Physics, Lecco, Italy ; <sup>3</sup>Ospedale Manzoni di Lecco, Department of Surgery, Lecco, Italy ; <sup>4</sup>Ospedale Manzoni di Lecco, Department of Clinical Oncology, Lecco, Italy

**Purpose or Objective**

Colorectal cancer (RC) is the most common gastrointestinal (GI) malignancy. More than half patients (pts) affected by RC consist in LARC and preoperative RT-CT followed by total mesorectal excision (TME) is the standard treatment in these pts.. The aim of this study was to evaluate pathological response and toxicities in pts affected by LARC underwent neoadjuvant RT-CT using two different doses.

**Material and Methods**

From January 2014 to September 2018 we analyzed 33 pts affected by LARC treated with neoadjuvant RT-CT followed by surgery. Fifteen pts were female (45,5 %) and 18 pts were male (55,5 %). The median age was 68 years old with a range wide from 36 to 80 years old. Twenty-two pts (Group 1) received 55 Gy in 28 FF (45 Gy to the pelvis and 55 Gy to the T, N+ and mesorectum in SIB technique) + Capecitabine 1650 mg/mq/day; 11 pts (Group 2) received 50.4 Gy to the pelvis in 28 FF + Capecitabina 1650 mg/mq/day. We evaluated clinicopathological characteristics of Tumour (T), Nodal (N), grading, margins, N-down-staging, T-down-staging, tumor regression and sphincter preservation. According to CTCAE vs 5 scale acute and late toxicity was evaluated.

**Results**

After a median follow-up of 38 months (range 3-48 months) the PFS at 2 and 4 years was 93,2% and 82,%, respectively. At histological examination 5 pts (15,2 %) had a T- complete response (CR), 21 pts (63.6%) had N-CR and 4 pts (12.2%) had both T and N-CR. There was no statistically differences between two groups (p-value > 0,05). Tumour down-staging was observed in 23 (66,6%) pts (68 % Group 1 and 63.5 % Group 2; p-value 0,78). Nodal down-staging was reached in 90 % of pts (100 % in Group 1 and 77 % in Group 2; with a trend in favor of Group 1, p-value= 0,082). Four pts had disease progression (2 pts in Group 1 and 2 in Group 2). Of them 3 pts distant metastases and one pt had locally and distant metastases. All pts underwent systemic treatment. Overall sphincter preserving was reached in 79,9 % (90% Group 1 and 65 % Group 2; p-value 0,012). Finally, GI and GU G2/3 acute toxicity was observed in 6 pts (18,2 %): 3/22 (13,6 %) Group 1 and 3/11 (27,2%) Group 2.

**Conclusion**

Neoadjuvant RT-CT with SIB technique and TD of 55 Gy/28ff (45 Gy to the pelvis and 55 Gy to mesorectum, T and N+) showed an advantage regarding N-down-staging and sphincter preserving compared to standard RT treatment (50.4 Gy/28ff). Acute and late toxicity was

acceptable with no statistically differences between two groups. The treatment was well tolerated without statistically differences between two groups. Randomized trials with higher number of pts and longer follow-up are needed to confirm our results

---

**Electronic Poster: Clinical track: Gynaecological (endometrium, cervix,vagina,vulva)**

---

**EP-1475 Radiotherapy Is a Safe and Effective Salvage Treatment for Recurrent Cervical Cancer**

H.J. Kim<sup>1</sup>, W.S. Koom<sup>2</sup>, G.E. Kim<sup>3</sup>, Y.B. Kim<sup>2</sup>

<sup>1</sup>Gil Medical Hospital, Department of Radiation Oncology, Incheon, Korea Republic of ; <sup>2</sup>Yonsei Cancer Center, Department of Radiation Oncology, Seoul, Korea Republic of ; <sup>3</sup>Jeju National University Hospital, Department of Radiation Oncology, Jeju, Korea Republic of

**Purpose or Objective**

The feasibility of salvage radiotherapy (RT) for patients with recurrent cervical cancer after definitive treatment is contentious. The purpose of this study was to investigate the feasibility and benefit of RT, particularly intensity-modulated RT (IMRT), for salvage treatment in patients with recurrent cervical cancer.

**Material and Methods**

We retrospectively analyzed 125 patients with recurrent cervical cancer treated with RT at Yonsei Cancer Center between January 2007 and December 2016. All patients received salvage RT for the recurred or metastatic tumor mass. Irradiating dose and volume were determined depending on initial treatment. IMRT was selected in challenging cases, such as re-irradiation or for patients for whom implementing a satisfactory 3-dimensional conformal RT plan was challenging.

**Results**

The median follow-up period was 5.5 years (range, 10.8 months to 41 years). The 5-year local failure-free survival (LFFS) and progression-free survival (PFS) rates were 63.9% and 39.6%, respectively. The 5-year overall survival (OS) rate was 66%; 10-year OS reached 51%. The median PFS rates in patients with locoregional failure, distant metastases, or both were 45.4, 29.1, and 14.7 months, respectively (p = 0.005). For the 45 patients that received re-irradiation, 5-year LFFS, PFS, and OS rates were 47.1%, 33.2%, and 66.5%, respectively. Late complications  $\geq$  grade 2 were observed in 12 patients (12/125, 9.6%).

**Conclusion**

Our data suggest that salvage RT is safe and effective against recurrent cervical cancer. IMRT is a safe and effective salvage modality for these patients, including those requiring re-irradiation.

**EP-1476 Validation of a combined PET and MRI radiomics model for prediction of recurrence in cervical cancer**

F. Lucia<sup>1</sup>, D. Visvikis<sup>2</sup>, M. Vallières<sup>2</sup>, M. Desseroit<sup>2</sup>, O. Miranda<sup>1</sup>, P. Robin<sup>3</sup>, P.A. Bonaffini<sup>4</sup>, J. Alfieri<sup>5</sup>, I. Masson<sup>6</sup>, A. Mervoyer<sup>6</sup>, C. Reinhold<sup>4</sup>, O. Pradier<sup>1</sup>, M. Hatt<sup>2</sup>, U. Schick<sup>1</sup>

<sup>1</sup>CHRU Brest, Radiation oncology, Brest, France ; <sup>2</sup>LaTIM-INSEERM- UMR 1101, University of Brest- ISBAM- UBO-UBL- Brest- France, Brest, France ; <sup>3</sup>CHRU Brest, Nuclear Medicine, Brest, France ; <sup>4</sup>McGill University Health Centre MUHC, Department of Radiology, Montreal, Canada ; <sup>5</sup>McGill University Health Centre MUHC, Department of Radiation Oncology, Montreal, Canada ; <sup>6</sup>Institut de Cancerologie de l'Ouest, Radiation Oncology, Nantes, France

**Purpose or Objective**

The aim of this study was to validate previously developed radiomics models relying on just two radiomics features from 18 F-fluorodeoxyglucose positron emission tomography (PET) and magnetic resonance imaging (MRI) images for prediction of disease free survival (DFS) and locoregional control (LRC) in locally advanced cervical cancer (LACC).

**Material and Methods**

Patients with LACC receiving chemoradiotherapy were enrolled in two French and one Canadian centers. Pre-treatment imaging was performed for each patient. Multicentric harmonization of the two radiomics features was performed with the ComBat method. The models for DFS (using the feature from apparent diffusion coefficient (ADC) MRI) and LRC (adding one PET feature to the DFS model) were tuned using one of the French cohorts (n=112) and applied to the other French (n=50) and the Canadian (n=28) external validation cohorts.

**Results**

The DFS model reached an accuracy of 90% (95% CI [79%-98%]) (sensitivity 92-93%, specificity 87-89%) in both the French (figure A) and the Canadian (figure B) cohorts. The LRC model reached an accuracy of 98% (95% CI [90%-99%]) (sensitivity 86%, specificity 100%) in the French cohort and 96% (95% CI [80%-99%]) (sensitivity 83%, specificity 100%) in the Canadian cohort. Accuracy was significantly lower without ComBat harmonization (82-85% and 71-86% for DFS and LRC, respectively). The best prediction using standard clinical variables was 56-60% only.

Figure A

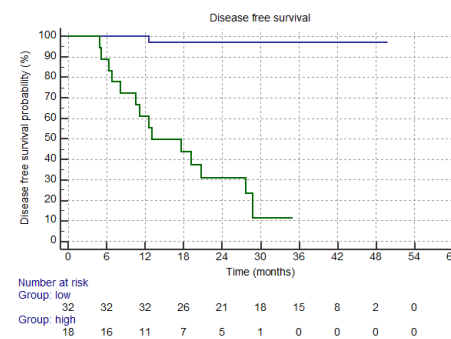
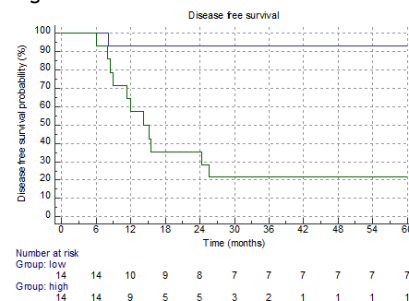


Figure B



**Conclusion**

The previously developed PET/MRI radiomics predictive models were successfully validated in two independent external cohorts. A proposed flowchart for improved management of patients based on these models should now be confirmed in future larger prospective studies.

**EP-1477 Image-guided Intensity Modulated Radiotherapy in cervical cancer: organ motion and geographical miss**

P. Ferrazza<sup>1</sup>, A. Delana<sup>2</sup>, L. Purpura<sup>3</sup>, E. Magri<sup>1</sup>, L. Bandera<sup>1</sup>, V. Vanoni<sup>1</sup>

<sup>1</sup>*Ospedale Santa Chiara di Trento, Radiation Oncology, Trento, Italy*; <sup>2</sup>*Ospedale Santa Chiara di Trento, Medical Physics, Trento, Italy*; <sup>3</sup>*Università degli Studi di Palermo, Radiation Oncology, Palermo, Italy*

**Purpose or Objective**

Volumetric Modulated Radiotherapy (VMAT) is increasingly used in order to minimize toxicity in cervical cancer. However, to prevent geographical misses caused by inter-fraction movement of uterus, the benefit of this approach is detracted by margins applied to Clinical Target Volume (CTV) to obtain Planning Target Volume (PTV). The aim of this retrospective analysis is to verify how variations in bladder filling may cause target miss and unnecessary organs at risk inclusion in high dose regions.

**Material and Methods**

From March 2016 to January 2018 10 patients (pts) with cervical cancer stage FIGO IIB underwent to concurrent radio-chemotherapy (total dose 45-50.4 Gy/25-28 fractions), followed by intrauterine high-dose brachytherapy. Full and empty bladder Computed Tomography (CT) scans were acquired prior the treatment to evaluate uterus, rectal and bowel motion. A VMAT plan based of the CT with full bladder was performed (by Montecarlo algorithm), after image fusion and delineation of the uterus in both CT scans (to create the uterus Internal Target Volume ITV). We applied isotropic margins of 7 and 10 mm respectively to lymph node-cervix and uterus ITV. Daily Cone Beam CT (CBCT) was performed.

We analysed 113 of 273 CBCT, due to the presence of artefacts in images. CBCTs were registered to CT simulation and an operator contoured bladder and uterus on each CBCT.

**Results**

The main cause of uterus motions in our analysis was bladder filling. The uterus shifts are wider in anterior-posterior and superior-inferior directions with larger movements of the fundus and lesser along the endocervical canal. Rectum filling or bowel interposition did not result in uterus motion outside the PTV

88% of CBCTs showed that uterus was included in PTV, especially in pts with correct bladder filling in simulation CT. A further analysis showed that an increase in superior-inferior and antero-posterior margins (anisotropic margins, 1.5 cm vs 1 cm) from uterus ITV, reduces by 9% the risk of target miss (from 12 to 3%). Dose constraints of bowel were respected despite the increase of PTV.

**Conclusion**

Pelvic organ motion is patient specific, and a correct bladder filling in CT simulation seems to reduce geographical misses during radiation treatment. The large CTV-PTV margins can increase gastrointestinal, genitourinary and hematological toxicity, but anisotropic margins in our preliminar analysis improve PTV coverage (respecting dose constraints of bowel and rectum). Due to the small sample size, Further validation of these results is necessary.

**EP-1478 Adjuvant small pelvic field radiotherapy in cervical cancer with intermediate risk factors**

J.A. Solis Campos<sup>1</sup>, B. Tudela Staub<sup>1</sup>, G. Veillon Contreras<sup>1</sup>, I. Perrot rosenberg<sup>2</sup>

<sup>1</sup>*Hospital Carlos Van Buren, oncology, Valparaiso, Chile*; <sup>2</sup>*Universidad de Valparaiso, School of Medicine, Valparaiso, Chile*

**Purpose or Objective**

Adjuvant radiotherapy improves outcomes in surgically treated cervical cancer patients with intermediate risk factors as defined by Sedlis. In our hospital, adjuvant

radiotherapy has been performed using a small pelvic field technique without brachytherapy since 2007. This report aims to analyze the results of those patients in terms of locoregional control, overall survival and acute toxicity.

**Material and Methods**

For this retrospective analysis, all patients treated at the Radiation Oncology Unit of our hospital between 2007 and 2014 were included. Adjuvant radiotherapy without concurrent chemotherapy was administered to FIGO IB1 cervical cancer patients with a combination of  $\geq 2$  of the following intermediate risk factors: lymph-vascular space invasion, deep stromal invasion and/or increased tumor size on pathology. Patients were treated with 3D-conformal radiotherapy, using a small pelvic 4-field box technique, with the upper limit at the inferior border of the sacroiliac joint. Acute genitourinary and gastrointestinal toxicities were classified according to the RTOG grading (G) system. Overall survival and relapse-free survival were analyzed using the Kaplan-Meier method.

**Results**

20 patients treated with small pelvic field radiotherapy were identified. Median follow-up time for the whole group was 37.5 months (IQR 20 - 66.5). Median age was 46 years (IQR 36.5 - 56). Nineteen patients underwent radical hysterectomy and 1 patient underwent radical trachelectomy. Median number of resected lymph nodes was 21.5 (IQR 18-28.5). Reported histologic types were squamous-cell carcinoma (15 patients), adenocarcinoma (2 patients), adenosquamous (2 patients), and clear cell carcinoma (1 patient). Median tumor size was 3 cm (IQR 2.3-3.5). Stromal invasion was 2/3 in 12 patients and 3/3 in 7 patients, and lymph-vascular space invasion was present in 16 patients. The prescribed dose was 50.4 Gy in 19 patients and 45 Gy in one patient. Acute genitourinary toxicity was G0 in 12, G1 in 6, G2 in 1 and G3/4 in 0 patients. Acute gastrointestinal toxicity was G0 in 10, G1 in 4, G2 in 6 and G3/4 in 0 patients.

Three-year relapse-free survival was 84.6%. 3 patients presented relapses; 1 classified as local relapse, 1 located in the retrovesical area, and 1 located lateral to L5 vertebra. Three-year overall survival was 100%.

**Conclusion**

Adjuvant small pelvic field radiotherapy is associated with good oncological outcomes and an excellent toxicity profile in patients with FIGO IB1 cervical cancer with intermediate risk factors. Only one patient experienced a relapse in a region that would have been treated with a standard pelvic field.

**EP-1479 The use of CT texture analysis in cervical cancer to predict response to chemoradiotherapy**

S. Otter<sup>1</sup>, A. Franklin<sup>1</sup>, P. Evans<sup>2</sup>, A. Stewart<sup>1</sup>

<sup>1</sup>*Royal Surrey County Hospital, St Luke's Cancer Centre, Guildford, United Kingdom*; <sup>2</sup>*University of Surrey, Centre for Vision- Speech and Signal Processing, Guildford, United Kingdom*

**Purpose or Objective**

Cervical cancer is the fourth most common cancer worldwide and the 5-year overall survival for stage IIIB disease is only 42%. Treatment for locally advanced cervical cancer (LACC) is chemoradiotherapy (CRT). It would be beneficial to identify at an early stage, patients who may not have a complete response to treatment so that they could have dose escalation or the addition of other systemic agents to improve the chance of cure. Texture analysis (TA) enables the quantification of the spatial heterogeneity of tumours thereby giving more information about a tumour than is available from visual analysis alone. The aim of this study was to apply TA to pre-treatment and brachytherapy CT scans of patients with LACC who were then treated with CRT.

### Material and Methods

46 consecutive LACC patients were included. Patients received CRT, 50.4Gy in 28 fractions and brachytherapy 21Gy in 3 fractions. Pre-treatment radiotherapy planning contrast enhanced CT scans and non-contrast enhanced brachytherapy CT scans (with the tandem and ovoids in situ) were exported from Aria (Varian, USA). The DICOM images were anonymised and imported into the TexRad system (Feedback Medical, UK). The CT slice which corresponded to the most FDG avid part of the tumour on staging PET-CT was used for contouring the region of interest (ROI). Laplacian of a Gaussian filters were applied to the image to highlight features between 2-6mm (labelled SSF 2 to SSF6). Mann-Whitney U test was used to compare TA values for mean, standard deviation (SD), mean positive pixels (MPP), entropy, kurtosis and skewness between a group of patients that achieved a complete response (CR) on the 3-month post-treatment MRI and those patients that achieved a partial response (PR).

### Results

Disease was staged as IB1 in 2%, IB2 in 13%, IIA 2%, IIB 52%, IIIB 13%, IVA 9% and IVB 9%. 33 patients achieved a CR and 13 patients achieved a PR. The TA parameters that yielded significant results from the pre-treatment CT were the SD, entropy and MPP at a spatial scaling factor of 4, 5 and 6 (see figure 1 and table 1) with partial responders having higher values for these parameters than complete responders. 36 patients had brachytherapy scans available which showed significant differences in entropy and skewness at SSF0 ( $p=0.038$  and  $0.017$ ), and in the mean at SSF2 ( $p=0.022$ ) between the patients achieving a CR and those achieving a PR.

TA parameter	SSF	Mean		AUC (95% CI)	P value (Mann-Whitney)
		Complete responders	Partial responders		
SD	4	33.7	42.0	0.69 (0.50-0.88)	0.05
	5	30.9	40.9	0.73 (0.56-0.91)	0.014
	6	28.3	39.9	0.77 (0.62-0.93)	0.005
Entropy	4	4.77	4.96	0.70 (0.51-0.88)	0.042
	5	4.66	4.91	0.75 (0.58-0.92)	0.008
	6	4.54	4.84	0.74 (0.57-0.91)	0.008
MPP	4	27.5	32.8	0.70 (0.52-0.88)	0.037
	5	25.3	32.3	0.75 (0.58-0.93)	0.008
	6	23.6	31.3	0.78 (0.62-0.94)	0.003

### Conclusion

In this cohort, mean values for SD, entropy and MPP from the pre-treatment CT scan were higher in patients who had a partial response compared to those who had a complete response to CRT. TA from the brachytherapy scans was less predictive of response. TA on pre-treatment CT scans could potentially be used in the future to identify patients who need an escalation of treatment. Further work is suggested to examine the correlation of TA parameters with other known prognostic factors for cervical cancer such as stage and nodal status. These results also need to be validated in an independent cohort of patients.

### EP-1480 Radiation therapy for Uterine Cervical Cancer with lung metastases including oligometastases

Y. Mukai<sup>1</sup>, I. Koike<sup>1</sup>, E. Miyagui<sup>2</sup>, M. Hata<sup>1</sup>

<sup>1</sup>Yokohama City University Graduate School of Medicine, Radiation Oncology, Yokohama, Japan; <sup>2</sup>Yokohama City University Graduate School of Medicine, Gynecology, Yokohama, Japan

### Purpose or Objective

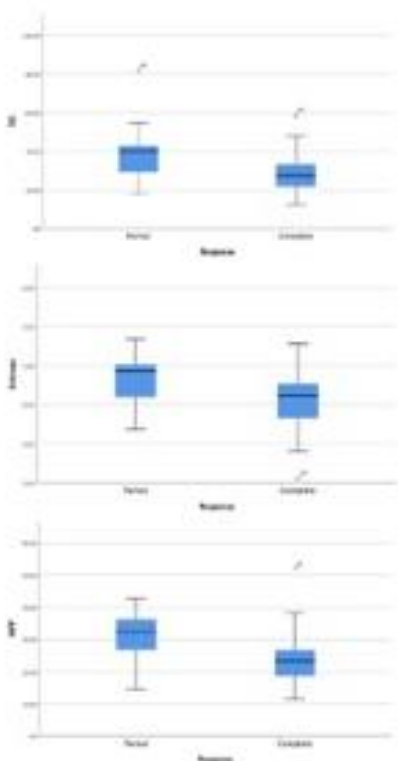
We investigated the role of, and optimal regimen for, radiation therapy (RT) for patients with lung (oligo) metastases from uterine cervical cancer.

### Material and Methods

We enrolled 23 consecutive uterine cervical cancer patients with lung metastases who received pelvic RT between November 2005 and July 2017 (median age: 52 years; range: 39-78 years). All patients had histopathological diagnoses of uterine cervical cancer (squamous cell carcinoma: n=13, 56.5%); 10 had lung metastases only (including 6 with oligometastases, defined as  $\leq 4$  lung metastases); 13 had distant metastases to other sites (para-aortic lymph node, liver, bones, peritoneum and ovary). All patients had bleeding from primary tumors; 5 patients received blood transfusions before RT (median total dose: 59 Gy; 2 Gy per fraction-equivalent dose [ $\alpha/\beta=10$ ], delivered to all patients' uterine cervical cancer tumors). Sixteen patients (69.6%) received concurrent chemotherapy (cisplatin: n=14, 40 mg/m<sup>2</sup> of body surface area; docetaxel/cyclophosphamide: n=2).

### Results

For the 22 patients (95.7%) who completed RT without interruption, 9 (39.1%) had complete response (CR) for primary tumors and 10 (43.5%) had partial responses (PR; initial CR+PR rate: 82.6%). The 1-year primary progression-free rate was 95.2%. Bleeding greatly decreased after treatment (objective hemostatic rate: 100% excluding 2 patients who discontinued RT or who had neuroendocrine carcinoma).



The 1-year overall survival rate was 47.2 % (estimated median survival: 9 months). Five patients were alive, of whom 4 were disease-free at last follow-up. Of 6 patients with oligometastases, 3 were alive and 2 were considered no evidence of disease at last follow-up (median survival time in this group: 31 months).

Significant prognostic factors for survival included <4 lung metastases ( $P = 0.035$ ), unilateral vs. bilateral lung metastases ( $P = 0.039$ ), primary tumor diameter <100 mm ( $P < 0.001$ ), and ECOG performance status <1 at initial treatment ( $P = 0.015$ ).

Lung metastases <10 mm ( $P = 0.14$ ) and concurrent chemotherapy ( $P = 0.07$ ) did not significantly affect survival. No acute or late toxicities > Grade 3 were associated with treatment.

#### Conclusion

RT is safe and effective for patients with lung metastases from uterine cervical cancer. Patients with oligometastases may especially benefit from aggressive treatment.

#### EP-1481 Leukocytosis and Neutrophil to Lymphocyte Ratio: Prognostic Factors in Uterine Cervical Cancer?

S. Garcia<sup>1</sup>, R. Costa Lago<sup>1</sup>, G. Almeida<sup>1</sup>, D. Rodrigues<sup>1</sup>, M.P. Fontes<sup>1</sup>, G. Pinto<sup>1</sup>

<sup>1</sup>Centro Hospitalar de São João, Serviço de Radioterapia, Porto, Portugal

#### Purpose or Objective

Even though the incidence and mortality of invasive uterine cervical cancer have steadily decreased, this disease is still the second most common type of cancer in females worldwide and the leading cause of cancer deaths in women in developing countries. Anemia has long been associated with poor prognosis in patients with cervical cancer. Recently, additional hematological parameters have emerged as potential indicators of a worse outcome in this patient group. In a cohort of cervical cancer patients treated with radiation therapy alone (RT) or concurrent chemoradiation therapy (CCRT) and brachytherapy, we report on prognostic significance of pretreatment hematologic parameters including leukocytosis and neutrophil to lymphocyte ratio (NLR).

#### Material and Methods

Ninety-seven cervical cancer patients were retrospectively identified from a single cancer institution's database (CHSJ - Centro Hospitalar de São João). A database was created with information obtained from patients' clinical records. Hematologic parameters were categorized as: leukocytosis (white blood cells count >  $10 \times 10^9/L$ ) and NLR (high ratio > 5). A demographic analysis of the study sample was performed. The impact of the hematological parameters on progression free survival (PFS) and overall survival (OS) was assessed using the Kaplan-Meier plots and the log rank test for univariate analysis and the Cox regression for multivariate analysis. Statistical analysis was performed with SPSSv24.

#### Results

Of the 97 patients, 10 were in the leukocytosis group and 31 were in the high NLR group. Median age at diagnosis was 58 years and median follow-up time was 56 months. Median PFS was 46 months and median OS was 54 months. Comparing the various groups of patients regarding hematological parameters, the high NLR was significantly associated with worse survival (PFS: 89 vs 118 months,  $p=0.009$ ; OS: 90 vs 118 months,  $p=0.004$ ). Leukocytosis did not show a statistically significant impact on PFS and OS. Multivariate analysis showed that both high NLR and leukocytosis were significant prognostic factors for OS ( $p=0.022$ , CI 95%).

#### Conclusion

Results showed that patients with a high NLR had significantly shorter PFS and OS than those with a low NLR. The leukocytosis and NLR may be promising parameters on which to base the choice of a therapeutic strategy to treat

uterine cervical cancer. This study involved a small sample size of a single institution, so further validation is required prior to incorporating the NLR as a prognostic indicator.

#### EP-1482 Stereotactic rt in ovarian cancer: multicentric retrospective pooled analysis (MITO-RT project)

G. Macchia<sup>1</sup>, G.R. D'Agostino<sup>2</sup>, A. Fodor<sup>3</sup>, A.M. Cerrotta<sup>4</sup>, R. Autorino<sup>5</sup>, D. Russo<sup>6</sup>, E. Perrucci<sup>7</sup>, A. Zamagni<sup>8</sup>, A. Di Stefano<sup>9</sup>, C. Iftode<sup>2</sup>, S. Cilla<sup>10</sup>, A.G. Morganti<sup>8</sup>, C. Aristei<sup>7</sup>, N. Di Muzio<sup>3</sup>, M. Scorsetti<sup>2</sup>, F. Deodato<sup>1</sup>, G. Scambia<sup>11</sup>, V. Valentini<sup>5</sup>, G. Ferrandina<sup>11</sup>

<sup>1</sup>Università Cattolica S. Cuore- Fondazione Giovanni Paolo II, Radiotherapy Unit, Campobasso, Italy;

<sup>2</sup>Humanitas Clinical and Research Hospital, Radiotherapy and Radiosurgery, Rozzano - Milan, Italy;

<sup>3</sup>San Raffaele Scientific Institute, Department of Radiotherapy, Milan, Italy;

<sup>4</sup>IRCCS Istituto Nazionale dei Tumori, Radiotherapy Unit, Milan, Italy;

<sup>5</sup>Policlinico Universitario "A. Gemelli"- Università Cattolica del Sacro Cuore, Department of Radiotherapy, Roma, Italy;

<sup>6</sup>Ospedale "Vito Fazzi", Radiotherapy Unit, Lecce, Italy;

<sup>7</sup>University of Perugia and Perugia General Hospital, Radiation Oncology Section, Perugia, Italy;

<sup>8</sup>Radiation Oncology Center, Department of Experimental-Diagnostic and Specialty Medicine - DIMES- University of Bologna-, Bologna, Italy;

<sup>9</sup>Fondazione di Ricerca e Cura "Giovanni Paolo II"- Università Cattolica del Sacro Cuore, Gynecologic Oncology Unit, Campobasso, Italy;

<sup>10</sup>Fondazione di Ricerca e Cura "Giovanni Paolo II"- Università Cattolica del Sacro Cuore, Medical Physics Unit, Campobasso, Italy;

<sup>11</sup>Fondazione Policlinico Universitario «A. Gemelli»- Università Cattolica del Sacro Cuore-, Department of Women's and Children's health, Rome, Italy

#### Purpose or Objective

Stereotactic body radiotherapy (SBRT) represents an interesting opportunity in the treatment of ovarian cancer (OC) isolated recurrences or residual lesions after systemic treatment, and a valid tool to lengthen the free time of re-challenge with platinum. Studies on this topic are sporadic and with few cases. Aim of this multicentric retrospective pooled analysis was to collect the largest unselected real-life dataset of OC patients treated with SBRT in the attempt to define the safety and efficacy. Secondary objectives were to identify the best dose/fractionation regimen in terms of local control as well as to describe acute and late toxicities.

#### Material and Methods

Eight Italian cancer Centers were firstly started the project giving their adhesion to this retrospective pooled analysis. A specific data-set for standardized data collection for ovarian cancer SBRT treatment was developed. Participants were required to fill a data sets including: age, histotype, site of irradiation, previous treatments, best response, toxicity as well as technical/dosimetric data about SBRT treatment.

#### Results

Data on 73 OC patients (median age: 63.5, range 40-83) carrying a total of 120 lesions were considered suitable for analysis. Between 2005 and 2018 all patients underwent SBRT in single or multiple fractions with a median biological equivalent dose (BED<sub>α/β 10</sub>) of 76.8 Gy (range 7.5-262.5). Patient and treatment characteristics as well as acute toxicity are detailed in Table 1. Safety. 52 patients (71.3%) did not experience acute toxicity, the others 21 (28.7%) experienced low grade acute toxicity with no patient showing > grade 2 toxicity. With a median follow-up of 18 months (range: 1 - 120), 68 patients (93.1%) did not experienced late toxicity, the others 5 (6.9%) experienced low grade late toxicity with no patient showing > grade 2 toxicity. Efficacy. On a per-lesion basis, the 12-and 24-months actuarial local control inside SBRT field were 88.3% and

86.2%, respectively. BED10 > 50Gy was correlated with a better 12-months local control (91.7% versus 72.9%, p=0.034).

Table 1. Patients' characteristics, treatment details and acute toxicity

	No. patients (%)	No. lesions (%)
	73	120
Age, years, median (range)	63.5 (40-83)	
Histotype		
Serous		85 (71.0)
Endometrioid		21 (17.5)
Clear cell		5 (4.1)
Mixed epithelial		2 (1.7)
Indifferentiated		5 (4.1)
Mixed malignant Mullerian tumor		1 (0.8)
Other		1 (0.8)
Type of lesion (%)		
Lymph Node metastases		62 (51.7)
Parenchymal lesions		56 (46.6)
Bone metastases		2 (1.7)
Patients treated by previous chemotherapy cycles	48 (95)	
N° of chemotherapy schedules, median (range)		3 (1-7)
Patients treated by previous surgery	73 (100)	
Gross tumor volume (cc), median (range)		3.9 (0.04-88.4)
Planning target volume (cc), median (range)		18.28 (0.04-224)
Median SBRT dose (Gy), range		36 (5-75)
Median SBRT dose BED 10 (Gy), range		78.8 (7.5-282.5)
Median SBRT dose per fraction (Gy), range		7.5 (5-30)
SBRT N° fractions		1-10
Reference dose		
ICRU 52/isocenter		54 (45.0%)
Target mean		51 (42.5%)
Specific isodose		55 (45.5%)
Acute toxicity		
Grade 0	52 (71.3)	
Grade 1: Gastrointestinal (11), pain (2), other (2)	15 (20.5)	
Grade 2: Gastrointestinal (2), pain (2), other (2)	6 (8.2)	

## Conclusion

Preliminary results on a population-level confirm that SBRT delivered in 1-10 consecutive fractions is safe and well tolerated notwithstanding several previous surgical and systemic treatments. Therefore, this treatment can be considered as a further resource in order to lengthen the free time of re-challenge with platinum.

## EP-1483 Stereotactic Body Radiation Therapy Boost for Stage IA - IIB Cancers of the Cervix: 5-Year Results

S. Dalwadi<sup>1</sup>, M. Ludwig<sup>1</sup>, N. Waheed<sup>1</sup>, D. Tran<sup>1</sup>, M. Bonnen<sup>1</sup>, C. Mantz<sup>2</sup>  
<sup>1</sup>Baylor College of Medicine, Radiation Oncology, Houston, USA ; <sup>2</sup>21st Century Oncology, Radiation Oncology, Fort Myers, USA

## Purpose or Objective

SBRT for cancers of the cervix may offer an alternative to brachytherapy for those patients who are not candidates for brachytherapy procedures. SBRT dose-fractionation schedules may be selected to approximate those of HDR in order to achieve similar radiobiologic dosing, while SBRT technique eliminates the need for applicator placement and sedation. Herein, we report health-related quality of life, toxicity and disease control outcomes of a multi-institutional series of SBRT for primary cervical cancers.

## Material and Methods

Eligible patients included those with (1) pathologically confirmed cervical squamous cell carcinoma or adenocarcinoma; (2) FIGO stage IA, IB, IIA or IIB disease; and (3) medical or technical contraindication to brachytherapy or patient refusal of brachytherapy. Prior to SBRT, all patients received pelvic EBRT to a prescribed dose of 45.0-50.4 Gy; pelvic nodal boost (total EBRT dose, 55.9-66.0 Gy) was permitted. All patients received cisplatin-based chemotherapy concurrent with EBRT. SBRT boost treatment planning then followed, and HR-CTV delineation was aided by co-registration of the boost planning CT to a post-EBRT MRI. A boost dose of 14.0-40.0 Gy was prescribed to the post-EBRT HR-CTV and delivered over 4-5 fractions. Assessments included (1) disease response assessed through post-treatment surveillance per institutional protocol; (2) acute and chronic toxicities assessed using the U.S. National Cancer Institute's CTCAE v3 toxicity scales; and (3) quality-of-life scored using FACT-G measurements.

## Results

Sixty-seven patients have been treated since June 2007 and have been followed for a median of 60 months (range, 5-120 months). Forty patients have been followed for a minimum of 5 years. Stage distribution was as follows: 2/67 stage IA, 6/67 stage IB1, 18/67 stage IB2, 3/67 stage

IIA1, 6/67 stage IIA2 and 32/67 stage IIB. Mean SBRT V100 was 95.3% (range, 75.0-99.8%), and mean total equivalent effective doses (EQD2) to 2 cc of bladder and rectum were 72.91 and 64.86 Gy, respectively. Post-SBRT complete response rate was 94.0% at 3 months for all patients based on clinical assessment with or without biopsy; among patients who underwent planned biopsy at 3 months, 52 of 55 demonstrated complete pathologic response. At 5 years, estimated local control at the SBRT boost site is 90.8% for all patients. Estimated failure-free survival and overall survival at 5 years are 83.1% and 74.7%, respectively. Two patients suffered grade 3 toxicities (urinary frequency, vaginal stenosis), and no patient experienced ≥ grade 3 bowel toxicity. Post-treatment FACT-G scores were available for 82% of cases and were statistically superior at 2 and 5 years compared to pre-treatment assessments for the following studied domains: physical, emotional and functional well-being.

## Conclusion

At a median followup of 5 years, SBRT appears to offer an effective and well-tolerated boost modality for selected stage IA-IIB cervix cancer patients who were otherwise contraindicated for brachytherapy.

## EP-1484 Neoadjuvant CT followed by chemoradiation in locally advanced cancer cervix : feasibility and QOL study

S. Singh<sup>1</sup>, S. Sadhan Sarangi<sup>1</sup>, P. Misra<sup>2</sup>, D. Kapoor<sup>3</sup>, A. Rani<sup>3</sup>, N. Rastogi<sup>1</sup>, S. Kumar<sup>4</sup>

<sup>1</sup>Sanjay Gandhi Postgraduate Institute of Medical Sciences, Dept. of Radiotherapy, Lucknow UP, India ;

<sup>2</sup>Sanjay Gandhi Postgraduate Institute of Medical Sciences, Dept. of Biostatistics, Lucknow UP, India ;

<sup>3</sup>Sanjay Gandhi Postgraduate Institute of Medical Sciences, Dept. of Gynecology- General Hospital, Lucknow UP, India ; <sup>4</sup>Sanjay Gandhi Postgraduate Institute of Medical Sciences, Dept. of Radiotherapy-Super Speciality Cancer Institute and Hospital, Lucknow UP, India

## Purpose or Objective

To assess feasibility, response rate and quality of life (QOL) in locally advanced cervical cancer patient treated by 3 weekly neoadjuvant chemotherapy (NACT) followed by chemoradiation (CCRT).

## Material and Methods

Between April 2016 - March 2017, 30 cervical cancer patients, FIGO stage IB2 to IVA, histopathologically proven, eligible and consented for the prospective study were included. Patients received 2 cycles of NACT using Inj. capecitabine 175mg/m<sup>2</sup> and Inj. cisplatin 35mg/m<sup>2</sup> or carboplatin AUC5 as 3 weekly schedule followed by definitive radiation therapy along with concurrent weekly cisplatin 35mg/m<sup>2</sup> or carboplatin AUC2 chemotherapy. The primary end point was to assess feasibility of NACT and overall response at 3 months post NACT-CCRT, toxicities, and QOL (using EORTC C30, CX 24 and OV 28 questionnaires). Analysis were intention to treat.

## Results

The median age was 53 years. 53% had FIGO stage III followed by stage II 40% with >50% having bulky disease. One fifth of patients had both regional and para aortic lymph nodes at presentation based on imaging criteria. 27/30 patients (90%) received planned 2 cycles of NACT while 3 received 1 cycle either due to side effects (n= 2) or administrative error (n=1). The overall clinical response rate post NACT was 76% with complete disappearance of disease seen in 1 patient (3%). 29/30 completed planned radiation treatment with 90% receiving concurrent chemotherapy with a median number of 5 cycles. At 3 months, post completion of all planned treatment 25/30 (84%) of patients had clinically complete disappearance of disease and 3(10%) had partial response using clinical and imaging findings. NACT was well tolerated with only 11% experiencing any grade 3/4 toxicities and no treatment-

related deaths. During CCRT 4% of patients had grade 3/4 hematological while 7% non hematological. With median follow-up of 21 months (Q1-Q3: 15-24 months) the 1 year progression free survival, distant disease survival and overall survival were 80%, 79% and 87% respectively.

The global health score showed moderate increment after treatment and at 6 months follow up (FU) suggesting an improvement in QOL post therapy. In general for both functional and symptom scales, QOL improved during FU from baseline but difference was not significant. Overall symptom experience declined significantly following completion of NACT and CCRT as compared to baseline score. There was trend towards significant difference in sexual activity score over four time period but sexual enjoyment and vaginal function scores could not be analyzed reliably as majority of patients chose not to answer the questions which highlights social stigma related to sex prevalent in society. There was a significant difference in financial difficulty as faced by patient during treatment period as compared to FU period.

#### Conclusion

2 cycles of 3 weekly NACT followed by CCRT in locally advanced cervical cancer had a good response and outcome with acceptable toxicities and without much impact on quality of life

#### EP-1485 Role of PET-CT in patients of recurrent carcinoma cervix treated with definitive chemoradiotherapy

M. Rastogi<sup>1</sup>, A.K. Gandhi<sup>1</sup>, R. Khurana<sup>1</sup>, S.S. Nanda<sup>1</sup>, H.B. Singh<sup>1</sup>, S. Rath<sup>1</sup>, P.C. Rai<sup>1</sup>, S. Kumar<sup>1</sup>, A. Bharati<sup>1</sup>, A.K. Srivastava<sup>1</sup>, S.P. Mishra<sup>1</sup>

<sup>1</sup>Dr. Ram Manohar Lohia Institute of Medical Sciences, Radiation Oncology, Lucknow, India

#### Purpose or Objective

We did this retrospective study to evaluate the role of positron emission tomography (PET-CT) in predicting the clinical outcome of patients with recurrent cervical carcinoma following definitive radiation therapy.

#### Material and Methods

Between July 2015 and June 2017, 40 histo-pathologically proven patients of carcinoma cervix treated with definitive radiotherapy or chemoradiotherapy and declared cured after the completion of their treatment were included. Patients were required to have a diagnosis of recurrent cervical cancer established by histopathology (biopsy or cytology) or clinically evident recurrent disease with a minimum of three months gap between recurrence and completion of radiotherapy. Patients with persistent residual disease and those having distant metastatic disease on conventional imaging (Abdominal CT scan or chest X-ray) were excluded from the study. 18-fluorodeoxyglucose (FDG) PET imaging was performed in each patient before the salvage therapy but was not used for guiding treatment decisions. The maximum standardized uptake value (SUV max) and metabolic tumor volume (MTV) were measured and correlated with cumulative progression free survival (PFS). The MTV was calculated as 60% of the volume covered by the SUV max. SPSS version 20.0 was used for statistical analysis.

#### Results

Median age of the patient was 47 years (Range 30-66 years). 22 patients had stage IIIB, 13 had stage II B, 3 patients had stage III A disease and 2 patients had stage IV disease in the pre-salvage workup. The median recurrence free period was 11 months (Range 3.5-36). 25 patients were treated with Re-irradiation (with EBRT doses of 20-36 Gy ± HDR interstitial brachytherapy of 10-20 Gy in 1-2 sessions), 4 patients underwent surgery (2 Radical hysterectomy and 2 Pelvic exenteration), 6 patients received palliative radiotherapy alone (Dose 5-20 Gray), 4 patient received palliative chemotherapy (with regimen consisting of Paclitaxel and Carboplatin, 3-6 cycles) and 1

patient was put on best supportive care. Median follow up period was 11 months (Range 3-29 months). Median SUVmax was 5.8 (range 2.9-56.2) and median MTV was 43 cm<sup>3</sup> (range 7.8-212). The cumulative PFS for all patients was 30% at 24 months. The one year PFS was 26 % for patients with SUVmax value of >5.8 versus 47 % for those with SUVmax value of <5.8 (P value 0.02). The one year PFS was 41% for patients with MTV of >43cm<sup>3</sup> versus 43% for those with MTV of <43 cm<sup>3</sup> (P value 0.8)

#### Conclusion

Post irradiated recurrent cervical carcinoma patients with SUVmax of <5.8 have a favourable outcome compared with those with SUVmax of >5.8 and should be selected for aggressive salvage therapy. Further prospective studies are needed to validate the findings of our study.

#### EP-1486 Role of HPV DNA testing and its influence on clinical outcomes in Cervical Cancer

P. Jayaprakash<sup>1</sup>, G. Narayanan<sup>1</sup>

<sup>1</sup>Vydehi Institute of Medical Sciences and Research Centre, Radiation Oncology, Bengaluru, India

#### Purpose or Objective

Persistent infection with Human Papillomavirus (HPV) is the major etiological factor for development of cervical cancer. Although the standard treatment of locally advanced cervical cancer includes Definitive Chemo Radiation, little is known about the impact of HPV on the response to chemo radiation and on the clinical outcome. Primary objective was to compare treatment response of cervical carcinoma patients infected with HPV 16 and HPV 18 who are treated with Definitive Chemo Radiation. Secondary Objectives was to find out the HPV positivity rate in diagnosed cervical cancer cases, to estimate the number of HPV high risk genotypes and to compare response between positive and negative cases of HPV in the same study group

#### Material and Methods

96 patients who presented to our institute were included for the study. Inclusion criteria were patients with biopsy proven carcinoma of the uterine cervix considered suitable for curative treatment with definitive radio-chemotherapy with Performance Status 0-2 (ECOG) and International Federation of Gynecology and Obstetrics (FIGO) Stages IB2 to IIIB. HPV testing was done using TRU PCR® HPV 16&18 Real-Time PCR kit. All the patients received External Beam Radiation therapy (EBRT) on Linear Accelerator with 3 Dimensional Conformal Radiotherapy (3DCRT) to a dose of 4600cGy in 23 fractions, 5 fractions per week and weekly Chemotherapy regimen consisted of Cisplatin 40 mg/m<sup>2</sup> during EBRT. Three fractions of High-dose rate Intracavitary Brachytherapy was delivered after completion of EBRT with a fraction dose of 7 Gy at point A. Treatment response assessment was done using Response evaluation criteria in solid tumors (RECIST) criteria. Clinical examination was performed at completion of EBRT and at 3rd month follow up. Radiological response was assessed using MRI at 3rd month follow up

#### Results

96 patients of Cervical Cancer were tested for HPV DNA, of which 79 (82.3%) patients were positive. 73 patients showed HPV genotype 16 and 6 patients were positive for genotype 18. The response was correlated with HPV genotype. There was a significant increase in radiological complete response in HPV16 compared to HPV 18 and HPV negative groups at 3 months, 80.8%, 50% and 52.9% respectively (x<sup>2</sup>=36.5, p<0.001). There was also a significant increase in clinical response at 3 months in HPV 16 group compared to HPV 18 and HPV negative groups, 87.5%, 50% and 50% respectively (x<sup>2</sup>=29.9, p<0.001). The age of the patient, volume of the disease, overall treatment time, and average Hemoglobin level and number of blood transfusions did not have any correlation.

HPV status/Genotype	Complete response	Partial response	Stable disease	Progressive disease	Pearson Chi Square	
<b>Response at completion of EBRT</b>						
HPV Negative	3 (17.6)	13 (76.5)	1 (5.9)		2.54	0.59
HPV 16 positive	13 (17.8)	57 (78.1)	3 (4.1)			
HPV 18 positive	0 (0)	5 (83.3)	1 (16.7)			
<b>Radiological response at 3 months</b>						
HPV Negative	9 (52.9)	8 (47.1)	0	0	36.5	P<0.001
HPV 16 positive	59 (80.8)	14 (19.2)	0	0		
HPV 18 positive	3 (50)	1 (16.7)	1 (16.7)	1 (16.7)		
<b>Clinical response at 3 months</b>						
HPV Negative	8 (50)	7 (43.8)	0	1 (6.2)	29.9	P<0.001
HPV 16 positive	63 (87.5)	9 (12.5)	0	0		
HPV 18 positive	3 (50)	2 (33.3)	1 (16.7)	0		

### Conclusion

HPV genotype 16 positivity shows higher complete response in Cervical Carcinoma patients treated with Definitive Chemo Radiation compared to HPV 18 genotype. Further, HPV genotyping could potentially help to stratify cervical cancer patients for more effective therapeutic regimens

### EP-1487 Prognostic value of 18F-FDG PET/CT parameters in patients with locally advanced cervical carcinoma

S. Cordoba Largo<sup>1</sup>, V. Garcia Jarabo<sup>1</sup>, D. Martinez<sup>1</sup>, M. Ramirez<sup>1</sup>, M. Gaztañaga Boronat<sup>1</sup>, C. De la Fuente<sup>2</sup>, G. Marquina<sup>1</sup>, A. Ortega<sup>1</sup>, R. Mendez<sup>1</sup>

<sup>1</sup>Hospital Clinico San Carlos, radiation Oncology, Madrid, Spain ; <sup>2</sup>Hospital Universitario Puerta de Hierro, radiation ONcology, Madrid, Spain

### Purpose or Objective

To investigate the value of pretreatment intensity-based 18F-FDG PET/CT parameters as predictors of outcome and para-aortic lymph node involvement in patients with locally advanced cervical carcinoma (LACC) treated with concurrent external beam radiotherapy and chemotherapy (CRT) followed by image-guided brachytherapy (IGBT-MRI).

### Material and Methods

From November 2010 to February 2016 we treated 65 patients with stages IB-III cervical carcinoma. Mean age: 54.6 y (30-88). TNM stage: I: 4 p, II: 54 p and III: 6 p. Histology: epidermoid: 49 p; adenocarcinoma: 15 p. All patients were treated with CRT and 3D-based planning intracavitary/interstitial IGBT, using the GEC-ESTRO recommendations for defining high-risk clinical target volume (HR-CTV). Equieffective doses at 2 Gy (EQD2) were calculated, applying linear quadratic model. In 34 p. (45%) a laparoscopic para-aortic lymphadenectomy was performed before treatment.

In all patients a pretreatment <sup>18</sup>F-FDG PET/CT was performed to determine the metabolic tumoral volume (MTV) and tumor standardized uptake value (SUVmax). In 56 p (87%) a second <sup>18</sup>F-FDG PET/CT before IGBT were used to classify patients as metabolic responders (MR) or non- metabolic responders (nonMR) according to the EORTC criteria.

Statistics: Student's T test for media comparison, chi-square test for comparing proportions and Kaplan Meier for survival analysis and log-rank for curve comparison.

### Results

After median follow-up of 30 months (10-90), 3-year overall survival (OS), 3-year disease-free survival (DFS), local relapse-free survival (LCFS), pelvic relapse-free survival (PRFS) and distant metastases disease-free survival (DMFS) were 83.7%, 58%, 84.2%, 86.3% and 86.8%, respectively.

Only 3/29 p with negative para-aortic PET/CT had pathologically involved nodes (negative predictive value, NPV: 89.6%). Treatment-related factors, D90/D98 HR-CTV and OTT, had no prognostic value. Patients with positive

para-aortic lymph node had a non-significant trend towards worse OS (54.7% vs 91.3%, p=0.06) and DMFS (75% vs 90.8%, p=0.06). Patients with a PET-CT MTV<24 cc had a better 3-y OS when comparing with MTV >24 cc (85% vs 56%, p=0.009). Pretreatment SUVmax did not influence outcome. Early <sup>18</sup>F-FDG PET/CT-based response assessment using the EORTC criteria was not correlated with disease control (3-y OS and LRFS), although patients with SUVmax < 5 had a non-significant trend towards better 3-y LRFS? (91% vs 78%, pNS).

### Conclusion

In our series pretreatment PET-CT MTV was a good predictor of OS. Owing the high NPV observed in our study, a para-aortic lymphadenectomy can be avoided in patients with negative para-aortic <sup>18</sup>F-FDG PET/CT. In our experience, early <sup>18</sup>F-FDG PET/CT-based response assessment before IGBT was not useful in predicting outcome.

### EP-1488 Treatment of early stage intermediate-risk endometrial cancer using MIS and adjuvant radiotherapy

J. Song<sup>1</sup>, T. Le<sup>2</sup>, M. Gaudet<sup>1</sup>, C. Ee<sup>1</sup>, K. Lupe<sup>1</sup>, R. Samant<sup>1</sup>  
<sup>1</sup>The Ottawa Hospital, Radiation Oncology, Ottawa, Canada ; <sup>2</sup>The Ottawa Hospital, Gynecologic Oncology, Ottawa, Canada

### Purpose or Objective

Modern series of technical skills in minimally invasive surgery (MIS) using robotic arm for total abdominal hysterectomy and bilateral salpingo-oophorectomy (TAH-BSO) have resulted in improvement in patient outcome with endometrial cancer. MIS has been increasingly used since its introduction in 2010 at our institution. Randomized prospective studies have shown that adjuvant radiotherapy (RT) following TAH-BSO significantly improves loco-regional control among stage I intermediate-risk patients. Our study aims to elucidate the current use and efficacy of MIS using robotic arm and adjuvant RT among these patients at our institution.

### Material and Methods

A single-center retrospective study was conducted on patients with FIGO stage I endometrioid-type endometrial cancer with intermediate risk factors as defined by PORTEC-1 (<50% myometrial involvement and Grade 2-3, or >50% myometrial involvement Grade 1-2), who have undergone TAH-BSO and adjuvant RT at our institution between 2010 and 2015. Data on surgical and radiation treatments, as well as patient and tumor characteristics were collected and correlated with clinical outcomes. Statistical analysis was carried out using Kaplan-Meier method to compare clinical outcomes to previously reported studies.

### Results

A total of 179 stage I intermediate-risk endometrial cancer patients were identified and 135 (75.4%) patients who received adjuvant RT were selected for study. Median age at diagnosis was 63 years (range 40-89 years) and median follow-up was 4.4 years. Surgical staging was performed with pelvic lymph node dissection on 107 (79.3%) patients, while 94 (69.6%) and 41 (30.4%) patients underwent MIS and traditional laparotomy, respectively. Twenty-eight (20.7%) patients received external beam radiotherapy (EBRT, 45Gy in 25 fractions) in the form of intensity-modulated radiotherapy (IMRT) and 107 (79.3%) patients received vaginal brachytherapy (VBT, 30Gy in 3 fractions). Five-year disease-free survival and overall survival rates were 92.8% and 94.8%, respectively. Estimated 5-year loco-regional relapse rate (vaginal, pelvic, or both) was 2.3%.

### Conclusion

Clinical outcomes for stage I intermediate-risk endometrial cancer at our institution remain excellent with few loco-regional recurrences, and are comparable

to that of previously published randomized studies. Our results confirm that MIS using robotic arm combined with adjuvant RT, especially VBT, should be offered for patients with stage I intermediate-risk endometrial cancer.

**EP-1489 How effective is adjuvant radiotherapy in the management of stage I high-risk endometrial cancer?**

J. Song<sup>1</sup>, T. Le<sup>2</sup>, M. Gaudet<sup>1</sup>, C. Ee<sup>1</sup>, K. Lupe<sup>1</sup>, R. Samant<sup>1</sup>  
<sup>1</sup>The Ottawa Hospital, Radiation Oncology, Ottawa, Canada ; <sup>2</sup>The Ottawa Hospital, Gynecologic Oncology, Ottawa, Canada

**Purpose or Objective**

A recent randomized controlled trial (PORTEC-3) has demonstrated that in endometrial cancer patients with high-risk features, compared to radiotherapy alone, addition of chemotherapy to radiotherapy results in a significant improvement on failure-free survival. However, in the study, the effect of chemotherapy was limited to stage III patients, while the benefit was less pronounced in stage I and II patients. Our study aims to investigate clinical outcome in stage I high-risk endometrial cancer patients who received radiotherapy only, and compare patient outcomes to those from the previous literature.

**Material and Methods**

A single-center retrospective study was conducted on women with high-risk endometrial cancer with FIGO 2009 stage I, endometrioid-type grade 3 with deep myometrial invasion or lymph-vascular space invasion, or both, who have undergone hysterectomy at our institution between 1998 and 2015. Data on surgical and radiation treatments, as well as patient and tumor characteristics were collected and correlated with clinical outcomes. Statistical analysis was carried out using Kaplan-Meier method to compare clinical outcomes to previously reported studies.

**Results**

A total of 46 stage I high-risk endometrial cancer patients were identified. Median age at diagnosis was 63 years (range 49-86 years) and median follow-up was 4.2 years. All patients underwent total abdominal hysterectomy and bilateral salpingo-oophorectomy (TAH-BSO). Surgical staging was performed with pelvic lymph node dissection on 38 (82.6%) patients, while 35 (76.1%) and 11 (23.9%) patients underwent minimally invasive surgery (MIS) and traditional laparotomy, respectively. Thirty-four (80.4%) patients underwent adjuvant radiotherapy alone (31 patients with external beam radiotherapy, EBRT, 45Gy in 25 fractions; and 3 patients with vaginal brachytherapy, 30Gy in 3 fractions), two (4.3%) patients underwent combined chemoradiotherapy (chemotherapy with 6 cycles of intravenous carboplatin and paclitaxel; radiotherapy with EBRT), and 9 (19.6%) patients received no adjuvant treatment. Five-year disease-free survival and overall survival rates were 74.2% and 80.2%, respectively. Five-year disease-specific mortality rate was 14.1%. Among 9 patients with recurrent disease, most disease relapse (89.9%) occurred outside pelvis in 8 patients, while only one patient had regional recurrence (perirectal lymph node). Five-year loco-regional relapse-free survival was 97.8%.

**Conclusion**

Clinical outcomes for stage I endometrial cancer patients with high-risk features in our study are consistent with the published literature. Adjuvant radiotherapy results in high rates of loco-regional disease control, and most recurrences occurred at distant sites. Systemic treatment with chemotherapy may be indicated in stage I endometrial cancer patients with high-risk features to further reduce the risk of distant relapses and improve survival.

**EP-1490 Bone mineral density correlates to pelvic fractures after radiotherapy for cervical cancer**

D. Kurrumeli<sup>1</sup>, B. Weidenbacher<sup>1</sup>, K. Borm<sup>1</sup>, M. Oechsner<sup>1</sup>, S.E. Combs<sup>1</sup>, C. Brams<sup>2</sup>, M. Löffler<sup>3</sup>, M.N. Duma<sup>1</sup>

<sup>1</sup>Klinikum rechts der Isar- TU München, Department of Radiation Oncology, München, Germany ; <sup>2</sup>Klinikum rechts der Isar- TU München, Department of Gynaecology, München, Germany ; <sup>3</sup>Klinikum rechts der Isar- TU München, Department of Neuroradiology, München, Germany

**Purpose or Objective**

The aim of this study was to investigate the risk factors for pelvic insufficiency fractures (PIF) after radiotherapy for cervical cancer.

**Material and Methods**

Medical records and imaging studies, including CT and MRI of 62 women with cervical cancer who received definitive or adjuvant radio(chemo)therapy between 2013 and 2017 were reviewed. 33 patients were treated with definitive radiochemotherapy, 22 with adjuvant radiochemotherapy and 7 patients were treated with radiotherapy alone. All patients received pelvic MRI during follow-up. The PIF were detected in the follow-up MRI. For each patient we manually contoured the sacrum and analyzed the bone mineral density (BMD) [ $\text{mg}/\text{cm}^3$ ] according to Schwaiger BJ, et al. AJNR Am J Neuroradiol 2014;35:1628-33. The BMD predicts osteoporotic vertebral fractures. We then registered the MRI of the PIF patients to the planning CT and contoured the PIF. Then, on the contralateral side of the fracture, a mirrored structure of the fracture was generated (mPIF). For the sacral bone as well as the fractures we analyzed the BMD, V50Gy, Dmean and Dmax. We also analyzed the BMD of three lumbar spine vertebral bodies (between the 1st and 5th) as well as the S1 and S2 sacral vertebrae for each patient.

**Results**

Out of 62 patients, 6 (9,7%) had a fracture. All of them were insufficiency fractures and all of them in the massa lateralis of the sacral bone. Two out of the 6 patients had a bilateral fracture with only one of them being symptomatic.

PIF patients showed a significantly lower BMD in the sacral bone ( $p < 0.026$ ) as well as in the lumbar vertebrae ( $p < 0.05$ ). The BMD of the PIF was  $70,4 \text{mg}/\text{cm}^3$  and of the mPIF on the contralateral side was  $84,2 \text{mg}/\text{cm}^3$ . However, the difference in the PIF compared to the mPIF was not significant ( $p < 0.49$ ). The Dmean/Dmax of the sacrum in the PIF group was  $40,3 \text{Gy}/55,4 \text{Gy}$  and in the other patients- i.e. without PIF-(OTH)  $39,7 \text{Gy}/53,9 \text{Gy}$ , respectively (with no significant difference between groups). Similarly, the V50Gy of the sacrum in the PIF group compared to OTH as well as the V50Gy of the PIF compared to the mPIF did not reach significance ( $p < 0.43$  and  $p < 0.12$  respectively).

**Conclusion**

PIF were detected in 9,7% of the patients. The dose does not seem to have a relevant impact on the incidence of PIF in our patients. One of the predisposing factors for developing PIF after radiotherapy seems to be the BMD which was significantly lower in the PIF group. For these patients preventive measures to improve BMD should be taken into account.

**EP-1491 Clinical outcome and toxicity of MRI-based vaginal cuff brachytherapy in endometrial cancer**

C. Jaisawang<sup>1</sup>, P. Alisanant<sup>1</sup>, K. Shotelersuk<sup>1</sup>, C. Khorprasert<sup>1</sup>, N. Amornwicheit<sup>1</sup>

<sup>1</sup>King Chulalongkorn Memorial Hospital, Division of Radiation Oncology- Department of Radiology, Bangkok, Thailand

**Purpose or Objective**

In the 3-dimensional image-guided brachytherapy era, the determination of vaginal thickness can be optimized for

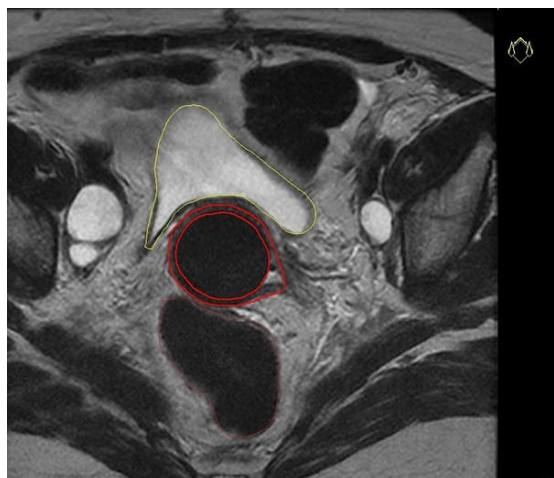
brachytherapy prescription in endometrial cancer. Thus, we conducted a review clinical outcome and toxicity of MRI-based brachytherapy based on post-operative anatomic variation in vaginal cuff (VC) anatomy, which can be visualized using T2W MRI.

#### Material and Methods

Retrospective analysis was done in resectable endometrial cancer patients (FIGO stage I-IV) treated with adjuvant MRI-based brachytherapy with or without external beam radiotherapy (EBRT) from January 2013 to December 2016 in King Chulalongkorn Memorial Hospital (KCMH). All patients in vaginal brachytherapy (VBT) alone group received high dose rate (HDR) brachytherapy with 3 fractions of 7 Gy. And the other group received 45-50.4 Gy of tumor-directed EBRT with 2 fractions of 5-7 Gy brachytherapy. Primary outcome was locoregional relapse free survival (LFRS). Secondary outcomes were toxicity, descriptive vagina doses represented by D90 of whole vaginal thickness in EQD<sub>2.10</sub> and D2cc doses of bladder and rectum in EQD<sub>2.3</sub>.

#### Results

Ninety-five patients and 218 brachytherapy plans were included in the analysis. 22 patients were treated with VBT alone and 73 patients received EBRT with VBT. Median age was 58 years old (IQR 52-72). Atypical forms of vaginal shape in MRI was found in 15 patients (16%). Median follow-up time was 40 months (range 23-50). No locoregional relapse was found in VBT alone group at 3 years. 1-yr, 2-yr and 3-yr LFRS in EBRT with VBT group were 93%, 90% and 88%, respectively. No grade 3-5 gastrointestinal (GI) and genitourinary (GU) toxicity was observed in both groups. Rate of grade 1-2 GI toxicity were significant lower in the VBT alone group than in EBRT with VBT group [0% (0/22) vs 11% (8/73)]. Rate of grade 1-2 GU toxicity was not different in both groups [4.5% (1/22) vs 4.2% (3/73)]. Mean D90 doses of whole vaginal thickness were 32.1 Gy EQD<sub>2.10</sub> for VBT alone and 63.9 Gy EQD<sub>2.10</sub> for EBRT with VBT. In VBT group, mean D2cc doses for bladder and rectum were 29.1 Gy EQD<sub>2.3</sub> and 28.0 Gy EQD<sub>2.3</sub>, respectively. In EBRT with VBT mean D2cc doses were 57.2 Gy EQD<sub>2.3</sub> for bladder and 58.4 Gy EQD<sub>2.3</sub> for rectum. Due to few numbers of events, the D2cc doses were insignificantly related to GI and GU toxicity.



#### Conclusion

The MRI-based brachytherapy for determination vaginal wall thickness provides good dose coverage, even in the atypical vaginal shape group. Additionally, this technique gives better chance to avoid adjacent organs. And the clinical results showed the high rate of tumor control and low gastrointestinal and genitourinary toxicities.

EP-1492 Comparison of 3DCRT and IMRT in endometrial cancer: efficacy, safety, and prognostic analysis

M. Ta<sup>1</sup>, A. Schernberg<sup>1</sup>, P. Giraud<sup>1</sup>, L. Monnier<sup>1</sup>, E. Darai<sup>2</sup>, S. Bendifallah<sup>2</sup>, M. Schlienger<sup>1</sup>, E. Touboul<sup>1</sup>, T. Challand<sup>1</sup>, F. Huguet<sup>1</sup>, E. Rivin Del Campo<sup>1</sup>

<sup>1</sup>Hôpital Tenon, Radiation Oncology, Paris, France ;  
<sup>2</sup>Hôpital Tenon, Gynecology, Paris, France

#### Purpose or Objective

Adjuvant Whole-Pelvic Radiation Therapy (WPRT) improves loco-regional control for stage I high-intermediate risk to stage III endometrial cancer. Nowadays Intensity Modulated Radiation Therapy (IMRT) tends to replace the standard 3D conformal radiation therapy (3DCRT) technique used in benchmark trials. The objective of this study was to compare 3DCRT versus IMRT in patients with endometrial cancer treated with post-operative WPRT.

#### Material and Methods

Patients with FIGO stage I to IIC2 endometrial cancer treated between 2008 and 2014 in our department with post-operative WPRT were included. The impact of the technique on local control, tolerance, and survival was assessed. Toxicity was graded weekly during radiation therapy, according to the Common Terminology Criteria for Adverse Events (CTCAE) version 3.0. The cumulative probabilities of OS and PFS rates were calculated using the Kaplan-Meier method and compared using a log rank test. Univariate and multivariate analyses were performed using Cox's regression

#### Results

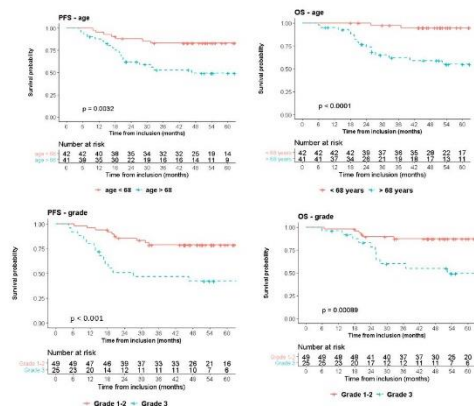
Among the 83 patients included, 47 patients were treated with 3DCRT and 36 with IMRT. There were no differences in patient characteristics between the two groups. Most of the women were menopausal (97.6%) with a median age of 68 years (range: 40-86), a myometrial invasion superior to 50% (66.3%) and no vaginal extension (90.4%). FIGO stage III (54.2%) and grade 1-2 (59%) cancers were the most represented in the population. The median dose was 45 Gy (41.4 - 55 Gy). Twenty-four patients (29%) with vaginal extension underwent Low-Dose Rate (LDR) vaginal brachytherapy after WPRT with a median dose at the reference isodose of 15 Gy (range: 10-20 Gy). Median follow-up was 50 months. The 5-year locoregional control and progression free survival (PFS) rates were 94.5% and 68%, respectively. No significant difference was found between the 3DCRT and IMRT groups in terms of survival, with a 5-year-overall survival (OS) rate of 74.6% and 78%, respectively. All locoregional relapses were associated with distant nodal metastasis, except a vaginal relapse. There was a trend towards lymphadenectomy as a prognostic factor of locoregional control but also in overall survival in univariate analysis (Table 1). The multivariate analysis found age over 68, stage > T1, and grade 3 as factors independently associated with shorter PFS and OS (Table 1, Figure 1). Five patients (10.6%) had grade 3-4 acute gastrointestinal (GI) toxicity in the 3DCRT group and two (5.4%) in the IMRT group. One (1.2%) late grade 3 GI toxicity of was observed.

Table 1. Predictive factors of overall survival.

Factor	n = 83	Deaths n = 20 (%)	5-year OS (%) (95% CI)	p		HR (95% CI)
				univariate analysis	multivariate analysis	
<b>Age (years)</b>						
≤ 68	42	3 (7.1)	95% (0.88-1)	<b>0.00065</b>	<b>0.0011</b>	9.7 (2.5-38.2)
> 68	41	17 (41.5)	55% (0.40-0.75)			
<b>T stage</b>						
T1	51	9 (17.6)	81.6% (0.71-0.94)	0.1	<b>0.025</b>	3 (1.15-8)
> T1	32	11 (34.4)	66.8% (0.52-0.86)			
<b>N stage</b>						
N0	31	7 (22.6)	79% (0.65-0.95)	0.43	--	--
N1	32	5 (15.6)	84% (0.7-0.98)			
<b>FIGO stage</b>						
I-II	38	7 (18.4)	80% (0.67-0.96)	0.35	--	--
III	45	13 (28.9)	72% (0.6-0.87)			
<b>Histology type</b>						
Type I	61	12 (19.7)	82% (0.73-0.93)	0.087	0.27	--
Type II	22	8 (36.4)	56% (0.37-0.86)			
<b>Grade</b>						
1-2	49	7 (14.3)	87.3% (0.78-0.97)	<b>0.0022</b>	<b>0.048</b>	1.7 (1.0-2.9)
3	25	12 (48.0)	49% (0.32-0.76)			
<b>LVSI</b>						
Yes	35	9 (25.7)	76.7% (0.63-0.94)	0.82	--	--
No	36	9 (25.0)	72% (0.59-0.89)			
<b>Lymphadenectomy</b>						
Yes	64	12 (18.7)	52% (0.3-0.88)	<b>0.0095</b>	0.94	--
No	19	8 (42.1)	82% (0.72-0.92)			
<b>EBRT technique</b>						
3D	47	13 (27.6)	75% (0.63-0.88)	0.74	--	--
IMRT	36	7 (19.4)	78% (0.65-0.94)			

Abbreviations: HR: Hazard ratio, 95% CI: 95% confidence interval; OS: overall survival; LVSI: lymphovascular space invasion; EBRT: external beam radiotherapy technique.

Figure 1. Subset analysis of progression free survival and overall survival for patients according to age and histological grade.



## Conclusion

These findings support IMRT as a safe technique for the treatment of endometrial cancer with no difference in efficacy and an apparently lower incidence of acute GI toxicities. Results of long-term prospective trials are needed to confirm these results.

## EP-1493 SBRT for oligometastatic gynecological cancer: a single institution experience

C. Iftode<sup>1</sup>, A. Tozzi<sup>1</sup>, G.R. D'Agostino<sup>1</sup>, T. Comito<sup>1</sup>, C. Franzese<sup>1</sup>, F. De Rose<sup>1</sup>, D. Franceshini<sup>1</sup>, L. Di Brina<sup>1</sup>, P. Navarra<sup>1</sup>, E. Clerici<sup>1</sup>, S. Tomatis<sup>1</sup>, M. Scorsetti<sup>1</sup>  
<sup>1</sup>Humanitas Research Hospital, Radiotherapy and Radiosurgery, Rozzano Milan, Italy

## Purpose or Objective

The aim of this study was to evaluate the role of stereotactic body radiotherapy (SBRT) in a series of oligometastatic gynecological malignancies.

## Material and Methods

Clinical records of patients affected by oligometastatic of any gynecological carcinoma treated with SBRT were

reviewed. From 2010 to 2018, a total of 49 patients with single or multiple metastases for a total of 96 lesions were treated in our Center. Primary cancer were 33 ovarian, 10 endometrial, 4 cervical, 1 vulvar and 1 tubal cancer. Toxicities were graded according to Common Terminology Criteria for Adverse Events version 4.0. Tumor response was evaluated by CT/ PET and/or MRI, according to Response Evaluation Criteria in Solid Tumors (version 1.1)

## Results

Median follow-up was 24 months (range 6-100). Most of treated lesions were located in lymph nodal sites 54.2%, lung in 22.9%, liver in 20.8% of cases, and soft tissue in 2.1%. Complete radiologic response, partial response, stable disease and progressive disease were observed in 57.3%, 26%, 10.4% and 6.3% of cases, respectively. The median LC was not reached. One year- and three year- LC were 96.6%. Median distant control was 35.5 months. Median OS was 59.9 months. All of patients completed the prescribed treatment with a low toxicity profile: only 12.5% experienced G2 acute toxicity, most common adverse effect was abdominal pain (5.2%), fatigue (4.2 %) and nausea and vomiting (3.1%). None of the patients had grade 3 or 4 acute or late toxicity.

## Conclusion

SBRT is a feasible and safe approach in selected cases of oligometastatic gynecological cancer with satisfactory results in terms of LC and DFS.

## EP-1494 Quality of life in women treated for gynecologic malignancies and dose-volume parameters correlation

A. Caroli<sup>1</sup>, L. Masini<sup>1</sup>, C. Pisani<sup>1</sup>, E. Gallizia<sup>1</sup>, I. Luciani<sup>1</sup>, M. Brambilla<sup>2</sup>, M. Krengli<sup>1</sup>  
<sup>1</sup>Hospital Maggiore della Carità, Department of Radiotherapy, Novara, Italy; <sup>2</sup>Hospital Maggiore della Carità, Medical Physics, Novara, Italy

## Purpose or Objective

The purpose of this study was to assess self-reported overall QoL and QoL related to genito-urinary and gastroenteric symptoms in patients affected by endometrial and cervical cancer after radiation therapy and in regular follow-up and to analyze a possible correlation with dose-volume parameters of organ at risks (OARs)

## Material and Methods

We administered the anonymous EORTC QLQ-C30 to 182 patients, 141 with endometrial cancer and 41 with cervical cancer, treated with pelvic radiotherapy from 2011 to 2017 and in regular follow-up in our center. The questionnaire was combined with EORT QLQ-EN24, in case of endometrial cancer, or with EORT QLQ-CX 24, in case of cervical cancer. There were no limitations regarding age or performance status. We analyzed overall health and overall quality of life (score from zero (low QoL) to seven (high QoL)), bladder symptoms, dysuria, bladder incontinence and fecal incontinence and their correlation with dose-volume parameters of OARs (whole bladder, bladder trigone, rectum and lumbosacral plexus).

## Results

QoL was very high (score 6-7) in many patients (88.5 % of patients). Relatively few patients referred urinary incontinence (12.6 %) or abdominal discomfort of high grade (7.2 %). We found a significant correlation between bladder V35, i.e., absolute percentage of bladder volume that received a dose of 35 Gy, and urinary incontinence (p<0.05, R=0.27, R<sup>2</sup> = 0.06), and abdominal pain (p<0.05, R= 0.16, R<sup>2</sup> = 0.02). We found also a correlation between urinary urgency and bladder V40, i.e., absolute percentage of bladder volume that received a dose of 40 Gy (p<0.05, R= 0.22, R<sup>2</sup> = 0.06).

## Conclusion

Women treated with surgery and radiotherapy for endometrial and cervical cancers have good QoL with

minimal limitations of daily activities. Parameters related to bladder function may be negatively affected by bladder V40 and V35.

#### EP-1495 Improved Disease-Free Survival with Radiotherapy in Early Stage Endometrial Cancer: 10-year outcome

S. Aytac Arslan<sup>1</sup>, I.P. Aral<sup>2</sup>, G. Altinşik Inan<sup>1</sup>, Y. Tezcan<sup>1</sup>, F. Avsar<sup>3</sup>, Y. Güney<sup>4</sup>

<sup>1</sup>Yildirim Beyazıt University, Radiation Oncology, Ankara, Turkey; <sup>2</sup>Elazığ Fethi Sekin Şehir Hospital, Radiation Oncology, Elazığ, Turkey; <sup>3</sup>Yıldırım Beyazıt University, Obstetric and Gynecology, Ankara, Turkey; <sup>4</sup>Ankara Memorial Hospital, Radiation Oncology, Ankara, Turkey

#### Purpose or Objective

The aim of this study is to evaluate the long term treatment outcomes of patients with early stage endometrial carcinoma.

#### Material and Methods

The data of 311 patients from 2 institutions with the international federation of gynecology and obstetrics (FIGO) stage 1-2 endometrial cancer whom received ±adjuvant treatment following surgery between June 2001 and December 2016 were retrospectively reviewed. Of these, 74 (24%) received no further treatment, 4 (1%) received only chemotherapy (CT), 233 (75%) received radiotherapy (RT) and 24 (7%) received both. RT was administered as pelvic + vaginal brachytherapy (n=128, 54.2%) or vaginal brachytherapy (n=106, 45.8%).

#### Results

The median follow-up was 102 months (range, 3 to 205 months). During this period, 68 (22%) patients died; of which 41 were disease related. Ten-year disease-free survival (DFS) and disease specific survival (DSS) were 73.9% and 82.7% respectively. The univariate analysis showed that nonendometrioid pathology, lymphovascular invasion (LVI) positivity, grad 3 histology, myometrial invasion <sup>3</sup>1/2, cervical stromal invasion (stage 2) and no adjuvant RT had negative significant impact on DSS. Cox multivariate analysis revealed that LVI (p:0.010, HR:2.96, CI:1.5-5.7) and stage (p:0.018, HR:2.1, CI:1.1-4) for DSS; RT (p:0.032, HR: 0.49, CI:0.2-0.9), LVI (p:0.02, HR:1.8, CI:1.09-3.1) and stage (p:0.04, HR: 1.8, CI:1.002-3.15) for DFS are as independent prognostic factors.

#### Conclusion

The findings of our cohort have affirmed the importance of adjuvant RT as a previously identified prognostic variable on long term early-stage endometrial carcinoma progression. RT can be suggested to LVI positive early stage endometrial carcinoma patients even without any other risk factors.

#### EP-1496 Feasibility of carbon ion radiotherapy for the melanoma of the lower genital tract

A. Barcellini<sup>1</sup>, V. Vitolo<sup>1</sup>, M.R. Fiore<sup>1</sup>, A. Iannalifi<sup>1</sup>, B. Vischioni<sup>1</sup>, P. Fossati<sup>1</sup>, S. Ronchi<sup>1</sup>, M. Bonora<sup>1</sup>, E. D'Ippolito<sup>1</sup>, R. Petrucci<sup>1</sup>, A. Facchetti<sup>2</sup>, A. Mirandola<sup>3</sup>, A. Vai<sup>3</sup>, S. Molinelli<sup>3</sup>, E. Mastella<sup>3</sup>, S. Russo<sup>3</sup>, G. Viselner<sup>1</sup>, L. Preda<sup>4</sup>, M. Ciocca<sup>1</sup>, F. Valvo<sup>1</sup>, R. Orecchia<sup>5</sup>

<sup>1</sup>National Centre of Oncological Hadrontherapy CNAO, Radiation Oncology, Pavia, Italy;

<sup>2</sup>National Centre of Oncological Hadrontherapy CNAO, Radiobiology, Pavia, Italy; <sup>3</sup>National Centre of Oncological Hadrontherapy CNAO, Department of Medical Physics, Pavia, Italy;

<sup>4</sup>National Centre of Oncological Hadrontherapy CNAO- University of Pavia- Pavia- Italy, Department of Clinical-Surgical- Diagnostic and Pediatric Sciences, Pavia, Italy; <sup>5</sup>National Centre of Oncological Hadrontherapy CNAO-

European Institute of Oncology- Milan- Italy, Radiation Oncology, Pavia, Italy

#### Purpose or Objective

Malignant mucosal melanoma (MMM) of the female genital tract is a rare and aggressive disease with a 5-years overall survival of 37-50% for vulvar (VuM), 13-32% for vaginal (VaM) and 10% for cervical melanoma (CM). MMM has been regarded as radioresistant tumors demonstrating unsatisfactory local control after photon radiotherapy. Based on the promising previous Japanese experience and in light of the well-known biological and therapeutic advantages of carbon ion radiotherapy (CIRT), we were prompted to use CIRT for gynecological MMM. The aim of the present study is to report our preliminary experience with CIRT in the treatment of gynecological MMM at the National Center of Oncological Hadrontherapy (CNAO).

#### Material and Methods

Between January 2016 and September 2018, 8 patients were admitted for CIRT at CNAO. Patient median age was 65 (range: 52-83). They had 6 VaM, 1 CM and 1 VuM. One patient with VaM had been previously irradiated with photons. GTV ranged from 1.13 to 380.96 cm<sup>3</sup> (median: 28.01 cm<sup>3</sup>). Two patients underwent to neoadjuvant and sequential anti-PD-1 immunotherapy. Due to their huge macroscopic diseases, the CM and VuM patients were irradiated with up to a total dose of 28 GyRBE in 3 fractions and 68.8 GyRBE in 16 fractions, respectively, and the CTV was defined as the GTV + uterine cervix and corpus for the CM and GTV + vulva for the VuM. Except one case, in the VaM the small pelvic space including GTV was irradiated with up to a total dose of 43 GyRBE (in 10 fractions) followed by a GTV boost of up to a total dose of 68.8 GyRBE in 16 fractions. One patient underwent to adjuvant CIRT on the small pelvic space up to a dose of 43 GyRBE after a radical surgery without lymphadenectomy. Acute and late toxicities were scored according CTCAE 4.0 scale. Time to event data was calculated from the end of CIRT.

#### Results

The treatment was well tolerated and no interruption was needed. During and at the end of CIRT only a patient experienced G3 erythema and 4 patients grade G1 vaginitis. For the evaluable patients (4) the median local control was 10.23 months for VaM and 7.26 months for CM. All these 4 patients experienced systemic progression. Data is still ongoing for the latest enrolled patients.

#### Conclusion

Because of the low incidence, there are no established guidelines for the management of gynecological MMM. Even if extensive surgery, when feasible, is the standard treatment due to high rate of distant metastases and unsatisfactory survival benefit, more conservative treatment approaches may be warranted. MMM is a radioresistant tumor, an ideal disease to test the biological efficacy of CIRT. Our preliminary results are encouraging, but a longer follow-up and large patient accrual are required. Patients should be encouraged to participate in clinical trials.

#### EP-1497 Particle radiotherapy for re-irradiation of pelvic recurrences of gynecological cancer

A. Barcellini<sup>1</sup>, V. Vitolo<sup>1</sup>, R. Lazzari<sup>2</sup>, M.R. Fiore<sup>1</sup>, A. Iannalifi<sup>1</sup>, B. Vischioni<sup>1</sup>, A. Facchetti<sup>3</sup>, S. Ronchi<sup>1</sup>, M. Bonora<sup>1</sup>, E. D'Ippolito<sup>1</sup>, R. Petrucci<sup>1</sup>, A. Mirandola<sup>4</sup>, A. Vai<sup>4</sup>, E. Mastella<sup>4</sup>, S. Russo<sup>4</sup>, G. Viselner<sup>1</sup>, M. Ciocca<sup>4</sup>, L. Preda<sup>5</sup>, F. Valvo<sup>1</sup>, R. Orecchia<sup>6</sup>

<sup>1</sup>National Centre of Oncological Hadrontherapy CNAO, Radiation Oncology, Pavia, Italy; <sup>2</sup>European Institute of Oncology, Radiation Oncology, Milano, Italy; <sup>3</sup>National Centre of Oncological Hadrontherapy CNAO, Radiobiology, Pavia, Italy; <sup>4</sup>National Centre of Oncological Hadrontherapy CNAO, Department of

*Medical Physics, Pavia, Italy ; <sup>5</sup>National Centre of Oncological Hadrontherapy CNAO- University of Pavia, Radiation Oncology- Department of Clinical-Surgical-Diagnostic and Pediatric Sciences, Pavia, Italy ; <sup>6</sup>National Centre of Oncological Hadrontherapy CNAO- European Institute of Oncology, Radiation Oncology, Pavia- Milano, Italy*

#### **Purpose or Objective**

Recurring gynecological tumors of the pelvic area within or at the edge of a previously irradiated field are often in close proximity to the intestinal tract. When surgery is not feasible, re-irradiation can be reasonably used. Re-irradiation presents challenges due to the high cumulative dose and the risk of severe toxicities in normal tissues. Particle therapy (with carbon ions and protons) is a promising alternative for these women.

#### **Material and Methods**

Between May 2014 and October 2018, 8 patients with gynecological recurrent tumor within or at the edge of the previously irradiated field were admitted for particle therapy at National Centre of Oncological Hadrontherapy (CNAO). They had recurrence of cervical (5), endometrial (2) and ovarian (1) cancer. Median age at the time of registration for particle RT was 58 years (range:35-72 years), and median GTV was 79 cm<sup>3</sup> (range: 34.99-172.80). Two patients, with marginal lymph node recurrence, were irradiated with protons up to a total dose of 25 GyRBE and 51 GyRBE respectively. The remaining women underwent to carbon-ion radiotherapy (CIRT) with a median total dose of 50.4 GyRBE (range: 36-57) administered in a median number of 12 fractions. Three patients with pelvic side wall recurrences received surgical spacer placement by open surgery to keep intestinal tracts apart from the tumor, since the distance between tumor and nearest intestinal tracts was not sufficient. Toxicity was scored according CTCAE 4.0 scale.

#### **Results**

All patients completed the planned treatment and no acute toxicities G>1 were observed. For the evaluable patients no grade 2 or higher late toxicities were reported. For the patients with a follow-up > 3 months, we observed 1 local recurrence and 5 patients died for systemic progression. The median local control was 10.26 months. Data is still ongoing.

#### **Conclusion**

Although the study's limitations, particle therapy showed no severe toxicities for recurrence of gynecological cancers after RT. Unfortunately, patients with large volume central or pelvic side wall recurrences have poor prognoses therefore efforts should be made to detect pelvic recurrences early. A strong collaboration between Gynecologic Oncologists and Radiation Oncologists is of utmost importance to make a step forward in the treatment of these diseases. Hence, hadrontherapy for pelvic recurrences should be further investigated in a prospective and multicenter trial.

#### **EP-1498 Reporting vaginal doses for cervical patients receiving external beam radiotherapy and brachytherapy**

T. Chan<sup>1</sup>, P.W. Tan<sup>1</sup>, J.I.H. Tang<sup>1</sup>

<sup>1</sup>The National University Cancer Institute- Singapore NCIS, Radiation Oncology, Singapore, Singapore

***This abstract is part of the media programme and will be released on the day of its presentation***

#### **EP-1499 The case selection for brachytherapy in cervical cancer patients after radical hysterectomy**

H. Xu<sup>1</sup>, Y. Lai<sup>2</sup>, Y. Jin<sup>1</sup>

<sup>1</sup>Ruijin Hospital- Shanghai Jiaotong University School of Medicine, Radiation Oncology, Shanghai, China ;

<sup>2</sup>XiaoShan Hospital, Oncology, Zhejiang, China

#### **Purpose or Objective**

To explore the suitable cases for brachytherapy as a component of adjuvant radiotherapy, and analyzed the relapse patterns of cervical cancer patients after radical hysterectomy.

#### **Material and Methods**

We retrospectively analyzed the clinical data of 213 cervical cancer patients (aged 28-78 years) with FIGO stage I A to II B admitted to our department who received adjuvant radiotherapy from January 2008 to December 2015. Squamous cell carcinoma (178 cases), adenocarcinoma(25 cases), adenosquamous carcinoma (9 cases) and undifferentiated carcinoma (1 case) were

included. Among them, 149 patients received EBRT (external beam radiation therapy) after radical hysterectomy, 64 received EBRT combined with intracavitary brachytherapy. There was no statistical difference in FIGO stage and pathological type distribution between the two groups. A dose of 45-50.4Gy in 25-28 fractions was prescribed to the planning target volume with IMRT. Those who underwent brachytherapy were supplemented with 18-30Gy/3-5Fx. Survival analyses were performed using Kaplan-Meier method, and Cox model was used to analyze prognostic factors.

#### Results

The median follow-up was 52 months (9-136 months), and 3 years PFS was 77%. Among them, 62 patients had local or distant recurrence, 31 cases in pelvic (including vaginal cuff), 10 cases with metastases to para-aortic or inguinal lymph nodes, and 21 cases with distant metastasis. The types of pathology, large mass, positive lymph node, FIGO stage and depth of invasion were all highly significantly and independently related to risk of recurrences ( $P=0.004$ ,  $0.023$ ,  $0.013$ ,  $0.003$  and  $0.035$ , respectively). However, the adjuvant chemotherapy was not a significant factor influenced PFS ( $P=0.88$ ), which did not reduce the risk of pelvic relapse or distant metastasis ( $P=0.27$ ,  $P=0.40$ ). We found that when the patients received EBRT with dose of 45Gy, 1) if the invasive depth reaching or exceeding the deep muscle layer, the brachytherapy could significantly reduce the recurrence ( $P=0.049$ ); 2) if the tumor size was more 4cm, the brachytherapy could reduce the recurrence (mean PFS,  $58.83\pm 9.28$  months vs.  $35.33\pm 6.78$  months), though the difference was not statistically significant ( $P=0.20$ ).

#### Conclusion

The pathology, stage, mass, lymph node status and depth of invasion were the prognosis factors of cervical cancer patients with radical hysterectomy in our study. Preliminary results showed that adjuvant chemotherapy did not improve the prognosis of these patients. In those who received prescribed dose of 45Gy for the EBRT, high risk factors such as depth of invasion and large tumor size would be the key factors for the case selection to additional intracavitary therapy. And more data is needed for further research.

#### EP-1500 Squamous Cell Carcinoma of unknown primary (CUP) in the Pelvis: A case series and review of literature

E. Connolly<sup>1</sup>, G. Rangaswamy<sup>1</sup>, O. Boycech<sup>1</sup>, C. Gillham<sup>1</sup>, O. McArdle<sup>1</sup>

<sup>1</sup>St Luke's Radiation Oncology Center, Radiation Oncology, Dublin, Ireland

#### Purpose or Objective

The diagnosis and management of Carcinoma of unknown primary (CUP) represents a challenge. Of the 3-5% of invasive cancers that are classified as CUP approximately 5%-10% are squamous cell carcinomas (SCCs), many of which are HPV +ve and are commonly located in the head and neck. HPV +ve SCCs CUP in the pelvis are extremely rare and there is not much known about the aetiology, pathogenesis, or ideal radiation therapy target coverage.

#### Material and Methods

Electronic medical records and patient charts registered as SCC CUP between 2014 and 2018 inclusive were reviewed. Those with a diagnosis of CUP in the Pelvis were included in our study. We also conducted a literature review to identify published data reporting treatment outcomes.

#### Results

Three patients with CUP in the Pelvis were identified at our institution. Case#1: A 62-year-old lady presented with a three-month history of progressive lower back pain. Imaging revealed a left pelvic sidewall mass, confirmed as p16 positive SCC. She was treated with chemoradiotherapy. Case#2: A 33-year-old lady, in her first

trimester presented with a deep vein thrombosis and found to have a right pelvic mass biopsy of which confirmed a SCC. She was treated with chemotherapy, external beam radiotherapy and a single dose of intracavitary brachytherapy. Case#3 A 40-year-old lady with a history of pelvic pain was diagnosed with p16 positive SCC after MRI showed a large infiltrative mass. She was treated with external beam radiotherapy with concomitant chemotherapy. We present treatment outcomes on all three patients and a review of the available literature.

#### Conclusion

Our case series highlights the complexities involved in the management of these rare CUP of the pelvis. Our three cases add to the very small number of previously reported cases in the literature to date. Identification of a primary site is important since therapy is potentially curative. We cannot deduce whether HPV/p16 caused these cancers but it may be that the HPV status can be helpful in identifying mucosal sites. It may thus prove a useful tool in developing a diagnostic and treatment paradigm for such patients.

#### EP-1501 Prognostic value of SCC-Antigen and SUVmax value in locally advanced cervix cancer

S. Pedraza Fernández<sup>1</sup>, P. Sarandeses<sup>2</sup>, D. Lora<sup>3</sup>, J.F. Pérez-Regadera<sup>1</sup>

<sup>1</sup>Hospital Universitario 12 de Octubre, Radiation Oncology, Madrid, Spain ; <sup>2</sup>Hospital Universitario 12 de Octubre, Nuclear Medicine, Madrid, Spain ; <sup>3</sup>Hospital Universitario 12 de Octubre, CIBER de Epidemiología y Salud Pública imas12-CIBERESP, Madrid, Spain

#### Purpose or Objective

The aim of this study is to combine tumour SUVmax (maximum standardized uptake) value at diagnosis and pretreatment squamous cell carcinoma antigen (SSC-Ag) level to evaluate the impact of both in predicting the response to combined chemoradiotherapy (CCRT) in locally-advanced cervix cancer (LACC).

#### Material and Methods

From March 2009 to October 2015, 114 consecutive patients (pts.) with LACC who underwent a 18F-FDG-PET/CT at diagnosis were enrolled in this retrospective study. Pts. were staged according to FIGO 2008 system. All received definitive radiotherapy in combination with weekly Cisplatin and endocavitary brachytherapy. A follow-up time, in the absence of an event, higher than 2 years (yrs) was required.

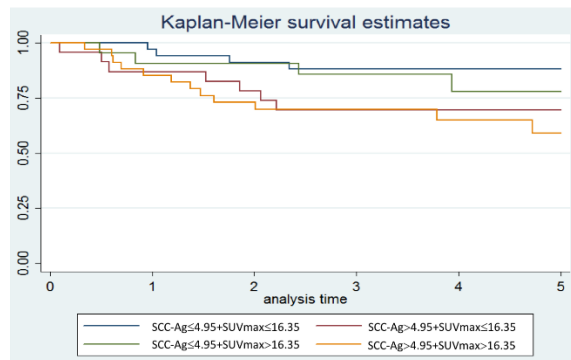
Univariate analysis was performed studying independently the differences in SCC-Ag group and tumor-SUVmax value group and clinic prognostic variables. Kruskal-Wallis test was used;  $p$  value  $\leq 0.05$  was considered statistically significant. Analysis of overall survival (OS) was performed with the Kaplan-Meier method and long-rank test. Statistical studies were performed using program Stata (Version 12, StataCorp, College Station, Texas).

#### Results

The mean age was 52(25-82)yrs. Histology specimens: 86(76%) squamous-cell carcinoma, 27(23.89%) non-squamous-cell carcinoma. FIGO stage: 25(21.93%) IB, 4(4%) IIA, 45(40%) IIB, 1(0.8%) IIIA, 33(29%) IIIB, 5(4.3%) IVA. Hydronephrosis was presented in 13(11.5%)pts. and 80(70%) had parametrial invasion. Pathological uptake in pelvic nodes was evidenced in 56.14%pts. Patients' distribution according to ECOG scale: 94(82.5%) 0 to 1 and 20(17.5%) 2 to 4. Mean follow-up was  $4\text{yrs}\pm 2.16(\text{SD})$ .

The average SSC-Ag pretreatment was  $17.9\text{ng/ml}\pm 36.19(\text{SD})$ . The median was  $4.95\text{ng/ml}$  (range: 0.5-221). There was significant correlation between SSC-Ag level and tumoral histology, FIGO stage, ECOG level and pelvic lymph node affectation ( $p=0.0001$ ,  $p=0.01$ ,  $p=0.01$ ,  $p=0.02$  respectively). No correlation was found with hydronephrosis or parametrial infiltration. Mean SUVmax of primary cervical tumour was  $16.9\pm 8.26$  (SD). The median was  $16.35$ (range: 4.2-48.32). Only pelvis lymph

nodes affectation was found to be statistically significant in prognosis prediction ( $p=0.003$ ). OS at 5yrs. was 73.7%. The 5-yrs OS for pts. with a SCC-Ag  $<4.95$  was higher compared to those with SCC-Ag  $>4.95$ ng/ml (84% Vs 63%,  $p=0.001$ ). Pts. with tumour SUVmax level  $\geq 16.35$  presented worse OS, although it was not statistically significant (80 Vs 66%,  $p=0.21$ ). When stratified pts. in four groups according to SCC-Ag and SUVmax level, the group with SCC-Ag  $>4.95$ ng/ml and SUVmax level  $\geq 16.35$  presented the worst OS at 5yrs ( $p=0.09$ ). Details are shown in figure 1.



### Conclusion

SCC-Ag pretreatment level and tumor SUVmax value can be useful for prognosis prediction in LACC. Further studies are required to establish the role of high level of both and if a more intensive therapy is required to this cohort.

### EP-1502 Endometrial cancer. Relapse free survival rates in our medium/large hospital in the UK

L. Price<sup>1</sup>, R. Allerton<sup>1</sup>

<sup>1</sup>Royal Wolverhampton Hospital, Oncology, Wolverhampton, United Kingdom

### Purpose or Objective

Endometrial cancer (EC) is common in developed countries (N. Colombo et al., 2013) and incidence is increasing in the UK and this is considered to be due to rising obesity rates (NCIN 2015), despite this survival rates have improved since 1990s (NCIN).

Endometrial cancer treatment is guided by the risk of recurrence, low medium or high.

Those with low-Intermediate risk Stage 1 disease have been shown to benefit from Radiotherapy following hysterectomy (PORTEC1). PORTEC2 looked at those with intermediate-high risk EC and demonstrated external radiotherapy is equivalent to vaginal brachytherapy (VT). Adjuvant Chemotherapy can be offered to those with high risk EC with Stage I-III any histology and no residual disease. (NSGO-9501/EORTC 55991 trial and MaNGO ILIAD III-study)

Our objective was to assess local outcomes of relapse free survival for those with low, intermediate and high risk EC treated in our local medium/large district general hospital and compare with published relapse free survival data from large multi-centre clinical trials, PORTEC1, 2 and 3.

### Material and Methods

179 patients with EC discussed at multi-disciplinary meetings (MDT) and actively treated between May 2010 to November 2013 were assessed retrospectively using electronic notes. Patients were followed up for a median of 4 years and 1 month (the minimum follow up was 3 years 3 months with the maximum follow up being 6 years 11 months).

### Results

Our cohort for low risk EC demonstrate a relapse free survival of 95% (62 of 64 patients) which is the same as that quoted by PORTEC1. All relapses were local relapses

within the vaginal vault and all were successfully salvaged with surgery.

Our cohort for intermediate / high risk EC demonstrate a 88% (53 of 60 patients) relapse free survival which is broadly in line with PORTEC2 trial (78 - 83% for endometrioid histology only). Tumour characteristics were broadly comparable by data we collected (See Figure 1). Recently, PORTEC3 reported a 76% failure free survival with chemo-radiotherapy (CRT) and 69% with radiotherapy at 5 years. We looked at 55 patients treated locally with high risk disease and found a 76% (42 of 55 patients) failure free survival rate, those patients were treated with a mixture of CRT, external beam radiotherapy, VT and adjuvant chemotherapy. (See Figure 2 for Kaplan-Meier curves for CRT with or without adjuvant chemotherapy versus radiotherapy alone). However of those with high risk disease only 4 had chemo-radiotherapy per PORTEC3 protocol (two cycles of cisplatin 50 mg/m<sup>2</sup> given during radiotherapy, followed by four cycles of carboplatin AUC5 and paclitaxel 175 mg/m<sup>2</sup>).

### Conclusion

We conclude that broadly our relapse rate for endometrial cancer are in line with those published in the seminal studies.

Importantly, when our cohort of high risk disease was compared to PORTEC3 data (ASCO June 2017), real life data is demonstrated. Only 4 of 55 patients received chemo-radiotherapy as per the PORTEC3 trial protocol because many patients could not be offered toxic CRT due to co-morbidities.

### EP-1503 Brachytherapy versus EBRT boost for cervical cancer: is the standard better?

D. Delgado<sup>1</sup>, A. Figueiredo<sup>1</sup>, J. Leitão Santos<sup>1</sup>, A. Florindo<sup>1</sup>, V. Mendonça<sup>1</sup>, M. Lemos<sup>1</sup>, M. Abdulrehman<sup>1</sup>, M.F. De Pina<sup>1</sup>

<sup>1</sup>Centro Hospitalar Lisboa Norte EPE, Serviço de Radioterapia, Lisbon, Portugal

### Purpose or Objective

Compare the outcomes of intracavity high-dose-rate brachytherapy (IC BT-HDR) boost and external beam radiotherapy (EBRT) boost of patients (pts) treated with concomitant chemoradiotherapy (CCRT) for cervical cancer.

### Material and Methods

Retrospective review of 92 pts with stage IB1-IVA cervical cancer treated with CCRT between 2008 and 2013 with at least 1 year follow-up. All pts received pelvic 3D-conformal EBRT (45-50,4Gy) concomitant with weekly cisplatin (40mg/m<sup>2</sup>) and an IC BT-HDR boost (24Gy/4 fractions prescribed to point A-A') to the tumor or a 3D-conformal EBRT boost (16,2Gy) if the former was not technically feasible. Pts with clinically positive paraaortic (PA) lymph nodes received PA lymph node irradiation. Parametrial EBRT boost was given when appropriate. Pts treated with at least one fraction of BT were included in the IC BT-HDR group. Characteristics of pts treated with and without IC BT-HDR were compared to evaluate for differences. The effect of the IC BT-HDR boost on recurrence free survival (RFS) and overall survival (OS) was examined with univariate and multivariate analyses.

### Results

Median age of all pts was 52 years (24-83). IC BT-HDR boost was given to 37 pts (40,2%) and an EBRT boost to 55 pts (59,8%). Patients treated with EBRT boost had larger tumors (mean 53mm vs 39mm -  $p < 0,001$ ) and more advanced disease at diagnosis (FIGO stage  $>IIB$  38,2% vs 5,4% -  $p < 0,001$ ), however roughly the same number of pts had stage  $\leq IIB$  (34 vs 35pts). There was no difference in age or clinically positive lymph nodes at diagnosis.

Ten pts (10,8%) received PA lymph node irradiation. Parametrial EBRT boost was given to 26 pts (74,6%) treated with IC BT-HDR boost. Median treatment time was

78 days (49-102 days) for IC-BT-HDR boost pts and 56 days (44-114 days) for EBRT boost pts.

The median follow-up time was 67 months (5-129 months) for all pts.

Pelvic failure was detected in 20,7% of pts and distant failure in 12%.

The 3-year RFS rate was 61% for all pts, 45% for EBRT boost pts and 84% for IC BT-HDR boost pts (Log-rank  $p < 0,001$ ). The 3-year OS rate was 76% for all pts, 66% for EBRT boost pts and 89% for IC BT-HDR pts (Log-rank  $p = 0,005$ ).

Multivaried Cox regression on PFS				
	HR	95% CI		p-value
<b>STAGE</b>				
≤IIB vs >IIB	0,693	0,302	1,59	0,387
<b>NI</b>				
N0 vs N1	0,371	0,177	0,777	0,009
<b>MTD</b>				
	1,015	0,99	1,04	0,241
<b>BOOST</b>				
EBRT vs BT	3,564	1,268	10,023	0,016
Multivaried Cox regression on OS				
	HR	95% CI		p-value
<b>STAGE</b>				
≤IIB vs >IIB	0,347	0,136	0,885	0,027
<b>NI</b>				
N0 vs N1	0,579	0,241	1,387	0,22
<b>MTD</b>				
	0,999	0,968	1,031	0,93
<b>BOOST</b>				
EBRT vs BT	3,14	0,969	10,171	0,056

Legend: Maximal Tumor Dimension (MTD); External Beam Radiotherapy (EBRT); Brachytherapy (BT)

In multivariate analysis controlling for maximum tumor dimension, lymph node status and FIGO stage (fig.1), EBRT boost was associated with a statistical significant increase in the risk of recurrence (HR 3,56; CI 95% 1,27-10,02  $p = 0,016$ ) and a trend towards an increase in the risk of death (HR 3,14; CI 95% 0,97-10,17  $p = 0,056$ ).

#### Conclusion

IC-BT-HDR boost is considered standard of care combined with CCRT in the treatment of cervical cancer not amenable by surgery.

In some cases IC BT-HDR boost is not technically feasible and department guidelines recommend an EBRT boost up to 66,6Gy.

This retrospective study demonstrates that the EBRT boost is associated with a three fold increase in the risk of recurrence. Better alternatives need to be studied for pts where a BT boost is not possible.

#### EP-1504 Role of PET/CT in assessing treatment response of cervical cancer after definitive RadioChemotherapy

A. Tsikkinis<sup>1</sup>, E. Vlaskou Badra<sup>1</sup>, N. Cihoric<sup>1</sup>, D. Aebersold<sup>1</sup>, K. Lössl<sup>1</sup>

<sup>1</sup>Inselspital- Universität Bern, Radiation-Oncology, Bern, Switzerland

#### Purpose or Objective

To evaluate the value of <sup>18</sup>FDG-PET/CT in the follow-up of patients (pts) with cervical cancer after definitive radio/chemotherapy (RChT).

#### Material and Methods

From 11/2010 to 08/2016, 53 (100%) patients (pts) with cervical cancer (FIGO stage IB1 to IVA) were treated with definitive radio-chemotherapy (RChT).. The median age at the time of diagnosis was 54 (29 -83) years. All pts were staged with a clinical exam and a pre-treatment <sup>18</sup>FDG-PET/CT. 29 (55%) pts were treated in our hospital and 24 (45%) in other referring institutions (n:7). 13 (25%) pts were lymph node (LN) negative and 40 (75%) LN positive. 12 (23%) pts had 1 positive LN, 9 (17%) two, 7 (13%) pts with 3-5 LN and 9 (17%) with >5 positive LN. 17 (32%) pts

had positive paraaortal LN. All pts were treated with image guided RChT. A dose of 50.4 Gy was prescribed to the elective pelvic nodal volume. Primary tumors smaller than 4 cm in diameter received an additional boost of 5.4 Gy, primary tumors larger than 4 cm in diameter received a boost of 9 Gy. Pts with positive LN detected with <sup>18</sup>FDG-PET/CT received a simultaneous integrated boost to a total dose of 64 Gy. Chemotherapy was administered according to institutional standards. After completion of the external beam RChT all pts were referred to our hospital for image guided HDR Brachytherapy in 4 once weekly fractions of 6-7 Gy. Follow up included clinical investigation at 6 weeks and at 3 months after therapy and a <sup>18</sup>FDG-PET/CT at 6 months.

#### Results

Median time to the first <sup>18</sup>FDG-PET/CT after therapy completion was 6 months (1 - 8 months). Pathological findings were found in 21 (40%) pts. 3 pts (6%) showed local tumor persistence and 2 pts (4%) were diagnosed with loco-regional persistence which were later histologically reclassified as benign. In 16 pts (30%) systemic metastasis was diagnosed, of those 12 received palliative systemic treatment and/or palliative radiation, 2 were operated upon and 2 were followed up. In total 19 (36%) pts were diagnosed and confirmed with having malignant disease, to date just 7/19 died as a direct consequence of their disease.

#### Conclusion

<sup>18</sup>FDG-PET/CT conducted 6 months after therapy completion is a valuable imaging tool in assessing treatment response of cervical cancer patients treated with definitive RChT. <sup>18</sup>FDG-PET/CT findings lead to therapeutic consequences in the majority of pts.

#### EP-1505 Is locally advanced cervix adenocarcinoma less radiosensitive than squamous cell carcinoma?

K. Vandecasteele<sup>1</sup>, E. De Jaeghere<sup>2</sup>, P. Tummers<sup>3</sup>, A. Makar<sup>3</sup>, P. De Visschere<sup>4</sup>, K. Van de Vijver<sup>5</sup>, E. Naert<sup>2</sup>, H. Denys<sup>2</sup>

<sup>1</sup>UZ Gent, Radiation Oncology, Gent, Belgium ; <sup>2</sup>UZ Gent, Medical Oncology, Gent, Belgium ; <sup>3</sup>UZ Gent, Gynaecology, Gent, Belgium ; <sup>4</sup>UZ Gent, Radiology, Gent, Belgium ; <sup>5</sup>UZ Gent, Pathology, Gent, Belgium

#### Purpose or Objective

Previous studies on cervical cancer reported a worse outcome for adenocarcinoma (AC) compared with squamous cell carcinoma (SCC). Nevertheless, standard treatment remains identical. Insight in the impact of histological types on biological behavior and pathological complete response rates might result in a treatment paradigm shift.

#### Material and Methods

Since 2006, 114 locally advanced (FIGO IB2-IVA and IVB in case of para-aortic/inguinal lymph nodes metastases only) cervical cancer (LACC) patients were treated consecutively with neo-adjuvant chemoradiation (NA-CRT) and surgery. RT was performed using an Intensity Modulated Arc Technique up to a minimal dose (D98) of 45Gy to the elective lymph nodes and primary target volume and 62/60Gy (SIB) to the tumor/affected lymph nodes. From 1/2/2009 onwards, para-aortic lymph node irradiation was performed in case of positive pelvic lymph nodes. Brachytherapy was applied in case of doubtful or positive margins after surgery or if surgery could not be performed. Chemotherapy was administered concomitantly (cisplatin or 5-FU). Six patients were excluded for analysis due to a synchronous second primary (n=5) or previous liver transplant (n=1). Clinicopathological characteristics, pathological response and survival rates were compared between AC (n=19) and SCC (n=89) LACC patients. Statistics were performed using SPSS vs 25.0.

#### Results

Clinicopathological characteristics before treatment are

described in table 1, only differentiation grade differed significantly between AC and SCC. In 8 SCC patients, surgery was not performed due to remaining unresectable disease after NA-CRT, they were considered as lack of pathological complete response (pCR). Adenocarcinoma patients treated with NA-CRT showed significantly less pCR compared with SCC patients (AC=10.5%, SCC=39%,  $p=0.017$ ) (table 1). Per FIGO stage, 5y OS and DSS was 100%/72%/50%/50% ( $p=0.012$ ) and 100%/85%/57%/50% ( $p=0.005$ ), for stage I/II/III/IV respectively. Per TNM stage, 5y-OS and DSS was 100%/75%/63%/69% ( $p=0.519$ ) and 100%/90%/71%/69% ( $p=0.258$ ) for stage I/II/III/IV respectively. Five-year OS and DSS were 80%/67% ( $p=0.285$ ) and 80%/78% ( $p=0.816$ ) for AC/SCC, respectively. Relapse pattern was not different between AC and SCC (table 1). Five-year locoregional relapse free survival (LRRFS) and DMFS (including distant nodal relapse) were 100%/83% ( $p=0.093$ ) and 52%/81% ( $p=0.024$ ) for AC/SCC, respectively. In AC, 2/6 patients metastasized in an oligometastatic way, 59m and 62m after treatment and were treated according to an oligometastasis protocol.

Table 1

	AC	SCC	p-value
N (%)	19	89	
Median Age, y (range)	53 (28-79)	54 (25-80)	0.800
Median Follow-up, m (range)	57 (5-131)	36 (7-145)	0.401
FIGO stage			
I	5 (26)	9 (10)	
II	11 (58)	52 (58)	
III	2 (10.5)	20 (22.5)	0.208
IV	1 (5)	8 (9)	
TNM-STAGE			
I	1 (5)	3 (3)	
II	8 (42)	34 (38)	
III	8 (42)	40 (45)	0.975
IV	2 (10.5)	12 (13.5)	
Node positive (%)	7 (37)	44 (49)	
Differentiation grade			
Good (%)	3 (16)	5 (6)	
Moderate (%)	6 (32)	37 (42)	
Bad (%)	3 (16)	33 (37)	0.039
Unknown (%)	7 (37)	14 (16)	
Chemotherapy (%)	18 (95)	83 (93)	1
Surgery (%)	19 (100)	81 (91)	0.201
Brachytherapy (%)	2 (10.5)	7 (8)	0.657
Pathological response			
Complete (%)	2 (10.5)	35 (39)	0.017
Incomplete (%)	17 (89.5)	54 (61)	
Locoregional relapse (%)	0 (0)	14 (16)	0.156
Distant Nodal relapse (%)	2 (10.5)	11 (12)	1
Distant Hematogenous (%)	6 (32)	13 (15)	0.098
Cause of Death (%)			
Cancer progression (%)	2 (10.5)	15 (17)	
Cancer related (%)	1 (5)	1 (1)	0.202
Intercurrent (%)	0 (0)	9 (10)	

### Conclusion

Patients with AC responded significantly less to NA-CRT as evidenced by a significantly lower pCR rate. After surgery, however, this did not result in a worse LRRFS for AC. AC patients had a significantly lower DMFS but this did not translate into a worse OS or DSS. These findings imply a need for a paradigm shift in the treatment of AC patients.

### EP-1506 Multi-institutional treatment and management of cervical cancer patients

A. Tsikkinis<sup>1</sup>, N. Cihoric<sup>1</sup>, E. Vlaskou Badra<sup>1</sup>, D. Aebersold<sup>1</sup>, K. Lössl<sup>1</sup>

<sup>1</sup>Inselspital- Universität Bern, Radiation-Oncology, Bern, Switzerland

### Purpose or Objective

Evaluation of treatment outcome, toxicity and patterns of failure in cervical cancer patients (pts) treated with image guided external beam radio(chemo)therapy (IG-EBRT)

and centralized image guided high dose rate brachytherapy (IG-HDR BT).

### Material and Methods

From 01/2012 to 06/2017, 96 (100%) pts with cervical cancer (FIGO IA2 - IVA) were treated with IG-EBRT in 10 national institutions. 74% of pts were diagnosed with positive lymph nodes, 21% after complete or sentinel-lymphadenectomy and 53% via <sup>18</sup>FDG-PET/CT. 81% of pts were diagnosed with tumors larger than 4 cm in diameter. 82% of the tumors were squamous cell carcinomas, 10% adenocarcinomas and 7% other histologies. All pts were treated with IG-EBRT. A dose of 50.4 Gy was prescribed to the elective pelvic nodal volume. Primary tumors smaller than 4 cm in diameter received an additional boost of 5.4 Gy, primary tumors larger than 4 cm in diameter received a boost of 9 Gy. Patients with positive lymph nodes detected with <sup>18</sup>FDG-PET/CT received a simultaneous integrated boost to a total dose of 64 Gy. Chemotherapy was administered according to institutional standards. After completion of IG-EBRT all pts were centrally referred to our hospital for IG-HDR BT treatment (4 x 6-7 Gy). Median EQD2 dose for the primary tumor was 81.6 Gy (62.6 - 93.2 Gy). Adverse events were coded according to the CTCAE version 4.0.

### Results

Survival data were available for 91 pts. During a median follow-up of 22 months (2-77 months) 28 (31%) pts developed disease relapse. 12 (13%) pts had loco-regional relapse, 7 (8%) local relapse and 5 (5%) nodal relapse. 22 (24%) pts developed systemic metastases. 13 (14%) pts died, 9 (10%) from cervical cancer. Median survival time was not reached. In total 89 acute adverse events (AE) were recorded (86 Gr. 1-2; 3 Gr. 3). Data on late AE were available for 83% of the pts. 68 late AE were recorded (37 Gr. 1; 26 Gr. 2; 5 Gr. 3).

### Conclusion

Satisfactory treatment outcomes were achieved while treatment-related toxicities were kept reasonably low.

### EP-1507 Radical radiotherapy/brachytherapy for cervix cancer in Alberta: who are treated, how do they fare?

N. Vawda<sup>1,2</sup>, S. Ghosh<sup>1,3</sup>, S. Menon<sup>4</sup>, A. Duimering<sup>1,2</sup>, J. Cuartero<sup>1,2</sup>, E. Wiebe<sup>1,2</sup>, C. Doll<sup>4,5</sup>, F. Huang<sup>1,2</sup>

<sup>1</sup>University of Alberta, Oncology, Edmonton, Canada ;

<sup>2</sup>Cross Cancer Institute, Radiation Oncology, Edmonton, Canada ;

<sup>3</sup>Cross Cancer Institute, Oncology, Edmonton, Canada ;

<sup>4</sup>University of Calgary, Oncology, Calgary, Canada ;

<sup>5</sup>Tom Baker Cancer Centre, Radiation Oncology, Calgary, Canada

### Purpose or Objective

To explore patterns of disease and outcomes of cervix cancer (CC) patients treated with radical (chemo)radiotherapy (RT), including brachytherapy (BT), in the province of Alberta (AB), Canada.

### Material and Methods

In this retrospective review, all patients with CC who received primary (chemo)RT (including BT) in AB were identified (by consultation date, January 1, 2013 - December 31, 2015). Descriptive statistics were performed on demographic and clinicopathologic data. The Kaplan Meier method was used to determine overall survival (OS) and cause-specific survival (CSS).

### Results

Over 3 years, 146 women received radical RT including BT in AB (2 tertiary cancer centres, 2:1 spread). Annual caseload was 52 and 55 for 2013 and 2014, respectively; less (39) for 2015. Over half (54.5%) lived within 50 km of their treatment centre, with 20 women residing > 350 km (one > 1000 km) away. Among AB residents (n=140), 32.1% lived in areas designated rural and/or remote (AB Health community profile). Mean age at diagnosis was 52.4 years. Only 19.2% reported a routine Pap smear within 2 years of CC diagnosis; 8.2% had never had a Pap and 24.7%, not in

at least 5 years. Half (55.5%) were current or ex-smokers. Squamous carcinoma (76.7%) was the most common histologic type (adenocarcinoma 16.4%, adenosquamous 1.4%). Clinical stage of the primary was distributed as: 30.1% IB, 11.0% IIA, 35.6% IIB, 3.4% IIIA, 15.8% IIIB, 3.4% IVA (n=1 missing). 63% had pelvic and/or para-aortic (PA) nodal involvement; 7.5% had clinical and/or radiological distant disease. Over 10% had another primary cancer diagnosis: n=7 (lymphoma, melanoma, sarcoma, breast, myelodysplastic syndrome) prior to, 2 (vulva, thyroid) concurrent with, and 6 (non-small cell lung, breast, vagina, bladder) after CC treatment. Most (n=125; 85.6%) had conventional chemoRT (pelvic±PA external beam RT with weekly cisplatin, and intracavitary±interstitial BT boost). N=14 received no chemotherapy; n=6, neoadjuvant±concurrent; n=1, concurrent+adjuvant. Four had BT only. Another 4 were treated after curative surgery was abandoned due to disease extent. An additional 11 had pelvic surgery: 1 pre-RT (nodal debulking), 1 post-BT (hysterectomy), 9 during follow-up (FU) (7 for salvage). Median FU was 28.5 months [3 - 54], with 2y-OS of 76.8% and CSS of 77.9%. By clinical stage, 2y-OS was 85.2% (IB), 82.5% (IIA/B), 55.3% (IIIA/B), 44.4% (IVA/B) and was statistically significant (p=0.001); this did not differ by nodal status. Those living < 50 km away fared worse, with 2y-OS of 71.4%, compared to 83.8% for those further away (p=0.054). Age and year of diagnosis had no appreciable effect.

#### Conclusion

In a heterogeneous CC cohort receiving primary RT/BT within a large integrated health system, outcomes are aligned with international reports. Mitigatable risk factors remain, as unrealized opportunities to optimize health outcomes in this population.

#### EP-1508 EQD2 and overall treatment time as prognostic factors in cervical cancer treated with definitive CRT

S.I. Perez Alvarez<sup>1</sup>, G.E. Trejo Durán<sup>1</sup>, J.C. Rodriguez Rosas<sup>1</sup>, C.H. Flores Balcazar<sup>1</sup>, J. Zamora Moreno<sup>1</sup>, G.B. Santiago Concha<sup>1</sup>, A. Mota Garcia<sup>1</sup>  
<sup>1</sup>Instituto Nacional de Cancerología, Radiation Oncology, Mexico City, Mexico

#### Purpose or Objective

Studies in cervical cancer treated with definitive (chemo)radiotherapy (dC(RT)) had reported the prognostic impact of hemoglobin before and during treatment, clinical response (CR), overall treatment time (OTT) and equivalent dose in 2Gy fractions (EQD2). We reported overall (OS) and disease free (DFS) survival by hemoglobin (Hb, cut-off 10 and 12g/dL), CR (complete or persistence), OTT (cut-off 52 and 56 days) and EQD2 (cut-off 75, 80 and 85Gy).

#### Material and Methods

Retrospective analysis of 898 patients with cervical cancer clinical stage I-IVA treated with complete dRT or dCRT from 2013 to 2017 at a single institution. Survival rates were calculated with Kaplan-Meier analysis and groups compared with log rank test.

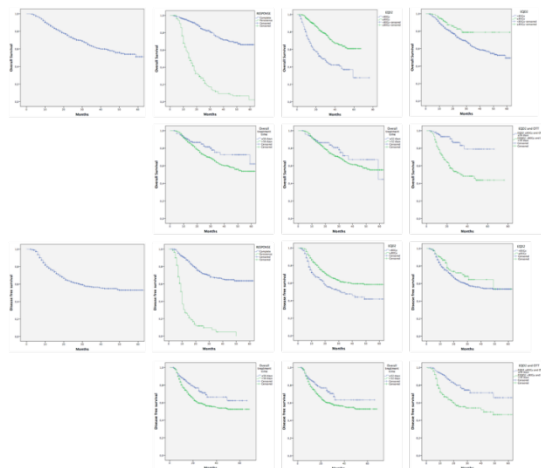
#### Results

More than a half were stage IIB, and 93.8% were treated with CRT (table 1). After treatment, response in 622 patients was complete (69.5%), in 172 stable/partial (19.1%) and in 104 progression (11.6%). With a median follow-up of 22 months (2-76), 317 patients recur or progress (35.3%) with a median time to recurrence of 11 months (1-50). At last follow-up, 69.3% were alive and 30.7% died.

Table 1. Clinico-pathological characteristics	
Median age	51.2 years (19-91 years)
Symptoms at diagnosis	803 (89.4%)
- Median months since symptoms	- 4 months (0-144 months)
Karnofsky performance status ≥90%	838 (96.3%)
Median Hemoglobin	
- On admission	- 12.9g/dL (3.8-16.7)
- Lowest before treatment	- 12.1g/dL (3-16.5)
- Lowest during treatment	- 10.7g/dL (3-15.4)
Clinical stage	
- IB	- 119 (13.3%)
- IIA vs IIB	- 52 (5.8%) vs 463 (51.6%)
- IIIA vs IIIB	- 21 (2.3%) vs 221 (24.6%)
- IVA	- 14 (1.6%)
Histology	
- Squamous cell carcinoma	- 734 (81.7%)
- Adenocarcinoma	- 98 (10.9%)
- Adenosquamous cell carcinoma	- 25 (2.8%)
Table 1. Treatment characteristics	
RT vs CRT	6.2% vs 93.8%
- Median time from admission to RT	- 11 weeks (0-50)
- Median total EQD2	- 82Gy (45-100)
- Median OTT	- 66 days (40-260)
Hemostatic RT	15 (1.7%)
- Median hemostatic radiotherapy dose	- 12Gy (6-24Gy)
Definitive RT	948 (100%)
- Median radiation therapy dose	- 50Gy (30-55.8Gy)
Boost RT	173 (19.3%)
- Median boost radiation therapy dose	- 10Gy (1.8-35Gy)
Brachytherapy	777 (86.5%)
- LDR vs HDR vs LDR and HDR	- 133 (14.8%) vs 655 (72.9%) vs 23 (2.5%)
- Median LDR dose	- 35Gy (15-35Gy)
- Median HDR dose	- 24Gy (5.3-42Gy)
Induction chemotherapy	94 (10.5%)
- Carboplatin / paclitaxel	- 85 (9.5%)
- Median number of cycles	- 6 cycles (1-8)
Concurrent CRT	842 (93.8%)
- Cisplatin vs gemcitabine	- 701 (78.1%) vs 107 (11.9%)
- Median number of cycles	- 5 cycles (1-7)

For all patients included 5-year OS was 51.2%. OS was significantly better within the first 4 years after treatment in patients with Hb before treatment ≥10g/dL (44% vs 30.2%, p<0.001) and ≥12g/dL (58% vs 41.9%, p=0.016). 5-year OS was better with complete CR (66.2% vs 2.3%); EQD2 ≥75Gy (61.5% vs 14.7%, p<0.0001), ≥80Gy (60.8% vs 27.6%, p<0.0001) and ≥85Gy (p=0.011); OTT ≤56 days (62.1% vs 53.7%, p=0.018) and ≤52 days (44.6% vs 50%, p=0.17). Patients with OTT ≤56 days and EQD2 ≥80Gy had a 5-year OS of 78.9% (vs 43.7%, p<0.0001).

For all patients 5-year DFS was 50%. DFS was significantly better within the first 4 years after treatment in patients with Hb before treatment ≥10g/dL (66.7% vs 35.9%, p<0.0001) and ≥12g/dL (65.1% vs 48.1%, p<0.005). 5-year OS was better with complete CR (63.6% vs 0%, p<0.0001); EQD2 ≥75Gy (59.9% vs 24%, p<0.0001), ≥80Gy (58.4% vs 41.7%, p<0.001) and ≥85Gy (54.3% vs 53.8%, p=0.099); OTT ≤56 days (62.3% vs 52.5%, p=0.003) and ≤52 days (63.2% vs 53.6%, p=0.26). Patients with OTT ≤56 days and EQD2 ≥80Gy had a 5-year OS of 65.8% (vs 46.5%, p<0.0001).



In univariate analysis, histological differentiation, Hb (≥10 and ≥12g/dL) before and during treatment, pelvic lymph nodes, concurrent CRT, EQD2 (≥75, ≥80 and ≥85Gy), OTT (≤56 and ≤52 days) and CR showed significance for OS and DFS.

#### Conclusion

Different factors impact negatively the oncologic outcomes. Hemoglobin, OTT and EQD2 are modifiable factors that must be considered for the treatment of patients with cervical cancer to achieve better oncological outcomes. Reducing OTT to ≤52 days and maintaining total

EQD2  $\geq 85$ Gy improves CR, OS and DFS in patients with cervical cancer treated with dCRT independent of other risk factors.

### EP-1509 “Young adult” and “geriatric” locally advanced cervix cancer in Alberta: same but different?

S. Menon<sup>1</sup>, S. Ghosh<sup>2,3</sup>, N. Vawda<sup>3,4</sup>, G. Menon<sup>2,3</sup>, M. Roumeliotis<sup>1,5</sup>, C. Doll<sup>1,5</sup>, E. Wiebe<sup>3,4</sup>, F. Huang<sup>3,4</sup>

<sup>1</sup>University of Calgary, Oncology, Calgary, Canada ;

<sup>2</sup>Cross Cancer Institute, Oncology, Edmonton, Canada ;

<sup>3</sup>University of Alberta, Oncology, Edmonton, Canada ;

<sup>4</sup>Cross Cancer Institute, Radiation Oncology, Edmonton, Canada ;

<sup>5</sup>Tom Baker Cancer Centre, Oncology, Calgary, Canada

#### Purpose or Objective

To review cervix cancer (CC) outcomes after radical (chemo(CH))radiotherapy (RT) including brachytherapy (BT), among women considered, in oncologic terms, younger and older.

#### Material and Methods

Of all CC patients seen in the province of AB (Canada), 01/2013-12/2015, for radical RT, including BT, we identified those aged <40 (young adult, YA) and >65 (geriatric, GA) at diagnosis. We excluded BT-alone cases. Health records were reviewed, abstracting demographic, clinicopathologic, patient-reported, treatment and outcomes data. Statistical analyses, descriptive and actuarial, were undertaken.

#### Results

N=30 YA women (median age 35.7 [23.6-39.1]) and n=26 GA (median age 71.1 [65.2-82.8]), 96% ECOG 0-1, were included. 40% of YA and 69% of GA were within 50 km of their treatment centre. Of the 9 coming from > 350 km away, 8 were YA. Four (all YA) did not live in AB. Age-adjusted Charlson Co-morbidity Index was 0 in all but n=3 YA (score  $\leq 2$ ); median was 3 [1-5] for GA. Most YA (73.3%) and GA (80.8%) had squamous histology, but adenocarcinoma was more common among YA (26.7%, vs. 11.5% for GA, p=0.15; a difference more pronounced between those aged <35 vs.  $\geq 70$ ). Older women had more advanced clinical tumor stage: (YA/GA) 46.7/30.8% IB, 13.3/19.2% IIA, 33.3/19.2% IIB, 0/11.5% IIIA, 6.6/11.5% IIIB, 0/7.7% IVA. YA and GA had similar (60% and 57.7%, respectively) pelvic and/or para-aortic (PA) nodal extent. Clinical/radiological distant metastasis was rare (2 YA, 1 GA). More YA had PET scan workup (76.7%, vs. 57.7%, p=0.13); more GA, EUA (61.5%, vs. 40.0%, p=0.11); MRI rates were similar. 93.3% YA (80.8% GA) received CHRT (pelvic $\pm$ PA external beam (EB)RT with weekly cisplatin, and intracavitary $\pm$ interstitial BT). 2 YA also had neoadjuvant CH. N=5 (all >70 years) had no CH; for those >70 who did, median 4 cycles [2-5]. Few had <3 cycles (3 YA, 2 GA). EBRT (40-50 Gy in 22-25 fractions, extra phase pre/post in 21.4%) preceded HDR-BT (3 fractions; less in n=4) or 1-fraction PDR-BT. BT complications were rare: all GA (3 procedural, 1 stroke). Overall treatment time (CHRT+BT) was 45.5 days median [41.0-84.0] in YA, GA not significantly different (51 [38-112]). Median HR-CTV D90 (Gy EQD2<sub>10</sub>) was 90.2 [53.4-107.1] for YA, 86.0 [54.6-105.5] for GA, p=0.30. Salvage surgery (1 YA, 2 GA) or RT (1 GA) were rare; palliative RT (4 YA, 4 GA) or CH (4 YA, 1 GA) more common. Patient reported outcomes (Table 1) evolved, pre-RT vs. at 6 months post-treatment. For a median 26 months [3-54] follow-up, 2-year overall (OS) for YA was 79.5% and for GA, 57.3% (p=0.473). Two-year cause-specific survival (CSS) was 74.5% for YA and 59.6% for GA (p=0.631) in this small cohort.

**Table 1.** Patient-reported items for YA and GA, from the ESAS-r (Edmonton Symptom Assessment System, revised) and the Canadian Problem Checklist (AB adaptation), administered at baseline and post-treatment (5-8 month visit data are shown).

	Baseline		5-8 months after treatment completion	
	Age < 40 (YA) (26 evaluable)	Age $\geq$ 65 (GA) (22 evaluable)	Age < 40 (YA) (25 evaluable)	Age $\geq$ 65 (GA) (22 evaluable)
<b>ESAS-r</b> (91 symptom items, scored 0 – 10, where 10 = worst possible outcome)				
2 most severe (>7/10) symptoms, ranked by median score	1. Depression, anxiety, well-being (8) 2. Tiredness (7.5)	1. Pain, tiredness, drowsiness, anxiety, well-being (7)	1. Tiredness, depression (8) 2. Drowsiness, anxiety (7.5)	1. Drowsiness (8) 2. Pain, well-being (7.5)
2 most frequent symptoms	1. Anxiety 2. Pain, Tiredness	1. Tiredness, anxiety 2. Well-being	1. Tiredness 2. Well-being	1. Tiredness 2. Pain, well-being
% women with top-rated severe symptom (any score)	76.9% - anxiety 57.7% - well-being 30.8% - depression	68.2% - tiredness 68.2% - anxiety 50.0% - well-being 40.9% - drowsiness 36.4% - pain	76.0% - tiredness 64.0% - depression	50.0% - drowsiness
<b>CPC</b> (54 named concerns, organized in 7 domains, scored yes/no)				
3 most flagged domains	1. Emotional 2. Practical 3. Physical	1. Physical 2. Practical 3. Informational	1. Physical 2. Emotional 3. Nutritional	1. Physical 2. Emotional 3. Social/Family/Spiritual
Most flagged item, within most common domain	Intimacy/sexuality	Bleeding/bruising	Sleep	Sleep
% women flagging most common domain	73.1% - emotional	40.9% - physical	52.0% - physical	40.9% - physical

#### Conclusion

CC seems more advanced in older women, who received less intense treatment in our provincial cohort. Patterns of care in primary RT for CC in AB differ in few but important ways among “oncologically” younger and older populations. How cancer outcomes might be improved by addressing the unique needs of each is not known.

### EP-1510 Phase I Trial of Stereotactic MR-guided Online Adaptive Radiotherapy for Ovarian Oligometastases

L. Henke<sup>1</sup>, O. Green<sup>1</sup>, A. Curcuru<sup>1</sup>, S. Mutic<sup>1</sup>, S. Markovina<sup>1</sup>, J. Schwarz<sup>1</sup>, P. Grigsby<sup>1</sup>, C. Robinson<sup>1</sup>, A. Chundury<sup>1</sup>

<sup>1</sup>Washington University/Barnes Jewish Hospital, Radiation Oncology, Saint Louis- MO, USA

#### Purpose or Objective

Delivery of ablative radiation dose using SBRT within the central thorax, abdomen, and pelvis risks toxicity due to target proximity to organs-at-risk (OARs). Stereotactic MR-guided online adaptive radiotherapy (SMART) has been previously shown to improve the therapeutic index of SBRT for abdominal cancers. The feasibility and safety of this approach to treat ovarian oligometastases has not been evaluated. We report the results of a Phase I prospective trial investigating the feasibility and safety of SMART for patients with oligometastatic ovarian cancer.

#### Material and Methods

10 patients with oligometastatic ovarian cancer were enrolled in a phase I trial (NCT02582931) between 9/2016 to 5/2018. All included patients had prior abdominopelvic resection and had received prior chemotherapy, including intraperitoneal chemotherapy in 5/10. Patients were treated with SMART using a 0.35T integrated MR-IGRT unit. 17 lesions were treated, at sites including the central thorax (3), the abdomen (5), and pelvis (9). The prescription was 35 Gy/5 fractions (goal of 95% PTV coverage), with optional dose escalation (DE) up to 50Gy/5 fractions, subject to strict maximum point dose (0.5cc) OAR constraints. During each fraction, physicians re-segmented a daily volumetric setup MRI. Initial plans were applied to daily anatomy to evaluate for OAR constraint violation, or if dose escalation (DE) > 7 Gy/fraction was possible. If either criterion existed, online re-optimization, QA, and delivery of a new plan were performed while the patient remained on-table. Feasibility of SMART was defined as delivery of >80% of planned fractions. Local control was evaluated by RECIST and acute toxicity (within 6 months of treatment) was evaluated by CTCAE v4.3 criteria.

#### Results

100% of SMART fractions were delivered, with a median on-table time of 63 minutes. Each patient received at least 1 adapted fraction and 38/65 (58%) of fractions were adapted, primarily for abdominal and pelvic sites (37/38).

Indications for adaptation included OAR constraint violation (n=32/38 fractions) or DE alone (n=6). 100% of OAR violations were reversed through adaptation. In 16/32 cases where OAR violation reversal was required, target coverage was simultaneously increased. RECIST control of the treated lesion was 100% at 3 months in evaluable patients; one patient did not have imaging at the required time point but had progression on imaging at 4.5 months post-treatment, consistent with 94% short-term lesion control. One treatment-related acute grade 3+ toxicity was observed (duodenal ulcer) with 100% of patients reporting.

#### Conclusion

SMART for patients with ovarian oligometastases is feasible, allowing for dose escalation and/or OAR sparing with low toxicity and promising efficacy. Daily imaging revealed motion primarily of abdominal and pelvic OARs that required frequent re-planning to avoid constraint violations. A phase II trial is planned to further evaluate SMART in this patient subset.

#### EP-1511 Investigation of prognostic factors of cervical squamous cell carcinoma using pre-treatment MRI

C. Tonoiso<sup>1</sup>, A. Haga<sup>2</sup>, A. Kubo<sup>1</sup>, T. Kawanaka<sup>1</sup>, S. Furutani<sup>1</sup>, H. Ikushima<sup>3</sup>, M. Harada<sup>1</sup>

<sup>1</sup>Tokushima University, Radiology, Tokushima, Japan ;

<sup>2</sup>Tokushima University, Medical Image Informatics,

Tokushima, Japan ; <sup>3</sup>Tokushima University, Therapeutic Radiology, Tokushima, Japan

#### Purpose or Objective

Diagnosis and prognostic prediction using features extracted from images have been reported recently. We analyzed MRI images before treatment to investigate prognostic factors of cervical cancer.

#### Material and Methods

100 consecutive patients with cervical squamous cell carcinoma who underwent chemoradiotherapy at Tokushima University Hospital from January 2005 to November 2013 were included in this study. The median age was 59 years old (range 30-79). The FIGO classification was I / II / III / IV in 16/42/34/8 cases, respectively. External irradiation and intracavitary brachytherapy was performed in all cases. The pretreatment T2WI images was transferred to the treatment planning device, and one radiologist defined gross tumor volume (GTV) for all cases. Then the MRI images was standardized with a minimum value of 0 and a maximum value of 1, 3-dimensional wavelet transformation was performed and 476 features were extracted for GTV region. Univariate analysis of prognostic factors was performed by Log-rank test using clinical information and features, and multivariate analysis was performed using Cox proportional hazard model.

#### Results

The median observation period was 55 months (range 2-123), and the 5-year survival rate of all cases was 77.7%. In the univariate analysis, significant differences were observed in the performance state, M factor, 7 features of GTV, and one feature of GTV was a significant factor in multivariate analysis.

#### Conclusion

Analysis using pretreatment MRI may be useful for prognostic prediction of cervical squamous cell carcinoma.

---

#### Electronic Poster: Clinical track: Prostate

---

#### EP-1512 Evaluation of target volume margins in prostate dose escalated VMAT by fiducial markers' technique

R. Fawzy<sup>1</sup>, R. Abdel-Malek<sup>1</sup>, M. Metwaly<sup>2</sup>, O. Abdel Aziz<sup>3</sup>, S. Alsirafy<sup>4</sup>, A. Selem<sup>4</sup>

<sup>1</sup>Kasr Al-Ainy Hospitals- Cairo University, Clinical Oncology Dept., Cairo, Egypt ; <sup>2</sup>United Lincolnshire Hospitals- NHS Trust, Department of Dosimetry & Imaging- Radiotherapy physics, Glasgow, United Kingdom ; <sup>3</sup>Kasr Al-Ainy Hospitals-cairo University, Diagnostic & Intervention Radiology Dept., Cairo, Egypt ; <sup>4</sup>Kasr Al-Ainy Hospitals-Cairo University, Clinical oncology Dept., Cairo, Egypt

#### Purpose or Objective

The study aims to investigate sources of errors in radiotherapy that cause uncertainty in the treatment delivery. Measurement of systemic & random errors introduced by the online marker match, the offline marker match & the offline bone match verification and consequently estimating the PTV needed if the verification was done guided by: (i) The fiducial markers match (PTV<sub>marker</sub>), (ii) The bone structure match (PTV<sub>bone</sub>) & (iii) The laser markers on the skin only (PTV<sub>laser</sub>).

#### Material and Methods

Thirty localized prostate cancer patients treated with dose escalated VMAT giving 78 Gy/35# to the whole prostate & 87Gy boost to the focal lesion. Three fiducial markers were inserted US guided; two at the base & the 3rd at the apex. For each patient, two daily MV images were acquired; 1<sup>st</sup> pre-online marker match was utilized for offline bone match, while the 2<sup>nd</sup> post-online marker match used for offline marker match as well. Systematic & random errors were calculated for each verification method to estimate the PTV needed. To composite the PTV<sub>marker</sub>, the online & offline marker matches were compared to check the uncertainty of the marker match, while CT scans were repeated weekly to estimate the marker migration. The PTV<sub>marker</sub> was then added to the evaluated PTV from the online marker match to obtain the PTV<sub>laser</sub>. The offline bone match was used to estimate the PTV due to skin marks migration (PTV<sub>skin marks migration</sub>), which was then deducted from the PTV<sub>laser</sub> to acquire the PTV<sub>bone</sub>.

#### Results

The comparison of the systemic & random errors for the online & offline marker match showed no major difference in the lateral & vertical direction (<0.5mm [p>0.38]), while it was significant with a maximum of 3mm [p=0] in the longitudinal direction. The outcome of the CT study revealed a mean of the maximum marker migration of 2<sub>mm</sub> ± 1.2, this was combined with the mean difference between the offline & the online marker match to produce the PTV<sub>markers</sub> of 2.7±0.6, 3.34±1.1 & 4.44±2.2<sub>mm</sub> in lateral, longitudinal & vertical directions respectively. The resulted PTV margin from the systematic & random errors data of the online marker match was added to the PTV<sub>markers</sub> to yield the PTV<sub>laser</sub> of 13±0.6, 17.7±1.1 & 15.8±2.2<sub>mm</sub> in the same directions respectively. On the other hand, the systemic & random errors equations for the offline bone match shifts revealed PTV<sub>skin marks migration</sub> of 7.1, 9.1 & 8.6<sub>mm</sub>, which implies PTV<sub>bone</sub> of 5.9±0.6, 8.6±1.1 & 7.2±2.2<sub>mm</sub> in the same directions respectively.

#### Conclusion

It was clarified that the PTV needed for fiducial marker image guided verification in dose escalated VMAT to the prostate ranged between 3<sub>mm</sub> and 4<sub>mm</sub> in the lateral, longitudinal & vertical directions; which is about 10<sub>mm</sub> smaller than that is guided by the laser skin marks only and tighter by about 5<sub>mm</sub> relative to that is based on the bone structure image matching only.

#### EP-1513 Patient-reported adverse events following trans-rectal ultrasound-guided prostate marker insertion

T. Rosewall<sup>1</sup>, A. Bayley<sup>1</sup>, P. Chung<sup>1</sup>, C. Catton<sup>1</sup>

<sup>1</sup>Princess Margaret Cancer Centre, Radiation Medicine Program, Toronto, Canada

### Purpose or Objective

Significant improvements in the precision of radiotherapy delivery have been made using radio-opaque intra-prostatic markers (IPM). Despite widespread clinical implementation, there is little information available on the frequency and severity of adverse events associated with IPM insertion. The purpose of this study was to quantify patient-reported adverse events following ultrasound-guided, trans-rectal implantation of IPM and to determine the factors that may influence the frequency and severity of those adverse events.

### Material and Methods

A cohort of 100 prostate cancer patients was prospectively accrued. Procedural parameters that may be associated with the risk of adverse events were documented in a data collection form by the interventional radiologist immediately after the IPM insertion. All patients completed an adverse events questionnaire immediately after IPM insertion and approximately 3 to 5 days later.

### Results

All patients were successfully implanted with 3 IPM following a course of prophylactic antibiotics. Local anaesthetic was used in only 2% of patients, and the radiologist reported that only 4% of patients complained of pain. Conversely, 49% of patients reported that the procedure was as painful as, or worse than, previous biopsies. There was no significant change in AUA prostate symptom score after IPM insertion. 23% to 30% of patients reported hematochezia, hematuria or hematospermia over a few days. Fever was reported by 8% of the patients, requiring a visit to their family doctor (6%) or the emergency department (2%) after which they were admitted to hospital for parenteral antibiotic therapy for Cipro-resistant infection. There were no detectable associations between pain during IPM insertion and pain later on, or between use of anticoagulants and bleeding events.

### Conclusion

IPM are a valuable tool for daily image-guidance during prostate radiotherapy but their utility must be balanced with the clinical safety of their implantation. The trans-rectal ultrasound-guided IPM insertion was well tolerated by most patients. Any bleeding or pain experienced was self-limiting. IPM insertion was however, associated with infrequent, but severe infections.

### EP-1514 Binary exponential model for the PSA fall after IMRT, dependency on initial PSA and Prostate volume

H. Nagano<sup>1</sup>, H. Yokoyama<sup>1</sup>, M. Kato<sup>2</sup>, H. Hashimoto<sup>1</sup>, T. Shimo<sup>2</sup>, M. Watanabe<sup>1</sup>, M. Nakanishi<sup>1</sup>, Y. Kaneko<sup>1</sup>, H. Suzuki<sup>1</sup>, A. Noguchi<sup>1</sup>, K. Kobayashi<sup>1</sup>

<sup>1</sup>Shonan Fujisawa Tokushukai Hospital, Radiation Oncology Department, Fujisawa, Japan; <sup>2</sup>Tokyo-West tokushukai Hp., Radiology, Akishima, Japan

### Purpose or Objective

PSA (prostate-specific antigen) kinetics for patients with localized prostate cancer after radiation therapy has been reported by some authors. These are mainly analysis of nadir or slopes of a certain period. We intended to fit data to binary exponential model mathematically to give away whole course kinetics of PSA after IMRT or VMAT.

### Material and Methods

Twenty one (T1c; 7, T2a; 10, T2b; 2, T2c; 2) patients with mean age 72.4 y. o. (range, 57 - 85 y. o.) and mean GS 6.5 (range, 5 - 8) were treated by IMRT or VMAT (76 Gy / 38 fractions / 8 weeks) without androgen ablation. Their prostate volume before treatment were ranged 13.0 to 68.7 ml with mean value of 39.0 ml. They had mean initial PSA (iPSA) as 7.28 ng/ml (range, 3.58 - 11.85 ng/ml) and had follow-up PSA examinations 2.5 to 8.2 years (mean 4.1 years) with about 3 months interval.

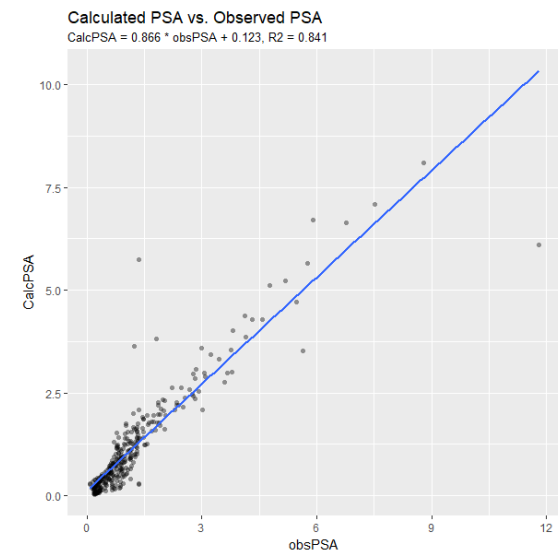
We supposed that PSA fall was composed of two steps, rapid and slow ones. Each fall may fit to exponential decay

with time constant T.rapid [month] or T.slow [month], and initial quantity Amp.rapid [ng/ml] or Amp.slow [ng/ml]. Mathematical expression of PSA at time t month is as this;  $PSA(t) = Amp.rapid * \exp[-t / T.rapid] + Amp.slow * \exp[-t / T.slow]$

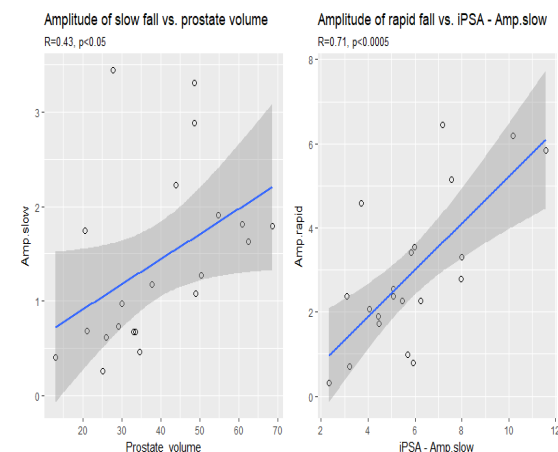
In the assumption that time constant, T.rapid and T.slow might be equal among the all patients, we can also estimate amplitudes of both falls (Amp.rapid and Amp.slow) of each patient using least square method comparing observed and calculated PSA.

### Results

Observed and calculated PSA values were well correlated (R = 0.92). Residuals were almost normally distributed with mean value 0.04 ng/ml and standard deviation 0.29 ng/ml excluding 5 outliers.



T.rapid and T.slow were 0.357 and 3.99 months, respectively. Amp.rapid ranged 0.31 to 6.46 ng/ml and mean was 2.93 ng/ml. Amp.rapid correlated well (R = 0.71) with iPSA - Amp.slow (p < 0.0005). Amp.slow ranged 0.26 - 1.42 ng/ml and mean was 1.42 ng/ml. Amp.slow correlated somewhat well (R = 0.43) with prostate volume (p < 0.05).



### Conclusion

PSA fall after IMRT or VMAT was well fitted to our binary exponential model. Amplitude of rapid fall (Amp.rapid) was related to iPSA - Amp.slow, and that of slow fall (Amp.slow) was relevant to prostate volume. We might speculate that slow fall may mainly related to normal prostate recovery after treatment, and rapid fall may represent elimination of cancer cells by radiation therapy.

**EP-1515 Substantial impact of 68Ga-PSMA-PET/CT on the radiotherapeutic approach for prostate cancer**  
N. Schmidt-Hegemann<sup>1</sup>, C. Eze<sup>1</sup>, M. Li<sup>1</sup>, P. Rogowski<sup>1</sup>, C. Schaefer<sup>1</sup>, C. Stief<sup>2</sup>, U. Ganswindt<sup>3</sup>, P. Bartenstein<sup>4</sup>, C. Belka<sup>1</sup>, H. Ilhan<sup>4</sup>

<sup>1</sup>Department of Radiation Oncology- University Hospital- LMU Munich, Department of Radiation Oncology- University Hospital- LMU Munich, München, Germany ; <sup>2</sup>Klinik und poliklinik für Urologie, Department of Urology - University hospital Munich, München, Germany ; <sup>3</sup>Department of Therapeutic Radiology and Oncology - Medical University Innsbruck, Department of Therapeutic Radiology and Oncology - Medical University Innsbruck, Innsbruck, Austria ; <sup>4</sup>Department of Nuclear Medicine- University Hospital- LMU Munich, Department of Nuclear Medicine- University Hospital- LMU Munich, München, Germany

#### Purpose or Objective

Prostate-specific membrane antigen positron emission tomography/computed tomography (PSMA PET/CT) offers unprecedented accuracy for staging of primary, persistent or recurrent prostate cancer. Thus, we hypothesized that PSMA PET/CT prior to radiotherapy significantly impacts the radiotherapeutic approach.

#### Material and Methods

Between February 2014 and December 2017, a total of 172 patients received PSMA PET/CT and were included in this retrospective analysis. Twenty-two (13%) patients were referred for primary definitive radiotherapy, 51% (88/172) for PSA persistence and 36% (62/172) for PSA recurrence after radical prostatectomy. The potential increase in diagnostic accuracy, and the subsequent change of radiotherapeutic approach was documented separately for PET/CT versus CT.

#### Results

Overall detection rate was 70% (120/172) in 68Ga-PSMA PET/CT. Patients with pre-PSMA PET/CT PSA-level >0.5 ng/ml (98/111; 88%) had significantly more often PET-positive results. Overall, PSMA PET/CT revealed a total of 171 lesions, PET alone 156 and CT alone 85. For all patients a continuous diagnostic increase in positive findings was observed for primary tumor/local recurrence (CT: 18% vs. PET/CT: 37%), pelvic lymph node (CT: 21% vs. PET/CT: 44%) and distant metastases (CT: 7% vs. PET/CT: 19%) when comparing CT vs. PET/CT. Compared to CT, the combination of PET/CT information resulted in a change of treatment in 107/172 (62%) patients, i.e. 8/22 (36%) patients prior to any treatment, 31/62 (50%) with PSA recurrence and 68/88 (77%) with PSA persistence. Comparing the different radiotherapy indications with each other, there was a higher change of management in postoperative patients vs. patients prior to any treatment.

#### Conclusion

Compared to conventional CT, PSMA PET/CT had a remarkable impact on radiotherapeutic approach especially in postoperative patients. Postoperative patients might benefit in particular from an improved staging method, as for patients with persistent or recurrent prostate cancer there are no nomogram-based radiotherapy treatment volumes.

**EP-1516 Macroscopic local relapse from prostate cancer: which role for salvage RT? An update analysis**

A. Bruni<sup>1</sup>, G. Ingrosso<sup>2</sup>, F. Trippa<sup>3</sup>, M. Di Staso<sup>4</sup>, L. Rubino<sup>1</sup>, G. Aluisio<sup>1</sup>, S. Parente<sup>4</sup>, L. Frassinelli<sup>1</sup>, E. Maranzano<sup>3</sup>, R. Santoni<sup>2</sup>, E. Mazzeo<sup>1</sup>, F. Lohr<sup>1</sup>  
<sup>1</sup>Az. Ospedaliero-Universitaria di Modena - Policlinico, Radiation Oncology Department, Modena, Italy ; <sup>2</sup>"Tor Vergata" University General Hospital, Radiotherapy Unit-, Rome, Italy ; <sup>3</sup>"Santa Maria" University Hospital, Radiotherapy Unit, Terni, Italy ; <sup>4</sup>"Nuovo San Salvatore" Hospital, Radiotherapy Unit, L'Aquila, Italy

#### Purpose or Objective

Radical prostatectomy (RP) is an effective and widely used curative treatment for localized prostate cancer while salvage radiotherapy (SRT) is recommended for biochemical relapse (BR) after prostatectomy (RP). Even if several studies showed that biochemical control can be achieved by SRT if it starts as soon as possible several patients (pts) are still referred to Radiation Oncologists when macroscopical recurrence has occurred. This is a final update analysis of a multicenter retrospective study to evaluate SRT efficacy and tolerability in pts with biopsy/imaging proven relapse.

#### Material and Methods

We retrospectively analyzed 105 pts with macroscopic relapse after RP who underwent SRT between 2001 and 2016. We identify subgroups by means of nodal involvement (N0 vs N1) at diagnosis, Gleason Score ( $\leq 7$  Vs  $> 8-10$ ), PSA value at relapse ( $\leq 2.0$  ng/mL Vs  $> 2.0$  ng/mL), restaging (biopsy Vs TC scan/MRI Vs Choline CT-PET) and concomitant hormone therapy (Yes/No). Survival curves were generated using Kaplan-Meier method and relationship with outcome were analyzed using univariate followed by Cox regression analysis.

#### Results

After a median follow up of 52 months, 89 pts were still alive. Total RT dose to macroscopic lesion was  $> 70$  Gy in 58 pts,  $\leq 70$  Gy in 43 pts. Exclusive SRT was used in 42 pts, while 63 received also concomitant ADT. Five and ten-year overall survival was 85,5% and 76,1% while distant metastasis free survival was 86,1% and 73,3% respectively. In 30 pts prophylactic RT was delivered to pelvic nodal stations. Five and 10-year-OS was 85,5% $\pm$ 4,4 Standard Error (SE) and 76,1% $\pm$ 5,9SE while MFS was 86,1% $\pm$ 3,6SE and 73,3% $\pm$ 5,9SE respectively. Five and 10-year-bPFS was 69.7% $\pm$ 5.2SE and 57.7% $\pm$ 6.6SE, respectively. Extrapelvic nodal relapse was found in 5 pts, bone metastasis in 12, both in 2. No grade 4/5 toxicities were found.

#### Conclusion

SRT even in pts with loco-regional macroscopic PCa relapse results in an excellent profile in terms of oncological outcome (OS, BFS, MFS) confirming the role of SRT even in this unfavorable subset of pts. In comparison with available series treated with ADT only, our data suggest that SRT may either postpone ADT or improve results over ADT alone in appropriately selected pts.

**EP-1517 The long-term result of stereotactic body radiotherapy for localized prostate cancer**

Y. Lin<sup>1</sup>, S. Wang<sup>1</sup>

<sup>1</sup>Chi Mei Medical Center, Department of Radiation Oncology, Tainan, Taiwan

#### Purpose or Objective

The understanding of radiobiology for prostate cancer suggested hypofractionation might achieve a higher therapeutic benefit. Stereotactic body radiation therapy (SBRT) is able to deliver a high dose per fraction precisely. SBRT for prostate cancer could escalate biological effective doses while without increasing toxicity. Here, we reported our long-term results of SBRT for localized prostate cancer.

#### Material and Methods

Between November 2008 and May 2018, a total of 232 patients with clinically localized prostate were enrolled for analysis. Patients were low-risk (11%), intermediate-risk (37%), and high-risk (52%). Low- and intermediate-risk patients were treated with SBRT to prostate and half of seminal vesicles (37.5Gy in 5 fractions). High-risk patients were treated with whole pelvic irradiation (45Gy in 25 fractions) and SBRT boost (21Gy in 3 fractions). The intermediate- and high-risk patients received hormone therapy with different duration. The toxicities of gastrointestinal (GI) and genitourinary (GU) tracts were scored by Common Toxicity Criteria Adverse Effect (CTCAE

v3.0). Patterns of prostate-specific antigen (PSA) response were analyzed. Biochemical failure was defined as Phoenix definition.

#### Results

The initial median PSA was 9.4 and 40.8 ng/ml for the low/intermediate-risk and high-risk patients, respectively. After SBRT treatment, median PSA at 60 months level was 0.16 and 0.07 ng/ml for the low/intermediate-risk and high-risk patients, respectively. In the low/intermediate-risk patients, there were four patients with biochemical failures within a median follow-up of 58 months. For the high-risk patients, seven patients with biochemical failure were disclosed in the median 46-month follow up. The estimated 10-year biochemical failure-free survival was 95.1% and 90.2% for low/intermediate-risk, and high-risk patients, respectively. In the low/intermediate-risk patients, late Grade 3 GU and GI toxicities were seen in 2.5% and 0%, respectively. In the high-risk patients, the incidence rate of late Grade 2 GU and GI toxicity were 5% and 2%. There was no late Grade 3 and GI toxicity in the high-risk patients. Most of acute toxicity effects in all the patients resolved within three to six months of treatment completion.

#### Conclusion

This is a 10-year experience of SBRT for localized prostate cancer in a single institution. SBRT with or without whole pelvic irradiation for localized prostate cancer is feasible with minimal toxicity and excellent biochemical failure-free survival. Continued accrual and follow-up would be necessary to confirm this long-term biochemical control and the late toxicity profiles.

#### EP-1518 A dosimetric comparison of treatment plans by using aaa/mc with vmat technique for prostate patients

P. Boydak<sup>1</sup>, K. Temizyurek<sup>2</sup>

<sup>1</sup>Istanbul Aydin University, Medical Physics, Istanbul, Turkey ; <sup>2</sup>Istanbul Aydin University, Medicine, Istanbul, Turkey

#### Purpose or Objective

In this study, it was aimed to compare the performance of two different algorithms on the VMAT technique. Twenty patients with prostate cancer were selected for comparison. Tomography images were scanned with a 3mm slices. Target volume PTV and at-risk organs (OAR) as bladder, rectum, right -left femur heads were defined. Doses of target volumes were prescribed as 70 Gy in 35 fractions for all treatment plans. In Varian technique patient plans are prepared using 6 MV energy, AAA algorithm, and double arc VMAT technique with the Eclipse Treatment Planning System (TPS), then in Elekta for same patients, treatment plans using 6 mV energy, the Monte Carlo algorithm and VMAT technique are made with the Monaco TPS. Dose distributions were obtained for each patient. These two different algorithms were compared in terms of critical organ dose values, target volume maximum dose values, HI, CI and MU values of PTV.

#### Material and Methods

Plans were normalized to cover 95% of the target volume. CI and HI values in Varian Rapidarc are 1.01±0.02 (1), 0.08±0.01 (0.08), respectively. For Elekta-VMAT CI and HI values are 0.96±0.02 (0,95) and 0.1±0.02 (0.09), respectively. Consequently RapidArc gave better result for CI and HI values. The monitor unit value of RapidArc 761,35 ± 94,29 was observed to be lower than that of Elekta-VMAT monitor unit 922,15 ± 93,4. In terms of bladder and rectum doses Elekta-VMAT technique give lower results than results of RapidArc technique. There was no significant difference (p>0.05) in the calculation of PTV Dmax and bladder 50% for each machine. When the critical organ doses were considered, the Elekta-VMAT technique has statistically significant lower values for bladder and rectum doses than those values of the

RapidArc technique. For right and left femurs, the RapidArc technique shows better results.

#### Results

RapidArc MU values are lower than MU values of Elekta-VMAT, so treatment duration was shorter in RapidArc. Clinically both VMAT-techniques for each machine were equally effective in producing acceptable plans.

#### Conclusion

As a result it can be said that these two techniques produce equivalent results by practice.

#### EP-1519 PSMA-PET/CT for guidance and response assessment of SABR for prostate cancer oligometastases

P. Dirix<sup>1</sup>, C. Mercier<sup>1</sup>, C. Billiet<sup>1</sup>, P. Vermeulen<sup>2</sup>, S.

Oeyen<sup>2</sup>, S. Van Laere<sup>2</sup>, P. Huget<sup>1</sup>, D. Verellen<sup>1</sup>

<sup>1</sup>Iridium Cancer Network, Radiation Oncology, Antwerp, Belgium ; <sup>2</sup>Oncologisch Centrum GZA, Translation Cancer Research Unit, Antwerp, Belgium

#### Purpose or Objective

Prostate-specific membrane antigen (PSMA) PET/CT is increasingly used to detect oligometastases in biochemical recurrent prostate cancer and subsequently guide metastasis-directed treatment such as SABR. However, limited prospective evidence is available.

#### Material and Methods

All patients were included in a prospective phase I dose-escalation trial on SABR for non-spine bone and lymph node oligometastases (NCT03486431). According to protocol, a new PMSA-PET/CT was performed at 6 months after treatment. Metabolic response was evaluated according to PERCIST 1.0 criteria. PSA progression was defined as a PSA increase of ≥ 25% and ≥ 2 ng/mL if PSA was ≥ 2 ng/mL at baseline, or a PSA increase of ≥ 25% if PSA was < 2 ng/mL. PSA response was defined as a decline from baseline of ≥ 80%, while complete response was defined as a decline from baseline of ≥ 90%. Toxicity was graded using Common Terminology Criteria for Adverse Event version 4.0.

#### Results

From July 2017 to March 2018, 15 consecutive patients had 1 (n = 12) or 2 (n = 3) metastases detected on PSMA-PET/CT and were prospectively included in the trial. They then received SABR to a total of 18 oligometastases. Four patients had non-spine bone only, 8 had node only, and 3 had mixed disease. The median age was 67 (52-78) years. Four patients received concomitant androgen-deprivation therapy (ADT) for 6 months. Eight patients were included in the first cohort (5x 7.0 Gy) and 4 in the second cohort (3x 10.0 Gy). SABR was feasible and delivered as planned in all cases.

At 6 months after SABR, 5 patients had a complete PSA response, while 7 patients showed PSA progression. Already 8 patients had new metastatic lesions visible on the second PSMA-PET/CT. Interestingly, only 5 of those patients had clear PSA progression at that time. Regarding local control, there was residual PSMA uptake in 6 patients (7 lesions in total). Remarkably, 3 of those 6 patients had a complete PSA response at the same time. All 4 patients who received concomitant ADT presented a complete metabolic response on PSMA-PET/CT as well as a complete PSA response.

Median follow-up was 11 (7 - 14) months. No grade ≥ 3 toxicity was observed. Progression-free survival at 1 year was 100% for patients who had received ADT versus 21% for patients who did not (p = 0.032). In total, 6 of the 11 patients not on ADT had started ADT at the last follow-up (1-year ADT-free survival of 32%).

A further 10 patients were included the second cohort, whose PSMA follow-up will be available at ESTRO.

#### Conclusion

Repeated imaging with PSMA-PET/CT could be incorporated into prospective clinical trials on SABR for prostate cancer oligometastases to evaluate the true

benefit of metastasis-directed therapy. However, specific response criteria for PSMA-PET/CT are urgently needed. Also, an interval of more than 6 months may be required to fully estimate the local efficacy of SABR in control PSMA-PET/CT in some patients.

**EP-1520 Acute and late toxicity of hypofractionated RT for localized prostate cancer: IMRT vs Tomotherapy**  
A. Rese<sup>1</sup>, F. Pastore<sup>1</sup>, G. Panelli<sup>1</sup>, A. Pepe<sup>1</sup>, D. Toledo<sup>1</sup>, F. Francomacaro<sup>1</sup>, V. Iorio<sup>1</sup>

<sup>1</sup>Emicenter, Radiotherapy, Casavatore NA, Italy

#### Purpose or Objective

To evaluate the incidence of acute and late toxicity after hypofractionated radiotherapy using Linac intensity-modulated radiotherapy (IMRT) compared with helical Tomotherapy.

#### Material and Methods

From September 2016 to March 2018, 110 consecutive patients with localized prostate cancer (cT1-2, GS< 8, PSA<10 ng/ml) were randomized to Linac IMRT and to helical Tomotherapy.

55 patients were treated with Linac IMRT and 55 with TOMO.

Patients were monitored before therapy, weekly during therapy, 2 weeks, three and six months after radiotherapy was completed, using RTOG GI and genitourinary toxicity grading scale.

Patients received radiotherapy schedule according to histology reports following international guidelines.

Doses were prescribed to planning target volumes (PTVs) as the followings: 72 Gy (2.4 Gy/fx) to PTV-whole prostate and 64.5 Gy (2.15 Gy/fx) to PTV-prostate and seminal vesicles in 30 fractions with SIB technique. Dose to abdominal cavity, both femoral heads, bladder and rectum were constrained below each tissue tolerance.

#### Results

Median age of the patients was 72.5 (range 55-86 years). At the end of the treatment (6 weeks), 16/55 (29%) patients in the TOMO group vs. 19/55 (34.5%) patients in the Linac IMRT group had G1-G2 grade of GI toxicity (p=0.009), while 2/55 (4%) patients in the TOMO group vs. 4/55 (7.3%) patients in the Linac IMRT group had G3 grade of GI toxicity.

27/55 (49%) patients in the TOMO group vs. 31/55 (56%) patients in the Linac IMRT group had G1-G2 grade of GU toxicity (p=0.04), while 1/55 (1.8%) patients in the TOMO group vs. 3/55 (5.5%) patients in the Linac IMRT group had G3 grade of GU toxicity.

No G4 grade of GI and GU toxicity was showed.

After 6 months from the end of the treatment, no patients in the TOMO group vs. 2/55 (3.6%) patients in the Linac IMRT group had G1-G2 grade of GI toxicity, while 1/55 (1.8%) patients in the TOMO group vs. 2/55 (3.6%) patients in the Linac IMRT group had G3 grade of GU toxicity.

#### Conclusion

Acute toxicity is very low. Most of the recorded symptoms decrease over time.

A small increase in mild toxicity, statistically significant, was observed in the Linac IMRT group when compared with TOMO group. Our study confirmed that Tomotherapy allows for safe moderate hypofractionation, offering a shorter overall treatment time, a lower rate of acute and late toxicities and providing potentially more economic health care.

**EP-1521 IMRT for prostate cancer with seminal vesicle involvement : A multicentric retrospective analysis**  
F. Goupy<sup>1</sup>, S. Supiot<sup>2</sup>, D. Pasquier<sup>3</sup>, I. Latorzeff<sup>4</sup>, U. Schick<sup>5</sup>, E. Monpetit<sup>6</sup>, G. Martinage<sup>3</sup>, C. Hervé<sup>1</sup>, B. Le Proust<sup>7</sup>, J. Castelli<sup>1</sup>, R. De Crevoisier<sup>1</sup>

<sup>1</sup>Centre Eugène Marquis, Radiotherapy, Rennes, France ;

<sup>2</sup>CLCC René Gauducheau, Radiotherapy, Nantes-Saint-Herblain, France ;

<sup>3</sup>CLCC Oscar Lambret, Radiotherapy, Lille, France ;

<sup>4</sup>Clinique Pasteur, Radiotherapy,

Toulouse, France ; <sup>5</sup>University Hospital Cavale Blanche, Radiotherapy, Brest, France ; <sup>6</sup>Centre Saint-Yves, Radiotherapy, Vannes, France ; <sup>7</sup>Centre Eugène Marquis, Medical Imaging, Rennes, France

#### Purpose or Objective

MRI can detect with high specificity prostate cancer with seminal vesicle involvement (ISV), classifying the tumor stage as T3b. Delivering high curative dose (> 70 Gy) in the ISV is particularly challenging, when respecting the dose constraints in the OARs. No studies have reported data of external beam radiotherapy for specifically T3b prostate cancer. The objective of this study was to analyze the dose distribution and the clinical outcome in a large series of patients having received IMRT for T3b prostate cancer.

#### Material and Methods

This retrospective analysis included all patients having received IMRT and androgen deprivation therapy for T3b prostate cancer, between 2008 and 2017 in six French institutions, with available MRI images and dosimetric data. A dosimetric analysis was performed, in particular regarding the ISV, divided in three thirds in the cranio-spinal axis. Recurrences, survivals and toxicities (CTCAE v4.03) were analyzed.

#### Results

A total of 276 T3b patients was included. The mean follow-up was 35 months. Only the first proximal third of seminal vesicle was involved for 64% of patients, and the entire for 16% of patients. Lymph node involvement was present for 26% of patients. The mean (range) prescribed doses to the prostate and to the ISV were 77 Gy (70-80) and 68 Gy (46-80), respectively. The prescribed doses to the ISV and the not-involved SV were equal to or greater than 70 Gy for 64% and 22% of patients, respectively. The pelvic lymph nodes without lymph node involvement were treated at a prophylactic dose in 90% of cases. The mean prescribed dose to the involved lymph node was 52 Gy (46-74), and equal to or greater than 60 Gy for 30%. The dose constraints recommendations were exceeded in less than 12% of patients for the rectum and the bladder. The 5 year risks of biochemical and clinical recurrences and cancer specific death were 24.8%, 21.7% and 10.3% respectively. The 5 year risks of local, pelvic lymph node and metastatic recurrences were 6.4%, 11.3% and 15%, respectively. Lymph node involvement was the only significant prognostic factor on clinical recurrence (HR 2.90, p=0.005) and cause specific survival (HR 4.45, p=0.017). Grade > 2 acute and 5 year late toxicity rates were 13.2% and 12% for digestive toxicity, and 34% and 31.5% for urinary toxicity. The dose to the pelvic lymph node was predictive of late digestive toxicity (HR 1.13, p=0.002).

#### Conclusion

We reported the most important series of IMRT for T3b prostate cancer. IMRT combined with IGRT allows delivering a high curative dose (> 70 Gy) in the ISV, while rarely exceeding dose constraints. Late digestive toxicity was low but urinary toxicity was slightly increased. Local control appears high and the main pattern of recurrence is metastasis, mostly related to lymph node involvement at diagnosis. More follow-up is needed to confirm the results due to the relative recent use of MRI allowing characterizing ISV. The combined MRI Linac may even more improves the results by a better IGRT targeting.

**EP-1522 Radiotherapy with or without antihormonal therapy for PSMA-positive oligorecurrent prostate cancer**

S. Kroeze<sup>1</sup>, C. Henkenberens<sup>2</sup>, N. Schmidt-Hegemann<sup>3</sup>, M. Vogel<sup>4</sup>, S. Kirste<sup>5</sup>, J. Becker<sup>6</sup>, H. Christiansen<sup>2</sup>, C. Belka<sup>7</sup>, S. Combs<sup>4</sup>, A. Grosu<sup>5</sup>, A. Müller<sup>6</sup>, M. Guckenberger<sup>8</sup>

<sup>1</sup>University Hospital Zürich, Radiation Oncology, Zurich, Switzerland ;

<sup>2</sup>Medical School Hannover, Radiotherapy and Special Oncology, Hannover, Germany ;

<sup>3</sup>University Hospital LMU, Radiation Oncology, Munich, Germany ;

<sup>4</sup>Technical University Munich, Radiation Oncology,

Munich, Germany ; <sup>5</sup>University of Freiburg, Radiation Oncology, Freiburg, Germany ; <sup>6</sup>University Hospital Tübingen, Radiation Oncology, Tübingen, Germany ; <sup>7</sup>University Hospital LMU Munich, Radiation Oncology, Munich, Germany ; <sup>8</sup>University Hospital Zürich, Radiation Oncology, Zürich, Switzerland

### Purpose or Objective

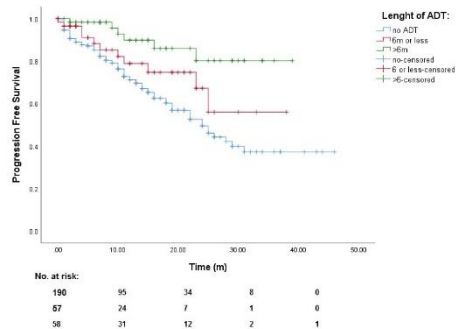
Based on <sup>68</sup>Ga-PSMA-PET imaging, approximately 20-40% of early biochemical recurrent prostate cancer after radical prostatectomy are oligometastatic and located outside the prostate bed, challenging the current standards of care. Definitive radiotherapy (RT) of these recurrences plays an increasingly important role, but it remains unknown whether patients benefit from the addition of antihormonal therapy (ADT) in this situation. This study aims to compare the efficacy of definitive radiotherapy (RT) of <sup>68</sup>Ga-PSMA-positive oligorecurrences (ORT) with or without additive antihormonal therapy (ADT).

### Material and Methods

Retrospectively, data of 305 patients who underwent definitive radiotherapy (RT) of 647 oligorecurrent <sup>68</sup>Ga-PSMA -positive metastatic sites were evaluated. Patients were treated between 04/2013 and 01/2018 in 6 academic centers. All oligorecurrent patients were treatment-naïve. PSA-progression free survival (PFS) and ADT-free survival was analyzed using Kaplan-Meier survival curves and log rank testing. Toxicity were analyzed with the CTCAE v4 score. Uni-, and multivariate analyses were performed to determine patient, disease and treatment factors influencing PFS.

### Results

Median age of patients was 70 (46-95) years, 96% were initially high-, or very high risk. Median PSA at time of <sup>68</sup>Ga-PSMA-PET was 1.05 (0.04-47.5) ng/ml and PSA-DT was 6.3 (1-56) months. A median of 1 (1-19) nodal, and 1 (1-5) distant metastatic lesions were irradiated. Overall, 93% of patients showed a PSA-decrease to median 0.07 (range 0-13.7) ng/ml after median FU of 16 (1-57) months. 37% of patients received additional ADT. Additional ADT resulted in a significantly improved PFS compared to RT alone, which remained significant in multivariate analysis (p=0.0001). However, the addition of ≤6 mo ADT did not significantly improve PFS compared to patients not receiving ADT (fig. 1). Other independent significant factors for better PFS were nodal-only metastases and biochemical recurrence ≥ 1 year. Patients without additional ADT required second salvage therapies more frequently (4% vs. 33%, p<0.001), but 1- and 3y ADT-free survival was 93% and 59%. Grade ≥3 acute toxicity was observed in 0.9% of patients, late toxicity in 2.3%.



### Conclusion

Definitive RT in this large cohort of mainly very high-risk, treatment-naïve oligorecurrent PCa patients was feasible and safe. Immediate addition of ADT improved PFS significantly, but two-third of patients treated with RT

only were spared from ADT for 3 years. Prospective trials with sufficiently long follow-up are needed evaluate the potential of ADT and its duration in addition to radical radiotherapy for PSMA-PET detected oligorecurrent prostate cancer.

### EP-1523 Predictors of severe late urinary toxicity after curative radiotherapy for localised prostate cancer

K. Takeda<sup>1</sup>, Y. Takayama<sup>2</sup>, N. Kadoya<sup>2</sup>, H. Takagi<sup>1</sup>, K. Ito<sup>2</sup>, T. Chiba<sup>2</sup>, K. Sato<sup>3</sup>, S. Dobashi<sup>1</sup>, R. Umezawa<sup>2</sup>, T. Yamamoto<sup>2</sup>, Y. Ishikawa<sup>2</sup>, K. Takeda<sup>2</sup>, H. Matsushita<sup>2</sup>, Y. Kawasaki<sup>4</sup>, K. Mitsuduka<sup>4</sup>, K. Jingu<sup>2</sup>

<sup>1</sup>Tohoku University School of Medicine, Health Sciences-Course of Radiological Technology, Sendai, Japan ;

<sup>2</sup>Tohoku University Graduate School of Medicine, Department of Radiation Oncology, Sendai, Japan ;

<sup>3</sup>Tohoku University Hospital, Department of Radiation

Technology, Sendai, Japan ; <sup>4</sup>Tohoku University Graduate School of Medicine, Department of Urology, Sendai, Japan

### Purpose or Objective

We aimed to assess the difference between planned and accumulated doses in prostatic urethra (PU) and bladder and to investigate the relationship between these differences and coexistent clinical status on severe late urinary toxicity following curative radiotherapy for patients with localised prostate cancer (PLPC).

### Material and Methods

Overall, 302 PLPC were treated with image-guided intensity-modulated radiation therapy (IMRT) between 2008 and 2015 in our institution. All PLPC had fiducial markers (FM) implanted in the prostate for daily set-up correction. For each PLPC, urethral catheter (UC) was temporarily used for the PU identification and delineation on planning CT (pCT) images. Moreover, cone-beam CT (CBCT) image was acquired on the first IMRT day and then approximately every 4 days, following daily set-up correction, throughout IMRT course (total 9-10 scans per PLPC). A radiation oncologist (RO) contoured the PU based on UC and the prostate, rectum, bladder, and seminal vesicles on pCT images. Among 302 PLPC, 8 who experienced grade 3 late urinary toxicities (according to the Common Terminology Criteria for Adverse Events version 4.0) within median follow-up period of 53 months (range, 6-118) were enrolled in the present study; the total dose administered was 80Gy in 40 fractions for 6 PLPC and 76Gy in 38 fractions for the remaining 2. Their median age was 65 years (range 59-73). Coexistent clinical status in the eight PLPC included antithrombotic therapy (AT) in four, diabetes mellitus in three, and prior transurethral prostate resection and high intensity focused ultrasound in two. All CBCT images were rigidly registered in the corresponding pCT images via matching FM and were exported to RayStation (version 4.5.1). Thereafter, the RO delineated the bladder on all CBCT images. The PU delineation conducted in each of the eight PLPC was transferred from pCT images to corresponding CBCT images. All CBCT images were then deformed to the corresponding pCT images using deformable image registration. Dose distributions were deformed and summed to estimate the following accumulated dosimetric factors: D<sub>98</sub>, D<sub>95</sub>, D<sub>mean</sub>, D<sub>50</sub>, D<sub>2</sub>, V<sub>75</sub> and D<sub>max</sub> of PU; and D<sub>98</sub>, D<sub>95</sub>, D<sub>mean</sub>, D<sub>50</sub>, D<sub>2</sub>, V<sub>35</sub>, V<sub>55</sub>, V<sub>65</sub>, V<sub>70</sub>, V<sub>75</sub> and V<sub>80</sub> of bladder. Mann-Whitney test was used to evaluate the difference of these dosimetric factors between planned and accumulated doses and to assess relationship between differences of dosimetric variables and coexistent status.

### Results

Marginally significant difference between planned and accumulated doses in D<sub>98</sub> and D<sub>95</sub> of PU were observed (p = 0.05). For PLPC treated with and without AT, the differences between both doses in D<sub>98</sub>, D<sub>95</sub>, D<sub>mean</sub>, D<sub>2</sub> and D<sub>max</sub> of PU were significant (p = 0.029). Differences of the

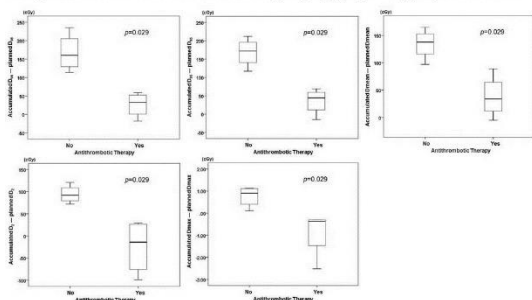
dosimetric factors were smaller in PLPC receiving AT than in PLPC did not undergo AT. Dosimetric factors of the bladder and other coexistent statuses were not significant.

Table. Relationship between the differences of dosimetric variables in  $D_{95}$ ,  $D_{90}$ ,  $D_{mean}$ ,  $D_2$  and  $D_{max}$  and coexistent clinical status in prostatic urethra

Difference of dosimetric parameters	Median (range)	AT (p value)	DM (p value)	Prior TURP and HIFU (p value)
Accumulated $D_{95}$ minus Planned $D_{95}$ (cGy)	86.5 (-18 to 235)	0.029*	0.571	0.286
Accumulated $D_{90}$ minus Planned $D_{90}$ (cGy)	93 (-15 to 212)	0.029*	0.571	0.286
Accumulated $D_{mean}$ minus Planned $D_{mean}$ (cGy)	93 (-5 to 165)	0.029*	0.571	0.286
Accumulated $D_2$ minus Planned $D_2$ (cGy)	107.5 (-8 to 168)	0.057	0.393	0.429
Accumulated $D_{max}$ minus Planned $D_{max}$ (cGy)	50.5 (-99 to 121)	0.029*	1.000	0.143
Accumulated $V_{15}$ minus Planned $V_{15}$ (%)	10.8 (-3.4 to 79)	0.114	0.393	0.071
Accumulated $D_{max}$ minus Planned $D_{max}$ (cGy)	-0.95 (-2.5 to 1.1)	0.029*	0.786	0.286

\* Statistical significance  
Abbreviation AT=antithrombotic therapy, DM=diabetes mellitus, TURP=transurethral resection of the prostate, HIFU=high intensity focused ultrasound.

Figure. For patients with localised prostate cancer treated with and without antithrombotic therapy, the differences between both doses in  $D_{95}$ ,  $D_{90}$ ,  $D_{mean}$ ,  $D_2$  and  $D_{max}$  of prostatic urethra



## Conclusion

PLPC with AT appeared to be more critical than doses in PU on severe late urinary toxicity.

## EP-1524 Differentiation between adenocarcinoma and prostatitis with multi-parametric MRI

S. Ken<sup>1</sup>, R. Aziza<sup>2</sup>, D. Portalez<sup>2</sup>, L. Chaltiel<sup>3</sup>, J. Gilhodes<sup>3</sup>, T. Brun<sup>4</sup>

<sup>1</sup>Institut Universitaire du Cancer - Oncopôle- Institut Claudius Regaud, Department of Engineering and Medical Physics, Toulouse, France ; <sup>2</sup>Institut Universitaire du Cancer - Oncopôle - Institut Claudius Regaud, Department of Medical Imaging, Toulouse, France ; <sup>3</sup>Institut Universitaire du Cancer - Oncopôle - Institut Claudius Regaud, Department of Clinical trial, Toulouse, France ; <sup>4</sup>Institut Universitaire du Cancer - Oncopôle - Institut Claudius Regaud, Department of Engineering and Medical Physics, Toulouse, France

## Purpose or Objective

In our institute, patients with low-to-moderate risk of prostate cancer could benefit from ultra-focal brachytherapy [1] as an alternative treatment to active surveillance. However, radiological diagnosis, which will guide the treatment strategy, remains challenging and still needs confirmed biopsies to distinguish between prostatic adenocarcinoma (PCa) and prostatitis (PT). This study aims at identifying imaging biomarkers derived from multi-parametric MRI (mpMRI) to help for the differentiation between PCa and PT.

## Material and Methods

Nineteen patients with low-to-moderate risk of prostate cancer underwent mpMRI on a 1.5T system (Magnetom Aera, Siemens Healthcare). Anatomical T2-weighted, IVIM diffusion (11b-values 0-800 s/mm<sup>2</sup>) and T1-weighted perfusion series were acquired. Volumes of interest (VOIs, in blue on Figure 1) were contoured on T2 images and reported on KTrans, ADC, D and computed b2000 maps. Distributions of voxel values inside the VOIs were compared to contralateral normal appearing tissue (CONTRO, in green on Figure 1) delineated with careful attention to get equivalent volume size for comparison. Volumes repartitions according to quartiles were compared between the biopsy confirmed groups of PCa

(N=12) and PT (N=7). All parameters values are given as median in the "Results" section.

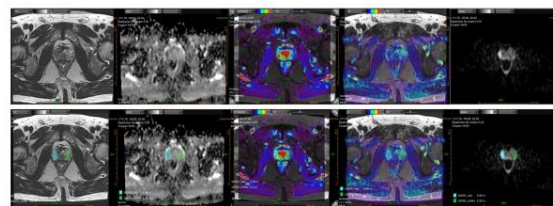


Figure 1: T2-weighted MR images, ADC, KTrans, D and computed b2000 maps (from left to right). Volumes of abnormal T2 are contoured in blue (VOI) and contralateral normal appearing tissues are contoured in green (CONTRO) and reported on ADC, KTrans, D and computed b2000 maps (bottom row).

## Results

Figure 2 presents the violin plots relative to parameters derived from mpMRI. Distributions of ADC, D (10<sup>-3</sup>mm<sup>2</sup>/s), KTrans (min<sup>-1</sup>) and computed b2000 (s/mm<sup>2</sup>) are shown according to the regions of interest (VOI or CONTRO) and the groups (PCa or PT).

For PCa group, ADC and D parameters inside the VOIs were significantly lower than in the CONTRO: 1.23 [0.66-1.62] vs. 1.48 [1.13-1.67] (p=0.0022) and 0.93 [0.59-1.49] vs. 1.33 [0.94-1.57] (p=0.0022), respectively. Voxels intensity of computed b2000 was significantly higher: 37.87 [28.29-87.11] vs. 27.63 [23.04-77.81] (p=0.0037). KTrans values were also significantly higher in the VOIs compared to CONTRO: 0.54 [0.05-1.10] vs. 0.36 [0.06-0.91] (p=0.0414). For PT group, ADC values were significantly lower inside the VOIs compare to CONTRO: 1.30 [0.98-1.43] vs. 1.43 [1.06-1.62] (p=0.0280). Computed b2000 values were significantly higher inside the VOIs: 46.45 [27.32-80.18] vs. 38.75 [25.66-70.20] (p=0.0180). D and KTrans were not significantly different between the VOIs and CONTRO: p=0.0630 and p=0.1282, respectively.

Volume of normal ADC (1<sup>st</sup> and 3<sup>rd</sup> quartile range) inside the VOIs were significantly smaller in the PCa group compared to the PT group: 12.2% [4.3-43.8] vs. 36.7% [8.7-50.9] (p=0.0346). Volume of low ADC (<1<sup>st</sup> quartile) was more important in the PCa group compared to the PT group: 72.7% [52.6-95.4] vs. 51.1% [16.7-84.4] but at the limit of significance (p=0.0519).

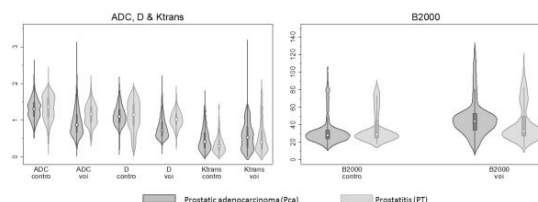


Figure 2: Violin plots of ADC, D, KTrans and computed B2000 parameters of prostatic adenocarcinoma (PCa) group in dark grey and prostatitis (PT) group in light grey. Distribution of these parameters are distinguished between the volume of interest (VOI) contoured according the abnormalities seen on the T2-weighted MR images and the contralateral normal appearing tissue (CONTRO).

## Conclusion

Abnormally low D parameters derived from IVIM and high KTrans parameters derived from perfusion MRI were found in the adenocarcinoma group but not in the prostatitis one. Percentage volumes distribution of ADC was also able to distinguish between the two groups.

[1] Brun et al. Brachytherapy 2018

<https://doi.org/10.1016/j.brachy.2018.01.011>

## EP-1525 Postoperative radiation therapy following radical prostatectomy in Stockholm County in 2008-2016

J. Falk<sup>1</sup>, M. Aly<sup>2</sup>, T. Nordström<sup>3</sup>, A. Valdman<sup>4</sup>

<sup>1</sup>Karolinska University Hospital, Department of radiation therapy, Stockholm, Sweden ; <sup>2</sup>Karolinska University Hospital, Department of Urology, Stockholm, Sweden ; <sup>3</sup>Danderyd Hospital, Department of Urology, Stockholm, Sweden ; <sup>4</sup>Karolinska University Hospital, Department of Radiation Therapy, Stockholm, Sweden

### Purpose or Objective

This is a large report including 714 consecutive patients who received postoperative radiotherapy following radical prostatectomy in Stockholm, Sweden. The aim of the study was to determine PSA outcomes in this patient cohort in relation of PSA values before radiotherapy.

### Material and Methods

During 2008-2016 all consecutive patients in the Stockholm area treated with postoperative radiotherapy were given 70 Gy to the prostatic bed and included in this study. After radiotherapy (RT) all patients have been monitored for biochemical failure with periodic PSA controls.

### Results

During median follow-up of 48 months, 49% of patients had no signs of biochemical failure (BcF), 13 % experienced BcF and 38 % never reached PSA nadir and subsequently progressed after RT. Five-year biochemical free survival was 47%. Patients who started RT at PSA < 0.28 ng/ml had the best 5-year bPFS of 58%. Patients who started RT at PSA values of 0.28-0.7 ng/ml had bPFS at 39%, and patients who started RT at PSA > 0.7 had the worst biochemical control at 33%.

### Conclusion

Low pre-RT PSA was an independent predictor of biochemical progression-free survival (HR=1.41, p<0.001). Median pre-RT PSA for the entire cohort was 0.28 ng/l (0.2-0.45) indicating the good standard of postoperative radiotherapy process from patient referral to start of postoperative radiotherapy in Stockholm County.

### EP-1526 PSMA-PET/CT validates Roach formula in 280 treatment-naïve prostate cancer patients

S. Koerber<sup>1,2,3</sup>, G. Stach<sup>4</sup>, C. Kratochwil<sup>4</sup>, M. Haefner<sup>1,2,3</sup>, S. Katayama<sup>1,2,3</sup>, H. Rathke<sup>4</sup>, K. Herfarth<sup>1,2,3,5</sup>, T. Holland-Letz<sup>6</sup>, U. Haberkorn<sup>4,7</sup>, J. Debus<sup>1,2,3,5,8,9</sup>, F.L. Giesel<sup>4,7,8</sup>

<sup>1</sup>Heidelberg University Hospital, Radiation Oncology, Heidelberg, Germany ; <sup>2</sup>National Center for Tumor diseases NCT, Radiation Oncology, Heidelberg, Germany ; <sup>3</sup>Heidelberg Institute of Radiation Oncology HIRO, Radiation Oncology, Heidelberg, Germany ; <sup>4</sup>Heidelberg University Hospital, Nuclear Medicine, Heidelberg, Germany ; <sup>5</sup>Heidelberg Ion-Beam Therapy Center HIT, Radiation Oncology, Heidelberg, Germany ; <sup>6</sup>German Cancer Research Center DKFZ, Biostatistics, Heidelberg, Germany ; <sup>7</sup>German Cancer Research Center DKFZ, Clinical Cooperation Unit Nuclear Medicine, Heidelberg, Germany ; <sup>8</sup>German Cancer Consortium DKTK, partner site Heidelberg, Heidelberg, Germany ; <sup>9</sup>German Cancer Research Center DKFZ, Clinical Cooperation Unit Radiation Oncology, Heidelberg, Germany

### Purpose or Objective

For radiotherapy planning, the Roach formula is a very useful tool when calculating the risk of lymph node metastases for patients with prostate cancer. However, several trials suggest a risk overestimation of this mathematical approach. Therefore, the present study aimed to evaluate the accuracy of the Roach formula using prostate-specific membrane antigen (PSMA) positron-emission tomography (PET)/computed tomography (CT).

### Material and Methods

Between July 2011 and July 2018, PSMA-PET/CT imaging was performed for almost 2500 patients. 280 patients with treatment-naïve prostate cancer and sufficient clinical data were enrolled in this study. The risk for lymph node metastases was calculated for all patients using Roach formula and PSMA data was analyzed retrospectively regarding lymph node metastases. For statistical analysis, the binary logistic regression was applied in various combinations of prostate-specific antigen (PSA), ln(PSA), Gleason score (GS) or WHO classification, to obtain new calculation methods. Afterwards, a comparison of all formulas was performed using receiver operating curves

(ROC).

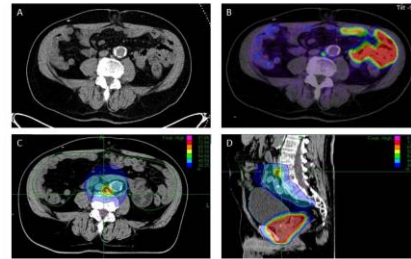


**Figure 1:** Personalized irradiation (C + D) of a 69-year old patient with prostate cancer and a risk of lymph node involvement of 20% according to Roach formula. While no suspect lymph node was observed in conventional CT scan (A), PSMA-PET/CT detected one positive lesion just above the bifurcation (B).

### Results

Most lymph node metastases appeared in the extern iliac vessels (28.95%). For patients with a higher GS (>7), there was a higher risk for presacral metastases or a spread outside the pelvis. For classical Roach formula and a cut-off of 20%, the area under the curve (AUC) was 0.781. In contrast, the binary logistic regression formula with ln(PSA) and GS had an AUC of 0.789.

### Conclusion

Although the AUC of the Roach formula is minimally smaller, the Roach formula can still be used for an initial assessment of the risk of lymph node metastases for patients with newly diagnosed prostate cancer undergoing radiotherapy.

### EP-1527 Proton therapy for prostate ca: Comparison of toxicity between mod-hypo and conventional fraction

T. Waki<sup>1</sup>, Y. Tominaga<sup>2</sup>, Y. Niwa<sup>1</sup>, H. Ihara<sup>1</sup>, D. Jin<sup>1</sup>, S. Sugiyama<sup>1</sup>, T. Kawabata<sup>1</sup>, K. Katsui<sup>3</sup>, M. Fujishima<sup>1</sup>, S. Kanazawa<sup>4</sup>

<sup>1</sup>Tsuyama chuo hospital, Radiology, Tsuyama-shi, Japan ; <sup>2</sup>Tsuyama chuo hospital, Radiological technology, Tsuyama-shi, Japan ; <sup>3</sup>Okayama university, Proton beam therapy, Okayama-shi, Japan ; <sup>4</sup>Okayama university, Radiology, Okayama-shi, Japan

### Purpose or Objective

To compare the acute toxicity between moderate hypofractionated (Mod-Hypo: 70 Gy (RBE) / 28 fr) and conventional fractionated (Conv: 74-78 Gy (RBE) / 37-39 fr) proton beam therapy (PBT) in patients with prostate cancer.

### Material and Methods

We evaluated consecutive 53 patients between April 2016 to December 2017. There were 21 Mod-Hypo and 32 Conv PBT cases. Retrospective analysis of the prospectively gathered data concerning gastrointestinal (GI), genitourinary (GU), skin and other toxicity was performed. Toxicity symptoms were scored weekly during treatment period and at 3 month after the completion of treatment by 1 radiation oncologist and 1 nurse. We compared the difference in the rate of acute adverse effect score between Mod-hypo and Conv cohorts using CTCAE.ver.4.03.

### Results

There was no severe (grade 3-4) acute toxicity. The rate of grade 1 / 2 GI toxicity in Mod-Hypo and Conv cohorts were 4.8 / 0.0% and 9.4 / 0.0%, respectively (p=0.82). The rate of grade 1 / 2 GU toxicity in Mod-Hypo and Conv cohorts were 57.1 / 9.5% and 50.0 / 25.0%, respectively (p=0.81). The rate of grade 1 / 2 skin toxicity in Mod-Hypo and Conv cohorts were 76.2 / 9.5% and 78.1 / 12.5%, respectively (p=0.87). The rate of grade 1 / 2 other toxicity in Mod-Hypo and Conv cohorts were 9.5 / 9.5% and

12.5 / 3.1%, respectively (p=0.94). There was no statistical difference between 2 cohorts for each toxicity.

#### Conclusion

Moderate hypofractionated proton beam therapy for prostate cancer is feasible. Further follow-up is needed to evaluate late toxicity.

#### EP-1528 Feasibility and toxicity of focal dose escalation on multimodally defined GTVs in prostate cancer

E. Haehl<sup>1</sup>, C. Zamboglou<sup>1</sup>, H.C. Rischke<sup>1</sup>, M. Bock<sup>2</sup>, S. Kirste<sup>1</sup>, M. Mix<sup>3</sup>, P.T. Meyer<sup>3</sup>, D. Baltas<sup>1</sup>, A.L. Grosu<sup>1</sup>  
<sup>1</sup>Medical Center - University of Freiburg, Department of Radiation Oncology, Freiburg, Germany ; <sup>2</sup>Medical Center - University of Freiburg, Department of Radiology, Freiburg, Germany ; <sup>3</sup>Medical Center - University of Freiburg, Department of Nuclear Medicine, Freiburg, Germany

#### Purpose or Objective

Introduction: The combination of MRI and PSMA PET/CT is a highly sensitive method to identify intraprostatic gross tumour volumes (GTV) in patients with prostate cancer (PCa). In silico studies already showed an improved tumour control for dose escalation through an intensity-modulated radiation therapy (IMRT) on multimodally defined GTV's. The present retrospective and monocentric analysis investigates the feasibility and acute toxicity of a focal IMRT dose escalation on multimodally defined target volumes.

#### Material and Methods

Methods: 31 patients with histologically ascertained PCa underwent insertion of intraprostatic gold markers followed by MRI imaging and a PSMA PET/CT planning scan. After image fusion target volumes were contoured based on MRI (GTV-MRI) and PET (GTV-PET defined as 30% of prostatic SUVmax) images. MRI and PET GTVs were merged (GTV-union) and the planning target volume for dose escalation (PTV-boost) was created by isotropic expansion with 4 mm. The clinical target volume (CTV) for the entire prostatic gland and the seminal vesicles was created according to the ESTRO guidelines and expanded isotropically with 6 mm to create the respective PTV. RT was performed using rapid-Arc and image guided RT (IGRT). During RT the doses applied to the target volumes and organs at risk were adapted considering cone beam CT scans. 6 patients received androgen deprivation therapy.

#### Results

Results: According to NCCN guidelines 18 respectively 13 patients have been classified as intermediate and high risk. A focal dose escalation could be realised in 21 patients (68%). Impending reasons were multifocal tumour lesions (>3), prolonged rectum contact and extensive tumour volume. Median volumes of GTV-MRI, GTV-PET, GTV-union and whole prostate were 2.1 ml (0-16,7 ml), 3.9 ml (0-11.13 ml), 5.5 ml (1-20.5 ml), and 58,2 ml (33-98 ml). Thereby GTV-union showed to be significantly larger than GTV-MRI (p<0.05).

Patients undergoing dose escalation received a mean dose of 74Gy on the PTV and 80Gy on the PTV-boost, both in 40 fractions. Acute grade 2 GI-toxicity occurred in 3 patients and acute grade 2 GU-toxicity in 4 patients, following CTCAE 5.0. One patient developed an acute grade 3 GU-toxicity most probably due to fiducial insertion, which was resolved completely.

#### Conclusion

Conclusion: Dose escalation to 80Gy based on multimodally defined target volumes could be performed in 68% of patients. Acute GI- and GU-toxicity seems to be tolerable. Further prospective studies are necessary to investigate this promising treatment regime.

#### EP-1529 Dosimetric parameters of radical radiotherapy for prostatic cancer: Targeting based on CT vs MRI

K. Nishiyama<sup>1</sup>, T. Toyofuku<sup>1</sup>

<sup>1</sup>Yao Municipal Hospital, Radiation Oncology, Yao, Japan

*This abstract is part of the media programme and will be released on the day of its presentation*

**EP-1530 Prostate volume reduction with neo-adjuvant hormones and its relation with bladder and rectal volume**

M. Sivanandan<sup>1</sup>, C. Vivekananthan<sup>1</sup>, Z. Ali<sup>1</sup>, S. Sundar<sup>1</sup>  
<sup>1</sup>Nottingham University Hospitals NHS Trust, Oncology and Radiotherapy, Nottingham, United Kingdom

**Purpose or Objective**

Androgen deprivation therapy (ADT) is routinely used in association with radical radiotherapy (RT) for intermediate and high risk prostate cancer. Neoadjuvant ADT has been shown to reduce the size of the prostate and hence target volume, thereby reducing the volume of normal tissue exposed to high radiation doses.

The purpose of our review was to examine whether prostate volume was associated with bladder and rectal volume as a surrogate of whether ADT-induced prostate volume reduction contributed to reduced normal tissue doses through changes in normal tissue volumes.

**Material and Methods**

Patients having radical prostate RT between January and May 2016 were identified from the hospital's RT database. Respective prostate volumes were calculated from diagnostic and planning MRI scans for each patient. Bladder and rectal volumes were calculated from each patient's planning CT scan. Statistical analysis was performed using the paired T-test and Pearson correlation.

**Results**

68 patients were identified. All patients had neoadjuvant ADT with median duration of ADT prior to planning MRI scan of 95 days. Mean reduction in prostate volume from diagnostic to planning MRI scan was 35.6% (95% CI: 32.0-39.3%) which was statistically significant ( $p < 0.01$ ). No correlation was seen between planning scan prostate volume and bladder volume ( $r = 0.0$ ;  $p = 0.97$ ) or rectal volume ( $r = 0.04$ ;  $p = 0.75$ ). Furthermore, no correlation was identified between percentage change in prostate volume and bladder volume ( $r = -0.07$ ;  $p = 0.60$ ) or rectal volume ( $r = 0.06$ ;  $p = 0.65$ ).

**Conclusion**

Our study confirms neoadjuvant ADT leads to a significant reduction in prostate volume. The reduction in high radiotherapy dose to bladder and rectum with ADT appears to be due to reduction in target volume alone rather than its interaction with normal tissue volumes. This work suggests that transurethral resection of the prostate (TURP) for patients with large prostate volumes before prostate RT with a view to specifically reducing bladder volumes would be of negligible benefit.

**EP-1531 SBRT for Prostate Cancer in 3 fractions: Acute Toxicity Rates from a Prospective Multicenter Study**

G. Sanguineti<sup>1</sup>, A. Farneti<sup>1</sup>, M. Trovò<sup>2</sup>, V. Landoni<sup>3</sup>, E. Moretti<sup>4</sup>, M. Ferriero<sup>5</sup>, F. Spasiano<sup>1</sup>, U. De Paula<sup>6</sup>, S. Gomellini<sup>6</sup>, A. Magli<sup>2</sup>

<sup>1</sup>irccs - Regina Elena National Cancer Institute, Radiotherapy, Rome, Italy ; <sup>2</sup>asiud, Radiotherapy, Udine, Italy ; <sup>3</sup>irccs - Regina Elena National Cancer Institute, Medical Physics, Rome, Italy ; <sup>4</sup>asiud, Medical Physics, Udine, Italy ; <sup>5</sup>irccs - Regina Elena National Cancer Institute, Urology, Rome, Italy ; <sup>6</sup>san Giovanni-Addolorata Hospital, Radiotherapy, Rome, Italy

**Purpose or Objective**

Five-fraction hypo-fractionated SBRT is an acceptable option for low/favorable intermediate risk prostate cancer (NCCN 2018). The aim of the present study was to further reduce the number of treatment sessions to 3. Here we report acute toxicity rates on the patients treated so far

**Material and Methods**

This phase I-II prospective study is enrolling patients with low/fav int risk prostate cancer at 3 Institutions since November 2015. The prescribed dose to the target (prostate+4 mm isotropic) is 40 Gy in 3 fractions while prioritizing a 30 Gy Dmax limit to the rectum (1cc), the bladder trigone (1cc) and the urethra (0.1cc). A gel spacer (along with gold fiducials) is placed before simulation to dislocate the rectum. Patients are simulated and treated with a urethral catheter and controlled bladder filling. Prostate had to be < 80 cc at diagnosis or after 3 months of androgen deprivation and IPSS < 16. Toxicity was graded according to the CTCAE v4.0 scale at the 3<sup>rd</sup> fraction and every 3 months afterwards. Toxicity developing within 3 months from treatment end is considered 'acute'.

**Results**

Twenty-eight patients (19, 7, 2 at each Institution) have been treated and have a 3-month minimum follow up. All patients had low (n=20) or intermediate risk (n=8) prostate cancer; mean (SD) age was 73 (5.2) years and mean (SD) PSA at diagnosis was 6.9 (2.8) ng/ml. At planning, average (SD) prostate volume (CTV) was 51.4 (17.8) cc, 3 patients after 3-month neoadjuvant androgen deprivation. On average (SD) 95% of the PTV was covered by the isodose 85.4 (4.7)% while the isodose 38 Gy covered 61.8 (19.0)% of the PTV. Mean (SD) Dmax to rectum (1cc), bladder trigone (1cc) and urethra (0.1cc) were 28.9 (1.9) Gy, 22.1 (9.0) Gy and 30.8 (1.6) Gy, respectively.

Peak acute GR0,GR1,GR2,GR3 gastrointestinal (GI) and genitourinary (GU) toxicity rates developed in 18,7,3,0 and 19,6,2,1 patients, respectively. Overall, 4 GR2+ GU events (2 urinary tract pain, 2 cystitis and 1 urinary retention) were recorded in 3 patients. The only grade 3 event consisted in urinary retention requiring transurethral resection 3 months after treatment completion. All three GR2 GI events consisted in mild proctitis. No GR4-5 GU or GI events were recorded as well as no other GR2+ event was observed.

**Conclusion**

Under the technical and dosimetric conditions set here, prostate SBRT in 3 fractions is associated with a favorable acute toxicity profile.

**EP-1532 Metastases directed SBRT using Ga68-PSMA for oligometastatic prostate cancer: TROD 09-002 Study**

G. Ozyigit<sup>1</sup>, S. Igdem<sup>2</sup>, B. Atalar<sup>3</sup>, H.B. Ozkok<sup>4</sup>, P. Hurmuz<sup>1</sup>, F. Akyol<sup>1</sup>

<sup>1</sup>Hacettepe University- Faculty of Medicine, Department of Radiation Oncology, Ankara, Turkey ; <sup>2</sup>Istanbul Bilim University, Department of Radiation Oncology, Istanbul, Turkey ; <sup>3</sup>Acibadem University, Department of Radiation Oncology, Istanbul, Turkey ; <sup>4</sup>Anadolu Medical Center, Department of Radiation Oncology, Istanbul, Turkey

**Purpose or Objective**

To evaluate the role of stereotactic body radiotherapy (SBRT) for oligometastatic prostate cancer (oPC).

**Material and Methods**

In current Turkish Radiation Oncology Group (TROD) study clinical data of 43 patients receiving metastases-directed SBRT between July 2014 and March 2017 from 4 institutions was retrospectively evaluated. Prior therapy was radical prostatectomy (RP) alone (30%), RP followed by adjuvant radiotherapy (28%) or definitive radiotherapy (RT) (42%). All of the patients should have biopsy proven prostate cancer with 5 or less metastases shown by Ga68-PSMA (Prostate Specific Membrane Antigen) PET-CT. SBRT was delivered in median 3 fractions (range, 1-5 fractions) to a total dose of median 27 Gy (range, 15-35 Gy).

**Results**

Median age was 64 years (range, 42-79 years). Median initial PSA was 21.5 ng/dL (range, 5-160 ng/dL) and Gleason score was 8 (range, 6-10). At the time of initial diagnosis, 18 patients had T3a, 12 patients had T3b disease and 7 patients were metastatic. Median 1 metastatic lesion located in regional lymph nodes (41%), bone (46%) and both lymph node plus bone (13%) was treated. Thirty three patients received androgen deprivation treatment (ADT). With a median follow up of 14.5 months (range, 1-45 months), 13 patients (30%) had progressive disease and 54% of them were oligometastatic progression. None of the patients had relapse in the treated region. Time to progression was median 13 months. One and two year progression free survival rates were 76% and 59%, respectively. No patients reported grade 3 or more acute or late radiation related gastrointestinal or genitourinary side effects.

**Conclusion**

This multi-institutional study shows that SBRT for oPCa seems to be safe and effective. Most of the relapses are oligometastatic, thus retreatment with SBRT might be an option for properly selected patients to avoid early ADT and its complications. Further prospective clinical studies should be done to evaluate this treatment option.

**EP-1533 Stereotactic Body Radiotherapy in Prostate Cancer: A Single Center Experience**

F. Akyol<sup>1</sup>, P. Hurmuz<sup>1</sup>, S. Sari<sup>1</sup>, A.E. Dogan<sup>1</sup>, D. Yuce<sup>2</sup>, S. Yazici<sup>3</sup>, B. Akdogan<sup>3</sup>, G. Ozyigit<sup>1</sup>

<sup>1</sup>Hacettepe University Ankara, Radiation Oncology, Ankara, Turkey; <sup>2</sup>Hacettepe University Ankara, Preventive Oncology, Ankara, Turkey; <sup>3</sup>Hacettepe University Ankara, Urology, Ankara, Turkey

**Purpose or Objective**

To evaluate our treatment results in patients with prostate cancer receiving definitive robotic stereotactic body radiotherapy (rSBRT).

**Material and Methods**

Between July 2007 and November 2016 135 patients were treated with CyberKnife® robotic radiosurgery treatment machine. According to our institutional treatment protocol we delivered 36.5 Gy in 5 fractions to prostate. According to D'Amico risk classification system 74 patients were in low-risk group and 61 patients were in intermediate-risk group. 'Phoenix definition' was used for biochemical relapse and Cavanagh definition was used for PSA bounce, respectively.

**Results**

Median follow-up time was 34 months (range, 3-111 months). Biochemical relapse was detected in 6 patients between the 26th and 56th months. PSA bounce was observed in 38 (29%) patients, and 30 of these patients had low-risk disease. Biochemical relapse was observed in 3 patients who experienced PSA bounce during the follow-up. For the whole group, 3-year biochemical relapse-free

survival (BRFS) and overall survival (OS) rates were 95% and 92%, respectively. Presence of PSA bounce did not have an effect on BRFS rates; however, OS rate was significantly higher in patients with PSA bounce, independent from the risk group (p=0.025). Treatment was well tolerated with no grade 3 or more acute toxicities. Late grade III gastrointestinal system and grade III genitourinary system toxicity was observed in 4 and 11 patients, respectively.

**Conclusion**

Prostate rSBRT is an effective and safe treatment for patients with low-intermediate risk prostate cancer with acceptable toxicity rates.

**EP-1534 Clinical Outcomes for Patients with Gleason Score 10 Prostate Adenocarcinoma: TROD 09-004 Study**

G. Ozyigit<sup>1</sup>, H.C. Onal<sup>2</sup>, P. Hurmuz<sup>1</sup>, A. Iribas<sup>3</sup>, I. Cetin<sup>4</sup>, I.B. Gorken<sup>5</sup>, D. Yalman<sup>6</sup>, F. Akyol<sup>1</sup>

<sup>1</sup>Hacettepe University- Faculty of Medicine, Department of Radiation Oncology, Ankara, Turkey; <sup>2</sup>Baskent University, Radiation Oncology, Adana, Turkey; <sup>3</sup>Istanbul University, Radiation Oncology, Istanbul, Turkey; <sup>4</sup>Marmara University, Radiation Oncology, Istanbul, Turkey; <sup>5</sup>Dokuz Eylul University, Radiation Oncology, Izmir, Turkey; <sup>6</sup>Ege University, Radiation Oncology, Izmir, Turkey

**Purpose or Objective**

Gleason score (GS) 10 disease is a rare and an aggressive form of prostate adenocarcinoma (PCa). In this national multi-institutional study we evaluated the treatment outcomes for this subgroup of patients.

**Material and Methods**

The clinical data of 30 patients receiving definitive radiotherapy (RT) plus androgen deprivation therapy (ADT) between January 2001 and March 2015 from 6 institutions was retrospectively evaluated in current Turkish Radiation Oncology Group (TROD) study. All of the patients had biopsy proven disease. Follow up duration of at least 24 months was mandatory. ASTRO Phoenix definition was used for biochemical relapse.

**Results**

Median age was 65 years (range, 58-78 years). Median initial PSA was 25 ng/dL (range, 4.5-150 ng/dL). Median RT dose was 75 Gy (range, 70-78 Gy) and 12 patients received pelvic radiation as a part of treatment protocol. All patients received ADT with median duration of 24 months (range, 9-48 months). With a median follow up time of 66.5 months, 13 patients (43%) had biochemical relapse, 2 patients (7%) had local relapse and 8 patients (27%) had distant metastases. Five-10 year overall survival (OS) and biochemical relapse free survival (BRFS) rates were 78%-66% and 56%-42%, respectively.

**Conclusion**

To our knowledge this is the first study to give BRFS in GS=10 prostate cancer patients treated with RT and long term ADT. Regarding the rarity of the disease multi-institutional studies are valuable in the further evaluation of this group of patients.

**EP-1535 Vessel-sparing prostate V-MAT with simultaneous integrated boost to dominant intraprostatic lesion**

S. Ciabatti<sup>1,2</sup>, M. Ntreta<sup>2</sup>, C. Gaudiano<sup>3</sup>, E. Sessagesimi<sup>3</sup>, V. Dionisi<sup>2</sup>, M. Buwenge<sup>2</sup>, M. Ferioli<sup>2</sup>, F. Deodato<sup>4</sup>, A. Ianiro<sup>5</sup>, G. Macchia<sup>4</sup>, M. Ferro<sup>4</sup>, S. Riga<sup>6</sup>, F. Romani<sup>6</sup>, A.L. Angelini<sup>6</sup>, V. Valentini<sup>7</sup>, S. Cammelli<sup>2</sup>, R. Golfieri<sup>3</sup>, G.P. Frezza<sup>1</sup>, A.G. Morganti<sup>2</sup>, S. Cilla<sup>5</sup>

<sup>1</sup>Radiation Therapy Department, Bellaria Hospital, Bologna, Italy; <sup>2</sup>Radiation Oncology Center, Dept. of Experimental- Diagnostic and Specialty Medicine - DIMES- University of Bologna- S. Orsola-Malpighi Hospital, Bologna, Italy; <sup>3</sup>Radiology Unit, Dept. of Diagnostic Medicine and Prevention- University of Bologna- S.

Orsola-Malpighi Hospital, Bologna, Italy ; <sup>4</sup>Radiotherapy Unit, Fondazione di Ricerca e Cura "Giovanni Paolo II", Campobasso, Italy ; <sup>5</sup>Medical Physics Unit, Fondazione di Ricerca e Cura "Giovanni Paolo II", Campobasso, Italy ; <sup>6</sup>Medical Physics Unit, Dept. of Experimental- Diagnostic and Specialty Medicine - DIMES- University of Bologna- S. Orsola-Malpighi Hospital, Bologna, Italy ; <sup>7</sup>Department of Radiotherapy, Policlinico Universitario "A. Gemelli"- Università Cattolica del Sacro Cuore, Rome, Italy

#### Purpose or Objective

New evidences suggested a vascular etiology for sexual impotence after prostate radiotherapy. Internal pudendal arteries (IPA), corpora cavernosa (CC) and penile bulb (PB) were identified as critical structures related to erectile function. We explored the potential of VMAT to spare the critical erectile structures with a SIB to the dominant intraprostatic lesion (DIL)

#### Material and Methods

Twelve patients were selected for this study. DILs were defined using T2-weighted, dynamic contrast-enhanced and diffusion-weighted MRI (multiparametric MRI). Vascular structures were contoured and expanded by a uniform 2 mm margin. The seminal vesicles, the prostate and DIL were expanded uniformly by 5 mm to create the planning target volumes (PTVsv, PTVpr and PTVdil, respectively). PTVsv, PTVpr and PTVdil dose prescription was 56.25, 67.50 and 75 Gy, respectively, in 25 fractions. The doses were prescribed to cover >95% of PTVs. All VMAT plans were generated in a dual-arc modality for a VersaHD linac. Original clinical plans (ST-VMAT) were created to fulfil targets coverage and Quantec constraints for non vascular OARs (NV\_OARs: rectum, bladder and femoral heads). For each patient, a new plan (SS-VMAT) based on the approved ST-VMAT plan was created. IPA, CC and PB were considered OARs related to sexual impotence (V\_OARs). All objectives for PTVs coverage and NV\_OARs sparing were left unchanged. New objectives were added for V\_OARs, with priority to minimize mean doses to IPA, CC and PB. A Wilcoxon signed-rank test was used to compare the two optimization techniques.

#### Results

For all plans, targets coverage was well within the predefined objectives for all metrics (D95, D98, Dmean). In particular, D98% was >95% of prescribed doses for all targets, patients and techniques. No significant differences were found in sparing rectum, bladder and femoral heads for all considered metrics (Dmean, V50, V60, V70). With regard to V\_OARs sparing, SS\_VMAT plans provided a major reduction of dose irradiation. Mean doses for IPA, CC and PB were reduced by 32.4% (11.2 Gy, p=0.002), 22.5% (4.1 Gy, p=0.006) and 10.0% (4.6 Gy, p=0.010), respectively. V30 decreased from 61.1% to 21.4% (p=0.02) for IPA and from 27.2% to 14.8% (p=0.04) for CC.

#### Conclusion

We showed that a significant dose sparing for IPA, CC and PB using VMAT-SIB strategy is feasible, allowing vessel-sparing and highly conformal plans, dose escalation to DIL and fast treatment delivery.

#### EP-1536 Influence of obesity in treatment outcomes in prostate cancer patients

J.L. Munoz Garcia<sup>1</sup>, F. Ropero Carmona<sup>1</sup>, M. Gonzalez Ruiz<sup>2</sup>, P. Simon Silva<sup>1</sup>, J. Quiros Rivero<sup>1</sup>, Y. Rios Kavadoy<sup>1</sup>, M.C. Cruz Muñoz<sup>1</sup>, J. Cabrera Rodriguez<sup>1</sup>  
<sup>1</sup>Badajoz University Hospital, Radiation Oncology, Badajoz, Spain ; <sup>2</sup>Punta de Europa Hospital, Radiation Oncology, Algeciras, Spain

#### Purpose or Objective

**Purpose/Objective:** obesity is related to worst pronostic factors after prostatectomy and lower prostate cancer specific survival (PCSS) after radiotherapy with low doses of external beam radiation (EBRT). Our objective is to

analyse the influence of obesity in treatment outcomes with high doses of external beam radiation therapy (HDEBRT) plus androgen deprivation therapy (ADT) in patients (pts) with prostate cancer (PC) treated with radical intention.

#### Material and Methods

**Material/methods:** Retrospective comparative study of 297 out of 531 pts with PC treated with EBRT+ADT in our hospitals from October 2001 to December 2011 with height and weight data available at baseline (56%). 168 were non-obese (57%) and 129 obese (43%). Baseline characteristics non-differed significantly between treatment groups in PSA level, tumour stage, risk group, percentage of positive cylinder, ADT duration and total dose of RT but more obese pts had cardiovascular events, high blood pressure and metabolic alterations. All pts were treated with 3DCRT at a median total dose of 78 Gy (range 74-78). Phoenix definition was used for biochemical failure. Survival rates were estimated with Kaplan-Meier and compared with Log Rank test. Prognostic factors such as age, primary tumour stage, Risk group, Gleason, percentage of positive cylinder, radiotherapy total dose and ADT duration have been related to BDFS, OS and PCSS using Cox regression.

#### Results

**Results:** The median follow-up was 84 months (range 11-175) in non-obese pts and 91 months (range 29-188) in obese pts. The 7-year BDFS, OS and PCSS in non-obese pts were 92.4%, 91.6%, and 99.9% respectively and in obese were 88.2% (p=0.147), 90.1% (p=0.384), and 96.6% (p=0.330) respectively. In the multivariate analysis, obesity was not a significant prognostic factor of BDFS, OS neither PCSS.

#### Conclusion

**Conclusion:** Regarding to our results, obesity in prostate cancer treated with high doses of EBRT did not have significantly influence in BDFS, OS and CSS. Studies with large sample of pts are recommended

#### EP-1537 Local Relapse after Radiotherapy for prostate cancer: is a second local treatment worthwhile?

C. Hennequin<sup>1</sup>, M. Pierre<sup>2</sup>, D.K. Eric<sup>3</sup>, V. Laetitia<sup>4</sup>, D. François<sup>2</sup>, C. Stéphane<sup>5</sup>, Q. Laurent<sup>1</sup>

<sup>1</sup>Hôpital Saint-Louis- AP-HP, Radiation Oncology, Paris, France ; <sup>2</sup>Hôpital Saint-Louis- AP-HP, Urology, Paris, France ; <sup>3</sup>Hôpital Saint-Louis- AP-HP, Radiology, Paris, France ; <sup>4</sup>Hôpital Saint-Louis- AP-HP, Nuclear Medicine, Paris, France ; <sup>5</sup>Hôpital Saint-Louis- AP-HP, Medical Oncology, Paris, France

#### Purpose or Objective

To compare the outcome of patients with an isolated local relapse (LR) after radiotherapy (RT) of prostate cancer treated with a salvage local treatment (SLT) with those only monitored

#### Material and Methods

Between January 2011 and December 2016, all consecutive patients presenting a biochemical relapse (BR: nadir+2ng/ml) after RT (external beam radiotherapy or brachytherapy) who had a staging including a 18-fluorocholine-PET-CT (FCH-PET/CT) were prospectively registered. Patients with an isolated LR had systematically a multiparametric magnetic resonance imaging (mpMRI) to confirm LR. After evaluation of comorbidities, life expectancy, functional status and discussion with the patient, a SLT (cryotherapy, stereotactic RT: SBRT or High-Intensity Focused Ultrasounds: HIFU) or a simple surveillance could be proposed. A salvage androgen deprivation therapy (ADT) was given in case of a PSA doubling-time ≤ 12 months or a PSA level higher than 10 ng/ml or if distant metastases are detected.

#### Results

Among the 134 patients with a BR, 67 had an isolated LR on FCH-PET/CT and mpMRI. Mean age was 67 yrs (53-86). Initial prognostic groups was: favourable: 20;

Intermediate: 28; High risk: 19. Mean PSA at the time of relapse was 6.3 ng/ml. Twenty-five had a SLT (cryotherapy: 23; SBRT:1; HIFU:1) and 42 a simple monitoring. Mean follow-up was 48 months. Three-year overall survival (OS: 93%) and distant metastasis-free survival (DMFS: 85%) were similar in both groups. But SLT postponed the use of ADT: at 3 year, 71% of the patients treated with SLT did not receive ADT versus 37% in the other group (p=0.001). We observed 24% of grade 3-4 side effects after cryotherapy, mainly incontinence, with two patients receiving an artificial urinary sphincter.

#### Conclusion

we did not observed an improvement in 3-year OS or DMFS after SLT for LR after RT. But it could delay the use of ADT. Due to the potential side effects of salvage treatments, a stringent selection of the patients based on imaging, analysis of prognostic factors and life expectancy must be recommended.

#### EP-1538 Where fail PC patients treated with limited RT to prostate and sv with 76-80 Gy +/- hormonotherapy?

J. Lopez Torrecilla<sup>1</sup>, P.P. J<sup>1</sup>, V. A<sup>2</sup>, G.H. T<sup>2</sup>, G.S. D<sup>1</sup>, A. P<sup>1</sup>, H.M. A<sup>1</sup>, G.M. E<sup>1</sup>, G.P. Jc<sup>1</sup>, B. L<sup>2</sup>, G. D<sup>2</sup>, R.F. J<sup>2</sup>

<sup>1</sup>H. General Univ Valencia, Radiation Oncology-ERESA, Valencia, Spain ; <sup>2</sup>H. General Univ Valencia, Radiofísica-ERESA, Valencia, Spain

#### Purpose or Objective

To analyse where they fail and what are the causes of death of patients treated with an "optimal" dose of radiotherapy.

#### Material and Methods

Between November 1997 and July 2007, 302 patients were treated with external radiotherapy +/- hormone therapy (29 with RTC-3D, 227 with IMRT and 52 with IMRT-IGRT). The average age of the series was 70.15 years (range of 51-87 years). Average follow-up 117.49 months, with a median of 130 months. The patients who died at the time of the analysis, the mean follow-up was 87.19 months, with a median of 87.5 months. Distribution by TNM: T: T1c: 80 (26.5%); T2a: 90 (29.8%); T2b: 36 (11.9%); T2c: 12 (4.0%); T3a: 42 (13.9%); T3b 38 (12.6%); T4: 2 (0.7%); Tx: 2 (0.7%). N: N0: 250 (82.7%); Nx: 52 (17.2%). M: M0: 233 (77.2%) ptes. Mx: 69 patients. Initial PSA <10 ng/ml: 177 (58.6%); 10-20: 87 (28.8%); > 20: 32 (10.6%), in 6 patients we do not know the PSA before any treatment. Gleason was <7: 225 (74.5%); 7:58 (19.2%); 8-10: 17 (5.6%). 2 patients unknown. Distribution by groups of risk (NCCN 2018 classification): Low risk 80 (26.55%), Intermediate risk: 86 (28.5%); high risk: 77 (25.5%), Very high risk 49 (16.2%), Unknown 10 (3.3%). The dose in prostate was 76 Gy in 119 (39.4%) patients and 80 Gy in 183 (60.6%). The dose in seminal vesicles was 50 Gy in 145 (47.9%) of the patients and 58 Gy in 152 (50.4%) patients. Patients were treated with 15 MV photons by 6 incidences with a rate of 200 cGy per session, 5 times per week. They did not receive hormone therapy 65 (21.5%) patients.

#### Results

**Survival at 5 and 10 years:** Global 84.4% and 65.0%. Free of biochemical failure (BQF): 89.1% and 82.0%. Free of metastasis: 96.4% and 94.3%, respectively. At the time of the analysis 143 (47.4%) patients are alive, 158 (52.3%) have died and one is lost. **BQF** has presented 54 (17.9%) patients, of them 30 (9.9%) have not developed clinical disease, 11 (3.6%) presented **local failure (LF)**, 4 (1.3%) **regional failure (RF)** and 17 (5.6%) **metastasis**. The cause of death was 106 (67.1%) intercurrent disease, 28 (17.7%) a second tumour, 24 (15.2%) due to prostate cancer. Of the 143 living patients 121 (84.6%) are disease-free, 22 (15.4%) with BQF (5 of them with associated LF, 1 LF + metastasis and 1 single metastasis). Of this group 5 patients (3.7%) are alive with a second tumour. **Late Complications (RTOG):** GU: G0: 40 (13.2%); G1: 134 (44.4%); G2: 98 (32.5%); G3: 27 (8.9%); G4: 3 (1.0%). GI:

G0: 237 (78.5%); G1: 45 (14.9%); G2: 10 (3.3%); G3: 8 (2.6%); G4: 2 (0.7%); Maximum haematuria in follow-up: G0: 257 (85.1%); G1: 16 (5.3%); G2: 18 (6.0%); G3: 11 (3.6%). Maximum rectal bleeding in follow-up: G0: 251 (83.1%); G1: 30 (9.9%); G2: 8 (2.6%); G3: 13 (4.3%).

#### Conclusion

**Conclusions:** Optimal dose of radiotherapy +/- Hormonotherapy in prostate cancer achieves a local control of the disease that translates into a low probability of death from cancer. The risk of regional failure has been extremely low (1.3%) despite not treating the pelvic lymph nodes.

#### EP-1539 Early experience and quality of life in SBRT prostate cancer boost of 9 Gy in a phase II trial.

F. Ferrer<sup>1,2,3</sup>, A. Pont<sup>4</sup>, R. De Blas<sup>5</sup>, A. Boladeras<sup>1,3</sup>, O. Garin<sup>4,6</sup>, M. Ventura<sup>1,3</sup>, E. Zardoya<sup>5</sup>, J. Delgado<sup>1</sup>, E. Condom<sup>7</sup>, E. Merino<sup>8</sup>, J. Mases<sup>1</sup>, M. Castells<sup>2,9</sup>, I. Guix<sup>1</sup>, J.F. Suarez<sup>10</sup>, J. Gonzalez<sup>1</sup>, S. Almendros<sup>1</sup>, M. Garcia<sup>11</sup>, M.A. Berenguer<sup>1,3</sup>, N. Garcia<sup>1</sup>, M. Stefanovic<sup>1</sup>, C. Gutierrez<sup>11</sup>, C. Picon<sup>5</sup>, M. Ferrer<sup>4,12</sup>, F. Guedea<sup>1,2,3</sup>

<sup>1</sup>Catalan Institute of Oncology, Radiation Oncology, L'Hospitalet Barcelona, Spain ; <sup>2</sup>Faculty of Medicine and Health Sciences. University of Barcelona, Clinical Sciences, L'Hospitalet Barcelona, Spain ; <sup>3</sup>IDIBELL, Cancer and Radiobiology Research Group, L'Hospitalet Barcelona, Spain ; <sup>4</sup>Institut Municipal d'Investigacions Mèdiques, Health Services Research Unit, Barcelona, Spain ; <sup>5</sup>Catalan Institute of Oncology, Medical Physics and Radiologic Protection, L'Hospitalet Barcelona, Spain ; <sup>6</sup>University Pompeu Fabra, Experimental Sciences, Barcelona, Spain ; <sup>7</sup>Bellvitge Hospital, Pathology, L'Hospitalet Barcelona, Spain ; <sup>8</sup>Institute for diagnostic with images IDI, Magnetic resonance imaging MRI, L'Hospitalet Barcelona, Spain ; <sup>9</sup>Bellvitge Hospital, Urology, L'Hospitalet Barcelona, Spain ; <sup>10</sup>Bellvitge Hospital, Urology, L'Hospitalet Barcelona, Spain ; <sup>11</sup>Catalan Institute of Oncology, Radiation Oncology-Brachytherapy Unit, L'Hospitalet Barcelona, Spain ; <sup>12</sup>Autonomous University of Barcelona, Health Sciences, Barcelona, Spain

#### Purpose or Objective

Extracranial stereotactic body radiation therapy (SBRT) allows delivering high doses per fraction with high accuracy to the prostatic gland in a low number of fractions. Dose escalation in normofractionated radiation prostate cancer trials showed an increased toxicity. In order to evaluate the feasibility and toxicity of a regimen of a single dose hypofractionated prostate stereotactic boost a phase II study was undertaken. Self-reported quality of life (QOL) measures were also obtained in order to better define the possible deleterious effect of treatment.

#### Material and Methods

Patients included were diagnosed of prostate cancer with T3aNOMO Gleason score 8 or less (N+risk<25%) and IPSS 0-12. Hormonal-therapy was prescribed according to risk classification. Image Guided RT with Cone Beam CT was mandatory. Dose SBRT was delivered at a prescribed planning target volume (PTV) 9 Gy after 60 Gy 2 Gy per fraction in 30 days, using with RapidArc VMAT, with 6 MV FFF photons. Equivalence of dose at 2 Gy per fraction, using Linear Quadratic Model is round 87Gy. RTOG-EORTC and CTCAE v4.0 morbidity scores were used to assess toxicities. Health-related quality of life questionnaire was administered centrally by telephone interview before treatment and during follow-up (at 3, 6 and 12 months). Study was planned following a Simon's 2-stage design. Due to a low recruitment rate firsts 22 evaluable patients were studied.

#### Results

First's 22 patients included were analyzed. Mean age was 69.6 years old. Median follow-up was 9 months (2-50) with more than 60% having at least 6 months of follow-up.

According to D'Amico risk classification for trial and inclusion criteria all of them were high risk. All patients completed the treatment as programmed with good tolerance. No toxicity greater than grade 2 was observed. EPIC urinary values were 81.26 and 80.49 at 6 and 12 months respectively. EPIC hormonal was 63.83 and 64.09 at 6 and 12 months respectively. EPIC bowel values for these points in time were 93.30 and 92.50. Non PSA relapse was seen during this short follow-up. Acute GI grade 2 toxicities were 9.2% for a week after treatment. At the 1<sup>st</sup> month GI Grade 2 toxicity showed the same percentage. At the 3<sup>rd</sup> month GI Grade 2 was reduced to 4.5%. Acute GU grade 2 toxicity was 31.8%. At the 1<sup>st</sup> month GU Grade 2 toxicity decrease to 9.1%. One patient showed late GU Grade 2 at 6 months.

#### Conclusion

SBRT regime of 9 Gy to the prostate after normofractionated 60 Gy for high risk prostate cancer is feasible and well tolerated in selected patients. Decline in QoL values are seen EPIC hormonal QLQ measures are related to prolonged hormonal treatment in high-risk patients. Long-term follow-up is needed for assessment of late toxicity and outcomes.

#### EP-1540 A bowel pathway for patients undergoing radiotherapy for prostate cancer

C. Perna<sup>1</sup>, C. Williamson<sup>1</sup>, S. Khaksar<sup>1</sup>

<sup>1</sup>Royal Surrey County Hospital, St Lukes cancer centre, Guildford, United Kingdom

#### Purpose or Objective

To investigate whether the introduction of a new bowel pathway, in patients undergoing radiotherapy to prostate (PRT), whole pelvis (WPRT) and prostate bed (PBRT), could improve the rate of repeated planning CT scans caused by faecal loading and rectal gas.

#### Material and Methods

Data were collected retrospectively from patient's notes and electronic records. From January 2015 until January 2016, 23% of patients underwent rescan due to faecal loading and rectal gas.

Patients underwent PBRT, traditionally did not receive bowel preparation, on the contrary, those underwent PRT and WPRT used micro enemas prescribed at the time of the fiducial markers insertion.

We introduced a new radiographer led clinic for all patients to discuss bowel habit and identify patients that needed additional laxatives. Patients underwent PBRT also received micro enemas routinely.

All patients received a bowel chart to record their bowel movement and type of stools. Sodium Docusate 100mg TDS was our laxative of choice. In addition, a record of off-line review was kept.

#### Results

A total of 195 patients were treated (18 PBRT and 177 between PRT and WPRT) from January 2017 until April 2017. They all received, a bowel chart and the prescription of micro enemas. 32 patients also received additional prescription of Sodium Docusate.

Sodium Docusate was well tolerated in all cases and therefore continued during the whole treatment helping in reducing faecal loading and rectal gas.

32 (16.4%) required a re-scan, because poor hydration, micro enema compliance and patient position. However, only 14 (7.1%) had large rectum with antero-posterior diameter >4 cm.

Of the 18 PBRT patients, 15 were assessed in the radiographer led clinic and did not require a second planning scan. The 3 patients who missed the clinic underwent re-scan.

The off-line review didn't show significant differences during the course of the treatment, but data are still too small.

#### Conclusion

The addition of a radiographer led clinic, with bowel habit assessment and prescription of laxatives, helped reducing the rate of planning rescan from 23% to 16.4% with only a 7.1% of rescan rate due to large rectum. This consequently reduced unnecessary radiation exposure to the patients and additional workload for the department.

#### EP-1541 Intention to treat analysis of 68Ga-PSMA/11C-choline PET/CT vs. CT for prostate cancer recurrences

A. Müller<sup>1</sup>, S. Olthof<sup>2</sup>, C. Pfannenber<sup>2</sup>, D. Wegener<sup>1</sup>, J. Marzec<sup>1</sup>, J. Bedke<sup>3</sup>, A. Stenzl<sup>3</sup>, C. La Fougère<sup>4</sup>, K. Nikolaou<sup>2</sup>, D. Zips<sup>1</sup>, J. Schwenck<sup>4</sup>

<sup>1</sup>Eberhard Karls University Tübingen, Department of Radiation Oncology, Tübingen, Germany; <sup>2</sup>Eberhard Karls University Tübingen, Department of Diagnostic and Interventional Radiology, Tübingen, Germany; <sup>3</sup>Eberhard Karls University Tübingen, Department of Urology, Tübingen, Germany; <sup>4</sup>Eberhard Karls University Tübingen, Department of Nuclear Medicine and Clinical Molecular Imaging, Tübingen, Germany

#### Purpose or Objective

Biochemical recurrence (BCR) after prostate cancer (PC) surgery is very common, even after additional salvage radiotherapy (SRT). This might be explained by target miss. Improved diagnostic accuracy provided by PET could potentially circumvent this therapeutic gap. Therefore, we evaluated the impact of simultaneous <sup>11</sup>C-choline and <sup>68</sup>Ga-PSMA PET/CT compared to standard CT imaging after surgery +/- SRT with regard to curative radiotherapy (RT) options including stereotactic body radiotherapy (SBRT) for oligometastases.

#### Material and Methods

The prospective register database (064 / 2013 BO1) was searched for patients receiving both <sup>68</sup>Ga-PSMA and <sup>11</sup>C-choline PET/CT within the same day. Inclusion in this analysis was restricted to patients after radical prostatectomy +/-SRT at time of BCR. <sup>11</sup>C-choline PET/CT was acquired with a contrast-enhanced CT and <sup>68</sup>Ga-PSMA was combined with a low-dose CT. TNM-stage was assessed by two blinded investigators (JS, SCO). Ten curative treatment routines were defined including SBRT for up to 5 oligometastases. Imaging-related changes of treatment and treatment intent as well as related costs depending on stage shift after imaging were analysed. Cost calculation for in-/correct treatment was performed using the German reimbursement catalogue ("Einheitlicher Bewertungsmaßstab"; EBM) and the German medicines compendium ("Rote Liste").

#### Results

Eighty-three patients were eligible (median PSA-level 1.9 ng/ml). Both PET-examinations led to concordant results in 72.3% of patients, while concordance of TNM-staging between <sup>68</sup>Ga-PSMA-PET and diagnostic CT was only 36.1%. Incorrect staging would lead to "wrong" treatment and therefore to additional treatment costs. A <sup>68</sup>Ga-PSMA-PET would be cost-effective if additional costs do not exceed 3,843 € (vs. CT). According to the "number needed to treat" we calculated the "number needed to image (NNI)" to avoid one "wrong" treatment for a patient. The NNI<sub><sup>11</sup>C-choline</sub> equals 4 and the NNI<sub>contrast enhanced CT</sub> equals 2 compared to <sup>68</sup>Ga-PSMA-PET to avoid one incorrect treatment. <sup>68</sup>Ga-PSMA-PET-staging enabled new curative options in half of the patients with previous SRT who otherwise always receive palliative ADT.

#### Conclusion

In this prospective analysis we compared the impact of three simultaneously performed imaging modalities on treatment of PC recurrences after surgery. Main findings include cost-efficacy of <sup>68</sup>Ga-PSMA-PET by calculating the additional costs of "wrong" intended treatment occurring in approximately 2/3 of patients after conventional staging. In addition, we were able to demonstrate that <sup>68</sup>Ga-PSMA-PET gave a high chance of curative treatment

for patients without previous RT (>90%) and new curative options in half of patients after SRT who usually would otherwise receive palliative ADT. Cost efficacy is further substantiated by the new measure NNI. Therefore, <sup>68</sup>Ga-PSMA PET/CT staging should become the standard method for staging of high risk prostate cancer patients with BCR, also after initial salvage therapy.

#### EP-1542 Long-term results and PSA kinetics after robotic SBRT for prostate cancer

Y. Park<sup>1</sup>, H.J. Park<sup>2</sup>, W.I. Jang<sup>3</sup>, B.K. Jeong<sup>4</sup>, H. Kim<sup>5</sup>, A.R. Chang<sup>1</sup>

<sup>1</sup>Soonchunhyang University Seoul Hospital, Radiation Oncology, Seoul, Korea Republic of ; <sup>2</sup>Hanyang University College of Medicine, Radiation Oncology, Seoul, Korea Republic of ; <sup>3</sup>Korea Institute of Radiological and Medical Sciences, Radiation Oncology, Seoul, Korea Republic of ; <sup>4</sup>Gyeongsang National University School of Medicine, Radiation Oncology, Jinju, Korea Republic of ; <sup>5</sup>Inha University Hospital, Radiation Oncology, Incheon, Korea Republic of

#### Purpose or Objective

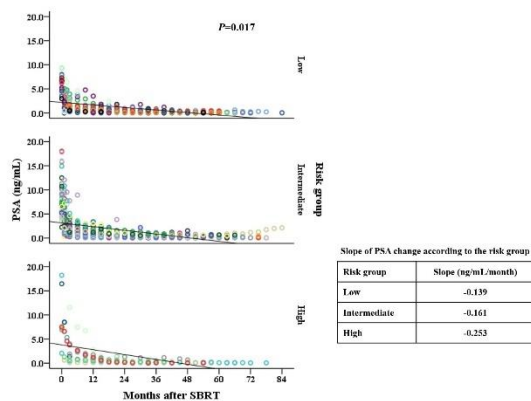
To evaluate the treatment outcome and prostate-specific antigen (PSA) change after stereotactic body radiotherapy (SBRT) for localized prostate cancer.

#### Material and Methods

Patients with localized prostate cancer treated with SBRT at three academic hospitals were enrolled. Treatment was delivered using Cyberknife with dose range from 35 to 37.5 Gy in 5 fractions. Biochemical failure (BCF) was assessed with Phoenix definition and toxicities were scored with Radiation Therapy Oncology Group (RTOG) toxicity criteria. The PSA kinetics were analyzed in patients who received no androgen deprivation therapy (ADT) and showed no recurrence.

#### Results

Of the total 88 patients, 14 patients (15.9%) received ADT. After median follow-up of 63.8 months, the 5-year BCF free survival (BCFFS) was 94.7%. Two patients experienced late grade  $\geq 3$  GI toxicities (2.2%). The median nadir PSA was 0.12 ng/mL and the median time to nadir was 44.8 months. Patients who reached nadir before 24 months showed poorer BCFFS than the others. The rate of PSA decline was maximum in the first year after treatment and gradually decreased with time. The pattern of PSA change was significantly different according to the risk groups ( $p=0.011$ ) with the slope of -0.139, -0.161 and -0.253 ng/mL/month in low-, intermediate- and high-risk groups, respectively (Figure)



#### Conclusion

SBRT for localized prostate cancer showed favorable efficacy with minimal toxicities. The time to PSA nadir was significantly associated with treatment outcome. PSA revealed rapid initial decline and slower decrease with

longer follow-up and the patterns of PSA changes were different according to the risk groups.

#### EP-1543 Early Results of a Phase 2 Multicentre Study of Linac-based Stereotactic Boost for Prostate Cancer

D. Pryor<sup>1</sup>, M. Sidhom<sup>2</sup>, S. Arumugam<sup>2</sup>, J. Buccicci<sup>3</sup>, J. Smart<sup>4</sup>, M. Grand<sup>2</sup>, P. Greer<sup>4</sup>, S. Keats<sup>2</sup>, L. Wilton<sup>4</sup>, M. O'Neill<sup>4</sup>, J. Martin<sup>4</sup>

<sup>1</sup>Princess Alexandra Hospital, Radiation Oncology, Brisbane, Australia ; <sup>2</sup>Liverpool Hospital, South Western Sydney Radiation Oncology, Sydney, Australia ; <sup>3</sup>St George Hospital, Radiation Oncology, Sydney, Australia ; <sup>4</sup>Calvary Mater Newcastle, Radiation Oncology, Newcastle- NSW, Australia

#### Purpose or Objective

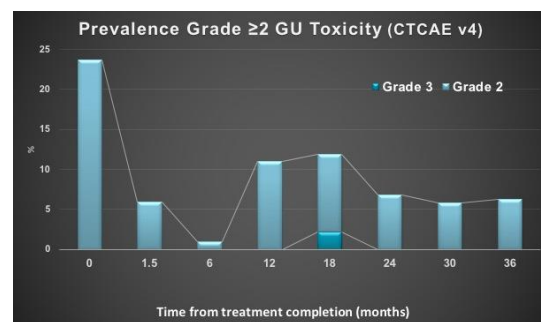
To report early toxicity and PSA kinetics following a novel, linac-based, stereotactic radiotherapy (SBRT) boost for a prospective multicentre phase 2 study (PROMETHEUS ACTRN12615000223538).

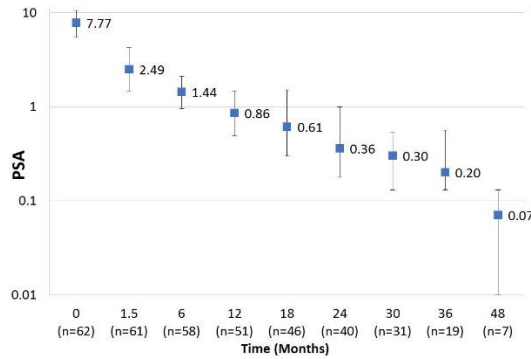
#### Material and Methods

Patients were treated with linac-based SBRT, 19-20 Gy in 2 fractions delivered one week apart, followed by conventionally fractionated IMRT/VMAT (46 Gy in 23 or 36 Gy in 12 fractions). MRI fusion for RT planning was mandated, as was rectal displacement during SBRT. Toxicity was prospectively graded using the Common Terminology Criteria for Adverse Events version 4.0 (CTCAE v4).

#### Results

Between 3/2014 and 10/2018, 134 patients (76% intermediate, 24% high-risk) with a median age of 70 years (range 53-85) have been treated across 5 centres. Short course ( $\leq 6$  m) ADT was used in 37%, long course in 17%. Rectal displacement method was SpaceOAR in 59% and Rectafix in 41%. 42 and 92 patients were treated at the 19 Gy and 20 Gy dose levels respectively. Median follow-up is 24 months. Acute G2 GI and GU toxicity occurred in 3% and 24% with no cases of acute G3 toxicity. Late  $\geq 2$  GI toxicity was 3%, 1% and 0% at 12, 24 and 36 months respectively. Only one G3 GI toxicity occurred (18 months post-RT). Late  $\geq 2$  GU toxicity at 6, 12, 18, 24 and 36 months was 1%, 11%, 12%, 7% and 6% respectively with only two G3 events (18 months post RT - figure 1). For patients not receiving ADT the median PSA value pre-treatment was 7.8 ug/L (range 1.1-20) and at 12, 24, 36 and 48 months post-treatment was 0.86, 0.36, 0.2 and 0.07 ug/L (figure 2).





### Conclusion

Delivery of linac-based SBRT boost is feasible and well tolerated with low rates of early toxicity and promising PSA responses. A second transient peak in moderate irritative GU toxicity was observed at 18 months. No urethral strictures have been reported to date. Longer term follow-up is required to document late toxicity and tumour control with this approach. A randomized trial comparing this approach with SBRT monotherapy is under development.

### EP-1544 Focal Linac-based SBRT Re-treatment for local recurrence of Ca P following previous definitive RT

G. Hruby<sup>1</sup>, A. Kneebone<sup>1</sup>, T. Eade<sup>1</sup>, A. Le<sup>1</sup>, J. Booth<sup>1</sup>, J. Hunter<sup>1</sup>, C. Kwong<sup>1</sup>, C. Brown<sup>1</sup>

<sup>1</sup>Royal North Shore Hospital, Radiation Oncology, Sydney, Australia

#### Purpose or Objective

to determine the safety and tolerability of focal linac based SBRT re-treatment with real time imaging for local only recurrence of prostate cancer after definitive RT

#### Material and Methods

A prospective, ethics approved feasibility and toxicity trial with nested sequential dose escalation component. In order to be eligible, men had to have biopsy proven recurrence limited to both PSMA-PET and mp-MRI region of suspicion and disease confined to less than half a lobe. We mandated a disease free interval of at least 4 years from initial RT and a PSA < 15 prior to enrolment.

#### Results

Between March 2016 and October 2018, 20 men were treated with 36 or 38Gy in 6 2nd to 3rd daily fractions. Two men had received LDR monotherapy and 2 HDR boost brachytherapy, the rest (16) EBRT. Median time from initial RT was 8 years (range 4.5-12). Original tumour details are presented in Table 1.

At focal SBRT, median age and PSA were 73 and 5.6 respectively. All 20 completed SBRT; 5, 3 and 2 men with grade 1 fatigue, GU and GI toxicity, respectively. All toxicity was self-limiting and to date there has been no late toxicity. 19 of 20 patients are biochemically controlled with PSA response. Nine men have undergone per-protocol repeat PSMA-PET at 12 months, only one (also with BF = PSA nadir +2) has failed within the prostate. Eight of 9 have demonstrated metabolic PSMA response to focal SBRT (see Figure 1).

Table 1: Tumour Features at original RT  
T stage NPSANGSNT190-10963T2910-204713T3220 or more783 91

Figure 1

16/11/2015 2 months before SBRT - local recurrence R lobe

3/6/2017: 12 months after SBRT re-treat

#### Conclusion

Our patients have tolerated treatment better than expected with no sub-acute or late toxicity. Biochemical and PSMA responses are promising. We continue to accrue patients at dose level 2 (38Gy in 6#).

### EP-1545 Prostate cancer EBRT: adaptive strategy and use of robust optimization for geometrical uncertainties

E. Ferrara<sup>1</sup>, D. Beldi<sup>1</sup>, J. Yin<sup>2</sup>, G. Loi<sup>3</sup>, M. Krengli<sup>1,4</sup>

<sup>1</sup>University Hospital "Maggiore della Carità", Radiotherapy, Novara, Italy; <sup>2</sup>Sichuan Cancer Center, Radiotherapy, Chengdu, China; <sup>3</sup>University Hospital "Maggiore della Carità", Medical Physics, Novara, Italy; <sup>4</sup>University of "Piemonte Orientale", Translational Medicine, Novara, Italy

#### Purpose or Objective

Intensity modulated radiotherapy is sensitive to errors, mainly due to steep beam dose gradients and organ motion. Conventional margins are often insufficient to ensure robustness of treatment plans. The aim of this work is to develop and validate a new adaptive treatment method for prostate cancer (PCa) radiotherapy (RT), using an off-line strategy to design a patient-specific internal target volume (ITV) based on the study of organ motion obtained by serial Cone-Beam CT (CBCT) images and management of the geometrical uncertainties with min-max robust optimization.

#### Material and Methods

20 patients (pts) with intermediate-high PCa treated with radical RT were enrolled in this study. The prescribed dose was 78 Gy to prostate (CTV78) and 60 Gy to prostate plus seminal vesicles (CTV60) delivering 2 Gy/fraction (fx). The CBCTs were acquired during the first 5 fxs, then once a week for the remaining treatment. The CBCTs were imported in the Raystation treatment planning system (TPS) and co-registered with the planning CT using the on-line match rigid transformations provided by the OBI system on the treatment unit (Varian Trilogy TX). Then the deformable image registration (DIR) algorithm ANACONDA was applied to propagate the CTV78 and CTV60 volumes from the reference planning CT to the first 5 CBCTs. The reliability of the DIR mapped ROIs was assessed by radiation oncologists and the contours were used to generate the ITV. The original plan was re-optimized using a min-max robust algorithm based on the worst scenario optimization assuming an isotropic 5 mm maximum setup error. Then CTV coverage and OARs sparing achieved with the robust plan (RP) were analyzed and compared with the original standard plan (SP) calculating the dose distributions on the residual CBCTs. For each isocenter perturbation of 1 mm, the dose was recalculated and the following parameters were acquired: D99, D98 and D95 to evaluate target volume coverage and mean dose and D2 to evaluate OARs doses.

#### Results

Our adaptive strategy and RP showed to achieve optimal coverage of CTV also in the worst scenario (geometric error up to 5 mm) with D99>95% of prescribed dose and significant less dose to rectum and bladder. The analysis on all the residual CBCT acquired during the treatment showed that CTV coverage of RP was statistically better than SP in terms of D99 and D98 (p=0.008 and p=0.02, Wilcoxon test). Statistically (T-student test) significant mean dose reduction and D2 reduction was noted for rectum (p<0.05) and for bladder (p<0.009). Moreover, RP appeared to be less sensitive to bladder and rectal filling.

#### Conclusion

Robust optimization is a feasible and safe approach in prostate treatment. It may be successfully used to adapt the treatment with better target coverage and OARs sparing than standard PTV based planning during the treatment course.

**EP-1546 Stereotactic radiotherapy for prostate bed recurrence after prostatectomy, a multicentric series**  
 G. Francolini<sup>1</sup>, B.A. Jereczek-Fossa<sup>2,3</sup>, V. Di Cataldo<sup>4</sup>, G. Simontacchi<sup>1</sup>, G. Marvaso<sup>3</sup>, M.A. Zerella<sup>2,3</sup>, C.I. Fodor<sup>3</sup>, L. Masi<sup>4</sup>, L. Livi<sup>5</sup>

<sup>1</sup>Azienda Ospedaliero Universitaria Careggi, Radiotherapy, Florence, Italy ; <sup>2</sup>University of Milan, Department of Oncology and Hemato-oncology, Milan, Italy ; <sup>3</sup>IEO European Institute of Oncology- IRCCS, Division of Radiotherapy, Milan, Italy ; <sup>4</sup>Istituto Fiorentino di Cura ed Assistenza, CyberKnife Center, Florence, Italy ; <sup>5</sup>Department of Experimental and Clinical Biomedical Sciences- University of Florence, Radiotherapy Unit, Florence, Italy

#### Purpose or Objective

Rate of biochemical recurrences in men affected by localized prostate cancer after radical prostatectomy (RP) ranges between 20 and 50%. Risk is particularly high for positive margins and poorly differentiated disease. Biochemical recurrence can be managed with curative purpose through salvage radiation therapy (SRT). However, Progression-free survival after conventional SRT approach, without concomitant androgen deprivation therapy (ADT), is 56% at 5 years. Moreover, likelihood of treatment failure in patients with pre-RT PSA values greater than 1.5 ng/ml is high, with PFS at 5 years of 18%. Positive metabolic imaging detecting local recurrence negatively impacts outcomes after SRT in this setting. Data from literature suggest that higher relapse-free survival is achieved by increasing radiation dose in patients undergoing SRT. Thus, when macroscopic recurrence is detected in prostatic bed through diagnostic imaging (MRI or CT-PET scan) improved local control may be achieved by extremely hypofractionated regimens. Here we present results from a multicentric retrospective experience including patients affected by macroscopic prostate bed recurrence and treated with stereotactic radiotherapy

#### Material and Methods

Data of 71 patients with prostate bed macroscopic recurrence treated in two institutions in Italy were reviewed. Recurrences were detected by MRI or CT-PET. Patients underwent stereotactic radiotherapy on prostate bed recurrence with a mean dose of 34.4 Gy (32.5-35 Gy) in 5 fractions, using Brainlab Veror<sup>®</sup> or Cyberknife<sup>®</sup> systems. Patients features, clinical outcomes and adverse events were reported. Biochemical failure after treatment was defined as increase of PSA levels of >10% if compared to pre-treatment value. Complete biochemical response after treatment was defined as PSA nadir <0.2 ng/ml. Univariate and multivariate analysis was performed through Cox regression model to explore the association between prognostic factors (Gleason score <7, Concomitant ADT, Time to recurrence <36 months and PSA at recurrence <1) and biochemical relapse-free survival (BRFS). Toxicity was reported according to CTCAE v

Mean age (years)	67,7
Gleason score at diagnosis	<7: 50 (70,4%)
	>7:19(26,8%)
pT Stage	N/A: 2 (2,8%)
	pT2: 37(52,2%)
	pT3: 32(45%)
	pT3a:20 pT3b:12 N/A: 2(2,8%)
pN Stage	N0/x: 64 (90,2%)
	N+: 5 (7%)
	N/A: 2 (2,8%)
Average PSA	Pre-RT: 2,3 ng/ml (0,14-16)
Concomitant ADT	Yes:12 (16,9%)*
	No:59 (83,1%)
TOTAL	71 (100%)

Table 1. Baseline population features

\*5 patients started ADT at SBRT, 7 patients had already ongoing ADT

#### 5.0

#### Results

71 patients were included, 16.9% were under ADT during treatment. Gleason score >7 and stage pT3 at diagnosis were reported in 26,8 and 45% of patients, respectively. Mean PSA at recurrence was 2,3 ng/ml, mean time to recurrence after RP was 98,6 months. Average volume of GTV was 10,8 cc (0,7-34,6). After an average follow up of 21.5 months 73

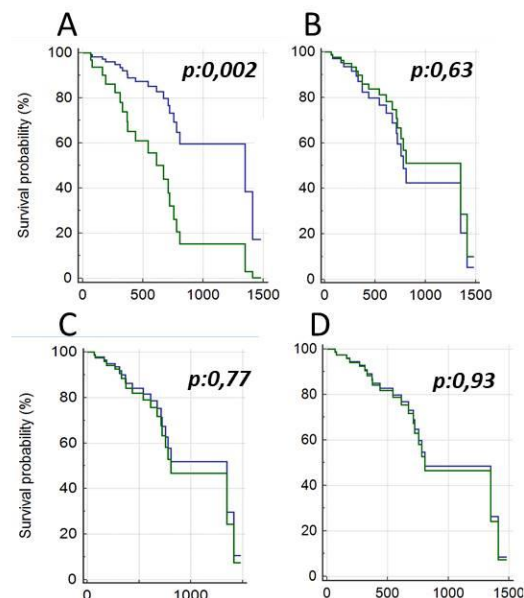


Fig.1: Multivariate analysis results. BRFS (days) in patients with Gleason score ≤/≥ 7(A), Time to macroscopic recurrence ≤/≥36 months (B), PSA at recurrence ≤/≥1 (C) and Concomitant ADT (D)

.1% of patients were free from recurrence and 49.3 % had complete biochemical response. Median BRF5 was 26 months (95% CI 23-46), Gleason score was the only prognostic independent factor associated with BRF5. Only 1 acute and 2 late G2 rectal and vesical toxicities were reported.

#### Conclusion

Stereotactic radiotherapy for prostate bed recurrence is safe and effective, regardless concomitant use of ADT and adverse prognostic factors. Prospective studies are needed to compare outcomes of conventional SRT to this technique

#### EP-1547 Developing an empirical nomogram for clinical visualization of DFS/OS for prostate cancer patients

R.M. Abdul<sup>1</sup>, E.P.P. Pang<sup>1</sup>, Y.S. Koh<sup>1</sup>, S.A. Gan<sup>1</sup>, J.K.L. Tuan<sup>1,2</sup>

<sup>1</sup>National Cancer Centre Singapore, Division of Radiation Oncology, Singapore, Singapore ; <sup>2</sup>Duke-NUS, Graduate Medical School, Singapore, Singapore

#### Purpose or Objective

To develop a predictive nomogram to provide clinical visualization on the probability of treatment outcomes [i.e. disease-free survival (DFS) and overall survival (OS)] for prostate cancer.

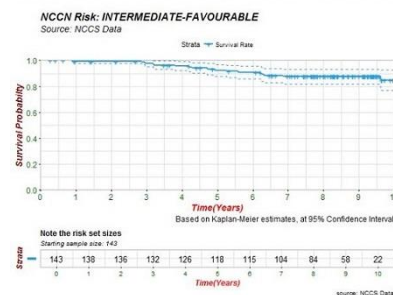
#### Material and Methods

This is a pilot longitudinal cohort study that analyzed 549 patients (enrolled in the DRO Cancer Registry) diagnosed with prostate cancer between 1998 and 2010. All the patients were stratified based on NCCN guidelines and have received radiotherapy up to 74Gy in 37# (+/- pelvic nodes irradiation). A multivariate analysis was conducted to predict DFS and OS as primary endpoints. Baseline prostate-specific antigen (PSA) level, T and N staging, Gleason scores (primary, secondary and total) were collected as independent prognostic factors in the building of this nomogram. Incidence of biochemical failure and death, along with its respective time from date of diagnosis to date of incidence, were tabulated to provide a binary predictor (SSMS, Microsoft). This is then input into a script utilizing R (survival), by using the Kaplan-Meier (K-M) survival estimate model. The resulting data output are then published on SQL Server Reporting Services (SSRS, Microsoft) to provide a visual representation of the model.

#### Results

Output from R provides a 95% Confidence Interval on DFS and OS based on input of the independent variables. A K-M survival curve (Figure 1), as well as a visual presentation based on a sample size of 100 patients of 5-year or 2-year survival estimates are displayed for facilitation of patients' meaningful understanding of the results (Figure 2). However, there were wide confidence variances for certain stratified groups with small sample size.

This graph is an estimation of survival rates up to 10 years after diagnosis. Results are based on selected inputs.

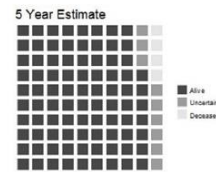


Probability of disease-free survival upon diagnosis, based on 143 patients:

At 2 years: ~98.5% (96.5% to 100.0%)

At 5 years: ~91.7% (87.0% to 96.4%)

At 10 years: ~More data required (Insufficient Data to compute accurately)



In a group of 100 patients with the same characteristics as selected, 87 to 96 of them are likely to not experience Biochemical Failure 5 years from their diagnosis.

These estimates are based on the real world outcome of patients treated in our institutions. Your exact experience may differ within the limits of this prediction. Survival estimates can be unreliable the further into the future prediction is made as there are less patients to base this estimate on

Report Generated on 15 Oct 2018, 08:16 AM

#### Conclusion

We have developed a cohort-based nomogram that served as a tool to facilitate the shared-decision making discussion between clinicians and patients on the management options.

#### EP-1548 Patterns of progression in metastatic prostate cancer: who might benefit from targeted radiotherapy? P. Patel<sup>1</sup>, N. Tunariu<sup>2</sup>, A. Tree<sup>1</sup>

<sup>1</sup>Royal Marsden NHS Foundation Trust- London and the Institute of Cancer Research, Clinical Oncology, London, United Kingdom ; <sup>2</sup>Royal Marsden NHS Foundation Trust- London and the Institute of Cancer Research, Radiology, London, United Kingdom

#### Purpose or Objective

Treatment for metastatic castrate-resistant prostate cancer (mCRPC) patients has rapidly changed since the introduction of androgen receptor targeted therapies (ART) such as Abiraterone and Enzalutamide. These treatments are better tolerated and have less toxicities compared to chemotherapies used. Therefore, methods of maintaining patients on these oral medications are of great interest. The aim of this study was to document patterns of progression of patients on ART and to identify the number of patients potentially amenable to Stereotactic body radiotherapy (SBRT) for oligo-progressive disease (OPD). OPD is a relatively newly described disease state whereby 1-3 metastatic lesions are progressing/new whilst all other sites of disease are well-controlled by a systemic agent. Theoretically SBRT to OPD lesions could allow continued therapeutic benefit of these oral treatments.

#### Material and Methods

This is a single centre retrospective cohort study. Data was collected from electronic patient records from the first 50 patients treated with ART for mCRPC between April 2015 - 2017. Data including patient demographics, tumour staging, radiological and symptomatic response to ART, PSA trend, and progression pattern on serial imaging were collected.

#### Results

This study analysed 50 patient records. The median age of patients was 81 years. Median PSA at presentation was 26. At the time of analysis 37 patients had progressed on ART, and 5 remained in remission. Four patients stopped treatment due to toxicity, 1 patient transferred care and 3 patients died due to other causes. Of those patients who had progressed 6 patients (12%) demonstrated OPD. Further details of the patients demonstrating OPD is represented in Table 1. Patient no.1 was treated with SBRT twice for OPD occurring 3 years apart. Patient no. 4 demonstrated further OPD 6 months later. The majority of patients remained asymptomatic at the time of OPD, 2 patients presented with related pain not requiring intervention. OPD lesions were detected by multiple different imaging modalities including CT, Whole body diffusion weighted MRI (WBDWMRI) and PET/CT.

Patient number	No. of sites of OPD	Sites of OPD	Type of scan detecting OPD	Suitability for SBRT	Treatment of OPD
1	1	Retroperitoneal lymph node	CT	Yes	SBRT 30Gy/5#
2	3	Thoracic vertebra T1, T6 Lumbar vertebra L1	WBDWMRI	Yes	Continuation of abiraterone + dexamethasone
3	1	Retroperitoneal lymph node	CT	Yes	Continuation of abiraterone
4	1	Prostate	Choline PET/CT	No-previous EBRT	Continuation of abiraterone + prednisolone
5	1	Pelvic lymph node	Choline PET/CT	Yes	Switched to abiraterone + dexamethasone
6	1	Inguinal lymph node	CT	Yes	Stopped systemic treatment

**Conclusion**

OPD is prevalent in mCRPC patients on Abiraterone/Enzalutamide. The majority of OPD occurred in non-bone metastases and a range of imaging techniques can be used to identify OPD. Most patients were asymptomatic at the time of OPD and had disease suitable for SBRT. The TRAP trial (NCT03644303) is currently testing the role of SBRT to sites of OPD in mCRPC.

**EP-1549 Clinical outcomes of image-guided radiotherapy in intermediate to high risk prostate cancer**

C. Chen<sup>1</sup>, H. Chuang<sup>2</sup>, M. Huang<sup>3</sup>

<sup>1</sup>Kaohsiung Medical University, Graduate Institute of Medicine- College of Medicine, Kaohsiung City, Taiwan ; <sup>2</sup>Kaohsiung Medical University, Faculty of Department of Public Health- College of Health Science, Kaohsiung City, Taiwan ; <sup>3</sup>Kaohsiung Medical University, Radiation Oncology, Kaohsiung City, Taiwan

**Purpose or Objective**

To report the long-term survival outcomes and late toxicities resulted from curative image-guided radiotherapy (IGRT) for prostate cancer patients with and without androgen deprivation therapy (ADT).

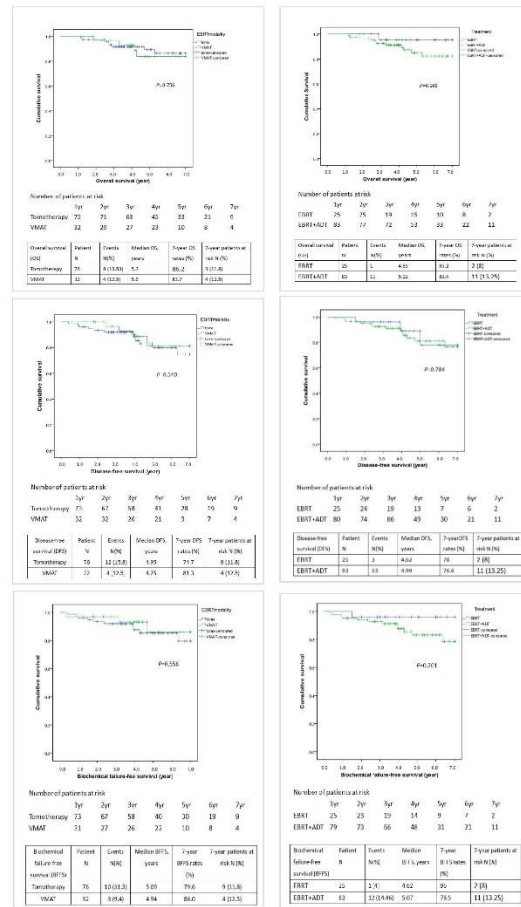
**Material and Methods**

The study included 108 patients with pathologically proven prostate adenocarcinoma who underwent IGRT between 2008 and 2014. Age ranged from 54 to 89 with a median age of 75 years. Twenty-nine patients were in the intermediate-risk group and 79 were in the high-risk group. The biochemical failure was defined by a rise of 2 ng/mL or more above the nadir PSA. The nadir was defined as lowest PSA value preceding a given threshold of 0.2 ng/mL or as absolutely lowest PSA before the transient bounce. Gastrointestinal (GI) and genitourinary (GU) toxicities were assessed and documented in agreement with the Common Toxicity Criteria Adverse Events version 3 (CTCAE v.3.0). Cox regression model and Kaplan-Meier curves were calculated, and the log-rank test was used to evaluate the differences of overall (OS), biochemical failure free (BFFS), disease free (DFS), locoregional failure free (LRFS) and distant metastases-failure free (DMFS) rates between two different modalities of radiotherapy.

**Results**

Among 108 patients, 32 patients (29.6%) were treated with RapidArc and 76 patients with Helical Tomotherapy. The mean radiation dose was 75 Gy. The median follow-up was 4.43 years (range, 417-3330 days). Two patients (2.8%, 2/72) in the EBRT-ADT group developed late GI complication 20 months after EBRT. There was no late GU complication. All patients tolerated the IGRT without any interruption. The 5-year OS, DFS, BFFS, LRFS and DMFS rates were 83.7%, 81.3%, 86.0%, 92.4% and 100.0% for the RapidArc group while 89.2% (P = 0.635), 80.1% (P = 0.747),

85.3% (P = 0.681), 95.5% (P = 0.338) and 91.7% (P = 0.129) for the Tomotherapy group.



**Conclusion**

There exists no statistically significant difference in the rates of locoregional recurrence, distant metastasis, biochemical control and overall survival when comparing RapidArc with Tomotherapy. IGRT was well tolerated with small late GU and GI toxicity.

**EP-1550 Give-me-five trial: toxicity assessment in ultra-hypofractionated prostate cancer radiotherapy**

D. Ciardo<sup>1</sup>, G. Marvaso<sup>1</sup>, S. Gandini<sup>2</sup>, M. Mambretti<sup>1</sup>, C. Fodor<sup>1</sup>, D. Zerini<sup>1</sup>, S. Volpe<sup>1,3</sup>, G. Riva<sup>1,3</sup>, D.P. Rojas<sup>1</sup>, G. Petralia<sup>4</sup>, R. Cambria<sup>5</sup>, R. Orecchia<sup>6</sup>, B.A. Jereczek-Fossa<sup>1,3</sup>

<sup>1</sup>IEO- European Institute of Oncology IRCCS, Department of Radiation Oncology, Milan, Italy ; <sup>2</sup>IEO- European Institute of Oncology IRCCS, Division of Epidemiology and Biostatistics, Milan, Italy ; <sup>3</sup>University of Milan, Department of Oncology and Hemato-Oncology, Milan, Italy ; <sup>4</sup>IEO- European Institute of Oncology IRCCS, Department of Radiology, Milan, Italy ; <sup>5</sup>IEO- European Institute of Oncology IRCCS, Unit of Medical Physics, Milan, Italy ; <sup>6</sup>IEO- European Institute of Oncology IRCCS, Scientific Direction, Milan, Italy

**Purpose or Objective**

To evaluate genitourinary (GU) and gastrointestinal (GI) toxicity after ultra-hypofractionated prostate cancer (PCa) radiotherapy.

**Material and Methods**

As a part of the prospective phase II Give-me-five trial, 65 PCa patients underwent volumetric modulated arc therapy with simultaneous integrated boost to the dominant

intraprostatic lesion (DIL). The treatment scheme was 36.25-37.5 Gy/5 fractions to the whole prostate gland and to the DIL, respectively.

Univariate and multivariate logistic regression models were applied to identify independent factors associated with toxicity adjusting for confounding factors. The systematic analysis of urinary bladder and rectum dose-volume histograms (DVHs) was performed with Fisher exact test. The correlation between the relative volume receiving a given absolute dose and acute toxicity was investigated, with cutoffs at grade G>0 and G>1.

**Results**

Sixty-five patients fulfilled the inclusion criteria. At 1-month after the end of radiotherapy, 42 patients (65%) had no GU toxicity, whereas 18 (28%), 4 (6%) and 1 (1%) patients had G1, G2 and G3 GU toxicity. As concerning GI toxicity, 54 (83%) patients had no toxicity, whereas 11 (17%) reported G1 toxicity.

IPSS changed significantly (P<0.05) from baseline to 1 month and changes during time are significantly different by symptomatic score at first month (mild, moderate and severe, P<0.0001).

At univariate analysis (Table 1), no relationship was found between the prostate volume and acute GU (P=0.97) or GI toxicity (P=0.83), nor between the urinary bladder volume and any grade of acute GU toxicity (P=0.60) whereas the correlation between the rectum volume and any grade of acute GI toxicity was at the boundary of statistical significance (P=0.05).

At multivariate analysis adjusting for age and the presence of severe concomitant disease, IPSS at 1 month is positively significantly associated with acute GU G≥1 toxicity (P=0.03), whereas rectum volume is only borderline significantly associated with GI G≥1 toxicity (P=0.06). Prostate volume is not significantly associated with any toxicity (P=0.78).

For urinary bladder, the area of DVH between 17-24 Gy vs. volume 12-22% was correlated with any acute GU toxicity and the region between 25-35 Gy vs. volume 2-6% was correlated with acute G>1 GU toxicity. As concerning the relation between rectum DVH and GI toxicity, the portion between 18-34 Gy was correlated with any acute GI toxicity (Figure 1).

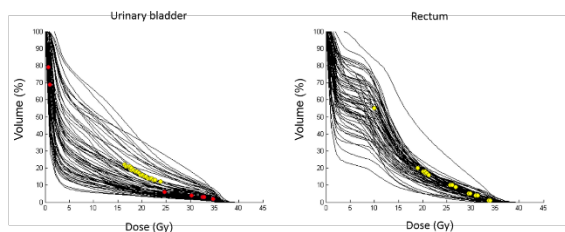


Figure 1 – Dose volume histograms of urinary bladder (left panel) and rectum (right panel) for all patients. Coloured points represent dose-volume combinations that statistically significantly correlate with acute genito-urinary (left panel) and gastro-intestinal (right panel) toxicity at Fisher's Exact Test. In particular, yellow points refer to any-grade toxicity (G>0) and red points refer to grade G>1 toxicity.

Table 1 - Univariate logistic regression evaluating the probability of acute genito-urinary (GU) and gastro-intestinal (GI) toxicity for urinary bladder and rectum, respectively. Values in table represent median and interquartile range, in brackets.

		All	No GU toxicity (n = 42)	Any GU toxicity (n = 23)	P-value
Urinary bladder	V <sub>18Gy</sub> (%)	12.4 (7.6, 18)	12.1 (7.6, 20.9)	12.4 (7.3, 17.4)	0.366
	V <sub>29Gy</sub> (%)	0.8 (0.36, 1.3)	0.8 (0.3, 1.3)	0.7 (0.36, 1.3)	0.269
	Bladder volume (cm <sup>3</sup> )	341 (226, 485)	354 (211, 470)	331 (242, 579)	0.602
	Prostate volume (cm <sup>3</sup> )	43 (33, 56)	41 (33, 53)	44 (33, 58)	0.828
Rectum	All		No GI toxicity (n = 54)	Any GI toxicity (n = 11)	P-value
	V <sub>18Gy</sub> (%)	20.9 (16.4, 23.5)	21 (16.4, 23.9)	19.6 (14.9, 21.2)	0.466
	V <sub>29Gy</sub> (%)	5.6 (4.0, 6.7)	5.8 (4.5, 7)	4.9 (3.7, 5.6)	0.164
	V <sub>35Gy</sub> (%)	1.5 (0.85, 2.9)	1.6 (0.9, 3)	1.1 (0.6, 1.6)	0.132
	V <sub>36Gy</sub> (%)	0.01 (0.0, 0.2)	0.02 (0.0, 0.3)	0.0 (0.0, 0.0)	0.146
	Rectum volume (cm <sup>3</sup> )	62 (50, 82)	56 (48, 81)	77 (69, 94)	0.051
	Prostate volume (cm <sup>3</sup> )	43 (33, 56)	43 (35, 53)	47 (26, 58)	0.969

Abbreviations: V<sub>18Gy</sub> = volume receiving 18 Gy; V<sub>29Gy</sub> = volume receiving 29 Gy; V<sub>35Gy</sub> = volume receiving 35 Gy; V<sub>36Gy</sub> = volume receiving 36 Gy; GI = genitourinary toxicity; GU = gastrointestinal toxicity.

**Conclusion**

The acute toxicity profile after ultra-hypofractionated radiotherapy for PCa is satisfactory. Prostate volume does not affect the toxicity probability.

The analysis will be extended to early and late toxicity (1-year minimum follow-up) and the systematic analysis of DVHs will be used to infer exploratory constraints for ultra-hypofractionated PCa radiotherapy.

**EP-1551 Interpretation of T3 found after MRI in low-intermediate risk patients with prostate adenocarcinoma.**

C. García Torres<sup>1</sup>, L.A. Glaría Enríquez<sup>1</sup>, A. Escribano Uzcudum<sup>1</sup>, R. Morera López<sup>1</sup>

<sup>1</sup>Hospital Universitario La Paz, Radiotherapy Oncology, Madrid, Spain

**Purpose or Objective**

Multiparametric magnetic resonance (mpMR) is the best imaging technique to achieve precise delimitation of disease-affected areas in PCa.

Urological guidelines do not systematically recommend MRI at low risk stage of prostate cancer, because of its low sensitivity to detect focal extra-prostatic extension (EPE) disease and cost.

After mpMR of low risk PCa patients, EPE data could be found (rmT3).

The finding of rmT3 upgrades the patient to high-risk group, which should change the type of treatment. This change of decision also implies exposing the patient to a greater risk of adverse events (AEs) related to the treatment. However in this group 85-95% is free of biochemical recurrence at 10 years, with any standard treatment.

Objective:

- 1- Determinate the percentage of low-risk patients studied with mpMR have EPE disease (T3)
- 2- Determinate factors associated to upstage of T after mpMR.

**Material and Methods**

We have retrospectively analyzed 58 patients diagnosed of low-risk prostate adenocarcinoma or favorable-intermediate risk, with PSA <20ng/ml and studied with mpMR.

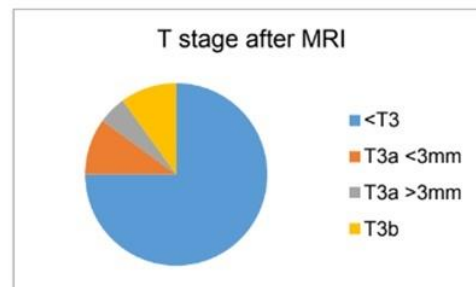
We use risk group classification according to NCCN 2018. Those with very low risk (VLR), low risk (LR) and favorable-intermediate (FI) were grouped as low risk. The definition of grade group (GG) according to AJCC 2010 was used.

Related to stage, we will group patients in <T3 (when none EPE is found after MRI), and T3 when there is some grade of EPE. The rmT3a was classified in focal T3a (<3mm of EPE) and extended T3a (>3mm of EPE) and T3b when seminal vesicle invasion is found.

**Results**

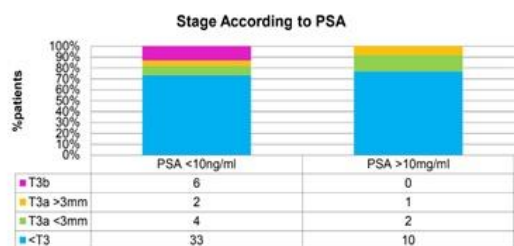
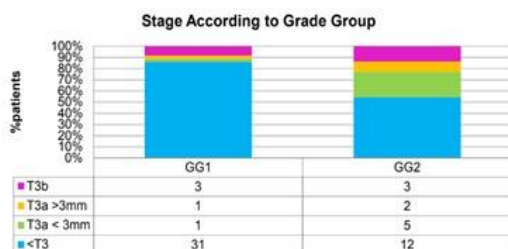
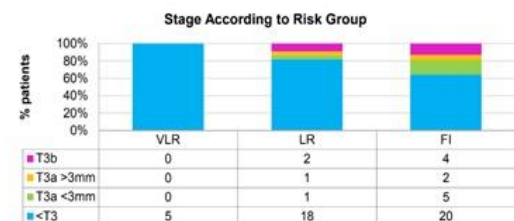
The mean age was 68.9 years (+/- 8.47 years). Among these patients, 36 (62.1%) belonged to GG1 and 22 (37.9%) corresponded to GG2.

After mpMR was performed 25% of patients presented some grade of EPE, becoming a locally advanced stage (T3a-T3b).



Patients were analyzed according to Risk Group: very low, low or intermediate. None very-low-risk patients (5 in total) increased their stage after mpMR. In low-risk

patients and in favorable-intermediate risk, 18.2% and 35.5% patients after mpMR upgrade to T3, respectively. We observe that among GG1 patients, 14 % and GG2 45.5% increased their stage. In patients with PSA <10ng/ml, 13.3% had an increase in stage. Between patients with PSA >10ng/ml, 23% upgrade to T3 after mpMR.



## Conclusion

According to the results obtained, we observed that 25% of patients diagnosed of localized prostate cancer with low-intermediate risk upgrade T stage after MRI. Switching to T3 stage of any type after MRI is more frequent in Grade 2 patients and favorable-intermediate risk groups. Grouping extended T3a and T3b we obtain 15.52.% (n=9). This percentage of more extended occult disease is close to historically reported recurrence (15- 25%). That is, with high reliability 15% of low- risk patients upgrade to high-risk groups. Without MRI, these patients could be undertreated according to a poor initial stage with the usual methods, which could be the cause of recurrence and subsequent metastasis.

## EP-1552 Impact of MRI on prostate cancer risk classification: game changer for therapeutic decision making?

C. Draulans<sup>1,2</sup>, W. Everaerts<sup>3,4</sup>, S. Isebaert<sup>1,2</sup>, G. Thomas<sup>4</sup>, R. Oyen<sup>5,6</sup>, S. Joniau<sup>3,4</sup>, E. Lerut<sup>6,7</sup>, L. De Wever<sup>5</sup>, B. Weynand<sup>6,7</sup>, E. Vanhoutte<sup>5</sup>, G. De Meerleer<sup>1,2</sup>, K. Haustermans<sup>1,2</sup>

<sup>1</sup>University Hospitals Leuven, Department of Radiation Oncology, Leuven, Belgium ; <sup>2</sup>KU Leuven, Department of Oncology, Leuven, Belgium ; <sup>3</sup>University Hospitals Leuven, Department of Urology, Leuven, Belgium ; <sup>4</sup>KU Leuven, Department of Development and Regeneration, Leuven, Belgium ; <sup>5</sup>University Hospitals Leuven, Department of Radiology, Leuven, Belgium ; <sup>6</sup>KU Leuven, Department of Imaging and Pathology, Leuven, Belgium ; <sup>7</sup>University Hospitals Leuven, Department of Histopathology, Leuven, Belgium

## Purpose or Objective

To investigate the impact of magnetic resonance imaging (MRI) information on clinical staging, risk stratification and treatment recommendations for prostate cancer (PCa) according to the European Association of Urology (EAU) guidelines.

## Material and Methods

We performed a single-centre analysis of 180 men with PCa, undergoing clinical staging by digital rectal examination (DRE) as well as MRI before their robot-assisted radical prostatectomy between April 2016 and December 2017. Patients were stratified according to the EAU guidelines based on their clinical T-stage assessed by either DRE or MRI, initial prostate specific antigen (iPSA) value and Gleason score. Furthermore, to combine the best of both world, we created a combined clinical T-stage definition and investigated its accuracy. This combined clinical T-stage takes into account the DRE-based clinical staging for peripheral zone tumours, except for anterior located tumours not detected by DRE (cT1c). In this case, as well as for tumours with a transitional zone tumour component, the combined clinical T-stage is determined by MRI-based clinical T-staging. Differences in risk classification and recommended optimal duration of concomitant androgen deprivation therapy (ADT) between DRE- and MRI-staging were analysed using a paired-samples sign test. In all analysis of differences, a statistical significance level of p<0.05 was used.

## Results

Use of MRI information instead of DRE information leads to significant upstaging of clinical T-stage (33%) and EAU risk grouping (31%). When comparing these results with the pT-stage after histopathological evaluation, MRI showed a significantly higher sensitivity than DRE to detect non-organ-confined PCa (59% vs. 41%; p<0.01). In contrast the specificity of MRI was significantly worse than DRE (69% vs. 95%; p<0.01). The combined clinical T-stage approach (DRE-MRI) showed a sensitivity of 58% and a specificity of 79% to detect non-organ-confined PCa. Incorporation of MRI only information in the treatment decision process based on the EAU guidelines would alter the choice of surgical treatment in 49/180 patients (27%) with in most cases less nerve-sparing surgery (46/180 patients (26 %)). When we focus on radiation treatment with concomitant ADT, the treatment would be intensified in 46/180 patients (26%) with ADT prolongation as a result of upstaging by MRI. When the combined clinical T-stage approach (DRE-MRI) would be used, treatment would be intensified in 36/180 patients (20%).

## Conclusion

The incorporation of MRI information substantially affects the treatment choice in PCa patients as compared to using the current available EAU guidelines based on DRE information. More specifically, treatment intensification would be recommended in 1 out of 4 patients. Hence, there is a clear need for contemporary, updated MRI-based stratification tools and treatment guidelines to avoid overtreatment. Currently, a combined DRE-MRI-based assesment could be a pragmatic approach for cT-staging of PCa tumours.

## EP-1553 High-dose hypofractionated helical IG-IMRT in high-risk prostate cancer patients

N.G. Di Muzio<sup>1</sup>, C.L. Deantoni<sup>1</sup>, F. Zerbetto<sup>1</sup>, C. Cozzarini<sup>1</sup>, S. Broggi<sup>2</sup>, P. Mangili<sup>2</sup>, A. Chiara<sup>1</sup>, I. Dell'Oca<sup>1</sup>, A.M. Deli<sup>1</sup>, R. Calandrino<sup>2</sup>, C. Fiorino<sup>2</sup>, A. Fodor<sup>1</sup>  
<sup>1</sup>San Raffaele Scientific Institute, Department of Radiotherapy, Milan, Italy ; <sup>2</sup>San Raffaele Scientific Institute, Medical Physics, Milan, Italy

## Purpose or Objective

Recently Kishan and co-workers (JAMA 2018) demonstrated that high-risk prostate cancer patients treated with dose-escalated external beam radiotherapy and more than 24 months of androgen deprivation have

better outcomes than surgical patients. Here we report the results of our experience with high-dose hypofractionated helical Image Guided-Intensity Modulated Radiotherapy (IG-IMRT) (Tomotherapy, Accuray, Wisconsin) in high-risk prostate cancer (HR PCA) patients (pts).

#### Material and Methods

One hundred thirty-three HR PCA pts treated with hypofractionated helical IG-IMRT from April 2006 to July 2015 were included in this analysis. HR PCA was defined as the presence of one or more of the following characteristics: Gleason Score  $\geq 8$ , and/or initial PSA  $\geq 20$  ng/ml, and/or clinical stage  $\geq$  T3b. Seventeen pts had radiologically positive nodes (N1). The median age of the patients was 75 (range: 57-90) years. They were treated on pelvic lymph nodes (including common iliac chain) to a total dose of 51.8 Gy, with simultaneous integrated boost (SIB) on prostate and seminal vesicles to 74.2 Gy in 28 fractions, delivered in 5 ½ weeks. The 2 Gy equivalent dose, considering the accepted a/b ratio of 1.5 for prostate cancer, is 88 Gy. Androgen deprivation therapy (ADT) was prescribed to 121/133 pts for a median of 38 (0-120) months (pts with biochemical failure during ADT continued the hormonal treatment). In NO pts ADT was prescribed for median of 32 months. Median initial PSA was 16 (1.41-826.00) ng/mL.

#### Results

With a median follow up of 60 (11.8-145.2) months, biochemical relapse free survival (bRFS) was 79.7% and distant metastasis free survival (DMFS) was 86.5%. Overall survival was 69.2%, and cancer specific survival (CSS) was 91.7%. Important differences were registered between NO and N1 pts (see Table 1). Gastro-Enteric (GE) acute grading (G)  $\geq 2$  toxicity was 6 %, G3 only 0.8%. Genito-Urinary (GU) acute G $\geq 2$  toxicity was 30.1%, G3 only 0.8%. Late toxicity was as follows: GE $\geq$  G2 12.8%, G3 3%; GU $\geq$  G2 21.1%, G3 9%, but with spontaneous or therapeutic resolution, thus only 3.8% of pts presented G3 GU toxicity at the last follow up.

Patients	bRFS	DMFS	CSS
High Risk, NO	82.8%	89.7%	94.8%
N1	52.9%	58.8%	70.6%

#### Conclusion

Our results confirm that high-risk prostate cancer patients, most of them not suitable for surgery due to comorbidities, irradiated on pelvic lymph nodes with dose-escalation on prostate, associated to androgen deprivation, obtain good 5-year biochemical control, with acceptable acute and late toxicity. Positive lymph nodes pts present worse outcomes.

#### EP-1554 Twice vs thrice-weekly moderate hypofractionated EBRT for PCa: does overall treatment time matter?

V. Achar<sup>1</sup>, S. Jorcano<sup>2</sup>, M. Rouzaud<sup>1</sup>, L. Escude<sup>2</sup>, R. Miralbell<sup>1</sup>, T. Zilli<sup>1</sup>

<sup>1</sup>Hopitaux Universitaires Geneve, Radio-oncology, Geneva, Switzerland ; <sup>2</sup>Teknon Oncologic Institute, Radiation Oncology, Barcelona, Spain

#### Purpose or Objective

For prostate cancer the influence of overall treatment time (OTT) remains a controversial issue. Although a protracted OTT may have a detrimental effect on long-term disease control with standard fractionation, its impact on outcome has never been explored in moderate hypofractionation. Furthermore, changes in dose per fraction and OTT can impact tolerance and treatment-related side-effects.

This study is aiming to evaluate the influence of OTT in disease control, acute, and long-term side effects with

moderate hypofractionated external beam radiotherapy (RT) for prostate cancer delivered either twice or thrice a week.

#### Material and Methods

From 2003 to 2017, 157 patients with localized prostate cancer and an estimated risk of nodal metastases of  $\leq 20\%$  were treated consecutively on the prostate  $\pm$  seminal vesicles with 56 Gy in 4 Gy-fractions delivered either twice (86 patients, from 2003 to 2010, group-1) or thrice (71 patients, from 2010 to 2017, group-2) a week using IMRT or VMAT techniques. Median OTT for group-1 and group-2 were 46 (range, 38-90) and 30 (range, 29 to 40) days, respectively. Sixty-one patients (39%) received, in addition, neoadjuvant and concomitant androgen deprivation (median duration of 6 months). Gastrointestinal (GI) and genitourinary (GU) toxicities were scored according to the Common Terminology Criteria for Adverse Events version 3.0 grading scale. Biochemical relapse-free survival (bRFS) was assessed using the Phoenix definition. The median follow-up time was 110 and 56 months for group 1 and 2, respectively.

#### Results

At 6 weeks, patients treated thrice-a-week experienced higher acute  $\geq$  grade-2 GU toxicity compared to those treated twice-a-week (25.4% vs 5.8%,  $p=0.001$ ) even though none presented  $\geq$  grade-3 GU or GI toxicity in the thrice-a-week group. Although, 5-year  $\geq$  grade-2 late GU toxicity-free survival was higher in group-1 (95.9% $\pm$ 2.3%) than in group-2 (81.5 $\pm$ 4.9%,  $p=0.003$ ), the long range GU toxicity was not different between both groups. Furthermore, no differences in  $\geq$  grade-2 late GI toxicity-free survival were observed between both groups (97.5 $\pm$ 1.7% vs. 97 $\pm$ 2.1% for groups1 and 2, respectively). The 5-year bRFS was not different for patients treated twice compared to those treated thrice-a-week (80.6 $\pm$ 4.5% vs. 85.3 $\pm$ 4.8%, respectively  $p=0.441$ ), as much as for patients treated in  $>5$  weeks vs. those treated in  $\leq 5$  weeks (81.3 $\pm$ 4.4% vs. 84.4 $\pm$ 5.1%, respectively  $p=0.584$ ).

#### Conclusion

Less vs. more than 5 weeks OTT may increase acute and late GU side effects without significantly improving bRFS in patients treated to high effective doses ( $>80$  Gy) with moderate hypofractionated RT for prostate cancer. However, the similar prevalence of side effects in the long range for both groups of patients may favor that patients find more convenient to be treated in 5 rather than 7 weeks. The role of OTT on long-term outcome and toxicity of prostate cancer patients treated with hypofractionation deserves further prospective evaluation.

#### EP-1555 Precision of deformable image registration for high-field MR-Linac treatment of prostate cancer

R.L. Christiansen<sup>1,2</sup>, L. Dysager<sup>3</sup>, O. Hansen<sup>2,3</sup>, C. Brink<sup>1,2</sup>, B. Uffe<sup>1,2</sup>

<sup>1</sup>Odense University Hospital, Laboratory of Radiation Physics, Odense, Denmark ; <sup>2</sup>University of Southern Denmark, Department of Clinical Research, Odense, Denmark ; <sup>3</sup>Odense University Hospital, Department of Oncology, Odense, Denmark

#### Purpose or Objective

Online radiotherapy (RT) plan adaption requires re-delineation of target and organs at risk (OAR), while the patient is on the treatment couch. Automated deformable image registration (DIR) resulting in deformation of the planned target and OAR delineations will potentially minimize time spent on re-planning if deformation of these structures is sufficiently accurate for clinical use. This study investigates the precision of automatically deformed structures with manually defined structures in high-risk prostate cancer patients.

#### Material and Methods

The study includes six high-risk prostate patients referred for curative RT and prescribed 78 Gy to the prostate and the proximal 2 cm of the seminal vesicles (SV) and 56 Gy

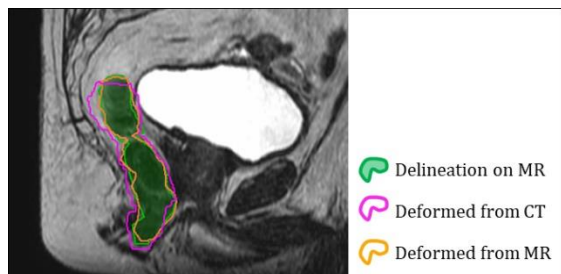
to the elective lymph node region (CTV56) in 39 fractions. The patients were CT- and MR-scanned (T2 weighted 3D sequence) for treatment planning and additionally MR scanned at the 10<sup>th</sup>, 20<sup>th</sup> and 30<sup>th</sup> treatment fraction. On each scan, target structures were defined by an experienced oncologist who also validated the OARs defined by an experienced RTT. For evaluation of intra-observer variability, all structures were re-delineated on one MR image set per patient at least 30 days after the initial delineations were performed.

Delineations and DIRs were performed in Monaco v 5.40 (Elekta AB, Sweden) treatment planning system (TPS) dedicated to the high field MR-Linac treatment. Structures defined on the planning CT and MR were deformed to the additional MR scans resulting in total 18 CT-MR and 18 MR-MR DIRs.

Agreement of deformed structures with the gold standard manual delineations was evaluated by mean surface distance (MSD) and Dice similarity coefficients (DSC). Differences between mean DSC and MSD of CT-MR and MR-MR deformation, respectively, were tested with paired t-tests for each structure set.

### Results

An example of a rectum structure delineation as well as CT- and MR-based deformation is shown in the figure. In total, 285 structures were deformed successfully, while three bladder structures were not created because the TPS' inability to deform ring structures. All mean DSC between deformed and manually delineated structures were better for MR-MR than CT-MR DIR, as seen in the table. Also, MSD was 0.6 - 1.3 mm lower for all deformed structures based on MR relative to CT. Overall, CT-MR deformed structures showed lesser DSC and higher MSD than the intra-observer variation. MR-MR deformed structures showed DSC and MSD of similar magnitude to those of intra-observer variations.



The figure shows the delineation of rectum made on an MR scan made at the 10<sup>th</sup> fraction along with deformed delineations originating from planning MR and CT scans.

Structure	DSC			MSD			Intra-obs. var.		
	Unit	CT-MR [index]	MR-MR [index]	p-value	CT-MR [mm]	MR-MR [mm]	p-value	DSC	MSD
Prostate		0.84	0.91	< 0.001	1.82	1.09	< 0.001	0.91	0.96
SV		0.63	0.77	0.02	2.01	1.00	0.06	0.78	1.06
CTV56		0.78	0.84	0.04	3.29	2.11	0.06	0.85	1.71
Rectum		0.73	0.86	0.005	3.06	1.80	0.006	0.93	0.85
Bladder		0.87	0.91	0.11	2.19	1.36	0.01	0.96	0.80
Femoral head R		0.90	0.94	0.03	1.46	0.91	0.03	0.93	1.06
Femoral head L		0.90	0.93	0.06	1.62	1.06	0.07	0.91	1.41
Penile bulb		0.61	0.76	0.23	1.75	1.07	0.33	0.80	1.02

DSC and MSD are given as the mean for all deformations within all patients for each structure. Resulting p-values for test of difference between CT-MR and MR-MR deformation are listed for DSC and MSD. DSC and MSD of each structure is given to evaluate intra-observer variation in delineation on MR.

### Conclusion

Intra-modally deformed OAR and target structures for daily plan adaptation in prostate cancer patients matched manually delineated structures more precisely than inter-modal deformations. Agreement of intra-modal deformations corresponded in magnitude to the intra-observer variation and is recommended for clinical use. However, some manual corrections of deformed structures should be expected.

### EP-1556 The effect of an endorectal balloon on GI toxicity after EBRT for localized prostate cancer

V. Groen<sup>1</sup>, L. Kerkmeijer<sup>1</sup>, E. Monnikhof<sup>2</sup>, M. Van Schie<sup>3</sup>, M. Kunze-Busch<sup>4</sup>, H. De Boer<sup>1</sup>, U. Van der Heide<sup>3</sup>, F. Pos<sup>3</sup>, K. Haustermans<sup>5</sup>, R.J. Smeenk<sup>4</sup>

<sup>1</sup>UMC Utrecht, Radiation Oncology, Utrecht, The Netherlands ; <sup>2</sup>UMC Utrecht, Epidemiology, Utrecht, The Netherlands ; <sup>3</sup>The Netherlands Cancer Institute, Radiation Oncology, Amsterdam, The Netherlands ; <sup>4</sup>Radboud University Nijmegen Medical Centre, Radiation Oncology, Nijmegen, The Netherlands ; <sup>5</sup>University Hospitals, Radiation Oncology, Leuven, Belgium

### Purpose or Objective

Gastro-intestinal (GI) toxicity is a common side effect following external beam radiation therapy (EBRT) in patients with localized and locally advanced prostate cancer. The introduction of IMRT and IGRT with subsequent margin reduction has shown to reduce the risk of GI toxicity. However, further reducing toxicity remains a challenge. Endorectal balloons (ERB) are applications initially developed to reduce intrafraction variations of the prostate during EBRT. In addition, studies have suggested the potential ability of an ERB to reduce EBRT related GI toxicity. The aim of this study was to compare GI toxicity in patients with and without an ERB after EBRT for localized prostate cancer.

### Material and Methods

We included 568 patients with intermediate and high risk prostate cancer of the phase 3 multicenter FLAME RCT in this observational analysis. The primary purpose of the FLAME trial is to compare EBRT in a standard treatment arm (n=284) of 77 Gy to the entire prostate + seminal vesicles in 35 fractions and a dose-escalation arm (n=284) consisting of an additional integrated boost up to 95 Gy to the macroscopic visible tumour on mpMRI. One of the participating centers applied an ERB during all radiation sessions (n=49). The ERB was filled with 100cc air.

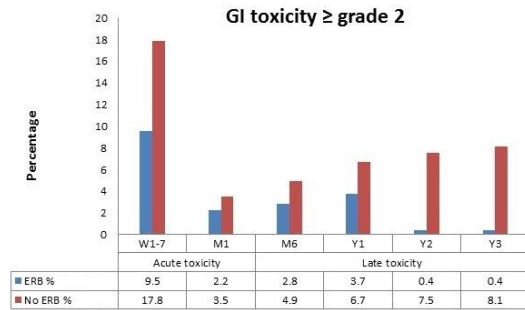
GI toxicity was scored by a physician using the CTCAE version 3.0 in all patients. The effect of the ERB in comparison to no ERB on cumulative GI toxicity  $\geq$  grade 2 was assessed by using a binary logistic regression model using the total study cohort irrespective of randomization. The model was adjusted for age, cardiovascular disease (CVD), diabetes mellitus (DM), T stage of prostate cancer, baseline toxicity, hormonal therapy and radiation dose received in 2cc of the rectum (D2cc). To account for missing data, multiple imputation was used. Furthermore, the prevalence of GI toxicity  $\geq$  grade 2 per follow-up moment was analyzed.

### Results

The incidence of cumulative GI toxicity  $\geq$  grade 2 within 3 years after treatment was lower in the ERB group compared to the group without ERB. After imputation the percentage of cumulative GI toxicity  $\geq$  grade 2 was 29.0% in the no ERB group versus 12.6% in the ERB group, p < 0.001. With adjustment for age, CVD, DM, T stage, baseline toxicity, hormonal therapy and rectum D2cc the daily application of an ERB showed a decreased risk of cumulative GI toxicity  $\geq$  grade 2 with an odds ratio of 0.35 (0.27 - 0.46 95% CI p < 0.001) (table 1). In figure 1 the prevalence of GI toxicity  $\geq$  grade 2 per FU moment is shown.

Imputed data	OR	95% CI
Without adjustment	0.353	0.272 - 0.459
Adjustment for baseline toxicity	0.361	0.277 - 0.470
Adjustment for all	0.353	0.271 - 0.461

Table 1. Binary logistic regression model imputed data. Adjusted for age, CVD, DM, T stage, baseline toxicity, hormonal therapy and rectum D2cc.



### Conclusion

Daily ERB application during EBRT for the treatment of localized prostate cancer may reduce GI toxicity  $\geq$  grade 2. However, the results above must be interpreted cautiously since the group of patients treated with ERB were all treated in the same center. Additional local protocol variations could have been confounders in the relation between ERB and GI toxicity. Further evaluation of the dosimetric parameters is necessary.

### EP-1557 Do metformin and statins play a role in localized high-risk prostate cancer?

G. Cadeddu<sup>1</sup>, F. López Campos<sup>1</sup>, M. Martín Martín<sup>1</sup>, L. Pelari Mici<sup>1</sup>, K. Ytuza Charahua de Kirschner<sup>1</sup>, A. Hernández Corrales<sup>1</sup>, E. Carrasco Esteban<sup>2</sup>, S. Sastre Gallego<sup>3</sup>, I. Císcar García<sup>1</sup>, S. Sancho García<sup>1</sup>, A. Hervás Morón<sup>1</sup>

<sup>1</sup>Hospital Ramón y Cajal, Radiation Oncology, Madrid, Spain ; <sup>2</sup>Hospital Central de la Defensa "Gómez Ulla", Radiation Oncology, Madrid, Spain ; <sup>3</sup>Hospital Beata María Ana, Radiation Oncology, Madrid, Spain

### Purpose or Objective

There is increasing evidence that statins and oral anti-diabetic drugs, such as metformin, can have a favourable role in the treatment of advanced prostate cancer. This study analyses the impact of metformin and/or statins on biochemical failure-free survival (BFFS) and on distant failure-free survival (DFFS) in high-risk prostate cancer treated with radiotherapy.

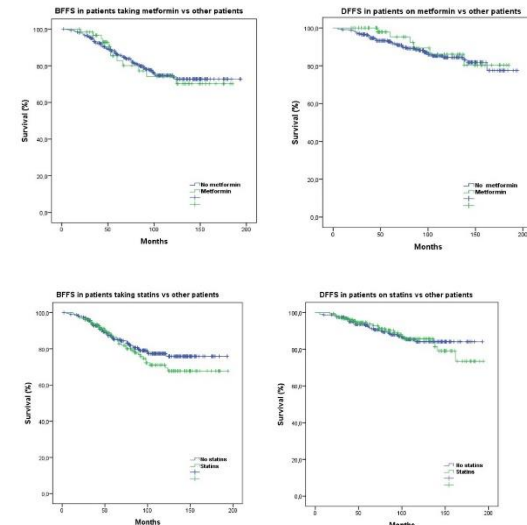
### Material and Methods

From 2002 to 2016, 393 patients with histologically confirmed high-risk prostate cancer defined by National Comprehensive Cancer Network (NCCN) risk group were retrospectively evaluated. All patients assumed androgen deprivation therapy and were treated with radiotherapy according to the institution protocol. Biochemical recurrence was determined by Phoenix criteria defined as a PSA rise of 2 ng/mL or more above the nadir PSA, metastatic patients were defined by the presence of radiological documented metastasis (CT scan, MRI, Choline-PET or bone scintigraphy) in nodes, bones, or visceral disease according to RECIST 1.0 criteria. Association with BFFS and DFFS was analysed using Kaplan and Meier method.

### Results

393 patients with a median age of 70 years (46-83) and median PSA at diagnosis of 34ng/ml (0.6-766) were studied. Of the patients included in this study, 40% (N=158) were treated with statins (64.6% with a dose  $\leq$  20mg/day) and 16% of patients (N=63) were treated with metformin (77.4% with a dose  $\leq$  1700mg/day). With a median follow-up of 97 months, no statistically significant differences were found in BFFS and DFFS between patients treated with metformin versus non-metformin treated patients: 74% versus 77% (p=0.92) and 89% versus 87% (p=0.52), respectively. BFFS and DFFS in patients receiving  $\leq$  1700mg/day versus  $\geq$  1700mg/day of metformin was 78% versus 56% (p=0.10) and 93% versus 71% (p=0.12), respectively. Regarding patients treated with

statins versus non-statins treated patients BFFS at 97 months was 74.6% versus 79% (p=0.31) and DFFS was 88% versus 87.2% (p=0.90). BFFS and DFFS in patients receiving  $\leq$  20mg/day vs  $\geq$  20mg/day of statins was 69.4% versus 77.8% (p=0.28) and 87.2% versus 88.3% (p=0.82), respectively.



### Conclusion

Metformin and statins treatments were not associated with an improvement of BFFS and DFFS in our analysis. Prospective studies are needed to define the role of metformin and statins in localized prostate cancer patients

### EP-1558 Updated results of a Phase II study on 5 fractions FFF SBRT for low and intermediate prostate cancer

F. Alongi<sup>1</sup>, L. Nicosia<sup>1</sup>, R. Mazzola<sup>1</sup>, N. Giaj-Levra<sup>1</sup>, F. Ricchetti<sup>1</sup>, V. Figlia<sup>1</sup>, M. Rigo<sup>1</sup>, G. Sicignano<sup>1</sup>, S. Naccarato<sup>1</sup>, R. Ruggieri<sup>1</sup>

<sup>1</sup>Ospedale Sacro Cuore "Don Calabria", Radiation Oncology, Negrar, Italy

### Purpose or Objective

SBRT had been shown to be a potential treatment option for localized prostate cancer (PC) in selected population. Usually, prostate SBRT has been delivered every other day in order to favour normal tissues recovery, minimizing side effects. Flattening Filter Free (FFF) delivery is a treatment modality able to reduce treatment beam-on time, decreasing patient positioning uncertainties. We reported feasibility, side effects and biochemical control of FFF SBRT delivered in 5 consecutive days in a cohort of patients affected by localized PC.

### Material and Methods

The study, approved by Ethical Committee, started on January 2014. Inclusion criteria were: age  $\leq$  80 years, World Health Organization performance status  $\leq$  2, histologically proven prostate adenocarcinoma, low-to-intermediate risk according to D'Amico criteria, no distant metastases, no previous surgery other than TURP, no other malignant tumor in the previous 5 years, a pre-SBRT International Prostatic Symptoms Score (IPSS) ranged between 0 and 7.

The SBRT-schedules were: 35Gy for low risk and 37.5Gy for intermediate risk PC in 5 fractions, delivered in 5 consecutive days. SBRT was delivered with volumetric modulated radiation therapy (VMAT). Toxicity assessment was performed according to CTCAE v4.0 scale. Neoadjuvant/concomitant hormonal-therapy was prescribed according to risk classification.

### Results

Fifty-two patients were enrolled at the time of analysis. Median age was 73 years (55-83), Median follow-up was 33 months (range: 6-55 months). Thirty-four (65.3%) had a low-risk PC and 18 (34.6%) an intermediate-risk PC. Median initial PSA was 5.9 ng/ml (range, 1.8-15.7 ng/ml). Median Gleason score was 6 (6-7). Median IPSS pre-SBRT was 4.5 (range, 0 - 7). All patients completed the treatment as planned.

Acute G1-2 toxicity occurred in 18 (34.6%) patients and was distributed as follows: 8 (15.3%) cases of G1 gastrointestinal toxicity, 1 (1.9%) patients had G2 gastrointestinal toxicity, 5 (9.6%) patients reported G2 genitourinary toxicity and 11 (21.1%) G1 genitourinary toxicity. Patients may have experienced more than one toxicity. Late G1 gastrointestinal toxicity occurred in 5 (9.6%) patients. No G3 toxicities occurred.

At the last follow-up median IPSS was 3 (1-19) and median PSA was 0.315 ng/ml (range 0.04-7.965 ng/ml). Biochemical control was 98%.

#### Conclusion

The results of our study showed that FFF SBRT in 5 fractions for low-to-intermediate PC is feasible and well tolerated. Longer follow-up is necessary to assess late toxicity and long-term effectiveness.

#### EP-1559 SBRT for lymph node metastases from prostate cancer: a multi-institutional retrospective analysis

F. Alongi<sup>1</sup>, L. Nicosia<sup>1</sup>, C. Francese<sup>2</sup>, G. D'Agostino<sup>2</sup>, L. Di Brina<sup>2</sup>, V. Figlia<sup>1</sup>, R. Mazzola<sup>1</sup>, S. Tomatis<sup>2</sup>, M. Scorsetti<sup>2</sup>  
<sup>1</sup>*Ospedale Sacro Cuore "Don Calabria", Radiation Oncology, Negrar, Italy*; <sup>2</sup>*Humanitas Clinical and Research Hospital, Radiotherapy and Radiosurgery Department, Milan, Italy*

#### Purpose or Objective

Metastases directed treatment is an emerging strategy for oligometastatic/oligorecurrent/oligoprogressive lymph node metastases from prostate adenocarcinoma. Aim of the present study was to evaluate outcome of patients treated with stereotactic body radiation therapy (SBRT) on lymph node metastases.

#### Material and Methods

This is a multi-institutional retrospective analysis, including patients affected by lymph node metastases from prostate adenocarcinoma treated with SBRT. Patients with a maximum of 5 lymph node metastases were included. Concomitant treatment with systemic therapy was allowed. End-points of the analysis were local control (LC), out-of-field progression-free survival (OFPFS), overall progression-free survival (PFS) and overall survival (OS).

#### Results

80 patients and 157 lymph node metastases, treated from 2009 to 2018 were evaluated. Median age was 70.2 years and median PSA before SBRT was 1.88 ng/ml. Median diameter of treated lesion was 37 mm (range 7 - 40 mm). Dose delivered ranged from 25 to 48 Gy in 5 to 12 Gy per fractions (median BED<sub>3Gy</sub> 116.67, range 66.67-240). Androgen deprivation therapy was administered concomitantly in 72 lesions. With a median follow-up of 16 months, LC rates at 1- and 3-years were 93% and 86%. In-field progression of disease was observed in 11 (7%) lesions. One and 3-years OFPFS were 59% and 29% while PFS were 49 % and 20%. Median values of OFPFS and PFS were 15 and 11 months, respectively. Rates of OS at 1- and 3-years were 100% and 95%.

#### Conclusion

SBRT in the management of lymph node metastases from prostate cancer seems to be an effective approach with high rates of in-field control. Prospective trials are necessary to better select patients who can benefit the most from this ablative focal treatment.

#### EP-1560 Quality of life after focal salvage high-dose-rate brachytherapy for radiorecurrent prostate cancer

M. Van Son<sup>1</sup>, E. Monnikhof<sup>2</sup>, M. Peters<sup>1</sup>, J. Van der Voort van Zyp<sup>1</sup>

<sup>1</sup>*UMC Utrecht, Radiotherapy, Utrecht, The Netherlands*; <sup>2</sup>*UMC Utrecht, Epidemiology, Utrecht, The Netherlands*

#### Purpose or Objective

Despite developments in radiotherapy, prostate cancer recurrences are common. Radiorecurrent disease is usually palliatively treated with androgen deprivation therapy (ADT), exposing patients to harmful side-effects and deterioration of quality of life (QoL). Focal ablative therapy is an emerging curative treatment option aiming to reduce toxicity and preserve QoL. Here, we present our longitudinal analysis of prospectively collected QoL data from recurrent prostate cancer patients treated with focal salvage high-dose-rate brachytherapy (HDR-BT).

#### Material and Methods

We included the first consecutive 100 patients who were treated with focal salvage HDR-BT at our institution. QoL was measured with the validated questionnaire EORTC QLQ-PR25, covering the domains urinary symptoms, bowel symptoms and sexual functioning (scoring scale from 0 - 100). Questionnaires were completed at baseline and after 1, 3, 6, 9, 12, 18 and 24 months, and yearly thereafter. All patients had completed at least 3 questionnaires at the time of analysis. A linear mixed effects model for repeated measures was used to assess the course of QoL over time. Furthermore, we assessed potential risk factors for QoL deterioration. For every domain, a separate model was built.

#### Results

Median follow-up time was 19.5 months (range 6-62). The mean questionnaire response rate was 86% (range 72-100% between follow-up time points). Median baseline QoL scores were 12 (urinary symptoms), 0 (bowel symptoms) and 50 (sexual functioning). Urinary symptoms and sexual functioning demonstrated clinically relevant changes over time with maximum score differences of 13 and 12 points respectively (>10 points generally being considered relevant change). Bowel symptoms showed small changes over time (<5 points). Figure 1 illustrates the modelled QoL trends per domain, without adjustment for covariates. Urinary symptoms increased in the first month, normalised afterwards and temporarily increased again after two years. Sexual functioning deteriorated in the first six months, but seemed to recover afterwards. Assessment of potential risk factors related to QoL deterioration was only performed for urinary symptoms and sexual functioning, since these domains showed relevant change over time. Urinary symptoms were related to the administered dose to the urethra, genitourinary toxicity (as graded by the CTCAE 4.0), baseline QoL score and biochemical failure after treatment. Sexual functioning was associated with age, size of the irradiated tumour volume, T-stage of the tumour, erectile dysfunction (as graded by the CTCAE 4.0), baseline QoL score and previous use of ADT.

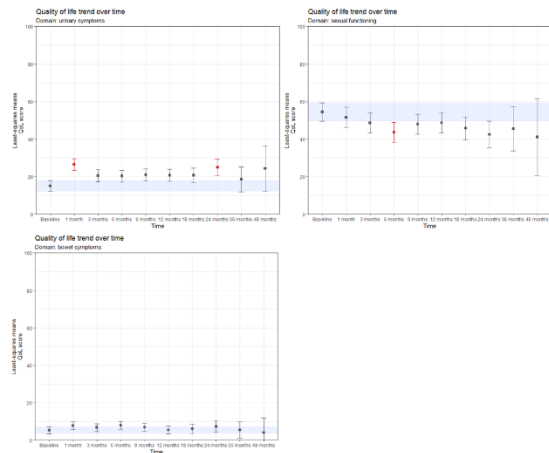


Figure 1: Modelled quality of life trends over time. Least-squares means are displayed with their 95% confidence intervals at each follow-up time point. As a reference, the estimated baseline score is highlighted in blue.

### Conclusion

Compared to baseline QoL, a transient increase of urinary symptoms was seen in the acute and late phase, and sexual function temporarily deteriorated in the first six months. Bowel symptoms did not increase after focal salvage HDR-BT. In contrast with the side-effects associated with ADT, this treatment has very low impact on QoL of recurrent prostate cancer patients.

### EP-1561 Prostate cancer radiotherapy: a systematic review about boost on the dominant intraprostatic lesion

S. Cammelli<sup>1</sup>, M. Buwenge<sup>1</sup>, S. Giambattista<sup>1</sup>, A. Zamagni<sup>1</sup>, E. Galafaro<sup>1</sup>, P. Valeria<sup>1</sup>, M. Ntreta<sup>1</sup>, E. Alexopoulou<sup>2</sup>, M. Ferro<sup>3</sup>, E. Arena<sup>3</sup>, G. Macchia<sup>3</sup>, F. Deodato<sup>3</sup>, S. Cilla<sup>4</sup>, I. Djan<sup>5</sup>, G.P. Frezza<sup>6</sup>, A.G. Morganti<sup>1</sup>  
<sup>1</sup>Radiation Oncology Center, Dept. of Experimental-Diagnostic and Specialty Medicine - DIMES- University of Bologna- S.Orsola-Malpighi Hospital, Bologna, Italy ; <sup>2</sup>Department of Radiation Oncology, University of Patras Medical School, Patras, Greece ; <sup>3</sup>Radiotherapy Unit, Fondazione di Ricerca e Cura "Giovanni Paolo II", Campobasso, Italy ; <sup>4</sup>Medical Physics Unit, Fondazione di Ricerca e Cura "Giovanni Paolo II", Campobasso, Italy ; <sup>5</sup>Institute of Oncology Vojvodina, Medical Faculty-University of Novi Sad, Novi Sad, Serbia ; <sup>6</sup>Radiation Oncology Unit, Bellaria Hospital, Bologna, Italy

### Purpose or Objective

Local recurrence has been shown to originate within the initial tumor in prostate cancer (PCa). Modern imaging allows identification of dominant intra-prostatic lesions (DIL). Evidence suggests that higher radiotherapy (RT) doses result in increased biochemical control, but dose escalation to the whole prostate is limited by the surrounding normal tissues tolerance. Therefore, a systematic review was conducted to analyse the current evidence of RT boost to DIL and assess toxicity and biochemical outcome.

### Material and Methods

PubMed Electronic database was searched through 9th April 2018 for clinical studies on DIL boost irradiation published in English. Established inclusion criteria were:  $\geq 15$  number of patients, localized PCa, and only clinical studies with planned boost to the DIL.

### Results

Thirteen studies with a total of 1044 patients (range: 15-239) reported on a boost to DIL. In all studies, functional imaging was used in DIL delineation to correlate with the histopathological findings. Boost RT to DIL-PTV was delivered using hypofractionated image-guided RT techniques. In series where boost RT was delivered by IMRT-SIB, median dose to DIL was 82.0 Gy (range: 74.0 -

83.2 Gy), while in series with BRT boost, median total dose was 78.0 Gy (range: 56.0-96.0 Gy). Median acute  $G \geq 3$  GU and GI toxicities were 2.0% (range: 0.0-7.0%) and 0.0% (0.0-5.0%), respectively. Median Late  $G \geq 2$  GU and GI toxicities reported were 7.5% (0.0-39.0%) and 6.3% (0.0-21.0%), respectively. Median 5-year bDFS was 94.0% (range: 70.5-98.0%).

### Conclusion

Based on our analysis, the strategy of boosting the DIL is correlated with reasonable toxicity and excellent results in terms of bDFS.

### EP-1562 CyberKnife or HDR Brachytherapy Alone for the Treatment of Prostate Cancer: A Matched Pair Analysis

P. Wojcieszek<sup>1</sup>, G. Głowacki<sup>2</sup>, T. Krzysztofciak<sup>1</sup>, P. Lelek<sup>1</sup>, M. Szlag<sup>3</sup>, A. Cholewka<sup>3</sup>, M. Fijałkowski<sup>1</sup>, S. Kellas-Ślęczka<sup>1</sup>, K. Krysiak<sup>1</sup>, L. Miszczyk<sup>4</sup>

<sup>1</sup>Maria Skłodowska-Curie Memorial Cancer Center and Institute of Oncology, Brachytherapy Department, Gliwice, Poland ; <sup>2</sup>COiDO, Radiotherapy, Tomaszów Mazowiecki, Poland ; <sup>3</sup>Maria Skłodowska-Curie Memorial Cancer Center and Institute of Oncology, Radiotherapy Planning Department, Gliwice, Poland ; <sup>4</sup>Maria Skłodowska-Curie Memorial Cancer Center and Institute of Oncology, Radiotherapy Department, Gliwice, Poland

### Purpose or Objective

To evaluate the efficacy and morbidity of CyberKnife (CK) compared to high-dose-rate (HDR) brachytherapy alone.

### Material and Methods

Two independent prospective trials were conducted in our cancer centre between 2008 and 2015. Outcome blinded patients from both trials exceeding six months of the follow-up were matched 1:1 with following criteria: Gleason score, maximum PSA, T stage, D'Amico risk, Age. No high-risk patients were allowed in this analysis. Wilcoxon rank test was used to assess the differences among the groups. Kaplan-Meier method, log-rank test and Cox regression model were used to analyse the biochemical recurrence-free survival.

### Results

One hundred ninety patients were enrolled in this study. There were no statistically significant differences among the two cohorts except for the age. Median follow-up for HDR and CK was 48 months (16-120 mo) and 52 months (9-74 mo), respectively. HDR was linked with higher mild genitourinary toxicity (p=0.03), while CK was associated with higher gastrointestinal morbidity (p=0.002). There was no difference in the time to achieve nadir PSA. Biochemical relapse-free survival was higher in the HDR cohort with no statistical significance (94% vs 88%; p=0.11). There were no differences in the overall survival.

### Conclusion

HDR alone and CK are safe with comparable outcomes. Less invasive treatment may be considered for older patients with good prognosis. A randomised controlled study should be designed to consider the best options for different groups of prostate cancer patients.

### EP-1563 PSMA-ligand based radiotherapy for lymph node relapsed prostate cancer after radical prostatectomy

C. Henkenberens<sup>1</sup>, N. Schmidt-Hegemann<sup>2</sup>, M.M.E. Vogel<sup>3</sup>, S. Kirste<sup>4</sup>, J. Becker<sup>5</sup>, C. Belka<sup>2</sup>, S.E. Coombs<sup>3</sup>, A. Grosu<sup>4</sup>, M. Arndt-Christian<sup>5</sup>, S.G.C. Kroeze<sup>6</sup>, M. Guckenberger<sup>6</sup>, H. Christiansen<sup>1</sup>, D. Walacides<sup>1</sup>

<sup>1</sup>Medical School Hannover, Department of Radiotherapy and Special Oncology, Hannover, Germany ; <sup>2</sup>University Hospital LMU, Department of Radiation Oncology, Munich, Germany ; <sup>3</sup>Technical University Munich, Department of Radiation Oncology, Munich, Germany ; <sup>4</sup>University of Freiburg, Department of Radiation Oncology, Freiburg, Germany ; <sup>5</sup>University Hospital Tübingen, Department of Radiation Oncology, Tübingen,

Germany ; <sup>6</sup>University Hospital Zürich, Department of Radiation Oncology, Zürich, Switzerland

#### Purpose or Objective

After initial curative treatment of prostate cancer with radical prostatectomy (RP) and salvage radiotherapy (sRT), a substantial number of patients develop lymph node metastases. The standard of care for these patients is the initiation of androgen deprivation therapy (ADT). PSMA-ligand PET imaging allows for individualizing the treatment concept. Radiotherapy (RT) of lymph node metastases aims to delay the initiation of ADT by improving the PSA-progression free survival (PSA-PFS). This study assessed the impact of RT on the PSA-PFS for lymph node recurrences after RP and sRT.

#### Material and Methods

Based on a multi-institutional databank of 379 patients from six academic radiation oncology departments, we performed a subgroup analysis of 41 patients who developed an isolated lymph node relapse after RP and sRT. All patients had a PSMA-ligand PET imaging for staging purposes. Patients were treated between 04/2013 and 01/2018 in six academic centers with definitive radiotherapy of all PSMA-ligand positive lymph node metastases.

PSA-PFS was analyzed using Kaplan-Meier survival curves and factors influencing PSA-PFS with cox regression Analysis.

#### Results

Median age of patients was 70 (52-79) years, median PSA at PSMA-ligand PET was 2.12 (0.12-22.08) ng/ml and PSA-DT was 8.0 (0-27) months. A median of 1 (1-10) lymph node metastases per patient was irradiated. After a median follow-up of 12 (2-31) months, 21 (51.2%) patients had biochemically progressive disease and 19 (46.3%) patients had no PSA progression. One (2.4%) patient was lost to follow-up. The median PSA-PFS was 15.0 months (95% CI 11.8-18.2). The median PSA-level prior to RT decreased significantly from 2.12 ng/ml to a median PSA-Nadir of 0.45 (<0.00-12.25; p=0.02). In 11 of 40 patients (27.5%) the PSA level decreased to 0.07 ng/ml or less. In multivariate cox-regression analysis no predictive factors for PSA-PFS were found.

#### Conclusion

Radiotherapy as a metastasis-directed therapy for PSMA-ligand positive lymph node metastases after RP and sRT improved PSA-PFS and is a considerably option in well-selected patients. Prospective trials are warranted to investigate which patients will benefit the most from and which RT technique, dose and field size are needed.

#### EP-1564 Evaluation of Quality of Life in men with prostate cancer after radiation therapy

B. Florenò<sup>1</sup>, C.G. Rinaldi<sup>1</sup>, P. Trecca<sup>1</sup>, P. Zuccoli<sup>1</sup>, M. Miele<sup>1</sup>, B. Santo<sup>1</sup>, G.M. Petrianni<sup>1</sup>, S. Gentile<sup>1</sup>, S. Palizzi<sup>1</sup>, L. Trodella<sup>1</sup>, R.M. D'Angelillo<sup>1</sup>, S. Ramella<sup>1</sup>  
<sup>1</sup>Campus-Bio Medico University, Radiotherapy Unit, Rome, Italy

#### Purpose or Objective

To evaluate health-related quality-of-life (QOL) outcomes in patients with prostate carcinoma after radiotherapy (RT) at a time-point during follow-up.

#### Material and Methods

QOL outcomes were assessed using the FACT-P QOL questionnaire administered during a whole month at a time-point during follow up. Mean scores of individual domains/scales were compared between different categories of patients (men in hormonal therapy or not, men who had undergone to radical prostatectomy and adjuvant RT or RT alone, men who had undergone to RT to pelvic nodes and men after RT to prostate or prostatic bed alone) using 't' test.

#### Results

60 patients (mean age 65.2 years) were included in the analysis. The median follow up was 46 months (range 3-134). 16 patients (25.8%) were taking hormonal therapy at the time of the examination, 26 patients (42.6%) underwent surgery before RT and 35 patients (57.4%) RT alone, and in 22 patients (36.1%) RT was delivered also to the pelvic lymph nodes. Several general (emotional functioning, role functioning, social contact) as well as prostate cancer-specific (sexuality, bowel and bladder function) QOL domains were analysed. Importantly, all the QOL domains were worse in patients in hormonal therapy, but only the functioning QOL domains in a significant way (p<0.05). Prostatectomy patients reported worse outcomes in bladder function and emotional well-being, but the difference wasn't statistically significant. There were no differences in the level of sexual activity between patients undergoing surgery and not, even if 16 patients (26.6%) didn't answer the question. Moreover, we didn't find QOL discrepancies between patients who had undergone to RT to pelvic nodes and men after RT to prostate or prostatic bed alone. There were no differences in all QOL domains in patients with > 75 years, even if emotional well being is worse in the younger group with a trend towards statistically significant. Patients with a follow up longer than 6 years didn't report worse QOL scores than those with a follow up of 6 years or less.

#### Conclusion

At a time point during follow up we didn't find significant discrepancies for all the QOL domains in the different categories of patients except for patients in hormonal therapy, who reported worse score in the functioning QOL domains. An analysis on a larger sample of patients is needed to confirm these preliminary data.

#### EP-1565 Quality of online information about radiotherapy for prostate cancer

L. Käsmann<sup>1</sup>, S. Janssen<sup>2</sup>, F. Fahlbusch<sup>3</sup>, D. Vordermark<sup>4</sup>, D. Rades<sup>2</sup>

<sup>1</sup>LMU University Hospital Grosshadern, Department of Radiation Oncology, Munich, Germany ; <sup>2</sup>University of Luebeck, Department of Radiation Oncology, Luebeck, Germany ; <sup>3</sup>Friedrich-Alexander-University of Erlangen-Nuernberg, Department of Pediatrics and Adolescent Medicine, Erlangen-Nuernberg, Germany ; <sup>4</sup>University Hospital Halle Saale, Department of Radiation Oncology, Halle Saale, Germany

#### Purpose or Objective

Prostate cancer represents the most common cancer in men. Radiotherapy is a major treatment option. It can either be used curatively in localized disease, adjuvant after radical prostatectomy or as an effective option in palliative setting. As patients increasingly seek medical information on the Internet, our goal was to evaluate the quality of websites regarding radiotherapy for prostate cancer.

#### Material and Methods

A simulated patients' search for the terms "prostate cancer" and "radiotherapy" was carried out in a time-staggered manner using the three most popular search-engines Google, Bing and Yahoo. The first 20 search results of each were evaluated using the validated DISCERN Plus instrument, the HON code certification, the JAMA benchmark criteria and the ALEXA global traffic rank.

#### Results

The quality of information on websites about prostate cancer and radiotherapy was good, with a mean DISCERN Plus score of 55.1 ± 10.0, 51.8 ± 10.3 and 50.7 ± 10.1 for Google, Yahoo and Bing, respectively. The scores ranged from a minimum of 34 to a maximum of 74. 13% of all websites were rated as excellent, 31%, 48% and 8% as good, fair and poor, respectively. The overall quality of websites was neither dependent on the choice of search engines nor did we observe a significant temporal change in quality. The main categories of websites retrieved from

the first search were charity/NGO sites (46%), followed by sponsored medical news sites (28%), hospital/university sites (20%) and governmental sites (6%). Websites operated by charity organizations had significantly higher DISCERN Plus scores (mean score:  $55.5 \pm 9.3$ ) compared to hospital sites (mean score:  $47.3 \pm 9.6$ ,  $p < 0.042$ ) and medical news sites (mean score:  $46.1 \pm 6.1$ ,  $p < 0.009$ ), respectively. The JAMA benchmark criteria were fulfilled for all four sections in 13%, for three, two and one in 13%, 31% and 40%, respectively. Only 13% of all websites were HON code certified. All analyzed websites had a focus on curative teletherapy, 76%, 51% and 22% of all websites mentioned brachytherapy, active surveillance and palliative radiotherapy, respectively. In 57% the procedure of radiotherapy was described in detail. Special radiation techniques like “hypo-fractionation”, “Intensity modulated Radiotherapy (IMRT)”, “Image guided Radiotherapy (IGRT)” and “proton therapy” were mentioned in 37%, 72%, 27% and 31% of all analyzed websites, respectively.

#### Conclusion

The quality of websites on radiotherapy and prostate cancer directed at laypersons is promising. The fact that we were unable to find a simple strategy for the identification of high quality websites (i.e. HON code certification, JAMA benchmark criteria, ALEXA ranking or different search engines) emphasizes the responsibility of the treating physicians to interpret and rank the vast quantity of information and value of personal contact with the treating radio-oncologist in order to integrate and interpret the information found online.

#### EP-1566 MR-guided online adaptive radiotherapy: First experience in the UK

A. Pathmanathan<sup>1</sup>, L. Bower<sup>1</sup>, H. Creasey<sup>2</sup>, A. Dunlop<sup>1</sup>, E. Hall<sup>3</sup>, I. Hanson<sup>1</sup>, T. Herbert<sup>2</sup>, R. Lawes<sup>2</sup>, D. McQuaid<sup>1</sup>, H. McNair<sup>2</sup>, A. Mitchell<sup>1</sup>, G. Smith<sup>2</sup>, R. Huddart<sup>1</sup>, U. Oelfke<sup>1</sup>, S. Nill<sup>1</sup>, A. Tree<sup>4</sup>

<sup>1</sup>The Institute of Cancer Research and The Royal Marsden NHS Foundation Trust, Radiotherapy and Imaging, Sutton, United Kingdom ; <sup>2</sup>Royal Marsden Hospital NHS Foundation Trust, Radiotherapy and Imaging, London, United Kingdom ; <sup>3</sup>Institute of Cancer Research, Clinical Trials and Statistics Unit, London, United Kingdom ; <sup>4</sup>Royal Marsden Hospital NHS Foundation Trust and the Institute Cancer Research, Radiotherapy and Imaging, London, United Kingdom

#### Purpose or Objective

The Elekta Unity<sup>1</sup> (Elekta AB, Stockholm, Sweden) combines a linear accelerator and 1.5T magnetic resonance imaging (MRI) scanner, allowing daily and real-time imaging for online adaptive radiotherapy (RT)<sup>2</sup>. Here we describe the first experience of MR-guided RT in the United Kingdom (UK).

#### Material and Methods

A 65 year-old man with localised prostate cancer on androgen deprivation therapy was recruited to the PRISM trial (Prostate Radiotherapy Integrated with Simultaneous MRI) NCT03658525, a non-randomised R-IDEAL phase I/IIa study<sup>3</sup>, to receive radical RT to the prostate and seminal vesicles (SV).

A week prior to imaging for reference planning, three gold fiducial markers (FM) were implanted. Planning computed tomography (CT) and MRI (standard T2-weighted and T2\*-weighted for FM visualisation) were registered using FM. Rectal preparation with micro-enemas and bladder filling were used prior to simulation imaging and each treatment as per trial protocol.

RT was planned using Monaco 5.4 treatment planning system (Elekta) to a standard UK dose of 60 Gy in 20 fractions with 7-field intensity modulated RT. Clinical target volume 1 (CTV1) was defined as the prostate and proximal 1 cm SV, planning target volume 1 (PTV1) was created by addition of a 5 mm isotropic margin, except 3

mm posteriorly. CTV2 was defined as the prostate plus proximal 2 cm SV with a 5 mm isotropic margin for PTV2. PTV1 and PTV2 were covered by 95% and 77% of the prescription dose respectively. Organ at risk constraints were defined as per institutional guidelines.

For each fraction, a daily session T2W MRI was acquired. CTV1/2 were re-contoured by a clinician each day for the ‘adapt to shape’ (ATS) workflow, whereby a new daily online plan was created with reoptimisation based on the anatomy of the day. Following plan adaptation and checking, a verification MRI was acquired before treatment to assess whether any additional adaptation was required to adjust for patient movement.

#### Results

A clinically acceptable reference CT-based plan was generated that achieved all mandatory and optimal dose constraints. Patient-specific electron densities were extracted for the daily MR-based adapted plans. (Figure 1). The patient received his first treatment on 18<sup>th</sup> September 2018 and completed all 20 fractions on the MR-Linac using the ATS online workflow. Prostate motion was visually monitored during treatment delivery using cine-MR.

Time taken for each stage of the adaptive workflow is summarised in Table 1. Over the treatment course, toxicity was assessed using RTOG and CTCAE criteria. Highest genitourinary toxicity was Grade 2 urinary frequency and cystitis (CTCAE). Highest gastrointestinal toxicity was Grade 2 diarrhoea (RTOG). Treatment was tolerated without any unexpected toxicity compared to standard treatment delivery.

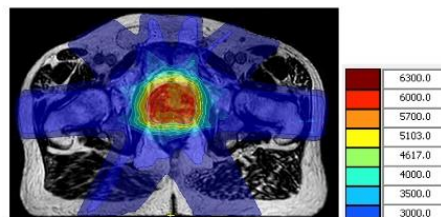


Figure 1: Example of a new daily online MR plan, 7-field IMRT prostate radiotherapy. This is created by adapting a CT-based reference plan, using the anatomy of the day. Red line- Prostate CTV.

Stage of online re-planning	Mean (standard deviation) time in minutes
Patient set-up time	4.9 (0.8)
Scan acquisition and image fusion	7.3 (1.4)
Clinician re-contouring	8.7 (0.8)
Plan adaptation	9.0 (1.2)
Physics checking	3.6 (0.9)
Verification imaging and review	7.3 (1.3)
Treatment delivery	5.1 (0.7)
<b>Total time from patient entering room to end of treatment delivery</b>	<b>45.9 (4.3)</b>

Table 1: Summary of the different stages of daily online adaptive radiotherapy for the prostate. Values reported here are for the first patient- mean (standard deviation) time in minutes over twenty fractions, reported to 1 decimal place.

#### Conclusion

Daily online adaptive RT for the prostate with MRI is feasible and well tolerated. The PRISM trial will recruit 30 patients, with a safety analysis after the first 10 patients.

#### EP-1567 Prospective longitudinal evaluation of quality of life after prostate cancer IMRT

A. Maggio<sup>1</sup>, T. Rancati<sup>2</sup>, P. Gabriele<sup>3</sup>, F. Munoz<sup>4</sup>, D. Cante<sup>5</sup>, B. Avuzzi<sup>6</sup>, C. Bianconi<sup>7</sup>, F. Badenchini<sup>8</sup>, B. Farina<sup>9</sup>, P. Ferrari<sup>10</sup>, E. Garibaldi<sup>3</sup>, T. Giandini<sup>11</sup>, G. Girelli<sup>12</sup>, V. Landoni<sup>13</sup>, A. Magli<sup>14</sup>, R. Spoto<sup>15</sup>, E. Moretti<sup>16</sup>, E. Petrucci<sup>17</sup>, P. Salmoiraghi<sup>18</sup>, G. Sanguineti<sup>19</sup>, E. Villa<sup>20</sup>, J.M. Waskiewicz<sup>21</sup>, R. Valdagni<sup>22</sup>, C. Fiorino<sup>23</sup>, C. Cozzarini<sup>24</sup>

<sup>1</sup>Istituto di Candiolo- Fondazione del Piemonte per

Oncologia FPO- IRCCS- Candiolo TO, Medica Physics, Candiolo, Italy ; <sup>2</sup>Istituto Nazionale dei Tumori- Prostate Cancer Program- Milano- Italy, Prostate Cancer Program, Milano, Italy ; <sup>3</sup>Istituto di Candiolo- Fondazione del Piemonte per Oncologia FPO- IRCCS- Candiolo TO, Radiotherapy, Candiolo, Italy ; <sup>4</sup>Ospedale Regionale U.Parini-AUSL Valle d'Aosta- Aosta, Radiotherapy, Aosta, Italy ; <sup>5</sup>Ospedale di Ivrea- A.S.L. TO4- Ivrea, Radiotherapy, Ivrea, Italy ; <sup>6</sup>Fondazione IRCCS Istituto Nazionale dei Tumori- Milano- Italy, Radiation Oncology 1, Milano, Italy ; <sup>7</sup>IRCCS Ospedale San Raffaele- Milano, Radiotherapy, Milano, Italy ; <sup>8</sup>Fondazione IRCCS Istituto Nazionale dei Tumori- Radiation Oncology 1- Milano- Italy, Prostate Cancer Program, Milano, Italy ; <sup>9</sup>Ospedale degli Infermi- Biella, Medical Physics, Biella, Italy ; <sup>10</sup>Comprensorio Sanitario di Bolzano, Medical Physics, Bolzano, Italy ; <sup>11</sup>Fondazione IRCCS Istituto Nazionale dei Tumori- Milano- Italy, Medical Physics, Milano, Italy ; <sup>12</sup>Ospedale degli Infermi- Biella, Radiotherapy, Biella, Italy ; <sup>13</sup>Istituto Nazionale dei Tumori "Regina Elena"- Roma, Medical Physics, Roma, Italy ; <sup>14</sup>Ospedale di Udine- Udine, Radiotherapy, Udine, Italy ; <sup>15</sup>Ospedale Regionale U.Parini-AUSL Valle d'Aosta- Aosta- Italy, Radiotherapy, Aosta, Italy ; <sup>16</sup>Ospedale di Udine- Udine- Italy, Medical Physics, Udine, Italy ; <sup>17</sup>Ospedale di Ivrea- A.S.L. TO4- Ivrea- Italy, Medical Physics, Ivrea, Italy ; <sup>18</sup>Cliniche Gavazzeni-Humanitas- Bergamo- Italy, Medical Physics, Bergamo, Italy ; <sup>19</sup>Istituto Nazionale dei Tumori "Regina Elena"- Roma- Italy, Radiotherapy, Roma, Italy ; <sup>20</sup>Cliniche Gavazzeni-Humanitas- Bergamo- Italy, Radiotherapy, Bergamo, Italy ; <sup>21</sup>Comprensorio Sanitario di Bolzano- Italy, Radiotherapy, Bolzano, Italy ; <sup>22</sup>University of Milan / Fondazione IRCCS Istituto Nazionale dei Tumori- Milano- Italy, Oncology and Hemato-oncology / Radiation Oncology 1 / Prostate Cancer Program, Milano, Italy ; <sup>23</sup>IRCCS Ospedale San Raffaele- Milano- Italy, Medical Physics, Milano, Italy ; <sup>24</sup>IRCCS Ospedale San Raffaele- Milano- Italy, Radiotherapy, Milano, Italy

### Purpose or Objective

To study the evolution of quality of life (QoL) in the first 5 years after IMRT for prostate cancer and to determine possible association with clinical/treatment data: age, presence and type of hormonal therapy, prescribed dose, acute intestinal (GI) and urinary (GU) toxicity

### Material and Methods

Patients were enrolled in a prospective multicentre observational trial in 2010-2014. They were treated at different prescription doses with conventional (74-80Gy-1.8-2Gy/fr) or moderately hypofractionated IMRT (65-75.2Gy-2.2-2.7Gy/fr) in 5 fractions/week. QoL was evaluated using the European Organization for Research and Treatment of Cancer (EORTC) QoL questionnaire (EORTC QLQ-C30) at baseline, at RT end and every 6 months up to 5 years after IMRT.

14 QoL dimensions were investigated separately: global health/QoL, physical functioning (func), role func, social func, emotional func, cognitive func, appetite loss, diarrhoea, fatigue, insomnia, dyspnoea, pain, constipation, nausea.

Longitudinal evaluation of QoL was analysed by means of ANOVA for multiple measures. Differences between groups were evaluated through Mann-Whitney test

### Results

281 patients with complete set of questionnaires across 5 years were available.

Figure 1 reports results from ANOVA in Table format, while Figure 2 presents longitudinal results for the 14 investigated QoL dimensions. A general trend toward significant worsening of QoL at RT end was detected for global health, physical and role func, fatigue, appetite loss, diarrhoea and pain. This worsening usually recovered within 6 months, with the only exception of

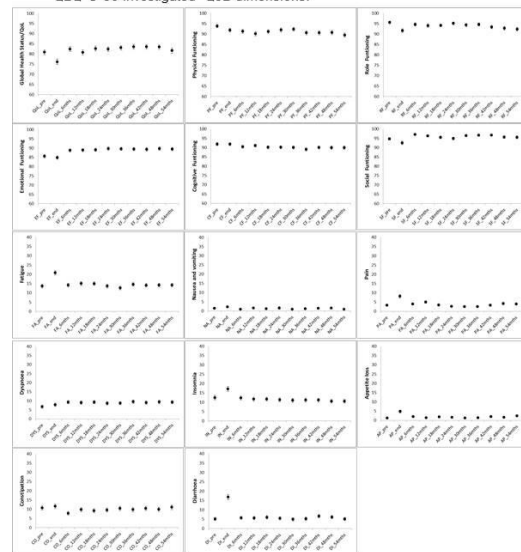
physical func which exhibited a further worsening at 5-year follow-up.

Detailed analysis was carried out for QoL dimension at RT end, which from ANOVA resulted as the most impaired time point. Acute Grade $\geq$ 2 GI toxicity significantly impacted global health, physical and role func, fatigue, appetite loss, diarrhoea and pain (p range: 0.02-0.0003, worsening range: 3-9 points). Pelvic irradiation resulted in significantly lower QoL for global health, fatigue, appetite loss and diarrhoea (p range: 0.05-0.0001, worsening range: 5-14 points). Acute Grade $\geq$ 2 GU toxicity resulted in lower role func and higher pain (p=0.03 and 0.002 respectively, worsening of 5 and 10 points). Prescription dose was associated to diarrhoea (cutoff at 81 2Gy-equivalent, p=0.0001, 23.9 vs 13 points). Use of any neoadjuvant/concomitant hormonal therapy was associated to lower pain (6.7 vs 11, p=0.01), while the use of anti-androgen was associated to lower fatigue (19.2 vs 24.8, p=0.01)

Figure 1: result of ANOVA analysis (over 5 years after the end of IMRT) on the 14 QoL dimensions investigated by EORTC QLQ C30 questionnaire

QoL dimension	significant trend with time from ANOVA	p-value	time and size	of significant variation
global health/QoL	quadratic	0.05	5 point worsening at RT end with respect to baseline, then recover	
physical functioning	cubic	0.04	4 point worsening at RT end with respect to baseline, then recover, further 4 point worsening at 5 years	
role functioning	cubic	0.04	5 point worsening at RT end with respect to baseline, then recover, further 5 point worsening at 5 years	
social functioning	linear	0.04	2 point increase in the 5 year period	
emotional functioning	linear	0.01	3 point increase in the 5 year period	
cognitive functioning	no significant trend			
appetite loss	quadratic	0.004	5 point worsening at RT end with respect to baseline, then recover	
diarrhoea	quadratic + linear decrease	0.05	14 point worsening at RT end with respect to baseline, then recover and at 5 years 1.5 points better with respect to baseline	
fatigue	quadratic	0.03	7 point worsening at RT end with respect to baseline, then recover	
insomnia	no significant trend			
dyspnoea	no significant trend			
pain	quadratic	0.03	5 point worsening at RT end with respect to baseline, then recover	
constipation	no significant trend			
nausea	no significant trend			

Figure 2: Longitudinal evolution (5-year time frame) of the EORTC QLQ C-30 investigated QoL dimensions.



### Conclusion

Modern IMRT delivered in conventional or hypofractionated regimens, at high dose, represents a modality that doesn't affect the long term QoL. A transient worsening of some QoL dimensions is associated to the presence of acute GI/GU toxicity, pelvic irradiation and higher prescribed doses. However, these detrimental effects are solved in the short term after RT end, within 6 months

**EP-1568 Long-term results of [18F] Fluorocholine PET/CT guided SBRT in patients with prostate cancer**  
 F. Pasqualetti<sup>1</sup>, M. Panichi<sup>2</sup>, P. Cocuzza<sup>3</sup>, A. Gonnelli<sup>3</sup>, D. Baldaccini<sup>3</sup>, A. Molinari<sup>3</sup>, M. Cantarella<sup>4</sup>, R. Mattioni<sup>3</sup>, S. Montrone<sup>2</sup>, A. Cristaudo<sup>3</sup>, A. Marciano<sup>5</sup>, R. Zanca<sup>5</sup>, M. Sollini<sup>6</sup>, A. Sainato<sup>2</sup>, P.A. Erba<sup>3</sup>, F. Paia<sup>3</sup>  
<sup>1</sup>Azienda Ospedaliero Universitaria Pisana, Oncology, Pisa, Italy ; <sup>2</sup>Azienda Ospedaliero Universitaria Pisana, Radiotherapy, Pisa, Italy ; <sup>3</sup>University of Pisa, Radiotherapy, Pisa, Italy ; <sup>4</sup>Casa di Cura Sanrossore, Radiotherapy, Pisa, Italy ; <sup>5</sup>University of Pisa, Nuclear Medicine, Pisa, Italy ; <sup>6</sup>Humanitas Cancer Centre, Nuclear Medicine, Milan, Italy

#### Purpose or Objective

**Aim:** In the last years, functional imaging has given a significant contribution to the clinical decision making of biochemical relapsed prostate cancer (PCa), allowing early diagnosis of metastatic disease with a limited tumor burden, the so-called oligometastatic patients, and driving local therapies like stereotactic body radiotherapy (SBRT). Herby, we present a prospective study aiming to validate the role of [<sup>18</sup>F]Fluoro-Methyl Choline ([<sup>18</sup>F]FMCH) PET/CT in the selection of PCa patients suitable for SBRT.

#### Material and Methods

**Materials and Methods:** Patients with biochemical recurrence were screened. Eligible patients were imaged with Endo-rectal Magnetic Resonance to exclude local recurrence inside the prostate bed and [<sup>18</sup>F]FMCH PET/CT to assess tumor burden. Patients with up to three synchronous active lesions identified by [<sup>18</sup>F]FMCH PET/CT were enrolled in the present study. All patients were treated with SBRT on all active lesions revealed by [<sup>18</sup>F]FMCH PET/CT. Systemic therapy free-survival since the [<sup>18</sup>F]FMCH PET/CT was considered as the primary endpoint.

#### Results

**Results:** 50 patients were included in the present study. Forty-five patients with oligometastatic PCa (castration sensitive in 34 patients, castration-resistant in 11) for a total of 66 lesions (lymph node and bone lesions, in 44 and 22 cases, respectively) were considered evaluable for the present analysis. After SBRT, five patients were lost at follow-up since they started ADT for personal reason. Patients' median age at the time of study entry was 70 years (range 50-81). The median length between PCA diagnosis and study enrollment was 69 months (range, 2-180 months). At the time of study entry, Median PSA value was 2,69 ng/mL (range 0.9-27,40). In-field progression was observed in 3 out of 66 irradiated lesions. After the detection of oligorecurrent disease following SBRT, 6 patients underwent further courses of SBRT on the active lesions revealed by [<sup>18</sup>F]FMCH-PET/CT (two, three, four, five courses respectively in 3,1,1,1 patients). Toxicity higher than grade 2 was not recorded. After a median follow-up of 22.3 months, systemic therapy was started in 24 patients (53,3%). Median systemic therapy free survival was 39.1 months (95%CI6.5-68.6) whereas systemic free survival ratios at 6, 12 and 24-month were 93.5%, 73.9%, and 63.1 %, respectively. At univariate Cox regression analysis, Delta PSA and Gleason Score (GS) demonstrated an impact on systemic therapy free survival (p=0.03 and p<0.001, respectively), being GS higher than 6 related to longer systemic therapy free survival. The Delta PSA remained statistically significant on multivariate analyses while the Gleason Score shows a trend to a statistically significant association (p<0.001 and p=0.18, respectively).

#### Conclusion

**Conclusion:** Based on our findings, [<sup>18</sup>F]FMCH PET/CT can identify oligometastatic patients suitable for SBRT, resulting in a systemic therapy free survival of 39.1 months.

**EP-1569 High-dose-rate brachytherapy boost in high-risk prostate cancer: results of two different schemes**

L. Pelari<sup>1</sup>, F. López<sup>1</sup>, G. Caddedu<sup>1</sup>, K. Ytuza<sup>1</sup>, A. Hernández<sup>1</sup>, I. Ciscar<sup>1</sup>, C. Vallejo<sup>1</sup>, M. Martín<sup>1</sup>, S. Sancho<sup>1</sup>, A. Hervás<sup>1</sup>  
<sup>1</sup>Ramón y Cajal Hospital, Radiation Oncology, Madrid, Spain

#### Purpose or Objective

To evaluate preliminary clinical results, acute and chronic genitourinary (GU) and gastrointestinal (GI) toxicity of a retrospective cohort of high-risk prostate cancer patients treated with External Beam Radiation Therapy (EBRT) and a boost of High-Dose-Rate Brachytherapy (HDR-BT).

#### Material and Methods

Patients with histologically confirmed high risk prostate cancer defined by National Comprehensive Cancer Network (NCCN) risk group were included. Patients received hypofractionated and image-guided EBRT by volumetric IMRT technique to a dose of 37.5 Gy in 15 fractions combined with a single 15 Gy HDR-BT (<sup>60</sup>Co multi-source) dose (Arm-1) or 60 Gy in 30 fractions combined with a single 9 Gy HDR-BT (<sup>60</sup>Co multi-source) dose (Arm-2). All patients assumed androgen deprivation therapy for two years. Biochemical recurrence was defined by Phoenix criteria (PSA concentration superior than nadir plus 2 ng/ml). Acute and chronic toxicity (according to the CTCAE Version 4.0) were collected. Toxicity was considered "acute" if occurred until 3 months after the treatment and "chronic" if occurred after 6 months of the end of the treatment.

#### Results

From February 2008 to July 2015, 78 patients were treated by the reported schedules. Median age was 72 years (range 42-83 years). With a median follow-up of 49 months (range 23 -126 months) the median biochemical progression-free survival rates were 91,5% for the 15 Gy HDR group (Arm 1) and 93,8% for the scheme of treatment of 9 Gy HDR (Arm 2). No post-HDR procedure complications were detected in all patients.

**Arm-1:** Acute GU toxicity grade I occurred in 8 patients (50%). No patients developed acute GI toxicity. Chronic GU toxicity grade I occurred in 2 patients (12,5 %). Chronic GI toxicity grade I was observed in 2 patients (12,5 %). No patients developed GU or GI acute or chronic toxicity ≥ GII.

**Arm-2:** Acute GU toxicity grade I occurred in 25 patients (40,3%), grade II in 7 patients (11,3 %) and grade III in 3 patients (4,8 %). Acute GI toxicity grade I were observed in 16 patients (25,8 %). No patient developed GI toxicity ≥ GII. Chronic GU toxicity occurred as follows: grade I in 13 patients (20,9 %), grade II in 4 patients (6,45 %) and grade III in 2 patients (3,22 %). Chronic GI toxicity grade I was observed in 4 patients (6,45%) and grade II in 1 patient (1,6 %). No late gradeIV GU or GI toxicity was detected.

#### Conclusion

Hypo-RT combined with HDR-BT produces acceptable acute and chronic toxicity rates with promising outcomes of biochemical control for high risk prostate cancer. Longer term follow-up should be analysed to confirm these data and to compare possible differences between both arms.

**EP-1570 Stereotactic body radiation therapy for oligometastatic prostate cancer. Our experience.**

C. García Aguilera<sup>1</sup>, A. Méndez Villamón<sup>1</sup>, I. Guerrero Fernández de Alba<sup>2</sup>, D. Villa Gazulla<sup>3</sup>, A. Miranda Burgos<sup>1</sup>, J.M. Ponce Ortega<sup>1</sup>, M.M. Puertas Valiño<sup>1</sup>, C. Escuin Troncho<sup>1</sup>, B. García Gimeno<sup>1</sup>, M.J. Irún Cuairán<sup>1</sup>, C. Borbonada Martínez<sup>1</sup>, M. Tejedor Gutiérrez<sup>1</sup>  
<sup>1</sup>Hospital Universitario Miguel Servet, Servicio de Oncología Radioterápica, Zaragoza, Spain ; <sup>2</sup>Hospital Universitario Miguel Servet, Servicio de Medicina Preventiva, Zaragoza, Spain ; <sup>3</sup>Hospital Universitario Miguel Servet, Servicio de Física y Protección Radiológica, Zaragoza, Spain

### Purpose or Objective

To analyze the survival and toxicity in patients with oligometastatic prostate cancer treated in our center with stereotactic body radiation therapy (SBRT).

### Material and Methods

We retrospectively reviewed 51 patients with oligometastatic prostate cancer that received SBRT to treat malignant adenopathies and bone metastasis between March 2014 and August 2018. We analyzed metastasis control (MC), disease-free survival (DFS), biochemical progression-free survival (BPFS), distant progression-free survival (DPFS), and overall survival (OS).

#### Patient and disease characteristics (n=51)

Characteristics	Value (%)
Age at diagnosis in years (median)	68,59
Gleason	9 (17,65)
	6 (22)
	7 (43,14)
	8 (11)
	9 (21,57)
10	8 (15,69)
	1 (1,96)
Regions treated	47 (69)
Lymph node	22 (68,12)
Bone	22 (31,88)
PSA pre-treatment (ng/ml)	35 (68,63)
0-5	8 (15,69)
>5-10	3 (5,88)
>10-20	5 (9,80)
>20	13 (25,49)
TNM	T1 (11)
	T2 (21,57)
	T3 (22)
	T4 (43,14)
Unkonwn	3 (5,88)
	2 (3,92)
Nx	4 (7,84)
N1	47 (92,16)
N2	0 (0)
M0	46 (90,20)
M1a	1 (1,96)
M1b	3 (5,88)
Unknown	1 (1,96)
Primary treatment	20 (39,22)
RP	1 (1,96)
RP+LP	19 (37,25)
RT	7 (13,73)
RP+RT	7 (13,73)
BT	3 (5,88)
HT	1 (1,96)
Hormonal treatment	37 (72,55)
Yes	14 (27,45)
No	

Abbreviations: PSA = prostate-specific antigen; RP = radical prostatectomy; RT = radiation therapy; LP=lymphadenectomy; BT = Brachytherapy; HT = Hormonal treatment.

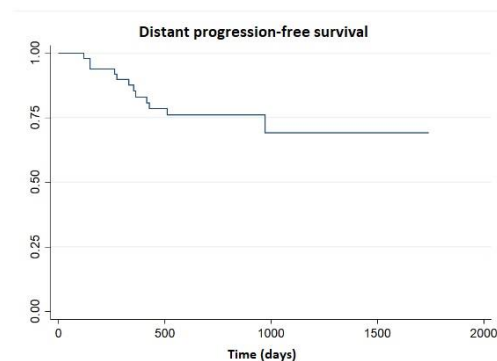
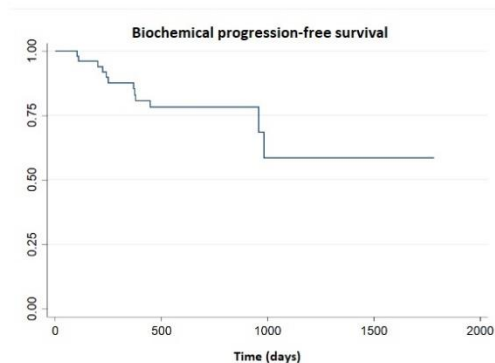
### Results

We included 51 patients with 69 lesions, of which 100% were hormone-sensitive. 72% were being treated with hormone therapy (analogue LHRH). 11.76% became castrate resistant during follow-up. The number of lesions treated was 22 bone metastasis and 47 malignant lymphadenopathies. The treatment was administered with intensity-modulated radiotherapy guided by daily image by cone-beam and simmetry device for respiratory control. The patients were immobilized by Body Fix system and the treatment dose used was 45Gy in 6 fractions of 7.5Gy, twice a week for lymph nodes and 16Gy single session for bone lesions.

Estimated Metastasis control at 2 years was 86.27%. Disease-free survival, biochemical progression-free

survival and distance-free relapse-free survival were 52,95%, 78,26%, 76,10% respectively, counting on a overall survival of 98,04%.

We used CTCAE 4.0 scale to measure toxicity. 46 patients (90.20%) had no acute gastrointestinal toxicity, 4 (7.84%) had acute grade 1 gastrointestinal toxicity. In case of acute genitourinary toxicity, 41 patients (80.39%) did not experience any toxicity while 8 (15.69%) had grade 1 toxicity. Only one patient suffered late toxicity, a pathological fracture, one year after administration of SBRT.



### Conclusion

Stereotactic body radiation therapy used in oligometastatic prostate cancer patients provided optimal control of metastasis and acceptable toxicity. It is a good therapy for bone and lymph nodes lesions.

### EP-1571 Pelvis Hypofractionarion in IMRT+IGRT:15 fractions and prostate HDR Brachytherapy. Toxicity analysis

P. Castro Peña<sup>1</sup>, E. Marinello<sup>1</sup>, P. Murina<sup>1</sup>, Y. Schworer<sup>1</sup>, L. Suarez Villasmil<sup>1</sup>, D. Venencia<sup>1</sup>, S. Zunino<sup>1</sup>  
<sup>1</sup>Instituto Zunino - Fundacion Marie Curie, Radiation Oncology, Cordoba, Argentina

### Purpose or Objective

To analyze urinary and rectal toxicity in patients with prostate cancer undergoing combination treatment with High Rate Dose Prostate Brachytherapy (HDR-B) plus External Beam Radiation Therapy IMRT + IGRT in 15 fractions, with pelvic lymph nodes irradiation.

### Material and Methods

Between June '15 and August '18, 38 patients with positive prostate cancer biopsy were treated. The average initial PSA was 22.34 ng/ml [4.19-84]. The average prostate volume was 40.5 g [15-75]. The distribution of patients by risk groups was: Low risk 0% (0), Intermediate risk 10.5% (4), High risk 73.7% (28), Locally advanced 13% and Metastatic 2%.

100% of the patients received neoadjuvant, concomitant and adjuvant hormonal treatment. All the patients were

irradiated with combined treatment, first with HDR Brachytherapy = 15 Gy in a single fraction, with Ir-192, Microselectron v2 Nucletron-Elekta. In that same act, 4 fiducial markers of intra-prostatic titanium were implanted for posterior IGRT. Two weeks later, IMRT+IGRT was performed on 15 fractions of the Novalis Tx linear accelerator (BrainLab-Varian), high resolution multilane collimator (HDMLC) with 2.5 mm wide slices. IGRT (intra and interfraction) were based on ExacTrac (BrainLab) localization system. The CTscan was performed every 2.5 mm at the prostate level. Drawing volumes and dosimetry planning were performed in the Eclipse (Varian system). Prescribed dose at 95% PTV-prostate + seminal vesicles and Pelvic Lymph nodes was = 39 Gy. Genitourinary toxicity (GU) was assessed using the IPSS (International Prostate Symptom Score) and gastrointestinal (GI) scale according to the RTOG criteria. The PSA was recorded systematically during the follow-up.

#### Results

The mean age was 66.7 years [47.1-76.7]. Average follow-up of 9 months [0.0-37.4]. The mean IPSS pre HDR-B was 7.4 [0-28]. Post IMRT + IGRT = 6.9 [1-25]; 6.4 [1-22] and 5.4 [1-22] for 2; 6 and 12 months respectively. The rate and degree of rectal toxicity after HDR-BQT + IMRT-IGRT was at 2 months G0 = 0%; G1 = 100%; G2 = 5.4% and G3 = 0%; G4 = 0% At 6 months: G0 = 0%; G1 = 100%, G2 = 0%; G3 = 0% and G4 = 0%. At 12 months: G0 = 0%; G1 = 100%; G2 = 0%, G3 = 0% and G4 = 0%. The mean PSA at 6 months was 0.28 ng / ml [0-1.2] and at 12 months 0.15 ng / ml [0-1.1]

#### Conclusion

According to the results presented, we didn't see any moderate or severe urinary nor rectal toxicity. Related to these results, lymph nodes irradiation in a hypofractionation schedule, could be a safe option for patients. Due to the limitations of these report, related to low patient volume and short follow up, these results should be confirmed in a prospective trial.

#### EP-1572 How multiparametric magnetic resonance changes the staging and treatment of prostate cancer

S. Fernandez Alonso<sup>1</sup>, S. Guardado González<sup>1</sup>, J. Durá Esteve<sup>1</sup>, A. Rodríguez Antolín<sup>2</sup>, M.J. Buj Pradilla<sup>3</sup>, I. Alda Bravo<sup>1</sup>, M. Alarza Cano<sup>1</sup>, J.F. Pérez-Regadera Gómez<sup>1</sup>, M.Á. Cabeza Rodríguez<sup>1</sup>

<sup>1</sup>Hospital Universitario 12 de octubre, Radiation Oncology, Madrid, Spain ; <sup>2</sup>Hospital Universitario 12 de Octubre, Urology, Madrid, Spain ; <sup>3</sup>Hospital Universitario 12 de Octubre, Radiodiagnosis, Madrid, Spain

#### Purpose or Objective

To determine the implication of multiparametric magnetic resonance (mpMRI) in the management of localized prostate cancer (PCa) and the correlation between PIRADS and histological grade.

#### Material and Methods

A retrospective study and a correlation statistical analysis were carried out in 149 patients diagnosed with localized PCa who underwent mpMRI +/- MR-guided biopsy (MRGB) before receiving treatment between 2015 and 2018.

#### Results

The mean age was 66 years and the mean PSA was 10.02 ng/ml. The mean time interval between diagnosis and mpMRI was 14 weeks.

The indication for mpMRI was staging in 73% cases, diagnostic in 16% and follow - up in 10%.

Rectal examination, transrectal ultrasound (TRUS) and transrectal biopsy did not found disease in 22 cases (14%). In cases where illness was found, 67% were T1c, 21% T2a, 10% T2b-c and 2% T3a. After MpMRI 15% were T1c, 15% T2a, 20% T2b-c and 40% T3-4. Spearman's correlation coefficient was 0.33.

Regarding GS, before MRGB 22 cases had not got histological confirmation; 60% were GS6, 19% GS7 and 7% GS8-10. MpMRI detected more clinically significant

prostate cancer, being after MRGB 57% GS6, 26% GS7 and 17% GS8-10. Kendall's correlation coefficient was 0.8.

MRGB gave the diagnosis of the 22 initially negative patients; 2 of them were GS6, 6 GS7, 13 GS8-9; about patients initially GS6, 5 of them were finally GS7 and 2 GS8.

Also, it confirmed histological suspicious lesions located on the anterior and transitional zone (considered as higher risk) seen in mpMRI but not in TRUS in 17 patients (11%). Grades GS8-9 were related to stages T3a, T3b and T4 by mpMRI with a Spearman's correlation coefficient of 0.42. Correlated with PIRADS classification, 16% of GS 6 were PIRADS 2-3, 63% PIRADS-4 and 20% PIRADS-5. Among GS7, 8% were PIRADS2-3, 33% PIRADS-4 and 58% PIRADS-5.

Of the GS8-9, 44% were PIRADS-4 and 56% PIRADS-5.

The GS 8-9 values were associated with higher PIRADS, with a Spearman correlation coefficient of 0.287.

Regarding the risk group, after mpMRI +/- MRGB, 52% belonged to high risk, to medium risk 27.5% and to low risk 20.5 %, while initially 14% did not have diagnosis, 11% belonged to high risk, 36 % to intermediate and 39% to low risk group. Spearman's correlation coefficient was 0.5.

As a result, mpMRI changed the treatment in 54% patients; 41% left active surveillance, brachytherapy was rejected in 5% and surgery in 8%, being finally treated with radiotherapy plus hormone therapy.

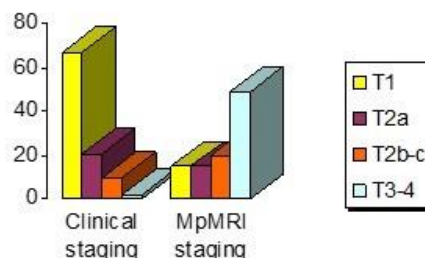


Figure 1: Prostate cancer staging.

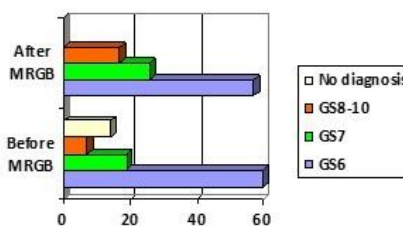


Figure 2: Gleason score.

#### Conclusion

Through clinical staging with TRUS and TRUS-guided biopsy, histological grade and staging of a part of tumors may be underestimated

In our experience, mpMRI modified histological grade in a third of patients, risk group in 50% and treatment decision in 54% cases.

Therefore, we recommend the use of mpMRI in PCa staging to carry out an adequate management of the disease according to its characteristics.

#### EP-1573 Is there an optimal OAR-filling protocol reducing G2+-toxicity for prostate IMRT?

J. Marzec<sup>1</sup>, F. Paulsen<sup>1</sup>, S. Westbomke<sup>1</sup>, Z. Outaggarts<sup>1</sup>, D. Wegener<sup>1</sup>, D. Thorwarth<sup>2</sup>, D. Zips<sup>1</sup>, A. Müller<sup>1</sup>

<sup>1</sup>Department of Radiation Oncology, University Hospital, Tübingen, Germany ; <sup>2</sup>Section for Biomedical Physics Department of Radiation Oncology, University Hospital, Tübingen, Germany

#### Purpose or Objective

Prediction of genitourinary (GU) and gastrointestinal (GI) toxicity after prostate cancer intensity modulated radiotherapy (IMRT) based on organs at risk (OAR) prescriptions is limited. Therefore, we investigated the potential impact of bladder-, rectal- and target volumes on acute side-effects of patients treated in a prospective study.

#### Material and Methods

Twenty-eight patients received a dose-escalated IMRT of localized prostate cancer (257/2007B01). Radiotherapy was performed using the coverage probability concept to a total dose of 78Gy in 39 fractions. All patients underwent at least three planning CTs and were instructed according to a bladder-rectal filling protocol (aim: bladder volume of 250-500ml, empty rectum). Contouring of OARs and target volumes was performed in each CT and three OAR-volumes per patient were measured. Incidence of acute GU/GI-toxicities (RTOG) was correlated with bladder-, rectal- and PTV-volumes. The volumes of 28 patients were descriptively evaluated by SPSS and subdivided in 4 quartiles (i.e. 7 patients per quartile).

#### Results

Acute toxicity was predominately detected in patients with small bladder volume, large or small rectal volume and large target volume.

**GU-toxicity** (G0/G1/G2: 5/15/8): Patients with the smallest bladder volume quartile (<188.41ml) represented with G2 (n=3) and G0/1 (n=1/3) toxicity. This equals 37.5% of G2-toxicities and 20% of G0- and G1-toxicities. The largest target volume quartile (>271.17ml) was connected to toxicity of grade G2 (4/7), G1 (2/7) and G0 (1/7) accounting for 50% (G2), 20% (G1) and 13% (G0) of GU-toxicities. Combination of adverse factors i.e. small bladder volume (<188.41ml) and large target volume (>271.17ml) was only present in 33% of patients experiencing G2 toxicity.

**GI-toxicity** (G0/G1/G2: 6/16/6): Considering the lowest (<63.36ml) and highest quartile (>166.87ml) of rectal volume 66% of patients experiencing G2-toxicity were in these quartiles compared to G1 with 50% and G0 with 33%. The largest quartile of PTV (>271.17ml) was always connected to GI-toxicity of at least G1 (n=5) and higher (G2=2). Presence of even small rectal maxima exceeding 80Gy (rectal V80>0.26ml) were related to G2-toxicity (83%, n=5/6). Combination of adverse factors i.e. small/large rectal volume and rectal V80>0.26ml were associated with increased toxicity (G1=31%, G2=50%).

#### Conclusion

GU-toxicity was reduced in case of a minimal bladder volume  $\geq 188.41$ ml and a target volume <271.17ml. GI-toxicity was less apparent in patients with intermediate rectal volumes between 63.36-166.87ml and absence of rectal hot spots >80Gy. Combination of these adverse factors was always connected to toxicity (no G0) and should therefore be avoided during treatment planning. These findings need to be substantiated in a larger cohort.

#### EP-1574 Four-year outcomes of hypofractionated proton therapy for localized prostate cancer

A. Grewal<sup>1</sup>, C. Schonewold<sup>1</sup>, S. Both<sup>2</sup>, S. Lam<sup>1</sup>, S. Mazzoni<sup>1</sup>, J. Bekelman<sup>1</sup>, J. Christodouleas<sup>1</sup>, N. Vapiwala<sup>1</sup>

<sup>1</sup>University of Pennsylvania, Department of Radiation Oncology, Philadelphia, USA ; <sup>2</sup>University Medical Center of Groningen, Department of Radiation Oncology, Groningen, The Netherlands

#### Purpose or Objective

Moderately hypofractionated radiation therapy represents an effective treatment for localized prostate cancer.

Hypofractionated proton therapy (HFPT) has not been extensively studied. The purpose of this study was to determine the toxicity profile and biochemical-clinical failure (BCF) rates for patients with localized prostate cancer treated with HFPT.

#### Material and Methods

Between 2010 and 2017, 184 men were enrolled on a prospective trial of 70Gy in 28 fractions of proton therapy for localized low- to intermediate-risk prostate cancer. Short-term androgen suppression (AS) was allowed, per institutional practice. Acute and late toxicity was evaluated using the Common Terminology Criteria for Adverse Events, version 4.0 (CTCAEv.4.0). Patient-reported urinary quality-of-life changes and erectile changes were captured using the International Prostate Symptom Score (IPSS) and the International Index of Erectile Function (IIEF-5) Questionnaire, respectively.

#### Results

Median follow-up was 49.2 months. Enrolled patients had low-risk [LR] (n=18), favorable intermediate-risk [FIR] (n=78), and unfavorable intermediate-risk [UIR] (n=88) disease. Twenty-six percent of patients received neoadjuvant and concurrent AS, with a median duration of 6 months.

Four-year rates of BCF free survival were 95.7%, 94.4%, 98.7%, and 93.2% in the overall group and the LR, FIR, and UIR cohorts, respectively (p=.21). Overall survival at 4 years was 97.3%. All 5 deaths were unrelated to prostate cancer.

Median IPSS before treatment and at 1 year after treatment were 6 and 7 for LR patients, 6 and 6 for FIR patients, and 8 and 7 for UIR patients. Median IIEF-5 before treatment and at 1 year after treatment were 21 and 18 for LR patients, 18 and 16.5 for FIR patients, and 15 and 10.5 for UIR patients.

The incidence of acute CTCAE v4.0 grade 2 or higher gastrointestinal (GI) and urologic toxicities were 3.8% (7 events) and 12.5% (23 events), respectively. Only one acute grade 3 GI toxicity was reported. The estimated cumulative 4-year incidence of late grade 2 or higher urologic toxicity was 7.6% (14 events), with no grade 3 or 4 events reported. The estimated cumulative 4-year incidence of late grade 2 or higher GI toxicity was 13.6% (25 events), with one grade 3 event and no grade 4 events. The predominant late grade 2 GI toxicity was rectal bleeding, and late grade 2 urologic toxicity was urinary frequency, accounting for 79% and 57% events, respectively. All late grade 2 and 3 events were transient. There were no associations between risk group, anticoagulation use, or history of transurethral resection of the prostate and incidence of acute or late toxicity.

#### Conclusion

HFPT for the treatment of prostate cancer is associated with low rates of urologic and GI toxicity, and low rates of patient-reported urinary bother post-treatment. Further analyses are warranted to assess long-term toxicity and understand differences between proton and photon hypofractionated radiation therapy in the treatment of prostate cancer.

#### EP-1575 Stereotactic Body Radiotherapy in bone oligometastatic prostate cancer patients

F. Trippa<sup>1</sup>, F. Arcidiacono<sup>1</sup>, A. Di Marzo<sup>1</sup>, L. Draghini<sup>1</sup>, P. Anselmo<sup>1</sup>, S. Terenzi<sup>1</sup>, M. Casale<sup>1</sup>, S. Fabiani<sup>1</sup>, E. Maranzano<sup>1</sup>

<sup>1</sup>Radiotherapy Oncology Centre, Santa Maria Hospital, Terni, Italy

#### Purpose or Objective

The first line treatment of metastatic prostate cancer (PC) is androgen-deprivation therapy (ADT). A subgroup of patients (pts) with disease progression can present few lesions (i.e., oligometastases). Stereotactic body radiotherapy (SBRT) delivers high ablative doses of radiotherapy while sparing adjacent tissues. We used SBRT

in selected PC oligometastatic pts with bone metastases (BM) to improve local control and delay the start of ADT or pharmacologic second-line therapy.

#### Material and Methods

Between October 2010 and July 2018, in 17 oligometastatic PC pts with a total of 20 BM local control (LC) rate, biochemical progression free-survival (b-PFS) and time to beginning of ADT were evaluated. Median age was 72 years (range, 57-87), median Gleason score at the primary diagnosis was 7 (range, 5-9). Median time from primary treatment to SBRT was 53 months (range 2-134 months). Diagnosis of BM was documented by Choline-PET/CT. Median PSA value before SBRT was 2.25 ng/ml (range, 0-46.8). Ten (59%) oligometastatic ADT-free pts underwent SBRT alone, while the other 7 (41%) oligometastatic castration-resistant prostate cancer (CR-PC) pts, continued ADT. Three (18%) pts underwent SBRT for two synchronous BM. The BM sites were: pelvis in 12 (60%), spine and ribs in 6 (30%), and in 2 (10%) cases, respectively. Gross tumor volume (GTV) was delineated using Choline-uptake and planning target volume was defined as the GTV plus a 5 mm isotropic margin. Radiotherapy schedules adopted were 5 × 5-8Gy in 13 (65%) BM and 3 × 9-10Gy in 7 (35%) BM. Response was assessed with PSA evaluation every 3 months during the first year and then every 6 months. Pts with a reduction or a stability of PSA level were considered responders, Choline-PET-CT was done in case of an increase of PSA level.

#### Results

The median follow-up was 10 months (range 3-96). All (100%) patients had a decrease of PSA level after SBRT. Nine (53%) pts remained b-PFS, while 8/17 (47%) pts had new PSA increase after a median time of 8 months (2-48). Among biochemical progression pts, Choline-PET/TC showed LC in 100% of the treated lesions and a disease progression in other sites. At last follow-up one (6%) patient has died for PC, the other 16 (94%) were alive. Of note, 7 CR-PC pts before SBRT continued ADT but they did not have to start second-line therapy; 2/10 (20%) ADT-free pts before SBRT had to start ADT due to disease progression for an ADT-free survival of 9 months (3-96). No SBRT related acute or late toxicities were observed.

#### Conclusion

Our experience showed that SBRT of BM was highly effective with an excellent risk-benefit profile. SBRT in PC bone oligometastases pts should be evaluated to improve response rate and delay ADT or pharmacologic second-line therapy.

#### EP-1576 Middle Half Body Radiotherapy in bone metastases from prostate cancer: a phase I study

A. Zamagni<sup>1</sup>, M. Buwenge<sup>1</sup>, G. Siepe<sup>1</sup>, A. Arcelli<sup>1</sup>, C.M. Donati<sup>1</sup>, S. Bisello<sup>1</sup>, G. Macchia<sup>2</sup>, F. Deodato<sup>2</sup>, S. Cilla<sup>3</sup>, M. Ferro<sup>2</sup>, V. Picardi<sup>2</sup>, M. Boccardi<sup>2</sup>, E. Arena<sup>2</sup>, A. Ianiro<sup>2</sup>, P. Farina<sup>4</sup>, C. Pozzo<sup>4</sup>, A.A. Woldemariam<sup>5</sup>, T. Wondemagegnhu<sup>5</sup>, G.P. Frezza<sup>6</sup>, A.G. Morganti<sup>1</sup>, S. Cammelli<sup>1</sup>

<sup>1</sup>Radiation Oncology Center- Department of Experimental- Diagnostic and Specialty Medicine - DIMES, University of Bologna- Sant'Orsola-Malpighi Hospital, Bologna, Italy ; <sup>2</sup>Radiotherapy Unit, Fondazione di Ricerca e Cura "Giovanni Paolo II", Campobasso, Italy ; <sup>3</sup>Medical Physics Unit, Fondazione di Ricerca e Cura "Giovanni Paolo II", Campobasso, Italy ; <sup>4</sup>Medical Oncology Unit, Fondazione di Ricerca e Cura "Giovanni Paolo II", Campobasso, Italy ; <sup>5</sup>Department of Radiotherapy, Black Lion Hospital, Addis-Ababa, Ethiopia ; <sup>6</sup>Radiation Oncology Unit, Bellaria Hospital, Bologna, Italy

#### Purpose or Objective

In 2001 a clinical randomized trial from IAEA tested 2D Half Body Irradiation (HBI) for palliative treatment of multiple bone metastases demonstrating that a dose of 12

Gy in 4 fractions, twice a day, had the same effectiveness and tolerability of a total dose of 15 Gy in 5 daily fractions. However, the 2-days treatment was more comfortable and time-saving for patients (pts), in a variety of metastatic malignancies, with the exception of prostate cancer. In fact, in metastatic prostate disease, better outcome and lower toxicity were observed with a longer therapeutic schedule. Aim of our study was to evaluate the possibility to deliver the higher dose (15 Gy) in 4 fractions twice a day, in the specific setting of HBI defined as middle half body (MHB: pelvis, femurs and lumbar spine) by using a multiple field 3D-conformal technique to reduce toxicity.

#### Material and Methods

A phase I trial in 3-dose escalation steps was designed: 13 Gy (3.25 Gy-fractions), 14 Gy (3.5 Gy-fractions), and 15 Gy (3.75 Gy-fractions). The eligibility criteria included prostate cancer with painful bone metastatic disease in MHB fields, ECOG performance status ≤ 3, life expectancy > 3 months, no severe bone marrow dysfunction. Treatment was delivered in 2 days with twice-daily fractionation and at least 6 hours interval. Pts were treated in cohorts of 6-12 to define the maximum tolerated dose (MTD). The dose-limiting toxicity (DLT) was defined as any acute toxicity of grade 3 or greater, using the RTOG scale. Pain was recorded using a visual analogue scale. IAEA pain and drug score were also registered.

#### Results

25 patients were enrolled. Only grade 1-2 acute toxicity was recorded. No pts experienced DLT. With a median follow-up of 7.4 months, only two cases of G1 skin late toxicity were observed. The overall (complete plus partial) response rate for pain was 84% (21/25 pts): 9 pts had complete pain relief (VAS=0), 10 pts showed at least 30% VAS reduction, 2 pts showed an improvement in pain score and drug score with 20 and 25% VAS reduction respectively.

#### Conclusion

The MTD of short course MHB radiotherapy in patients with bone metastases is 15 Gy. Preliminary data on palliative efficacy are promising.

#### EP-1577 Prostate SBRT with Gantry-based LINAC without ConeBeam. Toxicity outcomes of 205 patients

P. Castro Peña<sup>1</sup>, A. Henao<sup>1</sup>, P. Murina<sup>1</sup>, O. Muriano<sup>1</sup>, L. Suarez Villasmil<sup>1</sup>, A. Giraudo<sup>1</sup>, J.C. Archilla<sup>1</sup>, D. Venencia<sup>1</sup>, S. Zunino<sup>1</sup>

<sup>1</sup>Instituto Zunino - Fundacion Marie Curie, Radiation Oncology, Cordoba, Argentina

#### Purpose or Objective

To describe the technique of SBRT in 5 fractions, with IGRT ExacTrac only based, in patients with prostate cancer. Analyze of toxicity and biochemical response, in patients with age of 6 months of follow-up

#### Material and Methods

Between Nov / 13 and Jun / 15, 223 patients with a positive prostate cancer biopsy were treated; Mean initial PSA = 25 ng / ml [0.42-1890] and mean prostate volume = 52.8 g [18.1-134]. All were irradiated with SBRT technique in 5 fractions (alternate days), following the institutional protocol. For IGRT (intra and interfraction) based on ExacTrac, 4 intraprostatic fiducial markers were implanted 2 weeks before. Virtual simulation based on CT with 1mm cuts at the prostate level. Drawing of volumes and dosimetry with planning system iPLAN-Net (BrainLab) and Eclipse (Varian). Prescribed dose in 95% PTV-prostate = 40 Gy (95.6%) and 36.25 Gy (4.4%), according to institutional medical criteria. The patients were irradiated with Novalis Tx technology (BrainLab-Varian), high resolution multilamellar collimator (HDMLC) with 2.5mm plates. They were planned and irradiated with IMRT-dynamics technique, using 9 beams of 6 MV. Genitourinary toxicity (GU) was evaluated using the IPSS (International Prostate Symptom Score) (0-35 points) and

gastrointestinal (GI) scale according to the RTOG criteria (Grade 0-5). The PSA was systematically registered.

#### Results

We analyzed 205 patients with follow-up longer than 6 months. The average age was 69 years [48-86.6]. The distribution by risk group was: 12.6%, 62.2%, 23.3% and 1.9% for low, medium, high and metastatic respectively. Average follow-up: 24.7 months [5.7-46.3]. The mean of the IPSS prior to SBRT was = 6.1 [0-35]. After SBRT: 5.1 [0-31], 5.5 [0-30], 4.7 [0-22], 4.7 [0-19] and 5.5 [0-26] to 6, 12, 18, 30 and 42 months respectively. The rate and degree of rectal toxicity at the end of SBRT was: G0 = 96.6%; G1 = 2.4% and G2 = 1%. At 6 months: G0 = 84.2%; G1 = 9.2%, G2 = 5.1% and G3 = 1.5%. At 12 months: G0 = 89.3%; G1 = 5.3%; G2 = 2.4%, G3 = 1.8% and G4 = 1.2%. At 18 months: G0 = 90.8%; G1 = 6.8%; G2 = 0.8% and G4 = 0.8%. At 30 months: G0 = 90.7%, G1 = 8.5 and G4 = 0.8%. At 42 months: G0 = 99.2%, G4 = 0.8%. The mean PSA value in ng / ml, Pre-SBRT was = 16.54 [0.01-1890] and after 24 months = 5.32 [0.03-115].

#### Conclusion

According to the presented results we can suggest that SBRT Prostate based on a Novalis platform with IGRT ExacTrac based, is convenient for the patient, has acceptable toxicity rate, without significant difference with the Cone-Beam results published. The assessment of the impact on disease control deserves longer follow-up.

#### EP-1578 Hypofractionated postoperative imrt-igrt in prostate cancer single-institution preliminary results

J. Valero Albarran<sup>1</sup>, E. Pérez Sanchez<sup>2</sup>, A. Montero<sup>1</sup>, O. Hernando Requejo<sup>3</sup>, E. Sanchez<sup>1</sup>, R. Ciervide<sup>1</sup>, M. Lopez<sup>1</sup>, M.D.L.O. Garcia Aranda<sup>3</sup>, X. Chen<sup>1</sup>, B. Alvarez<sup>4</sup>, A. Acosta<sup>1</sup>, R. Alonso<sup>5</sup>, J. Palma<sup>1</sup>, M. Nuñez Baez<sup>4</sup>, P. Fernandez Leton<sup>6</sup>, J. Martin Asenjo<sup>7</sup>, J.M. Perez<sup>8</sup>, J. Garcia<sup>8</sup>, D. Zucca<sup>9</sup>, M. De la Casa<sup>9</sup>, M. Serrano<sup>10</sup>, L. Osorio<sup>11</sup>, C. Escaleras<sup>11</sup>, M.D. Fenor<sup>12</sup>, C. Rubio<sup>13</sup>

<sup>1</sup>Hospital University HM Sanchinarro, Radiation Oncology, Madrid, Spain ; <sup>2</sup>Hospital University Nuestra Señora de la Candelaria, Radiation Oncology, Tenerife, Spain ;

<sup>3</sup>Hospital University HM Sanchinarro, Radiation Oncology, Madrid, Spain ; <sup>4</sup>Hospital University HM Sanchinarro, Radiation Oncology, Madrid, Spain ;

<sup>5</sup>Hospital University HM Puerta del Sur, Radiation Oncology, Madrid, Spain ;

<sup>6</sup>Hospital University HM Sanchinarro, Hospital University HM Sanchinarro- Radiophysic, Madrid, Spain ;

<sup>7</sup>Hospital University HM Sanchinarro, Radiophysic, Madrid, Spain ;

<sup>8</sup>Hospital University HM Sanchinarro, Radiophysic, Madrid, Spain ;

<sup>9</sup>Hospital University HM Sanchinarro, Radiophysic, Madrid, Spain ;

<sup>10</sup>Hospital University HM Sanchinarro, Urology, Madrid, Spain ;

<sup>11</sup>Hospital University HM Sanchinarro, Urology, Madrid, Spain ;

<sup>12</sup>Hospital University HM Sanchinarro, Medical Oncology, Madrid, Spain ;

<sup>13</sup>Hospital University HM Sanchinarro, Radiation Oncology, Spain, Spain

<sup>14</sup>Hospital University HM Sanchinarro, Radiation Oncology, Madrid, Spain ;

<sup>15</sup>Hospital University HM Sanchinarro, Radiation Oncology, Madrid, Spain ;

<sup>16</sup>Hospital University HM Sanchinarro, Radiation Oncology, Madrid, Spain ;

<sup>17</sup>Hospital University HM Sanchinarro, Radiation Oncology, Madrid, Spain ;

<sup>18</sup>Hospital University HM Sanchinarro, Radiation Oncology, Madrid, Spain ;

<sup>19</sup>Hospital University HM Sanchinarro, Radiation Oncology, Madrid, Spain ;

<sup>20</sup>Hospital University HM Sanchinarro, Radiation Oncology, Madrid, Spain ;

<sup>21</sup>Hospital University HM Sanchinarro, Radiation Oncology, Madrid, Spain ;

<sup>22</sup>Hospital University HM Sanchinarro, Radiation Oncology, Madrid, Spain ;

All patients underwent treatment with IMRT up to a total dose of 62.5Gy/2.5Gy/day in 25 fractions (EQD2Gy for a/b=1.5 of 70 Gy). Daily verification was performed with IGRT. Eight p (10%) received androgen deprivation. Acute Toxicity was assessed according to CTCAE 5.0. Late toxicity was scored with RTOG/EORTC criteria. Biochemical relapse was defined as PSA increase of 0,2 ng/mL or greater from the post-RT nadir (confirmed with a second increase). Institution review board approved this study

Gleason score:	n	%
6		
7(3+4)	13	30
7(4+3)	16	37
8-10	26	11
	33	14
<b>Seminal vesicles invasion:</b>	n	%
-Yes	14	66
-No	66	82
<b>Extracapsular extension:</b>	n	%
-Yes	30	38
-No	50	62
<b>Positive Margin:</b>	n	%
-Yes	38	48
-No	42	52
<b>Perineural invasion:</b>	n	%
-Yes	40	50
-No	50	50
<b>Linfovascular invasion:</b>	n	%
-Yes	12	15
-No	68	85

#### Results

All patients received complete treatment. There were no complications during marker placement. Follow-up: 17 months (range 3-39 months). Of the 80 patients, 68 demonstrated a continuous biochemical response after treatment. Three patients had regional lymph nodes and 3 p distant metastasis. Only one patient died for lung cancer. All remaining patients were alive at the last follow up visit. The cancer specific survival is 100%. The estimated actuarial SLRB rate at 1, 2 and 3 years was 88%, 78% and 72% respectively. A pre salvage PSA level no significant prognostic factor for biochemical control (Breslow p = 0.075), log-rank (p=0.251). Maximal acute urinary (GU) toxicity: G2 in 4% (3 p) of patients. Maximal acute gastrointestinal (GI) toxicity: G2 in 1% of patients (1p). There was no grade 3, 4 or 5 acute toxicity. Neither urinary stress nor incontinence was influenced by radiation therapy. Late toxicities were evaluated in all patients. No G3 or greater late toxicities were observed. Late G2-GU: 2%; G2-GI: 0. No relationship was found between acute and late GU or GI adverse effects and any of the analyzed parameter> age, androgen deprivation or urinary incontinence pre/treatment.

#### Conclusion

Hypo-IMRT with IGRT for postoperative PC is feasible and well tolerated showing encouraging rates of BRFS although longer follow up is required.

#### EP-1579 Prior prostatectomy MRI improves target coverage of adjuvant radiotherapy for pT3bNo prostate cancer

G. Kacsó<sup>1</sup>, T. Popescu<sup>2</sup>, P. DAniel<sup>2</sup>, C. Iacob<sup>3</sup>, R. Zahu<sup>3</sup>, A. Eva<sup>4</sup>, D. Dordai<sup>4</sup>

<sup>1</sup>Radiotherapy Center AMETHYST- UMF Iuliu Hatieganu Cluj, Radiotherapy, Cluj, Romania ; <sup>2</sup>The Institute of Oncology "Prof Dr Ion Chiricuta" Cluj-NAPOCA, Radiotherapy, Cluj-Napoca, Romania ; <sup>3</sup>Radiotherapy Center AMETHYST, Radiotherapy, Cluj, Romania ; <sup>4</sup>Radiotherapy Center AMETHYST, Radiotherapy- Physics, Cluj, Romania

#### Purpose or Objective

Seminal vesicle (SV) invasion (pT3b) is accepted by all guidelines as criteria for adjuvant radiotherapy (aRT) after radical prostatectomy (RP). Our hypothesis was that the delineation of the tumour bed as per ESTRO guidelines might be improved by MRI fusion into the planning.

#### Material and Methods

Twelve pT3bNo, cM0 prostate adenocarcinoma patients (50 % with peri-vesicular extension) having received aRT in our institution during 2016-2017 were retrospectively contoured by fusing the preoperative prostate MRI into the treatment planning. The treated (postoperative) CTV and PTV (+5 mm) were according to the ESTRO delineation guidelines; 66Gy/33 fr IMRT/VMAT with daily IGRT were delivered. The preoperative MRI SV length was divided in 3 levels (lower, middle and upper third), expanded to PTV with the same margin as in the actual plan (5mm). We analysed the "geographic miss" of the postoperative dosimetry applied to the "preoperative SV adapted" delineation.

#### Results

Assuming all of them would have had peri-vesicular extension, the coverage of the SV bed was suboptimal for 8.3 % of the lower third, 25 % of the middle third and 16.6 % of the upper third of the SV, leaving only 50 % accurate PTV coverage!

#### Conclusion

Integrating the preoperative MRI into the RT planning might improve the target coverage in a substantial number of pT3b cases. We suggest that future ESTRO guidelines shall consider fusion of the prior prostatectomy prostate MRI into the treatment planning for adjuvant or salvage RT.

#### EP-1580 Adjuvant radiotherapy in prostate cancer patients-bRFS and toxicity using adaptive IMRT technique

P. Toncheva<sup>1</sup>, N. Volegova - Neher<sup>1</sup>, K. Henne<sup>1</sup>, A. Grosu<sup>1</sup>, S. Kirste<sup>1</sup>

<sup>1</sup>Uniklinik Freiburg, Radiation Oncology, Freiburg, Germany

#### Purpose or Objective

In this retrospective study we assessed local tumor control and biochemical recurrence free survival (bRFS) in a single center cohort of prostate cancer patients who underwent postoperative radiation therapy in adaptive IMRT technique. Furthermore we investigated acute and long - term genitourinary and gastrointestinal toxicities.

#### Material and Methods

We evaluated 140 high risk prostate cancer patients who were treated between 2010 and 2014 within 6 months after radical prostatectomy. Depending on bladder and rectum volumes the planning target volume (PTV) was adapted. Median prescription dose applied to the prostate bed was 66,6 Gy in 37 fractions. 39 out of 62 node positive patients received up to 54 Gy to the pelvic lymph nodes. Descriptive statistics as well as uni- and multivariate analysis were performed.

#### Results

Median follow up was 48 months (2 - 86 months). The 4 - year overall survival rate was 94%. 4 - year bRFS was 55%. 51 out of 140 patients developed a recurrence. Biochemical recurrence was observed in 15 patients, 30 patients developed a recurrence outside the treatment field and 6 patients had a recurrence inside the treatment field. Acute grade 3 genitourinary toxicity occurred in 3

patients (2%) and late grade 3 genitourinary toxicity was observed in 2 patients (1%). Acute and late grade 3 gastrointestinal toxicities occurred in 5 patients (4%) and 2 patients (1%). Lymph node status, pelvic lymph node irradiation, Gleason score, neoadjuvant and concomitant hormonal therapy were significant variables in univariate analysis for bRFS (p<0,05). Multivariate cox regression analysis identified lymph node status as having significant influence on bRFS.

#### Conclusion

Postoperative radiotherapy is able to deliver long - term biochemical disease free survival in a substantial number of patients with prostate cancer and high risks features. The majority of recurrences occur outside the treatment field. Modern radiotherapy techniques including IMRT and plan adaptation can reduce toxicity to < 4% in the postoperative setting.

#### EP-1581 Good tolerability of hypofractionated radiation therapy for localized prostate cancer

I. Navarro<sup>1</sup>, R. Correa<sup>1</sup>, A. Otero<sup>1</sup>, A. Roman<sup>1</sup>, I. Zapata<sup>1</sup>, A. Fernandez<sup>1</sup>, P. Prieto<sup>1</sup>, S. Segado<sup>1</sup>, C. Jodar<sup>1</sup>, C. Garrido<sup>1</sup>, J.A. Medina<sup>1</sup>, J. Gomez<sup>1</sup>

<sup>1</sup>Hospital Virgen de la Victoria, Radiation Oncology, Malaga, Spain

#### Purpose or Objective

Radiobiological models have determined a low  $\alpha/\beta$  value for prostate cancer (1.5Gy), which suggests a good response with fewer and larger fractions. Some randomized studies of hypofractionation in prostate cancer have been published, reported a high differences in patients selection and in the risk, dose and technical groups used; unable to establish as standard treatment. To analyze the efficacy and toxicities of localized prostate cancer (LPC) patients treated with curative hypofractionated radiotherapy, with a long follow up. These patients were treated outside of a clinical trial. We also evaluate the results in subgroups of patients to determine possible prognostic factors.

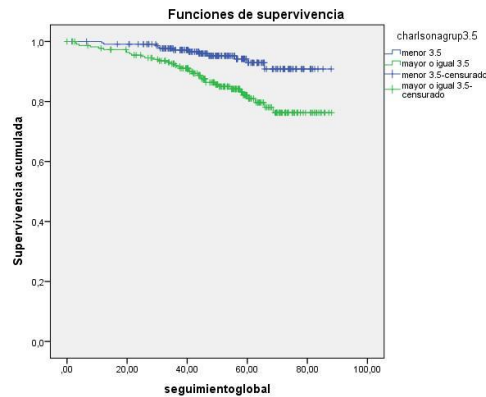
#### Material and Methods

Retrospective study of 451 patients with LPC treated with hypofractionated radiotherapy, in our institution, between January 2011 and May 2016. The scheme used was 60Gy to 3Gy/fraction, using 3D and volumetric arc therapy techniques (VMAT). We analyzed the Charlson Comorbidity Index (CCI) as a predictor of survival at 10 years. We also analyzed the age, Gleason score, stage and NCCN risk factors, as well the use of androgen deprivation therapy. Toxicity was evaluated using Common Terminology Criteria for Adverse Events (CTCAE) Version 4.0. The overall survival (OS) was defined as the time from the last day of radiotherapy until the date of last revision. We considered biochemical progression (BP) as Phoenix's definition of more 2ng/dl of PSA nadir; and clinical recurrence (CR) as progression to locoregional lymph-nodes or distant metastases.

#### Results

With a median follow-up of 51 months (1.6-88 months), only 1.6% (7 patients) died due to the disease, 89.6% remained alive, 8.4% with biochemical disease, and 3.3% with clinical disease. We observed a high rate of any grade of acute genitourinary toxicity (72.7%), most of them grade 1. But only 20% of chronic genitourinary toxicity was observed. The acute and chronic rectal toxicity showed a low rate, 19.1% and 2.7%, respectively. The radiotherapy technique was significantly associated with acute rectal toxicity. Thus, patients treated with VMAT presented toxicity in 23.9% versus 13.5% with RT3D (p=0.005). The OS at 2, 5 and 7 years was 97%, 88% and 83% respectively. Disease-free survival until BP was 96%, 83.8% and 77.9%. And for the CR, it was 99%, 94% and 92%, respectively. Regarding the survival analysis, the CCI was the only factor with statistical significance for OS (p = 0.00), with a greater number of events being observed in

the patients with CCI  $\geq$  to 3.5 (Image 1). Moreover, those patients with high or very high risk, presented a lower survival ( $p=0.032$ ), as well as patients with higher Gleason ( $p=0.04$ ).



### Conclusion

Hypofractionated radiotherapy with escalated doses in prostate cancer is a well-tolerated treatment, with a low rate of chronic toxicity and with a high efficacy. The hypofractionation benefits allow reducing the number of sessions thus improving the quality of life, the use of resources and decreases the cost of treatment.

### EP-1582 Differences between 3d and vmat in hypofractionated radiation therapy for localized prostate cancer

I. Navarro<sup>1</sup>, R. Correa<sup>1</sup>, A. Roman<sup>1</sup>, A. Otero<sup>1</sup>, A. Fernandez<sup>1</sup>, P. Prieto<sup>1</sup>, M.J. Garcia<sup>1</sup>, I. Garcia<sup>1</sup>, R. Ordoñez<sup>1</sup>, I. Jerez<sup>1</sup>, J.A. Medina<sup>1</sup>, J. Gomez<sup>1</sup>  
<sup>1</sup>Hospital Virgen de la Victoria, Radiation Oncology, Malaga, Spain

### Purpose or Objective

External beam radiotherapy (RT) is an appropriate treatment option for patients with localized prostate cancer. Some studies have shown superiority of dose escalation in the control of the disease. However, an increase in toxicity has been described with these regimens. The use of intensity modulated radiotherapy (IMRT) with volumetric arc therapy (VMAT) and image-guided radiotherapy (IGRT) makes possible to carry out the treatment without increasing side effects. The objective is to analyze the differences between 3D and VMAT techniques in the toxicity profile, biochemical failure and clinical recurrence.

### Material and Methods

Retrospective study of a large number of patients with localized prostate cancer treated with hypofractionated radiotherapy (60Gy to 3Gy per fraction) with radical intention using 3D and VMAT techniques, both with daily image verification with cone beam CT (XVI), in our institution, between January 2011 and May 2016. After analyzing dose-volume histogram (DVH), those cases with satisfactory coverage of planning target volume (PTV) and dose constraints for organ at risk, were treated with 3D technique. More complex cases were treated performing VMAT. From May 2015, due to the better conformation treatment planning, translated into better DVH results and a shorter treatment time, all patients were treated with VMAT. The variables analyzed were the age, stage, Gleason score, NCCN risk group and seminal vesicles treatment, using univariate and multivariate analysis.  $P$  values  $< .05$  were considered statistically significant.

### Results

We analyzed 451 men with prostate cancer with a range of age between 45 and 81 (median 68 years). 208 patients (46.1%) were treated with 3D radiotherapy, and 243

patients (53.9%) with VMAT. The median follow-up was 51 months (maximum 88 months). The volume and the mean rectal and bladder doses were slightly higher in VMAT compared to 3D (Table 1). Regarding toxicity, we found differences between both groups. An increased acute rectal toxicity (any grade) was seen in 58 patients (23.9%) in VMAT group, compared to the group of 3D-RT with 28 patients (13.5%) ( $p = 0.005$ ). No statically difference was found in the rest of parameters analyzed, and no difference in chronic toxicity between both techniques (Table 2). The percentage of patients in the VMAT group had higher risk factors with significant differences (age  $> 68$  years, seminal vesicles included, Gleason score  $> 7$ , stage and NCCN group risk), in univariate and multivariate test. No difference in biochemical and clinical failure were observed.

Table 1.

		VMAT	3D
RECTUM	VOLUME	54.13 cc	55.16 cc
	MEAN DOSES	35.65 Gy	28.60 Gy
	V40	43.73%	25.10%
	V50	15.28%	11.85%
	V60	0.88%	1.15%
BLADDER	VOLUME	83.02 cc	86.75 cc
	MEAN DOSES	40.38 Gy	31.41 Gy
	V40	53.86%	36.10%
	V50	40.26%	25.85%
	V60	17.27%	5.60%

Table 2.

		RADIOTHERAPY TECHNIQUE		
		VMAT	3D	P
BIOCHEMICAL FAILURE	YES	27 (11.1%)	33 (15.9%)	0.13
	NO	216 (88.9%)	175 (84.1%)	
CLINICAL RECURRENCE	YES	7 (2.9%)	12 (5.8%)	0.12
	NO	236 (97.1%)	196 (94.2%)	
RECTAL ACUTE TOXICITY	NO	185 (76.1%)	180 (86.5%)	0.005
	YES	58 (23.9%)	28 (13.5%)	
GENITOURINARY ACUTE TOXICITY	NO	67 (27.6%)	56 (26.9%)	0.87
	YES	176 (72.4%)	152 (73.1%)	
RECTAL CHRONIC TOXICITY	NO	238 (98.3%)	199 (96.1%)	0.14
	YES	4 (1.7%)	8 (3.9%)	
GENITOURINARY CHRONIC TOXICITY	NO	192 (79.3%)	166 (80.2%)	0.82
	YES	50 (20.7%)	41 (19.8%)	

### Conclusion

We did not find significant differences between the two techniques used, except in acute rectal toxicity. This apparent difference may be due to the fact that the VMAT technique was considered to be the choice in those cases that required a greater volume of irradiation, when including the seminal vesicles, so that this increased toxicity could be more related to the total volume rather than to the technique employed.

### EP-1583 Feasibility of postprostatectomy dose escalated salvage radiotherapy by reduction of bladder dose

G. Sancho Pardo<sup>1</sup>, E. Acosta<sup>1</sup>, L. Tilea<sup>1</sup>, A. Soto<sup>1</sup>, A. Nuria<sup>1</sup>, G. Gómez de Segura<sup>1</sup>, J. Craven-Bartle<sup>1</sup>  
<sup>1</sup>Hospital de la Santa Creu i Sant Pau, Radiation Oncology, Barcelona, Spain

### Purpose or Objective

After radical prostatectomy, salvage RT with doses over 66 Gy to the prostate bed may confer a benefit but also an increased risk of genitourinary (GU) toxicity. In this setting, we analyse the acute and late GU toxicity and their association with dosimetric parameters.

### Material and Methods

We performed a retrospective study in 190 patients (pt) with prostate cancer who had biochemical failure after radical prostatectomy. Since June 2011, all patients underwent a multiparametric-MRI to investigate the site of recurrence before planning the radiation treatment. Clinical and planning target volumes (CTV and PTV) were contoured according to the EORTC guidelines. Elective pelvic irradiation was indicated in patients without

lymphadenectomy. We have progressively increased the dose delivered to the prostate bed from 66 to 71 Gy. In patients with visible recurrence, we registered the mpMRI and the simulation CT images to define a recurrence and to intensify the dose on it. The series include the first 25 pt treated with IMRT and moderate hypofractionation (2.1 to 2.35 Gy per fraction). For the analyses, total doses were converted into 2Gy-equivalent doses (EQD2) according to the linear quadratic model taking  $\alpha/\beta=1.5$  for the tumor and  $\alpha/\beta=3$  for bladder. Acute and late toxicity were scored according to the RTOG and CTCAE v4.0 scales. We have investigated the association among the dosimetric parameters and toxicity.

### Results

The multiparametric-MRI was positive in 79 pt (41.5%). Local recurrences were mostly located at the perianastomotic site. Lymph node recurrence occurred in 22 pt (11.5%). Median radiation doses (Gy) for pt treated with normofractionation were: 70.2 (64-71) in prostate bed, 73.8 (71-76) on local recurrence location, and 60.90 (56-75.2) on positive lymph nodes. The doses for hypofractionation were: 65 (63.8-70.2) in prostate bed, 68.5 (63.8-70.2) on local recurrence location and 60.9 (58.8-62.35) on positive lymph nodes. With a median follow-up of 40 months (2-75 months) 75% of pt showed biochemical and clinical control. We observed acute grade 2-3 GU toxicity in 3pt (3.2%). Grade 2, 3 and 4 GU late toxicity (mainly haematuria) was observed in 9 (5.1%), 7 (3.9%) and 1 (0.5%) pt respectively. Late haematuria grade  $\geq 2$  was higher in those patients with mean bladder dose > 50 Gy (10.8% vs 1.4%;  $p=0.017$ ) and/or bladder V70 > 30 Gy (20.8% vs 2.3%;  $p < 0.001$ ). None of the patients treated with IMRT showed late grade  $\geq 2$  haematuria.

### Conclusion

We recommend a very strict evaluation of bladder dose-volume histogram to decide whether or not to intensify the radiation dose after prostatectomy.

### EP-1584 Radium-223 treatment in Metastatic Prostate Cancer: Prognostic Factors: Real-world Outcome

R. Pearson<sup>1</sup>, X. Jiang<sup>1</sup>, S. Atkinson<sup>2</sup>, S. Cumming<sup>1</sup>, A. Burns<sup>3</sup>, J. Frew<sup>1</sup>, R. McMenemin<sup>1</sup>, I. Pedley<sup>1</sup>, A. Azzabi<sup>1</sup>  
<sup>1</sup>Newcastle upon Tyne Hospitals NHS Foundation Trust, Northern Centre for Cancer Care, Newcastle upon tyne, United Kingdom ; <sup>2</sup>Newcastle upon Tyne Hospitals NHS Foundation Trust, Dept of Nuclear Medicine, Newcastle upon tyne, United Kingdom ; <sup>3</sup>Newcastle upon Tyne Hospitals NHS Foundation Trust, Dept of Radiotherapy Information Technology, Newcastle upon Tyne, United Kingdom

### Purpose or Objective

Radium 223 (Ra-223) is a radiopharmaceutical used to treat men with metastatic castrate resistant prostate cancer (mCRPC) with symptomatic bone metastases. We aim to evaluate factors impacting survival outcomes from a heterogeneous cohort of 228 patients treated in a single UK centre.

### Material and Methods

We prospectively collected data from 228 men underwent Ra-223 therapy for mCRPC between April 2014 and August 2018. Survival outcomes were analysed and prognostic factors were extracted.

### Results

Medium age = 72 (51-87) years. Most patients (90.3%) whose baseline haemoglobin > 10g/dl (n=160) managed to complete 5-6 cycles of treatment in contrast to 13.2% if it was 8-10 g/dl (n=19) or 0% if < 8 g/dl (n=4). Key findings are summarised in table below.

Variables	Patient No (%)	Median Survival (mths)	p-value (log rank)	HR (log rank)	95% CI
Overall	228	11.1	n/a	n/a	n/a

PS 0-1	160 (70.2%)	15.7	<0.0001	0.38	0.24 - 0.6
PS >2	53 (23.2%)	7.8	<0.0001		
No of mets <6	32 (14%)	28	<0.0001		
No of mets 6-20	64 (28.1%)	5.9	<0.0001		
No of mets >20	67 (29.4%)	5.4	<0.0001		
Baseline ALP <220	107 (46.9%)	13.5	0.0014	0.57	0.39 - 0.83
Baseline ALP >220	80 (35.1%)	8.4	0.0014		
Baseline Hb >/= 10	161 (70.6%)	13	<0.0001	0.32	0.15 - 0.7
Baseline Hb <10	22 (9.6%)	5	<0.001		
Baseline PSA <50	49 (21.5%)	19.5	0.006		
Baseline PSA 50-100	27 (11.8%)	15.8	0.006		
Baseline PSA >100	112 (49.1%)	8.9	0.006		
Cycles completed 5-6	144 (63.2%)	15.8	<0.0001	0.25	0.15 - 0.4
Cycles completed 1-4	62 (27.2%)	4.7	<0.0001		
PSA fall /= 30%	33 (14.5%)	25.1	0.0066	0.51	0.34 - 0.77
PSA other	152 (66.7%)	10.5	0.0066		
Neutrophil/lymphocyte ratio post Ra223 <3.89	84 (36.8%)	17.5	0.0005	0.52	0.35 - 0.75
Neutrophil/lymphocyte ratio post Ra223 >/= 3.89	85 (37.3%)	8.6	0.0005		

### Conclusion

Our data showed patients with fewer metastases, completion of 5-6 cycles of Ra-223 and those who had PSA reduction of 30% or more at the end survive significantly longer. Fitness but not age was significant. Lower baseline ALP, PSA, neutrophil/lymphocyte ratio and higher baseline haemoglobin are positive prognostic biomarkers for survival.

### Electronic Poster: Clinical track: Urology-non-prostate

### EP-1585 Modified BEP chemotherapy regimen in testicular germ cell tumors: Outcome and toxicity

N. Thakur<sup>1</sup>  
<sup>1</sup>Post Graduate Institute of Medical Education and Research, Radiotherapy and Oncology, Chandigarh, India

### Purpose or Objective

Bleomycin, Cisplatin and Etoposide (BEP) is established as standard treatment for Testicular Germ cell Tumours. Standard BEP regimen consist of Bleomycin 30 IU DAY 1,8 and 15, cisplatin 20 mg/m2 day1-5 and etoposide 100 mg/m2 day1-5. As these tumours are highly curable, so management is crucial in terms of long term toxicity particularly lung toxicity. With standard BEP there is increased toxicity which leads to poor compliance so we at a tertiary care centre assessed modified BEP regimen in such patients and evaluated its effectiveness in terms of response and toxicity as compared to standard BEP. The original intent is to explore the cost-effectiveness and improved patient compliance of this modified protocol without losing efficacy in treatment.

### Material and Methods

Forty nine patients of testicular tumours were enrolled in this study from January 2012 to December 2016. Of them, 43 patients were of non-seminomatous germ cell tumor

(NSGCT) and 5 patients were of pure seminoma. The mean age at diagnosis was 30 years. Pretreatment staging consisted of physical examination, determination of serum tumor marker levels and radiological examination. The modified BEP regimen consisted of bleomycin 30 IU Day 1, Cisplatin 20 mg/m<sup>2</sup> Day 1-5 and Etoposide 100mg/m<sup>2</sup> Day 1 to 5, given every three weeks. Therefore, the planned drug intensities were 33.3 mg/m<sup>2</sup>/week for cisplatin, 166.7 mg/m<sup>2</sup>/week for etoposide and 10 IU/body/week for bleomycin. The schedule for chemotherapy was as follows: four courses of modified BEP for stage I patients and six courses of modified BEP for stage I S, II and III patients.

#### Results

Out of 48 patients, 16 (33.3%) patients had complete response and 23 (47.9%) patients had partial response. Overall Response rate in our study was seen to be 81.2% which was comparable with the available evidence. The complete biochemical response was seen in 35 (72.9%) patients. Only 5 (10.4%) patients had febrile neutropenia and only two (4.1%) patients showed clinically evident Bleomycin induced pulmonary toxicity during chemotherapy. In this study no clinically evident neuropathy was seen. Lower toxicity seen in these patients led to better overall compliance as 40 (83.3%) patients completed 6 cycles within a stipulated overall treatment time of 16 weeks.

#### Conclusion

Modified BEP protocol is a good alternative to standard BEP with comparable efficacy, reduced toxicity and better compliance. We strongly believe that this modified BEP regimen improving the quality of life of these patients during chemotherapy will replace the conventional mode of administration if randomized trials will validate that this is achieved without jeopardizing the excellent response rates of the standard regimen.

#### EP-1586 FDG PET-CT based risk-adapted radiotherapy for post-chemotherapy residual mass in advanced seminoma

V. Murthy<sup>1</sup>, C. Johnny<sup>1</sup>, R. Krishnatry<sup>1</sup>, A. Joshi<sup>2</sup>, G. Prakash<sup>3</sup>, M. Pal<sup>3</sup>, G. Bakshi<sup>3</sup>, S. Menon<sup>4</sup>, A. Agarwal<sup>5</sup>, V. Rangarajan<sup>5</sup>, V. Noronha<sup>2</sup>, K. Prabhaskar<sup>2</sup>

<sup>1</sup>Tata Memorial Hospital, Radiation oncology, Mumbai, India; <sup>2</sup>Tata Memorial Hospital, Medical Oncology, Mumbai, India; <sup>3</sup>Tata Memorial Hospital, Surgical Oncology, Mumbai, India; <sup>4</sup>Tata Memorial Hospital, Pathology, Mumbai, India; <sup>5</sup>Tata Memorial Hospital, Nuclear Medicine, Mumbai, India

#### Purpose or Objective

There is a lack of consensus regarding the management of postchemotherapy residual mass in advanced seminoma. Surgery for these masses is technically challenging and often morbid. FDG PET CT has aided in identifying viable disease based on size and SUVmax values. The aim of this study is to evaluate if risk stratification based in FDG PET CT residual mass size and SUV uptake can help in identifying patients who would benefit with locoregional radiotherapy in advanced seminoma.

#### Material and Methods

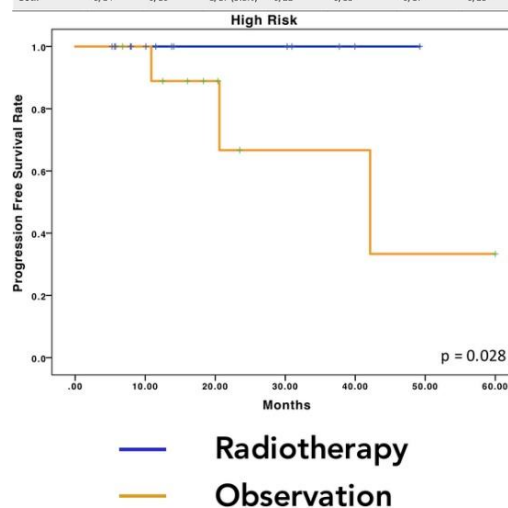
This is a retrospective study of patients with advanced classical seminoma primarily treated with platinum-based first-line chemotherapy. All patients had routine response assessment FDG PET CT after chemotherapy. Patients were stratified into three subgroups based on FDG PET-CT residual nodal size and SUV max. The low-risk group (LR) consisted of SUV max  $\leq 3$  and size  $\leq 3$ cm, intermediate and high-risk groups (HR) consisted of patients with SUV max  $\geq 3$  or size  $\geq 3$ cm and SUV max  $\geq 3$  and size  $\geq 3$ cm respectively. There were 2 intermediate risk groups (based on Size  $> 3$ cm with any SUV (IR-Size) and SUV $>3$  with any size (IR-SUV)). Patients were either kept on observation after chemotherapy or received radiotherapy to the PET positive nodal mass in the intermediate and

high-risk groups. Low-risk group patients did not receive radiotherapy. Patients who underwent surgery were excluded. Locoregional control, overall survival, and patterns of failure were compared between the two groups.

#### Results

Seventy-three patients were included in the study, 51 patients were observed and 22 patients received radiotherapy after chemotherapy. The median pre-chemotherapy node size between the radiotherapy and observation cohort was 8.9cm (IQR 7.6-11.6) and 8.6cm (IQR 5.6-11). Median post-chemotherapy node size in the radiotherapy and observation cohort was 4 cm (IQR:2.7-5.5) and 2.5 cm (IQR:1.4-5.5) respectively while the post-chemotherapy SUVmax in the 2 groups was 4.1 (IQR 3.2-5.8) and 0 (IQR 0-3.6) respectively. Median time to PET CT was 7 weeks (IQR 4-10). Locoregional failures in the radiotherapy and observation cohort were 0% and 30% in the HR (p = 0.028), 0% and 18% (p = 0.295) in IR-Size and 5.5% and 29% (p = 0.076) in IR-SUV respectively. The benefit of loco regional control failed to translate into overall survival benefit. The patterns of failure and failure rates by risk group are shown in table 1.

	SUV > 3 and size > 3cm (High Risk)		Any SUV and size > 3cm (Intermediate Risk, IR Size)		SUV > 3 and any size (Intermediate Risk, IR-SUV)		SUV < 3 and size < 3cm (Low Risk)	
	RT	No RT	RT	No RT	RT	No RT	RT	No RT
All failures	1/14 (7%)	4/10 (40%)	2/17 (12%)	6/22 (27%)	3/18 (16.6%)	6/17 (35%)	2/25 (8%)	
		p=0.05		p=0.176		p=0.14		
Loco regional failure only	0/14	3/10 (30%)	0/17	4/22 (18%)	1/18 (5.5%)	5/17 (29%)	2/25 (8%)	
		p=0.028		p=0.295		p=0.076		
Distant failure only	1/14 (7%)	1/10 (10%)	1/17 (5.8%)	2/22 (9%)	2/18 (11%)	1/17 (6%)	0/25	
Both	0/14	0/10	1/17 (5.8%)	0/22	0/18	0/17	0/25	



#### Conclusion

FDG PET CT can help in stratifying postchemotherapy masses based on size, SUVmax and hence can help in tailoring treatment appropriately. Residual masses  $\geq 3$ cm and SUVmax  $\geq 3$  (high-risk group) are likely to benefit the most with radiotherapy. A prospective study to address this question is planned.

#### EP-1587 Conservative strategy with concomitant chemoradiation for bladder cancer: analysis of a 313 patients

E. Fabiano<sup>1</sup>, H. Martin<sup>1</sup>, M. Arnaud<sup>2</sup>, G. Philippe<sup>1</sup>, K. Sarah<sup>1</sup>, T. Hélène<sup>1</sup>, B. Jean Emmanuel<sup>1</sup>, S. Antoine<sup>1</sup>, D. Catherine<sup>1</sup>

<sup>1</sup>Hôpital Européen Georges Pompidou, Radiation Department, Paris, France; <sup>2</sup>Hôpital Européen Georges Pompidou, Urology Department, Paris, France

#### Purpose or Objective

To evaluate trimodal conservative treatment as an alternative to radical surgery for urothelial invasive bladder carcinoma (IBC).

### Material and Methods

This retrospective study reported the carcinologic and functional results of patients (pts) presenting a cT2/T3 NOMO operable IBC, treated by a conservative strategy. Treatment consisted of a transurethral resection, as complete as possible, followed by concomitant bifractionated split-course chemoradiation (CCR) with 5FU-Cisplatin chemotherapy. A control cystoscopy was performed 6 weeks after the first part CCR (eq45Gy) with systematic biopsies. Pts with complete histologic response achieved CCR protocol. Salvage surgery was proposed to pts with persistent tumor.

### Results

313 patients (83% cT2, 17% cT3) treated between 1988 and 2013 were included in this study, with a median follow-up of 59 months and 67 year mean age. After the first part of CCR histologic response rate was 83%. After 5 years, overall, disease-free, metastasis-free and functional bladder-intact survival rates were respectively 69%, 61%, 78% and 69%, significantly better for patients in complete response after induction CCR ( 77% vs 32%, p= 0,001 for 5 years OS). Late urinary and digestive toxicities were limited, with respective rates of 3.2% and 1.3% of grade 3 toxicity.

### Conclusion

Chemoradiation after transurethral resection is a good treatment option, especially for older or frail pts.

### EP-1588 The preliminary result of combination of chemoradiotherapy and arterial infusion for bladder cancer

H. Yoshioka<sup>1</sup>, T. Shimbo<sup>1</sup>, Y. Tanaka<sup>1</sup>, A. Hori<sup>1</sup>, M. Nakata<sup>1</sup>, N. Yoshikawa<sup>1</sup>, K. Yoshida<sup>1</sup>, Y. Uesugi<sup>2</sup>, K. Yamamoto<sup>1</sup>

<sup>1</sup>Osaka Medical College, Department of Radiology, Takatsuki, Japan ; <sup>2</sup>Kansai University of Welfare Sciences, Rehabilitation, Kashiwara, Japan

### Purpose or Objective

We present the preliminary results from our clinical study evaluating the effectiveness of combination of chemoradiotherapy with balloon-occluded arterial infusion (BOAI) and hemodialysis (HD) for bladder cancer

### Material and Methods

We investigated 200 patients and the median age was 66 (range; 32-85) . According to the UICC classification, 4 patients were at clinical stage Tis, 19 at T1, 120 at T2, 40 at T3, and 17 at T4. About N stage, 167 patients had no lymph node metastasis. All patients received external beam radiation therapy (EBRT) of 40- 50 Gy to the whole pelvis with 10 Gy to the bladder as a boost. During EBRT, combination chemotherapy of gemcitabine (GEM) and cisplatin (CDDP) was described. After chemoradiotherapy, BOAI of CDDP was administered from bilateral internal iliac arteries with simultaneous HD to prevent back-flow of CDDP into the systemic circulation.

### Results

The median follow-up time was 38 months(range; 4-58). Complete response (CR) rate was 78% after 2 months of treatment. Three-year local control (LC) and overall survival (OS) rates were 72% and 87%, respectively, and 3-year bladder preservation rate was 99%.Grade 3 acute complication occurred in 25 patients (13%) (genitourinary: 9; gastrointestinal: 17) and Grade 4 acute complication was not observed.

### Conclusion

Combination of chemoradiotherapy with BOAI and HD may be regarded as a curative therapy for patients with bladder cancer.

### EP-1589 Establishing international variation in target delineation using MRI for bladder radiotherapy.

A. Hunt<sup>1</sup>, A. Chan<sup>2</sup>, L. Delacroix<sup>3</sup>, L. Dysager<sup>4</sup>, A. Edwards<sup>5</sup>, J. Frew<sup>6</sup>, A. Gordon<sup>3</sup>, A. Henry<sup>7</sup>, R. Huddart<sup>1</sup>,

M. Koh<sup>1</sup>, V. Kong<sup>8</sup>, Y. Nagar<sup>9</sup>, O. Parikh<sup>10</sup>, R. Pearson<sup>6</sup>, Y. Rimmer<sup>11</sup>, T. Schytte<sup>4</sup>, M. Serra<sup>1</sup>, M. Sidhom<sup>12</sup>, A. Sohaib<sup>13</sup>, I. Syndikus<sup>14</sup>, A. Tan<sup>15</sup>, S. Treece<sup>16</sup>, M. Varughese<sup>17</sup>, S. Hafeez<sup>1</sup>

<sup>1</sup>Institute of Cancer Research- The Royal Marsden NHS Foundation Trust, Radiotherapy and Imaging, London, United Kingdom ; <sup>2</sup>University Hospitals Coventry and Warwickshire, Clinical Oncology, Coventry, United Kingdom ; <sup>3</sup>The Royal Marsden NHS Foundation Trust, Radiotherapy, London, United Kingdom ; <sup>4</sup>Odense University Hospital, Oncology, Odense, Denmark ; <sup>5</sup>Maidstone and Tunbridge Wells NHS Trust, Clinical Oncology, Canterbury, United Kingdom ; <sup>6</sup>The Northern Centre for Cancer Care, Clinical Oncology, Newcastle, United Kingdom ; <sup>7</sup>The Leeds Teaching Hospitals NHS Trust, Clinical Oncology, Leeds, United Kingdom ; <sup>8</sup>Princess Margaret Cancer Centre, Oncology, Toronto, Canada ; <sup>9</sup>Queen Alexandra Hospital, Clinical Oncology, Portsmouth, United Kingdom ; <sup>10</sup>Lancashire Teaching Hospitals NHS Trust, Clinical Oncology, Preston, United Kingdom ; <sup>11</sup>Cambridge University Hospital NHS Foundation Trust, Clinical Oncology, Cambridge, United Kingdom ; <sup>12</sup>Liverpool Hospital, Oncology, Sydney, Australia ; <sup>13</sup>The Royal Marsden NHS Foundation Trust, Radiology, London, United Kingdom ; <sup>14</sup>The Clatterbridge Cancer Centre NHS Foundation Trust, Clinical Oncology, Liverpool, United Kingdom ; <sup>15</sup>Townsville Cancer Centre, Oncology, Townsville, Australia ; <sup>16</sup>North West Anglia NHS Foundation Trust, Clinical Oncology, Peterborough, United Kingdom ; <sup>17</sup>Taunton and Somerset NHS Foundation Trust, Clinical Oncology, Taunton, United Kingdom

### Purpose or Objective

MRI has an established diagnostic role in local staging of muscle invasive bladder cancer (MIBC). Improved soft tissue definition with MRI compared to CT should facilitate radiotherapy target definition. However, experience of MRI in bladder radiotherapy planning is limited, with no current guidance available on its use. This multicentre, international study aims to establish current inter-observer variability of target delineation for MIBC using MRI in order to develop future consensus.

### Material and Methods

24 participants with a specialist interest in MIBC (19 radiation oncologists, 2 radiologists and 3 treatment radiographers) from 15 institutions (11 UK, 1 Danish, 2 Australian, 1 Canadian) were provided with MRI scans of 3 patients with MIBC. One CT based case was also included. Consultant radiation oncologists also completed a questionnaire on their MIBC radiotherapy experience and MRI use. Case vignettes were given but participants were not coached on MRI or CT interpretation. CTV and GTV delineation was performed on T2W images and outer bladder wall (BW) delineation completed on T1W images. Diffusion weighted images were also available for reference. For the CT benchmark case, only CTV and GTV were defined. Delineation was carried out on the MONACO treatment planning system research version v5.10 (Elekta AB, Stockholm, Sweden).

On completion of all contours a Simultaneous Truth and Performance Level Estimate (STAPLE) was created for each structure set. Individual contours were compared to this, enabling inter-observer comparisons. Four variability tests were performed using ADMIRE research version v2.0 (Elekta AB, Stockholm, Sweden).

### Results

Participating consultant radiation oncologists had a median 10 years of experience (IQR 7-15) in MIBC radiotherapy. Use of MRI in the radiation pathway was mixed, 53% (9/17) of clinicians had access to diagnostic MRIs, 18% had access to radiotherapy planning MRs, while 41% did not routinely use MR in their radiotherapy pathway.

In total, 264 contours were completed, of which 2 could not be analysed due to technical reasons.

Table 1 shows the combined median variability indices across the MRI based cases with the CT based case as a comparator.

Variability Index	MRI GTV	MRI CTV	MRI Bladder Wall	CT GTV	CT CTV
Median DICE coefficient (IQR)	0.69 (0.59-0.76)	0.94 (0.94-0.95)	0.95 (0.93-0.96)	0.70 (0.6-0.8)	0.97 (0.97-0.97)
Median Cohen Kappa (IQR)	0.65 (0.54-0.73)	0.91 (0.90-0.92)	0.91 (0.89-0.93)	0.67 (0.57-0.78)	0.95 (0.94-0.95)
Median Hausdorff Distance (mm)	15.04 (11.99-30.3)	7.70 (6.27-11.22)	7.95 (6.39-10.29)	12.12 (9.83-14.47)	4.02 (3.51-5.19)
Median mean distance (mm)	3.08 (1.80-6.38)	1.22 (1.07-1.43)	1.43 (1.06-1.75)	2.21 (1.13-2.98)	0.60 (0.57-0.71)

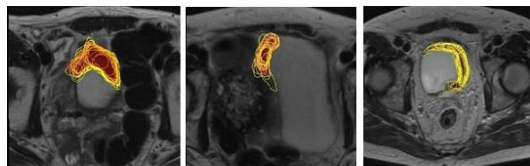


Figure 1 GTV inter-observer variation on T2 image. L-R cases 1-3, STAPLE in red colourwash, participants yellow contour

## Conclusion

Current use of MRI in MIBC radiotherapy is mixed. Some institutions have access to MRI for the majority of their patients, others have restricted or no access to these scans.

Despite this, MRI delineated volumes on average show reasonable concordance between participants, this is similar to CT where there is greater experience. Greatest variance was seen in GTV delineation with a median DICE of 0.69.

Further work will now include an education/consensus meeting followed by the production of guidance for the proposed use of MRI in MIBC radiotherapy target delineation with particular attention paid to GTV boost volume delineation.

## EP-1590 Hyperthermia-radiotherapy in frail bladder cancer patients unfit for cystectomy or chemoradiotherapy

E. Stutz<sup>1,2</sup>, B. Eberle<sup>1</sup>, E. Puric<sup>1</sup>, A. Meister<sup>1</sup>, O. Timm<sup>1</sup>, D. Marder<sup>1</sup>, S. Rogers<sup>1</sup>, S. Wyler<sup>3</sup>, N.R. Datta<sup>1</sup>, S. Bodis<sup>1</sup>  
<sup>1</sup>Center for Radiation-Oncology KSA-KSB, Kantonsspital Aarau, Aarau, Switzerland ; <sup>2</sup>Department of Radiation Oncology, Inselspital- Bern University Hospital, Bern, Switzerland ; <sup>3</sup>Department of Urology, Kantonsspital Aarau, Aarau, Switzerland

### Purpose or Objective

Radiotherapy (RT) combined with radiosensitizers such as chemotherapy (CRT) or hyperthermia (HTRT) with curative intent shows superior local tumour control (LC) compared with RT alone in muscle-invasive bladder cancer (MIBC). We aimed to evaluate the LC rate, overall survival, MIBC-specific survival, acute and late toxicity of RT with concomitant deep hyperthermia (HT) in MIBC patients who are too frail for or decline radical cystectomy (RC) or CRT.

### Material and Methods

From 12/2012 to 03/2018 we treated 17 patients with unifocal or multifocal MIBC (T1-4, cN0-1, cM0, G3) with HTRT after maximal TURBT. Multifocal MIBCs received 50 Gy/20 fx (5x/week) to the whole bladder. Unifocal MIBCs were treated with 36 Gy/12 fx (3x/week) to the full bladder and a 12 Gy/4 fx boost (once a week) to the resected tumour region to a total of 48 Gy/16 fx (4x/week). HT was delivered weekly over 60 minutes with a mean temperature of 41.3°C using a BSD-2000 applicator. LC was assessed by cystoscopy every 3 months if possible.

### Results

One patient did not tolerate HTRT and was excluded from the analysis. Thus 16/17 patients (94.1%) completed HTRT

as per protocol. The median age in these 16 patients (6 unifocal, 10 multifocal) was 81 years (range, 52 - 88 years) while the median age-adjusted Charlson comorbidity index was 5 (range 1 - 9). LC was achieved in 100% (12/12) of patients at 3 months and in 87.5% (7/8) of patients at 12 months (Tab. 1). Median cystoscopic follow-up was 7.5 months (range, 2 - 59 months). Two local recurrences were detected. One local relapse was a noninvasive papillary carcinoma (pTa) at 9.5 months, which was successfully salvaged by TURBT. The other relapse presented at 17 months with lymph node and bone metastases. MIBC-specific survival during follow-up was 100%. Overall survival at 1 year was 71.4% (95% CI 47.7% - 95.1%) (Fig. 1). Grade 3 gastrointestinal (GI) and genitourinary (GU) toxicity (CTCAE v4.0) was evident in 12.5% (2/16) patients while none had grade 4 toxicity. During follow-up, only one grade 3 (CTCAE v4.0) late toxicity occurred. This was a transient episode of macrohematuria under anticoagulation due to bladder telangiectasia and was locally treated by coagulation. Bladder function was well preserved in all patients.

### Assessed at 3 months

<b>Patients available:</b>	12/16 (75%)
<b>not available due to:</b>	<ul style="list-style-type: none"> <li>• 2/16; not yet reached follow-up timepoint</li> <li>• 2/16; unable for cystoscopy due to health deterioration</li> </ul>
<b>Local control:</b>	12/12 (100%)

### Assessed at 12 months

<b>Patients available:</b>	8/16 (50%)
<b>not available due to:</b>	<ul style="list-style-type: none"> <li>• 3/16; not yet reached follow-up timepoint</li> <li>• 1/16; declined further cystoscopic follow-up</li> <li>• 4/16; died (not MIBC-related)</li> </ul>
<b>Local control:</b>	7/8 (87.5%)
	• 1/8 with recurrence at 9.5 months

Tab. 1. Cystoscopic local disease control

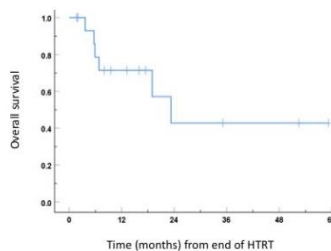


Fig. 1. Kaplan-Meier plot for rates of overall survival

## Conclusion

Elderly, polymorbid patients with MIBC have limited therapeutic options. To preserve quality of life, treatment achieving LC with a minimum of adverse effects is required. Several hypofractionated RT schedules have been reported for this population group, but this is the first report of RT combined with HT as radiosensitizer. Our results showed good tolerance of HTRT, minimal late toxicity and an excellent LC. These data are comparable or even better than those from hypofractionated RT alone in this population of frail patients unfit for definitive surgery or CRT.

## EP-1591 Dose mapping local failure following radical image guided bladder radiotherapy

S. Hafeez<sup>1</sup>, H. Abdel-Aty<sup>1</sup>, K. Warren-Oseni<sup>2</sup>, A. Dunlop<sup>2</sup>, K. Chan<sup>3</sup>, D. McQuaid<sup>2</sup>, K. Jones<sup>1</sup>, V. Harris<sup>4</sup>, M. Tan<sup>1</sup>, V. Hansen<sup>5</sup>, R. Huddart<sup>1</sup>, S. Hafeez<sup>1</sup>

<sup>1</sup>Institute of Cancer Research and The Royal Marsden NHS Foundation Trust, Radiotherapy and Imaging, London,

United Kingdom ; <sup>2</sup>Institute of Cancer Research and The Royal Marsden NHS Foundation Trust, Joint Department of Physics, London, United Kingdom ; <sup>3</sup>The Royal Marsden NHS Foundation Trust, Radiotherapy and Imaging, London, United Kingdom ; <sup>4</sup>Guys and St Thomas' Hospital NHS Foundation Trust, Radiotherapy, London, United Kingdom ; <sup>5</sup>Odense University Hospital, Radiotherapy and Medical Physics, Odense, Denmark

### Purpose or Objective

Recurrences after radical bladder radiotherapy occur predominantly within the bladder. Accurate dose mapping is important to determine whether cause of local failure is due to geographical miss, and or insufficient dose. To assess the success of image guided bladder radiotherapy strategies and margin reduction, we aim to determine the dose prescribed and received by the volume that harboured the local failure.

### Material and Methods

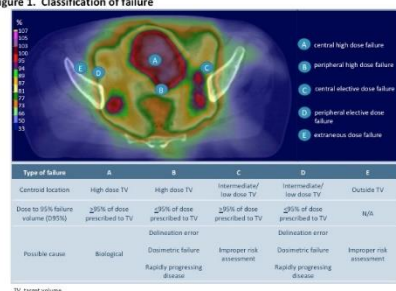
Thirty-eight patients with T2 (high risk pathology) or T3-4N0-3M0 bladder cancer recruited prospectively to an ethics approved phase II radiotherapy protocol treating whole bladder and pelvic lymph nodes with IMRT were retrospectively evaluated. Expansions to create the PTVs are shown Table 1. Soft tissue imaging was acquired prior to treatment with CBCT and registered to bony anatomy followed by soft tissue registration to whole bladder if necessary. Use of neo-adjuvant and concurrent chemotherapy was recommended.

Diagnostic imaging (CT/MRI) identifying the site of local recurrence was used to reconstruct the relapse volume (GTV<sub>relapse</sub>). This was co-registered with the planning CT. GTV<sub>relapse</sub> was compared dosimetrically and spatially to the PTV using centroid based approach. Patterns of failure were classified as in Figure 1. Time to local failure was defined from the start of radiotherapy to pathological confirmation of relapse, and was estimated using Kaplan Meier method.

Table 1. Applied expansions

Structure	Applied expansion to create corresponding PTV (cm)					PTV	Planned dose (Gy)
	Superior	Inferior	Lateral	Anterior	Posterior		
Bladder tumour	1.0	1.0	1.0	1.0	1.0	PTV <sub>Tumour bed</sub>	64
Whole bladder	1.5	0.5	0.5	1.5	1.0	PTV <sub>Whole bladder</sub>	52
Involved nodes	0.5	0.5	0.5	0.5	0.5	PTV <sub>Involved LN</sub>	60
Uninvolved nodes	0.5	0.5	0.5	0.5	0.5	PTV <sub>Pelvic LN</sub>	52

Figure 1. Classification of failure



### Results

27/38 (71%) of all patients had disease recurrence. 18/38 (47%) patients experienced first relapse within the bladder following radiotherapy. Median time to local relapse was 9.0 months (95% CI, 6.3-11.7 months). 15/18 (83%) of these patients received neo-adjuvant chemotherapy and 10/18 (57%) had received concurrent chemotherapy. 9/18 (50%) patients relapsed with  $\geq$ T2 local disease, and 7/18 (28%) with  $<$ pT1 disease. Based on endoscopic evaluation alone, 13/18 (72%) patients were reported to

have relapsed clinically at the original tumour site.

2 patients were excluded from further analysis because no axial imaging identifying relapse was available. Median volume of GTV<sub>relapse</sub> was 33.9cc (range 7.5-142.5). Median GTV<sub>relapse</sub> D<sub>95%</sub> was 56.4Gy (range 50.1-63.8Gy), 88.1% (78.3-99.6) of the prescribed dose (64Gy). Six patients (38%) were classified as experiencing type A failure, 9 patients (56%) as type B failure, and 1 (6%) as type C failure. No other types of local failure were identified.

### Conclusion

Relapse patterns following bladder radiotherapy suggest local failure occurs at or within close proximity of the original tumour (PTV<sub>Tumour bed</sub>). Work is on-going to expand the patient numbers and to determine actual radiotherapy dose delivered to GTV<sub>relapse</sub> from on-line CBCT data using the deformable registration techniques. This will inform whether dose escalation, and or margin modification could improve reported outcomes.

### EP-1592 Consolidative radiotherapy after loco regional relapse in muscle invasive bladder cancer

D. Santamaria Vasquez<sup>1</sup>, X. Maldonado<sup>2</sup>, M. Altibas<sup>2</sup>, D. Moreno<sup>2</sup>, S. Micó<sup>2</sup>, C. Raventós<sup>3</sup>, F. Lozano<sup>3</sup>, R. Morales<sup>4</sup>, J. Giralt<sup>2</sup>

<sup>1</sup>Vall D'Hebron hospital, Radiation Oncology, Barcelona, Spain ; <sup>2</sup>Hospital Universitario Vall d'Hebron, Radiotherapy, Barcelona, Spain ; <sup>3</sup>Hospital Universitario Vall d'Hebron, Urology, Barcelona, Spain ; <sup>4</sup>Hospital Universitario Vall d'Hebron, Medical Oncology, Barcelona, Spain

### Purpose or Objective

The aim of this study is to report the outcomes of consolidative radiotherapy after cystectomy in locoregional relapse of muscle invasive bladder cancer (MIBC) patients.

### Material and Methods

We performed a retrospective analysis of eighty-eight patients with MIBC that had been treated at our institution from January 1999 to August 2018.

Forty-nine patients underwent radical cystectomy followed by platinum-based chemotherapy (cisplatin / carboplatin). We identified 31 patients that had loco-regional relapse that received consolidative radiotherapy. These patients are the subject of our study.

Overall survival (OS) was calculated using the Kaplan-Meier method. OS was defined as the time from the start of radiotherapy to death.

The toxicity was evaluated according to the RTOG toxicity criteria.

### Results

In the select group of 31 patients with loco-regional relapse treated with consolidative radiotherapy, 25 were men, the median age was 65.3 years (range 44-87). Eight patients had local recurrence, 12 patients had regional recurrence, and 11 patients both.

All patients completed their radiotherapy course. Treatment volume was local recurrence or positive lymph nodes and regional pelvis. The mean dose of radiotherapy was 54.4 Gy (range 37.5 Gy - 64.8 Gy). No patient received concurrent chemotherapy.

Two patients (6%) developed grade 3 gastrointestinal toxicity. No grade 4 toxicity has been reported.

No grade  $\geq$ 2 genitourinary toxicity has been reported.

With a median follow-up of 27 months, there was no evidence of disease in 14 patients (45%) after consolidative radiotherapy. Seventeen patients presented metastatic distant progression: 5 hepatic, 4 bone and 4 pleuropulmonary.

One patient had local relapse, one patient had nodal relapse and one patient had loco-regional and metastatic relapse.

Overall survival was 21.8m (3-149m)

### Conclusion

These data suggest that consolidative radiotherapy after loco-regional relapse is feasible and could contribute to the long-term control in up to half of the treatments, with acceptable toxicity rates.

---

### Electronic Poster: Clinical track: Skin cancer / malignant melanoma

---

#### EP-1593 The impact of Radiotherapy combined with immunotherapy on local control in mucosal melanoma patients

H.J. Kim<sup>1</sup>, S.J. Shin<sup>2</sup>, K. Woong Sub<sup>3</sup>

<sup>1</sup>Gil Medical Hospital, Department of Radiation Oncology, Incheon, Korea Republic of ; <sup>2</sup>Yonsei Cancer Center, Division of Medical Oncology- Department of Internal Medicine, Seoul, Korea Republic of ; <sup>3</sup>Yonsei Cancer Center, Department of Radiation Oncology, Seoul, Korea Republic of

#### Purpose or Objective

Mucosal melanoma is an aggressive malignancy with a poor response to conventional therapies. The efficacy of immunotherapy (IMT), especially combined with radiotherapy (RT), has not been reported in this rare subtype. We investigated the impact of RT combined with IMT in mucosal melanoma patients.

#### Material and Methods

Forty-two patients with mucosal melanoma who were treated with RT at Yonsei Cancer Center between Jul 2008 and Feb 2017 were identified from our database. Patients who received postoperative RT, had no response evaluation, and expired during RT were excluded. A total of 18 patients with 22 lesions were included in this analysis. All patients received RT for primary or metastatic gross tumor mass. The median dose of radiation was 45 Gy (range, 20-69 Gy) with a median fractional dose of 3 Gy (range, 1.8-7.5 Gy). Eleven patients with 14 lesions were treated with RT alone, while 7 patients with 8 lesions were administered IMT sequentially or concurrently; pembrolizumab in 6 patients and nivolumab in 1. The local control (LC) rate, infield failure-free survival (IFFS), and outfield failure-free survival (OFFS) were compared between two groups (no-IMT vs. IMT group). IFFS and OFFS was determined from the date of RT finish, while overall survival (OS) was calculated from the date of diagnosis.

#### Results

Common anatomic sites of primary tumors were the head and neck (59%), anorectal region (31.8%), and female genital tract (9.1%). Patient characteristics including sex, age, primary site, tumor stage, BRAF mutation, adjuvant interferon, and RT site (primary vs. metastatic mass) were not significantly different between two groups. The median OS was 50.2 months with a median follow-up of 39.7 months (range, 7.3-102.1 months) for all patients. The LC rate was 59.1% for 22 lesions and the median time to local progression was 4.8 months (range, 0.5-20.3 months). Although RT dose was not significantly different between two groups, the LC rate was better in the IMT group than no-IMT group. (57.1% versus 12.5%; P = 0.074). The outfield failure rate was 87.5% in IMT group and 100% in no-IMT group (P = 0.364). Dividing lesions according to RT dose in terms of EQD2 ( $\alpha/\beta=10$ ), higher dose group (> 45 Gy) showed better tumor control; the LC rates were 53.8% vs. 22.2% and the median IFFSs were 20.3 vs. 7.3 months for >45 Gy vs. ≤45 Gy group, respectively. The OFFS was not significantly different between the IMT and no-IMT group.

#### Conclusion

RT combined with IMT improved local tumor control compared to RT alone. Combination treatment with RT and IMT can be an effective treatment option in patients with mucosal melanoma.

#### EP-1594 Two years' experience of electronic brachytherapy for basal cell carcinomas in selected patients

H. Westenberg<sup>1</sup>, R. Keus<sup>1</sup>, M. Van Hezewijk<sup>1</sup>, B. Oosterveld<sup>2</sup>

<sup>1</sup>Radiotherapiegroep, radiotherapy, Arnhem, The Netherlands ; <sup>2</sup>Radiotherapiegroep, medical physics, Arnhem, The Netherlands

#### Purpose or Objective

In 2016 electronic brachytherapy (EB) by low kilovoltage energy (69,5 kV Esteya®/Elekta, Sweden) was introduced in our department as addition to our radiation facilities for treating basal cell skin cancer. Due to the maximum applicator diameter of 3 cm, only small lesions are eligible. Maximum depth for dose prescription is 4 mm. After 2 years we evaluated toxicity, outcome and patient comfort.

#### Material and Methods

Patients with basal cell carcinoma referred for radiotherapy with curative intent were selected for EB. From March 2016 to September 2018 56 patients with 66 lesions were treated with electronic brachytherapy. All lesions received 6 fractions, twice a week, of 7 Gy prescribed to a depth of 3 mm (in 92% of the lesions) from the skin surface. In 2 patients the dose was prescribed to a depth of 4 mm, because of the tumour thickness, and in 3 patients to 2 mm because of superficial growth of the tumour. Before the first fraction the lesion (gross tumour volume GTV) and the treatment margin (GTV was expanded by 5- 10 mm to clinical target volume CTV, depending on size and histology) was delineated on the skin by the radiation oncologist. Dermatoscopy was used for precise GTV delineation. Photographs were routinely taken before the 1<sup>st</sup>, 4<sup>th</sup> and 6<sup>th</sup> fraction and during follow-up.

#### Results

One patient, in poor medical condition, was treated with palliative intent and one patient discontinued treatment because of a pneumonia. The remaining 54 patients with 64 lesions were evaluated. All lesions were ≤ 20 mm and 90% were histologically confirmed basal cell carcinoma, either of solid (67%), morpheaform (17%) or superficial growing (5%) type. Mean age was 75.7 years and despite high age and comorbidities, the treatment was well tolerated. Most lesions were localised in the head and neck area, with the majority on the nose (in 65% of the patients). The most common acute toxicity was a mild erythema and nasal mucositis, both self-limiting. In one patient, with a lesion on the tibia, delayed wound healing for several months occurred. Follow-up ranges from 0.5-26 months with an average FU of 5 months. There were 2 recurrences, one in and therefore a true recurrence, and one recurrence close to the radiation field.

#### Conclusion

In our two years' experience electronic brachytherapy offers an effective, comfortable and simple method for the curative treatment of small basal cell skin cancers in elderly patients with lesions in areas where surgery is complicated or mutilating. Our preliminary results are comparable to the published results with EB.

#### EP-1595 In operable SSSC, radiotherapy schedules could be chosen using dermoscopic features?

F. Pastore<sup>1</sup>, A. Rese<sup>1</sup>, G. Panelli<sup>1</sup>, A. Pepe<sup>1</sup>, D. Toledo<sup>1</sup>, V. Iorio<sup>1</sup>

<sup>1</sup>Emicenter, Radiation Oncology, Casavatore, Italy

#### Purpose or Objective

Radiotherapy is an optimal option for unoperable SSCC (Skin Squamous Cell Cancer) with excellent local control and good cosmetic outcomes. A lot of different fractionation and total doses had been used to treat SSCC, according to several clinical and histological parameters. Dermoscopically, these kind of lesion are characterized, by atypical vascular pattern and/or deep ulceration that some authors correlate with the severity of the neoplasm. In our study, we decide to use different radiotherapy schedules for our patients with SSCC, performing a “dose escalation” in those who had negative dermoscopic features.

#### Material and Methods

28 patients (age > 60yo) with unoperable SSCC were enrolled in this study. Based on negative dermoscopic features (ulceration, bleeding, irregular vessels), signed by a skilled dermatologist, we divided them in two groups: those with no negative dermoscopic features (15 patients) and those with negative one (13 patients). All the lesions were on the trunk or on upper/lower limbs. None of these lesions had nodal involvement (N0). No lesions were >4cm. In the first group we use an electron beam schedule of 2 Gy/30fx (60Gy) while in the second group we prescribe 2Gy/33fx (66Gy).

#### Results

All the patients ended treatment. In the group A (standard) the LC was observed (at 1 year follow up) in 13 patients (86%) and in 11 patients (73%) at 2 years follow up. Skin toxicity > grade 3 was not seen in these patients. No late toxicity was registered, with good cosmetic outcome. In the group B (negative features) the LC was observed in 12 patients (92%) at 1 year follow up and in 10 patients (77%) at 2 years follow up. 3 patients had grade 3 skin toxicity in this group with 2 cases of hypopigmentation.

#### Conclusion

Dermoscopic examination could be used to perform a dose escalation schedule in unoperable SSCC, with similar LC and acceptable toxicity. More patients and a longer follow up are the main future topics to enhance this kind of approach.

#### EP-1596 Radiotherapy and Ipilimumab as first-line immunotherapy: A comparative study on 63 patients

N. Benziane<sup>1</sup>, V. Atallah<sup>1</sup>, F. Amestoy<sup>1</sup>, E. Gerard<sup>2</sup>, N. Leduc<sup>1</sup>, A. Huchet<sup>1</sup>, M. Beylot Barry<sup>2</sup>, C. Dupin<sup>1</sup>, S. Prey<sup>2</sup>, L. Dousset<sup>2</sup>, N. Ouabrache<sup>1</sup>, M. Martin<sup>1</sup>, P. Gillon<sup>1</sup>, C. Dutriaux<sup>2</sup>, R. Trouette<sup>1</sup>, V. Vendrely<sup>1</sup>

<sup>1</sup>University Hospital Bordeaux, Radiation Oncology, Bordeaux, France ; <sup>2</sup>University Hospital Bordeaux, Dermatology, Bordeaux, France

#### Purpose or Objective

A combination of immune-checkpoint inhibitors and radiation therapy (RT) represents a promising therapeutic strategy in part mediated by the abscopal effect, but clinical experience related to this combination remains scarce (1). Abscopal effects have been observed with association of radiotherapy concomitantly to Ipilimumab (2). Shaverdian *et al.* showed that patients receiving radiotherapy before immunotherapy presented better survival rates (3). Radiotherapy used concomitantly to immunotherapy showed better survival outcomes. But all of series pooled heterogeneous cancer types or lines of treatment (1). Our study evaluated clinical outcomes for patients treated by radiotherapy or not concomitantly to cytotoxic T-lymphocyte-associated protein 4 (CTLA-4) inhibitor ipilimumab in a homogeneous cohort of patients.

#### Material and Methods

Clinical data and patterns of treatment were retrospectively collected from all consecutive patients with metastatic melanoma and receiving ipilimumab after one line of chemotherapy exclusively. Patients receiving Tyrosine Kinase inhibitor or other immunotherapies before Ipilimumab were excluded. Survival data and toxicities

were compared between patients receiving concurrent RT (CIR) or no concurrent irradiation (NCIR). Patients who received RT before immunotherapy were secondly pooled in the analysis.

#### Results

Sixty-three patients received Ipilimumab between June 2007 and May 2017 at our institution. Among these, 50.8% (n=32) received RT before immunotherapy (at least four weeks before immunotherapy) and 20.6% (n=13) received RT concurrently to immunotherapy. Sixty-six % (n=42) received RT both before and/or concurrently to immunotherapy (RT group). RT schedules were heterogeneous. After a 12.0 months median follow-up, median Progression-free survival (PFS) after initiation of immunotherapy for the NCIR group was 3.2 months versus 3.1 months for the CIR group (P=0.863). Overall Survival (OS) was also non-significant between these groups (P=0.141). For RT group (n=42), median PFS were 3.2 months compare to 3.0 months for unirradiated patients (P= 0,802). OS was also non-significant between RT group and unirradiated patients (P=0.080). Acute and late “in-field” or “out-of-field” immunologic toxicity profiles were similar in the two groups.

#### Conclusion

Despite the homogeneity of our series (we selected exclusively all patients receiving Ipilimumab as first-line immunotherapy after chemotherapy), we failed to show that combination of RT and Ipilimumab increase PFS or OS. These results could be explained by the heterogeneity of the RT schedules in our series. However, combination of RT and Ipilimumab were well tolerated and did not increase toxicities rates within and outside the irradiated field.

#### EP-1597 Radiotherapy of monstrous squamous cell carcinoma of the head and scalp in elderly: our series

G. Lazzari<sup>1</sup>, A. Terlizzi<sup>2</sup>, G. Silvano<sup>1</sup>

<sup>1</sup>Azienda Ospedaliera SS. Annunziata Presidio Osped, Radiology, Taranto, Italy ; <sup>2</sup>Azienda Ospedaliera SS. Annunziata Presidio Osped, Physics, Taranto, Italy

#### Purpose or Objective

Squamous cell carcinoma of scalp and skin head is a common clinical tumor in elderly population, mainly complicated by bleeding, necrotic masses with tissue loss. Most of them are very difficult to treat and little has been documented regarding treatment or outcomes due to low survival of these patients (pts). Herein we present our retrospective cases treated with customized electron beam radiotherapy analyzing factors impacting on local control .

#### Material and Methods

Fifty pts entered into this analysis. Elderly pts treated for giant and necrotic T3-T4 squamous skin lesions of the scalp and other skin regions of the head (occipital, face, nasal, retroauricular) between 2005-2015 were retrospectively studied. Age, sex, comorbidity, extension of the lesions, site , deep tissue involvement, necrosis, electron energies and radiation doses were analysed with t-test for univariate analysis assuming p< 0.05 for statistical significance. The Pearsons covariance test was adopted for multivariate analyses. The patients were primarily male (60%) with a median age of 83 years (75-93 years). A total of 60 lesions were treated. There were an high proportion of tumours of the scalp ( 55 %) and lesions with a maximum diameter over mean 6 cm (5- 9 cm) mainly showing a deep tissue involvement with bleeding (40%). Treatment consisted of one field with a customized electron beam. Energies ranged within 8- 15 MeV with or without a customized bolus according to deep involvement which was assessed by a simulation CT scan. The clinical target volume (CTV) was created adding 10 to 20 mm margins around the lesions. The dose schedules were 60 Gy in 30 fractions for lesions over 8 cm maximum diameter and 50 Gy in 20 fractions for the others.

## Results

Median follow up from treatment was 5 years. Bleeding control was obtained in all symptomatic lesions (100%). Local control consisted of a partial regression or resolution of necrotic skin cavities in 70 % of the lesions . A durable ( over 2 years) complete resolution was obtained in 40% of the treated lesions . The 5-year cumulative incidence of local relapse and local progression were 15% and 30% respectively . At univariate analysis statistically significant prognostic factors for local relapse were diabetes, age over 80 years, diameter > 5 cm, necrosis , deep invasion with a tissue loss and site; the scalp was the most significant site for a good and durable local control ( $p < 0.03$ ) ; fractionations and energies were not significant. At Pearson's multivariate the diameter , necrosis and the site were confirmed the most significant poor prognostic factors.

## Conclusion

Customized electron beam radiotherapy for head skin and scalp lesions is effective for palliation as bleeding or resolution with a good local control appearing an easy modality to treat monstrous and complicated lesions of very old population ameliorating quality of life.

### EP-1598 Efficient use of a modified Stanford TSEBT technique in the treatment of MF patients

E. Csiki<sup>1</sup>, M. Simon<sup>1,2</sup>, J. Papp<sup>1,2</sup>, P. Árkosy<sup>3</sup>, Á. Kovács<sup>1,2</sup>  
<sup>1</sup>University of Debrecen Med. and Health Science Centre- Clinic of Oncology, Department of Radiotherapy, Debrecen, Hungary ; <sup>2</sup>University of Pécs- Faculty of Health Sciences, Doctoral School of Health Sciences, Pécs, Hungary ; <sup>3</sup>University of Debrecen Med. and Health Science Centre- Clinic of Oncology, Department of Oncology, Debrecen, Hungary

## Purpose or Objective

Mycosis fungoides (MF) has the highest incidence in cutaneous T-Cell lymphomas, although it is a very rare entity amongst lymphomas. TSEBT is one of the most effective skin directed therapy for MF and can be used after other type of therapies (PUVA, topical steroids, etc.). In early stage disease (IIB) the intent of therapy is curative, at later stages (stage IV) it is mostly palliative to mitigate skin symptoms. We have treated two patients with modified Stanford Total Skin Electron Body Radiotherapy (TSEBT) technique. As a result of their condition these patients are barely suitable to hold the treatment position during treatment. We have developed a method to easily move, treat and re-position the patients during radiotherapy to ensure the effective and safe treatments.

## Material and Methods

During TSEBT entire skin homogeneous radiotherapy is carried out. Patients are irradiated with a nominal 6 MeV energy beam in High Dose Rate mode with a special applicator. In the treatment plane the beam energy decreased to 3.5 MeV, but it was sufficient to treat the skin surface and the underlying tissues. The beam size allowed by the special applicator in the plane of the isocenter was 40X40 cm. Patients were positioned in a special treatment frame, which had a rotating base plate, allowing the staff to easily re-position the patients between positions without removing them from the frame. An 8 mm thick Perspex had been attached to the frame to ensure the desired homogeneity of the electron beam in the treatment plane. The distance between the source and the Perspex was 360 cm, therefore a single beam was not sufficient. We matched two beams horizontally to perform the treatments. Geometrical matching was not plausible because of the extremely wide penumbra, a dosimetrical analysis was necessary to ensure the homogeneous border. The necessary angle to tilt the head was 18.5 °. Both dosimetrical and geometrical

parameters of the matched beams found to be fulfilling the recommendations.

## Results

Between February 2017 and July 2018 we have treated two patients. The first case was a young male patient with Stage IV. MF with erythroderma, Sezary syndrome. The second case was a Stage III. male patient with mental retardation, this circumstance made the treatments even more difficult. Prescribed dose was: 30-36 Gy/1,8-2 Gy at  $D_{max}$ . None of the patients have developed severe (grade III-IV) side effects during or following treatment. We perceived a grade II radio dermatitis in one of the cases, but treatment brake insertion was not necessary. Additional fields were used to complement the soles and perineal regions.

## Conclusion

At 3 months follow-up both patients were in a remission regarding the skin symptoms, no late side effects were observed. The method we implemented in the clinic was suitable to manage and treat both patients with dementia and severe skin symptoms.

### EP-1599 Electronic brachytherapy for non-melanoma skin cancers: preliminary results of a pilot trial

F. Maurizi<sup>1</sup>, G. Capezzali<sup>1</sup>, M. Mazza<sup>1</sup>, C. Blasi<sup>1</sup>, G.L. Moroni<sup>1</sup>, M. La Macchia<sup>1</sup>, A. Ciarmatori<sup>2</sup>, F. Palleri<sup>2</sup>, E. Argazzi<sup>2</sup>, S. Giancaterino<sup>2</sup>, M. Bono<sup>2</sup>, F. Bunkheila<sup>1</sup>  
<sup>1</sup>A.O. Ospedali Riuniti Marche Nord, Radiotherapy, Pesaro, Italy ; <sup>2</sup>A.O. Ospedali Riuniti Marche Nord, Medical Physics, Pesaro, Italy

## Purpose or Objective

Surface electronic brachytherapy (EBT) is an emerging alternative radiotherapy (RT) solution to external beam electron RT and high-dose-rate radionuclide-based brachytherapy for non-melanoma skin cancers. It can also be used as an alternative treatment to surgery for selected patients (pts). This prospective, single-center, non-randomized, pilot trial shows the clinical implementation of a new EBT system named Esteya® evaluating dosimetric features, the clinical safety and efficacy of this approach. Preliminary results are presented.

## Material and Methods

Flatness and symmetry of X-Ray beams have been evaluated using a high definition 2D array equipped of liquid filled ionization chambers. Half Value Layer (HVL), PDD and absolute dose have been measured for each applicator with a soft x-ray parallel plate chamber and solid water. Dose distributions have been compared with the ones calculated for conventional electron treatments (Fig.1). Between November 2016 and August 2018, 47 lesions of 36 consecutive pts (mean age: 78 years, range: 55-96) with non-melanoma malignant skin cancer have been enrolled and analyzed. Fifteen pts presented primary squamous cell carcinomas (SCC) of eyelids and scalp and 12.8 % recurrent SCC of the scalp and nose, 10.6 % showed recurrent basal cell carcinomas (BCC) of the nose and forehead, 44.7 % BCC of nose and temporal area. Only lesions with a maximum diameter < 2,5 cm were treated with radiation dose of 40 Gy (5 Gy fraction, 2/week). Acute toxicity has been measured according to CTCAE (Common Terminology Criteria for Adverse Events) v4.03 scales and RTOG-EORTC scales were used to assess cosmetic results.

## Results

All pts underwent clinical examination and photographs during RT, 4 weeks, 8 weeks, 3 months, and 6 months after treatment. Toxicity started after the 4<sup>th</sup> fraction and worsened between the end and 4-6 weeks after RT. All pts presented erythema: moderate to brisk grade was scored in 66% cases (G2 CTCAE). Moist desquamation and crusting were shown by 6 pts, 2 patient presented moderate edema. Late toxicity was scored in 42.4 % pts: 10 pts showed slight pigmentation changes (G1 Late RTOG-EORTC) and 4 pts presented moderate telangiectasia (G2).

No residual pain has been scored at the site of irradiation. A clinical complete response was observed in 95.7% of cases at 3 months, 2 patient presented residual disease at 3 months. After a median follow up of 6 months (1-21 months), local control rate is 95.6%: 1 patient experienced in-field recurrence at 6 months and one patient marginal recurrence at 4 months.

#### Conclusion

Our preliminary results show that EBT is an effective, simple, safe, and comfortable treatment associated with good cosmetic outcomes for non-melanoma skin cancers. Even if a longer follow-up and a bigger sample size are needed to confirm these preliminary findings, EBT can be an alternative solution for elderly pts, for pts refusing or presenting contraindications for surgery or when surgical treatment would result in a more disfiguring outcome.

**EP-1600 Implementing TG100: an FMEA for superficial radiotherapy at Wellington Blood and Cancer Centre**  
 A. Williams<sup>1</sup>, B. Steer<sup>1</sup>, D. Paterson<sup>1</sup>, J. Evans<sup>1</sup>, R. Dew<sup>1</sup>  
<sup>1</sup>Wellington Blood and Cancer Centre, Radiation Oncology, Wellington, New Zealand

#### Purpose or Objective

Prospective risk analysis is recommended in radiotherapy to identify high risks and implement safety interventions before adverse events occur [1-4]. In this project, a multidisciplinary team (MDT) conducted a Failure Modes and Effects Analysis (FMEA) for superficial radiotherapy (SXR) with the aim to identify risks in our SXR process and to recommend safety interventions for the highest risks. The process for SXR treatments has marked differences to that for MV photon treatments, for example, patient immobilisation is limited, there is no computerised planning on CT datasets, and there is no on-board imaging during treatment, so the results of the FMEA were expected to differ considerably from those of an advance linac-based technique such as IMRT as presented in TG 100 [1].

#### Material and Methods

We followed our department's own FMEA procedure, closely based on that of Ford [5]. It was planned that the MDT meet six times to perform the FMEA: 1) a general FMEA education session, 2) generate the SXR process map, 3) identify possible failure modes (FMs), 4) generate risk priority number (RPN) scores for identified FMs (all FMs were scored twice by different team members), 5) group review of FM scoring, 6) develop safety recommendations.

#### Results

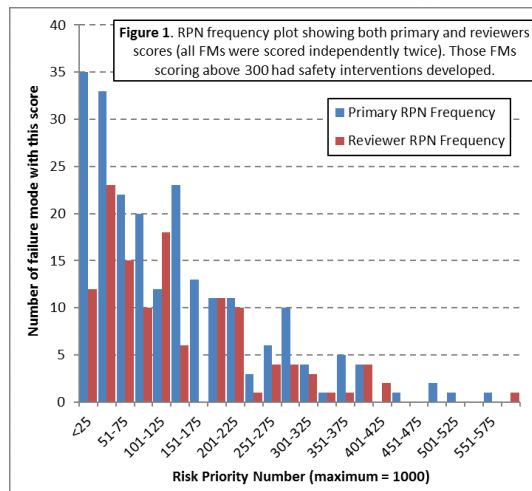
In total, 220 FMs were identified, of which 24 had an RPN greater than 300 (Figure 1) for which the team recommended 27 safety interventions. The recommendations were grouped according to TG100's Table III, *Ranking of QM tools based on effectiveness* as shown in table 1. The top three scoring FMs were 1) Lesion extends into hairline and difficulty seeing the margin, 2) plan parameters and treatment time checked incorrectly and 3) shielding not in place when marking up GTV e.g. under lip, so wrong GTV delineated. The recommended safety interventions for these FMs were 1) hair to be removed from lesion, 2) replace one manual treatment time calculation with a Radcalc QC check, do a reverse treatment time calculation, and scan-in the contour of irregularly shaped cut-outs to a computer for automated equivalent square calculation, and 3) mark-up GTV with shielding / cut-out / applicator in place.

Table 1. Number of interventions grouped according to effectiveness as per TG 100 Table III

QM Tools	Number of interventions (FMs)
1 - Forcing functions	0
2 - Automation and computerisation	5 (9)
3 - Protocols, standards and information	13 (18)
4 - Independent double check systems	1 (3)

5 - Rules and policies  
 6 - Education and information

6 (6)  
 2 (2)



#### Conclusion

The FMEA has facilitated a better understanding of the risks in the SXR process, however, it was time-consuming, requiring around ten hours of meetings (with four more meetings than planned) and many hours of supplementary work outside of the meetings. Listing FMs was challenging and their scoring highly subjective, and some of the recommended interventions e.g. a move to electronic prescribing, will affect our whole radiotherapy service, not just the SXR process.

The recommended interventions for failure modes scoring greater than 300 are now being reviewed by senior management with a view to their implementation.

#### References

- [1] Hug M, et al (2016) Applications of Risk Analysis Methods to Radiation Therapy Quality Management. American Association of Physicists in Medicine Task Group 100 Report. Med. Phys. 43:4209-4262. DOI: 10.1118/1.4947547
- [2] Ortiz Lopez P, et al (2009) Preventing Accidental Exposures from New External Beam Therapy Technologies. International Commission on Radiological Protection Publication 112, Annals of the ICRP 39(4):1-86. DOI: 10.1016/j.icrp.2010.02.002
- [3] Zielman A, et al (2012) Safety is no Accident: A framework for Quality Radiation Oncology and Care. American Society for Radiation Oncology.
- [4] Malicki J, et al (2015) General Guidelines on Risk Management in External Beam Radiotherapy. EU Radiation Protection Report 181, European Commission. DOI: 10.2833/867305
- [5] Ford EC, et al (2009) Evaluation of safety in a radiation oncology setting using failure mode and effects analysis. Int. J. Radiation Oncology Biol. Phys. 74(3):852-858. DOI: 10.1016/j.ijrobp.2008.10.038

#### Electronic Poster: Clinical track: Sarcoma

##### EP-1601 Radiotherapy in resectable Intrathoracic Sarcomas. A Rare Cancer Network Study

C. Solé<sup>1</sup>, F. Larsen<sup>2</sup>, M. Terlizzi<sup>3</sup>, P. Sargos<sup>3</sup>, V. Linacre<sup>4</sup>, F. Suarez<sup>5</sup>, Y. Kirova<sup>6</sup>, P. Van Houtte<sup>7</sup>, D. Lerouge<sup>8</sup>, T. Zilli<sup>9</sup>

<sup>1</sup>Instituto de Radiaciones Médicas, Radiotherapy, Santiago, Chile ; <sup>2</sup>Clinica IRAM, Santiago, Chile ; <sup>3</sup>Institut Bergonie, Bordeaux, France ; <sup>4</sup>Instituto Nacional del Torax, Thoracic Surgery, Santiago, Chile ; <sup>5</sup>Clinica Santa Maria, Thoracic Surgery, Santiago, Chile ; <sup>6</sup>Institut Curie, Paris, France ; <sup>7</sup>Institut Bordet, Bruxelles, Belgium ; <sup>8</sup>Centre Baclesse, Caen, France ; <sup>9</sup>Hôpitaux Universitaires de Genève, Geneva, Switzerland

#### Purpose or Objective

Intrathoracic sarcomas (ITS) are considered rare tumors and have a dismal prognosis. We investigated outcomes and risk factors for local control (LC), disease free survival (DFS) and overall survival (OS) in patients with resected non-metastatic ITS treated with or without adjuvant radiotherapy (RT) and or chemotherapy (CT).

#### Material and Methods

Patients from the Rare Cancer Network database were studied. Kaplan Meier estimate was used to assess survival curves and Cox proportional hazards regression was used to assess risk factors for LC, DFS and OS.

#### Results

Between 2000 and 2017, 121 patients met inclusion criteria. Primary site was lung in 30%, mediastinum 34% and pleura in 36%. 39 % and 32% received RT and CT. Median follow-up was 34 months (range, 2-141). Local control, DFS and OS at 10 years was 52%, 18.7% and 7.2%, respectively. In multivariate analysis RT (P=0.003) and R1 margin status (P=0.041) retained a significant association with local control. Only R1 resection (P=0.002) remained associated with a decreased risk of death in multivariate analysis. Overall, 7 patients (6%) developed grade 3 treatment-related chronic toxicity events

#### Conclusion

This joint analysis revealed that OS remains modest in this group of patients, mainly given by the high risk of local and distant failure. Our results suggest that resected ITS can benefit from adjuvant RT.

#### EP-1602 Role of clinical networks in sarcomas: The Scottish Sarcoma Network(SSN)Experience

J. Nixon<sup>1</sup>, F. Cowie<sup>1</sup>, J. White<sup>2</sup>, P. Chong<sup>3</sup>, S. Lo<sup>4</sup>, D. Bodie<sup>5</sup>, L. Hayward<sup>6</sup>, M. Ferguson<sup>7</sup>, L. Campbell<sup>8</sup>

<sup>1</sup>the beatson west of scotland cancer centre, Oncology, glasgow, United Kingdom ; <sup>2</sup>the beatson west of scotland cancer center, oncology, glasgow, United Kingdom ; <sup>3</sup>gartnaval hospital, surgery, glasgow, United Kingdom ; <sup>4</sup>glasgow royal infirmary, plastic surgery, glasgow, United Kingdom ; <sup>5</sup>aberdeen royal infirmary, surgery, aberdeen, United Kingdom ; <sup>6</sup>edinburgh cancer center, oncology, edinburgh, United Kingdom ; <sup>7</sup>nhs tayside, oncology, dundee, United Kingdom ; <sup>8</sup>national health services, nsd, glasgow, United Kingdom

#### Purpose or Objective

The Scottish Sarcoma Network(SSN) is one of the few National Managed Clinical Networks (MCNs) in Scotland. It was established in November 2004 with its core aim being to improve communication and collaboration between treating centres and promote patient care for sarcoma patients across Scotland. MCNs are virtual entities designed to drive upwards the standards of patient care through integration of services and collaboration. They are defined as "linked groups of health professionals and organisations from primary, secondary and tertiary care, working in a co-ordinated manner, unconstrained by existing professional and Health Board boundaries, to ensure equitable provision of high quality clinically effective services throughout Scotland." We aim to share our experience to achieve better care for sarcoma patients across Scotland.

#### Material and Methods

The National Network Lead rotates across centres and works closely with the National Manager, Subspecialty Leads and sub-groups, NHS staff, patients, carers, charities, Universities and Local Authorities to enhance patient care.

Ambition and Action (2016) details a commitment to delivering the national cancer quality programme across NHS Scotland, with a recognised need for national cancer Quality Performance Indicators(QPIs) to support a culture of continuous quality improvement. The sarcoma QPIs were implemented for patients diagnosed in 2014/15, refined based on the first year's results and reported for years two and three, reviewed after three years and will be reported for year four in December 2018. A weekly National Sarcoma MDT hosted by the SSN is ensuring same standards of care for all sarcoma patients. SSN plays a pivotal role in the QPI process and decision making regarding steps towards continuous improvements. In addition, three education days are organised by the network and are hosted in each of the

three regions treating sarcoma patients across Scotland. Medical Education is used by the network to promote clinical excellence, share clinical practice in transparency and learn through mistakes. A Mortality and Morbidity session is introduced into each of the education days to enable all members of the network to share their practices and share key learning points with peers.

#### Results

The data on QPIs is collected locally by each NHS Board and the analysis is performed locally, regionally and nationally with the resultant actions being assigned to the local NHS Board, the sarcoma specialist centre (there are five) or the Scottish Sarcoma Network. Education sarcoma days are well attended and based on evaluation are connecting specialists and health care professionals with patients, carers, charities, universities and local authorities, all working along the lines of promoting care and raising awareness for sarcomas.

#### Conclusion

SSN is an example that successful networking, which is enhanced through the education days can utilise limited resources by coordination and collaboration to provide best possible and uniform services closer to patient's home in challenging geographical circumstances.

#### EP-1603 Survival after adjuvant radiotherapy for aggressive fibromatosis depend upon time and B-catenin

J.S. Kim<sup>1</sup>, H.J. Kim<sup>1</sup>, M. Lee<sup>2</sup>, K.C. Moon<sup>3</sup>, S.G. Song<sup>3</sup>, H. Kim<sup>4</sup>, I. Han<sup>4</sup>, I.H. Kim<sup>1</sup>

<sup>1</sup>Seoul National University Hospital, Department of Radiation Oncology, Seoul, Korea Republic of ; <sup>2</sup>Hallym University College of Medicine, Department of Radiation Oncology, Seoul, Korea Republic of ; <sup>3</sup>Seoul National University Hospital, Department of Pathology, Seoul, Korea Republic of ; <sup>4</sup>Seoul National University Hospital, Department of Orthopaedic Surgery, Seoul, Korea Republic of

#### Purpose or Objective

We identified the prognostic factors influencing progression-free survival (PFS) of patients with aggressive fibromatosis (AF) after postoperative radiotherapy (PORT). We also assessed the correlation between immunohistochemistry (IHC) features of B-catenin/SMA and PFS.

#### Material and Methods

The records of 37 patients with biopsy-proven AF treated by PORT from 1984 to 2015 were retrospectively reviewed. Fifteen patients underwent wide excision for AF and 22 patients received debulking operation. The median total dose of PORT was 59.4 Gy. IHC of B-catenin and SMA were evaluated in available 11 and 12 patients, respectively. IHC staining intensity was graded and compared between low and high intensity. Log-rank test and Cox proportional hazard model were performed.

#### Results

The median follow up duration was 105.9 months. The 5-year PFS rate was 70.9%. The tumor size and margin status were not related to PFS in univariate analysis (p=0.197; p=0.716, respectively). Multivariate analysis showed that increased interval from surgery to PORT was independent risk factors for PFS (HR 1.303, 95% CI 1.023-1.650, p=0.032). PORT after recurrence had marginal significance (HR 7.550, 95% CI 0.964-59.110, p=0.054). Patient with 2 risk factors, AF recurrence and interval from surgery to PORT >5 weeks, had significantly lower 5-year PFS than patients with no risk factor (43.8% vs. 100.0%, p=0.022). Nuclear B-catenin intensity had a tendency to inversely correlate with 5-year PFS, although it did not have statistically significance (low intensity, 44.4% vs. high intensity, 100.0%, p=0.260). SMA intensity was not related to PFS (p=0.700).

#### Conclusion

PORT should be performed immediately after surgery as initial treatment of choice, irrespective of margin status and tumor size. B-catenin staining intensity of IHC might correlate with local recurrence. Further investigations to validate its prognostic value are needed.

**EP-1604 Feasibility of preoperative radiotherapy in localized sarcoma of the limb: a single center experience**

B. Durand<sup>1</sup>, G. Decanter<sup>2</sup>, M. Jafari<sup>2</sup>, W. Tessier<sup>2</sup>, Y. Robin<sup>3</sup>, A. Renaud<sup>4</sup>, M. Ben Haj Amor<sup>4</sup>, L. Basson<sup>5</sup>, D. Pannier<sup>6</sup>, T. Ryckewaert<sup>6</sup>, N. Penel<sup>6</sup>, A. Córdoba Largo<sup>7</sup>  
<sup>1</sup>Centre Oscar Lambret, Department of Radiotherapy, Lille, France ; <sup>2</sup>Centre Oscar Lambret, Surgery Department, Lille, France ; <sup>3</sup>Centre Oscar Lambret, Pathology department, Lille, France ; <sup>4</sup>Centre Oscar Lambret, Imaging department, Lille, France ; <sup>5</sup>Centre Oscar Lambret, Academic Radiation Department, Lille, France ; <sup>6</sup>Centre Oscar Lambret, Medical Oncology department, Lille, France ; <sup>7</sup>Centre Oscar Lambret, Department of Radiation Oncology, Lille, France

**Purpose or Objective**

To report feasibility and first clinical and toxicity data from a retrospective series of patients treated with the association of preoperative radiotherapy and radical surgery for a localized sarcoma in the limbs in our referenced center.

**Material and Methods**

All patients with soft tissue sarcoma of the limbs treated consecutively in our institution by preoperative radiotherapy and surgery combination. The combined treatment of preoperative radiotherapy and surgery was decided in a multidisciplinary consultation meeting depending on the histological type, the relationship of the tumor to the blood vessels and the size of the tumor. Principal objective: Feasibility of pre-operative radiotherapy followed by surgery at 4-6 weeks; Secondary: Resection quality (R0, R1, R2), Post-operative complication rate, Survival without local recurrence, Histological response (necrosis rate) to preoperative radiotherapy.

**Results**

31 patients were enrolled on a 4-year period. In 25 patients (80.6%) tumor was in lower limb. Vascular relation < 5mm on MRI was observed in 19 patients (61.3%), 27 patients (87.1%) were classed T2b and the median largest axis was initially 12 cm (1.7-30), the median depth was 7cm. Initial biopsy was performed in our center in 22 patients (71%). Histology based on biopsy was: sarcoma indifferenced in 11 patients (35.5%), adipocytic tumor in 10 patients (32.3%) and autre in 10 patients (32.3%). Preoperative radiotherapy delivered 45 to 50,4 Gy at 1,8 Gy fractions; IMRT for 26 patients (83,9%) and 3D-CRT for 5 (16.1%) patients. All patients were operated with a conservative intent with 49 days (24-83) median after the end of the radiotherapy. In 28 patients, (90.3%) we performed image, MRI in 25 (89.3%) patients or CT (9.7%) in 3 patients, before surgery. In 25 patients (80.6%) surgery was R0 and in the other six patients (19.4%) was R1. Histology after surgery was: sarcoma indifferenced in 13 patients (41.9%), adipocytic tumor in 9 patients (29%) and autre in 9 patients (29%). Flap was needed in 11 patients (35.5%), 5 (16.1%) immediately and 6 (19.4%) remote flap because delayed healing. Bone fracture was observed in 3 patients (9.7%). Three patients presented chronic pain (1 patient grade 1 and 2 patients grade 2). At the end of our median follow-up of 18 months, there were 6 relapses, 5 metastatic and 1 local), 2 of them died of the disease evolution.

**Conclusion**

Preoperative radiotherapy in locally advanced sarcoma of the limb is feasible, when achieved in a reference center, with a satisfactory early clinical and toxicity data.

**EP-1605 Adjuvant RT for soft tissue sarcomas: volumetric modulated arc therapy vs 3D conformal radiotherapy**

L. Di Brina<sup>1</sup>, P. Navarria<sup>1</sup>, G.R. D'Agostino<sup>1</sup>, F. De Rose<sup>1</sup>, C. Iftode<sup>1</sup>, E. Clerici<sup>1</sup>, F. Lobefalo<sup>1</sup>, A. Bertuzzi<sup>2</sup>, V. Quagliuolo<sup>3</sup>, M. Scorsetti<sup>4</sup>

<sup>1</sup>Humanitas Clinical and Research Center, Radiotherapy and Radiosurgery, Rozzano, Italy ; <sup>2</sup>Humanitas Clinical and Research Center, Medical Oncology, Rozzano, Italy ; <sup>3</sup>Humanitas Clinical and Research Center, Surgical Oncology, Rozzano, Italy ; <sup>4</sup>Humanitas University, Biomedical Sciences, Rozzano, Italy

**Purpose or Objective**

Soft tissue sarcomas (STS) represent rare tumors of mesenchymal origin, frequently detected to the extremities. Nowadays limb-sparing surgical resection followed by radiation therapy (RT) is considered the standard treatment in large, high-grade sarcomas. Recent RT technological advances allow to improve the tumor coverage with maximum sparing of normal tissues. Aim of this study is to assess the impact of VMAT compared with 3DCRT in patients with diagnosis of STS of the extremities and treated with surgery and adjuvant RT in terms of toxicity, local control (LC), disease free survival (DFS) and overall survival (OS).

**Material and Methods**

This analysis included patients with diagnosis of STS of the extremity treated with limb-sparing surgery and submitted to adjuvant RT for one or more of the following risk factors: deeply located tumors, grade II-III, maximum diameter larger than 5 cm and marginal surgical resection. From 2004 to 2010 plans were processed using 3DCRT. Starting from 2011 to 2016, all patients were treated with VMAT. Response was recorded with contrast-enhanced MRI and thoracic and abdominal CT scan every 3 months. Toxicity was evaluated with Common Terminology Criteria for Adverse Events (CTCAE) scale version 4.3.

**Results**

From 2005 to 2016, 109 patients were treated in our center and included in the analysis. Median age was 55 years (range 15-84 years). The majority of patients had disease of the lower extremity (95 patients, 87%). The most frequent histotype was liposarcoma (57,7%). Fifty-three patients received chemotherapy (CT). Radical surgical resection was performed in 76% of patients, 24 patients received R1 resection and 2 patients R2. 3DCRT was performed in 38 cases and VMAT in 71 cases. The administered total dose was 66 Gy in 33 fractions. Median follow-up was 70 months for the entire cohort, 121 months for the 3DCRT group, 61 months for the VMAT group. Actuarial LC at 3 years were 83.0% in 3DCRT group and 92.7% for patients in VMAT group. Actuarial DFS at 3 years were 74.0 % and 79.2% for patients who underwent 3DCRT and VMAT respectively. Actuarial OS at 3 years were 70.0% for patients who underwent 3DCRT, and 79.2% for VMAT group. Grade 1-2 acute skin toxicity occurred in 58% of the patients in 3DCRT group and 48% of VMAT group. One patient in each group presented grade 3 acute skin toxicity. Late toxicity was recorded in 38 patients (35%): nine patients treated with 3DCRT had grade 1 toxicity while in VMAT group 17 patients and 1 patients had G1-G2 and grade 4 skin toxicity respectively. Between VMAT patients 4 of them had G1 joint toxicity. Only margins and grade were significant factors for LR after univariate analysis (p=0.002). The technique influenced significantly OS both at univariate and multivariate analysis (p=0.006).

**Conclusion**

The availability of modern RT technique permit a better conformity on the target with maximum sparing of normal tissue and acceptable side effects. Results on local control and survival of VMAT are encouraging. More perspective

studies are needed to better define the use of arc therapy in this setting of patients.

#### EP-1606 Stereotactic Ablative Radiotherapy for oligometastatic soft tissue sarcoma patients

D. Greto<sup>1</sup>, M. Loi<sup>1</sup>, D. Pezzulla<sup>1</sup>, M. Lo Russo<sup>1</sup>, M.A. Teriaca<sup>1</sup>, V. Maragna<sup>1</sup>, S. Lucidi<sup>1</sup>, D.A. Campanacci<sup>2</sup>, G. Beltrami<sup>2</sup>, G. Scoccianti<sup>2</sup>, L. Livi<sup>1</sup>

<sup>1</sup>University of Florence-Azienda Ospedaliera Universitaria Careggi AOUC, Department of Biomedical- Experimental- and Clinical Sciences, Firenze, Italy ; <sup>2</sup>Azienda Ospedaliera Universitaria Careggi- University of Florence, Department of Orthopaedic Oncology and Reconstructive Surgery, Florence, Italy

#### Purpose or Objective

Stereotactic Body Radiotherapy (SBRT) is emerging as a novel treatment option in oligometastatic cancer patients ( $\leq 3$  synchronous lesions), but it is unclear whether this treatment option could be applied to bone and soft tissue sarcoma due to theoretical intrinsic radioresistance. The aim of our study was to evaluate the effectiveness and safety of SBRT in oligometastatic sarcoma.

#### Material and Methods

We collected data from a consecutive cohort of oligometastatic sarcoma patients treated in our Institution. Toxicity, Local Control (LC) rates and prognostic role of clinical and treatment-related characteristics (primary tumor type and location, synchronous or metachronous onset, SBRT site, dose delivered expressed as Biologically Effective Dose [BED], use of concurrent systemic treatment) were assessed.

#### Results

Thirty-four consecutive patients, accounting for 56 metastases (including 38 lung, 16 bone and 2 lymph node metastases), were treated at our institution with SBRT. Eight (23.5%) patients had metastatic disease at diagnosis. Nine (26.5%) patients in treatment with chemotherapy for metastatic disease received associated SBRT in case of oligoprogression. Median follow-up from first SBRT was 10 months (range 1-112). Median number of metastases treated per radiation course was 2 (range 1-3). Median number of SBRT fractions was 4.5 (range:3-12). Median prescribed dose was 40 Gy (range: 25-54 Gy) and median BED was 75 Gy (range 48-151). LC at 6 months, 1 year and 2 years was 85.4% [CI95% 73.8-92.4], 82.3 [CI95% 69.1-90.6], and 73.6% [CI95% 56.8-86.5] respectively. At statistical analysis, only trunk primary tumor identified patients with poorer LC ( $p=0.02$ ). Fifteen patients received 2 courses of SBRT while 1 patient received 3 courses of SBRT. No acute or chronic grade  $\geq 3$  toxicity was observed in the treated site, only 2 patients experienced minor toxicity consisting of 1 acute grade 1 skin reaction and 1 grade 1 late fibrosis, respectively.

#### Conclusion

In patients with oligometastatic sarcoma, SBRT yields satisfying LC with minimal toxicity regardless of concurrent treatment, metastasis timing location, and dose schedule. Repeated SBRT is feasible and may be considered to extend disease-free interval.

#### EP-1607 Preoperative Radiation Therapy and IORT in Retroperitoneal Soft Tissue Sarcomas. Long Term Outcome

F. Navarria<sup>1</sup>, S. Basso<sup>2</sup>, E. Palazzari<sup>1</sup>, R. Innocente<sup>3</sup>, A. Lauretta<sup>4</sup>, F. Matrone<sup>1</sup>, G. Fanetti<sup>1</sup>, A. Revelant<sup>1</sup>, A. Buonadonna<sup>5</sup>, C. Belluco<sup>2</sup>, V. Canzonieri<sup>6</sup>, J. Polesel<sup>7</sup>, G. Bertola<sup>2</sup>, A. De Paoli<sup>1</sup>

<sup>1</sup>Centro di Riferimento Oncologico CRO - IRCCS- Aviano-Italy, Radiation Oncology, Aviano, Italy ; <sup>2</sup>Centro di Riferimento Oncologico CRO - IRCCS- Aviano- Italy, Surgical Oncology, Aviano, Italy ; <sup>3</sup>Centro di Riferimento Oncologico CRO - IRCCS- Aviano-Italy, Radiation Oncology, Aviano, Italy ; <sup>4</sup>Centro di Riferimento Oncologico CRO - IRCCS- Aviano-Italy, Surgical Oncology,

Aviano, Italy ; <sup>5</sup>Centro di Riferimento Oncologico CRO - IRCCS- Aviano- Italy, Medical Oncology, Aviano, Italy ; <sup>6</sup>Centro di Riferimento Oncologico CRO - IRCCS- Aviano-Italy, Pathology, Aviano, Italy ; <sup>7</sup>Centro di Riferimento Oncologico CRO - IRCCS- Aviano- Italy, Cancer Epidemiology, Aviano, Italy

#### Purpose or Objective

Local control in patients (pts) with RPS is still challenging. Local recurrence after gross total resection remain the major issue. To improve local control radiation therapy (RT) was used. Post-op RT was not successful due to limited dose-tolerance of surrounding normal structure. Pre-op RT and IORT, allowing dose-escalation to high risk areas after resection, could overcome such limitations. Their use has been evaluated at our Institution.

#### Material and Methods

Long-term outcome of a consecutive series of 93pts(M/F ratio 50/40, median age 60yrs range 24-81) treated with preop RT +/-IORT at our Institute, from February 1999 to December 2017, is reported. Three pts had R2 resection and were excluded from this analysis. Fifty-five had primary 35 had recurrent disease. Pre-op RT consisted of 45-50.4 Gy in 25-28 frs after through-cut biopsy or initial operation. Conformal 3D-RT was used to include the tumor with a 3-5 cm margin (PTV1) with 45 Gy, followed by a reduced volume with a 2 cm margin (PTV2) up to 50.4 Gy. Concurrent chemotherapy (CT) with 3 cycles of c.i. Ifosfamide (1 gr/mq for 14 days, q 4 wks) was given to 31pts From 2012, IMRT with 45Gy/25frs and a SIB up to 52.5 Gy to posterior area at high risk, was used to optimize RT program. Pre-op RT ( $\pm$  CT) was followed by surgical resection after 4-6 weeks. A IORT boost was given to high risk area, if applicable, with a dose ranging from 10-18 Gy based on the completeness of surgical margins. Median tumor size was 16 cm (3-33 cm) and the most common histotypes were Liposarcoma (55%) and Leiomyosarcoma (21%). Tumor grade was G1:28.8%, G2: 27.7% and G3: 43.5%.

#### Results

All pts completed the planned pre-op RT at the median dose of 50.4 Gy (range 45-52.5Gy). Tolerance to pre-op RT was acceptable with G3 toxicity (15%) only in pts who received concurrent CT. Surgical operation was performed in all 90 with complete gross total resection in all operated pts. IORT at the median dose of 12 Gy (10-15Gy) was given to 79 of 90 resected pts. IORT was not given to 11 pts, in 3 because of wide complete resection and in 8pts for IORT technical reasons. At a median follow-up of 3.5 years (02-18 years) the cancer specific survival (CSS), LDFS and DFS were 57.1%, 54.6% and 41.1% respectively. Status of surgical margins, R0 vs R1, resulted of borderline significant for LDFS (71.4% vs 41.4% and 65% vs 37.3% at 5 and 10 yrs, respectively,  $p=0.047$ ). In the subset of 11 no-IORT pts, no difference in LDFS was reported. Complications occurred in 2 pts (3%) who had bowel perforation after pre-op RT  $\pm$  CT; 4 pts (10%) developed G2-3 IORT related neuropathy and 3 pts (3.3%) IORT urethral injury.

#### Conclusion

Pre-op RT and IORT in RPS was feasible with an acceptable toxicity profile. This approach allows a favourable complete resection rate and long-term outcome in disease control and survival with low rate of complications. IORT allows dose escalation to high-risk areas and in pts with R0 resection yields excellent local tumor control.

#### EP-1608 Results of an aggressive local strategy after R1 or R2 unplanned surgery for soft tissue sarcomas

P. Paul<sup>1</sup>, M. Laurence<sup>2</sup>, V. Gualter<sup>3</sup>, R.C. Isabelle<sup>4</sup>, M. Pierre<sup>3</sup>, B. Jean Yves<sup>4</sup>, P. Patrice<sup>3</sup>, B. Mehdi<sup>4</sup>, K. Marie<sup>5</sup>, D. Armelle<sup>4</sup>, S. Marie Pierre<sup>1</sup>

<sup>1</sup>Centre Léon Bérard, Radiation Oncology, Lyon, France ;

<sup>2</sup>CHRU Besançon, Radiation Oncology, Besançon, France ;  
<sup>3</sup>Centre Léon Bérard, Surgery, Lyon, France ; <sup>4</sup>Centre  
 Léon Bérard, Medical Oncology, Lyon, France ; <sup>5</sup>Centre  
 Léon Bérard, Pathology, Lyon, France

#### Purpose or Objective

To compare outcomes of soft tissue sarcomas (STS) with and without residual disease subsequent to re-excision in our institution after primary unplanned surgery.

#### Material and Methods

Between 1996 and 2015, 180 patients with extremities or trunk wall STS were referred to our center after unplanned R1 or R2 surgery for local treatment including re-excision with or without post-operative irradiation. Cutaneous and lipoma-like sarcomas were excluded. Re-excision was considered R0 if margins were  $\geq 1$  mm and R1 when margins were closer. Re-excision found microscopic residual disease in 93 patients, and no residual disease in 87 patients. Median time between unplanned surgery and re-excision was 2 months (range 1-8). Adjuvant radiotherapy was performed for 133 patients (74%) with a median delivered dose of 50 Grays in 25 fractions.

#### Results

Median follow-up was 78 months (range 3-244). Median age was 62 years old. In the group of patients with residual disease (R group), STS were more likely to be of higher grade ( $p=0.043$ ) and larger volume ( $p<0.01$ ) than the group of patients without residue (No-R group). Radiotherapy was more frequently performed in R group (74/93 patients) than No-R group (59/87 patients) ( $p=0.045$ ). In R-group, re-excision was R1 for 65% of patients and R0 for 35%. Achieving R0 margins was associated with better LRFs, MFS, DSS and OS on univariate ( $p=0.024$  for LRFs) and multivariate analysis ( $p=0.027$  for LRFs); grade 3 sarcomas were associated with worse MFS on multivariate analysis ( $p=0.044$ ).

Whether or not residual disease was remaining at the time of re-excision did not impact local-recurrence-free survival (LRFs), which was similar in the 2 groups : 62.4 months in R-group vs 73.4 months in No-R group ( $p=0.092$ ). In an analogous way, metastasis-free survival (MFS), overall and disease-specific survival (OS and DSS) were not different in the 2 compared groups.

In No-R group, radiotherapy was associated with better LRFs on univariate analysis ( $p=0.014$ ); tendency to better LRFs was observed on multivariate analysis ( $p=0.08$ ); grade 3 sarcomas had worse MFS on univariate analysis ( $p=0.014$ ).

#### Conclusion

Achieving R0 re-excision after primary unplanned surgery is essential. Our results suggest that radiotherapy should be performed after re-excision even if no residual disease is observed.

Engineering- Human Health Sciences, Kyoto, Japan ;  
<sup>6</sup>Kyoto University Graduate School of Medicine,  
 Department of Neurosurgery, Kyoto, Japan

#### Purpose or Objective

In pediatric patients, permanent alopecia occurred in a grave late complication of multi-drug chemotherapy (CTx) plus cranial irradiation, reducing both patient self-esteem and quality of life. To prevent permanent alopecia, we started to use craniospinal irradiation (CSI) using the volumetric-modulated arc whole-brain radiotherapy (VMAT-WBRT) for pediatric patients, and their hair had fully recovered without disease progression. As the threshold to prevent permanent alopecia is still unknown, we evaluated the dose distribution of VMAT-WBRT and compared the dosimetric parameters between VMAT-WBRT and conventional whole-brain radiotherapy (WBRT).

#### Material and Methods

Four consecutive patients (4-11 years old) who received CSI using VMAT-WBRT from June 2015 to December 2016 were included. One patient with embryonic carcinoma received radiotherapy (RT) with concurrent CTx; three patients with medulloblastoma (two patients with standard risk, and one patient with high risk) received RT followed by CTx. The prescribed doses of CSI were 23.4-35.2 Gy in 13-22 fractions, respectively. 5 mm thickness of the hair follicles bearing scalp was created (Fig. A). VMAT-WBRT was delivered with double arcs, and optimization was performed to reduce doses to the hair follicles with keeping the dose coverage to the planning target volume. For the dosimetric study, the conventional WBRT plans were retrospectively created, and the dose distributions were compared between VMAT-WBRT and conventional WBRT. Doses to the planning target volume for whole brain [PTV(WB)] and organs at risk (OARs), including hair follicles, cochlea, lacrimal glands, lens, eyes, parotid glands, oral cavity, hypopharynx, and thyroid, were evaluated.

#### Results

Although all patients experienced temporary alopecia, their hair fully recovered over the whole scalp within 8 months after finishing RT. None had disease progression at least 23.9 months after completing CTx or RT. In the dosimetric study, the mean doses to the hair follicles, parotid glands, and left lacrimal glands were lower in the VMAT-WBRT group. On the other hand, the mean doses to the oral cavity, hypopharynx, and thyroid were higher in the VMAT-WBRT group than in the conventional WBRT group. The average mean equivalent doses in 2-Gy fractions (EQD2) to the hair follicles were 19.5 and 13.3 Gy in the conventional WBRT and VMAT-WBRT groups, respectively. In this study, the mean EQD2 to the hair follicles of all patients who received VMAT-WBRT were lower than 15.1 Gy. The D2 of other OARs and the D2, D98, D50, mean doses, V90, V95, and V107 of PTV(WB) were similar between the two groups.

---

Electronic Poster: Clinical track: Paediatric tumours

---

#### EP-1609 Volumetric-modulated arc whole-brain radiotherapy prevents permanent alopecia for pediatric patients

M. Uto<sup>1</sup>, K. Ogura<sup>2</sup>, K. Umeda<sup>3</sup>, T. Katagiri<sup>4</sup>, K. Takehana<sup>1</sup>, M. Nakamura<sup>1,5</sup>, N. Mukumoto<sup>1</sup>, Y. Miyabe<sup>1</sup>, T. Kamitori<sup>3</sup>, A. Iwai<sup>3</sup>, Y. Arakawa<sup>6</sup>, Y. Mineharu<sup>6</sup>, M. Tanji<sup>6</sup>, I. Kato<sup>3</sup>, H. Hiramatsu<sup>3</sup>, T. Mizowaki<sup>1</sup>

<sup>1</sup>Kyoto University Graduate School of Medicine, Department of Radiation Oncology and Image-Applied Therapy, Kyoto, Japan ; <sup>2</sup>Kobe City Medical Center General Hospital, Department of Therapeutic Radiology, Kobe, Japan ; <sup>3</sup>Kyoto University Graduate School of Medicine, Department of Pediatrics, Kyoto, Japan ; <sup>4</sup>Shizuoka City Shizuoka Hospital, Department of Radiation Oncology, Shizuoka, Japan ; <sup>5</sup>Kyoto University Graduate School of Medicine, Division of Medical Physics Department of Information Technology and Medical

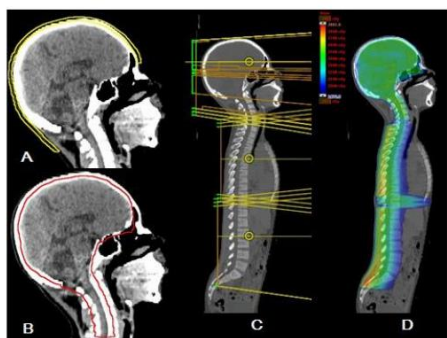


Figure.

The contours of hair follicles (A), and planning target volume of whole brain and cervical spinal cord (B). The sum of all fields for craniospinal irradiation using volumetric-modulated arc whole brain radiotherapy (C), and dose distribution (D) in a representative case. The area receiving more than 80 % of the prescribed dose was shown in (D).

Table. The indices about the planning target volume (PTV) for whole brain and organs at risk.

Contour	indices	Conventional WBRT		p-value
		Mean	SD	
PTV for whole brain	D2 (%)	106.2 ± 0.7	106.4 ± 1.8	0.869
	D98 (%)	95.2 ± 2.1	90.8 ± 2.5	0.107
	D50 (%)	100.7 ± 0.6	101.5 ± 1.3	0.313
	V90 (%)	99.4 ± 0.5	98.3 ± 1.7	0.625
	V95 (%)	98.1 ± 1.4	92.8 ± 3.8	0.113
	V107 (%)	1.1 ± 0.9	2.4 ± 2.9	0.625
Hair follicles	D2 (%)	106.2 ± 0.9	92.4 ± 5.7	0.023
	mean (%)	79.8 ± 2.1	61.0 ± 4.6	0.004
	mean (Gy)	23.6 ± 5.6	17.8 ± 3.0	0.021
Lt. eye	D2 (%)	102.5 ± 1.0	94.3 ± 8.2	0.125
Rt. lens	D2 (%)	25.2 ± 5.4	27.1 ± 2.8	0.436
Lt. lens	D2 (%)	27.5 ± 6.4	29.1 ± 5.0	0.239
Hypopharynx	mean (%)	47.2 ± 10.1	61.0 ± 8.4	0.003
Rt. cochlea	mean (%)	95.6 ± 1.0	87.5 ± 8.5	0.125
Lt. cochlea	mean (%)	96.1 ± 0.4	86.6 ± 8.6	0.125
Thyroid	mean (%)	63.2 ± 6.7	72.1 ± 4.6	0.012
Oral cavity	mean (%)	16.5 ± 2.2	36.8 ± 4.3	0.002
Rt. parotid gland	mean (%)	93.6 ± 5.8	50.2 ± 8.7	0.002
Lt. parotid gland	mean (%)	93.7 ± 5.8	50.1 ± 11.3	0.006
Bilateral parotid gland	mean (%)	93.7 ± 5.8	50.1 ± 9.8	0.003
Rt. lacrimal gland	mean (%)	93.8 ± 7.3	64.4 ± 6.2	0.125
Lt. lacrimal gland	mean (%)	91.9 ± 5.8	60.3 ± 9.0	0.002

Abbreviations: WBRT, whole brain radiotherapy; VMAT-WBRT, volumetric-modulated arc whole brain radiotherapy; SD, standard deviation; DX (%) means the relative dose to the X % of the PTV or the organs at risk; VX (%) means the relative volume of the PTV receiving X % of the prescribed dose; Rt., right; Lt., left.

## Conclusion

Our study showed that the mean EQD2 to the hair follicles lower than 15.1 Gy seemed to be associated with prevention of permanent alopecia. More cases are needed to verify the efficacy and more accurate threshold to prevent permanent alopecia for pediatric patients who receive multi-drug CTx and cranial irradiation.

## EP-1610 Cranio Spinal Axis irradiations using Pencil Beam Scanning: the PSI experience

D. Siewert<sup>1</sup>, F. Belosi<sup>1</sup>, R. Gonzalo Gleyzes<sup>1</sup>, L. Mikroutsikos<sup>1</sup>, D. Correia<sup>2</sup>, A. Pica<sup>1</sup>, F. Albertini<sup>1</sup>, A.J. Lomax<sup>1</sup>, D.C. Weber<sup>1</sup>, A. Bolsi<sup>1</sup>

<sup>1</sup>Paul Scherrer Institute, Center for Proton Therapy, Villigen, Switzerland ; <sup>2</sup>Bern University Hospital, Department of Radiation Oncology- University of Bern, Bern, Switzerland

## Purpose or Objective

Cranio Spinal Irradiation (CSI) is a promising indication for pencil beam scanning (PBS) proton therapy. In this study we present the clinical and dosimetric evaluation of CSI treatments delivered at PSI, with special focus on tumour recurrences.

## Material and Methods

20 CSI patients, treated between 2004 and 2017, have been included in this study. 17/20 were positioned prone (Gantry1), and 3 supine (Gantry 2). The primary tumors were: medulloblastoma (10pts), PNET (4pts), anaplastic ependymoma (3pts), choroid plexus carcinoma (1pt) and others (2pts). 3 of 20 patients received CSI for local failure after a first course of local fractionated RT, thus requiring accurate sparing of pre-irradiated brain tissue. Daily imaging was performed based on orthogonal topograms acquired once along the full length of the spine before delivery, and a single positioning correction vector for the entire CSI PTV applied. Dose delivery on the other hand consists of a number of patched subfields. As such, inaccuracies of couch movements between sub-fields during delivery might result in under- or over-dosage. For all cases we analysed: i) planning approach; ii) target coverage (V95, D98) and OAR sparing; iii) dose averaged LET distributions and iv) robustness (range errors and set-up scaling for fractionation). Accuracy of prone (G1) vs. supine (G2) setup was evaluated. During follow-up, 6 patients (30%) presented with tumor recurrences, of which 5 (25%) could be considered high risk patients at diagnosis - 3 with leptomeningeal dissemination at the time of CSI, 1 with a recurrent PNET at the time of irradiation and one case where the tumor was an "in-field" relapse of an anaplastic ependymoma after re-irradiation. For all 6 relapsing patients, a detailed localization of the recurrence and any spatial relationship with field patching was performed.

## Results

Clinical dosimetric data are summarized in Table 1. Supine positioning resulted in lower systematic and random errors as compared to prone (systematic residual errors < 0.1mm for supine as compared to 0.5mm for prone; random errors in PA direction were reduced from 1.7mm for prone to 1.1mm for supine). For the relapsing patients, the recurrences did not overlap with patch lines and were not correlated with setup or range error. Indeed, all recurrences were either located in the high risk PTV or were leptomeningeal dissemination. We observed two vascular radiation induced toxicities: one with Moya-Moya syndrome and one with multiple cerebral cavernomas. These observed vascular toxicities were not related to high-LET areas.

## Conclusion

PBS CSI treatments can be safely delivered, as the plans are robust considering range and setup uncertainties. The pattern of recurrences was not correlated with potential dose inaccuracies in the patch lines or lack of robustness, and no correlation of toxicities to enhanced LET have been observed.

Table 1. Summary of dosimetric data.

Prescribed dose (GyRBE)	32.6±5.2	
CSI series		
Prescribed dose (GyRBE) full treatment	54.4±1.7	
Field approach of CSI series	2 narrow fields (16/20)	
	Single field (1/20)	
	3 narrow fields (1/20)	
	Multiple fields with lateral approach for the head (2/20)	
Statistical parameters		
	CSI series	
V95 CTV (%) (*)	99.0±1.2	
V95 PTV (%) (*)	89.7±3.3	
D98 CTV (%) (*)	96.5±2.5	
D98 PTV (%) (*)	83.3±7.3	
Robustness		
	CSI series	Boost series
PTV vol. err-> 5% (%)	14.8±4.0	19.2±11.5
CTV vol. err-> 5% (%)	5.5±3.8	5.0±11.2
PTV vol. err-> 5% (%) <sup>(#)</sup>	14.1±6.2	22.0±18.4
CTV vol. err-> 5% (%) <sup>(#)</sup>	4.2±2.5	10.9±20.2
Recurrence vol. err-> 5% (%)	16.7 (**)	0±0 (***)

(\*) excluding pre irradiated patients

(#): calculated only on patients presenting with recurrence

(\*\*) calculated for a single patient presenting with recurrence in the CSI PTV

(\*\*\*) calculated for two patients presenting with recurrence in the boost PTV

boost PTV

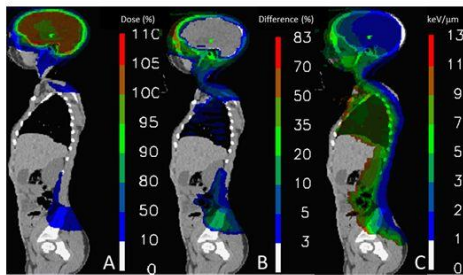


Figure 1. For a patient who presented with recurrence (green contour) different distributions are reported: A. CSI series dose distribution (% of CSI series prescription dose). B. CSI series robustness distribution (error bars as % of the prescribed dose, considering setup and range error for the delivered 20 fractions of the CSI series). C. LET distribution of the CSI series plan.

### EP-1611 Experience of uninterrupted radiotherapy for pediatric hodgkin's disease in a developing country

B.M. Qureshi<sup>1</sup>, Y. Ahmed<sup>1</sup>, F. Shaikat<sup>1</sup>, A.N. Abbasi<sup>1</sup>, M.R. Khan<sup>2</sup>, M.A. Mansha<sup>1</sup>, M.U. Karim<sup>1</sup>, A. Hafiz<sup>1</sup>, A.M.H. Khan<sup>1</sup>, B. Mir Khan<sup>1</sup>, N. Ali<sup>1</sup>, M.S. Ashraf<sup>3</sup>

<sup>1</sup>The Aga Khan University, Radiation Oncology Section- Department of Oncology, Karachi, Pakistan ; <sup>2</sup>The Indus Hospital, Department of Pediatric Oncology- Indus Children Cancer Hospital, Karachi, Pakistan ; <sup>3</sup>The Indus Hospital-, Department of Pediatric Oncology- Indus Children Cancer Hospital, Karachi, Pakistan

#### Purpose or Objective

Radiation therapy is an essential component of patients treated on Euronet protocol who have not responded to initial chemotherapy. The Purpose of the study is to report the planning and delivery experience of radiation therapy for pediatric Hodgkin's disease patients at our tertiary care university hospital in Pakistan.

#### Material and Methods

All the patients with Hodgkin's disease are discussed in site specific pediatric leukemia / lymphoma tumor board meeting. Patients having residual disease on interim evaluation after initial cycles of chemotherapy are treated with radiation therapy after the completion of appropriate chemotherapy according to treatment group. Radiation therapy is planned and delivered according to radiotherapy guidelines of Euronet PHL-C1 study treatment protocol. Children requiring radiation therapy are treated with a dose of 19.8 Gy in 11 fractions to the initial involved site with 1.8 Gy per fraction. A boost of 10 Gy in 5 fractions with 2 Gy per fraction is given to the residual disease seen on interim scan.

#### Results

From January 2017 till October 2018, a total of 18 patients of Hodgkin's disease were identified who required

radiotherapy according to the protocol. Out of 18 children, 14 (78%) were male and 4 (22%) were females. Mean age of the children was 11 years (6 - 17years).

All the patients were discussed in departmental peer review meeting with at least two radiation oncologists and a team of residents before starting radiotherapy. A total of 14 patients (77.8%) received both supra and infra diaphragmatic radiotherapy while two patients each had supra diaphragmatic and infra diaphragmatic radiation alone in phase I with total dose of 19.8Gy.

Out of 14 patients who received radiation to both supra and infra-diaphragmatic regions, 9 (64%) patients received simultaneous supra & infra diaphragmatic radiation whereas 5 (35.7%) received sequential radiotherapy to the other region.

Neck was irradiated in 16 (88.9%) patients, among them 9 patients received bilateral neck radiation. RT to axilla was given in 13 (72.2%) patients out of which bilateral axilla was treated in 9 patients. Spleen was treated in 12 (66.7%) patients. A phase II boost of 10 Gy was given to the regions of neck in 8 patients, axilla to 3 patients and spleen to 3 patients.

None of these patients had a treatment gap during the course of radiation therapy. Also, no severe acute hematologic toxicity was observed after completion of treatment.

#### Conclusion

Radiation therapy for children with Hodgkin's disease was planned by peer reviewed team and delivered according to the protocol without any treatment interruption. Long term toxicity needs to be evaluated, possibly in a larger prospective study.

### EP-1612 Radiation induced hypothyroidism in pediatric tumours of central nervous system

C. Satragno<sup>1</sup>, E. Tornari<sup>1</sup>, S. Barra<sup>2</sup>, F. Giannelli<sup>2</sup>, L. Belgioia<sup>1</sup>, M. Giaccardi<sup>3</sup>, N. Di Iorgi<sup>3</sup>, M.L. Garrè<sup>4</sup>, R. Haupt<sup>5</sup>, R. Corvò<sup>1</sup>

<sup>1</sup>University of Genoa and San Martino Hospital, Health Science Department DISSAL and Radiation Oncology, Genoa, Italy ; <sup>2</sup>San Martino Hospital, Radiation Oncology, Genoa, Italy ; <sup>3</sup>Istituto Giannina Gaslini, Department of Pediatrics, Genoa, Italy ; <sup>4</sup>Istituto Giannina Gaslini, Department of Neurooncology, Genoa, Italy ; <sup>5</sup>Istituto Giannina Gaslini, Epidemiology and Biostatistics Unit, Genoa, Italy

#### Purpose or Objective

To investigate primary and secondary hypothyroidism in pediatric patients affected by central nervous system (CNS) tumors.

#### Material and Methods

From January 1999 to September 2015 we retrospectively analyzed all patients with CNS tumors treated by IMRT or 3D-CRT. We analyzed hypothyroidism from direct thyroid damage (primary hypothyroidism) with FT4 value and hypothyroidism from direct damage to the pituitary gland and hypothalamus (considering them as a single organ at risk - central hypothyroidism) with TSH detection.

#### Results

Sixty-four consecutive pts with a median age of 10 years (range: 2 to 17) were identified. Nineteen (29,7%) and 45 (70,3%) pts received IMRT and 3DCRT respectively. 39 (60.9%) patients underwent craniospinal irradiation (CSRT) ± boost; all other patients were treated with involved field radiation therapy (IFRT) ± boost (39.1%). Histology was represented by medulloblastoma, gliomas, germinoma, ependymomas and others in 50%, 26.5%, 11%, 4.6% and 7.8% of patients, respectively. Sixty-one (95,3%) patients received chemotherapy (CT) and 42 (65,6%) patients surgery. Thyroid dose evaluation was possible in 20 of 39 patients who received CSRT, whereas a documented pituitary gland dose was available in 64 pts. 19/64 pts presented a TSH deficit and 6/64 FT4 deficit. Sixteen of 19 patients with TSH deficiency were treated with CSRT (dose

range: 23.4 to 39.0 Gy)  $\pm$  boost, and 3/19 with IFRT (dose range: 21.0 to 54.0 Gy)  $\pm$  boost. All patients with central and peripheral hypothyroidism underwent CSRT (dose range: 23.40 to 39.0 Gy)  $\pm$  boost. Three of 6 patients with FT4 deficiency were treated with CSRT (dose range: 23.40 to 36.00 Gy)  $\pm$  boost, 3/12 with IFRT (dose range: 50.40 to 60, 00 Gy)  $\pm$  boost.

#### Conclusion

Our data confirm the frequency of hypothyroidism post-RT in pediatric patients; the relationship between dose to pituitary gland and to thyroid and damage is ongoing.

#### EP-1613 A dosimetric comparison of Proton and VMAT for Pediatric Ewing sarcoma of pelvis and spine

F. Meniai-Merzouki<sup>1,2</sup>, M. Vigan<sup>3</sup>, F. Goudjil<sup>4</sup>, S. Helfre<sup>1,2</sup>  
<sup>1</sup>Institut Curie, Radiation oncology Department, Paris, France ; <sup>2</sup>centre de protontherapie, Radiation oncology Department, Orsay, France ; <sup>3</sup>Biostatistic Department, , France ; <sup>4</sup>Physics department, Orsay, France

#### Purpose or Objective

To compare the dosimetric results of proton radiation with volumetric modulated arc therapy (VMAT) for pediatric Ewing Sarcoma of pelvis and spine. The goal was to assess the potential advantage of proton over VMAT planning in pelvis and spine Ewing's sarcoma.

#### Material and Methods

Ten patients with Ewing sarcoma of the pelvis and spine treated with proton beam at Protontherapy center (CPO) at Institut Curie. VMAT plans had generated and analyzed. To facilitate dosimetric comparisons, clinical target volumes and normal tissue volumes were held constant. Plans were optimized for target volume coverage and normal tissue sparing.

#### Results

The average dose coverage values for CTV were comparable in PROTON and VMAT plans. Whereas the Proton plans achieved a higher conformity index compared to the VMAT plans (conformity index  $1.2 \pm 0.2$  vs. 1,  $p=0.009$ ), The index of homogeneity (IH) did not differ significantly. For the bladder, Kidney, head femoral and testis Dmean were significantly reduced in Proton plans. For the bowel and rectum, there was no significant difference in Dmean. The volume of normal tissue receiving at least 5 Gy (V5) was significantly higher in VMAT plans compared with Proton, whereas at high dose levels (V30) it was significantly lower.

#### Conclusion

Compared to VMAT, Proton showed significantly better results regarding dose conformity ( $p=0.009$ ) and mean Dose of bladder ( $p=0.004$ ), kidney ( $p=0.01$ ). Proton delivered a lower healthy tissue dose than VMAT. Thus, dose escalation in the radiotherapy of pelvic and spine Ewing's sarcoma can be more easily achieved using proton.

#### EP-1614 Incidence of second malignancies among pediatric patients treated with helical Tomotherapy

E. Coassin<sup>1</sup>, A. Drigo<sup>2</sup>, L. Barresi<sup>2</sup>, G. Fanetti<sup>3</sup>, C. Elia<sup>1</sup>, G. Sartor<sup>2</sup>, G. Franchini<sup>3</sup>, M. Mascarin<sup>1</sup>  
<sup>1</sup>IRCCS Centro di Riferimento Oncologico CRO di Aviano, Pediatric Radiotherapy and AYA Unit, Aviano, Italy ; <sup>2</sup>IRCCS Centro di Riferimento Oncologico CRO di Aviano, Medical Physics, Aviano, Italy ; <sup>3</sup>IRCCS Centro di Riferimento Oncologico CRO di Aviano, Radiation Oncology, Aviano, Italy

#### Purpose or Objective

Intensity modulated radiation therapy (IMRT) delivered with helical Tomotherapy (HT) has been increasingly applied in young patients with cancer. Concerns about a potential increase of radiation-induced malignancies (SMN) exist. The purpose of this study was to determine the incidence of SMN among pediatric patients treated with HT.

#### Material and Methods

We performed a retrospective study of 146 patients less than 24 years of age treated with HT since its introduction in 2006 to September 2013 at Centro di Riferimento Oncologico CRO in Aviano, Italy. The main outcome measure was the incidence of SMN after radiation.

#### Results

Seventy-eight patients with a follow-up of at least 5 years after the end of radiotherapy were included in the analysis. The median follow-up was 7.6 years (range, 5-12.2). Forty-seven and 14 patients were followed for at least 7 and 10 years, respectively. The median age at treatment was 13.5 years (range, 1.5-24). Forty-five patients were males and 33 were females. Patients were irradiated with HT alone or in combination with other radiation techniques for CNS tumors (n=33), lymphomas (n=21), sarcomas (n=17), H&N carcinomas (n=4), or other histologies (n=3). Treatment sites were brain (n=21, 2 whole ventricular), mediastinum (n=20), craniospinal (n=12), H&N (n=6), pelvis (n=6), thorax (n=5, 2 total pleural), limbs (n=4), abdomen (n=3, 1 whole abdomen), spine (n=1). Median prescribed doses were 54 Gy (range, 8-59.4) for CNS tumors, 25.2 Gy (range, 9-50) for lymphomas, 50.4 Gy (range, 41.4-66) for sarcomas, 66 Gy (range, 63-70) for H&N carcinomas, and 15-21 Gy for the remaining cases. At a median follow-up of 7.3 years (range, 5-12.2), 57 patients (73%) were alive in complete remission. Among these long-term survivors, a 17.5-year-old female affected by Hodgkin lymphoma developed a recurrent fibromatosis of the soft tissues of the breast region close to the central venous catheter insertion site within the irradiated area 5 years after HT (prescribed dose, 14.4 Gy in 8 fractions). At a median follow-up of 7.2 years (range, 5-8.9), 10 patients (13%) were died of disease. One patient died because of esophageal cancer 7 years after total pleural irradiation delivered for an Ewing sarcoma of the right thoracic wall (prescribed dose, 36 Gy in 20 fractions). The tumor arose in the high-dose radiation volume and was considered a SMN. No other SMN occurred. Eleven patients (14%) were alive with disease without evidence of SMN at the time of the study. A 6-year-old girl affected by Li-Fraumeni syndrome irradiated to a dose of 50.4 Gy in 28 fractions for an anaplastic rhabdomyosarcoma of the right masticator space was alive in first complete remission without SMN 9.6 years after HT.

#### Conclusion

At a median follow-up of more than 7 years, IMRT delivered with HT resulted not associated with an increased risk of SMN due to low-dose irradiation to normal tissues as previously reported. Longer follow-up is needed to confirm this finding.

---

#### Electronic Poster: Clinical track: Palliation

---

#### EP-1615 Impact of pretreatment imaging modality on the response to palliative radiation for bone metastases

Y. Wada<sup>1</sup>, E. Okuyama<sup>1</sup>, S. Kumagai<sup>1</sup>, M. Sasajima<sup>1</sup>, T. Tozawa<sup>1</sup>, N. Takagi<sup>1</sup>, A. Anbai<sup>1</sup>, M. Hashimoto<sup>1</sup>  
<sup>1</sup>Akita University Graduate School of Medicine, Radiology, Akita, Japan

#### Purpose or Objective

MRI, bone scintigraphy, and 2-deoxy-2-(<sup>18</sup>F)-fluoro-D-glucose positron emission tomography (<sup>18</sup>FDG-PET) have been reported to be more sensitive than CT for detecting malignant bone lesions. Therefore, it was thought that gross tumor volume (GTV) contoured on MRI, bone scintigraphy, or <sup>18</sup>FDG-PET is more accurate than that on CT. The aim of the present study was to evaluate whether the imaging modality before irradiation affects the

response to palliative radiation therapy of painful bone metastases from solid malignant carcinomas.

#### Material and Methods

Consecutive patients with painful bone metastases treated with palliative radiation between 2013 and 2017 in our institution were enrolled. Patients without pain and those with vertebral bone metastases were excluded. The reason for excluding vertebral bone metastases was that it was usual to contour the whole body of metastatic vertebra as the clinical target volume (CTV), and, thus, the effect of how to contour GTV for vertebral bone metastases was thought to be much less than that for long or flat bone metastases. The imaging modality used between one month before and the start of palliative radiation, primary sight of carcinoma, histological type, metastatic lesion type (osteolytic, osteoblastic, or mixed) and the biological equivalent dose of  $\alpha/\beta=10$  (BED10) were retrospectively investigated, and the relationships between these factors and treatment response were evaluated. "Response" was defined as the condition in which patients achieved pain relief or reduced their use of analgesic medications. All radiation plans were three-dimensional conformal radiation therapy based on simulation CT images according to the guideline of the Japanese Society for Radiation Oncology. Briefly, GTV was defined as the bone metastatic lesion according to physical and any imaging examinations. CTV was defined as GTV plus about 1 cm, and planning target volume (PTV) was defined as CTV plus about 0.5-2 cm.

#### Results

Forty-three patients were included in the present study (median age 67 years; age range 37-85 years; 27 males, 16 females). Prescribed doses were 8-50 Gy/1-25 fractions with 2-8 Gy/fraction. Response was seen in 36 (response rate, 84%). The number of each imaging modality before irradiation was 43 CT scans (all patients, including simulation CT for radiation planning), 10 MRI scans, 17 bone scintigraphies, and 6 <sup>18</sup>FDG-PET images. Welch's *t*-test, Mann-Whitney test and the chi-squared test showed that only BED10 was significantly related to treatment response ( $p<.01$ ) (Table 1), and multiple logistic regression analysis also showed that only BED10 was a significant predictor ( $p=.02$ ) (Table 2). No significant relationship was observed with imaging modality before irradiation.

Table 1. Predictive factors; univariate analysis

	Response	Non-response	P value
Age	Median 67 (range: 37-85)	Median 67 (range: 57-73)	0.82
Sex (Male: Female)	22:14	5:2	0.93
Primary Sight (Lung: Uro: GI: HN: Thyroid: Gyne: Unknown)	6:10:11:3:2:2:2	3:2:2:0:0:0:0	0.88
Histology (SCC: Adeno: Small: CC: others: unknown)	2:19:0:6:8:1	1:4:0:1:1:0	0.58
Bone metastases type (Osteolytic: Osteoblastic: Mixed)	26:6:4	5:2:0	0.92
BED10	Median 39 (range: 24.7-61.2)	Median 39 (range: 14.4-39)	<0.01
MRI	7 (19%)	3 (43%)	0.18
Bone scintigraphy	13 (36%)	4 (57%)	0.30
<sup>18</sup> FDG-PET	5 (14%)	1 (14%)	0.98

Uro: urology, GI: gastrointestinal, HN: head and neck, Gyne: gynecology, SCC: squamous cell carcinoma, Adeno: adenocarcinoma, Small: small cell carcinoma, CC: clear cell carcinoma, BED10: biological effective dose ( $\alpha/\beta=10$ )

Table 2. Predictive factors; multivariate analysis

	Odds ratio	95% CI	P value
BED10	1.187	1.007-1.399	0.02
MRI	0.131	0.015-1.108	0.19
Bone scintigraphy	0.555	0.081-3.792	0.31
<sup>18</sup> FDG-PET	1.000	0.060-16.578	0.98

BED10: biological effective dose ( $\alpha/\beta=10$ ), CI: confidence interval

#### Conclusion

The results of the present study suggest that appropriate radiation field setting according to CT images and physical assessment could avoid further imaging before palliative radiation for painful bone metastases.

#### EP-1616 Population-based Phase II Trial of Stereotactic Radiotherapy for up to 5 Oligometastases: SABR-5

R. Olson<sup>1</sup>, M. Liu<sup>2</sup>, A. Bergman<sup>3</sup>, S. Lam<sup>4</sup>, F. Hsu<sup>5</sup>, B. Mou<sup>6</sup>, T. Berrang<sup>7</sup>, A. Mestrovic<sup>8</sup>, N. Chng<sup>9</sup>, D. Hyde<sup>10</sup>, Q. Matthews<sup>9</sup>, C. Lund<sup>11</sup>, D. Glick<sup>7</sup>, H. Pai<sup>7</sup>, P. Basran<sup>8</sup>, H. Carolan<sup>2</sup>, B. Valev<sup>12</sup>, S. Tyldesley<sup>2</sup>, D. Schellenberg<sup>11</sup>  
<sup>1</sup>BC Cancer Agency - Centre for the North, Radiation Oncology, Prince George, Canada ; <sup>2</sup>BC Cancer, Radiation Oncology, Vancouver, Canada ; <sup>3</sup>BC Cancer, Medical Physics, Vancouver, Canada ; <sup>4</sup>BC Cancer, Clinical Trials, Vancouver, Canada ; <sup>5</sup>BC Cancer, Radiation Oncology, Abbotsford, Canada ; <sup>6</sup>BC Cancer, Radiation Oncology, Kelowna, Canada ; <sup>7</sup>BC Cancer, Radiation Oncology, Victoria, Canada ; <sup>8</sup>BC Cancer, Medical Physics, Victoria, Canada ; <sup>9</sup>BC Cancer, Medical Physics, Prince George, Canada ; <sup>10</sup>BC Cancer, Medical Physics, Kelowna, Canada ; <sup>11</sup>BC Cancer, Radiation Oncology, Surrey, Canada ; <sup>12</sup>BC Cancer, Radiation Oncology, Prince George, Canada

#### Purpose or Objective

Oligometastases refer to a state of disease where cancer has spread beyond the primary site, but is not yet widely metastatic, often defined as 1-3 or 1-5 metastases in number. Stereotactic ablative radiotherapy (SABR) is an emerging radiotherapy technique to treat oligometastases that require further prospective population-based toxicity estimates.

#### Material and Methods

This is a non-randomized phase II trial in a setting where SABR for oligometastases is not available off clinical trial. All participants receive SABR treatment to all sites of newly diagnosed or progressing oligometastatic disease. We have accrued 150 of a planned 200 patients to assess toxicity associated with this experimental treatment. The study was powered to give a 95% confidence on the risk of late grade 4 toxicity, anticipating a < 5% rate of grade 4 toxicity.

#### Results

We have accrued 150 patients within 18 months, and anticipate completion of study accrual by December 2018. The majority (65%) had a solitary metastasis, followed by 26%, 7%, and only 2% who had 2,3, or 4-5 metastases, respectively. Within the 150 patients, 220 metastases were treated, with the most common locations being lung (35%), non-spine bone (24%), spine (21%), lymph nodes (9%), and liver (7%). The majority of primary tumour sites were prostate (27%), colorectal (21%), breast (11%), renal cell carcinoma (11%), and head and neck cancer (9%). To date, no SABR related deaths have occurred, but there has been 1 grade 4 serious adverse event related to SABR reported (biliary duct stenosis resulting in jaundice). Updated adverse event rates will be presented.

#### Conclusion

SABR treatment of oligometastases is occurring off-trial at a high rate, without sufficient evidence of its efficacy or toxicity. We will present toxicity data from this population-based cohort, using standardized doses and organ at risk constraints.

#### EP-1617 Palliative radiotherapy for lung cancer from patients' perspective: a quality of life (QoL) study W. Majewski<sup>1</sup>, M. Wyduba<sup>2</sup>

<sup>1</sup>Maria Skłodowska-Curie Memorial Cancer Center and Institute of Oncology, Radiotherapy Department, Gliwice, Poland ; <sup>2</sup>Maria Skłodowska-Curie Memorial Cancer Center and Institute of Oncology, Anaesthesiology Department, Gliwice, Poland

### Purpose or Objective

To evaluate the results of palliative radiotherapy for lung cancer with prospective assessment of quality of life (QoL).

### Material and Methods

The study group comprises 162 patients with lung cancer undergoing palliative radiotherapy in 2014-2016. The mean patients' age was 66 years (46-89 years). There were 43 female (27%) and 27 male (73%) patients. A total of 115 patients (71%) were in a good performance status ZUBROD 0-1, whereas the rest was in a poor general condition: 36 (22%) ZUBROD-2 and 11 patients (7%) ZUBROD-3. Stage IIIA was diagnosed in 27 patients (17%), Stage IIIB in 17 (10%) and stage IV in 40 patients (73%). Radiotherapy was performed with 6 or 20 MV photons, using 2D technique and two opposed AP-PA fields in 131 patients (81%), whereas 3DCRT technique with 3- or 4- fields was utilized in remaining patients. The radiation schedules were as follows: 20 Gy with 4 Gy per fraction- 96 patients (59%), 20-30 Gy with 2 Gy per fraction- 34 patients (21%), 30 Gy with 3 Gy per fraction- 27 patients (17%) and 5 patients did not completed the planned RT. The prospective evaluation was based on QLQC30, RSCL and Pain questionnaires filled by each patient before, at the completion of radiotherapy and 3-4 months post-treatment.

In this study the evaluation of changes of pain intensity (NRS scale 0-10), global QoL (scored 0-100) and dyspnea was performed. With NRS scale- the higher point means more pronounced pain. With general QoL scale the higher point means better QoL. The intensity of dyspnea is scored on a 4-point scale (never, sometimes, often, very often), with higher score meaning more pronounced symptom. The comparison was performed with non-parametric Wilcoxon test.

### Results

The mean intensity of pain before treatment was 3.3 points. At the completion of radiotherapy it was 5.7 points. At the last measurement 3-4 months post-treatment it was 2.8 points. The differences with respect to the pre-treatment value were significant ( $p=0.0002$  and  $p=0.009$ ).

The mean global QoL was scored 56 points before treatment. At the completion of radiotherapy it was 35 points, at the last measurement 3-4 months post-treatment it was 62 points. The differences as compared to the pre-treatment value were significant ( $p=0.000$  and  $p=0.000$ ).

The mean dyspnea score before radiotherapy was 2.4 points. At the completion of radiotherapy it was 3.3 points, at the last measurement 3-4 months post-treatment it was 2.3 points. The difference between pre-treatment and post-treatment value was significant, and there was a trend to improvement between pre-treatment and 3-4 month post-treatment value ( $p=0.000$  and  $p=0.06$ ).

### Conclusion

Shortly after palliative radiotherapy for lung cancer a decrease in general status and increase in existing symptoms may be expected. At longer follow-up an improvement as compared to the pre-treatment status is reported. Patients with expected survival of at least 3-4 months seem to benefit from palliative radiotherapy.

### EP-1618 Early clinical results and feasibility of amplitude-gated DIBH for SBRT: A multi-centre experience

K. Chufal<sup>1</sup>, I. Ahmed<sup>1</sup>, C.P. Bhatt<sup>2</sup>, R. Chowdhary<sup>1</sup>, R. Singh<sup>1</sup>, A. Pahuja<sup>1</sup>

<sup>1</sup>Rajiv Gandhi Cancer Institute & Research Centre, Radiation Oncology, Delhi, India ; <sup>2</sup>Sarvodaya Hospital & Research Centre, Department of Radiation Oncology, Faridabad, India

### Purpose or Objective

This analysis reports our initial experience with amplitude-gated DIBH technique for SBRT in patients with oligometastases treated on an institutional review board approved prospective protocol.

### Material and Methods

Between 2016 and 2018, 21 consecutive patients with oligometastatic disease to lung and liver were treated with SBRT utilizing amplitude-gated DIBH technique and were included in this analysis. After being coached for 3-4 days to achieve a reproducible breath hold in terms of amplitude and duration, simulation CT scans and orthogonal fluoroscopy images were acquired in free breathing and DIBH phases. The gated amplitude was set at +/- 2mm from the recorded baseline DIBH pattern. Target delineation and plan evaluation was performed in accordance with the ongoing RTOG BR001 protocol. Treatment planning was performed with co-planar 6MV FFF 2-3 Arc VMAT technique on Eclipse v13.5. The dose was escalated in consecutive patients from BED<sub>10</sub> of 75 Gy<sub>10</sub> up to 132 Gy<sub>10</sub>. Patient-specific pre-treatment QA was performed for all patients. Pre- and intra-treatment positioning verification was performed with DIBH CBCT for all patients for each treatment fraction and corrected on a 6D treatment couch. The primary endpoints of the analysis were local control (LC) and time to local progression (TTLP).

### Results

**Results:** A total of 21 metastatic sites were treated, with 90.6% sites being located in lung and liver. 1 year LC rate was 88.9% ( $\pm 2$  SD = 0.148) and mean TTLP was 16.8 months (95% CI = 15.5 to 18 months). The median overall survival was 16.0 months (95% CI: 15.1 to 16.8 months). Breath-hold duration across all patients varied from 25 to 45 seconds. Maximum measured tumor motion during fluoroscopy in free breathing varied from 8-15 mm (Mean, 95% CI = 10.5 mm, 9.3 to 11.8 mm) and in DIBH it reduced to 1-2 mm (Mean, 95% CI = 1.7 mm, 1.6 to 2 mm), which permitted a reduction in PTV margins from 5mm to 3mm. DIBH CBCT acquisition was time-consuming, as it required two consecutive breath-holds within a short duration. We noted a significant degradation in image quality with three consecutive breath-holds or two breath-holds with a long gap in between. The Dose Gradient Index for all DIBH SBRT plans varied from 0.73 to 1.49 cm (Mean, 95% CI = 0.998, 0.883 to 1.112 mm). Total MU's varied from 1794 to 4765 (Mean, 95% CI = 3168 MU, 2651 to 3685 MU), with beam-on time varying from 120 to 537 seconds (Mean, 95% CI = 334 sec, 263 to 407 sec). Implementation time for the first treatment session (including imaging and verification) varied from 693 to 2488 seconds (Mean, 95% CI = 1464 sec, 1184 to 1744 sec).

### Conclusion

**Conclusions:** Amplitude-gated DIBH technique for SBRT in oligometastatic disease yielded equivalent results to reports previously published in the literature. Reduced target motion with DIBH resulted in reduction of PTV margins. The main limitation of this technique is long patient-on-table time, which is directly dependent on the patient's breath-hold duration.

### EP-1619 SBRT and the treatment of adrenal gland metastasis

D. Georgiev<sup>1</sup>, N. Gesheva-Atanasova<sup>1</sup>, S. Lalova<sup>1</sup>, A. Balabanova<sup>1</sup>, I. Mihaylova<sup>1</sup>, B. Antonov<sup>1</sup>, K. Ormankova<sup>1</sup>  
<sup>1</sup>National Oncological Center Hospital, Radiotherapy, Sofia, Bulgaria

### Purpose or Objective

The purpose of the study is to evaluate our experience in the use of stereotactic body radiation therapy (SBRT) for treatment of adrenal glands metastasis and in particular the dosimetry planning, clinical outcomes and toxicity.

### Material and Methods

From 6/2016 to 6/2018, 8 patients were treated with 10 lesions of the adrenal gland - 7 of the lesions were located

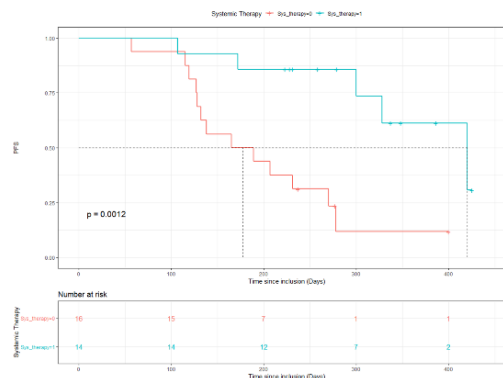


previously irradiated area). Twelve patients had non-spine bone lesions only, 16 had lymph node metastases, and two had mixed disease. Patient and tumor characteristics are presented in table 1.

Characteristics	n (%)	
<b>Mean age (range)</b>	<b>69 (48-86) years</b>	
<b>Gender</b>	<b>30</b>	<b>100%</b>
Male	24	80%
Female	6	20%
<b>Metastatic site</b>	<b>32</b>	<b>100%</b>
Non-spine bone	14	44%
Lymph node	18	56%
<b>Primary cancer</b>	<b>30</b>	<b>100%</b>
Prostate (AdenoCa)	18	60%
RCC	2	7%
NSCLC	2	7%
Breast (IDA)	2	7%
Ovarium	2	7%
Melanoma	1	3%
Cholangiocarcinoma	1	3%
Stomach (AdenoCa)	1	3%
Ureter (TCC)	1	3%
<b>Timing</b>	<b>30</b>	<b>100%</b>
Synchronous	3	10%
Metachronous	27	90%
<b>Concomitant systemic treatment</b>	<b>30</b>	<b>100%</b>
None	16	53%
Hormonal Therapy	11	37%
Chemotherapy	1	3%
Immunotherapy	2	7%
<b>Treatment characteristics</b>		
PTV_D50% (Gy); mean (range)	37,75	34,42-43,86
PTV_D2% (Gy); mean (range)	40,48	36,22-48,07
PTV_D98% (Gy); mean (range)	31,51	20,66-35,5

**Table 1.** Patient, tumor and treatment characteristics  
**NOTE.** Data presented as No. (%) unless otherwise indicated.  
**Abbreviations:** AdenoCa, adenocarcinoma; RCC, renal cell carcinoma; NSCLC, non-small cell lung carcinoma; IDA, invasive ductal adenocarcinoma; TCC, transitional cell carcinoma; PTV, planning target volume; D50%, median absorbed dose; D2%, near-maximum absorbed dose; D98%, near-minimum absorbed dose;

Median follow-up after SBRT was 9 (2 - 14) months. LC at 6 months was 100%. At 12 months, 2 local relapses were observed, both in lesions >4cm. The median PFS was 8 months. There was a significant difference between PFS in patients who received concomitant systemic treatment and those who did not (median 5.8 vs 13.8 months, p = 0.0012) (figure1). No significant difference in PFS between patients with bone and lymph node metastases was observed. There was no grade ≥ 3 toxicity observed. During follow-up, QoL scores didn't change significantly.



Limitations include small sample size, limited duration of follow-up, and lack of a control arm. **Conclusion** SABR in 5 fractions appears extremely safe and feasible, resulting in excellent local control but rather limited progression-free survival. Consequently, 30 more patients were included in the second cohort (3 fractions of 10 Gy), now including translational research to tailor future patient selection. Patients with oligometastases should probably not be withheld systemic treatment.

#### EP-1622 Stereotactic Body Radiation Therapy for Oligometastatic Disease: A single-institution experience

L.P. Guzman Gomez<sup>1</sup>, J. Luna Tirado<sup>1</sup>, D. Gonsalves Pieretti<sup>1</sup>, A. Ilundain Idoate<sup>1</sup>, M. Montero Feijoo<sup>1</sup>, W.A. Vasquez Rivas<sup>1</sup>, E. Lopez Ramirez<sup>1</sup>  
<sup>1</sup>Hospital Universitario Fundación Jiménez Díaz, Radiation Oncology Department, Madrid, Spain

#### Purpose or Objective

To report clinical outcome and treatment-related toxicity of SBRT in the treatment of oligometastatic disease in patients no suitable for surgery or unresectable metastases.

#### Material and Methods

Between May 2015 and December 2017, 68 patients with 1-3 inoperable metastases were treated with SBRT. Medical records were retrospectively reviewed. Patients with liver/abdominal lesions were immobilized with Vac-Q-Fix™ Cushions including BodyFix Diaphragm™ for abdominal compression to minimize respiratory organ motion. No abdominal compression was applied to lung patients, in these cases, 4D planning was required. Dose prescription ranged from 27 to 60 Gy in 3 - 8 fractions. In particular, 27 Gy in 3 fractions was prescribed to bone metastases, 60 Gy in 8 fractions to liver lesions, 50-60 Gy in 4 - 6 fractions to lungs lesions and 40-45 Gy in 4 - 6 fractions to adrenal metastases and abdominal lymph nodes. Dose reductions were allowed if judged necessary to cope with organs at risk (OAR) sparing. Treatment was delivered on Elekta Beam Modulator™ linear accelerator, using volumetric modulated arc therapy (VMAT) with 6-10 MV photon beam energy. Daily image guidance (IGRT) was performed by means of CBCT acquisitions prior to each treatment. After conclusion of SBRT, all patients were assessed at 1.5 months and every 3 months during the first year and every 6 months after 1 follow-up year, with a CT scan and/or RM at each follow up. The primary end points were local control (LC) and treatment-related toxicity.

#### Results

Sixty-eight patients with 82 total metastases were treated. Median age at treatment was 64 years (ranged, 28-87 years). 67% were men. 82% of patients presented an ECOG performance status 0-1. Primary tumors were 30 GI, 12 lungs, 10 breasts, 7 prostates, 4 gynecological, 2 melanomas, 2 sarcomas and 1 unknown tumor. 52 patients (76%) had a single lesion; the remaining patients had 2-3 lesions. 48% of the lesions were localized in bones; 28.7%

in the lungs; 16.3% in the liver; 5% in lymph nodes and 2% in adrenal glands. Median diameter of the lesions was 8 mm for bone lesions, 14 mm for lung, 24 mm for liver, 12 mm for adrenal and 13 mm for lymph nodes metastases. Median follow-up was 12.1 months (ranged 2 - 35 months). Local control at 1-year (inclusive of complete, partial and stable response) was achieved in 86.5% of the treated lesions. Treatment-related grade 2-3 toxicity was observed in 4.2% of patients; grade 1 toxicity in 10.8% and no toxicity was observed in 85% of the cases.

#### Conclusion

SBRT is a safe and effective therapeutic option for the treatment of oligometastatic patients not suitable for surgery or unresectable metastases, with high local control rates, good tolerance and low treatment-related toxicity.

#### EP-1623 KORTUC for lytic bone metastasis

S. Obata<sup>1</sup>, O. Yukihiro<sup>1</sup>, T. Tatsuya<sup>1</sup>, M. Shigeki<sup>1</sup>, O. Yohiaki<sup>1</sup>, K. Tsunehiko<sup>1</sup>, K. Shinya<sup>1</sup>, I. Yohta<sup>1</sup>, K. Akira<sup>1</sup>, I. Kayo<sup>1</sup>, W. Kumiko<sup>1</sup>, O. Hitomi<sup>1</sup>

<sup>1</sup>Nagasaki Prefecture Shimabara Hospital, Department of Radiology and Radiotherapy, Shimabara, Japan

#### Purpose or Objective

To improve the effects of radiation for lytic bone metastasis, we directly injected a new radio-sensitizer into the lesion (KORTUC) under image guidance after obtaining approval from our ethics committee and informed consent. We herein report the retrospective clinical data from 25 consenting patients since 2010.

#### Material and Methods

We selected 20 eligible patients our hospital followed up. Patient age was 42-83 years, the ratio of men to women was 12: 8. As for the primary lesion, lung was 12 cases, 3 rectums, 2 esophaguses, and others. Uncontrolled primary lesion was 16 cases. 16 cases accompanied other metastasis. Affected bone was 9 pelvic bones, extremities bone 5, thorax 2, and others. Performance status 3-4 was 7 cases, uncontrollable pain was recognized in 18 cases. We performed KORTUC in all cases. In half of the patients, chemotherapy, molecular targeted drug or immunotherapy was administered.

#### Results

Radiation dose was 8-54 Gy and the number of times of radio-sensitizer injection was 1-12 times. The palliative rate was 94%. 95% of the targets did not enlarge in size and half of the cases presented bone re-formation. The treatment took effect after 1-17 days and it continued for 7-630 days. The survival time was 30-1680 days. There was no severe adverse event. Neither univariate nor multivariate analysis of the local control recognized significant difference.

#### Conclusion

KORTUC for lytic bone metastasis was thought safe and effective. And a further accumulation of many cases is needed for recognition of a clinical option.

#### EP-1624 First clinical experiences with SBRT on the 1.5 T MR-linac for pelvic lymph node oligometastases

A.M. Werensteijn-Honingh<sup>1</sup>, P.S. Kroon<sup>1</sup>, D. Winkel<sup>1</sup>, E.M. Aalbers<sup>1</sup>, B. Van Asselen<sup>1</sup>, G.H. Bol<sup>1</sup>, K.J. Brown<sup>2</sup>, W.S.C. Eppinga<sup>1</sup>, M. Glitzner<sup>1</sup>, E.N. De Groot-van Breugel<sup>1</sup>, S.L. Hackett<sup>1</sup>, M. Intven<sup>1</sup>, J.G.M. Kok<sup>1</sup>, A.N. Kotte<sup>1</sup>, J.J.W. Lagendijk<sup>1</sup>, M.E.P. Philippens<sup>1</sup>, R.H.N. Tijssen<sup>1</sup>, J.W.H. Wolthaus<sup>1</sup>, S.J. Woodings<sup>1</sup>, B.W. Raaymakers<sup>1</sup>, I.M. Jürgenliemk-Schulz<sup>1</sup>

<sup>1</sup>University Medical Center Utrecht, Department of Radiotherapy, Utrecht, The Netherlands; <sup>2</sup>Elekta AB, Scientific Research, Stockholm, Sweden

#### Purpose or Objective

The 1.5 Tesla (T) MR-linac (Unity, Elekta AB, Stockholm, Sweden) has been available for clinical use at our institute since August 2018. Our aim is to present the first clinical

experience with the onboard workflow as provided in the system including daily contour adaptation and online treatment planning based on the daily anatomy as visualized on online MRI.

#### Material and Methods

Starting August 2018, we have been treating on average 2 patients per month for pelvic and low abdominal lymph node oligometastases. Seven-beam step-and-shoot IMRT (FFF 7 MV) was used to deliver 35 Gy in 5 fractions, with a maximum of 3 fractions per week.

The pre-treatment workup and actual online workflow for these treatments is illustrated in Figure 1 and consists of the following steps:

- 1) Pre-treatment preparation consists of CT and MR imaging, contouring based on CT and MRI, treatment planning, patient QA including film measurement and independent 3D dose calculation for the pre-treatment plan;
  - 2) Treatment session consists of online MRI, deformable registration from pre-treatment CT to the online MRI scan, manual adaptation of GTV and organs at risk (OAR) from deformed contours if needed, full online re-planning ('adapt to shape' workflow with most extensive re-planning option), position verification MRI, independent 3D dose calculation, radiation delivery with intra-fraction MRI and post-fraction MRI;
  - 3) Post treatment steps are patient QA and dose reconstruction on the intra- and post-fraction MRIs.
- All patients are asked to participate in a prospective observational study that investigates treatment issues and clinical outcome data, including acute toxicity and patient-reported quality of life.

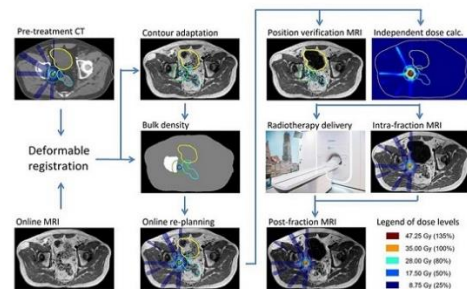


Figure 1: flow chart of online MR-linac workflow

Anatomical contours: yellow: bladder; light blue: sigmoid; pink: ureter; light green: GTV; dark blue: PTV; green circle: PTV + 2 cm. Images are shown for the first fraction of the second patient.

#### Results

As of October 2018, three patients have completed their full treatment course with Unity and two are currently being treated. The average daily online session duration was 41 minutes (range 33-49) including an average 34 minutes on-couch time (range 27-39). Time to completion for individual workflow items is shown in Figure 2.

Target lymph nodes and surrounding tissues and organs were well visible at each treatment session allowing for contour adaptation of GTV and OAR and full online re-planning to the daily anatomy. All online treatment plans satisfied the predefined target and OAR constraints. The online independent dose calculations resulted in an average Gamma pass rate (3%/3 mm) of 97.5% (range 90.4-99.2%). For all treatment fractions, the entire GTV received 100% of the prescribed dose (35 Gy) based on reconstruction on all online MRI scans (position verification, intra- and post-fraction).

Clinical outcome data including acute toxicity and patient-reported quality of life are being collected.

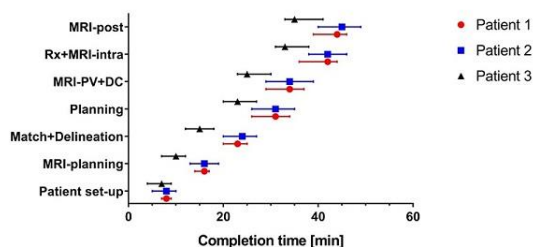


Figure 2: visualization of online session duration  
Average and range of time to completion (from session start) for the different workflow items.  
Rx: radiotherapy delivery; PV: position verification; DC: independent dose check.

## Conclusion

The onboard clinical workflow of the 1.5 T MR-linac, with daily contour adaptation and full online re-planning, can successfully be used to treat patients with pelvic and low abdominal lymph node oligometastases using an SBRT approach.

## EP-1625 Patterns-of-care and outcome-analysis of the stereotactic body RT (SBRT) of adrenal-gland-metastases

T. Voglhuber<sup>1</sup>, S.E. Combs<sup>1</sup>, K.A. Kessel<sup>1</sup>, M. Oechsner<sup>1</sup>  
<sup>1</sup>Technical University of Munich TUM, Department of Radiation Oncology, München, Germany

### Purpose or Objective

High-precision stereotactic body radiotherapy (SBRT) has proven to be a valuable method in the curative and palliative treatment of different tumor entities and is meanwhile an established keystone in the field of neoadjuvant tumor-therapy.

In this study, we evaluate the effect of SBRT in patients with metastases in the adrenal gland focused on progression-free-survival (PFS), overall survival (OS), and acute as well as late toxicity.

### Material and Methods

A cohort of 24 patients was analyzed treated with SBRT for metastases in the adrenal gland between 2006 and 2018. Treatment-planning was performed through contrast-enhanced CT followed by the image-guided radiation therapy (IGRT) using Cone-beam-CT (CBCT). SBRT was applied with a cumulative median dose of 35 Gy (range: 25-40 Gy) and a single dose of 5 Gy in five fractions per week.

### Results

The evaluation is still ongoing. Primary tumors of the patients were: NSCLC 45.8 %, Mamma-Ca 12.5 %, Melanoma 12.5 %, Sarcoma 8.3 %, and others 20.9 %. At the time of analysis, 7 patients (29.2 %) experienced local failure (LF) of the neoplasia in the adrenal gland (mean LF: 52.0 months, 95%-KI: 26.2-77.8 months, median not reached), 19 (79.2 %) faced a distant progression (median-PFS: 2.2 months, 95%-KI: 1.8-2.6 months). 12 patients were still alive (50 %), 5 of them without LF (41.7 %), 4 of them (33.3 %) without any tumor progression (median OS: 12.9 months, 95%-KI: 6.3-19.5 months).

Our results showed that there occurred no treatment-related side-effects  $\geq$  grade 2, which reflects the overall low-grade-toxicity of SBRT used for adrenal-gland-metastases.

Toxicity rates  $\geq$  grade 2 were as follows: 41.7 % suffered from acute ( $\leq$  6 months) gastrointestinal disorders like nausea (29.2 %), vomiting (8.3%), and abdominal pain (4.2 %); 29.2 % also reported acute fatigue, constipation, throbbing pain in the renal area and increase of the retention parameters. Only 20.8 % of the patients faced late-toxicities like loss of weight (4.2 %), fatigue (4.2 %) and gastrointestinal medical conditions (12.5 %) persisting or appearing after the 6-month-period.

### Conclusion

SBRT is a safe and effective method for treating metastases in the adrenal gland. None of the patients had treatment-related acute or late toxicities  $\geq$  grade 2, and 70.8% of the patients were progression-free after RT.

## EP-1626 "TEACHH MODEL" as a tool for decision-making in palliative patients: Our experience

A. Miranda Burgos<sup>1</sup>, C. Escuin Troncho<sup>1</sup>, G. Molina Osorio<sup>1</sup>, C. García Aguilera<sup>1</sup>, L. Alled Comín<sup>1</sup>, J.M. Ponce Ortega<sup>1</sup>, R. Ibáñez Carreras<sup>1</sup>

<sup>1</sup>Hospital Universitario Miguel Servet, Radiation Oncology, Zaragoza, Spain

### Purpose or Objective

Radiotherapy is an effective and cost-effective treatment when patients have symptoms such as metastatic bone pain, hemorrhages or cerebral edema. Up to 16% of planned patients do not receive treatment for causes such as clinical worsening or death. It is important to estimate the life expectancy to make appropriate decisions according to radiotherapy treatment. Our objective is to introduce in our clinical practice a scale of prognostic assessment that will help us decide on the relevance of palliative radiotherapy indication and thus reduce the rate of untreated planned patients below 10%.

### Material and Methods

After the review of literature, we considered the TEACHH model suitable as a support tool for decision making in palliative radiotherapy. The TEACHH model divides patients into three life expectancy groups (1.7, 5, and 19.9 months) based on the score obtained according to the patient's clinical characteristics (type of cancer, Eastern Cooperative Oncology Group performance status, age, prior palliative chemotherapy, prior hospitalizations, and hepatic metastases).

We decided to use the TEACHH model in all the patients that were hospitalized and needed palliative radiotherapy.

### Results

We selected 147 patients candidates for palliative radiotherapy. We administered radiotherapy for metastatic bone pain in 42% of the patients, with hemostatic intention in 10%, for brain metastases in 28% and finally, for spinal cord compression in 20% of the patients.

Of the total of treated patients, 22% were in the life expectancy group of 1.7 months; 74% in 5 months and 4% in 19.9 months. The use of the model allowed us to reject the treatment in 33 (22.5%) patients (18 in the group 1.7 months, 14 in 5 months and 1 in 19.9 months). We planned 21 (14%) patients who were not treated for death (3 in 1.7 months and 18 in 5 months).

### Conclusion

It is a tool that allows us to administer a palliative treatment or dismiss it individually to each patient considering their life expectancy and thus reduce the rate of planned patients not treated by improving the use of resources of our Service.

## EP-1627 Impact of body morphology on survival in patients with bone metastases: A prospective cohort study

B. Pielkenrood<sup>1</sup>, P. Van Urk<sup>2</sup>, J. Van der Velden<sup>1</sup>, N. Kasperts<sup>1</sup>, J. Verhoeff<sup>1</sup>, G. Bol<sup>1</sup>, L. Verkooijen<sup>1</sup>, J. Verlaan<sup>2</sup>

<sup>1</sup>UMC Utrecht, Radiotherapy, Utrecht, The Netherlands ;

<sup>2</sup>UMC Utrecht, Orthopedic Surgery, Utrecht, The Netherlands

### Purpose or Objective

An increasing number of patients is diagnosed with spinal metastases due to more effective treatment and better survival of cancer. Patients with painful spinal metastases are treated with radiotherapy, combined with surgical

stabilization in case of spinal instability or neurological deficit. Patients with a life expectancy less than 3 months are deemed unfit for surgery because quality of life is considered to be hampered too much by surgery and revalidation to justify the procedure. Therefore, adequate assessment of expected survival is necessary. The aim of this study was to evaluate whether abdominal fat and muscle distribution, and muscle attenuation are associated with overall survival.

#### Material and Methods

Within the UMC Utrecht PRospective Evaluation of interventional StudiEs on bone meTastases (PRESENT) cohort, we identified all 310 patients who received radiotherapy for thoracic or lumbar spinal metastases. Using an in-house developed delineation tool (VolumeTool), a single transverse slice at the L3 vertebra was used to (semi automatically) segment the visceral fat area, subcutaneous fat area, total muscle area and muscle attenuation (figure 1). Muscle attenuation was defined as the density of the muscle, which decreases with increased lipid content. Subsequently the ratio between visceral and subcutaneous fat was calculated. Cox regression analyses was performed to determine the association between the variables of interest and survival at 90 and 365 days, adjusted for potential confounders (age, sex, primary tumor, Karnofsky performance scale, number of bone metastases, non-bone metastases and neurological symptoms).

#### Results

Patients had a median age of 67 years, and 63% were male. The most common primary tumors were lung (28%), prostate (27%) and breast (18%). Median follow-up was 197 days, overall survival rates at 90 and 365 days were 71% and 36% respectively. In univariable analysis, subcutaneous fat area, fat ratio and muscle attenuation were significantly associated with survival at 90 and 365 days. After adjustment, only muscle attenuation was significantly associated with 90 and 365 days survival, HR: 0.89 (95% CI 0.84-0.94) and HR: 0.93 (95% CI 0.89-0.97) respectively.

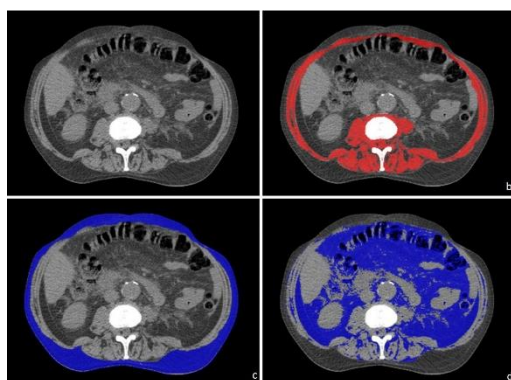


Figure 1. Example of a CT-analysis. a) base CT-scan b) total muscle area measurement c) subcutaneous fat area measurement d) visceral fat area measurement.

#### Conclusion

This study showed that muscle attenuation was significantly associated with the overall survival of patient with spinal metastases. CT-scans, which are routinely available in the majority of patients with spinal metastases, contain useful information and can contribute to better selection of patients for surgical stabilization of spinal metastases.

#### EP-1628 Stereotactic Ablative Radiotherapy for non-spinal bone metastasis. A single institution experience

A. Acosta Rojas<sup>1</sup>, M. Nuñez<sup>1</sup>, A. Montero-Luis<sup>1</sup>, E. Sanchez-Saugar<sup>1</sup>, O. Hernando-Requejo<sup>1</sup>, R. Ciervide-Jurio<sup>1</sup>, M. Lopez-Gonzalez<sup>1</sup>, M. Garcia-Aranda<sup>1</sup>, J. Valero-Albarran<sup>1</sup>, M.C. Rubio-Rodriguez<sup>1</sup>

<sup>1</sup>University Hospital Madrid Sanchinarro, Radiation Oncology, Madrid, Spain

#### Purpose or Objective

To evaluate the effectiveness and toxicity of stereotactic ablative radiation therapy (SART) for non-spinal bone metastases.

#### Material and Methods

From May 2013 to August 2017, 48 non-spinal bone metastasis of 43 patients were treated with SART, 47 metastasis underwent 30 Gy in 3 fractions and 2 lesions received 35 Gy in 5 fractions, delivered every single day in a Linear Accelerator Novalis with inter and intra-fraction orthogonal X-ray imaging guidance (IGRT). Intensity-modulated radiotherapy (IMRT) was performed in 44 lesions (90%) and 3D-conformal radiotherapy in 5 treatments (10%).

Patients were reviewed at the end of treatment and one, three and six months afterward. Pain control was documented with the Visual Analogue Scale (VAS) and the radiological response was determined with the MD Anderson Cancer Center Criteria (MDA criteria).

#### Clinical features of irradiated patients.

Characteristics		Cases	%
<b>Primary tumor n=43</b>			
- Breast	Infiltrating ductal carcinoma	11	25.58
	Infiltrating lobular carcinoma	1	2.33
- Lung	Adenocarcinoma	7	16.28
	Atypical carcinoid	1	2.33
	Prostate adenocarcinoma	14	32.56
- Urothelial	Renal	2	4.65
	Kidney	1	2.33
	Ureter	4	9.30
- Thyroid papillary		1	2.33
- Cholangiocarcinoma		1	2.33
<b>Location of the Metastasis n=48</b>			
- Sacrum		1	2.33
- Sacroiliac		6	13.95
- Iliac crest		13	30.23
- Ischium		3	6.98
- Pubis		2	4.65
- Acetabulum		5	11.63
- Femoral head		4	9.30
- Femoral diaphysis		5	11.63
- Acromion		1	2.33
- Ribs		6	13.95
- Sternum		1	2.33
- Skull		1	2.33
<b>MDA radiological response criteria</b>			
1 <sup>st</sup> control N=38	Stable disease	19	50
	Partial response	10	26.32
	Complete response	8	21.05
	Progression disease	1	2.63
2 <sup>nd</sup> control N=26	Stable disease	16	61.54
	Partial response	3	11.54
	Complete response	5	19.23
3 <sup>rd</sup> control N=19	Progression disease	2	7.69
	Stable disease	9	47.37
	Partial response	1	5.26
	Complete response	5	26.32
	Progression disease	4	21.05

#### Results

With a median follow-up of 14.5 months (1-64 month) 27 patients (56.25%) are alive, 20 patients (41.6%) death for progression of the disease and 1 patient (2.33%) death related to comorbidity.

Complete local pain control was reported in vast majority of patients (graphic 1).

38 lesions (79.17%), 26 lesions (54.17%) and 19 lesions (39.58%) were radiologically evaluated with MDA criteria at 3, 6 and 9 months respectively (table 1).

Local progression free survival was 92.1% at 12 months; 83.3% at 24 and 36 months.



The software is accessed remotely via Citrix and includes Pinnacle treatment planning system (TPS) V14 (Philips), Mosaic Record and Verify (R&V) System V2.62 (Elekta) together with RADCALC (RC) V 6.3 (Lifeline software Inc) and PerFRACTION™ 3D from SunNuclearCorporation.

**Plan production, Plan quality assessment and Plan metrics using Dose Volume Protocol (DVP) and Quality Checks(QC)**- A suite of scripts run within TPS based on the institutes clinical protocols and planning guidelines.

**Plan production** - Palliative Scripted class solution

**DVP** - reports the plan and DVH dose metrics independently extracted in a tabular format enables the planner to review OAR and PTV constraints using a visual traffic light system. Once plan is locked the report is auto generated and attached into the correct patient in R&V.

**QC**-Checks plan integrity against planning guidelines such as beam energy, normalisation and calculation grid which can be configured. QC interrogate R&V for information such as patient demographics and compare to TPS.

**RadCalc®** - independent MU check and creates a configurable QA reports which is auto loaded into R&V for approval if it meets the tolerance.

**RadCalc® Reconciler** - Ensures accurate reconciliation between the planning data in TPS and R&V. Comparison occurs in RC. prerequisites require data export of the final Clinical plan from TPS to RC and R&V to RC. The RTP-Filter informs the user of any differences and the report can be configured to display discrepancies only.

**PerFRACTION™3D** - independent automated phantom-less end to end QA solution for all patient plans and fractions. A report is automatically compiled and accessed via the web user interface. A traffic light system efficiently flags any issues with the option of viewing more information if needed.

## Results

Learning from the trial period from November 2018 to be presented together with detailed process map as well as Clinical case studies.

Activity Name	Activity	Comments
08:00-09:00	Patient preferences and finance details	Consent and book any patient experience appointments or preferences for day (including taxi, therapy table, appointment times, and patient finance details)
09:00-09:30	Checklist review	Appointment must be booked for open the day before to PAO
09:30-10:00	Checklist review	Appointment time to be communicated to patient at the point of arrival (email or text) to the patient - communication any delay
10:00-10:30	Checklist review	Appointment time to be communicated to patient at the point of arrival (email or text) to the patient - communication any delay
10:30-11:00	Checklist review	Appointment time to be communicated to patient at the point of arrival (email or text) to the patient - communication any delay
11:00-11:30	Checklist review	Appointment time to be communicated to patient at the point of arrival (email or text) to the patient - communication any delay
11:30-12:15	QC - RC calculation to TPS via parallel to 2nd check	QC - RC calculation to TPS via parallel to 2nd check
12:15-12:45	QC - RC calculation to TPS via parallel to 2nd check	QC - RC calculation to TPS via parallel to 2nd check
12:45-13:15	QC - RC calculation to TPS via parallel to 2nd check	QC - RC calculation to TPS via parallel to 2nd check
13:15-13:30	QC - RC calculation to TPS via parallel to 2nd check	QC - RC calculation to TPS via parallel to 2nd check
13:30-1:00	QC - RC calculation to TPS via parallel to 2nd check	QC - RC calculation to TPS via parallel to 2nd check
1:00-2:00	QC - RC calculation to TPS via parallel to 2nd check	QC - RC calculation to TPS via parallel to 2nd check
2pm	QC - RC calculation to TPS via parallel to 2nd check	QC - RC calculation to TPS via parallel to 2nd check

Some sequence applies for subsequent patients but start time to each patient 30 mins apart, no more than 4 patients per day

## Conclusion

Using Standardisation as a prerequisite automation can be achieved. The automation allows production of consistently good plans and streamline of checks. The time saving can be utilised to support a Rapid Access Palliative clinic.

**EP-1631 AIRO Palliative Study Group investigation on prognostic score in clinical practice: PROPHET Trial**  
F. Cellini<sup>1</sup>, V. Masiello<sup>1</sup>, S. Manfrida<sup>1</sup>, E. Lattanzi<sup>2</sup>, L. Marino<sup>3</sup>, F. Arcidiacono<sup>4</sup>, A. Santacaterina<sup>5</sup>, L. Cervone<sup>1</sup>, A. Diroma<sup>1</sup>, A. Romano<sup>6</sup>, R. Di Franco<sup>7</sup>, F. Pastore<sup>8</sup>, G. Siepe<sup>9</sup>, C. Donati<sup>9</sup>, R. Cassese<sup>10</sup>, M. Santarelli<sup>10</sup>, F. Deodato<sup>11</sup>, S. Pergolizzi<sup>12</sup>, E. Maranzano<sup>4</sup>, P. Muto<sup>13</sup>, S. Parisi<sup>14</sup>, V. Valentini<sup>1</sup>

<sup>1</sup>Fondazione Policlinico Gemelli IRCCS, Radioterapia Oncologica, Roma, Italy ; <sup>2</sup>Università di Parma, Radioterapia Oncologica, Parma, Italy ; <sup>3</sup>REM Center, Unità di Radioterapia, Catania, Italy ; <sup>4</sup>Ospedale Santa Maria, Centro di Radioterapia Oncologica, Terni, Italy ; <sup>5</sup>Azienda Ospedali Riuniti Papardo-Piemonte Messina., Unità Operativa di Radioterapia, Messina, Italy ;

<sup>6</sup>Università Federico II, Radioterapia Oncologica, Napoli, Italy ; <sup>7</sup>Seconda Università di Napoli, Radioterapia Oncologica, Napoli, Italy ; <sup>8</sup>Emicenter, Radioterapia Oncologica, Napoli, Italy ; <sup>9</sup>Università di Bologna Ospedale Sant'Orsola, Radioterapia Oncologica, Bologna, Italy ; <sup>10</sup>Azienda Sanitaria Locale Rieti, Radioterapia Oncologica, Rieti, Italy ; <sup>11</sup>Fondazione di Ricerca e Cura 'Giovanni Paolo II'- Catholic University of Sacred Heart, Unità Operativa di Radioterapia, Campobasso, Italy ; <sup>12</sup>Università di Messina, Dipartimento di Diagnostica per Immagini e Radioterapia, Messina, Italy ; <sup>13</sup>Istituto Nazionale Tumori di Napoli- IRCCS Fondazione Senatore Pascale, Radioterapia Oncologica, Napoli, Italy ; <sup>14</sup>IRCCS "Casa Sollievo della Sofferenza", Unità di Radioterapia Oncologica, San Giovanni Rotondo, Italy

## Purpose or Objective

Palliative Radiotherapy (PR) for bone metastases is a possible treatment for metastatic patients but often clinical practice and absence of shared guidelines can limit choice of correct regimen. Prognostic scores can help clinician to tailor time, dose and volume in PR. In this study we investigate about decision variance after application of Mizumoto Prognostic Score (MPS) to different clinical cases

## Material and Methods

Nine clinical cases were selected with a complete indication of MPS parameters: 3 cases were of A class (prognosis > 6 months), 3 of B class (prognosis between 6 and 12 months) and 3 of C class (prognosis between 12 and 24 months). Radiotherapy Oncologists (ROs) with different grade of experience [in training RO (IT), Junior RO (JRO), Senior RO(SRO), Junior RO Team Palliative member (JRPO), Senior RO Team Palliative member (SP)] underwent a questionnaire to explore what RT regimen would choose before and after MPS application. The questionnaire were administered on blind by phone. Results were recorded on CRF Excel format and analyzed on RStudio. Descriptive statistical analysis and concordance Fleiss' kappa test were used to discriminate variance of answers between groups.

## Results

The questionnaire was administered to 75 ROs (12 IT; 13 JRPO; 17 JRO; 25 SRO; 8 SP). Median conversion rate of RT dose prescription after MPS application was 9.3% (1.3-18.6%). In particular median conversion rate was: 13.8% for IT; 11.1% for JRPO; 8.5% for JRO; 10.2% for SRO; 15% for 15%. According to Fleiss' kappa parameters, evaluation of agreement in dose prescription showed an improving in 5.18% at the overall analysis after MPS application. Analytical case evaluation of agreement showed a basal good level of concordance between ROs in C class cases (46.8-66.6%), with an implement of agreement between 5.6 and 15.6%. A and B class cases showed a poor level of basal agreement (25-35.2%), that after MPS rise since to 38.6%. MPS score application resulted in increase of the agreement in the choice of pattern of care, beyond clinician's experience and actual patient's prognosis.

## Conclusion

This preliminary investigation about prognostic score used in palliative radiotherapy has showed that MPS application can change RT prescription in 9.3% of participant with different grade of experience in palliative care. Globally, there was also an increase of the agreement in final dose prescription, although only of 5.18%. Further analysis on subgroups, experience in palliation and clinical cases stratification would be reported in extensive publication, together with more questionnaire results.

## EP-1632 Response prediction of palliative radiotherapy to painful spinal bone metastases

J. Akhgar<sup>1</sup>, J.C. Peeken<sup>2</sup>, S.U. Pigorsch<sup>3</sup>, S.E. Combs<sup>2</sup>  
<sup>1</sup>Klinikum rechts der Isar - Technical University of Munich TUM, Department of Radiation Oncology, Munich, Germany ; <sup>2</sup>Klinikum rechts der Isar - Technical

University of Munich TUM - Institute of Innovative Radiotherapy iRT - Department of Radiation Sciences DRS - Helmholtz Zentrum München - Deutsches Konsortium für Translationale Krebsforschung DKTK - Partner Site Munich, ; <sup>3</sup>Klinikum rechts der Isar - Technical University of Munich TUM - Deutsches Konsortium für Translationale Krebsforschung DKTK - Partner Site Munich, Department of Radiation Oncology, Munich, Germany

### Purpose or Objective

Palliative radiation therapy of painful spinal bone metastases (SBM) triggers a pain response in only two-thirds of treated patients. A reliable prediction model of pain may help to personalize the decision for radiation therapy. In this retrospective study, we investigated the relationship between several pretherapeutic data and pain response in SBM patients.

### Material and Methods

A cohort of 190 patients with SBM treated with radiation was analyzed. Patients with non-solid tumors and previous invasive procedures were excluded. Pretherapeutic information about basic patient characteristics, staging information, treatment modalities, radiation-specific regimens, Karnofsky Performance Index (KI) and Spinal Instability Neoplastic Score (SINS) was collected. SINS was determined using radiotherapy planning CT scans. Pain response was categorized as complete pain response, partial pain response, indeterminate pain response or progression of pain according to previous studies. For statistical analysis, binary variables were created: complete response and any response (complete or partial pain response). Patients with indeterminate pain response were excluded. Univariate and multivariate binary logistic regression (IBM SPSS Statistics 20) was used to test for associations.

### Results

Univariate logistic regression revealed significant associations between complete response and multiple pretherapeutic parameters: SINS (Odds-Ratio [OR] 0.879; 95% confidence interval [CI] 0.784-0.985;  $p < 0.027$ ), KI (OR 1.032; 95% CI 1.006-1.058;  $p < 0.014$ ), neurological dysfunction (OR 0.459; 95% CI 0.232-0.909;  $p < 0.025$ ), tumor type (prostate or mammary carcinoma [OR 0.411; 95% CI 0.235-0.720;  $p < 0.002$ ] vs lung cancer [no significance (ns)] vs others [reference category;  $p < 0.008$ ]), tumor histology (adenocarcinoma [OR 0.127; 95% CI 0.024-0.672;  $p < 0.015$ ], squamous cell carcinoma [ns] and others [ns]), simultaneous systemic therapy (chemotherapy [ns], hormone therapy [ns], targeted [OR 0.344; 95% CI 0.154-0.767;  $p < 0.009$ ], no therapy [reference category;  $p < 0.002$ ]). There was no significant association between complete response and age, gender, grading, localization, spinal cord compression, soft tissue involvement, metastasis type (blastic/lytic/mixed), opioid/steroid medication and radiation dose. KI (OR 1.053; 95% CI 1.014-1.094;  $p < 0.008$ ) and neurological dysfunction (OR 0.320; 95% CI 0.103-0.997;  $p < 0.049$ ) were also significantly associated with complete response in multivariate logistic regression. Only age (OR 0.974; 95% CI 0.949-0.999;  $p < 0.043$ ) and steroid medication (OR 3.314, 95% CI 1.254-8.757;  $p < 0.016$ ) were significantly associated with any response in univariate and multivariate logistic regression.

### Conclusion

Our results indicate that spinal stability, higher KI, no simultaneous therapy, no neurological dysfunction, specific tumor histologies, and tumor types may be associated with pain response in patients with spinal bone metastases treated with radiation.

<sup>1</sup>Vall D`Hebron Hospital, Radiation Oncology, Barcelona, Spain

### Purpose or Objective

The role of radiotherapy as a supportive treatment in the palliative care of patients with advanced stages of cancer is well known. However, the decision to carry out these treatments is influenced by the benefit that could be obtained in the last days of life. The aim of this study was to analyze the factors that could influence death within 30 days after a palliative radiotherapy (RT) treatment was initiated.

### Material and Methods

We retrospectively collected data from patients treated with palliative intention radiotherapy in our department between January and June of 2018 in order to identify factors related to mortality in the first 30 days after start of the treatment. Clinical features of gender, age, Eastern Cooperative Oncology Group performance status (PS), Karnofsky index, presence of visceral metastases, the indication of radiotherapy treatment (antalgic, haemostatic, whole brain radiotherapy [WBRT], spinal cord compression or any other) and the prescribed doses. Follow-up was made up to 3 months after the RT was performed, but we decided to set our cut-off point in 30 days.

### Results

A total of 353 palliative treatments were performed in 284 patients. The main characteristic of our population are describe in table 1. The mean age was 64 years (5-90). At the end of the follow up period, 27 patients (9.5%) receiving 120 different treatments during the follow up, died within 30 days after the last treatment was performed, with a median of 16 days (13-22 days) after the start of the treatment. In the 27 deaths, single doses were administered in 37% of the cases (10), 9 with antalgic intentions. Typical fractionation schemes as 20Gy in 5 fractions and 30Gy in 10 fractions occurred in 7 patients (25.9%) in both cases, being 60% for pain control and 60% for WBRT, respectively. A higher mortality rate was observed in those who had worse performance status (ECOG 0= 18% vs ECOG 3= 69%  $p < 0.005$ ; KPS > 70= 24.2% vs KPS < 70= 49.3%  $p < 0.005$ ). Likewise, a difference was observed between the group with visceral metastasis and those that did not have it. Regarding the primary tumour, the lowest mortality was observed in the patients with breast, prostate, gynecologist and myeloma without finding a statistical significance. Greater mortality was found in WBRT and the cases of spinal cord compression (46.8% and 51.8% respectively,  $p$  NS) and in those who received single dose RT (44.8%  $p < 0.005$ ). Of these patients, 57.5% had a partial or completed response to treatment ( $p < 0.005$ ).

EP-1633 Profile of patients who die in the first 30 days after palliative radiotherapy in our center

D.C. Moreno Santiago<sup>1</sup>, M. Vázquez Varela<sup>1</sup>, M. Altabas Gonzalez<sup>1</sup>, J. Giralt<sup>1</sup>

**Table 1.** Clinical features of death and alive patients in the first 30 days after radiotherapy initiation (n = 347).

		Dead	Alive	p
Gender	Male	83 (23,9)	126 (36,3)	<0.005
	Female	37 (10,6)	101 (29,1)	
ECOG <sup>1</sup>	0	5 (1,4)	22 (6,3)	<0.005
	1	41 (11,8)	141 (40,6)	
	2	58 (16,7)	16 (4,6)	
	3	16 (4,6)	7 (2,0)	
KPS <sup>3</sup>	≥70	49 (14,1)	153 (44,1)	<0.005
	<70	71 (20,4)	73 (21,0)	
Primary tumour	Lung	47 (13,5)	60 (17,2)	NS**
	Colon and rectum	12 (3,4)	9 (2,5)	
	Urothelial	11 (3,1)	29 (8,3)	
	Breast	8 (2,3)	43 (12,3)	
	Liver and Bile duct	7 (2,0)	5 (1,4)	
	Head and Neck	6 (1,7)	1 (0,2)	
	Melanoma	5 (1,4)	4 (1,1)	
	Gynaecologists	2 (0,5)	14 (4,0)	
	Prostate	4 (1,1)	28 (8,0)	
	Gastroesophageal	4 (1,1)	6 (1,76)	
	Unknown	3 (0,8)	5 (1,4)	
	Myeloma	2 (0,5)	8 (2,3)	
	Lymphoma	4 (1,1)	2 (0,5)	
	Others	5 (1,4)	13 (3,7)	
Visceral metastasis	Present	39 (11,2)	115 (33,1)	<0.005
	Absent	81 (23,3)	111 (31,9)	
Indication	Antalgic	66 (19,0)	129 (37,1)	NS**
	Haemostatic	2 (0,5)	14 (4,0)	
	WBRT*	30 (8,6)	34 (9,7)	
	Spinal cord compression	13 (3,7)	14 (4,0)	
	Other	9 (2,5)	36 (10,3)	
Dose Prescribed	8Gy	39 (11,2)	48 (13,8)	<0.005
	10-20Gy	36 (10,3)	70 (20,1)	
	>20Gy-30Gy	38 (10,9)	83 (23,9)	
	>30Gy	6 (1,7)	25 (7,2)	
Completed radiotherapy	Yes	112 (32,2)	218 (62,8)	NS**
	No	8 (2,3)	9 (2,5)	

Quantitative variables expressed in median (percentile 25<sup>th</sup>, percentile 75<sup>th</sup>). Qualitative variables expressed in total amount and percentages. \*Whole brain radiotherapy. \*\*p>0.05, <sup>1</sup>Karnofsky performance status, <sup>2</sup>Eastern cooperative oncology group.

## Conclusion

As expected, the highest mortality incidence at 30 days was found in patients with worse PS, which in the majority of cases were treated with single doses, and in those with presence of visceral metastases. The largest fractionation schemes included in this group were prescribed in patients with WBRT intention.

Knowing these data is useful for treatment decision making as well as selection of dose-fractionation prescription. This could help to avoid futility and non-beneficial treatment during the end of life.

## EP-1634 Stereotactic Body Radiotherapy (SBRT) for bone metastases: Preliminary experience

E. González Del Portillo<sup>1</sup>, O. Alonso-Rodríguez<sup>1</sup>, A. Nieto-Palacios<sup>1</sup>, C. Martín-Rincón<sup>1</sup>, L.A. Pérez-Romasanta<sup>1</sup>

<sup>1</sup>Complejo Asistencial Universitario de Salamanca, Radiation Oncology, Salamanca, Spain

### Purpose or Objective

Bone metastases (BM) are common in patients with advanced solid tumours causing pain, disability, increased fracture risk, and having a negative impact on patient's quality of life. Stereotactic body radiotherapy (SBRT), also referred to as stereotactic ablative radiotherapy (SABR), is an emerging option of treatment for these metastases. It is characterized by either a single or limited number of dose fractions, and a high biological effective dose, often above 100 Gy. Its effects are higher cell death, lower DNA repair mechanisms, damage to tumour vasculature, and activation of immune system. Our goal is to evaluate local control, survival, pain control and complications.

### Material and Methods

This is a prospective study from 2014 to 2018. We included 31 oligometastatic patients and 44 BM treated with SBRT. Patients received a total dose of 20-35 Gy, typically in 5 consecutive fractions. Most treatments included an extended volume with simultaneous integrated boost on the macroscopic tumor, following standardized consensus for volume definition. Daily 3D imaging for verification purposes was done before treatment. The endpoints were radiological response and local control (control included complete response, partial response and stable disease), survival rate by Kaplan-Meier method, and pain control

evaluated with visual analogic scale (VAS) (0-3: light; 4-6: moderate; 7-10: intense).

## Results

Mean age at the bone metastases diagnoses was 56 years (range: 32-85 years). The most common primary tumour was breast cancer (58%), followed by lung cancer (16%), renal cell carcinoma (9%) and prostate cancer (6%). For metachronous metastases the mean interval between primary tumour diagnoses and bone metastasis diagnoses was 4,5 years (range: 0-18 years). Synchronous primaries and metastases appeared in 30% of patients. Most metastases (80%) were located in the spine, especially thoracic and lumbar vertebrae. Others sites were pelvis, breastbone, ribs and femur. Radiologically, 52% were sclerotic, 30% were lytic and 18% were mixed metastases. The maximum number of treated lesions per patient was 4. The mean total dose for macroscopic tumour was 29 Gy (range: 18-35 Gy) and for adjacent bone was 22 Gy (range: 20-30 Gy). Local control rate, including complete response, partial response and stable disease was 75%. Two year overall survival was 73,7%. The mean following time was 386 days. Four patients died during the follow-up. Before treatment, 16% suffered moderate pain and 30% intense pain. After treatment, 8 patients achieved complete control (VAS 0); 7 presented partial control (lower VAS); 12 kept stable; 4 patients did not achieve symptomatic control. The mean reduction of VAS after SBRT was 2 points. Forty-two percent achieved reduction of VAS ≥3 (range 3-8). No spinal cord toxicity was observed.

## Conclusion

SBRT is a treatment option for BM because local control and pain control without toxicity are achievable in most of cases.

## EP-1635 Stereotactic ablative radiation therapy for non-spine bone metastases

K.S. Kim<sup>1</sup>, C. Choi<sup>1</sup>

<sup>1</sup>Dongnam Institute of Radiological and Medical Sciences, Radiation Oncology, Busan, Korea Republic of

### Purpose or Objective

To report the treatment outcome of stereotactic ablative radiation therapy (SABR) for non-spine bone metastases in a single institution

### Material and Methods

From Jul. 2011 to Jan. 2017, thirty-three patients with non-spine bone metastatic disease were treated with SABR. Treatment intent were categorized as follows (1) Single metastasis or oligometastases, for which the goal was to irradiate all sites of disease; (2) Oligoprogression, for which the goal was to irradiate only those tumors that were progressing while a systemic therapy was controlling all other sites of disease; (3) Dominant areas of progression, for which the goal was to irradiate dominant tumors usually for palliation. A total of 38 lesions were treated and responses were evaluated according to University of Texas MD Anderson (MDA) cancer center criteria.

### Results

The most common primary cancer was non-small cell lung cancer (n=12) following breast cancer (n=8), hepatocellular carcinoma (n=3) and renal cell carcinoma (n=3). Twenty-five lesions (66%) were located in the pelvis following femur (n=5) and ribs (n=5). Majority of the lesions were lytic bone metastases (n=25, 66%). Prescribed radiation doses and fractions were 18 Gy/1 fraction (Fx) to 3 lesions, 24-60 Gy/3 Fx to 16 lesions, 28-48Gy/4 Fx to 15 lesions and 40-50 Gy/5 Fx to 4 lesions. Median follow up periods was 10.4 months (2.5-47.4). One-year local control rate was 94.2%. Median overall survival was 25.1 months (95% CI 14.7-35.5 month) for single metastasis or oligometastasis (n=24), 25.7 months (95% CI 0-54.2) for oligoprogression (n=3) and 5.8 months (95% CI 2.0-9.6) for

dominant areas of progression (n=6). No grade 3 or greater toxicity was reported.

#### Conclusion

Although heterogeneous patients populations, SABR to non-spine bone metastases showed high local control rate with acceptable toxicity. Appropriate treatment indication and unified response evaluation are important for the future clinical trials and wide application of SABR to non-spine bone metastases in the clinic.

---

#### Electronic Poster: Clinical track: Elderly

---

#### EP-1636 Linac-based radiosurgery in elderly patients: mono-institutional experience on 110 brain metastases

F. Gregucci<sup>1</sup>, A. Fiorentino<sup>1</sup>, S. Corradini<sup>2</sup>, V. Figlia<sup>1</sup>, R. Mazzola<sup>1</sup>, F. Ricchetti<sup>1</sup>, R. Ruggeri<sup>1</sup>, F. Alongi<sup>1,3</sup>

<sup>1</sup>Hospital Sacro Cuore Don Calabria- Cancer Care Center, Radiation Oncology, Negrar, Italy ; <sup>2</sup>LMU University Hospital, Radiation Oncology, Munich, Germany ;

<sup>3</sup>University of Brescia, Radiation Oncology, Brescia, Italy

#### Purpose or Objective

To analyze the feasibility and clinical results of linac-based stereotactic radiosurgery (SRS) or fractionated stereotactic radiotherapy (SFRT) with Flattening Filter Free (FFF) volumetric modulated arc therapy (VMAT) in elderly patients affected by Brain Metastases (BMs) with the idea of improving patients' compliance at treatment and their quality of life.

#### Material and Methods

Patients selected for the present analysis were > 65 years old with a life expectancy of > 3 months, good performance status, a controlled or synchronous primary tumor, a number of BMs <10 with a diameter <3 cm. All patients were treated with FFF Linac-based SRS/SFRT. The prescribed total dose (15-30Gy/1-5 fractions) was based on BMs size, proximity to organs at risk and intent of treatment. Acute and late toxicity was assessed according to CTCAE v4.0. A retrospective analysis of patients, BMs, treatment characteristics and outcomes included toxicity, local control (LC), overall survival (OS) and intracranial progression free survival (iPFS), were performed. MedCalc v18.2 was utilized for statistical analysis.

#### Results

From April 2014 to December 2017, 40 elderly patients with 110 BMs were treated by FFF-VMAT Linac-based SRS/SFRT. Median age was 70 years (range 65-83). The median number of BMs was 2 (range 1-10). The median PTV was 1 cc (0.1-42) and the median diameter of BMs was 1 cm (0.6-3). In case of multiple BMs, the median cumulative PTV was 10.3 cc (range 0.9-65.9 cc). Median biologically effective dose (BED) calculated with an alfa/beta value of 12 Gy was 47.2 Gy, with 87% of BMs receiving an efficacy dose  $\geq$  40 Gy. The median beam on time was 2 min (range 1,5-4) for lone lesion, while for multiple BMs, the treatment time was 11 min (range 9-15). With a median follow-up time of 28 months (range 6-50), median and 1-year OS were 9 months and 39%, respectively; median iPFS was 6 months. No difference in terms of outcomes were observed between patients under or over the age of 70 years ( $p=0.2$  and  $p=0.18$ ). At the time of the analysis, LC was reported in 109/110 BMs (99.1%): 12 BMs had a complete response; 51 a partial response; 46 a stable disease. One BM (0.9%) progressed after 2 months. The analysis of LC profile stratified by clinical and treatment variables has shown that BM volume (<1cc) and higher SRS/SFRT dose ( $\geq$  40 Gy) correlated to positive treatment local response ( $p=0.01$ ;  $p=0.0017$ ). No adverse events more than grade 2 were observed.

#### Conclusion

The present findings highlight the feasibility, safety and effectiveness of FFF Linac-based SRS/SFRT in elderly patients with BMs.

#### EP-1637 Validation of a predictive model for survival in elderly patients treated with radiotherapy

H. Park<sup>1</sup>

<sup>1</sup>Dankook University Hospital, Radiation Oncology, Cheonan, Korea Republic of

#### Purpose or Objective

Elderly patients are more likely to have poor performance status and comorbidities. There is a reluctance to extensively investigate and treat elderly patients. Patient selection based on prognosis is necessary to provide appropriate treatment. This study was conducted to validate a predictive model for survival of elderly patients treated with palliative radiotherapy.

#### Material and Methods

From February 2015 to February 2018, a total 41 patients aged 80 and older underwent palliative radiotherapy. Prognosis in Palliative care study predictor (PiPS), Palliative prognostic index (PPI) and Delirium-Palliative prognostic score (D-PaP) were used for prediction of survival. The Clinical prediction of survival (CPS) was excluded from the D-PaP score. The median biologically effective dose (BED) was 39 Gy<sub>10</sub> (range, 28-75 Gy<sub>10</sub>) with dose-per-fraction of 2.5-7.0 Gy.

#### Results

Among 41 patients, 1 patient didn't receive the scheduled treatment. During the median follow-up duration of 1.8 months (range, 0.2-27.5 months), 20 patients referred to hospice care center and 6 patients died. The 1- and 6-months overall survival (OS) rates were 97.0% and 87.3%, respectively. The 1- and 6-months OS of patients who were predicted to live more than a month according to PiPS were 100% and 90.7%, respectively. Patients with PPI and D-PaP without CPS less than 4 points, the 1- and 6-months OS were 100% and 93.8% each. The 1- and 6-month OS were 80.0% and 0% in the patients with D-PaP without CPS 4 points or more ( $p<0.001$ ). D-PaP without CPS score showed significant correlation with survival ( $p=0.033$ ).

#### Conclusion

The prognostic prediction models can be used to predict prognosis in elderly patients who need palliative radiotherapy. These models can be used to guide clinical decisions, including patient selection, total dose and schedule of radiotherapy. Further studies are needed to develop a more appropriate prediction models for elderly patients.

#### EP-1638 Radiotherapy and Immunotherapies in elderly: a systematic literature review

L. Belgioia<sup>1</sup>, I. Desideri<sup>2</sup>, A. Errico<sup>3</sup>, C. Franzese<sup>4</sup>, A. Daidone<sup>5</sup>, L. Marino<sup>6</sup>, M. Fiore<sup>7</sup>, P. Borghetti<sup>8</sup>, D. Greto<sup>2</sup>, A. Fiorentino<sup>9</sup>

<sup>1</sup>AIROGiovani Italian Association of Radiation Oncology-Young Members Working Group., Department of Health Science DISSAL, Genoa, Italy ;

<sup>2</sup>AIROGiovani Italian Association of Radiation Oncology-Young Members Working Group., Department of Biomedical-

Experimental and Clinical Sciences "Mario Serio"-Section of Radiation Oncology, Florence, Italy ;

<sup>3</sup>AIROGiovani Italian Association of Radiation Oncology-Young Members Working Group., Mons. R. Dimiccoli Hospital- Radiation Oncology, Barletta, Italy ;

<sup>4</sup>AIROGiovani Italian Association of Radiation Oncology-Young Members Working Group., Department of Radiotherapy and Radiosurgery, Rozzano, Italy ;

<sup>5</sup>AIROGiovani Italian Association of Radiation Oncology-Young Members Working Group., Radiation Oncology, Mazara del Vallo, Italy ;

<sup>6</sup>AIROGiovani Italian Association of Radiation Oncology-Young Members Working Group., Rem- Radiation Oncology, Catania, Italy ;

<sup>7</sup>AIROGiovani Italian Association of Radiation Oncology-Young Members Working Group., Campus Bio-Medico University-

Radiation Oncology, Rome, Italy ;

<sup>8</sup>AIROGiovani Italian

*Association of Radiation Oncology-Young Members Working Group., University and Spedali Civili - Radiation Oncology, Brescia, Italy ; <sup>9</sup>AIROGiovani Italian Association of Radiation Oncology-Young Members Working Group., General Regional Hospital " F. Miulli" - Radiation Oncology, Acquaviva delle Fonti Bari, Italy*

#### **Purpose or Objective**

In USA 53% of new cancer cases are diagnosed in people over 65 years, and in the next decade the incidence of cancer in elderly people will continue to grow up. Radiotherapy (RT), chemotherapy and more recently immunotherapy have favorably changed the outcome of various cancers. Nevertheless, elderly people are under-represented in clinical trials. Aim of the present review is to assess the present data about the use of the association of Radiotherapy and immunotherapy in elderly people.

#### **Material and Methods**

PubMed database was searched for English literature published up to December 2017 using keywords "radiotherapy" combined with "immunotherapy" and "ipilimumab" or "pembrolizumab" or "nivolumab". Studies performing radiotherapy and immunotherapy in people aged > 65 years were evaluated focusing on safety, toxicity and, if possible, efficacy. Studies eligible for inclusion in this review were: (a) case reports, retrospective or prospective studies in which RT and new drugs were used concomitantly or sequentially; (b) studies in which the evaluation of elderly sub-group was reported.

#### **Results**

The systematic search identified 363 records from PubMed. After exclusion of duplicates, full-text review, cross-referencing and paper that do not respect the inclusion criteria, 20 studies were included in this review. As regard Ipilimumab, data seems to indicate a longer OS in patients with metastatic melanoma treated with ipilimumab +RT vs those treated with ipilimumab alone, suggesting a possible RT role in enhancing ipilimumab-induced immune response (Stokes WA et al 2017, Tazi K et al 2015). In NSCLC a prospective phase II trial of neoadjuvant ipilimumab followed by radical or post operative surgery demonstrated excellent tolerance with no observed G3 or more side effects (Boyer MJ et al 2016) and in prostate cancer ipilimumab + palliative RT seems to improve OS in subgroups of pts (high risk) (Kwon ED et al 2015). As regards Pembrolizumab it seems to improve PFS and OS in NSCLC previous treated with RT without increasing in side effects (Shaverdian N et al 2017). On the other hand there are some data on immunotherapy related pneumonitis during anti PD1 treatment combined to RT, reported both for pembrolizumab and for nivolumab with development also later after RT end (Lu CS et al 2017, Manapov F et al 2018, Yoshida Tet al 2017).

#### **Conclusion**

Immunotherapies in association of RT seems to be safe, but in elderly patients data concerning safety and toxicity are limited. The tolerance of combined RT and immunotherapy seems similar among older and younger people. To date many data underline the immune stimulation of RT, so it might be interesting evaluate if the two combined treatment might improve the response also in elderly patients. Specific clinical trials on this population are encouraged.

#### **EP-1639 Socioeconomic Status and Mortality in Elderly Cancer Patients:A National Elderly Sample Cohort Study**

B. Jang<sup>1</sup>, J.H. Chang<sup>2</sup>

<sup>1</sup>Seoul National University Hospital, Radiation Oncology, Seoul, Korea Republic of ; <sup>2</sup>SNU-SMG Boramae Medical Center, Radiation Oncology, Seoul, Korea Republic of

#### **Purpose or Objective**

We hypothesized that lower socioeconomic status (SES) was associated with higher all-cause mortality in patients newly diagnosed with cancer, particularly with respect to the elderly (age  $\geq$  60 years). There are no previous studies evaluating the relationship between individual/regional-level SES and all-cause mortality in cancer patients more than 60 years in the context of national health care coverage.

#### **Material and Methods**

We collected study patients from the stratified random sample of Korean National Health Insurance Elderly Cohort (2002-2015). Patients who were newly diagnosed with cancer between 2003 and 2015 were included. Those living in a newly created city ('Sejong' city) or with other/ill-defined/sex-specific cancer at diagnosis were excluded. A total of 108,626 patients were collected. Cox's proportional hazard regression model was used to investigate risk factors of mortality. Individual SES position (insurance type, income level) and regional-level SES from composite deprivation index (CDI) 2010 were derived. The comorbidities were measured using Charlson Comorbidity Index score.

#### **Results**

Patients with disability or residing in a deprived region were found more in the low-income level group. In patients  $\leq$ 80 years, multivariate Cox hazard regression model revealed that low-income status was associated with higher risk of mortality compared to high-income status (HR 1.08, 95% CI 1.05-1.11,  $P < 0.001$ ). Contrary to patients > 80 years, those  $\leq$ 80 years and living in a deprived region at diagnosis showed worse survival (HR 1.10, 95% CI 1.08-1.12,  $P < 0.001$ ). Male, lowest insurance

#### **Conclusion**

Low individual/regional SES at the time of cancer diagnosis is associated with increased mortality in elderly patients. Further understanding causes of the phenomena and accordingly providing support for elderly cancer patients with low SES or residing in deprived regions would be necessary.

#### **EP-1640 Radical radiotherapy in elderly prostate cancer patients: a monoinstitutional experience**

C.L. Deantonj<sup>1</sup>, A. Fodor<sup>1</sup>, C. Fiorino<sup>2</sup>, C. Cozzarini<sup>1</sup>, F. Zerbetto<sup>1</sup>, P. Mangili<sup>2</sup>, C. Calandrino<sup>2</sup>, N.G. Di Muzio<sup>1</sup>  
<sup>1</sup>San Raffaele Scientific Institute- Milano- Italy, Department of Radiotherapy, Milano, Italy ; <sup>2</sup>San Raffaele Scientific Institute- Milano- Italy, Medical Physics, Milano, Italy

#### **Purpose or Objective**

Continuous or intermittent androgen deprivation therapy (ADT) is generally prescribed in elderly prostate cancer (PCa) patients (pts) with under 10 years life expectancy. Unfortunately, 18-24 months later many pts become castration resistant and only palliative therapies are available. Here we report toxicity and outcomes obtained in elderly ( $\geq$ 80 years old at diagnosis) PCa (pts) treated with radical radiotherapy in a monoinstitutional experience

#### **Material and Methods**

From December 2006 to July 2014, 34 elderly PCa pts underwent radiotherapy with radical intent. Three pts, affected by a low risk cancer, were treated on prostate and seminal vesicles only, to 71.4 Gy in 28 fractions (EQD2 80.8 Gy, considering  $\alpha/\beta=1.5$  for prostate cancer). Intermediate and high-risk PCa pts underwent prophylactic irradiation on pelvic nodes to 51.8 Gy in 28 fractions (EQD2 52.2 Gy), with simultaneous integrated boost to seminal vesicles up to 65.5 Gy (77.7 Gy EQD2) and to prostate up to 74.2 Gy (88 Gy EQD2). Neoadjuvant and/or adjuvant androgen deprivation therapy (ADT) was prescribed in 25/34 pts for a median of 27.9 months (2-79 months). All patients were treated with helical IMRT

(Tomotherapy®, Accuray, Wisconsin) and daily IGRT (MVCT). Patients' characteristics are reported in Table 1.

Median ( range) age at diagnosis	82 (80-90) years
Median (range) iPSA	10.09 (3.74-300.0) ng/ml
	6: 9
	7: 11
Median ( range) Gleason Score	8: 6
	9: 9
	cT1c: 16
	cT2a: 3
	cT2b: 2
T Stage	cT2c: 10
	cT3: 2
	cT4: 1

## Results

Median follow up was 61 (13.3-128.6) months. Acute and late toxicity were mild, with only one late G3 rectal toxicity (2.94%) registered, eventually solved by Argon Plasma applications, and 1 G3 urinary stenosis (2.94%), solved with temporary catheterization. Late G2 toxicity were 14.7% (5 pts) for urinary tract and 5.88% (2 pts) for the rectum.

Five-year biochemical relapse-free survival (bRFS) was 73.5% (25/34 pts) and clinical relapse-free survival was 79.4% (27/34 pts). Median bRFS and distant progression-free survival (calculated from the last day of RT) were 56.3 and 61.1 months respectively Eighteen pts were dead at the last follow up, six of whom with a prostate cancer progression.

## Conclusion

Radical radiotherapy with a curative intent even in elderly pts demonstrated good results in terms of both biochemical control and progression-free survival, with a good toxicity profile. In our opinion, radical treatment in elderly pts could improve their life expectation and quality of life.

### EP-1641 Radiotherapy for prostate cancer patients over 80 years: 95 patients treated in a single institution

P. Méré<sup>1</sup>, C. Dalban<sup>2</sup>, E. Peynet<sup>2</sup>, A. Guignot<sup>1</sup>, J. Droz<sup>3</sup>, P. Pommier<sup>1</sup>

<sup>1</sup>Centre Léon Bérard, Department of Radiation Oncology, Lyon, France ; <sup>2</sup>Centre Léon Bérard, Department of Research and Innovation, Lyon, France ; <sup>3</sup>Centre Léon Bérard, Department of Medical Oncology, Lyon, France

## Purpose or Objective

The benefit of radiotherapy alone or associated with hormonal treatment is still debated in men aged 80 years or more, due to competitive risk of death and the fear to induce more often severe acute or late toxicities than younger men. The objectives were to assess if the standard of care could be applied in that population

## Material and Methods

A retrospective study has been conducted in all consecutive patients (pts) aged 80 years or more, treated with a curative intent from January 2003 to December 2013 in a single radiotherapy center for a non-metastatic prostate adenocarcinoma (prostatectomy excluded). All patients received external beam radiotherapy (EBRT) or brachytherapy (BT) with or without associated hormonal therapy (HT) according to the cancer status, co-morbidities, and physician decision.

95 pts aged from 80 à 91 Years (median 81.9 Years) have been included. The majority of patients (92.2%) were in the 80 to 85 years age group.

The Performance Status was 0 in 84% and 1 in 16%. The majority of patients had 1 or 2 co-morbidities, but most were rated CIRS-G-1 or 2 and therefore not severe. All patients had an assessment of their overall health based on medical record data according to Balducci classification and G8 oncology and item distribution. 83.2% were considered as "fit elderly" according to

Balducci classification, and the G8 score was > 14 in 56.8 %.

The distribution according to d'Amico and Zumsteg Score was: low (4 pts), favorable intermediate (10 pts), unfavorable intermediate (28pts) and high risk (53 pts).

91 pts were treated with EBRT and 4pts with Iodine seeds BT. 21 pts previously receive a palliative HT before the decision to propose radiotherapy with a curative intent. HT was used concomitantly with EBRT in 36 pts.

Regarding EBRT techniques, a conformational 3D was used for the first 50pts, before the technique moved to IMRT (standard in 10; VMAT in 31 pts). The mean and median dose delivered to the prostate were respectively 69.7 and 74 Gy (Range 24 - 78) to the prostate volume. Pelvic nodes were irradiated in 15 patients.

## Results

The median follow-up time was 5.1 years (CI95%:4.6- 5.9). EBRT was prematurely stopped in 8 pts because of a grade >=3 acute toxicity in 5 (urinary in 4; diarrhea in 1), a fall at home in 2 and a breakdown in 1 pt. Three patients experienced a grade 3 late toxicity: Bladder in 2 pts; Rectal in 1pt. No grade 4 was reported. The median overall survival was 9.9 years. Event Free Survival according to d'Amico and Zumsteg classification are presented in figure 1.

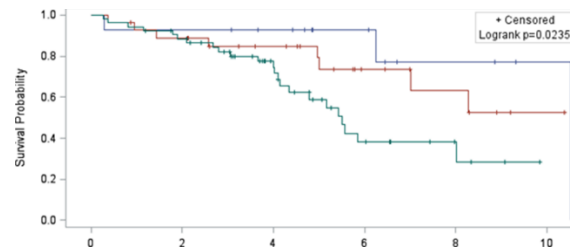


Figure 1: Event free survival (death, recurrence) according to D'Amico/Zumsteg classification 1: Low and Favorable Intermediate risk ; 2: Unfavorable Intermediate risk; 3: High risk

## Conclusion

Radiotherapy with a curative intent may be proposed in selected patients of 80 years or more, providing an accurate geriatric oncology evaluation to evaluate the benefit of this treatment in term of overall survival and quality of life.

### EP-1642 Short-course accelerated palliative EBRT for advanced head and neck cancer in elderly patients

M. Ferro<sup>1</sup>, G. Macchia<sup>1</sup>, S. Cilla<sup>2</sup>, A. Ianiro<sup>2</sup>, V. Picardi<sup>1</sup>, M. Boccardi<sup>1</sup>, E. Arena<sup>1</sup>, M. Ferro<sup>1</sup>, S. Cammelli<sup>3</sup>, F. Romani<sup>4</sup>, S. Riga<sup>4</sup>, E. Farina<sup>3,5</sup>, M. Buwenge<sup>3</sup>, M.A. Sumon<sup>6</sup>, A. Kamal Uddin<sup>6</sup>, P. Assalone<sup>7</sup>, V. Valentini<sup>8</sup>, A.G. Morganti<sup>3</sup>, F. Deodato<sup>1</sup>

<sup>1</sup>Fondazione di Ricerca e Cura "Giovanni Paolo II", Radiotherapy Unit, Campobasso, Italy ; <sup>2</sup>Fondazione di Ricerca e Cura "Giovanni Paolo II", Medical Physics Unit, Campobasso, Italy ; <sup>3</sup>Dept. of Experimental- Diagnostic and Specialty Medicine - DIMES- S.Orsola-Malpighi Hospital, Radiation Oncology Center, Bologna, Italy ; <sup>4</sup>Dept. of Experimental- Diagnostic and Specialty Medicine - DIMES- S.Orsola-Malpighi Hospital, Medical Physics Unit, Bologna, Italy ; <sup>5</sup>Maria Cecilia Hospital-GVM Care & Research, Radiation Oncology Unit, Cotignola RA, Italy ; <sup>6</sup>United Hospital Limited- Gulshan, Radiation Oncology Department, Dhaka, Bangladesh ; <sup>7</sup>Veneziale Hospital, Oncology Unit, Isernia, Italy ; <sup>8</sup>Policlinico Universitario "A. Gemelli"- Università Cattolica del Sacro Cuore, Department of Radiotherapy, Roma, Italy

## Purpose or Objective

To assess the safety and efficacy of a Short-course Accelerated Radiation therapy (SHARON) regimen in the

palliative treatment of H&N locally advanced or metastatic cancer in elderly patients.

#### Material and Methods

Eligibility criteria for the analysis were: 1) histological confirmed H&N cancers, 2) age  $\geq$  80 years, 3) expected survival  $>$  3 months and 4) Eastern Cooperative Oncology Group (ECOG) performance status of  $\leq$  3. A total dose of 20 Gy was delivered in 2 consecutive days with a twice daily fractionation (5 Gy per fraction) and at least 6-8 hour interval. Primary endpoint was the symptoms response rate.

#### Results

Thirty-four patients (male/female: 18/16; median age: 85.0 years; range: 80-98) were included in the analysis. ECOG performance status was  $<$  3 in 17 patients (50%). Patients with different cancer types were included in the analysis, in particular the primary were: oral cavity (N<sup>o</sup>=13; 38.2%), larynx (N<sup>o</sup>=5; 14.7%), oropharynx (N<sup>o</sup>=4; 11.7%), salivary gland (N<sup>o</sup>=3; 8.8%), lip (N<sup>o</sup>=3; 8.8%), nasal cavity (N<sup>o</sup>=2; 5.8%), maxillary sinus (N<sup>o</sup>=3; 8.8%) and ethmoid sinus cancer (N<sup>o</sup>=1; 2.9%). With a median follow-up time of 4.5 months (range 1 to 28 months), two patients (5.9%) developed  $\geq$ G3 acute toxicities: one patient had a G3 mucositis and one had a G3 dysphagia requiring N-G feeding tube and G4 dyspnoea requiring tracheostomy. Moreover, 9 (26.4%) G1-G2 acute pharyngeal toxicities, 8 (23.5%) G1-G2 acute skin toxicities and 9 (26.4%) G1-2 mucositis were recorded. Overall palliative response rate was 76.5%. Moreover, among 24 symptomatic patients for pain, 21 showed an improvement or resolution with an overall pain response rate of 87%. No detrimental effects in terms of quality of life (CLAS 1,2,3) were observed after the treatment. The median survival time was 9 months, with a median palliative progression free survival of 8 months.

#### Conclusion

Short-course accelerated radiotherapy in palliative setting of Head & Neck cancers is effective in terms of symptom relief and well tolerated even in elderly patients.

#### EP-1643 Short-course accelerated palliative radiotherapy for advanced lung cancer in elderly patients

M. Ferro<sup>1</sup>, M. Ferro<sup>1</sup>, F. Deodato<sup>1</sup>, S. Cilla<sup>2</sup>, A. Ianiro<sup>2</sup>, V. Picardi<sup>1</sup>, M. Boccardi<sup>1</sup>, E. Arena<sup>1</sup>, S. Cammelli<sup>3</sup>, M. Ferioli<sup>3</sup>, A. Zamagni<sup>3</sup>, S. Bisello<sup>3</sup>, E. Farina<sup>3,4</sup>, M. Buwenge<sup>3</sup>, P. Assalone<sup>5</sup>, A.A. Woldemariam<sup>6</sup>, T. Wondemagegnhu<sup>6</sup>, V. Valentini<sup>7</sup>, A.G. Morganti<sup>3</sup>, G. Macchia<sup>1</sup>

<sup>1</sup>Fondazione di Ricerca e Cura "Giovanni Paolo II", Radiotherapy Unit, Campobasso, Italy; <sup>2</sup>Fondazione di Ricerca e Cura "Giovanni Paolo II", Medical Physics Unit, Campobasso, Italy; <sup>3</sup>Radiation Oncology Center, Dept. of Experimental- Diagnostic and Specialty Medicine - DIMES- S.Orsola-Malpighi Hospital, Bologna, Italy; <sup>4</sup>Maria Cecilia Hospital- GVM Care & Research, Radiation Oncology Unit, Cotignola RA, Italy; <sup>5</sup>Veneziale Hospital, Oncology Unit, Isernia, Italy; <sup>6</sup>Black Lion Hospital, Department of Radiotherapy, Addis-Ababa, Ethiopia; <sup>7</sup>Policlinico Universitario "A. Gemelli"- Università Cattolica del Sacro Cuore, Department of Radiotherapy, Roma, Italy

#### Purpose or Objective

To assess the safety and efficacy of a Short-course Accelerated Radiation therapy (SHARON) regimen in the palliative treatment of locally advanced or metastatic lung cancer in elderly patients.

#### Material and Methods

Eligibility criteria for the analysis were: 1) histological confirmed lung cancers, 2) age  $\geq$  80 years, 3) expected survival  $>$  3 months and 4) Eastern Cooperative Oncology Group (ECOG) performance status of  $\leq$  3. A total dose of 20 Gy was delivered in 2 consecutive days with a twice daily fractionation (5 Gy per fraction) and at least 8 hour

interval. Primary endpoint was the symptom response rate.

#### Results

Forty patients (male/female: 29/11; median age: 84.0 years; range: 80-96) were included in the analysis. ECOG performance status was  $<$  3 in 36 patients (90%). Patients with different cancer histology were included in the analysis, in particular: adenocarcinomas (N<sup>o</sup>=22; 55%), squamous cells (N<sup>o</sup>=15; 37.5%), small cell lung cancer (N<sup>o</sup>=3; 7%). With a median follow-up time of 1.2 months (range, 1 to 20 months), no G3 acute toxicities were observed, 2 (5%) G2 acute lung toxicity, 2 (5%) G1-G2 acute skin toxicities and 2 (5%) G1 esophagus toxicities were recorded. Among overall 26 symptomatic patients, 25 showed an improvement or resolution of baseline symptoms (overall palliative response rate: 96%). With a median survival time of 6 months, the median symptom free survival was 4 months. No differences in terms of quality of life was recorded after the treatment. Two of 40 (5%) patients required a retreatment that was performed in median after 5 months (range: 3-7 months) from the previous one.

#### Conclusion

Short-course accelerated radiotherapy in palliative setting of lung cancers is effective in terms of symptom relief and well tolerated even in elderly patients.

#### EP-1644 Elderly patients with non-melanoma skin cancer: results of accelerated hypofractionated treatment

M. Ferro<sup>1</sup>, G. Macchia<sup>1</sup>, E. Arena<sup>1</sup>, S. Cilla<sup>2</sup>, A. Ianiro<sup>2</sup>, V. Picardi<sup>1</sup>, M. Boccardi<sup>1</sup>, S. Cammelli<sup>3</sup>, A. Veraldi<sup>3</sup>, F. Bertini<sup>3</sup>, A. Arcelli<sup>3</sup>, M. Buwenge<sup>3</sup>, M.A. Sumon<sup>4</sup>, A. Kamal Uddin<sup>4</sup>, V. Valentini<sup>5</sup>, A.G. Morganti<sup>3</sup>, F. Deodato<sup>1</sup>, M. Ferro<sup>1</sup>

<sup>1</sup>Fondazione di Ricerca e Cura "Giovanni Paolo II", Radiotherapy Unit, Campobasso, Italy; <sup>2</sup>Fondazione di Ricerca e Cura "Giovanni Paolo II", Medical Physics Unit, Campobasso, Italy; <sup>3</sup>Radiation Oncology Center, Dept. of Experimental- Diagnostic and Specialty Medicine - DIMES- University of Bologna- S.Orsola-Malpighi Hospital, Bologna, Italy; <sup>4</sup>United Hospital Limited, Radiation Oncology Department, Gulshan- Dhaka, Bangladesh; <sup>5</sup>Policlinico Universitario "A. Gemelli"- Università Cattolica del Sacro Cuore, Department of Radiotherapy, Roma, Italy

#### Purpose or Objective

To assess the safety and efficacy of an accelerated radiotherapy schedule (Short Skin) in elderly patients with early stage non-melanoma skin cancer (NMSC).

#### Material and Methods

Eligibility criteria for the analysis were: 1) Patients with NMSC  $\leq$  3 cm, without infiltration of deep structures; 2) aged  $\geq$ 80 years; 3) Eastern Cooperative Oncology Group (ECOG) performance status of  $\leq$  3. Exclusion criteria were as follows: T3-T4 disease stage, prior RT on the same anatomical site, and poor compliance. Radiotherapy was delivered using electrons (6-9-12 MeV) or megavoltage photons (6MV) depending on tumor site and characteristics. The field size choice depended on the lesion size and location. For basal cell tumors of stage T1, the field size included a 1.5-cm normal tissue margin, while for stage T2 and/or squamous cell carcinomas, a 2.5-3-cm margin was included. A total dose of 30 Gy was delivered in 5 Gy fractions throughout six consecutive days. Primary endpoint was the local control rate.

#### Results

Forty patients (male/female: 24/16; median age: 87.0 years; range: 80-98) were included in the analysis. ECOG performance status was  $<$  3 in 37 patients (92.5%). The histology of skin cancer was squamous cell in 19 (47.5%) and basal cell in 19 (47.5%) patients, while 2 patients had mixed histology (5%). With a median follow-up time of 10 months (range, 2-63 months), no G3 acute skin toxicity

was recorded, while G2 skin toxicity was recorded in 20 patients (50%) and G2 mucositis was recorded in one patient (2,5%). The complete response of lesion was obtained in 18 (45%) patients, with a partial response in 9 (22,5%) patients. In 7 (17,5%) patients the response was not evaluable and in 6 (15%) patients was registered a stable disease. The 1-year actuarial local control was 82,5% with median local control not reached.

#### Conclusion

Short-course RT in elderly patients affected by early stage NMSC is able to produce more than 80% disease local control with excellent tolerability

#### EP-1645 Short-course accelerated palliative radiotherapy for advanced skin cancer in elderly patients

M. Ferro<sup>1</sup>, F. Deodato<sup>1</sup>, S. Cilla<sup>2</sup>, A. Ianiro<sup>2</sup>, V. Picardi<sup>1</sup>, M. Boccardi<sup>1</sup>, E. Arena<sup>1</sup>, S. Cammelli<sup>3</sup>, E. Galofaro<sup>3</sup>, V. Panni<sup>3</sup>, A. Arcelli<sup>3</sup>, M. Buwenge<sup>3</sup>, M.A. Sumon<sup>4</sup>, A. Kamal Uddin<sup>4</sup>, A.L. Angelini<sup>5</sup>, S. Riga<sup>5</sup>, V. Valentini<sup>6</sup>, A.G. Morganti<sup>3</sup>, G. Macchia<sup>1</sup>

<sup>1</sup>Fondazione di Ricerca e Cura "Giovanni Paolo II", Radiotherapy Unit, Campobasso, Italy ; <sup>2</sup>Fondazione di Ricerca e Cura "Giovanni Paolo II", Medical Physics Unit, Campobasso, Italy ; <sup>3</sup>Dept. of Experimental- Diagnostic and Specialty Medicine - DIMES- University of Bologna- S.Orsola-Malpighi Hospital, Radiation Oncology Center, Bologna, Italy ; <sup>4</sup>United Hospital Limited- Gulshan, Radiation Oncology Department-, Dhaka, Bangladesh ; <sup>5</sup>Dept. of Experimental- Diagnostic and Specialty Medicine - DIMES- University of Bologna- S.Orsola-Malpighi Hospital, Medical Physics Unit, Bologna, Italy ; <sup>6</sup>Policlinico Universitario "A. Gemelli"- Università Cattolica del Sacro Cuore, Department of Radiotherapy, Roma, Italy

#### Purpose or Objective

To assess the efficacy and safety of a Short-course Accelerated Radiation therapy (SHARON) regimen in the palliative treatment of non-melanoma skin cancers in elderly patients.

#### Material and Methods

Patients with histological confirmed non-melanoma skin cancers, age  $\geq$  80 years, expected survival  $>$  3 months and Eastern Cooperative Oncology Group (ECOG) performance status of  $\leq$  3 were considered eligible for this analysis. The primary endpoint was to evaluate the symptom response rate. Radiotherapy regimen was based on the delivery of 4 radiotherapy fractions (5 Gy per fraction) with a twice daily fractionation in two consecutive days. Three different level of dose were administered according to organ at risk constraints: 20 Gy (1 cycle), 40 Gy (2 cycles) and 60 Gy (3 cycles).

#### Results

Twenty-seven patients (male/female: 13/14; median age: 87.0 years; range: 80-98) were included in this analysis. ECOG performance status was  $<$  3 in 18 patients (66.6%).

Histology were squamous cell carcinoma (N<sup>o</sup>=21, 77.8%), basal cell carcinoma (N<sup>o</sup>=3, 11.1%), baso-squamous carcinoma (N<sup>o</sup>=2, 7.4%) and Bowen's Disease (N<sup>o</sup>=1, 3.7%). Among 14 patients who completed the 1 cycle, only one (7%) experimented acute G3 skin toxicity; two (14%) G2 skin toxicities were observed. Nine patients reported an improvement or resolution of baseline symptoms (overall palliative response rate: 64%). When more cycles were administered, mean time between cycles was 28 days. Six patients underwent to 2 RT cycles: of these, no G3 toxicities were recorded; four patients (66%) showed G2 mucosal toxicity and G2 skin toxicity. In this subset of patients the overall response rate was 100%. Six patients received 3 RT cycles: none of them experienced G3, but all of them showed G2 skin toxicity. Even in this case, overall response rate was 100%. With a median survival

time of 15 months, the median symptom free survival was 10 months.

#### Conclusion

Short-course accelerated radiotherapy in palliative setting of non-melanoma skin cancers is effective in terms of symptom relief and well tolerated even in elderly patients. High doses seem to be more effective in terms of response rate against a reasonable toxicity profile.

#### EP-1646 Radiation Oncology for the Older Person: Defining international standards for trainee education

L. Morris<sup>1,2</sup>, S. Turner<sup>1</sup>, N. Thiruthaneeswaran<sup>3</sup>, A. O'Donovan<sup>4</sup>, M. Agar<sup>2</sup>, R. Simcock<sup>5</sup>

<sup>1</sup>Crown Princess Mary Cancer Centre, Radiation Oncology, Westmead, Australia ; <sup>2</sup>IMPACCT Centre Improving Palliative- Chronic and Aged Care through Clinical Research and Translation, University of Technology Sydney, Sydney, Australia ; <sup>3</sup>University of Manchester, Manchester Academic Health Science Centre, Manchester, United Kingdom ; <sup>4</sup>Applied Radiation Therapy Trinity, Trinity College Dublin, Dublin, Ireland ; <sup>5</sup>Brighton and Sussex University Hospitals NHS Trust Department, Sussex Cancer Centre, Sussex, United Kingdom

#### Purpose or Objective

To define an internationally applicable geriatric radiation oncology curriculum competency set for radiation and clinical oncology training. The purpose of developing a curriculum in geriatric radiation oncology is to address the gap in education in this increasingly important area of oncology practice.

#### Material and Methods

Stage 1 (completed): An Expert Reference Panel comprised of inter-professional experts in geriatric and radiation oncology was formed. Members of the panel performed an initial needs assessment by reviewing the literature. The candidate competency set was then developed via a comprehensive review of geriatric oncology literature, related international guidelines and consultation with international experts. Items were grouped into key learning themes.

Stage 2 (results pending): A modified Delphi Consensus methodology will be employed to further refine the ideal geriatric oncology competency set for radiation and clinical oncology trainees worldwide. Two formal Delphi rounds delivered online will be conducted with an intervening Expert Reference Panel Round (n = 9). Participants (n = 40) will review and rank potential curriculum competencies as well as providing free text comments.

Medical specialists looking after elderly patients from radiation oncology, geriatrics, surgery, medical oncology and palliative care will be invited to participate, as well as radiation and clinical oncology trainees, radiation therapists, specialist nurses and consumers. Rounds will commence in November 2018.

Geographic spread of participants aims at widespread relevance of the final competency set. This study is an international collaboration supported by the Global Radiation Oncology Collaboration in Education in conjunction with the Faculty of Radiation Oncology (RANZCR) and the UK Macmillan ER (Expert Reference Group) for the Older Person with Cancer.

#### Results

Stage 1: The Expert Reference Panel identified 70 potential knowledge & skill-based 'candidate' competencies across 12 domains. Concepts range from the epidemiology and biology of ageing and cancer, general geriatric medicine, geriatric assessment in oncology, approaches to planning and delivery of radiation therapy in the older person with cancer and special considerations regarding the role of systemic therapy, surgery and palliative care. Skills in communication, research, education and health advocacy are also included.

Stage 2: Modified expert Delphi Consensus results are pending. **Conclusion**

Development of the first international dedicated geriatric radiation oncology curriculum is underway. This educational framework will support radiation oncology training bodies around the world in ensuring future radiation and clinical oncologists are able to provide high quality and appropriate care to the rapidly increasing numbers of elderly people with cancer.

#### EP-1647 Neoadjuvant chemoradiotherapy in elderly rectal cancer patients in a mono-institutional experience

L. Gasparini<sup>1</sup>, C. Rosa<sup>1</sup>, S. Di Biase<sup>1</sup>, C. Di Carlo<sup>1</sup>, A. Allajbej<sup>1</sup>, F. Patani<sup>1</sup>, D. Fasciolo<sup>1</sup>, A. Porreca<sup>2</sup>, M. Di Nicola<sup>2</sup>, L. Caravatta<sup>1</sup>, D. Genovesi<sup>1</sup>  
<sup>1</sup>SS. Annunziata Hospital- "G. D'Annunzio" University, Department of Radiation Oncology-, Chieti, Italy ; <sup>2</sup>"G. D'Annunzio" University, Laboratorio di Biostatistica-Dipartimento di Scienze Biomediche, Chieti, Italy

#### Purpose or Objective

Colorectal cancer affects similarly both young and elderly patients. The improving mean life expectancy increases the number of rectal cancer patients in good performance status (PS), permitting to achieve a curative intent. Furthermore, modern radiotherapy (RT) allows a better coverage to the tumor, preserving the adjacent organs at risk, decreasing acute and late toxicities. The aim of this study was to evaluate the impact of neoadjuvant chemoradiotherapy (CRT) in elderly patients.

#### Material and Methods

Between 2000 and 2018, 117 (M:80;W:37) locally advanced rectal cancer patients, with  $\geq 70$  years, were treated in our Radiotherapy Department and retrospectively analysed. They received concurrent fluoropyrimidine based chemotherapy. RT was performed by 3D conformal technique, with a dose of 4500 cGy, on the pelvic nodes, followed by a sequential boost or a concomitant boost. Mandard tumor regression grade (TRG) score was used to evaluate the pathologic response. The evaluation of anal sphincter function was obtained according to the Memorial Sloan-Kettering Cancer Center (MSKCC) score. Acute and late toxicities were assessed using the Radiation Therapy Oncology Group (RTOG) scale and the RTOG/European Organization for Research and Treatment of Cancer (EORTC) late radiation scoring system. The 3-year and 5-year local control (LC), disease-free survival (DFS) and overall survival (OS) rates were calculated using the Kaplan-Meier method.

#### Results

Median follow-up was 45 months (range:1-163). The median age was 75 (range: 70-88). One hundred and three (88%) patients had ECOG PS 0. Sixty (51.3%) patients were staged as T3-T4 and/or N+. Eighty-three (70.9%) patients were treated with a sequential boost, with a total dose of 5040 cGy, whereas 34 (29.1%) received a concomitant boost of 1000 cGy (100 cGy/die, 2 times/week, total dose 5500 cGy). A pathological complete response (TRG 1) was obtained in 23 patients (19.7%). Acute toxicities were reported in Table 1. Twenty-four patients (20.5%) were lost to the follow-up. Ninety-four (80.3%) patients were evaluated for late toxicities. Overall sphincter function resulted excellent in 23 (24.5%) patients, good in 3 (3.2%), fair in 6 (6.4%) and poor (incontinence) in 11 (11.7%) patients. Twenty-three (24.5%) patients presented stoma. One patient presented late skin toxicity  $\geq G3$  and 2 late GI toxicity  $\geq G3$ . The 3-year DFS and OS rates were  $82.8\pm 4.2\%$  and  $86.5\pm 3.8\%$ , respectively. The 5-year LC, DFS and OS rates were  $89.5\pm 3.9\%$ ,  $73.3\pm 5.2\%$  and  $78.1\pm 5.0\%$ , respectively.

Table 1. Acute Toxicities

Acute Toxicities	G0	G1	G2	G3
Skin Toxicity	63 (53.8%)	22 (18.8%)	31 (26.5%)	1 (0.9%)
GI Toxicity	37 (31.6%)	39 (33.3%)	39 (33.3%)	2 (1.8%)
GU Toxicity	88 (75.2%)	26 (22.2%)	3 (2.6%)	0 (0%)
Hematologic Toxicity	94 (80.4%)	10 (8.5%)	10 (8.5%)	3 (2.6%)

#### Conclusion

Our results reported good tolerability, in terms of acute and late toxicities and clinical outcomes, of neoadjuvant CRT in patients 70 years. Based on our analyses, elderly patients with good PS can be also considered to be treated with a concomitant boost intensification in presence of very unfavourable prognostic factors.

#### EP-1648 Radio-chemotherapy with temozolomide in elderly patients with glioblastoma: our experience

A. Molinari<sup>1</sup>, F. Pasqualetti<sup>1</sup>, A. Gonnelli<sup>1</sup>, M. Cantarella<sup>2</sup>, S. Montrone<sup>1</sup>, F. Paleari<sup>1</sup>  
<sup>1</sup>University Hospital of Pisa, Radiotherapy Unit, Pisa, Italy ; <sup>2</sup>Casa di Cura San Rossore, Radiotherapy, Pisa, Italy

#### Purpose or Objective

Glioblastoma multiforme (GBM) is the most aggressive brain tumor in adults and the second most common brain cancer after meningioma with a peak of incidence on the fifty decades of life. Due to the progressive ageing of the developed country population, more than a half of new cases occurs in patients older than 65 years. The aim of the present study was to evaluate the clinical outcome of radio-chemotherapy with temozolomide in patients with glioblastoma aged more than 65 years.

#### Material and Methods

Sixty-three patients treated with radiotherapy and chemotherapy at Pisa University Hospital between September 2004 and November 2017 were enrolled in this retrospective analysis. All patients had a proven diagnosis of glioblastoma grade IV WHO, ECOG PS 0-2, age  $\geq 65$ . Radiotherapy was delivered in daily fractions of 2 Gy given 5 days per week for 6 weeks, for a total of 60 Gy. During radiotherapy, temozolomide was administered at a dose of 75 mg per square meter of body-surface area per day from the first to the last day of radiotherapy. 5-6 weeks after the end of radiotherapy, adjuvant temozolomide was administered at 150-200 mg per square meter for five consecutive days, every 28 days. A maximum of 12 cycles were prescribed if MRI showed no disease progression and temozolomide was well tolerated.

#### Results

Data analysis was performed in April 2018. The present study was performed in 37 male and 26 female patients with a median age at diagnosis of 72,5 years (range=65-89). Fifty-seven patients underwent surgical resection, four patients stereotactic diagnostic biopsy, two patients had a radiologic diagnosis only. During follow up, we recorded 46 cases of disease progression with a median progression-free survival (PFS) of 12 months (range 1-88 months). Median overall survival (OS) were 25 months (range 1-107 months); at data analysis, 65 patients were died. After disease recurrence, based on ECOG, tumor burden and age, patients were treated with surgery (15 cases), chemotherapy (30 cases) and re-irradiation (11 cases).

#### Conclusion

In our experience, progression free survival and overall survival were similar to those reported in literature for younger patients. We think that radiochemotherapy is a good option for older patients with a good performance status in glioblastoma treatment.

### EP-1649 Patterns of care and survival in elderly patients with advanced soft-tissue sarcoma

D. Greto<sup>1</sup>, S. Calogero<sup>2</sup>, M. Lo Russo<sup>1</sup>, D. Pezzulla<sup>1</sup>, M. Loi<sup>1</sup>, M.A. Teriaca<sup>1</sup>, V. Maragna<sup>1</sup>, S. Lucidi<sup>1</sup>, D.A. Campanacci<sup>3</sup>, G. Beltrami<sup>3</sup>, G. Scocianti<sup>3</sup>, L. Livi<sup>1</sup>

<sup>1</sup>University of Florence-Azienda Ospedaliera Universitaria Careggi AOUC, Department of Biomedical-Experimental- and Clinical Sciences, Firenze, Italy ;  
<sup>2</sup>Molecular and Nutritional Epidemiology Unit, Cancer Research and Prevention Institute ISPO, Florence, Italy ;  
<sup>3</sup>University of Florence-Azienda Ospedaliera Universitaria Careggi AOUC, Department of Orthopaedic Oncology and Reconstructive Surgery, Firenze, Italy

#### Purpose or Objective

Elderly people represent more than 50% of sarcoma patients and they often present many differences compared to younger patients. In fact, older patients experience increased cancer-related morbidity and mortality compared to younger patients: this is shown in several studies pointing out that older age is associated to poorer outcomes. Nowadays, there are no data regarding the management of advanced soft-tissue sarcoma (STS) in elderly patients. The aim of this study is to analyze clinical outcome and treatment related toxicity of elderly STS patients in a single Institution.

#### Material and Methods

We retrospectively collected data of patients  $\geq 65$  years old diagnosed with localized advanced STS between 1998 and 2017 in a single institution.

#### Results

The study included 111 patients. Mean Charlson Index was 7.5 (2-12). One hundred five (94.6%) patients underwent surgery, ninety-one patients (82%) received radiotherapy, 23 (20.7%) patients received concurrent radiochemotherapy and 20 (18.1%) patients received chemotherapy alone. Grade  $>3$  acute skin toxicity was recorded in 38 (52.8%) patients out of 72 patients who received postoperative radiotherapy, age  $> 80$  years correlated with higher incidence of toxicity compared to younger patients (63.6% vs 33.3%,  $p=0.02$ ). Late fibrosis, late edema and joint stiffness occurred in 10.4%, 11.8% and 4% of patients, respectively. Age did not correlate to late toxicity incidence. At a mean follow up of 4.1 years (0.1-17.7) twenty-four (22%) patients recurred, 3- and 5-year local recurrence free survival was 80.3% and 75.7%, respectively. At statistical analysis no treatments and patients characteristics affected local recurrence. Fifty-five (52.9%) patients developed distant metastasis, 3- and 5-year distant metastasis free survival (DMFS) was 59.6% and 44.6%, respectively. At univariate analysis no delivered of adjuvant radiotherapy and no surgery correlated with higher local recurrence ( $p=0.043$  and  $p=0.002$ ). On multivariate analysis, undifferentiated pleomorphic sarcoma histology was the only independent factors associated with DMFS ( $p=0.026$ ). Overall survival (OS) was 62% and 46.6% at 3 and 5 years, respectively. On multivariate analysis, surgery was the only independent factor associated with OS ( $p=0.006$ ).

#### Conclusion

Older patients have worse outcomes because they tend to present with worse tumors and are treated less aggressively. In this study elderly STS patients were treated with a tailored treatment comprising surgery, radiotherapy and/or chemotherapy resulted in a good efficacy and safe.

### EP-1650 Elderly glioblastoma patients:role of multidimensional assessment of frailty in predicting outcomes

L. Giaccherini<sup>1</sup>, P. Ciammella<sup>1</sup>, M. Galaverni<sup>1</sup>, M. Manicone<sup>1</sup>, I. Renna<sup>1</sup>, M. Galeandro<sup>1</sup>, G. Timon<sup>1</sup>, F. Bellafiore<sup>1</sup>, D. Ramundo<sup>1</sup>, F. Vigo<sup>1</sup>, A. Rosca<sup>1</sup>, T. Palmieri<sup>1</sup>, M.P. Ruggieri<sup>1</sup>, A. Botti<sup>2</sup>, R. Sghedoni<sup>2</sup>, E. Cagni<sup>2</sup>, M. Orlandi<sup>2</sup>, M. Iori<sup>2</sup>, M. Russo<sup>3</sup>, C. Iotti<sup>1</sup>

<sup>1</sup>Radiation Oncology Unit, Azienda USL-IRCCS di Reggio Emilia, Reggio Emilia, Italy ; <sup>2</sup>Medical Physics Unit, Azienda USL-IRCCS di Reggio Emilia, Reggio Emilia, Italy ; <sup>3</sup>Clinical Neurology, Azienda USL-IRCCS di Reggio Emilia, Reggio Emilia, Italy

#### Purpose or Objective

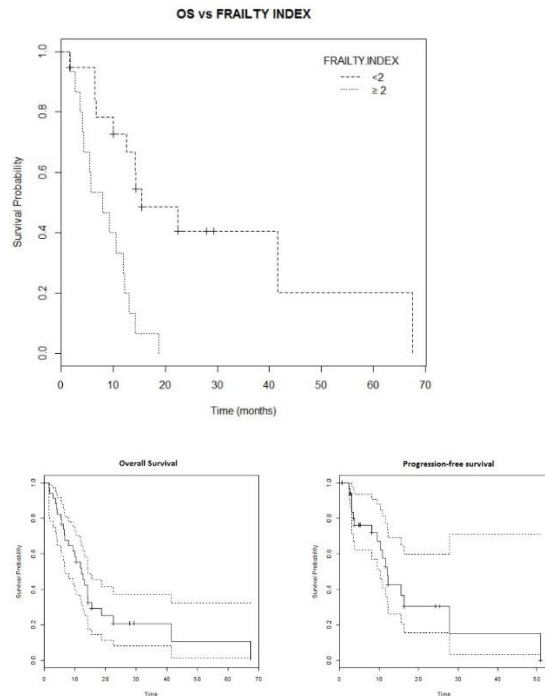
To evaluate the impact of comorbidities, clinical and biological factors on outcomes in elderly glioblastoma (GBM) patients (pts) treated with surgery followed by concurrent radiation (RT) and Temozolomide (TMZ).

#### Material and Methods

Elderly pts with GBM treated from January 2013 to December 2017 were included in the study. We collected data regarding age, extension of surgery, use of current medications, Karnofsky Performance Status (KPS), presenting symptoms, Prognostic Nutritional Index (PNI), Charlson Co-morbidity Index (CCI) and Frailty Index (FI). All of these parameters, measured before the start of RT-TMZ, were linked to clinical outcomes.

#### Results

Thirty four pts (male/female: 23/11; median age: 70 years), were retrospectively analysed. After a median follow-up of 9.7 months (range 2.0 - 30.6), the median OS was 12.1 months (range 6.7-14.3), and 1-year OS was 50% (range 31-64%). Median PFS was 12.1 months (range 10.3 + NA), 1-year PFS was 48% (range 30-73%). Four pts (11,76%) experienced G1-2 neurological symptoms during RT. No pts showed G3 events. At univariate analysis high KPS and total surgery were significantly associated with better OS ( $p=0.0339$  and  $p=0.00782$ ) and only the type of surgery with PFS ( $p=0.0182$ ). Using log rank test we identified as the optimal PNI cut-off level the value of 42; the best cut-off value of CCI was 2 for OS and 3 for PFS. Univariate analysis showed that 14 pts with a PNI  $< 42$  had a median survival of 13.10 months versus 8.38 months for those pts with a PNI  $\geq 42$  ( $p=0.63$ ). The 1 year OS rate for pts with a PNI  $< 42$  was 25% while the corresponding value for pts with PNI  $> 42$  was 54%. Univariate analysis showed that pts with a CCI  $>2$  had a median OS of 8 months versus 14.2 months for pts with CCI  $<2$  ( $p= 0.076$ ). The 1-year OS rate was 33% and 54% for pts with CCI  $<2$  and  $\geq 2$ , respectively. Pts with CCI  $\geq 3$  showed a median PFS of 5.9 months versus 12.3 months for those with CCI  $<3$  ( $p=0.0113$ ). The 1-year PFS rate for pts with a CCI  $<3$  was 52%, while no pts with CCI  $> 3$  was alive at one year. At the multivariate analysis FI alone remained significant in predicting OS: presenting with a FI  $>2$  compared with FI  $<2$  was significantly associated with an increased risk of death [( $p= 0.023$ , HR = 3.330 (1.96 - 5.66)]. At multivariate analysis KPS, type of surgery and FI remained a significant predictors of OS and, based on these parameters, we generated a prognostic score that, dividing pts into three risk categories, has proven to be a survival predictor, with an increase of the risk of death by 2.2 times for each increment of the score (HR 2.2,  $p=0.0004$ ).



### Conclusion

The appropriate management of elderly cancer pts with GBM is an important concern in oncology. Our data suggest that in elderly pts in good clinical conditions and with a low FI score, extensive surgery, when feasible without adding neurological impairment, followed by adjuvant RT-TMZ, should be considered.

### EP-1651 Geriatric oncology for decision-making in women over 75 years with breast cancer

M.D. De las Peñas-Cabrera<sup>1</sup>, J. Martínez Peromínguez<sup>2</sup>, P.M. Samper Ots<sup>1</sup>, E. Amaya Escobar<sup>1</sup>, M. Hernández Miguel<sup>1</sup>, C. Oñoro Algar<sup>2</sup>, M.E. Baeza Monedero<sup>2</sup>, C. González de Villambrosia<sup>2</sup>, J. Zapatero Ortuño<sup>1</sup>, S. Hoyos Simón<sup>3</sup>, M.R. Noguero Meseguer<sup>4</sup>, E. Abreu Griego<sup>4</sup>, M. De Matias Martínez<sup>4</sup>, R. Fernández Huertas<sup>4</sup>, A.B. Cuesta Cuesta<sup>4</sup>  
<sup>1</sup>Hospital Rey Juan Carlos, Radiation Oncology, Mostoles - Madrid, Spain ; <sup>2</sup>Hospital Rey Juan Carlos, Geriatric Oncology, Mostoles - Madrid, Spain ; <sup>3</sup>Hospital Rey Juan Carlos, Clinical Oncologist, Mostoles - Madrid, Spain ; <sup>4</sup>Hospital Rey Juan Carlos, Oncology Gynecology, Mostoles - Madrid, Spain

### Purpose or Objective

Geriatric Oncology Unit helps us to make oncological decision making, through a Comprehensive Geriatric Assessment (CGA). The objective of the present study is to describe how our patients are categorized, decisions made and the impact on oncological treatments.

### Material and Methods

It's a retrospective study on data prospectively recorded. From January 2017 to September 2018, 114 oncology patients, older than 75 years, were diagnosed in the University Hospital Rey Juan Carlos, Mostoles, Spain. Of them 42 patients (37.5%, 42/112) had breast cancer. All of them received a Comprehensive Geriatric Assessment. Data are shown as number and percentages and chi-squared was used for comparisons.

### Results

Age was  $83.90 \pm 4.83$  (range 75-94). Histology was invasive ductal carcinoma 81.0% (34/42). Immunophenotype was: Luminal A and B in 28 cases, 66.6%. Clinical stages were: I-II in 28 cases and IV, only in 11.9%. Comprehensive Geriatric Assessment was as follows: **Functional reservation**, with Barthel scale, only 31% were

independent; minor dependents, 31%. A high comorbidity according to Charlson score: 47.6% was present. **Polypharmacy** (> 5 drugs), was present in 64.3%. According to **Frail Frailty Questionnaire**: Non fragile 64.3% and fragile 35.7%. The **SPPB**: serious limitation, 33.3% Criteria for malnutrition according to the **MNA scale**: 54.8%, normal nutritional status; risk of malnutrition 40.5% and were only malnutrition 4.8%. And according to the body mass index, normal 42.9%. The presence of cognitive impairment on the **Pfeiffer scale**: normal were 54.8% and severe only 5 patients, 11.9%. Classification of patients, clinical decisions and main outcomes according to CGA were: **Robust**: 35.7% (15/42), decided: Endocrine therapy (ET): 40%, alive with disease. All of patients, were Luminal A or B. Full-oncological treatment: 60% (Surgery+/-CT+/-RT), alive without disease. Of them, 44.44%, (4/9) were triple negatives. One patient received chemotherapy neoadjuvant and 3, surgery was initial treatment. **Frail patients**: 50% patients, Refused[CdS1] treatment[B2] , 23.8%. Of them, 80% were triple negatives ET: 42.85%, alive with disease. **Bad prognostic patients**: 28.57%, of them, refused treatment 1 patient, 16.6%, palliative treatment with ET, 66.66%. The period of **follow up** was  $19.43 \pm 26.09$  months (Range 0.10-129.97). The 54.66% (23/42) were alive with disease. After the recommendation of the CGA, the proportion of patients in whom a curative treatment was decided was higher in the group of robust patients. This difference was statistically significant ( $p = 0.03$ ) when comparing robust patients with both poor prognosis and fragile groups considering these together.

### Conclusion

The CGA, the Immunophenotype and the participation of the patient and their families were determinants of the oncological treatment decision. Exclusive endocrine therapy was the most recommended treatment, in 45.23%. Comprehensive Oncogeriatric Assessment allows oncological treatments to be personalized without reducing the quality of life.

### EP-1652 Stability and survival of elderly patients after palliative radiotherapy of spinal bone metastases

T. Bostel<sup>1,2,3</sup>, R. Förster<sup>1,4</sup>, I. Schlamp<sup>1</sup>, T. Sprave<sup>1</sup>, S. Akkaba<sup>1</sup>, D. Wollschläger<sup>5</sup>, J. Debus<sup>1,3</sup>, H. Schmidberger<sup>2</sup>, H. Rief<sup>1</sup>, N.H. Nicolay<sup>1,3,6</sup>

<sup>1</sup>University Hospital of Heidelberg, Radiation Oncology, Heidelberg, Germany ; <sup>2</sup>University Medical Center Mainz, Radiation Oncology, Mainz, Germany ; <sup>3</sup>German Cancer Research Center DKFZ, Clinical Cooperation Unit Radiation Oncology, Heidelberg, Germany ; <sup>4</sup>University Hospital of Zurich, Radiation Oncology, Zurich, Switzerland ; <sup>5</sup>University Medical Center Mainz, Medical Biostatistics- Epidemiology and Informatics IMBEI, Mainz, Germany ; <sup>6</sup>University Hospital of Freiburg, Radiation Oncology, Freiburg, Germany

### Purpose or Objective

This retrospective study aimed to evaluate the stability of spinal bone metastases (SBM) in elderly patients resulting from various solid tumors following palliative radiotherapy (RT).

### Material and Methods

A total of 322 patients aged at least 70 years received palliative RT at two major University Hospitals. Stability assessment was based on the validated Taneichi score based on CT-imaging acquired prior to RT as well as at 3 and 6 months after RT. Furthermore, the survival time after RT (bone survival, BS) and prognostic factors for stability and survival were assessed.

### Results

Prior to RT, 183 patients (57%) exhibited unstable SBM. Among the surviving patients, significant re-calcification and stabilization were evident in 19% (23/118) and 40% (31/78) at the follow-up examinations at 3 and 6 months after RT. In breast cancer patients, the stabilization rates

were significantly higher than in patients with SBM derived from other histologies such as lung cancer, malignant melanoma or urothelial cancer. The median survival time and 6-months-survival rates following RT were 5.4 months (95% CL 4.4 - 7.2 months) and 48%, respectively. To predict BS, the Karnofsky performance status (KPS) was the strongest predictive factor in our study; further statistically significant factors were the application of chemotherapy, number of SBM and primary tumor classification.

#### Conclusion

Prognostic assessment of elderly patients with SBM should be at least based on the primary tumor classification and the KPS. In the event of palliative RT, more hypofractionated radiation schedules are advisable for patients with a very poor prognosis to reduce hospitalization times and to maintain the residual quality of life.

---

#### Electronic Poster: Clinical track: Health services research / health economics

---

#### EP-1653 Evaluation of Italian Radiotherapy research: preliminary analysis

A. Fiorentino<sup>1</sup>, R. Mazzola<sup>2</sup>, V. Lancellotta<sup>3</sup>, S. Saldi<sup>3</sup>, S. Chierchini<sup>3</sup>, A.R. Alitto<sup>4</sup>, P. Borghetti<sup>5</sup>, F. Gregucci<sup>2</sup>, M. Fiore<sup>6</sup>, I. Desideri<sup>7</sup>, L. Marino<sup>8</sup>, D. Greto<sup>7</sup>  
<sup>1</sup>General regional Hospital "F. Miulli", Radiation Oncology Department, Acquaviva delle fonti BA, Italy ; <sup>2</sup>Ospedale Sacro Cuore Don Calabria, Radiation Oncology, Negrar, Italy ; <sup>3</sup>University of Perugia, Radiation Oncology, Perugia, Italy ; <sup>4</sup>Fondazione Policlinico Universitario A. Gemelli IRCCS, Radiation Oncology, Roma, Italy ; <sup>5</sup>University and Spedali Civili, Radiation Oncology, Brescia, Italy ; <sup>6</sup>Campus Bio-Medico University, Radiation Oncology, Rome, Italy ; <sup>7</sup>University of Florence, Radiation Oncology, Firenze, Italy ; <sup>8</sup>REM- Viagrande, radiation Oncology, Catania, Italy

#### Purpose or Objective

The difficulty in conducting meaningful clinical research is a multifactorial issue, involving political, financial and cultural problems, which can lead to unexpected negative long-term consequences, in terms of knowledge advancement and impact on patient care. Aims of the present review were to evaluate the publications of Italian Radiotherapy (RT) groups during a 20-year period and to verify if research is still appealing to young radiation oncologists (RO) in Italy.

#### Material and Methods

PubMed database was searched for English-language articles published by Italian groups by 2 independent RO, from January 1985 to December 2015 using as keywords "radiotherapy" combined with "Italy" [(radiotherapy) AND (Italy)]. Studies eligible for inclusion in this analysis were: case reports, radiobiological studies, clinical and dosimetric retrospective or prospective studies (Phase I-II-III) in which RT was used, systematic or not reviews and meta-analyses. Exclusion criteria were: study not conducted in Italy, study in which RT was not used or was not investigated, study in which no Italian RO was in the authors list. Analyzed variables were: publication/year, kind of study, geographic area and age of the first Author.

#### Results

The systematic review identified 3291 articles: 1207 papers fulfilled the inclusion criteria. The number of Italian published papers increased during the examined period. Retrospective analyses, prospective Phase I-II trials and literature reviews were 44%, 20% and 14.5% of all published manuscripts, respectively. Randomized trials showed a mild increase from 2000 to 2005, but their absolute number remained low respect to other type of

studies (4%). Northern Italy produced the very most of Italian research papers (58.7%). The age of the first/second Author was evaluated on 716 papers: in more than 50% of cases, the first author was younger than 40.

#### Conclusion

Despite a general gradual improvement, RT clinical research suffers in Italy (as elsewhere) from insufficient funding, with a negative impact on evidence production. It is worth noticing that clinical research is still appealing and accessible to junior Italian RO.

#### EP-1654 Hypofractionation in breast cancer: possible advantages and logistical implications

I. Meaglia<sup>1</sup>, M. Paolini<sup>1</sup>, C. Bocci<sup>1</sup>, G.B. Ivaldi<sup>1</sup>, M. Liotta<sup>2</sup>, P. Tabarelli de Fatis<sup>2</sup>

<sup>1</sup>ICS Maugeri Società Benefit SpA, Servizio di Radioterapia, Pavia, Italy ; <sup>2</sup>ICS Maugeri Società Benefit Spa, Servizio di Fisica Sanitaria, Pavia, Italy

#### Purpose or Objective

In the last three decades, hypofractionation has been an interesting and promising field of investigation. The primary and most important benefit of treating, for instance, breast and prostate cancer with a hypofractionated regimen is the improved therapeutic index that can be obtained; moreover, there are other advantages in terms of logistics, patient convenience and resource allocation. Here, we present our speculations about a routinely use of a hypofractionated regimen in breast after conserving surgery, and how its introduction in our Department has had an impact on our waiting list.

#### Material and Methods

From 2010 to 2017 we used a hypofractionated regimen of 20 fractions, 5 fractions a week, with a weekly concomitant boost. In February 2018, we started a new 15 fractions regimen (5 fractions a week, and weekly concomitant boost), reducing overall treatment time to 3 weeks. In both cases the weekly concomitant boost follows whole breast irradiation immediately. Considering that we scheduled to keep 13 daily slot for breast radiotherapy in a dedicated linear accelerator, we estimated how many patients could be treated with the 15 fractions regimen in one year, assuming 250 working days. Then, we calculated the expected reimbursement (according to the current rates used in the Lombardy social reimbursement based Health System) and compared with the old 20 fractions schedule. We also checked if our waiting list changed during the six months since the introduction of the new fractionation regimen, comparing with historic data from our scheduling activity.

#### Results

In one year we estimate to treat 217 patients using the 15 fractions schedule compared to 162 patients that can be irradiated with the 20 fractions regimen in the same time. The expected reimbursement for each patient is 3200 euro for the 20 fractions schedule and 2750 for the 15 fractions regimen. With almost the same number of daily treatments performed, in the first 6 months of the 15 fractions schedule, we registered an average waiting time to start radiotherapy ranging from 16,3 to 30,1 days (median 24 days) for breast cancer patients. Previously, these patients had to wait at least one month in most of the cases (range: 24,6 - 37,5 days, median 29 days). The introduction of the 15 fractions regimen also affected the waiting list for other clinical scenario such as palliative treatments: in 2016 we calculated an average waiting time of 20,2 days (more than twice than the 10 days suggested by ISTISAN). From February to July 2018 palliative patients had a waiting time less than 10 days for 3 out of 6 months.

#### Conclusion

A hypofractionated regimen allows to treat more patients in the same interval of time with a reduction of the cost for each treatment. The potential increase in number of treated patients can affect the waiting list in a positive

way. These improvements should be additional justification for clinical implementation.

#### EP-1655 Cost-effectiveness analysis of stereotactic radiotherapy in colorectal cancer brain metastases

A. Paix<sup>1</sup>, F. Thillays<sup>2</sup>, J. Biau<sup>3</sup>, N. Vulquin<sup>4</sup>, I. Pop<sup>5</sup>, K. Debbi<sup>6</sup>, A.L. Grosu<sup>5</sup>, E.A. Sauleau<sup>7</sup>, G. Noël<sup>1</sup>

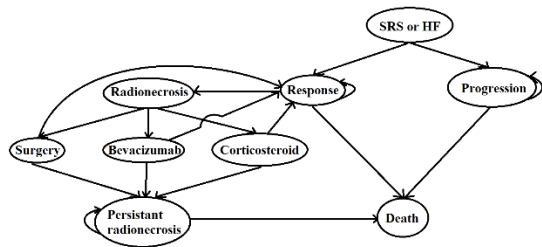
<sup>1</sup>Centre Paul Strauss, Radiothérapie, Strasbourg, France ; <sup>2</sup>Institut Cancérologique de l'ouest, Radiothérapie, Saint Herblain, France ; <sup>3</sup>Centre Jean Perrin, Radiothérapie, Clermont-Ferrand, France ; <sup>4</sup>Centre Georges-François Leclerc, Radiothérapie, Dijon, France ; <sup>5</sup>Universitätsklinikum Freiburg, Klinik für Strahlenheilkunde, Freiburg, Germany ; <sup>6</sup>Centre Henry Kaplan - CHU Tours, Radiothérapie, Tours, France ; <sup>7</sup>CHU Strasbourg, Methodological and clinical research group, Strasbourg, France

#### Purpose or Objective

Colorectal cancer (CRC) is the third most common cancer in developed countries and brain metastases only occur in 1% of CRC patients, however this rate is likely to raise due to the increase of the overall survival as new systemic drugs became available. Stereotactic radiosurgery (SRS) and hypofractionated stereotactic radiotherapy (HFSRT) are treatment options. We developed a Markov model to evaluate the cost-effectiveness of SRS and HFSRT in patients with CRC brain metastases.

#### Material and Methods

We designed a Markov model, reported Figure 1, to simulate the clinical trajectory of a patient with a single CRC brain metastasis using data retrospectively collected in 6 hospitals in France and Germany.

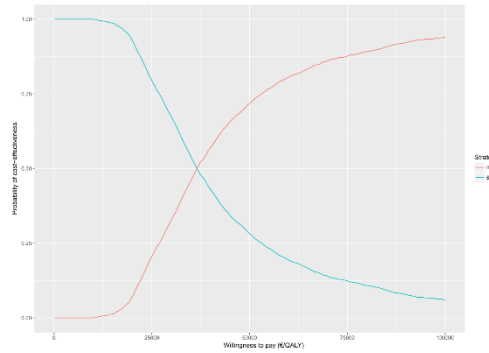


This analysis was conducted in a French payer perspective on a lifetime horizon. Utility values, recurrence risks, and costs were adapted from the literature. Deterministic (DSA) and probabilistic (PSA) sensitivity analyses were performed to assess the influence of the assumptions made.

#### Results

In the base case analysis, SRS and HFSRT total costs were 4,404.76€, and 5,921.34€ and the quality-adjusted life expectancies were 1.2545 and 1.2589.

In the probabilistic sensitivity analysis, SRS and HFSRT were associated with a mean total cost of 4,407.80 € and 5,817.33€, and quality-adjusted life expectancies 1.2597 and 1.2987 QALYs, respectively. SRS appeared to be 1,409.53€ cheaper than HFSRT with a decrease of quality-adjusted life expectancy of 0.039 QALYs. HFSRT had a probability of cost-effectiveness for the willingness-to-pay threshold of 30,000€ and 100,000€ of 33.2% and 94% respectively, as reported on the acceptability curves in Figure 2.



#### Conclusion

This is the first medico-economic evaluation of SRS and HFSRT in CRC brain metastases, and its results suggest that HFSRT is cost-effective compared to SRS, in the French payer perspective.

#### EP-1656 Prevention of heterotopic ossification after total hip replacement: a cost-effectiveness analysis

A. Paix<sup>1</sup>, T. Stévignon<sup>2</sup>, N. Baudrier<sup>3</sup>, G. Noël<sup>1</sup>

<sup>1</sup>Centre Paul Strauss, Radiothérapie, Strasbourg, France ; <sup>2</sup>Hôpital Saint Joseph, Orthopedic surgery, Paris, France ; <sup>3</sup>Centre chirurgical Emile Gallé, Orthopedic surgery, Nancy, France

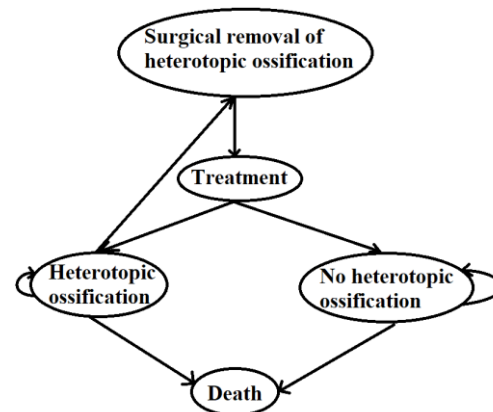
#### Purpose or Objective

Heterotopic ossifications (HO) following total hip replacement can severely impact the quality of life of patients. While there are no guidelines for HO prophylaxis, non-steroidal anti-inflammatory drugs (NSAIDs) are widely used. However, radiotherapy delivered in a single fraction has also proven its efficacy.

We conducted a medico-economic evaluation of NSAIDs and radiotherapy in the prevention of HO following total hip replacement.

#### Material and Methods

We designed a Markov model to simulate the clinical trajectory of a patient at risk for HO following total hip replacement. Two prevention strategies were compared: 3 x 25 mg per day for three weeks and a single radiation dose of 7 Gy. Patients treated with NSAIDs could experience upper digestive bleeding. In both cases, HO could occur despite prophylaxis and be treated with painkiller and physical therapy or surgery.



Our study was conducted from a French payer perspective, using payment data applicable in public hospitals in 2017. All the costs used are expressed in 2017 euros, and costs and Quality Adjusted Life Years (QALYs) were discounted at an annual rate of 4%.

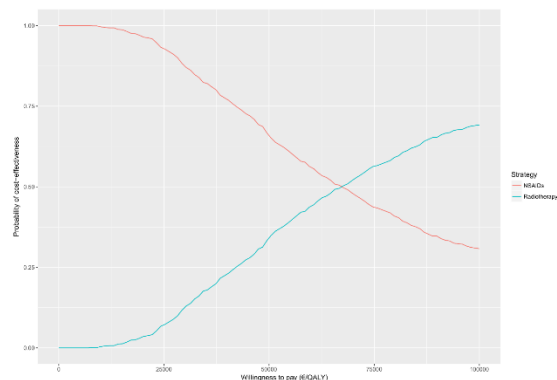
## Results

In the base case analysis total cost for the NSAIDs and the radiotherapy, strategies were 258.81€ and 702.01€ respectively. Utilities for the NSAIDs and radiotherapy strategies were 12.42332 QALY and 12.43608 QALY respectively. The ICER of radiotherapy compared to NSAIDs was 65,545€/QALY.

The deterministic sensitivity analysis reveals that the incremental cost-effectiveness ratio (ICER) is mainly sensitive to the probability of surgery in case of HO, to the relative risk of HO between NSAIDs and radiotherapy, to the probability of HO following radiotherapy, to the probability of upper digestive bleeding for NSAIDs and to the cost of surgery in case of HO.

In the probabilistic sensitivity analysis, the total cost for the NSAIDs and the radiotherapy strategies were 356.87€ and 777.36€ respectively. The utilities related to the NSAIDs and radiotherapy strategies were 14.58905 QALY and 14.59614 QALY respectively. The ICER of radiotherapy compared to NSAIDs was 59,286.17€/QALY. Most of the simulations were in the north-east quarter.

For a willingness to pay threshold of 30,000€/QALY, and 100,000€/QALY, the probability of cost-effectiveness of NSAIDs was 87.3%, and 30.8% respectively.



## Conclusion

We report the results of the first medico-economics evaluation of NSAIDs and radiotherapy in HO prophylaxis. Our analysis suggests that from a French payer perspective, radiotherapy is cost-effective for HO prophylaxis following total hip replacement.

### EP-1657 Overcoming appointment delay in radiotherapy: a single institution experience

M. Ait Erraïsse<sup>1</sup>, O. Masbah<sup>1</sup>, T. Bouhafa<sup>1</sup>, K. Hassouni<sup>1</sup>  
<sup>1</sup>CHU Hassan II, Radiothérapie, Fez, Morocco

#### Purpose or Objective

Delay to access to radiation therapy in developing countries is challenging and compromising the cancer prognosis. In our department there was one linear accelerator for a whole region in the country. 50 to 60 patient a day were treated and appointments were for more than 3 months. The medical and psychological impact on patients was important. Our objective was to shorten this delay.

#### Material and Methods

The radiotherapy department goal was to treat 50 to 60 patients from Monday to Friday as the majority of radiation therapy departments. Treatments started at 8 AM to finish at about 7 to 8 PM. The idea was to treat more patients and efficiently. Therefore, actions were taken on three axes : 1st Before radiotherapy, we had to shorten the time from first consultation to first radiotherapy fraction. 2nd during radiation, we extended treatment period to above 8 PM. and 3rd axis concerns fractionation regimens.

## Results

The hospital executive decided to transform the oncology hospital to an emergency hospital with the possibility to treat 24/7. In this way, we could treat up to 100 patient a day or more. we also treat on weekends especially palliative patients. Concerning the patient workflow, patients were seen immediately when they arrive at the department, and if medical file is complete and ready to radiation, CT scan simulation was done within a week, countouring, dosimetry, and validation with safety checks were done within 3 days. and finally, when possible, we chose hypo-fractionated regimens (Breast, rectum, single fraction for palliative, etc ...).

The appointment time started to drop from more than 3 months to almost 2 weeks.

## Conclusion

In developing countries, access to radiotherapy is a real problem. The number of linear accelerators per capita is very low. Therefore delays are very long. This kind of approach, if sufficient human resources, could solve the problem while waiting for a second and maybe other machines.

### EP-1658 Stereotactic Ablative Body Radiotherapy:UK implementation and current practices.Progress since 2012

G. Distefano<sup>1</sup>, S. Garikipati<sup>2</sup>, H. Grimes<sup>3</sup>, M. Hatton<sup>2</sup>  
<sup>1</sup>University of Surrey, Centre for Vision- Speech and Signal Processing, Guildford, United Kingdom ; <sup>2</sup>Weston Park Hospital, Oncology, Sheffield, United Kingdom ; <sup>3</sup>University College London Hospitals, Radiotherapy Physics, London, United Kingdom

#### Purpose or Objective

In 2012 a UK SABR Consortium survey reviewed the implementation of SABR treatment programmes in the UK, obtaining details of practice and varying techniques used in centres with an active treatment programme, evaluating the workload and assessing projected future provision<sup>1</sup>. A second survey was designed and implemented to update those results aiming to continue to drive forwards techniques, aid standardisation and assist in highlighting issues to be addressed within the NHS to improve access to SABR services and trials in the UK.

#### Material and Methods

An online questionnaire was sent by the UK SABR Consortium to over 65 UK radiotherapy institutions. The questionnaire covered current service provision and collected data on patient numbers, clinical sites, immobilisation, motion management, CT scanning protocols, target and OAR delineation, treatment planning, image-guidance, treatment protocols, QA methods and expected service development over the next couple of years.

#### Results

48 centres responded to the questionnaire. The number of centres with an active SABR program has doubled since 2012 (36 vs 15) with a further 12 centres indicating the intention of starting SABR in the next couple of years. 28 treating centres deliver SABR to non-lung sites, with 17 centres able to offer the range of sites required for treating oligometastatic disease. The number of patients treated has significantly increased since 2012 with 25 centres now treating above the minimum UK recommended level (25 patients per year).

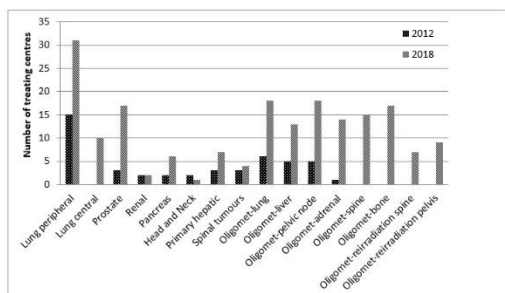


Figure 1: Results from survey in 2012 and 2018 indicating the number of centres treating a variety of sites with an active SABR program.

The survey indicates that treatment techniques remain reasonably standard across the UK with all centres using 4D-CT and 85% delineating their ITV to contain respiratory-induced tumour motion. The most popular immobilisation devices in the UK remain the wing board, vacuum bag and knee support in use by 70% of centres. 90% use inverse planning solutions together with VMAT delivery and > 80% of treating centres are still performing patient specific QA for all patients.

	Mode (2012)	Mode (2018)
4D-CT	30-40mins	50-60mins
Target and OAR delineation	30-60mins	30-60mins
Treatment planning	>91mins	>120mins
Patient-specific plan QA <sup>a</sup>	30-45mins	30-45mins
Daily treatment delivery	21-30mins	Lung 21-30mins Other 31-40mins

Table 1 Summary of the most frequent time at each stage of the SABR process in the UK (<sup>a</sup>quicker if several plans batched together).

Documented changes in practice since 2012 include the development of Linac delivered SABR to non-lung sites and notable increase in number of centres using abdominal compression as part of the immobilisation process (14 vs 2 centres). An increase in time spent at some stages of the SABR process (table 1) was also seen which is likely to be a reflection on the increased complexity of cases treated.

#### Conclusion

The 2018 survey shows a welcome increase in SABR provision across the UK with an ongoing commitment to Quality Assurance within centres. However, with emerging data it is clear that the UK SABR program need to continue its expansion to ensure that patients with oligometastatic disease have access and SABR for early stage lung is deliverable in all centres.

#### Reference

<sup>1</sup> Distefano G, Baker A, Scott AJ, Webster GJ; UK SABR Consortium Quality Assurance Group. Survey of stereotactic ablative body radiotherapy in the UK by the QA group on behalf of the UK SABR Consortium. Br J Radiol. 2014; 87:1037

#### EP-1659 Trends in industry payments to radiation oncologists from 2014-2017

D. Marshall<sup>1</sup>

<sup>1</sup>Mount Sinai Hospital, Radiation Oncology, New York, USA

#### Purpose or Objective

Physician-industry relationships are common and introduce conflicts of interest. This study investigates recent trends in industry payments to radiation oncologists in a population-based national sample.

#### Material and Methods

Open Payments records of general payments to radiation oncologists in the United States were included. We describe the number of payments, total amount of payments and annual percent change over 2014 to

2017. This excludes research payments and ownership interest.

#### Results

Radiation oncologists received 91,804 payments totaling \$25.6 million (USD) over the four-year period, representing 0.31% of payments to oncology specialties (46.4 million payments totaling \$8.3 billion USD). For radiation oncologists, the number of payments grew 6.9% over the period and the total number of payments grew 9.1%, while these numbers decreased by about 1% for all oncology specialties.

#### Conclusion

Industry-physician financial relationships are substantial and have grown over time. Further research is needed to determine the effect of these relationships on physician decision making.

General industry payments to physicians in Open Payments, 2014-2017

Specialty	Measure	Year				Total
		2014	2015	2016	2017	
Radiation oncology	number of payments	18,534	23,329	25,779	24,162	91,804
	total amount (USD)	\$ 4,676,365	\$ 7,228,094	\$ 7,069,081	\$ 6,620,594	\$ 25,594,134
All oncology specialties	number of payments	11,755,185	11,717,589	11,823,905	11,135,359	46,432,038
	total amount (USD)	\$ 2,093,715,892	\$ 2,077,188,495	\$ 2,117,974,615	\$ 2,060,608,391	\$ 8,349,487,394

#### EP-1660 Patterns of acute brain metastases related admissions: Opportunity amongst recurring themes

R. Bentley<sup>1</sup>, M. O'Cathail<sup>1</sup>, L. Aznar-Garcia<sup>1</sup>, V. Crosby<sup>2</sup>, A. Wilcock<sup>2</sup>, J. Christian<sup>1</sup>

<sup>1</sup>Nottingham University Hospitals NHS trust, Oncology and Radiotherapy, Nottingham, United Kingdom ;

<sup>2</sup>Nottingham University Hospitals NHS trust, Palliative Care, Nottingham, United Kingdom

#### Purpose or Objective

Brain metastases (BM) affect up to 40% of patients with metastatic disease. They are associated with a wide range of symptoms and significant morbidity. Though the symptoms are known the health care provider burden is not. We aim to describe the patterns of BM related admissions in a large oncology centre.

#### Material and Methods

Over a two year period (1<sup>st</sup> Jan 2016 - 31<sup>st</sup> Dec 2017), adult patients with a new radiologically confirmed diagnosis of BM were identified by retrieving all MRI and CT head scans that contained the words 'metastases', 'metastasis' or 'met' in the on-line scan report. Only patients with a confirmed primary cancer were included. Information recorded included patient demographics, primary cancer site, treatment received and survival. Number, duration of and reasons for hospital admissions were recorded if they were attributable to BM.

#### Results

236 cases of newly diagnosed BM identified. The median age at diagnosis was 65 years (range 30-87). The median survival across all groups was 115 days (range 1-829). There were more females (58%) than males (42%). Lung cancer represented the most common primary site (49%), followed by breast (20%) and melanoma (13%). Median survival varied by primary site with lung carrying the worst prognosis (95 days) and breast (202 days) the best. Sixty-nine percent of patients had a BM related admission. There were 305 admissions accounting for 2318 bed days. The first diagnosis of BM occurred as a direct result of an admission in 63 patients (27%). The median length of stay was 7 days. The most common reasons for admission were seizures (18%) headaches, (17%) confusion (16%) and weakness (14%). Patients with lung primaries had the longest median stay (12 days) and the largest number of admissions (50% of all admissions)

Bed days varied depending on the treatment received. Patients who received Stereotactic Radiosurgery (SRS) had the fewest bed days as a proportion of total follow up days. They had 63 admissions and 491 bed days, which represented 3% of the total follow up days.

	SRS	Whole Radiotherapy	Brain Surgery	BSC
Number	50	50	27	118
Median Survival	NR	202	210	55
Follow days up	16,107	11,111	7,218	10,058
Admissions	63	80	67	113
Bed Days	491	584	459	899
Bed days: follow up	3%	5.3%	6.4%	8.9%

The estimated cost of the bed day varies from £306 for an excess stay bed day to £1609 for an emergency admission. Based on these figures the cost range for admissions is between £709,308 at the low end and £3,729,662 at the top.

#### Conclusion

The four most common reasons for admission were seizure, confusion, weakness and headaches. Knowing this, it may be possible to better educate patients on the symptoms and, with proper support, avoid admission. Fifty-two admissions (17%) were related to headaches: patient education with telephone support may help avoid many of these admissions. We suggest there is scope to avoid unnecessary admissions and make significant cost savings with a dedicated BM nurse specialist supporting patients and we recently have appointed one.

---

#### Electronic Poster: Clinical track: Communication

---

##### EP-1661 Teleconsultations: Bringing specialist radiotherapy services to patients

M. O'Cathail<sup>1</sup>, L. Aznar-Garcia<sup>1</sup>, R. Bentley<sup>1</sup>, P. Patel<sup>1</sup>, J. Christian<sup>1</sup>

<sup>1</sup>Nottingham University hospital NHS trust, oncology and radiotherapy, Nottingham, United Kingdom

#### Purpose or Objective

As part of its 'Five year forward view' in 2014, NHS England recognised the changing needs of patients and the need to capitalise on the opportunities new technologies present. Teleconsultations have the ability to deliver greater access to specialist care and advice. Our centre provides a regional stereotactic radiosurgery (SRS) service to treat patients with brain metastases. These patients are prohibited from driving thus potentially limiting access to this service. We have established a teleconsultation service to support the management and follow-up of patients with brain metastases. We aim to assess the feasibility and acceptability of this service. Here we present the results of a pilot. Patients had a choice of teleconsultation or face to face (FTF) appointment for assessment

#### Material and Methods

Participants provided feedback via a previously validated set of questions which assesses clarity of audio-visual connection, ease of communication, perception of privacy, overall satisfaction, patient preference for future appointments and patient reported expense. Data is also collected on round trip distance and predicted travel time saved. A baseline survey of face-to-face consultations acts as a control. The pilot ran for 6 months.

#### Results

There were 123 attendances to the brain metastases clinic, of which 45 (36.5%) were teleconsultations. Twenty-four (11 female & 8 male) individual patients have participated with feedback received on 28 separate teleconsultations. Feedback from FTF clinics was received from 14 patients. The median age was 59 years (Range 32-

88) compared with 65 (range 23-84) in the FTF group. Participants avoided travelling 2520 miles (61.5 per consult) and 70 hours of travel time (1hr 42 mins per consult). FTF patients travelled 2362 miles (30.5 per consult) and spent 86 hours travelling (1hr 6mins per consult). Satisfaction, ease of communication and privacy measured on a Likert scale was universally high or very high in both surveys. 95% of respondents wished to continue further follow up via teleconsultation with 4/13 respondents wishing to try teleconsultations for future appointments. All respondents felt they received satisfactory care. Most common reasons for preferring video clinics were that it was less disruptive to daily life and saved time.

#### Conclusion

Teleconsultations are feasible means of assessing and following up patients for SRS and is acceptable to patients as a means of accessing specialist care although patient choice appears to be driven by distance and travel considerations. This clinic model has worked well in a patient cohort with distance and transport restrictions.

---

#### Electronic Poster: Clinical track: Other

---

##### EP-1662 Multicentric structured medical data production on an OIS for modeling of radiotherapy effects

J. Clavier<sup>1</sup>, R. Eugene<sup>2</sup>, J. Thariat<sup>3</sup>, D. Antoni<sup>1</sup>, V. Beneyton<sup>4</sup>, L. Claude<sup>4</sup>, J. Fontbonne<sup>5</sup>, N. Gaillot<sup>6</sup>, V. Ganansia<sup>1</sup>, C. Jamain<sup>7</sup>, A. Lepinoy<sup>8</sup>, C. Laude<sup>4</sup>, C. Mazzara<sup>1</sup>, C. Noblet<sup>1</sup>, S. Racadot<sup>4</sup>, A. Ruffier<sup>9</sup>, S. Servagi<sup>6</sup>, P. Truntzer<sup>1</sup>, S. Guihard<sup>1</sup>

<sup>1</sup>Cancer Center Paul Strauss, Radiation oncology, Strasbourg, France ; <sup>2</sup>Elekta, Consultancy Services Specialist, Boulogne Billancourt, France ; <sup>3</sup>Cancer Center François Baclesse / Archade, Radiation Oncology, Caen, France ; <sup>4</sup>Cancer center Léon Bérard, Radiation Oncology, Lyon, France ; <sup>5</sup>Laboratoire de Physique Corpusculaire, Research - Industrial and medical applications, Caen, France ; <sup>6</sup>Cancer center Jean Godinot, Radiation oncology, Reim, France ; <sup>7</sup>Unicancer, Basic and pre clinical research, Paris, France ; <sup>8</sup>Institut de Cancérologie de Bourgogne, Radiation Oncology, Dijon, France ; <sup>9</sup>Cancer center Gustave Roussy, Radiation Oncology, Villejuif, France

#### Purpose or Objective

We developed a model of structured medical charts. Three objectives were defined: collection of structured data during consultations, real-time production of medical letters and massive data extraction for clinical analysis feedback on a daily-basis.

#### Material and Methods

Twenty-three forms were created in MOSAIQ® oncology information system (OIS) related to the phase of patient journey (pretherapeutic, during irradiation and post-irradiation) and localization (brain, head and neck, breast etc.). Three hundred features were defined based on international scales (CTCAE, TNM, ICD-10 code, histology code, etc.), classical endpoints (date of local relapse), tumor-specific needs (use of gastrotomy, etc.) or case report forms of ongoing clinical trials. Ergonomics were adapted for fast entry during consultations without decreasing social contact. Consensus on the content of forms was reached between 17 radiation oncologists from 4 centers of the French national comprehensive cancer center network. Automatic medical letter production from collected data was implemented for time-saving. The software allows massive export of patient, tumor and radiation treatments (dose, fractionation, etc.) data.

## Results

Sixty per cent of radiation oncologists at initiating center used the forms. From January 2016 to May 2018, 411 134 structured data were collected with a monthly median of 15 197 (811-24 015). The forms and tables were synchronized between two MOSAIQ® systems in different institution. Daily use was easy and produced 14 864 data between May and June 2018. Prospective evaluations were performed (dermatitis rate by physicians, by technique etc.). Post processing of data allowed development of algorithms that enabled early detection of unexpected toxicity patterns in patient populations.

## Conclusion

Such massive production of data, integrated in daily care offers great opportunities for improvement of the quality of data and large scale of exploitation to produce levels of evidence from routine practice. Modeling of radiation treatment (tumor control and toxicity) and creation of more automatic alerts is ongoing. The concept and format used in MOSAIQ® OIS (Elekta) can be implemented in other software (OIS and hospital-based electronic patient charts). On October 2018, three other departments will integrate the structured medical record system.

### EP-1663 REQUITE multicentre study of patients undergoing radiotherapy for breast, lung or prostate cancer

C. West<sup>1</sup>, D. Azria<sup>2</sup>, J. Chang-Claude<sup>3</sup>, D. De Ruyscher<sup>4</sup>, R. Elliott<sup>5</sup>, S. Gutiérrez-Enriquez<sup>6</sup>, T. Rancati<sup>7</sup>, B. Rosenstein<sup>8</sup>, P. Seibold<sup>9</sup>, C. Talbot<sup>10</sup>, A. Vega<sup>11</sup>, L. Veldeman<sup>12</sup>, A. Webb<sup>13</sup>

<sup>1</sup>The University of Manchester, Translational Radiobiology, Manchester, United Kingdom ; <sup>2</sup>Cancer Institute of Montpellier, Oncologic Radiotherapy, Montpellier, France ; <sup>3</sup>German Cancer Research Center, Unit of Genetic Epidemiology, Heidelberg, Germany ; <sup>4</sup>Maastrro, Radiotherapeut Oncoloog, Maastricht, The Netherlands ; <sup>5</sup>University of Manchester, Division of Cancer Sciences, Manchester, United Kingdom ; <sup>6</sup>Vall d'Hebron Institute of Oncology-VHIO, Institute of Oncology, Barcelona, Spain ; <sup>7</sup>Fondazione IRCCS Istituto Nazionale dei Tumori, Prostate Cancer Program, Milano, Italy ; <sup>8</sup>Mount Sinai, Icahn School of Medicine, New York, USA ; <sup>9</sup>German Cancer Research Center DKFZ, Unit of Genetic Epidemiology, Heidelberg, Germany ; <sup>10</sup>University of Leicester, Department of Genetics, Leicester, United Kingdom ; <sup>11</sup>Universitario de Santiago, Fundación Pública Galega Medicina Xenómica, Santiago de Compostela, Spain ; <sup>12</sup>University of Ghent, Department of Radiotherapy, Ghent, Belgium ; <sup>13</sup>University of Leicester, Department of Genetic and Genome Biology, Leicester, United Kingdom

## Purpose or Objective

REQUITE aimed to establish a resource for multi-national validation of models and biomarkers that predict a patient's risk of late toxicity and quality-of-life following radiotherapy. The purpose here is to provide an overview of the data available.

## Material and Methods

An international, prospective cohort study recruited patients in 26 hospitals in eight countries between April 2014 and March 2017. Target recruitment was 5,300 patients. Eligible patients had breast, lung or prostate cancer and planned potentially-curable radiotherapy. Radiotherapy was prescribed according to local regimens, but centres used standardised data collection forms including patient reported outcome measures available in multiple languages. Pre-treatment blood samples were collected. Patients were followed for a minimum of 12 (lung) or 24 (breast/prostate) months and summary descriptive statistics generated.

## Results

Between 2014 and 2017, the study recruited 2,069 breast (98% of target), 1,808 prostate (86%) and 561 lung (51%) cancer patients. 383 lung cancer patients from external cohorts were included for genotyping. The centralised, accessible database includes: physician- (45,881 forms) and patient- (52,691) reported outcomes; 11,383 breast photos; 17,107 DICOM and 12,684 DVH files. Raw genotype data are available for 4,634 and imputed data for 4,304 patients with European ancestry (1,948 breast, 1,728 prostate, 628 lung) patients. Baseline demographics tended to vary per tumour site, e.g., the percentages of current smokers were 18% (365 breast patients), 14% (249 prostate) and 43% (227 lung). Respective figure for diabetes were 6% (126 breast), 7% (136 prostate) and 17% (92 lung); for heart disease 7% (143 breast), 21% (371 prostate) and 31% (166 lung); and for a BMI>30 kg/m<sup>2</sup> 22% (454 breast), 23% (399 prostate) and 22% (118 lung). Radiation induced lymphocyte apoptosis (RILA) assay data are available for 1,290 patients. DNA (n=4,434 REQUITE patients) and Paxgene tubes (n=3,039) are stored in the centralised biobank. Example 2-year prevalences (1-year for lung) of ≥grade 3 toxicities are: 13% atrophy (breast), 26% dyspnea (lung), and 3% rectal bleeding (prostate).

## Conclusion

The comprehensive centralised database and linked biobank is a valuable resource for the radiotherapy community for validating models and biomarkers that predict for risk of the late effects that most effect long-term quality-of-life. Most cancer patients gave consent to share their data and samples with external researchers, and a formal process for requesting data access for specific research questions is in operation (32 projects approved). A data discovery platform to search on numbers of patients with various attributes collected by the consortium is available at [www.requite.eu](http://www.requite.eu).

### EP-1664 Inter-fractional urinary bladder filling variation during IGRT in pelvic malignancies

M. Shah<sup>1</sup>, S. Agarwal<sup>2</sup>, R. Agarwal<sup>2</sup>, B. Subramanian<sup>2</sup>, S. Gupta<sup>3</sup>, S. De<sup>1</sup>, S. Mishra<sup>2</sup>, S. Srinivasan<sup>4</sup>, P. Chaudhary<sup>2</sup>, A. Chabra<sup>2</sup>, R. Chandra<sup>2</sup>  
<sup>1</sup>Jaypee Hospital- Noida, Radiation Oncology, Noida, India ; <sup>2</sup>Max Hospital- Delhi, Radiation Oncology, New Delhi, India ; <sup>3</sup>All India Institute of Medical Science- Rishikesh, Radiation Oncology, Rishikesh, India ; <sup>4</sup>Tata Institute of Medical Science, Radiation Oncology, Mumbai, India

## Purpose or Objective

Organ motion is an important factor that limits the precision of radiation treatment. Bladder filling variation has a significant impact on the position of target volumes in pelvic malignancies. One of the approach to reduce the bladder motion influence on the target location is by controlling the bladder volume, a protocol instructing the patient to drink a certain amount of water before starting the treatment. This study was an effort to maintain a consistent bladder volume after following a bladder protocol, which was then analyzed by in-room CBCT imaging. The bladder volumes and bladder wall dimension were Image-guided comprehensively thus adding considerable understanding to the bladder wall motions.

## Material and Methods

This study was conducted on patients of pelvic malignancies excluding urinary bladder carcinoma. It was a single institution, non-randomised, prospective study and the duration of the study was of 6 months. All patients of pelvic malignancies undergoing IGRT (Image guided radiotherapy) with curative intent having urine holding capacity of at least half an hour were included in the study. In Bladder protocol patients were instructed to void the bladder 40 minutes prior to treatment and to drink 600 ml of water within 10 minutes. The patients were scanned after 30 minutes of taking the last glass of water. Time of

last glass of water and CBCT was noted. The bladder protocol was followed from the planning day and then on daily basis before treatment. The CBCT data set was fused to the planning CT and was used to characterize the bladder each day. Bladder contouring was done on all planning CTs and treatment CBCT images by the same oncologist. The volumetric changes of the bladder were measured to analyze the inter-fractional filling variation. Total 274 CBCT was contoured in 26 patients and were compared with the 26 planning CT to see the average bladder filling variation and standard deviation in transverse, anteroposterior and longitudinal diameter.

#### Results

The mean bladder volumes in-room 183.07 cc (range, 62-475cc) and SD were 90.43cc. Similarly, the mean time was 40.12 minutes with SD of 2.15 min and p-value 0.059 which was non-significant. Bladder wall motion of these patients was analyzed in transverse, anteroposterior and longitudinal diameter shown in Table-1.

Urinary bladder movements	N	Mean	Standard Deviation	p-Value	Significance
Transverse (in cm)	26	8.35	1.039	0.064	NS
Antero-posterior (in cm)	26	6.69	1.05	0.108	NS
Longitudinal (in cm)	26	5.59	1.798	0.973	NS

Table 1- Mean± SD of bladder wall movements

#### Conclusion

This study finds a possible answer to a very pertinent question on bladder wall motion and bladder volume variations during radiation therapy. Image-guided radiotherapy (IGRT) with verification of the organ position before the daily treatment after following bladder filling protocol has allowed for lessening of inter-fraction bladder wall motion and showed considerable benefits in terms of margin reduction on lateral side as there is less displacement on transverse diameter and more liberal margins should anteroposterior in anteroposterior dimension and longitudinal dimension.

#### EP-1665 Extra-pulmonary Neuroendocrine Carcinoma. Rarity of Brain Metastases

L. FERRO<sup>1</sup>, I. Golomb<sup>2</sup>, H. Ligumsky<sup>3</sup>, O. Gutfeld<sup>1</sup>, I. Wolf<sup>3</sup>, V. Soyfer<sup>1</sup>

<sup>1</sup>Sourasky Medical Center, Radiation oncology- Oncology Division, Tel Aviv, Israel ; <sup>2</sup>Tel Aviv University, Sackler school of medicine- Tel Aviv University, Tel Aviv, Israel ; <sup>3</sup>Sourasky Medical Center, Oncology Division, Tel Aviv, Israel

#### Purpose or Objective

Extra-pulmonary small cell carcinoma (EPSCC) is a rare clinical entity and while its management is usually extrapolated from small cell lung cancer (SCLC), this approach is controversial and is not evidence-based. Specifically, the current clinical practice in the management of SCLC involves prophylactic cranial irradiation (PCI). The PCI proved the decrease in incidence of brain metastases both in limited and extensive disease. We aimed to analyze the clinical characteristics of a relatively large cohort of patients treated at single tertiary center.

#### Material and Methods

A search of the entire database of the Center, consisting of over 25,000 patients, yielded 24 patients diagnosed with EPSCC or high-grade neuroendocrine carcinoma between 2015 and 2018. Clinical characteristics were obtained from the medical files. The overall median survival, response rate, and the incidence of local and distant progression were calculated.

#### Results

The primary sites were 17 (71%) gastrointestinal including seven (41%) pancreatic, genitourinary (5, 21%), or unknown primary sites (2, 8%). The median Ki67 was 90% for all patients.

Five patients were diagnosed with limited disease and operated, one received neoadjuvant treatment and is still free of disease 10 years later, while one patient received adjuvant treatment and had a DFS of 4.7 months.

Nineteen patients were diagnosed with extensive disease, 14 of them received Platinum based chemotherapy as first line of treatment, mostly (13, 93%) with Etoposide, same treatment protocol as in SCLC. 6 (31.6%) and 3 (15.7%) patients received second or more lines of systemic treatment respectively. Of the 10 patients we have an imaging test after first course of treatment we can determine that 3 (30%) had a partial response and 4 (40%) had a stable disease. For the total of patients with extensive disease the median survival was 8.2 months.

While no patient received prophylactic cranial irradiation, only one patient (4%), presenting with pancreatic SCC developed brain metastasis, compared to the 40-50% known in SCLC.

#### Conclusion

We report herein a relatively large number of patients. Our data demonstrates a relative efficacy for the classic platinum based treatment. While treatment of EPSCC is often extrapolated from SCLC, the rarity of brain metastasis in this cohort suggest that PCI should not be incorporated in the treatment protocol of these patients.

#### EP-1666 ARENA: Improving training in target volume delineation for radiotherapy

E. Evans<sup>1</sup>, C. Piazzese<sup>2</sup>, E. Spezi<sup>2</sup>, J. Staffurth<sup>1</sup>, S. Gwynne<sup>3</sup>

<sup>1</sup>Velindre Cancer Centre, Clinical Oncology, Cardiff, United Kingdom ; <sup>2</sup>Cardiff University, School of Engineering, Cardiff, United Kingdom ; <sup>3</sup>South West Wales Cancer Centre, Clinical Oncology, Swansea, United Kingdom

#### Purpose or Objective

Inter-observer variation radiotherapy (RT) Target Volume Delineation (TVD) may be considered the 'weakest link' in the RT planning process. Accurate outlining is imperative to ensure patients receive optimal outcomes with minimal toxicity. In response to this the ARENA project has been launched by clinical oncologists in South Wales to facilitate a standardised approach to TVD training. The project will develop tumour site-specific TVD instructional modules with corresponding outlining modules, offering test cases for trainees to outline, upload and receive semi-automated feedback on through software developed by Cardiff University. Experience has been drawn from the team's involvement with National Radiotherapy Trials Quality Assurance (RTTQA) group, providing feedback for submitted pre-trial RT outlining.

#### Material and Methods

To ascertain TVD training needs of clinical oncology trainees, 406 UK clinical oncology trainees were surveyed regarding TVD training quality and preferential format for TVD modules. Using the survey results, a TVD instructional module and corresponding series of cases of varying difficulty with semi-automated feedback have been developed using oesophageal cancer as a pilot site. 6 UK UGI oncologists outlined 6 oesophagus cases to develop a reference volume for each case. Software was developed in MATLAB to provide semi-automated on the cases outlined by trainees on their training centre's planning software. Feedback developed included trainee outline against a reference volume, over /under contoured regions, minimum and maximum acceptable volumes, a conformity score and a 'red flag' when volumes contoured inappropriately include normal tissue. The latter module with semi-automated feedback was piloted locally with 3 clinical oncology trainees.

## Results

131 trainees at different stages of training responded to the survey. The most common method of TVD training for trainees was consultant led (94%) followed by self-directed learning (83%). RT trial protocols were the most common self-directed used tool (89%). Most trainees (54%) report their supervising consultants spend only 1 hour per week reviewing their TVD. 20% of trainees felt highly competent in TVD for a recently completed tumour site, 55% of trainees reasonably confident and 20% insufficiently competent. Most trainees (61%) preferred step-by-step instructions for TVD modules with qualitative feedback for the cases outlined (51%). Trainees testing the model allocated each feedback method a usefulness score out of 10, with the 'red flag' tool deemed most useful (mean score 9.2) and over/under contoured regions least useful (mean score 7).

## Conclusion

Given current reliance upon self-directed learning, ARENA aims to support consultant-led TVD teaching through site-specific TVD modules. Software developed for outlining feedback will be further developed to reflect trainee opinion. Further site-specific modules are in development.

### EP-1667 Safety and efficacy of fiducial marker implantation for robotic SBRT with fiducial tracking

N. Scher<sup>1</sup>, G. Bouilhol<sup>1</sup>, R. Tannouri<sup>1</sup>, I. Khemiri<sup>1</sup>, A. Vouillaume<sup>1</sup>, N. Sellami<sup>1</sup>, R. Von Eyben<sup>2</sup>, L. Rotenberg<sup>3</sup>, H. Lamallem<sup>1</sup>, O. Bauduceau<sup>1</sup>, M. Bollet<sup>1</sup>, D. Foster<sup>3</sup>, A. Toledano<sup>1</sup>

<sup>1</sup>Hartmann Institute of Radiotherapy, Hauts de Seine, Levallois Perret, France ; <sup>2</sup>Stanford Cancer Center, California, Palo Alto, USA ; <sup>3</sup>American Hospital of Paris, Hauts de seine, Neuilly sur seine, France

## Purpose or Objective

The purpose of this study was to assess the feasibility, efficacy and toxicity of fiducial marker implantation and tracking in CyberKnife® stereotactic radiation therapy (SBRT) applied to extracranial locations.

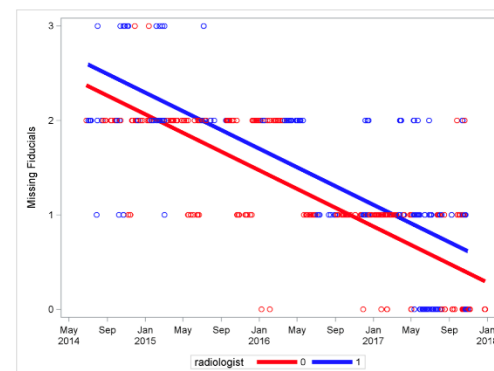
## Material and Methods

This was a retrospective, single-centre, observational study to collect the data of all patients treated by stereotactic radiation therapy with fiducial marker tracking at extracranial locations, conducted between June 2014 and November 2017 at the Hartmann Radiosurgery Institute. Information regarding the implantation procedure, the types of toxicity related to marker implantation and the number of markers implanted/tracked during treatment were collected. Complication rates were evaluated using the CTCAE [Common Terminology Criteria for Adverse Events] scale, version 4. The technical success rate was based on the ability to optimally track the tumour (during translation and/or rotation, depending on the type of target movement) throughout all treatment fractions.

## Results

2,505 patients were treated by stereotactic radiation therapy, 25% of whom received treatment with fiducial marker tracking. The total number of implantation procedures was 616, and 1,543 fiducial markers were implanted. The implantation-related complication rate was 3%, with 16 Grade 1 events and 4 Grade 2 events. The number of treated patients and the number of implanted markers has gradually increased since the technique was first implemented. The median treatment time was 27 minutes. 1,295 fiducials were actually tracked throughout all treatment fractions, representing a technical success rate of 84%. The difference between the number of fiducials implanted and those tracked during treatment decreased significantly as the site's experience increased.

Localization and number of patient (n)	Fiducial markers implanted Median, SD, range	Fiducial markers tracked Median, SD, range
Lung n=89	1 0.3 [1 ; 2]	1 0.3 [1 ; 2]
Prostate n=150	4 0.8 [2 ; 5]	3 0.5 [2 ; 4]
Liver n=151	4 1.3 [1 ; 6]	3 1 [1 ; 5]
Nodes n=85	1 0.6 [1 ; 3]	1 0.6 [1 ; 3]
Pancreas n=18	3 1.1 [1 ; 5]	3 0.5 [1 ; 3]
Bones n=57	1 0 1	1 0 1
Adrenal n=23	2 0.9 [1 ; 4]	2 0.9 [1 ; 4]



## Conclusion

Fiducial marker implantation and tracking is feasible, well-tolerated, and technically effective technique in SBRT for extracranial tumours.

### EP-1668 Creation and pilot-test of virtual cases for learning oncologic emergency management

Z.S. Fawaz<sup>1</sup>, P. Nancy<sup>1</sup>, J. Alfieri<sup>1</sup>

<sup>1</sup>McGill University Health Center, Radiation Oncology, Montreal, Canada

## Purpose or Objective

Management of radiation oncologic emergencies becomes critical at the start of the second year of a radiation oncology residency. Considering the limited exposure to oncology in the medical school curriculum, this knowledge gap needs to be filled prior to managing real patients. The aim of this project was to create virtual cases to ease this transition, improve readiness for managing oncologic emergencies on call, and to create viable alternatives to fulfill accreditation standards based on the Association of Faculties of Medicine of Canada (AFMC).

## Material and Methods

A curriculum mapping exercise was done to identify gaps. The main oncologic emergencies that needed to be addressed were selected for development of the modules. Review of the key concepts for management were

elucidated and validated. The learning concepts included history, physical examination, imaging interpretation, staging, as well as anatomy, epidemiology, pertinent literature, differential diagnosis, prognostication, radiation treatment planning, summarizing, and patient and peer communication skills.

Clinical vignettes were then designed, in collaboration with a virtual patient education expert, to mimic the clinical presentation and evolution of a typical patient for three common oncologic emergencies: spinal cord compression, superior vena cava syndrome, and hemorrhage.

#### Results

3 virtual cases were developed: spinal cord compression, superior vena cava syndrome, and tumour-induced hemorrhage. Each case includes 25 to 30 screens to progress through, with a total estimated completion time of 30 to 45 minutes. Each node branches out to provide a detailed answer and explanation of the key concept. Figures were included to mimic real patients and provide a more authentic learning environment.

The modules also included quantitative pre- and post-testing with multiple choice questions, true or false, fill in the blank, and text response. The cases were then transcribed onto a virtual patient simulation platform. The platform is accessible to the learner through his or her own personal sign-on. Following completion of the module, a report is generated for each individual learner to track all responses and can be used as an assessment tool. Qualitative data will also be collected regarding user-friendliness and learner satisfaction.

The pilot test showed an increase of 27% in the pre-to-post-test results in a cohort of 9 residents. The mean pre-test result of 64% increased to a mean post-test result of 91% (range: 70-100%) after completing the three modules.

#### Conclusion

Virtual patient cases can be used for the management of oncologic emergencies and can be done on a simulation-based learning platform. The modules can be used as an assessment and learning tool for junior residents. The preliminary results of the pilot-test show a significant improvement in competence after completion of the three modules.

#### EP-1669 Evaluation of Healthcare Quality Concepts in Radiation Oncology PG Training Programs

M. Uddin Karim<sup>1</sup>, A.N. Abbasi<sup>2</sup>, B.M. Qureshi<sup>2</sup>, N. Ali<sup>2</sup>, A. Hafiz<sup>2</sup>, B. Mir Khan<sup>2</sup>

<sup>1</sup>Aga Khan University Hospital, Oncology, Karachi, Pakistan ; <sup>2</sup>Aga Khan University, Oncology, Karachi, Pakistan

#### Purpose or Objective

Radiation Oncology (RO) Trainees (Post graduate Residents, Trainee medical physicists, Trainee Radiation Therapy Technologists RTTs) face ongoing challenges associated with the everyday reality of having demanding clinical workloads. They are expected to contribute to patient safety and quality improvement in RO, but prior studies suggest that training for this may be inadequate. In order to inculcate the basic concepts of healthcare quality in all three training programs, an evaluation of awareness was performed in our department. As per our team's deliberations, this evaluation will allow treatment idea sharing of quality systems and processes after training. As healthcare providers, these future carers will be looking after their professional development needs. It is important to identify weaker links and to learn core concepts of quality.

#### Material and Methods

An orientation lecture was designed to give a practical overview of quality RO practice concepts. The content was streamlined to fit into a single day activity and delivered through a lecture followed by interactive group discussion of the concepts.

A pre and post-test was developed comprising of 12 questions in order to assess the trainee's understanding of the knowledge of basic quality concepts deliberated in the lecture. The intent of tests was to provide qualitative feedback about the trainee's knowledge and understanding of these processes.

A total of 25 trainees (8 post graduate residents, 9 trainee medical physicists, 8 RTTs) participated. The class was led by a senior faculty who delivered a lecture and moderated the interactive discussion.

#### Results

There was an open and constructive interaction among the trainees during all four phases of this evaluation. Changes in trainee's knowledge and understanding was positive. The pretest scores of all 12 questions varied from 8% to 72%. This trend was positively changed to a score ranging from 84-100%.

#### Conclusion

The pretest survey results showed that most trainees have less than expected practical knowledge of healthcare quality concepts. Our team would recommend introduction of a well-constructed module for inclusion in these three training programs which can fill this knowledge gap.

#### EP-1670 Painful osteoarthritis responds to low-dose radiotherapy

B. Álvarez Rodríguez<sup>1</sup>, Á. Montero<sup>1</sup>, F. Calvo<sup>2</sup>, J. Valero<sup>1</sup>, F. Aramburu<sup>2</sup>, J. García<sup>3</sup>, R. Ciérvide<sup>1</sup>, M. López<sup>1</sup>, M.Á. De la Casa<sup>3</sup>, J. Martí<sup>3</sup>, E. Sánchez<sup>1</sup>, M. García-Aranda<sup>1</sup>, X. Chen<sup>4</sup>, O. Hernando<sup>4</sup>, R. Alonso<sup>4</sup>, S. Rodríguez<sup>2</sup>, P. García de la Peña<sup>2</sup>, C. Rubio<sup>1</sup>

<sup>1</sup>Hospital Universitario HM Sanchinarro, Radiation Oncology, Madrid, Spain ; <sup>2</sup>Hospital Universitario HM Sanchinarro, Rheumatology, Madrid, Spain ; <sup>3</sup>Hospital Universitario HM Sanchinarro, Radiophysics, Madrid, Spain ; <sup>4</sup>Hospital Universitario HM Puerta de Sur, Radiation Oncology, Madrid, Spain

#### Purpose or Objective

Evaluation of painful osteoarthritis response to low-dose irradiation based on previous positive evidence.

#### Material and Methods

With a median age of 67 years (range 45-89 years), 69 patients (56 women and 13 men) were enrolled in a prospective analysis between April 2015 and March 2018. 111 treatments were performed due to enrollment of patients affected with more than one location. Patients analyzed presented finger joints osteoarthritis, rhizarthrosis, wrist osteoarthritis, gonarthrosis, shoulder and hip arthritis or spondyloarthrosis. All patients underwent CT-based simulation. Planning target volume (PTV) contoured on CT scan included painful joint. Treatment was delivered in a LINAC and daily verified with orthogonal X-ray. 6 Gy were delivered in single fractions of 1 Gy every other day, however, if complete response wasn't reached, a second course of identical characteristics was delivered 6-8 weeks after finishing the first course. Pain was measured before and after radiotherapy using the visual analogue scale (VAS). Long term response was also evaluated with the functional scale proposed by von Pannewitz and determining the variation in the daily analgesic drugs intake.

#### Results

Most prevalent locations were fingers (47%), knees (30%), and shoulders (14%). With a median follow-up of 7 months (1-28 months), 52% of patients referred improvement, however, objectively, 74% of treated patients experienced pain relief in different degrees. According to the VAS scale, pain reported was greater or equal to 7 in 82% of the patients before treatment and 88% of this group showed response. After treatment, half of all patients showed grade 3 or less of pain even though, 86% of these patients had pain greater than 7 before treatment. 42% of the patients needed to take less analgesia after

treatment.

In 51 cases, a second course was needed to achieve better response, accomplishing it in 44 of them with a stable response in all except 2 cases. 55% of the cases were followed for more than 6 months and 90% of these patients maintained partial or total response after long follow-up.

#### Conclusion

Low doses of radiotherapy achieve significant pain relief in patients with osteoarthritis disorders, as well as subjective functional improvement and decrease in daily requirements of analgesia. All in all, this improvement can be translated in a better quality of life accomplished.

#### EP-1671 Radiotherapy: promising alternative treatment for painful enthesopathies and inflammatory diseases

B. Álvarez Rodríguez<sup>1</sup>, Á. Montero<sup>1</sup>, F. Aramburu<sup>2</sup>, E. Calvo<sup>2</sup>, J. Palma<sup>1</sup>, J. Valero<sup>1</sup>, J. García<sup>3</sup>, J. Martí<sup>3</sup>, R. Ciérvide<sup>1</sup>, E. Sánchez<sup>1</sup>, S. Rodríguez<sup>2</sup>, M.Á. De la Casa<sup>3</sup>, M. García-Aranda<sup>1</sup>, X. Chen<sup>4</sup>, O. Hernando<sup>4</sup>, R. Alonso<sup>4</sup>, M. López<sup>1</sup>, P. García de la Peña<sup>2</sup>, C. Rubio<sup>1</sup>

<sup>1</sup>Hospital Universitario HM Sanchinarro, Radiation Oncology, Madrid, Spain ; <sup>2</sup>Hospital Universitario HM Sanchinarro, Rheumatology, Madrid, Spain ; <sup>3</sup>Hospital Universitario HM Sanchinarro, Radiophysics, Madrid, Spain ; <sup>4</sup>Hospital Universitario HM Puerta del Sur, Radiation Oncology, Madrid, Spain

#### Purpose or Objective

Efficacy of low-dose radiotherapy for periarticular inflammatory diseases has been largely probed. We present the results after analyzing a series of patients enrolled in our protocol consisting of a prospective non-randomized study.

#### Material and Methods

From April 2015 to May 2018, 44 patients were enrolled in our protocol, including 32 women (70%) and 12 men (30%), with a median age of 59 y/o (range 30-89 y/o). The analysis was based on the number of treatments delivered, which were 70 because some patients referred pain at different locations. Most patients (77%) presented with bursitis, specifically trochanteritis (70.5%), followed by sacroiliitis (13%) and epicondylitis (6%).

Pre-treatment and post-treatment evaluation of the pain was based on the visual analogue pain scale (VAS), requirements of oral analgesic intake and the modified von Pannewitz pain score (MVPPS). Clinical response was evaluated 6 weeks after treatment and each 3 months thereafter. If less than major response was achieved, a second course was delivered 6-8 weeks after finishing the first course.

Treatment comprised low-dose radiation up to a total dose of 6 Gy (1 Gy/fraction) every other day. All patients underwent CT-based simulation. This was, sometimes, fused with the corresponding magnetic resonance image if available. Planning target volume (PTV) was contoured on CT scan including the painful periarticular soft tissue. Treatment was delivered in a LINAC and daily verified with orthogonal X-ray.

#### Results

Before treatment, 81% of the patients referred VAS equal or greater than 7, while only 7% of the patients maintained this VAS after treatment. On the other hand, no patients referred VAS equal or under 3 before treatment, but 66% of the patients did achieved it after radiotherapy; what is more, 13% of all cases referred complete response (VAS 0) after treatment.

The median follow-up was 8 months (range 1-29), and 54% of the patients were monitored for more than 6 months. In these cases, 89% maintained VAS < 7 and 37% showed VAS < 3 after long follow-up. Regarding functionality, 87% of the cases referred MVPPS 1-3 and 44% of patients referred less intake of analgesia.

A second course of radiotherapy was required in 44 cases (63%), obtaining response in 36 cases (81%) in the early analysis and response was maintained in 28 cases (77%) after 3 or more months.

#### Conclusion

Low-dose radiotherapy is an effective and well-tolerated approach for painful inflammatory periarticular disorders, achieving acceptable rates of pain control that seem to be maintained during follow-up and thus contributing to improve the quality of life of these patients. Further follow-up is required for ensuring these promising results.

#### EP-1672 Multimodality treatment in thymic tumors: a retrospective analysis and accordance with ESMO guidelines

A. Carnevale<sup>1</sup>, C. Greco<sup>1</sup>, M. Fiore<sup>1</sup>, E. Ippolito<sup>1</sup>, S. Silipigni<sup>1</sup>, C.G. Rinaldi<sup>1</sup>, A. Di Donato<sup>1</sup>, S. Gentile<sup>1</sup>, P. Trecca<sup>1</sup>, P. Zuccoli<sup>1</sup>, G. Petrianni<sup>1</sup>, S. Palizzi<sup>1</sup>, R.M. D'Angelillo<sup>1</sup>, L. Trodella<sup>1</sup>, S. Ramella<sup>1</sup>

<sup>1</sup>University Campus BioMedico of Rome, Radiation Oncology, Rome, Italy

#### Purpose or Objective

Surgery represents the mainstay treatment for Thymic Epithelial Tumors. Due to the lack of prospective randomized studies, the role of postoperative radiotherapy (PORT) is not supported by high levels of evidence. We retrospectively assessed whether the decision regarding the postoperative radiotherapy at Campus Bio-Medico University has been taken according to the new ESMO guidelines.

#### Material and Methods

All consecutive patients with Thymic Tumors from 2005 to 2018 were analyzed and a complete review of medical records was performed.

#### Results

51 patients underwent surgery up-front. Median age at diagnosis was 64 years (range 33-82). Tumors histology was thymoma (A-AB-B3) in 47 (92%) patients or thymic carcinoma in 4 (8%) patients. Complete resection (R0) was achieved in 35 (67%) patients. Other patients had R1 resection. Applying 8<sup>th</sup> TNM system edition, 1 patients with Masaoka stage III was reclassified to stage II and I stage and one IV A. Decision of delivering PORT was in accordance with ESMO guidelines in 94% of the 51 patients. Two patients with R1 resection, with B1 and B2 thymoma and negative postoperative CT scan, did not receive radiotherapy for excessive delay after surgery. Median total dose was 46 Gy and was variable depending of radical resection: median total dose was 45 Gy after R0 resection and 54 Gy after R1 resection. Only G1-2 acute esophageal and G1 acute lung toxicities were reported. No in-field local recurrences were reported; four patients had pleural and distance metastases. With a median follow up of 47 months (range 7.2-155 months), median overall survival was 9.7 years.

#### Conclusion

Our data suggest that PORT is a safe and effective treatment for Thymic Epithelial Tumors in patients with stage II (B2-B3), Stage III Masaoka-Koga, R1 resection and Thymic carcinoma, in accordance with ESMO guidelines.

#### EP-1673 Implementation of a Collaborative Fast Access Radiotherapy Program for Benign Disease

M. Rolfo<sup>1</sup>, R. Shaffer<sup>1</sup>

<sup>1</sup>Genesiscare Uk, Radiation Oncology, Berkshire, United Kingdom

#### Purpose or Objective

Benign diseases and non-malignant conditions may cause pain, loss of function and other symptoms that can impact on quality of life. Radiation may not be sought as first line treatment for benign conditions, but some studies have suggested the efficacy of RT as a valid treatment option for specific patient cohorts. Genesis Care Australia, Spain

and United Kingdom currently provide a benign RT service. A project was undertaken at GenesisCare UK to review all aspects of the patient pathway and to standardise RT delivery for Dupuytren's Disease, Ledderhose's Disease and Plantar Fasciitis across 12 centres with postulated endpoints to improve access, increase awareness and optimise clinical practice of the service to prospective patient and potential referrers.

#### Material and Methods

The project team was formed from a multi-disciplinary group consisting of a Medical Oncologist, Radiographers, Medical Physicist, Patient Experience Coordinator and a Referrer/Marketing Liaison Officer. A literature review was to be performed, and a clinical analysis of current practice initiated to identify potential quality improvement and efficiency gains. The efficacy of a dedicated heel pain clinic hypothesising a joint consulting model of a Medical Oncologist and a Musculoskeletal (MSK) Consultant, with access to multi-modality imaging and treatment to diagnose and treat Plantar Fasciitis (PF) and Achilles Tendonitis was investigated.

#### Results

The evaluation demonstrated that clinical quality improvement and efficiencies were warranted to improve service delivery

#### Findings included:

1. The patient pathway from consult to RT treatment was reduced from 10 to 14 days to 24 hours.
2. A fully electronic workflow was introduced
3. Evidence based clinical protocols were written for DD, LD, PF, AT.
4. Improved and standardised patient stabilisation for RT and Surface Guidance Radiotherapy was implemented for all benign treatments.
5. Introduction of a completed acrylic coated less toxic electron insert by sourcing an external supplier
6. Tattoo-less treatment was implemented for all benign RT treatment across all 12 centres
7. Extracorporeal Shockwave Treatments (EST) for newly diagnosed PF and AT and external beam for persistent and recurrent AT was introduced.
8. The Heel Pain clinic was implemented with a Medical Oncologist consulting with multimodality imaging available at the time of consult

#### Conclusion

The project resulted in i service delivery efficiencies, in reducing consult to treatment start time, through a collaborative and coordinated approach. Initiating mechanisms to develop external relationships with prospective patients and referrers have been implemented. Further investigation will continue evaluating the Benign Service and collect metrics on all aspects of the patient pathway. A joint consulting model for the heel pain clinic is anticipated to start in early 2018. Future goals are to initiate a centralised data base with an automated data transfer system for patient recorded outcomes measures and to expand the service

#### EP-1674 Early toxicity and outcome of 258 consecutive patients treated with CyberKnife in an Indian centre

D. Dutta<sup>1</sup>, R. Das<sup>1</sup>, A. Gupta<sup>1</sup>, K. Katakai<sup>1</sup>, T. Tarani<sup>1</sup>, A. Krishnan<sup>1</sup>, C. Oc<sup>2</sup>, R. Holla<sup>2</sup>

<sup>1</sup>Amrita Institute of Medical Science- Kochi, Radiation Oncology, Kochi, India ; <sup>2</sup>Amrita Institute of Medical Science- Kochi, Medical Physics, Kochi, India

#### Purpose or Objective

Demographic profile, patient parameters, early toxicity and response to treatment assessment of all consecutive patients treated with CyberKnife radiosurgery.

#### Material and Methods

258 consecutive patients [male 56%, mean age 52 (7-87 yrs)] treated with CK in an Indian dedicated radiosurgery unit. Brain tumour, GI tumour, oligo-metastasis, lung cancer and GU tumour patients were 146 (56%), 43 (17%), 41 (16%), 9 (4%) and 8 (3%) respectively. In brain tumour, 36 (14%) was meningioma, 26 (10%) AN, 23 (9%) AVM and 34 (12%) brain metastasis. 36 (14%) was HCC, 9 (4%) glomus tumour and only 6 (2%) were prostate cancer patient. In rare tumours, 6 (2%) were brainstem cavernoma, 2 patient each eye tumours, cholangiocarcinoma and pancreatic cancer. AVM dose 18-24Gy/1fr, meningioma & AN 12Gy/1fr. Lung cancer dose 45Gy/3fr, HCC 45Gy/5fr, prostate 36.25Gy/5fr. Four large AVM patients were treated in 'staged' SRS.

#### Results

Among 23 AVMs, 2 patient had acute oedema requiring admission and recovered with supportive care, 6 patients were on more than 1 month steroid after CK. Among 23 AN patients, 4 required steroid >3 months. One pituitary tumour patient had acute steroid insufficiency. 4% (7/146) of brain tumour patients required admission after CK. No treatment related death or permanent neurodeficit. Among 34 brain metastasis, 15 (44%) had controlled disease at last follow up [Estimated OS 284 days (95%CI: 234-328; SEM: 22.5); >6 month actuarial OS 89%]. 29.4% (10/34) had intra-cranial progression, 18% (6/34) patients had new lesions and 12% (4/34) had recurrence within high dose region. 27 HCC with PVT treated with CK [mean age 59 yrs, 94% male; CP A 63%; KPS>80: 81%]. 16% underwent TACE before SBRT. Mean follow up was 7 months (range 1.7-17.6 months). Mean actuarial OS was 10.8 months (SEM: 1.48; 95%CI: 7.8-13.7). At last follow up, 16/27(59%) were alive and 11/27(41%) expired. 22% (6/27) had complete PVT response, 11% had stable disease with partial PVT response. 30% had local progression & 27% had metastasis. No death due RILD. Post-CK, 2 patient underwent TACE and 1 had TARE. Mild GI toxicities (Gr I-II) in 40%, fatigue (Gr II-III) 28%. One (4%) patient had Gr III GI toxicity and one (4%) patient had decompensation (<4wk) after treatment. 36 patients (Male 92%, mean age 60.2 yrs, ECOG 0-1 92%, Child-Pugh A 89%) with HCCs underwent fiducial placement. Three patients (8%) had gross displacement (2 in lung, 1 in abdomen) immediate after placement. Poor post-fiducial pain score (3-4) was in 6% patients. 1/34(4%) patient expired after fiducial placement (<72 hours) with decompensation. Five patients (15%) had minor complications (pain abdomen 2, pneumothorax 2).

#### Conclusion

Early symptomatic toxicities after CK is less than 5%. Post-CK edema requiring long-term steroid is in 8%, procedure related mortality in 0.7% and admission required 4% patient. Recurrence rate after brain metastasis SRS is 29% at 6 month follow up. HCC with PVT response is in 27%. Acute toxicity and early outcome is acceptable with CK.

#### EP-1675 Club100 (student organization of DEGRO e.V.) - Current activities and future perspectives

L. Käsmann<sup>1</sup>, L. Bolm<sup>2</sup>, S. Knoedler<sup>3</sup>, T. Hoelscher<sup>4</sup>, F. Prött<sup>5</sup>

<sup>1</sup>LMU University Hospital Grosshadern, Department of Radiation Oncology, Munich, Germany ; <sup>2</sup>University Medical Center Schleswig-Holstein- Campus Luebeck, Department of Surgery, Luebeck, Germany ; <sup>3</sup>University Hospital Ulm, Department of Radiation Oncology, Ulm, Germany ; <sup>4</sup>University Hospital of Cologne, Department of Radiation Oncology, Cologne, Germany ; <sup>5</sup>St. Josefs-Hospital, Department of Radiation Oncology, Wiesbaden, Germany

#### Purpose or Objective

The Club 100 is an integral part of the German society of radiation oncology (DEGRO e.V.). The main goal of this subgroup is to actively support medical students as well as

biology and physics students in the field of radiation oncology. Several activities spread over the year are organized for students: special student program during the annual congress of the German society of radiation oncology, several training seminars as well as a "Journal Club". The Club 100 supports students in publishing their scientific work, gives advice for MD/PhD thesis, offers a mentorship as well as financial support for stays abroad. The aim of this survey was to characterize the Club 100, reveal students' interests as well as to gather ideas for future projects and activities to support the interest in the field of radiation oncology.

#### Material and Methods

We surveyed all members of the Club 100 (n=144), who joined the working group between 2015 and 2017 via an anonymous online questionnaire sent by e-mail. The questionnaire was based on 12 questions with a total of 42 items.

#### Results

The survey was sent to 144 members of the Club 100. A total of 44 responses (response rate: 31%) were completed and returned, and hence were eligible for further evaluation. A total of 36 (77.3%) students study medicine, 6 (13.6%) physics and 4 (9.1%) biology enrolled at 17 different universities. All medical students were all in an advanced stage of their studies. 15 (42%) medical students were in their final year. 39 (89%) of medical students reported participation in lectures during their study as previous experience, 27 (61%) undertook an elective, 22 (50%) chose a topic for their MD/PhD thesis in the field of radiation oncology, 17 (39%) undertook an internship (<6 weeks) during their studies and 9 (21%) had a rotation (2-4 months) during their final year. The majority of medical students were made aware of radiotherapy and the Club 100 during lectures (48%) or in conjunction with MD/PhD thesis. >90% of all students rate the activity and training seminars of the Club 100 as 'good' or 'very good'. For future projects, the students are interested in more information and opportunity of stays abroad, more interdisciplinary lectures and the organisation of an exclusive poster session during the annual meeting of the German society of radiation oncology.

#### Conclusion

Medical students represent the majority (77.3%) of all members in the Club 100 (subgroup of the German society of radiation oncology). The satisfaction of the Club 100 members is high concerning training seminars and the student programs at the annual meeting of the German society of radiation oncology. The ideas for future projects and improvements show that the students are interested in presentation of their scientific work as well as obtaining more information about internships and education opportunities abroad.

#### EP-1676 Importance of work-life balance among German students interested in the field of radiation oncology

L. Käsmann<sup>1</sup>, L. Bolm<sup>2</sup>, S. Knoedler<sup>3</sup>, T. Hoelscher<sup>4</sup>, F. Prött<sup>5</sup>

<sup>1</sup>LMU University Hospital Grosshadern, Department of Radiation Oncology, Munich, Germany ; <sup>2</sup>University Medical Center Schleswig-Holstein- Campus Luebeck, Department of Surgery, Luebeck, Germany ; <sup>3</sup>University Hospital Ulm, Department of Radiation Oncology, Ulm, Germany ; <sup>4</sup>University Hospital of Cologne, Department of Radiation Oncology, Cologne, Germany ; <sup>5</sup>St. Josefs-Hospital, Department of Radiation Oncology, Wiesbaden, Germany

#### Purpose or Objective

The Club 100 is an integral part of the German society of radiation oncology (DEGRO e.V.). The main goal of this subgroup is to actively support medical students as well as biology and physics students in the field of radiation oncology. Several activities spread over the year are

organized for students: special student program during the annual congress of the German society of radiation oncology, several training seminars as well as a "Journal Club". The Club 100 supports students in publishing their scientific work, gives advice for MD/PhD thesis, offers a mentorship as well as financial support for stays abroad. The aim of this survey was to reveal the importance of work-life balance as well as career and research ambitions of students interested in the field of radiation oncology.

#### Material and Methods

We surveyed all members of the Club 100 (n=144), who joined the working group between 2015 and 2017 via an anonymous online questionnaire sent by e-mail. The questionnaire was based on 10 questions with a total of 22 items.

#### Results

The survey was sent to 144 members of the Club 100. A total of 44 responses (response rate: 31%) were completed and returned, and hence were eligible for further evaluation. A total of 36 (77.3%) students study medicine, 6 (13.6%) physics and 4 (9.1%) biology enrolled at 17 different universities. All medical students were all in an advanced stage of their studies. 15 (42%) medical students were in their final year. 96% of all responders can imagine to work in the field of radiation oncology (physician, physicist or biologist). 71% of all students plan to work in the clinical field as well as to work in clinical or experimental research. 14% of all responders want to work fulltime in research and another 14% want to work fulltime in clinical field. Radiation oncology caught attention due to a good work-life-balance by 59% of all responders. The perspective to work in a private practise, in a clinic or university hospital is rates as 'very good' by 12%, 30% and 39% of all students. The opportunity to have a family with children and a career is seen as possible by 45%. The family situation is more important than a career by >90% of all responders.

#### Conclusion

The results of this survey show that >95% of all Club 100 members can imagine to start a career in radiation oncology and 71% of all responders want to work in the clinical field as well as in research. The work-life balance appears to be an important factor to start in radiation oncology. The family situation is an important part of career planning. Radiation oncology is perceived as family-friendly from a student perspective.

#### EP-1677 Low dose radiotherapy for painful joint and tendon disorders in elderly and risk for malignancies

R. Buecker<sup>1</sup>, R. Muecke<sup>2</sup>, U. Schaefer<sup>1</sup>

<sup>1</sup>Klinikum Lippe GmbH, Strahlentherapie / Radioonkologie, Lemgo, Germany ; <sup>2</sup>Strahlentherapie RheinMainNahe, Strahlentherapie / Radioonkologie, Bad Kreuznach, Germany

#### Purpose or Objective

Low-dose megavoltage or orthovoltage x-rays treatment for painful benign conditions in the locomotor system as arthrosis and chronic tendinopathy is still widespread in Germany, despite the theoretical risk of radiation-induced malignancies. The aim of this study was to investigate the rate of hematological malignancies, i.e. leukemia, non-Hodgkin's lymphoma, Hodgkin's disease and myeloma in patients treated with low dose x-rays

#### Material and Methods

A cohort of 3017 such patients (mean age 67 years, range 20 - 97 years), treated from 1995 -2007 at the General Hospital of Lippe (northern Germany) was analyzed with regard to the risk of hematologic malignancies suspected of emanating from red bone marrow. Therapy was applied on a conventional radiotherapy treatment with 200 kVorthovoltage x-rays in single fraction of 1 Gy to a total dose of 6 Gy in 6 fractions. Depending on the treated region, the absorbed red marrow dose was determined to be almost zero (elbow, hand, knee, foot; n= 1839),

intermediate (shoulder; n= 930), and high (mostly trochanteric bursa and hip, occasionally spine and sacroiliac joint; n= 248). The endpoints (hematological malignancies) were searched for by computer linkage with the hospital information system (the General Hospital of Lippe is the only oncological center for more than 350 0000 inhabitants). The rate of hematological malignancies has been assigned to the different dose groups.

#### Results

Median follow-up was 8.8 years (range: 0 - 22.7 years). In the zero dose group, the rates for all hematological malignancies, only leukemia, and only leukemia except chronic lymphocytic leukemia were 4 / 1839 (0.8%), 5 / 1839 (0.3%), and 4 / 1839 (0.2%). In the intermediate dose group (n= 929), the corresponding values were 11 / 930 (1.2%), 3 / 930 (0.3%), and 2 / 930 (0.2%). In the highest dose group (n= 248), corresponding values were 4 / 248 (1.6%), 2 / 248 (0.8%), and 1 / 248 (0.4%). The differences between the dose groups were not significantly different (chi-squared test). 332 (11 %) solid malignancies were detected.

#### Conclusion

No statistical evidence was provided in this cohort that a higher x-ray dose in the red bone marrow increases hematologic malignancies after low-dose radiotherapy of benign disease in middle-aged and older adults. However, in a larger number of patients, the differences between the dosage groups could reach the level of significance. Therefore, the extension of the cohort will be continued.

#### EP-1678 Modern radiotherapy learning: a scoping review of the literature

G. Walls<sup>1</sup>, S. McAleer<sup>2</sup>, G. Hanna<sup>1</sup>

<sup>1</sup>Queen's University Belfast, Centre for Cancer Research & Cell Biology, Belfast, United Kingdom ; <sup>2</sup>Queen's University Belfast, Centre for Medical Education, Belfast, United Kingdom

#### Purpose or Objective

The last two decades have seen revolutionary developments in both radiotherapy technology and postgraduate medical training. Trainees are expected to attain the required competencies over a period of five years using a mix of experiential learning, formal postgraduate teaching, self-directed learning and peer learning. Developing skills in radiotherapy relies on workplace-based learning in particular, and Radiation/Clinical Oncology is a recognised craft specialty where the apprenticeship model of education is applicable. The process of learning radiotherapy in its current form has not been comprehensively described.

#### Material and Methods

A systematic search of MEDLINE and EMBASE was undertaken to identify published studies of trainee and/or trainer experience of radiotherapy learning 1999-2018. Keywords used in the search included "radiotherapy", "radiation oncology", "postgraduate training", "postgraduate education" and "apprenticeship". Results pertaining to medical oncology, workforce trends, undergraduate radiotherapy exposure, academic training, global health, gender issues, non-medical staff, health service infrastructure and recruitment to training programmes were not included as they were out-with the focus of the research.

Publication Type	Freq (%)	Publication Timeframe	Freq (%)	Country	Freq (%)
Surveys	62	2015 - 2018	58	USA	59
Interventional	41	2011 - 2014	55	UK	21
Reports	28	2007 - 2010	21	Collaboration	20
Editorials	15	2003 - 2006	10	Canada	19
Pure research	8	1999 - 2002	2	Others	27
Interviews	3				

#### Results

Of 269 search results, 87 met the inclusion criteria. A further 59 publications cited in the search results were included in the synthesis. Only abstracts existed for 5

results. See table 1 below for a results summary. Surveys formed the greatest proportion of relevant manuscripts identified (n=62). The surveys were of trainees (n=32), trainers (n=11), both trainees and trainers (n=16) or were multidisciplinary (n=3).

#### Conclusion

Although studied since the emergence of Oncology as a specialty in the 1950s, there is a paucity of qualitative and quantitative research examining radiotherapy learning. Medical education is becoming a more popular focus in radiation oncology but no study has been designed to comprehensively assess the current status. A majority of the literature identified reports results of observational, local or national surveys with a tightly defined scope. The results of the search results indicate that variation has a major impact between different curriculum areas, within hospitals, within and between countries and over time. The important contributing factors were captured, as was the impact of suboptimal training. Emerging educational approaches to radiotherapy training were also proposed.

#### EP-1679 Modern radiotherapy learning: a qualitative study of trainer and trainee views

G. Walls<sup>1</sup>, G. Hanna<sup>1</sup>, S. McAleer<sup>2</sup>

<sup>1</sup>Queen's University Belfast, Centre for Cancer Research & Cell Biology, Belfast, United Kingdom ; <sup>2</sup>Queen's University Belfast, Centre for Medical Education, Belfast, United Kingdom

#### Purpose or Objective

Radiotherapy technology and postgraduate medical training have benefitted from considerable advances in recent decades. Trainees are expected to attain the required competencies over a period of five years using a mix of experiential learning, formal postgraduate teaching, self-directed learning and peer learning. Developing skills in radiotherapy relies on workplace-based learning in particular, and Radiation/Clinical Oncology is a recognised craft specialty where the apprenticeship model of education is applicable. The process of learning radiotherapy in its current form has not been comprehensively described, and it was postulated that a more accurate insight would be gained by including both stakeholders involved in the radiotherapy learning process.

#### Material and Methods

Five Clinical Oncology trainers and five Clinical Oncology trainees at a regional Cancer Centre were invited to undertake semi-structured interviews regarding their personal accounts of modern radiotherapy learning. All participants were treated as equal co-investors in the process of radiotherapy learning with the common ultimate aim of passing radiotherapy skills from trainers to trainees. Interviews lasted between 13 and 32 minutes. Following transcription, interpretative phenomenological analysis was performed.

#### Results

Trainee subjects had completed a median of 3 years of training, trainers had completed training for a median of 9 years, and 60% study participants female. With the increasing maturity of Clinical Oncology as a discipline, treatments are becoming more complex and cancer centres are becoming more busy, to the detriment of the apprenticeship model of learning. There is more onus on the trainee to navigate more advanced techniques in today's more rigorously structured training programme, whilst adapting to the increasingly time-pressured working environment. Moreover, insufficient confidence restricts new trainees. Despite this task, standardised, intra-centre factors are under-represented in the mandatory training requirements and owing to poor compatibility, the interface with the curriculum, ePortfolio, has not been fully engaged. The feedback on which competency-based training relies could be optimised, and increased both trainer and trainee commitment to radiotherapy learning

were insightfully suggested. A multitude of additional mechanisms were proposed to counter the challenges identified, not limited to enhanced induction, interdisciplinary teaching, trainee empowerment and mindfulness of collegiality. Both trainers and trainees offered tailored novel measures, illustrating the co-operative responsibility perceived in relation to RL, many of which would go some length to restoring a sense of apprenticeship in Clinical Oncology training.

#### Conclusion

It would be prudent for Clinical Oncologists with an interest in medical education to engage with both trainees and trainers to establish local challenges and opportunities.

#### EP-1680 The effectiveness and safety evaluation of radiotherapy for painful humeroscapular periarthritis (PHS)

T. Latusek<sup>1</sup>, G. Wozniak<sup>1</sup>, L. Miszczyk<sup>1</sup>

<sup>1</sup>Centrum Onkologii-Instytut im.M.Sklodowskiej-Curie Gliwice Branch, Radiotherapy, Gliwice, Poland

#### Purpose or Objective

Painful humeroscapular periarthritis (PHS) is a painful, degenerative skeletal disorder of unknown etiology. Among a large variety of treatment options, the radiotherapy (RT) represents a relevant method.

The aim of the study was to evaluate the efficacy and safety of radiotherapy for periarthritis of the shoulder.

#### Material and Methods

The research included a group of 60 patients with the Periarthritis of the shoulder irradiated in the Department of Radiotherapy in the Maria Sklodowska-Curie Memorial Cancer Center and Institute of Oncology Gliwice Branch. Patients' medical records have been analyzed retrospectively and a telephone survey has been carried out.

The following variables were assessed: pain duration before radiotherapy, shoulder function and pain evaluated using modified Constant- Murley and UCLA (University of California at Los Angeles) scales at the beginning of the therapy and during follow-up visits, the side effects after the irradiation in RTOG scale, duration of pain relief, the need for further treatment and necessity of analgesics use.

All patients were irradiated to a total dose of 6 Gy given in 6 fractions five times weekly. Cochran's Q test was used to assess the response to the therapy.

#### Results

The mean duration of follow-up was 3 years [range 2-6 years]. In 2012-2016, 60 patients were treated. 37% of the patients reported pain for months and 63% for years before radiotherapy. Nearly all patients had taken analgesics and had undergone physiotherapy.

During the first follow-up examination at the end of radiotherapy 60% of the patients reported pain relief and improvement of motility ( $p < 0.001$ ). In the telephone survey, 59% of the patients with pain relief stated that it had lasted for "years", in further 41% at least for "months". Necessity of analgesic use after radiotherapy was 10%. No radiation toxicity or secondary malignancies were observed.

#### Conclusion

The obtained results allow the conclusion that the low-dose radiotherapy for painful humeroscapular periarthritis may be an effective method of treatment; one that is often characterized by a long-lasting relief of pain and does not produce side effects.

#### EP-1681 Modern radiotherapy learning: a quantitative study of trainer and trainee views

G. Walls<sup>1</sup>, S. McAleer<sup>2</sup>, G. Hanna<sup>3</sup>

<sup>1</sup>Queen's University Belfast, Centre for Cancer Research & Cell Biology, Belfast, United Kingdom ; <sup>2</sup>Queen's University Belfast, Centre for Medical Education,

Belfast, United Kingdom ; <sup>3</sup>Queen's University Belfast, Centre for Cancer Research & Cell Biology, Belfast, United Kingdom

#### Purpose or Objective

Trainees in Clinical/Radiation Oncology previously learned radiotherapy skill in an apprenticeship model with their trainers. The last two decades have seen revolutionary developments in both radiotherapy technology and postgraduate medical training and therefore the current training landscape is different from that that current trainers experienced. The current state of radiotherapy training following this progress has not been explored comprehensively. As co-investors in the process of radiotherapy learning, passing radiotherapy skill from trainer to trainee, both the perspectives of trainers and trainees are important for this assessment.

#### Material and Methods

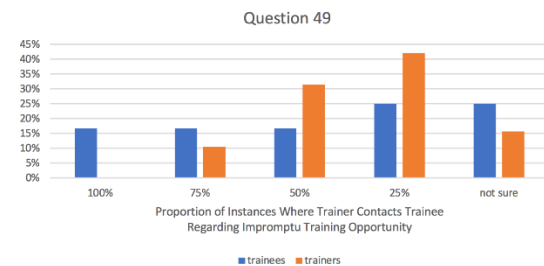
Clinical Oncology trainees and trainers at a regional Cancer Centre (n=34) were invited to undertake the same purpose-built questionnaire (69 questions). Four trainers (including two Educational Supervisors) and four trainees piloted the questionnaire, and input was sought from national leads in training Clinical Oncology training surveys. Significance testing was performed on pre-defined questions, and thematic analysis was performed on white space questions.

#### Results

Responses were received from 13 trainees and 19 trainers (96% invitees). The responses indicate that the training programme connects trainees to the necessary expertise and technology but several components could be optimised.

Discordance exists between some trainer and trainee views eg trainer and trainee responses were not aligned on how robust the programme induction is ( $p=0.005$ ), how encouraged trainees are to prioritise radiotherapy learning ( $p=0.009$ ) or how adequately equipped the First FRCR course prepares trainees for the physics ( $p=0.001$ ). Furthermore, trainees and trainers agreed on many points, such as Consultant observation of trainee volume delineation on a regular basis would optimise radiotherapy learning ( $p=0.182$ ) and peer teaching sessions increase trainee 'on the job' learning in the radiotherapy department ( $p=0.088$ ).

Additional differences between trainers and trainees were apparent from graphical representation of results eg graph 1 for 'proportion of instances where trainer contacts trainee regarding impromptu training opportunities'. Trainees are shown to have limited insight into the amount of plan analysis that occurs, and of the total components required for professional activity as a Consultant. Trainers on the other hand have poor awareness regarding trainee induction, general radiotherapy learning access outside their subspecialty, frequency of peer teaching and radiological anatomy teaching. A degree of validation of the bespoke questionnaire was achieved through comparison with RCR survey results.



#### Conclusion

The study demonstrated incomplete mutual understanding. Significant differences exist between the

perspective of trainers and trainees in radiation oncology and input from both stakeholders is needed for development. The survey tool should be validated in an external and large cohort for further evaluation.

## Physics E-posters

---

**Electronic Poster: Physics track: Radiation protection, secondary tumour induction and low dose (incl. imaging)**

---

### EP-1682 Fetal dose from head and neck tomotherapy versus 3D conformal radiotherapy

S.H. Park<sup>1</sup>, J. Choi<sup>1</sup>, Y.S. Kim<sup>1</sup>, J. Yoon<sup>2</sup>, S. Ahn<sup>3</sup>, W.H. Choi<sup>4</sup>

<sup>1</sup>Jeju National University Hospital, Department of Radiation Oncology, Jeju, Korea Republic of ; <sup>2</sup>Seoul National University Hospital, Department of Radiation Oncology, Seoul, Korea Republic of ; <sup>3</sup>Kangwon National University Hospital, Department of Radiation Oncology, Chuncheon, Korea Republic of ; <sup>4</sup>Gangnam Severance Hospital, Department of Radiation Oncology, Seoul, Korea Republic of

#### Purpose or Objective

To compare the dose of radiation received by the fetus in a pregnant patient irradiated for head and neck cancer using helical tomotherapy and 3-dimensional conformal radiation therapy (3DCRT).

#### Material and Methods

The patient was modeled with a humanoid phantom to mimic a gestation of 26 weeks. Radiotherapy with a total dose of 2 Gy in 20 fractions was delivered with both tomotherapy (2.5- and 5.0-cm jaw size) and 3DCRT. The position of the fetus was predicted to be 45 cm from the field edge at the time of treatment. The delivered dose was measured according to the distance from the field edge and the fetus using optically simulated luminescence dosimeters.

#### Results

The accumulated dose to the fetus was 1.6 cGy by 3DCRT and 2.0 and 2.3 cGy by the 2.5-and 5.0 cm jaw tomotherapy plans. For tomotherapy, the fetal dose with the 2.5-cm jaw was lower than that with the 5.0-cm jaw, although the radiation leakage was greater for 2.5-cm jaw plan due to the 1.5-fold longer beam-on time. At the uterine fundus, tomotherapy with a 5.0-cm jaw delivered the highest dose of 2.4 cGy. Considering that the fetus moves up to 35 cm at the 29th week of gestation, the resultant fetal doses for 3DCRT and tomotherapy with 2.5- and 5.0-cm jaws were estimated as 2.1, 2.7, and 3.9 cGy, respectively.

#### Conclusion

Fetal radiation dose was about 30% higher with tomotherapy than with 3DCRT, but this observed difference was tiny in absolute terms. For tomotherapy, scattering radiation was more important due to the high monitor unit values. Therefore, selecting a smaller jaw size for tomotherapy may reduce the fetal dose; however, evaluation of risk should be individually performed for each patient.

### EP-1683 Monte Carlo evaluation of organ doses from a proton gantry-mounted CBCT system

T. Henry<sup>1</sup>, O. Ardenfors<sup>1</sup>, I. Gudowska<sup>1</sup>, G. Poludniowski<sup>2</sup>, A. Dasu<sup>3</sup>

<sup>1</sup>Stockholm University, Medical Radiation Physics Department of Physics, Stockholm, Sweden ; <sup>2</sup>Karolinska University Hospital, Medical Radiation Physics and

Nuclear Medicine, Stockholm, Sweden ; <sup>3</sup>The Skandion Clinic, The Skandion Clinic, Uppsala, Sweden

#### Purpose or Objective

To simulate organ doses delivered by a proton gantry-mounted cone-beam computed tomography (CBCT) system using two Monte Carlo codes.

#### Material and Methods

The CBCT system at the Skandion Clinic, Uppsala, Sweden, was modelled using MCNP6 and GATE from measurements of depth doses in water and spatial profiles in air. The beam models were subsequently validated against absolute dose measurements in a CTDI phantom. Organ doses in a whole-body phantom from different CBCT scan modes (360° full scan, 190° posterior/anterior scans) and different protocols (Head, Thorax, Pelvis) were then evaluated with the validated Monte Carlo beam models. The influence of repeated imaging on organ doses was also investigated, taking into account different imaging schedules (weekly/daily imaging, based on a standard treatment schedule of 30 fractions).

#### Results

An agreement within 4% was observed between MCNP6, GATE and the measurements with regard to depth doses and beam profiles for all protocols. The resultant average agreement in absolute dose validation was 4%. In-field absorbed organ doses after a single 360° scan ranged between 6-8 mGy (Head protocol), 15-17 mGy (Thorax) and 24-54 mGy (Pelvis). The highest absorbed organ dose after a single scan (54 mGy) was deposited in the femoral heads for the Pelvis protocol. Total organ doses after repeated CBCT imaging ranged between 0.04 and 0.32 Gy for weekly imaging and 0.2-1.6 Gy for daily imaging, depending on the organ and protocol considered. An average increase of 24% in dose per mAs to the organs of interest was observed for the anterior scans in comparison to the 360° scans, while the posterior scans showed a 37% decrease.

#### Conclusion

An accurate model of a proton gantry-mounted CBCT system was implemented in the MCNP6 and GATE Monte Carlo codes and used to calculate organ doses in a whole-body phantom following CBCT acquisitions. Various protocols and acquisition modes were evaluated. Organ doses varied greatly depending on acquisition mode, favouring posterior scans.

### EP-1684 Radiation isocontour levels for shielding considerations of the Varian Halcyon linear accelerator

K. Caravani<sup>1</sup>, T. Jarema<sup>1</sup>, A. Kazi<sup>1</sup>, R. Murry<sup>1</sup>, G. Godwin<sup>2</sup>

<sup>1</sup>Radiation Oncology Centres, Physics, Toowoomba, Australia ; <sup>2</sup>Radiation Oncology Centres, Physics, Brisbane, Australia

#### Purpose or Objective

The purpose of this study was to create a radiation isocontour plot of the Varian Halcyon linear accelerator (Halcyon), within the bunker, with the aim of creating a Halcyon specific shielding design for future installations.

#### Material and Methods

A PTW 30013 Farmer chamber (with the manufacturer's supplied build-up cap) was positioned at predefined points in 15° increments around the room, in a horizontal plane at the height of the isocentre and at various radial distances. Static cardinal gantry angles were used, with collimator angle 45°, maximum field size 28 cm x 28 cm, 6 MV FFF beam, maximum dose rate 800 MU/minute and 1000 MU/reading. Room angles were defined as per Figure 1.

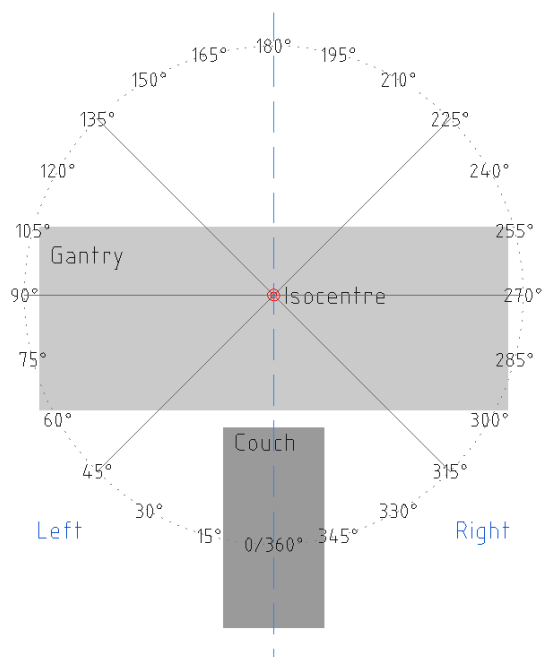


Figure 1: Illustration defining the room angles used for measurements.

Central axis (CAX) measurements in solid water, at depth of dose maximum, 100 cm SSD, for a 10 cm x 10 cm field, corrected for daily output variation, were used as a reference to give the relative reading [%]. Transmission through the beam stopper was measured for gantry 90° and 270° with the chamber at 1.5 m from the isocentre.

Head leakage measurements were made at 1 m behind the target, with closed MLC, collimator angle 0°, 1000 MU/reading, at room angles 90° and 270°.

#### Results

Initial horizontal plane measurement results at 1.5 m from the isocentre are shown in Figure 2.

The transmission through the beam stopper at a distance of 1.5 m from the isocentre was 0.003%. The inverse square law was used to calculate transmission at 1 m from the isocentre (0.007%). This agrees with the Varian Designers' Desk Reference, Halcyon Accelerator Edition (2017) which states that the transmission 1 m from the isocentre is < 0.1%.

The highest measurements were 0.28% and 0.27% at room angles 90° and 270° respectively, at 1.5 m from the isocentre. The average result of the head leakage measurements was 0.05%. Head leakage is required to be less than 0.1% as per IEC standard 60601-2-1. Gantry angles 0° and 180° provided similar results for the left and right (Figure 1) of the Halcyon, while Gantry angles 90° and 270° provided mirrored results.

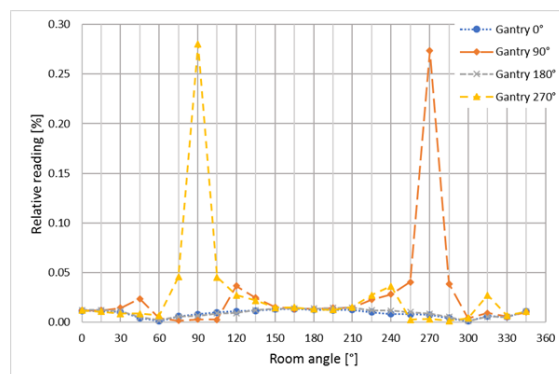


Figure 2: Relative readings [%] measured at a horizontal radial distance of 1.5 m from the isocentre at 15° increments.

Results at 2 m from isocentre follow the same trend as the results at 1.5 m.

Relative measurements in full scatter conditions are currently under investigation.

#### Conclusion

The relative radiation measurements in a horizontal plane throughout the bunker were plotted as a function of room angle for various distances from the Halcyon isocentre. Measurement results reported above fall within quoted reference values. These suggest that a primary barrier may not be required when designing a bunker for the Halcyon as the primary transmission through the primary beam stopper is negligible. This agrees with the Varian Designers' Desk Reference, Halcyon Accelerator Edition (2017) which states that a primary shielding wall is not required for the bunker.

#### EP-1685 Impact of acquisition mode of CBCT scans on size-specific dose estimates (SSDE) conversion factors

A. Abuhaimeid<sup>1</sup>, C. Martin<sup>2</sup>, O. Demirkaya<sup>3</sup>  
<sup>1</sup>King Abdulaziz City for Science and Technology, The National Centre for Applied Physics, Riyadh, Saudi Arabia ; <sup>2</sup>University of Glasgow, Department of Clinical Physics and Bioengineering, Glasgow, United Kingdom ; <sup>3</sup>King Faisal Specialist Hospital & Research Centre, Department of Biomedical Physics, Riyadh, Saudi Arabia

#### Purpose or Objective

This study aimed to investigate influence of an acquisition mode, namely the partial scan, which is used for cone-beam CT (CBCT) scans to image patients partially over 200°, on size conversion factors of size-specific dose estimates (SSDE), which were derived with the full 360° scan mode.

#### Material and Methods

The SSDE factors are used to account for patient size by converting a dose index that is measured in phantoms of reference sizes known as CTDI head and body phantoms. For a CBCT scan of nominal beam width > 40 mm, one of the dose indices, recommended by IEC, is called CTDI<sub>IEC</sub>. It is based on dose measurements at central and peripheral positions of the CTDI phantoms with a reference beam width of ≤ 40 mm, and free-in-air dose measurements for the beam of interest and the reference beam. SSDE factors for a Varian kV imaging system, namely on-board imaging (OBI), were derived to convert CTDI<sub>IEC</sub> values using Monte Carlo simulations with BEAMnrc and Cavity user codes under different conditions. SSDE factors were assessed in water phantoms of diameters ranging from 10 to 40 cm. The diameters range was selected to match the patient size that is given as a water equivalent diameter. Two clinical scan protocols, head and body, similar to those used in the clinic were employed. Four tube potentials of 80 - 140 kV and the full and partial scan modes were used to derive SSDE factors.

## Results

SSDE factors for the full scan mode were greater than those for the partial mode over all tube potentials studied using the head scan protocol (Fig.1). The full mode factors were higher by up to 7% for small sizes, and the differences were decreased as the phantom size increase reaching  $\pm 2\%$  for large sizes. The tube potential, however, was found to play a major role on factors of the body scan protocol (Fig. 1). For 80 kV, factors of the full and partial scan modes were comparable over all sizes, all being within  $\pm 1\%$ . However, for higher potentials, factors of the partial scan mode were greater than those for the full mode by (4 - 14%), (8 - 17%), and (9 - 17%) for 100, 120, and 140 kV, respectively. The body variations were also affected by the phantom size as the variations were raised by the size increase.

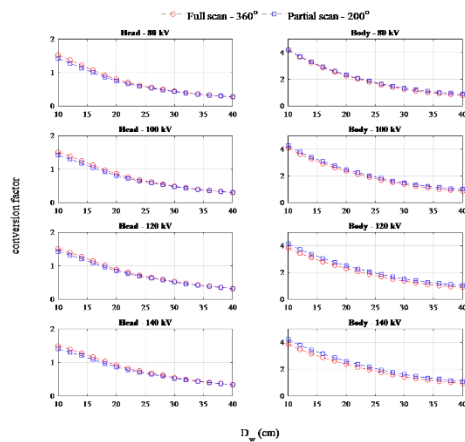


**Figure 1:** SSDE conversion factors for the head and body scan protocols using four tube potentials and the full and partial acquisition modes. The factors were derived for patients of sizes equivalent to a water phantom diameter ( $D_w$ ) in the range of 10 to 40 cm.

## Conclusion

Results of this study show that the SSDE factors derived for the full scan mode using the head scan protocol can be utilized for the partial mode with an over/underestimation reaching up to 7% over all sizes and for the tube potentials studied. For the body, negligible differences found for the lower tube potential, 80 kV, but attention to the differences should be paid if one uses the full mode factors for the partial mode at higher potentials. Moreover, influence of start point on CTDI measurements for partial scan should be taken into consideration.

## EP-1686 Assessment of patient size for size-specific dose estimates using two methods: a comparative study

A. Abuhaimed<sup>1</sup>, C. Martin<sup>2</sup>, O. Demirkaya<sup>3</sup>

<sup>1</sup>King Abdulaziz City for Science and Technology, The National Centre for Applied Physics, Riyadh, Saudi Arabia ; <sup>2</sup>University of Glasgow, Department of Clinical Physics and Bioengineering, Glasgow, United Kingdom ; <sup>3</sup>King Faisal Specialist Hospital & Research Centre, Department of Biomedical Physics, Riyadh, Saudi Arabia

## Purpose or Objective

Volume CT dose index ( $CTDI_{vol}$ ), which is assessed in cylindrical phantoms of reference sizes, is one of the main dose indices utilized for CT dosimetry. Since  $CTDI_{vol}$  is assessed in standard phantoms, it does not give the user an accurate indication of the dose absorbed by a patient of a specific size, which is different from the reference ones. As a result, the concept of size-specific dose estimates (SSDE) has been developed to overcome this limitation. SSDE is based mainly on determination of the

patient size. Aim of this study was to compare between two methods used to evaluate the patient size.

## Material and Methods

The first method is based on determination of the patient's dimensions for the region of interest (ROI). This includes anterior-posterior dimension and lateral dimension, from which effective diameter (ED) of the patient is calculated as suggested by AAPM TG-204. However, this method is limited as it does not distinguish between low and high attenuated regions. Therefore, an alternative method was suggested by AAPM TG-220 to account for attenuation of the ROI. It requires evaluating the mean CT number of the ROI, and number and area of pixels located in the same region. This allows estimation of the patient size as a water equivalent diameter (WED), from which a conversion factor can be applied to  $CTDI_{vol}$ . A MATLAB-based code was developed in house to import the ICRP reference adult phantoms, and to assess ED and WED for each slice of the two reference phantoms that represent an average male and female. Only the trunk was considered, and divided to three regions: thorax, abdomen, and pelvis.

## Results

Figure 1 shows variations between the methods studied for each slice. The variations were found to be comparable for both phantoms. WED values were higher than those for ED by 11% at the upper part of the thorax at most slices due to the higher attenuated area resulting from the shoulder. However, for the slices of the lower part, ED values became higher by up to 12% due to soft tissues existing in this part, e.g. lung and heart. Soft tissues were also spread largely over the abdomen region, which resulted in obtaining ED values that were higher. For the male phantom, ED values were higher by  $\sim 5\%$  over most of the slices, but the variations were reduced for the female phantom from 8 to 2% when the slices were moved down. WED values of the male phantom were lower over all the pelvic region by up to 6%. For the female phantom, however, WED values were within  $\pm 3\%$  of those for ED at most slices.

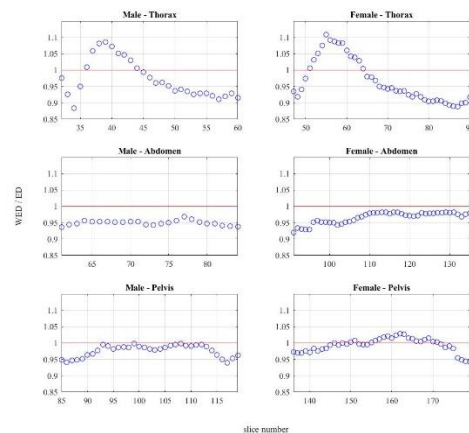


**Figure 1:** Variations between the ED and WED methods on the ICRP phantoms. Slice number is increased as the slice moves down of the body.

## Conclusion

The comparison shows that the variations between the methods investigated were within  $\pm 12\%$ ,  $\pm 8\%$ , and  $\pm 6\%$  for the thorax, abdomen, and pelvic regions, respectively. Since evaluation of the ED is relatively easier than that for the WED, one may use the ED method to obtain an approximate estimation for the patient dose, taking into consideration the uncertainty associated with this method, and that the WED is the accurate method to assess the dose.

### EP-1687 Variation of size-specific dose estimates (SSDE) of cone-beam CT (CBCT) scans with the scan length

A. Abuhaimeed<sup>1</sup>, C. Martin<sup>2</sup>, O. Demirkaya<sup>3</sup>

<sup>1</sup>King Abdulaziz City for Science and Technology, The National Centre for Applied Physics, Riyadh, Saudi Arabia ; <sup>2</sup>University of Glasgow, Department of Clinical Physics and Bioengineering, Glasgow, United Kingdom ; <sup>3</sup>King Faisal Specialist Hospital & Research Centre, Department of Biomedical Physics, Riyadh, Saudi Arabia

#### Purpose or Objective

Length of a cone-beam CT (CBCT) scan is defined mainly by the clinical need. Recently, size-specific dose estimates (SSDE) has been recommended to estimate the imaging dose received by a specific patient from a given scan. SSDE is based on determination of size of the area of interest for the patient, i.e. region being scanned. Since length of this area is varied by the scan length, this investigation aimed to study impact of the scan length on SSDE values for CBCT scans.

#### Material and Methods

Monte Carlo simulations with user codes, BEAMnrc and Cavity, that were based on EGSnrc system, were employed to model a Varian on-board imager (OBI) kV system integrated into a linear accelerator (Truebeam), and to assess doses in water phantoms of diameters ranging from 10 - 40 cm. This allowed derivation of size conversion factors required to assess SSDE. The factors were derived in water phantoms to be linked to the patient size, which is reported in terms of a water equivalent diameter ( $D_w$ ). SSDE of CBCT scans were assessed by applying the conversion factors to the dose index  $CTDI_{IEC}$ , which is recommended by IEC as a dose index for CBCT scans. A MATLAB-based code developed in house to calculate  $D_w$  of the region of interest was utilized. The ICRP adult male and female reference phantoms were used in this study to represent average sizes for adult patients. Impact of the scan length was investigated in the trunk, which was divided to three regions, thorax, abdomen, and pelvis. Eleven scan lengths ranging from 80 - 280 mm, with increments of 20 mm, were used for each region, and centers of each scan was set at middle of these regions. The protocol used in the clinic to scan the body was applied, and the beam widths in the z-axis for CBCT scans were set the scan lengths studied.

#### Results

Minimum, maximum, and mean values of  $D_w$  for the region of interest were assessed for each scan.  $CTDI_{IEC}$  of the body scan was evaluated to be 2.46 mGy/100 mAs, and this value was converted to SSDE using the different values of  $D_w$  as shown in Figure 1. Use of the mean and maximum values of  $D_w$  to assess SSDE indicated less dependency on the scan length, where SSDE values were only varied by up to  $\pm 5\%$  over all the scan lengths studied. However, SSDE values based on the minimum values of  $D_w$  were affected by the scan length, particularly for the thorax region, where extension of the scan length from middle of the region to the upper part included the shoulder that had a higher attenuation area. The lower variations in SSDE values based on the mean  $D_w$  values were found for the abdomen region, all being within  $\pm 1\%$ , as the attenuation values for the tissues in this region are comparable.

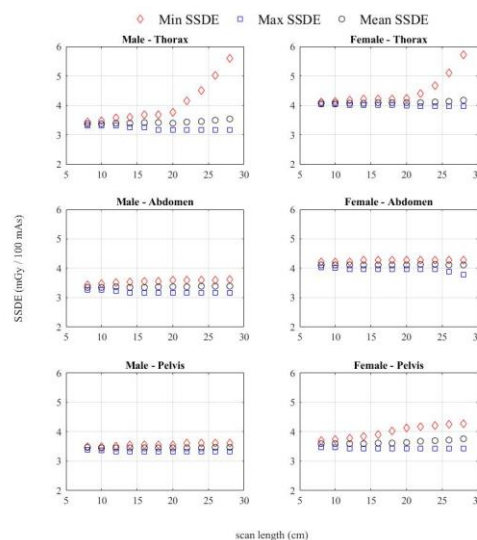


**Figure 1:** Influence of the scan length on SSDE values based on minimum, maximum, and mean values of  $D_w$  for the regions of interest.

#### Conclusion

Estimation of SSDE values based on the mean  $D_w$  for the regions of interest showed to give a good indication for the patient dose as the scan length had a minimal influence on SSDE values as well as it took into account the minimum and maximum values of  $D_w$ .

### EP-1688 Monte Carlo simulations to quantify out-of-field doses due to the electron streaming effect

V.N. Malkov<sup>1</sup>, S.L. Hackett<sup>1</sup>, J.W.H. Wolthaus<sup>1</sup>, B.W. Raaijmakers<sup>1</sup>, B. Van Asselen<sup>1</sup>

<sup>1</sup>UMC Utrecht, Department of Radiation Oncology, Utrecht, The Netherlands

#### Purpose or Objective

In the context of magnetic resonance guided radiation therapy (MRgRT), the influence of the magnetic field on surface doses has been an ongoing area of research. The electron return effect (ERE) can contribute to a significant increase in surface doses at boundaries (Raaijmakers et al.). In addition to the ERE, in orthogonal magnetic field orientations, electrons are swept out of the irradiated air volume. This leads to a reduction of in-field entry surface doses, but contaminant streaming electrons can contribute up to about 5.4% to out of field doses (Hackett et al., 2018). Further, Park et al. (2018) studied treatment accelerated partial breast plans with either a 0 or 0.35 T perpendicular magnetic field and found that the presence of the magnetic field induced out-of-field doses as large as 15% of the prescription dose to extend in the air along the magnetic field. In this work, the out-of-field surface doses contribution due to backscattered or ejected electrons, focused by the magnetic field, is studied. This electron streaming effect (ESE) can contribute to substantial out-of-field doses and requires detail study.

#### Material and Methods

The EGSnrc Monte Carlo package is used to simulate a water phantom with an incident  $10 \times 10 \text{ cm}^2$  7MV FFF beam. As shown in Figure 1, the phantom entry or exit surface is inclined with respect to the magnetic field, and an out-of-field water panel is positioned 10cm away from, and centered, on the isocenter. The surface dose profiles in the water panel are calculated with either a 0, 0.35, or 1.5 T magnetic field and inclines of 10, 30, or 45°.

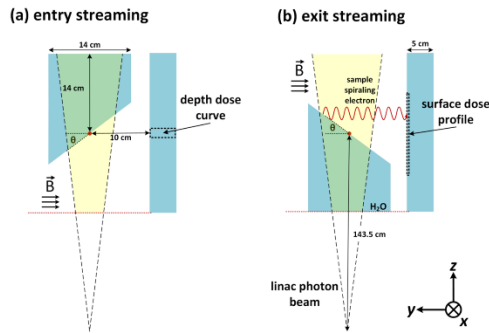


Figure 1: Schematic of EGSnrc simulation set-up of the (a) entry and (b) exit inclined phantoms.

## Results

As the magnetic field increases, in the entry and exit simulations, the dose distributions become sharper, as shown in Figure 2 for the exit streaming case. The maximum doses for the 0.35T exit simulations are 22.9%, 38.0%, and 42.8% for the respective 10, 30, and 45° simulations. For 1.5T, for the same angles, the maximum values are 16.7%, 29.6%, and 36.4%. Dose values drop to below 2% within the first 1cm of the out-of-field water phantom. For the entry simulation, the largest ESE doses were observed for the 45° simulation and were 4.5% and 8.0% for the 0.35 and 1.5T magnetic fields, respectively. Percentages are with respect to the maximum deliverable dose by the beam to a large water phantom.

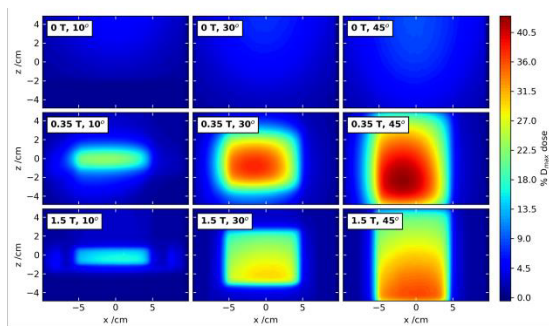


Figure 2: Surface dose profiles in the out-of-field for the exit streaming simulation

## Conclusion

The ESE can contribute to notable out-of-field doses and should be considered during treatment planning for MRgRT systems. Treatments often include several beams which will spread out the overall effect. In situation where ESE doses are unavoidable, a 1cm bolus or the already mounted RF coils would greatly reduce the effect. Further exploration is required into the capabilities of the treatment planning system to capture this effect.

### EP-1689 Implementation of ultra-low dose CBCT for children using an optimised bowtie filter

A. Bryce-Atkinson<sup>1</sup>, M.C. Aznar<sup>1</sup>, G. Whitfield<sup>2</sup>, M. Van Herk<sup>1</sup>

<sup>1</sup>The University of Manchester, Division of Cancer Sciences- School of Medical Sciences- Faculty of Biology Medicine and Health, Manchester, United Kingdom ; <sup>2</sup>The University of Manchester, Manchester Academic Health Science Centre- The Christie NHS Foundation Trust, Manchester, United Kingdom

### Purpose or Objective

Cone beam CT (CBCT) image guidance can lead to excessive doses to children undergoing radiotherapy due to incorrect use of imaging protocols designed for adults. But even with correct protocols, there are concerns of late effects due to imaging dose, affecting the use of image

guidance in children (e.g. choice of imaging modality and frequency of acquisition). The aim of this work is to implement ultra-low dose CBCT through use of a bowtie filter specifically designed for paediatric CBCT: it provides additional attenuation to reduce exposure and is shaped to fit the smaller body size of children. Here, we quantitatively evaluate the effect of implementing such a filter on image quality, registration accuracy and dose.

### Material and Methods

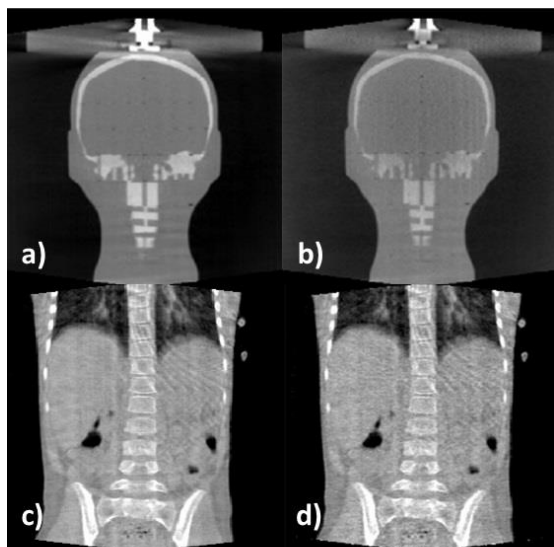
The paediatric bowtie filter (Fig.1) provides additional attenuation compared to the standard (adult) Elekta XVI bowtie filter and produces uniform X-ray intensity across the average paediatric patient in the lateral direction, as derived from 15 paediatric CBCT scans. This bowtie filter was used to scan an ATOM 10-year-old paediatric phantom at the lowest dose in the brain, thorax and abdominal regions. Registration accuracy was recorded as a measure of image quality and its suitability for IGRT. Each CBCT was automatically registered to the planning CT, matching on bony anatomy. The couch shift derived from the low dose scans was compared to that for the standard dose scans (100kV, 0.16mAs per frame, 200 frames). In addition, CBCT scans with the paediatric bowtie filter were simulated for 23 paediatric patients using a noise addition method, and the registration results were compared to that of the original acquisition.



Fig 1: The paediatric bowtie filter. The thick central part of the filter reduced exposure fivefold.

### Results

The lowest exposure acquired was equivalent to 15.6% of the standard low dose exposure used for children (0.8mGy to 0.13mGy). This dose level is well below the leakage dose of head and MLC. Bone-equivalent material in the phantom scans and bony anatomy in the simulated paediatric scans remained clearly visible, although increased noise was apparent in the images (Fig. 2). All acquired phantom scans and simulated patient scans had registration discrepancies of less than 1mm compared to the standard paediatric exposure. The filter can also be used at higher exposures, giving a greater range of ultra-low dose imaging protocols than is currently clinically available, such that optimised paediatric imaging protocols can be developed for different age groups.



**Fig 2:** Comparison of image quality of a) A typical paediatric exposure scan of the ATOM 10 year old phantom. b) The lowest dose phantom scan at 15% of this exposure (0.13 mGy). c) A typical paediatric patient scan (100kV, 0.16mAs). d) Same as c but with the new bowtie filter simulated by adding non-uniform noise.

### Conclusion

A bowtie filter optimised for children has been implemented and evaluated in phantom scans and simulated in patient CBCT data. Even at the lowest exposure setting, registration accuracy and image quality were sufficient, i.e., the filter provided considerable dose reduction to paediatric patients without affecting image guidance.

The authors are grateful to Elekta Oncology Systems for manufacture of the bowtie filter.

### EP-1690 Induced radioactivity as a (un)helpful effect of particle therapy

P. Sekowski<sup>1</sup>, I. Skwira-Chalot<sup>1</sup>, T. Matulewicz<sup>1</sup>

<sup>1</sup>University of Warsaw, Faculty of Physics, Warsaw, Poland

### Purpose or Objective

Particle therapy is a rapidly developing form of radiation therapy of tumours, but it still has many secrets which are continually discovered. The main purpose of our project is to measure radioactivity induced in the human body during hadron therapy tumour treatment and assessment of its influence on therapy effects and causation of secondary tumours.

### Material and Methods

In order to find the sources of induced radioactivity in the patient's body, the targets, which are very similar to humans tissues, have irradiated with commonly used beams in hadrontherapy. For that, the pig liver and bone meal were chosen and as projectiles, the proton beam of 60 MeV and neutron beam obtained from the neutron source were used. After irradiation, the samples measured using the low-background spectrometer, at INP PAS in Kraków. Based on Geant4, the Monte Carlo simulations were simultaneously performed. In our experiments, the proton beam of 60 MeV and neutron beam obtained from the neutron source were used.

### Results

Table 1 presents the list of isotopes which were identified after bone tissue irradiation of 60 MeV proton beam. One can see that the total dose from induced radioactivity for prescribed dose as 80 Gy in 100 c.c. tumour volume is approximately 30 µGy.

### Isotope Dose [pGy c.c. /Gy\_therapy]

Cl-34m 546 +/- 95

K-42 145.7 +/- 6.3

Sc-44 99.5 +/- 3.7

K-43 6.3 +/- 5.4

Sc-47 10.70 +/- 0.49

K-38 3100 +/- 1500

Sc-43 42.2 +/- 2.7

### Conclusion

As we can see above the additional dose using a low energetic proton beam is not significant. But for bigger tumours and highly energetic beams, the contribution of induced radioactivity could be higher. Moreover, as we can see in case of Proton Boron Cancer Therapy that even a small amount of specific element (in the case of PBCT - B-8) can significantly change the therapy effects. That is why the effect of induced radioactivity cannot be omitted and have to be estimated and taken into consideration during treatment planning.

### EP-1691 IORT and stray radiation: comparison of 2 commercial linacs

P. Stevens<sup>1</sup>, F. Van Hoof<sup>1</sup>, M. Holvoet<sup>1</sup>, E. Messens<sup>1</sup>, L. Grasso<sup>2</sup>, S. De Stefano<sup>2</sup>, G. Felici<sup>2</sup>, D. Verellen<sup>1</sup>

<sup>1</sup>GZA- Ziekenhuizen - St. Augustinus, Radiation Physics, Wilrijk, Belgium ; <sup>2</sup>SIT, Physics, Aprilia, Italy

### Purpose or Objective

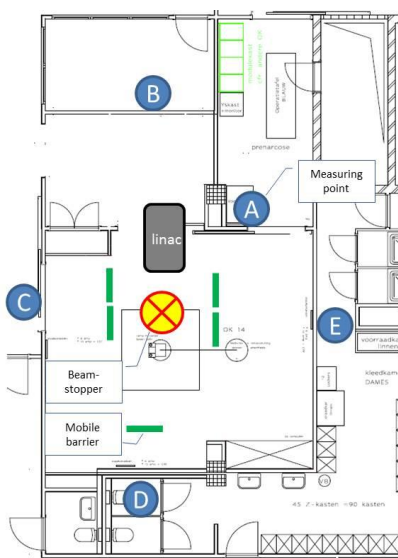
Intraoperative Radiation Therapy (IORT) is performed with a linear accelerator in a standard operating room mainly constructed with 7 cm drywall walls. An important safety issue of IORT is radiation protection and stray radiation. This stray radiation is mainly produced by the accelerator itself (leakage radiation) and the patient (Patient Stray Radiation), as per NCRP 151. Two IORT dedicated electron linacs (IntraOp Mobetron 1000 and SIT Liac HWL) have been installed in the same operating room in our institute, providing a unique opportunity to benchmark both with regard to radiation protection performances.

### Material and Methods

The 2 linacs were positioned in the center of the Operating Room; measurements have been performed with a reference applicator (100 mm applicator with bevel 0°) positioned on a 15 cm thick RW3 phantom, at a height of 100 cm above the floor with their beamstopper. Both linacs were set up at an energy of 12 MeV and a dose rate (DR) of 1000 MU/min or 550 MU/min. Measurements for the Liac HWL were performed with and without mobile barriers provided by the manufacturer. Instantaneous dose rate (IDR) was measured at 5 points against the wall of the surrounding rooms in the patient plane and at the hotspot at groundlevel beneath the OR with 3 survey meters: Canberra Babyline 81, Canberra Babyline 81\*, Fluke 451 P. Additional surveys were performed in the rooms surrounding the OR and personnel InLight dosimeters were placed at critical locations to assess the weekly dose equivalent during clinical use.

## Results

Device and set up	measuring point	Instant dose rate ( $\mu\text{Sv/h}$ )		
		Canberra babyline 81	Canberra babyline 81*	Fluke 451 P
MOBETRON	A	2000	200	/
DR 1000	B	300	50	/
12 MeV	C	1500	800	/
Without mobile barriers	D	300	100	/
	E	100	100	/
	downstairs	/	600	/
LIAC HWL for preliminary testing	A	200	150	200
DR 1000	B	60	30	60
12 MeV	C	200	200	200
with mobile barriers	D	40	100	40
beamstopper 70 cm	E	80	50	80
	downstairs	20	50	20
LIAC HWL 54	A	90	/	95
DR 500	B	15	/	20
12 MeV	C	50	/	60
with mobile barriers	D	30	/	35
beamstopper 90 cm	E	40	/	45
	downstairs	5	/	/
LIAC HWL 54	A	90	150	130
DR 1000	B	15	35	18
12 MeV	C	50	50	35
with mobile barriers	D	30	40	25
beamstopper 90 cm	E	40	40	25
clinical set up	downstairs	5	20	5
LIAC HWL 54	A	/	150	/
DR 1000	B	/	35	/
12 MeV	C	/	150	/
without mobile barriers	D	/	90	/
beamstopper 90 cm	E	/	100	/
	downstairs	/	20	/



The personnel dosimeters didn't register a monthly dose exceeding the minimal reporting limit (50  $\mu\text{Sv}$ ) for the treatment of 44 patients (480 Gy) over 5 months with the Liac HWL.

## Conclusion

In terms of stray radiation Liac HWL outperforms Mobetron 1000 both in the patient plane and the room beneath the OR. The Liac HWL produces an equal amount of stray radiation at a dose rate of 10 Gy/min or 5.5 Gy/min. The beamstopper was redesigned to reduce stray radiation below the limit of 10  $\mu\text{Sv/h}$  in the room under the OR. The mobile barriers reduce the stray radiation in patient plane. The personnel dosimeters confirm the survey measurements.

### Electronic Poster: Physics track: Basic dosimetry and phantom and detector development

#### EP-1692 Flatbed scanner stability for radiochromic film dosimetry

C. Laosa<sup>1</sup>, J.F. Calvo Ortega<sup>2</sup>, S. Moragues Femenia<sup>2</sup>, J. Casals<sup>2</sup>

<sup>1</sup>Hospital Quirónsalud, Radioterapia, 08035, Spain ;

<sup>2</sup>Hospital Quirónsalud Barcelona, Radiotherapy, Barcelona, Spain

## Purpose or Objective

To investigate the stability of a flatbed scanner used for radiochromic film dosimetry.

## Material and Methods

An Epson Pro V750 flatbed scanner and EBT3 films of a same batch were used. A piece of film exposed to 1 Gy was aged for 4 months so that its post-exposure change was considered as zero. The aged film and an unexposed film piece were simultaneously scanned in the center of the bed scanner. A 1 mm-thick glass sheet was used to avoid film curling. Transmission mode, RGB-48 bits and 72 dpi resolution were used. The scanner was warmed-up for at least 30 min before the scanning. For each scanning session, five empty scans were taken to stabilize the scanner lamp. After that, five consecutive scans were made. The first scan was discarded and the resulting image was the average of the remaining four. The film image was converted into a dose image using the triple-channel method implemented in Radiochromic.com software (<https://radiochromic.com>). The unexposed film piece was used to apply the inter-scan correction option of Radiochromic.com. Two approaches were considered to investigate the stability of the scanner: 1) the scanner was uninterruptedly powered on during 45 days. For each day, several scanning sessions were performed at different times. A total of 88 sessions were recorded. 2) During a period of 13 consecutive days, the scanner was powered on every day before the scanning session, and after finished, it was powered off. For each day, several scanning sessions were performed at different times. A total of 67 sessions were recorded. Average dose in a specific ROI over the aged film (DROI) was monitored over all scanning sessions for the two approaches. Fluctuation (SD to average ratio) of DROI was analyzed for each approach.

## Results

Fluctuations of 1.4% and 2.6% for  $D_{ROI}$  were observed for the approaches 1 and 2, respectively. 95<sup>th</sup> percentiles of 2.3% and 4.8% were respectively found for the deviation of  $D_{ROI}$  with respect to the average  $D_{ROI}$  over all scanning sessions.

## Conclusion

According to the results, keeping the scanner powered on improved its stability.

#### EP-1693 Determination of the angular dependence of a CC04 ion chamber

A. Prado<sup>1</sup>, Á. Gaitán<sup>2</sup>, M. Manzano<sup>2</sup>, M. Leonor<sup>2</sup>

<sup>1</sup>Hospital Universitario 12 de octubre, Oncología Radioterápica. Sección de Radiofísica., Madrid, Spain ;

<sup>2</sup>Hospital Universitario 12 de octubre, Radiofísica y Protección Radiológica., Madrid, Spain

## Purpose or Objective

Due to the specific geometry and design of each type of detector, its response when exposed to a radiation beam might vary with the angle of incidence. In the present work this angular dependence is quantified for a CC04 (IBA Dosimetry) ion chamber.

Due to the specific geometry and design of each type of detector, its response when exposed to a radiation beam might vary with the angle of incidence. In the present work this angular dependence is quantified for a CC04 (IBA Dosimetry) ion chamber. **Material and Methods**

Measurements were performed on a Varian Clinac iX using a 6MV beam energy. A CC04 ion chamber and a Bahnhofstrasse 5 (IBA Dosimetry) electrometer were utilized. A home-made phantom made of high-density

polyethylene with a cavity adapted to the size of the ion chamber used was employed (fig. 1). This cavity was constructed so as to make the center of the phantom coincide with the reference point of the chamber. The phantom is comprised of a half sphere joined to a cylindrical region. The center of the phantom was located at 10 cm depth from the spherical region surface. The phantom center was positioned at the unit isocenter. The phantom spherical region pointed upwards, being the chamber perpendicular to the couch plane. In this way, it was possible to rotate the gantry between 90° and 270° without moving the couch. In each measurement 200 MU were delivered using a 600 MU/min dose rate and a 4x4 cm<sup>2</sup> field size. Gantry angles between 90° and 270° in 10° steps were used, performing three measurements per angle and calculating the average and the standard deviation for each position. Results were normalized to the value obtained at 0° (ion chamber parallel to the radiation beam).



Figure 1: Home-made phantom used with a cavity adapted to the CC04 ion chamber size.

Measurements were performed on a Varian Clinac iX using a 6MV beam energy. A CC04 ion chamber and a Bahnhofstrasse 5 (IBA Dosimetry) electrometer were utilized. A home-made phantom made of high-density polyethylene with a cavity adapted to the size of the ion chamber used was employed (fig. 1). This cavity was constructed so as to make the center of the phantom coincide with the reference point of the chamber. The phantom is comprised of a half sphere joined to a cylindrical region. The center of the phantom was located at 10 cm depth from the spherical region surface. The phantom center was positioned at the unit isocenter. The phantom spherical region pointed upwards, being the chamber perpendicular to the couch plane. In this way, it was possible to rotate the gantry between 90° and 270° without moving the couch. In each measurement 200 MU were delivered using a 600 MU/min dose rate and a 4x4 cm<sup>2</sup> field size. Gantry angles between 90° and 270° in 10° steps were used, performing three measurements per angle and calculating the average and the standard deviation for each position. Results were normalized to the value obtained at 0° (ion chamber parallel to the radiation beam). Figure 1: Home-made phantom used with a cavity adapted to the CC04 ion chamber size. **Results** Results agree with the IEC 60731 document, which states that the angular dependence of an ion chamber should not exceed a 1% deviation in the angular interval comprised between ±40° (maximum deviation was 0.45% at -40°). However, for gantry angles greater than 40° an increasing angular dependence was found. In figure 2 the percent deviations of the normalized values as a function of the gantry angle is depicted. Some symmetry with respect to 0° is observed mainly due to the cylindrical geometry of the chamber as well as due to the irradiation geometry. Deviations up to 3.6% with respect to the 0° value were observed (at -90°). For each angle the standard deviation did not exceed 0.1%, so it was decided not to perform a higher number of measurements per gantry position.

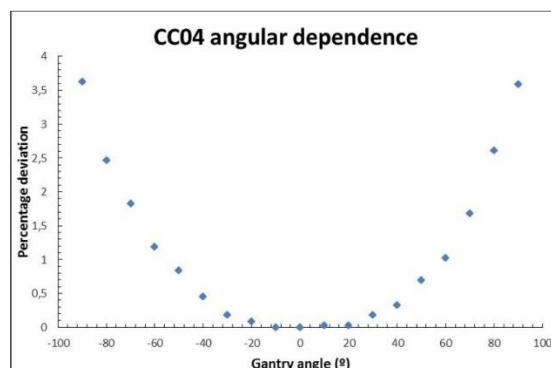


Figure 2: CC04 angular dependence in percentage deviation with respect to 0° value as a function of gantry angle.

Results agree with the IEC 60731 document, which states that the angular dependence of an ion chamber should not exceed a 1% deviation in the angular interval comprised between ±40° (maximum deviation was 0.45% at -40°). However, for gantry angles greater than 40° an increasing angular dependence was found. In figure 2 the percent deviations of the normalized values as a function of the gantry angle is depicted. Some symmetry with respect to 0° is observed mainly due to the cylindrical geometry of the chamber as well as due to the irradiation geometry. Deviations up to 3.6% with respect to the 0° value were observed (at -90°). For each angle the standard deviation did not exceed 0.1%, so it was decided not to perform a higher number of measurements per gantry position. Figure 2: CC04 angular dependence in percentage deviation with respect to 0° value as a function of gantry angle. **Conclusion**

The angular dependence of a CC04 ion chamber was obtained for an angular interval between 90° and 270°. This dependence is in accordance with the IEC 60731 document, but it increases as the angle deviates from 0° up to 3.6% at -90°. Considering these results it is recommended that the angular dependence of the detectors used be known by the user, being this data provided by the manufacturer or measured by the user itself. A proper characterization of this dependence could be employed to calculate correction factors to be applied when using an ion chamber.

The angular dependence of a CC04 ion chamber was obtained for an angular interval between 90° and 270°. This dependence is in accordance with the IEC 60731 document, but it increases as the angle deviates from 0° up to 3.6% at -90°. Considering these results it is recommended that the angular dependence of the detectors used be known by the user, being this data provided by the manufacturer or measured by the user itself. A proper characterization of this dependence could be employed to calculate correction factors to be applied when using an ion chamber.

#### EP-1694 Evaluation of a new portal dosimetry solution for dose quality control of Elekta and Varian linacs

S. Couespel<sup>1</sup>, N. Delaby<sup>1</sup>, S. Sorel<sup>1</sup>, C. Boutry<sup>2,3</sup>, C. Lafond<sup>1,4</sup>

<sup>1</sup>Centre Eugène Marquis, Ille-et-Vilaine, Rennes, France ;

<sup>2</sup>Groupe Oncorad Garonne, Tarn-et-Garonne, Montauban, France ; <sup>3</sup>Dream SAS, Haute-Garonne, Toulouse, France ;

<sup>4</sup>Univ Rennes- CLCC Eugène Marquis- Inserm- LTSI-UMR 1099, Ille-et-Vilaine, Rennes, France

#### Purpose or Objective

The aim of this study is to evaluate a new portal dosimetry solution (ARTISCAN Beam QA, AQUILAB - France) for independent QA of photon and electron beams on Elekta and Varian linacs.

## Material and Methods

ARTISCAN Beam QA software is based on EpiDream method (Boutry et al, Med Phys 2017) converting EPID signal in air into absorbed dose in reference conditions. The product is developed to perform dose quality control of photon and electron beams using EPID.

Our study was performed on 6 MV and 6 MV FFF photon beams from Elekta linac (Versa HD with iViewGT v3.4.1) and on 6 MV photon beam and 6 MeV electron beam from Varian linac (Clinac 2100C with EPID AS500). Intrinsic characteristics of the solution were first evaluated, including repeatability, reproducibility, dose linearity and dose consistency over the time. Then, we performed tests of our current internal QA program: daily X-Ray and electron output constancy, beam profiles constancy, wedge transmission factor constancy, monitor chamber linearity. Results were compared to those obtained with ionization chamber (0.6 cc, PTW) or with ionization chamber 2D-matrix (StarCheck, PTW).

## Results

The reproducibility of 10 EPID measurements was 0.09% for 6 MV (Elekta). Dose linearity for photon and electron beams for the Varian linac was better than 1% for MUs higher than 20 with EPID solution. From 3 to 15 MUs, dose linearity was between 1.3% and 2.4% for photon beam and 0.7% and 1.9% for electron beam EPID solution. A 4 months analysis showed a dose deviation for a square field between +0.05% and -1.25% for 6 MV beam and between +0.39% and -1% for 6 MV FFF beam (Elekta). For the daily output constancy on Elekta linac, the mean difference obtained for 32 QAs between EPID dosimetry and ionization chamber was -0.1% ( $\sigma=0.3\%$ ) for 6 MV and -0.6% ( $\sigma=0.3\%$ ) for 6 MV FFF beam. Beam profiles obtained with ARTISCAN Beam QA software and the StarCheck were plotted for 6 MV, 6 MV FFF and 6 MeV beams in Fig 1. The difference on wedge transmission factor obtained with EPID solution and ionization chamber was 0.2% for 6 MV (Varian). The maximal difference on monitor chamber linearity for 6 MV beam (Varian) between EPID solution and ionization chamber was 1.4% for MUs higher than 3, reaching 5% for 1 MU.

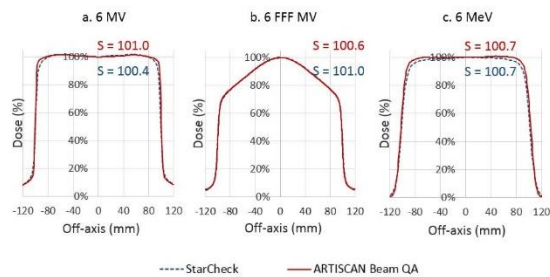


Fig 1: Inplane profiles for 6 MV (a), 6 FFF MV (b), photon beams and 6 MeV (c), electron beam, obtained with the StarCheck matrix (blue dashed curves) and with ARTISCAN Beam QA (red solid curves). The symmetry  $S$  is computed as  $S = 100 \times \left( \frac{D(x)}{D(-x)} \right)_{\max}$ ,  $D(x)$  and  $D(-x)$  being the symmetric points in the 80% isodose for the photon beams and in the 90% isodose -1 cm for the electron beam.

## Conclusion

Our results showed that the EPID dosimetry solution proposed by AQUILAB seems to be promising to perform QA programs on Elekta and Varian linacs for both photon and electron beams.

## Reference

A simple algorithm to convert EPID gray values into absorbed dose to water without prior knowledge. Boutry C, Sors A, Fontaine J, Delaby N, Delpon G. Med Phys. 2017 Dec; 44(12):6647-6653.

## EP-1695 Determining the dose per pulse dependence of a commercial synthetic diamond detector

D. O'Doherty<sup>1</sup>, J. Cross<sup>1</sup>, R. Plaistow<sup>1</sup>, K. Fathi<sup>1</sup>, S.J. Thomas<sup>1</sup>

<sup>1</sup>Addenbrooke's Hospital - Oncology Centre, Medical Physics Box 152, Cambridge, United Kingdom

## Purpose or Objective

When measuring percentage depth doses (PDD) using a radiation detector in a plotting tank, the dose per pulse decreases with depth in water. Since the recombination correction to be applied to the detector varies with dose per pulse, this requires corrections to be made to the PDD. At the small doses per pulse observed in conventional flattened field, these corrections are small (typically less than 0.2%); however with the larger doses per pulse seen in Flattening Filter Free (FFF) beams, corrections of up to 1.3% can be required, depending on the detector used (Budgell et al 2016). The PTW 60019 micro diamond (PTW, Freiburg, Germany) is a commercially available synthetic diamond detector, designed for the dosimetry of small radiotherapy fields. As there is a lack of consistent published data on the dose per pulse dependence of the Micro Diamond the purpose of the measurements described below is to determine whether a dose per pulse correction is needed for this detector.

## Material and Methods

We have performed measurements on two PTW 60019 Micro Diamond detectors to determine whether such a correction is necessary. Depth doses for a 10MV FFF beam were measured with the Micro Diamond, and compared with depth doses measured with an A1SL ion chamber which had been corrected for ion recombination.

## Results

For depths from 30mm to 300mm, the ratio of the depth dose to the corrected A1SL ion chamber depth dose was  $1.0005 \pm 0.001$  for one of the Micro Diamonds, and  $1.0001 \pm 0.001$  for the other. Both of these values are consistent with unity.

## Conclusion

For the measurement of depth doses on FFF beams with large dose per pulse, no correction for the variation with depth of dose per pulse is required when measuring with a PTW 60019 micro diamond.

## EP-1696 Microdosimetry assessment in cyclotron proton beamline with new 3D-microdetectors

J. Prieto-Pena<sup>1</sup>, A. Baratto-Roldán<sup>2</sup>, C. Fleta<sup>3</sup>, M.C. Jiménez-Ramos<sup>4</sup>, J. García López<sup>2</sup>, G. CONSUELO<sup>5</sup>, M. Cortés-Giraldo<sup>6</sup>, J.M. Espino<sup>6</sup>, F. Gómez<sup>1</sup>

<sup>1</sup>Univ. de Santiago de Compostela, Departamento de Física de Partículas, Santiago de Compostela, Spain ;

<sup>2</sup>Centro Nacional de Aceleradores, Univ. Sevilla- CSIC-JA, Sevilla, Spain ; <sup>3</sup>Centro Superior de Investigaciones Científicas CSIC, Instituto de Microelectrónica de

Barcelona IMB-CNM, Barcelona, Spain ; <sup>4</sup>Centro Nacional de Aceleradores, Univ. Sevilla- CSIC- JA, Sevilla, Spain ;

<sup>5</sup>Centre national de la recherche scientifique, Imagerie et Modélisation en Neurobiologie et Cancérologie, Orsay

Ville, France ; <sup>6</sup>Universidad de Sevilla, Dpto. Física Atómica- Molecular y Nuclear, Sevilla, Spain

## Purpose or Objective

Protontherapy achieves very high dose conformity around the target, allowing a better protection of the organs at risk (decreasing radiation side effect) [1]. The determination of the relative biological effectiveness (RBE) of protons depends on several factors, being the particle LET one of them. Therefore the use of devices that help to reduce any uncertainty is essential. Likewise, there is a rising interest in the medical-physics community in placing the enhanced LET of the beam within the tumor or removing it from the most sensitive normal structures around [2]. Nevertheless, there is no instrument to quantify the LET in clinical scenarios, but as the one we show herein. In this work we present direct microdosimetric measurements of 18 MeV proton beams

using novel silicon 3D-microdetectors [3]. Results were verified with both Geant4 and FLUKA simulations.

#### Material and Methods

The new 3D-microdetectors used are a type of diode with a 3D-cylindrical electrode etching (15  $\mu\text{m}$  diameter, 5  $\mu\text{m}$  depth) with an inner volume that matches a sensitive volume that simulates a subcellular structure. Details are described elsewhere [3,4]. The 18 MeV proton beams were generated in a Cyclone 18/9 cyclotron at flux rates of  $10^8$  p/cm<sup>2</sup>s. The proton beam average energy was modulated with an in-house wedge system formed by two equal 10° angle wedges made of 1.19 g/cm<sup>3</sup> Lucite that provides a continuously variable thickness from 3 mm up to 30 mm with an uncertainty of 30  $\mu\text{m}$  [5]. The cyclotron proton beamline was simulated with Geant4.10.4. The so simulated outgoing energy spectrum was used as input-file within Geant4 and FLUKA simulations of the 3D-microdetector performance.

#### Results

Fig. 1 shows the most probable lineal energy through the Bragg curve and measured microdosimetry spectra. The experimental silicon microdosimetric spectra showed clearly the variations of the lineal energy frequency distribution along the Bragg curve.

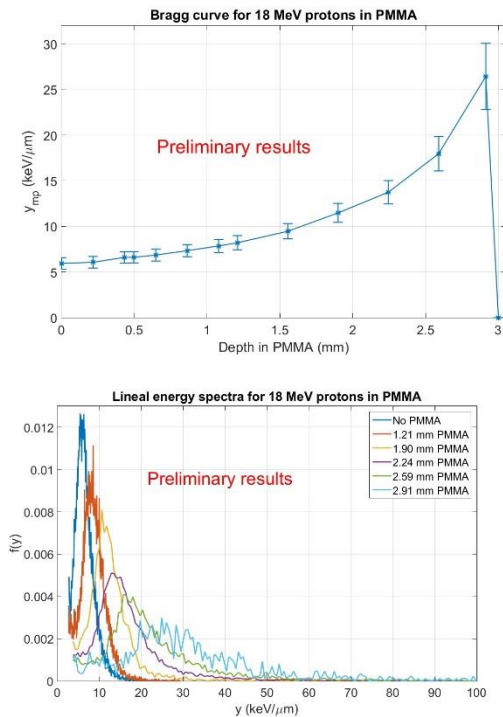


Figure 1: Left: Most probable lineal energy versus PMMA depth curve for the 18 MeV protons measured with the novel 3D-microdetector. Right: Measured microdosimetry spectra as a function of the PMMA thickness.

#### Conclusion

Measurements at various depths along the Bragg curve of a 18 MeV proton beam were performed at high fluence rate with a novel 3D-microdetector and both microdosimetric spectra and Bragg curves were obtained. The results show that this new device is useful to microdosimetry characterization of clinical proton beams.

[1] Schardt D. and Elsässer T., Reviews of Modern Physics, Vo. 82, 2010.

[2] Bassler N, Jäkel O., Sondergaard CS, et al. Acta Oncol. 2010 Oct;49(7):1170-6.

[3] C. Guardiola, F. Gómez, G. Pellegrini, et al., Applied Physics Letters 107, 023505 (2015).

[4] C. Fleta, S. Esteban, M. Baselga et al., 2015 JINST10 P10001

[5] F. Gómez, C. Fleta, S. Esteban, et al., Physics in Medicine and Biology 2016, 61 4036

#### EP-1697 Real time small animal irradiator dosimetry using Radioluminescence imaging

A. Spinelli<sup>1</sup>, E. D'Agostino<sup>2</sup>, S. Broggi<sup>3</sup>, C. Fiorino<sup>3</sup>, F. Boschi<sup>4</sup>

<sup>1</sup>San Raffaele Scientific Institute, Experimental Imaging Centre, Milano, Italy ; <sup>2</sup>DoseVue NV, Research and Development, Turnhout, Belgium ; <sup>3</sup>San Raffaele Scientific Institute, Medical Physics, Milano, Italy ; <sup>4</sup>University of Verona, Department of Computer Science, Verona, Italy

#### Purpose or Objective

The main objective of this work was the development of a novel real-time 2D dosimetry approach for small animal external radiotherapy using radioluminescence imaging (RLI) with a commercial CMOS detector. Radioluminescence light is generated by a flexible and thin scintillator composed of green-emitting rare earth phosphors.

#### Material and Methods

A CMOS detector was mounted on a photographic tripod and coupled with a F=1.4, 8 mm C-mount lens (Edmund Optics) facing the scintillator screen taped on the back side of the animal stage. Measurements were performed on the small animal image-guided platform SmART (Precision X-Ray Inc.). As shown in figure 1 the CMOS was inserted in the XRAD225Cx SmART cabinet, 40 cm away from the animal stage. The SmART cabinet was light-tight and, thus, allowed to investigate RLI with different lighting conditions by switching on/off the internal led during image acquisition.

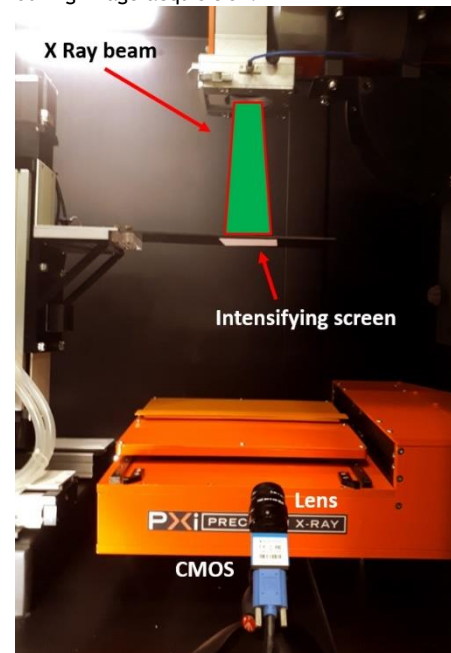


Figure 1 RLI acquisition setup.

The CMOS setting were as follow: gain=22, brightness=50 and exposure time=1/500 sec. A sequence of 60 images were acquired every 1 sec and summed. RLI data were corrected for perspective distortion with an home-made program written in Matlab. The SmART setting were as follow: tube voltage=225kV, current= 1, 3, 6, 9 and 13 mA, the corresponding dose rate at 13 mA was 4.2 Gy/min. Four fields were tested, 2 circular beams with diameter equal to 1 mm and 3 mm and 2 square fields (10x10 mm and 20x20 mm). Measured planar 2D dose distributions and dose profiles were compared against dose calculation performed with Monte Carlo (MC) simulations, including

FWHM estimate. Measurement repeatability was tested on the 20x20 mm beam by repeating by moving and positioning the CMOS for five times. Response linearity and noise variation against current were also measured.

### Results

The agreement of the measured dose profiles and beam sizes is fairly good, with maximum difference being less than 2% for all the four beams tested (see figure 2) with a maximum deviation for FWHM of 0.3mm for the 20x20 mm beam and of 0.1mm for the circular 1mm beam between MC and RLI.

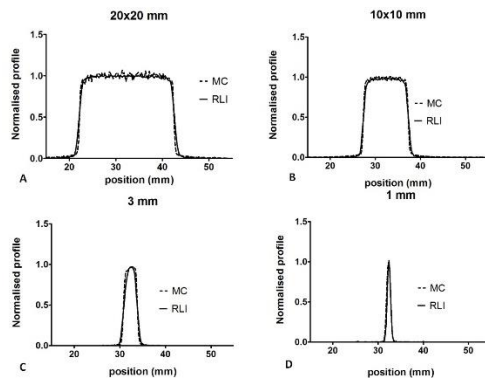


Figure 2 Normalized beams profiles from RLI and MC.

The image correction procedure was confirmed to be able to reduce the perspective distortion at a negligible level and, at the same time, is also robust and reproducible. RLI dose measurements were performed in both lights off/on conditions, the signal can be detected even in the light on condition making the RLI measurements possible even when light can not be removed (e.g. no light-tight irradiators) without relevant impact on dose profiles measurements. Linearity was confirmed ( $R^2=0.9996$ ) and the noise was found to be almost negligible and following Poisson-like behavior against the number of incident photons.

### Conclusion

A novel RLI approach for real time small animal dosimetry was developed. Results show a good agreement with MC dose calculations and linearity with respect to dose. We conclude that RLI can be an alternative approach to gafchromic films

### EP-1698 TRAPS upstream transmission detector for tracking mlc positions in VMAT and IMRT radiotherapy fields

S. Fletcher<sup>1</sup>, J. Haynes<sup>2</sup>, L. Beck<sup>3</sup>, J. Velthuis<sup>4</sup>, D. Crawford<sup>5</sup>

<sup>1</sup>University Hospitals Bristol, Medical Physics Radiotherapy, Bristol, United Kingdom ; <sup>2</sup>University Hospitals Bristol, Medical Physics- radiotherapy, Bristol, United Kingdom ; <sup>3</sup>University of Bristol, Physics, Bristol, United Kingdom ; <sup>4</sup>University of Bristol, Physics, Bristol, United Kingdom ; <sup>5</sup>University Hospitals Bristol, Medical Physics, Bristol, United Kingdom

### Purpose or Objective

Complex dynamic radiotherapy treatment techniques such as VMAT and IMRT present a challenge for beam delivery verification. The TRAPS detector is a prototype device designed for high precision detection of multi-leaf collimator position that could be suitable for real-time upstream monitoring of patients' treatments. We have evaluated its performance within a radiotherapy treatment beam.

### Material and Methods

The TRAPS detector comprises a Monolithic Active Pixel Sensor (MAPS), sensor readout electronics and DAQ, and can be mounted on a holder attached to the linac head. Raw pixel data is pre-processed (bad pixel removal,

background signal subtraction and Gaussian smoothing) and resulting images of the treatment beam is passed through a feature extraction process to locate leaf edges (SOBEL operator).

An Elekta Agility linear accelerator (linac) was used to assess four key characteristics of TRAPS detector performance: attenuation, linearity of signal with dose rate, positional accuracy and dynamic field response. Multi-leaf collimator defined field shapes for 6MV and 10MV photon beams were delivered whilst simultaneously acquiring TRAPS and EPID images (using the Elekta IViewTM amorphous silicon imaging panel).

EPID images were passed through the same feature extraction process and the resultant EPID leaf positions were used as 'standard' and compared with time matched TRAPS leaf positions. Deliberately introduced positional errors (0.5, 1, 2 and 3mm) for individual collimator leaves within thin rectangular fields were used to visually assess error detection capability.

A dynamic treatment plan (VMAT delivery) was devised to test the ability of TRAPS to track the linear leaf movement at varying speeds and under challenging beam scatter conditions.

### Results

The 6MV attenuation factor of the sensor was 1.04% +/- 0.03% for a 5x5cm field size.

Pixel values in TRAPS detector images responded linearly for dose rates up to 450 MU per minute for 6MV and 10MV photons (corresponding to a pulse repetition frequency (PRF) of 380 Hz). For a flattening filter free beam (6FFF) the response was linear to a dose rate of 600 MU per minute (PRF of 150 Hz) but the pixels saturated at higher beam intensities.

Positional accuracy of leaf edges in TRAPS images were within 1mm + 0.26mm of the corresponding EPID images (figure 1).

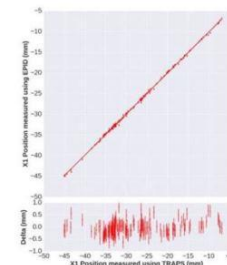


Figure 1 reconstructed leaf positions all segments of an IMRT field for EPID vs TRAPS

Visual examination of TRAPS images (thin rectangular fields with known errors) identified leaf positioning errors as small as 0.5mm, which is within the accuracy of leaf position calibration (1mm).

The dynamic leaf tests demonstrated that TRAPS is capable of tracking leaf movement at velocities up to 3.5cm/s Figure 2.

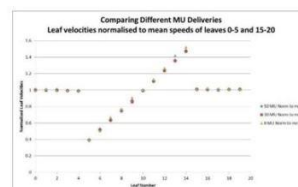


Figure 2 For each leaf, the average leaf velocity is plotted, normalised to the mean values of the outer leaf speeds. Shown for different MU monitor unit or dose deliveries of the same dynamic leaf pattern. The MU value relates to leaf speed, e.g. small MU deliveries require the leaves to travel faster than larger MU deliveries.

### Conclusion

The prototype TRAPS detector has a low attenuation, so is suitable for locating upstream in a treatment beam, and can accurately delineate leaf edges for a range of

clinically relevant scenarios. Modification of the data readout protocol could prevent saturation of sensor elements at the higher dose rates.

### EP-1699 Comparing water equivalent phantom materials using CT scans and conformal prostate treatment plans

M. Kirby<sup>1</sup>, P. Bridge<sup>1</sup>, J. Callender<sup>1</sup>

<sup>1</sup>University of Liverpool, Radiotherapy, Liverpool, United Kingdom

#### Purpose or Objective

Water is the standard reference material specified in national protocols for radiation dosimetry and QA. However solid phantoms are more versatile and easier to use - but materials must have a high water equivalency and/or equivalence to other human tissues to act as a true surrogate with similar attenuation and scattering characteristics. Good equivalence makes them ideal for QA and technique development in radiotherapy and especially for pre-treatment per-patient QA for both IMRT and VMAT.

Typical standard dosimetric characteristics of such materials are often determined by comparing measurements of percentage depth dose curves, build-up and attenuation factors with water. As a precursor to such measurements, we investigated 6 different water equivalent solid phantom materials for their equivalence by comparing analysis made in a treatment planning environment.

#### Material and Methods

Six water equivalent materials were investigated; PTW RW3 (PTW, Freiburg, Germany); Gammex SWHE and SW (Sun Nuclear, Middleton, WI, USA); CIRS PWDT and PW (CIRS, Norfolk, VA, USA) and BARTS SW (Phoenix Dosimetry Ltd., Berkshire, UK). All materials were CT scanned using a clinical pelvis scan protocol (120 kV, 260 mA, 55mAs, 2.5 mm slice thickness, 500mm RFOV) on a GE Lightspeed RT16 scanner. Slices were exported to Eclipse TPS (V13.8) for analysis. Ten-mm diameter ROIs were identified in the central portion of each phantom (9 on the central slice, 2 sup and 2 inf) ensuring that each ROI was in the middle of material slabs. ROI properties were used to measure the average HU in each and then compute (from all 13 ROIs) the min, max, mean and SD of the HU for each of the six types of material. Identical scans and measurements were made for real water.

The mean HU values were used to override existing values for soft-tissue on a real, three field (anterior and two post-oblique fields) conformal 6MV radical (74Gy/37#) prostate plan. Soft-tissue structures were all those within the patient excluding bony tissue. The plan was then recalculated for each of the six mean HU values from the phantom materials and the DVHs (PTV and rectum ORV) compared with the original clinical plan.

#### Results

The Mean (SD) of the measured HUs for each of the water equivalent materials were; PTW RW3 - 14.0 (14.1); Gammex SWHE - 15.1 (11.2); Gammex SW - 26.3 (11.9); CIRS PWDT - -8.5 (10.7); CIRS PW - 66.5 (14.8); BARTS SW - -5.8 (10.6); Water - -1.4 (3.5). The dosimetric impact of applying these mean HUs to the clinical plan is shown in Table 1.

**Table 1:** Dosimetric impact of water equivalent materials for the 6 MV 3-field prostate plan

	Original CT Data	PTW2	Gammex SWHE	Gammex SW	CIRS PWDT	CIRS PW	BARTS SW
D2%	100.3%	100.2%	100.2%	100.3%	100.2%	100.4%	100.2%
D98%	97.4%	97.6%	97.6%	97.5%	97.7%	97.3%	97.7%
V50	37.9%	38.1%	38.1%	38.0%	38.2%	37.9%	38.2%
V60	31.3%	31.5%	31.5%	31.4%	31.6%	31.3%	31.6%
V65	27.4%	27.7%	27.7%	27.6%	27.8%	27.4%	27.8%
V70	21.0%	21.6%	21.6%	21.4%	21.9%	20.9%	21.9%

#### Conclusion

Although the range of mean HUs for the six materials is wide (mean -5.8 to 66.5; range (across all ROIs) -41 to 121), there was little dosimetric impact on the three-field plan. All materials were within 0.3% of the target volume dose objectives (D2% and D98%) achieved in the clinical plan; all were within 1% of the ORV constraints (V50 to V70). All therefore would act as suitable equivalent materials to water/soft-tissue in the treatment planning setting.

### EP-1700 CyberKnife output factors from integral dosimetry

A. Kulmala<sup>1</sup>, J. Heikkilä<sup>2</sup>, A. Väänänen<sup>2</sup>, M. Tenhunen<sup>3</sup>

<sup>1</sup>Clinical Research Institute HUCH, Radiotherapy, Helsinki, Finland ; <sup>2</sup>Cancer Center Kuopio University Hospital, Radiotherapy, Kuopio, Finland ; <sup>3</sup>Helsinki University Hospital- Cancer Center, Radiotherapy, Helsinki, Finland

#### Purpose or Objective

The standard approach of determining output factors of small megavoltage beams has been the construction of smaller detectors to fit in the central area of the smallest fields of interest. As an alternative approach it has been shown that a large ionization chamber (IC) can be used for measuring output factor of a small (diameter 4-20 mm) conical collimator, when a radial response of the chamber and high resolution relative dose distribution (off-axis-ratio, OAR) of the field are known. In the current work we will apply this formalism to determine the output factors of the CyberKnife conical collimators.

#### Material and Methods

The 'radial response' of the PTW34001 (ROOS) parallel plate ionization chamber is deconvoluted from conical collimator OAR sets determined with the IC 'measured signal' and Gafchromic EBT2 film 'true signal' using a non-parametric super-resolution deconvolution method (Kulmala A and Tenhunen M 2012, Phys. Med. Biol. 57 7075-88). The output factors of the Cyberknife cone beams (diameter 5-30 mm) are estimated based on integral dose measurements with the IC, the deconvoluted radial response of the IC and relative dose distributions measured with the film. Finally, the output factors are compared to a reference set. As a reference method we use a direct measurement with the E60012 p-type

unshielded diode detector corrected with the published field-size dependency factors.

#### Results

The reference output factor data for conical collimators has a very close agreement, on average only 0.1 % larger, with output factor data obtained by the integral method. A difference minimum -0.8 % is found with a 25 mm collimator and maximum +0.9 % with a 12.5 mm cone.

#### Conclusion

We have demonstrated that the integral dosimetry can be used to determine the output factors of the CyberKnife conical collimators. The method seems suitable for verification the output factor results of the standard formalism.

#### EP-1701 Inverse square corrections for WAFACs

D. Rogers<sup>1</sup>

<sup>1</sup>Carleton University, Physics Department, Ottawa, Canada

#### Purpose or Objective

To derive systematically the corrections needed when using Wide Angle Free Air Chambers (WAFACs) to convert a value measured or calculated for a finite solid-angle-detector to the corresponding value on axis assuming an isotropic point source and no attenuation. Secondly, to verify these corrections using Monte Carlo simulations.

#### Material and Methods

Using published techniques, corrections for cylindrical, conical and square prisms are derived to give:

$$k_{r^2}^{\text{cyl}} = \frac{\alpha^2}{\left[ \ln(1 + \beta^2) + \frac{2R}{L}(\theta_c - \theta_m) - \frac{d}{L} \ln\left(\frac{1 + \alpha^2}{1 + \beta^2}\right) \right]}$$

$$k_{r^2}^{\text{cone}} = \frac{\alpha^2}{\ln(1 + \alpha^2)} \left( 1 + \frac{L}{d} + \frac{L^2}{3d^2} \right)$$

$$k_{r^2}^{\text{sq-prism}} = \frac{1}{d^2} \left[ \frac{2w^2}{12} + d^2 + dL + \frac{L^2}{3} \right]$$

where L = detector thickness, R = its front radius, d = its distance from point source,  $\alpha = R/d$ ,  $\beta = R/(L+d)$ ,  $\theta_c = \arctan(\alpha)$ ,  $\theta_m = \arctan(\beta)$  and w is the width of a square prism. Monte Carlo simulations are performed for a variety of detector geometries, (e.g., R large and R very small) using the egs\_brachy application based on EGSnrc (PMB 61 (2016) 8214) for a point source in vacuum and low density dry air in the detector volume. The average air kerma in the detector volume is calculated. Values are converted to the on-axis air-kerma values using the above corrections and compared to expected values.

#### Results

The corrections are dominated by the longitudinal  $1/r^2$  effects, e.g., the correction is 1.46 for a conical NIST-like WAFAC geometry. However, in practice NIST and other standards labs eliminate this longitudinal effect by using an effective detector volume rather than the true detector volume (J Res NIST 108 (2003) 337) and only the L = 0 correction is required. That said, for the cylindrical and conical corrections derived above, the Monte Carlo simulations verify their accuracy within the typical statistical uncertainty of 0.04%. However, for the square prism, the correction breaks down by up to 16% for values of L typical of actual detectors (e.g., 10 cm). However, for a detector with L=0.05 cm or less, the square prism corrections are accurate within the statistical uncertainties.

#### Conclusion

By explicit derivations and simulations, the standard correction factors for  $1/r^2$  effects with various WAFAC detectors have been shown to be accurate with the exception of that for thick square prism detectors. However, the corrections for square prism detectors using L=0.05 cm are shown to be accurate at the 0.04% level

which is important since dose-rate constants calculated using the egs\_brachy Monte Carlo application of EGSnrc (Med Phys 35 (2008) 4228) make use of this correction factor and these values have been clinically recommended for a variety of seeds by the AAPM's TG-43 (Med Phys 44 (2016) e297).

#### EP-1702 Examination of the real-time exposure dosimetry system using synthetic ruby on the radiation therapy

A. Maruyama<sup>1</sup>, T. Yamaguchi<sup>1</sup>, D. Ono<sup>1</sup>, T. Kikuchi<sup>1</sup>, Y. Kikuchi<sup>1</sup>, R. Sato<sup>1</sup>, S. Watanabe<sup>2</sup>, Y. Hosokai<sup>1</sup>

<sup>1</sup>International University of Health and Welfare, Department of Radiological Sciences, Otawara-city-Tochigi, Japan ; <sup>2</sup>South Miyagi Medical Center, Radiology, Shibata- Miyagi, Japan

#### Purpose or Objective

It is part of reason in the occurrence of medical accidents on the radiation therapy that the local exposure dose cannot be direct monitoring in real-time. Recently, we developed a real-time exposure dosimetry system using synthetic ruby for interventional radiology (IVR). This time, we discuss some character of the developed real-time radiation dosimetry system for use in radiation therapy condition.

#### Material and Methods

A synthetic ruby scintillator with a diameter of ~2mm was attached to the tip of a 10 m long optical acrylic fiber using quick setting adhesive. The emitted light from the synthetic ruby was measured in real time in terms of the number of photons recorded using a photon counter head. A calibrated ionization chamber with Roos Electron Chamber dosimeter was used as a reference dosimeter. The aims of this study were to measure the following items with synthetic ruby dosimeter.

1. Characteristic features of the percentage depth dose (X-ray)

The measuring devices were irradiated using 10 MV X-ray, at the center of 10×10 cm<sup>2</sup> and 15×15 cm<sup>2</sup> field, and monitor unit (MU) value was fixed 200 MU.

2. Characteristic features of the percentage depth dose (electron beam)

The measuring devices were irradiated using 6, 9 and 12MeV electron beam, at the center of 10×10 cm<sup>2</sup> field, and MU value was fixed 100 MU..

3. Characteristic features of coefficient of variance of MU value

The characteristic features of coefficient of variance (%CV) of MU value in terms of dose and number of photon were measured. The depth of measuring was 10 cm, the measuring number was 10 times.

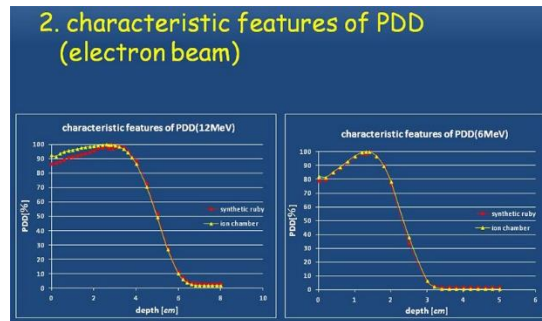
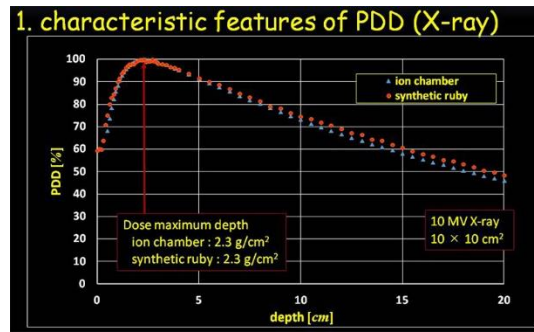
4. Linearity of the number of photons in terms of MU value  
The measuring devices were irradiated 10 MV X-ray, at the center of 10×10 cm<sup>2</sup> field, the depth of measuring was 10 cm. The MU value changed to 10 - 800 MU, the dose rate was fixed 500 MU/min.

#### Results

1, 2. The percentage depth dose (PDD) was same as the reference dosimeter. The dose maximum depth was no clear difference between the reference dosimeter and the ruby dosimeter.

3. The %CV of MU value in terms of dose and number of photon was ±0.67%.

4. There is a significant correlation between the MU value and the number of photons ( $r^2=0.9997$ ).



### Conclusion

The synthetic ruby system which we developed have high temporal resolution, thus, it is possible to measure the total exposure time to read the rise time and the fall time on the graph. The MU value increased linearly with the number of photons which was same as the reference dosimeter, the synthetic ruby system have a potential for the real-time exposure dosimetry system on the radiation therapy. However, we have to discuss the influence of the developed system in the exposure filed, pursuit of the precision, the possibility of multipoint measurement, the size and the covering material of dosimeter.

### EP-1703 Dose Evaluation of Build-up Region of Photon Beam using Thermoluminescence Dosimeter (TLD) Sheet

K. Sasaki<sup>1</sup>, Y. Shiota<sup>2</sup>, M. Miura<sup>2</sup>

<sup>1</sup>Gunma Prefectural College of Health Sciences, Graduate School of Radiological Technology, Maebashi, Japan ; <sup>2</sup>Iwata City Hospital, Medical Physics, Iwata, Japan

### Purpose or Objective

Although there are various devices for measuring high-energy radiation, radiographic films, Radiochromic films and parallel plate ionization chambers are generally used to obtain a dose of surface or build-up region with high accuracy. In this study, a new thermoluminescence dosimeter sheet (TLD) sheet dosimeter with effective atomic number close to water and high measurement flexibility was used to evaluate the dose in the build-up region after passing through the carbon couch. In addition, reduction of surface dose by sandwiching low-density material was also studied.

### Material and Methods

Percent depth dose (PDD) after passing through the carbon couch was measured using 6 MV, 10 MV photon from Novalis-TX (Varian Medical systems). The PDD from the phantom surface to the depth of 5 cm was measured by NACP-02 parallel plate ionization chamber (IBA), Gafchromic film EBT3 (Ashland) and TLD sheet (Toyo Medic). Changes in surface dose by sandwiching the Styrofoam between the phantom and the couch were also measured. The chemical formula of the TLD sheet is  $\text{LiB}_3\text{O}_5$  and its thickness is 150  $\mu\text{m}$ , about half that of Gafchromic film. In order to utilize this thinness as the

resolution of the depth, the measurement was carried out by stacking the TLD sheet.

### Results

The PDD showed consistent data between the ionization chamber and the TLD sheet, but the deviation was large in the TLD sheet. Due to the movement of the build-up region into the couch, the surface dose increased. This increase in surface dose could be evaluated in both the ionization chamber and the TLD sheet. The surface dose increased by approximately 80% by passing through the carbon couch. By sandwiching a 5 cm thick Styrofoam plate between the phantom and the carbon couch, it was possible to reduce the surface dose by 11.9% at 6 MV and 18.1% at 10 MV respectively. In these measurements, the TLD sheet was able to evaluate the dose closest to the surface of the phantom. The TLD sheet was able to evaluate the depth dose with the same variance as the Gafchromic film, and it was an advantage that the depth resolution in the stack measurement was higher. Although it takes time and effort to reduce the measurement interval in the depth direction using the parallel plate ionization chamber, it has been possible to quickly and conveniently measure by stacked method using the TLD sheet.

### Conclusion

We evaluated the dose in the build-up region using the TLD sheet which is a new material, and its usefulness was suggested. The TLD sheet was particularly useful for dose assessment on the surface of the phantom. In the TLD sheet, there is a fluctuation in the intensity of the signal depending on the position in the sheet, and the correction for this is currently under consideration. It was shown that the dose near the surface of the phantom is greatly increased by passing through the carbon couch but the surface dose can be reduced by placing a low density material between the phantom and the couch.

### EP-1704 A 2D reusable OSL-film for class solution specific QA of large modulated fields in the PART trial

R. De Roover<sup>1</sup>, C. Berghen<sup>1</sup>, G. De Meerleer<sup>1</sup>, T. Depuydt<sup>1</sup>, W. Crijs<sup>1</sup>  
<sup>1</sup>Catholic University of Leuven, Department of Oncology, Leuven, Belgium

### Purpose or Objective

The PART trial (NCT03079323) evaluates the effect of prophylactic para-aortic lymph node irradiation in addition to prostate (bed) and pelvic lymph node radiotherapy in histopathologically proven pelvic lymph node metastatic (pN1) prostate cancer. With treatment fields up to 35 cm, the inclusion of the para-aortic lymph nodes challenges the current in phantom patient-specific quality assurance (QA). As state-of-the art reusable dosimeters have a maximum field-of-view (FOV) of 25 cm for single shot measurements. Additionally, these dosimeters consist typically of an array of detectors with a resolution between 0.5 and 1.0 cm. Radiochromic films offer a sub-mm resolution, but these dosimeters are for single use, increasing the cost and excluding a dosimeter specific calibration. A large-sized (43 x 36 cm<sup>2</sup>) reusable optical-stimulated luminescence (OSL)-film may measure such large fields with sub-mm resolution in a single shot measurement. The potential of OSL-film as an absolute infield dosimeter in intensity modulated radiotherapy was previously reported. But the film's out-of-field-low-energy dependent overresponse requires additional modelling. This study investigates the use of such a modelling in a class solution specific calibration for the PART trial.

### Material and Methods

Ten patients currently included in the PART trial were selected for OSL measurements. Prescription was 70 Gy to the prostate bed in 35 fractions or 67.25 Gy to the prostate in 25 fractions and 45 Gy to the pelvic and para-aortic lymph nodes in 25 fractions. Treatment was delivered on

a Varian Clinac 2100CD using 10 MV dual arc VMAT with collimator angles  $350^\circ/10^\circ$ . All treatment plans passed our internal pre-treatment QA protocol.

Agfa HealthCare supplied the OSL-film and flying-spot CR-15-X-engine based reader used for these experiments. The OSL-film was positioned within a 20 cm stack of water-equivalent RW3 at 10 cm depth and the measured signal was scanned and erased 5 min after each irradiation. A class-solution specific OSL-calibration consisted of a uniformity correction and a linear out-of-field dose correction. Dose measurements were compared to the calculations using 3%/3mm gamma evaluation (both global and local normalization) with a low dose exclusion threshold set to 30% of the prescribed dose.

### Results

Plan properties and gamma agreement scores ( $\gamma$ AS) are compiled in Table 1. The median  $\gamma$ AS was 96.7% (range: 91.0% - 99.3%) and 93.0% (range: 87.0% - 96.6%) for global and local normalization respectively. The class solution specific calibration was able to model both the in-field dose and the dose gradients (Figure 1c-d). The zones with a mixture of in-field and out-of-field spectra (arrow in Figure 1b) performed typically worse for all patients.

**Table 1.** Plan properties and gamma agreement score for each patient case.

Patient case	Field size [cm <sup>2</sup> ]		Monitor units [MU] <sup>a</sup>	3%/3mm $\gamma$ AS [%] <sup>b</sup>	
	Arc 1	Arc 2		Global	Local
1	11.0 x 32.0	12.0 x 32.0	805	96.6	94.7
2	12.5 x 28.0	12.5 x 29.0	744	97.7	95.5
3	12.0 x 29.7	12.0 x 29.8	661	96.9	94.1
4	12.0 x 31.0	12.0 x 31.0	738	99.3	96.6
5	12.7 x 28.8	11.9 x 29.9	770	94.3	91.8
6	13.0 x 30.0	13.0 x 30.0	831	97.7	91.8
7	14.5 x 33.0	14.5 x 33.0	794	93.4	88.2
8	10.0 x 30.0	10.0 x 30.0	852	96.9	95.3
9	14.5 x 33.0	14.5 x 33.5	697	95.2	92.0
10	12.5 x 33.0	12.5 x 33.0	773	91.0	87.0

Abbreviations: OSL = optical stimulated luminescence,  $\gamma$ AS = gamma agreement score.  
<sup>a</sup>1 MU corresponds to 0.8 cGy at 10 cm depth delivered by a 10 x 10 cm<sup>2</sup> field at 90 cm source-surface distance.

<sup>b</sup>The  $\gamma$ AS was determined using a low dose exclusion threshold set to 30% of the prescribed dose.

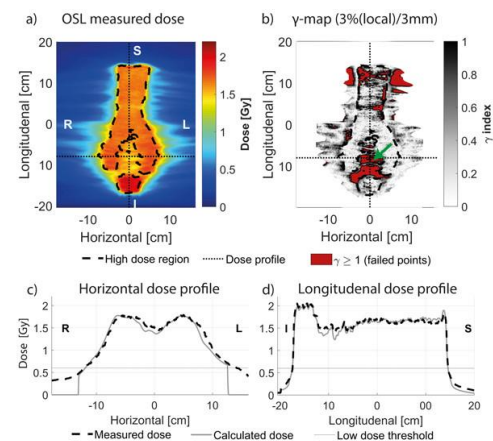


Figure 1. Depicts the OSL measurement and QA results for the worst case (patient 10, Table 1). (a) OSL measured dose map. (b) 3% (local)/3mm  $\gamma$ -map with a low dose exclusion threshold set to 30% of the prescribed dose (white region). (c) Horizontal and (d) longitudinal dose profiles. The location of the dose profiles are depicted as dashed lines on (a) and (b). The arrow in (b) indicates the zone that captures a mixture of in-field and out-of-field spectra, which performs typically worse in the OSL measurements.

### Conclusion

This study reports a class solution specific OSL-calibration for the large modulated fields encountered in the PART trial. This calibration adds a unique combination of reusability, sub-mm resolution and large FOV to the 2D dosimetry in radiotherapy.

### EP-1705 Quality assurance of micro-MLC based IMRT plans using patient-specific phantom

S. Sunel<sup>1</sup>, M. Yeginer<sup>1</sup>, F. Akyol<sup>1</sup>, F. BILTEKIN<sup>1</sup>, G. Ozyigit<sup>1</sup>  
<sup>1</sup>Hacettepe University, Department of Radiation Oncology, Ankara, Turkey

### Purpose or Objective

In this study, it is aimed to propose an alternative method to standard QA procedures by producing tissue-equivalent phantoms in the form of patient surface using 3D printing technology in micro MLC based brain and head&neck treatment techniques.

### Material and Methods

The outlines of the methodology of the study designed with the aims can be summarized as: (i) Transferring the CT images of selected Head&Neck patients to workstation, (ii) Transporting the CT images to 3D Slicer software and then preparing the model with the form of patient surface in computer environment, (iii) Transporting the parts of models to 3D printer and printing the crusts of the phantom, (iv) Filling the crusts with paraffin wax, (v) Taking the CT images of model and calculating the doses in the treatment planning system (TPS), (vi) Delivering the micro-MLC based IMRT treatment plans in Novalis unit by placing the EBT3 films between the phantom slices, (vii) performing the gamma analysis of 2D dose distributions acquired from EBT3 film and TPS. In the gamma analyses of treatment plannings of six head&neck patients, the four sets of criteria were used: 3% dose difference (DD) & 3 mm Distance to Agreement (DTA), 3% DD & 5 mm DTA, 5% DD & 3 mm DTA, and 5% DD & 5 mm DTA.

### Results

In the analysis with 3mm/3% criteria, it was observed that the dose distributions were agreed except for the dose reduction at the edge of the films induced from the deformation. When 5mm/5% criteria were chosen, the agreements between dose distributions of EBT3 film and TPS were found to be 95,7% in average (max. 96,4% and min. 93,4%). The threshold for success was accepted as 90%.

### Conclusion

Consequently, our study showed that the head&neck phantoms produced with 3D printing technology can be used for patient specific QA. By means of new technologies that accelerate the production process, 3D phantom applications including surface contour of patients can be routinely used in radiotherapy facilities.

### EP-1706 Production of samples with specified CT indices by 3D printing

I. Miloichikova<sup>1,2</sup>, Y. Cherepennikov<sup>1</sup>, A. Krasnykh<sup>3</sup>, S. Stuchebrov<sup>3</sup>

<sup>1</sup>Tomsk Polytechnic University, School of Nuclear Science & Engineering, Tomsk, Russian Federation ; <sup>2</sup>Cancer Research Institute of Tomsk National Research Medical Center of the Russian Academy of Sciences, Radiotherapy Department, Tomsk, Russian Federation ; <sup>3</sup>Tomsk Polytechnic University, Research School of High-Energy Physics, Tomsk, Russian Federation

### Purpose or Objective

This work is aimed at developing a method to produce tissue-equivalent phantoms with predetermined density distribution for the purpose of experimental planning and verification of radiotherapy treatments. The phantoms can be customized to mimic individual anatomical features of each patient.

It is advisable to manufacture such phantoms by fused deposition modeling using tomographic data.

The phantoms will make it possible to adjust the radiotherapy treatment plans directly on the radiation therapy machine. This will eliminate systematic errors of calculation algorithms. This becomes especially important with high-density implants installed in the region of interest, which do not allow accurate dose calculation due to artifacts in tomographic images. Customized phantoms will eliminate the inaccuracies of traditional experimental verification of radiotherapy plans based on mass-produced phantoms and thereby reduce the adverse effects of radiation therapy.

The purpose of this research is to develop modified materials for 3D printing with specified CT indices.

#### Material and Methods

Fused deposition modeling was chosen for the production of customized phantoms due to the possibility of simultaneously producing objects from several materials. To estimate the values of CT indices, test samples with a variety of infill values were manufactured on an UP! Plus 2 3D printer from pure polylactide (PLA) filaments and modified filaments. The 2-cm<sup>3</sup> samples were printed with a diamond infill pattern.

The modified filaments were made using a single-screw extruder SJ 45/25 with a diameter of 45 mm and an L/D ratio of 25 from a mixture of PLA and copper powder (particle size 10-20 µm).

The CT indices were measured using a Siemens Somatom Emotion computed tomography scanner. The data obtained were processed by the eFilm software.

#### Results

In the eFilm software, the tomograms were presented in the form of high-contrast black and white images. Each shade of gray was assigned a numeric value that corresponded to a specific value on a Hounsfield unit scale (CT indices). The samples were positioned parallel and perpendicular to the rotation axis for CT scanning.

Based on the processed data, a linear dependence of the CT indices on the sample infill values was obtained. It is shown that CT indices depend on the sample orientation in a CT scanner due to the different number of air gaps lying in the CT scanning plane.

#### Conclusion

The obtained results show that pure PLA can be used to simulate soft tissues with densities ranging from -600 to +200 on the Hounsfield scale. Metal-modified materials allow us to simulate muscle and bone tissue from +100 to -1100 HU.

The obtained dependences can be used to accurately determine the required material infill value for obtaining a specific CT index. That will allow applying the developed materials to produce customized tissue-equivalent phantoms.

#### EP-1707 Polymer gel-based tests for geometric accuracy in a 0.35 T MR-LINAC

S. Dorsch<sup>1,2</sup>, P. Mann<sup>1</sup>, A. Elter<sup>1,2</sup>, A. Runz<sup>1</sup>, S. Klüter<sup>3</sup>, C.P. Karger<sup>1</sup>

<sup>1</sup>German Cancer Research Center DKFZ, Medical Physics in Radiation Oncology, Heidelberg, Germany ; <sup>2</sup>University of Heidelberg, Faculty of Physics and Astronomy, Heidelberg, Germany ; <sup>3</sup>University Hospital Heidelberg, Department of Radiation Oncology, Heidelberg, Germany

#### Purpose or Objective

As MRgRT is becoming increasingly important in clinical applications, the development of new QA methods is needed. Besides the QA for dose delivery and dosimetry, also the machine-related geometric parameters like the alignment of the irradiation and imaging isocenters as well as the detection and measurement of geometric distortions of the MR are of key importance. Polymer dosimetry gels (PG) may offer a way to perform isocenter alignment tests as PG is visible in MR imaging. Additionally, PG may allow for online 3-dimensional (3D) evaluation. For this purpose we present first measurements of a dedicated phantom to measure both, isocenter alignment with a PG and geometric distortions with a regular 3-dimensional grid.

#### Material and Methods

The in-house developed phantom contains a PG (PAGAT<sup>1</sup>)-filled spherical glass flask embedded in 8 grid sheets building up a 3D grid of 996 control points. To measure the alignment of the irradiation and imaging isocenter, the phantom was irradiated with 5 beams separated by equidistant angles at a clinical MR-Linac (MRIdian, ViewRay) and was scanned immediately and 48 h after

irradiation at the MR-Linac using a double spin-echo sequence. The gel was additionally scanned on a 3 T MR device (Biograph mMR, Siemens) 5 h and 52 h after irradiation using multi spin-echo sequence with 32 equidistant echoes to evaluate the influence of different scanners on the star shot evaluation (Mephisto, PTW). To identify geometric distortions of the clinically used MR sequence (steady-state coherent sequence) of the MR-Linac, the individual control points of the grid were compared to CT-measurements as ground truth. The automatic determination of the control points was performed using the Weka segmentation (Image J, NIH).

#### Results

The evaluation revealed an isocircle radius of 0.5 mm for both imaging devices, image resolutions (0.5 x 0.5 mm<sup>2</sup> and 1.0 x 1.0 mm<sup>2</sup>) and time points after irradiation. The distance of the irradiation to the imaging isocenter was 0.25/0.65 mm (0.5 mm resolution) and 1.3/1.03 mm (1.0 mm resolution) for MR-Linac /3 T MRI respectively. Measurements of the grids of the QA-phantom revealed distortions below 1.2 mm (mean over all control points 0.35 mm) up to a distance along the bore of 102 mm from the isocenter.

#### Conclusion

The evaluation of a star shot measurement in a 0.35 T MR-LINAC is feasible, even immediately after irradiation. No significant differences for isocircle radii and isocentre distances between a diagnostic 3T MR scanner and the MR-Linac machine were found. As the PG can also be evaluated in 3D, future experiments will focus on a 3D isocenter alignment test where several slices along the y-direction will be evaluated. This would allow identifying any misalignment of Linac-components.

#### EP-1708 Organ motion impact on dose delivered with non-coplanar VMAT for lung SBRT

A. Bazani<sup>1</sup>, S. Comi<sup>2</sup>, F. Pansini<sup>1</sup>, F. Emiro<sup>1,3</sup>, D. Ciardo<sup>4</sup>, G. Piperno<sup>4</sup>, A. Ferrari<sup>4</sup>, B.A. Jercezek-Fossa<sup>4,5</sup>, F. Cattani<sup>1</sup>, C. Garibaldi<sup>6</sup>

<sup>1</sup>IEO- European Institute of Oncology IRCCS, Unit of Medical Physics, Milan, Italy ; <sup>2</sup>European Institute of Oncology, Radiotherapy, Divisione di Radioterapia pres, Italy ; <sup>3</sup>University of Milan, Physics, Milan, Italy ; <sup>4</sup>IEO- European Institute of Oncology IRCCS, Department of Radiation Oncology, Milan, Italy ; <sup>5</sup>University of Milan, Department of Oncology and Hemato-Oncology, Milan, Italy ; <sup>6</sup>IEO- European Institute of Oncology IRCCS, Radiation Research Unit, Milan, Italy

#### Purpose or Objective

To evaluate the effect of organ motion on dose delivered with non-coplanar VMAT for lung stereotactic treatment.

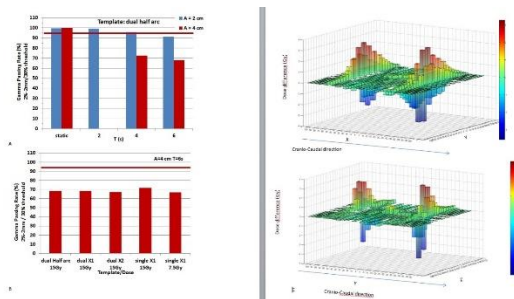
#### Material and Methods

Dynamic Wave Arc (DWA) is a novel non-coplanar VMAT technique implemented on the VERO SBRT system. The fluence modulation is achieved by a synchronized moving of gantry, ring and leaves at a fixed dose rate (400 MU/min). Seven DWA highly modulated VMAT treatments were planned for a single lung patient using Raystation TPS (v7.0, 0.2 mm dose grid) with Collapsed Cone Convolution Algorithm (v3.5) on a 4DCT scan (2.5 mm slice width). Plans were optimized on the mean CT obtained from 10 breathing phases. The goal prescription was D<sub>95%</sub>=95% for ITV+5mm. So far, 3 arc templates, simulating different combinations of gantry/ring speeds, 2 dose levels (15Gyx3 fr and 7.5Gyx8 fr) and 2 extreme organ motion amplitudes (2 and 4 cm) were considered to assess the impact of organ motion on dose delivery. Two ITVs were created from the original GTV to simulate a peak-to-peak tumor motion of 2 and 4 cm in cranio-caudal direction. Plans were delivered on the Delta4 with HexaMotion 6D Motion Platform. Dose distributions obtained with the phantom moving according to different 1D sinusoidal motion patterns (A = 2, 4 cm, T = 2, 4, 6 s, 3 phase shifts with respect to the start of the treatment) were compared with

the corresponding static dose map through a local gamma analysis (2%-2mm, 30% dose threshold) and absolute dose difference evaluation for each diode of both detector matrices.

**Results**

The agreement between static and calculated dose maps showed gamma > 98.5% for all plans. Figa shows that gamma passing rate of dynamic dose distributions is always acceptable (>95%) for the 2 cm peak-to-peak amplitude breathing pattern, for dual half arc template, except for the 6 s period motion for which a value of 91.2% was found. At the extreme peak-to-peak amplitude of 4 cm the gamma passing rate decreased to 70%. As shown in Figb, the gamma passing rates as a function of the different arc templates for the worst breathing pattern scenario (A=4cm, T=6s) are always < 75%. Analyzing the absolute dose deviations between dynamic and static measurements for both detector plates, the blurring effect is clearly predominant at the edge of the fields, but discrepancies up to 4 Gy were observed in the central high dose area, suggesting a possible interplay effect (Fig. c).



Dose level	ITV	Template	Description	Gantry Speed (deg/s)	Ring Speed (deg/s)	Breathing pattern (2Asino1)
15Gyx3fr	GTV+2cm cranio-caudal	dual X1	2 arcs Gantry (°)=184-176 Ring (°)=10-350	Arc1=5.5 Arc2=0.8	Arc1=1.4 Arc2=0.2	A = 4 cm T = 6 s
		dual X2	2 arcs Gantry (°)=184-176 Ring (°)=0-345*	Arc1=0.9 Arc2=1.7	Arc1=0.3 Arc2=0.6	
		dual Half arc	2 arcs Gantry (°)=184-0 Ring (°)=10-350	Arc1=1.2 Arc2=0.5	Arc1=0.6 Arc2=0.3	
		single X1	Single arc Gantry (°)=184-176 Ring (°)=10-350	0.5	0.1	
	GTV+1cm cranio-caudal	dual Half arc	2 arcs Gantry (°)=184-0 Ring (°)=10-350	Arc1=1.2 Arc2=0.5	Arc1=0.6 Arc2=0.3	A = 4 cm T = 4 s A = 4 cm T = 6 s
		dual Half arc	2 arcs Gantry (°)=184-0 Ring (°)=10-350	Arc1=1 Arc2=0.6	Arc1=0.5 Arc2=0.3	A = 2 cm T = 2 s A = 2 cm T = 4 s A = 2 cm T = 6 s
7.5Gyx8fr	GTV+2cm cranio-caudal	single X1	Single arc Gantry (°)=184-176 Ring (°)=10-350	1.1	0.3	A = 4 cm T = 6 s

**Conclusion**

Our preliminary results suggested that the DWA treatment could be safely implemented for lung SBRT without tumor tracking if the tumor motion does not exceed 2 cm. Further investigations are required to evaluate the impact of 3D irregular tumor motion on dose delivery, as well as the impact of the interplay effect inside the target. Nevertheless, we expect a low interplay effect due to the low dose rate, constant gantry and ring speed and high fraction doses.

**EP-1709 Dosimetric response of aSi1000 EPID continuous imaging of FFF beams for in vivo 3D SBRT verification**

A.R. Barbeiro<sup>1</sup>, L. Parent<sup>2</sup>, T. Younes<sup>1</sup>, L. Vieilleveigne<sup>2</sup>, F. Chatrie<sup>1</sup>, F. Younan<sup>3</sup>, X. Franceries<sup>1</sup>

<sup>1</sup>UMR-1037- Inserm- Université Toulouse III Paul Sabatier, Centre de Recherches en Cancérologie de Toulouse, Toulouse, France ; <sup>2</sup>UCT-Oncopole, Dpt. Ingénierie et physique médicale, Toulouse, France ; <sup>3</sup>Groupe Oncorad-Garonne- Clinique Pasteur, Service de Radiothérapie, Toulouse, France

**Purpose or Objective**

Electronic portal imaging device (EPID) dosimetry with flattening filter free (FFF) beams is still challenging, and is not supported by Varian commercial solution for aSi-1000 EPID model. Moreover, in order to develop a model for *in vivo* 3D verification of stereotactic body radiotherapy (SBRT) treatments, the continuous mode should be characterized for small field sizes and high dose-rates, which could saturate EPID response. This study aims at investigating the dosimetric response of an aSi-1000 EPID operating in continuous mode under these challenging conditions, for further *in vivo* SBRT verifications.

**Material and Methods**

An aSi-1000 EPID installed on a Varian TrueBeamSTx was irradiated with 6 and 10 MV FFF photon beams with the maximum available dose rates (1400 and 2400 MU/min, respectively), at variable source-detector distance (SDD) of 150 and 180 cm. Different EPID imaging sets were acquired in continuous mode (C.M.) and were also compared to the commonly used integrated mode (I.M.), in order to study relevant dosimetric characteristics, such as: dose linearity, repeatability and reproducibility of EPID response, ghosting effect and field-size dependence, where EBT3 film measurements were included for fields in the range of SBRT (0.5<sup>2</sup>-10<sup>2</sup> cm<sup>2</sup>). Dynamic arc fields were also measured to study EPID dose response dependence, when subject to potential fluctuations in dose-rate and compared to the static irradiation. In-house Matlab software was implemented to automatically process all data, and handling different image formats.

**Results**

Saturation of EPID response occurred only for continuous mode at higher dose-rate exposures, conversely to integrated mode, due to different reading schemes. Therefore continuous EPID imaging for 10 MV FFF beams and for larger field sizes (>15<sup>2</sup> cm<sup>2</sup>) of 6 MV FFF, should be done at 180 cm SDD. Dose response linearity was found to be similar for both modes, varying within 2.5% (I.M.) and 2.1% to 2.9% (C.M.) for static and dynamic arc fields, respectively, and for small MU values (≤5MU). Response repeatability was slightly better for I.M. and 6 MV FFF, due to lower dose-rate, being in all cases within 0.6%. Reproducibility (over 7 months) was well within 0.5% for both modes and energies. Field size dependence of EPID response in both modes agreed within 1%. However, when compared to EBT3 film, major discrepancies (>3%) were found for fields ≤ 1<sup>2</sup> and 1.5<sup>2</sup> cm<sup>2</sup>, in 6 and 10 MV, respectively. Signal increasing due to ghosting effect was within 1% to 1.2% for the configuration with the highest pre-irradiation dose (300MU), being comparable to the signal variations found between continuous acquisition frames (± 1.1, 1SD).

**Conclusion**

The dosimetric response of aSi-1000 EPID in continuous mode with FFF beams and high dose rates showed comparable results to the commonly used integrated mode, and dosimetric properties similar to those of FF beams. These results are promising to perform 3D verifications of SBRT with dynamic techniques using continuous EPID imaging.

**EP-1710 Update ADAM-pelvis phantom: New possibilities to simulate treatment scenarios in radiotherapy**

W. Johnen<sup>1,2</sup>, A. Runz<sup>1,2</sup>, N. Homolka<sup>1,2,3</sup>, N. Niebuhr<sup>1,2,3</sup>, P. Mann<sup>1,2</sup>, B. Beuthien-Baumann<sup>4,5</sup>, C. Gillmann<sup>1,2</sup>, A. Pfaffenberger<sup>1,2</sup>, A. Elter<sup>1,2,3</sup>, A.L. Hoffmann<sup>5,6,7</sup>, E. Troost<sup>2,7,8,9,10</sup>, S.A. Körber<sup>11</sup>, G. Echner<sup>1,2</sup>

<sup>1</sup>German Cancer Research Center, medical physics, Heidelberg, Germany ; <sup>2</sup>National Center for Radiation Research in Oncology NCRO, Heidelberg Institute for Radiation Oncology HIRO, Heidelberg, Germany ; <sup>3</sup>University of Heidelberg, Faculty for Physics and Astronomy, Heidelberg, Germany ; <sup>4</sup>German Cancer

Research Center DKFZ, Radiology, Heidelberg, Germany ;  
<sup>5</sup>National Center for Tumor Diseases NCT, Partner Site Heidelberg, Heidelberg, Germany ; <sup>6</sup>National Center for Radiation Research in Oncology, OncoRay, Dresden, Germany ; <sup>7</sup>Institute of Radiooncology - OncoRay, Helmholtz-Zentrum Dresden-Rossendorf, Dresden, Germany ; <sup>8</sup>German Cancer Consortium DTK, Partner Site Dresden, Dresden, Germany ; <sup>9</sup>National Center for Tumor Diseases NCT, Partner Site Dresden, Dresden, Germany ; <sup>10</sup>Technische Universität Dresden, Department for Radiotherapy and Radiation Oncology- Faculty of Medicine and University Hospital Carl Gustav Carus, Dresden, Germany ; <sup>11</sup>University Hospital Heidelberg, Radiation Oncology, Heidelberg, Germany

### Purpose or Objective

Radiotherapy needs anthropomorphic multimodality phantoms to simulate the treatment of cancer. In this work, we address two requirements and focus on the simulation of prostate cancer treatment: (i) A PSMA-PET/MRI based treatment planning should be simulated and for the following irradiation (ii) the phantom should be able to perform 3D dose measurement by using polymer gels (PG). We present a modified version of the ADAM-pelvis phantom [1] (Anthropomorphic, Deformable And Multimodal), the ADAM with PET extension (ADAM PETer). [1] Niebuhr et al. Med Phys 43(2), pp.908-16, 2016, Technical Note: Radiological properties of tissue surrogates used in a multimodality deformable pelvic phantom for MR-guided radiotherapy.

### Material and Methods

The same basic data as ADAM's is used for the rework of the construction. New possibilities in the 3D-printing made it possible to redesign the shape of the bone in more detail by using the software Geomagic® Freeform®. Now more details of the pelvis bone and all the parts of the joint are visible. For all other modifications, the software Autodesk inventor® was used. Bone tumors and the lymphatic system were integrated. The prostate was modified in such manner that subdivisions or internal spheres (tumor simulation) were created and filling operations from the outside of the segment are now possible.

All parts of the phantom are printed by means of a 3D-printer (Stratasys, Objet 300 Connex 3) from the material VeroClear™ and Agilus30™. Only the bladder, the muscle and adipose tissue are produced like in ADAM.

For PSMA-PET/MRI based treatment planning, gels of different agarose concentrations were mixed with gadolinium and radioactive tracers are added in variant 2 (fig 1b), in the lymphatic system (fig. 1c) and in the bone tumors (fig.1c). In a first irradiation experiment, the prostate variant 1 (fig. 1a) filled with PG was set as target and homogeneously irradiated.

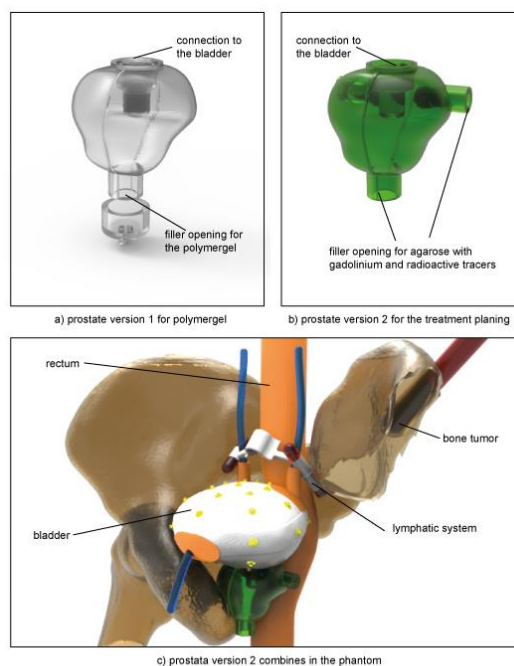


fig. 1: Update ADAM-pelvis phantom

### Results

The new version of ADAM, in which a bone tumor, the lymphatic system and prostates of different types were included, was produced in a 3D-printing process.

It is now possible to insert two bone tumors from outside the phantom. Thus, a simpler handling with radioactivity is facilitated. Further possibilities for tumor simulations with radiotracers are offered by the design of the lymphatic system and the prostate. Both are a closed system in the phantom, such that radiotracers are confined to within these structures.

An anthropomorphic multimodality phantom of the pelvis was created with modular prostate design in which, depending on the configuration, either gel dosimetry can be performed or patient-like PSMA-PET/MR data for treatment planning can be generated.

### Conclusion

With the revised ADAM-pelvis phantom, it was possible to extend the possibilities in simulating end-to-end in radiation therapy. This includes the use of radioactive tracers for treatment planning and the insertion of PG for dose verification in 3D.

### EP-1711 Discover Prostate SBRT or Validation of motion-tracked SBRT treatments with a transmission detector

M. Szegedi<sup>1</sup>, A. Paxton<sup>1</sup>, V. Sarkar<sup>1</sup>, P. Rassiah<sup>1</sup>, H. Zhao<sup>1</sup>, G. Nelson<sup>1</sup>, F. Su<sup>1</sup>, J. Huang<sup>1</sup>, J. Kunz<sup>1</sup>, D. Spitznagel<sup>1</sup>, B. Salter<sup>1</sup>

<sup>1</sup>University of Utah Huntsman Cancer Hospital, Radiation Oncology- Medical Physics, Salt Lake City, USA

### Purpose or Objective

IMRT treatments are typically validated prior to delivery to a patient. There is an assumption that after this initial validation, the patient treatments are delivered correctly. This work reports the patient treatment validation results during ultrasound (US)-image guided and tracked prostate SBRT treatments using a collimator-mounted diode transmission (CM DT) detector.

### Material and Methods

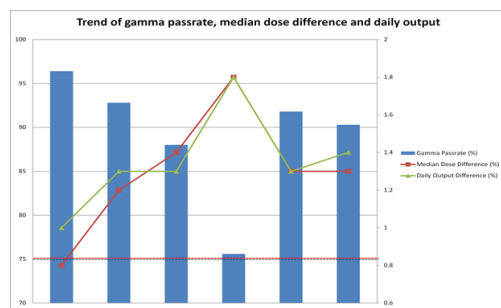
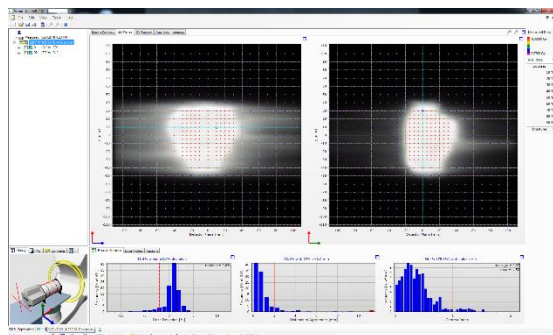
A recently introduced Delta<sup>4</sup> Discover (ScandiDOS) CM DT detector was commissioned for clinical use. Used as

standalone device during patient treatments, the Discover can measure the MLC positions, gantry- and collimator-angle and compare these measurements to the planned values. Combined with the Delta<sup>4</sup> Phantom+ (DP+) for pre-treatment plan validation, the subsequent Discover-only measurements during patient treatment can then be used to calculate the dose distribution for each treatment on the DP+. A gamma analysis can be used to evaluate the delivered treatment fractions the same way the pre-treatment delivery was evaluated.

Patient plans were developed according to our clinical protocol with two VMAT arcs. The attenuation of the Discover was determined for each photon beam energy during its commissioning and was accounted for in the patient plans. Each patient was localized and tracked using the Clarity US IG (Elekta). Tracking margins ensured that the PTV will be within 3 mm (maximum displacement) during beam-on time.

We present five SBRT patients, with five fractions for each patient that were all delivered with the Discover in place. Additionally, the Discover and DP+ were used for all pre-treatment IMRT validations. We accumulated the five dose-fractions into the planning CT data set and compared the Discover measured results that were converted to the total dose outcome with the actual plan. **Results**

To compensate for Discover attenuation, plan monitor units (MU) were increased by 1.3% for 6X flattened beams, 1.5% for 6X flattening filter free (FFF) beams and similarly for 10X for 1.0% and 10X FFF-beams for 1.2%. Figure 1 shows an example of the Discover gamma analysis with a criteria of 2%/2mm for the first fraction for one patient. As an example of our results, we found that the Discover device measured different gamma for each delivered fraction as shown in figure 2. The variation of gamma trended in line with the daily output difference.



**Conclusion**

Using US IG tracking, we assure that our patients have less than 3 mm motion of the prostate during their whole treatment course. Similarly as the US IG tracking assures treatment delivery in the correct position, the Discover device assures the delivery of the radiation plan is as intended. The combination of these techniques gives much greater confidence to the clinician that the dose seen in the treatment plan is the dose that is being delivered to the patient.

**EP-1712 Determination of photon output factors: implementation of the IAEA/AAPM TRS-483 Code of Practice**

P. De La Monja Rey<sup>1</sup>, C. Peraza<sup>1</sup>, M.L. Brosted<sup>2</sup>, A. Chaves<sup>3</sup>  
<sup>1</sup>GenesisCare Madrid - Hospital San Francisco de Asis, Medical Physics Department, Madrid, Spain ;  
<sup>2</sup>GenesisCare Madrid, Medical Physics Department, Madrid, Spain ;  
<sup>3</sup>GenesisCare Spain, Medical Physics Department, Madrid, Spain

**Purpose or Objective**

The aim of this work is to determine the output factors (OFs) measured with six different detectors for an Elekta Versa HD linear accelerator equipped with the Agility head. The measured output factors were subsequently corrected by applying the factors proposed in the Code of Practice International Atomic Energy Agency 483 (IAEA/AAPM TRS-483).

**Material and Methods**

The OFs for field sizes ranging from 1.0 x 1.0 cm<sup>2</sup> to 10 x 10 cm<sup>2</sup> at a depth of 10 cm and at 100 cm source to detector distance were measured for 6 MV and 6 MV Flattening Filter Free (FFF). Several types of detectors, all from PTW-Freiburg, were used for comparison: microDiamond, diode-P shielded, diode-E unshielded, diode SRS - unshielded, PinPoint 3D ionization chamber and 0.125 cm<sup>3</sup> Semiflex ionization chamber. Off-axis dose profiles (in-plane and cross-plane) measurements were performed with the PTW BeamScan water phantom to ensure detector alignment and determine the effective field size. Output correction factors from IAEA/AAPM TRS-483 were applied for all the detectors. In this study, the minimum field size analysed was 1.4 x 1.4 cm<sup>2</sup> for diode-p and 2 x 2 cm<sup>2</sup> for the chamber 0.125 cm<sup>3</sup> Semiflex. A daisy chaining approach was also utilised for the small OFs choosing the 4 x 4 cm<sup>2</sup> measurement as reference.

**Results**

For both energies, 6 MV and 6 MV FFF, the OFs measured for each detector as shown in Figure 1 and Figure 2. For the smaller field size of 1 x 1 cm<sup>2</sup> the maximum OF difference measured was 7.5% for 6 MV and 7.1% for 6 MV FFF, which, once corrected, lead to a maximum deviation respectively of 1.8% for 6 MV and 1.7% for 6 MV FFF. All detector response agree within 0.6 % except for the microDiamond where the OF measured were 1% higher than for other detectors. For field sizes greater than 2 x 2 cm<sup>2</sup>, the deviations of the corrected OFs were within 1% for both beams. The disparity between the direct and daisy-chain approach of OFs corrections was less than 0.3% for 6 MV and less than 0.5% for 6 MV FFF.

Figure 1. Output factors uncorrected and corrected with all detectors for different field sizes (6 MV).

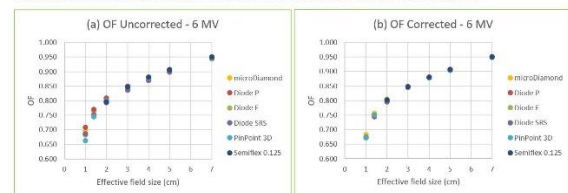
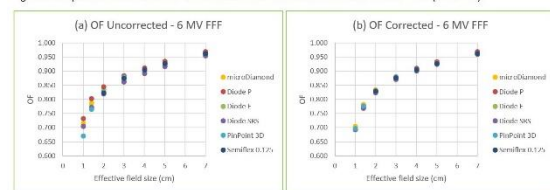


Figure 2. Output factors uncorrected and corrected with all detectors for different field sizes (6 MV FFF).



**Conclusion**

The results indicated that the diode-P overestimated OFs for fields smaller than 4 x 4 cm<sup>2</sup>. The microDiamond overestimated OFs for fields size smaller than 3 x 3 cm<sup>2</sup>,

but to a lesser extent than for the diode-P, while ionization chambers underestimated the OFs. The unshielded diodes for field sizes larger than  $1.5 \times 1.5 \text{ cm}^2$  underestimated OFs and for fields smaller than  $1.5 \times 1.5 \text{ cm}^2$  overestimated the OFs, this overestimation is likely due to density disturbance. The results of this study may assist in the selection of the appropriate method and type of detector to be utilised for small field dosimetry to ascertain the output factor. The variation observed in the output factors, with different detectors in fields size smaller than  $2 \times 2 \text{ cm}^2$ , requires further investigation which will be an ongoing project at our institution.

#### EP-1713 The implementation of 3D chemical dosimetry within a clinical radiotherapy department

J. Poxon<sup>1</sup>, M. Miquel<sup>1</sup>, N. MacDougall<sup>1</sup>

<sup>1</sup>Barts Health NHS Trust, Clinical Physics, London, United Kingdom

##### Purpose or Objective

A high-resolution 3D detector is recommended for the measurement of complex radiotherapy dose distributions, particularly during the commissioning of new techniques. 3D chemical dosimetry has been proposed but has not yet fully realised its potential within clinical radiotherapy departments.

We have developed an in-house method for Fricke gel dosimetry with MR readout and carried out a thorough dosimetric characterisation of this detector. This Fricke detector is energy, dose rate and volume independent and demonstrates adequate precision for a 3-20Gy dose range. When scanned between 10 and 90 minutes, the results are not influenced by chemical instability or diffusion. The aim of this study was to evaluate how the Fricke gel performed when applied to VMAT plans.

##### Material and Methods

Batches of Fricke gel detectors were manufactured in a basic laboratory situated within a clinical radiotherapy department. The T2 quantification of irradiated detectors was carried out using a 3T clinical MR scanner for multiple coronal, sagittal and transverse planes. T2 maps were created and converted to dose maps within OsiriX, an open source image processing application, by irradiating calibration samples to known doses. Measured dose maps were compared with TPS calculated doses in terms of dose profiles and gamma tests using relevant tolerances for dose difference and distance to agreement. The Fricke gel detector was used to measure two high dose VMAT plans delivered with a Varian TrueBeam Linac; for a brain metastasis and spine plan. Results were also compared with measurements carried out using a PinPoint ion chamber and Gafchromic<sup>TM</sup> EBT3 film.

##### Results

There was excellent agreement between measured and TPS dose distributions for coronal and transverse planes of the brain plan (figure 1), demonstrated by high gamma test pass rates (table 1). There was also good agreement in the high dose, steep gradient region of the spine plan. Small deviations between measured and calculated doses were seen in the low dose region for this plan, reflected in the gamma test results for the sagittal and coronal planes (table 1). Results also compared well with doses measured with the PinPoint ion chamber and radiochromic film.

Figure 1: Dose map analysis for the central transverse plane of the brain plan

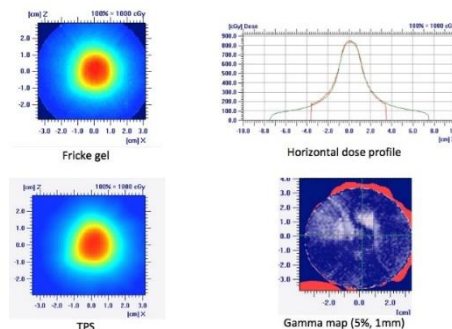


Table 1: Gamma pass rates (%) for the brain and spine VMAT plans

Gamma test settings	Brain Plan		Spine Plan		
	Central transverse plane	Central coronal plane	Central transverse plane	Central coronal plane	Central sagittal plane
3% 2mm	99.8	96.6	98.7	85.5	92.1
5% 1mm	99.8	99.1	98.4	84	92.9

##### Conclusion

The Fricke gel detector was demonstrated to be suitable for the 3D measurement of complex dose distributions. Excellent agreement was seen between measured and TPS calculated dose distributions. This method offers a simple option for 3D dosimetry within a clinical radiotherapy department.

#### EP-1714 Comparison of geometrical distortion of 1.5 T MR sim and 1.5 T MR linac

H. Jensen<sup>1</sup>, U. Bernchou<sup>2</sup>, U. Bernchou<sup>3</sup>, A. Bertelsen<sup>2</sup>, C. Brink<sup>2</sup>, C. Brink<sup>3</sup>, F. Mahmood<sup>2</sup>, F. Mahmood<sup>3</sup>

<sup>1</sup>Odense University Hospital, Afd R, Odense, Denmark ; <sup>2</sup>Odense University Hospital, Laboratory of Radiation Physics, Odense, Denmark ; <sup>3</sup>University of Southern Denmark, Department of Clinical Research, Odense, Denmark

##### Purpose or Objective

The supreme soft-tissue contrast given by the MR scanner has motivated a strong interest in using MR images for planning and guidance of radiation therapy (RT). With clinical introduction of MR linacs it is possible to adapt the plan to the anatomy at each treatment fraction using MR images.

MR imaging has several significant challenges. Among the most important for MR guided RT is the geometrical distortion that potentially could lead to mistreatments. In this study geometrical distortions are quantified for a standard clinical MR scanner as well as a high-field MR linac.

##### Material and Methods

An MR geometrical distortion phantom (Magphan RT, The Phantom Laboratory) in 35x27x21 cm configuration containing several hundreds of 1-cm spherical fiducials was used. The MR measured fiducial locations was used to generate a 3D distortion map (figure 1). The distortion magnitude was quantified within a radius of 100 mm and 175 mm from the iso-center, respectively. Also, the mean distortion of the 10 % most deviating points within 100 mm and 175 mm radius were evaluated.

A diagnostic 1.5 T MR-sim scanner (Ingenia, Philips Healthcare) was used as reference to evaluate the magnitude of distortion of a 1.5 T MR linac (Unity, Elekta Instrument AB).

Reference Ingenia sequence (MR-sim):

1. T1w 3D FFE (5 min, 34 sec), rBW 228.3 Hz/pix, WFS 0.951 pix, 1.1x1.1x2 mm, 2 averages.

Clinical MR linac sequences for pelvic imaging:

2. T2w 3D TSE (1 min 34 sec), rBW 786.2 Hz/pix, WFS 0.276 pix, 1.5x1.5x2.0 mm.

3. T1w 3D FFE (1 min 31 sec), rBW 433.5 Hz/pix, WFS 0.501 pix, 1.5x1.5x2 mm.
4. T2w 3D TSE (5 min 59 sec), rBW 752.3 Hz/pix, WFS 0.289 pix, 1.2x1.2x1.2 mm, 2 averages.
5. T1w 3D FFE (3 min 47 sec), rBW 431.9 Hz/pix, WFS 0.356 pix, 1.2x1.2x2 mm, 2 averages.

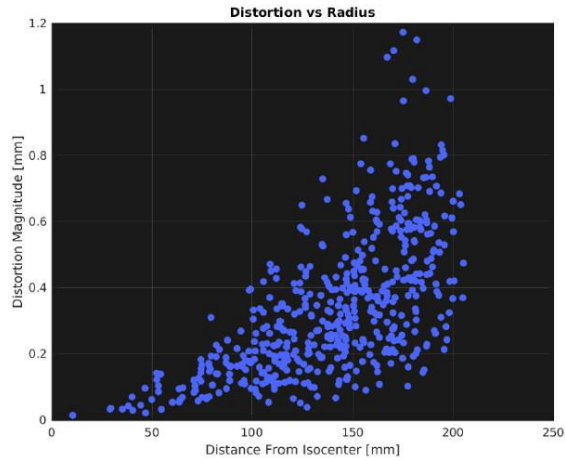


Figure 1 Distortions magnitude plot, Series Description [sequence 3]: T1w 3D FFE, high-field MR-linac Results

For the evaluated sequences the maximum distortions were in the range of 0.39-0.56 mm within a radius of 100 mm from iso-center. The MR linac performed slightly better than the MR-sim for most sequences. Likewise, the MR linac showed a maximum distortion of 0.96-1.28 mm within a radius of 175 mm, which is less than the MR-sim with a maximum distortion of 1.42 mm. Top 10 % most diverting points were analyzed and the mean distortions are listed in table 1, the MR linac shows respectively for 100 mm and 175 mm radius a distortion in the range of 0.28-0.35 mm and 0.68-0.70 mm. In comparison the MR-sim showed slightly more distortion (0.39 mm and 0.99 mm, respectively).

Sequence 3-5	<100 mm distance from isocenter		<175 mm distance from isocenter	
	Max Distortion [mm]	Mean Distortion Top 10% [mm]	Max Distortion [mm]	Mean Distortion Top 10% [mm]
1: 1.5T Ingenia T1w 3D (5m34s)	0.50	0.39	1.42	0.99
2: MR-linac T2w 3D (1m31s)	0.56	0.37	0.96	0.69
3: MR-linac T1w 3D (1m31s)	0.39	0.28	1.17	0.69
4: MR-linac T2w 3D (5m59s)	0.43	0.34	1.02	0.70
5: MR-linac T1w 3D (3m47s)	0.53	0.35	1.28	0.68

Table 1

**Conclusion**

The geometrical distortion on the MR linac was found to be less or similar to the distortions of a diagnostic MR scanner of same field strength. Distortions were of the magnitude of 0.5 mm which is needed to make precise dose delivery with the high-field MR linac. Patient induced susceptibility effects may add additional distortion and should be evaluated separately.

**EP-1715 Development of an antropomorphic brain phantom**

A. Bakhtiar<sup>1,2,3</sup>, A. Runz<sup>1,3</sup>, W. Johnen<sup>1,3</sup>, P. Mann<sup>1,3</sup>, G. Echner<sup>1,3</sup>

<sup>1</sup>DKFZ, Division of Medical Physics in Radiation Oncology E040, Heidelberg, Germany ; <sup>2</sup>Hochschule für Technik und Wirtschaft, Htw Saar, Saarbrücken, Germany ; <sup>3</sup>Heidelberg Institute for Radiation OncologyHIRO, National Center for Radiation Research in OncologyNCRO, Heidelberg, Germany

**Purpose or Objective**

In this work, we present the development of a reproducible anthropomorphic half-brain phantom for MRI, obtained with 3D printing techniques. We modelled the geometry, the shape and the size of the phantom on patient MRI data. The shape of the phantom aimed to reproduce as accurately as possible the shape of the patient brain. We adopted a T1 weighted sequence to obtain a good T1 contrast. We aimed to achieve in the phantom an equivalent contrast. This required the investigation of the concentration of the contrast agents. These are also required to reproduce a T1 relaxation time similar to the one in brain matter. The brain phantom is also foreseen to be used as training data for an automatic segmentation software. The different contrasts in the brain, that lead to the definition of the regions, could be exploited in the automatic segmentation. Moreover, this opens the possibility to compute the volume of the different regions in the brain. These values could be used in hospitals by the doctors to identify brain diseases, e.g. brain mass loss in Alzheimer patients.

**Material and Methods**

In first place, we cut the brain exactly at the center in the sagittal plane of the image. The model included a 1 mm external wall and two independent separated cavities. We produced the phantom with the Ultimaker3 FDM 3D-printer. Once printed, we put the phantom in an alcohol bath in order to make it watertight. In the following step, we filled the brain phantom with solutions made of water and the contrast agent Gadoteridol (0.5mmol/ml). The solutions have been prepared with precise mixing ratios to achieve different contrasts in the T1 weighted MRI. The objective of this experiment was to obtain an artificial contrast as close as possible to the literature values for grey (1124±50) and white (884±50) matter at MRI room temperature. We tested concentrations of 195 vs. 130 µmol/ml and 135 vs. 100 µmol/ml. To obtain the desired concentrations to insert in the phantom, we diluted the original solution of 200 µmol/ml. Finally, we performed MRI scans of the phantom with the support of the software Gel\_Evaluation and we computed the T1 times.

**Results**

The two different substances were recognizable in the MRI images, as shown in Figure 1. We obtained a clear contrast between the white and the grey matter. In agreement with the expectations, the T1-signal that we recorded showed the typical exponential decay.

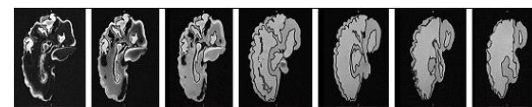


Figure 1.a. MPRAGE Scan for the concentrations 130 vs. 100 µmol/ml

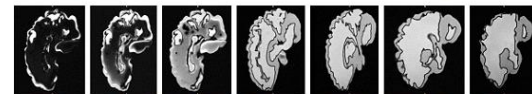


Figure 1.b. MPRAGE Scan for the concentrations 195 vs. 130 µmol/ml

**Conclusion**

Moreover, we compared the different concentration tests. We observed that the best contrast was obtained in the 195 vs. 130 µmol/ml case. In table 1 we restricted the investigation to the concentrations 135 vs. 100 µmol/ml, which have the closest T1 time to the grey and white brain matter. In our experiment, we observed a T1 relaxation time for the grey matter of (1190.1±8.3) ms for 100 µmol/ml, which differs of 5.87% from the literature value. On the other hand, the T1 relaxation time for the white matter was (985.2±84.6) ms, which differs by 11.43% from the literature.

Table 1. Comparison of measured and reference values

Tissue	Literature values [ms]	Measured values [ms]	Contrast agent concentration [ $\mu\text{mol/ml}$ ]	Relative deviation
White matter	884 $\pm$ 50	945.33 $\pm$ 7.5	135	6,93%
Grey matter	1124 $\pm$ 50	1190.12 $\pm$ 8.3	100	5,88%

### EP-1716 The Value of Independent Review in the Implementation of New Techniques at a New Radiotherapy Centre

R. Lally<sup>1</sup>, E. Reilly<sup>1</sup>, D. Stewart<sup>1</sup>, A. Reilly<sup>1</sup>

<sup>1</sup>Western Health and Social Care Trust, Radiotherapy Physics, Derry, United Kingdom

#### Purpose or Objective

Radiotherapy incidents have an adverse effect on treatment outcomes and consequently public perception of the safety of radiotherapy. Factors which contribute to incidents, as set-out in Towards Safer Radiotherapy, include: lack of training, competence or experience, fatigue and stress, poor design and documentation of procedures, over-reliance on automated procedures, poor communication and lack of team working, hierarchical departmental structure, staffing and skill levels, working environment and changes in processes. However, many of these factors are inherent to a new radiotherapy service established in a new centre, staffed by teams where individuals are often in a more senior position than they previously held. To mitigate risk, our centre added an additional safety layer to the commissioning process by requiring all new techniques, and significant changes to an existing technique, to be independently reviewed by a senior MDT. This work shares the benefits to this approach.

#### Material and Methods

Review teams consisted of senior representation from each professional group (i.e. Physics, Radiographers and Oncologists), ensuring no member had been directly involved in the implementation process. Reviews were primarily undertaken as tabletop exercises intended to address the salient points of Towards Safer Radiotherapy. Evidence reviewed included documentation (Process Documents, Records, End to End Test Reports etc.) embedded in the Quality Management System (QMS). To ensure staff were adequately trained, and service provisions adequate, competence matrices were reviewed to ensure sufficient numbers were trained to deliver the service. The teams also focused on legislative requirements. Findings were communicated verbally and tracked via email, alongside clear measurable objectives and milestones. The process was repeated until all outstanding actions had been addressed. A final implementation review report was published and made available in the QMS. Reviews have so far been undertaken for lung and head and neck radiotherapy.

#### Results

Lung radiotherapy was the first site implemented using independent review. The MDT identified n=12 findings, ranging from; the issue of entitlement records; update of competence matrices; documentation of end-to-end testing; through to work instruction changes. Findings were addressed within 13 days. Fewer findings were identified during the Head and Neck review.

#### Conclusion

Considering the many steps associated with radiotherapy, our centre found the implementation review process a valuable tool to identify any errors before they could propagate to an incident. The overall consensus was that the independent reviews provided valuable learning opportunities and reassurance to staff, thus reducing stress and consequently fatigue. Furthermore, through an increased overall awareness of how processes evolve, staff are less fearful of change and are more willing to constructively engage when changes are proposed.

### EP-1717 Challenges of Developing, Managing and Exploiting a National Radiotherapy Dataset - UK Experience

C. Roe<sup>1</sup>, U. Findlay<sup>1</sup>

<sup>1</sup>Public Health England, National Cancer Registration and Analysis Service, London, United Kingdom

#### Purpose or Objective

The Radiotherapy Dataset (RTDS) establishes a national standard for the collection of consistent and comparable data across radiotherapy (RT) providers in order to provide intelligence for service planning, commissioning, clinical practice and research and operational provision.

#### Material and Methods

RT providers are required to collect and submit the dataset and in turn, Public Health England (PHE) receive, validate, quality assure and integrate the data received to provide a timely and definitive analytical resource. This data is linked to data captured from other national cancer datasets (Cancer Outcomes and Services Dataset and Systemic Anti-Cancer Therapy) to support key service metrics to track progress in the provision of radiotherapy and other cancer services. This enables cancer site-specific analyses of outcomes by patient and treatment variables, and provide better understanding and appreciation of the specific role of radiotherapy in improving outcomes compared with other treatment modalities.

#### Results

Public Health England (PHE) took over full responsibility for the RTDS with effect from 1 April 2016. Dataset inclusions: the mechanism for extracting and uploading data; data processing and registration procedural processes internal to PHE; dataset QA; monthly reports to RT providers and additional examples of how the data is used to inform clinical practice and influence outcomes will be presented.

#### Conclusion

RTDS data is been used to inform RT service provision. This can only be achieved through direct partnership with key stakeholders from the RT community. Radiotherapy continues to be a rapidly evolving field. Therefore, there is a real need for a continual cycle of development, ongoing management and exploitation of radiotherapy datasets to ensure benefit to all.

### EP-1718 Determination of ion recombination correction factor by empirical and numerical methods

C. Anson Marcos<sup>1</sup>, P. Castro Tejero<sup>1</sup>, D. Hernández González<sup>1</sup>, M. Roch González<sup>1</sup>, P. García Castañón<sup>1</sup>, A. Viñals Muñoz<sup>1</sup>, R. Fayos-Sola Capilla<sup>1</sup>, S. Martín Juárez<sup>2</sup>, A. Valiente<sup>2</sup>, L. Pérez González<sup>1</sup>

<sup>1</sup>University Hospital La Princesa, Medical Physics, Madrid, Spain ; <sup>2</sup>University Hospital La Princesa, Radiation Therapist, Madrid, Spain

#### Purpose or Objective

Dose measurements using ionization chambers must take into account the effect of incomplete charge collection due to ion recombination as recommended by international protocols. The purpose of this work is to confirm the accuracy of ion recombination correction factor (k<sub>s</sub>) determined by empirical methods by evaluating its deviation to theoretical calculation.

#### Material and Methods

##### Equipment

The cylindrical chambers were studied were PTW: Farmer 30013, Semiflex 31010 and PinPoint 3D 31016 . The collected charge was measured with a PTW MP3 TANDEM electrometer. Varian Clinac 2100CD linear accelerator delivering 6MV flattened photon beam was used.

Measurement setup

Measurements were performed in a water phantom (PTW MP3 Phantom Tank) with vertical beam geometry. The source-to-surface distance was 100 cm and the field size 10 x 10 cm<sup>2</sup>. The chambers were situated at depth 10 cm in the centre of the field and integration time for collecting the charge (Q) was 60 s. Two readings of 100 MU set in 300MU/min rate were collected at each voltage for each measurement of ks. Nine different polarization voltages (V) were used (+50V, +100V, +150V, +200V, +250V, +300V, +350V, +400V). The chambers were at a fixed position and polarization voltage was changing giving enough time elapsed for the chamber to achieve stabilization.

#### Measurement

The ks value was determined; firstly plotting the data 1/Q and 1/V for each ionization chamber in a Jaffé curve (Eq. 1) in order to confirm their linearity and so the reliability of Boag's model for the beam in the range of voltages. A second value of ks was determined by means of two-voltage method (Eq. 2) measuring at polarization voltage +100V and +400V. This method assumes the linear dependence of 1/Q and 1/V. Value of ks was also determined by theoretical calculation taking into account the effects of initial recombination, diffusion and volume recombination (Roos and Derikum, 2000)(Eq.3)

$$\frac{1}{Q} = \frac{1}{Q_{sat}} + \frac{c}{V} \quad k_s = \frac{Q_{sat}}{Q(V)} \quad (\text{Eq.1})$$

$$k_s = \left( \frac{V_1}{V_2} - 1 \right) / \left( \frac{V_1}{V_2} - \frac{Q_1}{Q_2} \right) \quad (\text{Eq.2})$$

$$k_s \cong 1 + \frac{E_i \cdot d}{V} + 2 \frac{k_B \cdot T}{V \cdot e} + \frac{1}{2} \cdot \frac{\mu \cdot d^2 \cdot \rho}{V \cdot W/e} \cdot D_{DPP,a} \quad (\text{Eq. 3})$$

#### Results

Jaffé plots of the three chambers studied are shown in Figure 1. Farmer ionization chamber shows the highest linearity. Table 1 presents ks values determined by different approaches: Jaffé plot, two-voltage method and theoretical calculation, for each chamber. In theoretical calculation, the lowest ks is the one obtained from the PinPoint chamber, since it has smaller electrode distance. However, in the empirical methods ks obtained are larger, as well as deviation. This can be explained by the major instability of the measurements compared to the bigger chambers.

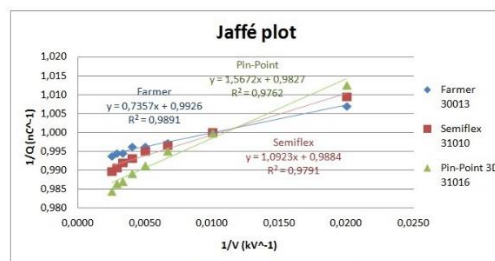


Figure 1. Jaffé plot of three ionization chambers

Farmer 30013			
	Jaffé plot	Two-voltage method	Theoretical
ks	1,0012	1,003	1,0021
Deviation to theoretical	-0,08%	0,09%	
Semiflex 31010			
	Jaffé plot	Two-voltage method	Theoretical
ks	1,0013	1,001	1,0016
Deviation to theoretical	-0,03%	-0,06%	
PinPoint 3D 31016			
	Jaffé plot	Two-voltage method	Theoretical
ks	1,0019	1,005	1,0006
Deviation to theoretical	0,12%	0,44%	

Table 1. ks values obtained from Jaffé plot, Two-voltage method and theoretical calculation

#### Conclusion

Ks value is specific for each ionization chamber and need to be estimated for absolute dosimetry measurements. Two-voltage method should be applied only after verification of the linearity of 1/Q and 1/V in the range of polarization voltage used. Jaffé curve must be measured for obtaining greater accuracy.

#### EP-1719 Automated data processing and BigData in radiation therapy

O. Schmidt<sup>1</sup>, N. Ballmann<sup>1</sup>, C. Bert<sup>1</sup>, R. Fietkau<sup>1</sup>  
<sup>1</sup>University Hospital Erlangen, Radiation Oncology, Erlangen, Germany

#### Purpose or Objective

The wide range of technologies and systems in radiation therapy produces a vast amount of heterogenic data sets. These are neither easy accessible nor processable for automated use in terms of clinical, technical or organizational issues. Therefore an IT-infrastructure has been developed which integrates the different parts of the treatment process in a single setup without a secondary data storage system. This project evaluates the effort, feasibility and validity of a single setup automatization approach with the oncology-information-system (OIS) Mosaiq (Elekta AB, Stockholm).

#### Material and Methods

The Mosaiq database is key to organizational issues and technical treatment delivery data in its role as record & verify system. Therefore a direct read-only access to the database was granted by Elekta. Topics of recurring interest can be displayed in a web application, accessible on every workstation in the institution, whereas non-regular issues are processed in a program within the infrastructure and given templates.

#### Results

The actual usage per treatment series of the different radiation techniques, as recorded in Mosaiq, was of interest for the year 2017. The distribution resulted in 3D-conformal (44%), VMAT (26%), StepNShoot-IMRT (22%) and Arc (8%) as shown in fig.1. Another issue was the identification of patient groups, which could be treated at the Linac VERO (Brainlab GmbH, Munich) without major changes to the treatment plan in order to increase the workload of that specific Linac considering the technical limitations (max. field size (x, y<15 cm), energy level (6 MeV) table rotation (<35°)). The evaluation was performed for the treatment parameters of all delivered series at the department in the given period. The result

showed that already 99% of the suitable prostate carcinoma patients, but only 61% of the lung carcinoma patients are treated at the VERO. This and further diagnoses offered options for a more balanced occupancy of the institution's Linacs. For better scheduling, the relevant tables of the Mosaik database are visualized in a web application within the network of the institution as shown in fig.2. The output can be selected by the timeperiod, ICD-10 diagnose and Linac.

#### Conclusion

As a prove of concept the Mosaik OIS was chosen, several questions have been answered and the result was validated. Currently, the Mosaik queries are integrated with queries to the treatment-planning-system Pinnacle<sup>3</sup> (Philips N.V., Amsterdam), the IMRT-verification systems ArcCHECK (Sun Nuclear GmbH, Neu-Isenburg) and Mobius3D (Mobius Medical Systems LP, Houston) allowing automated analysis of clinical parameters in large cohorts of patients. Including different data sources in a single setup is feasible for issues with the need of linking different data sets or processing vast amounts of data, which cannot be analyzed manually and reproducibly. BigData as well as machine learning applications are both in strong need for extensive and high quality data, therefore this approach is suitable.

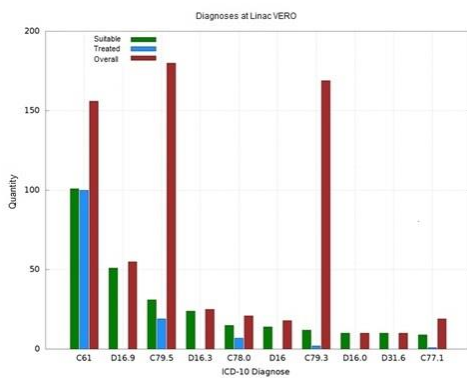


Figure 1: Identification of diagnoses suitable for treatment at the Linac VERO with its technical limitations regarding the plan parameters

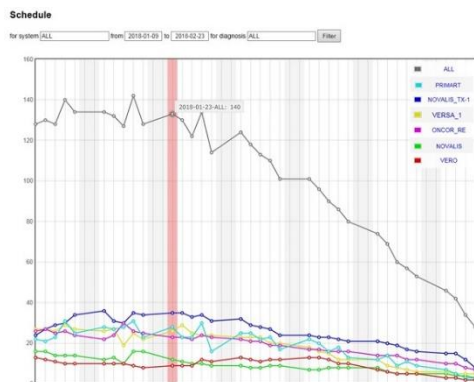


Figure 2: Web application based on Mosaik data for optimized scheduling

### Electronic Poster: Physics track: Dose measurement and dose calculation

#### EP-1720 Evaluation of dose perturbations for metal stent in photon and proton radiotherapy planning

H. Kim<sup>1</sup>, B. Lee<sup>1</sup>, S. Cho<sup>1</sup>, S. Jung<sup>1</sup>, Y. Han<sup>1</sup>, D. Lim<sup>1</sup>, H. Park<sup>1</sup>

<sup>1</sup>Samsung medical center, Radiation oncology, seoul, Korea Republic of

#### Purpose or Objective

This study was conducted to evaluate and apply dose influence of metal stent in photon and proton radiotherapy planning for hepatocellular carcinoma.

#### Material and Methods

Dose perturbations were evaluated by Monte Carlo simulation and Planning system in photon and proton. Computed tomography(CT) data sets of 1.25 mm slice thickness were obtained with containing metal stent in water equivalent solid phantom. The plan with and without metal stent consisting of nickel and titanium base alloys(Nitinol) was performed. We used Truebeam(Varian Medical System) and Pinnacle<sup>3</sup>(Philips Medical System) treatment planning system in photon and proton therapy system of Sumitomo and Raystation(Raysearch) treatment planning system in proton for dose calculation. The photon plan test are designed in an anterior-posterior/posterior-anterior (AP/PA) field technique using 6MV energy and proton plan are designed in AP field of Wobbling beam using 150 MeV energy. The Monte Carlo simulation was programed under same conditions for beam parameters, solid water phantom and metal stent of radiotherapy planning system and we compared the calculated dose distribution effects as with and without metal stent. The Monte Carlo was calculated using Geant4(v10.3) and GATE(v8.0).

#### Results

The thickness of the metal stent is about 0.1 mm. The stent appears blurred in the image because the stent is smaller than the size of the detector used in CT. In RTP, it was confirmed uncertainty for dose calculation that the image blurring of stent in CT can reconstruct the density of 1.08 - 1.3 g/cm<sup>3</sup>, which is much smaller than the actual density of 6.8 g/cm<sup>3</sup>. The treatment planning system cannot calculate dose perturbations due to stents. In the calculation of dose using Monte Carlo, dose enhance effect of photon was 1.6 - 3.0 % depending on the stent size due to multi scatter. The proton calculated dose reduction effect of -1.3 - 0.1% due to dose shadow.

#### Conclusion

Our study was performed to evaluate the uncertainty of dose calculations that could be caused by stents in radiotherapy planning and to apply them in clinical practice. In the Monte Carlo calculation, dose perturbations of 3.0% and -1.3% were observed with the use of metal stents in photons and proton. We confirmed the effect of dose change by metal stent through dose calculation and simulation. In case of RTP used in clinical practice, we can recommend to replace stent density to the average HU value of the surrounding normal tissue considering dose uncertainty by image blurring of stent that metal stent is not reflected in the planning system.

#### EP-1721 Sensitivity study between gamma index passing rate and clinical dose volume histogram

L. Szczurek<sup>1,2</sup>, R. Juszkat<sup>3</sup>, J. Szczurek<sup>4,5</sup>, P. Sosnowski<sup>3,4</sup>

<sup>1</sup>1st Department of Medicine, Poznan University of Medical Sciences, Poznan, Poland ; <sup>2</sup>The International Oncology Center Affidea, Poznan, Poland ; <sup>3</sup>Department of General and Interventional Radiology, Poznan University of Medical Sciences, Poznan, Poland ; <sup>4</sup>Affidea, Diagnostics Department, Poznan, Poland ; <sup>5</sup>Department of Endocrinology, Metabolism and Internal Medicine, Poznan University of Medical Sciences

#### Purpose or Objective

The sensitivity was analyzed to correctly identify the pre-treatment volumetric modulated arc therapy (VMAT) plans with high dose errors and to quantify the incidence of false negatives, for various the gamma index method.

#### Material and Methods

Twenty five high-risk prostate cancer patients and fifteen endometrial cancer patients treated with VMAT technique were analyzed. The percentage gamma passing rate (%GP) of two-dimensional (2D) and three-dimensional (3D) pre-

treatment VMAT dosimetric verification and their sensitivity with percentage dosimetric errors (%DE) between the planned dose volume histogram (DVH) and the patient's predicted DVH calculated by Compass and OmniPro system was calculated. Pre-treatment verifications were performed for all plans by acquiring the planar dose distribution with matrix detector. %GP of 2D and 3D with acceptance criteria 3%3mm was obtained by OmniPro and Compass software. %DE were calculated from planned dose volume histogram created in the treatment planning system (TPS) Monaco (Elekta) and the patient's predicted DVH which was calculated with Compass system. Analysis was performed for planning target volume (PTV) and some typical organs at risk (OAR). Parameters  $D_{2\%}$ ,  $D_{98\%}$ ,  $D_{\text{mean}}$  for target and dose in OAR, recommended by QUANTEC group and ICRU, were analyzed.

Sensitivity between %GP and %DE was investigated using receiver operating characteristics (ROCs). The number of false negative (FN) cases and true positive (TP) cases were calculated. FN had DVH errors >3% among those patients with %GP >95%. All the cases TP had DVH errors >3% and %GP <95%. From the FN and TP rates, receiver operating characteristic (ROC) curves were generated to investigate the ability of 2D and 3D methods to identify accurately the plan with dose errors 3%. The average area under curve (AUC) values of ROCs was analyzed.

#### Results

The t-test results between the planned and estimated DVH values for prostate and endometrial cancer group for PTV, bladder, rectum, femoral head, showed that mean values obtained from histograms were comparable ( $p > 0.05$ ). The %DE in PTV between 0.07 and 0.12 for prostate cancer patients, and from -0.14 to 0.21 for endometrial cancer group were observed. For the structures located in the low-dose region (e.g. bowel), a maximum difference of <8% was observed. For criterion 3%3mm the average %GP were acceptable in both groups, with average rates of 99.03% for 2D and 97.70% for 3D, respectively.

The average AUC value of ROCs was  $0.558 \pm 0.11$  and  $0.452 \pm 0.12$  for 3D and 2D, respectively. 3D had a better prediction on the %DE than did 2D, but the accuracy of both gamma index methods were not good enough for clinical acceptable with AUC values lower than 0.6.

#### Conclusion

Low sensitivity of 3%/3 mm 2D and 3D gamma method was confirmed. New approaches to evaluate QA plans need to be urgently implemented into clinical practice.

#### EP-1722 Development and validation of a strategy to use actual leaf positions as a patient QA tool

D. Den Boer<sup>1</sup>, K.M. Van Ingen<sup>1</sup>, Y.R.J. Van Herten<sup>1</sup>, J. Kaas<sup>2</sup>, J. Visser<sup>1</sup>, J. Wiersma<sup>1</sup>, A. Bel<sup>1</sup>

<sup>1</sup>Amsterdam UMC- location AMC, Radiotherapy, Amsterdam, The Netherlands ; <sup>2</sup>Netherlands Cancer Institute- NKI-AvL, Radiotherapie, Amsterdam, The Netherlands

#### Purpose or Objective

At our institute the actual leaf positions during VMAT delivery are stored in our record and verify (R&V) system ('actual values') for all VMAT treatments. This easily accessible information is present for all our patients, all fractions and all our Elekta linacs; an advantage as compared to using machine log files ("TRF") which are only present on newer models. Goal of this study is to develop and validate a strategy to use these actual values as a patient QA tool, which can be used pre-treatment (in a QA fraction), during treatment (for all fractions) and post-treatment (for population-based evaluation).

#### Material and Methods

Three types of data are analysed/compared: the treatment plan (TP), the actual leaf positions and the TRF file. The TRF data (with an entry every 40 ms) are used to validate the actual values (with an entry for every Control

Point, CP, Fig.1). The actual values are compared to the planned positions of the TP. In-house developed code was used to extract the data from these files, analysis was done in Matlab. The actual data per CP (red circles) cannot directly be compared to the TP (blue circles) as we found these are not registered at exactly the same point. We therefore interpolate the leaf positions of the TP between the CPs and compare the actuals to the interpolated plan with the lowest difference between these positions (least mean square). This can be regarded as a "best case scenario".

From the remaining differences we derive a "difference factor" (DF) in 3 steps: 1) Per leaf the difference between the actual value and the planned value (from the "best case scenario" interpolation) is taken. 2) This is normalised to the MU for this CP with respect to the total MU. 3) The top 10 percentile is taken of these MU scaled differences. **Results**

To determine a baseline we analysed the patients of two tumour sites at our institute part of clinically validated templates/class solutions, (prostate, 57 TPs, ~1700 fr and esophagus, 97 TPs ~1500 fr). We found a DF of 0.0031. We compared this to a tumour site where we were so far unable to validate a class solution (cervix, 30 TPs, ~700 fr) and got a significantly higher DF of 0.0040 (Fig.2). As a retrospective case study we examined cases where cervix TPs often led to replanning (due to complexity, n=6). The class solution/template was changed to reduce complexity and consequently we had less problems during Patient QA afterwards. Accordingly, the DFs went from 0.0054 to 0.0039. A higher value seems linked to more challenging patient QA.

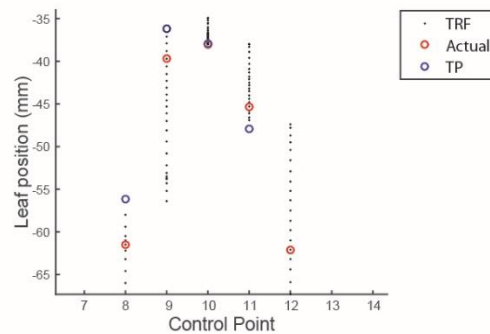


Figure 1 Leaf position for one leaf per CP in data file of actuals (red circle) and machine log file, TRF (black dots). It can be seen that they coincide. The blue dots represent the treatment plan for these CPs.

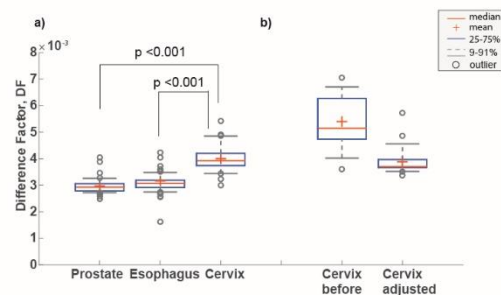


Figure 2 Difference factor (DF) from actuals.

a) For three tumor sites. Cervix is statistically higher than the class solution sites.

b) Case study: DF for cervix before (6 plans) and after (8 plans) an adjustment to decrease complexity that improved the patient QA results.

#### Conclusion

We have developed an approach to compare the actual leaf positions in the R&V software to the treatment plan. The DF difference parameters thus extracted can be used to analyse patient plans during treatment, post treatment and pre-treatment. Ideally such a factor will be monitored

for each fraction as an additional Quality Control. Our next step will be to study the DF with respect to the gamma analysis outcome of our patient QA.

#### EP-1723 Validation of EPID dose prediction and conversion models for flattening filter free beams

A. Ouakad<sup>1</sup>, M. Goubert<sup>1</sup>, L. Vieilleveigne<sup>1</sup>, F. Husson<sup>2</sup>, L. Parent<sup>1</sup>

<sup>1</sup>IUCT Oncopole, Department of Medical Physics, 1 avenue Irène Joliot-Curie-31059 Toulouse Cedex 9, France ; <sup>2</sup>Dosisoft, Department of Medical Physics, 45 Avenue Carnot- 94230 Cachan, France

##### Purpose or Objective

Electronic portal imaging devices (EPID) are interesting for pre-treatment quality assurance (QA) because of their high spatial resolution and ease of use. This study evaluated a new dosimetric portal method based on a superposition/convolution algorithm. It was tested for flattening filter free (FFF) photon beams.

##### Material and Methods

Dosisoft EPIbeam software compares an image prediction generated from the DICOM RT plan and a portal image converted into a dose map at 5 cm depth in water using kernels to account for output factors, field penumbra and arm backscatter. Irradiations were performed with a Varian TrueBeam STx linear accelerator equipped with HD120 MLC and associated with aSi 1000 EPID. Dose prediction from RT plan and EPID image conversion models were assessed in 6 and 10 MV FFF beams by comparing the model to measurements. For output factor measurements, PTW 31010 0.125 cm<sup>3</sup> ion chamber was used for output factors for 2x2 to 20x20 cm<sup>2</sup> field sizes at the isocentre. For clinical plans, prediction and conversion models were assessed with PTW 1000 SRS matrix (pixel resolution between 0.25 and 0.5 cm). Clinical plans were lung (6 MV FFF) and liver (10 MV FFF) stereotactic body radiotherapy plans using dynamic conformal arc technique.

##### Results

Predicted and converted output factors were within 2% of the measured values for field sizes between 2 and 20 cm<sup>2</sup>. For clinical cases, comparison of dose prediction to matrix measurements gave an average gamma passing rate (2%-2.5 mm, global, 10% threshold) of (99.77±0.26)% and (99.98±0.04)% for 6 and 10 MV FFF beams respectively. Comparison of converted EPID image to matrix measurements gave an average gamma passing rate (2%-2.5 mm, global, 10% threshold) of (99.28±0.97)% and (99.98±0.04)% for 6 and 10 MV FFF beams respectively. Both prediction and EPID image conversion model are therefore validated for dynamic conformal arc technique. When the EPID image is used for pre-treatment QA, EPIbeam gave excellent gamma passing rates (2%-2mm, local, 10% threshold): for 6 MV FFF, the average pass rates were (98.79±0.61)% and for 10 MV FFF, the average pass rates were (98.55±0.47)%. Tolerance and action limits were calculated irrespective of the energy and were set to 96% and 87% respectively.

##### Conclusion

For field sizes between 2 and 20 cm<sup>2</sup>, EPIbeam provided a good prediction of the dose in water at 5 cm depth and accurately converted the EPID image into a dose map in water. The software gave consistent results for the studied dynamic conformal arc clinical cases. This work should be extended to study more modulated beams, such as those used in volumetric modulated arc therapy and to study the sensitivity of the method to errors in delivery.

#### EP-1724 Delivery error sensitivity of an EPID based pre-treatment control for FFF dynamic arc therapy

A. Ouakad<sup>1</sup>, M. Goubert<sup>1</sup>, L. Vieilleveigne<sup>1</sup>, F. Husson<sup>2</sup>, L. Parent<sup>1</sup>

<sup>1</sup>IUCT Oncopole, Department of Medical Physics, 1 avenue Irène Joliot-Curie-31059 Toulouse Cedex 9,

France ; <sup>2</sup>Dosisoft, Department of Medical Physics, 45 Avenue Carnot- 94230 Cachan, France

##### Purpose or Objective

EPIbeam is a new algorithm based on a superposition/convolution algorithm and developed for pre-treatment quality control with electronic portal imaging device (EPID). It was tested in this study for dynamic conformal arc therapy with flattening filter free (FFF) photon beams in the context of stereotactic radiotherapy. Its sensitivity to delivery errors was assessed and compared to 3D phantom measurements.

##### Material and Methods

A Varian TrueBeam STx linear accelerator equipped with HD120 MLC was used for the measurements. EPID images were acquired with Varian aSi 1000 detector and analysed with Dosisoft EPIbeam software. 3D phantom measurements were performed with PTW 1000 SRS array inserted in PTW Octavius 4D phantom. Analysis was performed in PTW Verisoft software. Varian Eclipse treatment planning system (version 13.7 AAA algorithm) was used to calculate the reference dose distribution. EPID and phantom pre-treatment controls were first compared for ten 6 MV FFF lung plans (6.0 to 59.0 cm<sup>3</sup> PTV size) and ten 10 MV FFF liver plans (9.8 to 327.5 cm<sup>3</sup> PTV size).

Delivery error sensitivity was then tested by modifying the initial plans to introduce errors on dose (+1%, 2% and 3%), leaf bank shifts (1 mm and 2 mm), 10 mm central leaf shift, central leaf blockage, gantry rotation (+5° and +15°) as well as collimator rotation (+5° and 15°). For each energy, these errors were introduced for the largest and smallest PTV. Gamma agreement indices (GAI) were calculated with 2% local dose difference, 2 mm distance-to agreement and 10% threshold.

##### Results

EPIbeam gave gamma index passing rates similar to those with 3D phantom : for 6 MV FFF, the GAI were (98.79±0.61)% for EPIbeam and (99.86±0.26)% for 3D phantom and for 10 MV FFF, the GAI were (98.55±0.47)% and (99.55±0.86)% respectively.

Delivery error sensitivity varied with PTV size but not with energy. For small lesions (6-59 cm<sup>3</sup>), EPIbeam is more sensitive to dose errors compared with 3D phantom, spotting errors from 1% difference whereas for the largest lesion (327 cm<sup>3</sup>), a 3% difference was necessary. Leaf bank errors had to be at least 2 mm to fail the test with EPIBEAM whereas the 3D phantom test spotted a 1 mm error for small lesions. Central leaf 10 mm shift was spotted for the small lesions but not for the large lesion with both techniques. Leaf blockage was identified as error with both detectors. As expected, EPIbeam was completely insensitive to gantry rotation errors, unlike 3D phantom. EPIbeam is also less sensitive to collimator errors, compared to 3D phantom.

##### Conclusion

Once the treatment planning system has been validated with 3D phantom measurements, EPID based pre-treatment quality insurance can be achieved with EPIbeam for fluence verification, provided that independent QA of collimator and gantry rotations is performed on a regular basis on the machine.

#### EP-1725 Two years' experience with Esteya QA

M. Van het Loo<sup>1</sup>, W. Jansen<sup>1</sup>, A. Loopstra<sup>1</sup>

<sup>1</sup>Radiotherapiegroep, Department of Radiation Physics, Arnhem, The Netherlands

##### Purpose or Objective

Esteya® (Elekta AB, Sweden) is used to treat non-melanoma skin cancer. The QA results, since the installation in March 2016, have been reviewed to check the stability of the system.

##### Material and Methods

Esteya® is an electronic brachytherapy device with a 69.5 kV X-ray source enabling treatments up to 4 mm depth. In general the applied dose rate is 3.3 Gy/min and the maximum aperture is 30 mm. Esteya® QA consists of two parts: mandatory daily tests on radiation days carried out with the QA tool provided by Elekta and periodic QA tests. During the monthly tests reference dosimetry, energy, symmetry, flatness and penumbra size are checked for the 30 mm applicator. Annually the other applicator diameters are checked as well.

The reference dosimetry in air is performed with an ionization chamber (34013, PTW-Freiburg GmbH, Germany). Three fractions of 6 Gy prescribed at 0 mm depth are delivered for verification.

The energy consistency is determined by measuring at three depths. A Plastic Water Low Range (PWLRL, Cirs inc., USA) slab with a cavity for the ionization chamber is placed on top of 60 mm of PWRL backscatter material. As a reference a measurement without an additional slab is used. Besides we perform measurements with additional slabs of 5 and 10 mm PWLRL.

Flatness, symmetry and penumbra size are determined using Gafchomic EBT3 film (Ashland inc., USA) irradiated with a 5 Gy fraction. The film is placed on top of 60 mm PWLRL and covered with PWLRL slabs with a total thickness of 3 mm. The film is scanned with an Epson Perfection V750 Pro transmission scanner (Seiko Epson Corp., Japan) and analyzed using FilmQA Pro software (Ashland inc., USA). The penumbra size is determined as the distance between points representing 20% and 80% of the central axis dose.

#### Results

During acceptance measurements, the characteristics of Esteya® have been determined. Since acceptance neither the X-ray source, nor other major items have been replaced.

The results presented here are based on the monthly checks. The mean value of the reference dosimetry is 5.96 Gy (SD 0.03 Gy). All measurements are in tolerance of  $\pm 0.12$  Gy ( $\pm 2\%$ ). The mean value for the percentage depth dose at 5 mm is 72.8% (SD 0.7%) and at 10 mm 53.7% (SD 0.3%). This is well within  $\pm 2\%$  compared to the reference values of 73.1% and 53.9% at respectively 5 and 10 mm depth. The larger SD found at 5 mm depth is due to a difference in thickness of the slabs. All measurements of the symmetry and flatness are within the tolerance of  $\pm 3\%$ . The mean penumbra size is 0.3 mm (SD 0.1 mm).

#### Conclusion

All measurements are within the set tolerance limits. The physics characteristics of Esteya® have proven very stable and consistent. Hence, in combination with the sharp penumbra (mean size 0.3 mm) and steep dose fall off in depth, Esteya® enables a reliable and precise treatment of non-melanoma skin cancer.

#### EP-1726 Utilization of bolus in post-mastectomy radiation therapy

R. Chakarova<sup>1</sup>, D. Lundstedt<sup>2</sup>, H. Svensson<sup>1</sup>, M. Gustafsson<sup>1</sup>, M. Hällje<sup>1</sup>, P. Karlsson<sup>2</sup>

<sup>1</sup>Sahlgrenska University Hospital, Medical Physics and Biomedical Engineering, Göteborg, Sweden ;

<sup>2</sup>Sahlgrenska Academy, Dept. of Oncology- Institute of Clinical Sciences, Göteborg, Sweden

#### Purpose or Objective

Women receiving radiotherapy to the chest wall after mastectomy due to breast cancer usually have a bolus over the scar. The aim of this work is to evaluate the bolus effect on target coverage and in particular to determine if bolus recommendation should be related to the chest wall thickness and if different dose calculation algorithms estimate target coverage differently.

#### Material and Methods

The smallest thickness of the thoracic wall in the CTVT region was estimated for 160 consecutive patients

receiving radiation therapy after mastectomy. CT images were taken with bolus. CTVT and PVT were delineated according to national (SBRG) guidelines. 3DCRT plans were generated in Eclipse TPS using AAA and re-calculated with the same MU by Acuros XB and a Monte Carlo (MC) system based on EGSnrc. Calculations were performed on original CT scans and modified scans with bolus excluded. Dose distributions were obtained for three groups, (10 patients in each group), with selected chest wall thicknesses; below 15 mm (group 1), between 20 - 25 mm (group 2) and between 30 - 35 mm (group 3). Target coverage was evaluated in terms of DVH parameters; CTVT mean dose, CTVT\_V95%, PTV\_D98%, PTV\_V95% and PTV\_V105%.

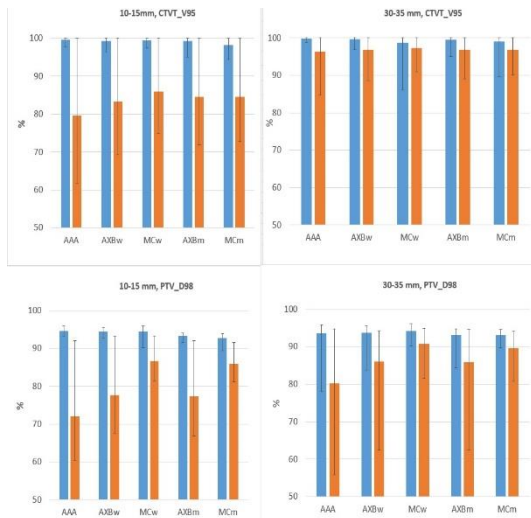
#### Results

The distribution of chest wall thickness for the 160 patients is shown in the Table. The bolus effect was most pronounced for patients in group 1. About 10-15% higher CTVT\_V95 and 10-20% higher PTV\_D98 values were obtained in case of bolus (Figure). For the patients in group 3, CTVT\_V95 differed by 4% and PTV\_D98 by 5-15% (Figure). CTVT mean dose for group 1 was 2% higher as estimated by Acuros XB and MC (4.5% for AAA) and 1% lower for groups 2 and 3 (negative bolus vs no-bolus difference). The increase of PTV\_V95% in absolute volume due to presence of bolus was comparable for the three groups: about 20 cm<sup>3</sup>; 15 cm<sup>3</sup> and 10 cm<sup>3</sup> as estimated by AAA; Acuros XB and MC, respectively. PTV\_V105% decreased in case of bolus by 5 - 10 cm<sup>3</sup> (group 1) and 20 - 40 cm<sup>3</sup> (group 3). The presence of bolus enhanced the agreement between the different algorithms and reduced the variation of the estimation within the group (max-min intervals in the figure).

**Table.** Chest wall thickness near CTVT for 160 patients undergoing post-mastectomy radiation therapy

Chest wall thickness, mm	Frequency, %
up to 15 mm	14
15 to 20	19
20 to 25	20
25 to 30	20
30 to 35	15
35 to 40	6
40 to 45	6
more than 45	6

**Figure.** CTVT\_V95% and PTV\_D98% for group 1 and 3 estimated by: AAA, Acuros XB dose to water and medium (AXBw, AXBm), Monte Carlo (MCw, MCm). Blue bars: bolus; red bars - no-bolus. Error bars indicate min-max interval.



### Conclusion

Bolus considerably improves the dose distribution in thin chest wall target. It is advisable also for other chest wall thicknesses to achieve better target coverage and decrease the overdose volume. Dose estimation in presence of bolus is more robust and less sensitive to the calculation algorithm. If the improved dose distribution with bolus translates into fewer chest wall recurrences needs to be verified in clinical trials.

### EP-1727 Validation of the Raystation Monte Carlo Code using dedicated ionization chambers

G. Pittomvils<sup>1</sup>, E. Bogaert<sup>1</sup>, P. Thysebaert<sup>2</sup>, C. De Wagter<sup>1</sup>, Y. Lievens<sup>1</sup>

<sup>1</sup>Ghent University Hospital, Dienst Radiotherapie, Gent, Belgium ; <sup>2</sup>Odisee Hogeschool-Universiteit, Campus Terranova, Brussels, Belgium

### Purpose or Objective

Electron Monte Carlo dose calculation algorithms are capable of predicting dose distributions within tolerances defined by international and national organizations for standard and non-standard setups, such as extended SSD treatments, oblique incidences and heterogeneous tissues. At Ghent University Hospital the Raystation planning system was introduced in 2016 and the electron Monte Carlo was also commissioned, allowing the dose prediction of electron dose deliveries for all treatment modalities.

### Material and Methods

Raystation Monte Carlo Code is verified using plane parallel chambers; Roos Chamber and a linear array using liquid filled plane parallel chambers (PTW, Freiburg, Germany) and an PTW Electron Diode type 6012. The clinical calculation grid size of 2mm<sup>3</sup> was selected using 250000 histories resulting in a statistical dose accuracy of 1.5%. The NCS15 protocol (Nederlandse Commissie Stralingsdosimetrie)[1] is used to validate the results. The dose output versus SSD (95.5-115cm) is evaluated for all applicators at Zref using the Roos chamber. The output of 19 different inserts is verified using de Electron Diode at SSD=100 cm. The dose reduction at the standard R50 value for a 14x14cm<sup>2</sup> applicator was verified for beam incidence angles ranging from 0° to 30°. The calculated dose is verified with a linear array for lung and air inserts of different dimensions with and without 1 cm build up material behind the 3D plus shaped cavity. The same linear array is used to verify the dose behind a cylindrical insert with three different bone density inserts.

### Results

Dose calculation and dose measurements remain within tolerances of NCS15 confirming the accuracy of the Monte Carlo Algorithm for different SSD's and all investigated inserts. Large fields remain in output very close to 1/(SSD)<sup>2</sup> and steeper measured dose fall off for small fields is predicted within tolerance with the Raystation Monte Carlo algorithm. The Distance To Agreement for the R50 values with increasing incidence angle remains 2 mm or smaller, again within NCS15 tolerances. The best fit for the line profiles behind the air, lung and bone cavities was obtained within 3 mm for the δ2 region (high dose gradient) and within 4% in dose for the δ4 region (photon tail), both within the tolerance of NCS15.

### Conclusion

According to NCS15 for non-standard treatment setups a dose agreement of 3 % in the d1 region of 4 % in de d4 region and for the d2 region a distance to agreement of 3 mm has to be obtained between measurements and calculations. This is investigated using different air filled and liquid field ionization chambers and diodes in several setups. This confirms the accuracy of the Monte Carlo code of Raystation for prediction of dose distribution within acceptable timeframes (<1000000 histories) for standard clinical treatment planning.

[1] Quality Assurance of 3-D treatment planning systems for external photon and electrons beams, NCS15, Bruinvis I.A.D. et all 2005

### EP-1728 1-year experience with automated transit in vivo dosimetry in a busy multicenter department

E. Bossuyt<sup>1</sup>, R. Weytjens<sup>1</sup>, S. De Vos<sup>1</sup>, R. Gysemans<sup>1</sup>, D. Verellen<sup>1</sup>

<sup>1</sup>Iridium Kankernetwerk Antwerpen, Physics department radiotherapy, Wilrijk, Belgium

### Purpose or Objective

Being a busy department with 5600 new patients/year and several satellite centers, efficiency, standardization and automation are key for a QC program. A web-based system was installed in our center early 2017, for pre-treatment and in-vivo QA based on phantomless EPID and/or log files (Sun Nuclear Corporation). DICOM data is pushed to the server. Images and log files are actively retrieved. Calculation and analysis occur automatically in the background. A clinical validation of the system's performance on detection of errors and reducing workload will be reported. Special attention was given to identify and mitigate false positive (FP) results.

### Material and Methods

In this study results are reported from an analysis for all patients treated between October 2017 and August 2018. During treatment every field or arc was controlled by means of logfiles for all patients receiving photon treatment. In addition, the first 3 days and then weekly, transit EPID images were generated. These were compared using relative 2D analysis. Recently absolute verification was introduced comparing the images to calculated data, further enhancing detectable errors. Appropriate actions were undertaken based on a decision tree derived from an initiating training period.

### Results

No relevant patient errors were detected with analysis of the logfiles, 15% of integrated images failed. One third were FP, due to incomplete dose accumulation (beam stop, 6%) or dispositioning of the imager (27%). Creating a report in Aria helps detecting these FP's. The remainder concerned patient related issues. Most common causes were patient positioning and anatomy changes such as weight loss (41%) and deviations in bladder or rectal filling (6%). Rare observations were shrinkage of tumor, hematoma, pneumonia, air cavity in the tumor and accidental translation of the table between fields. Actions to mitigate the most dominant causes of errors were

introduced such as adapting the imaging protocol, recalculating treatment plans on CBCT or a new CT, weekly weight control of patients at risk, adjusting rectal and bladder filling protocol. In 17% of cases no actions were taken. Due to the high resolution of transit images, most of the conventional portal images in non VMAT could be omitted. A learning curve was observed during feedback moments with staff, which resulted into a wide acceptance by repeated training using practical examples.

### Conclusion

A standardized transit dosimetry program using a decision tree was introduced in a busy department. Some treatment and imaging protocols were adjusted based on this experience and pre-treatment imaging could be omitted for some treatments. After 6 months half of the observed deviations could be reduced, contributing to a wide acceptance level in our department. A detailed report of further experience using an adapted workflow on the first years' experience will be presented as well as the preparatory work needed to establish a standardized QC program.

### EP-1729 Evaluation of beam modeling parameter variations among radiotherapy institutions using common TPS

M. Glenn<sup>1</sup>, D. Followill<sup>1</sup>, R. Howell<sup>1</sup>, J. Pollard-Larkin<sup>1</sup>, S. Zhou<sup>2</sup>, S. Kry<sup>1</sup>

<sup>1</sup>The University of Texas MD Anderson Cancer Center, Radiation Physics, Houston, USA ; <sup>2</sup>The University of Texas MD Anderson Cancer Center, Biostatistics, Houston, USA

### Purpose or Objective

Previous studies indicate that a major contributor to erroneous radiotherapy treatments is the inaccuracy of the dose calculation itself. This study evaluates the variation of several treatment planning system (TPS) beam modeling parameters to determine the degree to which the radiotherapy community shows consensus in how clinical beam models are established. Simultaneously, this study provides reference values for TPS parameters that can assist clinical physicists in the TPS commissioning process.

### Material and Methods

Beginning January 2018, TPS beam modeling parameter surveys were distributed to users of IROC services through online facility questionnaires. These surveys, designed for Eclipse, Pinnacle, and RayStation users, instructed physicists to report parameter values used to model the radiation source and multileaf collimator (MLC) for each treatment machine and beam energy used clinically for IMRT. Parameters collected included the effective source/spot size, MLC transmission, dosimetric leaf gap, tongue and groove effect, as well as other nondosimetric parameters specific to each TPS. To facilitate survey participation, instructions were provided on how to identify requested beam modeling parameters within each TPS environment. Survey results were then isolated according to calculation algorithm, beam energy, machine class, and MLC type, and then examined for trends.

### Results

To date, parameters for 2171 beam models from 533 radiotherapy institutions have been aggregated via online questionnaires. 76% of reported beam models were commissioned using Eclipse, 18% of responses were for Pinnacle, and 6% of responses reported values for RayStation beam models. Some parameters, such as the effective target spot size (Eclipse AAA and AcurosXB), exhibited very good uniformity (>75% reported the same value for a given machine class). Other variables presented broad distributions of values, especially for factors that are physically measured for the characterization of the MLC (e.g. MLC transmission and dosimetric leaf gap). These parameters that showed

remarkable variations tended to remain without strong consensus across different energies and machine classes.

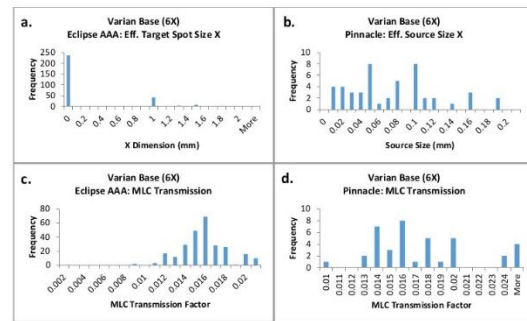


Figure 1. Histograms of several Eclipse and Pinnacle beam modeling parameter responses for 6 MV Varian Base Class models submitted: a) effective target spot size (Eclipse AAA), b) effective source size (Pinnacle), c) MLC transmission factor (Eclipse AAA), d) MLC transmission factor (Pinnacle).

### Conclusion

This study demonstrates that high variation exists in several TPS beam modeling parameters, thus highlighting the need for further exploration to determine what effects these discrepancies may have on dose calculations. These results can be employed by the radiotherapy community to compare parameter values obtained during commissioning to better inform what are considered reasonable values for model creation.

### EP-1730 Systematic Monte Carlo dose verification of VMAT treatment plans for TrueBeam linac using PRIMO

A. Sottiaux<sup>1</sup>, V. Baltier<sup>1</sup>, A. Monseux<sup>1</sup>, C. Leclercq<sup>1</sup>, D. Vanache<sup>1</sup>, M. Tomsej<sup>1</sup>

<sup>1</sup>CHU Charleroi, Radiotherapy, Montigny-leTilleul, Belgium

### Purpose or Objective

Complex techniques like VMAT require appropriate QA to check if the predicted dose is delivered to patient, including TPS dose verification. Regarding dose verification, Monte Carlo methods are often considered as gold standard. PRIMO is a Monte Carlo software self-containing (geometry included), publically available and able to handle VMAT plan for TrueBeam linacs.

The purpose of this study is to check if PRIMO is suitable for systematic VMAT plans dose verification.

### Material and Methods

PRIMO v0.3.1 combines linacs geometry, Graphical User Interface and 2 Monte Carlo engines: PENELOPE/PenEasy and DPM (Dose Planning Method, optimized for radiotherapy). DPM is faster but less accurate in low density materials. Download, Installation and PRIMO setup is very easy.

We used a PRIMO beta-version v0.3.1.1625 that provides 2 additional features: Macro mode and start from command line. Macro mode allows required task to simulate VMAT plan (load DICOM, set parameters, start simulation and perform Gamma Index (GI) analysis) to be executed with simple commands, without user action nor risk of error. We developed scripts to automate the process. After DICOM export from TPS, appropriate Macro file is generated, and simulation is launched (including GI) without any user action.

As TrueBeam head's geometry (beam production) is not implemented in PRIMO, Phase Space Files provided by Varian are used. They are designed to match TrueBeam standard tuning. We compared PRIMO simulation against PDD measurements for 3x3 cm<sup>2</sup> and 10x10 cm<sup>2</sup> beams, on 2 different TrueBeam.

50 VMAT plans (calculated with Eclipse/Acuros 13.7, dose to medium) have been compared for various cases and PTV size. All plans were calculated with DPM, and 8 recalculated with PENELOPE because they failed our criteria with DPM. We performed GI (3%/3mm and 2%/2mm, 95% passing

criteria), including noise reduction (integrated to PRIMO) in order to reduce underestimation of GI due to statistical noise in reference dose.

### Results

For all 4 PDD comparisons (2 beam sizes, 2 linacs), GI 1%/1mm is 99.7%-100%. With 3%/3mm criteria, all plans pass GI. 1 plan fails with DPM, but passes with PENELOPE. With GI 2%/2mm, 42/50 plans pass with DPM (6/8 failing plans are lung cases). Combining with PENELOPE recalculation, 45/50 plans pass GI. For 8 recalculated plans, mean GI is 90.5% and 95.2% for DPM and PENELOPE respectively. Average PTV median dose difference is +0.95% between PRIMO (DPM) and Acuros.

Calculation time varies from 19 min to 2 h 17 min (DPM), with an observed correlation with both PTV volume and Acuros calculation time. Calculation time with PENELOPE is -6-8 times longer.

### Conclusion

PRIMO can perform systematic VMAT plan dose verification for TrueBeam, using Varian Phase Space files. This requires low setup effort.

With enhancement regarding automation (PRIMO side and in-house developments), user time required is reduced to a few seconds.

### EP-1731 Using plane-parallel ionization chamber PPC40 to measure Dose Area Product Ratio

D. Mateus<sup>1,2</sup>, G. Mora<sup>3</sup>, M.J. Cardoso<sup>1,2</sup>, A. Martins<sup>1</sup>, A. Rocha<sup>1,2</sup>, C. Greco<sup>1</sup>

<sup>1</sup>Fundação Champalimaud, Radiotherapy, Lisboa, Portugal; <sup>2</sup>Mercurius Heath, Radiotherapy, Lisboa, Portugal; <sup>3</sup>Faculty of Sciences- University of Lisbon, Institute of Biophysics and Biomedical Engineering, Lisboa, Portugal

### Purpose or Objective

The introduction of Dose Area Product Ratio ( $DAPR_{20,10}$ ) as a new beam quality parameter for small field dosimetry to replace the traditional  $TPR_{20,10}$  have been suggested by several authors. These studies have been investigated the characteristics of  $DAPR_{20,10}$  for FF photon beam energies using large-area plane-parallel ionization chambers (IC), such as LACs, with diameter between 96.5 and 39.6mm. But LACs are not commonly used in the radiotherapy clinical centers and there is a lack of research about  $DAPR_{20,10}$  for FFF photon beam energies. In the present work, it was investigated the feasibility of using the common plane-parallel ionization chamber PPC40 (diameter of 16mm) instead of LACs for the  $DAPR_{20,10}$  measurements. In addition, it was studied the variation of  $DAPR_{20,10}$  with field size, beam energy and the diameter of the active area of IC. Finally, it was calculated correction factors to compensate the observed dependence of  $DAPR_{20,10}$  on the beam diameter of the IC (see Fig. 1).

### Material and Methods

Measurements of  $DAPR_{20,10}$  and  $TPR_{20,10}$  for photon beams emerging from the linear accelerator *Edge*, Varian, were performed using the PPC40 and PTW60019 microDiamond detector, respectively. Beam collimation included: 1) cones of different diameter (7.5mm, 10mm, 12.5mm, 15mm and 17.5mm) with jaws opening of 5x5 cm<sup>2</sup>; and 2) square field size of 1x1 cm<sup>2</sup>. Several energies were studied: 6MV (FF and FFF) and 10MV (FFF).

### Results

Our preliminar results indicate 1) using the PPC40, it is possible to properly measure DAP for the circular fields with diameter up to 12.5 mm and also the square field of 1x1cm<sup>2</sup> defined by the jaws; 2) differences between  $DAPR_{20,10}$  and  $TPR_{20,10}$  are around 2% (see Table 1); 3)  $DAPR_{20,10}$  does not depend practically on field size (maximum difference of 0.5%); 4)  $DAPR_{20,10}$  and  $TPR_{20,10}$  have similar variation with energy (difference around 7% between the energies 6MV-FFF and 10MV-FFF).

Table 1. -  $DAPR_{20,10}$  and  $TPR_{20,10}$  measurements acquired with PPC40 and microDiamond, respectively, for the cones of 7.5mm, 10mm, 12.5mm of diameter and the square field size of 1x1 cm<sup>2</sup>, for the energies 6MV, 6MV-FFF and 10MV-FFF.

Field Sizes	$DAPR_{20,10}$			$TPR_{20,10}$		
	6MV	6MV-FFF	10MV-FFF	6MV	6MV-FFF	10MV-FFF
Cone 7.5mm	0.627	0.593	0.668	0.614	0.581	0.647
Cone 10mm	0.622	0.591	0.665	0.617	0.585	0.653
Cone 12.5mm	0.622	0.590	0.665	0.621	0.589	0.658
1x1 cm <sup>2</sup>	0.626	0.592	0.666	0.622	0.590	0.658

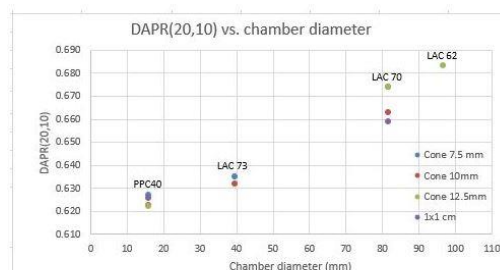


Fig. 1 – Variation of the  $DAPR_{20,10}$  with the diameter of the PPC40, LAC 70 (J. Niemela, 2017), LAC 73 (J. Niemela, 2017), M. Pimpelino, 2017; T. Kupfer, 2014) and LAC 62 (M. Pimpelino, 2017) for 6MV energy.

### Conclusion

The characteristics of  $DAPR_{20,10}$  determined for the circular fields up to 12.5 mm and square field of 1x1 cm<sup>2</sup> using the common clinical PPC40 are similar to those reported by previous studies which used LACs. We are conducting more research to validate our calculated correction factors by Monte Carlo method.

### EP-1732 The effect of different table top models on patient-specific QA

L. Paelinck<sup>1</sup>, E. Wuyts<sup>1</sup>, B. Vanderstraeten<sup>1</sup>, C. De Wagter<sup>1</sup>, Y. Lievens<sup>1</sup>

<sup>1</sup>University Hospital Ghent, Radiotherapy, Ghent, Belgium

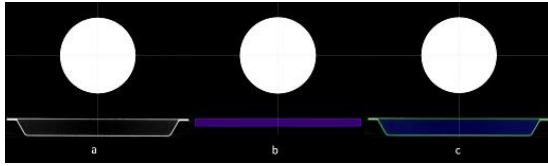
### Purpose or Objective

The purpose of this study was to investigate the effect of different table top models on the agreement between calculations and measurements on the Delta4 phantom (Scandidos) for different beam configurations. Also, 8 full arc prostate plans were measured and compared with calculations without the table model and with the three different table models included.

### Material and Methods

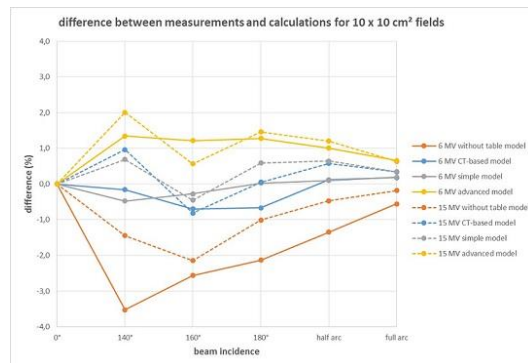
Our Elekta linear accelerators are equipped with the iBeam evo carbon fiber table top. Three different models for this table were considered in our TPS RayStation 6 (RaySearch): a CT-based, a simple and an advanced geometric model. For the CT-based model the treatment table was removed from the linear accelerator and scanned with a Toshiba Aquilion LB CT simulator. Thereafter, the part of the CT-images where the table-pixels are located, were extracted and injected in the artificial CT-images of the Delta4 phantom with a home-made java program. The result of this operation is seen in fig 1a. The simple geometric model is represented by a slab with a density of 0.25 g/cm<sup>3</sup> (fig 1b). The advanced geometric model is represented by a thin outer surface layer mimicking the table contour composed of carbon fiber (1.18 g/cm<sup>3</sup>) and an inner core composed of foam (0.055 g/cm<sup>3</sup>) (fig 1c).

Different beam configurations of 3x3 cm<sup>2</sup>, 5x5 cm<sup>2</sup> and 10x10 cm<sup>2</sup> at angles of 0°, 140°, 160° and 180° as well as a half arc of 180° crossing the table and a full arc of 360° for 6 and 15 MV were measured and calculated on the Delta4 phantom without and with the three table models included. The same was done for the 8 full arc prostate plans. All measurements were performed on the same day and a proper daily correction factor was applied. For the analysis of the prostate plans, a gamma criterion of 3%/3mm was used.



## Results

The percentage difference between measurements and calculations in the centre (at isocentre) of the Delta4 phantom is shown in fig 2 for 10 x 10 cm<sup>2</sup> field configurations both for 6 MV and 15 MV. Graphs for the other investigated field sizes are similar. The percentage differences for the CT-based and simple model are fluctuating around zero, whereas the percentage differences without table and with the advanced table model are all either negative or positive and have a larger range. This means that the CT-based and simple table model are equivalent to each other and superior to the others. Gamma analysis of the prostate plans shows little variances between the different models. This can be declared by the observation in fig 2 that the differences between measurements and calculations are below 1% for full arcs.



## Conclusion

The quality of the simple model and the CT-based model are equivalent. It is surprising that the quality of the advanced model is not satisfying. We prefer to use the simple model in routine clinical practice since it is more user-friendly than the CT-based model.

## EP-1733 CFR-PEEK vs titanium spinal stabilization implants in photon and proton therapy: A phantom study

R. Poel<sup>1</sup>, F. Belosi<sup>1</sup>, N. Klippel<sup>2</sup>, F. Albertini<sup>1</sup>, M. Walser<sup>1</sup>, A. Gisep<sup>3</sup>, D. Terribilini<sup>2</sup>, A. Joosten<sup>2</sup>, H. Hemmatzad<sup>2</sup>, K. Zaugg<sup>4</sup>, D. Aebersold<sup>2</sup>, P. Manser<sup>2</sup>, D. Weber<sup>1</sup>

<sup>1</sup>Paul Scherrer Institute, Center for Proton Therapy, Villigen, Switzerland ; <sup>2</sup>Inselspital University Hospital, Medical Radiation Physics and Radiation Oncology, Bern, Switzerland ; <sup>3</sup>Cotec AG, Clinical Research, Altstätten, Switzerland ; <sup>4</sup>Stadtspital Triemli, Radiation Oncology, Zurich, Switzerland

## Purpose or Objective

High density implants cause artefacts in CT and MRI which is problematic for the delineation process and dose calculation. The high density titanium implants are not properly accounted for in the dose calculation algorithms of the treatment planning system (TPS). This can result in an incorrect computation of the dose on TPS. Implants made from carbon fiber reinforced polyetheretherketone (CFR-PEEK) are radiolucent, non-magnetic and have a low density. Therefore, they do not produce artefacts and should be more compatible with the TPS algorithms. This study aims to assess the advantages of CFR PEEK vs. titanium implants in both photon and pencil beam scanning proton therapy (PT) for spinal treatment.

## Material and Methods

A unique phantom was developed with 4 interchangeable inserts at spine level Th 7-11: one reference case with a native spine and three with a spinal stabilization implant consisting of: titanium, CFR-PEEK and a hybrid composition of both materials. These 4 scenarios were irradiated with both proton and photon plans with a fraction dose of 2 Gy. A single field and a clinical scenario with 3 fields Intensity Modulated PT (IMPT) plan with spinal cord sparing were applied with protons. Static field plans and VMAT plans were created with the Varian Eclipse planning system and applied with a Varian linac with 6 MV photons. The severity of the artefacts was measured by size, contouring time and overlap with other structures. The delivered dose was measured with GafChromic films.

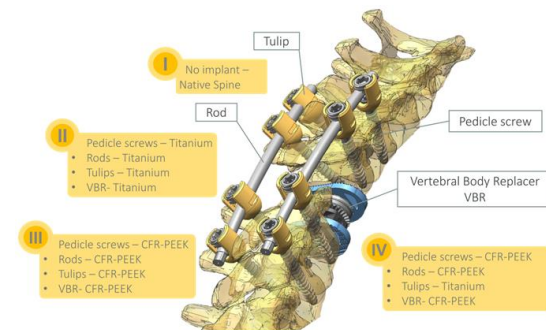


**Figure 1:** Design schematic of the interchangeable insert of the phantom. The 4 different inserts exist of: A native spine (case I), a full titanium implant (case II), an implant completely out of CFR-PEEK (case III) and a hybrid implant where the tulips are made of titanium (case IV).

## Results

The total volume of artefacts on CT was 390.6 cc, 174.2 cc and 33.9 cc for the titanium, hybrid and CFR-PEEK case respectively; with 7.5% of the spinal cord and 58.2% of the GTV affected by artefacts for the titanium while these structures were not affected in the CFR-PEEK cases. This resulted in a delineation time 4 times shorter for CFR-PEEK case (43.7 ± 36.5 min) compared to the titanium case (172.0 ± 111.6 min). The single field proton plans showed a large deviation of measured dose in the titanium containing cases. In the clinical plans this improved slightly, but cold spots still exceeded clinical acceptance levels of >5%. Photon plans showed the same effect for a single dorsal static field. The disturbance by titanium results in hot and cold spots with dose deviations up to 25% of the prescribed dose. The applied VMAT plans showed no detectable dose deviations compared to the reference case. The CFR-PEEK showed in all plans a result comparable to reference. The maximum deviation measured by GafChromic films with respect to the prescribed dose for all cases an both planning techniques are presented in Table I.

	Protons		Photons	
	Single field	3 field SC sparing	single field	VMAT SC sparing
Reference	4.4%	4.6%	5.5%	10.0%
Titanium	14%	10.8%	25.0%	10.0%
CFR-PEEK	4.0%	4.7%	7.0%	10.0%
Hybrid	17.5%	13.5%	11%	10.0%

**Table 1:** Represented is the maximum relative deviation of the prescribed dose as measured with the GafChromic films for the different plans. The single field plans and the 3 field and VMAT plan with spinal cord (SC) sparing for proton and photons respectively. Results of all the 4 phantom cases implant are presented.

## Conclusion

Whereas titanium leads to severe artefacts, prolonged planning time and incorrect dose calculations, use of CFR-PEEK implants solved all these issues. As such, CFR-PEEK implants should be used during the surgical procedure if adjuvant PT is considered for a patient.

### EP-1734 Dosimetric effects due to uncertainties in tissue segmentation for prostate cancer treatments

M. Krantz<sup>1</sup>, A. Lund<sup>1</sup>, R. Chakarova<sup>1,2</sup>

<sup>1</sup>Sahlgrenska University hospital, Department of Medical Physics and Biomedical Engineering- Sahlgrenska University Hospital- Gothenburg- Sweden, Gothenburg, Sweden ; <sup>2</sup>Sahlgrenska University hospital, Department of Radiation Physics- Sahlgrenska Academy at the University of Gothenburg- Sweden, Gothenburg, Sweden

#### Purpose or Objective

In a previous work, presence of gold markers, contrast in the bladder and rectum interpretation were identified as potential factors influencing tissue segmentation and causing discrepancies between dose distributions from the TPS and a Monte Carlo (MC) system [Phys Med 51 (2018) 32]. Thus, the objective of this work is to quantify dosimetric effects on the target dose determination due to uncertainties in tissue segmentation for prostate cancer treatments.

#### Material and Methods

CT scans of more than 200 consecutive VMAT plans for prostate cancer were reviewed. Three groups of plans were selected: (i) 18 plans with enhanced CT artifacts in the PTV due to presence of gold markers but no contrast in the bladder or visible air in the rectum as a part of the PTV; (ii) 15 plans with contrast in the bladder as a part of the PTV but no marker artifacts or air in the rectum in the PTV; (iii) 15 plans with air in the rectum as a part of the PTV but no contrast in the bladder in the PTV. Calculations were carried out by Eclipse™ TPS algorithms, AAA and Acuros XB (dose to medium ( $AXB_m$ )) and by an MC system (dose to water/medium ( $MC_w$ )/( $MC_m$ )) based on the EGSnrc. Dose distributions were obtained on the original CT scans as well as on the modified scans by setting HU to zero in the PTV, the bladder and the rectum for groups (i), (ii) and (iii), correspondingly. DVH estimates such as the mean dose to the CTV, PTV,  $D_{98\%}$  PTV and  $D_{2\%}$  PTV were compared to evaluate the effect of the various factors.

#### Results

The parameter  $D_{98\%}$  PTV was most sensitive to uncertainties in tissue segmentation, notably gold markers and air in the rectum. The maximum difference between AAA and  $MC_w$  was 2.8% (i) and 5.4% (ii) and between  $AXB_m$  and  $MC_m$  1.1% (i) and 4.5% (ii) (Figure 1). The variations were reduced to  $\pm 2.1\%$  when  $D_{98\%}$  PTV was determined on modified scans with HU=0 in the PTV or the rectum. A more detailed investigation showed that the TPS dose domination may be distributed in larger parts of the PTV volume with markers and visible CT artefacts (Figure 2). For group (ii), AAA may dominate locally, in the air part of the PTV, whereas the dose to the rest of the PTV may be lower compared to  $MC_w$ . In the case of contrast in the bladder, all DVH parameters showed similar results for calculations on original and modified CT scans. The median difference between AAA,  $AXB_m$ ,  $MC_w$  and  $MC_m$  estimations of the mean dose to the CTV and the PTV was within 0.5% for all cases. Mean dose deviations up to 2.4% were observed for individual plans.

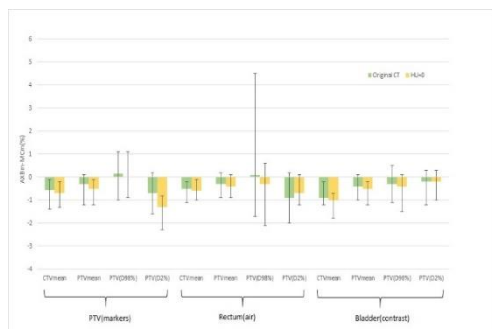


Figure 1. The median difference between DVH parameters estimated by  $AXB_m$  and  $MC_m$  for the three groups. Green bars - original scans, yellow bars - modified scans. Error bars; min-max variation of the difference.

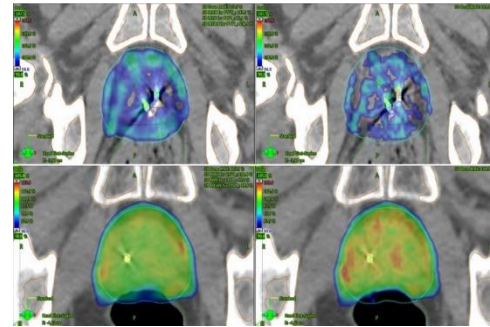


Figure 2. Dose distributions for selected plans from (i) and (ii). Color scale starts with 98%.

#### Conclusion

The presence of gold markers and inclusion of rectum air in the PTV may increase the variations in the  $D_{98\%}$  PTV estimation. However, no clinically relevant dosimetric effects were detected.

### EP-1735 Dosimetric verification of single isocenter VMAT for multiple brain metastases

E. Decabooter<sup>1</sup>, A. Swinnen<sup>1</sup>, R. Canters<sup>1</sup>

<sup>1</sup>Maastricht Radiation Oncology Maastrro, Physics Innovation, Maastricht, The Netherlands

#### Purpose or Objective

To verify the dose delivered by a single isocenter volumetric modulated arc therapy (VMAT) for stereotactic radiosurgery (SRS) of multiple brain metastases.

#### Material and Methods

Verification measurements were performed on single isocenter SRS plans of patients with 4-10 brain metastases treated on a Varian TrueBeamSTx. The 3x8Gy plans, calculated with Varian Eclipse treatment planning system (TPS) (Acuros version 15.5.11, 1mm grid size), consisted of 2 coplanar arcs and were normalized to deliver 100% of the prescription dose to all lesions.

Firstly, the dosimetric agreement between radiochromic EBT-XD film and the calculation by the TPS was investigated. Films were placed in an Alderson radiation therapy head phantom (ART-200) in 2 transverse planes both intersecting high dose regions. The phantom was positioned using a CBCT and 6 degrees of freedom (6D) couch. The film dosimetry measurement was analysed by Film QA pro software (Ashland) using the one-scan method with a dose threshold of 50% and a local gamma criterion of 2%, 2mm[1].

Secondly, to check the consistency of the film measurement, portal dose measurements were done by acquiring MV pre-treatment greyscale value images per field using a Varian aS1000 flat panel and converting them to full-scatter portal dose images using the dosimetric calibration model described in [2]. These measured portal dose images were converted to fluence and reconstructed to a 3D dose distribution in the CT data set. The evaluation was performed using a gamma criterion of 3%, 3mm.

#### Results

Comparison between film and calculation show a mean agreement of 96.3% for both measurement planes for all plans with 4-10 brain lesions. The gamma analysis of the reconstructed 3D dose distribution resulting from the portal dose measurements shows a mean agreement score of 99.7%.

#### Conclusion

We have found that both film as well as portal dose based dosimetry show comparable agreements with TPS

calculations. This study indicates that electronic portal imaging is suitable as a routine quality assurance tool for VMAT SRS for 4-10 brain metastasis using a single isocenter in combination with 6D couch.

[1] Lewis D, et al. An efficient protocol for radiochromic film dosimetry combining calibration and measurement in a single scan, *Med Phys.* 2012; 39:6339-50

[2] Nijsten SM, et al. A global calibration model for a-Si EPIDs used for transit dosimetry. *Med Phys.* 2007;34(10):3872-84

#### EP-1736 Study VMAT modulation to predict DQA results and have an efficient DQA workflow

S. Chiavassa<sup>1</sup>, A. Moignier<sup>1</sup>, A. Batista Camejo<sup>1</sup>, M. Wahl<sup>1</sup>, G. Delpon<sup>1</sup>

<sup>1</sup>Institut de cancerologie de L'Ouest, physic department, Saint-Herblain, France

#### Purpose or Objective

For complex treatment such as VMAT, a patient-specific DQA (PS-DQA) is usually systematically performed. Debate is set up around the efficiency of controlling all plans. The goal of this study is to improve the efficiency and the workload of DQA for VMAT treatment using modulation indexes.

#### Material and Methods

Nine indexes have been studied considering 303 VMAT plans splitted in four groups (prostate, prostatic bed, female and male pelvis with lymph nodes). Each plan had DQA results based on  $\gamma$ -analysis (3%/3mm criteria and  $\gamma$  passing rate  $\gamma_{PR} \geq 95\%$ , PTW 2Darray and Octavius). First, correlation test between indexes and  $\gamma_{PR}$  (R from Spearman Test), ROC analysis (AUC) and sensitivity score with 100% specificity were performed. Simultaneously, a study aimed to identify the machine parameters (leaves gap (DLG), gantry angle, dose rate and leaves offset) impacting the delivery accuracy. Finally, the use of automated planning optimization was investigated to adapt the degree of modulation to the clinical requirements.

#### Results

Only two modulation indexes out of 9 (MCSv<sup>1</sup> and LOIC<sup>2</sup>) provide good results: the thresholds of MCSv=0.38 and LOIC=1.03% give R=0.44, AUC=0.73, sensitivity=36% and R=-0.52, AUC=0.79, sensitivity=33% respectively. Moreover, these indexes reflect the clinical plan complexity: mean values of MCSv/LOIC were 0.50±0.11/0.97±0.53%, 0.35±0.07/1.37±0.44%, 0.28±0.07/1.41±0.50% and 0.28±0.05/1.80±0.39% for prostate, prostatic bed, female and male pelvis with lymph nodes respectively. Therefore, DQA could be skipped for plans with indexes below the thresholds. For plans with indexes beyond the thresholds,  $\gamma_{PR}$  are scattered and not correlated with indexes. LOIC reflects the plan sensitivity to DLG. The machine parameter study happens to show that the dosimetric impact is maximal with DLG whereas negligible for other parameters within the machine tolerance. For plans with a high LOIC, results of single day PS-DQA would depend on the DLG, which parameter varies over time. Therefore, a systematic DQA for these plans could be efficiently replaced by a daily DLG QA.

Our TPS (RaystationV7) allows to create automated optimization standardizing processes and dosimetric objectives. Such a protocol was created for prostatic bed to limit optimization on femoral heads. Testing it on 10 plans, mean values of MCSv were increased from 0.33±0.05 to 0.47±0.04 and corresponding PS-DQA results were improved from 94.8±2.9% to 99.2±1.3%. Moreover, a TPS script calculates MCSv and LOIC during and after optimization process to manage the degree of modulation.

#### Conclusion

This study shows that systematic PS-DQA for VMAT is not useful for low-modulated plans and not efficient for high-modulated plans. A daily DLG QA should ensure the

dosimetric accuracy for the most sensitive plans. Moreover, the workflow can be improved by adapting the degree of modulation to the clinical requirements.

1. Masi L. et al. *Med.Phys.* 2013
2. Dechambre D. et al., *Radiother. Oncol.* 2018

#### EP-1737 "End-to-end test" for setting up multiple brain metastases SRS

E. Graulieres<sup>1</sup>, S. Ken<sup>1</sup>, S. Kubler<sup>1</sup>, R. Ferrand<sup>1</sup>

<sup>1</sup>Institut Universitaire du Cancer de Toulouse - Oncopôle - Institut Claudius Regaud, Department of Engineering and Medical Physics, Toulouse, France

#### Purpose or Objective

Multiple brain metastases Stereotactic Radiosurgery (SRS) has proven its benefits over Whole Brain Radiotherapy for treating patients with a better prognosis<sup>1</sup>. SRS has become routine practice in a large number of centers thanks to advances in linear accelerators technology and dedicated software can now be used to treat Multiple Brain Metastases with one isocenter and several dynamic arcs. However, there are two major issues before setting up SRS for multiple brain metastases:

- How can we control the positioning for metastases that are at a certain distance from the isocenter?
- How can we realize dose quality assurance as targets are spread all over the brain?

We performed an "end-to-end test" at our center using an anthropomorphic brain phantom filled with polymer-based gel in order to realize a complete control with 3D dosimetry.

#### Material and Methods

An anthropomorphic brain phantom was 3D-printed and irradiated with the same treatment plan as the patient it was originated from. The phantom was scanned and images were exported into the treatment planning system Elements Multiple Brain Mets SRS (Brainlab). Six non-coplanar dynamic arc beams were placed to generate the single isocenter SRS plan to treat 5 metastases with the prescription dose of 9 Gy. Dose calculation was realized with a 1 mm resolution. This phantom was positioned on a linear accelerator TrueBeam (Varian) via the Brainlab ExacTrac imaging system and the six arc beams were delivered (Fig 1). After the treatment, 1 mm resolution multi-echo magnetic resonance images of this anthropomorphic phantom were acquired on a 1.5T system. MR images were remotely analyzed by RTsafe in order to provide profiles, 2D, 3D gamma index and Dose Volume Histogram (DVH) comparisons between measured and calculated dose distributions.

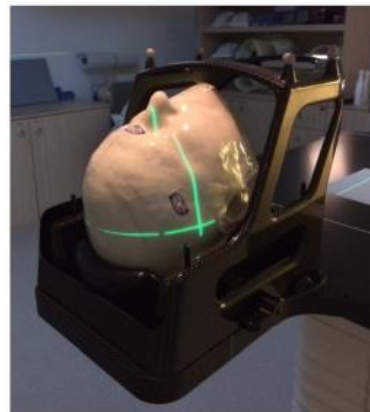


Figure 1: Anthropomorphic phantom positioned on the TrueBeam couch

#### Results

Plans comparison showed slightly narrower profiles of 1 mm at half maximum for measured dose (Fig 2). 2D gamma index calculations also showed a shift on the edge of the target when looking at the cartographies. The 3D gamma

index for 2 mm - 3% was over 97% for all the targets except for one which was at 94.7%. Measured DVHs showed a loss of dose coverage of 10% for targets when looking at 95% of volume.

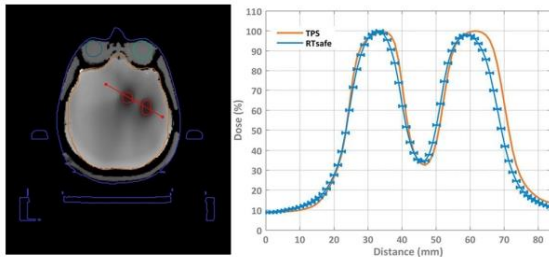


Figure 2: Profile of two targets (left). Superposition of calculated (TPS, in orange) and measured (RTSafe, in blue) profiles (right).

### Conclusion

The 3D gamma index passed the acceptance criteria. However, other data showed a slight underdosage and a slight dose distribution shift of all targets. Tests are still undergoing to understand the origin of these discrepancies. This study demonstrates the need to perform “end-to-end tests” before setting up complex treatments such as multiple brain metastases SRS.

### EP-1738 Validation of the electron Monte Carlo (eMC) algorithm in Eclipse 13.6

D. Kelly<sup>1</sup>, S. Meara<sup>2</sup>, K. Fogarty<sup>1</sup>, L. Gately<sup>1</sup>

<sup>1</sup>The Clatterbridge Cancer Centre NHS Foundation Trust, Medical Physics, Wirral, United Kingdom ; <sup>2</sup>The Christie NHS Foundation Trust, Medical Physics, Manchester, United Kingdom

### Purpose or Objective

To commission and evaluate the eMC 13.6.23 algorithm in Eclipse. To replace the manual calculation of MU for electron treatments for a TrueBeam linac.

### Material and Methods

Beam models at 6, 9, 12 and 16 MeV were built using the Varian representative data for TrueBeam linacs, with calibration points on the PDDs derived from measured values. A block of water was simulated in Eclipse and used to compare to measurements taken in a water tank or phantom. Profiles, PDDs, absolute dosimetry, applicator factors, cut-out factors and stand-off factors were compared using this method.

20 patients, previously treated with manually calculated MU, were re-planned using eMC and the calculated monitor units compared.

End-to-end tests were performed at 12 and 16 MeV. This was to test the accuracy of the beam model in conditions where the previously treated patients had large differences in the number of MUs between eMC and manual calculation. A wax dome was used to test curvature (figure 1) whereas stacked sheets of different density material (plastic, wood, cork and solid water) tested inhomogeneity.

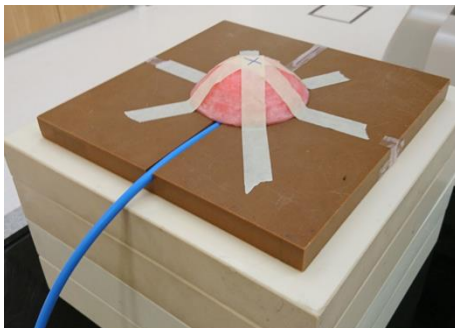


Figure 1 - Wax dome setup with Roos chamber for end-to-end test of curvature.

In-vivo skin surface measurements are performed at first fraction of treatment using TLDs according to local standard protocol. A retrospective audit of these measurements was performed to compare agreement to the predicted dose between manually and eMC calculated plans.

### Results

The profiles and PDDs were compared using the Venselaar criteria [1]. All were acceptable but approach tolerance close to surface, where Eclipse systematically overestimates the dose in the first 1-5 mm by up to 3%. The doses to a point in reference conditions matched to  $\pm 0.8\%$ . Applicator factors agreed to  $\pm 1.2\%$ . Cut-out factors agreed to  $\pm 1.9\%$ . Stand-off factors agreed to  $\pm 1.4\%$ .

The average difference between eMC and the manually calculated MU for the previously treated patients was 6.2% with a maximum difference of 14.7%. Patients with large differences had significant curvature and/or inhomogeneity, hence the need for the end-to-end tests. Eclipse calculated doses matched Roos measurements underneath the wax dome to  $\pm 2.0\%$  and TLD measurements at various points underneath the dome to  $\pm 0.7\%$ . The inhomogeneity measurements agreed to  $\pm 3.3\%$  with the plastic sheet and to  $\pm 0.9\%$  in all combinations without the plastic sheet. A CT artefact in the plastic contributed to the poorer result when the plastic sheet was included.

The results of the TLD audit are shown in figure 2. All measurements so far are within the local tolerance level of  $\pm 5\%$ .



Figure 2 - TLD audit results showing the difference between measured and predicted doses.

### Conclusion

All tests performed to validate the eMC beam model had satisfactory results, including in non-standard conditions. For some patients the eMC calculated MUs are significantly different to previous manual calculation. Patients planned using eMC in Eclipse have shown good agreement with skin dose TLD measurements.

### EP-1739 Indicators evaluation for robust dose prescription in SBRT of peripheral non-small cell lung cancer

G. Beldjoudi<sup>1</sup>, V. Bernard<sup>2</sup>, R. Tanguy<sup>1</sup>

<sup>1</sup>Centre Léon Bérard, Radiotherapy, LYON, France ;

<sup>2</sup>ORLAM, Radiothérapie, Lyon, France

### Purpose or Objective

Lung SBRT is a well-established alternative to surgery for inoperable early stage lung cancers. In our center, small peripheral lesions are mainly treated on a Cyberknife (CK) device at a dose of 3x18Gy (RTOG0236 study) usually prescribed on the isodose 80% with a type A algorithm (RayTracing [RT]). However, ESTRO ACROP recommendations are to use type B or type C algorithms when calculating doses in situations of small lesions surrounded by low density tissues and to prescribe 3x15Gy to D<sub>95-99%</sub>PTV. Nevertheless, these recommendations do not

question the usefulness of changing the volume of interest (PTV or GTV) for dose prescription as suggested by Lacornerie et al. (2004). The purpose of our study is to define a method that ensures robustness when prescribing dose using a MonteCarlo [MC] algorithm.

#### Material and Methods

Treatment plans of 30 patients were recalculated from RT algorithm to MC algorithm and three different indicators to prescribe dose were studied:  $D_{95\%PTV}$  (ESTRO ACROP),  $D_{50\%GTV}$  (Lacornerie et al.) and  $D_{98\%GTV}$  ( $D_{near-minGTV}$ ). On these indicators, overall doses prescription deviations were analyzed in function of tumor volume. Dose ratios to the indicator between MC and RT were calculated as it reflects the dose degradation. In a second part, using the same data, a prescription of  $3 \times 15\text{Gy}$  to  $D_{95\%PTV}$ , as recommended by ESTRO ACROP, with MC algorithm is calculated and the doses to the three indicators are compared to the ones determined in the first part.

#### Results

When prescribing  $D_{95\%PTV}=54\text{Gy}$  with a type A algorithm, doses to  $D_{95\%PTV}$ ,  $D_{50\%GTV}$  and  $D_{98\%GTV}$  with a MC algorithms are respectively, for  $GTV \leq 10\text{cm}^3$  (21 patients)  $41.3 \pm 3.2\text{Gy}$ ,  $53.8 \pm 3.5\text{Gy}$  and  $49.1 \pm 3.0\text{Gy}$  and when  $GTV > 10\text{cm}^3$  (9 patients)  $43.7 \pm 3.5\text{Gy}$ ,  $56.2 \pm 1.5\text{Gy}$  and  $50.2 \pm 1.7\text{Gy}$ .

Mean dose ratio between MC and RT algorithms are respectively  $77.4 \pm 6.1\%$ ,  $86.8 \pm 4.2\%$  and  $84.6 \pm 4.1\%$ . Prescribing doses of  $3 \times 15\text{Gy}$  to  $D_{95\%PTV}$  with a MC algorithm results, for  $GTV \leq 10\text{cm}^3$ , in doses to  $D_{95\%PTV}$ ,  $D_{50\%GTV}$  and  $D_{98\%GTV}$  of respectively  $45\text{Gy}$ ,  $58.7 \pm 2.6\text{Gy}$  and  $53.6 \pm 2.0\text{Gy}$  and for  $GTV > 10\text{cm}^3$  to  $45\text{Gy}$ ,  $58.2 \pm 4.0\text{Gy}$  and  $51.9 \pm 3.1\text{Gy}$ . Thus, following ESTRO ACROP prescription results in a dose increase to each indicator, for  $GTV \leq 10\text{cm}^3$  of respectively  $8.2$ ,  $8.3$  and  $8.4\%$  and for  $GTV > 10\text{cm}^3$  of  $2.9$ ,  $3.4$  and  $3.3\%$ .

#### Conclusion

Despite ESTRO ACROP recommendation, it has been shown in this study that  $D_{95\%PTV}$  is not a robust indicator to prescribe dose as, for a unique dose prescription, large doses fluctuations received by the tumors are observed depending on their volume: doses of  $3 \times 18\text{Gy}$  ( $GTV \leq 10\text{cm}^3$ ) and of  $3 \times 17\text{Gy}$  ( $10\text{cm}^3 < GTV < 20\text{cm}^3$ ) are obtained to  $D_{98\%GTV}$  when prescribing a unique dose of  $3 \times 15\text{Gy}$  to  $D_{95\%PTV}$ .  $D_{50\%GTV}$  indicator appears as the most robust indicator with the tumor volume, but it is not relevant to visually evaluate a treatment plan by looking at this criteria.  $D_{98\%GTV}$  indicator represents a good tradeoff between prescription robustness and clinical meaning as it represents the near-minimum dose the target.

**EP-1740 GLAaS absolute dose calibration for EPID on Halcyon: from algorithm validation to multi-center QA**  
G. Nicolini<sup>1</sup>, D. Nguyen<sup>2</sup>, C. Marais<sup>3</sup>, D. Lojko<sup>4</sup>, E. Vanetti<sup>1</sup>  
<sup>1</sup>Radiqa Developments, Medical Physics Team, Bellinzona, Switzerland ; <sup>2</sup>Groupe ORLAM, Service de Radiothérapie, Mâcon, France ; <sup>3</sup>Busamed Hillcrest Oncology Centre, Yenzakahle Consulting, Durban, South Africa ; <sup>4</sup>Nemocnica Komárno, Radiotherapy Department, Komárno, Slovakia

#### Purpose or Objective

The introduction of very recent technologies in clinical practice could require a more demanding QA program to guarantee safe treatments. In case of IMRT/VMAT treatments, a robust pre-treatment patient specific verification is a key-point. Amorphous silicon EPID technologies are particularly interesting since a very efficient timing solution is combined with high spatial resolution, large area, stability, dynamic range, and real-time acquisition capabilities.

Limited to standard C-arm linacs, the GLAaS algorithm (MedPhys 2006) has proved capable to meet a variety of applications with a simple direct calibration process to convert EPID raw readings into absorbed-dose-to-water. The purpose of this study was to verify the applicability of

the GLAaS principles to a new delivery system, Varian Halcyon, a 6FFF linac mounted on an O-ring gantry, equipped with a dual-layer stacked MLC with an effective shaping capability of 5mm at isocenter.

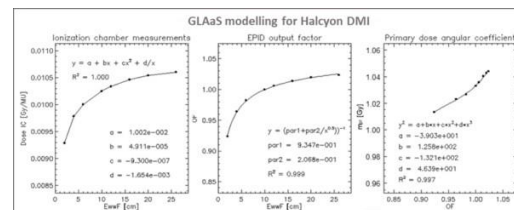
#### Material and Methods

Dosimetric data from 3 institutes were collected at dmax for primary and transmitted radiation to be correlated with Halcyon digital megavoltage imager (DMI) signal: pixel-by-pixel response changes were modelled on time basis, differentiating on segment sizes and beam quality, i.e. primary or below MLC radiation. The satisfactory GLAaS algorithm configuration allowed pre-treatment QA verifications in all the centers. For 3 different sites (prostate, head-and-neck and breast), each center pooled 5 patients from its own database to be acquired with DMI and other QA devices locally available (ArcCHECK, MapCHECK, Octavius, ion chamber point dose). For all centers, DMI images were analysed versus TPS dose water matrices with GLAaS algorithm and predicted fluences with Varian Portal Dosimetry (VPD).

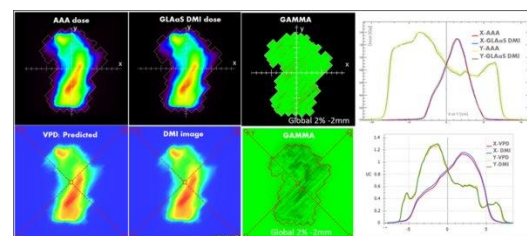
Among the previous 45 plans, a sub-set of 6 was shared among all to investigate the single machine delivery behavior respect to calculation based on the same pre-configured and not customizable beam modelling (Varian AAA dose algorithm).

#### Results

Adapting the GLAaS principles to Halcyon technology, it was possible to conveniently model the DMI dose response. Although in the CIAO area the global result is mainly affected by primary radiation modelling (ima1) due to the low MLC transmission (0.5% per layer), a dedicate model for transmission guarantees a more robust and accurate evaluation of the measured dose.



Overall, pre-treatment QA was fully satisfactory, with differences in terms of specific results depending on the devices; in case of DMI images, the gamma agreement index (GAI) was greater in comparison versus predicted /VPD than versus calculated /GLAaS doses (e.g GAI for 3%-3mm: global VPD>99% vs GLAaS>97%, local VPD>98% vs GLAaS>92%).



#### Conclusion

The extension of GLAaS to Halcyon offers the opportunity to easily set-up flexible and reliable verification, allowing a straight but independent comparison between EPID measurements and TPS water dose maps.

#### EP-1741 Evaluation of the application of NIPAM gel dosimeter to quantify dynamic dose effects

J.C. Sun<sup>1,2</sup>, Y.W. Tsang<sup>1</sup>, B.T. Hsieh<sup>2</sup>, K.Y. Cheng<sup>2</sup>  
<sup>1</sup>Department of Radiation Oncology, Chia-Yi Christian hospital, Chiayi City, Taiwan ; <sup>2</sup>Department of Medical

*Imaging and Radiological Sciences, Central Taiwan University of Science and Technology, Taichung, Taiwan*

#### Purpose or Objective

To evaluate the feasibility of N-isopropylacrylamide (NIPAM) polymer gel dosimeter in combination with MRI (magnetic resonance imaging) on dynamic dose distribution.

#### Material and Methods

The gel preparation was prepared with a composition of 5% NIPAM monomer, 5% gelatin and 3% BIS. 5 mM THPC was added to the solution to reduce the oxygen content and to improve sensitivity and reproducibility. The test treatment plan was a 4x5 cm<sup>2</sup> single-field treatment plan created using the Eclipse treatment planning system with an exposure angle of 180. A cylindrical acrylic model and a dynamic phantom were then selected to simulate the moving target with a motion period of 4 seconds and a range of 2 cm. The gel was irradiated with 0, 1, 2, 5, 8 and 10 Gy absorbed doses using a Varian iX linac with 6 MV X-rays. After the polymerization was completed, a slice image of the gel was extracted using a GE 1.5 Tesla MRI scanner. The slice images were analyzed using MATLAB and the results of the gamma test ( $\gamma$ -test) were performed on the treatment planning system and the NIPAM gel dosimeter. Since the estimated dynamic dose distribution is reduced, 4x4 and 4x3 cm<sup>2</sup> treatment plan are made to perform the gamma test together and the passing rate is evaluated.

#### Results

The gel results were compared to the 4x5, 4x4, and 4x3 cm<sup>2</sup> treatment plans. To verify the dose, the gamma-test was performed according to the gamma standards of 3% and 3 mm. The comparison results showed that the passing rates in the coronal section images were 60.76%, 95.07%, and 50.02%, respectively. Further analysis found that the dynamic dose distribution was the closest to the 4x4 cm<sup>2</sup> result and the highest passing rate. Shows that the dynamic dose distribution range is reduced, and the reduction range is 50% of the motion range.

#### Conclusion

The results demonstrate that it is feasible to validate the dynamic dose distribution using NIPAM gel and MRI scanners, and the dynamic dose range can be quantified by evaluating dynamic effects. In this study, the gel dosage and dynamic phantom simulate the breathing state of the human body, and the real situation is more complicated. It is recommended that future research can evaluate more types of treatment plans and design more impact parameters, such as: motion period and range, and get more careful assessment of dynamic effects, which can provide a more precise definition of treatment margin.

#### EP-1742 In vivo EPID dosimetry for prostate cancer treatments with an endorectal balloon

M. Wendling<sup>1</sup>, B. Sterckx<sup>1</sup>, I. Steinseifer<sup>1</sup>

<sup>1</sup>Radboud university medical center, Radiotherapy, Nijmegen, The Netherlands

#### Purpose or Objective

*In vivo* dose verification is an ideal QA method, because the dose distribution is verified during the actual treatment and no additional time for a pre-treatment measurement is needed. The commercial solution iViewDose (Elekta, Crawley, UK) offers EPID-based *in vivo* dose verification and has been proven for various treatment sites. Because large tissue inhomogeneities are not accurately handled by the algorithm, *in vivo* dose verification of lung cancer treatments is done “*in aqua*”, i.e. before dose reconstruction the images are first converted to a situation as if the patient consisted entirely of water [“*In aqua vivo* EPID dosimetry,” Med. Phys. 39, 367-377, 2012]. In this study we demonstrate that the *in aqua* method also leads to improvements in the verification of prostate cancer treatments, in case an air-

filled endorectal balloon is used to spare part of the rectal wall.

#### Material and Methods

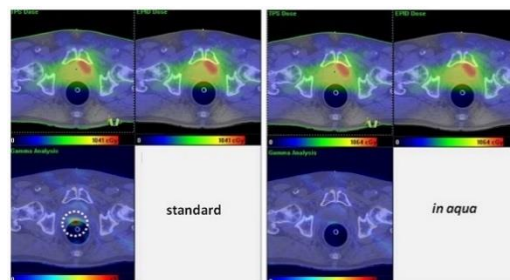
Six clinical hypo-fractionated prostate cancer treatments (5 x 7 Gy to the prostate with/without seminal vesicles, 5 x 10 Gy to the dominant intraprostatic lesion) were investigated. Treatment planning was done in Pinnacle (version 9.10, Philips, Fitchburg, WI, USA) using auto-planning with 2 VMAT arcs of 10 MV photons. Before treatment, the plans were verified with a pre-treatment measurement on a Delta4 phantom; all plans fulfilled our clinical gamma-criterion, i.e. 95% of the measured points within the 50% isodose surface were within 3%/3mm.

After position verification with cone-beam CT and correction for translational errors, the patients were treated and EPID dose measurements were done *in vivo* (3 to 4 fractions per patient were measured). The measured dose distributions were compared “as such” to the clinical plan and also *in aqua* to the *in aqua* plan, i.e. with a density override equal to 1 on the whole CT dataset.

#### Results

In the figure the TPS dose, the EPID-reconstructed dose and the gamma analysis are shown for both the standard EPID-based dose reconstruction and for the *in aqua* method. With the standard reconstruction and comparison, the disagreement in the region of the endorectal balloon can clearly be seen in the gamma analysis (white dotted circle). This is due to the large density inhomogeneity caused by the endorectal balloon. The agreement improves considerably, when the *in aqua* method is used.

On average (over fractions and patients) the percentage of points in agreement within the 50% isodose surface improves from 91%±2% (1SD) to 98%±2% for the clinical plan and the *in aqua* plan, respectively. The mean gamma improves from 0.46±0.05 to 0.36±0.05, respectively.



#### Conclusion

Although originally developed for lung cancer treatments, the *in aqua* method for EPID dosimetry also works as a correction for other large density inhomogeneities. EPID-based dose verification with iViewDose can therefore be used for *in vivo* dose verification of prostate cancer treatments with an endorectal balloon.

#### EP-1743 Dosimeter selection for small field percentage depth dose and tissue maximum ratio measurements

S. Crowe<sup>1,2</sup>, E. Whittle<sup>2</sup>, C. Jones<sup>3</sup>, K. Tanya<sup>1,2</sup>

<sup>1</sup>Royal Brisbane and Women's Hospital, Cancer Care Services, Herston, Australia ; <sup>2</sup>Queensland University of Technology, Science and Engineering Faculty, Brisbane, Australia ; <sup>3</sup>Princess Alexandra Hospital, Radiation Oncology, Brisbane, Australia

#### Purpose or Objective

The measurement of small field tissue-maximum ratio (TMR) and percentage depth dose (PDD) data is necessary for the calculation of dose for stereotactic radiotherapy treatments. The measurement of beam configuration data, including TMRs and PDDs, is complicated by a loss of lateral charged particle equilibrium in small fields and

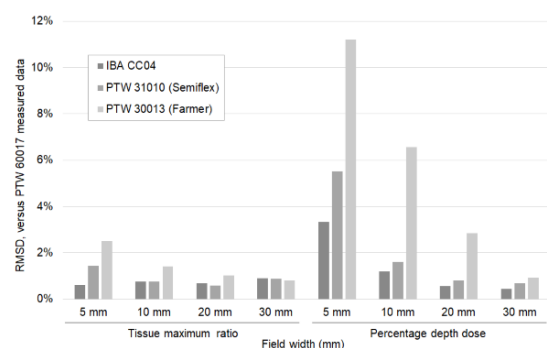
volume averaging effects. For this reason, various small-field-suitable dosimeters (e.g. diodes, scintillators) are recommended in the literature in place of the large ionisation chambers typically used for beam configuration data measurements in larger fields. The objective of this study was to evaluate whether relatively large volume ionisation chambers, that are unsuitable for other small field applications, might be used for accurate TMR or PDD measurements.

#### Material and Methods

PDD and TMR measurements were performed in an IBA BluePhantom 3D water tank with 100 cm source-to-surface distance and 100 cm source-to-detector distance, respectively; using four dosimeters: PTW 60017 (Diode E), IBA CC04, PTW 31010 (Semiflex) and PTW 30013 (Farmer); with active volumes of 0.00003, 0.04, 0.125 and 0.6 cc. Data was acquired for four field sizes (0.5×0.5, 1×1, 2×2 and 3×3 cm<sup>2</sup>) produced using an Elekta linear accelerator. Lateral scans were repeated for each field size to verify the positioning of the dosimeter in the centre of the field. Dose was measured to depths of 25 cm. Measurement data was resampled to a resolution of 0.5 mm, where necessary, and smoothed with a mean filter with a 2 mm window. Root-mean-square deviations (RMSD) were calculated between diode measurements (the "gold standard" data) and measurements acquired using the other dosimeters.

#### Results

PDD and TPR measurement data varied with detector volume (see figure). The largest disagreement in PDD profiles existed between the PTW 60017 diode and PTW 30013 chamber measurements at the smallest field size, with an RMSD of 11.2%. The corresponding RMSD for TMR data was 2.5%. The impact of a larger active volume is reduced when measuring TMRs, where the field size varies minimally with depth.



#### Conclusion

The results indicate that accurate TPR measurements may be obtained using dosimeters otherwise considered unsuitable for small field applications. While the PTW 30013 is not suitable for small field dosimetry, it provides a useful example of how TMR measurements are less sensitive to the active volume of the dosimeter than PDD measurements. If small-field-suitable dosimeters are unavailable, TMR measurements may provide more accurate beam characterisation data than PDD measurements.

#### EP-1744 Enhancing the accuracy in VMAT dose verification by the use of EPID-based commercial software

Y. Md Radzi<sup>1</sup>, R.S. Windle<sup>2</sup>, G.D. Lewis<sup>2</sup>, E. Spezi<sup>3</sup>  
<sup>1</sup>Universiti Sains Malaysia, School of Physics, Penang, Malaysia ; <sup>2</sup>Velindre Cancer Centre, Department of Medical Physics, Cardiff, United Kingdom ; <sup>3</sup>Cardiff University, School of Physics, Cardiff, United Kingdom

#### Purpose or Objective

Advanced radiotherapy dose verification using an EPID-based method such as a commercial software, Dosimetry Check (DC) has been extensively highlighted in recent years and its validity in verifying dose has become the major topic of interest in avoiding dosimetric errors [1-4]. In this work, we emphasised on the implementation of the commercial available DC [5-6] dose reconstruction system to address the significant of nonuniform backscatter effect from the Varian aS1000 EPID arm [4-5] to clinical VMAT pretreatment Head-and-Neck.

#### Material and Methods

The feasibility of applying the developed backscatter correction method [7] to a clinical VMAT Head-and-Neck case was investigated. A phantom was used with an optimised VMAT irradiation beams and all plans were calculated in local TPS. The assessment included, i) improvement of the beam profiles along in-line direction for dose reconstructed by DC, ii) pass-rate of the gamma criteria of 3%/5mm and 3%/3mm and iii) pass rate for gamma volume index.

#### Results

By using the correction method, an average percentage difference for DC dose relative to TPS dose improved from 4.2% to 1.7% in the in-line profiles (Fig.1). For gamma evaluation of 3%/5mm calculated in DC, about 95% and 97% of points passing gamma at coronal and sagittal planes respectively whereas more than 85% of points passing gamma for 3%/3mm gamma criterion at both planes. Gamma volume index calculated by DC for a ROI outlined within the Head-and-Neck phantom also improved from 73% before correction to 87% after correction and from 89% to 95% for a 3%/3mm and 3%/5mm gamma criterion respectively (Table1).

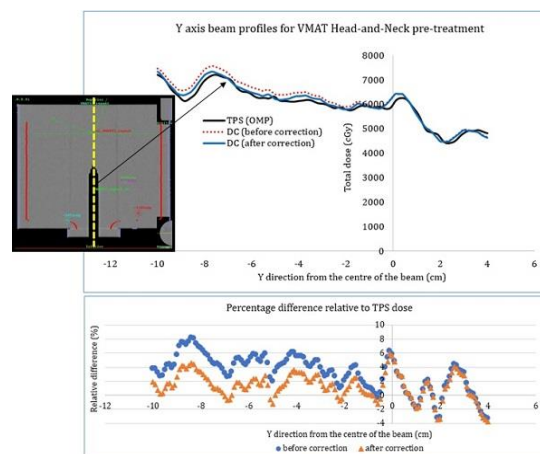


Fig. 1

VMAT Head-and-Neck pre-treatment plane	Gamma criteria pass rate (%)			
	3%/3mm		3%/5mm	
	Before	After	Before	After
Coronal	69.63	86.47	84.33	95.25
Sagittal	75.16	90.02	87.84	97.12
Average	72.40	<b>88.36</b>	86.09	<b>96.19</b>
Gamma criteria	Cumulative Gamma Volume index on ROI			
	Before correction		After correction	
	3%3mm	72.62%	3%5mm	87.03%
	88.52%		95.42%	

Table 1

#### Conclusion

This 'proof-of-concept' of the novel correction shown to give benefit to pretreatment VMAT verification techniques especially to critical plan such as Head-and-Neck using DC as a dosimetric verification tool. Ultimately, the software

effectively reduces verification inaccuracy caused by backscatter from the affected Varian EPID arm.

#### EP-1745 Performance of ArcCHECK based quality assurance in helical tomotherapy with TomoEdge technology

B. Yang<sup>1</sup>, H. Geng<sup>1</sup>, W.W. Lam<sup>1</sup>, K.Y. Cheung<sup>1</sup>, S.K. Yu<sup>1</sup>  
<sup>1</sup>Hong Kong Sanatorium & Hospital, Medical Physics and Research Department, Happy Valley, Hong Kong SAR China

#### Purpose or Objective

As a useful 3D quality assurance (QA) tool, ArcCHECK has gained wide application in helical tomotherapy (HT), but most of the studies were based on old models. This study is to report our experience in ArcCHECK based QA for HT with TomoEdge technique including the establishment of the action level.

#### Material and Methods

A total number of 303 clinical plans in different treatment regions in our hospital were retrospectively studied. The tomotherapy plan verification was conducted using the ArcCHECK diode array with an acrylic insert for placing an A1SL ionization chamber. DQA plans were created by situating the target at the center of ArcCHECK for point dose measurement and meanwhile, making sure the electronic part of the device was not under the main beam. Gamma analysis method was then used to quantitatively compare the dose measured by ArcCHECK and that calculated from the treatment planning system (TPS). The criteria of 3mm distance to agreement (DTA), 3% dose difference, 10% threshold and absolute dose comparison were chosen. According to AAPM TG 119, the recommended action level of gamma passing rate was calculated as  $AL = Gm - 1.96\sigma$ , where  $Gm$  was the mean of the gamma passing rate and  $\sigma$  was the standard deviation (SD).

#### Results

Details of our data are shown in table 1. A value pitch of 0.287 was used for almost all cases except for some brain treatments with values of 0.143 and 0.215. Jaw width of 2.5cm and 5cm with dynamic technique took up 95.7% of total cases and only fixed setting was used for 1cm jaw width. Good point dose agreements between measurements and TPS data were obtained with a mean deviation of 0.75%. Absolute gamma comparison gave an averaged passing rate of 96.6% with the SD of 4.7%, which resulted in an action level of 87.4%. Cases with lower gamma passing rate appeared to be in thorax and abdomen regions, which were suspected to be related to high MF and off-axis induced diode over-response. Our limited data showed that the gamma passing rate could be larger than 92% after a new DQA plan was created by locating the ArcCHECK close to the isocenter.

Table 1. Plan parameters for different treatment regions including planned actual MF, couch speed, proportion of different jaw widths, pitch value, measured point dose deviation and gamma passing rate.

Ta Region	No. of cases	Planned MF	Actual MF	Couch Speed (mm/s)	Proportion of Jaw Width (cm)			Pitch	Point Dose Deviation (%)	Gamma Passing Rate (%)
					103	2.5/5/0	5/0			
Abdomen	40	2.8128.51	2.96120.37	0.42710.213	2.5%	79.0%	22.3%	0.287	0.8720.08	96.1(67.5-100)
Breast/Chest Wall	47	3.5710.56	2.96350.29	0.60610.186	0.0%	42.4%	57.4%	0.287	1.0000.00	96.8(85.1-100)
Proba	52	2.7610.51	2.1770.39	0.60710.143	2.0%	86.3%	11.8%	0.287	0.9811.03	97.2(88.1-100)
Head/Neck	62	3.320.47	2.29120.30	0.99710.217	6.5%	93.3%	0.0%	0.287	0.7612.27	97.5(85.9-100)
Thoran	52	3.0210.46	2.17410.29	0.63010.243	1.0%	88.9%	17.3%	0.287	0.8751.08	94.8(81.8-100)
Brain	27	2.7620.80	2.13220.67	0.84120.215	22.2%	74.1%	3.7%	0.287(0.875)	0.4751.16	97.6(84.6-100)
Abdomen-Proba	9	2.8510.44	2.16910.33	0.51810.106	0.0%	77.8%	22.2%	0.287	1.1211.24	97.0(80.1-99.9)
Thoran-Abdomen	11	2.8710.50	2.80310.29	0.53110.190	0.0%	63.6%	36.4%	0.287	0.6110.78	96.9(86.8-100)
Spine	3	2.2201.18	1.8810.87	1.04710.008	0.0%	0.0%	100.0%	0.287	0.8810.37	94.8(89.4-99.5)
Overall	303	3.010.59	2.15310.38	0.67710.300	4.3%	77.9%	17.8%	0.287(0.875)	0.7311.08	96.6(4.7)

#### Conclusion

The clinical action level of treatment plan verification using absolute gamma comparison can be established at 87.4% with 95% confidence level. High MF values and large off-axis setup might be the possible reason for low absolute gamma passing rate in some cases.

#### EP-1746 GLAaS absolute dose calibration for iViewGT EPID with flat and FFF beams: multicenter experience

E. Vanetti de Palma<sup>1</sup>, J.M. Perez<sup>2</sup>, S. Ren Kaiser<sup>3</sup>, G. Nicolini<sup>1</sup>

<sup>1</sup>Radiqa Developments, Medical Physics Team, Bellinzona, Switzerland; <sup>2</sup>Hospital Universitario HM Puerta del Sur, Servicio de Radiofísica, Móstoles - Madrid, Spain; <sup>3</sup>Fondazione Poliambulanza Istituto Ospedaliero, Servizio di Fisica Sanitaria, Brescia, Italy

#### Purpose or Objective

Intensity modulation radiotherapy requires the implementation of adequate pre-treatment QA programs to guarantee safe treatments. Amorphous silicon EPIDs are particularly suitable for this task, due to their main characteristics: high spatial resolution, large area, stability, dynamic range and real-time acquisition. The GLAaS algorithm showed to adapt to a variety of applications with a simple direct calibration process to convert raw detector readings into absorbed-dose-to-water; nevertheless, up to now GLAaS validations were limited to Varian EPIDs technology. To test its feasibility out of single manufacturer environment, in this study GLAaS algorithm was applied to Elekta iViewGT images, using both flat and FFF beams.

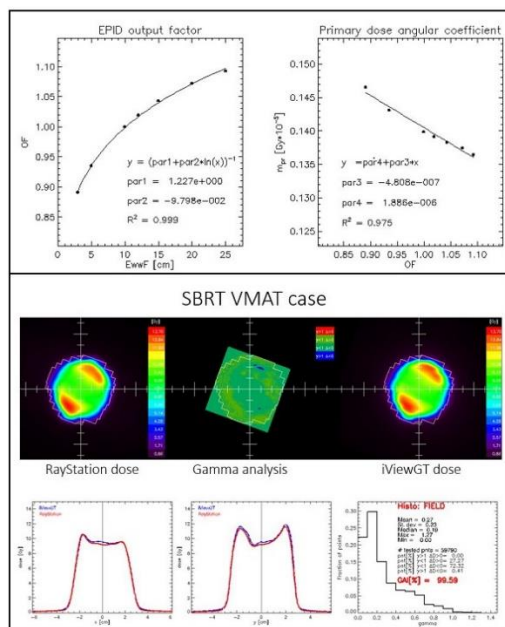
#### Material and Methods

Dosimetric data for 6MV, 10MV, 6FFF and 10FFF beams, delivered from 2 Elekta linacs both equipped with FFF (Synergy and Versa HD) belonging to 2 different institutes, were collected at maximum dose depth. Primary and transmitted radiation were correlated with iViewGT pixel reading and GLAaS algorithm was configured for both flattened and unflattened beams. For open and modulated fields, comparison respect to TPS dose maps (Monaco-MonteCarlo, RayStation-Collapsed Cone) was assessed through profiles and gamma analysis (local and global dose normalization criteria). Concerning modulated fields, 15 IMRT/VMAT plans were pooled from the clinical database of each institute, according to the following stratification: 5 breast, 5 H&N and 5 SBRT cases.

#### Results

As already observed for Varian EPIDs, the response of iViewGT was confirmed linear. Similarly, pixel-by-pixel response changes in time differentiating on field and/or segment sizes and beam quality basis, i.e. primary or transmitted through MLC radiation component, were properly modelled. FFF beams operated at high dose-rates showed saturation effect of the detector: in order to overcome such behaviour, attenuators were placed on the detector front cover during irradiation.

The satisfactory GLAaS algorithm configuration for both the linac models allowed pre-treatment QA in a variety of cases, IMRT and VMAT, flat and FFF beams, small and large fields. Analysis performed in field area showed an average gamma agreement index > 95% (global 3%-3mm) and > 90% (local 3% - 3mm).



### Conclusion

GLAaS algorithm application to iViewGT EPID is a smart tool to easily set-up flexible and reliable pre-treatment verification QA. Moreover, the high resolution of the EPID is of interest in highly demanding conditions such as in SRS/SBRT treatments and/or complicate fluence patterns. Indeed, the GLAaS approach allows a straight comparison between EPID measurements and TPS water dose maps (calculated with the same algorithm used clinically for the patient). The GLAaS compatibility with the two main EPID manufacturers could offer a valid measurement tool in multicentric studies dealing with treatment delivery and dose calculation aspects.

### EP-1747 In vivo dosimetry with electronic portal imaging device in VMAT for prostate cancer

S. Inui<sup>1</sup>, Y. Ueda<sup>1</sup>, S. Ono<sup>1</sup>, S. Ohira<sup>1</sup>, M. Isono<sup>1</sup>, Y. Nitta<sup>1</sup>, S. Murata<sup>1</sup>, M. Miyazaki<sup>1</sup>, T. Teshima<sup>1</sup>  
<sup>1</sup>Osaka International Cancer Institute, Radiation Oncology, Osaka, Japan

#### Purpose or Objective

This study aimed to identify inhomogeneity regions such as those with rectal gas during volumetric modulated arc therapy (VMAT) by using electronic portal imaging device (EPID)-based *in vivo* dosimetry (IVD).

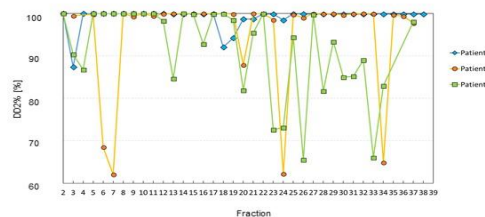
#### Material and Methods

All measurements were performed using TrueBeam STx system (Varian Medical Systems) by determining the radiation fluence using an EPID and analysed using PerFRACTION (version 1.7.3, SunNuclear) commercial software. Two phantom studies were performed to assess EPID-based IVD in prostate cancer patients. The anthropomorphic phantom was correct setup and irradiated while radiation fluence data were captured using EPID images. Systematic setup errors were simulated by moving this phantom 1, 3, and 5 mm in each translational direction. In the cube phantom attached to the Quasar phantom (Modus Medical), single-arc VMAT plan was used for baseline measurements after correct setup. An air cavity of 12 (2 × 2 × 3) cm<sup>3</sup> and 48 (4 × 4 × 3) cm<sup>3</sup> was created 1 cm below the center of the cube phantom. The presence of small and large air cavities was controlled by moving the Quasar phantom after single-arc VMAT quarter (T<sub>25%</sub>), half (T<sub>50%</sub>), and three quarter times (T<sub>75%</sub>). A complete air cavity (T<sub>0%</sub>) was also measured. From April 2017 to May 2018, 30 prostate cancer patients [median age: 76 (64-81)] received EPID-based IVD during

single-arc VMAT in our institute. X-ray images after the treatment of 16 patients were acquired to confirm the presence of rectal gas via offline reviews (Varian Medical Systems).

### Results

In the phantom study, no systematic setup error was detected. The 2% dose difference (DD2%) in small and large air cavities were 75.62% and 58.11%, 92.79% and 62.63%, 93.19% and 72.64%, and 99.40% and 80.71%, respectively, in the appearance of the air cavity after T<sub>0%</sub>, T<sub>25%</sub>, T<sub>50%</sub>, and T<sub>75%</sub>. The mean rectal diameter was 3 cm, which was between the sizes of the large and small air cavities in the phantom studies. We decided to assess the occurrence of rectal gas for DD2% < 90% in the clinical study by calculating the mean values of T<sub>75%</sub> in the large and small air cavities. In the clinical study, some fractions caused a sharp decline in the DD2% pass rate (Figure 1). The amount of DD2% < 90% was almost as same as that of the fraction confirmed with a rectum full of rectal gas (Table 1). The average DD2% values of the fractions with an empty rectum and a rectum full of rectal gas after irradiation were 96.12% and 86.13%, respectively.



	Fraction (%)
All patients (n=30, 1102 fractions)	
DD2% ≥ 90%	961 (87.21)
DD2% < 90%	141 (12.79)
Patients confirmed rectal gas after VMAT (n=16, 589 fractions)	
Empty rectum	524 (88.96)
Rectum full of rectal gas	65 (11.04)

### Conclusion

This study suggests that EPID-based IVD is better for the identifying of inhomogeneity regions such as those with rectal gas than for detecting systematic setup errors in VMAT for prostate cancer patients. There is a high possibility that rectal gas may occur in ~13% of the fractions in the clinical study.

### EP-1748 Adaptive solution for an improved treatment verification using Dosimetry Check system

Y. Md Radzi<sup>1</sup>, R.S. Windle<sup>2</sup>, D.G. Lewis<sup>2</sup>, E. Spezi<sup>3</sup>  
<sup>1</sup>Universiti Sains Malaysia, School of Physics, Penang, Malaysia ; <sup>2</sup>Velindre Cancer Centre, Department of Medical Physics, Cardiff, United Kingdom ; <sup>3</sup>Cardiff University, School of Engineering, Cardiff, United Kingdom

#### Purpose or Objective

Advanced radiotherapy such as IMRT and VMAT require an accurate and precise QA dose verification to avoid dosimetric errors [1-2]. In recent years, the use of one of the commercially available EPID-based method such as Dosimetry Check (DC) has been growing and demanded for an accuracy in treatment validation [3]. In this work, an Adaptive Arm Backscatter Solution (AdABS) [4-5] to accommodate the future application of DC allied with the widespread use of Varian aSi EPID was investigated.

#### Material and Methods

An existing feature in DC facility was investigated for a practical and more convenient way of routinely applying

the developed backscatter correction matrix (Fig.1 (a)). This provide an easy-to-apply method to correct for backscatter from the linac arm that may be applied to all clinical images before dose reconstruction (Fig. 1 (b)). Dose profiles of some static fields were then being assessed for the effectiveness of AdABS application against the Matlab-based scripted system externally to DC. TPS profiles were compared with (i) DC profiles without backscatter correction, (ii) DC profiles corrected with the Matlab script and (iii) DC profiles corrected with AdABS.

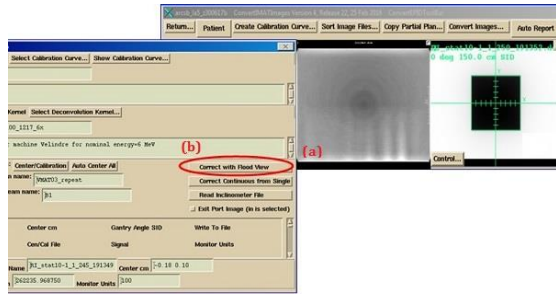
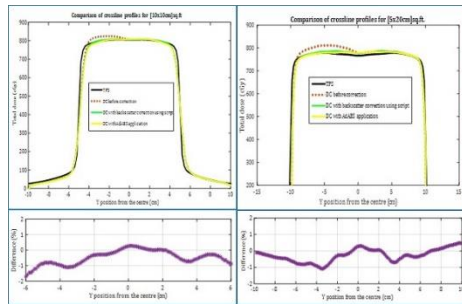


Fig. 1 (a) and (b)

**Results**

Profiles corrected for backscatter with the scripted method and with AdABS showed excellent agreement, with percentage differences of less than 1.5% relative to each other suggesting that AdABS is a feasible correction method that may be applied in the clinic for more accurate treatment verification (Fig. 2).



**Conclusion**

This technique provided a feasible way of applying the correction within DC without the need to generate corrected images using external software (Matlab) scripts for every plan. Ultimately, this will benefit clinical advanced radiotherapy treatment plan verification by providing a ready solution that will help in implementing a quick and efficient workflow in Dosimetry Check.

**References:**

- [1] Antonuk, L. E. 2002. Electronic portal imaging devices: a review and historical perspective of contemporary technologies and research. *Phys Med Biol*, 47, R31-R65.
- [2] Mijnheer, B., et al. 2013b. 3D EPID-based in vivo dosimetry for IMRT and VMAT. *Journal of Physics: Conference Series*, 444, 1-7.
- [3] Narayanasamy, G., Zalman, T., Ha, C. S., Papanikolaou, N., & Stathakis, S. 2015. Evaluation of Dosimetry Check software for IMRT patient-specific quality assurance. *J Appl Clin Med Phys*, 16, 329-338.
- [4] Md Radzi, Y., Windle, R. S., Lewis, D. G., & Spezi, E. 2017. EP-1473: Improving the accuracy of dosimetry verification by non-uniform backscatter correction in the EPID. *Radiotherapy and Oncology*, 123, S787-S787.
- [5] Md Radzi, Yasmin 2018. *Development of techniques for verification of advanced radiotherapy by portal dosimetry*. PhD Thesis, Cardiff University.

**EP-1749 Relation between depth dose and HVL for electronic brachytherapy systems: a Monte Carlo study**

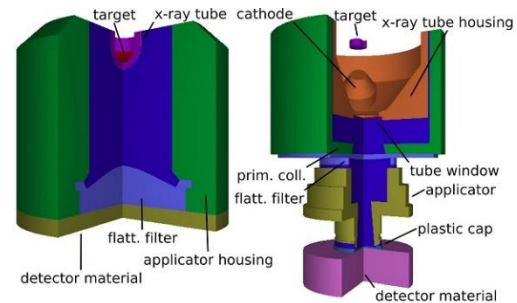
C. Valdés<sup>1,2</sup>, F. Ballester<sup>1</sup>, J. Vijande<sup>1</sup>, J. Perez-Calatayud<sup>1,3</sup>  
<sup>1</sup>Universitat de Valencia, Departamento de Física Atómica- Molecular y Nuclear, Valencia, Spain ; <sup>2</sup>Centro Oncológico de Antofagasta, Radioterapia, Antofagasta, Chile ; <sup>3</sup>La Fe Hospital, Radiofísica, Valencia, Spain

**Purpose or Objective**

There is a consensus on the use of the HVL (mm of Al) as an indicator of the beam quality for electronic brachytherapy equipments (eBT). Usually, the manufacturer supplies dosimetric data as percent depth dose (PDD) and HVL among others, being the responsibility of the final user to verify this information. HVL is obtained through a cumbersome procedure, which requires absorbent layers of high purity with very accurate thickness. The aim of this work is to investigate the relation between PDD and HVL for two eBT systems widely used in surface skin treatments, to evaluate the plausibility of verifying the PDD and the HVL supplied with a single measurement in water (or water-equivalent material).

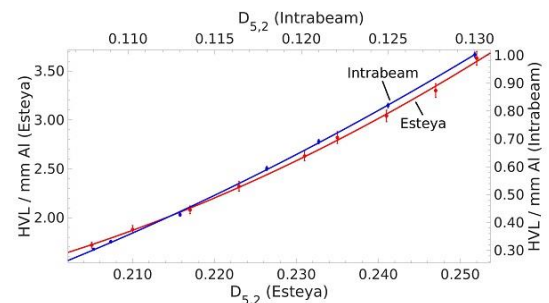
**Material and Methods**

The simulations of the Intrabeam® (Carl Zeiss Meditec AG, Oberkochen, Germany) and the Esteya® (Elekta Brachytherapy, Veenendaal, The Netherlands) systems; which emit flattened bremsstrahlung beams of 50 kVp and 69.5 kVp, respectively; were performed with penEasy for PENELOPE2014. In both cases, surface applicators of 10 mm in diameter were used. To obtain beams with different HVLs, the original beams were filtered (filtered beams) with different amounts of Al, calculating the new HVL and the ratio of the absorbed doses at 5 cm and 2 cm depth (D<sub>5,2</sub>), for both the original and the filtered beams.



**Results**

HVLs of the original beams were 0.304 ± 0.004 mm and 1.72 ± 0.04 mm for the Intrabeam and the Esteya systems, respectively. The D<sub>5,2</sub> of the original beams were 0.108 ± 0.002 and 0.205 ± 0.005 for the Intrabeam and the Esteya systems, respectively. We found that a change of 5% in D<sub>5,2</sub> deviates the HVL by approximately 40% and 20% in the Intrabeam and Esteya systems, respectively.



**Conclusion**

The present work has proven that small deviations detected in a PDD measurement can predict noticeable changes in the HVL for the eBT investigated. The finding

of optimum depth dose indexes, the effects of the depth dose measurement uncertainties on the HVL determination and the sensitivity of this method to safely predict changes in the dose calibration factors are some of the areas that require more investigation. These topics will be studied in a second step in this project.

#### EP-1750 Evaluation of Acuros XB in the presence of metallic elements

R. Chipana<sup>1</sup>, T. Younes<sup>1,2</sup>, L. Vieilleigne<sup>1,2</sup>

<sup>1</sup>Institut Claudius Regaud- Institut Universitaire du Cancer de Toulouse, Department of Medical Physics, Toulouse, France ; <sup>2</sup>Centre de Recherche en Cancérologie de Toulouse- UMR 1037 INSERM- Université Toulouse 3- ERL5294 CNRS- Oncopole, Department of Medical Physics, Toulouse, France

#### Purpose or Objective

The aim of this work was to evaluate Acuros XB (AXB) in presence of metallic elements, such as hip prosthesis and dental implants. Comparisons against Monte Carlo (MC), Anisotropic Analytical Algorithm (AAA) calculations and measurements were undertaken.

#### Material and Methods

In order to challenge AXB algorithm, radiation photon beams were selected to transit through metallic elements. Firstly, AXB calculations were performed in simple virtual phantoms constituted of water, Titanium and stainless steel and were compared with AAA and with GATE (Geant4 Application for Tomography Emission) platform based Monte Carlo as the benchmark. Secondly, measurements were undertaken in water tank phantom containing hip prosthesis (in Titanium, and in stainless steel) and dental implants (in stainless steel alloy). The PTW PinPoint 3D T31016 ion chamber was used to measure profiles and absolute doses at different depths beyond the metallic implants. The measured doses were then compared to the predicted ones by AXB and AAA. AXB and MC dose calculations were reported to dose-to-medium.

#### Results

In the virtual phantoms, AXB calculations were in good agreement with GATE. AAA failed predicting the backscatter in front of water/Titanium or water/stainless steel and exhibited differences up to 11%. Beyond 2 mm after the metallic heterogeneity, AXB differed by 1% and 4% for Titanium and stainless steel respectively, whereas AAA differed by 3% and 12%. The absolute dose measurements (around 2 cm after the metallic implants) for 6 and 10 MV photons beams indicated maximum differences of 1.5% and 5.8% for AXB and AAA, respectively. The PinPoint 3D dose profiles presented good agreement (<1% on average) compared with AXB calculations, in contrary to AAA calculations, as shown in the figure 1.

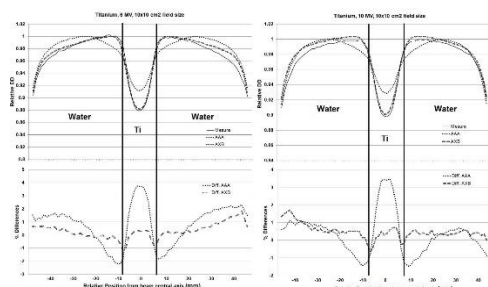


Fig. 1: Comparison of dose profiles: measurements with the PinPoint 3D and calculations with AXB and AAA at around 2 cm beyond the titanium hip prosthesis for 6 MV and 10 MV photon beams.

#### Conclusion

Even when the beams transited through the metallic implants, AXB has been shown to handle perturbations as

well as Monte Carlo calculations. AXB calculations were in good agreement with profile and absolute dose measurements, highly better than AAA calculations.

#### EP-1751 Topical skin agent application-thickness

influence on surface dose in external radiation therapy

K. Miko<sup>1</sup>, J. Kobayashi<sup>1</sup>, Y. Ono<sup>1</sup>, T. Tanino<sup>2</sup>, N. Uchida<sup>2</sup>

<sup>1</sup>Tottori University Hospital, Radiology, Yonago, Japan ;

<sup>2</sup>Tottori University Hospital, Radiology- Department of Pathophysiological Therapeutic Science, Yonago, Japan

#### Purpose or Objective

Radiation dermatitis during radiotherapy sometimes affects patients' quality of life or continuity of treatment. Topical skin agents such as ointments, lotions or creams may be prescribed. However, there remain concerns of a bolus effect due to the applied thickness or of beam scattering due to trace-metal components, possibly increasing irradiating surface doses. The purpose of this study was to investigate the effects of varied application thicknesses of topical agents, and their base ingredients or trace-metals on the surface dose, experimentally.

#### Material and Methods

The calibration curves in the range of 0 cGy to 500 cGy of 6, 10 MV-X-ray were acquired using Gafchromic dosimetry Film (EBT 3). Next, the films were placed on the surface of a water-equivalent phantom, then polyethylene wrap sheet. Various topical agents were applied on the sheet in varying thickness ranging from 0 mm to 5.00 mm. 100 MU of 6 MV or 10 MV X-ray was exposed to the film with SSD 100 cm, 10 × 10 cm<sup>2</sup> field size. The topical agents were simple creams or ointments, with ingredients such as silver, zinc, sodium and iodine. Each entrance surface dose was calculated by conventional Gafchromic dosimetry film method.

#### Results

The surface-absorbed dose increased with increasing thicknesses of simple cream. Simple regression analysis revealed a strong correlation between thickness of topical agent and surface dose ( $y = -0.088x^2 + 0.868x + 1.000$ ,  $R^2 = 0.996$ ). The surface dose with cream containing trace-metal was greater than that with simple cream ( $p < 0.05$ ). The difference between the dose with simple cream and the dose with trace-metal cream became greater with a decrease of application thickness. The surface dose difference between simple cream and trace-metal cream was greater in cases of 6 MV-X ray than that in 10 MV-X ray, especially when the application thickness was thin. Even at a thickness of 0.27 mm, which is similar to clinical use, elevations of surface dose were observed.

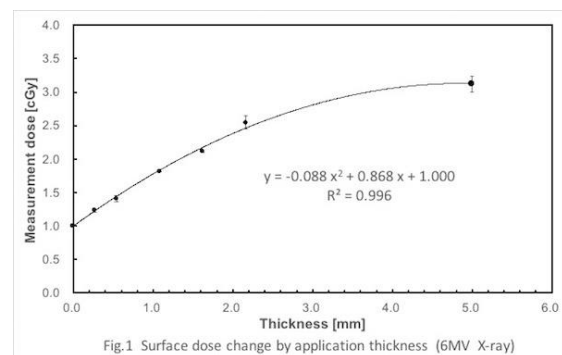
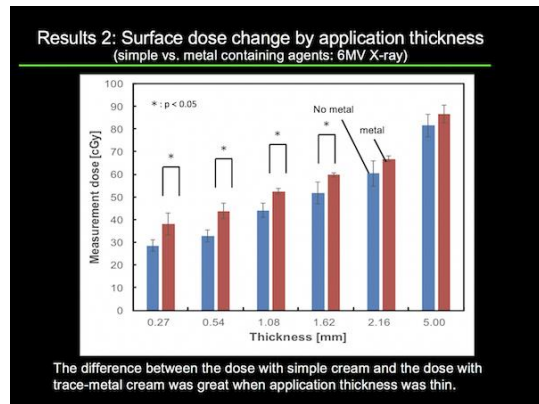


Fig.1 Surface dose change by application thickness (6MV X-ray)



### Conclusion

Thickness of the topical agent influenced surface dose, regardless of metallic composition or the base ingredient, even when applied in a very thin layer. It is necessary to consider appropriate application and timing in cases where topical agents are applied to the radiation treatment site.

### EP-1752 Impact of Leaf Spread Function on Fluence Reconstruction from Exit Detector Signals in TomoTherapy

H.H.F. Choi<sup>1</sup>, T.Y. Lee<sup>1</sup>, Y.W. Ho<sup>1</sup>, W.K.R. Wong<sup>1</sup>, K.Y. Cheung<sup>1</sup>, S.K. Yu<sup>1</sup>

<sup>1</sup>Hong Kong Sanatorium & Hospital, Medical Physics and Research Department, Happy Valley, Hong Kong SAR China

### Purpose or Objective

The onboard exit detector of TomoTherapy has been proposed as a tool to detect errors in fluence delivery during treatment. Many fluence reconstruction methods require a deconvolution of the collected signal with a leaf spread function (LSF). Measuring the LSF for all leaves and all jaw openings will yield the most accurate results, but may be time-consuming and unnecessarily complicated. Conversely, relying on a single LSF for the deconvolution of all data may be an oversimplification. This study aims to investigate the impact of the leaf spread function as measured with different jaw widths and different multileaf collimator (MLC) opening.

### Material and Methods

During the projections 6000-6599 in the TomoTherapy Quality Assurance (TQA) DailyQA module, blocks of eight neighbouring leaves were opened successively with a narrow jaw opening (J7, corresponding to a width of 1 cm at isocentre). The LSF was then taken to be the signals received in the exit detector channels corresponding to the fifteen unopened leaves next to the block of opened leaves. The central and edge LSFs were measured when the block of opened leaves was located at the centre and the edge of the beam, respectively. This was repeated for a similar MLC opening pattern with a wider jaw opening (J20, corresponding to a width of 2.5 cm at isocentre) in projections 7000-7599. Finally, a third "average LSF" was constructed by averaging the J7 and J20 LSFs. This was to observe the effects of jaw opening on LSF profiles. Next, the exit detector signals were collected for three standard plans (TomoPhant) supplied by the manufacturer, with the couch retracted from the bore. Fluence was then reconstructed using the J7, J20 and average LSFs for the TomoPhant plans. The deconvolution and fluence reconstructions were done with MATLAB.

### Results

The central and edge LSFs were found to be very similar (see Figure 1). The J20 LSF exhibited a slower drop-off than that measured with J7. The leaf opening times calculated from deconvolving with a J7 LSF were

consistently higher than that with a J20 LSF (see Table 1). The average LSF yielded reconstructed leaf opening times that lay between J7 and J20 LSFs for all jaw openings.

Figure 1: Leaf spread function profiles for different opened leaves and different jaw openings

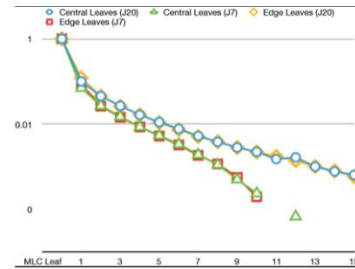


Table 1: Leaf opening errors (%) compared with the planned leaf opening patterns as calculated with different leaf spread functions for TomoPhant plans with different jaw openings

	Leaf opening errors (%)		
	Plan_01	Plan_03	Plan_05
Jaw opening at isocenter	5.0 cm	2.5 cm	1.0 cm
Reconstructed with average LSF	0.16 ± 1.47	-4.26 ± 1.94	-6.03 ± 2.39
Reconstructed with J7 LSF	1.77 ± 1.22	-2.52 ± 1.49	-4.25 ± 1.87
Reconstructed with J20 LSF	-1.97 ± 1.91	-6.06 ± 2.47	-7.88 ± 2.97

### Conclusion

The position of the opened leaf was not found to affect the measured LSF profile; however, different jaw openings were found to influence the fluence reconstruction. Measuring LSF for all clinically applicable jaw widths may yield a more accurate reconstruction.

### EP-1753 A dual detector system for in-vivo dosimetry: transit dose verification and error identification

O. Brace<sup>1</sup>, S. Alhujali<sup>1</sup>, S. Deshpande<sup>2</sup>, P. Vial<sup>2</sup>, P. Metcalfe<sup>1</sup>, M.L.F. Lerch<sup>1</sup>, M. Petasecca<sup>1</sup>, A.B. Rosenfeld<sup>1</sup>  
<sup>1</sup>University of Wollongong, Centre for Medical Radiation Physics, Wollongong, Australia ; <sup>2</sup>Liverpool and Macarthur Cancer Therapy Centres, Department of Medical Physics, Sydney, Australia

### Purpose or Objective

This work tests the ability to perform real time transit dosimetry and MV imaging with a dual detector system for radiotherapy. The system's ability to accurately measure water equivalent dose, predicted by the TPS for a heterogeneous phantom will be validated. Further the dual detector will be used for the identification of dose errors though co-registration of dose and imaging profiles.

### Material and Methods

The dual detector comprises of a silicon diode array detector (MP) and standard a-Si EPID. The MP is between two sheets of 5 mm thick water equivalent material and mounted directly above the EPID. The dual detector was placed at 150 cm SSD and aligned beneath the LINAC couch. The lung phantom has at its centre a 2 cm diameter water equivalent sphere to represent a tumour volume, surrounded by lower density lung equivalent material. With the target positioned at isocentre an ELEKTA LINAC was used to deliver 250 MU with a 6MV beam for a 5x5 cm<sup>2</sup> field. Transit dose was compared to both TPS calculations and measurements taken with the EBT3 film substituted for the MP in the dual detector system. Two deliberate dose errors were also introduced. Firstly a 5.2% increase of monitor units (263 MU) was delivered. Additionally, with the nominal 250 MU delivery the target was laterally shifted 7 mm from isocentre. EPID images taken were co-registered to MP profiles through physical markers present in the EPID images. Prior to transit measurements the MP

response was calibrated to dose at the machines reference condition.

### Results

Transit dose profiles of the MP, film and TPS are displayed in Fig. 1a) with the dose difference calculated in respect to the MP (Fig. 1b)). The MP measured dose agrees within error to both TPS and film across the inter-umbra region. A drop in dose at the centre of the field, in correspondence with the position of the target is present in all three profiles. The deliberate overdose delivery of 5.2% resulted in an increase in dose measured by the MP at the centre of the field of ( $5.4 \pm 1.8$ )%. Fig. 2 displays normalised profiles of the EPID and the MP when the target was at isocentre and laterally shifted. In Fig. 2a) the decrease in dose at the centre of the MP profile is aligned with the position of the target observed in the EPID image. The registration of the profiles in Fig. 2b) confirms deviation in the transit dose profile for the misalignment error delivery is due to a shift in the target position.

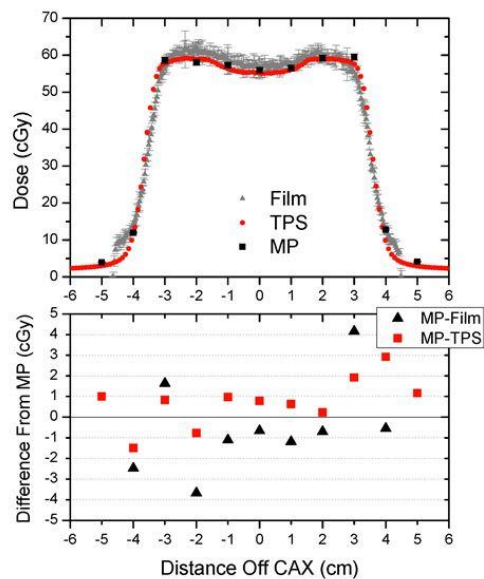


Figure 1. a) Profile of central axis transit dose for heterogeneous phantom for MP, film and TPS. b) Dose difference between film and TPS profiles in respect to the MP measured dose.

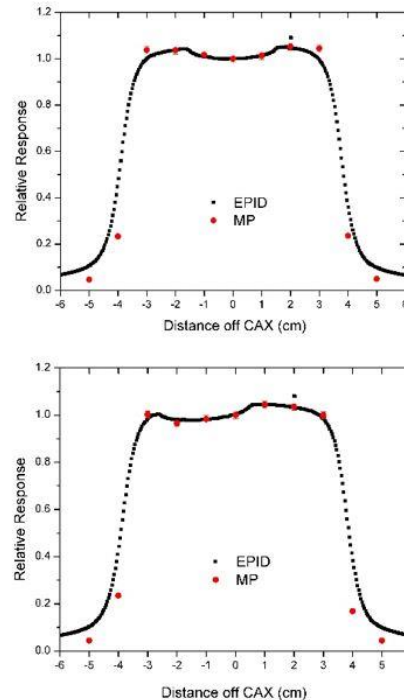


Figure 2. a) Normalised profiles for MP and EPID with target correctly aligned at isocentre. b) Profiles when target is shifted laterally 7 mm from isocentre.

### Conclusion

The dual detector system is capable of verifying the transit dose in water, predicted by the TPS for a heterogeneous phantom in real time. The mechanical mounting of an array detector above the EPID would create an easy to implement and low cost in-vivo dosimeter. Development of an array detector with improved spatial resolution would further effectiveness of the system. The dual detector system has been shown to be able to identify potential in-vivo dose errors of incorrect MU delivery and target misalignment with the aid of imaging and dose co-registration.

### EP-1754 High-resolution assessment of dose calculations in small MV photon beams on and off central axis

G. Biasi<sup>1</sup>, N. Hardcastle<sup>2</sup>, M. Petasecca<sup>1</sup>, S. Guatelli<sup>1</sup>, V.L. Perevertaylo<sup>3</sup>, A.B. Rosenfeld<sup>1</sup>, T. Kron<sup>2,4</sup>

<sup>1</sup>University of Wollongong, Centre for Medical Radiation Physics, Wollongong, Australia ; <sup>2</sup>Peter MacCallum Cancer Centre, Department of Physical Sciences, Melbourne, Australia ; <sup>3</sup>SPA-BIT, n/a, Kiev, Ukraine ; <sup>4</sup>University of Melbourne, Sir Peter MacCallum Cancer Institute, Melbourne, Australia

### Purpose or Objective

There is an increasing use of standard treatment planning systems (TPSs) for stereotactic radiosurgery (SRS), as opposed to dedicated SRS TPSs. In the literature, investigations have assessed their accuracy, and that of dose calculation algorithms, in clinical stereotactic situations with multiple fields combined, but not in small static fields. Small static fields are also not considered for beam modelling in TPS commissioning, since measurement accuracy cannot be guaranteed owing to a mix of uncertainties in effective field size, detector positioning and field-size dependent correction factor. The present work aimed at investigating the accuracy of calculations

by the Eclipse™ TPS in small static fields in homogeneous medium.

**Material and Methods**

We considered square fields in the range from 5 mm to 30 mm side produced by a multi-leaf collimator (MLC). Fields were centred on machine central axis (CAX) or off-CAX by 100 mm; collimators set to 0° or 90°. All fields were produced by a 6 MV flattening filter free beam delivered by a Varian TrueBeam STx® linear accelerator equipped with an HD-MLC. TPS plans were generated by Eclipse 15.5, independently commissioned and optimized for IMRT/VMAT deliveries. Calculations were performed, using the same beam model as input, a single isocentre and 1.0 mm grid, by the analytic anisotropic algorithm (AAA) and the Acuros-XB algorithm (AXB). Calculations were compared in terms of output factors (OFs) and off-axis ratios (OARs) (FWHM and penumbral width at 20%-80%) against measurements with a prototype 2D solid-state dosimeter 'Octa' and Gafchromic™ EBT3 films.

**Results**

In a 10 mm field on CAX, calculated and measured OFs (Table 1) were in agreement within 1.4% (AAA) and 1.5% (AXB) with collimators at 90°, and within 1.7% (AAA) and 1.8% (AXB) with collimators at 0°. In this same field off-CAX, agreement was within 5.1% (AAA) and 8.9% (AXB). In-line FWHMs (Fig. 1) were overestimated by calculations, with largest differences in 5 mm and 10 mm fields. In the latter field, overestimations were of comparable magnitude regardless of collimators rotation and position with respect to CAX. In-line penumbral widths (Fig. 1) were overestimated by calculations, with largest differences in off-CAX fields.

Square field	OF		
	AAA	AXB	Octa
5 mm 0° on-CAX	54.2	53.3	52.2
10 mm 0° on-CAX	71.0	71.1	69.8
10 mm 90° on-CAX	71.0	71.1	70.1
10 mm 0° off-CAX	54.0	55.9	51.4
20 mm 0° off-CAX	60.9	62.1	58.5
30 mm 0° off-CAX	63.8	64.5	61.8

Table 1. Output factors, normalized to the 100 mm side square field defined by the jaws, calculated by AAA and AXB algorithms and measured with the Octa.

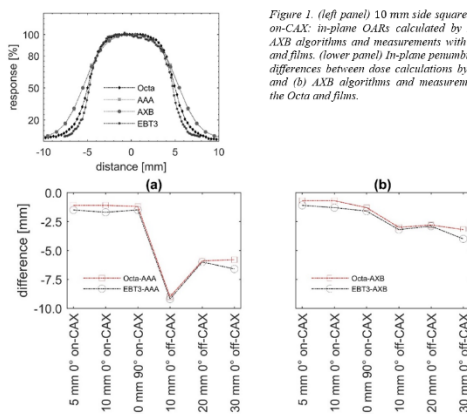


Figure 1. (left panel) 10 mm side square field 90° on-CAX: in-plane OARs calculated by AAA and AXB algorithms and measurements with the Octa and films (lower panel) In-plane penumbral width: differences between dose calculations by (a) AAA and (b) AXB algorithms and measurements with the Octa and films.

**Conclusion**

Calculation errors, which may be enhanced in small static fields, are expected to be smoothed out in dynamic multi-field clinical planning. In the present study, differences between calculations and measurements were affected by field size, position with respect to CAX and collimators rotation. Wider calculated FWHMs and penumbral widths were likely the result of a beam modelling aimed at ensuring modulated fields were accurately delivered, at the potential expense of inaccuracies in static fields. Our results emphasized the necessity of a thorough verification of a TPS in small static fields. The study had the limitation of not investigating the influence of parameters such as different back-up jaws settings, beam energy and depths in water.

**EP-1755 Implementation of EPID in vivo dosimetry for SBRT: setting tolerance levels for routine clinical use**

M. Esposito<sup>1</sup>, A. Ghirelli<sup>1</sup>, S. Pini<sup>1</sup>, S. Russo<sup>1</sup>, G. Zatelli<sup>1</sup>, P. Alpi<sup>2</sup>, R. Barca<sup>2</sup>, B. Grilli Leonulli<sup>2</sup>, L. Paoletti<sup>1</sup>, F. Rossi<sup>1</sup>, P. Bastiani<sup>2</sup>

<sup>1</sup>Azienda USL Toscana Centro, S.C. Fisica Sanitaria, Bagno a Ripoli, Italy ; <sup>2</sup>Azienda USL Toscana Centro, S.C. Radioterapia, Bagno a Ripoli, Italy

**Purpose or Objective**

Electronic portal imaging device (EPID) transit in vivo dosimetry is a powerful tool for patient specific quality assurance (QA), however there is a lack of consensus about which dose difference metric should be used for alert and action level. The aim of this work is to analyze results of transit EPID dosimetry of stereotactic treatment in the abdominal and pelvic sites, and establish tolerance levels for clinical routine use that are sensitive enough to find relevant errors but have also high specificity.

**Material and Methods**

64 stereotactic VMAT treatments (113 fractions) with target in the abdomen or pelvis were analyzed (15 liver, 10 adrenal gland, 7 spine, 32 lymph nodes). In vivo 3d doses were reconstructed with the back-projection EPID commercial algorithm Dosimetry Check 4.10. The differences between planned and in vivo doses were evaluated using Gamma Agreement Index (GAI) 3%/3mm (20% Dose threshold), and dose volume histogram (DVH) differences in prescription target volume (PTV) and clinical target volume (CTV). Initial tolerance levels were set to GAI<85% in PTV. Fractions exceeding tolerance levels (OTL) were checked by experienced Medical Physicists and were classified as due to set-up errors, incorrect use of immobilization devices, 4d errors, transit EPID algorithmic error, and unknown/unidentified errors.

**Results**

44% of total fractions were out of tolerance levels and were classified as: set-up errors (5%), incorrect immobilization device (3%), 4d errors (3%). 50% of OTL were due to transit EPID algorithm failure. In the remaining 28% the OTL causes were not identified. Average difference of PTV and CTV mean dose (± standard deviation) were -3.4%±3.4% and -2.4%±3.2% Average GAI (81.8±20.6) % in PTV and (72.8±31.2) % in CTV. Setting the tolerance level to ΔCTV mean dose > 5.5% the percentage of OTL decrease to 15% and only in one case (6%) EPID algorithmic error occurred.

	85% GAI PTV	3.5% ΔPTV <sub>mean</sub>	5.5% ΔCTV <sub>mean</sub>
Out of tolerance	50 (44%)	58 (51%)	17 (15%)
Residual set-up	5 (10%)	5 (9%)	5 (29%)
4d-intrafraction	3 (6%)	3 (5%)	3 (18%)
Immobilization devices	3 (6%)	3 (5%)	3 (18%)
Algorithm failure	24 (49%)	32 (56%)	1 (6%)
Unknown/unidentified	14 (29%)	14 (25%)	5 (29%)

Table1 In this table, results of the application of three different alert criteria are shown.

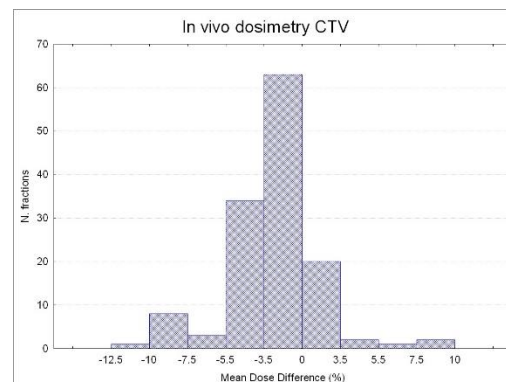


Figure1 Histogram of  $\Delta$  CTV  $D_{mean}$  for 113 fractions is shown in this figure.

#### Conclusion

Results of in vivo transit dosimetry using a commercial system are reported in this paper. A new tolerance level for abdominal and pelvic SBRT was established in this work.

#### EP-1756 Ion recombination and polarity correction for a plane-parallel ionization chamber in hadrontherapy

D. Maestri<sup>1</sup>, A. Mirandola<sup>1</sup>, G. Magro<sup>1</sup>, A. Mairani<sup>1</sup>, E. Mastella<sup>1</sup>, S. Molinelli<sup>1</sup>, S. Russo<sup>1</sup>, A. Vai<sup>1</sup>, M. Ciocca<sup>1</sup>  
<sup>1</sup>Fondazione CNAO, Medical Physics, PAVIA, Italy

#### Purpose or Objective

In order to physically characterize the particle beams clinically used in hadrontherapy, the integrated depth-dose-distributions (IDDs) are measured and implemented as basic input data for commissioning of commercial TPSS, usually compared against Monte Carlo (MC) simulations. The IDD curves are typically acquired as a ratio of readings of two large parallel-plate ionization chambers mounted on a variable depth water column detector. The purpose of this work is the evaluation, in terms of ion recombination and polarity effect, of the dosimetric correction for both proton and carbon ion curves as a function of depth in water, hence of LET variation.

#### Material and Methods

Dose-averaged LET values were calculated with a MC code for some selected IDD. Several points were investigated: the beam entrance, the initial slope, the Bragg peak position, the distal falloff and the practical range position. The charge produced was measured with the plane-parallel Bragg ionization chamber mounted on the PTW Peakfinder by delivering a fixed number of particles, with the maximum current level available. For each measurement, the field chamber was alternatively supplied with +400, +200, +100, -400 Volt. Ion recombination and polarity correction factors were then punctually calculated. Three different beam energies, representative of the clinical commissioned range, were investigated for this study, for both protons and carbon ions. The IDD's, corrected for the aforementioned factors, were then compared against MC simulations, for the same experimental setup.

#### Results

Ion recombination correction factors were both LET and energy dependent, ranging from 1.000 to 1.035 with uncertainties  $\leq 0.5\%$  for carbon ions, while they were found to be nearly negligible for protons. Moreover, no corrections need to be applied due to polarity effect, being  $< 0.5\%$  along all the measured IDD for both particle types. Corrected IDD's (IDD<sup>b</sup>) showed a better agreement than uncorrected curves when compared to MC simulations.

#### Conclusion

In this study, correction factors due the ion recombination and polarity effect were estimated and applied along the pristine IDD for protons and carbon ions. The IDD's were then compared against MC simulations showing a very good agreement. All results confirmed that corrections cannot be completely neglected.

#### EP-1757 Comparison of geometrical accuracy of different SRS delivery systems with end-to-end tests

G. Stelczer<sup>1,2</sup>, D. Szegedi<sup>1</sup>, T. Major<sup>1,3</sup>, C. Polgár<sup>1,3</sup>, C. Pesznyák<sup>1,2</sup>

<sup>1</sup>National Institute of Oncology, Center of Radiotherapy, Budapest, Hungary ; <sup>2</sup>Budapest University of Technology and Economics, Institute of Nuclear Techniques, Budapest, Hungary ; <sup>3</sup>Semmelweis University, Department of Oncology, Budapest, Hungary

#### Purpose or Objective

Purpose: at our institution in the last decades stereotactic radio surgery (SRS) treatments have been performed with frame-based targeting methods on linear accelerators. Recently a CyberKnife M6 (CK) with InCise2 MLC collimator has been installed in our department. Simultaneously the transition from frame-based to frameless SRS treatments was started on a TrueBeam v2.5 (TB) linear accelerator. The aim was to implement a unified method for quantification of spatial accuracy for these delivery systems.

#### Material and Methods

Materials and methods: on the CK the end-to-end tests were implemented according to the AAPM TG135 report with an antropomorphic phantom and Ball-cube insert. The concept of the method is to plan and deliver 4,2 Gy (70% isodose line) as conformal and symmetrically centered on the ball inside the phantom as possible, then calculate the distance between the mass center of the irradiated circle on EBT3 films and the center of the ball. For measurements pre-cut Gafchromic EBT3 Ball Cube II films were orthogonally placed inside the phantom and Accuray developed Matlab software was used for analysis. This way vertical, longitudinal and lateral targeting errors can be measured. The total targeting error is the vectorial sum of these three values. 7 deliveries were performed with both CK and TB. MLC collimator and 6DSkull tracking were used on CK. Rapid Arc delivery with KV-CBCT verification and 6DoF couch were used on TB. 3 of 7 TB deliveries were coplanar arcs without couch movement, while the others had 4 different couch angles, to evaluate the possible errors originating from couch movement during treatment.



#### Results

Results: the end-to-end test method dedicated to CK system was implemented also on the TB system successfully. Both systems' spatial accuracy was far below the tolerances. The average targeting errors in vertical, longitudinal and lateral directions for CK and TB in mm were 0,14±0,22; 0,13±0,18; -0,07±0,18 and -0,15±0,22; -0,24±0,14; -0,29±0,18, respectively. The average total targeting errors in mm for CK and TB were 0,36±0,09 and 0,48±0,13. Average total targeting errors with TB regarding coplanar and non-coplanar techniques were similar, with the values of 0,43±0,14 mm and 0,53±0,13 mm respectively.

		Vertical [mm]	Longitudinal [mm]	Lateral [mm]	Total targeting error [mm]	
CyberKnife	Average	0,14	0,13	-0,07	0,36	
	SD	0,22	0,18	0,18	0,09	
TrueBeam	Average	-0,15	-0,24	-0,29	0,48	
	SD	0,22	0,14	0,18	0,13	
TrueBeam	Non-coplanar	Average	-0,25	-0,15	-0,37	0,53
		SD	0,24	0,09	0,16	0,13
	Coplanar	Average	-0,01	-0,36	-0,19	0,43
		SD	0,05	0,09	0,15	0,14

#### Conclusion

Conclusion: the AAPM TG135 report recommended end-to-end test with the head phantom of CK is also feasible on

other SRS delivery systems such as TB. The test results are reproducible and consistent. The spatial accuracy of the CK's 6DSkull tracking with MLC is better than TB's kV-CBCT verification and 6DoF couch, but the difference is small. These results confirm that both systems are appropriate for safe SRS deliveries.

**EP-1758 A validation and criticality assessment of imaging dose calculation discrepancies of Halcyon MVCBCT**

Y. Zhang<sup>1</sup>, Y. Huang<sup>1</sup>, M. Wang<sup>1</sup>, R. Wang<sup>1</sup>, W. Wang<sup>1</sup>, H. Wu<sup>1</sup>

<sup>1</sup>Key Laboratory of Carcinogenesis and Translational Research Ministry of Education/Beijing- Department of Radiation Oncology- Peking University Cancer Hospital & Institute, Department of Radiotherapy, Beijing, China

**Purpose or Objective**

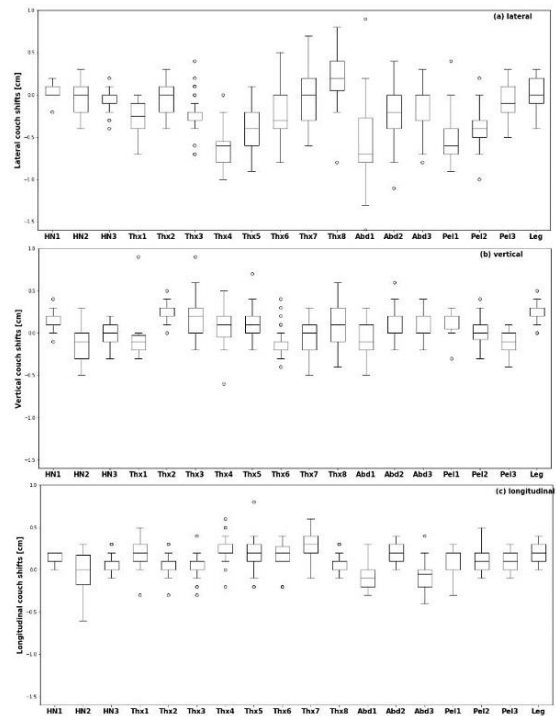
By using identical 6MV flattening-filter-free photons for both imaging and treatment on Varian Halcyon system, the total dose of the two can be incorporated automatically in Eclipse Treatment Planning system, which, however, uses treatment isocenter to calculate the imaging dose. This work aims to assess the criticality of the calculation deviations induced by fractional image-guided-couch-shifts for Halcyon MV cone beam CT (CBCT) imaging dose, based on real patient data.

**Material and Methods**

Eclipse-calculated imaging dose was first validated using a calibrated A1SL chamber in the 'Cheese Phantom' by measurement. Then, the actual imaging dose ( $D_{act}$ ) for 18 historical patients of various sites were recalculated based on 513 MV CBCT-guided-couch-shift data, and compared with the reference computations based on treatment isocentre ( $D_{ref}$ ). 'High Quality' and 'Low Dose' MV CBCT modes were applied in 382 and 131 fractions, delivering 10 MU and 5 MU per scan respectively. Patient- and plan-specific dose from treatment fields was integrated with  $D_{act}$  and  $D_{ref}$  respectively for comparison (Total Dose). More efficient computation was achieved by the automation using Eclipse Scripting Application Programming Interface.

**Results**

The average unsigned relative disagreements between the measured and Eclipse-calculated dose in Cheese phantom were less than 1.23%, hence the following studies were based on Eclipse simulations. Figure 1 displays the couch shifts on the lateral (a), vertical (b) and longitudinal (c) directions of 18 patients as guided by 513 MV CBCT scans. The bottom and top of the boxes indicate the first and third quartiles. The bands inside the boxes show the second quartile (the median). The whiskers display the lowest/highest datum still within 1.5 interquartile ranges of the lower/upper quartiles. The circles indicate the outliers.



As shown in table 1, the Gamma passing rates of the accumulated imaging dose were all better than 95.08% based on 3mm/3%/global/10% threshold criteria, and the mean±1SD was 97.54%±1.42%. The accumulated errors of minimum imaging dose to PTV were no larger than -14.38 cGy, which were reduced to -0.82 cGy after the heterogeneous treatment dose was overlaid. The mean relative discrepancies of PTV minimum dose were -0.61 cGy (-0.71%) and -0.00 (0.00%), before and after incorporating the treatment dose respectively.

**Table 1** Imaging dose deviations accumulated from the whole treatment course: comparisons between the calculations based on the treatment isocentre ( $D_{act}$ ) and the actual dose with fractional couch shifts included ( $D_{ref}$ ). The negative sign (-) indicates lower  $D_{act}$  than  $D_{ref}$ . Total dose (integration of imaging and treatment dose) were also compared.

	Imaging Dose			Total Dose	
	Gamma* [%]	PTV <sub>min</sub> cGy (%)	PTV <sub>mean</sub> cGy (%)	PTV <sub>min</sub> cGy (%)	PTV <sub>mean</sub> cGy (%)
HN1	96.37	0.15 (0.17)	-0.19 (-0.17)	0.48 (0.02)	-0.19 (0.00)
HN2	99.32	-0.03 (-0.25)	0.07 (0.03)	0.24 (0.01)	0.07 (0.00)
HN3	99.07	-14.38 (-14.32)	-0.15 (-0.05)	-0.82 (-0.02)	-0.15 (0.00)
Thx1	98.60	1.17 (6.32)	0.48 (0.19)	2.33 (0.03)	0.48 (0.00)
Thx2	99.35	0.23 (0.16)	-0.54 (-0.27)	-0.09 (0.00)	-0.54 (-0.01)
Thx3	98.81	-0.08 (-0.52)	-0.79 (-0.31)	0.39 (0.01)	-0.79 (-0.01)
Thx4	95.08	2.48 (1.08)	-0.77 (-0.27)	-0.70 (-0.01)	-0.77 (-0.01)
Thx5	97.74	-2.55 (-1.14)	-0.56 (-0.21)	-2.26 (-0.04)	-0.56 (-0.01)
Thx6	97.52	-0.17 (-4.74)	0.35 (0.37)	0.83 (0.01)	0.35 (0.00)
Thx7	95.89	-1.58 (-1.53)	0.14 (0.11)	-1.70 (-0.02)	0.14 (0.00)
Thx8	95.49	-0.44 (-3.18)	-0.53 (-0.10)	0.92 (0.01)	-0.13 (0.00)
Abd1	96.65	0.84 (0.45)	0.11 (0.05)	1.24 (0.01)	0.11 (0.00)
Abd2	98.22	3.07 (2.58)	-0.30 (-0.16)	-0.10 (0.00)	-0.30 (0.00)
Abd3	98.36	-0.43 (-2.73)	-0.46 (-0.26)	-0.87 (-0.01)	-0.46 (-0.01)
Pel1	95.70	-0.23 (-4.46)	-0.16 (-0.27)	-0.35 (0.00)	-0.16 (0.00)
Pel2	96.58	0.79 (0.80)	-0.11 (-0.08)	-0.10 (0.00)	-0.11 (0.00)
Pel3	98.09	-0.56 (-4.04)	0.29 (0.20)	0.92 (0.01)	0.29 (0.00)
Leg1	98.81	0.75 (12.66)	-0.32 (-0.28)	-0.37 (-0.01)	-0.32 (0.00)
Mean	97.54	-0.61 (-0.71)	-0.19 (-0.08)	-0.00 (0.00)	-0.17 (-0.00)
SD	1.42	3.67 (5.34)	0.38 (0.20)	1.08 (0.02)	0.37 (0.00)

\*The criteria used for the Gamma passing rate calculations were 3mm/3%/global/10% threshold. The relative errors (data in the brackets) were normalized to the reference dose as calculated on the treatment isocentre.

**Conclusion**

The Eclipse-calculated Halcyon MV CBCT dose was validated by measurement. Although the isocentre displacement-induced imaging dose calculation discrepancies for Halcyon MV CBCT were partially cancelled out by couch shifts of various directions and distances, especially after the incorporation of

heterogeneous treatment dose, it is still advisable to minimize unnecessary and avoidable uncertainties by recalculating the imaging dose using the fractional couch shifts.

#### EP-1759 Patient plan QA using EBT3 GafChromic film for the Unity MRI-Linac system

J. Wolthaus<sup>1</sup>, S. Hackett<sup>1</sup>, B. Asselen- van<sup>1</sup>, W. Vries- de<sup>1</sup>, S. Woodings<sup>1</sup>, J. Kok<sup>1</sup>, P. Kroon<sup>1</sup>, B. Raaymakers<sup>1</sup>

<sup>1</sup>UMC Utrecht, Department of Radiation Oncology, Utrecht, The Netherlands

##### Purpose or Objective

In our department an Elekta Unity MRI-Linac was installed, accepted and commissioned prior to start clinical patient treatments in August 2018. Individual treatment plan QA on the Unity is performed for both pre-treatment and online adapted plans. The presented work describes our patient plan QA procedure of absolute film dosimetry using EBT3 film obtaining high resolution, high accuracy dose measurements to compare to TPS dose calculations.

##### Material and Methods

Plan QA measurements using EBT3 film were performed for more than 30 7-field IMRT plans (optimized to deliver 800 cGy in a single pelvic lymph node). An associate OD-to-Dose model has been determined in advance for the conversion of the pixel values of the film (optical density) to absorbed dose. For each box of films, an additional dose calibration was performed by cutting four small pieces of film (5x10 cm<sup>2</sup>, film orientation specified) and irradiating three of the films with defined doses (650, 800 and 1100 cGy) on the Unity system. The OD-to-Dose model is updated with the results of this measurement.

On the Monaco TPS, the patient plan is calculated (2mm grid, MCVar 1%) on a 19x30x30 cm<sup>3</sup> RW3 slab phantom. Subsequently, the point location of the maximum dose is determined and the height defines the coronal film measurement plane. The 3D dose file is exported for TPS to film comparison. The RW3 phantom is positioned isocentrically on the couch. The film is placed at the determined height using slabs of various thicknesses (1-10mm). A few droplets of water are spread below and above the film to prevent any (small) airgaps. The plan is delivered.

Films are digitized the next day (Epson10000XL), to reduce the effect of post-exposure OD growth. Film images are corrected for scanner distortions and converted to absolute dose with the updated OD-to-Dose model, using in-house developed software. The same software is used for image registration of the 3D TPS dose file to the 2D film dose. Profiles can be extracted in both data sets to evaluate the similarity. A 2D local Gamma analysis (5%/2mm, stereotactic clinical criteria) in the film plane is performed.

##### Results

Currently, 34 patient plans have been analysed with this method: 12 prior to clinical introduction with varying tumour size and location and 22 clinical plans from 4 LN patients. The figure shows an example of the dose images, profiles and gamma distribution. All plans fulfilled the clinical criteria for an acceptable treatment plan and measured and calculated plans agreed well, the average pass rate was 99.7% using a 60% target dose threshold (mean gamma 0.3±0.2).

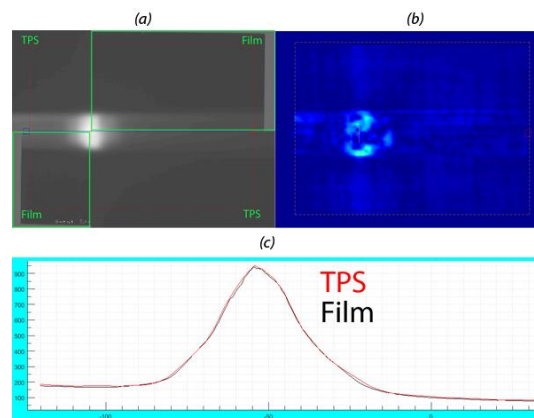


Figure. Example of a patient QA result: a) TPS and Film dose, b) Gamma distribution 5%/2mm (green = 0.9) and c) Absolute dose profiles

##### Conclusion

A patient plan QA procedure using film was developed for the MRI-linac. No additional ion chamber measurements are required to normalise the film dose. The methodology can readily be extended to conventional linacs or ViewRay systems. The results showed excellent agreement between planned and delivered doses for the Elekta Unity system.

#### EP-1760 Impact of cranial implants on proton dose distributions

A. Sjögren<sup>1</sup>, K. Andersson<sup>2</sup>, L. Stolarczyk<sup>2</sup>, U. Granlund<sup>1</sup>, C. Vallhagen Dahlgren<sup>2</sup>

<sup>1</sup>Örebro University, Department of Medical Physics-Faculty of Medicine and Health, Örebro, Sweden ; <sup>2</sup>The Skandion Clinic, The Skandion Clinic, Uppsala, Sweden

##### Purpose or Objective

The presence of metallic implants in patients can cause considerable uncertainties in proton therapy treatment planning. The purpose of this study was to investigate the impact of cranial implants on proton dose distributions calculated with Eclipse v13.7 (Varian) using pencil beam scanning technique. Experiments were focused on verification of range calculations for plans based on CT series with and without metal artefact reduction.

##### Material and Methods

The four implants were investigated; a 0.3 mm and a 0.4 mm Ti mesh, a 0.5 mm burr-hole cover and a craniofix implant with a diameter of 16 mm. Each implant was attached to a bone equivalent plate (CIRS) and scanned on a solid water phantom with a Siemens SOMATOM Definition AS Open CT. The images were reconstructed with and without the metal artefact reduction algorithm iMAR. In addition, reference images without implants were acquired. A treatment plan with 35 mm WET range shifter, field size 8 x 8 cm, range 10 cm and modulation 8 cm was created in Eclipse 13.7 using PCS beam model and a calculation grid size of 1 mm. Measurements of depth dose distributions were performed in a water phantom (BluePhantom2, IBA) using Roos IC (PTW) to verify the calculations. In addition, a theoretical value for the proton range shift introduced by a titanium plate was calculated using the equation proposed by Moskvina et al:

$$\Delta(t_m, Z) = t_m [\rho_m (1.192 - 0.158 \ln(Z) - 1)]. \quad [1]$$

Where  $t_m$  is the thickness of the titanium plate,  $\rho_m$  is the plate density and  $Z$  the atomic number of titanium.

Due to the structure of the craniofix implant, film measurements were performed instead. For this purpose Gafchromic EBT3 film, calibrated in a proton beam with the red channel method, was used to determine the dose at several different depths within a solid phantom setup.

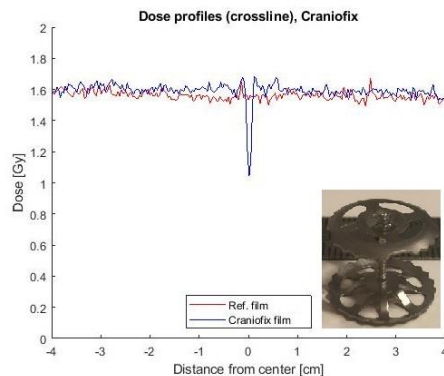
## Results

Table 1 shows the measured and theoretical range shifts, and also the range shifts calculated in Eclipse for CT series with and without iMAR. The calculations based on both the uncorrected and the iMAR images showed higher  $\Delta R_{50}$  values compared to the measured deviations. Also the theoretical  $\Delta R_{50}$  using equation (1) were higher the the measured values.

**Table 1:** Results from the measurements of the range shifts ( $\Delta R_{50}$ ) for three cranial implants.

Implant	$\Delta R_{50}$ measured [mm]	$\Delta R_{50}$ theoretical [mm]	$\Delta R_{50}$ Eclipse [mm]	$\Delta R_{50}$ Eclipse iMAR [mm]
Ti mesh (0.3 mm)	0.2	0.7	0.5	1.5
Ti mesh (0.4 mm)	0.5	0.9	1.4	2.0
Burr-hole cover	0.9	1.1	3.8	3.1

In Fig. 1 the result of the film measurement for the solid water setup with and without the craniofix can be seen. It can clearly be seen that the center of the craniofix caused a reduction in dose in the area where the titanium rod connects the two plates of the implant.



**Figure 1:** Crossline dose profiles for film measurements with and without the craniofix implant (inserted image) at a depth of 1.6 cm

## Conclusion

The cranial implants investigated were shown to reduce proton ranges by up to 0.9 mm. Calculated ranges in treatment plans showed an overestimation of the deviations due to metal artifacts.

## References:

[1] Moskvina V, Cheng C, Fanelli L, Zhao L, Das I. A semi-empirical model for the therapeutic range shift estimation caused by inhomogeneities in proton beam therapy. JACMP. 2012;13(2):3-12.

## EP-1761 Single isocenter multiple brain mets SRS with Elekta VersaHD and Monaco: end-to-end accuracy study

A. Nevelsky<sup>1</sup>, E. Borzov<sup>1</sup>, S. Daniel<sup>1</sup>, R. Bar Deroma<sup>1</sup>  
<sup>1</sup>Rambam Health Care Campus, Oncology, Haifa, Israel

## Purpose or Objective

The advantages of stereotactic radiosurgery (SRS) to multiple intracranial targets with a single isocenter have been well described. However, the efficiency of this approach strongly depends on the dosimetric and geometric accuracy at all steps of the workflow. In this work we report on the results of the end-to-end accuracy study of SRS treatment of multiple brain mets using Elekta VersaHD linac and Monaco TPS.

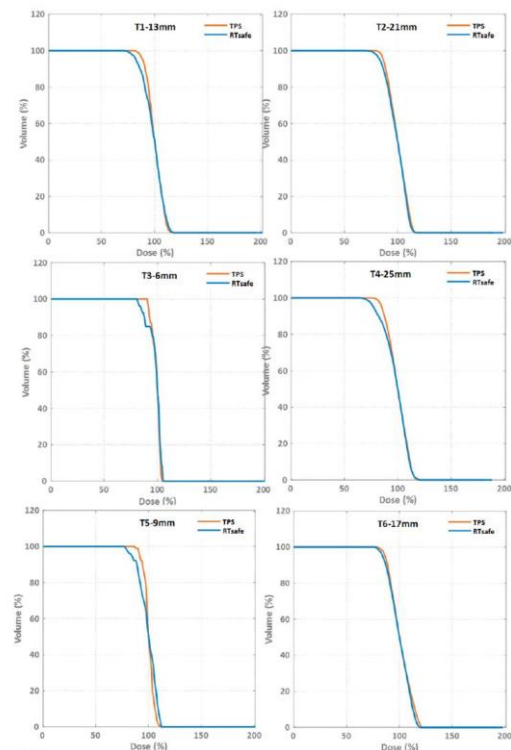
## Material and Methods

A CT simulation scan from a previously treated patient was used as the data set for definition of six clinical targets (ranging in diameter from 6mm to 25 mm) and one QA target in the brain. Based on this set, pseudo-patient phantom filled with dosimetric gel was constructed by

RTSafe company (RTsafe P.C, Athens, Greece). In addition, two phantoms of same size and shape as above but with ionization chamber and film inserts at location of QA target were created. A VMAT treatment plan with 5 non-coplanar VMAT arcs (lateral, vertex and 45°) was devised using Monaco. Using this plan, all three phantoms were irradiated at VersaHD linac. Forty-eight hours after the irradiation, the gel phantom was scanned on a 1.5 T MRI unit in order to obtain 3D dose distribution. In addition, absolute point dose was measured with PTW PinPoint ion chamber and 2D dose distribution at the QA target was measured with film dosimetry.

## Results

The difference between absolute point dose measured with ion chamber and the corresponding dose calculated with Monaco was 0.9%. The gamma passing rate in the film plane using 3D global gamma analysis was 98.2% (3%/2mm). For all clinical targets, the 3D gamma passing rate measured with gel dosimetry was more than 94.5%, with passing rate 97.1% averaged for all targets (3%/2mm). Comparison between planned and measured relative dose distributions in terms of DVHs for all clinical targets is presented in Figure 1 (all dose distributions were normalized to the corresponding D50% metric of each target).



## Conclusion

The end-to-end accuracy of SRS to multiple intracranial targets with a single isocenter at our center has been successfully validated using patient-like phantoms and 3D gel dosimetry.

## EP-1762 in vivo skin dosimetry correction factors for IMRT

P. Carrasco de Fez<sup>1</sup>, M.A. Duch<sup>2</sup>, N. Jornet<sup>1</sup>, P. Delgado-Tapia<sup>1</sup>, M. Lizondo<sup>1</sup>, C. Cases<sup>1</sup>, A. Latorre-Musoll<sup>1</sup>, A. Ruiz<sup>1</sup>, M. Ribas<sup>1</sup>

<sup>1</sup>Hospital de la Santa Creu i Sant Pau, Servei de Radiofísica i Radioprotecció, Barcelona, Spain ;

<sup>2</sup>Universitat Politècnica de Catalunya, Institut de Tècniques Energètiques, Barcelona, Spain

### Purpose or Objective

In IMRT any point at the patient's skin can be at the same time the entrance for some beam angles and the exit for others. Pure entrance correction factors ( $CF_{\text{entrance}}$ ) for skin *in vivo* dosimetry do not apply if some beams exit through the detector surface or in case of a mixed entrance-exit scenario. This study was aimed to establish a method to perform reliable skin *in vivo* dosimetry for IMRT techniques.

### Material and Methods

Ultra-thin TLDs with an effective point of measurement (EPOM) at a depth  $< 5 \text{ mg/cm}^2$  and EBT3 radiochromic films (RCF) with EPOM-120  $\text{mg/cm}^2$  were compared against the results of a PTW23392 Extrapolation Chamber (EC) with an entrance window  $\sim 0.7 \text{ mg/cm}^2$  TLD and RCF were enclosed inside sleeves of LowDensityPolyEthylene (LDPE) to allow placing them in contact to patient skin.  $CF_{\text{entrance}}$  for TLD and RCF were derived by comparing measured doses with the detectors against those measured with the EC. Devic *et al* showed that RCF correction factors for exit dose measurements  $CF_{\text{exit}}=1$ . This value was also applied to ultrathin TLDs when enclosed in LDPE, as their sensitive layer laid at a water equivalent depth of 70  $\mu\text{m}$ . A cumulative correction factor ( $CF^*$ ) was proposed for integrated dose measurements using 6 MV photon beams as a linear combination of  $CF_{\text{entrance}}$  and  $CF_{\text{exit}}$ . The combination coefficients were 1-PDD and PDD being PDD the depth dose for the average field size at the depth of the average phantom thickness for all beams.  $CF^*$  was tested with two phantom experiments:

1-Irradiation by two opposed fields of a *Plastic Water* slab phantom of 30X30  $\text{cm}^2$ . Three different thickness (10,15 and 20cm) of the phantom were considered. Measurements with only the entrance field and with both fields allowed us to know the delivered skin doses and compare them with those predicted by the model.

2-Delivery of a breast IMRT treatment plan on a QUASAR phantom. We compared the measurements of TLD and RCF in 8 consecutive points along the central axis at 2.5 cm distance one another.

### Results

Table 1 shows cumulative skin doses derived from measurements,  $D_{\text{skin,cumulative}}$ , and those calculated by the model ( $D_{\text{skin,cumulative}}^*$ ) as a function of the slab phantom thickness for 6MV photon beams. Differences between the skin doses derived from TLD measurements and those derived from RCF measurements were between 0 and 10%, with a RMS=5%. The RMS of the differences between the values derived from measurements and those calculated by the model was 2%.

Table 1. Cumulative skin doses derived from measurements ( $D_{\text{skin,cumulative}}$ ) and calculated by the model ( $D_{\text{skin,cumulative}}^*$ ) as a function of the slab phantom thickness for 6MV photon beams. The correction factors for *in vivo* cumulative measurements ( $CF^*$ ) are also shown.  $D_{\text{det,cumulative}}$  is the integrated dose measured by the detector without any correction.  $D_{\text{det,cumulative}}$  is the "true" cumulative dose, i.e., the entrance dose corrected by  $CF_{\text{entrance}}$  + the exit dose.  $D_{\text{skin,cumulative}}^*$  is  $D_{\text{det,cumulative}}$  multiplied by  $CF^*$ . Uncertainties are shown in brackets and expressed with  $k=1$ .  $\Delta_1$  are the percentage differences between skin doses determined from measurements and those calculated by the model.  $\Delta_2$  are the differences in skin doses determined by the model, comparing results calculated with EBT3 measurements to those calculated with TLD measurements.

Det.	Thickness (cm)	$CF^*$	$D_{\text{det,cumulative}}$ (Gy)	$D_{\text{skin,cumulative}}$ (Gy)	$D_{\text{skin,cumulative}}^*$ (Gy)	$\Delta_1$ (%)	$\Delta_2$ (%)
EBT3	10	0.895 (27)	0.351 (10)	0.992 (13)	0.872 (19)	0.888 (17)	1.8
	15	0.842 (26)		0.844 (13)	0.724 (19)	0.710 (16)	-1.9
	20	0.800 (24)		0.738 (13)	0.618 (19)	0.590 (15)	-5
TLD	10	1.00 (10)	0.231 (2)	0.804 (09)	0.802 (25)	0.802 (25)	0
	15	1.00 (10)		0.679 (07)	0.678 (24)	0.677 (24)	-0.1
	20	1.00 (10)		0.691 (11)	0.590 (26)	0.589 (26)	-0.1

Table 2 shows skin doses measured with TLD and RCF in eight points of the QUASAR phantom after delivering an IMRT treatment plan. Raw doses measured with TLDs and with EBT3 RCF, and corrected skin cumulative doses for EBT3 RCF are shown. The application of the proposed cumulative correction factor  $CF^*$  improved the Root Mean Square (RMS) of the differences between TLD measurements and RCF measurements from 19% to 5%.

Table 2. Cumulative doses measured with TLD and EBT3 radiochromic films after the delivery of a breast IMRT treatment plan, cumulative skin doses calculated from EBT3 measurements by applying  $CF^*$  ( $D_{\text{skin,cumulative}}$ ) for the same plan, and differences between doses measured with EBT and TLDs before ( $\Delta$ ) and after applying the correction ( $\Delta^*$ ). Uncertainties are shown in brackets and expressed with  $k=1$ .

Point #	$D_{\text{TLD,cumulative}}$ (Gy)	$D_{\text{EBT3,cumulative}}$ (Gy)	$\Delta$ (%)	$D_{\text{skin,cumulative}}^*$ ( $\Delta^*$ (%))	
				EBT3 (Gy)	
1	0.581 (8)	0.739 (13)	21	0.591 (29)	2
2	0.530 (6)	0.724 (13)	27	0.579 (26)	9
3	0.588 (2)	0.763 (13)	23	0.610 (27)	4
4	0.649 (11)	0.838 (09)	22	0.67 (3)	3
5	0.824 (14)	1.007 (07)	18	0.81 (4)	-2
6	0.795 (7)	0.954 (24)	17	0.76 (4)	-4
7	0.779 (13)	1.053 (20)	19	0.84 (4)	-1
8	0.853 (19)	1.047 (15)	26	0.84 (4)	7

### Conclusion

The proposed  $CF^*$  enables us to perform integrated skin dose measurements for IMRT with the lowest uncertainty reported to date.

### EP-1763 Monitoring total skin electron therapy using optically stimulated luminescence dosimeters

T. Kairn<sup>1</sup>, R. Wilks<sup>1</sup>, L. Yu<sup>1</sup>, S. Crowe<sup>1</sup>

<sup>1</sup>Royal Brisbane and Women's Hospital, Radiation Oncology- Cancer care Services, Herston, Australia

### Purpose or Objective

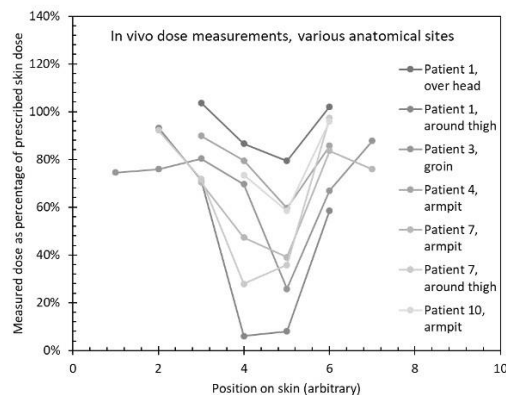
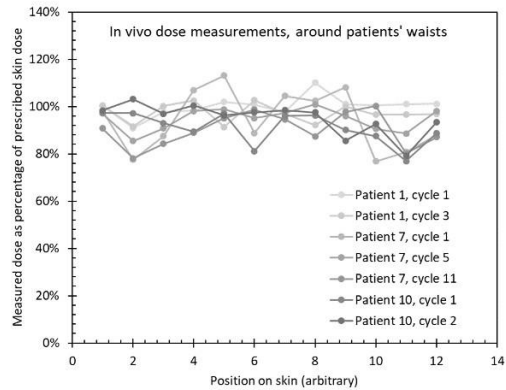
Total skin electron therapy (TSET, sometimes called TSEI or TSEBT) is delivered to patients who are standing in a series of well-established poses, rather than lying on a treatment couch. This unusual treatment geometry means that the dose received by each patient needs to be calculated without the use of a planning CT and usually without the use of a computerised treatment planning system. The treatment dose must therefore be verified, monitored and potentially adjusted throughout the treatment course, using *in vivo* dosimetry measurements. The aim of this study was to retrospectively examine a set of *in vivo* optically stimulated luminescence dosimetry (OSLD) measurements, and thereby provide an indication of the value of OSLD measurements for establishing and improving the dosimetric accuracy of TSET treatments, as well as proposed guidelines for completing such measurements in future.

### Material and Methods

Treatment records, including *in vivo* OSLD measurement data, were obtained for the ten patients who received TSET treatments during the last five years, at one large, metropolitan radiotherapy facility. Prescription doses ranged from 12 to 32.5 Gy, over 6 to 15 treatment cycles. Between 4 and 40 OSLD measurement points were used for each patient, at each cycle, depending on the number of areas of dosimetric concern identified by the prescribing oncologist or the physics team. All OSLDs were Landauer nanoDots, which were read out using a microStar reader (Landauer Inc, Glenwood, USA).

### Results

The *in vivo* dose measurements resulted in MU adjustments in five of the ten cases, to compensate for dose differences of 3.5% to 16% that resulted from changes in patient stance between treatment planning and delivery. Doses measured on the chest, back and around the waist were relatively consistent (see figure 1), under-doses were frequently identified at the top of the head, around the thighs and groin and in the armpits (see figure 2), and over-doses requiring the use of additional shielding were occasionally identified at extremities.



### Conclusion

OSLDs can be used to obtain measurements of TSET dose with sufficient accuracy to justify treatment dose adjustments and indicate the need for additional shielding or boost treatments. The identification and consistent use of a specific set of measurement points would increase the value of future in vivo measurement data, as a local audit and quality improvement resource.

### EP-1764 Portal dosimetry of the new O-ring system (Halcyon™): validation against a diode array

D. Nguyen<sup>1</sup>, F. Jossierand-Pietri<sup>1</sup>, G. Langeron<sup>1</sup>, M. Khodri<sup>1</sup>  
<sup>1</sup>Radiotherapie MACON, Medical Physics, Mâcon, France

### Purpose or Objective

The new fully pre-configured system dedicated for the fast delivery of IMRT/VMAT, Varian Halcyon™, a 6MV-FFF linac mounted on an O-ring gantry was installed in our centers. The Anisotropic Analytical Algorithm v15.6 (AAA) has been pre-configured to allow the calculation of patient dosimetry. It is also used to predict the dose in EPID for patient pre-treatment quality assurance (QA) with IMRT technique. With this one it is not possible to customize the beam modeling.

The purpose is to validate the Varian Portal Dosimetry (VPD) system against the standard QA system (diode array 2D), in order to use it for routine QA.

### Material and Methods

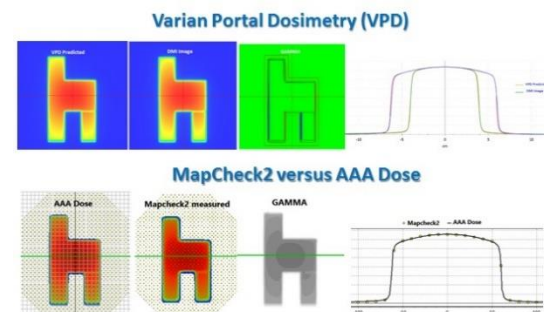
Dosimetric data were collected using the linac Varian Halcyon 2.0 with the 2D diode matrix Sun Nuclear MapCHECK2™ and the VPD with the AAA algorithm. Treatment Planning System (TPS) Eclipse™ version 15.6 was used to generate 26 alphabetical letters (A to Z) with the fluence brush tool (for example graph below for the letter h), 7 sweeping gaps (2, 4, 6, 10, 14, 16, 20mm) and 10 breasts cancers treatment with IMRT technique. The measured fluences with MapCHECK2™ were analyzed versus TPS dose water matrices (AAA V15.6) with the SNC software (V6.7.8) and predicted fluences with VPD (AAA V15.6).

### Results

For alphabetical letters and sweeps gaps, the mean passing rates of the global gamma evaluation were  $99.04 \pm 2.47\%$  and  $88.10 \pm 5.37\%$  and the local gamma evaluation were  $98.82 \pm 2.47\%$  and  $86.98 \pm 5.13\%$ , for the 2%/2 mm and 1%/1 mm criteria, respectively, for MapCHECK2.

In the case of the portal dosimetry, the mean passing rates of the gamma evaluation were  $99.18 \pm 3.73\%$  and  $90.75 \pm 8.77\%$  and the local gamma evaluation were  $99.15 \pm 3.75\%$  and  $89.72 \pm 8.77\%$  for the 2%/2 mm and 1%/1 mm criteria respectively.

For breast IMRT treatments, the mean passing rates of local gamma evaluation were  $99.9 \pm 0.28\%$  and  $99.9 \pm 1.68\%$  for VPD and  $99.56 \pm 0.65\%$  and  $97.49 \pm 1.86\%$  for MapCHECK2 for the 3%/3 mm and 2%/2mm criteria, respectively.



Example of h test results for mapcheck2 and VPD

### Conclusion

The pre-configured portal dosimetry beam modeling gives a very good results and close to the 2D array detector. It seems enough robust to use for routine QA without any need to customize.

### EP-1765 Adapted Delta4 phantom for EBT3 film based pre-treatment QA for lung SBRT VMAT: proof of concept

E. Bogaert<sup>1</sup>, F. Vanhoutte<sup>1</sup>, D. Dechambre<sup>2</sup>, Y. Lievens<sup>1</sup>, C. De Wagter<sup>1</sup>

<sup>1</sup>Ghent University Hospital, Radiotherapy and Oncology, Gent, Belgium ; <sup>2</sup>Cliniques Universitaires Saint-Luc, Radiotherapy and Oncology, Brussels, Belgium

### Purpose or Objective

Implementation of Lung SBRT in clinical routine requires an extensive quality control program to assure patient safety. Patient-specific evaluation of the measured dose against the treatment planning calculated dose is essential in this context. While several commercial 3-D detector arrays are available, they do not provide alone sufficient information to analyze complex dose distribution of highly conformal radiotherapy. Given the high resolution of Gafchromic films, we developed a proof of concept for a pre-treatment QA procedure using EBT3 films placed inside the body of a commercial X-shaped 3-D detector arrays phantom.

### Material and Methods

The Delta4 phantom has been modified by replacing the three detector plates (main board and wings) by EBT3 film placed in between 5mm thick PMMA slabs (Figure 1). Dose distribution of a three-arc VMAT (RayStation Version 6.0) plan for Lung SBRT (fraction dose of 15Gy, 6MV) was calculated on the homogeneous cylindrical body of the phantom and delivered using Elekta Synergy machine with Agility head. Calculated dose in the film planes (main plane 50° to the sagittal plane) was exported via a home-made script and compared to the measured film dose using FilmQPro software (Ashland ISP, USA) three-channel dosimetry. All specific film handling precautions were followed [1,2]. For quantitative evaluation, the gamma

index metric with 2%/2mm and 3%/3mm criteria was used in Film QA pro.

### Results

Relative and absolute dose comparison was performed with 2%/2mm gamma analysis of 92, 85 and 86% for the main and the wing films respectively; increasing up to 98, 93 and 96% using conventional 3%/3mm criterion. Results are presented in Figure 2 with vertical and horizontal line profiles couple to an isodose map of the main film. Having high resolution data into two perpendicular planes in a cylindrical phantom is advantageous against the classical setup in a cubic slab phantom. It provides more information than a single film in a coronal plane and reflects a geometry closer to the anatomical region treated as recommended by the NCS report 28 [3].

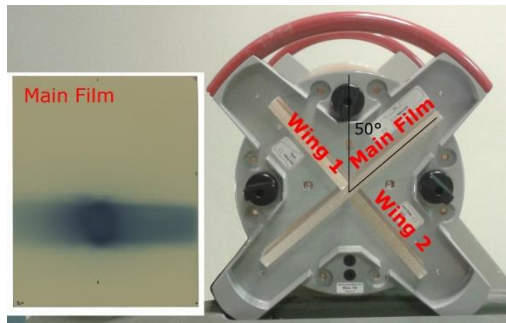


Figure 1. Adapted Delta4 phantom with film slabs. Left: Main film scanned image

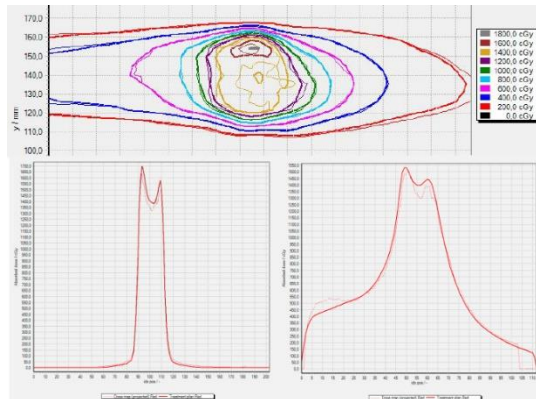


Figure 2. Film versus planned (solid line) isodose map and perpendicular dose profiles in the main plane

### Conclusion

Pre-treatment QA for Lung SBRT VMAT based on EBT3 film inside the body of the Delta4 phantom is feasible. Advantages are high spatial resolution and two-plane dose information in a cylindrical phantom. Further evaluation for more cases and different prescription doses is necessary.

[1] Borca VC, Pasquino M, Russo G, et al. Dosimetric characterization and use of GAFCHROMIC EBT3 film for IMRT dose verification. *Journal of Applied Clinical Medical Physics*. 2013;14:158-71.

[2] Paelinck L, De Neve W, De Wagter C. Precautions and strategies in using a commercial flatbed scanner for radiochromic film dosimetry. *Phys. Med. Biol.* 2007;52:231-242

[3] NCS Report 28-National Audit of Quality Assurance for Intensity Modulated Radiotherapy and Volumetric Modulated Arc Therapy- 2018

### EP-1766 Application of Extended CT Scale and Metal Artefact Reduction Methods on Radiotherapy Planning

H. Yucel<sup>1</sup>, F. Biltekin<sup>1</sup>, G. Ozyigit<sup>1</sup>, G. Yazici<sup>1</sup>

<sup>1</sup>Hacettepe University, Department of Radiation Oncology, Ankara, Turkey

### Purpose or Objective

The main purpose was to investigate the effects of extended computed tomography (ECT) scale and single energy metal artifact reduction (SEMAR) algorithm on dose distribution during the use of metal implants in radiotherapy treatments using 3D-printed individualized phantoms.

### Material and Methods

In this study, measurement was performed for both mandible and spinal titanium alloy implants. To evaluate the effect of these implants on real treatment case, three individualized phantoms were printed using MakerBot Replicator Z18 3D printer. In the first case, mandible implant was fixed to sawbone mandible model and it was placed inside of the individualized phantom. In the second and third case, two different spinal implants for C1-C3 and C4-C7 vertebra were instrumented to bone equivalent sawbone cervical vertebra model and these model were placed into the 3D-printed phantoms. CT scans of these phantoms were performed in two different step, with and without SEMAR methods, using Toshiba Aquilion LB CT simulator. In the treatment planning Varian Eclipse Version 7.1.3 TPS was used and measurement was performed on Varian Clinac DHX High Performance linear accelerator. In the first case, IMRT plans were created for both standard CT Scale (from -1024 HU to 3071 HU) and ECT scale (from -1024 HU to 64.511 HU). In the second and third case, in addition to CT scale comparisons for 3D-CRT and IMRT techniques, effect of SEMAR methods on dose distribution were analyzed for 3D-CRT treatment plans. Measurements were performed with EBT3 gafchromic film and 5mm DTA/%5 DD criteria was used for gamma analysis criteria.

### Results

In the first case, significant difference was not observed for SEMAR +/-, ECTS +/- since the implant used in the mandible phantom was thin and small so that it did not create dominant artifacts in the CT image. However, in C1-C3 and C4-C7 scenarios, it was observed that the ECT scale results were generally better (2-16% better) than SCT scale. When analyzing the gamma analysis data obtained for the planning of vertebral phantoms, no significant difference could be obtained from SEMAR +/- conditions.

### Conclusion

in case of significant metal artefact, use of ECT scale can improve the dosimetric accuracy of treatment planning. However, in mandible implant dosimetric differences were not found, since thin and small implants were preferred in clinical use.

### EP-1767 Validation and clinical use of a commercial Monte Carlo algorithm for Cyberknife patient-specific QA

M.T.W. Milder<sup>1</sup>, M. Sohn<sup>2</sup>, M. Alber<sup>2</sup>, M.S. Hoogeman<sup>1</sup>

<sup>1</sup>Erasmus MC Cancer Center, Radiotherapy, Rotterdam, The Netherlands ; <sup>2</sup>Scientific RT GmbH, GmbH, Munich, Germany

### Purpose or Objective

To ensure safe dose delivery in radiotherapy, uncertainties and errors have to be minimized by an extended quality assurance (QA) protocol. An established part of this chain is pre-treatment verification of monitor units, which can be performed by an independent dose recalculation. Especially for complex non-isocentric treatment plans as delivered by the Cyberknife with multi-leaf collimator (MLC), the traditional point-based MU verification does not suffice and a 3D dose recalculation is preferred for plan QA. The purpose of this work was to commission the first commercially available 3D Monte

Carlo dose engine for Cyberknife offered by SciMoCa and to report on the clinical utility of the SciMoCa model for MLC by benchmarking it with our standard patient-specific QA procedure for 100 patients.

#### Material and Methods

A beam model was developed by SciMoCa based on the standard commissioning data set for the Cyberknife treatment planning system. The beam model was validated by comparing measured and calculated output factors (OFs), percentage depth dose curves (PDDs), off-centre ratios (OCRs) and a set of clinically relevant, irregular and off-axis MLC segments. For the clinical evaluation, treatment plan files of 100 consecutive patients were re-calculated using the SciMoCa dose engine. In parallel, our standard procedure for patient specific-QA was carried out by overlaying the beams on a slab phantom for SRS1000 (PTW, Germany) measurements. The measurements and SciMoCa recalculations were analysed respectively by 2D and 3D gamma analysis. Clinical results were evaluated with 3% dose difference (DD) and 3 mm distance to agreement (DTA). For the purpose of this study the data was re-evaluated using for measurements and recalculations 2%/1 mm gamma criteria.

#### Results

The agreement between measured and modelled beam data is shown in table 1 and is mostly within 2%.

Altogether, 5 QA plans that were measured with the SRS1000 failed the 90% pass rate using 3%/3mm criteria. All failures were attributed to measurement problems and inaccuracies and were clinically approved. Re-evaluation of the measurements with tighter criteria of 2%/1 mm resulted in 17 failed plans, 16 of which were attributed to measurement inaccuracies. However, one was identified to have a problem in the plan calculation. Independent of the measurements, the SciMoCa recalculations identified only 1 failed plan with the tight criteria of 2%/1 mm. Both in measurements and recalculations the same plan failed the criteria.

**Table 1:** Agreement between measured and modelled data, averaged over three collimators and two Cyberknife systems. The largest deviations in PDD are correlated to the smallest field sizes and are within 5%.

#### OF PDD OCR (0.5 mm DTA)

<1% 81% 26% 84%

<2% 97% 76% 100%

#### Conclusion

A commercially available 3D dose re-calculation for individual Cyberknife MLC plan QA has been successfully implemented in the clinic, replacing time-consuming SRS1000 measurements, with fewer false alarms and similar sensitivity.

#### EP-1768 A Feasibility Study of EPID-Based In-Vivo Dosimetry System in Machine Specific Quality Assurance

F.Y. Yedekci<sup>1</sup>, F. Biltekin<sup>1</sup>, G. Ozyigit<sup>1</sup>

<sup>1</sup>Hacettepe University - Oncology Institute, Radiation Oncology, Ankara, Turkey

#### Purpose or Objective

The main purpose of this study was to evaluate performance of iViewDose (Elekta AB, Stockholm, Sweden) in machine-specific quality assurances.

#### Material and Methods

Measurement were carried out on Versa HD linear accelerator (Elekta AB, Stockholm, Sweden) using iViewDose Version 1.0.1 EPID-based in-vivo dosimetry tool. In this study, three sets of measurement were performed for 6 MV and 6 MV-FFF photon beams. In the first step, the output factor correction as a function of the photon beam field size were measured with iViewDose

system, then results were compared with the beam commissioning data. In the second step, measured and calculated percentage depth dose differences between iViewDose and beam commissioning data at the depth of 1.5, 5, 10 and 15 cm were evaluated. In the last step, linear accelerator dose calibration was set to cause a dose differences of 2% and 4% to evaluate the sensitivity of iViewDose in detecting dose calibration errors in daily check.

#### Results

The measured and calculated output factor comparison between iViewDose and beam data commissioning was illustrated in Figure 1. It was found that the results were compatible within 1% for all field sizes and photon energies. The percentage depth dose differences were generally maintained within 3% until the depth of 10 cm. However, the deviations increase up to 6% at the depth 15 cm. In the last step of measurement, the output differences for 2% and 4% was detected as 2.25% and 4.25% for 6 MV, 2.25% and 4.4% for 6 MV-FFF, respectively.

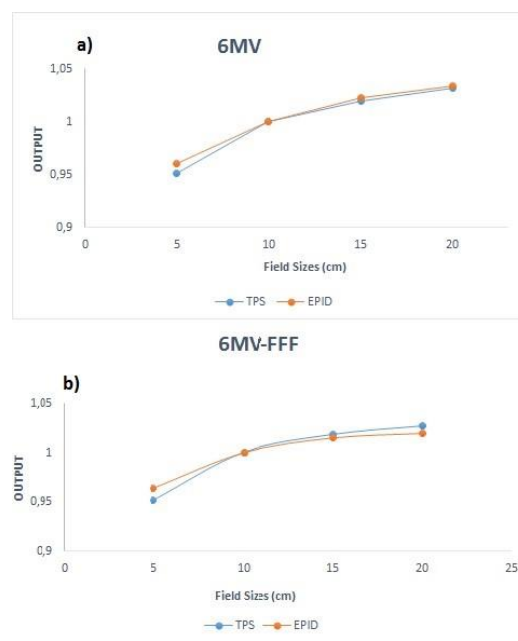


Figure 1. The measured and calculated output factor comparison between iViewDose and beam data commissioning

#### Conclusion

The EPID-based iViewDose tool proved to be a useful in daily check of output correction factors for different field size, depth dose at reference point and dose calibration constancy of linear accelerator.

#### EP-1769 Pre-treatment VMAT verification with SunCHECK Fraction 0 and Varian Portal Dosimetry - a comparison

N.I. Hoven<sup>1</sup>, J. Kalsnes<sup>1</sup>, P. Lønne<sup>1</sup>

<sup>1</sup>Oslo University Hospital, Department of Medical Physics, Oslo, Norway

#### Purpose or Objective

Varian Portal Dosimetry (PD) is routinely used for pre-treatment VMAT verification in our clinic. We are considering replacing this system with SNC SunCHECK Fraction 0 (FZ), and want to explore the difference between the two systems.

#### Material and Methods

36 clinical VMAT plans with a total of 70 arcs were evaluated using FZ and PD, on a Varian Clinac with the aS1000 EPID (46 arcs) and a Varian TrueBeam with the

aS1200 EPID (24 arcs). The plans were created in Eclipse v13.6, and calculated with the AAA13.6 algorithm. For each linac, the dosimetric output was calibrated to within 0.3%, and the beam flatness and symmetry was confirmed to be within specs (103% and 101%, respectively). The two verification systems were calibrated according to vendor instructions. Treatment plans were verified with PD according to our clinical practice, and the same acquired EPID image was analyzed with FZ within the SunCHECK software. The measured dose was compared to the predicted dose using the gamma analysis method with 3 precision levels:  $\Gamma$  3%/3 mm (3% dose difference and 3 mm DTA),  $\Gamma$  2%/2 mm and  $\Gamma$  1%/1 mm (global normalization, dose threshold 10%). To pass the analysis, the pass rate (points with  $\Gamma \leq 1$ ) should be  $\geq 95\%$  for  $\Gamma$  3%/3 mm and  $\Gamma$  2%/2 mm, and  $\geq 90\%$  for  $\Gamma$  1%/1 mm.

**Results**

For both methods and both machines/EPIDs, all arcs passed the  $\Gamma$  3%/3 mm analysis used in clinical routine. With stricter criteria, there is a number of arcs where one method passes while the other fails, as shown in Figure 1. There is a tendency of more arcs passing with FZ than with PD.

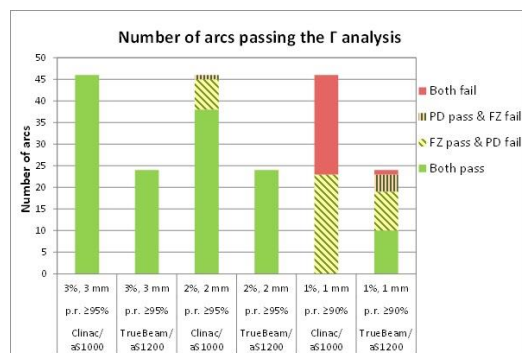


Figure 1: Number of arcs passing the gamma analysis with both methods, one of the methods or none of the methods, for various precision levels and pass rate settings.

The numbers of arcs that pass with one method but fail with the other were compared using Pearson's  $\chi^2$  test under the null hypothesis that "FZ pass & PD fail" is equally probable to "PD pass & FZ fail". The difference is statistically significant for measurements performed with Clinac/aS1000, as presented in Table 1.

**Table 1: Pearson's  $\chi^2$  comparison of numbers of arcs that pass one method but fail the other**

Precision Level	Machine/EPID	FZ pass & PD fail	PD pass & FZ fail	Significant ?
$\Gamma$ 2%/2 mm	Clinac/aS1000	7	1	Yes (p = 0,03)
$\Gamma$ 1%/1 mm	Clinac/aS1000	23	0	Yes (p = 0,00)
$\Gamma$ 1%/1 mm	TrueBeam/aS1200	9	4	No (p = 0,17)

The average  $\Gamma$  pass rate is higher with FZ than with PD for all precision levels (Figure 2), but the difference is not statistically significant. However, it's worth noting that most arcs have a higher pass rate with FZ than with PD.

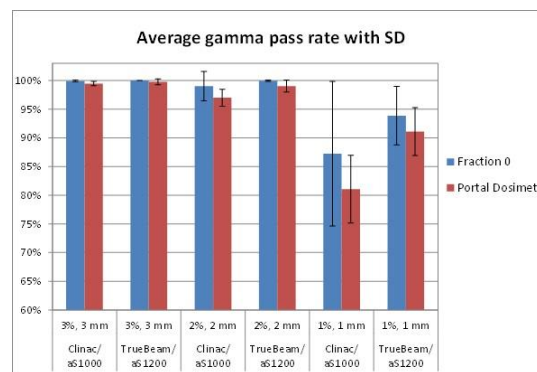


Figure 2: Average gamma pass rate with 1 standard deviation for various precision levels and pass rate settings.

**Conclusion**

Regardless of precision level, there's no significant difference between the average gamma pass rates from the two methods. For the criteria used in clinical routine, the two methods appear equivalent.

For the more stringent criteria there is a number of arcs where one method passes while the other fails, with a tendency of more arcs passing with FZ than with PD. This may be caused by the different approach to absolute calibration of the EPID. Future work will include 2D phantom measurements to determine which method corresponds better to the actual dose delivered.

**EP-1770 Investigation of Electronic Portal Imaging Based In-Vivo Dose Verification for Prostate SBRT**  
 F. Biltekin<sup>1</sup>, F.Y. Yedekci<sup>1</sup>, G. Ozyigit<sup>1</sup>  
<sup>1</sup>Hacettepe University - Oncology Institute, Radiation Oncology, ankara, Turkey

**Purpose or Objective**

The main purpose was to investigate electronic portal imaging based new in-vivo dosimetry tool iViewDose (Elekta AB, Stockholm, Sweden) for SBRT prostate cancer treatment in clinical use.

**Material and Methods**

The study was performed on Versa HD linear accelerator (Elekta AB, Stockholm, Sweden) and feasibility of iViewDose Version 1.0.1 tool was analyzed for prostate SBRT plans in clinical use. To validate this new quality assurance system in clinical facilities, fifteen prostate cancer patients were selected and iViewDose based in-vivo EPID dosimetry was performed. Treatment plans were generated with RayStation treatment planning system (RaySearch Lab., Stockholm, Sweden) and dose prescribed as 36.5 Gy in five fraction. For all SBRT patient, three dimensional gamma analysis results were evaluated. Additionally, measured and calculated dose in reference point (DRP) for CTV, rectum, bladder and femur heads were compared for all fraction.

**Results**

According to measurement results, mean gamma analysis ( $\gamma \leq 1$ ) passing rate of fifteen patient was found as 95.58% for  $\gamma 3D$  (criteria: 3% global dose difference/3 mm distance to agreement, threshold 50%). Additionally, mean DRP difference between measurement and calculated in treatment planning system for CTV, rectum, bladder, left and right femur heads were found as 1.97%, 10.04%, 18.318%, 3.19% and 4.56%, respectively. Maximum dose differences were found in rectum and bladder reference point due to the high dose gradient in these region. However, in medium and low dose gradient region measurements were compatible in 1% with calculated dose in treatment planning system.

**Conclusion**

iViewDose EPID-based in vivo dosimetry software provides an efficient safety check on the accuracy of dose delivery

during radiotherapy facilities. This is especially important in SRS/SBRT modalities which employ higher therapeutic doses in daily fraction.

### EP-1771 Measuring the influence of magnetic fields on the dose distributions of clinical electron beams

R. Kueng<sup>1</sup>, B.M. Oborn<sup>2</sup>, N. Roberts<sup>2</sup>, T. Causer<sup>2</sup>, M.F.M. Stampanoni<sup>3</sup>, P. Manser<sup>1</sup>, P. Keall<sup>4</sup>, M.K. Fix<sup>1</sup>

<sup>1</sup>Inselhospital- University Hospital Bern, Division of Medical Radiation Physics, Bern, Switzerland ; <sup>2</sup>University of Wollongong, Centre for Medical Radiation Physics, Wollongong, Australia ; <sup>3</sup>University of Zurich and Swiss Federal Institute of Technology ETH, Institute for Biomedical Engineering, Zurich, Switzerland ; <sup>4</sup>Sydney Medical School- University of Sydney, ACRF Image X Institute, Sydney, Australia

#### Purpose or Objective

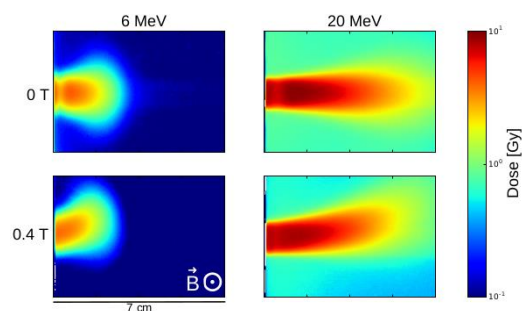
MRI-Linacs are a fast-growing area of cancer radiotherapy. To date only MRI-Linac photon beams have been investigated. However, radiotherapy quality can be improved for a wide range of clinical indications by using electron beams alone or in combination with photon beams. The objective of this work is to investigate the dosimetric impact of a magnetic field with different field strengths and orientations on therapeutic electron beams for three beam energies. For this purpose, an experimental setup for measuring dose distributions of clinical electron beams generated by a conventional linac in the presence of a magnetic field is established.

#### Material and Methods

A permanent magnet device was used to generate a magnetic field surrounding a solid water slab phantom. The magnetic field including maximal field strength  $B_{max}$  was varied by moving the permanent magnet banks and by insertion of focusing steel cones. Electron beams (6, 12 and 20 MeV) from a clinical linear accelerator (Varian Clinac 2100C) were incident perpendicular (transverse setup) and parallel (inline setup) to the main magnetic field direction. The magnet device was placed at a source to isocenter distance of 150 cm and the electron beams were collimated to a circle of 1 cm diameter and a square of 1.5 cm side length, respectively. Gafchromic EBT3 film was placed inside the homogeneous slab phantom, parallel to the beam (transverse setup) and perpendicular to the beam (inline setup) to measure two-dimensional dose distributions. Reference conditions with zero magnetic field were established by using identical collimation in an aluminum frame setup.

#### Results

As expected, for the transverse setup, substantial deflection of the electron beam was observed in the magnetic field, as indicated in figure (1). Consequently, a shift of lateral dose profiles and shift in distal dose fall-off (R50 up to -5 mm) was measured for all three electron beam energies. For the inline setup, focusing of electron beams was observed in magnetic fields compared to the zero field reference setup. An increase of measured dose of up to 100% (6 MeV beam, 0 vs. 0.7 T magnetic field) was shown, yielding a steeper lateral penumbra for a given dose level (FWHM -1.5 mm in 2 cm depth).



### Conclusion

Propagating in a magnetic field, substantial deflection (transverse setup) and focusing (inline setup) of all measured electron beams was observed. The inline setup shows steeper lateral penumbra of electron fields and thus the potential for enhanced plan quality for electron treatments.

### EP-1772 MLC parameters evaluation in a RT-dedicated MC environment (PRIMO) from static fields to VMAT plans

L. Paganini<sup>1</sup>, G. Reggiori<sup>1</sup>, A. Stravato<sup>1</sup>, V. Palumbo<sup>1</sup>, P. Mancosu<sup>1</sup>, F. Lobefalo<sup>1</sup>, A. Gaudino<sup>1</sup>, S. Tomatis<sup>1</sup>, M. Scorsetti<sup>1,2</sup>

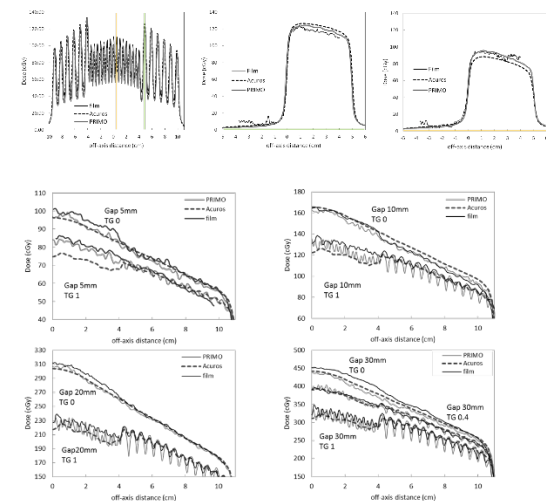
<sup>1</sup>Humanitas Clinical and Research Center, Radiosurgery and Radiotherapy, Rozzano, Italy ; <sup>2</sup>Humanitas University, Department of Biomedical Sciences, Rozzano, Italy

#### Purpose or Objective

PRIMO is a graphical environment for MonteCarlo (MC) simulations based on the Dose Planning Method (DPM), a fast MC algorithm specifically built for the simulation of the deposited dose in radiotherapy. The objective of this work was to validate the beams calculated by DPM against the ones from our Linac EDGE (Varian) and to compare PRIMO with the clinical algorithm Acuros (Varian) and film measurements with particular focus on the MLC parameters.

#### Material and Methods

In a first phase a full characterization of the 10MV FFF beam was performed. Then the 120 HD MLC modeling, particularly the Tongue and Groove effect, was investigated with two types of tests: static MLC fields in different settings and MLC plans configured in 'dynamic fence patterns'. These dynamic tests were planned with increasing leaf-ends, gap size and degree of TG effect. The dose distributions were measured using the IBA MultiCube phantom with GafChromic films positioned horizontally at 10cm depth. Finally a set of four clinical plans was selected from our database. All VMAT plans were optimized with 10MV FFF beam in Eclipse and calculated with Acuros. The DICOM files (plan, structures and images) were imported in PRIMO. DPM was used to calculate dose distribution in patients. The dose distributions were compared in terms of gamma analysis within BODY and PTV.



#### Results

Concerning the MLC modelling, static fields showed a good agreement between Acuros, PRIMO and film measurements, with slight differences in transmitted dose (Fig1). The comparison between dose profiles for the

dynamic fields highlighted differences between measurements and calculations. Discrepancies are higher for the MLC central region where leaves are thinner, and thus TG effect more consistent, with differences up to 8% for Acuros and 4% for PRIMO (Fig2). Differences in the external part of the MLC are below 3% for both algorithms. The differences in handling the MLC parameters between PRIMO and Acuros don't consistently affect the dose distribution resulting in Gamma Agreement Index (GAI) values (3%,2mm) always >97.5% for the PTV volume and 99.5% for the Body region. With more selective thresholds, however, these differences start to be noticeable, with mean GAI values of 98% (2%,2mm) and 90% (1%,1mm) for the Body and 92.2% (2%,2mm) and 65.5% (1%,1mm) for the PTV, confirming possible issues for the thinner leaves.

#### Conclusion

This study highlighted some critical issues in the MLC handling in both static and dynamic settings. PRIMO showed a better agreement with measurements compared to Acuros in all settings. In the considered clinical plans however, these differences lead to acceptable dose distributions for both Acuros and PRIMO though these results should be verified on a larger dataset of patients. In conclusion PRIMO can be an interesting tool to help the fine tuning of the TPS parameters in conditions where experimental measurements have high uncertainties and could benefit from simulations.

#### EP-1773 Radioiodine therapy: a dosimetric study in a patient with DTC after rhTSH stimulation

S. Mazzaglia<sup>1,2</sup>, L. Barone Tonghi<sup>2</sup>, A.M. Gueli<sup>1,3</sup>, C.N. Tuve<sup>1,3</sup>, G. Pellegriti<sup>1,4</sup>

<sup>1</sup>Specialization School of Medical Physics- University of Catania, Department of Medical- Surgical and Advanced Technologies "G. F. Ingrassia "DGFI, Catania, Italy ; <sup>2</sup>ARNAS Garibaldi - Catania, Medical Physics, Catania, Italy ; <sup>3</sup>University of Catania, Department of Physics and Astronomy, Catania, Italy ; <sup>4</sup>ARNAS Garibaldi - Catania, Endocrinology, Catania, Italy

#### Purpose or Objective

The main approach to the Differentiated Thyroid Cancer (DTC) therapy is still empiric, consisting of fixed activities administration, generally besides 1.1 GBq and 7.4 GBq. Repeated treatments, however, may cause stunning effect. An individualized dosimetric study may represent an important tool to determine the best activity to prescribe, in particular for patients with distant metastases or when therapy with rhTSH stimulation is deemed necessary.

We present the case of a patient underwent rhTSH stimulation before radioiodine therapy. This study illustrates the necessity of measuring both red marrow (RM) and blood (BL) absorbed dose during the treatment, because of estimating the activity that could be administered to the patient, in order to not exceed the dose limit of 2 Gy to RM, so as to avoid repeating radioiodine treatment several times. Afterward a variety of dosimetric approaches has been proposed.

#### Material and Methods

To calculate the absorbed dose to the RM it is necessary to know both the BL and whole-body (WB) residence times ( $\tau_{BL}$  and  $\tau_{WB}$ ) and the weight of patient,  $m_p$ , in kg. In this study, the BL absorbed dose was calculated using the EANM formulations and the dose to RM using the AIFM and the Traino methods. Dosimetry to the RM and BL were performed during the treatments, after administration of nominal therapeutic activity  $A_0$  of  $^{131}I$  equal to 3.7 GBq ( $3.3 \pm 0.2$  GBq measured), without modifying the fixed activity schema. Dosimetric calculations were carried out on blood samples of 3 ml at 2, 6, 24, 48, 144 hours after administration of the therapeutic activity, measured through a dose calibrator. Moreover, the patient underwent to WB measurements with an environmental ionization chamber at 2, 6, 24, 48, 144 hours after

therapeutic administration, with a full bladder. The first data after 2 hours correspond to effective administered activity  $A_0$ .

#### Results

$\tau_{BL}$  and  $\tau_{WB}$  by decreasing mono and bi-exponential fit of the experimental data were obtained [Fig.1-2]. Following the RM calculated dose was of  $411.53 \pm 14.68$  mGy for AIFM method,  $395.54 \pm 12.69$  mGy for Traino method, instead the BL calculated dose was  $527.32 \pm 19.48$  mGy, under the dose limit of 2 Gy. This result allows to estimate the maximum administrable activity, considering all approaches. The value obtained confirms that could have been administered to the patient an activity at least 4 times higher in a single treatment, after evaluation of the specialist.

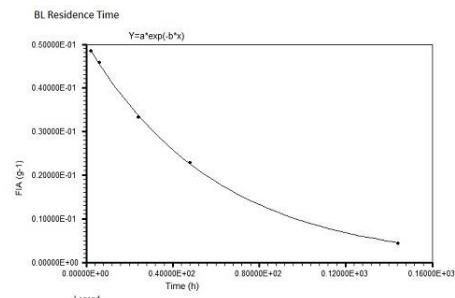


Fig.1

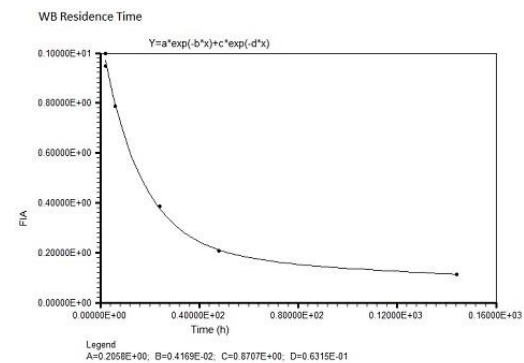


Fig. 2

#### Conclusion

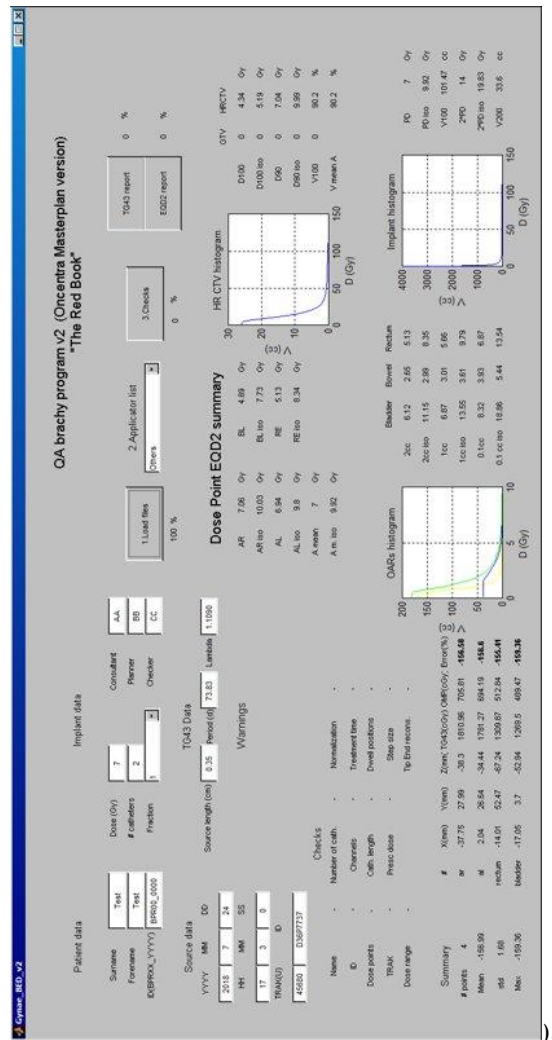
The results suggests the possibility to restrict the number of treatments, so reduced the risk of stunning effect and, where possible, eliminate an additional source of stress and dejection for patients. This is the most important result of this preliminary work. In fact, thanks to dosimetric study it was highlighted that it is possible to administrate individualized activities for DTC patients, in particular after rhTSH stimulation.

#### EP-1774 Independent dose verification of brachytherapy TPS and automation of EQD2 reports using Matlab Code

S. Esteve Sánchez<sup>1</sup>, A.B. Mohamed Yoosuf<sup>2</sup>, G. Workman<sup>1</sup>  
<sup>1</sup>Northern Ireland Cancer Centre, Radiotherapy Physics, Belfast, United Kingdom ; <sup>2</sup>King Abdulaziz Medical City, Radiation Oncology, Riyadh, Saudi Arabia

#### Purpose or Objective

To study the accuracy of an independent dose calculation of gynaecological treatments and develop an automated EQD2 report using a Matlab program (Figure 1



**Material and Methods**

For each fraction, DICOM RP and DVH text files are exported from the TPS, OncentraBrachy v4.5. The matlab program uses the source coordinates from the RP file along with published source data (Ir-192) as the primary input for dose calculation following TG 43 protocol and accounts for 2D anisotropy. The independent dose calculation was performed on point A and bladder/rectum dose points. The results were compared to the TPS calculation. Furthermore, the program verifies other treatments parameters which includes: total reference air kerma, dose prescription, applicator type, dwell positions, catheter length, total treatment time and a comparison to known standard time if appropriate.

The Matlab program also imports the tabular DVH file to interpolate the 2cc, 1cc and 0.1cc dose values of bladder, rectum and bowel and D100, D90 and V100 for the HRCTV. The program automatically exports the results to a patient report (Figure 2), and sums all doses at final fraction. Sensitivity of the program was studied by introducing deliberate errors.

**Results**

552 dose points have been checked with the independent dose calculation since the program was implemented in clinical practice. The EQD2 report created with Matlab has been used for 30 patients. The mean error in dose calculation between the Matlab code and TPS was  $-0.02\% \pm 0.61\% [-5.12, 1.51][YA1]$ . Largest errors were found on points created on the same plane as the ring applicator due to the different vectors used for each dwell position by the manufacturer and our measured ring path that affect the TG 43 interpolations. The OARs and HRCTV

values interpolated from the DVH text file agreed within 1% with the values calculated by the TPS.

The program was also found to be sensitive to errors created deliberately in dummy cases such as incorrect dose prescription, inconsistent catheter lengths and dwell positions and wrong reference source data. The process of exporting the files, running the program and creating the reports can be completed in less than 5 minutes.

**Conclusion**

The program is a useful tool to independently verify the dose calculation in brachytherapy treatments and had led to a more efficient workflow in the clinical sessions. The automated EQD2 report has reduced the possibility of transcription errors. The use of DICOM and DVH text files offers the possibility of extending the program to other TPS.

**EP-1775 Determination of tolerance criteria for the sliding leaf gap dynamic IMRT test**

S. Weston<sup>1</sup>, C. Thompson<sup>1</sup>, A. Esmail<sup>1</sup>, P. Rixham<sup>1</sup>, D. Paynter<sup>1</sup>

<sup>1</sup>Leeds Cancer Centre, Medical Physics and Engineering, Leeds, United Kingdom

**Purpose or Objective**

In the sliding leaf gap test a dynamic narrow field is moved across an ion chamber and the charge collected is normalised by an open field delivered using the same number of monitor units. This work determines clinically relevant tolerance criteria by introducing MLC errors into the delivery, and comparing VMAT verification results performed using Delta4 and ion chamber measurements within a phantom with sliding window output factor (SWOF) measurement.

**Material and Methods**

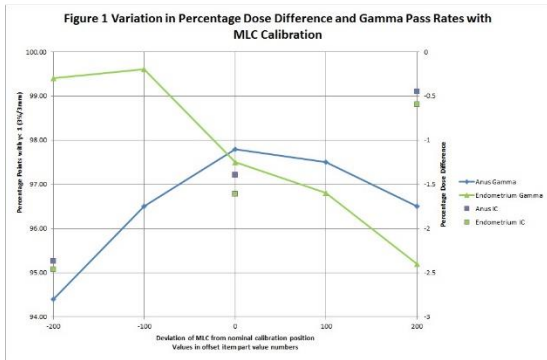
The MLC leaves on the LINAC were first calibrated and QA'd to ensure that the MLCs were performing optimally. The accuracy of treatment delivery was assessed by a measurement using Delta4 and by an ion chamber measurement in a phantom at the isocentre. Each leaf bank was adjusted by modifying the MLC calibration such that the subfields were made larger by 0.1 mm on each leaf. The verification measurements were repeated. This process of modifying the leaf bank calibration and verifying the VMAT deliveries was repeated until one of the deliveries failed the verification. The MLC calibration was restored and the process repeated this time reducing the subfield size.

A water phantom was placed at 100 cm SSD with an ion chamber on the CAX at depth of 5cm. The chamber was irradiated with a 200 MU 10x10 cm<sup>2</sup> field. The chamber was irradiated with a dynamic 200 MU 10 x 1 cm<sup>2</sup> field which moved across the field from -4.5 cm to 4.5 cm. The ratio of the dynamic field output to the open field is the sliding window output factor (SWOF). The SWOF was recorded for range of leaf calibration settings assessed as being clinically acceptable using the verification measurements of the two VMAT solutions.

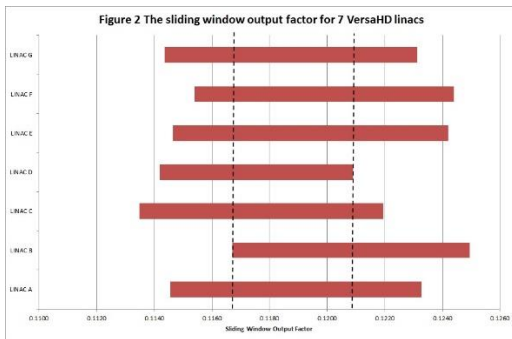
This process was repeated across 7 linear accelerators and the results from all linacs used to determine the clinical tolerances for the SWOF.

**Results**

The verification results for both anus and endometrium for LINAC A are shown in figure 1. The figure shows that as the leaf calibration is extended or withdrawn the verification results become poorer until eventually the verifications fail..



Note that this LINAC is resilient to leaf calibration changes of 200 item part value numbers, which equates to 0.2 mm, on each bank. This process was repeated on 7 linear accelerators in total.



By determining the SWOF at extremities of the leaf calibration range of each LINAC it is possible to determine the tolerance range for the SWOF. Figure 2 shows the SWOF tolerances for seven linear accelerators. The figure shows that sufficient overlap in the results to allow a single tolerance range for the whole fleet. The fleet wide SWOF tolerance range is 0.1169 to 0.1211, or 0.119 +/- 1.8 %.

### Conclusion

The sliding window output test can be used to monitor the MLC calibration. The sliding window output test has been benchmarked against standard verification measurements using two complex VMAT deliveries across seven linear accelerators. A single tolerance range for the sliding window output factor has been established that can be used across the fleet.

### EP-1776 Automated proton plan QA via independent Monte Carlo simulations

G. Guterres Marmitt<sup>1</sup>, A. Pin<sup>2</sup>, J.A. Langendijk<sup>1</sup>, S. Both<sup>1</sup>, A. Knopf<sup>1</sup>, A. Meijers<sup>1</sup>

<sup>1</sup>University Medical Center of Groningen, Department of Radiation Oncology, Groningen, The Netherlands ; <sup>2</sup>Ion Beam Applications, Research Group, Louvain-la-Neuve, Belgium

### Purpose or Objective

For radiation therapy, it is crucial to guarantee that the delivered dose matches the planned dose. Uncertainties in the dose calculations done in the treatment planning system (TPS), delivery errors or data corruption during transfer might lead to significant differences between predicted and delivered doses. As such, patient specific quality assurance (QA) of dose distributions, through experimental validation of individual fields, is currently necessary. In this work, we investigate the potential to replace the measurement-based patient specific QA with a simulation-based patient specific QA using a Monte Carlo (MC) code as independent dose calculation engine in order

to develop a fast, automated and accurate patient specific QA.

### Material and Methods

The QA platform is composed of a web interface, servers and computation scripts, and is capable to autonomously launch simulations, identify and report dosimetric inconsistencies. After plan approval in TPS, data are exported to a dedicated DICOM server, that triggers the QA workflow for the TPS-based plan. A preliminary dose recalculation automatically takes place and gamma analysis results, comparing original and recalculated dose maps, become available at the website. After review, the dry-run of the plan is performed to generate machine log files and, upload of the logs, triggers the log-based plan QA workflow. A log-based plan is reconstructed from the retrieved log files, and after the dose calculation, results for the 2<sup>nd</sup> workflow are available for review. For validation purposes of the MC beam model, a set of standardized plans (SOBPs) were designed and in-water calculations were compared between TPS and QA platform. Also, for a set of 10 clinical plans the QA results obtained from the QA platform were compared to the QA results from standard measurement-based approach.

### Results

To perform patient QA according to the proposed methodology 0-15 min of in-treatment-room time are required and additional 5-10 min for data export from TPS and retrieval of the log files. Independent MC calculations require 15-20 minutes. In-water simulations over 30 SOBPs plans with varying range and modulation showed a 99% ± 0.5% gamma pass ratio (2 mm, 2%) when compared to the TPS calculated dose maps. Comparison between QA platform and measurement-based results for 10 clinical cases, including the following indications: craniospinal axis, intracranial and head and neck, is summarized in Fig. 1. An example of calculated dose distributions for case #10 is shown in Fig. 2.

Patient	Measurement-based (gamma pass ratio %)	TPS-plan based recalculation (gamma pass ratio %)	Log-plan based recalculation (gamma pass ratio %)
#1	100	97.43	97.71
#2	99.81	98.75	-
#3	100	98.6	91.56
#4	100	98.43	98.59
#5	98.31	95.37	93.3
#6	98.55	96.05	95.54
#7	99.44	99.05	97.98
#8	99.12	99.14	98.99
#9	99.52	99.3	99.14
#10	99.31	96.02	94.97

Fig. 1. Gamma pass ratios for measurement-based plan QA, and the proposed TPS-based plan QA.

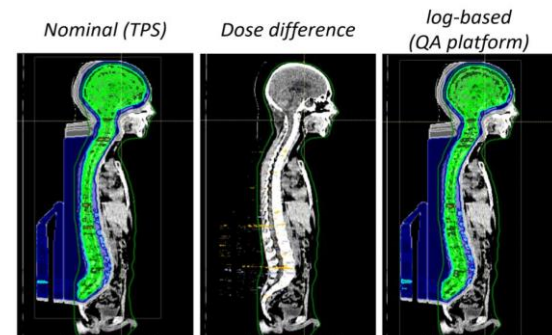


Fig. 2. Dose maps for the TPS calculated plan (left), the log-based recalculation (right) and the dose difference (center). For visualization purpose, recalculated dose maps have been imported in TPS. The dose maps are compared with gamma analysis (2 mm, 2%) and pass ratio is 95%.

### Conclusion

A new patient specific QA workflow was developed inside an automated web platform. The clinical application of this method has the potential to greatly reduce QA time. Validation with calculations in water shows great consistency of the MC engine over a wide range of beam-sets. The retrospective application of the approach for a set of 10 clinical plans implicate that the same decisions

would have been reached for either recalculation or measurement-based method.

### EP-1777 Improvements in pencil beam algorithm in proton therapy: do we still need Monte Carlo in brain?

L. Widesott<sup>1</sup>, S. Lorentini<sup>1</sup>, F. Fracchiolla<sup>1</sup>, P. Farace<sup>1</sup>, M. Schwarz<sup>1</sup>  
<sup>1</sup>APSS, Protonterapia, Trento, Italy

#### Purpose or Objective

Dose accuracy in presence of heterogeneities and range shifter (RS) modelling are some of the reasons that have made in the last years Monte Carlo (MC) dose calculation algorithm increasingly present in the clinical routine in proton therapy. On the other hand, MC brings with it significantly higher calculation times, especially if you want to do robust optimization/evaluation and/or frequent re-planning. The purpose of this work is to evaluate the last version of the pencil beam (PB7) present in our TPS comparing it with measurements and observe how it behaves with respect to the previous version of the pencil beam algorithm (PB6) and MC.

#### Material and Methods

We compared the new RayStation 7 pencil beam (PB7) algorithm vs. MC dose engine and the previous one (PB6) clinically implemented so far, in critical conditions such as superficial targets (i.e. in need of range shifter), different air gaps and different gantry angles to simulate both orthogonal and tangential beam arrangements. For every plan the PB7, PB6 and MC dose calculation were compared to measurements using a gamma analysis metrics with passing criteria of 3% of maximum dose, 3mm distal-to-agreement, global approach, and dose threshold of 5%. Measurements were performed with a 2D ion chamber array detector (MatriXX PT, IBA Dosimetry GmbH) placed underneath the following targets: 1) anthropomorphic head phantom (with two different thickness) and 2) a biological sample (i.e. half lamb's head).

#### Results

For both the configurations of the head phantom (i.e. one and two slabs) the gamma passing rate (GPR) was almost always better for PB7 compared to PB6 (on average >92% for PB7 vs >85% for PB6) but still below MC GPR (on average >99%). Overall the PB6 algorithm tends to overestimate the dose to the target (up to 25%) and underestimate the dose to the organ at risk (up to 30%). PB7 performed significantly better but an overestimation of the hot spot compared to MC was found (Figure). We found similar results for the two targets of the lamb's head where only two beam gantry angles were simulated (Table). Each field was optimized with PB6, the final dose calculation time was the same for PB6 and PB7 (about 20 seconds) and ten times greater for MC (about 200 seconds).

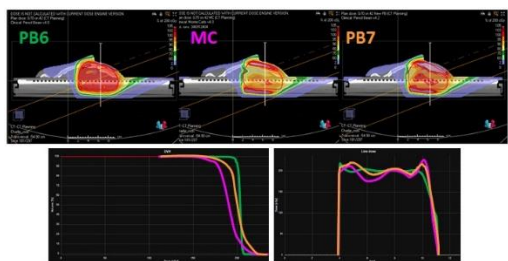


**Figure .** PB6 optimized dose distribution on 1/6 head phantom (top left), MC recalculation (top center) and PB7 recalculation (top right), with proton field angle of 70° and range shifter 42 cm from ISO (i.e. air gap ~ 24 cm). The white lines represent the dose profiles (bottom right) extraction plans. In the bottom left of the figure, DVH of each dose distribution is displayed.

Gantry angle	Snout position (cm)	Gamma Analysis results – Passing Rate (%)		
		PB6	MC	PB7
60°	42	70.1	95.6	93.8
	30	81.6	97.0	90.6
	18	87.6	97.0	89.0
	Split	90.6	99.3	90.4
0°	42	85.0	100	86.3
	30	86.8	100	93.1
	18	89.5	100	94.1
	Split	95.4	100	99.5

**Table .** PB6 vs MC and PB7  $\gamma$  analysis (3%,3mm) comparison on transversal planes for eight fields with target in the brain region of the lamb's head.

#### Conclusion

Our data show very promising results with PB7 and much lower computation time than MC. Questions remain about the use of PB7 for brain tumors only for some specific scenarios as use of RS with very large air gaps and beam directions tangential to the patient surface. On the contrary, speed gained with PB7 is a very important issue in the context of multi-criteria-optimization and/or robust optimization and/or on-line re-planning.

### EP-1778 Accumulated dose prediction from pre-treatment dosimetric parameters in cervical cancer PotD method

S. Heijkoop<sup>1</sup>, J. Godart<sup>1</sup>, E. Novakova<sup>1</sup>, J.W. Mens<sup>1</sup>, B. Heijmen<sup>1</sup>, M. Hoogeman<sup>1</sup>

<sup>1</sup>Erasmus Medical Center Cancer Institute, Radiation Oncology, Rotterdam, The Netherlands

#### Purpose or Objective

In our institute locally advanced cervical cancer patients are treated with an online adaptive Plan-of-the-Day (PotD) protocol. Daily CBCT scans are used to select a plan from the plan library that best fits the observed anatomy for that day. This radiotherapy technique allows for better sparing of organs at risk (OAR). However, due to organ motion and daily plan selection, accurate a-priori prediction of the total dose received at the end of the treatment course is challenging, which can lead to inaccurate prediction of normal tissue complications. The aim was to investigate whether pre-treatment established treatment plan parameters can predict accumulated OAR doses for the fractionated treatment.

#### Material and Methods

Treatment plans and daily CBCTs of 24 patients were included in the study. 14 patients had a tip of uterus displacement of more than 2.5 cm as measured with a full and empty bladder planning CT scan ('movers') and 10 patients had a motion less than 2.5 cm ('non-movers'). The movers had 3 plans in the plan library to cover the range of motion (full and empty-bladder IMRT plans with minimal adequate margins and a backup plan with an enlarged margin), whereas the non-movers had 2 plans in the plan library (1 IMRT plan with a minimal/adequate margin and a backup plan with enlarged margin). In all daily CBCT scans the bowel cavity, bladder and rectum were contoured. To calculate accumulated OAR doses non-rigid registration was used (1).

In clinical practice, the movers were on average in 50% of fractions irradiated with the full bladder plan and in the other 50% with the empty bladder plan. Therefore, in this study we investigated correlations ( $R^2$ ) between mean *planned* OAR dose parameters for the full and empty structure sets with the corresponding estimated *delivered* parameters derived with the CBCTs and dose accumulation.

### Results

Obtained  $R^2$  are presented in the Table with an overall average of 0.68. For rectum and bladder, V30 showed the strongest correlation. For the small bowel V20 correlated best, while  $R^2$  for V30 was still 0.74. The V40  $R^2$  for bladder, rectum and bowel were 0.75, 0.78 and 0.64, respectively. For bowel cavity V45,  $R^2$  was rather low. This may be related to the involved relatively small volumes combined with large mobility.

Table 1. Correlations between accumulated dose in bladder, rectum and bowel cavity with planned dose.

$R^2$	
<b>Bladder</b>	
• V20	0.39
• V30	0.76
• V40	0.75
• V45	0.67
<b>Rectum</b>	
• V20	0.45
• V30	0.90
• V40	0.78
• V45	0.67
<b>Bowel</b>	
• V20	0.90
• V30	0.74
• V40	0.64
• V45	0.48

### Conclusion

Especially the planned bladder, rectum and bowel cavity V30 and V40 correlated with accumulated dose.

Reference:

1. A symmetric nonrigid registration method to handle large organ deformations in cervical cancer patients. *Med Phys.* 2010 Jul;37:3760-3772.

### EP-1779 Impact of calculation grid resolution and CT slice thickness on TPS calculated small fields OF

M.D. Falco<sup>1</sup>, M. Fusella<sup>1</sup>, C. Fiandra<sup>1</sup>, S. Clemente<sup>1</sup>, C. Garibaldi<sup>1</sup>, M. Casati<sup>1</sup>, F.R. Giglioli<sup>1</sup>, E. Gallio<sup>1</sup>, T. Malatesta<sup>1</sup>, A. Delana<sup>1</sup>, C. Marino<sup>1</sup>, A. Soriani<sup>1</sup>, S. Linsalata<sup>1</sup>, P. Bagalà<sup>1</sup>, G. Benecchi<sup>1</sup>, R. Consorti<sup>1</sup>, M. Casale<sup>1</sup>, G. Reggiori<sup>1</sup>, E. Villaggi<sup>1</sup>, S. Russo<sup>1</sup>, P. Mancosu<sup>1</sup>  
<sup>1</sup>SBRT Working Group, AIFM - Italian Association of Medical Physics, Piazza della Repubblica- Milan, Italy

### Purpose or Objective

Stereotactic Body Radiation Therapy (SBRT) is increasing thanks to modern technologies and integrated image-guided systems. The main objective of the study was to assess the influence of calculation grid size resolution and CT slice thickness on calculated small fields output factors (OFs) among a large number of centers, equipped with a wide variety of Linacs and Treatment Planning System (TPS).

### Material and Methods

A total of 700 measurements from twenty centers were collected. On three homogeneous phantoms of different slice thickness, i.e. 1,2 and 3 millimetres, small fields OFs were calculated using data commissioned in the TPS. OFs for 1x1 cm<sup>2</sup>, 2x2 cm<sup>2</sup>, 3x3 cm<sup>2</sup> were calculated in the following combination of grid-slice thickness (G-S): G1-S1, G1-S2, G2-S2, G1-S3, G2-S3 and G3-S3, respectively. Four different calculation algorithms were analyzed: AcurosXB (AXB), Analytical Anisotropic Algorithm (AAA), Collapsed Cone Convolution (CCC) and VMC MonteCarlo (MC). The measurement set-ups were: SSD=90,95,100 cm with depth= 10, 5 and 10 cm, respectively. Calculated and measured OFs were compared and the Dev[%]=ABS[(OF<sub>meas</sub>-

OF<sub>calc</sub>)/OF<sub>meas</sub>] was considered. A Multivariate analysis of Variance was performed to test the effect of G, S, field size (FS), calculation algorithm and measurements setup on the uncertainties of OF (Dev [%]) giving the p-values of each variance component. For each factor identified as a significant predictor, a post-hoc test was carried out in order to assess the significance of intragroup differences.

### Results

Results showed that OFs calculated by TPSs were generally larger than OFs measured. Statistical analysis shows that the uncertainties on OFs are not correlated with slice thickness alone, while they increase as the size of the calculation grid increases with a greater dispersion of the data dependent on the algorithm (Fig. 1 panel a) ( $p < 0.01$ ) and as the FS decreases (Fig. 1 panel b) ( $p < 0.001$ ). Also algorithm and measurement setup affect results ( $p < 0.01$ ) with a lower dependence on the setup for systems that have the collapse cone as an algorithm (Fig. 1 panel c). A post-hoc test has confirmed the effect on OF's calculation of field, grid, algorithm and measurement setup ( $p < 0.01$ ).

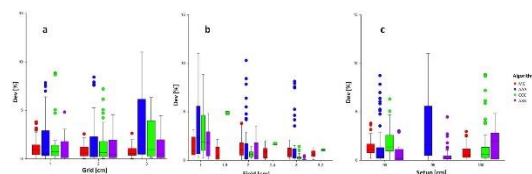


Fig 1. Box-Plot of the absolute difference of calculated and measured OFs in terms of calculation grid (panel a), field size (panel b) and measurement setup (panel c), grouped by algorithm.

### Conclusion

Our results indicate that modern TPS overestimate the calculated small fields OFs compared with measured ones. The overestimation increases with the grid resolution and decreases with the FS. Therefore, we suggest to use, in the SBRT treatment plans, a dimension of the calculation grid as lowest as possible taking account of the hardware capability of TPS and the calculation algorithm.

### EP-1780 Correlation between VMAT plans complexity indices and gamma passing rate by using three QA phantoms

I. Vacchieri<sup>1</sup>, P. Tabarelli De Fatis<sup>2</sup>, M. Liotta<sup>2</sup>  
<sup>1</sup>University of Milan, post graduate Medical Physics School, Milan, Italy ; <sup>2</sup>IRCCS Istituti Clinici Scientifici Maugeri, Medical Physics Unit, Pavia, Italy

### Purpose or Objective

to compare the correlation between VMAT plans complexity indices and local gamma passing rate obtained from three phantoms: ArcCHECK™ -Sun Nuclear Corp. (A), Octavius® 4D-PTW (O) and Delta4-ScandiDos (D<sup>4</sup>).

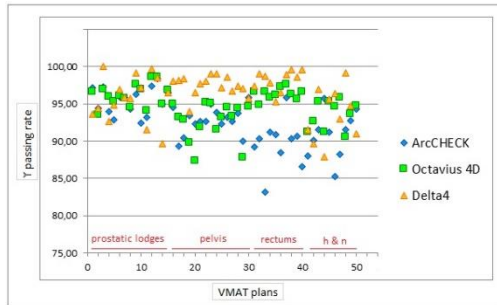
### Material and Methods

50 VMAT clinical plans that include 15 prostate tumor bed, 15 pelvis, 10 rectums and 10 head and neck have been planned with Philips Pinnacle<sup>3</sup> v9.0 for Varian Clinac iX with 120 Millenium MLC. For all plans, pre-treatment verifications have been performed with the three devices and a local gamma analysis (3%-3mm) has been made with a threshold of 10%. RTPlan files were analyzed with a homemade MATLAB (MathWorks®) program to obtain plan complexity indices: Modulation Complexity Score (MCS) and Normalize Leaf Travel LT<sub>i</sub> defined by Masi et al. [1], and Monitor Units (MU). Then, the correlations between gamma passing rate of the three devices and MCS, LT<sub>i</sub> and MU have been investigated by Pearson coefficient. The correlation were considered weak for  $|r| < 0.4$ , moderate for  $0.4 \leq |r| \leq 0.7$  and strong for  $|r| > 0.7$ . Furthermore statistical significance of the difference between the means of the gamma passing rate of the three phantoms

were assessed in pairs by employing a Student's T-test ( $p < 0.05$ ).

### Results

As the complexity of the plan grows the differences between the results obtained by the three instruments increase considerably (Fig. 1).



r Pearson	Device	Loggia	Pelvi	Retto	Testa-collo	Totali
MCS vs $\gamma$ passing rate	ArcCHECK	0,62	0,42	0,56	0,01	0,31
	Octavius 4D	0,90	0,58	0,22	0,17	0,71
	Delta4	0,72	0,20	0,07	0,65	0,51
MU vs $\gamma$ passing rate	ArcCHECK	-0,76	-0,51	0,02	-0,13	-0,08
	Octavius 4D	-0,84	-0,76	-0,21	-0,11	-0,76
	Delta4	-0,51	-0,30	-0,06	-0,73	-0,31
LTi vs $\gamma$ passing rate	ArcCHECK	0,36	-0,02	0,27	0,01	0,13
	Octavius 4D	0,35	-0,29	0,12	0,08	0,39
	Delta4	0,64	-0,60	-0,09	0,54	0,13

For the prostate tumor bed the correlation found with MCS and MU for the three devices were moderate and strong. With LTi the correlation was weak except for D<sup>4</sup>. For pelvis a moderate correlation was found with MCS for A and O while for the MU the correlation was moderate for A and strong for O. In the rectums a moderate correlation was found with MCS for A, the other correlations were weak or absent. For head and neck plans, the only device who found a moderate correlation with MCS and LTi and a strong one with MU was Delta<sup>4</sup>. Considering all 50 plans for A the correlation with MCS, MU and LTi was weak, a strong correlation was found for O with MCS and MU and a moderate one with LTi and finally for D<sup>4</sup> the correlation was moderate with MCS and weak for the other parameters.

A T-test was computed for the pairs: A-O, A-D<sup>4</sup> and O-D<sup>4</sup>. Considering all the 50 plans, we found statistically significance for all the pairs suggesting that the averages of the two distributions compared are different. Performing the test for individual anatomical districts, the results obtained show that for the prostate tumor bed all three devices seem to provide the same information ( $p > 0.05$ ). The same result was achieved in the pelvis for the couple A-O and for the head-neck for couples O-D.

### Conclusion

A strong dependence of the result of the gamma analysis from the instrument used was found. In fact the correlation was found only in few cases bringing out the limitations of the gamma metric, including the volumetric reconstruction algorithms and the differences in the measured dose.

### EP-1781 Ability of Modulation Complexity Score to predict the result of pre-treatment QA for VMAT plans

L. Vacchieri<sup>1</sup>, M. Liotta<sup>2</sup>, A. Malovini<sup>3</sup>, P. Tabarelli De Fatis<sup>2</sup>

<sup>1</sup>University of Milan, post graduate Medical Physics School, Milan, Italy; <sup>2</sup>IRCCS Istituti Clinici Scientifici Maugeri, Medical Physics Unit, Pavia, Italy; <sup>3</sup>IRCCS Istituti Clinici Scientifici Maugeri, Computer Science and Systems Laboratory for Clinical Research, Pavia, Italy

### Purpose or Objective

to evaluate the ability of the Modulation Complexity Score (MCS) to predict the result of the pre-treatment QA in

order to understand whether is necessary to perform the verifications for each VMAT plans or whether these can be replaced by a brief calculation of one or more parameters.

### Material and Methods

168 VMAT clinical plans that include 48 prostate tumor bed, 40 prostate pelvis, 40 rectums and 40 head and neck have been planned with Philips Pinnacle<sup>3</sup> v9.0 for Varian Clinac iX with 120 Millenium MLC. For all plans, pre-treatment verification have been performed with ArcCHECK (Sun Nuclear Corp.) with 2D local gamma analysis (3%-3mm) with a threshold of 10%. RTPlan files were analyzed with a homemade MATLAB (MathWorks®) program to obtain plan complexity indices: MCS and Leaf Travel LTi defined by Masi et al. (2013), and Monitor Units (MU). The correlations between gamma passing rate and MCS, LTi and MU have been investigated by Pearson coefficient. The correlations were considered weak for  $|r| < 0.4$ , moderate for  $0.4 \leq |r| \leq 0.7$  and strong for  $|r| > 0.7$ . Three ranges of values of the passing rate have been established:

- $\gamma < 88\%$  rejection area;
- $88\% \leq \gamma \leq 92\%$  verification area;
- $\gamma > 92\%$  acceptability area;

A machine-learning algorithm known as classification trees was used to identify threshold values for the calculated parameters that could predict at which range the study plane belongs. The discriminative performances were tested with the Leave One Out cross validation procedure. The accuracy of the results was expressed in terms of sensitivity and specificity, choosing to impose the values of 95% and 90% respectively.

### Results

The table shows the Pearson coefficients obtained.

r Pearson	Prostate tumor bed	Pelvis	Rectums	Head-Neck	Total
MCS vs $\gamma$ passing rate	0,69	0,38	0,48	0,41	0,51
Mu vs $\gamma$ passing rate	-0,77	-0,43	0,34	-0,40	-0,29
LTi vs $\gamma$ passing rate	0,50	-0,05	0,27	0,24	0,35

For the prostate tumor bed the correlations found with MCS and LTi were moderate and strong with MU. For the other districts,  $r$  is around 0.4 for MCS while MU appears to be moderately correlated with the exception of the rectum plans. The correlation with LTi was found to be weak or absent. Considering all plans the correlation with MCS is moderate while it appears weak for the other two parameters. The results show that the correlation found between complexity parameters and  $\gamma$  passing rate is strongly dependent on the anatomical district analyzed. For each parameter, it was possible to identify a threshold value. The best results, analyzing the data by categories, were obtained with MCS and MU in the pelvis district in identifying the rejected category: for MCS a threshold of 0.20 identifies the rejected plans with specificity 97% and sensitivity 46%; for MU, the threshold 752 achieves a specificity of 83% and a sensitivity of 46%. Analyzing all the data, the best result is achieved by LTi, whose threshold identifies the plans to be accepted with specificity 97% and sensitivity 50%.

**Conclusion**  
It was not possible to predict the results of the pre-treatment QA through MCS, LTi and MU with statistical reliability, not allowing us to avoid making the verification for each VMAT plans.

### EP-1782 Comparison of two commercial detectors and the influence of grid spacing calculations in SBRT

R. Gómez Pardos<sup>1</sup>, E. Ambroa Rev<sup>1</sup>, D. Navarro Giménez<sup>1</sup>, A. Ramírez Muñoz<sup>1</sup>, J. García-Miguel Quiroga<sup>1</sup>, M. Colomer Truyols<sup>1</sup>

<sup>1</sup>*Consorti Sanitari de Terrassa CST, Radiotherapy, Terrassa, Spain*

**Purpose or Objective**

With the increasing use of Stereotactic Body Radiation Therapy (SBRT) combined with VMAT technique the complexity of treatments has increased significantly. Now the dose distributions are less homogenous than with 3DCRT and the dose gradients are higher. We need to calculate and measure these dose distributions as accurately as possible.

The first objective of this work is to compare the dose distributions measured with two commercial array detectors against the calculated dose in Monaco TPS. The second objective is to evaluate the influence of the grid spacing used in the TPS calculation for the SRS1000 detector. In both we analyze lung and spinal SBRT cases separately.

**Material and Methods**

The SBRT plans were calculated in Monaco 5.10 TPS and did the QA with 1% statistical uncertainty and 2 and 1mm grid spacing. All the plans were delivered with an Elekta Synergy with Agility ML linac. We verified both 29 lung and 6 spinal SBRT cases.

The QA measurements were done with the PTW Octavius4D 1500 (1405 ionization chambers (ICs) of 0.06 cm<sup>3</sup> arranged in a 27x27cm matrix with a detector spacing of 7.1 mm) and PTW Octavius4D 1000SRS (977 liquid-filled ICs of 0.003 cm<sup>3</sup> arranged in a 10x10cm matrix with a detector spacing of 2.5 mm in the center area). We used the 3D gamma index  $\gamma(\%dose,DTA)$  to compare the measured and calculated dose distributions. Due to the special characteristics of SBRT treatments, we used  $\gamma(2\%,2mm)$  and  $\gamma(3\%,1mm)$  for the evaluations in the grid spacing case. In the 1500vs1000 comparison we evaluated just the  $\gamma(2\%,2mm)$ .

**Results**

Results are shown in Table 1. For the statistical comparison in both Lung and Spinal patients we first evaluated if the data was normally distributed. Lung data resulted not normally distributed so we did a Mann-Whitney-Wilcoxon test. Spinal data were normally distributed so we did a paired t test with a 95% confidence interval. For the 1000SRS grid comparison (2 vs 1mm) we found in both lung and spinal patients that the differences in the comparisons were statistically significant. For the 1500 vs 1000SRS gamma comparison, we had the same conclusion although the significance was weak.

TABLE 1

LUNG					
Detector: 1500 vs 1000		Grid spacing (with 1000 SRS): 2mm vs 1mm			
$\gamma(2\%,2mm)$ grid spacing 2mm		$\gamma(2\%,2mm)$		$\gamma(3\%,1mm)$	
	Octavius 1500	Octavius SRS1000	GS - 2mm	GS - 1mm	GS - 1mm
Mean (%)	95.3%	98.4%	98.4%	99.3%	94.9%
SD (%)	0.6%	1.0%	1.6%	0.8%	3.1%
Median (%)	99.0%	99.3%	99.1%	99.7%	95.7%

SPINAL					
Detector: 1500 vs 1000		Grid spacing (with 1000 SRS): 2mm vs 1mm			
$\gamma(2\%,2mm)$ grid spacing 2mm		$\gamma(2\%,2mm)$		$\gamma(3\%,1mm)$	
	Octavius 1500	Octavius SRS1000	GS - 2mm	GS - 1mm	GS - 1mm
Mean (%)	97.6%	94.3%	94.1%	96.1%	88.2%
SD (%)	0.6%	3.0%	3.0%	1.2%	4.5%
Median (%)	97.5%	94.2%	94.2%	96.3%	89.1%

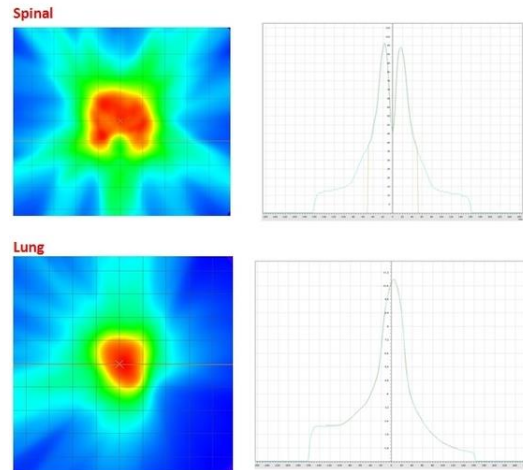
**Conclusion**

Comparing the 1000SRS measurements with 2 and 1mm calculation grids, we can conclude that for spinal cases 1mm grid represents better the dose delivered than 2mm grid. However, in lung cases that does not happen. We think that this happens because both dose distributions are in general very different. While in spinal SBRT we usually have large dose concavities with the corresponding dose fall-off, in lung SBRT we usually have approximately-rounded targets, were we hypothesize that spatial resolution is not that extremely crucial in calculations (Figure 1). In spite of that, both lung and spinal comparisons show statistically different results in both  $\gamma(2\%,2mm)$  and  $\gamma(3\%,1mm)$ .

In the 1500 vs 1000SRS comparison, assuming a grid of

2mm, we cannot assure that one matrix results are superior to the other ones.

Figure 1. Spinal and Lung SBRT examples



**EP-1783 Implementation of a fast method for routine linac-QA for VMAT with EPID dosimetry**

*P. Cambraia Lopes<sup>1</sup>, J. Van Egmond<sup>1</sup>, M. De Goede<sup>1</sup>, J. Van Santvoort<sup>1</sup>*

*<sup>1</sup>Haaglanden Medisch Centrum- Antoniusshove, Medical Physics, Leidschendam, The Netherlands*

**Purpose or Objective**

VMAT plans are rather complex and require continuous and synchronized change of many variables in time. It would therefore be desirable to regularly assess the quality of dynamic delivery, independent of any particular (patient) plan. We have developed a fast and simple method intended to detect suboptimal VMAT delivery by the linac, using EPID dosimetry.

**Material and Methods**

VMAT test plans were developed that contained relatively extreme dose rates (DR, range: -65-500 MU/min), gantry speeds (GS, range: -1-5 deg/sec), and MLC-leaf speeds (LS, up to 3.5 cm/sec), which can be found in clinical practice. The following linac states were constructed for the Pinnacle treatment planning system (TPS), by specifying for each VMAT segment the corresponding MU's and leaf positions: High-DR/High-GS (HH, 1.67 MU/deg), High-DR/Low-GS (HL, 10 MU/deg), and Low-DR/High-GS (LH, 0.22 MU/deg). Plans contained sharp transitions between these states, which also allowed to test for inertia effects (acceleration/deceleration) of the gantry, DR control, and for proper synchronization. Beam 1 contains linac states HH/HL, together with MLC movement, while beam 2 contains linac states HL/LH with static MLC (figure 1). The gantry travel between linac states was varied and kept as a multiple of 2 degrees. These plans were delivered on a cylindrical phantom while EPID frames were recorded. The delivered dose was then reconstructed with the iViewDose software from Elekta and the reconstructed dose was compared in 3D to the TPS dose. In addition, the test plans were benchmarked by independent dose measurements using a dedicated phantom for pretreatment patient-QA (ArcCHECK phantom), and by monitoring the linac parameters DR, GS, and LS, during delivery.

**Results**

It is necessary to explicitly define control points (CP) every 2 degrees, to get sufficiently detailed dose calculations from the TPS. By doing so, the agreement between the benchmark dose measurement and the TPS dose was found to be 78% for beam 1, and 95% for beam 2 (% gamma pass rate with criteria 3%/3mm). The agreement between iViewDose and the TPS was 97% for beam 1 (mean gamma

= 0.47) and 74% for beam 2 (mean gamma = 0.77), while the dose differences at the isocenter were 9.9% for beam 1, and -6.6% for beam 2 (iViewDose compared to TPS). These differences may be at least in part attributable to the presence of very small (=2 degrees) segments with different linac states, which may be challenging for accurate dose reconstruction. Except for some deviations in leaf position and speed for the very small segments at the end of beam 1, the linac accurately delivers the control points.

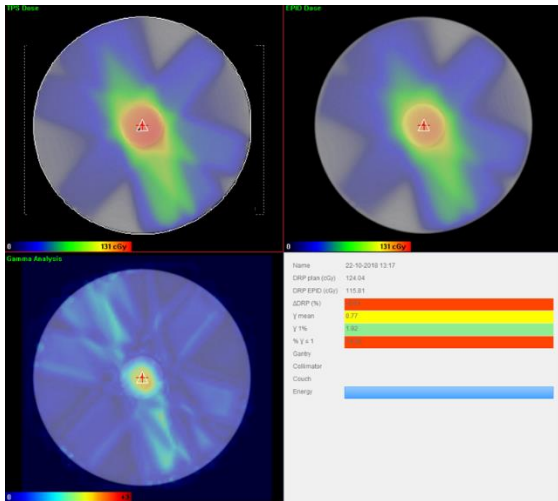
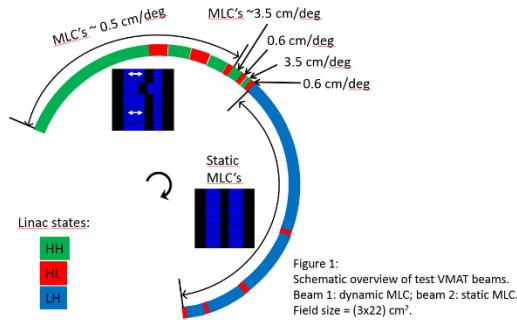


Figure 2: iView result for beam 2.

**Conclusion**

We have described a method to implement simple linac QA for VMAT using EPID dosimetry. The test beams have been successfully constructed and tested with benchmark measurements. The next step will be to determine reproducibility of results based on repeated measurements, in order to establish baseline values and possible action levels.

**EP-1784 ArcCheck HU setting influence on the uncertainty of pre-treatment verification results**  
 M. Giżyńska<sup>1,2</sup>, M. Bukat<sup>1</sup>, D. Szałkowski<sup>1</sup>, A. Walewska<sup>1</sup>  
<sup>1</sup>Maria Skłodowska-Curie Memorial Cancer Center and Institute of Oncology, Medical Physics Department, Warsaw, Poland ; <sup>2</sup>University of Warsaw Faculty of Physics, Department of Biomedical Physics, Warsaw, Poland

**Purpose or Objective**

ArcCheck (SunNuclear) should be characterized in TPS by the HU value that would provide the best agreement of TPS vs measurement entrance to exit dose ratio (ratio test) for 10x10 field size. The purpose of this work was to examine whether the best ratio test results depend on the beam quality and field size. The influence of the HU setting on the results for gamma analysis made for clinical plans was also examined.

**Material and Methods**

Array and dose calibration was performed prior to measurement. ArcCheck was irradiated with 5x5, 10x10, 15x15 and 20x20 field sizes on TrueBeam machine (Varian) with different beam energies used: 6WFF, 15WFF, 6FFF and 10FFF. The ratio test was done for all beam qualities and field sizes. Calculations of TPS dose distribution was done in Eclipse (AAA 13.6.23) with different HU assigned for ArcCheck phantom. Entrance and exit dose for measurement was calculated from six diodes surrounding entrance/exit points. Standard deviation was treated as measurement uncertainty. In the second step of our study we performed analysis for clinical plans. We evaluated 10 IMRT and VMAT plans with different beam geometries: full and half arcs, IMRT with small and large field sizes. Dose calculations were performed for two different HU values - one recommended (246HU) and one achieved in former step of our work (150HU). In order to do the bias-free evaluation artificial measurements were created based on the calculations performed with 150HU and compared with dose distributions calculated for 246 HU. Artificial measurement is a file created with a Python script on the basis of TPS dicom dose distribution which mimics the real measurement file. Comparisons were done with the SNCPatient (SunNuclear, v.6.7.3) software. The 3mm/3%; 2mm/2%; 1mm/1% parameters for global and local gamma evaluation were used. Dose threshold was set to 5%.

**Results**

For 10x10 field size the HU achieved from the ratio test varies between 150HU and 246HU depending on the beam quality (see Figure 1). The ratio test gives also incoherent results for evaluated field sizes: 200-280HU for 6WFF, 160-190HU for 15WFF, 160-230HU for 6FFF, 130-160HU for 10FFF (see Figure 2). The difference in gamma evaluation between 150HU and 246HU dose distributions depended on patient geometry and was mostly observed in exit dose region, though influencing the local gamma evaluation. Percent of passing points varied between 100% and 93% for 3mm/3% local gamma analysis and between 100% and 79% for 2mm/2% local gamma analysis.

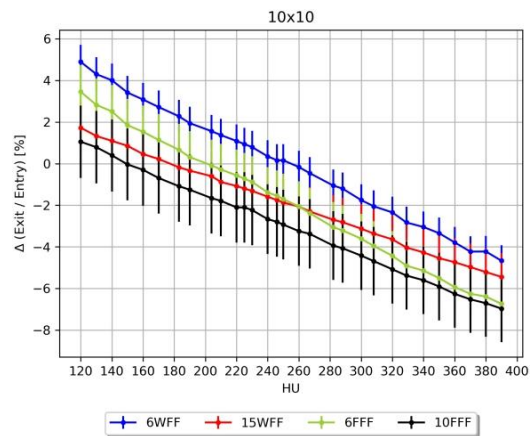


Figure 1. Ratio test result for 10x10 field and different beam qualities.

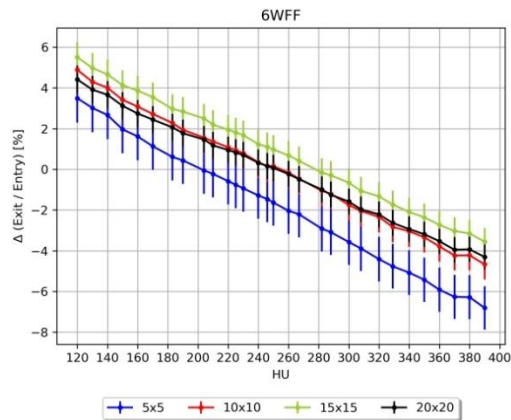


Figure 2. Ratio test result for 6WFF beam and different field size.

### Conclusion

Ratio tests performed for different beam qualities leads to range of HU values (150HU-250HU) which should be used to define ArcCheck phantom in TPS during preparation of pre-treatment verification plan. Choosing single HU value despite of beam quality can cause false negative result of pre-treatment verification if local gamma analysis is used. Special care should be taken while using ArcCheck for pre-treatment verification of multienergetic plans.

### EP-1785 Dosimetric verification of stereotactic treatment plans using 3D-printed phantom and GafchromicEBT3

M. Kruszyna<sup>1,2</sup>, A. Skrobala<sup>1,2</sup>, B. Pawalowski<sup>1</sup>, H. Szweda<sup>1</sup>  
<sup>1</sup>Greater Poland Cancer Centre, Medical Physics Department, Poznan, Poland ; <sup>2</sup>Poznan University of Medical Science, Department of Electroradiology, Poznan, Poland

### Purpose or Objective

The verification of stereotactic plans is usually performed with 2D-array of detectors, in the coronal projection. However, for complex cases, where localization of targets is proximity to organs at risk, there is necessity to use detectors with higher resolution and verification in other projections. The aim of this work was to design and build the 3D-printed phantom for verification with films dosimetry and evaluate the correctness of CyberKnife (CK) stereotactic plans' realization.

### Material and Methods

3D-printed phantom (PLA material) it is open cube (10x10x10cm<sup>3</sup>), filled with water, with the possibility to insert films in two projections: transversal and sagittal. The phantom was used in measurements on CK. The set of 3 to 5 sheets of Gafchromic EBT3 (Ashland) films were simultaneously placed and irradiated in the phantom, the films was placed at the center of target volume (reference position) and at distance of 1 to 2 cm from the reference position. A group of 10 intracranial cases with target's localization close to optical path (5 pts.) and close to brain stem (5 pts.) were evaluated. According to our clinical workflow all plans were verified and passed gamma criteria L2%/2mm, Th5% using the 2D-array SRS1000 (PTW, Freiburg) with mean result of 97,98%, additionally all were measured in 3D-printed phantom. Analysis were done in OmniProl<sup>m</sup>RT software (IBA Dosimetry, v1.6) using gamma evaluation method with criteria: 2%/2mm, 3%/3mm and threshold 5% and 20% of maximum dose, respectively.

### Results

The results for most distributions of planned doses showed high compliance with the obtained measurement data,

however, larger discrepancies were observed in areas of high dose gradients. For center position, score values were (2%/2mm: Th5%, Th20%): 93,73±6,95%, 96,66±5,00%; (3%/3mm: Th5%, Th20%): 98,57±2,04%, 99,14±1,89%, respectively. For others film's position, the results were (2%/2mm: Th5%, Th20%): 87,51±11,92%, 91,88±10,37%; (3%/3mm: Th5%, Th20%): 96,43±5,78%, 95,79±7,83%. The results presented above, confirm the usefulness of such specially design phantoms for more detailed dosimetric verifications.

### Conclusion

The 3D-phantom verification allows compact dosimetry with simultaneous measurements (saving time) in several planes and different than coronal projection. It's especially important for complicated intracranial cases (proximity to OARs) and multi-metastasis cases.

### EP-1786 Towards real-time Monte Carlo dose computation: muscle or brain?

M. Alber<sup>1</sup>, N. Saito<sup>1</sup>, M. Sohn<sup>2</sup>

<sup>1</sup>Heidelberg University Hospital, Department of Radiation Oncology, Heidelberg, Germany ; <sup>2</sup>Scientific RT, GmbH, Munich, Germany

### Purpose or Objective

Real-time Monte Carlo (MC) dose computation will soon be an essential pre-requisite for quality assurance of online-adapted treatment plans. Due to a surge in computation power by parallelization both in GPUs (muscle) and CPUs (brain), this goal is in reach. However, muscle and brain need very specific code optimization for full performance. Realistic benchmarks must be obtained with complete source and collimator models to avoid severe bias in timings. Here, we present how the capacity of CPUs to execute complex code can be harnessed by variance reduction (VR) techniques for high-accuracy MC calculations.

### Material and Methods

The SciMoCa code combines elements of the VMC/XVMC/VMC++ and EGSnrc family of codes with a 4D generic MLC model and a five-element virtual source model. Being optimized for CPU, it employs VR such as history repetition, particle splitting and their counterpart, Russian roulette. Source and collimator models can be much accelerated by VR, however, strong use of VR leads to widely varying particle weights, which slows down dose convergence. Ideally, all elementary energy deposition events (tallies) have the same magnitude. SciMoCa reduces the width of the tally distribution by dynamically adjusting the VR methods on the fly, from the particle source to full absorption. The code is further optimized for memory access, especially by an optimized representation of ICRU-derived cross-section tables.

### Results

In benchmarks against EGSnrc, SciMoCa agrees within statistical uncertainty, with a maximum error of 1.8% recorded for a 6 MeV pencil beam in a lung phantom. A density uncertainty of 1% in this geometry would produce a similar error magnitude. SciMoCa was experimentally validated for Elekta VersaHD, Varian TrueBeam and Accuray Cyberknife accelerators. Typical dose errors in commissioning conditions are in the order of 0.5%. Depending on plan and linac complexity, simulation of the source and collimators accounts for 3-20% of overall computation time, an acceleration by a factor 2-40 by dynamic VR tuning. Timing benchmarks show that SciMoCa is 2.5 times faster than XVMC. More importantly, performance scales almost linearly with logical CPU count (10% performance drop between 4 and 96 cores). This allows clinical dose computations with 1% uncertainty on 2 mm grid size in typically 10-60 seconds on contemporary entry-level server hardware (ca. 24 cores).

### Conclusion

Full source and collimator simulation increases the complexity of MC to an extent that puts GPUs at a

disadvantage, but can be addressed by leveraging the capabilities of CPUs. The advantages of dynamic VR tuning would be offset by thread divergence issues on GPU. The essential metric of code performance is its scaling capability with the number of CPU cores to be ready for the next level of parallelization in hardware. Real-time MC is rapidly becoming reality both with muscle and brain.

### EP-1787 Commissioning of the RayStation treatment planning system in a multi-vendor context

A. Savini<sup>1</sup>, F. Rosica<sup>2</sup>, V. D'Errico<sup>1</sup>, T. Licciardello<sup>1</sup>, E. Menghi<sup>1</sup>, F. Bartolucci<sup>2</sup>, F. Christian<sup>2</sup>, G. Orlandi<sup>2</sup>, A. Sarnelli<sup>1</sup>

<sup>1</sup>Istituto Scientifico Romagnolo per lo Studio e la Cura dei Tumori IRST IRCCS, Medical Physics Unit, Meldola, Italy ; <sup>2</sup>Ausl 4, Medical Physics Unit, Teramo, Italy

#### Purpose or Objective

To present our procedure and results regarding the commissioning of the RayStation treatment planning system (TPS) in a multi-vendor context with several LINACs, beam qualities and multi-leaf collimators (MLCs).

#### Material and Methods

RayStation clinical version 7.0 was considered in this work. The available dose calculation algorithm was the collapsed cone convolution (version 3.3). LINACs, beam qualities, MLCs and radiotherapy techniques considered for implementation are reported in Tab.1. The clinical commissioning included several steps such as the acquisition of basic dosimetric measurements (i.e. percentage depth doses, profiles and output factors), the dosimetry of ad-hoc abutted fields for modeling the MLC, the beam modeling for reproducing experimental measurements and, finally, the validation of the model for each radiotherapy technique. Validation for basic dosimetry was conducted using the  $\gamma$ -confidence limit (CL) between measured and calculated dosimetric curves as addressed in the ESTRO booklet n.7. Validation for intensity modulated techniques was conducted following the AAPM-TG119 protocol. Finally, for each beam quality considered for implementation of intensity-modulated techniques, pre-treatment verifications of ten clinical cases were performed as end-to-end test.

ID	Linac	MLC	Wedge	Couch	Beam quality - Technique
SYN1	Elekta Synergy	MLC1	MW	iBEAM Evo	6MV SMLC, VMAT, 3DCRT 18MV 3DCRT
SYN2	Elekta Synergy	MLC2	MW	iBEAM Evo	6MV SMLC, VMAT, 3DCRT 15MV 3DCRT
TRI	Varian Trilogy	Millenium 120	PW, EDW	IGRT Couch	6MV SMLC, DMLC, VMAT 15MV 3DCRT
TRU	Varian Truebeam	Millenium HD	EDW	IGRT Couch	6MV VMAT, 3DCRT 10MV VMAT, 3DCRT 15MV 3DCRT 6FFF VMAT 10FFF VMAT

Tab.1 List to the LINACs, accessories, beam qualities and radiotherapy techniques considered within this work. MW: motorized wedge; PW: physical wedge; EDW: enhanced dynamic wedge.

#### Results

$\gamma$ -CL evaluation is reported in Fig. 1a. The RayStation beam modeling was able to satisfy the required criteria ( $\gamma$ -CL < 1) for 99.4% of the analyzed dosimetric curves. Out of tolerances results were found for large fields (i.e. 30x30 and 40x40 cm<sup>2</sup>) at large depth (i.e. 20 cm) with little clinical relevance. For TG119 verifications,  $\gamma$ -index pass-rates calculated with TG119 criteria (3%, 3mm, global normalization) are reported in Fig. 1b (only VMAT results are shown). For all cases the pre-treatment verifications gave clinical acceptable results (i.e. pass-rate > 95%). For pre-treatment verifications of VMAT clinical cases,  $\gamma$ -index pass-rates with stricter criteria (3%, 3mm local) were all above 90%.

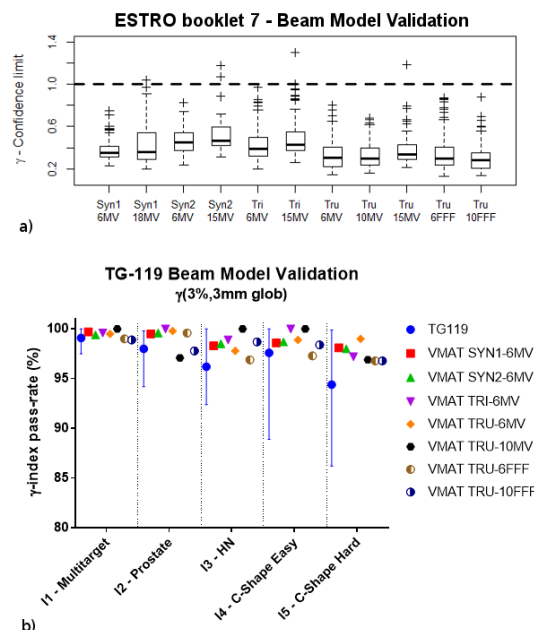


Fig.1

#### Conclusion

The RayStation TPS was modeled for different LINACs, beam qualities, MLCs and irradiation techniques. Following the presented procedure for modeling, we found a final accuracy that was comparable across the considered devices and clinically acceptable for each combination.

### EP-1788 Dose distribution for electron beam using Monte Carlo simulation with GATE

J. Leste<sup>1</sup>, M. Chauvin<sup>1</sup>, T. Younes<sup>1</sup>, L. Vieilleuvre<sup>1</sup>, M. Bardies<sup>1</sup>, X. Franceries<sup>1</sup>, R. Ferrand<sup>1</sup>, N. Pierrat<sup>2</sup>, L. Bartolucci<sup>2</sup>, L. Simon<sup>1</sup>

<sup>1</sup>CRCT, UMR 1037 Inserm, Toulouse, France ; <sup>2</sup>Institut Curie, Dpt. de Radiothérapie, Paris, France

#### Purpose or Objective

Limits of Treatment Planning Systems (TPS) for dose calculation of photon beams have been widely studied. There are fewer studies using Monte Carlo (MC) for electron beams. Although the use of advanced variance reduction technique (Macro Monte Carlo, MMC) to meet time clinical requirements leads to limited results in complex cases (heterogeneity, irregular surfaces). This study aims to assess a commercial algorithm, Fast electron Monte Carlo (eMC, Varian, Palo Alto, CA), based on MMC, and an in-house GATE model of a radiotherapy linac (TrueBeam, Varian) for electrons beams in complex cases. Algorithms are also evaluated for clinical cases (head & neck, breast).

#### Material and Methods

Validation of GATE model is performed with homogenous water phantom. Percentage depth dose curves (PDD) and lateral dose profiles (LDP) are compared with experimental measurement (6, 9, 12 and 18 MeV). For complex cases including heterogeneities (lung, bone) and irregular surface (step), results of dose calculation for eMC and GATE are compared using Gafchromic EBT3 (Ashland ISP, Wayne, NJ) films. LDPs are acquired at two different depths and normalized in a homogenous water region. Global Gamma Index Pass Rate (GIPR) 1D is computed to compare the data sets. For clinical case an absolute dose calibration of our MC model is achieved. Ten clinical cases are tested for several energies and for different inserts

(square, circular and personalized). The results of eMC and GATE dose distribution are compared using the GIPR 3D.

### Results

When comparing GATE and measurements, GIPR<sub>2%/2mm</sub> for PDD and LDP in homogenous water phantom is always superior to 96% for all energies. Field size difference is always inferior to 1%. GIPR<sub>3%/3mm</sub> for most of complex cases (lung, bone and step) is superior to 98.5% for GATE (6, 9, 12 MeV). In all configurations GIPR of eMC are always inferior to GATE except for two cases: 12 MeV at 20 mm for lung (100% and 96.1% for eMC and GATE respectively) and bone (68.9% and 66.2%). First results of clinical cases show discrepancies between GATE and eMC dose distribution calculation (especially in high density regions). GIPR<sub>3%/3mm</sub> ranged from 74.63 % to 77.25% for first tested patients.

### Conclusion

GATE model for electron beams is validated in reference conditions. When comparing to measurements for heterogeneous media and irregular surfaces, eMC was limited while GATE was satisfactory in almost all configurations. First dosimetric results of clinical cases show also relevant discrepancies with eMC. These differences must be confirmed by experimental investigations. The study shows that GATE could be proposed as a 3D dose check solution for complex electron beams. Using our regional meso-computer (>13000 cores) GATE computation takes less than 4 minutes.

### EP-1789 Repetitive use of TLD-100 without annealing for imaging doses in radiotherapy

M. Clausen<sup>1,2</sup>, P. Kuess<sup>1,2</sup>, D. Georg<sup>1,2</sup>, H. Palmans<sup>3,4</sup>

<sup>1</sup>Medical University of Vienna, Department of Radiotherapy, Vienna, Austria ; <sup>2</sup>Medical University of Vienna, Christian Doppler Laboratory for Medical Radiation Physics for Radiation Oncology, Vienna, Austria ; <sup>3</sup>MedAustron GmbH, EBG MedAustron, Wiener Neustadt, Austria ; <sup>4</sup>National Physical Laboratory, National Physical Laboratory, Teddington, United Kingdom

#### Purpose or Objective

Due to their small size and reusability thermoluminescence detectors (TLDs) are very practical and commonly used in various fields of radiation dosimetry. Before reusing the detectors, it is generally recommended to heat them in a TLD oven to achieve a complete reset via thermal annealing. This study investigates the repetitive use of TLDs, type TLD-100 (LiF:Mg,Ti, Thermo-Fischer Scientific), without intermediate annealing to improve the efficiency of measurements for the imaging doses (~ 50 mGy) in radiotherapy. Using the TLDs without the annealing process is time efficient. Moreover, since the consistency in the process of treating TLDs is a very crucial aspect, this can simplify the use and avoid possible errors coming from annealing.

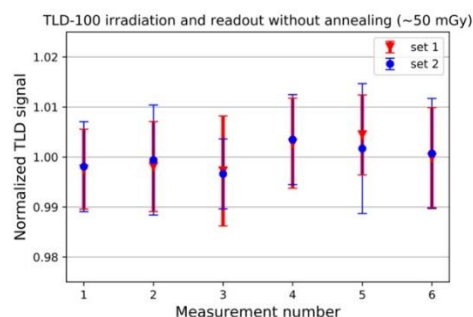
#### Material and Methods

20 TLDs were repetitively irradiated and read in a special-purpose reader (Risø, DTU Nutech, Denmark), with an inbuilt radiation (<sup>90</sup>Sr/<sup>90</sup>Y beta irradiator) source. For readout the temperature was increased at a rate of 5 °C/s up to the final temperature of 400 °C, in 400 steps. For the analysis, a region of interest (20 measurement points) around the dominant peak of the glow curve (5<sup>th</sup> peak, 250 °C) was evaluated. Individual sensitivity factors were applied for each specific TLD. The reproducibility of the dose measurements were studied as a function of irradiation time, and comparisons were made between TLD measurements with or without initial annealing.

#### Results

As a first step, TLDs were readout without irradiation. The TLD responses after the repetitive measurements without intermediate annealing are shown in figure below. Two

different measurement days (sets) are shown. The time between the six repetitions ranged from 1-3 hours. TLD signal was normalized to the mean of a measurement set. Calibration of TLDs was performed in a <sup>60</sup>Co beam. The precision of measurements was improved from 3% to 1.7% by applying the individual TLD sensitivity correction factors. By using the approach of repetitive measurements of the same dose (50 mGy) without annealing, the standard deviation was improved, in average from 1.7% to 1% compared to a readout process with prior annealing. Doses higher than 120 mGy led to an accumulated signal, for which the signal reset by readout was not sufficient. The number of repetitions, alternation of doses and the dose limits for the repetitive measurements need to be further investigated.



### Conclusion

The results indicate that the heating of the TLDs inside the reader for signal readout suffices to reset the TLDs to an acceptable level in the low dose range, which is typical for kV imaging procedures. Utilizing TLDs without annealing for this dose range can be beneficial for the dose assessment of imaging doses during X-rays, CT or microCT imaging, as this increases the workload efficiency and precision of measurements and simplifies the use of TLDs.

### EP-1790 TPS out of field dose accuracy: impact on dose volume histogram calculation of pacemaker devices

A. Delana<sup>1</sup>, A. Barbareschi<sup>2</sup>, F. Maria Daniela<sup>3</sup>

<sup>1</sup>S. Chiara Hospital- Azienda Provinciale Per I Servizi Sanitari-, Department of Medica Physics, Trento, Italy ;

<sup>2</sup>University of Roma Tor Vergata, Scuola di Specializzazione in Fisica Medica, Trento, Italy ;

<sup>3</sup>SS. Annunziata Hospital, Department of Radiation Oncology, Chieti, Italy

#### Purpose or Objective

As always more people carrying an electronic device such as pacemakers (PMK) undergo radiotherapy, an evaluation to the dose received by PMKs has to be made. As stated in AAPM TG 158, Treatment Planning Systems (TPS) show large error in the out of field region where PMK is typically placed, and the magnitude of dose calculation error should be known to ensure the proper categorization and clinical patients management. Aim of this multicenter study is to evaluate the behavior of three TPSs in the out of field dose region, comparing the dose volume histogram (DVH) of PMK placed in in-house built phantoms.

#### Material and Methods

Two phantoms were created with a PMK embedded in a PMMA slab with 2 cm or 1 cm of PTW Real Water 3 (RW3) over and 10 cm of RW3 under, to account for PMK depth inside the body and to ensure backscatter. CT datasets were acquired, PMK structure delineated, density corrections for the CT artifact performed; the CT datasets were then sent to the centers. TPSs considered are: Elekta-Monaco v.5.11 (C1), Philips-Pinnacle3 v.8 (C2) and Elekta-Oncontra Masterplan (C3). Linac commissioned is an Elekta Sinergy Agility; dose calculation algorithms are

XVMC for C1, collapsed cone convolution for the others. Each TPS calculated the dose for two plans (both with 6MV beams at DFA 95cm): a 10x10cm<sup>2</sup> beam and a dynamic multileaf collimator plan DMLC 10x10cm<sup>2</sup> field as a series of 10 rectangular strips in the lateral direction of 10 cm x 1 cm each. Each plan delivered 2Gy in one fraction, with a grid resolution of 2mm. TPSs calculated DVH for the PMK structure when its proximal edge was 1 cm to 10 cm to the field edge. Results are expressed as cGy/Gy. TPSs comparison is performed on the PMK maximum dose (D1cc) and mean dose (Dmean). An analysis is performed on the difference between these doses and the maximum discrepancies were evaluated.

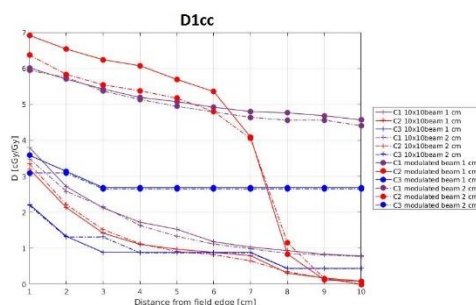


Figure 1: D1cc to the PMK as calculated by the TPSs at 1 cm and 2 cm depth for the two plans considered.

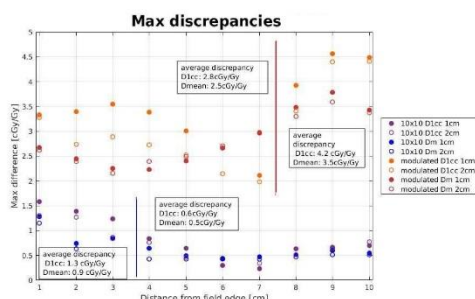


Figure 2: Highest discrepancies between TPSs calculation.

## Results

Out of field doses calculated at 1 cm and 2 cm depth are slightly the same for all TPSs: dose differences are less than 1 cGy/Gy for D1cc and Dmean, for both plans (see fig1). Discrepancies between D1cc and Dmean calculated from TPSs were higher for the DMLC plan than the 10x10cm<sup>2</sup> field as shown in fig2. For the square beam and DMLC plan, we identified two different regions of behavior calculations, as shown in fig2: for the square beam differences in D1cc and Dmean are higher close to the beam edge (distances  $\leq 3$  cm), whereas for the DMLC plan the discrepancies are greater at distances  $\geq 7$  cm from the beam edge. in the TPS

## Conclusion

While with the square beam all TPSs are in good accordance in the out of field dose calculation (maximum difference 1.6 cGy/Gy), in the DMLC plan the difference between TPSs is higher (up to 4.5 cGy/Gy). TPSs show different behavior in out of field dose for the square beam with respect to the DMLC plan, probably related to collimator scatter and head leakage modeling. All centers are currently working on measurements of such doses to better understand and evaluate TPS's reliability in estimating dose to a PMK.

## EP-1791 Correcting dose distributions to the magnetic field of a high-field MR-Linac using deep learning

R. Rozendaal<sup>1</sup>, W. Van den Wollenberg<sup>1</sup>, S. Van Kranen<sup>1</sup>, J. Sonke

<sup>1</sup>Netherlands Cancer Institute, Department of Radiotherapy Physics, Amsterdam, The Netherlands

## Purpose or Objective

The Elekta Unity MR-Linac integrates a high-field MR with a state of the art Linac. In order to exploit the potential of this device, the effect of the magnetic field must be taken into account when calculating dose. This is typically done using a Monte Carlo (MC) method, which is accurate but also computationally expensive. The associated computation time adds to the daily treatment time slots. The purpose of this study was to evaluate the potential of a convolutional neural network (CNN) to account for the presence of a magnetic field.

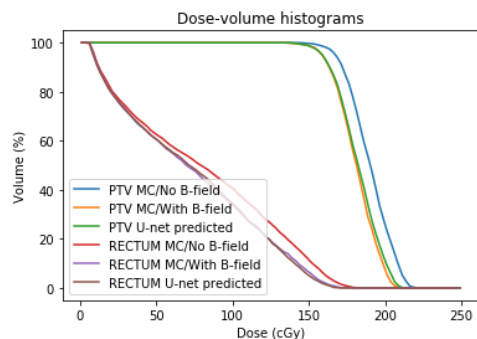
## Material and Methods

The CNN architecture chosen was a 3D U-net [1] like with 3-fold downsampling. Input data consisted of beam specific 3D dose distributions calculated using Unity treatment planning system (Monaco, Elekta AB, Stockholm) with the magnetic field effects switched off, desired output data were the same dose distributions with the magnetic field on. In total 7 patients, each with one treatment plan, were included; training and validation was done using leave-one-out cross validation. Training samples consisted of a full 3D dose distribution composed of 9 beams and were generated on the fly. Each plan had 27 treatment beams available: 9 beams at the (fixed) gantry angles used for plan optimization, and then each beam offset by +/- 10 degrees. By not using the anatomy of the patient as an input to the network, 18<sup>9</sup> possible dose distributions available for training: 6 (patients) \* 3 (beams per gantry angle) for 9 gantry angles. The loss function was a weighted mean squared error, with higher weights for higher doses. The network was implemented using python/keras; training was done on a NVIDIA GTX-1080 GPU. After training, the predicted dose distribution for validation was evaluated by inspecting parameters of the dose-volume histogram (DVH): D2 (near-maximum dose), D50 (median dose) and D98 (near-minimum dose) for the planned target volume (PTV); mean dose for two organs-at-risk (OARs), the rectum and the anal sphincter. Values were calculated for the baseline-situation (no magnetic field corrections) and the CNN-predicted dose distribution, both versus ground truth, MC with magnetic field on.

## Results

Training converged typically after ~2000 iterations, taking ~900s. A single prediction of the magnetic-field corrected dose took 1.64 ± 0.04 s. Table 1 shows average results, Figure 1 shows typical dose-volume histogram (DVH) curves. Average correspondence in the PTV is within 1%, correspondence in the OARs is at -3% and -2%. In general, the effect of the magnetic field is better modelled for higher dose regions.

Region	Parameter	Dose	Mean	S.D.
PTV	D2	MC, no magnetic field	+4.8%	±1.2%
PTV	D2	CNN prediction	+0.8%	±1.1%
PTV	D50	MC, no magnetic field	+4.5%	±2.0%
PTV	D50	CNN prediction	+0.7%	±2.3%
PTV	D98	MC, no magnetic field	+4.1%	±3.6%
PTV	D98	CNN prediction	-0.5%	±3.3%
Rectum	Dmean	MC, no magnetic field	+6.1%	±7.5%
Rectum	Dmean	CNN prediction	-1.7%	±8.1%
Anal Sphincter	Dmean	MC, no magnetic field	+7.1%	±9.0%
Anal Sphincter	Dmean	CNN prediction	-3.0%	±9.9%



## Conclusion

Even with a limited number of patients, a CNN can be quickly trained to accurately determine the magnetic field corrections on the dose distributions for the target volume of IMRT prostate treatments. In the lower dose regions, additional effort is still required. The ease and speed of training indicates that training patient-specific CNNs before treatment starts is also an option.

## EP-1792 Straightforward and easy way to determine MLC parameters (DLG, T) for FFF beams in Eclipse TPS

A. Walewska<sup>1</sup>, M. Giżyńska<sup>1,2</sup>, M. Fillmann<sup>1</sup>, P. Janiak<sup>1</sup>, M. Gruda<sup>1</sup>

<sup>1</sup>Maria Skłodowska-Curie Memorial Cancer Center and Institute of Oncology, Medical Physics Department, Warsaw, Poland ; <sup>2</sup>University of Warsaw Faculty of Physics, Department of Biomedical Physics, Warsaw, Poland

## Purpose or Objective

In order to perform dose calculations for dynamic techniques in Eclipse TPS (Varian) user has to set MLC parameters: Dosimetric Leaf Gap (DLG) and MLC Transmission (T). The values of DLG and T are usually obtained in trial and error process minimizing the difference between measurements and calculations in TPS [1]. Alternatively we propose to use gradient optimization method.

## Material and Methods

Chair shape plans were prepared for 6FFF and 10FFF beams for two SSD/depth setups (90/10cm and 95/5cm). Dynamic MLC pattern calculated on the basis of optimal fluence was saved. Measurements, corrected for beam stability, were done in water phantom with Semiflex Chamber (PTW 31010) on two TrueBeam machines. The chair shape dose distribution was divided into 9 regions (Fig. 1). The cost function  $F$  was defined as  $F = \sum_i w_i (D_c - D_m)^2$ , with  $i$  number of evaluated points,  $w$  - point priority,  $D_m$  - measured dose,  $D_c = D_c(DLG, T)$  - calculated dose being a function of DLG and T. Starting values for optimization were taken from sweeping gap measurements recommended by Varian to determine DLG and T values.  $F$  was calculated for 9 points surrounding starting value and  $gradF$  was calculated in both directions leading to a next iteration direction and step. Procedure was repeated until the global minimum was found. Priorities  $w$  were chosen arbitrarily (Fig. 1). Regions B, C and H in which the T has the higher role were given priority 3. Region A with higher DLG influence was given priority 9. Regions D, E and F for which both DLG and T have impact were given priority 2. Regions G and I with weak T impact get priority 1. Priorities used at both setups were the same. For each recalculation of dose distribution in TPS the same MLC pattern was used. Verification of optimized value of DLG and T was performed by comparing measured and calculated dose for sweeping gap performed with dynamic MLC (width: 0.2-20.0 mm). Pretreatment verifications for ten clinical IMRT/VMAT plans were performed as well. We used Octavius device with PTW729, EPID and measurement

done with ionization chamber in water and solid phantom.

6FFF			10FFF		
A	B	C	A	B	C
Priority: 9	Priority: 3	Priority: 3	Priority: 9	Priority: 3	Priority: 3
90cm: -0.2%	90cm: 0.9%	90cm: -2.3%	90cm: -0.2%	90cm: 1.6%	90cm: -2.3%
95cm: 0.1%	95cm: 2.6%	95cm: 0.4%	95cm: 0.2%	95cm: 2.9%	95cm: -0.6%
D	E	F	D	E	F
Priority: 2					
90cm: 0.0%	90cm: -0.1%	90cm: -0.2%	90cm: -0.4%	90cm: -0.4%	90cm: 0.0%
95cm: 0.1%	95cm: -0.3%	95cm: -0.2%	95cm: -0.1%	95cm: -0.2%	95cm: 0.3%
G	H	I	G	H	I
Priority: 1	Priority: 3	Priority: 1	Priority: 1	Priority: 3	Priority: 1
90cm: 0.5%	90cm: 0.3%	90cm: 0.8%	90cm: 0.2%	90cm: 1.4%	90cm: 1.0%
95cm: 0.5%	95cm: -0.8%	95cm: 0.9%	95cm: 0.5%	95cm: 1.4%	95cm: 1.4%

Figure 1. Chair shape test divided into regions. Agreement between measurements and TPS calculations for 6FFF (left) and 10FFF (right) for two setups and optimal DLG and T are shown. Comparisons were done for points located in the center of each region.

## Results

The shape of quadratic cost function used in optimization procedure can be seen in Fig 2. The optimal values of DLG and T were: 0.75mm and 1.35% for 6FFF, 0.90mm and 1.60% for 10FFF beam. For chair pattern the greatest difference between measurement and TPS are obtained for regions strongly influenced by T (up to 2.6% for 6FFF, 2.9% for 10FFF). Dose difference between measurement and TPS for sweeping gap fields was not greater than 0.3%. Results of pretreatment verification for all clinical plans passed our institution QA criteria.

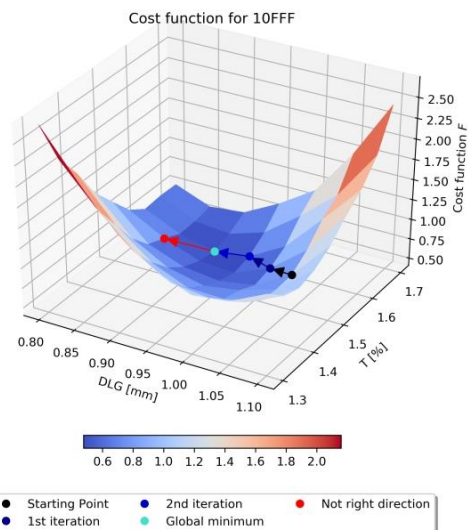


Figure 2. Shape of cost function. Starting point and points achieved in 3 following iterations are shown. Arrows indicate steps of iteration. The red dot is showing the next iteration step which would lead to a greater cost function and therefore was neglected.

## Conclusion

Proposed method of DLG and T determination is straightforward, easy, low time consuming and leads to a very good agreement between calculations and measurements confirmed in independent verification. The same methodology can be used for WFF beams.

[1] Van Esch et al., Radiotherapy and Oncology 65 (2002), 53-70

## EP-1793 Verification and Measurement of the Tongue and Groove Effect in an Electronic Portal Imaging Device

J. Saez Beltran<sup>1</sup>, L. Alba<sup>2</sup>, B. Clara<sup>2</sup>, L. Vieilleveigne<sup>3</sup>, C. Khamphan<sup>4</sup>, V. Hernandez<sup>5</sup>  
<sup>1</sup>Hospital Clinic i Provincial, Radiation Oncology Department, Barcelona, Spain ; <sup>2</sup>Hospital Clinic de Barcelona, Radiation Oncology Department, Barcelona, Spain ; <sup>3</sup>Institut Claudius Regaud - Institut Universitaire du Cancer de Toulouse, Department of Medical Physics-, Toulouse, France; <sup>4</sup>Institut Sainte Catherine, Medical

Physics Unit, Avignon, France ; <sup>5</sup>Hospital Sant Joan de Reus, Medical Physics Department, Reus, Spain

### Purpose or Objective

Varian's Portal Dosimetry prediction algorithm was recently updated to improve the re-sampling of the fluence in the portal dose calculation algorithm (PDC). From version 13.5, the fluence resolution used in PDC inherits the dose calculation resolution used in AAA. Recently, the asynchronous sweeping gap (aSG) tests were introduced [1] to test the Tongue and Groove (TG) effect in the TPS with dynamic beams. The goal of this study is twofold: On one hand to perform a measurement of the TG effect with the EPID and on the other hand to study how the resolution used in AAA affects the agreement of the PDC with measurement.

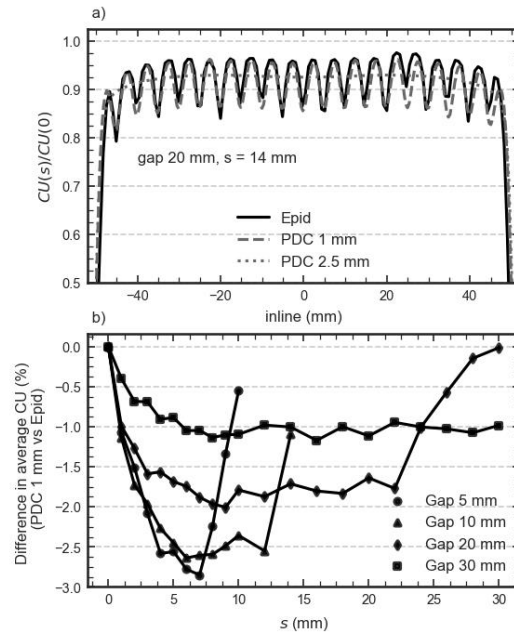
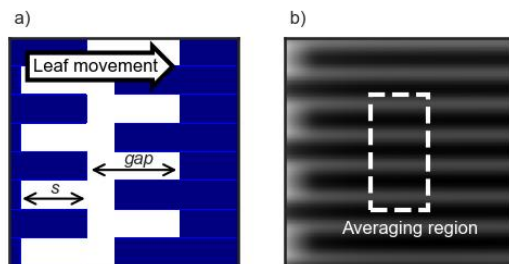
### Material and Methods

The aSG tests consist in different sweeping gaps where adjacent leaves are shifted a given amount  $s$  (see Figure 1a). When  $s=0$ , the standard sweeping gap test is recovered. We tested version 13.6 of the algorithms (PDC & AAA) with a Millennium MLC. First, we calculated the aSG tests in a water phantom in isocentric conditions for two resolutions: 2.5 and 1 mm. From the AAA calculation, verification plans were generated with the PDC algorithm (Fig1b shows the predicted planar dose for a 20 mm gap and  $s=14$  mm). The predicted planar dose distributions were exported and analyzed externally with an in-house software in MatLab that parsed the information contained in the \*.dxf files and calculated an average central value (see Fig1b) for each gap and leaf side  $s$ . In order to isolate the TG effect, for each gap, the ratio of dose for a given  $s$  to  $s=0$  was obtained. This ratio also allows to compare AAA with PDC despite the different dose units (Gy and CU).

Finally, the tests were irradiated on an aS500 EPID. The measured planar distributions were also exported for analysis and to obtain average values to compare with the PDC prediction.

### Results

The largest difference due to TG between PDC and AAA was  $<0.5\%$  regardless of the gap and dose resolution used. The predicted portal dose distributions with the 1 mm resolution exhibited excellent spatial agreement with the EPID measurements as shown in Fig2a. However, the average values obtained with the PDC algorithm overestimated the dose reduction due to the TG effect (see Fig2b). In particular, for the 1 mm-generated PDC the largest relative difference is  $-2.6\%$ , while for the 2.5 mm-generated PDC the largest difference is  $-1.6\%$  in both cases for the 10 mm gap and  $s=6$  mm. The overestimation of the average TG effect is particularly significant within the first 10 mm of  $s$  regardless of the gap and uncovers the fine details of the leaf tip model.



### Conclusion

The TG model of the MLC as used in AAA was adequately transferred to the fluence used in the PDC algorithm regardless of the resolution used. The response of the EPID captures the TG effect that causes a dose reduction for increasing sin the aSG tests. The agreement between PDC and EPID is excellent for a 1 mm dose resolution. PDC would thus benefit from always using a 1 mm fluence resolution regardless of the resolution used in AAA. [1] Phys Med Biol 62;2017:6688-6707

### EP-1794 Bias-free comparison of PTW arrays in terms of ability to detect clinically significant MLC errors

A. Walewska<sup>1</sup>, M. Giżyńska<sup>1,2</sup>, A. Paciorkiewicz<sup>1</sup>, D. Blatkiewicz<sup>1</sup>

<sup>1</sup>Maria Skłodowska-Curie Memorial Cancer Center and Institute of Oncology, Medical Physics Department, Warsaw, Poland ; <sup>2</sup>University of Warsaw Faculty of Physics, Department of Biomedical Physics, Warsaw, Poland

### Purpose or Objective

There are several types of pre-treatment verification QA devices with different types of detectors, resolution and design. Woon et al. (2018) and Saito et al. (2018) used the method of introducing known errors into the RT plans in order to analyze the sensitivity of various gamma index passing rates using different types of detectors with different resolution. To the best of our knowledge there is no work comparing three types of PTW arrays (Octavius: 729, 1500, 1000SRS). The aim of our study was to test ability of these arrays to detect clinically significant MLC errors.

### Material and Methods

We used 40 clinical plans (10 plans for each: brain, prostate, head & neck, gynecology) in the analysis. MLC errors: gap width (both banks moved in opposite direction) and shift error (both banks moved in the same direction) were introduced for all plans. Magnitudes of errors were 0.5 - 3.0 mm. Dose distributions were recalculated in patients' CT and Octavius 4D phantom (diameter 32cm) was used to create verification plans for all analyzed plans. Dose distributions were calculated in Eclipse (13.6.23 AAA, Varian). In order to get the bias-free comparison Python script was used to change the TPS dose distribution into the artificial measurement file mimicking the real measurement. So created artificial measurements

created are not biased by measurement uncertainty and have the same resolution as real measurements. Artificial measurement files were compared to the clinical (original) verification plan using gamma analysis (Verisoft v.6.1) with criteria: 1%/1mm, 2%/2mm, 3%/3mm both for local and max gamma. Dose threshold was set to 5%. DVHs for plans with introduced errors were also analyzed in order to find: 2% change in PTV mean dose, PTV D98%<95% and PTV D2%>107% (considered as clinically relevant).

### Results

Wilcoxon signed rank test was used to perform statistical comparison between array, p-value less than 0.005 was considered as significant. Significant difference between 729 and 1500 array was observed for most of the error types for 3%/3mm and 2%/2mm gamma analysis. It might be explained by impact of interpolated points included in evaluation. There is no significant differences between 1000SRS and 729 array for most of plans with shift error. However significant difference is noticed for gap width error showing greater capability for 1000SRS to detect plan with error (Fig. 1). The MLC errors without clinically relevant effect are marked in the Figure.

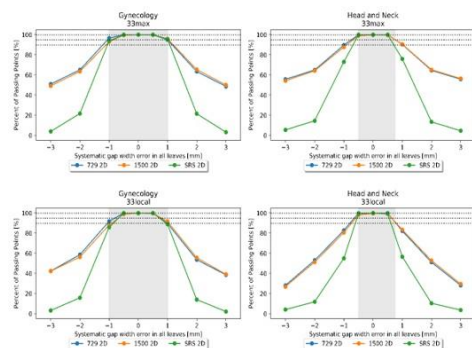


Figure 1. Example of gamma analysis results for gap width error for gynecology and head&neck plans.

### Conclusion

Analysis results for array 1500 and 1000SRS with Verisoft 6.1 may lead to false negative result (plan rejection with correct linac performance) due to including into gamma analysis not only measurement points but interpolated also. Higher detector resolution matters for gap width error but has no effect in case of systematic shift in MLC. The 1000SRS array, although dedicated to verification SRS plans, can also be used for larger PTV plans with high dose gradient even if it does not cover all irradiation area.

### EP-1795 HyperArc™ commissioning necessitates high-resolution measurements

M. Sjölin<sup>1</sup>, J.M. Edmund<sup>1</sup>

<sup>1</sup>University Hospital Herlev, Oncology, Herlev, Denmark

### Purpose or Objective

An integrated solution for linac-based stereotactic radiosurgery (SRS) has recently been introduced by Varian Medical Systems with an automated multiple non-coplanar arc beam arrangement. This technique calculates a high dosimetric target conformity with a rapid dose fall-off to critical organs and therefore requires careful dosimetric evaluation. The purpose of this study was to experimentally establish the accuracy of the dose modeling performed in the Eclipse treatment planning system (TPS) of this small target dosimetry technique manifested by high resolution measurements.

### Material and Methods

A set of 10 HyperArc™ treatment plans with single and multiple metastasis were optimized in Eclipse (v. 15.6) with the millennium MLC and 6 MV flattening filter free (FFF) beamlets. The planning target volume (PTV) measured as the effective equivalent sphere diameter,

ranged between 0.2 and 2.7 cm. The Acuros dose calculation algorithm was used after optimization with a dose grid resolution of 1.25 mm. Patient-specific measurements were carried out in the CIRS film QA phantom with GafChromic EBT3 film (Ashland Specialty Ingredients) located centrally in the frontal slice of the GTV and used for evaluation. The film calibration was cross-validated with ionization chamber (measurements) according to the IAEA TRS-398 protocol prior to measurements.

Fine-tuning of the calculation model was performed by varying the dosimetric leaf separation (dls) in the algorithm to best fit the measured dose distribution by visually inspection of the dose gradient together with gamma evaluation. A gamma criterion of 5%/1mm and 2%/2mm local normalization was used.

### Results

The mean fraction of  $\gamma_{5\%,1\text{mm}} \leq 1$  and of  $\gamma_{2\%,2\text{mm}} \leq 1$  was 94.5 % and 93.8 %, respectively, for all measurements after modifying the dls in the beam model. An adjustment of +0.5 mm was carried out on the dls parameter compared to the measured value at the machine, which corresponds to an increase in the effective MLC field size. Before dls adjustment, the measured maximum dose deviated around 8% as compared to the planned dose.

For the case with smallest target size (0.2 cm), an overestimation of about 4% in the maximum calculated dose as compared to measurements was observed. A tolerance of 5 mm in minimum equivalent sphere diameter of the PTV has therefore been introduced for treatment of SRS with the millennium MLC.

### Conclusion

For accurate modeling of the beam penumbra, which may have influence on the critical organ dosimetry, adjustments are warranted on the MLC modeling in the calculation model. High spatial resolution measurements therefore play an essential part in a safe delivery of HyperArc™.

### EP-1796 Comparison of Treatment Planning Systems' shallow depth dose prediction for IMRT

E. Bogaert<sup>1</sup>, G. Pittomvils<sup>1</sup>, C. De Wagter<sup>1</sup>

<sup>1</sup>Ghent University Hospital, Radiotherapy and Oncology, Gent, Belgium

### Purpose or Objective

Validation of a Treatment Planning System (TPS) for IMRT is well described e.g. NCS 22 report [1], but challenging. Dose contribution from outside IMRT segments' edges needs to be predicted correctly. QA patterns like Inverse Pyramids [2] are recommended at reference depths of 10 and 5 cm. However, at shallow depths primary scattered electron contamination causes head scatter conditions to differ. During photon beam modelling in RayStation v6.1 a rather high electron contribution was found to be necessary for modelling large open fields' depth dose curves. Our goal was to validate the need of this higher electron contribution by assessing the effects at shallow depths and by comparing RayStation planned doses to those retrieved from the two other TPS in use at our department.

### Material and Methods

For a Varian Clinac-IX (Millennium MLC; 6 and 18 MV), beam models were available in RayStation v6.1 (RaySearch Laboratories) and Eclipse v8.1 (Varian), whereas for Elekta Synergy (MLCi2; 6 and 15MV) models were available in RayStation v6.1 and Pinnacle v9.8 (Elekta). Predicted line dose profiles were evaluated against those measured in a polystyrene slab phantom with a PTW linear array LA48. Calculation grids were 2x2x2mm<sup>3</sup> for Synergy and 2.5x2.5x2.5mm<sup>3</sup> for Clinac-IX. The effective point of measurement (0.75mm below surface) was taken into account in all profiles. A local criterion of 3%/3mm (max dose) was used. For high energies and 1 cm depths, the effect of 0.5 mm shift in depth on the position for

extracting the line dose was evaluated. Cross calibration on reference field (10x10 cm<sup>2</sup>) and depth (10 cm) was applied on LA48-measured dose values.

#### Results

Figures 1 and 2 show Inverse Pyramid profiles for Elekta and Varian linac respectively. TPS beam modelling for head scatter conditions and MLC and jaw transmission are well within the criterion for all energies at depth of 3 cm. The modelling in Eclipse and Pinnacle show larger differences with measurements both at primary field dose region and scattered only regions for high energy and 1 cm depth. Beam modelling in RayStation shows agreement with the measurements within 3%/3mm for all regions, taken the spread-out of 0.5mm shift into account, whereas for the models in Eclipse and Pinnacle a 5%/5mm is met.

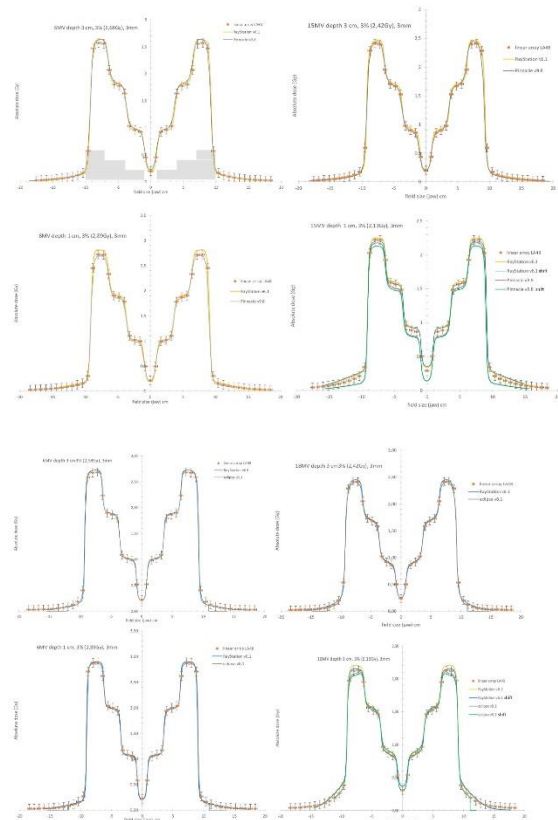


Figure 1 and 2. Inverse pyramid line dose profiles at 3- and 1-cm depths.

#### Conclusion

The higher electron contamination contribution in RayStation v6.1 modelling did not cause overdosage at shallow depths. Even for high energy and depths as low as 1 cm, the criterion of 3%/3mm was met. Extension of a QA protocol for IMRT beam model validation with dose calculation tests outside the fields at shallow depths is relevant.

[1] Code of Practice for the Quality Assurance and Control for Intensity Modulated Radiotherapy -Report 22 of the Netherlands Commission on Radiation Dosimetry - June 2013

[2] Srivastava RP, De Wagter C. The effects of incidence angle on film dosimetry and their consequences in IMRT dose verification. Med Phys. 2012;39:6129-38

#### EP-1797 Skin dose in HDR brachytherapy for breast cancers: our in vivo dosimetry protocol and data analysis

S. Fabiani<sup>1</sup>, M. Casale<sup>1</sup>, M. Italiani<sup>1</sup>, M. Muti<sup>1</sup>, E. Maranzano<sup>2</sup>

<sup>1</sup>"S.Maria" Hospital, Department of Radiation Oncology - Medical Physics Unit, Terni, Italy ; <sup>2</sup>"S.Maria" Hospital, Department of Radiation Oncology, Terni, Italy

#### Purpose or Objective

The aim of this work is to evaluate the skin dose in partial breast high dose rate brachytherapy (PB-BRT), developing a novel protocol for *in-vivo* dosimetry (IVD) and using two different dosimeter types.

#### Material and Methods

Currently there is not a general acknowledged constraint for skin dose in PB-BRT. Because of our center's experience (20 PB-BRT patients treated/year) we achieve a good cosmetic outcome if the TPS calculated skin dose is below 55% of the prescription of 32 Gy (4 Gy/fraction, twice daily). The skin dose, calculated by a TPS, is overestimated, assuming a homogeneous water medium and not accounting for the finite patient dimensions. IVD was performed on patients treated with multi-catheter brachytherapy, which involves the placement of 9-15 catheters through the breast. Both thermoluminescent dosimeters (TLDs) and MOSFET detectors were used in the IVD sessions and placed in five specific points on the skin: one close the nipple, two next to the entrance of the catheters (upper breast area) and two next to the exit (lower breast area). After a preliminary study using TLDs (IVD-TLD sessions), we performed MOSFET real time measurements to compare with TLD results and to further improve the estimation of the skin dose. We are currently implementing optical fiber real time measurements to test a new system based on the use of luminescent materials.

#### Results

The doses measured by both dosimeters were compared to those calculated by the TPS in the specific regions of interest. For a first group of three patients two IVD-TLD sessions were performed for each of them. A Gaussian fit of the percentage differences between measured and calculated doses yielded a mean overestimation value of 25% by the TPS. For a second group of seventeen patients IVD sessions were performed using MOSFET dosimeters, which were placed on the skin following the previous arrangement of TLDs. For each patient five IVD sessions were performed. Results showed a mean overestimation value of 28% by the TPS. The more accurate doses measured by MOSFETs indicated a different value when the dosimeter was placed on the upper or the lower breast area: the latter showed a smaller overestimation of the skin dose by the TPS.

#### Conclusion

We performed IVD on twenty patients, using two different dosimetry systems. We obtained a clear overestimation of skin dose by the TPS using both systems, because the TPS does not take into account the tissue-air interface. The different distribution obtained for MOSFETs placed on the lower breast area, is due to a possible reduction of the tissue-air interface. Preliminary measurements demonstrated the requirement to implement real time dosimeters in the *in vivo* sessions instead of using TLDs. Quantifying skin dose accurately does contribute to define a reliable constraint in PB-BRT, to achieve not only the tumor control but also a good cosmetic outcome to improve the quality of patient's life.

#### EP-1798 Calibration of the new RefleXion biology-guided radiotherapy unit in the context of the TRS-483 CoP

L. Mirzakhani<sup>1</sup>, R. Bassalow<sup>2</sup>, D. Zaks<sup>2</sup>, C. Huntzinger<sup>2</sup>, J. Seuntjens<sup>1</sup>

<sup>1</sup>McGill University, Medical Physics, Montreal, Canada ;

<sup>2</sup>Reflexion Medical, 25841 Industrial Blvd- Suite 275, Hayward- CA, USA

### Purpose or Objective

The design of the new Reflexion biology-guided radiotherapy (BgRT) system restricts the maximum field size to 2 cm in the International Electrotechnical Commission (IEC) Y dimension at the source-to-axis distance (SAD) of 85 cm. The closest field size to the conventional reference field in this machine is 2×10 cm<sup>2</sup> at the isocenter. The energy of the beam is 6 MV and the beam is flattening filter free (FFF). The 2×10 cm<sup>2</sup> field size does not meet the lateral charged particle equilibrium condition of the machine-specific reference (*msr*) field introduced in the IAEA TRS-483 Code of Practice (CoP). Therefore the IAEA TRS-483 CoP cannot be directly used for the calibration of this machine. In this study, two methods of calibration are proposed for the reference dosimetry of the BgRT Unit. The BgRT Unit is calibrated using the two methodologies and the results are compared.

### Material and Methods

The percent depth dose (PDD) and profile were measured in the BgRT unit using the Exradin A14SL chamber for the 2×10 cm<sup>2</sup> field size at SSD 85 cm. The BgRT system was modeled using the EGSnrc/BEAMnrc Monte Carlo (MC) code and the PDD and profile were calculated using EGSnrc/DOSXYZnrc. The beam model was tuned to achieve good agreement with the 2×10 cm<sup>2</sup> PDD and profile measurements. Two methods of calibration are suggested in this study. In the first method, the generic correction factors ( $k_{Q,F}, k_{Q,0}^{f,F}, f_{ref}$ ) are calculated directly using MC for Exradin A14SL. In this study the "F" Field refers to both *msr* and *non-msr* fields. In the second method, the IAEA TRS-483 protocol is extended to fields as small as 2 cm. The beam quality specifier and equivalent square field (S) are calculated and used to determine the beam quality correction factor ( $k_{Q,Q_0}$ ) using the analytical approach (IAEA TRS-398 CoP). The volume averaging and water to air stopping power ratio corrections are also applied to the  $k_{Q,Q_0}$  values to correct for the differences between the With Flattening Filter (WFF) and FFF beams.

### Results

The measured and calculated  $dd(10,S)$  are 57.15±0.40% and 57.06±0.07% respectively. When using the first method, the calculated  $k_{Q,F}, k_{Q,0}^{f,F}, f_{ref}$  value for Exradin A14SL is found to be 0.9965±0.0011. The equivalent field size S for the 2×10 cm<sup>2</sup> field size is determined as 3.5 cm. The  $k_{Q,Q_0}$  value corresponding to TPR<sub>20,10</sub>(10,3.5) in the TRS-398 CoP corrected for the volume averaging and water to air stopping power ratios is 0.9951.

### Conclusion

Good agreement is achieved between measured and MC calculated  $dd(10,S)$  values (0.16%). The correction factors determined using the two proposed approaches are in very good agreement (0.14% for Exradin A14SL). While the results of this study are promising, further studies are required to confirm that these two methodologies can be used for other small ionization chambers used in the calibration of BgRT.

### EP-1799 Characterisation of a commercially available large-area IC for dosimetry of scanned proton beams

S. Berke<sup>1,2,3</sup>, E. Almhagen<sup>3,4</sup>, L. Stolarczyk<sup>3,5</sup>

<sup>1</sup>The Clatterbridge Cancer Centre NHS Foundation Trust, Physics Department, Bebington, United Kingdom ; <sup>2</sup>The Royal Liverpool and Broadgreen University Hospitals NHS Trust, Department of Medical Physics and Clinical Engineering, Liverpool, United Kingdom ;

<sup>3</sup>Skandionkliniken, Physics Department, Uppsala, Sweden

<sup>4</sup>Uppsala University, Department of Immunology-Genetics and Pathology - Medical Radiation Science,

Uppsala, Sweden ; <sup>5</sup>Institute of Nuclear Physics PAN, Cyclotron Center Bronowice, Krakow, Poland

### Purpose or Objective

Large-area plane-parallel ionisation chambers are used to measure integrated depth dose curves (IDDCs) of proton pencil beams [1]. They have also been proposed for reference dosimetry, using the dose-area product of a single pencil beam instead of the dose at the centre of a broad field [2]. The larger the IC's diameter, the greater the part of the low-dose "halo" of proton pencil beams caused by scattered protons that is covered [1]. On the other hand, potential inhomogeneities in the chamber construction may influence measured doses and limit its usage in reference dosimetry [3].

A Stingray (IBA Dosimetry) IC with a diameter of 12cm has been characterised with respect to the measured proton range and IDDC shape compared to IDDCs measured with the 8cm Bragg Peak chamber (PTW 34070), and its response homogeneity. A method of chamber heterogeneity verification doable in clinical conditions has been proposed.

### Material and Methods

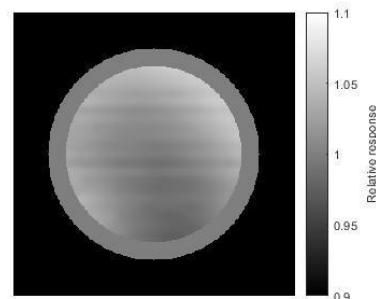
IDDCs were acquired for pencil beams with energies between 60 and 226 MeV using the 12cm and 8cm diameter ICs and a BP<sup>2</sup> water phantom (IBA Dosimetry). Differences in range parameters (R90, R80, R50, R20) and the relative dose difference between IDDCs measured with the two chambers were evaluated.

The chamber response homogeneity was examined by scanning the chamber across a 226MeV pencil beam in air and calculating the ratio between the measured signal at each position and the expected signal, assuming a 2D-Gaussian beam profile with  $\sigma_x=3.0\text{mm}$  and  $\sigma_y=3.1\text{mm}$  determined in air.

### Results

The range parameters measured with the two chambers agreed within 0.5mm. Relative dose differences between IDDCs measured with the two chambers were up to 4%. Generally, the difference was greater for higher energies and the maximum difference was observed at approximately half the proton range.

The IC homogeneity measurements revealed that differences between the expected and measured signal across the chamber area ranged from about -3% to +6% (ignoring points within 10mm of the chamber edge, where inaccurate assumptions about the beam profile might impact on the results; a relative response of unity was assumed there). The response variations were not symmetrical, as seen in the figure below (the stripes are a result of the scanning technique).



### Conclusion

The examined large-area plane-parallel ionisation chamber is suitable for its intended application of measuring IDDCs for routine QA.

For potential future use in reference dosimetry using a single proton pencil beam instead of a broad field, the observed inhomogeneities in the chamber response across its sensitive area require a correction map. The presented in air scanning of the sensitive chamber area provides a quick check of its response but with a limited accuracy. The observed -3% to +6% inhomogeneities had no significant effect on the measurement of IDDCs. References:

1. Bäumer *et al.* 2015 *J. Appl. Clin. Med. Phys.* **16** 151.
2. Gomà *et al.* 2017 *Phys. Med. Biol.* **62** 4991.
3. Kuess *et al.* 2017 *Phys. Med. Biol.* **62** 9189.

#### EP-1800 An Evaluation of Techniques for Dose Calculation on Cone Beam CT

V. Giacometti<sup>1</sup>, R.B. King<sup>2</sup>, C.E. Agnew<sup>2</sup>, D.M. Irvine<sup>2</sup>, S. Jain<sup>1</sup>, A.R. Hounsell<sup>2</sup>, C.K. McGarry<sup>2</sup>

<sup>1</sup>Centre for Cell Biology and Cancer Research- Queen's University Belfast, School of Medicine- Dentistry And Biomedical Sciences, Belfast, United Kingdom ;

<sup>2</sup>Northern Ireland Cancer Centre, Radiotherapy Physics, Belfast- Northern Ireland, United Kingdom

#### Purpose or Objective

This investigation assessed efficiency, accuracy and feasibility of four different techniques adopted to recalculate the dose delivered to the patients based on cone beam CT (CBCT) images acquired prior to treatment.

#### Material and Methods

Four established techniques (standard planning CT calibration curve, CBCT site specific calibration curve, HU density override and deformable registration) were investigated. Each technique was applied to 15 CBCT patients' images (5 prostate and pelvic nodes, 5 lung and 5 head and neck), and treatment planning dose calculations were performed in order to assess accuracy and efficacy of each technique. The patients were receiving volumetric modulated arc therapy to one of three treatment sites. Dose volume histogram metrics and 2.0% / 0.1 mm volumetric gamma analysis were employed to provide a quantitative analysis of the differences between planning CT and CBCT dose distributions.

#### Results

Dose volume histogram analysis indicated that all techniques yielded differences from expected results between -5.4% and +3.8% for both target volumes and organs at risk: -1.4% to 1.8% for prostate and pelvic nodes, -5.4% to 1.0% for head and neck, and -1.8% to 3.8% for lung. With volumetric gamma analysis, the median pass-rates at 10% threshold were 95.5%-97.2%, 92.6%-95.1%, and 85.2%-88.2% for prostate, head and neck and lung patients, respectively. Figure 1 shows the median pass-rates for standard planning CT calibration curve, CBCT site specific calibration curve, HU density override and deformable registration at 10% threshold for each treatment site. Deformed images yielded the highest pass-rates for prostate and head and neck patients, while site-specific calibration curve yielded the highest median pass-rate for lung patients.

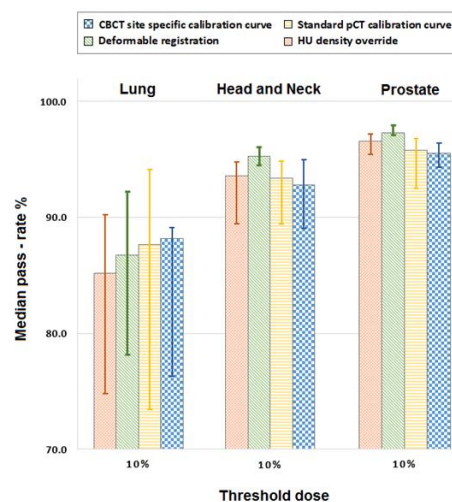


Figure 1: Median 2% / 0.1 mm gamma pass-rates (%) for dose thresholds of 10% for thorax, head and neck, and pelvis acquisitions. Note that the median pass-rate (y-axis scale) starts from 70%.

#### Conclusion

All four investigated techniques were identified as dosimetrically accurate and efficient methods to perform dose calculation based on CBCT images. The differences observed were treatment site dependent.

#### EP-1801 Automatic EPID based Beam QA : measurements become pleasure

A. Sors<sup>1</sup>, D. Perez<sup>1</sup>, P. Dudouet<sup>1,2</sup>, D. Franck<sup>2</sup>, M. Macé<sup>1</sup>, P. Boucarut<sup>1</sup>, C. Boutry<sup>1</sup>

<sup>1</sup>Clinique du Pont de Chaume - Groupe Oncorad Garonne, Service de Radiothérapie, Montauban, France ; <sup>2</sup>Clinique Pasteur - Groupe Oncorad Garonne, Service de Radiothérapie, Toulouse, France

#### Purpose or Objective

To demonstrate interest of automation for photon and electron beams Quality Assurance (QA) using EPID with a simple approach of absorbed dose to water reconstruction: the EpiDream method [1], integrated in the ARTISCAN Beam QA software (AQUILAB, France). The final aim of this study is to validate the use of EPID as a potential substitute to ionization chamber (IC) for routine beam QA.

#### Material and Methods

The study was performed on Clinac 2100CD and 2100EX (Varian Medical Systems, Palo Alto, CA) respectively equipped with on board As500 and As1000 EPID imager (pixel size of 0.784x0.784mm<sup>2</sup> and 0.392x0.392mm<sup>2</sup>). EPID has been calibrated based on EpiDream method and ARTISCAN software used to convert Grey Level integrated images into dose to water matrix for 6-25MV photons and 6-9-12-15-18MeV electron beams. A 4-month study was conducted to compare output constancy (including 5-10mm sliding windows (SW) for photons beams) and beam parameters (flatness, symmetry, penumbra and field size) obtained with EPID method and IC. Comparison was performed using MATLAB (MathWorks Inc., Natick, MA) between radial and transverse profiles measured with a 0.125cm<sup>3</sup> IC (PTW31010) and extracted from EpiDream converted matrices. Robustness of EPID vs. IC QA was estimated using standard deviation of each parameter. Time dedicated to daily and monthly QA for all energies using both methods was also evaluated.

#### Results

Table 1 reported the mean deviation for 6-25MV and 6-9-12-15-18MeV between EPID and IC for output constancy results (a), the mean deviation of EpiDream profiles with IC profiles (b) and robustness of EPID vs IC QA results (c).

As expected, our results show that with decreasing detector size, the measured penumbra width and therefore the distance to the point of inflection decreases [2]. Considering all energies, the mean time duration for linac output constancy daily measurement using EPID and IC was respectively 16 and 30 minutes. The mean time duration for beam parameters measurement using EPID and IC was respectively 14 and 200 minutes.

1. a	6MV				25MV				6MeV	9MeV	12MeV	15MeV	18MeV
	Sw5mm	Sw10mm	Sw5mm	Sw10mm	Sw5mm	Sw10mm	Sw5mm	Sw10mm					
Clinac	0.76%	-0.55%	-0.69%	0.10%	-0.21%	-0.43%	-0.53%	0.57%	0.38%	0.40%	0.56%		
2100CD	±0.59%	±0.64%	±0.71%	±0.41%	±0.75%	±0.89%	±0.54%	±0.50%	±0.49%	±0.44%	±0.51%		
Clinac	-0.41%	0.30%	0.04%	0.8%	0.59%	0.50%	0.16%	0.28%	0.31%	0.03%	-0.19%		
2100EX	±0.43%	±0.56%	±0.59%	±0.35%	±0.62%	±0.48%	±0.59%	±0.41%	±0.28%	±0.26%	±0.29%		

Table 1: Mean deviation for 6-25MV and 6-9-12-15-18MeV between EPID and IC for output constancy results (a), Mean deviation of EPIDream profiles with IC profiles considering flatness, symmetry, penumbra and field size values (b), Standard deviation of flatness, symmetry, penumbra and field size values of EPIDream and IC profiles (c).

## Conclusion

The use of automatic EPID based beam QA dramatically decreases the time dedicated to QA, eliminates manual steps in the process, reducing human errors, improving efficiency, robustness and productivity for radiotherapy providers with a significant decrease in waiting time for patients. In our institution we have chosen to use daily EPID QA to verify output constancy and beam uniformity without any modification on quality or tolerances of our QA process.

[1] Boutry C, Sors A, Fontaine J, Delaby N, Delpon G. A simple algorithm to convert EPID gray values into absorbed dose to water without prior knowledge. *Med Phys.* 2017 Dec ; 44(12):6647-6653.

[2] Laub WU and WongT The volume effect of detectors in the dosimetry of small fields used in IMRT *Med Phys.* 2003 Mar ; 30(3):341-347

## EP-1802 Dosimetry verification of IntraOperative Radiation Therapy (IORT): a Monte Carlo Study

H. Alhamada<sup>1</sup>, S. Simon<sup>2</sup>, C. Philippson<sup>2</sup>, C. Vandekerckhove<sup>2</sup>, Y. Jourani<sup>2</sup>, N. Pauly<sup>3</sup>, N. Reynaert<sup>2</sup>, D. Van Gestel<sup>2</sup>

<sup>1</sup>Institut Jules Bordet ULB, Radiotherapy, Brussels, Belgium ; <sup>2</sup>Institute Jules Bordet, Radiotherapy Department, Brussels, Belgium ; <sup>3</sup>Nuclear Metrology, Université Libre de Bruxelles, Brussels, Belgium

## Purpose or Objective

Most of intraOperative Radiation Therapy (IORT) clinics have not a treatment planning system (TPS). High dose (up to 24 Gy) is given in one session depending only on manual calculation. This study investigates the feasibility of doing 3D dosimetry of IORT patients using post operation patient's CT images with Monte Carlo (MC) code.

## Material and Methods

Mobetron 1000® is a mobile linear accelerator was modeled using BEAMnrc MC code. MC model validation was done for 12, 9 and 6 MeV energies by comparing MC results with measurements according to MC model tuning of Laccarino et al (2011). Absolute dose calibration was done using methodology of Popescu et al (2005). CTCREATE code and home-made code were used to convert post operation CT DICOM images to MC phantom. Each voxel in patient's MC phantom is one of these materials (Air521ICRU, Lung521ICRU, Tissue521ICRU, Bone521ICRU, PMMA521ICRU, AL521ICRU, Steel521ICRU). Contouring of the planning target volume (PTV) and the organs at risk was done by the radiation oncologist. IORT parameters (applicator size and position, energy, Monitors Units, shielding disk, Bolus, ....) as they were used in the operation room simulated using BEAMnrc and DOSXYZnrc for each patient. Finally, dose calculation was done in each patient's MC phantom. This study was done for 20

patients with different tumor locations, applicator sizes, and with different energies.

## Results

MC model validation process ended with good match between measurement and MC PDDs, Profiles and Output factors as the maximum value of the root mean square deviation (RMSD) was less than 3% between them. Absolut and relative doses in PTVs and in Organ at risks were verified using DVH and color wash like any classical linear accelerator TPS. Alhamada et al (2018) and Kamomae et al (2017) have studied new shielding disks and tungsten paper for organs at risk protection, but they did their studies in water phantom. It is possible to study any shielding disk design in clinical usage. Dosimetry impact verification of using customized applicator or beam shaper is available using our methodology. Summation of 3D IOERT dose with other radiotherapy plans is possible and helpful for total overdose avoidance.

## Conclusion

This study provides a step forward for dosimetry verification of IOERT patients. More accurate dosimetry could be achieved by using DICOM images of CBCT inside the operation room which it will be available next year in our clinic.

## EP-1803 Advances in the Patient Specific QA applied to VMAT and Tomotherapy

M. Piccoli<sup>1</sup>, K. Torzsok<sup>1</sup>, A. Ruiz Plata<sup>1</sup>, F. Marangoni<sup>1</sup>, J. Aponte<sup>1</sup>, H. Broque<sup>1</sup>

<sup>1</sup>Fundacion Arturo Lopez Perez, Medical Physics, Santiago, Chile

## Purpose or Objective

It has been more than 20 years (1998) that patient specific quality assurance (PSQA) is playing an important role to verify plan deliverability and reliability for modulated treatments. Since then, there have been massive improvements in machine accuracy in terms of mechanic and dosimetric parameters. Likewise TPS algorithms and experience with these techniques has grown exponentially. However, the verification methodologies kept being almost the same over these years. In this work we have shown the factibility of an alternative prediction index for potential plan failure for Tomotherapy and VMAT.

## Material and Methods

A retrospective analysis over 1000 patients already treated was carried out for an Elekta Synergy equipped with Agily MLC and a Tomotherapy HD. Patient Specific QA have been measured for every single patient before treatment and results from both machines were analyzed and registered using IBA MatriXX Evolution and the criteria of 3%, 3mm, 10% threshold have been applied. Although both machines have different delivery procedures, the modulation factor calculated during planning have being shown to be the main predictive factor of plan complexity and had a direct impact on gamma results. As an example, the following equation describes the way the Modulation factor is calculated for VMAT plans:

$$MF = \frac{MONITOR\ UNITS}{\sum_{n=1}^N \left[ \frac{SEGMENT\ AREA \times SEGMENT\ MU}{TOTAL\ AREA\ FOR\ THE\ ARC} \right]}$$

On the other hand, for Tomotherapy, leaf open time (LOT) is the major factor used for calculating modulation in the TPS. Regardless the system being used, reducing the modulation during planning might be the most effective way of having more representative plans with better gamma values. For a better understanding on how it would affect QA results, modulation factors were classified in

terms of technique (VMAT or Tomotherapy), anatomic region, prescription and ordered from 1 to 6 to better filter the data.

### Results

As expected, results based on previous treatments shows that as higher the modulation factor gets, lower is the number of pixels passing the gamma criteria. For VMAT, minimum and maximum values of 94,6% y 99,9% in gamma were found to be related to plans having modulation factors of 3,56 y 1,24 respectively. For Tomotherapy the same behaviour was observed. Applying a class solution is also important to take into account prescription and volume of the targets. For Tomotherapy reducing the expected value for modulation factor during calculation also impacts plan quality, so a good bias must be found. Whilst for VMAT, rising the segment size during planning was determinant to reduce modulation factor.

### Conclusion

Currently, modern machines are capable of delivering modulated plans in better accordance with the planning theoretical data. Performing PSQA for every single patient might be evaluated depending on internal statistics for each department. More effective and representative plans yielding better QAs results could be achieved if there is a better understanding of the factors provided by treatment planning systems.

### EP-1804 Experimental validation of a novel technique to derive stopping power ratio from MRI in soft tissue

J. Scholey<sup>1</sup>, D. Chandramohan<sup>1</sup>, T. McClave<sup>1</sup>, A. Sudhyadhom<sup>1</sup>

<sup>1</sup>The University of California- San Francisco, Radiation Oncology, San Francisco, USA

### Purpose or Objective

to experimentally validate the Unified Composition (UC) method and compare to "ground truth" measurements for determining mean ionization potential ( $I_m$ ) and stopping power ratio (SPR) using MRI for dose calculation in proton therapy for soft tissues.

### Material and Methods

Porcine soft tissue types (muscle, liver, brain, and spleen) were cryoground to produce homogeneous samples. Tissues were divided into two groups for determination of  $I_m$  and SPR using 1) Bragg's additivity rule (BAR), considered the ground truth (GT) method, and 2) the Unified Compositions (UC) method. For the GT method,  $I_m$  values were calculated directly using BAR with elemental composition determined from chemical combustion analysis of each tissue, as shown in equation 1. SPR values were determined by the Bethe-Bloch equation through measurements of physical density and atomic composition. For the UC method, phantoms were created containing each tissue type and pure water, isopropyl alcohol, acetone, and propargyl alcohol, which were used for proton density and water fraction calibration curves for MRI. Phantom images were acquired using kVCT, MVCT, and 3T MRI.  $I_m$  values were calculated from percent water/organic material by mass and hydrogen content of organic material computed using water/organic <sup>1</sup>H separation and proton-density weighted MRI scans, respectively, as shown in equation 2. For calculation of SPR, relative electron density ( $P_e^{rel}$ ) was determined from MVCT using calibration of an electron density phantom. For comparison, SPR was also calculated for each tissue using kVCT and the stoichiometric calibration method.

$$\ln(I_m) = \left( \sum_i \frac{w_i Z_i^2}{A_i} \ln I_i \right) \left( \sum_i \frac{w_i Z_i}{A_i} \right)^{-1} \quad (1)$$

$w_i$  is fraction by mass,  $Z_i$  is atomic number, and  $A_i$  is atomic mass of element  $i$ .

$$\ln(I_m) \approx (w_{H_2O} \ln(I_{H_2O})) + (w_{org,total} [\ln A - B \frac{H_{org}}{w_{org,total}}]) \quad (2)$$

$w_{H_2O}$  is fraction by mass of water,  $I_{H_2O}$  is the mean ionization potential of water,  $w_{org,total}$  is fraction by mass of organic material, and  $B \frac{H_{org}}{w_{org,total}}$  is total organic molecule hydrogen density by fractional mass in the voxel.  $A$  and  $B$  are constants relating hydrogen content in organic molecules to mean ionization potential of organic materials.

Figure 1: Equations for (1) Bragg's Additivity Rule used for Ground Truth computation and (2) Unified Composition Method.

### Results

Of the tissues evaluated, SPR values computed with the UC method agreed on average to within 0.7% of the GT method, with results shown in table 1. SPR values computed from the stoichiometric calibration saw greater disagreement to GT values, with percent differences of 5.3, 5.2, 3.8, and 4.5% for muscle, liver, brain, and spleen, respectively.

	$P_e^{rel}$			$I_m$ (eV)			SPR		
	GT	UC	% diff	GT	UC	% diff	GT	UC	% diff
Muscle	1.022 ± 0.006	1.020	-0.17	77.55 ± 0.8	77.86	0.39	1.018 ± 0.06	1.016	-0.22
Liver	1.036 ± 0.006	1.030	-0.63	77.06 ± 0.8	77.73	0.87	1.033 ± 0.06	1.026	-0.73
Brain	1.016 ± 0.006	1.007	-0.90	75.55 ± 0.8	77.79	2.97	1.016 ± 0.06	1.003	-1.24
Spleen	0.986 ± 0.006	0.990	0.42	77.81 ± 0.8	77.73	-0.11	0.982 ± 0.06	0.987	0.43

Table 1: Relative electron density ( $P_e^{rel}$ ), mean ionization potential ( $I_m$ ), and stopping power ratio (SPR) calculated using Ground Truth (GT) and UC methods, along with percent difference.

### Conclusion

It is possible to achieve sub-percent accuracy using the UC method for determination of  $I_m$  and SPR from MRI and MVCT imaging as compared to direct computation using GT principles for soft tissues evaluated in this study. All SPR values determined by the UC method were within experimental error of GT determination. Of note,  $P_e^{rel}$  is a predominant source of error in SPR calculations (as SPR varies linearly with  $P_e^{rel}$  and logarithmically with  $I_m$ ) and ongoing investigations are looking to improve this accuracy. SPRs computed via the UC method saw closer agreement with those computed by GT than the widely-used stoichiometric calibration method.

### EP-1805 The Effect of Material Heterogeneity in Endorectal Brachytherapy with <sup>192</sup>Ir, <sup>75</sup>Se and <sup>169</sup>Yb Sources

T. Shoemaker<sup>1,2</sup>, T. Vuong<sup>3,4</sup>, H. Glickman<sup>1</sup>, S. Kaifi<sup>3</sup>, G. Famulari<sup>1</sup>, S.A. Enger<sup>1,2,4</sup>

<sup>1</sup>McGill University, Medical Physics Unit, Montreal, Canada; <sup>2</sup>McGill University Health Centre, Research Institute, Montreal, Canada; <sup>3</sup>Jewish General Hospital-McGill University, Department of Radiation Oncology, Montreal, Canada; <sup>4</sup>McGill University, Department of Oncology, Montreal, Canada

### Purpose or Objective

Differences between prescribed and administered dose in high dose rate endorectal brachytherapy (HDR-EBT) were investigated by evaluating dose to clinical target volume (CTV) and organs at risk (OARs) calculated with a Monte Carlo based dose calculation tool, RapidBrachyMC. In addition, dose coverage, conformity and homogeneity were compared between the radionuclides <sup>192</sup>Ir, <sup>75</sup>Se and <sup>169</sup>Yb for use in HDR-EBT.

### Material and Methods

RapidBrachyMC, which builds on the Geant4 MC-toolkit, was used to perform postimplant dosimetry using computed tomography (CT) images for 8 patients, each treated with 3 fractions of HDR-EBT at the Jewish General Hospital in Montreal, Canada. In the HDR-EBT treatment a <sup>192</sup>Ir MicroSelectron v2 source was used with a flexible intracavitary applicator capable of fitting a tungsten rod in its central lumen for OAR shielding. In combination with this applicator, two balloons filled with iodine solution were used, one used to fix the applicator to the rectum and the other to displace the contralateral rectal wall. Four segmentation schemes were simulated. 1) According

to the TG-43 formalism. 2) Applicator, shield, source and balloon materials with nominal densities specified, but patient geometry consists of water. 3) Tissue materials assigned to contoured organs in addition to foreign structures, densities overridden with nominal densities. 4) Materials specified as per segmentation 3, with organ densities based on CT densities. In addition, two novel sources were investigated and dosimetrically compared with <sup>192</sup>Ir: <sup>75</sup>Se and <sup>169</sup>Yb. The clinical TG-43 based plan optimized for <sup>192</sup>Ir was used for all simulations. The TG-43 results for <sup>169</sup>Yb and <sup>75</sup>Se were normalized to give the same D<sub>90</sub> as the clinical plan.

**Results**

CTV coverage and dose to the OARs, pelvic and femur bone are overestimated for <sup>192</sup>Ir TG-43 based dosimetry, while for <sup>175</sup>Se and <sup>69</sup>Yb dose to CTV and OARs are overestimated, but pelvic and femur bone doses are significantly underestimated. <sup>75</sup>Se delivers similar dose to OARs as <sup>192</sup>Ir but delivers slightly increased bone doses. <sup>169</sup>Yb delivers lower dose to the rectum but significantly higher bone dose. Dosimetric indices and comparisons between segmentation schemes for the CTV, rectum, and pelvis are given in Table 1. Colorwash comparison between segmentation schemes for <sup>192</sup>Ir is given in Figure 1.

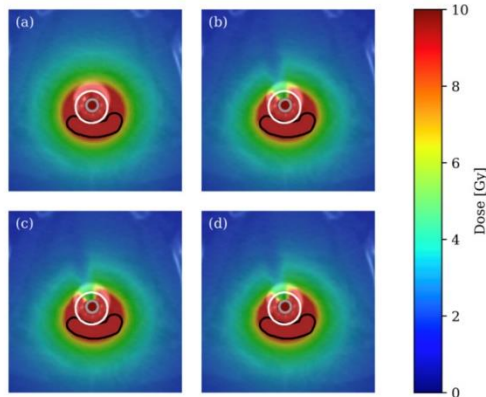


Figure 1: Colorwash comparison of four segmentation schemes for <sup>192</sup>Ir, with applicator contoured in white, tungsten shielding rod in gray and the CTV in black. (a) Segmentation scheme 1, (b) segmentation scheme 2, (c) segmentation scheme 3, (d) segmentation scheme 4.

Contour and Index	Mean Value ± σ <sub>mean</sub> [Gy]	% Difference from Segmentation 1	p-Value	
CTV D <sub>90</sub> <sup>192</sup> Ir [Gy]	Segmentation 1	-	-	
	Segmentation 2	10.8 ± 0.2	-5	0.00003
	Segmentation 3	10.8 ± 0.2	-6	0.00003
	Segmentation 4	10.8 ± 0.2	-6	0.00003
Rectum D <sub>90</sub> <sup>192</sup> Ir [Gy]	Segmentation 1	4.0 ± 0.5	-	-
	Segmentation 2	2.9 ± 0.4	-29	0.00003
	Segmentation 3	2.9 ± 0.4	-29	0.00003
	Segmentation 4	2.9 ± 0.4	-29	0.00003
Pelvis D <sub>90</sub> <sup>192</sup> Ir [Gy]	Segmentation 1	0.46 ± 0.04	-	-
	Segmentation 2	0.38 ± 0.03	-18	0.00003
	Segmentation 3	0.43 ± 0.04	-8	0.0004
	Segmentation 4	0.43 ± 0.04	-6	0.002
CTV D <sub>90</sub> <sup>75</sup> Se [Gy]	Segmentation 1	11.4 ± 0.2	-	-
	Segmentation 2	10.5 ± 0.3	-9	0.00004
	Segmentation 3	10.1 ± 0.3	-11	0.00003
	Segmentation 4	10.5 ± 0.3	-8	0.00003
Rectum D <sub>90</sub> <sup>75</sup> Se [Gy]	Segmentation 1	4.2 ± 0.5	-	-
	Segmentation 2	2.9 ± 0.4	-32	0.00003
	Segmentation 3	2.7 ± 0.4	-36	0.00003
	Segmentation 4	2.8 ± 0.4	-34	0.00003
Pelvis D <sub>90</sub> <sup>75</sup> Se [Gy]	Segmentation 1	0.52 ± 0.04	-	-
	Segmentation 2	0.40 ± 0.03	-22	0.00003
	Segmentation 3	0.54 ± 0.05	4	0.3
	Segmentation 4	0.58 ± 0.05	12	0.0008
CTV D <sub>90</sub> <sup>169</sup> Yb [Gy]	Segmentation 1	11.4 ± 0.2	-	-
	Segmentation 2	9.6 ± 0.3	-16	0.00003
	Segmentation 3	9.5 ± 0.3	-17	0.00003
	Segmentation 4	9.4 ± 0.3	-18	0.00003
Rectum D <sub>90</sub> <sup>169</sup> Yb [Gy]	Segmentation 1	4.1 ± 0.5	-	-
	Segmentation 2	2.6 ± 0.4	-38	0.00003
	Segmentation 3	2.5 ± 0.4	-41	0.00003
	Segmentation 4	2.4 ± 0.4	-41	0.00003
Pelvis D <sub>90</sub> <sup>169</sup> Yb [Gy]	Segmentation 1	0.55 ± 0.04	-	-
	Segmentation 2	0.41 ± 0.03	-25	0.00003
	Segmentation 3	0.65 ± 0.06	19	0.0002
	Segmentation 4	0.75 ± 0.07	37	0.00003

Table 1: Mean dosimetric index values for three selected contours and three radionuclides, with percent differences from segmentation scheme 1. D<sub>90</sub> is the dose received by xx percentage of the contour.

**Conclusion**

Ignoring patient geometry and in particular high-Z materials such as the iodine radiographic contrast, bone and tungsten shielding in dose calculations contributes to significant inaccuracies which lead to sub-optimal dose optimization and disagreement between prescribed and

delivered dose, specifically for radionuclides with lower average energy than <sup>192</sup>Ir. In addition, our results show that with a future MRI-based treatment planning for HDR-EBT, loss of CT-density data will not significantly affect dosimetry if material composition and nominal mass densities are used.

**EP-1806 Commissioning an Independent Dose Calculation System for the Unity MR-Linac**

E. Goodwin<sup>1</sup>, S. Nill<sup>1</sup>, U. Oelfke<sup>1</sup>

<sup>1</sup>Royal Marsden / Institute of Cancer Research, Joint Department of Physics, London, United Kingdom

**Purpose or Objective**

An independent secondary monitor unit check is a quality assurance measure used throughout the radiotherapy community, and is a legal requirement in many European countries. The first patients on the Unity MR-Linac (Elekta AB, Stockholm, Sweden) have recently been treated at The Royal Marsden Hospital. There is no commercial software for performing an independent calculation for a 1.5 T MR-Linac. Therefore a solution using scripting tools for the RayStation (RaySearch, Stockholm) treatment planning system was developed.

**Material and Methods**

The primary dose calculation for the MR-Linac is carried out in Monaco 5.4 (Elekta) using a Monte Carlo algorithm that has been benchmarked against beam data. This was used to generate a series of square and rectangular fields on a model of water phantom, with a 2mm voxel size and 0.5% uncertainty per beam. Depth dose curves and dose profiles were extracted and used as the basis for the RayStation model.

An FFF beam model was created which matched the dose curves as closely as possible. RayStation requires that MLC-Y machines have a backup jaw, so a 'dummy' Y-jaw open beyond the MLCs was placed in each plan. Profiles from the MR-Linac are asymmetric due to the effect of the magnetic field on secondary electrons. This could not be modelled in RayStation. To first approximation, the difference could be accounted for by translating the fields laterally. Each beam isocentre was offset by an empirically derived factor of 0.16 cm (see fig. 1). Beam attenuation through MR components varies with gantry angle, so a monitor unit correction was applied to each beam.

Point dose measurements and qualitative comparisons of profiles were made between simple fields (from 1.5 x 1.5 cm<sup>2</sup> to 22 x 58.6 cm<sup>2</sup>), complex field shapes and IMRT fields calculated in Monaco and RayStation. Ten protocol prostate plans (6 offline, 4 adapted) were created in Monaco.

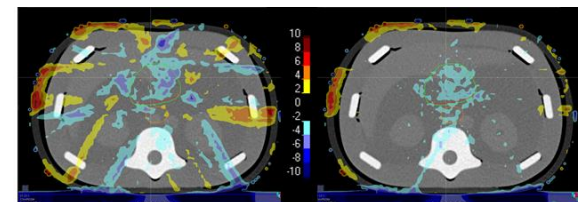


Figure 1: Dose difference (Monaco - RayStation) before the isocentre was offset perpendicular to the gantry angle, and in the direction of the Lorentz force (Left) and after (Right). Percentages are expressed relative to the prescribed dose (60 Gy).

**Results**

The RayStation profile and depth dose curves were in good qualitative agreement with Monaco for simple fields. In the centre of large fields, the dose difference was comparable to the statistical uncertainty of the Monaco calculation (0.5%). Elsewhere, agreement was worse due to the lack of asymmetry in RayStation. For complex field shapes the agreement was generally good, except near thin segments where RayStation would underestimate in-field dose by up to 3%. The RayStation calculated treatment plans yielded DVHs that were consistent with

Monaco for the OARs, but were approximately 1.5% hotter than the Monaco for the PTVs (see fig. 2).

Ratio of PTV DVH statistics (RayStation/Monaco)			
Dose at Volume (%)	Minimum	Mean	Maximum
5	1.002	1.012	1.018
50	1.007	1.017	1.027
95	1.006	1.016	1.025

Figure 2: The RayStation PTV DVH is approximately 1.5% hotter than the Monaco PTV DVH for the ten plans calculated. However, this is fairly consistent between patients and across the DVH.

**Conclusion**

It is possible to create a RayStation beam model for the Unity MR-Linac which is sensitive enough to detect gross errors in monitor unit calculations. With the prototype version of the MR-Linac beam model, the gynae and head and neck treatment sites had similar PTV DVH statistics to the prostate, however, additional sites will require validation before clinical implementation head and neck will require validation with this beam model. As the magnetic field is not modelled, care is required when interpreting doses near air interfaces.

**EP-1807 Use of SPC techniques to generate assessment criteria for transit dosimetry analysis**

A. Pyett<sup>1</sup>, C. Holmes<sup>1</sup>, C. Enever<sup>1</sup>, A. Fryer<sup>2</sup>, D. Paynter<sup>2</sup>, P. Rixham<sup>2</sup>, S. Weston<sup>2</sup>

<sup>1</sup>Leeds Cancer Centre, Radiotherapy Department, Leeds, United Kingdom ; <sup>2</sup>Leeds Cancer Centre, Medical Physics and Engineering, Leeds, United Kingdom

**Purpose or Objective**

When introducing a transit dosimetry programme the analysis criteria and the failure thresholds must be established. Conventional assessment of delivery using quasi-3D phantoms is usually performed using the  $\gamma$  parameter. A common threshold for gamma success is 95% of points with a  $\gamma < 1$  using parameters of 3%/3mm. However any transit dosimetry analysis must allow for clinically insignificant variation in the patient setup and the patients anatomy, effects which do not affect phantom measurement.

The aim of this work is to use measured data to establish clinically relevant parameters for the analysis of Lung SABR treatments

**Material and Methods**  
At X lung SABR treatments are planned on Elekta Monaco and delivered using a single arc 6MV FFF VMAT technique on Elekta VersaHD linacs. The patient position is verified using CBCT before every fraction. A portal movie image measured during the treatment is used to reconstruct the delivered dose distribution on the 3D planning CT using the Elekta iViewDose software.

iViewDose provides analysis of the delivered dose distribution in terms of

- Dose at the Dose Reference Point (DRP)
- Percentage of points that have a  $\gamma < 1$
- Mean  $\gamma$
- Near maximum  $\gamma$

During a pilot phase dose reconstructions were analysed using  $\gamma$  parameters of 3%/3mm. Mean values and confidence limits for all analysis parameters were calculated using SPC methodologies. The means and confidence limits were measured from the first twenty fractions to be analysed, ignoring the obvious outliers.

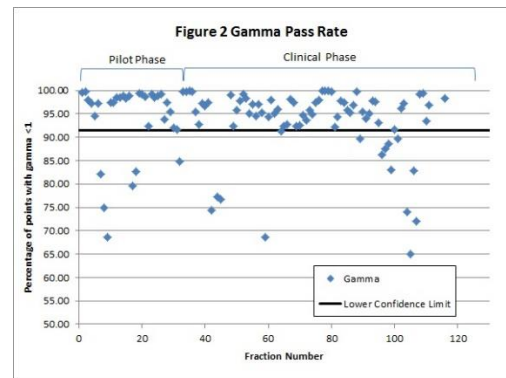
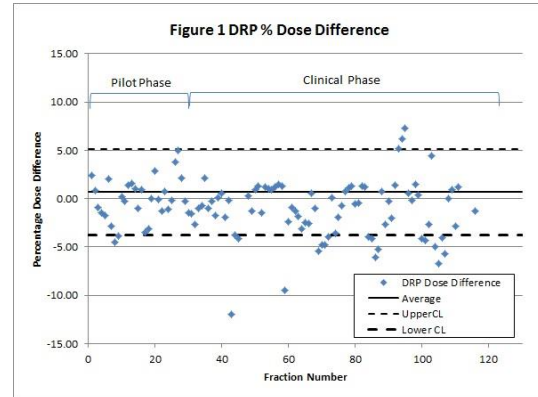
Following clinical implementation the reconstructions were analysed against the criteria established in the pilot phase. Where fractions passed all the criteria no further action was taken. Where one or more of the criteria failed the fraction was investigated.

**Results**

Parameter	Target	LCL	UCL	iViewDose	Tolerance
% DRP Deviation	0.67	-3.7	5.1	4%	

Gamma % < 1	100	91%	-	91%
Mean Gamma	0.42	0.28	0.55	0.6
Gamma > 1 %	1.09	0.72	1.46	1.5

84 fractions were analysed in the clinical phase. DRP and gamma results are shown in figures 1 and 2.



All of the fractions that failed at least one test were investigated. Almost all of the failures were true positives in that a reason could be identified for their failure: tumour motion, contour change, or oedema. One patient exhibited a failure which could not be explained due to anatomical changes. This was verified using a Delta4 system and the delivered distribution was found to be in good agreement with the planned distribution

**Conclusion**  
Transit dosimetry can be an effective tool in determining deviations from intended treatment. Errors identified using transit dosimetry correlated well with anatomical changes identified using CBCT. No errors were identified due to treatment delivery errors.

SPC techniques can be used to develop assessment criteria for transit dosimetry analysis. This should be performed on a site by site basis as different anatomical sites will yield different expected results and confidence levels depending upon the accuracy of the reconstruction and the normal anatomical variability of the site

**Electronic Poster: Physics track: Treatment plan optimisation: algorithms**

**EP-1808 Impact of the optimization-convergence errors on lung IMRT-SBRT plans computed with the Eclipse TPS**

J.F. Calvo Ortega<sup>1</sup>, H. Marcelino<sup>2</sup>, S. Moragues Femenia<sup>1</sup>, C. Laosa-Bello<sup>1</sup>, J. Casals<sup>1</sup>

<sup>1</sup>Hospital Quirónsalud Barcelona, Radiotherapy, Barcelona, Spain ; <sup>2</sup>Hospital Universitario Valle de Hebrón, Servicio de Física y Protección Radiológica, Barcelona, Spain

### Purpose or Objective

To investigate the accuracy of the dynamic MLC patterns derived for lung IMRT-SBRT plans with normalization values differing in more than 5% respect to the inverse optimization calculation.

### Material and Methods

Ten cases of lung SBRT planned using Sliding and Window IMRT technique were included. IMRT optimizations were performed using the Dose Volume Optimizer (DVO, version 10.0.28) algorithm of the Varian Eclipse TPS (version 13.7.14). The Anisotropic Analytical Algorithm (AAA, version 10.0.28) was applied for the final dose calculation (2 mm grid size). Photons beams of 6 MV from a Varian linac equipped with the Millennium 120 MLC were used. Due to optimization-convergence errors [J Appl Clin Med Phys. 2009 Oct 14;10(4):3061], the final plans needed to be re-normalized to insure that 95% of the PTV received the prescribed dose. The required final re-normalization values (62%-85%) varied in more than 5% respect to the 100% value of DVO-base target DVH. To detect potential violations of the MLC operating limits, Varian advises to verify the MLC leaf sequence for normalization variations larger than 5%.

Each original SBRT plan (Plan\_Orig) was delivered onto the linac EPID (Varian PortalVision aS500) to evaluate the accuracy of the dynamic MLC patterns created by the Eclipse for these re-normalization values (62%-85%). Two kinds of verifications were done: 1) the actual field fluences of the Plan\_Orig were verified using the Varian Portal Dosimetry software (version 13.7.14). The 3%/3 mm and 2%/2 mm criteria, both with 10% of maximum dose as dose threshold, were applied for 2D global gamma-evaluation. A total of 85 IMRT fields were analyzed. 2) The Plan\_Orig was recalculated by keeping the MUs but using the MLC files reconstructed from the Dynalog files recorded by the MLC controller (Plan\_Actual). This DynaLog-to-MLC conversion was performed using a MATLAB-based code developed by Teke et al. [Radiother Oncol. 2007;84(Suppl 2):S92]. The reconstructed dose distribution was verified against the original dose distribution using a 1%/1 mm 3D global gamma-evaluation for the PTV structure. The Computational Environment for Radiotherapy Research (CERR) software was used for this task.

### Results

1. The average  $\pm$  1 SD of the 2D gamma passing rates were  $99.4\% \pm 0.9\%$  (range: 96.1%-100%) and  $97.6\% \pm 2.5\%$  (range: 89.2%-97.6%) at 3%/3 mm and 2%/2 mm criteria, respectively.
2. A 1%/1 mm 3D gamma passing rate of 100% was obtained for the PTV in all plans.

### Conclusion

The results demonstrated the reliability and accuracy of the IMRT-SBRT plans designed by the Eclipse TPS with normalization values differing in more than 5% respect to the inverse optimization calculation.

### EP-1809 Comparison of Photon Optimizer (PO) and Progressive Resolution Optimizer (PRO) for SRS VMAT Plans

Y. Akdeniz<sup>1</sup>, G. Ugurluer<sup>2</sup>, E.B. Ispir<sup>1</sup>, I. Kaptan<sup>1</sup>, M. Serin<sup>2</sup>

<sup>1</sup>Acibadem Adana Hospital, Department of Radiation Oncology, Adana, Turkey ; <sup>2</sup>Acibadem Mehmet Ali Aydinlar University, Department of Radiation Oncology, Adana, Turkey

### Purpose or Objective

Linac-based stereotactic radiosurgery (SRS) of brain lesions is typically performed by using volumetric modulated arc therapy (VMAT) technique. For SRS of small target SRS, the optimization algorithms might influence the treatment quality significantly as they model the 3D space in different way. In this study, we aimed to compare a new optimizer "photon optimizer" (PO) with its predecessor "progressive resolution optimizer" (PRO) for SRS VMAT plans.

### Material and Methods

For ten patients with single brain metastases planning-CT scans were acquired with a slice thickness of 1 mm. Planning Target Volume (PTV) which was converted to high resolution segment had a mean volume of 14.85 cm<sup>3</sup> (range 8.6-20 cm<sup>3</sup>). Each patient's treatment was planned using PO and PRO optimizers on version 13.6 of the Eclipse treatment planning system with 6 MV FFF photon beams. A template using the same objectives was used for each optimized plan without any intervention. For PO the highest resolution (1.25 mm) was selected and during optimization with PRO the point cloud model resolution for PTV was set to 1 mm. The prescribed dose was 18 Gy in a single fraction. Volumetric dose normalization was adopted, by normalizing 100% D<sub>p</sub> to 99% of the PTV. Plans which were optimized with PO and PRO were calculated with anisotropic analytical algorithm (AAA, v.13.6), with the same dose grid resolution (1 mm). PO and PRO plans were compared in terms of total number of monitor units (MU), Paddick conformity (CI) and gradient index (GI) for PTV and V<sub>12</sub> (the volume receiving more than 12 Gy) and D<sub>mean</sub> (mean dose) for the healthy brain tissue. Statistical analysis was performed using SPSS.

### Results

The values of the plan quality metrics for both PO and PRO plans are shown for all patients in Table 1. For CI<sub>Paddick</sub> significant advantage in favour of PRO plans were achieved. While mean CI<sub>Paddick</sub> value increased significantly from  $0.89 \pm 0.009$  (for PO plans) to  $0.941 \pm 0.017$  (for PRO plans) ( $p < 0.05$ ), there was no statistically significant difference between PO ( $3.084 \pm 0.242$ ) and PRO ( $3.031 \pm 0.184$ ) plans in terms of GI<sub>Paddick</sub>. We had significant reduction in V<sub>12</sub> from  $12.74 \pm 3.61$  cm<sup>3</sup> (for PO plans) to  $11.52 \pm 3.22$  cm<sup>3</sup> (for PRO plans) ( $p < 0.05$ ). Also, we found that the D<sub>mean</sub> decreased in favor of PRO in statistical analysis from  $124.2 \pm 41.3$  cGy (for PO plans) to  $119.7 \pm 39.6$  cGy (for PRO plans) ( $p < 0.05$ ). There was no significant difference between PO and PRO in terms of total number of MU.

Table 1. Values of plan quality metrics

Pt # / Plan	Total # of MU		D <sub>mean</sub> (cGy)		V <sub>12</sub> (cc)		CI <sub>Paddick</sub>		GI <sub>Paddick</sub>	
	PO	PRO	PO	PRO	PO	PRO	PO	PRO	PO	PRO
1	5204	4991	90.1	87.5	9.73	8.95	0.885	0.962	3.157	3.163
2	4574	4953	121.6	124.8	12.6	11.5	0.895	0.931	2.682	2.722
3	7473	6607	161.2	149.4	15.37	13.58	0.906	0.939	3.242	3.150
4	4512	4590	154.4	140.6	17.13	15.12	0.899	0.951	3.202	3.224
5	4956	4950	152.5	151.9	18.9	17.25	0.889	0.933	2.957	2.974
6	5904	5605	35.4	33.3	7.08	6.42	0.883	0.929	3.376	3.298
7	4630	4725	144.1	137.7	12.95	11.82	0.890	0.937	2.876	3.028
8	5592	5341	147	144.1	10.77	9.92	0.894	0.977	2.839	2.936
9	5684	5079	85.1	80.6	9.95	8.74	0.875	0.923	3.387	3.318
10	4614	4652	144.3	138.7	12.87	11.85	0.885	0.938	3.041	2.999
mean	5330	5150	124.2	119.7	12.74	11.52	0.890	0.941	3.084	3.081
sd	919	598	41.3	39.6	3.61	3.22	0.009	0.017	0.242	0.184
min	4512	4590	35.4	33.3	7.08	6.42	0.875	0.923	2.682	2.722
max	7473	6607	161.2	151.9	18.9	17.25	0.906	0.977	3.387	3.318
	NS		p<0.05		p<0.05		p<0.05		NS	

### Conclusion

This study compared plan optimization outputs for the two optimization algorithms (PO and PRO) which models 3D space differently in SRS VMAT plans. Our study showed that SRS VMAT plans optimized with PRO's point cloud model yield better results in terms of both target volume coverage and organ protection than PO. PRO might be preferred to newer algorithm PO in optimization of small target volumes.

### EP-1810 Comparison of absorbed dose between medium and water on Monte Carlo algorithm for VMAT plan

N. Bhalla<sup>1</sup>, M. Palanisamy<sup>1</sup>, G. Anand<sup>1</sup>, C. Saravanan<sup>1</sup>, T. Thangaraj<sup>1</sup>, P. Abhishek<sup>1</sup>  
<sup>1</sup>Fortis Cancer Institute, Radiation Oncology, Mohali, India

#### Purpose or Objective

A comparison of absorbed dose to water ( $D_w$ ) and absorbed dose to medium ( $D_m$ ) on Monte Carlo (MC) dose calculation algorithm used in Monaco™ treatment planning system (TPS) for different clinical sites.

#### Material and Methods

Four patients from each site, a total of 20 patients, namely, larynx, lung, prostate, and brain treated with VMAT technique were chosen for this study. All plans were generated using 6MV photon beam in Monaco™ TPSV5.10 for Elekta Synergy™ linear accelerator with leaf width of 1cm. The reference plan was generated using the MC dose calculation algorithm with absorbed dose to water during final dose calculation. By keeping all other parameters constant, plans were recalculated by changing the absorbed dose to medium. Plans were evaluated using dose-volume histogram (DVH). For plan comparison, conformity index (CI), homogeneity index (HI), planning target volume (PTV) covered by 98% prescribed dose, mean and maximum dose to PTV ( $PTV_{max}$ ) and organ at risk (OAR) dose was compared. In addition, the normal tissue volume receiving dose  $> 5Gy$  &  $> 10Gy$ , normal tissue integral dose (NTID), calculation time (mins), point dose measurement and gamma pass rate was compared.

#### Results

In all four sites, CI and HI value was 4.24%-12.4% and 3.49%-19.63% increased in  $D_w$  as compared to  $D_m$  with significant difference ( $p < 0.05$ ). The dose received by 98% volume and  $D_{max}$  to PTV was 0.42%-2.23% and 0.9%-6.2% increased in  $D_w$  as compared to  $D_m$  ( $p > 0.05$ ). No significant dose difference was observed in  $D_{mean}$  to PTV, OAR, normal tissue volume receiving dose  $\geq 5Gy$  &  $\geq 10 Gy$  and NTID. Similarly, no significant difference was observed in calculation time, gamma pass rate and point dose measurements ( $p > 0.05$ ).

#### Conclusion

The choice of either  $D_m$  or  $D_w$  during dose calculation was based on significant clinical effect in tumor control and OAR sparing. In all clinical sites, during MC dose calculation, there was a significant increase in the point dose and inhomogeneous dose in  $D_w$  as compared  $D_m$  within the target. However,  $D_m$  will be the preferred option to achieve better accuracy in future for Monaco™ TPS.

### EP-1811 Volumetric modulated arc therapy with robust optimization for larynx cancer

H. Miura<sup>1</sup>, D. Yoshiko<sup>2</sup>, O. Shuichi<sup>1</sup>, N. Minoru<sup>1</sup>, O. Keiichi<sup>2</sup>, K. Masahiko<sup>2</sup>, N. Yasushi<sup>2</sup>

<sup>1</sup>Hiroshima High-Precision Radiotherapy Cancer Center, Medical Physics, Hiroshima, Japan ; <sup>2</sup>Hiroshima High-Precision Radiotherapy Cancer Center, Radiation oncology, Hiroshima, Japan

#### Purpose or Objective

In the case of larynx cancer using 3D-CRT, common carotid arteries receive radiation doses essentially equivalent to the prescription due to their close proximity to the target. VMAT has been used to reduce the dose to the carotid arteries. Robust optimization plan provides significantly more robust dose distributions to targets and OAR than the PTV-based optimization plan. We speculated that a larynx cancer patient may benefit from a partial-arc VMAT robust optimization plan due to its location. The aim of this study was to perform a comparison between robust optimization and planning target volume PTV-based optimization plans using VMAT by evaluating perturbed doses induced by

localization offsets for setup uncertainties in larynx cancer radiation therapy.

#### Material and Methods

Ten patients with early-stage (T1-2N0) glottis carcinoma were selected. The CTV, carotid arteries, and spinal cord were contoured by an oncologist. PTV-based and robust optimization plans were normalized at  $D_{95\%}$  to the PTV and  $D_{98\%}$  to the CTV, respectively. Both optimization plans were evaluated using perturbed doses by specifying user defined shifted values from the isocenter. CTV dose ( $D_{98\%}$ ,  $D_{50\%}$ , and  $D_{2\%}$ ), homogeneity index (HI) and conformity index ( $CI_{95\%}$ ,  $CI_{80\%}$ , and  $CI_{50\%}$ ), as well as doses to the carotid arteries and spinal cord were compared between PTV-based and robust optimization plans. Monitor Unit (MU) was also investigated.

#### Results

In the original plan, the CTV doses, HI, CI, OAR doses and MU using PTV-based and robust optimization plans are shown in Table 1. The robust optimization plans exhibited superior CTV coverage and a reduced dose to the carotid arteries compared to the PTV-based optimization plans ( $p < 0.05$ ). HI,  $CI_{95\%}$  and the dose to the spinal cord did not significantly difference between the PTV-based and robust optimization plans ( $p > 0.05$ ). The robust optimization plans showed better  $CI_{80\%}$  and  $CI_{50\%}$  compared to the PTV-based optimization plans ( $p < 0.05$ ). The robust optimization plans were on average 18.6% less than the total MU compared to the PTV-based optimization plans ( $p < 0.05$ ). Table 2 compares the doses to the CTV, carotid arteries, and spinal cord obtained from the rigidly shifted plan between the PTV-based and robust optimization plans. Plan perturbed evaluations showed that the robust optimization plan has small variations in the doses to the CTV, carotid arteries, and spinal cord compared to the PTV-based optimization plan.

Table 1  
Doses to the CTV and OAR, HI, CI, and MU using PTV-based and robust optimization plans.

	PTV based plan	robust plan	p value
CTV: $D_{98\%}$ (cGy)	194.8 ± 2.0 (191.0 - 198.0)	200.0 ± 0.0 (200.0 - 200.0)	0.002*
CTV: $D_{50\%}$ (cGy)	202.1 ± 1.9 (200.0 - 207.0)	206.1 ± 1.4 (204.0 - 209.0)	0.002*
CTV: $D_{2\%}$ (cGy)	208.8 ± 1.7 (206.0 - 212.0)	211.6 ± 2.2 (209.0 - 216.0)	0.025*
carotid artery_left: average dose (cGy)	88.1 ± 9.0 (81.0 - 105.0)	82.6 ± 6.5 (75.0 - 93.0)	0.006*
carotid artery_left: $D_{2\%}$ (cGy)	121.2 ± 13.2 (98.0 - 147.0)	108.7 ± 7.8 (99.0 - 123.0)	0.004*
carotid artery_right: average dose (cGy)	92.9 ± 13.6 (81.0 - 125.0)	86.5 ± 13.0 (74.0 - 118.0)	0.002*
carotid artery_right: $D_{2\%}$ (cGy)	127.0 ± 17.2 (111.0 - 168.0)	116.0 ± 19.6 (100.0 - 169.0)	0.004*
spina cord: average dose (cGy)	33.7 ± 5.2 (26.0 - 42.0)	32.0 ± 4.4 (24.0 - 38.0)	0.254
spinal cord: $D_{2\%}$ (cGy)	42.2 ± 4.9 (34.0 - 48.0)	39.6 ± 4.0 (32.0 - 47.0)	0.152
HI	0.069 ± 0.016 (0.043 - 0.099)	0.056 ± 0.011 (0.044 - 0.077)	0.160
CTV: $CI_{95\%}$	1.801 ± 0.355 (1.282 - 2.564)	1.713 ± 0.366 (1.249 - 2.433)	0.125
CTV: $CI_{80\%}$	2.988 ± 0.581 (1.907 - 4.175)	2.784 ± 0.551 (1.939 - 3.879)	0.020*
CTV: $CI_{50\%}$	5.276 ± 1.004 (3.484 - 7.265)	4.688 ± 0.864 (3.484 - 6.640)	0.004*
MU	308.5 ± 43.6 (238.3 - 394.8)	260.1 ± 14.7 (235.0 - 287.1)	0.004*

\*The Wilcoxon signed-rank test resulted in a statistically significant difference ( $p < 0.05$ ).  
HI, homogeneity index; CI, conformity index; MU, Monitor unit.

Table 2. Doses to the CTV and OAR for each plan at offset locations using PTV-based and robust optimization plans.

	PTV based plan	robust plan	p value
CTV: D <sub>95%</sub> (cGy)	193.7 ± 2.4 (185.0 - 199.0)	195.6 ± 2.9 (188.0 - 200.0)	< 0.001*
CTV: D <sub>50%</sub> (cGy)	201.1 ± 1.8 (196.0 - 207.0)	205.7 ± 1.9 (202.0 - 209.0)	< 0.001*
CTV: D <sub>2%</sub> (cGy)	209.8 ± 2.8 (205.0 - 218.0)	211.4 ± 2.7 (206.0 - 216.0)	0.003 *
carotid artery_left average dose (cGy)	89.5 ± 13.3 (72.0 - 130.0)	83.2 ± 9.7 (69.0 - 110.0)	< 0.001*
carotid artery_left: D <sub>2%</sub> (cGy)	126.8 ± 23.4 (92.0 - 177.0)	113.0 ± 16.5 (88.0 - 159.0)	< 0.001*
carotid artery_right: average dose (cGy)	94.3 ± 16.6 (74.0 - 140.0)	86.9 ± 14.6 (69.0 - 134.0)	< 0.001*
carotid artery_right: D <sub>2%</sub> (cGy)	133.7 ± 25.2 (96.0 - 190.0)	120.1 ± 22.8 (91.0 - 184.0)	< 0.001*
spina cord: average dose (cGy)	34.5 ± 6.0 (23.0 - 50.0)	32.7 ± 6.5 (21.0 - 66.0)	0.002 *
spinal cord: D <sub>2%</sub> (cGy)	45.5 ± 8.3 (30.0 - 69.0)	40.8 ± 5.3 (30.0 - 52.0)	< 0.001*

\*The Wilcoxon signed-rank test resulted in a statistically significant difference at the all parameter ( $p < 0.05$ ).

## Conclusion

The robust optimization plans yielded higher doses compared to the CTV and more spared dose to the carotid artery compared to the PTV-based optimization plans. With respect to the perturbed evaluation, the doses to the carotid arteries and spinal cord showed less variation with the robust optimization plans compared to the PTV-based optimization plans. The robust optimization plan may be a suitable treatment method in radiotherapy for larynx cancer patient.

**EP-1812 Outcome-optimized radiotherapy planning using risk modeling for lymphoma - a preliminary study**  
 L. Rechner<sup>1</sup>, A. Modiri<sup>2</sup>, L.B. Stick<sup>1</sup>, M.V. Maraldo<sup>1</sup>, S.R. Rice<sup>3</sup>, A. Sawant<sup>2</sup>, S.M. Bentzen<sup>4</sup>, I.R. Vogelius<sup>1</sup>  
<sup>1</sup>Rigshospitalet- University of Copenhagen, Department of Oncology- Section of Radiotherapy, Copenhagen, Denmark ; <sup>2</sup>University of Maryland- School of Medicine, Department of Radiation Oncology, Baltimore, USA ; <sup>3</sup>University of Maryland Medical Center, Radiation Oncology, Baltimore, USA ; <sup>4</sup>University of Maryland School of Medicine, Comprehensive Cancer Center and Department of Epidemiology and Public Health, Baltimore, USA

## Purpose or Objective

In current radiotherapy planning, a set of predefined, aggregated, population-based dose-volume constraints are used to maximize the therapeutic ratio. In this study, we introduce a novel radiotherapy planning approach which instead aims to maximize overall survival by incorporating risk of recurrence and mortality from late effects into inverse optimization.

## Material and Methods

We retrospectively analyzed 38 Hodgkin lymphoma patients (ages: 16-76) with mediastinal disease who were treated with 3D conformal radiotherapy. We used published data to develop risk models for lymphoma recurrence and late normal tissue complications, where we considered radiation-induced mortality from coronary heart disease, secondary lung cancer, and secondary breast cancer. Patient age, sex and cardiac risk factors (CRFs) as well as doses to heart, lung, breast, and tumor target were incorporated in the models. Patients were planned twice, once assuming the presence of CRFs and once assuming no CRFs. 16 co-planar gantry angles were chosen and 4 beam options per gantry angle were created and used for optimization. The dose from each beam option was calculated in a commercial treatment planning system and monitor units were optimized in our MATLAB-based, in-house, particle swarm optimization code to create outcome-optimized plans.

## Results

Outcome-optimized plans were created for 38 patients (Figure 1). The maximum reduction of the total risk (summed probabilities of recurrence and normal tissue complication) achieved by outcome-optimized plans compared to clinical plans was 8.1% for patient cases with cardiac risk factors (CRF) and 10.9% for cases without CRF (Figure 2). The total risk was reduced more than 1% for 9/38 patient cases with CRF and 10/38 patient cases without CRF. The results are, however, sensitive to the definition of risk models, in particular models of tumor control under inhomogeneous target coverage.

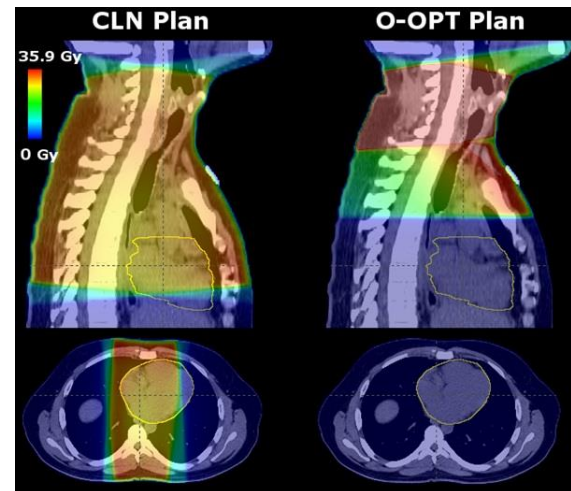


Figure 1. Example of a clinical (CLN) plan compared to an outcome-optimized (O-OPT) plan where the optimizer compromised the coverage of the target to spare the heart and lungs and improved risk of 9.9%.

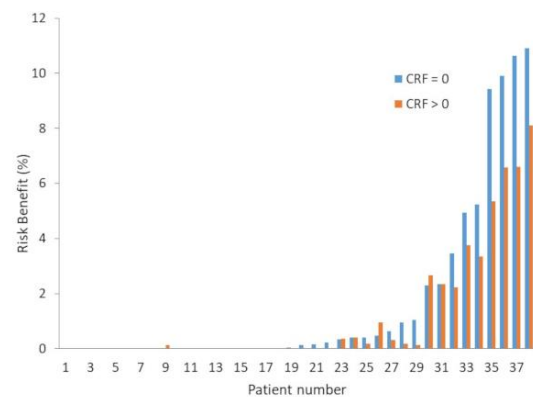


Figure 2. Reduction in risk (of recurrence and normal tissue complications) for outcome-optimized plans compared to clinical 3D conformal plans for the 38 patients with mediastinal Hodgkin lymphoma in this study with and without the presence of cardiac risk factors (CRF).

## Conclusion

We present a study of an individualized outcome-optimized radiotherapy planning technique based on metrics related to overall survival. A substantial potential benefit was observed in some patients, but the underlying knowledge of dose-response models is an important limitation.

**EP-1813 AAA vs Monte Carlo Dose Calculation Algorithm for Lung SABR**

I. Badrigan<sup>1</sup>, V. Huang<sup>1</sup>, D. Shellenberg<sup>2</sup>, A. Krauze<sup>2</sup>  
<sup>1</sup>BC Cancer Surrey, Medical Physics, Surrey, Canada ; <sup>2</sup>BC Cancer Surrey, Radiation Oncology, Surrey, Canada

### Purpose or Objective

To evaluate the dose calculation accuracy of the Varian Eclipse anisotropic analytical algorithm (AAA) for stereotactic ablative body radiotherapy (SABR) in comparison with Monte Carlo (MC) in order to investigate the dosimetric consequences to organs at risk (OAR) and coverage of planning target volume (PTV) in lung SABR plans.

### Material and Methods

25 cases of non-small-cell lung cancer (NSCLC) that were previously treated with SABR to 48 Gy in 4 fractions at our center were selected for this study. These cases were treated from March 2016 to February 2018 and were selected such that the PTV size covers a wide range, from 8.9 cc to 163.2 cc. The internal gross target volume (IGTV) has been contoured from the 4DCT and a 5 mm isotropic expansion was applied to form PTV. The original treatment plans were calculated with 6 MV flattening filter free (FFF) beams using AAA in Eclipse treatment planning system (TPS). The same plans were recalculated using MC for the purpose of this study. Dose volume histogram (DVH) data has been exported for all cases and later processed using in-house code developed in the R programming language. The following dose-volume parameters were used for the comparison:  $V_{100\%}$ ,  $V_{90\%}$  and  $D_{min}$ , to the PTV; conformity index ( $V_{100\%}/V_{PTV}$ ), low dose conformity ( $V_{50\%}/V_{PTV}$ ) and  $D_{2cm}$ ;  $V_{100\%}$  to IGTV;  $V_{20Gy}$  for the lung; dose parameters to OARs including chest wall, esophagus, great vessels, brachial plexus, trachea, heart, bronchial tree, skin and cord. The statistical comparison has been done by paired t-test analysis.

### Results

Comparable results were obtained for AAA and MC calculations except for  $V_{100\%}$  to the PTV ( $p < 0.001$ ), conformity index ( $p = 0.008$ ), low dose conformity ( $p < 0.001$ ) and lung  $V_{20Gy}$  ( $p < 0.001$ ). The largest difference was observed for  $V_{100\%}$  to PTV which in turn impacts the conformity index too. AAA calculations underestimated dose to lungs and PTV compared to MC. The dose differences in PTV  $D_{min}$  and PTV  $V_{90\%}$  as well as  $D_{2cm}$  were not statistically significant. No correlation has been observed between the PTV size and the dose differences between AAA and MC. Occasionally, MC revealed hot and cold spots which were not present in the AAA calculations.

### Conclusion

Our results demonstrate good agreement between AAA and MC doses to OARs for the most part. Lung is an exception as AAA underestimates  $V_{100\%}$  to PTV. AAA emerges a good choice for routine planning, but occasionally MC reveals hot or cold spots in sensitive places, e.g. the PTV center and therefore any plan-specific QA strategy should employ better algorithms to detect such instances. Further investigations are necessary in larger patient cohorts to determine whether AAA is still appropriate for dose calculations in cases of very small field size lung SABR treatment plans.

### EP-1814 On the aperture shape controller and the air cavity correction for lung plans using AcurosXB and AAA

L. Fog<sup>1</sup>, K. Offer<sup>1</sup>, N. Hardcastle<sup>1</sup>

<sup>1</sup>The Peter MacCallum Cancer Centre, Physical Sciences, Melbourne, Australia

### Purpose or Objective

Volumetric modulated arc therapy (VMAT) plan optimisation for radiotherapy in the thorax is subject to uncertainties in dose calculation algorithms during optimisation and to variations in plan complexity. The Eclipse™ v15.5 (Varian Medical Systems) Photon Optimiser incorporates two features: Air Cavity Correction (ACC) to improve the accuracy of scattered dose in the optimiser, and Aperture Shape Controller (ASC) to increase contiguity of apertures during VMAT delivery. We investigate the

effect of these features on dosimetry and delivery metrics for radiotherapy to locally advanced lung tumours.

### Material and Methods

12 randomly selected locally advanced NSCLC patients planned to 60 Gy in 30 fractions were prospectively re-optimised. All geometry and optimisation settings were constant except for ACC ('On' vs 'off') and ASC ('off', 'moderate', 'very high'). Two ipsilateral VMAT arcs were used and plans were calculated with AcurosXB (AXB,  $D_m$ ) and AAA (both version 15.5.11). To facilitate comparison of near minimum and near maximum doses the plans were normalised to median PTV dose received prescription dose. Intermediate dose was calculated during the optimisation. The following parameters were extracted: MU/Gy, edge metric (MLC open leaf edges/area), D98% for GTV and PTV, mean heart dose, D0.33cc for the oesophagus, and D5Gy and D20Gy for the (lungs-CTV) structure. Within each algorithm, ASC 'moderate' and 'very high' was compared with ASC 'off', and ACC 'off' was compared with ACC 'on', using paired two tailed t-test.

### Results

Table 1 shows the dosimetry variation for target and OARs, and plan complexity metrics. For AXB and AAA, as ACC was changed from 'off' to 'moderate' and 'very high' there was no statistical difference in GTV D98%, PTV D98%, PTV D2%, mean heart or oesophagus D0.33cc. Lung dose however increased slightly. Use of aperture shape controller decreased plan complexity (edge metric and MU/Gy). Turning ACC 'off' resulted in no difference in treatment plans for AXB, but worse GTV D98% for AAA. ACC had no impact on plan complexity.

Algorithm	ASC	ACC	GTV_D88[%]	PTV_D88[%]	PTV_D02[%]	Lungs <sup>1</sup> V <sub>100</sub> [%]	Lungs <sup>1</sup> V <sub>90</sub> [%]	Heart Mean [Gy]	Oesophagus D0.33cc [Gy]	Edge Metric	MU/Gy
AXB	Off	On	88.2 ± 1.4	90.0 ± 14.2	103.9 ± 1.5	91.9 ± 19.8	131 ± 3.9	9.4 ± 2.2	28.0 ± 2.7	0.74 ± 0.05	203 ± 94
		Off	88.2 ± 1.5	90.0 ± 12.5	104.0 ± 2.4	92.5 ± 19.5	133 ± 4.0	9.5 ± 2.5	29.0 ± 2.7	0.09 ± 0.03	204 ± 106
		Very high	87.0 ± 2.5	90.3 ± 11.0	104.7 ± 4.0	93.1 ± 19.6	142 ± 4.4	9.9 ± 2.6	28.8 ± 2.4	0.07 ± 0.04	202 ± 143
	On	Off	87.9 ± 1.9	90.5 ± 11.7	104.1 ± 2.2	92.9 ± 19.5	133 ± 4.1	9.5 ± 2.3	28.8 ± 2.7	0.76 ± 0.05	207 ± 104
		Moderate	88.2 ± 1.9	90.4 ± 14.2	104.4 ± 2.1	92.9 ± 19.5	133 ± 4.1	9.5 ± 2.3	28.8 ± 2.7	0.76 ± 0.05	207 ± 104
		Very high	88.2 ± 1.9	89.4 ± 13.7	104.4 ± 1.5	93.3 ± 19.0	133 ± 4.0	9.9 ± 2.7	29.6 ± 2.6	0.09 ± 0.03	202 ± 104
AAA	Off	On	88.2 ± 1.9	89.4 ± 13.7	104.4 ± 1.5	93.3 ± 19.0	133 ± 4.0	9.9 ± 2.7	29.6 ± 2.6	0.09 ± 0.03	202 ± 104
		Off	87.0 ± 3.2	89.0 ± 11.2	104.8 ± 2.9	93.8 ± 19.3	142 ± 4.4	10.2 ± 3.0	29.3 ± 2.7	0.07 ± 0.04	200 ± 142
		Moderate	87.0 ± 3.2	89.0 ± 11.2	104.8 ± 2.9	93.8 ± 19.3	142 ± 4.4	10.2 ± 3.0	29.3 ± 2.7	0.07 ± 0.04	200 ± 142
	On	Off	87.9 ± 1.9	90.5 ± 11.7	104.1 ± 2.2	92.9 ± 19.5	133 ± 4.1	9.5 ± 2.3	28.8 ± 2.7	0.76 ± 0.05	207 ± 104
		Moderate	88.2 ± 1.9	89.4 ± 13.7	104.4 ± 1.5	93.3 ± 19.0	133 ± 4.0	9.9 ± 2.7	29.6 ± 2.6	0.09 ± 0.03	202 ± 104
		Very high	88.2 ± 1.9	89.4 ± 13.7	104.4 ± 1.5	93.3 ± 19.0	133 ± 4.0	9.9 ± 2.7	29.6 ± 2.6	0.09 ± 0.03	202 ± 104

Table 1: Mean ± st. dev. dosimetry and plan efficiency metrics for AXB and AAA plans optimised with varying ASC and ACC settings. Blue cells represent statistical significance at  $p < 0.0005$ , green at  $p < 0.005$  and red at  $p < 0.05$ , relative to ASC 'Off' for ASC variation and comparing ACC 'Off' against 'On'

### Conclusion

The Air Cavity Correction is useful for improving target coverage with AAA but not with AXB. Use of Aperture Shape Controller results in no difference in target coverage, but slightly worse lung dose. ASC reduces treatment plan complexity and monitor units.

### EP-1815 MCO in VMAT treatment planning for locally advanced head and neck cancer

B. Farnault<sup>1</sup>, V. Favre<sup>1</sup>, L. Moureau-Zabotto<sup>1</sup>, J. Rolland<sup>2</sup>, A. Tallet<sup>1</sup>, P. Fau<sup>1</sup>

<sup>1</sup>Institut Paoli Calmettes, Radiotherapy Oncology, Marseille, France ; <sup>2</sup>Centre Hospitalier Intercommunal des Alpes du Sud, Radiotherapy Oncology, Gap, France

### Purpose or Objective

Efficacy of inverse planning is becoming increasingly important for advanced radiotherapy techniques, and especially for head and neck cancer to decrease radiation therapy toxicity. However, the inverse planning process can create a suboptimal plan despite meeting all constraints. Multicriteria optimization (MCO) may improve doses at organs at risk (OARs) and provides better treatment planning without being time consuming. The aim of this study was therefore to evaluate the benefit of VMAT with multi-criteria optimization (MCO) in RayStation (v6.1.1.2, RaySearch Laboratories, Sweden) for head and neck cancer patients and compare the DVH difference

between MCO VMAT plans and standard optimization (SO) VMAT plans.

#### Material and Methods

SO VMAT plans and MCO VMAT plans were created for 15 patients with head and neck cancer. Three levels of dose were prescribed to all patients: PTV 70Gy, 63Gy, 56Gy in 35 fractions. Acceptable SO VMAT plans with minimal average dose to OARs were chosen for comparison with deliverable MCO VMAT plans. All the plans were reviewed, and the dose-volume parameters were compared between the MCO plans and the SO plans. VMAT pretreatment QA are performed comparing measured and calculated dose distribution in phantom (ArcCheck, SunNuclear) by means of gamma index (3% 3mm, Threshold 10%). A complexity metric of the MLC, calculated as a function of the shape and the aperture of MLC, and the monitor units (MU) number were compared.

#### Results

For both types of optimization, the dose values required to validate target coverage (D98% and D2%) were respected (< 1% difference). The dose to OARs and the conformation number (CN) for each PTV were compared, and a Wilcoxon signed-rank test was performed. MCO provided statistically significant reduction of Dmean (10% to 20%) for: parotid gland, larynx, oral cavity and Dmax for brainstem ( $p < 0.05$ ) in which the magnitude was related to the overlapping volume of the corresponding OAR and targets. The CN with MCO allowed a gain between 5% and 15%, and especially on the PTV 56Gy ( $p < 0.05$ ). For the spinal cord and the brachial plexus, the study did not show a significant difference ( $p > 0.05$ ). The active planning time was the same. The QA passing rate with gamma analysis was > 99% for both types of optimization. The complexity metric and the MU number are higher with MCO plans compared to SO plans (5% and 10% respectively).

#### Conclusion

MCO is feasible in head and neck cancer treatments and MCO plans significantly reduced the dose of OARs, without compromising the target coverage comparing to standard VMAT optimization. All the plans are deliverable by a Linac. MCO, with the navigation of Pareto plan, enables physicians to provide greater active clinical input into the VMAT planning process.

#### EP-1816 A robustness comparison of margin based and robust plans for head and neck VMAT patients

J. Robbins<sup>1</sup>, E. Vasquez Osorio<sup>1</sup>, A. Green<sup>1</sup>, A. McWilliam<sup>1</sup>, A. McPartlin<sup>2</sup>, M. Van Herk<sup>1</sup>

<sup>1</sup>University of Manchester, Radiation Related Research, Manchester, United Kingdom ; <sup>2</sup>The Christie NHS Foundation Trust, Clinical Oncology, Manchester, United Kingdom

#### Purpose or Objective

PTV margins do not account for organs at risk (OARs). Using more advanced techniques such as robust or probabilistic planning can potentially help spare OARs close to the CTV while still guaranteeing CTV coverage. In this study we compared the robustness for random and systematic errors of head and neck (H&N) VMAT patients for PTV-based and robust plans.

#### Material and Methods

Data from 8 H&N cancer patients, all treated with 2 dose levels of 66Gy and 54Gy over 30 fractions were used. Delineations for CTV1, CTV2, brainstem, spinal cord (SC), and parotids were used for planning, using RayStation v6.99. Margin plans were created following clinical guidelines using 4mm isotropic PTV margins and 5mm PRV margins for the SC and brainstem. Robust plans included an isotropic robustness setting of 3mm for both CTVs and kept the rest of the objectives the same as the margin plan.

A plan evaluator was implemented to simulate treatments with different random and systematic translational set-up errors and collect relevant DVH parameters. For each

simulated treatment, one systematic error and 30 random errors were selected from a Gaussian distribution, and 100 treatments were simulated for each combination of random and systematic error SDs of 1, 2, 3 mm. The number of treatments achieving the clinical goals (Figure 1) were counted.

Structure	Constraint Type	Dose after 30 fractions
CTV1	Min 1cc	>90% prescribed (59.4Gy)
CTV2	Min 1cc	>90% prescribed (48.6Gy)
Spinal cord	Max	<4800
Brainstem	Max	<5400
Lt parotid	Mean	<2600
Rt parotid	Mean	<2600

Figure 1. Table showing the main clinical goals for the plan

#### Results

Figure 2 shows the mean and SD (over all patients) of the percentage of simulated treatments reaching the clinical goals for CTV1 and the SC as function of random and systematic error SD. These percentages decrease as the errors increase for both the OARs and the targets, with systematic errors having more effect than the random errors, as expected.

Comparing the two sets of plans, the margin plans have a consistently higher percentage of treatments in which the minimum dose across 1cc of CTV1 was above 90% of the prescribed dose. This same trend was seen in CTV2. At an SD combination of (1, 2 mm) the margin plans have ~90% of simulated treatments meeting the CTV1 constraint, which is consistent with the PTV margin used (2.5\*1mm + 0.7\*2mm = 4mm). The lower CTV coverage in the robust plan indicates that the robustness setting was too narrow compared to the utilised margin, and the closest to 90% coverage is the SD combination (1, 1 mm).

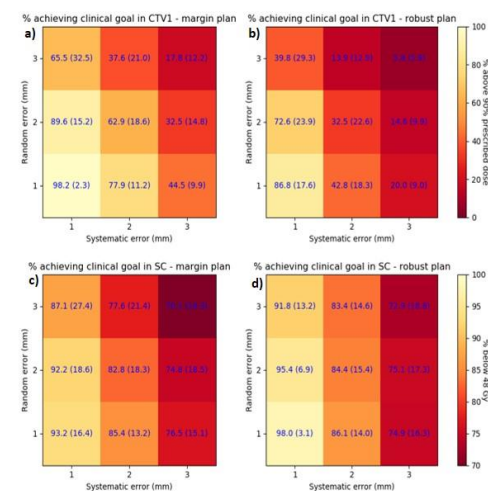


Figure 2. Colour plots showing the number of simulated treatments that achieve the clinical goal. The values for each error are displayed as 'mean (SD)' across all 8 patients. a) and c) show the margin plan, b) and d) the robust plan. a) and b) show the percentage with a minimum value across 1cc of CTV1 of at least 90% of the prescribed dose. c) and d) refer to the percentage with a maximum dose to the spinal cord less than 48Gy.

Comparing the SD combinations with close to 90% CTV probability, the percentage reaching a max dose of <48Gy

to the SC is 92.2% for the margin plan and 98% for the robust plan. This same trend was seen for the other OARs. That is, at a similar probability of CTV coverage the robust plan gives a higher probability of sparing the OARs.

#### Conclusion

A 3mm robustness setting is narrower in terms of CTV coverage compared to a 4mm margin plan. However, at a similar probability of CTV coverage, the robust plan gives a higher probability of sparing OARs. Future work will include analyses for varying robustness settings and include more complex uncertainties.

#### EP-1817 Comparison of 2 VMAT optimization algorithms using complexity metrics for breast cancer radiotherapy

L. Bartolucci<sup>1</sup>, E. Costa<sup>1</sup>, M. Robilliard<sup>1</sup>, A. Mazal<sup>1</sup>  
<sup>1</sup>Institut Curie, Radiation Oncology Department, Paris, France

#### Purpose or Objective

To compare 2 recent VMAT optimization algorithms used by 2 separated TPS for the radiotherapy treatment of breast cancer. For this purpose, complexity of each optimized plan was evaluated using complexity metrics and pre-treatment QA measurements.

#### Material and Methods

10 patients treated for non-metastatic breast cancer were included in the study. All patients received breast and lymph nodes irradiation along with a simultaneous integrated boost to the tumour bed. Prescription dose was 50.4 Gy in 28 fractions to the breast/lymph nodes, and 63 Gy in 28 fractions to the tumour bed. For all patients, VMAT plans were generated with 4 partial arcs of 230° amplitude each using both Eclipse (v.13.6) and RayStation (RS, v.7) TPS. Eclipse and RS optimization were respectively performed using Photon Optimizer and RS VMAT optimization algorithms. Plan optimization objectives, consistent for both TPS, were set to ensure acceptable PTV coverage and minimize dose to the surrounding OAR. For all plans, the following complexity metrics were calculated: MU (mean monitor unit per plan), MI (Park et al., 2014), MCSv, LT and LTMCS (Masi et al., 2013), and SAS with threshold 2 and 5 mm (Crowe et al., 2014). Pre-treatment QA were calculated using Varian's Portal Dose Image Prediction (PDIP) algorithm and delivered on a Varian TrueBeam. Agreement between planned and measured dose was evaluated using Varian Portal Dosimetry (PD) tool with global gamma index analysis (criteria: 3%/3mm). In order to use PD for both TPS, RS plans were recalculated with fixed MU on Eclipse. Statistical significance ( $p < 0.05$ ) was evaluated using a paired two-sided Wilcoxon signed-rank test.

#### Results

All plans were considered clinical acceptable and no statistical significance was observed between Eclipse and RS plans for PTV coverage and mean doses to the main OAR ( $p > 0.05$ ). Significant differences were found between Eclipse and RS for the metrics MU, MCSv and LT indicating that plans optimized with RS may be less complex than plans optimized with Eclipse and PO algorithm, unless for LT which showed more important leaf travel for RS plans ( $p < 0.05$ ). However, no statistical significances were found for MI, LTMCS and SAS metrics (Fig. 1). Pre-treatment PD QA showed significantly better gamma passing rate for RS plans ( $p < 0.005$ ) indicating a better agreement between calculated and measured dose (Fig. 2).

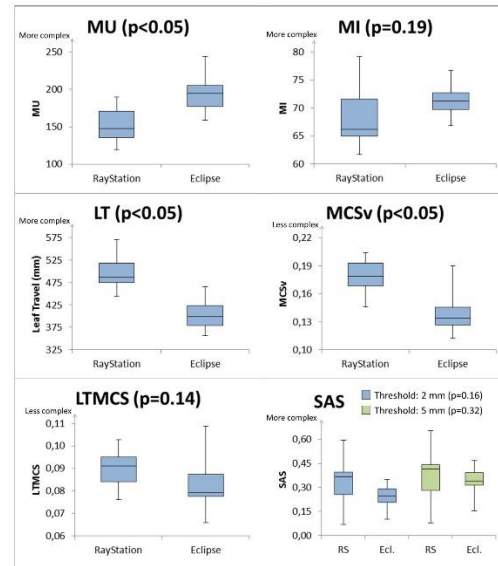


Fig. 1: Box plots for MU, MI, LT, MCSv, LTMCS and SAS complexity metrics for RayStation and Eclipse.

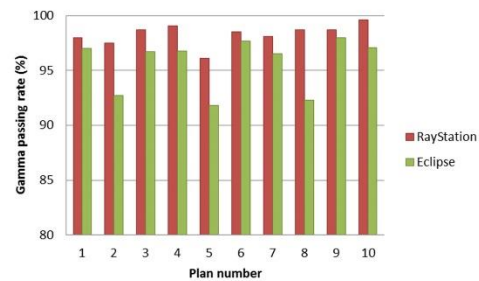


Fig. 2: Comparison of percentage gamma passing rates between RayStation and Eclipse using global 3%/3mm gamma index criteria.

#### Conclusion

Both VMAT optimization algorithms can produce equivalent dose plans regarding target coverage and OAR sparing for all patients of the study. Part of the complexity metrics analyzed in this work shows that, for a comparable dosimetric result, plans optimized with RS may be less complex than plans optimized with Eclipse and PO algorithm. PD results showed a higher degree of agreement for RS plans, indicating the influence of VMAT optimization algorithms on plan deliverability. Further work will include in depth analysis of the complexity metrics to better understand the impact of optimization algorithms on treatment delivery.

#### EP-1818 Comparison of two optimisation algorithms in Eclipse for VMAT in prostate: which one to choose?

D. Jurado-Bruggeman<sup>1</sup>, E. Sansalvador Boadas<sup>2</sup>, A. Onés Segarra<sup>1</sup>, D. Lambisto Castro<sup>1</sup>, M. Buxó<sup>3</sup>  
<sup>1</sup>Institut Català d'Oncologia, Medical Physics and Radiation Protection, Girona, Spain ; <sup>2</sup>Universitat de Barcelona, Física, Barcelona, Spain ; <sup>3</sup>Girona Biomedical Research Institute, IdibGi, Girona, Spain

#### Purpose or Objective

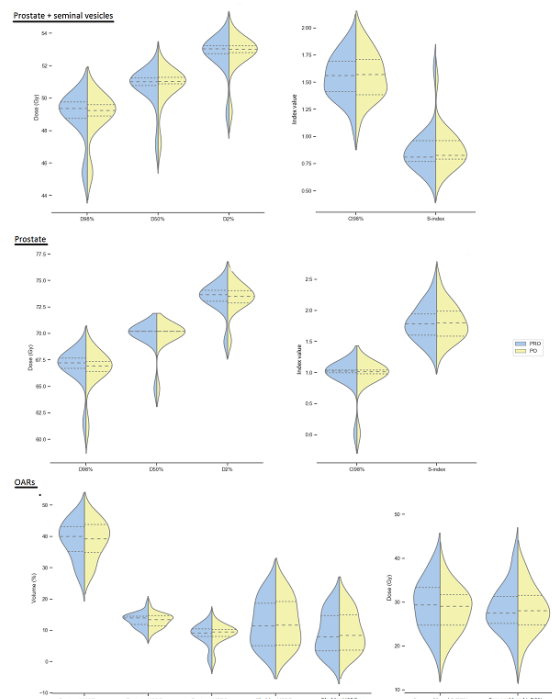
Eclipse TPS version 13.7 introduced Photon Optimizer (PO) optimisation algorithm. The previous Progressive Resolution Optimizer (PRO) engine is also available. The aim of this work is to evaluate the performance of PO against PRO for prostate VMAT treatments, both in terms of dosimetric quality and plan complexity, to aid choosing which one to use in clinical practice.

#### Material and Methods

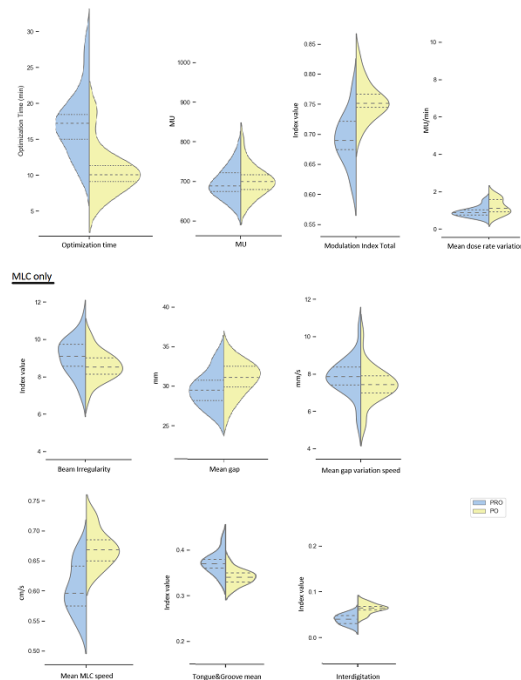
Twenty-two prostate cancer patients were randomly selected, all of them with seminal vesicles and a simultaneous integrated boost to the prostate. For each patient, two identical VMAT plans were created in Eclipse v13.7 using 2 arcs and 6 MV photons. One of the plans was optimised using PO v13.7 and the other using PRO v13.7 with the same optimisation goals. The dose distribution was calculated with Acuros XB in terms of dose-to-water and normalised to the median dose to the prostate. The dosimetric comparison of both plans was done for the PTVs by using Conformity Index (CI), Homogeneity Index (HI) and S-index, D98%, D50%, and D2%. Doses to OAR were also compared for the rectum (V44, V61, V65), bladder (V61, V65), and femoral heads (D2%, V50). Plan complexity was evaluated with a software developed in MATLAB by our National Society that returns several complexity indices and parameters: MUs, MLC information (speed and acceleration, gap and its variation speed), tongue-and-groove effect (T&G), interdigitation, Modulation Index Total, Modulation Complexity Score, Beam Irregularity, leaf travel, and dose rate and gantry speed variations. Optimisation times were also compared. The statistical analysis of the paired differences was performed using Wilcoxon tests.

### Results

The dosimetric differences are shown in Figure 1 as violin plots (median, quartiles, and density for each algorithm).



All these differences were not clinically relevant (below 1%). Optimisation time and plan complexity differences are shown in Figure 2.



Optimisation times were lower for PO (42%) than for PRO. Plan complexity was handled differently. PO plans had more MU and higher dose rate variations, total modulation, and MLC speed. Nevertheless, the MLC shape was simpler for PO: lower Beam Irregularity, higher and more stable (lower variation speed) mean gap between opposed leaves, and lower T&G. The interdigitation was higher for PO due to the pairs of leaves partially included in the limits in Y direction: PO moves its touching point outside the jaws whereas PRO puts it in the middle. There were no gantry speed variations in any case.

### Conclusion

PO and PRO optimisation algorithms implemented in Eclipse were analysed for prostate VMAT treatments in terms of dosimetric quality and plan complexity. PO optimisation times were much lower than PRO's. There were no clinically relevant differences in the dose distributions, but plan complexity was handled differently, with PO moving it from MLC shape to MLC speed and dose rate variations. Overall, PO is preferable over PRO for prostate VMAT treatments.

### EP-1819 Robustness to shifts in patient position with either knowledge based or multi-criteria optimisation

P. Houston<sup>1</sup>, D. Keiller<sup>1</sup>

<sup>1</sup>Beatson West of Scotland Cancer Centre, Radiotherapy, Glasgow, United Kingdom

### Purpose or Objective

To perform a comparison of the robustness of two treatment planning optimisation methods to shifts in patient position for VMAT Pancreas Planning. The optimisation methods investigated were a knowledge based planning solution, RapidPlan (RP v15.5), and a multi-criteria optimisation solution (MCO v15.5).

### Material and Methods

Knowledge based planning was performed with RP. Multi-criteria optimisation was performed with MCO. All plans were two arc axial VMAT and were normalised to a PTV mean of 100% dose.

RP generates estimated DVHs and planning objectives based on the library of plans it is built from. MCO is a planning trade off tool that calculates multiple plans for each planning objective; this allows the planner to explore the Pareto surface of the ideal dose distribution to

determine the optimal trade off between PTV coverage and OAR doses.

RP and MCO were applied to 10 Pancreas planning cases. Previous work, Houston P., Laverick N. *Planning comparison of knowledge based planning and multi-criteria optimisation for VMAT pancreas planning. ESTRO 2017* compared the plans with regards to plan quality. The treatment plans were here investigated for robustness to patient set-up by shifting the patient and re-measuring dose volume statistics. Plans were shifted  $\pm 0.3\text{cm}$  and  $\pm 0.5\text{cm}$  in the x, y and z directions and worst case dose values recorded for each PTV and OAR.

## Results

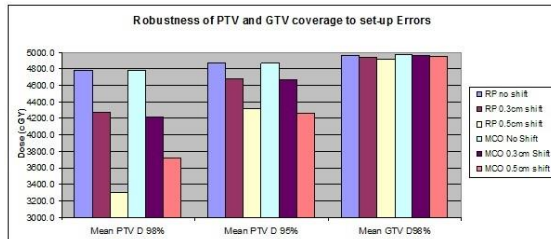


Figure1: Comparison of PTV and GTV coverage when shifts of 3mm and 5mm from planned position are applied.

MCO v15.5 and RP v15.5 plans show comparable robustness to 0.3cm shifts. MCO v15.5 gives higher PTV D98% coverage after a 0.5cm shift than RP v15.5. GTV coverage is not significantly affected by either a 0.3cm or 0.5cm shift, as expected due to GTV to PTV margins of 1cm.

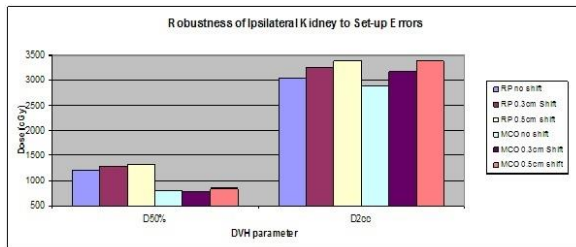


Figure 2: D50% and D2cc for ipsi-lateral kidney when shifts of 3mm and 5mm from planned position are applied.

The improvements in plan quality with MCO conferred a significant advantage in the robustness of OAR dose to shifts in patient position. Average ipsilateral kidney D50% was lower with MCO v15.5 shifted 0.5cm when compared to unshifted RP plans, 837cGy and 1200cGy respectively. Duodenum, which is often the dose limiting organ in pancreas planning, did not display a significant change in robustness of D33% or D2cc.

## Conclusion

MCO treatment planning does not degrade the robustness of PTV coverage to shifts in patient position and may in some cases improve that robustness. OAR doses are either comparable or improved when planned with MCO and possible shifts in patient are accounted for. This general robustness to changes in patient shifts indicates that current margins, imaging and set-up protocols are appropriate for MCO planned pancreatic radiotherapy treatments.

## EP-1820 Preliminary results of using artificial neural networks for prediction CK planning parameters

A. Skrobała<sup>1,2</sup>, J. Ginter<sup>3</sup>, B. Pawalowski<sup>1,4</sup>, M. Skowron<sup>3</sup>,

M. Adamczyk<sup>1</sup>, A. Jodda<sup>1</sup>, J. Litoborska<sup>1</sup>

<sup>1</sup>Greater Poland Cancer Centre, Department of Medical Physics, Poznan, Poland ; <sup>2</sup>Poznan University of Medical Sciences, Department of Electroradiology, Poznan, Poland ; <sup>3</sup>University of Warsaw, Department of

Biomedical Physics, Warsaw, Poland ; <sup>4</sup>Poznan University of Technology, Faculty of Technical Physics, Poznan, Poland

## Purpose or Objective

Optimal values of treatment plans parameters for CyberKnife (CK) prostate's treatment, could varied from patients-to-patients. An artificial neural network (ANN) could be powerful tool for a radiotherapy technique for mapping individual patient anatomy and other treatment plan's parameters. ANN could be support tools for prediction optimal parameters for CK's treatment. This study was performed to investigate the feasibility of ANN in prediction CK treatment planning parameters for prostate cancer.

## Material and Methods

A set of retrospective clinical data from 200 patients with prostate cancer were used to build and train the ANNs to predict radiotherapy treatment plan parameters. 22 new patients were used to test the models. Inputs were chosen from general parameters such as: prescription dose, volumes of PTV and six OARs and geometry parameters defining distance between mass centers of PTV and OARs, respectively.

A fully connected ANN was used with two hidden layers of 150 neurons, 18 input and 14 output neurons. As an activation function the Rectified Linear Units (ReLU) were used, with 0.4 dropout rate in order to avoid over fitting. The net was trained in 2000 epochs, with mean squared error as a loss function.

## Results

Errors of ANN's prediction of the plans parameters for patients from test set were evaluated in terms of mean absolute value of differences (mean(abs(diff))) between predicted and original values and root-mean-squares (rms (diff)) of these values. Table 1 presents mentioned errors for chosen parameters (prescribed isodose (%), number (#) of nodes, beams and collimators, estimated treatment time (minutes), PTV CI and PTV Coverage (%)) in comparison with original mean values (mean test) of parameters in the test set.

Table 1. Values of evaluated parameters: mean absolute value of differences (mean(abs(diff))) between predicted (ANN) and original values, root-mean-squares (rms (diff)) and mean values (mean(test)) of parameters in the test set of these values for seven predicted treatment planning parameters for CyberKnife prostate's treatment.

parameters	isodose (%)	# of nodes	# of beams	# of collimators	time (minutes)	PTV CI	PTV Coverage(%)
mean(abs(diff))	2.7	6.2	20.3	0.4	2.4	0.04	3.2
rms(diff)	3.2	7.4	23.9	0.7	3.1	0.04	3.7
mean(test)	79.4	33	162.2	4.3	33	1.08	95.8

## Conclusion

This investigation was preliminary and lead us to confirm the feasibility of artificial neural network in prediction CyberKnife treatment planning parameters for prostate cancer. The errors in comparison with mean values of parameters in test set were not high, but not yet good enough to be useful for clinical purposes: the errors were comparable with standard deviations of parameters of test set. Moreover several steps have to be undertaken in future. In order to predict features of treatment planning parameters, the crucial information is in geometry dependencies of PTV and OARs, which could be found specially tailored parameters. We suppose it could be obtained by convolutional neural network with bigger amount of training examples.

## EP-1821 Fast Robust Optimization using a Patient-Specific Scenario Selection Methodology

G. Buti<sup>1</sup>, K. Souris<sup>1</sup>, J.A. Lee<sup>1</sup>, E. Sterpin<sup>2</sup>

<sup>1</sup>Université Catholique de Louvain, Molecular Imaging-Radiotherapy & Oncology, Brussels, Belgium ;

<sup>2</sup>Katholieke Universiteit Leuven, Experimental Radiotherapy & Oncology, Leuven, Belgium

### Purpose or Objective

In proton therapy treatments, physical uncertainties can cause both aiming and range errors. Current planning strategies aim at achieving robust plans by optimizing an objective function over a discrete set of scenarios. As the problem complexity scales exponentially with the number of considered uncertainty sources, a pre-selection of scenarios is necessary to limit the computational burden and keep the computation time within clinically acceptable timescales.

The set of scenarios in conventional treatment planning is statistically inconsistent due to the use of unlikely scenarios (large setup error (SE) of 5 mm AND proton range error (PRE) of +/-3%) that lie outside of the planned confidence interval (CI), potentially compromising plan quality. This study aims to establish a novel treatment planning methodology that produces plans of acceptable robustness and guarantees coverage of a certain percentage of beam positions and proton ranges, defined by a priori chosen CI. The focus is to make the methodology statistically sound, fast and computationally cheap by efficiently pre-selecting relevant scenarios which are later fed to the robust optimizer.

### Material and Methods

We consider lung treatments with motion characterized by a 4DCT binned in ten breathing phases; robustness should be achieved for all phases. SE and PRE are distributed as Gaussian distributions with standard deviations of 2 mm and 1.6%, respectively. We perform two successive steps to determine the relevant scenarios: first, 12 scenarios are selected that cover extreme positions reached by the tumor during breathing together with spatial shifts of 5 mm and image density scaling of +/-2.5% (sampling of a 4D isoprobability hypersurface). The second selection is based on the magnitude of the PRE, estimated from maps of water-equivalent path lengths, computed for scenarios randomly sampled according to the distributions defined above. 20 scenarios are selected that produce the largest PRE evaluated for each voxel inside the CTV (see Fig. 1). All treatment plans were calculated for a lung tumor case and plan optimization was performed using the robust optimizer in RayStation 6. The dose prescription was 60 Gy (minimum coverage of 57 Gy). Conventional robustness optimization with SE of 5 mm, PRE of +/-3% and inhale/exhale breathing phases, was used as a reference. Plan robustness was evaluated with the MCsquare code by recalculating the dose distribution on a set of 100 randomly sampled error scenarios.

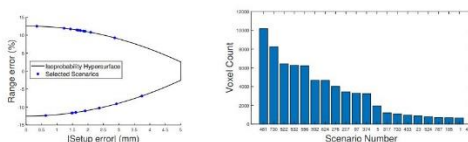


**Figure 1:** Scenario selection procedure. The left panel illustrates the isoprobability hypersurface with the selected scenarios. The right panel shows the scenario statistics, i.e. scenario  $i$  was counted as the worst case in  $x$  number of voxels of the CTV.

### Results

As shown by Table 1, an average right lung dose reduction of 3.1 Gy reduction is achieved, whilst reducing the average target dose ( $D_{98}$ ) by 2.1 Gy, with the scenario selection method as compared to a conventional one. Moreover, half of the number of optimization scenarios are necessary to produce this plan. Hence, the plan calculation time was reduced by half.

**Table 1:** DVH metrics for plans produced using the scenario selection (S.S.) and conventional (Conv.) methods.  $\bar{D}$  denotes the mean dose level.

	CTV		Heart	R. Lung
	$\bar{D}_{98}$ [Gy]	$\bar{D}_2$ [Gy]	$\bar{D}_{mean}$ [Gy]	$\bar{D}_{mean}$ [Gy]
Conv.	54.8 (53.8, 58.1)	65.2 (65.4, 62.5)	2.8 (3.5, 2.7)	16.3 (18.1, 16.3)
S.S.	52.7 (50.2, 55.6)	64.4 (64.6, 62.0)	2.6 (3.5, 2.4)	13.4 (15.0, 13.3)

\*The values between brackets ( $D_{worst}$ ,  $D_{nom}$ ) represent the worst case and nominal case scenarios, respectively, evaluated from the 90% best perturbed scenarios.

### Conclusion

Serious reduction of plan calculation time is achieved using the scenario selection methodology without significant compromise in treatment plan quality.

### EP-1822 Evaluation of plan robustness against tumor motion for lung SBRT treatment with non-coplanar VMAT

C. Garibaldi<sup>1</sup>, A. Bazani<sup>2</sup>, F. Pansini<sup>2</sup>, F. Emiro<sup>2</sup>, S. Trivellato<sup>2</sup>, S. Comi<sup>2</sup>, G. Piperno<sup>3</sup>, A. Ferrari<sup>3</sup>, B.A. Jereczek-Fossa<sup>3,4</sup>, M. Cremonesi<sup>1</sup>, F. Cattani<sup>2</sup>

<sup>1</sup>IEO-European Institute of Oncology IRCCS, Unit of Radiation Research, Milano, Italy; <sup>2</sup>IEO-European Institute of Oncology IRCCS, Unit of Medical Physics, Milano, Italy; <sup>3</sup>IEO-European Institute of Oncology IRCCS, Dept. of Radiation Oncology, Milano, Italy; <sup>4</sup>University of Milan, Department of Oncology and Hemato-Oncology, Milan, Italy

### Purpose or Objective

to investigate robust optimization for lung SBRT treatment using a non-coplanar VMAT technique, taking into account tumor motion due to respiration. Plan robustness was evaluated against variation in time spent in each breathing phase and variation of the mean tumor position. Robust plan was compared with the ITV-based plan for 3D dose and 4D dose accumulation.

### Material and Methods

Dynamic Wave Arc (DWA) is a novel non-coplanar VMAT technique implemented on the VERO system. The fluence modulation is achieved by a synchronized moving of gantry, ring and leaves at a fixed dose rate (400 UM/min). 4D CT of 2 patients treated for lung SBRT and CIRS phantom moving with 9 different breathing patterns (6 sinusoidal with A=5-15 mm and 3 with real patient breathing) were used for robust optimization using minimax optimization method in Raystation v8A (0.2 mm dose grid, Collapsed Cone Convolution Algorithm v3.5). Robust plan was calculated on the CT end-exale (CT<sub>EXP</sub>) and optimized on the GTV+5 mm on each respiratory phase, while ITV-based plan was calculated on the CT average intensity projection (CT<sub>AVE</sub>), obtained from all breathing phases, and optimized on ITV+5 mm with a prescription dose of 54 Gy in 3 fractions with a goal of  $D_{95\%}=95\%$  for GTV + 5 mm and ITV+5mm, respectively. Doses were calculated on each phase, deformed onto both CT<sub>AVE</sub> and CT<sub>EXP</sub> and accumulated over all phases. To assess robustness against realistic variation in time spent in each breathing phase, 3 methods of 4D dose accumulation were used: equivalent weight to all phases ( $\Sigma_{EQUI}$ ), more weight to expiration phases ( $\Sigma_{EXP}$ ), and more weight to the inspiration phases ( $\Sigma_{EQUI}$ ). To evaluate plan robustness against a baseline shift of the tumor, perturbed doses with a shift from the isocentre of  $\pm 5$  mm in CC and AP direction independently were calculated. Both 3D and 4D doses of the robust plan were compared with the conventional ITV-based approach.

### Results

Preliminary results for two patients and phantom with a tumor motion in CC direction of 10 and 15 mm are reported. All Robust and ITV-based plans satisfied criteria

for clinical acceptability. A reduced number of MU was obtained for the robust plan with a mean variation of -18% (-32%/-10%) compared to the conventional plan. Very small variation of dose metrics for GTV and OARs were obtained considering the 3 dose accumulation methods, as well as the perturbed doses. Small differences non clinically relevant were found between 3D and 4D dose calculation for both robust and ITV-based plan.

Plan	Dose difference (Gy)		GTV Dmin	GTV Dmean	GTV Dmax	Dmean lung	Dmax PRV cord
Robust	3D- $\Sigma_{EQUI}$	mean	-0.42	-0.06	0.26	-0.30	0.04
		SD	0.82	0.54	0.37	1.21	0.13
	$\Sigma_{EQUI} - \Sigma_{EXP}$	mean	0.08	0.08	0.09	-0.03	0.03
		SD	0.15	0.14	0.14	0.04	0.02
	$\Sigma_{EQUI} - \Sigma_{NSP}$	mean	-0.01	-0.06	-0.13	0.13	0.12
		SD	0.32	0.43	0.49	0.16	0.22
ITV-based	3D- $\Sigma_{EQUI}$	mean	0.29	0.19	0.62	-0.15	0.02
		SD	0.14	0.05	0.37	0.55	0.04
	$\Sigma_{EQUI} - \Sigma_{EXP}$	mean	-0.10	-0.04	-0.02	-0.03	0.01
		SD	0.07	0.10	0.23	0.04	0.03
	$\Sigma_{EQUI} - \Sigma_{NSP}$	mean	-0.08	-0.14	-0.34	-0.01	-0.03
		SD	0.19	0.24	0.27	0.04	0.05
Robust	perturbed dose (0, 0, $\pm$ 5mm)	mean	0.50	0.07	0.05	0.02	0.01
		SD	0.18	0.13	0.27	0.25	0.16
	(0, $\pm$ 5mm, 0)	mean	0.42	0.11	-0.04	0.04	0.01
		SD	0.35	0.11	0.34	0.27	0.12

## Conclusion

Robust optimization to account for respiratory motion was investigated for DWA lung SBRT. Our preliminary results confirmed the robustness against realistic variation in respiratory motion. Further investigations are warranted to confirm the clinical effectiveness of this novel approach compared to the conventional margin-based approach.

**EP-1823 Analysis of treatment plans robustness for dynamic techniques in external beam radiotherapy**  
 E. Dabrowska-Szewczyk<sup>1,2</sup>, M. Bukat<sup>1</sup>, P. Kukolowicz<sup>1</sup>, D. Szalkowski<sup>1</sup>, A. Paciorkiewicz<sup>1</sup>, A. Zawadzka<sup>1</sup>  
<sup>1</sup>Maria Skłodowska-Curie Memorial Cancer Center and Institute of Oncology, Department of Medical Physics, Warsaw, Poland ; <sup>2</sup>University of Warsaw, Department of Biomedical Physics, Warsaw, Poland

## Purpose or Objective

Uncertainty of patient positioning during treatment session have a significant impact on dose distribution in clinical target volume (CTV) and organs at risk (OARs). However, usually some discrepancy between DRR and daily set-up of the patient's position during the treatment are acceptable. The aim of our study was to evaluate the robustness of dynamic techniques dose distributions against isocentre shifts and to verify whether threshold used in patient position verification were chosen correctly.

## Material and Methods

For this study, plans prepared for 400 patients treated with VMAT or IMRT were retrospectively analyzed (50 plans per the following cases: brain-IMRT, head and neck-IMRT, head and neck-VMAT, breast-IMRT, breast VMAT, lung-VMAT, gynecology-IMRT, canal anal-VMAT). To estimate the robustness of analyzed plans against simulated isocenter shifts, tool named "Plan Uncertainty" was used (Eclipse TPS, Varian, version 15.6). For each plan the new 6 dose distribution were re-calculated with taking into account the positive and negative maximally acceptable threshold in our clinic during patient position verification. The values of acceptable shifts are as follow: 3 mm in case of brain and head and neck patients, 6 mm in case of breast patients and 4 mm in case of lung, gynecology and anal canal patients. For 400 references and 2400 re-calculated plans, near to minimum doses (D98%, D99%) and near to maximum doses (D1%, D2%) for CTV were investigated. Tolerance doses for relevant OARs were also evaluated according to our clinical protocol.

## Results

The dose distribution in CTV was not essentially affected by the isocenter shifts and still fulfilled constraints to be used in our clinic, regardless of tumor location, dynamic technique used and shift direction. Only in few cases CTV constraints were slightly violated on average by: 0,7%, 1,1%, 0,9, 0,3% of re-calculated plans for D98%, D99%, D1% and D2%, respectively. In case of rectum (gynecology, IMRT), jaw (head and neck, VMAT) and lungs (lung, VMAT) overdosage caused by isocenter shift was observed in more than 7% of re-calculated plans. For bladder and pelvic bones (gynecology IMRT), jaw (head and neck IMRT), optic nerves, optic chiasm and brainstem (brain IMRT) discrepancies below 3.3 % of simulated plans were observed. More detailed information was included in Table 1. No relevant impact was observed on rest of OARs, important in analyzed tumor locations.

Table 1. Percentage of re-calculated plans in which OARs tolerance doses were exceeded

TUMOR LOCATION	OAR	CONSTRAINTS	PERCENTAGE OF NUMBER OF PLANS (%)	MAXIMUM OAR'S OVERDOSAGE
brain (IMRT)	optic nerve left	d_max<54Gy	3.00	54.80y
	optic nerve right	d_max<54Gy	3.33	54.80y
	optic chiasm	d_max<54Gy	2.00	54.70y
brainstem	brainstem	d_max<54Gy	2.18	54.80y
	jaw	d_max<30Gy	7.00	74.3 Gy
head and neck (IMRT)	jaw	d_max<30Gy	12.57	74.3 Gy
	lungs	V20<15%	7.00	17.8%
lung (VMAT)	lungs	d_mean<20Gy	7.67	21.2 Gy
	rectum	V45<20%	13.37	73.01%
gynecology (IMRT)	bladder	V65<20%	2.00	92.3%
	pelvic bones	V20<75%	2.67	78.5%

## Conclusion

Based on 2400 simulated plans, dosimetric treatment plan parameters robustness was analyzed in the context of the daily patient positioning error. For all plans the dose distribution in the CTV fulfilled all investigated criteria. Analysis of OARs showed that in some cases isocenter displacement cause dose restrictions exceeding, however it is the worst-case scenario, when the systematic error would occur. In case of serial OARs, for which PRV concept was used, the maximum overdosage not exceed more than 1 Gy. Thresholds used in our clinic in patient position verification seem to be well adjust as to treat patients properly.

## Electronic Poster: Physics track: Treatment planning: applications

### EP-1824 Hybrid-Volumetric Modulated Arc Therapy in the Upper Thoracic Esophageal Cancer: A Planning Study

Y.E. Choi<sup>1</sup>, K. Sung<sup>1</sup>, H.J. Kim<sup>1</sup>, Y.K. Lee<sup>1</sup>  
<sup>1</sup>Gil Medical Hospital, Radiation Oncology, Incheon, Korea Republic of

## Purpose or Objective

To compare the dosimetric differences and lung sparing of three different treatment techniques - three-dimensional conformal radiotherapy (CRT), volumetric modulated arc therapy (VMAT) and Hybrid-VMAT (H-VMAT) in the treatment of upper thoracic esophageal cancer.

## Material and Methods

CRT, VMAT, and H-VMAT plans were regenerated for 14 upper thoracic esophageal cancer patients with T3N0-1M0. The target prescription dose was 50.4 Gy. All plans were optimized to reach clinically acceptable levels by the departmental plan criteria: the maximum dose for the spinal cord was less than 45 Gy, whereas the volume of the lung irradiated by a dose of 20 Gy (V<sub>20</sub>) and 30 Gy (V<sub>30</sub>) was less than 30% and 20%, respectively. For PTV coverage, 95% of PTV should be covered by 95% of the prescription dose, unless the spinal cord limit was violated. Plan quality was evaluated using: conformity index (CI), homogeneity index (HI), mean lung dose (MLD), lung volume receiving >5-30 Gy (lung V<sub>x</sub>), and maximum spinal cord dose (cord D<sub>max</sub>). The Wilcoxon Signed-Rank test was used to determine any differences between datasets with a Bonferroni's adjustment for multiple comparisons (p < 0.017).

## Results

In comparison with CRT, VMAT and H-VMAT yielded a better conformity and significantly lower MLD, cord  $D_{max}$ , and lung volume receiving >10-30 Gy. No differences were observed in lung  $V_5$  between CRT and VMAT (41.59% and 44.59%, respectively). VMAT plans represented the best conformity and the lowest cord  $D_{max}$ , whereas H-VMAT plans gave the lowest MLD and lung volume receiving 5-10 Gy.

## Conclusion

The H-VMAT technique was superior in lung sparing with comparable dose coverage for treating upper thoracic esophageal cancer compared to CRT and VMAT.

## EP-1825 Variability of PTV volume and target coverage for hypofractionated prostate treatments

E.M. Ambroa Rey<sup>1</sup>, A. Ramirez Muñoz<sup>1</sup>, J. Garcia-Miguel Quiroga<sup>1</sup>, R. Gómez Pardos<sup>1</sup>, D. Navarro Giménez<sup>1</sup>, N. Feltes<sup>2</sup>, J. Lozano<sup>2</sup>, A. Muñoz<sup>2</sup>, M. Galdeano<sup>2</sup>, M. Colomer Truyols<sup>1</sup>

<sup>1</sup>Consorti Sanitari de Terrassa, Medical Physics Unit-Radiation Oncology, Terrassa, Spain ; <sup>2</sup>Consorti Sanitari de Terrassa, Radiation Oncology, Terrassa, Spain

## Purpose or Objective

To study the variability of PTV volume and PTV coverage depending on the Radiation Oncologist (RO) who performs the contours and the Medical Physicist (MP) who executes or reviews the treatment plan, and to evaluate if the different combinations of MP and RO have an influence on the PTV coverage.

## Material and Methods

175 patients with low or intermediate risk prostate cancer were selected for this study. Patients were recruited following a strict protocol. The hypofractionated scheme was 60Gy in 20 fractions. VMAT plans were carried out using Monaco TPS (v5.10) based on a single arc arrangement.

Every patient was delineated by one RO and planned/reviewed by one MP. A total of 4 RO and 5 MP were evaluated. The same protocol for delineation, treatment planning and plan evaluation was used for all patients.

At least 98% of the PTV covered by 95% of the dose prescription is required and the OAR must satisfy a certain constraints otherwise patient is changed to another fractionation scheme.

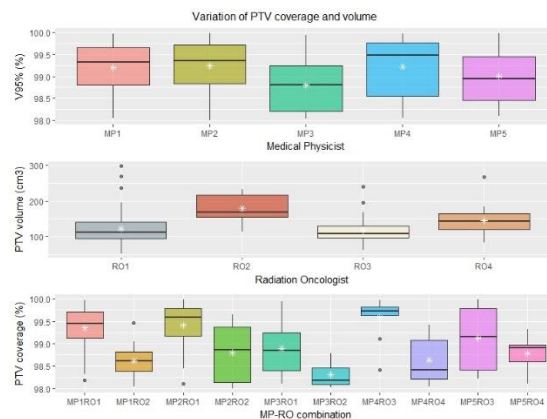
## Results

The number of patients contoured by each RO and reviewed by each MP is summarized in Table I; along with the different combinations of MP-RO (combinations with less than 5 patients were excluded).

Number of patients for each observer					
Medical physicist	Mean V95% (%)	Radiation oncologist	Mean PTV volume (cm <sup>3</sup> )	MP-RO combination	Mean V95% (%)
MP1: 48	99.2	RO1:106	122	MP1-RO1: 37	99.3
MP2: 57	99.2	RO2: 28	179	MP1-RO2: 9	98.6
MP3: 34	98.8	RO3: 25	118	MP2-RO1: 43	99.4
MP4: 18	99.2	RO4: 16	145	MP2-RO2: 12	98.8
MP5: 18	99.0			MP3-RO1: 26	98.9
				MP3-RO2: 7	98.3
				MP4-RO3: 11	99.6
				MP4-RO4: 7	98.6
				MP5-RO3: 12	99.1
				MP5-RO4: 6	98.8

Table I

Figure I show the median, mean, upper quartile and lower quartile for each RO, MP and combination of both.



A statistical analysis (Kruskal-Wallis test) was performed to analyze the differences between groups. The results show that there are significant differences in the PTV volume between different RO (p-value: 5.774e-09). No differences were found between MP in the PTV coverage. From the output of the test, we know that there is a significant difference in the average of the PTV volume between pairs of RO, but we don't know which pairs are different. To that end a pairwise comparisons using Wilcoxon rank sum test were performed. The results show that there are significant differences between RO1-RO2 (p-value: 8.1e-09), also between RO3-RO2 (p-value: 5.2e-06). Moreover, a medium effect size was found:  $d_{Cohen}=0.52$  (RO1-RO2),  $d_{Cohen}=0.66$  (RO3-RO2). In addition, 10 different combinations of MP-RO were analyzed and significant differences in the PTV coverage between groups were found (p-value = 3.595e-08).

## Conclusion

A strict treatment planning protocol helps to achieve a more homogeneous treatment plan with regardless of the MP that reviews the plan.

Target delineation is overall a major source of uncertainty in radiotherapy and delineation variation depends, among other things, on the observers and the delineation protocol. Thus, having a protocol helps to prevent these variations. From the results we can conclude that although we found similar results in the PTV volume for each RO, a review of the delineation protocol must be done in order to improve these differences.

Also, certain combinations of MP-RO could result in a slightly better target coverage.

## EP-1826 Comparison of two Volumetric Arc Therapy techniques for hippocampal sparing whole brain radiotherapy

A.I. Milanés<sup>1</sup>, A. Prado<sup>1</sup>, G. Pozo<sup>1</sup>, A. Ferrando<sup>1</sup>

<sup>1</sup>Hospital Universitario 12 de octubre, Radiofísica, Madrid, Spain

## Purpose or Objective

Whole brain radiotherapy (WBRT) is one of the main treatments for patients with multiple brain metastases. However, several studies showed that usual WBRT produces damage to hippocampi, entailing dementia and neurocognitive function decline. Nowadays, with the introduction of volumetric-modulated arc therapy (VMAT) it is possible to spare hippocampal regions maintaining PTV coverage. The aim of this study is to compare two different beam arrangements for hippocampal sparing WBRT utilizing VMAT.

## Material and Methods

A total of ten patients were selected for this study. Imaging of each patient consisted of a 3 mm slice thickness CT scan. Hippocampi were contoured according to RTOG 0933 contouring atlas. Hippocampal avoidance regions were defined as a 5 mm expansion of both hippocampi.

PTV was defined as the usual WBRT PTV minus the hippocampal avoidance regions.

Treatment plans were created in Eclipse v.11.0 TPS (Varian Medical Systems, Palo Alto, CA) using a 6MV Varian Unique linac with a maximum dose rate of 600 MU/min. The Anisotropic Analytical Algorithm (AAA) was used with the Progressive Resolution Optimizer (PRO3) for VMAT optimization.

The prescription dose was 30 Gy to the PTV in 10 fractions. The techniques compared are shown in table 1.

	Gantry angles (°)	Collimator angle (°)	Couch angle (°)
Technique 1	A1: 181 to 179 (CW)	30	0
	A2: 179 to 181 (CCW)	330	0
Technique 2	A1: 181 to 179 (CW)	30	0
	A2: 179 to 181 (CCW)	330	0
	A3: 21 to 179 (CW)	150	90
	A4: 179 to 21 (CCW)	210	90

Table 1: Beam arrangement, collimator angles and couch angles for both techniques studied

Regarding PTVs  $V_{25}$ ,  $V_{30}$ ,  $D_{50\%}$ ,  $D_{2\%}$ ,  $D_{98\%}$ , the Homogeneity Index (HI) and the Paddick Conformity Factor (CF) were evaluated for both techniques. For both eyes  $D_{max}$  and  $D_{avg}$  were considered.  $D_{max}$  for lenses and  $D_{max}$  and  $D_{100\%}$  for both hippocampi were also evaluated. Dose limits for OARs and dose objectives for PTVs were defined following the RTOG 0933 protocol.

### Results

Table 2 shows results obtained for evaluated parameters regarding PTV and OARs.

As it is shown in table 2, technique 2 achieved a better PTV coverage ( $p < 0.04$ ) and a more homogeneous and conformed dose distribution ( $p < 0.002$  and  $p < 0.005$ , respectively). Besides, hippocampi  $D_{max}$  and  $D_{100\%}$  are reduced compared to technique 1 results ( $p < 0.045$  and  $p < 0.04$ , respectively). Lenses and eyes  $D_{max}$  were also reduced ( $p < 0.003$ ). Technique 1 delivered a lower number of monitor units ( $683 \pm 38$ ) in a shorter time ( $2.49 \pm 0.2$  min), mainly due to the reduced number of arcs and the absence of couch angles different from  $0^\circ$  ( $p < 0.0012$ ). Plan 2 technique delivered 842 MU in 4.57 min.

PTV							
	$V_{25}$ (%)	$V_{30}$ (%)	$D_{50\%}$ (cGy)	$D_{2\%}$ (cGy)	$D_{98\%}$ (cGy)	HI	CF
Technique 1	98.9	91.1	3129.3	3250.2	2716.6	0.17	0.84
Technique 2	99.2	94.1	3126.3	3248.8	2847.9	0.13	0.89
Left eye		Right eye		Left Lens		Right Lens	
	$D_{max}$ (cGy)	$D_{avg}$ (cGy)	$D_{max}$ (cGy)	$D_{avg}$ (cGy)	$D_{max}$ (cGy)	$D_{max}$ (cGy)	$D_{max}$ (cGy)
Technique 1	1994.8	1347.0	2053.4	1099.1	799.9	810.9	
Technique 2	1755.5	897.7	1740.1	861.2	740.7	752.6	
Left hippocampus		Right hippocampus					
	$D_{100\%}$ (cGy)	$D_{max}$ (cGy)	$D_{100\%}$ (cGy)	$D_{max}$ (cGy)			
Technique 1	883.3	1559.2	891.8	1549.9			
Technique 2	864.9	1509.4	875.1	1440.5			

### Conclusion

In both cases, the RTOG 0933 dose criteria were achieved, not incurring in any acceptable or unacceptable deviation. Technique 2 was the best in terms of PTV coverage, HI and CF. Besides, it achieved a better sparing of hippocampi, lenses and eyes. On the contrary, the analysis of MU and treatment time indicated that technique 1 delivered the lowest number of MU in the shortest time. The election of one of these techniques also involves considering the workload of every specific institution.

### EP-1827 Influence of the optimization PTV structure on hippocampal sparing radiation therapy using VMAT

A. Prado<sup>1</sup>, A. Milanés<sup>1</sup>, R. Díaz<sup>1</sup>, E. Cabello<sup>1</sup>

<sup>1</sup>Hospital Universitario 12 de octubre, Oncología Radioterápica. Sección de Radiofísica, Madrid, Spain

### Purpose or Objective

Whole brain radiotherapy (WBRT) is one of the main treatments for patients with multiple brain metastases. However, several studies showed that usual WBRT produces damage to hippocampi, entailing dementia and neurocognitive function decline. Nowadays, it is possible to spare hippocampal regions maintaining PTV coverage using intensity modulation. The aim of this study is to compare how PTV coverage and hippocampi doses depend on the distance between hippocampi and the PTV optimization structure employed.

### Material and Methods

Hippocampi were contoured according to RTOG 0933 contouring atlas. Hippocampal avoidance regions were defined as a 5 mm expansion of both hippocampi. PTV was defined as the usual WBRT PTV minus the hippocampal avoidance regions. Treatment plans were created in Eclipse v.11.0 (Varian Medical Systems, Palo Alto, CA) using a 6MV Varian Unique linac with a maximum dose rate of 600 MU/min. The Anisotropic Analytical Algorithm (AAA) was used with the Progressive Resolution Optimizer (PRO3) for VMAT optimization. The prescription dose was 30 Gy to the PTV in 10 fractions. Two full arcs were used with collimator settings of  $30^\circ$  and  $330^\circ$ , respectively. PTV optimization structures were defined as the WBRT PTV minus the hippocampi avoidance regions plus a margin between 0 and 5 mm. Hence, PTVX represents the optimization structure which is at X mm from the hippocampi. Each PTV optimization structure was considered as the objective structure in the optimization process but the dose evaluation was always performed using the PTV. All parameters regarding the cost functions were set to the same values when optimizing using different PTVX structures as objective structures. To evaluate differences between plans  $D_{2\%}$  and  $D_{100\%}$  were considered for hippocampi and  $V_{25}$ ,  $V_{28}$  and  $V_{30}$  for PTV

### Results

Figure 1 depicts hippocampi and PTV results when optimizing using distinct PTV optimization structures. As the distance X is increased, PTV coverage decreased as a result of dose reduction nearby the hippocampal avoidance regions (table 1). Also, hippocampi  $D_{2\%}$  and  $D_{100\%}$  both decreased. This reduction in  $D_{2\%}$  and  $D_{100\%}$  seemed to be greater from PTV5 to PTV7 (210 cGy and 48 cGy, respectively) than from PTV7 to PTV9 (75 cGy and 27 cGy, respectively). For X values from 5 to 7 mm there was little reduction in PTV coverage (Table 1), increasing these differences for higher X values.

HIPPOCAMPI	PTV5	PTV6	PTV7	PTV8	PTV9
$D_{2\%}$ (cGy)	1515	1455	1305	1281	1257
$D_{100\%}$ (cGy)	891	843	816	801	789
PTV	PTV5	PTV6	PTV7	PTV8	PTV9
$V_{25}$ (%)	99,7	99,5	99,2	98,9	98,5
$V_{28}$ (%)	98,6	98,4	98	97,5	96,9
$V_{30}$ (%)	93,5	93,4	93,2	92,2	92

Table 1: Evaluated parameters for hippocampi and PTV when optimizing utilizing distinct PTVX objective structures. X stands for the distance between PTVX optimization structure and hippocampi in mm.

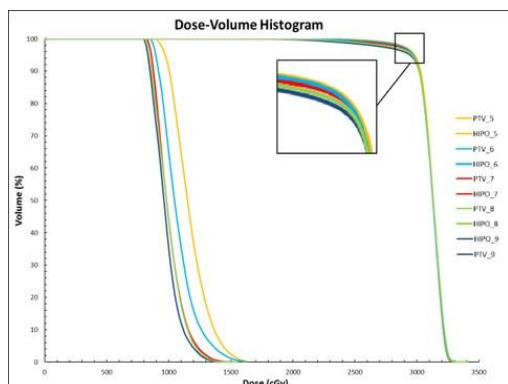


Figure 1: Dose volume histogram for the results obtained for PTV and hippocampi when optimizing utilizing distinct PTVX structures. X stands for the distance in mm from the PTVX structure to the hippocampi.

#### Conclusion

Optimizing using PTV7 structure as objective structure and evaluating final results on PTV implies maintaining PTV coverage and the achievement of an important reduction on hippocampi maximum dose.

#### EP-1828 Treatment plan comparison between SBRT techniques for recurrent nasopharyngeal carcinoma

Y. Lin<sup>1</sup>, H. Ho<sup>1</sup>

<sup>1</sup>Chi Mei Medical Center, Department of Radiation Oncology, Tainan, Taiwan

#### Purpose or Objective

To evaluate the potential benefit of HyperArc (HA) in previous treated, recurrent nasopharyngeal cancer treated with stereotactic body radiation therapy (SBRT).

#### Material and Methods

The twenty patients with recurrent nasopharyngeal cancer who were treated using CyberKnife (CK) for salvage treatment were enrolled. The median dose for the previous treatments for the twenty patients was 70Gy in 35 fractions. CK was delivered with a median 35 Gy in 5 fractions. The HA treatment plans were created for each patient to meet the same treatment plan criteria for CK. These two SBRT treatment plans were compared with target coverage, sparing of organs at risk, and dose distribution metrics, including conformity index, heterogeneity index, dose gradient index, and high/intermediate dose spillage. Monitor units (MU) were compared to assess as delivery efficiency.

#### Results

The HA plans consistently exhibited similar CTV and PTV coverage and significantly reduced the dose to organs at risk. The mean CTV coverage for CK and HA was 97.3% and 98.3%; the mean PTV coverage for CK and HA was 94.7% and 96.1%. Using HA plans, mean doses to the spinal cord, brainstem, optic nerves, and optic chiasm were reduced by 64%, 62%, 61% and 68%, respectively. The conformity and heterogeneity metrics of the HA plans were significantly better than the CK plans. With HA plans, the mean high dose spillage volumes were decreased by 54%. In average, the HA plans resulted in 56% less MUs than the CK plans (HA, 20643 MUs vs. CK, 47464 MUs).

#### Conclusion

Excellent sparing of organs at risk and good dosimetric distribution make HA an attractive SBRT technique for the treatment of recurrent nasopharyngeal cancer.

#### EP-1829 Clinical validation of knowledge-based planning for multiple brain metastases

N. Kishi<sup>1</sup>, M. Nakamura<sup>1,2</sup>, H. Hirashima<sup>1</sup>, N. Mukumoto<sup>1</sup>, K. Takehana<sup>1</sup>, M. Uto<sup>1</sup>, Y. Matsuo<sup>1</sup>, T. Mizowaki<sup>1</sup>

<sup>1</sup>Kyoto University Graduate School of Medicine, Department of Radiation Oncology and Image-Applied Therapy, Kyoto, Japan ; <sup>2</sup>Kyoto University Graduate School of Medicine, Department of Information Technology and Medical Engineering Human Health Sciences, Kyoto, Japan

#### Purpose or Objective

Recently, single isocenter volumetric modulated arc therapy (VMAT) has arisen as an alternative to whole brain radiotherapy when treating multiple brain metastases (BMs). The aim of this study was to evaluate the clinical validation of knowledge-based planning (KBP) for multiple BMs.

#### Material and Methods

Consecutive 56 patients treated with single isocenter VMAT for multiple BMs between October 2015 and September 2018 in our institute were enrolled into this study. The patient cohort was divided into two groups according to the number of BMs; model training (50 cases with 2-4 BMs) and validation (6 cases with 12-20 BMs). Four KBP models (M1-4) with different number of BMs per case were constructed using RapidPlan™ (Varian Medical Systems, Palo Alto, USA): M1, using all 50 cases with 2-11 BMs; M2, 40 cases with 2-6 BMs; M3, 30 cases with 2-4 BMs; and M4, 20 cases with 2-3 BMs. Then, the four KBP models were applied to each case in the validation group with the same beam arrangements as in a clinical plan (CL). The total number of BMs in the validation group was 96, whereas the clinical plans consisted of 88 planning target volumes (PTVs). One time of optimization per KBP model was performed for each case. The dosimetric differences between the KBP plans and CLs were assessed for PTVs and organs at risk (OARs). OARs included brain-PTVs, brainstem, chiasm, optic nerves, eyes, lens and skin. The following dose-volumetric parameters were recorded: PTV D<sub>2%</sub>, D<sub>50%</sub> and D<sub>98%</sub>, the maximum dose to OARs and V<sub>20Gy</sub> of brain-PTVs. Friedman test were performed for statistical analysis at  $\alpha = 0.05$ , followed by Wilcoxon signed-rank test with Bonferroni correction for multiple comparisons as a post hoc test. Statistical significance was set at  $p < 0.01$ .

#### Results

Three to seventeen (median, 7) optimizations were required until the CLs were obtained. Interquartile ranges were smaller in the KBPs than in the CLs for any dose-volumetric parameters (Fig. 1). The difference between the median values in the CLs and those in the KBPs was within  $\pm 1.7\%$  points and  $\pm 0.4\%$  points for PTV D<sub>50%</sub> and D<sub>98%</sub>, respectively. No significant difference was observed among these dose-volumetric parameters ( $p > 0.05$ ). Although the PTV D<sub>2%</sub> was significantly higher in the KBPs than in the CLs ( $p < 0.01$ ), the difference of its median value between the CLs and the KBPs ranged from 1.7 to 2.3% points. The maximum dose of brain-PTVs in the KBPs were decreased by 4.9% points (range, 1.5-11% points), compared with the CLs. The median values of difference in the maximum dose to other OARs and V<sub>20Gy</sub> of brain-PTVs between the CLs and KBPs were ranged from -5.6% points to +0.5% points.

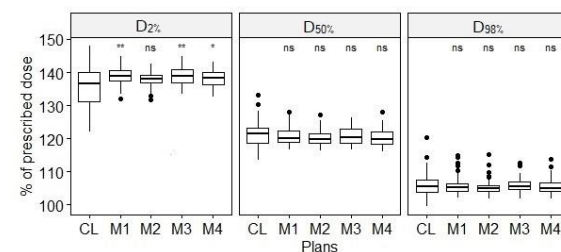


Fig. 1 Box-and-whisker plots of the difference between the CLs and the KBPs for the PTV D<sub>2%</sub>, D<sub>50%</sub>, and D<sub>98%</sub> for the planning target volumes. Notes: \* =  $p < 0.01$ ; \*\* =  $p < 0.001$ ; ns = not significant.

#### Conclusion

We have demonstrated that the KBPs for multiple BMs was dosimetrically equivalent to the CLs with a single time of optimization, even if the number of BMs included in the model training group was different from that in the validation group.

#### EP-1830 Dosimetric comparison of planning techniques in Radiosurgery for Arteriovenous Malformation

R. Chauhan<sup>1</sup>, V. Mhatre<sup>1</sup>, K. Talapatra<sup>1</sup>, P. Chadha<sup>1</sup>, P. Shree<sup>1</sup>, A. Balasubramaniam<sup>2</sup>, A. Kumar<sup>1</sup>  
<sup>1</sup>Kokilaben Dhirubhai Ambani Hospital, Radiation Oncology, Mumbai, India ; <sup>2</sup>Yashoda Hospital, Neurosurgery, Hyderabad, India

##### Purpose or Objective

To investigate the dosimetric indices employing different techniques such as Static Conformal Fields(SCF), Intensity-Modulated Radiosurgery (IMRS), Dynamic Conformal Arc (DCA), Volumetric Modulated Arc Therapy (VMAT).

##### Material and Methods

Fifteen patients of Arteriovenous Malformations were included in the study of which 2 patients were grade 1, 7 patients were grade 2 and 6 patients were grade 3 by Spetzler Martin grading system. Thirteen out of 15 patients were unruptured and 2 were ruptured for which partial embolisation was done followed by radiosurgery. Range of target volume (0.7cc to 12.28cc Mean=7.94cc). A plan each of SCF, DCA, IMRS and VMAT were generated for each patient using MLC 2.5mm. For every patient fixed dose of 22Gy prescribed at 80%. All plans were compared using standard dosimetric indices. Dosimetric comparison includes target coverage, conformity index(CI), homogeneity index(HI), gradient index(GI). In addition maximum doses to OARs i.e Brainstem.

##### Results

Paddick CI for SCF is (0.58±0.08), DCA Paddick CI (0.580±0.09), IMRT Paddick CI (0.66±0.09) and VMAT Paddick CI (0.68±0.01), best Paddick CI observed in VMAT, P<0.05. HI for SCF is (1.05±0.04), HI for DCA (1.046±0.04), HI for IMRT (1.044±0.03), HI for VMAT (1.043±0.03) best HI observed in VMAT. Primary goal is to achieve 99% of target coverage by 1760cGy, minimum dose to target is 17.5Gy to V99%, VMAT had improved coverage but no significant difference, P>0.05. Best GI observed in DCA(3.13±0.5), GI for SCF is (3.22±0.55), GI for IMRT is (4.34±1.16), GI for SCF is (3.45±0.64), P<0.05. Dose Heterogeneity Index for SCF is (0.079±0.01), for DCA is (0.08±0.01), for IMRT (0.108±0.02), for VMAT DHI is (0.08±0.01), P<0.01. The dose received by 1 cc volume of brainstem were (5.33±5)Gy, (5.72±5)Gy, (5.85±5)Gy and (5.08±4)Gy for SCF, DCA, IMRS, VMAT plans respectively.

##### Conclusion

We have found that VMAT has shown better coverage as compared to other plans and it spares OARs, It is better in terms of 1 cc volume dose to the brainstem. This dosimetric comparison provides insight into selection of the right modality for the current treatment scenario.

#### EP-1831 Avoidance sector strategy to reduce healthy tissue dose in locoregional breast planning with VMAT

S. Thengumpallil<sup>1</sup>, J. Bezar<sup>1</sup>, K.H. Spruijt<sup>1</sup>, N. Peguret<sup>1</sup>, C. Vrieling<sup>1</sup>

<sup>1</sup>Clinique des Grangettes, Radiation Oncology, Geneva, Switzerland

##### Purpose or Objective

The benefit of the avoidance sector strategy for breast only VMAT radiotherapy planning has been proven to reduce significantly the healthy tissue dose levels (Fogliata A. Br J Radiol. 2017). Our aim is to explore whether this strategy leads to similar results in

locoregional breast planning, a more complex treatment volume.

##### Material and Methods

Two approaches were compared: VMAT partial arcs (without avoidance sectors) and VMAT with avoidance sectors. The latter was set in such a way that the arc arrangement was mimicking the tangential technique, thus allowing an optimal sparing of the heart and contralateral OARs. An avoidance arc of about 40 degrees was chosen for each patient based on particular clinical objectives. The same arc trajectory and same dose objectives were applied for both. The two approaches were evaluated based on DVH for both PTVs and OARs for 15 locoregional left breast patients. Homogeneity and conformity indices for PTVs, V5 for OARs as measure for low dose and number of monitor units (MU) were also compared.

##### Results

VMAT with avoidance sectors demonstrates a significant reduction of the low dose for almost all OARs with major impact on the contralateral OARs. From the preliminary results, we found a mean volume reduction for the V5 of 18% for the contralateral lung, 14% for the contralateral breast, 4% for the heart, 3% for the body-PTV (healthy tissues) and 0.4% for the ipsilateral lung. The trade-off was a slight increase of the V20 to the ipsilateral lung by 2% for the plan with avoidance sectors as expected due to the more tangential-like arc arrangement. However, the two approaches were able to fulfill the same initial dose objectives. The PTV criteria were met with both techniques, the V95 for the total PTV (breast + regional lymph node) were about 95%. The mean homogeneity index was 0.96 and 0.94 for the complete partial arcs and avoidance sectors, respectively. The mean conformity index was 0.88 and 0.87, respectively. The mean number of MU were similar between the two approaches.

##### Conclusion

The avoidance sector strategy shows significant improvement in decreasing the low-dose-bath to OARs while keeping an acceptable PTV coverage in agreement with the ICRU criteria. We encourage the use of VMAT with avoidance sectors as a solution to reduce possible late toxicities and secondary cancer induction in locoregional breast treatments. However, in the planning process, a complex anatomy and/or specific dosimetric objectives would require careful evaluation in the choice of the approach to use.

#### EP-1832 Dosimetric comparison of IMRT for early-stage glottic cancers with and without air cavity in the PTV

D. Asher<sup>1</sup>, W. Amestoy<sup>1</sup>, M. Studenski<sup>1</sup>, S. Samuels<sup>1</sup>, M. Abramowitz<sup>1</sup>, L. Freedman<sup>1</sup>, N. Elsayyad<sup>1</sup>, M. Samuels<sup>1</sup>  
<sup>1</sup>University of Miami, Radiation Oncology, Miami, USA

##### Purpose or Objective

For early-stage glottic cancers, intensity-modulated radiation therapy (IMRT) has been shown to have comparable local control to 3D-conformal radiotherapy with the advantage of decreased dose to the carotid arteries. The planning target volume (PTV) for early glottic cancers typically includes the entire larynx, plus a 3-5 mm uniform margin. The air cavity within the larynx creates a challenge for the inverse optimization process as the software attempts to "build up" dose within the air. This unnecessary attempt at dose build-up in air can lead to hot spots within the rest of the PTV and surrounding soft tissue. We hypothesized that removal of the air from the PTV would decrease hot spots and allow for a more homogeneous plan while still maintaining adequate coverage of the PTV.

##### Material and Methods

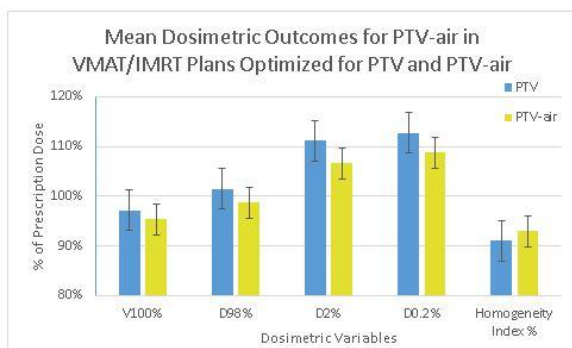
We analyzed 20 consecutive patients with early-stage glottic cancer, T1-2N0, who received IMRT at our institution from April 2015, to December, 2016. Each patient received 63-65.25 Gy in 2.25 Gy per fraction. Two

plans were created for each case: one in which the PTV included the laryngeal air cavity and one in which the air cavity was subtracted from the PTV to create a new PTV-air structure. Acuros XB (Varian Medical Systems, Palo Alto, CA) dose calculation algorithm was utilized. Dosimetric variables were collected for PTV-air structure from both IMRT plans, including V100% (volume that received the prescription dose), D98% (dose received by 98% of the volume), D2%, and D0.2%. Dosimetric variables for organs at risk (OARs), including spinal cord and the carotid arteries were also recorded. Homogeneity index (HI) defined as D98%/D2% was calculated. Two-sided t-tests were used to compare dosimetric variables.

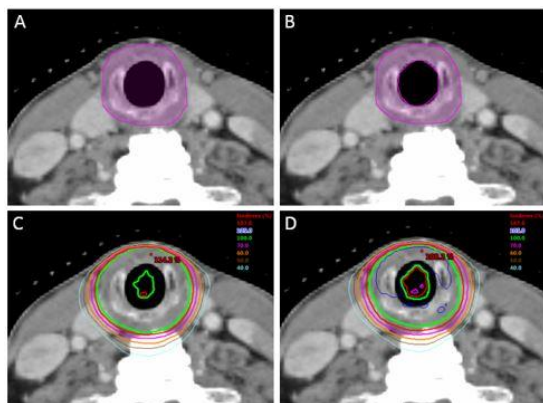
#### Results

The mean V100% was  $95.1 \pm 2.5\%$  for the PTV plans and  $95.4 \pm 0.9\%$  for the PTV-air plans, demonstrating adequate target coverage and no statistical difference between the plans ( $p=0.584$ ). The mean D0.2% (maximum dose) within PTV optimized plan was significantly lower for the PTV-air optimized plans at  $108.8 \pm 2.1\%$  compared to  $111.4 \pm 3.3\%$  ( $p=0.0002$ ). The HI also improved from  $0.90 \pm 0.03$  up to  $0.93 \pm 0.02$  ( $p<0.0001$ ). Even with these gains, there were no significant differences in any of the OARs.

When the PTV-air contour was superimposed onto the PTV plan, the V100% was significantly higher at  $97.2 \pm 2.3\%$  compared to  $95.4 \pm 0.9\%$  ( $p=0.003$ ), showing that the PTV plan was unnecessarily hot. The D2% and D0.2% were also significantly higher ( $p=0.0002$ ).



IMRT optimization using PTV-air (yellow) maintained adequate PTV-air coverage with reduction in V100%, D98%, D2%, and D0.2% and improvement in Homogeneity Index (D98%/D2%) compared to optimization using PTV (blue).



Representative case demonstrating dosimetric benefit of removal of air from PTV. On this planning CT with IV contrast, PTV and PTV-air are shown in (A) and (B). Isodose lines for VMAT/IMRT plans optimized for PTV (C) and PTV-air (D) are shown below. By removing air from the PTV, the hot spot within this single axial slice (shown in red located within the anterior cricoid cartilage) decreases from 114.2% of the prescribed dose to 108.2%.

#### Conclusion

The removal of the air cavity from the PTV for early-stage glottic cancers does not compromise PTV coverage or

sparing of OARs and can result in a more homogeneous IMRT plan.

#### EP-1833 Impact of physicist clinical practice on the quality of head and neck IMRT and VMAT plans

S. David<sup>1</sup>, M. Hermida-López<sup>1</sup>

<sup>1</sup>Hospital Universitari Vall d'Hebron, Servei de Física i Protecció Radiològica, Barcelona, Spain

#### Purpose or Objective

During treatment plan design many decisions are taken based on the planner's own experience and potential biases. Although the treatment planning system (TPS) is plenty of similar plans that could help in the decision making, it is not easy to access to all this information. These data can be more accessible using Mobius3D (Mobius Medical Systems, LP), an independent dose calculator, own database. We aimed to assess differences in treatment plan quality for head and neck IMRT and VMAT plans between three experienced physicists in our center.

#### Material and Methods

After a plan is created, the RTplan, the planning CT and the RTdose DICOM files are exported to Mobius3D (M3D) database. Using a Python script provided by M3D (slightly modified), an Excel file was created for every plan in M3D database. A Matlab script was used to filter the head and neck plans with only two dose levels (54 Gy for the nodes and 70 Gy for the high-dose PTV). Plans from replannings and clinical trials were excluded to ensure there was no bias during plan creation. Sixty-three plans approved by one of our three physicists (16, 15 and 6 years of experience, respectively) were studied. Monitor units (MU) and 40 dosimetric parameters for PTVs and OARs, the most common reported in the literature, were evaluated. Statistically significant differences were analyzed with two-tailed two-samples unpaired t-tests ( $\alpha=0.05$ ).

#### Results

As expected, IMRT plans resulted in a bigger amount of MU ( $1211 \pm 423$ ) than VMAT plans ( $556 \pm 89$ ). A statistically significant difference was found between physicists A and C for IMRT plans. Although VMAT MU values are consistent with those reported in the literature, IMRT MU values are higher with those published by Cozzi et al. [JROBP, 2004, 58.2]. A possible reason could be different fluence-smoothing procedures among physicists

Statistically significant differences were found between physicist A and physicist C for the mean dose and conformity index for the high-dose PTV and for the mean dose, homogeneity, D(2%) and V(107%) for the low-dose PTV.

Statistically significant differences were found between physicist A and physicist C for D(50%) and D(66%) for the left parotid, while between physicist A and B for mean dose, D(33%), D(50%) and D(66%) for the right parotid.

Physicist A achieved the best result in the 45% of the evaluated parameters, physicist B in the 40%, and physicist C in the 15% left. The standard deviation, taken as a surrogate for the planning consistency, was the smallest in 52.5% of the parameters for physicist A, in 20% for physicist B, and in 22.5% for physicist C.

#### Conclusion

Analyzing plan quality parameters have showed differences between physicists, which leads to an opportunity to share practices to improve dosimetric results and decrease self-bias, thus resulting in a better and more homogeneous treatment plan quality. The developed procedure can be easily implemented for other sites and prescriptions.

#### EP-1834 Feasibility study of extreme hypofractionated proton treatment planning for prostate cancer

P. Klinker<sup>1</sup>, C. Brouwer<sup>1</sup>, C. Roos<sup>1</sup>, C. Hammer<sup>1</sup>, H.

Vanhauten<sup>1</sup>, S. Bijmolt<sup>1</sup>, J. Langendijk<sup>1</sup>, S. Both<sup>1</sup>, A. Van den Bergh<sup>1</sup>, S. Al-Uwini<sup>1</sup>

<sup>1</sup>UMCG University Medical Center Groningen, Radiotherapy, Groningen, The Netherlands

### Purpose or Objective

Extreme hypofractionated radiotherapy is an efficient and convenient treatment option for prostate cancer (PCa) patients, mostly delivered by stereotactic body radiotherapy (SBRT). Recent improvements in proton planning techniques like robust proton pencil beam scanning (PBS) has the potential to deliver the same quality hypofractionated plans as SBRT with much lower exposure dose to the surrounding tissues. The purpose of this study is to investigate the feasibility of delivering clinically acceptable extreme hypofractionated proton plans.

### Material and Methods

Planning CT scans of 4 representative PCa patients treated at our department were used in this study. The organs at risk (OARs) (rectum, anal canal, urethra and bladder) and the CTV (prostate) were delineated by a radiation oncologist according to our SBRT protocol. For each CT scan, 4 plans were created: two fractionation regimen (4x9.5 Gy and 5x7.5 Gy) each having two different setup margins (3 and 5 mm). Treatment plans were robustly evaluated for the corresponding setup and  $\pm 3\%$  density changes. The considered protocol for target coverage and OAR constraints is listed in Table 1. For proton planning robust optimization and Monte Carlo based dose calculation in Raystation v6.99 was used. Target coverage was optimized without violating the OAR dose constraints. Clinically acceptable plans were those which met the protocol constraints with minor violation of max 5%. The endpoint of the study was percentage of acceptable plans for each fractionation regimen and each robustness setup margin.

Table 1. Clinical goals in treatment planning

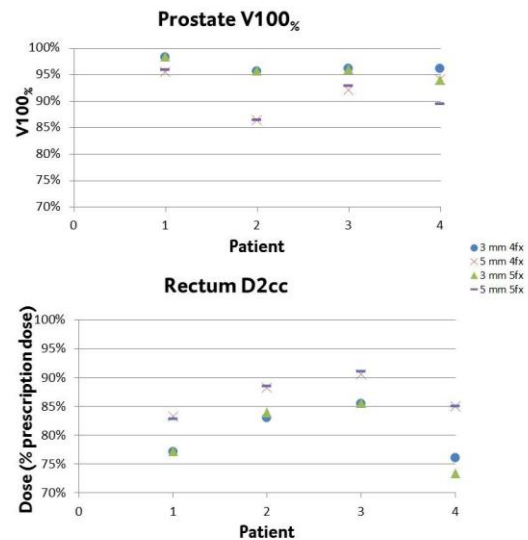
Organ	Parameter	Constraint
Prostate	V100%	$\geq 95\%$
	D90%	$\geq 100\%$
Rectum	D2cc	<100% PD
Anterior rectal wall	Dmax	<100% PD
Posterior rectal wall	Dmax	<40% PD
Anal canal	D5cc	<40% PD
	Dmax	<70% PD
Urethra	Dmax	<105 PD
Bladder	D20cc	<60% PD
	Dmax	<105 PD

PD= prescribed dose

### Results

The target coverage was acceptable in 7/8 plans with 3-mm margin, while only 3/8 plans (two in 4-fraction and one in 5-fraction regimen) with 5 mm margin were acceptable. Bladder constraints were acceptable in all plans with 3-mm margin, and in only 4/8 when 5-mm plans were used. In two patients, dose constraints were met in not any plan. All rectum constraints met the protocol constraints in both setup margin groups. There were no significant differences in target coverage and OAR constraints between 4 and 5 fractions regimen.

Figure 1. Prostate V100% and Rectum 2cc for the four different treatment plans



### Conclusion

Both fractionation regimen of 4 and 5 fractions met the dose constraints and are considered clinically feasible if 3-mm setup margin are used. The target coverage was suboptimal in most plans for 5 mm setup margin. A larger cohort of patients is needed to confirm our results.

### EP-1835 Use of the gEUD in modern TPSs for prostate radiotherapy with VMAT technique

L. Grimaldi<sup>1</sup>, V. Morandini<sup>1</sup>, S. Berlinghieri<sup>1</sup>, E. Castrezzati<sup>1</sup>, P. Frata<sup>1</sup>, N. Pasinetti<sup>1</sup>

<sup>1</sup>Esine Hospital, Radiation Oncology Service, Esine, Italy

### Purpose or Objective

Aim of this study is to find a starting point for gEUD parameters in the Philips Pinnacle<sup>3</sup> TPS to reach a comparable dose distribution to target and to maximize the OARs sparing irradiation in a normo-fractionated prostate RT schedule (74 Gy-2 Gy/fr).

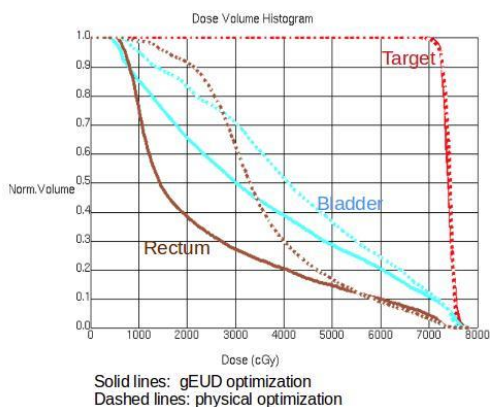
### Material and Methods

For 10 patients treated with prostate radiotherapy, two RT plans were optimized using VMAT technique. For the first plan only physical parameter was used, instead for the other one, the biological gEUD parameter were replaced to all OARs. The TPS was Philips Pinnacle<sup>3</sup> v9.10.

### Results

For the targets volumes the two plans show an equivalent dosimetry in term of Conformity Index ( $COIN = (V_{T,pi})^2 / (V_T * V_{pi})$ ), Homogeneity Index ( $HI = 100 * (D_{2\%} - D_{98\%}) / D_{pi}$ ) and Gradient Index ( $GI = V_{50\%} / V_{100\%}$ ). Instead for the principals OARs: the femoral heads don't put in evidence substantial differences, at absorbed doses of 30-40 Gy, the rectum volumes involved are halved and for bladder the reduction of absorbed medium doses are of about 30%. There isn't a significant reduction for absorbed dose of 65-70 Gy. To optimize a VMAT plan by using the Pinnacle<sup>3</sup> radiobiological function and obtain a dose distribution comparable to that based on a physical optimization, the following parameters have been set:

	Objective (Gy)	Weight	Parameter a
Target (ie 74 Gy)	74	14	-20
Rectum	32	3	1.5
Rectum OUT Target	35	5	3.6
Bladder	23	2	1.0
Bladder OUT Target	22	4	1.7
Head Fem DX	22	1	1.2
Head Fem SN	22	1	1.2



When using VMAT optimization based on the gEUD, the following differences emerge: the programmed number of MU increases by over 40%; on average, the size of the equivalent square field decreases by more than 13%; the absorbed dose at the middle and lower levels of the rectum and bladder are considerably decreased.

#### Conclusion

The use of gEUD parameters produce an increase in the mean times for the optimization of the treatment plan, but a considerable OARs sparing. Despite the risk of complications is predominantly determined by the high doses, it is necessary not to neglect the control over the low- and mid-dose range. The optimization with cost functions based on the gEUD concept is straightforward and numerically expedient. In fact, with the only parameter gEUD you can control both high and low dose values; however, the need remains to better determine the parameter “a” for these OARs.

**References:** Report of AAPM, *The Use and QA of Biologically Related Models for Treatment Planning*, (2012) TG 166 of the Therapy Physics Committee

#### EP-1836 Validation of a novel knowledge-based planning (KBP) model for lung cancer treatments with VMAT

N. Tambe<sup>1,2</sup>, C. Moore<sup>1</sup>, I.M. Pries<sup>2</sup>, C. Cawthorne<sup>3</sup>, A.W. Beavis<sup>1,2,4</sup>

<sup>1</sup>Hull and East Yorkshire Hospitals NHS Trust, Radiation Physics, Cottingham, United Kingdom ; <sup>2</sup>University of Hull, Faculty of Health Sciences, Hull, United Kingdom ; <sup>3</sup>KU Leuven, Nuclear Medicine and Molecular Imaging-Department of Imaging and Pathology- Biomedical Sciences Group, Leuven, Belgium ; <sup>4</sup>Sheffield-Hallam University, Faculty of Health and Well Being, Sheffield, United Kingdom

#### Purpose or Objective

Radiotherapy plan design can vary widely and is dependent on the experience of the treatment planning staff. Plans meeting planning objectives may still be suboptimal where there is scope to reduce OAR doses without compromising target coverage and deliverability.

This study aimed to develop a novel KBP model to reduce lung cancer plan variability, by predicting minimum achievable (or ideal) lung volume-dose measures  $V_5/V_{20}$  (volume of lungs receiving 5Gy/20Gy dose) and mean lung dose (MLD) based on previously treated patients using our VMAT technique. The effect of the KBP model on treatment plan complexity and treatment delivery was assessed.

#### Material and Methods

36 previously treated lung cancer patients were randomly selected from the Eclipse database and their dosimetric data and normal and target structures analysed. The three lung metrics,  $V_5$ ,  $V_{20}$  and MLD, were correlated against residual lung volume (RLV) defined having iteratively searched for a lung volume construct that provided maximal correlation with all three metrics. It was found to be equal to the total lung volume excluding an isotropic 5 cm expansion of the PTV. A straight line was manually fitted to the correlation plots that demonstrated the lowest achieved dose metric values as a function of RLV. This was hence referred to as the lower-bound model.

The model was tested by re-planning a further 39 patients, using the model predicted values as ideal constraints to replace protocol values. Treatment plan complexity metrics (MU/Gy, islands <1cc, small aperture scores) for the KBP plans were extracted. The effect of the models application on treatment deliverability was assessed by measurements. Treatment beams were measured with EPID panel and processed in portal dose image prediction software within Eclipse.

#### Results

A significant reduction in mean (maximum)  $V_5$ ,  $V_{20}$  and MLD of 6.6% (19.8%), 1.1% (7.8%), and 0.7Gy (2.3Gy) respectively was achieved whilst maintaining optimal target coverage. The application of the model resulted in a 5.1% reduction in the number plans failing clinical constraints. A single observer study showed considerable reduction of variability in treatment plans. Plan complexity was observed to increase for KBP plans compared to the original plans, resulting in a small increase in measured delivery errors. Two of the 78 arcs failed the local optimal gamma pass criteria (3%/2mm $\geq$ 98%) however they passed the hard criteria (3%/2mm $\geq$ 95) and were therefore considered clinically acceptable.

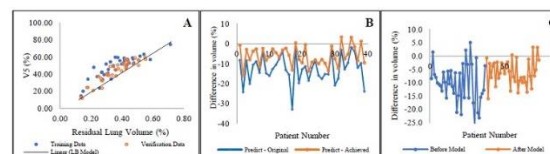


**Figure 1:** Plots showing reduction in Lung  $V_5$  (Volume of Lung receiving 5Gy) pre- and post- model implementation. A - Lower bound model (straight line) and with training and verification data set. B - Reduction in the volume of lung receiving 5Gy with and without model. C - Reduction in variability in plans with the model.

#### Conclusion

Our study showed that our novel in-house KBP models allowed a reduction in heterogeneity in treatment plan quality, with a concurrent decrease in dose to lung volume for VMAT-treated patients. Treatment delivery verifications demonstrated the KBP model plans were deliverable. The model has been implemented clinically using Eclipse scripting.

#### EP-1837 A new hybrid approach to allow robust Monte Carlo-based multi-field optimization in proton therapy

F. Tommasino<sup>1</sup>, L. Widesott<sup>2</sup>, F. Fracchiolla<sup>2</sup>, S. Lorentini<sup>2</sup>, R. Righetto<sup>2</sup>, C. Algranati<sup>2</sup>, E. Scifoni<sup>3</sup>, F. Dionisi<sup>2</sup>, D. Scartoni<sup>2</sup>, D. Amelio<sup>2</sup>, M. Cianchetti<sup>2</sup>, M. Schwarz<sup>2</sup>, M. Amichetti<sup>2</sup>, P. Farace<sup>2</sup>

<sup>1</sup>University of Trento, Physics, Trento, Italy ; <sup>2</sup>Azienda Provinciale per i Servizi Sanitari APSS, Protontherapy Department, Trento, Italy ; <sup>3</sup>Istituto Nazionale di Fisica

### Purpose or Objective

Protontherapy treatments with pencil beam scanning (PBS) offer the highest flexibility when proton fields are optimized simultaneously (i.e. with multi-field optimization, MFO). Due to the high in-field dose gradients obtained with MFO, this might come at the price of reduced robustness. Robust optimization techniques have been proposed to handle this issue, but they require extensive computational power. Therefore, they are hardly compatible with the clinical application of Monte Carlo (MC) dose calculation algorithms, which have been demonstrated to significantly improve the accuracy of proton treatment plans. The purpose of this work is to implement a robust MFO technique compatible with the application of MC algorithm and to evaluate its robustness to both physical and biological uncertainties.

### Material and Methods

9 patients (3 brain, 5 head-and-neck, 1 spine) underwent proton treatment generated by a novel robust MFO technique. A hybrid (hMFO) approach was implemented, planning dose coverage on a PTV compensating for setup errors, whereas range calibration uncertainties are incorporated in PTV robust optimization process as CT calibration uncertainties (i.e.: three scenarios are optimized, corresponding to nominal and  $\pm 3.5\%$  uniform mass density scaling). A commercial MC dose calculation engine was adopted. hMFO was compared with single-field optimization (SFO), both by robustness analysis (considering both CT calibration uncertainties and isocenter shifts due to setup errors, for a total of 16 perturbed scenarios) on CTV and organs at risk (OARs) and by assessing in the nominal plans the potential impact of variable relative biological effectiveness (RBE).

### Results

Nominal hMFO plans were superior compared to SFO in terms of target coverage ( $p=0.004$ ), without difference for OARs sparing ( $p=0.280$ ). The improvement in target coverage obtained with hMFO is preserved in worst-case scenarios ( $p=0.004$ ), confirming that hMFO is as robust as SFO to physical uncertainties in terms of target coverage. This is summarized in the boxplots of Figure 1, showing the difference between prescription and actual CTV doses for the patients considered in the study. Similarly, the difference between OARs planning and prescription dose for the different scenarios is shown in Figure 2. On OARs, physical (i.e. worst-case scenario) and biological (i.e. variable RBE) uncertainties resulted into significant ( $p<0.01$ ) dose increase for both hMFO and SFO (by 3-7 Gy), but without significant difference between these two techniques.

### Conclusion

hMFO allows improving plan quality compared to SFO, without affecting robustness to setup, range and RBE uncertainties. We show that hMFO is compatible with the application of MC-based robust optimization with minimal impact on computation time. Our data also indicate that uncertainties due to variable RBE, even though generally neglected in clinical practice, might be comparable with those resulting from physical uncertainties.

### Figure 1

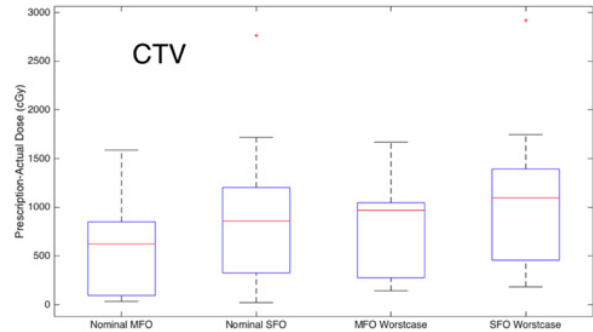
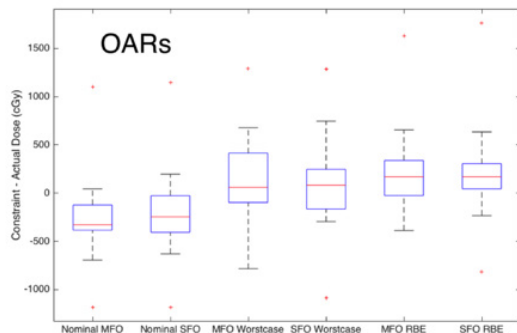


Figure 2



### EP-1838 Dosimetrical comparison of brain SRS treatment plans using IRIS and InCise 2 MLC of the CyberKnife

M. Vekas<sup>1</sup>, G. Stelczer<sup>1</sup>, L. January<sup>1</sup>, T. Major<sup>1</sup>, C. Polgar<sup>1</sup>  
<sup>1</sup>National Institute of Oncology, Center of Radiotherapy, Budapest, Hungary

### Purpose or Objective

A Cyberknife M6 (CK) system was installed at our institution in 2018 January. The aim was to compare the dosimetrical properties of the treatment plans and treatment times with IRIS and MLC collimator.

### Material and Methods

Ten patients with single brain tumours were selected for this study. For each patient three treatment plans were made. Optimal treatment plans were created with MLC and IRIS. Due to the big differences in treatment time between these two plans, one additional IRIS plan was made with time reduction (IRIS TR), to get as short treatment time as possible for a clinically still acceptable plan. The dose prescription of each IRIS plan was set in order to have the same target coverage as the MLC plan. MLC plans were compared to IRIS and IRIS TR plans pairwise with respect to PTV coverage ( $V_{100\%}$ ), treatment time, ICRU 83 homogeneity index (HI), conformity index (nCI), monitor units (MU),  $D_{0,04ccm}$ ,  $D_{0,5ccm}$  for brainstem,  $D_{0,2ccm}$ ,  $D_{0,04ccm}$  for optic pathway and maximum dose of a shell (one voxel thick ring ROI around the target at 10 mm distance). Wilcoxon matched pair test of Statistica 7 software was used for statistical analysis.

### Results

The average volume of PTVs was 13,4 cm<sup>3</sup>. There were no differences between the target coverages of the three plans. However, average MUs were significantly lower for the MLC plans compared to IRIS ( $p=0,005$ ) or to IRIS TR ( $p=0,005$ ) plans, 7908 MU, 23109 MU and 19467 MU respectively. The mean calculated treatment time was significantly less with MLC (18 mins) compared to IRIS (27 mins,  $p=0,008$ ) or IRIS TR (23 mins,  $p=0,008$ ). There was a trend for average HI where the IRIS plans had better values (0,15) than MLC (0,18), while IRIS TR (0,19) values were similar. IRIS plans resulted better nCI values (1,27) than

MLC plans (1,31), but the difference was not significant. The MLC plans had significantly ( $p=0,02$ ) lower average maximum doses for the shell (1282 cGy) compared to IRIS TR plans (1473 cGy), while IRIS plans (1281 cGy) showed similar maximum dose in the lower dose region. The  $D_{0,04ccm}$ ,  $D_{0,2ccm}$  for Optic Pathway and the  $D_{0,04ccm}$  and  $D_{0,5ccm}$  values for Brainstem were 733 cGy, 491 cGy, 761 cGy, 593 cGy with MLC and 744 cGy, 549 cGy, 828 cGy, 630 cGy with IRIS and 785 cGy, 578 cGy, 817 cGy, 633 cGy with IRIS TR, without significant differences.

#### Conclusion

The InCise 2 MLC offers shorter treatment time, less MU, higher conformality for low doses with same or better organs at risk protection. However, the IRIS plans had a slightly better homogeneity and conformity index values. The treatment time of IRIS TR plans are still more than MLC plans' if we insist on clinically acceptable plans. The further reduction of treatment time of IRIS TR plan results in a much worse plan quality, except with large spherical targets where the treatment time of IRIS plans could be reduced to the level of MLC plans, maintaining the same plan quality.

#### EP-1839 Development of Cardiac Avoidance Treatment Planning for Non-Small Cell Lung Cancer Patients

S. De Vos<sup>1</sup>, C. Rowbottom<sup>1</sup>, M. Gilmore<sup>1</sup>

<sup>1</sup>Clatterbridge Cancer Centre, Radiotherapy, Birkenhead, United Kingdom

#### Purpose or Objective

Lung cancer is the deadliest type of cancer, and eight in 10 lung cancers are non-small cell lung cancers (NSCLC). There is evidence that cardiac dose contributes to reduced overall survival in NSCLC patients. If cardiac dose can be minimised in the treatment of these patients, without impacting on planning target volume (PTV) dose, or other organs at risk (OARs), this may improve their prognosis. This study will aim to develop cardiac avoidance treatment planning techniques for NSCLC patients.

#### Material and Methods

Twenty-three patients who have received the standard Clatterbridge Cancer Centre (CCC) volumetric modulated arc therapy (VMAT) NSCLC protocol of 55Gy in 20 fractions (#) were included in the study. Three new plans were created retrospectively: a second plan (B) was morphed from the original delivered plan (A), where the cardiac dose objectives (mean heart dose (MHD), V5Gy and V30Gy) were pushed harder in the optimiser. For the third plan (C), the full or half arcs were replaced by partial arcs, with cardiac avoidance sectors, in a coplanar orientation. The fourth plan (D) has the same partial arcs as the third plan, but in a noncoplanar orientation, to further drive heart dose down. For a small subset of patients, a more extreme noncoplanar arc configuration (seven partial arcs) was created. Plans were compared and evaluated with statistical analysis, using a range of PTV and OAR dosimetric parameters.

#### Results

MHD, V5Gy and V30Gy were improved for all three new plans, compared with the clinical plan (A). The largest improvements in heart dose were observed for the noncoplanar partial arc geometry (D), followed by the coplanar full/half arc geometry with tighter planning objectives (B). MHD reduced by 32.4% for Plan D, compared with Plan A ( $P < 0.001$ ), whereas heart V5Gy and V30Gy saw a reduction of 26.1% ( $P < 0.001$ ) and 38.8% ( $P < 0.001$ ) respectively. For Plan B, compared to A, the mean reduction in MHD, heart V5Gy and V30Gy was 25.7% ( $P = 0.001$ ), 17.6% ( $P = 0.002$ ) and 35.7% ( $P < 0.001$ ) respectively. Oesophagus dose increased significantly for Plan B (2.2%,  $P = 0.009$ ), and Paddick Conformity Index (CI) decreased significantly for Plan D (3.3%,  $P = 0.02$ ) but on the whole OAR doses and PTV coverage either improved or remained similar between plans.

#### Conclusion

It is possible to develop cardiac avoidance treatment planning for NSCLC patients undergoing VMAT treatment (55Gy in 20#) without significantly compromising other OARs or PTV coverage.

#### EP-1840 comparing the dosimetric impact of omentum spacer in carbon-ion, proton and photon radiotherapy

M. Yamada<sup>1</sup>, H. Sato<sup>1</sup>, T. Ono<sup>2</sup>, Y. Ieko<sup>1</sup>, T. Kanai<sup>1</sup>, N. Yano<sup>1</sup>, H. Akamatsu<sup>1</sup>, M. Harada<sup>1</sup>, M. Ichikawa<sup>1</sup>, Y. Kikuchi<sup>2</sup>, K. Nemoto<sup>1</sup>

<sup>1</sup>Yamagata University Faculty of Medicine, Department of Radiation Oncology, Yamagata, Japan ; <sup>2</sup>Southern Tohoku Proton Therapy Center, Department of Radiation Oncology, Koriyama, Japan

#### Purpose or Objective

This study was an *in silico* planning study to compare carbon-ion (C-ion), proton and photon radiotherapy (RT) plans regarding dose reduction of the gastrointestinal (GI) tract by the greater omentum spacer (GO spacer).

#### Material and Methods

A total of 10 patients who received surgical spacer placement for abdominal and pelvic tumors were included in this study. In all patients, the tumor was adjacent to the GI tract, and GO spacer was inserted between the tumor and the surrounding GI tract. Simulation plans were created on pre-spacer CT and post-spacer CT for C-ion, proton and photon RT respectively. All plans prescribed 70 Gy (relative biological effectiveness (RBE) equivalent) delivered in 35 fractions to the PTV. They were normalized so that at least 95% of the PTV received the prescribed dose. The dose constrain for the spinal cord was maximum dose ( $D_{max}$ ) < 45Gy. All plans were created with the dose to the GI tract reduced as much as possible under the condition of meeting the dose constrains for the PTV and spinal cord. The GI tract to be evaluated was defined as that most adjacent to the PTV. We aimed to satisfy the dose constraints of the minimum dose received by the most exposed 2 cc volume of the organ ( $D_2$  cc) of the GI tract < 50 Gy. C-ion RT plans and proton RT plans were calculated by a spot scanning technique and photon RT plans were calculated employing fixed-field intensity-modulated radiation therapy (IMRT). We tested the difference in mean values of the  $D_2$ cc, the volume receiving 10 Gy or more (V10), V15, V20, V25, V30, V35, V40, V45, V50, V55, V60, V65 and V70 of the GI tract on pre-spacer CT and post-spacer CT for all three RT modalities. Statistical analysis was performed by the paired t-test.

#### Results

GO spacer significantly reduced  $D_2$  cc of the GI tract for C-ion RT (mean±SD: 65.4±5.2 vs 6.4±2.4 Gy,  $p < 0.0001$ ), proton RT (63.3±6.1 vs 6.4±2.9 Gy,  $p < 0.0001$ ) and photon RT (58.8±4.5 vs 24.4±5.2 Gy,  $p < 0.0001$ ). Reduction of  $D_2$  cc of the GI tract by GO spacer was more effectively achieved by C-ion RT and proton RT than by photon RT (C-ion vs photon  $p = 0.001$ , proton vs photon  $p = 0.002$ ). There was no significant difference between C-ion RT and proton RT in reduction of  $D_2$  cc of the GI tract by GO spacer (C-ion vs Proton  $p = 0.992$ ). In one patient on photon RT plan,  $D_2$  cc of the GI tract did not meet the constrain. The GTV of that patient was the left acetabular and sacral bone metastasis of uterine body cancer. In that patient, the GI tract most adjacent to the PTV on post-spacer CT was sigmoid colon and the separation distance from the PTV to the GI tract was 0.43 cm and  $D_2$  cc of the GI tract of C-ion RT, proton RT and photon RT were 22.4, 29.2 Gy and 61.3 Gy respectively.

#### Conclusion

GO spacer significantly reduced  $D_2$  cc of the GI tract for C-ion RT, proton RT and photon RT. Reduction of  $D_2$  cc of the GI tract by GO spacer was more effectively achieved by C-ion RT and proton RT than by photon RT.

### EP-1841 Couch modeling optimization for TomoTherapy planning and delivery

M. Tanooka<sup>1</sup>, W. Okada<sup>1</sup>, K. Sano<sup>2</sup>, S. Mayuri<sup>2</sup>, H. Doi<sup>3</sup>, M. Miyazaki<sup>1</sup>, R. Nakahara<sup>1</sup>, M. Sueoka<sup>1</sup>, H. Suzuki<sup>1</sup>, M. Fujiwara<sup>1</sup>, N. Kamikonya<sup>1</sup>, Y. Inomata<sup>2</sup>, K. Yamakado<sup>1</sup>  
<sup>1</sup>Hyogo College of Medicine, Department of Radiology, Nishinomiya, Japan ; <sup>2</sup>Takarazuka City Hospital, Department of radiotherapy, Takarazuka, Japan ; <sup>3</sup>Kindai University Faculty of Medicine, Department of Radiation Oncology, Sayama, Japan

#### Purpose or Objective

Carbon-fiber flat top couches have been widely used for radiotherapy. It was reported that the beam intensity attenuation inside the couch should be taken into account in treatment-planning system. From the start, TomoTherapy planning system (Accuray Precision) has been provided such a capability. However, this couch model does not have appropriate physical densities. Furthermore, it is not possible to correct these physical densities. Therefore, we performed a novel couch modeling optimization for TomoTherapy planning and delivery.

#### Material and Methods

The beam intensity attenuation caused by the TomoTherapy Radixact couch unit was evaluated by creating and adding a new optimized couch model in a planning support system (MIM Maestro). The couch modeling started with acquiring CT images, the images were transferred to the planning support system for contouring. Then these DICOM images data and a created DICOM RT structure set for couch modeling were transferred to the TomoTherapy planning system. Additionally, dose was compared between calculation and measurement in order to optimize the appropriate densities for the contoured couch region. To do this, a Exradin A17 chamber was placed on the couch. Doses were measured at gantry angles ranging from 0° to 355° in 5° increments for a 6 MV photon beam. This setup was replicated in the TomoTherapy planning system and dose was calculated using collapsed-cone-convolution (CCC) algorithm (TomoDirec plan, Forward Planning, dynamic jaw mode, Field size: 10×5 cm<sup>2</sup>). Interactive appropriate physical density optimization was performed by comparing calculated and measured doses in order to minimize the discrepancies. Finally, the optimized appropriate physical densities were employed in the typical QA plan of 14 patients to evaluate the impact of the treatment couch on the dosimetry validation.

#### Results

The presence of the treatment couch in a plan resulted in a decrease ranging from 3.0% up to 11.1%, depending on the beam angles. The conventional modeling decreased at isocenter dose discrepancy in the range of 0.9% to 2.3%. However, our modeling decreased dose discrepancy less than 0.5% except for gantry angles 115° and 245° (Figure 1). Our simple shape model with optimized physical densities was selected among the models considered, and the optimized physical densities of the treatment couch were 1.3 g/cm<sup>3</sup> and 2.5 g/cm<sup>3</sup>. A total average decrease in absolute dose at a selected point of 0.2% was calculated in the QA plans. Additionally, the dose distribution our modeling yielded an average pass rate using gamma index (3%, 2 mm) of 96.5% (max 99.7%, min 91.7%), and the pass rate was higher than conventional modeling (Table 1).  
**Figure 1**

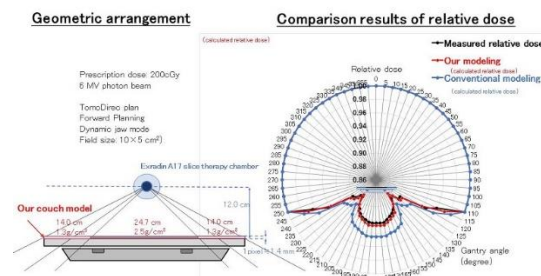


**Table 1**

	Average absolute dose difference	Average pass rate of ArcCHECK using gamma index (3%, 2 mm)
Conventional modeling	0.0%	94.9%
Our modeling	0.2%	96.5%

#### Conclusion

We could successfully obtain an accurate couch model for TomoTherapy planning system by interactively optimizing the physical density of the couch using planning support system. Furthermore, this modeling proved to be an efficient way of correcting the dosimetric effects of the treatment couch in TomoTherapy planning and delivery.

### EP-1842 Automated treatment planning of prostate cancer using prioritized clinical-goal based optimization

R. Kierkels<sup>1</sup>, A. Fredriksson<sup>2</sup>, E. Hynning<sup>2</sup>, S. Both<sup>1</sup>, J.A. Langendijk<sup>1</sup>, B. Vanhauten<sup>1</sup>, E.W. Korevaar<sup>1</sup>  
<sup>1</sup>University Medical Center Groningen, Radiation Oncology, Groningen, The Netherlands ; <sup>2</sup>RaySearch Laboratories, Stockholm, Sweden

#### Purpose or Objective

To increase departmental efficiency and achieve high quality treatment plans for prostate cancer patients. Therefore, we implemented fully automated prioritized clinical-goal based treatment planning (ATP) for intensity modulated radiotherapy (IMRT) and volumetric modulated arc therapy (VMAT) and evaluated the ATP plans with the clinical dosimetrist-optimized treatment plans.

#### Material and Methods

The clinical goals of prostate radiotherapy (patients containing gold markers) were extracted from our medical protocol and ordered by priority into a wishlist. The order and priorities of the clinical goals were fine-tuned based on the dosimetrist-optimized clinical VMAT plans of two previously treated prostate cancer patients. The final version of the wishlist was used by the ATP solution (RayStation v6.1, RaySearch Laboratories AB, Stockholm, Sweden) to automatically optimize treatment plans for novel patients. The ATP optimization is a lexicographic method that tries to fulfill the goals of the wishlist iteratively. A goal of higher priority will not be compromised to fulfill goals of lower priority.

To assess the quality of the wishlist, prostate IMRT and VMAT plans were automatically optimized by the ATP algorithm for eight previously treated prostate cancer patients. From these patients a dosimetrist-optimized prostate VMAT plan was also available. The treatment planning time of a representative dosimetrist-optimized prostate case was approximately 180 minutes. Target coverage, conformity index (CI95%) and homogeneity index (HI98%) as well as organ at risk dose values were compared between the ATP plans and the dosimetrist-optimized plans.

## Results

The wish list for prostate IMRT/VMAT comprised of 10 priority levels (see table 1). The first few levels focused on target coverage, followed by target homogeneity and conformity. The subsequent priority levels mainly accounted for organ sparing. The lowest priority further reduced the average organ at risk dose as much as possible. Studying ATP-IMRT an ATP-VMAT plans of the eight evaluation patients, we found similar target coverage (all ATP plans:  $V95 > 98.2\%$  for  $PTV_{77}$  and  $PTV_{70}$ ), target conformity (range:  $CI95\%_{PTV_{70}} = 0.64 - 0.81$ ), target homogeneity (range:  $HI98\%_{PTV_{77}} = 0.92 - 0.94$ ) as compared to the dosimetrist-optimized VMAT plans. Furthermore, ATP resulted in an averaged dose reduction of 3.3 Gy (range: Gy -0.8 - 11.9 Gy) to the bladder and 4.6 Gy (range: -2.6 - 6.3 Gy) to the rectum (representative case in figure 1). Preparation and post-processing took approximately 45 minutes for the ATP plans. All plans were approved by an experienced radiation-oncologist in prostate cancer treatments.

Table 1. Wishlist for prostate prioritized auto planning

Priority	Volume of Interest	Clinical goal
1	$PTV_{70}$	$D99 \geq 66.5$ Gy
	$PTV_{77}$	$D98 \geq 73.2$ Gy
2	$PTV_{70min}PTV_{77}$	$Dmax \leq 82.0$ Gy
	$PTV_{77}$	$Dmax \leq 75.0$ Gy
3	External	$V39 < 20000$ cc
4	Bladder	$Dmean \leq 40$ Gy
	Small bowel	$D2 \leq 58.0$ Gy
5	Rectum	$Dmean \leq 40.0$ Gy
	Bladder	$V80 \leq 1.0$ cc; $V75 \leq 25.0$ cc; $V70 \leq 35.0$ cc; $V65 \leq 50.0$ cc; $Dmean \leq 35.0$ Gy
6	Small bowel	$Dmax \leq 68.0$ Gy
	Rectum	$V77 \leq 1.0$ cc; $V72 \leq 25.0$ cc; $V70 \leq 35.0$ cc; $V65 \leq 50.0$ cc; $V60 \leq 50.0$ cc; $D50 \leq 50.0$ Gy; $Dmean \leq 35.0$ Gy
6	Hips	$Dmax \leq 50$ Gy
7	Bladder	$Dmean \leq 30.0$ Gy
	Rectum	$Dmean \leq 30.0$ Gy
8	$PTV_{70min}PTV_{77}$	$D2 \leq 75$ Gy
9	Bladder	$Dmean \leq 25$ Gy
	Rectum	$Dmean \leq 25$ Gy
10	Bladder	Reduce average dose
	Rectum	Reduce average dose

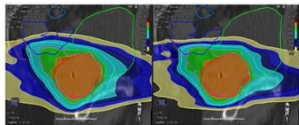


Figure 1. Sagittal view of a CT scan of a prostate cancer patient overlaid with a dose distribution of the (left) automated treatment plan and (right) dosimetrist-optimized treatment plan. The dose is indicated from low to high by a yellow to orange dose wash.

## Conclusion

The prioritized clinical-goal based ATP algorithm led to high quality IMRT and VMAT plans for prostate cancer patients. The plans were fully automatically optimized in the background resulting in an increased departmental efficiency (approx. 135 minutes reduction per prostate case).

## EP-1843 Evaluation of treatment efficiency for helical tomotherapy with TomoEdge technology

B. Yang<sup>1</sup>, W.W. Lam<sup>1</sup>, H. Geng<sup>1</sup>, K.Y. Cheung<sup>1</sup>, S.K. Yu<sup>1</sup>  
<sup>1</sup>Hong Kong Sanatorium & Hospital, Medical Physics and Research Department, Happy Valley, Hong Kong SAR China

## Purpose or Objective

Some previous studies analyzed the impact of modulation factor (MF) on both plan quality and treatment time by varying MF and pitch. Those studies usually drew conclusions based on a series of reference plans and focused on specific treatment region, e.g. head and neck. This study aims to evaluate the treatment efficiency based on large amount of clinical plans in different treatment regions by analyzing the treatment plan parameters of helical tomotherapy with TomoEdge technology, especially the correlation between actual modulation factor (MF) and gantry period.

## Material and Methods

A total number of 303 patients treated in head and neck (HN), breast/chest wall (BCW), brain, thorax, abdomen (ABD) and pelvis regions in our hospital using tomotherapy with TomoEdge technique were retrospectively studied. All treatment plans involved in this study were approved by oncologists with clinical goals achieved. The treatment

plan parameters including planned MF, actual MF, couch speed, gantry period, average leaf open time (LOT), pitch and jaw width were analyzed. Pearson correlation coefficient was calculated between the actual MF and the gantry period.

## Results

The distribution of actual MF for total cases is plotted in figure 1(a) and detailed data are listed in table 1. The mean value of actual MF didn't show much difference for different treatment regions. As shown in figure 1(b)-(c), the actual MF correlates with the gantry period with Pearson correlation coefficients of 0.70 and 0.84 for BCW(2.5D) and BCW(5D) respectively while  $p < 0.01$ . The minimum rotation time of 12s was not reached for any BCW case. If the gantry period less than 13s was taken as the end point for a conventional 2Gy/fr treatment when optimizing treatment efficiency, the current planned MF for BCW could be further decreased. Besides, the planning efficiency might also be improved by reducing the iteration based on the large discrepancy between planned and actual MF. Figure 1(d)-(e) show the correlation for HN(2.5D) and abdomen(2.5D) as well. A few HN cases with the maximum gantry speed indicated the current lower limit of 2 for the planned MF was proper, which had to be increased to 3 for some critical cases. However, the linear trend in figure 1(d) indicated the upper limit should be decreased and a value of 3.4 could be reasonable. Those outliers with gantry period larger than 20s were caused by large prescription dose. The same conclusions were drawn for thorax and pelvis region. For abdomen and brain cases, no linear correlation could be observed which meant the current planned MF had a reasonable range from 1.8 to 3.6 and 1.4 to 3.2, respectively.

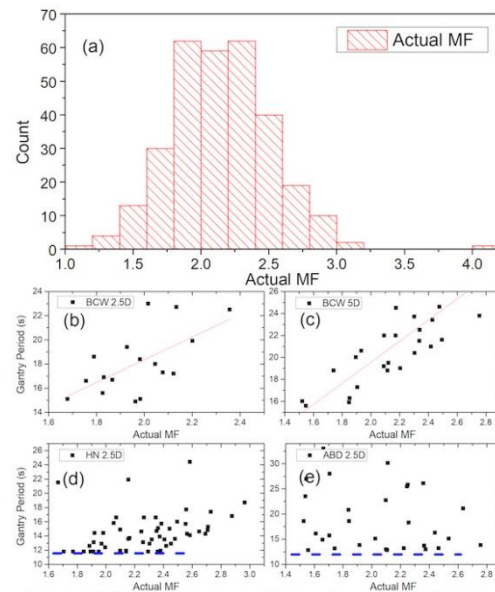


Figure 1 (a) Histogram of actual MF for all cases;(b)-(e) Scatter plots of gantry period versus actual MF for breast/chest wall, head and neck, and abdomen cases. Blue dash lines indicate the gantry speed limit

Table 1. Plan parameters for different treatment regions including planned actual MF, couch speed, gantry period, average LOT, proportion of different jaw widths and pitch value.

Tx Region	No. of cases	Planned MF	Actual MF	Couch Speed (mm/s)	Gantry Period (s)	Average LOT (°)	Proportion of Jaw Width (mm)			Pitch
							1(F)	2.5(D)	5(D)	
Abdomen	40	2.8110.51	2.06110.37	0.42720.213	24.613.3	0.24020.131	2.5%	75.0%	22.5%	0.287
Breast/Chest Wall	47	3.5710.56	2.06510.29	0.60610.188	19.515.8	0.18610.052	0.0%	42.6%	57.4%	0.287
Pelvis	52	2.7810.51	2.17710.39	0.40720.141	21.8110.4	0.20410.115	2.0%	86.3%	11.8%	0.287
Head&Neck	62	3.1310.45	2.29110.30	0.49710.217	16.217.4	0.13910.082	6.5%	93.5%	0.0%	0.287
Thorax	52	3.0210.46	2.17410.29	0.45810.543	23.7111.0	0.21710.106	1.9%	80.8%	17.3%	0.287
Brain	27	2.7910.80	2.11210.67	0.34110.215	29.1125.0	0.33210.359	22.2%	74.1%	3.7%	0.287(85.2%)
Abdomen+Pelvis	9	2.9310.46	2.16910.33	0.5110.106	17.415.8	0.16110.071	0.0%	77.8%	22.2%	0.287
Thorax+Abdomen	11	2.8710.50	2.00310.29	0.53310.190	19.916.8	0.19710.070	0.0%	83.6%	36.4%	0.287
Spine	3	2.2010.16	1.8810.07	1.16710.088	12.511.0	0.13010.066	0.0%	0.0%	100.0%	0.287
Overall	303	3.010.59	2.15310.38	0.47710.360	21.4112.2	0.20510.147	4.3%	77.9%	17.8%	0.287(98.7%)

## Conclusion

Actual MF values for BCW positive correlations with the gantry period, which indicates the treatment time could be potentially reduced by decreasing the planned MF value. Proper range of planned MF was present for HN, thorax, ABD, brain and pelvis regions based on the clinical data in our center.

## EP-1844 Re-irradiation with SBRT for pancreatic cancer: dose summation and toxicity

X. Zhu<sup>1</sup>, C. Yangsen<sup>1</sup>, Z. Xianzhi<sup>1</sup>, S. Yuxin<sup>1</sup>, J. Xiaoping<sup>1</sup>, Q. Shuiwang<sup>1</sup>, C. Fei<sup>1</sup>, J. Zhen<sup>1</sup>, F. Fang<sup>1</sup>, G. Lei<sup>1</sup>, Z. Huojun<sup>1</sup>

<sup>1</sup>Changhai Hospital, Radiation Oncology, Shanghai, China

## Purpose or Objective

A significant number of patients with pancreatic cancer may develop local recurrence after treatment. These patients may not be amenable for surgery due to its high complication rates. In addition to second-line chemotherapy regimens, re-irradiation with stereotactic body radiation therapy (SBRT) may be an alternative, which has been used in few studies. However, the techniques were conventional radiotherapy prior to re-irradiation with SBRT in previous studies and the dose constraints of organs at risk (OAR) were never reported. Therefore, the goal of the study was to determine the cumulative dose-volume parameters to OAR after two courses of SBRT.

## Material and Methods

All patients received two courses of SBRT for the same region with a partial or complete overlap of two previous dose distributions were enrolled. The maximum dose of OAR was calculated as 50% more than the normal constraint. Secondly, we allowed a dose reduction of 50% for a re-irradiation 12 months after the last radiation. A dose reduction of 25% was allowed for a re-irradiation after 6-12 months. No dose reduction was used when re-irradiation was done within 6 months. Due to different doses to target regions and OAR and fractionation schemes, all treatment schedules were recalculated to an Equivalent Dose of 2 Gy per fraction (EQD<sub>2</sub>). An  $\alpha/\beta$  value of 10 Gy (Gy<sub>10</sub>) was employed for the tumor dose and acute effects, and the value determined as 3 Gy (Gy<sub>3</sub>) concerning late effects. Dose distributions, structures sets and CT scans of two treatment plans were extracted from Multiplan<sup>®</sup> System (version: 4.0.2) and sent to MIM<sup>®</sup> System (version: 6.6.8) for analysis. Firstly, two CT scans were aligned rigidly via automatic bone matches (translation and rotations). Therefore, for each plan before summation, each of the contoured OARs was registered rigidly. Subsequently, a non-rigid registration was followed in dose summations. After non-rigid registration, the dose distributions of the first plan were projected to the second treatment with both of doses converted to EQD<sub>2</sub>, which were summed up finally.

## Results

A total of 41 patients were identified. The median accumulated D<sub>max</sub>, D<sub>1</sub> and V<sub>10</sub> of the stomach, duodenum

and the bowel were 36.75Gy<sub>3</sub>, 27.87 Gy<sub>3</sub> and 66.41cc; 30.36 Gy<sub>3</sub>, 22.13 Gy<sub>3</sub> and 18.66cc; 35.76 Gy<sub>3</sub>, 28.06 Gy<sub>3</sub> and 119.48cc, respectively. The median accumulated D<sub>max</sub> of the spinal cord was 6.42 Gy<sub>3</sub>. The median cumulative D<sub>mean</sub> and D<sub>2/3</sub> of the left and right kidney were 4.62 Gy<sub>3</sub> and 3.03 Gy<sub>3</sub>; 2.67 Gy<sub>3</sub> and 2.10 Gy<sub>3</sub>, respectively. The median cumulative D<sub>mean</sub> and D<sub>50%</sub> of the liver was 4.28 Gy<sub>3</sub> and 3.03 Gy<sub>3</sub>, respectively. The median summed dose to the radiation field was 93.38 Gy<sub>3</sub>. No grade 3-4 toxicity occurred. Partial response and a stable disease to the second irradiation was found in 4 and 33 patients.

## Conclusion

The cumulative doses to OAR as dose constraints were acceptable and safe, which could be used as a reference in the decision for re-irradiation with SBRT after prior SBRT for pancreatic cancer but required further validations with radiobiological models in cohorts.

## EP-1845 Proton beam therapy vs best photons for the management of mediastinal Hodgkin lymphoma: step by step

L. Abbassi<sup>1</sup>, F. Goudjil<sup>1</sup>, A. Arsène-Henry<sup>1</sup>, M. Amessi<sup>1</sup>, R. Dendale<sup>1</sup>, Y.M. Kirova<sup>1</sup>

<sup>1</sup>Institut Curie, Département Oncologie-Radiothérapie, Paris, France

## Purpose or Objective

Reducing treatment-related toxicity among survivors of Hodgkin lymphomas (HL) has been the cornerstone of recent advances in the treatment of hematologic malignancies. The purpose of this presentation is to describe the practical procedure inspired by the recently published ILROG Guidelines of treatment decision, preparation and treatment, illustrated with the presentation of the first reported case of localized HL treated with Protontherapy (PT) in Europe.

## Material and Methods

We present the case of 24 years old female patient with a mediastinal Bulky localized mixed cellularity classic HL who required an Involved-Site Radiation Therapy (ISRT) after complete response acquired with polychemotherapy. The 3D conformal radiotherapy (RT) was not acceptable due to high doses to breasts, heart and lungs. The first step was realizing a 4D CT-scan to evaluate target movements and another one with respiratory control (gating and breath-hold technique) by spirometer. Step 2: Delineation was realized on the 4D CT-scan as well as on the deep inspiration breath-hold CT-scan after images registration between initial PET-scan and the CT in treatment position, for photon RT and PT respectively. CTV/ITV and organs at risk (OAR) were delineated the same way for both technics, following ILROG Guidelines. Step 3: Realization of 2 dosimetric plans: one with rotational intensity modulated radiation therapy (IMRT) with a Helical Tomotherapy (HT) with the Tomotherapy Treatment Planning System (TPS) and one with conformational PT with Eclipse TPS.

## Results

The step 4 consisted of the choice of the best plan treatment for this patient after discussion between 2 senior radiation oncologists with comparison of the treatment volume coverage and evaluation of doses to OAR. Step 4a: volume coverage was good with 95% of PTV covered by 98% and 99% of the prescribed dose with PT and HT, respectively. Step 4b: sparing of OAR was better with PT for lungs, in terms of the mean dose (3.7Gy vs 8.4Gy), median dose (0.002Gy vs 6.9Gy) and low dose (V5 Gy = 17.8% vs 54.18%). Mean dose to the heart was higher with HT (3.7Gy) compared to PT (2.6Gy). Breast sparing was better with PT, with a mean dose of 2.4Gy to the right breast and 1.9Gy to the left breast versus 4.4Gy and 4.6Gy. Total dose chosen was 30Gy in 15 fractions of 2Gy with PT with direct anterior field using Pencil Beam Scanning (PBS). Step 5: Treatment delivery and follow-up during PT. We observed only grade 1 skin erythema, no

dysphagia, and no other symptom. Step 6: follow-up after PT. Three months after PT, the patient is PS 0, with no symptom, normal blood tests and metabolic CR according to the LUNAGO criteria on PET-scan (DEAUVILLE score at 2).

#### Conclusion

The use of PT for HL engaging the mediastinum is promising and there is a dosimetric advantage of reducing the dose to OAR. However, the limited availability of PT calls for case selection based on a clear understanding of which patient will most benefit from PT compared to advanced photon techniques.

#### EP-1846 Cloud-based contouring education system supporting access from multi-devices

H. Takegawa<sup>1,2</sup>, S. Nakamura<sup>1,2</sup>, N. Tanigawa<sup>1</sup>

<sup>1</sup>Kansai Medical University, Department of Radiology, Osaka, Japan ; <sup>2</sup>Kansai Medical University Hospital, Division of Radiation Oncology, Osaka, Japan

#### Purpose or Objective

Contouring uncertainties is sensitive to clinical outcomes in intensity-modulated radiation therapy due to its steep dose gradient around tumors and organs at risk. To reduce contour uncertainties among radiation oncologists and institutions, contouring seminars and workshops are held. However, contouring education systems used in those seminars does not often support access from multi-devices and multi-platform environments. The purpose of this study was to develop a cloud-based contouring education system supporting access from multi-devices.

#### Material and Methods

The system overview is shown in figure 1. A fundamental desktop application of the system was developed in MATLAB language and basic functions of contouring education were implemented as described below. It is considered that the system is used by experts (teachers) and beginners (students). Experts prepare educational data with their treatment planning systems (TPS) at their institution and send them to the cloud system and then beginners can access these data according to their privilege. Educational image resources such as treatment planning CT, MR and PET/CT are imported, and image fusion are performed based on a DICOM image registration object exported from a TPS to ensure same image registration results as those of TPS. Data of structure sets which experts prepared are also imported to the system. Beginners draw contours on planning images without any contours in the structure sets and experts can modify beginners' contours to give them feedback. Educational effects can be measured by evaluating dice similarity coefficients of contours between experts and beginners. To allow users access the developed desktop application from multi-devices, it was deployed to a cloud system, Amazon Workspaces, which is a virtual desktop infrastructure (VDI) on Amazon Web Services. Access from desktop and laptop computers, and tablet with the VDI client application and from HTML5-compatible web browsers to the system were verified.

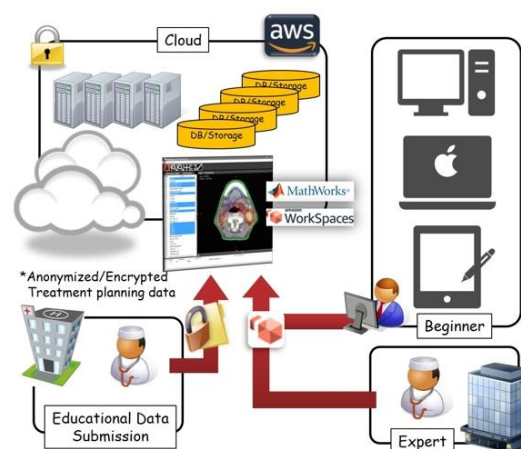


Figure 1. Overview of the cloud-based contouring education system.

#### Results

All devices successfully accessed the system with the VDI client and the deployed application worked without any problems. A modern input device such as a stylus pen also worked and so it was possible to contour targets and organs at risk as drawing pictures. The delay in display and input were quite less even though the access was performed through 4G mobile network. Not all the web browsers accessed the system and input with a touch screen did not work.

#### Conclusion

The cloud-based contouring education system supporting access from multi-devices was developed and its access from multi-devices was verified.

#### EP-1847 Automatic optimization of Head and Neck treatments with multicriteria radiobiological cost functions

M. Esposito<sup>1</sup>, A. Ghirelli<sup>1</sup>, S. Pini<sup>2</sup>, S. Russo<sup>1</sup>, G. Zatelli<sup>3</sup>, P. Alpi<sup>4</sup>, R. Barca<sup>4</sup>, S. Fondelli<sup>4</sup>, B. Grilli Leonulli<sup>4</sup>, L. Paoletti<sup>4</sup>, F. Rossi<sup>4</sup>, P. Bastani<sup>4</sup>

<sup>1</sup>Azienda Sanitaria USL Centro, S. C. Fisica Sanitaria-Firenze Empoli, Bagno a Ripoli, Italy ; <sup>2</sup>Azienda Sanitaria USL Centro, S. C. Fisica Sanitaria-Firenze Empoli, Bagno a Ripoli, Italy ; <sup>3</sup>Azienda Sanitaria USL Centro, S. C. Fisica Sanitaria-Firenze Empoli, Bagno a Ripoli, Italy ; <sup>4</sup>Azienda Sanitaria USL Centro, S. C. Radioterapia, Bagno a Ripoli, Italy

#### Purpose or Objective

The optimization of Head and Neck treatments is one of the most complex task for planners; skills and experience can influence planning results. Automatic planning can help standardize plan quality and is needed for adaptive radiotherapy. Aim of this study is to construct and evaluate a template for automatic optimization of Head and Neck treatments using multicriteria radiobiological cost function of the treatment planning system Monaco 5.10.

#### Material and Methods

The automatic workflow was tested on ten previously treated Oropharyngeal Head and Neck cases. Each treatment consisted in multiple prescription target volumes (PTV): high dose PTV (between 66 and 70 Gy), intermediate dose PTV of 60 Gy and a low dose PTV of 54 Gy in 32 fractions. Constraints for organ at risk (OAR) were: Parotid  $D_{\text{mean}} < 26$  Gy, Cord planning risk volume (PRV)  $D_{1\text{cm}^3} < 50$  Gy, esophagus  $D_{\text{mean}} < 34$  Gy, the patient  $D_{\text{max}} < 110\%$  of the higher PTV dose. Planning objectives were to cover at least the 95% of each PTV with the 95% of the prescription dose. The radiobiological functions used in the template are shown in Table1. To each function a dosimetric objective was assigned; when all

objectives were fulfilled the multi-criterial optimizer reduced the dose to all organs at risk until doses to PTVs were not affected. For each case, the automatic plan was compared with the approved plan manually optimized. The following dosimetric parameters were recorded: PTV D95, Parotid D<sub>mean</sub>, PRV Cord D<sub>1cm3</sub>, esophagus D<sub>mean</sub>. For each plan a modulation degree index (MD) was computed: MD= Total MU/[Sum of (Segment Area x Segment MU)/Total Beam Area].

Contour	Cost function	Objective	Multicriterial
Parotids	Mean dose	30 Gy	yes
Parotids	Serial	22 Gy (20)	yes
Cord	Serial	37 Gy (18)	yes
Esophagus	Serial	40 Gy (15)	yes
Larynx	Serial	42 Gy (19)	yes
PTV	Target EUD	Prescription dose	no

Table1 Cost function used in automatic template. In brackets the exponents of the serial cost functions are shown

### Results

The plans produced automatically fulfilled OAR constraints and reach objectives in 9/10 case. In the remaining case the plan produced automatically was not able to reach a minimum requirement of PTV coverage. Plan comparison is shown in table2. Automatic plans achieved lower dose to both parotids at the cost of a little reduction of dose to the high dose PTV and increase of dose to PRV cord. Modulation degrees of automatically produced and approved plans were not statistically different.

	Approved Plans	Automatic plans	p
PTV 70 D <sub>95</sub>	68.5 (1.4) Gy	66.5 (2.4) Gy	0.02
PTV 54 D <sub>95</sub>	51.1 (1.1) Gy	53.6 (1.2) Gy	0.001
Parotid Ipsilateral	29.3 (12) Gy	25.3 (6.4) Gy	0.06
Parotid Controlateral	26.5 (4.1) Gy	23.4 (3.7) Gy	0.03
PRV Cord 1cm <sup>3</sup>	39.5 (3.7) Gy	43.5 (1.5) Gy	0.001
Esophagus	39.3 (9.1) Gy	34.7 (3.7) Gy	0.09
Larynx	37.6 (1.7) Gy	42.5 (2.4) Gy	0.001
MD	6.2 (0.5)	5.8 (0.5)	0.22

Table2 Comparison of automatic vs approved plans. Average value are shown, in bracket standard deviations are reported.

### Conclusion

In this study the feasibility of the automatic plan generation using the multicriteria function of Monaco has been shown.

### EP-1848 Inaccuracies in proton dose calculation may be as significant as setup and range uncertainties

M. Schwarz<sup>1,2</sup>, M. Innocenzi<sup>1,3</sup>, I. Giacomelli<sup>1</sup>, F.

Fracchiolla<sup>1</sup>, V. Patera<sup>3</sup>, R. Righetto<sup>1</sup>

<sup>1</sup>Centro di Protonterapia, Protontherapy, Trento, Italy ;

<sup>2</sup>TIFPA-INFN, Medical Physycs, Trento, Italy ; <sup>3</sup>Università degli Studi di Roma, Basic and Applied Sciences for Engineerin, Roma, Italy

### Purpose or Objective

Plan robustness with respect to setup and range errors is considered a priority in protontherapy. However, geometrical uncertainties are not the only source of error in proton treatment planning. In this work we evaluate the effects of setup errors, range uncertainties and dose calculation algorithms on protontherapy dose distributions, to assess which uncertainties affect the most the difference between the nominal and actual dose distribution.

### Material and Methods

12 treatment plans used for clinical treatment at our centre were selected, covering four treatment sites: brain, head&neck, chordoma of the spine, and craniospinal axis. The plans, which were initially optimized with a PTV-based single field optimization technique and pencil beam (PB) dose algorithm, were

recalculated with a validated Monte Carlo(MC) code with a statistical uncertainty of 1%. We evaluated the effect of setup and range uncertainties on the planned dose distribution with an in-house software simulating 8 setup errors and 2 range errors (16 calculations per plan in total), to estimate near worst-case scenarios for target volume and organs at risks (OAR). We evaluated the differences between MC and PB distributions and the plan robustness using the same dosimetric indices used to optimize the plan (e.g. D1 and D99 for the target volume, D1 for serially responding OARs, etc.).

### Results

For the intracranial lesions, the differences between PB and MC was small (mostly <1%) and setup&range error were causing the largest differences between nominal and actual(perturbed) dose. For the remaining treatment sites, CTV coverage in MC plans was always lower than in PB plans, in some cases with difference in CTV D99 by more than 10%(Table1). The differences were the largest when a preabsorber was needed to irradiate the shallowest part of the target. Concerning the OAR, the differences between MC and PB algorithm were typically lower than in CTV coverage, without a very clear trend in the differences (Table1).Except for intracranial treatments, the differences in the CTV due to the dose calculation algorithm MC dose were in general larger than the difference between the nominal plan and worst-case scenario after robustness evaluation (see example in fig. 1).

Site	ROI	Dose Index	PB(cGy(RBE))	MC(cGy(RBE))	PB-MC(%)
Brai n	CTV	D99	5623	5601	0.4
H&N	CTV	D99	5917	5592	6%
CSI	PTVBrain	D99	3456	3124	11
Brai n	Brainstem	D1	5770	5823	-1%
H&N	Lacrimal gland	Mean dose	1993	1829	9%
CSI	Kidney	Mean dose	597	586	2%

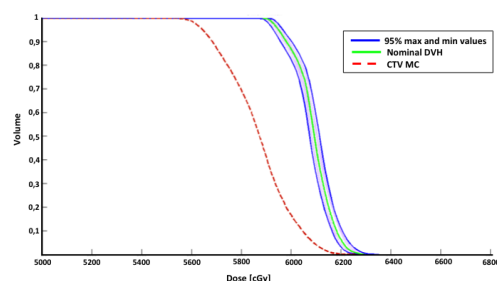


Fig. 1 - Comparison between the nominal DVH calculated with PB, the overall variations due to setup and range error (band between the blue lines) and recalculation with MC for a head and neck case.

### Conclusion

In protontherapy, the effect of using two dose calculation algorithms may be larger than the effect of setup errors and range uncertainties, especially in CTV coverage for shallow targets. The minimum dose to the CTV is not guaranteed when plans are designed with PB, in particular for shallow targets. Ensuring plan robustness is important, but it should not come at the cost of less accurate dose calculation.

With significant tissue heterogeneities and/or shallow

targets, robust optimization should be performed with Monte Carlo to provide reliable results.

**EP-1849 Evaluation of plan modulation parameters on pre-treatment QA results during VMAT and SABR**

M. Chun<sup>1</sup>, J. Kim<sup>1</sup>, C.H. Choi<sup>1</sup>, J. Yoon<sup>1</sup>, H.J. An<sup>1</sup>, J. Son<sup>1</sup>, O. Kwon<sup>1</sup>, J.M. Park<sup>1</sup>

<sup>1</sup>Seoul National University Hospital, Department of Radiation Oncology, Seoul, Korea Republic of

**Purpose or Objective**

To rigorously demonstrate how well the plan parameters and modulation indices impact on the pre-treatment quality assurance on gamma passing rates (GPR) for patient-specific quality assurance of volumetric modulated arc therapy (VMAT) and stereotactic ablative body radiotherapy (SABR).

**Material and Methods**

A total of 332 VMAT and 339 SABR patients' plan with TrueBeam STx linear accelerator (Varian Medical System) was selected. Two-dimensional gamma analysis were performed between calculated and measured dose distribution with 2 mm/2% criteria for VMAT, and 1 mm/2% for SABR, respectively. Modulation indices by considering the speed of MLC (MI<sub>s</sub>), acceleration of MLC (MI<sub>a</sub>), both MLC properties, gantry rotation, and dose rate variation (MI<sub>t</sub>), and also modulation complexity score for VMAT (MCS<sub>v</sub>), and leaf travel MCS (LTMCS) were obtained. Plan parameters of mean aperture, total monitor unit (MU), and the percentage of jaw tracking (%JT) were also acquired. Statistical analysis between GPR and plan modulation parameters were performed with Spearman's rank correlation coefficient ( $r_s$ ) with respect to single and multiple parameter regressions to find the most influencing parameters for each treatment technique.

**Results**

In VMAT plans, the  $r_s$  to GPRs with MI<sub>s</sub>, MI<sub>a</sub>, and MI<sub>t</sub> were -0.392, -0.374, and -0.375, respectively, which showed the MLC, gantry rotation, and dose rate variation largely impacted on the GPR while the majorities were with speed of MLC. MCS<sub>v</sub> and LTMCS showed  $r_s$  to GPR of -0.155 and -0.028, relatively less than MI<sub>s</sub>, MI<sub>a</sub>, and MI<sub>t</sub>. In SABR plans, MCS<sub>v</sub> and LTMCS showed  $r_s$  to GPR of 0.261 and 0.310, which was higher than those with MI<sub>s</sub>, MI<sub>a</sub>, and MI<sub>t</sub> (-0.044, -0.108, and -0.102), presenting the definition of modulation complexity score highlighted more on MU in MCS<sub>v</sub> and LTMCS. The  $r_s$  to GPR for MU and the %JT were -0.299 and -0.265 in SABR while those in VMAT were -0.116, and -0.036, respectively. The highest  $r_s$  to GPR in multiple parameter regression was 0.425 with MI<sub>s</sub> and %JT combination in VMAT, while those in SABR was with MU and %JT combination (0.376).

**Conclusion**

The MLC modulation mostly affected the GPR when delivering the VMAT plans, while these representing tendencies moved to total monitor unit, and the percentage of jaw tracking for SABR.

**EP-1850 Intensity modulated protons: feasibility for hypofractionated hepatocellular carcinoma treatment**

L. Cozzi<sup>1</sup>, T. Comito<sup>2</sup>, A. Fogliata<sup>2</sup>, C. Franzese<sup>2</sup>, S. Tomatis<sup>2</sup>, M. Scorsetti<sup>1</sup>

<sup>1</sup>Humanitas Research Hospital and Humanitas University, Radiation Oncology Dept and Biomedical Science Dept, Milan-Rozzano, Italy ; <sup>2</sup>Humanitas Research Hospital, Radiation Oncology Dept, Milan-Rozzano, Italy

**Purpose or Objective**

The radiation treatment of hepatocellular carcinoma HCC with a spot scanning protonic approach is challenging due to the respiratory induced motion of the target. In the absence of complex rescanning and gating procedures, a simple approach is here explored, based on the combination of an abdominal compression to reduce the internal motion, and a robust optimization in the planning

phase of the intensity modulated proton treatment, IMPT. A plan uncertainty analysis was carried out to assess the feasibility, at planning level, compared to the consolidated VMAT photonic approach.

**Material and Methods**

Twenty patients presenting advanced stage HCC, unsuitable to other loco-regional therapies, and treated with VMAT 60 Gy in 6 fractions, were selected from the institutional database for this study. They were all immobilized with thermoplastic body mask including a styrofoam block as abdominal compressor. 4D-CT was acquired to evaluate and account for any residual respiratory related motion, and CTV delineated after co-registration with MRI. CTV to PTV margin was 4 to 7 mm. IMPT plans were generated for a Varian ProBeam system using spot scanning, optimized with the Nonlinear Universal Proton Optimizer (v. 15.07) using the robust optimization tool Proton Dose Perturbation PDP, and calculated with the Proton Convolution Superposition algorithm with a 2.5 mm grid. Two to three fields were arranged, according to the patient anatomy. The perturbation features used for the robust optimization were the CT calibration variation of  $\pm 3\%$ , and the isocentre localisation uncertainty of 6 mm to cover the worst case scenario.

VMAT plans were designed for a Varian TrueBeam linac, with two 10MV FFF partial arcs, optimized with PRO (v. 15.07) and calculated with Acuros dose calculation algorithm with a 2.5 mm grid.

Quantitative metrics to compare IMPT and VMAT plans were derived from the DVHs.

**Results**

The target coverage was fully achieved by both VMAT and IMPT plans, as well as all the OAR objectives. The inclusion of the uncertainties in the IMPT optimization lead to some deterioration in the target dose homogeneity, while none of the coverage parameters or OAR objective was violated. Comparison, in the worst case scenario of 3% HU and 6 mm isocentre position errors, between robust IMPT and VMAT yield to PTV coverage in terms of D<sub>98%</sub> of 58.7 $\pm$ 0.6 and 58.8 $\pm$ 0.4 Gy, respectively. For the liver deducted the PTV volume, the V<sub><21Gy</sub> (goal <70 cm<sup>3</sup>) was 1081  $\pm$ 105 and 965 $\pm$ 120 cm<sup>3</sup>, the integral dose was 2.8 $\pm$ 1.2 and 7.5 $\pm$ 2.9 Gy $\cdot$ cm<sup>3</sup> $\cdot$ 10<sup>5</sup> for IMPT and VMAT, respectively.

**Conclusion**

Robust optimization IMPT with the support of abdominal compression, can be considered a viable solution also for advanced HCC patients.

**EP-1851 VMAT versus 3D-CRT for the irradiation of left breast or chest wall plus supra/infraclavicular nodes**

M.A. Gilio<sup>1</sup>, R. Bagnoli<sup>2</sup>, M. Mignogna<sup>2</sup>, A. Tofani<sup>3</sup>, S. Linsalata<sup>3</sup>

<sup>1</sup>University of Pisa, Medical Physics, Pisa, Italy ; <sup>2</sup>Azienda USL Toscana nord ovest, Radiotherapy, Pisa, Italy ;

<sup>3</sup>Azienda USL Toscana nord ovest, Medical Physics, Pisa, Italy

**Purpose or Objective**

The aim of the present study is to compare a dual arc VMAT technique and half beam block 3D-CRT technique for the irradiation of left breast or postmastectomy chest wall plus supra- and infraclavicular lymphnodes. The two techniques were compared in terms of target coverage, doses to OAR and total MU.

**Material and Methods**

26 planning CT were segmented for left breast or chest wall, supra/infraclavicular nodes, heart, omolateral and controlateral lungs, spine and controlateral breast. For every CT two plans were generated: a 3D-CRT with two tangential half beam block for the breast or chest wall and two nearly opposed half beam block for the supra/infraclavicular lymphnodes, using the same isocenter for all the beams (6MV, 10MV or 15MV - Philips

Pinnacle3 TPS) and a dual arc VMAT of  $240^\circ \pm 20^\circ$  starting from gantry at  $180^\circ$  (6MV - Elekta Monaco TPS). Both plans were optimised in order to obtain the best compromise between target dose distribution and OAR sparing. For each planning CT were registered: target coverage of the two PTVs in terms of  $V_{95}$ ,  $V_{98}$ , mean dose, Conformity Index (CI) and Homogeneity Index (HI);  $V_{20}$ ,  $V_5$  and mean dose for ipsilateral, contralateral and total lung;  $V_{30}$ ,  $V_5$  and mean dose for heart; right breast  $V_5$  and mean dose; spine maximal dose; total MU. In order to encompass the inter-subjects variability, for each planning CT the differences of each parameter in the two competitive plans were evaluated by means of two tailed paired t-test.

**Results**

Mean  $\pm$  SD of each parameter in each group of 26 plans (3D and VMAT) are reported in Table, together with the statistical analysis. VMAT plans show highly significant better coverage both for breast or chest wall and lymphnodes and result in highly significant better CI and HI. Moreover, in VMAT, due to the better conformity of the technique, heart  $V_{30}$  is significantly lower than in 3D ( $p=0.002$ ) and  $V_{20}$  of ipsilateral and total lung are lower, although not significant, than in 3D. OAR low doses are higher for VMAT:  $V_5$  for ipsilateral, contralateral and total lung are significantly higher ( $p<0.001$ ), similarly heart  $V_5$  and mean dose ( $p<0.001$ ) and also right breast  $V_5$  and mean dose ( $p<0.001$ ). Finally, total MU are significantly higher in VMAT ( $p=0.01$ ).

**Conclusion**

Our results show that VMAT technique for the irradiation of left breast or chest wall plus supra\infraclavicular nodes offers better target coverage and superior CI and HI than 3D-CRT. VMAT shows better  $V_{30}$  for heart and  $V_{20}$  for lung and higher low dose parameters for all the observed OAR. In our department VMAT is becoming the favourite technique because of its better target conformity and coverage and considering that, as reported in recent literature, nor low dose bath, nor MU increase, with consequent out-of-field dose, observed in VMAT, seems to determine higher detriment to healthy tissues, which is instead frequently reported in the medium-high dose region usually larger in the 3D technique.

	VMAT	3D	Probability
	MEAN $\pm$ SD	MEAN $\pm$ SD	
BREAST OR POSTMASTECTOMY CHEST WALL	$V_{95}$ =93,343,4	$V_{95}$ =76,147,4	$p=1,9E-6^*$
	$V_{98}$ =72,948,2	$V_{98}$ =60,243,7	$p=2,3E-2^*$
	$D_{95\%}$ =449,540,33Gy	$D_{95\%}$ =448,440,71Gy	$p=9,9E-3^*$
	HI=0,11 $\pm$ 0,03	HI=0,44 $\pm$ 0,1	$p=9,7E-6^*$
	CI=1,1 $\pm$ 0,1*	CI=1,6 $\pm$ 0,3*	$p=5,4E-7^*$
SUPRA- AND INFRACLAVICULAR LYMPHNODES	$V_{95}$ =93,943,2	$V_{95}$ =84,448,1	$p=6,7E-8^*$
	$V_{98}$ =75,4410,4	$V_{98}$ =70,5412,8	$p=1,6E-2^*$
	$D_{95\%}$ =449,540,43Gy	$D_{95\%}$ =449,341,21Gy	$p=5,6E-3^*$
	HI=0,12 $\pm$ 0,04	HI=0,34 $\pm$ 0,2	$p=1,0E-7^*$
	CI=1,11 $\pm$ 0,1*	CI=1,64 $\pm$ 0,3*	$p=5,4E-7^*$
IPSI LATERAL LUNG	$V_{20}$ =15,544,9	$V_{20}$ =24,047,0	$p=1,5E-1^*$
	$V_{30}$ =0,10 $\pm$ 5,7	$V_{30}$ =43,0111,8	$p=1,0E-9^*$
	$D_{95\%}$ =49,841,59Gy	$D_{95\%}$ =113,143,71Gy	$p=6,7E-2^*$
CONTRALATERAL LUNG	$V_{20}$ =0,05 $\pm$ 0,11	$V_{20}$ =0,004 $\pm$ 0,02	$p=4,6E-2^*$
	$V_{30}$ =18,3410,2	$V_{30}$ =0,09 $\pm$ 0,18	$p=2,0E-4^*$
	$D_{95\%}$ =3,340,88Gy	$D_{95\%}$ =30,440,11Gy	$p=3,0E-17^*$
TOTAL LUNG	$V_{20}$ =7,242,4	$V_{20}$ =10,643,3	$p=2,2E-1^*$
	$V_{30}$ =33,147,1	$V_{30}$ =19,115,0	$p=6,1E-14^*$
	$D_{95\%}$ =46,341,09Gy	$D_{95\%}$ =45,241,51Gy	$p=1,3E-11^*$
	$V_{50}$ =0,11 $\pm$ 0,3	$V_{50}$ =1,44 $\pm$ 1,0	$p=2,3E-3^*$
HEART	$V_{50}$ =12,246,4	$V_{50}$ =9,845,0	$p=1,4E-4^*$
	$D_{95\%}$ =3,340,71Gy	$D_{95\%}$ =3,241,11Gy	$p=6,3E-6^*$
SPINE	$D_{95\%}$ =22,043,31Gy	$D_{95\%}$ =19,048,01Gy	$p=8,0E-5^*$
	$V_{50}$ =9,245,3	$V_{50}$ =4,741,8	$p=8,5E-9^*$
CONTRALATERAL BREAST	$D_{95\%}$ =42,640,59Gy	$D_{95\%}$ =41,140,31Gy	$p=4,5E-18^*$
MU	767497	7866149	$p=1,6E-2^*$

Table. Statistical analysis in terms of two tailed paired t test ( $\alpha=0.05$ ); \* where  $p<0.05$ . \*\*CI was calculated accordingly to ICRU 83:  $CI=V_{95\%}/V_{PTV}$ , where  $V_{95\%}$  is the treated volume and  $V_{PTV}$  is the PTV total volume.

**EP-1852 Dosimetric comparison of techniques for left-sided breast and regional lymph node radiotherapy**  
 T. Joslin-Tan<sup>1</sup>, R. Maggs<sup>1</sup>, C. Pembroke<sup>2</sup>, J. Lambert<sup>3</sup>, K. O'Neill<sup>3</sup>, J. Staffurth<sup>2</sup>

<sup>1</sup>Velindre Cancer Centre, Medical Physics, Cardiff, United Kingdom ; <sup>2</sup>Velindre Cancer Centre, Clinical Oncology, Cardiff, United Kingdom ; <sup>3</sup>Rutherford Cancer Centre South Wales, Physics, Newport, United Kingdom

**Purpose or Objective**

Inclusion of supraclavicular fossa (SCF), axillary, and internal mammary nodes (IMN) as target volumes in breast cancer radiotherapy (RT) has been shown to give clinical benefits for certain patient cohorts. However, heart and ipsilateral lung doses have been shown to increase when treating the nodes with 3D conformal radiotherapy (3D-CRT) using a wide tangent and matched field approach. Concerns also exist over planning complexity with 3D-CRT. Deep inspiration breath hold (DIBH) has been shown to reduce heart and lung doses while maintaining target coverage. Intensity modulated radiotherapy (IMRT), volumetric modulated arc therapy (VMAT), and spot scanning proton beam therapy (PBT) have been shown to improve plan quality over 3D-CRT with free-breathing patients. A dosimetric study was performed to compare these three techniques in DIBH.

**Material and Methods**

CT datasets of 10 patients previously treated with RT in DIBH for left-sided breast cancer were used in the study. IMRT (four-field), VMAT (two  $200^\circ$  arcs), and PBT (anterior and 'en-face' beams) plans were created in Nucletron Oncentra Masterplan v4.3 with a view to creating class solutions to treat the breast (40Gy [100%] in 15 fractions) and regional nodes (36Gy [90%] in 15 fractions). Target coverage, organ at risk (heart, lungs, contralateral breast), and other normal structure (including the left anterior descending coronary artery and brachial plexus) doses were reviewed and statistical significance was evaluated using paired two-tailed t-tests.

**Results**

Plans were created for 9/10 patients. VMAT and PBT plans met all mandatory planning objectives compared with 7/9 IMRT plans. PBT plans had lower mean heart dose, left lung V17Gy, and mean contralateral breast dose than IMRT and VMAT while achieving better coverage. VMAT had superior target coverage, conformity, and breast PTV uniformity over IMRT with similar heart and left lung doses, but with increased contralateral breast mean dose and V5Gy. Dosimetric values are summarised in Table 1.

Structure	Metric	Mean $\pm$ S.D.			Paired t-test p-values		
		IMRT	VMAT	PBT	IMRT v VMAT	IMRT v PBT	VMAT v PBT
Heart	Mean (Gy)	4.4 $\pm$ 0.6	4.1 $\pm$ 0.4	0.6 $\pm$ 0.4	0.172	<0.001	<0.001
Left Lung	V17Gy (%)	30.9 $\pm$ 3.3	32.1 $\pm$ 0.1	11.0 $\pm$ 1.6	0.158	<0.001	<0.001
Contralateral Breast	Mean (Gy)	2.7 $\pm$ 0.5	3.2 $\pm$ 0.1	0.1 $\pm$ 0.1	0.017	<0.001	<0.001
	V5Gy (%)	6.7 $\pm$ 3.1	12.9 $\pm$ 2.6	0.2 $\pm$ 0.2	0.005	<0.001	<0.001
Breast PTV	V38Gy (%)	94.1 $\pm$ 2.8	96.7 $\pm$ 1.7	99.1 $\pm$ 0.5	0.005	0.001	0.007
IMN PTV	V36Gy (%)	93.2 $\pm$ 2.3	98.5 $\pm$ 1.6	99.6 $\pm$ 1.1	<0.001	<0.001	0.022
L1-L4 Nodes PTV	V36Gy (%)	93.2 $\pm$ 3.2	98.0 $\pm$ 1.4	99.7 $\pm$ 0.6	0.002	<0.001	0.024

Table 1 - Summary of dosimetric parameters for OARs considered during plan optimisation and PTVs.

**Conclusion**

PBT gave better overall plan quality than both photon modalities but is not currently available to all regional nodal RT patients in the UK. The dosimetric benefits in target coverage coupled with a more robust class solution made VMAT the preferred choice over IMRT. Where VMAT is not possible and lower nodal target coverage is acceptable IMRT may be suitable for most patients. Lower contralateral breast doses may make IMRT advantageous when secondary cancers are of concern.

**EP-1853 Dosimetric comparison of helical tomotherapy and intensity-modulated radiotherapy in cervical cancer**

J. Liu<sup>1</sup>, L. ZHU<sup>1</sup>, S. Li<sup>1</sup>, S. Gao<sup>1</sup>, J. Yan<sup>1</sup>, L. Xie<sup>1</sup>, Z. Hou<sup>2</sup>, X. Zhou<sup>1</sup>, B. Liu<sup>1</sup>

<sup>1</sup>Nanjing Drum Tower Hospital- Medical School of Nanjing University, The Comprehensive Cancer Centre, Nanjing, China ; <sup>2</sup>School of Biological Sciences and Medical Engineering, Southeast University, State Key Laboratory of Bioelectronics

### Purpose or Objective

To compare the dosimetric differences between helical tomotherapy (HT) and seven-field intensity-modulated radiotherapy (7F-IMRT) in the pelvic irradiation of patients with cervical cancer.

### Material and Methods

Twenty-five patients with cervical cancer who received pelvic external beam radiation therapy by HT from March 2015 to October 2017 were retrospectively studied. Total dose of 4600 to 5000 cGy was delivered in 23 to 25 equal fractions. The 7F-IMRT planning was inversely carried out for comparison using Pinnacle<sup>3</sup> 9.10 planning system according to the original computed tomographic simulation data of each patient. Dose to target volumes, organs at risk, homogeneity, and conformity indexes were evaluated for each case according to the dose volume histogram.

### Results

1) For planning target volumes (PTV) in HT vs. 7F-IMRT, average conformity index (CI) was  $0.898 \pm 0.017$  vs.  $0.834 \pm 0.013$  ( $P < 0.001$ ) and average homogeneity index (HI) was  $0.062 \pm 0.012$  vs.  $0.109 \pm 0.019$  ( $P < 0.001$ ), both of which were significantly higher in HT planning than in IMRT planning. The maximal doses of 1% and 2% target volume ( $D_1$ ,  $D_2$ ) in HT group were lower than those in IMRT group ( $P < 0.001$ ), while mean dose ( $D_{mean}$ ), and minimal doses of 95% and 98% target volume ( $D_{95}$ ,  $D_{98}$ ) were higher than IMRT group ( $P = 0.048$ ,  $P = 0.015$ ,  $P < 0.001$ ). 2) For OARs, HT had superior organ sparing advantages. The maximal dose ( $D_{max}$ ),  $D_{mean}$ ,  $V_{30}$  and  $V_{40}$  of small bowel, colon, rectum and bladder in HT group were all significantly lower than IMRT group ( $P < 0.001$ ,  $P < 0.001$ ,  $P < 0.001$ ,  $P = 0.001$ ).  $V_{50}$  was slightly lower in HT group without statistical difference ( $P = 0.13$ ). As for femoral head,  $V_{25}$ ,  $D_5$ ,  $D_{mean}$  and  $D_{max}$  in HT group were lower than those in IMRT group ( $P < 0.001$ ). The treatment linac outputs of HT were significantly higher than those of the IMRT group.

Dosimetric comparison for PTV parameters between HT and 7F-IMRT (x±s)

	CI	HI	$D_{mean}$ (Gy)	$D_1$ (Gy)	$D_2$ (Gy)	$D_{95}$ (Gy)	$D_{98}$ (Gy)
HT	0.898±0.017	0.062±0.012	50.25±2.00	51.19±2.12	50.99±2.11	48.68±1.95	47.85±1.98
7F-IMRT	0.834±0.013	0.109±0.019	50.47±1.97	52.44±2.18	52.34±2.19	48.39±1.86	47.03±1.81
P	$P < 0.001$	$P < 0.001$	$P = 0.048$	$P < 0.001$	$P < 0.001$	$P = 0.015$	$P < 0.001$

Dosimetric comparison for OARs between HT and 7F-IMRT (x±s)							
Organs	Project	$V_{30}$ (%)	$V_{40}$ (%)	$V_{50}$ (%)	$D_{mean}$ (Gy)	$D_{max}$ (Gy)	
Small bowel	HT	12.08±9.67	4.80±5.84	1.37±2.95	19.42±5.04	50.35±4.56	
	7F-IMRT	15.11±11.84	5.64±6.46	1.56±3.49	20.38±5.22	51.31±3.71	
	P	$P < 0.001$	$P = 0.001$	$P = 0.130$	$P < 0.001$	$P < 0.001$	
Colon	HT	18.72±11.30	11.00±8.73	2.96±3.97	20.26±5.34	51.11±2.15	
	7F-IMRT	22.48±11.95	11.82±1.64	3.14±4.04	21.19±5.63	52.10±2.24	
	P	$P < 0.001$	$P = 0.006$	$P = 0.051$	$P < 0.001$	$P < 0.001$	
Rectum	HT	80.58±19.76	55.70±17.56	15.93±16.90	40.61±5.44	51.14±2.10	
	7F-IMRT	96.70±7.72	85.07±13.41	25.85±24.99	45.59±3.63	52.51±2.46	
	P	$P < 0.001$	$P < 0.001$	$P = 0.006$	$P < 0.001$	$P < 0.001$	
Bladder	HT	68.99±12.73	52.84±11.40	23.26±19.86	39.10±3.31	51.67±2.06	
	7F-IMRT	70.17±9.02	60.03±9.32	23.69±19.60	40.44±2.86	53.13±2.17	
	P	$P < 0.001$	$P < 0.001$	$P = 0.309$	$P < 0.001$	$P < 0.001$	

Note: PTV: planning target volume; CI: conformity index; HI: homogeneity index;  $D_{mean}$ : mean dose;  $D_1$ ,  $D_2$ : the maximal doses of 1% target volume ( $D_1$ ) and 2% target volume ( $D_2$ );  $D_{95}$ ,  $D_{98}$ : the minimal doses of 95% target volume ( $D_{95}$ ) and 98% target volume ( $D_{98}$ ); HT: helical tomotherapy; 7F-IMRT: seven-field intensity-modulated radiotherapy; OARs: organs at risk

### Conclusion

HT achieved better conformity, uniformity and OARs protection than IMRT. The treatment outputs were higher for the HT group compared with the IMRT group indicating less beam utilization. As a conclusion, HT showed dosimetric advantages and great promise in the clinical application of image-guided radiotherapy in patients with cervical cancer.

### EP-1854 Application of a tool for bulk treatment plan evaluation in advanced treatment planning training

M. Van Herk<sup>1</sup>, N. Burnet<sup>2</sup>, N. Dinapoli<sup>3</sup>, G. Meijer<sup>4</sup>, U. Nestlé<sup>5</sup>, D. Van den Bongard<sup>4</sup>, M. Stock<sup>6</sup>

<sup>1</sup>Christie Hospital NHS, Division of Molecular & Clinical Cancer Sciences, Manchester, United Kingdom ; <sup>2</sup>The University of Manchester, Division of Cancer Sciences, Manchester, United Kingdom ; <sup>3</sup>Agostino Gemelli University Polyclinic Foundation, Polo Oncology and Hematology Sciences, Rome, Italy ; <sup>4</sup>University Medical Center Utrecht, Department of Radiotherapy, Utrecht, The Netherlands ; <sup>5</sup>Medical Center - University of Freiburg, Department of Radiation Oncology, Freiburg, Germany ; <sup>6</sup>EBG MedAustron GmbH, Division of Medical Physics, Wiener Neustadt, Austria

### Purpose or Objective

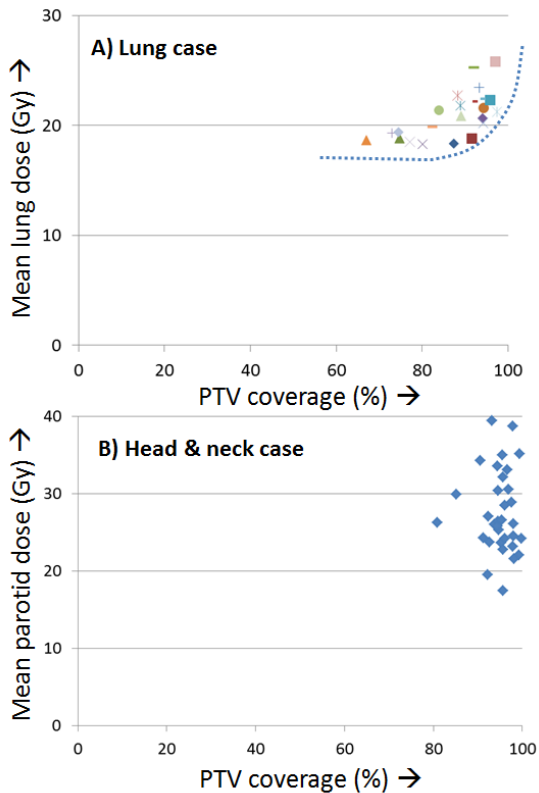
Hands-on training and group review is an essential part of learning how to create a good treatment plan. In an international training course, students tackled challenging study cases each day and 3 selected plans were reviewed together. So far, by necessity, plan selection was performed rather qualitatively by the faculty. It is the purpose of this work to develop and test a tool for bulk plan evaluation - applied in the context of training. The system aims to evaluate all plans, extract statistics in terms of target coverage and organ at risk (OAR) sparing, illustrate compromises made, and select most interesting plans for review and group discussion.

### Material and Methods

98 students worked in pairs on 48 treatment planning systems provided by 5 vendors for 4 complex cases: locally advanced breast cancer with involved internal mammary lymph nodes, locally advanced lung cancer, bilateral oropharyngeal cancer and meningioma. Dose cubes (RTDose files) were collected for all finalized plans - albeit finalized in limited time and often on unfamiliar planning systems. These were then loaded into the tool and processed. For selected structures, DVHs and previously defined DVH parameters were re-calculated. By plotting parameters for target coverage against OAR dose, plan quality could be estimated taking trade-offs into account. In addition, by highlighting plan-parameter combinations where the parameter is clinically acceptable and/or reasonable close to the best plan, the 'winner' could be selected, i.e., the plan with most highlights.

### Results

23 plans were collected for the breast case, 23 for the lung case, 34 for the head and neck case, and 29 for the meningioma case. All plans could be read, although student identification was sometimes difficult. Students often modified structures as part of the planning process, showing the importance of evaluating against identical structures. Some planning systems showed significant differences in coverage of superficial PTVs, which was mainly due to differences in dose grid voxel assignment at the patient surface (up to 2 mm). Most but not all cases showed a Pareto-front like trade-off of PTV coverage versus OAR dose for different planners (Fig. 1). The qualitative selected best plan never coincided with the best plan based on quantitative analysis of all parameters. General observations were that recently introduced automatic planning tools tended to perform quite well under time constraints, and different planning systems excelled at different cases.



### Conclusion

In conclusion, it is feasible and useful to collect and compare plans in bulk in a teaching situation, as it allows selection of good plans taking trade-offs into account and can be used to illustrate behaviour of different planners and treatment planning systems. It also allows individual participants to benchmark their results to the others. Lastly, it gives important feed-back to the faculty on the complexity of the study cases.

### EP-1855 Retrospective review of brain dose from cranial stereotactic radiosurgery treatments of metastases

T. Kairn<sup>1</sup>, Y. Ikeda<sup>2</sup>, M. West<sup>2</sup>, D. Schlect<sup>2</sup>, S. Crowe<sup>1</sup>  
<sup>1</sup>Royal Brisbane and Women's Hospital, Radiation Oncology- Cancer care Services, Herston, Australia ;  
<sup>2</sup>Genesis Care, Genesis Cancer Care Queensland, Auchenflower, Australia

### Purpose or Objective

The planning and delivery of cranial stereotactic radiosurgery (SRS) treatments is changing. New treatment planning and delivery technologies are extending the numbers of lesions that can be treated using linacs without shifting the patient position. In order to understand the potential benefits or relative limitations of these new "single-isocentre" techniques, it is important to understand the plan quality achievable using older, more-established techniques, for comparison. This study therefore investigated achievable SRS treatment plan quality, in terms of dose to planning target volumes (PTVs) and to healthy brain tissue, using a retrospective analysis of cranial metastasis treatment plans.

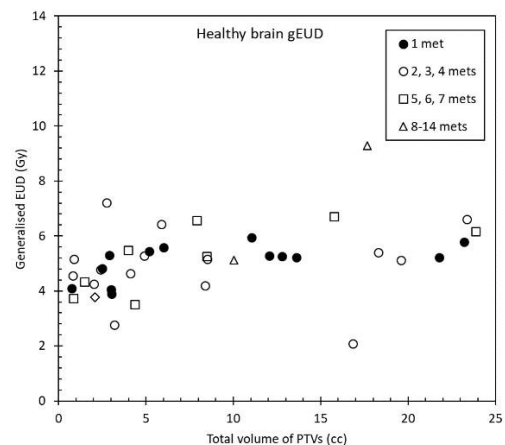
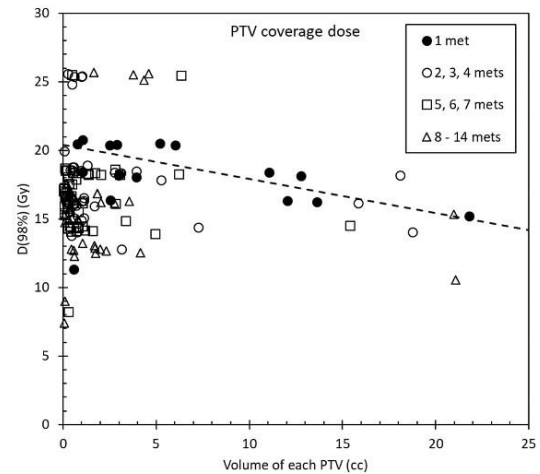
### Material and Methods

In-house Treatment and Dose Assessor (TADA) software was used to evaluate 60 single-fraction stereotactic radiosurgery treatment plans, 46 of which were identified as involving multiple metastases. All treatments were planned using a multiple-isocentre technique (one isocentre per metastasis), with the Brainlab iPlan treatment planning system, for delivery using a linac

equipped with a Brainlab m3 microMLC (Brainlab AG, Munich, Germany). Having previously established that iPlan's pencil beam algorithm provides a useful worst-case estimate (slight over-estimate) of the out-of-field dose, we used DICOM dose files exported from the planning system to calculate fractionation-insensitive generalised equivalent uniform doses (gEUDs) for brain structures with PTVs subtracted, while also evaluating the dose to the PTVs and other relevant structures.

### Results

For cases with one metastasis, the PTV coverage dose trended downward with increasing metastasis volume (Figure 1), conforming with the established local practise of optimising prescription doses to minimise dose to the healthy brain, which would otherwise increase with increasing metastasis volume. Prescribed PTV doses were generally lower for multiple metastases cases, and similarly followed the trend of decreasing with increasing PTV volume (Figure 1). The effects of this careful optimisation of prescription dose are apparent in the comparatively low brain doses that were produced by these treatment plans, even for relatively large PTV volumes (Figure 2).



### Conclusion

The results of this retrospective analysis of cranial SRS treatment plans provide a valuable example of the plan quality that can be achieved using a multiple-isocentre technique, and may therefore stand as a useful baseline for comparing the results of single-isocentre treatment planning techniques, in the future.

### EP-1856 Dose escalation potential for hypofractionated radiotherapy in locally advanced pancreatic cancer

J. Bertholet<sup>1</sup>, A. Hunt<sup>2</sup>, A. Dunlop<sup>1</sup>, T. Bird<sup>2</sup>, A. Mitchell<sup>1</sup>, U. Oelfke<sup>1</sup>, S. Nill<sup>1</sup>, K. Aitken<sup>2</sup>  
<sup>1</sup>The Institute of Cancer Research and The Royal Marsden NHS Foundation Trust, Joint Department of Physics, London, United Kingdom ; <sup>2</sup>The Royal Marsden NHS Foundation Trust, Department of Radiotherapy, London, United Kingdom

### Purpose or Objective

Dose escalation to a biological effective dose (BED<sup>10</sup>) of 100 Gy may improve overall survival in locally advanced pancreatic cancer (LAPC). The ability to dose escalate is limited by the risk of toxicity for organs-at-risks (OAR) close to the planning target volume (PTV). A BED of 100Gy may be easier to achieve in a moderate hypofractionated regimen (15 fractions (#)) compared to 5# stereotactic body radiotherapy (SBRT). We evaluated the potential for dose escalation in 5 or 15# for 10 LAPC patients and investigated the correlation between OAR/PTV overlap and achievable PTV coverage.

### Material and Methods

The study included ten LAPC patients (table). The PTV was defined as the gross-tumour volume (GTV) plus 3 mm isotropic margin, assuming treatment delivery in breath-hold under active breathing coordination. The duodenum, bowel (large and small), stomach, spinal cord, liver and kidneys were delineated as OAR. Two regimens, 5 and 15#, were compared. The aim was to cover 95% of the PTV with a BED of 54Gy (base dose=33Gy in 5#, 42.5Gy in 15#) while respecting OAR constraints. For duodenum, stomach and bowel, previously published constraints (table) were used: V<sub>15Gy</sub><9cc, V<sub>20Gy</sub><3cc, V<sub>33Gy</sub><1cc in 5# and D<sub>0.5cc</sub><45Gy in 15#. Once the highest PTV coverage while respecting OAR constraints was achieved, dose escalation to a BED>98Gy (prescription dose=50Gy in 5#, 67.5Gy in 15#) was attempted up to 95% PTV coverage, limiting the PTV maximum dose to 130% of the prescription. Plans were generated using Raystation 6.99 (RaySearch Laboratories) with a single 6MV FFF VMAT arc (179-181° gantry rotation, collimator rotation 5°).

The OAR/PTV overlap (PTV<sub>OAR</sub>) and proximity (OAR<sub>prox</sub>) volumes were calculated using eq.1 and 2 respectively (table) and their effect on PTV coverage was evaluated using Pearson's correlation coefficients (significance level of 5%).

### Results

The patients presented a range of PTV<sub>OAR</sub> and OAR<sub>prox</sub> volumes leading to varying PTV coverage (table, Fig1). In 5#, 95% PTV coverage by the escalated dose was only achievable for patient 1 with PTV<sub>OAR</sub>=0. In all other patients, coverage even by 33Gy had to be compromised to comply with OAR constraints. In 15#, 95% PTV coverage by 42.5Gy was feasible for all patients and coverage by the escalated dose was higher than in 5# in eight patients. The target coverage by the base dose was correlated with PTV<sub>OAR</sub> in 5 and 15# and with OAR<sub>prox</sub> in 15#. The target coverage by the escalated dose was correlated with PTV<sub>OAR</sub> in 15# (Fig2).

Table: Patient characteristics and target coverage by base and prescription dose.

Patient	PTV volume [cc]	PTV <sub>OAR</sub> [%] (eq. 1)	OAR <sub>prox</sub> [%] (eq. 2)	5# [1] base dose = 33Gy, prescription = 50Gy		15# [2] base dose = 42.5Gy, prescription = 67.5Gy	
				PTV V <sub>33Gy</sub> [%]	PTV V <sub>50Gy</sub> [%]	PTV V <sub>42.5Gy</sub> [%]	PTV V <sub>67.5Gy</sub> [%]
				1	12.38	0	2.02
2	58.41	12.10	43.21	66.77	22.83	95.1	24.2
3	37.58	7.98	67.78	76.28	12.74	95.54	54.06
4	58.05	19.67	56.16	59.44	30.48	95.00	8.53
5	101.33	1.36	29.45	82.50	8.42	98.81	70.49
6	212.36	5.10	24.58	67.70	11.84	96.10	17.34
7	83.99	7.89	32.19	81.86	52.62	95.80	41.51
8	105.85	11.19	15.31	57.63	6.33	97.40	21.40
9	63.72	11.39	42.31	73.83	20.79	96.20	38.17
10	237.27	4.76	23.54	63.26	6.31	95.44	12.05
Mean (SD)	97.09 (73.07)	8.14 (5.79)	33.66 (19.38)	72.93 (12.87)	26.74 (27.85)	96.54 (1.68)	38.28 (27.91)

OAR constraints: [1] Alliance trial A021501 (NCT02839343) [2] ABC-07 Trial (EudraCT 2014-003656-31)

PTV<sub>OAR</sub> = 100 \*  $\frac{\text{volume}(PTV \cap OAR)}{\text{volume}(PTV)}$  (eq. 1)      OAR<sub>prox</sub> = 100 \*  $\frac{\text{volume}(PTV_{min} \cap OAR)}{\text{volume}(PTV)}$  (eq. 2)  
 where PTV<sub>rim</sub> = (PTV + 1cm) \ PTV and OAR = (duodenum U stomach U bowel).

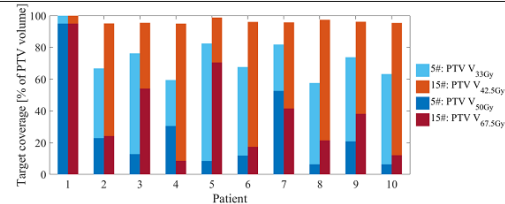


Figure1: PTV coverage by the base dose (BED=54Gy) and by the escalated dose (BED>98Gy) in 5 (blue) or 15 (red) #.

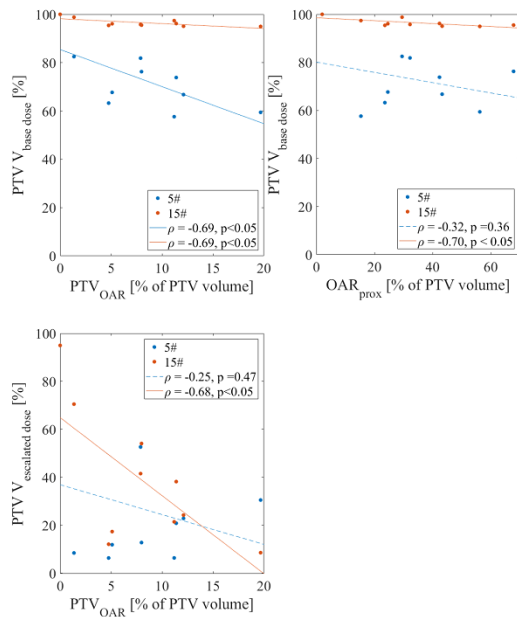


Figure2: Correlation between PTV/OAR overlap (left) or proximity (right) and target coverage by the base dose (top) or escalated dose (bottom).

### Conclusion

The potential for dose escalation was higher in 15 than in 5# except for patients 4 and 7. Patient 4 had the largest PTV<sub>OAR</sub> volume and would likely benefit from the improved coverage by BED=54Gy in 15# compared to 5# (table). Patients with favourable anatomy (OAR>1cm away from PTV) can be treated in 5# to a high BED. Moderate hypofractionation is better suited if the PTV is overlapping with OARs. Using a daily adaptive approach, the PTV coverage by the escalated dose can be increased on days with favourable anatomy.

I. Miloichikova<sup>1,2</sup>, Y. Cherepennikov<sup>1</sup>, B. Gavrikov<sup>3</sup>, A. Krasnykh<sup>4</sup>, S. Stuchebrov<sup>4</sup>

<sup>1</sup>Tomsk Polytechnic University, School of Nuclear Science & Engineering, Tomsk, Russian Federation ; <sup>2</sup>Cancer Research Institute of Tomsk National Research Medical Center of the Russian Academy of Sciences, Radiotherapy Department, Tomsk, Russian Federation ; <sup>3</sup>Moscow municipal oncological hospital №62, 1st Radiological Department, Moscow, Russian Federation ; <sup>4</sup>Tomsk Polytechnic University, Research School of High-Energy Physics, Tomsk, Russian Federation

### Purpose or Objective

For electron beam radiation therapy of irregularly shaped tumors adjacent to critical organs, it is necessary to form complex fields with due consideration of the patients' anatomical features. Consequently, there is a need to apply special tools in addition to standard applicators and blocks that come with a clinical electron accelerator. For example, customized complex-shape metal collimators produced by melting or cutting.

This study proposes an alternative approach where polymer objects produced by rapid prototyping serve as electron beam-forming elements.

The purpose of this study is to assess the applicability of the proposed approach. For this purpose numerical simulation of the clinical electron beams interaction with tissue-equivalent media, including polymeric materials suitable for the products creation by fused deposition modeling (FDM) was carried out.

### Material and Methods

A numerical model simulating the external electron beam of a clinical accelerator and parameters of the polymer materials under study was developed on the basis of the GEANT4 mathematical and physical modeling libraries.

For verification of the electron beam model, we used clinical dosimetry data of the ONCOR Impression Plus medical linear accelerator obtained in the 3D Scanner water phantom.

To construct a model of polymer materials, we manufactured a set of products by fused deposition modeling from ABS, PLA and HIPS plastics and determined their actual density.

The depth dose distributions of clinical electron beams in polymer objects were studied experimentally on the ONCOR Impression Plus accelerator using GafChromic EBT3 dosimetry films. Then we compared the results obtained with the calculated data.

### Results

The developed numerical model of a clinical electron beam with near-real radiation parameters makes it possible to evaluate such characteristics of the depth dose distribution curve in a water phantom as  $R_{50}$  (cm) with an accuracy of 0.05 cm,  $R_{90}$  (cm) with an accuracy of 0.1 cm,  $d_{max}$  (cm) with an accuracy of 0.2 cm and  $R_p$  (cm) with an accuracy of 0.3 cm.

The calculated and experimental data are in good agreement, which makes the numerical model suitable for determining the minimum thickness of a polymer absorber for developing collimating devices in the range of electron beam energies from 6 to 18 MeV.

It was shown that the polymer thickness required for the absorption of the electron beam with an energy of 6 MeV is 4 cm, for an energy of 12 MeV, it is 8 cm, and for 18 MeV, 11 cm. The difference in thickness depending on the type of plastic (ABS, PLA and HIPS) is  $\pm 0.5$  cm.

### Conclusion

The numerical model of a clinical electron beam developed in this study allows estimating the distribution of ionizing radiation in tissue-equivalent media, exploring new approaches to the generation of irregularly shaped therapeutic fields with complex geometry, and predicting the dimensions to produce forming objects by fused deposition modeling.

**EP-1858 Inter-observer variability in rectal target delineation on MRI for MR image-guided radiotherapy**  
I. White<sup>1</sup>, A. Hunt<sup>1</sup>, T. Bird<sup>2</sup>, S. Settatree<sup>3</sup>, H. Soliman<sup>3</sup>, S. Bhide<sup>3</sup>

<sup>1</sup>Royal Marsden NHS Foundation Trust and Institute of Cancer Research, Academic Radiotherapy, London, United Kingdom ; <sup>2</sup>University Hospitals Bristol NHS Foundation Trust, Oncology, Bristol, United Kingdom ; <sup>3</sup>Royal Marsden NHS Foundation Trust and Institute of Cancer Research, Oncology, London, United Kingdom

### Purpose or Objective

Evaluate inter-observer variability (IOV) in mesorectum and pelvic lymph node clinical target volume (CTV) delineation on 2D and 3D MRI sequences optimised for MR image-guided radiotherapy.

### Material and Methods

Radiotherapy treatment planning MRI were acquired in 3 rectal radiotherapy patients. MRI sequences, which had been optimised for MR image-guided radiotherapy on a 1.5T Siemens radiology scanner, included high resolution 2D T2W and 3D T2W sequences with field of view to encompass the entire pelvis. 5 experienced radiation oncologists in rectal radiotherapy contoured the mesorectum, pre-sacral and right and left pelvic lymph node (LN) CTV regions of interest (ROI) on each 2D and 3D MRI sequence using Elekta MR Linac consortium rectal contouring guidelines. A simultaneous truth and performance level estimation (STAPLE)<sup>(1)</sup> was created for each ROI, on each MRI data set using Monaco ADMIRE software v2.0 (Research version, Elekta AB). Observer contours on each image data set were compared to the STAPLE contour by calculating the Dice similarity coefficient (DSC) and the mean and maximum distance to agreement (DTA). Analysis between MRI sequences was performed using Wilcoxon signed-rank test with GraphPad Prism,  $p < 0.05$  was considered statistically significant.

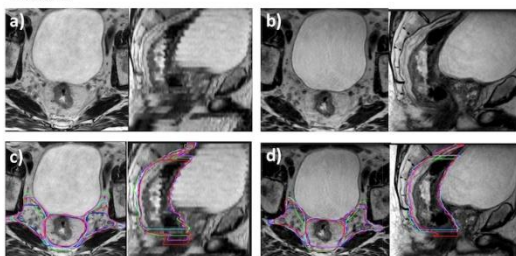
### Results

IOV for the different target volumes on 2D T2W MRI and 3D T2W MRI is illustrated in table 1. There was very good agreement between observers and the STAPLE reference contours for both MRI sequences (Figure 1). DSC  $> 0.8$  was observed for all CTV ROIs, except for the presacral LN region when delineated on the 2D T2W MRI sequence (DSC 0.69).

**Table 1.** Inter-observer variability for the different clinical target volume regions of interest (ROIs) when delineated on 2D T2W MRI and 3D T2W MRI. The median and range for the Dice similarity coefficient (DSC) and the mean and maximum distance to agreement (DTA) are reported.

Target ROI	Interobserver variability measure	MRI sequence	
		2D T2W MRI Median (range)	3D T2W MRI Median (range)
Mesorectum	DSC	0.92(0.86- 0.95)	0.94 (0.87- 0.95)
	Mean DTA (cm)	0.12 (0.08- 0.12)	0.1 (0.10- 0.18)
	Maximum DTA (cm)	1.05 (0.97- 1.33)	0.14 (0.13- 0.15)
Right pelvic LN	DSC	0.87 (0.81- 0.88)	0.87 (0.84- 0.88)
	Mean DTA (cm)	0.13 (0.10- 0.14)	0.12 (0.10- 0.12)
	Maximum DTA (cm)	1.09 (0.99- 1.21)	1.14 (1.08- 1.27)
Left pelvic LN	DSC	0.86 (0.80- 0.87)	0.88 (0.85- 0.88)
	Mean DTA (cm)	0.14 (0.10- 0.14)	0.11 (0.11- 0.11)
	Maximum DTA (cm)	1.37 (0.87- 1.44)	1.09 (1.02- 1.15)
Pre-sacral LN	DSC	0.69 (0.63- 0.72)	0.82 (0.77- 0.82)
	Mean DTA (cm)	0.08 (0.08- 0.09)	0.07 (0.05- 0.08)
	Maximum DTA (cm)	0.74 (0.73- 0.97)	0.78 (0.67- 0.93)

**Figure 1.** Example axial and sagittal imaging in a) 2D T2W MRI and b) 3D T2W MRI. c) and d) show the same images with observer contours for the mesorectum and right and left pelvic lymph node CTVs



## Conclusion

Very good IOV is seen in mesorectum and pelvic lymph node CTV delineation for rectal radiotherapy when using consensus contouring guidelines and MRI sequences optimised for MR image-guided radiotherapy.

## References

1) Warfield SK, Zou KH and Wells WM. Simultaneous truth and performance estimation (STAPLE): an algorithm for the validation of image segmentation. *IEEE Trans Med Imaging*. 2004 Jul;23(7):903-21.

**EP-1859 Investigating the feasibility of boosting 18F-FLT-PET-CT volumes to 75 Gy in oropharyngeal cancer**  
 J. Wyatt<sup>1</sup>, G. Petrides<sup>2</sup>, C. Kelly<sup>1</sup>, R. Maxwell<sup>3</sup>, R. Plummer<sup>1,3</sup>, R. Pearson<sup>1</sup>

<sup>1</sup>Newcastle upon Tyne Hospitals NHS Foundation Trust, Northern Centre for Cancer Care, Newcastle upon Tyne, United Kingdom ; <sup>2</sup>Newcastle upon Tyne Hospitals NHS Foundation Trust, Department of Nuclear Medicine, Newcastle upon Tyne, United Kingdom ; <sup>3</sup>Newcastle University, Northern Institute of Cancer Research, Newcastle upon Tyne, United Kingdom

## Purpose or Objective

Radioresistance is a major cause of radiotherapy failure within Head And Neck Squamous Cell Carcinoma (HNSCC), with many tumour recurrences occurring within the gross tumour volume. Dose escalation to the active tumour sub-volume may overcome this problem. <sup>18</sup>F-FLT-PET-CT is a proliferation biomarker which has been investigated for staging and treatment response for HNSCC. This was a planning study investigating the technical feasibility of treating <sup>18</sup>F-FLT-PET-CT identified boost volumes to 75 Gy in 30 fractions.

## Material and Methods

Five patients diagnosed with HNSCC received <sup>18</sup>F-FLT-PET-CT scans in the radiotherapy planning position. 2.59 MBq/kg <sup>18</sup>F-FLT was administered between 45-60 minutes before imaging started. The 75 Gy boost volume was defined as 70% of the maximum Standard Uptake Volume (SUVmax) plus a 5 mm isotropic margin. Gross Tumour Volumes, Clinical Target Volumes and Organs at Risk were contoured according to the clinical routine.

Two treatment plans were created for each patient. Plan 1 delivered the clinical standard 65 Gy to the primary tumour and involved lymph nodes and 54 Gy to the prophylactic lymph nodes. Plan 2 included 75 Gy to the PET-defined boost volume in addition to the clinical standard dose prescriptions. Both plans were created with a 6 MV dual 360° arc Volumetric Modulated Arc Therapy (VMAT) technique with a 5° collimator rotation. The plans were compared for each patient on the doses to the targets and Organs At Risk (OAR), the body integral dose and beam delivery time.

## Results

The mean boost volume was 16 ± 9 cm<sup>3</sup> (sd, range 7 - 27 cm<sup>3</sup>). The mean dose differences to the targets and OAR's are shown in table 1. An example dose distribution is shown in figure 1. The dose differences to the targets were within 1 Gy except for the boost PTV.

The mean difference in dose statistics for all OAR's was ≤ 1 Gy. OARs that did not meet dose constraints in Plan 2 did not meet them in Plan 1. The mean body integral dose was 3 ± 1 % lower for Plan 2 than for Plan 1. There was no difference in beam delivery time (mean difference 0.00 ± 0.02 minutes).

**Table 1** Mean differences (Plan 2 - Plan 1) between Plan 2 and Plan 1 in dose statistics for targets and organs at

Structure	Dose Statistic	Mean Difference/Gy
Boost PTV (75 Gy)	D5	9.6 ± 1.0
Boost PTV (75 Gy)	D50	9.0 ± 0.4
Boost PTV (75 Gy)	D95	8.3 ± 0.6
Primary PTV (65 Gy)	D5	1.0 ± 1.1
Primary PTV (65 Gy)	D50	0.0 ± 0.2
Primary PTV (65 Gy)	D95	-0.6 ± 0.8
Prophylactic PTV (54 Gy)	D5	0.1 ± 0.5
Prophylactic PTV (54 Gy)	D50	0.0 ± 0.3
Prophylactic PTV (54 Gy)	D95	-0.4 ± 0.9
Spinal Cord	D0.1cc	-0.3 ± 1.2
Brain Stem	D0.1cc	0.8 ± 2.2
Ipsilateral Parotid Gland	Mean	0.2 ± 0.7
Contralateral Parotid Gland	Mean	0.3 ± 1.0
Ipsilateral Submandibular Gland	Mean	-1.0 ± 1.4
Contralateral Submandibular Gland	Mean	-0.2 ± 1.2
Larynx	Mean	0.3 ± 2.6

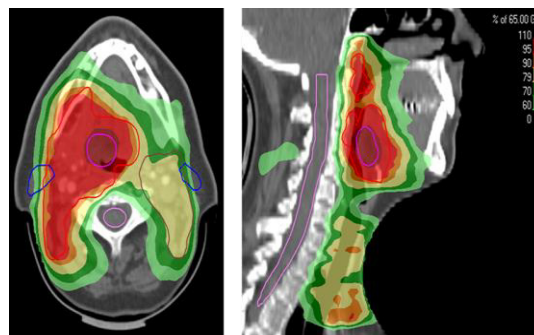


**Figure 1** Example dose distribution showing dose to boost volume (pink structure), primary target (red), and prophylactic target (brown), and OAR's spinal cord (pink) and parotid glands (blue).

## Conclusion

Doses to <sup>18</sup>F-FLT-PET-CT identified boost volumes can be escalated to 75 Gy without substantially impacting other target doses, OAR doses, body integral dose or beam delivery time using VMAT. Treating patients with <sup>18</sup>F-FLT-PET-CT boost volumes could improve local recurrence rates for HNSCC patients. A prospective trial is required to assess the safety of delivering the boost plan.

**EP-1860 Dosimetric and physical aspects of APBI techniques: External Beams vs IntraOperative Radiotherapy**

P. Tabarelli de fatis<sup>1</sup>, M. Liotta<sup>1</sup>, I. Meaglia<sup>2</sup>, M. Paolini<sup>2</sup>, C. Bocci<sup>2</sup>, G.B. Ivaldi<sup>2</sup>

<sup>1</sup>Istituti Clinici Scientifici Maugeri, Medical Physics, Pavia, Italy ; <sup>2</sup>Istituti Clinici Scientifici Maugeri, Radiotherapy, Pavia, Italy

## Purpose or Objective

To evaluate dosimetric and physical aspects of two techniques used in ICS Maugeri hospital to deliver Accelerated Partial Breast Irradiation (APBI).

## Material and Methods

From 2012 to 2018 we treated 57 APBI patients (pts). 26 with Photon Beam Radiotherapy (EPBRT) and 31 with electron Intra Operative Radiotherapy (eIORT). 25 EPBRT pts were treated with multiple no-coplanar 6 MV 3DCRT and 1 patient with IMRT technique. The irradiation geometry has been planned on pt's CT images (5 mm spaced) by Philips Pinnacle treatment planning system to fulfill dosimetric criteria on organs at risk (ORs): <50% and 100% of prescribed dose received by 60% and 35% of omolateral breast respectively, <30% prescribed dose received by 15% omolateral lung, <5% prescribed dose on

40% of heart (PBI on left breast), and on 5% of the heart (PBI on right breast). Homogeneity index (HI: ratio between D2% and D98%) and conformity index (CI: ratio between 95% isodose volume and PTV volume) for PTV coverage and OR dosimetric criteria have been calculated. The 31 eIORT pts were treated with a single dose (21 Gy prescribed to 90%). During eIORT a shielding disc, with diameter 2-3 cm larger than electron applicator, has been placed between the gland and pectoralis muscle to spare internal structures. In vivo dosimetry with gafchromic films has been performed to check accelerator output accuracy and the alignment between electron field and shielding disc. One piece of film has been positioned on the tumour bed and another circular films with the same dimension of the shielding disc has been put on the upper surface of the disc (immediately below the tumour bed). The HI (ratio between maximum and mean dose received by tumour bed) has been computed and the agreement between expected and measured entrance and exit dose on the tumour bed and the alignment of the shielding disc with the irradiation beam, considering isodoses > 85% inside the film, have been evaluated.

#### Results

Concerning EPBRT the mean HI is  $1.12 \pm 0.13$  while for CI is  $1.8 \pm 0.7$ . The OR doses have been always below the criteria except for the omolateral breast volume receiving 50% of prescribed dose in the range from 82.6% to 37%. 38% of the pts have been exceeded the limit due to the large PTV volumes respect to the whole breast. For eIORT the average HI value is  $1.12 \pm 0.07$ , the mean entrance dose is  $2.8 \pm 2\%$ , while the median difference between expected and measured dose (corrected for backscatter factor estimated in phantom) on the shielding disc is 2.7% (from 0.1 to 12.3%). For 68% of the pts the shielding disc has been aligned to the electron applicator.

#### Conclusion

Both APBI techniques give good and similar homogeneous irradiations. In EPBRT the irradiation is poorly conformed, but OR doses are well observed. Instead eIORT is well conformed to tumour bed but the sparing of normal tissue is not always satisfied for the critical alignment of shielding disc to electron applicator.

#### EP-1861 Simultaneous truth and performance level estimation method for contouring assessment in radiosurgery

H. Sandstrom<sup>1</sup>, I. Toma-Dasu<sup>2</sup>, C. Chung<sup>3</sup>, H. Jokura<sup>4</sup>, A. Dasu<sup>5</sup>

<sup>1</sup>Medical Radiation Physics, Stockholm University and Karolinska Institutet, Stockholm, Sweden; <sup>2</sup>Medical Radiation Physics, Department of Physics- Stockholm University, Stockholm, Sweden; <sup>3</sup>University of Texas, MD Anderson Cancer Center, Houston, USA; <sup>4</sup>Jiro Suzuki Memorial Gamma House, Furukawa Seiryō Hospital, Osaka, Japan; <sup>5</sup>The Skandion Clinic, The Skandion Clinic, Uppsala, Sweden

#### Purpose or Objective

Target contouring variability has shown to be an intrinsic problem for stereotactic radiosurgery. Several methods have been developed for evaluating the contouring accuracy. The aim of this work was to analyse and quantify the contouring variability and to estimate the true volume based on multiple delineations using the Simultaneous Truth and Performance Level Estimation (STAPLE) algorithm. In addition, the analysis of the robustness of the STAPLE method for the assessment of the true target with respect to the number of contours available as input was also assessed.

#### Material and Methods

A multicentre analysis of the variability in contouring of three metastases (diameters 30 mm, 20 mm and 13 mm) and three common targets treated with Gamma Knife radiosurgery, a cavernous sinus meningioma, a vestibular schwannoma and a pituitary adenoma was performed with

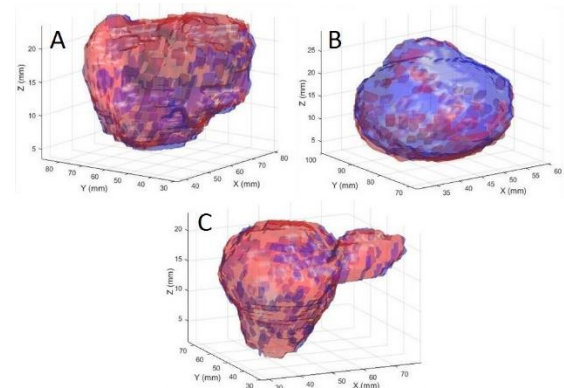
the STAPLE approach, an iterative algorithm which generates an estimate of the true volume together with the sensitivity and specificity of each segmentation input. Twelve contours were provided for each case by experienced planners for Gamma Knife. The robustness of the STAPLE method, with respect to the number of contours, was analyzed by randomly and repeatedly selecting sets of 6-12 contours for each case. A previously developed method based on the agreement volume was also applied. The STAPLE true volume was compared to the 50% agreement volume, AV50.

#### Results

In the evaluation when all 12 available contours were used as input, the similarity between the STAPLE true volume and the 50% agreement volume was high (90-100% similarity). A graphical illustration of the results for the cavernous sinus meningioma (A), the pituitary adenoma (B) and the vestibular schwannoma (C) showing the 3D surface plots of the STAPLE true volume (red) using all the segmentations available as input together with the AV50 (blue) is displayed in Figure 1. The similarity decreased as the number of contours included in the calculations decreased. Random removal of up to 5 input contours might lead to a difference between the STAPLE-generated true target and the 50% agreement volume between 10-70% for all cases. The magnitude of the actual variability in the contours is directly impacting the robustness as the minimum number of input contours required increases with a higher variability.

#### Conclusion

The STAPLE method is a valuable tool for the estimation of a true target based on multiple contours if a high enough input number of contours is available. The robustness of the STAPLE method for rendering the true target volume depends on the number of contours provided as input and their variability with respect to shape, size and position. The additional benefit of employing this method for contouring variability analysis is the simultaneous generation of sensitivity and specificity for each input, thus for each delineated structure, relative to the true volume of that structure.



#### EP-1862 A comparative study of male pelvis CT auto-segmentation and its clinical utility

J. Wood<sup>1</sup>, M. Aznar<sup>2</sup>, P. Whitehurst<sup>1</sup>

<sup>1</sup>The Christie NHS Foundation Trust, Christie Medical Physics & Engineering, Manchester, United Kingdom; <sup>2</sup>The University of Manchester, Radiotherapy Related Research, Manchester, United Kingdom

#### Purpose or Objective

This work investigated the geometric accuracy of auto-segmented structures from multiple providers within the male pelvis and their utility for prostate VMAT treatment planning.

#### Material and Methods

SPICE (Philips Radiation Oncology, Andover MA), Mirada RTx (Mirada Medical, Oxford UK) and ADMIRE (Elekta, Stockholm Sweden) were used to segment the bladder, rectum, femoral heads, prostate and SV in 11 pelvic CT scans. For Mirada RTx and ADMIRE atlases were generated from local manual outlines. Atlases in SPICE cannot be customised and so the proprietary 'Male Pelvis' atlas was used.

DICE and mean distance to agreement (DTA) were used to assess the geometric accuracy of the auto-segmented structures compared to 'ground-truth' manual outlines drawn by expert clinical oncologists and treatment planners. Manual contours were drawn purely on CT without MR fusion.

PTVs and optimisation volumes were expanded and VMAT treatment plans generated using each set of auto and manual structures in the Pinnacle TPS. Hybrid-plans were also created using manual targets (prostate and SV) and auto OARs. The same optimisation objectives and beam parameters were used for all plans. Auto- and hybrid-plan dose distributions were compared to manual-plans using standard prostate VMAT DVH statistics (all reported to the 'ground-truth' manual outlines) and gamma analysis at 3% / 3 mm inside the 30% and 50% isodoses - the two lowest doses reported on clinical treatment plans based on the CHHiP protocol.

### Results

In terms of DICE and mean DTA, SPICE and ADMIRE performed the best for the bladder, rectum and SV. Mirada RTx and ADMIRE performed the best for the femoral heads and all three packages were comparable for the prostate. Figure 1 shows boxplots for each structure and variation across the 11 patients.

Gamma analysis pass rates are presented in Table 1 and show that the dose distributions for all hybrid-plans are comparable to the corresponding manual-plans at doses > 50%. For the hybrid-plans, all reported DVH statistics were within 3% of those achieved with the manual outlines (mostly within 2%). No correlation was found between any of the geometric evaluations of the auto-segmented structures and treatment plan doses.

### Conclusion

Overall, SPICE and ADMIRE gave the best geometric agreement with manual outlines. The utility of auto-segmented target volumes for treatment planning is severely limited. However, hybrid-plans using manual target volumes and auto-segmented OARs demonstrate good agreement with manual-plans. Further work is required to refine the hybrid treatment planning solution, but this work demonstrates promise for the approach, which could generate significant treatment planning efficiencies.

### EP-1863 Semi-Automatic Planning in head and neck VMAT treatments

A.F. Monti<sup>1</sup>, M. Brambilla<sup>1</sup>, C. Carbonini<sup>1</sup>, M.B. Ferrari<sup>1</sup>, H.S. Mainardi<sup>1</sup>, S. Nici<sup>1</sup>, A. Lassy Taty<sup>1</sup>, D. Zanni<sup>1</sup>, A. Torresin<sup>1</sup>

<sup>1</sup>ASST Ospedale Niguarda, Medical Physics, Milano, Italy

### Purpose or Objective

Automation or semi-automation greatly facilitate IMRT and VMAT planning potentially removing some biases afflicting manual procedures. Such biases are mainly related to operators' skills and the level of stress they accumulate during the working day. In this work, we evaluated the (semi)automatic abilities of a biological constrained based TPS (Monaco 5.11 - Elekta, SWE).

### Material and Methods

Monaco is a double step TPS (S1, optimization - S2, segmentation) which tries to fulfil the PTVs and OARs dose requirements in two modalities: the "Constrained" (C) and the Pareto (P) one. In C modality the cost function is optimized to fulfil OARs dose limitations; in P modality the priority is focused in PTVs coverage. In both modalities it

is possible to activate a Multicriterial (M) option for OARs. In M, the cost function is treated as a multicriterial objective and the optimizer works harder on the constraints to lower them beyond what the user set. In this work manual procedures (C-C), based on consolidated H&N templates, were compared to two semi-automated approaches: the CM-CM, in which the C modality with M is used in S1 and S2, and the CM-P, in which the C modality with M is used in S1 and the P one for S2. The first combination should reduce the dose to OARs, while the second should guarantee a better PTV coverage than CM-CM. H&N cases were divided into different groups (G) of complexity in order to explore the potentialities of each combination. G1 is a light case group with only one PTV far or not so near many OARs; G2 is a more complex situation, with two or more PTVs near many OARs and overlapping them, but without compromising dose constraints; G3 is a harder situation similar to G2, with a very large overlapping of the PTVs and one or more OARs.

### Results

Table 1 regards preliminary results of ten cases. The comparison is between each group/combination plan and the corresponding manual plan. G1 shows a dramatic decrease in dose to OARs, the PTV coverage is also decreased but still acceptable and none of the automatic plans was rejected. G1 CM-CM combination is surprisingly better than CM-P also in PTV coverage, due to the easy situation that promotes OARs' sparing. In group G2 improvements versus manual treatments are clearly evident even if not as in G1. G2 gives OARs better results in all combinations with a light superiority of CM-P particularly on parotids and brain stem. When the situation gets worse, as in G3, the semi-automatic approach fails, giving conflicting results: the PTVs coverage increases but some OARs receive higher doses.

		AG1 (%)		AG2 (%)		AG3 (%)	
		CM-CM	CM-P	CM-CM	CM-P	CM-CM	CM-P
PTVt	D98%	-3.6	-3.9	0.0	-0.7	0.7	1.2
	D2%	1.6	3.0	0.6	0.7	-0.8	-0.8
PTVn	D98%			0.0	-1.0	0.9	0.9
	D2%	-55.2	-53.6	-6.0	-4.7	-6.9	-7.5
Brain St.	D2%	-74.7	-73.4	-12.4	-17.5	13.4	10.4
Parotids	Dmean	-55.4	-51.7	-17.6	-19.0	-3.8	3.7
	Oral C.	Dmean	-12.7	-9.3	-2.1	-2.5	-10.1
Mandibula	Dmean	-18.6	-17.4	-2.6	-3.3	1.3	4.0
	Tyroid	Dmean	-0.4	0.2	-2.6	-3.7	1.1
Larinx	Dmean	-46.6	-42.9	-1.0	-1.6	7.3	0.8
RVR	Dmean	-18.5	-17.9	-5.8	-6.5	1.8	1.3

### Conclusion

This approach is a semi-automatic one, having to manually select C or P modality and the M option. A semi-automatic plan is usually better than a manual one, if a small reduction in PTV coverage can be accepted when occurring. Very complex cases are not easily automated, as the results are often conflicting and even worse than in a manual approach.

### EP-1864 Dose optimization research of esophageal cancer with automatic treatment planning module

M. Mingchang<sup>1</sup>, W. Ma<sup>1</sup>, R. Zhang<sup>1</sup>, Z. Chi<sup>1</sup>

<sup>1</sup>Fourth Hospital of Hebei Medical University, Department of Radiation Oncology, Shijiazhuang, China

### Purpose or Objective

Compared with the manual planning, evaluating the dosimetric characteristics of the esophageal cancer planning based on the automated planning module and the feasibility of clinical application.

### Material and Methods

Ten treated IMRT plans of upper thoracic esophageal cancer and ten treated IMRT plans of thoracic esophageal cancer were re-planned with Auto-planning module. Only one cycle of automated optimization of the Auto-Planning module was performed for each plan without any manual intervention. Compare the dosimetric parameters of the two IMRT plans, paired t-test was used for statistical analysis.

## Results

All esophageal cancer plans generated with the auto-planning module met the clinical dose requirements. In comparison group of upper thoracic esophageal cancer plan, homogeneity index has no significant differences between two groups ( $P=0.115$ ), the conformity Index of targets was superior in the automated plans than in manual plans ( $P=0.027$ ). In addition, the automated plans had significantly reduced the dose of lung received, lung's  $V_5$ ,  $V_{10}$ ,  $V_{20}$ ,  $V_{30}$  was reduced by 2.1%, 1.6%, 3%, 1.2% respectively ( $P=0.001$ , 0, 0, 0.01). The dose of cord received was not significant differences between two groups ( $P=0.892$ ). In comparison group of thoracic esophageal cancer plan, homogeneity index was not significant differences between two groups ( $P=0.428$ ), the conformity Index of targets was superior in the manual plans than in automated plans ( $P=0.048$ ). Lung's  $V_5$  had no significant differences ( $P=0.053$ ), lung's  $V_{10}$ ,  $V_{20}$ ,  $V_{30}$  was reduced by 2%, 3.1%, 1.3% ( $P=0.032$ , 0, 0.008). The dose of cord and heart received has no significant differences between two groups ( $P=0.204$ , 0.894).

## Conclusion

Auto-Planning module can improve the overall quality of treatment plans, reduced plans quality differences due to inexperienced planners. Compared with the manual planning, the Auto-planning have substantially shorter manual planning time and improved planning efficiency. It is feasible to generate automated IMRT plans with automated planning module for esophageal cancer patients. The relatively complex esophageal cancer plans still needs to be manually optimized after an automatic planning of optimization.

## EP-1865 A feasibility study: 6 VMAT arcs full collimator opening for hippocampal sparing

M. Maffei<sup>1</sup>, S. Bou Selman<sup>1</sup>, H. Stefan<sup>2</sup>, M. Haller<sup>2</sup>, P. Ferrari<sup>2</sup>

<sup>1</sup>Azienda Sanitaria dell'Alto Adige, Servizio di radioterapia oncologica, Bozen, Italy ; <sup>2</sup>Azienda Sanitaria dell'Alto Adige, Servizio di fisica sanitaria, Bozen, Italy

## Purpose or Objective

to assess the feasibility of 6 arcs with full collimator opening for an efficient VMAT planning approach for hippocampal-avoidance whole-brain radiation therapy

## Material and Methods

11 patient were considered, prescribed dose was 30 Gy in 10 fractions. Contouring was in accordance to RTOG 0933. VMAT Treatment Planning Techniques was applied using 6 coplanar arcs. Full collimator opening was used with the following parameters: arc1 181°-179° clockwise and 95° collimator, arc2 179°-181° counterclockwise and 265° collimator, arc3 181°-300° clockwise and 350° collimator, arc4 60°-179° clockwise and 350° collimator, arc5 179°-60° counterclockwise and 10° collimator and arc6 300°-181° counterclockwise and 10° collimator. Specific physical objective were used for PTV coverage and hippocampal sparing as RTOG protocol suggested. Conformity and homogeneity index were calculated. Statistical analysis was performed.

## Results

The coverage of PTV was warranted  $D_{90\%} = 28.8 \pm 0.3$  Gy,  $D_{2\%} = 31.6 \pm 0.4$  Gy and for Hippocampal  $D_{100\%} = 8.5 \pm 0.6$  Gy, max dose =  $14.9 \pm 0.3$  Gy. Conformity and homogeneity index were equal to  $1.11 \pm 0.01$  and  $0.86 \pm 0.03$  respectively.  $600 \pm 10$  segments and a total of  $1170 \pm 150$  MU were used. Total delivery time  $516 \pm 16$  sec.

## Conclusion

6 VMAT arcs full collimator opening for hippocampal sparing was feasible and showed a easy coverage in PTV saving hippocampal in accordance of RTOG 0933 constrains. The specific rotation of collimator in the 6 arcs, warranted a easy calculation and deliverability of the plan, with 1000 MU and 500 sec of delivery time.

## EP-1866 An interplay effect study comparing two different VMAT techniques for free-breathing moving targets

M. Gil Conde<sup>1</sup>, Á. Seguro<sup>1</sup>, F. Campos<sup>1</sup>, M.J. Albertos<sup>1</sup>, M.A. Iborra<sup>1</sup>, L. Díaz<sup>2</sup>

<sup>1</sup>Hospital de Jerez, Radiation Physics and Radiological Protection, Jerez de la Frontera, Spain ; <sup>2</sup>Hospital de Jerez, Radiation Oncology, Jerez de la Frontera, Spain

## Purpose or Objective

Dosimetric impact due to interplay effect is studied in VMAT plans for lung tumors in free-breathing patients. The magnitude of this effect is compared in two treatment planning techniques: pure VMAT and hybrid VMAT.

## Material and Methods

A programmable respiratory motion phantom was used, simulating a typical breathing pattern with a maximum longitudinal amplitude of 20 mm and a variable period around 5 s. A Pinpoint chamber (0.016 cc) was introduced inside the phantom in a methacrylate holder that moved in the longitudinal direction following the mentioned pattern.

5 VMAT plans that had been previously planned for real patients were used as irradiation technique in a Varian Truebeam. They used 6 MV, variable dose rate of maximum 600 MU/min and 2 half-arcs of  $180.1^\circ-0^\circ/0^\circ-180.0^\circ$ , depending on the laterality of the tumor.

Alternatively, a hybrid plan (80% 3DCRT - 20% VMAT) was designed for each patient, consisting of 3 conformal 6 MV static fields plus a 6 MV half-arc to homogenize the plan. The phantom was positioned aligning the chamber with the Linac isocenter so during the breathing cycle the chamber moved around this point. Absolute dose was measured under these conditions for each plan in 5 treatment fractions.

## Results

Measured dose per fraction and after the 5 fractions of each plan was obtained separately. For all the patients studied, the mean deviation of the measured dose ( $D_{meas}$ ) from the expected one ( $D_{exp}$ ) after 5 fractions for VMAT and hybrid plans was 0.43% and -0.64%, respectively. Mean standard deviation of  $D_{meas}$  in all fractions was of 4.85 cGy for VMAT versus 2.96 cGy for the hybrid plans, however. Maximum deviation found of  $D_{meas}$  in one fraction between all the VMAT and hybrid plans was of -4.00% and -3.58%, respectively. The maximum mean dose deviation along 5 fractions in a single beam was of 16.7% with VMAT and -8.50% when using the hybrid technique. This last deviation was observed in an arc. Maximum mean dose deviation found between all the 3DCRT beams was of 3.18%, being the average standard deviation for the 5 patients 0.14 cGy.

	$\overline{D_{meas}}$ dev. %	$\sigma$ ( $\overline{D_{meas}}$ ) cGy	Max( $D_{meas}$ dev./fr) %	Max( $\overline{D_{meas}}$ dev./beam) %
VMAT	0,43	4,85	-4,00	16,7
Hybrid	-0,64	2,96	-3,58	-8,50
3DCRT	-	0,14	-	3,18

## Conclusion

Despite the standard deviation of absolute dose values between fractions for the same patient is higher with VMAT than with the hybrid technique and even higher when compared to 3DCRT, differences in the mean dose after 5 treatment fractions between both cases are not significant. Interplay effect when combining VMAT with respiratory movement is observed in single arcs. Nevertheless, the random character of this effect makes deviation of different arcs in the same plan or inter-fraction dose deviation cancel out, not being clinically relevant after adding all the fractions.

### EP-1867 SBRT automatic treatment planning as a dose escalation strategy in pancreatic cancer

S. Cilla<sup>1</sup>, A. Ianiro<sup>1</sup>, F. Deodato<sup>2</sup>, G. Macchia<sup>2</sup>, V. Picardi<sup>2</sup>, P. Viola<sup>1</sup>, M. Craus<sup>1</sup>, M. Buwenge<sup>3</sup>, S. Cammelli<sup>3</sup>, V. Valentini<sup>4</sup>, A.G. Morganti<sup>3</sup>

<sup>1</sup>Fondazione di Ricerca e Cura "Giovanni Paolo II"- Università Cattolica del Sacro Cuore, Medical Physics Unit, Campobasso, Italy ; <sup>2</sup>Fondazione di Ricerca e Cura "Giovanni Paolo II"- Università Cattolica del Sacro Cuore, Radiation Oncology Unit, Campobasso, Italy ;

<sup>3</sup>Department of Experimental- Diagnostic and Specialty Medicine - DIMES- University of Bologna- S. Orsola-Malpighi Hospital, Radiology Oncology Department, Bologna, Italy ; <sup>4</sup>Fondazione Policlinico Universitario A. Gemelli - Università Cattolica del Sacro Cuore, Radiation Oncology Department, Roma, Italy

#### Purpose or Objective

Stereotactic body radiation therapy (SBRT) has been suggested as a new treatment strategy for locally advanced pancreatic cancer. However, the close proximity of highly radiosensitive organs prevent the administration of high doses to the vascular infiltration areas, aiming for a radical resection. Aim of this study was to perform a planning feasibility analysis of an automated planning system (Pinnacle<sup>3</sup> AutoPlanning) using a VMAT-SIB technique as a dose escalation strategy.

#### Material and Methods

Twelve patients with unresectable pancreatic head adenocarcinoma due to vascular infiltration, were included in this study. CTV<sub>v</sub> was defined as involved vessels plus 5 mm or contact between the gross tumor volume (GTV) and vessels. The vascular PTV (PTV<sub>v</sub>) was obtained adding an anisotropic margin (5 mm craniocaudal direction, 3 mm in other directions). The tumor PTV (PTV<sub>t</sub>) was defined as the GTV plus an anisotropic margin (5 mm craniocaudal direction, 3 mm in other directions) and including the PTV<sub>v</sub>. A duodenum-PRV was defined by adding an isotropic 5 mm margin. SBRT was delivered in 5 fractions with a SIB strategy. For each patient 3 plans were optimized. Plan 1: 30 Gy (6 Gy/fraction) to PTVs; plan 2 and plan 3 escalated PTV<sub>v</sub> dose to 40Gy (8 Gy/fraction) and 50Gy (10 Gy/fraction), respectively. Corresponding EQD2 were 40Gy, 60Gy and 83.3Gy (a/b equal to 10). The dose-volume constraints for OARs were based on the AAPM TG101 recommendations. Automated plans were generated by Pinnacle AutoPlanning module by means of VMAT dual-arc. A progressive optimization algorithm is used to continually adjust initial targets/OARs objectives while tuning structures are automatically added to increase the dose fall-off outside targets. The primary endpoint was to achieve PTV<sub>t</sub> and PTV<sub>v</sub> coverage in terms of D95%>95%, respecting all OARs constraints.

#### Results

OARs constraints were achieved in all patients. PTV<sub>v</sub> D95% was 30.8±0.1Gy, 36.1±5.4Gy and 39.2±12.0Gy at level 1, 2 and 3, respectively. In particular, the primary endpoint D95%> 95% was achieved in 12 patients (100%), 8 patients (67%) and 7 patients (58%) for level 1, 2 and 3, respectively. The mean dose to PTV<sub>v</sub> was 40.6±1.1 Gy and 49.7±2.3 Gy at level 2 and 3, respectively. PTV<sub>v</sub> mean dose was >90% in all patients.

#### Conclusion

AutoPlanning reported a great potential for a tailored SBRT in advanced pancreatic cancer, allowing dose escalation and showing the feasibility to administer in all patients strongly differentiated doses.

### EP-1868 Automated VMAT planning in Pinnacle3: a dosimetric study in high-risk prostate cancer

S. Cilla<sup>1</sup>, A. Ianiro<sup>1</sup>, P. Viola<sup>1</sup>, G. Macchia<sup>2</sup>, M. Buwenge<sup>3</sup>, A. Arcelli<sup>3</sup>, S. Cammelli<sup>3</sup>, V. Valentini<sup>4</sup>, A.G. Morganti<sup>3</sup>, F. Deodato<sup>2</sup>

<sup>1</sup>Fondazione di Ricerca e Cura "Giovanni Paolo II"- Università Cattolica del Sacro Cuore, Medical Physics Unit, Campobasso, Italy ; <sup>2</sup>Fondazione di Ricerca e Cura "Giovanni Paolo II"- Università Cattolica del Sacro Cuore, Radiation Oncology Unit, Campobasso, Italy ;

<sup>3</sup>Department of Experimental- Diagnostic and Specialty Medicine - DIMES- University of Bologna- S. Orsola-Malpighi Hospital, Radiation Oncology Department, Bologna, Italy ; <sup>4</sup>Fondazione Policlinico Universitario A. Gemelli - Università Cattolica del Sacro Cuore, Radiation Oncology Department, Roma, Italy

#### Purpose or Objective

Treatment plans for high-risk prostate cancer are highly complex due to large irregular shaped target volumes, multiple dose prescription levels and several OARs close to the target. The quality of these plans is highly inter-planner dependent. We aimed to assess the performance of the Auto-Planning module present in the Pinnacle TPS (version 16.0), comparing automatically generated VMAT plans (AP) with the historically clinically accepted manually-generated ones (MP).

#### Material and Methods

Twelve consecutive patients treated with VMAT-SIB for high-risk prostate cancer were re-planned with the Auto-Planning engine. The PTV1 included the prostate and the seminal vesicles; the PTV2 included the pelvic lymph nodes. Both PTVs were simultaneously irradiated over 25 daily fractions at 65Gy (2.6 Gy/fraction) and 45Gy (1.8 Gy/fraction). All manually (MP) and automatically (AP) generated plans were created by means of the "dual arc" feature. For the MP plans, additional non-anatomical structures needed to be delineated in order to interactively guide the optimization process. For AP plans, a progressive optimization algorithm is used to continually adjust initial targets/OARs objectives; tuning structures are automatically added during optimization to increase the dose fall-off outside targets. Various dose and dose-volume metrics (D98%, D95%, D50%, D2%, Dmean, V95% for target volumes; Dmean, Dmax and various Vx% for OARs), as well as conformity (CI) indexes and healthy-tissue integral dose (ID) were evaluated. A Wilcoxon paired test was performed for plan comparison with statistical significance set at p<0.05.

#### Results

Differences in all dose coverage metrics (in terms of V95%, D98%, D50%, D2% and Dmean) for both PTVs were not statistically significant (p<0.05). Differences in CI reached significance only for PTV2 (MP:1.59 vs. AP:1.48). Differences in DVHs were no significant in overall dose range for rectum, bladder and small bowel (rectum: V<sub>50Gy</sub>: 31.7 vs. 32.2Gy, V<sub>60Gy</sub>: 21.1 vs. 22.5Gy, Dmean: 40.6 vs. 40.5Gy; bladder: V<sub>65Gy</sub>: 19.6 vs. 20.6, Dmean: 44.3 vs. 43.8Gy). For small bowel: V<sub>15Gy</sub>: 105.0 vs 119.1cc, Dmean: 13.3 vs. 12.8cc. AP plans provided a decrease in Integral Dose of 5.1%. The mean number of MUs was not statistically different: MP (537) and AP (546), p=0.887.

#### Conclusion

The Pinnacle Auto-Planning module achieved highly consistent treatment plans in the cases of complex anatomical sites. The working time was substantially reduced with Auto-Planning.

### EP-1869 Automated VMAT planning in Pinnacle3: a dosimetric study in head-neck cancer

S. Cilla<sup>1</sup>, A. Ianiro<sup>1</sup>, G. Macchia<sup>2</sup>, F. Romani<sup>3</sup>, A.L. Angelini<sup>3</sup>, M. Buwenge<sup>4</sup>, S. Cammelli<sup>4</sup>, V. Valentini<sup>5</sup>, A.G. Morganti<sup>4</sup>, F. Deodato<sup>2</sup>

<sup>1</sup>Fondazione di Ricerca e Cura "Giovanni Paolo II"- Università Cattolica del Sacro Cuore, Medical Physics Unit, Campobasso, Italy ; <sup>2</sup>Fondazione di Ricerca e Cura "Giovanni Paolo II"- Università Cattolica del Sacro Cuore, Radiation Oncology Unit, Campobasso, Italy ;

<sup>3</sup>Department of Experimental- Diagnostic and Specialty Medicine - DIMES- University of Bologna- S. Orsola-

*Malpighi Hospital, Medical Physics Unit, Bologna, Italy ;  
 4Department of Experimental- Diagnostic and Speciality  
 Medicine - DIMES- University of Bologna- S. Orsola-  
 Malpighi Hospital, Radiation Oncology Department,  
 Bologna, Italy ; 5Fondazione Policlinico Universitario A.  
 Gemelli - Università Cattolica del Sacro Cuore, Radiation  
 Oncology Department, Roma, Italy*

#### **Purpose or Objective**

Treatment plans for head-neck cancer are highly complex due to large irregular shaped target volumes, multiple dose prescription levels and to several OARs close to the target. We assessed the performance of the Auto-Planning module present in the Pinnacle TPS (version 16.0), comparing automatically generated VMAT plans (AP) with the historically clinically accepted manually-generated ones (MP) for head-neck cancer patients.

#### **Material and Methods**

Twelve consecutive patients treated with VMAT-SIB for bilateral head-neck cancer were re-planned with the Auto-Planning engine. The PTV1 included the primary tumor, PTV2 and PTV3 included the high-risk and low-risk lymph-nodal areas, respectively. PTV1, PTV2 and PTV3 were simultaneously irradiated over 30 daily fractions at 67.5Gy, 60.0Gy and 55.5 Gy, respectively. All manually (MP) and automatically (AP) generated plans were created by means of the 'dual arc' feature. For the MP plans, additional non-anatomical structures needed to be delineated in order to interactively guide the optimization process. For AP plans, a progressive optimization algorithm is used to continually adjust initial targets/OARs objectives; tuning structures are automatically added during optimization to increase the dose fall-off outside targets and improve the dose conformity. Various dose and dose-volume metrics (D98%, D95%, D50%, D2%, Dmean, V95% for target volumes; Dmean, Dmax and various Vx% for OARs), as well as conformity (CI) indexes and healthy-tissue integral dose (ID) were evaluated. A Wilcoxon paired test was performed for plan comparison with statistical significance set at  $p < 0.05$ .

#### **Results**

Differences in all dose coverage metrics (in terms of V95%, D98%, D50%, D2% and Dmean) for all PTVs were not statistically significant ( $p < 0.05$ ). AP plans reported a better CI for PTV3 (MP:1.43 vs. AP:1.35,  $p = 0.01$ ). No significant differences in maximum doses were found for eyes, lens and optic chiasm. AP plans reduced maximum doses to PRV spinal cord and brainstem by 1.3Gy ( $p = 0.04$ ) and 4.3Gy ( $p = 0.02$ ), respectively, and mean dose for parotids by 3.4Gy ( $p = 0.02$ ). In addition, AP plans provided a significant decrease in Integral Dose of 6.6%. The mean number of MUs was higher for AP (586 vs. 451,  $p = 0.01$ ), suggesting an increased degree of fluence modulation.

#### **Conclusion**

The Pinnacle Auto-Planning module was able to produce highly consistent treatment plans for this complex anatomical sites. The working time was substantially reduced with Auto-Planning.

#### **EP-1870 Dosimetric assessment of metal artefact corrected CT images use for pelvis treatment planning**

*E. Jaegle<sup>1</sup>, E. Cordier<sup>2</sup>, M. Alayrach<sup>1</sup>, A. Badey<sup>1</sup>, V. Bodez<sup>1</sup>, C. Khamphan<sup>1</sup>, P. Martinez<sup>1</sup>, R. Garcia<sup>1</sup>*

*<sup>1</sup>Institut Sainte Catherine, Physique, Avignon, France ;*

*<sup>2</sup>Institut National des Sciences et Techniques Nucléaires, Medical physics, Gif sur Yvette, France*

#### **Purpose or Objective**

Single Energy Metal Artefact Reduction algorithm (SEMAR, Canon Medical Systems) provides modified Hounsfield Unit (UH) Computed Tomography (CT) images by correcting artefacts related to photon starvation induced by metallic prostheses. The aim of this study is to assess the dosimetric impact of using such images for treatment planning with Eclipse™ (Varian Medical Systems VMS).

#### **Material and Methods**

Gammex RMI@465 CT Electron Density Phantom (Gammex Inc.) with titanium insert was used to get SEMAR-off and SEMAR-on HU-Electron Density (HU-ED) calibration curves for both voltages: 120 kVp and 135 kVp. 8 patients with metallic prosthesis, divided in 2 groups (limbs, prostate), were selected to the compare following dose calculation conditions (Anisotropic Analytical Algorithm 13.5, VMS):  
 Condition 1 : SEMAR<sup>off</sup> CT // SEMAR<sup>off</sup> UH-ED (clinical use)  
 Condition 2 : SEMAR<sup>on</sup> CT // SEMAR<sup>off</sup> UH-ED  
 Condition 3 : SEMAR<sup>on</sup> CT // SEMAR<sup>on</sup> UH-ED  
 Monitor Units (MU) resulting from the condition 1 were used for each calculation.

Mean, minimal and maximal PTV dose were recorded. Results were expressed as prescription percentage.

UH-ED curve impact

Dose Comparison between conditions 2 and 3.  
 UH modification impact

Dose Comparison between conditions 1 and 2.

For VMAT prostate patients, results from inverse planning (Photon Optimizer 13.5,VMS) with SEMAR<sup>on</sup> CT // SEMAR<sup>off</sup> UH-ED were also compared to the reference plan (clinical use). For identical PTV coverage, MUs and global Gamma index passing rates with [2% / 2 mm criteria] (Portal Dose Image Prediction 13.5, VMS) were compared.

#### **Results**

The difference between SEMAR<sup>off</sup> and SEMAR<sup>on</sup> is smaller than the difference between 120 kV and 135 kV regarding the UH value of Titanium. No differences were recorded around pelvis densities.

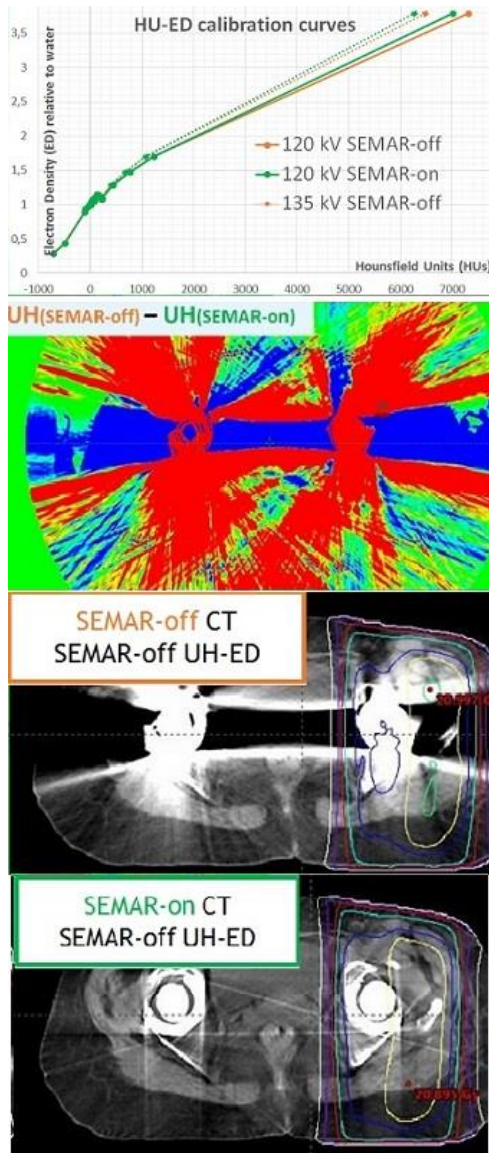
UH-ED curve impact

Adapting the UH-ED did not modify the average mean dose calculated over the 8 patients.

UH modification impact

Mean PTV dose increased by 0.5% for the 8 patients. Concerning limbs group, the minimal dose was strongly impacted (+1.9%). Prostate cases for which beams do not enter through metal, did not show such differences even if higher dose indices were recorded comparing to clinical use.

Results from optimizing on SEMAR<sup>on</sup> followed the same trend found with dose indices, with fewer MUs needed to get identical coverage. Gamma passing rates remained in our tolerance.



Patient	Technique	PTV(Dose) (%) prescription			Dose difference (%) prescription						
		Dose/ID	1	2	3	UH-ED impact		UH modification impact		UH modification impact	
						condition 1-3	Average over the 4 patients group	condition 1-3	Average over the 4 patients group	condition 1-3	Average over the 4 patients group
Limb	Left Hip 3DCRT	Mean Dose	100.1	100.9	100.9	0.1	0.0	0.0	0.8	0.5	0.6
		Min Dose	93.1	94.5	94.3	-2.2	-0.2	0.8	1.4	1.0	1.3
		Max Dose	109.0	104.8	104.9	-0.1	-0.1	-0.2	0.4	0.3	
	Left Femur 3DCRT	Mean Dose	100.0	101.1	101.1	0.1					
		Min Dose	99.3	101.1	101.1	0.0					
		Max Dose	100.6	106.5	106.0	-0.1					
	Left Hip 3DCRT	Mean Dose	101.1	101.9	101.9	0.0					
		Min Dose	101.1	101.9	101.9	0.0					
		Max Dose	101.1	101.9	101.9	0.0					
	Left Hip 3DCRT	Mean Dose	102.8	103.5	103.4	0.1					
		Min Dose	101.1	101.9	101.9	0.0					
		Max Dose	102.8	103.5	103.4	0.1					
Pelvis	Prostate UMAT*	Mean Dose	100.0	100.0	100.0	0.0					
		Min Dose	99.7	99.5	99.5	-0.1					
		Max Dose	100.3	100.4	100.5	-0.2	-0.1	0.7	0.3		
	Prostate UMAT*	Mean Dose	100.0	100.0	100.0	0.0					
		Min Dose	99.9	99.5	99.5	-0.1					
		Max Dose	100.3	100.4	100.5	-0.2	-0.1	0.9	0.4		
	Prostate UMAT*	Mean Dose	100.0	100.0	100.0	0.0					
		Min Dose	99.9	99.5	99.5	-0.1					
		Max Dose	100.3	100.4	100.5	-0.2	-0.1	0.9	0.4		
	Prostate UMAT*	Mean Dose	100.0	100.0	100.0	0.0					
		Min Dose	99.9	99.5	99.5	-0.1					
		Max Dose	100.3	100.4	100.5	-0.2	-0.1	0.9	0.4		
Prostate 3DCRT*	Mean Dose	100.0	100.0	100.0	0.0						
	Min Dose	99.8	99.5	99.5	-0.1						
	Max Dose	100.3	100.4	100.5	-0.1						

\* bears acid entering through prosthesis

**EP-1871 Can the use of a hydrogel spacer enable intra-prostatic boosts without increasing rectal doses?**  
 N. Laverick<sup>1</sup>, S. Currie<sup>1</sup>  
<sup>1</sup>Beatson West of Scotland Cancer Centre, Radiotherapy Physics, Glasgow, United Kingdom

**Purpose or Objective**

To assess the impact of using a hydrogel spacer (SpaceOAR®, Augmenix Inc. Waltham, MA, USA) on plan quality in prostate patients when including an intra-prostatic focal boost.

**Material and Methods**

Treatment plans were created on scans of ten patients pre- and post-implantation of the hydrogel spacer. All plans used VMAT with two coplanar arcs to treat the prostate to 60Gy in 20 fractions (PTV60) and the seminal vesicles to 47Gy (PTV47). All plans were optimised using the Centre’s RapidPlan model (Varian Medical Systems, Palo Alto, CA, USA). A boost volume was then identified for each patient and outlined on both the pre- and post-scan sets with the aid of MRI imaging. These boost volumes were planned to two separate dose prescriptions, 67Gy and 78Gy. Plans were compared in terms of target coverage and doses to bladder and rectum. Paired two-tailed t-tests were used to examine for statistical significance.

For the plans without the focal boost and the 78Gy boost plans, the robustness of the OAR doses was also assessed by inducing a 5mm target shift in all directions and recording the poorest rectal and bladder doses.

**Results**

Target coverage was not affected by the presence of the hydrogel spacer; however rectal doses were reduced post-implantation. As Figure 1 shows, the volume of rectum receiving both intermediate and higher doses is reduced with the spacer. The implantation of the spacer has allowed boosting of in intra-prostatic volume to 78Gy whilst still achieving lower rectal doses than the treatment plans produced on the pre-implantation scans with no boost volume. Using p<0.01 as the limit for statistical significance, significant increases were found in rectal dose when boosting without the hydrogel spacer, whereas increases with boosting with the spacer in place were not significant.

The mean dose to the rectum, which is associated with faecal incontinence and high stool frequency following radiotherapy, is also reduced; the reduction is such that similar levels (p = 0.04) are achieved for the pre-implantation with no boost (median 19.6Gy) and the post-implantation with 78Gy boost (median 17.0Gy). No overall change in bladder dose was seen.

Median Rectal DV Statistics

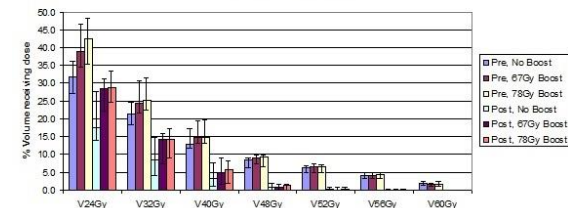


Figure 1: Median values of rectal DV statistics pre and post implantation of hydrogel spacer for different boost dose prescriptions. Error bars represent the IQR.

As seen in Figure 2, the worst-case increase in rectal doses was reduced when using the hydrogel spacer, especially the volume of rectum receiving the higher dose levels which are associated with rectal bleeding. No meaningful change in the robustness of bladder dose was observed.

**Conclusion**

SEMAR dedicated UH-ED curves don’t seem necessary to compute dose with SEMAR<sup>ON</sup> CT.

When beams do not enter through metallic implants, slight dosimetric differences caused by UH modification are negligible. When PTV encompasses metal and beams pass through it, PTV coverage may be strongly modified. Further investigations (Acuros® XB dose calculation, Monte Carlo simulation) need to be done to improve the real irradiation knowledge.

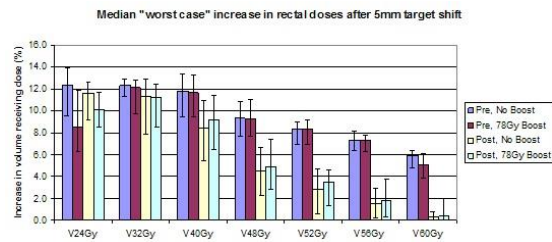


Figure 2: Median "worst case" increases in rectal DV statistics when shifting target by 5mm. Error bars represent the IQR.

#### Conclusion

The implantation of the hydrogel spacer enables the use of intra-prostatic focal boosts whilst maintaining similar or reduced rectal doses to those achieved pre-implantation and also improving the robustness of these doses to PTV shifts.

#### EP-1872 Combining multi-criteria optimisation and a hydrogel spacer for intra-prostatic focal boosts

N. Laverick<sup>1</sup>, S. Currie<sup>1</sup>

<sup>1</sup>Beatson West of Scotland Cancer Centre, Radiotherapy Physics, Glasgow, United Kingdom

#### Purpose or Objective

To assess whether using multi criteria optimisation alone or in combination with a hydrogel spacer (SpaceOAR®, Augmenix Inc. Waltham, MA, USA) can improve plan quality in prostate patients when including an intra-prostatic focal boost.

#### Material and Methods

Multi-criteria optimisation (MCO) is a planning tool which creates multiple treating plans for each planning objective; the aim is to enable the planner to explore the Pareto surface to find the optimum clinical planning solution. Plans created using MCO may be able to achieve lower OAR doses whilst maintaining target coverage. Hydrogel spacers are also of interest in prostate radiotherapy, aiming to lower rectal doses and therefore toxicity by increasing the separation between the prostate and rectum.

Plans were created on patient (n=10) scans pre- and post-implantation of a hydrogel spacer which treated the prostate to 60Gy and seminal vesicles to 47Gy using the Centre's RapidPlan model (Varian Medical Systems, Palo Alto, CA, USA). Boost volumes were identified on both sets of scans with the aid of MRI imaging and further plans created treating these volumes to 78Gy. Finally, MCO was used to further optimise all plans. Plan quality was compared through target coverage and doses to bladder and rectum and paired two-tailed t-tests were used to examine for statistical significance.

#### Results

PTV coverage and bladder doses were similar across all plan types. When MCO was applied to the pre- hydrogel plans, the rectal doses were significantly reduced across all dose levels ( $p < 0.01$ ) for both plans with and without the focal boost. Applying MCO to the focal boost plans reduced doses to the same level as the standard plans without the boost.

When the hydrogel spacer was implanted, MCO was found to only significantly affect the lower dose metrics (V24Gy and V32Gy) and the mean dose. However, this is likely due to the extremely low volumes of rectum receiving the higher dose levels when the spacer is present. Figures 1 and 2 show the median pre- and post-implantation dose statistics. The combination of using the hydrogel spacer and MCO in the focal boost plans resulted in significantly lower rectal doses than were achieved in the standard pre-implantation plan without the boost ( $p < 0.01$ ).

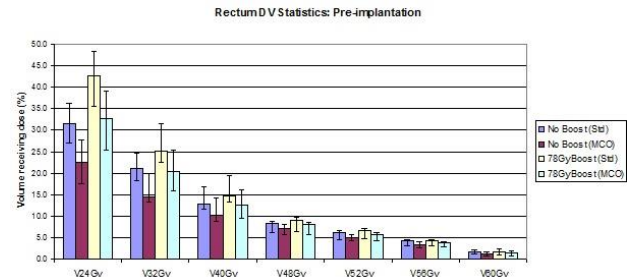


Figure 1: Median Rectal DV statistics pre-implantation of hydrogel spacer. Error bars represent IQR

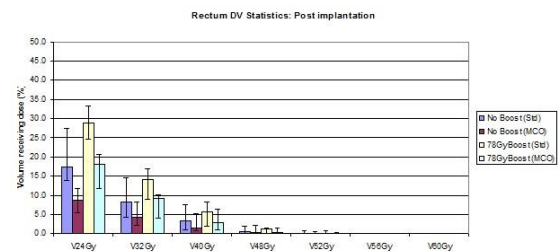


Figure 2: Median rectal DV statistics post-implantation, Error bars represent IQR

#### Conclusion

Using multi-criteria optimisation allows for boosting of an intra-prostatic volume up to 78Gy without significantly increasing rectal doses. Rectal doses are further reduced when MCO and the hydrogel spacer are used in combination.

#### EP-1873 Reducing OAR doses in prostate patients: use of a hydrogel spacer and multi-criteria optimisation

N. Laverick<sup>1</sup>, D. Church<sup>1</sup>, S. Currie<sup>1</sup>

<sup>1</sup>Beatson West of Scotland Cancer Centre, Radiotherapy Physics, Glasgow, United Kingdom

#### Purpose or Objective

To assess the impact of using a hydrogel spacer (SpaceOAR®, Augmenix Inc. Waltham, MA, USA) with and without multi-criteria optimisation on bladder and rectum doses in moderately hypo-fractionated prostate treatments.

#### Material and Methods

Plans were created using Eclipse v15.5 (Varian Medical Systems, Palo Alto, CA, USA) on ten patient scans pre- and post-implantation of the hydrogel spacer treating the prostate to 60Gy in 20 fractions in accordance with the CHHiP trial protocol. All plans were optimised using the Centre's RapidPlan™ model. Finally, the post-implantation plans were further optimised using multi-criteria optimisation. Plans were compared in terms of target coverage and doses to bladder and rectum. Paired two-tailed t-tests were used to examine for statistical significance.

#### Results

PTV coverage was similar between all plan types. The table below shows the mean rectal doses across the ten patients. Statistically significant differences between plan types are highlighted in green.

Test	Rectum						Bladder			
	V25	V32	V41	V49	V53	V57	V60	V41	V49	V60
	<65%  < <80%	<60%  < <65%	<50%  < 60%	<30%  < <50%	<20%  < <30%	<10%  < 15%	<3%  < <2%	<30%  < <50%	<20%  < <25%	<3%  < 5%
Mean Std	47.0	35.6	23.4	14.2	9.7	4.8	0.0	23.9	17.3	0.9
Mean SpaceOAR	48.1	29.5	15.8	7.6	4.3	1.8	0.0	20.2	14.0	0.8
Mean Space+MCO	27.9	18.1	10.5	5.4	3.4	1.8	0.1	17.6	12.4	0.9
Std vs Space	0.864	0.066	0.010	0.003	0.004	0.013	0.223	0.419	0.337	0.352
Std vs Space + MCO	0.000	0.000	0.001	0.001	0.002	0.009	0.378	0.209	0.187	0.869
Space vs Space+MCO	0.000	0.000	0.000	0.002	0.004	0.430	0.306	0.005	0.000	0.788

The hydrogel spacer was effective at reducing rectal doses in the intermediate dose range, with very little volume receiving 60Gy and above for all plan types. Using MCO on the post-implantation plans resulted in even lower rectal doses alongside a significant reduction in bladder doses compared to the spacer alone.

#### Conclusion

The implantation of a hydrogel spacer can significantly reduce rectal doses for patients treated with moderately hypofractionated prostate radiotherapy without compromising PTV coverage. Using multi-criteria optimisation alongside the hydrogel spacer can further reduce these rectal doses and results in lower bladder doses than are achieved using the spacer only.

#### EP-1874 Multiple brain metastasis radiosurgery using dedicated treatment planning system: a dosimetric study

M. Biston<sup>1</sup>, M. Ayadi<sup>1</sup>, P. Dupuis<sup>1</sup>, T. Baudier<sup>2</sup>, C. Malet<sup>1</sup>, M. Sunyach<sup>1</sup>

<sup>1</sup>Léon Bérard Cancer Center, Radiotherapy, Lyon, France ; <sup>2</sup>Lyon university, Creatis, Lyon, France

#### Purpose or Objective

The objective was to compare the performances of conventional versus dedicated linear accelerator for the stereotactic treatment of multiples brain metastases. Cyberknife® plans were compared to those obtained with a treatment planning system (TPS) designed for treating multiple brain metastases on conventional linac and to another one used in routine for volumetric modulated arc therapy planning (VMAT).

#### Material and Methods

Eight previously treated patients with 2 to 8 tumors representing 37 gross target volumes (GTV) were selected. GTV-to-Planning target volume (PTV) margins were 2 mm in all directions. PTV sizes were under 2 cm<sup>3</sup>. The prescribed dose was 20 Gy in single fraction prescribed at the isodose 80% and covering 96-99% of the PTVs. The original treatments planned with Multiplan® (V3.2.0, Accuray) delivered on a Cyberknife® (Accuray) using 2 or 3 fixed-size collimators were replanned in dynamic conformal arctherapy (DCAT) with dedicated automated brain metastases TPS Elements® (v.1.5, Brainlab) and with Monaco TPS (V 5.11.02, Elekta) using VMAT. Plans were delivered using 6-MV photons with an Agility® MLC consisting of 80 paired leaves each measuring 5 mm in width at the isocenter. The dose distributions were compared using Paddick conformity index (CI), mean dose to the PTVs, and volume of healthy brain receiving 10 (V10), 12 (V12) and 5 (V5) Gy. Delivery efficiency was compared throughout the number of monitor units (MUs), delivery time and logfiles analyses.

#### Results

A better CI was found with the Cyberknife (1.26 ±0.06) than with Elements® DCAT (1.29 ±0.12) or Monaco VMAT (1.33 ±0.11). Mean dose to the PTVs were found higher for Cyberknife (22.47 Gy±0.29) and VMAT (22.27 Gy±0.43) plans than for DCAT plans (22.06 Gy±0.55). The healthy

brain was better spared with Elements® DCAT than with the Cyberknife and VMAT. VMAT gave significantly higher doses to the brain than the 2 other techniques (Table 1). Mean estimated delivery time was 78 min, 20 min and 25min for the Cyberknife®, DCAT and VMAT techniques, respectively. Logfile analysis showed that VMAT plans had more MUs than DCAT plans (8477±1651 vs 5037±1090), smaller segments, and more important fluctuations in dose rate and gantry speed.

	Multiplan® Cyberknife	Elements®DCAT	Monaco® VMAT
V5 Gy (±SD)	94 (74.02)	82.75 (67.07)	146.16 (133.6)
V10 Gy (±SD)	22.22 (12.7)	19.43 (11.11)	30.58 (18.04)
V12Gy (±SD)	16.09 (8.90)	13.78 (7.76)	20.73 (11.65)

Table 1: Volume (cm<sup>3</sup>) of healthy brain receiving a critical dose level for each technique

#### Conclusion

Elements® DCAT is a robust automatic planning solution for treating multiple brain metastasis. The planning time is considerably reduced compared to the 2 other techniques, and the system is nearly operator independent. For clinically acceptable plan quality the delivery efficiency is considerably better with linac-based stereotactic radiosurgery than with Cyberknife. Further investigations are in progress to examine whether tumor size/location and number of lesions have an impact on the results.

#### EP-1875 Compare OAR dose of breast cancer using sequential boost and simultaneous integrated boost technique

L. Chou<sup>1</sup>, T. Wang<sup>2</sup>, C. Shiau<sup>1</sup>, P. Huang<sup>1</sup>, Y. Lin<sup>1</sup>, C. Lin<sup>1</sup>  
<sup>1</sup>Taipei Veterans General Hospital, Oncology, Taipei City, Taiwan ; <sup>2</sup>China Medical University Hospital, Radiation Oncology, Taichung, Taiwan

#### Purpose or Objective

Thanks to advances in treatment and diagnosis, the mortality of breast cancer has decreased. Radiotherapy is an indispensable part in adjuvant treatment for patients undergoing breast-conserving surgery. However, inevitable radiation exposure to the heart and lung may cause serious long-term toxicities. Besides whole breast irradiation, tumor bed boost can be delivered in sequential (SEQ) or simultaneously integrated boost (SIB) techniques. This study aimed to compare the dosimetric outcome of two techniques.

#### Material and Methods

Eighty node-negative left breast cancer patients receiving breast-conserving surgery were evaluated, of which 47 patients received 45Gy in 25 fractions to the whole breast and then 10 Gy in 5 fractions to tumor bed, while 33 patients received 55Gy to tumor bed and 45Gy to whole breast in 25 fractions using SIB technique. All treatment plans were based on CT imaging and consisted of two tangential fields with 6MV photon to whole breast and 1-2 beams to tumor bed. If necessary, we used 1-2 additional beams to improve whole breast homogeneity and normal organ sparing. Conformal index, homogeneity index, heart dose, ipsi-lateral lung dose were compared between SEQ and SIB technique. (Table 1)

#### Results

The median age of SEQ and SIB group were 48 (25-71) and 54 (33-74) respectively and the PTV<sub>boost</sub> volume were similar (110.7±84.6 c.c. for SEQ and 108.7±66.4 c.c. for SIB). Both SEQ and SIB plans demonstrated similar homogeneity (p>0.05) but significant difference of conformity (p<0.01). In addition, SEQ plans provided significantly less lung radiation exposure (V5, V10 and mean left lung dose) than SIB plans (p<0.05). Heart dose were similar in two groups crossing V5, V10, V30, and mean heart dose (all p>0.05).

Table 1. Dosimetric parameters of Heart and Lung

		SEQ	SIB	difference	P value
PTV <sub>boost</sub>	Volume	110.7±84.6	108.7±66.4	2	0.91
	CI	2.19±0.56	1.35±0.29	0.84	<0.01
	HI	1.09±0.01	1.09±0.02	0	0.73
Heart	V <sub>10</sub> (%)	10.7±12.0	8.6±7.9	2.1	0.34
	V <sub>20</sub> (%)	5.8±5.6	4.2±3.4	1.6	0.12
	V <sub>30</sub> (%)	3.1±3.8	1.8±2.1	1.3	0.06
	mean(Gy)	1.6±1	1.3±0.8	29	0.15
Heart	V <sub>10</sub> (cc)	120.8±466.4	37.1±40.3	83.7	0.34
	V <sub>15</sub> (cc)	71.8±293.6	17.7±15.8	54.1	0.12
	V <sub>20</sub> (cc)	41.7±178	7.8±9.7	33.9	0.06
Ipsi-lateral lung	V <sub>10</sub> (%)	27.1±9.2	34.1±7.8	-7	0.0005
	V <sub>20</sub> (%)	16.3±5.5	19.4±4.5	-3.1	0.007
	V <sub>30</sub> (%)	12.1±4.8	13±3.5	-0.9	0.33
	V <sub>40</sub> (%)	10.2±4.3	10.7±3.2	-0.5	0.52
	V <sub>50</sub> (%)	7.4±3.6	7.1±2.7	0.3	0.62
	mean(Gy)	2.2±1	2.8±1.1	62.4	0.01

### Conclusion

Although SIB technique is more convenient due to the shorter treatment time and well tolerated in previous study, we found that lung dose was higher than in SEQ technique. More efforts should be made when using this technique.

### EP-1876 Level II volume and parotid doses during nasopharyngeal radiotherapy: what relationship?

Z. Fessi<sup>1</sup>, N. Fourati<sup>1</sup>, W. Mnejja<sup>1</sup>, L. Farhat<sup>1</sup>, T. Sahnoun<sup>1</sup>, W. Siala<sup>1</sup>, J. Daoud<sup>1</sup>  
<sup>1</sup>Hopital Habib Bourguiba, Radiation Oncology, Sfax, Tunisia

### Purpose or Objective

High dose to parotid gland may increase the risk of xerostomia during radiotherapy for nasopharyngeal carcinoma (NPC). This dose is essentially correlated to the proximity of the target volume, mainly linked to the level II lymph node invasion. The aim of this study was to evaluate the relationship between parotid doses and level II lymph node volume.

### Material and Methods

Retrospective study of 45 patients with NPC treated by intensity modulated radiotherapy (IMRT) in our institution during 2 years (2016-2018). The 2 parotid glands were delineated as a single structure and we noted the mean doses (Dmean) received at their level. We then retrospectively delineated Level II lymph node separately to determine its volume. The results were analyzed by SPSS v20. Pearson Test was used to determine the correlation between Dmean and Level II lymph node volume. We then determine the function that links the 2 variables according to a linear model: Dmean = a + b Level II lymph node volume.

### Results

Median Dmean dose was 35.54 Gy (23.36-53.34). Median Level II lymph node volume was 9.8 cc (0-93 cc). The correlation between the two variables showed a proportional relationship with a Pearson r coefficient of 5.23 (p <0.001). According to the linear model, the relationship between Dmean and level II lymph node volume was as follows: Dmean = 33.56 + 0.15 Level II lymph node volume.

### Conclusion

Level II lymph node involvement is common in NPC and is found in more than 80% of cases. The results of our study found that parotid mean doses, which represent a significant risk organ during IMRT planning, are correlated with level II lymph node volume. It is therefore difficult to respect parotid doses in the presence of a level II invasion. In this situation, the choice would be between excluding the part of the target volume extending at the parotid and taking into account only the superficial lobe of the parotid.

### EP-1877 Proton vs photon deep inspiration breath-hold planning study for left-sided breast cancer patients

K. Czernska<sup>1</sup>, P. Winczura<sup>2</sup>, J. Wejs-Maternik<sup>2</sup>, A. Blukis<sup>2</sup>, M. Antonowicz-Szydlowska<sup>2</sup>, A. Rucinski<sup>3</sup>, P. Olko<sup>3</sup>, R. Kopec<sup>1</sup>, A. Badzio<sup>2</sup>

<sup>1</sup>Institute of Nuclear Physics PAN, Cyclotron Center Bronowice, Krakow, Poland ; <sup>2</sup>Radiotherapy Center Elblag, Radiotherapy, Elblag, Poland ; <sup>3</sup>Institute of Nuclear Physics PAN, Proton Radiotherapy Group, Krakow, Poland

### Purpose or Objective

Deep inspiration breath-hold (DIBH) is an effective approach to reduce the dose to the heart and coronary vessels in left-sided breast radiotherapy. The aim of this study was to compare doses to organs at risk between 3D photon DIBH technique and an Intensity Modulated Proton Therapy (IMPT) planning using a deep inspiration and free breathing (FB).

### Material and Methods

Six patients with early left-sided breast cancer were planned on a computed tomography datasets acquired for FB and DIBH, with a 3D photon (6 MeV tangential fields with additional lower weight fields to ensure homogeneity of the plan) and IMPT proton technique (with the application of 3 anterior-oblique fields). All cases were planned to the whole breast only. Prescribed dose was 50 Gy for photons and 50 Gy(RBE) for protons in 25 fractions. Main goal was to achieve acceptable target coverage with dose reduction to the organs at risk, which could reflect to the clinical satisfactory plans. Dosimetric comparison was made by using a paired, two-tailed Student's t-test and Wilcoxon signed rank test.

### Results

With regard to doses to the heart and coronary vessels, there was no difference between DIBH and FB for proton plans. However proton FB technique, as compared to the photon DIBH, ensured significant dose reduction to the organs at risk. Mean heart dose was lower in proton plans comparing to photons (0,5 Gy(RBE) vs 1,6 Gy; p=0,0096). Also the mean dose to the ipsilateral lung was reduced from 9,0 Gy to 5,4 Gy(RBE); (p=0,0006) for photons and protons, respectively. Several parameters were taken into account to depict the benefit for the Left Anterior Descending Artery (LAD): mean, maximum dose, D<sub>max</sub>0,2cm<sup>3</sup> and V45Gy. We found profound decrease of the D<sub>max</sub>0,2cm<sup>3</sup> by a factor of 3 for proton plans comparing to photons (8,2 Gy(RBE) vs 22,0 Gy; p=0,0687). The volume of LAD receiving dose of 45 Gy was very low for both techniques. Detailed dosimetric comparison between both techniques is presented in table 1.

		PHOTONS (A)	PROTONS (B)	p-Value
		Breath-hold	Free breathing	
heart	Dmean	1,6 ± 0,6 Gy	0,5 ± 0,2 Gy(RBE)	0,0096
	Dmax	9,0 ± 1,3 Gy	5,4 ± 0,8 Gy(RBE)	0,0006
left lung	V20Gy	17,2 ± 4,5%	9,5 ± 1,5%	0,0114
	Dmean	9,9 ± 6,8 Gy	4,1 ± 2,3 Gy(RBE)	0,0509
LAD	Dmax	29,2 ± 18,3 Gy	23,5 ± 11,8 Gy(RBE)	0,3470
	V45Gy	0,1 ± 0,2 cm <sup>3</sup>	0,0 ± 0,0 cm <sup>3</sup>	0,3008
	Dmax 0,2 cm <sup>3</sup>	22,0 ± 19,3 Gy	8,2 ± 6,1 Gy(RBE)	0,0687

### Conclusion

Breath-hold approach for photon planning already ensures a significant dose reduction to the heart and coronary vessels. This study shows that the application of proton FB technique leads to better dose reduction to the organs at risk. No further benefit was achieved with proton DIBH technique. Proton FB radiotherapy could be a promising solution for patients with more demanding anatomies, these with serious cardiac comorbidities or patients unable to perform deep inspiration breath-hold.

**EP-1878 PRV brainstem during the nasopharyngeal IMRT: margin calculation and dosimetric implications**  
 N. Fourati<sup>1</sup>, L. Farhat<sup>1</sup>, W. Mnejja<sup>1</sup>, Z. Fessi<sup>1</sup>, T. Sahnoun<sup>1</sup>, W. Siala<sup>1</sup>, J. Daoud<sup>1</sup>  
<sup>1</sup>Hopital Habib Bourguiba, Radiation Oncology, Sfax, Tunisia

#### Purpose or Objective

According to the ICRU 83 recommendations, a margin around the organ at risk is necessary to define the planning organ at risk volume (PRV). However, for brain stem this margin is not well defined in the literature and remains non-consensual. The aim of this study was to evaluate the margin around the brainstem in relation to setup errors in intensity modulated radiotherapy (IMRT) of nasopharyngeal carcinomas (NPC) and determine the dosimetric implication of this additional margin.

#### Material and Methods

Data from 33 patients with NPC treated by IMRT in our institution was analyzed. A five points mask was used for patient's immobilization. For the definition of the optimization objectives an artificial structure was created by adding 5 mm margin around the brain stem whereas for the dosimetric validation the doses were noted at the level of the brainstem. From the portal imagery (PI) database, we retrospectively calculated the margin for set up errors required for the brain stem PRV using the McKenzie formula. We then noted the volumes, maximum doses (Dmax) and the dose received by 2% (D2%) of the brain stem and the PRV brain stem.

#### Results

A total of 1250 PIs were analyzed. The mean antero-posterior, right-left and super-inferior movements were +0.39 mm (-5mm to 8 mm), +0.24 mm (-5 to 18 mm) and +0.15 mm (-7 to 7 mm), respectively. Calculated PRV margin was 2mm. The median volume was 27.5 mm (18.7-37.3) for the brainstem and 40.9 mm(29.7-56.8) for the PRV brainstem with a median increase of 5.68% (13.46-62.44). The median Dmax was 54.45 Gy (48.42-60.78) for brain stem and 58.7 Gy (53.49-65) for PRV brain stem with a median variation of 3.23 Gy (0-9.15) between brain stem and PRV brain stem. The median D2% was 51.84 Gy (43.91-58.66) for brain stem and 53.07 Gy (45.46-59.23) for PRV brain stem.

#### Conclusion

The brainstem is a critical organ that deserves special attention when planning NPC radiotherapy especially in cases of massive posterior invasion. The creation of a PRV brainstem to account setup errors is necessary. The dose analysis must be done on the PRV especially as the doses respected at the level of the brainstem can be exceeded on the PRV. But, given the increase in volume during the creation of the PRV, we can evaluate the D2% of the PRV before deciding whether or not to validate the treatment plan.

**EP-1879 HyperArc for stereotactic radiosurgery: comparison of planning options**

D. Kearns<sup>1</sup>

<sup>1</sup>Beatson West of Scotland Cancer Care, Treatment Planning, Glasgow, United Kingdom

#### Purpose or Objective

To evaluate treatment plan quality metrics produced for four different plans for stereotactic radiosurgery treatments using HyperArc and investigate the optimal choice. The methods investigated were two different energy modes 6FFF and 10FFF and different multi-leaf collimators systems, standard 120 leaves and high definition (HD-MLC) 120 leaves.

#### Material and Methods

Ten multiple metastatic cranial patients previously treated with HyperArc utilizing 10FFF and HD-MLC were retrospectively planned using the Eclipse Treatment

Planning System v15.5 [Varian Medical Systems, Palo Alto, CA, USA]. The following planning options were investigated: 6FFF, 10FFF with both MLC standard and high definition MLCs.

The cohort of patients included a range of patients with two to ten lesions. Total PTV volumes varied from 2.9cc to 21.0cc. All plans included four non-coplanar arcs with a single isocentre placed at the centre of mass of the total target volume whilst respecting the delivery capabilities of the treatment linear accelerator. All plans were optimised using standard objectives to meet clinical constraints based on SRS guidelines. All plans were normalized such that 80% of the highest prescription target volume (primary target volume) received the prescribed dose.

Plan quality was evaluated by; volume of the brain receiving 20%, 40% and 60% of the maximum PTV prescription for that patient; and median brain dose.

#### Results

Primary target volume coverage was achieved by normalisation in each case. All plans met local constraints and were suitable for treatment.

The dose to brain was reduced in all plans using 6FFF together with HD MLC for all metrics. When compared with 10FFF HD-MLC selection, this was significant statistically at both the 20% and 40% values (p<0.05). There was no significant statistical variation in brain optimized when comparing the 10FFF HD-MLC plan and 6FFF standard MLC plan, however the median dose was reduced with the 10FFF plan.

The least conformal plan was the 10FFF plan with the standard MLC. This showed a significant statistical increase in brain center when compared with the 6FFF HD-MLC plan. The median dose was also higher than the other plan situations, however this was not found to be significant. The number of PTVs did not influence optimal plan selection and plan quality metrics.

#### Conclusion

The use of 6FFF and a HD-MLC provided the optimal solution to provide the sharpest dose gradient and to minimise brain dose but all plan types provided clinically acceptable plans. The disadvantage of 6FFF in relation to 10FFF is the treatment delivery time with dose rates being reduced from 24Gy to 14Gy per minute that may impact the selected PTV margins. This is equivalent to an increase in treatment delivery time of 41%. The reduction in dose rate would however allow increased MLC modulation. Current practice is being reviewed to produce two HD MLC plans at both energies to help determine plan selection.

**EP-1880 A planning study evaluating the use of 4DCT vs 3DCT in pancreas planning, both conventional and SABR**

E. Tait<sup>1</sup>, O. Byrne<sup>1</sup>, D. O'Doherty<sup>1</sup>, B. Evans<sup>1</sup>, T.

Ajithkumar<sup>2</sup>, G. Begum<sup>2</sup>, A. Ho<sup>2</sup>

<sup>1</sup>Addenbrookes Hospital, Medical Physics, Cambridge, United Kingdom ; <sup>2</sup>Addenbrookes Hospital, Radiation Oncology, Cambridge, United Kingdom

#### Purpose or Objective

Acquiring a 4DCT scan in pancreas planning allows the use of an ITV to PTV margin which is smaller than the GTV to PTV margin used in conventional 3D planning, generally leading to a smaller PTV. We aim to evaluate the dosimetric difference between plans created where the PTV was created using 4DCT or 3DCT only and to review the impact of this on SABR planning.

#### Material and Methods

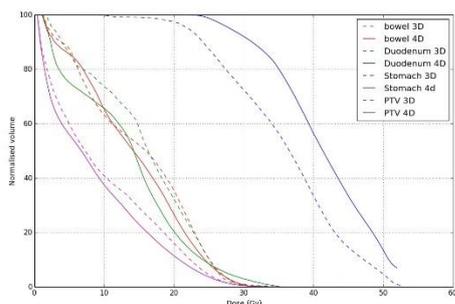
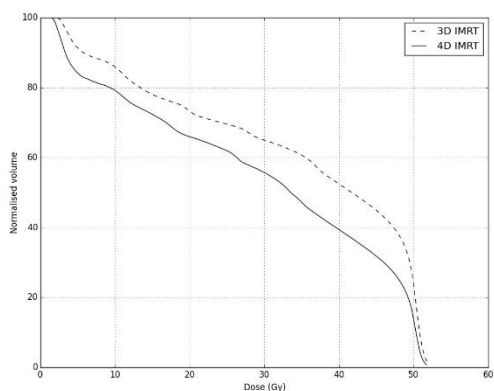
Patients who had previously been treated for pancreatic cancer planned using 4DCT were retrospectively outlined using 3D scans only and the volume of the new PTVs was assessed. 6MV conformal IMRT plans were then re-created in Pinnacle; plans were created using the same beam

parameters and conventional fractionation (50.4Gy in 28 fractions) as originally used but optimised to the new PTV. In order to investigate the dosimetric difference between 4DCT and 3DCT for pancreas SABR planning patients were outlined according to the SPARC protocol. The PTV was prescribed 35Gy in 5 fractions and the area at risk (PTV\_M) was prescribed a dose of 45-50Gy in 5 fractions and the OAR constraints from the SPARC trial were used. PTV coverage was compromised to meet mandatory OAR constraints in both the 3D and 4D plans.

### Results

The average PTV volume dropped by 33% and we saw reductions to the mean dose of all OARs in the conventional fractionation. There was no correlation observed between the magnitude of the tumour motion and the reduction in OAR dose. The drop in dose to OAR is highly dependent on tumour position. The most significant OAR improvement was seen in the duodenum with an average mean dose difference of 5.3Gy (range 2.4-6.9Gy), other OAR mean dose reductions are as follows: spine 2.6Gy, bowel 2.9Gy, stomach 4.3Gy, liver 2.2Gy and kidneys 1.4Gy. Figure 1 shows the mean duodenum DVH for conventional 3D and 4D plans.

The dose constraints for the SABR plans were challenging for both 3D and 4D as the majority of patients had OARs overlapping the PTV which had to be carved out. As expected PTV coverage was improved in the 4D plan as there was less overlap with the OARs and OAR doses were generally lower. The mean V95% dropped from 85.5% using the 4D plan to 62.4% using the 3D plan when all mandatory OAR constraints were met. Figure 2 shows the mean DVH for the dose limiting OARs and the PTV receiving 35Gy for SABR 3D and 4D plans. PTV\_M coverage was very similar for both plan types. This level of PTV coverage could lead clinicians to dose deescalate, the SPARC protocol also allows 30Gy in 6 fractions and 6.5Gy in 6 fractions.



### Conclusion

The use of a 4DCT in pancreas planning results in lower dose to the OARs, improved PTV coverage in the case of SABR planning and the potential for dose escalation.

### EP-1881 Sequentially- versus co-optimized plans for pelvis and prostate bed: time efficacy and plan quality

A. Gulyban<sup>1</sup>, E. Marques<sup>1</sup>, O. Michel<sup>1</sup>, A. Rijnders<sup>1</sup>, C. Salembier<sup>1</sup>

<sup>1</sup>Europe Hospitals - Site St Elisabeth, Radiation department, Brussels, Belgium

### Purpose or Objective

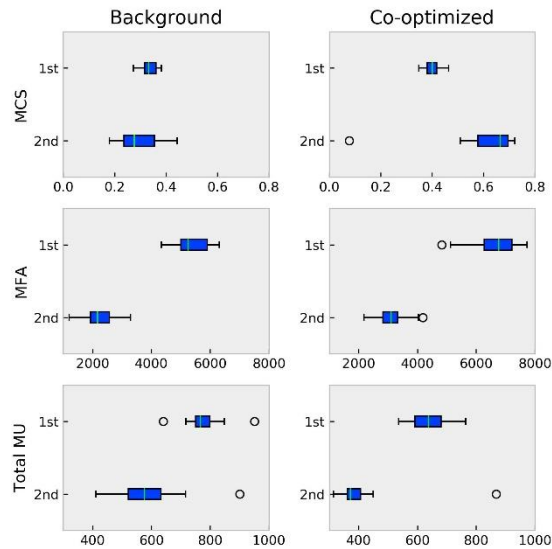
To evaluate the performance of sequentially- and co-optimized treatment planning approaches for pelvic lymph node and prostate bed irradiation in terms of required time, plan quality and modulation complexity.

### Material and Methods

Twenty consecutive patients were included in this investigation. For all patients the prescription dose consisted of 50 Gy in 25 fractions for the pelvic lymph node region planning target volume (*1<sup>st</sup> phase, PTV\_LD*), followed by 16 Gy in 8 fractions for the prostate bed (*2<sup>nd</sup> phase, PTV\_HD*). Rectum, bladder and small bowel were delineated as organs at risk (OARs), and used for optimization (by excluding the area overlapping with PTV\_LD+2mm). Sequential and combined planning were performed. The sequential approach (background dose based "BG") consisted in a standalone *1<sup>st</sup> phase* planning, followed by a linked *2<sup>nd</sup> phase* and total plan optimization, while the combined one (co-optimized "CO") used separate and pooled planning objectives simultaneously for the *1<sup>st</sup>, 2<sup>nd</sup>* and *combined* phases. For all treatment planning Raystation (version 6.1.1.2, Stockholm, Sweden) was used by the same planner with identical initial optimization parameters. Seven field (45 segments) Direct Machine Parameter Optimization (DMPO) class solutions were used for the *1<sup>st</sup> phase*, while single full rotation modulated ARC (37 segments, sector size of 10° and 4° arclets/sector) for the *2<sup>nd</sup> phase*, with five field (40 segments) DMPO as backup in case initial arc sequencing failed. Time required to achieve a clinically acceptable plan was measured, followed by a qualitative comparison of relevant dose parameters and assessment of plan Modulation Complexity Score (MCS). Results were compared using paired t-test with p<0.05 significance level

### Results

Eighty plans were analyzed. The average (range) time (min:sec) required for BG based planning was 7:29 (4:20-10:02), 5:27 (3:50-07:36) and 12:56 (8:19-16:17) for *1<sup>st</sup> phase*, *2<sup>nd</sup> phase* and total planning respectively. For CO on average 4:24 (-2:42-23:29) more time was required, leading to an average planning time of 17:20 (10:46-39:46)(p=0.01). For *2<sup>nd</sup> phase* all BG plans consisted of a mARC, while for CO only one plan succeed with proper arc sequencing. On average (±standard deviation) 26.9±9.5%, 40.5±15.8% and 3.3±1.6% of the rectum, bladder and small bowel were overlapped with the PTV\_LD+2mm respectively. Statistically significant (p<0.01) differences were observed in MCS (Figure): 0.32 (0.18-0.44) vs. 0.51 (0.08-0.72) between BG and CO respectively without significant differences neither in PTV coverage nor in integral dose (Body V5/20Gy). Furthermore majority of OAR parameters were significantly better using the BG approach (Table).



ROI	Dose parameter	Plan Phase	Background planning Mean (SD)	Co-optimized planning Mean (SD)	p-value
Rectum	V50Gy(%)	Total	25.9 (7.9)	33.2 (9.2)	<0.001
	V60Gy(%)	Total	15.8 (5.8)	19.8 (7.5)	<0.001
	V64Gy(%)	Total	10.9 (4.3)	14.0 (6.1)	<0.001
	Dmean (Gy)	Total	35.7 (3.5)	40.9 (4.1)	<0.001
Bladder	V20Gy(%)	Total	77.6 (10.5)	85.2 (10.7)	<0.001
	V35Gy(%)	Total	54.2 (15.1)	59.0 (15.2)	<0.001
	V50Gy(%)	Total	37.2 (14.5)	40.0 (14.3)	<0.001
	V60Gy(%)	Total	27.1 (12.7)	28.8 (12.6)	<0.001
	Dmean (Gy)	Total	40.0 (6.7)	42.5 (6.4)	<0.001
Small bowel	V20Gy(%)	Total	60.2 (13.8)	65.5 (16.8)	0.028
	V35Gy(%)	Total	19.2 (7.0)	24.3 (10.7)	<0.001
	V50Gy(%)	Total	0.7 (0.6)	0.9 (0.7)	0.036
	Dmean (Gy)	Total	23.6 (3.4)	25.3 (4.7)	0.006
Body	V5Gy (cc)	1st Phase	1500 (289)	1696 (330)	0.059
	V5Gy (cc)	2nd Phase	10781 (1838)	10956 (1799)	0.765
	V5Gy (cc)	Total	11494 (1960)	11300 (1800)	0.101
	V20Gy (cc)	Total	5364 (914)	5492 (780)	0.240
PTV_LD	D98%(Gy)	1st Phase	46.9 (0.3)	46.8 (0.5)	0.782
	D2%(Gy)	1st Phase	52.0 (0.1)	52.1 (0.2)	0.116
	V47.5Gy(%)	1st Phase	96.3 (0.8)	96.2 (1.2)	0.741
	V53.5Gy(%)	1st Phase	0.0 (0.1)	0.0 (0.1)	0.381
PTV_HD	D98%(Gy)	2nd Phase	15.2 (0.3)	15.1 (0.2)	0.301
	D2%(Gy)	2nd Phase	16.4 (0.2)	16.6 (0.2)	0.002
	V15.2Gy(%)	2nd Phase	96.2 (5.1)	97.0 (2.1)	0.562
	V17.12Gy(%)	2nd Phase	0.0 (0.1)	0.1 (0.3)	0.449
	D98%(Gy)	Total	64.1 (0.4)	64.7 (0.3)	<0.001
	D2%(Gy)	Total	68.0 (0.3)	67.7 (0.4)	0.003
	V62.7Gy(%)	Total	99.7 (0.4)	100.0 (0.1)	0.004
V70.62Gy(%)	Total	0.0 (0.0)	0.0 (0.0)	0.330	

**Conclusion**

Sequential plan optimization should be preferred for pelvic lymph node irradiation of 50 Gy followed by 16 Gy boost for the prostate bed, as it resulted in significantly better plan quality in shorter time compared to combined optimization. Modulation Complexity Scores were higher with sequential plans.

**EP-1882 Dosimetric comparison between proton SFUD, IMPT and SBRT Boost in clivus chordoma radiotherapy**

M. Vidal<sup>1</sup>, A. Gerard<sup>1</sup>, C. Barnel<sup>1</sup>, C. Peucelle<sup>1</sup>, D. Maneval<sup>1</sup>, A. Claren<sup>1</sup>, F. Guedea Edo<sup>2</sup>, J. Doyen<sup>1</sup>  
<sup>1</sup>Centre Antoine Lacassagne, Institut Méditerranéen de Protonthérapie, Nice, France ; <sup>2</sup>Institut Català d'Oncologia, Servicio de Oncología Radioterápica, Barcelona, Spain

**Purpose or Objective**

Clivus chordoma is a recognized indicator for protontherapy treatment [1]. Dose escalation is very challenging in this localization due to chiasma, optic nerves and brainstem proximity and their low dose tolerance. The idea of this work is to dosimetrically test different treatment techniques available at Centre Antoine Lacassagne (Nice, France) to reach the therapeutic dose (72-74 Gy RBE), including proton therapy

single-field uniform dose (SFUD) and intensity modulated protontherapy (IMPT) both for sequential and integrated proton boost (SIB) and stereotactic body radiotherapy (SBRT) (Cyberknife®) for sequential boost. The hypothesis was that SBRT could achieve better coverage and conformity than IMPT for the boost.

**Material and Methods**

10 patients with a clivus chordoma were included in this study. Protontherapy SFUD and IMPT plans were computed with RayStation 6.0 (RaySearch Laboratories, Sweden) and realized with a CTV-based robust optimization with parameters as follow: 3% of the range for range uncertainties and 3 mm for metric uncertainties (patient positioning, contouring, robot couch accuracy...). SBRT treatments were planned with Multiplan (Cyberknife®, Accuray, USA). Plans were calculated for sequential boost with proton SFUD, IMPT and SBRT with 50.4 Gy RBE (1.8Gy RBE/fraction) delivered to the low dose CTV and 23.4 Gy RBE (1.8Gy RBE /fraction) for PT plans or 22 Gy RBE (2Gy RBE /fraction) for SBRT plans to reach 73.8 Gy RBE for PT plans and 72.4 Gy RBE in SBRT. SIB plans were computed to deliver 73.5 Gy RBE (2.1 Gy RBE /fraction) to this volume, the low dose CTV receiving 56 Gy RBE (1.6 Gy RBE /fraction). SBRT was not used for the planning of the low dose CTV because of its large size.

**Results**

The dose constraints to the OAR were evaluated following the ICRU91 recommendations for SBRT plans and ICRU78 recommendations for PT plans. All plans were performed to be clinically deliverable and to respect the OAR constraints - the difference between the plans is about the tumor coverage, conformity and homogeneity. In general, plans comparison showed that IMPT SIB achieved better tumor coverage for the boost than SFUD SIB (50.8% vs 70.9% for the example patient shown in Fig.1 and Fig.2); this was also better than sequential SFUD (60.4% vs 70.9%); the best tumor coverage was however reached with SFUD + SBRT technique (80.2% tumor coverage for the example patient). This tendency was observed for 7 patients over 10. For the other patients the SIB strategy was adopted due to the CTV geometries (large high dose target volume).

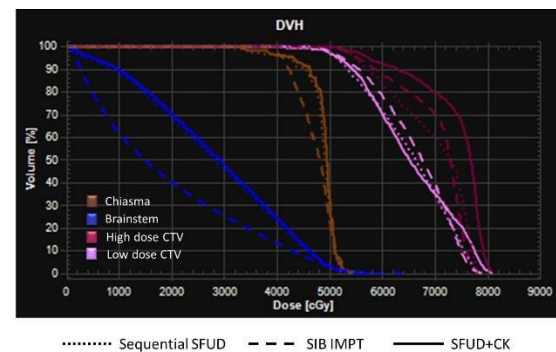


Figure 1. Dose Volume Histogram for sequential SFUD, IMPT SIB and SFUD combined with SBRT plans computed for 2 critical OAR (brainstem, chiasma) and the 2 target volumes for one patient of the cohort.



Figure 2. Dose distribution for IMPT SIB (left), sequential SFUD (center) and SFUD combined with SBRT (right) plans computed for one patient of the cohort.

**Conclusion**

7 over 10 patients were treated with the SBRT technique to reach the therapeutic dose of 73.8 Gy RBE in addition to the SFUD irradiation for the low dose volume, due to

the better coverage of the high dose CTV, while respecting the constraints of the critical OAR (brainstem, chiasma, optic nerves).

**References:** [1] Amichetti M., et al. *Neurosurg Rev.* 2009;32:403-16.

#### EP-1883 Lung tumor target delineation: different segmentation strategies

C. Gasperi<sup>1</sup>, S. Borghesi<sup>2</sup>, L. Noferini<sup>1</sup>, C. Sottocornola<sup>1</sup>, A.S. Curion<sup>1</sup>, F. Zenone<sup>1</sup>, P. Pernici<sup>2</sup>, R. De Majo<sup>2</sup>, S. Nucciarelli<sup>2</sup>, S. Nanni<sup>2</sup>, S. Bertocci<sup>2</sup>, P.G. Gennari<sup>2</sup>, A. Rampini<sup>2</sup>, L. Lastrucci<sup>2</sup>, C. Iermano<sup>2</sup>, E. Tucci<sup>2</sup>  
<sup>1</sup>San Donato Hospital, Health Department Staff - Medical Physics, Arezzo, Italy ; <sup>2</sup>San Donato Hospital, Radiotherapy Department, Arezzo, Italy

#### Purpose or Objective

Precise definition of the target volume is one of the crucial factors in the management of Non-Small Cell Lung Cancer (NSCLC) with Stereotactic body radiotherapy (SBRT). It is widely recognized that the motion pattern of lung tumors varies greatly among patients. Therefore tumor motion should be assessed with patient specific image acquisition, to ensure adequate tumor coverage and minimizing dose to the Organs at Risk. The "gold standard" approach for defining an Internal Target Volume (ITV) is to use gross tumor volume (GTV) delineated over several phases in course of one respiratory cycle. It is a time consuming method and different Institutions have adopted several alternative techniques which compress all temporal information into one CT image set, to optimize work flow efficiency. The purpose of this study is to evaluate alternative target segmentation strategies with respect to the gold standard.

#### Material and Methods

Twenty lung cancer SBRT patients, treated on a linac with 4 mm width multileaf-collimator (MLC), were analyzed retrospectively. From the acquisition of a low-pitch helical CT scan (Untag CT) combined with a respiratory monitor system signal, four-dimensional CT (4D-CT) scans were reconstructed for each patient. GTV was delineated based on 4 single respiratory phases and on Maximum Intensity Projection (MaxIP), Minimum Intensity Projection (MinIP), Mean Intensity Projection (MeanIP) CTs and Untag CTs. Comparison was performed on Dice similarity coefficient (DSC). The relative position between the delineated target was evaluated calculating the centroid distance between volumes.

#### Results

GTVs derived from different MaxIP and MeanIP image sets were at least comparable with the single phase ITV delineation, with DSC values varying from 0.551 to 0.936 for Untag, from 0.331 to 0.877 for MaxIP, from 0.354 to 0.877 for MeanIP. MinIP GTV delineation was less comparable to the 4D-CT ITV with DSC range between 0.07 and 0.8. The differences in relative position of target volume localization were small and in all cases < 3mm. The mean differences  $\pm$  SD of the centroid distances for ITV and GTV\_Untag, GTV\_maxIP, GTV\_meanIP, GTV\_minIP were 0.18 $\pm$ 0.16 cm, 0.18 $\pm$ 0.16 cm, 0.23 $\pm$ 0.19 cm, 0.26 $\pm$ 0.19cm respectively.

#### Conclusion

Our results indicate that the delineated targets were comparable for Untag, MaxIP and MeanIP CT with respect to the standard ITV from 4DCT single phase method. The use of the MinIP leads to an underestimation of the contoured volume. The spatial accuracy of the tumor volume is limited to a range within 3 mm (mean distance of the volume centroids) and this leads to a good spatial agreement between PTVs, if generated by expanding an uniformly isotropic 5 mm margin from ITV and GTVs. Among various techniques used for image segmentation, Untag, MaxIP and MeanIP GTVs could be considered as a geometrical surrogate of the standard ITV.

#### EP-1884 Commissioning and clinical validation of FRED: Monte Carlo on GPU for proton beam therapy

M. Garbacz<sup>1</sup>, J. Baran<sup>1</sup>, G. Battistoni<sup>2</sup>, M. Durante<sup>3</sup>, J. Gajewski<sup>1</sup>, N. Kraha<sup>4</sup>, K. Krzempek<sup>1</sup>, V. Patera<sup>5</sup>, M. Pawlik-Niedzwiecka<sup>1</sup>, I. Rinaldi<sup>6</sup>, B. Sas-Korczynska<sup>7</sup>, E. Scifoni<sup>3</sup>, A. Skrzypek<sup>8</sup>, A. Schiavi<sup>3</sup>, F. Tommasino<sup>9</sup>, A. Rucinski<sup>1</sup>  
<sup>1</sup>Institute of Nuclear Physics PAN, Proton Radiotherapy Group, Krakow, Poland ; <sup>2</sup>INFN, Sezione di Milano, Milan, Italy ; <sup>3</sup>TIFPA, Trento Institute for Fundamental Physics and Applications, Trento, Italy ; <sup>4</sup>CNRS/CREATIS, Umr 5220, Lyon, France ; <sup>5</sup>Sapienza Università di Roma, Dipartimento di Scienze di Base e Applicate per Ingegneria, Rome, Italy ; <sup>6</sup>ZonPCT/Maastro Clinic, ZonPCT/Maastro Clinic, Maastricht, The Netherlands ; <sup>7</sup>Maria Skłodowska-Curie Institute - Oncology Center, Oncology Clinic, Krakow, Poland ; <sup>8</sup>AGH University of Science and Technology, Faculty of Physics and Applied Computer Science, Krakow, Poland ; <sup>9</sup>University of Trento, Department of Physics, Trento, Italy

#### Purpose or Objective

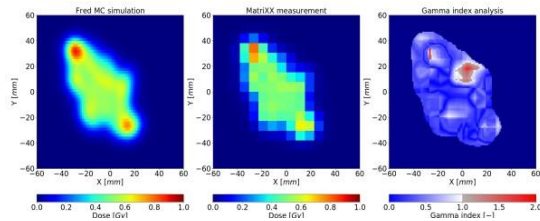
This work presents commissioning and validation of GPU-accelerated Monte Carlo (MC) code FRED at proton beam therapy (PBT) facility in Krakow. The aim of this study was to develop fast proton beam model phase space implementation method exploiting experimental data acquired during the facility start-up. We validate FRED simulations against patient quality assurance (QA) measurements following clinical acceptance procedures. Ultimately we utilize time performance of FRED for recalculation of clinical treatment plans with variable radiobiological effectiveness.

#### Material and Methods

A GPU-accelerated MC tool FRED (Fast pArTicle thErapy Dose evaluator; Schiavi et al. 2017) was developed at Sapienza University of Rome and is investigated at Krakow PBT centre. FRED was already validated against FLUKA and GEANT4, as well as clinical data from CNAO facility. The depth-dose distributions (DDD) of single pencil beams measured in water phantom and lateral beam profiles in air for 17 energies in 70-226.1 MeV range were used to build a FRED dedicated phase space library. The validation procedures included QA measurements of spread out Bragg peak (SOBP) of different range in water and comparison of more than 182 measurements of Krakow patient treatment fields. The gamma index (GI) analysis were used to evaluate the dosimetric results of MC calculations.

#### Results

The DDDs of a single proton pencil beam in water for various energies simulated in FRED MC code were in agreement with the commissioning measurements: the range (R80%) of the pencil beams agreed within 0.1 mm, the absolute dose difference along the pencil beam profile was below 5%, the FWHM of the Bragg peak agreed within 0.3 mm, the distal fall-off width between 80% and 20% Bragg peak dose agreed within 0.07 mm. The simulations of verification plans in water were performed and evaluated against measured data using GI method with 3%/2mm passing criteria (see example field in Figure). The dose distributions from FRED fulfill the Krakow facility QA acceptance criteria (passing rate > 90% for dose > 10% of maximum dose) with average passing rate 96.28(3.3)% (1 sigma). For a patient verification treatment plan the average tracking rate was 8.5(1.6)x10<sup>6</sup> protons / sec (1 sigma).



### Conclusion

FRED was commissioned and validated against the experimental data acquired during the start-up of PBT centre in Krakow. A fast procedure for phase space library implementation was developed. FRED passed clinical acceptance tests required to admit certified TPS for clinical use. Once commissioned and tested with patient CT data, FRED can be used for fast recalculation of clinical treatment plans.

### EP-1885 Neutron beam design and dosimetric evaluation for accelerator-based Boron Neutron Capture Therapy

S. Bortolussi<sup>1</sup>, I. Postuma<sup>2</sup>, N. Protti<sup>2</sup>, S. Fatemi<sup>2</sup>, C. Magni<sup>1</sup>, S. Gonzalez<sup>3</sup>, S. Altieri<sup>1</sup>

<sup>1</sup>University of Pavia and INFN, Department of Physics, PAVIA, Italy ; <sup>2</sup>INFN, Unit of Pavia, Pavia, Italy ; <sup>3</sup>CNEA, Computational Dosimetry and Treatment Planning group, Buenos Aires, Argentina

### Purpose or Objective

Boron Neutron Capture Therapy (BNCT) is a form of hadrontherapy based on the administration of a drug able to concentrate adequate quantities of <sup>10</sup>B into the tumour and on the subsequent irradiation with low-energy neutrons. At these energies, the neutron capture reaction in <sup>10</sup>B occurs with a cross section of almost 4000 b. The reaction produces two high-LET, short-range particles (alpha particle and <sup>7</sup>Li ion) that cause non-reparable damage only to the cell where they are created. If <sup>10</sup>B concentration is higher in the tumour than in normal cells, it is possible to deliver a therapeutic dose to the malignancy while sparing the healthy tissues. A project to build a clinical BNCT facility in Italy based on a proton accelerator is underway. The proton beam produces neutron by (p,n) reaction in a Be target and a Beam Shaping Assembly (BSA) has been designed to obtain an epithermal neutron beam to treat deep-seated tumours. To optimize the beam, the geometry of BSA was first set-up to comply with physical in-air figures of merit, traditionally used to evaluate the suitability of a neutron facility for BNCT. The beam has been then improved according to its dosimetric performance in real cases of deep-seated tumours and taking into account peripheral dose in-patient and in the environment.

### Material and Methods

The clinical neutron beam has been designed by MCNP. The BSA geometry and materials have been selected among different possibilities according to the in-air physical characteristics of the beam, such as epithermal flux and contaminations from thermal and fast dose components and from gamma. The selected beams have been tested on a real case of limb osteosarcoma to evaluate the potentiality to deliver a high radiation dose with a uniform distribution in the tumour while keeping the dose to the most radiosensitive organ below the tolerance limit. The treatment planning system NCTPlan, already used for clinical BNCT, has been employed. Finally, radioprotection calculation in the treatment room and peripheral dose in a human model in the irradiation position has been used to further optimize the beam.

### Results

An epithermal beam peaked around 1 keV has been obtained with a BSA whose main component is aluminum

fluoride, a material obtained by an original procedure based on powder sintering. Dosimetric results obtained with the final beam design show that BNCT can deliver high doses to tumour respecting the dose constraints in the critical organs.

### Conclusion

As the selectivity of BNCT is due to boron uptake more than to the neutron beam itself, BNCT can be an option to treat tumours that are too large or infiltrated into the normal tissues or too close to very radiosensitive organs. Moreover, it could be exploited for metastatic spreads. Clinical experience show that a favorable dose distribution is possible also for tumours that have no other treatment options, and treatment planning simulations with this neutron beam demonstrate that clinical BNCT is possible with this technology.

### EP-1886 Efficacy of a hydrogel spacer in 3D-CRT for prostate cancer

M. Ogita<sup>1</sup>, H. Yamashita<sup>1</sup>, S. Sawayanagi<sup>2</sup>, W. Takahashi<sup>1</sup>, K. Nakagawa<sup>1</sup>

<sup>1</sup>The University of Tokyo Hospital, Radiology, Tokyo, Japan ; <sup>2</sup>Teikyo University Hospital, Radiology, Tokyo, Japan

### Purpose or Objective

Intensity-modulated radiotherapy (IMRT) can reduce the toxicity of prostate RT, but three-dimensional conformal radiotherapy (3D-CRT) is still used in many facilities. Insertion of a hydrogel spacer creates the space between prostate and rectum. We aimed to evaluate the 3D-CRT plan using a hydrogel spacer can fulfill the dose constraints of IMRT for prostate cancer.

### Material and Methods

From April 2017 to July 2018, the planning computed tomography (CT) scans of 39 consecutive prostate cancer patients received stereotactic body radiotherapy in our institution were used in this analysis. All patients inserted a hydrogel spacer before the treatment and underwent CT scans before and after the hydrogel insertion. The planning CT scan was taken with a full bladder and empty rectum. The 3D-CRT plan was made based on three types of risk groups based on NCCN classification; low, intermediate, and high risk. CTV included prostate + seminal vesicle (SV) 2cm for high risk, prostate + SV 1cm for intermediate, and prostate only for low risk. PTV margin of 7 mm except for 5 mm posterior around the CTV were added. The 3D-CRT plan included 10 MV of coplanar seven photon beams, and 76 Gy/38fr delivered to isocenter. Dose constraints for rectum and bladder were V70 Gy ≤ 15%, V65 Gy ≤ 30%, V40 Gy ≤ 60%, and V50 ≤ 50% for femoral head.

### Results

Thirteen (33%), 19 (49%) and 35 (90%) patients before the spacer insertion fulfilled the rectum dose constraints, and 34 (87%), 38 (97%), and 38 (97%) after the spacer fulfilled rectum dose constraints for high, intermediate, and low risk planning, respectively. A hydrogel spacer use significantly increased the dose constraints fulfilment rate in high risk (P < 0.001) and intermediate risk (P = 0.004), but no difference was found in low risk planning (P = 0.25). The mean rV70 Gy, rV50 Gy, and rV40 Gy were 12% vs 23%, 17% vs 29%, and 52% vs 62% in high risk group (with vs without spacer, P < 0.001, P < 0.001, P < 0.001, respectively). Thirty-three (85%) vs 23 (59%) in high risk, 35 (90%) vs 29 (74%) in intermediate risk, and 38 (97%) vs 36 (92%) in low risk planning fulfilled bladder dose constraints, (with vs without spacer, P = 0.006, P=0.03, P = 0.25, respectively). Mean PTV D95 was 72 Gy, 72 Gy and 71 Gy in high, intermediate and low risk with a spacer, respectively. The patient who had a large prostate had difficulty to fulfill the dose constraints even with a spacer.

### Conclusion

Most of the 3D-CRT plan fulfilled IMRT dose constraints by using a hydrogel spacer. If IMRT is not available, a

combination of 3D-CRT and a hydrogel spacer may become a treatment option for prostate RT.

**EP-1887 Dosimetric and volumetric evaluation of MR-only planning for radiotherapy of rectal cancer**  
 S. Vieira<sup>1</sup>, O. Pares<sup>1</sup>, N. Loução<sup>2</sup>, J. Stroom<sup>1</sup>, I. Santiago<sup>3</sup>, C. Greco<sup>1</sup>, C. Matos<sup>3</sup>  
<sup>1</sup>Fundação Champalimaud, Radiotherapy, Lisboa, Portugal; <sup>2</sup>Philips Iberia, Radiology, Lisbon, Portugal; <sup>3</sup>Fundação Champalimaud, Radiology, Lisboa, Portugal

#### Purpose or Objective

MR delineations in radiotherapy are generally more accurate than on CT but for dose calculations CT data are mandatory. However, software has become available that transforms MR data into pseudo-CT data. In this abstract we study the pros and cons of switching to MR-only planning for radiotherapy of rectal cancer.

#### Material and Methods

Preliminary data of five patients with locally advanced rectal cancer were available. Radiotherapy VMAT plans (Varian) were developed using our clinical simulation protocol that includes the use of FDG PET/CT. Magnetic Resonance for Calculating Attenuation (MRCAT, Philips®) images with five different grey values were generated from 3D T1-weighted mDIXON images (outside the clinical protocol). We used 2 echoes, 1x1x2.5 mm spatial resolution, TR/TE1/TE2 1.64/3.8/5.7(ms), and scan time 3min16s. Two aspects of the new procedure were studied: Part 1: We compared dose calculation on the MRCAT and on the planning CT. MRCAT was matched with the planning CT and the treatment plan with tumor and OAR delineations was copied to the MRCAT. Then the dose was recalculated on the MRCAT (figure 1a/b).

Part 2: A radiation oncologist and radiologist, both specialists in rectal cancer, together delineated MRI-only target volumes and OARs (figure 1c/d). New radiotherapy plans were then generated and compared with the existing clinical plans.

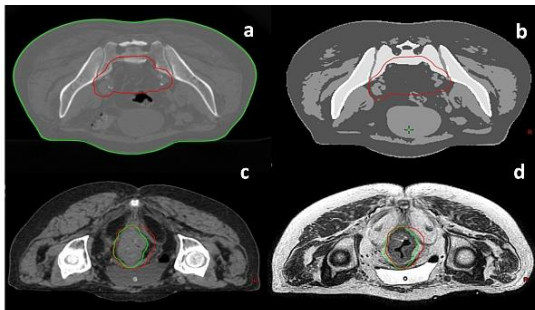


Figure 1—Part1: Target volume in the planning CT (a) and copied to the MRCAT (b) for patient 1. Part2: Target volume boost segmented by the radiologist (green) and the radiation oncologist (red) for patient 4.

#### Results

Part 1: Regarding the dose comparison, doses in target volumes and critical organs calculated on MRCAT differed only slightly from clinical doses: on average mean doses in target and OARs <1%, with standard deviations of 0.4-2.2% (figure 2). Deviations could be explained more by differences in patient anatomy between planning CT and MRCAT than by differences in Hounsfield units.

Part2: MRI-only pelvic PTV volumes were on average 14% ( $\pm 19\%$ , 1SD) smaller than clinical volumes. Just one case actually presented a larger MRI-only target volume due to better visualisation of the anterior mesorectal fascia. MRI-only boost PTV volumes were on average 40% ( $\pm 5\%$ , 1SD) smaller. Dose coverage of tumor volumes was similar in both MRI-based and clinical plans.

A disadvantage of the MRCAT-based planning was that online matching with CBCT on the linac appeared hardly feasible due to the limited number of grey values in the

MRCAT CT. Therefore, rectum cancer cases are now being tested with improved MRCAT software which is able to generate pseudo-CT images with infinite number of grey levels.

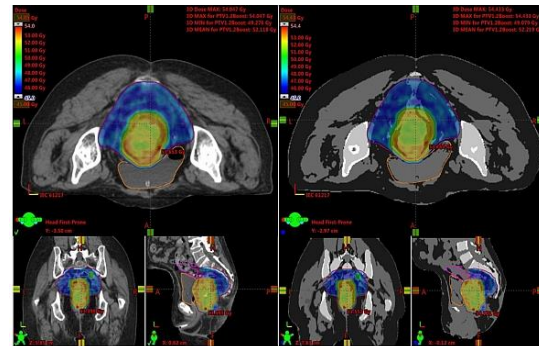


Figure 2—Part1: Dose distribution of the clinical plan calculated on the planning CT (left) and on the MRCAT (right) for patient 1.

#### Conclusion

Dosimetrically even low-resolution MRCAT images are suitable for planning rectum cancer patients. Using MRI only for target delineation reduced the CTV size considerably. When higher resolution MRCAT images become available for better online matching, planning CTs may be discarded completely for rectum radiotherapy.

#### EP-1888 Validation of automated planning with RapidPlan for prostate bed VMAT radiotherapy

B.L. Rekstad<sup>1</sup>, P. Lønne<sup>1</sup>

<sup>1</sup>Oslo University Hospital, Department of Medical Physics, Oslo, Norway

#### Purpose or Objective

RapidPlan is a module for automated planning (AP) in the Varian Eclipse treatment planning system based on DVH-estimation from previous treatment plans. We wanted to explore and validate the module for prostate bed VMAT, prescribed with only one target volume dose level and rectum, bladder, anal canal, femoral heads and penile bulb as organs at risk (OARs). The aim of the study was to investigate possible use of AP and to what extent AP is comparable to or better than manual treatment planning regarding target volume coverage, dose to OARs.

#### Material and Methods

A model was built in Eclipse 13.6 based on 70 clinical prostate bed VMAT plans. Treatment was given with 6 MV on a Varian Clinac 2300iX equipped with Millennium 120 MLC. Either one (n=55) or two (n=15) full arcs were used. Prescribed dose to the prostate bed CTV was 66 - 70 Gy delivered in 33 -35 fractions. The model was tuned by slightly varying the normal tissue objective (NTO) function parameters and also adding a maximum dose constraint to rectum, bladder and anal canal. A validation of the model was then performed by applying the model to 30 other prostate bed cases and comparing with manual clinical plans. Isocenter was the same in clinical and AP plans. All AP plans were made with one arc. With AP the model was applied and run through optimization once without further interaction.

#### Results

Target volume doses were comparable for manual and AP plans. Mean CTV D<sub>98%</sub> was 98.3 % and 98.5 % and mean PTV D<sub>98%</sub> was 95.8 % and 95.3 % for manual and AP plans respectively. This equal target volume coverage is also evident from the mean DVHs for CTV and PTV for the 66 Gy cases (n=23) (Figure 1). For OARs mean DVHs show lower AP doses for rectum, anal canal, femoral heads and penile bulb in medium dose regions, and slightly higher AP doses for bladder (Figure 1). Also, the rectal dose tends to be higher in the high dose region for some of the AP plans. This should be explored more before clinical use. For

clinical and AP plans mean rectal dose was 40.2 Gy and 36.8 Gy, mean bladder dose was 44.6 Gy and 44.1 Gy, and mean anal canal dose was 29.9 Gy and 27.7 Gy.

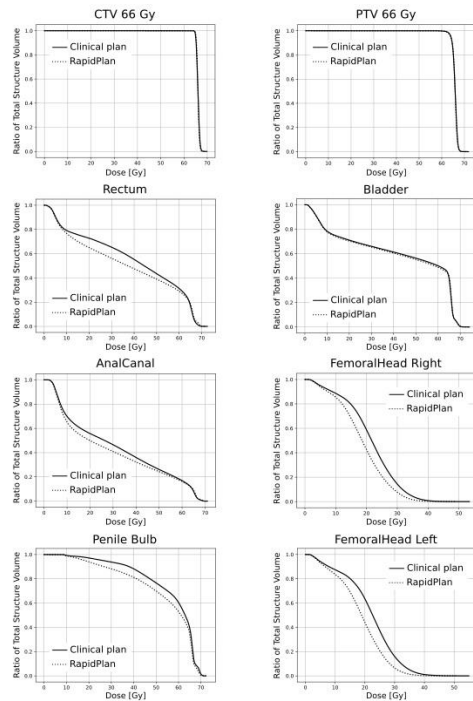


Figure 1. Mean dose volume histograms for prostate bed target volumes and organs at risk for clinical plans and RapidPlan plans.

#### Conclusion

Automated prostate bed VMAT planning with RapidPlan results in clinically acceptable and possibly favorable treatment plans from a DVH perspective. Dose distributions should also be thoroughly analyzed before clinical implementation.

#### EP-1889 Evaluation of organ-motion based robust optimisation for RT of the breast, axilla, and IMC

I. Blasiak-Wal<sup>1</sup>, A. Dunlop<sup>1</sup>, R. Colgan<sup>1</sup>, A. Ranger<sup>2</sup>, A. Kirby<sup>2</sup>

<sup>1</sup>The Institute of Cancer Research and The Royal Marsden NHS Foundation Trust, Radiotherapy Physics, Sutton, United Kingdom ; <sup>2</sup>ICR and Royal Marsden NHS Foundation Trust, Clinical Oncology, Sutton, United Kingdom

#### Purpose or Objective

Simultaneous irradiation of the internal mammary chain (IMC) alongside treating the whole breast and axilla nodes using VMAT (in breath-hold) is increasing. A concern of VMAT delivery for breast RT is the lack of skin flash that is utilised in tangent-based delivery to account for setup uncertainties and increases in the patient contour. We aimed to develop and validate a methodology using organ-motion based robust optimisation, to generate VMAT plans for simultaneous irradiation of the whole breast, IMC, and axilla nodes.

#### Material and Methods

Non-robust plans were initially generated in order to determine a patient-specific optimal objective function. In order to account for changes in position, size, and shape of the breast target tissue, organ-motion simulation available within a commercial treatment planning system (TPS) (RayStation 7.0, RaySearch Laboratories, Stockholm) was used to simulate CTs exhibiting worst-case breast swelling scenarios. Robustly-optimised plans were generated using the simulated CTs and the objective function from the non-robust plan. For five patients,

including one who demonstrated significant breast swelling, the robust plans were compared to the corresponding non-robust plans by comparing the nominal dose distributions on the planning CT and by calculating daily delivered doses using cone beam CT (CBCT) images (n = 67) taken prior to each treatment delivery.

#### Results

No significant differences were observed between the robust and non-robust plans for the nominal dose distributions on the planning CT with both techniques able to meet all mandatory clinical goals taken from the HeartSpare Plus trial. Figure 1 illustrates the skin flash that can be achieved using organ-motion based robust optimisation.

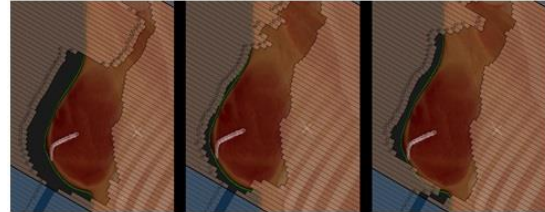


Figure 1: Beams-eye-view of typical segment for: (left) robustly-optimised plan; (centre) non-robust plan; and (right) plan generated using a virtual bolus technique. The patient external region of interest is shown as a green contour.

When considering the daily delivered doses, the robust plans demonstrated significantly better whole breast clinical target volume (CTV) coverage (Table 1) and this is particularly evident in the patient who demonstrated significant breast swelling. The robust plans demonstrated a significant advantage in covering the superficial part of the breast CTV with prescription dose. Delivered doses to organs at risk and IMC and Axilla CTVs were similar for the robust and non-robust plans (Table 1).

Table 1: Estimation of delivered dose statistics for the robust and non-robust plans. Both plans were calculated on 67 CBCTs using bulk-density overrides for dose calculation. The superficial breast region of interest consisted of the outermost 5 mm of the breast CTV.

ROI	Statistic	Dose statistics for all CBCT-based delivered dose estimation			
		Robust plans		Non-robust plans	
		Average	SD	Average	SD
Breast CTV	D98 (Gy)	38.3	0.5	37.6	1.2
	D95 (Gy)	38.7	0.4	38.3	0.7
	D50 (Gy)	40.1	0.3	40.0	0.3
	D2 (Gy)	41.7	0.3	41.4	0.3
Axilla CTV	D98 (Gy)	39.0	0.9	39.1	0.9
	D95 (Gy)	39.4	0.7	39.5	0.6
	D50 (Gy)	40.3	0.5	40.4	0.6
	D2 (Gy)	41.4	0.6	41.6	0.7
IMC CTV	D98 (Gy)	37.7	1.6	38.1	2.0
	D95 (Gy)	38.2	1.4	38.6	1.6
	D50 (Gy)	40.2	0.8	40.5	0.7
	D2 (Gy)	41.7	1.0	41.8	0.8
Superficial Breast	D98 (Gy)	37.4	1.6	35.9	2.4
	D95 (Gy)	38.3	0.6	36.8	1.7
Heart	mean (Gy)	4.5	1.3	4.5	1.2
Ipsi-lateral Lung	V17G (%)	31.0	1.9	31.0	1.7
	mean (Gy)	13.3	0.6	13.2	0.6
Contra-lateral Lung	mean (Gy)	3.1	0.1	3.0	0.2
Contra-lateral Breast	mean (Gy)	3.3	0.1	3.3	0.1
Humeral Head	mean (Gy)	11.5	5.1	11.0	4.7

#### Conclusion

Organ-motion-based robust optimisation available within a commercial TPS is able to generate plans that are clinically acceptable in the nominal (planning CT) scenario and are more robust, when compared to the non-robustly optimised plans, to both typical changes in patient shape and cases of significant breast swelling.

#### EP-1890 Patient specific conversion of CBCT images for proton therapy treatment planning

N. Krah<sup>1</sup>

<sup>1</sup>CNRS / University Lyon, Creatis lab UMR 5220, Lyon, France

### Purpose or Objective

Cone beam CT (CBCT) is becoming a commonly available imaging technology in radiotherapy. However, the presence of artifacts and poor accuracy of Hounsfield Units (HU) preclude its use for treatment planning purposes in proton therapy where range accuracy is crucial. We investigate whether a sufficiently accurate proton relative stopping power (RSP) map can be obtained from a CBCT image when using a patient specific calibration of the HU-RSP conversion curve based on proton radiographic images.

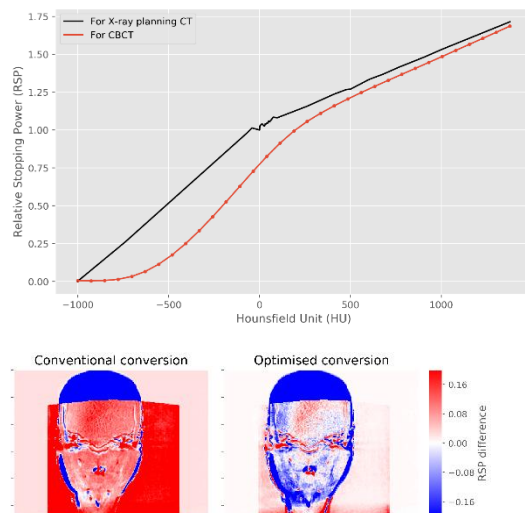
### Material and Methods

We employ a calibration procedure which on one hand uses a proton radiographic image potentially acquired with readily available detector hardware in pencil beam scanning delivery and on the other hand a proton digitally reconstructed radiography based on a CBCT image. The difference between the two is minimized using a recently developed regularized optimization method. The result is a HU-RSP curve which can be used as input to the treatment planning system in combination with the CBCT image instead of the conventional X-ray planning CT.

We applied the calibration to head and neck patient cases who were scheduled for proton therapy and received regular CBCT scans prior to treatment sessions. The CBCT images were rigidly registered to the planning CT. Tomographic reconstruction of the CBCT images was performed with the vendor software including only basic artifact correction for now. Proton radiographies were simulated with the GPU accelerated Monte Carlo code "Fred" using an idealized range telescope set-up and the same data processing chain which we apply to experimental data. The X-ray planning CT converted to RSP through a stoichiometric HU-RSP conversion curve was used as simulation input.

### Results

Figure 1 shows an example of an optimized HU-RSP conversion curve to be applied to a CBCT image. It differs noticeably from the conventional one especially in the range of lower HU values. The HU intervals of the curve, which are usually chosen in accordance with human tissue properties, need to be adjusted in this special application and a regular spacing appeared to yield most reasonable results. Figure 2 shows the difference of RSP values between the CBCT and the planning CT. Agreement is overall much better when using the optimized curve, although spatially dependent discrepancies are still visible. We are currently investigating to which extent more advanced artifact correction during the CBCT reconstruction can improve this. Preliminary results of treatment plan recalculation on CBCT images already showed great improvement when using the optimized HU-RSP.



### Conclusion

Our results suggest that this novel way of converting and correcting CBCT images to RSP for the use in proton therapy treatment planning is feasible. The use of readily available artifact correction techniques are expected to further improve RSP accuracy. The technique could be easily employed in practice using readily available detector hardware.

### EP-1891 A new hotspot correction algorithm in Modulated Electron Radiation Therapy utilizing 3D printed boli

B. Basaric<sup>1</sup>, J. Robar<sup>2</sup>, R. Orbovic<sup>1</sup>, A. Dennis<sup>1</sup>, C. Majcher<sup>1</sup>

<sup>1</sup>Adaptiiv Medical Technologies Inc., Research and Development, Halifax, Canada ; <sup>2</sup>Nova Scotia Health Authority, Department of Medical Physics, Halifax, Canada

### Purpose or Objective

Modulated Electron Radiation Therapy (MERT) modulates the electron beam by changing the thickness of the bolus resulting in a 3D printed non-uniform thickness bolus that conforms the prescribed dose to the distal part of the PTV. However, there may be a certain trade-off between the resulting conformity and dose homogeneity to the PTV depending on shapes of the PTV and modulated bolus and on the energy of the beam. The objective of this work is to introduce a new hotspot algorithm that changes the shape of the modified electron bolus in such a way it reduces hotspots and keeps dose conformity to the PTV similar to the initial modified electron bolus.

### Material and Methods

Initial modulation of the 3D printed bolus that insures the conformity of the prescribed dose to the distal part of the PTV was designed in the "3D Bolus" software (Adaptiiv Medical Technologies Inc.). Overall, 6 MERT plans were calculated in Eclipse TPS (Varian Medical Systems, Inc.). 5 plans were calculated on a phantom where different shaped PTVs were drawn which RT plans ultimately resulted in different dose homogeneity and an overall good conformity in all cases. Hotspots ranged from 114% (1 small peak case) to 142.2% (1 large peak case). A new hotspot correction algorithm uses PTV, contoured hotspot and modulated bolus RT Structures to estimate the location of peaks in a 3D modulated bolus winged edge mesh in order to reduce the height of these peaks in respect to the corresponding valleys resulting in less scattered radiation toward the hotspot area. The amount of peak reduction on the modulated bolus was scaled from 100% (intact modulated bolus) to 0% (completely reduced peaks resulting in flattened modulated bolus). For each of the 6 cases, hotspot corrected modulated bolus was produced using peak reduction scaling factors of 80%, 60%, 40%, 20% and 0%.

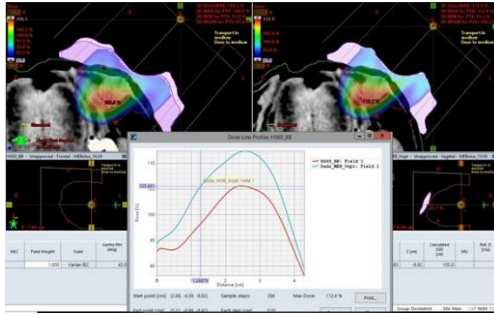
### Results

In all cases, a significant hotspot reduction was noticed which ranged from 23-40% in the 1 large case, 24-33% in the 2 large peaks case, 6-15% in the 1 small peak case, 8-22% in the 2 small peaks case, 10-20% in the no-peaks case and 6-9% in the patient case. In all cases, a progressive reduction of maximum dose to the plan was noticed as the peak reduction scaling factor was closer to 0% while at the same time a progressive loss of conformity of the prescribed dose to the PTV was also noticed. All cases produced at least 1 plan (with one particular peak reduction scaling factor) that satisfied both clinically acceptable level of maximum dose to the plan and conformity of the prescribed dose to target volume that was comparable to the initial modulated bolus electron plan.

### Conclusion

The new hotspot correction algorithm showed in all cases that by scaling the height reduction of the bolus peaks, a clinically acceptable plan can be achieved that satisfies

both the maximum dose to the PTV as well as the conformity of the prescribed dose to the PTV.



Picture 1: Dose comparison before hotspot correction (right) and after (left)

**Electronic Poster: Physics track: Radiobiological and predictive modelling, and radiomics**

**EP-1892 Predictive Response To Radiotherapy Of Head And Neck Cancer Using Radiomics Analyses Of Cbct.**

S. Sellami<sup>1</sup>, D. Bouzid<sup>2</sup>, M. Hatt<sup>2</sup>, D. Visvikis<sup>2</sup>, F. Lucia<sup>1</sup>, O. Pradier<sup>1</sup>, U. Schick<sup>1</sup>

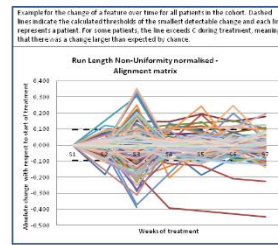
<sup>1</sup>University Hospital- Brest Morvan, Radiation Oncology Department, Brest, France ; <sup>2</sup>LaTIM- University of Brest, Imaging Research Laboratory- INSERM- UMR 1101, Brest, France

**Purpose or Objective**

Radiotherapy for head and neck cancer (HNC) is now guided by cone-beam computed tomography (CBCT). Advanced imaging features (radiomics) extracted from diagnostic imaging have already been shown to predict outcome in several tumor models. The aims of this study were to investigate a methodology for feature selection of a longitudinal radiomics approach and to develop a radiomics signature based on CBCT to predict response to radiotherapy.

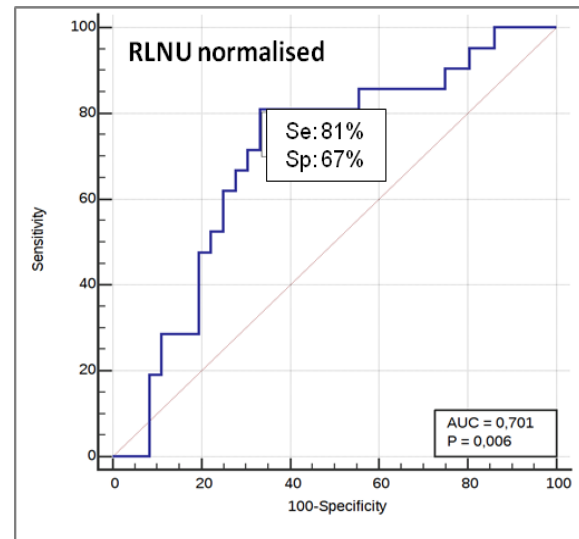
**Material and Methods**

In 102 HNC patients grouped in a training (=68) and validation (=34) cohorts, Gross Tumor Volumes of the primary tumor (GTVT) and metastatic lymph nodes (GTVN) used for the planning were registered to the weekly CBCT images using a deformable registration followed by manual correction. 88 features were extracted from the GTVs on each CBCT. Receiver operating characteristic (ROC) curves were plotted at each week to evaluate the predictive power of response of each feature. Only significant features at each week and independent of volume were pre-selected (AUC) >0.65). Absolute differences (CBCTn-CBCT1, called delta-radiomics) were calculated between features from each weekly CBCT images and the baseline CBCT1 performed before the first fraction. The smallest detectable change (C) with his confidence interval (95%) was determined for each radiomics using the formula  $C=1.96 \cdot SD$ , SD being the standard deviation of differences between features values calculated on CBCT1 and CBCT2. We then selected the features for which the change was more than C for at least 10% of patients at least for one week (Fig.1). A radiomics-based model was built at the time-point that showed most changes. Finally, we compare the prognostic performance of 3 models: clinical, radiomics, and combined.



**Results**

For GTVT, four radiomics features met all criteria. For GTVN, none of the radiomics had an AUC>0.65 at each week, so that we selected the two features with the highest and significant AUC. The number of patients having an absolute delta features variation out of the boundaries was the highest at the third week, thus, this time point was chosen to drive our models. For GTVT, AUCs for predicting the therapeutic response were 0.782 (p<0.001), 0.701 (p=0.0059) and 0.740 (p<0.001) for clinical, CBCT3-radiomics (Run Length Non-Uniformity (RLNU) normalized)(Fig.2) and combined models, respectively. For GTVN, the clinical based model (AUC 0.736, p<0.001) did better than the combined model (AUC 0.563, p=0.143) or the radiomics based model (Elongation, AUC : 0.569). On the validation cohort, the best prediction was given by radiomics for GTVT (AUC:0.639) and by clinical parameters for GTVN (AUC:0.685).



**Conclusion**

We described a feature selection methodology for longitudinal radiomics that is able to select reproducible delta radiomics features which are informative due to their change during treatment. Nonetheless, the prognostic value of the selected delta radiomics features did not seem to improve the prediction already given by the clinical data.

**EP-1893 A machine learning based stain-free method for classification of cell apoptosis stages**

J. Feng<sup>1</sup>, P. Wang<sup>2</sup>, N. Zhang<sup>1</sup>, S. Yu<sup>1</sup>

<sup>1</sup>Tianjin University, Biomedical Engineering, Tianjin, China ; <sup>2</sup>Tianjin Medical University Cancer Institute and Hospital, Radiation Therapy, Tianjin, China

### Purpose or Objective

Cell apoptosis plays critical roles in cancer research and treatment. The most commonly used methods for high-throughput detection of cell apoptosis are based on flow cytometry (FCM) in combination with the dyes which bond to different components in the cells. Despite of the accuracy, these methods are characterized with higher cost and time consuming associated with staining cells. Here we represent a stain-free method based on diffraction imaging flow cytometry and machine learning techniques for detecting cell in different apoptosis stages.

### Material and Methods

For apoptosis induction, human erythroleukemia K562 cells were treated with cisplatin (DDP) in a concentration of 25 mg/ml for 24. And the cell samples without any treatment were used as the control group. Annexin V-PE and SYTOX® Green Dead cell stain were used for cell sorting using fluorescence activated cell sorting (FACS). After cell sorting K562 cells were separated into three sub-groups which were viable, early apoptotic, and late apoptotic/necrotic cells. These sub-groups were measured with our polarization diffraction imaging flow cytometry (p-DIFC) system and the cell images were acquired. In processing the image pairs with s and p polarizations of single cells, a new method based on uniform and rotation invariant local binary patterns (LBP) algorithm for feature extraction was developed. This algorithm has advantages in gray-scale and rotation invariant and dimension reduction of the features. Each image was separated into 100 sub-images, features of each sub-image were extracted and then all features from the 100 sub-images were put together sequentially as a representation (feature vector) of the diffraction image. 2000 feature vectors were constructed for each image pair of a cell. A software tool based on support vector machine (SVM) with linear kernel and radial basis function (RBF) kernel were developed for classification. The training dataset consisted of samples of 2000 early apoptotic cells, 2000 viable cells and 1000 apoptotic/necrotic cells. In the test dataset, numbers of cell samples of these three sub-groups were 250, 250 and 80. After 10-fold cross validation, precision, Kappa statistic, mean absolute error and the area under the curve of the receiver operating characteristic (ROC area) were introduced to evaluate the prediction and classification model.

### Results

Fig.1 shows typical diffraction images of K562 cells in different apoptotic stages. The Kappa statistic, mean absolute error and ROC area showed that the RBF kernel performed better than the linear kernel on the dataset (Table 1). Classification precision of 93.276% on the independent test dataset was obtained.

### Conclusion

With the new method, stable and accurate classification of cells in different apoptotic stages can be achieved.

### EP-1894 On the possibility of estimating the radiosensitivity range in a cell mixture

N. Stavreva<sup>1</sup>, P. Stavrev<sup>1</sup>, D. Penev<sup>1</sup>, A. Nahum<sup>2</sup>, R. Ruggieri<sup>3</sup>, D. Pessyanov<sup>1</sup>

<sup>1</sup>SRD Sofia University "St. Kliment Ohridski", Scientific Research Dpt, Sofia, Bulgaria ; <sup>2</sup>Liverpool University, Physics Department, Liverpool, United Kingdom ; <sup>3</sup>Sacrocuore - don Calabria<sup>1</sup> Hospital, Department of Radiation Oncology, Negrar VR, Italy

### Purpose or Objective

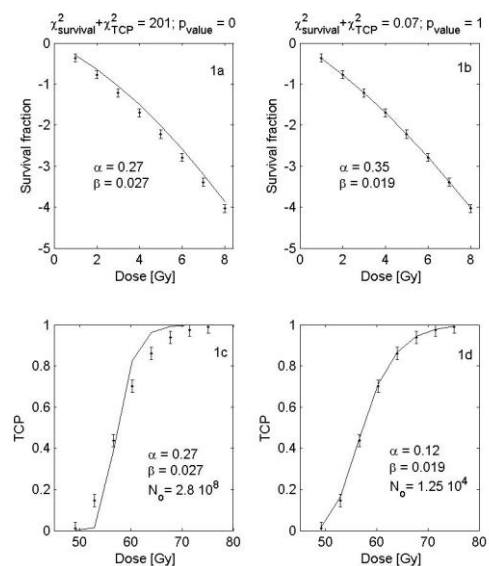
To expand a previous study [1] on tumours that are heterogeneous in cell radiosensitivity and on the observed differences between the values of the effective cell radiosensitivity extracted from fits to pseudo-experimental cell survival data and from fits to pseudo-experimental tumour control probability (TCP) data.

### Material and Methods

A heterogeneous tumour is assumed to consist of the following mixture of cells varying only in  $\alpha$  :  $\alpha_i = [0.1; 0.15; 0.2; 0.25; 0.3; 0.35]$  Gy<sup>-1</sup>,  $\log(N_{0,i}) = [3.7; 4; 4.3; 5; 7; 8]$  with  $B = 0.02$  Gy<sup>-1</sup>; sub-population 'i' consists of initial cell number  $N_{0,i}$  with radiosensitivity  $\alpha_i$ . For this tumour a theoretical cell survival curve is constructed according to the linear-quadratic (LQ) model of cell killing. Also a TCP vs (total) dose curve is constructed based on the Poisson TCP model for  $n = 20$  equal fractions. Both curves consist of 8 points corresponding to different doses. The error in the cell-survival data was considered to be 10% and the error in the TCP data 3%. In this study the two data-sets are then *simultaneously* fitted with a single-component (homogeneous) LQ model of cell killing and a single-component Poisson TCP model respectively. The  $\chi^2$  method of fitting is used on whose basis a p-value is calculated serving as a measure of the goodness of the fit.

### Results

Two different versions of fitting were used. It was firstly assumed that the two data sets may be described with one unique value of the radiosensitivity  $\alpha$ . The result is shown in figs 1a) and 1c) respectively. The p-value is 0. In figs 1b) and 1d) are shown a fit of the LQ model to the pseudo-experimental cell-survival curve and a simultaneous fit of the TCP model to the TCP curve, where two separate values of  $\alpha$  for the two models are assumed. The p-value of the fit is 1. The pseudo-experimental data points are shown in the figures with their assumed error bars.



### Conclusion

A p-value of 0 renders the first version statistically unacceptable. This means that cell survival and the TCP experiments cannot be both described with a single a radiosensitivity value. This conclusion is confirmed by the high p-value (p=1) of the second fit, where two distinctly different best-fit values of  $\alpha$  were obtained. A high value of  $\alpha=0.35$  Gy<sup>-1</sup> from the fit to the cell-survival curve corresponds to the most sensitive sub-population and a relatively low value of  $\alpha=0.12$  Gy<sup>-1</sup> from the fit to the TCP curve corresponds approximately to the most resistant cell subpopulation of the heterogeneous tumour. It should be noted that the best fit value of  $N_0$  also corresponds to the number of cells of the most resistant component of the tumour.

1. Stavrev et al. Phys Med Biol 2015;60(15):N293-9.

Supported by the Bulgarian National Science Fund under contract: DN 18/4 (10.12.2017).

### EP-1895 Multicenter CT phantoms public dataset for radiomics reproducibility studies

P. Kalendralis<sup>1</sup>, A. Traverso<sup>1</sup>, Z. Shi<sup>1</sup>, I. Zhovannik<sup>1,2</sup>, R. Monshouwer<sup>2</sup>, M.P.A. Starmans<sup>3</sup>, S. Klein<sup>3,4</sup>, P. Elisabeth<sup>5</sup>, R. Boellaard<sup>6</sup>, A. Dekker<sup>1</sup>, L. Wee<sup>1</sup>

<sup>1</sup>Maastricht Clinic, Department of Radiation Oncology Maastricht- GROW School for Oncology and Developmental Biology- Maastricht University Medical Centre+- Maastricht- The Netherlands, Maastricht, The Netherlands ; <sup>2</sup>Radboud University Medical Center- Nijmegen- The Netherlands, Department of Radiation Oncology, Nijmegen, The Netherlands ; <sup>3</sup>Erasmus Medical Centre- Rotterdam- The Netherlands, Department of Radiology and Nuclear Medicine, Rotterdam, The Netherlands ; <sup>4</sup>Erasmus Medical Centre- Rotterdam- The Netherlands, Department of Medical Informatics, Rotterdam, The Netherlands ; <sup>5</sup>University Medical Center Groningen- Groningen- The Netherlands, University Medical Center Groningen- Groningen- The Netherlands, Groningen, The Netherlands ; <sup>6</sup>VU Medical Center- Amsterdam- The Netherlands., Department of Radiology and Nuclear Medicine- VU Medical Center- Amsterdam- The Netherlands., Amsterdam, The Netherlands

#### Purpose or Objective

Reproducibility is a fundamental requirement for radiomics-based clinical prediction models. The aim of this study is to describe and provide an open-access Computed Tomography (CT) phantoms image dataset acquired at three different Dutch centers. The data was acquired for radiomics reproducibility studies with respect to variations in acquisition settings, scanners and reconstruction algorithms.

#### Material and Methods

The CT images of the Catphan 700, COPDGene Phantom II (Phantom Laboratory, Greenwich, NY, USA), and the Triple-modality 3D Abdominal Phantom (CIRS, Norfolk, Virginia, USA) were exported in Digital Imaging and Communications in Medicine (DICOM) format from Siemens and Philips scanners. Participating centres were MAASTRO Clinic (Maastricht, NL), Radboud University Medical Center (Nijmegen, NL), and University Medical Center Groningen (Groningen, NL). The scans were acquired by varying the parameters of slice thickness, reconstruction kernels, and tube current. The regions of interest (ROIs) of the COPDGene and Abdominal phantoms were delineated manually in MIRADA DBx (version 1.2.0.59, Mirada Medical, Oxford, United Kingdom). The Catphan700 was used for quality assessment of the scans. Representative axial slices of phantoms and the delineated ROIs of the scans are shown in Figure 1.

#### Results

The scans are publically accessible and reusable via an instance of the eXtensible Neuroimaging Archive Toolkit (XNAT) hosted within the national Dutch research infrastructure (TraIT, www.ctmm-trait.nl). The Phantom Laboratory images have been uploaded to the XNAT collection STW-STRATEGY-Phantom\_Series1: (<https://xnat.bmia.nl/data/projects/stwstrategygs1>). The CIRS multimodality Abdominal Phantom images have been uploaded to the SNAT collection STW-STRATEGY-Phantom\_Series2: (<https://xnat.bmia.nl/data/projects/stwstrategygs2>). An overview of the parameters and protocols used is presented in Table 1.

**Conclusion**  
The phantoms dataset are offered to the radiomics community for the comparison of simple features extracted with different software pipelines. The dataset could be potentially useful for the identification of unstable features with respect to different scanning and acquisition parameters.

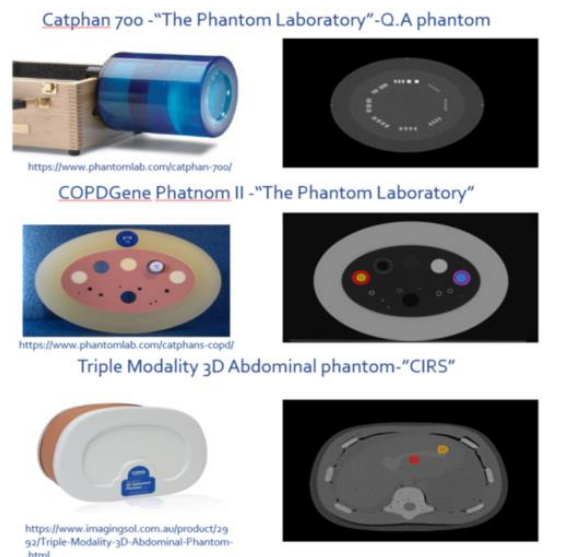


Figure 1. The three different phantoms used in the multicenter study with the delineated spherical ROIs.

Catphan 700/ COPDGene Phantom II				
Parameters	DICOM tags	MAASTRO Clinic, Maastricht	Radboud University Medical Center Nijmegen	University Medical Center Groningen
Institution protocol name		RT_Thorax3mm	THORAX/Thorax	Thorax_1
Slice thickness (mm)	(0018, 0050)	3	3	3
KVP (KV)	(0018, 0060)	120	120	80
Reconstruction diameter (mm)	(0018, 1100)	500	255	239
Exposure time (msec)	(0018, 1150)	500	923	500
Tube current (mA)	(0018, 1151)	39	134	149
mAs	(0018, 1152)	24	124	53
Convolution kernel	(0018, 1210)	B31f	B(Standard)	l3of

Triple Modality 3D Abdominal Phantom				
Parameters	DICOM tags	MAASTRO Clinic, Maastricht	Radboud University Medical Center Nijmegen	University Medical Center Groningen
Institution protocol name		RT_Abdomen3mm	ABDOMEN/Abdomen	Onco_Abdomen_1
KVP (KV)	(0018, 0060)	120	120	120
Reconstruction diameter (mm)	(0018, 1100)	500	385	300
Exposure time (msec)	(0018, 1150)	500	923	500
Tube current (mA)	(0018, 1151)	118	190	18
mAs	(0018, 1152)	73	175	9
Convolution kernel	(0018, 1210)	B3of	B(Standard)	l3of

Table 1. Imaging acquisition parameters and protocols used for the baseline scans across the three different scanners.

### EP-1896 A TCP-based early-regression index predicts outcome of rectal cancer patients better than pCR

C. Fiorino<sup>1</sup>, P. Passoni<sup>2</sup>, C. Gumina<sup>2</sup>, A. Palmisano<sup>3</sup>, S. Broggi<sup>1</sup>, G.M. Cattaneo<sup>1</sup>, A. Di Chiara<sup>3</sup>, M. Mori<sup>1</sup>, R. Rosati<sup>4</sup>, N. Slim<sup>2</sup>, F. De Cobelli<sup>3</sup>, R. Calandrino<sup>1</sup>, N.G. Di Muzio<sup>2</sup>

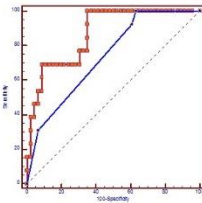
<sup>1</sup>San Raffaele Scientific Institute, Medical Physics, Milano, Italy ; <sup>2</sup>San Raffaele Scientific Institute, Radiotherapy, Milano, Italy ; <sup>3</sup>San Raffaele Scientific Institute, Radiology, Milano, Italy ; <sup>4</sup>San Raffaele Scientific Institute, Gastroenterology Surgery, Milano, Italy

#### Purpose or Objective

A radiobiological parameter (early regression index,  $ERI_{TCP}$ ) based on early tumor (GTV) regression was previously found to predict pathological complete remission (pCR) after neo-adjuvant radio-chemotherapy (RCT) of locally advanced rectal cancer (Rca). In current investigation,  $ERI_{TCP}$  was tested against conventional clinical and pathological biomarkers in predicting long-term outcome after RCT delivered within an observational study testing an early regression- guided adaptive boosting technique (ART).

### Material and Methods

Complete data of 65 patients (pts), including overall, loco-regional relapse and distant metastasis-free survival (OS, LRFS, DMFS) information were available. Pts received 41.4Gy in 18 fr (2.3 Gy/fr) delivering ART concomitant boost on the residual GTV in the last 6 fr (3 Gy/fr, GTV  $D_{mean}$ : 45.6Gy). Chemotherapy consisted of oxaliplatin (OXA) 100 mg/m<sup>2</sup> on days -14, 0 (start of RT), and +14, and 5-fluorouracil (5-FU) 200 mg/m<sup>2</sup>/d from day -14 to the end of RT. Uni- and multi-variable Cox regression models for OS, LRFS and DMFS were assessed considering several clinical (age, sex, OXA dose, 5-FU dose, time to surgery, stage) and histological (pCR, pCR or clinical complete response (cCR) followed by surgery refusal (pCR/cCR), Tumor regression grade, Residual vital cells <5%, <10%) variables. High resolution T2-weighted MRI taken before RT (MRI<sub>pre</sub>) and at half RT (MRI<sub>half</sub>) were available and GTVs were contoured by a single clinician ( $V_{pre}$ ,  $V_{half}$ ). The parameter  $ERI_{TCP} = -\ln[(1 - (V_{half}/V_{pre}))^{V_{pre}}]$ , previously introduced to quantify early response, was considered. Models including/not including  $ERI_{TCP}$  (CONV\_model and REGR\_model respectively) were assessed and their ability in discriminating relapsing pts compared.

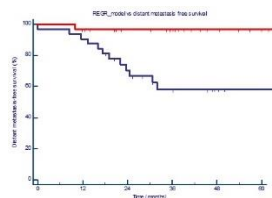


### Results

The median time between RCT and surgery was 11w (range:7-19); 63 pts were operated and two refused surgery after cCR; pCR were 20/63 (32%). The median follow-up was 30 months (range: 5.5-100). OS, LRFS and DMFS at 30 months were 96%, 97% and 80% respectively. Due to the few events the analysis was focused on DMFS: the best CONV\_model included pCR/cCR (HR:0.12,p=0.038) and 5-FU dose>90% (HR: 0.35,p=0.039), with AUC=0.73 (95%CI: 0.62-0.83). The best REGR\_model included  $ERI_{TCP}$  (HR:1.019, p<0.0001) and 5-FU dose>90% (HR:0.18,p=0.005); AUC was 0.87 (95%CI: 0.76-0.94), significantly higher than CONV\_model (p=0.03, Figure 1). When grouping pts according to the best cut-off value for REGR\_model, DMFS at 30 months was 97 % vs 63 % (p=0.0006) for pts below (n=33, 1 event) and above (n=32, 12 events) this value (Figure 2). Higher  $ERI_{TCP}$  values were also associated to worse OS (p=0.036).

### Conclusion

Early regression during RCT for Rca pts as modeled by a Poisson-based TCP formula predicted DMFS better than pCR. An independent impact of the individually administered drug dose was also quantified.  $ERI_{TCP}$  should be considered as a strong outcome predictor with large potentials in treatment individualization.



**EP-1897 Texture analysis of the initial CT to predict the response to neoadjuvant CRT in rectal cancer**  
B. Vandendorpe<sup>1</sup>, C. Durot<sup>2</sup>, L. Lebellec<sup>3</sup>, M. Le Deley<sup>3</sup>, D. Sylla<sup>3</sup>, A. Bimbai<sup>3</sup>, K. Amroun<sup>4</sup>, F. Ramiandrisoa<sup>1</sup>, A. Cordoba<sup>5</sup>, X. Mirabel<sup>5</sup>, C. Hoeffel<sup>2</sup>, D. Pasquier<sup>5</sup>, S. Servagi-Vernat<sup>1</sup>

<sup>1</sup>Institut Jen Godinot, Radiation Oncology, Reims, France ; <sup>2</sup>Centre Hospitalier Universitaire de Reims, Radiology, Reims, France ; <sup>3</sup>Centre Oscar Lambret, Biostatistics unit, Lille, France ; <sup>4</sup>Institut Jen Godinot, Surgery, Reims, France ; <sup>5</sup>Centre Oscar Lambret, Radiation Oncology, Lille, France

### Purpose or Objective

Baseline contrast-enhanced Computed Tomography (CT)-derived texture analysis in locally advanced rectal cancer could be useful in order to offer the best personalised treatment. The purpose of this study was to determine the value of baseline-CT texture analysis in the prediction of downstaging in patients with locally advanced rectal cancer.

### Material and Methods

We retrospectively included all consecutive patients treated with neoadjuvant chemoradiation therapy (CRT) followed by surgery for locally advanced rectal cancer. Tumour texture analysis was performed on the baseline pre-CRT contrast-enhanced CT. Based on the selected model of downstaging with a penalized logistic regression in a training set, a radiomics score (Radscore) was calculated as a linear combination of selected features. A multivariable prognostic model was built including Radscore and clinical factors.

### Results

Among the 121 patients included in the study, 109 patients (90%) were T3-T4 and 99 (82%) N+ at diagnosis. A downstaging response was observed in 96 patients (79%). In the training set (79 patients), the best model (ELASTIC-NET method) reduced the 36 texture features to a combination of 6 features. The multivariate analysis retained, as independent factors, the Radscore (Odds Ratio, OR=13.25; 95%-Confidence Interval, 95%CI, 4.06-71.64; p<0.001) and the age (OR=1.10/1 year; 1.03-1.20; p=0.008). The model was evaluated in the test set leading to an area under the curve of 0.70 (95%CI, 0.48-0.92).

### Conclusion

This study presents a prognostic score for downstaging, from initial computed tomography derived texture analysis in locally advanced rectal cancer, which may lead to a more personalised treatment for each patient.

### EP-1898 Encouraging the use of decision support systems in routine clinical practice

R. Fijten<sup>1</sup>, B. Reymen<sup>2</sup>, R. Houben<sup>3</sup>, P. Fick<sup>4</sup>, T. Hendrik<sup>4</sup>, S. Puts<sup>1,4</sup>, J. Veugen<sup>4</sup>, A. Dekker<sup>1</sup>

<sup>1</sup>Maastricht University Medical Centre, Department of Radiation Oncology Maastricht, Maastricht, The Netherlands ; <sup>2</sup>Maastricht Clinic, Department of Radiotherapy, Maastricht, The Netherlands ; <sup>3</sup>Maastricht Clinic, Data Center Maastricht, Maastricht, The Netherlands ; <sup>4</sup>Maastricht Clinic, Informatisering and Services, Maastricht, The Netherlands

### Purpose or Objective

In the current era of machine learning, many new predictive models are generated yearly. In routine clinical practice, predictive models can assist physicians in interpreting multidimensional clinically relevant data and therefore aiding the (shared) decision making process. However, their use is not widespread due to a number of reasons, such as time constraints during consultations and the difficulty of accessing relevant models. In order to alleviate these concerns and encourage the use of predictive models in routine clinical practice, we have developed an easily accessible web-based interface to host clinically relevant models.

### Material and Methods

A linear regression model was created to determine the survival probability of small-cell lung cancer patients 26 weeks after the start of Prophylactic Cranial Irradiation (PCI). The model was based on data from 151 patients and was internally validated.

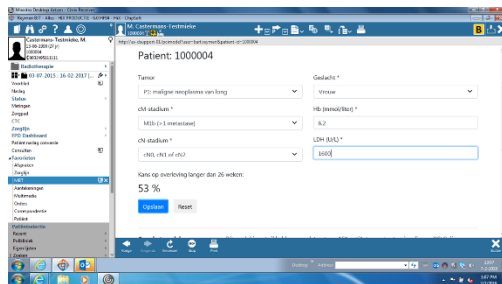
A web-based interface was then created to incorporate this model and make it accessible to physicians. A Java service was built at the back-end of the interface to allow direct communication between the model and the EHR system (HiX, Chipsoft, The Netherlands). Communication was performed by SOAP (Simple Object Access Protocol) queries through a business intelligence software suite (BusinessObjects) which acted as an intermediary. This allowed for automated filling of the input parameters and subsequent calculations.

### Results

The internally validated AUC was 0.71 and provides the probability of surviving 26 weeks after the start of PCI radiation. Input parameters included the tumour N- and M-staging, gender, and concentrations of lactate dehydrogenase (LDH) and haemoglobin (HB) in the blood upon diagnosis.

A web-based interface was created in which the model was plugged in. The architecture of the interface was set up in such a way that other models could be plugged in easily. Because of the direct communication with the HiX EHR system, real-time retrieval of the most recent information was possible so that the model input parameters are up-to-date at any time. Additionally, even though the input parameters are filled in automatically, clinicians are able to adjust all input parameters, after which the model instantly recalculates the outcome. Finally, accessibility of the model was improved by adding it as an option inside the HiX EHR system, allowing physicians to access the model directly from within the system that they use during the consultation. The interface is currently being tested in a prospective clinical trial.

Fig 1: Screenshot of the interface inside the HiX EHR system



### Conclusion

The interface described in this abstract allows for automated generation of model outcomes at a moment's notice with up-to-date information and within the EHR system. By increasing the usability of a model using this interface, clinicians are encouraged even more to utilize the added benefit that predictive models can bring in routine clinical practice.

### EP-1899 Prediction of outcomes in lung SBRT with dosimetric variables and machine learning techniques

D. Sevillano<sup>1</sup>, C. Martín<sup>2</sup>, C. Vallejo<sup>3</sup>, M. Martín<sup>3</sup>, R. Colmenares<sup>1</sup>, R. Morís<sup>1</sup>, B. Capuz<sup>1</sup>, J.D. García<sup>1</sup>, M. Cámara<sup>1</sup>, A. Martínez<sup>1</sup>, F. Orozco<sup>1</sup>, M.J. Béjar<sup>1</sup>, D. Prieto<sup>1</sup>, S. Sancho<sup>3</sup>, F. García-Vicente<sup>1</sup>

<sup>1</sup>Hospital Universitario Ramón y Cajal, Medical Physics, Madrid, Spain ; <sup>2</sup>ETSIT. Universidad Politécnica de Madrid, Biomedical Engineering, Madrid, Spain ; <sup>3</sup>Hospital Universitario Ramón y Cajal, Radiation Oncology, Madrid, Spain

### Purpose or Objective

To find models based on dosimetric variables that allow prediction of outcomes in primary lung tumor SBRT.

### Material and Methods

94 patients with primary lung tumor treated with SBRT from September 2010 to December 2016 were retrospectively analysed (mean follow-up time= 2.6 years). All patients were treated with a 3DCRT technique and a dose prescription of 60 Gy in 3, 5 or 8 fractions. Three dosimetric/radiobiological variables of the PTV, ITV and GTV were used in the analysis (BED<sub>2</sub>, BED<sub>mean</sub>, BED<sub>98</sub>, with  $\alpha/\beta=10$ ) as well as their volumes. Treatment outcomes analysed were local recurrence (LR, 13 cases), nodal recurrence (NR, 13 cases), distant recurrence (DR, 33 cases) and death from disease (DD, 23 cases). Three different machine learning techniques were used in this work: logistic regression, linear Support Vector Machines (SVM) and decision trees (DT).

Validation of the machine learning techniques were performed with 10-fold cross validation due to the limited data available, while Lasso regularization was employed for feature selection. The objective was to use no more than two variables for the model.

In all outcomes but DR, Synthetic Minority Over-sampling Technique (SMOTE) was employed. This technique creates new instances of positive cases from real ones in order to balance the number of positive and negative cases.

### Results

Areas under receiving operating characteristics curve (AUC) of different outcomes with the three methods are shown in Table 1. Best results of AUC are highlighted. For LR, the features used where PTV volume and GTV BED<sub>mean</sub> and the best method was logistic regression with AUC close to 0.75. In case of NR, selected features were ITV volume and GTV BED<sub>mean</sub>, and the method with a best performance was again logistic regression. In the case of DR, none of the methods were able to predict it, as values of AUC close to 0.5 are obtained. Finally, the best AUC obtained for DD was 0.67 for both Decision Trees and SVM using PTV volume and PTV BED<sub>2</sub>. In this case, we can see that the method clearly benefits from using SMOTE.

	AUCs (SD) using SMOTE			AUCs (SD) without SMOTE		
	Logistic Regression	Decision trees	Linear SVM	Logistic Regression	Decision trees	Linear SVM
Local Recurrence	<b>0.75 (0.01)</b>	0.67 (0.03)	0.72 (0.03)	0.737 (0.009)	0.66 (0.04)	0.70 (0.04)
Nodal Recurrence	<b>0.73 (0.01)</b>	0.60 (0.04)	0.72 (0.02)	0.705 (0.006)	0.57 (0.02)	0.52 (0.08)
Distant recurrence				0.49 (0.02)	0.51 (0.05)	0.48 (0.06)
Death from disease	0.62 (0.01)	0.67 (0.02)	<b>0.67 (0.01)</b>	0.586 (0.009)	0.56 (0.03)	0.56 (0.08)

Table 1. AUCs of different methods for all treatment outcomes analysed

For those outcomes where we found AUCs>0.7, we will be able to develop models for treatment outcome probabilities. In this case, we developed models for LR and NR with the method with a better performance, which is logistic regression. To do this, we trained the model with the whole dataset using the hyperparameters and features obtained during cross validation. Models are shown in Table 2.

	Recurrence prob $\frac{1}{1 + e^{-\beta_0 - \beta_1 x_1 - \beta_2 x_2}}$				
	$\beta_0$	$\beta_1$	$x_1$	$\beta_2$	$x_2$
Local Recurrence	-0.57	0.018	PTVvol (cm <sup>3</sup> )	-0.014	GTVBEDmean (Gy <sub>2D</sub> )
Nodal Recurrence	-0.7	0.033	ITVvol (cm <sup>3</sup> )	-0.015	GTVBEDmean (Gy <sub>2D</sub> )

Table 2. Final models for local recurrence and nodal recurrence probability

### Conclusion

Machine learning techniques permit to obtain fair predictions of LR and NR in our clinical practice. Furthermore, those models yield reasonable conclusions regarding tumor volume (volume of PTV and ITV) and dose prescription (GTV BED<sub>mean</sub>).

Logistic regression was the most accurate method, being also the one with a closest relationship to recurrence probability.

These results should be considered as preliminary considering that only cross validation was performed, the

inclusion of more patients would allow a for better validation of the model.

#### EP-1900 Predictive parameters for long-term cardiac mortality excess related to left breast radiotherapy

N. Pasinetti<sup>1</sup>, V. Morandini<sup>1</sup>, S. Berlinghieri<sup>1</sup>, E. Castrezzi<sup>1</sup>, S. Pedretti<sup>2</sup>, L. Spiazzi<sup>3</sup>, P. Frata<sup>1</sup>, L. Grimaldi<sup>1</sup>

<sup>1</sup>Esine Hospital, Radiation Oncology service, Esine, Italy ;

<sup>2</sup>Spedali Civili Hospital, Department of Radiation Oncology, Brescia, Italy ; <sup>3</sup>Spedali Civili Hospital, Department of Medical Physics, Brescia, Italy

#### Purpose or Objective

As shown by Early Breast Cancer Trialists' Collaborative Group(\*) breast cancer radiotherapy is considered mandatory in patients treated with breast conserving surgery or in mastectomy to improve cancer death rate and disease recurs. However, treatment of patients with left breast cancer is burdened by the risk of long-term secondary cardiac effects that may be added to those known induced by chemotherapy (anthracyclines, trastuzumab). Consequently, careful evaluation of the heart-absorbed dose is necessary and, although a risk of cardiac death <1% after breast RT is considered acceptable, the QUANTEC constraint  $V_{25Gy}<10\%$  is not sufficient to limit the excess cardiac mortality risk for each patient and for every RT schedule of tangential beams left sided breast RT. Aim of this work is to find a group of patient for which the dose constraint, above mentioned, is respected, but at a further investigation the excess cardiac mortality probability results greater than 1%. Correlation with new "predictive" dosimetric parameters and cardiac mortality risk was investigated and verified on a control group of patients.

#### Material and Methods

Analyzing the DVHs on TPS Philips Pinnacle<sup>3</sup> of 240 women, who underwent to left sided breast tangential beams RT, came out that the constraint  $V_{25Gy}<10\%$  was always respected. By inspecting the integral DVHs some patients were individuated as "probable false negatives". For each heart absorbed dose distribution the EQD2 was calculated and the Relative Seriality model ( $\alpha/\beta=3Gy$ ,  $s=1$ ,  $D_{50}=52.4Gy$  and  $g=1.28$ ) was used as method to evaluate the probability of late cardiac mortality.

#### Results

For 19 patients the  $V_{25Gy} <10\%$  was satisfied, but by analyzing the differential DVHs the probability of long-term cardiac mortality was found >1% and up to 6%. The dosimetric heart constraints  $V_{40Gy}$  and  $D_{2\%}$  showed a good correlation ( $R=0.97$  and  $R=0.90$  respectively) with the risk of cardiac death. To keep the probability lower than 1%, the cut off levels were determined by the simultaneous occurrence of the conditions:  $V_{40Gy}<2\%$ , and  $D_{2\%}<38Gy$ . On a control group of 15 other patients (or whom  $V_{25Gy}<10$  was satisfied) these parameters were tested. What emerged is that if both parameters were satisfied the long term cardiac mortality probability resulted, with an explicit calculation, <1%.

Application of the new constraints on 15 pz (control group)				
#pz	$V_{25Gy}<10\%$	$V_{40Gy}<2\%$	$D_{2\%}<38Gy$	$P<1\%$
Pz 01	OK	NO	NO	NO
Pz 02	OK	NO	NO	NO
Pz 03	OK	OK	OK	OK
Pz 04	OK	NO	NO	NO
Pz 05	OK	NO	NO	NO
Pz 06	OK	NO	OK	NO
Pz 07	OK	OK	OK	OK
Pz 08	OK	NO	NO	NO
Pz 09	OK	OK	NO	NO
Pz 10	OK	OK	NO	NO
Pz 11	OK	NO	OK	NO
Pz 12	OK	NO	NO	NO
Pz 13	OK	NO	NO	NO
Pz 14	OK	NO	NO	NO
Pz 15	OK	NO	OK	NO

Constraint extrapolated by patients data analysis			
parameters	relationship	Dose constraint	Volume constraint
$D_{2\%}$	<	38 Gy	
$V_{40Gy}$	<		2%

#### Conclusion

Our "predictive" parameters, although they are only a calculation and not an observation of mortality, are closely connected to the irradiation technique used and aimed to specific end-points. Anyway modern TPSs should promote, even more, the use of either radiobiological DVHs or algorithm optimization, especially in the era of hypofractionation.

(\*) Early breast cancer trialist collaborative group, Lancet 2011; 378: 1707-16

#### EP-1901 Identifying organs at risk for radiation-induced dysphagia in head and neck cancer patients

J. Hedström<sup>1</sup>, L. Tuomi<sup>1</sup>, C. Finizia<sup>1</sup>, C. Olsson<sup>2</sup>

<sup>1</sup>Inst of Clinical Sciences, Dept of Otorhinolaryngology, Göteborg, Sweden ; <sup>2</sup>Inst of Clinical Sciences, Dept of Radiation Physics, Göteborg, Sweden

#### Purpose or Objective

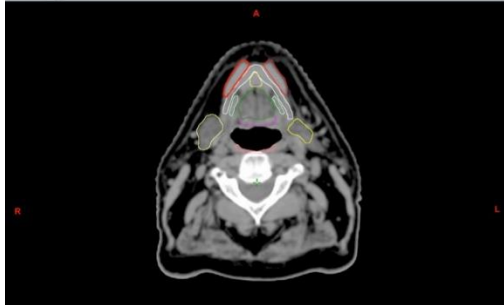
Dysphagia is a common and severe dose-limiting toxicity after oncological treatment of head and neck cancer (HNC). This study aims to investigate the relationship between radiation dose to structures involved in normal swallowing and patient-reported as well as clinically measured swallowing function in HNC patients after curative (chemo)radiotherapy (RT).

#### Material and Methods

Patients (n=90) with tumours of the tonsil, base of tongue, hypopharynx, and larynx curatively treated with radiation therapy +/- chemotherapy in 2007-2015 were assessed for dysphagia post-treatment by telephone interview and videofluoroscopy (VFS). A study-specific symptom score, accounting for presence of drinking, eating, swallowing difficulties, and coughing when eating/drinking, was used to determine patient-reported dysphagia (DESdC). The penetration-aspiration scale (PAS) was applied to determine swallowing function by VFS. Anatomical structures involved in normal swallowing were individually delineated on the patients' original planning CT scans. Radiation dose-volume relationships for these structures were investigated, including ipsi- and contralateral structure dose for the bilateral structures. Univariate logistic regression analysis was performed with structure mean and maximum absorbed doses as predictors for dysphagia. Multivariate regression analysis was subsequently performed to identify the most statistically critical structures associated with swallowing impairment according to DESdC and PAS. Potential effects by relevant clinical factors (comorbidity as scored by ACE-27, age, smoking and BMI) were accounted for.

**Figure 1.** Delineation of organs-at-risk. One representative cross-sectional slice of a pre-treatment planning CT with OARs delineated. A=anterior; R=patient's

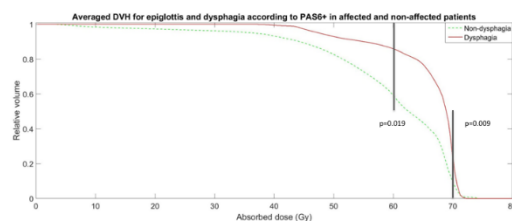
right; L=patient's left. Dark green=Genioglossus muscle/Tongue; Dark yellow=Submandibular gland; Light green=Hyoglossus muscle; Light yellow=Geniohyoideus muscle; Pink=Upper pharyngeal constrictor muscle; Purple=Base of tongue; Red=Anterior digastric muscle; White=Mylohyoideus muscle.



## Results

Dose to several swallowing structures was associated with dysphagia post-RT in univariate analysis. When applying a multivariate model, the mean dose to the larynx and the epiglottis as well as the maximum dose to the contralateral submandibular gland were associated with  $PAS \geq 4$ ,  $PAS \geq 6$  and  $PAS \geq 4$  as well as  $PAS \geq 6$  respectively. The mean dose to the contralateral submandibular gland and the maximum dose to the contralateral anterior digastric muscle were associated with  $DESdC \geq 3$ .

**Figure 2.** Dose-volume histogram for epiglottis, the structure with the best discrimination power for dysphagia according to MVA and associated statistically significant volume differences between dysphagia and non-dysphagia patients.



## Conclusion

Dose-response relationships were found for specific dysphagia endpoints.

### EP-1902 S32: A decision Support System to predict radiation toxicity in lung cancer patients

F. Núñez Benjumea<sup>1</sup>, J. Moreno Conde<sup>1</sup>, A. Moreno Conde<sup>1</sup>, S. González García<sup>1</sup>, M.J. Ortiz Gordillo<sup>2</sup>, J. Riquelme<sup>3</sup>, M.D.C. Fernández Fernández<sup>2</sup>, C.L. Parra Calderón<sup>1</sup>, J.L. Lopez Guerra<sup>2</sup>

<sup>1</sup>Hospital Universitario Virgen del Rocío, Group of Technological Innovation, Sevilla, Spain; <sup>2</sup>Hospital Universitario Virgen del Rocío, Radiation oncology, Sevilla, Spain; <sup>3</sup>University of Sevilla, Department of Computer Language and Systems, Sevilla, Spain

### Purpose or Objective

Decision support systems are a growing class of tools with the potential to impact healthcare. The S32 project aims to develop an informatics infrastructure oriented towards

standardizing, analyzing and reusing retrospective lung cancer patients' information to generate radiation-induced toxicity predictive models that could be actioned in real-time during the treatment planning process. A prospective trial will be developed in a real environment in order to elucidate the accuracy of the predictions yielded by the system and its impact in health-related quality of life, among other endpoints. In this work, the preliminary results of the feature selection methods and prediction models investigated for this purpose are presented.

### Material and Methods

As a preliminary step for the radiation-induced toxicity prediction process, several Feature Selection (FS) methods based on either feature sub-setting or forward selection techniques have been tested along with two different prediction models based on Support Vector Machines (SVM) and Artificial Neural Network (ANN) for predicting radiation-induced acute esophagitis and pneumonitis. The following sub-setting algorithms were applied to both SVM and ANN prediction models: 1) Correlation-based Feature Selection (CFS); 2) Random Forest-based (Boruta); and 3) Chi-Squared filter. In addition, the prediction models were also trained with those features which appeared in two or more of the FS methods listed above (which we called the "polling" method). In addition, the following forward selection techniques were applied only to the SVM-based prediction model for exploratory purposes: 1) Minimum Redundance-Maximum Relevance (mRMR); 2) Relief; 3) Random Forest (RF); and 4) Information Gain (IG). The SVM-based prediction model was also trained with those features which appeared in two or more of the FS methods listed above. Furthermore, and for comparison purposes, the performance of the SVM-based prediction method was also tested without applying any FS method, i.e., with all the available features.

### Results

FS methods and predictive models have been tested with a retrospective dataset with information gathered during routine care for the last 5 years. Radiation-induced prediction models were developed for the two most common side effects found in the dataset: acute esophagitis (N = 406) and acute pneumonitis (N = 408). The models were trained with the 80% of the samples, leaving the remaining 20% for testing purposes. Accuracy of the prediction was measured in terms of AUC (Table).

	ACUTE ESOPHAGITIS			ACUTE PNEUMONITIS			
	Algorithm	Features selected	SVM	ANN	Features selected	SVM	ANN
Sub-setting	CFS	9	0.60	<b>0.71</b>	8	0.61	0.66
	Boruta	21	0.58	0.50	24	0.67	0.59
	Chi-Squared	33	0.57	0.42	23	0.59	0.62
	Polling	15	0.57	0.57	15	<b>0.88</b>	0.47
	mRMR	20	0.63	N/A	120	0.55	N/A
Forward selection	Relief	14	0.51	N/A	72	0.60	N/A
	RF	66	0.62	N/A	27	0.67	N/A
	IG	15	0.60	N/A	67	0.56	N/A
	Polling	17	0.63	N/A	46	0.54	N/A
None	172	0.61	N/A	172	0.51	N/A	

### Conclusion

The best prediction model found for predicting acute esophagitis was the ANN trained with the features yielded by the CFS method. The highest AUC found for predicting acute pneumonitis was related to the model built upon the SVM and Polling of the sub-setting algorithms investigated. This tool could help to define new lung patients care protocols based on predictive models for patient toxicity.

### EP-1903 Learning from scanners: radiomics correction modeling

I. Zhovannik<sup>1,2</sup>, J. Bussink<sup>1</sup>, R. Fijten<sup>2</sup>, A. Dekker<sup>2</sup>, R. Monshouwer<sup>1</sup>

<sup>1</sup>Radboud University Medical Center, Radiation Oncology,

Nijmegen, The Netherlands ; <sup>2</sup>Maastricht University Medical Center +, Radiation Oncology - Maastricht Clinic, Maastricht, The Netherlands

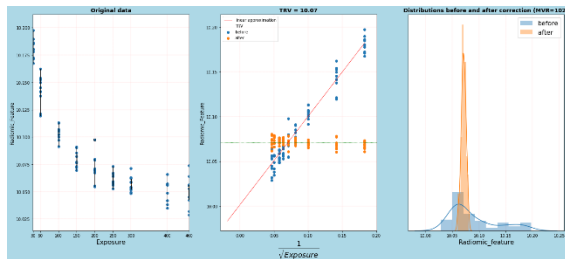
### Purpose or Objective

Every cancer patient treated with radiotherapy undergoes imaging. This is imaging intended primarily for staging and treatment planning, however, there is increasing interest to use this data to support clinical decision making based on imaging. To build a reliable model 'big data' are necessary, involving data from hospitals located in different locations and countries to generalize well across the patient population.

Cancer prediction modeling based on image biomarkers is referred to as radiomics. Although radiomics have predictive power, generalizability is often poor in cross-institutional studies because the institutions have different scanners with various acquisition protocols. The question in this study is whether there is a way to correct for the influence of these image acquisition parameters on the radiomics?

### Material and Methods

We used a Gammex 467 CT phantom to build a training (default configuration) and validation (home-made plugs) sets for radiomics. As an example for scanner variation, we varied the X-ray tube exposure (mAs) used in the scans. To extract radiomic features we used an open-source tool PyRadiomics. Linear regression with X-ray tube exposure as a predictor was used to predict the relationship between X-ray tube exposure and a radiomic feature target value (TRV). Spearman rank was used to evaluate the relationship monotony between a radiomic feature and the X-ray tube exposure. Mean variance ratio (MVR) - variance ratio before and after correction averaged for each delineation - was used to evaluate the correction model.



### Results

In 88 out of 92 radiomic features we found a positive correction in both training and validation sets (MVR > 1). Spearman rank test showed to be a good metric of correctability.

### Conclusion

There is a straightforward way to correct on redundant radiomics variance caused by X-ray tube exposure variation. Radiomics correction modeling may be used to pre-process local institutional data to reduce scanner induced noise in cross-institutional studies involving radiomics.

### EP-1904 3T CE-MRI (peri)tumoral radiomics for prediction of lymphovascular invasion in early breast cancer

M. Avanzo<sup>1</sup>, L. Vinante<sup>2</sup>, G. Pirrone<sup>1</sup>, J. Stancanello<sup>3</sup>, A. Revelant<sup>2</sup>, A. De Paoli<sup>2</sup>, A. Drigo<sup>1</sup>, L. Barresi<sup>1</sup>, L. Balestrieri<sup>4</sup>, M. La Grassa<sup>4</sup>, M. Urbani<sup>4</sup>, N. De Pascalis<sup>4</sup>, S. Massarut<sup>5</sup>, M. Mileto<sup>5</sup>, G. Franchin<sup>2</sup>, G. Sartor<sup>1</sup>

<sup>1</sup>Centro di Riferimento Oncologico di Aviano CRO IRCCS, Medical Physics Department, Aviano, Italy ; <sup>2</sup>Centro di Riferimento Oncologico di Aviano CRO IRCCS, Department of Radiation Oncology, Aviano, Italy ; <sup>3</sup>Oncoradiomics SA, Oncoradiomics SA, Liege, Belgium ; <sup>4</sup>Centro di Riferimento Oncologico di Aviano CRO IRCCS,

Department of Radiology, Aviano, Italy ; <sup>5</sup>Centro di Riferimento Oncologico di Aviano CRO IRCCS, Breast Surgery Unit, Aviano, Italy

### Purpose or Objective

The presence of lymphovascular invasion (LVI) in early stage breast cancer patients is related to worse outcome. For patients undergoing partial breast irradiation with intraoperative radiotherapy (IORT), if LVI is found in pathological examination, then the local treatment is completed with external beam whole breast irradiation. The purpose of this investigation was to predict presence of LVI in patients with early-stage invasive breast cancer by use of radiomics of tumor and peritumoral volume (PV) in 3.0-T, contrast enhanced MRI (CE-MRI).

### Material and Methods

50 patients diagnosed with early-stage invasive breast carcinoma had bilateral 3.0-T breast CE-MRI before surgery and IORT, which was delivered using low-energy photon source, the Intrabeam System (Carl Zeiss, Oberkochen, Germany). The gross target volume (GTV) was contoured by an experienced radiation oncologist in the T1-MRI series with maximum contrast enhancement. The PV was automatically contoured by generating a 1 cm thickness shell around the GTV. The 3D images were pre-processed with re-sampling and 3-D filtering using Gaussian, Laplacian of Gaussian, and Median filters.

A total of 228 radiomic histogram-based and textural features were calculated in the GTV and PV (456 in total). Sequential feature selection was used to identify a subset of features that best predicts the data and remove redundant or not significant predictors. A support vector machine learning classifier was trained on the patient dataset for prediction of presence of LVI in the treated site assessed by pathology (positive classifier for presence of LVI).

The predictive power of the model was assessed using sensitivity (probability that test is positive on patients with LVI), specificity, and Youden's index in five-fold cross validation.

### Results

In 20 out of 50 patients (40.0%) LV was found in pathology. The features selected for prediction of LV were 8 from the PV, 3 from GTV, all of which were textural features derived from the GLRLM, GLCM, NGTDM, and GLSZM matrices. The classifier scored sensitivity 90.0%, specificity 80.0%, and Youden's Index of 0.7 in the cross validation.

### Conclusion

These preliminary findings show that radiomic variables extracted from the PV and GTV in 3.0-T CE-MRI can predict LVI and may help to better select patients candidate to exclusive partial breast irradiation with IORT.

### EP-1905 CT /PET based dosiomics and radiomics model predicts local control of nasopharyngeal carcinoma

M. Avanzo<sup>1</sup>, G. Pirrone<sup>1</sup>, C. Avigo<sup>2</sup>, G. Fanetti<sup>3</sup>, J. Stancanello<sup>4</sup>, A. De Paoli<sup>3</sup>, P. Elisa<sup>3</sup>, A. Drigo<sup>1</sup>, P. Chiovati<sup>1</sup>, A. Dassie<sup>1</sup>, E. Borsatti<sup>5</sup>, T. Baresic<sup>5</sup>, G. Franchin<sup>3</sup>, G. Sartor<sup>1</sup>

<sup>1</sup>Centro di Riferimento Oncologico di Aviano CRO IRCCS, Medical Physics Department, Aviano, Italy ; <sup>2</sup>ULSS 1 Dolomiti - S. Martino Hospital, Medical Physics Department, Belluno, Italy ; <sup>3</sup>Centro di Riferimento Oncologico di Aviano CRO IRCCS, Department of Radiation Oncology, Aviano, Italy ; <sup>4</sup>Oncoradiomics SA, Oncoradiomics SA, Liege, Belgium ; <sup>5</sup>Centro di Riferimento Oncologico di Aviano CRO IRCCS, Department of Nuclear Medicine, Aviano, Italy

### Purpose or Objective

to develop and validate a model predictive for local control, based on CT-PET radiomics and planning CT

dosiomics features, of nasopharyngeal carcinoma (NPC) treated by Intensity Modulated Radiation Therapy (IMRT).

#### Material and Methods

Patients diagnosed with NPC treated with RT were included in this study. Clinical and instrumental follow-up was performed every month for the first 2 years, then every 6 months. Pre-treatment PET and CT-scans were collected as well as the three dimensional dose distribution calculated on the CT. The CT, PET images and the calculated dose distribution were pre-processed with re-sampling and 3-D filtering using Gaussian, Laplacian of Gaussian, and Median filters. 728 radiomic shape, size, histogram-based and textural features were calculated from the filtered and unfiltered images and dose in the gross target volume, which was contoured using CT and PET. Sequential feature selection was used to identify a subset of features that best predict the data and remove redundant or not significant predictors. An ensemble learning classifier with adaptive boosting was trained on the patient dataset for prediction of local control (positive classifier for appearance of disease in the treated site during follow-up, negative otherwise). The predictive power of the model was assessed using sensitivity (probability that test is positive on patients with recurrence) and specificity in five-fold cross validation. The area under ROC curve (AUC) was used to investigate correlation of features with recurrence.

#### Results

After a median follow-up of 31.4 (95%CI 3.8-86.7) months, 49 out of 60 (82.6%) patients were free from local recurrence. The features selected were 1 shape (solidity), 1 CT (Low Gray level zone emphasis from GLSZM), 1 PET (Second measure of information correlation of GLCM) and 3 dose features (Percentile area 90, Strength of NGTDM, Small Zone high grey level emphasis of GLSZM). The classifier scored sensitivity 72.7% and specificity 89.8% in the cross validation. The single most predictive feature for recurrence was PET (AUC=0.712). The category with highest AUC was dose, as the combined features had AUC of 0.735.

#### Conclusion

These findings show that PET radiomic and dosiomic variables are correlated with local control of NPC. The model incorporating radiomic features from imaging and dose can predict local control in this type of head and neck cancer.

#### EP-1906 CBCT delta-radiomics for predicting complete pathological response of rectal cancer after CT-RT

G. Pirrone<sup>1</sup>, E. Palazzari<sup>2</sup>, F. Navarra<sup>2</sup>, R. Innocente<sup>2</sup>, J. Stancanello<sup>3</sup>, G. Fanetti<sup>2</sup>, G. Franchin<sup>2</sup>, C. Cappelletto<sup>1</sup>, A. De Paoli<sup>2</sup>, G. Sartor<sup>1</sup>, M. Avanzo<sup>1</sup>

<sup>1</sup>Centro di Riferimento Oncologico di Aviano CRO IRCCS, Medical Physics Department, Aviano, Italy; <sup>2</sup>Centro di Riferimento Oncologico di Aviano CRO IRCCS, Radiation Oncology Department, Aviano, Italy; <sup>3</sup>Oncoradiomics SA, Oncoradiomics SA, Liege, Belgium

#### Purpose or Objective

The study of the variation of radiomic features extracted from cone-beam CT (CBCT) acquired for Image-Guided Radiotherapy (IGRT) opens a promising scenario for assessing tumor response during chemo-radiotherapy (CT-RT). The objective of this study is to determine whether variation of radiomic features (delta-radiomics) predicts complete pathological response (pCR) of patients treated with RT for rectal cancer.

#### Material and Methods

The analysis was conducted on daily-setup imaging data of a total of 19 patients diagnosed with rectal cancer who received preoperative volumetric arc therapy (VMAT) with a prescribed dose of 54 Gy in 25 fractions. All the CBCT images were acquired with 125 kVp and 80 mA with a Varian Trilogy LinAc. An expert radiation oncologist contoured the gross volume target (GTV) for each patient

on three CBCTs acquired on the first, middle (12<sup>th</sup> fraction) and last fraction of the treatment. The image intensity levels were normalized using the mean value of a region of interest in the bladder, and a voxel re-sampling was performed to obtain isotropic voxel spacing. To denoise images and enhance image characteristics all the CBCTs were convolved with different kernels (Gaussian, Laplacian of Gaussian, and Median). Radiomic features were extracted from 3D tumor regions and the delta-features, i.e. the relative feature values change were evaluated between the mid and last fraction of the RT (Delta1), the first and mid-fraction of the CT-RT (Delta2), and the first and last fraction of CT-RT (Delta3). Wilcoxon signed-rank test was used to evaluate if delta-features in patients with pCR after CT-RT were significantly different from patients with partial or no response.

#### Results

Nine patients had pCR after CT-RT. Eleven Delta1, five Delta2, and twelve Delta3 features were significantly different ( $p < 0.05$ ) in patients with pCR.

#### Conclusion

These preliminary results show the potential of delta-radiomics for predicting pCR of rectal cancer patients early during the CT-RT.

#### EP-1907 Which FDG-PET features are robust enough for Radiomic studies in pancreatic cancer patients?

L. Presotto<sup>1</sup>, M. Mori<sup>2</sup>, P. Passoni<sup>3</sup>, M.L. Belli<sup>4</sup>, S. Broggi<sup>2</sup>, G.M. Cattaneo<sup>2</sup>, M. Picchio<sup>1</sup>, N.G. Di Muzio<sup>3</sup>, V. Bettinardi<sup>1</sup>, C. Fiorino<sup>2</sup>

<sup>1</sup>IRCCS San Raffaele Scientific Institute, Nuclear Medicine, Milano, Italy; <sup>2</sup>IRCCS San Raffaele Scientific Institute, Medical Physics, Milano, Italy; <sup>3</sup>IRCCS San Raffaele Scientific Institute, Radiotherapy, Milano, Italy; <sup>4</sup>IRST Istituto Scientifico Romagnolo per lo Studio e la Cura dei tumori, Medical Physics, Meldola, Italy

#### Purpose or Objective

FDG-PET Radiomics is promising for the characterization of pancreatic cancer (Pca). However, uncertainties due to delineation/segmentation and to acquisition/processing may affect its reliability. Aim of this study was to assess robust radiomic features (RF) based on the impact of delineation uncertainty and of parameters affecting image acquisition/processing.

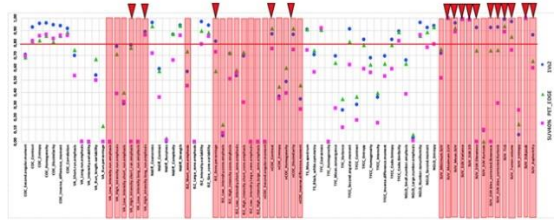
#### Material and Methods

Twenty-five Pca patients previously treated with IMRT were considered. Four PET Pca contours were available: 2 manual, 1 semi-automatic (based on SUV maximum gradient: PET\_Edge) and 1 automatic (40%SUV\_max thresholds); 72 RF were extracted with CGITA software (v. 1.4). The stability of RF against inter-observer variability was quantified by Intra-Class Correlation Coefficient (ICC); the robustness of RF for PET\_Edge and 40%SUV was assessed against manual delineation. The impact of acquisition/processing on RF was tested on uniform and purpose built heterogeneous phantoms. Statistical effect size indicators were used to determine: i) the impact of each nuisance factor (discretization, acquisition statistics, reconstruction algorithm, filtering), and ii) the discriminating power. Based on the robustness with respect to all factors, we categorized RF based on repeatability and on heterogeneous PET patterns discrimination, leading to the definition of a list of robust RF. Among them, the ones showing an ICC $\geq$ 0.80 (for "inter-observer variability") in the delineation study were finally defined as suitable for Pca Radiomics.

#### Results

Inter-observer agreement was moderate (median DICE: 0.73); 35 (47%) RF showed an ICC $<$ 0.80, mostly in the Voxel-Alignment (VA) matrix and in the Intensity-Size Zone (ISZ) matrix families. The number of RF with ICC $<$ 0.80 for PET\_Edge and SUV40% (considering the worst ICC value against observers) increased to 44 and 54 respectively. Regarding image acquisition/processing,

the discretization method based on relative range outperformed those based on bins of fixed width in units of SUV and was then adopted. The less robust families considering repeatability and discrimination were the Gray Level Run Length Matrix (GLRLM) and the Neighborhood Gray Tone Difference (NGTD) while the Grey Level Cooccurrence Matrix (GLCM) and the SUV first order RF were the most suitable. In Figure 1, the red bars indicate the most robust RF considering acquisition/processing, 14 of first and 20 of higher order. The resulting RF suitable for radiomic studies shown in Figure 1 were 11 of first and only 5 of higher order. Relaxing the limit for delineation agreement to  $ICC \geq 0.60$ , the numbers increased to 12 and 8 respectively.



### Conclusion

Based on a large set of phantom experiments, a list of 34 FDG-PET RF (from 72) was suggested as sufficiently robust against both repeatability and pattern discrimination. Delineation uncertainty for Pca is quite large, reducing the number of robust RF to 16/34, increased to 20 for a lower ICC threshold (0.60) for contouring agreement.

### EP-1908 A Guide For Predicting Normal Tissue Dose in Stereotactic Radiosurgery

D. Cummins<sup>1</sup>, C. Skourou<sup>1</sup>, S. O'Sullivan<sup>2</sup>, P. Davenport<sup>1</sup>, D. Fitzpatrick<sup>2</sup>, C. Faul<sup>2</sup>, M. Javadpour<sup>3</sup>, M. Dunne<sup>4</sup>  
<sup>1</sup>St. Luke's Radiation Oncology Network, Radiotherapy Physics, Dublin, Ireland; <sup>2</sup>St. Luke's Radiation Oncology Network, Radiation Oncology, Dublin, Ireland; <sup>3</sup>St. Luke's Radiation Oncology Network, Beaumont Hospital National Centre for Neurosurgery, Dublin, Ireland; <sup>4</sup>St. Luke's Radiation Oncology Network, Clinical Trials, Dublin, Ireland

### Purpose or Objective

The defining factors for selecting a prescription dose for intracranial metastases in stereotactic radiosurgery (SRS) are the size of the target and consequently the dose received by surrounding normal brain tissue. Prescription dose is recursively adjusted [24Gy-18Gy] following completion of a plan, until the normal brain tissue dose constraints are met. The availability of a nomogram to inform dose selection from the time of diagnosis would reduce planning time by eliminating the recursive adjustment of the prescription. This paper describes the development of such a guide using a knowledge-based method for predicting normal tissue dose as a function of target diameter in SRS.

### Material and Methods

Data from 50 previous SRS treatment plans (completed on iPlan with non-co-planar dynamic conformal arcs) was used to extract the terms for the key planning metrics (conformity index and gradient index) and define them as a function of target volume.

The relationship between the measured target diameter and the dose to normal tissue volume (NTV) was established by approximating a spherical target volume covered by the prescription dose which could inform the expected  $V_{40\%}$ . A scaling parameter described by a modeled non-linear fall-off of dose beyond the target was then used to scale  $V_{40\%}$  in order to provide a first order approximation of the resulting NTV

The predictive model was retrospectively validated against calculated NTV (chosen as  $V_{12Gy}$  for this study)

obtained from a total of 26 single fraction clinical plans created for solitary lesions ranging in diameter (equivalent sphere) from 0.5cm to 3cm.

### Results

For the 26 plans investigated, the model predicted the  $V_{12Gy}$  to within 0.67cc on average with a standard deviation of 0.53cc. Predictions were found to be most sensitive to the sphericity and size of the target, where small changes in gradient and conformity had the largest impact on the final NTV volume.

### Conclusion

This knowledge-based method for NTV prediction in intracranial SRS could be used as a guide for deciding the prescription dose to targets prior to treatment planning in a busy clinical environment.

### EP-1909 Delta-radiomics signature predicts outcomes after preoperative chemoradiotherapy in rectal cancer

C. Song<sup>1</sup>, J. Seung Hyuck<sup>1</sup>, K. Bohyoung<sup>2</sup>, K. Jae-Sung<sup>1</sup>  
<sup>1</sup>Seoul National Univ. Bundang Hospital, Radiation Oncology, Seongnam- Gyeonggi-Do, Korea Republic of; <sup>2</sup>Hankuk University of Foreign Studies, Division of Biomedical Engineering, Yongin, Korea Republic of

### Purpose or Objective

To develop and compare delta-radiomics signatures from 2- (2D) and 3-dimensional (3D) features that predict treatment outcomes following preoperative chemoradiotherapy (CCRT) and surgery for locally advanced rectal cancer.

### Material and Methods

In total, 101 patients (training cohort, n = 67; validation cohort, n = 34) with locally advanced rectal adenocarcinoma between 2008 and 2015 were included. We extracted 55 features from T2-weighted magnetic resonance imaging (MRI) scans. Delta-radiomics feature was defined as the difference in radiomics feature before and after CCRT. Signatures were developed to predict local recurrence (LR), distant metastasis (DM), and disease-free survival (DFS) from 2D and 3D features. The least absolute shrinkage and selection operator regression was used to select features and build signatures. The delta-radiomics signatures and clinical factors were integrated into Cox regression analysis to determine if the signatures were independent prognostic factors.

### Results

The radiomics signatures for LR, DM, and DFS were developed and validated using both 2D and 3D features. Outcomes were significantly different in the low- and high-risk patients dichotomized by optimal cutoff in both the training and validation cohorts. In multivariate analysis, the signatures were independent prognostic factors even when considering the clinical parameters. There were no significant differences in C-index from 2D vs. 3D signatures.

### Conclusion

Delta-radiomics signatures from both 2D and 3D features successfully predicted the outcomes and were independent prognostic factors irrespective of other conventional clinicopathologic factors. External validation is warranted to ensure their performance.

### EP-1910 CT image standardization is superior to larger but heterogeneous datasets for robust radiomic models

D. Vuong<sup>1</sup>, M. Bogowicz<sup>1</sup>, J. Unkelbach<sup>1</sup>, R. Foerster<sup>1</sup>, S. Denzler<sup>1</sup>, A. Xyrafas<sup>2</sup>, M. Pless<sup>2</sup>, S. Thierstein<sup>2</sup>, S. Peters<sup>3</sup>, M. Guckenberger<sup>1</sup>, S. Tanadini-Lang<sup>1</sup>  
<sup>1</sup>University Hospital Zurich and University of Zurich and Swiss Group for Clinical Cancer Research SAKK, Radiation Oncology, Zürich, Switzerland; <sup>2</sup>Swiss Group for Clinical Cancer Research SAKK, Coordinating Center, Bern, Switzerland; <sup>3</sup>Centre Hospitalier Universitaire Vaudois CHUV, Oncology, Lausanne, Switzerland

### Purpose or Objective

Radiomics is a promising tool for identification of new prognostic biomarkers. Radiomic models are often based on single-institution data. However, multi-centric data that are highly heterogeneous due to different scanning protocols reflect better the clinical reality. Robustness studies are crucial to find features independent from e.g. scanner settings. We studied if a CT radiomics overall survival (OS) model trained on multi-centric data with prior robust feature selection can achieve a similar performance as a model on standardized data.

### Material and Methods

Pre-treatment CT data from 121 stage IIIA/N2 NSCLC patients from a prospective Swiss multi-centric randomized trial (SAKK 16/00, neoadj. chemo- or radiochemotherapy prior to surgery) were used to calculate 1404 radiomic features on the primary tumor. Two OS radiomic models were trained on (1) a patient sub-cohort characterized by standardized imaging protocol (native CT, standard kernel,  $n = 84$ ) and on (2) the entire heterogeneous patient cohort but with pre-selection of robust radiomic features. Robust features were extracted from four distinct robustness studies (contrast, convolution kernel, motion, delineation). Stability measure was the intra-class correlation coefficient ( $> 0.9$  considered stable). Principal component (PC) analysis was performed for feature selection and PCs describing in total 95% of data variance were selected. Features were selected separately for the entire and standardized dataset. The feature with highest correlation to the PCs served as a surrogate for the multivariate Cox model. Finally, backward selection was performed. Model performance was quantified using Concordance Index (CI). 10-fold cross-validation and bootstrap with resampling were used both to verify and compare model performances.

### Results

Robustness studies revealed 113 stable features ( $n_{\text{shape}} = 8$ ,  $n_{\text{intensity}} = 0$ ,  $n_{\text{texture}} = 7$ ,  $n_{\text{wavelet}} = 98$ ). The convolution kernel was the largest influence on the robustness of the radiomic features. The final OS model on the entire non-standardized dataset consisted of four and the model on standardized data of six features (all identified as unstable). The model on standardized imaging data showed significant better prognostic performance compared to the model with robust feature pre-selection based on the entire heterogeneous imaging data (CI = 0.64 and 0.61,  $p < 0.05$ , resp.).

### Conclusion

For our prognostic NSCLC radiomic models, image protocol standardization appears superior to using larger but heterogeneous imaging data combined with robust feature selection.

### EP-1911 Treatment response on MR during radiotherapy in patients with head and neck squamous cell carcinoma.

B. Peltenburg<sup>1</sup>, M. Philippens<sup>1</sup>, R. De Bree<sup>2</sup>, C. Terhaard<sup>1</sup>  
<sup>1</sup>UMC Utrecht, Radiotherapy, Utrecht, The Netherlands ;  
<sup>2</sup>UMC Utrecht, Head and Neck Surgical Oncology, Utrecht, The Netherlands

### Purpose or Objective

In head and neck radiotherapy, early recognition of patients with poor response to treatment is important and might allow for treatment modification. Conventionally, tumor volume changes are used to assess treatment response. Recently, apparent diffusion coefficient (ADC) determined by diffusion weighted magnetic resonance imaging (DW-MRI) has been introduced as a prognostic factor in patients with head and neck squamous cell carcinoma. Aim: To follow treatment response on DWI and T2 weighted images of head and neck tumors.

### Material and Methods

Twenty patients with stage II, III or IV head and neck squamous cell carcinoma were included in the PREDICT study. Two patients had HPV positive tumors. Treatment consisted of radiotherapy with or without concurrent chemotherapy. All patients underwent MRI prior to and during week 2, 3, 4 and 5 of the radiotherapy treatment. Imaging was obtained with the patient positioned in the radiotherapy mask. Tumor delineation was performed on T2 weighted images for the baseline MRI and each subsequent MRI. Volume changes were determined using these delineations. For the ADC changes the tumor was again delineated on the baseline  $b=800$  s/mm<sup>2</sup> images using a semi-automatic method. This delineation was copied to the corresponding ADC map and ADC maps of subsequent weeks. Median ADC values for each available delineation were extracted. A follow up of at least 3 months was available for all patients.

### Results

During (chemo)radiotherapy tumors generally reduce in size with each passing week. On average the tumors were only 50% of their original size at the end of the third week of treatment. However due to the treatment effects, tumors are increasingly harder to differentiate from nonmalignant tissues in the treatment area. At the end of the fifth week only 20% of the original tumor volume was visible on T2. In one patient the tumor visibly increased in size from the third week onward. This patient had a local recurrence within 3 months after treatment. In total four patients had a recurrence. ADC generally increases during therapy. The fractional change in median ADC between the baseline and third week of treatment ( $fADC_3$ ) was on average 1.25 and the most discriminating between patients with recurrence and with response. A cutoff of 32% increase in ADC at week 3 resulted in a sensitivity of 100% and specificity of 81%.

### Conclusion

During (chemo)radiotherapy, T2 images can be used to measure tumor volume. Generally tumors decrease in size during treatment. A large increase at week 3 however, might predict a recurrence of tumor. Figure 1. Fraction tumor change volume of patients (black), average of all patients with recurrence (red) and average of patients without recurrence (green).

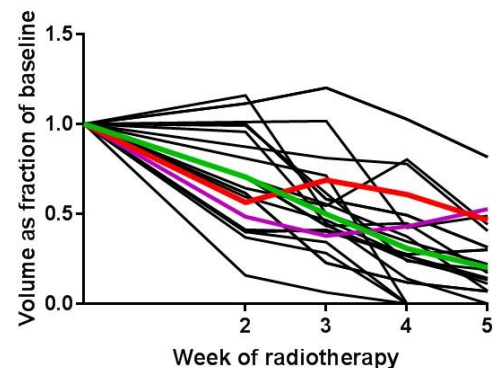
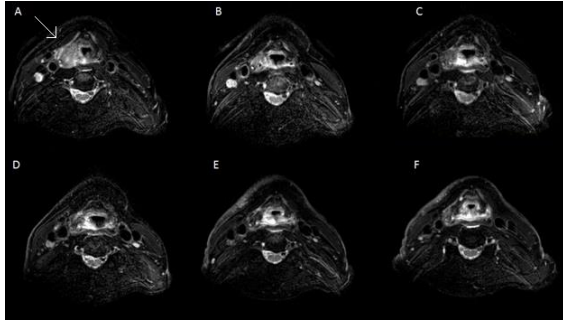


Figure 2. T2 weighted MRI images of the patient with a local recurrence within 3 months after treatment. A) Pretreatment MRI with the tumor in the hypopharynx (white arrow). B) Week 2 C) Week 3, D) Week 4, E) Week 5 of radiotherapy. F) MRI of local recurrence 3 months after radiotherapy.



### EP-1912 Outcome prediction with CT radiomics and random forests in primary lung tumor treated with SBRT

C. Martín<sup>1</sup>, D. Sevillano<sup>2</sup>, C. Vallejo<sup>3</sup>, M. Martín<sup>3</sup>, J. .D. García<sup>2</sup>, R. Colmenares<sup>2</sup>, R. Moris<sup>2</sup>, B. Capuz<sup>2</sup>, M. Cámara<sup>2</sup>, A. Martínez<sup>2</sup>, F. Orozco<sup>2</sup>, M.J. Béjar<sup>2</sup>, D. Prieto<sup>2</sup>, S. Sancho<sup>3</sup>, F. García-Vicente<sup>2</sup>

<sup>1</sup>ETSIT. Universidad Politécnica de Madrid, Biomedical Engineering, Madrid, Spain ; <sup>2</sup>Hospital Universitario Ramón y Cajal, Medical Physics, Madrid, Spain ; <sup>3</sup>Hospital Universitario Ramón y Cajal, Radiation Oncology, Madrid, Spain

#### Purpose or Objective

To predict treatment outcomes from radiomics information of tumor images in the planning CT.

#### Material and Methods

87 patients treated from September 2012 to December 2016 (median follow-up time=25.2 months) were retrospectively analyzed for this work. Radiomic features from the tumor contoured by the radiation oncologist in the planning CT were obtained with IBEX software (Zhang *et al*, *IBEX: an open infrastructure software platform to facilitate collaborative work in radiomics*, *Med Phys* 2015 (42)3, 1341-53). From there, 766 features regarding tumor shape, intensity levels, Co-occurrence matrix, gradient orientations and intensity difference between neighboring voxels were obtained. Analyzed treatment outcomes were Distant recurrence (DR, 26 cases) and death from disease (DD, 23 cases)

For feature selection, a Random Forests algorithm was used with the whole dataset features. Importance of each feature was obtained by permuting the values of each variable and calculating the variation in Out-of-Bag (OOB) error prediction. This process was repeated ten times and mean error increase calculated. Those features with higher mean error increase are those with more prediction power. Once features are selected, Random Forests with only those features was used for prediction. Area under the ROC curves (AUC) were obtained from OOB predictions of the algorithm

Kaplan-Meier (K-M) plots were obtained by dividing our patient population in half according to median score of the random forests algorithm. Logrank test was performed in order to check if there was a significant difference between both patient populations.

#### Results

For DR, two features regarding Co-occurrence Matrix maximum probability and local standard deviation of intensity values were selected. The algorithm achieved an AUC of 0.76 (SD= 0.02).

Also, a value of  $p=3.10^{-5}$  was obtained in the logrank test. In the case of DD, features selected were related to information measure of the Co-occurrence matrix and maximum probability in co-occurrence matrix. The value of AUC was 0.79 (SD= 0.01) and logrank test yielded a value of  $p=0.03$ . K-M plots are shown in Figure 1.

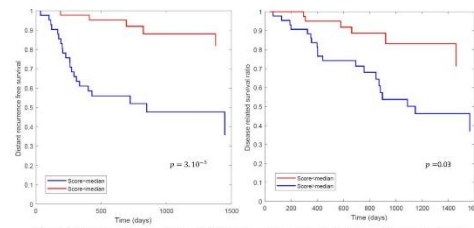


Figure 1. K-M plots of the population divided by the median score of the Random Forests algorithm for distant recurrence and death from disease.

### Conclusion

Random Forests performed well in the prediction of DR and DD with Radiomics features. The nature of Random Forests and the use of OOB prediction prevents for overfitting. Also the low standard deviation of AUC values when repeating the training are encouraging. Nevertheless, patient population needs to be enlarged in order to be able to perform validation in an independent dataset.

### EP-1913 Distributed rapid learning made easy: a user-friendly dashboard for model development and execution

J. Van Soest<sup>1</sup>, C. Masciocchi<sup>2</sup>, P. Fick<sup>1</sup>, T. Hendriks<sup>1</sup>, R. Negro<sup>2</sup>, A. Damiani<sup>2</sup>, V. Valentini<sup>2</sup>, A. Dekker<sup>1</sup>  
<sup>1</sup>Maastricht Radiation Oncology Maastricht Clinic, Knowledge Engineering, Maastricht, The Netherlands ;  
<sup>2</sup>Università Cattolica del Sacro Cuore, Radiotherapy, Rome, Italy

#### Purpose or Objective

Data analysis is becoming more apparent in radiotherapy and medicine in general. Next to the technical skills, interpretation and clinical usefulness of results is of major importance. Hence, visual representations of data and outcomes (plots, charts, nomograms) can help in exploring the data and analysis results. However, the number of people managing both technical and clinical skills is limited, introducing a challenge to leverage from all available (and continuously updated) data. The aim of this abstract is to develop a user-friendly dashboard to ask different types of questions (e.g. showing basic cohort statistics or learning a prediction model). This dashboard triggers these tasks on multiple routine clinical datasets; performing a distributed and privacy-preserving analysis without requiring in-depth technical skills.

#### Material and Methods

The datasets available in participating institutes contained 2469 and 837 routine clinical rectal cancer patients. Information regarding age, gender, clinical TNM stage, prescribed RT dose, overall survival status and time were available for inclusion and/or analysis. Three distributed algorithms were developed to perform: a) general statistics, b) plotting one integrated Kaplan-Meier graph, c) learning a Cox proportional hazards model. We developed a dashboard to select the distributed algorithm (A, B or C) and define inclusion criteria. The dashboard also shows previous executions of algorithms (including selected inclusion criteria) and visualizes the result (tables/figures/text) for every algorithm execution. When Algorithm C is selected, the dashboard can show an interactive prediction model executor. In this model executor, users can enter patient-specific criteria whereafter the predicted probabilities over time are shown.

#### Results

The developed dashboard is publicly available at <http://coraldashboard.jvsoest.eu>. Results of algorithms are visualized (e.g. variable distributions, KM curve for inclusion criteria, prediction model), and stored in the history of algorithm executions. This means users can

come back at a later convenient time to e.g. apply the trained model in practice.

#### Conclusion

We developed an easy to use distributed learning dashboard. Statistical information about the datasets available can be requested using algorithm A. Algorithm B gives users the opportunity to search for treatment outcomes for similar patients treated in the past. Definition of clinical similarity can be set by the user him/herself using broader/smaller inclusion criteria. Algorithm C can be triggered, and afterwards directly applied for new patients, as a true rapid learning platform. All algorithms can be triggered as often as needed, to update when new information becomes available. Furthermore, both algorithms and connected hospitals are configurable, allowing dashboards for specific collaborations and algorithms.

#### EP-1914 A method to deal with highly correlated explanatory variables in the development of NTCP models

A. Van Der Schaaf<sup>1</sup>, L. Van den Bosch<sup>1</sup>, S. Both<sup>1</sup>, E. Schuit<sup>2</sup>, J.A. Langendijk<sup>1</sup>

<sup>1</sup>University of Groningen- University Medical Center Groningen, Radiation Oncology, Groningen, The Netherlands ; <sup>2</sup>Julius Center for Health Sciences and Primary Care, University Medical Center Utrecht- Utrecht University, Utrecht, The Netherlands

#### Purpose or Objective

Data-driven modelling of patient outcomes is often impeded by high correlation between explanatory variables (EVs), resulting in unstable variable selection and inflated variance. This problem can lead to models that highly depend on specific correlations between EVs and, therefore, generalise poorly to other populations. We modified a frequently used model development method (MDM) to deal with this problem and tested the performance and generalizability of the resulting models in realistic simulations.

#### Material and Methods

As reference MDM we used stepwise logistic regression with forward variable selection based on the Bayesian Information Criterion (BIC). To deal with high correlation between EVs we modified this MDM using four steps. First, the EVs were assigned to overarching EV groups with mutual correlations  $\leq 0.8$  and that were as large as possible. Second, for each such group, a prediction model was developed using the reference MDM. Third, models with good performance were selected based on the BIC with a range equivalent to one degree of freedom. Finally, we combined all models with good performance into a single logistic model by averaging their linear predictors. We simulated random datasets with 10 EVs drawn from a standard Gaussian distribution with autoregressive correlation structure and a correlation of 0.9 between neighbouring EVs. A binary response variable was added according to a logistic response relation with 5 randomly chosen EVs with coefficients drawn from a standard uniform distribution. Datasets of varying size of 100 up to 500+ observations were generated and used to develop prediction models using the reference and modified MDM. Using the same response relation we generated 3 validation sets, each containing 1000 observations. The first validation set had the same correlation structure of the EVs as the training set, to test the model performance in the same population. The other validation sets had 0.5 and 0 correlation between EVs, to test model generalizability. Calculated measures included the mean absolute prediction error (MAE), loss of log-likelihood (LoLL), and loss of area under the receiver operating characteristic curve (LoAUC). Of these measures we calculated the average relative difference between the

modified and reference MDM, and how often each MDM was better than the other.

#### Results

On average, for data set sizes up to 500 observations, the modified MDM performed and generalized better than the reference MDM, but not in each single simulation, as shown in the Table and Figure. For larger data sets the performance of both MDMs stabilized at a constant high level, with only small differences between both methods, which were on average slightly in favour of the reference method.

Table: Relative performance of the modified MDM compared to the reference MDM, expressed as mean relative difference (positive means an improvement), and the percentage of simulations in which the modified MDM was better, equal, or worse than the reference MDM.

	Performance in same population	Generalizability to 0.5 correlation	Generalizability to 0 correlation
MAE	+14% Better: 69% Equal: 11% Worse: 20%	+15% Better: 61% Equal: 13% Worse: 26%	+16% Better: 62% Equal: 12% Worse: 26%
LoLL	+28% Better: 73% Equal: 7% Worse: 21%	+32% Better: 64% Equal: 11% Worse: 25%	+34% Better: 66% Equal: 10% Worse: 24%
LoAUC	+35% Better: 65% Equal: 13% Worse: 22%	+26% Better: 55% Equal: 15% Worse: 30%	+13% Better: 51% Equal: 12% Worse: 37%

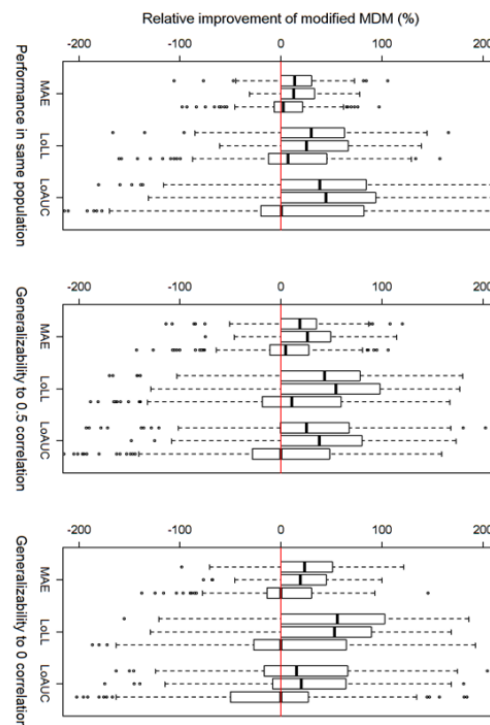


Figure: Boxplot of all results of all simulations with data set sizes up to 500 observations. The grouped bars represent data set sizes of 100-200 (upper), 300 (middle), and 400-500 (lower) observations.

#### Conclusion

We modified an existing MDM to deal with high correlation between EVs. On average, the modified models predict and generalize better than the reference models, up to the point where sufficient data is available to reliably estimate all model parameters.

### EP-1915 Modelling framework for FMISO and FDG PET imaging tailored dose prescription

M. Lazzeroni<sup>1</sup>, A. Ureba<sup>2</sup>, D. Baltas<sup>3</sup>, A.L. Grosu<sup>3</sup>, I. Toma-Dasu<sup>1</sup>

<sup>1</sup>Stockholm University, Medical Radiation Physics- Dept. Physics, Stockholm, Sweden ; <sup>2</sup>Skandionkliniken, Skandionkliniken, Uppsala, Sweden ; <sup>3</sup>Medical Center-Medical Faculty Freiburg- German Cancer Consortium DTK Partner Site Freiburg, Department of Radiation Oncology-, Freiburg, Germany

#### Purpose or Objective

Positron emission tomography (PET) may play a central role in personalized radiation therapy when aiming at a dose prescription based on the functional and biological properties of the tumor, such as hypoxia. Hypoxia is well known for increasing cell radioresistance and it is considered as one of the main determinants of locoregional failure.

This study aims at setting the modelling framework for combining the metabolic tumor information derived from fluorodeoxyglucose (FDG) PET images together with tumor hypoxia imaging with fluoromisonidazole (FMISO) PET to quantify the tumor clonogenic cell and oxygen distributions for a tailored dose prescription.

#### Material and Methods

A modelling approach for assessing the dose to be prescribed in order to achieve a predefined level of tumour control probability accounting for hypoxia and density of clonogens was proposed. Two scenarios were considered regarding the initial distribution of clonogens in the clinical target volume, a homogeneous density of the clonogens and a heterogeneous one. The heterogeneous distribution of clonogens was hypothesized that could be derived based on the FDG avidity extracted from PET images. Linear and non-linear conversion functions of FDG uptake into number of clonogenic cells were considered. For each of these scenarios, the required radiation doses to counteract the increased tumor cell radioresistance at voxel level were calculated based on maps of oxygen partial pressure derived from FMISO PET images by the use of conversion functions of radiotracer uptake.

#### Results

The framework for dose calculation was implemented as a scripted module to a research version of a treatment planning system, RayStation (RaySearch Laboratories AB, Stockholm). For exemplifying the results of applying the proposed formalism for personalised treatment planning, the distribution of oxygen partial pressure in one of the clinical target volumes for a head and neck cancer patient, the clonogenic cell distribution obtained when a linear and a sigmoidal conversion function of uptake into clonogenic cell number and the corresponding dose distributions to counteract the radiation resistance at voxel level are shown in Figure 1.

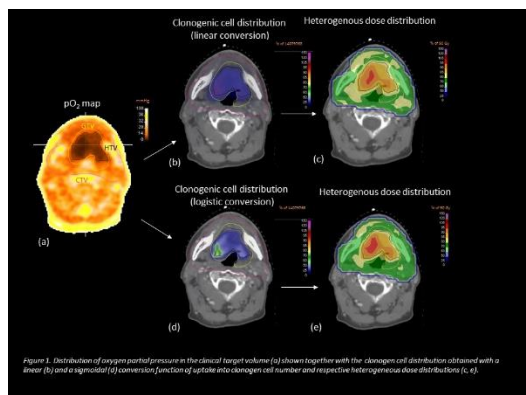


Figure 1. Distribution of oxygen partial pressure in the clinical target volume (a) shown together with the clonogen cell distribution obtained with a linear (b) and a sigmoidal (c) conversion function of uptake into clonogen cell number and respective heterogeneous dose distributions (d, e).

#### Conclusion

A modelling framework was developed and implemented in a research version of a treatment planning system allowing for different radiobiology-based strategies for dose prescription at voxel level targeting hypoxia and enhanced density of tumour clonogens. This modelling framework could be used for further development of individualized radiation therapy dose prescription approaches. Further validation based on patient treatment outcome is however warranted and it is pursued in an ongoing study.

### EP-1916 Predictive model of the dose to the heart based on geometry evaluation in left breast radiotherapy

S.M. Tomatis<sup>1</sup>, E. Esposito<sup>1,2</sup>, A. Gaudino<sup>1</sup>, F. Lobefalo<sup>1</sup>, P. Mancosu<sup>1</sup>, L. Paganini<sup>1</sup>, V. Palumbo<sup>1</sup>, A. Stravato<sup>1</sup>, E. Tomatis<sup>3</sup>, M. Rossi<sup>3</sup>, E. Merati<sup>3</sup>, F. De rose<sup>1</sup>, G. Reggiori<sup>1</sup>, M. Scorsetti<sup>1,4</sup>

<sup>1</sup>Humanitas Research Hospital, Medical Physics of Radiotherapy, Rozzano Milan, Italy ; <sup>2</sup>Università degli studi di Milano, facoltà di medicina, Milano, Italy ; <sup>3</sup>liceo classico giosuè carducci, alternanza scuola lavoro, Milano, Italy ; <sup>4</sup>Humanitas University, Department of Biomedical Sciences, Rozzano MI, Italy

#### Purpose or Objective

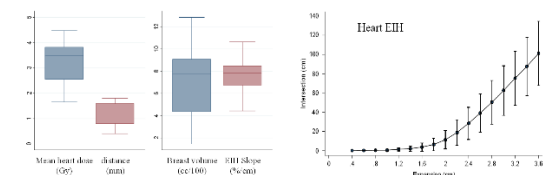
Radiotherapy treatment of the left breast can be difficult due to heart proximity. Conservative dose constraint with mean heart dose (MHD) < 4 Gy was suggested for minimizing heart late effects. Deep Inspiration Breath Hold (DIBH) was demonstrated to help in reducing MHD. In this study a predictive model was developed to correlate MHD to the patient geometry aiming to select the best patients that would benefit to DIBH.

#### Material and Methods

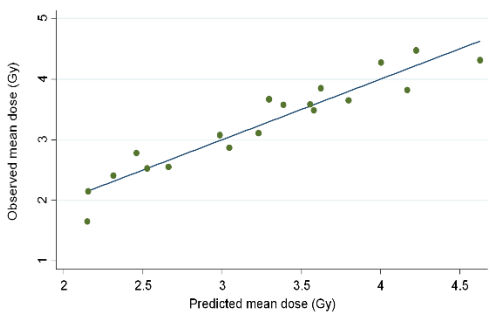
Nineteen patients treated in our facility for left breast cancer were randomly selected and considered in this study. All cases were subjected to a treatment course of 15 fractions for a total dose of 48 Gy to the surgical bed and 40.5 Gy to the whole breast. Patients were treated with volumetric modulated arc therapy (VMAT) with two or four arcs. The model was developed by target expansion and overlap procedure following the Expansion Intersection Histogram (EIH) method (1). This procedure operates by progressive target isotropic expansions and mapping the corresponding intersection with the critical organ into the EIH graph. From this graph the distance (max non zero overlap expansion) and slope (mean EIH derivative) are extracted and added to the target volume as input variables for a simple linear model. All variables are subjected to function transforms in order to approach a gaussian shaped distribution. All calculations and tests were made with stata software and the "ladder" function was used to generate the proper variable transform.

#### Results

Parameter distribution and overall EIH graph (mean ± SD) for the 19 patients are represented in figure 1.



After data extraction, variables were selected by the ladder command as follows: 1) square root of breast volume. 2) distance (not modified). 3) 1/average slope. All variables resulted to be Gaussian ( $p > 0.05$ ).



The linear model, adjusted by the number of arcs, resulted to have a  $R^2$  of 0.9. All three input parameters were significant ( $P < 0.05$ ). A representation of the linear fit is reported in figure 2

**Conclusion**

These data could be used as predictive model to assist in risk evaluation and decision for appropriate technique, such as breath hold or other suitable techniques

**EP-1917 Variable versus conventional inter-fraction intervals in SBRT**

P. Stavrev<sup>1</sup>, N. Stavreva<sup>1</sup>, A. Nahum<sup>2</sup>, R. Ruggieri<sup>3</sup>, P. Tsonev<sup>1</sup>, D. Pressyanov<sup>1</sup>  
<sup>1</sup>SRD Sofia University “St. Kliment Ohridski”, Scientific Research Dpt, Sofia, Bulgaria ; <sup>2</sup>Clatterbridge Cancer Centre, Formerly at Physics Dpt, Bebington, United Kingdom ; <sup>3</sup>Sacrocuore - don Calabria’ Hospital, Department of Radiation Oncology, Negrar VR, Italy

**Purpose or Objective**

To investigate theoretically the maximal possible difference in local tumor control that can be achieved with SBRT regimens with conventional and with variable inter-fraction intervals.

**Material and Methods**

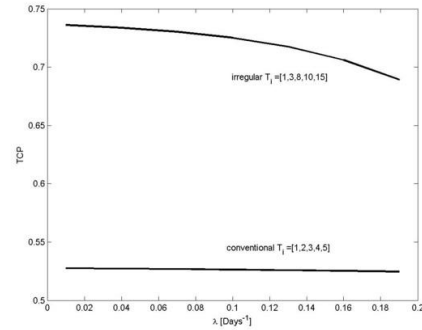
This study was stimulated by [1] which reported that a higher local tumor control (by 30%) was observed clinically for a SBRT regimen employing non-consecutive, i.e. irregular rather than consecutive (conventional) inter-fraction intervals. The fractionation schemes compared in [1] are  $T_{i,1} = \{1,2,3,4,5\}$  and  $T_{i,2} = \{1,3,8,10,15\}$ , delivering otherwise equal total dose to the tumor. They are studied here employing a TCP model accounting for tumor hypoxia [2,3,4]; this TCP model includes re-sensitization of the tumor cells through re-oxygenation during a prolonged treatment and therefore may potentially explain the improved treatment outcome of the non-conventional SBRT schedule.

The parametric space of the applied TCP model was searched in order to investigate the dependence of the obtained TCP difference on the values of the model parameters. A dose per fraction of 11 Gy was assumed, consistent with [1].

**Results**

There exist a parameter set presented in the table for which the difference in the predicted TCPs is around 20%. The TCP dependence on the repopulation rate for both schedules is shown in the figure.

$N^0_a$	$N^0_{sb}$	$N^0_{ah}$	$\alpha_a$ (Gy <sup>-1</sup> )	$\beta_a$ (Gy <sup>-2</sup> )	$\alpha_{sb}$ (Gy <sup>-1</sup> )	$\beta_{sb}$ (Gy <sup>-2</sup> )	$\alpha_{ah}$ (Gy <sup>-1</sup> )	$\beta_{ah}$ (Gy <sup>-2</sup> )	$\alpha$	$C$
$1.4 \cdot 10^7$	$1.0 \cdot 10^6$	$6 \cdot 10^6$	0.18	0.02	0.08	0.012	0.05	0.005	0.08	0.1



**Conclusion**

Although the maximal TCP difference obtained theoretically in this study is lower than the one reported in [1], where a difference of 30% was obtained, it supports the reported clinical finding. A more detailed investigation will be carried out with this and an alternative model [5] which also accounts for re-oxygenation of the tumor during treatment in order to investigate whether the observed TCP difference can be predicted by existing TCP models.

- Alite, Fiori et al. *Radiotherapy and Oncology*, 121, 1, 9 - 14, 2016
- Ruggieri R. *Phys Med Biol* 2004;49:4811-4823.
- Ruggieri R, Nahum AE. *Med Phys* 2006;33:4044-4055.
- Ruggieri R et al. 2012, *Int J Radiat Oncol Biol Phys.* 2012 Aug 1;83(5):1603-8.
- Stavreva NA et al. *Med Phys.* Mar;32(3):720-5. 2005 Supported by the Bulgarian National Science Fund under contract: DN 18/4 (10.12.2017).

**EP-1918 Active bone marrow identification in the pelvis using texture analysis of CT features**

E. Gallio<sup>1</sup>, S. Rosati<sup>2</sup>, C. Fiandra<sup>3</sup>, F. Arcadipane<sup>3</sup>, A. Lesca<sup>4</sup>, P. Silveti<sup>3</sup>, G. Balestra<sup>2</sup>, U. Ricardi<sup>3</sup>, P. Franco<sup>3</sup>  
<sup>1</sup>A.O.U. Città della Salute e della Scienza, Medical Physics Unit, Turin, Italy ; <sup>2</sup>Politecnico of Turin, Department of Electronics and Telecommunications, Turin, Italy ; <sup>3</sup>University of Turin, Radiation Oncology-Department of Oncology, Turin, Italy ; <sup>4</sup>A.O.U. Città della Salute e della Scienza, Nuclear Medicine Unit, Turin, Italy

**Purpose or Objective**

For anal cancer patients, hematologic toxicity (HT) may influence compliance to therapy (concurrent chemoradiation). It is crucial to implement strategies able to identify and spare active bone marrow (aBM). Several methods exist to locate aBM, based on PET or MR images. The aim of this study is to evaluate the feasibility of detecting aBM on CT images with radiomics.

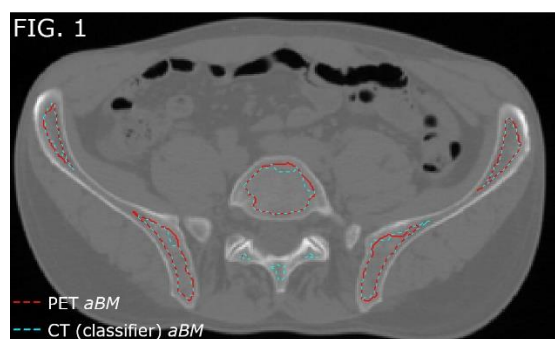
**Material and Methods**

Five patients were included in the study. For all patients, aBM was manually drawn on PET images (pixel size: 4x4mm<sup>2</sup>, spatial resolution: 6 mm) and divided in three ROIs (subregions): iliac bone marrow (iBM), lower pelvis (LPBM) and lumbosacral (LSBM) one. For identifying aBM on CT (pixel size: 1x1mm<sup>2</sup>), three classifiers were implemented. For training of the classifiers, pelvic bone marrow (PMB) was segmented on CT images according to Mell L.K. et al. (*Int.J.Radiat.Oncol.*, 2006, p. 1356-1365) procedure. The aBM was selected by PMB applying k-means algorithm (k=2), removing the pixel with the highest mean intensity (corresponding to cortical bone) and overlapping with PET aBM ROIs (after deformable registration). For all elements overlapping PET aBM, a set of 36 radiomics features was calculated: 4 first-order statistical features and 32 second-order ones. For each aBM subregion, a training set was obtained by randomly selecting 1/4 of elements from five slices for each subject.

Each training set was used for constructing a Support Vector Machine (SVM) classifier that was employed to segment the specific *aBM* subregions on CT images of the five patients. A comparison between PET *aBM* ROIs and CT ones was carried out with respect to DICE index, precision and recall for elements with at least 64 pixels.

### Results

Fig.1 shows an example of *aBM* manually drawn on PET and the segmentation of the classifier on CT images. Tab. 1 sums the values of DICE index, precision and recall found for the five patients for *LSMB*, *IBM* and *LPBM* ROIs. The highest indices values were obtained for *LSMB* and *IBM* subregions, where the DICE index was  $\geq 0.75$  and precision was  $\geq 0.80$  in 4 out of 5 patients. The high values of recall for these two subregions (average values: 0.80 and 0.73 respectively) means that the *aBM* was correctly recognized by the classifier on CT images. For the *LPBM*, supoptimal results were achieved (average DICE index was 0.5). The identification of *aBM* in the *LPBM* might be influenced by the presence of the coxa.



Patients	LSBM			IBM			LPBM		
	DICE	Precision	Recall	DICE	Precision	Recall	DICE	Precision	Recall
1	0.86	0.89	0.86	0.85	0.87	0.85	0.62	0.55	0.89
2	0.84	0.90	0.80	0.85	0.91	0.82	0.38	0.29	0.68
3	0.79	0.82	0.79	0.75	0.78	0.74	0.48	0.37	0.80
4	0.90	0.90	0.92	0.82	0.94	0.74	0.50	0.43	0.66
5	0.67	0.86	0.62	0.64	0.96	0.51	0.53	0.43	0.74
Mean	0.81	0.87	0.80	0.78	0.89	0.73	0.50	0.41	0.76
± S.D.	± 0.09	± 0.03	± 0.11	± 0.09	± 0.07	± 0.14	± 0.09	± 0.09	± 0.09

### Conclusion

A classifier based on texture analysis features for the automatic segmentation of active bone marrow in pelvic region was created. The obtained results were promising, especially for the lumbosacral and iliac structures. A larger population of patients will be included in future studies, to better test the generalization capability of this approach. Furthermore, to improve the detectability in the *LPBM* subregion, other classifiers, may be employed and/or combined among them.

### EP-1919 Voxel-based assessment of proton RBE in paediatric brain cancer radiotherapy from multimodal imaging

M. Skaarup<sup>1</sup>, A. Appelt<sup>2</sup>, M. Lundemann<sup>1</sup>, S. Darkner<sup>3</sup>, M. Jørgensen<sup>4,5</sup>, C. Thomsen<sup>6</sup>, I. Law<sup>7</sup>, D. Mirkovic<sup>8</sup>, R. Mohan<sup>9</sup>, D. Grosshans<sup>3</sup>, C. Peeler<sup>3</sup>, I. Vogelius<sup>1,9</sup>

<sup>1</sup>The Finsen Center - Rigshospitalet, Clinic of Oncology, Copenhagen, Denmark ; <sup>2</sup>University of Leeds and Leeds Cancer Centre- St. James's University Hospital, Institute of Cancer and Pathology, Leeds, United Kingdom ; <sup>3</sup>University of Copenhagen, Department of Computer Science, Copenhagen, Denmark ; <sup>4</sup>Rigshospitalet, Clinic of Nephrology, Copenhagen, Denmark ; <sup>5</sup>Sjællands Universitetshospital, Radiology department, Roskilde, Denmark ; <sup>6</sup>Rigshospitalet, Department of Radiology, Copenhagen, Denmark ; <sup>7</sup>Rigshospitalet, Department of Clinical Physiology- Nuclear Medicine and PET, Copenhagen, Denmark ; <sup>8</sup>The University of Texas- MD Anderson Cancer Center, Department of Radiation

Physics- Division of Radiation Oncology, Houston, USA ; <sup>9</sup>Copenhagen University, Faculty of Health and Medical Science, Copenhagen, Denmark

### Purpose or Objective

Clinical proton radiotherapy (RT) currently assumes constant spatial relative biological effectiveness (RBE). In vitro data have demonstrated a dependence of RBE on local linear energy transfer (LET), but in vivo data are lacking. In order to model the relationship between dose, LET and RBE in clinical settings, tissue response must be assessed on the same voxel-to-voxel level as the 3D treatment plan information. We investigated a hybrid image registration methodology that utilizes multimodal anatomical imaging to deform functional images (diffusion tensor imaging [DTI] and 18F-FET-PET) between different timepoints, to relate local tissue response to dose and LET on a voxel-to-voxel basis.

### Material and Methods

Multimodal MRI sequences were acquired at baseline and in follow-up as part of a prospective study. Here we present the first results of multimodal hybrid image registration on a single patient with suspicion of progression due to anatomical changes leading to 18F-FET-PET scans on clinical indication in addition to the protocol MRI scans. All anatomical scans at a given timepoint were rigidly co-registered to create a hybrid template. Multimodal deformable image registration was used to relate templates between timepoints. The resulting deformation matrix was used to map functional imaging between baseline and all follow-ups. Functional imaging response was related to dose and LET on a voxel-by-voxel basis by co-registering planning CT to baseline MRI. Dose cubes were corrected for fraction size effects and LET RBE dependence by calculating:

$$EQD(d_x)_x = D_p \cdot [((\alpha/B)_x \cdot RBE_{max} + RBE_{min}^2 \cdot d_p) / ((\alpha/B)_x + d_x)]$$

(where  $d_x$  is dose per fraction,  $d_p$  is the proton dose per fraction and  $D_p$  is the total proton dose,  $(\alpha/B)_x = 2.1Gy$ ,  $RBE_{max} = \alpha_p/\alpha_x$  and  $RBE_{min}^2 = \beta_p/\beta_x$ ). Two models for dose correction were examined, in order to evaluate the impact of LET variation on RBE: (1) Fixed  $RBE_{max} = RBE_{min} = 1.1$ ; and (2) model-based (McNamara et al 2015)  $RBE_{max} = 0.99 + LET \cdot 0.36 / (\alpha/B)_x$ ,  $RBE_{min} = 1.10 - 0.0039 \cdot (\alpha/B)_x^{0.5} \cdot LET$ . Response was evaluated using change in fractional anisotropy (FA) MRI (loss of signal related to white matter changes) as well as 18F-FET-PET.

### Results

The image registration pathway is illustrated in Figure 1. For the example patient, imaging changes were noted at follow-up nine months after start of treatment (FU2), where multimodal MRI and FET-PET were performed. Average change in FA from baseline (DFA) and 18F-FET-PET signal as function of EQD2 are shown in Figure 2: Fig 2a for constant RBE (1), and Fig 2b for LET-dependent RBE (2). The constant RBE (1) dose shows very limited dose-response relations, while the LET-dependent RBE dose

seems to relate to local response in high dose regions.

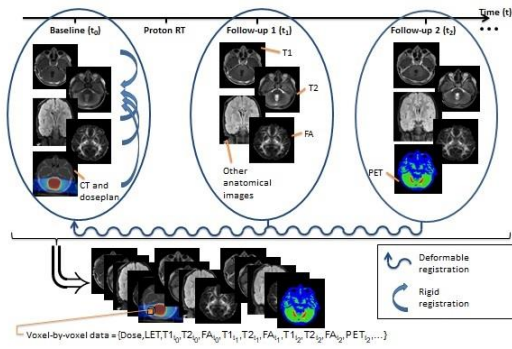


Figure 1. Schematic overview of the registration process. Time-interval between follow-ups was 3 months. Anatomical MRIs (T2 FLAIR, T1) and functional MRIs (diffusion tensor) were co-registered to a hybrid template, and then each hybrid template was registered with deformable image registration.

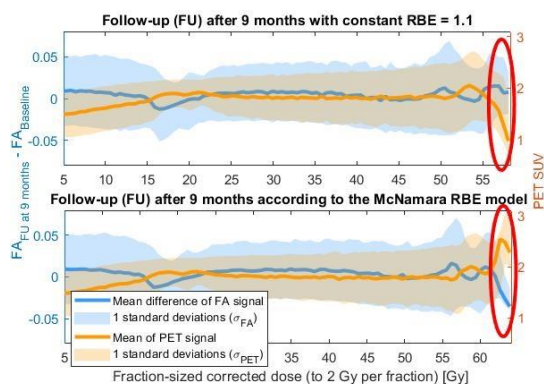


Figure 2. The difference between (1) the fixed RBE model with RBE=1.1 (top plot) and (2) the McNamara model for RBE dependence on LET (bottom plot) in terms of proton radiation response as measured by loss of fractional anisotropy signal (light-blue) and increase in 18F-FET-PET uptake (orange). Mean values of the signals are shown as solid lines while one standard deviation is shown as the corresponding highlighted regions.

## Conclusion

This framework uses multimodal deformable anatomical image registration to relate functional imaging changes to treatment information (dose and LET). This may allow in vivo assessment of RBE dependence on LET for proton RT in larger patient cohorts.

## EP-1920 ADC mean versus fractional volume to predict radiation sensitivity of HNSCC xenografted in nude mice

S. Leibfarth<sup>1</sup>, R.M. Winter<sup>1</sup>, S. Böke<sup>1,2</sup>, P. Mena-Romano<sup>1</sup>, E.C. Sezgin<sup>2</sup>, M. Krüger<sup>3</sup>, B. Pichler<sup>3,4</sup>, D. Zips<sup>2,4</sup>, D. Thorwarth<sup>1,4</sup>

<sup>1</sup>Section for Biomedical Physics- Department of Radiation Oncology, University Hospital Tübingen, Tübingen, Germany ; <sup>2</sup>Department of Radiation Oncology, University Hospital Tübingen, Tübingen, Germany ;

<sup>3</sup>Department of Preclinical Imaging and Radiopharmacy- Werner Siemens Imaging Center, Eberhard Karls University Tübingen, Tübingen, Germany ; <sup>4</sup>German Cancer Consortium DKTK- partner site Tübingen, and German Cancer Research Center DKFZ, Heidelberg, Germany

## Purpose or Objective

Pre-therapy diffusion weighted MR imaging (DW-MRI) has been associated with clinical RT outcome in various studies. In most studies the mean apparent diffusion coefficient (ADC) in the gross tumor volume (GTV) has been investigated for patient stratification. To further explore the potential of pre-therapeutic ADC, ADC maps obtained in pre-clinical head and neck squamous cell carcinomas (HNSCC) tumor models were studied for their

potential to stratify for cell line-specific radiation sensitivity.

## Material and Methods

The study was performed on immuno-deficient nude mice with tumors from different HNSCC cell lines grown in the hind leg (n=46) that had been measured on a 7T-PET/MR scanner (Bruker Biospec). The imaging protocol included anatomical T2w MRI and DW-MRI using 8 b-values between 0 and 800 s/mm<sup>2</sup>. Based on previously published tumor control doses 50% (TCD50) [1], the cell lines were grouped into three categories of radiation sensitivity: high (H), medium (M), and low (L) (cf. Table 1).

The GTV was defined manually on T2w MRI for each mouse by an experienced radiation oncologist. ADC maps were derived from the DW-MRI images by a mono-exponential fit. Two methods were used to define ADC-based variables for stratification according to radiosensitivity: mean ADC (M1) and volume fraction of ADC voxels below a pre-determined threshold (M2). For M2, the threshold was determined on a sub-group of the total cohort (n=30) based on optimal separation of the groups H-M and M-L. Final analysis of stratification potential using the determined threshold was performed on all samples.

## Results

The optimal threshold derived for M2 was ADC = 450E-6 mm<sup>2</sup>/s. The results of the two ADC-based variables for each sample are shown in Figure 1. M1 could stratify groups M and L (p = 7.83E-5, U-test), but not groups H and M (p = 0.17). M2 allowed to stratify all three groups (H-M: p=9.82E-5, M-L: p=7.83E-5). UTSCC-45 seems to have higher volume fractions in M2 compared to other high-sensitive cell groups (cf. Figure 1, M2). Possibly this is due to the fact that this cell line is HPV positive in contrast to all other cell lines.

## Conclusion

ADC was found to be a good biomarker for stratification of GTVs into different radiosensitivity groups in small-animal tumors. Particularly, the fractional volume of low ADC (M2) outperformed mean ADC (M1). These findings are being translated into a currently running clinical study to explore the performance of fractional volumes of low ADC against the more commonly used mean ADC. [1] Yaromina et al., Radiother Oncol 96:116 (2010) Acknowledgements: Research has received funding from the European Research Council (ERC).

radio-sensitivity	cell line	TCD50 in Gy (mean + CI)	number of tumors	tumor volume in mm <sup>3</sup> (mean ± SD)
H	UTSCC-45	45 [38,52]	9	926 ± 179
H	XF354	47 [40,55]	4	871 ± 227
H	UTSCC-14	52 [46,59]	4	740 ± 291
H	UTSCC-8	52 [40,61]	4	424 ± 137
M	FaDu	85 [77,96]	12	1317 ± 474
L	SAS	127 [114,140]	13	989 ± 547

Table 1: Characteristics of the small animal cohort. TCD50 values were taken from [1].

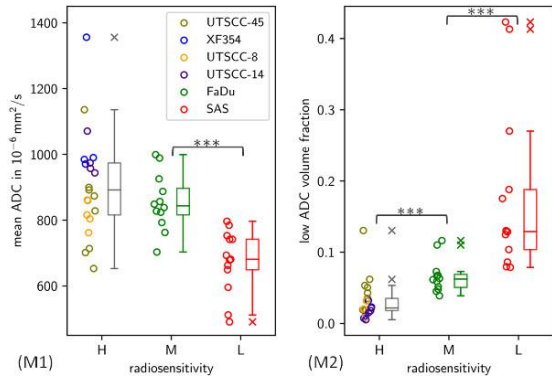


**Figure 1:** Plot of mean ADC (M1) and volume fraction of low ADC (ADC < 450E-6 mm<sup>2</sup>/s, M2) evaluated in the GTV for each mouse. Grouping is by radiosensitivity (H-high, M-middle, L-low). Groups H-M and M-L were tested for significant difference based on the U-test, with \*\*\* indicating p < 0.0001.

**EP-1921 Phase II AIRC-IG13218: Association of MRI-based radiomics with prognostic factors in prostate cancer**

D. Ciardo<sup>1</sup>, G. Marvaso<sup>1</sup>, S. Raimondi<sup>2</sup>, S. Volpe<sup>1,3</sup>, F. Botta<sup>4</sup>, L. Bianchini<sup>5</sup>, G. Riva<sup>1,3</sup>, D.P. Rojas<sup>1</sup>, G. Petralia<sup>6</sup>, S. Alessi<sup>6</sup>, P. Pricolo<sup>6</sup>, O. De Cobelli<sup>7</sup>, R. Orecchia<sup>8</sup>, M. Cremonesi<sup>9</sup>, M. Bellomi<sup>6</sup>, B.A. Jereczek-Fossa<sup>1,3</sup>  
<sup>1</sup>IEO- European Institute of Oncology IRCCS, Department of Radiation Oncology, Milan, Italy ; <sup>2</sup>IEO- European Institute of Oncology IRCCS, Division of Epidemiology and Biostatistics, Milan, Italy ; <sup>3</sup>University of Milan, Department of Oncology and Hemato-Oncology, Milan, Italy ; <sup>4</sup>IEO- European Institute of Oncology IRCCS, Unit of Medical Physics, Milan, Italy ; <sup>5</sup>University of Milan, Department of Physics, Milan, Italy ; <sup>6</sup>IEO- European Institute of Oncology IRCCS, Department of Radiology, Milan, Italy ; <sup>7</sup>IEO- European Institute of Oncology IRCCS, Department of Urology, Milan, Italy ; <sup>8</sup>IEO- European Institute of Oncology IRCCS, Scientific Direction, Milan, Italy ; <sup>9</sup>IEO- European Institute of Oncology IRCCS, Radiation Research Unit, Milan, Italy

**Purpose or Objective**

To decode tumour phenotype in prostate cancer (PCa) using a radiomic approach based on multiparametric magnetic resonance imaging (MRI).

**Material and Methods**

Give-me-five trial is a prospective phase II study designed for the treatment of PCa patients with ultra-hypofractionated radiotherapy scheduled in 5 fractions with 36.25 Gy delivered to the whole prostate and a concomitant boost of 37.5 Gy to the dominant intraprostatic lesion (DIL) identified by multiparametric MRI. T2-weighted (T2W) MRI sequences acquired on a 1.5T Magnetom Avanto<sup>Fit</sup> scanner (Siemens) with homogenous characteristics in terms of acquisition protocol were selected and the prostate gland contours were analysed. The extraction of radiomic features (shape, first-order statistics and textural features) was performed using the IBEX software after applying a 8 bit 3-sigma normalization and hierarchical clustering was applied to reduce features redundancy. We tested univariate association of each feature with Gleason score (GS, 3+3 vs 3+4 vs 4+3), extracapsular extension (ECE, 1/2 vs 2 vs 3) score, Prostate Imaging - Reporting and Data System (PIRADS, 2/3 vs 4 vs 5) score and risk class (intermediate vs low) by Kruskal-Wallis test and selected the feature with the lowest p-value in each cluster. We calculated both original p-values and False Discovery Rate (FDR) corrected p-values to adjust for multiple testing. We performed multinomial cumulative logistic regression models and

reported the c-statistic for model discrimination (results not shown). Statistical analysis was performed with SAS/STAT® software.

**Results**

Of the 65 prospectively enrolled patients, 49 T2W-MRI sequences fulfilled the inclusion criteria. Baseline characteristics of the study population are reported in Table. For each patient, 636 radiomic features were identified and then grouped in 10 clusters to reduce dimensionality. At univariate analysis, higher GS was associated with higher values of the texture feature GLRLM25\_LongRunLowGrayLevelEmpha (p=0.005, FDR adjusted p=0.05) and lower values of the shape feature Compactness2 (p=0.02, FDR adjusted p=0.08). Higher ECE score was associated with lower values of the histogram feature ID\_GlobalEntropy (p=0.03, FDR adjusted p=0.10). Higher PIRADS score was associated with lower values of the texture feature GLCM25\_45-4Entropy (p=0.01, FDR adjusted p=0.06). Higher risk class was associated with higher values of the texture feature GLCM25\_135-4Energy (p=0.01, FDR adjusted p=0.06). Boxplots in Figure show the distribution of these radiomic features according to the prognostic factors.

Table – Baseline characteristics of the study population (N=49).

Characteristic	N (%)
PSA*	6.47 (3.07)
T stage	
cT1	7 (14%)
cT2	42 (86%)
Gleason score	
3+3	26 (14%)
3+4	17 (86%)
4+3	6 (14%)
ECE score	
1	3 (6.3)
2	12 (24.5)
3	15 (30.6)
4	19 (38.8)
PIRADS score	
2	1 (2.0)
3	4 (8.2)
4	27 (55.1)
5	17 (34.7)
Risk class	
Low	8 (16.3)
Intermediate	41 (83.7)

Legend: PSA = prostate specific antigen, T= tumor, ECE = extracapsular extension, PIRADS = Prostate Imaging – Reporting and Data System.  
 \*Mean (standard deviation)

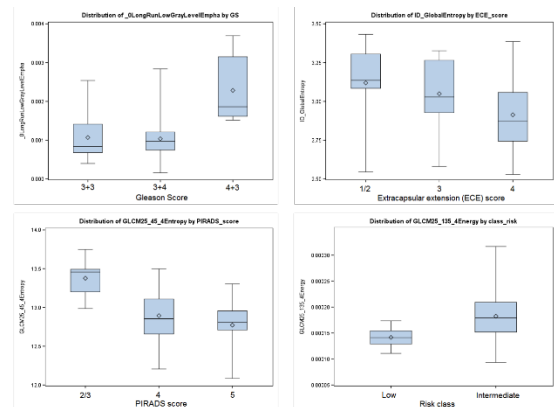


Figure – Boxplot representing the distribution of radiomic features according to prognostic factors.

**Conclusion**

MRI-based radiomics in PCa for the prediction of tumour phenotype is a feasible and promising approach. It might lead to a semi-automated definition of tumour characteristics and thus reduce the intra/inter-operator variability in the radiologic image interpretation. We plan to increase the dataset dimensionality in order to strengthen the statistical power and to validate results.

**EP-1922 Comparing biological and conventional dose accumulation using daily imaging of head and neck and pelvis cases**

N. Niebuhr<sup>1,2,3</sup>, T. Bostel<sup>3,4,5</sup>, K. Harrison<sup>6</sup>, R. Jena<sup>7,8</sup>, N.H. Nicolay<sup>4,9</sup>, D.J. Noble<sup>7,8</sup>, L.E.A. Shelley<sup>7,10,11</sup>, M. Splinter<sup>3,12</sup>, A. Pfaffenberger<sup>3,12</sup>

<sup>1</sup>German Cancer Research Center DKFZ, Department of Medical Physics in Radiation Oncology, Heidelberg, Germany ; <sup>2</sup>Heidelberg University, Department of Physics and Astronomy, Heidelberg, Germany ; <sup>3</sup>National Center for Radiation Research in Oncology NCRO, Heidelberg Institute for Radiooncology HIRO, Heidelberg, Germany ; <sup>4</sup>German Cancer Research Center DKFZ, Clinical Cooperation Unit "Radiation Oncology", Heidelberg, Germany ; <sup>5</sup>University Hospital Heidelberg, Department of Radiation Oncology, Heidelberg, Germany ; <sup>6</sup>University of Cambridge, Cavendish Laboratory, Cambridge, United Kingdom ; <sup>7</sup>Cambridge University Hospitals NHS Foundation Trust, Department of Oncology, Cambridge, United Kingdom ; <sup>8</sup>University of Cambridge, Department of Oncology, Cambridge, United Kingdom ; <sup>9</sup>Freiburg University Medical Center, Department of Radiation Oncology, Freiburg, Germany ; <sup>10</sup>University of Cambridge, Department of Engineering, Cambridge, United Kingdom ; <sup>11</sup>Cambridge University Hospitals NHS Foundation Trust, Department of Medical Physics and Clinical Engineering, Cambridge, United Kingdom ; <sup>12</sup>German Cancer Research Center DKFZ, Medical Physics in Radiation Oncology, Heidelberg, Germany

### Purpose or Objective

Daily imaging facilitates investigation of the impact of anatomical changes on the delivered dose. Conventional dose accumulation averages the fraction dose which introduces a systematic mathematical underestimate of the achieved biological effect in the presence of dose variations. To overcome this inconsistency in the use of the total delivered dose for biological models, we introduce an EQD-based formalism to accumulate the total biological dose. The difference with respect to conventional dose accumulation is investigated for two different patient cohorts using daily imaging.

### Material and Methods

We adapted the standard EQD-formalism to compare a treatment of constant fraction dose  $d$  to a treatment of daily varying doses  $d_i$ . The derived  $EQD_d(d_i)$  yields the total biological dose under consideration of the varying delivered doses and the tissue radiosensitivity. An initial cohort of 9 patients treated for prostate carcinoma with IMRT was studied using daily imaging with an in-room CT-on-rails system. Gamma index analysis (3%/3mm) is used to compare both the conventionally accumulated ( $D_a$ ) and the biologically accumulated ( $EQD_d$ ) with the planned dose. The second test cohort consisted of 30 out of 194 available patients treated for head and neck (H&N) tumours recruited in the VoxTox programme that underwent TomoTherapy and daily MVCT imaging.

### Results

$EQD_d$  is systematically higher than  $D_a$  with highest deviations in dose gradient regions around the target and in areas of strong motion amplitudes. In the pelvic cases, deviation hot spots in the bladder and rectum wall around 4 Gy were found for 5/9 patients. In 6/9 cases for both bladder and rectum using  $EQD_d$ , 2-4 Gy are added up locally in regions where the gamma criterion already failed using  $D_a$ , and furthermore leading to a failure rate increase of up to 3%. H&N patients showed an overall smaller difference between the two accumulation methods. Deviations are below 1 Gy for most volumes but deviation hotspots between 1 Gy and 8 Gy in OARs around the target volume were found in 20% of cases.

### Conclusion

The systematic underestimation of the biological effect from dose accumulation can potentially impair dose-response modelling and treatment adaptation. The presented approach of biological dose accumulation can avoid this inaccuracy. Stronger day-to-day motion amplitudes in the pelvic region compared with the H&N cases resulted in higher deviations of several Gy. Individual cases of high local deviation occurred in both

cohorts, highlighting the importance of daily imaging and the use of  $EQD_d$  rather than  $D_a$ . The impact of  $EQD_d$  on NTCP outcome is being investigated. Building on the results presented, the study of pelvic and H&N cases is being extended, exploiting the 194 available H&N cases as well as a dataset of 250 pelvic cases from the VoxTox programme. For local analysis, dose surface maps of the rectum are obtained for both  $D_a$  and  $EQD_d$ , and are compared for dose-response modelling.

### EP-1923 Dimensionality reduction of radiomic features using a clustering coherence-based approach

C. Tenconi<sup>1,2</sup>, T. Rancati<sup>3</sup>, F. Palorini<sup>3</sup>, A. Cerrotta<sup>4</sup>, B. Pappalardi<sup>4</sup>, F. Piccolo<sup>4</sup>, A. Messina<sup>5</sup>, M. Carrara<sup>6</sup>, T. Giandini<sup>6</sup>, C. Fallai<sup>4</sup>, E. Pignoli<sup>6</sup>, L. Licitra<sup>1,7</sup>, R. Valdagni<sup>1,2,3</sup>

<sup>1</sup>University of Milan, Department of Oncology and Haemato-oncology, Milan, Italy ; <sup>2</sup>Fondazione IRCCS Istituto Nazionale dei Tumori, Radiation Oncology 1, Milan, Italy ; <sup>3</sup>Fondazione IRCCS Istituto Nazionale dei Tumori, Prostate Cancer Program, Milan, Italy ; <sup>4</sup>Fondazione IRCCS Istituto Nazionale dei Tumori, Radiation Oncology 2, Milan, Italy ; <sup>5</sup>Fondazione IRCCS Istituto Nazionale dei Tumori, Radiology, Milan, Italy ; <sup>6</sup>Fondazione IRCCS Istituto Nazionale dei Tumori, Medical Physics, Milan, Italy ; <sup>7</sup>Fondazione IRCCS Istituto Nazionale dei Tumori, Head and Neck Medical Oncology Unit, Milan, Italy

### Purpose or Objective

Radiomic features (RFs) dimensionality represents a critical challenge to be addressed to lower the overfitting risk in radiomic studies. Assess a methodology for a-priori selection of non-redundant RFs from MR acquisitions and investigate its robustness over different clinical scenarios.

### Material and Methods

T2-weighted (T2W) images of 20 patients (pts) with locally advanced cervical cancer, treated with 4 session MR-guided adaptive brachytherapy were considered. Within ~12days, all pts underwent multiple MR with a standardized acquisition protocol. Fig. 1 illustrates study workflow: 77scans acquired with 2 different 1.5T scanners (same manufacturer) were uploaded to Image Biomarker EXplorer (IBEX) for RF extraction. Cylindrical regions of interest (ROIs) were manually drawn on 3 different anatomical regions, possibly representing 3 different radiomic scenarios: the left gluteus muscle (ROIg), outside treatment region (variation in RFs due to factors other than treatment); the cervix tumor target volume (ROIc), (variation in RFs induced by treatment); the bladder (ROIb), which is usually filled before each scan (uniform texture). From these ROIs 279 RFs were extracted for *Gray Level Cooccurrence Matrix 25 (GLCM25)*, *Gray Level Run Length Matrix 25 (GLRLM25)*, *Gradient Orient Histogram (GOH)* categories.

To explore linear associations among RFs and to investigate clustering coherence under different clinical/technical scenarios (inter-scanners, intra-patient, inter-ROIs), correlation matrices were computed for the whole dataset and for data grouped according to MR scanner, to ROI type (i.e.: ROIg/ROIc/ROIb) and to acquisition session. For each correlation matrix, clusters of highly correlated RFs (threshold  $r=0.85$ ) were identified and a "class label" assigned to the RF with the simplest mathematical definition. Redundant RFs (i.e., RFs with similar definition) were filtered out from the dataset for further analyses.

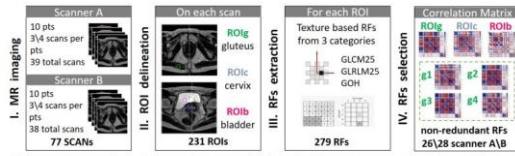


**Fig 1.** Study workflow: I, for each patient (pts) multi-MR scans were acquired, at different times, with 2 different scanners (A/B); II: on each scan 3 ROIs (regions of interest) were manually delineated; III: selected categories of texture based radiomic features (RFs) were extracted; IV: correlation matrices for different scenarios, i.e.: different ROI type (ROIg/ROIc/ROIb) and acquisition session (g1/g2/g3/g4,...), were computed and clustering coherence was investigated. Non-redundant sets of 26 and 28 RFs were obtained for scanner A and B, respectively.

## Results

Correlation analysis on the whole dataset highlights presence of several disjoint clusters made up of many highly correlated RFs, see **Fig. 2A**. Intra-scanner analysis, **Fig. 2B-C**, also revealed similar structures. Using a threshold of 0.85, 27 and 25 nonredundant RFs were selected for ROIg, considering, separately, data acquired with scanner A and B. The selected RFs were 27 and 30 for ROIc, 26 and 30 for ROIb. Strong clustering coherence was observed for GLRLM25 features (all the examined ROIs have the same class label set in common). Also, GOH RFs have a higher number of stable clusters in common among all the ROIs compared to GLCM25. Likewise, preliminary intra-patient analysis confirmed the same clustering coherence for GLCM25 and GOH features.

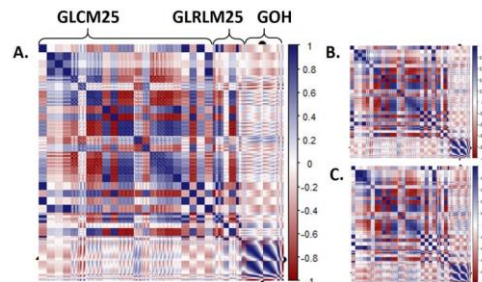


**Fig 2.** A. Correlation matrix computed on the whole dataset (20pts, 231ROIs); B.-C. Correlation matrices obtained for scanner A and B, respectively. Blu blocks along the diagonals represent highly positively correlated clusters of features.

## Conclusion

The proposed methodology of clustering coherence analysis allowed to reduce to about 1/10 the number of RFs to be used for further analyses. A-priori reduction of RF number will enhance generalization capability of radiomic signatures and speed up implementation of radiomic approaches into clinical practice.

### EP-1924 Are spatial dose metrics predictive of oral mucositis duration in oropharyngeal cancer?

A. Carver<sup>1</sup>, M. Hickman<sup>2</sup>, S. Warren<sup>1</sup>, M. Ward<sup>1</sup>, A. Thomas<sup>2</sup>, P. Sanghera<sup>3</sup>, C. Fong<sup>3</sup>, A. Hartley<sup>3</sup>

<sup>1</sup>University Hospital Birmingham NHS Foundation Trust, Medical Physics, Birmingham, United Kingdom ;

<sup>2</sup>University Hospital Birmingham NHS Foundation Trust, Radiotherapy, Birmingham, United Kingdom ; <sup>3</sup>University Hospital Birmingham NHS Foundation Trust, Clinical Oncology, Birmingham, United Kingdom

### Purpose or Objective

In patients with oropharyngeal cancer treated with chemoradiotherapy oral mucositis is very likely to occur at a significant grade and the pertinent question is the duration rather than the probability of occurrence. It has been established that simple dosimetric parameters do not correlate well to the duration of toxicity in these patients (Hickman, M. 2017). This study uses spatial dose metrics to try to establish whether there is a more complex relationship between dose and toxicity duration.

## Material and Methods

The duration of significant mucositis in 81 patients with oropharyngeal cancer was measured via four outcome metrics (CTCAE versions 3 and 4 (grade 3 or greater), patient reported duration of interference in daily activities (quite a bit or very much) and patient reported duration of severity (severe or very severe)). The oral mucosa volume was outlined according to international consensus guidelines. The section of the dose grid intersecting the oral mucosa was extracted and converted to BED. Thirty nine intensity and spatial metrics were extracted from the dose grid using Pyradiomics (van Griethuysen, J. J. M et al, 2017). Varimax rotated PCA was used to de-correlate the data and reduce the thirty nine dimensions down to the ten dimensions with the greatest variance. These ten variables were combined into a single model predicting the duration of toxicity. The dose bin width for the calculation of dose metrics was set to be 1 Gy<sub>10</sub> BED wide.

## Results

The median duration was 7 weeks for all toxicities except for patient reported severity which was 6 weeks. The interquartile range was 4-5 weeks with outliers ranging from 0 to 15 weeks. When correlating the principal components against toxicity duration two components remained statistically significant after applying a Benjamini-Hochberg correction namely CTCAE V4 and the patient reported duration of severity outcomes. These two features were strongly anti-correlated although the dominant features in the components were different. The first component was dominated by metrics related to the spread of doses such as variance. The other component was dominated by the median and image coarseness, a measure of the rate of change of the dose. A third component was also significant until the multiple comparison correction. Lasso regression identified similar metrics to be important as those found by varimax rotated PCA analysis.

## Conclusion

Spatial metrics were not found to correlate any more strongly to the duration of mucositis than simpler metrics. The most strongly correlated factors were metrics such as median dose and variance rather than the spatial metrics. Factor analysis suggested metrics related to the variance in the dose delivered to the oral mucosa and the rate of change in dose within a region was correlated to duration of toxicity. Outcome modelling with regression and classification is difficult with no strong classifiers. Work is ongoing to try and create a model to identify patients at risk of long toxicity duration.

### EP-1925 Association of MRI-based radiomic features with prognostic factors in oropharyngeal cancer

G. Marvaso<sup>1</sup>, C. Delia<sup>1</sup>, D. Alterio<sup>1</sup>, F. Botta<sup>2</sup>, C.

Giannitto<sup>3</sup>, S. Volpe<sup>1,4</sup>, F.A. Maffini<sup>5</sup>, S. Raimondi<sup>6</sup>, M.

Ansarin<sup>7</sup>, M. Bellomi<sup>3</sup>, B.A. Jereczek-Fossa<sup>1,4</sup>

<sup>1</sup>IEO- European Institute of Oncology IRCCS,

Radiotherapy, Milan, Italy ; <sup>2</sup>IEO- European Institute of

Oncology IRCCS, Unit of Medical Physics, Milan, Italy ;

<sup>3</sup>IEO- European Institute of Oncology IRCCS, Radiology,

Milan, Italy ; <sup>4</sup>University of Milan, Department of

Oncology and Hemato-oncology, Milan, Italy ; <sup>5</sup>IEO-

European Institute of Oncology IRCCS, Division of

Pathology, Milan, Italy ; <sup>6</sup>IEO- European Institute of

Oncology IRCCS, Epidemiology and Biostatistics, Milan,

Italy ; <sup>7</sup>IEO- European Institute of Oncology IRCCS,

Otolaryngology and Head and Neck Surgery, Milan, Italy

### Purpose or Objective

Radiomics focuses on extracting a large number of quantitative imaging features correlated with clinical characteristics. We propose a radiomic approach using magnetic resonance imaging (MRI) to decode tumour phenotype and treatment response in oropharyngeal squamous cell carcinoma (OPSCC).

### Material and Methods

The T1-weighted MRI sequences of OPSCC patients treated between 2008 and 2016 were retrospectively selected. The extraction of radiomic features was performed using the IBEX software, and hierarchical clustering was applied to reduce features redundancy. The association of each radiomic feature with grading, HPV status and loco-regional recurrence within 2 years, considered as main endpoints, was assessed by univariate analysis and then corrected for multiple testing. Statistical analysis was performed with SAS/STAT® software

### Results

Thirty eligible cases were identified. For each patient, 1286 radiomic features were extracted, subsequently grouped into 16 clusters. Higher grading (G3 vs. G1/G2) was associated with higher values of *GLCM3/0-1MaxProbability* and lower values of *GLCM25/135-1ClusterShade* ( $p=0.03$  and  $0.04$ , respectively). Positive HPV status was associated with higher values of *GLCM3/11-4Contrast*, *GLCM3/6-1ClusterProminence*, *GLCM25/180-1InformationMeasureCorr2* ( $p=0.03$ ,  $0.02$  and  $0.04$ , respectively) and lower values of *GLCM3/11-4Correlation* and *GLCM3/11-7Correlation* ( $p=0.04$  and  $0.01$ , respectively). Loco-regional recurrence within 2 years was associated with higher values of *GLCM3/4-7Correlation* ( $p=0.04$ ) and lower values of *GLCM3/2-1InformationMeasureCorr1* ( $p=0.04$ ). Results lost statistical significance after correction for multiple testing.

### Conclusion

MRI-based radiomics in OPSCC for the prediction of tumour phenotype and treatment response is a feasible and promising approach. Larger collaborative studies are warranted in order to increase the statistical power and to obtain robust and validated results.

### EP-1926 Radiomics in rectal cancer: prognostic significance of 3D features extracted from diagnostic MRI

C. Piazzese<sup>1</sup>, P. Whybra<sup>1</sup>, E. Qasem<sup>2</sup>, D. Harris<sup>2</sup>, R. Gtaes<sup>3</sup>, K. Foley<sup>4</sup>, E. Spezi<sup>1</sup>

<sup>1</sup>Cardiff University, School of Engineering, Cardiff, United Kingdom ; <sup>2</sup>Singleton Hospital, Department of Surgery, Swansea, United Kingdom ; <sup>3</sup>Singleton Hospital, Medical Physics, Swansea, United Kingdom ; <sup>4</sup>Cardiff University, School of Medicine, Cardiff, United Kingdom

### Purpose or Objective

Many radiomic studies have successfully demonstrated the potential value of PET and CT image features to predict patient outcomes. MRI can be susceptible to greater technical heterogeneity during its acquisition but, compared to PET and CT, relatively few studies have assessed the added value of MRI radiomics. In this work, we aimed at assessing the prognostic value of 3D textural features extracted from MR images of patients with locally advanced rectal cancer (LARC).

### Material and Methods

A cohort of 29 patients with LARC were investigated in this study. All patients underwent anatomical T2 MRI examination before preoperative chemoradiotherapy (CRT) and were followed up for at least 98 months. All MRI scans were processed using the CERR package<sup>1</sup> and a range of radiomics features developed in-house and compliant with the IBSI initiative<sup>2</sup>. The voxels within the tumour region with intensities outside the range  $\mu \pm 3\sigma$  were rejected and the intensity range obtained was then quantized to 6 bits. Radiomic features were automatically extracted using in-house developed image and data analysis software<sup>3</sup>. Pearson coefficient was computed and used to rank the features so to retain the 25 most variant ones. Each feature was then compared to the remaining ones and if the Pearson correlation coefficient was outside the range  $[-0.4, 0.4]$  the feature with the highest rank was removed. A prognostic model (Cox regression) was

developed by using filtered features and clinical characteristics. The calculated median prognostic score was used to separate patients into two groups and differences in overall survival (OS) were evaluated.

### Results

A total of 138 3D imaging features were computed for each patient. Six uncorrelated features were used to construct a Cox regression model together with 3 clinical variables (age, pre-treatment tumour stage and tumour regression grade). The model identified 1 feature (morphologic elongation) that was significantly associated with OS ( $p$ -value  $< 0.05$ , HR = 0.004, 95% CI = 0 - 1.17). There was a significant difference ( $X^2= 8.485$ , df = 1,  $p$ -value  $< 0.05$ ) in OS according to the median prognostic score (Figure 1).

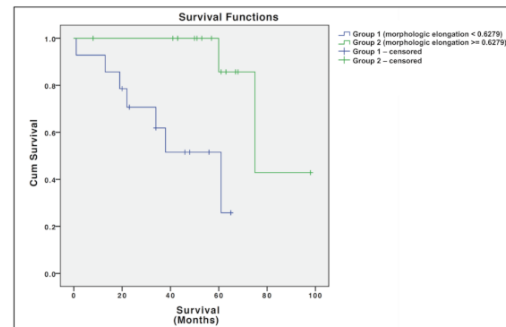


Figure 1. Kaplan-Meier plot of the patients separated in two groups based on the prognostic score.

### Conclusion

MRI radiomics could provide additional information in LARC patients before preoperative CRT. Although based on a relatively small sample size, these preliminary results show that morphologic elongation are correlated with OS. Further work is needed to test the stability of MRI radiomic features and validate their predictive potential in larger cohorts of patients with LARC.

### References:

1. Deasy JO et al. CERR: a computational environment for radiotherapy research. *Med Phys.* 2003 May;30(5):979-85.
2. Zwanenburg A et al. Image biomarker standardisation initiative, <https://arxiv.org/abs/1612.07003v7>
3. Gwynne S et al. Toward semi-automated assessment of target volume delineation in radiotherapy trials: the SCOPE 1 pretrial test case. *Int J Radiat Oncol Biol Phys.* 2012 Nov 15;84(4):1037-42.

### EP-1927 Mechanistic modelling of RT damage to microvasculature and of its effect on tumour microenvironment

A. Cicchetti<sup>1</sup>, F. Laurino<sup>2</sup>, E. Pascucci<sup>2</sup>, T. Rancati<sup>1</sup>, P. Zunino<sup>2</sup>

<sup>1</sup>Fondazione IRCCS Istituto Nazionale dei Tumori, Prostate cancer program, Milan, Italy ; <sup>2</sup>Politecnico di Milano, MOX - Department of Mathematics, Milan, Italy

### Purpose or Objective

There is evidence that radiotherapy affects the morphology and the function of small vessels, such as capillaries, of healthy and neoplastic tissues exposed to radiation. However, the underlying mechanisms of this effect are still poorly understood. Here, we present a mathematical model for the tumor microenvironment, with the unique ability to describe (i) realistic vasculature; (ii) capillary flow with non-Newtonian blood rheology and capillary leakage; (iii) coupling of capillary flow and interstitial flow; (iv) capillary deformation and occlusion; (v) mass, heat and particle transport. This model embraces enough of the fundamental physics regulating the tumor microenvironment such that it is

suitable to describe the effects of radiation on the fluid balance at the microvascular level. We will discuss different scenarios that illustrate this dependence.

**Material and Methods**

The model describes the tumor microenvironment in a three-dimensional setting representing a tissue slab of about 0.5 mm size (Fig.2). The model consists of a system of coupled partial differential equations that are solved numerically, by means of an in house code based on the finite element method. This approach has been already successfully applied to model drug delivery and hyperthermia (*Int J Numer Meth Biomed Engng* 2014).

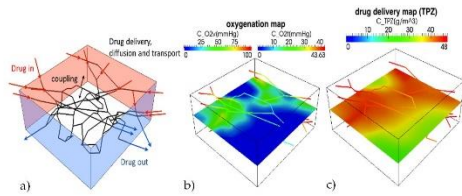


Fig. 1: the in-silico model consists of a tumour slab of R3230AC mammary carcinoma in rat dorsal skin flap preparation. The boundary conditions (inflow/outflow) are shown in panel (a); the simulated map of oxygen released from the vasculature to the tissue is shown in panel (b); Panel (c) shows the drug injected at the inflow points and delivered to the tissue.

**Results**

We study interplay between radiotherapy and microcirculation in the early phase, namely within 24 hours from treatment. The effect of radiation on microvasculature is primarily represented in the model by means of an increase of vascular permeability and degradation of the mechanical properties of the vascular walls (in terms of thinning and decrease of the Young modulus). We show that the combination of these effects entails a cascade of phenomena involving interstitial hypertension, capillary constriction and finally occlusion of the weakest channels, which correspond to the observed outcomes of radiotherapy, such as decrease of the volumetric density of functional capillaries.

More precisely, the fundamental governing equations (Fig.2) are solved with numerical simulations. Possible effects of radiation on the functional parameters are also shown.

The exact tuning of the parameters describing damage as a function of dose/dose fractionation (for example the constitutive relation for  $L_p$  increasing with increasing RT dose) will be performed by measuring damage to microvessels on microfluidic chips as a function of dose, using a clinical linear accelerator.

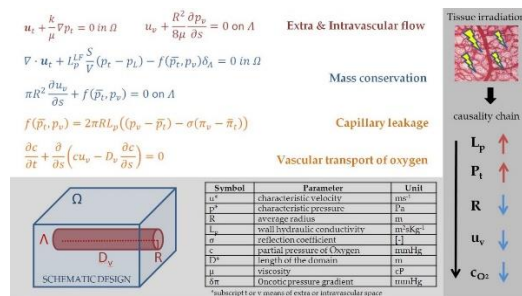


Fig.2: Set of equations (and parameters) included into the simulation code. On the right side a possible causality chain activated by the irradiation of the intra and extravascular space.

**Conclusion**

The results of this study represent a first step towards the challenging objective of understanding, and describing in a mechanistic way, the effect of radiation on the vascular microenvironment. Combining such mechanistic causality laws with patient specific data about the vascular environment, will enable prescription of radiotherapy treatment based on additional/patient specific guidelines that improve the treatment efficacy and preserve the

functionality of tissue/structures/organs neighboring the treated region.

**EP-1928 Radiomic features and local response in Lung Cancer treated with Stereotactic Radiation Therapy**

S. Chiesa<sup>1</sup>, R. Gatta<sup>2</sup>, A. Martino<sup>1</sup>, A. Piras<sup>1</sup>, D. Cusumano<sup>1</sup>, L. Boldrini<sup>1</sup>, C. Masciocchi<sup>1</sup>, M. Massaccesi<sup>3</sup>, N. Dinapoli<sup>3</sup>, F. Cellini<sup>1</sup>, A. D'Aviero<sup>1</sup>, G.C. Mattiucci<sup>1</sup>, G. Mantini<sup>1</sup>, M. Balducci<sup>1</sup>, V. Valentini<sup>1</sup>

<sup>1</sup>Fondazione Policlinico A. Gemelli IRCCS- Università Cattolica Sacro Cuore, Dipartimento Scienze Radiologiche- Radioterapiche ed Ematologiche- Istituto di Radiologia, Rome, Italy ; <sup>2</sup>Università Cattolica del Sacro Cuore- Roma Italia, Dipartimento Scienze Radiologiche- Radioterapiche ed Ematologiche- Istituto di Radiologia, Rome, Italy ; <sup>3</sup>Fondazione Policlinico A. Gemelli IRCCS, Dipartimento Scienze Radiologiche- Radioterapiche ed Ematologiche- Istituto di Radiologia, Rome, Italy

**Purpose or Objective**

Stereotactic ablative radiation therapy (SABR) is a treatment option for early-stage lung cancer. This study investigates the prognostic performance of radiomic features for disease recurrence in early stage non-small cell lung cancer (NSCLC) patients treated with stereotactic ablative radiation therapy (SABR).

**Material and Methods**

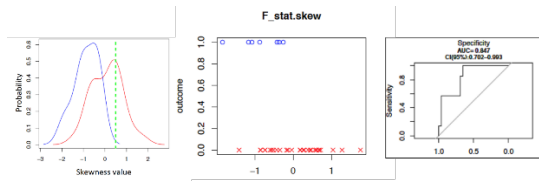
Patients with early stage NSCLC, treated with SABR were considered for this study. The lung lesions received a total dose of 42 Gy in 3 fractions or 50 Gy in 5 fractions according to the site.

A 4D-CT was performed to delineate the internal target volume (ITV) and the radiomic features were extracted from the ITV reported on average intensity projection (AIP), through the use of a dedicated software. The Wilcoxon Mann Whitney test was applied to evaluate the significance of the radiomic features; afterwards a Logistic Regression model was built for each significant feature. We considered as main outcome the response to SABR according to RECIST Criteria. The clinical response was evaluated during the follow up through the CT and PET-CT scans.

**Results**

Forty-two early stage NSCLC patients and 47 lesions, receiving SABR, were considered for this analysis. Thirteen lesions presented a local recurrence.

Ninety-four features were extracted using a dedicated software. The correlation between the radiomic features and the local recurrence at 12-24 and 36 months was investigated. Seventeen features showed a significant correlation ( $p < 0.01$ ) with local recurrence at 12 and 24 months at Wilcoxon Mann Whitney test: 3 intensity based statistical features; 2 Grey level co-occurrence based features-Texture features (GLCM); 6 Grey level run length based features-Texture features (GLRLM); 6 Grey level size zone based features-Texture features (GLDZM), according to Image biomarker standardization initiative v.7 (<https://arxiv.org/abs/1612.07003>). No correlation was found between radiomic features and local recurrence at 36 months. At the kernel density estimation of Skewness ( $p < 0.01$  at the Mann Whitney test) is shown on the picture on the left for both, the positive (blue) and negative (red) lesions, on Figure 1. In the middle the distribution of positive and negative outcomes (same colors) depending on the value of Skewness and on the right the ROC curve of the associated Logistic Regression model (AUC = 0.847).



## Conclusion

These results suggest that radiomics can help in detecting, under specific circumstances (e.g. Skewness greater or equal than 0.5) local recurrence at 12 months after SABR and that this decision support system could potentially allow for early salvage therapy. A multicentric study in order to increase the number of patients and to confirm the interesting results is ongoing.

## EP-1929 Prediction of voxelwise mandibular osteoradionecrosis maps in HNC patients using deep learning

L. Humbert-Vidan<sup>1</sup>, I. Oksuz<sup>2</sup>, V. Patel<sup>3</sup>, A.P. King<sup>2</sup>, T. Guerrero-Urbano<sup>4</sup>

<sup>1</sup>Guy's and St Thomas' NHS Foundation Trust / King's College London, Radiotherapy Physics, London, United Kingdom ; <sup>2</sup>King's College London, School of Biomedical Engineering & Imaging Sciences, London, United Kingdom ; <sup>3</sup>Guy's and St Thomas' NHS Foundation Trust, Oral Surgery, London, United Kingdom ; <sup>4</sup>Guy's and St Thomas' NHS Foundation Trust, Clinical Oncology and Radiotherapy, London, United Kingdom

### Purpose or Objective

Head and neck cancer (HNC) incidence accounts for 3% of all cancers in the UK. Radiotherapy is one of the main treatments for HNC, either alone or combined with chemotherapy, surgery or hormones. Radiation-induced toxicity to healthy tissue can be a limiting factor for the successful treatment of HNC. Mandibular osteoradionecrosis (ORN) is one of the most severe complications in patients with HNC undergoing radiation therapy. Normally, the risk of toxicities such as ORN is assessed using dose-volume histograms (DVH), but DVH-based parameters ignore the spatial component of radiation dose distribution. We propose the use of deep learning to predict 3D ORN toxicity maps based on 3D dose distribution maps and CT volumes using a U-net convolutional neural network. The ability to predict spatial toxicity maps has the potential to assist decision making in the radiotherapy treatment planning process.

### Material and Methods

Our current deep CNN design is based upon the original U-net deep CNN (see Figure 1). Our model is trained to predict 2D ORN toxicity maps based on corresponding slices extracted from 3D dose distribution maps and CT volumes. The CT and dose map imaging data were used as two channels of input to the network. A total of 232, 59 and 16 sets of slices (i.e. dose map, CT slices and ORN masks) were used for training, validation and testing respectively. Data augmentation was implemented on the training dataset.

The Dice Similarity Coefficient loss function was used to train and validate the CNN and the Adam optimiser was used to minimise the loss function. Dropout regularisation (20%) was used to prevent the model from overfitting. A basic manual grid search of parameter values was performed to find the optimal combination of training parameters for the CNN. Based on this search, the best performance was achieved by training the network for 500 epochs with a batch size of 40 and a learning rate of 0.00001.

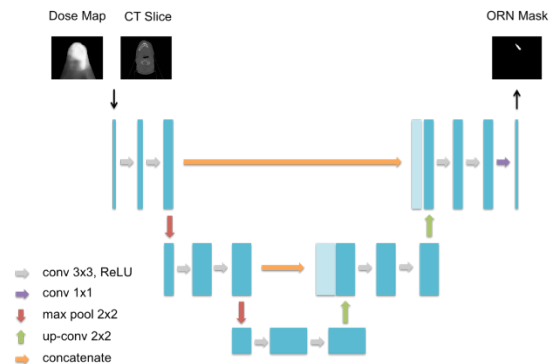


Figure 1. Schematics showing our U-net deep CNN design.

## Results

The training, validation and testing Dice coefficients obtained so far are 0.90 (max), 0.51 (max) and 0.13 (mean), respectively. An improvement in all three coefficients was observed when training the network with the augmented dataset. A maximum test dice coefficient of 0.83 was obtained (see Figure 1). However, in the current ORN predictions of the network, some segmentations appear on the wrong side of the mandible; adding more training cases could help to improve the prediction of ORN location. In addition, some predictions do not contain any ORN at all. A custom loss function could be considered to try to improve performance in such cases.

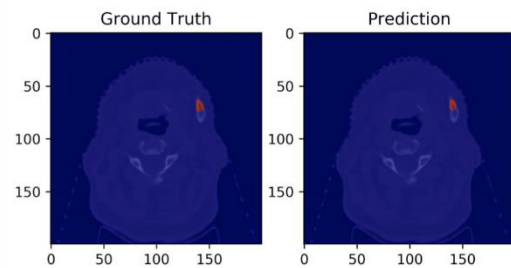


Figure 2. Example of a good agreement (test Dice coefficient of 0.83) between the ground truth (left) and predicted (right) segmentations.

## Conclusion

Our current design of the U-net is able to produce ORN masks based on CT images and dose distribution maps. The results obtained so far are encouraging but the accuracy of the ORN predictions could be improved. Further work is required in both data processing, CNN design and parameter optimisation to achieve these improvements. The predicted toxicity spatial maps will provide more specific information on what normal tissue regions are at a higher risk.

## EP-1930 Hypoxia induced by vascular damage could impact on the outcome of stereotactic body radiotherapy

E. Lindblom<sup>1</sup>, A. Dasu<sup>2</sup>, I. Toma-<sup>3</sup>

<sup>1</sup>Stockholm University, Medical Radiation Physics, Stockholm, Sweden ; <sup>2</sup>The Skandion Clinic, The Skandion Clinic, Uppsala, Sweden ; <sup>3</sup>Stockholm University and Karolinska Institutet, Department of Physics and Department of Oncology and Pathology, Stockholm, Sweden

### Purpose or Objective

Recent years have seen an increasing interest in studying the vascular response from large fractional doses delivered in stereotactic body radiotherapy (SBRT). While the vascular effect is extensively discussed as a potential source for tumour cell kill, the observed vascular response after doses of 10-15 Gy appears to be highly dynamic. With an initial reduction in blood flow that persists for various lengths of time, the actual vascular effect could be highly dependent on the time point at which treatment fractions are delivered with respect to each other. Thus, rather than leading to an increased cell kill, an increased radioresistance could be expected during the limited SBRT treatment if the total fraction of acutely hypoxic cells is increased. This study investigated the impact of temporary vascular collapse on tumour control probability (TCP) in SBRT, taking into account the different radiosensitivity of chronically and acutely hypoxic cells.

### Material and Methods

Three-dimensional tumours were simulated based on tumour vessel distributions assuming different fractions of collapsed vessels at every treatment fraction. Thus, the simulated tumours contained both chronically and acutely hypoxic regions before the start of the treatment, the chronically hypoxic subvolume having a size of 30-60% of the tumour diameter, and a hypoxic fraction <5mmHg of 30-50%. The rest of the tumours were in general well-oxygenated at the start of the treatment. A radiation-induced increase in the acutely hypoxic fraction was simulated following the first fraction. SBRT-fractionation schedules of 3, 5, and 8 fractions were considered, and cell survival was calculated with a modified linear-quadratic model taking into account different radiosensitivities of chronically and acutely hypoxic cells. The simulated treatments were evaluated by calculating the TCP.

### Results

A complex interplay between the radiation-induced and chronic hypoxia was observed for different fractionation schedules. For an eight-fraction treatment, for example, delivering 60 Gy in total, the TCP for a tumour with no treatment-induced vascular collapse in the well-oxygenated region and a chronically hypoxic subvolume with a diameter corresponding to 30% of the tumour size, was 97%. Assuming a vascular collapse of 35% induced by the first fraction and persisting throughout the remainder of the treatment resulted in a TCP of only 2% while the TCP was 83% for an identical tumour except for a much larger chronically hypoxic subvolume with a diameter of 60% of the tumour size. Thus, radiation-induced increase in acute hypoxia had a worse impact on the outcome of the treatment than an increase diameter of the chronically hypoxic subvolume.

### Conclusion

The timing of SBRT fractions leading to vascular damages and thus increased acute hypoxia could impact on the efficacy of the treatment, and should be considered together with the tumour oxygenation to avoid loss of TCP for SBRT treatments.

### EP-1931 Photon vs proton therapy for reduction of cardiac toxicities in locally advanced lung cancer

S. Teoh<sup>1</sup>, F. Fiorini<sup>1</sup>, B. George<sup>1</sup>, K.A. Vallis<sup>1</sup>, F. Van den Heuvel<sup>1</sup>

<sup>1</sup>CRUK/MRC Oxford Institute for Radiation Oncology, Oncology, Oxford, United Kingdom

### Purpose or Objective

Identify a sub-group of patients with locally advanced lung cancer who would benefit most from proton therapy compared to photon therapy for reduction of cardiac toxicities using the model-based approach.

### Material and Methods

Dual-arc volumetric modulated arc photon therapy (VMAT) and robust-optimised intensity modulated proton

therapy (IMPT) plans were created in twenty proxy patients with locally advanced lung cancer to a physical dose of 70Gy in 35 fractions. Proxy patients were selected to represent varying anatomical locations of the primary tumour and nodal involvements (15/20 had nodal involvement). Contouring, treatment planning and organs-at-risk constraints followed RTOG 1308 trial. The following cardiac sub-structures were delineated- right and left: atriums, ventricles and coronary arteries, and sino-atrial node. Dose calculation and optimisation of IMPT plans were done using Monte-Carlo dose engine. Dose to the heart and sub-structures were compared. Risk estimates of grade 3+ cardiac toxicities were calculated based on normal tissue complication probability models which incorporated dose metrics and patients' risk-factor - pre-existing cardiac disease (CD). Wilcoxon signed-rank test was used to assess statistical significance of the difference.

### Results

There was no statistically significant difference in target coverage between VMAT and IMPT. Overall IMPT delivered lower doses to the heart (mean heart dose (MHD), V5 and V30). In VMAT plans, there were statistically significant positive correlations between heart dose and thoracic vertebral level (MHD, V5 and V30; Pearson correlation coefficient,  $r$ : 0.67, 0.79, 0.48,  $P < 0.05$ ). Between VMAT vs IMPT, there was no statistically significant difference in the mean cardiac dose or its sub-structures when the tumour (primary and nodes) extended above T7 vertebrae ( $n = 4$ ). When tumour extended to and below T7 vertebrae ( $n = 16$ ) IMPT delivered lower cardiac doses (MHD, V5 and V30, and mean dose to all sub-structures,  $P < 0.001$ ). Risk of G3+ cardiac toxicities when tumour extended to and below T7 vertebrae are presented in Table 1.

Table 1: Risk estimates of G3+ cardiac toxicities with tumour extension to and below T7 vertebrae

Cardiac Risk	VMAT (95% CI)	IMPT (95% CI)
Pre-existing CD		
AR (based on MHD, %)	19 (16-20)	11 (10-13)
AR (based on V5, %)	25 (20-30)	9 (8-10)
RR reduction (based on MHD)		0.39 (0.31-0.47)
RR reduction (based on V5)		0.59 (0.50-0.69)
No pre-existing CD		
AR (based on MHD, %)	7 (4-9)	3 (3-4)
AR (based on V5, %)	11 (8-13)	3 (3-4)
RR reduction (based on MHD)		0.45 (0.34-0.57)
RR reduction (based on V5)		0.62 (0.51-0.73)

CI - confidence interval, CD - cardiac disease, AR - absolute risk, MHD - mean heart dose, RR - relative risk

### Conclusion

Proton therapy has the potential to reduce cardiac toxicities compared to photon therapy. This analysis suggests that patients with tumour extension to and below T7 vertebrae would benefit most from proton therapy over photon therapy. The absolute benefit is higher in patients with underlying cardiac disease.

### EP-1932 Development of a deep learning network using a pre-trained convolutional neural network

M. Rooney<sup>1</sup>, J. Mitchell<sup>2</sup>, D.B. McLaren<sup>2</sup>, W.H. Nailon<sup>1,3</sup>

<sup>1</sup>NHS Lothian, Department of Oncology Physics-Edinburgh Cancer Centre, Edinburgh, United Kingdom ;

<sup>2</sup>NHS Lothian, Department of Clinical Oncology-Edinburgh Cancer Centre, Edinburgh, United Kingdom ;

<sup>3</sup>The University of Edinburgh, School of Engineering, Edinburgh, United Kingdom

### Purpose or Objective

The use of machine and deep learning is rising in oncology. Discrimination of tissue types using texture analysis is a long standing technique. Texture features are often used to train machine learning models. Deep learning, a subfield of machine learning, overcomes the need to calculate features by allowing the machine to learn directly from the image. However, a large amount of labeled image data is required to train deep learning models, this is a difficulty in oncology. The aim of this

work was to investigate the feasibility of applying a pre-trained CNN to a set of medical T2 MRI images with the intent to identify areas of disease in the prostate using texture analysis as a baseline.

#### Material and Methods

T2 MRI studies of 16 patients with localised prostate cancer were studied. The MRI images were rigidly registered to the planning CT and the OAR's, prostate and the focal lesion were contoured by a consultant oncologist. Using Matlab, three workflows were investigated. Firstly, 32 texture features were calculated to characterise the image properties of healthy and diseased tissues and used to train four different machine learning algorithms. Secondly AlexNet, a CNN trained on > 1 million images containing 1,000 classes was used as a feature extractor for later classification. Lastly, AlexNet was adapted for use on MRI images using transfer learning. Each was initially developed on Brodatz images containing strong textural features. This was then translated onto a set of 40 prostate MRI images published as part of a MICCAI grand challenge, Figure 1, to test performance on a set of medical images. The models were assessed in terms of accuracy, sensitivity, specificity and AUC (Table 1).

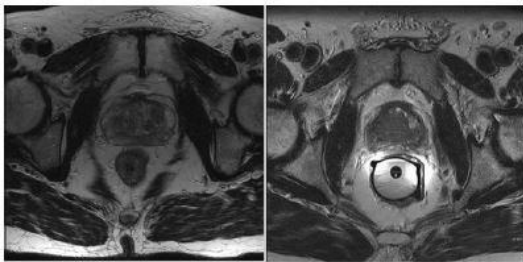


**Figure 1:** An example of the T2 MRI images included in the MICCAI dataset with and without an endorectal coil, only cases without an endorectal coil were considered.

#### Results

Findings from Brodatz images showed the ability to obtain high levels of classification accuracy using texture analysis and CNNs. Application to the MICCAI data showed that superior sensitivity can be achieved using a fine-tuned CNN over texture analysis. Transfer learning was successful in identifying prostate from surrounding structures in T2 prostate MRI images with the hypothesis being that the CNN would identify generic features common to most images such as colour, contrast and repetitive patterns. Application to the local dataset showed promise. Using AlexNet, the results were on par with those of machine learning but low sensitivity was observed. This is likely due to the high level of imbalance inherent to this data type.

Data Set	Method	Accuracy	Sensitivity	Specificity	AUC
Brodatz	Texture Features	0.924	0.924	0.924	0.978
	CNN Derived Features	0.818	0.701	0.867	0.899
	Fine-tuned CNN	0.966	0.918	0.989	0.996
MICCAI	Texture Features	0.595	0.492	0.716	0.651
	CNN Derived Features	0.529	0.241	0.867	0.568
	Fine-tuned CNN	0.593	0.830	0.367	0.635
T2 Prostate Cancer Positive	Texture Features	0.682	0.454	0.710	0.641
	CNN Derived Features	0.674	0.632	0.679	0.682
	Fine-tuned CNN	0.783	0.227	0.852	0.663

**Table 1:** Results of each method on all datasets. Overall, the AUC indicates that the performance of the CNN is on par with machine learning methods. These data strengthen the claim that pre-trained CNN's are suitable to identify prostate cancer on MRI images.

#### EP-1933 A deep learning approach for identifying focal prostate cancer from multi-parametric MRI

M. Rooney<sup>1</sup>, A. Killean<sup>2</sup>, J. Mitchell<sup>2</sup>, D.B. McLaren<sup>2</sup>, W.H. Nailon<sup>1,3</sup>

<sup>1</sup>NHS Lothian, Department of Oncology Physics-Edinburgh Cancer Centre, Edinburgh, United Kingdom ;

<sup>2</sup>NHS Lothian, Department of Clinical Oncology-Edinburgh Cancer Centre, Edinburgh, United Kingdom ;

<sup>3</sup>The University of Edinburgh, School of Engineering, Edinburgh, United Kingdom

#### Purpose or Objective

There are no technical barriers to delivering radiotherapy to small focal lesions within the prostate gland, however, reliably identifying focal disease is challenging. Multi-parametric magnetic resonance imaging (mp-MRI) has significant potential for this and in addition because of the improved image resolution may be combined with machine learning techniques to assist with tumour delineation. The aim of this work was to combine information from T2 weighted, apparent diffusion coefficient (ADC), and diffusion weighted (DW) MRI to train machine learning models to automatically identify focal disease within the prostate.

#### Material and Methods

Two datasets were utilised from previously treated patients with localised prostate cancer. The first included 16 patients with diagnostic T2 MRI, the second included 12 patients with diagnostic T2 and ADC studies. The planning CT, T2 and ADC images, where available, were registered rigidly using a Varian Eclipse workstation. An experienced clinician contoured the prostate and focal lesion on both images, Figure 1. Matlab was used to process the images in this study, where sub images were extracted from each before 32 texture features were calculated. These features were used to train SVM, k-NN, decision tree and Ada-boost classification algorithms. In addition, AlexNet, a pre-trained convolution neural network was fine-tuned to classify each sub image as healthy or diseased tissue. The performance of each model was assessed in terms of sensitivity, specificity and AUC (Table 1).

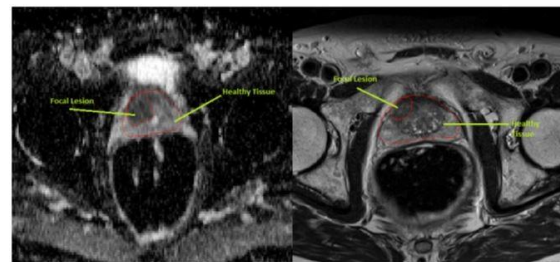


**Figure 1:** An example of the clinically defined area of disease on both ADC (left) and T2 (right) MRI scans used in this study.

#### Results

The results demonstrate that multimodality imaging data, in the form of T2 MRI and ADC images, can be successfully combined to build models for the identification of focal disease within the prostate. This was achieved through the creation of co-trained classification models using texture and CNN image features derived from the MRI sequences from a cohort of 12 patients. Overall, it can be noted that texture features yield more sensitive results versus the fine-tuned CNN. This novel approach achieved very high classification performance when tested on T2 images with a maximum AUC of 0.935 compared to the highest result of 0.663 AUC found using single sequence MRI studies.

Data Set	Method	Sensitivity	Specificity	AUC
T2	Texture features + classification	0.454	0.710	0.641
	Fine-tuned CNN	0.227	0.852	<b>0.663</b>
Mp-MRI	Texture features + classification	0.384	0.976	<b>0.935</b>
	Fine-tuned CNN	0.244	0.892	0.892

**Table 1:** Summary of classification results from both data groups testing using T2 images

### Conclusion

These results are promising, a larger data set is required to further develop these approaches. However, in the absence of this, there are many areas of improvement still to be explored.

### EP-1934 A study of RBE and NTCP uncertainties underlying model-based patient selection to proton therapy

S.N. Fly<sup>1</sup>, J. Pedersen<sup>1</sup>, J.B. Petersen<sup>1</sup>, C.H. Stokkevåg<sup>2</sup>, L.P. Muren<sup>1</sup>

<sup>1</sup>Aarhus University Hospital, Department of Medical Physics, Aarhus, Denmark ; <sup>2</sup>Haukeland University Hospital, Department of Oncology and Medical Physics, Bergen, Norway

### Purpose or Objective

Normal tissue complication probability (NTCP) models have been proposed for patient selection to proton therapy (PT). NTCP model parameters from different (mostly photon-based) studies often show large variability with wide confidence intervals. PT dose distributions should also be corrected for the higher and variable relative biological effectiveness (RBE) of protons. A number of different models for variable RBE are available, with their inherent model parameter dependencies. The aim of this study was to investigate how the choice of RBE model and their uncertainties relate to the uncertainties of current NTCP model parameters.

### Material and Methods

Three published variable RBE models (McNamara et al., Wedenberg et al., and Carabe et al.) - as well as the generic (constant RBE = 1.1) alternative - were applied when analysing spot scanning PT plans of six prostate cancer patients (prescription doses of 78 Gy (RBE = 1.1)). The RBE corrected dose volume histograms of the rectum and bladder were adjusted for fractionation effects using the linear-quadratic model (EQD<sub>2Gy</sub>) before entered into the Lyman-Kutcher-Burman (LKB) NTCP model. Nine different published LKB parameter sets (including the QUANTEC parameters, Michalski et al) were used for the rectum and three sets for the bladder. The effect of varying  $\alpha/\beta$ -ratio within the range of published values was investigated. Uncertainties in the NTCP values were calculated from the confidence intervals of the published NTCP parameters using both error propagation and Monte Carlo simulations.

### Results

The choice of NTCP model parameter sets had a much larger influence on the resulting NTCP predictions than the choice of variable RBE model (Fig. 1). The value of the  $\alpha/\beta$ -ratio had a considerable effect on the resulting NTCP estimates for the variable RBE models (Fig. 1). The McNamara model resulted in higher NTCP values than the Wedenberg and Carabe models (Fig. 1) while all three variable RBE models resulted in higher NTCPs than the generic constant RBE alternative, with the differences increasing for lower  $\alpha/\beta$ -ratios. The uncertainty in the NTCP parameters had a large impact on the NTCP values, with differences up to 5% for the rectum (with the QUANTEC parameters) and more than 10% for the bladder (Fig. 2).

**Figure 1:** NTCP values for four different parameter sets (in papers of Michalski et al., Söhn et al., Tucker et al., and Rancati et al.) of the rectum and four different RBE scenarios (McNamara, Carabe, and Wedenberg models as well as the generic RBE = 1.1) are plotted against  $\alpha/\beta$ -ratio for six patients (in different colours). The differences in NTCP between the different NTCP parameter sets were larger than between the variable RBE models. The NTCPs calculated with the variable RBE models increased for decreasing  $\alpha/\beta$ -ratio. Two of the five other NTCP parameter sets (data not shown) also resulted in NTCP = 0 (as for the Rancati et al. parameters).

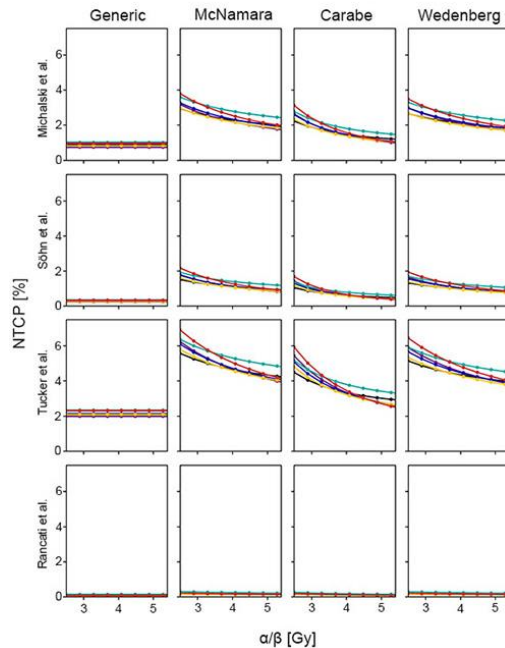
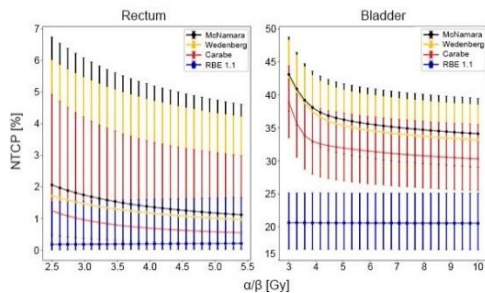


**Figure 2:** NTCP values and their confidence intervals for one parameter set of the rectum (Michalski et al.) and one parameter set of the bladder (Thor et al.), for four different RBE scenarios (McNamara, Carabe, and Wedenberg models as well as the generic RBE = 1.1) plotted against  $\alpha/\beta$ -ratio for one patient. The confidence intervals of the NTCPs from the variable RBE models have some overlap with the corresponding intervals for constant RBE for the rectum (left), but not for the bladder (right).



### Conclusion

The choice of NTCP model parameters has a much larger influence on resulting risk predictions than the choice of variable RBE model, even for the rectum where there are more published morbidity studies than for most other organs. The three variable RBE models resulted in higher NTCPs than the generic constant RBE, with the differences increasing for lower  $\alpha/\beta$ -ratios. Even without considering implications of potential differences in volume effects between photons and protons (due to the reduced dose bath of PT), this study clearly shows that model-based patient selection to PT should be performed with caution, taking current model and parameter uncertainties into account.

### EP-1935 Delta radiomics Features Analysis in Glioblastoma multifome GLI.F.A. Project. A multi-centric study

S. Chiesa<sup>1</sup>, F. Beghella Bartoli<sup>1</sup>, I. Palumbo<sup>2</sup>, R. Barone<sup>1</sup>, M. Lupatelli<sup>2</sup>, C. Masciocchi<sup>1</sup>, R. Tarducci<sup>2</sup>, A. Rongoni<sup>2</sup>, D. Cusumano<sup>1</sup>, R. Russo<sup>3</sup>, P. Floridi<sup>2</sup>, S. Longo<sup>1</sup>, N. Dinapoli<sup>3</sup>, M. Balducci<sup>1</sup>, V. Valentini<sup>1</sup>, C. Aristei<sup>2</sup>

<sup>1</sup>Fondazione Policlinico A. Gemelli IRCCS- Università Cattolica Sacro Cuore, Dipartimento Scienze Radiologiche- Radioterapiche ed Ematologiche- Istituto di Radiologia, Rome, Italy ; <sup>2</sup>Università di Perugia- Ospedale S. Maria della Misericordia- Sezione di Radioterapia Oncologica, Dipartimento di Chirurgia e Scienze Biomedicali, Perugia, Italy ; <sup>3</sup>Fondazione Policlinico A. Gemelli IRCCS, Dipartimento Scienze Radiologiche- Radioterapiche ed Ematologiche- Istituto di Radiologia, Rome, Italy

#### Purpose or Objective

Different investigations have focused on the GBM's heterogeneous features to develop an individualized patient management. A multi-institutional study, the GLI.F.A. (Glioblastoma: advanced Imaging Features Analysis) Project, was performed for a comprehensive analysis of GBM heterogeneity in order to create a multidimensional map for predictive models (PM) and decision support systems (DSS) in GBM

#### Material and Methods

Adult patient with newly diagnosed GBM, that undergo surgery and chemo-radiotherapy according to EORTC 26981-22981-NCIC trial were analyzed in this first phase of the study. Gross Tumor Volume (GTV) was contoured in the T1 post contrast and T2-FLAIR weighted images. A brain ontology and a platform for sharing and combining multiple datasets (BOA-WEB System) were created in order to standardize data. MRI features were extracted by the dedicated software. Two analysis were conducted: the study of imaging features of MRI at diagnosis and a delta radiomics study oriented to evaluate the evolution of imaging features, considering all MRI performed. In both of the studies, the Wilcoxon Mann Whitney test and the Log-rank test for Kaplan-Meier curves were applied to evaluate the significance of the radiomic features on the T2-Flair and T1 images, using the median value of the radiomic features to categorize the continue variables. We considered as main outcomes the local control (LC), the progression free survival (PFS) and the response to radio-chemotherapy (RTCT).

#### Results

We enrolled in this study 43 patients, treated from July 2014 to February 2018. Median age was 63 years (45-80) and 27 patients were still alive at the time of the analysis. The MODDICOM software analyzed image features. Significant features of MRI images at diagnosis divided by MRI sequence and outcome are reported in Fig1. The second order, textural features order, describing the spatial correlation between images voxel, resulted significant for PFS, LC and response to RTCT on the contrast-enhanced T1 weighted MRI. Regarding the delta radiomics features analysis, 18 patients were considered and the CTV segmentation and feature extraction was performed on 68 post contrast T1 weighted MRI. After extracting 92 features, we observed a significant correlation, defined by the adjusted p value, for PFS and LC on pre-RT MRI and on MRI after the 6th chemotherapy cycle. The significant features belong to the first, the second and the third order are reported in Fig2. Almost significant features are morfological and could describe quantitatively something that usually is only qualitatively described

#### Conclusion

This preliminary univariate analysis suggests that the radiomic features relates to survival and clinical outcomes and that is possible to stratify patients according MR based quantitative imaging. A higher number of patients, multivariate analysis and external validation are next steps for getting reliable predictive model.

#### EP-1936 PET/CT Radiomics predict local recurrence in patients treated with SBRT for early-stage NSCLC

G. Dissaux<sup>1</sup>, M. Hatt<sup>2</sup>, D. Visvikis<sup>2</sup>, O. Pradier<sup>1</sup>, E. Chajon<sup>3</sup>, I. Barillot<sup>4</sup>, L. Duverge<sup>3</sup>, I. Masson<sup>5</sup>, R. Abgral<sup>6</sup>, M. Santiago-Ribeiro<sup>7</sup>, A. Devillers<sup>8</sup>, F. Kraeber-Bodéré<sup>9</sup>, M. Mahé<sup>3</sup>, R. De Crevoisier<sup>3</sup>, U. Schick<sup>1</sup>

<sup>1</sup>University Hospital, Radiation Oncology department, Brest, France ; <sup>2</sup>Univ Brest, LaTIM- INSERM- UMR 1101, Brest, France ; <sup>3</sup>Centre Eugène Marquis, Radiation Oncology department, Rennes, France ; <sup>4</sup>University Hospital, Radiation Oncology department CORAD, Tours, France ; <sup>5</sup>Institut de Cancérologie de l'Ouest Cancer Center, Radiation Oncology department, Nantes, France ; <sup>6</sup>University Hospital, Nuclear Medicine department, Brest, France ; <sup>7</sup>University Hospital, Nuclear Medicine department, Tours, France ; <sup>8</sup>Centre Eugène Marquis, Nuclear Medicine department, Rennes, France ; <sup>9</sup>Institut de Cancérologie de l'Ouest Cancer Center, Nuclear Medicine department, Nantes, France

#### Purpose or Objective

The aim of this French multicentric study was to develop and validate an FDG PET/CT radiomics signature with prognostic value in patients treated with stereotactic radiotherapy (SBRT) for early-stage non-small cell lung cancer (NSCLC) and to assess its incremental value with respect to the standard clinical and imaging features.

#### Material and Methods

Patients from Rennes (n=27), Tours (n=29) and Brest (n=8) were pooled to constitute the training set, whereas the patients from Nantes (n=23) were used as the testing set. The primary endpoint of study was local control. For each patient, the primary tumour was delineated automatically in the PET images using the FLAB algorithm, and manually in the low-dose CT images, and IBSI-validated radiomic features were extracted. A total of 184 radiomic features (92 in both FDG PET and low-dose CT), 7 clinical and histopathological parameters (age, gender, tumour size, stage, localization, OMS status, histology) and one treatment parameter (biologically equivalent dose, BED) were included. In order to pool together radiomics features extracted from the four institutions relying on different PET/CT scanners and associated protocols, we used the posteriori harmonization method ComBat. In the training set, variables found significant in the univariate analysis were fed into a multivariate Cox proportional hazard regression model. The area under the ROC curve (AUC) was used to evaluate the performance of the resulting model in the testing set.

#### Results

Median follow-up was 22.7 (3.2 - 63.4) and 22.2 (1.7 - 58.1) months, in training and testing sets respectively. In univariate analysis, none of the clinical variables, 2 PET features and 3 CT features were significant. The best performance in the training set was obtained with the model combining the two PET features, reaching an AUC of 0.94 (sensitivity 100%, specificity 88%) to predict local recurrence, with a HR undefined (p<0.001). This model obtained an accuracy of 0.91 (sensitivity 100%, specificity 81%), with a HR undefined (p = 0.023) in the testing set. The models relying on CT radiomics features or the combination of PET and CT features reached lower accuracy.

#### Conclusion

We showed that two radiomic features derived from FDG PET were independently associated with local control in patients with NSCLC undergoing SBRT and could be combined in an accurate predictive model. This model could provide recurrence-related information and could be helpful in clinical decision-making, especially regarding dose escalation.

### EP-1937 Distributed AUC algorithm: a privacy-preserving approach to measure the performance of Cox models

C. Masciocchi<sup>1</sup>, A. Damiani<sup>1</sup>, N.D. Capocchiano<sup>1</sup>, J. Van Soest<sup>2</sup>, J. Lenkovicz<sup>1</sup>, E. Meldolesi<sup>1</sup>, G. Chiloiro<sup>1</sup>, M.A. Gambacorta<sup>1</sup>, A. Dekker<sup>2</sup>, V. Valentini<sup>1</sup>

<sup>1</sup>*Policlinico Universitario Agostino Gemelli - Divisione di Radioterapia Oncologica - Gemelli ART, Roma, Italy* ;

<sup>2</sup>*GROW School for Oncology and Developmental Biology, Department of Radiation Oncology Maastricht, Maastricht, The Netherlands*

#### Purpose or Objective

Recent years have brought both a notable rise in the ability to efficiently harvest vast amounts of information, and a concurrent effort in preserving and actually enforcing the privacy of patients and their related data, as evidenced by the European GDPR. In these conditions, the Distributed Learning Ecosystem has shown great potential in allowing researchers to pool the huge amounts of sensitive data need to develop and validate prediction models in a privacy preserving way and with an eye towards personalized medicine.

The aim of this abstract is to propose a privacy-preserving strategy for measuring the performance of Cox Proportional Hazard (PH) model.

#### Material and Methods

A privacy-preserving AUC strategy has been proposed, developed and tested. The algorithm is mainly composed of 4 distinct steps:

- Each site calculates the vector of the linear predictor based on the sites' local data and sends to the results to the master.
- The master merges the received lists of linear predictors and sorts them by calculating the threshold values. This vector is then sent back to each site.
- All sites then calculates the confusion matrix for each value of the threshold and sends the results back to the master;
- The master sums up the confusion matrices for each value of the threshold, and subsequently calculates the true positives and false negatives to plot the ROC points. The area under the ROC curve is finally computed by using trapezoidal approximation.

The proposed method has been tested on a centralized and a distributed infrastructure, with real rectal cancer clinical data, with the data split into 2 random and independent datasets. Age, gender, clinical TNM stage, overall survival status and time were considered in the analysis. The resulting ROC and AUC from both the centralized and distributed infrastructure have then been analyzed and compared.

#### Results

A total number of 945 rectal cancer patients (pts) were selected to develop and validate the proposed model. The whole dataset was split into two distinct sites: site A with 473 pts and site B with 472 pts. A description of the available data is summarized in figure 1.

Once set up and launched, 9 iterations were needed for all sites to converge on a result and compute a distributed Cox model and an additional 2 iterations for the algorithm to calculate the ROC and AUC, for a total of 11 iterations over the course of 172 seconds. The results of the computation are shown in figure 2 with an additional comparison between the distributed and centralized approaches.

Death	0	1	Gender	
Split1	429 (90,70%)	44 (9,30%)	Split1	170 (35,94%) 303 (64,06%)
Split2	436 (92,37%)	36 (7,63%)	Split2	179 (37,92%) 293 (62,08%)

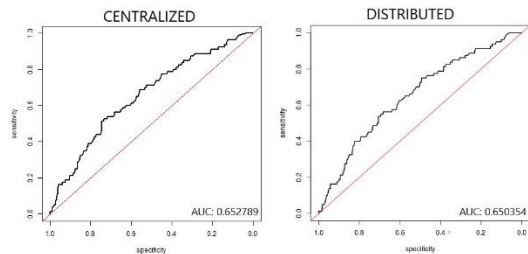
cT	1	2	3	4
Split1	1 (0,21%)	47 (9,94%)	355 (75,05%)	70 (14,80%)
Split2	3 (0,64%)	51 (10,81%)	358 (75,85%)	60 (12,71%)

cN	0	1	2	3
Split1	92 (19,45%)	215 (45,45%)	165 (34,88%)	1 (0,21%)
Split2	92 (19,49%)	229 (48,52%)	148 (31,36%)	3 (0,64%)

age	min	median	max
Split1	0	63	95
Split2	0	60	93



#### Conclusion

The distributed AUC algorithm we developed fills an important void in the current distributed learning environment, as up until now there was, to the best of our knowledge, no practical way of measuring the performance of a privacy preserving and distributed Cox model. This additional step is fundamental to evaluate the model performance of final distributed models.

### EP-1938 A high precision irradiation system for in vivo RBE measurements with ion beams

J. Besuglow<sup>1,2,3</sup>, G. Echner<sup>4</sup>, A. Mairani<sup>3,5,6</sup>, M. Alber<sup>1,2,3</sup>, E. Bahn<sup>1,2,3,7</sup>

<sup>1</sup>*Department of Radiation Oncology, Heidelberg University Hospital, Heidelberg, Germany* ; <sup>2</sup>*NCT, National Center for Tumor Diseases, Heidelberg, Germany* ; <sup>3</sup>*HIRO, Heidelberg Institute of Radiation Oncology, Heidelberg, Germany* ; <sup>4</sup>*Division of Medical Physics in Radiation Oncology, German Cancer Research Center DKFZ, Heidelberg, Germany* ; <sup>5</sup>*Heidelberg Ion-Beam Therapy Center HIT, Department of Radiation Oncology- Heidelberg University Hospital, Heidelberg, Germany* ; <sup>6</sup>*National Centre of Oncological Hadrontherapy CNAO, Medical Physics, Pavia, Italy* ; <sup>7</sup>*Clinical Cooperation Unit Radiation Oncology, German Cancer Research Center DKFZ, Heidelberg, Germany*

#### Purpose or Objective

Research platforms for experimental small animal irradiation can foster to the acute need of robust in vivo data for current challenges in radiotherapy, such as the determination of the RBE of high-LET radiation in the brain. Due to the strong dependence of dose response on the volume of the small irradiation fields employed in these experiments, highly identical dose distributions are required for inter-comparison of different ion types, which presents a major challenge for experimental design.

We devised a multi-component system that meets the requirements of a precise comparative RBE measurement within the pristine Bragg peak of ion beams. Via a passive collimation system, we obtain range adjustment to sub-millimetre precision and sharp lateral beam collimation, combined with precise and rapid animal positioning.

#### Material and Methods

The model requires irradiation of the frontal lobe of a mouse brain with a pristine Bragg peak while sparing sensitive adjacent regions. The dose volume is a 3.5 mm x 7 mm wide cuboid of 4 mm depth for proton, helium, carbon and oxygen ion irradiation. This is achieved via passive collimation with a 3D printed bolus that can be

accurately adjusted relative to the fixated animal head. The collimator was optimized by Monte Carlo (FLUKA) based beam simulation in water and on CT scans. Doses were weighted by LEM I and IV model predictions. Lateral and depth dose distributions in the original collimation geometry were validated by combined dosimetry with gafchromic films and ionization chambers.

### Results

Placement of animals and collimators is rapid, precise and easily reproducible. The entrance field exhibits a lateral dose fall off  $x_{80-x_{20}} = 0.3$  mm (oxygen) to 1.1 mm (protons), see also Fig. 1a. We obtain highly pristine Bragg peaks with very low ion beam energies of 48.12, 50.57, 88.83 and 103.77 MeV/u for protons, helium, carbon and oxygen ions respectively, requiring range shifting by 11.15, 12.59, 10.93 and 10.78 mm PMMA for a residual range R80 of 4 mm. The Bragg peaks are highly similar in beam direction for all ion types (distal dose fall off  $z_{80-z_{20}} = 1.24 \pm 0.02$  mm and peak width  $w_{80} = 2.15 \pm 0.01$  mm), only protons show a slightly wider peak (2.51 mm) and a steeper fall off (1.11mm), see Fig. 1b. Very high LET variations can be achieved. Dosimetric film measurements show a dose homogeneity of  $\pm 2.0\%$ .

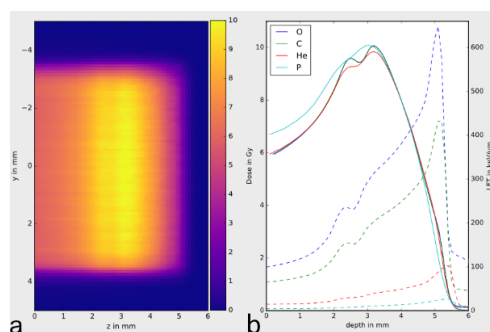


Fig. 1: Dose distribution obtained by Monte Carlo simulation in water. a) Projected dose distribution for He ions. b) Depth-dose curves (solid lines) and depth-LET curves (dotted lines) for the four studied ion types.

### Conclusion

We have shown that conformity of dose distributions between highly different ion types is achievable. The proposed setup allows a detailed examination of biological effects at the distal end of the Bragg peak, thus providing valuable in-vivo data of high RBE irradiation.

### EP-1939 Repeatability of FDG PET/CT based radiomic features using wavelet and Laplacian of Gaussian filters

S. Kyzalas<sup>1</sup>, L. Nygård<sup>2</sup>, B.M. Fischer<sup>3</sup>, J.M. Edmund<sup>1,4</sup>, I.R. Vogelius<sup>2</sup>

<sup>1</sup>Niels Bohr Institute, University of Copenhagen, Copenhagen, Denmark ; <sup>2</sup>Rigshospitalet, Department of Oncology, Copenhagen, Denmark ; <sup>3</sup>Rigshospitalet, Department of Clinical Physiology- Nuclear Medicine & PET, Copenhagen, Denmark ; <sup>4</sup>Copenhagen University Hospital, Radiotherapy Research Unit- Department of Oncology, Herlev, Denmark

### Purpose or Objective

Pre-processing of medical images prior to radiomics feature analysis is an important step which is often under-analyzed or documented. One aspect is the use of filtering, which has sometimes been applied to yield (more) significant correlations [1]. Here we analyze the value of a filtering process in terms of repeatability of radiomics features in a prospective scan-rescan study of non-small cell lung cancer (NSCLC) patients [2]. Furthermore, we report how the features depend on the applied filtering.

### Material and Methods

We compare the repeatability of 51 radiomic features, extracted from unfiltered and filtered images, using 8 commonly applied wavelet and 10 Laplacian of Gaussian (LoG) filters. 19 patients were included in a previously published study of both free-breathing PET/CT and deep inspiration breath hold PET/CT. Both breathing modalities were repeated a few days apart without any active therapy in between to form a scan-rescan study [2]. CT images were discretized in 64 bins with saturation thresholds at  $\pm 465$  Hounsfield Units [HU]. The PET images were converted into square root SUV maps, and discretized in 64 bins with saturation thresholds at  $\sqrt{\text{SUV}} = \pm 3.2$ . For the computation of the features, a Matlab radiomics package was used, originally developed by Martin Vallieres [3], although several adjustments to the original script were introduced. Repeatability of the features was based on Pearson's intraclass correlation coefficient (ICC), and the dependence between features with different filters was assessed with Spearman's rank correlation coefficient.

### Results

Most features were found to be more robust on original scan than features based on commonly used, LoG or wavelet filters, cf. Figure 1. On CT, the average ICC for the LoG-based features was  $0.91 \pm 0.12$ ,  $0.81 \pm 0.30$  for the wavelet-based, and  $0.92 \pm 0.10$  for the unfiltered. The ICC differences across the different filters were consistent between PET and CT. Features extracted from images based on the same filter type, were found to be highly correlated, as shown in figure 2.

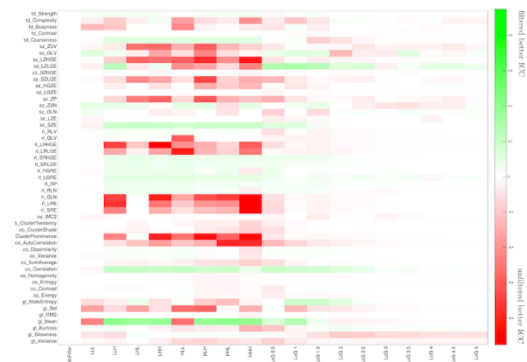


Figure 1: Comparison of repeatability of filter-based features to unfiltered. The values of the heatmap are produced by subtracting the ICC (Pearson) of the filtered features from the unfiltered ones, on CT.

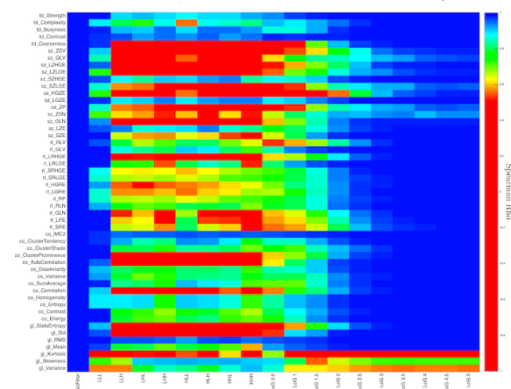


Figure 2: Spearman's rank correlation between features obtained from differently filtered images, in relation to unfiltered, on CT.

### Conclusion

Most of the investigated radiomic features were found to be more robust without the use of any image filters.

Because of the high dependence across features extracted from images based on the same filter type, the number of redundant features may be reduced in future studies.

#### References

1. Vishwa Parekh and Michael A. Jacobs. Radiomics: a new application from established techniques. *Expert Rev Precis Med Drug Dev.* 2016; 1(2): 207226.
2. Nygård L, Aznar MC, Fischer BM, et al. American Journal of Nuclear Medicine and Molecular Imaging. 8(2), 127-136.
3. <https://github.com/mvallieres/radiomics>.

#### EP-1940 Impact of respiratory motion on the robustness of 18F-FDG PET/CT radiomic features

S. Kyzalas<sup>1</sup>, L. Nygård<sup>2</sup>, B.M. Fischer<sup>3</sup>, J.M. Edmund<sup>1,4</sup>, I.R. Vogelius<sup>2</sup>

<sup>1</sup>Niels Bohr Institute, University of Copenhagen, Copenhagen, Denmark ; <sup>2</sup>Rigshospitalet, Department of Oncology, Copenhagen, Denmark ; <sup>3</sup>Rigshospitalet, Department of Clinical Physiology- Nuclear Medicine & PET, Copenhagen, Denmark ; <sup>4</sup>Radiotherapy Research Unit- Department of Oncology, Herlev, Denmark

#### Purpose or Objective

We investigate the repeatability of 18F-FDG PET/CT radiomic features, based on scans obtained in deep inspiration breath-hold (DIBH) and free breathing (FB) in a prospective scan-rescan study of patients with non-small-cell lung cancer (NSCLC) [1].

#### Material and Methods

18F-FDG PET/CT scans from 19 NSCLC patients were analyzed. DIBH and FB scans were obtained twice, a few days apart, with the same fixation in a prospective study without any active treatment between scans [1]. CT images were discretized in 64 bins with saturation thresholds at  $\pm 465$  Hounsfield Units [HU]. The PET images were converted into square root SUV maps, and discretized using a fixed bin width of 0.03  $\sqrt{\text{g/ml}}$ . For the computation of the features, a Matlab radiomics package was used, originally developed by Martin Vallieres [2], although several adjustments to the original script were introduced. The evaluation of the feature repeatability was based on Fisher's intraclass correlation coefficient (ICC).

#### Results

Breathing modality (FB or DIBH) affected the value of many features. However, DIBH vs. FB have negligible impact on the repeatability, as long as the respiratory patterns are not interchanged. The results on the repeatability of the most stable, and least codependent features, are shown in table 1, while the mean effect is shown in figure 1. Additionally, CT-based features were found to be more stable as compared to PET-based features.

CT			
Features	DIBH	FB	Mixed
sh volume	0.992	0.995	0.993
gl Variance	0.965	0.976	0.906
co Entropy	0.950	0.970	0.873
co Correlation	0.910	0.919	0.869
rl LRHGE	0.982	0.993	0.695
sz GLN	0.980	0.984	0.962
sz SZHGE	0.936	0.968	0.916
td Complexity	0.949	0.905	0.912
td Strength	0.966	0.956	0.983

PET			
Features	DIBH	FB	Mixed
sh volume	0.989	0.993	0.994
sh solidity	0.939	0.741	0.692
co Entropy	0.934	0.947	0.902
co Homogeneity	0.905	0.933	0.884
co Variance	0.838	0.864	0.841
rl RP	0.876	0.946	0.856
rl SRLGE	0.887	0.933	0.907
sz SZLGE	0.948	0.854	0.694
td Strength	0.935	0.873	0.811

Table 1: Feature ICC (Fisher) values, calculated from DIBH and FB scans on PET and CT, of the most stable and least codependent features. "Mixed" corresponds to interchanged patterns, where the ICC is calculated between one day of DIBH and one of FB.

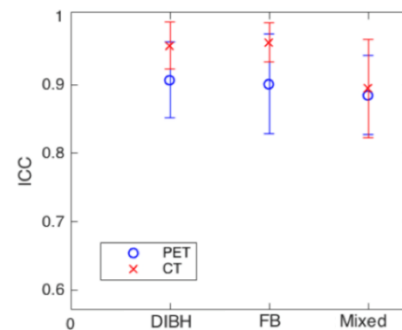


Figure 1: Mean ICC comparison of the features extracted from different respiratory patterns and imaging modalities (shown in table 1), where the errorbars represent  $\pm$ one standard deviation. "Mixed", corresponds to interchanged patterns, where the ICC is calculated between one day of DIBH and one day of FB.

#### Conclusion

The majority of feature values are affected by the use of different respiratory patterns. When it comes to feature robustness, our data found no support to choose DIBH over FB. To maximize feature reproducibility upon multiple scanings, it is advisable to maintain a consistent respiratory pattern.

#### References

- [1] Nygård L, Aznar MC, Fischer BM, et al. Repeatability of FDG PET/CT metrics assessed in free breathing and deep inspiration breath hold in lung cancer patients. *American Journal of Nuclear Medicine and Molecular Imaging.* 2018;8(2):127-136.
- [2] <https://github.com/mvallieres/radiomics>.

#### EP-1941 MRI-based radiogenomics analysis of 1p/19q codeletion in grade II and III gliomas

W. Takahashi<sup>1</sup>, T. Nakamoto<sup>1</sup>, H. Akihiro<sup>2</sup>, T. Satoshi<sup>3</sup>, T. Shota<sup>3</sup>, S. Aoki<sup>1</sup>, T. Kiritoshi<sup>1</sup>, M. Ogita<sup>1</sup>, H. Yamashita<sup>1</sup>, K. Nakagawa<sup>1</sup>

<sup>1</sup>University of Tokyo, Department of Radiology, Tokyo, Japan ; <sup>2</sup>Tokushima University, Department of Medical

*Image Informatics, Tokushima, Japan ; <sup>3</sup>University of Tokyo, Department of Neurosurgery, Tokyo, Japan*

#### **Purpose or Objective**

Gliomas with 1p/19q codeletion are diagnosed as oligodendrogliomas and associated with better prognosis than their 1p/19q nondeleted counterparts. The purpose of this study was to investigate feasibility for predicting the 1p/19q codeletion status of the gliomas based on the radiogenomic analysis using T2-weighted magnetic resonance (MR) images (T2WIs).

#### **Material and Methods**

We analyzed the institutional database, for adult patients with a diagnosis of World Health Organization grade II and III gliomas from 1995 to 2017. Based on multiplex ligation-dependent probe amplification (MLPA) or microsatellite analysis, 38 patients underwent testing for 1p/19q codeletion (23 with codeleted and 15 with nondeleted). Pretreatment T2WIs of all patients were retrospectively evaluated. Gross tumor volumes (GTVs) were manually contoured and radiogenomic features (shape, size, histogram, and texture features) were extracted in the GTVs. Data were analyzed using L1-norm regularized logistic regression. A leave-one-out cross validation was employed in order to evaluate performance of a prediction model. Accuracy, sensitivity, specificity, and area under the receiver operating characteristics (ROC) curve (AUC) value were calculated as evaluation indices. This retrospective data evaluation was approved by the local ethics committee.

#### **Results**

Total number of the radiogenomic features was 476. Accuracy, sensitivity, specificity, and AUC values of the prediction models were 0.711, 0.697, 0.733, and 0.736, respectively. The 1p/19q codeletion could be moderately predicted using the proposed framework.

#### **Conclusion**

We developed a radiogenomics-based framework for non-invasively predicting the 1p/19q codeletion in grade II-III gliomas using the T2WIs. The proposed framework would be feasible to preoperatively predict genomic status of the gliomas using the MR images. Further validation studies at multi-centric level are mandatory and scheduled to confirm our findings.

#### **EP-1942 Combining radiomic and dosimetric parameters to predict chemoradiation response of EC patients**

X. Jin<sup>1</sup>, C. Xie<sup>1</sup>

<sup>1</sup>The 1st Affiliated Hospital of Wenzhou Medical University, Radiation and Medical Oncology, Wenzhou, China

#### **Purpose or Objective**

The treatment response prediction capability of radiomics features extracted from PET and CT images had been extensively investigated. However, radiotherapy dosimetric parameters, which are the key parameters that affect the treatment response, were not included in the response studies. The purpose of this study is to investigate the prediction feasibility and accuracy of an integrated model with combined radiomic features and dosimetric parameters for esophageal cancer (EC) patients underwent concurrent chemoradiation (CRT) using machine learning techniques.

#### **Material and Methods**

Ninety-four patients underwent CRT for primary EC between Oct 2012 and Oct 2015 were enrolled in this study. The primary target volumes (GTVs) of these patients were delineated by two expert oncologists. DICOMs files were exported from TPS to an open infrastructure software platform: IBEX for preprocessing and feature extraction. Dosimetric parameters were extracted from DVH. The response of these patients to treatment was evaluated three months after the

treatment. Xgboost was applied to build a model to predict the correlation between parameters and treatment response.

#### **Results**

There were total of 42 radiomics features and 18 dosimetric parameters extracted for these 94 cases, together with sex, age and radiotherapy modalities were included in the modeling. According to the results of data visualization using parallel coordinates, prescription dose, GTV, heart and cord related dosimetric parameters, as well GlobalMean X.33.1, Correlation, Coarseness, Skewness have a strong correlation with treatment response. The prediction accuracy and precise of training and validation data were 0.9, 0.86 and 0.54, 0.6, respectively. Remodeling after principal components analysis (PCA), the prediction accuracy and precise of training and validation data were 0.79, 0.76 and 0.75, 0.76, respectively. According to the Gain calculated for each parameter in the prediction model, image features of GlobalMean X.333.1, Coarseness, Skewness, GlobalStd were contributed most to the model. Dosimetric parameters of PTV HI, Cord Dmax, Prescription dose, Heart-Dmean and Heart-V50 also have a strong contribution to the model. The Area under curve (AUC) of receiver operating characteristics (ROCs) for dosimetric features alone and combined dosimetric features and dosimetric parameters were 0.6 and 0.75, respectively.

#### **Conclusion**

Models combining radiomics features and dosimetric parameters is capable of and outperform those with radiomics features alone in predicting the treatment response for EC patients underwent CRT.

---

#### **Electronic Poster: Physics track: Intra-fraction motion management**

---

#### **EP-1943 Intra-fractional respiration monitoring for patients undergoing lung SBRT**

E.P.S. Sande<sup>1</sup>, T.P. Hellebust<sup>1</sup>

<sup>1</sup>Oslo University Hospital, Dep. of Medical Physics, Oslo, Norway

#### **Purpose or Objective**

The Varian TrueBeam (TB) Respiratory Gating System (RGS) tracks respiratory motion via a reflector block placed on the patient's chest. The system may interrupt the beam when detected motion exceeds pre-defined thresholds, due to sudden or gradual involuntary patient motion - such as coughing or baseline drift. The purpose of this study was to investigate the feasibility of using the TB RGS for intra-fractional monitoring during free breathing (FB) stereotactic lung radiotherapy (SBRT) to possibly increase the accuracy in dose delivery.

#### **Material and Methods**

Firstly, intra-fractional respiratory motion curves were recorded for 31 lung SBRT treatment sessions (9 patients). Thresholds were not applied, ensuring no RGS-related beam interruptions. Post-treatment analysis assessed the fraction of treatment sessions in which the beam would have been interrupted due to sudden motion or baseline drift, if thresholds had been set prior to treatment. Findings were used to determine suitable thresholds, given possible clinical implementation of RGS intra-fractional monitoring. Secondly, possible dosimetric disadvantages of interrupting the delivery of SBRT plans were investigated. A 6 MV FFF VMAT plan and a 10 MV FFF static plan (PTV D<sub>min</sub> 15 Gy/fraction) were delivered to a stationary ArcCheck phantom (Sun Nuclear Corp.). Respiratory motion of the reflector block was simulated during delivery using a CIRS (CIRS Inc.) respiratory motion phantom. Plans were delivered using three duty cycles (DC) - defined as the ratio of beam-on time to the total

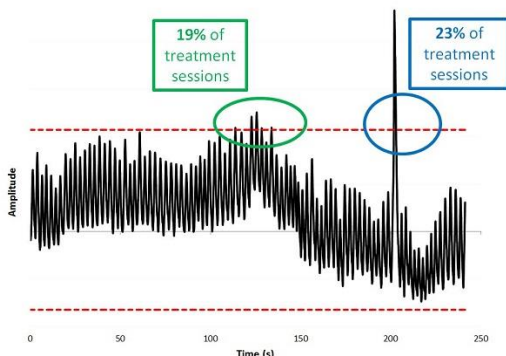
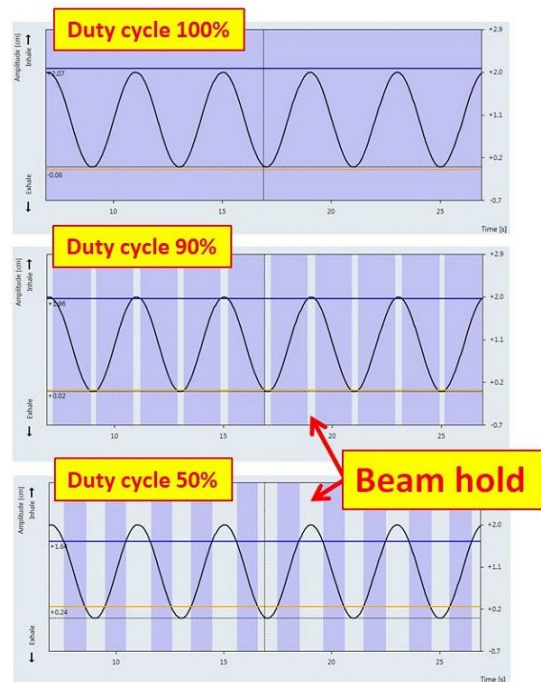
beam time: 100% (no beam interruptions), 90% and 50% (Fig. 1).

**Results**

Post-treatment analysis of recorded motion curves was done assuming upper and lower thresholds of 3 mm above normal inhale and below normal exhale, respectively. Normal inhale and exhale was defined as the average maximum and minimum block positions, respectively, based on the first four respiratory cycles following setup. Results are summarized in Fig. 2, illustrated by a recorded curve. Thresholds are shown as red dotted lines. 19% and 23% of treatment sessions had gradual intra-fractional drift or sudden motion, respectively, which would lead to beam interruption given the above mentioned thresholds. Gamma passing rates for plans delivered to the ArcCheck phantom, using different DC, are shown in Table 1. A 3%/3 mm criterion was used. Gamma passing rates for plan delivery using different DC differed less than 0.5%, even with only a 50% DC - the latter implying an unlikely high rate of beam interruptions.

	γ passing rate (%):		
	100% DC	90% DC	50% DC
6 FFF VMAT	99.5	99.5	99.0
10 FFF static	97.5	97.4	97.4

**Table 1:** Gamma passing rates for plans delivered to the ArcCheck phantom using different DC.



**Conclusion**

It seems feasible to use the TB RGS as a system detecting patient motion during delivery of FB lung SBRT - with the additional benefit of pausing the beam when motion exceeds pre-defined thresholds. Repeated beam interruptions during delivery appear to have little dosimetric impact.

**EP-1944 Automated respiratory cycle binning for liver 4D-MR imaging**

B. L'Home<sup>1</sup>, L. Parent<sup>1</sup>, O. Bieri<sup>2</sup>, Z. Celicanin<sup>3</sup>, P. Cattin<sup>4</sup>, S. Ken<sup>1</sup>

<sup>1</sup>Institut Universitaire du Cancer de Toulouse, Department of Engineering and Medical Physics, Toulouse, France ; <sup>2</sup>University Hospital Basel, Department of Radiology, Basel, Switzerland ; <sup>3</sup>Intuitive Therapeutics SA, Radiotherapy and Radiosurgery Planning Treatments, Saint-Sulpice, Switzerland ; <sup>4</sup>University of Basel, Department of Biomedical Engineering, Basel, Switzerland

**Purpose or Objective**

Stereotactic body radiation therapy (SBRT) has proven its benefit for local control of liver lesions<sup>1</sup>. Because high dose per fraction is delivered on small volume, very accurate lesion segmentation is necessary and respiratory gating enables safe margin reduction on the planning target volume (PTV). MRI is the preferred imaging modality for detection and characterization of hepatic lesions, but it is prone to motion artifacts if breathing is not managed. As external device for breathing movement detection may be inaccurate, the tracking of the sub-diaphragmatic organs movements with very fast 2D sagittal images appeared to be an interesting retrospective strategy using a previously validated 4D-MRI sequence for the liver<sup>2</sup>. In this study, an automated method was developed to sort images according to the respiratory phases with the sub-diaphragmatic organ movements.

**Material and Methods**

The 4D-MRI acquisition is performed with an experimental sequence (bSSFP TrueFISP<sup>3</sup>) on a 1.5T system (Magnetom Aera, Siemens). This sequence allows very fast interleaved axial and sagittal 2D acquisition (0.44 sec/slice) during free breathing. In order to correctly sample the entire breathing magnitude, 20 axial acquisitions are collected every 2.5 mm in the cranio-caudal direction. A sagittal slice (the navigator) is always acquired at the same position in the imaging volume and at 0.44 sec from the associated axial slice. According to the sub-diaphragmatic organs position on navigators, axial slices are automatically sorted in 6 phases (0% = inspiration, 16%, 33%, 50% = expiration, 66%, 83%). Automatic binning is performed by comparing the relative translation (white arrow on Figure 1) of each navigator (green slice, Figure 1) regarding a reference navigator (purple slice).

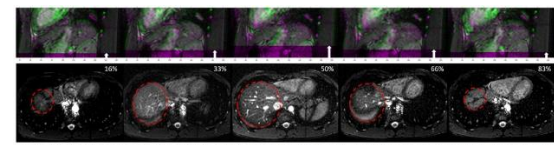


Figure 1: Axial slice sorting (with liver movement highlighted with red contour) by sub-diaphragmatic organs tracking on navigators

The sequence was evaluated on 5 volunteers with an audio coaching (5 and 6 sec period) and 2 patients without audio coaching.

**Results**

Retrospective axial slices binning according to their positions in the breathing cycle was achieved by automated motion tracking of sub-diaphragmatic organs on navigators. All axial slices of the 6 respiratory phases were imported into the treatment planning system (TPS) Eclipse 13.7 (Varian) allowing the reconstruction of the sagittal and coronal images. The 50% phase appears as the

most reproducible phase (with the lowest standard deviation on all respiratory cycles, *figure 2*) confirming the treatment strategy to target the PTV on the phase 50% during the expiratory phase.

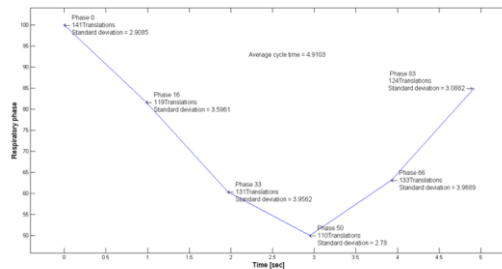


Figure 2: Average cycle calculated from all the navigators of the exam.

### Conclusion

Images from volunteers and patients were acquired using a 4D-MRI bSSFP (TrueFISP) sequence. After automated sorting with the method developed in this study, all the respiratory phases were imported into our TPS. Patient 4D-MRI could be registered with 4D-CT to capture the entire organs movements (liver cranio-caudal movements in red, Figure 1) during respiratory cycles and improve lesion delineation.

### References

1. Scorsetti *et al.* 2014
2. Nemtanu *et al.* 2017
3. Celicanin *et al.* 2015

### EP-1945 Cost-effectiveness of the No Action Level Protocol for Head and Neck cancer patients

P. Kukolowicz<sup>1</sup>, M. Mietelska<sup>2</sup>

<sup>1</sup>The Maria Skłodowska-Curie Memorial Cancer Center, Medical Physics, Warsaw, Poland ; <sup>2</sup>Warsaw University, Faculty of Physics, Warsaw, Poland

***This abstract is part of the media programme and will be released on the day of its presentation***

**EP-1946 First french clinical experience using the Calypso tracking system for the prostate treatment**  
 J. Prunaretty<sup>1</sup>, D. Cirella<sup>1</sup>, P. Debuire<sup>1</sup>, N. Ailleres<sup>1</sup>, A. Morel<sup>1</sup>, S. Simeon<sup>1</sup>, S. Valdenaire<sup>1</sup>, P. Fenoglio<sup>1</sup>  
<sup>1</sup>CRLC Val d'Aurelle - Paul Lamarque, Radiotherapy, Montpellier, France

### Purpose or Objective

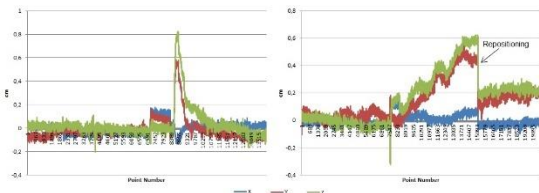
To report the intrafraction prostate displacement using the Calypso system through a randomized phase II study (RCMI-GI).

### Material and Methods

The Calypso System consists in an electromagnetic detection of implanted transponders. It is a real-time target tracking system that takes into account both inter- and intrafractional target motion. The RCMI-GI study will include 166 patients into arm 1 and arm 2 in 1:1 ratio. 83 patients will be treated with standard set-up margins (1 cm all around the prostate except 5mm in the posterior direction) and conventional IGRT protocol (daily CBCT). For the other ones, the treatment will be performed with reduced margins (3mm all around the prostate) using the Calypso® system. The prescribed dose is 80Gy in 40 fractions. To date, 21 patients were treated in arm 2 using VMAT and Calypso. At the beginning of each fraction, a CBCT was performed and "Set zero and track" function of the Calypso was applied. A 3mm-gating threshold was used during the treatment. The displacements  $\geq 3$ mm in all directions were evaluated qualitatively and quantitatively.

## Results

A total of 787 sessions were analyzed. An intrafraction motion  $\geq 3$ mm was detected for 77 fractions (9.8%). Visually, the shifts were unpredictable and varied from a transient evolution (left figure) continuous drift to a continuous drift (right figure). For each patient, from 0% to 23% of fractions were impacted by a displacement  $\geq 3$ mm. 12,4% of movements were in the lateral direction, 48,8% in the axial direction and 38.8% in the longitudinal one. The mean time of the treatment interruption was ranged from 0.01' to 09.52 minutes and increased the mean session time of 24.7% in comparison with a fraction without motion. Forty six percent of 77 fractions required couch shift corrections using kV imaging (as mandatory in our protocol) and explained a longer treatment.



## Conclusion

The intrafraction motions of the prostate are unpredictable and not negligible during the treatment. The Calypso system performs an accurate and continuous monitoring of the target and allows a safe margin reduction.

### EP-1947 RCMIGI randomized phase II study using Calypso system. First dosimetric results on CBCT acquisitions

P. Debuir<sup>1</sup>, J. Prunaretty<sup>1</sup>, N. Ailleres<sup>1</sup>, O. Riou<sup>1</sup>, D. Azria<sup>1</sup>, P. Fenoglietto<sup>1</sup>

<sup>1</sup>Institut du Cancer de Montpellier ICM, Radiothérapie, Montpellier, France

### Purpose or Objective

In the RCMIGI randomized phase II study, two treatment techniques of prostate cancer are compared in terms of radiation late toxicities, depending on the irradiated volumes. One of these techniques is a non-irradiative real-time tracking which uses electromagnetic implanted transponders (Calypso, Varian Medical System) to detect and follow submillimetric motions of a target. This way, the margin around the prostate can be reduced and a correlation may be found with late toxicities by studying the daily patient treatment deliveries. Here we present the results of dose calculation on daily CBCT images leading to the real treatment delivery knowledge.

### Material and Methods

25 prostate cancer patients were treated using RapidArc technique on a TrueBeam linear accelerator (Varian Medical System). In each arm of the study, 80 and 56 Gy were prescribed to the prostate and seminal vesicles (SV) in 40 fractions. The Calypso arm included 14 patients, each with 3 transponders implanted in the prostate that can be tracked before and during the irradiation. This allows to reduce the margin used to create the Planning Target Volume (PTV<sub>2</sub> = Prostate + 3 mm). Eleven patients were included in the standard arm, without real-time tracking and with standard margins (1 cm, 0.5 cm posterior). For every patient, Cone Beam Computed Tomography (CBCT) imaging was performed at each fraction before irradiation. Target volumes and Organs at Risk (OAR) were contoured and the original Eclipse (Varian medical system) treatment plan was calculated on the CBCT images. Thus 40 daily Dosimetric Volume Histograms (DVHs) were obtained per patient (1000 CBCTs in total). The averaged prostate, SV, bladder and rectum DVHs were then compared to the original treatment plan DVHs, for both arms of the study.

## Results

Figure 1 shows the averaged target volumes' DVHs on CBCTs and original dosimetry CT match each other in both arms. There are some discrepancies for rectum and bladder in both arms. DVHs of the CBCTs bladder are always lower than dosimetry because the bladder is empty during the original dosimetric scanner (CBCTs mean volume is 125 cc and 97.4 cc for the original CT), leading to higher relative volume doses. Rectum DVHs are on average higher on CBCTs, with an important uncertainty due to the high variation in rectum shape. Calypso SV, bladder and rectum DVHs are lower than those of the standard arm because of the lower irradiated volume induced by the reduced PTV margin. For instance, Calypso bladder D50 is 14 Gy (23 Gy for standard arm) and V70 is 5% (13%). There is also a 6 Gy lower rectum D50% on the Calypso patients, and V72 is 6% versus 10.5% for the standard arm.

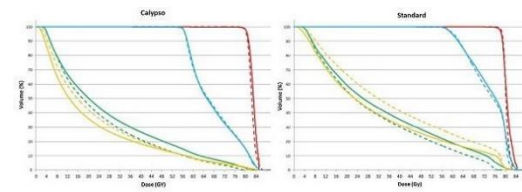


Figure 1: Average CBCTs DVHs vs dosimetry in Calypso arm (left) and standard arm (right)

## Conclusion

Calypso system allows submillimetric tracking of the prostate and therefore a reduction in the irradiated volume as shown in these first patient dosimetric results. Associated with long-term life quality follow-up, this could lead to the correlation of late toxicities versus dose statistics.

### EP-1948 Deep-inspiration breath-hold and free-breathing in left breast cancer irradiation: a dosimetric study

D. Aiello<sup>1</sup>, G.R. Borzi<sup>2</sup>, L. Marino<sup>2</sup>, V. Umina<sup>2</sup>, A.M. Di Grazia<sup>2</sup>

<sup>1</sup>Fondazione Istituto Oncologico del Mediterraneo, Radiotherapy, Viagrande, Italy; <sup>2</sup>REM Radioterapia, Radiotherapy, Viagrande, Italy

### Purpose or Objective

To analyze organs at risk dose reduction between voluntary deep inspiration breath hold (DIBH) and free-breathing (FB) techniques in left breast irradiation.

### Material and Methods

Between January 2018 and October 2018, eighty RT plans, based on DIBH and FB scans, were generated for forty breast left cancer patients who received three-dimensional conformal (3D) adjuvant RT and were retrospectively analyzed. Treatment plans were generated on both DIBH and FB CT scans. The scans were monitored by the Varian RPM™ respiratory gating system. The patients were asked to breathe freely and then inhale and hold their breath at a comfortable level, for at least 15 seconds. The treatment planning was performed with conformal tangential fields by means of 6, 10, or 15 MV photon fields. Treatment schedule were 40.05 Gy in 15 fractions (hypofractionated schedule) or 50 Gy in 25 fractions (conventional schedule) with or without sequential boost to tumor bed. Dose-volume histograms (DVHs) were compared for all plan. For the comparison, we considered: the mean dose to the heart (D<sub>meanheart</sub>), left anterior descending coronary artery (D<sub>meanLADCA</sub>) and ipsilateral lung (D<sub>meantlung</sub>), the volume receiving 20 Gy (V<sub>20Gylung</sub>) and the volume receiving 30 Gy (V<sub>30Gylung</sub>) for the ipsilateral lung, the volume receiving 20 Gy for LADCA (V<sub>20GylADCA</sub>) in conventional schedule, the volume receiving

19 Gy for LADCA ( $V_{19GyLADCA}$ ) in hypofractionated schedule. Quantitative statistical analysis of plan dose differences were generated. Maximum heart distance (MHD) was defined as the maximum distance between the anterior cardiac contour and the posterior tangential field edges. In order to correlate each measure of cardiac dose with MHD a linear regression model was used. Statistical level significance was set with a p-value <0.05.

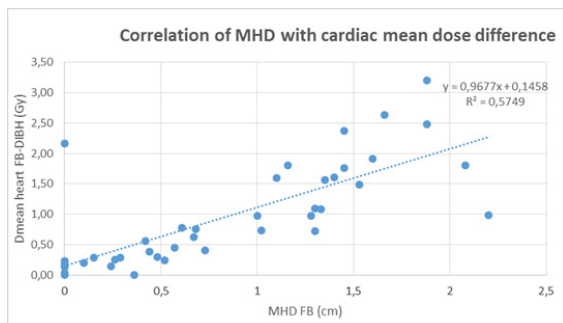
### Results

A statistical significant reduction of cardiac and pulmonary doses was achieved using DIBH technique compared to FB plans (Table 1) maintaining an equal coverage of planning target volume (PTV). A positive correlation was found between MHD and mean heart dose reduction (Fig.1).

Table 1

Organ	Technique	Mean dose (Gy)	SD	Mean difference dose (Gy)	p-value	Mean dose reduction (%)
Heart Dmean	FB	2.25	1.27	0.98	0.0000	43.5
	DIBH	1.27	0.65			
Heart Dmax	FB	39.61	12.57	19.09	0.0000	48.2
	DIBH	20.52	16.17			
LADCA Dmean	FB	13.39	10.02	8.39	0.0000	62.7
	DIBH	5.00	5.69			
LADCA Dmax	FB	39.17	11.04	20.29	0.0000	51.8
	DIBH	18.88	14.97			
Mean Lung Dose	FB	7.82	2.76	1.16	0.0354	14.8
	DIBH	6.66	2.02			
		Mean volume (%)		Mean difference volume (%)		Mean volume reduction (%)
Lung left V20Gy	FB	13.56	5.70	2.35	0.0390	17.3
	DIBH	11.21	4.20			
Lung left V30Gy	FB	11.52	5.58	2.18	0.045	18.9
	DIBH	9.34	3.83			
LADCA V20Gy	FB	27.64	27.72	21.93	0.0025	79.4
	DIBH	5.71	15.98			
LADCA V19Gy	FB	20.25	19.02	18.14	0.0004	89.6
	DIBH	2.11	5.54			

Fig. 1



### Conclusion

Our study confirms literature data about DIBH technique advantage in terms of reduction of cardiac and pulmonary doses for tangentially treated left sided breast cancer patients. Further research is warranted to evaluate potential long-term clinical implications of these relevant dosimetry results.

**EP-1949 Heart position reproducibility in deep inspiration breath hold radiotherapy for lung cancer**  
M. Josipovic<sup>1</sup>, M.C. Aznar<sup>1,2,3</sup>, J.B. Thomsen<sup>1</sup>, J. Scherman<sup>1,4</sup>, S.M.S. Damkjær<sup>1</sup>, L. Nygård<sup>5</sup>, L. Specht<sup>3,5</sup>, M. Pöhl<sup>5</sup>, G.F. Persson<sup>1,3,6</sup>

<sup>1</sup>Rigshospitalet, Dept. of Oncology\Section of Radiotherapy, Copenhagen, Denmark ; <sup>2</sup>Manchester Cancer Research Centre, Division of Cancer Science, Manchester, United Kingdom ; <sup>3</sup>University of Copenhagen, Department of Clinical Medicine- Faculty of Health and Medical Sciences, Copenhagen, Denmark ; <sup>4</sup>Skåne University Hospital, Dept. of Radiation Physics, Lund, Sweden ; <sup>5</sup>Rigshospitalet, Dept. of Oncology, Copenhagen, Denmark ; <sup>6</sup>Herlev Hospital, Dept. of Oncology, Copenhagen, Denmark

### Purpose or Objective

Heart dose has been linked to both increased mortality (McWilliam 2017) and cardio-vascular toxicity (Wang 2017) in patients with locally advanced non-small cell lung cancer (NSCLC), treated with modern chemo-radiotherapy. Residual setup errors, with tumour position closer to the heart than planned, had negative impact on overall survival (Johnson-Hart 2018).

We have shown, that treating this patient group in deep inspiration breath hold (DIBH) is well tolerated, improves image guidance and, in majority of patients, facilitates reduced dose to the heart (REF XXX).

The purpose of this study was to assess the reproducibility of the heart position between the consecutive DIBHs.

### Material and Methods

Patients participating in a single institution DIBH radiotherapy trial (2015-2017) were included. Voluntary DIBHs were supported by use of an optical marker system and a visual feedback of the patient's DIBH level. The patients underwent three consecutive DIBH CT scans as part of the imaging for radiotherapy planning. DIBH CT no. 2 and no. 3 were rigidly registered on DIBH CT no.1 with focus on the heart. In 15 patients, all registrations were repeated after two months to evaluate the uncertainty of the manual registration process.

The positional variations of the heart position were compared to previously evaluated variations in position of the peripheral tumour (T) and the lymph nodes (N).

### Results

In total 60 patients were available for the analysis. Mean ± standard deviations (SD) in the heart position between the DIBH CTs were 0.3±1.2 mm in left-right (LR), -0.1±1.3 mm in antero-posterior (AP) and 0.0±2.0 mm in cranio-caudal direction (CC). Over 90% of the deviations were < ±3mm (Figure 1). Intra-observer variation of the manual registration was 0.8mm in LR, 0.7mm in AP and 1.0mm in CC direction.

Heart-to-T position deviations were (mean±SD): 0.1±1.4 mm in LR, 0.3±1.8 mm in AP and -0.4±1.8 mm in CC, with 79% of deviations < ±3mm. Heart-to-N position deviations were 0.2±1.2mm in LR, 0.2±1.4mm in AP and -0.1±1.4 mm in CC direction, with 90% of deviations < ±3mm (Figure 1). During the image registration process, differences in heart circumference of >1cm were observed in some patients, despite reproducible lung volume and chest elevation (Figure 2).

Largest heart position deviation was in the CC direction and may only in part be explained with higher observer uncertainty in this direction. It was possibly a result of cardiac motion, its impact on image quality and heart deformations between the consecutive DIBHs.

Figure 1 – Box & beeswarm plot of variation in the heart position between consecutive DIBHs (top panel), and differences between the position of the heart and the peripheral tumour (middle panel) and between the heart and the lymph nodes (bottom panel). Thick line represents the median, box the 1<sup>st</sup> & 3<sup>rd</sup> quartile, whiskers are set at the 1.5 times interquartile range of the lower and upper quartiles. Points above and below the whiskers are considered outliers (deviating more than 2.7SD from the median).

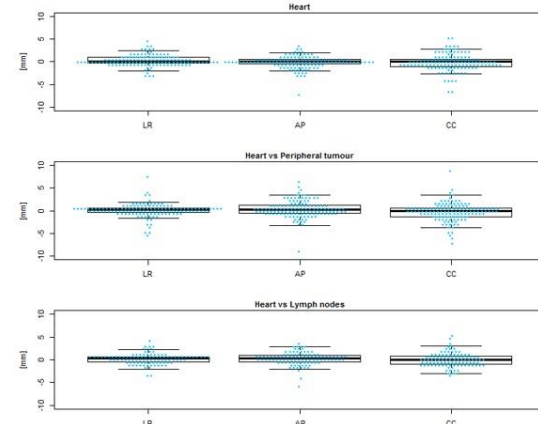
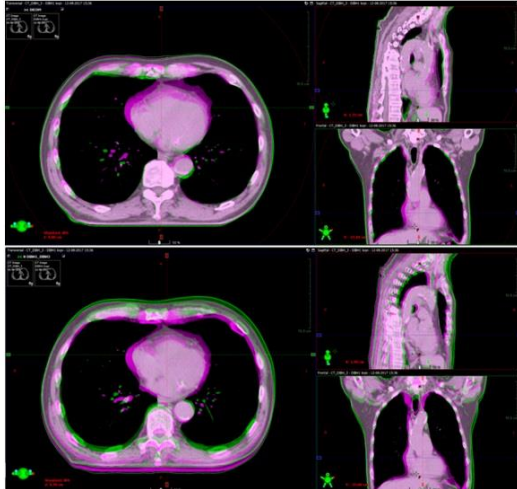


Figure 2 – green/magenta overlay of 1<sup>st</sup> (green) and 3<sup>rd</sup> (magenta) DIBH CT in patient #44. Top panel: registration between DIBH1 and DIBH3, based on DICOM origin: bones are well aligned, no major differences in lung volume or thorax surface, but clearly extended heart volume anteriorly. Bottom panel: CT scans are registered on the heart (3<sup>rd</sup> DIBH CT shifted 0.9 mm to the right, 7.4mm shift posteriorly and 3 mm cranially). There is still clear difference in heart circumference on both scans, while it fits well in cranio-caudal direction. DIBH lung volume increased by 54% compared to FB.



### Conclusion

The position of the heart was reproducible between consecutive DIBHs. Deviations between heart and N were smaller than between heart and T.

Further investigations on the variations in the position and shape of the heart and its substructures are warranted, for both free breathing and DIBH, and in combination with the variation in the position of the lung tumour (due to the baseline shift and anatomical changes).

### EP-1950 Phase gated lung SBRT verified by fluoroscopy

P. Wright<sup>1</sup>, S. Ramadan<sup>1</sup>, S. Suilamo<sup>1</sup>, P. Mali<sup>1</sup>, H. Minn<sup>1</sup>  
<sup>1</sup>Turku University Central Hospital, Radiotherapy and Oncology, Turku, Finland

### Purpose or Objective

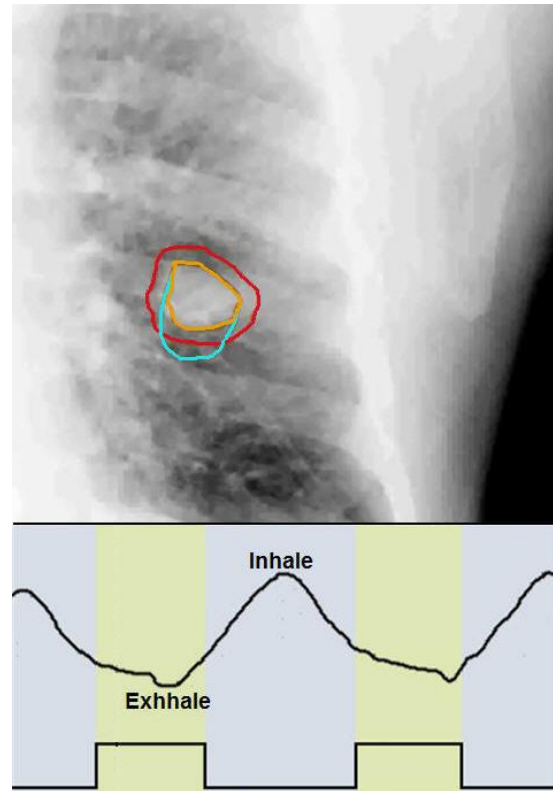
Diaphragm motion may cause large motion of lung tumours. A resulting large internal target volume (ITV) may limit the possibility of stereotactic body radiotherapy (SBRT). By delivering radiotherapy phase gated during the mid-vent breathing phase the resulting ITV may be remarkably reduced thus enabling SBRT for otherwise unsuited patients. This retrospective study presents treatment management and reproducibility of free breathing mid-vent phase gated lung SBRT.

### Material and Methods

During 2014-2018 30 patients have been treated for either primary lung cancer or metastatic disease with mid-vent phase gated lung SBRT. Treatment was planned on the average 4D-CT image created from the 30-70% breathing phases. The achieved reduction in ITV and resulting planning target volume (PTV) as compared with the full breathing cycle 4D-CT volumes were recorded for all patients. During treatment the patients breathed freely while their breathing amplitude was monitored with the Varian respiratory management system. Treatment was delivered mid-vent gated i.e. during the 30-70% phases of the breathing cycle (figure 1). Patient positioning was based on on-line cone beam computed tomography (CBCT) reconstructed with a 2 mm slice thickness and transaxial resolution of 1 x 1 mm. Following initial CBCT the match results was verified with on-line fluoroscopic images. A total of 198 fluoroscopic breathing cycles, acquired from 12 of the patients, were available for off-line analysis. From these images the tumours' cranio-caudal motion relative to that in the planning 4D-CTs was measured

(figure 1). All individual cycles were controlled for the tumour being within the PTV during the gating interval as well as if the tumour's exhale maximum deviated from its position in the 4D-CT. Furthermore, it was analysed if the observed deviations from the exhale baseline correlated with variation in either the patient's cycle time or monitored breathing amplitude.

Figure 1: Fluoroscopic view (top) with ITV mid-vent (orange), ITV full cycle (blue) and PTV (red). Mid-vent gating interval (lower) indicated by yellow bars.



### Results

The median ITV and PTV reductions were 40% (SD. 10%) and 30% (SD. 10%), respectively. The ITVs relative cranio-caudal motion between fluoroscopic images and planning 4D-CTs was on median 1.0 (SD. 0.2, p-value 0.82). Of the analysed fluoroscopic breathing cycles the tumours fitted into the ITV outline of the average 30-70% 4D-CT within  $\pm 1$  mm and  $\pm 2$  mm in 70% and 85% of the cycles, respectively. Thus a deviation larger than the CBCT resolution was observed in 15% of the cycles. In one patient the tumour moved outside the PTV during the gating interval. Deviations of the tumour's exhale maximum position did neither correlate with variations in breathing cycle length nor breathing amplitude.

### Conclusion

Free-breathing mid-vent phase gated lung SBRT was clinically feasible and the exhale maximum was stable. Due to its better resolution fluoroscopic images may be used for correcting the on-line CBCT match.

### EP-1951 Clinical feasibility of whole brain radiation therapy without a mask

J. Dekker<sup>1</sup>, T. Rozema<sup>2</sup>, F. Böing-Messing<sup>3</sup>, W. De Kruijff<sup>1</sup>, M. Garcia<sup>4</sup>, D. Washington<sup>4</sup>  
<sup>1</sup>Instituut Verbeeten, Klinische fysica & instrumentatie, Tilburg, The Netherlands ; <sup>2</sup>Helios Radiotherapie B.V., Radiotherapie, Tilburg, The Netherlands ; <sup>3</sup>Jheronimus Academy of Data Science, n/a, 's-Hertogenbosch, The Netherlands ; <sup>4</sup>Instituut Verbeeten, Radiotherapie, Tilburg, The Netherlands

### Purpose or Objective

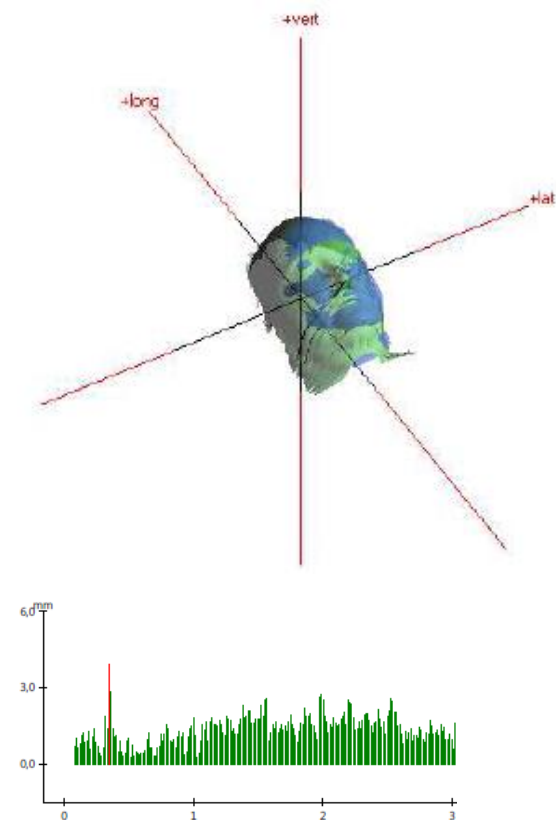
Patients complain about the tightness of thermoplastic masks and experience anxiety when the mask tightly encloses the head. Especially for patients suffering from claustrophobia, wearing a mask can be intolerable. Hence, a treatment method without the necessity of fixating the head is of advantage for patients. In order to ensure a reproducible position and to control intra-fraction motion, an alternative is needed. For this purpose, optical surface imaging is used. The aim of the study is to investigate the clinical feasibility of whole brain radiation therapy without a mask.

### Material and Methods

In total 30 patients received palliative, whole brain radiation therapy (5 fractions of 4 Gy) with the intention not to use a thermoplastic mask. The CTV-PTV margin is 5 mm. In case of participation, informed consent was signed. The surface scanner used for this study is the Catalyst™ (C-RAD AB, Sweden). Patients are instructed to lie as still as possible on the treatment couch. Positioning is done using surface scanning (see Figure 1) and an online matching procedure is performed. This is verified by making an anterior-posterior and a medio-lateral kV image. Motion monitoring starts as soon as the patient is positioned. The threshold for motion of the head is set to 3 mm, since this is an acceptable deviation taking the CTV-PTV margin of 5 mm into account. Figure 2 gives an example of the calculated iso-center shift. If the movement exceeds the threshold the radiation beam is interrupted and the patient may be repositioned. When more than two repositioning procedures are required, the fraction is labelled unsuccessful. Success of the treatment is defined when three or more fractions of one patient have been successful. Clinical feasibility in this study is defined as: more than 70% of the patients can complete the radiation treatment successfully, which is tested by using a one-tailed binomial test ( $p$  value  $< 0.05$ ).

### Results

Two patients out of the total population were not able to lie still and continued the treatment by using a mask. For one of them it was already decided at the CT to make a mask. The other patient completed a successful and an unsuccessful fraction without mask, before it was decided to use a mask for the remaining fractions. All other patients completed their treatment successfully with only one unsuccessful fraction (4 repositioning procedures) for one of these patients. With a probability of success of 93,3% (28 out of 30), we accept the hypothesis that more than 70% of the patients can complete radiation treatment successfully ( $p$  value is 0.0021, 95%-confidence interval 0.80-1.0). Intra-fraction motion data is available for further analysis.



### Conclusion

Patients receiving whole brain radiation therapy have been treated without a thermoplastic mask. In this study it is observed that patients are able to lie still below the threshold of 3 mm. Hence, it can be concluded that irradiation without a mask is a clinically feasible method for whole brain radiation therapy.

### EP-1952 Intra-fraction motion assessment of frameless intracranial radiosurgery using 1.5T MR simulator

J. Yuan<sup>1</sup>, G.G. Lo<sup>2</sup>, O.L. Wong<sup>1</sup>, K.F. Cheng<sup>3</sup>, W.W.K. Fung<sup>3</sup>, Y.H. Zhou<sup>1</sup>, G. Chiu<sup>3</sup>, K.Y. Cheung<sup>1</sup>, S.K. Yu<sup>1</sup>

<sup>1</sup>Hong Kong Sanatorium & Hospital, Medical Physics and Research Department, Hong Kong, Hong Kong SAR China ;

<sup>2</sup>Hong Kong Sanatorium & Hospital, Department of Diagnostic & Interventional Radiology, Hong Kong, Hong Kong SAR China ;

<sup>3</sup>Hong Kong Sanatorium & Hospital, Department of Radiotherapy, Hong Kong, Hong Kong SAR China

### Purpose or Objective

The intra-fraction motion of intracranial radiosurgery is usually investigated by using the online X-ray-based imaging. We aim to retrospectively assess the intra-fraction motion shift of a thermoplastic mask immobilized intracranial radiosurgery using MRI data acquired on a 1.5T MR-simulator by taking the advantage of superior MRI image contrast.

### Material and Methods

The simulation MRI scan data at 1.5T of 27 patients (brain metastases  $n=23$ , others  $n=4$ ) prior to Cyberknife intracranial radiosurgery were retrospectively assessed. All patients were scanned in the identical treatment position with a thermoplastic mask fixation. MRI protocol included at least two (T2w and post-contrast T1w+c, ~10min) sequences for all patients. A third T1w+c sequence (~5min) was included in 10 patients. All MRI images had isotropic 1mm voxel size. T1w+c MRI (represented the position at 5min and 10min respectively)

was rigidly registered to T2w (represented the position at 0min) based on mutual information and the intra-fraction motion shifts were calculated from transformation matrix.

#### Results

At the time point of 5min, the intra-fraction translation shifts (mm) were  $0.03 \pm 0.29$  (mean $\pm$ SD),  $0.08 \pm 0.11$ ,  $-0.53 \pm 0.72$  and  $0.71 \pm 0.62$  in LR, AP, SI and 3D, and rotational shifts ( $^{\circ}$ ) were  $-0.06 \pm 0.19$ ,  $0.00 \pm 0.00$ , and  $-0.01 \pm 0.20$  in roll, pitch and yaw, respectively. At the 10min point, the corresponding translation became  $0.02 \pm 0.35$  (mean $\pm$ SD),  $0.10 \pm 0.15$ ,  $-0.96 \pm 0.72$  and  $1.03 \pm 0.72$  in LR, AP, SI and 3D, and rotation ( $^{\circ}$ )  $-0.09 \pm 0.37$ ,  $-0.00 \pm 0.01$ , and  $-0.26 \pm 0.33$  in roll, pitch and yaw. The 3D intra-fraction shift at two time points was illustrated in Fig. 2. Most patients had excellent positional stability during the first 5min, but an apparent time trend of shift was observed at 10min. 7 out of 10 patients exhibited a much larger shift at 10min than at 5min. The superior soft tissue contrast of MRI facilitated more precise image registration and assessment of intra-fraction motion than X-ray skull tracking. So, our results might faithfully reveal the true intra-fraction shift magnitude of the intracranial target during radiosurgery and be helpful for planning margin setting. The limitations of this study included the off-line nature, small sample size, and limited duration and time points.

#### Conclusion

Our results suggested that thermoplastic mask immobilized frameless intracranial radiosurgery could achieve excellent positional stability within the initial 5min of treatment. The frameless immobilization might have high possibility of larger positional shifts that should be substantially compensated after 10min of treatment.

#### EP-1953 Lung tumour dynamics during SABR: Analysis of 415 CBCTs using a semi-automated contouring technique

E. Chandu<sup>1</sup>, L. Conway<sup>2</sup>, G. Distefano<sup>2</sup>, J. Earley<sup>2</sup>, K. Lamont<sup>2</sup>, M. Long<sup>2</sup>, I. Phillips<sup>3</sup>, H. Saxby<sup>2</sup>, C. South<sup>2</sup>, C. West<sup>2</sup>, V. Ezhil<sup>2</sup>

<sup>1</sup>Royal Marsden Hospital, Clinical Oncology, London, United Kingdom ; <sup>2</sup>Royal Surrey County Hospital, Radiotherapy, Guildford, United Kingdom ; <sup>3</sup>Western General Hospital, Clinical Oncology, Edinburgh, United Kingdom

#### Purpose or Objective

SABR (Stereotactic Ablative Body Radiotherapy) is an effective and increasingly utilised treatment in patients with early lung cancer. Because it relies on hypofractionation and a steep dose gradient, the ability to precisely target the tumour with tight margins is of paramount importance. Cone-Beam computed tomography allows online soft tissue matching during SABR to lung cancers. The data from these scans can be harvested to formally verify geometrical conformity and to extract radiobiological information about early response to treatment.

#### Material and Methods

415 CBCTs of 44 lung cancer patients treated with SABR were contoured using a semi-automated technique. The volume of tumour at each CBCT was determined in order to verify geometric conformity with the planning scan and to elucidate the radiobiology of tumours during SABR. The contoured CBCT was registered to the planning CT scan with the online match used at radiation delivery. Formal geometric verification was performed and any volume of tumour not within the reference planning structures was recorded. Counterfactual planning tumour volumes (PTVs) with reduced margins were created to evaluate the potential consequences of smaller PTV margins in clinical practice. (Figure 1)

#### Results

Lung tumours increased before reducing in volume during SABR. The mean volume of tumour at fraction 5 was

significantly smaller than at fraction 2 (6.07 vs. 7.25 cm<sup>3</sup>,  $p = <0.04$ , figure 2). Formal geometric verification confirmed that an isotropic 5 mm PTV margin reliably captured tumour, despite changes in volume and shape during treatment. The volume of tumour not captured by the PTV was trivial (range = 0.00-0.70 cm<sup>3</sup>, median = 0.00 cm<sup>3</sup>). 3 mm and 4 mm margins also consistently captured tumour and may be appropriate in clinical practice. Reasons for tumour falling outside the ITV included change in geometry, imperfect online match and CBCT artefact.

#### Conclusion

Semi-automated contours are effective for analysing Cone Beam CTs scans during SABR.

Our cancer centre delivers SABR with excellent geometrical precision.

5 mm PTV contours effectively capture change in tumour dynamics during treatment.

Smaller PTV margins may be appropriate in SABR for thoracic tumours.

#### EP-1954 The role of 4D cone beam CT and abdominal compression in motion management for Liver SABR

M. Nix<sup>1</sup>, G. Ward<sup>1</sup>, R. Goody<sup>2</sup>, J. Lilley<sup>1</sup>, N. Casanova<sup>2</sup>, R. Garratt<sup>3</sup>, K. Picken<sup>3</sup>, B. Al-Qaisieh<sup>1</sup>

<sup>1</sup>Leeds Cancer Centre, Radiotherapy Physics, Leeds, United Kingdom ; <sup>2</sup>Leeds Cancer Centre, Clinical Oncology, Leeds, United Kingdom ; <sup>3</sup>Leeds Cancer Centre, Radiotherapy, Leeds, United Kingdom

#### Purpose or Objective

Liver SABR relies on IGRT to ensure liver motion and organ at risk (OAR) position are reproducible from simulation through the treatment course. Motion management may include abdominal compression where possible. 4D cone beam CT (4DCBCT) on-set imaging allows verification of motion extent at each fraction and may lead to modifications prior to treatment delivery.

#### Material and Methods

A review of 19 patients treated with 5 fraction SABR for primary or metastatic liver cancer was performed. Total doses delivered were individualised based on OAR constraints and ranged from 40-50Gy. At simulation a multi-phase CT scan was obtained in voluntary exhale breath hold (ExBH), with bolus tracking to obtain arterial, portal venous and delayed phase scans. Oral contrast or water helped visualise duodenum. A 4DCT was acquired to determine extent of tumour motion. When required for target delineation, a treatment position contrast enhanced MRI was obtained. Where possible a CIVCO abdominal compression device was used for all imaging. The GTV was delineated on contrast enhanced ExBH CT or, where obtained, on MRI registered to ExBH CT. In most cases GTV was not visible on 4DCT datasets; ITV margins were determined based on assessment of surrogate liver motion. Maximum inhale and exhale liver contours were generated from 4DCT to aid motion assessment at 4DCBCT. As fiducials are not available in this centre, liver position was used as a surrogate for tumour location. Matching of liver position on maximum exhale phase of 4DCBCT to planning contour was performed. When a full liver match could not be obtained, accuracy of the match in the target region was favoured. A review of the motion and position of any dose-limiting OARs was then performed. Two pre-treatment 4DCBCTs were performed to ensure positioning and motion were stable. 4DCBCT was repeated after each fraction to ensure no change occurred during treatment. Cases were reviewed to assess impact of 4DCBCT.

#### Results

All 19 patients completed treatment. 6 (32%) patients were unsuitable for abdominal compression due to abdominal girth or intolerance of the device. 5 (38%) of the abdominal compression patients required modification to the compression device setting during treatment, to ensure liver motion observed on 4DCBCT was within limits

of motion observed at simulation. The mean absolute paddle height modification required was 7.4 mm (range 4-13 mm). 3 cases were modified prior to the first fraction, 2 later in treatment. Of the patients treated without compression, 3 required coaching to improve breathing to match liver motion limits based on 4DCBCT.

#### Conclusion

4DCBCT IGRT identified 5/13 cases where modifications to abdominal compression were required to achieve liver and OAR motion equivalent to simulation. For patients unsuitable for abdominal compression, 3/6 cases were identified where coaching was required. 4DCBCT is a valuable tool in ensuring the planned dose is successfully delivered.

#### EP-1955 Increased accuracy in setup position by using surface scanning

M. Garcia<sup>1</sup>, J. Dekker<sup>2</sup>

<sup>1</sup>Dr. Bernard Verbeeten Institute, Radiotherapy, Tilburg, The Netherlands ; <sup>2</sup>Dr. Bernard Verbeeten Institute, Medical Physics, Tilburg, The Netherlands

#### Purpose or Objective

The radiotherapy lung patients are traditionally setup using permanent tattoos en laser. During the setup the positioning of the arms can be difficult to position. Depending on the GTV and PTV repositioning can be necessary. The objective of this study was to investigate the accuracy and reproducibility of the arm and body position using surface scanning, compared with our standard positioning method using lasers and pointguards.

#### Material and Methods

- Twenty healthy test subjects participated in this study.
- Initial position: The test subjects were first positioned on the treatment couch according to our standard setup protocol for lung patients. The body and arms were marked in the Z (vertical), Y1, Y2 (longitudinal), and X (lateral) direction. The marked direction are showed in figure 1
- Positioning: Two positioning methods were compared, both using absolute table positions<sup>1</sup> :
  - Standard method: Positioning with laser alignment and pointguards.
  - Surface scanner: Positioning with a Catalyst™ surface scanner.
- Analysis: For both positioning methods, the deviation of the markings in the Z, Y1, Y2, and X directions was measured. To establish the efficiency of both positioning methods, the setup time per positioning method was also measured.

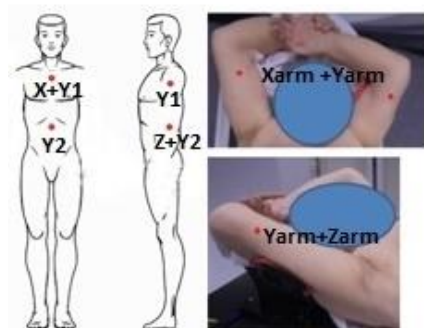


Figure 1. Location of the pointguards in the Z, Y1, Y2 and X direction on the body and arms.

#### Results

A tolerance margin of 3 mm (millimeters) was applied as a criterion for an accurate setup position.

#### Results:

- Body position: The deviation in X, Y and Z direction was within the tolerance margin for 78% of the measurements using the standard positioning method, compared to 75% using the surface scanner.
- Y<sub>2</sub> longitudinal body deviation: With 59% of the measurements, the positioning using laser alignment and pointguards showed a deviation that was smaller than or equal to 3 mm. When using the surface scanner, this occurred in 76% of the measurements.
- Arm position: In 27% of the measurements, the deviation was within the tolerance margin when using the standard method, while this was increased to 42% when using the surface scanner. The results of the arm positioning are showed in figure 2.
- Setup time: The average setup time was 1 minute and 7 seconds for the standard positioning. This was increased to 2 minutes and 17 seconds for the setup using the surface scanner.

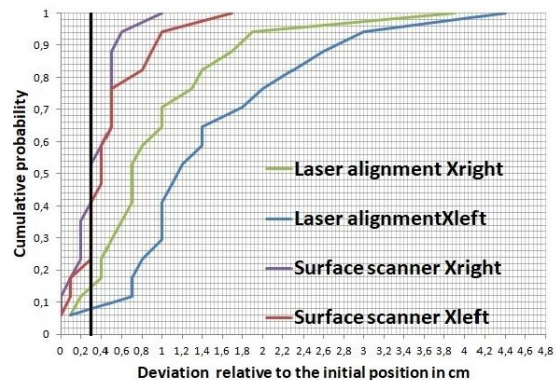


Figure 2. Cumulative histogram for the arm laser positioning in the X right direction (green) and X left direction (blue) and for the arm surface scanner positioning in the X right direction (red) and X left direction (violet). The vertical line (black) mark the 3 mm tolerance margin. This tells what percentage of the total number of measures has a deviation equal to 3 mm or smaller than 3mm.

#### Conclusion

The positioning method using the surface scanner showed an improved body (Y<sub>2</sub> direction) position, especially with regard to the arm position. As the positioning method with the surface scanner entails a new positioning technique, it took relatively longer to set up the patient than with the positioning standard method using laser alignment and pointguards.

<sup>1</sup>Kruijff de, W., & Martens, R. (2015). *Reducing patient posture variability using the predicted couch position*

#### EP-1956 Image quality of in-treatment 4D-CBCT obtained at various doses in VMAT for SBRT: a phantom study

Y. Shimohigashi<sup>1</sup>, Y. Doi<sup>1</sup>, M. Maruyama<sup>1</sup>, Y. Yotsuji<sup>1</sup>, Y. Kai<sup>1</sup>, R. Toya<sup>2</sup>

<sup>1</sup>Kumamoto University Hospital, Radiological Technology, Kumamoto, Japan ; <sup>2</sup>Kumamoto University Hospital, Radiation Oncology, Kumamoto, Japan

#### Purpose or Objective

In-treatment four-dimensional cone beam computed tomography (4D-CBCT) is a useful tool for assessing the intra-fractional location of a moving tumor and determining planning target volume (PTV) margin. However, in-treatment 4D-CBCT projection data acquired during volumetric modulated arc therapy (VMAT) depends

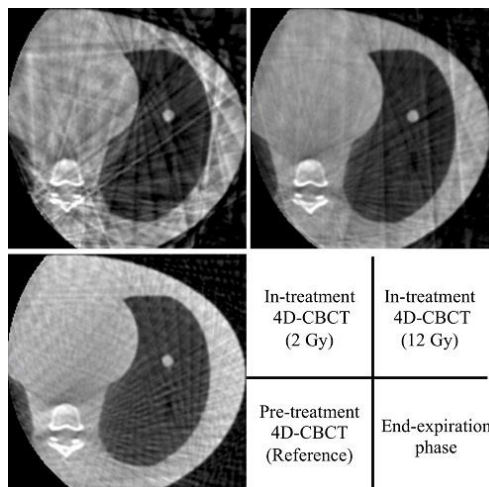
on the delivery time and includes a scatter component arising from treatment using MV beams. These factors may affect the image quality of in-treatment 4D-CBCT. This study aimed to quantitatively evaluate the image quality of in-treatment 4D-CBCT with various prescription doses (PDs) for accurately assessing tumor location in VMAT for stereotactic body radiation therapy (SBRT) of lung tumor.

#### Material and Methods

Spherical targets of diameters 10, 20, and 30 mm inserted in a dynamic thorax phantom moved sinusoidally with respiratory cycles of 4 s and amplitudes (A) of 5 and 10 mm along the superior-inferior direction. The target volumes were contoured from 4D-CT and merged into internal target volume (ITV). The PTV was defined by adding a uniform 5-mm margin to the ITV. The treatment plan was created with a D95 prescription of 2, 6, 7.5, 10, and 12 Gy for PTV using a single-arc VMAT with 6 MV. Pre-treatment 4D-CBCT (Elekta Symmetry™) scans were performed with an acquisition time of 3 min for the phantom setup, and those images were defined as reference images. The in-treatment 4D-CBCT images with various PDs were compared with the reference images using image quality metric. The image quality was evaluated by using signal-to-noise ratio (SNR), contrast-to-noise ratio (CNR), and dice similarity coefficient (DSC; to evaluate the spatial overlapping of target volumes with pre- and in-treatment 4D-CBCT). A Kruskal-Wallis test was performed for the statistical analysis of the results obtained with various PDs, and a P value < 0.05 was regarded as a significant difference.

#### Results

The figure shows representative images of pre- and in-treatment 4D-CBCT for the 10 mm target with A of 10 mm. The streak artifacts on the in-treatment 4D-CBCT images decreased as the PDs increased from 2 Gy to 12 Gy. For the 10 mm target with A of 10 mm, the mean values ( $\pm$  SD) of the SNR and CNR increased from  $9.8 \pm 0.8$  to  $17.4 \pm 1.5$  and from  $6.4 \pm 1.1$  to  $8.3 \pm 1.4$ , respectively, as the PDs increased from 2 to 12 Gy. The mean values ( $\pm$  SD) of the DSC were not statistically significant from  $0.75 \pm 0.15$  to  $0.7 \pm 0.11$  ( $P = 0.669$ ) as the PDs increased from 2 to 12 Gy. A similar tendency was observed for target sizes of 20 and 30 mm with A of 5 and 10 mm, respectively.



#### Conclusion

PD is an important factor that affects the image quality in in-treatment 4D-CBCT image acquisition. Moreover, in-treatment 4D-CBCT obtained with PDs > 2 Gy is acceptable for assessing tumor location in VMAT for SBRT of lung tumor.

#### EP-1957 An MR-based simulation procedure for individual assessment of tumor motion in MR-guided lung SABR

M. Palacios<sup>1</sup>, J.R. Van Sornsens de Koste<sup>1</sup>, F.O.B. Spoelstra<sup>1</sup>, C.J.A. Haasbeek<sup>1</sup>, A.M.E. Bruynzeel<sup>1</sup>, B.J. Slotman<sup>1</sup>, F.J. Lagerwaard<sup>1</sup>, S. Senan<sup>1</sup>  
<sup>1</sup>VU University Medical Center, Radiation Oncology Department, Amsterdam, The Netherlands

#### Purpose or Objective

To evaluate a simulation protocol to account for irregular breathing patterns in MR-guided SABR for lung tumors, and to report on the reproducibility of GTV position and duty-cycle efficiency during treatment.

#### Material and Methods

A workflow for initial simulation for MR-guided SABR was developed using MR-planar acquisitions (TR/TE = 2.41ms/1.09ms, FA=60°, 4 frames-per-second) in sagittal, coronal and axial planes, allowing for an individualized assessment of tumor motion in three directions for each patient. MR-planar acquisitions allowed the choice of the most suitable breathing-phase for SABR delivery and evaluation of the tracking performance during simulation. A 4D-CT scan was omitted. Ten patients who exhibited variable tumor motion and were treated using two dose schemes (8x7.5Gy and 5x11.0Gy) were identified for this study.

Treatment was delivered with GTV contour tracking during repeated breath-holds based on real-time deformable image registration using MR-planar acquisitions in the sagittal plane. PTV (GTV+3mm) was used as gating window. Treatment delivery performance was analyzed by quantifying the fraction of GTV inside the PTV in each frame during beam-on and corresponding duty-cycle efficiency for a total of 67 fractions.

#### Results

Substantial and variable tumor motion during respiration was observed: range 0.3 - 6.5 mm (AP), 0.2 - 4.7 mm (LR) and 1.5 - 27.1 mm (CC). Five patients were treated during shallow inspiration and five during expiration breath-hold. Reasons for expiration breath-hold were: lateral tumor movements, irregular tumor trajectories, and fast and substantial tumor motion in CC-direction.

Patients treated in expiration breath-hold with MR-guided SABR exhibited better reproducibility of the GTV inside the PTV and higher duty-cycle efficiencies, than patients treated during shallow inspiration. On average across all fractions, 96.9% (SD: 2.1%) and 94.3% (SD: 2.2%) ( $p < 0.001$ ) of the GTV area displayed on the MR-cine during treatment beam-on was inside the PTV for expiration and inspiration patients, respectively. Corresponding duty-cycle efficiencies were 71.9% (SD: 10.5%) and 64.5% (SD: 16.0%) ( $p = 0.016$ ), respectively.

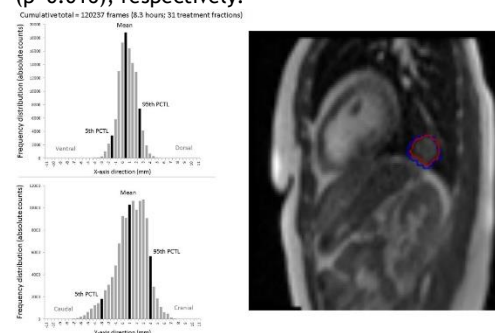


Figure: Frequency distribution of GTV-centroid position with respect to PTV-centroid in AP- and CC-direction for five patients treated with expiration breath-hold (left panel). Example of an MR-sagittal frame during treatment delivery (right panel).

#### Conclusion

An MR-based workflow for simulation prior to SABR for lung patients allowed individualized assessment of tumor motion and irregular breathing trajectories. Complex motion patterns observed led to use of SABR in expiration

breath-holds, and such patients exhibited higher reproducibility for the GTV position and duty-cycle efficiencies than patients treated in inspiratory phase.

#### EP-1958 Eight different open face masks compatibility with surface guided radiotherapy

M. Kügele<sup>1</sup>, E. Konradsson<sup>1</sup>, M. Nilsing<sup>2</sup>, S. Ceberg<sup>3</sup>

<sup>1</sup>Skåne University Hospital, Department of Hematology-Oncology and Radiation Physics, Lund, Sweden ; <sup>2</sup>C-rad Positioning AB, Research and development, Uppsala, Sweden ; <sup>3</sup>Lund University, Medical Radiation Physics-Department of Clinical Sciences, Lund, Sweden

#### Purpose or Objective

Open face masks can be combined with optical surface scanning (OSS) for patient positioning and real time monitoring during radiotherapy treatment. For the open mask, the OSS system aims to detect the patient skin surface only and any unwanted signal from the mask might affect the OSS performance. An increasing number of mask materials are about to be introduced to the radiotherapy environment, but few studies have been carried out investigating the compatibility with OSS system. Also, in this study we had access to new masks which are not yet available on the commercial market.

The aim of this study was to evaluate 1) eight different open face masks compatibility with the optical surface scanning system Catalyst™ (C-RAD Positioning AB, Uppsala, Sweden) and 2) the positioning accuracy using a novel surface algorithm for stereotactic radiosurgery (SRS).

#### Material and Methods

Eight open face masks from several vendors were molded onto a head phantom (Little Junior, Laerdal Medical, Orpington, UK). The OSS system automatically cropped away the mask and only used the skin surface for positioning. Markers were placed onto the skin surface of the phantom for CBCT evaluation purposes. Due to the different designs of the masks, the area of the surface visible for the OSS system varied (figure 1). The phantom was initially positioned on the treatment couch in an open mask at the reference position in isocenter and a CBCT was acquired to register the position. In order to test the novel SRS algorithms accuracy, an offset in the phantom position of 1 cm in all translational directions was introduced. The OSS system calculated couch shifts were sent over to the linac and was automatically shifted, using the auto couch function. A CBCT was acquired to verify the phantom position. For each mask, the marker position was evaluated using the Hounsfield unit profile extracted from the image registration in the treatment planning system (Eclipse 13.6, Varian Medical Systems, Palo Alto, CA). The position of the marker was evaluated in Matlab (Toolbox Release 2015b, The MathWorks, Inc., Natick, MA) in anterior-posterior (AP-PA), left-right (L-R), superior-inferior (S-I) position, respectively.

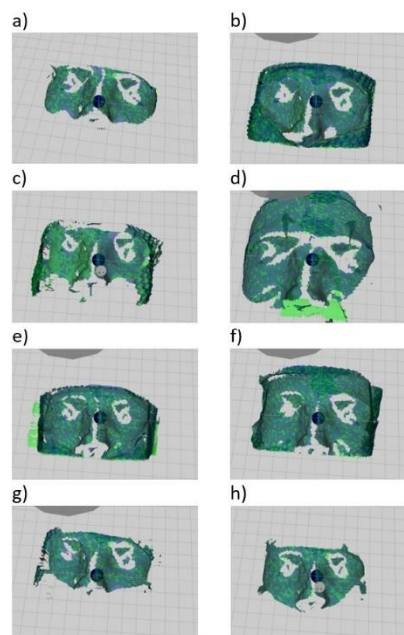


Figure 1. Surface scanned by the optical surface scanning (OSS) system for eight open masks, showing the different sized surfaces the OSS system used for the positioning. The novel stereotactic radiosurgery (SRS) algorithm was used to match the live surface (green) and the reference surface (blue) for positioning.

Table 1. The positioning result from the CBCT for eight different open masks positioned with the OSS system.

	Anterior- Posterior (mm)	Left- Right (mm)	Superior- Inferior (mm)
Mask a	-0.1	0.1	-0.1
Mask b	0	0	0
Mask c	0.1	0	-0.1
Mask d	0	0	0.5
Mask e	-0.1	0.1	0
Mask f	0	0.1	0.1
Mask g	0	0.1	0.1
Mask h	0	-0.1	0.1

#### Results

The range of the width and height of the masks were 6-12 cm and 12.5-29 cm, respectively, which resulted in different sized surfaces for the OSS system to use for the positioning calculation (figure 1). The median (range) position of the marker on the phantom surface for all masks were 0.0 (-0.1 - 0.1), 0.1 (-0.1 - 0.1), 0.1 (-0.1 - 0.5) mm in AP-PA, L-R and S-I directions, respectively (table 1).

#### Conclusion

Overall, all of the masks were compatible in combination with the OS system and the novel SRS algorithm. Regardless of the size of the skin surface, a high accuracy for surface based positioning using the novel SRS algorithm was observed.

#### EP-1959 Performance of Marker-less Tracking for Gimbaled Dynamic Tumor Tracking

M. Ziegler<sup>1</sup>, S. Lettmaier<sup>1</sup>, R. Fietkau<sup>1</sup>, C. Bert<sup>1</sup>

<sup>1</sup>University Hospital Erlangen, Radiation Oncology, Erlangen, Germany

### Purpose or Objective

Dynamic tumor tracking (DTT) is an advanced treatment technique to treat intra-fractionally moving tumors. Until now, the CyberKnife (Accuray Inc., Sunnyvale, CA, USA) and the Vero 4DRT system (BrainLab AG, Munich, Germany) are the only two commercially available systems which can perform a DTT treatment. Both systems detect the internal target position from X-ray images. Until recently, the Vero system required implanted fiducial markers to extract the target position from the X-ray images. Recently, marker-less DTT (MLDTT) was introduced to the Vero 4DRT system with ExacTrac 3.6.1. This work evaluates the accuracy of the new MLDTT method of the Vero 4DRT system and reports the results of the first patients treated with MLDTT at the Vero system.

### Material and Methods

The BrainLab Gating Phantom was used in combination with a QA-tool provided by the vendor (an inhomogeneous "egg" made from a gypsum-like material on an acrylic plate) to measure the detection accuracy of the new MLDTT software. The phantom consists of a vertical and a horizontal one-dimensional drive. A patient breathing curve was used as an input for the phantom and the accuracy was measured for all three spatial directions of the Vero system.

Three patients have been treated with MLDTT at the Vero system of the University Hospital Erlangen. During a MLDTT treatment additional kV images are acquired to determine a template of the day used for tumor detection during treatment delivery. The additional dose delivered by the additional images was determined using the CTDI Set for CT Dosimetry (PTW, Freiburg, Germany) and a log-file analysis was performed to evaluate the MLDTT treatment.

### Results

The accuracy of the MLDTT detection is  $0.12 \text{ mm} \pm 0.12 \text{ mm}$ ,  $0.12 \text{ mm} \pm 0.11 \text{ mm}$  and  $0.20 \text{ mm} \pm 0.21 \text{ mm}$  for the x-, y- and z-direction, respectively which is comparable to the accuracy of the marker-based DTT target detection ( $0.08 \text{ mm} \pm 0.09 \text{ mm}$ ,  $0.07 \text{ mm} \pm 0.08 \text{ mm}$  and  $0.07 \text{ mm} \pm 0.06 \text{ mm}$ ).

The median treatment time for the MLDTT patients was 18 min 25 seconds. On median 65 additional kV images were acquired per treatment fraction to determine the template for the target detection. In comparison to DTT, this results in an additional isocenter dose of 257.4 mGy over the course of the entire treatment.

### Conclusion

Three patients were treated with MLDTT at the University Hospital Erlangen. The accuracy of the MLDTT target detection and the treatment time of a MLDTT treatment were comparable to the marker based marker DTT of the Vero system. The additional imaging dose administered during the treatment can easily be justified since it spares the imaging dose of a CT guided marker implantation into the lung which is an interventional procedure carrying a great risk of pneumothorax.

### EP-1960 A comparison of positioning accuracy for frameless lung SBRT using two immobilization systems

J.M. Penedo Cobos<sup>1</sup>, J. Luna<sup>1</sup>, M.A. Garcia<sup>1</sup>, E. Lopez<sup>1</sup>, K. Aguilar<sup>1</sup>, R. Gonzalez<sup>1</sup>, A. Sanchez<sup>1</sup>, S. Gomez-Tejedor<sup>1</sup>, M. Rincon<sup>1</sup>, M. Alarcia<sup>1</sup>, S. Martin<sup>1</sup>, D. Gonsalves<sup>1</sup>, J. Olivera<sup>1</sup>

<sup>1</sup>Capio-Fundación Jimenez Diaz, radiotherapy oncology, Madrid, Spain

### Purpose or Objective

To quantify the localization accuracy and intrafraction stability of lung cancer patients treated with frameless stereotactic body radiotherapy (SBRT) using two different immobilization systems and to calculate the Internal Target Volume (ITV) margins in both cases to account for the setup errors.

### Material and Methods

19 patients with a single peripheral lung tumor, smaller than 30 cc, were included in this study. Two different immobilization systems were used: 9 patients were immobilized using the Elekta WingSTEP device (system1) and 10 patients using the Qfix Arm Shuttle with Vac-Qfix vacuum bag (system2). For each patient a 4dimensional-CT was acquired in a Philips Brilliance Big Bore CT. The ITV was delineated according to six breathing phases.

In total, 35 fractions were delivered in system1 and 32 fractions in system2. Two risk risk-adapted fractionation schemes were used: 3 fractions of 18 Gy and 5 fractions of 10 Gy. For each fraction, three 4-dimensional Cone Beam CT (4D-CBCT) scans were acquired: before treatment to measure and correct the mean tumor position (initial set-up), after correction to validate the correction applied, and after treatment to estimate the intrafraction stability. (In system2, after correction 4D-CBCT was not acquired).

These scans were volume registered with the localization CT, using a soft-tissue match, in the Elekta XVI software. Corrections were performed by a robotic patient positioning platform that enables sub-millimeter accuracy (Elekta HexaPOD evo RT system). Treatment was delivered using 6 MV photons generated from an Elekta Synergy Beam Modulator Linac.

Patient positioning data from all scans were recorded to determine systematic ( $\Sigma$ ) and random ( $\sigma$ ) set-up errors for initial set-up, after correction and after treatment imaging, in the left-right (X), craniocaudal (Y) and anteroposterior (Z) directions. The ITV to PTV margin (M) was also calculated for after correction and after treatment imaging, using the Van Herk formula:  $M=2.5 \Sigma + 0.7 \sigma$

### Results

A summary of patient set-up errors, intrafraction stability and ITV to PTV margins, in the three orthogonal directions, is shown in Table I.

Calculated margins do not account for target delineation and organ motion uncertainties and are consistent with our current 7 mm margins in all directions.

Table I. Summary of set-up errors and ITV margins

Immobilization system	Directions	CBCT initial Set-up(mm)		CBCT after correction(mm)			CBCT after treatment (mm)		
		$\Sigma$	$\sigma$	$\Sigma$	$\sigma$	M	$\Sigma$	$\sigma$	M
		WingSTEP	X	2.1	2.2	0.7	1.0	2.5	1.1
	Y	5.4	3.6	1.3	1.2	4.0	1.5	1.4	4.6
	Z	2.6	2.7	0.3	0.8	1.4	1.0	1.2	3.3
Vac-Qfix	X	3.4	2.9	---	---	---	0.8	0.8	2.5
	Y	3.9	2.0	---	---	---	1.0	0.7	3.0
	Z	2.3	3.8	---	---	---	1.0	0.7	3.0

### Conclusion

Patients treated using frameless SBRT are well immobilized in both systems studied. This is demonstrated with small intrafraction movements after initial set-up correction using imaging guidance. Therefore this technique can be safely administered using 4D-CBCT. ITV margins are smaller and intrafraction stability improves using the Vac-Qfix immobilization system compared to WingSTEP device.

Vac-Qfix immobilization system can be more convenient for patients with certain clinical conditions.

### EP-1961 Evaluation of dosimetric and anatomic parameters in Deep Inspiratory Breath Hold breast Radiotherapy

A. Nachankar<sup>1</sup>, A. Pawar<sup>1</sup>, A. Jadhav<sup>1</sup>, N. Burela<sup>1</sup>, A. Kakade<sup>1</sup>, P. Dandekar<sup>1</sup>

<sup>1</sup>Sir H N Reliance Foundation Hospital and Research Center, Radiation Oncology, Mumbai, India

### Purpose or Objective

Cardiovascular morbidity following radiotherapy to left sided breast cancers is significant. Several options have

been proposed to reduce cardiac morbidity. We evaluated dosimetric and anatomic characteristics of patient undergoing Deep Inspiratory Breath Hold Technique (DIBH).

#### Material and Methods

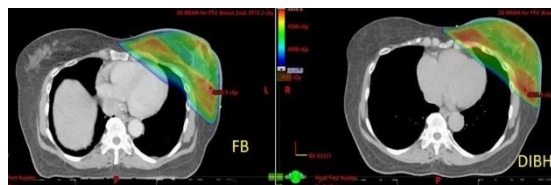
A total of 35 patients were analyzed retrospectively undergoing DIBH for adjuvant radiotherapy for left breast/ chest wall (CW) [BCS (n = 24) or CW (n= 11)] with or without regional nodes irradiation. 20/35 patients were treated with 40Gy/15 fractions and 15/35 patients were treated with 50Gy in 25 fractions +/- 12.5-15 Gy tumor bed boost. All patients trained for DIBH on Real-Time Position Management (RPM) system (Varian Medical Systems). All patients underwent Free Breathing (FB) and Breath-hold scans and were planned on both with tangential field in field technique. Doses to heart, left anterior descending artery (LAD), contralateral breast and lung were documented. Anatomical parameters like sternal angle, Haler's index, maximal heart distance (MHD) and heart and left ventricle to chest wall contact were calculated.

#### Results

Average Breath-hold amplitude was 1.96 cm (Breast), 1.75cm (CW) and average Breath hold duration was 20.8 sec (Breast), 21sec (CW). Average mean heart dose in DIBH patients receiving 50Gy/25fr is 2.24Gy vs 2.96 Gy in patients receiving 40Gy/15fr. Average reduction in mean heart dose in BCS was 56.5% vs 40.9% in CW patients. Average V30% of heart reduced from 6.58 to 1.36 % in 50Gy/25 fr subgroup (p= <0.001) and 7% to 3.03% in 40Gy/15fr subgroup (<0.001) from FB to DIBH respectively. Average MHD reduced from 1.35cm to 0.52cm in 50Gy/25fr subgroup (<0.001) and 1.89 to 1 cm in 40Gy/15fr subgroup (<0.001) from FB to DIBH respectively. Average reduction in irradiated volume of heart (50% isodose line) from 36.8 cc to 7.2cc in 50 Gy/25fr subgroup (<0.001) and 40.5cc to 18.2cc in 40Gy/15fr subgroup (<0.001) from FB to DIBH respectively. Average mean LAD dose reduced from 21.76Gy to 12.16 Gy in 50 Gy/25fr subgroup (<0.001) and 18.5 Gy to 13.4Gy in 40Gy/15fr subgroup (<0.001) from FB to DIBH respectively. Average maximum LAD dose reduced from 40.9 Gy to 32.4 Gy in 50 Gy/25fr subgroup (p=0.04) and 37.6 Gy to 31.9Gy in 40Gy/15fr subgroup (p=0.03), from FB to DIBH respectively. Average reduction in Mean LAD was 42.25 % in BCS patients compared to 25.96% in CW patients. There was statistically significant difference between sternal angle (p= 0.003), MHD (p=<0.001) and heart and left ventricle to chest wall contact (p=<0.001) in FB vs DIBH which correlated with decrease in cardiac and LAD doses. No significant difference in lung V20, mean lung dose & dose to the contralateral breast between FB and DIBH.

Table (1): Anatomical and Morphologic parameters significant for cardiac sparing DIBH for 50Gy/25fr vs 40 Gy/15fr subgroup

	50Gy/25#				40Gy/15#			
	BCS		CW		BCS		CW	
	FB	DIBH	FB	DIBH	FB	DIBH	FB	DIBH
Mean Heart Dose (Gy)	8.65	2.55	5.89	2.67	3.74	2.17	7.32	5.33
Heart V5%	35.03	8.55	13.53	8.13	12.66	6.39	21.33	16.37
Heart V25%	20.1	2.93	7.15	2.27	6.29	1.79	13.55	9.14
Heart V30%	18.31	2.36	6.31	1.87	5.19	1.33	12.45	8.11
Maximal heart Distance (cm)	1.61	0.55	1.46	0.69	1.73	0.88	2.08	1.38
Irradiated Heart Volume (cc)	113.70	13.60	30.07	8.52	33.06	11.25	63.00	39.16
LAD Mean Dose (Gy)	19.82	9.41	24.53	16.29	16.45	11.18	24.56	20.06
LAD Max (Gy)	37.11	26.16	46.62	41.71	36.04	28.62	45.00	42.00
LAD V25% (Gy)	40.20	14.39	49.08	20.85	40.32	19.92	56.50	44.37
Lung V20	22.98	16.24	17.77	16.18	14.09	14.69	18.97	18.27
Mean Lung dose (Gy)	10.99	8.78	9.30	8.80	6.91	7.03	8.88	8.58



#### Conclusion

DIBH is effective tool for cardiac sparing showing significant dose reduction to heart, and LAD. Changes in anatomical parameters in FB and DIBH scan, like MHD, Sternal angle and heart/ left ventricle contact with chest wall can be helpful in predicting the dose reduction.

#### EP-1962 A simple and low-cost method of deep inspiration breath-hold irradiation for breast cancer

Y. Koide<sup>1</sup>, T. Kitagawa<sup>1</sup>, T. Aoyama<sup>1</sup>, H. Shimizu<sup>1</sup>, H. Tanaka<sup>1</sup>, H. Tachibana<sup>1</sup>, T. Kodaira<sup>1</sup>

<sup>1</sup>Aichi Cancer Center, Radiation oncology, Nagoya, Japan

#### Purpose or Objective

Voluntary deep inspiration breath-hold (DIBH) was useful technique for cardiac dose reduction in left-sided breast cancer radiotherapy. It usually needs some devices to trace patients' respiratory cycle. However, there is a problem of expense and technical challenges of its implementation. Our institution started DIBH with the combination of video-monitoring thoracic motion and the setup using cine-images on an electronic portal imaging detector (EPID) and digitally reconstructed radiograph (DRR). The purpose of this study is to evaluate the accuracy and the reproductivity of this DIBH technique and to compare dose metrics of DIBH and free-breathing (FB) plans.

#### Material and Methods

Ten patients with left-sided breast cancer were included in this study. They were coached and must voluntarily hold their breath during the treatment. Each patient was performed DIBH and FB computed tomography (CT) and created both treatment plans. Patients' thoracic motion was traced with video-monitoring, and the treatment beam was delivered manually when their surface marker was within the acceptable position. Treatment setup was verified comparing DRR and an EPID image. The inter-fractional variation was measured using DRR and the first frame of cine-EPID images acquired during each irradiation. The intra-fractional variation was measured from comparing cine-EPID images from the first frame to the last one at each irradiation. The dose metrics of breast planning target volume (PTV), heart, left ascending artery (LAD), and lung contours were compared between the DIBH plan and the FB plan. Reported results are mean ± SD (DIBH plan vs. FB plan).

#### Results

Eligible patients were all completed planned treatment. The average median inter-fractional movement in the left-right direction (X axis in our study) and in the cranio-caudal direction (Y axis in our study) was  $-0.05 \pm 1.61$  mm and  $1.2 \pm 1.58$  mm, and median intra-fractional movement was  $0.01 \pm 0.49$  mm and  $-0.2 \pm 0.27$  mm. The mean volume of PTV, heart, LAD, and lung between DIBH and FB plan were  $500 \pm 232$  mL vs.  $475 \pm 224$  mL (p = 0.42),  $587 \pm 153$  mL vs.  $584 \pm 130$  mL (p = 0.48),  $2.5 \pm 0.58$  mL vs.  $2.3 \pm 0.62$  mL (p = 0.26), and  $3591 \pm 574$  mL vs.  $2246 \pm 418$  mL (p = 0.0003), respectively. The mean PTV dose was  $42.3 \pm 0.40$  Gy vs.  $42.1 \pm 0.64$  Gy (p = 0.25) and conformity index of PTV was  $0.3 \pm 0.094$  vs.  $0.29 \pm 0.079$  (p = 0.42). The mean heart dose was  $0.76 \pm 0.11$  Gy vs.  $1.33 \pm 0.52$  Gy (p = 0.02), the mean LAD dose was  $2.6 \pm 0.85$  Gy vs.  $7.8 \pm 5.6$  Gy (p = 0.03), and the mean lung dose was  $1.7 \pm 0.42$  Gy vs.  $1.8 \pm 0.45$  Gy (p = 0.29).

#### Conclusion

As only minor inter-fractional and intra-fractional movements were observed, this simple low-cost DIBH technique could ensure a feasible method of voluntary DIBH irradiation. It could reduce the mean heart dose and mean LAD dose with maintaining PTV coverage compared to FB plans.

#### EP-1963 IGRT to improve accuracy in lung SBRT

C. Anson Marcos<sup>1</sup>, D. Hernández<sup>1</sup>, P. Castro Tejero<sup>1</sup>, M. Roch González<sup>1</sup>, A. Valiente González<sup>2</sup>, P. García Castañón<sup>1</sup>, A. Viñals Muñoz<sup>1</sup>, R. Fayos-Sola Capilla<sup>1</sup>, L.

Pérez González<sup>1</sup>, M.T. Murillo González<sup>3</sup>  
<sup>1</sup>University Hospital La Princesa, Medical Physics, Madrid, Spain ; <sup>2</sup>University Hospital La Princesa, Radiation Therapist, Madrid, Spain ; <sup>3</sup>University Hospital La Princesa, Radiation Oncology, Madrid, Spain

### Purpose or Objective

Patient motion and breathing cause misalignment of the tumor and toxicities to the healthy tissue during lung Stereotactic Body Radiation Therapy (SBRT). In order to ensure the accuracy of dose delivering, correction motion can be applied by using Image-Guided Radiation Therapy (IGRT). The aim of this work is to describe our IGRT Protocol for Lung SBRT.

### Material and Methods

Data from 31 patients undergoing SBRT for lung cancer have been analysed for this study. Our IGRT protocol involves the use of time-resolved four-dimensional CT (4DCT) scanning technique (Real-Time Position Manager by Varian) in a Toshiba AquilionLB unit in the simulation phase, and the use of Cone Beam Computed Tomography (CBCT) and fluoroscopy images (On-Board Image by Varian) in the treatment phase in a Clinac 2300 iX.

- Simulation phase: during the scan, the patient is instructed to breathe normally. A 4DCT scan of 10 respiratory phases is reconstructed using phase sorting. After that, contour of the target volume in the 10 sets of CTs is performed. The used approach is creating an internal target volume (ITV) which encompasses the entire tumor displacement in a breathing cycle. ITV is expanded with a margin of 5 mm to create the PTV.

- Treatment phase: radiation delivery consists on three coplanar dynamic hemi-arc fields with RapidArc. Before dose deliver, a full rotation pre-CBCT is performed in the OBI system. Our deviation tolerance in the tumor from the reference setup, determined in three dimensions, is 1cm. Between field activation, intra-fraction anterior-posterior projection fluoroscopy imaging is performed to confirm tumor motion within the PTV contour. If the tumor is not visualized in the fluoroscopy image or the motion exceeds the PTV contour, intermediate CBCT image is performed. Finally, after treatment a post-CBCT assesses intra-fraction tumor displacement.

### Results

For the group of 31 patients, the 84% were able to be performed intra-fraction fluoroscopy against 16% in which the image contrast was low for visualization of the tumor. By using fluoroscopy imaging tumor motion within the session was verified in 61% of the patients. On the other hand, fluoroscopy images showed intra-fraction tumor displacement, and therefore the need of reposition, in 23% of the patients (Figure 1).

The average and standard deviation of the setup errors for all the patients are showed in Table 1. Pre-CBCT presents larger setup errors than post-CBCT, since tumor position is verified, and corrected if necessary, with the fluoroscopy imaging.

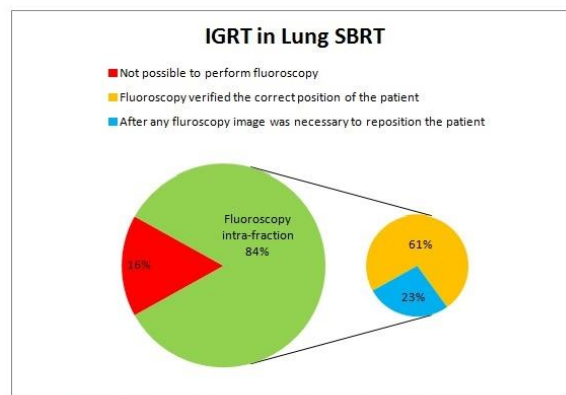


Figure 1. Intra-fraction fluoroscopy imaging performed to verify tumor position.

	IGRT Registration					
	pre-CBCT			post-CBCT		
	X (cm)	Y (cm)	Z (cm)	X (cm)	Y (cm)	Z (cm)
Average	-0,03	-0,18	0,01	-0,01	-0,07	-0,02
Σ	0,29	0,33	0,30	0,06	0,10	0,08

Table 1. Errors in position in CBCT images before and after fractions

### Conclusion

IGRT is an important motion management strategy for tumor motion, as in SBRT lung cancer. Fluoroscopy manages to verify tumor position accuracy and in comparison to CBCT intra-fraction, it involves reducing treatment duration and minimizing dose to patient.

Even though fluoroscopy depends on high contrast for visualization, in conjunction with CBCT, it may be used to confirm motion during the treatment.

### EP-1964 Setup verification and Intrafraction motion monitoring with Optical Surface Imaging for frame-less SRS

A. Nachankar<sup>1</sup>, A. Pawar<sup>1</sup>, A. Jadhav<sup>1</sup>, P. Dandekar<sup>1</sup>  
<sup>1</sup>Sir H N Reliance Foundation Hospital and Research Center, Radiation Oncology, Mumbai, India

### Purpose or Objective

Accurate positioning, rigid immobilization and image verification is crucial in high precision stereotactic radiosurgery. We evaluated setup accuracy using frameless open mask stereotaxy system with optical surface monitoring (OSMS) as an adjunct to gold standard Cone Beam CT (CBCT) scan.

### Material and Methods

We retrospectively analyzed 12 patients treated with frameless cranial stereotactic radio surgery (SRS) during August 2016 and June 2018, at our institution. Patients were immobilized using Q fix immobilization system (Q-fix Aquaplast mask, Head & Neck base plate, MOLDCARE® Cushion & Silverman head support). All patients were aligned to the isocenter with lasers on Perfect Pitch 6 DoF couch. Set up errors were calculated by OSMS prior to acquiring CBCT by comparing surface data to planning CT scan in translational and rotational directions. All the patients underwent CBCT based for correction of setup errors pretreatment and posttreatment verification CBCT. OSMS continuously monitored for intrafraction motion and threshold for beam holding for translational motion was 3 mm and rotational motion was 2 degrees. Data was analysed by Paired T test and Pearson correlation coefficient.

### Results

A total of 24 CBCT scans were analyzed for 12 patients undergoing cranial SRS. Setup errors documented by CBCT were compared with the shifts computed by OSMS. Mean translational errors documented by pretreatment OSMS

are comparable to CBCT setup errors [1.4 +/-1mm vs 1.3 +/-0.09mm in vert (p= 0.87), 1.4 +/-1mm, vs 1.7 +/-0.8mm in long (p= 0.75), 1.5 +/-1mm vs 1.6 +/- 1mm in lat (p= 0.53) directions respectively]. Mean rotational errors documented by OSMS and CBCT system are [1.02 +/-0.8° vs 1.2 +/-0.8° pitch (p= 0.12), 0.6 +/-0.4°, vs 0.7 +/-0.6° roll (p= 0.77), 0.96 +/-0.5° vs 0.98 +/- 0.6° in rotation (p= 0.82) directions respectively]. Mean translational errors documented by post treatment OSMS are comparable to CBCT setup errors (0.3 +/- 0.4 mm vs 0.5 +/-0.4 mm in vert, 0.5 +/-0.2 mm vs 0.6 +/-0.5mm in long and 0.3 +/- 0.4 mm vs 0.8 +/-0.3mm in lat direction respectively). Mean rotational errors post treatment documented with OSMS and CBCT (0.4 +/- 0.5° vs 0.3 +/-0.4° pitch, 0.3 +/- 0.4° vs 0.3 +/- 0.3° in roll, 0.3 +/- 0.2° vs 0.2 +/- 0.3° in rotation respectively). Average intrafractional translational errors were (0.5 +/- 0.3 mm in vert, 0.7 +/-0.2 mm in long and 0.5 +/- 0.4mm in lat directions respectively), and mean rotational errors (0.45 +/- 0.3°, in pitch, 0.3 +/- 0.3° in roll and 0.33 +/-0.2° in rotation respectively). Pearson's correlation coefficient for pretreatment setup verification by OSMS compared to CBCT was (r = 0.12) in vert, (r = 0.16) in long, (r=0.24) in lat, (r= 0.5) in pitch, (r = 0.04) in roll and (r= -0.41) in rotation.

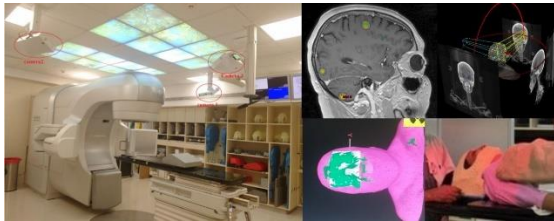


Figure (1): Frame-less, open mask Stereotactic Radiosurgery system with OSMS

#### Conclusion

Setup accuracy of shifts computed by OSMS is comparable to CBCT data. Overall, there is positive correlation between OSMS and CBCT documented setup errors ( $0 < r < 1$ ).

#### EP-1965 RealSense™ Camera Technology for Real Time Surface Monitoring During Radiotherapy

A. Fielding<sup>1</sup>, Y. Jonmohamadi<sup>1</sup>, S. Lee<sup>1</sup>, A. Pandey<sup>1</sup>  
<sup>1</sup>Queensland University of Technology, Science and Engineering Faculty, Brisbane, Australia

#### Purpose or Objective

The aim of this work is to investigate the use of the latest generation of the Intel® Real Sense™ SR300 camera technology for real-time measurement of radiotherapy patient positioning. The systems make use of optical camera technology that measures the distance to a surface; rapid image acquisition can then enable real time motion detection of the location of the surface. The measurement based study investigated the accuracy and precision of the camera system through a series of controlled measurements of static and moving objects.

#### Material and Methods

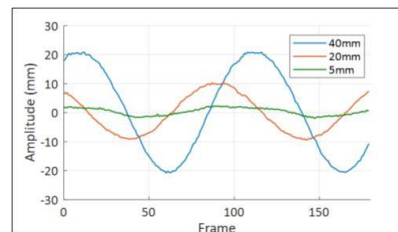
This work is a feasibility study of the use of an Intel® Real Sense™ SR300 camera for measuring patient position and motion for radiotherapy applications. The camera was connected to the USB port of a laptop running the Windows 10 operating system. Frame capture was performed using the free RealSense™ Software Development Kit (SDK 2.0) and cross-platform libraries. 30 frames were captured at a rate of 30 fps with each frame having 640x480 pixels. Measurements were performed on the flat surface of a static object with a range of camera-object distances between 100 and 1000 mm. The 30 frames were averaged and the mean and variance of the depth values in a 10 x 10 region of pixels was calculated

for each dataset. For each camera-object distance four repeat datasets were acquired to assess reproducibility. Further measurements were performed with the object moving on a Standard Imaging respiratory gating platform (Standard Imaging Inc, USA) with a range of 1D motion amplitudes (5, 20, and 40 mm) and frequencies (0.18, 0.22 and 0.29 cycles/sec).

#### Results

The results of the camera depth measurements on the static object are shown in table 1. For distances between 300 and 600 mm the camera was able to measure the distance to an accuracy better than 1 mm. The measured depth values over a 10 x 10 pixel region of interest on the object had a maximum variance of 5 mm (0.5%) at a camera-object distance of 1000 mm. The variance was less for shorter camera-object distances. Figure 1 shows the measured depth as a function of time for motion amplitudes of 5, 20, and 40 mm with a frequency of 0.29 cycles/sec. The measured amplitudes of the motion from the camera depth data in figure 1 were 4.2, 19.4 and 41.6 mm respectively.

Distance (mm)	Depth value (mm)				Variance (mm)				Percentage (%)			
	1	2	3	4	1	2	3	4	1	2	3	4
100	99.6	99.6	99.6	99.6	0.014	0.015	0.021	0.024	0.013	0.015	0.021	0.023
200	198.0	198.0	198.0	198.0	0.005	0.005	0.005	0.004	0.002	0.003	0.002	0.002
300	300.8	300.8	300.7	300.8	0.13	0.14	0.13	0.13	0.050	0.046	0.046	0.042
400	400.5	400.5	400.4	400.5	0.53	0.51	0.52	0.54	0.130	0.130	0.130	0.134
600	601.0	600.9	600.9	600.9	1.28	1.31	1.39	1.33	0.21	0.22	0.23	0.22
800	795.5	795.5	795.5	796.4	2.08	2.45	2.76	2.11	0.26	0.31	0.35	0.27
1000	995.6	995.5	995.5	995.5	5.13	5.00	4.13	5.50	0.51	0.5	0.42	0.55



#### Conclusion

The results of this preliminary work showed the Intel® RealSense™ SR300 camera to be able to measure the respiratory like 1D cyclical motion of a test object with an amplitude of 5 mm with an accuracy better than a mm. The camera was able to operate at camera-object distances of up to 1000 mm with pixel noise levels of 0.5% making the camera a feasible option for measuring patient position and motion during radiotherapy.

#### EP-1966 Deep inspiratory breath hold versus free breathing techniques in breast cancer radiotherapy

A.D. Tawfik<sup>1</sup>, A. Ali<sup>1</sup>, S. Talima<sup>1</sup>, M. Mousa<sup>1</sup>  
<sup>1</sup>Cairo University, Department of Clinical Oncology, Cairo, Egypt

#### Purpose or Objective

It has been theorized that radiation therapy to the breast using deep inspiratory breath hold (DIBH) technique can reduce cardiac doses by moving the heart away from the target volume. In addition, lung expansion during inspiration can decrease the relative volume of irradiated lung. To test this hypothesis, dosimetric and geometric comparisons were conducted between DIBH and conventional free breathing (FB) treatment delivery techniques in breast cancer patients.

### Material and Methods

Eligible patients, who had the intellectual and physical capacity to perform reproducible DIBH during training, underwent DIBH CT simulation and treatment delivery using the Varian surface-based real-time position management (RPM) tracking system. Treatment planning was carried out on the Varian Eclipse treatment planning system v.11. Patients received a prescription dose of 45Gy in 20 fractions. A second series of CT images was taken during FB for each patient, for which a second treatment plan was generated. Accordingly, a comparison between the DIBH and FB sets of plans, in terms of certain lung and heart dosimetric and geometric parameters, was conducted. Paired t-test was used to compare means for both data sets.

### Results

Thirty consecutive breast cancer patients were treated with DIBH radiation therapy technique. Twenty patients (67%) had left breast cancer, nine patients (30%) were right-sided and one patient (3%) had bilateral disease. Dosimetric comparison between DIBH and FB plans revealed a lower heart V18 with DIBH at  $4.7 \pm 4.7\%$  vs.  $12.1 \pm 11.1\%$  in FB ( $p=0.001$ ), a lower heart V28 with DIBH at  $3 \pm 3.3\%$  vs.  $10.3 \pm 10\%$  in FB ( $p=0.0002$ ) and a lower mean cardiac dose of  $4.1 \pm 3\text{Gy}$  with DIBH vs.  $6.7 \pm 4.9\text{Gy}$  in FB ( $p=0.009$ ). There was also a reduction in the left anterior descending coronary artery (LAD) V18 with DIBH at  $43.5 \pm 42.1\%$  vs.  $68 \pm 43.2\%$  in FB ( $p<0.0001$ ), a lower mean LAD dose of  $18.2 \pm 15\text{Gy}$  with DIBH vs.  $28.3 \pm 18\text{Gy}$  in FB ( $p=0.006$ ) and a lower maximum LAD dose of  $27.5 \pm 17.8\text{Gy}$  with DIBH vs.  $32.9 \pm 17.9\text{Gy}$  in FB ( $p=0.007$ ). In addition, DIBH yielded a lower ipsilateral lung V18 at  $20.5 \pm 4.8\%$  vs.  $25.7 \pm 8.1\%$  in FB ( $p<0.0001$ ) and a lower ipsilateral lung mean dose of  $11.1 \pm 3.7\text{Gy}$  vs.  $12.3 \pm 3.2\text{Gy}$  in FB ( $p=0.026$ ). With regard to the geometric parameters, DIBH reduced the cardiac contact distance with the chest wall, both in the axial ( $0.4 \pm 0.8\text{cm}$  vs.  $3.9 \pm 2.2\text{cm}$  in FB;  $p<0.0001$ ) and sagittal planes ( $2.5 \pm 1.9\text{cm}$  vs.  $4.2 \pm 2.1\text{cm}$  in FB;  $p<0.0001$ ), see figure 1. Moreover, DIBH significantly decreased the maximum heart distance inside the treatment field compared with FB ( $1.6 \pm 0.6\text{cm}$  vs.  $2.7 \pm 0.5\text{cm}$ , respectively;  $p<0.0001$ ).



### Conclusion

Compared to FB, DIBH technique results in marked reduction of the doses to the heart, LAD and lungs. In addition, it decreases the cardiac volume in contact with the chest wall as well as the maximum heart distance inside the treatment field. Thus, DIBH appears to be a promising technique to mitigate long-term cardiac and pulmonary toxicities in breast cancer survivors.

### EP-1967 Relationship of uncertainty due to respiratory motion with amplitude in SBRT treatments

J. García Ruiz-Zorrilla<sup>1</sup>, M.A. De la Casa de Julián<sup>1</sup>, P. García de Acilu Laa<sup>1</sup>, O. Hernando Requejo<sup>2</sup>, C. Rubio Rodríguez<sup>2</sup>, J. Martí Asenjo<sup>1</sup>, P. Fernández Letón<sup>1</sup>, D. Zucca Aparicio<sup>1</sup>, J.M. Pérez Moreno<sup>1</sup>

<sup>1</sup>Hospital Universitario HM Sanchinarro, Radiofísica, Madrid, Spain ; <sup>2</sup>Hospital Universitario HM Sanchinarro, Oncología Radioterápica, Madrid, Spain

### Purpose or Objective

Quantify the experimental relationship between the uncertainty due to respiratory motion (RM) and the peak to peak amplitude (A) of this movement in liver, lung, pancreas and breast tumors treated with stereotactic body radiation therapy (SBRT) and ExacTrac Adaptive Gating® with intra-fractional IGRT.

### Material and Methods

Fifty five fractions (15000 cycles) of liver, 41 fractions (14000 cycles) of lung, 76 fractions (34000 cycles) of pancreas and 70 fractions (14000 cycles) of breast tumors were treated with SBRT using ExacTrac Adaptive Gating® in a Novalis® linac. This system uses external markers to monitor the respiratory cycle and internal fiducial markers to set up the patient and measure the movement of the tumor.

All the magnitudes of the respiratory motion of tumor were analyzed through a linear regression between the motion of external markers and internal fiducial markers (surrogate to tumor motion).

The uncertainty due to respiratory motion (SD(RM)) is estimated measuring directly the standard deviation (SD) of the respiratory motion (RM).

### Results

Table 1 shows the amplitude (A), the standard deviation of the amplitude [SD(A)] and the uncertainty due to respiratory motion {SD(RM)}.

	Amplitude [SD(A)] [SD(RM)]		
	SI (mm)	AP (mm)	LAT (mm)
Liver	9.7 [5.1] [5,3]	4.0 [2.5] [2,3]	1.6 [1.3] [1,2]
Lung	3.9 [3.4] [3,2]	2.0 [1.7] [1,6]	1.7 [1.7] [1,6]
Pancreas	7.7 [4.6] [4,6]	2.6 [2.4] [2,2]	2.1 [1.5] [1,5]
Breast	1.5 [0.9] [1,1]	1.7 [1.0] [1,1]	1.1 [0.7] [0,9]

Table 1

The SD(RM) is usually estimated as A/3, this is valid for an ideal respiratory cycle represented by  $RM = A \cdot \sin^{2n}(wt)$ , in which the amplitude is not variable. But it may not be true if SD(A) is substantial.

In this study SD(RM) is significantly larger than A/3 ( $p<0.001$ ) in all directions of all localizations due to the intrafraction variability of A.

The univariate analysis revealed a statistical significant linear correlation between SD(RM) and A and between SD(RM) and SD(A) both with  $p<0.001$  in all directions of all localizations.

On the other hand, the multivariate regression  $SD^2(MR) = a \cdot A^2 + b \cdot SD^2(A)$  showed statistical significant correlation with  $SD^2(A)$  and  $A^2$  ( $p<0.05$ ) in all cases, except in lung tumors in which the  $A^2$  correlation was not significant. In addition, for liver and pancreas tumors the  $SD^2(A)$  contribution to the respiratory motion variance is the greatest but not in a significant way.

### Conclusion

Whereas for ideal respiratory cycles the uncertainty in tumor position due to respiratory motion can be estimated accurately with A/3, in real respiratory cycles is necessary to include the SD(A) beside A to avoid underestimation of this uncertainty. Further studies are necessary to demonstrate if those findings have any repercussion on PTV margin estimation.

### EP-1968 Respiratory-gated carbon-ion beam treatments of abdominal targets: clinical introduction of 4DMRI

A. Vai<sup>1</sup>, G. Meschini<sup>2</sup>, S. Molinelli<sup>1</sup>, C. Paganelli<sup>2</sup>, D. Maestri<sup>1</sup>, G. Magro<sup>1</sup>, E. Mastella<sup>1</sup>, A. Mairani<sup>1,3</sup>, A. Mirandola<sup>1</sup>, S. Russo<sup>1</sup>, L. Preda<sup>4</sup>, G. Viselener<sup>4</sup>, A. Barcellini<sup>5</sup>, V. Vitolò<sup>5</sup>, A. Mancini<sup>5</sup>, G. Fontana<sup>6</sup>, G.

Baroni<sup>2,6</sup>, M. Ciocca<sup>1</sup>  
<sup>1</sup>National Center for Oncological Hadrontherapy CNAO, Medical Physics Department, Pavia, Italy ; <sup>2</sup>Politecnico di Milano, Department of Electronics- Information and Bioengineering, Milan, Italy ; <sup>3</sup>Heidelberg Ion Beam Therapy Center HIT, Physics Department, Heidelberg, Germany ; <sup>4</sup>National Center for Oncological Hadrontherapy CNAO, Radiology Department, Pavia, Italy ; <sup>5</sup>National Center for Oncological Hadrontherapy CNAO, Radiotherapy Department, Pavia, Italy ; <sup>6</sup>National Center for Oncological Hadrontherapy CNAO, Bioengineering Department, Pavia, Italy

**Purpose or Objective**

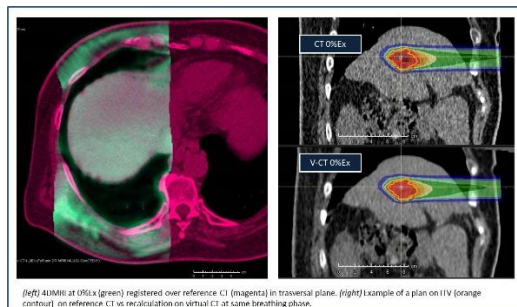
Irradiation geometry for abdominal targets in which a carbon-ion beam passes at the lung-diaphragm interface for a gated scanning treatment is not robust in our experience of plan recalculations on re-evaluative 4DCTs. In this work the potentialities of patient-specific virtual CTs, deformed on extracted 4DMRI vector fields (VFs) to quantify and mitigate the impact of motion pattern variations in respiratory-gated carbon ion treatments of the abdominal site were investigated.

**Material and Methods**

3 patients (2 liver, 1 pancreas) treated at CNAO with a respiratory-gated carbon-ion plan were selected. In addition to the 4DCT imaging workflow, 4DMRI images were obtained by retrospective sorting of multi-slice 2DMRI acquisition, covering a limited field-of-view of 10 cm in the L-R direction. Virtual CTs were generated by applying the 4DMRI-extracted motion fields (VFs) to the acquired 0%Ex (full-exhale) CT.

Range of motion (ROM) for the right kidney was calculated as centroid distance between 100%In (full-inhale) and 0%Ex phases, and the difference was computed between 4DMRI and 4DCT. GTV ROMs were also compared to a population of 10 patients (averaged ROM derived on 4DCT data) treated at our facility. The GTV was then warped from 0%Ex to the other breathing phases in the 4DMRI datasets and the ITV was defined.

For each patient, a single-beam carbon-ion plan was optimized delivering uniform dose to the ITV on the 0%Ex CT. Recalculations were carried out both on the 100%In CT and on virtual-CTs depicting 0%Ex and 100%In phases. D<sub>2%</sub>, D<sub>50%</sub>, D<sub>98%</sub> were calculated for ITV and GTV<sub>100In</sub>.



**Results**

ROM differences between 4DCT and 4DMRI for the kidney were <2% on average. GTV ROM were within the population range (2-12mm). ITV volume differences were <5%. Target DVH parameters discrepancies between dose distributions evaluated on acquired and virtual CT at corresponding phases were <1% on average.

Range of Motion (ROM) for right kidney [cm]				ITV (VX + 2018 + 10%) Volume <sup>1</sup>				Carbon-ion plan opt. for uniform dose on ITV (%) CT vs virtual CT					
Pt.	CT	MR	D19 (%)	CT	MR	D19 (%)		ITV			GTV <sub>100In</sub>		
#1	0.69	0.60	12.5%	19.02	19.40	-0.7%	D <sub>2%</sub>	85.9%	85.2%	0.8%	11.2%	10.9%	2.9%
#2	0.87	1.12	28.9%	17.34	16.18	5.6%	D <sub>50%</sub>	95.4%	94.9%	0.5%	91.6%	92.0%	1.1%
#3	0.87	0.77	11.0%	17.20	15.97	7.2%	D <sub>98%</sub>	98.9%	98.6%	0.3%	98.3%	98.3%	0.0%
Avg			1.8%			-4.5%				0.5%			0.6%

**Conclusion**

Consistency between 4DMRI and 4DCT was verified on kidney MR, ITV definition, and by plan recalculation on virtual CTs. Validation on a larger group of patients is needed.

**EP-1969 Dosimetric effect of diaphragm motion on target volume coverage for oesophageal cancer**

R. Stansbridge<sup>1</sup>, M. Borland<sup>1</sup>, B. Stewart Thomson<sup>2</sup>, M. Gilmore<sup>1</sup>

<sup>1</sup>Clatterbridge Cancer Centre, Physics, Liverpool, United Kingdom ; <sup>2</sup>Clatterbridge Cancer Centre, Radiation Services, Liverpool, United Kingdom

**Purpose or Objective**

Intra-fraction diaphragm motion for oesophageal cancers can result in dosimetric uncertainty due to changes in the electron density of individual voxels during the breathing cycle. The objective of this study is to quantify the dosimetric impact of diaphragm motion on PTV coverage over the breathing cycle to provide evidence for 3D planned VMAT.

**Material and Methods**

Radical oesophagus patients with significant diaphragm overlap of the PTV were identified to demonstrate the largest potential effect on plan dosimetry. All had received a prescription of either 50.4Gy/28# (n=2), 50Gy/25# (n=4) or 55Gy/20# (n=4). At our centre, for patients with a regular breathing trace, a 4DCT is acquired and a VMAT plan produced on the Average Intensity Projection (AIP) with a PTV margin of 0.5cm. For patients who do not have a regular breathing trace, a 3DCT scan is acquired as this may catch the diaphragm at an extreme that is not representative of the average diaphragm position during treatment, these patients are currently treated with a conformal plan. In order to verify the resilience of VMAT plans to this potential discrepancy, individual bins from the 4DCT were used as a surrogate for a 3DCT taken at the extremes of diaphragm motion (peak inspiration and peak expiration). A simulated plan was optimised on each of the two extreme cases with the PTV copied from the original plan. After optimisation, the plan was then recalculated on the AIP to represent the full respiratory motion during treatment delivery and assessed for changes in dosimetry.

**Results**

The mean peak to peak diaphragm motion was 2.3 ± 0.9cm with a maximum of 3.5cm. The mean difference from peak inspiration to AIP for D<sub>98%</sub> was -0.81 ± 0.45% and peak expiration to AIP was 0.48 ± 0.22%. All hotspots remained within the PTV as defined on the AIP with the mean change in D<sub>2%</sub> from peak inspiration to AIP was -0.26%. Hotspots were enhanced in the plans recalculated from peak expiration to AIP with an average increase of 1.83%. Doses to proximal OAR were also assessed, with minimal changes to mean dose and <0.3Gy change over the whole prescription. It should be noted, however, that structures were not changed from those outlined on the original AIP. Hotspots became apparent in the peak expiration plan onto AIP but still deemed clinically acceptable according to local protocols. The hotspots were the result of change in density from liver to lung tissue and created at the lung-tissue interface within the PTV, the maximum D<sub>2%</sub> was 106.9% (3.9% change between peak to AIP).

**Conclusion**

This study suggests that VMAT plans are sufficiently robust to diaphragm motion to allow VMAT planning of 3D scanned oesophagus patients. Patients will now be treated with an increased PTV margin of 1cm to account for PTV motion not captured. It is also recommended that diaphragm motion is monitored at treatment to ensure consistency. Further investigation is planned for patients with diaphragm motion >4 cm.

## EP-1970 2D and 3D dose verification for a gated irradiation on a 0.35 T MR-LINAC

P. Mann<sup>1,2</sup>, K. Spindeldreier<sup>2,3</sup>, G. Echner<sup>1,2</sup>, S. Klüter<sup>2,3</sup>, C. Karger<sup>1,2</sup>

<sup>1</sup>German Cancer Research Center DKFZ, Medical Physics in Radiation Oncology, Heidelberg, Germany ; <sup>2</sup>National Center for Radiation Research in Oncology NCRO, Heidelberg Institute for Radiation Oncology HIRO, Heidelberg, Germany ; <sup>3</sup>University Hospital Heidelberg, Department of Radiation Oncology, Heidelberg, Germany

### Purpose or Objective

As MRgRT becomes increasingly important in clinical applications, the development of new QA methods is needed. Especially for the verification of MR-based gating techniques, workflows tests with 2D and 3D dose verification prior clinical implementation are desirable. In this work, we present an MR compatible motion phantom that can hold both film and polymer gel (PG) inserts to perform 2D and 3D dose measurements for gated treatments.

### Material and Methods

A water-filled cylindrical phantom (d = 22 cm, l = 50 cm) holding a movable smaller water-filled cylinder (d = 9 cm, l = 50 cm) that can be combined with (1) film and (2) PG inserts was developed. For (1), an elliptical silicone insert with high MR contrast served as a target, while for (2), an oxygen sealed BAREX™ container filled with in-house produced PAGAT dosimetry gel was used as target. Both inserts were irradiated in separate experiments at an MR-Linac (MRIdian, ViewRay®) with a dose of up to 5 Gy. To test the influence of motion and gating on the target coverage with dose, three different irradiations were carried out:

- (i) Static target
- (ii) Dynamic target without gating
- (iii) Dynamic target with gating

For all experiments, the target volume was delineated in the Viewray TPS. Phantom motion for (ii) and (iii) was set to a cos<sup>4</sup> trajectory with an amplitude of 1.5 cm and a motion cycle of 10 cycles/min. For (iii) an additional gating margin of 3 mm was added allowing for 10% of the target being outside of the contour.

The film was scanned (10000XL, Epson) 1 h after irradiation and the red channel was evaluated. PG was scanned on a 3 T MR device (Biograph mMR, Siemens) 48 h after irradiation using a multi spin-echo sequence. Results were evaluated using the 2/3D -criterion (2%/2mm and 3%/3mm). For the film, the relative profiles were compared (using experiment (i) as reference) and the PG results were compared against TPS calculations.

### Results

For both film and PG measurements, results showed a homogeneous target coverage for (i), a significant dose smearing in motion direction for (ii) and a restored dose distribution with a homogeneous target coverage for (iii). The respective passing rates are shown in table 1.

Table 1: Comparison of film and PG measurements for three different experiments (i-iii).

Experiment	Insert	$\gamma_{2,3D}$ passing rate 3%/3mm; 2%/2mm
(i) Static target	Film	-
	PG	99.7%; 95.1%
(ii) dynamic target without gating	Film	61.1%; 50.9%
	PG	68.6%; 39.6%
(iii) dynamic target with gating	Film	100%; 99.1%
	PG	98.6%; 92.1%

### Conclusion

The developed phantom in combination with film and PG inserts has shown to be a valuable tool to test new treatment techniques like gating on a commercial MR-Linac device. Three different scenarios have been tested and gating revealed nearly the same accuracy as a static

treatment. Future experiments will focus on the verification of dose accumulation algorithms that are used to calculate the final dose in case of dynamic treatment.

## EP-1971 Comparison of pancreatic respiratory motion using three abdominal corsets for particle therapy

S. Schneider<sup>1,2</sup>, K. Dolde<sup>3,4,5</sup>, M. Alimusay<sup>6</sup>, B. Fluegel<sup>6</sup>, N. Saito<sup>7</sup>, A. Hoffmann<sup>1,2,8</sup>, A. Pfaffenberger<sup>3,4</sup>

<sup>1</sup>Helmholtz-Zentrum Dresden-Rossendorf, Radiooncology-OncoRay, Dresden, Germany ; <sup>2</sup>OncoRay - National Center for Radiation Research in Oncology, Medical Radiation Physics, Dresden, Germany ; <sup>3</sup>German Cancer Research Center DKFZ, Medical Physics in Radiation Oncology, Heidelberg, Germany ; <sup>4</sup>National Center for Radiation Research in Oncology, Heidelberg Institute for Radiooncology, Heidelberg, Germany ; <sup>5</sup>University of Heidelberg, Department of Physics and Astronomy, Heidelberg, Germany ; <sup>6</sup>Heidelberg University Hospital, Center for Orthopedic and Trauma Surgery, Heidelberg, Germany ; <sup>7</sup>University Clinic Heidelberg, Department of Radiation Oncology, Heidelberg, Germany ; <sup>8</sup>Faculty of Medicine and University Hospital Carl Gustav Carus at the Technische Universität Dresden, Radiotherapy and Radiation Oncology, Dresden, Germany

### Purpose or Objective

Particle therapy (PT) has the potential to reduce the risk of toxicity in patients with pancreatic cancer beyond that of photon therapy. Since PT is strongly susceptible to anatomical changes during dose delivery, strategies for pancreatic motion management are mandatory.

The purpose of this study was to compare the usability of different corsets for abdominal compression by measuring their effect on the respiration-induced motion of the pancreas as well as their water equivalent ratio (WER) for PT. **Material and Methods**

Three types of abdominal corsets were used that differed in material composition (polyethylene (PE) vs. polyurethane (PU)), material thickness (2.5mm - 24mm), and construction method (patient individual vs. patient independent). A healthy volunteer was scanned on a 1.5T MR scanner (Magnetom Aera, Siemens Healthineers) on two consecutive days for four subsequent scenarios: with and without wearing the three corsets. A gradient echo sequence with radial golden angle acquisition (field of view = 384×384×288 mm<sup>2</sup>, voxel size = 1.5×1.5×3 mm<sup>3</sup>, spokes per partition = 2100, bandwidth = 610 Hz/pixel, TE = 1.5 ms, TR = 3.3 ms, ) was used and reconstructed to a 4D-MR data set comprising 20 breathing phases. The pancreas was delineated in the maximum inhale and exhale phases using the open-source software MITK (Fig. 1). Its centre of mass was calculated as a surrogate for the respiratory motion in each of the four scenarios for both days.

CT scans of the three corsets were acquired (field of view = 388×388×476mm<sup>3</sup>, voxel size = 0.73×0.73×2mm<sup>3</sup>, tube voltage = 120kVp, Tube current time product = 148mAs) to assess the material homogeneity and thickness constancy. WER measurements were performed at two different proton energies (150MeV, 200MeV) using a high-resolution multi-layer ionization chamber (Giraffe, IBA Dosimetry).

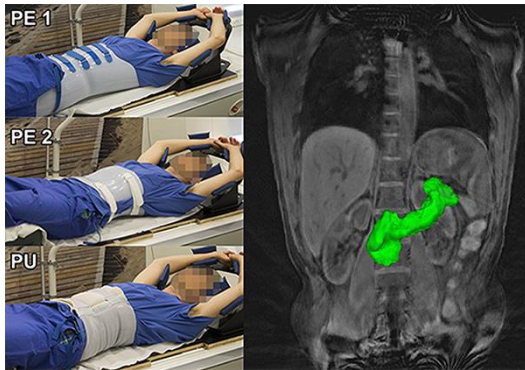


Figure 1. [left] Volunteer with three different abdominal corsets (PE1, PE2, PU) in scanning position. [right] Coronal slice of resulting 4D MRI in expiration phase with 3D segmentation of pancreas in green.

## Results

All three corsets reduced the pancreatic motion by a similar amount, mainly in inferior-superior direction (Table 1). As expected, the CT scan showed that the two PE corsets were made of homogeneous material that had a constant thickness of  $2.5 \pm 0.1$  mm and  $4.9 \pm 0.1$  mm, respectively. The PU corset was inhomogeneous due to the presence of small air inclusions throughout the whole corset. Furthermore, its thickness varied between 8.0 - 24.2 mm. The WER of the two PE corsets was 0.990 and 0.956, while the average WER of the PU corset was 0.298.

Table 1. Centre of mass motion of segmented pancreas between maximum inhale and maximum exhale. Motion was assessed while volunteer was wearing three different corsets as well as a free breathing scan for reference.

	No Corset	PE 1	PE 2	PU
Amplitude LR [mm]	$2.6 \pm 0.5$	$1.9 \pm 0.7$	$2.9 \pm 0.6$	$0.8 \pm 0.4$
Amplitude AP [mm]	$1.6 \pm 1.4$	$0.3 \pm 0.2$	$0.2 \pm 0.2$	$0.4 \pm 0.1$
Amplitude IS [mm]	$12.5 \pm 1.4$	$5.6 \pm 1.4$	$4.0 \pm 0.2$	$3.5 \pm 1.7$

## Conclusion

While all three corsets significantly reduce the respiratory-induced pancreatic motion, the PU corset is not suitable for PT due to its irregular material structure and thickness. The two PE corsets both show stable material conditions which could easily be included in treatment planning. Preferences for any of the two PE corsets will mainly depend on differences in fit, flexibility, cost and the time required for preparation.

## EP-1972 Transit-Guided RadioTherapy (TGRT): a novel intra-fraction patient monitoring approach

A. Latorre-Musoll<sup>1</sup>, P. Delgado-Tapia<sup>1</sup>, M. Lizondo<sup>1</sup>, N. Jonet<sup>1</sup>, P. Carrasco<sup>1</sup>, A. Ruiz-Martinez<sup>1</sup>, I. Valverde-Pascual<sup>1</sup>, M. Barceló<sup>1</sup>, M. Ribas<sup>1</sup>  
<sup>1</sup>Hospital de la Santa Creu i Sant Pau, Servei de Radiofísica i Radioprotecció, Barcelona, Spain

## Purpose or Objective

IGRT is an effective tool to reduce patient positioning uncertainties. However, intra-fraction motion component is not completely removed by conventional daily imaging protocols. We propose a novel approach to correct intra-fraction patient positioning shifts based on transit portal images (TGRT) which does not add extra time nor imaging dose.

## Material and Methods

We propose a pixel-based exponential model to relate the measured transit images ( $P_{ij}$ ), the pre-patient fluence ( $F_{ij}$ ) and the mass attenuation thickness map ( $x_{ij}$ ) for each field:

$$P_{ij} = P_0 F_{ij} \exp(-\mu x_{ij}),$$

where  $P_0$  and  $\mu$  are free scalar parameters. A first-order approximation of the directional derivatives of this model gives us the BEV shift estimation maps ( $s_{ij}$ ) as:  $s_{ij} = (P_{ij}/P_{ij}^0 - 1) \cdot [\mu(\partial x/\partial s)_{ij}]^{-1}$ , where  $P_{ij}^0$  is a convenient reference image (after IGRT corrections). Finally, the gantry angle is used to transform  $s_{ij}$  from the BEV reference frame to patient/couch coordinates  $s_{ij}'$ .

We validated the model for the following sites and techniques using a RANDO anthropomorphic phantom (Eclipse v13.5, Varian):

- A head-and-neck IMRT plan with 7 sliding-window 6 MV fields (1.6/1.8/2.12 Gy/fx @ low/intermediate/high risk areas).
- A whole-breast IMRT plan with 7 quasi-tangential sliding-window 6 MV fields (2 Gy/fx).
- A whole-breast 3DCRT plan with 2 tangential + 2 field-in-field 6 MV fields (2 Gy/fx).

We delivered these plans on a Clinac 2100C/D equipped with a Millenium 120 MLC (Varian). We shifted the phantom between fractions by moving the couch top from  $s = -10$  to 10 mm in 1 mm steps along the three axes. We acquired transit images ( $P_{ij}$ ) in integrated mode by placing the EPID at 140(150) cm for the head-and-neck(breast) plans.

We obtained  $F_{ij}$ ,  $x_{ij}$  and  $(\partial x/\partial s)_{ij}$  using the Eclipse Scripting API v13.5. We developed an in-house code (MATLAB v2015b, MathWorks) to fit  $P_0$ ,  $\mu$  and to obtain  $s_{ij}$ . Finally, we compared the per-beam pixel-averaged shift estimations  $\langle s_{ij}' \rangle$  against the real shifts  $s$  for all plans and irradiations.

## Results

Figure 1 compares the 723 model shift estimations against the real shifts. Estimations showed good linearity up to 5 mm (slope =  $0.854 \pm 0.016$ , RMS of residuals = 1.03 mm). Linearity decreased for larger shifts due to the first-order nature of the model (slope =  $0.820 \pm 0.011$ , RMS of residuals = 1.65 mm) but, even in this setting, estimations led to minimize positioning errors after correction. Figure 2 shows that only 12% of the estimations differed from the real shifts by more than 3mm (only 1% corresponded to shifts  $\leq 5$  mm). Therefore, cumulative corrections after each field irradiation may rapidly converge to target position.

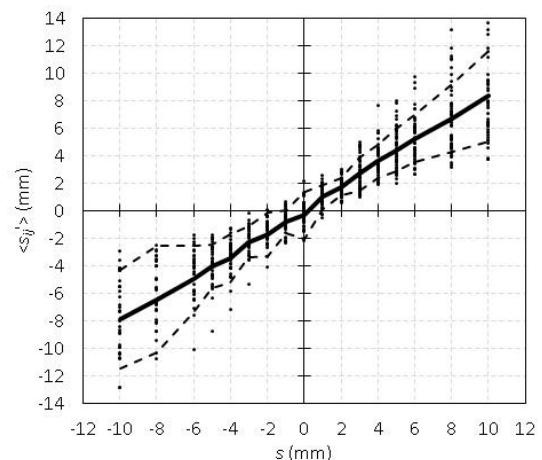
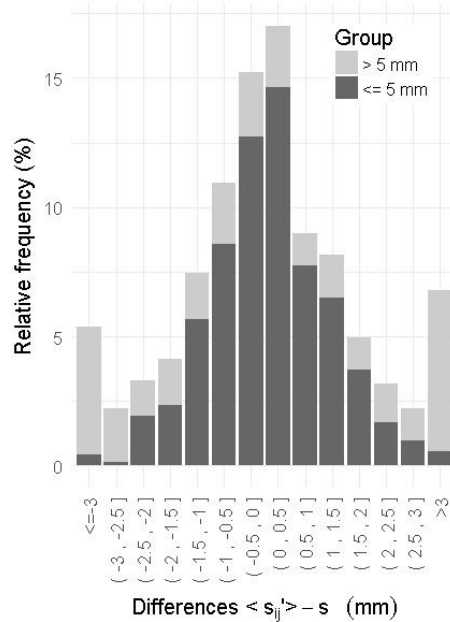


Figure 1. DOTS: model shift estimations  $\langle s_{ij}' \rangle$  against couch top shifts  $s$ , for all plans, fields and directions. LINES: mean (solid line)  $\pm$  standard deviation (dashed lines) of all data.



**Figure 2.** Distribution of residual differences between model shift estimations and real shifts. Data is split into two subsamples:  $s \leq 5$  mm and  $s > 5$  mm.

### Conclusion

A simple, robust and reliable approach (TGRT) has been validated to correct patient positioning shifts. TGRT may add intra-fraction monitoring capabilities to conventional IGRT by providing real-time convergent corrections after every beam irradiation. Initial testing in patients and model extrapolation to VMAT techniques are work in progress.

This work was partially financed by FIS PI15/00788.

### EP-1973 Cardiac dose sparing with active breath coordinator in breast radiotherapy: a dosimetric analysis

A. Ianiro<sup>1</sup>, M. Boccardi<sup>2</sup>, G. Macchia<sup>2</sup>, F. Deodato<sup>2</sup>, P. Viola<sup>1</sup>, M. Craus<sup>1</sup>, V. Picardi<sup>2</sup>, M. Ferro<sup>2</sup>, M. Ferro<sup>2</sup>, E. Arena<sup>2</sup>, A. Pjero<sup>3</sup>, M. Buwenge<sup>4</sup>, F. Romani<sup>5</sup>, A.L. Angelini<sup>2</sup>, V. Valentini<sup>6</sup>, A.G. Morganti<sup>4</sup>, S. Cilla<sup>1</sup>  
<sup>1</sup>Fondazione di Ricerca e Cura "Giovanni Paolo II"- Università Cattolica del Sacro Cuore, Medical Physics Unit, Campobasso, Italy ; <sup>2</sup>Fondazione di Ricerca e Cura "Giovanni Paolo II"- Università Cattolica del Sacro Cuore, Radiation Oncology Unit, Campobasso, Italy ; <sup>3</sup>Fondazione di Ricerca e Cura "Giovanni Paolo II"- Università Cattolica del Sacro Cuore, Radiology Department, Campobasso, Italy ; <sup>4</sup>Department of Experimental Diagnostic and Specialty Medicine - DIMES - University of Bologna, Radiation Oncology Department, Bologna, Italy ; <sup>5</sup>Department of Experimental Diagnostic and Specialty Medicine - DIMES - University of Bologna, Medical Physics Unit, Bologna, Italy ; <sup>6</sup>Fondazione Policlinico "A. Gemelli"- Università Cattolica del Sacro Cuore, Radiation Oncology Department, Roma, Italy

### Purpose or Objective

Cardiac toxicity is a major concern for left breast tangential field irradiation. Moderate deep inspiration breath hold (mDIBH) during radiation treatment delivery helps in reducing the cardiac dose. In this dosimetric study, the doses to heart were compared between free-breathing (FB) and mDIBH during tangential IMRT breast irradiation.

### Material and Methods

Twenty consecutive patients with left-sided breast cancer who underwent adjuvant tangential IMRT with ABC mDIBH were analyzed in this study. All patients underwent CT

simulation in both free breathing (FB) and mDIBH setup. The Elekta ABC spirometer was used for respiratory control and breath-hold period of 20-30 s. A simultaneously integrated boost (SIB) plan was created for both simulation CTs (FB and mDIBH) consisting of a prescription dose of 50 Gy to the whole breast and 60 Gy to tumor bed in 25 fractions. The heart and the left ventricle were contoured according to the Feng et al. heart atlas. Dose volume histograms were analyzed to assess the heart mean dose (MHD) and the volume of left ventricle receiving 5Gy (V5), since these dosimetric metrics have been demonstrated to be the best predictors of acute cardiac events. Data were analyzed using a Wilcoxon signed-rank test with a level of significance set at  $p < 0.05$ .

### Results

The use of ABC mDIBH resulted in similar target coverage with no significant statistical differences. For PTV1 median D95% and V95% were 58.5 Gy (range: 57.3-59.5 Gy) and 98.6% (range: 96.0-100.0%) in FB, and 58.5 Gy (range: 57.0-60.1 Gy) and 98.7% (range: 95.0-99.9%) in mDIBH. For PTV2 D95% and V95% were 48.8 Gy (range: 43.4-50.5 Gy) and 97.0% (range: 91.4-99.4%) in FB and 49.3 Gy and 98.0% (range: 92.3-99.8%) in mDIBH. Median MHD was 3.7 Gy (range: 2.8-6.2 Gy) in FB and 2.5 Gy (range: 1.6-4.1 Gy) in mDIBH ( $p < 0.05$ ), resulting in absolute and relative reduction of 1.3 Gy (range: 0.2-2.5 Gy) and 35.0% (range: 4.7-53.6%), respectively. Median LV-V5 was 27.4% (range: 1.8-44.0%) in FB and 8.2% (range: 0.0-25.9%) in mDIBH ( $p < 0.05$ ). The use of ABC mDIBH reduced MHD by 20% or greater and LV-V5 by 35% or greater in 90% of patients.

### Conclusion

The use of the ABC spirometer for mDIBH resulted in a significant reduction in cardiac dose for left sided breast radiotherapy. The significant cardiac dose sparing may translate in reduction of excess risk of acute cardiac events.

### EP-1974 Usage of computer generated 4D CTs for interplay effect studies in scanned proton therapy

T. Pfeiler<sup>1,2,3</sup>, C. Bäumer<sup>1,2,4</sup>, E. Engwall<sup>5</sup>, D. Geismar<sup>1,2,4,6</sup>, U. Mäder<sup>7</sup>, B. Spaan<sup>3</sup>, B. Timmermann<sup>1,2,4,6</sup>, J. Wulff<sup>1,2,7</sup>

<sup>1</sup>University Hospital Essen, West German Proton Therapy Centre Essen WPE, Essen, Germany ; <sup>2</sup>University Hospital Essen, West German Cancer Centre WTZ, Essen, Germany ; <sup>3</sup>TU Dortmund University, Experimental Physics 5, Dortmund, Germany ; <sup>4</sup>German Cancer Consortium DKTK, Radiation Oncology and Imaging, Heidelberg, Germany ; <sup>5</sup>RaySearch Laboratories AB, Development, Stockholm, Sweden ; <sup>6</sup>University Hospital Essen, Department of Particle Therapy, Essen, Germany ; <sup>7</sup>TH Mittelhessen, Radiation Protection Institute, Gießen, Germany

### Purpose or Objective

There is a need for realistic 4D data-sets in radiation therapy, especially in scanned proton therapy to systematically investigate interplay effects for moving targets. The production of physical phantoms representing the entire spectrum of patients is generally not feasible and the availability of suitable, clinical 4D CTs is limited. Recently, the 4D XCAT phantom, a whole-body computer model of human anatomy and physiology, became available and allows generation of virtual 4D CTs (v4D CTs). Their application was tested in a proof-of-concept study investigating the magnitude of interplay effects as a function of the target size for one patient with different CTVs.

### Material and Methods

A 4D XCAT chest CT was imported to RayStation 7. In addition to a set with typical clinical CT-numbers for treatment planning, a copy with image-values representing organ IDs was imported. The segmentation tools thereby allowed to perfectly map organs in all 4D CT

phases. The structures guided the deformable image registration (DIR). Five spherical liver tumours of radius  $R=1-5$  cm were manually delineated as CTVs in the end-exhale phase and mapped to other phases by DIR. A dose of 63 Gy<sub>RBE</sub> was prescribed to the CTVs in 15 fractions. The magnitude of interplay effects was analysed based on an experimentally validated 4D dose calculation routine including DIR and 50 interplay scenarios per plan with varying field delivery time structures [1]. The homogeneity index ( $HI=(D_5-D_{95})/D_{prescribed}$ ) and the percentage over- and underdosage ( $V_{107/95}=V_{107}+100-V_{95}$ ) of the CTV served as evaluation criteria.

### Results

All workflow steps from data import to interplay simulations were successfully completed for the v4D CT. The simulated CT data enabled fast, threshold-based segmentation of 48 anatomical structures in all 4D CT phases. Thus, 4D studies could be performed with perfect contouring, minimal DIR uncertainties and realistic image quality without the influence of CT artefacts. Fig. 1 shows exemplarily two 4D dose distributions. While the HI increased with growing target volume from  $11.5\% \pm 3.0\%$  (average value  $\pm$  standard deviation of all scenarios) for  $R=1$  cm to  $22.3\% \pm 2.4\%$  for  $R=5$  cm,  $V_{107/95}$  did not reproduce this trend.  $V_{107/95}$  was maximal for the largest CTV (39.9%  $\pm$  5.4%), but the smallest value was observed for  $R=3$  cm ( $22.3\% \pm 7.6\%$ ).

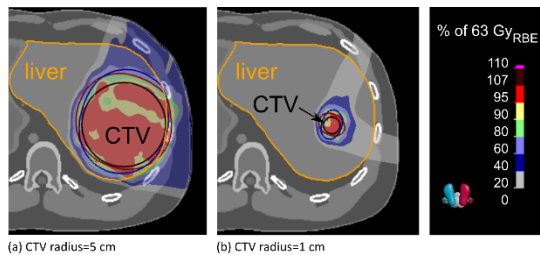


Figure 1: 4D dynamically accumulated dose distribution (overlayed as colour wash) of a random interplay scenario for the smallest and the largest CTV (transverse view): The beam-specific PTV margins are coloured dark blue and dark red.

### Conclusion

The results demonstrate the feasibility of 4D CT simulation based on XCAT phantoms for interplay evaluations. The manifestation of investigated interplay effects exhibited complexity, without clear correlation between the interplay level and the target size. Studies on larger scale must show whether a categorisation to influencing factors such as tumour motion or size into different treatment groups is possible and whether it can replace time consuming, individual interplay evaluations. The application of v4D CTs can facilitate these studies and furthermore allows investigation of mitigation strategies in a systematic approach.

[1] Pfeiler et al. Z Med Phys 2018;28:121-33.

EP-1975 Intra-fraction robustness evaluation of deep inspiration breath hold radiotherapy for lung cancer K. Håkansson<sup>1</sup>, M. Josipovic<sup>1</sup>, I.R. Vogelius<sup>1,2</sup>, G. Persson<sup>2,3</sup>, C. Behrens<sup>3</sup>

<sup>1</sup>Rigshospitalet- Copenhagen University Hospital, Department of Oncology- Section of Radiotherapy, Copenhagen, Denmark ; <sup>2</sup>Faculty of Health Science- University of Copenhagen, Department of Clinical Medicine, Copenhagen, Denmark ; <sup>3</sup>Herlev Hospital- Copenhagen University Hospital, Department of Oncology, Copenhagen, Denmark

### Purpose or Objective

Deep inspiration breath hold (DIBH) for radiotherapy (RT) of lung cancer has recently been shown to be feasible and can reduce dose to the heart and lungs. Robustness may be an issue, however, and built in tools in the treatment planning systems typically do not account for anatomical

changes between subsequent DIBHs. It is of clinical interest to be able to identify the patients where variations in anatomy between DIBHs would result in a sub-optimal treatment. The purpose of the current study was to develop a method for evaluating the intra-fraction robustness of DIBH-RT treatment plans. Two treatment plans were evaluated as a proof of principle.

### Material and Methods

We chose two example patients from a previous DIBH study, where three repeated DIBH scans were acquired before treatment. Patient 1 had good agreement between scans and was treated in DIBH, whereas patient 2 was treated in free breathing because of large variation in tumor position between scans. The DIBH plans (2 Gy x 33, volumetric modulated arc therapy with two partial arcs) were divided into four sub-arcs, each of duration of one DIBH (~20 s), using the Eclipse Scripting Application Programming Interface (ESAPI) version 15.5 (Varian). The three DIBH scans were assigned randomly to the four sub-arcs in a simulation of all 33 fractions, to evaluate the impact of intra-fraction variation throughout the treatment course. Subsequently, a plan with corresponding field weights was created for each DIBH scan, followed by deformable registration and dose summation in Velocity version 4.0. The resulting simulated sum dose was compared to the planned dose. The workflow is illustrated in Figure 1.

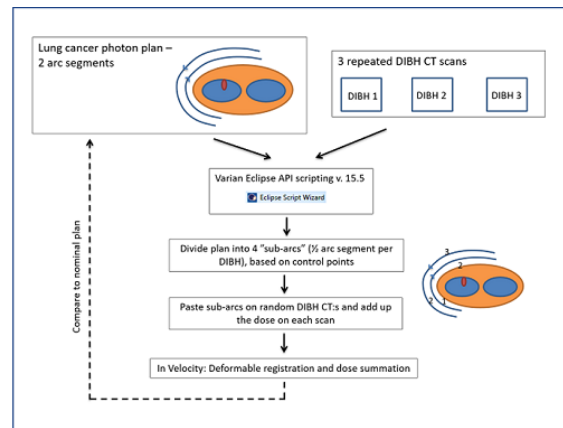


Figure 1. Workflow for the intra-fraction robustness evaluation of DIBH treatments

### Results

The ESAPI script could successfully divide a treatment plan into four sub-arcs. The robustness evaluation method showed small differences in target and organs at risk (OAR) doses between the original plan and the Velocity sum for patient 1. For patient 2, the dose differences were similar for OARs but large for the target. The difference was most pronounced for the coverage of the T-site lesion - V95% was 97.1% for PTV-T in the original plan but only 71.2% in the Velocity sum plan (Table 1).

Table 1. Dose metrics for comparison between original plan and Velocity sum, where the difference between three repeated DIBH scans have been applied in an intra-fraction robustness analysis. Patient 1 and 2 are example patients - patient 1 with small differences between DIBH scans and patient 2 with large differences.

		Patient 1		Patient 2	
		Original Plan	Velocity sum	Original Plan	Velocity sum
PTV-T	V95%	98.4 %	97.4 %	97.0 %	91.6 %
PTV-NI	V95%	97.7 %	97.1 %	97.1 %	71.2 %
Medulla	Dmax	43.7 Gy	44.0 Gy	28.5 Gy	28.3 Gy
Lungs - GTV	V20Gy	30.3 %	30.4 %	12.8 %	13.0 %
	Mean dose	17.2 Gy	17.2 Gy	7.8 Gy	7.9 Gy
Heart	V25Gy	0.3 %	0.1 %	24.8 %	23.5 %
Oesophagus	Dmax	69.3 Gy	67.9 Gy	68.8 Gy	66.8 Gy
Body	Dmax	73.2 Gy	72.3 Gy	71.1 Gy	72.3 Gy

### Conclusion

We demonstrated a method for dose-volume assessment of the impact of anatomical changes across consecutive DIBHs on a treatment plan. With the proposed method, a patient could be identified where the DIBH technique was sensitive to anatomical changes between repeated DIBHs

and could result in sub-optimal treatment. For a patient with small differences between DIBH scans, no concerning differences in dose due to intra-fraction uncertainty could be identified.

#### EP-1976 Clinical evaluation of two monitoring devices for prostate radiotherapy treatment

M. Biston<sup>1</sup>, L. Delcoudert<sup>1</sup>, T. Zaragori<sup>1</sup>, A. Munoz<sup>1</sup>, D. Sarrut<sup>2</sup>, P. Pommier<sup>1</sup>

<sup>1</sup>Léon Bérard Cancer Center, Radiotherapy, Lyon, France ; <sup>2</sup>Lyon university, Creatis, Lyon, France

#### Purpose or Objective

The objective of this work was to co-evaluate 2 in-beam monitoring devices for prostate radiotherapy: intra-prostatic electromagnetic transmitters (EM-T) (RayPilot®, Micropos Medical) and ultrasound imaging using transperineal probe (TP-US) (Clarity®, Elekta). We report the monitoring results obtained with the 2 devices used concomitantly on 9 patients.

#### Material and Methods

The accuracy of the 2 systems was first investigated in a phantom study. Then intra-fraction motions measured with the 2 devices used simultaneously were analyzed for 9 intermediate risk prostate cancer patients (155 sessions). They were implanted with the EM-T and 2 fiducial markers 8 days before the simulation CT. Pre-treatment positioning was performed with the TP-US and validated by a Cone Beam CT (CBCT) imaging (+ fiducial markers)/CT registration. During CBCT imaging the 2 devices monitoring mode were started. Irradiation was stopped and patient positioning adjusted for shifts above a threshold of 3mm for at least 15s for both devices. Each time threshold was exceeded a CBCT was performed to confirm the obtained shifts. The percent time the differences between TP-US and EM-T were >1, >1.5, >2, >2.5, >3 and 5mm, was scored for each direction and each patient.

	Left-Right (mm)	Supero-inferior (mm)	Antero-Posterior (mm)
Patient 1	0,16 ± 0,29	-0,11 ± 0,54	-0,02 ± 0,69
Patient 2	0,09 ± 0,38	0,55 ± 0,77	0,13 ± 0,69
Patient 3	0,05 ± 0,43	0,09 ± 0,56	0,04 ± 0,69
Patient 4	0,01 ± 0,50	-0,03 ± 0,33	0,05 ± 0,62
Patient 5	-0,04 ± 0,33	-0,09 ± 1,45	0,24 ± 0,74
Patient 6	0,41 ± 1,41	-1,77 ± 5,73	1,24 ± 3,51
Patient 7	0,11 ± 0,42	-0,53 ± 0,50	0,30 ± 0,43
Patient 8	0 ± 0,42	-0,19 ± 0,34	0,17 ± 0,45
Patient 9	0,02 ± 0,25	-0,10 ± 0,34	-0,33 ± 0,75

Table 1: Mean differences between displacements observed with EM-T and TP-US during all the treatment sessions.

#### Results

Experiments on phantom confirmed the lack of interference between the 2 systems, and showed deviations of less than 0.5mm when translations were applied progressively. In presence of rotations (5 to 15° around left-right (LR) and antero-posterior (AP) axis), each system compensated with systematic shifts up to 6.9 mm for the TP-US and up to 3.8 mm for the EM-T. Mean differences between displacements observed on patients with EM-T and TP-US were ≤0.55mm in all directions except for patient 6 (Table 1). A strong correlation was found in LR direction: differences >2mm were monitored only less than 0.22% of the time for all patients and differences >2.5 mm never exceeded 3s, except for patient 6 (>2.5 mm 9.3% of the time). More important differences were observed in supero-inferior (SI) and AP directions, where more intrafraction displacements occurred. In AP direction they were >2mm less than 3.8% of the time for all patients but patient 6 (26% of the time). They were >2mm less than 1% of the time for 6 patients

and more than 7% of the time (up to 19% (patient6)) for the 3 others. When intrafraction CBCT was performed, a strong correlation was observed with TP-US. While punctual differences could be explained by the differences in latency between the 2 systems, large prostate rotations, the presence of gas and EM-T location in the prostate are likely to explain more important differences.

#### Conclusion

TP-US is a promising option since it is non-invasive and enables visualization of the target and organs at risk. However the accuracy needs to be evaluated in presence of rotations. EM-T is a reliable technique for monitoring prostate. However location in the prostate volume is of important to be more accurate.

#### EP-1977 Intrafraction motion in CNS radiotherapy with an open mask system using an optical surface imaging

D. Reitz<sup>1</sup>, S. Schönecker<sup>1</sup>, M. Pazos<sup>1</sup>, P. Freislederer<sup>1</sup>, M. Reiner<sup>1</sup>, M. Niyazi<sup>1</sup>, U. Ganswindt<sup>2</sup>, C. Belka<sup>1</sup>, S. Corradini<sup>1</sup>

<sup>1</sup>University Hospital LMU Munich, Department of Radiation Oncology, München, Germany ; <sup>2</sup>University of Innsbruck, Department of Radiation Therapy, Innsbruck, Austria

#### Purpose or Objective

Intrafraction motion control is of special interest in modern radiotherapy. Open masks allow for a continuous patient monitoring, reduce claustrophobia and anxiety and improve patient's compliance compared to closed masks. In this prospective study we evaluated the magnitude of intrafraction motion in patients receiving radiotherapy for CNS tumors with an open mask system.

#### Material and Methods

Data of 114 fractions in 10 patients that underwent non-stereotactic radiotherapy for CNS tumors (primary or secondary) were analyzed. During each treatment session patients were monitored using the Catalyst™ optical surface scanner (C-RAD AB, Sweden). Three-dimensional deviations and relative position differences during the whole treatment fraction were calculated and analyzed statistically.

#### Results

Overall, the maximum magnitude of the mean deviation vector was 0.62 mm ± 0.62 mm (standard deviation) (95%-CI: [0.07 - 2.2] mm) and a median of 0.35 mm during dose application (beam-on time only).

Along the lateral (-0.12 ± 0.61 mm; 95%-CI: [-1.73 - 0.99] mm) and longitudinal (-0.07 ± 0.56 mm; 95%-CI: [-1.38 - 1.09] mm) axis changes were quite similar, while for the vertical axis deviation was tendentially lower (-0.03 ± 0.25 mm; 95%-CI: [-0.46 - 0.53] mm). 99% of the whole beam-on time the magnitude of the deviation vector was < 2.55 mm. The median net beam-on time of radiation therapy was 92 seconds.

According to Friedman's test differences in the distributions between the three possible directions (lateral, longitudinal and vertical) were significant (p<0.01), in Post-Hoc-analysis a dissimilarity between lateral and vertical as well as longitudinal and vertical direction could be verified (p<0.01) whereas between lateral and longitudinal direction a dissimilarity could not be verified (p=1.0).

#### Conclusion

Real-time intrafraction motion was < 2.5 millimeters in all directions and open masks can therefore be considered a suitable and reliable treatment option in clinical practice.

#### EP-1978 Surface guided coplanar and non-coplanar stereotactic radiotherapy with open masks - a phantom study

E. Konradsson<sup>1,2</sup>, M. Kügele<sup>1,2</sup>, K. Petersson<sup>2</sup>, L. Berg<sup>2</sup>, M. Gebre-Medhin<sup>2</sup>, S. Ceberg<sup>1</sup>

<sup>1</sup>Medical Radiation Physics, Department of Clinical Science- Lund University, Lund, Sweden ; <sup>2</sup>Department of Hematology- Oncology and Radiation Physics, Skåne University Hospital, Lund, Sweden

#### Purpose or Objective

For most on-board imaging techniques in radiotherapy, such as Cone-Beam Computed Tomography (CBCT), verification of patient position is only possible with the couch at an angle of 0°. Furthermore, patient position is often only verified before, and not during, treatment. The purpose of this study was to investigate if an optical surface scanning (OSS) system with a novel surface algorithm for stereotactic radiotherapy (SRT), in combination with open masks, provide sufficient accuracy for positioning and real-time monitoring of coplanar and non-coplanar SRT treatments.

#### Material and Methods

The study was performed using an Alderson RANDO phantom and a costume-made three-point open mask (Orfit Industries, Wijnegem, Belgium) on a TrueBeam system (Varian, Palo Alto, California, USA) with an OSS three camera Catalyst™ system with the novel SRT solution (C-RAD Positioning AB, Uppsala, Sweden). For coplanar treatments the agreement between the isocenter shift calculated by the OSS system and the isocenter shift suggested after image-verification with CBCT was evaluated. A total of 40 measurements were carried out, after positioning the phantom using the OSS system's auto-couch function

For non-coplanar treatments the accuracy of positioning and real-time monitoring was evaluated by separating any potential couch rotation offsets from the uncertainties in the OSS system's calculation of the isocenter shift. This was done by placing a high-Z marker on top of the phantom in line with the isocenter point in longitudinal and lateral direction and acquiring megavoltage (MV) images at different couch angles. By comparing the MV images acquired at each couch angle (45°, 90°, 270° and 315°) with images acquired at the standard position (0°), the couch rotation offset could be identified and thus the accuracy of the OSS system's calculation of the isocenter position could be determined.

#### Results

For coplanar treatments the median agreement in the isocenter shift calculation between the OSS system and the CBCT was 0.1/-0.2/0.0 mm (range: -0.2 to 0.3/-0.5 to 0.1/-0.3 to 0.2 mm) in the vertical/longitudinal/lateral direction, respectively. For all rotational directions the agreement was within 0.9°. For non-coplanar treatments the accuracy of the OSS system's calculation of the isocenter position was within 0.5 mm, with a median of -0.3 and -0.4 mm (range: -0.4 to 0.4/-0.5 to 0.4 mm) in the longitudinal and lateral direction, respectively.

#### Conclusion

The OSS system with its novel surface algorithm for SRT in combination with open masks show excellent agreement with the CBCT system and has the ability to validate the position of a phantom with 0.5 mm accuracy regardless of couch angle. The results of the study show that the system could be very useful as a complementary tool for verification and real-time monitoring of coplanar and non-coplanar stereotactic radiotherapy treatments.

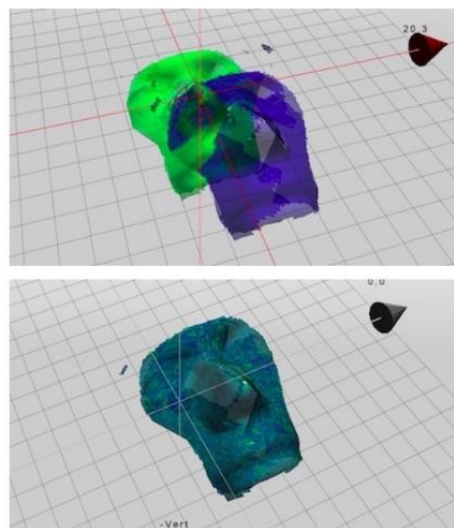


Figure 1: The live phantom surface (green) and the reference surface (blue) are displayed. The upper figure show a mismatch in position between the two surfaces and the lower figure show a perfect alignment.

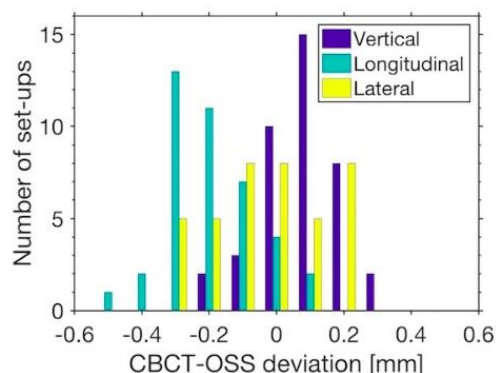


Figure 2: Translational deviations between the isocenter shift calculated by the OSS system and the isocenter shift suggested after image-verification with CBCT.

#### EP-1979 Intrafraction stability of 8526 deep inspiration breath holds in left-sided breast cancer

D. Reitz<sup>1</sup>, S. Schönecker<sup>1</sup>, M. Pazos<sup>1</sup>, P. Freislederer<sup>1</sup>, M. Reiner<sup>1</sup>, M. Niyazi<sup>1</sup>, U. Ganswindt<sup>2</sup>, C. Belka<sup>1</sup>, S. Corradini<sup>1</sup>

<sup>1</sup>University Hospital LMU Munich, Department of Radiation Oncology, München, Germany ; <sup>2</sup>University of Innsbruck, Department of Radiation Therapy, Innsbruck, Austria

#### Purpose or Objective

Patients with left-sided breast cancer often receive deep inspiration breath hold (DIBH) radiotherapy to reduce the risk of cardiac side effects. Data of a large study cohort receiving radiotherapy with DIBH were analyzed regarding intrafraction breath-hold stability.

#### Material and Methods

105 patients that underwent left-sided breast cancer radiotherapy with DIBH using the Catalyst™ optical surface scanner (C-RAD AB, Sweden) were analyzed. During each treatment session the vertical motion of the patient was continuously measured by the optical system and gating control (beam on/off) was performed by an audio-visual patient feedback system. The Catalyst™ system works through an optical surface scanning with LED light and

reprojection captured by a CCD camera, which provide target position control during treatment delivery. Dose delivery is automatically enabled when the tracking point is within a predefined gating window.

### Results

8526 breath-holds were analyzed. The mean amplitude of the gating window referred to the baseline breathing curve was 16.36 mm (SD 6.57 mm) (95%-confidence interval: [7.81 - 31.11] mm). The mean standard deviation of breath-hold inside the gating window was 0.42 mm (95%-CI: [0.05 - 0.94] mm). The gating window height had a mean value of 3.24 mm (95%-CI: [0 - 5] mm).

### Conclusion

The use of the Catalyst™ optical surface scanner enables stable and reliable breath-holds during radiotherapy for left-sided breast cancer the clinical routine.

### EP-1980 Randomised trial investigating breathing regularity: Audiovisual biofeedback vs free breathing

E. Steiner<sup>1</sup>, K. Makhija<sup>1</sup>, R. O'Brien<sup>1</sup>, J. Wolf<sup>2</sup>, J. Ludbrook<sup>2</sup>, P. Greer<sup>2</sup>, P. Keall<sup>1</sup>

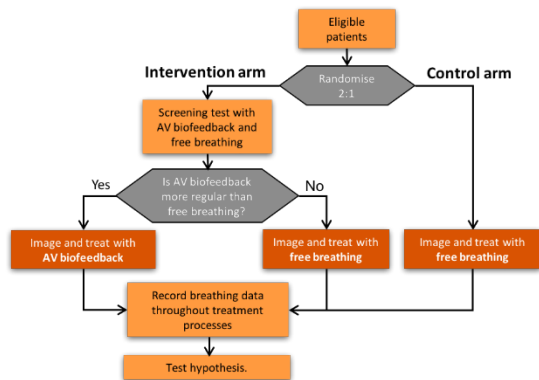
<sup>1</sup>The University of Sydney, Central Clinical School- ACRF Image X Institute, The University of Sydney, Australia ; <sup>2</sup>Calvary Mater Newcastle, Radiation Oncology, Newcastle, Australia

### Purpose or Objective

Irregular breathing leads to artefacts in 4DCT imaging and uncertainties during radiotherapy delivery. We present the early results of the first multi-institutional, randomised trial to investigate if breathing regularity improves with audiovisual biofeedback (AVBF) breathing guidance for lung cancer patients.

### Material and Methods

We report the data from the first eleven lung cancer patients recruited to the ethics-approved trial. Patients were randomised 2:1 to the intervention arm with AVBF screening or the free breathing (FB) control arm (Figure 1).



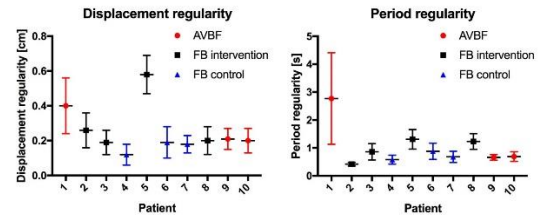
Breathing motion was measured with the Real-time Position Management (RPM) system (Varian Medical Systems). An in-house developed AVBF system provided breathing guidance to patients. Patients with AVBF screening were treated with AVBF if the AVBF-guided breathing was more regular during the screening session, or FB otherwise. Breathing regularity was quantified by the displacement regularity and the period regularity (as defined in Venkat *et al.* 2008) between the average breathing motion during the CT simulation session and the breathing motion during each treatment fraction. We tested the hypothesis that AVBF improves breathing displacement regularity and period regularity compared to FB using a one-sided t-test.

### Results

8 patients were recruited into the intervention arm, 3 patients into the control arm. In the intervention arm 3 patients were screened to be treated with AVBF, 5

patients were screened to be treated with FB. One patient treated with FB was excluded for analysis because the breathing traces could not be recorded for the treatment fractions. For the patients treated with AVBF and with FB the displacement regularity was  $0.27 \pm 0.09$  cm and  $0.25 \pm 0.14$  cm and the period regularity was  $1.4 \pm 1.0$  s and  $0.9 \pm 0.3$  s, respectively (Figure 2).

### Breathing regularity for all patients



Overall the FB arm had lower regularity values indicative of more regular breathing, but no significant difference between AVBF and FB could be shown (displacement regularity:  $p=0.41$ , period regularity:  $p=0.15$ ). Thus, our null hypothesis is not supported. Patient 1 treated with AVBF showed large variations in displacement and period regularity for different treatment fractions resulting from large changes in the daily performance. Patient 5's large displacement regularity values resulted from a different breathing pattern during CT simulation compared to the treatment fractions.

### Conclusion

At this stage, no difference in breathing regularity between AVBF and FB could be shown. Further investigations will be performed.

### EP-1981 Intrafractional baseline drift in SBRT of lung tumors

J. García Ruiz-Zorrilla<sup>1</sup>, M.A. De la Casa de Julián<sup>1</sup>, O. Hernando Requejo<sup>2</sup>, P. García de Acilu Laa<sup>1</sup>, C. Rubio Rodríguez<sup>2</sup>, J. Martí Asenjo<sup>1</sup>, P. Fernández Letón<sup>1</sup>, D. Zucca Aparicio<sup>1</sup>, J.M. Pérez Moreno<sup>1</sup>, X. Chen<sup>2</sup>

<sup>1</sup>Hospital Universitario HM Sanchinarro, Radiofísica, Madrid, Spain ; <sup>2</sup>Hospital Universitario HM Sanchinarro, Oncología Radioterápica, Madrid, Spain

### Purpose or Objective

To investigate the frequency and amplitude of baseline or drift of lung tumors treated with stereotactic body radiation therapy (SBRT) and ExacTrac Adaptive Gating® with intra-fractional IGRT. Methods and materials

### Material and Methods

Forty one fractions of 12 patients with lung tumors were treated with SBRT using ExacTrac Adaptive Gating® in a Novalis® linac. This system uses external markers to monitor the respiratory cycle and internal fiducial markers to set up the patient and measure the movement of the tumor. The tumor position is measured intermittently during the treatment via stereoscopic x-ray images to compensate the baseline drift. Therefore, the accumulative changes in the couch position correspond to the baseline drift in the tumor motion.

### Results

The average change in position of the treatment couch during the treatment time was  $-0.1 \pm 0.8$  mm (mean  $\pm$  standard deviation),  $-0.1 \pm 1.2$  mm, and  $0.2 \pm 1.9$  mm in the left-right (LR), antero-posterior (AP) and cranio-caudal (CC), directions respectively. Overall the baseline shift/drift occurs toward the cranial directions. The incidence of a baseline drift exceeding 1 mm was 43%, for the CC direction, within 15 minutes of the start of treatment, and 63% within 25 minutes. On the other hand, the incidence of a baseline drift exceeding 3 mm was 4% for the CC direction, within 15 minutes of the start of treatment, and 25% within 25 minutes.

The intra-fractional uncertainties due to baseline drift of lung tumors are:

Direction	M (mm)	$\Sigma$ (mm)	$\sigma$ (mm)
LR	-0.1	0.1	0.4
AP	-0.1	0.3	0.6
SI	0.1	0.5	0.8

M: the overall mean or group systematic error,  $\Sigma$ : the standard deviation (SD) of the systematic error,  $\sigma$ : the SD of the random error.

In the absence of intra-fraction IGRT, the baseline drift uncertainties does not imply the use of increased standardized margins in any direction in SBRT for lung tumors when the rest of uncertainties are minimized. Nevertheless this uncertainty can be very important in some patients leading to the needance of increased margins.**Conclusion**

Real-time monitoring and frequent adjustments of the couch position are suggested to be necessary to compensate for possible underdosage in CC direction due to baseline drift in SBRT for lung tumors in some patients.

---

#### Electronic Poster: Physics track: Adaptive radiotherapy and inter-fraction motion management

---

#### EP-1982 Pancoast tumours. A good candidate for proton spot scanning?

D. Sloth Møller<sup>1</sup>, L. Hoffmann<sup>1</sup>, M. Josipovic<sup>2</sup>, A.K. Berthelsen<sup>2</sup>, G. Persson<sup>3</sup>

<sup>1</sup>Aarhus University Hospital, Department of Medical Physics, Aarhus C, Denmark ; <sup>2</sup>Copenhagen University Hospital Rigshospitalet, Department of Oncology, Copenhagen, Denmark ; <sup>3</sup>Copenhagen University Hospital Herlev, Department of Oncology, Copenhagen, Denmark

#### Purpose or Objective

Large anatomical changes and respiratory motion during radiotherapy for lung cancer patients challenge precise delivery of proton spot scanning, with high risk of target under dosage. Upper-lobe pancoast tumors are less influenced by respiration and may be good proton-candidates, but setup-errors and longitudinal anatomical changes may still deteriorate the dose distribution.

#### Material and Methods

Nine patients with stage III NSCLC Pancoast tumours, treated with photon volumetric arc therapy (VMAT) were retrospectively planned using three-field intensity modulated proton therapy (IMPT) and single field uniform dose (SFUD) with field directions avoiding distal fall off in front of the spinal cord. The brachial plexus (BP) overlapped with the target for all patients and was delineated by an experienced radiologist (Fig 1). Target coverage and dose to oesophagus, lungs, BP and spinal cord of the initial treatment plans were compared. To evaluate the dose deterioration due to setup errors, all treatment plans were shifted 3 mm in each of the six directions and recalculated. To evaluate the dose deterioration due to tumor shrinkage, the daily CBCT scans acquired for setup were used. The tumor shrinkage present at the CBCT of the last treatment day was delineated and each plan was recalculated on a CT, where the HU inside the delineated structure were set to lung density. For both scenarios, CTV receiving 95% of the prescribed dose ( $V95\%_{CTV}$ ) and the dose to the hottest 1 cm<sup>3</sup> of the spinal cord ( $D1cm^3_{spinal}$ ) was analyzed.

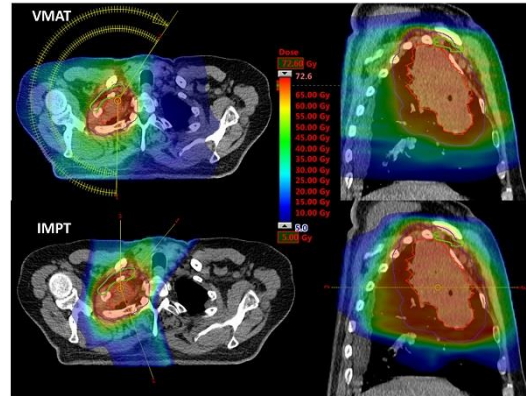


Figure 1: Patient example with GTV (red), PTV (blue) and Brachial Plexus (green) delineated. Dose color wash of doses above 5 Gy is shown for VMAT (upper panel) and IMPT (lower panel).

#### Results

Lung dose metrics (mean dose,  $V20Gy$  and  $V5Gy$ ) were significantly reduced (Fig 2), while no reduction was seen for the mean dose to oesophagus and BP (Fig 2) compared to VMAT. There were no significant differences in normal tissue dose between IMPT and SFUD. For target coverage, the  $V95\%_{PTV}$  differed between patients and planning strategies depending on target proximity to the spinal cord ( $D1cm^3_{spinal} < 45$  Gy for all plans). For SFUD  $V95\%_{PTV}$  was median[range] 93%[64-100], while IMPT and VMAT achieved 99%[97-100] and 94%[85-98]. Setup errors decreased target coverage of up to 3%, 4% and 10% and increased  $D1cm^3_{spinal}$  by 4Gy, 2 Gy and 6Gy for VMAT, SFUD and IMPT, respectively. Robustness towards tumor shrinkage was high for all SFUD/IMPT, where the field directions selected ensured  $<0.1$  Gy increase in  $D1cm^3_{spinal}$ . VMAT was less robust and  $D1cm^3_{spinal}$  increased 2-9 Gy, but low initial spinal cord doses prevented over dosage. All plans maintained initial target coverage regardless of tumor shrinkage.

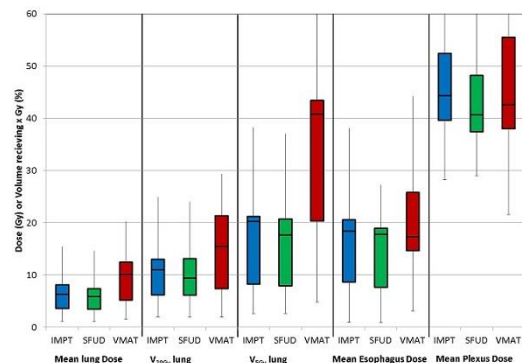


Figure 2: Difference in dose to organs at risk using IMPT, SFUD and VMAT presented as a boxplot. The box shows the range between 1<sup>st</sup> and 3<sup>rd</sup> inter quartile ranges, the vertical line in the middle indicates the median value and the whiskers range from minimum to maximum value. For both IMPT and SFUD the reduction in lung dose (mean,  $V_{20Gy}$  and  $V_{5Gy}$ ) compared to IMRT was statistically significant (Wilcoxon sign rank,  $p < 0.05$ ).

#### Conclusion

Pancoast tumours are candidates for proton spot scanning reducing lung dose significantly compared to VMAT. IMPT is preferred over SFUD due to superior target coverage. No sparing of the BP was seen due to large overlap with the target. For field directions avoiding distal fall off in front of the spinal cord, both IMPT and SFUD were highly robust towards tumor shrinkage, while setup errors posed a risk of target under dosage or spinal cord over dosage mainly for IMPT.

#### EP-1983 Inter and intra-fraction bowel motion during abdomino-pelvic stereotactic ablative radiotherapy

F. Slevin<sup>1</sup>, M. Beasley<sup>2</sup>, J. Lilley<sup>3</sup>, R. Speight<sup>3</sup>, L.J. Murray<sup>1</sup>, A.M. Henry<sup>1</sup>

<sup>1</sup>St James Institute of Oncology, Clinical Oncology, Leeds, United Kingdom ; <sup>2</sup>St James Institute of Oncology, Therapeutic radiography, Leeds, United Kingdom ; <sup>3</sup>St James Institute of Oncology, Medical physics, Leeds, United Kingdom

### Purpose or Objective

Abdomino-pelvic Stereotactic Ablative Radiotherapy (AP-SABR) is increasingly used to treat oligometastatic pelvic nodal disease. Bowel within or adjacent to the Planning Target Volume (PTV) is often the most significant organ at risk. Bowel motion is dynamic and unpredictable and could result in significantly different dose delivered than planned. This retrospective single centre study quantifies inter and intra-fractional changes in bowel using cone beam CT (CBCT) and calculates the impact on delivered bowel doses.

### Material and Methods

10 consecutive patients treated with AP-SABR delivered using flattening filter free (FFF) volumetric modulated arc therapy (VMAT) to a dose of 30Gy in 3 or 5 fractions were investigated (5 fractions used for re-irradiation cases). Delivery times are around 90 seconds. Median intra-fraction imaging time period was around 6 minutes. 84 CBCT images acquired immediately pre and post each SABR fraction were exported to Monaco Treatment Planning System and rigidly co-registered with the planning CT scan. Individual bowel loops within a 3cm expansion beyond the PTV were contoured on each CBCT (majority of dose fall off occurs within this region). Inter-fraction bowel changes were calculated by comparing the planning CT to each pre-treatment CBCT. Intra-fraction bowel changes were calculated by comparing each pre and post-treatment CBCT. Dosimetric consequences of changes in bowel volume and position were determined by superimposing the planned dose distribution onto each CBCT and generating dose volume histogram data. Bowel volume, maximum dose to 0.5cc (Dmax) and 5cc (D5cc) within 3cm of the PTV on planning CT and CBCT were compared using a Wilcoxon signed-rank test.

### Results

Significantly higher bowel volumes within a 3cm PTV expansion were consistently found on CBCT compared to planning images, resulting in greater delivered than planned bowel doses (Figures 1 and 2). Bowel volumes within 3cm of the PTV, Dmax and D5cc were greater on CBCT images compared to planning CT (all  $p < 0.0001$ ). Dmax of bowel on treatment CBCTs was greater than that planned in 37 of 42 (88.1%) pre-treatment CBCTs and 33 of 42 (78.6%) of post-treatment CBCTs. By summing the delivered Dmax per fraction for individual patients, the median net increase over the whole treatment course on pre and post-treatment CBCTs was 33.7% (range -18.5 to 133.1%) and 29.9% (range -23.8 to 135.9%) respectively. 5 of 10 (50%) patients had greater than 20% net increase in Dmax compared to planned doses. No significant difference was observed for intra-fraction variations in bowel volume, Dmax and D5cc within 3cm of the PTV.

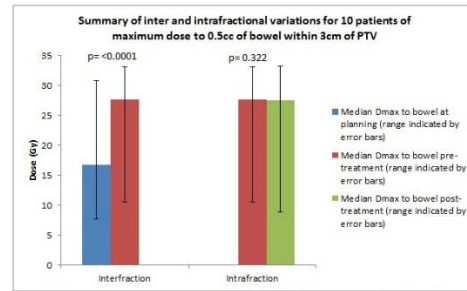


Figure 1: Bar chart showing median inter and intra-fraction maximum dose to 0.5cc of bowel (Dmax) within 3cm of the PTV for 10 patients with minimum and maximum ranges of Dmax indicated by error bars. Significantly greater inter-fraction variation in Dmax during treatment compared to planning was demonstrated ( $p < 0.0001$ ). Intra-fraction variation was non-significant.

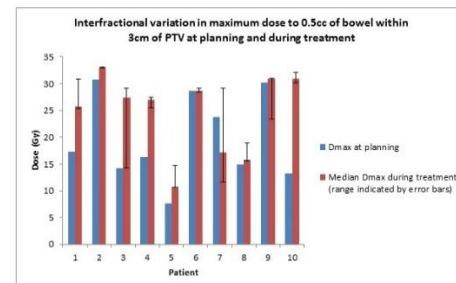


Figure 2: Bar chart showing inter-fractional variation in median maximum dose to 0.5cc of bowel (Dmax) for 10 patients with minimum and maximum ranges of Dmax indicated by error bars. Significantly greater median Dmax to bowel was observed during treatment compared to planning ( $p < 0.0001$ ).

### Conclusion

Significantly greater volume of bowel within a 3cm expansion of the PTV was observed during treatment than at planning, resulting in significantly higher than planned bowel doses. Little intra-fraction change in bowel was observed. Developing adaptive workflows that utilise plan-of-the-day or daily fast adaptive re-planning could compensate for inter-fraction bowel changes.

### EP-1984 Cone beam computed tomography (CBCT) interobserver variability in patient setup error evaluation

A. Delana<sup>1</sup>, V. Vanoni<sup>2</sup>, P. Ferrazza<sup>2</sup>, F. Coelli<sup>2</sup>, M. Maino<sup>2</sup>  
<sup>1</sup>S. Chiara Hospital- Trento, Dept. Medical Physics, trento, Italy ; <sup>2</sup>S. Chiara Hospital- Trento, Dept. of Radiation Oncology, trento, Italy

### Purpose or Objective

To evaluate the interobserver variability in registration of daily CBCT to treatment-planning-CT (TPCT) in patients treated in five different anatomical sites, with volumetric modulated arc therapy (VMAT).

### Material and Methods

In an off-line retrospective approach, 16 well-trained radiotherapy technicians/radiotherapists (RT) performed manual CBCT/TPCT registrations for five patients, treated with VMAT for head and neck, lung, breast, prostate and gastric tumors. An Elekta Synergy XVI linac was used for CBCT acquisition and CBCT/TPCT registration. Each RT quantified the patient setup error in all three axes, by manually matching CBCT and TPCT datasets after automatic pre-matching either based on a gray scale or bone algorithm. Matching results obtained by RTs were compared to those obtained by 1 board certified radiation oncologist with extensive experience in image guided radiotherapy: differences between technologists and radiation oncologist's results were quantified. A statistical analysis was performed to calculate the minimum threshold of agreement between the observers.

### Results

In total, 137 CBCT datasets were acquired and 2281 CBCT/TPCT registrations and setup error evaluations

performed. Table 1 summarizes the results obtained in terms of: number of CBCT acquired (#CBCT), number of CBCT/TPCT registrations (#REG) and threshold below which the agreement between the observers was 90% and 95% (Threshold\_mm95% and Threshold\_mm90%). The prostate patient had the largest threshold values, but always inferior to the planning target (PTV) margin and only 4% of the 713 differences evaluated were above the 5 mm or 7mm PTV margins used in the clinical routine for the respective VMAT treatment paradigms.

	#CBCT	#REG	Threshold_mm 95%			Threshold_mm 90%		
			AP mm	LL mm	CC mm	AP mm	LL mm	CC mm
Head&Neck	30	480	1.7	1.1	1.1	1	1	1
Lung	30	480	1.8	1.1	2	0.9	1.1	1.4
Prostate	39	713	4.2	5.4	2.8	3.2	2.5	1.5
Breast	12	192	1	2	2	0.9	1.6	1.1
Gastric	26	416	1.8	2	2.3	1	1.1	2

## Conclusion

Interobserver reproducibility between trained RTs and an expert radiation oncologist was very good. The largest variability was observed for prostate, probably as a consequence of the more difficult interpretation of the CBCT/TPCT fusion. The study will be extended to a larger number of patients and Radiation Oncologists to validate the results and provide a robust basis for the definition of IGRT protocols.

## EP-1985 Clinical feasibility of CBCT-based online plan adaptation for multiple lesion brain SRS

G. Wortel<sup>1</sup>, U. Stankovic<sup>1</sup>, J. Trinks<sup>1</sup>, G. Sotiropoulos<sup>1</sup>, S. Van Kranen<sup>1</sup>, S. Van de Water<sup>1</sup>, S. Van de Schoot<sup>1</sup>, L. Dewit<sup>1</sup>, E. Damen<sup>1</sup>, T. Janssen<sup>1</sup>, P. Remeijer<sup>1</sup>, J. Sonke<sup>1</sup>  
<sup>1</sup>Netherlands Cancer Institute, Department of Radiation Oncology, Amsterdam, The Netherlands

## Purpose or Objective

In the absence of a 6DoF couch, IGRT can correct for translation but is not able to manage more complex anatomical changes, including rotations. This study aims to develop and evaluate an online method to automatically adapt treatment plans to the anatomy of the day. As a first showcase, we apply the method to multiple lesion brain SRS.

## Material and Methods

All plans in this study are made with a GTV-PTV margin of 2 mm and a single isocentre, an approach we apply if the targets are < 4 cm apart.

The plan adaptation consists of 5 automated steps. 1) The CBCT is rigidly registered to the planning CT. A new CT, that represents the anatomy of the day, is created by applying the registration results to the original planning CT. 2) The treatment plan is transferred to the new CT in our TPS Pinnacle<sup>3</sup>. 3) A custom built script, based on Ahunbay et al. (2008), morphs the segment apertures to the new targets. 4) A segment weight optimization (SWO) is performed. 5) The plan is exported and checked. The method was evaluated by applying it 55 times (11 setup errors for 5 patients). 10 errors were randomly sampled from the typical setup error for this patient group ( $\sigma_{tx,ty,tz}=1.3\text{mm}, 1.6\text{mm}, 1.7\text{mm}, \sigma_{rx,ry,rz}=1.0^\circ, 1.1^\circ, 0.69^\circ$ ). A more challenging case ( $rx=10^\circ$ ) was also included. For comparison, the original plans were also recomputed on the new CTs, including table translations. The dose distributions were evaluated on the  $V_{100\%}$  to the PTVs and 5mm rings around the PTVs (conformity). We also recorded the duration of the process.

## Results

A DVH example for 1 setup error for 1 patient is shown in Fig. 1. The SWO results in an adapted plan that is more inhomogeneous (allowed for SRS) than the original and recomputed plan. An overview of all results is shown in Fig. 2. PTV coverage is slightly reduced, but acceptable, for most adapted (-1.9pp) and recomputed (-1.4pp) plans. Similarly, the plans are slightly less conformal, with the

recomputed plans performing 1.7pp better in ring  $V_{100\%}$  than the adapted. As can be seen in Fig. 2, the adaptation method is able to correct the large  $rx=10^\circ$  setup errors (with a plan quality similar to that for the small setup errors), whereas the table correction completely fails target coverage (average  $V_{100\%}$  of 65%). On average, the entire process from registration to plan export was completed within 14 (max 18) minutes.

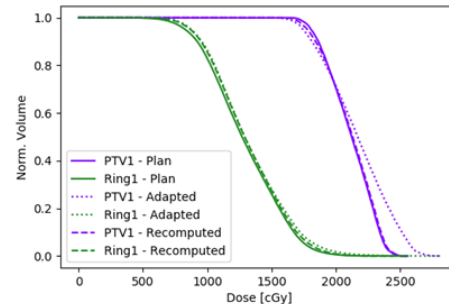


Fig. 1: DVHs for PTV and 5mm Ring (conformity) for one of the PTVs for the original, the adapted, and the recomputed plan.

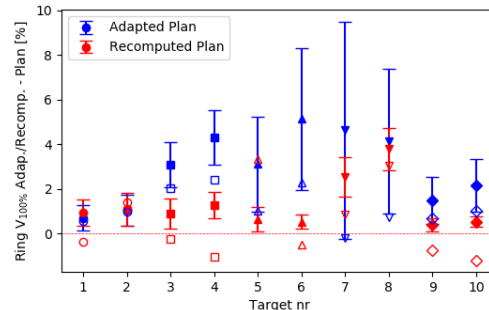
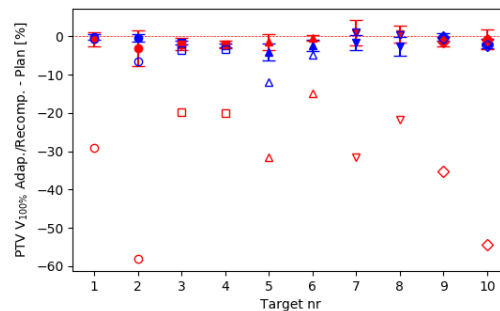


Fig. 2: The  $V_{100\%}$  (averaged over 10 realistic setup errors, with error bars representing  $\sigma$ , different symbols representing different patients) for the PTV (top) and 5mm Ring (bottom). The value of the  $V_{100\%}$  relative to the (original) Plan is plotted per target (2 targets for 5 patients). The open symbols represent a large setup error ( $rx=10^\circ$ ).

## Conclusion

We have successfully developed a method to adapt multiple lesion brain SRS plans online based on CBCT. Whereas this new method performs similar to a physical table correction for our current brain SRS protocol and setup errors, it greatly outperforms the table correction for larger geometrical differences. This ability to correct larger setup errors could allow a PTV margin reduction and extend the use of planning with a single isocentre. The introduced method is not limited to rigid corrections and can be applied to other tumor sites. Ultimately, we consider the development of this method an important step towards full online adaptive radiotherapy.

## EP-1986 Comparison of automatic OAR contour propagation from CT to MR lung images

M. Dubec<sup>1,2</sup>, S. Brown<sup>1</sup>, R. Chuter<sup>1</sup>, A. McWilliam<sup>1,3</sup>, D. Cobben<sup>1,3</sup>, C. Faivre-Flinn<sup>1,3</sup>, M. Van Herk<sup>1,3</sup>

<sup>1</sup>The Christie NHS Foundation Trust, Radiotherapy Related Research, Manchester, United Kingdom ;

<sup>2</sup>University of Manchester, Quantitative Biomedical Imaging Laboratory, Manchester, United Kingdom ;

<sup>3</sup>University of Manchester, Division of Cancer Sciences, Manchester, United Kingdom

### Purpose or Objective

For daily plan adaptation on the MR-Linac, fast and accurate methods of OAR contouring are required and it is envisaged that automatic contour propagation will play an important role.

MRI sequences differ in speed, with the DIXON VIBE being relatively quick, whilst acquiring multiple contrasts simultaneously. It is unknown whether contour propagation onto these images is as accurate as other slower sequences. The radial k-space stack-of-stars acquisition (STARVIBE) is commonly used in areas associated with motion, e.g. lungs, to reduce artefacts, while the DIXON sequence can be used as a basis for MR only planning.

This aim was thus to compare contour propagation from CT onto STARVIBE and DIXON images and to determine whether the fast DIXON would be a sufficient pre-treatment sequence.

### Material and Methods

5 NSCLC patients were imaged mid-treatment on a diagnostic 1.5T MR (MAGNETOM Aera, Siemens Healthcare, Erlangen, Germany) using non-triggered sequences: STARVIBE (time = 7:21, spokes = 1050, with fat sat) and DIXON VIBE (time = 1:51, averages = 4), both with matrix 1.25x1.25x3.5 mm<sup>3</sup>. Patients were scanned in the treatment position. The mean time between the two sequences was 25 mins. The DIXON water-only contrast was used for analysis.

MR images were first rigidly registered to the patients' CT planning scans in MONACO (Elekta AB, Stockholm, Sweden). Oesophagus, heart and spinal canal contours, drawn by radiation oncologist, were then propagated from the CT to each mid-treatment MR scan via deformable registration using ADMIRE (Elekta AB, Stockholm, Sweden). The resulting OAR contours were compared by volume, mean DTA and DICE index for both MR sequences.

### Results

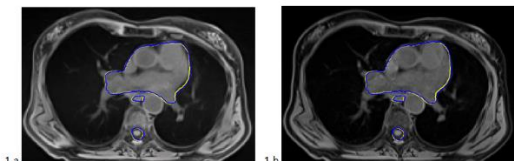


Figure 1. Oesophagus, heart and spinal canal contours overlaid on the STARVIBE (1.a, yellow contour) and DIXON (1.b, blue contour).

The average volume ratios (DIXON/STARVIBE) were 1.10, 1.01 and 1.00 for the oesophagus, heart and spinal canal respectively. Only the oesophagus volume was significant ( $p = 0.01$ ).

The mean DTAs  $\pm$  SD, were  $0.94 \pm 0.72$ ,  $1.23 \pm 1.00$  and  $1.24 \pm 1.70$  for the oesophagus, heart and spinal canal respectively. The mean DTAs for OARs across the 5 patients are shown in figure 2. All OARs were < 2 mm mean DTA except P1 heart (2.1 mm) and P5 spinal canal (2.2 mm). DICE indices of  $0.84 \pm 0.02$ ,  $0.96 \pm 0.02$  and  $0.87 \pm 0.05$  were obtained for the oesophagus, heart and spinal canal respectively.

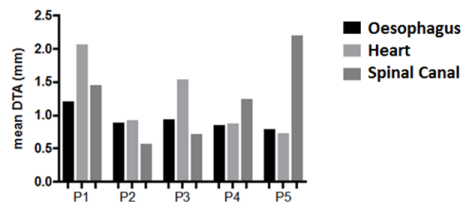


Figure 2. Mean DTA for oesophagus, heart and spinal canal contours on the STARVIBE and DIXON Images for the 5 patients.

### Conclusion

This work compared contours obtained via auto-contour propagation from CT to mid-treatment STARVIBE and DIXON VIBE images.

The mean volume difference for the oesophagus was significant. The mean DTA between the two MR scans was less than 2 mm in all but two instances. DICE was greater than 0.8 for all OARs. Differences could occur due to registration inaccuracies and also due to organ motion between scans.

The results indicate that the DIXON VIBE type sequence may be suitable for set up imaging on the MRL to reduce set-up times (DIXON <2 min, STARVIBE > 5 min). Auto-contour propagation must still be followed by clinician verification at this stage. Future work will compare OAR and GTV contours against clinician drawn contours in a larger sample.

### EP-1987 Dose accumulation assessing the validity of reduced PTV margins in head-and-neck radiotherapy

N. Lowther<sup>1</sup>, S. Marsh<sup>2</sup>, R. Louwe<sup>1</sup>

<sup>1</sup>Wellington Blood & Cancer Centre, Department of Radiation Oncology, Wellington, New Zealand ;

<sup>2</sup>University of Canterbury, Department of Medical Physics, Chirstchurch, New Zealand

### Purpose or Objective

**Purpose:** Emerging literature has reported reduced treatment toxicity while maintaining equivalent local-regional control rates after reducing planning target volume (PTV) margins from 5 to 3 mm for head-and-neck radiotherapy (HNRT). As we considered whether it was possible to implement reduced 3 mm PTV margins in our department, it was recognized that many aspects of HNRT including robustness of the planning solution for anatomical changes may influence treatment outcomes and should be considered when PTV margins are reduced. This retrospective study investigates the robustness of treatment plans using 3 or 5 mm PTV margins for anatomical changes. The results of this study can be used to develop strategies for treatment adaption based on objective criteria.

### Material and Methods

**Methods:** Volumetrically modulated arc therapy (VMAT) plans for 12 patients using 3 or 5 mm PTV margins (Prescribed dose 54 Gy and simultaneous integrated boost volumes to 60 and 66 Gy in 30 fractions) were optimized using the local planning protocol. The planning CT (pCT) was first registered to each daily cone beam CT using deformable image registration (DIR). Subsequently, the inverse registration was used to reconstruct and accumulate the delivered dose to target and organ-at-risk (OAR) structures in the pCT scan. For the initial analysis, the coverage of the PTVs, clinical target volumes (CTVs) and salivary glands were assessed using the  $D_{98\%}$ ,  $D_{99\%}$  and  $D_{mean}$  respectively. The uncertainty of the reconstructed dose was assessed using an *in silico* model based on clinically observed deformations to determine the 95% level of confidence.

## Results

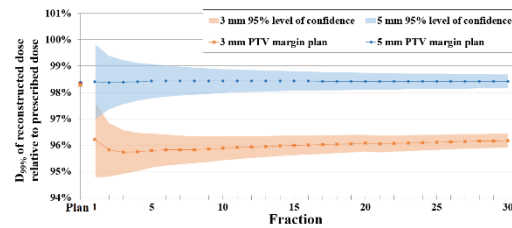


Fig. 1: Reconstructed dose relative to prescribed dose  $D_{99\%}$  for an individual patient's high-dose CTV.

**Results:** Preliminary results (4 patients) showed that for 4 out of 5 high-dose PTVs,  $D_{98\%}$  during treatment was at least 2% lower than planned in both margin plans. The high-dose CTVs'  $D_{99\%}$  generally changed less than 1% relative to the planned dose. However, for two 3 mm plans the high-dose CTV  $D_{99\%}$  was systematically 2% lower (Fig.1). For all high-dose CTVs, the  $D_{99\%}$  of the reconstructed dose at the end of treatment was always 96% of the prescribed dose or higher in both 3 and 5 mm margin plans. For the elective low-dose CTVs, the reconstructed  $D_{99\%}$  was at least 99% of the prescribed dose for all fractions in both plans. On average, the  $D_{\text{mean}}$  for the ipsilateral parotid glands was 4 Gy lower (range; 1 to 10 Gy) in 3 mm margin plans compared to the 5 mm plans. For submandibular glands, the average dose reduction was 2 Gy. The difference between reconstructed and planned  $D_{\text{mean}}$  of the parotid glands was not significantly different for the 3 mm (range; -1.2 to 1.1 Gy) and the 5 mm (range; -1.4 to 1.2 Gy) plans ( $p=0.67$ ).

### Conclusion

Changes in delivered dose due to anatomical changes can be accurately reconstructed using DIR. Initial results indicate that 3 mm PTV margins are robust for anatomical changes occurring during HNRT with CTV  $D_{99\%} \geq 96\%$  of the prescribed dose. PTV margin reduction resulted in increased OAR sparing.

### EP-1988 Statistical process control to monitor anatomical changes during head and neck radiotherapy

N. Lowther<sup>1</sup>, D. Hamilton<sup>1</sup>, H. Kim<sup>1</sup>, J. Evans<sup>1</sup>, S. Marsh<sup>2</sup>, R. Louwe<sup>1</sup>

<sup>1</sup>Wellington Blood & Cancer Centre, Department of Radiation Oncology, Wellington, New Zealand ;

<sup>2</sup>University of Canterbury, Department of Medical Physics, Christchurch, New Zealand

### Purpose or Objective

Reduced toxicity while maintaining loco-regional control rates have been reported after reducing planning target volume (PTV) margins for head-and-neck radiotherapy (HNRT). In this context, quantifying anatomical changes to monitor the patient during treatment is preferred. This retrospective feasibility study investigated the application of deformable image registration (DIR) and Exponentially Weighted Moving Average (EWMA) Statistical Process Control (SPC) charts for this purpose.

### Material and Methods

DIR was performed between the computed tomography for treatment planning (pCT) images of 12 patients and their daily on-treatment cone beam computed tomography (CBCT) images to quantify changes in patient pose and anatomy during treatment. EWMA charts were used to investigate trends in patient positioning reproducibility and soft tissue changes of various structures. The 90% confidence limits for both the EWMA trends and the SPC process limits were obtained using a comprehensive uncertainty analysis. These confidence limits were used to confirm whether a trend breached either an SPC limit or an *a priori* set clinical limit of 2 mm at a previous fraction or not.

### Results

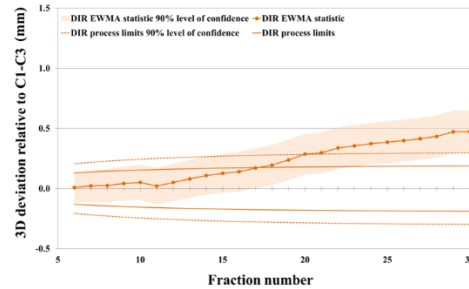


Figure 1: EWMA chart of the mandible deviation for patient 3 relative to week one of treatment

Trends in patient positioning reproducibility relative to the first week of treatment that were outside SPC process limits before the end of treatment week 4 occurred in 54% of cases. Only 24% of these cases could be confirmed at a 90% confidence level before the end of treatment. Using an *a priori* clinical limit of 2 mm, absolute changes in patient pose were detected in 39% of cases, of which 82% were confirmed. Soft tissue trends outside SPC process limits occurring before the end of treatment week 4 could be confirmed in 90% of cases.

### Conclusion

EWMA trends based on DIR data combined with structure specific action thresholds enabled detection of systematic changes in patient pose and anatomy during the first four weeks of treatment. This approach may facilitate timely treatment adaptation and provide a safety net for PTV margin reduction.

### EP-1989 Mesorectal variation and PTV margins for irradiation of rectal cancer patients using belly-board

M. Cox<sup>1</sup>, M. Wendling<sup>1</sup>, R. Van Leeuwen<sup>1</sup>, H. Rütten<sup>1</sup>, P. Braam<sup>1</sup>

<sup>1</sup>Radboud University Medical Centre, Radiation Oncology, Nijmegen, The Netherlands

### Purpose or Objective

In our centre rectal cancer patients are currently treated with VMAT in a prone position, using a belly-board and full bladder protocol. Current PTV margins are 15 mm in anterior direction and 10 mm in other directions. These margins are based on studies in which patients were irradiated either in supine position or prone position without the use of a belly-board. In the mesorectal part of the CTV, shape variation is expected to be most substantial and heterogeneous. Therefore, the purpose of this study was to investigate the inter-fraction shape variation of the mesorectum and determine PTV margins in rectal cancer patients irradiated in prone position using a belly-board.

### Material and Methods

For 18 patients a planning CT (pCT) and five cone-beam CT (CBCT) scans were acquired in prone position using a belly-board (Pelvic Prone Board, MacroMedics, The Netherlands). The mesorectal part of the CTV was delineated on all scans. These delineations were interpolated on the craniocaudal axis to 50 slices, and 100 equidistant dots were placed and numbered on each slice, starting at the posterior side of the patient via left, anterior, right and back to posterior. The mesorectal shape variation was quantified for each patient by measuring the 1D distance between corresponding dots on the pCT- and the five CBCT delineations. For dots on the left/right side the distance was measured in lateral direction and for the anterior/posterior side in ventrodorsal direction. For each patient the mean and standard deviation (SD) were calculated for each dot and stored in 2D surface maps. Subsequently, local group mean (signed for inside/outside), systematic- and random error maps of the total group were calculated (figure 1). In

order to derive PTV margins, we adapted the margin recipe described by Nijkamp et al (Radiother Oncol 2012).  
**Results**

Systematic- and random errors were ranging from 2 mm SD in the upper-lateral region of the mesorectum up to 5 mm SD in the upper-anterior region (figure 1). Local group mean variation was relatively small, ranging between -1 mm in the anterior region and 2mm in the lower-posterior region. Derived PTV margins were smallest in the upper-lateral region (6 mm) and largest in the upper-anterior region (16 mm).

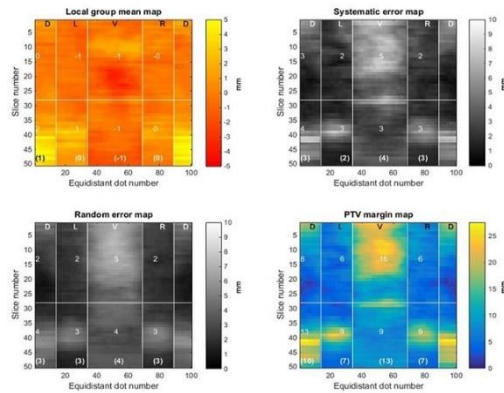


**Fig. 1.** Local group mean, systematic, random error and PTV margin for the total group of patients. The horizontal axis represents the 100 equidistant dots of each slice starting at posterior (P), via left (L), anterior (A), right (R) and back to posterior. The vertical axis represents the 50 slices ordered from cranial to caudal. The horizontal lines indicate the mean level of the apex of the os sacrum. The bold numbers in parentheses at the bottom represent the combined outcomes of the upper and lower mesorectum for each direction.

**Conclusion**

Even in rectal cancer patients irradiated in prone position and using a belly-board, mesorectal shape variation is heterogeneous and largest in the upper-anterior region. Derived PTV margins are less than described in literature, ranging from 7 mm in lateral direction up to 16 mm at the upper-anterior region of the mesorectum.

**EP-1990 Assessment of Inter-Sessional Positional Reproducibility in the HN Sub-Regions Using 1.5T MR-Sim**

Y. Zhou<sup>1</sup>, J. Yuan<sup>1</sup>, K.F. Cheng<sup>2</sup>, W.W.K. Fung<sup>2</sup>, O.L. Wong<sup>1</sup>, G. Chiu<sup>2</sup>, K.Y. Cheung<sup>1</sup>, S.K. Yu<sup>1</sup>

<sup>1</sup>Hong Kong Sanatorium & Hospital, Medical Physics and Research Department, Happy Valley, Hong Kong SAR China ; <sup>2</sup>Hong Kong Sanatorium & Hospital, Department of Radiotherapy, Happy Valley, Hong Kong SAR China

**Purpose or Objective**

We hypothesize that head-and-neck (HN) sub-regions might show different inter-fractional positional characteristics due to the complicated HN anatomies and different sub-regional motion flexibilities. As such, we attempt to utilize the superior MRI soft tissue contrast to assess these inter-fractional positional characteristics in the HN sub-regions at 1.5T.

**Material and Methods**

14 healthy volunteers were recruited. Each subject was immobilized with a 5-point thermoplastic mask, and received 4 MRI scans using a T1-SPACE sequence (TR/TE = 420/7.2ms, isotropic voxel size = 1.05mm, scan time = 301s) on a 1.5T MR-sim to simulate RT fractions. Sub-regions of brain, nasopharynx (NP), oropharynx, and hypopharynx were manually drawn on the reference images acquired in the first MRI scan. Inter-fractional positional variations in translation and rotation were assessed by rigidly registering the overall HN images and each sub-region to the reference images. Correlations of sub-region positional shifts with that of overall HN were assessed using Pearson correlation. The mean and SD of positional shifts, systematic error ( $\Sigma$ ) and random error ( $\sigma$ ) of each sub-regional anatomy were calculated, and compared using paired Wilcoxon signed rank test.

**Results**

Mean and SD of positional shifts, systematic and random errors of overall HN and all sub-regions were mostly within 1mm and 1° (Table I), indicating the excellent positional reproducibility achieved on the MR-sim. Inter-fractional positional shifts in sub-regions were highly correlated with (highest in SI, lowest in roll) and insignificantly different from those in overall HN except for roll in hypopharynx, mainly attributed to the high motion flexibility in the neck even under immobilization ( $p=0.039$ ). Sub-regions did exhibit notably different, although insignificant, shift patterns from the overall HN, in particular in roll and yaw, as shown by the box-plot in Fig. 1. Overall HN mainly underestimated the inter-fractional shift magnitude, range and variability in sub-regions. In terms of margin setting, according to van Herk target margin recipe of  $2.5\Sigma+0.7\sigma$ , larger target margins might be needed in NP for positional compensation than in overall HN and other sub-regions.

Overall												
Translation						Rotation						
	LR	AP	SI	3D	Roll	Pitch	Yaw	3D				
Mean (mm)	-0.04	0.05	0.27	0.27	-0.01	0.00	0.10	0.10				
SD (mm)	0.76	0.27	0.74	1.09	0.14	0.01	0.50	0.52				
Systematic Error $\Sigma$ (mm)	0.56	0.20	0.50	0.78	0.09	0.00	0.36	0.37				
Random Error $\sigma$ (mm)	0.54	0.20	0.55	0.80	0.09	0.00	0.36	0.37				
van Herk's Margin (mm)	1.78	0.65	1.64	2.50								

Brain												
Translation						Rotation						
	LR	AP	SI	3D	Roll	Pitch	Yaw	3D				
Mean (mm)	-0.17	0.06	0.23	0.29	-0.02	0.00	0.24	0.24				
SD (mm)	0.71	0.63	0.81	1.26	0.45	0.01	1.01	1.10				
Systematic Error $\Sigma$ (mm)	0.55	0.50	0.59	0.95	0.36	0.00	0.75	0.83				
Random Error $\sigma$ (mm)	0.56	0.49	0.61	0.96	0.35	0.00	0.77	0.84				
Correlation Coefficient $r$	0.76	0.59	0.90	0.26	0.59	0.85						
van Herk's Margin (mm)	1.95	1.63	2.16	2.41								

Nasopharynx												
Translation						Rotation						
	LR	AP	SI	3D	Roll	Pitch	Yaw	3D				
Mean (mm)	-0.21	0.10	0.23	0.32	-0.04	0.00	0.25	0.25				
SD (mm)	1.04	0.82	0.84	1.57	0.56	0.01	1.02	1.16				
Systematic Error $\Sigma$ (mm)	0.79	0.66	0.62	1.21	0.44	0.01	0.75	0.87				
Random Error $\sigma$ (mm)	0.80	0.65	0.64	1.21	0.43	0.01	0.77	0.88				
Correlation Coefficient $r$	0.79	0.53	0.89	0.22	0.59	0.85						
van Herk's Margin (mm)	2.54	1.99	2.23	3.03								

Oropharynx												
Translation						Rotation						
	LR	AP	SI	3D	Roll	Pitch	Yaw	3D				
Mean (mm)	-0.15	0.10	0.21	0.28	-0.05	0.00	0.21	0.21				
SD (mm)	0.97	0.60	0.73	1.35	0.46	0.01	0.92	1.03				
Systematic Error $\Sigma$ (mm)	0.70	0.48	0.56	1.02	0.36	0.01	0.64	0.73				
Random Error $\sigma$ (mm)	0.69	0.48	0.58	1.02	0.35	0.01	0.66	0.74				
Correlation Coefficient $r$	0.84	0.52	0.87	0.18	0.63	0.87						
van Herk's Margin (mm)	2.32	1.55	2.07	2.56								

Hypopharynx												
Translation						Rotation						
	LR	AP	SI	3D	Roll	Pitch	Yaw	3D				
Mean (mm)	-0.09	0.05	0.18	0.21	-0.10	0.00	0.11	0.15				
SD (mm)	0.79	0.57	0.85	1.29	0.31	0.01	0.74	0.80				
Systematic Error $\Sigma$ (mm)	0.60	0.41	0.63	0.96	0.18	0.01	0.49	0.52				
Random Error $\sigma$ (mm)	0.58	0.40	0.64	0.95	0.20	0.01	0.48	0.52				
Correlation Coefficient $r$	0.85	0.42	0.91	0.28	0.81	0.75						
van Herk's Margin (mm)	2.05	1.29	2.23	2.38								

Table I. Positional errors of the overall and four sub-regions and the statistical analysis of positional variation correlation in all translation and rotation directions.

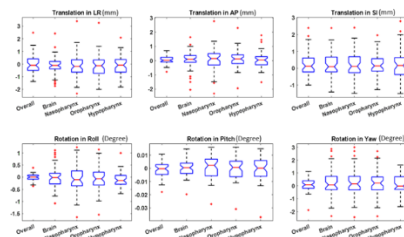


Fig. 1. Box-plot of sub-regions' translation and rotation displacements in every direction.

**Conclusion**

Sub-millimeter inter-fractional positional reproducibility could be achieved in HN sub-regionals on an MR-sim. HN sub-regions showed notably different inter-fractional positional characteristics and this should be taken into account for positional and motion compensation.

**EP-1991 PTV margin evaluation for pediatric craniospinal irradiation with 3D and 2D position verification**

E. Slooten<sup>1</sup>, N. Van Wieringen<sup>1</sup>, R. De Jong<sup>1</sup>, B. Balgobind<sup>1</sup>, S. Huijskens<sup>1</sup>, C. Windmeijer<sup>1</sup>, I. Van Dijk<sup>1</sup>, A. Bel<sup>1</sup>

<sup>1</sup>Academic Medical Center, Radiotherapie, Amsterdam, The Netherlands

### Purpose or Objective

Craniospinal axis irradiation (CSI) is important in specific brain tumors like medulloblastoma. This is a challenging tumor site due to the large size of the fields and complicated patient positioning. Little is known about these patients' inter and intrafraction motion, while these are important components of the PTV margin. The purpose of this study is to determine the magnitude of the inter and intrafraction motion for the thoracic and lumbar spine, and to compare these to the currently used PTV margins. Additionally, we investigate whether 2D kV/DRR position verification yields the same results as 3D CBCT/CT, as the 2D method would lead to lower imaging dose for the patients.

### Material and Methods

We retrospectively included 14 patients [median age 8.5y; range 5-14y] treated with CSI. The thoracic and lumbar CTVs were expanded with anisotropic margins of 0.8cm in LR direction, 1.0cm in caudal direction in the lumbar field and 1.0cm in AP direction for the thoracic and lumbar CTV.

All patients were treated in supine position on a thin mattress and knee support, immobilized with a 5 points mask. For clinical position verification, pre and post treatment CBCTs were acquired of the thoracic and lumbar CTV, using a hybrid offline/online protocol. Average time between the pre and post fractional CBCTs was 22min [range 17-33min]. In total 180 pre and 154 post fraction CBCTs were analyzed. Inter and intrafraction motion in LR, CC and AP directions were determined based on clinically used CBCT/CT automated matches of the bony anatomy. Distributions of systematic and random errors (standard deviations  $\Sigma$  and  $\sigma$ , respectively) were calculated. PTV margins were calculated using inter and intrafraction motion, without considering other sources of error.

We simulated 2D kV/DRR position verification by extracting two orthogonal radiographs from the CBCT series under angles with optimal visibility of the target. These were matched manually to the bony anatomy on DRRs of corresponding angles from the planning CT. The corrections resulting from these matches were compared to the corrections from the 3D CBCT/CT matches and Pearson correlation coefficients were calculated.

### Results

The systematic and random errors and resulting PTV margins for inter and intrafraction motion are shown in table 1 for the 3D CBCT/CT method. The clinically used PTV margins are sufficient for these uncertainties. In figure 1 the corrections from the 2D matches are plotted versus those from the 3D matches for all directions and linear regression lines are shown. A moderate to strong correlation was found as indicated by the Pearson correlation coefficients.

	Thoracic			Lumbar		
	LR	CC	AP	LR	CC	AP
$\Sigma_{interfraction}$ (cm)	0.14	0.20	0.13	0.13	0.28	0.19
$\sigma_{interfraction}$ (cm)	0.25	0.24	0.19	0.30	0.29	0.24
$\Sigma_{intrafraction}$ (cm)	0.15	0.09	0.07	0.13	0.11	0.19
$\sigma_{intrafraction}$ (cm)	0.26	0.20	0.18	0.24	0.18	0.23
PTV (cm)	0.8	0.8	0.6	0.8	1.0	0.9

Table 1:  $\Sigma$  and  $\sigma$  for the inter and intrafraction motion as found by CBCT.

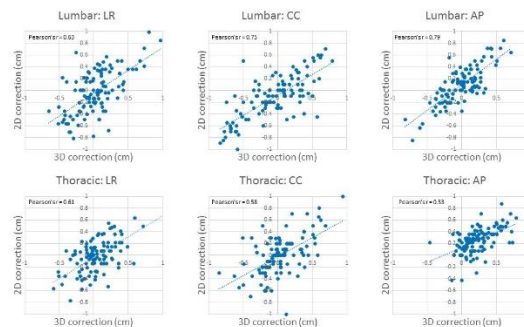


Figure 1: Correlation between corrections following from 2D position verification (i.e. 2D kV/DRR) and those following from 3D position verification (i.e. 3D CBCT/CT) for the lumbar and thoracic part of the target in all directions.

### Conclusion

The current PTV margins are sufficient to incorporate the inter and intrafraction motion measured on the CBCT for both the thoracic and lumbar CTV. The moderate to strong correlation between the 2D and 3D matches implies that larger margins may be needed when using 2D position verification to account for the additional uncertainty.

### EP-1992 Dose warping protocol for interfraction variation in Bladder filling in ano-rectal cancer patients

C. Fiandra<sup>1</sup>, E. Trino<sup>1</sup>, F. Arcadipane<sup>2</sup>, F. Olivero<sup>1</sup>, U. Ricardi<sup>1</sup>, P. Franco<sup>1</sup>

<sup>1</sup>University of Turin, Oncology, Turin, Italy ; <sup>2</sup>Città della Salute e della Scienza, Radiation Oncology, Turin, Italy

### Purpose or Objective

During pelvic radiotherapy (RT), bladder filling may randomly change during the course of treatment. The more reliable approach to account for this variation is represented by Plan of the Day approach; This relies on the robustness of deformable image registration (DIR) algorithms and software to match dissimilar volumes in different scansets. The main purpose of this work was to investigate a framework with 2 different algorithms to validate DIR performed between planning CT and each CBCT to explore the relationship between the "real" dose received by the Bladder and its volume change.

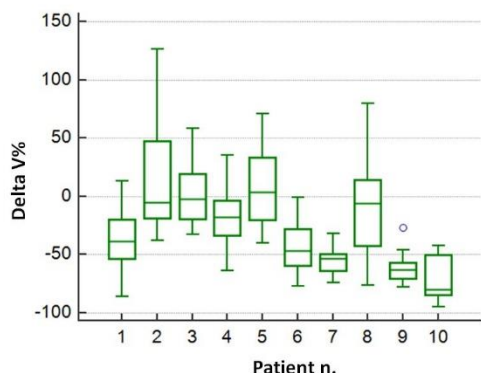
### Material and Methods

Ten patients were enrolled in the study; a total of 233 CBCTs were analyzed and contoured. Bladder, femoral heads and pubic symphysis were mapped from planning CT (pCT) to each CBCT and then verified by physicians. Each contour was then mapped back on the planning CT by means of specific deformable vector field (DVF) using both Hybrid and Biomechanical DIR algorithms. The goodness of the registration was double-checked first by visual inspection of each registration by physician and then by structures correspondence using Dice similarity coefficient (DSC) and Hausdorff distance (HD). The plan was then recalculated on each CBCT and dose warping was applied to accumulate dose on the planning CT with both algorithms, only in case of  $DSC \geq 0,8$  and  $HD \leq 3$ mm. Each re-calculated and deformed dose was used to evaluate the average dose (AD) and dose received by 2% volume ( $D_2$ ) of the Bladder for each treatment session and their correlation with percentage variation of volume of the Bladder (PVB) was investigated; Spearman's coefficient of rank correlation ( $r$ ) was calculated for both algorithms for AD and  $D_2$  in function of PVB

### Results

Percentage variation of Bladder volume compared to the pCT was  $-28.7 \pm 39\%$  showing a tendency for a smaller bladder volume during treatment than simulation CT. Figure 1 shows a box plot of the percentage variation of volume of bladder for each patient while Table 1 reports mean values and standard deviation of DSC and HD indexes for all structures for both algorithms;  $r$

values respectively of 0,171 and 0,140 for Hybrid algorithm were obtained for AD and for D<sub>2</sub>, while values of -0,164 and 0,041 were obtained for Biomechanical algorithm. Patient by patient analysis reveals higher correlation if volume of bladder has more limited variation like in the case of patient 3.



	DSC		HD (mm)	
	Hybrid	Biomechanical	Hybrid	Biomechanical
Bladder	0,929±0,135	0,951±0,025	0,967±1,261	0,776±1,111
Right femur	0,980±0,014	0,960±0,011	0,540±0,459	0,466±0,260
Left femur	0,976±0,020	0,967±0,01	0,560±0,497	0,572±1,902
Pubic symphysis	0,950±0,070	0,886±0,142	0,486±0,353	0,657±0,515

**Conclusion**

Dose warping protocol was applied for dose accumulation in the bladder during radiotherapy for pelvic cancers. Particular attention was addressed to the QA of the DIR involved for dose warping. Only deformable vector fields with a sufficient value of DSC or HD were considered, but random variations of Bladder volume shows poor or absent correlation with “real” dose received in terms of AD and D<sub>2</sub> compared to the original value of planning; an exception is represented by patients in which the volume variation of Bladder is more similar compared to the initial value on pCT.

**EP-1993 Evidence of CTV underdosing due to anatomical changes during breast Helical Tomotherapy**  
 P. Mangili<sup>1</sup>, M. Mori<sup>1</sup>, A. Fodor<sup>2</sup>, B. Longobardi<sup>1</sup>, P. Signorotto<sup>1</sup>, M. Pasetti<sup>2</sup>, F. Zerbetto<sup>2</sup>, N. Di Muzio<sup>2</sup>, R. Calandrino<sup>1</sup>, C. Fiorino<sup>1</sup>  
<sup>1</sup>San Raffaele Scientific Institute, Medical Physics, Milan, Italy ; <sup>2</sup>San Raffaele Scientific Institute, Radiotherapy, Milan, Italy

**Purpose or Objective**

Several planning studies claimed Helical Tomotherapy (HT) as a valid technique to optimize breast cancer radiotherapy due to potential improvements in dose homogeneity within PTV and sparing of Organs at risk (OARs), especially in case of concave-shaped PTVs. However, no studies dealt with the robustness of the delivered dose. In current study we quantified the dosimetry effects of anatomical changes on the delivered dose to breast CTV during post-operative HT.

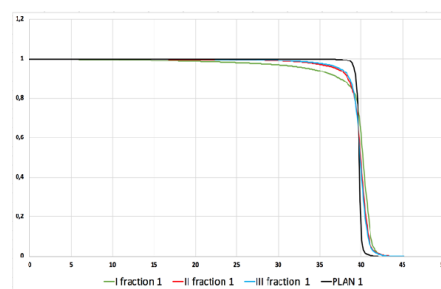
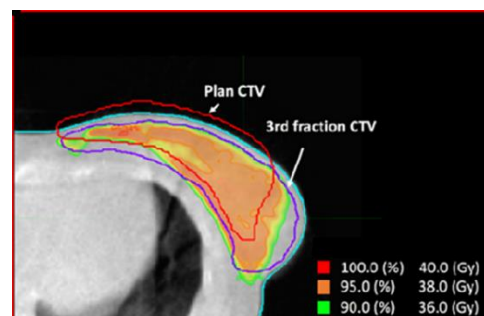
**Material and Methods**

Eleven patients (pts) previously treated with TomoDirect (TD) with post-operative radiotherapy to the whole breast were considered; HT treatment plans were optimized with the Tomotherapy planning station (Accuray Inc.) to deliver

a prescribed dose of 40Gy/15 fr. CTV and PTV were defined according to national guidelines (including a 5mm crop from body external contour); no additional PTV margins were added toward the body contour in order to avoid the inclusion of skin and the consequent delivery of high skin dose, expected in the HT mode. The changes of the dose distributions during treatment were weekly assessed in 3/15 fractions by dose-of-the-day recalculation on daily MVCT using the DQA TomoTherapy software. MVCTs were rigidly registered to the planning CT by matching chest bones position, according to our clinical procedure. CTV contours were then deformable registered from planning CT to the daily anatomy on MVCT, using a constrained-intensity-based algorithm (MIM software). Finally, after CTV fine-tuning manual correction, contours were cropped 5mm from MVCT body contour, consistently with the original definition. CTV DVHs during therapy were then obtained: for each patient, mean/min values of V32, V36, V38, V40, V43.2 over the three considered fractions were extracted (corresponding to 80%,90%,95%,100% and 105% of the prescribed dose) and compared against planning values.

**Results**

On average, the minimum values of V36 and V38 during therapy were 98.3% (92.8-99.9 %) and 97.1% (88.9-99.8 %) respectively against 100% at planning. For 3/11 pts (27%) there was an evidence of relevant local underdosing of CTV due to anatomical changes, with minimum values of V38 ranging between 95.4% and 88.9%. For two of these pts, local dose reduction >20% were visible: looking at V36, mean/min values for these pts were: 95.4/92.8 and 96.8/93.4 against planned values equal to 100%. The worst case is shown in Figure 1 (planning CTV in red, daily MVCT CTV in purple, dose delivered at fraction 4). The corresponding DVHs for the three fractions are compared against the planning DVH in Figure 2.



**Conclusion**

Although HT provides an optimal planned dose distribution, our results showed that breast HT is clinically associated to potentially dangerous underdosing of CTV during delivery, mostly due to relevant anatomical changes. Improved planning strategies need to be developed to improve delivery robustness and are actually under investigation.

### EP-1994 Lung Radiotherapy : Internal position reproducibility with spirometric DIBH

R. Garcia<sup>1</sup>, P. Mazars<sup>1</sup>, E. Jaegle<sup>1</sup>, V. Bodez<sup>1</sup>, C. Khamphan<sup>1</sup>, M.E. Alayrach<sup>1</sup>, A. Badey<sup>1</sup>, P. Martinez<sup>1</sup>  
<sup>1</sup>Institut Sainte Catherine, Physics, Avignon, France

#### Purpose or Objective

Deep Inspiration Breath Hold (DIBH) is an interesting method that provides a simple process with a single CT free from internal movements influences. The use of a spirometer has been the first way to implement a breathing control. With a calibrate system, the inspired air volume is well controlled but does not guaranty the internal organs positions. Lung radiotherapy benefit a lot from DIBH but IGRT is needed to evaluate the internal reproducibility.

#### Material and Methods

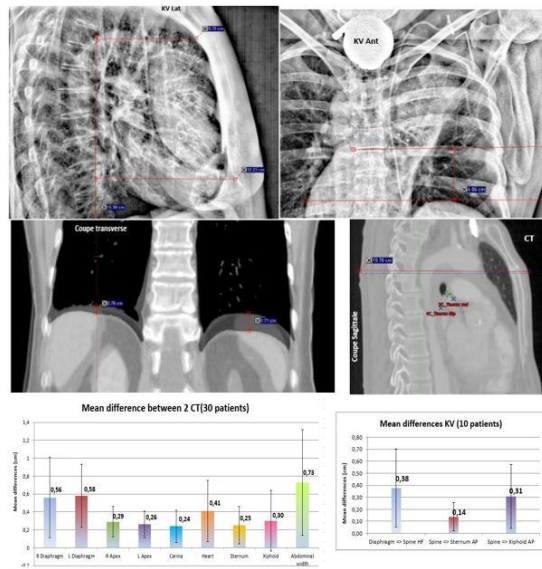
The lung radiotherapy is driven with the help of the SDX<sup>TM</sup> spirometer and video feed back assisting the patient to provide a deep inspiration breath hold during each imaging and delivery phase.

The anatomy position is evaluated with CT and KV images. The study is based on 30 patients who had a second CT during the course of treatment and 10 patients with KV images including the diaphragm.

Multiple distances were defined and measured on the whole set of data. They concern the diaphragm, the apex, the sternum, the xiphoid, the heart, the carina and the abdomen.

The lung volume, being and indicator of correlation with the dosimetry conditions, was measured and compared.

#### Results



The mean lung volume of the 30 cases studied is 5256 cm<sup>3</sup> ( $\pm$  928 cm<sup>3</sup>).

The mean lung volume difference between two CT acquisitions is 168 cm<sup>3</sup>  $\pm$  390 cm<sup>3</sup> (2 s), which represents a variation of 3.28% ( $\pm$ 3.81%).

The distances measurements carried out on CT images indicate a diaphragm mean displacement of 5.7 mm ( $\pm$  4 mm), the abdomen width (A-P) of 7,3mm (5,9mm), the apex (H-F) 2,8mm(1,6mm), the carina (R-L) 2,4mm(1,8mm), the sternum (A-P) 2,5mm (2,8mm), the xiphoid (A-P) 3mm (3,4mm) and the heart (perpendicular to the ribs 4,1mm (3,4mm).

The KV images measurements were obtained with the graphic rule on a stretched image area over the entire screen. The manual use of the graphic rule was evaluated

with a potential error of less than 2mm due to the mouse tool and the blurred edge of each anatomy image

The distances measurements carried out on KV images indicate a diaphragm mean displacement of 3.8 mm ( $\pm$  3.2 mm) in the cranio-caudal direction. The sternal position is pretty well reproducible with a mean variation of 1.4 mm ( $\pm$  1.2 mm). The xiphoid moves slightly more 3.1 mm ( $\pm$ 2.7 mm) in the anteroposterior direction.

#### Conclusion

The spirometric DIBH practice provides a reproducible lung volume which is important regarding the use of its DVH constraints. The distances measured on CT and KV images show an acceptable reproducibility and indicate the minimum PTV margins which have to be applied. Spirometric DIBH is safely used with high dose per session prescriptions often combined with VMAT and High Dose Rate FFF beams.

### EP-1995 Anisotropic definition of ITV-PTV margins according to the target position in lung SBRT with 4D-CBCT

S. Pini<sup>1</sup>, G. Della Gala<sup>2</sup>, S. Russo<sup>1</sup>, M. Esposito<sup>1</sup>, L. Paoletti<sup>3</sup>, P. Alpi<sup>3</sup>, R. Barca<sup>3</sup>, S. Fondelli<sup>3</sup>, F. Rossi<sup>3</sup>, P. Bastiani<sup>3</sup>

<sup>1</sup>Azienda USL Toscana Centro, S.C. Fisica Sanitaria di Firenze-Empoli, Firenze, Italy ; <sup>2</sup>Scuola di Specializzazione in Fisica Medica, Università degli Studi di Firenze, Firenze, Italy ; <sup>3</sup>Azienda USL Toscana Centro, S.O.C. Radioterapia, Firenze, Italy

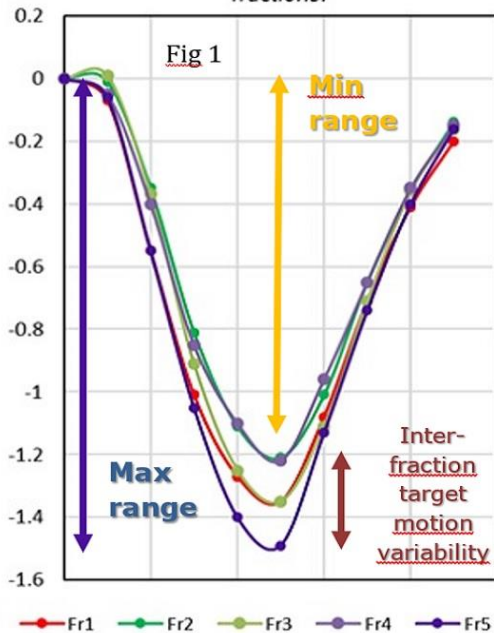
#### Purpose or Objective

4D-CBCT has been increasingly used to evaluate lung tumor position and to validate the PTV margins during SBRT treatments. The aim of this study was to estimate the inter-fraction variability of respiratory-induced motion of target volumes in lung SBRT treatments.

#### Material and Methods

This study is a retrospective analysis on 59 patients receiving lung SBRT (276 fractions in total). 4D-CT scans for planning were obtained on a GE 4D-CT scanner. For breath control a compression abdominal belt was used. GTV was contoured on each of the multi-phases reconstructed images to generate ITV and PTV (ITV plus 5mm). Prior to each fraction, in-room 4D-CBCT image scan was acquired and registered to the planning CT by the Symmetry XVI Elekta system using an automatic two steps image registration: first an anatomical landmarks-based clipbox was defined for setup correction and then a mask of 5mm around PTV was created for the soft tissue registration. Matching results were used to shift the table along the LL-SI-AP directions (respectively left-right, superior-inferior, and anterior-posterior) to correct daily patient setup and tumor baseline shifts. The dual registration results were always reviewed by the physician and manually adjusted if not correct. The baseline shifts were measured by subtracting the clipbox suggested correction from the applied table shift. Tumour motion was quantified for each fraction as the absolute range of the respiratory cycle. The inter-fraction variability of the target motion was then evaluated for each patient, first, by calculating the difference between the max and min range of the respiratory cycle for all treatment fractions and then extracting the value corresponding to the highest discrepancy (fig.1).

**Measure of the inter fraction target motion variability**  
 Example of respiratory cycles along SI for a patient treated with 10Gy in 5 fractions.



### Results

The inter-fraction target motion variability showed a distribution that ranges from zero to almost 1 cm in the worst case. SI direction was found to have the biggest discrepancy, followed by AP direction and LL. As expected, the variability was particularly significant for patients with a lesion in the lower lobe of the lung. For SI direction median values are respectively 0.9, 1.8 and 2.8 mm for upper, middle and lower lobe (fig.2). Target in the upper and medium lobe showed a stable motion along LL direction: for most of the patients the variability was less than 2 mm.

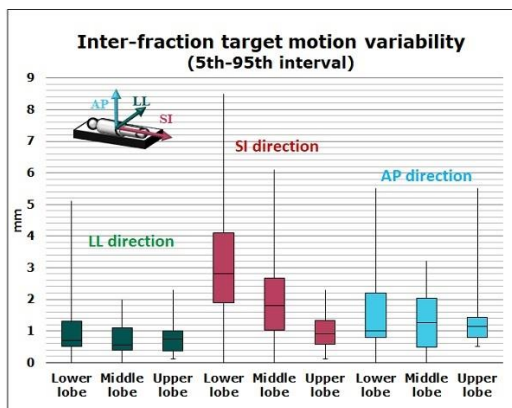


Fig.2: Box plot of the absolute inter-fraction target motion of the tumor along the three directions based on the position of the tumor in the lung. Higher ranges are visible for tumors positioned in the lower lobe of the lung and for SI direction.

### Conclusion

Targets in the lower lobe of the lung showed higher motion variability. SI direction, was found to have the biggest target motion discrepancy, followed respectively by AP and LL directions. Since the inter-fraction variability of the respiratory induced tumor motion contributes to the definition of the motion component of the PTV margin,

these results suggest the definition of anisotropic clinical ITV-to-PTV margins depending on target position: tighter margins for LL and AP directions and for lung tumors positioned in the upper lobe of the lung.

### EP-1996 Assessment of bulk-density CT accuracy for MR-guided proton therapy of prostate cancer

J. Handrack<sup>1,2</sup>, M. Bangert<sup>1,2</sup>, C. Möhler<sup>1,2</sup>, M. Ellerbrock<sup>2,3</sup>, S. Greilich<sup>1,2</sup>

<sup>1</sup>German Cancer Research Center DKFZ, Department of Medical Physics in Radiation Oncology, Heidelberg, Germany; <sup>2</sup>National Center for Radiation Research in Oncology, Heidelberg Institute for Radiation Oncology, Heidelberg, Germany; <sup>3</sup>Heidelberg University Hospital, Heidelberg Ion-Beam Therapy Center HIT- Department of Radiation Oncology, Heidelberg, Germany

### Purpose or Objective

Magnetic resonance (MR) imaging offers superior soft tissue contrast in comparison to computed tomography (CT) images and can be used to monitor anatomical changes in the patient during the treatment. Therefore, interest in MR guidance for proton therapy, which is highly susceptible to changes, is growing. However, the conversion of the MR image to so-called "synthetic CT (sCT)" images is necessary, since they lack stopping-power information. So far, mostly machine learning techniques have been applied to address this problem, but the required complexity of the sCT is still unknown. In this work, the influence of bulk density (BD) substitutes for different tissues was investigated for the male pelvis to identify the minimum number of BD classes necessary for accurate range prediction with a sCT.

### Material and Methods

The planning CT images from three prostate cancer patients irradiated with protons were retrospectively analysed by segmenting the CT into different tissue classes, which were replaced with mean BD values. Two types of BD-CTs were investigated: BD-CT1 contains four tissue classes, namely air, fat, non-fatty soft tissue and bone. For BD-CT2, the bone segment was further split into soft and hard bone. The clinical dose plans, consisting of two opposing beams, were re-calculated on the BD-CTs. The resulting dose distributions were compared to the original ones by means of gamma analysis (2mm/2%), dose volume metrics (DVMs), and proton range differences.

### Results

For BD-CT1, a mean absolute range difference ( $\pm$  mean s.d.) of (2.2 $\pm$ 2.7) mm was found. When splitting bone into soft and hard bone (BD-CT2), the mean absolute range difference was reduced to (1.4 $\pm$ 1.8) mm. Figure 1 shows this reduction exemplarily for the range shift maps of BD-CT1 and BD-CT2 for one patient. The mean gamma pass rates for the CTV and  $V_{>2\%presDose}$  (the volume where the dose was larger than 2% of the prescribed dose) were 99.6% and 98.8% for BD-CT1, and 99.9% and 99.6% for BD-CT2, respectively. For target volumes,  $D_2$ ,  $D_{50}$  and  $D_{98}$  were compared, which deviated less than 1.5% from the original plan for both BD-CT1 and BD-CT2, except for PTV- $D_{98}$  of one patient case, which deviated up to 2.9%. For the organs at risk,  $D_{50}$  and  $D_{15}$  were compared, which deviated up to 2.6%, however no RTOG dose constraints were exceeded.

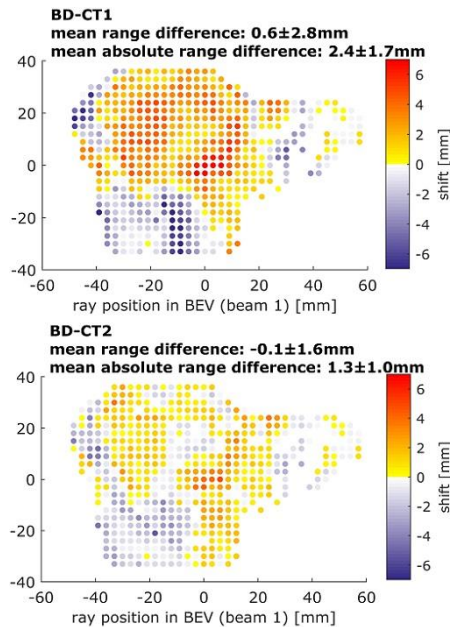


Figure 1: Proton range shift maps for one patient for BD-CT1 (top) and BD-CT2 (bottom). Each point represents one ray in the beam used during irradiation, the shift is color-coded.

## Conclusion

The deviations of the BD-CT dose distributions from the original dose distribution were small for the considered metrics in the three cases. It is necessary to include more patient cases to this work in progress for more significant results. However, our results indicate the applicability of a BD approach for sCT generation from MR for proton therapy. In a next step, we will identify MR sequences suited to identify respective tissue classes, transfer the gained knowledge to an MR-based workflow and compare the resulting predicted dose distribution to the calculation based on the planning CT.

## EP-1997 Daily adaptive proton therapy: A clear potential to reduce dose to healthy tissue and integral dose

L. Nenoff<sup>1,2</sup>, M. Matter<sup>1,2</sup>, J. Hedlund Lindmar<sup>1,2</sup>, T. Lomax<sup>1,2</sup>, D.C. Weber<sup>1,3,4</sup>, F. Albertini<sup>1</sup>

<sup>1</sup>Paul Scherrer Institute, Center for Proton Therapy, Villigen PSI, Switzerland ; <sup>2</sup>ETH Zurich, Department of Physics, Zurich, Switzerland ; <sup>3</sup>University Hospital Bern, Department of Radiation Oncology, Bern, Switzerland ; <sup>4</sup>University Hospital Zurich, Department of Radiation Oncology, Zurich, Switzerland

## Purpose or Objective

In some anatomical areas, for example the nasal cavities, anatomical changes can be observed on a daily base. This could lead to large dose distortions and is therefore covered by large target margins and a careful selection of field directions. However, this increases the dose to healthy tissue. With a daily 3D image in treatment position target coverage can be ensured by adapting on the daily geometry. Consequently, target margins can be reduced and alternative, less robust but more conformal field arrangements could be used. In this study we investigate the dosimetric effect of daily adaptive proton therapy (DAPT) combined with conformal field arrangements.

## Material and Methods

Planning CTs of 5 Patients with tumors involving parts of the nasal cavities were used to generate an anatomically robust “star” plan with the clinically used PTV margin and a “conformal” plan with a field specific PTV with covering 3% uncertainty in range and 1 mm in setup (60 GyRBE, 30 fx, figure 1) each. Also synthetic CTs with different nasal

cavity fillings were created by filling the nasal cavities onion layer wise from outside to inside. Each nasal cavity was filled separately ranging from empty to completely filled. Each artificial CT was combined with 5 random setup errors (1.57 mm  $\sigma$  for translation and 0.57°  $\sigma$  for rotation in all 3 directions), leading to between 180 and 625 clinical scenarios per patient and plan approach, depending on the size of the nasal cavities. Plans were recalculated and reoptimized for each scenario, simulating non-adapted and DAPT fractions, respectively. 100 times 30 randomly selected fractions were combined to treatment doses. Target coverage, dose to organs at risk (OARs) and integral dose were evaluated.

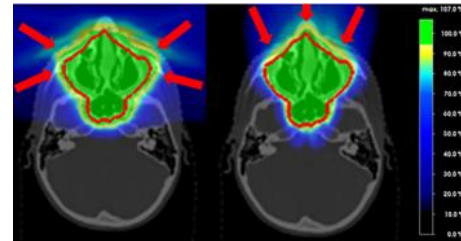


Figure 1: Example of planned “star” (left) and “conformal” (right) dose distribution.

## Results

By using conformal field directions the integral dose could be reduced by 43% on average (minimum reduction patient 4: 29%, maximum patient 2: 53%, figure 2a). Also OAR doses were reduced, if they were not directly attached or included in the target volume. In the non-adapted scenario the loss of target coverage is mainly patient dependent (V95 reduction of up to 34%, figure 2b) while the field direction has no systematic influence. DAPT can restore target coverage in all cases and in some cases even reduce the dose to OARs.

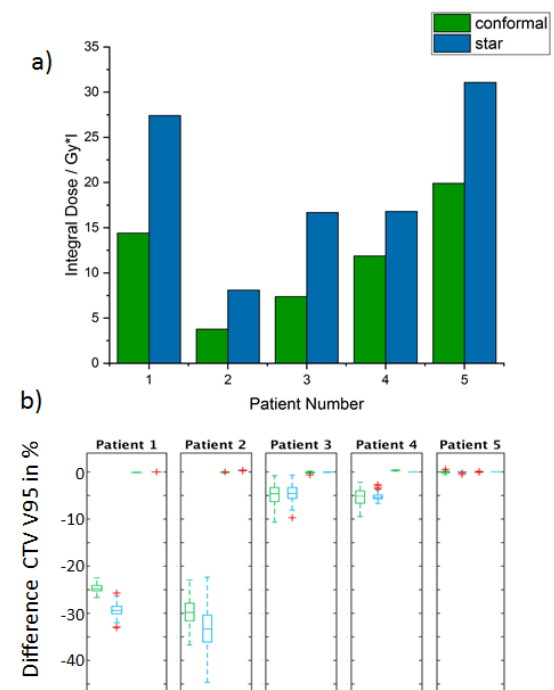


Figure 2: a) Integral dose of initial treatment plans. b) CTV V95 differences between treatment doses and initial treatment plan.

## Conclusion

DAPT combined with an adequate margin adaption and conformal field directions reduces the integral dose and

dose to OARs while ensuring robust target coverage. This will most likely translate to a clinical benefit for the patient.

#### EP-1998 Quality assurance criteria and anatomically plausible models for deformable image registration

C. Zachi<sup>1</sup>, B. Denis de Senneville<sup>2</sup>, B. Raaymakers<sup>1</sup>  
<sup>1</sup>University Medical Center Utrecht, Department of Radiotherapy, Utrecht, The Netherlands ; <sup>2</sup>Université de Bordeaux, Institut de Mathématiques de Bordeaux, Bordeaux, France

#### Purpose or Objective

Concepts in adaptive radiotherapy such as contour propagation and dose accumulation often rely on deformations provided by medical image registration algorithms. However, existing registration methods are often built upon elements originating from the computer graphics domain. Therefore, the anatomical plausibility of the estimated deformations may not be guaranteed. In this work we propose two quality assurance (QA) criteria, which assist in evaluating the anatomical plausibility of the deformations estimated by registration algorithms. In addition, a novel deformable image registration method is also proposed, specifically designed for biological soft tissue tracking.

#### Material and Methods

We propose assessing anatomical plausibility via two criteria: *the jacobian determinant* and *the curl magnitude* of the estimated deformations. Due to their high water content, most biological soft tissues are incompressible and therefore the jacobian determinant of their deformations is close to one. On the other hand, the local curl magnitude of the deformations should be close to zero, since local torsions inside most organs are unlikely to occur.

Two methods are evaluated against the proposed criteria: the state-of-the-art Evolution registration algorithm (EVO) and a novel method "Evolution Incompressible" (EVI) proposed here. The latter replaces the smoothness regularization of the former with a penalty on deviations from unity of the jacobian determinant of the deformations. By doing so, the new method constrains the estimated deformations to be incompressible.

The two methods were employed for the registration of five abdominal data batches, with each batch including five pairs of: (1) T1w MR - T1w MR, (2) CT - CT, (3) T1w MR - T2w MR, (4) CT - CBCT, (5) CT - MR images. The deformations estimated for the liver and kidneys were assessed both in terms the proposed QA criteria and the dice similarity coefficient (DSC). **Results** Table 1 reports the average DSC for the liver and kidneys before and after registration, with both methods leading to nearly identical improvements. However, a statistical analysis of the jacobian determinant of the deformations (see Fig. 1(a)) reveals high deviations from unity in the case of the EVO algorithm. A Mann-Whitney test indicates that this effect is significantly dampened by the EVI method at  $p = 0.05$ . Fig 1(b) illustrates an analysis of the vorticity of the deformations estimated by the two methods, with EVI providing overall lower values for the curl magnitude.

Data batch	Organ	Algorithm		
		None	EVO	EVI
T1w MR - T1w MR	Liver	0.91	0.96	0.96
	Kidneys	0.85	0.94	0.94
CT - CT	Liver	0.84	0.91	0.91
	Kidneys	0.83	0.92	0.92
T1w MR - T2e MR	Liver	0.89	0.94	0.94
	Kidneys	0.75	0.86	0.86
CT - CBCT	Liver	0.84	0.90	0.90
	Kidneys	0.83	0.90	0.90
CT - MR	Liver	-	-	-
	Kidneys	0.66	0.87	0.86

Table 1

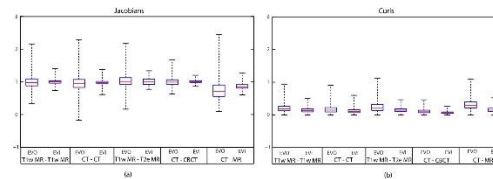


Figure 1

#### Conclusion

Both methods demonstrated a comparable performance for contour alignment. However, within the organ boundaries, the proposed method showcased an improved anatomical plausibility, with significantly lower compressions/expansions and vortices. This demonstrates both the importance of the proposed QA criteria for assessing the anatomical plausibility of deformations within the organ boundaries and that of adapting the registration model to the material properties of the observed tissues.

#### EP-1999 Robustness of IMPT plans towards anatomical variations for nasopharyngeal cancer

R. Argota Perez<sup>1</sup>, M.B. Sharma<sup>1</sup>, K. Jensen<sup>2</sup>, A. Vestergaard<sup>2</sup>, J.B.B. Petersen<sup>3</sup>, S. Korreman<sup>3</sup>  
<sup>1</sup>Aarhus University Hospital, Department of Oncology, Aarhus, Denmark ; <sup>2</sup>Aarhus University Hospital, Danish Center for Particle Therapy, Aarhus, Denmark ; <sup>3</sup>Aarhus University Hospital, Danish Center for Particle Therapy and Department of Oncology, Aarhus, Denmark

#### Purpose or Objective

Proton dose delivery is very sensitive to any variations during the treatment course. Setup uncertainties can be accounted for using robust optimization, whereas anatomical variations, e.g., changes in weight, tumour shrinkage, and filling or emptying of nasal cavities for head and neck cancer patients, are usually not accounted for. The present study evaluates the performance of a standard robust optimization technique towards anatomical variations.

#### Material and Methods

Proton treatment plans using simultaneous integrated boost (68/60/50 Gy) were optimized for five patients with nasopharyngeal cancer using the Eclipse TPS vs 13.7. Planning was performed using multiple-field optimization (MFO) with three beam directions, and robust optimization for the 68 Gy CTV (CTV1) with 5 mm perturbations in all directions. Anatomical changes were simulated by density overrides in the original CT scans. For weight gain and loss, 5 mm of water equivalent material (WEM) was added or subtracted to the body contour. Nasal cavity filling was simulated by overriding the entire cavity density with WEM. Setup errors were simulated using isocenter shifts of +/-5 mm in three orthogonal directions, separately and in combination with anatomical changes. The dose was recalculated with the original plans in each simulated situation, and plan robustness was evaluated comparing CTV1 coverage ( $V_{95}$ ) and OAR doses.

## Results

CTV1 coverage was not affected by the simulated isocenter shifts. For anatomical changes, weight gain and nasal cavity filling deteriorated CTV1 coverage, although  $V_{95}$  stayed above 95% in all cases (Fig. 1). When isocenter shifts and anatomical variations were combined, CTV1  $V_{95}$  dropped to unacceptable levels for a subset of patients. For weight gain combined with 5 mm setup errors, CTV1  $V_{95}$  dropped below 90% for 3/5 patients. For filling of the nasal cavity combined with 5 mm setup errors, CTV1  $V_{95}$  dropped below 95% for 2/5 patients. Weight loss did not affect CTV1 coverage even when combined with setup errors. The mean dose to the ipsilateral parotid gland was affected by all anatomic changes and setup errors, and the largest increases were seen for weight loss and filling of the cavities (Fig. 2). The maximum dose to the brainstem and the spinal cord had a similar behaviour for all the variations, but only for 1/5 patient the dose was above the clinical constraint.

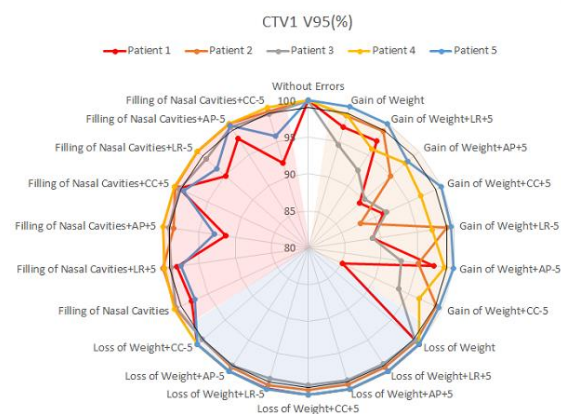


Figure 1. Spider plot of the dose coverage ( $V_{95\%}$ ) for CTV1. Doses are shown for the planned proton dose without errors (shown on top), for simulated weight gain, weight loss and cavity filling, separately and in combination with 5 mm setup errors. The black circle indicates the clinically acceptable level.

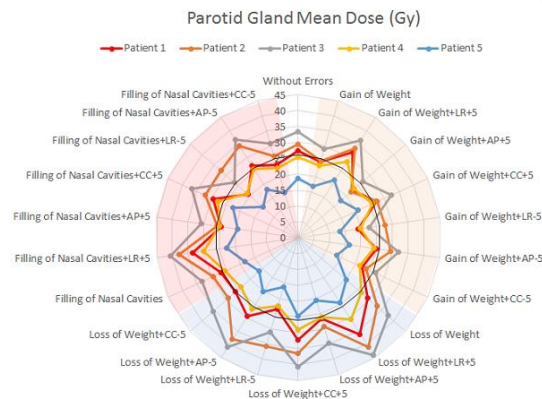


Figure 2. Mean dose to the ipsilateral parotid gland. Doses are shown for the planned proton dose without errors (shown on top), for simulated weight gain, weight loss and cavity filling, separately and in combination with 5 mm setup errors. The black circle indicates the opted clinical dose constraint.

## Conclusion

Target volume dose was not compromised by setup errors for robustly optimized proton plans in nasopharyngeal cancer patients. Weight gain and nasal cavity filling had detrimental effect on target doses, especially in combination with setup errors, reaching unacceptably low levels for several patients. Better robustness methods are needed to account for anatomical variations in order to minimize the need for plan adaptation.

## EP-2000 Dosimetric impact of setup errors and anatomical changes in breast cancer patients

E. Costa<sup>1</sup>, T. Bely<sup>1</sup>, M. Laurans<sup>1</sup>, S. Caneva Losa<sup>1</sup>, P. Poortmans<sup>1</sup>, Y.M. Kirova<sup>1</sup>

<sup>1</sup>Institut Curie Ensemble Hospitalier, Department of Radiation Oncology, Paris cedex 05, France

### Purpose or Objective

To evaluate the dosimetric impact of uncorrected setup errors and anatomical changes in stage I-III breast cancer (BC) patients during loco-regional radiation therapy (RT) with Helical Tomotherapy after adjuvant chemotherapy.

### Material and Methods

We studied the daily MVCT images acquired in patients treated to the breast or chest wall, internal mammary nodes (IMN), and axillary lymph nodes (levels II, III and IV). Setup corrections along the X, Y and Z directions and roll rotation were carried out after rigid registration of the bony anatomy and soft tissues between MVCT and planning CT. Pitch and yaw rotations were recorded only. Target volumes initially delineated on the planning CT were duplicated on every registered MVCT and adjusted by a physician in order to reflect the anatomical modifications of the day. Similarly, the external body contour was adapted to each MVCT and the volume of this structure was calculated. Using 1 MVCT/patient/week, we calculated the dose distribution on a total of 101 MVCT's. First, we analyzed the impact of the interval between chemotherapy and RT on the amplitude of anatomical changes. Subsequently, we quantified the changes in target volume coverage and we studied the correlation with the anatomical changes and with pitch and yaw uncorrected setup errors.

### Results

Dosimetric data of 19 patients with whole breast or chest wall RT were studied, of which 17 were treated to the regional lymph nodes as well. Spearman correlation analysis showed a significant correlation between the amplitude of the changes of the external body contour and the period between chemotherapy and RT ( $r_s=0.60$ ;  $p=0.01$ ).

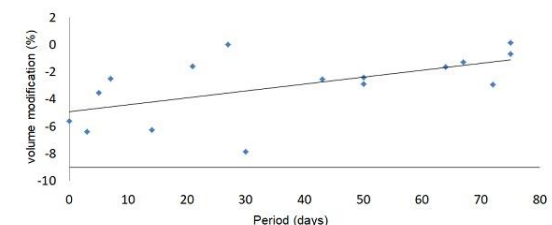


Figure 1. External body contour volume modification (%) vs. interval between completion of chemotherapy and start of radiation therapy.

The analysis of the calculated dose on the MVCT's showed that in 7% of studied fractions, the near maximum dose (D2%) increased by at least 2% in the breast, IMN and nodes level II and III. In 2% of studied fractions, the D2% increased by at least 5% in nodes level IV. In 5% of studied fractions, the D95% decreased by at least 5% in the breast, IMN and nodes level IV.

Pearson correlation analysis showed a significant correlation between the amplitude of external body contour changes and the influence on D2% in breast and IMN, D95% in nodes level IV and mean dose in breast. Pearson correlation analysis showed a significant correlation between pitch residual setup errors and modification of D2% in IMN and nodes level IV and the D95% in nodes level IV. We didn't note correlation between yaw residual setup errors and target coverage alteration ( $r<0.3$ ;  $p>0.01$ ).

		r (Pearson)	
		External body volume modification	Setup error for pitch rotation
Breast/chest wall	D2%	-0,51	
	Dmoy	-0,61	
IMN	D2%	-0,49	0,50
Lymph nodes level IV	D2%		0,51
	D95%	-0,52	0,51

**Table 1.** Pearson correlation coefficient between target coverage and setup errors or anatomical modifications ( $p < 0,01$ ).

### Conclusion

We demonstrated that, using our IGRT protocol with daily online corrections, anatomical changes, noted especially for patients with a shorter interval between chemotherapy and RT, affect target coverage in only a small proportion of the RT fractions. In addition, among the two uncorrected setup errors, pitch and yaw, only pitch is correlated to dose delivery changes. The clinical impact of these changes is likely negligible.

### EP-2001 Efficacy of CBCT guided IMRT for Head and Neck cancers and its dosimetric impact on other structures.

K. Talapatra<sup>1</sup>, C. Medichelme<sup>1</sup>, R. Chauhan<sup>1</sup>, P. Chadha<sup>1</sup>, V. Mhatre<sup>1</sup>, V. Muthu<sup>1</sup>

<sup>1</sup>Kokilaben Dhirubhai Ambani Hospital and Medical Research Institute, Radiation Oncology -, Mumbai, India

### Purpose or Objective

Online adaptive correction in image-guided intensity-modulated radiotherapy appears to be a promising approach for precision radiation treatment in head and neck tumors. This study is to evaluate the effect of online cone beam computed tomography (CBCT) guidance in Intensity Modulated Radiotherapy of Head and Neck Cancers.

### Material and Methods

38 Head and Neck cancer cases treated at our institute were selected for this study from prospectively maintained data (May 2017 to May 2018). Most of the cases were of Ca hypopharynx (23 cases). The Varian NovalisTx system which integrates an On Board Imager (OBI), was used to deliver radiation treatment. Daily/alternate day CBCT images were acquired and registered to the planning CT for online and offline analysis and to correct the patient setup errors. The setup errors were noted after matching of CBCT with planning CT images. New plans were generated in each patient using the mean lateral, vertical and longitudinal shifts. This DVH was compared to the original planning DVH and doses delivered to the target and various critical structures were evaluated. and the difference in doses received were computed. Statistical analysis was done using paired t-test.

### Results

The mean setup errors in three directions were : 1.4mm longitudinal, 1.2mm vertical and 1mm lateral. Analysis of dosimetric change due to a translational isocenter shift, if no correction was applied showed : Mean PTV1 V95% coverage to be dropped to 94.95% from the original of 96.37%, if shifts weren't applied ( $p < 0.0001$  with standard error 0.007 and 95% CI -1.4331 to -1.406). Similarly PTV2 V95% coverage reduced by -1.06% (97.39% to 96.33%) with  $p < 0.0001$  (standard error of 0.006 and 95% CI -1.0724 to -1.0476). There was also considerable dosimetric changes to critical organs as follows : ipsilateral parotid mean doses were increased by 0.54 Gy (42.06Gy to 42.60 Gy ;  $p = 0.94$ ) ; Contralateral parotid mean doses were increased by 1.74Gy (28.12 to 29.96Gy ;

$p = 0.5$ ). Dmax to spinal cord was increased by 1.6Gy (40.3 Gy to 41.90Gy ;  $p = 0.2$ ).

### Conclusion

Online CBCT correction ensures better coverage of targets (PTV) while reducing doses to normal tissue. There was significant reduction in PTV coverage if translational shifts wouldn't have been applied during the course of radiotherapy. CBCT-based online correction also increased the accuracy of IMRT in Head and neck cancer patients and provides scope to reduce irradiated margins, by decreasing the setup errors.

### EP-2002 Prostate treatment planning for the MR-linac: effect of online performance on template development

R.A. Mitchell<sup>1</sup>, A. Dunlop<sup>1</sup>, A. Pathmanathan<sup>2</sup>, S. Nill<sup>1</sup>, A.C. Tree<sup>2</sup>, U. Oelfke<sup>1</sup>

<sup>1</sup>The Institute of Cancer Research and The Royal Marsden NHS Foundation Trust, Joint Department of Physics, London, United Kingdom ; <sup>2</sup>The Royal Marsden NHS Foundation Trust and The Institute of Cancer Research, Clinical Oncology, London, United Kingdom

### Purpose or Objective

The MR-linac (Elekta AB, Stockholm) requires creation of an offline reference plan in Monaco 5.4 (Elekta) to enable propagation of planning parameters into an online workflow and adaptation of the existing plan. Consequently, the effect of parameters defined offline must be evaluated in the online setting during plan template development. We report on two areas for PRISM trial (NCT03658525) prostate planning: plan robustness with a-priori information and timing.

### Material and Methods

Monaco's constrained optimisation mode prioritises organs-at-risk (OAR) over target dose coverage; setting generic, effective OAR sparing IMRT objectives may adversely affect target coverage. Application of patient-specific objectives in Monaco, to lower OAR doses (Figure 1), is possible in our workflow using a-priori information derived from backup plans created upfront in RayStation 7.0 (RaySearch Laboratories, Stockholm). Two prostate patients, each with CT scan and four T2-weighted diagnostic MR scans, were used. CTVs (prostate and seminal vesicles), bladder and rectum were clinician-delineated, and RayStation and offline Monaco plans generated as per protocol. Monaco bladder and rectum IMRT objectives were set 5% higher than equivalent DVH values achieved by the backup plans. Online plans were generated on each MR image using an adapt-to-shape workflow (ATS); reference plans are adapted to each MR scan's anatomy. Further ATS plans were created using objective values at 10% above the backup plans to compare online plan robustness.

Planning time is affected by the number of shape changes during segment shape optimisation (SSO); more changes (SSO loops) may improve plan quality but with increased time, which is practical offline. Online, patients would be on-set for longer, with increased probability of intra-fraction motion. A reference plan was created for a prostate patient. Two ATS plans were generated on each of four MR scans, using our offline setting of ten SSO loops and then five to derive a suitable number for use online.

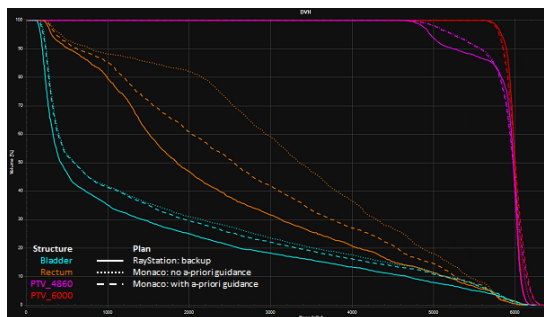


Fig. 1. Target and OAR DVHs comparison between: RayStation VMAT backup plan, Monaco IMRT plan without a-priori information and Monaco IMRT plan using a-priori guidance from the backup plan. All plans were prescribed to give 60Gy to the PTV\_6000 D<sub>50%</sub> in 20 fractions.

**Results**

Table 1 compares plans generated using differing a-priori information. For ATS plans, there were more PTV\_6000 coverage constraint violations (31% vs. 19%) when using more stringent objective values. All mandatory and optimal OAR constraints were satisfied except one optimal, which was likely due to randomness in Monaco's statistical-based optimisation.

Neither ten nor five SSO loops demonstrably changed the ATS plans in terms of distributions and DVH values. However, average planning time decreased by 40% (2.6 min) for five loops.

Table 1. Target and OAR results for reference plans and ATS plans generated with rectum and bladder optimisation objective values set to 5% and 10% above corresponding values achieved for backup plans. Results are averaged across plan types. Dose constraints are given as mandatory (optimal) where applicable.

Structure	Dose constraints	Plan						Units
		Reference		ATS @ 5%		ATS @ 10%		
		Average	SD	Average	SD	Average	SD	
Bladder	V6080cGy < 25 (3)	0.9	0.6	0.7	0.3	0.4	0.3	%
	V5676cGy < 35 (5)	5.5	0.9	3.7	1.3	3.4	0.9	%
	V5270cGy < 50	8.4	0.5	5.9	2.1	5.8	2.0	%
	V4870cGy < 25	10.9	0.3	7.7	2.8	7.6	2.7	%
	V4050cGy < 50	15.7	0.2	11.0	3.9	11.0	3.9	%
PTV_4860	D98% > 4617	5140	267	5030	189	5036	213	cGy
	D50% > 4860	5980	13	5968	17	5969	16	cGy
PTV_6000	D98% > 5700	5731	15	5685	31	5700	17	cGy
	D50% = 6000 ±60	6004	1	6005	2	6004	2	cGy
Rectum	V6080cGy < 5 (3)	0.7	0.6	0.8	0.6	1.2	0.8	%
	V5680cGy < 15	5.3	1.5	5.2	1.6	5.9	2.0	%
	V5270cGy < 30	9.5	1.7	9.2	2.5	10.3	2.8	%
	V4860cGy < 50 (35)	13.5	2.4	14.0	3.9	15.7	4.6	%
	V4050cGy < 60 (5)	23.1	3.2	23.4	5.1	26.9	6.9	%
	V3240cGy < 65	38.3	6.8	37.7	5.9	43.2	9.6	%
	V2440cGy < 80	55.6	9.1	56.0	5.8	61.7	7.4	%

**Conclusion**

MR-linac planning template development requires inclusion of IMRT objective flexibility to avoid the creation of highly optimised plans based on a particular geometry that will not exist online; more consistent target coverage requires allowances in OAR doses. On-set time reductions are also essential. It is possible to appreciably reduce online plan optimisation time by using five SSO loops without adversely affecting plan quality.

**EP-2003 Evaluation of three methods to calculate the dose on CBCT in case of IMRT for cervical cancer**

A. Barateau<sup>1</sup>, E. Trifard<sup>1</sup>, N. Perichon<sup>1</sup>, C. Hervé<sup>1</sup>, D. Guillaume<sup>1</sup>, J. Leseur<sup>1</sup>, A. Simon<sup>1</sup>, R. De Crevoisier<sup>1</sup>, C. Lafond<sup>1</sup>  
<sup>1</sup>Univ Rennes- CLCC Eugène Marquis- INSERM, Laboratoire Traitement du Signal et de l'Image - UMR 1099, Rennes, France

**Purpose or Objective**

To evaluate and compare the dose uncertainties of three methods to calculate the dose on CBCT in case of cervix carcinoma IMRT.

**Material and Methods**

A total of seven patients treated by IMRT for cervix carcinoma (45 Gy in 25 fractions) had 1 or 2 per-treatment couple(s) of CT and CBCT (corresponding to a total of 10 couples of images). The volumes of interests were delineated on CT. Reference dose distributions were calculated on the CTs, with Pinnacle TPS. CBCT images were first enlarged with assignment of water equivalent density to have the match with the corresponding CT body contour. Three methods of dose calculation on CBCT were compared: i) use of HU to density (HU-D) curve from phantom CBCT image, ii) density assignment method of three structures (air, soft tissues and bones) and iii) deformable image registration (DIR) method deforming the CT on CBCT, creating a deformed-CT (Admire research software, Elekta). As anatomy on CBCT can differ from CT, air pockets from reference CT were applied on CBCT of each method and contours (tumor volume, bladder and rectum) were rigidly registered from CT to CBCT. The dose distributions calculated on the CBCT by each method were compared to the reference CT dose calculation with DVH differences and 3D gamma analysis (local, 3%/3mm, 2%/2mm and 1%/1mm with a 10% dose threshold). The Wilcoxon test was used to compare the dosimetric endpoints.

**Results**

The figure shows the DVH differences for the tumor volume between dose calculation from CT and from CBCT using each of the methods. DVH differences were significantly lower when using the density assignment method or the DIR method, than when using the HU-D method.

The table shows the mean 3D gamma passrates (percentage of voxels with gamma <1) of each CBCT dose calculation method compared to the reference dose distribution on CT. Gamma passrates were significantly lower for the HU-D curve method than for the density assignment method or the DIR method.

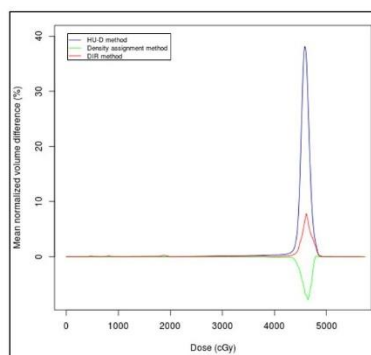


Figure. DVH differences of each CBCT dose calculation method compared to the reference CT for the tumor volume

Gamma criteria	HU-D method	Density assignment method	DIR method
1%/1mm	97 ± 2	100 ± 0.1	99.9 ± 0.1
2%/2mm	89 ± 5	99.3 ± 0.6	99.7 ± 0.3
3%/3mm	66 ± 11	94 ± 4	97 ± 2

Table. Mean 3D gamma passrates ± SD (in percentage) for each CBCT dose calculation method

**Conclusion**

The density assignment and DIR methods are the most accurate methods for CBCT-based dose calculation. Recently, more sophisticated methods based on deep learning lead to interesting results in MRI-based dose calculation. These methods could be evaluated with CBCT images to generate pseudo-CT. The next step is the dose accumulation to quantify the delivered dose during treatment (considering replanning or plan treatment library, if any) for comparison with the planned dose.

**EP-2004 Online rotation correction for MR-guided prostate radiotherapy**

W. Van den Wollenberg<sup>1</sup>, C. Carbaat<sup>1</sup>, P. De Ruiter<sup>1</sup>, P. Remeijer<sup>1</sup>, T. Janssen<sup>1</sup>, J. Sonke<sup>1</sup>  
<sup>1</sup>Netherlands Cancer Institute, Radiation Oncology, Amsterdam, The Netherlands

### Purpose or Objective

The MR-Linac (Elekta Unity, Elekta AB, Stockholm, Sweden) integrates a 7MV linac with a 1.5T MRI scanner. Currently, translational target misalignment can be corrected for using plan adaptations but rotational errors cannot. The purpose of this work was to develop and evaluate a method to correct for inter-fractional target rotation in prostate cancer patients.

### Material and Methods

In this retrospective study, 4 prostate cancer patients with seminal vesicles (SV) invasion were included. Per patient, a planning CT scan, delineations of the prostate+SV (CTV), PTV (5mm margin), rectum, and anal sphincter, and a 9-beam step-and-shoot IMRT (20x3Gy) MR-linac treatment plan were available. The plans were created using the clinical version of Monaco 5.4.

For each patient, delineations were rigidly transformed to simulate prostate rotations around the LR axis (-15° to +15° in 1° steps). To avoid rotation into organs-at-risk (OARs) the rectum and anal sphincter were deformed by the same rotation that dampens with PTV distance (maximal within 5mm then drops off linearly over 1cm). Two adapt-to-shape (ATS) workflows available on the MR-linac were tested:

1.  $ATS_{seg}$  starts with the segments of the original plan but uses the rotated structure set. It then tries to satisfy the planning constraints as best as possible. Per structure, electron density is set to the median density on the planning CT.
2.  $ATS_{flu}$  works as  $ATS_{seg}$ , but starts from scratch with a fluence optimization.

We evaluated the anal sphincter and rectum  $D_{mean}$ , and the PTV  $D_{98\%}$  and  $D_{2\%}$ . In addition we expanded the CTV into a dose evaluation volume (DEV) with increasing margins accounting for residual uncertainties and calculated the DEV  $D_{99\%}$ . We compared these values to those obtained by the adapt-to-position (ATP) workflow, which does not correct for rotations.

### Results

Distributions of DVH parameters are shown in figure 1. Figure 2 shows the CTV (plus margins) coverage as a function of rotation angle. Unlike the ATP method, the ATS methods maintained CTV coverage ( $D_{99\%} > 95\%$ ) up to a margin of 3mm in all tested cases. CTV+4mm coverage was maintained in the large majority of cases. PTV coverage is lost incidentally for negative rotations, but often for positive ones ( $>5^\circ$ ); positive rotations wrap the rectum around the PTV hindering plan optimization. Median adaptation times were 4.0 min (ATP), 9.9 min ( $ATS_{seg}$ ) and 10.9 min ( $ATS_{flu}$ ). These were measured on a research computer and clinical times are expected to be faster.

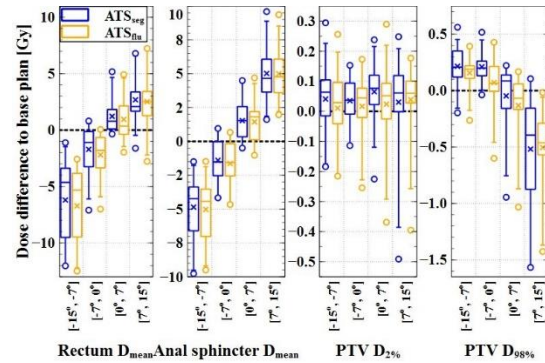


Figure 1 - Distribution of different DVH parameters for  $ATS_{seg}$  and  $ATS_{flu}$  in bins of rotation angle where all patients have been included. The whiskers denote the 2/98 percentile points. Note the different y-axis scales.

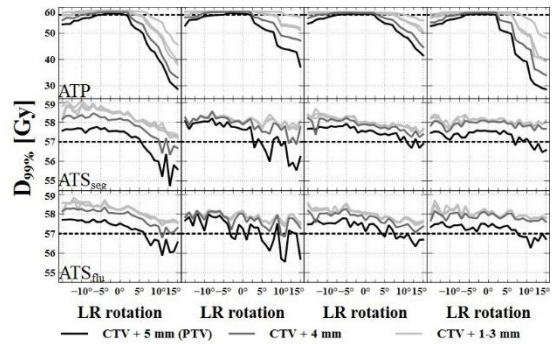


Figure 2 -  $D_{99\%}$  of the CTV expanded by various margins as a function of LR rotation angle for four patients (columns). Shown are ATP (top),  $ATS_{seg}$  (middle), and  $ATS_{flu}$  (bottom). The 5 mm expansion coincides with the PTV. The 57 Gy (95% of prescription dose) line is also shown (black dashed line). Note the different y-axis scales between ATP and ATS.

### Conclusion

The ATP method fails to adequately correct for larger prostate rotations, while ATS does account for such rotations.  $ATS_{seg}$  is faster than  $ATS_{flu}$ , but  $ATS_{flu}$  appears to be slightly better in terms of OAR sparing and target coverage. ATS is the preferred correction method for prostate rotations larger than a few degrees. The potential for PTV margin reduction following daily ATS is the subject of future studies.

### EP-2005 A novel method for rectal wall dose accumulation for prostate cancer patients

F. Kamp<sup>1</sup>, H. Liu<sup>1</sup>, L. Ermoschkin<sup>1,2</sup>, M. Di Biase<sup>1,3</sup>, C. Kurz<sup>1</sup>, G. Landry<sup>4</sup>, C. Belka<sup>1,5</sup>, M. Li<sup>1</sup>

<sup>1</sup>University Hospital LMU Munich, Department of Radiation Oncology, München, Germany; <sup>2</sup>HELIOS Hospital Krefeld, Department of Radiation Oncology, Krefeld, Germany; <sup>3</sup>"G. D'Annunzio" University of Chieti-SS. Annunziata Hospital, Department of Radiation Oncology, Chieti, Italy; <sup>4</sup>Faculty of Physics- Ludwig-Maximilians-Universität München, Department of Medical Physics, Munich, Germany; <sup>5</sup>German Cancer Consortium DKTK, Munich, Munich, Germany

### Purpose or Objective

Due to inter-fractional changes in rectum and bladder filling, precise dose estimation for the rectal wall over all fractions of a prostate treatment remains a major challenge. We developed a novel dose accumulation workflow for rectal wall dose, explicitly accounting for the daily changing geometry as well as physiological properties of this elastic organ, without the need for deformable image registration (DIR).

### Material and Methods

In order to facilitate dose recalculations on the patient geometry of the day, the daily cone beam CT (CBCT) was intensity corrected using a previously published method. This method exploits the planning CT (pCT) as a prior to correct the projections yielding intensity corrected  $CBCT_{cor}$ . All necessary structures are contoured on  $CBCT_{cor}$ .

images. The dose of the day is calculated with the isocenter of the original treatment plan shifted according to the clinically applied IGRT table shift. The rectum wall dose is accumulated in several steps, partly illustrated in fig. 1.

- 1) The whole rectum is contoured. Axial rectum slices are numbered starting at the caudal end at the tuber ischiadicum going cranially.
- 2) The rectal wall in every slice is represented in polar coordinates (around the center of mass "CoM") and subdivided into equal angles (e.g. with a resolution of  $1^\circ$ ).
- 3) The dose is extracted in every axial slice for every arc length element and every daily fraction.
- 4) Dose accumulation is performed for every small arc length element and transferred back to the corresponding pCT rectum wall element.

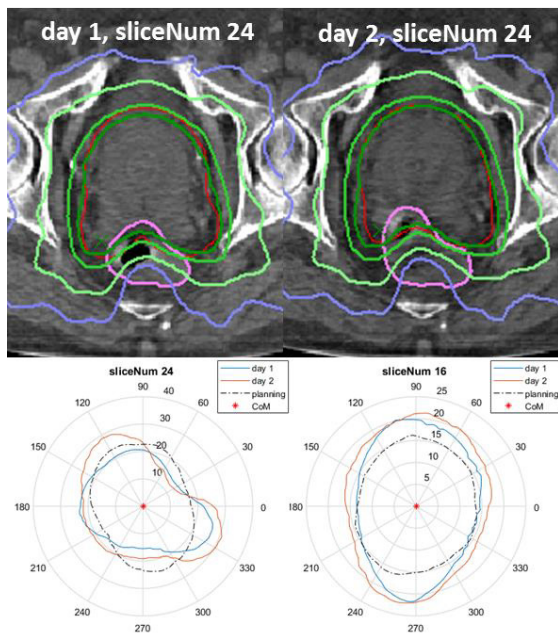


Fig.1: Axial slice through the CBCT<sub>cor</sub> of an exemplary patient. Isodoselines are shown together with the PTV (red) and rectum wall (pink). The second row depicts the corresponding rectum wall in polar coordinates around their center of mass (CoM) for two axial slices. Dose accumulation is performed in arc length elements with an angle resolution of  $1^\circ$  over all fractions and mapped back to rectum wall of the planning CT.

#### Results

In fig. 2 resulting dose-volume-histograms (DVH) are shown for an exemplary patient case irradiated with 37 fractions of 2 Gy. For this particular patient the dose to the rectum wall was higher in the planning CT than in the single fractions. Differences between the mean DVH over all fractions ("spatially not resolved accumulation") and the accumulated DVH in fig. 2 indicate the effect of the improved geometrical accuracy of the novel method. The developed dose accumulation approach is robust against changes in the angle resolution ( $0.1^\circ$ - $5^\circ$ ).

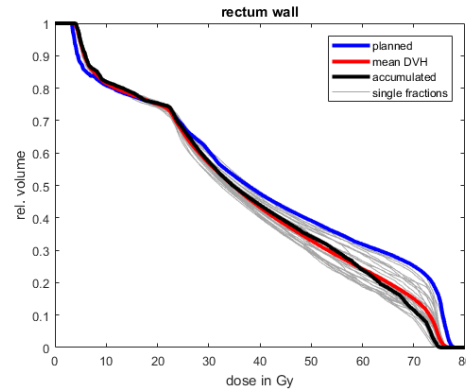


Fig.2: DVHs of the rectum wall. Doses are scaled to the treatment dose of 74 Gy.

#### Conclusion

The developed dose accumulation approach is a promising tool for dose estimations to the rectum wall, as it has a high geometrical precision and does not rely on potentially inaccurate DIR for dose accumulation. The method is applied to several patient cases which will be presented at the congress. A future goal is to validate the accumulated rectum wall doses by correlating them with patient reported side effects.

#### EP-2006 Dosimetric benefit of the first clinical SBRT of lymph node oligometastases on the 1.5T MR-linac

D. Winkel<sup>1</sup>, G.H. Bol<sup>1</sup>, A.M. Werensteijn-Honingh<sup>1</sup>, M.P.W. Intven<sup>1</sup>, W.S.C. Eppinga<sup>1</sup>, B. Van Asselen<sup>1</sup>, J. Hes<sup>1</sup>, B.W. Raaymakers<sup>1</sup>, I.M. Jürgenliemk-Schulz<sup>1</sup>, P.S. Kroon<sup>1</sup>

<sup>1</sup>UMC Utrecht, Department of Radiotherapy, Utrecht, The Netherlands

#### Purpose or Objective

The 1.5T MR-linac system (Unity, Elekta AB, Stockholm, Sweden) recently became available for clinical use in august 2018 and allows for MR-guided external beam radiotherapy. At our department, SBRT using the Unity has been initiated for patients with pelvic lymph node oligometastases. The purpose of this study was to compare the clinical dosimetric outcomes of online re-planning based on the new contours with an alternative online plan adaptation based on the online patient position with pre-treatment contours as well as with CBCT-linac VMAT back-up plans.

#### Material and Methods

In August 2018 clinical treatment with the Unity commenced in our clinic. At this time three patients received SBRT of 5x7Gy prescribed to 95% of the PTV with a 3mm PTV margin. For each patient a 7-beam pre-treatment IMRT plan was created using Monaco TPS (Elekta AB, Stockholm, Sweden), taking into account the 1.5T magnetic field. Also, CBCT-linac VMAT back-up plans were created with the clinical PTV margin (8, 3 and 3 mm for patient 1, 2 and 3, respectively, based on target visibility). With online MR imaging as provided in the Unity, the pre-treatment plan can be adapted by either 1) taking the new target position into account (adapt to position) and optimizing on the pre-treatment CT and contours or 2) using the new patient anatomy (adapt to shape) and optimizing on the daily image and adapted contours (Figure 1). Optimization was done by optimizing both segment shapes and weights for both methods. We compared these clinical plans with adapt to position plans and with VMAT CBCT back-up plans, using the daily anatomy of all online MRIs. All plans were evaluated using clinical dose criteria: PTV V<sub>35Gy</sub> >95%, PTV D<sub>0.1cc</sub> <47.25Gy, ureter D<sub>max</sub> <40Gy and bladder, bowel bag, rectum and sigmoid V<sub>32Gy</sub> <0.5cc.

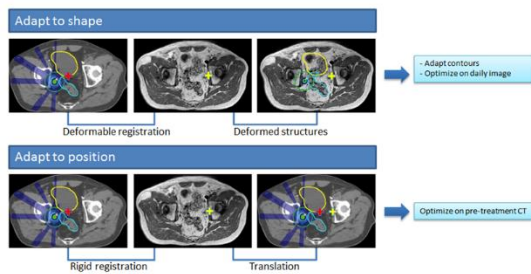


**Figure 1:** Schematic overview of the differences between the MR-linac Unity "adapt to shape" method in which online plan adaptation is performed on the new patient anatomy and optimized on the daily MRI and adapted contours, and the "adapt to position" method in which online plan adaptation is performed based on the new patient position and optimized on the pre-treatment CT and contours.

**Results**

The clinically delivered (adapt to shape) plans show the highest target coverage with an average PTV  $V_{35Gy}$  of  $99.2 \pm 1.5\%$  [range, 96-100%] (Figure 2). The clinical prescribed dose criteria were met for all fractions. The adapt to position strategy would result in the lowest PTV coverage with an average PTV  $V_{35Gy}$  of  $87.3 \pm 6.8\%$  [range, 72-99%], which is below dose criteria for three fractions for patient 1 and all fractions for patients 2 and 3. With the CBCT-linac back-up plans the PTV  $V_{35Gy}$  was on average  $94.5 \pm 2.1\%$  [range, 90-97%] which would be below criteria for 1, 5 and 2 fractions for patient 1, 2 and 3, respectively. For both the adapt to position and CBCT-linac back-up plans, small violations would have occurred for the ureter for patients 1 and 2, with a maximum  $D_{max}$  of 40.9Gy.

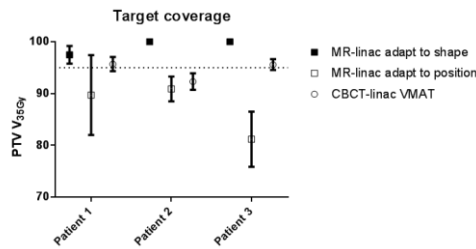


**Figure 2:** Target dose coverage (average and range) described as PTV  $V_{35Gy}$  in % evaluated on the daily anatomy for SBRT of lymph node oligometastases on the 1.5T MR-linac. Online plan optimization for the MR-linac plans was done through segment shape and weight optimization after segment aperture morphing. The 95% line depicts the minimum target coverage following the clinical dose constraints.

**Conclusion**

Evaluation of the first clinical SBRT treatments of pelvic lymph node oligometastases on the 1.5T MR-linac using the full re-planning approach yields beneficial DVH parameters compared to conventional treatment. The adapt to position option yields equal or worse DVH parameters compared to conventional treatment. This emphasizes the dosimetric benefit of online contour adaptation.

**EP-2007 Analysis of MRgRT treatment adaptation strategies with a high-field MR-Linac**

M. Nachbar<sup>1</sup>, D. Mönnich<sup>1,2,3</sup>, C. Marks<sup>2</sup>, A. Stolte<sup>2</sup>, O. Dohm<sup>2</sup>, D. Thorwarth<sup>1,3</sup>, D. Zips<sup>2,3</sup>, C. Gani<sup>2</sup>, S. Boeke<sup>1,3</sup>  
<sup>1</sup>University Hospital Tübingen, Section for Biomedical Physics- Department of Radiation Oncology, Tuebingen, Germany ; <sup>2</sup>Department of Radiation Oncology, University Hospital and Medical Faculty- Eberhard Karls University Tübingen, Tübingen, Germany ; <sup>3</sup>German Cancer Consortium DKTK, partner site Tübingen- and German Cancer Research Center DKFZ, Heidelberg, Germany

**Purpose or Objective**

MR-Linac systems are a promising technology with the capability of online plan adaptation. Here we evaluate the first treatment at our institution and compare

different adaptation workflows and their impact on target coverage and OAR sparing.

**Material and Methods**

A 55 year old patient with a single recurrent pararectal lymphnode metastasis of a prostate cancer was treated with the Unity 1.5 T MR-Linac (Elekta AB, Stockholm, Sweden) with 35/30 Gy to the GTV (10 mm<sup>3</sup>)/PTV in five fractions using eight step-and-shoot IMRT beams. The reference plan and all adapted plans were created with Monaco 5.4 (Elekta AB, Stockholm, Sweden). For daily online adaptation, the adapt-to-position (ATP) workflow was applied consisting of an isocenter shift for each segment followed by a segment weight optimization. Later, OARs were delineated offline on the daily pretreatment MR (T2w 3D). Retrospectively, the online adapt-to-shape (ATS) workflow was simulated, with a complete reoptimization starting from the fluence map based on the daily anatomy. In addition, a workflow consisting of using original segments (OS) only was simulated, in which the shift of the patient was not taken in account. The different workflows were compared with respect to the rectum  $D_{1.4ccm}$ , which corresponds to the  $D_{2\%}$  of the rectum in the reference plan, as well as PTV and GTV  $D_{98\%}$ . Plan conformity was evaluated based on  $V_{20Gy}$  of the total patient volume. To estimate the applied cumulative dose, the DVH parameters were averaged over all fractions.

**Results**

Table 1 shows the daily shift of the patient with respect to the PTV position in the reference plan. Table 2 shows the evaluated DVH parameters for each workflow. The rectum  $D_{1.4ccm}$  for the reference plan was slightly lower on the daily contoured and accumulated parameters (22.9 Gy) compared to the initial planning CT (23.5 Gy). The OS workflow shows a strong decrease of tumor coverage. Even for the minimal absolute shift (fx 5, 0.45 cm) the PTV  $D_{98\%}$  dropped from 29.2 Gy to 21.6 Gy. In the ATP workflow tumor coverage was maintained for all fractions, with minimal differences in the averaged PTV  $D_{98\%}$  of 29.2 Gy and 28.9 Gy for the reference plan and ATP, respectively, and equivalent OAR-sparing. The ATS workflow shows decreased rectum  $D_{1.4ccm}$ . with respect to the reference plan, equivalent tumor coverage with respect to PTV  $D_{98\%}$  (28.7 Gy) and GTV  $D_{98\%}$  (34.6 Gy) and the highest conformity ( $V_{20Gy} = 18.1$  Gy).

Fraction	Lateral	Cranial-caudal	Anterior-posterior	Absolute distance
1	0.63 cm	-0.01 cm	1.34 cm	1.481 cm
2	0.41 cm	-0.01 cm	0.47 cm	0.624 cm
3	0.62 cm	-0.03 cm	0.14 cm	0.636 cm
4	1.17 cm	0.30 cm	0.00 cm	1.208 cm
5	0.16 cm	0.12 cm	-0.40 cm	0.447 cm

**Table 1:** Changes in patient positioning per treatment fraction. The absolute distance is calculated based on the Euclidean distance.

		Reference plan	OS	ATP	ATS
Rectum $D_{1.4ccm}$ [Gy]	Fraction 1	22.42	20.26	21.79	21.70
	Fraction 2	24.74	22.62	25.47	20.84
	Fraction 3	22.43	19.73	22.51	20.48
	Fraction 4	21.57	18.22	22.24	18.58
	Fraction 5	22.19	22.00	23.48	22.09
	<b>Average</b>	<b>22.87</b>	<b>20.57</b>	<b>23.10</b>	<b>20.74</b>
PTV $D_{98\%}$ [Gy]	Fraction 1	29.23	1.77	28.16	29.09
	Fraction 2	-	19.91	29.12	29.00
	Fraction 3	-	23.43	29.11	28.99
	Fraction 4	-	20.44	29.05	28.44
	Fraction 5	-	21.60	29.05	28.18
	<b>Average</b>	<b>29.23</b>	<b>17.43</b>	<b>28.90</b>	<b>28.74</b>
GTV $D_{98\%}$ [Gy]	Fraction 1	34.16	33.75	34.86	34.48
	Fraction 2	-	29.06	34.26	34.48
	Fraction 3	-	29.50	34.30	34.83
	Fraction 4	-	22.98	34.37	34.54
	Fraction 5	-	32.32	34.21	34.50
	<b>Average</b>	<b>34.16</b>	<b>23.94</b>	<b>34.18</b>	<b>34.64</b>
Skin $V_{20Gy}$ [cm <sup>3</sup> ]	Fraction 1	20.98	21.00	17.31	20.50
	Fraction 2	-	20.61	24.00	17.71
	Fraction 3	-	20.78	23.96	18.77
	Fraction 4	-	20.41	20.45	17.67
	Fraction 5	-	20.77	21.87	16.07
	<b>Average</b>	<b>20.98</b>	<b>20.71</b>	<b>21.44</b>	<b>18.14</b>

**Table 2:** Analyzed DVH-parameters for the different workflows Original Segments (OS), Adapt-to-position (ATP) or Adapt-to-shape (ATS) for all treatment fractions.

**Conclusion**

Here we show with our initial experience that virtual couch shift with ATP is feasible to deliver high-precision MRgRT in a difficult-to-treat situation. Given the higher

complexity of ATS compared to ATP, further evaluation of the dosimetric and clinical benefit is ongoing.

### EP-2008 Positioning errors in free breathing and DIBH breast cancer radiotherapy: SGRT vs. skin markers

A.M. Acosta Roa<sup>1</sup>, S.G. Mikalsen<sup>1</sup>, T.P. Hellebust<sup>1</sup>  
<sup>1</sup>Oslo University Hospital, Department of Medical Physics, Oslo, Norway

#### Purpose or Objective

The purpose of this study was twofold: 1) To compare positioning errors in patient alignment for surface guided radiotherapy (SGRT) and skin markers (SM), both for free-breathing (FB) and deep inspiration breath hold (DIBH) breast cancer radiotherapy (BCRT). 2) To calculate the required PTV margins due to setup uncertainties in the same patient groups, if no corrections are applied prior to treatment.

#### Material and Methods

Data from 83 whole breast or chest wall BCRT patients was retrospectively analyzed. Due to different equipment available at two different sites in our department the procedure for patient alignment and pre-treatment imaging is different: SGRT with cone beam CT (CBCT) or SM with extended no-action limit protocol (eNAL) from portal images. Thereby, four patient groups were identified: SM DIBH, SGRT DIBH, SM FB, and SGRT FB with 25, 14, 19, and 25 included patients, respectively. Varian's RPM system was used for DIBH at the SM site while AlignRT (VisionRT) was used at the SGRT site.

Mean positioning shifts (MPS) in the vertical (Vrt), longitudinal (Lng), and lateral (Lat) directions were found from the pre-treatment image registration (matched to planning CT following bony anatomy), and the vector length  $|r^2|$  of the shifts was calculated. Data from every treatment fraction was analyzed for patients undergoing the CBCT imaging protocol, whereas only the 3 first fractions were included for those following the eNAL protocol.

Minimum PTV margins for 95% dose coverage to the CTV in 90% of the patients were calculated using van Herk's equation.

#### Results

The MPS from initial setup in the Vrt, Lng, and Lat directions together with the mean displacement vector  $|r^2|$  for all patient groups are shown in Figure 1. A tendency towards larger positioning errors was observed in  $|r^2|$  for patients aligned with SGRT in comparison to SM, for both DIBH and FB (0.45 to 0.41 cm, and 0.49 to 0.45 cm, respectively). These differences are not statistically significant ( $p > 0.05$ ) according to a two-sample t-test assuming unequal variances.

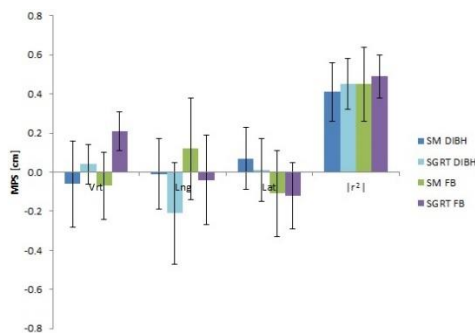


Figure 1. Mean positioning shifts in the four patient groups. Error bars correspond to one SD.

The results from calculation of the PTV margins for 95% dose coverage of the CTV in 90% of the patients are shown in Table 1. It can be observed that margins do not necessarily correlate to MPS, since margin calculation depend strongly on the size of the standard deviation (SD), and not on the average. SGRT yielded smaller margins in

the vertical direction for FB and DIBH, but larger for the longitudinal direction when used in combination with DIBH. Otherwise, margins agreed within 1 mm for both techniques.

Table 1. Mean positioning shifts ± SDs, and calculated PTV margins accounting for setup errors if no corrections are applied prior to treatment.

	MPS [cm]				PTV margin [cm]		
	Vrt	Lng	Lat	$ r^2 $	Vrt	Lng	Lat
SM DIBH	-0.06 ± 0.22	-0.01 ± 0.18	0.07 ± 0.16	0.41 ± 0.15	0.65	0.54	0.49
SGRT DIBH	0.04 ± 0.10	-0.21 ± 0.26	0.01 ± 0.16	0.45 ± 0.13	0.34	0.82	0.54
SM FB	-0.07 ± 0.17	0.12 ± 0.26	-0.11 ± 0.22	0.45 ± 0.19	0.57	0.77	0.68
SGRT FB	0.21 ± 0.10	-0.04 ± 0.23	-0.12 ± 0.17	0.49 ± 0.11	0.36	0.76	0.57

#### Conclusion

Patient alignment by SM seems to be generally more accurate but less precise than SGRT. Larger SDs in the MPS lead to increased PTV margins. A wider spread in SD was however expected for the SM patient group, as fewer image registrations could be included due to use of eNAL protocol. Calculated margins account only for setup uncertainties, and are required if no correction is effectuated prior to treatment.

### EP-2009 Inter-fractional Motion of Intact Cervical Cancer Treated On A MR-Guided Radiation Therapy System

D. Asher<sup>1</sup>, K. Padgett<sup>1</sup>, R. Llorente<sup>1</sup>, E. Mellon<sup>1</sup>, A. Wolfson<sup>1</sup>, B. Farnia<sup>1</sup>, G. Simpson<sup>1</sup>, N. Dogan<sup>1</sup>, L. Portelance<sup>1</sup>

<sup>1</sup>University of Miami, Radiation Oncology, Miami, USA

#### Purpose or Objective

Treatment verification has improved significantly over the past decade, with on-board MRI-guidance now available. MRI provides superior soft tissue contrast compared to CT-based imaging, allowing for identification of the tumor on daily imaging. Consensus contouring guidelines for IMRT of cervical cancer advise including the whole uterus in the target volume and adding large planning volume margins to account for motion. The primary objective of our analysis was to assess the inter-fractional GTV motion for those with an intact cervix using a MRI-guided-Radiation-Therapy (MRgRT) system and investigate the benefit of reducing the primary PTV to the GTV with a margin for microscopic disease and target motion.

#### Material and Methods

We analyzed 125 daily set-up MRIs from five patients with cervical cancer who received MRgRT. The GTV, bladder, uterus, and rectum were contoured on all 125 MRIs, then the positional and volume changes of the OARs were calculated to assess their effect upon the displacement of the tumor. Using these data, margin calculations were performed to account for the daily inter-fraction motion and compared to the consensus guidelines for margin expansions.

#### Results

The GTV decreased in size during the course of treatment for all patients, 34.0%-85.2%. The median GTV displacement range was 0.69cm-1.04cm. The margins calculated were: 0.78cm Left-Right, 1.31cm Anterior-Posterior and 1.38cm for the Superior-Inferior directions. The formalism presented here reduces the PTV by 36% compared to consensus guidelines sparing both the sigmoid and bowel.

#### Conclusion

Including the whole uterus in the target and adding large margin expansions, to account for inter-fractional motion, is the standard practice. However, by utilizing daily on-board MRI-guidance the GTV becomes readily visualized allowing for a reduction of margins and potentially excluding a portion of the uterine fundus from the PTV with the ultimate goal of decreasing treatment toxicity while maintaining tumor control.

**EP-2010 A QA method for evaluation of deformable image registration in head and neck adaptive radiotherapy**

E. Cagni<sup>1</sup>, A. Botti<sup>1</sup>, M. Orlandi<sup>1</sup>, M. Galaverni<sup>2</sup>, R. Sghedoni<sup>1</sup>, C. Iotti<sup>2</sup>, E. Spezi<sup>3</sup>, M. Iori<sup>1</sup>

<sup>1</sup>Azienda USL-IRCCS di Reggio Emilia, Medical Physics Unit, Reggio Emilia, Italy ; <sup>2</sup>Azienda USL-IRCCS di Reggio Emilia, Radiotherapy Department, Reggio Emilia, Italy ; <sup>3</sup>Cardiff University, School of Engineering, Cardiff, United Kingdom

**Purpose or Objective**

This study aimed to assess a method for evaluation of delivered VMAT dose based on multimodal deformable image registration (DIR) using for head and neck (HN) adaptive radiotherapy.

The main goal was to develop the proof-of-concept to be used as QA registration tool for adaptive radiotherapy.

**Material and Methods**

The HN phantom, "ATOM Max TM Dental and Diagnostic Head Model-711"(CRS, Virginia) was scanned with CT and and cone-beam computed tomography (CBCT).

Firstly, CT images of the phantom were artificially deformed in a warped CT (wCT) by using 20 clinical representative deformable vector fields (DVF), considered the ground truth (gt-DVF). These DVFs were created by deformable registration between the planning CT (pCT) and two CBCTs of the 16<sup>th</sup> and 26<sup>th</sup> fraction of 10 HN patient treated in our Institute with VMAT plans. The CT-CBCT deformable registration was performed using Velocity AI (Varian Medical System, Palo Alto, CA) software, version 3.2.

Secondly, the phantom CBCT was registered with the wCT resulting in a test-DVF and generated a warped CBCT (wCBCT) (Figure1).

Quality of the registration was assessed as the ability of the test-DVF to recover the artificially induced gs-DVF..

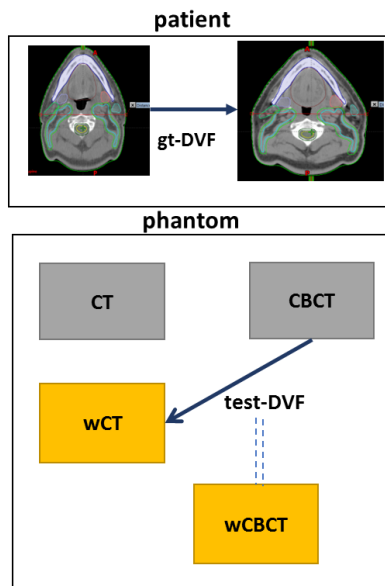


**Figure1.** Workflow for validation of CT –CBCT DIR. The HN phantom was scanned with CT and CBCT devices. CT images were digitally warped using 20 realistic patient-based DVF, considered as ground truth ( gt-DVF) resulting in a warped CT (wCT). The CBCT was then registered with wCT generating a test-DVF. Test-DVF was compared with the gt-DVF to quantify the target registration error (TRE).

To assess dosimetric errors, adaptive-CT was created for each patient gs-DVFs to overcome the limitation related

to unconventional Hounsfield Unit (HU) numbers of CBCT, by reshaping the pCT into CBCT. VMAT treatment plans were recomputed on each adaptive-CT and back-projected to the pCT via both the gt-DVF (gs-dose) and test-DVF (test-dose), respectively. The differences between gs-dose and test-dose on pCT were evaluated. The following organs at risk (OARs) were considered in the analysis:

- spinal canal and mandible (inserted in the original phantom manufacture);
- oral cavity, left and right parotids (digitally created by post-processing CT and CBCT image sets with real patient HU contrast).

**Results**

DIR error statistics were quantified using the target registration error (TRE) between gt-DVF and test-DVF, on a voxel basis. In both fractions of all patients, we found a TRE (mean±std(max)) of 2.5±1.0(5.5) mm, 2.9±0.7(3.9) mm, 1.4±0.4(2.6) mm, 1.8±0.6(3.1) mm, 2.0±0.9(4.0) mm and 1.5±0.5(2.7) mm for body, spinal cord, mandible, left and right parotid and oral cavity respectively.

The difference between the two dose propagation methods (mean±std(max)) were 1.1±0.5(2.0) Gy, 0.9±0.3(1.6) Gy, 1.0±0.4(2.0) Gy, 1.6±0.7(3.7) Gy, 1.7±1.0(4.1) Gy and 1.1±0.5(2.6) Gy for body, spinal cord, mandible, left and right parotid and oral cavity respectively. Table 1 reports TRE and dose errors for all OARs, for each patient and in each fraction, in terms of mean±std calculated on a voxel basis.

	gt-DVF – test-DVF TRE (mm)											
	body		spinal cord		mandible		left parotid		right parotid		oral cavity	
	16th fr	26th fr	16th fr	26th fr	16th fr	26th fr	16th fr	26th fr	16th fr	26th fr	16th fr	26th fr
patient 1	1.2±0.2	1.3±0.2	2.0±0.2	2.0±0.9	0.9±0.3	1.6±0.8	0.8±0.2	1.2±0.4	1.0±0.9	1.6±0.8	1.1±0.2	1.1±0.5
patient 2	3.7±0.8	3.3±0.3	3.2±0.7	3.7±0.8	1.5±0.7	1.6±0.8	3.4±1.1	3.1±1.2	1.5±0.7	1.6±0.8	1.3±0.7	2.6±1.6
patient 3	0.5±0.9	1.8±0.2	1.0±0.9	2.8±0.2	1.5±0.5	1.4±0.6	1.2±0.4	0.9±0.5	1.5±0.5	1.4±0.6	1.3±0.4	1.1±0.3
patient 4	2.4±0.5	1.5±0.4	3.9±0.4	3.5±0.8	1.2±0.5	1.7±0.1	3.2±0.3	4.9±0.8	1.6±0.5	1.7±1.0	2.1±0.3	2.2±0.4
patient 5	1.8±0.2	2.1±0.3	3.0±0.2	3.3±0.3	1.5±0.7	2.6±0.9	1.2±0.5	1.4±0.8	1.5±0.7	2.6±0.9	1.5±0.7	1.9±0.8
patient 6	2.5±0.6	3.1±0.2	3.4±0.5	2.2±0.8	1.1±0.4	1.2±0.6	3.8±0.7	4.3±0.2	1.3±0.4	1.2±0.6	0.9±0.3	1.1±0.5
patient 7	3.1±0.4	2.6±0.2	3.2±0.3	2.6±0.2	1.3±0.7	1.5±0.5	1.3±0.5	1.3±0.6	1.3±0.7	1.5±0.5	1.3±0.7	1.2±0.5
patient 8	2.1±0.2	2.2±0.2	3.0±0.2	3.6±0.3	1.1±0.5	1.2±0.6	2.1±0.9	1.9±0.5	1.3±0.5	1.2±0.6	0.9±0.4	1.6±0.7
patient 9	2.1±0.3	2.8±0.2	3.0±0.4	3.0±0.4	1.5±0.7	1.1±0.6	2.7±1.3	2.4±1.0	1.5±0.7	1.3±0.6	1.4±0.5	1.0±0.5
patient 10	2.9±0.7	2.8±0.2	3.2±0.6	2.9±0.3	1.2±0.5	1.2±0.6	1.8±0.9	1.4±1.0	1.2±0.5	1.2±0.6	1.7±0.6	1.4±0.6

	gt-Dose – test-Dose difference (Gy)											
	body		spinal cord		mandible		left parotid		right parotid		oral cavity	
	16th fr	26th fr	16th fr	26th fr	16th fr	26th fr	16th fr	26th fr	16th fr	26th fr	16th fr	26th fr
patient 1	0.7±0.2	0.7±0.2	0.8±0.1	0.6±0.6	0.8±0.8	0.8±1.1	0.4±0.5	0.8±0.9	1.3±1.0	1.4±2.0	0.6±0.3	0.9±0.8
patient 2	1.8±0.4	2.0±0.4	0.6±0.8	1.2±0.2	1.3±1.1	2.0±0.3	1.8±1.8	2.5±2.6	4.3±3.5	3.9±4.2	0.8±0.7	1.9±1.7
patient 3	0.5±0.4	1.3±0.3	0.6±0.5	1.1±0.9	1.0±0.9	1.1±1.0	0.8±1.1	1.3±0.8	1.7±0.8	2.0±0.3	1.2±0.1	1.6±0.4
patient 4	1.1±0.4	1.4±0.4	1.0±0.5	1.0±0.4	1.0±1.2	1.7±0.2	1.5±1.7	1.7±0.2	1.2±0.5	2.0±0.4	0.9±0.1	0.9±0.2
patient 5	0.7±0.2	0.8±0.2	1.2±0.4	1.2±0.2	1.0±1.5	1.5±1.6	1.1±1.0	2.3±2.7	1.3±1.3	1.8±2.2	0.9±0.8	1.0±1.0
patient 6	1.7±0.9	1.9±0.5	1.6±0.9	1.0±1.2	0.8±0.8	1.0±1.7	1.1±1.1	1.5±1.8	1.3±2.0	1.5±2.1	0.8±0.7	0.9±1.0
patient 7	0.3±1.3	1.0±0.3	0.2±0.2	0.6±0.9	0.2±0.1	0.7±0.6	0.1±0.1	0.9±0.8	0.3±0.1	1.1±0.5	0.1±0.1	0.6±0.6
patient 8	0.7±0.2	0.7±0.2	1.1±0.3	1.2±0.4	0.4±0.6	0.6±0.9	1.4±1.6	1.5±2.3	2.0±2.7	1.1±1.3	0.6±0.6	0.9±0.9
patient 9	0.6±0.2	0.7±0.2	0.9±0.6	0.8±1.6	1.1±1.5	0.8±0.9	3.7±4.5	1.6±2.1	1.5±2.1	0.9±1.1	2.6±2.8	1.0±0.8
patient 10	0.9±0.2	0.9±0.2	0.9±0.3	0.9±1.3	0.9±1.4	0.9±1.4	1.9±1.9	1.9±1.9	1.2±1.8	1.2±1.8	1.1±0.3	1.1±0.3

**Conclusion**

The proposed method based on the use of an anthropomorphic phantom was able to evaluate spatial and dosimetric errors of CT -CBCT DIR. This method could be applied as a patient specific based DIR QA tool which is a necessary step toward image-guided adaptive radiotherapy process.

**EP-2011 Dose calculation accuracy of using tailored synthetic CT for MR-guided online adaptive radiotherapy**

D. Cusumano<sup>1</sup>, L. Placidi<sup>1</sup>, S. Teodoli<sup>1</sup>, L. Boldrini<sup>2</sup>, F. Greco<sup>1</sup>, S. Longo<sup>2</sup>, F. Cellini<sup>3</sup>, N. Dinapoli<sup>3</sup>, V. Valentini<sup>2</sup>, M. De Spirito<sup>1</sup>, L. Azario<sup>3</sup>

<sup>1</sup>Fondazione Policlinico Universitario A.Gemelli IRCCS, U.O.C. Fisica Sanitaria- Dipartimento di Diagnostica per immagini- Radioterapia Oncologica ed Ematologia, Roma, Italy ; <sup>2</sup>Università Cattolica del Sacro Cuore, Istituto di Radiologia, Roma, Italy ; <sup>3</sup>Fondazione Policlinico Universitario A.Gemelli IRCCS, U.O.C. Radioterapia- Dipartimento di Diagnostica per immagini- Radioterapia Oncologica ed Ematologia, Roma, Italy

**Purpose or Objective**

The online MR-guided adaptive Radiotherapy (MRgART) workflow relies on the assignment of the water relative electron density (RED) map to the daily MR image (dMRI), to allow the dose calculation. The actual approach consists in co-registering the CT image acquired during the simulation procedure with the dMRI and then transferring the RED values obtained from the CT to the dMRI.

This approach can result misleading in clinical situations where the inter-fraction variability, the different organs filling and the changes in patient's anatomy (i.e. weight loss) can lead to considerable variations in RED map. A possible approach to overcome this variability consists in the daily generation of a synthetic CT (sCT) by segmenting the dMRI in 5 density levels (air, lung, fat, tissue and bone) and assigning a RED bulk value to each level according to ICRU 46 recommendations. Aim of this study is to evaluate the dose calculation accuracy of this approach in MRgART and to evaluate if assigning patient specific RED values can improve such accuracy.

#### Material and Methods

26 patients treated in the pelvic and abdominal sites were retrospectively enrolled.

For each patient, a planning CT (pCT) was acquired and segmented in 5 density levels, then median RED (mRED) values were calculated for fat, soft tissue and bone. Correlation between mREDs and clinical parameters (age, sex, body mass index) was investigated by using the Pearson Correlation Coefficient (PCC). Two sCTs were generated by assigning RED bulk values to the segmented levels on pCT: the sCT<sub>ICRU</sub> uses the RED values recommended by ICRU 46, the sCT<sub>tailor</sub> uses the median patient

specific RED values. The sCTs were generated from the CT image and not from MRI in order to avoid any potential bias due to the different MR and CT patient positioning. The same treatment plan was calculated on the sCTs and compared to those calculated on pCT in terms of 1%/1mm gamma analysis and dose volume histogram (DVH) parameters. The statistical significance of the difference between the sCTs was evaluated using Wilcoxon Mann Whitney test.

#### Results

A significant correlation between the clinical parameters and the mRED values was observed only between bone and age in women (PCC=-0.71), probably due to osteoporosis and menopausal status of the enrolled women (Figure 1).

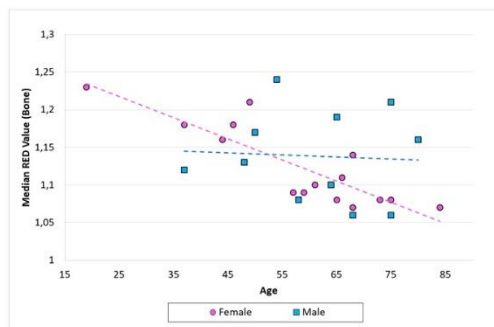


Figure 1 – Plot of the median RED values of the bone density for women and men in function of the age

For the dosimetric analysis, high agreement was found between dose calculated on sCTs and pCT:  $\gamma$  passing-rate was  $91.2\% \pm 6.9\%$  for sCT<sub>ICRU</sub> and  $93.7\% \pm 5.3\%$  for sCT<sub>tailor</sub>. A statistically significant gain in using sCT<sub>tailor</sub> respect to sCT<sub>ICRU46</sub> was found ( $p = 0.0013$ ). As shown in Figure 2, in 8 cases out of 26 the use of a personalised approach lead to an improvement in dosimetric accuracy higher than 4%.

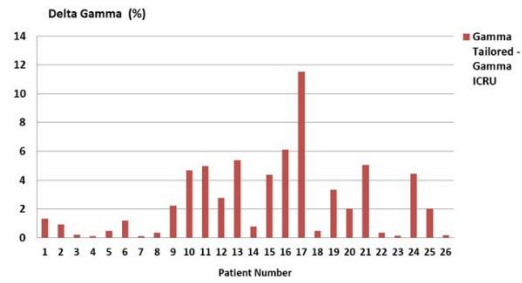


Figure 2 – Difference in gamma passing rates (1%/1mm) between the gamma analysis carried out between sCT<sub>tailor</sub> and pCT, and between sCT<sub>ICRU</sub> and pCT

#### Conclusion

The use of bulk synthetic CT achieves a high level of dose calculation accuracy, allowing its reliable use for online adaptive MR-guided Radiotherapy. In particular, assigning patient specific RED values to sCT allows to improve the accuracy of this approach.

#### EP-2012 MR-guided online adaptive radiotherapy for pancreatic cancer: where are we and where are we going?

L. Placidi<sup>1</sup>, D. Cusumano<sup>1</sup>, L. Boldrini<sup>2</sup>, V. Chiloiro<sup>2</sup>, S. Teodoli<sup>1</sup>, A. Capotosti<sup>1</sup>, S. Manfreda<sup>2</sup>, F. Cellini<sup>2</sup>, L. Azario<sup>1</sup>, M. De Spirito<sup>1</sup>, V. Valentini<sup>2</sup>

<sup>1</sup>Fondazione Policlinico A. Gemelli IRCCS - Università Cattolica Sacro Cuore, Medical Physics, Rome, Italy ;

<sup>2</sup>Fondazione Policlinico A. Gemelli IRCCS - Università Cattolica Sacro Cuore, Radiation Oncology, Rome, Italy

#### Purpose or Objective

Magnetic Resonance guided -Radiotherapy (MRgRT) represents to date the most suitable IGRT technique for Online Adaptive (OA) RT, due to the superior soft tissue contrast and the real-time gating approaches achievable using cineMRI images. Aim of this study is to perform a process optimization analysis for the evaluation of the robustness and reliability of the OA workflow implemented in our institution for locally advanced pancreatic cancer (LAPC) patients (pts) undergoing low tesla MRgRT.

#### Material and Methods

Our OA workflow is characterised by different steps: for each fraction, OaR re-contouring is performed within a distance of 3 cm from the PTV surface on the daily acquired MR image scan. The dose distribution of the original plan is firstly calculated on the anatomy of the day and, if the dose constraints are not met, treatment plan is re-optimised. Online Quality Assurance (QA), based on an independent Monte Carlo (MC) calculation, is finally performed before delivery starts. Ten (pts) affected by LAPC were retrospectively enrolled after being treated with the OA workflow, for a total amount of 50 delivered fractions. Several parameters have been registered for the analysis: single fraction couch shifts after daily MRI registration, OaRs and target volumes variation, number of delivered OA fractions with a predicted or re-optimised dose, beam-on time for each adaptive fraction, online QA 3%/3mm gamma passing rate, DVH metrics (target coverage as PTV V95% and CTV V98%, and OaRs specific dose-volume constraint) and single fraction distance between CTV and duodenum/stomach centre of mass.

#### Results

Lateral, longitudinal and vertical single fraction couch shifts result in (mean $\pm$ SD (range min/max) for all patients, for all 50 fractions)  $-0.18\pm 0.58$ cm ( $-1.49/0.96$ cm),  $-0.11\pm 0.72$ cm ( $-2.81/1.38$ cm),  $-0.02\pm 0.31$ cm ( $-0.80/0.68$ cm) respectively. OaRs and targets volume variation are summarised in Figure 1. Out of a 50 fractions, 34 fractions were re-optimised and 16 delivered using the

original plan. Single fraction treatment time duration, including also the fraction with re-optimised dose distribution, was  $8.8 \pm 2.8$  min : 4.7/17.3min. When the plan underwent re-optimisation, a reduction of the beam-on time in comparison with the original plan has been detected in 44% of the cases (15 plans). Online QA 3%/3mm gamma passing rate was  $97.5 \pm 1.5\%$  (94.8/100.0%), comparable with the offline QA performed on a dedicated phantom ( $98.7 \pm 1.1\%$  (96.7/100.0%)). DVH metrics results are shown in Table 1 for a subgroup of 6 (pts) with same dose per fraction prescription (8 Gy). Maximum single fraction CTV to duodenum/stomach centre of mass distance was 2.4cm and 1.8cm respectively; SD of CTV to duodenum/stomach centre of mass distance for all the evaluated 50 fractions is 0.9cm and 0.8cm respectively.

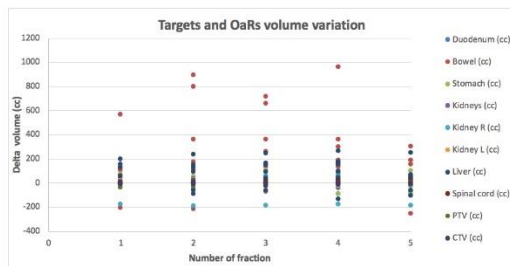


Figure 1 – Targets and OaRs single fraction volume variation

	$\Delta d$ V33 (cc)	$\Delta d$ V25 (cc)	$\Delta d$ V18 (cc)	$\Delta d$ V12.5 (cc)	$\Delta b$ V33 (cc)	$\Delta b$ V25 (cc)	$\Delta s$ V33 (cc)	$\Delta s$ V25 (cc)	$\Delta s$ V28 (cc)	$\Delta kr$ V12 (cc)	$\Delta kl$ V12 (cc)	$\Delta l$ V21 (cc)	$\Delta PTV$ V95 (%)	$\Delta CTV$ V98 (%)
Min	-0.7	-2.4	-2.2	-5.2	-1.0	-0.6	-0.3	-11.8	-16.9	-2.5	-5.4	-6.6	-17.7	-16.9
Max	0.7	5.5	11.2	10.7	0.7	15.1	0.3	5.7	13.0	9.2	2.3	47.8	0.9	22.1
Mean	0.1	1.1	3.0	2.8	0.2	5.3	0.0	-0.5	-0.1	4.0	-0.1	15.8	-4.5	0.8
SD	0.4	2.2	4.0	5.2	0.6	4.9	0.2	4.1	8.2	3.8	1.9	24.1	5.8	5.5

Table 1 – Targets and OaRs DVH metrics in terms of minimum, maximum, mean and standard deviation (SD) of the difference between the planning DVH parameters and the daily registered one, after the online adaptation of the plan for a subgroup of 6 pts. d = duodenum, b = bowel, s = stomach, kr = right kidney, kl = left kidney, l = liver, PTV = planning target volume, CTV = clinical target volume

## Conclusion

The results of this evaluation emphasize that different parameters can affect the entire workflow. Most of them can be improved to optimise the current workflow in order to better perform the OA strategy.

## EP-2013 Lung tumor motion based on 4D-CBCT: baseline shift, interfraction amplitude and volume variation

F. Oger<sup>1</sup>, P. Dupuis<sup>1</sup>, E. Mesny<sup>1</sup>, T. Baudier<sup>2</sup>, S. Rit<sup>2</sup>, R. Tanguy<sup>1</sup>, M. Ayadi<sup>1</sup>

<sup>1</sup>Léon Bérard Cancer Center, Radiotherapy, Lyon, France ; <sup>2</sup>INSA-Lyon- Université Lyon 1, CREATIS- CNRS UMR5220- Inserm U1044, Lyon, France

## Purpose or Objective

4D-Cone Beam Computed Tomography (CBCT) allows the accurate positioning of moving targets and the study of tumor motion. In this work based on clinical data, we first compared the Internal Target Volume (ITV) volumes and motion amplitude between 4D-Computed Tomography (4D-CT) and 4D-CBCT. Secondly, we estimated the interfraction baseline shift and motion amplitude variations.

## Material and Methods

Patients with early non-small cell lung cancer treated with SBRT were included in the study. Patients were installed in a Bodyfix (Elekta) and underwent a 4D-CT scan (Big Bore, Philips). Treatment plans based on an ITV strategy were delivered on a Versa HD linac (Elekta). Before each fraction, a 4D-CBCT was acquired. A bone registration followed by an automatic region-of-interest (ROI) registration of the tumor were then computed with the

on-line reconstruction software Symmetry (Elekta). For each patient, baseline shifts were obtained by the difference between bone and ROI registrations. Mean tumor motion amplitudes were estimated from the 4D-CT by subtracting the 3D tumor centroid coordinates on extreme breathing phases, and automatically from 4D-CBCT images. A physician delineated the ITV on average images (4D-CT and 4D-CBCT) using a MonacoSim workstation (Elekta) to analyze the variations of the ITV volume.

## Results

A total of 280 4D-CBCT images from 58 tumors (52 patients) were retrospectively analyzed. The repartition of the tumors in the lungs was: 53% of tumors located in the upper lobe (UL), 9% in the middle lobe (ML) and 38% of tumors located in the inferior lobe (IL). The grand mean (GM) baseline shifts (SD) in the cranio caudal (CC) direction were 0.16 cm (0.12) for UL, 0.53 cm (0.26) for ML and 0.31 cm (0.28) for IL. In the other directions, GM baseline shifts were under 0.21 cm. 13% of UL tumors, 100% of ML tumors and 67% of IL tumors had a baseline shift above 0.30 cm in the CC direction. The mean [range] of amplitude differences between 4D-CT and 4D-CBCT was less than 0.10 cm [-0.93 cm; 1.70 cm] in all directions. 27% of UL tumors, 40% of ML tumors and 52% of IL tumors had amplitude differences larger than 0.30 cm in all directions. The median [range] of ITV volume deviation between 4D-CT and 4D-CBCT was -1.0% [-196.0%; +82.7%].

## Conclusion

The largest baseline shifts were observed for tumors located in the middle and inferior lobes. After a review of these cases, those tumors were mainly located on the fissure (ML), close to the chestwall, or in areas influenced by gastric filling (left IL). The same observation was found for amplitude variations. The variability of ITV volume between 4D-CT and 4D-CBCT was, in some cases, large and mainly due to delineation difficulties on average CBCT (image quality or atelectasis) or breathing artefacts (duplication) on the 4D-CT.

## EP-2014 Decision Support System for Checking Online Adaptive Treatments on the Elekta Unity

D. McQuaid<sup>1</sup>, R. Niliwar<sup>1</sup>, J. Mohajer<sup>1</sup>, E. Goodwin<sup>1</sup>, S. Nill<sup>1</sup>, U. Oelfke<sup>1</sup>

<sup>1</sup>The Institute of Cancer Research and The Royal Marsden NHS Foundation Trust, Joint Department of Physics, Sutton, United Kingdom

*This abstract is part of the media programme and will be released on the day of its presentation*

### Purpose or Objective

Reproducible patient positioning and image guidance are crucial aspects for effective particle therapy. Proper immobilization of patients with limb-extremities tumors can be challenging and existing guidelines on this topic are not univocal.

The aim of this study is to analyze positional interfraction reproducibility of limb-extremities when multiple combinations of immobilization devices are used in particle therapy.

### Material and Methods

Data of 12 patients treated at our institute between 2014 and 2017 were retrospectively recorded. Patient, treatment and setup data are enlisted in Table 1.

**Table 1. Patient characteristics, treatment data and details on patient setup and immobilization devices used. \*NA= not available**

Patient and Treatment data							Patient Setup				
Gender (M/F)	Weight (Kg)	Age (years)	Histology	Site	Particle	Decubitus	N° point tattoos	Thermoplastic mask	AccuForm™ cushions	Foot rest/ Additional supports	
P1	F	71.0	61	Chondrosarcoma	Femur	Carbon Ion	Prone	3	body	60x60 cm	-
P2	F	NA	62	Osteosarcoma	Hip	Carbon Ion	Prone	4	body	40x60 cm	Combitrill™
P3	M	82.5	57	Musfibrosarcoma	Thigh	Carbon Ion	Prone	3	body	60x60 cm	Combitrill™
P4	M	82.6	17	Ewing's sarcoma	Tibia	Proton	Supine	5	body	60x60 cm	-
P5	M	77.4	56	Liposarcoma	Knee	Carbon Ion	Supine	3	body	40x60 cm	-
P6	M	76.0	59	Liposarcoma	Thigh	Carbon Ion	Supine	4	body	60x60 cm	Feettrill™
P7	M	68.0	51	Rabdomiosarcoma	Thigh	Carbon Ion	Supine	6	body	60x60 cm	ankle support
P8	M	NA	75	Chondrosarcoma	Hand	Carbon Ion	Prone	4	head	20x25 cm	hand support
P9	F	80.0	80	Desmoplastico melanoma	Arm	Carbon Ion	Supine	5	body	40x60 cm	Combitrill™+ Wingstep
P10	F	63.8	44	Leiomiomasarcoma	Shoulder	Carbon Ion	Lateral	5	body	60x60 cm	-
P11	M	66.8	33	Sarcoma MPNIT	Brachial plexus	Proton	Lateral	6	body	60x60 cm	-
P12	F	77.6	68	Sarcoma MPNIT	Brachial plexus	Carbon Ion	Lateral	4	body	40x60 cm	head/rest+ cushions

All patients were immobilized using multiple combinations of immobilization devices: personalized AccuForm™ cushions, thermoplastic mask hooked on an indexed plate plus, when needed, either foot or ankle rest or head support. Tattoos setup points were drawn on patient skin to provide a reference for daily positioning. Before treatment, patients were first aligned according to the skin tattoos using localization laser. Daily orthogonal x-ray images were acquired prior irradiation and patient setup correction vectors were assessed by 2D-3D image registration. The correction of the set-up errors was performed using a 6-degree robotic positioning system. Sperman's correlation coefficient was used to investigate correlation between patient data and correction vector. Analysis of variance (ANOVA) was performed to investigate the 3D correction vector across patients and treatment site (lower and upper limbs).

### Results

A total of 156 treatment fractions were analyzed. The distribution of interfraction correction vectors is shown in Figure 1 for each patient (P1, P2, .., P12) and for the whole population. Median (interquartile range) correction vector over all patients was -0.6 (4.1) mm in latero-lateral direction, 1.2 (5.0) mm in cranio-caudal direction, -3.0 (4.8) mm in antero-posterior while rotations around the above mentioned axis were -0.2 (1.0)°, 0.0 (0.8)°, 0.0 (0.7)° respectively.

### EP-2015 Interfraction setup error using multiple immobilization devices for limb-extremity particle therapy

R. Ricotti<sup>1</sup>, B. Tagaste<sup>1</sup>, A. Pella<sup>2</sup>, G. Fontana<sup>3</sup>, G. Elisei<sup>1</sup>, S. Tampellini<sup>4</sup>, M. Ciocca<sup>5</sup>, F. Valvo<sup>6</sup>, G. Baroni<sup>7,8</sup>

<sup>1</sup>Centro Nazionale di Adroterapia Oncologica CNAO, Clinical Department- Bioengineering Unit, Pavia, Italy ;

<sup>2</sup>Centro Nazionale di Adroterapia Oncologica CNAO, Clinical Department- Bioengineering Unit, Pavia, Italy ;

<sup>3</sup>Centro Nazionale di Adroterapia Oncologica CNAO, Clinical Department- Bioengineering Unit, Pavia, Italy ;

<sup>4</sup>Centro Nazionale di Adroterapia Oncologica CNAO, Clinical Department- RTTs Unit, Pavia, Italy ;

<sup>5</sup>Centro Nazionale di Adroterapia Oncologica CNAO, Clinical Department- Medical Physics Unit, Pavia, Italy ;

<sup>6</sup>Centro Nazionale di Adroterapia Oncologica CNAO, Clinical Department, Pavia, Italy ;

<sup>7</sup>Centro Nazionale di Adroterapia Oncologica CNAO, Clinical Department- Bioengineering Unit, Pavia, Italy ;

<sup>8</sup>Politecnico di Milano, Department of Electronics Information and Bioengineering, Milano, Italy

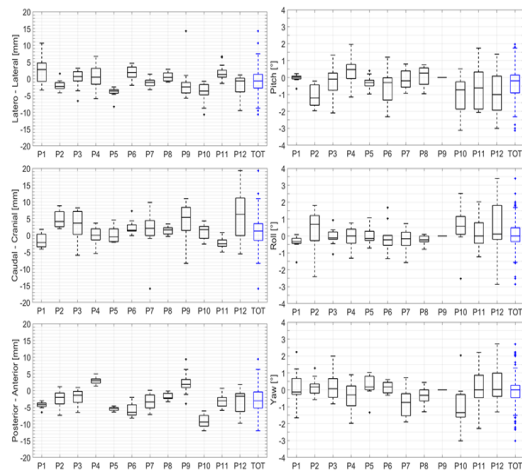


**Figure 1.** Distribution of correction vectors applied for each patient and over all patients (blue boxplot). According to clinical decision Patient 9 (P9) were positioned not applying rotations.

No correlation between the 3D translation correction vector and patient weight and age was found ( $r < 0.3$ ). No statistically significant difference between 3D correction vector in lower (P1-P7) and upper (P8-P12) limb was found ( $p$ -value=0.07) while it was significantly patient-dependent ( $p$ -value $<0.001$ ). **Conclusion**

The use of multiple combinations of immobilization devices for limb-extremities allowed for relatively small setup errors. This report might contribute to an Institutional standardization of limb-extremities positioning guidelines.

#### EP-2016 Evaluation of 4D cone beam CT-based dose calculation for SBRT lung cancer treatment

S. Bellefqih<sup>1</sup>, B. Benadon<sup>1</sup>, A. Roque<sup>1</sup>, N. Gaillot<sup>1</sup>, S. Servagi-Vernat<sup>1</sup>

<sup>1</sup>Institut Jean Godinot, Radiotherapy, Reims, France

#### Purpose or Objective

Stereotactic body radiation therapy (SBRT) has become a standard treatment for patients with medically inoperable early-stage non-small cell lung cancer (NSCLC). Daily image-guidance is crucial to ensure correct patient set-up prior to treatment delivery, with 3D-CBCT the conventional method used in image guidance. More recently, 4D-CBCT has been used to take into account tumor motion induced by respiration. Another potential use of 4D-CBCT is to determine the actual dose received by the tumor during treatment by using 4D-CBCT intra-fraction.

#### Material and Methods

This study included five patients treated with stereotactic body radiotherapy. Radiation treatments were delivered on an Elekta Versa HD linear accelerator. Prior to each radiotherapy treatment fraction, a 4D-CBCT was performed using XVI 4.5. Symmetry (from Elekta package of software solutions for IGRT). All translational errors were corrected prior to the treatment and then a 3D-CBCT was acquired to measure the residual error. Finally, a pre-treatment 4D-CBCT was acquired to verify intra-fraction motion. The intra fraction 4D-CBCT was used to delineate the GTV, and the ten GTV merged to form an ITV. A 5-mm margin was added to define a planning target volume (PTV). Finally, the initial plans were recomputed on the CBCT images using a patient specific stepwise curve (Hounsfield units to density). Internal target volumes (ITVs; D98%, D95%, D2%) were compared between simulation CT-derived treatment plans and 4D-CBCT-based plans.

#### Results

The ITV's volume was raised by an average of 26% [8.1%-44.6%]. The difference in ITV mean dose was 3.91% [0.2%-6.2%], D2% was 0.5% [0.2%-4.5%], D50% was 4.2% [1%-6.7%], D95% was 7.2% [3.3%-11.4%] and D98% was 8.3% [3.7%-12.1%]. Differences in dose distribution were less important for patients with less variation in volume of ITV

#### Conclusion

In this study 4D-CBCT based dose calculations was mainly affected by limited CBCT image quality. Improvement of CBCT image quality is necessary to accurate dose calculations.

#### EP-2017 GANs covert CBCT to CT for head-neck, lung and breast: paired vs unpaired; single-site vs generic

M. Maspero<sup>1</sup>, M.H.F. Savenije<sup>1</sup>, T.C.F. Van Heijst<sup>1</sup>, A.N.T.J. Kotte<sup>1</sup>, A.C. Houweling<sup>1</sup>, J.J.C. Verhoeff<sup>1</sup>, P.R. Seevinck<sup>1</sup>, C.A.T. Van den Berg<sup>1</sup>

<sup>1</sup>UMC Utrecht, Radiation Oncology, Utrecht, The Netherlands

#### Purpose or Objective

CBCT offers a representation of daily anatomy that may be used for online dose calculation and adaptation. However, dose calculations cannot be performed on CBCT due to lack of HU calibration, limited FOV and presence of image artefacts. This study investigates the use of generative adversarial networks (GANs) to convert CBCT into CT. Such networks allow very fast image conversion and thus facilitate online adaptation. However, CBCT to CT conversion using paired learning is problematic given the possible anatomical interscan differences breaking the "paired" (PA) assumption of data consistency. Here, we investigate the use of unpaired (UP) training, which obviates the need for consistent pairwise datasets (e.g. registered, anatomically matched) in the training. In this explorative study, we investigated the performance of PA vs UP learning and compared site-specific vs generic trained network.

#### Material and Methods

CBCTs of 88 patients diagnosed with head-neck (HN, 31), lung (29) and breast (28) cancer undergoing radiotherapy were rigidly registered according to the clinical procedure and resampled to the planning CT (XVI, Elekta). PA vs UP

To perform PA training, we used a conditional GAN (cGAN), while for UP training, we used a cycle-consistent GAN (cycleGAN). The two networks were trained in 2D transverse planes mapping CBCT to CT Hounsfield Units. For each anatomical site, the networks were trained on 15 patients (training set) and evaluated on the remaining patients (test set).

#### Single vs generic

To verify whether a single network could be used for all the patients independently of the anatomical site, we trained both the cGAN and the cycleGAN on the data of 45 patients.

Image comparison in terms of mean absolute error (MAE) and mean error (ME) in the FOV of the CBCT vs planning CT was performed on the test set for both the experiments.

#### Results

cGAN and cycleGAN training required about 1 and 5 days, respectively, on a GPU Tesla P100 (NVIDIA). Forward evaluation took about 20 s.

#### PA vs UP

For all the three sites, discontinuities between 2D transverse slices were more visible after PA compared to UP training (Fig1). In the case of UP training, some residual image artefacts were present in the transverse plane, especially for the breast cases. Mean MAE and ME were for UP and PA are reported in Fig2.

#### Single vs generic

For all the anatomical sites, training with all the patients resulted in mean MAE and ME within  $1\sigma$  respect to training on patients of each site (Fig2).

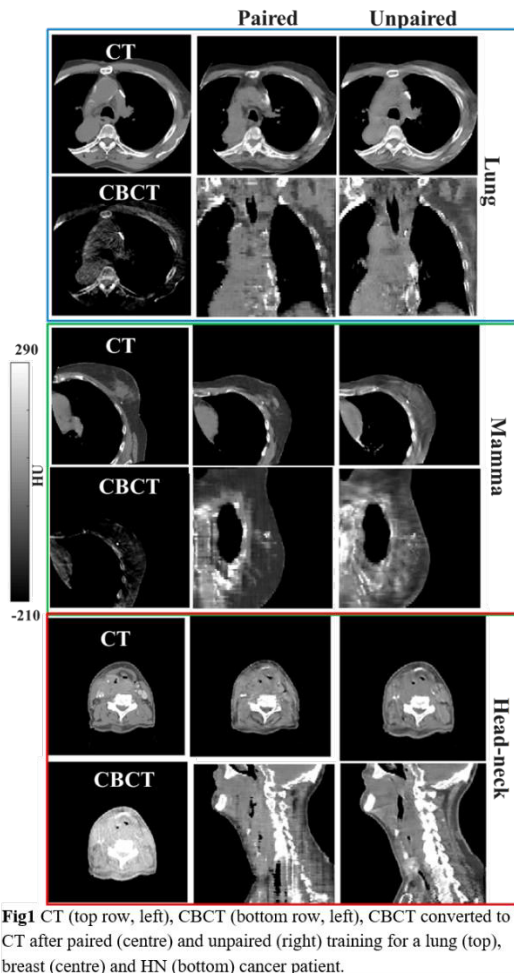


**Fig1** CT (top row, left), CBCT (bottom row, left), CBCT converted to CT after paired (centre) and unpaired (right) training for a lung (top), breast (centre) and HN (bottom) cancer patient.

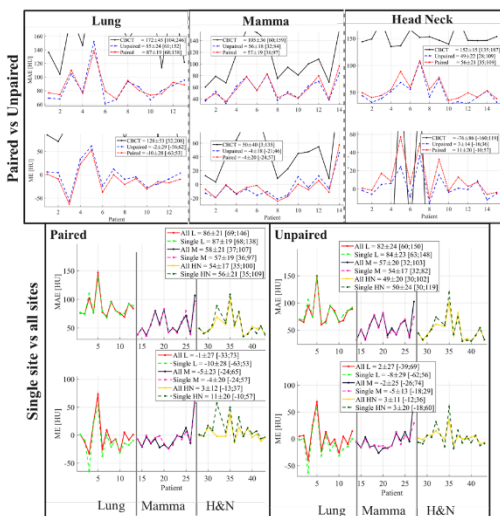


**Fig2** Top Mean absolute error (MAE, first row), and ME (mean error, second row) of original CBCT (black) paired wise translation of CBCT to CT (blue dashed), and unpaired conversion of CBCT to CT (red continuous). Bottom MAE (first row) and ME (second row) of the networks trained on all the sites (continuous lines) and single sites (dashed lines) for paired (left) and unpaired training (right) against CT. The insets display average  $\pm 1\sigma$  and range [min,max].

## Conclusion

Visually, UP training resulted in slightly better image quality although residual artifacts were present. Quantitatively PA and UP were comparable; however, a fundamental problem in the evaluation is the lack of a good reference considering that anatomical changes between CT and CBCT may have taken place. Investigations to verify the accuracy of dose calculations

is still needed to justify the use of GANs to enable CBCT-based dose calculations. In general, the use of a generic network for all the sites seems to be a viable option and the time necessary to convert CBCT into CT justifies the use of GANs for online ART.

**EP-2018 Actual delivered boost dose for gynecological cancer patients treated with image-guided IMRT**  
 S. Vieira<sup>1</sup>, M. Possanzini<sup>1</sup>, M. Silva<sup>1</sup>, J. Stroom<sup>1</sup>, C. Greco<sup>1</sup>  
<sup>1</sup>Fundação Champalimaud, Radiotherapy, Lisboa, Portugal

## Purpose or Objective

A phase I/II study of image-guided IMRT for intermediate and high risk endometrial cancer (EC) as brachytherapy replacement is ongoing in our department. The main rationale is to shape and deliver the high boost dose while overcoming the short range of brachytherapy sources without compromising normal tissue.

Our aim is to: (a) provide actual delivered dose for our endometrial and cervical cancer (CC) patients (pts) by non-rigidly deforming the planning CT (pCT) based on CBCT images acquired prior treatment delivery and (b) assess the applied CTV-PTV margins.

## Material and Methods

23 pts were included (14 EC and 9 CC). Patient set-up consisted of a rectal balloon, a vaginal cylinder and a full bladder (fig1). Intra-fraction motion was monitored by electromagnetic beacons (Calypso®) inserted in the vaginal cylinder (limiting beacon motion to <2mm). Operated pts received 3 fractions of 7.5-10.5Gy, non-operated 5 fractions of 4-5Gy after whole pelvis irradiation. For both schemes a CTV-PTV margin of 3mm was used. The 3 fraction scheme comprised of two dose levels: (1) 3x5-7Gy to PTV1 and (2) 3x7.5-10.5Gy to CTV2 (without PTV margin). VMAT boost treatment delivery included 4 arcs using 10MV FFF beams. Patient set-up was confirmed by CBCT on each fraction. The CBCT image acquired just prior to delivery of each treatment fraction served as reference for non-rigidly deforming the pCT using a structure guided multi-pass algorithm (Velocity® V3.2.0). Delineation of balloon, bladder, and vaginal cylinder on the CBCT improved deformation accuracy. Dose re-calculation (Eclipse™) was performed for each fraction on the reshaped pCT using the original plan parameters. The actual dose delivered was then obtained by inversely deforming dose map followed by a dose sum of all fractions. Fractions with obvious misfits after registration (bladder and rectal filling, cylinder placement) were rejected and replaced by worst-case fraction of the same patient. PTV coverage was evaluated for CTV-PTV margins review.

## Results

Planned and delivered doses are shown in Table1. Deformation acceptance rate was 93% and 73% for the 3 and 5 fractions scheme, respectively. Doses in the organs at risk (OAR) are within the constraints as defined in our protocol for both schemes, except for small bowel outliers due to poor CBCT image quality. All pts presented less PTV and CTV coverage than planned, as expected. For the 5 fraction scheme (cases without surgery), lower coverage was observed due to the OAR in the vicinity and larger tumor size ( $160 \pm 76cc$ ) as compared with the 3-fraction scheme ( $64 \pm 17cc$ ). Following the results shown for the 3-fraction scheme, a PTV margin of 3 mm was added to the CTV2 for new pts.

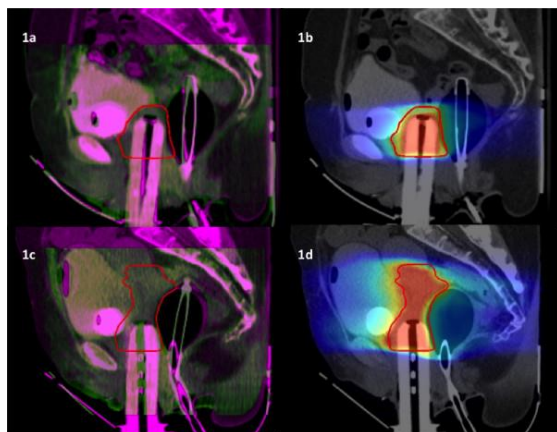


**Figure 1.** Sagittal view of two patients with a vaginal cylinder, rectal balloon and planning PTV (red). **1(a) and 1(c)** CBCT (green, without proper Hounsfield units) of one fraction overlaid on planning CT (purple), in treatment position. **1(b) and 1(d)** Measured dose map non-rigidly deformed overlaid on planning CT. **Upper images:** Patient 1 with CBCT-planning CT match leading to a CTV coverage difference between planned and measured of 0.5%; **Lower images:** Patient 2 with difficult patient set-up leading to a CTV coverage difference between planned and measured of 13.4%.

Table 1. Average dose planned and delivered for 23 patients. Delivered doses derived from CBCT anatomy for all fractions. Dose constraints as indicated in our clinical protocol. Data for the 3 and 5 fractions scheme is shown.

3 Fractions	Mean treatment	Mean planned	Dose volume constraints
D2cc Bladder wall (Gy)	15.7 ± 3.0	15.9 ± 3.0	V21.6 Gy/2cc
Dmax Small bowel (Gy)	5.5 ± 7.2	7.0 ± 10.0	Dmax = 80y (7.50y/fraction)
V PTV (%)	86.0 ± 6.3	99.8 ± 0.3	V15 or 21 Gy) ≥ 99%
V CTV1 (%)	96.8 ± 2.8	99.4 ± 2.2	V15 or 21 Gy) ≥ 99%
V CTV2 (%)	89.4 ± 10.8	99.6 ± 0.4	V22.5 or 31.5 Gy) ≥ 99%
D2cc Rectal wall (Gy)	16.2 ± 2.4	16.2 ± 2.6	V16.8 Gy < 2cc
5 Fractions	Mean treatment	Mean planned	Dose volume constraints
D2cc Bladder wall (Gy)	24.7 ± 1.6	24.9 ± 1.7	V25 Gy/2cc
Dmax Small bowel (Gy)	15.0 ± 6.5	7.5 ± 3.7	Dmax = 90Gy
V PTV (%)	58.8 ± 11.9	72.9 ± 11.0	V15 Gy) ≥ 99%
V CTV (%)	71.9 ± 14.2	82.0 ± 13.2	V15 Gy) ≥ 99%
D2cc Rectal wall (Gy)	19.6 ± 2.7	19.3 ± 1.2	V20.5Gy < 2cc

## Conclusion

Image-guided VMAT boost for gynecological cancer pts has been implemented. Patient set-up and CBCT image quality is a challenge for the low prognostic pts (5 fraction scheme). PTV margins used are adequate but evaluation of the added PTV margin to the 3 fraction scheme is needed.

## EP-2019 Does the use of an endorectal balloon improve seminal vesicle stability for prostate radiotherapy?

S. Chin<sup>1</sup>, A. McWilliam<sup>1,2</sup>, D. Brand<sup>1</sup>, S. Barton<sup>1</sup>, Y.P. Song<sup>1,2</sup>, M. Van Herk<sup>1,2</sup>, A. Choudhury<sup>1,2</sup>

<sup>1</sup>The Christie NHS Foundation Trust, Department of Radiotherapy Related Research, Manchester, United Kingdom ; <sup>2</sup>The University of Manchester, Division of Cancer Sciences, Manchester, United Kingdom

## Purpose or Objective

Endorectal balloons have been used for prostate immobilisation and rectal wall sparing during radiotherapy for prostate cancer. However, inter-fraction motion of the seminal vesicles (SVs) is larger than for the prostate, and reducing their motion may lead to improved target volume coverage and/or decreased rectal dose when SVs are included in the clinical target volume. In this study, we assessed whether the use of an endorectal balloon (ERB) improved stability of the SVs.

## Material and Methods

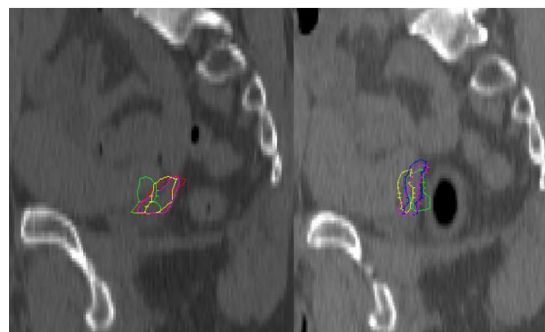
Ten patients undergoing radiotherapy for prostate cancer participated in a feasibility study of a RectalPro ERB filled with 100cc of air inserted at radiotherapy planning and 4 subsequent visits during treatment. SVs were contoured on the radiotherapy planning CT and subsequent cone

beam CTs (CBCT) with and without an ERB. SV stability was assessed by comparison of their displacement on CBCT compared to the radiotherapy planning CT by centre of mass, keeping the prostate aligned using soft tissue registration. Comparison of means and standard deviations were assessed using two-tailed unpaired t-tests and f-tests respectively.

## Results

34 and 37 CBCTs with and without ERB were assessed. Four patients were not able to complete all four pairs of cone beam CBCTs. Mean SV displacement without and with ERB for left-right direction was -0.6mm vs 0.6mm (p=0.070), superior-inferior -0.1mm vs -0.1mm (p=0.987) and anterior-posterior 0.7mm vs -0.3mm (p=0.476). Corresponding standard deviations of SV displacement without and with ERB were left-right 3.6mm vs 2.0mm (p=0.001), superior-inferior 2.8mm vs 2.0mm (p=0.132) and anterior-posterior 6.7mm vs 5.0mm (p=0.101). Seminal vesicles were more difficult to visualise on CBCT than radiotherapy planning CTs, especially with ERB in situ, and variation in ERB insertion angle affected positioning of pelvic soft tissue organs.

Seminal vesicle displacement	Endorectal balloon	Left-right	Superior-inferior	Anterior-posterior
Mean	Without	-0.6mm	-0.1mm	0.7mm
	With	0.6mm	-0.1mm	-0.3mm
Standard deviation	Without	3.6mm	2.8mm	6.7mm
	With	2.0mm	2.2mm	5.0mm



Left: Seminal vesicle positioning without endorectal balloon. Right: Seminal vesicle positioning with endorectal balloon.

## Conclusion

The insertion of an endorectal balloon for prostate radiotherapy improves stability of the seminal vesicles relative to the prostate. The largest seminal vesicle displacement is seen in the anterior-posterior direction. However, ERBs may impair soft tissue visualisation and alter soft tissue anatomy, so utilisation of daily image guided radiation therapy is recommended when ERBs are used.

## EP-2020 Assessment of treatment margins for breast radiotherapy evaluated using CBCT

S. Nørring Bekke<sup>1</sup>, C.F. Behrens<sup>1</sup>, F. Mahmood<sup>2</sup>

<sup>1</sup>Radiotherapy Research Unit, Department of Oncology-Herlev and Gentofte Hospital - University of Copenhagen, Herlev, Denmark ; <sup>2</sup>Research Unit for Oncology, Department of Clinical Research- University of Southern Denmark- Department of Oncology- Odense University Hospital, Odense, Denmark

## Purpose or Objective

In the clinical routine patients are often positioned based on planar x-ray images prior to irradiation in external beam breast radiotherapy. The objective of the present study was to find the treatment margins from a setup

based on planar kV-MV, in-room lasers or surface scans. The different setup techniques were evaluated using cone beam computed tomography (CBCT) as the ground truth.

#### Material and Methods

This prospective clinical trial included 39 patients, from which 102 treatment fractions were analysed. Patients were treated with deep inspiration breath-hold radiotherapy after breast conserving surgery, without lymph node involvement. The initial setup was based on in-room lasers and tattoo marks. A surface scan was acquired (Catalyst and Sentinel, from C-RAD Positioning AB, Uppsala, Sweden) followed by a CBCT scan. Lastly, the patient was moved to the planned treatment position based on anterior-posterior kV and tangential MV images (kV-MV), and treatment was delivered. In off-line analysis, the planned treatment position was found based on the acquired surface scans and on the acquired CBCTs scans (soft tissue, semi-automatic rigid registration in six degrees of freedom). The treatment position found from the CBCT scans were used as the ground truth. The CTV to PTV margins were calculated according to van Herk [1] using the systematic ( $\Sigma$ ) and random ( $\sigma$ ) errors between the different setup techniques (kV-MV, in-room lasers and surface scans) and the CBCT.

#### Results

CTV to PTV margin required to ensure dose coverage of the CTV were largest in the vertical direction for all setup techniques (Table 1). Overall the margins were smaller for patient positioning based on kV-MV compared to in-room lasers and surface scans. The margins were smaller in the lateral and vertical direction using surface scans compared to in-room lasers. Of the 102 treatment fractions, the number of treatment fractions with a setup error above 1 cm in either direction was 6, 4 and 1 for in-room lasers, surface scans and kV-MV, respectively.

Table 1

	$\Sigma$ [mm]	$\sigma$ [mm]	CTV to PTV margin [mm] ( $2.5\Sigma + 0.7\sigma$ ) [1]
<b>Planar x-rays (kV-MV)</b>			
Lateral	1.8	2.3	6.2
Longitudinal	2.0	2.7	6.8
Vertical	2.7	2.4	8.5
<b>Tattoos and in-room lasers</b>			
Lateral	3.5	2.5	10.6
Longitudinal	3.0	3.1	9.8
Vertical	4.3	3.0	12.8
<b>Surface scans</b>			
Lateral	2.7	1.9	8.0
Longitudinal	3.3	2.9	10.3
Vertical	3.3	2.5	10.1

#### Conclusion

The study shows that the CTV to PTV margin is smallest for a kV-MV setup and suggests that a CTV to PTV margin of 6, 7 and 9 mm should be applied in the lateral, longitudinal and vertical directions, respectively. The margins from the initial setup based on in-room lasers can be reduced in the lateral and vertical direction using surface scans; in the longitudinal direction the margins are similar.

[1] van Herk M, Remeijer P, Rasch C, et al. The probability of correct target dosage: Dose-population histograms for deriving treatment margins in radiotherapy. *Int J Radiat Oncol Biol Phys* 2000;47:1121-1135.

#### EP-2021 Commissioning and clinical implementation of dose accumulation and adaptive radiotherapy

K. Brock<sup>1</sup>, M. McCulloch<sup>1</sup>, G. Cazoulat<sup>1</sup>, A. Ohrt<sup>1</sup>, P. Balter<sup>1</sup>, H. Bahig<sup>1</sup>, S. Ping<sup>1</sup>, A. Mohamed<sup>1</sup>, H. Elhalawani<sup>1</sup>, B. Elgohari<sup>1</sup>, S. Frank<sup>1</sup>, J. Wang<sup>1</sup>, D. Rosenthal<sup>1</sup>, C. Fuller<sup>1</sup>  
<sup>1</sup>The University of Texas MD Anderson Cancer Center, Imaging Physics, Houston, USA

#### Purpose or Objective

Purpose/Objective: To commission a commercial deformable registration and dose accumulation system to

enable accurate and efficient adaptive radiotherapy for head and neck cancer patients.

#### Material and Methods

Material/methods: Patients treated on an IRB approved adaptive radiotherapy trial using weekly CT and MR and daily CBCT guidance were evaluated. The accuracy of a commercial deformable registration algorithm, using correlation coefficient and weighted Dirichlet energy, was evaluated for CT to CT and CT to CBCT DIR. For CT to CT DIR, 9 patients with mid-treatment repeat CT scans were obtained. Normal tissues were contoured on both images. The contours were propagated using DIR from the planning CT onto the mid-treatment CT and compared to the clinician drawn contours using the Dice similarity coefficient (DSC). The performance of the CT to CBCT DIR was evaluated relative to the CT to CT DIR, by rigidly registering the CBCT obtained the same day as the mid-treatment CT and copying the contours onto the CBCT. DIR was performed between the planning CT and the mid-treatment CBCT and the propagated contours were compared using DSC. The accuracy of dose calculation on the CBCT was evaluated by comparing the difference in the clinically relevant metrics between the dose calculated on the CT and the CBCT obtained on the same day. Dose accumulation was performed based on only weekly CTs and based on daily CBCTs. Differences in total accumulated dose over treatment was evaluated.

#### Results

Results: CT to CT DIR accuracy was evaluated for the brainstem, larynx, parotids submandibular glands, mandible and esophagus using DSC. The average DSC was 0.80 (SD 0.05), range: 0.73 (esophagus) to 0.91 (mandible). CT to CBCT registration accuracy was evaluated for 10 image pairs. The average DSC, relative to the CT to CT DIR, was 0.91 (SD 0.04), range: 0.89-0.94. Dose difference using CT or CBCT was evaluated for 10 image pairs based on the GTV, CTV, submandibular glands, larynx, mandible, and parotids. The average difference of clinical metrics was 0.6 cGy (SD 2.7 cGy) or 0.07% of the planned fraction dose (SD 2.7%). The maximum difference was 8 cGy, observed for a single image pair for the mean larynx dose. Based on daily CBCT dose accumulation, the average difference between the planned dose and the delivered dose for the targets was -170 cGy (SD: 51, range: -260 - -97) and for the normal tissues was -51 cGy (SD: 143 cGy, range: -277 - 181 cGy). For the target structures, the average difference between the dose accumulated using daily CBCT compared to weekly CT was 114 cGy (SD: 39 cGy, range: 55 - 180 cGy). For the normal tissues, the average difference between the dose accumulated using daily CBCT compared to weekly CT was 53 cGy (SD: 93 cGy, range: -101 - 175 cGy).

#### Conclusion

Conclusion: Dose accumulation is clinically feasible and can be used to guide adaptation to ensure target coverage and normal tissue sparing and to improve understanding of delivered dose and outcomes.

#### Electronic Poster: Physics track: Quantitative functional and biological imaging

#### EP-2022 Dose-dependent changes in T2w-MRI texture of obturator muscles after prostate cancer radiotherapy

E. Scalco<sup>1</sup>, T. Rancati<sup>2</sup>, A. Mastropietro<sup>1</sup>, A. Cicchetti<sup>2</sup>, B. Avuzzi<sup>3</sup>, R. Valdagni<sup>2,3,4</sup>, G. Rizzo<sup>1</sup>

<sup>1</sup>Istituto di Bioimmagini e Fisiologia Molecolare, CNR, Segrate Milano, Italy; <sup>2</sup>Fondazione IRCCS Istituto Nazionale dei Tumori, Prostate Cancer Program, Milano, Italy; <sup>3</sup>Fondazione IRCCS Istituto Nazionale dei Tumori, Radiation Oncology 1, Milano, Italy; <sup>4</sup>Università degli Studi di Milano, Department of Oncology and Hemato-oncology, Milano, Italy

### Purpose or Objective

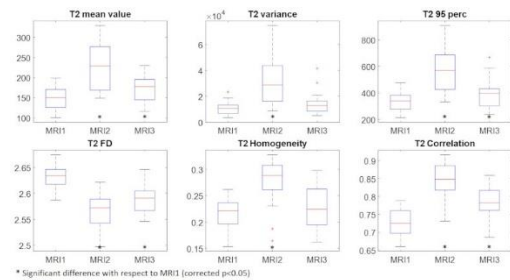
To investigate radiation-induced alterations in internal obturator muscles in prostate cancer patients treated with external-beam radiotherapy (RT), considering T2w-MRI images, acquired before treatment and at one and two years of follow-up.

### Material and Methods

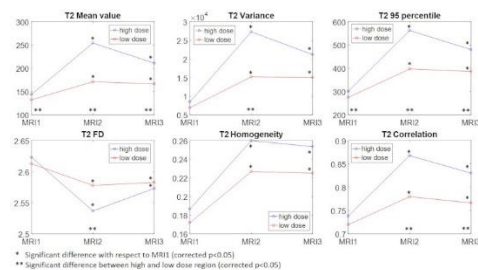
T2-weighted MRI were acquired in fourteen patients before RT (MRI1), about 12 months (MRI2) and 24 months (MRI3) of follow-up. Images were corrected for bias field inhomogeneities, normalized and spatially registered to automatically propagate obturators contours, which were manually delineated on MRI1. The following textural features were extracted: histogram-based indices (mean intensity, variance, 95<sup>th</sup> percentile, entropy, skewness, kurtosis), GLCM (Grey-Level Co-occurrence Matrix)-based indices (energy, correlation, homogeneity, entropy, contrast, dissimilarity), NGTDM (Neighborhood Grey-Tone Different Matrix)-based indices (coarseness, contrast, busyness, complexity, strength) and fractal dimension (FD). The dose map associated with the planning CT was deformed on each MRI and two regions were identified within the obturator: a high dose region (receiving >55 Gy) and a low dose region (receiving <55 Gy). To assess significant changes in internal obturator muscles, a comparison of the parameters extracted at each time point in the two regions was carried out by repeated-measure ANOVA and post-hoc t-test, with significant p-value < 0.05, after Bonferroni correction for multiple comparisons.

### Results

For several features (such as mean value, variance, 95<sup>th</sup> percentile, GLCM homogeneity and correlation, FD) it was found a significant increase or decrease at MRI2 and a gradual recovery at MRI3, in some cases still significantly different from MRI1 (see Figure 1).



Looking at regional results, different trends were found for the two regions. The high dose region presented highly different values at MRI2 with respect to MRI1 and a rapid but incomplete recovery at MRI3. The low dose region presented lower and less significant differences at MRI2, with respect to the high dose region, followed by a plateau at MRI3 (see Figure 2).



### Conclusion

In patients who underwent RT for prostate cancer treatment, a dose-dependent behaviour was observed regarding changes in T2w-MRI signal intensity and texture

of the internal obturator muscles. Specifically, the increased signal intensity and homogeneous pattern at MRI2, compatible with an inflammatory status, was more evident in the region receiving high dose. Two years after the end of RT, a relatively high recovery was observed in the high dose region, indicating a partial resolution of the inflammation; however, the plateau found in the low dose region may indicate that this altered status could not be completely recovered.

Other analyses at further time-points should be performed and correlations with genito-urinary toxicity scores should be investigated, considering the involvement of the pelvic floor muscles in the urinary dysfunctions.

### EP-2023 Predictive value of delta-radiomics features extracted from MR Images in image-guided liver SBRT

N. Dogan<sup>1</sup>, D. Asher<sup>1</sup>, B. Farnia<sup>1</sup>, C. Ford<sup>1</sup>, F. Yang<sup>1</sup>, L. Portelance<sup>1</sup>, G. Simpson<sup>1</sup>

<sup>1</sup>University of Miami- Sylvester Comprehensive Cancer Center, Department of Radiation Oncology, Miami-Florida, USA

### Purpose or Objective

With a projection of 600,000 deaths each year, liver cancer is a leading cause of cancer deaths worldwide and is very difficult to treat. A predictive model that could identify patients whose tumors are not responding to the treatment could be beneficial for improved personalized care. On-board MRI-guided radiotherapy which allows real-time tumor tracking presents a potential to utilize daily setup MR images to predict response and as well as safe dose escalation. The objective of this study was to determine the changes in image texture features (delta-radiomics) measured on daily low-field MR images and if delta-radiomics features could be used to assess treatment response and predict patient outcomes.

### Material and Methods

We conducted a retrospective analysis of ten patients with liver cancer treated with MR-guided SBRT (27 Gy to 50 Gy in 3 to 5 fractions). Radiomics features extracted from set-up images were acquired with an onboard 0.35 T MRI. The predictive capabilities of texture features extracted from daily set-up images for patients with liver lesions treated with SBRT were assessed using delta-radiomics which track changes in texture features through treatment. Five classes of texture features containing 42 features were extracted from the gross tumor volume (GTV). Gray-level Size Zone Matrix (GLSZM), Neighborhood Gray-level Difference Matrix (NGLDM), Gray-level Co-occurrence Matrix (GLCOM), and Gray-level Run Length Matrix (GRLRM) based features were selected. After extraction of texture features, the difference in feature value between first and last fraction set-up images was calculated. Patients were grouped into non-responders (three patients) who had local failure (disease progression) and responders (seven patients) who achieved local control. Patients were classified using follow-up PET images with modified RECIST criteria. The delta-radiomics features for each group were compared using Wilcoxon signed-rank test.

### Results

A univariate analysis identified three delta-radiomics texture features (*p*-value < 0.05) that were able to differentiate between responders and non-responders groups. The difference between dissimilarity (GLCOM), homogeneity (GLCOM), and busyness (GLNDM) features, was statically significant (*p*-value < 0.05) between the two groups. Entropy (GLCOM), complexity (GLNDM), and gray-level non-uniformity (GLSZM) features approached significance (*p* = 0.0874). No GRLRM or GLSZM features in the analysis were found to be significant.

### Conclusion

The ability to continually inform physician decisions during treatment would significantly advance the move towards personalized care. Delta-radiomics has the potential to

monitor patient response non-invasively during treatment, which could help inform physicians about whether a patient may require treatment adaption. This study demonstrated that three delta-radiomics texture features extracted from low-field MR images during SBRT in liver were able to differentiate between local disease control and local control failure.

**Table 1:** The table below displays the mean delta-radiomic texture features for each group of patients along with the standard deviation. Busyness, dissimilarity, and homogeneity were the only significant features selected, while entropy and complexity were trending towards significant.

Texture Feature	Responder (n=7)		Non-responder (n=3)		p-value
	Mean	STD	Mean	STD	
Busyness	0.05	0.09	-0.05	0.04	0.0167
Dissimilarity	1.25	2.01	-1.85	0.69	0.0304
Homogeneity	0.00	0.01	0.01	0.01	0.0167
Entropy	-0.09	0.22	0.62	0.74	0.0874
Complexity	-7933	36145	107588	141951	0.0874

### EP-2024 Assessment of ADC value when comparing two methods to reduce geometrical distortion in DWMRI

A. Lopez Medina<sup>1</sup>, A. Garcia<sup>1</sup>, C. Perez<sup>1</sup>, P. Montesinos<sup>2</sup>, I. Nieto<sup>3</sup>, A. Nieto<sup>4</sup>, V. Ochagavia<sup>3</sup>, M. Arias<sup>4</sup>, F.J. Salvador<sup>1</sup>, M. Salgado<sup>1</sup>, V.M. Muñoz<sup>3</sup>

<sup>1</sup>Hospital do Meixoeiro, Radiofisica y PR, Vigo Pontevedra, Spain ; <sup>2</sup>Philips Iberia, Healthcare, Madrid, Spain ; <sup>3</sup>Hospital do Meixoeiro, Radioterapia, Vigo Pontevedra, Spain ; <sup>4</sup>Complejo Hospitalario Universitario de Vigo, Diagnóstico por Imaxe, Vigo, Spain

#### Purpose or Objective

One of the most promising methods to determine tumor response during treatment using functional imaging is apparent diffusion coefficient (ADC), derived from diffusion-weighted imaging (DWI) in MRI. We investigate the use of reversed gradient (RG) algorithm in DWI for reduction in geometric distortion when using echo-planar imaging (EPI), and DWI using turbo spin echo (TSE) acquisition method, that reduces the distortion, but implies longer acquisition times. We compare the ADC values for water, ethanol and propanol using both methods and images for the phantom and for one patient from the HeNeBra project (continuation of ARTFIBio project).

#### Material and Methods

ADC was measured for RG corrected and original images of a specific phantom containing water, ethanol and propanol. The phantom (Fig. A) was scanned in a 3T Philips Ingenia magnet and for EPI images, b-values were set at 0, 50, 100, 200, 500 and 1000 s/mm<sup>2</sup>, reverting the phase encoding direction (AP: antero-posterior; PA: postero-anterior), while for TSE images, b values were: 0, 500, and 1000 s/mm<sup>2</sup>. Differences in b are because this protocol is being used in HeNeBra project to evaluate tumor response in radiotherapy patients during treatment (Fig. B) and compared results from ADC maps and PET/CT, and we wondered how acquisition method would influence in the obtained ADC. More b-values in TSE protocol are difficult to be considered, because its penalty in acquisition time.

#### Results

Figure shows how distortion is corrected by RG method in the phantom (Fig. A) and in the patient (Fig. B) and corrected RG images are similar to those obtained by TSE technique. Undistorted images (RG & TSE) from ADC maps and b=0 images can be compared with patient's PET/CT scan and the correspondence between the affected right node in all the image datasets is observed.

No significant difference in calculated ADC in water, ethanol and propanol for corrected and raw images of the phantom were observed, neither from EPI or TSE images. The table shows obtained mean values and one standard deviation from the images considering all the volumes. For low values of ADC, RG images have a greater variability

and associated standard deviation increases for ethanol and propanol. However, values from images are very close to expected values measured experimentally.

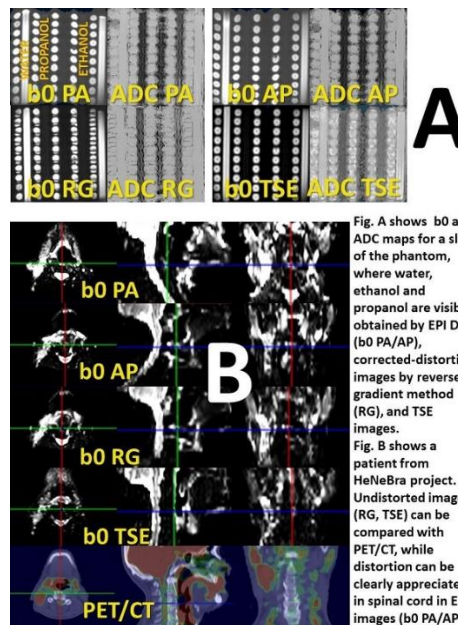


Fig. A shows b0 and ADC maps for a slice of the phantom, where water, ethanol and propanol are visible, obtained by EPI DWI (b0 PA/AP), corrected-distortion images by reversed gradient method (RG), and TSE images.

Fig. B shows a patient from HeNeBra project. Undistorted images (RG, TSE) can be compared with PET/CT, while distortion can be clearly appreciated in spinal cord in EPI images (b0 PA/AP).

	Water	Ethanol	Propanol
Measured diffusion Coefficient at 274,2 K (10 <sup>-9</sup> m <sup>2</sup> /s)	2,085	0,999	0,555
<small>Tofu, P. S. et al. 2000. Test liquids for quantitative MRI: measurements of self-diffusion coefficient in vivo. MR in Med 368-374.</small>			
<ADC> ± σ from DWI corrected by Reversed Gradients (10 <sup>-9</sup> m <sup>2</sup> /s)	2,20 ± 0,03	0,94 ± 0,28	0,56 ± 0,22
Difference respect to expected value	5,5%	-5,9%	0,9%
<ADC> ± σ from DWI corrected (Phase Encoding direction: AP) (10 <sup>-9</sup> m <sup>2</sup> /s)	2,21 ± 0,03	0,99 ± 0,19	0,56 ± 0,07
Difference respect to expected value	6,0%	-0,9%	0,9%
<ADC> ± σ from DWI corrected (Phase Encoding direction: PA) (10 <sup>-9</sup> m <sup>2</sup> /s)	2,18 ± 0,02	0,98 ± 0,10	0,56 ± 0,10
Difference respect to expected value	4,6%	-1,9%	0,9%
<ADC> ± σ from DWI obtained by TSE (10 <sup>-9</sup> m <sup>2</sup> /s)	2,15 ± 0,02	0,92 ± 0,09	0,51 ± 0,07
Difference respect to expected value	3,1%	-11,9%	0,9%

#### Conclusion

Both methods: RG from DWI-EPI and DWI-TSE can be used to evaluate ADC changes in the full range (0.555·10<sup>-9</sup> m<sup>2</sup>/s - 2.085·10<sup>-9</sup> m<sup>2</sup>/s) of the expected ADC changes of tumor during radiotherapy treatment and an important reduction of distortion can be observed in both cases, but the RG method introduces more noise in the final corrected image and can make more difficult to evaluate changes, especially in ADC range for tumors. Finally, we would like to highlight that if only ADC (not intravoxel incoherent motion) is used to evaluate tumor response and few values of b are required, TSE can be successfully used to measure the desired data.

Funded by ISCIII PI17/01735 grant (cofunded by FEDER).

### EP-2025 Predicting midtreatment FDG PET in head and neck cancer

Z. Gouw<sup>1</sup>, K. Lonning<sup>1</sup>, M.D. La Fontaine<sup>1</sup>, S. Van Kranen<sup>1</sup>, O. Hamming-Vrieze<sup>1</sup>, J. Van de Kamer<sup>1</sup>, A. Al-Mamgani<sup>1</sup>, J. Sonke<sup>1</sup>

<sup>1</sup>Netherlands Cancer Institute, Department of Radiation Oncology, Amsterdam, The Netherlands

### Purpose or Objective

There are multiple ways to improve radiation therapy for head and neck cancer. One is by dose painting, using the baseline FDG PET. Another is adaptive response assessment, using a midtreatment FDG PET scan. Good predictability of the midtreatment PET is a reason to pursue baseline dose painting. Contrary, if the midtreatment PET does add substantial new information, adaptive response assessment would need further investigation. Therefore, we evaluated the predictability of the midtreatment PET scan, using pretreatment information.

### Material and Methods

We analyzed 39 patients with squamous cell cancer of the oropharynx, oral cavity and hypopharynx. Patients were treated with radiotherapy with curative intent, in combination with cisplatin or Cetuximab. Pretreatment imaging consisted of planning CT, MRI and FDG PET/CT. Patients received a second FDG PET and CT during treatment. All scans were deformable registered to the midtreatment CT. A neural network was formed for a voxel based prediction of the midtreatment FDG PET within the gross tumor volume. We used the mean square error as a loss function. The input were the imaging modalities, dose and the marked variables in table 1. A 6-fold cross-validation was used to create the artificial PET scans (example in figure 1). We compared the real and artificial midtreatment  $SUV_{max}$ ,  $SUV_{mean}$  and the area encompassed by 50% of the  $SUV_{max}$  ( $SUV_{50\%}$ ). The dice coefficient between the 2  $SUV_{50\%}$  segmentations was calculated. Last, we expanded the artificial  $SUV_{50\%}$  or lowered the segmentation threshold to encompass the entire real  $SUV_{50\%}$ .

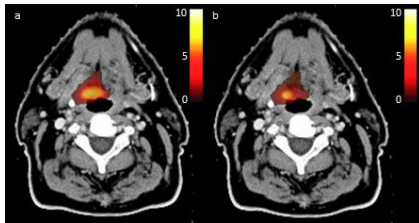


Figure 1. Patient with a cT4N2b base of tongue carcinoma. On the left is the planning CT with an overlay of the artificial midtreatment FDG PET. On the right an overlay of the real midtreatment PET. The colorbar represents range of SUV.

### Results

Patient and tumor characteristics are depicted in table 1. The artificial PET underestimated the real midtreatment  $SUV_{max}$ , the median difference was 3.4 points (interquartile range 4.1 points). The artificial PET underestimated the real  $SUV_{max}$  more when the real  $SUV_{max}$  increased (Pearson's  $r = 0.94$ ). The predicted  $SUV_{mean}$  was also lower, with a median difference of 2.2 points (interquartile range 2.7 points). The artificial  $SUV_{50\%}$  segmentations were larger, the median volume was 12.3 cc (interquartile range 15.1) vs 4.6 cc (interquartile range 4.7) for the real  $SUV_{50\%}$ . The median dice coefficient between the segmentations was 0.53 (interquartile range 0.18). To encompass the real  $SUV_{50\%}$ , the SUV threshold of the artificial scans had to be lowered till  $SUV_{38\%}$  (interquartile range of 15%) or a median expansion was needed of 3 mm (interquartile range 2 mm).

		n
Age (years)	average	59
	range	35-69
T-stage*	2	1
	3	14
	4	24
N-stage*	0	6
	1	7
	2	24
	3	2
Site	Oropharynx	33
	Oral cavity	4
	Hypopharynx	2
HPV-status*	Negative	15
	Positive	24
Concurrent systemic therapy*	Cisplatin	33
	Cetuximab	6
Days between PET and start RT*	average	13
	range	7-28
Fractions until midtreatment PET	average	8.5
	range	7-11

The variables marked \* are included in the neural network.

### Conclusion

This pilot study indicates that midtreatment PET scans can be partially predicted. Model improvements through increased sample size and modified loss functions are subject of further studies.

### EP-2026 Diffusion weighted textural differences between p16 positive and negative oropharyngeal carcinoma

S. Deschuymer<sup>1</sup>, V. Vandecaveye<sup>2</sup>, F. De Keyzer<sup>2</sup>, S. Nuyts<sup>1</sup>

<sup>1</sup>University Hospital Gasthuisberg, Radiotherapy, Leuven, Belgium ; <sup>2</sup>University Hospital Gasthuisberg, Radiology, Leuven, Belgium

### Purpose or Objective

To explore the feasibility and diagnostic performance of radiomic features (RF) based on diffusion weighted (DW) MRI in differentiating among p16 positive and negative oropharyngeal carcinoma (OPC).

### Material and Methods

Sixty-six patients with histologically proven OPC were prospectively analysed. OPC were considered p16 positive if more than 70% diffuse nuclear and cytoplasmic immunohistochemistry staining was present. 1.5 T MRI with echo-planar DW sequences at 6 b-values (0, 50, 100, 500, 750 and 1000 s/mm<sup>2</sup>) were acquired before treatment. The region of interest (ROI) encompassing the entire primary tumor volume was manually drawn on the apparent diffusion coefficient (ADC) map by an experienced head and neck radiologist.

One hundred and five RF (Table 1), including shape, size, first-order-histogram and textural analysis (TA), were extracted from the ROI with Pyradiomics software and were compared between p16 positive and p16 negative OPC with the two-tailed unpaired Student t-test. The significance threshold was set at a p-value of <0.05. In addition, receiver operating characteristic (ROC) curves were generated to determine the discrimination performance and the optimal cut-off value of the RF.

### Results

Fourteen (21%) tumors were p16 positive. A total of 34 RF were significantly different including volumetric parameters with smaller and more sphere shaped tumors

in the p16 positive group. There was no significant difference in ROI-based mean and minimum ADC value between p16 positive and p16 negative OPC (ADC<sub>mean</sub> = 1.11 ± 0.38 × 10<sup>-3</sup> mm<sup>2</sup>/s and 1.26 ± 0.57 × 10<sup>-3</sup> mm<sup>2</sup>/s, respectively, GLCM\_Joint\_Entropy, showed significant differences suggesting that p16 negative tumors are more heterogeneous than p16 positive tumors (Table 1\*). ROC curves of all significant RF were generated of which the volumetric parameters major\_axis and maximum\_3D\_diameter had the best AUC, both 0.80, followed by GLDM\_dependence\_non\_uniformity\_parameter (AUC=0.77). The optimal cut-off value of 6.78 mm 7.81 mm and 5.89 respectively, provided 80.3% accuracy for these three radiomic features.

	p16 Mean ± SD	p16+ Mean ± SD	p-value
<b>1. Volumetric (11 of 14 features)</b>			
Least Axis	4.39 ± 1.89	3.27 ± 1.27	0.0420
Major Axis	19.98 ± 5.62	8.50 ± 2.41	0.0005
Maximum 2D Diameter: Column	20.77 ± 5.25	6.82 ± 2.42	0.0084
Maximum 2D Diameter: Row	11.51 ± 6.58	6.70 ± 2.61	0.0078
Maximum 2D Diameter: Slice	15.85 ± 6.44	7.77 ± 2.40	0.0015
Maximum 3D Diameter	14.89 ± 6.60	8.71 ± 2.99	0.0013
Minor Axis	1.32 ± 0.67	9.24 ± 3.61	0.0189
Sphericity	0.68 ± 0.11	0.73 ± 0.08	0.0278
Surface Area	363.42 ± 305.39	146.41 ± 87.60	0.0111
Surface Volume Ratio	1.37 ± 0.40	1.33 ± 0.39	0.0359
Shape Volume	200.04 ± 489.05	113.97 ± 65.61	0.0937
<b>2. First Order (8 of 18 features)</b>			
Entropy	1.99 ± 0.61	1.82 ± 0.45	0.0375
Kurtosis	3.44 ± 2.81	2.78 ± 0.79	0.1919
Mean ADC	1.16 ± 0.37*10 <sup>-3</sup>	1.11 ± 0.38*10 <sup>-3</sup>	0.3595
Median ADC	1.26 ± 0.64*10 <sup>-3</sup>	1.07 ± 0.35*10 <sup>-3</sup>	0.2837
Minimum ADC	0.56 ± 0.33*10 <sup>-4</sup>	0.69 ± 0.34*10 <sup>-4</sup>	0.1868
Range	1.52 ± 0.90*10 <sup>-4</sup>	0.85 ± 0.62*10 <sup>-4</sup>	0.0449
Skewness	0.18 ± 0.67	0.17 ± 0.49	0.9002
Uniformity	0.31 ± 0.11	0.40 ± 0.13	0.0176
<b>3. GLCM: Gray Level Co-occurrence Matrix (9 of 23 features)</b>			
Correlation	0.26 ± 0.22	0.09 ± 0.17	0.0085
Joint Energy	0.14 ± 0.08	0.20 ± 0.12	0.0415
Joint Entropy	3.58 ± 1.10	2.88 ± 0.77	0.0289
Maximum Probability	0.24 ± 0.11	0.51 ± 0.16	0.0422
Sum Entropy	2.50 ± 0.77	2.01 ± 0.55	0.0292
<b>4. GLDM: Gray Level Dependence Matrix (4 of 14 features)</b>			
Dependence Entropy	3.12 ± 0.87	4.42 ± 0.70	0.0077
Dependence Non-Uniformity	30.49 ± 34.92	9.82 ± 5.37	0.0321
Large Dependence High Gray Level: Emphasis	934.19 ± 723.55	444.85 ± 345.65	0.0172
Low Gray Level: Emphasis	0.16 ± 0.13	0.24 ± 0.13	0.0311
<b>5. GLRLM: Gray Level Run Length Matrix (7 of 16 features)</b>			
Gray Level Non-Uniformity	70.89 ± 71.94	29.49 ± 21.39	0.0414
Gray Level Non-Uniformity Normalized	0.39 ± 0.10	0.36 ± 0.10	0.0483
Long Run Low Gray Level: Emphasis	0.34 ± 0.23	0.51 ± 0.33	0.0328
Low Gray Level Run Emphasis	0.16 ± 0.13	0.25 ± 0.13	0.0275
Run Entropy	1.97 ± 0.59	2.52 ± 0.43	0.0080
Run Length Non-Uniformity	178.13 ± 110.16	103.83 ± 50.97	0.0179
Short Run Low Gray Level: Emphasis	0.14 ± 0.11	0.21 ± 0.11	0.0320
<b>6. GLSZM: Gray Level Size Zone Matrix (4 of 16 features)</b>			
Gray Level Non-Uniformity	3.35 ± 3.98	2.62 ± 0.94	0.0139
Gray Level Non-Uniformity Normalized	0.23 ± 0.09	0.32 ± 0.09	0.0026
Low Gray Level: Zone Emphasis	0.25 ± 0.14	0.32 ± 0.11	0.0187
Zone Entropy	3.97 ± 0.93	2.82 ± 0.44	0.0050
<b>7. NGTDM: Neighboring Gray Tone Difference Matrix (0 of 4 features)</b>			
			NS

Table 1: Seven different classes of radiomic features. Between brackets ( ) the number of displayed features and the total number of investigated features is shown. P-value was calculated with the two-tailed unpaired Student's t-test; significant values are in bold. The asterisk \* indicates significant values specifying tumor hetero/homogeneity. SD=standard deviation, NS = Not significant

**Conclusion**

Evaluating the global primary tumor volume, we could not establish a significant difference in ADC value between p16 positive and p16 negative OPC. However, analysing the ADC based TA features at DW-MRI, there was a significant difference with p16 positive OPC having a more uniform and homogeneous distribution. Future research should investigate if these TA differences have a prognostic and predictive value and if they can be used in a DW-MRI based individualized treatment strategy.

**EP-2027 FDG-PET/CT-based assessment of hematologic toxicity in anal cancer patients following chemoradiation**

J. Kalsnes<sup>1</sup>, E. Rusten<sup>1</sup>, A. Abravan<sup>2</sup>, B.L. Rekstad<sup>1</sup>, E. Hernes<sup>3</sup>, M.G. Guren<sup>4</sup>, E. Malinen<sup>5</sup>

<sup>1</sup>Oslo University Hospital, Department of Medical Physics, Oslo, Norway; <sup>2</sup>The University of Manchester, Division of Cancer Sciences, Manchester, United Kingdom; <sup>3</sup>Oslo University Hospital, Department of Radiology and Nuclear Medicine, Oslo, Norway; <sup>4</sup>Oslo University Hospital, Department of Oncology, Oslo, Norway; <sup>5</sup>University of Oslo, Department of Physics, Oslo, Norway

**Purpose or Objective**

The standard treatment of concurrent chemoradiotherapy (CRT) for anal cancer patients is known to cause high rates of severe haematologic toxicity (HT) such as lymphopenia. HT is associated with longer treatment times and/or reduction in chemotherapy dose, and may lead to

suboptimal treatment outcome. Previous studies have hypothesized that irradiation of active bone marrow (ABM), as defined by [<sup>18</sup>F]fluorodeoxyglucose (FDG)-PET, is the principal radiation-induced cause of HT, but the results have been inconclusive. This study tests the same hypothesis on a larger patient cohort than the previous studies.

**Material and Methods**

84 patients with anal squamous cell carcinoma were included. All patients underwent a FDG-PET scan prior to curative CRT. Lymphocyte counts were collected during and after treatment on a weekly to monthly basis. Lymphopenia was defined as lymphocytes nadir (LN) lower than 0.5 × 10<sup>9</sup> cells/L (≥ grade 3, CTCAE v5.0). The pelvic bones from the top of the iliac crest to 1-2 cm below the lesser trochanter of femur, as defined by CT, was used as a surrogate for total bone marrow (TBM). ABM<sub>x</sub> was defined as the subvolume of TBM that exhibited the X% highest FDG-uptake, respectively (Figure 1). Median dose to the volumes was calculated. Linear and logistic regression were used to assess the correlation between dose to BM and LN and lymphopenia, respectively. The bootstrap technique was used to generate 95% confidence intervals (CI) for model comparison.

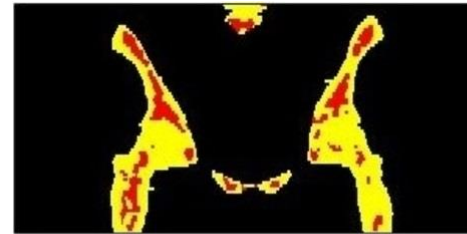


Figure 1: Delineation of ABM<sub>25</sub>. ABM<sub>25</sub> is the subvolume of TBM with the highest 25% FDG-uptake. Red = ABM<sub>25</sub>, yellow = TBM-ABM<sub>25</sub>. Abbreviations: ABM = active bone marrow, TBM = total bone marrow, FDG = [<sup>18</sup>F]fluorodeoxyglucose.

**Results**

Median lymphocytes nadir was 0.3 × 10<sup>9</sup> cells/L (range; 0.0 - 0.8 × 10<sup>9</sup> cells/L). Table 1 shows results from univariate linear regression analyses. All dose metrics were significantly associated with LN (p < 0.001). The model with the highest r<sup>2</sup> was that for ABM<sub>25</sub>, but 95% CIs for adjusted r<sup>2</sup> were [0.03, 0.28] and [0.07, 0.44] for TBM and ABM<sub>25</sub>, respectively, showing that the best ABM model was not superior to the TBM model. Lymphopenia occurred in 71 (85%) patients. The incidence of lymphopenia was associated with median dose to TBM, ABM<sub>75</sub>, ABM<sub>50</sub>, ABM<sub>25</sub> and ABM<sub>10</sub> (p < 0.05), with ABM<sub>75</sub> being the strongest predictor. Bootstrapping gave log-likelihood 95% CIs of [-36.6, -15.7] and [-35.0, -13.7] for TBM and ABM<sub>75</sub>, respectively, showing that the best ABM model did not significantly outperform the TBM model.

Table 1: Univariate linear regression with lymphocytes nadir (x10<sup>9</sup> cells/L) as response variable and median dose (Gy) to bone marrow volume as predictor variable.

Dosimetric parameter	β	95% CI	p value	Adjusted R <sup>2</sup>
TBM	-0.010	[-0.016, -4.5e-3]	5.9e-4	0.124
ABM <sub>75</sub>	-9.0e-3	[-0.013, -5.1e-3]	1.3e-5	0.199
ABM <sub>50</sub>	-8.1e-3	[-0.011, -4.8e-3]	4.7e-6	0.217
ABM <sub>25</sub>	-7.4e-3	[-0.010, -4.6e-3]	1.2e-6	0.242
ABM <sub>10</sub>	-6.0e-3	[-8.5e-3, -3.5e-3]	6.8e-6	0.210

Abbreviations: TBM = total bone marrow, ABM<sub>x</sub> = subvolume of TBM that exhibited the X% highest FDG-uptake, β = regression coefficient, CI = confidence interval, FDG = [<sup>18</sup>F]fluorodeoxyglucose.

**Conclusion**

Irradiation of pelvic bone marrow was associated with risk of developing lymphopenia following treatment. However, models using ABM, defined by FDG uptake, did not significantly improve model performance compared to models using TBM. One reason for this might be the strong

correlation between median dose to TBM and ABM (Pearson's  $r = 0.78$  between TBM and ABM<sub>25</sub>). In future works a clinical trial can be considered where one group is treated according to standard clinical practice and the other with an ABM sparing dose plan. This will reduce the correlation between TBM and ABM volumes, making it easier to evaluate the predictive power of FDG-PET-based models for HT.

**EP-2028 Pilot study: Textural features of mpMRI for response assessment in prostate cancer patients**  
M. Daniel<sup>1,2</sup>, P. Kuess<sup>1,2</sup>, P. Andrzejewski<sup>3</sup>, T. Nyholm<sup>4</sup>, G. Goldner<sup>1</sup>, M. Heilmann<sup>1</sup>, T. Helbich<sup>2</sup>, S. Polanec<sup>2,5</sup>, P. Baltzer<sup>2,5</sup>, D. Georg<sup>2</sup>

<sup>1</sup>Medical University of Vienna, Department of Radiation Oncology, Vienna, Austria ; <sup>2</sup>Medical University of Vienna, Christian Doppler Laboratory for Medical Radiation Research for Radiation Oncology, Vienna, Austria ; <sup>3</sup>EBG MedAustron GmbH, Medical Physics, Wr. Neustadt, Austria ; <sup>4</sup>Umeå University, Department of Radiation Sciences, Umeå, Sweden ; <sup>5</sup>Medical University of Vienna, Department of Biomedical Imaging and Image-Guided Therapy, Vienna, Austria

**Purpose or Objective**

Multiparametric (mp)MRI is a well-established tool for response assessment in radiation oncology. In view of the upcoming analytical methodology of radiomics, the potential of Haralick textural features (TF) in the context of response assessment has so far not been fully explored. The aim of this study is thus to investigate the added value of Haralick textural features for response assessment in prostate cancer (PCa) radiotherapy.

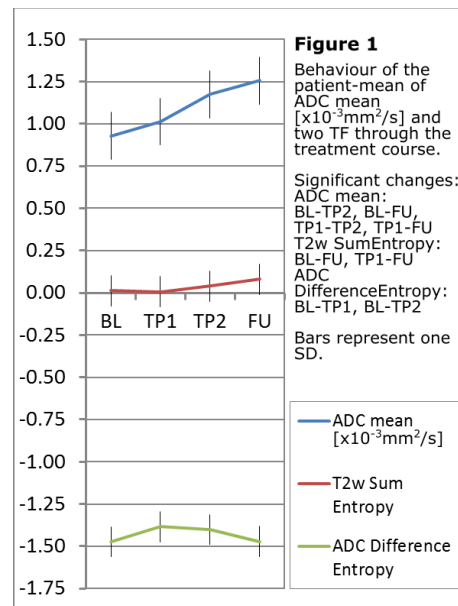
**Material and Methods**

21 PCa patients were enrolled in this longitudinal prospective IRB approved response assessment study, consisting of mpMRI at four time points (TP): at baseline (BL), in week 2 of treatment (TP1), in week 4 of treatment (TP2) and 3 months after end of EBRT as follow up (FU). Inclusion criteria were biopsy proven primary PCa, external beam radiotherapy (EBRT) and no contraindications to MRI. mpMRI was performed on a 3T scanner (MAGNETOM® Trio Tim, Siemens). For TF analysis T2-weighted (T2w) and apparent diffusion coefficient (ADC) MRI data were used.

Data collection of seven patients could be completed so far. The preliminary results are based on these 7 full datasets. The tumour lesion was delineated by an experienced radiologist on the BL T2w image dataset. The lesion was propagated to the other TP via rigid registration of the T2w images. Manual adaptations were performed on both T2w and ADC images in cases of tumour shrinkage, image distortions or artefacts caused by air in the rectum or movement. Both image datasets were normalized. Mean T2w and ADC values were extracted. After histogram equalization, 20 grey level invariant Haralick TF [1] were calculated for each modality. Data handling, visualization, image registration, pre-processing and feature extraction were carried out using MICE Toolkit® (© 2018 NONPI Medical AB). All features were tested for significant changes between TP with a Student's t test. **Results** Mean T2w grey level did not change significantly between TP. In total, for five T2w and 13 ADC TF significant changes could be identified during or after EBRT. Significance levels of the corresponding TF and the mean ADC for  $p < 0.05$  are presented in table 1 for each pair of TP. For better comparability, the behaviour of mean ADC, T2w SumEntropy and ADC DifferenceEntropy is plotted in figure 1.

T2w	BL	BL	BL	TP1	TP1	TP2
	TP1	TP2	FU	TP2	FU	FU
mean						
Entropy					0.05	
Correlation	None	None		None	0.001	None
SumEntropy			0.04		0.007	
InformationMeasureOfCorrelation1			0.02			
InformationMeasureOfCorrelation2			0.02			
ADC	BL	BL	BL	TP1	TP1	TP2
	TP1	TP2	FU	TP2	FU	FU
mean		0.01	0.01	0.04	0.02	
InverseDifference	0.01					
Entropy	0.02					
Energy	0.05					
DifferenceVariance	0.04	0.001				
DifferenceEntropy	0.02	0.005				
Contrast	0.02	0.005				
Homogeneity	0.02	0.007				None
Dissimilarity	0.01	0.04				
DifferenceAverage	0.01	0.04				
ClusterShade		0.03				
SumAverage			0.02			
Autocorrelation			0.03			
SumEntropy				0.05		

**Table 1** Significant changes of T2w and ADC TFs for each pair of time points. Non-significant TF are not listed.  $p < 0.01$  is highlighted as bold.



Nine ADC TF showed very early changes already in the second week of treatment (TP1). Three T2w features and two ADC features (SumAverage and Autocorrelation) differed significantly with respect to FU. Correlation to clinical outcome was not assessed in the scope of this preliminary analysis, but will be part of the final evaluation.

**Conclusion**

This pilot study demonstrated that T2w and ADC TF of PCa lesions change during EBRT. The results might suggest that some TF reflect very early response mechanisms while others could aid mid-term response assessment. These primary findings motivate further analysis of the remaining patient datasets.

**EP-2029 Principal component analysis for quantitative and robust analysis of dynamic PET/MR imaging data**

R. Winter<sup>1</sup>, S. Leibfarth<sup>1</sup>, S. Boeke<sup>1,2</sup>, P. Mena-Romano<sup>1</sup>, M. Krueger<sup>3</sup>, E. Cumhur Sezgin<sup>2</sup>, G. Bowden<sup>3</sup>, J. Cotton<sup>3</sup>, B. Pichler<sup>3,4</sup>, D. Zips<sup>2,4</sup>, D. Thorwarth<sup>1,4</sup>

<sup>1</sup>University Hospital Tübingen, Radiation Oncology-Section for Biomedical Physics, Tübingen, Germany ; <sup>2</sup>University Hospital Tübingen, Radiation Oncology, Tübingen, Germany ; <sup>3</sup>Werner Siemens Imaging Center, Preclinical Imaging and Radiopharmacy, Tübingen, Germany ; <sup>4</sup>German Cancer Consortium DKTK- partner

site Tübingen, and German Cancer Research Center DKFZ, Heidelberg, Germany

### Purpose or Objective

To investigate principal component analysis (PCA) as an alternative strategy to pharmacokinetic modelling for quantitative and more robust analysis of dynamic PET or contrast-enhanced (DCE) MRI data on a voxel level.

### Material and Methods

In 31 immuno-deficient nude mice, five different ectopic head and neck squamous cell carcinoma xenografts (subcutaneous, hind leg) were investigated with simultaneous PET/MRI (7T, Bruker Biospec). Tumor radiation sensitivity, i.e., tumor control dose 50% (TCD<sub>50</sub>) to clinically relevant irradiation with 30 fractions in 6 weeks have been previously published [1]. The imaging protocol included dynamic FMISO-PET over 90 min, T2-weighted (T2w) MRI and DCE T1-weighted MRI (750 s, 139 frames).

Tumor tissue was delineated on T2w MRI data. Necrotic tissue was excluded based on DCE-MRI information (low temporal median enhancement). The Brix model was fitted to the DCE-MRI tumor data on the voxel level. Standard deviations (SD) obtained from the fit covariance matrix were used to estimate the robustness of the fit parameters.

For PCA, DCE signal data  $S(t)$  was converted to relative signal increase  $RSI(t) = (S(t) - S_0) / S_0$ , where  $S_0$  represents the mean signal before contrast agent injection. PCA was then applied to the RSI data of the total set of tumor voxels of all animals.

Finally, parameter maps were calculated for both Brix and PCA. For each map, different thresholds were tested to identify volume fractions that would allow for stratification in terms of TCD<sub>50</sub>.

### Results

DCE-derived Brix parameters presented with highly varying SDs resulting in large fit inaccuracies on the voxel level.  $A_{Brix}$  was found to be more robust than  $K_{ep}$ . However,  $35 \pm 14\%$  of the voxels within a tumor (mean  $\pm$  SD over all tumors) showed a relative SD of  $A_{Brix}$  greater than 0.3. Both visual and mathematical examination of voxel curve data indicated that PCA allows for dimensionality and noise reduction in the recorded DCE data. Reconstructing the data with just the first two principle components reduced the number of variables extremely (139 time points) while most of the temporal information was still captured. Further principal components seem to rather depict noise (Figure 1). The percentage of the total variability expressed by the principal components PC1 to PC5 was 94.22, 1.95, 0.18, 0.11 and 0.10%, respectively. In a first analysis, similar results were found for PCA of dynamic FMISO-PET data.

Threshold-based analysis of parameter maps indicated that the relative volume presenting with  $PC2 < -0.12$  correlates with TCD<sub>50</sub> (Figure 2). No such correlation was found for Brix parameters, other principal components, or any mean parameter values.

### Conclusion

PCA may be a more robust alternative to pharmacokinetic modelling for the analysis of functional image data on a voxel level and may reveal relevant information e.g. in terms of prediction of tumor response to therapy. Further investigation of PCA on patient data seems promising. [1] Yaromina et al., Radiother Oncol 96:116 (2010)

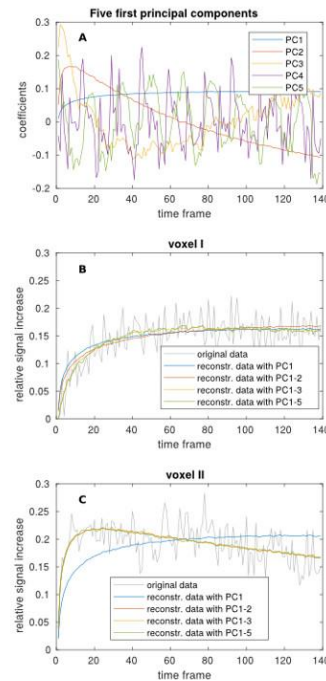


**Figure 1:** PCA on DCE RSI data. A: Five first principal components in descending order of component variance. B, C: The accuracy of data reconstruction with principal component coefficients is demonstrated for two different tumor voxels by successively increasing the number of principal components.

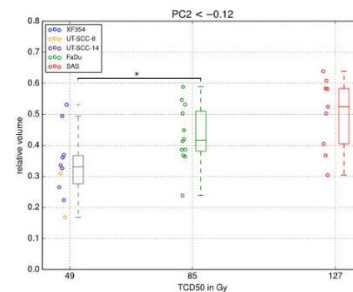


**Figure 2:** Relative volume of  $PC2 < -0.12$  seems to correlate with radiation sensitivity (TCD<sub>50</sub>) of the different tumor models. A Wilcoxon rank sum test was used for statistical analysis. Note that the one FaDu and one SAS tumors with volume fractions  $\leq 0.3$  were much smaller in size ( $< 600$  voxels) compared to the rest of the ensemble (mean  $\pm$  SD:  $1938 \pm 721$  voxels).

**Acknowledgements:** Research has received funding by the European Research Council (ERC).

### EP-2030 Multiparametric MRI and FMISO PET in HNSCC and its relation with outcome

N. Wiedenmann<sup>1,2</sup>, H. Bunea<sup>1,2</sup>, H. Rischke<sup>1,2</sup>, A. Bunea<sup>1,2</sup>, N.H. Nicolay<sup>1,2</sup>, L. Majerus<sup>1</sup>, L. Biela<sup>3</sup>, A. Protopopov<sup>3</sup>, U. Ludwig<sup>2,3</sup>, M. Büchert<sup>2,3</sup>, C. Stoykova<sup>2,4</sup>, M. Mix<sup>2,4</sup>, M. Bock<sup>2,3</sup>, A. Grosu<sup>1,2</sup>

<sup>1</sup>University of Freiburg, Department of Radiation Oncology- Medical Center University of Freiburg, Freiburg, Germany; <sup>2</sup>German Cancer Research Center DKFZ- German Cancer Consortiumion DKTK, Partner Site Freiburg, Heidelberg, Germany; <sup>3</sup>University of Freiburg, Department of Radiology- Medical Physics- Medical Center University of Freiburg, Freiburg, Germany; <sup>4</sup>University of Freiburg, Department of Nuclear Medicine- Medical Center University of Freiburg, Freiburg, Germany

### Purpose or Objective

Purpose of the current study was to assess the effect of radiochemotherapy (RCT) on tumour hypoxia assessed by <sup>18</sup>F-misonidazole PET/CT (FMISO PET) and on multiparametric (mp) MRI parameters in HNSCC at an early (week 2) and late (week 5) time point during treatment and to analyse the relation between mpMRI and PET parameters with local control.

### Material and Methods

Thirty-four patients with stage III to IVb HNSCC (UICC 7th edition) undergoing definitive RCT (total dose 70 Gy, 3 cycles of cisplatin administered over 7 weeks) were included in this study. Patients were prospectively imaged with <sup>18</sup>F-FDG PET/CT at baseline and with serial FMISO PET and serial 3 Tesla mpMRI for T1w-, T2w-TSE, dynamic contrast enhanced (DCE) perfusion measurements ( $k_{trans}$ ,  $v_e$ ) and diffusion weighted measurements (DWI) including apparent diffusion coefficient (ADC) maps in weeks 0, 2 and 5. Gross tumour volumes for tumour (GTV-T) and normal tissue (NT) were contoured. For MRI and FMISO PET analysis, mean values and SUVmax were obtained within GTV-T and NT. Patients were identified as responders or non-responders during follow-up. SUVmax FMISO PET and mean values for mpMRI parameters at weeks 0, 2, and 5 were compared between responders and non-responders with the t-test at a significance level of  $p \leq 0.05$ .

### Results

20 patients met inclusion criteria for image analysis by presenting a complete set of serial FMISO PET data and serial 3T MRI data. Mean follow-up time was 9.5 months. 11 patients were diagnosed with local recurrence. For GTV-T, responders showed less tumour hypoxia on FMISO PET than non-responders for weeks 0 and 2 (SUVmax=2.15±0.39 vs. 2.48±1.28 and 1.95±0.39 vs. 2.05±0.39,  $p > 0.05$ ). Baseline tumour volume was larger for non-responders than for responders (54.4±57.5ml vs. 31.0±15.1ml,  $p > 0.05$ ) and decreased at week 5 to 25.3±36.3 ml vs. 13.6±9.4 ml,  $p > 0.05$ . On mpMRI, tumour apparent diffusion coefficient ADC increased over time for both responders and non-responders from week 0 to 5. The increase was higher for responders than non-responders (51.1% vs. 5.7%,  $p = 0.094$ ). The volume transfer constant  $k_{trans}$  increased from week 0 to 5 for both responders and non-responders. The increase was higher for non-responders than responders (27.4% vs. 11.3%,  $p > 0.05$ ) and differed in pattern, as for non-responders the increase in  $k_{trans}$  reached a maximum at week 2 and then dropped, while for responders a steady increase in  $k_{trans}$  was found until week 5 (non-responders vs. responders (week 2 to 5:  $-0.107 \text{ min}^{-1}$  vs.  $+0.021 \text{ min}^{-1}$ ). Interstitial space volume fraction  $v_e$  was increased between week 0 and 5 by 37.8% for responders vs. 27.1% for non-responders,  $p > 0.05$ .

### Conclusion

Tumour volume and FMISO-PET-derived tumour hypoxia were higher among patients with local relapse as compared to locally controlled patients ( $p > 0.05$ ). DCE parameters  $k_{trans}$  and  $v_e$  and DW parameter ADC differed between relapsing and non-relapsing patients, however without reaching statistical significance in this cohort. Further studies are ongoing.

### EP-2031 <sup>18</sup>F-Choline-PET-CT to guide simultaneous integrated boost in prostate cancer

R. Pearson<sup>1</sup>, R. Samuel<sup>2</sup>, H. McCallum<sup>3</sup>, J. Frew<sup>3</sup>, E. Howell<sup>4</sup>, R. Maxwell<sup>4</sup>

<sup>1</sup>Newcastle University, Northern Institute for Cancer Research, Newcastle upon Tyne, United Kingdom ; <sup>2</sup>Leeds Cancer Centre, Dept of Clinical Oncology, Leeds, United Kingdom ; <sup>3</sup>Newcastle upon Tyne Hospitals NHS Foundation Trust, Northern Centre for Cancer Care, Newcastle upon Tyne, United Kingdom ; <sup>4</sup>Newcastle University, Centre for In Vivo Imaging, Newcastle upon Tyne, United Kingdom

### Purpose or Objective

<sup>18</sup>F-fluorocholine positron emission tomography (PET-CT) has an established role in detecting recurrent prostatic carcinoma but is not routinely used to guide radiotherapy delineation in the UK. Radiotherapy dose escalation to a boost volume has potential to improve tumour control and is the focus of current research protocols using MRI. A suitable boost volume may be defined as <50% of the total prostate volume on MRI, however quantitative PET may

also hold utility in defining targetable boost regions. The aim of this study was to evaluate the feasibility of defining a deliverable simultaneous integrated boost (SIB) to a dominant intraprostatic lesion (DIL) in the context of intensity modulated radiotherapy using automated thresholding of <sup>18</sup>F-fluorocholine PET within a radiotherapy treatment planning system.

### Material and Methods

Five prostate cases were selected. All patients had high risk prostate cancer and were on androgen deprivation therapy. DILs were defined automatically by 60%, 70% and 80% of maximum prostatic uptake of <sup>18</sup>F-fluorocholine on PET-CT using the RayStation 7 Treatment Planning System. A comparison of prostate gross tumour volumes (GTV), planning target volumes (PTV) and SUVmetrics between DIL and prostate gland was undertaken. PTVprostate was defined on MRI/CT as whole prostate GTV plus 5mm, (posterior margin 3mm). PTV DIL was defined as GTV plus 3mm. Median values for PTVs with ranges are reported.

### Results

Median SUVmax of prostate gland was 8.5 (range 4.9 - 18.1). All patients had Gleason 9 disease. Median prostate GTV was 44.6 cm<sup>3</sup> (range 21.0 - 73.4 cm<sup>3</sup>). Median GTV for DIL defined by 60% SUVmax was 9.2 cm<sup>3</sup> (range 2.6 - 24.9 cm<sup>3</sup>) accounting for 16% of the prostatic GTV (range 6 - 33.9%). Median GTV for DIL defined by 70% SUVmax was 4.4 cm<sup>3</sup>, 8.2% of prostatic GTV (range 2.9 - 17.2). Median DIL defined by 80% SUVmax was 1.5 cm<sup>3</sup>, 2.7% of prostatic GTV (range 0.4 - 5.9%).

Region of Interest	Median volume cm <sup>3</sup> (range)	Median % prostate (range)	volume PTV
PTV prostate (manual)	83.2 (45.6 - 124.6)	-	-
60% SUVmax (automated PTV)	13 (8.6 - 46.2)	18.9 (8.5 - 37)	
70% SUVmax (automated PTV)	7.9 (4.7 - 31.1)	10.3 (5.4 - 24.9)	
80% SUVmax (automated PTV)	3.8 (1.2 - 15.6)	4.5 (2.6 - 16)	

### Conclusion

DIL defined using automated thresholding of 60% and 70% of SUVmax was technically feasible using readily available treatment planning software. 60% of SUVmax defined a suitable boost volume with DILs <50% of the total prostate volume. The impact of this metric on organ-at-risk constraints in the context of dose escalation is being studied in a larger cohort. Ongoing work is examining how these PET-derived boost volumes compare with MR lesions and how PET-MRI may have utility in this context.

### EP-2032 Automated Bone Scan Index (aBSI) as an Imaging Biomarker in Castration Sensitive Prostate Cancer

A. Alshehri<sup>1,2</sup>, J. O'Sullivan<sup>2,3</sup>, K. Prise<sup>2</sup>, S. Jain<sup>2,3</sup>, P. Turner<sup>3</sup>, C. Campfield<sup>1</sup>, S. Biggart<sup>1</sup>, C. Chatzigiannis<sup>1</sup>, A. Cole<sup>2,3</sup>

<sup>1</sup>Northern Ireland Cancer Centre- Belfast Health and Social Care Trust, Nuclear Medicine Department, Belfast, United Kingdom ; <sup>2</sup>Centre for Cancer Research and Cell Biology- Queen's University Belfast, Cancer Research and Cell Biology, Belfast, United Kingdom ; <sup>3</sup>Northern Ireland Cancer Centre- Belfast Health and Social Care Trust, Oncology, Belfast, United Kingdom

### Purpose or Objective

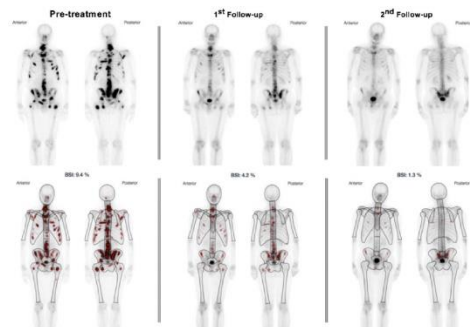
There is an unmet need for monitoring response to prostate cancer therapeutics in the management of bony metastases. A number of modalities including whole body MRI, PSMA-PET, CT scanning and Isotope Bone Scans (IBS) are used dependent on resources and centre preference.

Of these IBS is the most widely used in staging and initial management decisions. Often decisions regarding treatment are based on changes in ALP and PSA in the absence of radiological information. We present preliminary data from a Phase II trial exploring the use of Radium-223 (Ra-223) in combination with prostate and pelvic radiotherapy post docetaxel in a metastatic castration sensitive prostate cancer (mCSPC) (> 3 bone metastases, no lymph node or visceral disease T4N0/1M1b).

#### Material and Methods

Twenty-eight metastatic castration sensitive prostate cancer (mCSPC) patients were treated with monthly injections of radium-223 along with castration therapy and Volumetric Modulated Arc Therapy (VMAT) to the prostate and pelvic lymph nodes. Fifteen of the eligible mCSPC patients had baseline bone scans and treatment follow-up bone scans (during and post-treatment) available for automated aBSI analysis. The EXINI aBSI software programmed was used to retrospectively analyse the IBS and generate the aBSI value. Alkaline phosphatase (ALP) and Prostate Specific Antigen (PSA) values were collected. **Results**

Fifteen patients had at least 2 pre and post Ra-223 IBS available for analysis. All 15 patients had a reduction or stability in the aBSI reading. There was a median reduction of 71.5% (-350-88.9%) in the aBSI with a number of patients having almost complete resolution of quantifiable disease on bone scan as evidenced in Figure 1. All 15 patients included had a reduction in ALP from Cycle 1 to Cycle 6 with treatment, median reduction from cycle 1 90 (65-236) to cycle 6 59 (37-165). Over a median follow up period of 25.9 months the median overall survival and progression free survival have not yet been reached.



#### Conclusion

aBSI allows quantitative measurement of response to bone targeted therapies. It is more standardised, readily available and more economically sustainable than other modalities as a post therapeutic monitoring tool in bony metastatic setting. It's use in the castration sensitive prostate cancer setting with Ra-223 has not been previously documented, two-thirds of the patients in this study have prolonged reductions in aBSI in excess of 2 years post commencement of LHRHa. Further comparison with wbMRI in this study will allow comparison of response and prognostic information.

#### Electronic Poster: Physics track: Imaging acquisition and processing

#### EP-2033 Impact of CBCT roll rotation artifact on adaptive online cranial SRS of multiple targets

J. Casals Farran<sup>1</sup>, J.F. Calvo-Ortega<sup>1</sup>, S. Moragues Femenia<sup>1</sup>, C. Laosa<sup>1</sup>

<sup>1</sup>Hospital Quirónsalud Barcelona, Radiotherapy, Barcelona, Spain

#### Purpose or Objective

Roll artifacts up to 1° in CBCT scans have been described in the literature for the Varian OBI system [Phys Med Biol. 2013 Feb 21;58(4):1059-73]. Our aim is to investigate the dosimetric impact of this artifact on cranial SRS planning using an online adaptive procedure developed by our group [Med Dosim. 2013 Autumn;38(3):291-7].

#### Material and Methods

A Varian Clinac 2100 CD equipped with an OBI system was used. After placing a phantom (Easy Cube phantom, Scanditronix.....) on the treatment couch, 2 CBCT scans (CCW and CW directions) were acquired with the SRS protocol used for our CBCT-based SRS procedure. Proper leveling of the phantom was done before CBCT imaging by using a digital level with ± 0.1° accuracy (Smart Tool, M-D Building Products), and it was not moved between both scans. The differences between both CBCT scans were analyzed and the roll error observed in the axial reconstructed images was measured. Ten (10) independent measurements for each acquisition direction (CCW and CW) were performed to know the roll error inherent to the CBCT images (θ).

We randomly selected 10 cases of multiple brain metastases planned with a single isocenter. For each one, the CBCT scan acquired during patient setup (CBCTref) was corrected by applying a rotation of -θ° to the axial planes (CBCTcorr). A single-isocenter reference plan was calculated over the CBCTref (Plan\_ref), and then was also re-calculated over the generated CBCTcorr scan (Plan\_corr). Both plans were compared in order to know the dosimetric impact of these rotations in the target coverage (D99%) when the uncorrected CBCTref scan is used for adaptive SRS planning. Differences in D99% were given respect to the prescription dose (PD) of each target: [D99%@Plan\_corr - D99%@Plan\_ref]/PD. **Results**

Average roll errors of 0.3° (range: 0.1° to 0.4°) and 0.5° (range: 0.3° to 0.8°) were found for the CCW and CW-CBCT acquisitions, respectively. Target coverage differences (mean ± SD) of -1.0% ± 1.1% and -2.9% ± 2.1% were found for the CCW and CW-CBCT acquisitions, respectively.

#### Conclusion

Roll artifacts of less than 0.5° were detected in the CCW-CBCT direction acquisition. A negligible dosimetric impact (-1%) in the target coverage whether the CCW-CBCT scan is used for adaptive SRS planning. Only the CCW acquisition direction was selected for our SRS online procedure.

#### EP-2034 Evaluation of a web-based software for "Winston-Lutz" test analysis

J.F. Calvo Ortega<sup>1</sup>, M. Hermida-López<sup>2</sup>, S. Moragues Femenia<sup>1</sup>, J. Casals<sup>1</sup>

<sup>1</sup>Hospital Quirónsalud Barcelona, Radiotherapy, Barcelona, Spain ; <sup>2</sup>Hospital Universitario Valle de Hebrón, Servicio de Física y Protección Radiológica, Barcelona, Spain

#### Purpose or Objective

The popular "Winston-Lutz (WL)" test is a well established procedure to check the congruency between the center of a target to be irradiated and the radiation linac isocenter.

In this work, we investigated the performance of a free web-based software to quantitatively analyze this test.

#### Material and Methods

A Varian Clinac 2100 CD equipped with the Millennium 120 MLC and the aSi-500 Portal Vision (EPID) was used (Varian Medical Systems, Palo Alto, CA). The EPID was placed with a source-detector-distance of 180 cm (0.4 mm/pixel at the isocenter plane). A tungsten ball (5 mm-diameter) was used as a target in the 2x2 cm<sup>2</sup> MLC-based WL test performed in our department.

One hundred fifty portal images (WL images) were retrieved from the Aria system to be analyzed using a web-based application ("Winston-Lutz-Automatic Analyzer", <http://winston-lutz.herokuapp.com/>), and also with a FDA (U.S. Food and Drug Administration) accredited software (DoseLab Pro v. 6.40, Mobius Medical Systems, LP, Houston, TX). DoseLab was used as reference.

Both softwares calculate on each portal image the distance between the centroid of the tungsten ball shadow and the radiation field center ("delta"). Different image processing tools and algorithms are implemented in each software. Delta values given by both softwares were compared, and agreement between both softwares was assessed using the Bland-Altman method.

#### Results

An average difference (bias) in "delta" metric of -0.01 mm (SD: 0.13 mm) was found. The 95% limits of agreement between both softwares were from -0.28 mm to 0.25 mm.

#### Conclusion

The 95% limits of agreement found were comparable to the pixel size of the portal images analyzed (0.4 mm). Therefore, the results given by Winston-Lutz-Automatic Analyzer are comparable to those reported by DoseLab Pro for WL test analysis.

#### EP-2035 Robust optimization of CT reconstruction and scanning parameters

S. Alani<sup>1</sup>, E. Gez<sup>1</sup>, J. Zidan<sup>1</sup>

<sup>1</sup>*ziv medical center, radiation oncology, zefad, Israel*

#### Purpose or Objective

CT simulation has become an integral component of modern RT planning and therefore needs to be continually optimized. We improved the detection of small and low-contrast regions in images obtained during CT simulation by optimization of CT reconstruction and scanning parameters. For potential applications involving detection of low-contrast tumor structures

#### Material and Methods

A CT phantom containing a contrast detail modulus for detection of low-contrast structures was used to optimize the CT protocol. The parameters (A) Pitch, (B) Reconstruction Filter, and (C) Rotation Time type were varied for assessment of image quality. Three factors, three levels, and nine experiments were identified. According to the Taguchi approach an L9 orthogonal array was selected. The reconstruction parameters of the CT scanner Toshiba aquilion Pitch, Reconstruction Filter type, and Rotation Time, were iteratively scanned according to the orthogonal array. A Catphan 604 CT phantom was used to characterize low-contrast resolution (CPT730 module). All CT scan images were analyzed by IMAGE-OWL software. The objective of the study was to identify parameters that maximize the low-contrast resolution of the images. The ANOVA and F-tests were used to analyze results using JMP 14.1.0 statistical software.

#### Results

The optimal settings and predicted optimal values for low-contrast resolution were determined. The ANOVA was used to determine the optimum combination of process parameters more accurately by investigating the relative importance of each process parameter. We determined that Pitch (61.3%) had the most significant influence on low contrast resolution, followed by the Reconstruction Filter type (31.3%). The optimal setting level is A1-B1-C3,

0.68 pitch, smooth filter, and gantry rotation time 1.5 sec, respectively. In the phantom model of this study, optimal Contrast Detail Values were determined to be: 1% contrast, 2mm; 0.5% contrast, 4mm; 0.3% contrast, 7mm. Additional measurements were made to confirm the prediction error model is justified and the results are validated.

#### Conclusion

Protocol was improved comparing to those using the standard clinic protocol. CT image quality can be improved with the protocol created in this study, to provide better soft tissue contrast, which would be beneficial for RT contouring for SBRT and stereotactic radiosurgery in which accurate delineation of small-sized, low-contrast regions are important.

#### EP-2036 Visualization of prostate fiducial markers using phase-cycled bSSFP MRI

Y. Shcherbakova<sup>1</sup>, S. Mandija<sup>1</sup>, L.W. Bartels<sup>1</sup>, L.G.W. Kerkmeijer<sup>2</sup>, J.R.N. Van der Voort van Zyp<sup>2</sup>, C.A.T. Van den Berg<sup>2</sup>

<sup>1</sup>*UMC Utrecht, Center for Image Sciences/Imaging Division, Utrecht, The Netherlands*; <sup>2</sup>*UMC Utrecht, Department of Radiotherapy, Utrecht, The Netherlands*

#### Purpose or Objective

The existing manual techniques for visualization of gold fiducial markers (FMs) are mostly based on spoiled gradient-echo imaging (SPGR). FMs appear as signal voids in magnitude images, which makes it difficult to distinguish them from hemorrhages/calcifications. Being able to distinguish FMs in MR images is crucial for MR-only RT, where CT images are not available. Automatic FMs detection methods are available, but require special software which is not available at the MR console. Here we investigated a new method for distinctive FMs visualization in the prostate for MR-only RT which facilitates FMs detection at the MR console.

#### Material and Methods

A dynamic bSSFP scan is performed with RF phase cycling, where for each dynamic acquisition the phase of the RF excitation pulse is increased stepwise according to a certain incrementing scheme.

Complex phase-cycled bSSFP images were acquired on a phantom (agar phantom with 4 gold FMs GM1054 implanted) and on 8 patients at 3T: TR 9.2 ms, TE 4.6 ms, FA 20°, FOV (phantom) 200x200x80mm<sup>3</sup>, FOV (patients) 320x320x60 mm<sup>3</sup>, acquisition voxel size 2x2x2 mm<sup>3</sup>, reconstruction voxel size 1x1x1 mm<sup>3</sup> for both setups, 6 dynamics acquisitions with RF phase increment of , scan time 01:48 min (phantom) and 02:12 min (patients).

On each dynamic acquisition the manifestations of the magnetic field distortions around the FMs (the artifacts) are different due to different frequency offset related to the corresponding RF phase. Thus, the contrast from FMs in the images appears different for each dynamic acquisition.

CT scans of the phantom and patients were acquired. The distances between the centers of the markers were measured both on MRI and CT images by 1 observer. The accuracy of detecting FMs by was assessed by comparing the measured distances between FMs on MRI and CT images.

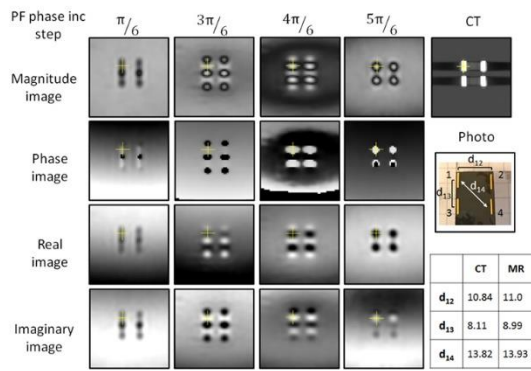


Figure 1. Experimental results in the phantom: MR images (Magnitude, Phase, Real, and Imaginary) acquired using 6 phase-cycled bSSFP, CT image for comparison for one coronal slice. The measured distances between the FMs using CT and MR images.

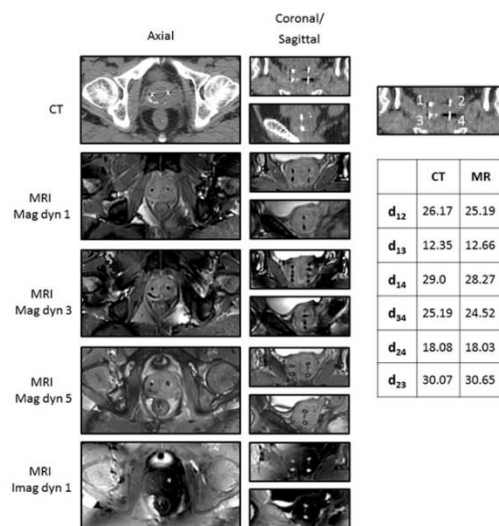


Figure 2. Experimental results in prostate: CT images and MR images acquired using 6 phase-cycled bSSFP (Magnitude Dynamics 1,3,5, Imaginary Dynamic 1) for axial, Coronal and sagittal planes. The measured distances between the FMs using CT and MR images.

## Results

The experimental results in the phantom are shown in Figure 1. Complex MR images are shown on one coronal slice for different dynamic acquisitions. These images show a distinct MR contrast given by the FMs for each dynamic. A CT image is shown as comparison. The differences between the distances between all FMs measured using MR and CT are within 1mm, proving correct FMs detection.

The CT and MR images of the prostate with implanted FMs are shown in Figure 2 for one patient. The same variable contrast of the FMs can be seen dependent on the RF phase increment used. FMs can be clearly seen on the acquired images. Similar results were observed in the other 7 patients. The < 1 mm differences in the distances between all FMs measured using MR and CT proves correct FMs detection.

## Conclusion

We have presented a method for direct FMs visualization at the MR console. The method is based on phase-cycled bSSFP imaging, providing different contrast of FMs dependent on RF phase increment used. This method does not require any additional post processing or software and can be easily done directly at the scanner. This is relevant especially for MR-only prostate RT.

## EP-2037 Digital phantom for evaluating the dosimetric impact of MRI Geometric inaccuracy in MR only based RT

T. Torfeh<sup>1</sup>, R. Hammoud<sup>1</sup>, S. Paloor<sup>1</sup>, S. Aouadi<sup>1</sup>, N. Al-Hammadi<sup>1</sup>

<sup>1</sup>National Center for Cancer Care & Research, Radiation Oncology, Doha, Qatar

### Purpose or Objective

Magnetic Resonance Imaging (MRI) is increasingly being used in radiotherapy applications for tumor delineation and tracking in the presence of respiratory motion. The purpose of this work is to investigate the impact of magnetic resonance distortions on dose distributions during respiratory motion.

### Material and Methods

An in-house motion platform and a control point based phantom were used to calculate an MR distortion map during motion for a Cine sequence which is the standard sequence for target delineation in liver cancer RT.

The calculated distortion map was used to distort original images generated from a 3D virtual phantom as shown in figure 1 which is composed of a C shape target of 5 and 7 mm of inner and outer diameters respectively. This C shape is surrounding a spherical target shape of 5 mm diameter. Another ellipsoidal organ shape with a width of 6 mm and a height of 5 mm is also included.

A dataset of 42 dicom images was finally generated with a resolution of 512X512 pixels, a 3 mm slice thickness, a 0 mm gap between slices and a pixel size of 0.97x0.97 mm.

Targets on the original and distorted datasets were automatically delineated. A treatment plan for liver cancer treatment was computed on EclipseTM TPS using the distorted dataset. This plan was then copied on the original dataset and the dose distribution was analysed. A highly conformal volumetric modulated arc therapy (VMAT) technique using multiple noncoplanar arcs was used. Dose Volume Histograms (DVH) including  $D_{95}$ ,  $D_{50}$ ,  $D_{min}$  and  $D_{mean}$  were benchmarked for accuracy measurements.

### Results

The mean magnitude of the geometric distortion was 0.5, 0.7 and 0.9mm for radial distances of 50, 100 and 150 mm respectively. Blurring was observed during motion causing an increase in the FWHM of  $\approx 30\%$ . Our results showed differences of less than 5% in the DVH parameters distorted and undistorted treatment plans. Results also showed that the difference in the DVH is sensitive to the size and position of the tumor. Higher differences were recorded as the distance to the isocentre increases and/or the tumor size decreases.

### Conclusion

The present work is a preliminary study aimed at putting in place an infrastructure allowing addressing the dosimetric impact of image deformation with any anatomy of interest.

Further investigations using more realistic shapes will be carried out with the idea of producing 3D patient specific models for SBRT evaluation.

## EP-2038 Use of deformable image registration for automatic outlining of the rectum

S. Hunt<sup>1</sup>, S. Thomas<sup>1</sup>, J. McClelland<sup>2</sup>, K. Harrison<sup>3</sup>, C. Rose<sup>1</sup>, J. Scaife<sup>4</sup>, M. Sutcliffe<sup>5</sup>, N. Burnet<sup>4</sup>, R. Jena<sup>6</sup>

<sup>1</sup>Cambridge University Hospitals NHS Foundation Trust, Medical Physics Box 152, Cambridge, United Kingdom ;

<sup>2</sup>University College London, Centre for Medical Image Computing, London, United Kingdom ;

<sup>3</sup>University of Cambridge, Department of Physics, Cambridge, United Kingdom ;

<sup>4</sup>University of Cambridge, Department of Oncology, Cambridge, United Kingdom ;

<sup>5</sup>University of Cambridge, Department of Engineering, Cambridge, United Kingdom ;

<sup>6</sup>Cambridge University Hospitals NHS Foundation Trust, Oncology, Cambridge, United Kingdom

## Purpose or Objective

We have evaluated deformable image registration (DIR) as a method of automatically outlining the rectum on pelvic megavoltage CT (MVCT) scans.

The rationale for this work is to retrospectively correlate the dose delivered to the rectum with the toxicity patients experience from external beam radiotherapy for prostate cancer. To calculate the dose delivered to the rectum, it must first be delineated on MVCT images acquired at the time of the patient's treatment. However, the study recruited 529 prostate patients who each received 20 or 37 treatment fractions; manual outlining for such a large number of images would clearly be impractical.

Our group currently uses a purpose-built automatic segmentation algorithm to outline the rectum on these images. However, DIR presents a potential alternative method of doing this, and we wished to investigate its performance for this purpose.

## Material and Methods

On six MVCT images from six different patients, the rectum was independently outlined by ten oncologists, according to our departmental protocols. They were also outlined using the automatic segmentation algorithm. The rectums on patients' original planning CT scans had been outlined by one oncologist at the time of treatment planning.

Three pieces of DIR-capable software were tested as part of this project:

- Prosoma (MedCom, Darmstadt, Germany)
- Pinnacle (Philips, Amsterdam, The Netherlands)
- RTx (Mirada, Oxford, United Kingdom)

Each piece of software was used to deformably register the patients' planning CT scans to their MVCT scans. The calculated deformations were then applied to the original rectum outline on the planning CT to propagate it to the MVCT dataset.

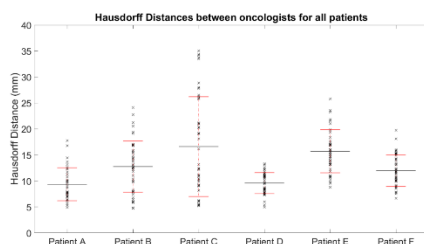
Contours were compared to one another using the Jaccard Index and Hausdorff Distance, to assess general volume overlap and gross spatial variation. Each oncologist's outline was compared to all others for each patient, to assess inter-observer variation in outlining. The outlines produced using DIR and automatic segmentation were then compared to each of the oncologists' outlines to assess the performance of the software.

## Results

The mean Jaccard Indices (JI) and Hausdorff Distances (HD) between the oncologists' outlines, and between outlines from each piece of software and each oncologist, are displayed in Table 1.

Table 1		Oncologists	Prosoma	Pinnacle	RTx	Auto. Seg.
Jaccard	Mean	0.68	0.62	0.60	0.62	0.58
Index	S.D.	0.06	0.09	0.07	0.08	0.10
Hausdorff	Mean	11.9	13.5	15.0	18.0	15.6
Dist. (mm)	S.D.	4.8	4.0	5.1	7.3	3.0

The figure below displays the variation in HD between each pair of oncologists for each of the six patients in this study. The central bar indicates the mean HD for that patient, while the smaller bars indicate the range of the mean  $\pm$  one standard deviation.



## Conclusion

The above results show that there is significant inter-observer variation in outlining of the rectum on MVCT images. In the context of this variation, DIR appears to produce outlines that are comparable to those of oncologists. These outlines may also be a superior alternative to the automatic segmentation algorithm currently used for this purpose.

## EP-2039 Validation Of The Direct Density™ Ct Image Reconstruction Algorithm

I. Peiro Riera<sup>1</sup>, E. Fernandez-Velilla Ceprià<sup>1</sup>, J. Quera Jordana<sup>1</sup>, O. Pera Cegarra<sup>1</sup>, N. Anton Comelles<sup>1</sup>, M. Prieto Carballo<sup>1</sup>, M. Algara López<sup>1</sup>

<sup>1</sup>Hospital del Mar, Radiotherapy Oncology, Barcelona, Spain

## Purpose or Objective

The standard kV setting for Simulation CT images in radiotherapy is 120kV. Planning Systems (TPS) use calibration curves at that energy for associating electron densities to Hounsfield units (HU). For contrast and radiation protection reasons, in some situations a different kV may be recommendable. This requires the commissioning of one calibration curve for each kV. In our work we analyze the Siemens reconstruction algorithm Direct Density™ (DD), which gives CT numbers proportional to relative electron densities (RED), independent of the kilo-voltage used. DD is evaluated and compared to the standard Filtered Back-Projection (FBP) in order to verify its accuracy to be introduced in the radiotherapy workflow.

## Material and Methods

A Siemens Somatom Confidence RT Plus CT system was used to acquire the images at 70, 80, 100, 120 and 140kV. Slice thickness and pitch were the same used in clinical protocols for pelvis and brain patients. mAs were adjusted at all kV in order to keep CTDI unchanged from the reference 120kV studies.

A Catphan CTP 604 phantom was scanned in order to evaluate image quality in terms of high and low contrast resolutions, uniformity and noise. Additionally, a Gammex 467 Tissue Characterization Phantom was scanned to obtain calibration curves and to confirm that they were kV independent when DD was applied. CTDI doses were verified with an RTI Piranha to assure they were unchanged. Finally, a comparison between 3D doses using FBP at 120kV and DD images was done by means of a Varian Eclipse v. 13.6 TPS in real patients, using both AAA and Acuros XB 13.7 algorithms.

## Results

The observed differences in calibration curves were maximal at 70kV for the cortical bone and the 50% CaCO<sub>3</sub> rods (highest densities). For the other values of kV, HU and electronic density showed the same linear relationship whatever the kV was.

Image quality was slightly better in FBP than in DD images (Table 1). Spatial resolution in high contrast showed a worsening from 0.71mm to 0.83mm, and in low contrast no circles of the Catphan module could be detected in DD images at energies over 70kV. A slight difference in uniformity was observed, always being FBP better than DD. Noise was significantly higher in the DD images, around 3 times higher.

As expected, DD does not result in significant differences in dose calculations in comparison with FBP. Using AAA, the maximum differences were 0.1% in pelvis and 0.7% in brain. For Acuros the same differences were found.

Pelvis	Filtered Back-Projection					DirectDensity™				
	70 kV	80 kV	100 kV	120 kV	140 kV	70 kV	80 kV	100 kV	120 kV	140 kV
Spatial Resolution in High Contrast (mm)	0.71					0.83				
Spatial Resolution in Low Contrast with a contrast level of 1.0 % ( $\pm 1$ mm)	4	5	6	2	4	7	>15	>15	>15	>15
Uniformity - Relative differences in HU from the central pixels (%)	0.022	0.028	0.032	0.037	0.052	0.039	0.044	0.045	0.042	0.055
Noise level (HU)	3.2	3.4	3.2	3.3	3.4	10.2	11.6	9.1	9.6	10.0
Brain	Filtered Back-Projection					DirectDensity™				
	70 kV	80 kV	100 kV	120 kV	140 kV	70 kV	80 kV	100 kV	120 kV	140 kV
Spatial Resolution in High Contrast (mm)	0.71					0.83				
Spatial Resolution in Low Contrast with a contrast level of 1.0 % ( $\pm 1$ mm)	4	2	2	2	2	>15	>15	>15	>15	9
Uniformity - Relative differences in HU from the central pixels (%)	0.014	0.026	0.038	0.020	0.043	0.053	0.036	0.049	0.041	0.048
Noise level (HU)	3.4	3.2	2.9	3.0	3.1	11.6	9.8	9.1	10.4	10.2

### Conclusion

DD allows the acquisition of CT images at different kV settings with only one calibration curve in the planning system, with a minimum impact in dose calculations. However it needs matching with the original FBP images for volume delineation due to the lower image quality. Consequently Direct Density™ is accurate enough to be introduced in clinical routine.

### EP-2040 IDose4 algorithm for radiotherapy planning process: how reduce the dose without image quality loss

A. Clivio<sup>1</sup>, E. Barletta<sup>2</sup>, C. Bonacini<sup>1</sup>, R. Graeter<sup>1</sup>  
<sup>1</sup>Zentrum für Radiotherapie Rüti, Radiotherapy, Rüti ZH, Switzerland ; <sup>2</sup>Zentrum für Radiotherapie Rüti / KSW Kantonsspital Winterthur, Radiotherapy, Rüti ZH / Winterthur, Switzerland

### Purpose or Objective

With the software upgrade on the Big Bore CT (Philips), we have the opportunity to use the iDose<sup>4</sup> Algorithm (iDA) to reduce the patient dose during the CT acquisition. The aim of our study is to verify that, applying this Algorithm, the CTs are compatible for the radiotherapy planning process in terms of image quality and physical aspects

### Material and Methods

We used three different phantoms. The Catphan CTP504 and CIRS O62M phantom to measure the parameters linked to the image quality analysis (as Hounsfield Unit (HU), Homogeneity, and Resolution). The anthropomorphic Alderson RANDO phantom (AP) to evaluate the image quality on a 'real' patient. Using the iDA we have to select one of the seven available strength levels. With the level one we have to reduce about 20% the nominal mAs and for each higher level the reduction is 10% more. We took into account 4 different iDose<sup>4</sup> level (1 to 3 and 6) and we tested those applying nominal mAs value from 100 to 500, with a step of 50 mAs for the first 2 phantom. For the AP phantom, we acquired CT in three regions (Head, Thorax, and Pelvis) with our standard internal protocol and with the above four iDose<sup>4</sup> levels. We evaluate qualitatively the resolution and the image quality and we calculate some standard plans on the AP scan to compare the dose distributions

### Results

For the HU analysis, we found very small differences in the inserts of the CatPhan Phantom between the values obtained with the standard scan and with the iDA. For the scans with 150 mAs or more, the maximal difference is 5.1 HU (for Teflon). When we applied iDose<sup>4</sup> level 3, we had as mean difference in terms of HU over all the inserts (in the square bracket the range),  $1.4 \pm 0.8$  [0.3;2.3] with

500mAs,  $1.7 \pm 0.9$  [0.5;3.3] for 250mAs and  $1.3 \pm 2.2$  [-1.5;5.1] for 150mAs. We noted the maximal difference about 10.1HU with the iDose<sup>4</sup> level 3 and 100mAs in one of the two air insert. We obtain the same results also for the CIRS phantom: maximal difference about 6.5 HU and for iDose<sup>4</sup> level 3  $-1.0 \pm 1.9$  [-4.8;1.2],  $0.4 \pm 2.1$  [-2.4;3.8] and  $1.2 \pm 3.6$  [-3.9;6.5] HU mean difference respectively with 500, 250 and 150mAs. About the resolution and the homogeneity in the Catphan no difference is visible if we apply more than 200 mAs. With high iDose<sup>4</sup> level and less than 200mAs we lost 2 low constants inserts, with level 6 we lost one more. The qualitative evaluation on the AP CT didn't show any relevant difference and the same result we had with the test plans calculation. We calculated also the CT dose sparing and for Head region we had -30% respect our standard protocol with the level 2, for Thorax -22% with level 3 and for Pelvis -29% with iDose<sup>4</sup> level 3

### Conclusion

With the iDA we have the possibility to reduce the dose for the planning CT keeping a good resolution and without significant difference in the HU numbers. For the region in which we don't need a very high resolution, for example for simple breast or prostate Patients, suggest to use iDose<sup>4</sup> level 3 and for the other level 1 or 2 are recommended

**EP-2041 A comparison between 120kv and virtual mixed images in dual energy CT for RT simulation**  
 E. Fernandez-Velilla Cepria<sup>1</sup>, J. Quera Jordana<sup>1</sup>, O. Pera Cegarra<sup>1</sup>, M. Prieto Carballo<sup>1</sup>, N. Anton Comelles<sup>1</sup>, M. Algara Lopez<sup>1</sup>

<sup>1</sup>Hospital del Mar, Radiotherapy Oncology, Barcelona, Spain

### Purpose or Objective

Dual Energy CT (DECT) is being introduced in RT simulation due to its special features. DECT combines low kV (typically 80kV) and high kV (140kV) in order to enhance iodine contrast detection. So far radiotherapists needed two acquisitions in the simulation process: one with contrast for delineation and one without it for calculation. DECT allows the creation of Virtual Non Contrast Images (VNC) at 120kV (standard kV used for simulation), eliminating the need of the non contrast acquisition. The accuracy of this approach depends on the ability of the algorithm to calculate virtual 120kV images from the real 80 and 140kV acquisitions. The so called 120Mixed images are obtained with a weighted formula which uses HU at both kV and a single weighting parameter. A first step in the verification of this formula is applying it to non contrast images to prove whether it works properly. The objective of this study is checking the reliability of that calculation in real patients without injected iodine.

### Material and Methods

CT Simulation images were acquired by means of a Siemens Confidence RT Plus CT. For each patient two series were imaged: the standard 120kV (used for simulation) and the DECT (composed of 2 consecutive series at 80 and 140kV). For the 120kV series, the acquisition protocol was the one used in clinical routine. For the DECT acquisition, parameters were modified in order to keep the same CTDI as that of the 120kV. Slice thickness was 2mm in all cases. No iodine contrast was used, in order to avoid changes in Hounsfield Units of soft tissues.

For each patient, 6 tissues of interest (TOI) were delineated: lung, fat, blood, muscle, liver and cortical bone. Mean HU and standard deviations were calculated for each TOI in the 120kV, 120 Mixed, 80 kV and 140kV series. Comparisons were done in the Contouring module of a Varian Eclipse 13.6 TPS.

### Results

Mean differences in HU between 120kV and 120Mixed series were less than 3 HU in all tissues except bone (see table). 120kV were the series with less noise, followed by

120Mixed and 140kV. The highest noise and deviations were observed in bone, where a mean difference of 52HU appears and the difference between maximum and minimum deviations is 129.5HU.

The analysis of all patients and tissues one by one shows that even Lung has a mean at 120kV (-763.6HU) only 2.4HU different to the 120Mixed, the extreme values are separated by 50.7HU, and the standard deviations are 84.6 and 94.3HU respectively.

Fat, blood, muscle and liver show very small differences and deviations between 120kV and 120Mixed images, always under 6HU.

	120kV		120kV Mixed		Dif (HU)	Difference 120MIX-120KV	
	Mean	StDev	Mean	StDev		Max	Min
Lung	-763,6	84,6	-761,1	93,0	2,4	17,8	-32,9
Fat	-104,5	10,0	-105,6	12,0	-1,1	3,2	-2,8
Blood	41,5	9,4	42,8	9,5	1,3	3,1	-0,6
Muscle	51,8	10,9	54,6	13,3	2,8	5,7	1,3
Liver	55,5	8,6	57,4	12,7	1,9	3,6	0,6
Bone	800,4	276,8	853,1	302,0	52,7	92,8	36,7

### Conclusion

The calculation of 120Mixed images from 80kV and 120kV DECT images is accurate enough for soft tissues. Deviations increase at high HU tissues as bone. A fixed weighting factor seems to have some limitations to calculate 120Mixed images in all the HU range. More studies are needed to find the impact of such a limitation in dose calculation, and to find the factor dependency on density and composition.

### EP-2042 A clinically applicable deep learning model for segmentation in the prostate region

M. Nakamura<sup>1</sup>, H. Enno<sup>2</sup>, T. Kabasawa<sup>2</sup>, Y. Shido<sup>2</sup>, Y. Okunishi<sup>2</sup>, K. Muguruma<sup>2</sup>, H. Hirashima<sup>3</sup>, T. Mizowaki<sup>3</sup>  
<sup>1</sup>Kyoto University, Department of Information Technology and Medical Engineering, Kyoto, Japan ;  
<sup>2</sup>Rist- Inc., Department of Research and Development, Tokyo, Japan ;  
<sup>3</sup>Kyoto University, Department of Radiation Oncology and Image-Applied Therapy, Kyoto, Japan

### Purpose or Objective

The purpose of this study was to evaluate the accuracy of a deep learning segmentation model using FusionNet architecture, to delineate the prostate, seminal vesicles, rectum, and bladder in pelvic CT images.

### Material and Methods

The clinical data used in this study were obtained from randomly chosen from 469 prostate cancer patients who underwent IMRT or VMAT in prone position between July 2007 and October 2016. Regions of interest (ROIs), including the prostate, seminal vesicles, rectum, and bladder, were manually drawn by radiation oncologists and medical physicists. All CT images were acquired with a 512x512 matrix and 2.5-mm slice thickness (voxel size, 1.07 mmx1.07 mmx2.5 mm). A total number of CT images of 14,301 and their corresponding structural images were randomly assigned to either training (60%), validation (20%) or testing (20%) sets. A deep neural network, FusionNet, was implemented as the segmentation model. The CT image data set for training was augmented by performing rotation and shear on the original images. The model was then trained using the CT image data set with corresponding ROIs label data set. The optimization algorithm called Adam (adaptive moment estimation optimizer, learning rate=2e-5) was used to train the network weights. The trained model was evaluated with

test data set to segment the final ROIs slice by slice. The segmentation was conducted on a workstation with Intel(R) Xeon(R) CPU E5-2686 v4 2.30GHz, the NVIDIA Tesla V100 GPU accelerator (64 GB GPU Memory), and 244 GB Main Memory.

### Results

Median (interquartile range) dice similarity coefficient was 0.95 (0.85-1.00), 1.00 (1.00-1.00), 1.00 (0.97-1.00), 0.94 (0.87-0.96) for the prostate, seminal vesicles, rectum, and bladder, respectively. An averaged computation time to complete segmentation was 0.12 s per slice.

### Conclusion

Our proposed method, which employs the FusionNet architecture, was highly accurate for automated ROI segmentation.

### EP-2043 Efficiency Boosting of HN Positional Verification Using Highly Accelerated 3D MR Imaging in MRgRT

Y. Zhou<sup>1</sup>, W.W.K. Fung<sup>2</sup>, K.F. Cheng<sup>2</sup>, J. Yuan<sup>1</sup>, O.L. Wong<sup>1</sup>, G. Chiu<sup>2</sup>, K.Y. Cheung<sup>1</sup>, S.K. Yu<sup>1</sup>

<sup>1</sup>Hong Kong Sanatorium & Hospital, Medical Physics and Research Department, Happy Valley, Hong Kong SAR China ;  
<sup>2</sup>Hong Kong Sanatorium & Hospital, Department of Radiotherapy, Happy Valley, Hong Kong SAR China

### Purpose or Objective

We aim to evaluate the performance of highly accelerated 3D MRI scan for head and neck (HN) in MR-guided-radiotherapy (MRgRT) on efficiency enhancement and inter-fractional positional error measurement.

### Material and Methods

18 healthy volunteers immobilized with a customized 5-point thermoplastic mask received 183 scans on a 1.5T MR-sim to simulate MRgRT fractions. Each scan included a high-resolution (voxel-size=1.05x1.05x1.05mm<sup>3</sup>, duration=5min) and a highly-accelerated low-resolution (acceleration-factor=9, voxel-size=1.4x1.4x1.4mm<sup>3</sup>, duration=59s) T1w spin-echo sequence (TR/TE=420/7.2ms) (Fig.1). The high-resolution images of the first session were used as the reference to mimic planning MRI. Rigid image registration was used to pairwise register the following sessional high-resolution and low-resolution images to the reference using 3D-slicer, named HHR and LHR respectively. Disagreement of inter-sessional positional shift calculated from HHR and LHR were analyzed using Bland-Altman plot. Systematic and random errors were also compared.

### Results

In efficiency, accelerated MRI, although with artifacts and lower image quality, considerably reduced scan time from 5min to 1min. LHR also reduced the automated registration time on a personal computer from ~45s to ~15s. The calculated translation shifts (mm) were 0.00±0.76 (mean±SD), 0.23±0.33, -0.23±0.69 and 0.33±1.08 in LR, AP and SI from HHR, and correspondingly -0.01±0.78, 0.26±0.31 and -0.32±0.71 from LHR (Table 1). The calculated rotation shifts (°) were -0.04±0.14, 0.00±0.00, and 0.16±0.44 in roll, pitch and yaw from HHR, and correspondingly -0.07±0.15, 0.00±0.00, and 0.13±0.43 from LHR. Bland-Altman analysis showed the calculated shift difference from LHR to HHR was small, i.e. -0.01 95%CI: [-0.23, 0.21], 0.03 [-0.14, 0.19], and -0.09 [-0.36, 0.18] in LR, AP and SI translation (mm) respectively, and -0.03 [-0.14, 0.09], 0.03 [-0.003 to 0.003], and -0.02 [-0.26, 0.21] in roll, pitch and yaw (°). The calculated systematic error and random error from HHR and LHR were also highly consistent, showing negligible differences (Table 1).

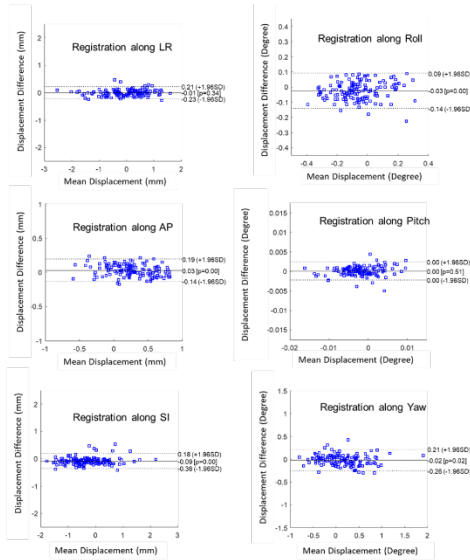


Fig 1. Altman-Bland plot of the positional shift difference in translation and rotation calculated from LHR to HHR

#### High-High Registration (HHR)

	3D Translation			3D Rotation		
	LR	AP	SI	Roll	Pitch	Yaw
Mean (mm)	0.00	0.23	-0.23	-0.04	0.00	0.16
SD (mm)	0.76	0.33	0.69	0.14	0.00	0.44
Group Systematic Error M (mm)	-0.16	0.14	-0.09	-0.01	0.00	0.05
SD of Systematic Error $\Sigma$ (mm)	0.64	0.25	0.43	0.14	0.00	0.31
RMS of Random Error $\sigma$ (mm)	0.63	0.27	0.73	0.11	0.00	0.25

#### Low-High Registration (LHR)

	3D Translation			3D Rotation		
	LR	AP	SI	Roll	Pitch	Yaw
Mean (mm)	-0.01	0.26	-0.32	-0.07	0.00	0.13
SD (mm)	0.78	0.31	0.71	0.15	0.00	0.43
Group Systematic Error M (mm)	-0.15	0.16	-0.16	-0.04	0.00	0.07
SD of Systematic Error $\Sigma$ (mm)	0.68	0.24	0.55	0.13	0.00	0.28
RMS of Random Error $\sigma$ (mm)	0.61	0.24	0.72	0.10	0.00	0.25

Table 1. The mean, standard deviation, systematic error and random error of translation and rotation shift calculated from HHR and LHR registrations.

## Conclusion

Highly-accelerated 3D-MRI could enhance positional verification efficiency in the HN MRgRT without compromising guidance accuracy.

## EP-2044 CT number estimation techniques for the stoichiometric method to predict proton stopping power

V. Taasti<sup>1</sup>

<sup>1</sup>Memorial Sloan Kettering Cancer Center, Medical Physics, New York, USA

### Purpose or Objective

The stoichiometric method is a well-established method, often used in proton therapy planning to estimate the stopping power ratio (SPR) of a patient's tissue. This method includes a CT scanner characterization and a subsequent CT number estimation for reference human data from the literature. The method originally proposed for these steps is based on a parametrization of the x-ray attenuation coefficient with fixed parameters for the target material dependency. However, other CT number estimation methods exist, which can equally well be used

for the stoichiometric method. This study investigated whether the SPR accuracy of the stoichiometric method could be improved by applying other CT number estimation methods.

### Material and Methods

Six published CT number estimation methods (Table 1) were investigated, including the method originally proposed for the stoichiometric method. All methods proposed a calibration method to characterize the x-ray energy spectrum based on CT scans of an electron density phantom, without the need for direct measurements of the x-ray spectrum. Therefore, these methods can all be used in the first steps of the stoichiometric method to estimate the CT numbers for reference human tissues, which in the last step is used to fit an empirical piecewise linear conversion curve from CT numbers to SPRs. CT scans of a tissue equivalent phantom (Cone-Beam Electron Density Phantom, Gammex, Middleton, WI, Fig. 1) were acquired at 120 kVp with a Flash scanner (Siemens Healthineers, Forchheim, Germany). The CT number estimation accuracy of the six methods was tested in a fully self-calibrated evaluation for the twelve insert materials used in the calibrations (measured vs estimated CT numbers), as well as theoretically for the reference human tissues (theoretical vs estimated CT numbers). Stoichiometric conversion curves were fitted based on each set of estimated CT numbers for the reference human tissues, applying the same curve fitting recipe for all six conversion curves (Fig. 2). The SPR accuracy was evaluated for published proton range measurements of organic beef and pork tissue samples, which had been scanned with the same CT scanner.

Table 1: Naming convention for the six methods, and references to the original publications. Parameters:  $\mu$  – x-ray attenuation coefficient;  $\sigma_e$  – electron cross section; Z – atomic number.

Name	Note	Reference
Method A	Parametrization of $\mu$	Schneider <i>et al.</i> , PMB, 41 (1996)
Method B	Parametrization of $\sigma_e$	Bourque <i>et al.</i> , PMB, 59 (2014)
Method C	Z-space	Lalonde and Bourchard, PMB, 61 (2016)
Method D	Effective energy	Han <i>et al.</i> , Med Phys, 43 (2016)
Method E	Effective energy	Taasti <i>et al.</i> , Med Phys, 43 (2016)
Method F	Two effective energies	Taasti <i>et al.</i> , Med Phys, 45 (2018)

Table 2: Results for the six CT number estimation methods. Column two and three are for the self-calibrated CT number ( $J_t$ ) estimation of the Gammex inserts, stated as the root-mean-square error (RMSE) and the mean error, both in percentage relative to the experimentally measured CT numbers for the twelve inserts. On the right in column four and five, the results for the stopping power estimation (SPR) of the fourteen pork and beef tissue samples are listed; the results are stated relative to the experimentally measured SPR values.

	RMSE $J_t$ (%)	Mean $J_t$ (%)	RMSE SPR (%)	Mean SPR (%)
Method A	3.1	-1.2	0.7	-0.2
Method B	2.9	-1.0	0.9	-0.3
Method C	2.1	-0.6	1.3	0.3
Method D	0.6	0.0	0.7	-0.3
Method E	0.5	0.0	0.6	-0.1
Method F	0.2	0.0	0.5	-0.1

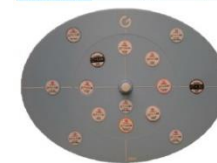


Figure 1: Gammex electron density phantom used in this study containing twelve tissue equivalent inserts. The measured CT numbers for the inserts were used to perform the CT scanner characteristic in each of the six methods, and in the self-calibrated CT number evaluation.

## Results

The CT number estimation method originally proposed for the stoichiometric method provided the least accurate CT number estimates with a root-mean-square error (RMSE) of 3.1% (Table 2). The lowest RMSE was 0.2%; this was obtained with a method based on two effective energies to characterize the CT scanner energy spectrum. In the theoretical evaluation, the deviations for the original method were found to increase with density for bone tissues (Fig. 3). The SPR accuracy for the organic tissues varied between the methods, with RMSEs between 1.3% and 0.5% (0.7% for the original method).

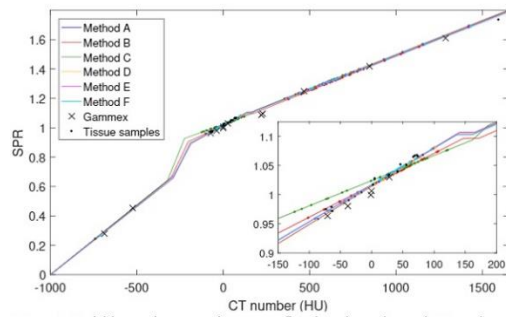


Figure 2: Stoichiometric conversion curves fitted on the estimated CT numbers for the reference human tissues for each of the six methods. The data points for the Gammex inserts and for the organic tissue samples are also shown.

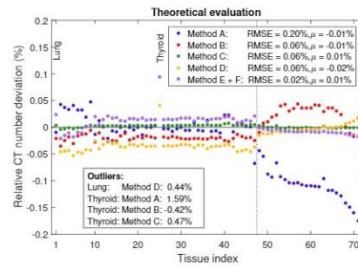


Figure 3: Relative deviations for the estimated CT numbers,  $\Delta H$ , for the reference human tissues in theoretical evaluation. The vertical dashed line separates soft and bone tissues. Data points for method E and F overlaps.

**Conclusion**

The accuracy of the SPR estimation in the stoichiometric method could be improved by changing the CT number estimation method. For the optimal method, the SPR accuracy (RMSE = 0.5%) was close to values obtained for dual energy CT.

**EP-2045 Tumor profile matching at the end of 8x7,5 Gy SBRT treatment: CBCT vs Untagged Image Reconstruction**

G. Pozo Rodriguez<sup>1</sup>, P. Garcia<sup>2</sup>, A. Ferrando<sup>1</sup>, M. Leonor<sup>1</sup>, A. Gaïtan<sup>1</sup>

<sup>1</sup>Hospital Universitario 12 de Octubre, Medical Physics Department, MADRID, Spain ; <sup>2</sup>Hospital Universitario de La Princesa, Medical Physics Department, Madrid, Spain

**Purpose or Objective**

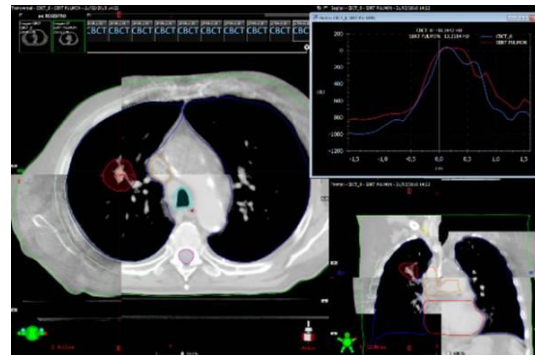
To assess and quantify correlation between tumor images by comparing Hounsfield Unit (HU) profiles of 4DCT acquisition and CBCT image acquired at last therapy fraction.

**Material and Methods**

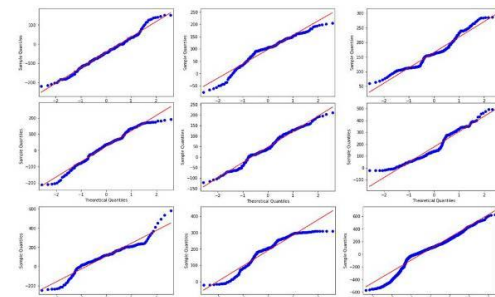
A cohort of 15 NSCLC patients treated with SBRT and dose administration delivered in 8 fractions of 7,5Gy (BED=105Gy) was selected for this study. SBRT treatments were performed on a Varian Clinac 2300 iX (Varian Medical Systems, Palo Alto.CA). This linear accelerator includes an On Board Imager (OBI) unit to perform planar or CBCT KV image, with a aSi digital panel detector model PaxScan 4030CB. In each fraction, 2 CBCT are acquired for patient positioning and intra-fraction movement tracking, with an average acquisition time (tacq) of 13,02s ( $\sigma=0.21s$ ). 4DCT was acquired with a Philips Brilliance Big Bore CT of 64 detector rows (Philips Healthcare, Amsterdam.The Netherlands), using a nominal slice thickness of 2mm. Respiratory cycle was binned into 10 phases and ITV was generated by means of merging 10 contoured GTV. This structure is expanded 5mm isotropically and determines PTV to be treated. CT utilized for planning is an averaged reconstruction called Untagged Series. Image analysis has been performed with Image Registration tool implemented in ARIA R&V System (Varian Medical Systems)

**Results**

Performing a rigid registration between CT image acquired with CBCT at the eighth fraction (last treatment's fraction) and CT Untagged, a HU Profile has been plotted referred to PTV's centroid of in both images as seen in Figure 1.



Since qualitative profile depicts analogous behaviour between both images, statistical analysis has been performance to quantify whether or not are correlated. Normality tests were performed to decide the best fit model. Attempt to correlate CBCT and Untag profiles was carried out by performing and ordinary least square (OLS) linearity model with Python 3.7. This analysis was done for each individual and also considering 'all in one' bulk data. R2 for individuals ranged from 0,736 to 0,980, yielding an average R2=0.872 for individuals ( $\sigma=0.074$ ) and R2=0.739 for bulk analysis. In fact, 75% of patients had an R2>0.850, showing a strong correlation that only fails in HU ranges linked to air and intrinsic variability of acquisition process as seen in Quantile Quantile Plot (Figure 2).



1) to 8) Examples of good linearity accordance, centered in high density area. Deviations are linked to lung tissue and extreme values.  
9) Bulk QQPlot Analysis

**Conclusion**

CBCT and planning Image matching in lung has been evaluated in terms of HU profile since acceptable contrast can be obtained. Focusing on target shape, in despite of apparent artifacts frequently seen in CBCT, profile analysis exhibits good correlation between initial and final image (R2=0.872). Apparently, HU topography of the tumor represented is not device-dependent as averaged target is displayed in both cases: Untagged CT and CBCT acquisition ( $t_{aq}=13,02s$  evolving several respiratory cycles), although inherent noise may be present (OAR proximity, respiration). Even when considering bulk data analysis, an R2 of almost 0,750 reveals a predictable model at least concerning to tumor surrounding.

**EP-2046 Patient setup verification using synthetic DRRs in an MR only workflow for head and neck cancer**

E. Palmér<sup>1</sup>, A. Karlsson<sup>1,2</sup>, F. Nordström<sup>1,2</sup>, K. Petruson<sup>3</sup>, M. Ljungberg<sup>1,2</sup>, M. Sohlín<sup>1,2</sup>

<sup>1</sup>University of Gothenburg, Department of Radiation Physics- Institute of Clinical Sciences- Sahlgrenska Academy, Gothenburg, Sweden ; <sup>2</sup>Sahlgrenska University Hospital, Department of Medical Physics and Biomedical

Engineering, Gothenburg, Sweden ; <sup>3</sup>University of Gothenburg, Department of Oncology and Radiotherapy- Institute of Clinical Sciences- Sahlgrenska Academy, Gothenburg, Sweden

### Purpose or Objective

The MR only radiotherapy workflow is based solely on MR data, hence there is no CT data available. Instead a synthetic CT (sCT) generated from the MR data is used as Hounsfield Unit (HU) map for dose calculation. Consequently, the Digital Reconstructed Radiograph (DRR) originating from CT data is replaced with synthetic DRR (sDRR) (Figure 1). The purpose of this observer study was to investigate the precision of patient positioning for head and neck cancer using sDRR, compared to the today clinical used DRR.

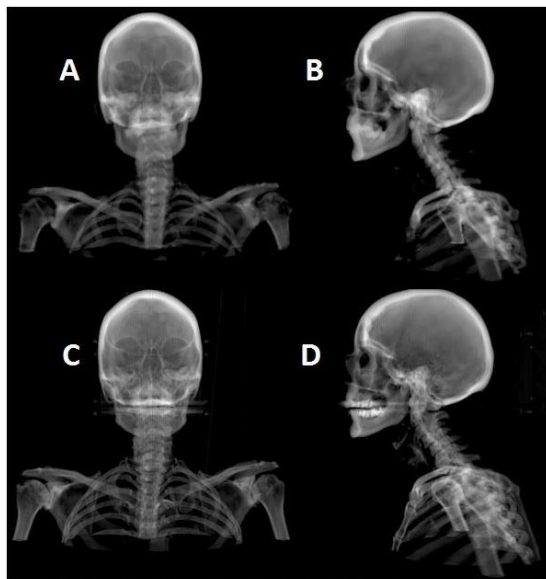


Figure 1. Illustration of synthetic DRR (A and B) and today clinical used DRR (C and D), in 0° and 90°.

### Material and Methods

Pre-treatment CT and MR from four patients, as well as kV-images (0° and 90°) from the linac mounted imaging device were used. sCT data was generated using MriPlanner (Spectronic Medical AB). A second CT data set was created by deformable registration of the CT to the MR using Velocity (Varian Medical Systems). The deformed CT data was used to mitigate anatomical differences between the pre-treatment imaging sessions. For each patient, orthogonal kV images from 4 fractions were retrospectively manually registered in five degrees of freedom against 3 different image sets (DRR, sDRR and deformed DRR (defDRR)) by 6 observers, resulting in a total of 288 registrations. None of the observers were informed about which type of DRR they worked with.

### Results

Differences between patient positioning with sDRR and the clinically used DRR, as well as differences between defDRR and DRR, in vertical (vrt), longitudinal (lng) and lateral (lat) directions, for all observers, are presented in Figure 2. The mean differences and the standard deviations between patient positioning with sDRR and DRR were  $-0.79 \pm 1.75$  mm,  $-0.59 \pm 0.79$  mm and  $0.96 \pm 1.20$  mm in vrt, lng and lat direction respectively. For pitch and rotation (rtn), a difference of  $-0.61 \pm 1.41^\circ$  [ $-4.0$  2.6] and  $-0.22 \pm 0.83^\circ$  [ $-2.7$  1.7] were noticed. The differences between defDRR and DRR concluded in a mean difference of  $-1.08 \pm 2.36$  mm,  $-0.53 \pm 1.08$  mm and  $0.53 \pm 1.26$  mm in vrt, lng and lat directions and in pitch and rtn of  $-0.68 \pm 1.33$  [ $-3.8$  2.4] and  $-0.31 \pm 0.87^\circ$  [ $-3.5$  1.6].

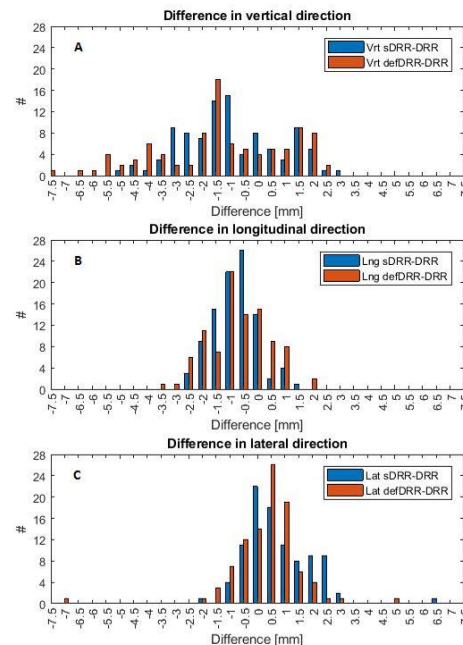


Figure 2. Histograms presenting differences between patient positioning with sDRR and DRR (blue) and with defDRR and DRR (red). Histogram A illustrates differences in vertical direction, histogram B differences in longitudinal direction and histogram C differences in lateral direction.

### Conclusion

Differences in all degrees of freedom for sDRR-DRR are found to be similar to the differences for defDRR-DRR, i.e. the generation of sCT is not introducing any large additional uncertainties or errors that propagates to the sDRR. The similarity indicates that the dominating factor contributing to the observed differences is repositioning between the CT and MR scan. Supplementary phantom measurements, enabling fixed coordinate systems, could be valuable.

### EP-2047 Investigating a new MR sequence combined with radiologist training for prostate delineation

J. Wyatt<sup>1</sup>, J. Frew<sup>1</sup>, A. Henry<sup>2,3</sup>, L. Murray<sup>2,3</sup>, R. Pearson<sup>1</sup>, A. McNeil<sup>4</sup>, E. Johnstone<sup>2</sup>, R. Speight<sup>3</sup>, H. McCallum<sup>1</sup>  
<sup>1</sup>Newcastle upon Tyne Hospitals NHS Foundation Trust, Northern Centre for Cancer Care, Newcastle upon Tyne, United Kingdom ; <sup>2</sup>University of Leeds, Leeds Institute of Cancer and Pathology, Leeds, United Kingdom ; <sup>3</sup>Leeds Teaching Hospitals NHS Trust, Leeds Cancer Centre, Leeds, United Kingdom ; <sup>4</sup>Newcastle upon Tyne Hospitals NHS Foundation Trust, Radiology, Newcastle upon Tyne, United Kingdom

### Purpose or Objective

MR is increasingly being used for prostate delineation in radiotherapy due to its superior soft-tissue contrast. However the literature is scarce regarding the optimal sequence for prostate definition and many oncologists are unfamiliar with using MR images for delineation. This study aimed to investigate the variability of prostate delineation for two different MR acquisition sequences both prior to and after expert radiologist training.

### Material and Methods

CT and MRI scans for radiotherapy planning were acquired in the treatment planning position for 15 patients in two cohorts (5 and 10 respectively). Two MR sequences were acquired in the same scanning session, a 3D T2-weighted turbo spin echo sequence (SPACE) and a 2D T2-weighted combined multiple gradient echo sequence (MEDIC). Three consultant oncologists from two institutions delineated the prostate and seminal vesicles on each image set independently for the first cohort using the same treatment planning system. These delineations were then

reviewed by an expert urology radiologist and discussed with the oncologists. The same oncologists subsequently delineated the second cohort.

The delineation variability was quantified using a generalised conformity index for each image and patient. This is the intersection volume divided by the union volume generalised to be independent of the number of observers. The delineation variability for each MR sequence was compared to the CT within each cohort using a paired t-test. The mean ratio of volumes delineated on each MR sequence to the volumes delineated on CT was calculated.

### Results

The radiologist training substantially improved the delineation variability for all three image data sets (see figure 1). Prior to radiologist training, the delineation on MEDIC sequence showed a similar variability to CT and the SPACE sequence significantly more ( $P = 0.05$ ). Post-training delineation on the MEDIC sequence showed a significantly reduced variability compared to CT ( $P = 0.01$ ) and the SPACE sequence similar to CT. The MEDIC sequence gave the least delineation variability in 9/10 post-training patients (figure 2) and was preferred by all delineators.

The volumes on both MR sequences were consistently smaller than on CT. Post-training the SPACE volume was  $87 \pm 2\%$  of the CT (mean  $\pm$  s.e.m.). The MEDIC volume was  $96 \pm 3\%$  of the CT. Further work will investigate the reason for differences in volume size between the two MR sequences.

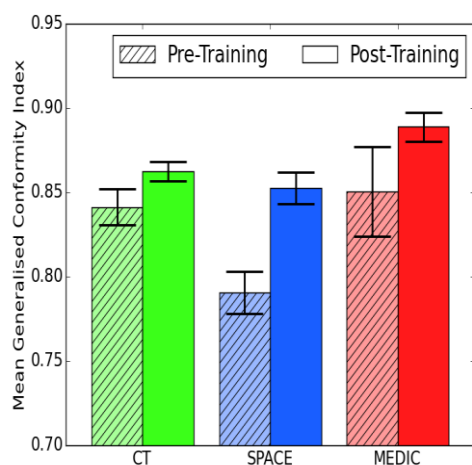


**Figure 1** Mean conformity index pre and post radiologist training. 1 indicates perfect agreement. Error bars are one s.e.m.

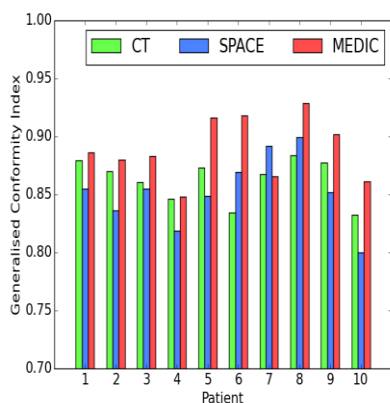


**Figure 2** Conformity index for each post-training patient.

### Conclusion

Radiologist training reduced delineation variability on all sequences and particularly on the MR sequences. Post-training the MEDIC sequence had the least delineation variability, was preferred by all delineators and produced slightly smaller volumes compared to CT. This study suggests the MEDIC sequence in conjunction with radiologist training can reduce the variability in prostate delineation.

**EP-2048 Development and implementation of a cost-effective technique to improve CT scans for contouring**  
D. Nash<sup>1</sup>, A.T. Davis<sup>1</sup>, A.L. Palmer<sup>1</sup>

<sup>1</sup>Queen Alexandra Hospital, Medical Physics, Portsmouth, United Kingdom

### Purpose or Objective

Radiotherapy CT scans are generally of inferior image quality (IQ) to a diagnostic CT scan. However, for IMRT and VMAT, more intricate structures need to be visualised, thus needing superior IQ. This is particularly true considering that the clinician outlining can be the most significant uncertainty in radiotherapy. This work was to develop a method of enhancing IQ for contouring without impairing the dose calculation, introducing any motion error or any additional imaging dose.

### Material and Methods

The proposed method was to provide a second reconstruction of the planning CT raw data with alternative, optimised, parameters specifically to improve the image for contouring. The second scan was to be fused with the planning scan but never used for planning dose calculations.

The preferred parameters were determined, with an initial focus on head and neck (H&N) scans. These were determined qualitatively by two experienced physicists by reconstructing previous scans acquired on a Canon Aquilion LB CT scanner, with a particular focus on edge and contrast enhancement. Reconstruction of the same data set meant no induced error due to motion between two scans, nor any additional radiation dose. Parameters changed included the reconstruction kernel to a head-specific one from the standard body one (FC13) and reduction of the reconstruction FOV diameter. The scan was then fused onto the planning CT scan and guidance sought from two experienced radiation oncologists.

For the chosen parameters, the next 11 (6 with IV contrast) head and neck patients had this second scan reconstructed. Each oncologist was provided with a short questionnaire asking to qualitative opinions on the additional scan, whether there was any reduction in outlining time, their degree of confidence in images and how they compared to diagnostic scans stored for the patient on the PACS system. Comments were also requested.

### Results

The selected image parameters for the secondary reconstruction were to reduce the FOV to approximately 20cm, from the usual 55 or 80 cm, and changing the reconstruction kernel to a sharper head kernel (FC44). An example is shown in fig. 1.

For 9 of the 11 scans the Oncologists reported a reduction in outlining time, with no change for 2. For all scans the Oncologists had more confidence in their outlining. When compared against PACS, 9/11 were superior, 1/11 equivalent and 1 poorer (which was acquired at a different hospital). In terms of the comments given, all were positive. Based on these results the technique was adopted for all H&N patients and performed automatically with little workflow impact.

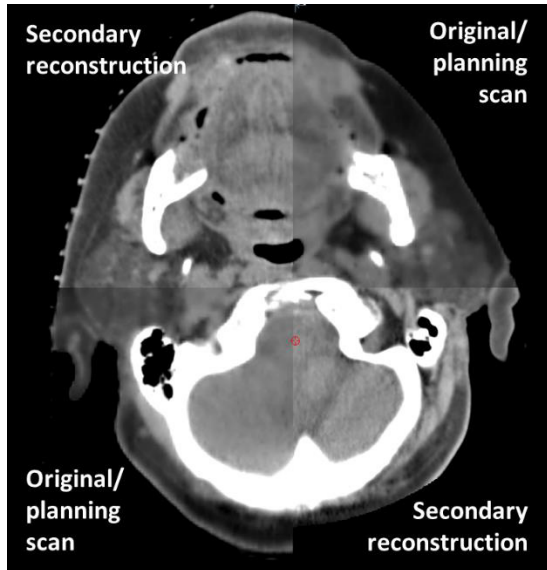


Fig. 1. Example image.

### Conclusion

A technique to provide enhanced IQ from a radiotherapy CT scanner has been developed and demonstrated qualitatively to be superior to conventional scans. Major benefits of the technique include no additional time required for the scan, no extra radiation dose and no motion effects introduced with use of the second scan. Further work including a contouring study is planned.

### EP-2049 Patient specific pixel-based weighting factor bone-only dual-energy x-ray imaging

S. Darvish-Molla<sup>1</sup>, M. Reno<sup>2</sup>, M. Sattarivand<sup>1,2,3</sup>

<sup>1</sup>Nova Scotia Health Authority, Radiation Oncology - Medical Physics, Halifax, Canada ; <sup>2</sup>Dalhousie University, Physics and Atmospheric Science, Halifax, Canada ; <sup>3</sup>Dalhousie University, Radiation Oncology, Halifax, Canada

### Purpose or Objective

Implement the novel pixel-based weighting factor dual energy (DE) algorithm for effective soft-tissue suppression throughout the image to enhance the bone-only image quality and to overcome the limitation of the conventional DE algorithm with constant weighting factor, which is restricted to regions with uniform patient thickness.

### Material and Methods

A step phantom was constructed consisting of slabs of solid water and average bone materials. Thicknesses of bone ranged from 0 to 6 cm in one direction, and solid water from 5 to 30 cm in the other direction, creating 7 by 7 regions of interest (ROIs). The slabs were stacked and placed on a custom-made plastic stand, angled at 42°, such that the central axis of the x-ray beam was perpendicular to the phantom surface. Using Brainlab's ExacTrac system, projection images of the step phantom were acquired at (60 kVp, 40 mAs) and (140 kVp and 12 mAs). Using an in-house Matlab code, the optimal pre-calculated weighting factors ( $\omega$ ) were found by varying values in the range 0-2 for each ROI such that the soft tissue contrast-to-noise ratio (CNR) reached zero. CT images of Rando phantom were acquired using thorax protocol. Ray tracing technique was used to calculate the bone and soft-tissue DRRs (digitally reconstructed radiographs) (Figure 1b,c). Weighting factors for different pixel locations on the DRRs were interpolated (or extrapolated) using the pre-calculated weighting factors and the  $\omega$  image for Rando phantom was generated. By applying the  $\omega$  image into the DE algorithm and utilizing noise suppression algorithm, the bone-only DE image was generated and compared to the clinical single energy x-

ray image and conventional DE image which uses a constant  $\omega$  throughout the image. Signal-to-noise ratio (SNR) of regions with different soft-tissue and bone thicknesses in step phantom was investigated for both DE techniques.

### Results

The optimal pre-calculated  $\omega$  values were found to be in a range [0.82, 1.19] depending on the region thickness in step phantom (Figure 1a). The  $\omega$  values that cancels 25 cm (ROI1) and 10 cm (ROI2) soft-tissue overlapped with 3 cm bone were calculated as 0.93 and 0.83, respectively. Figure 1d demonstrates the  $\omega$  image of Rando for the given projection view. Figure 2 demonstrates the effectiveness of the PP-DE algorithm compared to the clinical single energy x-ray image and conventional DE images (with  $\omega=0.93$  and  $\omega=0.83$ ). The SNR of DE image for ROI1 and ROI2 of the step phantom was 45 and 674 for PP-DE compared to 43 and 203 for conventional DE, respectively.

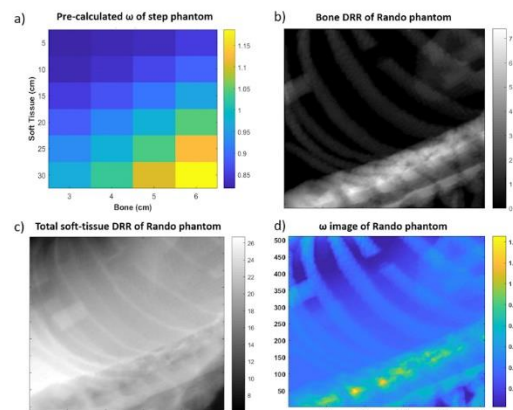


Figure 1. Generating pixel-based  $\omega$  image (d) from precalculated  $\omega$  values of step phantom (a) and Bone and soft-tissue DRRs (b,c)

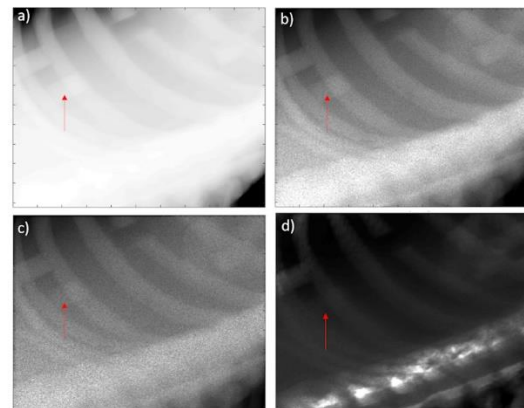


Figure 2. a) Single Energy clinical x-ray image, b) Conventional DE image with  $\omega=0.83$ , c) Conventional DE image with  $\omega=0.93$ , d) the novel pixel-based bone-only DE image that effectively suppresses different thicknesses of soft-tissue simultaneously. Note that the red arrow pointed to the solid water plug, inserted to the lung of Rando Phantom, which should not appear in the bone-only DE images.

### Conclusion

Bone-only patient specific pixel-based algorithm was successfully implemented, which could have clinical interests for image guidance for spine SBRT patients. Compared to the conventional DE, this novel technique creates images with improved bone contrast, specifically in soft tissue overlapping regions, improved SNR, thus enhanced image quality for precise tumor localization.

### EP-2050 Implementation of CT-based attenuation maps of RT positioning devices in PET/MRI - online vs offline

L. Taeuber<sup>1,2,3</sup>, A. Pfaffenberger<sup>1,3</sup>, Y. Berker<sup>4</sup>, B. Beuthien-Baumann<sup>5,6</sup>, A.L. Hoffmann<sup>7,8,9</sup>, E. Troost<sup>6,7,8,9,10</sup>, S.A. Koerber<sup>3,6,11</sup>, M. Kachelrieß<sup>4</sup>, C. Gillmann<sup>1,3</sup>

<sup>1</sup>German Cancer Research Center, Division of Medical Physics in Radiation Oncology, Heidelberg, Germany ; <sup>2</sup>University of Heidelberg, Faculty for Physics and Astronomy, Heidelberg, Germany ; <sup>3</sup>Heidelberg Institute for Radiation Oncology, National Center for Radiation Research in Oncology, Heidelberg, Germany ; <sup>4</sup>German Cancer Research Center, Division of X-Ray Imaging and Computed Tomography, Heidelberg, Germany ; <sup>5</sup>German Cancer Research Center, Division of Radiology, Heidelberg, Germany ; <sup>6</sup>National Center for Tumor Diseases, Partner Site Dresden, Dresden, Germany ; <sup>7</sup>Helmholtz-Zentrum Dresden-Rossendorf, Institute of Radiooncology - OncoRay, Dresden, Germany ; <sup>8</sup>Technische Universität Dresden, Faculty of Medicine and University Hospital Carl Gustav Carus Dresden-Department for Radiotherapy and Radiation Oncology, Dresden, Germany ; <sup>9</sup>OncoRay, National Center for Radiation Research in Oncology, Dresden, Germany ; <sup>10</sup>German Cancer Consortium, Partner Site Dresden, Dresden, Germany ; <sup>11</sup>Heidelberg University Hospital, Department of Radiation Oncology, Heidelberg, Germany

#### Purpose or Objective

Integrating PET/MR hybrid imaging into radiation treatment (RT) planning has great potential to improve tumor delineation and dose prescription. Since these scans must be acquired under treatment conditions, attenuation correction of RT positioning devices is necessary. Attenuation maps can be implemented either online (directly at the PET/MRI scanner) or offline (at another PC). In this study, we compare both methods and assess their impact on PET image quality using a CT-based user-generated attenuation map of an RT table overlay.

#### Material and Methods

CT images of an RT table overlay (in-house construction) were acquired on a stand-alone CT (Somatom Definition Flash, Siemens Healthineers, Erlangen, Germany) at 120 kV and 360 mAs. Based on the CT images, an attenuation map of the RT table overlay was calculated via the bilinear approach [1].

The RT table overlay was then mounted onto the patient table of the PET/MRI (Biograph mMR, Siemens Healthineers) and two sets of PET-measurements were taken using an active <sup>68</sup>Ge phantom (32 MBq, 10 min scan time). The phantom was scanned with the RT table overlay (RT scan), and without the RT table overlay (reference scan).

PET reconstructions of the phantom scans were performed online at the PET/MRI scanner and offline using the e7tools (Version VA20, Siemens Healthineers) with identical reconstruction parameters. For the PET-reconstructions of the RT scan, the attenuation map of the RT table overlay was implemented. Attenuation correction accuracy was evaluated by comparing PET activities between RT and reference scans in 10 ROIs placed every 10 slices along the phantom in longitudinal direction, both for the online and the offline reconstruction methods.

#### Results

The RT table overlay attenuation map was successfully added to the hardware attenuation maps produced online and offline. Table 1 compares measured PET activities. For the online reconstruction, a mean percentage difference of 0.7% was found between the reference and the RT scan. For the offline reconstruction, a mean percentage difference of 1.4% was found. A systematic difference of around 500 Bq/ml was found between the online and offline reconstructions.

#### Conclusion

For the integration of PET/MRI in RT planning, attenuation correction of RT positioning devices is viable. The online

reconstruction seems to be more accurate, but it has the disadvantage that the attenuation map must be removed from the system after every RT measurement to prevent an incorrect reconstruction of patient data that were not scanned in RT setup. Alternatively, offline reconstruction can be implemented at any PC via e7tools, and the reconstruction could be automated, thereby diminishing human error. The cause of the systematic signal difference in online and offline reconstruction needs to be investigated further.

[1] Carney et al. doi: 10.1118/1.2174132

**Table 1: Comparison of measured PET activities for online and offline reconstruction of the RT and the reference scans.**

Slice location	Online reconstruction			Offline reconstruction		
	RT scan [Bq/ml]	Reference scan [Bq/ml]	Difference [%]	RT scan [Bq/ml]	Reference scan [Bq/ml]	Difference [%]
10	2607	2627	-0.8	2142	2140	0.1
20	2645	2612	1.3	2149	2126	1.1
30	2588	2571	0.7	2121	2103	0.8
40	2595	2601	-0.2	2136	2115	1.0
50	2571	2553	0.7	2113	2078	1.7
60	2566	2555	0.4	2103	2071	1.5
70	2571	2567	0.1	2094	2067	1.3
80	2591	2600	-0.3	2089	2078	0.5
90	2653	2635	0.7	2105	2076	1.4
100	2690	2688	0.0	2053	2029	1.2

#### EP-2051 A comparative analysis of MR signal normalization methods during proton therapy treatment

G. Buizza<sup>1</sup>, C. Paganelli<sup>1</sup>, G. Fontana<sup>2</sup>, A. Franconeri<sup>3</sup>, M.V. Raciti<sup>3</sup>, A. Pella<sup>2</sup>, L. Anemoni<sup>4</sup>, A. Iannalfi<sup>5</sup>, L. Preda<sup>3</sup>, F. Valvo<sup>5</sup>, G. Baroni<sup>1</sup>

<sup>1</sup>Politecnico di Milano, DEIB - Department of Electronics Information and Bioengineering, Milano, Italy ; <sup>2</sup>National Centre of Oncological Hadrontherapy CNAO, Clinical Bioengineering Unit, Pavia, Italy ; <sup>3</sup>National Centre of Oncological Hadrontherapy CNAO, Diagnostic Imaging Unit, Pavia, Italy ; <sup>4</sup>National Centre of Oncological Hadrontherapy CNAO, Medical Radiology Technicians Unit, Pavia, Italy ; <sup>5</sup>National Centre of Oncological Hadrontherapy CNAO, Radiation Oncology Unit, Pavia, Italy

#### Purpose or Objective

To compare typical normalization strategies applied to T1- and T2-weighted MR images in patients affected by meningioma for evaluating the MR signal intensity (SI) during proton therapy (PT).

#### Material and Methods

55 exams consisting of contrast-free T1w (VIBE, 3D GRE, TR=5.16 ms, TE=2.09 ms, flip angle=9°, resolution=1.02x1.02x1.02 mm) and T2w (TSE, 2D SE, TR=11.9-14.5 s; TE=104 ms, flip angle=80°, resolution=0.47x0.47x3 mm) MRI were acquired on a 3T scanner during PT for 17 patients. Gross tumour volumes (GTV) were manually delineated on T2w images, whereas white matter (WM) contours were obtained by an automatic algorithm, post-processed and visually checked. T1w images were rigidly registered on T2w images, to allow their evaluation on the same regions. Three normalization methods based on histogram matching (M1,[1]), WM-driven standardization (M2,[2]) and min-max (M3) were implemented. Two metrics computed in WM areas were considered for the evaluation: the Jeffreys' divergence between any combination of mode-aligned histograms (JD) and the ratio between interquartile range and median computed on the median SI values (npCV). Medians and percentiles (5<sup>th</sup>-95<sup>th</sup>) from WM and GTV regions were also compared.

#### Results

For T1w-images, JD (median[IQR]) was 0.029[0.023], 0.035[0.041] and 0.056[0.074] for M1, M2 and M3, with respect to 0.045[0.045] derived from raw ones. According to JD and npCV (Tab. 1), M1 was the best-performing

method. For T2w-images, JD was 0.182[0.496], 0.036[0.038] and 0.095[0.152] for M1, M2 and M3, with respect to 0.090[0.142] in raw images. M2 was found to outperform all the other methods according to JD, whereas the use of M1 was supported by npCV (Tab. 1). For both T1w- and T2w-images it was noticed that WM variability measured by npCV was lower than the GTV one, apart from M2 for which median values were close to zero. Differences in variability varied for different normalization methods, but all of them qualitatively kept the WM-GTV relation observed in raw images (Fig.1).

**Conclusion**

Overall, M1 showed better performance for T1w-images and both M1 and M2 for T2w-images. M3 is the simplest method but it does not seem to guarantee a comparison between MRI acquisitions. The evaluation of the performance of different MR normalization methods is not trivial but required for MRI analysis in longitudinal studies, as well as for applications in feature extraction for patient classification or stratification. Harmonized evaluation of such (and other) pre-processing method is therefore needed.

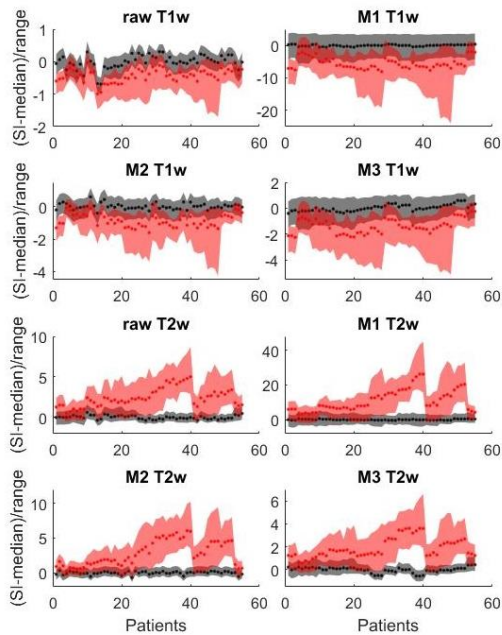


Figure 1 - Median distributions for T1w- (up) and T2w- (down) raw images and normalized by M1, M2 and M3, in WM (black) and GTV (red) regions.

npCV	WM	GTV	npCV	WM	GTV
T1w			T2w		
raw	0.077	0.107	raw	0.096	0.281
M1	0.016	0.108	M1	0.081	0.619
M2	1.790	-0.710	M2	2.359	1.291
M3	0.066	0.204	M3	0.109	0.342

Table 1 - Values of npCV for T1w- (left) and T2w- (right) raw images and normalized by M1, M2 and M3, in both WM and GTV (regions).

**Bibliography:**

[1] L.G. Nyul, J.K. Udupa, and Xuan Zhang, "New variants of a method of MRI scale standardization," *IEEE Trans. Med. Imaging*, vol.19, no.2, pp.143-150, 2000.

[2] R.T. Shinohara, E.M. Sweeney, J. Goldsmith, N. Shiee, F. J. Mateen, P. A. Calabresi, S. Jarso, D. L. Pham, D. S. Reich, and C. M. Crainiceanu, "Statistical normalization techniques for magnetic resonance imaging," *NeuroImage Clin.*, vol.6, pp.9-19, 2014.

**EP-2052 Commissioning monoenergetic CT images for optimal proton dose calculations using TwinBeam scans**

P. Randers<sup>1</sup>, M. Fuglsang<sup>1</sup>, V. Trier Taasti<sup>1</sup>  
<sup>1</sup>Aarhus University Hospital, Danish Centre of Particle Therapy, Aarhus, Denmark

**Purpose or Objective**

Monoenergetic CT images derived from two CT images acquired at different kVps offer the potential of reducing the beam hardening (BH) effect compared to single energy CT (SECT) images. Commissioning monoenergetic CT images for proton dose calculations could therefore lead to a reduced range uncertainty. The first step is to determine the optimal energy leading to the lowest possible BH effect, and then to establish stoichiometric calibration curves from CT numbers to proton stopping power ratios (SPRs) and mass densities.

**Material and Methods**

CT scans of a tissue equivalent electron density phantom (Gammex, Middleton, WI) were acquired with a SOMATOM Definition Edge dual energy CT (DECT) scanner (Siemens Healthineers, Forchheim, Germany). This is a single source scanner with a TwinBeam (TB) mode (Fig.1), which enables simultaneous dual energy acquisition, which reduces the risk of motion blurring. CT scans were acquired in both TB and SECT mode. Seven different clinically relevant configurations were used and fifteen different tissue equivalent inserts were scanned individually within each configuration (Fig 1). All remaining positions were filled with solid water inserts of the same composition as the bulk phantom, to avoid interference between the different inserts. Monoenergetic images were generated using the Siemens syngo.via software at different energies (monoEs). The size of the BH effect was quantified as the standard deviation of the monoenergetic CT numbers over the various configurations for a specific insert at a given monoE. The BH effect was analysed for all inserts together by summing over the inserts, as well as for each insert separately. The CT number differences for the SECT scans of the seven configurations were also extracted and used to investigate if the TB monoenergetic CT images decreased the BH compared to SECT. After obtaining the optimal monoE, stoichiometric calibration curves were fitted for the small and the large phantom, respectively.

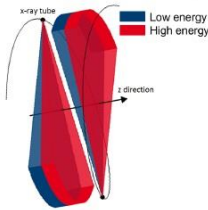
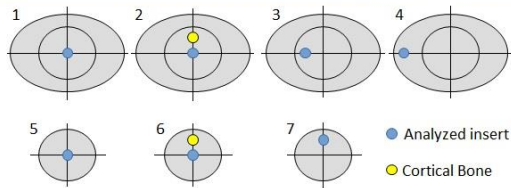
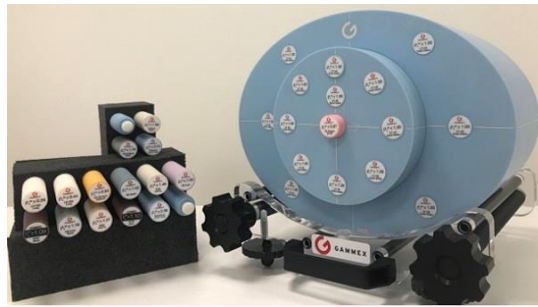


**Figure 1:** *Upper:* Electron density calibration phantom, with fifteen tissue equivalent insert materials. The phantom consists of an inner head sized phantom, and an outer torso shaped phantom. *Middle:* The seven clinically realistic configurations used to investigate the beam hardening effect. *Bottom:* TwinBeam mode, the x-ray spectrum is split in two by different prefiltration materials to obtain DECT scans with two different energies.

**Results**

The CT number variance was very small for the low- to medium-density inserts and could be assumed to originate from CT noise rather than BH. In contrast, large differences were seen for the CT number of the high-density bone inserts. The lowest BH effect was found at slightly different monoEs for the four high-density bone inserts. The average optimal monoE was found at 90 keV. At this monoE, the BH was at least reduced by half compared to SECT. The resulting calibration curves for the small and large phantom differed only slightly at very high monoenergetic CT numbers, above the clinically relevant region (Fig. 2)

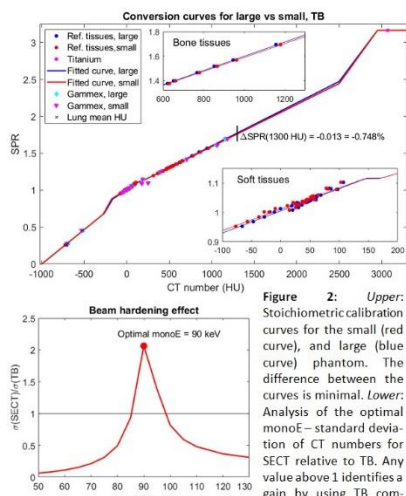


**Figure 2:** *Upper:* Stoichiometric calibration curves for the small (red curve), and large (blue curve) phantom. The difference between the curves is minimal. *Lower:* Analysis of the optimal monoE—standard deviation of CT numbers for SECT relative to TB. Any value above 1 identifies a gain by using TB compared to SECT, as TB then reduces the BH effect.

**Conclusion**

Using monoenergetic images at 90 keV derived from TB DECT scans, the BH effect can be markedly reduced compared to SECT. The difference between the calibration curves for the small and large phantom was minor, which would decrease the SPR deviation when

patients' sizes differ from the size of the calibration phantom used to generate the curves.

**EP-2053 Pelvic plan adaptation to manage systematic rotations without CT re-imaging**

A. Licup<sup>1</sup>, S. Van Kranen<sup>1</sup>, M. Buijs<sup>1</sup>, F. Koetsveld<sup>1</sup>, J. Sonke<sup>1</sup>, P. Remeijer<sup>1</sup>  
<sup>1</sup>Netherlands Cancer Institute, Radiotherapy, Amsterdam, The Netherlands

**Purpose or Objective**

In IGRT workflows for pelvic treatments, rotations often remain uncorrected. Especially for large target volumes (TVs), e.g. cervical tumors that include pelvic and para-aortic lymph nodes, large CTV to PTV margins are required to account for the residual errors. Replanning on a repeat CT (rCT) scan may correct for systematic rotations, however this increases clinical workload and patient imaging dose and may still fail to image the systematic rotational error. Therefore we propose to simulate an rCT scan based on the clinical (rigid) registrations of TVs in CBCT scans. To overcome large displacements outside the registered region, often seen as considerable displacements of the patient skin contour, we developed and validated a technique that restricts skin deformations while correcting for the observed systematic rotations in the pelvic area.

**Material and Methods**

To simulate an rCT scan, we propose to use compactly-supported radial basis functions (CSRBF) [1]. CSRBF is a method in which rigid registrations are confined in a local region, outside of which non-rigid deformations reduce smoothly to zero within a set RBF radius. Figure 1 illustrates this method for a cervical cancer patient model.

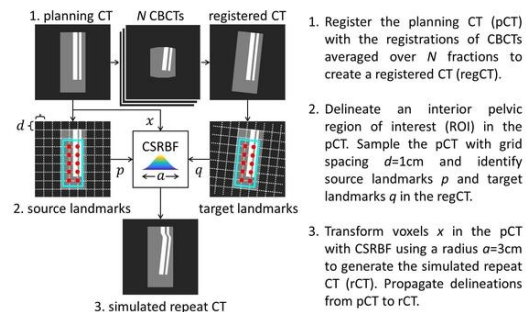


Figure 1. Schematic to simulate a repeat CT with CSRBF. The blue delineation encloses the interior pelvic region of interest (ROI) marked by source and target landmarks *p* and *q* (red grid points).

We validated the simulated rCT scan based on a single fraction (*N*=1) on the following aspects:

- (1) skin contour preservation,
- (2) interior pelvic anatomy rigid registration, and
- (3) delineation shape preservation.

**Results**

Offline simulation of the rCT took 6mins on a 64-bit 3.40GHz Intel® Xeon® PC. Figure 2A shows a translation-only registration between the planning CT (pCT) and a single CBCT with a large rotation, the effect of uncorrected rotations are clearly seen. Figure 2B shows an example where we simulate an rCT on the same CBCT. The patient outline is preserved while the internal anatomy rotations are corrected. Figure 2C is a grey level difference image between pCT and rCT registered on the skin. We evaluated the root mean squared differences (RMSD). An RMSD=0 suggests high similarity. Figure 2C shows minimal RMSD outside the ROI, validating (1). To validate (2), the entire rCT was rigidly registered back to the pCT (figure 2D), with minimal RMSD inside the ROI. Figure 2E summarizes the RMSD statistics. Finally, to

validate (3), We evaluated Dice's coefficient to verify shape similarity between pCT and rCT delineations (figure 2F). Values near 1 indicate shape preservation except for kidneys, as these intersect the ROI superior boundary where non-rigid transformations were applied.

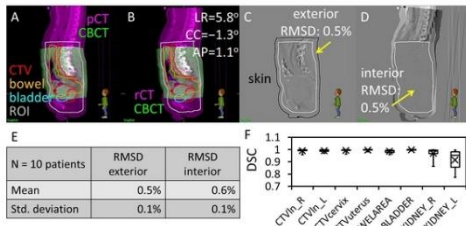


Figure 2. (A) Overlay of planning CT (pCT) with CBCT and (B) simulated rCT with CBCT. (C) Grey value differences between pCT and rCT, show minimal RMSD in the region exterior to the ROI. (D) Registration of rCT back to the pCT shows minimal RMSD within the ROI. (E) Summary RMSD statistics for 10 patients. (F) Dice similarity coefficient (DSC) close to 1 verifies shape similarity between pCT and rCT delineations.

**Conclusion**

Simulation of a repeat CT scan based on RBFs successfully corrects pelvic rotations, while maintaining minimal skin displacement and preserving tumor and OAR shapes. To manage systematic rotations, the simulated rCT should be based on the average registration of N CBCTs. The proposed method is a highly efficient alternative for repeat CT scanning to adapt pelvic treatment plans for systematic rotations.

Reference:

1. M. Fornefett, K. Rohr and H.S. Stiehl. Image and Vision Computing 19, 87-96 (2001).

**EP-2054 Potential role of dual-energy CT imaging modality in the neoadjuvant radiotherapy: a phantom study**

P. Gallo<sup>1</sup>, A. D'Alessio<sup>2</sup>, F. Padelli<sup>3</sup>, M.L. Fumagalli<sup>1</sup>, E. D'ippolito<sup>2</sup>, T. Giandini<sup>2</sup>, C. Tenconi<sup>2</sup>, C. Cavatorta<sup>2</sup>, M.G. Bruzzzone<sup>3</sup>, E. Pignoli<sup>2</sup>, E. De Martin<sup>1</sup>

<sup>1</sup>Fondazione IRCCS Istituto Neurologico Carlo Besta, Health Department, Milan, Italy ; <sup>2</sup>Fondazione IRCCS Istituto Nazionale dei Tumori di Milano, Medical Physics Unit, milan, Italy ; <sup>3</sup>Fondazione IRCCS Istituto Neurologico Carlo Besta, Neuroradiology Department, Milan, Italy

**Purpose or Objective**

**Purpose/Objective:**

Dual-energy CT (DECT) is a more and more widespread technique based on the merging of two CT scans acquired at different tube potentials (80 and 140 kVp) to improve differentiation of materials and patient tissues. Images obtained through virtual monoenergetic reconstruction (MONO) can improve image quality compared with conventional single-energy CT scanning (SECT). The purpose of this study is to investigate potential applications of MONO reconstructions to improve soft-tissue contrast with no need of contrast medium injection, and consequent repercussions on target volume identification and delineation.

**Material and Methods**

The CIRS® Electron Density Phantom containing different tissue-equivalent inserts was imaged using two CT scanners: Siemens Somatom Confidence (sequential scanning at two tube voltages) and General Electric (GE) Revolution GSI (rapid switching of tube voltage). SECT and DECT acquisitions were performed maintaining a similar dose level and MONO images were then reconstructed at various energies levels (40, 50, 70, 100, 120, 140, 190 keV). In the first step of our analysis, both SECT and DECT images were reconstructed through a Filter Back Projection (FBP) algorithm. CT numbers and their standard deviations were measured within the CIRS® inserts to

evaluate different contrasts (breast-adipose, muscle-adipose, liver-adipose) of MONO reconstructions with respect to SECT images.

**Results**

In general, a soft-tissue signal enhancement was observed with the decrease of MONO images reconstruction energy. The greatest signal enhancement is observed at 40 and 50 keV compared to SECT for adipose and breast inserts for both scanners (Figure 1). Moreover, at 40 keV breast-adipose CT number contrast results in +48% and +45% for GE and Siemens respectively when compared to SECT data. At 50 keV this contrast enhancement is still observable (+19% and +14% for GE and Siemens respectively). As expected, higher energy MONO reconstructions show less contrast with respect to SECT data (Table1).

**Conclusion**

**Conclusion:**

Low energy (40-50 keV) DECT MONO reconstructions increase soft-tissue contrast, potentially allowing a better radiotherapy target volume identification and delineation, in particular when breast and pelvic anatomy are involved. The increased image noise associated with lower MONO energies could be at least partially compensated by using iterative reconstruction algorithms. Our results suggest that a great advantage might be achievable for example in the neoadjuvant radiotherapy of breast cancer, especially in the partial breast irradiation with ablative intent.

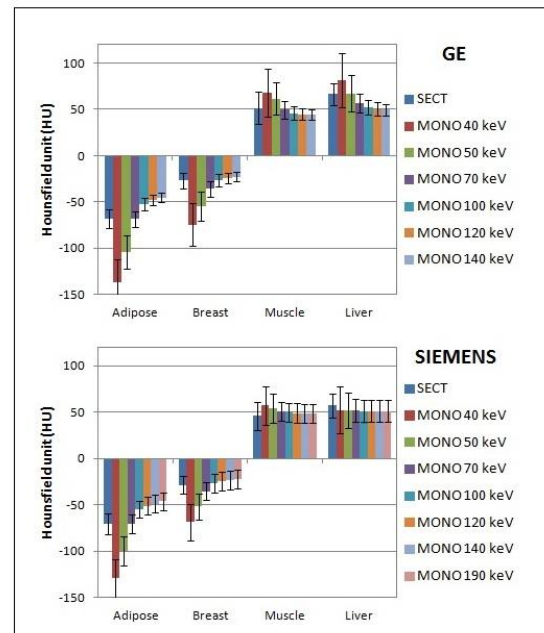


Figure 1: CT numbers measured on SECT and DECT images of CIRS® Electron Density Phantom

Table1: Contrast variation between Dual Energy CT and Single Energy CT acquisitions.

CT Scanner	Tissue contrast	Contrast variations (%) between DECT and SECT acquisition.						
		40 keV	50 keV	70 keV	100 keV	120 keV	140 keV	190 keV
SIEMENS	BREAST-ADIPOSE	45%	14%	-16%	-32%	-36%	-39%	-41%
	MUSCLE-ADIPOSE	60%	32%	4%	-10%	-14%	-16%	-18%
	LIVER-ADIPOSE	42%	19%	-4%	-17%	-20%	-22%	-24%
GE	BREAST-ADIPOSE	48%	19%	-22%	-39%	-43%	-46%	//
	MUSCLE-ADIPOSE	70%	38%	-2%	-18%	-23%	-26%	//
	LIVER-ADIPOSE	61%	27%	-7%	-23%	-27%	-30%	//

**EP-2055 Impact of patient-specific MRI distortion correction for stereotactic cranial target definition**

T. Gevaert<sup>1</sup>, B. Engels<sup>1</sup>, C. El Aisati<sup>1</sup>, M. De Ridder<sup>1</sup>

<sup>1</sup>Universitair Ziekenhuis Brussel, Radiotherapy, Brussels, Belgium

### Purpose or Objective

The accuracy of a stereotactic treatment is primarily limited by the least accurate process in the whole chain of events from patient scanning to patient treatment. The total error is accumulated through the processes of a) target localization and planning using medical imaging (computed tomography (CT) and magnetic resonance imaging (MRI), image fusion, dose planning, and b) dose delivery using image guidance patient positioning, immobilization devices and a radiation dose delivery system.

QA is often performed on the dose delivery and planning section rather than the localization. This targeting is primarily limited by the accuracy of the CT and MRI images. In theory CT scans are precise. In contrast, MRI datasets are subjected to distortions, due to nonlinearity of gradient fields, and may cause incorrect target definition.

This study aimed to analyze the impact of a patient-specific algorithm, Cranial distortion Elements (Brainlab, München, Germany), rather than a manufacture-specific, to correct spatial distortion in cranial magnetic resonance images.

### Material and Methods

Twelve trigeminal patients treated with a single dose of 90 Gy with a 4mm collimator were studied retrospectively. A radiosurgery target (gross target volume (GTV)) was defined on a 1.0mm T1 MPRAGE and T2 MRI corrected for distortion with a machine-specific algorithm.

For this study, the manufacture-specific corrected MRI was further corrected using a patient-specific distortion correction algorithm that references the treatment planning CT. The GTV were then mapped onto this newly created patient specific corrected MRI dataset. The original defined target and the corrected deformed object were mutually compared by means of several quantitative measures such as Dice, Jaccard, and Hausdorff indices. The average distance between the two centers of the two GTV was also calculated.

### Results

On average, a good agreement was found between both GTV resulting in a Dice index of 0.76 (SD 0.23) ranging between 0.13 and 0.92. The Jaccard index, which is an intersection over Union was similar ( $p > 0.1$ ) to the Dice with an average of 0.66 (SD 0.23) ranging between 0.09 and 0.86. The greatest of all the distances from a point in GTV to the closest point in the other GTV, called the Hausdorff distance, was 0.73 on average (range 0.50 - 1.80), reflecting good similarity between both GTVs. Average distance between both GTV was 0.43 mm (SD 0.26mm), with a minimum of 0.20 mm and a maximum of 1.10 mm. One out of the 12 patients met criteria of "geometric miss", which was not correlated with clinical outcome.

### Conclusion

Although MRI distortion is often corrected manufacture specific, distortion may persist due to patient specific conditions. Our study showed that the cranial distortion Elements correct all images even when manufacture-specific corrections fail. In order to avoid any geometrical miss, a patient specific distortion correction must be applied for all cranial indication.

### EP-2056 Feasibility of realistic Digitally Reconstructed Radiograph (DRR) rendering through shallow learning

J. Dhont<sup>1,2</sup>, J. Vandemeulebroucke<sup>1</sup>, I. Mollaert<sup>3</sup>, D. Verellen<sup>2,3</sup>

<sup>1</sup>Vrije Universiteit Brussel, Department of Electronics and Informatics ETRO, Brussels, Belgium ; <sup>2</sup>Vrije Universiteit Brussel, Faculty of Medicine and Pharmaceutical Sciences, Brussels, Belgium ; <sup>3</sup>GZA Ziekenhuizen Sint-Augustinus- Iridium

kankernetwerk, Department of Medical Physics, Antwerp, Belgium

### Purpose or Objective

Accurate DRRs with realistic soft-tissue contrast could aid markerless tumor tracking. Purpose of this study is to investigate the feasibility of accurate DRR rendering using a shallow neural network (NN) that models the CT-to-Xray intensity, including non-linear effects such as beam-hardening, omitting multiple phantom measurements and Xray source modeling.

### Material and Methods

To overcome the black box character of deep-learning (DL), this study was divided into several controlled steps. Initially, real-patient data was omitted to avoid object deformations, and input and output data was rendered using a static CIRS thorax phantom. One planning CT image (512\*512\*328, 1 mm slice thickness, 1.1x1.1 mm<sup>2</sup> in-plane res., Toshiba) and one full-fan CBCT image (TrueBeam STx, Varian) were acquired, of which only the anterior-posterior (AP) projection image (1024\*768 ppx, 0.39 x 0.39 mm<sup>2</sup> res.) was used.

To render input for the NN, a ray-tracing algorithm was developed in Matlab, see Figure 1. Taking into account the CBCT acquisition geometry, the nearest CT voxel was sampled every 1 mm on a straight line from the Xray source to each pixel in the AP projection image, resulting in 1024\*768 rays. Per ray, most surrounding was discarded, keeping 500 samples per ray centered around the phantom as input to the model.

Secondly, to determine the model topology and optimize the hyper-parameters while keeping other degrees of freedom to a minimum, the line integral over each ray was taken as the output target value for each ray, creating a raw DRR value. In total 1024\*768 input-output couples were generated, of which 24% were discarded to avoid imbalance. Of the remainder, 98% was used to determine model topology, for hyper-parameter optimization and for training, while 2% was used for validation, sampled randomly.

A shallow feed-forward regression network, see Figure 1, was created using TensorFlow, consisting of an input layer of 500 nodes, one single-node fully-connected hidden layer with rectified linear activation (ReLU) function, and a single-node output layer. Stochastic gradient descent was used to optimize the network weights and the loss function was minimized based on the mean squared error (MSE). The network accuracy was evaluated using student's t-test to determine the statistical significance of the difference between the predicted and ground-truth output values in the validation data-set.

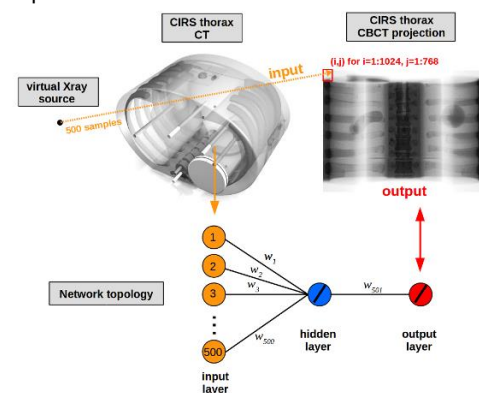


Figure 1: A ray-tracing algorithm was used to sample the CT image and generate 500 input samples per ray, for every pixel in the corresponding projection image, whose values will be used as targets in the illustrated network topology.

### Results

Student's t-test showed no significant difference between the predicted and ground-truth output values ( $p < 0.001$ ), with maximum intensity differences of 0.1%.

## Conclusion

The first steps in this feasibility study, implemented to avoid the black box nature of DL, allowed to render useful and sufficient training and validation data, and to construct an accurate NN with optimized hyper-parameters. In a next step, the pixel intensity in the projection image corresponding to each ray will be used as output target value, to include the non-linearities into the model and to render realistic DRRs.

## EP-2057 Influence of implanted metals in new CT reconstruction algorithm for radiotherapy treatment planning

T. Kamomae<sup>1</sup>, T. Nakaya<sup>2</sup>, F. Kawabata<sup>2</sup>, K. Okudaira<sup>2</sup>, M. Kumagai<sup>1</sup>, H. Oguchi<sup>3</sup>, Y. Itoh<sup>1</sup>, S. Naganawa<sup>1</sup>

<sup>1</sup>Nagoya University Graduate School of Medicine, Department of Radiology, Aichi, Japan ; <sup>2</sup>Nagoya University Hospital, Department of Radiological Technology, Aichi, Japan ; <sup>3</sup>Nagoya University Graduate School of Medicine, Department of Radiological and Medical Laboratory Sciences, Aichi, Japan

## Purpose or Objective

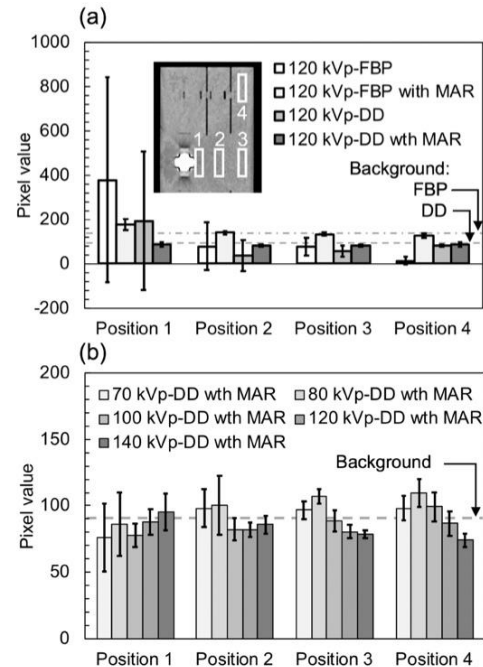
Computed tomography (CT) imaging is used to delineate organs and calculate the dose distributions for treatment planning. To calculate the dose distributions, the CT numbers are converted to relative electron density (RED) or mass density by using the conversion curve that depends on the X-ray tube voltage. A recently developed algorithm directly reconstructs the CT images constructed from the RED values, which are independent of the tube voltage. This algorithm offers the freedom to choose the tube voltage to obtain higher contrast images. We have recently clarified the feasibility of using this algorithm for accurate dose calculations in the low- to middle-density regions correspond to the human body tissues. In this work, we evaluate this algorithm in the regions containing high-density implanted metals, which lead to the metal artifacts.

## Material and Methods

Gammex phantom with various rods inserted was scanned to evaluate the CT number to RED conversion curves. These rods contained titanium and steel. All raw data were reconstructed with the standard filtered back-projection (FBP) and the novel DirectDensit™(DD) algorithms, and additionally, the metal artifact reduction (MAR) algorithm was applied. Furthermore, the CT images of the experimental oral phantom that contained a mock metal crown and tooth were obtained with various tube voltages to evaluate the impact of metal artifacts and dose perturbations.

## Results

For the rods correspond to the human body tissues (i.e., lungs, soft tissues, and bones), the mean differences in pixel values between the present and absent metal rods were  $-6 \pm 31$ ,  $2 \pm 8$ ,  $-2 \pm 25$ , and  $3 \pm 6$  for 120 kV-FBP, 120 kV-FBP with MAR, 120 kV-DD, and 120 kV-DD with MAR, respectively. The maximum pixel value became saturated at about 2500 at the region of titanium and steel for DD images. The artifact indices at 10 mm apart from the metal in the experimental oral phantom were 464, 23, 318, and 8 for 120 kV-FBP, 120 kV-FBP with MAR, 120 kV-DD, and 120 kV-DD with MAR, respectively. For varied tube voltages in DD with MAR images, the artifact indices were 25, 23, 0, 8, and 13 for 70 kV, 80 kV, 100 kV, 120 kV, and 140 kV, respectively. The calculated dose differences between the 120 kV-FBP with MAR and DD with MAR images were in general less than 1% when the density override corrections for the remaining metal artifacts were performed.



## Conclusion

The metal artifacts and dose calculation results of the DD images were the approximation of standard FBP images, and the MAR was also beneficial in the DD algorithm. The restriction of the maximum pixel value in the DD image and the remaining metal artifact that tended to appear in the lower tube voltage need to be considered carefully. The DD algorithm can be used for treatment planning in the regions containing the high-density implanted metals, and lead to the benefit of an optimization of the tube voltage individually in the treatment planning process.

## EP-2058 Measuring eye deformation between planning and proton beam therapy position

M. Jaarsma-Coes<sup>1</sup>, M.S. Schuurmans<sup>2</sup>, M.K.M.A. Hassan<sup>2</sup>, E. Astreindou<sup>3</sup>, M. Marinkovic<sup>4</sup>, F.P. Peters<sup>3</sup>, J.W.M. Beenakker<sup>1</sup>

<sup>1</sup>LUMC, Radiology & Ophthalmology, Leiden, The Netherlands ; <sup>2</sup>LUMC, Radiology, Leiden, The Netherlands ; <sup>3</sup>LUMC, Radiotherapy, Leiden, The Netherlands ; <sup>4</sup>LUMC, Ophthalmology, Leiden, The Netherlands

## Purpose or Objective

Uveal melanoma (UM) is the most common primary malignant intraocular tumour. Proton beam irradiation (PBT) is often the therapy of choice for large tumours. MRI is essential not only for diagnosis but also for the clinical target volume (CTV) definition (shape and extension of the tumour) and PBT treatment planning. However, while PBT is performed with the patient in sitting position, the acquisition of the MRI images are done with the patient in supine position. This change in gravity direction potentially changes the shape of the eye and tumour. As even small geometrical deformation can lead to over- or underdose to the tumour and surrounding healthy tissues, we used MRI to investigate and quantify the effect of different patient positions on the shape of the eye.

## Material and Methods

Seven volunteers and one UM patient were scanned with closed eyes in two positions on a 3T Philips MRI scanner with a 47mm surface coil after giving informed consent. One set of images was acquired in supine position, while a second set was acquired mimicking the patient sitting for PBT (flexed position, figure 1). Additionally, two volunteers were scanned twice in the supine position to assess the reproducibility of the segmentation method.

For the healthy subjects, the analyses were performed on 3D T2-weighted images (0.9mm isotropic) as these provide optimal contrast to differentiate the sclera, while for the UM patients a post-contrast T1 (1.0mm) was used to differentiate between UM and retinal detachment (RD). The analysis strategy is described in figure 1. For the UM patient only the tumour-vitreous border could be accurately compared, as the fast retinal wash-out of the contrast agent changed the appearance of the eye-wall between both acquisitions.

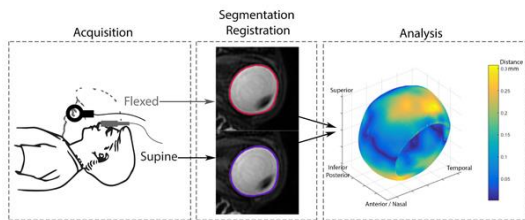


Figure 1. The image in flexed position is registered to the image in supine position and the sclera in both positions is segmented. Subsequently the distances between both segmented sclera meshes were calculated.

**Results**

In healthy controls the median difference between the supine and flexed scans was 0.1mm (95<sup>th</sup> percentile (P): 0.3mm), which is in the order of the reproducibility of the method (95<sup>th</sup> P: 0.3mm), figure 2-A. The slightly larger difference in eye-shapes of subjects 5 was caused by eye-motion artefacts. In the UM patient we found a median deformation of the tumour of 0.1mm (95<sup>th</sup> P: 0.4mm).

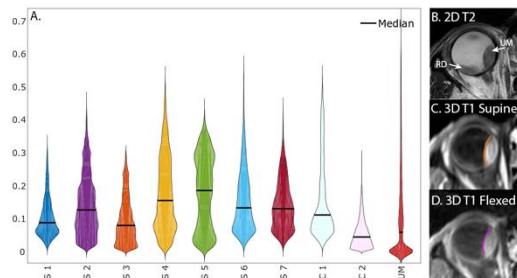


Figure 2: A. Violin plots of the measured distances. Controls (C1&C2) show a measurement reproducibility of 0.3mm. The subjects (S1-S7) and UM patient show similar distances as the controls. B. 2D T2 showing the UM and Retinal detachment (RD). C. 3D-T1 in supine position with segmented UM. D. Registered 3D-T1 in flexed position with segmented UM.

**Conclusion**

Changes in gravity direction produce no substantial changes in sclera and tumour shape. We are currently expanding the number of UM patients, but the results so far indicate that supinely acquired MR images can be used to accurately plan ocular PBT, which is performed in sitting position.

**EP-2059 Assessment of image quality in simulated low-dose paediatric cone beam CT**

J.W.H. Lindsay<sup>1</sup>, A. Bryce-Atkinson<sup>1</sup>, M. Van Herk<sup>1</sup>, M.C. Aznar<sup>1</sup>

<sup>1</sup>The University of Manchester, Faculty of Biology-Medicine and Health, Manchester, United Kingdom

**Purpose or Objective**

Reduction of dose to healthy tissue is imperative to limit the risk of secondary cancers in paediatric patients. Lower imaging dose would naturally reduce this risk and allow for more frequent imaging, which may reduce dose due to

positioning errors and (in proton therapy) range uncertainties. However, it is important to maintain sufficient image quality for position verification and visualisation of potential anatomical changes during the course of radiotherapy. In this work, we have evaluated the image quality for soft tissue visualisation of low-dose CBCT scans simulated for phantom and paediatric patient acquisitions.

**Material and Methods**

CBCT scans of a Catphan 503 phantom were acquired with Elekta XVI v5.02 using 16mA/10ms and 100 kV, 200 projection images. In addition, CBCT scans acquired as part of routine treatment were collected from 10 paediatric patients (aged 3 to 12 years) with tumours in the abdominal-pelvic region. All scans were acquired using the same exposure (16mA/10ms and 100 kV), small field of view, half rotation. Low-dose images were created by adding non-uniform Gaussian noise to the original projection images prior to reconstruction, accurately simulating exposures of 10mA/10ms, 10mA/8ms, and 5mA/5ms while keeping kV constant. In addition, the imaging dose was estimated as fraction of the CTDI for the acquisition dose (0.8 mGy). Contrast-to-noise ratio (CNR) was determined between subcutaneous fat and abdominal/pelvic muscle for the paediatric scans and between the acrylic and LDPE inserts (most similar to fat and muscle tissue, respectively) of the Catphan.

**Results**

Figure 1 shows an example of simulated low-dose (8mA/10ms and 5mA/5ms) scans compared to the original (16mA/10ms) image. Figure 2 shows the relationship between CNR and dose in paediatric scans and phantoms. Lower-dose simulations created images with more noise and artefacts than the original scans; however the muscle and subcutaneous fat could still be distinguished at all simulated exposures. CNR remained higher than 3 until around 0.5 mGy in paediatric simulations and above 0.4 mGy in the phantom images (sufficient for observation of the selected contrasts for small objects according to the Rose criterion) (Rose, 1974). There was considerable inter-patient variation in CNR for the same dose, which does not seem to correlate with patient age, suggesting these are related to image artefacts.



Figure 1: Original 0.8 mGy pelvic CBCT scan of patient 4 (top) compared to simulated 0.4 mGy (centre) and 0.2 mGy scans (bottom).

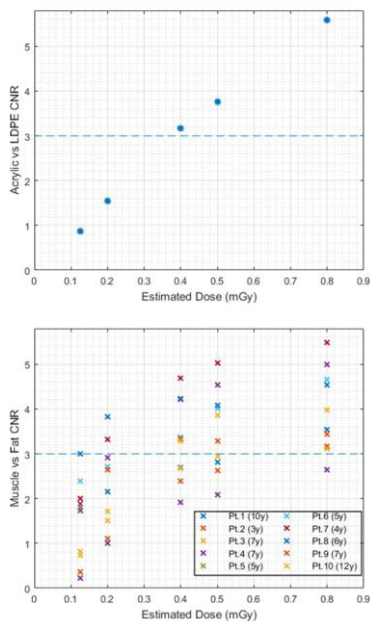


**Figure 2:** CNR in phantom (top) and paediatric CBCT simulations (bottom). The Rose criterion (CNR  $\geq 3$ ) is represented by a dashed line. Some patient CNRs are lower than the phantom, indicating the effect of artefacts.

### Conclusion

Simulations of low-dose paediatric CBCT scans show that a lower dose than is currently used clinically is sufficient for image evaluation in paediatric IGRT. As expected, a 50% reduction in dose leads to a 25% reduction in CNR. At 15% of clinically used doses CNR is reduced dramatically, but muscle and subcutaneous fat can still be distinguished. Investigation of the clinical impact of CNR reduction is planned.

### EP-2060 Feasibility of prostate rectum spacer in an MRI only radiotherapy workflow

M. Lerner<sup>1,2</sup>, E. Persson<sup>1,2</sup>, N. Eliasson<sup>1</sup>, M. Moreau<sup>1</sup>, H. Benedek<sup>1,3</sup>, C. Gustafsson<sup>1,2</sup>, P. Nilsson<sup>1</sup>, E. Kjellén<sup>1</sup>, L.E. Olsson<sup>1,2</sup>, A. Gunnlaugsson<sup>1</sup>

<sup>1</sup>Skåne University Hospital, Hematology- Oncology and Radiation Physics, Lund, Sweden ; <sup>2</sup>Lund University, Translational Sciences- Medical Radiation Physics, Malmö, Sweden ; <sup>3</sup>Lund University, Medical Radiation Physics, Lund, Sweden

### Purpose or Objective

A precondition for MRI only radiotherapy is the generation of a synthetic CT (sCT). Previous studies have successfully validated such methods for prostate radiotherapy. A prostate rectum spacer can reduce the dose to the main risk organs while maintaining high target dose. The aim of this clinical study was to validate the use of the spacer in an MRI only radiotherapy workflow by evaluating dose volume criteria and comparing Hounsfield Units (HU) within the spacer structure between the CT and sCT images. Since treatment planning is performed on the sCT, a validation of the spacer is required to ensure correct dose delivery.

### Material and Methods

This study was approved by the Ethical Review Board and informed consent was obtained from all patients. Study participation did not affect treatment prescription, and routine clinical workflow was followed. Eight patients with localized intermediate risk prostate cancer were included. A hydrogel prostate rectum spacer was injected during gold fiducial marker insertion, by an oncologist certified

by the spacer distributor. Besides a CT examination, dedicated MR examinations were performed on a GE Discovery 750w. A T2-weighted image, covering the full body contour, was added to the clinical protocol and was used for sCT generation.

A clinically approved VMAT treatment plan was created based on the CT and clinical local practice. For each patient, the generated sCT was resampled and rigidly registered to the CT. Structures were transferred to the sCT, including a structure delineating the spacer (see image for illustration). Separate body contours were generated based on the respective image. The CT based treatment plan was recalculated on the sCT, using the same number of MU. The dose distributions, based on sCT and CT, respectively, were compared based on the departments clinical DVH criteria. The mean HU value within the spacer structure was compared between the sCT and CT for all patients.

### Results

The median dose differences [95% CI] between sCT and CT for  $D_{mean,PTV}(\%)$  and  $D_{mean,CTV}(\%)$  were 0.45% [0.35, 0.80] and 0.48% [0.40, 0.90], respectively. The median [95% CI] difference between sCT and CT for the rectum dose-volume constraint  $D_{15\%}$  was 0.34% [0.26, 0.56]. Thus, the dose differences between sCT and CT plans for target structures and rectum were found to be small and not clinically significant.

The mean HU within the spacer structure was  $-11.8 \pm 26.7$  HU for sCT and  $7.6 \pm 32.0$  HU for CT.

### Conclusion

The use of a hydrogel prostate rectum spacer is a straightforward procedure which fits well into our MRI only radiotherapy workflow. Minimal differences were found between sCT and CT dose distributions for both target and rectum, comparable to previous studies evaluating the technique without a spacer. The small differences in dose and HU indicate that the use of a prostate rectum spacer in an MRI only workflow is feasible with no clinically significant effect on the dose calculations.

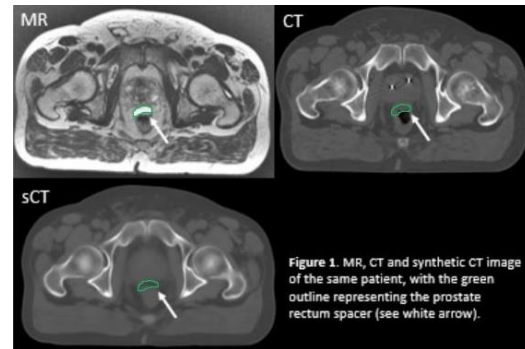


**Figure 1.** MR, CT and synthetic CT image of the same patient, with the green outline representing the prostate rectum spacer (see white arrow).

### EP-2061 Feasibility of MR-only planning in a commercial treatment planning system

H. McCallum<sup>1</sup>, N. Richmond<sup>1</sup>, C. Walker<sup>1</sup>, S. Andersson<sup>2</sup>, S. Svensson<sup>2</sup>

<sup>1</sup>The Newcastle Upon Tyne Hospitals NHS Foundation Trust, Northern Centre for Cancer Care, Newcastle upon Tyne, United Kingdom ; <sup>2</sup>RaySearch Laboratories, Research Department, Stockholm, Sweden

### Purpose or Objective

MR is of increasing interest in radiotherapy treatment planning due to its superior soft-tissue contrast compared to CT. An MR-only pathway improves delineation accuracy and removes uncertainty due to CT-MR fusion. This study aims to investigate the feasibility of an MR-only planning solution which relies on bulk-density assignment which is fully integrated within the commercial treatment planning system RayStation.

## Material and Methods

CT and MR images were acquired in the treatment position for five prostate cancer patients. The planning target and OARs were delineated according to the standard practice of the clinic. Conventional VMAT plans were generated for each patient based on the CT image. In order to create a tissue density map to calculate dose on the MR image, a bone ROI was created by a multi-atlas-based segmentation algorithm. To minimise the effect of anatomical differences between the CT and MR image, the external contour defined on the CT image was used for the MR image. The CT based plan was recalculated on the MR image by assigning bulk densities to the external contour and bone. The calculated dose for the CT based plan was compared to the recalculated dose based on the MR image.

In order to find the optimal bulk density assignments for soft tissue and bone, a range of soft-tissue and bone density pairs were evaluated for all patients. The soft-tissue density varied from 0.95-1.03 g/cm<sup>3</sup> in 0.01 increments and the bone density varied from 1.15 - 1.65 g/cm<sup>3</sup> in 0.05 increments. Dose differences between the CT and the bulk density based dose distributions were calculated for D1, D2, D50, D95, D98, D99 and average dose for the PTV, Rectum and Bladder. The density pair with the lowest dose difference between the CT and MR based calculations among all dose statistics and for all ROIs and patients was considered the best and used for the rest of the study. Further, the robustness of this bulk-density approach was investigated by looking at the average dose per ROI for all five patients. **Results**

With a mean absolute dose difference of 0.3% of the prescribed dose over all patients, ROIs and dose statistics, the best results were found with a density of 0.98 g/cm<sup>3</sup> for soft tissue and 1.25 g/cm<sup>3</sup> for bone. In Table 1 the average percentage dose difference of the prescribed dose is shown for each ROI and patient with these densities. The mean average dose was close to 0.0% and the standard deviation was 0.5% or less for all ROIs. Figure 1 shows the CT based dose distribution, MR based dose distribution and DVHs for PTV, Rectum and Bladder for Patient 1.

	PTV	BLADDER	RECTUM	Mean
Patient 1	-0.60	0.04	-0.01	-0.19
Patient 2	0.39	0.43	0.29	0.37
Patient 3	0.48	0.24	0.15	0.29
Patient 4	-0.50	0.01	-0.13	-0.21
Patient 5	0.14	0.14	0.16	0.15
<b>Mean</b>	<b>-0.02</b>	<b>0.17</b>	<b>0.09</b>	<b>0.08</b>
<b>MAE</b>	<b>0.42</b>	<b>0.17</b>	<b>0.15</b>	<b>0.24</b>
<b>SD</b>	<b>0.50</b>	<b>0.17</b>	<b>0.17</b>	<b>0.27</b>

Table 1: The average dose difference of the prescribed dose between the MR image and the CT image in percent.

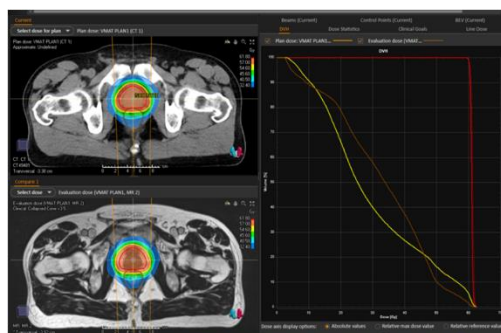


Figure 1: Top left - Dose distribution on CT. Bottom left - Dose distribution on MR. Right - DVH for PTV (red), bladder (yellow) and rectum (brown) CT based statistics solid lines, MRI statistics dashed lines.

## Conclusion

Using bulk-density assignment on MR images with dosimetrically optimized densities for bone and soft tissue results in small dose differences compared to dose calculated on the CT. This demonstrates that an integrated MR-only pathway utilizing a bulk density

assignment for two tissue types is a feasible approach for patients with prostate cancer.

## EP-2062 Feasibility of automatic detection of breast limits for auto-planning

J. Oliveira<sup>1</sup>, M.C. Aznar<sup>2</sup>, Y. Kirova<sup>3</sup>, A. Henry<sup>3</sup>, P. Aljabar<sup>1</sup>, M. Van Herk<sup>2</sup>, P. Poortmans<sup>3</sup>, M. Gooding<sup>1</sup>  
<sup>1</sup>Mirada Medical Ltd, Science department, Oxford, United Kingdom ; <sup>2</sup>University of Manchester, Division of Cancer Sciences, Manchester, United Kingdom ; <sup>3</sup>Institut Curie, Radiation Oncology, Paris, France

## Purpose or Objective

The planning of tangential breast radiotherapy requires the detection of the limits of the breast on CT imaging. The purpose of this abstract is to assess the feasibility of automated methods for detecting those limits without resorting to any manual annotations or markers (e.g., wires) for the patient.

## Material and Methods

Three automated methods were evaluated in this work. The first used a convolutional neural network (CNN) to predict the slice coordinate in a reference volume given a single slice of a query volume (e.g., finding slice location in the superior-inferior axis). Once these normalized coordinates are computed for the query volume, the breast limits can be predicted by matching the normalized coordinates with manual annotations of the limits in the reference volume.

The second method used a CNN to predict the normalized distance to the selected limits given an input slice. This approach is more focused on the limits, nonetheless it has the downside of requiring manual annotations for all the volumes in the training set.

The ground truth for training the CNNs of these two approaches was derived from the deformable registration of the reference volume to the query volumes. The third method predicts the limits of breast clinical target volumes (CTVs) through atlas-based segmentation. This is a simpler approach that requires less parameter tuning, but it requires manually contouring the CTVs for the whole training set.

The methods were evaluated in a database of 56 CT scans from breast cancer patients, including manual delineations of breast CTVs contoured according to the ESTRO guidelines. The delineations were used to define the cranial and caudal limits of each CTV. One CT scan was defined as the reference, while the remaining database was divided into 5 folds, where 4 were used for training and 1 for testing. The methods were evaluated on the 55 CT scans by rotating the training and test sets across folds.

## Results

The results for detecting the cranial and caudal limits of breast CTVs are presented in Table 1. Method 2 outperformed method 1 (Figure 1), which may be justified with the former method being more focused on detecting the limits, allowing the CNN to learn a more direct mapping between image features and breast limits. Methods 2 and 3 achieved comparable results, with method 2 performing better for the caudal limit but worse for the cranial limit.

Table 1 - Results of the evaluated methods. The metric used evaluation was the absolute error in number of slices, which is presented in the table in the form of mean absolute error ± standard deviation (lowest values in bold).

Limits	Proposed (approach 1)	Proposed (approach 2)	Atlas-based segmentation
Cranial	11.58 ± 6.56	3.56 ± 3.50	<b>2.95 ± 2.54</b>
Caudal	6.82 ± 5.43	<b>3.89 ± 3.07</b>	4.53 ± 3.43

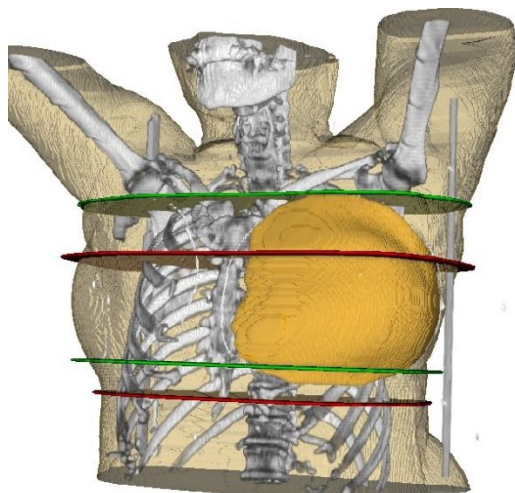


**Figure 1** – Visual representation of the results for a volume. The red and green planes represent the result of method 1 and 2, respectively. The volume corresponds to the manual delineation of the breast's CTV.

### Conclusion

The results demonstrate that CNN-based methods trained on a relatively small database of CT scans can detect the cranial and caudal limits of breast CTVs with an accuracy comparable to that of an atlas-based segmentation. Besides the accuracy level, a CNN-based method might be a better option than atlas-based segmentation for this application because it requires less manual effort for setup. In the future, methods 2 and 3 will be evaluated in larger datasets to observe how the accuracy and computation scale. Additionally, breast limits on other imaging planes will be considered.

### EP-2063 Treating prostate cancer with MRI-only radiotherapy

**E. Persson**<sup>1,2</sup>, **C. Gustafsson**<sup>1,2</sup>, **J. Nilsson**<sup>1</sup>, **S. Ceberg**<sup>3</sup>, **S. Engelholm**<sup>1</sup>, **S. Bäck**<sup>1</sup>, **L.E. Olsson**<sup>1,2</sup>, **A. Gunnlaugsson**<sup>1</sup>  
<sup>1</sup>Skåne University Hospital, Hematologi- Oncology and Radiation physics, Lund, Sweden ; <sup>2</sup>Lund University, Translational Sciences- Medical Radiation Physics, Malmö, Sweden ; <sup>3</sup>Lund University, Medical Radiation Physics, Lund, Sweden

### Purpose or Objective

The use of imaging has a crucial role in radiotherapy (RT), for localizing both tumours and organs at risk (OARs). Imaging is also an integral part of treatment planning, dose calculations and patient set-up. Magnetic resonance (MR) imaging provides excellent soft tissue contrast. A major argument for replacing CT with MR in the RT process (MRI-only technique) is the significantly improved spatial definition of the target and OARs. In addition, an MRI-only RT workflow may eliminate image registration uncertainties between MR and CT. Excluding CT will simplify the patient logistics process, reduce the number of appointments and may also decrease the workload and reduce costs. The purpose of the MR-PROTECT (The MR-only Prostate RadioTherapy Excluding CT) trial was to implement and prospectively study an MRI-only RT workflow for prostate cancer.

### Material and Methods

Preceding the clinical study and on different patient cohorts, the following tasks were performed: We validated and used the MRiPlanner (Spectronic Medical AB, Sweden) to generate syntheticCT (sCT) from T2w MR-sequence. Target delineation directly on the T2w image was compared to the traditional combined MR/CT delineation process. A dedicated gold fiducial detection tool for MR workflow was developed and tested. A QA method for using cone beam CT (CBCT) for quality control of the sCT was validated. For the clinical implementation study,

forty patients with localized prostate cancer were included for treatment according to an MRI-only workflow based on the validated methods. A CT was acquired after the MR examination, but only strictly used in the background for evaluation of the implementation process.

### Results

For the tasks preceding the clinical study, the following results were obtained: The validation study of the sCT confirmed that MRiPlanner can be used clinically with negligible differences between sCT and CT dose distributions for target and relevant organs at risk. The CTV using MRI-only for delineation was consistently smaller (18%) than using CTV for a combined CT/MR workflow. A dedicated multiecho gradient echo sequence was shown to be a feasible and reliable way for manual identification of fiducial markers (100%). CBCT was a clinically feasible QA procedure for MRI-only RT of prostate cancer patients. Thereby all the methods developed for the clinical study was working appropriately. In the clinical study, 39 of 40 patients completed their treatment with no major deviations. One patient was too large for the field of view of the MR-scanner.

### Conclusion

The results of this prospective clinical trial demonstrate that a successful MRI-only implementation can be achieved with a fine detailed work plan and thoroughly validated methods. One patient was excluded due to a large body contour, a problem that has been solved in a later process during our work. Our results confirm that the CT can successfully be entirely excluded. MRI-only RT enables a high precision RT technique with simplified logistics and less workload.

### EP-2064 A novel method for GTV generation for large-scale analysis of lung cancer patients planned with 4DCT

**A. Davey**<sup>1</sup>, **M. Van Herk**<sup>1</sup>, **C. Faivre-Finn**<sup>1</sup>, **S. Brown**<sup>2</sup>, **A. McWilliam**<sup>1</sup>

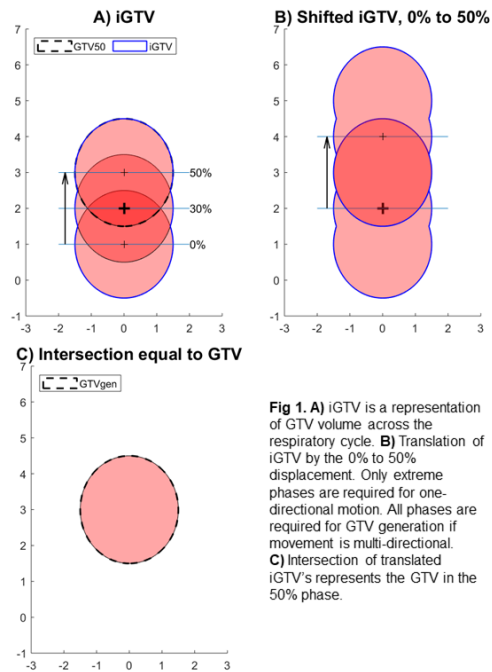
<sup>1</sup>The University of Manchester, Division of Cancer Sciences, Manchester, United Kingdom ; <sup>2</sup>The Christie NHS Foundation Trust, Clinical Oncology, Manchester, United Kingdom

### Purpose or Objective

Lung cancer patients undergoing stereotactic ablative body radiotherapy receive 4DCT for treatment planning. Often, an internal gross target volume (iGTV) is directly delineated without defining a GTV. However, the GTV volume and shape are important parameters for prognostic and dose modelling. In this study, we demonstrate and validate a new method to automatically generate the GTV, on any phase, directly from the iGTV.

### Material and Methods

Eleven 4DCT data-sets and delineations were collected from an institutional archive; each plan had a contoured iGTV. The method assumes deformation of the GTV is small compared to its motion. Rigid registration was therefore performed to map the tumour across all 4D phases to a reference phase, e.g. 50%. Registration performance was assessed by the mean and standard deviation (SD) of the correlation ratio cost function. Figure 1 demonstrates the GTV generation method. The iGTV should encompass the GTV volume at all positions across the respiratory cycle (A). Therefore, inversely, if the iGTV is translated by the registration displacements of each phase to the reference (B), the intersection of all translated iGTVs will recreate a GTV volume in the reference coordinate frame, GTVgen (C).



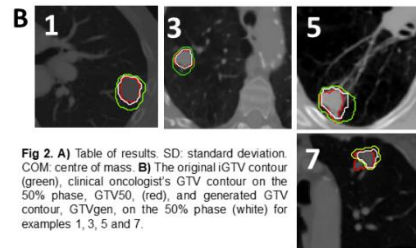
For validation, a radiation oncologist contoured the GTV on the 50% phase (GTV50). For comparison, surface distance to agreement (DTA) was calculated by extracting the absolute perpendicular distance from the surface of GTVgen to GTV50, with mean and SD recorded. For geometric comparison, the volume (V) and surface area (A) were extracted and ratios calculated. For shape, the ratio of sphericity,  $S = (\pi^{1/3}(6V)^{2/3})/A$ , was calculated. To assess position, the vector distance between centre of mass (COM) was extracted.

#### Results

Mean registration cost function was 0.95. The mean tumour motion amplitude calculated as vector of three directions was 7.47mm (range: 2.75-12.60mm). All tumours analysed were T-stage 1 or 2. Six patients had an upper lobe tumour and five had a lower lobe tumour.

Observer variation is reported as 1.2-1.8mm SD (Peulen et al., 2015). The distance variability, DTA SD, is within the range of observer variation (Fig. 2A). Pictorial examples (Fig. 2B) display good agreement. GTV shape was highly accurate. GTV volume was well estimated and a ratio change represents small volume difference.

A	GTV volume (cm <sup>3</sup> )	Volume ratio	Mean DTA (mm)	SD DTA (mm)	Sphericity ratio	COM distance (mm)
1	4.51	1.31	1.16	1.03	1.02	0.55
2	3.16	0.54	0.82	0.99	0.98	2.39
3	3.61	0.96	0.94	1.07	1.02	0.65
4	2.76	1.38	1.27	1.20	1.06	0.77
5	9.05	0.93	1.14	1.13	1.25	3.50
6	16.06	0.71	1.14	1.18	1.01	1.34
7	2.57	1.30	1.77	1.70	0.97	1.86
8	6.83	0.95	0.90	1.05	1.10	1.80
9	14.42	0.83	0.87	0.97	1.07	1.16
10	7.86	0.74	0.90	0.98	1.05	0.94
11	4.32	0.94	0.61	0.91	1.00	0.99



Patient 5 displayed worst results, with a 3.5mm COM deviation and largest sphericity ratio, however, the segmented volume is accurate. Patient 7 provides an example of higher DTA SD but this seems to be driven by observer disagreement, rather than issues with algorithm performance.

#### Conclusion

This study presents and validates a method for automatically generating the GTV from an iGTV. The technique provides a representation of the GTV that is accurate within observer variation. This method supports calculating delivered dose to the GTV without additional delineation and will facilitate large-scale retrospective analysis of patients treated in the routine setting.

#### EP-2065 Simulation PET-CT vs diagnostic PET-CT fusion in head and neck RT: volumetric and planning implications

S. Di Biase<sup>1</sup>, A. Ferretti<sup>2</sup>, E. Bellan<sup>2</sup>, F. Perrotti<sup>3</sup>, A. Augurio<sup>1</sup>, M. Nuzzo<sup>1</sup>, M. Trignani<sup>1</sup>, L. Caravatta<sup>1</sup>, D. Genovesi<sup>1</sup>, G. Mandoliti<sup>3</sup>

<sup>1</sup>SS. Annunziata Hospital, Department of Radiotherapy - G. D'annunzio University, Chieti, Italy; <sup>2</sup>Santa Maria della Misericordia Hospital, Medical Physics Unit, Rovigo, Italy; <sup>3</sup>Santa Maria della Misericordia Hospital, Radiotherapy Unit, Rovigo, Italy

#### Purpose or Objective

To evaluate the dosimetric impact of an automated threshold SUV based delineation method on simulation PET-CT (sPET-CT) compared to manual delineation target volumes on diagnostic PET-CT (dPET-CT) fused with simulation-CT in head and neck (H&N) radiotherapy.

#### Material and Methods

Ten consecutive H&N cancer patients underwent to sPET-CT in treatment radiotherapy set-up. A specific sPET-CT acquisition protocol was optimized by the medical physicist. All patients also underwent to whole body dPET-CT that was co-registered and fused with planning CT using a rigid algorithm (mutual information intensity-based metrics).

1. GTVs were delineated using an automated threshold method at 50% of the intra-lesion SUV max ( $t_{50\%GTV}$ ), both on sPET-CT and dPET-CT. GTVs differences were analyzed in terms of volumetric absolute values, Jaccard Index (JI) and distances from centroids, in order to evaluate shift errors. GTVs were manually

(mGTV) delineated both on sPET-CT and dPET-CT, too.

- CTV was obtained adding an isotropic margin of 9 mm respecting anatomical boundaries; a margin of 3 mm was added for PTV. Plans were then generated using IMRT or VMAT considering also elective nodal irradiation and different dose levels, in the following two steps:
  - First, plans were optimized on the PTVs generated from the manual delineation on dPET-CT; then the coverage of the PTVs deriving from  $t_{50\%}$ GTV on sPET-CT was assessed in terms of target coverage and conformity index (CI), without a plan re-optimization.
  - Secondarily, plans were optimized on PTVs deriving from  $t_{50\%}$ GTV on sPET-CT to evaluate organs at risk (OAR's) dose differences compared to dPET-CT plans.

#### Results

- The volumetric analysis showed a mean JI of 0.2 (0-0.5) between  $t_{50\%}$ GTV on sPET-CT vs  $t_{50\%}$ GTV on fused dPET-CT. Mean distance between centroid in these volumes was 1.05 cm (0.53-2.17cm). Comparing  $t_{50\%}$ GTV, in 6/10 cases the dPET-CT presented larger volumes respect to sPET-CT (mean: 3.7 vs 3.3 cc). Moreover, mGTV on dPET-CT were larger then  $t_{50\%}$ GTV on sPET-CT (mean: 13.2 vs 3.3 cc) in the totality of cases (table1).
- Planning evaluation:
  - In all cases a decrease of CI (mean reduction 18%, range 7%-35%) of PTVs deriving from  $t_{50\%}$ GTV on sPET-CT, introduced into the plans optimized on dPET-CT, was observed; although, in 7/10 cases a good coverage, defined as  $v_{95\%}>95\%$ , was obtained.
  - For plans optimized on sPET-CT, a slightly dose reduction, almost to one of OARs, was observed in all cases.

	Fusion with dPET-CT	sPET-CT
Mean $t_{50\%}$ GTV	3.7 cc	3.3 cc
Mean Jaccard Index	0.2	
Range Jaccard Index	0-0.5	
Mean centroid distance	1.05 cm	
Range centroid distance	0.53-2.17 cm	
Mean mGTV	13.2 cc	11.9 cc

Table 1. Volumetric analysis results

#### Conclusion

Shift errors, related to the image fusion process, negatively influenced concordance between target volumes obtained on sPET-CT and dPET-CT. An adequate coverage of sPET-CT volumes in plans optimized on dPET-CT volumes despite lower CI and a small reduction of dose to OAR's in sPET-CT plans were reported. Based on these preliminary evaluations, sPET-CT could be considered an optimization in RT workflow for H&N cancer management to reduce image fusion uncertainties and to standardize delineation.

#### EP-2066 Evaluation of ANACONDA performances varying the exploited subset of controlling ROIs (AIRC IG-14300)

C. Romano<sup>1,2</sup>, S. Trivellato<sup>1,2</sup>, P. De Marco<sup>1</sup>, S. Comi<sup>1</sup>, A. Bazani<sup>1</sup>, G. Marvaso<sup>3</sup>, D. Ciardo<sup>3</sup>, B.A. Jereczek-Fossa<sup>3,4</sup>, R. Orecchia<sup>5</sup>, F. Cattani<sup>1</sup>

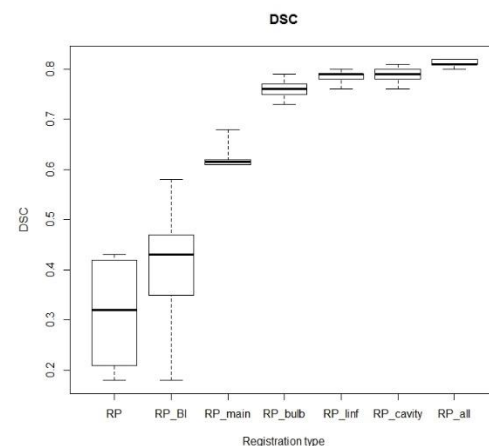
<sup>1</sup>IEO- European Institute of Oncology IRCCS, Unit of Medical Physics, Milan, Italy; <sup>2</sup>University of Milan, Department of Physics, Milan, Italy; <sup>3</sup>IEO- European Institute of Oncology IRCCS, Division of Radiation Oncology, Milan, Italy; <sup>4</sup>University of Milan, Department of Oncology and Hemato-oncology, Milan, Italy; <sup>5</sup>IEO- European Institute of Oncology IRCCS, Scientific Directorate, Milan, Italy

#### Purpose or Objective

To evaluate the influence of different controlling Regions Of Interest (ROIs) selection on Raystation ANatomically CONstrained Deformation Algorithm (ANACONDA) performances. This is an ancillary study for further investigations on deformable image registration (DIR) performances in assessing dose accumulation in mixed beam treatments (AIRC IG-14300).

#### Material and Methods

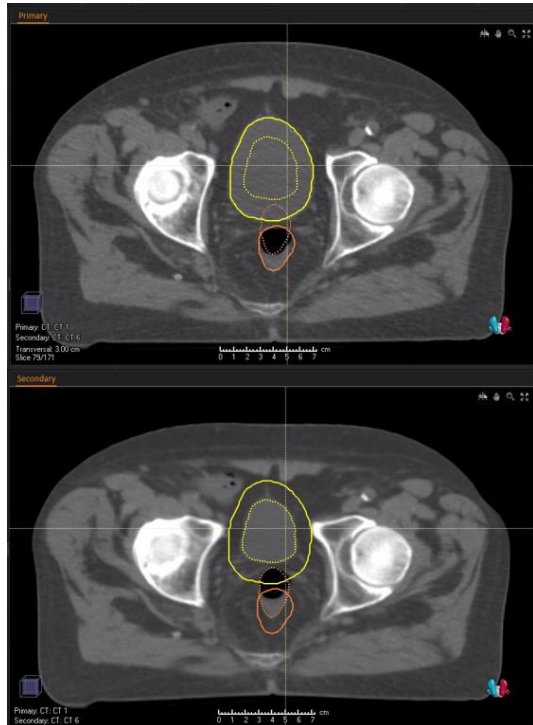
Two different deformed image datasets (target CTs) were computationally generated by applying proper Deformation Vector Fields (DVF) to an original synthetic man pelvis dataset and a real patient CT dataset (reference CTs). The target CTs were obtained by exploiting the ImSimQA package (Oncology System Limited, Shrewsbury, UK). These datasets were generated simulating different bladder filling levels. In both datasets, the bladder enlargement and shrinking were simulated preserving the femoral heads stiffness (figure 1). DIR performances were tested selecting different subset of controlling ROIs to guide the registration. The DIR deformed ROIs were mapped to the target CT and then compared to the ROIs returned from the ImSimQA software. A statistical test was performed to highlight DIR differences based on Correlations Coefficient (CC) and Dice Similarity Coefficient (DSC). This analysis was carried out on the global CC and DSC obtained for each bladder volume by multiplying the CC and DSC scored for all the contoured ROIs (body, bladder, prostate, rectum and femoral heads for the synthetic image case with the addition of penile bulb, peritoneal cavity, anal canal and lymph nodes for the real patient CT dataset).



#### Results

DIR performances improve increasing the number of controlling ROIs reaching a saturation level after the selection of bladder, rectum and prostate in the synthetic phantom case with the addition of the penile bulb in the real patient CT dataset (figure 2). The fluctuation of

bladder filling affects DIR performances only in the case where no controlling ROI is selected or when only the bladder is exploited as controlling ROI. The statistical test shows significant differences on the DSC results between the DIR obtained selecting as controlling ROIs all the available ROIs and the DIR obtained without controlling ROIs or only when a subset of controlling ROIs is selected (bladder or bladder, prostate and rectum). As far as the CC concern, significant differences were observed only between DIR computed exploiting as controlling ROIs all the delineated ROIs and DIR performed without the selection of controlling ROIs or, for the real patient CT case only, where the bladder was selected as controlling ROI.



### Conclusion

ANACONDA performances improve increasing the number of selected controlling ROIs approaching a saturation level after the selection of a defined ROIs subset. This would suggest to reduce the number of controlling ROIs delineated in clinical practice thus decreasing the time spent to contour each patient CT.

### EP-2067 Data driven region of interest respiratory surrogate signal extraction from CBCT data

A. Akintonde<sup>1,2</sup>, H. Grimes<sup>3</sup>, S. Moinuddin<sup>3</sup>, R.A. Sharma<sup>4</sup>, J. McClelland<sup>1</sup>, K. Thielemans<sup>2</sup>

<sup>1</sup>University College London, Centre for Medical Image Computing- Department of Medical Physics and Biomedical Engineering, London, United Kingdom ;

<sup>2</sup>University College London, Institute of Nuclear Medicine, London, United Kingdom ; <sup>3</sup>University College London Hospital, Department of Radiotherapy Physics, London, United Kingdom ; <sup>4</sup>University College London, Cancer Institute, London, United Kingdom

### Purpose or Objective

Cone-beam CT (CBCT) scans performed during a course of radiotherapy can be degraded by respiratory motion. 4D reconstruction or motion-compensated (MC) reconstruction can be used to visualise or compensate for the motion. Both techniques require a respiratory surrogate signal. Surrogate signals derived directly from the projection data are appealing as they require no extra

equipment and may have a stronger relationship to the internal motion than signals from external devices. In this study, we developed a novel method for extracting a surrogate signal directly from CBCT data, and we compared it to the Amsterdam Shroud technique.

### Material and Methods

A region of interest (ROI) corresponding to either the tumour or diaphragm was selected, and the ROI in the projection data was enhanced by digitally removing the rest of the anatomy. PCA was applied to groups of adjacent projections using a sliding-window approach, and a novel technique used to combine the extracted signals from each window to generate a coherent respiratory signal from the entire data set.

We evaluated our method using four simulated CBCT acquisitions (three standard, one extended) that emulate clinical conditions and were generated with the XCAT computer phantom and real patient respiratory traces as the ground truth (GT) signals. Simulations were performed using OpenRTK. We assessed the signals extracted from the tumour ROI (T-ROI) and the diaphragm ROI (D-ROI) by calculating the correlation coefficient (CC) with the GT signal. For comparison, we extracted a signal generated using a modified Amsterdam Shroud (M-AS) technique, which corrects for the drift that can be present in the original Amsterdam Shroud signal. Finally, phase sorted 4DCBCT images were reconstructed for the extended acquisition using the GT, T-ROI, and M-AS signals.

### Results

Figure 1 shows the different signals for the four simulated acquisitions, also shown are the corresponding CC obtained for each simulation. Figure 2 shows the 4DCBCT reconstructions generated using the different signals. It can be seen that the 4DCBCT images from the T-ROI signal closely resemble the images from the GT signal, whereas the images from the AS signal show clear motion artefacts.

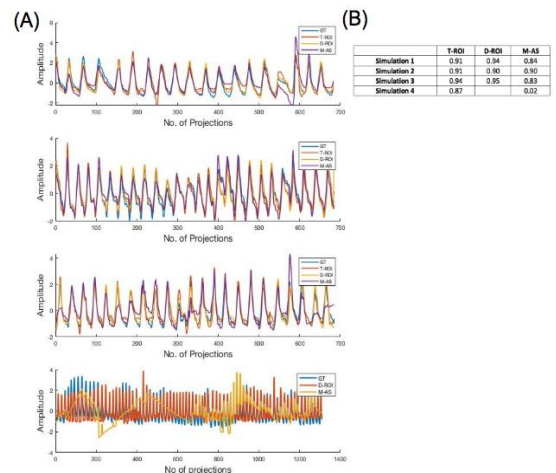


**Figure 1.0.** (A) Respiratory signals obtained from 4 different simulations. The first 3 simulations were standard acquisition with the tumour and diaphragm region in the FOV of the projections, where the last simulation corresponds to an extended acquisition where the diaphragm was not in the FOV. Plots show the signals obtained using our method from 2 ROIs (D-ROI and T-ROI), the M-AS method and the GT. For the last simulation, D-ROI is not shown as not available. (B) Correlation coefficients between the extracted signals, M-AS, and the ground truth signals for the different simulations

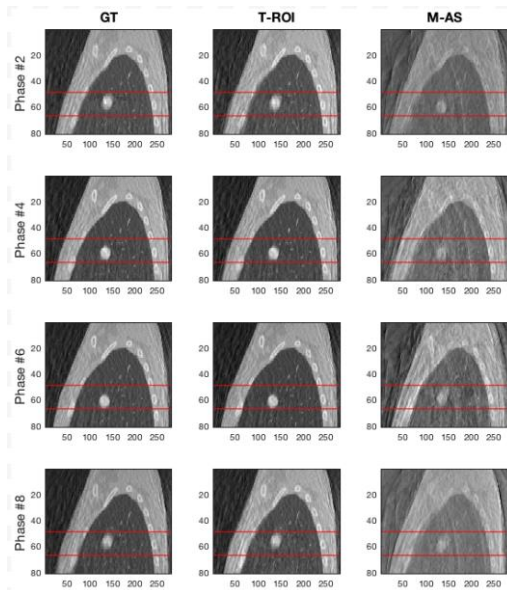


**Figure 2.0.** Sagittal planes of the images reconstructed from respiratory sorted phase bins using the GT motion, our proposed method and the M-AS technique respectively. Each row corresponds to a particular phase bin, shown here are the 2<sup>nd</sup>, 4<sup>th</sup>, 6<sup>th</sup> and 8<sup>th</sup> bins (out of 8) respectively. These phases were chosen to highlight the extent of the tumour motion. The red horizontal lines are positioned to show the extent of the tumour motion.

## Conclusion

We have developed a novel method of extracting respiratory motion from CBCT projection data. The method allows selecting a ROI to target the respiratory motion of interest. We evaluated our method on XCAT simulations and compared it to the well-known Amsterdam Shroud technique, combined with a simple method for baseline-drift correction. High correlations were obtained between signals from our proposed method and the ground truth for all simulations, achieving better correlations than when using AS. The preliminary evaluation shows that the proposed technique is therefore a potential candidate for a robust basis for respiratory motion management without need for external equipment. In future, we plan to apply this method to patient data.

**EP-2068 Scatter-corrected CBCTs for online water-equivalent path length calculations in proton therapy**  
 A.G. Andersen<sup>1</sup>, U.V. Elstrøm<sup>2</sup>, B. Winey<sup>3</sup>, J.B.B. Petersen<sup>2</sup>, M. Falk<sup>1</sup>, P. Skyt<sup>1</sup>, O. Nørrevang<sup>1</sup>, C. Grau<sup>4</sup>, L.P. Muren<sup>1</sup>

<sup>1</sup>Danish Centre for Particle Therapy, Department of Medical Physics, Aarhus, Denmark ; <sup>2</sup>Aarhus University Hospital, Department of Medical Physics, Aarhus, Denmark ; <sup>3</sup>Massachusetts General Hospital, Department of Medical Physics, Boston- MA, USA ; <sup>4</sup>Aarhus University Hospital, Department of Oncology, Aarhus, Denmark

## Purpose or Objective

Releasing the full potential of proton therapy requires mitigation of proton range variations caused by density/anatomy changes during the course of treatment. Cone-beam CT (CBCT) scanners are becoming available at proton gantries, but scatter and other artefacts deteriorate the accuracy of the Hounsfield unit representation in the CBCTs, with implications for online proton range or dose calculations. *A priori* scatter correction algorithms have shown promising results for reducing CBCT artefacts. Proton range calculations based on scatter corrected CBCTs have not yet been compared directly to calculations on conventional CTs in patients. The aim of this study was therefore to do such a

comparison using mid-course CTs of head and neck cancer patients.

## Material and Methods

Our scatter correction algorithm initially used rigid and deformable registration of the planning CT (pCT) to a raw reconstruction of the CB projections (rawCBCT). The deformed CT was then forward projected onto the same geometry as that of the CB projections, from which the forward projections were subtracted. The differential projections were then smoothed with a low-pass gaussian filter, to create a scatter map which was then subtracted from the original CB projection before a final reconstruction (corrCBCT). For comparison we also used our clinical reconstruction of the CB projection (clinCBCT), which used the adaptive scatter kernel superposition method (Varian iTools). The pCT, a mid-course CT (mCT) and CB projections acquired the same day as the mCT from four head and neck patients previously treated with photon-based radiotherapy were analysed. Proton ranges, i.e. water-equivalent path lengths (WEPLs), were calculated in planar projections of all voxels in the patients, using the pCT as reference. WEPL maps for the mCT were subtracted from both the corrCBCTs and the clinCBCTs, under the assumption that the patient anatomy changes between the mCT and the CBCT were negligible.

## Results

In three of the four patients, the WEPL maps based on the corrCBCT deviated less from the WEPL maps based on the mCT compared to the clinCBCT (Fig 1). In one case the average across the subtracted WEPL map was reduced from 7 mm to 2 mm, with the fraction of the WEPL maps with deviations exceeding +/- 10 mm reduced from 41% with clinCBCT to 19% using the corrCBCT. In the fourth case the averages were within 0.5 mm.

## Conclusion

Scatter correction of CBCTs translates into clinically relevant improvements in CBCT-based WEPL calculations, opening a potential for online proton range verification/monitoring.

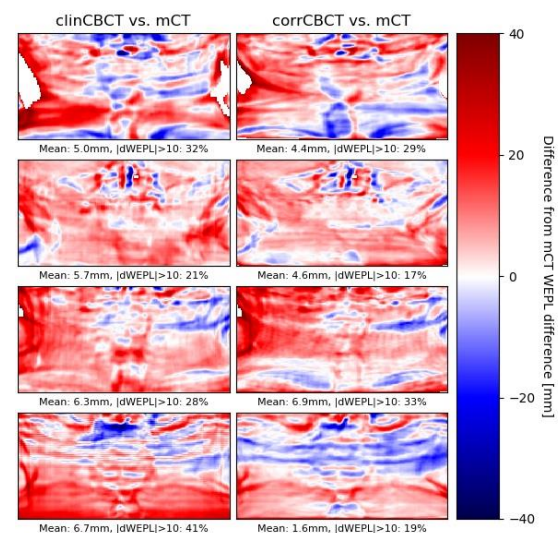


**Figure 1:**

The difference between the WEPL difference of the pCT and mCT, and the WEPL difference of the pCT and the two CBCT reconstructions, in units of mm WEPL. The corrCBCT reconstruction to the right and the clinCBCT to the left. Each row corresponds to one patient.

**EP-2069 Improved dose calculation on CBCT using polyenergetic quantitative (Polyquant) reconstruction**  
 J. Mason<sup>1</sup>, W. Nailon<sup>2</sup>, A. Perelli<sup>1</sup>, S. Andiappa<sup>2</sup>, M. Davies<sup>1</sup>

<sup>1</sup>The University of Edinburgh, School of Engineering, Edinburgh, United Kingdom ; <sup>2</sup>Edinburgh Cancer Centre-

Western General Hospital-, Department of Oncology Physics, Edinburgh, United Kingdom

### Purpose or Objective

The accuracy of radiotherapy dose calculation from cone beam computerised tomography (CBCT) depends on estimation of the electron density accounting for beam hardening, the effects of metal artefacts and inhomogeneous object scatter. However, this is made challenging by the inherent sampling deficit in CBCT and the desire to minimise patient dose. Several studies have considered this problem from the point of view of reconstruction, registration or a combination of the two. Here we present the enhanced electron density and dose planning accuracy made possible by a new direct quantitative reconstruction method called Polyquant.

### Material and Methods

The stereotactic end-to-end verification (STEEV) phantom patient, Model 038, was used for this study (CIRS, Norfolk, VA, USA). Using a 1 mm head protocol planning fan beam CT images were acquired on a Philips Brilliance Big Bore CT scanner fitted with a flat couch (Philips, Amsterdam, The Netherlands). Treatment plans were prepared using the Eclipse treatment planning system (Varian Medical Systems, Inc., Palo Alto, CA, USA) for a 200 MU 10x10 cm<sup>2</sup> field delivered at 9 gantry angles and the dose calculated at a predetermined reference point. The STEEV phantom was set up on a Varian Truebeam linear accelerator and CBCT images acquired using the on-board imager with the preset head acquisition protocol. Physical dose measurements were acquired using a Pinpoint ionization chamber (PTW, Freiburg, Germany) inserted into the dosimetry cavity of the STEEV phantom. Using the 'raw' CBCT projections standard Feldkamp, Davis and Kress (FDK) reconstruction was carried out. Quantitative reconstruction was also performed using our new Polyquant method. Dose calculation was carried out on the FDK-CBCT and the Polyquant-CBCT images on Eclipse and compared to the physical measurement.

### Results

Quantitative results from the physical measurements on the STEEV phantom compared to the calculated dose by Eclipse using the planning CT, FDK-CBCT and Polyquant-CBCT are shown in Table 1 and Figure 1. Not only is the error reduced from the FDK-CBCT result, but the Polyquant reconstruction significantly outperforms the planning CT accuracy with a 26.5% reduction in error. This may be a surprising result due to the usual superiority of fan-beam CT, from its heavily reduced scatter over CBCT, and the routine use of this modality in practice for planning. We would expect that if we had access to the raw data from the fan-beam CT also, the Polyquant applied to this would likely result in better accuracy still.

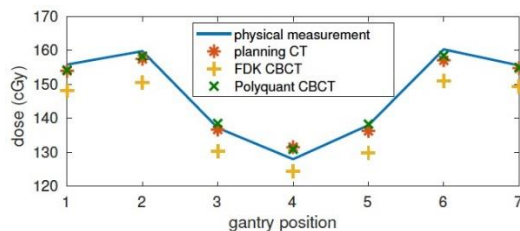


Figure 1: Graphical representation of dose results.

Gantry Angle (deg)	Dose (cGy) from			
	Measurement	Planning CT	FDK-CBCT	Polyquant-CBCT
270	155.84	154	148.2	154.2
300	159.78	157.5	150.6	158.3
330	137.18	136.7	130.4	138.5
0	127.98	131.5	124.4	130.9
30	137.98	136.3	129.9	138.3
60	160.31	157.1	151	158.5
90	155.58	154.8	149.3	155
RMSE	-	2.234	7.491	1.642

Table 1: Results from calculated and physical measurements.

### Conclusion

These preliminary results show that a significant increase in CBCT dose calculation accuracy is possible with the use of the new Polyquant method that we have developed. Further work is however required particularly on the utility of this approach on a range of different phantoms, with different dose calculation algorithms, and also in particle therapy.

### EP-2070 Comparison of multi-atlas based synthetic CT generation methods for radiotherapy for prostate cancer

C. Choi<sup>1</sup>, G. Sasso<sup>2</sup>, B. Pontre<sup>1</sup>

<sup>1</sup>The University of Auckland, Anatomy and Medical Imaging, Auckland, New Zealand ; <sup>2</sup>Auckland District Health Board, Radiation Oncology, Auckland, New Zealand

### Purpose or Objective

Magnetic resonance imaging (MRI) plays an important role in radiation therapy planning (RTP) due to its excellent soft tissue contrast. In recent years, there has been increasing interest in MR-only RTP to prevent registration errors between the MRI and computed tomography (CT) images, to minimise total radiation dose to patients, and to reduce the time and cost associated with planning and treatment. The goal of this study is to evaluate the performance of MRI-guided synthetic CT (sCT) workflows used in a commercial RTP software package.

### Material and Methods

A multi-atlas based sCT conversion workflow was developed using MIM's in-built deformable registration tools (MIM Software Inc., Cleveland, OH). MIM offers three types of deformable registration: one based on image intensities (intensity-based), one using contours of anatomical structures of interest (contour-based), and one using a combination of the intensity-based and contour-based methods (hybrid). The contours for contour-based and hybrid workflows (bladder, prostate, rectum and bone) were manually drawn with reference to axial, sagittal, coronal MR images and validated by a clinician.

The three workflows were tested on CT and T2 weighted MR atlases from six patients using a leave-one-out approach [1]. Once the atlas MR is registered to the target MR, sCTs were generated by applying the corresponding deformation vector field from the registration to atlas CTs, which were then fused to form a final sCT. Dice similarity coefficient (DSC) of the bone region and mean absolute error (MAE) of bone and tissue regions were computed in order to evaluate the performance of the three workflows.

### Results

The target planning CT and sCTs produced from the three workflows are shown in Figure 1. Among the three deformable registration methods, the hybrid deformable registration workflow produced the highest dice coefficient, followed by the intensity-based and contour-based workflows (Table 1). Furthermore, the lowest mean absolute error was also produced using the hybrid workflow. However, the results show a reduction in grey scale contrast due to fusion of multiple sCTs. More focus should be on examining techniques to address this issue.

	Intensity-based	Contour-based	Hybrid
DSC	0.73 ± 0.05	0.62 ± 0.02	0.75 ± 0.04
MAE (bone)	28.05 ± 5.90	37.90 ± 4.63	27.75 ± 4.85
MAE (tissue)	39.89 ± 3.27	44.34 ± 3.01	34.91 ± 2.66

Table 1: DSC and MAE computed between the sCTs and planning CT

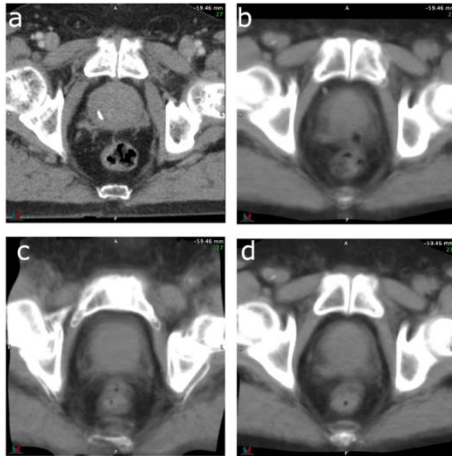


Figure 1: Typical example of a) planning CT b) intensity-based sCT c) contour-based sCT d) hybrid sCT

### Conclusion

In this project, we have tested multi-atlas based deformable registration workflows using commercially available RTP software. Our results indicate that hybrid of intensity- and contour-based deformable registration methods MIM provides the best solution for generating sCTs in the prostate region.

Reference:

1. Sjölund, J., Forsberg, D., Andersson, M., & Knutsson, H. (2015). Generating patient specific pseudo-CT of the head from MR using atlas-based regression. *Physics in Medicine & Biology*, 60(2), 825.

---

**Electronic Poster: Physics track: Implementation of new technology, techniques, clinical protocols or trials (including QA & audit)**

---

### EP-2071 Redefining the classical Winston-Lutz test for cranial radiosurgery in terms of dose

J.F. Calvo Ortega<sup>1</sup>, S. Moragues Femenia<sup>1</sup>, J. Casals<sup>1</sup>  
<sup>1</sup>Hospital Quirónsalud Barcelona, Radiotherapy, Barcelona, Spain

#### Purpose or Objective

To analyze the dosimetric impact of the deviations (ball center-field center) revealed by the traditional Winston-Lutz (WL) test.

#### Material and Methods

A pointer-based WL plan containing 15 non-coplanar fields is routinely delivered in our department for SRS QA purpose (Pointer-WL test). The maximum deviation between the ball center and the radiation field center ( $d_{\text{ball-center,max}}$ ) over the 15 taken portal images gives the result of this test. Two acrylic phantoms able to support a radiochromic film in coronal and sagittal orientations, respectively, were home-made. Both phantoms were CT-scanned and transferred to the Eclipse treatment planning system (TPS).

The WL plan was recreated in the Eclipse TPS over each phantom to be delivered (Dose-WL test). This film-based

test was generated to investigate whether the deviations reported by the Pointer-WL test are actually reflecting the geometrical shift of the measured prescription isodose line respect to the target center ( $d_{80\%-\text{center}}$ ). In addition, the film dose distributions were compared with the theoretical distributions computed by the Eclipse, to evaluate the entire delivery accuracy (E2E test) in terms of isodose shifts ( $d_{\text{E2E}}$ ). The Pointer-WL, Dose-WL and E2E tests were performed in 10 different sessions using CBCT imaging. For each session, the  $d_{\text{ball-field,max}}$  value was compared to the three patient's anatomical components (Left-Right or L/R; Anterior-Posterior or A/P; and Superior-Inferior or S/I) of the  $d_{80\%-\text{center}}$  and  $d_{\text{E2E}}$  vectors.

#### Results

The deviations (mean ± SD) found for the Dose-WL (L/R:  $0.5 \pm 0.4$  mm; A/P:  $0.5 \pm 0.4$  mm; S/I:  $0.6 \pm 0.2$  mm) and the E2E tests (L/R:  $0.7 \pm 0.5$  mm; A/P:  $0.5 \pm 0.4$  mm; S/I:  $0.6 \pm 0.2$  mm) were in most cases less than 1 mm, and they were quite less than the maximum deviations registered with the traditional Pointer-WL tests ( $d_{\text{ball-field,max}}$ :  $1.8 \pm 0.3$  mm). On average,  $d_{\text{ball-field,max}}$  exceeded 1.2 mm (in R/L and S/I) and 1.3 mm (in A/P) the deviations reported by the 10 Dose-WL tests. Analogously, an average excess of 1.0 mm (in R/L), 1.3 mm (in A/P) and 1.1 mm (in S/I) were noted for the 10 E2E tests.

#### Conclusion

In this study we have proved that deviations greater than 1 mm as reported by the analysis of a traditional WL test do not necessarily imply shifts greater than 1 mm in the prescription isodose line respect to the target to be treated. According to the results of this work, it is advisable to move to a dose-based WL test by replacing the classical WL test involving a metallic ball that only provides information about geometric misalignments of the isocenter.

### EP-2072 Automatic analysis of patient specific QA measurements made with the Octavius verification device

P. Haering<sup>1</sup>, M. Splinter<sup>1</sup>, C. Lang<sup>1</sup>  
<sup>1</sup>DKFZ, e040, Heidelberg, Germany

#### Purpose or Objective

Patient specific 3D QA measurements with the PTW Octavius phantom are well accepted. A small drawback of the method is, that only the 3d dose distribution can be evaluated what makes it difficult to understand possible deviations found. We present a tool that compares the measurement file to the DICOM RT plan file and detects deviations automatically.

#### Material and Methods

The measurement of the PTW Octavius system results in a time sample structured file, based on the settings given for the system. This file includes the dose matrix together with gantry and time information. The tool presented detects the dose information and puts them together as dose groups by eliminating the beam off times. Calibration and correction factors are also applied. The DICOM RT plan file is searched for MU, MLC, Gantry information which will be sorted to fit the order of the measurement data. Knowing the geometry, RT-plan data are transferred to dose matrixes using a simple scatter model (Gaussian curve based). Measured values are given in the Octavius/array resolution needing an interpolation and correction of partial volume effects, which is also taken care of by a scatter model. The tool now analysis both data sets for dose and position errors which are indicated only if given limitations are exceeded and finally calculates a gamma pass rate per segment/gantry step. 12 patient cases from a Siemens Artiste have been analyzed so far with the IDL (RSI) written tool. Excel sheets then help to understand and display the generated data.

#### Results

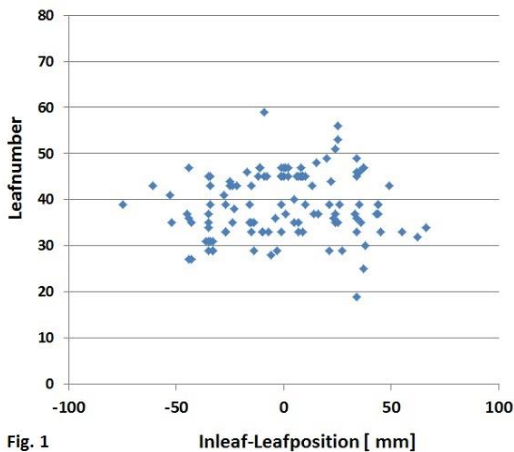


Fig. 1

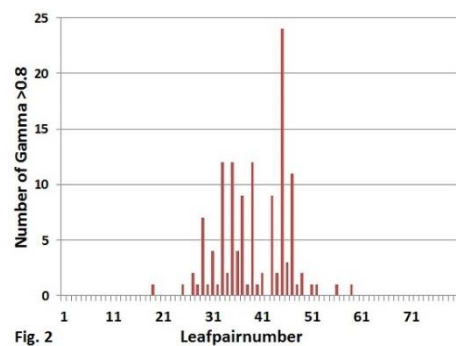


Fig. 2

The additional effort for the analyzation is quite low and just takes a few minutes for copying data and starting the tool. All results can be summarized in a printable report file or Excel sheets. The analyzation of the 12 cases with almost 1000 segmented fields resulted in a mean gamma value 0,549 while only 19 segment fields had a maximum gamma of more than 1, based on a 2mm/3% local criteria. Fig 1 shows positions of gamma values >0.8 in the dose. While here results are equally distributed the histogram of leaf pairs (Fig 2) indicates that the area of leaf pair 45 has highest number of >0.8 gamma values of the matrixes. Here it might be worth to look at the leaf calibration even though center leafs are more in use than others. Beside that, patient cases did show good results and thereby supported the positive 3d dose results. A manipulated test case (changed leaf positions and MU settings) was easily detected by gamma index and local dose error results.

#### Conclusion

The tool breaks up the complex 3D dose verification measurement to an understandable field based approach and automatically checks the dose delivery in a different way. This might have the potential to easier understand why some patient verification measurements might show higher or lower pass rates.

#### EP-2073 Reconstruction of the electron source distribution using in-air measurements and genetic algorithm

E. Borzov<sup>1</sup>, A. Nevelsky<sup>1</sup>, R. Bar-Deroma<sup>1</sup>, I. Orion<sup>2</sup>  
<sup>1</sup>Rambam Health Care Campus - Faculty of Medicine, Oncology, Haifa, Israel ; <sup>2</sup>Ben-Gurion University of the Negev, Nuclear Engineering, Beer Sheva, Israel

#### Purpose or Objective

The intensity distribution of a pre-target electron source in Monte Carlo accelerator model is needed for accurate reproducing of measured photon beam data. The purpose of this study is to develop an approach for the electron source reconstruction problem. The approach should

justify the selection of electron beam parameters in MC simulations aimed to model small fields and detector specific correction factors.

#### Material and Methods

Monte Carlo simulations were performed using the EGSnrc code system. The MC model for the Agility treatment head of the Elekta VersaHD linear accelerator was created and examined in our previous study. The IBA Stereotactic Field Diode was approximated as a silicon chip of relevant dimensions.

In the current study, the electron source was presented as a sum of square sub-sources. We divided the electron target area of 4.8 x 4.8 mm<sup>2</sup> into a number of squares of 0.2 x 0.2 mm<sup>2</sup> in the centre region and 0.4 x 0.4 mm<sup>2</sup> in the peripheral region. Then, each part was treated as an independent electron sub-source in (x,y) position on the target surface. The reconstruction of the source intensity distribution was based on a search of the best agreement between simulated and measured data. Measured data was obtained in the form of a 2D array where each value corresponds to an in-air measurement in a certain position of the SFD detector at SSD 100 cm.

The weights for each sub-source was optimized to minimize a least-square cost-function:

$$\text{CostFunction} = \sum_V (A_V^{\text{meas}} - A_V^{\text{MC}})^2$$

where  $A\{\text{meas},V\}$  is the measured dose at position V in the 2D array of measured doses;  $A\{\text{MC},V\}$  is the MC dose at position V in the 2D array of simulated doses. At position V in the plane of measurements,  $A\{\text{MC},V\}$  consists of a weighted sum of simulated dose  $A\{\text{MC},V\}(x,y)$  from each sub-source in the (x,y) position on the target surface:

$$A_V^{\text{MC}} = \sum_{(x,y)} \text{weight}(x,y) \cdot A_V^{\text{MC}}(x,y)$$

The search for weight factors was performed using a genetic algorithm optimization with rank scaling function and tournament selection function. For benchmarking the proposed technique, the whole procedure was applied in the case where the MC simulation data with the known electron source distribution was used instead of the measured data.

#### Results

The benchmark procedure demonstrated that the algorithm reconstructs the source dimensions with accuracy better than 0.01 cm. Using measured data, the matrix of electron intensity distribution was calculated. After a curve fitting procedure, the matrix was found to be elliptical in shape with Gaussian intensity distribution:  $\text{FWHM}_x = 0.08$  cm and  $\text{FWHM}_y = 0.17$  cm, where x and y correspond to inplane and crossplane directions. The found source dimensions with the current approach are similar to those found in our previous work using empirical method:  $\text{FWHM}_x = 0.10$  cm and  $\text{FWHM}_y = 0.20$  cm.

#### Conclusion

Our results demonstrate that the electron source of the Elekta Versa HD linear accelerator has Gaussian elliptical shape. The approach can be used for accurate parameter selection of the electron source when MC simulations are used for calculation of small field correction factors.

#### EP-2074 Can we use Effective Depth for deformable image registration QA alongside the AAPM recommendations?

M. Wilson<sup>1</sup>, J. Lui<sup>1</sup>, D. Noble<sup>2,3</sup>, G. Royle<sup>1</sup>, S. Holloway<sup>1,4</sup>

<sup>1</sup>University College London, Medical Physics and Biomedical Engineering, London, United Kingdom ;  
<sup>2</sup>Cambridge University Hospitals NHS Foundation Trust, Oncology, Cambridge, United Kingdom ;  
<sup>3</sup>University of Cambridge, Oncology, Cambridge, United Kingdom ;  
<sup>4</sup>NIHR University College London Hospitals Biomedical Research Centre, Medical Physics, London, United Kingdom

### Purpose or Objective

A common problem with the QA of deformable image registration (DIR) algorithms is the absence of ground truths with which to generate quantitative metrics for performance evaluation. It was hypothesised that Effective Depth (ED) calculations could be used as a surrogate ground truth for assessment of image warping using DIR for daily proton dose evaluations.

### Material and Methods

We compared two DIR algorithms, open-source software NiftyReg and commercial solution OnQ (Oncology Systems Ltd.), by deforming two head-and-neck CT scans to a repeated scan at the end of treatment for two different modalities: repeated CT (rCT) and image-guidance MVCT. Effective Depth (ED) Dose calculations were then performed using an in-house effective depth algorithm and stoichiometric calibration curves for the relevant modalities (MVCT and kVCT). The quality of the DIR performance was assessed according to APPM TG132 recommendations. By comparing the effective depth calculated, we can determine the range errors associated with the DIR that are relevant for dose calculations.

### Results

We performed ED calculations for an equally-spaced range of 32 coplanar and non-coplanar beam angles centred on the GTV centroid as shown in Figure 1.

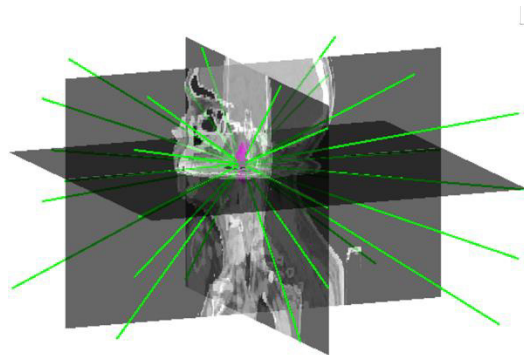


Figure 1: The selection of 32 beam angles used to calculate the Effective Depths. The isocentre was defined as the centroid of the gross tumour volume.

The EDs were calculated for the deformed CT and the ground truth rCT and MVCT for comparison of the percentage difference. For the standard DIR QA, we calculated the mean surface distance, dice similarity coefficient (DSC) and Hausdorff distance (95<sup>th</sup> percentile) for five organs at risk outlined on the CT, rCT and MVCT images: the parotid glands, submandibular glands and spinal cord.

The results are shown in Table 1.

Modality \ DIR Metric	Mean Surface Distance [mm]	DSC	Hausdorff Distance [mm]	Effective Depth MAE [%]
MVCT OnQ	1.92 (0.69)	0.75 (0.07)	5.63 (1.90)	4.00 (3.38)
MVCT NiftyReg	1.59 (0.66)	0.78 (0.07)	5.22 (2.14)	3.64 (3.06)
rCT OnQ	1.48 (0.48)	0.78 (0.05)	3.45 (0.96)	2.49 (3.65)
rCT NiftyReg	1.78 (0.31)	0.82 (0.02)	3.01 (0.62)	1.71 (2.09)
AAPM standards	~2-3mm	~0.80-0.90	N/A	N/A

Table 1: Results of the DIR evaluation metrics. For the contour-based metrics, the values are given as a mean over five organs at risk with the sample standard deviation in brackets. The ED is provided as a mean absolute error over 32 beam angles with the standard deviation in brackets.

The results show that when the DIR is within tolerance according to the APPM recommendations, the %ED error is also within 3%. When the DIR is just outside the tolerance, as observed for the MVCT, the mean %ED error is between 3-4%. NiftyReg performed better than OnQ for both standard QA metrics and ED error for both modalities. The large %ED errors (>3%) for both NiftyReg and OnQ occurred at similar beam angles for both MVCT and rCT. However, the ED difference for NiftyReg and OnQ was systematically greater than the ground truth for MVCT but with opposite signs with respect to the ground truth for rCT.

### Conclusion

This work highlights the potential for ED to be used as a QA measure for DIR for the purposes of proton dose calculations, which does not require labour-intensive manual contouring on the images involved. However, we also think this method would be useful for standard radiotherapy in centres using TomoTherapy with MVCT as daily IGRT. ED calculations could be used concurrently with contour propagation for QA of regular dose delivered assessments. Further work will be to implement this technique in a TomoTherapy centre and evaluating other commercial DIR software. A limiting factor to this work is that current proton centres use CBCT as their method of IGRT, which ED cannot be calculated on directly at present.

### EP-2075 mARC vs. IMRT prostate treatments: OAR dose distribution analysis stratified by PTV extent

R. Bermúdez Luna<sup>1</sup>

<sup>1</sup>Hospital Universitario de Fuenlabrada, Medical Physics, Fuenlabrada, Spain

### Purpose or Objective

mARC is the volumetric modulated arc therapy technique provided by Siemens. This technique was implemented in our centre during 2016.

Among the reported benefits of the volumetric modulated arc therapy plans is that they can yield dose distributions highly conformed to the target volumes with improved protection of the surrounding organs at risk (OAR).

The aim of this work has been to compare the dose distributions obtained with mARC plans with those corresponding to the IMRT technique in prostate cancer radiotherapy treatments. The analysis has been focused on the OARs and has been stratified according to seminal vesicle and pelvic lymph node involvement.

### Material and Methods

The dose-volume histograms (DVH) of 60 prostate cancer mARC plans have been analysed and compared to the

results corresponding to 60 seven-field step and shoot IMRT plans that had been previously delivered in our centre. Both samples were formed by 3 groups of 20 patients each, regarding the target volume extent: prostate (PR), prostate and seminal vesicles (PR+SV) and prostate, seminal vesicles and pelvic lymph nodes (PR+SV+PLN).

All treatments had a prescription dose to the prostate PTV of 70 Gy in 28 fractions (2.5 Gy/fraction). In case of seminal vesicle involvement, the corresponding PTV had a prescription dose of 56 Gy (2 Gy/fraction). If the pelvic lymph nodes were also considered for treatment, the prescribed dose to their PTV was 50.4 Gy (1.8 Gy/fraction). Plans were optimised to meet the dosimetric requirement of at least the 95% of each PTV receiving the 95% of its prescription dose, with the OARs being irradiated with the lowest dose as possible.

Several dosimetric quantities and the mean DVHs have been evaluated for the rectum, bladder and femoral heads.

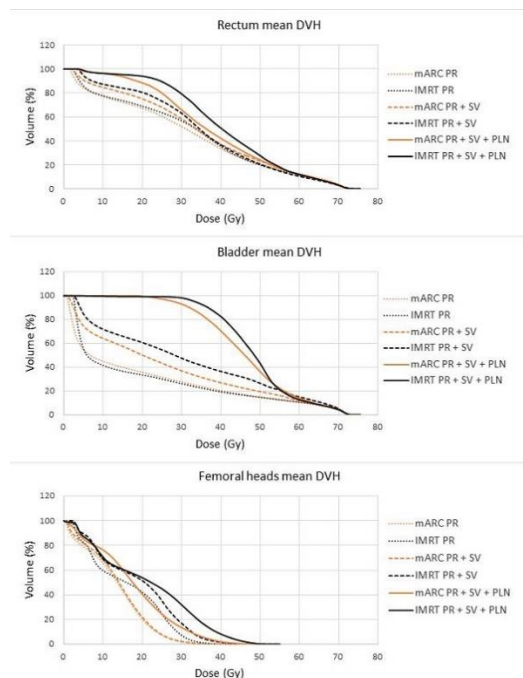
The unpaired t-test or the Mann-Whitney test have been conducted on the evaluated parameters to assess statistically significant differences among both techniques, with a 5% significance level.

### Results

Every plan was considered valid for treatment by the radiation oncologists.

The table lists the results of the analyses (mean values  $\pm$  standard deviations; n.s.: not significant). The mean DVHs are displayed in the figure.

Organ at risk	Plan parameter	Group	IMRT	mARC	p
Rectum	Mean dose (Gy)	PR	32.1 $\pm$ 3.7	31.4 $\pm$ 5.1	n.s.
		PR + SV	35.4 $\pm$ 3.8	34.5 $\pm$ 5.1	n.s.
		PR + SV + PLN	41.1 $\pm$ 2.7	38.1 $\pm$ 3.4	0.004
Bladder	Mean dose (Gy)	PR	19.1 $\pm$ 8.8	19.7 $\pm$ 8.6	n.s.
		PR + SV	32.4 $\pm$ 10.7	25.9 $\pm$ 5.7	0.043
		PR + SV + PLN	48.4 $\pm$ 3.3	46.6 $\pm$ 4.7	n.s.
Femoral heads	Mean dose (Gy)	PR	15.9 $\pm$ 3.1	13.3 $\pm$ 2.0	0.010
		PR + SV	19.1 $\pm$ 3.3	13.8 $\pm$ 1.9	< 0.001
	PR + SV + PLN	21.5 $\pm$ 3.4	18.0 $\pm$ 2.1	0.002	
	Maximum dose (Gy)	PR	41.0 $\pm$ 5.5	36.2 $\pm$ 6.6	0.016
		PR + SV	43.9 $\pm$ 7.4	35.5 $\pm$ 5.6	< 0.001
		PR + SV + PLN	50.9 $\pm$ 2.8	47.2 $\pm$ 4.4	0.007



### Conclusion

mARC prostate treatment plans have generated clinically acceptable dose distributions and have shown similar or better protection of the evaluated OARs.

Regarding the rectum, the greatest advantage of the mARC technique has been obtained in the PR+SV+PLN group, in which the mARC plans have yielded a statistically significant mean reduction in the mean dose of 3 Gy.

Considering the bladder, mARC plans have shown a systematic sparing over the entire dose range in the PR+SV group with a statistically significant mean reduction in the mean dose of 6.5 Gy.

With respect to the femoral heads, mARC dose distributions have yielded statistically significant reductions in the mean and maximum doses of every group, showing highly significant mean reductions of 5.3 Gy in the mean dose and 8.4 Gy in the maximum dose in the PR+SV group.

### EP-2076 Is there any advantage in using helium ions over protons for minibeam radiation therapy?

T. Schneider<sup>1</sup>, A. Patriarca<sup>2</sup>, Y. Prezado<sup>1</sup>

<sup>1</sup>Imagerie et Modélisation en Neurobiologie et Cancérologie IMNC, CNRS - Université Paris 11 - Université Paris 7, Orsay, France ; <sup>2</sup>Institut Curie - PSL Research University, Centre de Protonthérapie d'Orsay - Radiation Oncology Department, Paris, France

### Purpose or Objective

Hadron minibeam radiation therapy (hMBRT) is a novel concept combining the normal tissue sparing of submillimetric, spatially fractionated beams [1,2] with the improved dose deposition of ions. The increase of normal tissue tolerances may allow a safe dose escalation in the tumour. Along this line, proton minibeam radiation therapy [3] has already shown a widening of the therapeutic window for radioresistant tumours [4,5]. Next to protons, a possible choice for minibeam radiation therapy are helium ions. Their reduced multiple coulomb scattering compared to protons could lead to more favourable dose distributions, without the possible concerns related to nuclear fragmentation of heavier ions [6,7].

### Material and Methods

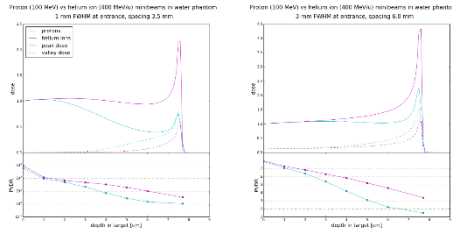
The dose distributions of protons and helium minibeam with the same range (7.7 cm) both in a water phantom and in the computer tomography images of an anonymized human patient (brain tumour) have been assessed by means of Monte Carlo simulations (GATE v.8.0 [7]). Two different full widths at half maximum (FWHM) at the entrance were considered: 1 and 3 mm. Different minibeam spacings and divergences were also evaluated. The peak-to-valley dose ratio (PVDR), entrance-to-Bragg peak dose ratio (EBDR) and lineal energy transfer (LET) were used as figures of merit.

### Results

It was found that the use of helium ions can significantly improve the EBDR yielding a two-fold increase for 3-mm beams and a more than three-fold increase for 1-mm beams, which favours tissue sparing. Due to their reduced lateral scattering, helium ions yield slightly larger PVDRs than proton minibeam, which ultimately might make it challenging to obtain a homogeneous lateral dose distribution at Bragg peak depth with only one array. However, in recent studies in pMBRT, tumour sterilization was achieved even in configurations leading to highly heterogeneous dose distributions [5]. Lastly, no significant difference was observed in terms of LET maps between protons and helium.

### Conclusion

Helium ions may be an optimum alternative for minibeam radiation therapy since they offer improved dose distributions with respect to protons without the possible drawbacks linked to nuclear fragmentations of heavier ions.



References:

- [1] <https://doi.org/10.1667/RR14018.1>
- [2] <https://doi.org/10.1073/pnas.0603567103>
- [3] <https://doi.org/10.1118/1.4791648>
- [4] <https://doi.org/10.1038/s41598-017-14786-y>
- [5] [https://doi.org/10.1016/S0167-8140\(18\)30879-X](https://doi.org/10.1016/S0167-8140(18)30879-X)
- [6] <https://doi.org/10.1118/1.4930960>
- [7] <https://doi.org/10.1002/mp.12175>
- [8] <https://doi.org/10.1088/0031-9155/49/19/007>

**EP-2077 De-intensification of radiotherapy dose to the elective neck in oropharyngeal squamous cell cancers**  
**R. Valentine<sup>1</sup>, A. Martin<sup>2</sup>, S. Currie<sup>1</sup>, C. Paterson<sup>2</sup>**  
<sup>1</sup>Beatson West of Scotland Cancer Centre, Radiotherapy Physics Department, Glasgow, United Kingdom ; <sup>2</sup>Beatson West of Scotland Cancer Centre, Radiation Oncology Department, Glasgow, United Kingdom

**Purpose or Objective**

The incidence of oropharyngeal squamous cell cancer (OPSCC) is rising due to Human Papilloma Virus (HPV) infection. HPV-positive (HPV+) OPSCC has a good prognosis and is sensitive to treatment. Standard of care is high dose radiotherapy which is very effective but causes significant and permanent toxicity. There is a consensus that investigation into less toxic treatments for these patients is required. A retrospective planning study was carried out evaluating the effect of delivering a reduced radiotherapy dose to the elective neck, known as Planning Target Volume (PTV\_LR) on dose received by the organs at risk (OARs).

**Material and Methods**

Ten representative patients (HPV+, non-smokers, OPSCC) were re-planned retrospectively using Eclipse TPS v15.5 [Varian Medical Systems, Palo Alto, CA, USA], RapidPlan<sup>®</sup> and multi-criteria optimisation (MCO). All plans consisted of two VMAT fields with two full rotational arcs at 6 MV and 600 MU/min. In our centre, head & neck squamous cancers are typically prescribed 65Gy in 30 fractions to gross disease; High Risk Planning Target Volume (PTV\_HR) while the PTV\_LR is treated to 54Gy in 30 fractions (50Gy equivalent). The original clinical plans were re-optimised with a locally published RapidPlan<sup>®</sup> model and MCO to achieve optimal PTV coverage while maintaining OAR sparing consistent with our centre's specified dose constraints. Subsequently, all plans were similarly re-optimised only this time PTV\_LR was prescribed 42.1Gy in 30 Fractions [40Gy (EQD2Gy)] while retaining 65Gy to PTV\_HR. Finally, plan deliverability for all plans was assessed using the modulation factor (MF) and MLC average leaf pair opening (ALPO).

**Results**

Table 1 highlights the dose differences found between PTV\_HR, PTV\_LR and pertinent OARs when comparing between the 54Gy and 42.1Gy prescriptions to PTV\_LR. Acceptable and within protocol, PTV\_HR coverage was still achieved for 42.1Gy with only a small % reduction found in the D99% and D95% constraints. Comparing between the prescriptions, the dose constraints for PTV\_LR were clinically acceptable with each of the appointed OAR doses significantly reduced for 42.1Gy (p<0.05). On average, we found the MF to be 0.40 and 0.46 and the ALPO to be 2.9 and 3.0 for the 54Gy and 42.1Gy plans, respectively, suggesting highly deliverable plans.

PTV	Coverage/Constraint	Dose Prescribed to PTV_LR		Reduction (%)
		54Gy	42.1Gy	
		Dose (%)		
	D99% > 90%	93.4 ± 0.9	90.6 ± 0.5	-3.0
PTV_HR	D95% > 95%	96.1 ± 0.5	95.2 ± 0.3	-0.9
65Gy	D5% < 105%	103.8 ± 0.3	103.8 ± 0.4	0.0
	D2% < 107%	104.5 ± 0.4	104.7 ± 0.5	0.2
	D99% > 90%	93.0 ± 0.7	90.8 ± 0.7	-2.4
PTV_LR	D95% > 95%	96.2 ± 0.4	95.5 ± 0.5	-0.7
	D5%	109.1 ± 0.8	116.9 ± 3.8	7.1
	D2%	113.6 ± 1.2	129.7 ± 3.7	14.2
OARs		Dmean (Gy)		
Ipsilateral Parotid		32.5 ± 11.4	29.3 ± 11.8	-9.8
Contralateral Parotid		20.6 ± 3.7	15.6 ± 2.6	-24.3
Larynx		42.8 ± 5.9	39.3 ± 6.2	-8.2
Constrictor Muscles		57.2 ± 2.2	50.9 ± 2.7	-11.0

**Conclusion**

By reducing the dose from 54Gy to 42.1Gy to PTV\_LR, we found a significant reduction in OAR doses while maintaining acceptable doses to the PTV\_HR. Due to steep dose response curves seen in OARS, we anticipate that this reduction in radiotherapy dose will translate into potentially important toxicity gains for patients. This approach is likely to be safe due to maintained dose to gross disease yet with potential clinically relevant reductions in dose received by OARS. On the basis of these results a larger dosimetric study is in progress and will form the basis for the radiotherapy protocol and QA work for a clinical trial investigating this strategy.

**EP-2078 Comprehensive risk assessment for the clinical introduction of an MR-linac**

**J. Geuze<sup>1</sup>, R. Bouwman<sup>1</sup>, U.A. Van der Heide<sup>1</sup>, S. Ten Hoeve<sup>1</sup>, M.E. Nowee<sup>1</sup>, T.M. Janssen<sup>1</sup>**  
<sup>1</sup>Netherlands Cancer Institute, Radiotherapy, Amsterdam, The Netherlands

**Purpose or Objective**

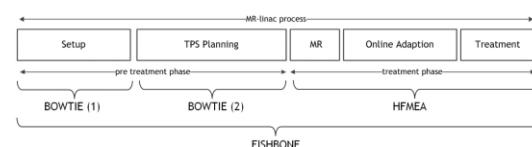
Bodies like Joint Commission International and Health & Safety Executive advise hospitals to use risk assessment methodologies like HFMEA (Healthcare Failure Mode Effect Analysis) to enhance patient safety and reduce unwanted incidents<sup>1</sup>.

A major event like the clinical introduction of the Unity MR-linac (Elekta AB, Stockholm, Sweden) has impact on the complete treatment chain. However, the scope and complexity of this process make a single HFMEA assessment inadequate for thorough identification of potential risks<sup>2</sup>. Alternatively, the execution of multiple HFMEA based risk assessments would be quite time consuming.

The aim of this work is to present a comprehensive risk assessment program, where multiple risk assessment methodologies are combined to ensure patients safety in a complex process like the introduction of an MR-linac.

**Material and Methods**

In the MR-linac treatment process 5 different sub processes are identified (fig. 1). Depending on whether a sub process was MR-linac specific or already clinically implemented, different risk assessment methodologies were chosen.



The sub processes of the pre-treatment phase are quite similar to those for a conventional linear accelerator. The

BOWTIE method is event based, which enables to focus on the distinctions. It is suitable to identify single hazards, root causes and measures that are MR-linac specific. The BOWTIE method has been used in the process of setup and planning.

The HFMEA method is process-based and more appropriate to identify potential failures and risks in the treatment phase. The steps of this process (MR acquisition, online plan adaptation and treatment) don't have an equivalent within the process of the conventional linac.

The final integral assessment is executed with the Fishbone method. By analyzing the 'process defects' based on 4 potential causes (treatment, technology, management/organization and environment) potential interface risks are included in the risk assessment.

### Results

The program resulted in 25 initiated outcome measures. (table 1a). The measures from the BOWTIES where more related with technology, materials, QA and SOP's, were the HFMEA and Fishbone resulted measures associated with task, responsibilities and authorizations.

The comprehensive risk assessment program was executed in five sessions with an average duration of 1h 40' with 19 different healthcare professionals (table 1b) over a period of 8 months (Oct'17 - Jun'18).

Process	Medical devices and supporting materials	Standard operation procedures	Quality Assurance	Training	Tasks, responsibilities and authorizations
Set-up	3	2	1	-	-
TPS Planning	1	2	3	-	1
Treatment	-	1	-	-	2
MR-linac (integral)	-	2	1	1	5
<b>Total</b>	<b>4</b>	<b>7</b>	<b>5</b>	<b>1</b>	<b>8</b>

Table 1a Overview of outcome measures

Process	Method	Involved people	Physician	Physicist	RTT	Session(s)	Total time
Set-up	BOWTIE	4	-	1	3	1	2h 00'
TPS Planning	BOWTIE	4	1	1	2	1	2h 00'
Treatment	HFMEA	5	1	1	3	2	3h 20'
MR-linac (integral)	FISHBONE	6	1	3	2	1	1h 00'
<b>Total</b>		<b>19</b>	<b>3</b>	<b>6</b>	<b>10</b>	<b>5</b>	<b>8h20'</b>

Table 1b Overview of risk assessments

### Conclusion

By tailoring the risk assessment methods for each sub process we able to thoroughly and efficiently identify root causes and potential risks relevant for the patient safety with respect to a complex chain process like MR-linac based radiotherapy. This avoids the need of multiple HFMEA assessments. The integral risk assessment, with the Fishbone method, ensured that overall logistics, interface and process based (potential) risks were identified. [1] Chatman I.J. (The Joint Commission, 2010) [2] Gould J, et al. (Health & Safety Laboratory, 2010)

### EP-2079 HyperArc™ RT for thyroid eye disease: a plan comparison with VMAT and parallel opposed techniques

R. Valentine<sup>1</sup>, S. Schipani<sup>2,3</sup>, P. Cauchi<sup>4</sup>, V. Chadha<sup>4</sup>, J. Connolly<sup>4</sup>, T. Mitchell<sup>2</sup>, D. Ritchie<sup>2</sup>, S. Currie<sup>1</sup>

<sup>1</sup>Beatson West of Scotland Cancer Centre, Radiotherapy Physics Department, Glasgow, United Kingdom ; <sup>2</sup>Beatson West of Scotland Cancer Centre, Radiation Oncology Department, Glasgow, United Kingdom ; <sup>3</sup>University of Glasgow, Institute of Cancer Sciences, Glasgow, United Kingdom ; <sup>4</sup>Gartnavel General Hospital, Tennent Institute of Ophthalmology, Glasgow, United Kingdom

### Purpose or Objective

To compare HyperArc™ (HA) radiotherapy with 2-Field VMAT (2F-V) and 2-Field Parallel Opposed (2F-PO) technique for the treatment of Thyroid Eye Disease (TED).

### Material and Methods

Patients with high dose steroid refractory TED were selected. The patients were immobilized with a stereotactic radiosurgery (SRS) encompass shell. A non-contrast enhanced CT was acquired with 1mm slices for planning purposes. CT was fused with a baseline diagnostic MRI to better define the Organs at Risk (OARs). CTV was

defined as the bilateral retro-ocular soft tissues including the ocular muscles and the retro-bulbar fat and excluding the lacrimal glands with a 3mm margin. CTV was expanded to PTV with a 2mm margin. Lenses, optic chiasm, brain, lacrimal ducts, brainstem, hippocampus, pituitary, nasal cavity and lacrimal glands were defined as OARs. HA, 2F-V and 2F-PO plans were generated with Eclipse TPS v15.5 (Varian Medical Systems, Palo Alto, CA, USA). HA used up to 4 arc fields, 3 of which were non-coplanar, optimised collimator angles and a SRS normal tissue objective (NTO) feature for plan optimisation. 2F-V plans consisted of two full rotational arcs. HA and 2F-V plans were generated using high definition 2.5 mm leaf width MLCs along with a 1.25 mm optimisation resolution and grid size. 2F-PO plans were constructed with both anterior field edges placed posterior to the lenses and the posterior field edges covering the orbital apex. All plans were generated using a photon beam energy of 6MV, a dose rate of 600 MU/min, and a dose prescription of 2004 cGy in 12 fractions to the PTV. Dosimetric parameters for PTV and organs at risk (OARs) were evaluated.

### Results

Ten patients were included in the study. HA plans offered superior PTV coverage (p<0.05) at particular dose metrics compared to 2F-V (D99%, D98%) and 2F-PO (D99%, D98%, D95%, D50%). For the HA plans, Dmean to the brain, brainstem, hippocampus, pituitary and nasal cavity were reduced (p<0.05) compared to the 2F-V plans. For the 2F-PO plans, Dmax to optic chiasm, Dmean to lacrimal ducts, nasal cavity and lacrimal glands was higher (p<0.05), while Dmax to lenses, Dmean to brain, brainstem, hippocampus and pituitary was lower (p<0.05) compared to the HA and 2F-V plans. HA gave an increased Dmean to brain, brainstem, hippocampus and pituitary in the range of 0.8-2.4Gy compared to 2F-PO. The dosimetric results are reported in Table 1.

	Constraint	HyperArc (HA)	2F-VMAT	2F-PO
		Dose (%)		
PTV	D99%	91.6 ± 3.9	89.0 ± 6.3	6.3 ± 2.1
	D98%	94.0 ± 2.1	92.4 ± 3.1	8.2 ± 3.4
	D95%	96.2 ± 1.5	95.1 ± 2.5	16.0 ± 7.6
	D50%	101.8 ± 0.6	101.5 ± 1.5	99.6 ± 0.8
	D5%	105.8 ± 1.1	105.8 ± 2.1	103.2 ± 0.8
	D2%	106.9 ± 1.3	106.9 ± 2.2	104.1 ± 1.0
		Dose (Gy)		
OARs				
Optic Chiasm	Dmax	5.1 ± 1.4	6.5 ± 3.2	10.2 ± 6.9
Left Lens		5.7 ± 1.9	5.9 ± 1.1	2.3 ± 1.8
Right Lens		5.8 ± 1.9	5.8 ± 1.3	1.6 ± 0.8
Brain	Dmean	2.5 ± 0.2	2.6 ± 0.2	1.0 ± 0.2
Lacrimal Ducts		8.4 ± 3.4	9.5 ± 3.2	11.4 ± 6.9
Brainstem		2.5 ± 0.5	3.4 ± 1.4	0.2 ± 0.02
Hippocampus		2.6 ± 0.4	3.9 ± 1.3	0.2 ± 0.02
Pituitary		2.8 ± 0.6	4.2 ± 2.3	2.0 ± 1.4
Nasal Cavity		7.8 ± 1.7	11.5 ± 2.8	13.5 ± 1.5
L Lacrimal Gland		8.6 ± 4.2	9.5 ± 3.9	17.1 ± 2.3
R Lacrimal Gland		8.6 ± 4.0	9.4 ± 4.0	16.8 ± 2.9

### Conclusion

HA offers better compromise between PTV coverage and OARs sparing especially for lacrimal glands with possible advantage in TED symptom control and long term complications (ocular dryness). A prospective study will be carried out in our institution.

### EP-2080 MC simulations on the dose enhancement effect of antibody conjugated AuNPs in targeted radiotherapy

A. Klapproth<sup>1</sup>, W. Li<sup>2</sup>, S. Stangl<sup>1</sup>, C. Diederichs<sup>1</sup>, M. Shevtsov<sup>1</sup>, V. Ntziachristos<sup>3</sup>, G. Multhoff<sup>1</sup>

<sup>1</sup>Klinikum Rechts der Isar, Department of Radiation Oncology, Munich, Germany ; <sup>2</sup>Helmholtz Zentrum

München, Institute of Radiation Protection, Munich, Germany ; <sup>3</sup>Helmholtz Zentrum München, Institute of Biological and Medical Imaging, Munich, Germany

### Purpose or Objective

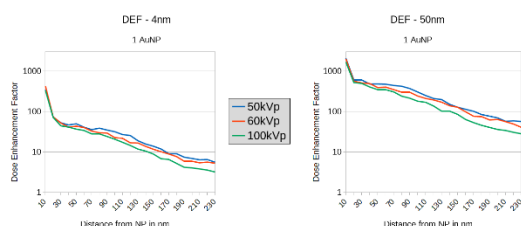
Different cell culture experiments and Monte Carlo simulations already showed that gold nanoparticles (AuNPs) can result in a dose enhancement of radiotherapy. Current *in vitro* results suggest an increased uptake of AuNPs into Hsp70-positive tumor cells after conjugation of AuNPs with cmHsp70.1 antibody. Before the start of *in vivo* investigation, the dose enhancement effect of functionalized cmHsp70.1 mAb AuNPs will be simulated.

### Material and Methods

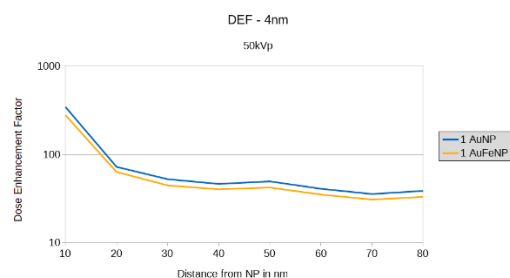
The Geant4-DNA toolkit was used to compute the dose enhancement effects of gold nanoparticles in different cellular compartments after x-ray irradiation. In particular, the amount of energy released by photon interactions will be analyzed after penetration of the x-ray beam through the cell. This energy is released by secondary electrons. Especially Auger-electrons contribute exceedingly to the dose enhancement effect for the tested energy spectra (50kVp, 60kVp, 100kVp). Different nanoparticle sizes (4nm, 10nm, 50nm, 100nm) and distribution patterns were used in the simulations. Simultaneously the same simulations are performed with the same geometry in water without AuNPs. The comparison provides the respective dose enhancement factor (DEF) in distinct areas within a cell. This work provides information about localization and energy deposition of the particle events and also the electron spectrum around the AuNPs.

To allow for tracking of the nanoparticles via MRI, we are planning to include an Fe<sub>3</sub>O<sub>4</sub> core at the center of the AuNPs used in experiments. Accordingly, we repeated the same set of simulations replacing the pure AuNPs with hybrid AuFeNPs.

### Results



The DEF is calculated by dividing the results from simulations containing AuNPs by results from respective simulations without AuNPs. Results of simulations with  $10^8$  photons shot directly at one AuNP are shown in the first figure. Due to the limited range of Auger-electrons, the DEF is at its maximum in immediate range to the AuNP and decreases with increasing range.



The second figure shows the comparison between the courses of the DEF for simulations with 1 AuNP and 1 AuFeNP respectively. A decrease in dose enhancement was expected, since iron-oxide is less likely to produce

secondary electrons under irradiation in comparison to a high-Z material like gold. Yet no decrease in functionality that would exclude the hybrid AuFeNPs from implementation could be found so far.

### Conclusion

The limited range of secondary electrons and fast decrease of the DEF with increasing range underlines the importance of developing techniques to deliver the AuNPs not only into the tumor cells but at best in close range to their nucleus to maximize the probability of cell death during irradiation.

The results of the simulations will be used to compute the overall dose in a phantom under irradiation. By this we determine optimal conditions for the subsequent *in vivo* experiments, where cmHsp70.1 conjugated GNPs will be tested in small animals treated with radiotherapy.

### EP-2081 Real time CyberKnife dosimetry using Radioluminescence imaging

A. Spinelli<sup>1</sup>, E. D'Agostino<sup>2</sup>, C. Fiorino<sup>3</sup>, S. Broggi<sup>3</sup>  
<sup>1</sup>San Raffaele Scientific Institute, Experimental Imaging Centre, Milano, Italy ; <sup>2</sup>DoseVue NV, Research and Development, Turnhout, Belgium ; <sup>3</sup>San Raffaele Scientific Institute, Medical Physics, Milano, Italy

### Purpose or Objective

The main objective of this work was the development and the preliminary test of a novel real-time 2D dosimetry approach for CyberKnife quality assurance using radioluminescence imaging (RLI) with a commercial CMOS detector. In particular, the possibility to verify collimators field size was investigated. Radioluminescence light was generated by two flexible and thin scintillators film composed respectively of green-emitting and red emitting rare earth phosphors.

### Material and Methods

A CMOS detector was mounted on a photographic tripod and coupled with a F=1.4, 8 mm C-mount lens (Edmund Optics) facing the scintillator film placed on the patient bed, as shown in figure 1. The scintillator film was placed under a 1 cm slab of PMMA.

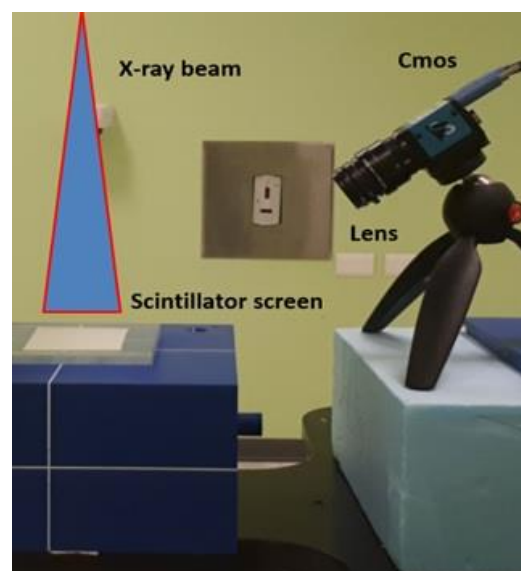


Figure 1 RLI acquisition setup in the CyberKnife treatment room. The CMOS is mounted on a tripod and coupled to a C-mount lens facing the film.

Dose measurements were performed using the CyberKnife system (Accuray) switching off the main treatment room light during RLI image acquisition; few led lights around the CyberKnife system were on. The CMOS setting was as follows: gain=22, brightness=50 and exposure time=1/100 sec. A sequence of 120 images was acquired every 1 sec

and summed using Fiji. RLI data were corrected for perspective distortion with a home-made program written using Matlab2018b. A perpendicular single beam (Source-Surface Distance = 80cm) was set with different field sizes. Two circular fields with diameter equal to 10 and 40 mm were tested.

Measured planar dose distributions and dose profiles were compared against radiochromic films (GC), including FWHM estimate. Measurement repeatability was tested on both beam by moving and repositioning the CMOS for three times.

### Results

The image correction procedure was confirmed to be able to reduce the perspective distortion at a negligible level and, at the same time, was reproducible. The agreement of the measured dose profiles and beam sizes is fairly good as shown in figure 2; light scattering due to the buildup slab slightly affected the flat region of the profile. The measured FWHM of the 40 mm beam obtained with RLI and CG were respectively equal to 42.4 mm and 42.7 mm.

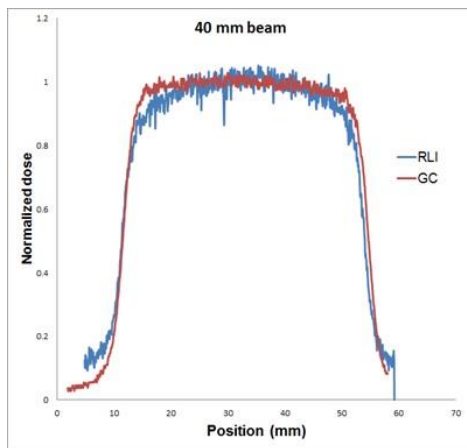


Figure 2 Comparison of normalized RLI and GC beams profiles.

The FWHM of the 10 mm beam were respectively equal to 10.9 mm and 11.3 mm: repeatability tests confirmed RLI values for FWHM within 0.3 mm. The RLI signal was detected in dimmed condition, showing the RLI dose measurements possible even when the lights in the treatment room cannot be totally removed.

### Conclusion

A novel RLI approach based on a thin scintillator screen and a CMOS detector was tested for CK dosimetry, in particular for periodic constancy checks, also allowing real time dose information. Preliminary results show a good agreement with GC dose measurements; the set-up of the measurement (positioning of the detector, fixation, PMMA slab optimization, light collection parameters) may likely be further improved and future investigation is warranted.

### EP-2082 An adapted use of the gamma index method for Monte Carlo dose distributions comparison

M. Cohilis<sup>1</sup>, S. Edmond<sup>1,2</sup>, L. John A.<sup>1</sup>, S. Kevin<sup>1</sup>

<sup>1</sup>Université Catholique de Louvain- Institute of Experimental & Clinical Research, Molecular Imaging- Radiotherapy and Oncology, Brussels, Belgium ;

<sup>2</sup>Katholieke Universiteit Leuven, Department of Oncology, Leuven, Belgium

### Purpose or Objective

In IMRT/IMPT, QA is essential. The quality of the treatment can be verified by comparing the TPS dose to measurements or to Monte Carlo (MC) simulations, which are slower and noisy due to their stochasticity, but more accurate. The most common method of dose comparison is the gamma test. However, this method is known to be

asymmetric and dependent on the noise level in dose distributions. When setting a noisy dose as reference (MCref) in the gamma test, the passing rate (PR) is underestimated, while setting a noisy dose as evaluated dose (MCEval) results in an overestimated PR. MC algorithms nowadays can be fast, but not enough to avoid substantial noise. This work proposes a method to correct the gamma test result when applied to MC doses, while keeping a tractable computation time.

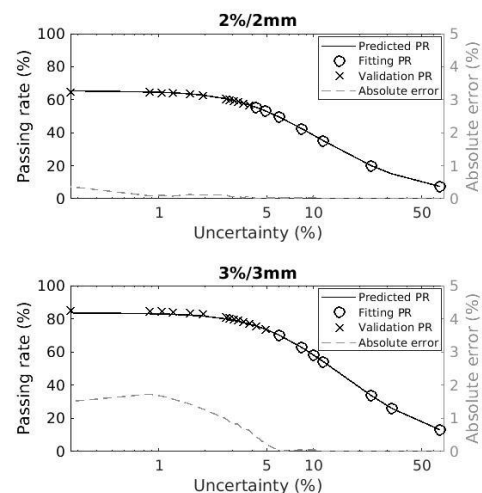
### Material and Methods

The method was derived thanks to the similarities observed between multiple patients. It consists of extrapolating the PR corresponding to a low noise MC dose from several PR computed for various high noise levels. We avoid this way a too costly MC computation. The fitting function has 7 parameters. This model being quite flexible, the optimization is performed with 50 random initial conditions uniformly distributed in a given interval, and the best solution is kept.

This method was applied to 5 PBS proton plans: prostate, lung, liver, brain, H&N. For each of them, using the fast code MCsquare, we computed 21 MC doses with different uncertainty levels: 7 for the fitting (high noise) and 14 for the validation (low noise). Gamma tests were performed between the MC and the TPS dose maps, for each available noise level and 4 different criteria. We then predicted the PR corresponding to the lowest MC uncertainty and compared our results with the actual PR previously calculated. Points used for the fitting corresponded to maximum 2E7 or 4E7 simulated protons in the MC calculation.

### Results

Only the results for MCref case are presented here, but MCEval case is similar. As the method is not deterministic, we applied it 60 times and report here the results as mean values with corresponding standard deviations (SD). Figure 1 illustrates the method for a brain case, showing the fit and the error in each point for two gamma criteria. Table 1 gives the results for all patients. The gain obtained with our method is defined as the difference between two errors: the error made by the classical gamma index for a MC dose calculated with uncertainty S, and the error made by our method when using a smallest fitting uncertainty S. We are thus comparing the methods at equal MC computation time. We see here that the error on the PR at the lowest uncertainty is most of the times between 1% and 3%, with a SD about 1%. The gain is between 0.5% and 12%.



Case		Mean error (%)	Mean gain (%)	SD (%)
Prostate	2%/2mm	1.86	2.38	1.27
	3%/3mm	0.47	5.14	0.74
	4%/4mm	0.94	2.58	0.69
	3%/1mm	1.42	3.17	0.11
Lung	2%/2mm	2.60	11.89	0.45
	3%/3mm	1.07	8.36	0.63
	4%/4mm	0.57	4.60	0.81
	3%/1mm	4.41	11.78	1.18
Brain	2%/2mm	1.07	8.51	0.99
	3%/3mm	2.75	12.19	1.15
	4%/4mm	2.20	8.74	1.11
	3%/1mm	0.86	9.96	1.01
Liver	2%/2mm	0.63	3.91	0.19
	3%/3mm	2.50	1.97	1.12
	4%/4mm	0.84	0.56	0.58
	3%/1mm	1.34	3.61	0.04
H&N	2%/2mm	2.28	1.46	0.01
	3%/3mm	0.57	4.06	0.02
	4%/4mm	0.76	2.91	0.53
	3%/1mm	0.95	3.05	0.18

Table 1: MC<sub>ref</sub> case : summary of the results. The table gives the case, the criterion, the mean errors and gains obtained at the lowest uncertainty available ( $2 \times 10^{10}$  particles) and the standard deviation over these mean values.

### Conclusion

The gamma test can be very sensitive to the noise of MC dose distributions. We propose here a method to correct this bias. The test remains fast (< 7 minutes including MC computations) and provides a PR way more reliable than the conventional gamma test.

### EP-2083 Evaluation of Deformable Image Registration and Dose Accumulation in Prostate SBRT Patients

J. Swamidás<sup>1</sup>, R. Phurailatpam<sup>1</sup>, S. Panda<sup>1</sup>, V. Murthy<sup>1</sup>, K. Joshi<sup>1</sup>, D. Deshpande<sup>2</sup>

<sup>1</sup>ACTREC- Tata Memorial Centre, Radiation Oncology, Mumbai, India ; <sup>2</sup>Tata Memorial Hospital, Medical Physics, Mumbai, India

### Purpose or Objective

To quantify the difference between planned and the delivered dose using deformable image registration (DIR) and deformable dose accumulation (DDA) for patients treated with Stereotactic Body Radiotherapy (SBRT) for prostate cancer.

### Material and Methods

Ten prostate cancer patients previously treated with SBRT (35Gy in 5 fractions) were retrospectively analysed for this study. All patients were treated with Rapid Arc using 10MV FFF beams (Varian Eclipse TPS v13.5.37, True Beam v 2.1, Varian Medical Systems, Palo Alto). Daily cone beam CT (CBCT) was carried out as per the institutional protocol, which includes a bladder filling and a bowel protocol which reproduces the anatomy on the treatment day as compared to the planning day. Delivered dose was calculated by accumulating the doses using DIR and DDA in Velocity DIR software (v 3.2.1). Daily CBCTs were also imported and deformably registered to the planning CT (pCT) and generated a synthetic CT (sCT). RT plan was recalculated on sCTs. The dose calculated on sCTs were deformed back and accumulated onto pCT to estimate the total delivered dose-DDA. The planned and delivered doses were compared using various dose volume parameters for PTV, CTV and OARs (bladder and rectum). Target coverage was estimated by comparing the differences between the planned and accumulated doses of PTV and CTV in terms of V<sub>95%</sub>(%), D<sub>mean</sub>(Gy) and D<sub>max</sub>(Gy). For OARs, D<sub>max</sub>(Gy), D<sub>mean</sub>(Gy), volume receiving various dose levels such as 30, 20, 10 and 5Gy were evaluated. Registration accuracy were also evaluated

using Dice Similarity Co-efficient (DSC) and Hausdorff distances (Hf avg).

### Results

Mean (±sd) volume of PTV, CTV of pCT was 60(±12)cc and 27(±7)cc respectively. Mean (±sd) volume of bladder and rectum of pCT vs CBCT averaged over 5 fractions were 368(±88) vs 345(±104)cc and 50(±14) vs 53(±14)cc respectively. Mean (±sd) DSC of bladder and rectum were 0.88(±0.7) and 0.92(±0.06), while Hfavg bladder and rectum were 2.6(1.4) mm and 1.2(1.0) mm respectively. Mean (±sd) difference in V<sub>95%</sub> between the planned and the delivered dose for PTV was 4(±3)%. However, maximum variation in V<sub>95%</sub> between the delivered and the planned dose was found to be correlating with the variation in bladder volume (r=0.42). Variation in other dose volume parameters was found to be negligible including for CTV. Mean (sd) difference between the planned vs delivered dose for bladder was 1.4 (5.7)%. However, patient wise analysis showed a maximum variation of 19% when the bladder volume variation was 138cc (patient-1). Mean (sd) difference between the planned vs delivered dose for rectum was 1.7 (±3.0)%, patient wise analysis showed a maximum variation of 4.0%, when the volume variation was 22 cc, and no correlation with rectal volume was observed.

### Conclusion

The difference between the planned and the delivered dose to target volumes and OARs were quantified. Bladder volume variation was found to be correlating with dose to PTV, however, no correlation was found for rectum.

### EP-2084 Arms-down versus arms-up positioning for breast cancer patients receiving proton beam radiation.

E. Batin<sup>1</sup>, N. Depauw<sup>2</sup>, S. MacDonald<sup>2</sup>, R. Jimenez<sup>2</sup>  
<sup>1</sup>UMC Groningen Proton Therapy Center, Radiation Oncology, Groningen, The Netherlands ; <sup>2</sup>Massachusetts General Hospital, Radiation Oncology, Boston, USA

### Purpose or Objective

Breast irradiation, with or without regional nodal involvement, is traditionally performed in an arms-up position. This is driven by the necessity to accommodate the photon treatment head while treating tangential fields in order to avoid collisions or treatment through the arms. This position can be uncomfortable for patients who, as a consequence of surgery, may have cording or contractures that limit arm mobility. Breast irradiation with proton therapy (PT) is performed using an enface approach, thus removing the treatment limitations of photons. This study evaluates the contouring, dosimetric, and practical challenges involved in performing PT breast irradiation in the arms-down position.

### Material and Methods

Ten breast patients underwent computed tomography (CT) simulation in both an arms-up and an arms-down position, following similar protocols for treatment. Contouring was performed on both arms up and arms down CT scans by two physicians with extensive proton breast treatment experience. Each set of contours was then verified by the non-contouring physician. Plans were generated with multi-criteria optimization and Pareto surface navigation using an in-house treatment planning system. Each treatment plan was generated using identical target coverage objectives, target constraints, and organs-at-risk (OAR) constraints, with each plan optimized by prioritizing target coverage within the confines of the a priori determined OAR constraints. No OAR objectives were used to avoid biasing the planning process. Two physicists was responsible for generating all plans. Each plan was then verified by the non-planning physicist.

## Results

At the time of CT simulation, all patients expressed a preference for the arms-down position in terms of comfort. Both physicians described a greater degree of difficulty when contouring the level I axilla in the arms-down position. Difficulty in plan generation between arms-up and arms-down cases was similar. Overall, the arms-down plans conferred a slightly lower target coverage, but within a clinically acceptable range. Treatment positioning using surface imaging presented equal challenges in either position.

## Conclusion

This study highlights the appropriateness of treating breast patients in an arms-down position when using proton therapy.

### EP-2085 PET/MR in GTV delineation in patients with carcinoma of the tongue

N. Samolyk-Kogaczewska<sup>1</sup>, E. Sierko<sup>2</sup>, K. Zuzda<sup>3</sup>, P. Gugnacki<sup>3</sup>, P. Szumowski<sup>4</sup>, M. Mojsak<sup>4</sup>, J. Burzyńska-Sliwowska<sup>5</sup>, T. Filipowski<sup>1</sup>, M.Z. Wojtukiewicz<sup>6</sup>, D. Jurgielewicz<sup>4</sup>

<sup>1</sup>Comprehensive Cancer Center of Białystok, Department of Radiotherapy, Białystok, Poland ; <sup>2</sup>Medical University of Białystok- Comprehensive Cancer Center, Department of Oncology- Department of Radiotherapy, Białystok, Poland ; <sup>3</sup>Medical University of Białystok, Scientific Student's Association affiliated with Department of Oncology, Białystok, Poland ; <sup>4</sup>Medical University of Białystok, Laboratory of Molecular Imaging- Nuclear Medicine Department, Białystok, Poland ;

<sup>5</sup>Comprehensive Cancer Center of Białystok, Department of Diagnostic Imaging, Białystok, Poland ; <sup>6</sup>Medical University of Białystok, Department of Oncology, Białystok, Poland

## Purpose or Objective

Evaluation of accuracy and usefulness of 18-fluor-labeled fluorodeoxyglucose (PET) and magnetic resonance (MR) hybrid in gross tumor volume (GTV) delineation during radiotherapy planning in patients with carcinoma of the tongue.

## Material and Methods

Computed tomography (CT) and PET/MR examination were made in group of 10 patients (pts) with squamous cell carcinoma (SCC) of the tongue. The GTV for primary tumor and lymph nodes (nGTV) were defined on CT (GTV-CT) and compared to GTVs obtained from PET (GTV-PET) and MR (GTV-MR) images. Two methods of GTV determination were used: visual interpretation of CT, PET (GTV-PET<sub>vis</sub>) and MR images and quantitative automatic method (Syngovia, Siemens) based on a chosen threshold value (20%, 30%, 40%, 50%) of SUV<sub>max</sub> from PET examination (GTV-PET<sub>20%</sub>, GTV-PET<sub>30%</sub>, etc.). Differences in GTV values obtained from CT, PET and MR studies were statistically analysed. The level of significance was considered as p<0.05. The GTV-CT was used as the reference.

## Results

The 80% of GTV-MR and 40% of GTV-PET<sub>vis</sub> were larger than GTV-CT. Respectively, 20% of GTV-MR and 60% of GTV-PET<sub>vis</sub> were smaller than GTV-CT. Taking into account all threshold measurements - 70% of volumes were smaller than GTV-CT. GTV-PET<sub>30%</sub> (p=0,2026) were the most closely related volumes to GTV-CT from all threshold method in 50% of patients. GTV-PET<sub>vis</sub> (p=0,5750) generated the most similar volumes in relation to GTV-CT from all PET measurements. Comparing to nGTV-CT - 70% of nGTV-MR and 20% of nGTV-PET<sub>vis</sub> were larger. Remaining nGTV-MR and nGTV-PET<sub>vis</sub> measurements were smaller than nGTV-CT. Measurements of all thresholds nGTVs were smaller than nGTV-CTV in 52,5% of cases. nGTV-PET<sub>20%</sub> were the most closely related volumes to nGTV-CT in 40% of the cases. Statistical analysis shown that nGTV-PET<sub>20%</sub> (p=0,0468), nGTV-PET<sub>vis</sub> (p=0,0166) and nGTV-PET<sub>50%</sub> (p=0,0166) diverge significantly from nGTV-CT results.

nGTV-MR (p=0,1141), nGTV-PET<sub>30%</sub> (p=0,2845) and nGTV-PET<sub>40%</sub> (p=0,5076) were the most significantly related with nGTV-CT.

## Conclusion

Combination of PET/MR provide better accuracy in GTV delineation in radiotherapy planning of pts with SCC of the tongue than other standard imaging methods. The most frequently matching threshold value in PET/MR was 30% of SUV<sub>max</sub> for primary tumor delineating and 30% and 40% of SUV<sub>max</sub> for nGTV estimation.

### EP-2086 Innovative hybrid 18FDG-PET/MR in GTV delineation in locally advanced oral cavity cancer patients

N. Samolyk-Kogaczewska<sup>1</sup>, E. Sierko<sup>2</sup>, D. Dziemiańczyk-Pakieta<sup>3</sup>, B. Nowaszewska<sup>3</sup>, K. Zuzda<sup>4</sup>, J. Burzyńska-Sliwowska<sup>5</sup>, P. Szumowski<sup>6</sup>, D. Jurgielewicz<sup>6</sup>, T. Filipowski<sup>1</sup>, M.Z. Wojtukiewicz<sup>7</sup>, M. Mojsak<sup>6</sup>

<sup>1</sup>Comprehensive Cancer Center of Białystok, Department of Radiotherapy, Białystok, Poland ; <sup>2</sup>Medical University of Białystok- Comprehensive Cancer Center, Department of Oncology- Department of Radiotherapy, Białystok, Poland ; <sup>3</sup>Medical University of Białystok, Department of Maxillofacial and Plastic Surgery, Białystok, Poland ; <sup>4</sup>Medical University of Białystok, Scientific Student's Association affiliated with Department of Oncology, Białystok, Poland ; <sup>5</sup>Comprehensive Cancer Center of Białystok, Department of Diagnostic Imaging, Białystok, Poland ; <sup>6</sup>Medical University of Białystok, Laboratory of Molecular Imaging- Nuclear Medicine Department, Białystok, Poland ; <sup>7</sup>Medical University of Białystok, Department of Oncology, Białystok, Poland

## Purpose or Objective

The aim of the study was to assess possibilities offered by innovative hybrid of <sup>18</sup>FDG-PET/MR in GTV definition during RT planning in patients (pts) with locally advanced carcinoma of the oral cavity.

## Material and Methods

A group of 15 pts with squamous cell carcinoma of the oral cavity underwent contrast-enhanced CT (Aquilion ONE, Toshiba) and PET/MR (3T Siemens Biograph mMR) examination. Delineation of GTV was made using two methods: visual interpretation of CT (GTV-CT), PET (GTV-PET<sub>vis</sub>) and MR (GTV-MR) images, as well as quantitative automatic method (Syngovia, Siemens) based on a chosen threshold value (20%, 30%, 40%, 50%) of SUV<sub>max</sub> from PET examination (GTV-PET<sub>20%</sub>, GTV-PET<sub>30%</sub>, etc.). Obtained volumes of primary tumor were compared and differences were statistically analyzed. The level of significance was considered as p<0.05. The GTV-CT was used as the reference.

## Results

In 80% of cases of GTV-MR and 100% of GTV-PET<sub>vis</sub> volumes were larger than reference GTV-CT. Only in three patients GTV-MR was smaller than GTV-CT. The 40% of all PET automatic threshold measurements were larger than results based on CT images. Respectively - 60% of volumes from quantitative automatic method were smaller than GTV-CT. Statistical analysis shown that the most closely related results to GTV-CT were obtained from MR imaging (p=0,0796), GTV-PET<sub>30%</sub> (p=0,8927), GTV-PET<sub>40%</sub> (p=0,3452) and GTV-PET<sub>50%</sub> (p=0,0796). On the other hand GTV-PET<sub>vis</sub> (p=0,0431) and GTV-PET<sub>20%</sub> (p=0,0431) diverge significantly from volumes based on CT images.

## Conclusion

Quantitative automatic method based on a chosen threshold value combined with MR imaging seems to be better delineation method in cases of locally advanced cancer of oral cavity. Hybrid PET/MR supports the optimal determination of volumes for RT treatment. Although, further studies are needed.

### EP-2087 Probabilistic Modeling of Patient Setup Time in VMAT Treatments Based on Anatomical Regions

T.Y. Lee<sup>1</sup>, M.W.K. Law<sup>1</sup>, V.C.W. Cheung<sup>1</sup>, K.K. Tang<sup>1</sup>, S.W.K. Chow<sup>2</sup>, L.W.M. Lee<sup>2</sup>, M.M.S. Wong<sup>2</sup>, S.H. Yoo<sup>1</sup>, P.P.H. Nam<sup>1</sup>, J.W.Y. Lee<sup>2</sup>, B.S.K. Yu<sup>1</sup>

<sup>1</sup>Hong Kong Sanatorium & Hospital, Medical Physics and Research Department, Happy Valley, Hong Kong SAR China ; <sup>2</sup>Hong Kong Sanatorium & Hospital, Department of Radiotherapy, Happy Valley, Hong Kong SAR China

**Purpose or Objective**

The patient setup time was analyzed to provide a statistical insight regarding the variation of setup time, including the most probable setup time and spread across treatments of different anatomical regions. The major benefit of the study is to facilitate treatment time slot allocation, so as to improve treatment machine throughput without increasing the patient waiting time.

**Material and Methods**

The statistics of 3069 fractions of 189 treatments, treated with 6MV photon-beam Volumetric-Modulated Arc Therapy (VMAT) by a linear accelerator (VersaHD, Elekta, Stockholm), were collected over a 25-month period. The setup time were inspected according to three treatment target regions: thorax (THX), breast (BRT) and head and neck (HN) as shown in Table 1. All first treatment fractions were excluded due to the high uncertainty in consultation and coaching time.

The Hypoexponential distribution (Eq.1.) was fitted to the setup time of each of the three concerned treatment regions based on maximum log likelihood.

**Results**

The observed setup time histograms were well-followed by the fitted distributions (Fig. 1). The probability distributions of the overall observed setup time were positively skewed with tails extending to longer setup time. BRT had a wider spread and appeared similar to a normal distribution, while HN was heavily skewed and asymmetrical. The distribution of THX was in between of the two. HN took the shortest time to setup, followed by THX then BRT, with medians of 4.18, 6.08 and 7.83 minutes respectively. The optimal value of K was empirically found to be 8 based on our data. The model parameters of the three studied regions were found dissimilar after fitting (Table 1).

$$pdf(t; \lambda_1, \lambda_2, \dots, \lambda_K) = \sum_{i=1}^K \lambda_i e^{-\lambda_i t} \left( \prod_{j=1, j \neq i}^K \frac{\lambda_j}{\lambda_j - \lambda_i} \right)$$

Eq. 1. The definition of Hypoexponential distribution of variable t, where  $\lambda_i$  is the model parameters to be found using maximum log-likelihood method.

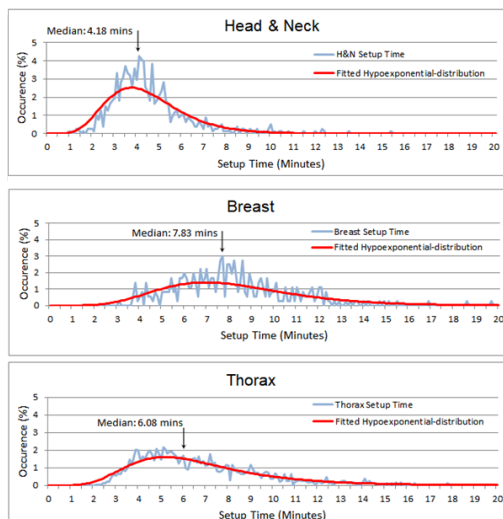


Fig. 1. The histograms of observed setup time for different treatment regions with the fitted Hypoexponential distributions.

The shaded area under the fitted Hypoexponential distributions (Fig.2) shows the most probable 68%

occurrence of setup time, mathematically the region of median  $\pm$  34%. Hypoexponential distribution (red area) offered a much closer agreement to the observed setup time range (purple area) in all cases, in contrast to the normal distribution (green area) which has a much wider spread.

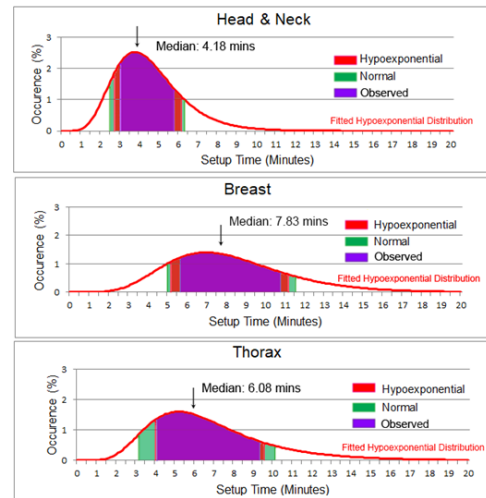


Fig. 2. The fitted Hypoexponential distributions with shaded regions showing the 68%-median samples in minutes for the three treatment regions respectively.

	Probability Density Function (pdf) with K=8								Median (mins)	Number of cases	Number of fractions
	$\lambda_1$	$\lambda_2$	$\lambda_3$	$\lambda_4$	$\lambda_5$	$\lambda_6$	$\lambda_7$	$\lambda_8$			
Head & Neck	0.80	1.65	2.01	2.20	2.29	2.32	2.30	2.25	4.18	40	786
Breast	0.48	0.98	1.14	1.22	1.23	1.20	1.14	1.06	7.83	27	364
Thorax	0.36	1.79	1.65	1.64	1.67	1.70	1.72	1.75	6.08	122	1919
Total Number of cases:										189	3069

Table 1. The fitted model parameters and details of studied treatments.

**Conclusion**

This study investigated the statistical distribution of the patients' setup time in 3069 fractions of VMAT treatments, categorized based on three anatomical regions. The setup time was shown to be effectively modeled by Hypoexponential distributions, a continuous probability model for describing the total finishing time of multiple sequential tasks such as queuing and logistic procedures. We have also shown the dissimilarity among the distributions of the three treatment regions, suggesting a treatment-region-based categorization scheme was essential for effective model fitting, so as to anticipate the patient setup time. In order to achieve a seamless and efficient treatment scheduling scheme, a representative probability model will help allocating treatment time slot based on treatment regions, thus achieving higher machine throughput while reducing patient waiting time simultaneously.

**EP-2088 Upright open-source cone beam CT imaging for radiotherapy**

J. Korte<sup>1</sup>, N. Hardcastle<sup>1,2</sup>, S. Everitt<sup>3,4,5</sup>, T. Kron<sup>1,4</sup>  
<sup>1</sup>Peter MacCallum Cancer Centre, Physical Sciences, Melbourne, Australia ; <sup>2</sup>University of Wollongong, Centre for Medical Radiation Physics, Wollongong, Australia ; <sup>3</sup>Peter MacCallum Cancer Centre, Radiation Therapy Services, Melbourne, Australia ; <sup>4</sup>The University of Melbourne, Sir Peter MacCallum Department of Oncology, Melbourne, Australia ; <sup>5</sup>Monash University, Department of Medical Imaging & Radiation Sciences, Melbourne, Australia

**Purpose or Objective**

Some patients receiving radiotherapy may benefit from treatment in the upright position due to inability to lay prone/supine and through improved tumour-organ at risk geometry. A major challenge of upright radiotherapy

however is the requirement of simulation volumetric imaging and image guidance imaging to be acquired in the upright position. In this work, we aim to acquire upright cone beam CT (CBCT) projections on a conventional digital linac and reconstruct images with an open-source toolkit.

#### Material and Methods

A phantom imaging study was conducted on a TrueBeam® linac (v2.5, Varian Medical Systems) in developer mode using a Catphan® 500 (The Phantom Laboratory). The kV imaging system was kept stationary at a gantry angle of 0° while the couch was rotated through a 180° arc. An extended field of view (FOV) was achieved by offsetting the kV detector in two half-rotation acquisitions (+13cm, -13cm) in continuous fluoroscopy mode (125kVp, 40mA, 11fps) with no bowtie filter. The 4cm wide region where the pair of offset projections overlaps was used for normalisation between image pairs, at each angle the mean intensity of a central patch was matched. A vertical shift correction was calculated by matching vertical line profiles in the overlap region. The corrected offset projections were combined into a single image frame (Fig.1) and header information modified using custom software. The combined projections were reconstructed with the Reconstruction Toolkit (RTK) using an alternating direction method of multipliers with total variation regularisation (ADMM-TV) algorithm. A standard CBCT of the Catphan® taken during routine quality assurance is included for comparison.

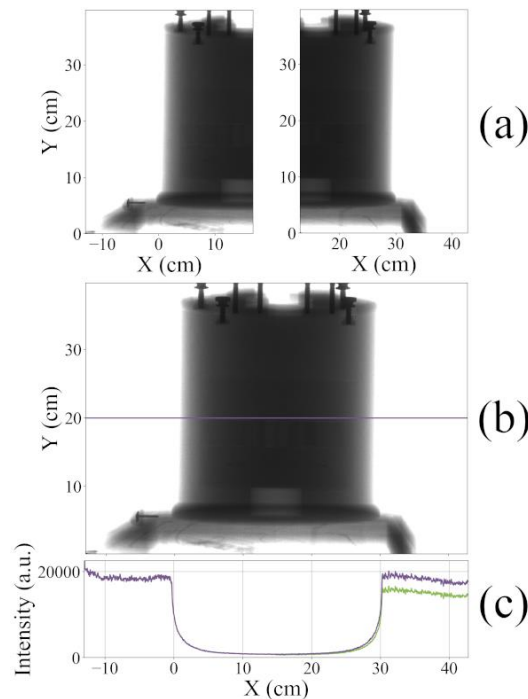


**Fig.1:** (a) offset projections (b) combined corrected projection (c) line profile of (green) uncorrected and (purple) corrected projection.

#### Results

Attenuation correction and vertical shift correction between the two offset projections improved the extended FOV projection (Figure 1c). A gradient from left to right is observed in regions of air and is attributed to anode heel effect and static flood field corrections. This will be addressed using a measured average flood field image in future experiments.

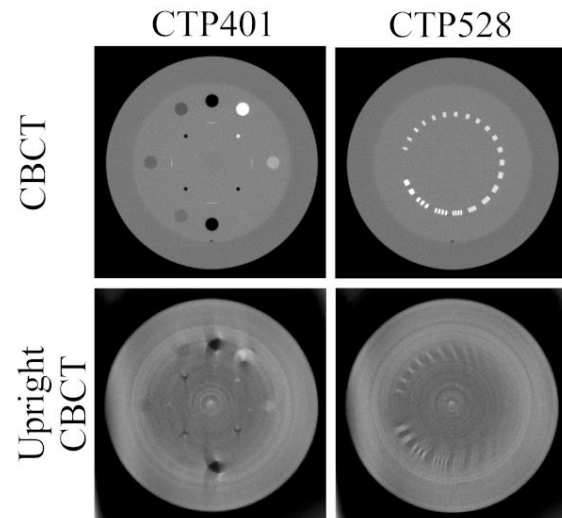


**Fig.2:** Comparison of CBCT and Upright CBCT images of a Catphan®

Reconstructed upright images (Fig.2) show a general agreement with the CBCT images. Expected intensity variations are observed in the spatial linearity module (CTP401) and some structures are visible in the high contrast resolution module (CTP528). The upright images suffer from ring artifact which may be reduced by median filtering or other methods. Further image improvements may arise from projection pre-processing methods and reconstruction options.

#### Conclusion

We have demonstrated upright CBCT can be acquired on a digital linear accelerator and reconstructed using an open source toolkit. Initial reconstruction results are promising, with future work to focus on improvement of image quality through projection space filtering.

#### EP-2089 Technical implementation of total marrow irradiation (TMI) using VMAT

J.M. Perez moreno<sup>1</sup>, C. Rubio Rodriguez<sup>2</sup>, J. Valero Albarrán<sup>2</sup>, P. Fernández Letón<sup>3</sup>

<sup>1</sup>Hospital HM Puerta del Sur, Radiofísica y Protección Radiológica, Mostoles, Spain ; <sup>2</sup>Hospital Universitario HM Sanchinarro, Radiation Oncology, Madrid, Spain ;

<sup>3</sup>Hospital Universitario HM Sanchinarro, Radiofísica y Protección Radiológica, Madrid, Spain

#### Purpose or Objective

To implement LINAC based total marrow irradiation (TMI) using VMAT in the first clinical case.

#### Material and Methods

Our first patient VMAT TMI case is reported. Treatment planning was performed on RayStation 7 using a VERSA HD LINAC.

Patient was immobilized using a head and neck mask and BodyFIX system. Two planning CT scans were performed to imaging whole target volume, head first and feet first supine (HFS and FFS). Target volume was defined in both scans and it included all bones in the body, whole brain, supraclavicular, axillary and paraaortic lymph nodes and spleen. A margin of 3 mm was used except in lower extremities and spleen, where 5 mm margin was used. Dose prescription was 12 Gy in 6 fractions twice a day.

Four factors were considered in plan design:

1. body and target geometry
2. encompass full target while limiting beam size to 27 cm in head-feet direction
3. force an overlap of 5-8 cm between beams of adjacent sectors
4. geometric viability of treatment

Patient's anatomy was split in 7 sectors: head, thorax, abdomen, pelvis and femoral using HFS patient orientation, and knee and tibial in FFS. One isocenter were used in each anatomic region except in abdomen and pelvis, where two coplanar isocenter were settled with a lateral shift between them. Two VMAT arcs were used in each anatomic area, except in tibial region where AP/PA field in field segmentation was performed.

Rigid and deformable registration between HFS and FFS scans were performed to map doses and calculate/optimize total dose in overlapping region of two CT studies.

QA was performed using with Octavius 4D system using 3%-2.5mm 3D gamma index analysis.

Patient setup was assured using one CBCT per isocenter with a 20 cm FOV in head-feet direction.

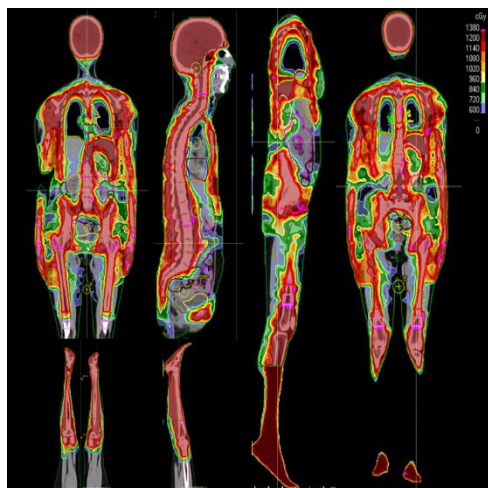
### Results

Total body volume of 55.8 litres and 43.8 cm body radius. Total PTV volume was 12.9 litres. This gives a ratio PTV/Body of 0.23. Plan was normalized to 95% of PTV be covered by 12 Gy. PTV Dmean, D98% and D2% were 12.8 Gy, 11.6 Gy and 14.1 Gy respectively.

Table 1 show dose statistics of main OARs.

ROI	ROI vol. [cm <sup>3</sup> ]	Dose [cGy]						
		D99	D98	D95	Average	D50	D2	D1
Bladder	193.38	388	401	427	712	641	1244	1279
Brainstem	30.88	1254	1257	1260	1284	1285	1314	1318
Colon	867.26	426	443	479	770	723	1221	1272
Esophagus	23.01	577	603	658	963	965	1254	1270
Eyes, Left	10.52	298	304	314	520	508	936	975
Eyes, Right	10.65	276	285	300	489	483	787	797
Heart	367.33	278	288	316	726	685	1255	1325
Kidney (Left)	196.9	760	772	800	1031	1022	1302	1315
Kidney (Right)	183.94	351	356	372	671	576	1246	1274
Larynx	23.66	344	361	395	692	639	1172	1204
Lens, Left	0.09	296	297	297	306	306	317	317
Lens, Right	0.08	273	274	276	294	294	310	311
Liver	1738.43	357	379	439	814	782	1273	1300
Lung_L	1022.69	429	441	475	872	871	1311	1340
Lung_R	1183.44	349	372	411	766	717	1270	1289
Mandible	54.97	177	186	210	621	635	1171	1254
Optic Nerve, Left	0.45	816	823	837	1128	1181	1294	1300
Optic Nerve, Right	0.57	638	659	673	1039	1107	1268	1274
OralCavity	36.28	190	195	207	442	428	818	855
ParotidGland (Left)	13.42	219	221	230	446	367	1104	1149
ParotidGland (Right)	13.79	210	212	215	448	352	1152	1229
Rectum	66.43	358	368	383	636	544	1261	1287
SmallBowel	1070.66	274	297	374	681	631	1175	1218
Stomach	157.87	347	362	384	713	551	1240	1256
ThyroidGland	7.24	455	472	494	782	761	1144	1175
Trachea	26.11	422	434	450	692	576	1145	1163

Figure 1 shows dose distribution in coronal and sagittal planes of HFS, FFS and composite plans.



Total gamma <1 passing rates are 92.4%, 97.4%, 96.3%, 95.7%, 93.5% and 96.8% in head, thoracic, abdominal, pelvic, femoral and knees areas, respectively. In 3D gamma analysis was observed that total results were

dominated by 10%-20% dose areas, where passing rates were lower.

Mean setup error was 0.21, 0.27 and 0.39 cm in LAT, INF-SUP and AP directions, averaged over all isocenters.

First fraction delivery took 112 minutes, while remaining sessions had a duration between 90-100 minutes.

### Conclusion

Proposed TMI method allows achieve planning, delivery and patient setup accuracy similar to conventional radiotherapy, even managing large volumes where two CT scans in different patient orientation are needed.

OARs doses values are lower than in conventional TBI as was demonstrated by previous studies. Showed case values are slightly higher than in those studies, probably due to higher PTV volume.

### EP-2090 Helical tomography radiation therapy for multiple brain lesions: in-phantom accuracy assessment

M. Zani<sup>1</sup>, L. Marrazzo<sup>1</sup>, S. Calusi<sup>1</sup>, C. Talamonti<sup>1</sup>, S. Scoccianti<sup>2</sup>, D. Greto<sup>2</sup>, L. Livi<sup>2</sup>, S. Pallotta<sup>1</sup>

<sup>1</sup>University of Florence, Medical Physics Unit- Azienda Ospedaliera Universitaria Careggi, Firenze, Italy ;

<sup>2</sup>University of Florence, Radiotherapy Unit- Azienda Ospedaliera Universitaria Careggi, Firenze, Italy

### Purpose or Objective

This study aimed to demonstrate the possibility of safely using helical tomography radiation therapy (HT) for the treatment of multiple brain metastases. Imaging and delivery accuracy of HT systems were investigated by performing End to End (E2E) tests on two different phantoms.

### Material and Methods

A two step analysis was followed in order to assess the reliability of the HT for the treatment of multiple brain metastasis. At first the imaging accuracy was tested. In HT systems target localization is provided by registering MegaVoltage CT (MVCT) and CT images and its precision depends on MVCT acquisition protocols as well as on image registration algorithms. These two aspects were investigated, for different registration options and MVCT slice thickness, by applying known misalignments to an ad-hoc developed phantom. The rotation detection of the imaging technique was also studied. E2E tests were then performed to assess the delivery accuracy in phantoms containing multiple targets by using radiochromic films. On the coronal plane 6 target were simulated on a phantom which consists of a PMMA plate 1cm thick with eight embedded glass spheres (GS-phantom) (fig.1a). On the axial plane 3 thin plastic sheets were cut thus to create 5 approximately circular holes, and then they were inserted and fixed between adjacent slices of an Alderson Rando phantom head (fig.1b): 5 targets in total, with the longest axis ranging from 4mm to 8mm (volumes ranging from 0.47cc to 1.79cc). Measured dose distribution centroids were compared with physical and calculated target positions. Moreover, along the axial plane, planned and measured dose maps were compared in terms of absolute values.

### Results

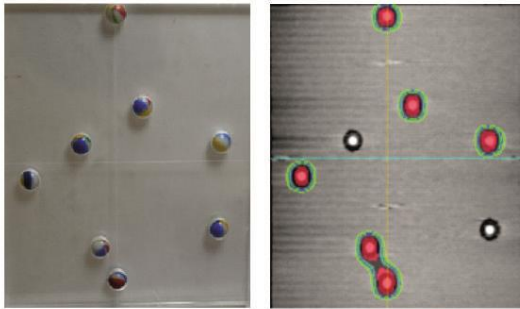
First Step: The algorithm focusing on bone and tissues with the fine MVCT reconstruction grid gave the best results among the automatic options. The most accurate registration modality resulted to be the manual one with a sub-voxel accuracy shifts and a capability in the detection of rotations within 0.3°.

Second Step: In fig.2a the results for the centroid shifts along the coronal plane (6 targets) are shown: the mean deviation between measured dose distribution centroids and physical barycenters is of 0.6 mm (range 0.1 mm-1.3 mm). Along the axial plane (5 targets), a mean deviation of 1.2 mm (range 0.7 mm-2.1 mm) was found for the centroid shifts. In fig.2b one dose profile is reported, corresponding to the dotted line in the EBT3 radiation

exposed map: calculated and measured values compare well. This is also reflected in the Gamma analysis: for each of the 3 films irradiated inside the Rando head phantom a passing rate higher than 97% (3%/2 mm, local) between planned and delivered dose distributions were measured.

Figure 1

a) Coronal Irradiation: 6 targets simulated in the GS-phantom



b) Axial Irradiation: 5 targets placed in 3 Rando Slices

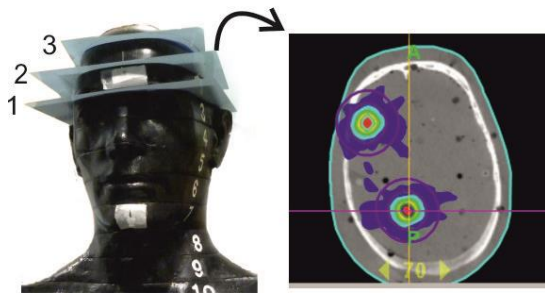
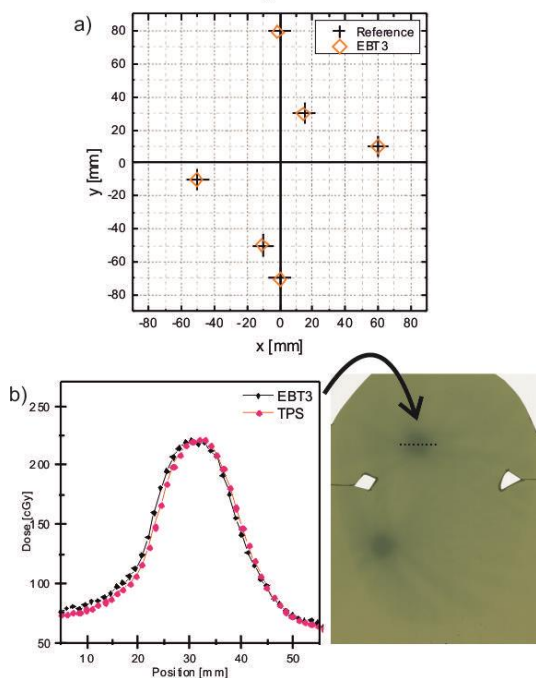


Figure 2



### Conclusion

These results give an in phantom demonstration that multiple brain lesions can be treated with the requested accuracy by HT. When treating real patients, contributions to the uncertainty in dose delivery such as intra-fraction motions have also to be taken into account.

### EP-2091 How to measure high dose in functional disorder treatment: an innovative silicon diode detector.

P. Gallo<sup>1</sup>, E. De Martin<sup>1</sup>, M.L. Fumagalli<sup>1</sup>, F. Ghielmetti<sup>1</sup>, M. Carrara<sup>2</sup>, S. Alhujaili<sup>3</sup>, M. Lerch<sup>3</sup>, A.B. Rosenfeld<sup>3</sup>, M. Marchetti<sup>1</sup>, L. Fariselli<sup>1</sup>, M. Petasecca<sup>3</sup>

<sup>1</sup>Fondazione IRCCS Istituto Neurologico Carlo Besta, Health Department, Milan, Italy; <sup>2</sup>Fondazione I.R.C.C.S. Istituto Nazionale dei Tumori di Milano, Health Department, Milan, Italy; <sup>3</sup>Centre for Medical Radiation Physics, University of Wollongong, Wollongong, Australia

### Purpose or Objective

**Purpose:** Stereotactic radiosurgery (SRS) of intra-cranial lesions is a treatment modality where a well defined target volume receives a high radiation dose in a short fractionation regimen. SRS is usually characterised by steep dose distributions achieved through the delivery of small radiation fields and therefore requires dosimetry performed with small active volume detectors. The purpose of this study is to validate the use of an innovative angular independent edgeless-diode detector, already characterised for standard Quality Assurance (QA) of Cyberknife, in stereotactic radiosurgery for brain functional disorders and trigeminal neuralgia.

### Material and Methods

**Methods and materials:** An anthropomorphic head phantom (RANDO, The Phantom Laboratory, Salem, NY) was CT imaged with three edgeless diodes inserted in central, 8 mm cranial and 26 mm caudal positions (Figure1) targeting the trigeminal nerve close to its root entry in the brainstem. The image set was transferred to the treatment planning system and a treatment volume was contoured by simulating a typical trigeminal target in correspondence of the central diode. In the framework of a dose escalation protocol, a radiosurgery plan (Rando) was optimized and delivered with the central diode receiving prescription doses respectively of 75, 100, 140 and 200 Gy in single fraction. Simultaneously to the 75 Gy - Rando delivery an EBT3 film, properly prepared and calibrated, was also arranged in correspondence with the caudal diode position, where a prescription dose of 12 Gy was delivered. The EBT3 reading was used to validate the corresponding diode's recorded value.

Quality-assurance (QA) verifications were also performed for three patient planes treated at different prescription doses. In this case the central diode was in correspondence with the contoured trigeminal target. Finally, the doses measured by the three diodes were compared to the planned ones.

### Results

The comparison between measured and planned doses is shown in the following table. The recorded values of the dose to the central diode (target) were within 3.6% of the plan for all the seven delivered plans (4 Rando plans and 3 patients). The difference between the EBT3 reading and the caudal diode's recorded value in the Rando-plan was smaller than 5%.

### Conclusion

**Conclusion:** The edgeless-diode detector was employed to measure the dose delivered by a full trigeminal stereotactic treatment. The obtained results combined with its mechanical and electrical characteristics make it a suitable choice for QA dosimetry of trigeminal neuralgia

functional treatments.



**Figure1:** the figure shows how the three diodes were inserted in Rando phantom in central, cranial and caudal position.

**Table:** the differences between planned and measures doses are reported for the three diodes.

	Prescribed Dose (Gy)	Plan Dose (Gy)			DIODE Dose (Gy)			Difference (%)		
		cranial	central	caudal	cranial	central	caudal	cranial	central	caudal
Rando plan	75	6.8	71.1	12.5	5.9	71.0	11.9	-13.1	-0.1	-4.7
	100	9.1	94.8	16.7	7.9	92.1	15.7	-12.7	-2.9	-5.5
	140	12.7	132.7	23.3	10.1	130.8	19.3	-20.7	-1.4	-17.2
	200	18.2	189.6	33.3	14.0	182.7	23.9	-22.7	-3.6	-28.2
QA- First Patient	90	4.9	85.6	3.6	4.6	83.3	3.5	-5.3	-2.0	-2.5
QA-Second Patient	90	11.1	92.4	3.0	11.3	94.9	2.6	1.9	2.6	-12.6
QA-Third Patient	100	9.8	74.6	2.3	9.5	71.3	2.1	-3.2	-1.7	-10.3

### EP-2092 Time-driven activity-based costing for competing treatments using different technology solutions

C.K. Torzsok<sup>1</sup>

<sup>1</sup>Foundation Arturo Lopez Perez, radiation therapy, santiago de chile, Chile

#### Purpose or Objective

##### Purpose

Adequate and equitable access to radiotherapy (RT) must be a reasonable health care goal worldwide. However, the provision of RT in low to middle income countries (LMIC) faces challenges such as lack of professionals, reimbursement schemes and public policies. Given that the costs of delivering state of the art RT care remain poorly described, this abstract reports results of time-driven activity-based costing (TDABC) for competing treatments using different technology solutions and opens the way for discussions on how to better account for and utilize resources.

#### Material and Methods

##### Methods

TDABC is an advanced cost calculation technique that iteratively allocates resource costs to products based on activity consumption weighed by treatment complexity factors. Process maps were developed for each phase of care from the initial visit to end of treatment through 2 years of clinical practice using Cyberknife Stereotactic body radiation therapy treatments (SBRT), Radiosurgery (SRS), Elekta Volumetric Arc therapy (VMAT), Tomotherapy (TOMO) and conformal RT (3D). The costs of materials, equipment, personnel, and space were calculated per unit of time and relative capacity used.

#### Results

##### Results

Substantial cost variation was observed over 2 years, with costs ranging from \$3,298 for TOMO, to \$10,565 for SBRT. TOMO was notably cheaper than VMAT \$4,648, and SRS \$3,665 was cheaper than VMAT, with the cost savings attributable to shorter procedure times and fewer fractions despite of higher initial capital costs. Both equipment costs and quality assurance contributed to the high cost of SBRT, where machine quality assurance (QA) and patient specific delivery quality assurance (DQA) costs range up to 54% when single fraction. 3D was only 20% cheaper than TOMO, largely because of workflow. RT costs are predominantly determined by personnel 38% and equipment cost 39%. Machine usage activities consume greatest proportion with treatment delivery 65%, QA 12% and DQA 8%.

#### Conclusion

##### Conclusions

The use of TDABC is feasible for cost estimation of RT and is converging with other studies when it comes to fractionation. It allows for analyzing cancer services and provides insights into cost-reduction tactics in an era focused on emphasizing value. By detailing all steps from diagnosis and treatment, this study demonstrates significant cost variation between competing treatments and highlights the impact of QA and DQA time on the actual cost structure. It impelled us to evaluate resource or practice changes in the 3 major cost drivers: fractionation, QA and DQA. Our aim is to develop a model that establishes a direct and transparent link between equipment, human resources, fractionation and quality assurance data and indications for RT to be used by LMIC when tackling the change of paradigm of using state of the art RT. Unlike published benchmarks for accelerator throughput to allow estimation of the number of Linacs per million people in each country, we vouch for considering the whole patient workflow.

### EP-2093 Heart sparing with deep inspiration breath hold (DIBH) in left breast treatment: a prospective study

V. Vanoni<sup>1</sup>, S. Mussari<sup>1</sup>, L. Bossi<sup>1</sup>, F. Coelli<sup>1</sup>, M. Maino<sup>1</sup>, A. Martignano<sup>2</sup>

<sup>1</sup>Ospedale Santa Chiara di Trento, Radiation Oncology, Trento, Italy ; <sup>2</sup>Ospedale Santa Chiara di Trento, Medical Physics, Trento, Italy

#### Purpose or Objective

The aim of the study was to prospectively assess the dosimetric benefit achievable with the use of the deep inspiration breath hold technique (DIBH) in left breast radiotherapy.

#### Material and Methods

101 patients with left-sided breast cancer underwent left breast irradiation with DIBH. Following an initial training period including the first 25 patients, the following 76 patients were included in the present study: patients were considered for DIBH if they were younger than 55 years or if the OAR-constraints (lung and heart) were unachievable with free breathing (FB). Both FB and DIBH simulation-CT were available for each patient and formed the basis of their dosimetric analysis. Mean heart dose (MHD), left ventricle V25Gy (V25V), V10Gy and V20Gy for ipsilateral lung (V10L, V20L), ipsilateral lung volume (LV) and minimum distance of the heart from the PTV (HDIST) were recorded and the differences ( $\Delta$ ) between FB and DIBH plans were calculated.

#### Results

The mean age of the enrolled patients was 50 years (range 31-66 y). 43.4% of the patients underwent VMAT radiotherapy and 55.3% 3D conformal radiotherapy; 1 patient was planned with a dMLC technique. In 39.5% of the patients, supraclavicular nodes were included in the treatment volume and 7.9% had supraclavicular and internal mammary lymph nodes involved. 72% of the patients enrolled in the study eventually underwent DIBH

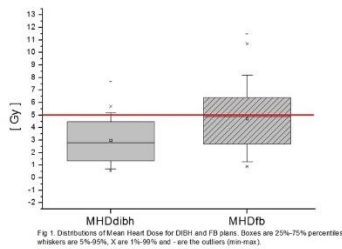
treatment. In the remaining patients the dosimetric benefit from DIBH was not considered sufficient to opt for this technique or (only 1 patient) they were not able to perform DIBH at the treatment sessions.

Mean DIBH inspiration threshold was 1.7 l (range 1.0-2.7 l). The results are reported in table 1. The percentage of plans with MHD inferior to the threshold of 5 Gy was 84.3 % for the DIBH technique, and 54.1 % for the FB plans.  $MHD_{DIBH}/MHD_{FB}$  and  $V25V_{DIBH}/V25V_{FB}$  distributions were significantly different ( $p < 0.001$ , paired T-test).

Table 1. Comparison of dose metrics in DIBH and FB plans.

Dose Metric	DIBH Mean [range]	FB Mean [range]	$\Delta$ of mean value of dose metric [range of $\Delta$ ] in DIBH and FB plans
MHD [Gy]	3.0 [0.5+7.7]	4.7 [0.9+11.5]	-1.9 [-6.9+0.1] $p < 0.001$
V25V [%]	1.3 [0+6.7]	4.3 [0+20.4]	-3.2 [-19.5+9.1] $p < 0.001$
V20L [%]	17.3 [1.2+37.8]	18.9 [0.1+59.4]	-2.6 [-29.6+6.7] $p = 0.009$
V10L [%]	26.3 [5.7+52.3]	27.1 [0.5+78.5]	-2.0 [-31.5+9.8] $p = 0.030$
HDIST [cm]	0.8 [0.0+3.0]	0.2 [0.0+1.4]	0.6 [-0.2+1.9] $p < 0.001$

MHD – mean heart dose, V25V – volume of left ventricle receiving 25 Gy, V20L – volume of ipsilateral lung receiving 20 Gy, DIBH – Deep Inspiration/Breath Hold, FB – Free Breathing, p – statistical significance (paired T-test).



## Conclusion

The use of DIBH in a routine clinical setting significantly reduced mean dose to the heart and the volume of the left ventricle that received 25 Gy, thus confirming that DIBH is an efficient technique that can be strongly recommended to lower the risk of ischemic heart disease after breast cancer radiotherapy.

## EP-2094 Machine QA Time Efficiency Savings with IBA Dolphin Detector

S. Loughlin<sup>1</sup>, R. Lally<sup>2</sup>, A. Reilly<sup>2</sup>

<sup>1</sup>NWCC, Department of Physics, derry, United Kingdom ;

<sup>2</sup>NWCC, Radiotherapy Physics, derry, United Kingdom

### Purpose or Objective

Machine availability is a precious commodity in a radiotherapy department when the burden of measurement based PS-QA and machine QA are considered, therefore vital that all links in the PS-QA and machine QA chains are streamline and accurate. Within our portfolio of dosimetry equipment, it was identified that further savings in time could be made by using the IBA Dolphin detector for measurement based PS-QA and machine QA.

### Material and Methods

Investigations were carried out on Varian TrueBeam linear accelerators (linacs) using the Dolphin detector and an appropriate chamber traceable to the National Physical Laboratory (NPL) in the UK. The Dolphin is a 2D detector array consisting of 1513 vented air ionisation chambers arranged across an area of 40 x 40 cm<sup>2</sup>. The spatial

resolution across the central area of the array (15 x 15 cm<sup>2</sup>) is 5 mm. Dose linearity was characterised between 1 MU and 500 MU under reference conditions (10 x 10 cm<sup>2</sup> field) at maximum dose-rate for all clinical MV photon energies (i.e. 6MV and 10MV in addition to flattening filter free 6FFF and 10FFF). Dose-rate response was characterised for all available dose-rates. The field size dependence of the array was assessed for all energies for square field sizes ranging from 1 x 1 cm<sup>2</sup> through to 25 x 25 cm<sup>2</sup>. Dose linearity and dose-rate response measurements were compared to that of a Farmer chamber whilst the field size dependence was compared to that of an IBA CC13 small volume ionisation chamber. PS-QA plan delivery time was compared to the SunNuclear ArcCheck solution. Deliberate errors (1.8%) were introduced by beam steering into the radial and transvers angles of the Varian linac to check if the array could detect an error.

## Results

The dolphin exhibited a linear response to dose. The dose-rate response of the Dolphin was comparable to that of the Farmer chamber (<1%) with the most significant dose rate dependence observed for the 6 MV delivery (0.87 ± 0.2%; mean ±2SD). Both the Dolphin and the CC13 exhibited field-size dependence below 5 x 5 cm<sup>2</sup> (i.e. a difference of 3% from the response at 10 x 10 cm<sup>2</sup>). The maximum difference between the response of the Dolphin and the CC13 was observed at 1 x 1 cm<sup>2</sup> for the 6FFF delivery (i.e. CC13 under responded by 21% in comparison to the 10 x 10 cm<sup>2</sup> field whilst the dolphin under responded by 43%). PS-QA time was reduced from 15 minutes on average for ArcCheck to 5 minutes on average for Dolphin. The Dolphin identified flatness and asymmetry in the beam for a 6 MV and 6 FFF delivery.

## Conclusion

The characteristics of this array make this detector suitable for PS-QA and machine QA, with the array demonstrating significant time savings.

## EP-2095 SBRT of prostate with integrated boost of Dominant Lesion. A crowd-knowledge based planning study

A. Savini<sup>1</sup>, S. Cilla<sup>1</sup>, M. Esposito<sup>1</sup>, E. Moretti<sup>1</sup>, E. Villaggi<sup>1</sup>, S. Russo<sup>1</sup>, M. Stasi<sup>1</sup>, P. Mancosu<sup>1</sup>

<sup>1</sup>SBRT Working Group, AIFM - Italian Association of Medical Physics, Italy, Italy

### Purpose or Objective

Stereotactic Body Radiation Therapy (SBRT) with large dose per fraction has gained increasing popularity in treatment of prostate cancer due to its low  $\alpha/\beta$  ratio (e.g. 1.5 Gy). Furthermore, a dose escalation to the dominant intra-prostatic lesion (DIL) has the potential to increase biochemical control whilst avoiding the enhance in side effects associated with whole gland dose escalation. There is a lack of consensus on optimization strategies and appropriate plan quality metrics for SBRT plans delivered in simultaneous integrated boost (SIB). The aim of this study was to evaluate and ultimately reduce the variability of planning strategies. A crowd-knowledge approach was adopted, where teacher/student hierarchy is not defined a-priori, but hierarchy is dynamically determined by the results.

### Material and Methods

Four radiation oncology centers experienced in performing SBRT participated to this study. The case with pre-delineated volumes was distributed among participating centers using an ad-hoc web-platform. Two plans were optimized. A preliminary homogeneous plan with a prescribed dose to the target of 35 Gy in 5 fractions. A second plan with prescribed dose to the target of 35 Gy in 5 fractions and 50Gy integrated boost to the DIL. Constraints on target coverage and dose to nearby organs at risk were set a priori. Plans were collected in DICOM-RT format. A grouped analysis was performed using crowd-

based (CB) DVHs which were generated using a script developed in R language. CB-DVHs were reported on the web-platform in order to allow centers to confront their results in a fast and intuitive way.

### Results

The most relevant variations were observed for the dose to the PTVs and to the rectum (Fig.1 and 2). In particular, for the homogeneous plan, observed dose ranges were: PTV mean dose, 35.5-38.4 Gy; PTV max dose, 37.3-42.6 Gy; rectum mean dose, 15.8-22.3 Gy; rectum max dose, 35.9-39.8 Gy. For the inhomogeneous plan, dose ranges were: PTV mean dose, 36.1-37.9 Gy; PTV max dose, 51.1-54.1Gy; PTV-DIL mean dose, 46.9-50.2 Gy; PTV-DIL max dose, 51.1-54.1; rectum mean dose, 15.9 - 23.6 Gy; rectum max dose, 37.4 - 49.0 Gy.

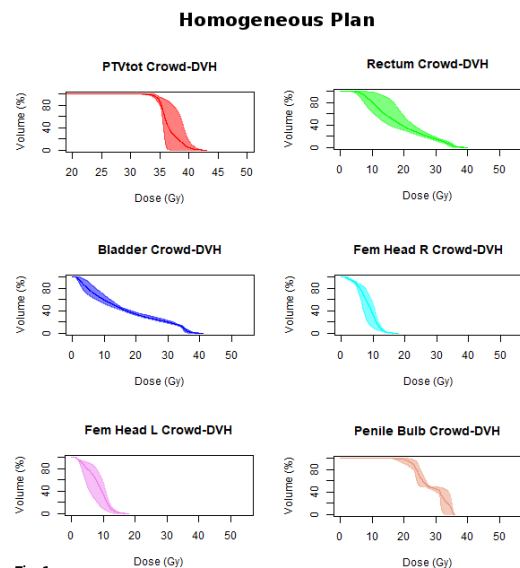


Fig.1

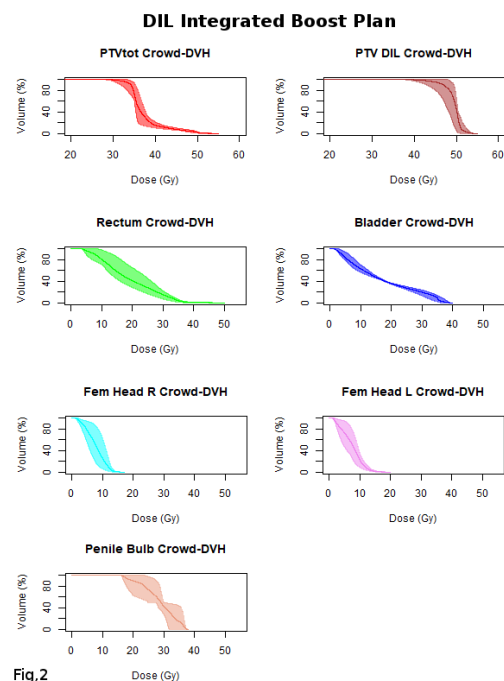


Fig.2

### Conclusion

A crowd-based method was applied for exploring different approaches in planning a novel treatment of prostate in SBRT. Variation of dose distributions for targets and organs at risk (especially rectum) showed the need of multicenter

comparison even among experienced centers. CB-DVHs could give a fast and intuitive overview of the variability of planning approaches. The analysis of CB-DVHs is propaedeutic for reviewing planning strategies of each center with the ultimate goal of uniforming treatment approaches in SBRT.

### EP-2096 Multi-institutional versus site-specific training data for a deep breast segmentation algorithm

J. Schreier<sup>1</sup>, H. Laaksonen<sup>1</sup>, F. Attanasi<sup>2</sup>  
<sup>1</sup>Varian Medical Systems Oy, Strategic Technologies, Helsinki, Finland ; <sup>2</sup>VMS International AG, Oncology Software Product Management, Steinhausen, Switzerland

### Purpose or Objective

Deep Learning techniques have demonstrated impressive performance in different medical image analysis applications, producing more accurate segmentation results and exhibiting significantly better generalization than traditional atlas or model-based approaches. In this study, we present results of training a deep neural network with a multi-institutional versus a site-specific dataset. This is done to evaluate the trade-off between generalizability versus specificity, meaning is it better for an institution to use a site-specific model or a multi-site one? For this, a deep neural network was developed that automatically contours organs-at-risk on CT images for breast cancer radiotherapy treatments.

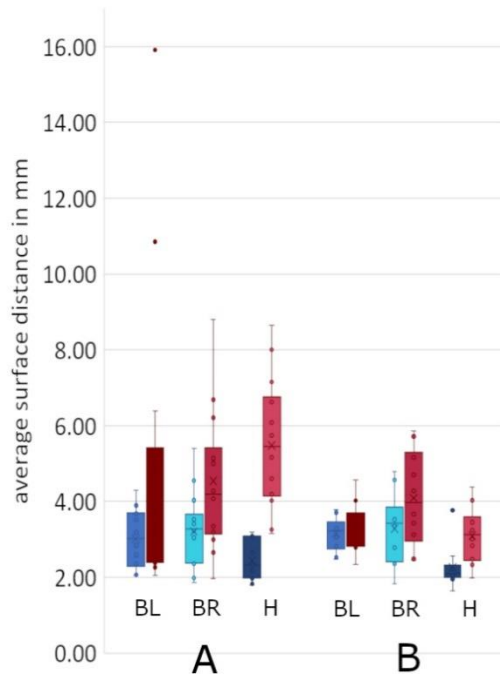
### Material and Methods

CT datasets from four institutions were selected, three from Europe (Clinic A, B and C) and one from the U.S. (Clinic D). The complete dataset consisted of 380 CT breast scans with heterogeneous characteristics to ensure balance with respect to diagnosis, age and body mass index. All patients were scanned in the supine position and immobilized either with breast boards or vacuum cushions. Patients from Clinic A, B and C were scanned with both arms up instead of the traditional one arm up used in Clinic D.

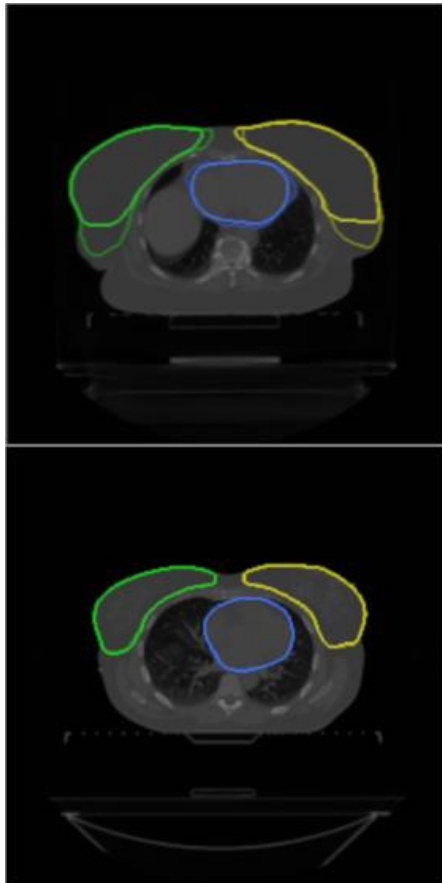
For each CT dataset, a team of experts reviewed the original contours and added missing structures to ensure both breasts and heart were delineated. Reviewed contours were used for representing the ground truth. Four site-specific models were trained. Additionally, one model was trained using data from all clinics. The models were evaluated using the average surface distance and the dice score on the test cases from the clinic trained on and compared to the multi-institutional model.

### Results

The average surface distance of the multi-institutional (blue) and the site-specific models (red) are shown for the two different clinics (A and B) for the left breast (BL), the right breast (BR) and the Heart (H). Preliminary results from model C are comparable.



The axial slices in Figure 2 show the comparison between the ground truth (solid) and the model-generated contours (faded) with the highest (upper) and lowest (lower) surface distance on the left breast among the test cases. The lowest average surface distance was produced by the multi-institutional model and the highest distance by a site-specific model.



**Conclusion**

A multi-site deep learning model for breasts and heart delineation was realized and compared against site-specific models showing that the multi-institutional model performs better than the site-specific model. Our results indicate that a deep learning model is able to generalize its output to apply to multi-site needs by using a broader training dataset. With deep learning, it is possible to overcome the current hurdles encountered in manual contouring and eliminate the need of creating site-specific deep learning-based models. Taken into use, this technology can have a huge impact on the workload of clinical staff and on the standardization of care.

#### EP-2097 Use of an a-Si EPID for routine QC of the Elekta Unity MR-Linac

J. Berresford<sup>1</sup>, J. Agnew<sup>1</sup>, T. Harriden<sup>1</sup>, G. Budgett<sup>1</sup>  
<sup>1</sup>The Christie NHS Foundation Trust, Christie Medical Physics & Engineering, Manchester, United Kingdom

#### Purpose or Objective

One challenge associated with the Elekta Unity MR-Linac is to develop a robust, time-efficient set of QC procedures. Accurate set-up of QC equipment and ion chambers takes longer than on conventional linacs and therefore making use of the onboard MV imager for QA purposes is attractive. This work investigates the use of the EPID panel for daily output checks, field size QC and a symmetry constancy check. Data was collected over six months of regular QC on the pre-clinical machine, with the intention of rolling out the checks on the final clinical version.

#### Material and Methods

Daily EPID images were acquired at the four cardinal gantry angles using a field size of 20x8cm. These four fields were always run immediately after a 1000 MU warm-up beam. A set of monthly images were also acquired at 4x4cm to provide a measure of field size scaling. For the daily images, code was written to extract the pixel factor from the log file and record the mean grayscale for the central square of 50x50 pixels (2x2cm at the level of the EPID). These output values were normalised against isocentric Farmer chamber measurements and the variation between the two investigated.

Symmetry was calculated on both axes discounting the penumbral region. A measure of flatness was also determined but, as the image is divided through by a flood field, this value is relative. The symmetry is also affected by this flood field but still gives a useful measure of constancy to complement periodic measurements with a beam profiler array.

Field size was calculated using both the 50% method and the point of maximum gradient.

#### Results

A comparison of normalised EPID output measurements at gantry angle (GA) 90° to those acquired with a Farmer chamber can be seen in Figure 1. The EPID results have a slightly larger variation (standard deviation of 0.6% vs 0.4% for the Farmer) but correspond with the low-level gradual trends measured using the Farmer.

The average symmetry value at GA0 was 101.9% (SD 0.1%) for the cross-plane axis and 100.8% (SD 0.2%) for the in-plane measurement.

The two techniques for measuring field size produced slightly different results with the averages at GA0 varying by up to 2mm for the in-plane field (8cm width). Both techniques however generated consistent results for a particular field size/orientation, with SD of <0.3mm for each set of measurements.

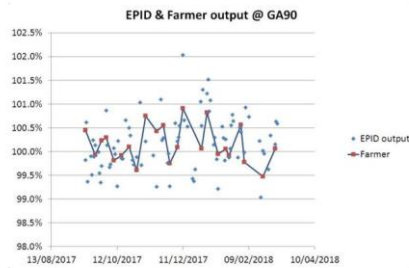


Figure 1: Normalised EPID output measurements at gantry angle 90° vs. those made using a Farmer chamber.

### Conclusion

The MV imager mounted on the Elekta Unity MR-Linac is a fast and reliable method of measuring daily output as a constancy check between weekly ion chamber measurements. The panel is also capable of performing field size QC for fields up to 20x8cm and generating values for beam symmetry. The Unity MR-Linac was found to be extremely stable for all QC parameters over a six-month period. For the clinical MR-Linac, the EPID will form a useful role in minimising time required for daily QC checks.

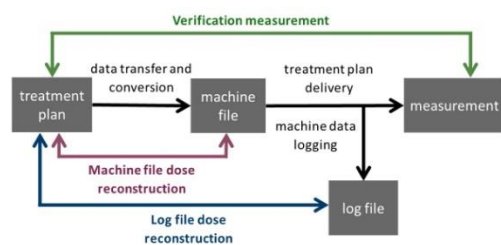
### EP-2098 Measurement free patient specific verification for PBS proton plans - a quantitative evaluation

M. Matter<sup>1,2</sup>, N. Fachouri<sup>1</sup>, L. Nenoff<sup>1,2</sup>, G. Meier<sup>1</sup>, A. Bolsi<sup>1</sup>, D.C. Weber<sup>1,3,4</sup>, A.J. Lomax<sup>1,2</sup>, F. Albertini<sup>1</sup>

<sup>1</sup>Paul Scherrer Institute, Center for Proton Therapy, Villigen PSI, Switzerland ; <sup>2</sup>ETH Zurich, Department of Physics, Zurich, Switzerland ; <sup>3</sup>University Hospital Bern, Department of Radiation Oncology, Bern, Switzerland ; <sup>4</sup>University Hospital Zurich, Department of Radiation Oncology, Zurich, Switzerland

### Purpose or Objective

Large clinical efforts and substantial beam time are invested in patient specific verification (PSV) measurements for pencil beam scanning (PBS) proton therapy. Despite the big expenditure to conduct these measurements the added value to ensure the treatment integrity is not given without doubt. Hence, there is an urgent need to remove the PSV-bottleneck in the clinical work-flow, while upholding the high safety standards. Capabilities of current PSV methods to ensure the treatment integrity are investigated and compared to an alternative approach of reconstructing the dose directly from the machine control- or delivery log files with the help of an independent dose calculation (IDC) (Figure 1). The results from this investigation motivate the design and implementation of a clinical measurement free PSV protocol.



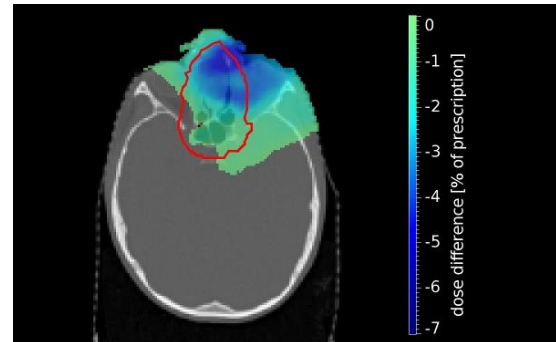
### Material and Methods

Six realistic delivery or work-flow failure scenarios based on in-depth assessment of the clinical procedures, were simulated on a varying range of patients and indications. Examples are patching miss alignment in a large head and

neck case or a simulation of imprecise spot positions during the delivery in a highly modulated IMPT plan surrounding the spinal cord. Investigating these scenarios is an important extension of the sensitivity analysis of the method on a single treatment field, conducted and published in prior. The failure simulations were realized by inclusion in the machine files. These altered machine files were delivered and measured with our clinical PSV measurement protocol. IDC machine- and log file checks were conducted and their sensitivity at detecting the errors was compared to the measurements. Further, a conclusive analysis of failure detection probability considering the whole clinical chain with measurements and with the alternative IDC checks was performed.

### Results

The PSV measurements showed a poor performance in detecting small, but clinically relevant alterations in the machine file. An example dose difference, which the PSV measurement was not able to detect, is displayed in Figure 2. The previously determined sensitivity of the IDC checks could be verified on the varying patient geometries and in combination the method was shown to out perform the measurements. The clinical PSV measurement protocol was able to correctly detect 2 out of 6 failure scenarios, while the IDC checks had a perfect detection record. The knowledge of the detection sensitivity and the failure detection probability highlighted the strengths and weaknesses of the investigated methods and enabled the definition of a new clinical measurement free PSV procedure.



### Conclusion

Machine- and log-file IDCs have been shown to represent a valuable and more sensitive addition to the QA procedure. The reported performance of the IDC yields a big potential for replacing PSV measurements, which would significantly streamline the quality assurance procedure. Currently in our clinic the defined measurement free PSV procedure is in the process of clinical implementation.

### EP-2099 The national approach to assign risk factors for failure modes and effects analysis in IMRT process

I. Koniarova<sup>1</sup>, V. Dufek<sup>1</sup>, I. Horakova<sup>1</sup>

<sup>1</sup>National Radiation Protection Institute, Department of Radiotherapy and X-Ray Laboratory, Praha, Czech Republic

### Purpose or Objective

It is mandatory with new legislation to perform risk analysis in the Czech Republic to prevent accidents or to minimize their occurrence in radiotherapy. The failure modes and effects analysis (FMEA) is a recommended tool to fulfil this requirement. The aim of this work was to estimate values of O (occurrence), S (severity), D (detectability), and RPN for possible failures in the IMRT process tree; and to describe systematic national approach to this problem.

### Material and Methods

The group of medical physics experts in radiation oncology in the Czech Republic is formed by representatives from hospitals, service companies, National Radiation Protection Institute (NRPI), and regulatory body. All members were asked to make the estimates for values of O (occurrence), S (severity), D (detectability), and RPN (risk priority number) used in the FMEA for IMRT process. Although there exist examples of these values published in literature, the analysis was performed to estimate independently the most appropriate and valid values corresponding to the national conditions, practices, and experience. Results from analysis of radiotherapy accidents was taken into account which NRPI performs on request of the regulatory body. The hospitals must report the most serious accidents to the regulatory body, but were asked to report also less serious accidents and near misses, which was voluntary based to cover accidents that happened in the Czech Republic in the period 2012 - 2017. The results from this analysis were used to modify and validate estimates of values for FMEA.

#### Results

Published values in AAPM TG 100 were confronted with the estimates based on experience of Czech physicists. The contribution shows differences in identification of the most hazardous steps on IMRT process tree. In total, more than 230 accidents in radiotherapy were evaluated. The most serious accidents in radiotherapy in the Czech Republic in previous years have been caused by software failures which was not included in 10 highest ranked failures by AAPM TG 100. The description of these most serious accidents caused mainly by data transfer and Record and Verify System failures will be included. The most frequent accidents in previous years were related to incorrect patient positioning, choice of incorrect treatment plan, and patient identification.

#### Conclusion

The contribution shows the results from performed analysis and helps local physicists to adopt legislative requirements. It also shows an effective way by grouping physicists to form an official body in the country to enable cooperation between professionals on the national level which is benefit especially in small countries where enough experts are not available to form different working groups. The results will be published in form of the national recommendation by the regulatory body and it is expected that particular departments will implement the method considering local conditions.

#### EP-2100 Quality in the implementation of stereotactic radiotherapy services on a national scale

T. Aland<sup>1</sup>, R. Fitzgerald<sup>2</sup>, M. Knesl<sup>1</sup>, A. Perkins<sup>3</sup>, D. Shannon<sup>1</sup>, L. Anderson<sup>1</sup>, M. Jones<sup>4</sup>, N. Bailey<sup>3</sup>, M. Foote<sup>1</sup>, M. Dally<sup>3</sup>

<sup>1</sup>Icon Group, Icon Cancer Centres, Brisbane, Australia ;

<sup>2</sup>Icon Group, Icon Cancer Centres - North Lakes,

Brisbane, Australia ; <sup>3</sup>Icon Group, Icon Cancer Centres - Richmond, Melbourne, Australia ; <sup>4</sup>Icon Group, Icon Plan, Brisbane, Australia

#### Purpose or Objective

Icon Group operates a network of 20 radiotherapy centres (Icon Cancer Centres) across Australia. A nationwide project was launched to implement a safe, high quality stereotactic radiotherapy programme, based on the extensive experience within our network already, for a variety of stereotactic radiotherapy (SRT) and stereotactic body radiotherapy (SBRT) treatment techniques including lung, liver, cranial, and oligo-metastases. The aim of this initiative was to provide these advanced treatments closer to patients in the community setting resulting in reduced travel time for treatment and associated financial and personal burden.

#### Material and Methods

Within the 20 Icon Cancer Centres, a mix of software and hardware exists including Varian, Elekta, Brainlab, and

RaySearch. Staffing across the network had varied levels of clinical and technical experience. Implementation was achieved using national multi-disciplinary project teams that developed a template for implementation to be used by other centres within our network. These project teams also developed draft clinical guidelines, which were then disseminated to wider staff groups for refinement. An endorsement program within a clinical governance structure was developed to facilitate implementation of a stereotactic service at a new Icon Cancer Centre. Endorsement for a centre to provide a specific stereotactic service involved the centre providing evidence of equipment commissioning, technique documentation (clinical and technical), staff training, and competency assessments.

The endorsement process is governed by national stereotactic "clinical streams", which are in-house physician led groups comprised of a mix of both senior and junior physicians, as well as key technical staff. To assist commencing junior physicians and to provide opportunities for learning and skill development, a mentorship program and national virtual stereotactic chart round was established and held weekly. To ensure quality control in treatment planning, a virtual treatment planning model was set up. This consisted of a mix of dedicated treatment planning staff, as well as remote planners, all operating within a virtual treatment planning room environment.

#### Results

To date, national clinical guidelines have been written for cranial metastases SRT, lung SBRT, liver SBRT, and bony/oligometastatic SBRT. To complement these guidelines, a series of national work instructions covering simulation, planning, and treatment processes have also been developed, and are based on what software / hardware is available on site. Stereotactic radiotherapy has been implemented in 13 of our centres. To date, 51 cases have been presented within our chart round.

#### Conclusion

Thus far, stereotactic radiotherapy services have been implemented at Icon Cancer Centres across Australia. Compliance with approved documents is monitored by the clinical streams via the endorsement programme and chart rounds, to ensure quality in stereotactic services on a national scale.

#### EP-2101 Evaluation of the feasibility of performing markerless tracking for lung SBRT patients

T. Gevaert<sup>1</sup>, A. Girardi<sup>1</sup>, C. El Aisati<sup>1</sup>, C. Collen<sup>1</sup>, B. Engels<sup>1</sup>, M. De Ridder<sup>1</sup>

<sup>1</sup>Universitair Ziekenhuis Brussel, Radiotherapy, Brussels, Belgium

#### Purpose or Objective

Tumor tracking based on fiducial markers using the VERO SBRT system uses a correlation model to estimate internal tumor position based on external surrogate motion. Previous studies in our department showed already the feasibility and accuracy of performing this marker-based tracking. The drawback of this technique is the implantation use of a marker as a surrogate for the tumor motion, as majority of patients are not eligible for marker implementation due to risk of pneumothorax in COPD patients and anatomical challenges. That is why we wanted to implement a less invasive technique eligible for a larger variety of patients using state of the art imaging. In this study, we want to report on the first simulation of a markerless real-time tumor tracking solution based on the Vero SBRT gimbaled Linac system for treatment of lung tumors.

#### Material and Methods

Twenty previously treated patients with a marker-based tracking were used to analyze the feasibility of markerless tracking. In these fluoroscopic images, the marker was erased in the image in order to analyze the markerless

environment of the ExacTrac v3.5 system (Brainlab, München, Germany). The density of the lesion was used as a surrogate for tracking. The accuracy of the target identification for a reference image pair, which is provided to the markerless tracking algorithm, was compared against the marker-based implants detection. The result gives an estimation of the manual target identification error. Additionally, the user-variability and the patient-variability of the manual target identification error were analyzed. Furthermore, 15 patients treated with internal target volume (ITV) were simulated for markerless tracking.

#### Results

Root mean square error between the markerless tracking and the marker-based tracking for all patients in LR, AP and SI directions were [0.1, 0.3] mm, [0.8, 0.9] mm and [1.2, 0.9] mm, respectively. This markerless tracking algorithm was able to track 87 % of all images. In the case of simulating real time patients treated with an ITV approach, 80% were eligible for markerless tracking.

#### Conclusion

In this study, we successfully implemented a markerless environment for dynamic tracking leading to a patient specific dose delivery.

#### EP-2102 Accurate software detection of light markers coincidence using a computed radiography system

M.A. Benito Bejarano<sup>1</sup>, A. Del Castillo Belmonte<sup>2</sup>

<sup>1</sup>Hospital Provincial de Zamora, Department of Radiation Physics, Zamora, Spain ; <sup>2</sup>Hospital Clínico Universitario, Department of Radiation Physics, Valladolid, Spain

#### Purpose or Objective

The current recommendations on quality assurance (QA) of medical accelerators set a monthly frequency for testing the coincidence of the light field crosshair projection and patient positioning lasers. Nowadays, the standard way of performing this test is by naked eye examination of the projection of those markers over graph paper. However, the accuracy of this method is compromised by interobserver variability. We propose a new method that allows a precision gain by means of a Computed Radiography (CR) system and an in-house developed analysis software.

#### Material and Methods

A Konica Regius model 140 CR System is used. The system has been previously tested to determine and correct geometric distortions. The CR cassette is irradiated with 16 MU in a 40x40 cm<sup>2</sup> 6MV field at isocenter distance to obtain a latent uniform background image. In our procedure, we use the sensitivity of the CR plate to visible light to acquire an impression of the optical indicators. The uncovered phosphor is directly exposed to the laser light for 20 s. The collimator is set to several angles, switching the light field on for 20 s in each one. The CR plate is put back inside the cassette and is read by the CR system. The result consists of a superposition of the image from the laser cross plus the image star from the different projections at each collimator position. An in-house software routine has been developed to analyse the images. It imports the image in RAW format and finds the laser crossing point. The lines of the star-shot pattern of the light crosshair are detected, and the minimum circle encompassing all the lines is determined. The software returns the radius as well as the distance of the circle centre to the laser cross point. The accuracy of this procedure has been tested by running it against synthetic images with intentional known shifts applied.

#### Results

Geometric distortions were found negligible, no image correction was needed. The coincidence of lasers with cross-hairs could be determined with an accuracy better than 0.2 mm with a 95% confidence interval. The image acquisition process takes less than 15 minutes, image processing less than 2 minutes.

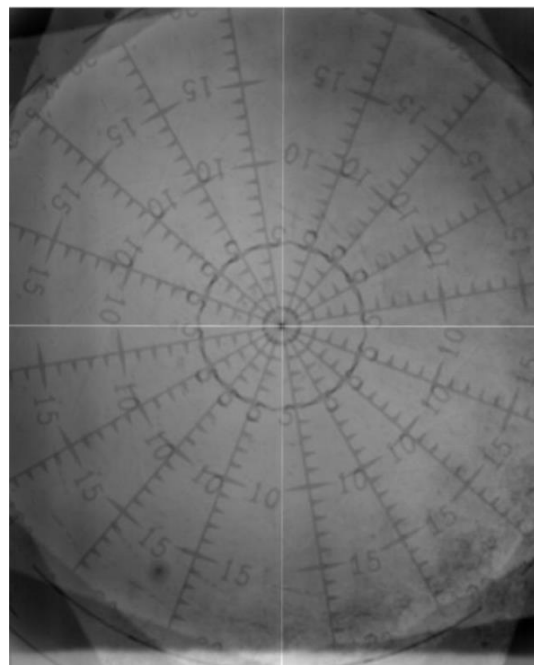


Figure1: Input image with laser marks in white, and crosshair star pattern in black

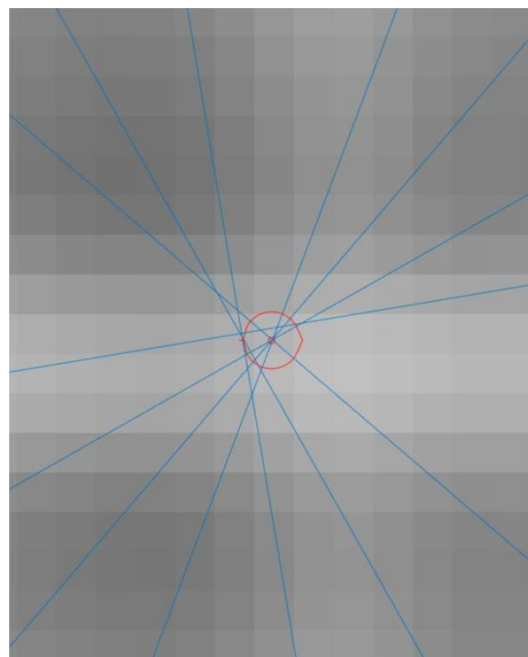


Figure2: Analysis results. Zoom of the area near the detected laser cross mark, showing the minimum encompassing circle and its centre.

#### Conclusion

This method allows the measurement of light crosshair and laser lines coincidence. The accuracy is improved, as it eliminates the inter-observer dependence. The resulting digital images can be archived after processing, for future reference. The materials involved are readily available in a modern hospital setting. The test is inexpensive as no consumables like film are used. This method has been proven useful when performing the light field crosshair to lasers coincidence test, mainly after a field service intervention in the linac, i.e. mirror or crosshair substitution.

**EP-2103 Development of a personalized, interactive patient decision aid for participation in clinical trials**  
 C. Offermann-Wulms<sup>1</sup>, C. Roumen<sup>1</sup>, A. Ankolekar<sup>1</sup>, J. Coenen<sup>1</sup>, I. Nijsten<sup>1</sup>, R. Fijten<sup>1</sup>, D. De Ruyscher<sup>1</sup>  
<sup>1</sup>*Maastrro Clinic, Department of Radiotherapy, Maastricht, The Netherlands*

#### Purpose or Objective

Performing clinical trials is a crucial step towards changing standard clinical practice.

Lack of statistical power is one of the major problems hampering clinical trials, thus ensuring that appropriate inclusion in trials takes place is crucial. However, cancer patients often do not make informed decisions regarding clinical trial participation. This is due to misconceptions and wrong beliefs that trial participants do not receive the best possible care, and due to the fact, that written or oral information about clinical trials is often incomplete, complex, unclear and confusing.

Therefore, patient-centered approaches in clinical trials call for support in the decision-making process, guiding patients to clarify their preferences and values, and helping patients make a well-informed decision about participation.

To this end, we developed a web-based patient decision aid for trial participation (tDAT).

#### Material and Methods

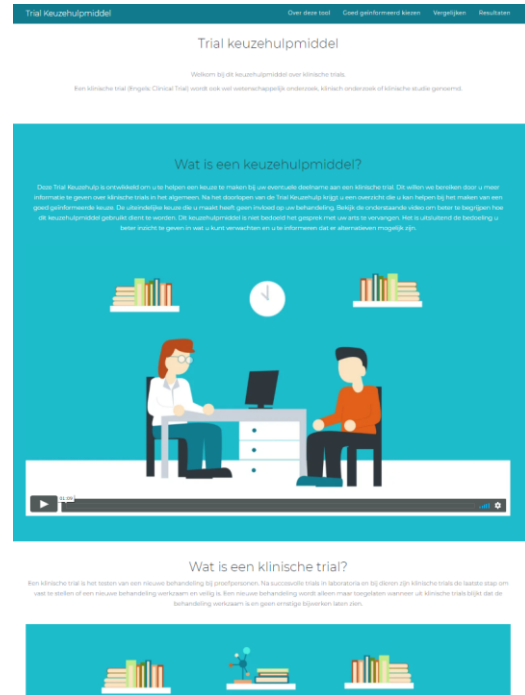
The tDAT was developed between April 2017 and April 2018 according to the international patient decision aid standard (IPDAS) guidelines. First, we identified views on decisional needs for trial participation of stakeholders (e.g. trial experienced patients, trial assistants, physicians) and verified these needs in scientific literature and by interviewing patients who were already participating in a clinical trial. Based on this evidence, a prototype was developed, which was subsequently tested by stakeholders using semi-structured interviews. This review by the stakeholders led to a redraft and redesign.

#### Results

The resulting tDAT displayed information about trial participation in an interactive manner and without medical jargon.

The general information on the definitions of clinical trials are given by using animations, videos and written text in which the trial participation process is explained. Additionally, a questionnaire is included that allows patients to test their gained knowledge. This is followed by multiple comparisons to determine what matters to them based on their personal preferences.

At the end, the patient receives an overview of their preferences which they can then discuss with the trial assistant and/or MD in order to make a founded and better-informed decision.



#### Conclusion

We have developed a tDAT that will enable us to test our hypothesis that well-informed patients are more likely to participate in a trial and less likely to drop-out of a trial. In the near future, we will be conducting a trial to evaluate the quality and effectiveness of our current web-based tDAT. This will be done after stakeholders tested the feasibility of the tool.

**EP-2104 Audit of the dosimetric impact of weight loss in head and neck patients to assess when a re-plan is required**

N. Lalli<sup>1</sup>, S. Khan<sup>2</sup>, L. Hong<sup>2</sup>, M. Daly<sup>2</sup>, D. Carnell<sup>2</sup>, R. Mendes<sup>2</sup>, A. Thompson<sup>2</sup>

<sup>1</sup>*University College London Hospital NHS Trust, Radiotherapy Physics, London, United Kingdom ;*

<sup>2</sup>*University College London Hospital NHS Trust, Radiotherapy, London, United Kingdom*

#### Purpose or Objective

Anatomical changes including weight loss can cause dosimetric changes over a course of VMAT radiotherapy for head and neck cancer, affecting target volume coverage or organ at risk dose. Adaptive re-planning can be used to mitigate these effects; however doing this can require additional time and resources. Repeat planning CTs can contribute concomitant radiation dose. Calculating the planned dose using on-treatment CBCT images helps quantify the dosimetric changes to OARs, facilitating decision-making when faced with weight loss during treatment.

At UCLH, when patient separation loss is observed on weekly CBCTs, a request is sent to the physics team to implement a dosimetric assessment. The planned patient external contour is amended to reflect the recent CBCT. The plan is re-calculated to document the changes in target coverage and OAR doses, and is reviewed by the clinician to determine if action is required. The purpose of this study was to audit the existing process and determine whether it could be streamlined within our department. Being able to identify patients where weight loss can have an undesired dosimetric impact and when and to take effective action was the endpoint of this study.

### Material and Methods

An institutional audit of head and neck patients undergoing radical arc radiotherapy was carried out for the period of April 2017 to March 2018. Specific time points during a patient's treatment were recorded including the date where dosimetric assessment query was raised to physics team and how long the evaluation took. The total number of dose re-calculations, and rescans were summarised and spinal cord doses were audited. The dosimetric impact of separation change was evaluated by recalculating the RT plans for a sample of 5 patients with irradiation of bilateral nodes, after reducing the external body contour on the TPS by 1cm in all directions. Using the typical fraction at which weight loss is seen a composite weight loss plan was created and spinal cord doses were evaluated.

### Results

Audit of Head and Neck patients in RT during April 2017 – Mar 2018	
Total no. of patients	99
No. of patients that required a plan recalculation, due to anatomical variations seen on CBCT	23
Average point of recal	17 fractions (out of 30)
No. that required a rescan/re-plan after recalculation	8
Average time between separation change CBCT and re-CT	5 days
Average time from re-CT to re-plan	5 days

The audit results are as shown in Table 1. In addition, it was found that patients requiring a re-scan were because of poor fitting shell, and thus variability of set-up, rather than the dosimetric impact.

### Conclusion

Where the planned cord PRV doses are within 0.5Gy of tolerance and with more than 50% treatment remaining, a rescan/re-plan should be actioned. This audit has shown that while the VMAT plan is robust to patient separation changes, if variability in set-up is seen a rescan pathway should be implemented immediately. IGRT is necessary to ensure accurate positioning throughout a course of treatment.

The results of this audit will help streamline local processes to implement an efficient adaptive pathway for head and neck patients. Further work is being carried out to implement deformable registration to facilitate this accurately and efficiently.

### EP-2105 Robustness comparison between 6- and 8-fields SIB proton plans on head and neck patients

N. Bizzocchi<sup>1</sup>, C. De Angelis<sup>1</sup>, J. Hrbacek<sup>1</sup>, A.J. Lomax<sup>1</sup>, D.C. Weber<sup>1</sup>, A. Bolsi<sup>1</sup>

<sup>1</sup>Paul Scherrer Institut, Center for Proton Therapy, Villigen, Switzerland

### Purpose or Objective

Pencil Beam Scanning (PBS) proton therapy, compared to conventional radiotherapy (CRT), can improve organs at risk (OAR) sparing in Head and Neck (H&N) patients, especially for median OARs like the spinal cord and brainstem. Nevertheless, plan robustness (PR) needs to be optimal and delivery time (DT) reasonable. For these reasons, bilateral H&N cases with involved lymph nodes chains could represent an issue due to the extension/complexity of the targets and the high number of OAR involved. The PSI standard approach for such cases uses an 8-field beam arrangement (BA) that was proven to satisfy PR specifications. However, with this approach the long delivery time (at least 30 minutes) still represents an issue for intra fractional setup. Therefore a new planning technique was studied to reduce fields number (and treatment time), without compromising the dose distribution. In this study, we report on a comparison of PR between the standard 8 field approach (8F) and a 6 field alternative (6F).

### Material and Methods

In H&N cases with lymph node involvement, a different BA is strongly advised between the cranial portion of the PTV and the PTV localized in the neck area. Different field directions are used to treat the different PTV portions, with overlapping junctions between the fields (8F, Figure 1). The 6F approach keeps also a different BA between head and neck regions, but the reduction in field numbers is reached by a different splitting of the PTV. In this way, 2 field directions are kept identical for both cranial and neck portions of PTV (6F, Figure 2). The 6F planning technique was studied for two H&N cases clinically treated at PSI using 8F BA and a Simultaneous Integrated Boost (SIB) fractionation of 3 dose levels (54, 60 and 69 Gy-RBE- at 1.8, 2 and 2.3 Gy-RBE- per fraction). 6F plans were designed to be clinically equivalent to the delivered 8F ones, and PR was computed for both 6F and 8F approaches (setup uncertainties for PSI patients positioned with mask:  $s_{85\%}=2.25$  mm) for PTVs, CTVs, spinal cord, brainstem, Parotids, chiasma and optic nerves. DT for 8F approach was over 35 minutes while for 6F between 25 and 30 minutes.

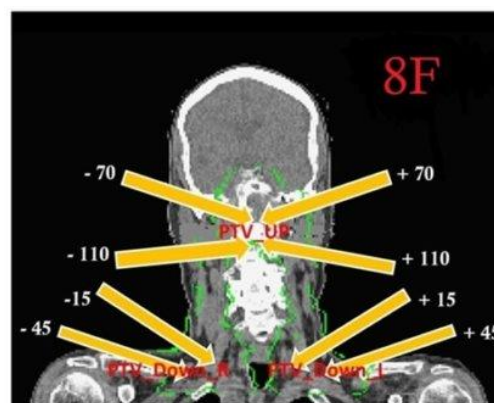


Figure 1: standard BA with 8 fields

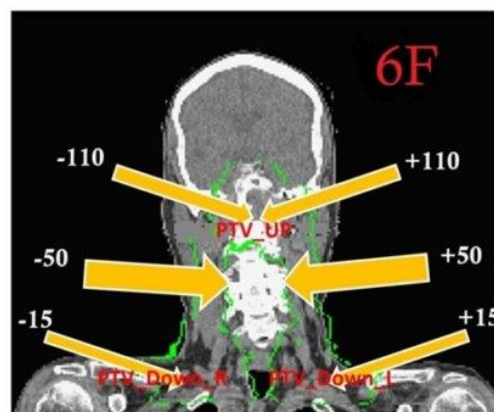


Figure 2: new BA with 6 fields

### Results

Table 1 shows the comparison between the 8F and 6F approaches. The values are for one of the 2 analyzed cases (also representative of the other). The fraction of PTV, CTV and OAR volumes (%) with dose errors over 5, 10 and 15% are reported. For OARs results are better for 6F for chiasma and brainstem while for the other VOIs there is no clear trend.

VOI	Brainstem			Chiasma			Spinal Cord		
	6F	8F	diff 6F-8F (%)	6F	8F	diff 6F-8F (%)	6F	8F	diff 6F-8F (%)
N° fields	70.97	77.36	-6.39	97.96	91.84	6.12	18.52	23.75	-5.23
V50% (%)	34.09	40.54	-6.45	3.06	4.08	-1.02	5.86	6.10	-0.25
V15% (%)	8.24	8.74	-0.50	0.00	0.00	0.00	0.75	0.00	0.75
VOI	Optic Nerve			Parotid L			Parotid R		
	6F	8F	diff 6F-8F (%)	6F	8F	diff 6F-8F (%)	6F	8F	diff 6F-8F (%)
N° fields	76.84	63.28	13.56	41.27	50.15	-8.88	52.77	43.00	9.78
V50% (%)	53.95	40.68	13.27	7.91	8.27	-0.37	1.65	4.12	-2.46
V15% (%)	20.62	1.13	19.49	2.91	1.54	1.37	0.00	0.04	-0.04
VOI	CTV 54 Gy			CTV 60 Gy			CTV 69 Gy		
	6F	8F	diff 6F-8F (%)	6F	8F	diff 6F-8F (%)	6F	8F	diff 6F-8F (%)
N° fields	23.95	23.10	0.85	16.53	13.69	2.84	9.72	6.36	3.36
V50% (%)	1.11	1.17	-0.06	1.13	0.77	0.36	0.31	0.27	0.04
V15% (%)	0.03	0.06	-0.03	0.23	0.05	0.18	0.09	0.03	0.06
VOI	PTV 54 Gy			PTV 60 Gy			PTV 69 Gy		
	6F	8F	diff 6F-8F (%)	6F	8F	diff 6F-8F (%)	6F	8F	diff 6F-8F (%)
N° fields	34.16	33.32	0.84	36.91	34.51	2.40	24.58	20.96	3.62
V50% (%)	4.43	4.38	0.05	7.80	5.76	2.04	3.03	2.46	0.57
V15% (%)	0.31	0.48	-0.17	1.30	0.79	0.51	0.59	0.39	0.20

Table 1: robustness evaluation in % of set-up error over % of the target/OAR volume. In green the results where 6F is better (lower PR values) over 8F, while in orange the cases where 8F has better values as 6F.

**Conclusion**

In terms of robustness, the 6F approach could be considered similar to the 8F one. Nevertheless, 6F delivery time is reduced by 20% compared to the 8F technique. Indeed, for a comparable amount of spots, the couch movements between fields are reduced from 7(8F) to 5(6F), thus reducing intrafraction motion. 6F approach should therefore be preferred over the 8F one, even if other cases should be investigated to strengthen our conclusion.

**EP-2106 Statistical process control analysis of pre-treatment VMAT QA for different anatomical sites**  
 H. Omar Ghafour<sup>1</sup>, S. Russo<sup>2</sup>, M. Esposito<sup>2</sup>, S. Pini<sup>2</sup>, A. Ghirelli<sup>2</sup>, G. Zatelli<sup>2</sup>

<sup>1</sup>Ministry of Health KRG / Sulaymani directorate of health of Health/ Zhiyanawa Cancer Center, Zhiyanawa Cancer Center, Sulaymaniyha, Iraq ; <sup>2</sup>Azienda USL Toscana Centro, Medical Physics Unit- Azienda USL Toscana Centro- Sede di Firenze-, Firenze-, Italy

**Purpose or Objective**

Pre-treatment patients specific QA are used to validate the dosimetry of VMAT plans and to evaluate dosimetric performance over time of VMAT QA process. Discrepancy tolerance limits between calculated and delivered radiation doses are neither well defined nor consistently applied. The aim of this work is to determine the Tolerance limit and the Action Limit for the dose delivery process for different anatomical sites.

**Material and Methods**

QA measurements were performed by PTW Octavius 4D 729 in the PTW Octavius 4D phantom for 464 VMAT plan for six anatomical sites: Head and Neck, Lung, Breast, Prostate, post prostatectomy, Abdominal and Pelvic case. Measurements were compared with TPS Elekta Monaco 5.1 computed doses via 3D global gamma analysis 3%/3mm (global normalization point value >90% of maximum dose) by using PTW VeriSoft software 6.1. The Action limit and tolerance limit were established, by using the concept of Statistical control process (SPC), as suggested by AAPM Task Group 218:

$$\Delta A = B \times \text{SQRT}(\sigma^2 + (\bar{x} - T)^2) \quad \text{Eq(1)}$$

$$\text{Action limit} = (100 - \Delta A) / 2 \quad \text{Eq(2)}$$

$$\text{Tolerance limit (LCL)} = \bar{x} - 2.66 \times (\text{mean moving range}) \quad \text{Eq(3)}$$

$$\text{Mean moving range (MR)} = 1 / (n - 1) \times \sum |X_i - X_{i-1}| \quad \text{Eq(4)}$$

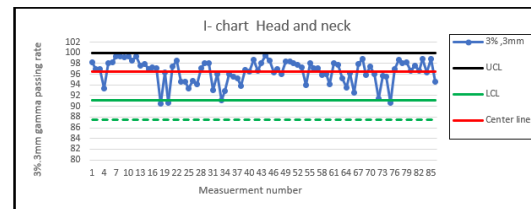
where ΔA is the difference between the upper and lower action limits (typically written as ± ΔA / 2); T is the process target value (100% for QA VMAT); σ<sup>2</sup> and  $\bar{x}$  are the process variance and process mean, respectively and B is a parameter whose suggested value is equal to 6. The moving range is absolute difference between two successive point data in the time ordered data and can be calculated according equation (4), where (X) is an

individual IMRTQA measurement. (n) is total number of measurements.

**Results**

The average pass rate of volumetric 3D gamma index for global normalization with criteria 3%,3mm, the specific tolerance limit and action limits for each anatomical site were shown in table 1. Gamma values resulted outside LCL only for about 6%, 2.5%, 4% of cases for Head and Neck, Prostate, post Prostatectomy and Pelvic case respectively. The chart control limit was constructed for each site based on the SCP. An example for Head and Neck patient is presented in

Site of patients	Patients	σ	( $\bar{x}$ ) of (γ) 3%,3mm	LCL	Action limit	Value over LCL
Head and neck	86	2.2	96.5	91.3	87.6	5
Lung	61	2.0	96.7	91.2	88.5	0
Breast	41	1.8	96.1	91.2	86.9	0
prostate	118	0.6	99.7	98.6	97.8	3
pelvic and abdominal	106	3.0	96.4	88.4	85.9	4
post prostatectomy	52	1.2	99.1	97.0	95.5	2



**Conclusion**

The action limits and tolerance limits for the specific couple of linac and measuring system used in this work were determined and stratified for different anatomical site. The Control chart limit approach indicates that the process is under control.

**EP-2107 DQA gamma Analysis evaluation criteria for prostate SBRT using MLC InCise 2 of a Cyberknife-M6**  
 A. Ruiz<sup>1</sup>, K. Torzsok<sup>1</sup>, M. Ribeiro<sup>1</sup>, H. Broqué<sup>1</sup>, J. Aponte<sup>1</sup>, F. Marangoni<sup>1</sup>

<sup>1</sup>Fundación Arturo López Pérez, Radiotherapy, Santiago de Chile, Chile

**Purpose or Objective**

A multileaf collimator (MLC) for radiosurgery on a robotic arm is new worldwide. The Cyberknife M6<sup>®</sup> shapes the beam in 3 ways, one through the MLC InCise2<sup>®</sup> consisting of 26 leaf pairs, each with a width of ≈ 2 mm. The maximum field size is 115 mm × 100.1 mm. Patient specific quality assurance evaluation criteria recommended internationally are scarce. The objective of this work is to determine tolerance criteria and gamma approval rates achievable for evaluation and validation of the gamma index and CC01 IBA<sup>®</sup> ionization chamber point dose measurements in prostate SBRT performed with the MLC InCise2<sup>®</sup> on a sample of 22 treated patients.

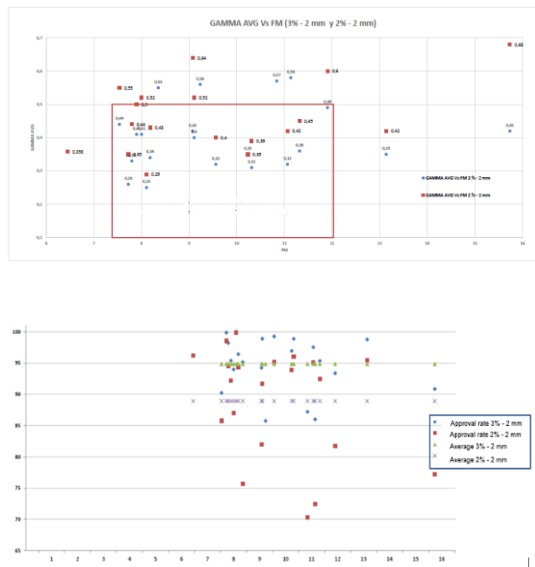
**Material and Methods**

A film dosimetry method was developed. A 24 hours calibration curve was made with EBT3 films and Omnipro software for evaluation of SBRT prostate plans, 2 dose planes and film background correction were used for each patient. Absolute and relative calculations were made, with different criteria to test approval rates ranges, as well as, the average gamma to obtain with this MLC with statistical parameters. Physics time investment per patient was ≈ 3.5 hours. The algorithm used by treatment planning system (TPS) is equivalent path length type A. MLC less collimation limits given by the manufacturer were evaluated, considering tests analogous to those proposed by James L Bedford et al.

**Results**

Different criteria of approval rate value, as well as modulation factor (MF) has not shown a defined trend

variation, with respect to the PTV volume. The values obtained from the point dose in a deviation range of  $\pm 3\%$  have corresponded to an approximate 8-13 range of the MF. The same range of MF is observed in figure 1, for those average gamma values that are less than 0.5, obtaining more points that fail as the criterion's rigor increases. When evaluating the approval rate with 2 different criteria, figure 2, the dispersion range of the points is much higher with the strictest criterion. It is not only that the approval rate is lower, which is not necessarily unfavourable, but points are more dispersed making it more difficult to establish an evaluation criterion based on a stable averaged behaviour. In addition, the values distribution of the approval rate was evaluated with Monte Carlo simulation. Minimum Gumbel type distribution was the best fit obtained.



## Conclusion

Regarding compliance of the objective, with the obtained data, it could be determined that most achievable criterion in DQA prostate SBRT with the use of this technology could be:  $\Delta D 2\%$  / DTA 3 mm in relative with an approval rate greater than 90% keeping an average Gamma of less than 0.5 and a point dose value in  $\pm 3\%$  between TPS calculated and ionization chamber measurement. Due to the high dispersion of the  $\Delta D 2\%$  / DTA 2 criterion, used with cones, it should not be used for the MLC, data shows that it is not possible to establish an evaluation criterion based on a stable behaviour averaging.

## EP-2108 Varian and Elekta quality assurance using artificial neural network based on portal imaging

F. Chatrie<sup>1</sup>, A. Vasseur<sup>2</sup>, A.R. Barbeiro<sup>3</sup>, F. Younan<sup>4</sup>, J. Mazurier<sup>4</sup>, M.V. Le Lann<sup>5</sup>, X. Franceries<sup>3</sup>

<sup>1</sup>CRCT- UMR 1037- INSERM- Université Toulouse III-Paul Sabatier- LAAS-CNRS, Disco, Toulouse, France ; <sup>2</sup>Institut de Cancérologie de Bourgogne, Physique Médicale, Auxerre, France ; <sup>3</sup>CRCT- UMR 1037- INSERM- Université Toulouse III-Paul Sabatier, Team 15, Toulouse, France ; <sup>4</sup>Atrium- Clinique Pasteur - Groupe Oncorad-Garonne, Service de Radiothérapie, Toulouse, France ; <sup>5</sup>Institut National des Sciences Appliquées- LAAS-CNRS, Disco, Toulouse, France

## Purpose or Objective

Artificial neural networks (ANN) applied to external beam radiation therapy, can be of great interest, especially for quality assurance (QA) based on electronic portal imaging device (EPID). As EPID images contain information about

the treatment delivery, they can be used to predict the delivered dose distribution, which can be compared to the planned one to ensure that the patient receives the correct treatment. Therefore, in this work we proposed the application of machine-learning algorithms to allow the reconstruction of 2D and further 3D absorbed dose maps based on EPID signal obtained from both, Varian and Elekta machines.

## Material and Methods

A supervised ANN algorithm consisting of a non-recurrent feed-forward multilayer model was employed, which works according to two phases - learning and recognition (like humans). In order to reconstruct 2D absorbed dose distribution from treatment delivery, during the learning phase, the creation of "neurons" was done by linking input and output data, taken from EPID images, and absorbed dose distributions from the TPS, respectively. Once the learning was over, new EPID signal (input data) was used to predict the delivered absorbed dose distribution (as output) in the recognition phase, to be compared to the TPS for treatment verification. The latter was done by means of global 2%/2mm gamma index (10% threshold). Although the learning phase was more time consuming while setting the ANN model, during the recognition phase, the model operated in an instantaneous way. Datasets from different EPID and TPS types were included, so that the developed model could be extended to Varian and Elekta machines. EPID images were taken from an aSi-1000 EPID on a Varian Clinac 23iX and an iViewGT on Elekta Synerg during 6MV treatment delivery, with a dose rate of 600 MU/min and 400 MU/min, respectively, while 2D dose distributions of IMRT plans were calculated in Eclipse<sup>TM</sup> and Pinnacle<sup>TM</sup>, at the maximum depth dose in a water phantom.

## Results

Learning was performed using 10 and 4 input/output datasets, respectively, from IMRT treatments. All of the used image datasets (both EPID inputs and absorbed dose distribution outputs) consisted of 384x512 and 1024x1024 pixels, respectively. In Figure 1 the result from one of the evaluated treatment plans is presented, showing the similarity between the absorbed dose distributions obtained by the implemented ANN and the originally planned. Gamma passing rates > 98% were obtained for the evaluated brain cases from Varian and Elekta instances, highlighting the ANN capability to predict the absorbed dose distribution based on EPIDs with different machines.

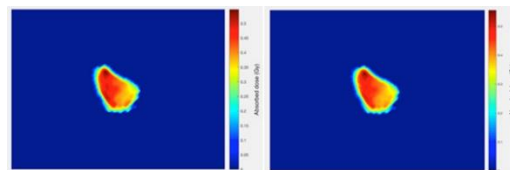


Figure 1: Comparison of 2D absorbed dose distributions calculated by ANN (left) and obtained from TPS (right) for a brain case of Varian instance.

## Conclusion

The ANN algorithm implemented in this work was able to perform IMRT treatment verification based on EPID, showing excellent gamma index results for the evaluated cases. Furthermore it was able to predict dose distributions with the same ANN model, depending of the training data, but regardless the machine type, which makes it extensible to Varian and Elekta QA.

EP-2109 Can we improve the dosimetric values with the experience? our results with vmat in lung cancer  
F.J. Luna Tirado<sup>1</sup>, M. Rincón<sup>1</sup>, D. Gonsalves<sup>1</sup>, L. Guzmán<sup>1</sup>, M. Montero<sup>1</sup>, J.M. Penedo<sup>1</sup>, A. Ilundain<sup>1</sup>, J. Olivera<sup>1</sup>, E. López<sup>1</sup>

<sup>1</sup>Capio-Fundación Jimenez Díaz, Radiation Oncology Department, Madrid, Spain

**Purpose or Objective**

RTOG 0617 trial established among other conclusions the advantages of IMRT/VMAT in locally advanced non small cell lung cancer (LA-NSCLC) mainly due to better dosimetric values comparing to 3DRT. Our objective is to determine if the better knowledge and experience in the development of VMAT in lung cancer is related with an improvement in dosimetric parameters.

**Material and Methods**

We started to employ VMAT for lung cancer in January 2014. Since then, 125 locally advanced non small cell lung cancer and limited disease small cell lung cancer have been treated with this technique.

All patients were treated following our protocol treatment. The simulation consisted in a 4D CT simulation (3mm slices) with an Elekta frame based immobilization system and free breathing. We delimited the planning target volume and organs at risk according to RTOG guidelines. For constraints, Quantitative Analyses of Normal Tissue Effects in the Clinic (QUANTEC) was used. The plan was designed using Volumetric Modulated Arc Therapy (VMAT) with one or two arcs and 6-10 MV photons. It was calculated by the Monaco treatment planning system (version 5.10).

The plan was delivered using Elekta Agility Linac with Precise treatment system (precise table) and Elekta XVI CBCT system for quality assurance.

We have analyzed and compared dosimetric values (lung V5-10-13-20 and mean lung dose; mean heart dose) between the first 20 patients treated with VMAT (group 1) and the last 20 patients treated with VMAT (group 2). To achieve an interpretable results a volume ratio have been employed to ensure homogeneous groups:  $V_{PTV} / V_{TOTAL}$  LUNG. Where  $V_{PTV}$  : Plannig target volume (cc) and  $V_{TOTAL}$  lung: Total lung volume (cc)

**Results**

Both groups were homogeneous with the same volume ratio: 0.16. Significant differences were registered between groups in all the dosimetric values analyzed, all of them in favour of group 2, mainly in mean heart dose, with a great difference of 28,6% for the group 2. Every lung dosimetric values were clearly better in group 2, especially Mean lung dose and V5 (see figure 1)

**Conclusion**

The implementation of every technical advance in radiation oncology requires a comprehensive formation and experience to achieve the best results.

In our experience, the dosimetric values in lung cancer have been clearly improved with the greater knowledge and use of VMAT technique.

**EP-2110 Developing a QA programme for the Elekta Unity MR-linac**

J. Chick<sup>1</sup>, I. Hanson<sup>1</sup>, S. Nill<sup>1</sup>, U. Oelfke<sup>1</sup>

<sup>1</sup>Royal Marsden Hospital NHS Trust and the Institute of Cancer Research, Joint Department of Physics, Sutton, United Kingdom

**Purpose or Objective**

In all modalities of treatment and diagnosis a well-structured Quality Assurance (QA) programme is necessary to ensure a high quality service and to minimise the risks to patients and staff. The Unity MR-linac (Elekta AB, Stockholm) has recently been brought into clinical service at the Royal Marsden Hospital (RMH), and requires a QA programme to include dosimetry, image quality and safety aspects. Here the RMH QA programme is outlined and initial results reported for the first month of clinical use.

**Material and Methods**

The QA programme is currently completed in daily 60-90 minute sessions before patient treatment, including daily mandatory tests (45minutes), and weekly and monthly tests on a rotating cycle. A summary of the programme is described in Table 1, detailing frequency and equipment used.

Many of the tests use a QA platform, which is a jig that fits onto the couch top, with set up marks to enable equipment to be set up reproducibly. The Syzygy phantom consists of spheres aligned along a plumb line and water level, to provide an absolute frame of reference (Hanson et al. ESTRO 37, QC-0079). The alignment of the MR and MV co-ordinate systems is measured daily using an Elekta Phantom which has 7 ZrO<sub>2</sub> spheres which are visible on MV, with corresponding signal voids on MR.

Further MR tests will be done quarterly, to include B0 homogeneity, B1 flip angle accuracy, dynamic stability, ghosting and spurious noise (Tijssen et al, ESTRO 36, QC-0257). Annual tests will include dose linearity, gantry angle attenuation, and MLC transmission/leakage.

FIGURE 1 (DOSIMETRIC VALUES VMAT LUNG CANCER)

	$V_{PTV} / V_{TOT}$	MEAN LUN G DOSE	LUNG V5	UNG V10	L LUN V13	LUN V20	HEART DOSE
GRO UP 1 (FIRST 20 PATIENTS)	0,24	16,24 Gy	74,67 %	55,29 %	45,17 %	28,91 %	15,09 Gy
GRO UP 2 (LAST 20 PATIENTS)	0,05	15,05 Gy	67,95 %	52,46 %	43,87 %	27,65 %	10,78 Gy
DIFFERENCE (%)	-7,3	9,0	5,1	2,9	3,3	4,28	28,6

**Table 1: RMH QA Programme for the MR-linac**

	Test	Equipment
DAILY	<b>Daily Radiation</b> (Consistency of output and field sizes)	EPID panel
	<b>MR-MV alignment</b> (Consistency of alignment of isocentres)	Elekta phantom
	<b>MR Image Quality</b> (SNR and scaling)	Philips PIQT
	<b>Safety</b> (e.g. interrupt/terminate buttons, patient communication)	n/a
WEEKLY	<b>Weekly Radiation</b> (Output, flatness and symmetry)	QA platform PTW StarCheck Maxi MR
	<b>MR Image Quality</b> (SNR, linearity, resolution, ghosting)	Philips PIQT ACR large phantom
	<b>Helium Level</b>	Philips Marlin
	<b>Weekly Safety</b> (Emergency Power Off buttons)	n/a
MONTHLY	<b>Monthly Radiation</b> (Absolute Output, TPR20/10, Output Factors)	QA platform PTW Watertank PTW Farmer 30013
	<b>Monthly Radiation with gantry angle</b> (Output, flatness and symmetry at cardinal gantry angles)	PTW Octavius 4D
	<b>MR Distortion</b>	Philips 3D Geometric Modus MRID phantom
	<b>System alignment</b> (Absolute gantry angle, EPID rotation, EPID iso-pixel, MLC/Jaw position & orientation)	QA platform Szyzyg phantom EPID panel
	<b>Radiation isocentre</b>	QA platform, StarShot film
	<b>Safety</b> (Interlocks, Emergency ventilation)	n/a
	<b>EPID</b> (image quality, image scaling)	QA platform, Las Vegas Phantom, Elekta Phantom
	<b>Couch</b> (level, slop and position)	QA platform, spirit level

**Results**

In the first month of clinical use, the daily output of the MR-linac, as measured by the EPID pixel factor, had a coefficient of variation (standard deviation/mean) of 0.22%. The mean RMS of the daily MR to MV alignment registration compared to the baseline registration was below 0.1mm. The results are summarised in Table 2, the MLC and Jaw positions reflected by the field size measurements were all within tolerance. All MR image quality tests passed Philips thresholds and were consistent. Further results will be reported including the weekly and monthly tests.

**Table 2: MR-linac Daily Tests (first 20 days of clinical use)**

	Mean (sd)
EPID pixel factor (a.u.)	0.01744 (0.00004)
MR to MV alignment (mm, RMS deviation)	0.08 (0.02)
Jaw defined field size @200 (mm)	199.68 (0.40)
Jaw defined field size @50 (mm)	49.47 (0.28)
MLC defined field size @80 (mm)	79.99 (0.39)
MLC defined field size @20 (mm)	20.04 (0.33)
MRI Signal to Noise Ratio (> 80)	122.43 (4.50)
MRI Scaling – axial (% , < 0.5)	0.09 (0.03)
MRI Scaling – coronal (% , < 0.5)	0.12 (0.03)

**Conclusion**

A comprehensive QA programme has been developed for the MR-linac, drawing on both Linear Accelerator and MRI methods. As more system data is collected, the programme will be optimised with respect to test frequency and methods, in order to reduce the overall time. The MR-linac performance in its first month of clinical use has been dosimetrically stable, geometrically stable with respect to the system alignment, with consistent MR image quality.

**EP-2111 Apex micromultileaf SRS Dynamic Conformal Arc treatment comparison with Agility multileaf collimator**

C. Ferrer<sup>1</sup>, C. Huertas<sup>1</sup>, R. Plaza<sup>1</sup>, R. Simón de Blas<sup>1</sup>, F. Sánchez<sup>1</sup>, E. Corredoirá<sup>1</sup>

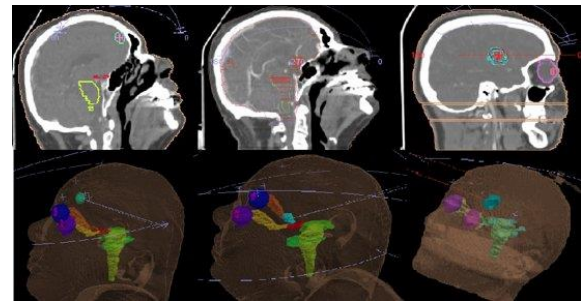
<sup>1</sup>Hospital universitaria La Paz, Radiofísica y Radioprotección, Madrid, Spain

**Purpose or Objective**

To evaluate the benefits of Apex micromultileaf collimator (mMLC) attached to the Agility multileaf collimator (MLC) against the same treatment without it attached when planning using Dynamic Conformal Arc (DCA) technique.

**Material and Methods**

Three brain metastases were prescribed to 18Gy, first one located in the central lobe, away from any critical structure. Second one located behind the optic nerves over the chiasm, and the third one in the right temporal lobe and showing irregular shape. The three locations are shown in Figure 1. Treatment was planned with Elekta Monaco treatment planning system (v. 5.11.02), and optimized using biological and physical based cost functions for isocentric DCA SRS treatment on an Elekta Synergy linear accelerator equipped with a 160-Agility MLC with of 5 mm nominal width leaves at the isocenter and an Elekta Apex mMLC attached, which has 56 pairs of tungsten alloy leaves with nominal width of 2.45 mm at the isocenter. Five non coplanar partial arcs were used, maintaining the same constraints when Apex was attached and when it wasn't. Additionally, a VMAT treatment was planned using only Agility MLC with another constraints, as with this technique a better modulation is possible. Conformation index (CI), conformation number (CN), Heterogeneity index (HI), Homogen



ity index (Hmi), Target coverage (TC), Monitor units MU, Modulation (UM/cGy) and Minimum Target Dose have been compared, as well as doses to organs at risk (OAR). Results Considering the TC, the Apex mMLC improves the treatment compared with the same DCA planning realized only with the Agility MLC, as it is shown in Table 1. Nevertheless VMAT planning achieves better TC at the cost of more MU. This better TC with Apex and DCA causes that some maximum doses are slightly higher, being the number of MU very similar. So as Apex is nearer to the patient, its penumbra is lower, and TC can be higher without increasing much the maximum doses to OAR. Conformation indexes are similar, being almost equal for Apex DCA and VMAT treatments.

INDEX	LESION 1		LESION 2		LESION 3		LESION 3	
	APEX	DCA	AGILITY	VMAT	APEX	DCA	AGILITY	VMAT
CI	1.42	0.94	1.00	1.56	1.22	1.72	1.08	1.08
CN (Padlock)	0.08	0.80	0.63	0.59	0.66	0.56	0.51	0.52
HI	1.05	1.08	1.04	1.07	1.14	1.07	1.09	1.12
TC (%)	98.80%	96.84%	100.00%	96.77%	89.83%	98.09%	97.82%	95.80%
MU	2407.69	2343.04	3017.72	2918.41	2927.27	4061.92	2384.86	3489.87
MODULATION (UM/cGy)	1.34	1.30	1.68	1.62	1.63	2.26	1.49	1.54
<b>ORGANS AT RISK</b>								
Minimum target dose (cGy)	0.98	0.92	1.01	0.95	0.89	1.02	0.94	0.89
Right optic lens (cGy)	52.70	40.60	54.80	40.50	83.50	66.80	11.30	22.80
Left optic lens (cGy)	70.80	84.20	90.60	20.20	81.00	25.50	8.00	5.00
Right optic nerve maximum dose (cGy)	87.90	62.80	92.90	1323.40	1382.50	1501.20	32.00	38.70
Left optic nerve maximum dose (cGy)	135.80	158.70	209.40	1516.50	1511.00	1641.50	19.80	16.20
Chiasm (cGy)	49.10	11.00	49.5	1811.60	1659.80	1748.20	69.40	51.40
Brain Stem (cGy)	29.20	8.80	37.00	284.00	193.20	143.20	90.20	73.50

**Conclusion**

The results achieved with Apex attached in SRS DCA treatments are superior then the same treatments are planned only with Agility. However VMAT treatments attain better results, at the cost of more MU. We will have to wait to be able to perform treatments with VMAT and APEX to have a full comparison.

**EP-2112 Automation of consistency and integrity checks in external radiotherapy plans**

M.A. Benito Bejarano<sup>1</sup>, F. Saez Beltran<sup>1</sup>  
<sup>1</sup>Hospital Provincial de Zamora, Department of Radiation Physics, Zamora, Spain

### Purpose or Objective

Modern external radiotherapy techniques rely on different computerised systems to design and deliver the treatments. Treatment plans are created in a Radiotherapy Planning System (RTPS), and upon approval they are sent to a Record and Verify System (R&V), where the plan data is stored for subsequent use in each treatment fraction. A quality assurance (QA) procedure must be applied to ensure that there have been no errors in the plan design, as well as inconsistencies or data corruption during the transmission or storage of the plan parameters. In the present, most QA procedures are based in manual and time-consuming verifications. We propose an automated system to check the plan integrity and validate its proper transmission to the R&V.

### Material and Methods

The plans were created in XiO RTPS. They were transmitted by means of DICOM RT PLAN protocol to the Mosaik R&V. A set of routines was developed in MATLAB. Those routines enable the extraction and analysis of data from DICOM files generated by the RTPS, as well from the OPENRTP text files exported by the R&V. The system works in a three stages sequence. In the first stage, the "verifydicomrt" routine analyses the DICOM file from the RTPS, to seek inconsistencies or plan errors. In the second stage, "dicomprocess" extracts data from the DICOM file to be used in our in-house secondary monitor unit (MU) verification spreadsheet. In the third stage, the "rtpdicomrtcomp" routine compares selected parameters from the RTPS-generated DICOM file with those in the OPENRTP file from the R&V. In any of those stages, when an issue is detected a warning message is displayed. DICOM and OPENRTP files with intentional errors were created to test the system.

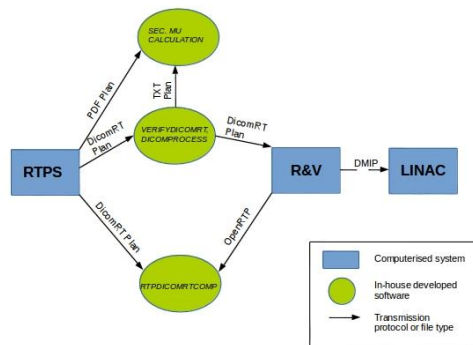


Figure 1: Plan transmission and automated QA procedures workflow

### Results

"verifydicomrt" was able to catch common planning errors in parameters related to the couch, collimator, gantry, MU, or others (see table 1). This allowed the early detection and correction of those errors before the plan was transmitted to the R&V. "dicomprocess" enabled the automatic extraction of the data needed for independent MU calculation, minimising the possibility of manual data input mistakes. "rtpdicomrtcomp" was able to compare the data generated by the RTPS with the actual parameters stored in the R&V database. This permitted tracking down any transmission errors, data corruption in the RTPS or R&V databases, or any mistakenly manual modification of parameters. "rtpdicomrtcomp" can be run in a weekly basis to keep track of unintended changes in the plans stored in the R&V database.

Parameters verified by verifydicomrt.m
Plan name
Plan approval status
Institution ID
Machine ID
Dose unit type
Collimator angle within machine definition limits
Couch isocentric angle within machine definition limits
MU value is integer
Positioning fields: Energy, MU
Conformality: Jaws and MLC aperture
Same isocentre for a dose site
MU minimum value

Parameters extracted for the secondary MU check
Patient ID
Patient name
Dose site
Fraction number
Dose/Fraction
Field ID
Field energy
Field size
MLC leaves position

Parameters compared by rtpdicomrtcomp.m
Patient ID
Dose site: Total dose
Dose site: Dose/Fraction
Dose site: Number of fractions
Dose site: Number of assigned fields
Machine ID
Field: Energy
Field: Gantry angle
Field: Collimator angle
Field: Couch isoc. angle
Field: MU
Field: Source to surface distance
Field: Jaws field size
Field: MLC leaf position

Table 1: Parameters processed by each routine

### Conclusion

The usage of this checking system enabled the automation of plan QA verification in a quick and reliable way. Errors could be detected during the treatment plan design, transmission and storage stages. The system could also detect data modifications in the R&V database.

### EP-2113 Congruence of mechanical, radiation, and imaging isocentres of two types of Elekta linacs

C. Mekala<sup>1</sup>, A. Naga<sup>1</sup>, N. Babu<sup>1</sup>, S. Kumar<sup>1</sup>, N. Khater<sup>1</sup>, C. Birch<sup>1</sup>

<sup>1</sup>Southampton University Hospital NHS Trust, Radiotherapy Physics, Southampton, United Kingdom

### Purpose or Objective

In this study we quantify the congruence of mechanical, radiation and imaging isocentres of two Elekta linear accelerator linacs as it is crucial for cranial hypofractionated stereotactic radiosurgery and radiotherapy deliveries where lesions of small volumes are treated with high-dose per fraction of 5 to 21 Gy.

### Material and Methods

Winston Lutz test was performed as a part of stereotactic pre-treatment linac quality control checks using a metal ball bearing phantom of diameter 5 mm which was set on the couch using in-room lasers which were originally calibrated to the MV isocentre. 2D planar MV images were acquired at 4 cardinal gantry angles and 4 couch angles with gantry set to 0° for a field size of 2.4x2.4 cm<sup>2</sup> on an Elekta Beam Modulator linac and 3x3 cm<sup>2</sup> using a recently commissioned 6MVFFF beam on Elekta Agility. The images were analysed using Pipspro software and the ball bearing was moved to match with the centre of the radiation isocentre based on optimal shifts calculated by the software. A cone beam computed tomography (CBCT) image and exactrac image of the ball bearing phantom were also acquired and the congruence of all the isocentres was evaluated based on the optimal 3D shifts of the centre of the ball bearing phantom to that of the MV isocentre. The data was acquired on both the linacs on 25 stereotactic treatment days over a period of six months.

### Results

Maximum systematic total deviation of 1.2 mm (0.6 mm radius) and 1.5 mm (0.75 mm radius) was found in the in

the Gun/Target (GT) direction for the MV isocentre for Elekta beam modulator and Elekta Agility linear accelerators respectively. The lateral and vertical errors were relatively smaller both under 0.8 mm diameter. The mechanical deviation of the couch was within 1.5 mm diameter on both the linacs. There were some outliers which were due to suboptimal beam steering and couch isocentric rotation setup which were picked up during this procedure and were corrected by our in-house engineers. The CBCT imaging isocentre was within 0.7 mm on the beam modulator linac whereas both the CBCT and exactrac isocentres were within 0.5 mm on the agility linac in comparison to the MV isocentres on each machine.

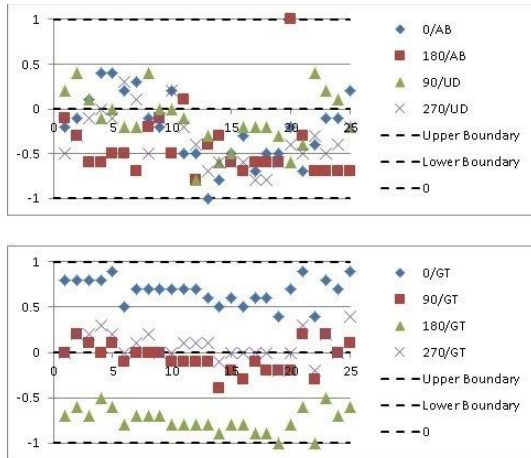


Fig.1. Gun/Target, Lateral and Vertical errors of position of the centre of the ball bearing to the central of the MV radiation isocentre for Elekta Agility linac (No. of fractions along x-axis and error in mm along y-axis)

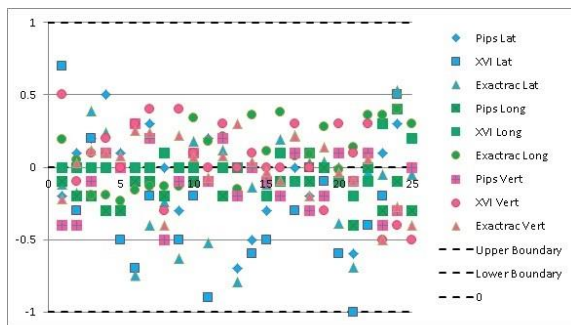


Fig.2. Lateral, longitudinal and vertical deviation between the centre of the ball bearing phantom and centre of MV, kV CBCT, and exactrac systems

**Conclusion**

Congruence of mechanical, radiation and imaging isocentres of two types of Elekta linear accelerator heads were quantified to ensure safe treatment of stereotactic patients and to assess if the planning target margins used are sufficient for target coverage.

**EP-2114 Predicting inaccuracy of overmodulated RapidArc plans using Machine Learning model**

A. Botti<sup>1</sup>, E. Cagni<sup>1</sup>, M. Orlandi<sup>1</sup>, R. Sghedoni<sup>1</sup>, D. Lambertini<sup>1</sup>, A. Barani<sup>1</sup>, V. Bertolini<sup>1</sup>, M. Iori<sup>1</sup>

<sup>1</sup>Azienda USL - IRCCS di Reggio Emilia, Medical Physics Unit, Reggio Emilia, Italy

**Purpose or Objective**

Significant differences between measured and calculated doses of RapidArc plans with very small PTV volume or overmodulated MLC pattern were observed [Fog et al - Phys. Med. Biol. 2011]. The aim of the study was to train a Machine Learning (ML) model to predict the calculated

dose inaccuracy for plan potentially affected by overmodulation issue.

**Material and Methods**

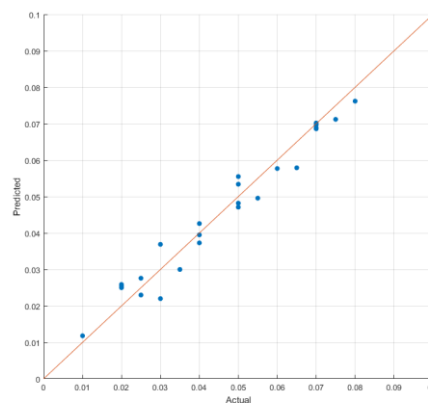
70 stereotactic RapidArc plans were planned in Eclipse v. 13.7 (Varian Medical System) and delivered on TrueBeam stx. Delivery Quality Assurances (DQA) of all plans were performed: delivered doses were measured with PTW SRS1000 chamber array combined with PTW Octavius 4D and compared with calculated dose using PTW Verisoft v.6.1. Each plan was characterized by 14 features extracted from RP-Dicom files describing different aspects of their complexity that could lead to dosimetric disagreements [Carlson et al - Phys Med Biol. 2016]. A subset of 45 plans (training set) was used to train a gaussian process regression model using the features as predictor inputs and the measured dose differences as response output. Training model was achieved with 5 fold cross validation and PCA for predictors reduction. Further open-loop validation was performed with the remaining 25 plans not belonged the training set (validation set). Features extraction, training process and validation analysis were performed using in-house Matlab ( the Mathworks) scripts. To evaluate an application of the model, a dose-painting plan was optimized in several steps with different plan complexity solutions, achieved by using different Max MU objective constraints, then DQA results were compared with prediction model.

**Results**

The cross validation analysis on the training set showed a Root Mean Square Error (RMSE) equal to 0.01 and R<sup>2</sup> equal to 0.92. The open loop-validation resulted in a RMSE equal to 0.003 and R<sup>2</sup> equal to 0.96, that indicate a good model generality. With PCA analysis the model was trained only by 3 principal components with an explained variance set to 95%.

The Figure 1 shows, for the evaluation set, a correlation plot of the predicted versus actual dose differences normalized to the maximum dose.

The dose-painting plan was optimized 3 times before to achieve a predicted dose difference within 3% of the maximum dose. In the Table1 prediction and actual values for each dose-painting plan are reported.



# Plans	total MU	predicted delta dose (%)	measured delta dose (%)	difference (%)
1	3596	5,3%	6,0%	-0,7%
2	2294	3,1%	3,5%	-0,4%
3	2091	2,8%	3,0%	-0,2%

**Conclusion**

The results indicate both a good accuracy and good generality of the trained model. ML model seems to be able to predict when a plan solution is deliverable during the planning processes, reducing the number of DQA failures, the re-optimizations due to failing DQA and the number of plans being rejected during the physics plan check because of overmodulation issue.

#### EP-2115 Semi-automated quality assurance of deformable registration in CT radiotherapy data

T. Mcgrath<sup>1</sup>, Z. Lawrence<sup>1</sup>, R. Farhad Salih<sup>1</sup>, Y. Peters<sup>1</sup>, J. Rawling<sup>1</sup>, M. Wilson<sup>2</sup>, C. Piazzese<sup>3</sup>, S. Holloway<sup>2</sup>

<sup>1</sup>The University of Manchester, School of Physics and Astronomy, Manchester, United Kingdom ; <sup>2</sup>University College London, Department of Medical Physics & Biomedical Engineering, London, United Kingdom ; <sup>3</sup>Cardiff University, School of Engineering, Cardiff, United Kingdom

#### Purpose or Objective

A common issue in many medical physics studies is the lack of data available in order to successfully train machine learning algorithms to be able to validate registrations where ground truths are not available. Usually large datasets are required, especially for inference on more intricate structures. The aim of this work was to establish the viability of performing quality assurance on Deformable Image Registration (DIR) through the use of Convolutional Neural Networks (CNNs) in CT images.

#### Material and Methods

A total of 94 head and neck cancer patients' 2D planning CT images converted to 3D Nifty images from The Cancer Imaging Archive (TCIA) were used in this study. Pairwise affine and deformable registrations were performed on this dataset using the open source NiftyReg software package, and the contours of the brain stem, spinal cord, and left & right parotid glands were propagated. A brief grid search was carried out to optimise the bending energy, a penalty term in the optimisation algorithm to avoid overfitting, and control point spacing of the registrations, to ensure a reasonable quality of the registrations. The results were evaluated with commonly used overlap and surface based similarity metrics that measure how well the propagated contour has been transformed compared to the ground truth. Examples of these metrics include the DICE score and the 95th percentile surface distance. Furthermore, a brief viability study was conducted using pre-existing architectures within NiftyNet, by segmenting structures within a 3D CT scan of a patient.

#### Results

Using NiftyReg, 2753 out of a possible 8742 registrations were obtained. The average values of the DICE scores between the ground truth segmentation of the reference image and the propagated contours of the executed registrations were in the range of 0.5 - 0.6. However, there were a significant number of outliers, revealing the abundance of poor registrations and further highlighting the necessity of quality assurance in DIR. For the viability study, the method that provided the best metric values involved training 2D U-Net on 2D slices of the image and for a segmentation of the spinal cord to be generated for each one. The concatenated 3D segmentation was compared to a ground truth contour provided by a clinician by means of the metrics mentioned previously, obtaining a DICE score of 0.92 and a 95th percentile distance of 1.12.

#### Conclusion

To develop the project, the 2D U-Net method could be tested on the other structures to determine the difference in segmentation quality between them. Ideally, a 3D segmentation method would be successfully employed, as the field of medical physics is progressing in that direction. Combined with the registration dataset produced, our research lays the groundwork for continued development of this project.

#### EP-2116 End-to-end dosimetry audits of Stereotactic Ablative Radiotherapy

M. Shaw<sup>1,2</sup>, A. Alves<sup>1</sup>, C. Davey<sup>1</sup>, M. Geso<sup>2</sup>, F. Kadeer<sup>1</sup>, J. Lehmann<sup>3,4</sup>, J. Supple<sup>1</sup>, J. Lye<sup>1</sup>

<sup>1</sup>ARPANSA, Australian Clinical Dosimetry Service, Yallambie, Australia ; <sup>2</sup>RMIT University, School of Health and Biomedical Sciences, Melbourne, Australia ; <sup>3</sup>Calvary Mater Hospital, Radiation Oncology, Melbourne, Australia ; <sup>4</sup>RMIT University, School of Science, Melbourne, Australia

#### Purpose or Objective

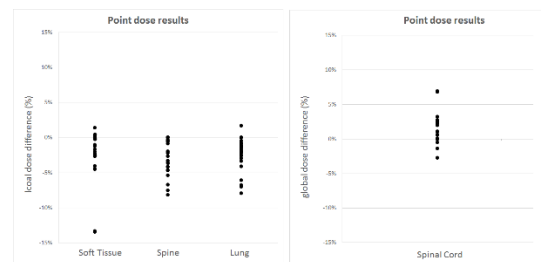
Stereotactic Ablative Radiotherapy (SABR) refers to radiotherapy treatment deliveries which give a high dose of radiation to an extra-cranial tumour, with high geometric precision (1). The risk to patients is increased with SABR techniques due to the increased dose per fraction, and as such specialised planning, treatment and QA practices are needed to ensure patient safety (1). Independent on-site audits are recommended by current SABR guidelines (1-3).

#### Material and Methods

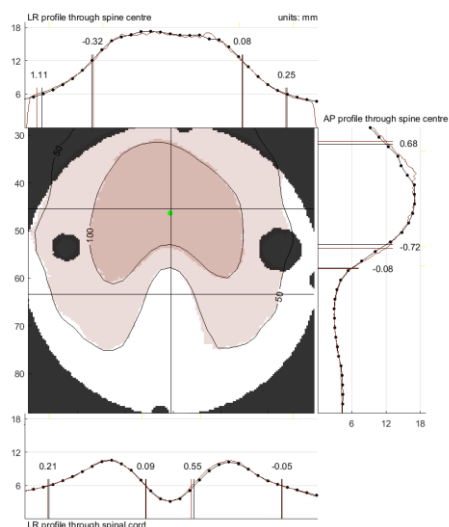
The Australian Clinical Dosimetry Service (ACDS) began SABR audits in March 2018. An end-to-end dosimetry audit was developed using a customised CIRS® humanoid thorax phantom. The audit planning cases include lung, spine and soft tissue targets, with delivery modality being at the discretion of the treating facility. Point dose measurements were taken at the centre of each target volume, and in the spinal cord using a PTW 60019 microDiamond. Gafchromic EBT3 Film measurements were taken and analysed with gamma criteria and distance-to-agreement between planned and measured dose profiles.

#### Results

To date, 59 SABR plans have been included in the audit. Figure 1 shows the local point dose variation for the target measurements and the global point dose variation for the spinal cord measurements. Large variations are seen in the vertebrae hard bone measurement point (average -3.6%, standard deviation 2.4%) and the lung measurement point (average -2.7%, standard deviation 2.4%). The measurements in the spine point in Figure 1 are with the detector calibrated in water. To account for measurement in bone, algorithm dependent Monte Carlo corrections are applied and the average improves to 0.0%, standard deviation 2.3%.



Film localisation accuracy within the phantom has been verified to <0.5 mm. The distance-to-agreement in the sagittal and coronal planes was analysed at the 50% isodose level. Figure 2 shows the results of a VMAT spine plan with maximum discrepancies of -0.08 mm (A-P) and 0.55 mm (L-R).



### Conclusion

The ACDS is developing a comprehensive audit for SABR treatments. Large discrepancies between calculated and measured dose in different medium such as bone are to be further explored.

### References/ Acknowledgements

1. Guidelines for safe practice of stereotactic body (ablative) radiation therapy. Faculty of Radiation Oncology, The Royal Australian and New Zealand College of Radiologists. (2015)
2. Solberg TD, Balter JM, Benedict SH et al. Quality and Safety Considerations in Stereotactic Radiosurgery and Stereotactic Body Radiation Therapy. PRO (2011) 2(1), p2-9.
3. Stereotactic Ablative Body Radiation Therapy (SABR): A resource. UK SABR Consortium. Version 4.0 (2013).

### EP-2117 Novel kV CBCT Imager on Ring Gantry Radiotherapy Unit Permits High Inter-rater Contour Uniformity

L. Henke<sup>1</sup>, B. Cai<sup>1</sup>, S. Rudra<sup>1</sup>, B. Fischer-Valuck<sup>1</sup>, P. Gabani<sup>1</sup>, P. Samson<sup>1</sup>, A. Srivastava<sup>1</sup>, M. Roach<sup>1</sup>, E. Laugeman<sup>1</sup>, J. Luo<sup>1</sup>, S. Mutic<sup>1</sup>, G. Hugo<sup>1</sup>, H. Kim<sup>1</sup>  
<sup>1</sup>Washington University/Barnes Jewish Hospital, Radiation Oncology, Saint Louis- MO, USA

### Purpose or Objective

A novel kV imaging system coupled with a ring gantry radiation treatment system is now commercially available. Improved on-board kV CBCT acquisition time (17-40 seconds) and image quality using this device may allow online adaptive radiotherapy. The purpose of this work was to evaluate the image quality of the on-board kV CBCT as defined by inter-rater contour variability across a spectrum of anatomical structures.

### Material and Methods

Seven patients undergoing routine external beam radiation therapy were enrolled on an IRB-approved, prospective imaging study. Patients were imaged with the ring gantry kV CBCT system at breath hold and/or free breathing. Imaged sites included the head & neck, thorax, abdomen, and pelvis. Patient anatomy was independently contoured by 7 radiation oncology physicians on both the original simulation CT (diagnostic quality) and kV CBCT images. Sequence of contouring was randomized across raters to minimize bias and all kV CBCT images were contoured prior to diagnostic scans to mitigate physician learning of patient anatomy. Inter-rater contour variability was assessed by computing a consensus contour with STAPLE and computing DICE between each individual rater contour and the consensus contour. Inter-rater

uncertainty was computed as the mean DICE over all raters for each organ and patient. Statistical analysis included paired t-testing to evaluate differences between visualization of organs on the planning CT and corresponding kV CBCT images.

### Results

Eighteen organs-at-risk were evaluated across seven patients; a total of 52 kV CBCTs were acquired and contoured by each rater for comparison. The median DICE were 0.85 +/- 0.21 (planning CT), 0.82 +/- 0.11 (breath hold CBCT), and 0.84 +/- 0.11 (free breathing CBCT). Neither breath hold (p=0.14) nor free breathing kV CBCT (p=0.88) were statistically significantly different from planning CT for the inter-rater delineation variability across all organs-at-risk and patients. Limiting to a selection of abdominal organs only, the median DICE values were 0.93 +/- 0.07 (planning CT), 0.93 +/- 0.10 (breath hold CBCT, p=0.53), and 0.92 +/- 0.16 (free breath CBCT, p=0.15).

### Conclusion

Inter-rater ability to delineate organs-at-risk was not statistically different between images acquired on a novel ring gantry kV CBCT unit versus diagnostic quality simulation CT images. Prospective evaluation of the utility of kV CBCT imaging to enable online adaptation applications is.

## E-posters Brachytherapy

### Electronic Poster: Brachytherapy: Breast

### EP-2118 Effects of interfraction uncertainty with Strut Adjusted Volume Implant applicator

K. Miyaoura<sup>1</sup>, T. Fujii<sup>2</sup>, T. Kubo<sup>2</sup>, H. Shinjoh<sup>1</sup>, M. Kato<sup>1</sup>, K. Toyofuku<sup>1</sup>, A. Niiya<sup>1</sup>, R. Kobayashi<sup>1</sup>, Y. Ozawa<sup>1</sup>, K. Murakami<sup>1</sup>, M. Morota<sup>1</sup>, Y. Ito<sup>1</sup>, A. Imai<sup>1</sup>, Y. Kagami<sup>1</sup>  
<sup>1</sup>Showa University, Radiation oncology, Tokyo, Japan;  
<sup>2</sup>Showa University, Department of Radiological technology, Tokyo, Japan

### Purpose or Objective

We started accelerated partial breast irradiation (APBI) after breast conservation surgery using Strut Adjusted Volume Implant (SAVI) from March 2014. As the SAVI applicator does not displace after implantation, planning only at treatment start. However, slight displacement of the SAVI applicator and its influence on the DVH parameter may be considered. We examined changes in the interfraction uncertainty and DVH parameters of the SAVI applicator using daily CT.

### Material and Methods

In this study, we examined 50 patients. We use checking CT for each treatment to confirm that the SAVI applicator is not displaced. Therefore, after contouring the objects to CT, imprinting of the initial plan was performed, and the change of the DVH parameter due to the interfraction uncertainty of the applicator was calculated. The region of interest to be evaluated is a PTV = "PTV\_EVAL" for dose assessment excluding the SAVI catheter, adding 2 mm from the skin side and 0 mm from the chest wall, adding a 3-dimensional margin of 10 mm to the SAVI catheter, Skin = "SKIN", chest wall = "CHESTWALL".

### Results

The average coefficient of variation was "PTV\_EVAL" V 90%: 1.0%, V 150%: 7.2%, V 200%: 8.1%, "SKIN" D 1 cm<sup>3</sup>: 5.6%, "CHEST WALL" D 1 cm<sup>3</sup>: 4.1%. In "PTV\_EVAL", the variation of V90% is small, and the influence by interfraction uncertainty is considered to be small. However, the variation was increased at a higher dose region. "SKIN" was more variant than "CHESTWALL".

### Conclusion

From this study, it was revealed that a change in the dosimetric index of DVH occurs in the interfraction uncertainty of the SAVI applicator. In the future, it is suggested that it is necessary to consider the robustness of the plan from the interfraction change and the necessity of re-planning.

**EP-2119 HDR BRT boost in breast cancer: postoperative vs intraoperative procedure, long-term outcomes**

F. Piro<sup>1</sup>, D. Cosentino<sup>1</sup>, A. Martilotta<sup>1</sup>, A. Massenzo<sup>1</sup>, U. Piro<sup>1</sup>, G. Tocci<sup>1</sup>, L. Marafioti<sup>1</sup>

<sup>1</sup>*Ospedale Mariano Santo, Radiotherapy Center, Cosenza, Italy*

**Purpose or Objective**

To evaluate which is the best BRT technique, we studied the impact on survival and longterm outcomes of two HDRBRT procedure boost: postoperative (POST) vs intraoperative (INTRA).

**Material and Methods**

From January 2001 to February 2005, 75 pts. with breast cancer were treated with intraoperative (29) or postoperative (46) implant consisting of 3 fractions of 350 cGy each, 6 hour apart, before or after Whole Breast Radiotherapy (50 Gy/5 weeks). To provide coverage of tumor bed implant done with afterloading catheters at the time of quadrantectomy or after the external beam. All pts. underwent CT to evaluate the needles insertion according this criteria: 3 cm at least around surgical cavity (when surgical clips available) or 3 cm around surgical scar in case of postoperative. If intraoperative: clips to mark the walls of the excision cavity same treatment volume. All implants had markers at the extremities of each catheter plus other marker on the apex of the implant out of the breast (skin points). Implants planned with a semi-3-D technique aided by simulator, target volume determined by surgical clips and dose to the skin by the catheter markers. Survival comparison with Kaplan Meier method

**Results**

Median follow up: 8,2 years (1-16 years). Age: median 57 (26-77). Survival comparison median 10,24 years (POST) vs median 2.74 (INTRA) P=0.95 (not significant). In POST group 11/46 pts. (24%) had relapse or metastasis vs INTRA 8/29 (27%). The rate of relapse: 6.5 INTRA vs 6.8 POST. Lymph node status (guidelines of ABS not available at the time of treatment) for relapse or metastasis not significant. Ten years local relapse-free rate was 90 INTRA vs 89% POST.

**Conclusion**

Comparing these different boost techniques we did not find any difference in loco-regional recurrence, in metastasis-free and overall survival. Although it is preferable to perform intraoperative boost, these data show that postoperative mode, if properly performed according to the guidelines, is alternative to the first one. Also the treatment volumes should not be underestimated. INTRA is easier to carry out.

**EP-2120 Analysis of our Accelerated Partial Brachytherapy Irradiation (APBI) learning curve**

S. Pinto<sup>1</sup>, A. Pereira<sup>1</sup>, P. Fernandes<sup>2</sup>, L. Trigo<sup>2</sup>

<sup>1</sup>*Instituto Português de Oncologia do Porto Francisco Gentil- EPE, Medical Physics, Porto, Portugal;* <sup>2</sup>*Instituto Português de Oncologia do Porto Francisco Gentil- EPE, Brachytherapy, Porto, Portugal*

**Purpose or Objective**

To analyse our learning curve of APBI treatments with multi-catheter image-guided brachytherapy (BT), based on the experience obtained with the 60 initial applications.

**Material and Methods**

We changed the APBI treatment technique in November 2016 from an applicator-based planning (with a dosimetry based on isodose curves according to the Paris system without an imaged target volume - theoretical plan with rigid needles), to a volume-based planning (with target volume and OAR contouring, as well the reconstruction of plastic catheters in a CT image). Following GEC ESTRO<sup>(1)(2)</sup>, ABS<sup>(3)</sup> and ASTRO<sup>(4)</sup> recommendations for the implant technique and the AAPM TG43 formalism for the dosimetry, all plans were made with inverse planning (IPSA) and, when necessary, with graphical optimization, in Oncentra Brachy (version 4.5.3 - Elekta). Patients were treated with a high dose rate (HDR) modality (8 fractions, 2 per day, with 32Gy of prescribed dose) in a microSelectron from Elekta, with a difference of at least 6 hours between the fractions. To evaluate our learning curve, the patients were chronologically divided into three groups of 20. The following parameters were analysed: V<sub>PD</sub>, V<sub>1.5xPD</sub>, V<sub>PTV</sub>, V<sub>100</sub>, V<sub>150</sub>, V<sub>200</sub>, DHI, COIN, dose to the skin (0.2cm<sup>3</sup> and 1cm<sup>3</sup>, defined 5mm below the body contour), and the number of implanted tubes.

**Results**

The following table shows the analyzed dose-volume parameters and the recommended limits.

**Conclusion**

Regarding the parameters related to the target coverage (V<sub>100</sub> and COIN), a significant improvement was observed over time. Regarding the parameters related to the implant (V<sub>PD</sub>, V<sub>1.5xPD</sub> and DHI), a loss in homogeneity and the consequent appearance of high dose points (V<sub>200</sub>) was observed over time. Following recommendations, an improvement in the homogeneity of our implants and a better compromise between all parameters involved (target coverage, dose homogeneity, excessive dose volumes and dose in the OAR) should be achieved. It is noteworthy that the skin dosimetric values have always remained well below the recommended limits. Our dosimetric quality indices evolution shows that we are on the right track.

**EP-2121 Intraoperative radiotherapy in early breast cancer: short-term outcomes**

J.R. Oliver<sup>1</sup>, E. Hernando Almudi<sup>1</sup>, C. Casamayor Franco<sup>1</sup>, C. Vallejo<sup>1</sup>, G. Molina Osorio<sup>2</sup>, A. Miranda Burgos<sup>2</sup>, M. Lanzuela Valero<sup>2</sup>, R. Ibáñez Carreras<sup>2</sup>

<sup>1</sup>*Hospital Universitario Miguel Servet, General Surgery, Zaragoza, Spain;* <sup>2</sup>*Hospital Universitario Miguel Servet, Radiation Oncology, Zaragoza, Spain*

**Purpose or Objective**

The aim of this abstract is to evaluate the short-term outcomes of using Intraoperative radiotherapy (IORT) in early breast cancer in our center.

**Material and Methods**

A prospective review was performed. 233 cases of early breast cancer were treated with breast conserving surgery (BCS)/oncoplastic surgery and IORT from 13/05/2015 to 16/08/2017. A low energy X-rays system (Axxent Xofter device) administered a 20-Gy dose at the tumor bed.

All patients were evaluated by a multidisciplinary Tumor Board. Selection criteria for IORT as radiotherapy alone were: age ≥50 y.o., no BRCA mutations, clinical tumor size up to 3cm, none linfovacular invasion, ER +, not multicentric or multifocal tumors, histology of IDC, cN0 and no neoadjuvant therapy.

The rest of the patients who did not meet the criteria were finally treated with IORT as a boost.

Clinical and radiological evaluations (ultrasound and mammographic exams) were performed routinely. Complications reported are: dermatitis, hematoma, seroma, infection, pain, fibrosis / fat necrosis, ulcer and fistula (delayed healing of a small side of the surgical wound).

## Results

During the study period, 233 patients were treated with BCS/oncoplastic surgery and IORT: 218 (93.6%) patients as monotherapy, 12 (5.1%) patients as a boost, and 3 (1.3%) patients were treated out of protocol, accepted by the Tumor board because of comorbidities, elderly and social issues.

Patients: mean age 67 y.o. (48.2-88.9)

Histology: IDC 205 (88.0%), ILC 8 (3.4%), other subtypes of IDC 20 (8.6%). ER + 225 (91.0%). HER-2/neu 3+ or SISH+ 7 (3.0%). Ki 67 >15% 160 (68.7%).

Surgery: average IORT time 11.2 min (9.5-16.5), average operation time 150.5 min (65-315). BCS 219 (94.0%), oncoplastic surgery 14 (6.0%).

SLNB 224 (96.1%): positive (micrometastases or macrometastases) 64 (28.3%)

Reinterventions 20 (8.6%): rescission 6 (2.6%), MRM 1 (0.4%), ALND 5 (2.1%), complications 8 (3.5%).

Adjuvant therapy: chemotherapy 50 (21.5%), hormone-therapy 220 (94.4%), EBRT 65 (27.9%).

Oncologic outcomes: local recurrences 3 (1.3%). Metastases (liver, bone) 2 (0.9%).

Major complications: RTOG 3-4: 2 (1.0%), seroma that required >3 drainages 2 (0.9%), infection that required intravenous antibiotic or surgical drainage 4 (1.7%), hematoma that required surgical drainage 4 (1.7%), fistula that required surgical fixing 4 (1.7%), palpable fibrosis 14 (6.1%).

Median follow up: 857.5d (215-1210). Cancer related mortality: 0. Non cancer related mortality 7 (3.0%).

## Conclusion

IORT is a feasible technique with several benefits and good short-term outcomes in selected patients.

**EP-2122 Outcome of exclusive RT for BC in older women according to age and comorbidity: A retrospective study**  
W. Lorraine<sup>1</sup>, K. Cao<sup>1</sup>, M. Carton<sup>2</sup>, A. Fourquet<sup>1</sup>, Y. Kirova<sup>1</sup>

<sup>1</sup>Curie institute, Radiotherapy, Paris, France; <sup>2</sup>Curie Institute, Biostatistics, Paris, France

## Purpose or Objective

Older women with breast cancer (BC) are less likely to receive standard care. In specific circumstances when surgery is omitted as first step of treatment, RT seems to be an adequate local solution as a non-invasive option. The aim of this study was to assess the efficacy, tolerance and impact of comorbidities on outcomes in older women treated by exclusive radiation therapy (RT) for non-metastatic breast cancer (BC)

## Material and Methods

We studied retrospectively women aged  $\geq 70$  years at diagnosis who received exclusive conformational RT for their BC between 2003 and 2012 in our Department. We calculated the Charlson Comorbidity Index (CCI) for each patient. Conventionally fractionated or hypofractionated RT was prescribed at the physician's discretion in a case-by-case basis. We analysed overall survival (OS), progression free survival (PFS), and specific survival (SS). Acute and late toxicities were assessed according to the Common Terminology Criteria for Adverse Events (CTCAE) v3.0.

## Results

On sixty-six patients included, median age was 84.8 years [71.3-91.7]. Most patients had a CCI score  $\geq 1$  (n = 41, 62.1%). Nearly half (47%) had T1-2N0M0 BC (n = 31). Surgery was omitted in most cases because of patients' refusal (54.2%) and/or patients' comorbidities (41.7%). Most of them (87.9%) were treated by hypofractionated RT and received hormonal therapy for their HR+ HER2- BC (84.8%). With a median follow-up of 6.8 years [1.3-12.3], OS, SS and PFS at 5 years were 65.5% CI95%[54.1-79.3], 86.3% CI95% [77.2-96.4], and 58.4% CI95%[46.9-72.7], respectively. Five-year OS was statistically different according to age younger or older than 85 years: 72.9%

CI95% [58.4-91.1] and 57.1%, IC 95% [40.8-79.8], (p = 0.0026). Similar results were found for 5-year PFS: 64.5% CI95% [49.5-84.1] for patients aged from 70 to 85 years, and 51.6% CI95% [35.8-74.5] for patients over 85 years old, respectively (p = 0.014). The 5-year OS was also statistically different according to the CCI score: 70.8% CI95% [57.0-87.9] for a CCI of 0, and only 59.8% CI95% [42.4-84.3] for patients with a CCI Score  $\geq 1$  (p = 0.039). 10.6% of the patients had no toxicities; of those who experienced side effects, the most frequent were grade 1 and 2 radio dermatitis (59%). Late toxicities were observed in 39.4% of the patients, mostly of grade 1 and 2. No late toxicity of grade  $\geq 3$  was observed.

## Conclusion

Exclusive radiation therapy for non-metastatic BC in older women is feasible and well-tolerated when adapted techniques are used, but the prognostic is poor in comparison with younger patients as the outcome is strongly impacted by age and comorbidities.

**EP-2123 APBI with Interstitial Brachytherapy versus Whole-Breast Irradiation for Early-Stage Breast Cancer**

A. Figueiredo<sup>1</sup>, D. Delgado<sup>1</sup>, J. Santos<sup>1</sup>, A. Florindo<sup>1</sup>, V. Mendonça<sup>1</sup>, M. Jorge<sup>1</sup>, M. Filomena de Pina<sup>1</sup>

<sup>1</sup>Centro Hospitalar Lisboa Norte, Serviço de Radioterapia, Lisboa, Portugal

## Purpose or Objective

To report long-term outcomes of adjuvant accelerated partial breast irradiation (APBI) with multicatheter interstitial high dose rate brachytherapy (HDR BT) at our department and compare these results to adjuvant whole-breast irradiation (WBI) with 3D external beam radiotherapy (EBRT).

## Material and Methods

Between 2004 and 2017, 25 patients (pts) with early-stage breast cancer (pT1-2 ( $\leq 30$  mm) pN0) were treated with interstitial HDR BT after breast-conserving surgery. The characteristics of these pts are presented in table 1. The prescribed dose was 8 fractions of 4 Gy, twice a day, in all patients. A propensity-score matching approach was performed to compare the survival outcomes of APBI to WBI using a database of 260 pts treated with adjuvant WBI at our center.

DEMOGRAPHIC DATA	
Median age (range)	74 (51-81)
CLINICAL DATA	
Histology	
Invasive Carcinoma	20 (80 %)
G1	10 (40 %)
G2	10 (40 %)
Ductal Carcinoma in Situ	5 (20 %)
Low-grade	2 (8 %)
Intermediate-grade	1 (4 %)
Not determined	2 (8 %)
T stage	
Median tumour size (range)	9 (5-30 mm)
pTis	5 (20 %)
pT1a	3 (12 %)
pT1b	13 (52 %)
pT1c	1 (4 %)
pT2	3 (12 %)
Hormone Receptors	
Positive	24 (96 %)
Negative	1 (4 %)
Ki-67	
< 15%	13 (52 %)
≥ 15%	2 (8 %)
Not determined	10 (40 %)
HER2	
Positive	0 (0 %)
Negative	18 (72 %)
Not determined	7 (28 %)
Lymphovascular invasion	
Present	1 (4 %)
Absent	16 (64 %)
Not determined	8 (32 %)
Surgical procedure	
Lumpectomy	21 (84 %)
Quadrantectomy	4 (16 %)
Axillary procedure	
Sentinel Lymph Node Biopsy	17 (68 %)
Axillary Lymph Node dissection	6 (24 %)
None	2 (8 %)
Surgical margin status	
Free	18 (72 %)
Involved	0 (0 %)
Not determined	7 (28 %)

*Table 1: demographic and clinical data of APBI group*

## Results

The median follow-up was 81 (3-167 months). There were no significant differences between the APBI and WBI groups in terms of age, stage, immunohistochemical analysis (hormone receptors, HER2, Ki-67), surgical margins, lymphovascular invasion and use of adjuvant hormone therapy. The 5-year recurrence-free survival and overall survival were 91.7 % and 100 %, respectively. No significant difference of recurrence-free ( $p=0.564$ ) and overall ( $p=0.113$ ) survival was found. The treatment with APBI was well tolerated with no late toxicity reported in 60 % of pts. Breast edema and fibrosis were the main

toxicities observed, but no grade 3 toxicity or higher was described.

## Conclusion

Several prospective trials demonstrated that the majority of local recurrences (69-90 %) arises at the vicinity (1-2 cm) of the tumor bed. Given that it seems rational the use of more conformational techniques with APBI. These techniques allow to spare organs at risk (heart, lung, chest wall and contralateral breast) without compromising the excellent survival outcomes in breast cancer, which is supported by recent results of randomized clinical trials. The interstitial HDR BT is the technique with the longest clinical experience and with strong evidences of non-inferiority in comparison with the standard WBI. These results are in line with our one-institutional analysis with the use of a propensity-score matching methodology. Careful selection of the pts who are most likely to benefit from such approach is crucial for the success of the treatment.

## Electronic Poster: Brachytherapy: Gynaecology

### EP-2124 Brachytherapy in the treatment of locally advanced cervical cancer: a single center study

J. Khalil<sup>1</sup>

<sup>1</sup>National Institute of Oncology Sidi Mohamed Ben Ab, Radiotherapy, Rabat, Morocco

#### Purpose or Objective

Concurrent chemoradiotherapy in combination with brachytherapy is the standard treatment of locally advanced cervical carcinoma. Brachytherapy has, in fact, become an integral component of cervical cancer treatment as it confers many dosimetric benefits insuring better local control and survival rates when compared to external beam radiation alone. Lately, a decline in brachytherapy use has been noticed either because of the lack of expertise or because of the radiation oncologist's trend to replace brachytherapy with the newest radiotherapy techniques. The aim of our study is to evaluate the role of brachytherapy as a boost technique in locally advanced cervical carcinoma.

#### Material and Methods

Our study is a retrospective one including 387 patients treated for locally advanced cervical carcinoma, between January 2007 and December 2007, in the national institute of oncology Morocco. 179 patients received external beam pelvic irradiation combined with brachytherapy, while 208 patients were treated with external beam radiotherapy alone (EBRTA).

#### Results

The mean age for the whole group was 47.7 (range 26-78 years), and the median age was 46 years, there was no significant difference between the two groups. The past medical history was also identical between the two groups. All patients received their treatment in our institution during the same time period, and by the same specialized gynecologic oncologists and radiotherapists. Differences between the two groups concerned tumor stage, tumor size, treatment doses and time duration. Local control rate at 5 years was of 80.7% in the brachytherapy group and 56.8% in the EBRTA arm (Pearson chi-square;  $p < 0.0001$ ). As to survival rates, there was a statistically highly significant difference in all of 5-year overall survival (73% and 57.3% for brachytherapy and EBRTA arms respectively,  $p < 0.001$ ), cancer-specific survival (63.5 % for the brachytherapy group and 47.6% in the EBRTA group,  $p=0.002$ ), and disease-free survival (log-rank test;  $p < 0.00001$ ). Patients in the brachytherapy arm showed less treatment related toxicities.

#### Conclusion

Our results are concordant with those previously reported in the literature and stating that brachytherapy should still

be considered as a standard of care in the treatment of locally advanced cervical carcinoma

#### EP-2125 High Dose Rate Brachytherapy in Brazil: Demand Estimation and Coverage in Public Healthcare System

G.H. Yoshinari<sup>1</sup>, M.P. Alvarenga<sup>1</sup>, H.H. Fernandes<sup>1</sup>, F. Nadur<sup>2</sup>, J. Domingues<sup>2</sup>, H.F. De Oliveira<sup>1</sup>  
<sup>1</sup>Hospital Marcio Cunha, Servico De Radioterapia, IPATINGA, Brazil; <sup>2</sup>Faculdade de Medicina de Itajuba, Graduação em medicina, Itajubá, Brazil

##### Purpose or Objective

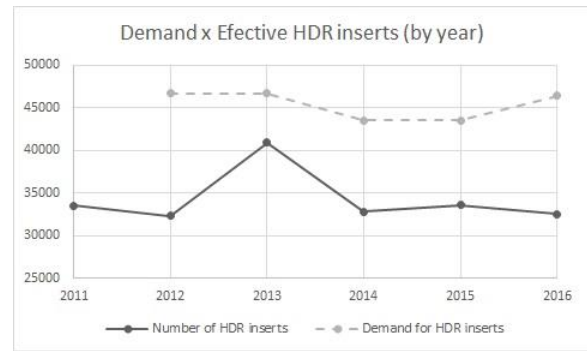
The Public Healthcare System (SUS) in Brazil allows high dose rate brachytherapy (HDR) for cervical and uterine cancers only. Objective: to characterize and compare the installed capacity and estimate the demand for HDR in the context of the public access.

##### Material and Methods

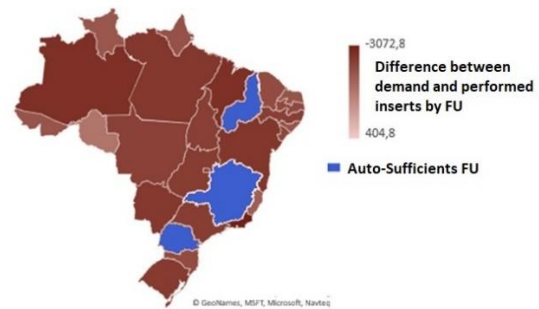
The number of services and HDR insertions is available in the SUS database. The official estimation of incidence for cervical and uterine malignancy by Federative Unit (FU) from 2011 to 2016 in a two-year basis was adjusted for the proportion of patients with HDR indication and the number of HDR insertions covered by SUS. We also compared the estimated demand for HDR inserts with the number of registered services from 2011 to 2016.

##### Results

In 2016, forty-five percent of all public radiotherapy services provided HDR, while four FUs did not offer HDR. There is a concentration in offer in the Southeast region (55%) which concentrates 38.6% of Brazil's population. For the year, the estimated demand for HDR insertions in the year was 46,400, but only 32,500 inserts were registered, generating a deficit of 13,900 inserts (coverage of 70%), even though 25% of the population afford private health insurance. Only three FUs met the estimated demand. We observe a tendency of decrease in the incidence of cervical cancer and a slight increase in the incidence of endometrial cancer, with an increment of services offering HDR in the past five years. Overall demand for HDR remained stable for the period. We detected a peak (superior to Median+2SD) of procedures registered in 2013 (40,939) for an expected need of 46,724 inserts, influenced by inserts carried out by only one FU (São Paulo). The cause of the peak of registered procedures carried out in São Paulo in 2013 should be investigated since it appears to be possible to increase the number of procedures without increasing the number of services providing HDR. There were no peaks detected in the estimated demand for HDR nor services offering the procedure in SUS.



Demand and Performed HDR inserts for 2016



##### Conclusion

Besides the consistent increase of services providing HDR in SUS the distribution of services along the country seems inadequate. There is a 30% deficit in the estimated demand coverage for HDR.

#### EP-2126 Cervix cancer treatments with electronic brachytherapy according to the EMBRACE protocol

S. Lozares<sup>1</sup>, A. Gandía<sup>1</sup>, J.A. Font-Gómez<sup>1</sup>, D. Villa<sup>1</sup>, A. Mendez<sup>2</sup>, A. Miranda-Burgos<sup>2</sup>, V. Alba-Escorihuela<sup>1</sup>, S. Jiménez-Puertas<sup>1</sup>  
<sup>1</sup>H.U. Miguel Servet, Física y Protección Radiológica, Zaragoza, Spain; <sup>2</sup>H.U. Miguel Servet, Oncología Radioterápica, Zaragoza, Spain

##### Purpose or Objective

In this study we present the first cervical cancer cases treated with interstitial electronic brachytherapy (eBT) in our hospital compared to plans made with high dose rate interstitial brachytherapy with Ir192.

##### Material and Methods

In our centre, 8 patients with cervical cancer have been treated with the Axxent (Xoft, Inc.) eBT equipment. The planning of all the patients has been carried out with MR image and CT image following the recommendations of the EMBRACE protocol. The dosimetric parameters of the recommended OAR for bladder, rectum and sigma have been evaluated: D2cc, D1cc, D0,1cc. In addition, the V150 and V200 of irradiated tissue are compared for each plan, both eBT and HDR-BT. The mean age of the patients was 59.8 years (27-70) with different tumor stages, all with good response to external radiotherapy and no parametrial involvement. All patients received IMRT with a regimen of 23 sessions of 2 Gy followed by 4 sessions of 7 Gy of eBT performed in two weeks (first two sessions and then another two a week later) following the EMBRACE recommendations.

##### Results

The doses in organs at risk for electronic brachytherapy plans were lower than for HDRBT plans. The dose in bladder with electronic brachytherapy was 62.8% of the prescribed dose for D2cc vs. 63.7% for HDRBT Ir 192, for D1cc was 69.7% vs. 70.1% and for D0.1cc was 85.4% vs. 84.9%. In rectum the D2cc was 27% vs. 34.3%, for D1cc was

32.9% vs. 39.5% and for D0.1cc was 52.4% vs. 46.7% and in sigmoid colon the D2cc was 49.5% vs. 53.6%, for D1cc was 57.7% vs. 61.5% and for D0.1cc was 78% vs. 81.9%. The results demonstrated lower doses to risk organs in all electronic brachytherapy plans. The acute toxicity for electronic brachytherapy in cases of mucositis was two cases with grade 1 toxicity and one case with grade 2 toxicity, without cases of rectal toxicity and one case with grade 1 urinary toxicity and no relapses have occurred to date.

#### Conclusion

The first results of treatment with the Axxent eBT unit for the 8 patients are very promising, as no recurrence has been observed and the toxicity of the treatment is very low. Despite the increase in V150 and V200 there has been no increase in the toxicity of the vaginal mucosa, and the doses in the OAR are lower than in the implemented plans of HDR-BT with Ir192. Electronic brachytherapy is a good alternative for treating cervical cancer in centers without the availability of conventional HDR. To date, there are few published studies reporting on the outcomes of patients treated with electronic brachytherapy, and none on patients treated for cervical cancer.

#### EP-2127 Hydrogel bladder and rectal spacer (TraceIT) for brachytherapy in locally advanced Cervical cancer

D. Najjari Jamal<sup>1</sup>, C. Gutiérrez<sup>1</sup>, L. Martí<sup>2</sup>, S. Marin<sup>1</sup>, A. Stocker<sup>1</sup>, G. Rodriguez<sup>1</sup>, S. Moreno<sup>3</sup>, M. Garcia<sup>1</sup>, F. Guedea<sup>1</sup>

<sup>1</sup>ICO Hospitalet, Radiation Oncology, Hospitalet de Llobregat, Spain; <sup>2</sup>Hospital de Bellvitge, Gynaecology, Hospitalet de Llobregat, Spain; <sup>3</sup>ICO Hospitalet, Physics, Hospitalet de Llobregat, Spain

#### Purpose or Objective

Treatment for locally advanced cervical cancer (LACC) comprises concomitant radiochemotherapy (RCHT) followed by brachytherapy (BT). Assessment of toxicity is important in radiotherapy, since is necessary to define therapeutic ratio and determine the specific benefit of a given treatment. The injection of an hydrogel to space the bladder and rectum from cervix may help to organ-at-risk (OaR) sparing during BT treatment and therefore reach higher doses to the D90 in the HR-CTV to improve local control. The aim of this study, therefore, is to place the hydrogel around cervix and evaluate the benefit on the plan dosimetry at time of BT. Appropriate approvals by local ethic committee was obtained.

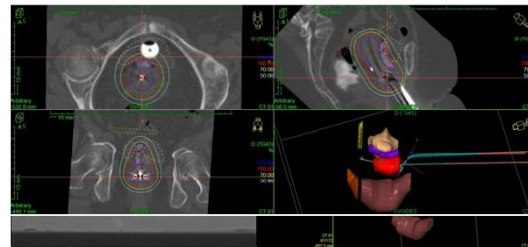
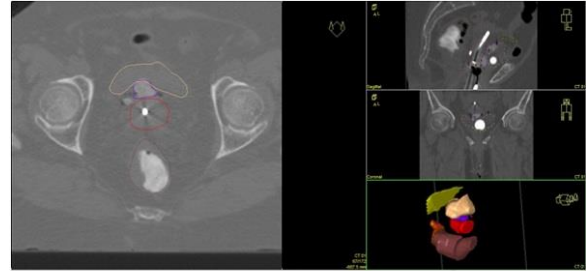
#### Material and Methods

The preliminary prospective study includes 3 patients diagnosed with LACC and treated with concomitant radio(chemo)therapy + IGABT. The radio-opaque hydrogel (TraceIT) is placed between rectum-cervix and bladder-cervix after conclude RCHT and at time of BT. We approached the technique using transrectal ultrasound (TRUS) and transvaginal injections. A stepper was used to stabilize the image and allow two hands to manipulate the needle and the speculum. A hydro-dissection technique with saline was used to open the space to advance the needle into this space 1cm at a time. Injection of 3-6ml of TraceIT created the space around cervix and bladder. The distance from cervix to OaR was measured before and after the hydrogel injection in CT-scan and (TRUS). At time of BT the distance was measured again in TRUS. A total nominal dose of 21Gy in 7Gy/fraction with HDR was prescribed. The D2cc for bladder and rectum and EQD2 (OaR alpha/beta=3 and tumor alpha/beta=10) HR-CTV D90 were calculated.

#### Results

TraceIT placement was performed in 2 of the 3 selected patients. The third patient was not a good candidate due to pouch of Douglas prolapse. The 2 performed cases were diagnosed with stage IIB cervical cancer. Before BT, the first patient had complete response and de second patient a partial response with more than >50%. At time of BT,

TraceIT was placed between cervix and bladder. A space of 8x20x38mm and 13x39x31mm (APxLLxCC), respectively, in each patient was created (Figure 1). The bladder D2cc were 6.20Gy and 5.11Gy, respectively, with a HR-CTV D90 >85Gy EQD2 in both cases (Figure 2).



#### Conclusion

TraceIT injection is easily reproducible in the 2 cases. In addition, the hydrogel can be easily identified in both MRI and CT-planning for BT. Compared to historical controls the rectum and bladder D2cc were lower without decreasing the HR-CTV D90 dose. Therefore, TraceIT can help to improve the dosimetry in IGABT for LACC and may help to raise the dose to D90 HR-CTV>85Gy without increasing the dose in bladder. No acute symptoms were described. Further investigations are needed to improve the technique and to perform rectum-cervix placement and furthermore to evaluate the benefit of TraceIT in dosimetry improvement at time of BT.

#### EP-2128 Rectal toxicity with MUPIT Interstitial Brachytherapy - Predictors, clinical and dosimetric outcomes

V. Pareek<sup>1</sup>, R. Bhalavat<sup>2</sup>, M. Chandra<sup>2</sup>, C. Bakshi<sup>3</sup>, N. Bhambhani<sup>4</sup>

<sup>1</sup>Jupiter Hospital, Radiation Oncology, Mumbai, India;

<sup>2</sup>Jupiter Hospital, Radiation Oncology, Thane, India;

<sup>3</sup>Jupiter Hospital, Medical Oncology, Thane, India;

<sup>4</sup>Jupiter Hospital, Surgical Oncology, Thane, India

#### Purpose or Objective

Late rectal toxicities are a concern associated with Interstitial Brachytherapy for various indications in pelvic malignancies. In this study we evaluate the rectal toxicities associated and look in to the clinical correlation with the predictive factors associated with such toxicities associated with high dose rate pelvic interstitial brachytherapy.

#### Material and Methods

From January 2010 to December 2016, 35 patients with residual or bulky cervical disease and vaginal vault recurrence were included in the study. Patients received

external radiation 50 Gy in 25 fractions over 5 weeks with weekly cisplatin. Rectum and rectal mucosa were delineated along with other organs at risk. The dose received by 0.1, 1, 2, 5 cc of rectum, RM, and sigmoid were assessed for dosimetric analysis. The 2Gy equivalent dose was evaluated for all the organs at risk. With assessment and grading of toxicities on the follow up, the predictive factors associated with rectal toxicities with brachytherapy were assessed using univariate analysis. The Coverage Index (CI), dose homogeneity index (DHI), overdose index (OI), dose non-uniformity ratio (DNR), external volume index (EI), conformity index (COIN) and dose volume parameters recommended by GEC-ESTRO were evaluated. The patients were followed up and toxicities were graded as per the RTOG scales and local control rates and disease-free survival were evaluated.

#### Results

The median follow-up of the patients was 30 months and grade II and grade III toxicities were seen in 5 (14.2%) and 1 (2.8%) patient respectively. The mean CTV volume was 154 cc. The median number of needles was 18 (Range 15 - 20). Median CI, DHI, V150, V200, DNR, OI, EI and COIN was 0.81 (range: 0.74 - 0.87), 0.7 (range: 0.59 - 0.79), 81cc, 29 cc, 0.42 (range: 0.25 - 0.47), 0.07 (range: 0.05 - 0.14), 0.12 (range: 0.06 - 0.16) and 0.81 (range: 0.69 - 0.89). On Univariate Analysis, D0.1-cc Rectal Mucosa dose >70 Gy ( $p = 0.02$ ), D1-cc Rectal Mucosa dose >67 Gy ( $p < 0.001$ ), D2-cc Rectal Mucosa dose and D5-cc Rectal Mucosa dose >60 Gy ( $p = 0.001$ ) correlated with Grade  $\geq$  II toxicity. The 2Gy equivalent dose for D2 cc rectum and rectal mucosa associated with 10 and 20% risk of rectal toxicity were found to be 56 and 67Gy and 54Gy and 64Gy respectively.

#### Conclusion

CT based planning using MUPIT for gynecological brachytherapy implants has good outcomes as assessed in our study. Plan evaluation and documentation using various indices and parameters recommended by GEC-ESTRO assist in objective evaluation and reproducibility and correlate with clinical outcomes in the disease. Limiting 2-cc RM and rectal doses within the proposed thresholds can minimize Grade  $\geq$  II toxicity for gynecological high-dose-rate interstitial brachytherapy.

#### EP-2129 A decision tool for interstitial needles implants in uterovaginal pulsed dose rate brachytherapy

M. Sandt<sup>1</sup>, F. Gassa<sup>1</sup>, P. Pommier<sup>1</sup>

<sup>1</sup>Centre Léon Bérard, Radiothérapie, Lyon, France

#### Purpose or Objective

Implants of interstitial needles (IN) in uterovaginal brachytherapy treatments has proved its efficiency in case of parametrial invasion<sup>[1],[2]</sup>. The aim of the present study is to analyze patient anatomy and to determine cases where interstitial needles implants could help to cover the high-risk volume.

#### Material and Methods

Fifteen patient plans with interstitial needles were considered. On MRI or CT images post implantation, following dimensions were reported: the smallest distance between uterin probe and the nearest organ at risk in the anterior direction (frequently the bladder), and secondly the biggest lateral dimension between uterin probe and the edge of high-risk CTV. The ratio of these two values is called  $r$ . PDR dose plans were calculated and optimized on Oncentra® TPS using the same dosimetric method by a single operator, with and without needles activation. CTV coverage (D90 of CTVHR and CTVIR) and organ at risk near-maximum doses (D2cc for bladder, rectum and sigmoid) were reported and compared.

#### Results

Doses comparison of CTV coverage showed that  $r=2$  is a threshold. Wilcoxon test for paired samples reveals that

below this value, IN implant did not significantly improve CTV coverage. But for cervix uteri for which  $r$  is higher than 2, IN implant was a great help to increase CTV doses (D90 of CTVHR increases by an average of 16Gy, and D90 of CTVIR by an average of 9,2Gy -  $p=0.00195$ ), without significant variation of doses received by OARs ( $p>0,2$ ).

#### Conclusion

Interstitial needles implants can improve target volumes coverage when the high risk volume presents a  $r$  ratio higher than 2, with no change on organ at risk near-maximum doses.

#### EP-2130 Dose integration of intensity-modulated arc therapy and interstitial brachytherapy of cervix cancer

G. Fröhlich<sup>1</sup>, J. Vizkeleti<sup>1</sup>, N. Anhhong Nguyen<sup>1</sup>, T.

Major<sup>1</sup>, C. Polgár<sup>1</sup>

<sup>1</sup>National Institute of Oncology, Centre of Radiotherapy, Budapest, Hungary

#### Purpose or Objective

Comparative analysis of EQD2 total doses resulted with intensity-modulated arc therapy (IMAT) complemented with image-guided adaptive interstitial brachytherapy (ISBT) versus conventional treatment techniques in cervix cancer using a personalised biological dose integration method.

#### Material and Methods

21 locally advanced cervical cancer patients, treated with IMAT with 2 full arcs plus manual optimised ISBT, were selected. Additional plans were created: conformal teletherapy (TT) plans and inverse optimised interstitial (is.), optimised intracavitary (ic.), non-optimised ic. brachytherapy (BT) plans. Since neither the rigid nor the deformable image registration result appropriate fit of interested volumes in the proximity of the applicator, manual registration method is needed. As the critical organs receive the maximal total dose in the region where the dose maximum is in BT, the most exposed 2 cc volume (D2) of bladder, rectum and sigmoid in BT were identified manually on TT CT images individually for every patient. Biological total doses (EQD2) of these volumes were calculated and compared between each combination of TT and BT plans using 2-way ANOVA and Fisher-LSD post hoc test. This dose integration method was compared with the GEC-ESTRO recommended method, uniform dose conception (UDC) in IMAT and conformal TT plans with Wilcoxon-matched pairs test.

#### Results

The D90 of High-Risk CTV, D2 of bladder and sigmoid were different in BT techniques only:  $p=0.0149$ ,  $<0.001$ ,  $<0.001$ , respectively. The most advantageous values were obtained in the manual optimised ISBT plans, inverse optimised is. plans did not differ dosimetrically from these, while optimized ic. plans resulted in worse dose-volume parameters, and the worst of all were ic. plans without optimization. The D2 of rectum was significantly lower with IMAT than with conformal TT plans ( $p=0.037$ ) and showed the same trend in BT plans than the other parameters ( $p<0.001$ ) (Table). The UDC dose summation method overestimates D2 of the bladder with 12% and 8.5%, the rectum with 55% and 26.5% and the sigmoid with 17.2% and 12% in the case of IMAT and conformal TT plans, respectively ( $p<0.001$  for all).

Table:

EQD2		Manual	Inverse	Manual	Non-	p*	p* (BT)
		opt. is. BT	opt. is. BT	opt. ic. BT	optimised ic. BT		
D90 (HR-CTV) (Gy)	IMAT	84.6	84.3	82.2	88.7	0.9899	0.0149
	Conf. TT	84.6	84.3	82.2	88.7		
D <sub>2</sub> (bladder) (Gy)	IMAT	62.9	62.5	71.5	88.4	0.434	<0.001
	Conf. TT	64.9	64.6	73.6	90.5		
D <sub>2</sub> (rectum) (Gy)	IMAT	40.0	38.4	44.9	72.1	0.037	<0.001
	Conf. TT	49.0	47.3	53.8	81.1		
D <sub>2</sub> (sigmoid) (Gy)	IMAT	55.3	54.4	60.5	71.2	0.2794	<0.001
	Conf. TT	57.9	56.9	63.5	73.8		

Table. Mean EQD2 total doses of different combinations of BT and TT plans. IMAT:

intensity-modulated arc therapy, Conf. TT: conformal TT, is.: interstitial, ic.:

intracavitary BT plans. D90: the minimum dose delivered to 90% of HR-CTV,

D<sub>2</sub>(bladder), D<sub>2</sub>(rectum), D<sub>2</sub>(sigmoid): the minimal dose of the most exposed 2

ccm of bladder, rectum and sigmoid. \*2-way ANOVA and Fisher-LSD post-hoc

test.

## Conclusion

Although optimization improves the quality of intracavitary BT plans, interstitial plans yield in significantly higher dose coverage of HR-CTV and lower doses to OARs. IMAT plans decrease dose to the rectum. The impact of BT technique for summarised biological total dose of HR-CTV and critical organs is much higher than that of TT. Based on the personalised biological dose integration method, UDC overestimates OARs doses.

## EP-2131 Venezia: New Advanced Brachytherapy Gynecological Applicator in cervical cancer. Our preliminary data

G. Riva<sup>1</sup>, V. Andrea<sup>1</sup>, R. Spoto<sup>1</sup>, S. Durante<sup>1</sup>, D. Ciardo<sup>1</sup>, S. Comi<sup>2</sup>, F. Cattani<sup>2</sup>, R. Lazzari<sup>1</sup>, B.A. Jereczek-Fossa<sup>1</sup>  
<sup>1</sup>Istituto Europeo di Oncologia - IEO, Radiotherapy, Milan, Italy; <sup>2</sup>Istituto Europeo di Oncologia - IEO, Medical Physics, Milan, Italy

## Purpose or Objective

The purpose of this work is to report our recent and preliminary experience with Elekta's Advanced Gynecological Applicator, Venezia™, a new applicator system that allows clinicians to treat different stages of cervical cancer as a hybrid brachytherapy (BT) applicator, combining characteristics of both ring and ovoid devices, with the possibility to perform interstitial BT.

## Material and Methods

Clinical data, BT parameters and acute toxicity (Radiation Therapy Oncology Group RTOG toxicity scale) of consecutive women treated in our institute with Venezia™ were examined.

Pulsed-dose-rate (PDR) was the technique chosen for all the patients. Clinical Target Volume (CTV) coverage and mean dose (D<sub>2cm<sup>3</sup></sub>) to 2cm<sup>3</sup> of bladder, rectum and bowel were assessed. The dosimetric parameters of a series of 10 consecutive patients treated previously at our center with interstitial PDR BT employing other applicators (MUPIT and Utrecht, unpublished data) served as a dosimetry benchmark for the Venezia™ patients. Two-sided Wilcoxon rank sum test was performed for statistical comparison

## Results

Since January 2018 to May 2018, 8 women, median age 51 years (27.2-64.2) affected by cervical cancer were treated with Venezia™. All but one underwent interstitial BT. Median dose prescribed to CTV was 30 Gy (range 30-35) with a median dose rate of 0.6 Gy/h (range 0.5 - 0.6).

Coverage of CTV and dose to organ at risk (OAR) was reported in table 1, along with the dosimetric parameters of PDR BT employing other applicators.

Apart from manageable acute genitourinary and gastrointestinal toxicities (2 patients with RTOG grade 1), no complications grade 3-2 were reported.

	Venezia™ applicator	Benchmark cohort	p-value
	Median (range)	Median (range)	
CTV90(%)	100 (90-108)	114 (102-128)	0.015
D2cm <sup>3</sup> bladder (%)	73 (53-78)	82 (63-93)	<<0.01
D2cm <sup>3</sup> rectum (%)	33 (23-53)	78 (28-90)	0.013
D2cm <sup>3</sup> bowel (%)	66 (17-89)	59 (36-105)	0.9

## Conclusion

The initial experience revealed that BT treatment with Venezia™ was well-tolerated and allows for adequate tumor coverage while satisfying the dose constraints for OARs. It also appears user friendly in positioning and removal time. A larger cohort of patients will be required for additional conclusions related to the long-term clinical benefits and late toxicity.

## EP-2132 Verification of vaginal cylinder position using bony landmarks

M. Zahra<sup>1</sup>, P. Drewell<sup>1</sup>, W. Keough<sup>1</sup>

<sup>1</sup>Edinburgh Cancer Centre, Oncology, Edinburgh, United Kingdom

## Purpose or Objective

To allow rapid assessment at time of treatment of the correct positioning of the vaginal cylinder using bony landmarks

## Material and Methods

A cohort of patients who had planning CT scans for their adjuvant post-hysterectomy vaginal vault brachytherapy also had a verification scan to assess the position of the organs at risk. These scans were reviewed and the distances between the position of the tip of the cylinder and S1 vertebra, the most proximal surface of the pubic bones and left and right femoral heads were measured using the planning software. The bladder volumes, the amount of soft tissue cranial to the cylinder and the angle of the cylinder to the treatment couch were also measured for each scan. Descriptive statistics along with differences in the measurements between the 2 scans, using T-test for 2 samples (2-tailed testing with p ≤ 0.05 for significance) were assessed. Correlations between differences in the bladder volumes and cylinder angle with the differences in the measurements were studied using a Pearson correlation test (p ≤ 0.05).

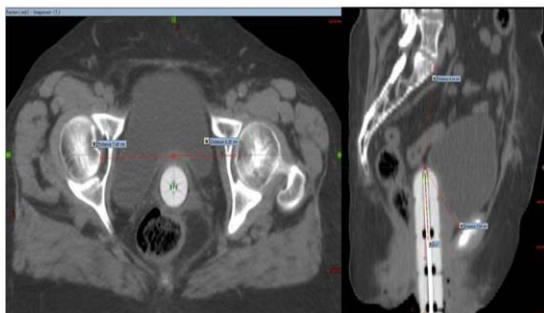
## Results

37 patients having had 2 CT scans were available for review.

	Planning CT	Verification CT	Difference between 2
	Median (range)± stdev.	Median (range)± stdev.	CT's Median (range)± stdev.
Tissue above cylinder (mm)	3(range: 0 to 9) ± 2.6	3(range: 0 to 9) ± 2.3	0 (range: -6 to 3) ± 1.48
Vaginal length (cm)	12 (range: 7-15.4) ± 1.8	11.8 (range: 7.6 to 16.8) ± 1.9	0 (range: -1.2 to 1.6) ± 0.65
S1 measurement (cm)	6.1 (range: 2 to 8.7) ± 1.48	6.5 (range: 2.5 to 8.9) ± 1.6	-0.3 (range: -1.9 to 1.2) ± 0.78
Pubic bone measurement (cm)	7.6 (range: 5.1 to 11.0) ± 1.3	7.4 (range: 5.3 to 10.2) ± 1.2	0.2 (range: -1.6 to 2.6) ± 0.78
Right measurement (cm)	6.8 (range: 4.5 to 7.5) ± 1.3	6.8 (range: 4.7 to 7.7) ± 0.7	-0.1 (range: -0.9 to 0.8) ± 0.4
Left measurement (cm)	6.6 (range: 4.3 to 7.7) ± 0.8	6.7 (range: 4.5 to 7.6) ± 0.7	0 (range: -0.6 to 0.9) ± 0.36
Angle of cylinder (degrees)	7 (range: -2.8 to 16.7) ± 4.8	4.5 (range: -3.2 to 13.7) ± 3.9	2.9 (range: -8.9 to 11.9) ± 5.6
Bladder volume (cc)	160 (range 40 to 891) ± 203	119 (range: 47 to 836) ± 202	3.1 (range: -184 to 277) ± 101

There was no significant difference between the 2 scans for the measurements done, T-test values for S1 -0.69 (p=0.48), pubic bone 1.05 (p=0.29), right -0.13 (p=0.89) and left -0.16 (p=0.87), showing a good degree of reproducibility in the cylinder insertions. There were 2

cases with a difference of >1.5cm in the S1 measurement and another 2 cases for the pubic bone measurement and in all cases there was no evidence of air gaps and no difference in the soft tissue measured above the cylinder. No correlation was identified between the bladder volume and the angle of the cylinder with any of the measurements or their differences.



### Conclusion

The use of verification imaging to assess the placement of vaginal cylinders using bony landmarks can provide a rapid confirmation of the correct position. From our cohort there was not much differences in the measurements used between the planning and the verification scans. Soft tissue evaluation showed that within the range of differences in the measurements using bony landmarks the cylinder remained correctly placed; these changes in measurements are likely due to elasticity of the vaginal walls.

### EP-2133 Interstitial brachytherapy for vaginal recurrence of pelvic gynecological cancers

A. Visy<sup>1</sup>, J. Charret<sup>1</sup>, F. Gassa<sup>1</sup>, A. Serre<sup>1</sup>, M. Sandt<sup>1</sup>, F. Lafay<sup>1</sup>, P. Pommier<sup>1</sup>

<sup>1</sup>Centre Leon Berard, Radiotherapy, Lyon, France

### Purpose or Objective

To date, there are no standard therapy for vaginal recurrences of pelvic gynecological cancers. Local treatment with surgery, External Beam radiotherapy (EBRT) and/or brachytherapy (BT) may be proposed taking into account previous treatments and the extent of the recurrence. Compared to plesioBT, an interstitial implant may permit to deliver a more homogeneous and a higher dose to the tumor. The aim of this study is to evaluate the outcomes of interstitial BT with Iridium192 alone or in addition to surgery, EBRT and/or chemotherapy (CT).

### Material and Methods

From 2011 to 2018, 25 consecutive patients with isolated vaginal recurrences from endometrial (n=15), cervical (n=7), ovarian (n=2) or vaginal cancer (n=1) have been included. The primary treatment included surgery in all but one, EBRT and BT in 1 pt, EBRT in 1pt, and BT in 1 pt. The median time to relapse was 20 months. The site of the recurrence was central (vaginal vault) in 16; lateral in 6, both in 3 pts, with an upper-vaginal "parametrium" extension in 5. A surgery was performed in 6 pts. EBRT (with concomitant CT in 14) was delivered in all patient but one (previously irradiated). Two types of applicators were used according to the site of the recurrence (figure 1 and 2). BT technique was LDR (Iridium wires) in 8 pts treated before 2014 (median dose 19 Gy); PDR in 15 (median dose: 20Gy; 50Gy for exclusive BT) and HDR in 2 pts (12-15Gy in 3 fractions). The cumulative EBRT and BT median dose was: 64 Gy.

### Results

Only 1 grade 2 acute toxicity was observed with BT: a cutaneous abscess on the stitch after BT. Regarding late toxicities, 1 patient required a surgical resection for a

small intestine radio-necrosis. One patient experienced a vaginal necrosis with a bladder fistula, associated with a peritoneal and local tumor progression. In addition vaginal adhesions were reported in 2 and chronic diarrhea in 1 pt. With a 35 months median follow-up (4 - 85 months), 7 patients experienced a local failure (median delay of 22 months after BT, range 11 to 70 months) within the treated volume, isolated in 2 and associated to metastatic progression in 5. Distant metastases alone occurred in 3 pts.

### Conclusion

Interstitial brachytherapy associated with EBRT (+/- concomitant CT) is an effective treatment for locally recurrent gynecological cancers, with favorable clinical outcomes and an acceptable toxicity profile.

### EP-2134 Developing a IC+IS applicator for treatment of advanced cancer cervix by image based brachytherapy

S. Banerjee<sup>1</sup>, V. K<sup>1</sup>, D. Kamaraj<sup>1</sup>, D. Gupta<sup>1</sup>, S. Goyal<sup>1</sup>, S. Bisht<sup>1</sup>, K. Narang<sup>1</sup>, S. Mishra<sup>1</sup>, M. Pinto<sup>2</sup>, P. Manderna<sup>2</sup>, T. Kataria<sup>1</sup>

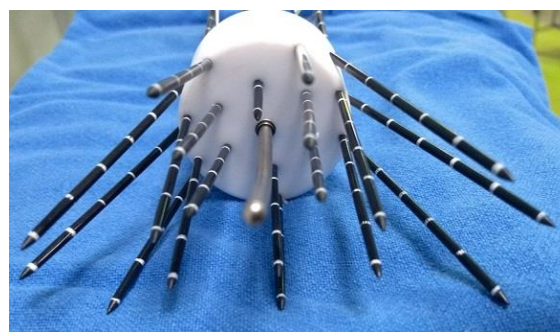
<sup>1</sup>Medanta The Medicity, Division of Radiation Oncology, Haryana, India; <sup>2</sup>Medanta The Medicity, Biomedical Engineering, Haryana, India

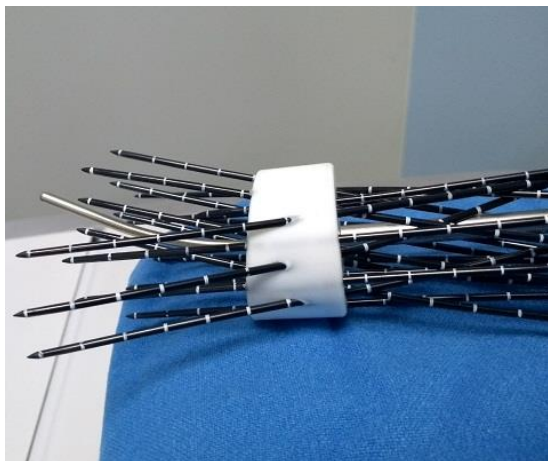
### Purpose or Objective

The GEC ESTRO initiatives have revolutionized the field of gynecological brachytherapy. Advanced applicators are capable of curative dose even to lateral parametria and allow modulation of dose to the critical organs. The outcomes are visible in terms of local control, and reduced toxicities. However in spite of all the advancements the practice of intracavitary + interstitial (IC+IS) is still restricted to select institutions. Due to limited resource and lack of training in IS techniques advanced applicators are not available where they are most needed. We have developed an IC+IS applicator that is easy to assemble and use.

### Material and Methods

A schematic planning diagram of the applicator was drawn on graphical paper. The size of the applicator, shape, position of the needles in the template (which also serves as fixed ovoid) was determined. First a virtual applicator was constructed in TPS and desired dose distributions were experimented keeping principles of IC + IS brachytherapy planning in mind. The applicator was constructed [Fig 1- End on view of the applicator with central tandem and needles, Fig 2- Lat view applicator with needles]. CT images of the applicator were acquired and the applicator was reconstructed in TPS. We selected 3 cases of interstitial brachytherapy treated in our institute and we contoured exact dimensions of HRCTV on the CT images of the applicator.





### Results

We have constructed a 3.5/ 4 cm cylindrical applicator with beveled surface (antero-posterior direction) to fit the plane of cervix, of length 2.5 cm with unique 6 Fr catheter insertion points at fixed distances within the applicator (acting both as template for needle inserting/guidance and ovoid for IC loading). Three needles in anterior oblique direction parallel and in same plane of the Central tandem and 3 needles in lateral oblique direction for distal parametria could be placed technically on each side. Other needles used were straight needles to achieve adequate coverage. The distance of the oblique catheters from central tandem is more than 3 cm at point A. We devised a loading pattern that can give IC + IS type of distribution.

Dummy plans was created to see coverage of HRCTV [Table 1].

volume	Max width (c.m)	Max Thickness (c.m)	Height (c.m)	Vol (c.c)	D90 (%)	V90 %
HRCTV A	5.6	3.9	5.3	45.5	114	98.2
HRCTV B	4.5	3.5	5.8	47.8	105.4	96.6
HRCTV C	5	4.5	5.1	25.3	127.3	98.4

### Conclusion

We have developed an IC+IS applicator capable of delivering dose up to > 3.5 cm from point A. A single cylinder functioning both as ovoid and template for interstitial needles makes the applicator easy to use. The needles used also do not need to be bent. The applicator will be clinically used after feedback from the scientific society.

### EP-2135 Exclusive brachytherapy in endometrial cancer: experience of an university hospital

C. Salas<sup>1</sup>, L. Gutiérrez Bayard<sup>1</sup>, M.J. Macias Lozano<sup>1</sup>, S. Garduño Sánchez<sup>1</sup>, R. Rodríguez Sanchez<sup>1</sup>, S. Sayago Gil<sup>1</sup>, V. Díaz Díaz<sup>1</sup>, E. Gonzalez Calvo<sup>1</sup>, I. Villanego Beltran<sup>1</sup>, A. Ruiz Herrero<sup>1</sup>, M. Lorente Sanchez<sup>1</sup>, J. Jaén Olásolo<sup>1</sup>  
<sup>1</sup>Hospital Universitario Puerta del Mar, Comprehensive Care Department Cancer- Radiation Oncology Service- University Hospital Puerta del Mar, Cadiz, Spain

### Purpose or Objective

To analyze the impact of two different fractionation regimens of postoperative treatment through exclusive endovaginal High Dose Rate Brachytherapy (HDRBT) in women intervened for endometrial cancer, and find

differences of chronic toxicity (LT), local recurrence (LR), locoregional relapse (LRR) and survival free metastases (SFM).

### Material and Methods

102 patients who were diagnosed and intervened of endometrial adenocarcinoma Grade I (G), GII and localized G3, with IA and IIB stage, exclusively treated with endovaginal HDRBT, with cylinders, between 2008-2015 with a minimum follow up of 30 months, were included in this retrospective analysis. Fédération Internationale de Gynécologie Obstétrique Stage (FIGO): IAa:37, IB:63, IIA:2. Brachytherapy: Group (Gp) I: 30 patients who received 5-6 fractions (fx)/3,8-4 Gy at 0,5 cm. surface cylinders, and Group II: 72 patients, who received 3fx/7Gy 0,5 surface cylinder. The mean days overall treatment time (OTT) was 11 and 8 respectively in Group I and II. Previously they had undergone hysterectomy plus salpingo-oophorectomy abdominal or assisted by laparoscopy ± lymphadenectomy.

Toxicity vaginal, bladder and rectal was evaluated using Common Terminology Criteria for Adverse Events v4.03 (CTCAE). The equivalent dose at 2 Gy (EQD2) and bioequivalent dose (BED) study was performed in vaginal mucosa surface with  $\alpha/\beta:3$ . The results from these two groups were then compared and analysed with SPSS 18.

LT, LR, LRR, SFM and OS were compared in both groups and were analyzed with the SPSS 18. Survival (OS) was defined for Test Long Rank (Mantel-Cox).

### Results

Histology of adenocarcinoma in 94 (92%), serous-clear cell in 6,8%. Well differentiated 35%, moderated 60% and poorly 7%. Lymphovascular space invasion (LVSI) positive in 1 patient of Gp I. Grouped by risk group, low risk 34 (9GpI/25GpII), intermediate risk 40 (10/30), high-intermediate risk: 25 (10/15) and high risk: 3 (1/2).

The EQD2 on the vaginal surface of Gp I patients was 72,19 Gy and Gp II: 95,42 Gy. The BED on the vaginal surface of Gp I patients was 120,32 Gy and Gp II 159,04 Gy.

Late toxicity appeared in 14/102 (14%): vaginal 8 Grade 1, 3 Grade 2; bladder 2 Grade 2; rectal 1 Grade 1. With a mean and median follow-up of 69 and 72 months (range, 20-96), none patient had vaginal relapse. 5 of 102 patient had locoregional relapse, 2 in Gp I and 3 in Gp II. 6 patient had distant metastases, 2 in Gp I and 4 in Gp II. Of them, 2 dead in Gp1 and 3 in Gp II. No differences were found in relation to OTT, LR, SFM and OS in Groups I and II. No differences were found in LT to relation BED Groups I and II.

### Conclusion

Six fractions of 3,8-4 Gy in 11 days or three fractions of 7 Gy in 8 days in patients receiving exclusive HDRBT was a safe treatment in relation to late toxicity, local and locoregional control and survival free metastases, but the 3-fractions scheme increases the comfort of the medical team and the patient by reducing the number of times they go to the hospital.

### EP-2136 Brachytherapy study between patients treated with HDR Ir-192 and Xofigo 50kVp source for uterus cancer

K. Asiev<sup>1</sup>, S. Devic<sup>2</sup>, B. Bahoric<sup>3</sup>

<sup>1</sup>Jewish General Hospital, Radiation Oncology Department G18.123, Montreal, Canada; <sup>2</sup>Jewish General Hospital, Radiation Oncology Department G18.121, Montreal, Canada; <sup>3</sup>Jewish General Hospital, Radiation Oncology Department G.002, Montreal, Canada

### Purpose or Objective

To evaluate the possibility of treating patients with low-energy electronic 50kVp brachytherapy beam modality instead of present standard of care High-Dose-Rate Brachytherapy (HDRBT) Ir-192 source for patients with uterus cancer.

### Material and Methods

Five female patients with uterus cancer were treated with HDR Ir-192 source using intra-cavitary Miami applicator with 7 channels. Brachytherapy plans were generated using IPSA inverse planning module of MasterPlan Treatment Planning System (TPS). For the purpose of this study the same five patients were re-planned with HDR Ir-192 source but using only the central channel of Miami Applicator. Next step was to export all five patients (CT datasets and structure sets) to BrachyVision (Eclipse) TPS (Varian, Palo Alto, USA) and plan them with Xofig Axxent 50kVp electronic x-ray source. Due to the fact that same CT datasets and structure sets were used for re-planning process with BrachyVision TPS patient geometry and applicator geometry did not change. The best mimic of Miami applicator in BrachyVision TPS was Straight Tandem (1 channel) applicator overlaid with Miami applicator central channel. Re-planning was performed in such a way so that dosimetric coverage of the planning clinical target volume (Planning\_CTV) achieved for two comparative treatment modalities (single-Iridium and 50 kVp) was matched with the plan patient was treated with.

### Results

Comparison of doses to critical structures (small bowel, bladder and rectum) was performed and summarized in Table 1. Dose values of D (0.1 cc), D (1.0 cc) and D (2.0 cc) are averaged over 5 patients and given in Table 1, together alongside with range of doses and standard deviations. Average times for delivery of the plans were: 8.24 min. for HDR Ir-192 with Miami applicator with 7 channels, 5.38 min. for HDR Ir-192 with Miami applicator with 1 central channel and 6.23 min. for Xofig Axxent 50kVp electronic x-ray source with Straight Tandem 1 channel.

Table 1: Summarizes averaged (over 5 patients) doses to the organs at risk for the three plans per patient investigated.

	Small Bowel			Bladder			Rectum		
	D (0.1cc) Gy	D (1.0cc) Gy	D (2.0cc) Gy	D (0.1cc) Gy	D (1.0cc) Gy	D (2.0cc) Gy	D (0.1cc) Gy	D (1.0cc) Gy	D (2.0cc) Gy
HDR Ir-192 Miami applicator 7 channels									
Average	8.09	6.11	5.43	8.41	7.13	6.59	9.02	7.61	6.97
Range	3.91 - 11.61	3.33 - 8.35	3.05 - 7.32	7.77 - 9.06	6.63 - 7.66	6.11 - 7.13	8.65 - 9.64	7.2 - 8.04	6.42 - 7.36
SD	3.19	2.07	1.76	0.48	0.44	0.46	0.43	0.34	0.41
HDR Ir-192 Miami applicator 1 channel									
Average	9.38	6.86	5.98	7.72	6.85	6.41	9.03	7.78	7.12
Range	4.47 - 13.87	3.75 - 9.66	3.4 - 8.34	7.08 - 8.31	6.15 - 7.34	5.68 - 6.89	8.15 - 9.76	7.07 - 8.37	6.36 - 7.52
SD	3.88	2.42	2.02	0.45	0.45	0.46	0.68	0.53	0.48
Xofig Axxent 50kVp Straight Tandem 1 channel									
Average	11.0	6.87	5.64	8.00	6.83	6.24	10.20	8.21	7.27
Range	4.03 - 16.45	3.12 - 8.78	2.72 - 7.11	7.51 - 8.35	6.09 - 7.14	5.42 - 6.58	8.61 - 12.00	7.36 - 9.31	6.27 - 8.05
SD	5.32	2.63	2.02	0.31	0.42	0.47	1.25	0.81	0.72

### Conclusion

Our results of retrospective dose comparison suggest that 50 kVp could potentially replace Ir-192 brachytherapy treatment modalities providing similar target coverage and similar maximum dose values to surrounding critical structures. Averaged treatment times are as well comparable between two treatment modalities. Further studies are needed however to investigate the impact of radio-biological effectiveness of 50 kVp photons when compared to Ir-192 emissions.

### EP-2137 Locally advanced cervical carcinoma treated with electronic brachytherapy: Our experience

A. Miranda Burgos<sup>1</sup>, A. Méndez Villamón<sup>1</sup>, R. Ibáñez Carreras<sup>1</sup>, M. Gascón Ferrer<sup>1</sup>, A. Campos Bonel<sup>1</sup>, B. García Gutierrez<sup>1</sup>, E. Muñoz Sanz<sup>1</sup>, S. Lozares Cordero<sup>2</sup>, J. José Gutiérrez<sup>3</sup>, I. Negro Quintana<sup>3</sup>, I. Escartín Martínez<sup>4</sup>, G. Riazuelo Fantova<sup>4</sup>, M. Tejedor Gutiérrez<sup>1</sup>  
<sup>1</sup>Hospital Universitario Miguel Servet, Radiation Oncology, Zaragoza, Spain; <sup>2</sup>Hospital Universitario Miguel Servet, Medical Physics and Radiation Protection, Zaragoza, Spain; <sup>3</sup>Hospital Universitario Miguel Servet, Gynecology, Zaragoza, Spain; <sup>4</sup>Hospital Universitario Miguel Servet, Radiology, Zaragoza, Spain

### Purpose or Objective

The standard treatment of locally advanced cervical carcinoma is radiochemotherapy, including concomitant external beam radiation (EBRT) with weekly Cisplatin and brachytherapy (BT). The electronic brachytherapy (XB) is a treatment option for breast, skin and gynaecological cancer.

Our objective is to present our experience using electronic brachytherapy for cervical cancer.

### Material and Methods

We present 8 patients with locally advanced cervical carcinoma. They were treated between May/2016 and August/2018 with EBRT, 46Gy in 200cGy fractions, using intensity-modulated radiation therapy (IMRT) and image-guided radiation therapy (IGRT) techniques concomitant with Cisplatin 40mg/m<sup>2</sup> followed by XB guided by magnetic resonance imaging (MRI). The total dose administered was 28Gy in 4 fractions given in two consecutive weeks (Thursday-Friday). We analysed the median dose in bladder, rectum and sigmoid D2cc with XB comparing the doses with Ir192. Toxicity was analysed according CTCAE 4.0 scale.

### Results

After EBRT, six of the patients presented a complete response and the other two a partial response with a residual tumour <3cm. The mean doses received were: CTV<sub>HR</sub> 90: 112,55%, CTV<sub>HR</sub> 98: 95,88%, CTV<sub>IR</sub> 90: 59,03%, CTV<sub>IR</sub>98: 63,67%. The mean V150 (cm<sup>3</sup>) with XB vs. Ir192 were: 23.4 vs. 20.7 and the V200 were: 13.8 vs. 11.8.

In organs at risk (OAR) the median dose in bladder with XB vs. Ir192 was: 2cc 60.4% vs. 60.7%. In rectum XB vs. Ir192 was: D 2cc 33.7% vs. 43.9. In sigmoid XB vs. Ir192 was: D 55.4% vs. 58.3%.

The mean following time is 13 months (range 2-29). Acute toxicity was observed: mucositis was observed in 4 patients (2 patients G1 and 2 G2); genitourinary (GU) toxicity was observed in 2 patients (G1) and gastrointestinal (GI) toxicity in 1 patient. At 3 months after treatment only 1 patient presents mucositis G1.

After the XB treatment 7 patients are in complete response and 1 patient died from systemic progression.

### Conclusion

The XB with tandem and ovoids is an appropriate technique on selected patients with residual tumour <3cm and without parametrial invasion. The dose received by the organs at risk with the XB is less compared to Ir192, with a good coverage of the PTV with excellent results as for toxicity.

### EP-2138 Rectal and urinary toxicity in patients with cervical carcinoma treated with brachytherapy

V. Garcia Jarabo<sup>1</sup>, S. Cordoba Largo<sup>1</sup>, M. Ramirez<sup>1</sup>, D. Martínez<sup>1</sup>, M. Gaztañaga Boronat<sup>1</sup>, C. De la Fuente<sup>2</sup>, G. Marquina<sup>1</sup>, A. Ortega<sup>1</sup>, R. Mendez<sup>1</sup>

<sup>1</sup>Hospital Clinico San Carlos, Radiation Oncology, Madrid, Spain; <sup>2</sup>Hospital Universitario Puerta de Hierro Majadahonda, Radiation Oncology, Madrid, Spain

### Purpose or Objective

To asses dosimetric factors predicting rectal and urinary morbidity and describe vaginal toxicity in patients treated with chemoradiation (CRT) and image-guide brachytherapy (IGBT-MRI) for locally advanced cervical cancer.

### Material and Methods

From November 2010 to February 2016 we treated 64 patients (p) with stages IB-III cervical carcinoma. Mean age: 54.6 years (30-88). TNM stage: I: 4p, II: 54p and III: 6p. Histology: epidermoid: 49p; adenocarcinoma: 15p. All patients were treated with CRT and 3D-based planning intracavitary/interstitial IGBT, using the GEC-ESTRO recommendations for defining high-risk clinical target volume (HR-CTV). Equieffective doses at 2 Gy (EQD2) were calculated, applying linear quadratic model. Statistical analysis: chi-square test for comparing

proportions and Kaplan Meier for survival analysis and log-rank for curve comparison. Toxicity was evaluated according to CTCAE v.4.0 criteria.

#### Results

After a median follow-up of 30 months, 3-year overall survival (OS), 3-year disease-free survival (DFS) and 3-year local relapse-free survival (LRFS) were 83.7%, 58% and 84.2%, respectively. The mean  $D_{2cc}$  in rectum and bladder were: 66.2Gy (47.8-87.9) and 76.3Gy (54.9-96), respectively. Rectal morbidity (diarrhea, proctitis and/or bleeding), was observed in 22p: G1: 13p (20%) and G2-3: 9p (14%). One patient presented with sigmoid perforation. Two-year G2-3 rectal toxicity-free survival (RTFS) and G2-3 rectal bleeding-free survival (RBFS) were 82.6% and 84.2%, respectively. In relation to dosimetric parameters, there were more rectal toxicity in patients with  $D_{2cc} > 65$ Gy, although differences were not significant (2y G2-3 RTFS of 65% vs 93%). A  $D_{2cc} > 65$ Gy was associated with more incidence of G2-3 proctitis (0% vs 100%,  $p = 0.05$ ). Urinary morbidity (urgency, incontinence, cystitis and/or hematuria) was observed in 17p (G2-3 cystitis: 2p and G2-3 hematuria: 6p). Two-year G2-3 hematuria-free survival was 91%. The probability of G2-3 hematuria was not related with  $D_{2cc} > 80$ Gy. G2-3 vaginal stenosis was observed in 25p (39.6%). Sacrum fracture was observed in 12p (19%). Two-year sacrum fracture-free survival was 84%.

#### Conclusion

Rectal complications remain as the main toxicity in modern brachytherapy. Efforts should be made to maintain rectal  $D_{2cc}$  below 65 Gy. Based in our results, early evaluation and intervention are recommended to detect and prevent sacral fractures.

#### EP-2139 Adjuvant brachytherapy for T1b1N0 cervical cancer: an alternative to postoperative EBRT

E. Bronsart<sup>1</sup>, C. Petit<sup>1</sup>, I. Fumagalli<sup>1</sup>, S. Gouy<sup>2</sup>, P. Morice<sup>2</sup>, C. Haie-Meder<sup>1</sup>, C. Chargari<sup>1</sup>

<sup>1</sup>Gustave Roussy, Radiation oncology, Paris, France;

<sup>2</sup>Gustave Roussy, Gynecologic Surgery, Paris, France

#### Purpose or Objective

Generally the treatment in early stage cervical cancer is upfront surgery. An adjuvant external beam radiation therapy (EBRT) is delivered according to histopathological risk factors (lymph node involvement, lymphovascular invasion, tumor > 4cm, deep stroma invasion, positive surgical margins, parametrial spread). In a Gynecologic Oncology Group (GOG) study, adjuvant EBRT was shown to reduce the risk of locoregional relapse by 46%, at the expense of an increase in severe morbidities.<sup>1</sup> We report our institutional experience of adjuvant vaginal wall brachytherapy as an alternative to EBRT in selected patient treated with upfront surgery for pT1b1N0 tumors.

#### Material and Methods

Medical records of consecutive patients treated for an early stage cervical by upfront radical colpohysterectomy and pelvic lymph node dissection for a pT1bN0 cervical cancer between 1991 and 2018 were examined. Patients were proposed adjuvant vaginal wall brachytherapy because of the following risk factors: tumor size  $\geq 2$ cm and/or lymphovascular involvement. Patients with parametrial spread, positive margins, or with nodal metastases were excluded and received adjuvant EBRT. Patients received a dose of 60 Gy and the dose was prescribed at 5 mm depth from the vaginal wall and the upper third of vagina was included in the target volume. The vaginal mould technique was used in all cases. Organ at risk point doses or dose/volume parameters followed ICRU dose constraints guidelines. Patients were followed clinically and toxicities were scored according to CTCAEv3.

#### Results

40 patients were included, mean age 50.3 years (range: 28.8-80.6 years). A total of 25 patients (62,5%) had a

squamous cell carcinoma and 15 (37.5%) had an adenocarcinoma. Eight patients (20%) had LVI, eight (20%) had a tumor size more than 3 cm and one (2.5%) had close resection margins (<2mm). Median follow-up time was 39.5 months. A total of four patients experienced tumor relapse (10%), all in the peritoneal cavity, associated with synchronous external iliac lymph node in one patient. No patient had vaginal relapse and no isolated pelvic nodal failure was reported. The median overall survival time was 42 months. The Kaplan-Meier estimated five-year probability of survival was 84% (CI95%:68%-100%). In univariate analysis, probability of relapse was significantly higher in patients with tumor size > 3cm ( $p=0.004$ ). Presence of LVI, margin distance, or histology (adenocarcinoma versus squamous cell) was not significant. No toxicity more than grade 1 was reported. During their follow-up, five patients (12.5%) presented telangiectasia grade 1, 2 (5%) had vaginal stenosis grade 1, 2 (5%) had vaginal bleeding grade 1, 1 (2.5%) had vaginal dryness grade 1. One patient had rectal bleeding and two had urinary toxicity. No bowel morbidity was reported.

#### Conclusion

This study suggests that adjuvant BT is an appropriate option for decreasing vaginal relapses in selected patients with pT1b pN0 cervical cancer with one or two of the following risk factors: size > 2cm and LVI.

---

#### Electronic Poster: Brachytherapy: Head and neck

---

#### EP-2140 HDR Brachytherapy in Reirradiation of Local Nasopharyngeal Recurrence

M. Ait Erraïsse<sup>1</sup>, W. Hassani<sup>1</sup>, T. Bouhafa<sup>1</sup>, K. Hassouni<sup>1</sup>

<sup>1</sup>CHU Hassan II, Radiothérapie, Fez, Morocco

#### Purpose or Objective

pharyngeal carcinoma (NPC) is a most cancer of head and neck in North Africa and South East Asia. Reirradiation of local recurrence is limited by the dose constraints. Brachytherapy alone or in combination with EBRT can be a good compromise. The aim of this study was to determine the role of brachytherapy in safety reirradiation of recurrent NPC.

#### Material and Methods

This is a retrospective study of 8 patients with nasopharyngeal cancer recurrence collected in the radiotherapy department of the University hospital Hassan II in Fez between January 2014 and December 2017.

#### Results

The average age of our patients is 42 years old. The average time to onset of relapse is 29 months. All patients received external radiation therapy at 70 Gy on macroscopic tumor volume (tumor and lymphadenopathy) during initial irradiation with or without chemotherapy. relapse was localized in 5 patients and associated with lymph node involvement in 3 patients. 2 patients received exclusive high-dose rate brachytherapy and 6 received external radiation radiotherapy followed by brachytherapy. The total radiation dose EQD2 was 60 to 66 Gy. With an average follow-up of 20 months, 37.5% of patients are alive and in complete remission.

#### Conclusion

Brachytherapy alone or after EBRT could play an important role in reirradiation of locally recurrent NPC with acceptable toxicity.

---

#### Electronic Poster: Brachytherapy: Physics

---

#### EP-2141 Recommendations for reporting the rectal dose during image guided HDR brachytherapy of prostate

M. Szlag<sup>1</sup>, A. Cholewka<sup>1</sup>, P. Wojcieszek<sup>2</sup>, S. Kellas-Ślęczka<sup>2</sup>, M. Stąpór-Fudzińska<sup>1</sup>, T. Krzysztofiak<sup>2</sup>, K. Ślosarek<sup>1</sup>

<sup>1</sup>Cancer Center and Institute of Oncology Gliwice Branch, Radiotherapy Planning Department, Gliwice, Poland;

<sup>2</sup>Cancer Center and Institute of Oncology Gliwice Branch, Brachytherapy Department, Gliwice, Poland

### Purpose or Objective

Imaging modalities, routinely used for 3D dose calculation for HDR prostate brachytherapy, are transrectal ultrasound (US) and computed tomography (CT). Depend on the imaging modalities, contours of the rectum contain: the whole rectum (when CT is used) or anterior rectal wall (for US based treatment plans). Contouring and rectum deformation by the transrectal probe modify the dose delivered to rectum. For different imaging types, the caution should be paid when using the same treatment plan evaluation protocol since some of the dosimetric parameters may be inconsistent. In this study we defined DVH regions where dosimetric parameters of the rectum and rectal wall differs significantly. The aim of this study was to specify dose-volume parameters for reporting the dose delivered to rectum and rectal wall during image guided brachytherapy of prostate and to indicate parameters which can be used for both imaging methods and these which should be used with caution. Clinical data are in relation to the set of physical dose parameters obtained from planning systems. Validation of dosimetric protocol is required to properly predict the clinical outcomes when new modalities are introduced to planning.

### Material and Methods

In our department prostate brachytherapy is performed in a real-time based on transrectal ultrasound (US) or computed tomography (CT). For the purpose of this study 33 randomly selected CT-based plans (OncentraBrachy ELEKTA) were compared with 33 US-based plans (OncentraProstate ELEKTA). Plans were calculated for patients treated with brachytherapy as a monotherapy with total dose of 26Gy delivered in two fractions. DVH parameters for prostate, rectum and rectal wall were selected for analysis (Table1). We evaluated statistically significant difference between mean values of dosimetric parameters for rectum and rectal wall.

Table 1. Mean DVH parameters for prostate, rectum and rectal wall

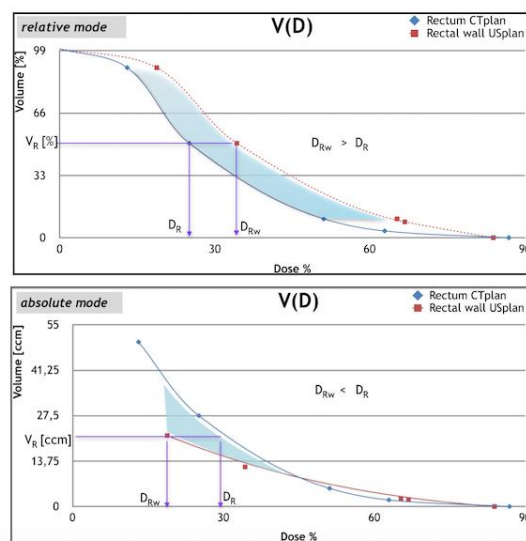
	V <sub>PTV</sub>	PTV <sub>100%</sub>	D <sub>90%</sub>	V <sub>rectum</sub>	D <sub>0.01ccm</sub>	D <sub>2ccm</sub>	D <sub>10%</sub>	D <sub>50%</sub>	D <sub>90%</sub>	V <sub>70%</sub>
CT	53.1ccm	95%	108%	55.3 ccm (whole rectum)	87%	63%	51%	25%	13%	3%
US	51.1ccm	95%	108%	23.9 ccm (rectal wall)	84%	67%	65%	34%	19%	7%
p value	0.59	0.76	0.13	<0.001	0.2	0.08	<0.001	<0.001	<0.001	<0.001

V<sub>PTV</sub> is the volume of the prostate gland, PTV<sub>100%</sub> is the volume of the prostate covered with 100% isodose, D<sub>90%</sub> is the dose that covers 90% of the organ (PTV, rectum or rectal wall), V<sub>rectum</sub> is the rectum or rectal wall volume (depend on the imaging used for treatment), D<sub>0.01ccm</sub> and D<sub>2ccm</sub> is the dose delivered to the 0.01 and 2 ccm of the rectum and rectal wall, D<sub>10%</sub> is the dose that covers 10% of the organ, D<sub>50%</sub> is the dose that covers 50% of the organ, V<sub>70%</sub> is the volume of the organ covered with 70% of the isodose. p value for t- test.

### Results

Table 1 presents dosimetry of prostate, rectum and rectal wall. Two groups of treatment plans were similar when comparing the PTV volume and PTV coverage, significant differences were observed for dose delivered to the 10%, 50% (intermediate-dose region) and 90% (low-dose region) of the rectum delineated based on CT and US. In the relative mode (Fig 1) rectal wall received higher dose in the low- and intermediate-dose regions but in absolute scale the dose delivered to the rectal wall covers larger volume when the whole rectum is delineated (Fig 1). The high dose regions for rectum and rectal wall (D<sub>0.01ccm</sub>, D<sub>2ccm</sub>) were comparable in US and CT plans and they

were consistent and independent on contouring methods.



### Conclusion

Dose delivered to rectal wall in the low- and intermediate-DVH region is underestimated in comparison to the dose delivered to the whole rectum. Only high dose region was comparable for both types of plan. CT and US plans should be evaluated with the use of different evaluation protocol for low and intermediate rectum doses.

### EP-2142 Analysis of dose distribution between TG-43 and TG-186 in lung cancer

M. Sawicki<sup>1</sup>, Ł. Jarosław<sup>2</sup>

<sup>1</sup>University of Rzeszów, Faculty of Medicine, Rzeszów, Poland; <sup>2</sup>Subcarpathian Cancer Center, Department of Brachytherapy, Brzozów, Poland

### Purpose or Objective

Standard treatment planning and dose calculation in brachytherapy HDR is based on water mass density. Human tissues has a different mass density than water. In the case of cancer located in the lung, the dose distribution is calculated mainly in the area of lung and critical organs (heart, esophagus, spinal cord). The OARs in lung, for example heart mass density is 1.05 which is very close to water density (1.0) and it seems correct to treat this area like a area of homogeneous water, but in case of lung there are such as areas like soft tissue and air. For lung (inflated) mass density is 0.2. in the area of lung cancer. The dose calculation algorithm should take into account the heterogeneity of the area, otherwise the calculated dose distribution will differ from the actual dose distribution in patient's body.

### Material and Methods

The material for this study included 15 patients with advanced inoperable non-small cell lung cancer treated with HDR Ir-192. The study group consisted 24 treatment plans with bronchial applicators (1-3 applicators). For each treatment fraction, two treatment plans were created. One for TG-43 and second one for TG-186. TP was created in the Oncentra MasterPlan Brachy 4.5.3 ® system. Dose distributions were compared in both treatment plans. First, the value of dose was compared at points at constant and same distance from the axis of the applicators (range 0.1-2.0 cm;). Then, the dose in the Target and critical organs (heart, oesophagus, spinal cord, healthy lung, lung) would have been evaluated. Parameters analysed for PTV are maximum and minimum value of median and V<sub>85</sub>, V<sub>100</sub> and V<sub>115</sub>. . In cases of the heart, spinal cord and oesophagus, the examined dosage equaled D<sub>0.1 cm<sup>3</sup></sub>, D<sub>1 cm<sup>3</sup></sub> and D<sub>2 cm<sup>3</sup></sub> for each of the structures.

Also, heart D20 was examined as well as D5 for the healthy lung

### Results

Comparison of both calculation methods presented differences in dose distribution in treatment plans. Were noted differences in dose points in distances from applicator axis as well as differences in dose distribution for PTV and OARs. Difference in value of median for the dose point in 1 cm distance from the applicator is 0,2%, maximal value was 41,78% and minimal value was 0,04%. For PVT V<sub>100</sub>, the difference was 2,6% and for the lung D5 was 3,6%.

### Conclusion

Differences in dose distribution in HDR brachytherapy for lung cancer between TG-43 and TG-186 prove that the we should consider the use of algorithms taking into account the tissue mass density.

### EP-2143 TRAK per unit reference dose as a QA tool is insensitive to finding cervix brachy planning errors

P. Gonzalez<sup>1</sup>, F. Koetsveld<sup>1</sup>, A. Mans<sup>1</sup>

<sup>1</sup>Netherlands Cancer Institute, Radiotherapy, Amsterdam, The Netherlands

### Purpose or Objective

To ensure the quality of a clinical treatment plan for HDR brachytherapy of the cervix, several checks can be made. Following the recommendations of the ICRU report 38, one of these checks is the calculation and reporting of the total reference air kerma (TRAK). This physical quantity, which is defined as the integral of the reference air kerma rate at 1 m distance from the source over the duration of treatment, is believed to be a reliable patient-specific QA tool in determining the treatment intensity. In our clinic the TRAK per unit reference dose, TRAK/D<sub>ref</sub>, as calculated from the TPS is compared to a predicted value. This predicted value is taken from a linear model relating the treatment volume (TV) to the TPS calculated TRAK/D<sub>ref</sub>. The TRAK check is passed if the predicted value does not differ more than 3% from the TPS calculated value. The purpose of this work is to test our hypothesis that the TRAK check is not sensitive enough in finding cervix brachy planning errors.

### Material and Methods

The linear model was determined by fitting TRAK/D<sub>ref</sub> to the treatment volume using a total of 51 clinical intra-cavitary/ interstitial plans. To determine the sensitivity of the TRAK check, several planning errors were introduced into a clinical plan using the Utrecht interstitial CT/MR applicator. All plans were made with the Oncentra treatment planning system. Planning errors were taken from an ASTRO white paper (Pract. Rad. Onc. (2014) 4, 65-70) and were complemented by several other error sources we check for in our institute. The errors included: wrongful addition of a dwell position, wrong dose optimization and wrong reference dose.

### Results

Table 1 shows the various types of errors introduced and the deviation of the predicted value of the TRAK per unit reference dose from the calculated value. Only 2 out of 13 planning errors were found using the TRAK check: using a wrong reference dose and wrongful positioning of a dwell position. The deviations in these cases were -15.5% and 4.7% respectively. All other deviations fall within 3% of the clinical no-error plan. In the first case it must be noted that this error will go undetected if the wrong reference dose is entered in *both* the planning and TRAK check, which is likely to occur in a clinical workflow. The second detected error was due to a misplaced dwell position. It was placed far outside of the high-dose region such that it contributed to the TRAK but not to the treatment volume. This planning error was only detected because we used a strict limit of 3%. We also placed additional dwell positions in the high-dose region. Evidently the treatment volume changed but the ratio TRAK/TV remained constant.

Introduced error	Treatment Volume [cc]	TRAK/D <sub>ref</sub>	Lin. Model	Deviation
No error plan	59.31	477.7	484.8	-1.5%
Wrong ref. dose in planning	59.31	409.6	484.8	-15.5%
Wrong isodose in planning	59.31	477.8	484.8	-1.5%
Additional dwell position in intra-uterine tube	66.54	518.6	518.0	0.1%
Additional dwell position in needle	67.66	518.6	523.2	-0.9%
Additional dwell position in needle	66.40	518.6	517.4	0.2%
Additional dwell position in needle	67.25	518.6	521.4	-0.5%
Additional dwell position in intra-uterine tube high	61.59	518.6	459.3	4.7%
Additional dwell position in intra-uterine tube low	66.40	518.6	517.4	0.2%
Accidentally displaced isodose line	92.07	645.6	635.5	1.6%
Accidentally displaced isodose line	130.9	828.1	814.1	1.7%
Offset intra-uterine tube -5 mm	59.28	477.8	484.7	-1.4%
Offset intra-uterine tube -15 mm	59.03	477.8	483.5	-1.2%
Offset needles +5 mm	59.23	477.8	484.5	-1.4%

Table 1. Calculated and predicted values of TRAK/D<sub>ref</sub> as a function of the treatment volume are shown. The last column shows the deviations of the predicted values from the TPS values after introducing several planning errors.

### Conclusion

We conclude that the TRAK check is not a sensitive QA tool since only two very specific planning errors were detected, one of which had a value just above the threshold, and the other could go undetected depending on the workflow.

### EP-2144 Feasibility of using Micro Silica Bead TLDs for 3D dosimetry in brachytherapy

S. Babaloui<sup>1</sup>, S. Jafari<sup>2</sup>, A. L. Palmer<sup>2</sup>, W. Polak<sup>2</sup>, M. W.J. Hubbard<sup>3</sup>, T. Skopidou<sup>3</sup>, A. Lohstroh<sup>3</sup>, R. Jaber<sup>4</sup>  
<sup>1</sup>Cancer Institute Tehran Univ. of Medical Science, Department of Medical Physics and Biomedical Engineering, Tehran, Iran Islamic Republic of;  
<sup>2</sup>Portsmouth Hospitals NHS Trust, Medical Physics Dept., Portsmouth, United Kingdom; <sup>3</sup>University of Surrey, Department of Physics, Guildford, United Kingdom;  
<sup>4</sup>Cancer Institute- Tehran University of Medical Sciences, Radiation Oncology Research Centre RORC, Tehran, Iran Islamic Republic of

### Purpose or Objective

Evaluation of the feasibility of using silica bead TLDs for 3D phantom dosimetry in brachytherapy (BT) for verification of treatment doses and routine quality control. Estimation of beam perturbation effect of TLDs and clinically relevant spatial resolution (SR) required for placing the beads at the organs' surface.

### Material and Methods

The TLDs were positioned with 2.5, 5 and 7.5mm spacing on the surface of a 5cc syringe (Fig1a) in a water tank of similar size to the pelvis of a medium patient. CT scans are taken and a 4field conformal radiotherapy (CRT) plan was created using 6MV beams. From the treatment planning system (TPS), 3dose planes were extracted at different depths, in the middle, bottom and below the syringe for every TLD's arrangement. By using a 2D-γ analysis, the TPS reports were compared with and without presence of the beads.

A novel anthropomorphic phantom was developed to position the TLDs. It consists of all pelvic organs which are relevant in gynaecology (GYN) BT. Organs were 3D printed using the CT scan datasets of handmade organs (Fig1 b & d). Acrylonitrile butadiene styrene (ABS) with 90% infill density was used with a CubePro printer (3D Systems Inc., U.S). Bones were made of PVC coated with clinical plaster. The phantom components were confirmed to have mass density and CT numbers similar to the relevant

tissues (solid water:  $CT\#=1012$ ,  $0.944 < \rho < 1.044$ ; Phantom organs:  $\rho=0.95$  and the  $CT\#=959$ ).

TLDs were threaded and placed on the organs' surface with 1cm resolution. Then whole assembly was placed inside the same water tank and irradiated with  $^{60}\text{Co}$  HDR source within a Vienna applicator (Eckert & Ziegler GmbH) to 7Gy prescribed to ICRU38 defined A-points. A TOLEDO TL system was used to readout the TLDs. Percentage difference of mean doses and dose surface histograms (DSH) of measured doses were compared against the TPS for the uterus as clinical target volume (CTV), bladder, rectum and sigmoid as organs at risk (OARs).

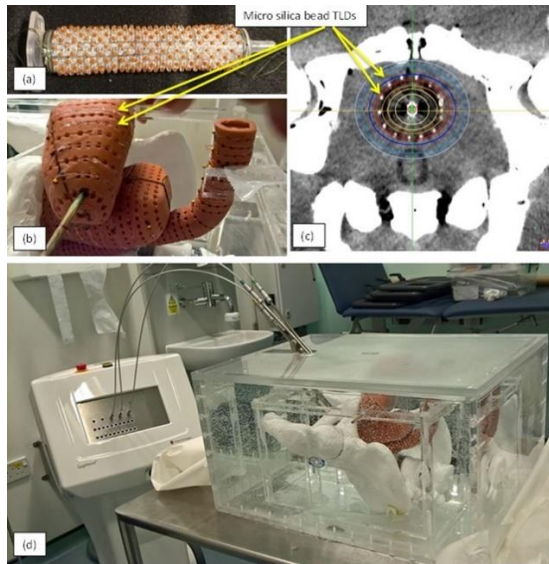


Fig1. (a) Syringe with a 2.5 mm spacing arrangement of silica bead TLDs. (b) 3D printed organs with placement of TLDs at the surface. (c) HDR plan on the CT scan of phantom; each TLD is clearly visible. (d) The anthropomorphic pelvis phantom in the water tank connected to the high dose rate (HDR) unit.

## Results

The 2D- $\gamma$  analysis on the syringe showed more than 99% points passed 3% and 3mm criteria at all source to plane distances which mean TLDs with different SR do not cause any perturbation effect.

Fig 2 shows the DSHs of measured doses with TLDs in comparison with those of the TPS dose calculation. By calculating the integral dose for the organs, % difference were found to be 3%, 4%, 10% and 45% for uterus, rectum, bladder and sigmoid respectively. Results showed, % difference of mean doses in the uterus is  $<1.4\%$  ( $SD=0.4$ ) for TLDs up to 4cm distance from the centre of ring vertically, 9% to 22% ( $SD=10.5$ ) above 6cm which is the low- dose region ( $<1\text{Gy}$ ).

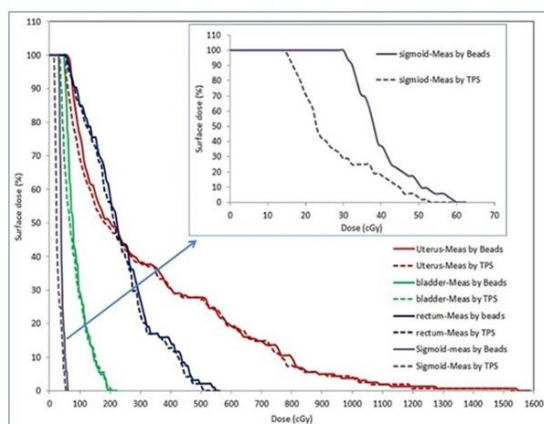


Fig2: Dose surface histograms obtained by TLDs readout and point doses calculations of TPS

## Conclusion

A customized anthropomorphic pelvis phantom was successfully built and clinically assessed to confirm properties similar to tissues. The small size of the TLDs together with negligible beam perturbation effect, suggest their further potential use as in-vivo dosimetry system which is the next step of this project. A careful calibration is needed, especially in the region of low doses.

## EP-2145 Biological comparison of $^{60}\text{Co}$ & $^{192}\text{Ir}$ brachytherapy sources: a possible need for correction factor

S. Abdollahi<sup>1</sup>, M. Dayyani<sup>2</sup>, H. Miri Hakimabad<sup>3</sup>, L. Rafat Motavalli<sup>3</sup>, E. Hoseinian Azghadi<sup>3</sup>

<sup>1</sup>Reza Radiotherapy and Oncology Center RROC, Medical Physics, Mashhad, Iran Islamic Republic of ; <sup>2</sup>Reza Radiotherapy and Oncology Center RROC, Radiation Oncology, Mashhad, Iran Islamic Republic of ; <sup>3</sup>Ferdowsi University of Mashhad, Physics, Mashhad, Iran Islamic Republic of

## Purpose or Objective

High Dose Rate Brachytherapy (HDR BT) has become a standard treatment as a boost or monotherapy for different tumors such as gynecological malignancies, prostate cancers, sarcomas, and breast cancers. In most of modern clinical studies in BT, one of the commercial Ir-192 sources was employed. Recently though, Co-60 HDR BT sources have been used worldwide. Co-60 with a lower dose rate (about one-half), can deliver the prescribed dose two times longer than Ir-192. Moreover, because of their different photon spectra, these two sources show some discrepancies in dose distributions. Before expanding the Iridium-based results to Cobalt-based clinical treatments, It may be questioned whether these differences can meaningfully influence the biologically effective dose (BED) distributions inside the tumor?

## Material and Methods

Dose rate distributions were estimated for Co-60 and Ir-192 sources (Eckert & Ziegler BEBIG) using TG-43 formalism for vaginal cylinder and Tandem-Ovoids used for gynecological tumors and interstitial needles for breast and prostate malignancies. The linear-quadratic (LQ) model was used to investigate probable biological differences made by dose and dose rate distributions of two sources. For the estimation of the incomplete recovery factor  $g$  in the LQ model which compares dose rate effects in one irradiation session, mono-exponential repair kinetics was assumed and the repair half-times ( $T_{1/2}$ ) were extracted from literature. BED distributions were then calculated considering site dependent  $\alpha/\beta$  values.

## Results

For all sites, DVH curves of clinical target volumes (CTVs) were in good agreement for two sources however dose distributions varied significantly in some dose points. Considering the physical dose, points on the vaginal cuff received higher dose up to about 40% from Co-60 as compared with Ir-192. In three other cases, discrepancies up to about  $\pm 10\%$  can be observed for some few points. For BED analysis,  $\alpha/\beta=10$  Gy and  $T_{1/2}=1$  h were selected for gynecological sites. However, several values of  $\alpha/\beta$  and repair time for prostate ( $\alpha/\beta=1.5$  and 3 Gy,  $T_{1/2}=16$  min) and breast tumors ( $\alpha/\beta=2, 3.5$ , and 5 Gy,  $T_{1/2}=0.1, 0.5$ , and 2 h) were examined. For gynecological sites, BED distribution patterns agreed with dose distributions except for the vaginal cuff in which Co-60 caused an increase from +10% to +90% in BEDs as compared with Ir-192. The patterns were different for prostate site because of the faster repair time and lower values of  $\alpha/\beta$ . BED values from Co-60 source showed -20% to -10% reduction in  $>70\%$  of CTV in comparison with Ir-192. For the breast site, the reduction to -10% can be observed only for  $T_{1/2}=0.1$ .

## Conclusion

The results were in agreement with the previous studies which clinically confirmed Co-60 as an HDR BT source for gynecological tumor management. However, one may be cautious for applying the Iridium-based prescribed dose into the Cobalt-based treatments in some cases such as prostate cancers which using a correction factor of about 1.2 might be reasonable.

#### EP-2146 Comparison of planning US HDR prostate on transversal or longitudinal ultrasound acquisitions

D. Aramburu<sup>1</sup>, V. Brennan<sup>2</sup>, G. Cohen<sup>1</sup>, A. Damato<sup>1</sup>  
<sup>1</sup>Memorial Sloan Kettering Cancer Center, Medical Physics, New York, USA; <sup>2</sup>Memorial Sloan Kettering Cancer Center, Radiation Oncology, New York, USA

##### Purpose or Objective

To investigate differences in planning using images acquired using different acquisition techniques in US-based HDR prostate brachytherapy.

##### Material and Methods

We analyzed the records of 20 patients who received real-time transrectal ultrasound (US) guided interstitial high-dose-rate brachytherapy at our institution. For each patient, two sets of US images were acquired with a digital stepper immediately after treatment: transUS using the transversal US transducer, acquired by retracting the TRUS probe during image acquisition; twistUS using the longitudinal US transducer, acquired by rotating the TRUS probe during image acquisition. For all patients, measurement from the template to the connector-end of each needle were recorded and used for relative confirmation of needle tip identification. The DICOM plans were analyzed using MATLAB routines to assess catheter shift (average distances between reciprocal dwell source positions at transUS and twistUS after rigid registration between all dwell positions is performed). Catheters were digitized on the transUS and the twistUS and the identified tip positions were verified against a reference needles using the measurement data. A subset of 13 patient records was recontoured; contours were rigidly registered based on implant geometry. Difference in target volume and kappa statistics were calculated.

##### Results

The average  $\pm 1$  standard deviation of the number of needle tip adjustments per patients performed due to discrepancies with measured data was  $4 \pm 2$  for transUS and  $3 \pm 3$  for twistUS. Average of the distance between reciprocal dwell source position between transverse transUS and twistUS were  $0.12 \pm 0.04$  cm with a range of  $(-0.03 - 0.03)$  cm. Difference in Target volumes between transUS and twistUS were  $-1.8 \pm 7.8$  cm<sup>3</sup>.

##### Conclusion

Based on the number of adjustment required to match the physical measurement, physical measurements are required for both twistUS and transUS to accurately identify the needle tips. On average, the digitization geometry was similar using the two imaging techniques, although differences up to 3mm were observed in some cases. This may be due to deformation of the anatomy and implant geometry occurring during retraction of the probe in transUS acquisitions. Further analysis will be performed on more patients and dose distributions to validate these results, which suggest similar dose delivered to the target using both acquisitions.

#### EP-2147 Commissioning of a novel brachytherapy device for diffusive alpha-particle radiation therapy

A. Damato<sup>1</sup>, B. Beattie<sup>1</sup>, G. Cohen<sup>1</sup>, B. Serencsits<sup>1</sup>, L. Dauer<sup>1</sup>, J. Humm<sup>1</sup>  
<sup>1</sup>Memorial Sloan Kettering Cancer Center, Medical Physics, New York, USA

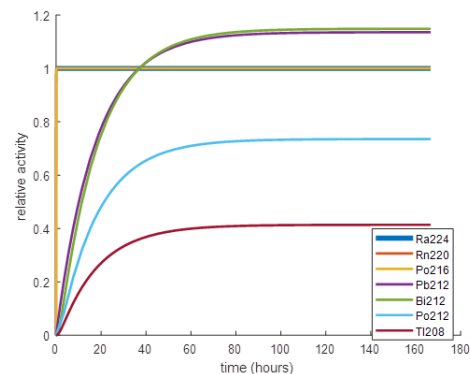
##### Purpose or Objective

To establish acceptance and commissioning of a novel brachytherapy device (DaRT, Alpha Tau Medical, Tel Aviv,

Israel) consisting of needles pre-loaded with stranded Ra224 sources. In the patient, each source delivers alpha radiation up to 3-6 millimeter in tissue through the diffusion of the daughter elements, emitted as a recoil from the source, and its progeny.

##### Material and Methods

Four devices were obtained, two "flex" (plastic catheters) devices, one with 3 sources and one with 6 sources; and two "needle" devices, one with 1 source and one with 3 sources. All sources were 1cm long. All devices were sealed against gas leaks at manufacturing and wrapped in sterile packages. The packages were tested upon arrival for contamination and leaks. A handheld Zinc Sulfide (ZnS(Ag)) detector and liquid scintillation counter, equipped with an alpha/beta discriminator, were used for the contamination survey. The gamma spectrum up to 2MeV of all devices were measured in their sterile packaging in a high purity Germanium detector (HPGe) and compared to the expected spectrum with equilibrium assumed (See Figure). Calibration of the HPGe was performed using a NIST calibrated Eu152 source with the same measurement geometry. Absolute calibration of the source activity was obtained from the 241 keV peak of Ra224, which was discriminated from the 238.6 keV peak of Pb212. Radiography of all devices was used to establish internal geometry and location of the active sources. Measurement of the devices in their sterile packaging in a well chamber was performed. The 1 source device was used to determine the sensitivity of the chamber (sweet spot), and correction factors were calculated based on the radiography measurements to account for geometry. Calibration factors were established using the HPGe absolute calibration.



##### Results

No contamination on the outer shipment packaging or inner shielding material was found. Preliminary measurements with an ionization chamber showed the external exposure rate on contact with the sealed sterile source packages to be 12.8 mR MBq<sup>-1</sup> hr<sup>-1</sup> for the metallic "needle" devices and 23.4 mR MBq<sup>-1</sup> hr<sup>-1</sup> for the plastic "flex" devices. Discrimination of the 238.6 keV and 241 keV peaks was possible using the HPGe. It was possible to visualize the sources inside the applicator and obtain a geometrical calibration factors for each type of device. Our measurements indicate that the use of a well chamber adds 1.8% uncertainty to source calibration when correction for geometry is used, and 2.5% otherwise.

##### Conclusion

Commissioning of this novel device is underway. A clinical protocol for routine source assay based in a standard well chamber has been established, using a HPGe measurements as reference. Absolute reference measurements will be performed at regular intervals.

**EP-2148 Brachytherapy on anal canal tumors**

C. Sousa<sup>1</sup>, M. Cruz<sup>1</sup>, K. Pereira<sup>1</sup>, A. Neto<sup>1</sup>, S. Gonçalves<sup>1</sup>, J. Brandão<sup>1</sup>, L. Khouri<sup>1</sup>, C. Alves<sup>2</sup>, P. Alves<sup>3</sup>

<sup>1</sup>Instituto Português de Oncologia de Coimbra, Radiotherapy, Coimbra, Portugal; <sup>2</sup>Instituto Português de Oncologia de Coimbra, Medical Physics, Coimbra, Portugal; <sup>3</sup>Instituto Português de Oncologia de Coimbra-Faculty of Medicine - University of Coimbra, Radiotherapy, Coimbra, Portugal

**Purpose or Objective**

Technological advancements in radiotherapy (RT) with improved volumetric conformation and accuracy of dose administration have resulted in better locoregional control (LCR) and lower toxicity. Brachytherapy (BT) is a technique that allows a greater dose escalation and can be used in combination with external RT to increase dosage in tumors of the anal canal, enabling the preservation of sphincter function and reducing the total treatment time. With this study, we intend to analyse the therapeutic approach and response to treatment of patients undergoing endorectal brachytherapy.

**Material and Methods**

Retrospective study of patients with anal canal tumors treated at our institution with endorectal high dose rate BT (HDR BT) with endocavitary applicator and Iridium-192 radioactive source, between 2008 and 2016. The toxicity evaluation was carried out according to the CTCAE4 and RTOG/EORTC scales. The response to therapy was assessed by clinical observation, imaging and histologically. Primary Endpoints: locoregional control (LCR), progression-free survival (PFS). Secondary Endpoint: overall survival (OS). Statistical analysis was performed using SPSS v20.

**Results**

We included 12 patients, all were female, with a median age of 67.5 (41-81) years; Histologically: 2 adenocarcinomas, 8 squamous carcinomas; As for the location of lesion and stage: 2 low rectal carcinomas, 1 stage I and 1 stage III; 10 anal canal carcinomas, 5 in stage I, 2 stage II, and 3 stage III; All patients had disease confined to  $\leq 50\%$  of the anal circumference, with 7  $\leq 25\%$ ; All tumors extension  $\leq 50$  mm, 9 with  $\leq 30$  mm and 1 with 50 mm; According to purpose of treatment, 9 patients under intensive, 2 patients in neoadjuvant and 1 in adjuvant intent; The main chosen chemotherapy regimen was MMC and 5-FU, concomitantly with external radiotherapy. 11 patients were subjected to external radiation, with the most frequent fractionation scheme 50.4Gy/28Fr/5.5weeks and dose increment by BT HDR endorectal, between 4.5 and 5Gy in a single fraction, on tumor volume; Concomitant treatment was well tolerated, with two major complications with need for treatment interruption: febrile neutropenia and herpetic lesions associated with G3 radiodermatitis; 10 patients obtained complete response and 2 partial response; The median follow-up time was 5.25 (1-9) years; 2 cases of disease progression have been reported, one in the liver, with a PFS of 47 months and 1 in a locoregional area with a PFS of 31 months. 3 colostomies were performed, 2 with abdominal-perineal amputation as treatment of rectal carcinoma and 1 in a palliative context due to locoregional recurrence. The median survival time was 8.7 years, with an overall survival of 77% at 5 years.

**Conclusion**

This type of malignant tumors with low incidence should be treated in centers with an experienced and differentiated team, allowing better results and control of the correlated morbidity. These results are in agreement with published literature. BT in association with external RT provides better LCR, allowing the preservation of sphincter function and better quality of life.

**Electronic Poster: Brachytherapy: Prostate****EP-2149 HDR brachytherapy as monotherapy for low and intermediate risk prostate cancer**

M. Gaudet<sup>1,2</sup>, M. Pharand-Charbonneau<sup>2</sup>, D. Wright<sup>2</sup>, M. Desrosiers<sup>2</sup>, A. Haddad<sup>1</sup>

<sup>1</sup>The Ottawa Hospital, Radiation Oncology, Ottawa, Canada; <sup>2</sup>Centre Intégré et de Services Sociaux de l'Outaouais, Radio-Oncologie, Gatineau- QC, Canada

**Purpose or Objective**

To determine biochemical disease-free survival, late toxicity and effect on health-related quality of life of a 2-fraction regimen of high dose-rate (HDR) brachytherapy for the treatment of prostate cancer.

**Material and Methods**

Patients with low or intermediate risk prostate cancer eligible for prostate brachytherapy were treated with HDR brachytherapy as monotherapy in 2 separate implants of 13.5 Gy spaced 7-14 days apart in a prospective REB-approved phase II clinical trial (NCT02077335). HDR brachytherapy was done with a CT-based planning with a template or freehand implant technique based on patient anatomy and prostate volume. Patients had evaluation with International Prostate Symptom Score (IPSS) and Expanded Prostate Index Composite (EPIC) questionnaires and serum PSA at 1,3,6, 9, 12, 16, 20, 24, 30, 36, 48 and 60 months post brachytherapy. Proportion of patients in each IPSS category (Mild=0-7, Moderate=8-18, Severe=19+) were evaluated at each of the intervals above. Paired t-tests with baseline values were done for IPSS and EPIC urinary, sexual, intestinal and hormonal domains. Biochemical disease-free survival was determined according to Phoenix criteria (Nadir + 2.0 ng/ml) and Kaplan-Meier method.

**Results**

30 patients were accrued to the study between June 2014 and February 2016. Median age was 66 (Range 54-82). Median PSA at diagnosis was 8,7 (Range 4.1-17.5). T stage was T1c=65%, T2a=21%, T2b=14%. 27% had Gleason 6 and 73% Gleason 7. Mean prostate volume at time of first implant was 45cc. IPSS categories at baseline, 6, 12 and 24, 36 and 48 months were respectively Mild(81%, 63%, 76%, 65%, 67%, 50%) Moderate (19%, 29%, 20%, 29%, 22%, 50%) and Severe (0%, 7%, 4%, 6%, 11%, 0%). There was a significant decrease in EPIC Sexual Summary Scores at 6 and 12 months with mean intra-patient differences of -18 points (p=0.02) and -17 points (p=0.01) respectively. Biochemical disease-free survival at 4 years was 94,7%. Median PSA (ng/ml) at 12, 24, 36 and 48 months were respectively 0.7, 0.3, 0.3 and 0.1. Overall survival at 4 years was 100%

**Conclusion**

This is the first report of biochemical disease-free survival in this cohort of patients treated with 2 fraction HDR monotherapy. This regimen shows rates of toxicity and health related quality of life that appear acceptable as compared to other treatment modalities. These results are also comparable with other reports with similar treatment regimens. Further study will be required to determine longer-term results of this cohort which can help guide determination of the optimal dose and fractionation for HDR prostate monotherapy.

**EP-2150 Re-salvage treatment for locally recurrent prostate cancer by HDR brachytherapy guided by MRI and US**

A. Garcia Perez<sup>1</sup>, P. Willisch Santamaria<sup>2</sup>, M. Martinez Agra<sup>2</sup>, A. Gonzalez Castro<sup>3</sup>, B. Andrade Alvarez<sup>1</sup>, E. Cespon Outeda<sup>1</sup>, A. Lopez Medina<sup>1</sup>, M. Salgado Fernandez<sup>1</sup>, V.M. Muñoz Garzon<sup>2</sup>

<sup>1</sup>Hospital Meixoeiro, Radiofísica y PR, VIGO, Spain;

<sup>2</sup>Hospital Meixoeiro, Radioterapia, Vigo, Spain; <sup>3</sup>Hospital

Universitario de Burgos, Radioterapia, Burgos, Spain;  
 4Hospital Meixoeiro, Urologia, Vigo, Spain

#### Purpose or Objective

Salvage IMRT is well established for recurrence of prostate cancer after radical prostatectomy. With the improvement in early diagnostics and the increase in survival it is possible to observe second local or distant recurrences, and hormonal therapy is the most common treatment in these cases. One challenge in patients with local recurrence is to delay the hormonal treatment and it can be achieved by re-salvage brachytherapy. In 2016 we started focal re-salvage high-dose-rate brachytherapy (HDR-BT) guided by MRI, registered with US [1,2], that is a novel treatment that minimizes side-effects. We describe the procedure carried out to our patients, evolution of the prostate specific antigen (PSA), and related toxicity.

#### Material and Methods

Ten patients were treated by focal HDR-BT because of a second local recurrence after undergoing radical prostatectomy and IMRT for primary recurrent prostate cancer. The mean age of the patients was 66,9 years (52-77). Dose prescription was 17 Gy for 6 patients and 20 Gy for 3 patients, given in two fractions. Delineation was performed using 1,5T MRI (T2-weighted) registered with US obtained by a transrectal probe. In order to reduce dose to rectum, hyaluronic acid was injected between rectum and target volume. Optimization (Figure 1) of the plan was performed by Oncentra Prostate® (Elekta) and based on the following constraints: CTV  $V_{100}$ : 95%,  $D_{90}$ : 100%,  $D_{min}$ : 80%; Urethra  $V_{120}$ : 0 cm<sup>3</sup>. Treatment was delivered by MicroSelectron HDR (Elekta). PSA was evaluated before and after treatment, and periodically every three months, and a follow-up consultation was carried out after each PSA evaluation.

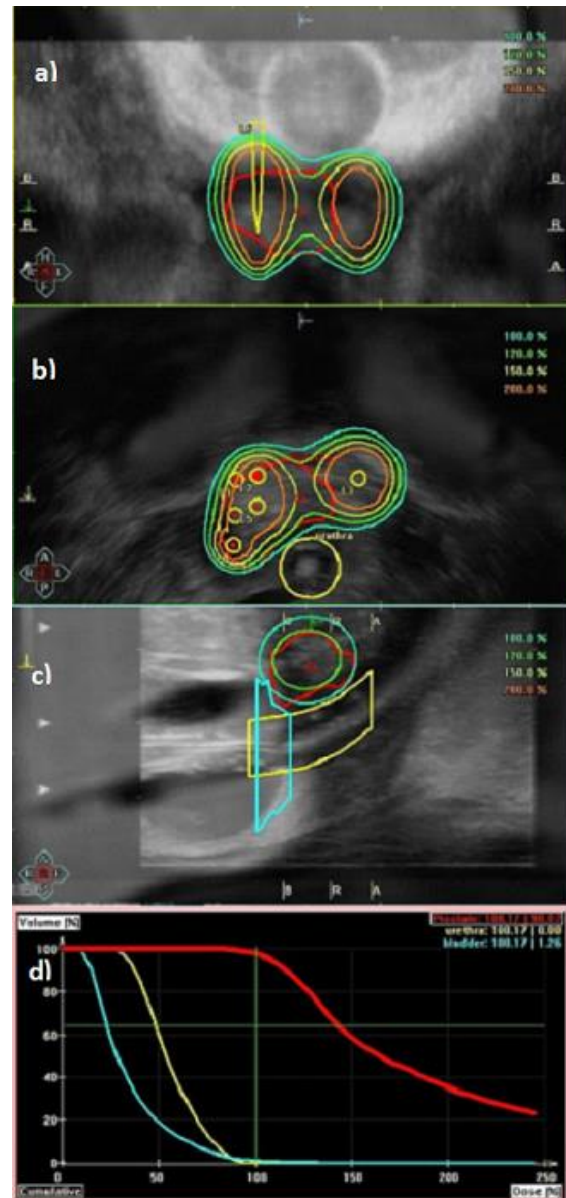


**Figure 1.** a) Coronal plane, b) transverse plane and c) sagittal plane showing delineations of the PTV, urethra and bladder, the reconstructed catheters and the isodose curves on the MRI-US registered images. d) Cumulative DVH.

#### Results

Average dosimetric parameters after optimization were: CTV  $V_{100}$ : 98,0%,  $D_{90}$ : 118,1%,  $D_{min}$ : 84,5%; urethra  $V_{120}$ : 0 cm<sup>3</sup>;  $V_{100}$ : 2,53 cm<sup>3</sup>. With a follow-up of 12 months, 7 patients do not show any side effects, 2 patients have urethral stricture and one had haematuria. PSA values for all patients are shown in Figure 2. 3 patients had stable values of PSA and 2 patients showed PSA <0,2. PSA after treatment increased in 5 patients because of new local recurrences in other localizations (3 patients), or metastatic nodes (1 patient), or unknown cause (1 patient) and were treated with hormonal therapy (7-17 months delay).

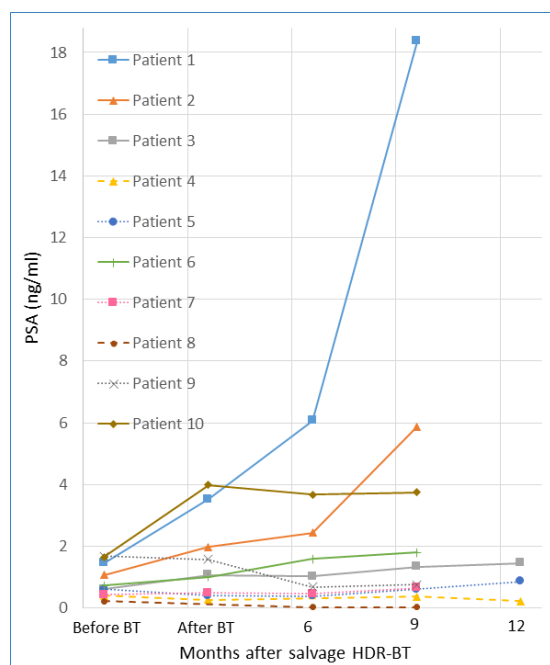


**Figure 2.** Prostate-specific antigen values of all 10 patients. Solid line: patients with biochemical recurrence. Dotted line: patients with stable values of PSA. Dashed line: patients that show PSA<0.2.

### Conclusion

Re-salvage for locally recurrent prostate cancer by focal HDR-BT guided by MRI-US is feasible and can be offered to patients as low-toxicity local treatment. Even in those cases where it does not represent a definitive cure, it can delay hormonal therapy. Therefore, we consider this technique to be recommended especially in patients with a long life expectancy.

[1] Van Son, M. J. *et al* (2018). Re-salvage MRI-guided Focal High-dose-rate Brachytherapy for Locally Recurrent Prostate Cancer. *Cureus* 10(4): e2429. DOI 10.7759/cureus.2429

[2] Maenhout, *et al* (2017). Second salvage high-dose-rate brachytherapy for radiorecurrent prostate cancer. *J Contemporary Brachytherapy* 9(2), 161-6. Funded by FIS PI17/01735 grant (cofunded by FEDER).

### EP-2151 Intermediate-risk prostate cancer with EBRT plus permanent 125-I seeds. Long term results

M. Peña<sup>1</sup>, J. Guinot<sup>1</sup>, R. Roncero<sup>1</sup>, B. Quiles<sup>1</sup>, P. Santamaria<sup>1</sup>, M.A. Santos<sup>1</sup>, C. Boso<sup>2</sup>, J.C. Sanchez-Relucio<sup>2</sup>, M.I. Tortajada<sup>1</sup>, L. Arribas<sup>1</sup>

<sup>1</sup>Fundación Instituto Valenciano de Oncología, Department of Radiation Oncology, Valencia, Spain;

<sup>2</sup>Fundación Instituto Valenciano de Oncología, Department of Radiation Physics, Valencia, Spain

### Purpose or Objective

To present long-term results in patients with intermediate-risk prostate carcinoma treated with combined treatment with external beam radiotherapy (EBRT) plus low dose brachytherapy with 125-I seeds.

### Material and Methods

From April 2008 to December 2010, 51 patients with intermediate risk prostate carcinoma according to EAU guidelines (T2b-c, Prostate Specific Antigen-PSA- between 10 and 20ng/ml or Gleason 7), underwent EBRT on prostate and seminal vesicles to a mean of 46Gy. In the next 3-4 weeks they received the permanent implantation of 125-I seeds, to a median dose of 108Gy, with real-time dosimetry planning and Bard ProLink™ system. Hormonal treatment (HT) was prescribed to 31% during 3-6 months.

Biochemical failure (BF) was considered according to Phoenix definition.

### Results

Mean age was 67, mean PSA was 9.34ng/ml (4.31-18.3) and Gleason score was 6 in 37.3% patients, 7 (3+4) in 45.1% and 7(4+3) in 17.6%. Clinical tumour stage was T1c in 51%, T2a in 27.5%, T2b in 11.7% and T2c in 9.8%. With a median follow-up of 99 months (range 24-124), 5 cases (9.8%) presented BF. Biochemical relapse free survival (bRFS) at 5 and 8 years was 98% and 89.3%. No differences according to Gleason (G), PSA, clinical T stage or HT. At 8 years, patients with Gleason 6 had bRFS of 94.7%, G7 (3+4) 89.5%, G7 (4+3) 75% (p=0.27). When we classify the risk of patients with Mount Sinai Criteria (intermediate or high), we appreciate differences in PSA control at 8 years, 94.3% vs 75% (p<0.06). Late genitourinary G1-G2 toxicity was observed in 9.8%, G3 in 5.8% (3 patients required Transurethral Resection (TURP). Late gastrointestinal G1-G2 toxicity was observed in 9.8%, G3 0%.

### Conclusion

Combined treatment in intermediate-risk prostate carcinoma offers good results on PSA control with low rates of late toxicity. The presence of several intermediate criteria marks a trend to worse results.

### EP-2152 Pre-rectal spacing w/. Blood Patch in HDR Prostate Brachytherapy, Feasibility and Dosimetric Analysis

D. Martinez Perez<sup>1</sup>, G. Sarria Bardales<sup>1</sup>, L. Pinillos Ashton<sup>1</sup>, F.A. Usuga Torres<sup>2</sup>, A. Salgado<sup>3</sup>, R.C. Chumbimuni Contreras<sup>1</sup>, L.A. Maya<sup>2</sup>, I. Veliz<sup>3</sup>, B. Carrion Peñafiel<sup>1</sup>, C. Flores<sup>4</sup>, L. Chirinos<sup>4</sup>

<sup>1</sup>Oncosalud - AUNA, Radiation Oncology, Lima, Peru;

<sup>2</sup>Instituto de Cancerología - Clínica las Américas, Radiation Oncology, Medellín, Colombia; <sup>3</sup>Instituto Nacional del Cancer, Radiation Oncology, Santiago de Chile, Chile; <sup>4</sup>Oncosalud - AUNA, Statistics and Traslational Investigation, Lima, Peru

### Purpose or Objective

Our main goal is to describe a useful technique to decrease rectal dose during high dose rate (HDR) prostate brachytherapy given either as boost or monotherapy, Evaluated in a multicentric initial Latin American first experience from Peru, Chile and Colombia using a blood patch as OAR spacer, as an alternative procedure to improve rectal toxicity in developing countries with limited resources.

### Material and Methods

60 patients, underwent HDR prostate brachytherapy in multiple institutions. Under spinal anesthesia and sedation, approximately 16 mL of blood was extracted from the patient via antecubital venopuncture and mixed with 4 ml of iodine venous contrast as the technique firstly described in 2008 by Morancy from Boston For prostate LDR brachytherapy.

The perineum was prepared for a sterile procedure. Under ultrasound guidance, an 18 gauges spinal needle was placed to open the space below the denonvilliers fascia for hydro-dissection, after the volume of blood was then instilled within the peri-rectal space on each side, as the needle was withdrawn, using the sagittal ultrasound image for guidance as the technique described by Hatiboglu in 2012 in Heidelberg.

After creation of the blood patch, a standard needle insertion to the prostate is performed under US guidance, followed by CT Simulation and then MR fusion is performed for treatment planning. The prescribed dose to PTV in monotherapy is 20.5 Gy and as Boost to EBRT is 15 Gy.

### Results

Patients median age were 71, volume most of them between 20-60 cc, stage II and III intermediate and high risk, Blood Patch was successfully apply in 60 patients, the other 9 are controls without blood patch. It's remarkable that the use of in vivo dosimetry to compare the dose

calculated in the TPS and the dose measured in vivo with over 98% of correlation among them. The blood patch thickness will decrease in 50% in 10 to 15 days after the application. All the rectal dose parameters above the V20 - V80 were significantly improved by the blood patch, also the Dmax and it was correlated with the homogeneity of the blood patch application, V5-V10 weren't significant because these isodoses are 5 to 6 cm far from target. The average pre rectal space obtained was 0.83 cm. The dosimetric potential advantages with the blood patch are that, the mean dose to 0.1 cc of rectum was limited to 57.4% and mean dose to 2 cc of rectum was 40%, also parameters such as D90 and V100 were significantly improved.

#### Conclusion

The use of a blood patch can reduce the integral radiation dose to the rectum and may help to decrease the amount of possible acute and late rectal toxicities due to prostate HDR brachytherapy procedure, letting us to do a safe dose escalation treatment in order to improve outcomes. This technique could be particularly beneficial in patients with minimal peri-rectal fat, appearing to be a cost-effective way to improve outcomes in developing countries with limited resources.

#### EP-2153 Late toxicity after single dose HDR-BT and EBRT for prostate cancer: clinical-dosimetric predictors

D. Büchser<sup>1</sup>, F. Casquero<sup>1</sup>, J.M. Espinosa<sup>1</sup>, F. Perez<sup>1</sup>, P. Minguez<sup>1</sup>, L. Martinez-Indart<sup>2</sup>, F. Suarez<sup>1</sup>, A. Gonzalez<sup>1</sup>, J. Cacedo<sup>1</sup>, I. San Miguel<sup>1</sup>, P. Bilbao<sup>1</sup>, A. Gomez-Isturriaga<sup>1</sup>

<sup>1</sup>Hospital de Cruces, Radiation Oncology, Baracaldo-Vizcaya, Spain; <sup>2</sup>Hospital de Cruces, Bioinformatics and Statistics Department, Baracaldo-Vizcaya, Spain

#### Purpose or Objective

To describe the genitourinary (GU) and gastrointestinal (GI) late toxicity profile and to analyse the clinical and dosimetric predictive factors in a prospective trial of the combination of EBRT and high-dose-rate (HDR) prostate brachytherapy (BT) for localized prostate cancer.

#### Material and Methods

Between January 2012 and May 2017, 210 patients were included in a prospective protocol. Treatment consisted in HDR-BT (15Gy single fraction) and supplemental 3DCRT (37.5Gy/15 fractions) +/- androgen deprivation therapy according to risk stratification. Exclusion criteria included previous pelvic radiotherapy and pubic arch interference. Acute and late urinary complications were assessed using the CTCv4.0 definition.

A descriptive analysis was performed. Univariate and multivariate logistic regression was used to analyse the impact of these variables into late toxicity. All variables with a P value <0.15 in the univariate analysis were selected and included in the stepwise selection procedure of the multivariate analysis. In this last analysis, a P value <0.05 was considered statistically significant. A Hosmer-Lemeshow test and receiver-operating characteristic analysis was performed to calculate area under the receiver operator curve (ROC) (AUC) to compare strength of predictors.

#### Results

Median age was 71 (56-82), 12.4% of patients had low, 44.3% intermediate and 41% high-risk prostate cancer. Median prostate volume was 28.4cc. Median V100, V150, V200 were 98.2%, 27% and 7.4% respectively. Median urethra Dmax, rectum D1cc and D2cc, were 113.5%, 62.2% and 54.2% respectively.

After a median follow-up of 41 months (5-75) late G2 GU and GI late toxicity was observed in 14.8% and 5.2% of patients respectively. Late G3 GU and GI toxicity occurred in 0% and 1% of patients respectively. No grade 4 or 5 events were recorded.

Out of the 31 patients with G2 events, 21 had a resolution of their symptoms by the time the current analysis was

performed. Median time to the development of G2 GU toxicity was 13.5 month (3-63.6). The median duration of G2 events was 8.3 months (3.6-30.6).

Of the 13 patients presenting with G<sub>≥2</sub> GI toxicity, 10 were free of toxicity by the time of the current analysis. Median time to the development of G<sub>≥2</sub> GI toxicity was 11 months (3-44.2). The median duration of the events was 6 months (0.2-9.5).

In univariate analysis, no variable studied was associated with late G<sub>≥2</sub> GU toxicity, whereas previous cardiovascular disease (p=0.042), rectum D2cc (p=0.016) and rectum D1cc (p=0.017) were associated with G<sub>≥2</sub> GI toxicity. Multivariate analysis showed that rectum D1cc (HR11.56; 95%CI 1.4-92.1; p=0.021) and prior history of cardiovascular disease (HR3.6; 95%CI 1-12.9; p=0.045) remained independent predictors of G<sub>≥2</sub> GI toxicity.

#### Conclusion

Single fraction 15Gy HDR-BT and hypofractionated EBRT is well tolerated with low incidence and prevalence of late GU and GI toxicity. Lower rectal D1cc doses may reduce GI toxicity.

#### EP-2154 Efficacy of LHRH agonist-free cytoreduction prior to prostate seed brachytherapy

N. Wallace<sup>1</sup>, A.M. Peoples<sup>1</sup>, S.J. O'Brien<sup>1</sup>, P.J. Kelly<sup>1</sup>  
<sup>1</sup>Cork University Hospital, Radiotherapy Department, Cork, Ireland

#### Purpose or Objective

Our institutional practice for patients planned for prostate brachytherapy is to first perform a TRUS volume study to assess for technical feasibility. For patients who are unsuitable due to a large gland size or pubic arch interference (PAI), cytoreduction with androgen-deprivation therapy may convert patients to suitability for brachytherapy. In an effort to spare patients the known side effects of LHRH agonists, particularly erectile dysfunction, we have adopted bicalutamide 50mg once daily combined with dutasteride 0.5mg once daily for 12 weeks as described by Gaudet et al in Radiotherapy and Oncology in 2016.

The purpose of this retrospective review was to establish the efficacy of this regimen in converting patients to suitability for a prostate seed implant.

#### Material and Methods

We treated 36 patients who were deemed unsuitable for brachytherapy based on their large gland volume and/or the presence of pubic arch interference at the time of their pre-treatment TRUS assessment. Patients received a combination of dutasteride and bicalutamide for 12 weeks. We repeated the TRUS for each patient after 12 weeks of therapy to assess for the presence of PAI, gland volume and whether the patient had become suitable for treatment with brachytherapy.

The data was collected prospectively at the time of the volume studies and analysed retrospectively.

#### Results

The median pre-cytoreduction prostate gland volume was 53.5cc (IQR 47-60cc). The median prostate volume after 12 weeks of dual agent cytoreductive therapy was 38cc (IQR:35-42cc). The median reduction in gland size was 29.0% (IQR 25-36.2%).

33 out of 36 patients (91.7%) had PAI on initial TRUS. Of those individuals with initial PAI, 13/35 (37.1%) had persistent PAI post cytoreduction and one had an obstructive pattern on uroflow studies so was not a suitable candidate. Of the 13 patients with persistent PAI post cytoreduction 9 were felt unsuitable to proceed to implant.

Overall, 26/36 (72.2%) were suitable candidates for brachytherapy following 12 weeks of cytoreductive therapy

#### Conclusion

The percentage of our patients who converted to suitability for brachytherapy following LHRH-free

cytoreduction is similar to those described previously in the literature. It is also comparable to those who report conversion to suitability using LHRH agonists, albeit with a more favourable side effect profile.

#### EP-2155 Optimising HDR Prostate Implant, Planning and delivery. A new centre experience

R. Farrell<sup>1</sup>, S. Jain<sup>1</sup>, P. Shiels<sup>1</sup>, G. Workman<sup>1</sup>, K. Crowther<sup>1</sup>, D. Mitchell<sup>1</sup>

<sup>1</sup>Belfast Health and Social Care Trust- City Hospital, Radiotherapy Department, Belfast, United Kingdom

#### Purpose or Objective

High dose rate prostate Brachytherapy (HDR) is a well-established method of dose escalation in combination with external beam radiotherapy (EBRT) and research in its use as a monotherapy continues.

Having optimised our permanent seed prostate brachytherapy pathway over 500 cases, we wished to prospectively review the HDR pathway from its implementation at our centre. The goal was to minimize anaesthetic time, optimise ultrasound-based planning and improve patient throughput.

#### Material and Methods

Following formal training, mentoring and development of all departmental policies, procedures, work instructions and treatment pathways, 19 steps were identified on the pathway from patient admission to theatre to discharge from recovery. A supernumerary therapeutic radiographer prospectively documented the time for each task and following the initial 10 cases a multi-disciplinary meeting was held to identify potential areas where time could be saved. This process was repeated to the point where procedural times were consistent and no further significant time gains were identified.

#### Results

To date 66 patients have been treated with HDR brachytherapy for prostate, 55 combination cases with External beam radiotherapy and 11 salvage or monotherapy treatments.

At the Plan, Do, Study, Act, (PDSA) review of the initial 10 cases, several tasks including pre-implant contouring and planning catheter position were felt to be unnecessary duplication and a standardised 'template' coordinate implant was adopted. Subsequent cohorts clarified dose constraint objectives and defined methods of prioritising dose to target volumes. When required, second check verification was moved to be a parallel process at each task rather than serially.

By the 30<sup>th</sup> case our procedure time had reduced from 280mins to 175mins, reduction in overall treatment time of 37.5%. Adoption of identified changes in initial implant procedure resulted in 52% reduction in time, from the average of 69mins (1<sup>st</sup> 10 cases) to 33mins (11<sup>th</sup>-30<sup>th</sup> case), from probe insertion to grid locking and hence commencement of planning.

Additional reviews of time for catheter reconstruction (simplified to a maximum of 4 waypoints along catheter length) and reduction in the number of treatment checks by radiographers saw a further improvement in procedure time, a reduction of 29% was gained from these changes in the process between the grid locking and treatment start, average of 129mins in the 1<sup>st</sup> cohort compared to 92mins 2<sup>nd</sup>.

#### Conclusion

This time and motion study has reduced overall anaesthetic exposure and improved theatre capacity for our HDR cases. We continue to see a reduction in overall treatment time and frequent PDSA reviews highlight any further issues thus ensuring we improve the overall patient experience.

#### Electronic Poster: Brachytherapy: Miscellaneous

#### EP-2156 Assessment of Role of ILRT as palliative treatment in advanced esophageal cancer

V. Pareek<sup>1</sup>, R. Bhalavat<sup>1</sup>, M. Chandra<sup>1</sup>

<sup>1</sup>Jupiter Hospital, Radiation Oncology, Mumbai, India

#### Purpose or Objective

This study aims to assess the improvement in dysphagia, associated complications and overall and disease-free survival with intraluminal brachytherapy (ILRT) as palliative care in advanced esophageal cancer

#### Material and Methods

Thirty-four patients were treated with high dose rate ILRT with or without external radiation therapy from 2009 to 2017 at our institute. Patients were assessed for various parameters including disease stage, length of lesion, KPS and as per grade of dysphagia at presentation. The patients received median dose of 6Gy at 1 cm off axis for 2 fractions one week apart. Fourteen patients were treated radically and 20 patients post EBRT. Multivariate analysis was used to assess the predictors for dysphagia improvement. Remissions of dysphagia and other clinical and radiological factors were assessed in the first month post-treatment, and then in the third, sixth, and twelfth months. The survival rate was compared with some chosen clinical factors using a log-rank test and the Kaplan-Meier method.

#### Results

Patients were followed up as per standard institute protocol. Median dysphagia free survival was 12 months. Stricture was seen in 3 patients and ulceration noted in another 2 patients. However, no tracheoesophageal fistula or procedure related complications were noted. Complications were seen with the post EBRT group. The overall survival in the cohort was 12 months and was better post EBRT as compared to radical ILRT ( $p < 0.001$ ). On multivariate analysis, stage of disease ( $p = 0.02$ ), size of lesion ( $p = 0.018$ ) and grade of dysphagia ( $p = 0.023$ ) were found to be predictors for improved outcomes with use of ILRT in palliation.

#### Conclusion

Brachytherapy in the form of ILRT in advanced esophageal cancer provides good palliation with minimal complications and improved survival and quality of life to patients.

#### EP-2157 Needle-based stepping source electronic brachytherapy - a feasibility study

A.M. Ruder<sup>1</sup>, L. Inghelram<sup>1</sup>, F. Schneider<sup>1</sup>, Y. Abo-Madyan<sup>1</sup>, M. Ehmann<sup>1</sup>, J. Hesser<sup>1</sup>, F. Wenz<sup>1</sup>, F. Giordano<sup>1</sup>

<sup>1</sup>Universitaetsklinikum Mannheim, Klinik für Radioonkologie und Strahlentherapie, Mannheim, Germany

#### Purpose or Objective

Electronic needle-based kilovolt (kV) brachytherapy (eBT) may resemble an economic alternative to multi-catheter (HDR) and permanent seed implantation (PSI) brachytherapy. We have evaluated whether tumors treated with seed implants would have been suitable for electronic brachytherapy.

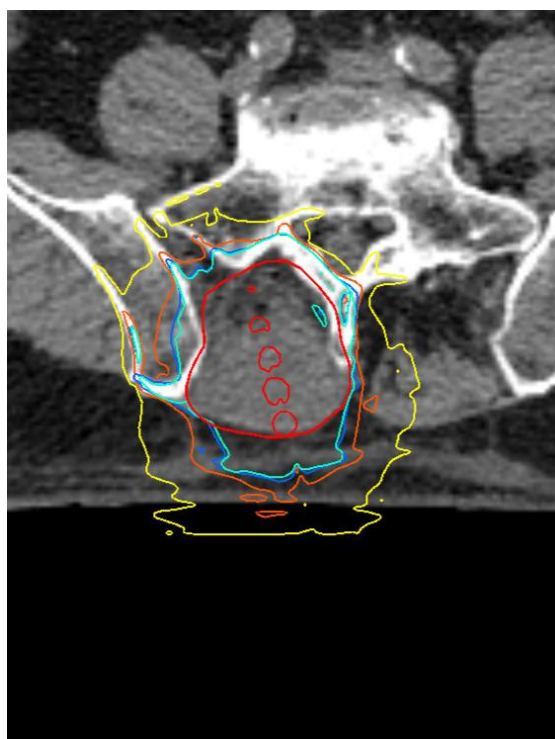
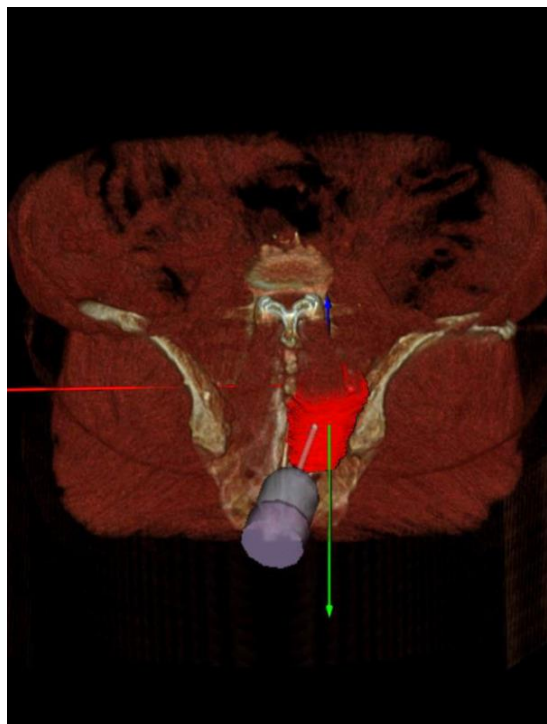
#### Material and Methods

N=5 post-interventional CT studies of patients who had received PSI with <sup>125</sup>I seeds in tumors were used as templates for planning. We then simulated treatment with a needle applicator (length = 94 mm) of a kilovoltage x-ray system (INTRABEAM, Carl Zeiss Meditec AG) using a dwell point stepping (DPS) approach. For planning the dwell points, an algorithm for kV-dose distribution in tissue of various density was used (Radiance®, GMV Innovating Solutions S.L., Madrid). For dose summation, Radiance dosimetry files were transformed and imported

into Velocity (Varian Medical Systems Inc., USA) for forward planning. DPS dose distributions achieved with eBT were then compared to those achieved with PSI.

#### Results

The total number of dwell points for eBT per patient ranged from 2 to 15. In all patients, dose coverages achieved with eBT were similar to the prescribed doses with those obtained in PSI. Dose constraints (e. g. D10, D1cc, Dmax) for organs at risk were met in all patients. The number of trajectories needed for adequate coverage was lower with eBT compared to PSI.



#### Conclusion

eBT with a DPS approach was feasible for tumors initially treated with PSI.

## E-posters Radiobiology

### Electronic Poster: Radiobiology track: Radiobiology of particles and heavy ions

#### EP-2158 The Apoptosis Mechanism and Injury of Heavy Ion Beam and X-ray Radiation on Malignant Melanoma Cell

S. Li<sup>1</sup>, Q. Jin<sup>1</sup>, Z. Chao<sup>1</sup>, G. Dong-Wei<sup>2</sup>, L. Qiang<sup>3</sup>, Z. Hong<sup>4</sup>, J. Xiao-Dong<sup>3</sup>, L. Yang<sup>4</sup>

<sup>1</sup>Lanzhou General Hospital of PLA, Radiotherapy, Lanzhou, China; <sup>2</sup>Northwest Normal University, Biology, Lanzhou, China; <sup>3</sup>Modern Physics- Chinese Academy of Sciences, Medical Physics, Lanzhou, China; <sup>4</sup>Modern Physics- Chinese Academy of Sciences, Radiation Medicine, Lanzhou, China

#### Purpose or Objective

This study aims to investigate the influence of high LET heavy ion ( $^{12}\text{C}^{6+}$ ) and low LET X-ray radiation on apoptosis and related proteins of malignant melanoma on tumor-bearing mice under the same physical dosage.

#### Material and Methods

C57BL/6J mice were burdened by tumors and randomized into three groups. These mice received heavy ion ( $^{12}\text{C}^{6+}$ ) and X-ray radiation under the same physical dosage, respectively; and their weights and tumor volumes were measured every three days post-radiation. After 30 days, these mice were sacrificed. Then, median survival time (MST) was calculated and tumors on mice were proliferated. In addition, immunohistochemistry was carried out for apoptosis-related proteins to reflect the expression level.

#### Results

After tumor-bearing mice were radiated by heavy ion, MST improved and tumor volume significantly decreased in conjunction with the upregulated expression of pro-apoptosis factors, Bax and Cytochrome C, and the downregulated expression of apoptosis-profilin (Bcl-2, Survivin) and proliferation-related proteins (PCNA). Results indicated that radiation can promote the apoptosis of malignant melanoma cells and inhibit their proliferation. This case was more suitable for heavy ion ( $^{12}\text{C}^{6+}$ ).

#### Conclusion

High LET heavy ion ( $^{12}\text{C}^{6+}$ ) radiation could significantly improve the killing ability for malignant melanoma cells by inducing apoptosis in tumor cells and inhibiting their proliferation. These results demonstrated that heavy ion ( $^{12}\text{C}^{6+}$ ) presented special advantages in terms of treating malignant melanoma.

#### EP-2159 Influence of L-Dopa pretreatment on cellular features in T98G cells

A. Facchetti<sup>1</sup>, C. Aprile<sup>2</sup>, M. Cavagnini<sup>1</sup>, M. Ciocca<sup>3</sup>, A. Iannalfi<sup>2</sup>, L. Lodola<sup>4</sup>, M. Marengo<sup>4</sup>, R. Nano<sup>5</sup>, F. Pasi<sup>6</sup>, M.G. Persico<sup>7</sup>, F. Valvo<sup>2</sup>, R. Orecchia<sup>8</sup>

<sup>1</sup>Fondazione CNAO, Radiobiology Unit, Pavia, Italy; <sup>2</sup>Fondazione CNAO, Radiation Oncology, Pavia, Italy; <sup>3</sup>Fondazione CNAO, Medical Physics Unit, Pavia, Italy; <sup>4</sup>Fondazione IRCCS Policlinico San Matteo, Struttura Complessa di Medicina Nucleare, Pavia, Italy; <sup>5</sup>Università degli Studi di Pavia, Dipartimento di Biologia e Biotecnologie "L. Spallanzani", Pavia, Italy; <sup>6</sup>Fondazione IRCCS Policlinico San Matteo, Struttura Complessa di Radioterapia, Pavia, Italy; <sup>7</sup>Università degli Studi di Pavia, Scuola Universitaria Superiore IUSS,

Pavia, Italy ; <sup>8</sup>Fondazione CNAO- Istituto Europeo di Oncologia, Radiation Oncology, Pavia- Milano, Italy

### Purpose or Objective

Recently, a role of L-Dopa for the diagnosis and treatment of glioblastoma has been hypothesized. Four hours pre-load with L-Dopa has been previously reported to increase incorporation of BPA (boron-phenyl-alanine) in tumors both in vivo and in vitro, likely activating the LAT system and thus increasing the efficacy of BNCT (Boron Neutron Capture Therapy). This approach looks very appealing because in theory it could be employed to increase the tumor accumulation of <sup>18</sup>F-DOPA in PET diagnostics or of the <sup>11</sup>B substrate in BPCT (Boron Proton Capture Therapy). In light of these experimental applications, the aim of this study was to assess the effects of pretreatment with L-Dopa on the biological behavior of human T98G cells, a chemo/radioresistant glioblastoma cell line.

### Material and Methods

Briefly, 4-hour pretreatment with 50 µg/mL or 100 µg/mL of L-Dopa can influence the morphology, the growth rate, the ability to form colonies, and the migratory capacity of T98G cell in exponential growth, in basal conditions and after carbon ion irradiation (2 and 4 GyRBE). Statistical analysis has been performed with ANOVA and paired t test.

### Results

After L-dopa pretreatment cells show a lower tendency to aggregate and a round-like pattern. Recovery of the scratched area was significantly faster and higher by T98G cells pretreated cells. Boyden Chamber test confirmed enhanced migration of the treated cells. Carbon ions irradiation increases the migratory efficiency either at 15 and 24 hours.

### Conclusion

The results show that L-Dopa induced significant changes in T98G cells behavior. These aspects have been never previously evaluated and open further questions about real utility of L-Dopa pre-load in BNCT and indicate a lack of experimental data for a possible application in PET with FDOPA and BPCT.

### Electronic Poster: Radiobiology track: Radiation-induced signalling pathways

#### EP-2160 Downregulation of Nrf2 promotes radiation-induced apoptosis in non-small cell lung cancer cells H. Zhang<sup>1</sup>

<sup>1</sup>Institute of Modern Physics- Chinese Academy of Sciences, Department of Radiation Medicine, Lanzhou, China

### Purpose or Objective

The nuclear factor erythroid-2-related factor 2 (Nrf2) is a crucial regulator of the cellular antioxidant system. Nrf2 is often constitutively activated in non-small cell lung cancer (NSCLC) cell lines, which promotes cytoprotection against oxidative stress and xenobiotics. Notch1 signaling is critically implicated in cell fate determination. It has been reported that Nrf2 strongly regulates Notch1 activity. However, the role of Nrf2 mediated Notch1 signaling in response to ionizing radiation (IR) remains elusive. We report that knockdown of Nrf2 promotes radiation-induced apoptosis through Nrf2 mediated Notch1 signaling in NSCLC cells.

### Material and Methods

The human lung cancer cells (A549, NCI-H1299 (H1299), NCI-H460 (H460)) were exposed to ionizing radiation at room temperature using Faxitron RX-650 X-rays (Faxitron Bioptics, LLC, USA). The dose rates were 0.765 Gy/min. siRNA against Nrf2, Notch1 and non-targeting negative control siRNA were purchased from Invitrogen (Invitrogen Life Technologies, Carlsbad, CA, USA).

Real-time fluorescent quantitative PCR assay the level of Nrf2 and Western blot to analyze the Nrf2, GCLC, HO-1, NQO1, Bax, Bcl-2. Cells were treated with siRNA-Nrf2 before X-irradiation (4 Gy) and incubated for 24 h. After staining with anti-Nrf2 antibody and Alexa Fluor 647-conjugated secondary antibody and were visualized under a fluorescence microscope. Immunofluorescence staining for Notch1 in A549 cells, Alexa Fluor 647-conjugated secondary antibody and nuclei were counterstained with DAPI.

### Results

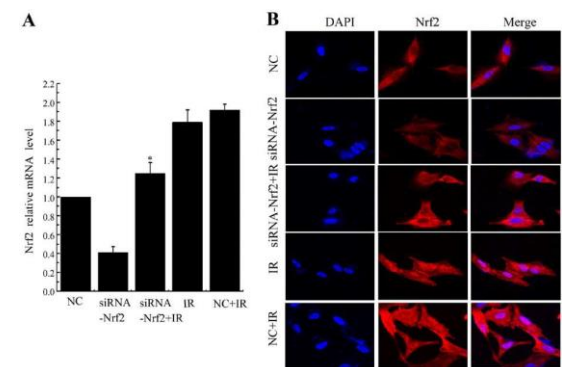


Figure 1. IR-induced nuclear translocation of Nrf2 is suppressed by siRNA-Nrf2 in A549 cells. (A) mRNA levels of Nrf2 at 24 h after 4 Gy of X-ray irradiation. (B) Cells were treated with siRNA-Nrf2 before X-irradiation (4 Gy) and incubated for 24 h. After staining with anti-Nrf2 antibody and Alexa Fluor 647-conjugated secondary antibody (red) and DAPI for nuclear staining (blue), cells were visualized under a fluorescence microscope. \* $p < 0.05$  versus NC+IR group.

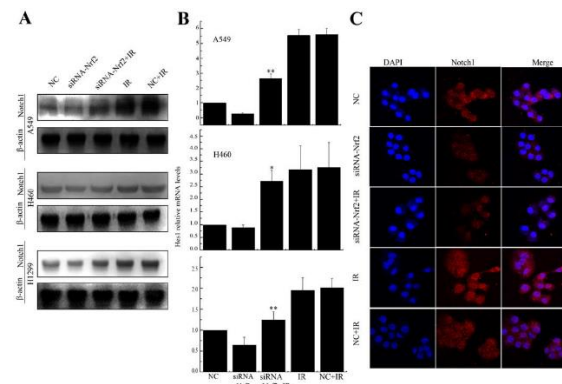


Figure 2. Expression of Notch1 and related gene in the knockdown of Nrf2 cells. (A) Quantification of protein expression. (B) Hes1 mRNA levels were measured by quantitative RT-PCR. (C) Immunofluorescence staining for Notch1 in A549 cells. \* $p < 0.05$  and \*\* $p < 0.01$  versus NC+IR group.

### Conclusion

- 1) Nrf2 is induced by ionizing radiation in A549 cells
- 2) Knockdown of Nrf2 decreases radiation-upregulated Nrf2 in A549 cells.
- 3) Knockdown of Nrf2 decreased Notch1 expression after IR

#### EP-2161 miR-454-3p regulates cellular radio-sensitivity by targeting to BTG1 in renal carcinoma cells J. Wang<sup>1</sup>

<sup>1</sup>Institute of Modern Physics- Chinese Academy of Sciences, Biophysics, Lanzhou, China

### Purpose or Objective

Our previous study showed that miR-454-3p decreased obviously after exposure of renal carcinoma 786-O cells to X-rays. miR-454-3p targeted to BTG1, which has long been recognized as a tumor suppressor gene, through a direct interaction with the 3'-UTR of BTG1 mRNA. Here, we try to explore the function and mechanisms of miR-454-3p in renal carcinoma cells responding to ionizing radiation and detect whether miR-454-3p contributes to the instability of genome after ionizing radiation exposure.

### Material and Methods

The human renal carcinoma 786-O cells were exposed to 2.5 Gy of X-rays. The mRNA levels and protein levels of BTG1 were analyzed by qRT-PCR and western blotting. The radio-sensitivity was quantified by assaying the number of micronuclei in binucleated cells with a fluorescence microscope after exposure.

### Results

We found that both the mRNA levels and protein levels of BTG1 were significantly increased at 4-8 hours in renal carcinoma 786-O cells exposed to 2.5 Gy of X-rays. The number of micronuclei increased significantly in binucleated 786-O cells at 36 hours when BTG1 were down-regulated by transfection of miR-454-3p mimics, implying that BTG1 contributed to maintain the genetic integrity after exposure of 786-O cells to ionizing radiation.

### Conclusion

Our results indicate that down-regulation of BTG1 renders tumor cells sensitive to radiation. These results support our previous report that miR-454-3p regulates cellular radio-sensitivity by targeting to BTG1. Our findings may shed light on the potential application of microRNA in tumor radiotherapy.

**Electronic Poster: Radiobiology track: Tumour microenvironment**

### EP-2162 Applying the Linear Quadratic Model to PC-3 cells irradiated under different O<sub>2</sub> conditions

T. McMullan<sup>1</sup>, J. Meehan<sup>2,3,4</sup>, S. Langdon<sup>2</sup>, D.B. McLaren<sup>3</sup>, S. McLaughlin<sup>5</sup>, W.H. Nailon<sup>1,6</sup>

<sup>1</sup>Edinburgh Cancer Centre, Oncology Physics, Edinburgh, United Kingdom; <sup>2</sup>University of Edinburgh, Institute of Genetics and Molecular Medicine, Edinburgh, United Kingdom; <sup>3</sup>Edinburgh Cancer Centre, Clinical Oncology, Edinburgh, United Kingdom; <sup>4</sup>Heriot Watt University, Institute of Sensors- Signals and Systems., Edinburgh, United Kingdom; <sup>5</sup>Heriot Watt University, School of Engineering and Physical Sciences, Edinburgh, United Kingdom; <sup>6</sup>University of Edinburgh, School of Engineering, Edinburgh, United Kingdom

### Purpose or Objective

Prostate cancer outcome is compromised by areas of tumour hypoxia, which can be three times more radioresistant than well oxygenated areas. However, taking account of hypoxia when estimating the  $\alpha/\beta$  ratio and the resulting surviving fraction of cells as a function of dose is challenging. The aim of this study was to use the linear quadratic (LQ) model to fit to cell survival data obtained from PC-3 cells irradiated under a range of different O<sub>2</sub> conditions.

### Material and Methods

Human prostate cancer PC-3 cells, 100 cells in each well of a 96 well plate, were cultured and prepared under normoxic (20% O<sub>2</sub>), hypoxic (0.5% O<sub>2</sub>), and oxic conditions close to those in the human body (7% O<sub>2</sub>). Additionally, groups of 0.5% O<sub>2</sub> and 7% O<sub>2</sub> cells were transferred to 20% O<sub>2</sub> conditions after irradiation (Re-Ox). Irradiation was performed 24 hours after seeding in a Faxitron RX-650 cabinet X-ray device with doses in the range 0.5 - 6 Gy. The cells were left for at least 13 days before fixation and

cell response to irradiation was measured using SRB assays. The LQ model was fitted to the surviving fraction of cells at the different O<sub>2</sub> conditions and the  $\alpha$  and  $\beta$  values estimated.

### Results

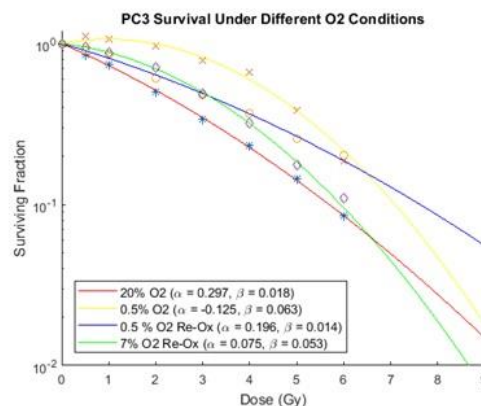


**Figure 1:** The LQ fit to the surviving fraction of cells obtained under different O<sub>2</sub> conditions.

The LQ fits for the single dose data are shown in Figure 1. As expected, the 20% O<sub>2</sub> had the lowest survival fraction up to 6 Gy. The 7% Re-Ox cells, which are closer to those found in the body, had greater cell-kill at higher doses due to the larger  $\beta$  component. At 6 Gy the survival fraction for the hypoxic 0.5% O<sub>2</sub> cells (irradiated at 0.5% O<sub>2</sub> and kept at 0.5% O<sub>2</sub> until fixation) was essentially the same as the 0.5% Re-Ox cells (irradiated at 0.5% O<sub>2</sub> and transferred to 20% O<sub>2</sub> at fixation).

Interestingly, the hypoxic cells show increased resistance to irradiation at low doses up to 1 Gy with their populations increasing. However, the dose increments are not sufficient to show the *low dose hyper-radiosensitivity* found by other researchers. Beyond 6 Gy, the  $\beta$  effect of cell-kill dominates in a similar manner to the 7% O<sub>2</sub> curve. Overall, in the dose range studied, there is a decrease in surviving fraction with increasing O<sub>2</sub> conditions. The 20% O<sub>2</sub> has an almost linear response, which is reflected in the high  $\alpha$  value.

**Table 1:** Resulting alpha/beta ratios for the different O<sub>2</sub> conditions.

O <sub>2</sub> Condition	$\alpha/\beta$	Description
20%	16.5	Normoxic
0.5%	14	Hypoxic (with re-ox)
7%	1.4	Normal Prostate

### Conclusion

The data presented demonstrates that it is possible to obtain estimates of  $\alpha$  and  $\beta$  that accounts for different levels of O<sub>2</sub> in the tumour microenvironment. However, it is important to take account of the impact of fractionation before considering the probability of tumour control.

**Electronic Poster: Radiobiology track: Immunoradiobiology**

### EP-2163 Combination therapy of microglia and radiotherapy in a rat model of spontaneous glioma

Y. Suzuki<sup>1</sup>, N. Okonogi<sup>2</sup>, H. Sato<sup>3</sup>, T. Oike<sup>3</sup>, Y. Yoshimoto<sup>3</sup>, K. Mimura<sup>4</sup>, S. Noda<sup>3</sup>, M. Okamoto<sup>3</sup>, T.

Tamaki<sup>1</sup>, Y. Morokoshi<sup>5</sup>, S. Hasegawa<sup>5</sup>, H. Ohgaki<sup>6</sup>, H. Yokoo<sup>7</sup>, T. Nakano<sup>3</sup>

<sup>1</sup>Fukushima Medical University School of Medicine, Department of Radiation Oncology, Fukushima-City, Japan; <sup>2</sup>National Institute of Radiological Sciences-National Institutes for Quantum and Radiological Science and Technology, Hospital, Chiba, Japan; <sup>3</sup>Gunma University Graduate School of Medicine, Department of Radiation Oncology, Maebashi, Japan; <sup>4</sup>Fukushima Medical University School of Medicine, Department of Gastrointestinal Tract Surgery, Fukushima-City, Japan; <sup>5</sup>National Institute of Radiological Sciences- National Institutes for Quantum and Radiological Science and Technology, Radiation and cancer biology team, Chiba, Japan; <sup>6</sup>International Agency for Research on Cancer, Section of Molecular Pathology, Lyon, France; <sup>7</sup>Gunma University Graduate School of Medicine, Department of Human Pathology, Maebashi, Japan

### Purpose or Objective

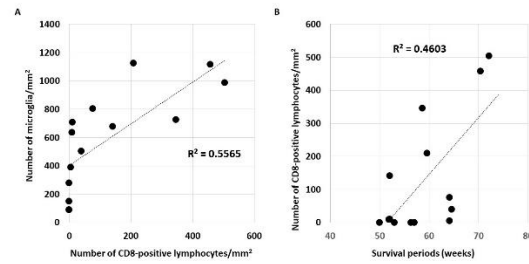
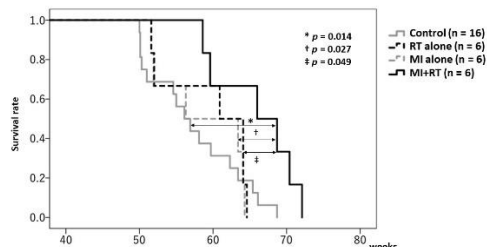
Glioblastoma multiforme (GBM) is the most common primary brain tumor in adults, accounting for approximately 70% of high-grade gliomas. The current standard of care is based on maximal safe surgical resection with concurrent chemoradiotherapy using temozolomide followed by 6 months of maintenance chemotherapy, resulting in median survival time of approximately just 15 months. Microglia are immune effector cells that play an important role in processes such as phagocytosis and antigen presentation in the CNS. The aim of this study was to investigate the efficacy of combination therapy with intravenously injected microglia (MI) and radiation therapy (RT) for malignant glioma in rats.

### Material and Methods

Transgenic rats expressing v-erbB and spontaneously developing malignant glioma were used. The rats were divided into 4 groups: control (n = 19), RT alone (n = 10), MI alone (n = 9), and combination MI and RT (MI + RT) (n = 10). Cranial x-ray irradiation (8 Gy per fraction; once per week) was performed at 50 and 51 weeks of age. Cultured rat microglial cells ( $5 \times 10^6$  cells/rat) were intravenously injected via the tail vein within 30 minutes after RT.

### Results

No evidence of side effects, including thrombosis or graft-versus-host disease, was noted. Rats treated with RT alone, MI alone, MI + RT, and control survived 60.9, 56.3, 66.0, and 56.1 weeks, respectively. The survival period of MI + RT was significantly longer than that of control (P = .014), MI alone (P = .027), and RT alone (P = .049). Immunohistochemical analysis showed a significantly higher number of tumor-infiltrated MI in the RT alone (P = .041) and MI + RT groups (P = .014) compared with the control. Significantly more CD8-positive lymphocytes were observed in the MI + RT group (P = .049) compared with the control. A positive correlation was found between the number of MI and CD8-positive lymphocytes ( $R^2 = 0.556$ ). A positive correlation was also found between CD8-positive lymphocytes and survival periods ( $R^2 = 0.460$ ).



### Conclusion

MI + RT increased infiltrated MI and CD8-positive T cells and prolonged survival in transgenic rats that spontaneously developed malignant glioma. Combined immunocellular therapy and RT may provide a novel treatment strategy for malignant glioma.

### EP-2164 Pilot Study: Systemic response after lung SBRT analyzing immune Cells phenotyping

A. Navarro-Martin<sup>1</sup>, I. Linares<sup>2</sup>, M.A. Berenguer<sup>2</sup>, R. Cañas<sup>3</sup>, F. Guedea<sup>4</sup>

<sup>1</sup>Instituto Catalan De Oncologia, Radiation Oncology Department, Hospitalet De Llobregat, Spain; <sup>2</sup>Instituto Catalan de Oncologia, Radiation Oncology Department, Barcelona, Spain; <sup>3</sup>ONCOBELL Program/IDIBELL, Radiation Oncology Department Barcelona, Barcelona, Spain; <sup>4</sup>Instituto Catalan de Oncologia, Radiation Oncology Department, Barcelona, Spain

### Purpose or Objective

To investigate changes of immune-phenotyping values in patients treated with Stereotactic Body Radiation Therapy (SBRT) over the lung in order to evaluate the immune response after radiation therapy.

### Material and Methods

From November 2016 to May 2018, 7 patients (p) with 7 lung lesions were enrolled in a translational sub-study. All of them underwent SBRT treatment.

Peripheral blood samples prior to the treatment for each patient (1month, 3 months and 6 months) were collected and analyzed. Peripheral mononuclear cells (PBMCs) were isolated from a heparinized venous blood sample by density gradient centrifugation. After centrifugation, PBMCs were collected from the plasma-Ficoll interphase and used for flow cytometry.

Three panels were used:

- Lymphocyte Phenotyping DuracloneTM, Beckman Coulter: CD16 Ab, CD56 Ab, CD19 Ab, CD14 Ab, CD4 Ab, CD8 Ab, CD3 Ab, CD45 Ab

- Regulatory T cells DuracloneTM, BeckmanCoulter: CD45RA Ab, CD25 Ab, CD39 Ab, CD4 Ab, Intracellular FOXP3 Ab, CD3 Ab, Helios Ab, CD45 Ab

- Myeloid Derived Suppressor Cells (MDSC) DuracloneTM, BeckmanCoulter: CD45, HLA-DR, CD14, CD33, CD11b.

Cell surface and intracellular staining were performed according to the manufacturer's protocols. Cell phenotypes were evaluated using the FACS Navios system (BeckmanCoulter).

### Results

Median age was 73r (65-80). 5 Males and 2 females. Primary lung tumor 5 cases, 1 CRC and 1 breast primary. None were a candidate to undergo surgery after evaluation in a multidisciplinary tumor board. Locations were: 2p right upper lobe, 3p right inferior lobe and 2p right medium lobe. Following the clinical protocol doses delivered were 60Gy (7.5Gy x 8fr) in 3p y 50Gy (12.5Gy x 4 fr) in 4 p. Mean follow up of 16 months r(2-20), 1p incomplete response, 2p in partial response and 4 in stable .

Lymphocyte Phenotyping showed that Natural Killer cells defined as CD56+high CD16+, increased among the follow up with initial values of 0.95% to 1.38% at 6 months. Statistical analysis using Friedman Test ( $p=0.18$ ) and Wilcoxon test don't showed significant differences.

Regulatory T cells activated defined as (CD4+-CD25+Foxp3+CD45RA) showed stable values during the follow up (baseline values 4.97% vs. 4.46% at 6 months). No statistical differences were detected.

Myeloid-derived suppressor cells (MDSC) CD33+CD11b+CD14-, showed a tendency to lower values during the follow up (basal 62.6% vs 66.1%). No statistical significance was detected.

#### Conclusion

High doses of radiation therapy over the lung can provide a systemic effect detected in peripheral blood samples. Even the small sample size, our study shows an increase of stimulatory immune populations with stability or decreasing suppressive populations.

---

#### Electronic Poster: Radiobiology track: Radiation and tumour metabolism

---

#### EP-2165 m6A RNA modification by METTL3 regulates chemo- and radioresistance in pancreatic cancer cells

S. Tatekawa<sup>1,2,3</sup>, M. Konno<sup>2,3</sup>, A. Asai<sup>2,3</sup>, J. Koseki<sup>2</sup>, K. Taketo<sup>1</sup>, H. Ishii<sup>2,3</sup>, K. Ogawa<sup>1</sup>

<sup>1</sup>Osaka University Graduate School of Medicine, Department of Radiation Oncology, Osaka, Japan; <sup>2</sup>Osaka University Graduate School of Medicine, Medical Data Science, Osaka, Japan; <sup>3</sup>Osaka University Graduate School of Medicine, Cancer Frontier Science, Osaka, Japan

#### Purpose or Objective

N6-methyladenosine (m6A) is the most prevalent internal modification of messenger RNA (mRNA) and long noncoding RNA (lncRNA) in the majority of eukaryotes. The m6A modification in RNA can be catalyzed by methyltransferases, or removed by demethylases, which are termed m6A writers and erasers, respectively. m6A mRNA methylation is a gene regulatory mechanism affecting cell differentiation and proliferation through regulation of RNA stabilities, mRNA splicing, microRNA processing and mRNA translation. Especially in cancer, however, it has been mostly unclear what means m6A is dynamically regulated or written by enzymatic components represented by methyltransferase-like 3 (METTL3) and how m6A is significant for each of the numerous genes. We focused on METTL3 in pancreatic cancer, because the prognosis of which is not satisfactory despite the development of multidisciplinary therapies including radiation therapy.

#### Material and Methods

To study the roles of m6A mRNA methylation in chemo- and radioresistance, we established METTL3-knockdown pancreatic cancer cell line using short hairpin RNA. We performed proliferation assay, sphere formation assay, chemo- and radiosensitivity assay. For the purpose of searching target genes affected by METTL3, we conducted cDNA expression analysis and anti-m6A antibody methylated RNA immunoprecipitation sequencing (MeRIP-Seq).

#### Results

Although there was no difference in morphology and proliferation rate between control and METTL3-depleted cells, METTL3-depleted cells in sphere formation assay showed significantly lower ability than control cells to form spheres. Furthermore, METTL3-depleted cells showed higher sensitivity to anticancer reagents such as gemcitabine, 5-fluorouracil, cisplatin and irradiation through enhancing apoptotic response. Our data suggest

that METTL3 is a potent target for enhancing therapeutic efficacy in patients with pancreatic cancer. In addition, we performed cDNA expression analysis followed by gene ontology and protein-protein interaction analysis using the Database for Annotation, Visualization, and Integrated Discovery and Search Tool for the Retrieval of Interacting Genes/Proteins databases, respectively. The results demonstrated that METTL3 was associated with mitogen-activated protein kinase cascades, ubiquitin-dependent process and RNA splicing and regulation of cellular process, suggesting functional roles and targets of METTL3. Finally, we confirmed methylation statuses of those genes were changed by METTL3 using MeRIP-Seq.

#### Conclusion

The present study demonstrates that METTL3 is associated with chemo- and radioresistance and is a potential therapeutic target of pancreatic cancer. Additionally, our findings suggest several critical pathways, including MAPK cascades, ubiquitin-dependent process, RNA splicing and regulation of cellular process, as possible targets of METTL3.

---

#### Electronic Poster: Radiobiology track: DNA damage response

---

#### EP-2166 Ro90-7501 is a novel radiosensitizer which inhibits ATM phosphorylation and DNA repair

K. Tamari<sup>1</sup>, Z. Li<sup>1</sup>, K. Otani<sup>1</sup>, Y. Takahashi<sup>1</sup>, K. Minami<sup>1</sup>, Y. Seo<sup>2</sup>, O. Suzuki<sup>1</sup>, F. Isohashi<sup>1</sup>, K. Ogawa<sup>1</sup>

<sup>1</sup>Osaka University Graduate School of Medicine, Radiation Oncology, Suita- Osaka, Japan; <sup>2</sup>Osaka University Graduate School of Medicine, Radiation Oncology, Suita-Osaka, Japan

#### Purpose or Objective

To explore new radiosensitizers, we have previously performed a cell-based high throughput screening by using 1280 compounds with irradiation, and found Ro90-7501 as a candidate for radiosensitizer. Ro90-7501 has been reported as an inhibitor of amyloid B42 fibril assembly which causes Alzheimer's disease. However, the radiosensitizing effect of Ro90-7501 was unknown. The purpose of this study was to validate the radiosensitizing mechanism of Ro90-7501.

#### Material and Methods

A human cervical cancer cell line, HeLa, was used for entire experiment. Radiosensitizing effect of Ro90-7501 were validated by clonogenic survival assay and tumor regression assay using female BALB/c nude mice. Flow cytometry was performed to evaluate the difference in apoptosis and cell cycle after irradiation with or without Ro90-7501. Western blot was performed to evaluate the expression of proteins, involved DNA damage response such as pATM, pH2AX, pChk1, and pChk2.

#### Results

Clonogenic survival assay showed significant radiosensitizing effects of Ro90-7501 not only in normoxia but also hypoxia. Tumor regression assay *in vivo* revealed that combination treatment group using radiotherapy with Ro90-7501 (RT+Ro) was significantly reduced tumor volume compared with no treatment group, Ro90-7501 group and radiotherapy group. Ro90-7501 did not induce apparent side effects. Apoptosis significantly increased in RT+Ro group compared with other groups. Cell cycle analysis showed that RT+Ro group increased G2/M arrest. Western blot analysis showed that Ro90-7501 suppressed phosphorylation of ATM, and also suppressed phosphorylation of several downstream proteins such as H2AX, Chk1, Chk2 after irradiation, indicating that DNA repair pathway was inhibited in Ro+RT group.

### Conclusion

Ro90-7501 was identified as a radiosensitizer, which represses ATM phosphorylation, inhibits DNA repair after irradiation, and then increases cell apoptosis.

### EP-2167 Radiosensitizing effect of eribulin mesylate in human cervical carcinoma cells in vitro

R. Benlloch Rodríguez<sup>1</sup>, J. Romero Fernández<sup>1</sup>, R. Castejón Díaz<sup>2</sup>, S. Rosado García<sup>3</sup>, P. Sánchez Rubio<sup>4</sup>, S. Sánchez García<sup>1</sup>, I. Martínez Montesinos<sup>1</sup>, I. Zapata Paz<sup>1</sup>, M. López Valcárcel<sup>1</sup>

<sup>1</sup>Hospital Universitario Puerta de Hierro, Radiation Oncology, Majadahonda - Madrid, Spain; <sup>2</sup>IDIPHIM, Internal Medicine, Majadahonda - Madrid, Spain; <sup>3</sup>IDIPHIM, Cellular Culture Unit, Majadahonda - Madrid, Spain; <sup>4</sup>Hospital Universitario Puerta de Hierro, Radiophysics, Majadahonda - Madrid, Spain

### Purpose or Objective

To determine the radiosensitizing properties of eribulin mesylate, a synthetic analogue of the marine natural compound halichondrin B, in human cervical carcinoma cells; and study the potential mechanisms of radiosensitization

### Material and Methods

Cell line: HeLa cells, derived from a human cervical carcinoma, were maintained in DMEM medium, supplemented with FCS and antibiotics. In vitro chemo- and radiosensitivity were assessed by the crystal violet method. To determine chemosensitivity, cells were treated with a 24 h. exposure time of eribulin at different concentrations and, after 10 days of incubation, a dose-response curve was constructed from which the IC10 and IC50 were calculated. Radiosensitivity was evaluated by irradiating the cells at different doses (1,2,4,6 and 8 Gy) in absence or presence of the drug at different concentrations. Survival data were adjusted to the LQ model by a least squares algorithm. Surviving fraction at 2 Gy (SF2) and 4 Gy (SF4) from each survival curve were calculated from the fitted data. Cell cycle changes for control and treated cells were assessed by propidium iodide (PI) staining and flow cytometry analysis. Apoptotic cells were detected by FITC-conjugated Annexin V labelling method using flow cytometry. The percentage of apoptotic cells was obtained from a bivariate histogram of Annexin V labelled-cells versus PI labeled cells for control, 1.5 nM and 3 nM eribulin exposure, irradiation (6 Gy) and combined eribulin-irradiation groups.

### Results

HeLa cells are sensitive to eribulin at nanomolar range. The IC10 and IC50 for 24 h eribulin exposure were 0.75 nM and 2.1 nM respectively. A dose-dependent radiosensitization was observed. The SF2 for control, eribulin 0.3 nM, 0.75 nM and 1.5 nM were 0.94; 0.96; 0.84; and 0.71, respectively. The corresponding figures for SF4 were 0.79; 0.85; 0.67; and 0.47, respectively. The dose enhancement factor (DEF) calculated at 2 and 4 Gy for 1.5 nM eribulin were 1.25 and 1.68, respectively. A G2M cell cycle arrest was induced by eribulin. In the time-course experiment, the percentage of cells in G2M phase for control and 8, 24 and 48 h after 24 h exposure to 1.5 nM eribulin were 11.6%, 20%, 26.3% and 74.7%. The cultures treated with 1.5 nM and 3 nM eribulin showed a percentage of apoptotic cells of 22.5 and 28.1%, respectively. The combined treatment of irradiation at 6 Gy with 3 nM eribulin produced a significant increase in the percentage of apoptosis up to 45% of cells.

### Conclusion

Eribulin mesylate confers radiosensitizing effect in HeLa cells in vitro. The potential mechanisms involved in this effect are an arrest in the most radiosensitive G2M cell cycle phase and an increase in apoptosis in combined radiation-drug treatment.

### EP-2168 Analysis of Chromosomal Aberrations by FISH in FaDu tumor cells after in vivo X-ray MRT irradiation

A. Porth<sup>1</sup>, A. Hunger<sup>1,2</sup>, T. Setzkorn<sup>2</sup>, N. Mehrabi<sup>1</sup>, K. Burger<sup>1,3,4</sup>, S.E. Combs<sup>1,2</sup>, T.E. Schmid<sup>1,2</sup>

<sup>1</sup>Technische Universität München, Klinik und Poliklinik für RadioOnkologie und Strahlentherapie, München, Germany; <sup>2</sup>Helmholtz Zentrum München, Institut für innovative Radiotherapie, Neuherberg, Germany; <sup>3</sup>Technische Universität München, Lehrstuhl für Biomedizinische Physik- Physik-Department, Garching, Germany; <sup>4</sup>Technische Universität München, Munich School of Bio Engineering, Garching, Germany

### Purpose or Objective

X-ray microbeam radiation therapy (MRT) is a new irradiation technique in which the dose is deposited spatially separated with high peak doses. Studies comparing this technique to conventional X-ray irradiation have shown reduced toxicity in normal tissue and a better tumor control. Requiring high dose rates and precise beam collimation, MRT studies are mainly performed at synchrotron radiation facilities. In contrast to these, more cost effective and compact novel X-ray sources like the Munich Compact Light Source, used in this study, overcome the main limitations for the transfer of MRT to a clinical setting. In this study fluorescence in situ hybridization (FISH) was performed to detect chromosomal aberrations in order to assess the cellular response to MRT.

### Material and Methods

The human head and neck cancer cell line (FaDu) was injected subcutaneously into the ear of immunocompromised NMRI nu/nu mice. Tumors were irradiated conventionally or with MRT at mean doses of 3 Gy or 5 Gy using 25 keV X-rays. Sham irradiated and unirradiated mice served as control group. When a tumor reached the 15-fold of its initial volume, the tumor cells were isolated and cultivated for further in vitro analysis. Applying standard protocols, metaphase chromosome spreads were prepared and then hybridized with probes staining chromosomes 2 and 4. For each cell line, 500 metaphases were counted manually under a fluorescence microscope and chromosome aberrations were evaluated, focusing on translocations and aneuploidy.

### Results

24 cell lines were successfully isolated and analyzed via FISH. Three to seven replicates constituted the control and experimental groups respectively. In the control group, 5 ±1% of the cells showed structural aberrations. In irradiated cells this portion was higher: 11 ±1% for cells treated conventionally with 3 Gy, 10 ±1% for cells treated conventionally with 5 Gy, 15 ±2% of the cells irradiated with 3 Gy MRT and 11 ±2% of those irradiated with 5 Gy MRT. Numerical aberrations were found in 4 ±3% of the cells in the control group, 1 ±2% in the group treated with 3 Gy conventional X-rays, 2 ±1% in the group treated conventionally with 5 Gy and 2 ±1% for both MRT irradiated groups.

### Conclusion

Our study demonstrated an overall higher percentage of stable chromosome aberrations in all irradiated groups, corresponding to the clastogenic effect of ionizing radiation. In respect to this effect, no difference was visible between conventional and microbeam X-ray irradiation. Aneuploidy rates were high, both in irradiated and non-irradiated cells, which is a typical finding for tumor cells. Interestingly, this rate was lower in conventionally irradiated groups but not in the MRT groups. This might indicate a different influence of conventional and MRT irradiation on genomic instability.

## E-posters RTT

---

### Electronic Poster: RTT track: Patient preparation, positioning and immobilisation

---

#### EP-2169 Are treatment times with breast DIBH comparable to free breathing?

D. Ledsom<sup>1</sup>, V. Acton<sup>1</sup>, R. Biggar<sup>1</sup>

<sup>1</sup>Clatterbridge Cancer Centre, Department of Radiotherapy, Bebington- Wirral, United Kingdom

#### Purpose or Objective

The use of deep inspiration breath hold (DIBH) at the author's centre was extended to treat all breast cancer patients irrespective of laterality or nodal status in March 2017. This audit investigated the duration of treatment before and after implementation of the DIBH technique for all breast cancer patients to determine if the standard 15 minute appointment slot was still achievable.

#### Material and Methods

Varian Aria reports (v13.6) was used to identify treatment start and end time for all breast cancer patients treated March 2016 to February 2017 (left DIBH, right free breathing (FB)) and April 2017 to March 2018 (right and left DIBH). Data from March 2017 was excluded due to crossover of techniques.

#### Results

For all breast patients treated between March 2016-February 2017 (n=801, right sided FB, left sided DIBH) median treatment time was 12m:08s (SD 5:09) compared to 12m:47s (SD 5:22) when all patients were treated in DIBH (n=1288, April 2017-March 2018).

Data was stratified by laterality to compare FB and DIBH treatment times. For FB (n=418), median treatment time was 11m:50s (SD 5:01), versus DIBH (n=610) 12m:56s (SD 5:27). The difference was statistically significant (p<0.01). Outliers were excluded from data.

#### Conclusion

Median treatment time increased by 1 minute with DIBH; although this was statistically significant it was not clinically significant as there was no substantial increase in treatment time and the 15 minute appointment slot was achieved. DIBH treatment time therefore does not impact on capacity or extend appointment times.

#### EP-2170 Scheduling optimization to reduce patient waiting beam times in four-room proton therapy center

C.Y. Lin<sup>1</sup>  
<sup>1</sup>Chang Gung Memorial Hospital, Radiation Oncology, Taoyuan, Taiwan

#### Purpose or Objective

In proton therapy, patients are required to lie flat and wait on the treatment bed for the conversion of the beam before treatment. The displacement resulted from maintaining the posture with long time might lose the advantages of proton therapy. This study attempts to use the time difference to reduce wait time and provide the stability of the treatment posture.

#### Material and Methods

We recorded patients' waiting time from rooms 1 and 2 with the same wobbling system (Sumitomo Proton therapy System) and rooms 3 and 4 with the same pencil beam system. There were 27 working days for each time-dividing and non-time-dividing. For non-time-dividing, number of patients in room 1, 2, 3, and 4 are 262, 289, 219, and 231 and number of irradiation fields in room 1, 2, 3, and 4 are 528,584, 523, and 533, respectively. For time-dividing, number of patients in room 1, 2, 3, and 4 are 222, 210, 260, and 261 and number of irradiation fields in room 1, 2, 3, and 4 are 466,464, 682, and 621, respectively. The waiting time difference of time-dividing or not between

the treatment rooms was analyzed by using the independent T-test of SPSS Vision18 software.

#### Results

In rooms 1 and 2 with the wobbling system, the waiting time without and with time-dividing in one work day are 60.84±10.52 and 45.36± 0.17 minutes (p=0.173). In rooms 1 and 2 with the pencil beam system, the waiting time without and with time-dividing in one work day are 56.58±3.42 and 48.02±6.70 minutes (p=0.249). With all four treatment rooms simultaneous operation, the waiting time without and with time-dividing in one work day are 58.71±6.85 and 46.70±4.16 minutes (p=0.024). In rooms 1, 2, 3, and 4, the waiting time without and with time-dividing in one work day are 52.37±17.32 and 44.63±13.25 minutes (p<0.05), 66.67±19.86 and 45.00±12.95 minutes (p<0.05), 54.37±16.81, 45.26±10.42 minutes (p<0.05), and 57.04±22.89 and 43.70±12.64 minutes (p<0.05), respectively. The percentages of waiting time more than 60 minutes without and with time-dividing are 35.2% and 16.7%, respectively.

#### Conclusion

In proton therapy, the use time-dividing could reduce the patient's waiting time, decrease the discomfort of patients, minimize the random error of treatment, and improve the stability.

#### EP-2171 Optimizing individual customized neck rests for proton therapy of brain tumors

A. Schouboe<sup>1</sup>, M. Gioertz<sup>1</sup>, P. Randers<sup>1</sup>, A. Harboell<sup>1</sup>, C.R. Hansen<sup>1</sup>, A. Vestergaard<sup>1</sup>

<sup>1</sup>Aarhus University Hospital, Danish Center for Particle Therapy, Aarhus N, Denmark

#### Purpose or Objective

To study the reproducibility of individually customized neck rests for positioning patients with brain tumors undergoing irradiation in a Proton Centre. The Head and Neck board (HN board) is designed with an indentation for positioning the neck rest which has smooth sloping surfaces to ensure no steep gradients related to proton therapy. The system could potentially introduce an error in positioning of the individually customized neck rests. The purpose of this study was to evaluate the use of two neck rests with respect to displacement, ease of use and patient comfort.

#### Material and Methods

Individual customized neck rests from two different manufactures (A and B) were tested on 5 healthy volunteers. One individual customized neck rest from each manufacture was customized for each volunteer. The volunteer was positioned on the HN board with the head in neutral neck position.

In customizing individually neck rest we focused on comfortable and adequate support to the neck with no gaps underneath the head or neck. The aim was to create a neck rest as homogenous as possible in order to avoid large abrupt density variations, which for proton treatments can reduce plan robustness.

The volunteer was immobilized with a thermoplastic mask. A Beekly spot was placed underneath the HN-board and defined as reference. Two Beekly spots were placed in the same longitudinal plan as the reference and two on the cranial part of the neck rest (Fig 1). To evaluate the reproducibility of the positioning of the neck rests, the volunteer was re-positioned and a MRI scan was performed.

#### Results

A total of 10 MRI were evaluated. The mean longitudinal shifts were 1.4 mm (range 0.2-2.3 mm) and 1.3 mm (range 0.9-1.0 mm) for neck rest A and B, respectively. The cranial markers revealed no significant rotational error in positioning. The staff's main experience was to be extremely watchful when customizing the neck rest to make sure the material fitted in the indentation of the HN board to avoid the neck rests from being displaced. They

also subjectively experienced differences in handling the neck rests from the two manufactures. The staff found the material in neck rest A easier to handle because the amount of material was more appropriate. The amount of material in neck rest B resulted in too much spare material around the head which could contribute to steep gradients. The volunteers experienced neck rest A more comfortable and provided better support. Some of the volunteers observed smell from neck rest B in their clothes and hair for hours.

#### Conclusion

Challenges in customizing the individually neck rests for positioning brain tumor patients for proton therapy can be solved by being alert to the indentation on the HN board, when customizing the neck rest. The study showed no significant displacement using either of the neck rests. The staff found neck rest A was easiest to handle and without smell and most of the volunteers found neck rest A more comfortable.

#### EP-2172 Evaluation of the pitch functionality and setup accuracy of the Solstice SRS Immobilization System

C.L. Ong<sup>1</sup>, K. Hunnago<sup>1</sup>, F. Gescher<sup>1</sup>, J. Franssen<sup>1</sup>, E. Franken<sup>1</sup>

<sup>1</sup>Hagaziekenhuis, Radiotherapy, Den Haag, The Netherlands

#### Purpose or Objective

For stereotactic treatment of brain metastases, a good patient immobilization is crucial to ensure a highly accurate dose delivery with a limited PTV margin of 1-2 mm. Various commercial products offer great solutions for patient fixation and in combination with online daily imaging, translational and yaw-rotational setup errors can be corrected. Pitch-rotational setup errors correction is however only feasible with a 6D-couch, which is not commonly available in all institutes. The purpose of this study was to investigate the accuracy of the new Civo Solstice™ SRS immobilization system which allows manual correction of the pitch-rotational setup errors.

#### Material and Methods

The solstice mask comprised of a carbon fiber head support, customizable cushion, thermoplastic mask and a thermoplastic mouth-bite. A CT-scan of a Kyoto head phantom fixated with the Solstice mask was acquired (fig 1). Two spacers were position at the anterior and posterior side of neck area in order to allow a controlled pitch-rotational motion of the phantom within the mask. At the LINAC, CBCT's were acquired and registered to the CT in order to determine the accuracy of the mask. Subsequently several pitch-rotational setup errors were introduced within the mask and a CBCT was acquired. Based on the match value, the pitch setup error was manually corrected with the head support (fig 1) and a new verification CBCT was made. Furthermore, this mask was also applied on one patient receiving whole brain irradiation. This patient was also fixated using thermoplastic mask and the customized cushion and mouth bite. For this patient, two CBCT's were acquired before the treatment and one after. All scans were automatically registered on bony anatomy.

Figure 1 shows the setup of the Kyoto head phantom within the Solstice mask. The mask is secured to the head support, and the phantom is positioned within the mask. The setup is shown from a top-down perspective, highlighting the alignment of the mask and the phantom.



#### Results

The match values of CBCT with planning-CT with the phantom placed within the mask un-rotated were smaller than 0.1mm/° in all directions. After the phantom was rotated within the mask, CBCT match showed pitch-rotational errors of 1.7° and -3.7° (Fig. 2). After manual adjustment of the pitch-rotation on the head support, the verification match showed rotational setup error of  $\leq 0.1^\circ$  and translational setup error of  $\leq 0.2\text{mm}$  (Fig.2). The rotational match values of the CBCT are independent of the location of the correction reference point and correspond to the pitch-rotational axis of the head support. For the first patient, the pre-treatment and post-treatment verification CBCT showed translational setup errors of  $\leq 0.4\text{mm}$  and  $\leq 0.3\text{mm}$ , which is close to the accuracy of the couch motion accuracy of 0.2mm.

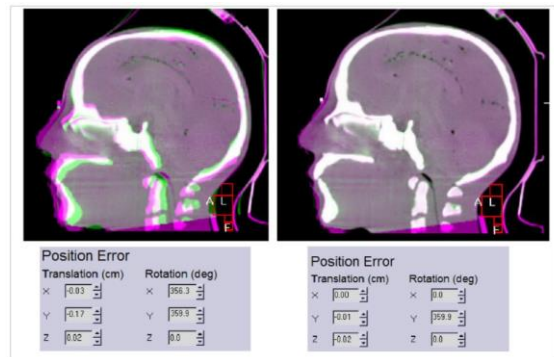


Fig 2. CBCT match to planning-CT (left) showed pitch-rotational setup error of 3.7°, the purple and green showed misalignment of the skull. After manual adjustment of the pitch rotation on the head support, CBCT match showed rotational setup error of  $\leq 0.1^\circ$  and translational setup error of  $\leq 0.2\text{mm}$  (right).

#### Conclusion

Manual adjustment of pitch-rotational setup error is feasible with the Solstice mask. This correction can be clinically importance for SRS treatment as it permits a more frequent use of single isocenter to treat patients with multiple brain metastases. The use of single isocenter has shorter treatment time and therefore is more patient friendly and reduce the risk of interfraction motion. These preliminary results warrant further investigation on more patients.

#### EP-2173 Bladder filling in patients undergoing prostate radiotherapy on the MR-linac

G. Adair Smith<sup>1</sup>, T. Herbert<sup>1</sup>, R. Lawes<sup>1</sup>, H. Creasey<sup>1</sup>, A. Dunlop<sup>2</sup>, A. Mitchell<sup>2</sup>, A. Pathmanathan<sup>1</sup>, L. Bower<sup>3</sup>, I. Hanson<sup>2</sup>, D. McQuaid<sup>2</sup>, R. Huddart<sup>1</sup>, U. Oelfke<sup>2</sup>, S. Nil<sup>2</sup>, A. Tree<sup>1</sup>, H. McNair<sup>1</sup>

<sup>1</sup>The Royal Marsden NHS Foundation Trust, Radiotherapy, Sutton, United Kingdom; <sup>2</sup>The Institute for Cancer Research, Medical Physics, Sutton, United Kingdom; <sup>3</sup>The Institute for Cancer Research, Radiotherapy and Imaging, Sutton, United Kingdom

#### Purpose or Objective

The first patient in the UK was treated for prostate cancer on the Elekta Unity (Elekta AB, Stockholm, Sweden) in September 2018. Due to the longer treatment times, departmental guidance for bladder filling was altered. An audit is being undertaken to evaluate if the bladder filling guidance is appropriate and reproducible; and to determine the rate of bladder filling and the effect on dose constraints across three time points during a treatment session.

#### Material and Methods

The first cohort of patients, under PRISM (Prostate Radiotherapy Integrated with Simultaneous MRI) trial

(NCT03658525), to be treated on the MR-linac will receive 60Gy in 20 fractions. These patients have been advised to drink 350ml of water 30 minutes before their MR-linac appointment time, to achieve a minimum bladder volume of 250ml during treatment (O'Doherty et al, 2006). The daily volume of water drunk, and time before treatment, was recorded.

A T2 weighted MR image was acquired at three time points: the start of each session, prior to treatment delivery and post treatment delivery. The bladder was retrospectively outlined for all three images. The volume of the bladder and time of MRI acquisition documented. The average rate of intrafraction filling was determined. The dose delivered to the re-outlined bladder at each timepoint was re-calculated and documented to assess if mandatory dose constraints were met with the initial bladder size and increased bladder size pre and post treatment. The effect on dose constraints will be investigated.

#### Results

The bladder filling guidelines were altered 11 times during the course of treatment. The patient drank 1 to 2 cups of water 25 to 35 minutes before treatment and had to partially empty his bladder 12 times prior to treatment. We will continue to assess the revised guidelines on future patients.

The median (range) percentage increase in bladder volume across 25 minutes from initial planning MRI to pre-treatment MRI was 62% (34% to 126%) and across 36 minutes from initial planning MRI to post treatment MRI was 89% (46% to 174%). The mean (SD) rate of bladder filling was 4.3cc per minute (1.5cc per minute) from initial planning MRI to post treatment MRI.

For the first fraction the mandatory bladder dose constraints were met for all three time points. Further fractions will be investigated.

#### Conclusion

Although the bladder filling guidelines were altered regularly, our initial analysis has indicated that the mandatory bladder dose constraints were achieved.

The rate of bladder filling during treatment delivery indicated the bladder volume was at recommended minimum for departmental guidance. The advantage of bladder filling displacing small bowel superiorly was noted across the course of treatment and will be investigated further.

#### EP-2174 Patients' experiences with whole body irradiation using Tomotherapy

P. Schon<sup>1</sup>, P. Lannerheim-Saure<sup>1</sup>, C. Hagstrom<sup>1</sup>, A. Löfgren<sup>1</sup>

<sup>1</sup>Skåne University Hospital, Department of Radiation Therapy, Lund, Sweden

#### Purpose or Objective

At our clinic, the traditional Total Body Irradiation treatment (TBI) using a linear accelerator has been replaced with Total Marrow Irradiation (TMI) with Tomotherapy, treating patients with leukaemia prior to stem cell transplantation. The reason to use TMI instead of TBI is to minimize dosage to healthy tissue. Total Skin Irradiation (TSI) is a similar treatment used for treating patients with severe mycosis fungoides. To be able to complete the treatment, the patient's well-being is crucial during the treatment. Therefore quality control that focus on the patient's experience is imperative. The purpose was to explore the patient's experience of full body irradiation, when treated with Tomotherapy.

#### Material and Methods

The oncology nurse perform the preparations, which includes giving information and support based on the patient's need prior to the start of the treatment. TMI- and TSI-treatments were similar to each other concerning immobilization and position of the patient. The patient was immobilized using a large vacuum cushion, from feet

to neck and a 5-point open-face thermoplastic mask. Fiducial markers and tattoos were used for positioning reference. In addition the patient receiving TSI was also wearing a wet suit for the bolus effect. It is important that the position is reproducible and comfortable to ensure the same position during 1,5-2 hours treatment time. A small break during change of position from head first to feet first is included. Four patients received a questionnaire with 37 questions after all radiotherapy sessions was finished, which included questions enquiring their experiences during their radiotherapy sessions. Five patients were also asked to rate their pain level and level of nausea using Visual Analog Scale after every session, and if so if they vomited. Their skin and mucous membrane were observed. They all received 12 Gy/6 sessions.



#### Results

All patients felt some level of pain and chafing during treatment (Fig 1). The TBI-patients felt more pain and nausea. The TSI-patient's skin improved during all sessions, but there were some bleeding. All patients felt safe, but the TBI-patients found the environment more frightening. The TSI-patient lacked information about side-effects and self-care, but found the overall information sufficient. None of the patients felt completely relaxed, but they all felt that the treatment sessions were manageable, though the treatment time was challenging.

#### Conclusion

The quality control revealed that the patient were lacking some information and support. The oncology nurses should focus on information and prevention to increase the patient's well-being. To minimize treatment time the nurse ought to develop skills handling the technology and treatment procedure. Based on the results, the patients' positioning was improved owing to some modifications, minimizing pressure and enhancing mobility of vulnerable parts of the body.

#### EP-2175 No more Lines - Omitting skin marks, safe to align with tattoo only for lung cancer patients?

L. Wiersema<sup>1</sup>, J. Stam<sup>1</sup>, T. Wiersma<sup>1</sup>, J. Belderbos<sup>1</sup>, A. Licup<sup>1</sup>, F. Koetsveld<sup>1</sup>, P. Remeijer<sup>1</sup>

<sup>1</sup>Netherlands Cancer Institute, radiotherapy, Amsterdam, The Netherlands

#### Purpose or Objective

In our department besides ink tattoos, skin marks are used for patient positioning treated within the thoracic area. The tattoos and skin marks are placed by RTT's during the Computed Tomography (CT) simulation. The added value of the skin marks is being questioned by physicians and RTT's. Patients are instructed to retrace the skin marks until the first day of treatment in case of fading, this introduces a risk of shifting the skin marks. Besides, there is also a degree of discomfort for the patients, because the skin marks might show from underneath their clothes, whereas some patients may also present with an allergic reactions to the ink. The purpose of this study was to see

whether omitting the skin marks and positioning based on tattoos only, would have an influence on the initial setup error within the context of image guided RT (IGRT). Within our department lung cancer patients will be treated according an online IGRT protocol, therefore the rotations are of most interest. In case an offline IGRT protocol is used in other departments, besides the rotations, the translations are also relevant when omitting skin marks.

#### Material and Methods

To analyze the results we selected 2 groups of lung cancer patients, treated with a fractionated radical dose prescription and a daily online IGRT protocol, aligned using 5 tattoos (3 anterior, 2 lateral) and positioned on a thorax support. Group A, the control group with skin marks, included 37 patients. Group B, a prospective cohort, included 30 patients irradiated without skin marks. For both groups, grand mean, systematic ( $\Sigma$ ) and random ( $\sigma$ ) errors were calculated using the initial set up errors from 1388 Cone Beam Computed Tomography (CBCT) scans. This study was communicated to all RTT's within the department, but no additional set up instructions were given. The statistical significance for the systematic and random errors were tested using Levene's test and Mann-Whitney U-test, respectively.

#### Results

The mean for the translations in both groups are  $< 0.1$  cm. The Levene's test and Mann-Whitney U test showed no statistically significant difference between the group standard deviations.

Setup error	LR (cm)	CC (cm)	AP (cm)	roll (°)	pitch (°)	yaw (°)
<b>With skin marks - Group A</b>						
Mean	-0.07	0.07	-0.09	0.8	-0.1	0.2
Systematic Error	0.30	0.38	0.26	1.2	0.9	0.8
Random error	0.34	0.47	0.15	0.6	0.7	0.9
<b>Without skin marks - Group B</b>						
Mean	-0.03	0.02	0.02	0.5	-0.1	0.0
Systematic Error	0.23	0.42	0.20	0.7	1.0	0.9
Random error	0.35	0.41	0.14	0.6	0.7	0.9
P-value ( $\Sigma$ ) Levene's test	0.54	0.60	0.07	0.24	0.92	0.30
P-value ( $\sigma$ ) Mann-Whitney U test	0.47	0.48	0.41	0.27	0.19	0.44

#### Conclusion

Omitting skin marks for patients treated in the thoracic area results in an equivalent initial setup error for both translations and rotations. Patients might benefit, as there will be no risk of any allergic reactions from the ink and they do not have to retrace the skin marks.

#### EP-2176 Analysis of inter-fraction tumor position variability in lung SBRT

A. Coral<sup>1</sup>, N. Espinosa<sup>1</sup>, A. Latorre<sup>1</sup>, S. Bermejo<sup>2</sup>, X. Nolla<sup>1</sup>, G. De Segura<sup>1</sup>, C. Diaz<sup>1</sup>, M. Mancera<sup>1</sup>  
<sup>1</sup>Hospital de la Santa Creu i Sant Pau, Servei de Radiofísica i Radioprotecció, Barcelona, Spain; <sup>2</sup>Hospital de la Santa Creu i Sant Pau, Servei d'Oncologia Radioteràpica, Barcelona, Spain

#### Purpose or Objective

The aim of our study was to compare the tumor position differences (*displacements*) between the simulation TC and the CBCT performed prior each treatment fraction. We also correlated the magnitude of the displacements and the tumor location (lobe) in the lung.

#### Material and Methods

We retrospectively analyzed 112 oligometastatic lung cancer patients between December 2013 and August 2018. The patients underwent a simulation 4D-TC with limited free breathing obtained by abdominal compression, using Respiratory Belt (CIVCO).

The positioning devices were a thorax support (Posirest-2, CIVCO) and vacuum mattress (Urethane MTVLPLV01, CIVCO). The positioning in the treatment unit was based on the simulation skin marks (tattoos) followed by the isocenter displacements as indicated by the treatment plan.

A CBCT was acquired before each treatment fraction to correct for inter-fraction positioning errors. We reported those position displacements for the three axes (AP, LR, SI). We finally correlated the magnitude of the displacements with the tumor localization (upper-, medium-, or low lung lobe).

#### Results

Figure 1 shows that the largest displacement was observed along the vertical direction.

The medium lung lobe was the localization with the lowest dispersion of the displacements. The largest range of displacements (in vertical direction between -1.8 cm and 0.3 cm and in lateral direction between -0.6 cm and 1.2 cm) was observed in the lower lobe.

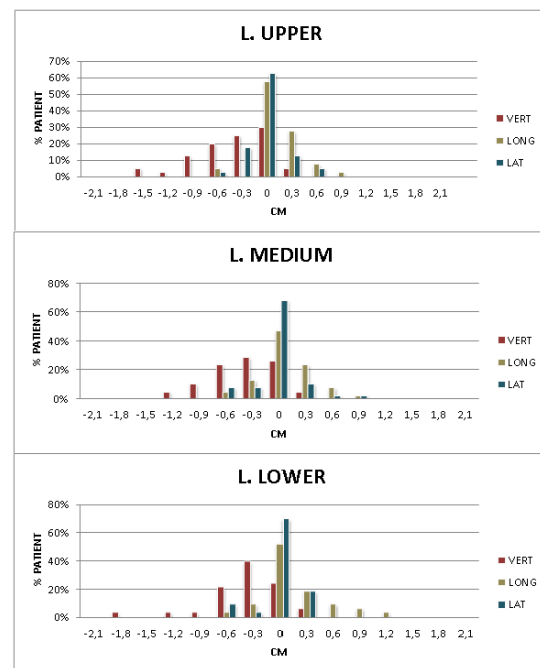


Figure 1. Distribution of displacements along the three axes for upper, medium and lower lung lobes.

#### Conclusion

Tumors located in the lower lobe have important mobility in all directions. We suggest performing a stronger diaphragmatic compression or other respiratory control strategies with the objective to reduce this movement. The largest displacements in all lung locations (upper-, medium-, lower lobe) were observed in the vertical axis. To reduce the displacement of the upper lobe, attributable to the positioning of the arms, implementation of the new systems of immobilization, as a thermoplastic mesh, or surface recognition systems are recommended. IGRT techniques are essential to ensure a good reproducibility of the treatment.

#### EP-2177 4D CBCT based determination of tumor amplitude variation in lung cancer SBRT

J. Papp<sup>1,2</sup>, M. Simon<sup>1,2</sup>, E. Csiki<sup>1</sup>, E. Csobán<sup>1</sup>, A. Molnár<sup>1</sup>, P. Árkosy<sup>3</sup>, Á. Kovács<sup>1,2</sup>

<sup>1</sup>University of Debrecen Med. and Health Science Centre-Clinic of Oncology, Department of Radiotherapy, Debrecen, Hungary; <sup>2</sup>University of Pécs Faculty of Health Sciences, Doctoral School of Health Sciences, Pécs, Hungary; <sup>3</sup>University of Debrecen Med. and Health Science Centre-Clinic of Oncology, Department of Oncology, Debrecen, Hungary

#### Purpose or Objective

Stereotactic Body Radiation Therapy (SBRT) is often performed with complex immobilization systems paired

with four-dimensional information to assess tumor motion in time. The aim of this study was to determine tumor amplitude variation based on 4D CBCT data.

#### Material and Methods

Between May 2015 and August 2018 a total of 46 patients received lung SBRT treatment in 359 fractions based on 4DCT data. Abdominal compression was used in 8 patients to reduce tumor motion at lower lobe tumors. GTV was defined during treatment planning at least in 3 breathing phases to generate an ITV. Translational position corrections were determined using pre-treatment 4D CBCT at each fraction. A second 4D CBCT data set had been acquired after the treatment fraction to assess intra-fractional motion. Amplitude values in three directions were recorded both pre- and post-fractional.

#### Results

Population mean values ( $\pm$ SD) for pre-treatment amplitudes were: 0.12( $\pm$ 0.09) cm, 0.44( $\pm$ 0.4) cm and 0.24( $\pm$ 0.17) cm in Superior-Inferior (SI), Left-Right (LR) and Anterior-Posterior (AP) directions respectively for the free breathing cohort. Patients with abdominal compression the values were: 0.18( $\pm$ 0.1) cm, 0.87( $\pm$ 0.13) cm, 0.25 ( $\pm$ 0.51) cm respectively. Post-fractional values were: 0.11( $\pm$ 0.09) cm, 0.4( $\pm$ 0.4) cm, 0.22( $\pm$ 0.15) cm for the free breathing and 0.18( $\pm$ 0.1) cm, 0.78( $\pm$ 0.12) cm, 0.24( $\pm$ 0.41) cm for the abdominal compression group.

#### Conclusion

Correlating pre- and post-treatment values in our patient cohort the complex immobilization systems combined with four-dimensional data are capable of handling tumor amplitude changes over a fraction and abdominal compression can mitigate tumor motion to a more manageable area which can lead to the reduction of the volume of ITV.

#### Electronic Poster: RTT track: Imaging acquisition and registration, OAR and target definition

#### EP-2178 Evaluation of a user-guided deformable registration workflow for multi-modal prostate imaging

A. Lastrucci<sup>1</sup>, A. Barucci<sup>2</sup>, S. Pini<sup>1</sup>, S. Russo<sup>1</sup>, R. Barca<sup>1</sup>, M. Coppola<sup>1</sup>, S. Fondelli<sup>1</sup>, L. Paoletti<sup>1</sup>, F. Rossi<sup>1</sup>, P. Bastiani<sup>1</sup>, M. Esposito<sup>1</sup>

<sup>1</sup>USL Toscana Centro, Radiotherapy, Florence, Italy; <sup>2</sup>Ifac CNR, Medical Physics, Sesto Fiorentino, Italy

#### Purpose or Objective

Reg-refine is a tool that adds human knowledge to deformable image registration (DIR) process. In this study a CT-MRI deformable registration workflow for prostate cancer was evaluated.

#### Material and Methods

Deformable and rigid alignments of axial CT and axial T2 weighted MRI scans of 8 patients were evaluated using Mim Maestro 6.7.10 (Mim Software Inc.). DIR workflow consisted of three rigid alignments, in the upper, middle, and lower prostate part, defined by two users in consensus using Reg-refine and converted in local alignments by the DIR algorithm. Dice coefficient and Hausdorff distance were computed for evaluation of deformable and rigid alignments.

#### Results

Dice resulted (0.78  $\pm$ 0.12; max 0.9, min 0.58) for rigid registration vs (0.89 $\pm$ 0.05; max 0.94, min 0.82). Hausdorff distance resulted (11.7 mm  $\pm$  4.5 mm; max 17.1, min 5.4) for rigid registration vs (7.6 mm  $\pm$  4.1 mm; max 13.5 mm, min 3.5 mm). Box plots are reported in Figure 1.

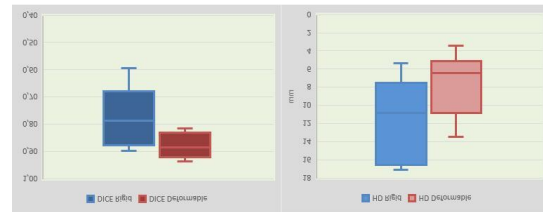


Figure 1: Box plot of Dice and Hausdorff distance (HD) for rigid and deformable CT-MRI alignments.

#### Conclusion

The DIR workflow evaluated in this study produced good results in all patients analyzed and was able to improve the registration accuracy of rigid alignments. Reg-refine based DIR of CT and MRI scans can be used for prostate contouring.

#### EP-2179 Estimation of intrafractional motion of intra-orbital optic nerve by MRI

S. Tsuruoka<sup>1</sup>, Y. Hamamoto<sup>1</sup>, Y. Kuribayashi<sup>2</sup>, H. Inata<sup>2</sup>, T. Matsuno<sup>2</sup>, T. Mochizuki<sup>1</sup>

<sup>1</sup>Graduate School of Medicine Ehime University, Radiology, Ehime, Japan; <sup>2</sup>Saiseikai Imabari Hospital, Radiology, Ehime, Japan

#### Purpose or Objective

Optic nerve is one of the most significant organs at risk in radiotherapy for the intra-and/or peri-orbital tumors. Although intra-orbital optic nerve is likely to move with eye-movement, intrafractional motion of the intra-orbital optic nerve has not been well documented. To determine the optimal planning organ at risk volume, intrafractional motion of the intra-orbital optic nerve was measured by magnetic resonance imaging (MRI).

#### Material and Methods

A total of five normal volunteers were underwent MRI around the orbit. (1) One of five volunteers was underwent MRI with maximally oriented in outward, inward, upward, and downward direction at the time of both opening and closing the eyes. The displacement in each direction at three points (the adhesive part of optic nerve and eyeball, 10 mm and 20 mm from the adhesive part) was measured. (2) For all volunteers, displacement in lateral direction of the intra-orbital optic nerve from the position when gazed at the front was measured by axial cine-MR imaging. The maximum displacement of the intra-orbital optic nerve was recorded.

#### Results

(1) At the time of opening the eyes, the average of maximal displacement in four directions (outward, inward, upward, and downward) at the adhesive part of optic nerve and eyeball, 10 mm and 20 mm from the attachment were 5.20 mm (standard deviations [SD]; 0.97), 3.23 mm (SD; 0.54), and 1.23 mm (SD; 0.55), respectively. At the time of closing eyes, those were 4.11 mm (SD; 1.31), 1.91 mm (SD; 0.82), and 0.53 mm (SD; 0.24), respectively. (2) For the right eye, the average of the maximal displacement inward and outward were 2.8 mm and 2.5 mm, respectively. For the left eye, the average of the maximal displacement inward and outward were 2.6 mm and 3.0 mm, respectively. The mean amounts displacement of right and left eye on cine-MR imaging were 2.65 mm (SD; 1.14) and 2.78 mm (SD; 1.62), respectively.

#### Conclusion

Based on our results, intrafractional margins of the intra-orbital optic nerve needed at least 3 mm in outward, inward, upward, and downward direction.

#### EP-2180 The effect of Rectal size and shape on Bladder deformation in Urinary Bladder Radiotherapy

N. Hutton<sup>1</sup>, J. Callender<sup>2</sup>, D. Hutton<sup>1</sup>, L. Williams<sup>1</sup>, S. Wong<sup>1</sup>, H. Wong<sup>1</sup>, I. Syndikus<sup>1</sup>

<sup>1</sup>Clatterbridge Cancer Centre, Radiotherapy, Bebington-Wirral, United Kingdom; <sup>2</sup>The University of Liverpool, School of Health Sciences, Liverpool, United Kingdom

**Purpose or Objective**

The urinary bladder is subject to variation in shape and size which, to some extent, be controlled using an empty bladder protocol for planning and treatment. Bladder can still be influenced by adjacent organs, notably the rectum.

Micro-enemas are used with a view to controlling the rectal volume. An earlier study, showed improve consistency in rectal diameter and content between planning and treatment with the use of a micro-enema. The aim of this study is to identify any significance in the relationship between rectal consistency and bladder deformation with a view to reconsidering appropriate treatment margins.

Utilising on treatment imaging technology for soft tissue visualisation enabled the variation in bladder and rectal volumes to be quantified.

**Material and Methods**

A control group consisted of patients asked to empty their bladder immediately before planning and treatment. No guidance was given on rectal state. An intervention group consisted of patients asked to use a micro-enema 20 mins prior to planning and each treatment and empty their bladder immediately before both.

Treatment CBCT images were analysed on-line using an automatic match algorithm to provide a rigid bone registration and a 3mm Action level and a CTV coverage check.

Retrospective analysis was carried out on 97 CBCT scans from 15 patients, control group (n = 41) and intervention group (n= 56). Volume and positional organ variations were determined from the rigid bone registration of CT and CBCT. Bladder and rectum volumes were manually contoured on planning CT and each CBCT using Varian Eclipse™ contouring module.

Centre of mass shifts for bladder and rectum were determined in the X,Y and Z axis and the magnitude of Centre of Mass shift calculated for the planning scan and all fractions. The Dice similarity coefficient was taken from the Eclipse planning system.

**Results**

Rectum volume (cm <sup>3</sup> )	Bladder volume (cm <sup>3</sup> )	150
Rectum volume (cm <sup>3</sup> )	Bladder volume (cm <sup>3</sup> )	308
Rectum volume (cm <sup>3</sup> )	Bladder volume (cm <sup>3</sup> )	0.10
Rectum volume (cm <sup>3</sup> )	Bladder volume (cm <sup>3</sup> )	0.01
Rectum volume (cm <sup>3</sup> )	Bladder volume (cm <sup>3</sup> )	0.02
Rectum volume (cm <sup>3</sup> )	Bladder volume (cm <sup>3</sup> )	0.02
Rectum volume (cm <sup>3</sup> )	Bladder volume (cm <sup>3</sup> )	0.02

Comparison test (z-test) of EYE/VA group

Rectum volume (cm <sup>3</sup> )	Bladder volume (cm <sup>3</sup> )	81.7
Rectum volume (cm <sup>3</sup> )	Bladder volume (cm <sup>3</sup> )	13.1
Rectum volume (cm <sup>3</sup> )	Bladder volume (cm <sup>3</sup> )	0.03
Rectum volume (cm <sup>3</sup> )	Bladder volume (cm <sup>3</sup> )	0.02
Rectum volume (cm <sup>3</sup> )	Bladder volume (cm <sup>3</sup> )	0.02
Rectum volume (cm <sup>3</sup> )	Bladder volume (cm <sup>3</sup> )	0.02
Rectum volume (cm <sup>3</sup> )	Bladder volume (cm <sup>3</sup> )	0.02

Comparison test (z-test) of CONTROL group

**Conclusion**

The introduction of a micro-enema shows significant worsening of bladder and rectum stability relevant to the control group. The significant result for correlation between rectum changes in the Y and Z directions and bladder centre of mass shift in the same direction suggest that the use of micro-enema may, in some cases, destabilise the rectum. It is acknowledged that the small study size may influence the results. Bladder radiotherapy may benefit from daily imaging with appropriate justification and optimization of imaging dose. The majority of target volumes in the pelvis are moving to daily online imaging acknowledging the physiological movements of organs.

**Electronic Poster: RTT track: Treatment planning and dose calculation / QC and QA**

**EP-2181 Use of treatment log-files for QA of cranial radiosurgery adaptive plans**

S. Moragues Femenia<sup>1</sup>, J.F. Calvo-Ortega<sup>1</sup>, M. Hermida-López<sup>2</sup>, J. Casals<sup>1</sup>

<sup>1</sup>Hospital Quirónsalud Barcelona, Radiotherapy, Barcelona, Spain; <sup>2</sup>Hospital Universitario Vall d'Hebron, Servicio de Física y Protección Radiológica, Barcelona, Spain

**Purpose or Objective**

To analyze the accuracy of delivered adaptive stereotactic radiosurgery (SRS) plans.

**Material and Methods**

Adaptive cranial SRS is performed in our department [Med Dosim. 2013 Autumn;38(3):291-7] as a strategy to compensate for the patient's roll and pitch rotational errors not supported by the 4D couch of the Varian 2100 CD linac used for treatment delivery. Our current adaptive SRS policy requires adapting the original treatment plan (Plan\_ref) when pitch and/or roll errors detected by CBCT imaging are ≥ 0.5 degrees. The beam fluences of the Plan\_ref are adapted to the actual patient's position such that an adaptive plan (Plan\_adapt) is created while patient is lying on the linac couch. Obviously, it is not possible to perform a fully patient-specific QA. In order to check the Plan\_adapt delivery, an off-line re-calculation of the Plan\_adapt is done using the Varian Dynalog files recorded by the linac during the delivery [J Appl Clin Med Phys. 2014 Mar 6;15(2):4665], such that a reconstructed plan is generated (Plan\_adapt\_Dyn). Dose calculations were done with the Analytical Anisotropic Algorithm (AAA) of the Eclipse v.13.6 treatment planning system using a 1 mm calculation grid size. The accuracy of this algorithm for SRS was previously investigated by our team [Med Dosim. 2014 Summer;39(2):129-33]. Plan\_adapt plans were computed with AAA modelled with the beam data (6 MV) of our linac, while the Plan\_adapt\_Dyn plans were calculated with the AAA modelled in an independent way with the Golden Beam Data (6 MV) supplied by Varian for our linac model. In order to assess the accuracy of the delivered dose, Plan\_adapt and Plan\_adapt\_Dyn plans were compared for 20 multitarget SRS cases using the 3D gamma tool of the Computational Environment for Radiotherapy Research (CERR) software. It was compiled from the source code available at <https://github.com/cerr/CERR> on July 8, 2018. 3D gamma calculations were focused on the planning target volumes (PTVs) and the OARs (brainstem, optic nerves and optic chiasma). Gamma passing rates were computed for several dose difference criteria (1%, 2% and 3% of the reference maximum dose), 1 mm distance-to-agreement-distance, and threshold of 10% of the reference maximum dose.

**Results**

Sixty PTVs were analyzed: average gamma passing rates were 87.4% (95% CI [81.9, 92.9]), 97.7% (95% CI [95.1, 100.0]) and 99.6% (95% CI [98.9, 100.0]) for 1%/1 mm, 2%/1 mm and 3%/1 mm criteria, resp. Minimum passing rate of 100% was reached for all 20 OARs of each type regardless of the gamma criteria used.

**Conclusion**

The proposed log-file-based method is a useful tool to assess the accuracy of the dose delivery when adaptive SRS is performed. A high agreement within 3% and 1 mm between the designed adaptive plans (Plan\_adapt) and the corresponding delivered ones (Plan\_adapt\_Dyn) was found for all cases.

**EP-2182 Skin dose calculation in breast cancer when the air surrounding the patient contour is considered**

I. Lorenzo<sup>1</sup>, J.F. Calvo-Ortega<sup>1</sup>, S. Moragues Femenia<sup>1</sup>, C. Laosa-Bello<sup>1</sup>, J. Casals<sup>1</sup>

<sup>1</sup>Hospital Quirónsalud Barcelona, Radiotherapy, Barcelona, Spain

#### **Purpose or Objective**

Skin dose calculations in plans of breast cancer have been performed with and without including the air surrounding the patient external contour.

#### **Material and Methods**

Wang et al have described the effect of considering the air surrounding the external patient contour ("body contour") in the accuracy of the calculated skin dose [J Appl Clin Med Phys. 2018 Mar;19(2):191-197]. They proved that an air extension of the body contour of at least 1 cm should be done in order to improve the skin dose calculation accuracy.

We have included 30 breast plans that were calculated for treatment without air extension of the body contour. Then, these plans were re-calculated for a 2 cm-extension towards the air of the body contour (Fig 1). The Eclipse v. 13.6 treatment planning system with the AAA dose calculation algorithm was used. Photons beams of 6 MV from a Varian Clinac 2100 CD with the Millennium 120 MLC were used. The skin structure was outlined in the axial slices where the PTV was present, and it consisted of a 5 mm thickness layer beneath the default body contour detected by the Eclipse (Fig 1). Skin dose is defined in this study as the mean dose registered in the skin structure as defined above. We compared the skin dose for the two type of plans computed with and without extension of the body contour.

#### **Results**

An average increase of 7% (range: 6% to 8.5%) in the skin dose was observed when a 2 cm-enlarged body contour was used.

#### **Conclusion**

The skin dose increase revealed by the 2 cm-enlarged body contour is considered during the dosimetric evaluation of the breast plans designed to patient treatments.

#### **EP-2183 Dosimetric impact of CBCT calibration curve on dose calculated by a radiotherapy TPS**

C. Laosa<sup>1</sup>, J.F. Calvo-Ortega<sup>1</sup>, S. Moragues Femenia<sup>1</sup>, J. Casals<sup>1</sup>

<sup>1</sup>Hospital Quirónsalud Barcelona, Radiotherapy, Barcelona, Spain

#### **Purpose or Objective**

A radiotherapy treatment planning system (TPS) requires a relationship between electron density and CT numbers (calibration curve) to account for tissue heterogeneities during dose calculations. In this work we investigated the dosimetric impact of variations of the calibration curve of a CBCT scanner used for online adaptive cranial radiosurgery.

#### **Material and Methods**

A Varian Clinac 2100 CD linac equipped with a kV-CBCT scanner was used. A half-fan protocol (655 projections, 125 kVp, 80 mA and 13 milisecc per projection, field of view of 260 mm, 384x384 matrix and 1 mm slice distance) is used in our department for adaptive cranial radiosurgery (Med Dosim. 2013 Autumn;38(3):291-7). A reference CBCT calibration curve was established in the Varian Eclipse TPS by using the CatPhan phantom containing seven inserts (air, PMP, LDPE, polystyrene, acrylic, Delrin and Teflon). After that, the CBCT calibration curve was monitored using the CatPhan phantom in a monthly-basis during a year. CBCT scanner was recalibrated when a variation greater than  $\pm 40$  HU was noted in any insert, according to the Varian recommendation. For each CBCT scan (obtained before re-calibration if needed), a box plan (6 MV) was planned and the mean dose and CT number were computed on each insert over an inner region of interest.

CT number and dose for each insert were compared to the values obtained for the reference CBCT scan.

#### **Results**

Maximum variations in the CT number and dose respect to the values of the reference CBCT scan were (CT#/dose): 3 HU/0.7%, 34 HU/0.7%, 32 HU/0.6%, 23 HU/0.5%, 34 HU/0.7%, 32 HU/0.6% and 96 HU/0.8% HU for air, PMP, LDPE, polystyrene, acrylic, Delrin and Teflon, respectively.

#### **Conclusion**

Small impact ( $< 1\%$ ) was observed in the dose quantity even for large absolute variations in the CT number ( $> 40$  HU). Some guidelines (TECDOC-1583; IAEA, Vienna 2008) recommend adjusting the calibration curve in the TPS or tuning the CT scanner when CT numbers vary by more than  $\pm 20$  HU. We propose to act when absolute dose differences greater than 1% are detected.

#### **EP-2184 A study on dose of the junction in radiotherapy of breast cancer including SCL**

W. Jung<sup>1</sup>

<sup>1</sup>Seoul National University Bundang Hospital, Department of Radiation Oncology, Seongnam-si, Korea Republic of

#### **Purpose or Objective**

In treatment planning with junction, heterogeneity is considered to be minimized, but if there are adjacent MLCs, dose distribution can be affected and heterogeneity can be increased. The aim of this study was to compare dose of junction between breast and SCL fields in radiation therapy by MLC located at the junction.

#### **Material and Methods**

With 6 MV of 21EX-S equipped with 120-leaf Millennium MLC, treatment plans were designed with 30 patients who underwent radiation therapy using tangential field technique. Plan 1 where the MLC was all used at the junction. In plan 2 and plan 3, MLC was retracted 5 mm from breast and SCL, respectively. Plan 4 with all of MLC retracted at the junction were designed. In all the plans, collimator angle for SCL field was divided into  $0^\circ$  and  $270^\circ$ . To verify junction dose, the dose at 3cm depth of junction was compared with average value by MapCHECK.

#### **Results**

In case of the SCL field with  $0^\circ$  collimator angle, average value of D3cm was 4131.1, 4215.9, 4351.4, and 4423.0 cGy. In case of the SCL field with  $270^\circ$  collimator angle, average value of D3cm was 4044.3, 4246.7, 4291.1, and 4441.2 cGy. In plan 1 and 3, change in average dose depending on collimator angle was changed more significantly than plan 2 and 4. Dose measured at 3cm depth of junction was similar to treatment plan.

#### **Conclusion**

As a result of the study, there was a difference of about 10% between the plan where all the MLC was applied to the junction and the retracted plan. In radiation therapy plan for breast cancer with SCL, retracting MLC from junction between breast and SCL fields will lead to reduce effect of dose of the junction.

#### **EP-2185 Study of the seroma volume changes in the patients who underwent Accelerated Partial Breast Irradiation**

D.H. Kim<sup>1</sup>, S.J. Son<sup>1</sup>, J.G. Mun<sup>1</sup>, S.J. Seo<sup>1</sup>, J.H. Lee<sup>1</sup>

<sup>1</sup>Seoul National University Hospital, radiation oncology, Seoul, Korea Republic of

#### **Purpose or Objective**

By analyzing seroma volume changes in the patients who underwent Partial breast radiation therapy after breast conserving surgery, we try to contribute to the improvement of radiotherapy effect.

#### **Material and Methods**

Enrolled 20 patients who underwent partial breast radiation therapy by ViewRay MRIdian System were subject.

After seeking for the size of the removed sample in the patients during surgery and obtained seroma volume changes on a weekly basis. On the Basis of acquired volume, it was compared with age, term from start of the first treatment after surgery, BMI (body mass index) and the extracted sample size during surgery. And using the ViewRay MRIdian RTP System, the figure was analyzed by PTV(=seroma volume + margin) to obtain a specific volume of the Partial breast radiation therapy.

### Results

The changes of seroma volume from MR simulation to the first treatment (a week) is 0~5% in 8, 5~10% in 3, 10 to 15% in 2, and 20% or more in 5 people. Two patients (A, B patient) among subjects showed the biggest change. The A patient's 100% of the prescribed dose volume is 213.08 cc, PTV is 181.93 cc, seroma volume is 15.3 cc in initial plan. However, while seroma volume decreased 65.36% to 5.3 cc, 100% of the prescribed dose volume was reduced to 3.4% to 102.43 cc and PTV also did 43.6% to 102.54 cc. [Fig. 1] In the case of the B patient, seroma volume decreased 42.57% from 20.2 cc to 11.6 cc. Because of that, 100% of the prescribed dose volume decreased 8.1% and PTV also did to 40% [Table 1]

### Conclusion

As the period between the first therapy and surgery is shorter, the patient is elder and the size of sample is smaller than 100 cc, the change grow bigger. It is desirable to establish an adaptive plan according to each patient's changes of seroma volume through continuous observation. Because partial breast patients is more sensitive than WBRT patients about dose conformity in accordance with the volume change.

### EP-2186 Feasibility planning study for hypofractionated salvage prostate bed radiotherapy

L. Koopman<sup>1</sup>, S. Van der Neut<sup>1</sup>, C. Roos<sup>1</sup>, C. Hammer<sup>1</sup>, H. Vanhauten<sup>1</sup>, S. Bijmolt<sup>1</sup>, A. Van den Bergh<sup>1</sup>, J. Lagendijk<sup>1</sup>, S. Both<sup>1</sup>, C. Brouwer<sup>1</sup>, S. Al-Uwini<sup>1</sup>  
<sup>1</sup>UMCG University Medical Center Groningen, Radiotherapie, Groningen, The Netherlands

### Purpose or Objective

Salvage radiotherapy treatment (SRT) can provide long-term disease control for recurrent prostate cancer patients after radical prostatectomy. Introducing hypofractionation will decrease the overall treatment time and may improve effectiveness of radiotherapy. The aim of this study was to evaluate the feasibility of target coverage and organ at risk (OAR) constraints of our proposed hypofractionated regimen as an experimental arm of a phase III randomized controlled trial.

### Material and Methods

Planning CT-scans of 5 representative patients who received standard conventional SRT of 35 fractions of 2 Gy were used to virtually create hypofractionated (HF) (20x3Gy) and standard fractionated (SF) (35x2Gy) SRT plans. For both treatment regimens a predetermined list of OAR constraints (Table 1) was tested for its feasibility. Target coverage was evaluated on PTV coverage (D95%).

	Hypofractionated Regimen	Standard Regimen
Rectum Dmax	< 100 % PD	< 100 % PD
Rectum D, 2 cc	< 100 % PD	< 100 % PD
Rectum < 15%	V60	V70
Rectum < 10%	V55	V65
Rectum V50 < 80%	V25	V30
Rectum V50 < 60%	V38	V41
Rectum V50 < 35 %	V50	V60
Rectum V50 mean	< 25 Gy	< 30 Gy
Anal Canal Dmax	< 24 Gy	< 25 Gy
Anal V50 < 10%	V25	V30
Bladder Dmax	< 102 % PD	< 102 % PD
Bladder < 40%	V50	V60
Bladder < 20%	V60	V70
Uterus V50 < 10%	V45	V55

### Results

The average D95% of the low dose PTV (LD PTV) was 99,3% for the standard regimen and 99,5% for the hypofractionated regimen. For the high dose PTV (HD PTV) the average D95% for the standard regimen was 98,6% and 99,2% for the hypofractionated regimen. In only one case 50% of the constraints was not met for both HF and SF regimen. In two cases, all constraints were met for the hypofractionated regimen, while the constraints for rectum Dmax and bladder Dmax where not met for the standard regimen. In one of these two cases, the rectum V65 was not met neither for the standard regimen. For the other 2 cases, only the rectum volume receiving 55 Gy for HF and 65 Gy for SF was more than the intended 15%, with an average of 18,2% of the rectum volume receiving 55 Gy for the HF regimen versus 17,2% of the rectum volume receiving 65Gy for the SF. The median rectum volume (70 cc, range 62-119) did not influence the probability to meet rectum constraints.

### Conclusion

For both target coverage and OAR constraints the hypofractionated regimen appears feasible except for one constraint (rectum V55) which needs further research. A larger number of patients is needed to confirm this feasibility.

### EP-2187 Metal artifact correction improves dose calculation of intensity modulated radiation therapy

H. Moriwaki<sup>1</sup>, T. Ikeda<sup>1</sup>, T. Kiyomiya<sup>1</sup>, H. Tajima<sup>1</sup>, K. Shiraishi<sup>1</sup>, A. Sakumi<sup>2</sup>

<sup>1</sup>Mitsui Memorial Hospital, Radiation oncology, Tokyo, Japan; <sup>2</sup>NTT medical center Tokyo, Department of Radiology, Tokyo, Japan

### Purpose or Objective

We evaluated the dose errors of Intensity Modulated Radiation Therapy (IMRT) between the calculated dose from the planning CT with a commercial CT metal artifact reduction algorithm and the measured dose by ion chamber and radio-chromic film in a water phantom with a cylinder of Titanium alloy

### Material and Methods

A prostate cancer patient with a unilateral right hip prosthesis was selected for this study. IMRT plans were created by Pinnacle3 (Philips Ltd.) v.9.10 using Synergy MLCi (Elekta Ltd.) beam models. We compared among three plans: 1) Five beams step and shoot IMRT plan, 2). Volumetric Modulated Arc Therapy (VMAT) plans with split arc segments thereby avoiding direct beam deliveries to the prosthesis (hereinafter referred to as avoidance VMAT), and 3) a single full-arc beam.

A Titanium alloy (Ti-6Al-4V, density = 4.43 g/cm<sup>3</sup>) cylinder object with a diameter of 30 mm was placed in a water phantom imitating right femoral position. CT images were taken with a single energy metal artifact reduction (SEMAR) algorithm, installed on the CT system (Aquilion ONE, Canon Medical Corporation). The patient treatment

plan was recalculated on the phantom CT images with SEMAR algorithm. Dose calculation results were compared between CT numbers in metal regions replaced with that for the density of Titanium alloy and 2) no correction. An ion chamber was placed at the phantom center for dose comparison to TPS calculation. A film was placed inside a water phantom with a metal object and beams were delivered. Gamma analysis was performed between the film measurements and the TPS dose calculation.

### Results

The dose difference of the measured those and the calculation using SEMAR without no correction are shown in Table.1. The avoidance VMAT did not show the metal effects in all the plans. The density correction improves the dose calculation. Differences in dose distributions with and without the metal was mainly observed in low dose regions due to back scattering from the metal object.

	Table 1 Isocenter dose in each plan				
	Measured dose (phantom)	SEMAR without density correction	%Difference	With density correction	%Difference
Step and Shoot	179.6 cGy	177.7 cGy	-1.00%	178.3 cGy	-0.70%
Avoidance VMAT	189.5 cGy	192.1 cGy	1.35%	190.9 cGy	0.76%
Single arc VMAT	186.3 cGy	182.1 cGy	-2.26%	183.2 cGy	-1.68%

### Conclusion

We observed a significant impact of a metal object on dose distributions in VMAT when a single full arc beam was delivered. However VMAT beams with the avoidance angles did not suffer from the metal effect. The CT with metal artifact reduction improves the dose calculation in IMRT.

### EP-2188 The risk of CIEDs damage by photon beams, define by neutron activation products of CIED materials

W. Szyszka<sup>1</sup>, E. Konstanty<sup>2</sup>, K. Brudecki<sup>3</sup>

<sup>1</sup>Greater Poland Cancer Center, Department of Radiotherapy II, Poznań, Poland; <sup>2</sup>Greater Poland Cancer Center, Department of Medical Physics, Poznań, Poland; <sup>3</sup>Kraków, Poland

### Purpose or Objective

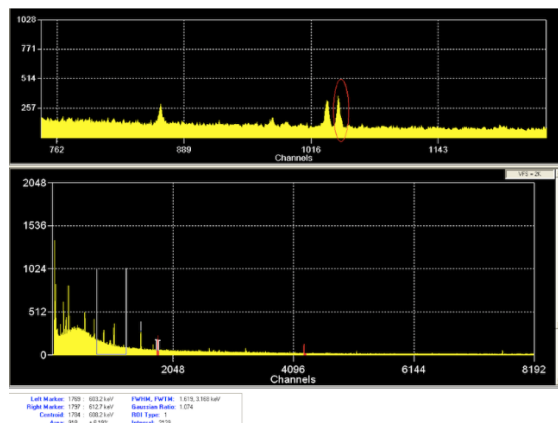
Epithermal or thermal neutron derived from photon beam radiation with energy above 10 MV could react with nuclei of the CIEDs materials. Threshold energies do not apply to (n;  $\gamma$ ) reactions. The study performance based on the risk of the pacemaker or cardioverter-defibrillator damage in a linear accelerator environment analyzing isotopes of elements of devices subjected to irradiation will depend only on the photon beam energy used during RT and the ensuing neutron contamination. The study is focused on understanding the mechanism causing devices malfunctions.

### Material and Methods

The study was performed based on the analysis of high-resolution gamma spectroscopy. Isotopes spectra allow establishing the occurrence of the reaction, and simultaneously determine the portion of emitted energy by detecting the type of the isotope and neutron contamination of the photon beam in linear medical accelerator environment. The study conducted for (i) 6 MV, (ii) 10MV, (iii) 15MV, (iv) 20 MV photon energy for 4 CIED distances relative to the radiation beam - 1) directly in the radiation beam, 2) 10 cm 3) 40 cm and 4) 100 cm from the edge of the radiation field. Each CIED received a dose of 2 Gy. The spectra of device material isotopes were detected using High Purity Germanium detector (HPGe).

### Results

For the samples of CIEDs, which has irradiated with high-energy photon beam (<15 MV) the different spectra of isotopes were observed. occurrence in samples spectra of long-lived isotopes on the energy of 350-360 keV confirmed neutron activation reaction.



### Conclusion

The CIEDs function in patients irradiated with above 10 MV photons should be avoided or if necessary closely monitored, especially in patients subject the increasing number of neutrons in high energies beams, the probability of malfunction increase with the energy of the beam, causing irreversible life-treating failures of the device. The appearance of long-lived isotopes explains the occurrence of CIEDs damages even after a long time from radiotherapy. Understanding the exact mechanism and all the factors of arising malfunctions of CIED is extremely important in consideration of the ever-increasing percentage of patients with CIEDs undergoing radiotherapy.

### EP-2189 Compare OARs dose in postoperative high-risk prostate cancer patients using IMRT and VMAT technique

Y. Chen<sup>1</sup>, L. Chou<sup>1</sup>, T. Wang<sup>2</sup>, Y. Liu<sup>1</sup>

<sup>1</sup>Taipei Veterans General Hospital, Department of Oncology, Taipei City, Taiwan; <sup>2</sup>China Medical University Hospital, Division of Radiation Oncology, Taichung City, Taiwan

### Purpose or Objective

For prostate cancer patients post radical prostatectomy with high risk features, post-operative radiotherapy improves biochemical progression-free survival at the cost of increased urinary and intestinal toxicities. Comparing to 3D conformal radiotherapy, step-and-shoot intensity-modulated radiotherapy (IMRT), volumetric modulated arc therapy (VMAT) both provide highly conformal dose distribution with good sparing of normal tissues in definitive setting. However, no comparison is done for the two techniques in post-operative radiotherapy setting.

### Material and Methods

Seventy-five consecutive post-operative prostate cancer patients were selected retrospectively for this dosimetric comparison study. nineteen patient received IMRT and 60 patient received VMAT radiotherapy using the Eclipse™ treatment planning system (Varian Medical Systems). Planning target coverage, monitor units (MU), dose to bladder and rectum were compared across techniques.

### Results

Overall, dose to the prostate bed, expressed as mean  $\pm$  standard deviation, was 74.7  $\pm$  1.1 (Gy). PTV coverage and total MU were 97.65  $\pm$  1.47 % and 1090.5  $\pm$  279.5 MUs for VMAT and 97.05  $\pm$  1.49 % and 913.3  $\pm$  441.1 MU for IMRT technique. For rectum, mean dose, V40, V45, V50, V55, V60, V65 were 46.2/46.75 Gy (p = 0.78), 35.4/35.6 % (p = 0.93), 27.2/26.9 (p = 0.92), 20.3/19.9 (p = 0.83), 14.2/13.4 (p = 0.68), 8.0/5.6 (p = 0.15), 1.4/1.7 (p = 0.77) % in VMAT and IMRT technique. For bladder, mean dose, V40, V45, V50, V55, V60, V65 were 63.1 /49.2 Gy (p = 0.04), 54.9/40.5 (p = 0.01), 45.9/32.6 (p = 0.02), 38.5/26.0 (p = 0.02), 32.0/20.5 (p = 0.02), 25.7/14.1 (p = 0.01), 7.4/4.2 (p = 0.17) % in VMAT and IMRT technique.

### Conclusion

Both techniques provided good target coverage and good organs-at-risk sparing. However, IMRT resulted in lower dose to the bladder.

### Electronic Poster: RTT track: Image guided radiotherapy and verification protocols

#### EP-2190 MVCT in pediatric craniospinal radiotherapy

F. Ferraro<sup>1</sup>, A. Lastrucci<sup>1</sup>, Y. Wandael<sup>2</sup>, C. Galeotti<sup>2</sup>, M. Vernaleone<sup>2</sup>, D. Greto<sup>2</sup>, G. Simontacchi<sup>2</sup>, P. Bonomo<sup>2</sup>, L. Livi<sup>1</sup>

<sup>1</sup>University of Florence, Department of biomedical-experimental and clinical sciences "Mario Serio", Florence, Italy; <sup>2</sup>A.O.U. Careggi, Radiotherapy, Florence, Italy

#### Purpose or Objective

This work reports the analysis of MVCT, system based on the image-guided radiation therapy (IGRT) in the tomography treatment, used for the initial setup verification in pediatric patients treated with craniospinal irradiation.

The duration of the MVCT scanning time on the entire craniospinal axis is high and anesthesia in pediatric patients is required during this period. For this reason, the reduction of the scanning time is a great interest. The final aim of this work is the comparison between the results obtained from the matching of MVCT and two different kind of patient centering on CT: one based on the scan of the entire craniospinal axis (case 1) and the other based on the acquisition average of the reduced volume at the end and at the beginning of the scanning (case 2).

#### Material and Methods

During this study 7 pediatric patients treated with craniospinal tomotherapy was investigated (total amount of 105 MVCT). Shifts (mm) along the three principal axes (X-lateral, Y-longitudinal and Z-vertical) were acquired for each single fraction associated to the different patients obtained during the matching. In the first case (matching between MVCT and CT scan of the entire craniospinal axis) the shifts were controlled by the operator and the results were acquired in the automatic mode; after the shifts were reset.

In the second case (matching between MVCT and the average CT scans of the reduced volume at the end and at the beginning of the scanning) the matching of MVCT and CT on two different parts was acquired. The analyzed sections were, respectively, the region from frontal sinus to the first thoracic vertebra and the region from the eleventh thoracic vertebra to the first lumbar vertebra. In this case the average of the scans at different positions was considered. The results obtained in the two different cases were compared. During the matching was only considered shifts of translations.

#### Results

The analysis confirms that there is only a slight difference between the two different methods, in some cases less than 1 mm, as reported in the table 1.

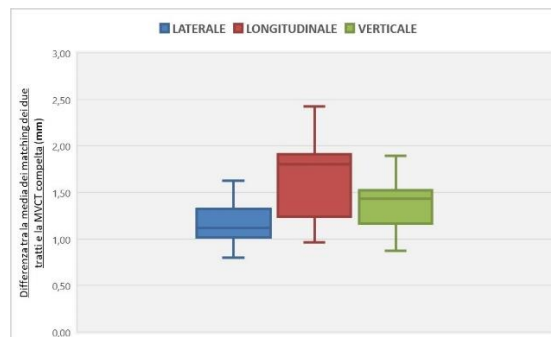


Table1

Box plot representation of the average values obtained from the two different matching on three different planes.

#### Conclusion

The good accordance of these data confirms the quality of the entire procedure, but other studies are necessary before the implementation of this procedure in the clinical protocols. In order to fulfill this goal the evaluation of the following parameters is mandatory:

*Accordance between the results obtained by two different operators:* evaluation of the matching of the data obtained by two different operators.

*Validation by third observer:* evaluation of the differences between the two kinds of MVCT obtained from the entire craniospinal axis and from the average of two reduced volumes (frontal sinus/ D1 and D11/L1).

#### EP-2191 Daily Image Guided Radiotherapy -the relevance for patients with metastatic spinal cord compression

L. Johansen<sup>1</sup>, D. Gasic<sup>1</sup>, V. Gram<sup>1</sup>

<sup>1</sup>The Finsen Center - Rigshospitalet, Radiation Oncology, Copenhagen, Denmark

#### Purpose or Objective

There are wide differences in pre-treatment verification for patients with metastatic spinal cord compression (MSCC). At our clinic, daily Image Guided Radiotherapy (IGRT) with cone beam computed tomography (CBCT) and volumetric modulated arc therapy has been standard practice for MSCC patients for almost a decade. It is seen as a great safety precaution that the treatment is delivered correctly. These patients often suffer from neurological and cancer related pain in various degrees, which can make precise positioning according to setup tattoos alone difficult. This setup uncertainty is compensated by daily setup correction in the form of a couch shift based on the pre-treatment CBCT scan.

For patients treated in the lumbar region of the vertebral column there are also added positional uncertainties as a result of the setup tattoos being placed on the side of the thorax wall, and therefore, far from the target. In addition, there are no fixations used for this anatomical site.

Daily IGRT with couch corrections for MSCC patients is not standard procedure for many radiotherapy clinics and the relevance of it is often discussed. Advantages of IGRT and couch corrections include the ability of reducing target volumes, as well as an added security in correct positioning-ensuring irradiation of the affected vertebra(s).

By looking at the setup corrections made for each fraction, it is possible to estimate the standard deviation and through this evaluate how far off mark a treatment would have been without the use of IGRT.

#### Material and Methods

A total of 30 consecutive patients from early 2018 with MSCC in the lumbar region (proximal thoracic vertebrae were sometimes included in the lumbar target) treated with 3 Gy X 10, 5 F/W were included. The CBCT based

couch shift for superior-inferior (SI), anterior-posterior (AP), medial-lateral (ML) and yaw (rotation around the AP-axis) for all fractions were examined and the mean, minimum, maximum shift and standard deviation (SD) of each parameter in each treatment course was calculated.

### Results

The mean couch shift following the 300 CBCT scans included (table 1) was 5.87 mm SI (Range: 0 - 30 mm, SD: 3.86), 3.96 mm AP (Range: 0 - 22 mm, SD 2.58), 6.51 mm ML (Range: 0 - 34 mm, SD 4.40) and 1.24° yaw (Range: 0 - 4.6°, SD .75). The greatest couch shifts and deviations were generally found in the ML direction.

**Table 1**

Table 1 shows the mean, minimum, maximum shift and standard deviation of each parameter of the 30 patients' treatment course. It should be noted that the couch corrections are not an expression of the direction the couch was moved, but an expression of the deviations corrected, regardless of direction.

	SI	mean	min	max	SD	AP	mean	min	max	SD
1		3.0	0.0	7.0	2.31		2.4	2.0	4.0	0.70
2		6.8	1.0	12.0	3.71		7.0	2.0	12.0	4.29
3		3.2	1.0	6.0	1.75		5.4	0.0	10.0	3.81
4		3.6	2.0	6.0	1.51		3.3	1.0	9.0	2.58
5		4.6	3.0	7.0	1.26		4.6	2.0	8.0	1.90
6		8.6	4.0	21.0	5.13		1.1	0.0	9.0	2.81
7		5.3	0.0	11.0	4.45		3.7	3.0	14.0	4.99
8		2.8	0.0	8.0	2.70		1.0	0.0	2.0	0.67
9		16.1	0.0	27.0	9.94		12.3	1.0	22.0	5.42
10		3.8	1.0	7.0	2.04		3.5	1.0	6.0	1.72
11		5.8	1.0	11.0	2.86		4.1	0.0	13.0	3.90
12		4.1	1.0	14.0	3.84		3.3	1.0	8.0	2.21
13		4.8	1.0	9.0	3.05		2.5	0.0	5.0	1.51
14		6.1	2.0	12.0	3.31		4.1	1.0	9.0	2.51
15		2.0	0.0	5.0	1.49		2.1	1.0	4.0	1.10
16		6.0	0.0	27.0	7.83		1.9	0.0	11.0	3.35
17		4.2	1.0	8.0	2.74		7.4	3.0	12.0	3.10
18		5.2	0.0	8.0	3.01		3.0	0.0	7.0	2.26
19		2.6	0.0	6.0	1.78		5.3	1.0	11.0	3.59
20		8.6	1.0	16.0	4.09		2.9	1.0	5.0	1.10
21		7.8	1.0	20.0	6.14		3.2	0.0	7.0	1.87
22		9.6	0.0	16.0	5.30		3.0	0.0	7.0	2.26
23		3.2	0.0	6.0	2.30		4.0	1.0	7.0	1.89
24		4.5	1.0	9.0	2.72		7.2	2.0	9.0	2.49
25		2.5	0.0	5.0	2.07		2.1	0.0	5.0	1.60
26		8.8	0.0	23.0	7.38		0.9	0.0	2.0	0.88
27		9.7	6.0	14.0	2.71		8.6	2.0	19.0	5.13
28		12.3	0.0	30.0	8.90		2.6	0.0	5.0	1.43
29		8.3	2.0	25.0	7.09		3.6	0.0	15.0	4.97
30		2.3	0.0	7.0	2.31		2.6	0.0	5.0	1.51
Mean of SD					3.86					2.58
Total		5.87	0.00	30.00			3.96	0.00	22.00	

	ML	mean	min	max	SD	Yaw	mean	min	max	SD
1		14.4	5.0	34.0	9.57		0.6	0.2	1.1	0.32
2		6.4	1.0	12.0	3.63		1.3	0.1	3.2	1.03
3		3.7	0.0	9.0	2.75		0.8	0.1	1.9	0.63
4		6.2	0.0	20.0	6.14		0.9	0.0	1.9	0.71
5		3.3	1.0	10.0	2.83		0.7	0.0	1.8	0.60
6		8.6	2.0	21.0	6.29		0.7	0.2	1.7	0.50
7		5.7	0.0	15.0	5.06		1.2	0.3	2.6	0.81
8		6.0	1.0	16.0	4.62		1.6	0.8	2.3	0.61
9		4.9	1.0	9.0	2.77		1.1	0.0	2.6	0.80
10		13.0	1.0	26.0	8.35		1.2	0.1	2.2	0.82
11		6.8	0.0	13.0	3.99		2.3	1.2	2.9	0.60
12		11.1	2.0	25.0	6.82		1.2	0.4	2.8	0.77
13		6.8	1.0	14.0	3.82		2.0	0.3	3.5	1.10
14		3.9	1.0	8.0	2.13		0.9	0.0	1.6	0.56
15		6.4	0.0	14.0	5.10		1.4	0.2	2.8	0.71
16		7.4	1.0	12.0	3.06		0.7	0.1	1.2	0.31
17		3.7	0.0	10.0	3.53		0.9	0.1	1.7	0.48
18		6.1	2.0	14.0	4.36		0.9	0.1	2.0	0.80
19		8.5	1.0	17.0	5.32		2.2	1.4	3.0	0.55
20		8.8	2.0	14.0	4.99		2.7	1.1	4.6	1.00
21		13.0	0.0	26.0	8.22		1.6	0.0	3.2	1.11
22		2.5	1.0	5.0	1.51		1.0	0.0	2.6	0.97
23		4.2	1.0	9.0	3.19		1.1	0.2	2.8	0.82
24		3.3	0.0	9.0	2.98		0.9	0.0	2.1	0.70
25		3.6	1.0	9.0	2.17		1.2	0.0	2.9	0.86
26		5.0	0.0	16.0	5.12		1.2	0.1	2.1	0.82
27		11.9	2.0	27.0	7.52		1.2	0.2	2.7	0.75
28		4.2	0.0	7.0	2.04		0.9	0.0	1.8	0.61
29		1.3	0.0	4.0	1.49		1.2	0.0	3.1	1.05
30		4.5	1.0	10.0	3.31		1.9	0.3	3.2	0.96
Mean of SD					4.40					0.75
Total		6.51	0.00	34.00			1.24	0.00	4.60	

### Conclusion

The CBCT based couch shifts showed, that IGRT is highly relevant and useful in ensuring correct treatment of patients with M SCC.

### EP-2192 A systematic approach aimed at reducing IGRT dose in paediatric patients

S. Stead<sup>1</sup>

<sup>1</sup>Clatterbridge Cancer Centre NHS Trust, Radiotherapy, Wirral, United Kingdom

### Purpose or Objective

Compared to adults, the higher survival rates and anticipated decades of longevity of paediatric patients heighten the concerns regarding late effects of radiotherapy and secondary malignancies. Much has changed in the way we plan and deliver radiotherapy and an understanding is required of the differences between adult and paediatric cancers and the consequences of treatment. With continual technological advances such as IMRT and VMAT the ability to optimise plans with sharp dose gradients has dramatically improved, reducing the amount of dose received by normal tissue. However, in order to minimise target volumes for these increasingly conformal techniques, there is a requirement for increased IGRT to ensure accurate tumour localisation and patient set up.

Over-utilization of RT verification systems and procedures could inflict a large amount of excessive radiation

exposure to our paediatric patients, who are already at greater risk of secondary malignancies. It is therefore essential to make sure that the dose delivered as part of any verification procedure is optimised such that the dose is high enough to produce a useable image, but no higher.

#### Material and Methods

A 1 year old patient was referred for RT with an upper lip rhabdomyosarcoma with metastatic neck nodes. The patient was anaesthetised for treatment with a nasogastric tube fitted and laryngeal mask. Daily CBCT was required as IMRT was to be used and also daily repositioning was difficult due to the position of the nasogastric tube and laryngeal mask.

A Varian TrueBeam linear accelerator with software version 2.0 was used for treatment. The CBCT mode editor was utilised and Varian default settings modified so that the gantry was forced to go under the couch, avoiding beam entry through radiosensitive structures such as the eyes. The mAs was reduced in steps to ensure image quality, such as homogeneity, contrast and noise were maintained in the reconstructed image. The geometry of a cone beam scan enables a large FOV to be viewed in one rotation. However this contributed to a large amount of scatter radiation. So in addition to a lower mAs, a smaller FOV was utilised to further reduce scatter radiation. Care was taken to not limit the total volume that could be reconstructed.

#### Results

CBCT images were reconstructed, evaluated, and compared. Visual comparison indicates that the image quality of CBCT(s) is comparable to that of the initial CBCT (#1-2). The results demonstrate that the scanning parameters can be manipulated to reduce the dose to the patient with minimal effect on the quality of the CBCT when comparing bony anatomy. This is done by employing lower mAs, less fps, smaller FOV, or by using 200° rotation below couch.

#### Conclusion

With optimal settings in use, the dose to the patient can be reduced by 95.5% when compared to the default setting with minimal impact on image quality. It is therefore safe and appropriate to use this optimised mode for all paediatric patients.

	kVp	mA	ms	Exposure time	Exposure	fps	Dag/se	Scan length	CTDIw ~mGy	% dose
#1-2 CCC Head	100	15	20	7350	14 6	15	6	185	3.0	100
#3-7 CCC image gently	80	11	13	7350	95	15	6	185	2.0	29
#8 CCC very image gently	80	10	10	4900	49	15	6	185	0.8	15
#9-10 CCC very image gently	80	10	10	4900	49	15	6	155	0.4	10
#11 CCC image very very gently	80	10	10	2310	23	7	6	185	0.4	7.5
#12-13 CCC image very very gently	80	10	10	2310	23	7	6	155	0.4	4.5

#### EP-2193 Influence of rotational setup errors on dose in target and organs at risk in cranial radiotherapy

A.S. Gerhardt<sup>1,2</sup>, M.N. Duma<sup>1,3</sup>, M. Düsberg<sup>1</sup>, J.J.

Wilkens<sup>1</sup>, S.E. Combs<sup>1,3</sup>, M. Oechsner<sup>1</sup>

<sup>1</sup>Klinikum Rechts der Isar, Department of Radiation Oncology, Munich, Germany; <sup>2</sup>Technical University Munich, Faculty of Medicine, Munich, Germany;

<sup>3</sup>Helmholtz Zentrum München, Institut für Innovative Radiotherapie, Munich, Germany

#### Purpose or Objective

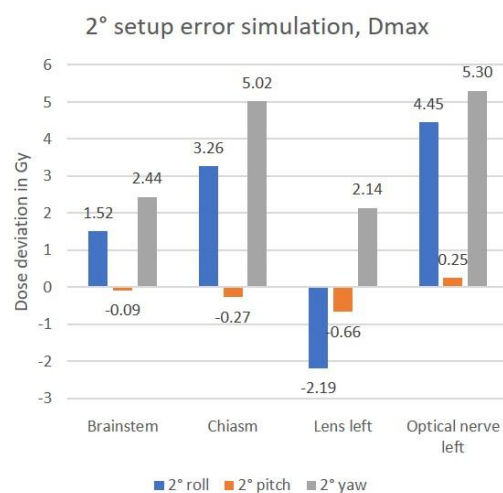
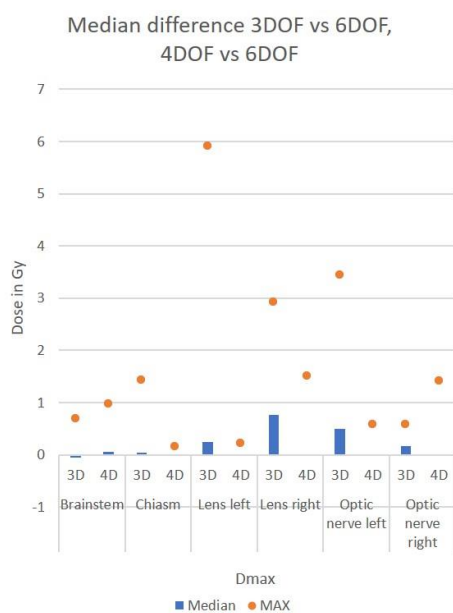
The aim of this study is to detect dose aberrations in cranial radiation therapy in the target volume and adjacent organs at risk (OARs) caused by insufficient rotational setup correction. 6 degrees of freedom (DOF) fusions were considered as the gold standard and compared to 4 DOF and 3 DOF registrations.

#### Material and Methods

Setup errors of 12 patients with cranial lesions undergoing radiotherapy and positioned with cone beam computed tomography (CBCT) were analyzed. The PTVs of the included patients were large and irregularly shaped and located near or overlapping cranial OARs such as brainstem, chiasm, optical nerves or lenses. A registration between planning CT and the first CBCT of the treatment course was performed using 6 DOF, 4 DOF and 3 DOF. Differences between the three registrations were implemented and the planning CT and associated structure set shifted and warped accordingly. To detect the DOF with the largest influence on the delivered dose a rotational error of 2°, 3° and 4° was simulated in one rotational dimension at a time. Using the original parameters, the treatment plan was copied and recalculated to the warped image set. Dmax and Dmean of the cranial OARs and D98 and D2 for the respective CTV and PTV were analyzed.

#### Results

Differences between 6 DOF and 4 or 3 DOF fusion ranged between -1.4° and 2° in pitch direction, -2.5° to 2° in yaw, and -4.4° to 4.2° in roll direction. Resulting median D98 in the PTV decreased by 0.7 Gy using only 3 DOF and increased by 0.08 Gy if 4 DOF were included. Maximum dose reduction of the PTV D98 was 2.96 Gy using 3 DOF and 0.39 Gy using 4 DOF. CTV dose decreased by 0.68 using only 3 DOF and by 0.03 Gy using 4 DOF. Resulting median dose effects in the OARs are displayed in Figure 1, with largest effects of additional 0.2 and 0.8 Gy for the left and right lenses, respectively. Doses for individual patients varied up to additional 6 Gy in the lenses and 3 Gy in the optic nerves. Effects on doses in the OARs and target volumes were generally larger with 3 DOF than with 4 DOF included, except for the brainstem with no visible difference. Pitch and roll setup errors had larger effects on the OARs compared to yaw setup deviations, as demonstrated in Figure 2. 2° roll setup errors caused more than 5 Gy dose effect on the ipsilateral optical nerve and chiasm, followed by 2° pitch errors resulting in over 3 Gy additional dose. The simulated 2° yaw error had an effect of under 1 Gy on dose delivery.



### Conclusion

For cases involving higher dose effects on the evaluated structures, 4DOF registration improved plan conformity compared to 3DOF. Clinically relevant dose deviations in the CTV were not found in this patient collective. While mean dose delivery to OARs increased only slightly, up to 6 Gy in additional dose occurred for individual patient cases in this collective because of rotational errors. Safety margins for OARs could be a solution to this matter.

### EP-2194 Do lower dose KV-CBCT protocols produce adequate quality images for head and neck cancer patients?

M. Forshaw<sup>1</sup>, A. Taylor<sup>2</sup>, S. Temple<sup>3</sup>, H. Wong<sup>4</sup>, A. Willet<sup>5</sup>, C. Rowbottom<sup>5</sup>

<sup>1</sup>The Clatterbridge Cancer Centre, Radiotherapy, Wirral, United Kingdom; <sup>2</sup>Sheffield Hallam University, Radiotherapy and Oncology, Sheffield, United Kingdom; <sup>3</sup>The Clatterbridge Cancer Centre, Physics, Wirral, United Kingdom; <sup>4</sup>The Clatterbridge Cancer Centre, Statistics, Merseyside, United Kingdom; <sup>5</sup>The Clatterbridge Cancer Centre, Physics, Merseyside, United Kingdom

### Purpose or Objective

Previous literature cites that patients treated with volumetric arc therapy (VMAT) for head and neck cancer necessitates Daily Cone Beam Computerised Tomography (CBCT) in order to ensure treatment accuracy. This is because throughout a course of radiotherapy for head and neck cancer anatomical changes occur within the patient due to the treatment delivered, resulting in geometric uncertainty. It is imperative the imaging dose is minimised in line with the Ionising Radiation (Medical Exposures) Regulations 2018 (IR(ME)R) and that images are fit for purpose.

Within the practice environment (PE) the imaging mode for KV CBCT is set by the manufacturer of the Linear Accelerators (Linac), Varian Medical Systems, Palo Alto, CA (Varian).

### Material and Methods

A service evaluation was undertaken to determine whether lower dose KV CBCT head imaging modes provided adequate imaging quality for the purpose of treatment verification, in comparison to the standard manufacturer settings. Optimization of images was completed via a reduction in the mAs. Two alternate settings were produced and tested on a phantom. The novel KV CBCT imaging protocols were then tested on patients who were receiving already justified for daily imaging. Daily KV CBCT scans were acquired and patients received one CBCT per week of a lower dose mode. Overall 304 KV CBCT images were scored independently using a graded scale by three independent multidisciplinary image observers. Qualitative analysis was used to evaluate the results of the study.

### Results

N=38 patients were included in the project. 304 KV CBCT scans were scored using a graded scale. Initial review of images allowed the grouping of image scores into good, moderate and poor categories based on the average image scores for all image reviewers. 56.57% of lower dose images were deemed good in quality in contrast to 1.31% were deemed poor in quality. 42.11% of the lower dose scans were grouped in the moderate quality category. This identified that poor quality images were infrequent. Statistical analysis was undertaken using parametric t-test analysis and provided comparison statistics between standard imaging and lower dose imaging for each individual score. Intra observer variability was also analysed using Kappa analysis. This identified that the physicist results were statistically different to the radiographer and clinician when scoring images.

### Conclusion

Findings identified that low dose imaging produce adequate quality imaging for the purpose that they are intended whilst benefiting the patient by minimising concomitant exposure. The very low dose imaging modes are not suitable for volumes that extend past cervical vertebrae seven, as this produces poor quality images with artefact and image distortion. Calculations were completed to obtain the effective dose that the patient would receive with the differing imaging modes throughout the course of radiotherapy and it was proven that the lower dose imaging reduced the dose received by the patient.

### EP-2195 Optimization of SABR lung CBCT verification

L. Turtle<sup>1</sup>, A. Willet<sup>2</sup>, C. Lee<sup>2</sup>, C. Fitzpatrick<sup>2</sup>, R. Biggar<sup>2</sup>  
<sup>1</sup>Clatterbridge Cancer Centre NHS Foundation Trust, Radiotherapy, Wirral, United Kingdom; <sup>2</sup>Clatterbridge Cancer Centre NHS Foundation Trust, Physics, Wirral, United Kingdom

### Purpose or Objective

CBCT verification is arguably more critical to ensure set-up accuracy in hypo-fractionated SABR regimens. At our clinic all SABR lung patients receive pre-treatment 4D-CBCT and post-treatment 3D-CBCT imaging. The current default is Varian TrueBeam 'thorax' mode (125kV, 15mA, 46cm FoV). This is a full trajectory scan, taking 60 seconds to acquire. To improve on-set efficiency and optimise imaging dose alternative 'spotlight' CBCT exposures were investigated. Spotlight offers a shorter 200° trajectory and the smaller 25cm FoV is sufficient for SABR lung PTV's. These modes were tested on the post-treatment imaging to determine if they are clinically suitable for verification.

### Material and Methods

Two thorax spotlight modes (A, B) were optimised using a CIRS lung phantom. Exposure parameters were reduced in both cases to 100kV and 10mA and 15mA for modes A and B, respectively. 5 patients were selected randomly for clinical testing (including gated and non-gated cases). For each patient, standard 'thorax' mode was replaced by 'spotlight' A or B, on subsequent fractions in no particular order. Treatment radiographers were blinded to which mode was of higher mA.

Images were reviewed and scored offline by 4 RTTs of various experience and 1 physicist. Scorers were blinded to which exposures had been used. The CBCTs were scored using an adapted 5-point scoring system, where 1 is the highest score. A score  $\leq 3$  was deemed clinically suitable. For each image, the highest and lowest scores were discarded.

### Results

CTDI<sub>w</sub> was established as 0.78 mGy (A) and 1.16 mGy (B). This represents a dose reduction of 71%-80% compared with the current standard 'thorax' mode (CTDI<sub>w</sub>=3.94mGy). This also corresponds to an effective dose of roughly 0.4mSv (A) and 0.6mSv (B) which is about a lifetime cancer risk of 1 in 42000 and 1 in 28000 respectively compared with the current standard 'thorax' mode which is 1 in 8000 (2.2mSv).

Spotlight A and B achieved an average scoring of 2.4 and 2.5 across all patients, respectively. Both would therefore be suitable for clinical use. With minimal scoring difference, the lower dose Spotlight A is preferable for its reduced dose.

CBCT delivery time was reduced from 60 seconds to 33 seconds.

### Conclusion

The use of spotlight mode for verification of lung SABR has been demonstrated. Imaging dose has been optimised as low as reasonably practicable whilst fulfilling the clinical requirement for verification. Delivery time has been reduced, improving patient experience and clinic throughput. The new mode will be introduced as the clinical standard.

---

### Electronic Poster: RTT track: Motion management and adaptive strategies

---

#### EP-2196 Dosimetric impact of anatomical changes during IMRT for prostate cancer

L. Farhat<sup>1</sup>, W. Mnejja<sup>1</sup>, H. Daoud<sup>1</sup>, F. Dhoubi<sup>1</sup>, T. Sahnoun<sup>1</sup>, W. Siala<sup>1</sup>, J. Daoud<sup>1</sup>

<sup>1</sup>Hbib Bourguiba Hospital, Radiotherapy, Sfax, Tunisia

### Purpose or Objective

During the treatment of prostate cancer with intensity modulated radiotherapy (IMRT), we observe geometric (volumetric and positional) variations. We proposed in this work to evaluate the dosimetric impact of these variations on prostate and organs at risk: bladder and rectum.

### Material and Methods

Ten patients treated with IMRT for prostate cancer were included in this study. For each patient, 3 to 5 control scans (CTc) were made during the treatment period and fused with the initial scan (CTi). We manually delineated the prostate, the bladder and the rectum on the CTc. A comparative study of the different volumes was performed to determine the percentage of variation. We recorded the minimum dose (Dmin) in the prostate and the maximal dose (Dmax) in the rectum and bladder on the various CT made. Comparison of averages deviations was done using the Wilcoxon Signed Rank test for associated samples.

### Results

We found a significant average variation of volume for the different structures. It was about 20.67% [-89, 198%] for the rectum (p<0.001), 16.69% [-66, 86%] for the bladder (p<0.001) and 5.81% [-23, 18%] for the prostate (p<0.001). The Dmin in the prostate was decreased by 4.05%, the Dmax in the rectum and the bladder by 0.16 and 0.51%. Two patients had an important decrease of Dmin in the prostate. It was about 18 and 13.75%. For those patients, the increase in prostatic volume was about 6.97% and 16.04% and the decrease in rectal volume about 27.96% and 48.91%.

### Conclusion

The anatomical variations during IMRT in the target volume and the organs at risk were not correlated with a major dose variation. However, in two cases, the significant reduction in rectal volume was associated with a decrease in prostatic Dmin which could have an impact on the control of the disease. We insist, then, on the need to perform the dosimetric scanner with an empty rectum.

#### EP-2197 EEBH as a method of managing respiratory movement in treating abdominal structures with SABR

J. Barber<sup>1</sup>, B. Taylor<sup>2</sup>, A. Gaya<sup>2</sup>, A. Qureshi<sup>2</sup>, C. Thomas<sup>3</sup>, C. Hartill<sup>1</sup>, V. Staykova<sup>3</sup>, C. Sisodia<sup>3</sup>

<sup>1</sup>Guys and St Thomas', Radiotherapy, London, United Kingdom; <sup>2</sup>Guys and St Thomas', Oncology, London, United Kingdom; <sup>3</sup>Guys and St Thomas', Radiotherapy Physics, London, United Kingdom

### Purpose or Objective

When treating abdominal structures with SABR, accounting for respiratory movement is mandated by the CORE and SARON trials and SABR CtE. The most common methods are to apply an ITV, meaning the target volume stays within the high dose area, or using Abdominal Compression to physically restrict the movement of abdominal structures. Utilising EEBH for delivering treatment will enable complete eradication of target volume movement and therefore the ITV.

### Material and Methods

Following the implementation of EEBH in pre-treatment resulting in improved CT image quality, the potential impact of treating in EEBH rather than using an ITV was assessed by quantifying the reduction in target volume and the impact on OAR doses when an EEBH plan was created. This showed clear benefits to treating in EEBH, with volumes being as much as halved and OAR doses being dramatically reduced.

### Results

Treating in EEBH has reduced target volumes by an average of 31% (values ranging from 8% to 51% in the 8 patients analysed), consequently allowing higher doses to be used in more patients and increasing the overall number of patients suitable for treatment with SABR.

### Conclusion

There are challenges involved in treating patients in EEBH, including reproducing breath-holds and verifying the level of hold. Techniques used with DIBH techniques proved ineffective as a result of the EEBH position being within the normal range of respiratory motion, meaning AlignRT was unable to detect this as they would the significant

contour change of DIBH. Instead, RPM was used as this system normalises to a baseline of 0, determined by the End Expiration amplitude. This breath hold was then verified by acquiring a CBCT while in EEBH and comparing to the planning CT acquired in EEBH. Flattening Filter Free (FFF) was utilised at treatment to cut delivery time, allowing patients to be treated in an achievable number of breath-holds. Further work will be carried out to determine the dosimetric impact on OARs of this volume reduction.

---

#### Electronic Poster: RTT track: Patient care, side effects and communication

---

##### EP-2198 Addressing treatment-related sexual side effects: Sub-optimal practice in radiation therapy

O. Lynch<sup>1</sup>, P. Murphy<sup>1</sup>, A. O'Donovan<sup>1</sup>

<sup>1</sup>Trinity College Dublin, Discipline of Radiation Therapy, Dublin, Ireland

#### Purpose or Objective

Sexual side effects of treatment are common among cancer patients receiving radiation therapy. Little attention has been given to the role of radiation therapists (RTs) in managing sexual issues. The current study sought to address this by assessing the provision of care for sexual issues by RTs in Ireland.

#### Material and Methods

Cross-sectional data were collected using an online questionnaire. Measures included: participant characteristics; sexuality-related practice, knowledge, awareness, and confidence in dealing with sexual issues; the sexual attitudes and beliefs survey; and opinions as to the 'ideal' management of sexual issues.

#### Results

Discussion of sexual issues with patients was rare, and most participants ( $N = 46$ ) did not feel these issues were addressed effectively in their departments. Barriers to the discussion of sexual issues included: low knowledge, awareness, and confidence, perceptions of professional role boundaries; and concerns about personal and patient discomfort. Nonetheless, participants indicated that RTs should ideally be equipped to discuss sexual side effects of treatment, as they would any other side effect.

#### Conclusion

This study has identified a sub-optimal provision of care for sexual issues by RTs. Training is needed if RTs are to effectively support the work of the multidisciplinary team in this area.

##### EP-2199 Attitudes of parents of female secondary school students towards the HPV vaccine

K. Lawless<sup>1</sup>, C. Poole<sup>1</sup>, P. Murphy<sup>1</sup>

<sup>1</sup>TCD Division of Radiation Therapy, Radiation Therapy, Dublin, Ireland

#### Purpose or Objective

Cervical Cancer is the seventh most common cancer worldwide. The HPV virus is responsible for 70% of invasive cervical cancers and the decision to vaccinate a child against HPV is made by their parents. Concerns over the safety of the vaccine has resulted in a decrease in the uptake of the HPV vaccine. The main purpose of this study was to identify the influences behind attitudes currently held by parents of Irish adolescent girls and the factors causing the drop-in uptake.

#### Material and Methods

An anonymous questionnaire was designed and circulated among the parents of first-year students in two all-girl secondary schools ( $n = 158$ ). The questionnaire included both quantitative and qualitative questions. Outcome

measures were HPV Knowledge, information sources and parental attitudes.

#### Results

The vaccine uptake according to this study was 63.4% ( $n=41$ ). The study showed that 68.3% of the parents had good knowledge of the HPV Virus/Vaccine. A strong trend towards significance in this study suggested that participants with lower knowledge were more likely to consent. Thematic analysis of the qualitative data revealed that parents wish to protect their child from cervical cancer and that worries about the vaccine safety were the main barrier to vaccination. Assumptions that more knowledge of HPV would lead to acceptability was not established in this study, instead it was suggested that those with lower knowledge were more likely to consent. Increased knowledge would indicate that the parents were more likely to do in-depth research and discover the well-publicised safety concerns.

#### Conclusion

Further efforts must be made to counteract the negative media available to parents to ensure they are fully informed in their decision making. Further research on the parents' knowledge of vaccine safety could be done to address this.

##### EP-2200 Understanding the impact of health literacy on self-efficacy in cancer patients undergoing treatment

R. Scanlon<sup>1</sup>, C. Gillham<sup>2</sup>, A. Craig<sup>1</sup>

<sup>1</sup>Trinity College Dublin, Discipline of Radiation Therapy, Dublin, Ireland; <sup>2</sup>St Luke's Radiation Oncology Network, Radiation Therapy, Dublin, Ireland

#### Purpose or Objective

Health literacy influences how cancer patients participate in self-care and disease management due to their level of knowledge in the area. As shown in other groups, greater levels of self-efficacy result in patients seeking information, thus improving levels of self-care. These factors are important to consider in cancer patients, who rely on disease management and self-care to improve quality of life.

The purpose was to investigate if a relationship exists between health literacy and self-efficacy in cancer patients undergoing radiotherapy and to identify if such a relationship can be affected by patients' sociodemographic factors.

#### Material and Methods

An anonymous survey combining sociodemographics with standardised instruments of health literacy and self-efficacy was distributed in a radiotherapy service. Quantitative analysis was used to determine if a relationship exists.

#### Results

From the 165 surveys distributed, 62 surveys were returned, yielding a 38% response rate. Health literacy moderately impacted on self-efficacy ( $r = 0.617, p < 0.001$ ), with the strongest correlation in participants asking questions and participating in treatment. Education ( $r = 0.39, p = 0.002$ ) and employment status ( $H(4) = 10.19, p = 0.04$ ) influenced health literacy. Of the sociodemographic data analysed, only employment status influenced self-efficacy ( $H(4) = 9.727, p = 0.045$ ).

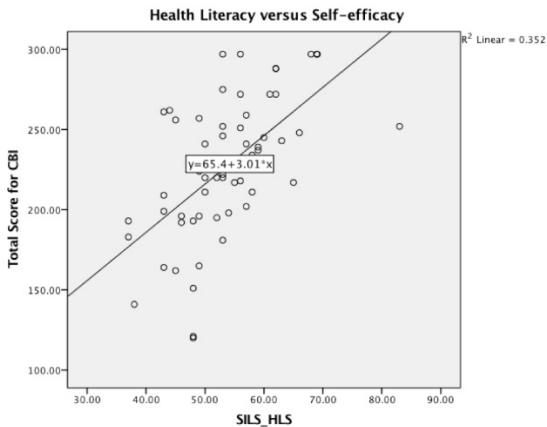


Figure 1. shows the moderate positive relationship between health literacy (SILS\_HLS) and self-efficacy (Total Score for CBI).

### Conclusion

Health literacy is related to self-efficacy in cancer patients. Education level positively impacts health literacy levels, highlighting the importance of tailoring patient information to patient education levels, in order to promote self-care and disease management.

### EP-2201 Auditing patient's radiotherapy medical file for improvement

S. Cucchiari<sup>1</sup>, M. Delgaudine<sup>2</sup>, P. Coucke<sup>1</sup>

<sup>1</sup>C.H.U. Sart Tilman, Radiotherapy Department, Liège, Belgium; <sup>2</sup>C.H.U. - Sart Tilman, STA Quality Department, Liège, Belgium

### Purpose or Objective

The patient's Radiation Therapy (RT) medical file is the place of collection and conservation of medical and paramedical information, recorded for any patient. The patient's record ensures the traceability of all actions performed. It is an important tool of communication, coordination and information between the multidisciplinary RT team. It makes it possible to follow and understand the patient's RT journey. This file must be complete and contain the information essential for the quality of the treatment. The purpose of this study is to draw up an objective inventory of the RT medical record and to propose improvement actions so that it is best documented as possible.

### Material and Methods

The methodology used is an internal audit of medical files. A grid was developed based on criteria used in the Quality Assurance Team for Radiation Oncology (QUATRO) reference, criteria recommended by Joint Commission International accreditation, and RT department-specific criteria derived from adverse event reporting for incomplete or erroneous patient records.

This grid (Figure 1) includes 19 observation items and one box for comments. The filling is simple and is carried out by "yes-no-partially-not applicable".

The analysis of files was carried out retrospectively by selecting patients treated by radiotherapy in the service between January and June 2018.

Figure 1: Assessment grid for chart review

Date:	Type	sheet 1	sheet 2	sheet 3	sheet 4	sheet 5	sheet 6	sheet 7	sheet 8	sheet 9	sheet 10
1	Is the pathology report included?										
2	Are Multidisciplinary Oncology Consultations (MOCs) decisions (taken)?										
3	Is the staging properly documented?										
4	Is the pathology clearly identified?										
5	Is the prescription evidence based?										
6	Are total dose, dose/fraction, and number of fraction stipulated?										
7	Was there any change during treatment?										
8	Are Chemos / surgery dates specified?										
9	Are the specific simulation features specified?										
10	Are the specific criteria of care completed? (allergy, pregnancy, sacral/prostate...)										
11	Is the irradiation technique as well as the laterality specified?										
12	Is performance status included?										
13	Is the first consultation completed?										
14	Are the follow up consultations completed?										
15	Is the end of treatment consultation completed?										
16	Is a geriatric assessment done?										
17	Is a pain assessment done?										
18	Is the patient's general consent stipulated?										
19	Is the information given to the patient and his family about his state of health, his examinations, his treatments (and possible changes) traced?										
	Comments										

### Results

10 patient files per doctor were randomly selected; there are 13 doctors in the department, so a total of 130 records were observed.

By analyzing the results obtained, it is noted that the files are quite complete, for example the pathology is clearly identified (100%), there is a trace of the first consultation (95%), the dose prescription is specified (99%). On the other hand, it is observed that in some cases important data for quality management care are missing, such as irradiation technique or tumor laterality are partially completed (65%), no systematic geriatric evaluation in patients over 75 (35%), no traceability of general consent (29%) and information given to the patient (39%). Various improvement actions were put in place following this analyze: setting up informed consent, check list to ensure that important issues are completed, use of a standard scale of pain identical to the one of the hospital. A half-yearly follow-up of these actions and a punctual audit during the year to verify the relevance of these actions will be realized.

### Conclusion

This RT patient chart review allows us to identify what is being done correctly and what needs improvement. Data contained within these files are extremely valuable for improving radiotherapy department efficiency and ensuring quality and safety of treatments. It is important that these files contain all the information necessary for good management.

Conducting internal audits such as medical records observation in the RT department is an effective tool for quality management in patient care.

### EP-2202 Iatrogenic sexual dysfunction following BRT. supportive therapy for better perception life quality

F. Piro<sup>1</sup>, D. Cosentino<sup>1</sup>, A. Martilotta<sup>1</sup>, A. Massenzo<sup>1</sup>, U. Piro<sup>1</sup>, G. Tocci<sup>1</sup>, L. Marafioti<sup>1</sup>

<sup>1</sup>Spedale Mariano Santo, Radiotherapy Center, Cosenza, Italy

### Purpose or Objective

BRT treatments can cause permanent sexual dysfunction due to shortening and vaginal shrinkage induced by fibrosis and post-treatment stenosis as a permanent toxic effect. We evaluated the introduction of supportive therapy (SuBRT) vs control group (CBRT).

### Material and Methods

From January 2010 to September 2017, 207 patients histologically proven endometrial carcinoma treated with BRT exclusively, with or without supportive therapy during treatment. BRT treatment involved a total dose of 30 Gy with a daily fraction of 6 Gy. Supportive therapy: daily endovaginal lavender with clorexidina and 12 hours after endovaginal ovules of hyaluronic acid low weight. We have formulated a psychological check-list for short interview to assess quality of life and impact on sexual activity after BRT, respecting privacy. We defined following areas: 1) social relationships and personal emotions, 2) intimacy of

couples and sexuality, 3) impact of treatment on sexuality, 4) relationship doctor-patient before BRT.

#### Results

Evaluable 199 pts.; median follow up 44 months (range 8-93); median age 62 years (40-88). Histological examination resulted 5 squamous and 194 adenocarcinoma; grading G1 for 15%, G2 for 65% and G3 for 20% of cases; all stage pT1B; lymph node status Negative in 149 (75%) and NX in other 50 (25%). Diameter of the cylinder used in 168 (84%) pts. it was 3-4 cm the remaining 31 (26%) diameter 1-2. Only 3 (1.5%) pts. disease progression. Psychological evaluation performed on 142 pts. (median age 61, range 44-71) the rest 57 not interested because not sexual active. Two groups: 69 CBRT vs 73 pts. SuBRT. First area the change of social activity recorded as "very, very much" was 33 of CBRT vs 22% of SuBRT, in the emotional state we found 42 of CBRT vs 29 % SuBRT. Second area: intimacy of couple; 71 vs 49% said they had undergone change; with repercussions on her relationship 49 vs 32 % and 81 vs 48 % of women reported decreased sexual desire.

Third area impact on sexuality: BRT changed your sex life? 46 vs 21% of SuBRT "very, very much". With sexual intercourse painful for 73 vs 48 % of the interviewees and to the question "Are sexual relations satisfactory?" 91 vs 60 % of respondents answered "NO".

Fourth area when we asked "Have you been informed that BRT could have an impact on sexuality?" 58 vs 80% of the patients answered "YES" while at the question "Did they advise you to have sex with your partner?" 71% vs 81 of the women received these indications. Unexpectedly, 13 vs 1 % SuBRT of patients explicitly requested psychological support.

#### Conclusion

Regardless of grading and lymph node depletion, BRT is effective in preventing disease recurrence. Although cylinders with larger diameter are used, the problem of post BRT toxicity management remains. Introduction of supportive therapy during treatment and best patient doctor relationship reduced the impact on quality of life of these patients.

#### EP-2203 DVH as predictor of acute skin toxicity, its clinical application in breast cancer radiotherapy

F. Piro<sup>1</sup>, D. Cosentino<sup>1</sup>, A. Martilotta<sup>1</sup>, A. Massenzo<sup>1</sup>, U. Piro<sup>1</sup>, G. Tocci<sup>1</sup>, L. Marafioti<sup>1</sup>

<sup>1</sup>Ospedale Mariano Santo, Radiotherapy Center, Cosenza, Italy

#### Purpose or Objective

The correlation between acute cutaneous toxicity and homogeneous dosimetry in breast cancer radiotherapy is now certain. For this reason, using the 3D conformational technique, we reviewed the dosimetry and DVH of each patient and recorded during the treatment the possible onset of acute cutaneous toxicity.

#### Material and Methods

from September 2017 to April 2018, 204 patients with breast cancer underwent 3D conformal radiotherapy on the breast. Tangential latero-medial technique, 6 MV photons, also using dynamic filters, two treatment schedules: single dose. 2.65 up to 42.40 Gy or single dose 2 to 50 Gy plus boost with electrons single dose 2.5 up to 10 Gy. So we evaluated the DVHs of each treated patient. Both during and after treatment, the onset, the location, and the degree of cutaneous toxicity were recorded.

#### Results

The evaluation of the DVH and of the dosimetry of each patient, regardless of the fractionation used, showed the presence of hot spots with respect to the prescribed dose for 51 of the 204 aforesaid patients even in the presence of normal dosimetrics for the remaining parameters that usually are considered. Reviewing the outlines made it was possible to highlight that the presence of such dose peaks may be due to various factors such as the size or shape of

the breast. 56 patients (27%) reported acute G2/G3 toxicity; 35 pts. in the ipsilateral axillary area and submammary line, 21 patients recorded (10% of total) G2 toxicity but affecting the whole breast. In any case, the presence of hot areas only in some points did not allow us to understand the onset of toxicity on the whole mammary area. From these data for this group of patients it was necessary to use a more aggressive topical therapy. No patient discontinued treatment. The post-treatment cosmetic result at a median follow-up of 8 months showed no permanent damage.

#### Conclusion

The possibility of having an instrument such as DVH to predict acute toxicity also allows to put in action for selected patients those actions useful to avoid the toxicity onset, first of all with the use of new treatment methods able to limit the number of hot spots. The combination of clinical and radiotherapy techniques knowledges allows the identification of new methodological approaches to avoid functional imperfections and limitations, limited to the duration of treatment. The 3D conformational technique used by us has allowed a decrease in toxicity compared to the data reported in the literature, but does not always allow homogeneity of the treatment. Even the continuous use of topical supportive therapy should not be underestimated.

#### EP-2204 The impact of breast irradiation using thermoplastic mask on quality of life

A. DINU<sup>1</sup>, T. Flonta<sup>1</sup>, L. Marcu<sup>2</sup>

<sup>1</sup>County Hospital "Gavril Curteanu", Radiotherapy, Oradea, Romania; <sup>2</sup>Faculty of Science- University of Oradea- Romania School of Physical Sciences- University of Adelaide- Australia, Medical Physics, Oradea- Adelaide, Romania

#### Purpose or Objective

The critical role of thermoplastic mask in patient immobilization during breast irradiation is well known. However, these immobilizing casts can have a buildup effect which augments the skin dose, thus leading to unwanted adverse events. The purpose of this study is to evaluate these adverse events and their impact on patient's quality of life (QoL).

#### Material and Methods

For patients with large and pendulous breasts the prone setup represents the ideal solution for an accurate immobilization, which can be achieved either with a designated board or using thermoplastic masks. The study included 42 patients, between the ages of 32-60, where 21 patients were irradiated with the mask, while the other 21 underwent breast irradiation without mask. Dose prescription for both groups was 50Gy in 25 fractions to the whole breast CTV and boost dose to the tumour bed of 60 Gy in 25 fractions. At the start of therapy all patients were informed about possible adverse events, particularly of radiodermatitis, as well as other risk factors (sun exposure, smoking, the use of inadequate ointments on the lesion). During the course of treatment, the radiation therapists used both verbal questioners and physical examination of the irradiated skin to be assured that the physicians' recommendations were followed. The main targeted aspects were: (1) the grade and time interval to radiodermatitis, (2) the impact of radiodermatitis on patient's quality of life. Radiodermatitis was visually evaluated using the RTOG criteria

#### Results

Without thermoplastic mask, skin erythema developed after 10-14 days from the start of treatment, all patients developing grade 1/2 radiodermatitis by the end of therapy. When irradiated with the thermoplastic mask, skin erythema was installed after the 7<sup>th</sup> day of treatment, grade 1 radiodermatitis after 26-30Gy, while by the 4<sup>th</sup> treatment week grade 2 radiodermatitis was present in all patients. By the end of treatment, 3 patients (14.3%)

developed grade 3 radiodermatitis. The QoL was directly proportional to the initiation of radiodermatitis. Local discomfort lead to insomnia, anguish and mild depression, with more pronounced depressive episodes in women aged 32-40 years. Five patients presented with skin telangiectasia. While irradiation-induced fatigue together with the above adverse events decreased their QoL on the short term, 6-month post-therapy radiodermatitis has cleared, leaving only a light depigmentation on the breast skin. All patients confirmed an increased QoL with the disappearance of dermatitis.

#### Conclusion

There is a clear dependence between radiodermatitis and breast cancer patients' QoL. The impact of adverse events on QoL can be diminished with the supportive care of the radiation therapists and physicians. The role of thermoplastic mask to reduce positioning errors and increase the therapeutic index outweighs the risk of adverse events and their impact on QoL.

#### EP-2205 Patient involvement in developing research-based patient information on proton therapy

A. Kristensen<sup>1</sup>, H. Hansen<sup>1</sup>

<sup>1</sup>Aarhus University Hospital, Danish Centre for Particle Therapy, Aarhus N, Denmark

#### Purpose or Objective

No previous patient information material on proton therapy has been developed in a Danish setting.

A new centre for particle therapy is currently being established, and patient involvement is a fundamental value both during this process and will be in the future running of the centre.

The purpose of this project was:

- To test whether patient involvement as a method can be used in the development of research-based patient information.
- To identify possible differences in patient information aimed at children, adolescents and adults.

#### Material and Methods

Qualitative semi-structured interviews were conducted with seven adults (18-55 years) and eight families with children and adolescents (2-18 years). The adult interviewees and the children/adolescents had received proton treatment abroad within the last two years.

Qualitative content analysis inspired by Ricoeur was used to analyse the collected data. The emerging themes were discussed by the authors and consensus was reached.

To ensure compliance between interview data and the actual patient information material and to ensure the quality, a user panel consisting of some of the interviewees will be organised.

#### Results

The following main themes needed to be covered in the patient information:

- The difference between proton and photon therapy; what protons are and when protons are preferred.
- Illustrations of the equipment used in the treatment, making of the mask, how scans and treatment are performed as well as arguments for deliberately planning sometime between first visit and start of treatment.
- Knowledge about possible side effects and their effect on the patient's life during and after end of treatment.
- Information about practical issues (transportation and accommodation during course of treatment).

#### Conclusion

Patient involvement as a method is useful to ensure representation of the patient perspective when developing research-based patient information.

#### EP-2206 How long should men abstain from receiving anal sex following treatments for prostate cancer?

S. Ralph<sup>1</sup>, C. Richardson<sup>2</sup>

<sup>1</sup>NHS, The Clatterbridge Cancer Centre NHS Foundation Trust, Bebington, United Kingdom; <sup>2</sup>University of Manchester, Division of Nursing- Midwifery and Social Work, Manchester, United Kingdom

#### Purpose or Objective

To develop UK guidance on how long men should abstain from receiving anal sex before, during, and after investigations and treatments for prostate cancer.

#### Material and Methods

A modified Delphi technique utilising two question rounds was employed in order to generate consensus opinion from a panel of 15 clinical oncologists and 11 urological surgeons who specialise in the diagnosis and treatment of prostate cancer.

#### Results

The overwhelming consensus from panel members was yes men should abstain from receiving anal sex before, during, and after investigations and treatments for prostate cancer (table 1). The consensus and consensus level for how long should men abstain was: 1 week before a PSA test (n=15 / 58%); 2 weeks after a transrectal ultrasound guided biopsy (n=6 / 55%); 1 week after a transperineal biopsy (n=6 / 60%); 6 weeks after a radical prostatectomy (n=5 / 45%); yes during external beam radiotherapy (n=11 / 73%) and for 2 months after (n=4 / 40%); and 2 months after high-dose rate brachytherapy (n=3 / 60%). Panel members failed to reach consensus on how long men should abstain from receiving anal sex after the insertion of fiducial marker and permanent seed brachytherapy.

Table 1: Consensus summary table for should men abstain from receiving anal sex...?

Should men abstain from receiving anal sex:	Consensus (n / %)
Following a transrectal ultrasound guided biopsy?	Yes (10 / 90.9%)
Following a transperineal biopsy?	Yes (8 / 72.7%)
Following a radical prostatectomy?	Yes (10 / 90.9%)
After the insertion of fiducial markers?	Yes (9 / 60.0%)
Whilst undergoing a course of external beam radiotherapy?	Yes (11 / 73.3%)
After completing a course of external beam radiotherapy?	Yes (11 / 73.3%)
Following permanent seed brachytherapy?	Yes (4 / 100.0%)
Following high-dose rate brachytherapy?	Yes (5 / 100.0%)

#### Conclusion

Men should abstain from receiving anal sex before, during, and after investigations and treatment for prostate cancer in order to avoid receiving a false positive PSA test; manage their side effects appropriately; minimise radiation exposure to sexual partners; and to minimise the risk of developing post-intervention complications. The data from this study has been used by the charity Prostate Cancer UK to update their patient information publication 'Prostate cancer tests and treatment: A guide for gay and bisexual men'.

#### EP-2207 PROMS: Transperineal insertion of prostate markers - results from a prospective clinical trial

A. O'Neill<sup>1,2</sup>, K. Crowther<sup>1</sup>, D. Mitchell<sup>1</sup>, S. Jain<sup>1,2</sup>, A. Hounsell<sup>1,2</sup>, J. O'Sullivan<sup>1,2</sup>

<sup>1</sup>Belfast Health and Social Care Trust, Radiotherapy, Belfast, United Kingdom; <sup>2</sup>Queens University Belfast, Centre for Cancer Research and Cell Biology, Belfast, United Kingdom

#### Purpose or Objective

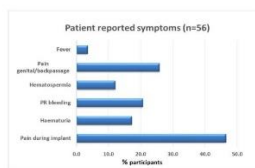
Surgical insertion of fiducial markers (FMs) is an important component of image guided radiotherapy for prostate cancer and has similar risks to that of prostate biopsy including pain, bleeding, and infection. The procedure is usually performed on an outpatient day case basis using a transurethral ultra-sound (TRUS). We report our experience of FM insertion and patient feedback on acute effects from a prospective clinical trial.

### Material and Methods

A prostate prospective clinical trial required all participants to have prostate FMs. All participants were invited to complete a simple questionnaire designed to capture their experience of FM insertion and any side effects they experienced within 1 week of implantation. FM insertion was performed trans-perineally under TRUS guidance using local anaesthetic and antibiotic prophylaxis.

### Results

58 participants were each implanted with three gold FMs, verified on CT planning scan. A total of 56 out of 58 (97%) questionnaires were returned. An overall summary of patient reported symptoms following FM implantation are given in Figure 1.



### Conclusion

In our centre, FM insertion is well tolerated. Acute side effects were mild to moderate and in general were transient, resolving within a few days. Grade >3 toxicity was rare and self-managed with the use of simple analgesics. Efforts to standardise patient preparation, implantation procedures and data collection to allow meaningful comparison and inform best practice are needed.

### EP-2208 Evaluating the efficacy of the Cancer Nurse Consultant Role for Radiotherapy Oncology inpatients

M. Rolfo<sup>1</sup>, T. Pearce<sup>2</sup>, J. Armstrong<sup>3</sup>, M. Guiney<sup>4</sup>, S. Ryan<sup>3</sup>  
<sup>1</sup>Genesiscare UK, Radiation Oncology, Berkshire, United Kingdom; <sup>2</sup>GenesisCareUnited Kingdom, Radiation Oncology Berkshire, United Kingdom; <sup>3</sup>GenesiCare Australia, Radiation Oncology, Melbourne, Australia; <sup>4</sup>GenesisCare Australia, Radiation Oncology, Melbourne, Australia

### Purpose or Objective

A pilot study to validate the implementation of a Cancer Nurse Consultant (CNC) role in a busy tertiary cancer centre in improving the patient experience, providing clinical expertise and coordinating all aspects in relation to the delivery of radiotherapy treatment to inpatients.

### Material and Methods

This pilot study was conducted in 2017 in a major tertiary hospital with over 800 inpatient beds and a comprehensive oncology program covering many tumour streams. In this evaluation, the CNC participated in the Multi-Disciplinary Team Meetings (MDTM) to initiate timely interventions and proactively manage the continuum of care for inpatients undergoing radiotherapy (RT). Participation of the CNC in MDTMs was postulated to enable better coordination and implementation of earlier interventions and create a efficient pathway for the patient to access care. Inpatients satisfaction termed a Net Promoter Score (NPS) metrics were taken

### Results

The evaluation demonstrated that the CNC was able to intervene earlier in the patient pathway and ensure that the time from MDT to treatment initiation was reduced by an average of 2 days. Findings included:

1. Collaborative model of care and engagement between Oncologists, CNC and the treating team to optimise patient outcomes.
  2. Patients were able to be identified earlier in the pathway, with a radiotherapy care plan initiated immediately post MDTM.
  3. Inpatient nursing reviews identified patient care needs which were incorporated into the treatment pathway.
  4. Toxicity management was assessed and initiated by the CNC who collaborated with inpatient clinicians, influencing earlier discharge.
  5. Coordination of multimodality treatment and providing education to patients, carers and MDT members and other relevant stakeholders.
  6. Minimising the administrative responsibility and burden on the Medical/Radiation Oncologists guides the appropriate skillset utilisation of all members of the MDT, and efficiently manages the process requirements associated with treatment initiation.
  7. Tumour specific initiatives such as a Head & Neck Allied Health MDTM were established to able the MDT to collaboratively manage toxicities and patient supportive measures.
- NPS improved from 67% to 100%.

### Conclusion

The study indicated that the RT CNC demonstrated significant efficiencies, in reducing diagnosis to treatment start time through a collaborative and coordinated approach. The results suggest that the CNC plays a key role in providing clinical expertise, establishing and embedding external relationships and integration within a large tertiary hospital. After the pilot evaluation the CNC role has been implemented at other affiliated institutions. Further investigation will continue evaluating metrics on all aspects of the inpatient oncology service.

### Electronic Poster: RTT track: Education and training/role development

### EP-2209 Non-medical prescribing for Therapeutic Radiographers - extending roles and advancing practice

H. Nisbet<sup>1</sup>  
<sup>1</sup>Oxford University Hospitals NHS Foundation Trust, Radiotherapy Department, Oxford, United Kingdom

### Purpose or Objective

Legislation has been in place in the UK to allow Therapeutic Radiographers to train as supplementary prescribers (SP) and the role has been successfully undertaken since 2005. Since March 2016 Therapeutic Radiographers can train as independent prescribers and this has been supported by the Royal College of Radiologists citing a positive patient experience, a more streamlined patient pathway and a sharing of the pressures of the clinical team's workload as just some of the very substantial benefits. One Advanced and two Consultant Therapeutic Radiographers at our Cancer Centre completed their qualification to become independent prescribers (IP) in June 2017. The objective of this poster is to outline the training pathway, scope of practice and clinical model for Therapeutic Radiographer non-medical prescribers (NMP) and to detail the advantages of this role.

### Material and Methods

The NMP must undergo an approved post-registration training programme that meets the prescribing standards set by the Health Professions Council before being annotated as an IP/SP on the register in order to be able to prescribe. As with most Trusts, the NMP must also be accepted into the role by the Trust's NMP lead for indemnity purposes. They may prescribe any licensed medicine for any condition within national and local

guidelines, the practitioner's area of expertise and competence, and the overarching framework of the treatment of cancer. NMPs within our cancer centre run independent clinics to review and treat patients who require the support and management of radiotherapy treatment related conditions and toxicities before, during and after their course of radiotherapy treatment. NMPs work in close liaison with other healthcare professionals to ensure safe and effective treatment is prescribed and administered to patients to manage common radiotherapy toxicities and complications such as skin reactions, oral mucositis, pain, diarrhoea, constipation and emesis.

#### Results

The introduction of NMPs supports the delivery of a seamless review service within this Cancer Centre. This benefits the patient by improving the patient pathway, reducing the need for repeated assessment and review, enhancing patient care, supporting the multi-disciplinary team and using the skills of the workforce more effectively. Since June 2017 NMP prescribing practice has averaged upwards of 10 prescriptions a week equating to a minimum saving of 3 hours of oncologist time otherwise spent in consultation and prescribing activity.

#### Conclusion

NMPs can provide a more holistic approach to patient care, a smoother patient pathway, provide improved accessibility to appropriately prescribed medication and release pressures on the oncologists' workload.

#### EP-2210 Building a respiratory synchronization model in the CK System during the RT session of liver metas

K. Szczepanik<sup>1</sup>, A. Grzadziel<sup>2</sup>, B. Jochymek<sup>1</sup>, D. Bodusz<sup>1</sup>, E. Telka<sup>1</sup>, M. Kijonka<sup>3</sup>

<sup>1</sup>Maria Sklodowska-Curie Memorial Cancer Center and Institute of Oncology, Radiotherapy, Gliwice, Poland;

<sup>2</sup>Maria Sklodowska-Curie Memorial Cancer Center and Institute of Oncology, Planning Radiotherapy and Brachytherapy, Gliwice, Poland; <sup>3</sup>Maria Sklodowska-Curie Memorial Cancer Center and Institute of Oncology, Medical Physics, Gliwice, Poland

#### Purpose or Objective

The aim of this work is to show the building of a respiratory model used for radioablation of liver metastases using tracing of implanted markers using the Synchrony Respiratory Tracking System.

#### Material and Methods

The CyberKnife system (Accuray Inc., Sunnyvale, CA) enables irradiation of patients using the internal markers tracking method with respiratory synchronization.

The patients who are qualified for radioablation of liver metastases are implanted with 3 markers. After preparing the external stabilization, performing the CT (the patient should wear the Synchrony Tracking Vest) and performing the treatment plan in the MultiPlan system, and then can start irradiation. The process of preparing the patient for treatment includes the implementation of an individual external stabilizer and treatment planning based on the CT examination in the Synchrony Tracking Vest System. To build a respiratory model, it is necessary to put on the Synchrony Tracking Vest patient's vest and attach to it three external markers (Tracking Markers), whose movement, consistent with the patient's breathing movements, is recorded by means of X-ray lamps. After locating external and internal markers, it is possible to start building a breathing model. This is done using the Synchrony Respiratory Tracking System. The respiratory model is built on the basis of 6-8 verification imagines.

#### Results

Irradiation of metastases to respiratory organs (including the liver) using the Synchrony System enables precise treatment of the appropriate radiation dose with the saving of healthy tissues. Continuous control of the patient's position and correlation of the respiratory movements with the motion of the accelerator head are

the main advantages of the Synchrony Respiratory Tracking System of the CyberKnife System.

#### Conclusion

Irradiation of metastases to respiratory organs (including the liver) using the Synchrony System enables precise treatment of the appropriate radiation dose with the saving of healthy tissues. Continuous control of the patient's position and correlation of the respiratory movements with the motion of the accelerator head are the main advantages of the Synchrony Respiratory Tracking System of the CyberKnife System.

#### EP-2211 Impact of virtual learning environment on students' satisfaction, engagement, recall and retention

E. Ryan<sup>1\*</sup>, C. Poole<sup>1</sup>

<sup>1</sup>TCD Division of Radiation Therapy, Radiation Therapy, Dublin, Ireland

#### Purpose or Objective

Virtual Learning Environments (VLEs) were introduced to progress students from passive to active learners. Active learning promotes the critical thinking skills essential for the transfer/use of classroom-acquired knowledge into the clinical setting. Virtual reality forms an increasingly vital component of clinical skills development in a range of disciplines.

#### Material and Methods

A randomised control trial was conducted with students randomly attending one of two teaching sessions about radiation therapy. Both sessions were identical except a VLE was used in the second talk with the first being solely didactic. Anonymous questionnaires were distributed. Two weeks after the talks, participants were required to complete the same knowledge questionnaire to determine retention. Mann-Whitney, means, standard deviations and chi-squared tests were employed according to data characteristics. Qualitative data (open-ended questions) was analysed thematically.

#### Results

Virtual learning seemed to significantly improve students' satisfaction/engagement and recall (n40). The student group taught using the VLE had higher mean scores for retention compared to the didactic group however this was not statistically significant. Students' learning styles seemed to have no effect on their satisfaction/engagement and ease of learning. Three key themes emerged from the qualitative data, (1) the visuals were good/helpful, (2) the talk was informative, and (3) more detail/visuals were required.

#### Conclusion

Incorporating virtual learning into education suggests an enhanced student experience with increased levels of engagement, satisfaction and recall. This study adds to and supports current research which illustrates there is a role for VLEs in teaching. Future research is required to determine if VLEs produce a long-term impact on student's retention of knowledge.

#### EP-2212 Piloting an educational framework for the enhanced role of RTTs in MRI-guided adaptive radiotherapy

C. Eccles<sup>1</sup>, J. Webb<sup>1</sup>, A. Flynn<sup>1</sup>, A. McWilliam<sup>2</sup>, A.

Sanneh<sup>1</sup>, M. Van Herk<sup>2</sup>, A. Choudhury<sup>2</sup>, M. Aznar<sup>2</sup>

<sup>1</sup>The Christie, Radiotherapy, Manchester, United Kingdom; <sup>2</sup>University of Manchester, Radiotherapy Related Research, Manchester, United Kingdom

#### Purpose or Objective

To develop and implement a framework to support the enhanced role RTTs delivering MRI-guided adaptive radiotherapy.

### Material and Methods

A team of MRI radiographers and RTTs was assembled to realise radiotherapy treatments on a hybrid MRI-linear accelerator (MR-Linac) and to pilot a program of learning, for safe, effective MR-Linac based research and treatment. We followed a scoping exercise to determine a framework of knowledge, skills and competence required for the enhanced role of RTTs working in MRI-guided adaptive radiotherapy. A gap analysis and survey of existing educational programs that could bridge gaps in knowledge were undertaken. Where no didactic or practical programs were available an in-house program was developed to fulfill the framework requirements. The program includes directed self-study, didactic and practical competency-based experiences.

### Results

From the scoping exercise it was determined the framework should include: a) MRI safety and screening, b) MR image formation/acquisition, c) MRI image interpretation, d) multi-modality image registration, e) radiotherapy specific imaging needs (e.g., geometric fidelity), f) MRI safe patient positioning, g) target and normal tissue segmentation and/or segment manipulation, and h) treatment plan evaluation. The survey of existing educational programs found a) several UK-based higher education institutions (HEIs) with suitable courses offering graduate level modules in MRI physics and clinical applications, that include basic MRI safety, with some including MRI-based anatomy, b) an international peer-to-peer MRinRT program and c) online MRI/multi-modality anatomical atlases that are suitable for inclusion in this framework of blended learning. All HEI programs included knowledge assessments, however, it was decided online-based learning and MRI screening should be appraised as competencies gained through practical experience. Formal programs in the specific imaging and positioning for radiotherapy were lacking, therefore tutorials and practical competencies will be developed to teach and assess this body of knowledge and skills. To date 12 tutorials are available, each with a question-based assessment, and competency profile to be included in each learner's portfolio of evidence. To embed competence in image registration, segmentation, and treatment plan assessment, practical tutorials and inter-observer variability studies supplemented by interdisciplinary discussions with clinicians and physicists experienced in treatment planning are planned.

### Conclusion

The safe, effective realisation of MRI-linear accelerator technologies requires an enhanced RTT portfolio, a formal framework for which does not yet exist in the UK. Using a scoping exercise and gap analysis, we have been able to define a preliminary framework for a blended learning experience that is currently being piloted in our institution. Following the pilot, a mixed method model will be used to evaluate its effectiveness and inform the program's evolution.

### EP-2213 An evaluation of radiotherapy students' perceptions of research and evidence-based practice

S. Ketterer<sup>1</sup>

<sup>1</sup>University of Liverpool, Department of Radiotherapy-School of Health Sciences, Liverpool, United Kingdom

### Purpose or Objective

Engagement with research is recognised as a pre-requisite for professional registration as a therapy radiographer. Educational programmes have an obligation to support and develop autonomous and reflective thinking, and evidence-based practice, as modern careers in radiotherapy require active engagement in research, and the generation of primary research data, in order to challenge the current evidence base and to optimise approaches to both treatment delivery and patient care. This study aims to evaluate how all three year groups

within a radiotherapy undergraduate degree course perceive the role of research within their future clinical practice, and looks to identify any changing attitudes of students to research as they progress through their undergraduate studies. A further objective is to examine if there are particular learning interventions that maximise student engagement with research.

### Material and Methods

A qualitative approach was adopted with students from all three years of an undergraduate BSc Radiotherapy programme invited to participate in individual year group focus group sessions. Each session was audio recorded, transcribed into an anonymous script, and subjected to thematic analysis.

### Results

A total of 17 students participated. Students recognised research as part of the role of a therapy radiographer, but did not always explicitly identify research activities within day-to-day work. Each year group had a strong focus on current academic research tasks, for example dissertation projects. Some could see the benefits of laying foundations in research methodology, although this was generally seen as an arduous process. Motivation and excitement around research had been observed in the clinical setting, but students felt this was largely amongst a minority of staff. There were multiple references to utilisation of practical, interactive, "real-world" examples in order to make research learning more relevant.

### Conclusion

The evidence-based nature of radiotherapy was welcomed, but only a minority of students appeared eager to accept active research involvement as part of their future roles. The challenge for educators, which emerged, is to inject excitement for research into the academic setting, so students feel ownership of and immersed in the topic, and can develop positive attitudes towards continuous questioning of practice to carry forward into the clinical environment.

---

### Electronic Poster: RTT track: Risk management/quality management

---

### EP-2214 Assessing the evidence for proton therapy in prostate cancer

T. Chan<sup>1</sup>, P.W. Tan<sup>1</sup>, J.I. Tang<sup>1</sup>

<sup>1</sup>The National University Cancer Institute- Singapore NCIS, Radiation Oncology, Singapore, Singapore

### Purpose or Objective

Proton beam therapy (PBT) has evolved significantly with respect to its use in prostate cancer. Pencil beam scanning, an advanced technique of PBT is often used in many centers. Growing interest and controversy regarding its use has resulted in PBT being closely scrutinized. The plethora of evidence suggests that PBT is effective and safe for early stage prostate cancer. However, it is still unknown whether the theoretical dosimetric advantages of PBT translate into meaningful clinical improvements over routine intensity-modulated radiation therapy, which is commonly used for this patient group.

### Material and Methods

A systematic search using MEDLINE/PubMed and MeSH headings was used to identify articles addressing RT techniques with for early stage prostate cancer. The headings were prostate cancer, radiation therapy, proton therapy and intensity modulated radiation therapy. Eligible articles include articles about 1) prostate cancer RT; 2) RT associated toxicities; 3) advances in treatment delivery and 4) published in an English language peer-reviewed journal. Articles were excluded if they provided

pilot data, descriptions of a study design and articles on non-prostate cancer data.

**Results**

85 eligible articles were identified. Early trials on prostate cancer utilizing PBT demonstrated mixed results upon comparison with the routinely used IMRT. The systematic search highlighted the growing popularity and interest in PBT, demonstrated controversy on the efficacy of PBT, compared its clinical and cost-effectiveness and revealed advances in its delivery.

Table 1: Comparing treatment rates in Dose Escalation Randomized Controlled Trials

Study	Beam Modality	Planning Technique	Low dose Arms Gy	High dose Arms Gy	Median follow up (mo)	No of patients analyzed	Toxicity Scale	Grade 1-2 Toxicity, %		Grade 3-5 Toxicity, %	
								Low dose	High dose	Low dose	High dose
Zalman et al (2005) <sup>10</sup>	Protons	Conformal	70.2	79.2	5.5	385	RTDQ	1.9	8.0	1.0	1.0
Zalman et al (2015) <sup>11</sup>	Protons	Conformal	70.2	79.2	8.9	385	RTDQ	9	1.0	2.0	2.0
Cheer et al (2011) <sup>12</sup>	Protons	Conformal	No comparison available	82.0	2.6	85	RTDQ/ORTC	No comparison available	1.6	No comparison available	2.0
Peters (2006) <sup>13</sup>	Protons	Conformal/IMRT	80.0	76.0	4.2	669	RTDQ	4.9	8.0	12.0	13.0
Chen et al (2007) <sup>14</sup>	Protons	Conformal	84.0	74.0	5.3	843	RTDQ/LENTISSOM/ UCLA PCI	6.9	10.3	2.0	4.0
Al-Mangest et al (2006) <sup>15</sup>	Protons	Conformal	80.0	76.0	5.6	666	RTDQ/ORTC	4.9	6.0	12.0	13.0
Kilian et al (2008) <sup>16</sup>	Protons	3D Conformal	70.0	76.0	6.7	304	RTDQ/ENT	1.9	7.0	5.0	3.0
Snyder et al (2010) <sup>17</sup>	Protons	Conformal	84.0	74.0	5.0	843	RTDQ/LENTISSOM/ RMI	6.9	8.0	No results available	No results available
Backlund et al (2011) <sup>18</sup>	Protons	Conformal	70.0	80.0	5.1	306	RTDQ	1.9	6.9	2.6	1.9

RTDQ: Radiation therapy toxicity group; ORTC: European Organization for Research and Treatment of Cancer; LENTISSOM: Late Effects of Normal Tissue: Subjective, Objective, Management; RMI: Royal Marsden Hospital assessment score; UCLA PCI: University of California, Los Angeles Prostate Cancer Index; UCLA PCI score.

**Conclusion**

Literature demonstrated that the unique physical properties of protons allow dose escalation to the prostate while effectively sparing neighboring normal tissue structures. Theoretically, this allows for better disease control while minimizing toxicities and second malignancies. This allows a dosimetric advantage over photon IMRT. Existing literature consist of prospective Phase II trials and retrospective studies. These articles demonstrated favorable outcomes for early stage prostate cancer utilizing PBT. PBT is significantly expensive. This remains a barrier to its widespread use. To date, the cost-effectiveness of PBT remains conflicting. Its cost-effectiveness requires more study. More studies are needed for a better estimation. Ongoing trials directly comparing PBT with photon EBRT will hopefully elucidate the value of PBT for early stage prostate cancer. Unless there is overwhelming evidence for the clinical superiority of PBT over present advanced techniques, the case for PBT remains questionable.

# Radiotherapy & Oncology

Journal of the European Society for  
Radiotherapy and Oncology

## INFORMATION FOR AUTHORS

ARTICLES should deal with original research or reviews of topics defined in the aims of the journal. Radiotherapy and Oncology publishes original material only. It is therefore understood that the content of the paper has not previously been published in the same or a similar form and that it is not under consideration for publication elsewhere. The act of submitting a manuscript to the journal carries with it the right to publish that paper.

Radiotherapy and Oncology uses an online manuscript submission and peer review process.

Papers and correspondence should be submitted online at <http://www.ees.elsevier.com/ro> and the instructions on the site should be closely followed. Authors may submit manuscripts and track their progress to final decision. Reviewers can download manuscripts and submit their reports to the Editors electronically.

The full contact details for the Editorial Office are shown below:

**Professor Michael Baumann, Editor-in-Chief, Radiotherapy & Oncology Editorial Office, Deutsches Krebsforschungszentrum (DKFZ), Im Neuenheimer Feld 280, 69120, Heidelberg, Germany (E-mail: [RadioTherOncol@dkfz.de](mailto:RadioTherOncol@dkfz.de)).**

### TYPES OF PAPERS

#### 1. Full length original papers (max. 3000 words)

Describe original scientific work in the field of radiation oncology or related areas. The content of the paper should be sufficient to reach valid conclusions. Full papers should include a structured abstract and be divided into sections (Introduction; Materials and Methods; Results; Discussion; References; Tables; Figures) and should not normally exceed 6 printed pages, including references and a maximum of 6 tables/figures. Additional material can be submitted as supplementary files.

#### 2. Short communications and Technical notes (max. 2000 words)

Provide a brief but complete account of a particular piece of work, e.g. Phase I or II study, and should in total be no longer than 4 printed pages, normally including a maximum of 2 figures or tables. A summary of not more than 50 words should be included (not a structured abstract), but the manuscript can have fewer subheadings (e.g. short introduction; materials and methods; results and discussion). Authors are advised to see a recent issue of the journal for size and lay-out.

#### 3. First in Human – Translational innovations in radiation oncology (max. 3000 words)

These papers should follow the same format as for short communications or full length original research articles. The introduction must focus on the clinical translational need for further clinical studies and the preclinical translational history for the benefit of a general audience; recent papers illustrating the problems with the current clinical situation should underpin this. Materials and Methods may be brief. Only prospective trials that have undergone review by the appropriate review board or ethical committee and, if applicable by national or European law, will be considered. Statements indicating compliance with these laws need to be included in the materials and methods sections. Results may be brief but must show (with practical examples, photos, other appropriate illustrations) how this innovation is applied in the clinic. Discussion may be brief, does not need to discuss the limitation given by low patient numbers (as this applies to all papers in this section) but must end with a brief and very clear statement on "clinical translational relevance" also including an outlook on the necessary next steps. Please avoid terminology such as "pilot trial" – make clear that this is a significant innovation (and why).

#### 4. Review articles

Rigorous critical assessment of clinical and/or laboratory research in a field of interest to the journal and its subscribers. Reviews are normally solicited by the editors, and it is suggested that authors wishing to contribute a review article contact the editor-in-chief.

#### 5. Editorials and commentaries

Editorials and commentaries relate to articles in the journal or to issues of relevance for the readership. This type of communication is normally solicited by the editors.

#### 6. Letters to the Editor

On topics of current interest or comment upon material previously or simultaneously published in the journal. They should be limited to 500 words and may include 1 table or figure.

#### 7. Announcements

The inclusion of announcements, etc. is at the discretion of the Editors and the Publisher and subject to space availability. Request for inclusion of meeting announcement should be sent to the ESTRO secretariat (see address in journal).

### Author inquiries

For inquiries relating to the submission of articles (including electronic submission where available) please visit this journal's homepage at <http://www.elsevier.com/locate/radonc>. For detailed instructions on the preparation of electronic artwork, please visit <http://www.elsevier.com/artworkinstructions>. Contact details for questions arising after acceptance of an article, especially those relating to proofs, will be provided by the publisher. You can track accepted articles at <http://www.elsevier.com/trackarticle>. You can also check our Author FAQs at <http://www.elsevier.com/authorFAQ> and/or contact Customer Support via <http://service.elsevier.com>

**Language services.** Authors who require information about language editing and copyediting services pre- and post-submission please visit <http://webshop.elsevier.com/languageediting> or our customer support site at <http://service.elsevier.com>.

A full and complete Guide for Authors is available online at  
<http://www.thegreenjournal.com>

